Effect of Triacylglycerol Structure on Absorption and Metabolism of Isotope-Labeled Palmitic and Linoleic Acids by Humans

E.A. Emken[a,*], R.O. Adlof[a], S.M. Duval[a], J.M. Shane[b], P.M. Walker[b], and C. Becker[c]

[a]USDA, ARS, NCAUR, Peoria, Illinois 61604, [b]Illinois State University, Normal, Illinois 61790, and [c]Pelikan Technologies, Inc., Palo Alto, California 94303

ABSTRACT: The effect of dietary TAG structure and fatty acid acyl TAG position on palmitic and linoleic acid metabolism was investigated in four middle-aged male subjects. The study design consisted of feeding diets containing 61 g/d of native lard (NL) or randomized lard (RL) for 28 d. Subjects then received an oral dose of either 1,3-tetradeuteriopalmitoyl-2-dideuteriolinoleoyl-*rac*-glycerol or a mixture of 1,3-dideuteriolinoleoyl-2-tetradeuteriopalmitoyl-*rac*-glycerol and 1,3-hexadeuteriopalmitoyl-2-tetradeuteriolinoleoyl-*rac*-glycerol. Methyl esters of plasma lipids isolated from blood samples drawn over a 2-d period were analyzed by GC–MS. Results showed that absorption of the ^{2}H-fatty acids (^{2}H-FA) was not influenced by TAG position. The ^{2}H-FA at the 2-acyl TAG position were 85 ± 4.6% retained after absorption. Substantial migration of ^{2}H-16:0 (31.2 ± 8.6%) from the *sn*-2 TAG position to the *sn*-1,3 position and ^{2}H-18:2n-6 (52.8 ± 6.4%) from the *sn*-1,3 position to the *sn*-2 position of chylomicron TAG occurred after initial absorption and indicates the presence of a previously unrecognized isomerization mechanism. Incorporation and turnover of the ^{2}H-FA in chylomicron TAG, plasma TAG, and plasma cholesterol esters were not influenced by TAG acyl position. Accretion of ^{2}H-16:0 from the *sn*-2 TAG position in 1-acylphosphatidylcholine was 1.7 times higher than ^{2}H-16:0 from the *sn*-1,3 TAG positions. Acyl TAG position did not influence ^{2}H-18:2n-6 incorporation in PC. The concentration of ^{2}H-18:2n-6-derived ^{2}H-20:4n-6 in plasma PC from subjects fed the RL diet was 1.5 times higher than for subjects fed the NL diet, and this result suggests that diets containing 16:0 located at the *sn*-2 TAG position may inhibit 20:4n-6 synthesis. The overall conclusion is that selective rearrangement of chylomicron TAG structures diminishes but does not totally eliminate the metabolic and physiological effects of dietary TAG structure.

Paper no. L9356 in *Lipids 39,* 1–9 (January 2004).

A long-standing question has been whether the *sn*-1, *sn*-2, and *sn*-3 positions of TAG influence the physiological and metabolic properties of dietary fatty acids (FA). Animal and human studies indicate that 75–80% of the FA in the *sn*-2 TAG position of dietary fats are retained during absorption and incorporation into chylomicron TAG (1–4). This positional stereospecificity is subsequently lost during chylomicron TAG clearance and incorporation into lipoprotein TAG. However, the various hydrolysis and reacylation reactions responsible for chylomicron TAG clearance and plasma TAG synthesis are nonrandom (5), and stereospecific TAG structures are produced that contain mainly saturated FA at the *sn*-1,3 positions and unsaturated FA at the *sn*-2 TAG position (4–9). This TAG restructuring process is complex, and the relative contribution and specificity *in vivo* of the lipoprotein and hepatic lipase enzymes involved have not been well-characterized.

A number of studies have investigated the effect of fatty acid position on lipoprotein and serum cholesterol concentrations. Results from recent human (10–14) and animal (15–18) studies show that differences between the fatty acid acyl position distribution in native and randomized dietary fats do not influence lipoprotein and serum cholesterol concentrations. A few studies have used specific dietary TAG structures, such as 1,3-dioleoyl-2-palmitoylglycerol, 1-palmitoyl-2,3-dioleoylglycerol, 1,3-dioleoyl-2-stearoylglycerol, and 1-stearoyl-2,3-dioleoylglycerol, to compare the influence of the *sn*-1,3 and *sn*-2 positions on fatty acid metabolism (3,19,20). The authors of these studies concluded that the *sn*-1,3 and *sn*-2 locations of FA on the glycerin backbone did not affect their metabolism.

However, dietary TAG structure has been linked to various physiological and biological effects. For example, rabbit studies have shown that increasing the saturated fatty acid content at the *sn*-2 acyl position of dietary fats increased arterial lesion formation (21,22). In rats, FA located at the *sn*-2 position were reported to be the primary source of desaturated and elongated fatty acid metabolites, and interesterified (randomized) lard diets containing less 16:0 in the *sn*-2 position produced lower TAG levels than native lard (NL) diets (23). Palmitic acid absorption by young animals (20,24,25) and infants (26,27) is higher when 16:0 is located at the *sn*-2 TAG position than at the *sn*-1,3 position. Plasma TAG clearance is reported to be slower in both animals and humans when dietary fats contain saturated FA at the *sn*-2 TAG position (4,28–31). These and other related studies are summarized and discussed in various reviews (32–34).

In this isotope tracer study, we used TAG containing ^{2}H-16:0 and ^{2}H-18:2n-6 at the regiospecific *sn*-1,3 and *sn*-2 acyl positions to investigate the metabolic effect of acyl position in human subjects that had been prefed diets containing either NL or randomized lard (RL). Lard diets were chosen because about

*To whom correspondence should be addressed at Midwest Research Consultants, 11422 Princeville-Jubilee Rd., Princeville, IL 61559.
E-mail: eaemken@npoint.net

Abbreviations: AUC, area-under-curve; CE, cholesterol ester; FA, fatty acids; ^{2}H-FA, deuterated FA; L2P4L2, 1,3-dideuteriolinoleoyl-2-tetradeuteriopalmitoyl-*rac*-glycerol; NL, native lard; P4L2P4, 1,3-tetradeuteriopalmitoyl-2-dideuteriolinoleoyl-*rac*-glycerol; P6L4P6, 1,3-hexadeuteriopalmitoyl-2-tetradeuteriolinoleoyl-*rac*-glycerol; PC, phosphatidylcholine; PC-1, 1-acyl PC; PC-2, 2-acyl PC; RL, randomized lard; TAG, triacylglycerol.

65% of the 16:0 in food-grade lard (NL) is located at the *sn*-2 TAG position vs. 33% in RL. The objectives of this human study were threefold: (i) to determine whether the location of FA at the *sn*-1,3 and *sn*-2 positions influenced their incorporation and turnover in plasma lipid classes; (ii) to investigate the effect of fatty acid position on chain-shortening, elongation, and desaturation; and (iii) to address the question of whether diets enriched with 16:0 at the *sn*-2 TAG position (NL) influence 16:0 and 18:2n-6 metabolism.

EXPERIMENTAL PROCEDURES

Study design. Four male Caucasian subjects who had participated in an NL vs. RL diet study (14) volunteered for this stable isotope study. Two subjects were from the NL group, and two were from the RL group. Each subject had consumed diets containing 61 g/d (25% of total energy) of either NL or RL for 28 d. The composition of the diets and the fatty acid distribution at the *sn*-1,3 and *sn*-2 TAG positions of the NL and RL are summarized in Table 1. Physical examinations and clinical blood profile data indicated that all subjects were in good health. Medical histories indicated no evidence of congenital ailments. The fatty acid composition of the NL and RL and the physical characteristics and plasma lipid profiles for the subjects are summarized in Table 2. The plasma lipid data listed are for blood samples drawn at the end of the 28-d diet period. Complete information on the study design, diet compositions, and other details has been described previously (14). Institutional approval was obtained for the study protocol from the Institutional Review Board for research involving the use of human subjects at Illinois State University (Normal, IL). All subjects signed written consent forms before the onset of the study.

Deuterated FA and TAG. Deuterium-labeled methyl *cis*-9,*cis*-12-octadecadienoate-12,13-d_2 (9*c*,12*c*-18:2-d_2), methyl *cis*-9,*cis*-12-octadecadienoate-15,15,16,16-d_4 (9*c*,12*c*-18:2-d_4), methyl hexadecanoate-13,13,14,14-d_4 (16:0-d_4), and methyl hexadecanoate-12,12,13,13,15,16-d_6 (16:0-d_6) were synthesized by using general procedures described previously (35). Reported procedures (36,37) were used to synthesize and purify 1,3-tetradeuteriopalmitoyl-2-dideuteriolinoleoyl-*rac*-glycerol (P4L2P4), 1,3-dideuteriolinoleoyl-2-tetradeuteriopalmitoyl-*rac*-glycerol (L2P4L2), and 1,3-hexadeuteriopalmitoyl-2-tetradeuteriolinoleoyl-*rac*-glycerol (P6L4P6).

Stable isotope study design. A mixture containing P6L4P6 (8.5 g) and L2P4L2 (15.5 g) was blended for 1 min with a warm (80°C) mixture containing 30 g of glucose, 35 g of sucrose, and 42 g of calcium-sodium caseinate in 200 mL of distilled water. After a 12-h overnight fast, each NL diet group subject was fed an equal portion of the total mixture. The weight of deuterated FA fed to each NL diet group subject was 2.57 g of 16:0-d_6, 2.36 g of 16:0-d_4, 4.04 g of 18:2-d_2, and 1.35 g of 9*c*,12*c*-18:2-d_4. Equal portions of a second mixture containing 17 g of P4L2P4, 30 g of glucose, 35 g of sucrose, 42 g of calcium-sodium caseinate, and 200 mL of distilled water were fed to each of the two subjects from the RL diet group following a 12-h overnight fast. The weight of deuterated FA fed to each RL diet group subject was 5.14 g of 16:0-d_4 and 2.22 g of 18:2-d_2. All of the above ^{2}H-fatty acid weights were adjusted for chemical and isotopic purity. All subjects were fed the deuterated fat mixture 10 min prior to receiving a no-fat breakfast at 8:00 AM. A low-fat (*ca.*15% fat calories) lunch was provided at 12:00 noon. The normal NL and RL study diets were provided for the 5:30 PM and subsequent meals. The amount of labeled fatty acid and TAG fed per kg of body weight is summarized in Table 3. Different numbers of deuterium atoms were used to label the palmitic and linoleic acids in the TAG mixture (P6L4P6 and L2P4L2) fed to the NL subjects. This multiple-isotope approach allowed identification of which FA were at the *sn*-1,3 and *sn*-2 TAG positions and provided a direct comparison of their metabolism.

Blood sampling times, lipid class isolation techniques, and analytical methods used were similiar to the procedures from a previous study (38). The positional stereospecificity of chylomicron TAG and NL and RL samples was determined by incubating the TAG with pancreatic lipase and analyzing of the isolated 2-acylmonoglycerol fraction as described previously (39).

Statistical analysis and calculations. A two-tailed, unpaired *t*-test was used to test for significant differences between NL

TABLE 1
Nutrient Content and Fatty Acid Composition of Lard Diets

Native and randomized lard diets			Fatty acid TAG position (mol%)					
			Native lard			Randomized lard		
Macronutrients	Amount	Fatty acid	Total	*sn*-1 + -3	*sn*-2	Total	*sn*-1 + -3	*sn*-2
Protein (en%)	13	14:0	1.7	1.8	1.6	2.0	2.1	1.8
Total fat (en%)	35	16:0	29.8	16.2	57.1[a]	31.4	31.9	30.6[a]
Carbohydrate (en%)	52	16:1	2.6	2.1	3.7	2.3	2.4	2.1
Cholesterol (mg/d)	272	18:0	16.4	20.3	8.5	15.5	15.6	15.2
Saturated fat (g)	38.9[b]	*t*-18:1	1.9	1.3	3.1	2.4	2.3	2.6
Monounsaturated fat (g)	38.8[b]	*c*-18:1	38.1	47.2	19.8	37.5	36.9	38.5
Polyunsaturated fat (g)	8.8[b]	18:2n-6	8.1	9.6	5.1	7.8	7.5	8.3
Lard (g)	60.7	18:3n-3	0.3	0.3	0.3	0.3	0.3	0.2
Lard (% of total fat)	71	20:1	0.6	0.7	0.4	0.5	0.5	0.5
Total energy (kcal/d)	2224	Other	0.5	0.6	0.4	0.4	0.4	0.3

[a]Percentage of 16:0 at the *sn*-2 triacylglycerol (TAG) position in native lard and randomized lard is 64 and 33%, respectively.
[b]Based on analysis of duplicate diet composites.

TABLE 2
Physical Characteristics and Plasma Lipid Profiles of Subjects

Subject[a] (number)	Age (yr)	Diet[b]	Body wt (kg)	BMI[c] (kg/m^2)	Plasma lipids: TAG (mg/dL)[d]	TAG (mg/dL)[e]	Cholesterol mg/dL)[d]	Cholesterol (mg/dL)[e]
1	35	NL	72.6	25.2	188	129	205	171
2	49	NL	99.9	23.1	155	139	268	233
3	50	RL	96.3	24.3	114	78	225	186
4	52	RL	85.8	26.3	192	173	229	234

[a]Males, nonsmokers, normal hypertensive.
[b]NL, native lard diet; RL, randomized lard diet.
[c]BMI, body mass index.
[d]Fasting plasma lipid concentrations at start of 28-d diet period.
[e]Fasting plasma lipid concentrations at end of 28-d diet period. See Table 1 for other abbreviation.

TABLE 3
Deuterated Fats Fed

Deuterated fats fed	Diet groups and subject number: Native lard Subject 1	Native lard Subject 2	Randomized lard Subject 3	Randomized lard Subject 4
^{2}H-fatty acid		(mg/kg body wt)		
16:0-13,13,14,14-d_4 (P4)	32.53	23.66	53.45	59.95
16:0-12,12,13,13,15,16-d_6 (P6)	35.41	25.75		
18:2-12,13-d_2 (L2)	55.63	40.46	23.02	25.83
18:2-15,15,16,16-d_4 (L4)	18.54	13.48		
TAG[a]				
L2P4L2	88.16	64.12		
P6L4P6	53.95	39.23		
P4L2P4			76.47	85.78

[a]L2P4L2, 1,3-dideuteriolinoleoyl-2-tetradeuteriopalmitoyl-*rac*-glycerol; P6L4P6, 1,3-hexadeuteriopalmitoyl-2-tetradeuteriolinoleoyl-*rac*-glycerol; P4L2P4, 1,3-tetradeuteriopalmitoyl-2-dideuteriolinoleoyl-*rac*-glycerol.

and RL diet group data for the same fatty acid. A two-tailed, paired *t*-test was used to test for significant differences between data for different ^{2}H-FA and for labeled FA located at different *sn* TAG positions (40). The concentration data (μg/mL) for the deuterated FA and their metabolites were normalized and area-under-curve (AUC) data calculated from time-course plots as described previously (41)

RESULTS

Absorption. The time-course curves for labeled 16:0 and 18:2n-6 incorporation into chylomicron TAG from subjects fed the NL and RL diets are shown in Figure 1. These curves provide a comparison of the relative absorption and clearance of the labeled FA in the *sn*-1,3 and *sn*-2 TAG positions. The curves for incorporation of labeled FA from the *sn*-1,3 and *sn*-2 TAG positions are essentially identical and show that TAG acyl position has no effect on 16:0 and 18:2n-6 absorption. The concentration of the ^{2}H-fatty acid at maximal incorporation (4 h) was about 25% lower for the subjects fed the RL diet than for the NL diet subjects; this observation suggests the RL diet facilitates TAG clearance.

The ^{2}H-16:0 and ^{2}H-18:2n-6 content of the chylomicron 2-acyl TAG position is plotted as the percentage of total ^{2}H-fatty acid in Figure 2 (data are normalized to 100% to facilitate comparison). The 4-h chylomicron data for both the NL and RL subjects show that 80–90% of the FA at the *sn*-2 TAG position is initially incorporated into the 2-acyl position of chylomicron TAG. The 6- and 8-h data for the NL subjects show that 31.2 ± 8.6% of the ^{2}H-16:0 incorporated at the *sn*-2 TAG position migrated to the *sn*-1 position and that 52.8 ± 6.4% of the ^{2}H-18:2n-6 incorporated at the *sn*-1 position migrated to the *sn*-2 TAG position. In contrast, ^{2}H-16:0 incorporated at the *sn*-1 and ^{2}H-18:2n-6 incorporated at the *sn*-2 positions of chylomicron TAG did not migrate and the percentages remained constant. The change in percentages was not due to preferential removal of *sn*-2 ^{2}H-FA. Relative percentage for the ^{2}H-FA in chylomicron total TAG did not change with time.

Plasma lipid class results. The time-course curves for incorporation of the ^{2}H-fatty acid in plasma TAG, cholesterol ester (CE), and phosphatidylcholine (PC) are shown in Figures 3, 4, and 5, respectively. Comparison of the plasma lipid class results for the NL and RL diet subjects suggests that the NL and RL diets did not alter the incorporation and clearance of the ^{2}H-FA. The plasma TAG curves in Figure 3 for ^{2}H-16:0 and ^{2}H-18:2n-6 from the *sn*-1 and *sn*-2 TAG positions are similar except for a small difference in concentration of ^{2}H-18:2 that was in the *sn*-1,3 TAG position (NL diet group). The plasma CE curves in Figure 4 for the *sn*-1 and *sn*-2 ^{2}H-18:2n-6 are similar, and the expected strong discrimination against

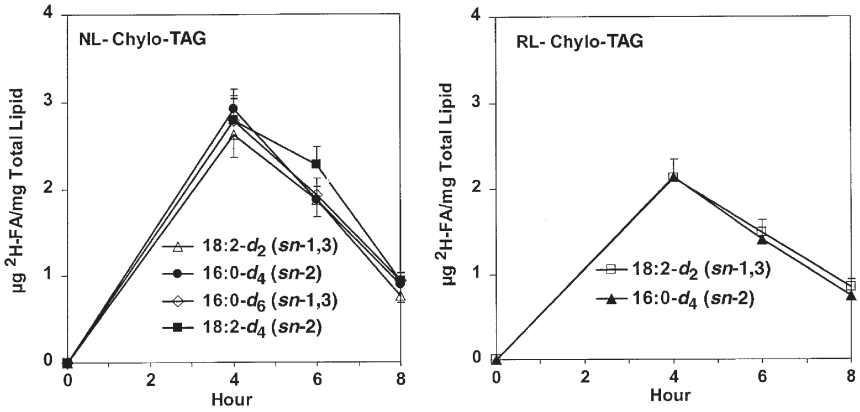

FIG. 1. Time-course plots for incorporation of deuterium-labeled 16:0 and 18:2n-6 in total chylomicron of subjects fed native (NL) and randomized lard (RL) diets. NL subjects were fed a mixture of (P6L4P6 + L2P4L2). RL subjects were fed a single deuterium-labeled triacylglycerol (TAG) (P4L2P4). Each data point is the average for data from two subjects. Error bars equal SE. Error bars are not shown when less than the size of the symbol. Data are plotted as micrograms of ^{2}H-fatty acid/mg of total chylomicron TAG/mg of ^{2}H-fatty acid fed. P4L2P4, 1,3-tetradeuteriopalmitoyl-2-dideuteriolinoleoyl-*rac*-glycerol; L2P4L2, 1,3-dideuteriolinoleoyl-2-tetradeuteriopalmitoyl-*rac*-glycerol; P6L4P6, 1,3-hexadeuteriopalmitoyl-2-tetradeuteriolinoleoyl-*rac*-glycerol.

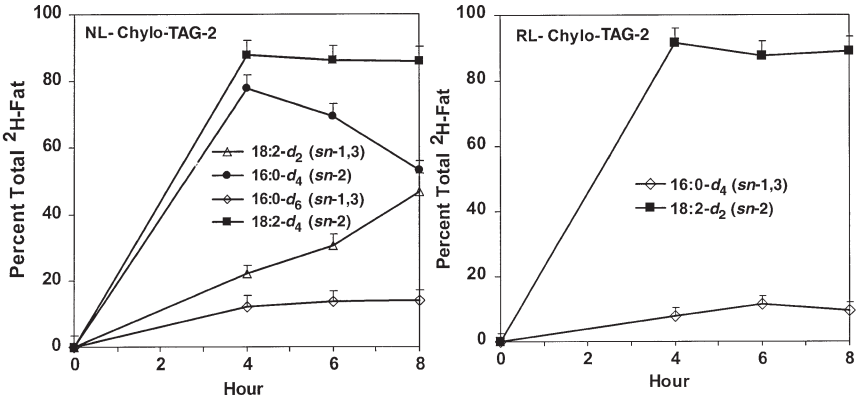

FIG. 2. Time-course plots for incorporation of deuterium-labeled 16:0 and 18:2n-6 in the *sn*-2 position of chylomicron TAG of subjects fed NL and RL diets. Each data point is the average for data from two subjects. NL subjects were fed a mixture of (P6L4P6 + L2P4L2). RL subjects were fed a single deuterium-labeled TAG (P4L2P4). Error bars equal SE. Error bars are not shown when less than the size of the symbol. For abbreviations, see Figure 1.

incorporation of ^{2}H-16:0 is nearly identical for ^{2}H-16:0 fed as *sn*-1,3 and *sn*-2 TAG. The plasma PC data in Figure 5 show that neither the *sn* positions of the FA nor dietary treatment influenced the *ca*. twofold preferential incorporation of 18:2n-6 relative to 16:0. Overall, the time-course curves for the plasma lipid classes show that the TAG acyl position had little influence on accretion or turnover of ^{2}H-16:0 or ^{2}H-18:2n-6

The total AUC data for the plasma TAG, CE, and PC time-courses (Figs. 3–5) are tabulated in Table 4. The AUC data represent a weighted average for the ^{2}H-16:0 and ^{2}H-18:2n-6 concentration data in samples collected at the seven time-points. AUC concentration data are included also for 1-acyl and 2-acyl PC (PC-1 and PC-2). Neither the dietary treatment nor the *sn* position of the ^{2}H-fatty acid significantly influenced the accretion of 16:0 and 18:2n-6 in plasma TAG and CE. However, the AUC data for ^{2}H-16:0 in PC-1 were 40.5% lower ($P < 0.09$) for the RL diet group than the NL diet group data. For the NL diet group, the ^{2}H-16:0 (*sn*-2) concentration in PC-1 was 24.5% lower ($P < 0.09$) than for ^{2}H-16:0 (*sn*-1,3). These results suggest that the NL diet structure enhanced 16:0 incorporation in PC-1 but not because 16:0 at the *sn*-2 acyl position is preferentially incorporated relative to *sn*-1,3 16:0. In contrast, the concentrations of ^{2}H-18:2n-6 in PC-2 and PC were not influenced by *sn* acyl position or by dietary treatment; these results show that *sn* acyl position did not significantly influence accretion of ^{2}H-18:2n-6 in PC.

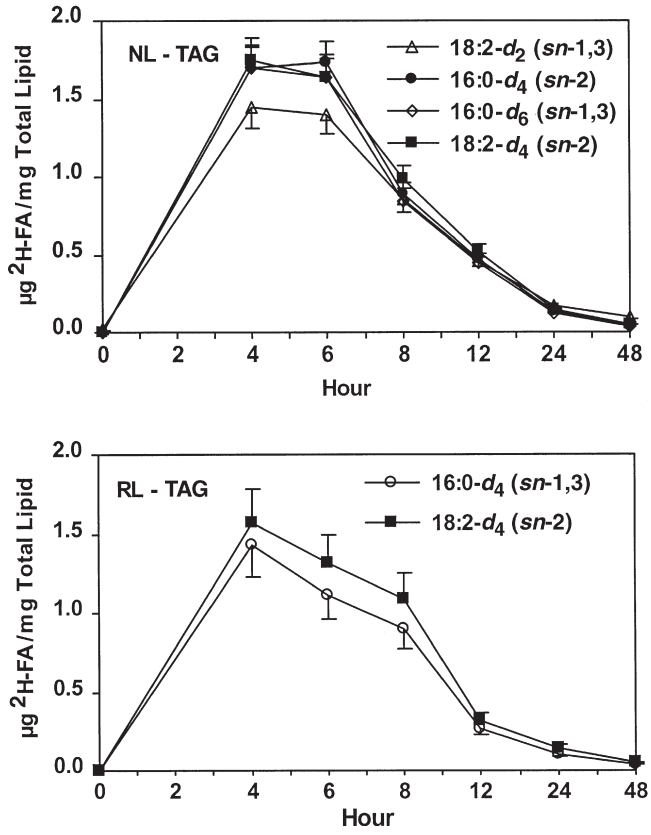

FIG. 3. Time-course plots for incorporation of deuterium-labeled 16:0 and 18:2n-6 in plasma TAG of subjects fed NL and RL diets. NL subjects were fed a mixture of (P6L4P6 + L2P4L2). RL subjects were fed a single deuterium-labeled TAG (P4L2P4). Each data point is the average for data from two subjects. Error bars equal SE. Error bars are not shown when less than the size of the symbol. Data are plotted as micrograms of ^{2}H-fatty acid/mg of total TAG/mg of ^{2}H-fatty acid fed. For abbreviations, see Figure 1.

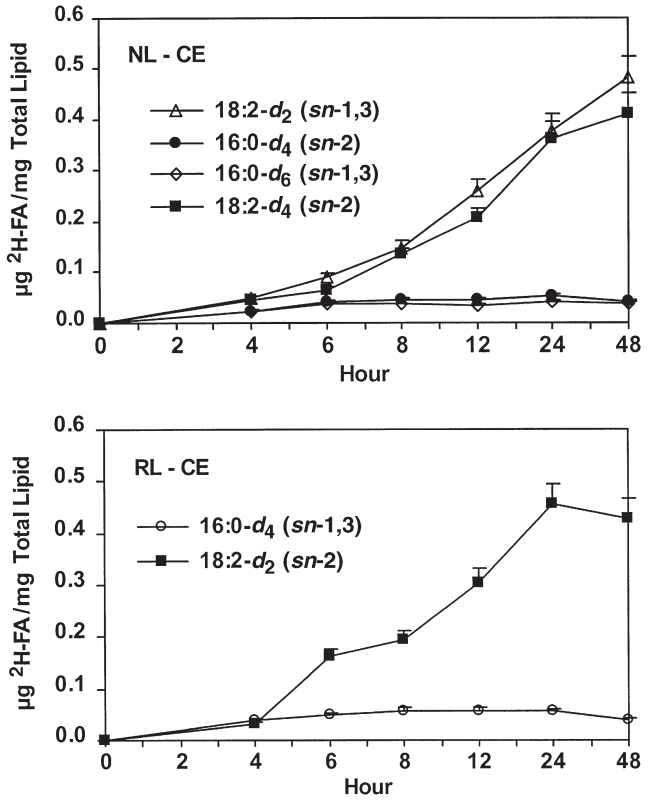

FIG. 4. Time-course plots for incorporation of deuterium-labeled 16:0 and 18:2n-6 in plasma cholesterol ester (CE) of subjects fed NL and RL diets. NL subjects were fed a mixture of (P6L4P6 + L2P4L2). RL subjects were fed a single deuterium-labeled TAG (P4L2P4). Each data point is the average for data from two subjects. Error bars equal SE. Error bars are not shown when less than the size of the symbol. Data are plotted as micrograms of ^{2}H-fatty acid/mg of total CE FA/mg of ^{2}H-fatty acid fed. For other abbreviations, see Figure 1.

Metabolites. Concentrations for the major metabolites (^{2}H-16:1, ^{2}H-18:0, ^{2}H-20:3n-6, and ^{2}H-20:4n-6) of ^{2}H-16:0 and ^{2}H-18:2n-6 in plasma TAG, CE, and PC are summarized in Table 5. These metabolite data are a measure of the effect of the *sn*-1 vs. *sn*-2 TAG position and of the NL vs. RL diet treatment on desaturation and elongation of 16:0 and 18:2n-6. Neither the *sn* acyl position of ^{2}H-16:0 and ^{2}H-18:2n-6 nor diet influenced accretion of fatty acid metabolites in plasma TAG and CE. In plasma PC, the concentration of the ^{2}H-16:1 metabolite from *sn*-1,3 ^{2}H-16:0 was 2.8 times higher ($P < 0.03$) than ^{2}H-16:1 from *sn*-2 ^{2}H-16:0. ^{2}H-16:1 accretion in PC samples from the NL diet subjects was four times higher ($P < 0.03$) than for the RL diet subjects. The concentration of ^{2}H-20:4n-6 in plasma PC from subjects fed the RL diet was 2.6 times higher ($P < 0.1$) than for the NL subjects. No other *sn*-1,3 vs. *sn*-2 and NL vs. RL comparisons of data in Table 5 are significant at $P < 0.1$. For total plasma, the average percent conversion for all subjects was 2.6 ± 1.0% for 16:0 to 16:1 and 3.5 ± 1.2% for 16:0 to 18:0.

Total plasma lipid AUC concentration data are plotted in Figure 6 for ^{2}H-20:3n-6 and ^{2}H-20:4n-6 metabolites and reflect the total amount of these metabolites synthesized from ^{2}H-18:2n-6. The average percent conversion of 18:2n-6 to 20:4n-6 for all subjects was 11.7 ± 4.9%. The NL subject data for ^{2}H-20:4n-6 synthesized from *sn*-1,3 and *sn*-2 ^{2}H-18:2n-6 are not significantly different and show that the *sn* TAG position of the ^{2}H-18:2n-6 precursor does not have a large effect on n-6 metabolite synthesis. In contrast, the ^{2}H-20:4n-6 synthesized from *sn*-2 ^{2}H-18:2n-6 data in Figure 6 [^{2}H-20:4n-6 (*sn*-2)] for the RL diet subjects is 2.36 times higher ($P < 0.09$) than the NL diet group data. The ^{2}H-20:3n-6 (*sn*-2) RL subject data are also about two times higher than the NL subject 20:3n-6 (*sn*-2) data. These differences suggest that the NL diet inhibited the synthesis of n-6 metabolites from 18:2n-6.

DISCUSSION

The multiple-isotope tracer methodology used in this study provides a more accurate comparison of fatty acid incorporation and metabolite synthesis than a single-isotope tracer design because all the ^{2}H-FA in the mixture fed to a subject are influenced equally by the same metabolic variables. Thus, the *sn*-1,3 vs. *sn*-2 position comparisons are highly accurate for

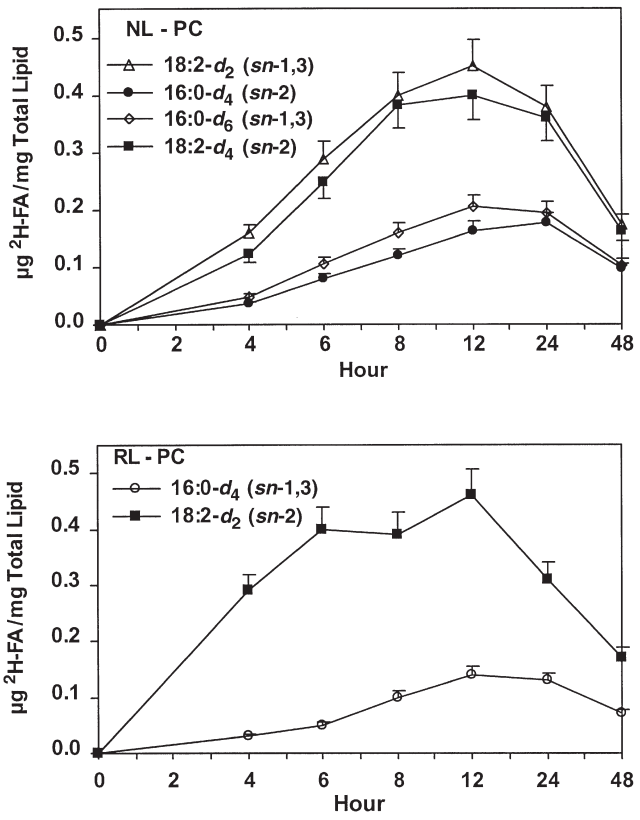

FIG. 5. Time-course plots for incorporation of deuterium-labeled 16:0 and 18:2n-6 in plasma phosphatidylcholine (PC) of subjects fed NL and RL diets. NL subjects were fed a mixture of (P6L4P6 + L2P4L2). RL subjects were fed a single deuterium-labeled TAG (P4L2P4). Each data point is the average for data from two subjects. Error bars equal SE. Error bars are not shown when less than the size of the symbol. Data are plotted as micrograms of ^{2}H-fatty acid/mg of total PC fatty acid/mg of ^{2}H-fatty acid fed. For abbreviations, see Figure 1.

individual subjects, but the small number of subjects studied limits the conclusions that can be drawn for the NL vs. RL diet group comparisons because subject variability may mask small but real differences.

Absorption and fatty acid migration. The chylomicron total TAG plots (Fig. 1) show that ^{2}H-16:0 and ^{2}H-18:2n-6 located at the *sn*-1,3 and *sn*-2 positions were equally well absorbed by these adult male subjects. As expected, the 16:0 results are typical for adults and contrast with the lower absorption by infants of 16:0 located at the *sn*-1,3 position (23–26). The percent total isotopic enrichment for the 4-h chylomicron TAG samples from the NL diet subjects was 33.4 ± 1.81% and is consistent with results from previous studies with deuterium-labeled 18:1 isomers (42). Since a total of 10.3 g of ^{2}H-fat and no unlabeled fat was present in the meal fed to the NL diet subjects, the enrichment data indicate that substantial (*ca.* 30 g) amounts of unlabeled FA were incorporated into chylomicron TAG during absorption of the labeled FA. Similar results were observed for the RL diet subjects. Residual chylomicron TAG is not responsible for the isotopic dilution observed since the 0 h (fasting) data show that the total plasma pool contained less than 0.2 g of residual chylomicron TAG. The amount of unlabeled FA incorporated into chylomicron TAG during absorption is not trivial and undoubtedly compromises results from studies that use unlabeled fats to investigate TAG absorption and the metabolic effect of TAG structure.

The source of the unlabeled FA remains unclear. Three possible sources are plasma TAG, residual intestinal TAG, and mobilized stored TAG. Exchange between plasma TAG and chylomicron TAG is not a probable explanation because insufficient plasma TAG was present to achieve the level of isotopic dilution observed. Residual intestinal TAG is an unlikely source of the unlabeled FA because the fatty acid compositions of the chylomicron TAG samples and the diets were different. For example, the chylomicron TAG contained 1.0 ± 0.1% 20:4n-6, which is about seven times higher than the percentage of 20:4n-6 in the NL and RL diets. Thus, mobilization of stored TAG is the most probable source of the unlabeled FA present in the chylomicron TAG.

The chylomicron 2-acyl TAG plots (Fig. 2) show that 80–90% of the fatty acid in the *sn*-2 position of P6L4P6 and L2P4L2 was retained during absorption and, by default,

TABLE 4
Concentration of Deuterated Palmitic and Linoleic Acids in Plasma Lipid Classes[a]

Lipid class[c]	Diet[d]	Deuterated fatty acid and *sn* TAG position[b]			
		16:0 (*sn*-1,3)	16:0 (*sn*-2)	18:2n-6 (*sn*-1,3)	18:2n-6 (*sn*-2)
		(µg/mg ^{2}H-fatty acid fed/mg lipid/kg body wt ± SD)			
TAG	NL	16.01 ± 0.64	15.75 ± 2.15	15.58 ± 1.76	18.01 ± 1.79
TAG	RL	12.34 ± 2.19	No data	No data	14.36 ± 1.14
CE	NL	1.39 ± 0.50	1.62 ± 0.25	12.48 ± 1.01	11.19 ± 1.65
CE	RL	2.05 ± 0.05	No data	No data	15.31 ± 4.84
PC	NL	6.87 ± 2.54	5.74 ± 1.01	14.65 ± 5.11	13.04 ± 3.47
PC	RL	3.73 ± 0.62	No data	No data	11.26 ± 2.52
PC-1	NL	7.47 ± 1.88 *,†	5.64 ± 0.10*	0.40 ± 0.10	0.24 ± 0.17
PC-1	RL	4.45 ± 0.98†	No data	No data	0.70 ± 0.17
PC-2	NL	0.12 ± 0.01	0.24 ± 0.04	11.18 ± 3.15	12.03 ± 3.63
PC-2	RL	0.11 ± 0.05	No data	No data	14.23 ± 3.13

[a]Based on area-under-curve time-course data.
[b]*sn*-1,3 and *sn*-2 indicate acyl position of ^{2}H-fatty acid in the TAG fed.
[c]PC-1, 1-acyl PC; PC-2, 2-acyl PC; CE, cholesterol ester. See Table 1 for other abbreviation.
[d]NL and RL, native lard and randomized lard diets, respectively.
[e]*$P < 0.1$ for *sn*-1 vs. *sn*-2; †$P < 0.1$ for NL vs. RL.

TABLE 5
Concentrations of Labeled Palmitic and Linoleic Acid Metabolites in Plasma Lipid Classes[a]

		Lipid class and diet group					
	Precursor's	TAG		CE		PC[c]	
FA	*sn* position[b]	NL	RL	NL	RL	NL	RL
		(μg/mg ^{2}H-fatty acid fed/mg lipid/kg body wt ± SD)					
16:1	*sn*-1,3	0.262 ± 0.026	0.166 ± 0.023	0.049 ± 0.012	0.056 ± 0.011	0.028 ± 0.003*,†	0.007 ± 0.005†
16:1	*sn*-2	0.173 ± 0.040	No data	0.020 ± 0.027	No data	0.010 ± 0.004*	No data
18:0	*sn*-1,3	0.216 ± 0.001	0.145 ± 0.021	0.003 ± 0.001	0.018 ± 0.005	0.564 ± 0.115	0.498 ± 0.051
18:0	*sn*-2	0.225 ± 0.052	No data	0.004 ± 0.006	No data	0.591 ± 0.022	No data
20:3n-6	*sn*-1,3	0.040 ± 0.006	No data	0.010 ± 0.006	No data	0.510 ± 0.086	No data
20:3n-6	*sn*-2	0.025 ± 0.008	0.007 ± 0.009	0.028 ± 0.040	0.021 ± 0.017	0.633 ± 0.412	1.416 ± 0.111
20:4n-6	*sn*-1,3	0.045 ± 0.009	No data	0.265 ± 0.176	No data	1.849 ± 0.073	No data
20:4n-6	*sn*-2	0.050 ± 0.216	0.054 ± 0.085	0.341 ± 0.026	0.283 ± 0.152	2.61 ± 0.113†	6.75 ± 0.95†

[a]Based on area-under-curve time-course data.
[b]*sn*-1,3 and *sn*-2 indicate acyl position of ^{2}H-fatty acid in the TAG fed.
[c]*$P < 0.05$ for *sn*-1 vs. *sn*-2; †$P < 0.05$ for NL vs. RL. For abbreviations, see Tables 1, 2, and 4.

80–90% of the ^{2}H-fatty acid originally at the *sn*-1,3 TAG positions is retained at the *sn*-1,3 positions. These results are reasonably consistent with results from animal and nontracer human studies that report over 75% retention of the FA in the *sn*-2 acyl position of dietary fats during absorption (1–4). However, the results of this study suggest that previous studies may have underestimated the percent *sn*-2 retention owing to co-incorporation of stored fat into chylomicron TAG and/or fatty acid migration between the *sn*-1,3 and *sn*-2 TAG positions.

The chylomicron 2-acyl TAG time-course curves (Fig. 2) show that ^{2}H-16:0 at the *sn*-2 chylomicron TAG position migrates to the *sn*-1 chylomicron TAG position and that the ^{2}H-18:2n-6 at the *sn*-1,3 acyl positions of chylomicron TAG migrates to the *sn*-2 position. In contrast, there was no significant migration of ^{2}H-16:0 from the *sn*-1,3 position to the *sn*-2 chylomicron TAG position or migration of ^{2}H-18:2n-6 from the *sn*-2 chylomicron-TAG position to the *sn*-1,3 position. Thus, extensive fatty acid migration occurred only when the

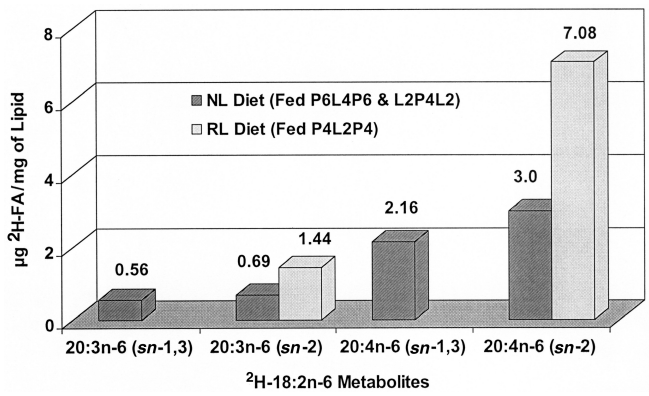

FIG. 6. Influence of dietary TAG structure on accretion of deuterium-labeled 20:3n-6 and 20:4n-6 in plasma total lipid. The *sn*-1,3 and *sn*-2 notation associated with the 20:3n-6 and 20:4n-6 metabolite designates the position of the ^{2}H-18:2n-6 precursor in the TAG fed. Data are plotted as micrograms of ^{2}H-fatty acid metabolite/mg of total lipid fatty acid/mg of ^{2}H-18:2n-6 fed and are the average of area-under-curve data for two subjects. For abbreviations, see Figure 1.

^{2}H-FA in the fed TAG were at a position that differed from their normal position in human chylomicron TAG samples. These results suggest the presence of an isomerization mechanism that converts the positional distribution of FA in chylomicron TAG to "normal" TAG structures prior to clearance. This fatty acid isomerization or rearrangement process appears to be an initial step in the overall metabolic sequence that is ultimately responsible for human plasma TAG structures containing mainly saturated FA at the *sn*-1,3 positions and unsaturated FA at the *sn*-2 position.

It is interesting that ^{2}H-16:0 fed as an *sn*-2 TAG migrates from the chylomicron *sn*-2 TAG position, but ^{2}H-16:0 fed as an *sn*-1,3 TAG does not seem to migrate when incorporated at the chylomicron *sn*-2 TAG position. It appears that 16:0 equilibrates between the *sn*-2 and *sn*-1,3 positions in an approximate 15:85 ratio. Selective clearance is not a factor since both 16:0 tracers were present at about the same concentrations in the chylomicron total TAG at all time points, and the relative percentages of the ^{2}H-FA did not change with time. From the curves in Figure 2, it appears that some restructuring of chylomicron TAG may have occurred prior to collection of the first (4 h) sample. Thus, retention of the *sn*-2 FA in dietary TAG during absorption may be higher than the 80–90% observed in this study and the 75–80% values reported by others (1–4).

Incorporation and turnover in plasma lipid classes. The *sn* position of ^{2}H-16:0 and ^{2}H-18:2n-6 in L2P4L2, P6L4P6, and P4L2P4 did not influence incorporation and turnover of these ^{2}H-FA in plasma TAG and CE. This is the expected result if the locations of the ^{2}H-fatty acid in the majority of the chylomicron TAG structures were rearranged to similar positions before subsequent incorporation into plasma TAG and CE.

An effect of fatty acid *sn* position on incorporation of 16:0 into plasma PC was observed. The *sn*-1,3 and *sn*-2 16:0 data for the NL subjects provide a direct comparison of the influence of position since the TAG mixture fed contained labeled 16:0 at both the *sn*-1,3 and *sn*-2 positions. These data show that accumulation of *sn*-2 TAG ^{2}H-16:0 in the 1-acyl position of PC was 24.5% lower ($P < 0.1$) than labeled palmitic acid fed as an *sn*-1,3 TAG. This result suggests that ^{2}H-16:0 migration from

the *sn*-2 to the *sn*-1,3 position does not totally eliminate the influence of the *sn*-2 position before a portion of the chylomicron TAG is converted to PC. The results also suggest a possible diet effect because the ^{2}H-16:0 concentration in PC-1 was 46.5% lower ($P < 0.1$) for RL subjects than for NL subjects. These combined results demonstrate that less 16:0 is incorporated into the 1-acyl position of PC when dietary TAG contain 16:0 at the *sn*-2 position. Presumably, this occurs because a portion of plasma PC is synthesized from chylomicron TAG that still retain elements of the dietary TAG structure. On the basis of the later time for maximal incorporation in PC compared with chylomicron TAG, we can rule out the possibility that synthesis of PC by intestinal mucosal cells during absorption is a significant source of plasma PC.

Metabolite synthesis and accretion. The AUC data summarized in Table 5 show that concentrations of the major metabolites of 16:0 and 18:2n-6 (16:1, 18:0, 20:3n-6, 20:4n-6) in plasma TAG and CE were not significantly influenced by the *sn* position of the ^{2}H-FA in L2P4L2, P6L4P6, and P4L2P4 nor by dietary treatment. The *sn* acyl position of ^{2}H-18:2n-6 did not influence accumulation of the ^{2}H-20:4n-6 metabolite in plasma PC and plasma total lipid (Fig. 6). However, ^{2}H-20:4n-6 accretion was higher ($P < 0.1$) in plasma PC and plasma total lipid for the RL diet group subjects than for the NL subjects and suggests that intake of dietary fats enriched at the *sn*-2 acyl position with 16:0 may reduce both 20:3n-6 and 20:4n-6 synthesis. Dietary treatment and *sn* position also influenced the accretion in plasma PC of 16:1 synthesized from 16:0. The concentration of ^{2}H-16:1 in plasma PC for subjects fed the RL diet was 75% lower ($P < 0.05$) than for the NL diet subjects, and ^{2}H-16:1 derived from *sn*-2 was 64% lower ($P < 0.05$) than ^{2}H-16:1 derived from *sn*-1,3 ^{2}H-16:0. Overall, these metabolite data are consistent with the possibility that dietary TAG molecular structure has physiological importance.

This study provides evidence for a previously unrecognized migration of *sn*-2 16:0 to the *sn*-1,3 position and *sn*-1,3 18:2n-6 to the *sn*-2 chylomicron TAG position. The *sn* TAG position and dietary fat containing 16:0 in the *sn*-2 position have little influence on 16:0 and 18:2n-6 incorporation into TAG and CE. Both results are consistent with the view that isomerization of TAG structures following their initial absorption reduces the metabolic influence of TAG regiospecificity. The results also suggest that the postabsorption lipid-related physiological effects of dietary TAG structures would be diminished. This concept is consistent with observations that dietary TAG structure does not significantly influence serum cholesterol and lipoprotein levels in humans (10–14). However, the effect of TAG structure on 16:0 and 20:4n-6 incorporation into PC and the possible inhibition of 20:4n-6 synthesis by the NL diet treatment are findings that suggest possible physiological importance of TAG structure and warrant further study.

ACKNOWLEDGMENTS

Lynne C. Copes and Erin L. Walter are acknowledged for assistance with laboratory procedures and sample analyses.

REFERENCES

1. Mattson, F.H., and Volpenhein, R.A. (1964) The Digestion and Absorption of Triglycerides, *J. Biol. Chem. 239*, 2772–2777.
2. Kayden, H.J., Senior, J.R., and Mattson, F.H. (1967) The Monoglyceride Pathway of Fat Absorption in Man, *J. Clin. Invest. 46*, 1695–1703.
3. Summers, L.K.M., Fielding, B.A., Herd, S.L., Ilic, V., Clark, M.L., Quinlan, P.T., and Frayn, K.N. (1999) Use of Structured Triacylglycerols Containing Predominantly Stearic and Oleic Acids to Probe Early Events in Metabolic Processing of Dietary Fat, *J. Lipid Res. 40*, 1890–1898.
4. Yli-Jokipii, K., Kallio, H., Schwab, U., Nykkanen, H., Kurvinen, J.P., Savolainen, M.J., and Tahvonen, R. (2001) Effects of Palm Oil and Transesterified Palm Oil on Chylomicron and VLDL Triacylglycerol Structures and Postprandial Lipid Response, *J. Lipid Res. 42*, 1618–1625.
5. Agren, J.J., Ravandi, A., Kuksis, A., and Steiner, G. (2002) Structural and Compositional Changes in Very Low Density Lipoprotein Triacylglycerols During Basal Lipolysis, *Eur. J. Biochem. 269*, 6223–6232.
6. Myher, J.J., Kuksis, A., Breckenridge W.C., McGuire, V., and Little, J.A. (1985) Comparative Studies of Triacylglycerol Structure of Very Low Density Lipoproteins and Chylomicrons of Normolipemic Subjects and Patients with Type II Hyperlipoproteinemia, *Lipids 20*, 90–101.
7. Myher, J.J., Kuksis, A., Breckenridge W.C., and Little, J.A. (1984) Studies of Triacylglycerol Structure of Very Low Density Lipoproteins of Normolipemic Subjects and Patients with Type III and Type IV Hyperlipoproteinemia, *Lipids 19*, 683–691.
8. Kuksis, A., and Myher, J.J. (1990) Gas–Liquid Chromatographic Profiling of Plasma Lipids Using High-Temperature-Polarizable Capillary Columns, *J. Chromatogr. 500*, 427–441.
9. Abia, R., Pacheco, Y.M., Perona, J.S., Montero, E., Muriana, F.J.G., and Ruiz-Gutierrez, V. (2001) The Metabolic Availability of Dietary Triacylglycerols from Two High-Oleic Oils During the Postprandial Period Does Not Depend on the Amount of Oleic Acid Ingested by Healthy Men, *J. Nutr. 131*, 59–65.
10. Nestel, P.J., and Homma, Y. (1976) Effect of Dietary Polyunsaturated Pork on Plasma Lipids and Sterol Excretion in Man, *Lipids 11*, 42–48.
11. Zock, P.L., de Vries, J.H.M., de Fouw, N.J., and Katan, M.B. (1995) Positional Distribution of FA in Dietary Triglycerides: Effects on Fasting Blood Lipoprotein Concentrations in Humans, *Am. J. Clin. Nutr. 61*, 48–55.
12. Nestel, P.J., Noakes, M., Belling, G.B., McArthur, R., and Clifton, P.M. (1995) Effect on Plasma Lipids of Interesterifying a Mix of Edible Oils, *Am. J. Clin. Nutr. 62*, 950–955.
13. Mascioli, E.A., McLennan, C.E., Schaefer, E.J., Lichtenstein, A.H., Høy, C.E., Christensen, M.S., and Bistrian, B.R. (1999) Lipidemic Effects of an Interesterified Mixture of Butter, Medium-Chain Triacylglycerol, and Safflower Oils, *Lipids 34*, 889–894.
14. Shane, J.M., Walker, P.M., and Emken, E.A. (1999) Effect of Randomization of Lard Triglyceride Structure on Plasma Lipids, *J. Appl. Nutr. 51*, 68–77.
15. Zsinka, A.J.N., Peredi, J., Szepvolgyi, J. Maucha, E., Foldes, V., and Biro, G (1989) Effect of Interesterified Fat Mixtures on Certain Lipid Indices in Experimental Fat Metabolism Disturbance, *Nahrung 33*, 107–118.
16. Pfeuffer, M., DeGreyt, W., Schoppe, I., Barth, C.A., and Huyghebaert, A. (1995) Effect of Interesterification of Milk Fat on Plasma Lipids of Miniature Pigs, *Int. Dairy J. 5*, 265–273.
17. Pufal, D.A., Quinlan, P.T., and Salter, A.M. (1995) Effect of Dietary Triacylglycerol Structure on Lipoprotein Metabolism: A Comparison of the Effects of Dioleoylpalmitoylglycerol in

Which Palmitate Is Esterified to the 2- or 1(3)-Position of the Glycerol, *Biochim. Biophys. Acta 1258*, 41–48.
18. Becker, C., Lund, P., and Holmer, G. (2001) Effect of Randomization of Mixtures of Butter Oil and Vegetable Oil on Absorption and Lipid Metabolism in Rats, *Eur. J. Nutr. 40*, 1–9.
19. Hunter, K.A., Crosbie, L.C., Weir, A., Miller, G.J., and Dutta-Roy, A.K. (1999) The Effects of Structurally Defined Triglycerides of Differing Fatty Acid Composition on Postprandial Haemostasis in Young, Healthy Men, *Atherosclerosis 142*, 151–158.
20. Sanders, D.J., Howes, D., and Earl, L.K. (2001) The Absorption, Distribution and Excretion of 1- and 2-[^{14}C]Palmitoyl Triacylglycerols in the Rat, *Food Chem. Toxicol. 39*, 709–716.
21. Kritchevsky, D. (1995) Fatty Acids, Triglyceride Structure, and Lipid Metabolism, *Nutr. Biochem. 6*, 172–178.
22. Kritchevsky, D. (2000) Overview: Dietary Fat and Atherosclerosis, *Asia Pacific J. Clin. Nutr. 9*, 141–145.
23. Renaud, S.C., Ruf, J.C., and Petithorny, D. (1995) The Positional Distribution of Fatty Acids in Palm Oil and Lard Influences Their Biological Effects in Rats, *J. Nutr. 125*, 229–237.
24. Innis, S.M., and Dyer, R. (1997) Dietary Triacylglycerols with Palmitic Acid (16:0) in the 2-Position Increase 16:0 in the 2-Position of Plasma and Chylomicron Triacylglycerols, but Reduce Phospholipid Arachidonic and Docosahexaenoic Acids, and Alter Cholesterol Ester Metabolism in Formula-Fed Piglets, *J. Nutr. 127*, 1311–1319.
25. Innis, S.M., Dyer, R., and Lien, E.L. (1997) Formula Containing Randomized Fats with Palmitic Acid (16:0) in the 2-Position Increases 16:0 in the 2-Position of Plasma and Chylomicron Triglycerides in Formula-Fed Piglets to Levels Approaching Those of Piglets Fed Sow's Milk, *J. Nutr. 127*, 1362–1370.
26. Filer, L.J., Mattson, F.H., and Fomon, S.J. (1969) Triglyceride Configuration and Fat Absorption by the Human Infant, *J. Nutr. 99*, 293–298.
27. Carnielli, V.P., Luijendijk, I.H.T., van Goudover, J.B., Sulkers, E.J., Boerlagge, A.A., Degenhart, H.J., and Sauer, P.J.J. (1996) Structural Position and Amount of Palmitic Acid in Infant Formulas: Effects on Fat, Fatty Acid, and Mineral Balance, *J. Pediatr. Gastroenterol. 23*, 553–560.
28. Yli-Jokipii, K.M., Schwab, U.S., Tahvonen, R.L., Kurvinen, J.P., Mykkanen, H.M., and Kallio, H.P.T. (2002) Triacylglycerol Molecular Weight and, to a Lesser Extent, Fatty Acid Positional Distribution, Affect Chylomicron Triacylglycerol Composition in Women, *J. Nutr. 132*, 924–929.
29. Zampelas, A., Williams, C.M., Morgan, L.M., and Wright, J. (1994) The Effect of Triacylglycerol Fatty Acid Positional Distribution on Postprandial Plasma Metabolite and Hormone Responses in Normal Adult Men, *Br. J. Nutr. 71*, 401–410.
30. Hodge, J., Li, D., Redgrave, T.G., and Sinclair, A.J. (1999) The Metabolism of Native and Randomized Butterfat Chylomicrons in the Rat Is Similar, *Lipids 34*, 579–582.
31. Mortimer, B.C., Holthouse, D.J., Martins, I.J., Stick, R.V., and Redgrave, T.G. (1994) Effects of Triacylglycerol-Saturated Acyl Chains on the Clearance of Chylomicron-Like Emulsions from the Plasma of the Rat, *Biochim. Biophys. Acta 1211*, 171–180.
32. Small, D.M. (1991) The Effects of Glyceride Structure on Absorption and Metabolism, *Ann. Rev. Nutr. 11*, 413–434.
33. Kubow, S. (1996) The Influence of Positional Distribution of Fatty Acids in Native, Interesterified and Structure-Specific Lipids on Lipoprotein Metabolism and Atherogenesis, *J. Nutr. Biochem. 7*, 531–541.
34. Hunter, J.E. (2001) Studies on Effects of Dietary FA as Related to Their Position on Triglycerides, *Lipids 36*, 655–668.
35. Adlof, R.O. (1998) Isotopically Labelled Fatty Acids, in *Lipid Synthesis and Manufacture* (F. Gunstone, ed.), pp. 46–93, Sheffield Academic Press, Sheffield, England.
36. Kodali, D.R., Atkinson, D., Redgrave, T.G., and Small, D.M. (1987) Structure and Polymorphism of 18-Carbon Fatty Acid Triacylglycerols: Effect of Unsaturation and Substitution in the 2-Position, *J. Lipid Res. 28*, 403–413.
37. Adlof, R.O. (2003) Synthesis and Analysis of Symmetrical and Nonsymmetrical Disaturated/Monounsaturated Triacylglycerols, *J. Agric. Food Chem. 51*, 2096–2099.
38. Emken, E.A., Adlof, R.O., Duval, S., Nelson, G., and Benito, P. (2002) Effect of Dietary Conjugated Linoleic Acid (CLA) on Metabolism of Isotope-Labeled Oleic, Linoleic, and CLA Isomers in Women, *Lipids 37*, 741–750.
39. Neff, W.E., Zeitoun, M.A.M., and Weisleder, D. (1992) Resolution of Lipolysis Mixtures from Soybean Oil by a Solid-Phase Extraction Procedure, *J. Chromatogr. 589*, 353–357.
40. Statistical Analysis System Institute (1987) *SAS Guide for Personal Computers*, 6th edn., SAS Institute, Cary, NC.
41. Emken, E.A., Adlof, R.O., Duval, S.M., and Nelson, G.J. (1998) Effect of Dietary Arachidonic Acid on Metabolism of Deuterated Linoleic Acid by Adult Male Subjects, *Lipids 33*, 471–480.
42. Emken, E.A. (1986) Absorption of Deuterium-Labeled *cis*- and *trans*-Octadecenoic Acid Positional Isomers in Man, in *Fat Absorption* (Kuksis, A., ed.), Vol. 1, pp. 159–175, CRC Press, Boca Raton, FL.

[Received July 25, 2003; accepted November 19, 2003]

Trans, Saturated, and Unsaturated Fat in Foods in the United States Prior to Mandatory *Trans*-Fat Labeling

Subramaniam Satchithanandam*, Carolyn J. Oles, Carol J. Spease, Mary M. Brandt, Martin P. Yurawecz, and Jeanne I. Rader

Division of Research and Applied Technology, Office of Nutritional Products, Labeling and Dietary Supplements, U.S. Food and Drug Administration, College Park, Maryland 20740

ABSTRACT: On July 11, 2003, the U.S. Food and Drug Administration published a final rule amending its food-labeling regulations to require that *trans* FA be declared in the nutrition label of conventional foods and dietary supplements. The effective date of this final rule is January 1, 2006. This places some urgency on increasing the number and types of currently available foods for which there are *trans*-fat data. Compositional databases on *trans* fat content of food are currently limited. The purpose of this study was to determine the *trans*-fat content of a wide range of foods prior to the effective date of the new regulation. AOAC Official Method of Analysis 996.01 was modified for the analysis of *trans* fat in noncereal products. Food products for analysis were selected on the basis of market share and data from the USDA's 1994–1996 Continuing Survey of Food Intake by Individuals. Foods were purchased from local supermarkets, weighed, hydrolyzed, converted to FAME, and analyzed by GC. The results showed that *trans* fat (g/100 g fat) ranged from 0.0 to 48.8 in bread, cake, and related products; from 14.9 to 27.7 in margarines; from 7.7 to 35.3 in cookies and crackers; from 24.7 to 38.2 in frozen potatoes; from 0.0 to 17.1 in salty snacks; from 0.0 to 13.2 in vegetable oils and shortenings; from 0.0 to 2.2 in salad dressings and mayonnaises; and from 0.0 to 2.0 in dry breakfast cereals. Serving sizes for the foods included in this survey ranged from 12 to 161 g, and *trans*-fat levels ranged from 0.0 to 7.2 g/serving. The significant differences in *trans*-fat content in products within each food category are due to differences in the type of fats and oils used in the manufacturing processes.

Paper no. L9382 in *Lipids 39*, 11–18 (January 2004).

Hydrogenated fats and oils are used in foods to improve texture and stability for a longer shelf life. Some unhydrogenated fats and oils are less suitable for use in food because of their low m.p. and the ease with which they are oxidized. *Trans* FA are formed during industrial hydrogenation of dietary fats and oils. Food products made with such hydrogenated fats and oils also contain *trans* FA. Such foods are the primary source of *trans* fat in typical U.S. diets (1). *Trans* FA also are formed as a result of biohydrogenation in the rumen of animals such as cows and sheep. Thus, dairy products and meat also contain small quantities of *trans* FA (1).

Evidence from a number of persuasive studies using a range of test conditions and across different geographical regions and populations is strong for an adverse relationship between *trans*-fat intakes and risk of coronary heart disease (reviewed in Refs. 2 and 3). The evolving state of scientific knowledge regarding *trans* fat prompted the U.S. Food and Drug Administration (FDA) to issue a proposed rule in 1999 (4), which was published as a final rule on July 11, 2003 (5), that will require manufacturers to list *trans* FA or *trans* fat on the Nutrition Facts and Supplement Facts panels of food and dietary supplement labels by January 1, 2006. This declaration is to be placed on a separate line immediately under the declaration for saturated fat (SF). A declaration of amounts of *trans* fat on a separate line is not currently required on the Nutrition Facts panel. Rather, amounts of *trans* fat are currently "captured" in the declaration of total fat.

Both in its proposal and in its final rule (4,5), FDA used nationally representative dietary intake data and a U.S. Department of Agriculture (USDA) food composition database containing data on *trans* fat content of foods (6) to estimate *trans*-fat intakes in the U.S. population. Estimation of the current consumption of *trans* fat has been problematic because of the limited quantitative data available on the *trans*-fat content of foods (i.e., the currently available USDA *trans*-fat database contains relatively few foods).

The purpose of this work was to determine the FA content of a wide range of foods, particularly those foods that have been shown to be important dietary sources of *trans* fat. In this study, food samples were selected from among market-leader products within eight food groups. AOAC Official Method 996.01 "Fat Analysis in Cereal Products" (7), originally developed for analysis of FA in cereal products, was modified for quantification of FA, including *trans* fat, in a much wider range of food products.

EXPERIMENTAL PROCEDURES

Sample selection. Food products were identified on the basis of market share and were purchased from local supermarkets in

*To whom correspondence should be addressed at Office of Nutritional Products, Labeling and Dietary Supplements, Food and Drug Administration, HFS-840, 5100 Paint Branch Pkwy., College Park, MD 20740-3835. E-mail: Ssubrama@cfsan.fda.gov

Definitions and abbreviations: CFR, Code of Federal Regulations; FDA, U.S. Food and Drug Administration; IOM/NAS, Institute of Medicine of the National Academy of Sciences; IRI, Information Resources, Inc.; MUFA, the sum of all *cis*-monounsaturated FA; PUFA, the sum of all *cis*,*cis* methylene-interrupted PUFA; SF, saturated fat, all FA containing no double bonds; SRM, Standard Reference Material; total fat, total lipid FA expressed as TG. *Trans* fat is defined in FDA's final rule (Ref. 5) as follows: All unsaturated FA that contain one or more isolated (i.e., nonconjugated) double bonds in a *trans* configuration.

2002. A total of 117 food products were analyzed. Food items were selected using data derived from USDA's Continuing Survey of Food Intakes by Individuals 1994–1996 Diet and Health Knowledge Survey database and technical support databases (8). Food samples were sorted into groups as follows: bread, cake, and related products; margarines; cookies and crackers; frozen potato products; salty snacks; vegetable oils and shortenings; salad dressings and mayonnaise; and ready-to-eat breakfast cereals.

Sample preparation. Foods were stored at appropriate temperatures until homogenized. Quantitative label information and fat sources listed on the labels were recorded. Individual foods were homogenized in a food processor and frozen in plastic jars. At least 0.5 kg (or one consumer unit, e.g., 1 package of cookies, 1 pound of margarine) was used for each composite. Samples of oils for analysis were stored at room temperature. At least two independent analyses of each homogenized sample were conducted. About 2 g of the homogenized samples was weighed and transferred to test tubes (25 × 200 mm). Ethyl alcohol (2 mL) was added to prevent lumping of the sample during hydrolysis. Internal standard (1 mL) (tritridecanoate, 5 mg/mL in hexane) was added. The samples were mixed and digested with 8 N HCl in a water bath at 80°C for 40 min. Ethanol (10 mL) was added, and the samples were cooled in tap water. Each digested sample was transferred to a separatory funnel and extracted once with 30 mL of diethyl ether, once with 30 mL of petroleum ether, and twice with 30 mL of ethyl ether/petroleum ether (1:1). The diethyl ether, petroleum ether, and mixed ether extracts were combined in a 125-mL flat-bottomed flask, evaporated under nitrogen, saponified with methanolic sodium hydroxide, and methylated with boron trifluoride (7). FAME were dried with anhydrous sodium sulfate.

Sample analysis. A Hewlett-Packard 5890 Series II gas chromatograph equipped with an HP 7673 autosampler, a split injector (20:1), an FID, and a Hewlett-Packard ChemStation Data System (Hewlett-Packard Co., Palo Alto, CA) was used for the analyses. A CP Sil 88 fused-silica capillary column (100 m × 0.25 mm i.d.; 0.20 μm film thickness; Chrompack, Raritan, NJ) was used to separate the FA. Operating conditions were as follows: injector temperature, 250°C; detector temperature, 280°C; temperature programmed at 75°C for 2 min and increased to 175°C at a rate of 5°C /min and held at 175°C for 33 min, increased to final temperature of 225°C at a rate of 5°C/min and held at 225°C for 8 min. Hydrogen was used as the carrier gas at a flow rate of 1.5 mL/min, linear velocity, 29.2 cm/s. One (1) microliter injections, ideally representing 1–2 mg FAME/mL, were made. In some injections, however, we recognized that the column was overloaded and there was a loss of resolution due to this overloading. All samples in which peak shapes were found to be distorted on the initial run were diluted and reanalyzed. Using the operating conditions just described, we saw the same pattern of peaks in the same elution order as is reported in American Oil Chemists' Society Official Method Ce 1f-96 (9). FAME, including *trans* compounds, were identified by isomer retention time areas as indicated in the figures in Method Ce 1f-96 (9). The responses of components in the lipid standard mixture containing 37 FA (Sigma Chemical Co., St. Louis, MO) were used to calculate response factors for individual FA. Use of the 13:0 internal standard to set response factors indicated that, on average, 96% of the weighed FAME were accounted for in the GC analysis.

Calculations. The amounts of each FA were calculated from the corresponding peak areas. Total fat was calculated as the sum of all individual FA (including *trans* FA) expressed as TG. Saturated fat, monounsaturated fat, polyunsaturated fat, and *trans* fat were calculated as the sums of all FA and expressed as FA in accordance with 21 CFR §101.9 (10). Conversion factors (11) were used for conversion of FAME to their corresponding TG and FA.

Presentation of results. Results for the 117 food products are grouped in eight tables by food category. Each listing represents a single product. Serving size obtained from the label and total fat content determined by analysis are listed for each product. Values for *trans*, saturated, and unsaturated (mono- and poly-) fats, expressed as gram/labeled serving size and as g/100 g fat, are also listed. The final column in each table lists the sum of *trans* + SF expressed as g/100 g fat. Because of the differences in the way the various classes of fat are calculated, the value for total fat expressed as TG will differ slightly from the sum of saturated + monounsaturated + polyunsaturated + *trans* FA expressed as FA.

RESULTS AND DISCUSSION

Modification of AOAC Official Method 996.01. Samples in this study were analyzed according to a modification of AOAC Official Method 996.01 (7). This method was originally developed for the analysis of FA composition in cereal products. We modified the chromatographic conditions as follows to allow for the analysis of FA in a much wider range of foods: We used a split injector ratio of 20:1 rather than 100:1 as specified in AOAC 996.01. A CP Sil 88 fused-silica capillary column measuring 100 m was used instead of the 30-m column specified in AOAC 996.01. This greatly increased resolution of the peaks. The operating conditions called for in AOAC 996.01 (i.e., temperatures: injector, 250°C; detector, 275°C; hydrogen flow, 34 mL/min; air flow, *ca.* 300 mL/min; split ratio, 100:1; carrier gas, He; linear velocity, 21 cm/s at 175°C; initial temperature, 120°C (hold 4 min); rate 5.0°C/min; final temperature, 230°C; final time, 5.0 min) were modified as stated in the foregoing section. Hydrogen, rather than helium as specified in AOAC 996.01, was used as the carrier gas. This increased response resolution. These changes in length of column, temperature program, and carrier gas increased the run time to 73 min/sample but greatly increased the resolution of FAME.

AOAC Official Method 996.01 was modified previously for the recovery of total fat and FA in milk-based Standard Reference Material (SRM) 1846 (12). The results of the study with SRM 1846 (12) confirmed that the mean analyzed values were highly reproducible as indicated by CV of <5% for all major FA (excluding *trans* FA). Mean analyzed values for individual

TABLE 1
Total, *trans*, Saturated, and Unsaturated Fat in Bread, Cake, and Related Products[a]

Food	Total fat g/serving	Serving size, g	*Trans* fat g/serving	*Trans* fat g/100 g fat	SF g/serving	SF g/100 g fat	MUFA g/serving	MUFA g/100 g fat	PUFA g/serving	PUFA g/100 g fat	*Trans* + SF g/serving	*Trans* + SF g/100 g fat
Cake, iced and filled	21.0	74	7.2	34.5	3.8	18.3	6.2	29.5	1.5	7.0	11.1	52.8
Cake rolls, iced and filled	17.0	61	4.7	27.4	3.8	22.6	6.2	36.5	1.5	9.0	8.5	49.9
Biscuits, butter-flavored	9.4	58	3.1	32.7	2.8	30.1	2.9	30.5	0.3	3.1	5.9	62.8
Taco dinner kit	16.0	161	2.6	16.3	2.1	13.4	6.3	39.5	4.3	26.9	4.7	29.7
Sponge cake, filled	12.6	57	2.5	19.7	3.5	28.0	4.4	35.2	1.4	11.1	6.0	47.8
Flaky biscuits	8.7	56	1.8	20.8	2.8	31.5	2.8	32.3	0.9	10.8	4.6	52.3
Buttermilk biscuits	4.9	34	1.7	34.1	1.2	24.4	1.6	32.5	0.3	5.9	2.9	58.5
Butter-flavored biscuits	4.9	34	1.7	34.4	1.2	23.5	1.5	31.3	0.3	5.9	2.8	57.9
Cornbread	4.5	41	1.4	32.1	1.2	27.6	1.4	32.1	0.4	7.9	2.7	59.8
Cereal bars	2.9	22	1.4	48.8	0.8	27.2	0.5	16.4	0.1	2.4	2.2	76.0
Cake, iced and filled	9.2	64	1.4	15.3	2.5	27.3	2.9	31.7	2.2	24.0	3.9	42.6
Pizza kit	4.9	27	1.1	22.8	1.3	25.8	1.9	38.8	0.7	13.6	2.4	48.6
Taco dinner kit	4.4	51	1.1	24.9	0.8	18.1	0.8	18.6	1.5	33.7	1.9	43.0
Fig bars	3.9	31	1.1	27.8	0.6	16.2	1.0	26.2	1.0	25.7	1.7	44.0
Crescent rolls, reduced fat	5.6	28	1.1	19.3	1.8	31.7	1.9	33.5	0.7	12.8	2.9	51.0
Flour tortillas	5.1	42.5	0.9	18.0	1.5	29.8	1.6	31.2	0.9	17.0	2.4	47.8
Taco dinner kit	4.3	82	0.9	20.7	1.1	24.4	1.6	36.9	0.6	13.6	2.0	45.2
Sponge cake, filled	4.3	43	0.9	20.8	1.1	24.8	1.7	38.2	0.5	11.6	2.0	45.6
Apple cobbler bars	3.1	37	0.8	25.4	0.7	22.8	1.1	35.5	0.4	11.7	1.5	48.2
Cereal bars with strawberry	2.8	37	0.7	26.0	0.6	19.6	1.1	38.1	0.3	12.1	1.3	45.6
Oatmeal bars	3.3	37	0.7	22.4	0.8	25.5	1.2	35.3	0.4	12.6	1.6	47.9
Tortillas	3.7	41	0.7	19.5	1.0	27.4	1.3	35.9	0.5	12.6	1.7	46.8
Biscuits, Texas-style	2.6	34	0.7	26.2	0.7	26.6	0.2	8.4	0.9	34.2	1.4	52.9
Cake, chocolate-covered	8.2	38	0.5	6.6	5.0	60.8	1.1	13.8	0.6	7.8	5.5	67.4
Dinner rolls	3.2	40	0.5	16.6	0.9	29.1	1.1	35.3	0.5	14.4	1.5	45.6
Cereal bars	2.3	37	0.5	21.0	0.5	23.6	0.9	37.1	0.3	13.1	1.0	44.5
Mini cake snacks, iced	4.3	38	0.5	10.9	1.3	28.9	1.1	25.2	1.3	28.9	1.7	39.7
Flour tortillas	3.4	50	0.5	13.3	0.7	19.2	1.2	34.5	1.0	28.3	1.1	32.5
Granola bars, with chocolate chips	4.7	28	0.4	7.6	1.4	29.8	2.0	42.3	1.0	20.5	1.8	37.4
Granola bars with peanut butter, chocolate chunks	3.2	28	0.2	7.1	0.9	29.0	1.2	38.0	0.7	20.1	1.2	36.1
Cake, peanut butter-covered	9.3	38	0.1	0.9	4.9	52.4	2.0	21.0	1.9	20.8	5.0	53.3
Tortillas, fat-free	0.8	33	0.1	9.8	0.2	24.4	0.2	22.0	0.3	40.2	0.3	34.2
Flour tortillas	2.7	51	0.1	1.9	0.6	23.0	0.5	19.6	1.5	55.6	0.7	24.8
Chocolate cookie cake	0.3	17	0.0	3.8	0.1	38.5	0.1	23.1	0.1	30.8	0.1	42.3
Corn tortillas	0.8	26	0.0	0.0	0.1	17.9	0.2	23.1	0.4	55.1	0.1	17.9
Granola bars with brown sugar	6.8	42	0.0	0.0	0.7	10.6	3.6	52.5	2.5	36.7	0.7	10.6
Sponge cake, filled	1.4	43	0.0	0.0	0.6	42.4	0.3	22.9	0.4	25.7	0.6	42.4

[a]Values are means of two determinations of each sample. SF, saturated fat; MUFA, monounsaturated FA; PUFA, polyunsaturated FA.

TABLE 2
Total, *trans*, Saturated, and Unsaturated Fat in Margarine Products[a]

Food	Total fat g/serving	Serving size, g	*Trans* fat g/serving	*Trans* fat g/100 g fat	SF g/serving	SF g/100 g fat	MUFA g/serving	MUFA g/100 g fat	PUFA g/serving	PUFA g/100 g fat	*Trans* + SF g/serving	*Trans* + SF g/100 g fat
Soft margarine, soybean oil	8.7	14	2.4	27.7	0.7	8.5	2.8	32.6	2.3	26.6	3.1	36.2
Spread, 70%, soybean oil	9.5	14	2.1	22.4	1.9	19.6	2.9	30.8	2.3	24.2	4.0	42.0
Margarine, soybean oil	10.5	14	1.6	15.6	2.4	22.8	2.8	26.6	3.5	33.4	4.0	38.4
Spreadable sticks, 60%, soybean oil	8.3	14	1.6	19.0	1.7	20.6	2.5	30.3	2.4	29.1	3.3	39.6
Margarine, corn oil	10.4	14	1.5	14.9	1.9	17.9	3.2	30.4	3.4	32.8	3.4	32.8
Spread, 70%, soybean oil	9.3	14	1.5	16.4	1.8	19.8	2.5	26.7	3.1	33.5	3.4	36.2
Spread, 65%, soybean oil	8.3	14	1.3	15.1	2.0	23.4	2.3	27.6	2.7	32.4	3.2	38.5

[a]Values are means of two determinations of each sample. For abbreviations see Table 1.

FA in SRM 1846 analyzed by modified method AOAC 996.01 fell within ±1 SD or less of the certified values. The mean analyzed value for total fat as TG was equal to the mean certified value. This method was then used to determine the total fat and FA content of powdered and liquid infant formulas (13). The results demonstrated the applicability of the method to the analysis of fat and FA in other food matrices. Therefore, this method was employed in the analysis of FA in this study. Mossoba *et al.* (14) recently reviewed the most common GC and IR spectroscopic official methods for the determination of *trans* FA for food-labeling purposes.

Food sources of trans *fat.* In FDA's *trans*-FA labeling proposal (4) and in the final rule (5), the agency estimated the average *trans*-fat intakes of adults in the United States from, among other sources, the USDA Continuing Survey of Food Intake by Individuals 1994–1996 (8). Estimates were provided for food groups based on product type. The contribution to *trans*-fat intake based on food groups is as follows: bread, cake, cookies, crackers, and related products, 41%; margarine, 17%; animal products (meat, milk, butter, cheese, cream, sour cream), 21%; fried potatoes, 8%; potato chips, corn chips, popcorn (salty snacks), 5%; household shortening, 4%; salad dressing, 3%; candy, 1%; breakfast cereal, 1% (5).

We used these groups as the basis for our purchase of foods for analysis. We queried the Information Resources, Inc. (IRI) InfoScan (15) database to identify the market leader brands within those product types. The IRI InfoScan database contains dollar and sales information from food and dietary supplement products from a sample of more than 32,000 grocery, drug, and mass merchandiser stores with annual sales of $2 million and above across the continental United States. IRI applies projection factors to the sample store data to estimate total sales in the continental United States. We selected the market leader products in eight of the groups, purchased the identified products, and conducted analyses to determine total FA composition.

The groups and number of products we analyzed were as follows: Table 1, bread, cake, and related products, 37; Table 2, margarines, 7; Table 3, cookies and crackers, 23; Table 4, frozen potatoes, 6; Table 5, potato chips, corn chips, and popcorn (salty snacks), 16; Table 6, vegetable oils and shortenings, 12; Table 7, salad dressings and mayonnaise, 14; and Table 8, dry breakfast cereal, 2. We did not analyze meat or dairy products, or, with the exception of two breakfast cereals, those products that provide only about 1% of total *trans* intake (e.g., candy, cream, sour cream, butter, breakfast cereals).

Overview of results. We calculated the sum of *trans* fat + SF for each product because there is strong agreement among expert panels (2,5) that the available evidence is sufficiently compelling to conclude that intakes of *trans* fat and SF increase risk of coronary heart disease. Accordingly, expert panels recommend, in addition to the long-standing recommendations regarding limitation in SF intake, that consumers also reduce their intake of *trans* fat.

The highest level of *trans* fat, expressed as gram/serving or as g/100 g fat, was found in foods in the bread, cake, and related products group (Table 1). In 11 of 37 (30%) of the products

TABLE 3
Total, *trans*, Saturated, and Unsaturated Fat in Cookies and Crackers[a]

Food	Total fat g/serving	Serving size, g	*Trans* fat g/serving	*Trans* fat g/100 g fat	SF g/serving	SF g/100 g fat	MUFA g/serving	MUFA g/100 g fat	PUFA g/serving	PUFA g/100 g fat	*Trans* + SF g/serving	*Trans* + SF g/100 g fat
Soft wafers	7.7	32	2.6	34.0	1.6	20.2	3.0	38.7	0.2	3.0	4.2	54.2
Cheese sandwich crackers	9.7	31	2.5	25.7	2.2	22.8	4.2	43.1	0.4	4.0	4.7	48.5
Cheese sandwich crackers	7.4	31	2.1	29.0	2.0	27.1	2.9	39.3	0.4	5.4	4.1	56.2
Chocolate sandwich cookies	8.4	29	2.1	25.0	1.9	22.5	3.5	42.1	0.5	5.7	4.0	47.5
Cookies	6.3	28	2.0	31.4	1.4	22.6	2.2	35.4	0.4	6.5	3.4	54.0
Baked snack crackers	5.7	31	1.9	33.7	1.2	21.5	2.1	36.5	0.2	3.9	3.1	55.2
Crackers	7.9	31	1.9	23.8	2.4	29.9	2.9	37.4	0.4	4.8	4.2	53.6
Lemon filled cookies	5.7	32	1.6	28.3	1.2	21.6	2.2	39.1	0.4	6.5	2.8	49.9
Whole wheat crackers	4.8	28	1.5	31.5	0.9	19.3	1.8	37.3	0.3	7.0	2.5	50.7
Assorted cookies	5.0	28	1.4	27.7	1.5	30.5	1.5	30.9	0.3	6.2	2.9	58.2
Chocolate chip cookies	5.9	32	1.4	23.1	1.8	30.2	2.3	38.3	0.2	4.1	3.1	53.2
Cheese-baked snack crackers	6.3	30	1.3	20.8	1.6	24.8	2.4	38.3	0.7	11.8	2.9	45.6
Chocolate sandwich cookies	5.9	32	1.2	20.7	1.3	21.2	2.4	40.5	0.8	13.3	2.5	42.0
Chocolate chip cookies	4.7	33	1.2	25.1	1.4	29.1	1.7	36.8	0.2	4.9	2.6	54.3
Crackers	3.5	16	1.1	33.0	0.7	19.4	1.3	37.7	0.2	6.1	1.8	52.5
Peanut butter sandwich crackers	6.5	31	1.1	16.4	1.5	22.8	2.5	38.9	1.2	17.6	2.6	39.2
Sandwich cookies	3.0	26	1.1	35.3	0.6	19.3	1.1	36.0	0.2	7.7	1.6	54.7
Baked snack crackers	5.3	30	0.9	17.7	1.5	27.7	2.0	37.1	0.7	12.4	2.4	45.4
Vanilla sandwich cookies	4.0	26	0.8	21.0	0.9	23.0	1.7	43.3	0.4	9.3	1.8	44.0
Oatmeal cookies	5.7	28	0.8	13.2	1.5	26.7	1.7	30.3	1.4	24.7	2.3	39.9
Saltine crackers	1.9	15	0.5	28.6	0.4	21.7	0.8	40.7	0.2	7.9	1.0	50.3
Saltine crackers	1.3	15	0.5	35.1	0.3	20.9	0.4	31.3	0.1	9.0	0.8	56.0
Strawberry-filled cookies	3.7	25	0.3	7.7	1.6	43.7	1.3	35.8	0.3	8.7	1.9	51.4

[a]Values are means of two determinations of each sample. For abbreviations, see Table 1.

TABLE 4
Total, *trans*, Saturated, and Unsaturated Fat in Frozen Potato Products[a]

Food	Total fat g/serving	Serving size, g	*Trans* fat g/serving	*Trans* fat g/100 g fat	SF g/serving	SF g/100 g fat	MUFA g/serving	MUFA g/100 g fat	PUFA g/serving	PUFA g/100 g fat	*Trans* + SF g/serving	*Trans* + SF g/100 g fat
Frozen potato product	13.2	84	3.3	24.7	2.8	21.5	5.5	41.7	1.0	7.7	6.1	46.2
Frozen potato product	6.9	86	2.0	28.9	1.3	18.7	3.2	46.2	0.2	3.0	3.3	47.6
Frozen potato product	5.1	84	1.4	27.1	1.0	19.8	2.3	44.8	0.2	3.0	2.4	46.9
Frozen potato product	4.5	84	1.2	27.7	0.9	19.5	2.0	45.0	0.2	3.4	2.1	47.2
Frozen potato product	3.7	84	1.0	28.4	0.7	19.7	1.4	38.5	0.3	8.7	1.8	48.1
Frozen potato product	2.5	84	1.0	38.2	0.5	20.5	0.7	27.7	0.2	9.2	1.5	58.6

[a]Values are means of two determinations of each sample. For abbreviations, see Table 1.

TABLE 5
Total, *trans*, Saturated, and Unsaturated Fat in Salty Snacks[a]

Food	Total fat g/serving	Serving size, g	*Trans* fat g/serving	*Trans* fat g/100 g fat	SF g/serving	SF g/100 g fat	MUFA g/serving	MUFA g/100 g fat	PUFA g/serving	PUFA g/100 g fat	*Trans* + SF g/serving	*Trans* + SF g/100 g fat
Tortilla chips	7.9	28	1.1	14.3	1.3	16.1	2.9	36.7	2.2	28.1	2.4	30.4
Tortilla chips	6.9	28	1.0	14.6	1.3	18.1	2.6	38.2	1.7	24.7	2.3	32.7
Tortilla chips	6.9	28	0.9	12.8	1.3	18.8	2.4	34.5	2.1	30.3	2.2	31.6
Tortilla chips	5.2	42.5	0.9	17.1	1.6	30.5	1.6	30.7	0.9	16.7	2.5	47.6
Potato chips	9.3	28	0.9	9.3	2.3	24.3	2.5	26.6	3.3	35.1	3.1	33.6
Tortilla chips	3.4	49.5	0.5	13.3	0.7	19.2	1.2	34.5	1.0	28.3	1.1	32.4
Potato chips	11.1	28	0.1	0.7	1.3	11.7	2.8	25.5	6.8	61.8	1.4	12.4
Tortilla chips	0.8	33	0.1	9.8	0.2	24.4	0.2	22.0	0.3	40.2	0.3	34.1
Potato chips	7.2	28	0.1	0.9	1.8	24.7	1.1	15.9	4.2	58.5	1.8	25.6
Potato chips	11.8	28	0.0	0.2	2.9	24.7	1.7	14.7	7.1	60.4	2.9	24.9
Potato chips	10.9	28	0.0	0.2	2.6	23.6	1.6	14.2	6.2	56.7	2.6	23.8
Potato chips	10.3	28	0.0	0.2	1.4	14.0	2.9	28.2	5.5	53.2	1.5	14.2
Potato chips	11.3	28	0.0	0.2	2.6	23.3	1.6	14.2	6.5	57.7	2.7	23.5
Potato chips	9.9	28	0.0	0.2	2.4	24.3	1.4	14.1	5.6	56.9	2.4	24.5
Tortilla chips	0.8	26	0.0	0.0	0.1	17.9	0.2	23.1	0.4	55.1	0.1	17.9
Tortilla chips	2.1	28	0.0	0.0	0.3	13.8	0.5	23.8	1.2	59.0	0.3	13.8

[a]Values are means of two determinations of each sample. For abbreviations, see Table 1.

TABLE 6
Total, *trans*, Saturated, and Unsaturated Fat in Vegetable Oils and Shortenings[a]

Food	Total fat g/serving	Serving size, g	*Trans* fat g/serving	*Trans* fat g/100 g fat	SF g/serving	SF g/100 g fat	MUFA g/serving	MUFA g/100 g fat	PUFA g/serving	PUFA g/100 g fat	*Trans* + SF g/serving	*Trans* + SF g/100 g fat
Shortening, soybean and cottonseed oils	12.3	13	1.6	12.6	2.9	23.5	4.0	32.3	3.3	27.0	4.4	36.1
Shortening, soybean and cottonseed oils	11.4	12	1.5	13.2	2.7	24.0	3.8	33.1	2.8	24.9	4.3	37.2
Canola oil	13.5	14	0.1	0.5	1.0	7.5	7.9	58.6	3.9	28.7	1.1	8.1
Soybean oil	14.3	14	0.1	0.3	2.0	13.9	3.0	20.9	8.7	60.9	2.1	14.3
Safflower oil	12.4	14	0.0	0.3	1.1	9.0	1.6	12.9	9.1	73.3	1.2	9.3
Soybean oil	13.5	14	0.0	0.3	2.0	15.1	2.8	20.6	8.0	59.4	2.1	15.4
Canola oil	13.4	14	0.0	0.1	1.0	7.5	7.9	59.2	3.8	28.8	1.0	7.6
Olive oil	12.0	14	0.0	0.1	2.3	19.1	6.9	57.5	2.3	18.8	2.3	19.2
Extra virgin olive oil	12.8	14	0.0	0.0	1.8	14.3	9.2	71.9	1.2	9.4	1.8	14.3
Spanish olive oil	11.8	13	0.0	0.0	1.8	15.4	8.8	74.6	0.9	7.9	1.8	15.4
Virgin olive oil	11.9	14	0.0	0.0	1.8	14.8	8.7	73.4	0.9	7.4	1.8	14.8
Corn oil	15.9	14	0.0	0.0	1.9	11.8	4.1	25.8	9.2	57.5	1.9	11.8

[a]Values are means of two determinations of each sample. For abbreviations, see Table 1.

TABLE 7
Total, *trans*, Saturated, and Unsaturated Fat in Salad Dressings and Mayonnaise[a]

Food	Total fat g/serving	Serving size, g	*Trans* fat g/serving	*Trans* fat g/100 g fat	SF g/serving	SF g/100 g fat	MUFA g/serving	MUFA g/100 g fat	PUFA g/serving	PUFA g/100 g fat	*Trans* + SF g/serving	*Trans* + SF g/100 g fat
Creamy ranch dressing	14.0	30	0.1	0.6	2.3	16.0	3.0	21.4	8.7	62.1	2.3	16.6
Italian dressing	9.9	30	0.1	0.6	1.9	18.7	2.7	27.6	5.2	53.0	1.9	19.4
Olive oil and vinegar dressing	27.6	27	0.1	0.2	4.2	15.2	12.1	43.7	10.1	36.6	4.2	15.4
Mayonnaise	11.5	14	0.1	0.4	1.7	14.9	2.5	21.3	6.8	58.7	1.8	15.4
Ranch dressing	27.6	30	0.0	0.1	2.8	10.0	4.0	14.6	19.5	70.6	2.8	10.2
Italian dressing	23.7	29	0.0	0.2	3.1	13.1	5.7	24.1	13.8	58.2	3.1	13.2
Ranch dressing	25.1	29	0.0	0.1	4.1	16.4	5.3	21.0	14.6	58.1	4.2	16.6
Mayonnaise	6.3	15	0.0	0.5	0.9	14.8	1.4	22.1	3.7	58.1	1.0	15.3
Italian dressing	9.5	30	0.0	0.2	1.3	14.1	1.8	19.3	5.9	62.4	1.4	14.3
Mayonnaise	12.1	14	0.0	0.2	2.7	22.7	2.7	22.2	6.7	55.0	2.8	22.8
Italian dressing	0.5	33	0.0	2.2	0.3	65.2	0.1	23.9	0.0	2.2	0.3	67.4
Reduced-fat dressing	5.4	32	0.0	0.0	0.9	15.7	1.2	22.4	3.1	58.1	0.9	15.7
Fat-free ranch dressing	0.5	32	0.0	0.0	0.2	43.8	0.1	22.9	0.2	33.3	0.2	43.8
Light mayonnaise	4.7	15	0.0	0.0	0.8	16.3	1.0	21.4	2.7	57.7	0.8	16.3

[a]Values are means of two determinations of each sample. For abbreviations, see Table 1.

TABLE 8
Total, *trans*, Saturated, and Unsaturated Fat in Breakfast Cereal[a]

Food	Total fat g/serving	Serving size, g	*Trans* fat g/serving	*Trans* fat g/100 g fat	SF g/serving	SF g/100 g fat	MUFA g/serving	MUFA g/100 g fat	PUFA g/serving	PUFA g/100 g fat	*Trans* + SF g/serving	*Trans* + SF g/100 g fat
Cereal	1.5	30	0.0	2.0	0.4	23.6	0.4	29.7	0.6	39.9	0.4	25.7
Cereal	1.1	53	0.0	0.0	0.2	20.9	0.2	15.5	0.6	57.3	0.2	20.9

[a]Values are means of two determinations of each sample. For abbreviations, see Table 1.

analyzed, *trans*-fat levels exceeded 25 g/100 g fat, and in 28 of 37 products analyzed (76%), the sum of *trans* fat + SF exceeded 40 g/100 g fat. Levels of *trans* fat and SF in margarine products (Table 2) ranged from 15 to 28 and 9 to 23 g/100 g fat, respectively. The sums of *trans* fat + SF for these products fell within a relatively narrow range of 33–42 g/100 g fat. Cookies and crackers contained 8–35 g *trans* fat/100 g fat, and the sum of *trans* fat + SF for these products ranged from 39 to 58 g/100 g fat (Table 3). All frozen potato products examined contained 25–38 g *trans* fat/100 g fat (Table 4). The sum of *trans* fat + SF was in the range of 46–59 g/100 g fat for these products. Low levels of *trans* fat, expressed as g/100 g fat, were found in salty snacks, vegetable oils and shortenings, salad dressings and mayonnaise, and breakfast cereals (Tables 5, 6, 7, and 8, respectively). There was considerable variability in the *trans*-FA content of foods within each food category.

One of the problems addressed in FDA's final rule was the inadequacy in assessment of intakes of *trans* FA by the U.S. population. This is because current USDA data for the *trans*-FA content of foods are limited to a few foods with a relatively small number of samples (5, page 41445). The available database provides analytical data on the *trans*-FA content of 214 foods obtained under USDA contract. The samples analyzed for this data set were collected between 1989 and 1993. It is important to note that the formulations for these products may have changed, and USDA advised that caution be exercised when using the values (http://www.nal.usda.gov/fnic/foodcomp).

Estimating the amounts of *trans* FA in the food supply has been hampered by the lack of an accurate and comprehensive database for use in deriving consumption data. The trend toward reformulation of products over the last decade also has made it difficult to develop satisfactory intake data. Additionally, the variability noted above in the *trans*-FA content of foods within a food category is extensive and can introduce substantial error when calculations are based on food-frequency questionnaires that rely heavily on groupings of similar foods.

The Institute of Medicine of the National Academy of Sciences (IOM/NAS) noted in its recent report (3) that additional research was needed in the area of *trans* fat. Among the research needed was the development of a comprehensive database for the *trans*-fat content of the U.S. food supply. Such a database could be used to determine *trans*-FA intakes in different age and socioeconomic groups. IOM/NAS (3) also noted that efforts should be made to assess major sources of *trans* FA currently in the marketplace and to develop alternatives similar to those made for foods high in saturated FA. It is anticipated that the current database and updates to USDA's database will contribute to both of these needs.

ACKNOWLEDGMENTS

The authors thank Cory Fominaya, University of Maryland, College Park, Maryland, and Daniel Brecher, Wootton High School, Rockville, Maryland, for their assistance in sample analysis and data handling.

REFERENCES

1. Craig-Schmidt, M.C. (1992) Fatty Acid Isomers in Foods, in *Fatty Acids in Foods and Their Health Implications* (Chow, C.K., ed.), pp. 365–398, Marcel Dekker, New York.
2. Expert Panel on Detection, Evaluation and Treatment of High Blood Cholesterol in Adults, Third Report of the National Cholesterol Education Program (NCEP) Expert Panel on Detection, Evaluation and Treatment of High Blood Cholesterol in Adults (Adult Treatment Panel III), Chapter II, "Rationale for Intervention," and Chapter V, "Adopting Healthful Lifestyle Habits to Lower LDL Cholesterol and Reduce CHD Risk," http://www.NHLBI.nih.gov (accessed August 2003).
3. Institute of Medicine, National Academy of Sciences (IOM/NAS) (2002) Dietary Reference Intakes for Energy, Carbohydrate, Fiber, Fat, Fatty Acids, Cholesterol, Protein and Amino Acids (Macronutrients), Chapters 8 and 11, National Academy Press, Washington, DC, http://www.nap.edu (accessed August 2003).
4. Department of Health and Human Services, FDA (1999), Food Labeling: *Trans* Fatty Acids in Nutrition Labeling; Nutrient Content Claims, and Health Claims; Proposed Rule, *Federal Register 64*, No. 221, November 17, 1999, pp. 62746–62825.
5. Department of Health and Human Services, FDA (2003) Food Labeling; *Trans* Fatty Acids in Nutrition Labeling; Nutrient Content Claims, and Health Claims; Final Rule, *Federal Register 68*, No. 133, July 11, 2003, pp. 41434–41506.
6. Fat and Fatty Acid Content of Selected Foods Containing *trans* Fatty Acids, USDA Nutrient Database, www.nal.usda.gov/fnic/foodcomp (accessed August, 2003).
7. AOAC International, Official Method 996.01 (2002) Fat (total, saturated, unsaturated and monounsaturated) in Cereal Products, *Official Methods of Analysis of the AOAC*, 17th edn., revised, AOAC International, Gaithersburg, MD (revisions, 2002).
8. USDA, ARS (1998) Continuing Survey of Food Intake by Individuals (CSFII) and 1994–1996 Diet and Health Survey and Technical Support Databases, National Technical Information Service, Springfield, VA.
9. American Oil Chemists' Society (AOCS) (1999) Official Method Ce 1f-96 (revised 2002), Determination of *cis*- and *trans*-Fatty Acids in Hydrogenated and Refined Oils and Fats by Capillary GLC, *Official Methods and Recommended Practices of the AOCS*, 5th edn. (Firestone, D., ed.), Champaign.
10. *Code of Federal Regulations (CFR)* (2003); Part 21, § 101.9. U.S. Government Printing Office, Washington, DC.
11. DeVries, J.W., Kjos, L., Groff, L., Martin, B., Cernohous, K., Patel, H., Payne, H., Leichtweis, H., Shay, M., and Newcomer, L. (1999) Studies in Improvement of Official Method 996.06, *J. AOAC Int. 82*, 1146–1155.
12. Satchithanandam, S., Fritsche, J., and Rader, J.I. (2000) Extension of AOAC Official Method 996.01 to the Analysis of Standard Reference Material (SRM) 1846 and Infant Formulas, *J. AOAC Int. 84*, 805–813.
13. Satchithanandam, S., Fritsche, J., and Rader, J.I. (2002) Gas Chromatographic Analysis of Infant Formulas for Total Fatty Acids, Including *trans* FA, *J. AOAC Int. 85*, 86–89.
14. Mossoba, M.M., Kramer, J.K.G., Delmonte, P., Yurawecz, M.P., and Rader, J.I. (2003) *Official Methods for the Determination of* trans *Fat*, AOCS Press, Champaign, 22 pp.
15. Information Resources, Inc. (1999) *Infoscan 1999 Annual Data*, Information Resources, Chicago.

[Received September 15, 2003; accepted December 23, 2003]

Variations of *trans* Octadecenoic Acid in Milk Fat Induced by Feeding Different Starch-Based Diets to Cows

S. Jurjanz[a,]*, V. Monteils[a], P. Juaneda[b], and F. Laurent[a]

[a]Laboratoire de Sciences Animales, Institut National de la Recherche Agronomique–Ecole Nationale Supérieure d'Agronomique et des Industries Alimentaires (INRA–ENSAIA), Vandoeuvre-lès-Nancy, France, and [b]Unité de Nutrition Lipidique, INRA de Dijon, France

ABSTRACT: The impact of starch sources differing in their velocities of ruminal degradation on the milk fat of dairy cows was studied. The animals received diets containing a slowly degradable (potatoes) or rapidly degradable (wheat) starch concentrate (40% of the dry matter) in a total mixed diet. Milk fat was the only animal performance factor affected: Cows produced significantly less milk fat when fed the wheat diet than the potato diet (–3.3 g/kg, –122 g/d; $P < 0.05$). With the wheat diet, milk fat was poorer in short-chain FA and richer in unsaturated long-chain FA, especially in *trans* octadecenoic acid (4.4 vs. 2.7% of the total FA, $P < 0.05$). A very large increase in the isomer *trans*-10 18:1 (+1.46% of the total FA) was observed. Because no difference in volatile FA concentrations in the rumen was revealed, the increase in *trans* octadecenoic acids, and particularly the isomer *trans*-10 18:1, was associated with the larger postprandial drop in ruminal pH with wheat. Similar concentrate levels and FA profiles in both diets indicated that the decrease in milk fat was due to changes in the ruminal environment. Quicker degradation of wheat starch, and hence a greater drop in pH with this diet associated with the absence of any effect on volatile FA, strengthen the hypothesis developed in the literature of enzyme inhibition *via* increased levels of *trans* octadecenoic acids, especially the *trans*-10 isomer. Hence, milk fat can be decreased with rapidly degradable starch sources and not only with high levels of concentrates in the diet or added fat. More detailed work is necessary to elucidate the microorganisms involved and to determine whether metabolic pathways similar to those reported for high-concentrate diets are involved.

Paper no. L9325 in *Lipids 37,* 19–24 (January 2004).

Trans FA (TFA) have often been associated with a risk of coronary heart disease (1,2) and an increase in arterial cholesterol content in humans (3–5). With current eating habits, the main source of TFA in human nutrition is partially hydrogenated vegetable oils (6,7). Milk fat and its FA are another source, even though low proportions of animal TFA in the total intake often make it difficult to prove the relationship between animal TFA and health risks in epidemiological studies. However, controlling the TFA concentration in milk makes it possible to avoid an undesirable increase in the TFA content of dairy products.

*To whom correspondence should be addressed at Laboratoire de Sciences Animales, INRA-ENSAIA, B.P. 172, 2 Avenue de la Forêt de Haye, 54505 Vandoeuvre cedex, France. E-mail: jurjanz@ensaia.inpl-nancy.fr

Abbreviations: IPE, isopropyl esters; TFA, *trans* FA; VFA, volatile FA.

The presence of TFA in milk fat is closely linked to incomplete biohydrogenation of PUFA in the rumen. The main *trans* forms in milk fat are octadecenoic acids; other FA represent only small proportions of TFA in milk (6). *Trans* double bonds are mainly synthesized during hydrogenation of unsaturated FA by enzymes of different rumen bacteria (8,9). Ruminal conditions, especially a precipitous postprandial drop in pH, enhances biohydrogenation, leading to *trans* bonds in the FA chain (10,11). The reduction of *trans*-18:1 is generally rate limiting for the complete hydrogenation of unsaturated octadecenoic acids. Hence, there is often a ruminal accumulation of *trans*-18:1 but rarely of CLA containing *trans* double bonds (12). CLA can be absorbed in the small intestine or synthesized in the mammary gland by desaturation of TFA (13).

A high level of concentrate in the diet has been shown to be a determining factor for a sharp drop in ruminal pH and increased TFA contents in milk fat (10,14–16). Recently, it has been shown that rapid starch degradation also can accelerate the postprandial drop in pH (17). The objective of this study was to determine whether differences in the velocity of starch degradation in the rumen of dairy cows caused a decrease in milk fat provoked by TFA accumulation. Specifically, this work studied the effects of *trans* octadecenoic acid and its isomers on milk fat and also the effect of CLA by focusing on rumen fermentation.

MATERIALS AND METHODS

Animals, diets, and experimental design. This trial was conducted during winter 2001 (January to March) at our experimental station near Nancy (East France). Four multiparous Holstein cows were assigned to a single reverse design to study the effect of starch source (i.e., velocity of ruminal degradation) on milk composition. Animals were housed in a free-stall barn and were milked twice daily (6 AM and 5 PM). At the start of the trial, cows weighed 653 kg (±57 kg) on average and had been in lactation for at least 21 d. Cows were fitted with ruminal cannulas (#3; Bar Diamond, Parma, ID) at least 6 wk before the trial in accordance with French animal care guidelines. Each cow received a corn silage-based total mixed diet completed with wheat straw, soybean meal, urea, wheat or potatoes as the starch source, and a mineral–vitamin mix. Diets were designed to meet the requirements of high-yielding dairy cows according to the French system (18). The

composition and nutritive value of both diets are presented in Table 1.

Each experimental period consisted of 1 wk of transition, 2 wk of adaptation, and 1 wk for sampling and measurement.

Sampling. Cows were fed once daily in the morning (*ad libitum* intake) using electronic feed gates (SEFER Co., Neuville de Poitou, France). Feed intake and the corresponding dry matter intake were recorded daily by an individual transponder providing access to one of the gates for each cow. A sample of each feedstuff was taken during each measurement week. Milk yield was recorded automatically at each milking time (system ISALAIT 2045; Bou-Matic, Saint-Nom-la-Bretêche, France). During the measurement week of each period, milk was sampled at four consecutive milking times (from Tuesday PM to Thursday AM). After the last milk sampling on Thursday morning, a kinetic assay of the rumen fluid composition was carried out. At each experimental period, the rumen fluid of each cow was sampled immediately before access to the diet after the morning milking (time 0) and was subsequently sampled at 1, 2, 4, 5, 6, 8, 10, and 12 h using a rigid tube *via* the rumen cannula to ensure that samples were taken from the same rumen layer. Thus, the ruminal fluid was sampled every hour after the main intake peaks (after morning milking: time 0; after the distribution of the daily ration: time 4) and every 2 h for the rest of the day. Ruminal pH was determined immediately by a portable pH meter (electrode Xerolyt Ingold M6-DXK S7/25, Portamess 751; Knick, Darmstadt, Germany). The liquid phase was separated from the bacteria and solid particles by centrifugation ($4000 \times g$ for 20 min) and was frozen immediately.

Analytical methods and calculations. Because the composition of both tested diets was very similar (Table 1), only the FA composition of the starch concentrates was analyzed, according to the method of Gontier *et al.* (19).

The concentrations of volatile FA (VFA) in the ruminal fluid were determined after thawing by GC according to the method of Jouany (20).

The milk was analyzed by the IR method (Fossomatic; Fosselectric, Hillerød, Denmark) to determine fat and protein contents. Milk fat was separated by centrifugation ($4500 \times g$ for 45 min) and dissolved in hexane (10 mL for 10 g of fat) to determine the FA composition.

FA were analyzed using two different esterification procedures to ensure that all FA were analyzed. Because heating and acid esterification modified the CLA, isopropyl esters (IPE) were used for analysis of FA only up to 18:0. Longer FA such as CLA were analyzed in the form of methyl esters (FAME) with a soft transesterification.

The IPE were prepared by treating the milk fat with isopropanol/H_2SO_4 (87.5:12.5, by vol) at 100°C for 1 h (21). The IPE were then extracted twice with hexane, and the phases were clarified by centrifugation for 3 min at $3000 \times g$. The IPE were analyzed by GC (Hewlett-Packard model 5890, Series II; Hewlett-Packard, Palo Alto, CA) fitted with a split–splitless injector (250°C) and an FID (280°C). A BPX-70 column (60 m, 0.25 mm i.d., 0.25 μm layer thickness; SGE, Melbourne, Australia) was used. The carrier gas was hydrogen. The temperature program was as follows: 5 min at 50°C, an increase of 5°C/min from 50–190°C, 15 min at 190°C, an increase of 20°C within 1 min, and maintained 10 min at 210°C.

FAME were prepared by dissolving the milk fat in toluene and heating this solution with sodium methanolate (16.499-2; Aldrich, St. Quentin Fallavier, France) for 5 min at 50°C. The reaction was stopped by adding 0.1 mL of acetic acid, cooling the mixture to approximately 20°C, and extracting the FAME with hexane as described above for IPE. The GC column used was a 100 m CP Sil 88 column (0.25 mm i.d., 0.2 μm layer thickness; Varian, Les Ulis, France). The oven temperature was increased by 20°C/min from 60–200°C, and the final temperature was maintained for 55 min.

The areas of IPE were transformed into areas of FAME using the following relationship: FAME = (area FAME 18:0/area IPE 18:0) × area IPE. Stearic acid was used as a reference peak, and all areas were reported as the sum of detected esters of the total fat.

To analyze the positional isomers of *trans* octadecenoic acids (22), FAME samples were dried under nitrogen and dissolved in acetone. The *trans* octadecenoic acids were then separated from the other FA esters by RP-HPLC using two Kromasil C18 columns (250 mm length, 10 mm i.d., 5 μm layer thickness; ThermoHypersil, Les Ulis, France) in series. The mobile phase was acetonitrile (100%) at a flow rate of 4 mL/min. The detector was a differential refractometer (RI 410; Waters, St. Quentin-en-Yvelines, France). The samples were collected manually and dried under nitrogen before again dissolving them in hexane. The positional isomers of the separated *trans* octadecenoic acids were analyzed using the same GC column as described above for the analysis of FAME but using a different temperature program: 1 min at 60°C, increased at 20°C/min to 160°C, and held there for 29 min.

TABLE 1
Composition and Nutritive Values of Diets

Feedstuff (% of dry matter)	Wheat diet	Potato diet
Corn silage	55.3	52.2
Wheat straw	2.9	2.7
Cracked wheat	29.9	0
Potatoes[a]	0	28.8
Soybean meal	10.4	14.3
Urea	0	0.4
Mineral and vitamin mix	1.6	2.0
Nutritive values (per kg dry matter)		
Net energy lactation[b] (Mcal)	1.58	1.51
Crude protein[c] (g)	130	127
Ether extract[d] (g)	18.0	13.7
Starch[e] (g)	410	404
Crude fiber[f] (g)	114	109

[a]Potatoes: screening®, Farm Frites Group, Montigny-le-Roi, France.
[b]Calculated according to Jarrige Co. (see review in Ref. 15).
[c]Kjeldahl method.
[d]Norm V 18-117, AFNOR 1997, Paris, France.
[e]Norm V 18-121, AFNOR 1997, Paris, France.
[f]Weende method (Norm V 03-040, AFNOR 1993, Paris, France).

Statistics. The weekly averages of dry matter intake, milk yield, and milk composition were treated statistically with ANOVA using the MIXED procedure of SAS (SAS Institute, Cary, NC). The model included the fixed factor "starch concentrate" (wheat or potatoes) and the randomized factor "cow." The FA composition of milk was analyzed in the same way except for FA representing less than 0.05% of milk fat, which were excluded from statistical analyses and considered as traces.

VFA concentrations and pH of the ruminal fluid were analyzed by ANOVA using the MIXED procedure of SAS (SAS Institute) with the repeated-time option. The fixed factors included in the model were: starch concentrate (wheat or potatoes), sampling time, and the interaction between them, as well as the randomized factor "cow." The covariance structure between the different sampling times was defined in the model as being autoregressive after verification of Akaike and Schwarz–Bayesian criteria (23).

RESULTS

The compositions of the diets were similar except for the starch source (Table 1). The FA composition of both starch sources was also similar (Table 2). Only traces of short- and medium-chain FA and high proportions of linoleic acid (9*c*,12*c*-18:2) were revealed; linoleic acid can therefore be considered as the main lipid source for ruminal biohydrogenation.

On average, the pH of the ruminal fluid (Table 3) was significantly lower (–0.17 units, $P < 0.05$) with the wheat diet compared with the potato diet. This difference in pH was clearly evident in the postprandial pH time course (Fig. 1); with the potato diet the pH dropped first after the beginning of intake and rose again after 2 h, in contrast with the wheat diet. From the second intake peak at 4 h, the pH remained lower with wheat. This difference was significant at 4 (–0.32, $P < 0.05$) and 5 h (–0.34, $P < 0.05$). On the other hand, the starch source had no effect on VFA concentration or proportion of the main VFA (acetate, propionate, or butyrate) in the ruminal fluid, nor generally for the time course (Table 3) at a specific sampling time. Although slight differences existed at time 0 and persisted the first hour (time course not shown), differences never reached the significance threshold. Hence, the total VFA levels during the time course were very similar. Generally, the low proportion of acetate and high proportion of propionate characterized well these corn silage-based diets containing 40% concentrate.

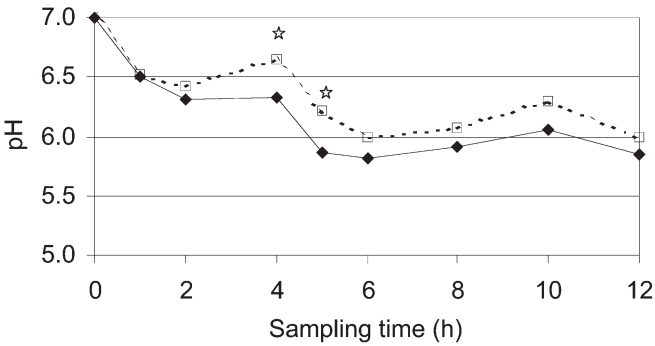

FIG. 1. Effect of type of starch concentrate in the diet on ruminal pH during the time course of the experiment ($n = 4$ at each sampling time). ◆, Wheat; □, potatoes. A star (☆) marks a significant ($P < 0.05$) difference between means at a given sampling time.

The dry matter and starch intakes, milk yield, milk protein content, and protein yield were not affected by either kind of starch concentrate in the diet (Table 4). Nevertheless, milk fat (content and yield) was significantly lower with the wheat diet than with the potato diet (–3.3 g/kg and –122 g/d, respectively, $P < 0.05$).

The FA composition of milk fat from cows fed the wheat diet had significantly less short-chain FA (<10:0) and medium-chain FA (14:0 and 16:0) than milk fat from cows fed the potato diet (Table 5). Saturated medium-chain FA (14:0 and 16:0) were affected in the same way. Conversely, milk fat from cows fed the wheat diet had significantly more unsaturated long-chain FA such as 18:1, 18:2, 18:3, and 20:1n-9 without affecting saturated long-chain FA (Table 5). This effect was particularly evident for the content of *trans* octadecenoic acids, which was nearly twice as high in milk

TABLE 2
FA Composition (wt%) of Starch Concentrates Used

FA	Wheat	Potato
16:0	18.1	17.9
18:0	1.9	1.6
18:1[a]	12.3	12.1
18:2n-6	62.6	63.4
18:3n-3	5.1	5.1

[a]Sum of 18:1n-9 and 18:1n-7.

TABLE 3
Effect of Starch Source on Ruminal Fermentation Profile (average values of the kinetics)[a]

	Wheat diet	Potato diet	Root mean SE
pH	6.19[b]	6.36[a]	0.30
Total VFA (mmol/L)	93	95	19
Acetate (mol/100 mol)	46.0	47.2	5.2
Propionate (mol/100 mol)	27.3	27.2	5.6
Butyrate (mol/100 mol)	18.9	18.0	5.0

[a]Means within a row with different superscript roman letters are significantly ($P < 0.05$) different. VFA, volatile FA.

TABLE 4
Effect of Starch Source on Animal Performance Factors[a]

	Wheat diet	Potato diet	Root mean SE
Dry matter intake (kg/d)	19.6	19.2	1.4
Starch intake (kg/d)	8.0	7.7	0.56
Milk yield (kg/d)	32.1	32.3	3.3
Fat content (g/kg)	31.4[b]	34.7[a]	2.7
Protein content (g/kg)	29.9	30.1	1.3
Fat yield (g/d)	1022[b]	1144[a]	98
Protein yield (g/d)	942	983	99

[a]Means within a row with different superscript roman letters are significantly ($P < 0.05$) different.

TABLE 5
Effect of Starch Source on Milk Fat Composition (wt%)[a]

FA	Wheat diet	Potato diet	Level of significance	Root mean SE
4:0	3.05[b]	3.36[a]	0.05	0.35
6:0	2.18[b]	2.46[a]	0.01	0.28
8:0	1.22[b]	1.46[a]	0.01	0.14
10:0	3.40[b]	3.69[a]	0.05	0.36
10:1	0.30[b]	0.37[a]	0.01	0.05
11:0	0.16	0.15		0.03
12:0	4.11	4.36		0.45
13:0	0.21	0.20		0.04
anteiso 14:0	0.04[b]	0.06[a]	0.01	0.01
14:0	11.6[b]	12.2[a]	0.01	0.41
14:1	1.45	1.49		0.18
iso 15:0	0.46	0.51		0.08
15:0	1.64	1.56		0.29
16:0	31.9[b]	33,8[a]	0.01	1.76
16:1	2.27	2.14		0.23
anteiso 17:0	0.40[b]	0.44[a]	0.05	0.05
iso 17:0	0.79	0.78		0.09
17:0	0.79	0.72		0.14
17:1	0.36[a]	0.33[b]	0.05	0.04
18:0	5.94	5.95		0.62
18:1*t*	4.41[a]	2.68[b]	0.01	0.91
18:1*c*	19.0[a]	17.7[b]	0.01	1.30
9*c*,11*t*-18:2	0.55	0.61		0.10
9*c*,12*t*-18:2	0.25	0.24		0.03
9*c*,13*t*-18:2	0.19[a]	0.16[b]	0.01	0.02
9*c*,12*c*-18:2	2.53[a]	1.98[b]	0.01	0.32
9*t*,12*c*-18:2	0.10	0.09		0.02
9*c*,12*c*,15*c*-18:3	0.24[a]	0.19[b]	0.01	0.04
20:0	0.07	0.07		0.01
11*c*-20:1	0.07[a]	0.04[b]	0.01	0.02

[a]Means within a row with different superscript roman letters are significantly different at the level indicated in the specific column.

TABLE 6
Effect of Starch Source on the Composition of *trans* 18:1 Isomers in Milk Fat (wt%) Isolated by HPLC[a]

	Wheat diet	Potato diet	Level of significance	Root mean SE
Δ6 *trans* to 8 *trans*	0.31[a]	0.19[b]	0.05	0.11
Δ9 *trans*	0.34[a]	0.21[b]	0.01	0.08
Δ10 *trans*	2.12[a]	0.66[b]	0.01	0.95
Δ11 *trans*	1.20	0.93		0.29
Δ12 *trans*	0.32	0.28		0.05
Δ13 *trans*	0.25	0.22		0.08
Δ14 *trans*	0.23[a]	0.19[b]	0.01	0.02
Δ15 *trans*	0.14[a]	0.12[b]	0.01	0.02
Δ16 *trans*	0.12	0.12		0.04
Δ17	0.04	0.04		0.01

[a]Means within a row with different superscript roman letters are significantly different at the level indicated in the specific column.

fat from cows fed the wheat diet than those fed the potato diet (4.4 vs. 2.7 g/100 g of milk fat, $P < 0.01$).

Analysis of milk fat also revealed traces (<0.05%) of saturated medium-chain FA (anteiso 13:0, iso 13:0, iso 14:0, iso 16:0) and several long-chain FA (9*c*,11*c*-18:2, 18:3n-6, 20:5n-3, 22:0, 24:0; data not shown).

The composition of positional isomers of *trans* octadecenoic acid also showed significant differences between the two starch sources: There were significantly more *trans* octadecenoic acids with the double bond at positions 6 to 10 as well as positions 14 and 15 in the milk fat of cows fed the wheat diet than in the milk fat of those fed potatoes (Table 6). This effect was particularly high (by nearly three times) for *trans*-10 18:1. None of the positional isomers of *trans* 18:1 was higher in the milk fat of cows fed the potato diet.

DISCUSSION

Animal performance values showed that the type of starch concentrate did not induce differences in dry matter intake, milk yield, or milk protein. The main effect of these dietary treatments was on milk fat, confirming previous results with starch intakes over 7 kg/d (24). Similar observations have been reported for comparisons of other starch sources with different ruminal degradation rates fed in high amounts (25–28). Variations in fat synthesis in the udder have been explained previously by differences in the production of lipid precursors by the ruminal fermentation of starch (27–30). Nevertheless, the glucogenic-insulin theory (31) cannot fully explain the diet-induced decrease in milk fat found in this study. Indeed, the altered VFA composition is more reflective of a shift in the ruminal process than in a shortage of lipogenic precursors for mammary gland synthesis (32). With our starch sources, we observed a milk fat decrease without a difference in VFA concentrations, which confirms previous observations (17).

The second explanation for differences in milk fat synthesis is based on the inhibition of key enzymes for mammary fat synthesis by *trans* FA. Gaynor *et al*. (33) showed that cows responded to an increased level of barley starch (a rapidly degradable starch) with decreased milk fat synthesis, and the content of *trans* octadecenoate in milk fat increased substantially (up to 3.6%). The relationship between a decrease in milk fat and increased levels of *trans* octadecenoic acids in milk fat has been reported previously (34,35). In our study, the milk fat decrease in cows fed wheat could be explained by the much higher content of *trans* octadecenoic acid for the wheat diet compared with the potato diet. The *trans* 18:1 content of milk fat from cows fed the potato diet was in accordance with the values of 2–3% generally reported (33,36–38). However, the 4.4% content recorded for cows fed the wheat diet was much higher than the percentages observed in trials using classical dietary conditions.

More recently, a diet-induced decrease in milk fat was associated with a specific increase in *trans*-10 18:1 rather than an increase in the total *trans* octadecenoic acids (39,40), especially in low-fiber diets (41). The level of this positional isomer increased in fat-added low-fiber diets over the normally dominant *trans*-11 isomer (41,42) at the same time as the fat content decreased. In our study, *trans*-11 18:1 was the main isomer found with the potato diet, even though the proportion of *trans*-10 18:1 was quite high. With the wheat diet, the *trans*-10 isomer represented 44% of all *trans* octadecenoic acid isomers. A highly negative correlation with the fat content also has been shown with the *trans*-6 to *trans*-8 and

trans-9 isomers (43), but this is contrary to the results of other authors (7,32). However, Piperova *et al.* (42) reported reduced activity of key enzymes for milk fat synthesis in the udder, such as FA synthetase and acetyl-CoA carboxylase, with diets inducing a decrease in milk fat and an increased content of *trans*-10 18:1. Similar inhibitory effects were reported with *trans* bonds in position 10 of CLA (41,45,46). Conversely, *trans*-11 18:1 had only a minor effect on these enzymes (47) but generally represented the main form of this FA in milk fat (47,48). This distribution of the positional isomers, and especially the greatly increased content of *trans*-10 18:1, indicated that in our study enzyme inhibition in the mammary gland was the main reason for the decrease in milk fat with our diets containing similar fiber contents and without added fat.

Because *trans* octadecenoic acids are formed as intermediates in ruminal biohydrogenation, variations in the isomer composition of TFA have to be associated with an altered ruminal environment, which is clearly reflected in pH differences (41). Indeed, a lower ruminal pH led to higher TFA contents in milk fat, mainly of the *trans*-10 isomer, and scarcely affected the *trans*-11 isomer (41). Several studies (10,11,49) have shown that high levels of starch concentrates in the diet cause a drop in pH. These high levels of concentrates were generally based on corn grains, a slowly degradable starch. With similar concentrate levels in both diets, we observed a greater drop in pH with the more rapidly degraded wheat starch, especially around the fermentation peak of 4–5 h after feed intake. The increase of *trans*-10 18:1 with the wheat diet could therefore be associated with ruminal fermentation. Indeed, both diets had a similar composition; the starch sources compared here supplied similar profiles of FA and were rich in the main source of biohydrogenation (18:2). The greater drop in ruminal pH observed with the rapidly degraded wheat diet and the very high proportion of *trans*-10 18:1 in milk fat suggest an effect on biohydrogenation in our study similar to that reported in the literature for fat-added high-concentrate diets (7,10,11,13,33). Further studies are needed to determine whether differences in the drop in pH affect the population of ruminal microbes and also to understand their consequences for the different biohydrogenation steps.

This study showed that dietary starch sources with different velocities of degradation induced a change in the amount and composition of milk fat. Hence, not only the forage/starch concentrate ratio and fat addition can be used to control these parameters. The diet containing rapidly degraded wheat starch led to a stronger postprandial drop in pH without affecting the VFA concentration or composition in the rumen. In other dietary conditions, an incomplete biohydrogenation of PUFA in the rumen has been shown to increase *trans*-10 18:1 levels and decrease milk fat. We also observed a large increase in the octadecenoic acid content of milk fat in our study, especially the *trans*-10 isomer. The observed decrease in milk fat can be explained by enzyme inhibition *via* these TFA in the mammary gland, an effect which was shown in the literature.

More detailed work is necessary to demonstrate how variations in the velocities of starch degradation in diets with identical starch concentrate levels could change the pH, thereby affecting biohydrogenation and resulting in high TFA levels. These studies should focus especially on ruminal processes to elucidate the microorganisms involved. Finally, the inhibition of specific enzymes in the mammary synthesis of lipids by isomers of TFA—which have been only partially studied in the literature—should be confirmed.

REFERENCES

1. Willet, W.C., Stampfer, M.J., Manson, J.E., Colditz, G.A., Speizer, F.E., Rosner, B.A., Sampson, L.A., and Hennekens, C.A. (1993) Intake of *trans* Fatty Acids and Risk of Coronary Heart Disease Among Women, *Lancet 341*, 581–585.
2. Kris-Etherton, P.M., Emken, E.A., Allison, D.B., Dietschy, J.M., Nicolosi, R.J., and Denke, M.A. (1995) *Trans* Fatty Acids and Coronary Heart Disease Risk, *Am. J. Clin. Nutr. 62*, 655S–707S.
3. Mensink, R.P., and Katan, M.B. (1990) Effect of Dietary *trans* Fatty Acids on High Density Lipoprotein Cholesterol Levels in Healthy Subjects, *N. Engl. J. Med. 323*, 439–445.
4. Judd, J.T., Clevidence, B.A., Muesing, R.A., Wittes, J., Sunkin, M.E., and Podczasy, J.J. (1994) Dietary *trans* Fatty Acids: Effects on Plasma Lipids and Lipoproteins of Healthy Men and Women, *Am. J. Clin. Nutr. 59*, 861–868.
5. Ascherio, A., Hennekens, C.A., Buring, J.E., Master, C., Stampfer, M.J., and Willet, W.C. (1994) *Trans*-Fatty Acid Intake and Risk of Myocardial Infarction, *Circulation 89*, 94–101.
6. Ledoux, M., Laloux, L., and Sauvant, D. (2000) Les isomères *trans* d'acides gras. Origines et présence dans l'alimentation, *Sci. Aliments. 20*, 393–411.
7. Wolff, R.L., Combe, N., Destaillats, F., Boué, C., Precht, D., Molketin, J., and Entressangles, B. (2000) Follow-Up of Δ4 to Δ16 *trans*-18:1 Isomer Profile and Content in French Processed Foods Containing Partially Hydrogenated Vegetable Oils During the Period 1995–1999. Analytical and Nutritional Implications, *Lipids 35*, 815–825.
8. Rindsing, R.B., and Schultz, L.H. (1974) Effects of Abomasal Infusions of Safflower Oil or Elaidic Acid on Blood Lipids and Milk Fat in Dairy Cows, *J. Dairy Sci. 57*, 1459–1466.
9. Harfoot, C.G., and Hazlewood, G.P. (1997) Lipid Metabolism in the Rumen, in *The Rumen Microbial Ecosystem* (Hobson, P.N., ed.), pp. 382–426, Elsevier Applied Science, London.
10. Kalscheur, K.F., Teter, B.B., Piperova, L.S., and Erdman, R.A. (1997) Effect of Dietary Forage Concentration and Buffer Addition on Duodenal Flow of *trans*-C18:1 Fatty Acids and Milk Fat Production in Dairy Cows, *J. Dairy Sci. 80*, 2104–2114.
11. Kucuk, O., Hess, B.W., Ludden, P.A., and Rule, D.C. (2001) Effect of Forage:Concentrate Ratio on Ruminal Digestion and Duodenal Flow of Fatty Acids in Ewes, *J. Anim. Sci. 79*, 2233–2240.
12. Griinari, J.M., and Bauman, D.E. (1999) Biosynthesis of Conjugated Linoleic Acid and Its Incorporation into Meat and Milk in Ruminants, in *Advances in Conjugated Linoleic Acid Research* (Yurawecz, M.P., Mossoba, M.M., Kramer, J.K.G., Pariza, M.W., and Nelson, G.J., eds.), Vol. 1, pp. 180–200, AOCS Press, Champaign.
13. Chilliard, Y., Ferlay, A., Mansbridge, R.M., and Doreau, M. (2000) Ruminant Milk Fat Plasticity: Nutritional Control of Saturated, Polyunsaturated, *trans* and Conjugated Fatty Acids, *Ann. Zootech. 49*, 181–205.
14. Piperova, L.S., Sampugna, J., Teter, B.B., Kalscheur, K.F., Yurawecz, M.P., Youh, K.U., Morehouse, K.M., and Erdman, R.A.

(2002) Duodenal and Milk *trans* Octadecenoic Acid and Conjugated Linoleic Acid Isomers Indicate That Postabsorptive Synthesis Is the Predominant Source of *cis*-9-CLA in Lactating Dairy Cows, *J. Nutr. 132*, 1235–1241.
15. Van Soest, P.J. (1963) Ruminant Fat Metabolism with Particular Reference to Factors Affecting Low Milk Fat and Feed Efficiency. A Review, *J. Dairy Sci. 46*, 204–216.
16. Hoden, A., Coulon, J.B., and Faverdin, P. (1988) Alimentation des vaches laitières, in *Alimentation des bovins, ovins et caprins* (Jarrige, R., ed.), pp. 135–158, INRA, Paris.
17. Monteils, V., Jurjanz, S., Colin-Schoellen, O., Blanchart, G., and Laurent, F. (2002) Kinetics of Ruminal Degradation of Wheat and Potato Starches in Total Mixed Rations, *J. Anim. Sci. 80*, 235–241.
18. Jarrige, R. (1988) *Alimentation des bovins, ovins et caprins,* 1st edn., 476 pp., INRA, Paris.
19. Gontier, E., Boussouel, N., Terrasse, C., Jannoyer, M., Ménard, M., Thomasset, B., and Bourgaud, F. (2000) *Litchi chinensis* Fatty Acid Diversity: Occurrence of the Unusual Cyclopropanic Fatty Acids, *Biochem. Soc. Trans. 28*, 578–580.
20. Jouany, J.P. (1982) Volatile Fatty Acid and Alcohol Determination in Digestive Contents, Silage Juices, Bacterial Cultures and Anaerobic Fermentor Contents, *Sci. Aliments. 2*, 131–144.
21. Wolff, R.L., and Fabien, R.J. (1989) L'extraction de la matière grasse de produits laitiers pour l'estérification subséquente des acides gras, *Le lait 69*, 33–42.
22. Juaneda, P. (2002) Utilisation of Reversed-Phase High-Performance Liquid Chromatography as an Alternative to Silver-Ion Chromatography for the Separation of *cis*- and *trans*-C18:1 Fatty Acid Isomers, *J. Chromatogr. 954*, 285–289.
23. Littell, R.C., Milliken, G.A., Stroup, W.W., and Wolfinger, R.D. (1996) *SAS System for Mixed Models*, 633 pp., SAS Institute Inc., Cary, NC.
24. Jurjanz, S., Colin-Schoellen, O., Gardeur, J.N., and Laurent, F. (1998) Alteration of Milk Fat by Variation in the Source and Amount of Starch in a Total Mixed Diet to Dairy Cows, *J. Dairy Sci. 81*, 2924–2933.
25. Omwubuemeli, C., Huber, J.T., King, K.J., and Johnson, C.O. (1985) Nutritive Value of Potato Processing Wastes in Total Mixed Rations for Dairy Cattle, *J. Dairy Sci. 68*, 1207–1214.
26. Faldet, M.A., Bush, L.J., and Adams, G.D. (1986) Effect of Different Levels of Wheat in Concentrate Mixture on Production Responses of Lactating Dairy Cows Fed Sorghum Silage as the Only Forage, *Oklahoma Anim. Sci. Res. Rep.*, 66–70.
27. Herrera-Saldana, R., and Huber, J.T. (1989) Influence of Varying Protein and Starch Degradabilities on Performance of Lactating Cows, *J. Dairy Sci. 72*, 1477–1483.
28. Casper, D.P., Schingoethe, D.J., and Eisenbeisz, W.A. (1990) Response of Early Lactation Dairy Cows Fed Diets Varying in Source of Nonstructural Carbohydrate and Crude Protein, *J. Dairy Sci. 73*, 1039–1050.
29. Aldrich, J.M., Muller, L.D., Varga, D.A., and Griel, L.C. (1993) Nonstructural Carbohydrates and Protein Effects on Rumen Fermentation, Nutrient Flow, and Performance of Dairy Cows, *J. Dairy Sci. 76*, 1091–1105.
30. Sauvant, D., Chapoutot, P., and Archimède, H. (1994) La digestion des amidons par les ruminants et ses conséquences, *INRA Prod. Anim. 7*, 115–124.
31. McClymont, G.L., and Vallance, S. (1962) Depression of Blood Glycerides and Milk-Fat Synthesis by Glucose Infusion, *Proc. Nutr. Soc. 21*, 41–42.
32. Bauman, D.E., and Griinari, J.M. (2001) Regulation and Nutritional Manipulation of Milk Fat: Low-Fat Milk Syndrome, *Livest. Prod. Sci. 70*, 15–29.
33. Gaynor, P.J., Waldo, D.R., Capuco, A.V., Erdman, R.A., Douglass, L.W., and Teter, B.B. (1995) Milk Fat Depression, the Glucogenic Theory, and *trans*-C18:1 Fatty Acid, *J. Dairy Sci. 78*, 2008–2015.
34. Davis, C.L., and Brown, R.E. (1970) Low-Fat Milk Syndrome, in *Physiology of Digestion and Metabolism in the Ruminant* (Phillipson, A.T., ed.), pp. 545–565, Oriel Press, Newcastle upon Tyne, United Kingdom.
35. Selner, D.R., and Schultz, L.H. (1980) Effects of Feeding Oleic Acid or Hydrogenated Vegetable Oils to Lactating Cows, *J. Dairy Sci. 63*, 1235–1241.
36. Jahreis, G., Fritsche, J., and Steinhart, H. (1996) Monthly Variations of Milk Composition with Special Regards to Fatty Acids Depending on Season and Farm Management Systems—Conventional Versus Ecological, *Fett/Lipid 98*, 356–359.
37. Fritsche, J., and Steinhart, H. (1997) Contents of *trans* Fatty Acids in German Foods and Estimation of Daily Intake, *Fett/Lipid 99*, 314–318.
38. Joy, M.T., DePeters, E.J., Fadel, J.G., and Zinn, R.A. (1997) Effects of Corn Processing on the Site and Extent of Digestion in Lactating Dairy Cows, *J. Dairy Sci. 80*, 2087–2097.
39. Griinari, J.M., Dwyer, D.A., McGuire, D.A., Bauman, D.E., Palmquist, D.L., and Nurmela, K.V.V. (1998) *Trans*-Octadecenoic Acids and Milk Fat Depression in Lactating Dairy Cows, *J. Dairy Sci. 81*, 1251–1261.
40. Griinari, J.M., Nurmela, K.V.V., and Bauman, D.E. (1997) *Trans*-10 Isomer of Octadecenoic Acid Corresponds with Milk Fat Depression, *J. Dairy Sci. 80* (Suppl. 1), 204 (abstract).
41. Griinari, J.M., and Bauman, D.E. (1999) Biosynthesis of Conjugated Linoleic Acid and Its Incorporation into Meat and Milk in Ruminants, in *Advances in Conjugated Linoleic Acid Research* (Yurawecz, M.P., Mossoba, M.M., Kramer, J.K.G., Pariza, M.W., and Nelson, G.J., eds.), Vol. 1, pp. 180–200, AOCS Press, Champaign.
42. Piperova, L.S., Teter, B.B., Bruckental, I., Sampugna, J., Mills, S.E., Yurawecz, M.P., Fritsche, J., Ku, K., and Erdman, R.A. (2000) Mammary Lipogenic Enzyme Activity, *trans* Fatty Acids and Conjugated Linoleic Acids Are Altered in Lactating Dairy Cows Fed a Milk Fat-Depressing Diet, *J. Nutr. 130*, 2568–2574.
43. Precht, D., Hagemeister, H., Kanitz, W., and Voigt, J. (2002) Milk Fat Depression and the Role of *trans* and CLA Fatty Acid Isomers by Feeding a High Fiber Diet with Calcium Soaps of Fatty Acids in Early Lactating Dairy Cows, *Milchwissenschaft 57*, 518–522.
44. Corl, B.A., Baumgard, L.H., Dwyer, D.A., Griinari, J.M., Phillips, D.S., and Bauman, D.E. (2001) The Role of Δ9-Desaturase in the Production of *cis*-9,*trans*-11 CLA, *J. Nutr. Biochem. 12*, 622–630.
45. Baumgard, L.H., Matitashvili, E., Corl, B.A., Dwyer, D.A., and Bauman, D.E. (2002) *Trans*-10,*cis*-12 Conjugated Linoleic Acid Decreases Lipogenic Rates and Expression of Genes Involved in Milk Lipid Synthesis in Dairy Cows, *J. Dairy Sci. 85*, 2155–2163.
46. Bauman, D.E., and Griinari, J.M. (2003) Nutritional Regulation of Milk Fat Synthesis, *Annu. Rev. Nutr. 23*, 203–207.
47. Ledoux, M., Laloux, L., and Sauvant, D. (2002) Occurrence of *trans*-$C_{18:1}$ Fatty Acid Isomers in Goat Milk: Effect of Two Dietary Regimens, *J. Dairy Sci. 85*, 190–197.
48. Precht, D., and Molketin, J. (1995) *Trans* Fatty Acids: Implications for Health, Analytical Methods, Incidence in Edible Fats and Intake, *Nahrung 39*, 343–375.
49. Jiang, J., Bjoerck, L., Fonden, R., and Emanuelson, M. (1996) Occurrence of Conjugated *cis*-9,*trans*-11-Octadecadienoic Acid in Bovine Milk: Effect of Feed and Dietary Regimen, *J. Dairy Sci. 78*, 438–445.

[Received May 23, 2003, and in revised form November 10, 2003; revision accepted December 14, 2003]

Dietary Protein Modulates the Effect of CLA on Lipid Metabolism in Rats

Asuka Akahoshi[a,*], Kazunori Koba[b], Fumika Ichinose[a], Mai Kaneko[a], Asako Shimoda[a], Kikuko Nonaka[a], Masao Yamasaki[c], Toshio Iwata[d], Yoshie Yamauchi[d], Kentaro Tsutsumi[d], and Michihiro Sugano[a]

[a]Faculty of Environmental and Symbiotic Sciences, Prefectural University of Kumamoto, Kumamoto 862-8502, Japan, [b]Faculty of Nursing and Nutrition, Siebold University of Nagasaki, Nagayo, Nagasaki 851-2195, Japan, [c]Laboratory of Food Chemistry, Department of Bioscience and Biotechnology, Graduate School Kyushu University, Fukuoka 812-8581, Japan, and [d]Department of Research and Development, Rinoru Oils Mills Co., Tokyo 104-0033, Japan

ABSTRACT: The effect of the interaction of CLA and type of dietary protein on lipid metabolism was studied in male rats by feeding diets containing casein (CAS) or soy protein (SOY) as dietary protein and either linoleic acid (LA, a control FA) or graded levels of CLA at 0, 0.1, 0.5, and 1.0% for 28 d. CLA reduced the weight of perirenal adipose tissue in a dose-dependent manner, but the magnitude of the reduction was greater when rats were fed SOY. Feeding SOY resulted in a significant reduction of the concentrations of serum total and HDL cholesterol, TG, glucose, and insulin irrespective of dietary CLA. The concentration of serum leptin tended to be lower on the SOY diet free of CLA than in the corresponding CAS diet, but it fell with an increasing dietary level of CLA in the CAS groups. In contrast, serum leptin tended to increase when CLA was added to SOY diets. The concentration of serum adiponectin was higher in the CAS than in the SOY groups, and it tended to increase in response to dietary CLA levels in the CAS-fed rats, whereas CLA showed no effect in SOY-fed rats. The activity of liver mitochondrial carnitine palmitoyltransferase was higher in the SOY than in the CAS groups, but it tended to increase with an increasing dietary level of CLA in both protein groups. Although the body fat-reducing activity of CLA was more effective when the protein source was SOY, rats fed CAS appeared to be more susceptible to CLA than in those fed SOY with respect to cytokines examined. These results suggest that the type of dietary protein may modify the antiobesity activity of CLA.

Paper no. L9369 in *Lipids 39*, 25–30 (January 2004).

CLA has various beneficial physiological functions such as anticarcinogenic, antiobesity, and antiatherogenic activities (1–5). However the response of animals to CLA differs from species to species, and humans appear to be the least responsive animal (6). From the threshold level of CLA in the inhibition of mammary carcinogenesis in rats (7), an estimated intake of approximately 5 g/d is recommended for humans (4). However, a series of human studies on the body fat-reducing activity of CLA showed no unequivocal results over a wide range of dosages (8–13). It is therefore appropriate to examine the ability of dietary components to enhance the activity of CLA to reduce dietary CLA levels, because CLA may also produce unfavorable side effects such as an elevation of blood glucose (14–17). If the reinforcing effects of various food ingredients on the physiological functions of CLA can be defined, the administration of CLA can be made more beneficial for humans. In a previous study, we showed that the weights of white adipose tissues in rats fed CLA were low when the protein source was soy protein (SOY) compared to casein (CAS) (18).

In this context, we studied the modifying effect of dietary protein type on the body fat-reducing activity of CLA in rats in more detail. Thus, growth parameters, adipose tissue size, concentration of serum components related to lipid metabolism, and hepatic FA β-oxidation activities were measured in rats fed either SOY or CAS diets with graded levels of CLA.

MATERIALS AND METHODS

Animals and diets. Four-week-old male Sprague-Dawley rats were purchased from Seac Co. (Fukuoka, Japan) and housed individually in stainless steel cages in an air-conditioned (22–23°C) and light-controlled (lights on 0800–2000) room. During a an acclimation period of 1 wk, commercial pellets (Type NMF; Oriental Yeast Co., Tokyo, Japan) and water were given freely. Thereafter, rats were randomly allocated to one of the eight different diets (eight rats per group), stratified for the content of CLA and the source of dietary protein. Experimental diets were prepared as a powder according to the AIN-93G formula and contained 7% dietary fat (6% soybean oil and 1% high-linoleic safflower oil) (19). CLA (0, 0.1, 0.5, and 1.0%) was added at the expense of safflower oil (both donated by Rinoru Oil Mill Co., Tokyo, Japan). CLA containing 34.1% 9*c*,11*t*-, 35.9% 10*t*,12*c*-, 2.5% *c,c*-, and 1.6% *t,t*-isomers was used. Dietary protein sources were CAS (Seac Co.) and SOY (Fujipro R; Fuji Oil Co., Osaka, Japan) at the 20% level. Diets and water were freely given for 28 d. At the end of the feeding period, blood was withdrawn from the abdominal aorta of the animals under diethyl ether anesthesia, and serum was harvested. The blood was drawn from 9 AM without food deprivation. The visceral tissues were

*To whom correspondence should be addressed at the Faculty of Environmental and Symbiotic Sciences, Prefectural University of Kumamoto, 3-1-100 Tsukide, Kumamoto 862-8502, Japan.
E-mail: a-asuka@pu-kumamoto.ac.jp

Abbreviations: CAS, casein; CPT, carnitine palmitoyltransferase; GOT, glutamic-oxaloacetic transaminase; GPT, glutamic-pyruvic transaminase; LA, linoleic acid; SOY, soy protein.

excised immediately, rinsed, and weighed. This study was done in accordance with the Guidelines for Animal Experiments approved by the Prefectural University of Kumamoto.

Analyses. The concentrations of serum glucose, total and HDL cholesterol, and TG, and the activities of glutamic-oxaloacetic transaminase (GOT) and glutamic-pyruvic transaminase (GPT) were measured using commercial enzymatic kits (all from Wako Pure Chemicals, Osaka, Japan). HDL cholesterol was measured by precipitating lipoproteins other than HDL with heparin in the presence of manganous (Mn^{2+}) ions. The concentration of serum insulin was measured by a rat insulin enzyme immunoassay kit (SPI-BIO, Massy Cedex, France). The concentration of serum leptin was measured by a commercial rat ELISA kit (Yanaihara Institute Inc., Shizuoka, Japan). The concentration of serum adiponectin was measured by a mouse/rat ELISA kit donated by Otsuka Pharmaceutical Co. (Tokyo, Japan). The activity of carnitine palmitoyltransferase in liver mitochondria was measured by the method of Bieber *et al*. (20).

Statistics. Results were presented as means ± SE. Data were analyzed by two-way ANOVA to test statistical difference of the means among groups followed by the Tukey–Kramer test to identify significant differences using a StatView software system (version 5.0, SAS Institute Inc., Cary, NC). Differences were considered significant at $P < 0.05$.

RESULTS

Effects on growth parameters and tissue weights. There was no difference in food intake among the groups (Table 1). However, body weight gain and food efficiency were significantly higher in rats fed CAS than in those fed SOY (both $P < 0.001$), although the difference became small with an increasing dietary level of CLA due to a reduction of weight gain in the CAS groups. CLA did not influence weight gain and food efficiency when the protein source was SOY.

No demonstrable differences were observed in relative weights (g/100 g body weight) of liver, heart, lung, and spleen, but the weight of kidney was significantly higher in rats fed SOY ($P < 0.01$). There was a significant difference in the weight of kidney only in the case of the 0.1% CLA diet between CAS and SOY groups. The liver weight of the SOY groups tended to be heavier as dietary CLA increased, but no such CLA effect was observed in the CAS groups.

There was a significant effect of dietary protein on perirenal adipose tissue weight, which was lower in the groups of rats fed SOY compared with the corresponding groups of rats fed CAS as shown in Figure 1. The weight of perirenal adipose tissue decreased in response to the dietary CLA level in both protein groups, but the magnitude of the reduction was comparable in terms of both the absolute and relative effects. Thus, the weight of perirenal adipose tissue reached a plateau at 0.5% CLA in the SOY group, whereas it was lowest at 1.0% CLA in the CAS group. In contrast, the protein effect was less marked in epididymal adipose tissue weight, although the 1.0% CLA diet tended to reduce it in either protein group. There was no

TABLE 1
Interactions of Dietary Protein and CLA Content on Growth Parameter and Tissue Weights of Rats[a]

	CAS				SOY				Two-way ANOVA		
	CLA-0	CLA-0.1	CLA-0.5	CLA-1.0	CLA-0	CLA 0.1	CLA-0.5	CLA-1.0	Protein	CLA	Protein × CLA
Growth parameter											
Initial (g)	111 ± 2	110 ± 2	111 ± 2	111 ± 2	107 ± 7	107 ± 7	111 ± 3	110 ± 3	NS	NS	NS
Gain (g/26 d)	240 ± 8	237 ± 15	225 ± 9	224 ± 9	205 ± 4	204 ± 9	198 ± 9	200 ± 9	$P < 0.0001$	NS	NS
Food intake (g/d)	21.3 ± 0.6	20.9 ± 1.2	21.1 ± 0.6	20.7 ± 0.7	21.2 ± 0.5	20.6 ± 0.6	20.2 ± 0.6	20.3 ± 0.7	NS	NS	NS
Food efficiency (g gain/g intake)	0.44 ± 0.01*	0.44 ± 0.01**	0.41 ± 0.01	0.42 ± 0.01	0.37 ± 0.01*	0.38 ± 0.01**	0.38 ± 0.01	0.37 ± 0.01	$P < 0.0001$	NS	NS
Tissue weight (g/100 g body weight)											
Liver	4.47 ± 0.11	4.53 ± 0.17	4.44 ± 0.20	4.35 ± 0.15	4.29 ± 0.16	4.52 ± 0.14	4.68 ± 0.17	4.69 ± 0.31	NS	NS	NS
Kidney	0.77 ± 0.02	0.75 ± 0.03*	0.78 ± 0.02	0.83 ± 0.03	0.85 ± 0.02	0.85 ± 0.01*	0.84 ± 0.02	0.85 ± 0.03	$P < 0.01$	NS	NS
Heart	0.35 ± 0.02	0.36 ± 0.02	0.37 ± 0.01	0.39 ± 0.01	0.36 ± 0.02	0.35 ± 0.01	0.35 ± 0.01	0.39 ± 0.02	NS	NS	NS
Lung	0.41 ± 0.02	0.41 ± 0.02	0.43 ± 0.01	0.44 ± 0.02	0.45 ± 0.04	0.41 ± 0.01	0.42 ± 0.02	0.42 ± 0.01	NS	NS	NS
Spleen	0.23 ± 0.02	0.26 ± 0.02	0.22 ± 0.01	0.22 ± 0.01	0.24 ± 0.01	0.23 ± 0.01	0.24 ± 0.01	0.24 ± 0.01	NS	NS	NS

[a]Means ± SE of eight rats. Values sharing the same symbol (*, **) are significantly different at $P < 0.05$. CAS, casein diet; SOY, soy protein diet; NS, not significant; CLA-0, -0.1, -0.5, -1.0, supplementation level of CLA to CAS or SOY pellets (= 0, 0.1, 0.5, and 1%).

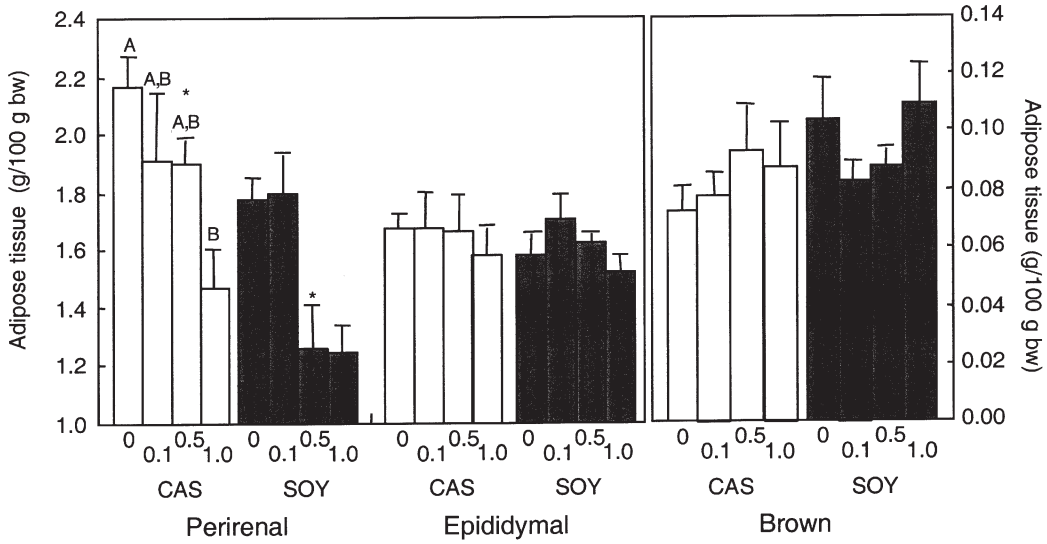

FIG. 1. Effects of dietary protein and CLA on adipose tissue weight. Values are means ± SE of six rats per group. The results of the two-way ANOVA indicated significant protein ($P < 0.05$) and CLA ($P < 0.01$) effects in the body weight (bw) of perirenal adipose tissue, but not in the weight of epidydimal and brown adipose tissue. Different letters (A,B) or the same symbol (*) indicates a significant difference at $P < 0.05$ among groups.

significant difference in the weight of intrascapular brown adipose tissue, but it tended to be higher in the SOY groups than in the corresponding CAS groups. CLA tended to increase the weight of brown adipose tissue in both groups of rats.

Effects on serum components. As shown in Table 2, the concentrations of serum total and HDL cholesterol, TG, glucose, and insulin were demonstrably higher in the CAS groups in relation to the SOY groups, whereas the concentration of serum total protein was comparable between these protein groups. Although the concentrations of total and HDL cholesterol were higher in the groups of rats fed CAS, there was a trend toward a reduction when the diet containing 1.0% CLA was fed. The GOT and GPT activities were modified neither by the type of dietary protein nor by the dietary CLA level.

As Figure 2 shows, the concentration of serum leptin was higher in the CAS than in the SOY groups when no CLA was added to the diets. It tended to fall with an increasing dietary level of CLA in rats fed CAS (801 ± 65, 795 ± 144, 623 ± 92, and 537 ± 102 pg/mL for rats fed CAS and 0, 0.1, 0.5, and 1.0% CLA). No such effect was observed in rats fed SOY, and leptin tended to increase when CLA was included in the diets. There was apparently no effect of dietary protein on the concentration of serum adiponectin, but it tended to increase when the dietary CLA level was above 0.5% in the CAS group and at 1.0% in the SOY group.

Reflecting these response patterns in serum cytokines, a weak negative correlation was observed between serum concentrations of adiponectin and leptin when rats were fed CAS

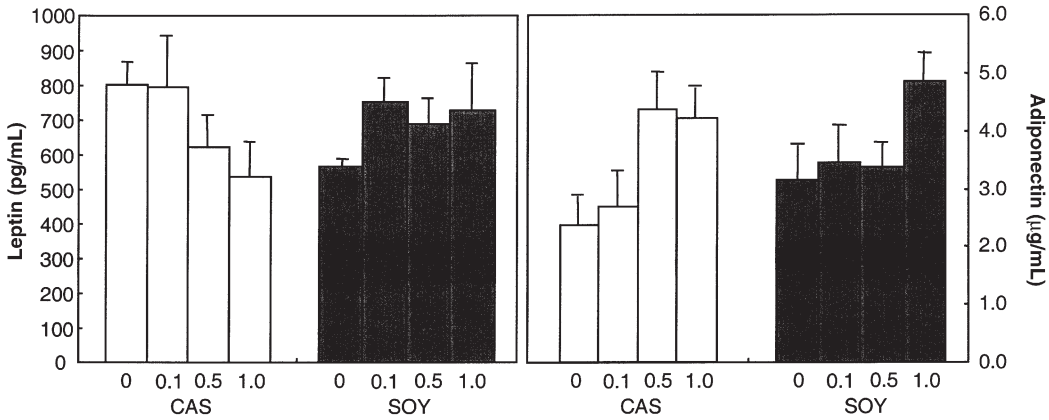

FIG. 2. Effects of dietary protein and CLA on serum leptin and adiponectin. Values are means ± SE of six rats. The results of the two-way ANOVA indicated a significant protein effect ($P < 0.05$) on the concentration of serum adiponectin, whereas CLA did not affect it. There were no significant effects of protein or CLA in the concentration of serum leptin, although it tended to decrease with an increasing CLA level in the CAS group.

TABLE 2
Interactions of Dietary Protein and CLA Content on Serum Components of Rats[a]

	CAS				SOY				Two-way ANOVA		
Serum components	CLA-0	CLA-0.1	CLA-0.5	CLA-1.0	CLA-0	CLA-0.1	CLA-0.5	CLA-1.0	Protein	CLA	Protein × CLA
Total cholesterol (mg/dL)	102 ± 6	119 ± 7	102 ± 6	95.8 ± 6.4	78.5 ± 3.5	78.2 ± 2.4	69.8 ± 1.2	82.8 ± 9.2	P < 0.0001	NS	NS
HDL cholesterol (mg/dL)	63.7 ± 4.4	73.5 ± 6.6	63.0 ± 6.2	52.2 ± 5.3	41.3 ± 3.6	41.5 ± 1.8	37.8 ± 2.2	43.0 ± 9.0	*P* < 0.001	NS	NS
HDL/total cholesterol	0.63 ± 0.04	0.61 ± 0.03	0.61 ± 0.03	0.54 ± 0.03	0.52 ± 0.03	0.54 ± 0.01	0.51 ± 0.02	0.50 ± 0.04	*P* < 0.01	NS	NS
TAG (mg/dL)	172 ± 39	169 ± 21	202 ± 24	181 ± 19	131 ± 12	133 ± 18	136 ± 13	176 ± 25	*P* < 0.05	NS	NS
Glucose (mg/dL)	188 ± 4	197 ± 10	202 ± 8	186 ± 4	178 ± 6	181 ± 4	182 ± 3	176 ± 7	*P* < 0.01	NS	NS
Insulin (ng/dL)	752 ± 87	863 ± 46	713 ± 80	743 ± 112	599 ± 0.5	599 ± 0.8	598 ± 0.9	596 ± 2.7	*P* < 0.01	NS	NS
Total protein (g/dL)	5.22 ± 0.19	5.30 ± 0.17	5.28 ± 0.18	5.03 ± 0.18	5.28 ± 0.21	5.43 ± 0.17	5.40 ± 0.14	5.35 ± 0.14	NS	NS	NS
GOT (IU)	62.3 ± 3.3	63.5 ± 5.4	62.0 ± 4.9	58.7 ± 3.2	69.3 ± 5.6	58.7 ± 3.8	53.8 ± 4.2	58.8 ± 2.8	NS	NS	NS
GPT (IU)	7.83 ± 2.15	9.50 ± 3.68	12.3 ± 3.9	8.33 ± 1.41	8.83 ± 2.20	5.80 ± 1.70	4.00 ± 1.13	7.83 ± 1.89	NS	NS	NS

[a]Means ± SE of eight rats. GOT, glutamic-oxaloacetic transaminase; GPT, glutamic-pyruvic transaminase; for other abbreviations see Table 1.

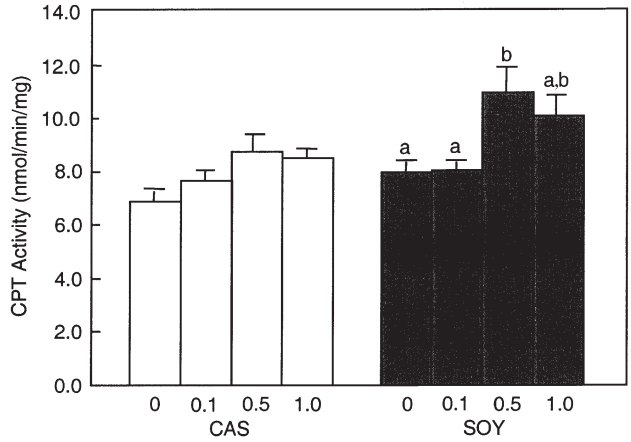

FIG. 3. Effects of dietary protein and CLA on activities of the FA oxidation pathway in rat liver. Values are means ± SE of six rats. The results of the two-way ANOVA indicated significant protein ($P < 0.05$) and CLA ($P < 0.01$) effects in the carnitine palmitoyltransferase (CPT) activity. Different letters (a,b) show significant differences at $P < 0.05$ in the SOY group.

($R^2 = 0.160$). In contrast, the correlation coefficient was positive in rats fed SOY ($R^2 = 0.028$). It is interesting that different correlations were shown by the different dietary protein sources, although the correlation coefficients were weak.

Effects on hepatic FA β-oxidation. Figure 3 summarizes the effects of protein and CLA on the rate of FA β-oxidation in rat liver. The activity of mitochondrial carnitine palmitoyltransferase (CPT), a key enzyme in mitochondrial FA β-oxidation, was higher in the SOY than in the CAS groups, but it increased with an increasing dietary level of CLA in both protein groups. CPT activity appeared to reach a plateau at a 0.5% level of CLA in both protein groups.

DISCUSSION

Dietary protein modifies several parameters of lipid metabolism, and SOY in relation to CAS reduces serum cholesterol and stimulates FA oxidation in several animal species including humans (21–23). Therefore, the use of SOY as a dietary protein source is expected to augment the body fat-reducing potential of CLA. In the previous study (18), we found that SOY, compared with CAS, reduced the weight of white adipose tissue and that sesamin, a lignan abundant in sesame seed and oil, when fed simultaneously, further stimulated the reduction of body fat in rats fed CAS. In the present study, the antiobesity effect of SOY compared with CAS was confirmed. In addition, the antihypercholesterolemic effect of SOY was not affected by CLA, indicating the benefit of this combination. However, the dose-dependent response of body fat to dietary CLA was more marked in rats fed SOY than in those fed CAS, although the effect of CLA on other parameters related to adipogenesis, such as measured concentrations of serum cytokines, was rather marked when rats were fed CAS in relation to SOY.

Dietary CLA induces liver enlargement in experimental animals, particularly in mice (24). The effect is not consistent in

rats (25). The liver weight tended to increase with an increasing dietary level of CLA in the SOY group, whereas no such effect was observed in the CAS group (Table 1). This observation again indicates the importance of dietary protein type in evading the untoward effects of CLA.

In this study, the concentration of serum glucose tended to increase with increasing dietary CLA level in the CAS group, whereas no such effect was observed in the SOY group. The concentration of serum glucose reportedly increased with increasing dietary level of CLA in adult male rats (14). In contrast, the SOY diet decreased body fat content and plasma glucose levels more effectively than the isocaloric CAS diet in obese mice (26). SOY may blunt the serum glucose-raising effect of CLA in rats.

When rats were fed diets free of CLA, the serum concentration of leptin was low in rats fed SOY (Fig. 2), but a dose-dependent reduction with feeding of CLA was observed only in rats fed CAS. No such CLA effect was confirmed in rats fed SOY. The response of serum adiponectin to dietary CLA was noted in both groups of rats, and it was increased by dietary CLA. Adiponectin, in contrast to leptin, has been shown to produce situations favorable for health maintenance, such as regulation of insulin sensitivity, antiarteriosclerotic activity, and an increase in FA β-oxidation (23,27,28). Thus, these beneficial effects of adipocytokine may be expected when the protein source is CAS. A positive correlation has been shown between white adipose tissue weight and serum leptin concentration, whereas there is a negative correlation between visceral adipose tissue size and serum adiponectin concentration (29,30). Thus, the ratio of leptin to adiponectin may serve as an obesity index (31,32). In the present study, however, a weak negative correlation was observed in the concentrations of serum cytokines when rats were fed CAS, but not SOY. In the SOY groups, the correlation was rather positive, although the correlation coefficient was negligibly small in both cases. In the obese mouse model, dietary protein did not significantly influence the plasma adiponectin concentration and adiponectin mRNA level in adipose tissue (26). In this context, the different diurnal rhythms between adiponectin and leptin should be taken into consideration for the response to dietary manipulations of these cytokines (33). The observation that the concentration of serum glucose did not increase with increasing dietary CLA level in the SOY group may indicate the importance of the dietary protein source in the regulation of glucose metabolism (34,35). These observations indicate that dietary protein influences the response of these cytokines differently, suggesting a probable role of dietary protein in the manifestation of a CLA effect.

The hepatic activity of CPT, the key enzyme in FA β-oxidation, was higher in rats fed SOY than in those fed CAS, in accordance with our previous observation (18). However, the activity increased in both protein groups by feeding CLA, although it still tended to be higher in the SOY groups than in the corresponding CAS groups.

These observations suggest that SOY itself has the potential to reduce body fat, and that CLA exhibited a limited additional effect when SOY was fed simultaneously. In contrast, the body fat-increasing potential of CAS can be controlled by CLA.

Serum chemistries related to indices of antiobesity activity were found to depend largely on the dietary level of CLA in rats fed CAS. In rats fed SOY, the CLA effects were obscure, probably owing to the potent body fat-reducing activity of SOY in relation to CAS (20), although this plant protein reduced perirenal adipose tissue weight more than animal protein did. Thus, an appropriate selection of dietary protein is important to reinforce the favorable health effects of CLA. When considering a current trend in the developed countries of ingesting more animal foods, CLA may serve to ameliorate various health hazards.

ACKNOWLEDGMENT

Supported by a Grant-in-Aid for Scientific Research (C) (11660130) from the Ministry of Culture, Sports, Science and Technology, Japan.

REFERENCES

1. Pariza, M.W., Park, Y., and Cook, M.E. (1999) Conjugated Linoleic Acid and the Control of Cancer and Obesity, *Toxicol. Sci. 52*, 107–110.
2. Kritchevsky, D. (2000) Antimutagenic and Some Other Effects of Conjugated Linoleic Acid, *Br. J. Nutr. 83*, 459–465.
3. Pariza, M.W., Park, Y., and Cook, M.E. (2001) The Biologically Active Isomers of Conjugated Linoleic Acid, *Prog. Lipid Res. 40*, 283–298.
4. Siems, W.G., Grune, T., Hasselwander, O., and Kramer, K. (2001) Conjugated Linoleic Acid, in *Nutraceuticals in Health and Disease Prevention* (Kramer K., Hoppe, P.P., and Packer, L., eds.), pp. 257–288, Marcel Dekker, New York.
5. Parodi, P.W. (2002) Conjugated Linoleic Acid, *Food Aust. 54*, 96–99.
6. Kelly, G.S. (2001) Conjugated Linoleic Acid: A Review, *Altern. Med. Rev. 6*, 367–382
7. Ip, C., Chin, S.F., Scimeca, J.A., and Pariza, M.W. (1991) Mammary Cancer Prevention by Conjugated Dienoic Derivative of Linoleic Acid, *Cancer Res. 51*, 6118–6124
8. Terpstra, A.H.M. (2001) Differences Between Humans and Mice in Efficacy of the Body Fat-Lowering Effect of Conjugated Linoleic Acid: Role of Metabolic Rate, *J. Nutr. 131*, 2067–2068.
9. Zambell, K.L., Keim, N.L., Van Loan, M.D., Gale, B., Benito, P., Kelley, D.S., and Nelson, G.J. (2000) Conjugated Linoleic Acid Supplementation in Humans: Effects on Body Composition and Energy Expenditure, *Lipids 35*, 777–782.
10. Mougios, V., Matsakas, A., Petridou, A., Ring, S., Sagredos, A., Melissopoulou, A., Tsigilis, N., and Nikolaidis, M. (2001) Effect of Supplementation with Conjugated Linoleic Acid on Human Serum Lipids and Body Fat, *J. Nutr. Biochem. 12*, 585–594.
11. Smedman, A., and Vessby B. (2001) Conjugated Linoleic Acid Supplementation in Humans—Metabolic Effects, *Lipids 36*, 773–781.
12. Thom, E., Wadstein, J., and Gudmundsen, O. (2001) Conjugated Linoleic Acid Reduces Body Fat in Healthy Exercising Humans, *J. Int. Med. Res. 29*, 392–396.
13. Riserus, U., Arner, P., Brismar, K., and Vessby, B. (2002) Treatment with Dietary *trans*10,*cis*12 Conjugated Linoleic Acid Causes Isomer-Specific Insulin Resistance in Obese Men with the Metabolic Syndrome, *Diabetes Care 25*, 1516–1521.

14. Stangl, G.I. (2000) High Dietary Levels of a Conjugated Linoleic Acid Mixture Alter Hepatic Glycerophospholipid Class Profile and Cholesterol-Carrying Serum Lipoprotein of Rats, *J. Nutr. Biochem. 11*, 184–191.
15. Yamasaki, M., Mansho, K., Ogino, Y., Kasai, M., Tachibana, H. and Yamada, K. (2000) Acute Reduction of Serum Leptin Level by Dietary Conjugated Linoleic Acid in Sprague-Dawley Rats, *J. Nutr. Biochem. 11*, 467–471.
16. Roche, H.M., Noone, E., Sewter, C., McBennett, S., Savage, D., Gibney, M.J., O'Rahilly, S., and Vidal-Puig, A.J. (2002) Isomer-Dependent Metabolic Effects of Conjugated Linoleic Acid: Insight from Molecular Markers Sterol Regulatory Element-Binding Protein-1c and LXRα, *Diabetes 51*, 2037–2044.
17. Clement, L., Poirier, H., Noit, I., Bocher, V., Guerre-Millo, M., Krief, S., Staels, B., and Besnard, P. (2002) Dietary *trans*10-, *cis*-12 Conjugated Linoleic Acid Induces Hyperinsulinemia and Fatty Liver in the Mouse, *J. Lipid Res. 43*, 1400–1409.
18. Sugano, M., Akahoshi, A., Koba, K., Tanaka, K., Okumura, T., Matsuyama, H., Goto, Y., Miyazaki, T., Murao, K., Yamasaki, M., *et al.* (2001) Dietary Manipulations of Body Fat-Reducing Potential of Conjugated Linoleic Acid in Rats, *Biosci. Biotechnol. Biochem. 65*, 2535–2541.
19. Reeves, P.G., Nielsen, F.H., and Fahey, G.C. (1993) AIN-93 Purified Diets for Laboratory Rodents: Final Report of The American Institute of Nutrition *ad hoc* Writing Committee on the Reformulation of the AIN-76A Rodent Diet, *J. Nutr. 123*, 1939–1951.
20. Bieber, L.L., Abraham, T., and Helmrath, T. (1972) A Rapid Spectrophotometric Assay for Carnitine Palmitoyltransferase, *Anal. Biochem. 50*, 509–518.
21. Volgarev, M.N., Vysotosky, V.G., Meshcheryakova, V.A., Yatsyshina, T.A., and Steinke, F.H., (1989) Evaluation of Isolated Soy Protein Foods in Weight Reduction with Obese Hypercholesterolemic and Normocholesterolemic Obese Individuals, *Nutr. Rep. Int. 36*, 61–72.
22. Anderson, J.W., Johnstone, B.M., and Cook-Newell, M.E. (1995) Meta-analysis of the Effects of Soy Protein Intake on Serum Lipids, *N. Engl. J. Med. 333*, 276–282.
23. Tonstad, S., Smerud, K., and Hoie, L. (2002) A Comparison of the Effects of 2 Doses of Soy Protein or Casein on Serum Lipids, Serum Lipoproteins, and Plasma Total Homocysteine in Hypercholesterolemic Subjects, *Am. J. Clin. Nutr. 76*, 78–84.
24. DeLany, J.P., and West, D.B. (2000) Changes in Body Composition with Conjugated Linoleic Acid, *J. Am. Coll. Nutr. 19*, 487S–493S.
25. Jones, P.A., Lea, L.J., and Pendlington, R.U. (1999) Investigation of the Potential of Conjugated Linoleic Acid (CLA) to Cause Peroxisome Proliferation in Rats, *Food Chem Toxicol. 37*, 1119–1125.
26. Nagasawa, A., Fukui, K., Funahashi, T., Maeda, N., Shimomura, I., Kihara, S., Waki, M., Takamatsu, K., and Matsuzawa, Y. (2002) Effects of Soy Protein Diet on the Expression of Adipose Genes and Plasma Adiponectin, *Horm. Metab. Res. 34*, 635–639.
27. Pajvani, U.B., and Scherer, P.E. (2003) Adiponectin: Systemic Contributor to Insulin Sensitivity, *Curr. Diab. Rep. 3*, 207–213.
28. Tschritter, O., Fritsche, A., Thamer, C., Haap, M., Shirkavand, F., Rahe, S., Staiger, H., Maerker, E., Haring, H., and Stumvoll, M. (2003) Plasma Adiponectin Concentrations Predict Insulin Sensitivity of Both Glucose and Lipid Metabolism, *Diabetes 52*, 239–243.
29. Akahoshi, A., Goto, Y., Murao, K., Miyazaki, T., Yamasaki, M., Nonaka, M., Yamada, K., and Sugano, M. (2002) Conjugated Linoleic Acid Reduces Body Fats and Cytokine Levels of Mice, *Biosci. Biotechnol. Biochem. 66*, 916–920.
30. Yannakoulia, M., Yiannakouris, N., Bluher, S., Matalas, A.L., Klimis-Zacas, D., and Mantzoros, C.S. (2003) Body Fat and Macronutirent Intake in Relation to Circulating Soluble Leptin Receptor, Free Leptin Index, Adiponectin, and Resistin Concentrations in Healthy Humans, *J. Clin. Endocrinol. Metab. 88*, 1730–1736.
31. Stiger H., Tschritter, O., Machann, J., Thamer, C., Fritsche, A., Maerker, E., Schick, F., Haring, H.U., and Stomvoll, M. (2003) Relationship of Serum Adiponectin and Leptin Concentrations with Body Fat Distribution in Humans, *Obes. Res. 11*, 368–372.
32. Chen, Y., Ogawa, H., Narita, H., Ohtoh, K., Yoshida, T., and Yoshikawa, Y. (2003) Ratio of Leptin to Adiponectin as an Obesity Index of Cynomologus Monkeys (*Macaca fascicularis*), *Exp. Anim. 52*, 137–143.
33. Gavrila, A., Peng, C.K., Chan, J.L., Mietus, J.E., Goldberger, A.L., and Mantzoros, C.S. (2003) Diurnal and Ultradian Dynamics of Serum Adiponectin in Healthy Men: Comparison with Leptin, Circulating Soluble Leptin Receptor, and Cortisol Patterns, *J. Clin. Endocrinol. Metab. 88*, 2838–2843.
34. Silha, J.V., Krsek, M., Skrha, J.V., Sucharda, P., Nyomba, B.L., and Murphy, L.J. (2003) Plasma Resistin, Adiponectin and Leptin Levels in Lean and Obese Subjects: Correlation with Insulin Resistance, *Eur. J. Endocrinol. 149*, 331–335.
35. Wolf, G. (2003) Adiponectin: A Regulator of Energy Homeostasis, *Nutr. Rev. 61*, 290–292.

[Received August 15, 2003; accepted December 29, 2003]

Hepatic Lipid Characteristics and Histopathology of Laying Hens Fed CLA or n-3 Fatty Acids

Gita Cherian* and Mary P. Goeger

Department of Animal Sciences, Oregon State University, Corvallis, Oregon 97331-6702

ABSTRACT: The effect of dietary CLA and n-3 PUFA on hepatic TAG accumulation, histopathology, and FA incorporation in lipid classes by laying chickens was investigated. One hundred twenty 30-wk-old single-comb white leghorn laying hens were distributed randomly to four treatments (3 replications of 10 birds) and were fed diets containing CLA and animal fat (Diet I), 18:3n-3 (Diet II), or long-chain n-3 FA (Diet III). A sunflower oil (n-6 FA)-based diet was the control. Feeding Diet I resulted in an increase in hepatic total lipids ($P < 0.05$). The liver TAG content was 32.2, 18.9, 29.4, and 18.7 mg/g for hens fed Diet I, Diet II, Diet III, and the control diet, respectively ($P < 0.05$). The serum TAG was lowest in birds fed Diet II ($P < 0.05$). Diet I resulted in an increase in the total number of fat vacuoles and lipid infiltration in hepatocytes ($P < 0.05$). The number of cells with 75% or higher lipid vacuolation was observed only in birds fed Diet I. Feeding diets containing CLA resulted in an increase in the content of the *c*9,*t*11 CLA isomer in liver TAG and PC ($P < 0.05$). No difference was observed in the CLA concentration of hepatic PE fractions. The content of DHA (22:6n-3) was higher in the TAG, PC, and PE of hens fed Diet II and Diet III than Diet I and the control ($P < 0.05$). Feeding CLA resulted in an increase in total saturated FA in the TAG and PC fractions ($P < 0.05$). Long-term feeding of CLA in laying birds leads to an increase in liver TAG and may predispose birds to fatty liver hemorrhagic syndrome.

Paper no. L9344 in *Lipids 39,* 31–36 (January 2004).

The health-promoting effects of certain FA such as n-3 PUFA and CLA have recently attracted great attention. This includes the TAG-lowering, antiatherosclerotic, and antiarrhythmic properties of n-3 PUFA (1,2), as well as the anticarcinogenic and antiatherogenic properties of CLA (3). Other beneficial effects of CLA include body fat reduction, immunomodulation, and antioxidant properties (3–5). Animal products contribute up to 70% of the total FA in typical Western diets. This includes CLA and n-3 PUFA. CLA are contributed predominantly by food lipids of ruminant animals, and n-3 PUFA are contributed by marine products and plant sources such as flaxseed and canola oils. Current intake of CLA is estimated to be several hundred milligrams per day (6). Based on animal data, it is estimated that approximately 3 g/d of CLA would be required to produce beneficial effects in humans (7). However, as Americans are opting for low-fat dairy and beef products and choosing more poultry products than beef, it is likely that the dietary contribution of CLA and n-3 PUFA will be further reduced in a typical U.S. diet. As a result, feeding strategies have been adopted by the poultry industry to enrich poultry meat and egg lipids with n-3 PUFA and CLA (8). However, the reported studies were short-term feeding trials—under 6 wk—and focused on CLA and PUFA enrichment in egg lipids with little emphasis on potential adverse effects on bird health.

Dietary FA in poultry are contributed by animal- or vegetable-blend oils that are high in saturated and n-6 FA. Liver is the primary site of *de novo* FA synthesis in avians. The major route of FA absorption in birds is by mixed micelle formation. The rudimentary lymphatic system in birds causes the chylomicrons to be absorbed directly into the portal blood for transport to liver. Such a feature also predisposes laying birds to a pathological condition called fatty liver hemorrhagic syndrome (FLHS). FLHS is characterized by increased abdominal fat, multiple hemorrhages, and hematomas of an overtly fatty liver. A high percentage of commercial layers and companion birds develop FLHS, causing the hepatocytes to distend with fat vacuoles, resulting in rupture and death (9). Long-term feeding of n-3 PUFA from flaxseed (10) and fish oils (11) has been reported to increase the incidence of FLHS. Recent studies from our laboratory demonstrated increased hepatic lipid infiltration and lipidosis when CLA, a naturally occurring *trans* FA, was included in hen diets (12). In broiler birds, feeding CLA has been reported to reduce hepatic lipid and TAG content (13). These results suggest that FA chain length, number of double bonds of FA, type of bond (*cis* vs. *trans*), and the metabolic status of birds may affect lipid partitioning by hepatic tissue leading to FLHS. The objectives of the present study were to investigate the long-term effects of feeding CLA and n-3 PUFA on TAG content, hepatic histopatholgy, and pattern of FA incorporation in hepatic tissue lipid classes in a biological system in which the liver plays a key role in fat metabolism, as in laying hens. Both land-based and marine-based n-3 PUFA were used along with an n-6 FA-based control diet.

MATERIALS AND METHODS

These experiments were reviewed by the Oregon State University Animal Care Committee to ensure adherence to Animal Care Guidelines.

Diets. Isocaloric (2900 kcal/kg feed) and isonitrogenous (16% crude protein) experimental rations were formulated with

*To whom correspondence should be addressed at 122-Withycombe Hall, Department of Animal Science, Oregon State University, Corvallis, OR 97331-6702. E-mail: Gita.Cherian@oregonstate.edu

Abbreviation: FLHS, fatty liver hemorrhagic syndrome.

2% animal fat and 1% CLA (Diet I), 1% flaxseed oil + 2% canola oil (Diet II), 3% menhaden (fish) oil (Diet III), and 3% sunflower oil (Control). The composition of the diet is shown in Table 1. Flaxseed and canola oils were used as a source of 18:3n-3, and fish oil was used as a source of >20-carbon n-3 FA. A sunflower oil rich in n-6 FA was used in the control diet. The FA composition of the diets is shown in Table 2. The flaxseed, canola, and sunflowerseed oils were purchased from the local market, and fish oil was donated (Omega Protein, Inc., Reedville, VA). The CLA oil containing 75% FFA was donated from a commercial source and was made up of equal amounts of *c*9,*t*11 and *t*10,*c*12 CLA isomers (Pharmanutrients, Lake Bluff, IL). The diets were mixed weekly and stored before use in a cold room (4°C) in airtight containers.

Birds. A total of 120 thirty-week-old single-comb white leghorn laying hens were weighed and distributed randomly to the experimental diets (3 replications of 10 birds each). The birds were kept individually in cages and were maintained on a 16-h/8-h light/dark photoperiod and standard conditions of temperature and ventilation as per Oregon State University Poultry Farm standard operating procedures. Water and feed were provided *ad libitum*. Feed intake was measured on a weekly basis. The experiment was conducted for 80 d.

Sample collection. After 80 d of feeding the experimental diets, 6 birds per treatment (2 birds per replicate) were randomly selected. The birds were killed by decapitation, and liver tissue was harvested by a veterinary pathologist at the Oregon State University Veterinary Hospital. Liver weights were recorded. On day 40 of feeding, a total of 6 eggs per treatment (2 per replicate) were collected.

Hepatic histopathology and criteria for fat scoring. A slice of liver about 1 × 1 × 0.5 cm thick was taken from the right lobe of each hen, fixed in 10% neutral buffered formalin for 48 h, embedded in paraffin, sectioned (8 μm), and stained with hematoxylin and eosin stain prior to microscopic examination as reported previously (12). For each section of liver, three randomly located areas were graded at 40× magnification using a grid within a 10× ocular piece. Approximately 20 hepatocytes would be expected to fall within the limits of the grid. Fat content of each grid was assessed in two patterns: (i) total number of fat vacuoles in the grid and (ii) number of cells within the grid having >75% lipid vacuolation of cytoplasm. For each method, the sum total from each bird was divided by three to give an average value per grid (12). A fat vacuole was considered to be any nonstaining area of cytoplasm with a sharply defined border. The two methods were used, as it is common for lipid-laden cells to be largely occupied by only one or two vacuoles in severe fatty metamorphosis. A single section from each bird was assessed in this manner. A final average for each group was then calculated. The remaining liver tissue was kept frozen (–20°C) for further lipid analysis.

Lipid analyses. Total lipids were extracted from feed, egg yolk, and liver tissues by the method of Folch *et al.* (14). One gram of sample was weighed into a screw-capped test tube with 20 mL of chloroform/methanol (2:1, vol/vol), and homogenized with a polytron (Type PT10/35; Brinkman Instruments, Westbury, NY) for 5 to 10 s at high speed. After an overnight incubation at 4°C, the homogenate was filtered through Whatman #1 filter paper into a 100-mL graduated cylinder, and 5 mL of 0.88% sodium chloride solution was added and mixed. After phase separation, the volume of lipid layer was recorded, and the top layer was completely siphoned off. Total lipids were determined gravimetrically after evaporating the solvent.

About 5 mL of the lipid extract was put in a glass scintillation vial, was concentrated under nitrogen at 40°C, and was redissolved with an appropriate amount of chloroform to provide a sample with 100 mg lipid. This was applied to precoated silica gel G plates (20 × 20 cm) that had been previously activated by heating at 70°C for 1 h. Lipid standards (TAG, PC, and PE) were applied beside the lipid extracts. The plates were developed in chloroform/methanol/water (65:25:4) (15) to 10 cm from the origin (25 min) and then in hexane and diethyl ether (4:1) to 17 cm from the origin (20 min). The plates were air-dried and then sprayed with 0.1% (wt/vol) 2′,7′-dichlorofluorescein in ethanol. The spots corresponding to TAG, PC, and PE were identified under UV light and were scraped off into screw-capped tubes. The total lipid, TAG, PC, and PE were redissolved in 2 mL boron trifluoride/methanol methylation solution and were incubated in a boiling water bath for 1 h at 90–100°C (12). After cooling to room temperature, the FAME were separated with hexane and distilled water.

Analysis of FA composition was performed with an HP 6890 gas chromatograph (Hewlett-Packard Co., Wilmington, DE) equipped with an autosampler, FID, and fused-silica capillary column, 100 m × 0.25 mm × 0.2 μm film thickness (SP-2560; Supelco, Bellefonte, PA). Sample (1 μL) was injected with helium as a carrier gas onto the column programmed for ramped oven temperatures (initial temperature was 110°C, held for 1.0 min, then ramped at 15.0°C/min to 190°C and held for 55.0 min, then ramped at 5.0°C/min to 230°C and held for 5.0 min). Inlet and detector temperatures were both 220°C (12). Peak areas and percentages were calculated using Hewlett-Packard ChemStation software. FAME were identified by comparison with retention times of authentic standards (Matreya, Pleasant Gap, PA). FA values and total lipids are expressed as weight percentages.

Liver TAG were estimated by adapting an enzyme-based procedure with colorimetric end point, originally developed for serum. The liver tissue total lipid extract served as substrate. A glycerol standard (G1394-5ML; Sigma Diagnostics, St. Louis, MO) was used for calibration of the assay, and Accutrol normal control serum (2034-1 VL; Sigma) was used for quality control.

Statistical analysis. The effect of dietary oils on hepatic lipid class FA and hepatic histopathology were analyzed by ANOVA using SAS (version 8.2) (SAS Institute, Cary, NC). The Student–Newman–Keuls multiple range test (16) was used to compare differences among treatment means ($P < 0.05$). Mean values and SEM are reported.

TABLE 1
Composition of Experimental Diets

Ingredients	Percentage	Calculated analyses	
Corn	38.5	Metabolizable energy (kcal/kg)	2900
Wheat middling	29.5	Crude protein (%)	16
Wheat grain	10.0	Calcium (%)	3.7
Soybean meal	9.0		
Limestone	6.5		
Dicalcium phosphate	2.5		
Salt	0.5		
Oil source[a]	3.0		
Layer premix[b]	0.5		

[a]Oil source includes 2% animal fat + 1% CLA (Diet I), 1% flax oil + 2% canola oil (Diet II), 3% menhaden (fish) oil (Diet III), and 3% sunflower oil (Control).
[b]Supplied per kg feed: vitamin A–12,500 IU; vitamin D_3–4000 IU; vitamin E–25 IU; vitamin B_{12}–0.014 mg; riboflavin–8 mg; pantothenic acid–12 mg; niacin–40 mg; menadione–2.5 mg; choline–500; thiamine–1.75 mg; selenium–0.264 mg; folic acid–0.75 mg; pyridoxine–2 mg; D-biotin–0.15 mg; ethoxyquin–2.5 µg.

RESULTS AND DISCUSSION

The FA composition of the diets reflected the supplemented oil source (Table 1). CLA was present only in the CLA-supplemented diet (Diet I) and consisted of *c*9,*t*11 and *t*10,*c*12 at 4.1 and 2.9%, respectively. Inclusion of flaxseed oil and fish oil resulted in the incorporation of 18:3n-3 and 22:6n-3 in Diets II and III, respectively. Linoleic acid (18:2n-6) was the major FA in the control diet and constituted 55.2%. The addition of different oils also kept the total n-6/n-3 ratio in the test diets at an average of 2.7 compared with 26.6 for the control diet (Table 2). Performance of hens was measured for 120 d (test period). The average feed consumption/bird/d was 107 g for Control and Diet I and 106 g for Diet II and Diet III, respectively ($P > 0.05$). The hen day egg production was 88.5, 91.3, 90.8, and 90.9 for Control, Diet I, Diet II, and Diet III, respectively ($P > 0.05$). Hen day production is calculated from the following formula:

$$\frac{(100 \times \text{number of eggs laid})}{(\text{number of hens} \times \text{days on diet})} \quad [1]$$

No difference was observed in the egg weight among different treatments ($P > 0.05$).

Gross necropsy findings. No significant abnormalities were noted in any of the birds examined with the exception of hepatic changes. The liver tissues from Diet I fed hens were pale and swollen with hemorrhages along the edges. Livers from Diet II and Diet III had normal to good color. Livers of the control diet had a mild pallor with yellowing and focal hemorrhages at the edges in three cases.

TABLE 2
Major FA Composition of Laying Hen Diets

	Dietary treatments[a]			
FA	Control	Diet I	Diet II	Diet III
16:0	13.9	16.3	13.8	13.6
16:1	0.0	0.0	0.0	7.2
18:0	4.6	4.4	4.8	4.7
18:1	22.8	26.4	32.2	18.2
18:2	55.2	32.5	35.0	29.5
18:3n-3	2.1	2.1	11.9	2.5
*c*9,*t*11 CLA	0.0	4.1	0.0	0.0
*t*10,*c*12 CLA	0.0	2.9	0.0	0.0
20:5n-3	0.0	0.0	0.0	4.4
22:5n-3	0.0	0.0	0.0	0.8
22:6n-3	0.0	0.0	0.0	3.4
Total SFA	20.0	21.6	20.9	32.6
Total MUFA	22.8	26.4	32.2	25.5
Total PUFA	57.2	52.0	46.9	41.9
Total CLA	0.0	7.0	0.0	0.0
Total n-6 PUFA	55.2	32.5	35.0	29.5
Total n-3 PUFA	2.1	2.1	11.9	11.0
Total n-6/total n-3	26.6	2.6	2.9	2.8

[a]The control diet contained 3% sunflower oil. Diet I—2% animal fat + 1% CLA; Diet II—1% flax oil + 2% canola oil, Diet III—3% fish oil. Values are reported as percent total FA. SFA, saturated FA (14:0 + 16:0 + 18:0 + 20:0 + 22:0 + 24:0); MUFA, monounsaturated FA (16:1 + 18:1 + 20:1 + 22:1 + 24:1); CLA includes *c*9,*t*11 and *t*10,*c*12. Total PUFA includes total n-6 + total n-3 + total CLA.

Hepatic histopathology. The liver tissue from hens fed Diet I had the most significant pathology, including the most extensive fat deposition and numbers of cells with 75% vacuolation. Extensive hepatocytic vacuolation due to fat deposition was observed in hens fed Diet I (Table 3). Large vacuoles containing fat distended many hepatocytes. The total number of fat vacuoles per grid and the number of hepatocytes with greater than 75% cytoplasmic vacuolation were higher ($P < 0.05$) in Diet I (Fig. 1). The control diet resulted in the fewest vacuoles per grid, at 0.67, when compared with the 36.7 for Diet I ($P < 0.05$). In addition to scoring the liver for fat deposition, the sections were examined for other lesions. The pathology report indicated other abnormalities associated with fatty liver, such as dilated sinusoids, intrasinusoidal fibrin deposition, telangiectasis and lymphocyte aggregates, and an increased

TABLE 3
Hepatic Total Lipid and TAG Content of Laying Hens Fed CLA or n-3 FA[a]

	Dietary treatments				
	Control	Diet I	Diet II	Diet III	SEM
Total lipid (g/g of liver)	0.070[b]	0.170[a]	0.066[b]	0.087[b]	0.02
Liver TAG (mg/g)	18.69[b]	32. 21[a]	18.86[b]	29.42[a,b]	2.94
Serum TAG (mg/dL)	403.17[a,b]	426.50[a]	357.50[b]	380.80[a,b]	12.68
Number of fat vacuoles/grid	0.67[b]	36.7[a]	1.10[b]	5.6[b]	3.045

[a]Means with different superscripts within a row differ significantly ($P < 0.05$), $n = 6$. The control diet contained 3% sunflower oil. Diet I—2% animal fat + 1% CLA; Diet II—1% flax oil + 2% canola oil; Diet III—3% fish oil.

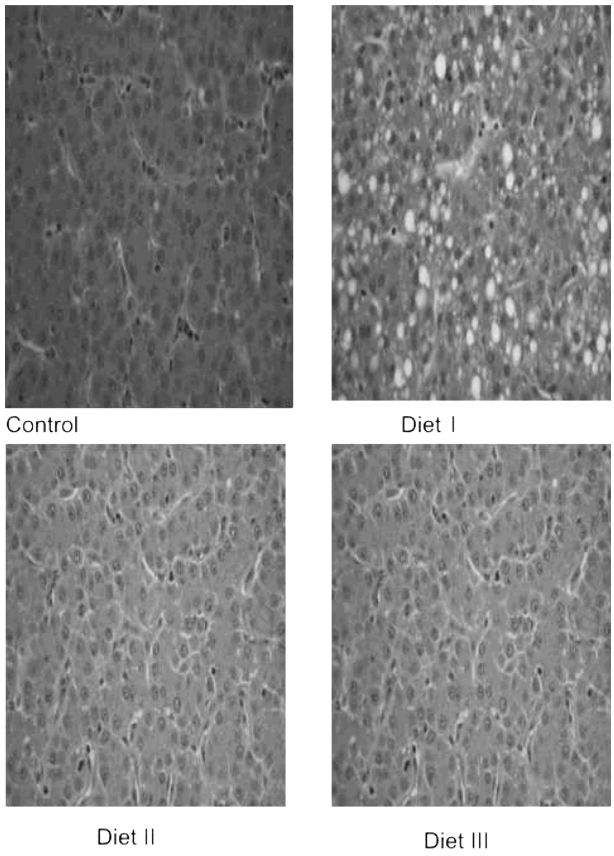

FIG. 1. Histological sections of liver tissue from hens fed Control, Diet I, II, or III. The control diet contained 3% sunflower oil; Diet I—2% animal fat + 1% CLA; Diet II—1% flax oil + 2% canola oil; Diet III—3% fish oil.

incidence of single-cell necrosis in the hepatic tissue from hens fed Diet I. Although no difference was found in liver weight as a percentage of body weight, lipid infiltration was significantly altered in hens fed Diet I. These results corroborate our previous research (12).

Liver lipids, TAG, and FA. A significant effect of dietary CLA on hepatic total lipid was noted. Livers from hens fed Diet I contained approximately 2.5 times the total lipids found in the other diets ($P < 0.05$) (Table 3). The increase in total lipid corroborates our previous findings (12) and those reported in mice (17) and fish (18). Profound *t*10,*c*12-CLA-mediated changes in the pattern of hepatic gene expression, contributing to fat accumulation leading to hepatomegaly, were reported in mice (19). The increase in liver lipids was associated with an increase in hepatic TAG concentration ($P < 0.05$) (Table 3). The birds fed the control diet had lower liver TAG ($P < 0.05$) than Diet I, but no difference was observed between the serum TAG of these two treatments, suggesting that dietary CLA may affect TAG channeling in the hepatic tissue. In broiler chickens, feeding CLA has been reported to reduce hepatic TAG and total lipids (13). The reduction in hepatic total lipids in broiler birds fed diets containing CLA reported by Badinga *et al.* (13) was also observed in our laboratory (Cherian, G., and Goeger, M.P., unpublished data). Unlike mammalian species, *de novo* FA synthesis occurs exclusively in the liver in avian species. This discrepancy observed between laying birds and broiler birds may possibly be due to the physiological state of laying birds. The increase in liver total lipids and hepatic lipidosis was observed from our previous research when CLA was fed to laying birds for a short-term (6-wk period) feeding trial (12), simulating the time span over which broiler birds are usually fed or raised. The high lipid turnover in laying birds imposes an extra metabolic demand, suggesting that a species- and strain-specific CLA-responsiveness leading to enhanced TAG accumulation may exist in laying birds. The significant changes in hepatic histopathology and TAG accumulation observed in Diet I birds suggest that dietary CLA, even at a low level, may influence hepatic lipid metabolism and subsequently may contribute to FLHS. Understanding how dietary FA control lipid partitioning in egg-laying birds is critical to formulating diets that can minimize FLHS. To our knowledge, effects of dietary CLA on liver TAG concentrations in laying birds have not been previously reported. The CLA oil used in the present study contained both *t*10,*c*12 and *c*9,*t*11 isomers at 4.1 and 2.9% and were in an FFA form. The effects of using CLA in other forms such as TAG need to be investigated. A positive energy balance has been reported to cause FLHS in hens and companion birds (20). In the current study, the experimental diets were isocaloric, and the total fat in the laying hen ration was 3%, which is within the range for laying chickens.

The FA composition of liver TAG, PC, and PE was significantly affected by diet ($P < 0.05$) (Table 4). The *c*9,*t*11 isomers were higher ($P < 0.05$) in liver from hens fed Diet I in the TAG and PC fractions and were not detected in PE. The *c*9,*t*11 isomer was the only isomer detected in liver tissue. The increase in CLA was at the expense of oleic acid (18:1) in TAG. The saturated FA content increased in TAG and PC of birds fed Diet I ($P < 0.05$). Even a minor increase in CLA resulted in a dramatic change in the concentration of palmitic (16:0) and stearic acids (18:0) in TAG and PC ($P < 0.05$). However, the reduction in oleic acid and the increase in saturated FA by incorporating CLA were not detected in PE suggesting that CLA feeding may have differential effects on hepatic phospholipid classes in birds. Inclusion of n-3 FA from fish oil and the flaxseed oil–canola oil mix resulted in an increase in 22:6n-3 in TAG, PC, and PE with a preferential channeling in PE.

The FA composition of egg yolk is shown Table 5. The FA composition of egg yolk reflected the liver FA of the hens from which the eggs came, which is not surprising because, in avians, liver is the primary site of lipogenesis. CLA was present only in Diet I and constituted up to 3.5%. The major CLA isomer in the yolk lipids was *c*9,*t*11 and constituted 2.5% in the yolk lipids of hens fed Diet I. Addition of 1.5% CLA resulted in a significant increase in saturated FA with a concomitant reduction in monounsaturated FA. These results corroborate our previous results and those of others (21,22). Feeding a sunflowerseed oil to the control resulted in a significant increase in 18:2n-6 and 20:4n-6. Diets II and III resulted

TABLE 4
Major FA Composition of Hen Liver TAG, PC, and PE[a]

FA	Dietary treatments				
	Control	Diet I	Diet II	Diet III	SEM
	TAG				
16:0	15.4^{c}	26.2^{a}	15.4^{c}	20.2^{b}	1.55
16:1	0.16^{c}	2.2^{b}	1.8^{b}	3.7^{a}	0.27
18:0	11.3^{b}	18.5^{a}	8.1^{c}	11.2^{b}	0.88
18:1n-9	40.6^{b}	32.9^{c}	50.8^{a}	44.9^{b}	1.38
18:2n-6	28.5^{a}	16.6^{b}	17.6^{b}	16.8^{b}	1.59
18:3n-3	0.0^{c}	0.4^{b}	1.7^{a}	0.4^{b}	0.01
20:4n-6	3.1^{a}	0.9^{b}	1.7^{a,b}	0.3^{b}	0.48
cis-9,*trans*-11 CLA	0.0^{b}	0.5^{a}	0.0^{b}	0.0^{b}	0.08
22:6n-3	0.0^{b}	0.0^{b}	0.95^{a}	1.1^{a}	0.28
Total SFA	27.3^{b,c}	45.8^{a}	24.4^{c}	32.6^{b}	5.12
Total MUFA	40.8^{c}	35.2^{d}	53.4^{a}	48.5^{b}	1.56
Total n-6 PUFA	31.7^{a}	17.5^{b}	19.4^{b}	17.2^{b}	1.84
Total n-3 PUFA	0.2^{c}	0.9^{b,c}	2.7^{a}	1.7^{a,b}	0.46
	PC				
16:0	33.3^{b}	36.1^{a}	29.9^{c}	33.8^{b}	0.49
16:1	0.9^{a}	0.98^{a}	1.2^{a}	1.6^{a}	0.35
18:0	15.8^{b}	22.4^{a}	15.1^{b}	14.2^{b}	0.91
18:1n-9	24.3^{b}	23.1^{b}	29.4^{a}	29.7^{a}	1.03
18:2n-6	17.0^{a}	10.4^{c}	13.6^{b}	10.8^{c}	0.83
20:4n-6	5.8^{a}	2.1^{c}	5.1^{a}	3.1^{b}	0.33
cis-9,*trans*-11 CLA	0.0^{a}	0.2^{b}	0.0^{a}	0.0^{a}	0.09
22:6n-3	0.6^{b}	0.0^{b}	4.6^{a}	4.2^{a}	0.33
Total SFA	49.7^{b}	60.7^{a}	45.0^{c}	48.6^{b,c}	1.24
Total MUFA	25.2^{b}	24.0^{b}	30.7^{a}	31.4^{a}	0.74
Total n-6 PUFA	24.0^{a}	13.7^{c}	19.4^{b}	15.0^{c}	1.07
Total n-3 PUFA	0.9^{b}	1.3^{b}	4.9^{a}	4.9^{a}	0.45
	PE				
16:0	16.1^{b}	17.7^{b}	15.0^{b}	20.9^{a}	0.73
16:1	0.7	0.6	0.8	0.5	0.20
18:0	32.2	32.9	32.6	36.2	1.06
18:1n-9	15.7	16.3	17.5	15.1	0.50
18:2n-6	15.9^{a}	15.5^{a}	11.7^{b}	7.8^{c}	0.77
20:4n-6	14.6^{a}	12.2^{a}	11.8^{a}	5.3^{b}	0.85
22:6n-3	3.1^{b}	2.4^{b}	8.6^{a}	10.4^{a}	0.86
Total SFA	48.3^{b}	50.6^{b}	47.8^{b}	57.1^{a}	1.64
Total MUFA	16.6	16.8	18.3	15.6	0.82
Total n-6 PUFA	31.6^{a}	28.8^{a}	24.1^{b}	15.7^{c}	0.77
Total n-3 PUFA	3.5^{b}	3.6^{b}	9.8^{a}	11.6^{a}	1.02

[a]Means with different superscripts within a row differ significantly ($P < 0.05$). Values are reported as percent total FA, $n = 6$. The control diet contained 3% sunflower oil. Diet I—2% animal fat + 1% CLA, Diet II—1% flax oil + 2% canola oil, Diet III—3% fish oil. For abbreviations, see Table 2.

in a significant increase in n-3 FA such as 18:3n-3 and 22:6n-3. Most of the reported studies on CLA and PUFA in poultry were short-term feeding trials investigating tissue enrichment and body fat reduction properties. The long-term potentially adverse effect of PUFA and CLA on hepatic tissue has been largely ignored. The results from the present study suggest that CLA feeding is associated with preferential channeling of liver TAG toward hepatic storage. Whether the dietary CLA-associated TAG accumulation observed in this study is a phenomenon peculiar to laying hens or one that might occur in any situation in which the metabolic activity of the liver is enhanced or chronically stressed, as in laying hens, is not known. The results from the present study suggest the need for further investigations on the long-term use of CLA in animal health and also on the long-term clinical use of CLA supplementation as a means of weight management in humans.

ACKNOWLEDGMENTS

The Ott Professorship awarded to G. Cherian is acknowledged. The CLA used in this study was kindly supplied by Pharmanutrients (Lake Bluff, IL). The generous donation of menhaden oil from Omega Protein Inc, Reedville, Virginia, is appreciated. The assistance of Irene Pilgrim and Ramesh Selvaraj, Oregon State University, is acknowledged.

TABLE 5
Major FA Composition of Eggs[a]

FA	Dietary treatments				
	Control	Diet I	Diet II	Diet III	SEM
16:0	25.8[b]	32.7[a]	24.0[c]	26.5[b]	0.18
16:1	2.5[c]	1.1[d]	3.3[b]	4.2[a]	0.16
18:0	10.8[b]	19.9[a]	9.1[c]	10.8[b]	0.14
18:1n-9	36.3[b]	25.2[c]	42.8[a]	41.7[a]	0.20
18:2n-6	22.6[a]	15.4[b]	15.3[b]	12.3[c]	0.15
18:3n-3	0.0[c]	0.0[c]	2.6[a]	0.3[b]	0.08
20:4n-6	2.1[a]	1.3[b]	1.3[b]	0.6[c]	0.08
cis-9,*trans*-11 CLA	0.0[b]	2.4[a]	0.0[b]	0.0[b]	0.14
trans-10,*cis*-12 CLA	0.0[b]	1.1[a]	0.0[b]	0.0[b]	0.13
22:6n-3	0.0[c]	0.0[c]	1.4[b]	3.0[a]	0.07
Total SFA	36.6[b]	52.6[a]	33.1[c]	37.2[b]	0.18
Total MUFA	38.7[b]	27.1[c]	46.2[a]	46.3[a]	0.18
Total n-6 PUFA	24.7[a]	16.8[b]	16.6[b]	12.8[c]	0.15
Total n-3 PUFA	0.0[c]	0.0[b]	4.0[a]	3.7[a]	0.13

[a]Means with different superscripts within a row differ significantly ($P < 0.05$), $n = 6$. Values reported as percent total FA. Control diet contained 3% sunflower oil. Diet I—2% animal fat + 1% CLA, Diet II–1% flaxseed oil + 2% canola oil, Diet III—3% fish oil. For abbreviations see Table 2.

REFERENCES

1. Laidlaw, M., and Holub, B.J. (2003) Effects of Supplementation with Fish Oil-Derived n-3 FA and γ-Linolenic Acid on Circulating Plasma Lipids and Fatty Acid Profiles in Women, *Am. J. Clin. Nutr. 77*, 37–42.
2. Nair, S.D.S., Leitch, J.W., Falconer, J., and Garg, M.L. (1997) Prevention of Cardiac Arrhythmia by Dietary (n-3) Polyunsaturated Fatty Acids and Their Mechanism of Action, *J. Nutr. 127*, 383–393.
3. Pariza, M.W., Park, Y., and Cook, M.E. (2001) The Biologically Active Isomers of Conjugated Linoleic Acid, *Prog. Lipid Res. 40*, 283–298.
4. Cook, M.E., Miller, C.C., Park, Y., and Pariza, M.W. (1993) Immune Modulation by Altered Nutrient Metabolism: Nutritional Control of Immune-Induced Growth Depression, *Poult. Sci. 72*,1301–1305.
5. Palacios, A., Piergiacomi, V., and Catala, A. (2003) Antioxidant Effect of Conjugated Linoleic Acid and Vitamin A During Nonenzymatic Lipid Peroxidation of Rat Liver Microsomes and Mitochondria, *Mol. Cell. Biochem. 250*, 107–113.
6. Fritsche, J.R., Rickert, H., Steinhart, M.P., Yurawecz, M.M., Mossaba, N., Roach, J.A.G., Kramer, J.K.G., and Ku, Y. (1999) Conjugated Linoleic Acid (CLA) Isomers: Formation, Analysis, Amounts in Foods and Dietary Intake, *Fett/Lipid 101*, 272–276.
7. Ha, Y.L., Grimm, N.K., and Pariza, M.W. (1989) Newly Recognized Anticarcinogenic Fatty Acids: Identification and Quantification in Natural and Processed Cheeses, *J. Agric. Food Chem. 37*, 75–81.
8. Cherian, G. (2002) Lipid Modification Strategies and Nutritionally Functional Poultry Foods. Food Science and Product Technology, Ch. 4 in *Food Science and Product Technology* (Nakano, T., and Ozimek, L. eds.), pp. 77–92, Research Sign Post, Trivandrum, India.
9. Squires, J., and Leeson, S. (1998) Etiology of Fatty Liver Syndrome in Laying Hens, *Br. J. Vet. Med. 144*, 602–609.
10. Bean, L.D., and Leeson, S. (2003) Long-Term Effects of Feeding Flaxseed on Performance and Egg Fatty Acid Composition of Brown and White Hens, *Poult. Sci 82*, 388–394.
11. Van Elswyk, M.E., Hargis, B.M., Williams, J.D., and Hargis, P.S (1994) Dietary Menhaden Oil Contributes to Hepatic Lipidosis in Laying Hens, *Poult. Sci. 73*, 653–662.
12. Cherian, G., Holsonbake, T.B., Goeger, M.P., and Bildfell, R. (2002) Dietary Conjugated Linoleic Acid Alters Yolk and Tissue Fatty Acid Composition and Hepatic Histopathology of Laying Hens, *Lipids 37*, 751–757.
13. Badinga, L., Selberg, K.T., Dinges, A.C., Comer, C.W., and Miles, R.D. (2003) Dietary Conjugated Linoleic Acid Alters Hepatic Lipid Content and Fatty Acid Composition in Broiler Chickens, *Poult. Sci. 82*, 111–116.
14. Folch, J., Lees, M., and Sloane-Stanley, G.H. (1957) A Simple Method for the Isolation and Purification of Total Lipids from Animal Tissues, *J. Biol. Chem. 226*, 497–507.
15. Cherian, G., and Sim, J.S. (1992) Preferential Accumulation of n-3 Fatty Acids in the Brain Tissue of Chicks from n-3 Fatty Acid Enriched Eggs, *Poult. Sci. 71*, 1658–1668.
16. Steel, R.G.D., and Torrie, J.H. (1980) *Principles and Procedures of Statistics: A Biometrical Approach*, 2nd edn., McGraw-Hill, Toronto.
17. Belury, M.M., and Kempa-Stezko, A. (1997) Conjugated Linoleic Acid Modulates Hepatic Lipid Composition in Mice, *Lipids 32*, 199–204.
18. Twibell, R.G., Watkins, B.A., and Brown, P.B. (2001) Dietary Conjugated Linoleic Acids and Lipid Source Alter Fatty Acid Composition of Juvenile Yellow Perch, *J. Nutr. 131*, 2322–2328.
19. Clément, L., Poirier, H., Niot, I., Bocher, V., Guerre-Millo, M., Krief, K., Staels, B., and Besnard, P. (2002) Dietary *trans*-10,*cis*-12 Conjugated Linoleic Acid Induces Hyperinsulinemia and Fatty Liver in the Mouse, *J. Lipid Res. 43*, 1400–1409.
20. Butler, E.J. (1976) Fatty Liver Disease in the Domestic Fowl—A Review, *Avian Pathol. 5*, 1–14.
21. Du, M., Ahn, D.U., and Sell, J.L. (1999) Effect of Dietary Conjugated Linoleic Acid on the Composition of Egg Yolk Lipids, *Poult. Sci. 78*, 1639–1645.
22. Raes, K., Huyghebaert, G., Smet, S.D., Nollet, L., Arnouts, S., and Demeyer, D. (2002) The Deposition of Conjugated Linoleic Acids in Eggs of Laying Hens Fed Diets Varying in Fat and Fatty Acid Profile, *J. Nutr. 132*, 182–189.

[Received July 8, 2003, and in revised form November 4, 2003; revision accepted December 2, 2003]

Dietary Diacylglycerol Prevents High-Fat Diet-Induced Lipid Accumulation in Rat Liver and Abdominal Adipose Tissue

Xianghe Meng[a], Dongya Zou[a], Zhongping Shi[a,*], Zuoying Duan[a], and Zhonggui Mao[a,b]

[a]School of Biotechnology, Southern Yangtze University, Wuxi, 214036, P.R. China, and [b]Key Laboratory of Industrial Biotechnology, Ministry of Education, Southern Yangtze University, Wuxi 214036, P.R. China

ABSTRACT: The inhibitory effects of 1,3-diacylglycerol (DAG) on diet-induced lipid accumulation in liver and abdominal adipose tissue of rats were investigated in the present study. Male Sprague-Dawley rats were given free access to diets containing 7 wt% TAG (low TAG), 20 wt% TAG (high TAG), or 20 wt% DAG (high DAG), respectively, for 8 wk. The body weight of rats in the 20% high-TAG group increased significantly, and the weights of their abdominal adipose tissue and liver also showed a significant increase compared with rats in the low-TAG group. However, the high-DAG diet resulted in both a significant reduction in body weight gain (with a decrease of 70.5%) and an increase in the ratio of abdominal fat to body weight (by 127%) compared with the high-TAG diet. As well, the liver TAG and serum TAG levels of the high-DAG group were significantly lower than those of the high-TAG group. These effects were associated with up-regulation of acyl-CoA carnitine acyltransferase (ACAT) and down-regulation of acyl-CoA DAG acyltransferase (DGAT) in the liver. However, no significant difference was observed in the activities of alanine aminotransferase and aspartate aminotransferase among the groups ($P > 0.05$). The present results indicate that dietary DAG reduced fat accumulation in viscera and body, and these effects may be involved with up-regulation of ACAT and down-regulation of DGAT in the liver.

Paper no. L9396 in *Lipids 39*, 37–41 (January 2004).

Diseases such as diabetes mellitus, cardiovascular diseases, and other so-called lifestyle-related diseases are all related to obesity, especially to abdominal obesity (1–3). Moreover, intra-abdominal distribution of fat in body is associated with disease risks (4,5). Overaccumulation of fat in the liver can lead to liver infiltration and fatty liver. Obesity characterized by excessive body fat accumulation is generally associated with enhanced lipid consumption, although the factors that cause obesity are various and complex. Therefore, many studies have focused on food ingredients, medicinal drugs for prevention, and reduction of obesity (6–8).

With respect to lipid metabolism, several studies (9,10) have shown that dietary DAG can lower the magnitude of postprandial increase in serum and chylomicron-TAG levels. In a single administration study in men, dietary DAG prevented body fat accumulation, especially in visceral fat in healthy men, and improved serum profile and anthropometric parameters in free-living subjects (11). However, Sugimoto *et al.* (12) suggested that dietary DAG does not have any anti-obesity and lipid-lowering effects. The lower DAG oil level (10 wt%) in their experiment, and the lower total DAG (of 80 wt%) and 1,3-DAG content (55%) in their DAG oil could be the reason for the observation of the opposite result. Moreover, Hase and colleagues (13) investigated the reduction of body fat by α-linolenic acid-rich DAG. These results highlighted the synergistic interaction of the 1,3-DAG structure and n-3 FA. In addition, the effects of DAG on up-regulation of acyl-CoA oxidase (ACO), acyl-CoA synthase (ACS), and medium-chain acyl-CoA dehydrogenase mRNA in intestine and in liver were investigated by Murase and others (14,15). However, they did not study the relationship between dietary DAG and the activity of hepatic acyl-CoA DAG acyltransferase (DGAT), and acyl-CoA carnitine acyltransferase (ACAT). ACAT is a key enzyme involved in the β-oxidation reaction. DGAT catalyzes the acyl-CoA-dependent acylation of *sn*-1,2-DAG to generate TAG, which is the final step and also a common pathway in TAG biosynthesis process. Therefore, we hypothesized that DAG would reduce fat accumulation in the body by suppressing DGAT activity and/or stimulating ACAT activity. The present study focused on the mechanisms leading to reduced body fat accumulation by DAG, by investigating the effects of dietary DAG on the activities of hepatic DGAT, ACAT, abdominal fat, and hepatic lipid in rats.

MATERIALS AND METHODS

Experimental oils. DAG oil was prepared by esterification of rapeseed oil-derived FA with glycerol using 1,3-specific Lipozyme RM^{IM} (Novo Nordisk Co, Bagsvaerd, Denmark) as biocatalyst. The molar ratio of 1,3-acylglycerol to 1,2-acylglycerol was about 7:1. TAG oil was prepared by mixing rapeseed oil and soybean oil so that the FA composition was similar to that of DAG oil. The composition of test oils is shown in Table 1.

*To whom correspondence should be addressed. E-mail: zpshi@sytu.edu.cn

Abbreviations: ACAT, acyl-CoA carnitine acyltransferase; ACO, acyl-CoA oxidase; ACS, acyl-CoA synthase; ALT, alanine aminotransferase; AST, aspartate aminotransferase; DGAT, acyl-CoA DAG acyltransferase; MGAT, MAG acyltransferase; PPAR, peroxisome proliferator-activated receptor(s); TC, total cholesterol.

TABLE 1
FA and Acylglycerol Compositions of TAG Oil and DAG Oil

	TAG oil	DAG oil
FA	g /100 g FA	
16:0	0.21	0.30
16:1	4.63	5.14
18:0	3.34	3.55
18:1	56.20	55.68
18:2	22.42	22.99
18:3	7.56	6.99
Others	5.64	5.35
Acylglycerols	g /100 g oil	
DAG	0.98	90.2
TAG	97.50	8.43
Others	1.52	1.37

Animals and treatments. Five-week-old male Sprague-Dawley rats were obtained from the animal experimental center of Nanjing University of Traditional Chinese Medicine. The animal room was maintained at 23 ± 2°C, with 40–70% RH. The air was changed at 12-h intervals. A light/dark cycle of 12 h (light on from 7:00 AM to 7:00 PM) was maintained. After a 7-d acclimation period, the rats were divided into three groups (10 rats/group). The rats were given free access to food and tap water. The composition of purified feeds specified by the formula of AOAC and AIN93 are shown in Table 2. The low-TAG feed contained 7 wt% TAG, the high-TAG feed contained 20 wt% TAG, and the high-DAG feed contained 20 wt% DAG. All measurements were initiated after a 7-d acclimation period. The amount of food consumed in a 24-h period was measured every day for 1 wk to calculate fat digestibility. Measurements of body weight were made weekly.

At the end of the experiments (after 8 wk of feeding), the rats were fasted for 12 h, anesthetized with sodium pentobarbital, and then subjected to surgery. Blood was collected from the vena cava, and the serum was used for various biochemical analyses. Under the same condition of anesthesia, abdominal adipose (epididymal, mesentery, and perirenal fats) and liver were removed and then weighed. Crude fat content of the experimental diets and feces was extracted according to the method of Folch *et al.* (16). Calculation of fat digestibility was based on the fat content of diets and feces. Hepatic lipids were extracted with chloroform/methanol (1:2, vol/vol) (17).

TABLE 2
Composition of the Different Diets[a] (g/100 g diet)

Ingredients	Low TAG	High TAG	High DAG
Casein	20.0	20.0	20.0
Cornstarch	64.5	51.5	51.5
TAG oil	7.0	20.0	—
DAG oil	—	—	20.0
Cellulose	4.0	4.0	4.0
Vitamin mixture[b]	1.0	1.0	1.0
Mineral mixture[b]	3.5	3.5	3.5
Total	100	100	100

[a]DL-Methionine and choline tartrate were further added to the pre-prepared diets (100 g) at the rate of 0.3 g/100 g diet and 0.2 g/100 g diet, respectively.
[b]Vitamin mixture and mineral mixture refer to the AIN93 prescription.

The following indexes were determined using an Automatic Biochemical Analyzer (Hitachi 7600-020; Hitachi Co., Tokyo, Japan): alanine aminotransferase (ALT), aspartate aminotransferase (AST), total cholesterol (TC), and total TAG in serum. VLDL and the chylomicron fraction were isolated by sequential ultracentrifugation. Liver phospholipids were measured by phosphorus analysis (18). DGAT activity was detected according to the method of Middleton *et al.* (19) and Lozeman *et al.* (20). The activity of ACAT was determined by the method described by Bieber *et al.* (21).

Statistical analysis. The results were expressed as means ± SD for 10 rats unless otherwise indicated. The differences among the three groups were analyzed by ANOVA, and each group was compared with the others by Fisher's protected least-significant difference (PLSD) test (statistical package of STATISTICA 6.0; StatSoft, Tulsa, OK). Statistical significance was defined as $P < 0.05$.

RESULTS AND DISCUSSION

Effect of DAG on the body weight and visceral fat weight of rats. No significant differences were observed in initial body weight among the groups (Table 3). All of the groups showed a gain in body weight. Compared with the low-TAG group, the high-TAG group showed a significant difference in the increase in body weight (47.6 g, $P < 0.01$) and abdominal adipose tissue weight (3.86 g, $P < 0.05$). On the other hand, the high-DAG group had a lower body weight gain and abdominal adipose tissue increase compared with the high-TAG group. The significance test levels of indexes between the high-DAG group and the high-TAG group were as follows: body weight gain ($P < 0.01$), abdominal adipose tissue weight ($P < 0.01$), ratio of abdominal adipose tissue weight to body weight ($P < 0.05$), mesenteric fat ($P < 0.01$), perirenal fat ($P < 0.01$), and epididymal fat ($P < 0.01$). During the experiments, no significant difference was observed in fat digestibility among the groups. The rats in the high-TAG group took in more energy than those in the low TAG-group ($P < 0.05$). This could be one of the reasons for the differences between the two groups. However, there was no significant difference in energy intake between the high-TAG group and the high-DAG group. In addition, the FA composition of the DAG oil was similar to that of the TAG oil.

Other studies have shown that the extent of postprandial serum TAG increases after administration of the DAG emulsion, especially chylomicron TAG. This was less than that observed after administration of the TAG emulsion (9,10). Impaired postprandial serum TAG clearance also was associated with visceral obesity (22,23). The higher postprandial serum TAG caused a higher load of postprandial serum TAG clearance. Since DAG feeding could suppress the postprandial TAG increase, this may explain, at least in part, the reduction of visceral obesity by DAG. In addition, recent research suggested that dietary DAG could affect peroxisome proliferator-activated receptors (PPAR) (24). However, liver PPAR plays a role in regulating TAG homeostasis and preventing the damages of other tissues caused by TAG accumulation (25).

TABLE 3
Effects of Different Diets on the Body Weight and Abdominal Fat[a] of Rats Fed for 8 wk

Parameters	Low TAG	High TAG	High DAG
Body weight			
Initial weight (g)	145.5 ± 10.3	145.4 ± 6.4	146.3 ± 7.3
Final weight (g)	394.6 ± 32.1	442.1 ± 26.2[A]	409.2 ± 25.6[a,b]
Gain (for 8 wk, g)	249.1 ± 21.3	296.6 ± 19.9[A]	262.9 ± 23.6[a,b]
Abdominal adipose tissue weight			
Absolute (g)	15.70 ± 2.38	19.54 ± 3.49[a]	15.76 ± 3.02[b]
Relative (g/100 g body weight)	4.0 ± 0.5	4.4 ± 0.4[a]	3.8 ± 0.3[a,b]
Mesenteric fat (g)	5. 98 ± 1.62	7.46 ± 1.18[A]	6.16 ± 1.20[a,b]
Perirenal fat (g)	7. 46 ± 1.18	9.19 ± 1.85[a]	7.28 ± 2. 63[b]
Epididymal fat (g)	2. 23 ± 0.57	2.89 ± 0.46[A]	2.32 ± 0.37[b]
Fat digestibility (%)	95.70 ± 0.46	95.62 ± 0.37	95.44 ± 0.34
Energy intake (kJ/rat/d)	347.40 ± 12.10	422.90 ± 12.60[A]	421.90 ± 11.80[A]

[a]Values are means ± SD (n = 10). [a]$P < 0.05$, [A]$P < 0.01$, significant difference from the low-TAG group. [b]$P < 0.05$, significant difference from the high-TAG group.

Effect of DAG on the blood lipids of rats. As expected, plasma total TAG concentrations were raised after consumption of TAG feed and lowered by the high-DAG diet when compared with the low-TAG diet (Table 4). The rats fed the high-DAG diet had lower chylomicron-TAG and VLDL-TAG (TAG in VLDL) concentrations than the rats fed the high-TAG diet. However, there were no significant differences in TC and phospholipid concentrations between the high-DAG and the high-TAG groups. The activities of AST and ALT were similar for all the groups.

In general, blood from animals with free access to food has high levels of chylomicrons and VLDL, both of which are rich in TAG. TAG are thought to be metabolized to FFA and 2-MAG by digestion, absorbed into epithelial cells of the small intestine, and then reassembled *via* a 1,2-DAG generation process. On the other hand, 1,3-DAG are metabolized to 1-MAG and FFA by digestion, but it is difficult to regenerate 1(3),2-DAG because the affinities of 1(3)-MAG for MAG acyltransferase (MGAT) in epithelial cells of the small intestine are lower than that of 2-MAG for MGAT (26). The FA from 1,3-DAG digestion would be assimilated primarily through the glycerol-3-phosphate pathway instead of the 2-MAG pathway. Furthermore, TAG formed through the glycerol-3-phosphate pathway, in contrast to that reassembled through the 2-MAG pathway, was mainly stored in the cytoplasm of intestinal mucosal cells rather than being directly used as the building block for chylomicron assembly. Hence, dietary DAG contributed to the decrease in chylomicron TAG. On the other hand, VLDL, which is rich in TAG (as mentioned before), is generally produced in hepatic mesenchymal cells and then secreted into blood circulation. Studies of the mechanism of the incorporation of TAG into secreted VLDL in the liver suggest that the route from cytosolic droplet TAG to VLDL-TAG involves the hydrolysis to 1,2-*sn*-DAG and then reesterification of the remodeled DAG to TAG before secretion (27,28). Hence, activities of DGAT in liver microsomes can affect VLDL-TAG secretion (29). Lower VLDL-TAG maybe due to the decrease of DGAT activity down-regulation by DAG dietary (shown in Table 5). These observations may explain the differences in serum TAG concentration between the high-DAG and the high-TAG groups.

Effect of DAG on liver weight, hepatic lipid, and hepatic enzymes in rats. Table 5 shows the differences in liver weight and hepatic lipid composition in rats fed the different diets. The weight of liver increased significantly (by 18.9%) in the high-TAG diet group, but the increase was suppressed by the high-DAG diet. However, there was no significant difference in the ratio of the liver to body weight. This suggests that the increase in liver weight is proportional to body weight gain. The changes of hepatic lipid levels after feeding the high-TAG and the low-TAG diets to the rats were similar to those of plasma lipid levels, as well as those of fat pad weights.

TABLE 4
Influence of Different Diets on Plasma Lipid[a] of Rats Fed for 8 wk

Parameters	Low TAG	High TAG	High DAG
TC (mmol/L)	1.56 ± 0.25	1.65 ± 0.31	1.58 ± 0.32
Total TAG (mmol/L)	3.01 ± 0.17	3.47 ± 0.29[a]	2.76 ± 0.25[b]
Chylomicron-TAG (mmol/L)	1.89 ± 0.25	2.13 ± 0.25[a]	1.72 ± 0.29[a,b]
VLDL-TAG (mmol/L)	0.86 ± 0.09	1.22 ± 0.21[a]	0.64 ± 0.12[a,b]
Phospholipid (mmol/L)	2.42 ± 0.14	2.75 ± 0.30	2.57 ± 0.50
AST (U/L)	114.67 ± 15.63	104.58 ± 19.45	101.90 ± 13.49
ALT (U/L)	29.22 ± 4.58	25.72 ± 3.56	27.40 ± 3.27

[a]Values are means ± SD (n = 10). [a]$P < 0.05$, significant difference from the low-TAG group; [b]$P < 0.05$, significant difference from the high-TAG group. TC, total cholesterol; AST, aspartate aminotransferase; ALT, alanine aminotransferase.

TABLE 5
Effects of Different Diets on Liver Weight, Hepatic Lipid Concentration, and Activity of Hepatic Enzymes[a] in Rats Fed for 8 wk

Parameters	Low TAG	High TAG	High DAG
Liver weight (g)	13.65 ± 2.00	16.22 ± 3.52[a]	14.24 ± 2.77[a,b]
Liver weight/body weight (%)	3.46 ± 0.40	3.67 ± 0.26	3.48 ± 0.12
Hepatic lipid content (μmol/g)			
Total TAG	41.8 ± 0.30	48.5 ± 0.25[A]	42.64 ± 0.32[b]
TC	9.48 ± 0.20	10.06 ± 0.46	9.88 ± 0.37
Phospholipid	35.24 ± 1.48	33.60 ± 1.32	38.95 ± 1.50[a]
DGAT (nmol/min/mg protein)	7.01 ± 0.32	7.68 ± 0.84[a]	6.40 ± 0.41[a,b]
ACAT (nmol/min/g liver)	1.01 ± 0.15	1.21 ± 0.26[a]	1.69 ± 0.18[A,b]

[a]Values are means ± SD (n = 10). [a]$P < 0.05$, [A]$P < 0.01$, significant difference from the low-TAG group; [b]$P < 0.05$, significant difference from the high-TAG group. ACAT, acyl-CoA carnitine acyltransferase; DGAT, acyl-CoA DAG acyltransferase; for other abbreviations see Table 4.

To examine further the effect of the high-DAG diet on the liver, we measured the activity of hepatic ACAT and DGAT in rats fed with high DAG (Table 5). After 8 wk of feeding, ACAT activity of the high-DAG-fed rats was stimulated to 1.4 times ($P < 0.05$) that of the high-TAG-fed rats, whereas DGAT activity was decreased 1.2 times. ACAT is the key enzyme of the β-oxidation reaction. It controls transportation of long-chain FA through the mitochondrial membrane. DGAT catalyzes the acyl-CoA dependent acylation of 1,2-*sn*-DAG to generate TAG (30,31), which is the final step in all TAG biosynthesis pathways (MAG pathway, dihydroxy-acetone phosphate pathway, and glycerol phosphate pathway). This suggests that dietary DAG affects FA metabolism in the liver by stimulating β-oxidation and repressing anabolism of TAG. Murase *et al.* (32) showed that high-DAG feeding up-regulated mRNA expression of ACO, ACS, medium-chain acyl-CoA dehydrogenase, and uncoupling protein-2 in intestinal tissue but not in liver, skeletal muscle, or brown fatty tissue of C57BL/6J mice. They thought that the effect of DAG lies in its contribution to intestinal lipid metabolism (32). However, different from Murase's conclusion, Murata *et al.* (33) observed that dietary DAG could affect the activity of ACO and FA synthase in mouse liver. These observations suggest that stimulation of FA oxidation and suppression of TAG synthesis may be partially responsible for the beneficial effects of dietary DAG. In addition, lower hepatic TAG content in the high-DAG-fed rat may be related to this fact.

The results in this study showed that DAG could reduce fat accumulation in viscera and body, and the reduction effect was closely related to the activity of DGAT and ACAT. However, the regulation mechanism of DGAT and ACAT by DAG remains unknown.

ACKNOWLEDGMENTS

We greatly appreciate Dr. Duo Li of the College of Food Science, Biotech. & Environment Engineering, Hangzhou University of Commerce, China, for his kind comments and suggestions in reviewing our manuscript. We also greatly appreciate Terry Pickett of the Department of English, Southern Yangtze University, China, for his kindness in editing our manuscript.

REFERENCES

1. Lakka, H.M., Lakka, T.A., Tuomilehto, J., and Salonen, J.T. (2002) Abdominal Obesity Is Associated with Increased Risk of Acute Coronary Events in Men, *Eur. Heart J. 23*, 706–713.
2. Okosun, I.S., Prewitt, T.E., and Cooper, R.S. (1999) Abdominal Obesity in the United States: Prevalence and Attributable Risk of Hypertension, *J. Hum. Hypertens. 13*, 425–430.
3. Seidell, J.G., Verschuren, W.M., Van Leer, E.M., and Kromhout, D. (1996) Overweight, Underweight and Mortalty: A Prospective Study of 48,287 Men and Women, *Arch. Intern. Med. 156*, 958–963.
4. Matsuzawa, Y., Nakamura, T., Shimomura, I., and Kotani, K. (1995) Visceral Fat Accumulation and Cardiovascular Disease, *Obes. Res. 3*, 645–647.
5. Kannel, W.B., Cupples, L.A., Ramaswami, R., Stokes, J., 3rd, Kreger, B.E., and Higgins, M. (1991) Regional Obesity and Risk of Cardiovascular Diseases: The Framingham Study, *J. Clin. Epidemiol. 44*, 183–190.
6. Bray, G.A., and Tartaglia, L.A. (2000) Medicinal Strategies in the Treatment of Obesity, *Nature 404*, 672–677.
7. Greenberg, I., Chang, S., and Blackburn, G.L. (1999) Nonpharmacologic and Pharmacologic Management of Weight Gain, *J. Clin. Psychiatry 60*, 31–36.
8. Scheen, A.J., and Lefebvre, P.J. (1999) Pharmacological Treatment of Obesity: Present Status, *Int. J. Obes. Relat. Metab. Disord. 23*, 47–53.
9. Hara, K., Onizawa, K., Honda, H., Otsuji, K., Ide, T., and Murata, M. (1993) Dietary Diacylglycerol-Dependent Reduction in Serum Triacylglycerol Concentration in Rats, *Ann. Nutr. Metab. 37*, 185–191.
10. Murata, M., Hara, K., and Ide, T. (1994) Alteration by Diacylglycerols of the Transport and Fatty Acid Composition of Lymph Chylomicrons in Rats, *Biosci. Biotechnol. Biochem. 58*, 1416–1419.
11. Nagao, T., Watanabe, H., Goto, N., Onizawa, K., Taguchi, H., Matsuo, N., Yasukawa, T., Tsushima, R., Shimasaki, H., and Itakura, H. (2000) Dietary Diacylglycerol Suppresses Accumulation of Body Fat Compared to Triacylglycerol in Men in a Double-Blind Controlled Trial, *J. Nutr. 130*, 792–797.
12. Sugimoto, T., Kimura, T., Fukuda, H., and Iritani, N. (2003) Comparisons of Glucose and Lipid Metabolism in Rats Fed Diacylglycerol and Triacylglycerol Oils, *J. Nutr. Sci. Vitaminol. 49*, 47–55.
13. Hase, T., Mizuno, T., Onizawa, K., Kawasaki, K., Nakagiri, H., Komine, Y., Murase, T., Meguro, S., Tokimitsu, I., Shimasaki, H., and Itakura, H. (2001) Effects of α-Linolenic Acid-rich Diacylglycerol on Diet-Induced Obesity in Mice, *J. Oleo Sci. 50*, 701–710.

14. Murase, T., Mizuno, T., Omachi, T., Onizawa, K., Komine, Y., Kondo, H., Hase, T., and Tokimitsu, I. (2001) Dietary Diacylglycerol Suppresses High Fat and High Sucrose Diet-Induced Body Fat Accumulation in C57BL/6J Mice, *J. Lipid Res. 42*, 372–378.
15. Murase, T., Nagasawa, A., Suzuki, J., Wakisaka, T., Hase, T., and Tokimitsu, I. (2002) Dietary α-Linolenic Acid-rich Diacylglycerols Reduce Body Weight Gain Accompanying the Stimulation of Intestinal β-Oxidation and Related Gene Expressions in C57BL/KsJ-db/db Mice, *J. Nutr. 132*, 3018–3022.
16. Folch, J., Lees, M., and Sloane Stanley, G.H. (1957) A Sample Method for the Isolation and Purification of Total Lipids from Animal Tissue, *J. Biol. Chem. 226*, 497–509.
17. Bligh, E.G., and Dyer, W.J. (1959) A Rapid Method for Total Lipid Extraction and Purification, *Can. J. Biochem. Physiol. 37*, 911–917.
18. Bartlett, G.R. (1959) Phosphorus Assay in Column Chromatography, *J. Biol. Chem. 234*, 466–468.
19. Middleton, C.K., Kazala, E.C., Lozeman, F.J., Hurly, T.A., Mir, P.S., Bailey, D.R.C., Jones, S.D.M., and Weselake, R.J. (1998) Evaluation of Diacylglycerol Acyltransferase as an Indicator of Intramuscular Fat Content in Beef Cattle, *Can. J. Anim. Sci. 78*, 265–270.
20. Lozeman, F.J., Middleton, C.K., Deng, J., Kazala, E.C., Verhaege, C., Mir, P.S., Laroche, A., Bailey, D.R.C., and Weselake, R.J. (2001) Characterization of Microsomal Diacylglycerol Acyltransferase Activity from Bovine Adipose and Muscle Tissue, *Comp. Biochem. Physiol. Biochem. Mol. Biol. 130*, 105–115.
21. Bieber, L.L., Abraham, T., and Helmrath, T. (1972) A Rapid Spectrophotometric Assay for Carnitine Palmitoyltransferase, *Anal. Biochem. 50*, 509–518.
22. Couillard, C., Bergeron, N., Prudhomme, D., Bergeron, J., Tremblay, A., Bouchard, C., Mauriege, P., and Despres, J.P. (1998) Postprandial Triacylglycerol Response in Visceral Obesity in Men, *Diabetes 47*, 953–960.
23. Mekki, N., Christofilis, M.A., Charbonnier, M., Atlan-Gepne, C., Defoort, C., and Juhel, C. (1999) Influence of Obesity and Body Fat Distribution on Postprandial Lipemia and Triacylglycerol-rich Lipoproteins in Adult Women, *J. Clin. Endocrinol. Metab. 84*, 184–191.
24. Yanagizawa, Y., Kawabata, T., Tanaka, O., Kawakami, M., Hasegawa, K., and Kagawa, Y. (2003) Improvement in Blood Lipid Levels by Dietary *sn*-1,3-Diacylglycerol in Young Women with Variants of Lipid Transporters 54T-FABP2 and -493g-MTP, *Biochem. Biophys. Res. Commun. 302*, 743–748.
25. Gavrilova, O., Martin, H., Matsusue, K., Jaime, J.C., Johnson, L., Dietz, K.R., Nicol, C.J., Vinson, C., Gonzalez, F.J., and Reitman, M.L. (2003) Liver Contributes to Hepatic Steatosis, Triglyceride Clearance, and Regulation of Body Fat Mass, *J. Biol. Chem. 278*, 34268–34276.
26. Bierbach, H. (1983) Triacylglycerol Biosynthesis in Human Small Intestinal Mucosa. Acyl-CoA:Monoacylglycerol Acyltransferase, *Digestion 28*, 138–147.
27. Zammit, V.A. (1996) Role of Insulin in Hepatic Fatty Acid Partitioning: Emerging Concepts, *Biochem. J. 314*, 1–14.
28. Yang, L.Y., Kuksis, A., Myher, J.L., and Steiner, G. (1996) Contribution of *de novo* Fatty Acid Synthesis to Very Low-Density Lipoprotein Triacylglycerols: Evidence from Mass Isotopomer Distribution Analysis of Fatty Acids Synthesized from [$^2H_6$] Ethanol, *J. Lipid Res. 37*, 262–274.
29. Owen, M.R., Corstorphine, C.C., and Zammit, V.A. (1997) Overt and Latent Activities of Diacylglycerol Acytransferase in Rat Liver Microsomes: Possible Roles in Very-Low-Density Lipoprotein Triacylglycerol Secretion, *Biochem. J. 323*, 17–21.
30. Lehner, R., and Kuksis, A. (1996) Biosynthesis of Triacylglycerols, *Prog. Lipid Res. 35*, 69–201.
31. Dircks, L., and Sul, H.S. (1999) Acyltransferases of *de novo* Glycerophospholipid Biosynthesis, *J. Lipid Res. 38*, 461–479.
32. Murase, T., Aoki, M., Wakisaka, T., Hase, T., and Tokimitsu, I. (2002) Anti-obesity Effect of Dietary Diacylglycerol in C57BL/6J Mice: Dietary Diacylglycerol Stimulates Intestinal Lipid Metabolism, *J. Lipid Res. 43*, 1312–1319.
33. Murata, M., Ide, T., and Hara, K., (1997) Reciprocal Responses to Dietary Diacylglycerol of Hepatic Enzymes of Fatty Acid Synthesis and Oxidation in the Rat, *Br. J. Nutr. 77*, 107–121.

[Received October 21, 2003, and in revised form December 28, 2003; revision accepted January 6, 2004]

Alterations of Fatty Acid Metabolism and Membrane Fluidity in Peroxisome-Defective Mutant ZP102 Cells

Michiaki Nagura[a], Makiko Saito[a,*], Masao Iwamori[b], Yoichi Sakakihara[a], and Takashi Igarashi[a]

[a]Department of Pediatrics, Graduate School of Medicine, The University of Tokyo, Tokyo, Japan, and
[b]Department of Biochemistry, Faculty of Science and Technology, Kinki University, Osaka, Japan

ABSTRACT: We investigated lipid composition and FA metabolism in Chinese hamster ovary (CHO-K1) cells and *Pex5*-mutated CHO-K1 (ZP102) cells to clarify the biochemical bases of peroxisome biogenesis disorders (PBD). ZP102 cells have defective peroxisomes and exhibit impairments of peroxisomal β-oxidation of FA and plasmalogen biosynthesis. In addition, we identified FA metabolic alterations in the synthesis of several classes of lipids in ZP102 cells. The concentration of FFA in ZP102 cells was twice that in CHO-K1 cells, but methyl esters and TAG were decreased in ZP102 cells in comparison with control cells. Also, ceramide monohexoside (CMH) concentration with ZP102 cells was significantly increased compared with the control cells. The FA molecular species, particularly the saturated to unsaturated ratios, of individual lipids also differed between the two cell types. The rate of incorporation of [^{14}C]-labeled saturated acids into sphingomyelin (SM) and CMH in ZP102 cells was higher than that in CHO-K1 cells. Lignoceric acid incorporated into cells was predominantly utilized for the synthesis of SM at 24 h after removal of [^{14}C]lignoceric acid from the culture medium. ZP102 cells showed higher fluorescence anisotropy of 1,3,5-diphenylhexatriene, corresponding to lower membrane mobility than in CHO-K1 cells. In particular, alteration of lipid metabolism by a *Pex5* mutation enhanced metabolism of saturated FA and sphingolipids. This may be related to the reduced membrane fluidity of ZP102 cells, which has been implicated in the dysfunction of membrane-linked processes in PBD.

Paper no. L9315 in *Lipids 39,* 43–50 (January 2004).

Peroxisome biogenesis disorders (PBD), such as Zellweger syndrome and neonatal adrenoleukodystrophy, are caused by *Pex* gene mutations. Peroxisomal dysfunctions in PBD are known to cause alterations of lipid metabolism including β-oxidation of FA, synthesis of ether phospholipids, and degradation of pipecolic acid (1). Accordingly, patients with PBD exhibit various biochemical abnormalities, such as the accumulation of very long chain FA (VLCFA) and defects of the plasmalogens (2,3). To date, the relationship of these biochemical abnormalities to the impaired differentiation and migration of neural cells, which are the major central nervous system (CNS) findings in patients with PBD, remains unclear. Recently, two transgenic mouse models of Zellweger syndrome were generated [*Pex5* (4) and *Pex2* (5) knockout mice]. It was suggested that the synthesis of ether phospholipids and the degradation of straight-chain FA might be necessary for normal embryonic development, based on the results of investigations of the peroxisomal lipid-metabolizing pathway in normal and *Pex5* knockout mice embryos (6). Later, it was reported that lack of peroxisomal β-oxidation itself did not cause the defect in neuronal migration in *Pex5* knockout mice (7). One can expect that other metabolic alterations, which occur secondarily, play roles in the pathological changes in PBD. We previously attributed the accumulation of glycosphingolipids in *Pex2* mutant Z65 cells [*Pex2*-mutated Chinese hamster ovary (CHO)-K1 cells] and PBD patients' fibroblasts to *Pex2* mutations (8,9). The expression of ceramide glucosyltransferase (GlcT), which is located at the first step in elongation of the carbohydrate chains of glycolipids, was significantly increased, and accumulation of ceramide also occurred in Z65 cells cultured in the presence of a GlcT inhibitor (10).

The expression of ganglioside molecular species is strictly regulated in the CNS during development in the gestational stages (11), and the growth or differentiation of neural cells is affected by the presence of glucosylceramide and gangliosides (12,13). Also, ceramide is well known to exhibit bioactivity that induces cellular apoptosis (14). Taken together, these observations indicate that the altered glycosphingolipid metabolism in Z65 cells might be related to the pathogenesis of PBD. Moreover, it is necessary to confirm that alterations of lipid metabolism similar to those observed in Z65 cells occur in peroxisome-deficient cells belonging to other genetic classes.

A *Pex5* mutation was introduced into ZP102 cells (*Pex5*-mutated CHO-K1 cells), which were previously isolated as peroxisome-defective CHO cells by Tsukamoto *et al.* (15). The *Pex5* gene encodes the receptor for the peroxisome targeting signal-1 (PTS-1) sequence exhibiting affinity with the C-termini of many peroxisomal proteins including acyl-CoA oxidase (16).

*To whom correspondence should be addressed at Dept. of Pediatrics, Graduate School of Medicine, The University of Tokyo, 7-3-1 Hongo, Bunkyo-ku, Tokyo 113-8655, Japan. E-mail: makisaito-tky@umin.ac.jp

Abbreviations: CE, cholesterol ester(s); CHO-K1 cells, Chinese hamster ovary K1 cells; CMH, ceramide monohexoside; CNS, central nervous system; DHAP, dihydroxyacetone phosphate; DPH, 1,6-diphenyl-1,3,5-hexatriene; GlcT, ceramide glucosyltransferase; PBD, peroxisome biogenesis disorders; PTS-1, peroxisome targeting signal-1; SM, sphingomyelin; VLCFA, very long chain FA; Z65 cells, *Pex2*-mutated CHO-K1 cells; ZP102 cells, *Pex5*-mutated CHO-K1 cells.

Our goal was to identify pathogenic factors contributing to peroxisomal dysfunction in the severe PBD phenotype. We analyzed changes in lipid metabolism and membrane fluidity attributable to defective functioning of the PTS-1 receptor in ZP102 cells.

EXPERIMENTAL PROCEDURES

Materials. 1-[^{14}C]Palmitic (50 mCi/mmol), 1-[^{14}C]lignoceric (50–60 mCi/mmol), 1-[^{14}C]oleic, and 1-[^{14}C]arachidonic acids (each 40–60 mCi/mmol) were obtained from NEN, PerkinElmer Life Science, Inc. (Boston, MA). TLC plates (silica gel 60) were obtained from Merck (Darmstadt, Germany). All other chemicals were of the highest grade available.

Cell culture. ZP102 cells (15) were maintained at 37°C under 5% CO_2 in Ham's F12 medium supplemented with 10% FCS containing penicillin G (100 U/mL) and streptomycin sulfate (100 mg/mL), and were used for experiments when they reached subconfluence (80–90%).

Analysis of the lipid compositions of ZP102 and CHO-K1 cells. Cells were harvested from a plate with PBS, and then lyophilized. After measurement of the dry weight, the lipids were extracted successively with 2 mL of chloroform/methanol/water, 20:10:1, 10:20:1, and 1:1:0 (by vol) at 40°C for 20 min. The crude lipid extracts were analyzed by TLC with solvent systems of chloroform/methanol/water (65:35:8, by vol) and *n*-hexane/diethyl ether/acetic acid (80:20:1, by vol). The spots were visualized with a cupric acetate–phosphoric acid reagent. The densities of the spots of samples and various known amounts of each standard lipid were determined with a dual-wavelength TLC densitometer (CS-9000; Shimadzu Co., Kyoto, Japan). The amounts of samples were determined from a standard curve obtained with the values for standard lipids.

Analysis of the FA composition. PC, sphingomyelin (SM), and PE were isolated by preparative TLC with a solvent system of chloroform/methanol/water (65:35:8, by vol). FFA, TG, and cholesterol esters (CE) were isolated by preparative TLC with a solvent system of *n*-hexane/diethyl ether/acetic acid (80:20:1, by vol). Individual lipids were then methanolized with 1 N HCl–methanol at 100°C for 30 min. The liberated FAME were extracted with *n*-hexane and then analyzed by GLC (GC700 Shimadzu) on a capillary column (Omegawax 320, 0.32 mm × 30 m; Supelco, Bellefonte, PA). The injection and detection port temperatures were 250 and 300°C, respectively. The column temperature was raised from 170 to 250°C at a rate of 5°C per min. Each peak was identified by comparing the retention time with those of standard FAME.

Incorporation of [^{14}C]-labeled FA. Each radiolabeled FA dissolved in ethanol was added directly to Ham's F12 medium supplemented with 10% FCS. The amount of ethanol was less than 0.2% of the total medium volume. Cells at the subconfluence stage (90% of the dish) were cultured in medium containing 12.0 μM 1-[^{14}C]palmitic, 12.5 μM 1-[^{14}C]oleic, 2.5 μM 1-[^{14}C]arachidonic, and 12.0 μM 1-[^{14}C]lignoceric acid for 6 h. The cells were then harvested and ultrasonically homogenized in PBS. The protein contents of the cell homogenates were measured by the method of Lowry *et al.* (17). Lipids in cell homogenates were extracted with 1.5 mL of chloroform/methanol (2:1, vol/vol) at 40°C for 20 min. After centrifugation, the radioactivity of the supernatant was determined with a liquid scintillation counter, followed by separation by TLC as described above. The radioactivity incorporated into each lipid fraction was visualized and quantified with a BAS 2000 imaging analyzer (Fuji Film, Tokyo, Japan).

Membrane fluidity of ZP102 and CHO-K1 cells. Membrane fluidity was monitored according to the method of Kawato *et al.* (18). CHO-K1 and ZP102 cells at the subconfluence stage, scraped from plates after washing three times with PBS, were centrifuged at 125 × *g* for 10 min and then resuspended in 0.5 mL of PBS (pH 7.4) with 0.15 mM EDTA. The resulting cell suspensions were homogenized ultrasonically. After centrifugation at 100 × *g* for 10 min, the supernatants were removed and centrifuged at 15,000 × *g* for 20 min, and then at 100,000 × *g* for 60 min. The 100,000 × *g* membrane pellets were homogenized and resuspended in PBS (pH 7.4). A lipophilic probe, 1,6-diphenyl-1,3,5-hexatriene (DPH), was dissolved in THF and added to homogenates of CHO-K1 and ZP102 cells to give a final concentration of 1 μM. The membrane suspensions were then incubated at 37°C for 20 min. The fluorescence intensity of each membrane suspension was measured with a fluorescence spectrophotometer (FP-2070; JASCO, Tokyo, Japan) at an excitation wavelength of 360 nm and an emission wavelength of 426 nm. The vertical (I_v) and horizontal (I_h) fluorescence intensities were measured with a polarizing filter, and steady-state emission anisotropy (r) was calculated as follows.

$$r = I_v - I_h/I_v + 2I_h \quad [1]$$

The anisotropy parameter $[(r_0/r) - 1]^{-1}$ was calculated using an r_0 value of 0.365 for DPH (19). The temperature dependence of $[(r_0/r) - 1]^{-1}$ was determined over the range of 4–37°C. Membranes were initially heated to 37°C for 20 min until the fluorescence intensity was stable, and fluorescence polarization was then estimated every 1–2°C as the suspension cooled slowly to 4°C. Plots of log $[(r_0/r) - 1]^{-1}$ vs. $1/T$ were constructed to detect thermotropic transitions (19).

RESULTS

Lipid compositions of ZP102 and CHO-K1 cells. Figure 1 shows the TLC results of lipids in ZP102 and CHO-K1 cells. Although the concentrations of the major phospholipids, i.e., PC, PE, and SM, in CHO-K1 cells were the same as those in ZP102 cells, ceramide monohexoside (CMH) was present at a higher concentration in ZP102 cells than in CHO-K1 cells. Also, there were no differences in the amounts of cholesterol and CE between CHO-K1 and ZP102 cells, whereas amounts of TAG, FFA, and FAME in CHO-K1 cells differed significantly from those in ZP102 cells: 1.15 ± 0.21 μg/mg dry weight in ZP102 cells and 1.98 ± 0.14 μg/mg dry weight in CHO-K1 cells

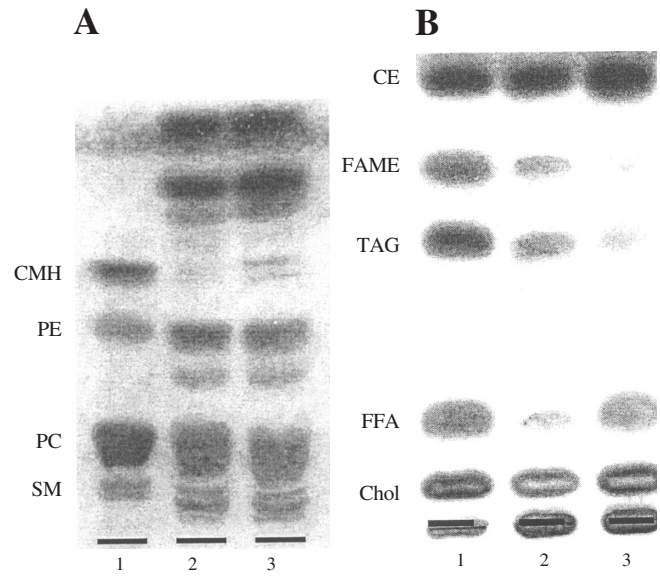

FIG. 1. TLC of phospholipids (A) and neutral lipids (B). Portions of the lipids extracted from freeze-dried Chinese hamster ovary (CHO)-K1 (lane 2) and ZP102 (*Pex5*-mutated CHO-K1) cells (lane 3) (equivalent to 0.5 mg dry weight) were developed with chloroform/methanol/water (65:35:8, by vol) (A) and *n*-hexane/diethyl ether/acetic acid (80:20:1, by vol) (B), and the spots were detected with a cupric acetate–phosphoric acid reagent. Standard lipids were run in lane 1. SM, sphingomyelin; CMH, ceramide monohexoside; CE, cholesterol ester; Chol, cholesterol.

for TAG; 0.58 ± 0.12 μg/mg dry weight in ZP102 cells and 0.27 ± 0.14 μg/mg dry weight in CHO-K1 cells for FFA (Fig. 1B). On the other hand, FAME were detected only in CHO-K1 cells, i.e., not in ZP102 cells, as shown in Figure 1B.

FA compositions of lipids in ZP102 and CHO-K1 cells. The FA compositions of lipids in ZP102 and CHO-K1 cells are presented in Table 1. In the FFA fraction, the relative ratio of saturated to unsaturated FA in ZP102 cells was significantly decreased, due mainly to the increases in oleic, arachidonic, and docosahexanoic acids, in comparison with CHO-K1 cells. The ratio of saturated to unsaturated FA in SM of ZP102 cells was also lower than that in CHO-K1 cells but that in TAG of ZP102 cells was higher than in CHO-K1 cells. A distinct difference in the distribution of lignoceric acid (24:0) was observed between the FFA and TAG fractions. Lignoceric acid was negligible in the FFA fraction of ZP102 cells but constituted 2.77 ± 0.18% of that in CHO-K1 cells. On the other hand, as for TAG, 6.27 ± 0.32% and a trace amount of lignoceric acid were found in ZP102 and CHO-K1 cells, respectively. When the ratios of lignoceric acid to behenic acid (C_{24}/C_{22}) were compared, those in the TAG, SM, and PE fractions were significantly increased in ZP102 cells. Arachidonic acid was present in higher proportions in the FFA and phospholipid fractions of ZP102 cells than in those of CHO-K1 cells. Oleic acid also was present in higher proportions in the FFA and SM fractions of ZP102 cells than in those of CHO-

TABLE 1
FA Composition of Lipids in ZP102 and CHO-K1 Cells[a]

	FFA		TAG		Cholesterol ester		Sphingomyelin		PC		PE	
FFA	ZP102	CHO-K1	ZP102	CHO-K1	ZP102	CHO-K1	ZP102	CHO-K1	ZP102	CHO-K1	ZP102	CHO-K1
12:0	1.24	2.66	1.76	1.8	1.04	1.32	0.47*	1.75	0.37	0.26	0.73	1.67
14:0	2.84	3.81	4.67	4.22	8.93	8.04	2.21	4.63	1.12	1.65	2.55	4.56
16:0	24.38	24.85	30.22	31.97	30.95	32.18	30.85	33.78	17.28	20.4	16.97	21.20
16:1	3.98	3.4	1.44	1.15	3.16*	2.54	2.47	1.49	1.3	1.24	1.45	0.26
18:0	**13.89***	**23.42**	22.76	19.06	16.92	18.94	19.06	19.49	24.78	24.89	28.62	27.24
18:1n-9	**25.67***	**12.57**	16.7*	21.33	25.66	23.44	**28.26***	**21.12**	22.85	23.84	21.87	18.04
18:2n-6	6.26	5.14	4.37	4.23	2.36	2.22	3.42	3.03	3.88	4.00	3.50	3.42
18:3n-3	0.40	<0.01	0.34*	<0.01	0.73	0.84	0.11	0.15	0.17	<0.01	<0.01	<0.01
20:0	0.83*	1.77	2.32	1.78	1.53	1.50	0.72	1.19	0.9	1.05	1.10	1.19
20:1	1.20	<0.01	1.02	1.64	1.71	1.41	1.52	0.76	1.69	2.66	0.53	1.83
20:2	1.91	2.19	<0.01	<0.01	<0.01	<0.01	<0.01	<0.01	0.41	<0.01	0.84*	<0.01
20:3n-9	<0.01	<0.01	<0.01	<0.01	<0.01	<0.01	<0.01*	0.47	0.65	<0.01	<0.01	<0.01
20:3n-6	0.75	<0.01	<0.01	<0.01	<0.01	<0.01	0.65*	1.30	1.75	2.16	1.11*	<0.01
20:4n-6	3.65*	<0.01	<0.01	<0.01	<0.01	<0.01	0.48*	<0.01	**11.03***	**7.87**	6.79	5.36
20:5n-3	0.59	<0.01	<0.01	<0.01	<0.01	<0.01	<0.01	<0.01	0.43*	<0.01	<0.01	<0.01
22:0	1.04*	4.73	4.99*	2.62	2.2	2.45	2.22	3.37	1.97	2.38	2.43	3.50
22:1n-9	9.59	12.69	3.16*	10.26	3.22	3.85	2.62	1.54	2.83	2.28	3.84*	5.69
22:4n-6	<0.01	<0.01	<0.01	<0.01	<0.01	<0.01	<0.01	<0.01	1.14	1.23	1.23*	<0.01
22:5n-3	1.28	<0.01	<0.01	<0.01	0.89*	<0.01	<0.01	<0.01	2.26	1.69	2.03	2.04
24:0	**<0.01***	**2.77**	**6.27***	<0.01	1.44	1.27	3.31	3.49	1.04	1.08	**3.02***	**2.04**
22:6	**1.51***	**<0.01**	<0.01	<0.01	<0.01	<0.01	<0.01	<0.01	2.17	1.35	1.39	1.96
24:1n-9	<0.01	<0.01	<0.01	<0.01	2.42*	<0.01	1.53	2.44	<0.01	<0.01	<0.01	<0.01
24:0/22:0	<0.01*	0.58	1.25*	<0.01	0.64	0.52	1.48	1.04	0.52	0.45	1.25*	0.58
Saturated (S)	44.23*	64.01	72.98*	61.44	63.43	64.72	58.85*	67.68	47.47	51.67	55.41	61.4
Unsaturated (U)	55.77*	35.98	27.02*	38.55	36.57	35.28	41.06*	32.32	52.53	48.34	44.56	38.57
S/U	**0.79***	**1.78**	**2.71***	**1.59**	1.76	1.84	**1.43***	**2.09**	0.90	1.06	1.24	1.60

[a]Data represent mean weight percentages of total FA from each glycerolipid class in three different experiments. The major findings are shown in boldface type. Each SD was less than 15% of the mean value. *, $P < 0.05$. CHO-K1, Chinese hamster ovary K1 cells; ZP102, *Pex5*-mutated CHO-K1 cells.

K1 cells. Palmitic and stearic acids constituted about half of the total FA in all lipid classes examined, and the relative concentrations were essentially the same in ZP102 and CHO-K1 cells. Taking into account the FA composition of each lipid class, we next investigated the differences in FA utilization in both cell types using radiolabeled FA.

Incorporation of ^{14}C-labeled FA into the lipids in ZP102 and CHO-K1 cells. The radioactivity of each lipid class in ZP102 and CHO-K1 cells after incubation with 1-[^{14}C]-labeled palmitic, oleic, arachidonic, and lignoceric acids is shown in Figure 2. In accord with the above results, FAME synthetic potential was observed in CHO-K1 cells but not in ZP102 cells. The rates of incorporation of palmitic and lignoceric acids into CMH in ZP102 cells were significantly higher than those in CHO-K1 cells, but unsaturated FA were scarcely incorporated into CMH. Higher radioactivity in ZP102 cells than in CHO-K1 cells on incubation with lignoceric acid was also observed in SM, indicating the enhanced utilization of longer saturated FA for sphingolipids. TAG in CHO-K1 cells incorporated all radioactive FA at higher rates than those in ZP102 cells. On the other hand, although oleic, arachidonic, and lignoceric acids were incorporated into PC of CHO-K1 cells at higher rates than into ZP102 cells, the radioactivity of PC with palmitic acid in CHO-K1 cells was lower than in ZP102 cells (Fig. 2B). These differences in the incorporation experiments were not consistent with the results of the FA composition analysis (Table 1). For example, there was no difference in the lignoceric acid content of the SM fraction between CHO-K1 and ZP102 cells.

Pulse-labeling experiment with [^{14}C]lignoceric acid. As shown in Figure 2, when the rates of incorporation of palmitic, oleic, arachidonic, and lignoceric acids were compared between CHO-K1 and ZP102 cells, that of lignoceric acid was found to differ between the two cell types as follows. In contrast to palmitic, oleic, and arachidonic acids, the majority of lignoceric acid incorporated into cells with a 6-h incubation was retained in FFA, the highest level being observed in ZP102 cells, and the radioactivity of the conjugated form of lignoceric acid in ZP102 was higher in the sphingolipids SM and CMH, lower in PC and TAG, and similar in PE and CE as compared with CHO-K1 cells. These findings indicate altered metabolism of saturated longer-chain FA in ZP102 cells in comparison with CHO-K1 cells. Accordingly, a pulse-labeling experiment was conducted as follows. After incubation of cells with [^{14}C]lignoceric acid for 6 h, the medium was changed to that without the radioactive

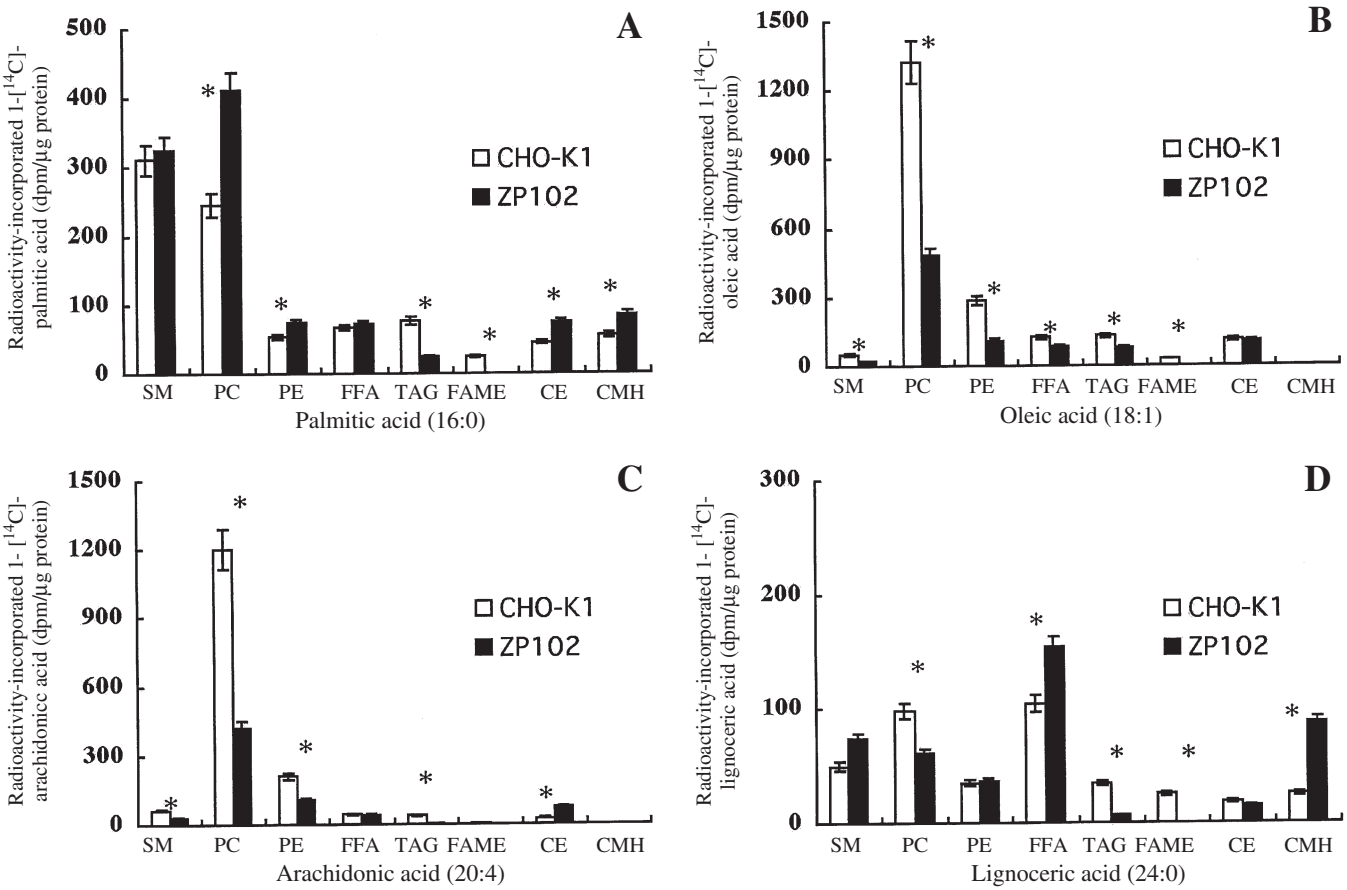

FIG. 2. Incorporation of ^{14}C-labeled FA into each lipid. Nearly confluent CHO-K1 and ZP102 cells were labeled with 1-[^{14}C]palmitic (A), 1-[^{14}C]oleic (B), 1-[^{14}C]arachidonic (C), and 1-[^{14}C]lignoceric (D) acids for 6 h. The cells were then harvested, and total lipids were extracted. Total lipid extract equivalent to 10,000 dpm radioactivity was separated by TLC. The radioactivity incorporated into individual lipids was determined with an imaging analyzer. Data are the means ± SD (shown by error bars) of three independent experiments, each performed in duplicate. Values with an asterisk differ significantly from the control (CHO-K1): $P < 0.01$. For abbreviations see Figure 1.

FA, and the incubation was then continued for an additional 24 h. As shown in Figure 3, the bulk of [^{14}C] was present in the phospholipid pool after a 6-h incubation as well as after a 24-h chase. Lignoceric acid incorporated into CMH was substantially lowered in CHO-K1 cells, and the percentage of radioactivity of the CMH fraction decreased from 3.3 to 1.2%. The lignoceric acid incorporated into CMH was also decreased in ZP102 cells, but the rate of reduction was slower than that in CHO-K1 cells. The radioactivity of the SM fraction after 24 h had increased in both cell types. The rate of increase in the SM fraction in CHO-K1 cells was higher than that in ZP102 cells, resulting in higher radioactivity in the SM fraction at 30 h in CHO-K1 cells. The lignoceric acid, once incorporated into PE, FFA, and CE during a 6-h incubation, was retained well after 24 h. However, a reduction in radioactivity after 24 h was observed in PC in both cell types. Also, a marked reduction in radioactivity after 24 h was observed in TAG of CHO-K1 cells, i.e., less than 2% of total radioactivity was in TAG. On the other hand, the radioactivity incorporated into TAG in ZP102 cells was negligible throughout the incubation period.

Membrane fluidity of ZP102 and CHO-K1 cells. The anisotropic values for CHO-K1 and ZP102 cells at 37°C were 0.151 ± 0.006 and 0.178 ± 0.004 (mean ± SD for separate determinations), respectively. The value for ZP102 cells was significantly higher than that for CHO-K1 cells ($P < 0.001$), showing the decreased membrane fluidity of ZP102 as compared with control cells. The effect of temperature on the fluorescence anisotropy parameter, $[(r_0/r) - 1]^{-1}$, of DPH in membranes is illustrated by representative Arrhenius plots in Figure 4. An increase in temperature produced a concomitant decrease in the $[(r_0/r) - 1]^{-1}$ value, which meant an increase in membrane fluidity. However, the evolution of fluidity was not linear; a thermotropic transition temperature was indeed observed at 30.9 ± 1.5°C for ZP102 cells. The $[(r_0/r) - 1]^{-1}$ value of CHO-K1 cells was significantly ($P < 0.01$) decreased as compared with that of ZP102 cells. The thermotropic transition temperature of CHO-K1 cells was 26.4 ± 1.2°C. The temperature of lipid phase separation of the membranes of ZP102 cells was elevated as compared with that of CHO-K1 cells.

DISCUSSION

We demonstrated several changes in lipid composition and FA metabolism due to defective functioning of peroxisomes. First, the finding that the amount of TAG was decreased in ZP102 cells demonstrated the altered TAG metabolism. The *sn*-glycero-3-phosphate pathway represents a *de novo* route to TAG formation. FA are converted into acyl-CoA esters before they are esterified to *sn*-glycero-3-phosphate, and the resulting phosphatidate is converted to TAG. Dihydroxyacetone phosphate (DHAP) is a known substrate for ether lipid synthesis but can act as an alternative acyl acceptor for TAG biosynthesis. DHAP acyltransferase, which is one of the per-

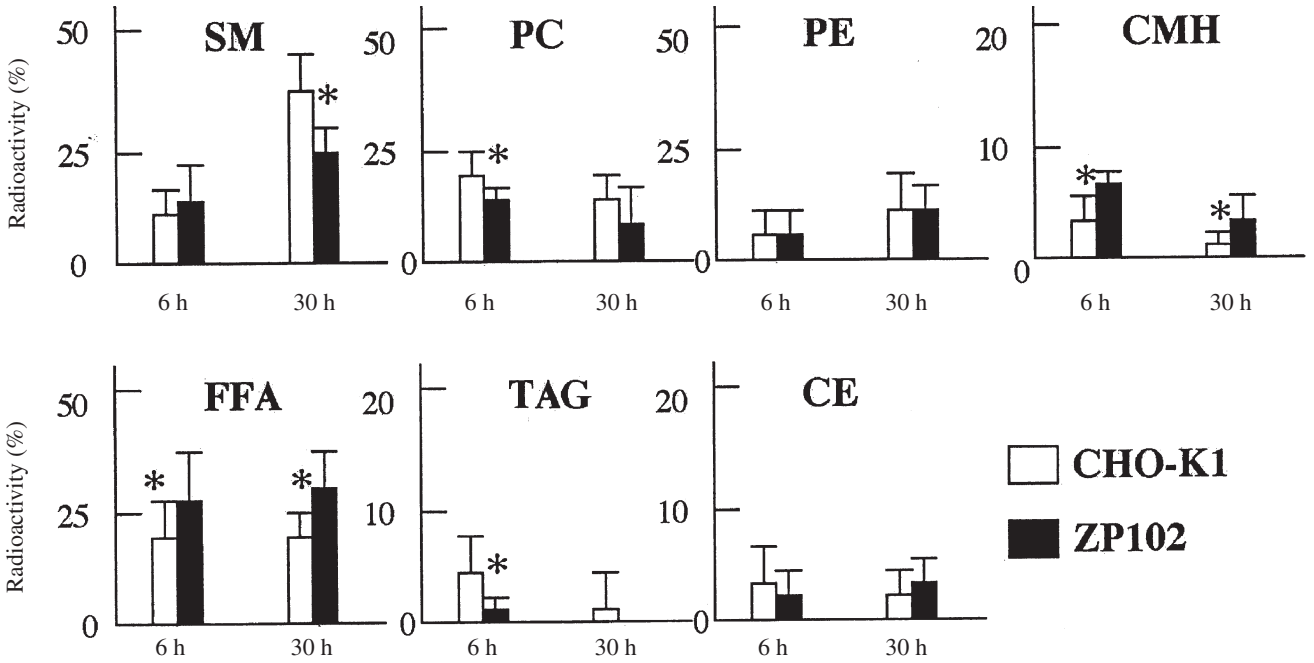

FIG. 3. Pulse-labeling with [1-^{14}C]lignoceric acid in CHO-K1 and ZP102 cells. Nearly confluent CHO-K1 and ZP102 cells were labeled with 1-[^{14}C]lignoceric acid for 6 h, and the medium was then changed to that without the radioactive FA. Cultivation was continued for an additional 24 h, and total lipids were then extracted as described in the text. The radioactivity of the total lipid extract was counted with a scintillation counter. Lipid extract equivalent to 10,000 dpm was developed with a solvent system, either chloroform/methanol/water (65:35:8, by vol) or *n*-hexane/diethyl ether/acetic acid (80:20:1, by vol). The ordinate represents the percentage of radioactivity of each lipid fraction compared to the total radioactivity. Data are the means ± SD (shown by error bars) of three independent experiments, each performed in duplicate. Values with an asterisk differ significantly from the control (CHO-K1) value: $P < 0.01$. For abbreviations see Figure 1.

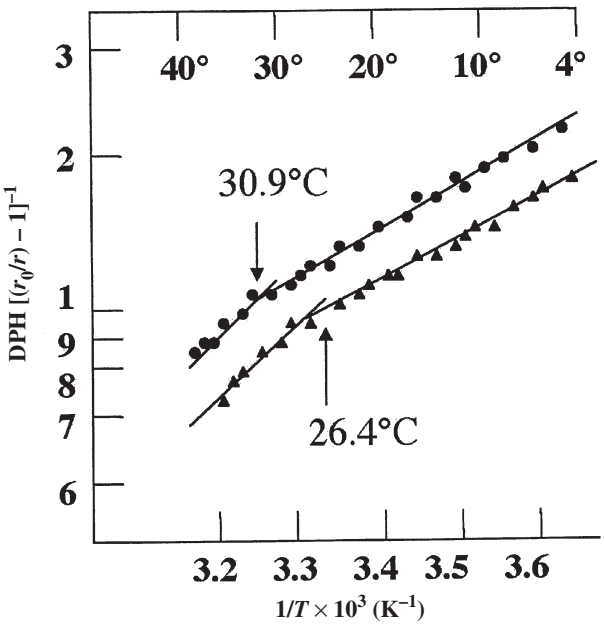

FIG. 4. Temperature dependence of the fluorescence anisotropy of 1,6-diphenyl-1,3,5-hexatriene (DPH) in control cells (▲) and ZP102 cells (●). The ordinate is fluorescence anisotropy. The abscissa is the reciprocal of the absolute temperature. Experimental details are given in the text. This experiment is representative of the three that were performed.

oxisomal enzymes, catalyzes the acylation of DHAP to form 1-acyl DHAP. This reaction leads to glycerol ester lipids following the enzymatic reduction of the reaction product by NADPH to 1-acyl-*sn*-glycerol-3-phosphate (20). Although changes in TAG metabolism have not yet been demonstrated in PBD, peroxisomal glycerolipid-synthesizing enzymes including DHAP acyltransferase were recently reported to be induced during the differentiation of adipocytes, in which half of the TAG is synthesized *via* the DHAP acyltransferase pathway (21). If the same DHAP acyltransferase pathway for the synthesis of TAG exists in the peroxisomes of CHO-K1 cells, the decreased TAG content in ZP102 cells may be explained by decreased DHAP acyltransferase activity. Furthermore, PUFA reportedly reduce hepatic synthesis and the secretion of TAG by lowering the activity of acyl-CoA 1,2-DAG acyltransferase (22,23). Since total FFA and the *n*-3 unsaturated FA content in ZP102 cells were higher than those in CHO-K1 cells, the synthetic potential for TAG might be suppressed in ZP102 cells. Moreover, not only the total TAG content but also the molecular species of TAG were altered in ZP102 cells, which had a significantly higher concentration of lignoceric acid (24:0) than that of CHO-K1 cells. In this regard, VLCFA have been reported to accumulate primarily in the form of esterified lipids, i.e., in the CE fraction, in peroxisomal disorders (24), suggesting them to be pathogenic factors in some of these disorders (25,26). In addition, it has been hypothesized that VLCFA are more likely to be esterified to lipids than are shorter-chain FA (27). The esterified form of lignoceric acid was found in TAG of ZP102 cells at a significantly higher concentration than in that of CHO-K1 cells. However, the rate of incorporation of labeled lignoceric acid, as well as other FA, into TAG was lower than that in CHO-K1 cells, indicating that the higher content of lignoceric acid in TAG of ZP102 cells is not attributable to increased incorporation. Since the metabolism of [^{14}C]lignoceric acid-labeled TAG in CHO-K1 cells was rapid in comparison with that in ZP102 cells, lignoceric acid was suspected to be lost from TAG of CHO-K1 cells. TAG are the main form of energy within the cell, but are also a source of DAG. DAG are also generated from phospholipids. The cross-talk between TAG and phospholipids occurs *via* the metabolic pathway for DAG (28–30). In consequence, the altered TAG metabolism in ZP102 cells might reflect altered phospholipid metabolism, such as the absence of ether phospholipids, which have frequently been observed in the tissues of patients with primary peroxisomal dysfunction.

Lipid composition analysis also demonstrated a higher concentration of FFA in ZP102 than in control cells. FFA have been confirmed to be responsible for the opening of potassium and calcium ion channels, for changes in the intracellular pH, and also in acting as signal mediators (31–34). Consequently, the altered metabolism and accumulation of FFA in ZP102 cells might modify several bioactivities. In radiolabeling experiments, the rates of incorporation of labeled unsaturated FA into glycerophospholipids in ZP102 cells were significantly lower than those in CHO-K1 cells. Consequently, unsaturated FA might accumulate in the FFA fraction of ZP102 cells as demonstrated in Table 1. Labeled lignoceric acid remained in a free form in ZP102 cells in a higher amount than in CHO-K1 cells after a 6-h incubation, whereas the amount of lignoceric acid in the FFA fraction was definitely lower than that in CHO-K1 cells (Table 1). These observations imply that lignoceric acid might be utilized for the synthesis of lipids, such as CMH and TAG, on longer incubation. In fact, lignoceric acid incorporated into ZP102 cells was utilized for the synthesis of CMH at a significantly higher level than in control cells. In addition, the CMH concentration was higher in ZP102 than that in the control cells, and ganglioside GM3 was found to be increased in ZP102 cells (Saito, M., and Iwamori, M., unpublished results), consistent with findings in Z65 cells, which have a *Pex2* mutation (9). Palmitic acid was also incorporated at a higher rate into CMH of ZP102 cells than into that of control cells, indicating that saturated FA are preferentially utilized for the metabolism of CMH in ZP102 cells. The pulse labeling experiment demonstrated that lignoceric acid incorporated into both cell types with a 6-h incubation was continuously utilized for the synthesis of SM and PE, leading to the higher radioactivity at 30 h than at 6 h, although the radioactivity of the other lipids at 30 h was essentially the same as or lower than that at 6 h. The rate of continuous utilization of labeled lignoceric acid for SM synthesis in CHO-K1 cells was higher than that in ZP102 cells, resulting in the higher radioactivity of the SM fraction at 30 h in CHO-K1 cells. It is noteworthy that higher radioactivity was restricted to the SM and CMH fractions of ZP102 cells after a 6-h incuba-

tion. Taken together, these results indicate that saturated FA tend to be incorporated into membrane phospholipids more quickly in ZP102 than in control cells. Furthermore, sphingolipid metabolism, which preferentially utilizes saturated FA, is significantly enhanced in ZP102 cells.

To date, it has been shown that abnormal metabolism of VLCFA alters membrane fluidity (24–26). Whitcomb *et al.* (26) hypothesized that cells exposed to VLCFA exhibit increased membrane microviscosity, with a consequent decrease in hormone sensitivity. In PBD patients, multiple peroxisomal enzymatic defects make it difficult to unravel the mechanism underlying altered membrane fluidity. In fact, higher mobility of membrane lipids has been demonstrated in fibroblasts from a patient with PBD (36). Hermetter *et al.* (35) stressed that factors influencing membrane fluidity (19) such as the cholesterol/phospholipid ratio, the protein/phospholipid ratio, and the FA composition were essentially identical in PBD and control cells. They speculated that the higher membrane fluidity in PBD patients' fibroblasts might be due to lipid asymmetry or plasmalogen protein interactions. In the present study, we showed decreased membrane fluidity in peroxisome-defective cells, findings inconsistent with those of previous studies. Possible explanations for this discrepancy are the cell types examined, whether the experiments were conducted on whole living cells or plasma membrane fragments, and the kind of fluorescence probe used. In ZP102 cells, the saturated/unsaturated FA ratio in the SM fraction was lower than that in control cells. The amount of lignoceric acid in the PE fraction was higher in ZP102 than in control cells. These factors have adverse effects on membrane fluidity. Other factors, such as the molecular species of phospholipids, may be responsible for the effect on membrane fluidity observed in ZP102 cells. We did not obtain direct evidence that the spectrum of severe symptoms observed in PBD patients is causally linked to alterations of FA metabolism and membrane fluidity. However, our analyses of the stability, fluidity, and permeability of biomembranes of peroxisome-defective cells should provide clues for clarifying the effects of peroxisomal deficiency on lipid metabolism in the pathogenesis of PBD. Based on these results, experiments involving cells with *Pex2* or *Pex5* mutations, *Pex5* knockout mice, and tissues from patients with PBD are now in progress in our laboratory.

ACKNOWLEDGMENT

This study was supported by grant 15501086 from the National Institute of Science and Education of Japan to the corresponding author.

REFERENCES

1. Gould, S.J., Raymond, G.V., and Valle, D. (2001) The Peroxisome Biogenesis Disorders, in *The Metabolic and Molecular Bases of Inherited Disease* (Scriver, B.V.S., Beaudet, V.S., Sly, W., Valle, D., Childs, B., Kinzler, K., and Vogelstein, B., eds.), pp. 3181–3217, McGraw-Hill, New York.
2. Moser, A.B., Kreiter, N., Bezman, L., Lu, S., Raymond, G.V., Naidu, S., and Moser, H.W. (1999) Plasma Very Long Chain Fatty Acids in 3,000 Peroxisome Disease Patients and 29,000 Controls, *Ann. Neurol. 45*, 100–110.
3. Powers, J.M., Tummons, R.C., Caviness, V.S., Jr., Moser, A.B., and Moser, H.W. (1989) Structural and Chemical Alterations in the Cerebral Maldevelopment of Fetal Cerebro-hepato-renal (Zellweger) Syndrome, *J. Neuropathol. Exp. Neurol. 48*, 270–289.
4. Baes, M., Gressens, P., Baumgart, E., Carmeliet, P., Casteels, M., Fransen, M., Evrard, P., Fahimi, D., Declercq, P.E., Collen, D., *et al.* (1997) A Mouse Model for Zellweger Syndrome, *Nature Genet. 17*, 49–57.
5. Faust, P.L., and Hatten, M.E. (1997) Targeted Deletion of the *PEX2* Peroxisome Assembly Gene in Mice Provides a Model for Zellweger Syndrome, a Human Neuronal Migration Disorder, *J. Cell Biol. 139*, 1293–1305.
6. Huyghe, S., Casteels, M., Janssen, A., Meulders, L., Mannaerts, G.P., Declercq, P.E., van Veldhoven, P.P., and Baes, M. (2001) Prenatal and Postnatal Development of Peroxisomal Lipid-Metabolizing Pathways in the Mouse, *Biochem. J. 353*, 673–680.
7. Baes, M., Gressens, P., Huyghe, S., De, N.K., Qi, C., Jia, Y., Mannaerts, G.P., Evrard, P., Van, V.P., Declercq, P.E., and Reddy, J.K. (2002) The Neuronal Migration Defect in Mice with Zellweger Syndrome (*Pex5* knockout) Is Not Caused by the Inactivity of Peroxisomal β-Oxidation, *J. Neuropathol. Exp. Neurol. 61*, 368–374.
8. Tatsumi, K., Saito, M., Lin, B., Iwamori, M., Ichiseki, H., Shimozawa, N., Kamoshita, S., Igarashi, T., and Sakakihara, Y. (2001) Enhanced Expression of a-Series Gangliosides in Fibroblasts of Patients with Peroxisome Biogenesis Disorders, *Biochim. Biophys. Acta 1535*, 285–293.
9. Saito, M., Iwamori, M., Lin, B., Oka, A., Fujiki, Y., Shimozawa, N., Kamoshita, S., Yanagisawa, M., and Sakakihara, Y. (1999) Accumulation of Glycolipids in Mutant Chinese Hamster Ovary Cells (Z65) with Defective Peroxisomal Assembly and Comparison of the Metabolic Rate of Glycosphingolipids Between Z65 Cells and Wild-Type CHO-K1 Cells, *Biochim. Biophys. Acta 1438*, 55–62.
10. Saito, M., Fukushima, Y., Tatsumi, K., Bei, L., Fujiki, Y., Iwamori, M., Igarashi, T., and Sakakihara, Y. (2002) Molecular Cloning of Chinese Hamster Ceramide Glucosyltransferase and Its Enhanced Expression in Peroxisome-Defective Mutant Z65 Cells, *Arch. Biochem. Biophys. 403*, 171–178.
11. Svennerholm, L., Rynmark, B.M., Vilbergsson, G., Fredman, P., Gottfries, J., Mansson, J.E., and Percy, A. (1991) Gangliosides in Human Fetal Brain, *J. Neurochem. 56*, 1763–1768.
12. Uemura, K., Sugiyama, E., and Taketomi, T. (1991) Effects of an Inhibitor of Glucosylceramide Synthase on Glycosphingolipid Synthesis and Neurite Outgrowth in Murine Neuroblastoma Cell Lines, *J. Biochem. 110*, 96–102.
13. Tettamanti, G., and Riboni, L. (1993), Gangliosides and Modulation of the Function of Neural Cells, *Adv. Lipid Res. 25*, 235–267.
14. Hannun, Y.A. (1996) Functions of Ceramide in Coordinating Cellular Responses to Stress, *Science 274*, 1855–1859.
15. Tsukamoto, T., Bogaki, A., Okumoto, K., Tateishi, K., Fujiki, Y., Shimozawa, N., Suzuki, Y., Kondo, N., and Osumi, T. (1997) Isolation of a New Peroxisome-Deficient CHO Cell Mutant Defective in Peroxisome Targeting Signal-1 Receptor, *Biochem. Biophys. Res. Commun. 230*, 402–406.
16. Dodt, G., Braverman, N., Wong, C., Moser, A., Moser, H.W., Watkins, P., Valle, D., and Gould, S.J. (1995) Mutations in the PTS1 Receptor Gene, PXR1, Define Complementation Group 2 of the Peroxisome Biogenesis Disorders, *Nature Genet. 9*, 115– 125.
17. Lowry, O.H., Rosebrough, N.J., Farr, A.L., and Randall, R.J. (1951) Protein Measurement with the Folin Phenol Reagent, *J. Biol. Chem. 193*, 265–275.
18. Kawato, S., Jr., Kinosita, K., and Ikegami, A. (1977) Dynamic Structure of Lipid Bilayers Studied by Nanosecond Fluorescence Techniques, *Biochemistry 16*, 2319–2324.

19. Shinitzky, M., and Barenholz, Y. (1978) Fluidity Parameters of Lipid Regions Determined by Fluorescence Polarization, *Biochim. Biophys. Acta 515*, 367–394
20. Lehner, R., and Kuksis, A. (1996) Biosynthesis of Triacylglycerols, *Prog. Lipid Res. 35*, 169–201.
21. Hajra, A.K., Larkins, L.K., Das, A.K., Hemati, N., Erickson, R.L., and MacDougald, O.A. (2000) Induction of the Peroxisomal Glycerolipid-Synthesizing Enzymes During Differentiation of 3T3-L1 Adipocytes. Role in Triacylglycerol Synthesis, *J. Biol. Chem. 275*, 9441–9446.
22. Rustan, A.C., Nossen, J.O., Christiansen, E.N., and Drevon, C.A. (1988) Eicosapentaenoic Acid Reduces Hepatic Synthesis and Secretion of Triacylclycerol by Decreasing the Activity of Acyl-Coenzyme A:1,2-Diacylglycerol Acyltransferase, *J. Lipid Res. 29*, 1417–1426.
23. Strum-Ordin, R.B., Adkins-Finke, W.L., Blake, W.L., Phinney, S.D., and Clarke, S.D. (1987) Modification of the Fatty Acid Composition of Membrane Phospholipids in Hepatocyte Monolayers with n-3, n-6, and n-9 Fatty Acids, *Biochim. Biophys. Acta 921*, 378–391.
24. Brown, F.R., III, Chen, W.W., Kirschner, D.A., Frayer, K.L., Powers, J.M., Moser, A.B., and Moser, H.W. (1983) Myelin Membranes from Adrenoleukodystrophy Brain White Matter—Biochemical Properties, *J. Neurochem. 41*, 341–348.
25. Knazek, R.A., Rizzo, W.B., Schulman, J.D., and Dave, J.R. (1983) Membrane Microviscosity Is Increased in the Erythrocytes of Patients with Adrenoleukodystrophy and Adrenomyeloneuropathy, *J. Clin. Invest. 72*, 245–248.
26. Whitcomb, R.W., Linehan, W.M., and Knazek, R.A. (1988) Effects of Long-Chain, Saturated Fatty Acids on Membrane Microviscosity and Adrenocorticotropin Responsiveness of Human Adrenocortical Cells *in vitro, J. Clin. Invest. 81*, 185–188.
27. Ho, J.K., Moser, H., Kishimoto, Y., and Hamilton, J.A. (1995) Interactions of a Very Long Chain Fatty Acid with Model Membranes and Serum Albumin. Implications for the Pathogenesis of Adrenoleukodystrophy, *J. Clin. Invest. 96*, 1455–1463.
28. Igal, R.A., Caviglia, J.M., de Gomez Dumm, I.N., and Coleman, R.A. (2000) Diacylglycerol Generated in CHO Cell Plasma Membrane by Phospholipase C Is Used for Triacylglycerol Synthesis, *J. Lipid Res. 42*, 88–95.
29. Igal, R.A., and Coleman, R.A. (1998) Neutral Lipid Storage Disease: A Genetic Disorder with Abnormalities in the Regulation of Phospholipid Metabolism, *J. Lipid Res. 39*, 31–43.
30. Igal, R.A., and Coleman, R.A. (1996) Acylglycerol Recycling from Triacylglycerol to Phospholipid, Not Lipase Activity, Is Defective in Neutral Lipid Storage Disease Fibroblasts, *J. Biol. Chem. 271*, 16644–16651.
31. Ordway, R.W., Jr., Walsh, J.V., and Singer, J.J. (1989) Arachidonic Acid and Other Fatty Acids Directly Activate Potassium Channels in Smooth Muscle Cells, *Science 244*, 1176–1179.
32. Huang, J.M., Xian, H., and Bacaner, M. (1992) Long-Chain Fatty Acids Activate Calcium Channels in Ventricular Myocytes, *Proc. Nat. Acad. Sci. USA 89*, 6452–6456.
33. Nishizuka, Y. (1992) Intracellular Signaling by Hydrolysis of Phospholipids and Activation of Protein Kinase C, *Science 258*, 607–614.
34. Hamilton, J.A., Civelek, V.N., Kamp, F., Tornheim, K., and Corkey, B.E. (1994) Changes in Internal pH Caused by Movement of Fatty Acids into and out of Clonal Pancreatic β-Cells (HIT), *J. Biol. Chem. 269*, 20852–20856.
35. Hermetter, A., Rainer, B., Ivessa, E., Kalb, E., Loidl, J., Roscher, A., and Paltauf, F. (1989) Influence of Plasmalogen Deficiency on the Membrane Fluidity of Human Skin Fibroblasts: A Fluorescence Anisotropy Study, *Biochim. Biophys. Acta 978*, 151–157.

[Received May 8, 2003, and in revised form November 7, 2003; revision accepted November 25, 2003]

Interaction of Bile Salts with Gastrointestinal Mucins

Timothy Scott Wiedmann*, Wei Liang, and Heather Herrington

Department of Pharmaceutics, University of Minnesota, Minneapolis, Minnesota 55455

ABSTRACT: The properties of three mucins were examined to identify the structural features responsible for their functional differences. Bovine submaxillary mucin (BSM), porcine gastric mucin (PGM), and rat intestinal mucin (RIM) were each characterized, and high carbohydrate contents were found for RIM and PGM. The amino acid compositions were typical of mucin glycoproteins, with over half comprising small, neutral amino acids. Thereafter, each mucin was equilibrated with three different series of concentrations of the bile salts sodium taurocholate, sodium taurodeoxycholate, and sodium taurochenodeoxycholate. Following multiple centrifugations, the supernatant and mucin pellet concentrations of the bile salts were measured. The bile salt pellet concentration was plotted as a function of supernatant concentration, and from the slopes, the excluded volumes were calculated as 25, 29–44, and 28–55 mL/g for BSM, RIM, and PGM, respectively. The intercepts were 8–10, 2–3, and 1–3 mM for BSM, RIM, and PGM, respectively, which represents an estimate of the bound concentration of bile salt. Differences among the bile salts were observed in the excluded volume and amount bound, but no trends were evident. The bile salts may interact as aggregates with the hydrophobic areas and carbohydrate side chains of the mucins, providing favorable sites for association. The binding at low concentrations with exclusion at high concentrations is significant for modulating the absorption of lipid aggregates from the intestine. Finally, the differences among the mucins reflect the unique structure–function relationship of these gastrointestinal mucins.

Paper no. L9332 in *Lipids 39*, 51–58 (January 2004).

Mucus represents a biologically significant but complicated material (*cf.* 1). Mucus is secreted at the surface of all mucous membranes and is widely distributed at body–environment interfaces. This includes the eye, respiratory tract, vaginal tract and cervix, bladder, gallbladder, and along the entire length of the gastrointestinal tract. The mucous gel is primarily water, but contains mucin-type glycoproteins that are responsible for the characteristic viscoelasticity. These glycoproteins are large-M.W. species ($>10^6$ D), typically consisting of about 20–30% protein and 70–80% carbohydrate. Our interest has been in the gastrointestinal (GI) mucins. In particular, the properties of salivary, gastric, and intestinal mucins were examined to identify unique structural features that would relate to the functional differences. As is well known, salivary mucin provides a lubricant activity for ingested food, gastric mucin prevents the self-digestion of the stomach, and intestinal mucin provides a coating for facilitating the passage of the luminal contents.

Based on recent genomic investigations, more detailed structures of the protein core of secreted mucins have been proposed (1–3). The linear, central protein core is highly glycosylated and is flanked by regions of globular protein that are rich in cysteine residues and may be involved in inter- and intramolecular disulfide bonds. The variability in M.W. arises from the central region that contains tandem repeats, which are amino acid sequences that are repeated a variable number of times. Along the GI tract, MUC5B is expressed in the salivary gland, MUC5AC is highly expressed and MUC6 expressed to a lesser extent in the stomach, and MUC2 and MUC3 are expressed in the small intestine. From the known models of these mucins, there is considerable homology among them despite their disparate functions. Nevertheless, the tandem repeats and cysteine-rich regions are distinct among these mucins (3).

In addition to the distinct protein cores, the carbohydrate side chains also differ. Although the O-glycosidic side chains of all mucins contain the same monosaccharides, the length of the side chains varies among GI mucins (1). Bovine submaxillary mucins (BSM) have relatively short chains with an average length of two units (4). Rat intestinal mucins (RIM) have intermediate chains with lengths most often in the range of three to four units (5). Human gastric mucins are believed to have much longer side chains extending as long as 19 units (6,7). The terminal sugar is often sialic acid, although sulfate groups are found on gastric mucins. Finally, whereas RIM is typically isolated in its pure native form, many investigators rely on commercially available preparations for BSM and porcine gastric mucin (PGM). These contain impurities, and their native 3-D structures may be altered due to lyophilization.

Transport of bile salts through mucin is a critical step in the absorption of fat and poorly water-soluble drugs. Therefore, bile salt aggregates were used to probe the interaction of micelles with these three mucins. Although fully expecting a significant size and charge exclusion of the bile salt micelles from the mucin gels (8–15), a specific association became evident. In this work, the interaction of three different bile salts with three distinct mucins of the GI tract was examined, from which the magnitude of association and exclusion by the glycoprotein networks was obtained.

*To whom correspondence should be addressed at University of Minnesota, Department of Pharmaceutics, 308 Harvard St. SE, Minneapolis, MN 55455. E-mail: wiedm001@tc.umn.edu

Present address of second author: Biophysical Institute of Chinese Academy of Science, Beijing, China.

Abbreviations: BSM, bovine submaxillary mucin; CMC, critical micelle concentration; GI, gastrointestinal; PGM, porcine gastric mucin; RIM, rat intestinal mucin; TC, taurocholate; TCDC, taurochenodeoxycholate; TDC, taurodeoxycholate.

EXPERIMENTAL PROCEDURES

Materials. Sodium taurocholate (TC), sodium taurodeoxycholate (TDC), sodium taurochenodeoxychoate (TCDC), 11α-hydroxyprogesterone, pilocarpine, PGM-III, and BSM IS were purchased from Sigma Chemical Co. (St. Louis, MO). Sodium trimethylsilyl-tetradeutero-propionate was purchased from Aldrich Chemical Co. (Milwaukee, WI). Water was deionized and then distilled, and methanol was HPLC grade. All other chemicals were reagent/analytical grade or better. RIM was isolated from male Sprague-Dawley rats (250–500 g). This study was approved by the Institutional Animal Care and Use Committee. Rats were given a 0.4-mL intraperitoneal injection of pilocarpine (160 mg/mL) and were sacrificed 30 min later (16). Mucin was then isolated and characterized by the extraction method of Carlsted *et al.* using 4 M guanidine (5,12). The amino acid analysis was conducted by the Microchemical Facility at the University of Minnesota.

Methods. (i) Centrifugation. The mucins and bile salts were prepared in aqueous solutions containing 0.9% sodium chloride and 0.1% sodium azide adjusted to pH 7.0. BSM and PGM, at initial concentrations of 1%, were centrifuged at 17,000 × *g* for 90 and 120 min, respectively, in tared, skirted, screw-capped microcentrifuge tubes in a refrigerated centrifuge. RIM, *ca.* 0.003%, required centrifugation at 13,000 × *g* for 5 min for complete recovery owing to its aggregated state. A known mass of bile salt solution, ranging in concentration from 2 to 50 mM, was added to each. The dispersion was briefly vortexed and centrifuged. The supernatant was removed and the remaining mass determined. Another aliquot of the bile salt solution was added, and the dispersion was again vortexed and centrifuged. The addition and centrifugation process was repeated a third time, after which the mass of supernatant and pellet were each measured.

The bile salt concentration was determined by HPLC in the supernatant and also in the pellet following dilution with 150 μL of water and vigorous vortexing using a modified published procedure (12). The mobile phase for sodium TC was 50 mM potassium phosphate buffer (pH 3.4)/methanol/water (1:4:1 by vol) and for TDC and TCDC, 10 mM sodium dihydrogen phosphate/methanol (3:7 vol/vol). The column was a Supelcosil LC-18 (25 × 0.46 cm, 5 μm particle size; Supelco, Bellefonte, PA). The system consisted of a Shimadzu C-R5A integrator, SPD-6AV detector at 220 nm, SIL-10Advp autoinjector, and an LC-10Atvs pump running at 1 mL/min.

The mucin concentration in the remaining pellet was determined gravimetrically after drying. The concentration of mucin was corrected for the presence of bile salt, sodium chloride, and sodium azide. Since no trend was evident in the mucin concentration as a function of bile salt concentration, the mucin concentration was reported as the mean of all samples. The effect of salt on the final pellet weight was determined by centrifuging different salt concentrations with mucin in a manner similar to the one described for the bile salt solutions. The measured mass of the dried sample was corrected for the presence of sodium chloride.

We intended the series of samples to vary with respect to bile salt concentration but have a constant mucin concentration. However, the samples were determined experimentally to have slightly different mucin concentrations. To correct the observed concentration of bile salt in the pellet to the same mucin concentration, the following approach was taken: The measured concentration of bile salt in the pellet was first plotted as a function of that measured in the supernatant. The data were initially fit by linear regression, and the average mucin concentration in the samples was calculated. The corrected pellet concentration of bile salt, $BS_{p,corr}$, was calculated as follows:

$$[BS]_{p,corr} = [BS]_p + (slope)(1 - M_{ave}/M_s)[BS]_s + (intercept)(1-M_s/M_{ave}) \quad [1]$$

where $[BS]_p$ and $[BS]_s$ are the measured bile salt concentrations in the pellet and supernatant respectively, M_{ave} is the average mucin concentration, and M_s is the mucin concentration of the sample; the slope and intercept were obtained from the initial linear regression. The corrected bile salt concentrations in the pellet were then plotted as a function of the supernatant bile salt concentrations. This inherently assumed that the slope and intercept were linearly proportional to the mucin concentration over a small range of values. The linear regression was repeated, and the 95% confidence limits of the slope and intercept were calculated. For statistical analyses, comparisons of the slopes and intercepts were carried out in a pair-wise manner using a Microsoft Excel spreadsheet with 95% confidence intervals.

(ii) Diffusion coefficient measurement and analysis. The diffusion coefficients of the bile salts were determined in the supernatants by pulsed field gradient spin-echo NMR spectroscopy as described previously (12). The results were analyzed by assuming a two-state model for the observed diffusion coefficient of the bile salt, D_{obs},

$$D_{obs} = f_i D_i + f_m D_m \quad [2]$$

where f_i and D_i are the fraction and diffusion coefficients of bile salt as a monomer, and f_m and D_m are the fraction and diffusion coefficients of bile salt in the aggregated form. The fractions may be written in terms of the total bile salt concentration, $[TC]_t$, and monomer concentration, critical micelle concentration (CMC), as follows:

$$D_{obs} = (CMC/[TC]_t)D_i + \{1 - (CMC/[TC]_t)\}D_m \quad [3]$$

This may be rearranged as

$$D_{obs}[TC]_t = CMC(D_i - D_m) + D_m[TC]_t \quad [4]$$

so that a plot of the product of the observed diffusion coefficient and total bile salt concentration as a function of the total bile salt concentration will yield a straight line with a slope equal to the diffusion coefficient of the bile salt micelle. A viscosity of 1 cP was assumed to allow calculation of the

hydrodynamic radius from the inferred diffusion coefficients of the aggregates using the Stokes–Einstein equation (17).

RESULTS AND DISCUSSION

The composition of each mucin is given in Table 1. The protein concentration was determined by both Lowry's assay using albumin as a standard and amino acid analysis. The differences among the results are reasonable given the nature of these assays. PGM had the lowest protein content, at about 17% of the dry weight. BSM had the highest content, with as much as 50% of the mass due to protein. The carbohydrate content ranged from a low value of 51% for BSM to more than 86% for RIM. The low content of BSM was unexpected, but indicates that the material purchased from Sigma is a relatively poor model for native salivary mucins. The results for RIM reported in this study are distinct from those given in an earlier work (12). The difference likely arises from the use of pilocarpine, which stimulated the release of mucin (16).

The sialic acid content is important, as this amino sugar bears a negative charge. BSM had the highest value at 10% and PGM the lowest at just over 1%. It should be noted that PGM is expected to contain sulfate groups, which provide the negative charge in gastric mucins (1). Neither BSM nor RIM has been reported to contain a significant amount of sulfate (1).

The results of the amino acid analyses are given in Table 2, which were very similar overall. In analyzing the composition, PGM had about 10% negatively charged amino acids, whereas RIM and BSM had just over 15%. For the small, neutral amino acids, RIM had 46%, BSM had 54%, and PGM had 68%. For hydrophobic amino acids, PGM had the least at 10%, BSM had 20% and RIM had just under 30%. Finally, all three mucins had about 10% positively charged amino acids.

In Figure 1, the corrected concentration of TDC in the mucin pellet is given as a function of the supernatant bile salt concentration for RIM, PGM, and BSM. The solid lines represent the best fits for supernatant concentrations of 10 mM and greater. This concentration range was chosen for analysis, since it lies above the consensus values of the CMC reported for the bile salts, which are 5, 2, and 4 mM for TC, TDC, and TCDC, respectively (18). As can be seen, the concentration of TDC in the pellet rose linearly with the concentration in the supernatant for concentrations greater than 10 mM. The low concentrations fell below the regression line for all three mucins. The slopes of the lines were less than unity, indicating that the bile salt pellet concentration was lower than the supernatant concentration. However, most interestingly, the intercepts of the regression line were greater than zero. The results for each mucin were distinct as well. PGM was found to have the smallest intercept for TDC, whereas RIM had the largest slope. The slope for BSM was intermediary, but the line had the highest intercept.

In Figure 2, the corrected RIM pellet concentration of the three bile salts is given as a function of the supernatant bile salt concentration. As mentioned, the data could be fit to a straight line at concentrations greater than 10 mM. In each case, the slope was less than unity, and the intercept was greater than zero. For RIM, the intercept of TCDC was significantly lower than the intercepts obtained with TC and TDC. Moreover, the slope of TDC was greater than the slopes of TC and TCDC at 95% confidence. Analogous relationships were examined for the other two mucins, BSM and PGM; the slopes and intercepts of the fitted lines, along with the 95% confidence limits, are shown in Tables 3 and 4. In general, similar results were observed with BSM and PGM. The two exceptions were that the intercept of TDC in BSM was greater than that of TC, and none of the slopes or intercepts was significantly different for PGM.

The average value of the concentration of mucin was calculated from the dry weights and is given in Table 5. The RIM was low, being less than 0.1%, whereas BSM and PGM ranged between 2 and 3%. This difference suggests that the aggregated state of isolated RIM is distinct in comparison with the commercial preparations of BSM and PGM. In this study, RIM appeared as a fine dispersion, where floccules of mucin had a domain size on the order of 100 μm. BSM and PGM yielded hazy, moderately viscous dispersions indicative of a mucin solution in the presence of insoluble material. The lower-weight fraction obtained with RIM presumably was a result of cross-linking that limited the concentration that could be achieved with centrifugation.

Before discussing the implications of these results, a question may arise as to whether equilibrium was achieved by using

TABLE 2
Percent Amino Acid Composition of Mucins[a] as Determined by Amino Acid Analysis

	RIM	PGM	BSM
Asp	7.1	3.8	6.2
Glu	8.2	6.2	9.5
Thr	14.0	20.8	10.8
Ser	9.1	12.5	11.8
Pro	8.5	16.8	9.2
Gly	8.1	10.4	12.0
Ala	5.8	7.5	10.1
Cys	0.7	0.2	0.3
Val	5.9	4.6	6.6
Met	1.8	0.2	0.7
Ile	5.4	1.5	2.8
Leu	8.5	2.9	6.6
Tyr	3.1	0.0	1.6
Phe	4.4	0.8	2.2
His	2.5	4.2	1.8
Lys	3.9	4.4	3.8
Arg	3.0	3.2	4.1

[a]For abbreviations see Table 1.

TABLE I
Properties of Rat Intestinal Mucin (RIM), Bovine Submaxillary Mucin (BSM), and Porcine Gastric Mucin (PGM) Expressed as Dry Weight

	RIM	PGM	BSM
Protein (g/100 g, Lowry's assay	33.9 ± 2.0	16.63 ± 0.49	36.9 ± 3.6
Protein (g/100 g, amino acid analysis)	25.4	18.9	49.4
Carbohydrate (g/100 g)	86.5 ± 9.1	76 ± 20	51.59 ± 0.72
Sialic acid (g/100 g)	5.16 ± 0.54	1.19 ± 0.22	9.95 ± 0.18

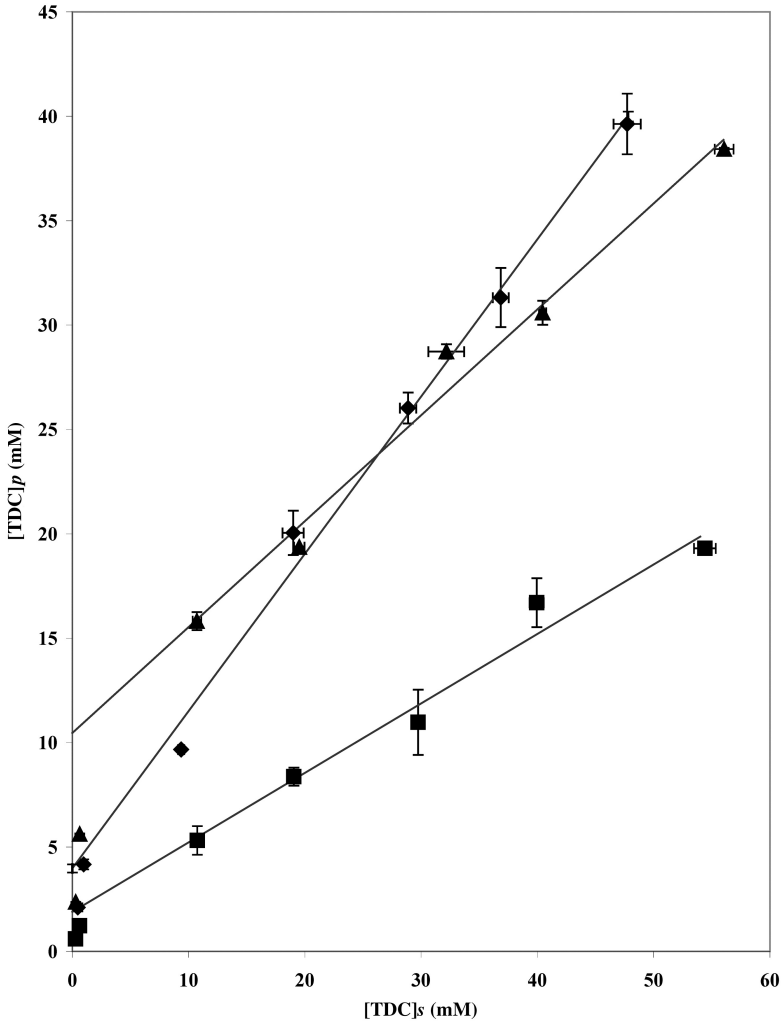

FIG. 1. Concentration of sodium taurodeoxycholate (TDC) in the supernatant (*s*) as a function of the concentration of sodium TDC in the mucin pellet (*p*) for three different mucins, (◆) rat intestinal mucin, (■) porcine gastric mucin, and (▲) bovine submaxillary mucin.

multiple centrifugations. Although binding experiments involving centrifugations are commonly performed with small-M.W. solutes and proteins, the aggregated state of mucin along with the presence of micelles raises a concern. In addition, previous work in this laboratory using equilibrium dialysis of phospholipid/bile salt dispersions with mucins (11,12,19) as well as the work of other researchers using dialysis (20–22) have repeatedly demonstrated that long equilibration times are required to achieve equilibrium between lipid aggregates and mucins.

Two key factors in earlier publications are distinct from the present work. The first is the presence of PC. PC can be considered to exist exclusively in an aggregated form, since the solubility of monomeric PC is quite low. As such, exchange among aggregates would occur only by a collision process. This is inherently slow, especially for large aggregates. In the present study, no phospholipids were present. The second is the resistance of the dialysis membrane. In earlier studies, the 500 MWCO membrane allowed the passage of bile salts but only slowly, since their M.W. actually exceeds 500 Da (11,20). Therefore, a high resistance would be encountered in the diffusion of bile salts through the pores. In this study, there was no diffusion across a dialysis membrane.

The equilibration time in centrifugation studies is determined by the exchange rates and the associated diffusivity of the bile salt monomers. Micelles containing only bile salts undergo rapid exchange between the monomers and aggregates (23). Moreover, the exchange occurs on the millisecond time frame, since NMR spectra contain only peaks representing a time average of the two environments, monomer and micelle (11). Diffusion of bile salt monomers is relatively fast as deduced from the measured micelle diffusion coefficients. Finally, owing to the fast exchange, diffusion of a micellar aggregate into the mucin gel particles is not necessary.

Binding to proteins or glycoproteins is also characterized by fast on/off rate constants, since there is no high-affinity binding.

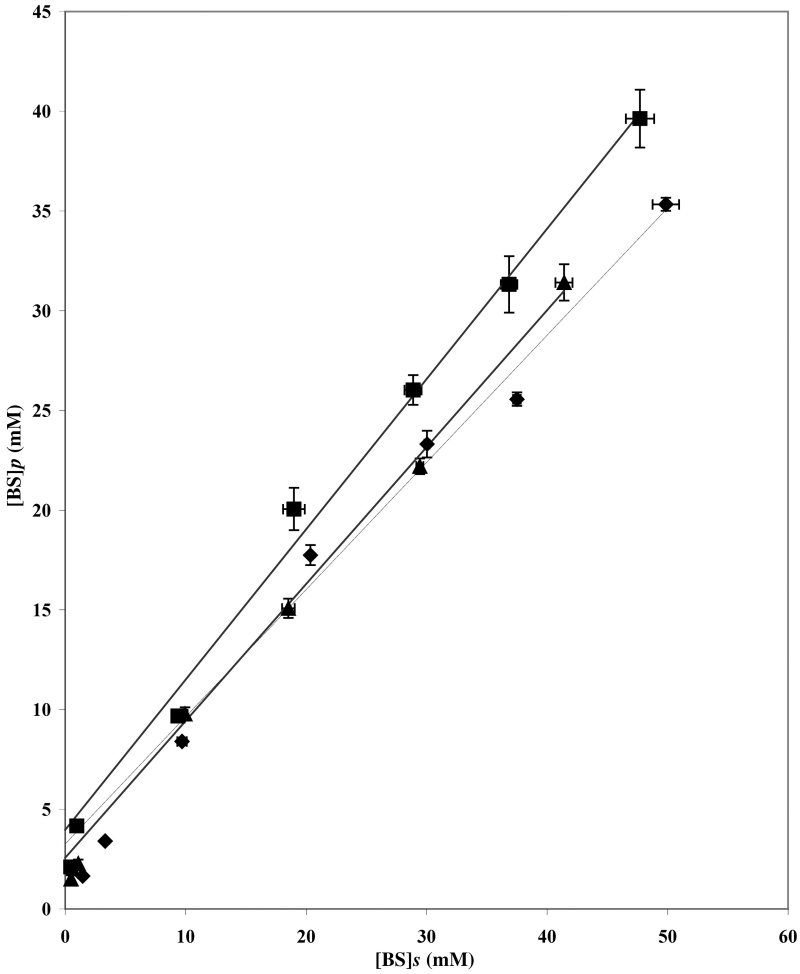

FIG. 2. Concentration of bile salt (BS) in the supernatant (*s*) as a function of BS concentration in the rat intestinal mucin pellet (*p*) for three different bile salts, (◆) taurocholate (TC), (■) taurodeoxycholate (TDC), and (▲) taurochenodeoxycholate (TCDC).

Only when very high-affinity binding is encountered do equilibration times become a concern. This is not the case in this study. Thus, given the rapid exchange of bile salts with micelles, the rapid diffusion between the micelle and glycoprotein surface, and the rapid exchange between the monomer and glycoprotein, there was ample equiliberation time in the multiple centrifugations that were performed to allow equilibration of the bile salts with the mucin aggregates.

In examining the results, the concentration of bile salt in the mucin pellet appears to be a linear function of the bile salt concentration in the supernatant where the slope is less than unity. The slope is related to the excluded volume of mucin. Although the excluded volume effect may be expected to be a nonlinear function of mucin concentration, it is not unreasonable to have the same excluded volume effect as the concentration of solute being excluded is varied. Thus, the linear function is reasonable, although expanding the range of concentrations could very well yield nonlinearity.

From the dry weights and the slopes of the bile salt concentrations in the pellet given as a function of the supernatant concentration, the volume excluded per gram of mucin was calculated. For RIM, the values ranged from 29 to more than 44 mL/g, suggesting a very large exclusionary boundary layer. The values for PGM were similar, ranging from 28 to 55 mL/g. Thus, following correction for the mucin concentration, the excluded volume per gram was similar for RIM and PGM. These large excluded volumes correlate with the high carbohydrate content. In contrast, the excluded volume of BSM was smaller, with values less than 25 mL/g, and BSM also had a relatively low carbohydrate content.

TABLE 3
Intercepts (± 95% confidence limit) of Plots of the Supernatant Concentration as a Function of Pellet Concentration of Bile Salts

	RIM	PGM	BSM
TC	3.26 ± 0.94	2.13 ± 0.48	8.77 ± 0.78
TDC	3.97 ± 0.82	1.89 ± 0.64	10.47 ± 0.78
TCDC	2.57 ± 0.39	1.53 ± 0.54	10.1 ± 4.1

[a]TC, taurocholate; TDC, taurodeoxycholate; TCDC, taurochenodeoxycholate; for other abbreviations see Table 1.

TABLE 4
Slopes (± 95% confidence limit) of the Plots of the Supernatant Concentration as a Function of the Pellet Concentration of Bile Salts[a]

	RIM	PGM	BSM
TC	0.638 ± 0.049	0.398 ± 0.027	0.449 ± 0.072
TDC	0.754 ± 0.044	0.333 ± 0.031	0.507 ± 0.038
TCDC	0.687 ± 0.025	0.332 ± 0.036	0.409 ± 0.014

[a]For abbreviations see Tables 1 and 3.

TABLE 5
Average Dry Weight of Mucin (mean ± SD, g/g) Measured in Samples Used in the Centrifugation Experiments[a]

	RIM	PGM	BSM
TC	0.0081 ± 0.0017	0.021 ± 0.001	0.027 ± 0.003
TDC	0.0083 ± 0.0019	0.020 ± 0.001	0.032 ± 0.002
TCDC	0.0090 ± 0.0019	0.012 ± 0.002	0.023 ± 0.002

[a]For abbreviations see Tables 1 and 3.

Other factors were also considered in addition to carbohydrate content, but they did not appear to have a major effect on the excluded volume. As noted, RIM retained its cross-linked network, whereas PGM and BSM were hazy, viscous dispersions representative of simple physical entanglement. Nevertheless, there was no dramatic difference in the excluded volumes between RIM and PGM. This suggests that chemical cross-links did not dramatically influence the excluded volume.

Another factor that was examined was electrostatic interaction. For this purpose, the mucin weight fraction was determined as a function of sodium chloride concentration following centrifugation. From 5 to 100 mM NaCl, there was a substantial increase in the dry weight corresponding to a decrease in pellet volume. However, above 100 mM, no significant changes in the mucin weight fraction were observed. Thus, at physiological concentrations of salt (i.e., 150 mM), electrostatic repulsion appears to be of little importance in determining the molecular conformation. This is also consistent with the view that the steric hindrance of the oligosaccharide side chains is most important in determining molecular inflexibility (1).

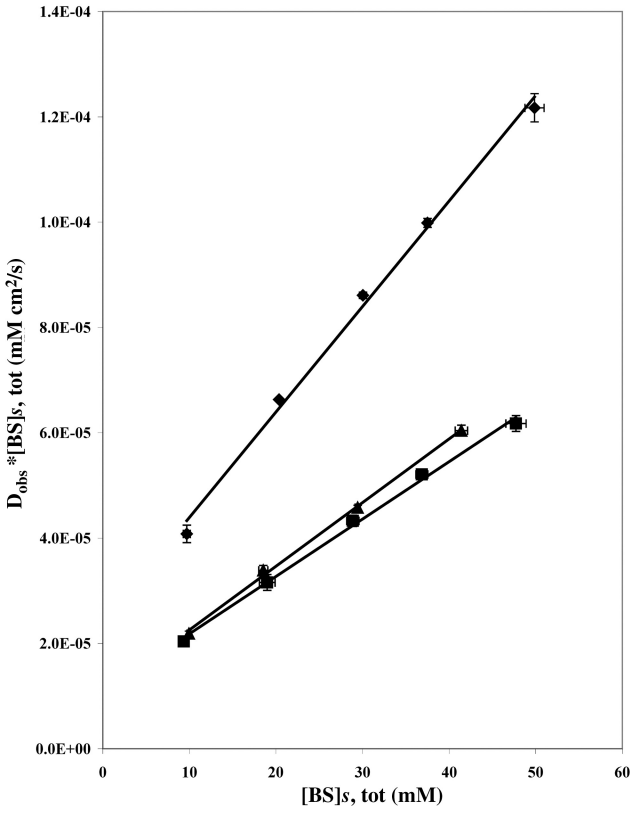

FIG. 3. Plot of the product of the BS concentration and observed diffusion coefficient, D_{obs}, as a function of the total BS concentration (*s*, tot) for (◆) TC, (■) TDC, and (▲) TCDC. For abbreviations see Figures 1 and 2.

In principle, the excluded volume should depend on the micelle size of the bile salt. To address this aspect in more detail, the diffusivity of the micelle in the supernatant was determined as a function of concentration; the results are shown in Figure 3. From the slopes, the diffusion coefficients of the micelles were obtained, which are given in Table 6. In the supernatant above RIM, these were 2.00, 1.09, and 1.21×10^{-6} cm^2/s for TC, TDC, and TCDC, respectively. From the bile diffusivities, the corresponding hydrodynamic radii were calculated with the Stokes–Einstein equation, which yielded 11, 20, and 18 Å for TC, TDC, and TCDC, respectively. These values correspond well with the aggregation numbers reported in the literature (18). TC is known to be relatively small, with an aggregation number between 4 and 5. TDC and TCDC form larger aggregates, which are found to depend strongly on the bile salt concentration and ionic strength of the solution. Since the hydrodynamnic radii were less than twice that observed with TC, the aggregation number for TDC and TCDC was expected to be less than 30.

From the diffusion coefficients, the rank order of micelle size is given as TC < TCDC < TDC, which in principle should dictate the order of the excluded volume. However, as shown in Table 4, the slopes, which represent the free volume, do not follow any trend. Thus, excluded volume was not found to correlate with micelle size. It may be that the differences in micelle size are too small to have a significant effect. Alternatively, the association of bile salts with the mucin represents a confounding influence on the excluded volume. Overall, the carbohydrate content appears to be the most influential factor in determining the excluded volume of mucins with bile salt micelles.

In addition to the slopes, the positive intercepts are of interest. One possible explanation is that bile salts associate with mucin. The intercepts had values that ranged from 1 to more than 10 mM, which allowed calculation of the moles of bile salt bound per gram of mucin. For RIM, the values ranged from 0.28 to 0.48 mmol/g; BSM also had relatively high values at 0.32–0.43 mmol/g, whereas PGM had values in the range of 0.096–0.127.

Other investigators have found that mucin can bind solutes. Early work by Smith and LaMont (24) indicated that there were about 42.5 binding sites per gallbladder mucin molecule for a hydrophobic fluorescent probe. This translates into 0.0425

TABLE 6
Fitted Bile Salt Diffusion Coefficients ($\times 10^{-6}$ cm^2/s) in the Supernatant[a]

	RIM	PGM	BSM
TC	2.00	2.10	2.07
TDC	1.09	1.17	1.16
TCDC	1.21	1.22	1.24

[a]For abbreviations see Tables 1 and 3.

mmol of binding sites/g of mucin, which is an order of magnitude less than the values just given for the bile salts. Given the large discrepancy, it is unlikely that the binding phenomena are similar. One possibility is that bile salts associate with mucin as micellar aggregates rather than binding as monomers to specific sites, as was suggested for the fluorescence probe. Since only data above the CMC were only analyzed, it is not possible to evaluate the binding of monomers. Nevertheless, the magnitude of the binding suggests that micelle binding occurs at concentrations above the CMC.

In comparing the binding by mucins, BSM and RIM had two and three times the content of hydrophobic amino acids, respectively, relative to PGM. As such, hydrophobicity may contribute to their greater binding. As noted, mucin possesses a long central protein backbone from which carbohydrate side chains extend. Based on a chemical analysis of RIM, carbohydrate side chains occur about every third to fourth amino acid and have an average length of 3.4 units (1). It is well known that this region is well hydrated with water. Bile salts, in turn, are believed to undergo back-to-back self-association. This allows their hydrophobic surface to be shielded from water yet permits the α-hydroxyl moieties to interact freely with water. The oligosaccharides also may promote accumulation of bile salt micelles. That is, bile salt aggregates are located among the carbohydrate side chains of mucin. In this site, the water hydrating the bile salt micelle and carbohydrate side chains would be released as the bile salt and carbohydrates underwent intermolecular hydrogen bonding.

Such an explanation is supported by the observation that the two mucins, RIM and BSM, which are rich in short carbohydrate side chains, had considerably more binding of bile salts. This is in contrast with PGM, which has relatively long side chains. It is also consistent with the relative insensitivity of the binding number to the type of bile salt. All three mucins had an equivalent content of positively charged amino acids, so this does not appear to be a decisive factor in the different amounts bound. However, the negatively charged micelles were not expected to associate readily with the mucin that also bore a net negative charge. Nevertheless, the presence of 150 mM NaCl would greatly minimize the electrostatic repulsion. Clearly, more studies examining the effect of ionic strength would be of interest (25).

In this study, both the association and exclusion of bile salts by GI mucins have been suggested. The exclusionary effect of mucin on phospholipid/bile salt aggregates has been addressed previously (11,12,20,25); however, study designs did not allow for quantitative assessment of the simultaneous association and exclusion. Moreover, the use of equilibrium dialysis membranes precluded examination of high concentrations of mucin, which are experimentally necessary to measure the binding. Thus, the past results presented a clouded picture where at times binding dominated, at other times exclusion dominated, and very often the binding and exclusion were similar and no effect was observed (11,12,25). In the present study, the use of centrifugation provided a means to generate high concentrations of mucin.

In summary, the interaction of bile salts with three GI mucins was studied. Bile salts were found to associate with mucin at low concentration, but were excluded at high concentrations. The composition and structural information on each mucin were used to explain the results, which indicated that the carbohydrate content correlated with a high excluded volume but that the hydrophobic amino acid content was related to the extent of binding.

ACKNOWLEDGMENT

The support of National Institutes of Health grant DK54359 is acknowledged.

REFERENCES

1. Perez-Vilar, J., and Hill, R.L. (1999) The Structure and Assembly of Secreted Mucins, *J. Biol. Chem. 274*, 31751–31754.
2. Reid, C.J., and Harris, A. (1998) Developmental Expression of Mucin Genes in the Human Gastrointestinal System, *Gut 42*, 220–226.
3. Dekker, J., Rossen, J.W.A., Buller, H.A., and Einerhand, A.W.C. (2002) The MUC Family: An Obituary, *Trends Biochem. Sci. 27*, 126–131.
4. Tsuji, T., and Osawa, T. (1986) Carbohydrate Structures of Bovine Submaxillary Mucin, *Carbohydr. Res. 151*, 391–402.
5. Carlstedt, I., Herrmann, A., Karlsson, H., Sheehan, J., Fransson, L.A., and Hansson, G.C. (1993) Characterization of Two Different Glycosylated Domains from the Insoluble Mucin Complex of Rat Small Intestine, *J. Biol. Chem. 268*, 18771–18781.
6. Slomiany, B.L., Zbebska, E., and Slomiany, A. (1984) Structural Characterization of Neutral Oligosaccharides of Human H + Le^{b+} Gastric Mucin, *J. Biol. Chem. 259*, 2863–2869.
7. Slomiany, A., Zbebska, E., and Slomiany, B.L. (1984) Structures of the Neutral Oligosaccharides Isolated from A-Active Human Gastric Mucin, *J. Biol. Chem. 259*, 14743–14749.
8. Lukie, B.E. (1977) Studies of Mucus Permeability, *Mod. Probl. Paediatr. 19*, 46–53.
9. Nimmerfall, F., and Rosenthaler, J. (1980) Significance of the Goblet-Cell Mucin Layer, the Outermost Luminal Barrier to Passage Through the Gut Wall, *Biochem. Biophys. Res. Comm. 94*, 960–966.
10. Saltzman, W.M., Radomsky, M.L., Whaley, K.J., and Cone, R.A. (1994) Antibody Diffusion in Human Cervical Mucus, *Biophys. J. 66*, 508–518.
11. Wiedmann, T.S., Deye, C., and Kallick, D. (2001) The Interaction of Sodium Taurocholate and Phospholipids with Bovine Submaxillary Mucin, *Pharm. Res. 18*, 45–53.
12. Wiedmann, T.S., Herrington, H., Deye, C., and Kallick, D. (2001) Analysis of the Diffusion of Bile Salt/Phospholipid Micelles in Rat Intestinal Mucin, *Chem. Phys. Lipids 112*, 81–92.
13. Winne, D., and Verheyen, W. (1990) Diffusion Coefficient in Native Mucus Gel of Rat Small Intestine, *J. Pharm. Pharmacol. 42*, 517–519.
14. Wikman-Larhed, A., Artursson, P., Grasjo, J., and Bjork, E.

(1997) Diffusion of Drugs in Native and Purified Gastrointestinal Mucus, *J. Pharm. Sci. 86*, 660–665.
15. Wikman Larhed, A., Artursson, P., and Bjork, E. (1998) The Influence of Intestinal Mucus Components on the Diffusion of Drugs, *Pharm. Res. 15*:66–71.
16. Phillips, T.E. (1992) Both Crypt and Villus Intestinal Goblet Cells Secrete Mucin in Response to Cholinergic Stimulation, *Am. J. Physiol. 262*, G327–G331.
17. Long, M.A., Kaler, E.W., Lee, S.P., and Wignall, G.D. (1994) Characterization of Lecithin–Taurodeoxycholate Mixed Micelles Using Small-Angle Neutron Scattering and Static and Dynamic Light Dcattering, *J. Phys. Chem. 98*, 4402–4410.
18. Cabral, D.J., and Small, D.M. (1989) The Physical Chemistry of Bile, in *Handbook of Physiology: The Gastrointestinal System* (Schultz, S.G., Forte, J.G., and Rauner, B.B., eds.), Vol. 3, Section 6, pp. 621–662, Waverly Press, New York.
19. Wiedmann, T.S., Herrington, H., Deye, C., and Kallick, D. (2001) Interaction of Sodium Taurocholate and Egg Phosphatidylcholine with Rat Intestinal Mucin, *Pharm. Res. 18*, 1489–1496.
20. Higuchi, W.I., Arakawa, M., Lee, P.H., and Noro, S. (1987) Simple Micelle–Mixed Micelle Coexistence Equilibria for the Taurocholate–, Taurochenodeoxycholate–, and Tauroursodeoxycholate–Lecithin Systems, *J. Colloid Interface Sci. 119*, 30–37.
21. Duane, W.C. (1977) Taurocholate– and Taurochenodeoxycholate–Lecithin Micelles: The Equilibrium of Bile Salt Between Aqueous Phase and Micelle, *Biochem. Biophys. Res. Commun. 74*, 223–229.
22. Nagadome, S., Yamauchi, A., Miyashita, K., Igimi, H., and Sugihara, G. (1998) Transport Behavior of Four Bile Salt Micelles and Cholesterol Solubilized by Their Micelles Across Porous Membrane, *Colloid Polym. Sci. 276*, 59–65.
23. Li, C.-Y., Zimmerman, C., and Wiedmann, T.S. (1996) Diffusivity of Bile Salt/Phospholipid Aggregates in Mucin, *Pharm. Res. 13*, 535–541.
24. Smith, G.F., and LaMont, J.T. (1984) Hydrophobic Binding Properties of Bovine Gallbladder Mucin, *J. Biol. Chem. 259*, 12170–12177.
25. Lichtenberger, L.M. (1995) The Hydrophobic Barrier Properties of Gastrointestinal Mucus, *Annu. Rev. Physiol. 57*, 565–583.

[Received June 4, 2003, and in revised form October 3, 2003; revision accepted January 8, 2004]

Fatty Acids of Serine, Ethanolamine, and Choline Plasmalogens in Some Marine Bivalves

Edouard Kraffe[a], Philippe Soudant[b], and Yanic Marty[a,*]

[a]Unité mixte Centre Nationale de la Recherche Scientifique (CNRS) 6521, Université de Bretagne Occidentale CS93837, 29238 Brest Cedex 3, France, and [b]Unité mixte CNRS 6539, Institut Universitaire Européen de la Mer, Université de Bretagne Occidentale, 29280 Plouzané, France

ABSTRACT: The FA composition of glycerophospholipid (GPL) classes and subclasses was investigated in whole animals of three marine bivalve mollusks: the Japanese oyster *Crassostrea gigas*, the blue mussel *Mytilus edulis*, and the Manila clam *Ruditapes philippinarum*. Individual organs (gills, mantle, foot, siphon, and muscle) of the Manila clam also were examined. The PS plasmalogen (PSplsm), PE plasmalogen (PEplsm), and PC plasmalogen (PCplsm) subclasses were isolated by HPLC, and their individual FA compositions were examined using GC. Plasmalogen forms of PS and PE, when compared to their respective diacyl forms, were found to be specifically enriched with non-methylene-interrupted (NMI) FA (7,15-22:2, 7,13-22:2, and their precursors) and 20:1n-11 FA. Such a clear specific association was not found for PCplsm. Interestingly, this trend was most apparent in PSplsm, and the above FA were found to be, respectively, the predominant PUFA and monounsaturated FA in the PSplsm isolated from the three species. This specificity was maintained in all the analyzed organs of the Manila clam but varied in proportions: The highest level of plasmalogens, NMI FA, and 20:1n-11 was measured in gills and the lowest was in muscle. These results represent the first comprehensive report on a FA composition of the PSplsm subclass isolated from mollusks. The fact that NMI FA and 20:1n-11, which are thought to be biosynthesized FA, were mainly associated with aminophospholipid plasmalogens (PE and PS) is likely to have a functional significance in bivalve membranes.

Paper no. L9385 in *Lipids 39*, 59–66 (January 2004).

Ether glycerophospholipids (GPL) are subclasses of phospholipids found in animal cells. The two predominant forms have either an alkyl or an alkenyl ether linkage at the *sn*-1 position of the glycerol moiety and an acyl linkage at the *sn*-2 position. The 1-alkenyl-2-acyl ether GPL are commonly called "plasmalogens." The biological activity of plasmalogens is not fully understood, although a number of functions have been proposed. Plasmalogens are supposed to be important in membrane dynamics, allowing the formation of inverted hexagonal structures (H_{II}) (1). Several recent studies have led to the proposal that these ether lipids also may serve as endogenous antioxidants to protect cells from oxidative stress (2–4). One other function proposed is as sinks for PUFA, to maintain high levels of these FA in some tissues (1).

It is well established that marine invertebrates are especially rich sources of plasmalogens whereas they contain only small amounts of 1-alkyl-2-acyl GPL (see Refs. 5 and 6 for reviews). Indeed, they generally have higher concentrations of plasmalogens than other well-known rich sources such as mammalian brain (7) and heart (1). In a variety of human tissues, high proportions of plasmalogen forms were found in PE and to a lesser extent in PC (see Ref. 1 for review). In winter-collected marine invertebrates, Dembitsky and Vaskovsky (8) concluded that these animals can be grouped according to the distribution of plasmalogens in their phospholipids. Plasmalogens of Coelenterata and Echinoidea exist only as PE; those of Annelida, Arthropoda, Ascidia, and most of the Echinodermata, as both PE and PC; and those of Mollusca, as PE, PC, and PS. Later, Dembitsky (9) repeated this investigation with animals collected during the summer and confirmed that, among all examined invertebrates, only mollusks contained PS plasmalogen (PSplsm).

Very few analyses of the FA composition of marine mollusk plasmalogens have been carried out. In fact, the separation of the plasmalogen subclasses from the analogous diacyl subclass in a GPL extract of molluscan tissues is quite difficult owing to the complexity of the mixture of various molecular species as well as to the similarities between their chemical structures. However, in previous investigations, the acid-catalyzed hydrolysis of the *sn*-1 position combined with a phospholipid separation by HPLC has rendered possible the determination of the FA composition, by GC, of the bulk of plasmalogen forms in the great scallop *Pecten maximus* (10–13). GC–MS identification, after enzymatic hydrolysis of phospholipid polar heads, also has been applied to describe the detailed fatty acyl chain compositions of PE plasmalogen (PEplsm) and PC plasmalogen (PCplsm) from the Japanese oyster *Crassostrea gigas* (14,15). In these studies, noticeable amounts of non-methylene-interrupted (NMI) FA were found in PEplsm. These unusual FA have been previously described in different phyla of marine invertebrates (6,16). More recently, high levels of 22:2 NMI FA were found in the polar lipids of *C. gigas* and *Ruditapes philippinarum* (17,18), but the FA composition of plasmalogen and diacyl GPL were not determined in these studies. Pathways for the biosynthesis of 20:2 NMI (5,11 and 5,13) and 22:2 NMI (7,13 and 7,15) FA have been reported in the bivalve mollusks *Scapharca broughtoni* and *Mytilus edulis* (19,20). These results indicated that mollusks have active FA elongation and desaturation systems permitting

*To whom correspondence should be addressed at Unité mixte CNRS 6521, Université de Bretagne Occidentale, CS93837, 29238 Brest Cedex 3, France. E-mail: Yanic.Marty@univ-brest.fr

Abbreviations: CL, cardiolipin, common name of diphosphatidylglycerol; GPL, glycerophospholipid(s); MUFA, monounsaturated FA; NMI, non-methylene-interrupted; ΣNMI, sum of all non-methylene-interrupted fatty acids; PCplsm, PC plasmalogen; PEplsm, PE plasmalogen; PSplsm, PS plasmalogen; SFA, saturated fatty acid(s).

the *de novo* synthesis of these NMI FA. The unknown biological roles of both plasmalogens and NMI FA in marine invertebrates have motivated investigations of the distribution patterns of plasmalogens (21) and NMI FA among different organs (22). Unfortunately, analysis of plasmalogens and NMI FA were always conducted separately, and speculations on the putative biological functions of these membrane components were never related.

Because information on the composition of FA in the *sn*-2 position of molluscan plasmalogens is very scarce, or nonexistent in the case of PS plasmalogen (PSplsm), an HPLC procedure was developed to separate the plasmalogen forms of PE, PS, and PC. In the present study, the proportions and the fatty acyl chain compositions of both 1-alkenyl-2-acyl and 1,2-diacyl analogs were investigated in whole-animal extracts of *C. gigas*, *M. edulis*, and *R. philippinarum*. For the latter, the investigation was also conducted on different organs. We demonstrate that a specific association of particular FA with plasmalogen exists in these three bivalve species.

MATERIALS AND METHODS

Chemicals. Boron trifluoride (BF_3, 10% by wt in methanol) was obtained from Supelco (St. Quentin Fallavier, France). Other reagents and solvents were purchased from Merck (Darmstadt, Germany).

Sample preparation and lipid extraction. Adult *C. gigas, M. edulis,* and *R. philippinarum* were collected from the Bay of Brest during spring and summer 2001. After removing the digestive tract, whole animals of each species were pooled and homogenized with a Dangoumeau homogenizer at –180°C. Samples were analyzed in triplicates of three pooled individuals for the three species. Also, the mantle, foot, siphon, gills, and adductor muscle of *R. philippinarum* were excised, pooled, weighed, and homogenized as above (triplicate of three pooled individuals). Lipid extraction was conducted on tissue homogenates according to the method described by Folch *et al.* (23). To ensure the complete extraction of tissue lipids, a solvent-to-tissue ratio of 70:1 was used as described by Nelson (24). After removing the organic phase, the residue was washed with a mixture of $CHCl_3$/MeOH (2:1, vol/vol) to exclude any solvent retention. The final extract was stored at –20°C under nitrogen after 0.01 wt% BHT (antioxidant) was added.

Separation of polar lipids on a silica gel microcolumn. An aliquot of the lipid extracts was evaporated to dryness, and lipids were recovered with three washings of 500 µL of $CHCl_3$/MeOH (98:2, vol/vol) and deposited at the top of a silica gel microcolumn (30 × 5 mm i.d., packed with Kieselgel 60; 70–230 mesh, Merck) previously heated at 450°C and deactivated with 6 wt% H_2O (25). Neutral lipids were eluted with 10 mL of $CHCl_3$/MeOH (98:2, vol/vol). The polar lipid fraction was recovered with 20 mL of MeOH and stored at –20°C. An aliquot of this fraction was taken for the direct determination of the total GPL FA composition by GC; the rest was used for GPL class separations by HPLC and their FA composition analysis.

Separation of phospholipid classes and FA analysis. Separation of the GPL classes and subclasses was achieved using a combination of two successive HPLC separations with two different mobile phases.

(i) Non acid HPLC separation. A rapid gradient elution separation was achieved, based on a method previously described by Soudant *et al.* (26), on a Merck HPLC system (UV detection at 206 nm) equipped with a Diol phase column (OH-bound silica gel column, Lichrosorb Diol 5 µm, 250 × 4 mm i.d.; Merck). The former method was modified as follows: The initial mobile phase was an isocratic 9:1 ratio of solvent A (*n*-hexane/2-propanol/water, 40:52:1, by vol) and solvent B (*n*-hexane/2-propanol/water, 40:52:8, by vol) run for 11 min. This solvent ratio was then followed by a 1-min linear gradient to 100% solvent B. The column was maintained on solvent B for 18 min to complete the separation, then finally reactivated with 20 min of the initial 9:1 ratio of solvent A to B. The solvent flow rate was 1 mL/min during the entire elution program. This separation allowed the collection of a first fraction (within 3–19 min) containing PE (diacyl + plasmalogen form) and PC (diacyl + plasmalogen form), and a second fraction (within 19–25 min) containing cardiolipin (CL), PI, lysophosphatidylcholine (LysoPC), and PS (diacyl + plasmalogen form).

(ii) Acidic HPLC separations (Fig. 1). First and second fractions were treated separately. After evaporation to dryness under nitrogen, each fraction was recovered with two washings of 50 µL each of $CHCl_3$/MeOH (98:2, vol/vol) before being manually injected in the 200-µL loop of the second HPLC system. The separation was achieved as previously described (27). This method, based on the use of an acidic mobile phase, allows the hydrolysis of the vinyl ether bond at the *sn*-1 position of the glycerol backbone of the plasmalogen forms (10) and

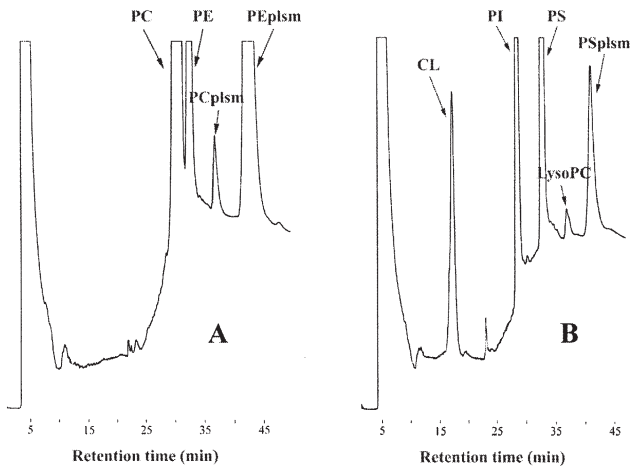

FIG. 1. Further acidic HPLC separations of the glycerophospholipid classes and subclasses. The two fractions (A) and (B) were obtained by a previous non acidic HPLC separation (not represented). Chromatographic conditions and properties for non acidic and acidic HPLC separations are indicated in the Materials and Methods section. PC and PE: phosphatidylcholine and phosphatidylethanolamine diacyl forms; PCplsm and PEplsm, phosphatidylcholine and phosphatidylethanolamine plasmalogen forms; CL: cardiolipin; PI: phosphatidylinositol; LysoPC: naturally occuring lysophosphatidylcholine; PS: phosphatidylserine diacyl form; PSplsm: phosphatidylserine plasmalogen form.

creates lyso analogs that elute later than the intact diacyl forms. This offers the possibility of analyzing separately diacyl and plasmalogen subclasses of PE and PC from the first fraction and diacyl and plasmalogen subclasses of PS from the second fraction. Each PS, PE, and PC subclass, jointly with CL, PI, and LysoPC, was collected and, after transesterification ($MeOH/BF_3$), analyzed by GC for FA composition. FA were expressed as molar percentages of the total FA content of each class or subclass. For PEplsm, PSplsm, and PCplsm subclasses, the total percentage was adjusted to 50% to take into account the alkenyl chains of the *sn*-1 position hydrolyzed by the acid mobile phase. The quantities of each class and subclass of GPL were determined from their respective quantitative spectrum of FA obtained by GC. To obtain the molar content of each analyzed fraction, a corrective factor was applied to their respective total FA molar contents: ×1 for the PSplsm, PEplsm, and PCplsm fractions and for the natural LysoPC fraction; ×1/2 for the PE-, PC-, PS-, and PI-diacyl fractions, and ×1/4 for the CL fraction.

RESULTS

Contents of plasmalogen and diacyl PE, PS, and PC in C. gigas, M. edulis, *and* R. philippinarum. PEplsm and PCdiacyl were the two major subclasses and accounted for two-thirds of the total GPL of *C. gigas*, *R. philippinarum,* and *M. edulis* (Table 1). The PSplsm, PSdiacyl, PEdiacyl, and PCplsm subclasses, together with PI, LysoPC, and CL, constituted the other third. The PEplsm subclass was more prominent than the PE-diacyl subclass, accounting for most of the PE (77.8 to 85%), whereas the PCplsm constituted only 3.1 to 10.9% of PC. The PS class contained plasmalogen and diacyl forms in similar proportions, with PSplsm accounting for 43.4, 44.8, and 66.4% of total PS in *C. gigas, R. philippinarum,* and *M. edulis,* respectively (Table 1). The same general features were also observed in the different organs isolated from the *R. philippinarum* (Table 1). Nevertheless, the proportions of plasmalogens in PS, PE, and PC varied according to the organs. PEplsm, PSplsm, and PCplsm proportions ranged, respectively, from 66.1, 28.9, and 5 in the muscle to 85.6, 67.2, and 14.6% in gills (Table 1). The sum of the plasmalogen subclasses (PSplsm + PEplsm + PCplsm) was found to reach a mean value of 41.4% of the GPL of the three species when analyzed as whole animal. Analysis of *R. philippinarum* organs indicated that the sum of plasmalogen subclasses ranged from a minimum of 28.4% in muscle to a maximum of 52.1% in gills (Table 1).

FA composition of the plasmalogen and diacyl forms of PE, PS, and PC. In the three bivalve species analyzed as whole-animal extract, the total saturated FA (SFA) ranged between 34 and 47.6% in the diacyl fractions of PS, PE, and PC. SFA content was found to be very low in PEplsm and PSplsm (<2.5 and <7%, respectively; Tables 2 and 3) and slightly higher in PC-plsm (from 12.1 to 18.1% of the total FA; Table 4). The 16:0 and 18:0 acids were generally predominant in the SFA of all fractions. The MUFA content was lower in PEplsm and PC-plsm than in their respective diacyl forms for the three species (Tables 2 and 4). However, the MUFA content was lower in the PSplsm compared to the PSdiacyl only for *M. edulis* (Table 3). The 20:1n-11 FA was the main MUFA of PSplsm and of PE-plsm, accounting, respectively, for 55 to 79.2% and 41.5 to 60.9% of the total MUFA in the three species analyzed as whole animal (Tables 2 and 3). No such specific association was observed for PCplsm (Table 4). The variation of 20:1n-11 content in PS, PE, and PC subclasses followed a similar pattern in all organs analyzed from *R. philippinarum* (Fig. 2). The characteristic 20:1n-11 enrichment of the PSplsm MUFA was observed in all organs. The lowest percentage was measured in muscle and the highest percentages in mantle and gills (Fig. 2). In addition, while maintaining such a specificity, the GPL content of 20:1n-11 in organs ranged from a higher value in gills (4%) to a lower value in muscle (1.7%) (Table 5).

TABLE 1
Composition of Glycerophospholipids[a] and Plasmalogen Content of PE, PS, and PC Classes in the Whole Body of *Crassostrea gigas, Mytilus edulis,* and *Ruditapes philippinarum* and in Separated Organs from *R. philippinarum*

	Glycerophospholipid composition (mol%)[a]							
	Whole body			Organs				
	C. gigas	*M. edulis*	*R. philippinarum*	Mantle	Foot	Siphon	Gills	Muscle
PEdiacyl	5.8 ± 0.9	8.0 ± 1.0	8.1 ± 0.2	8.0 ± 1.2	8.8 ± 0.1	6.9 ± 0.5	6.1 ± 0.4	11.3 ± 0.7
PEplsm	33.6 ± 4.7	28.1 ± 1.5	31.5 ± 2.0	30.7 ± 2.2	35.1 ± 0.8	31.6 ± 1.9	36.5 ± 2.8	22.1 ± 2.6
PSdiacyl	7.2 ± 0.6	4.8 ± 1.3	8.5 ± 2.0	9.2 ± 1.1	7.2 ± 1.7	11.7 ± 2.1	5.3 ± 2.0	9.8 ± 3.0
PSplsm	5.8 ± 2.2	9.5 ± 1.8	6.9 ± 1.7	6.3 ± 2.3	5.9 ± 1.9	7.2 ± 2.5	10.6 ± 0.5	4.0 ± 1.1
PCdiacyl	36.5 ± 2.4	40.5 ± 1.7	33.9 ± 1.8	33.1 ± 0.1	33.5 ± 3.8	30.4 ± 2.5	28.9 ± 2.9	42.0 ± 5.1
PCplsm	4.7 ± 0.7	1.3 ± 0.5	2.8 ± 0.7	2.9 ± 0.7	1.9 ± 0.7	2.5 ± 0.4	5.0 ± 2.4	2.3 ± 0.8
PI	5.5 ± 1.7	5.3 ± 1.4	5.8 ± 0.9	6.9 ± 0.7	4.9 ± 1.5	6.5 ± 0.8	4.9 ± 0.3	6.6 ± 0.4
CL	1.1 ± 0.2	1.3 ± 0.8	0.9 ± 0.2	1.0 ± 0.4	1.3 ± 0.1	1.0 ± 0.2	0.8 ± 0.2	0.6 ± 0.2
LysoPC	2.2 ± 1	2.5 ± 0.9	1.7 ± 0.1	1.9 ± 0.5	1.3 ± 0.2	2.2 ± 0.1	1.9 ± 0.7	1.3 ± 0
Total plasmalogen	44.1	38.9	41.2	39.9	42.9	41.3	52.1	28.4
Plasmalogen content of the class[b]								
PE	85.0 ± 3.8	77.8 ± 1.3	79.6 ± 0.6	79.4 ± 1.2	80.0 ± 0.3	82.1 ± 2.0	85.6 ± 1.7	66.1 ± 4.1
PS	43.3 ± 11.9	66.4 ± 10.4	44.8 ± 0.3	39.9 ± 6.2	44.8 ± 2.2	37.6 ± 4.2	67.2 ± 7.6	28.9 ± 0.8
PC	10.9 ± 2.1	3.1 ± 1.3	7.5 ± 1.3	7.9 ± 1.9	5.2 ± 1.5	7.5 ± 0.3	14.6 ± 7.4	5.0 ± 1.2

[a]Expressed as mol% of total moles of glycerophospholipids, calculated as indicated in the Materials and Methods section. Results are mean ± SD (n = 3).
[b]Ratio (in %) of the plasmalogen form to the diacyl + plasmalogen forms of a class.

TABLE 2
FA Composition of PEdiacyl and PEplsm in the Whole Animals *C. gigas, M. edulis*, and *R. philippinarum*[a]

	C. gigas		*M. edulis*		*R. philippinarum*	
FA	Diacyl[b]	Plsm[c]	Diacyl	Plsm	Diacyl	Plsm
Branched[d]	2.2 ± 0.3	0.2 ± 0.1	1.2 ± 0.1	0.1 ± 0.0	7.4 ± 0.8	1.0 ± 0.2
14:0	0.8 ± 0.4	0.1 ± 0.1	0.8 ± 0.1	0.1 ± 0.1	0.6 ± 0.0	0.0 ± 0.0
15:0	0.6 ± 0.2	0.1 ± 0.0	0.4 ± 0.0	0.0 ± 0.0	0.3 ± 0.0	0.0 ± 0.0
16:0	13.6 ± 0.2	1.2 ± 0.2	12.5 ± 0.5	0.6 ± 0.2	8.0 ± 0.0	0.7 ± 0.1
17:0	3.2 ± 0.7	0.2 ± 0.0	2.8 ± 0.2	0.1 ± 0.0	2.5 ± 0.1	0.2 ± 0.0
18:0	19.4 ± 3.5	0.8 ± 0.1	17.6 ± 1.0	0.6 ± 0.1	15.0 ± 2.4	0.4 ± 0.0
16:1n-7	0.7 ± 0.1	0.1 ± 0.1	1.2 ± 0.8	0.5 ± 0.2	3.0 ± 0.1	0.8 ± 0.1
18:1n-9	2.2 ± 1.7	0.3 ± 0.2	1.2 ± 0.2	0.2 ± 0.0	4.8 ± 0.7	1.8 ± 0.4
18:1n-7	3.3 ± 1.2	0.3 ± 0.2	3.4 ± 0.6	0.2 ± 0.0	1.8 ± 0.1	0.2 ± 0.0
20:1n-11	1.5 ± 0.0	2.8 ± 0.1	0.8 ± 0.1	1.7 ± 0.0	3.6 ± 0.6	3.1 ± 0.3
20:1n-9	0.8 ± 0.1	0.3 ± 0.0	4.0 ± 0.3	1.2 ± 0.0	2.6 ± 0.3	0.7 ± 0.0
20:1n-7	4.4 ± 0.1	0.6 ± 0.1	1.3 ± 0.1	0.3 ± 0.0	5.2 ± 1.0	0.4 ± 0.0
18:3n-3	0.7 ± 0.1	0.2 ± 0.0	1.4 ± 0.0	0.3 ± 0.0	0.3 ± 0.2	0.1 ± 0.0
18:4n-3	0.6 ± 0.2	0.3 ± 0.0	1.0 ± 0.0	0.1 ± 0.0	0.3 ± 0.2	0.1 ± 0.1
20:2NMI(5,11)	0.0 ± 0.0	0.2 ± 0.1	1.4 ± 0.2	7.0 ± 0.2	0.1 ± 0.0	0.1 ± 0.0
20:2NMI(5,13)	0.4 ± 0.0	0.3 ± 0.0	0.4 ± 0.1	2.9 ± 0.1	0.2 ± 0.0	0.1 ± 0.0
20:4n-6	5.6 ± 0.5	1.3 ± 0.1	2.6 ± 0.3	2.5 ± 0.2	5.0 ± 0.1	1.0 ± 0.0
20:5n-3	23.9 ± 0.6	9.3 ± 0.1	22.9 ± 0.6	17.2 ± 0.6	5.3 ± 0.4	2.1 ± 0.2
22:2NMI(7,13)	0.6 ± 0.0	1.9 ± 0.0	0.2 ± 0.0	0.9 ± 0.2	1.4 ± 0.1	3.7 ± 0.3
22:2NMI(7,15)	4.6 ± 0.5	9.2 ± 0.2	1.0 ± 0.0	3.5 ± 0.4	3.8 ± 0.2	10.2 ± 0.3
22:3NMI(7,13.16)	0.2 ± 0.0	0.5 ± 0.0	0.3 ± 0.0	1.4 ± 0.1	0.5 ± 0.1	1.6 ± 0.2
22:4n-6	0.4 ± 0.1	0.9 ± 0.0	0.3 ± 0.1	0.7 ± 0.1	2.2 ± 0.1	4.3 ± 0.1
22:5n-6	0.3 ± 0.0	0.8 ± 0.0	0.3 ± 0.0	0.4 ± 0.0	1.1 ± 0.0	1.4 ± 0.1
22:5n-3	1.1 ± 0.2	2.9 ± 0.1	0.9 ± 0.1	1.6 ± 0.0	3.0 ± 0.0	4.4 ± 0.1
22:6n-3	6.9 ± 0.6	14.4 ± 0.6	18.5 ± 0.8	5.3 ± 0.4	17.1 ± 0.8	8.9 ± 0.6
Others[e]	1.4 ± 0.8	0.8 ± 0.2	1.5 ± 0.6	0.5 ± 0.4	4.2 ± 0.7	2.4 ± 0.3
Total NMI	5.7 ± 0.5	12.1 ± 0.3	3.3 ± 0.1	15.7 ± 0.4	6.0 ± 0.0	15.8 ± 0.3
Total SFA	40.3 ± 3.3	2.5 ± 0.6	35.3 ± 0.9	1.4 ± 0.0	34.0 ± 1.7	2.3 ± 0.3
Total MUFA	13.0 ± 3.2	4.6 ± 0.5	12.0 ± 1.3	4.1 ± 0.3	22.4 ± 2.9	7.3 ± 0.8
Total PUFA	46.7 ± 0.1	42.9 ± 1.0	52.7 ± 0.5	44.5 ± 0.4	43.6 ± 1.2	40.3 ± 1.1

[a]Results expressed as mol% are mean ± SD (n = 3). For abbreviations see Table 1.
[b]"Diacyl" refers to both *sn*-1 and *sn*-2 fatty acyl chains of the diacyl form.
[c]"Plsm" refers to *sn*-2 fatty acyl chains of the plasmalogen form; the total percentage was adjusted to 50% to take into account the alkenyl chains of the *sn*-1 position hydrolyzed by the acid mobile phase as described in Materials and Methods section.
[d]Branched-chain FA (mainly 15:0 and 17:0 iso and anteiso).
[e]Total of 11 FA detectable (16:1n-5, 18:1n-5, 18:2n-6, 18:2n-4, 18:3n-6, 18:3n-4, 20:2n-6, 20:3n-6, 20:4n-3, 21:4n-6, and 21:5n-3, none of which was more than 1.0% in any subclasses).

Long-chain PUFA with 20 and 22 carbons were found to be the dominant PUFA in the plasmalogen and diacyl fractions. They were principally constituted by NMI FA as well as 22:6n-3, 20:5n-3, and 20:4n-6. The different NMI FA were the 20:2 NMI (5,13-20:2 and 5,11-20:2) and the 22:2 NMI (7,15-22:2 and 7,13-22:2). Low levels of 22:3 NMI (7,13,16-22:3) were also detected in the FA of the three bivalves. Considering the sum of these NMI FA (ΣNMI), *C. gigas, M. edulis*, and *R. philippinarum* showed a high percentage of ΣNMI in PSplsm (12.7, 20.2, and 20.3% of the total FA, respectively) and in PEplsm (12.1, 15.7, and 15.8% of the total FA, respectively). ΣNMI in PSplsm and PEplsm were generally higher than those measured, respectively, in PSdiacyl and PEdiacyl, except in the PS of *C. gigas,* where it reached 13.9% of total FA in PSdiacyl (Tables 2 and 3). The predominant NMI FA was the 7,15-22:2 isomer, which was the major PUFA of PSplsm in the three species. *Mytilus edulis* plasmalogens also contained a high proportion of 20:2 NMI, these isomers being predominantly localized in PEplsm (Table 2). In *R. philippinarum* organs, as in the whole body of the three bivalves, the three plasmalogen subclasses showed a specific association with ΣNMI when compared to their diacyl analogs (Fig 3). This specificity was especially important in PSplsm and PEplsm and to a lesser extent in PCplsm. Such specificity was maintained, whereas the content of ΣNMI in GPL ranged from a higher value in gills (16.1%) to a lower value in muscle (4.3%). As in the whole body, the predominant NMI of *R. philippinarum* organs was the 7,15-22:2 isomer, along with minor amounts of 7,13-22:2; the ratio of these two FA was unchanged whatever the organ (data not shown).

DISCUSSION

Importance of plasmalogen subclasses. Plasmalogens constituted a high proportion of GPL, in *C. gigas*, *R. philippinarum,*

TABLE 3
FA Composition of PSdiacyl and PSplsm in the Whole Animals *C. gigas, M. edulis*, and *R. philippinarum*[a]

	C. gigas		*M. edulis*		*R. philippinarum*	
FA	Diacyl[b]	Plsm[c]	Diacyl	Plsm	Diacyl	Plsm
Branched[d]	1.1 ± 0.3	0.2 ± 0.1	1.2 ± 0.0	0.3 ± 0.0	2.3 ± 0.2	0.5 ± 0.1
14:0	0.3 ± 0.0	0.2 ± 0.0	0.3 ± 0.0	0.4 ± 0.0	0.1 ± 0.0	0.0 ± 0.1
15:0	0.2 ± 0.0	0.1 ± 0.1	0.0 ± 0.0	0.1 ± 0.0	0.0 ± 0.0	0.0 ± 0.0
16:0	5.2 ± 0.4	2.8 ± 0.8	8.7 ± 2.9	2.7 ± 0.6	5.2 ± 0.9	1.5 ± 0.2
17:0	2.6 ± 0.5	0.6 ± 0.2	4.1 ± 0.3	0.2 ± 0.0	3.6 ± 0.2	0.3 ± 0.0
18:0	32.0 ± 5.0	3.1 ± 0.3	26.4 ± 0.8	1.8 ± 1.1	36.1 ± 0.6	2.3 ± 0.3
16:1n-7	0.1 ± 0.1	0.1 ± 0.1	0.9 ± 0.0	0.4 ± 0.0	0.8 ± 0.0	0.2 ± 0.0
18:1n-9	0.8 ± 0.7	0.3 ± 0.2	0.7 ± 0.0	0.1 ± 0.0	1.8 ± 0.4	0.5 ± 0.1
18:1n-7	1.3 ± 0.8	0.5 ± 0.5	1.9 ± 0.0	0.2 ± 0.0	0.7 ± 0.1	0.1 ± 0.0
20:1n-11	4.6 ± 0.4	12.5 ± 1.9	0.7 ± 0.1	2.5 ± 0.1	2.2 ± 0.1	8.4 ± 0.2
20:1n-9	0.8 ± 0.1	1.5 ± 1.4	5.8 ± 1.6	1.0 ± 0.1	0.7 ± 0.1	0.6 ± 0.1
20:1n-7	7.2 ± 1.8	1.3 ± 0.6	1.0 ± 0.5	0.2 ± 0.0	1.0 ± 0.1	0.3 ± 0.0
18:3n-3	0.3 ± 0.0	0.0 ± 0.1	1.0 ± 0.0	0.1 ± 0.0	0.1 ± 0.2	0.0 ± 0.0
18:4n-3	0.1 ± 0.2	0.1 ± 0.1	0.5 ± 0.0	0.1 ± 0.0	0.1 ± 0.1	0.0 ± 0.0
20:2NMI(5,11)	0.1 ± 0.1	0.1 ± 0.0	1.0 ± 0.0	2.1 ± 0.1	0.1 ± 0.1	0.1 ± 0.0
20:2NMI(5,13)	0.3 ± 0.2	0.2 ± 0.1	0.5 ± 0.0	0.9 ± 0.1	0.1 ± 0.0	0.1 ± 0.0
20:4n-6	5.7 ± 0.3	1.2 ± 0.3	2.3 ± 0.6	1.2 ± 0.0	5.5 ± 0.4	0.9 ± 0.1
20:5n-3	20.1 ± 1.4	4.7 ± 0.2	8.1 ± 0.6	6.2 ± 0.6	5.7 ± 0.0	1.0 ± 0.1
22:2NMI(7,13)	1.8 ± 0.1	2.2 ± 0.0	0.4 ± 0.0	1.2 ± 0.1	1.5 ± 0.0	6.1 ± 0.2
22:2NMI(7,15)	11.6 ± 1.2	10.1 ± 2.6	6.0 ± 0.0	14.9 ± 4.0	4.6 ± 0.3	13.6 ± 0.8
22:3NMI(7,13,16)	0.1 ± 0.0	0.2 ± 0.1	0.5 ± 0.0	1.1 ± 0.1	0.2 ± 0.1	0.5 ± 0.2
22:4n-6	0.2 ± 0.1	0.5 ± 0.1	0.4 ± 0.0	0.7 ± 0.1	2.0 ± 0.0	1.9 ± 0.0
22:5n-6	0.2 ± 0.0	0.5 ± 0.2	0.6 ± 0.0	0.7 ± 0.1	1.2 ± 0.0	1.5 ± 0.0
22:5n-3	0.4 ± 0.2	1.1 ± 0.1	1.5 ± 0.2	1.7 ± 0.2	3.5 ± 0.1	1.6 ± 0.1
22:6n-3	2.4 ± 0.7	5.7 ± 1.1	23.9 ± 0.1	8.6 ± 2.1	18.3 ± 0.6	6.4 ± 0.2
Others[e]	0.3 ± 0.3	0.2 ± 0.1	1.5 ± 0.1	0.4 ± 0.0	2.0 ± 0.5	1.1 ± 0.2
Total NMI	13.9 ± 1.1	12.7 ± 2.7	8.4 ± 0.1	20.2 ± 4.2	6.5 ± 0.3	20.3 ± 0.8
Total SFA	41.8 ± 5.3	7.0 ± 0.4	40.8 ± 3.9	5.5 ± 1.6	47.6 ± 0.2	4.7 ± 0.6
Total MUFA	14.8 ± 3.2	16.4 ± 1.9	11.0 ± 2.3	4.5 ± 0.1	7.5 ± 0.9	10.6 ± 0.0
Total PUFA	43.4 ± 2.1	26.6 ± 1.5	48.1 ± 1.6	40.0 ± 1.5	44.9 ± 0.7	34.6 ± 0.6

[a–f]For footnotes see Table 2.

and *M. edulis*. Plasmalogens were found in especially high proportions in PE (>78%) and in fairly low proportions in PC (<11%). Although PSplsm was a minor GPL component (about 7% of the total GPL), it represented an important part of PS, ranging from 45% in *C. gigas* and *R. philippinarum* to 67% in *M. edulis.* These results were in good agreement with those first reported on 14 bivalve species by Dembitsky and Vaskovsky (8) and those reported on *C. gigas* (59.8% of PEplsm in PE and 7.2% of PCplsm in PC) by Koizumi *et al.* (14).

FA composition of plasmalogen subclasses. A new combination of two HPLC separations allowed the analysis of the FA profile of the different GPL classes and subclasses in three bivalve species. To date, very little information is available on the FA composition of plasmalogen subclasses from marine bivalves. Only two studies described the FA composition of PEplsm and PCplsm of *C. gigas* (14,15), but the FA composition of the PSplsm has never been studied. To the best of our knowledge, the present study represents the first comprehensive report on the FA composition of the PS plasmalogen subclass in marine bivalves and, in fact, in marine mollusks as well. The FA pattern of PSplsm clearly showed a high specificity for NMI FA and 20:1n-11, and this characteristic was very consistent in the three bivalve species analyzed. The 7,15-22:2 isomer, a NMI FA, was the main PUFA encountered in the PSplsm subclass. Although present in a smaller proportion than the 7,15-22:2, the 7,13-22:2 isomer also showed also a specific association with the PSplsm compared to the PSdiacyl form. The other noticeable point was the very high percentage of 20:1n-11, accounting for more than half of the MUFA in PSplsm. Compared to the FA composition of PSplsm, the composition of PEplsm presents a lower but significant specificity for NMI FA and 20:1n-11, whereas in PCplsm these FA are present only as traces. Koizumi *et al*. (14) also indicated that, in *C. gigas*, most of the 22:2 NMI occurred in PEplsm. Although their results clearly showed the specific presence of 20:1n-11 in the PEplsm, this characteristic had not been discussed. In the erythrocyte membrane of the marine bivalve *S. broughtoni* (28), taking into account the corrections published later (29), the high concentrations of 22:2 NMI found in PE and PS were both demonstrated to be constituted mainly by the plasmalogen form. In mollusk and mammalian erythrocytes, the aminoglycerophospholipids (PE and PS) are primarily localized in the inner layer of the membrane (28,30). Since additional evidence is available for such asymmetry of phospholipids in other biomembranes (30), one may conclude that NMI and 20:1n-11

TABLE 4
FA Composition of PCdiacyl and PCplsm in the Whole Animals *C. gigas, M. edulis,* and *R. philippinarum*[a]

	C. gigas		*M. edulis*		*R. philippinarum*	
FA	Diacyl[b]	Plsm[c]	Diacyl	Plsm	Diacyl	Plsm
Branched[d]	1.6 ± 0.1	1.2 ± 0.0	1.5 ± 0.4	0.9 ± 0.5	4.1 ± 0.1	2.3 ± 0.1
14:0	2.7 ± 0.4	0.7 ± 0.1	2.4 ± 0.2	1.5 ± 1.2	1.1 ± 0.2	0.2 ± 0.0
15:0	1.9 ± 0.2	0.7 ± 0.1	1.1 ± 0.1	0.2 ± 0.2	1.0 ± 0.0	0.2 ± 0.0
16:0	24.0 ± 2.3	7.4 ± 0.7	25.0 ± 1.0	9.8 ± 4.7	22.1 ± 0.8	5.1 ± 0.7
17:0	1.6 ± 0.2	0.8 ± 0.0	1.1 ± 0.0	1.1 ± 0.6	1.8 ± 0.1	0.6 ± 0.0
18:0	3.8 ± 0.0	2.7 ± 0.0	3.1 ± 0.1	4.6 ± 1.7	4.4 ± 0.0	3.5 ± 0.3
16:1n-7	2.2 ± 0.1	0.7 ± 0.0	3.1 ± 0.8	0.7 ± 1.0	3.3 ± 0.4	0.8 ± 0.0
18:1n-9	3.7 ± 0.1	1.8 ± 0.0	1.7 ± 0.1	0.9 ± 0.3	5.0 ± 0.3	2.0 ± 0.0
18:1n-7	8.1 ± 0.5	2.2 ± 0.3	3.4 ± 0.4	0.5 ± 0.8	1.9 ± 0.1	0.4 ± 0.0
20:1n-11	0.8 ± 0.1	0.9 ± 0.1	0.3 ± 0.0	0.6 ± 0.2	0.6 ± 0.1	1.3 ± 0.2
20:1n-9	0.6 ± 0.0	0.2 ± 0.0	2.7 ± 0.4	1.0 ± 0.0	0.6 ± 0.1	0.4 ± 0.1
20:1n-7	3.1 ± 0.5	1.1 ± 0.1	0.9 ± 0.2	0.5 ± 0.1	0.9 ± 0.2	1.0 ± 0.1
18:3n-3	1.5 ± 0.1	0.8 ± 0.1	1.6 ± 0.1	0.3 ± 0.4	0.2 ± 0.0	0.0 ± 0.0
18:4n-3	2.0 ± 0.2	1.0 ± 0.2	2.5 ± 0.2	0.5 ± 0.6	0.9 ± 0.1	0.4 ± 0.2
20:2NMI(5.11)	0.1 ± 0.0	0.0 ± 0.0	0.4 ± 0.0	1.1 ± 0.6	0.0 ± 0.0	0.0 ± 0.0
20:2NMI(5.13)	0.6 ± 0.1	0.2 ± 0.0	0.2 ± 0.0	0.6 ± 0.2	0.1 ± 0.0	0.1 ± 0.1
20:4n-6	4.7 ± 0.2	2.4 ± 0.0	2.2 ± 0.4	1.8 ± 0.2	3.9 ± 0.1	1.5 ± 0.0
20:5n-3	17.9 ± 1.2	10.1 ± 0.5	19.3 ± 0.1	11.3 ± 1.7	8.5 ± 0.4	2.5 ± 0.2
22:2NMI(7,13)	0.2 ± 0.0	0.3 ± 0.0	0.1 ± 0.0	0.1 ± 0.0	0.3 ± 0.0	1.0 ± 0.0
22:2NMI(7,15)	1.9 ± 0.1	2.0 ± 0.1	0.6 ± 0.0	0.8 ± 0.2	0.7 ± 0.0	2.5 ± 0.1
22:3NMI(7,13,16)	0.0 ± 0.0	0.0 ± 0.0	0.3 ± 0.0	0.1 ± 0.1	0.2 ± 0.0	0.3 ± 0.0
22:4n-6	0.3 ± 0.0	0.3 ± 0.0	0.2 ± 0.0	0.1 ± 0.1	2.8 ± 0.3	2.5 ± 0.4
22:5n-6	0.4 ± 0.0	0.3 ± 0.0	0.2 ± 0.0	0.1 ± 0.2	1.5 ± 0.0	1.1 ± 0.1
22:5n-3	1.4 ± 0.0	1.2 ± 0.1	1.9 ± 0.0	1.2 ± 0.3	5.0 ± 0.2	3.3 ± 0.3
22:6n-3	10.3 ± 0.1	8.9 ± 0.6	20.3 ± 1.3	9.4 ± 1.1	24.7 ± 0.7	14.5 ± 0.1
Others[e]	3.5 ± 0.6	2.2 ± 0.3	3.1 ± 0.3	0.4 ± 0.6	3.9 ± 0.5	1.7 ± 0.6
Total NMI	2.9 ± 0.1	2.4 ± 0.1	1.9 ± 0.1	2.7 ± 0.7	1.4 ± 0.1	3.8 ± 0.2
Total SFA	35.9 ± 3.3	13.6 ± 0.5	34.1 ± 0.8	18.1 ± 1.0	34.6 ± 0.5	12.1 ± 0.5
Total MUFA	19.4 ± 1.5	6.9 ± 0.1	12.9 ± 1.7	4.2 ± 1.2	13.2 ± 0.5	6.7 ± 0.7
Total PUFA	44.7 ± 1.8	29.5 ± 0.4	52.9 ± 1.0	27.7 ± 2.2	52.3 ± 1.0	31.2 ± 0.2

[a–f]For footnotes see Table 2.

FA also are asymmetrically distributed in the lipid bilayer and involved in specific cellular functions of the inner membrane.

The most striking results were that plasmalogen and diacyl subclasses of PS and PE can be distinguished according to the origin of their unsaturated FA. The 22:6n-3, 20:5n-3, and 20:4n-6, which were the predominant FA of the PSdiacyl and PEdiacyl, originate mainly from the phytoplanktonic diet of bivalves. Indeed, bivalves have a limited or total inability to synthesize 20–22-carbon PUFA with more than three double bonds (31,32). On the other hand, the NMI FA, which were the predominant PUFA of the PSplsm, are synthesized *de novo* by bivalves, as first proposed by Ackman and Hooper (16) and demonstrated by Zhukova (19,20). The pathway consists of a Δ9 desaturation and elongation of 16:0 and 18:0, respectively, into 20:1n-7 and 20:1n-9. A C_{20}Δ5 desaturation converts them, respectively, into 5,13-20:2 and 5,11-20:2, which are finally elongated, respectively, into 7,15-22:2 and 7,13-22:2. Similarly, 20:1n-11, found only as traces in microalgae (33), could also be of endogenous origin, although there is no demonstration of that in the literature. Only a few studies have indicated the presence of a high concentration of 20:1n-11 in bivalves (34,35). It might be possible that a Δ9 desaturase acting on 20:0 produces 20:1n-11 in the same way as Δ9 desaturase(s) acting on 16:0 and 18:0 produce the two precursors 20:1n-7 and 20:1n-9. Unlike these NMI precursors, 20:1n-11 did not appear to be subjected to further Δ5 desaturation, suggesting the C_{20}Δ5 desaturase may be "Δ13 and Δ11 specific."

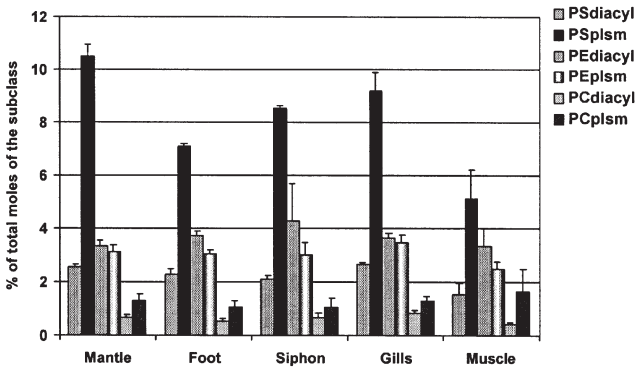

FIG. 2. Percent composition (in mol%, mean ± SD, $n = 3$) of 20:1n-11 from diacyl and plasmalogen forms of glycerophospholipid PS, PE, and PC of *Ruditapes philippinarum* organs.

TABLE 5
ΣNMI and 20:1n-11 Compositions in Organs of *R. philippinarum* (in mol% of the total FA of glycerophospholipids)

	Mantle	Foot	Siphon	Gills	Muscle
ΣNMI[a]	10.6 ± 0.2	10.9 ± 0.5	9.3 ± 0.1	16.1 ± 1.1	4.3 ± 0.8
20:1n-11	3 ± 0.1	2.8 ± 0.1	3 ± 0.2	4 ± 0.3	1.7 ± 0.1

[a]Sum of all non-methylene-interrupted FA [20:2NMI(5.11), 20:2NMI(5.13), 22:2NMI(7,13), 22:2NMI(7,15), and 22:3NMI (7.13.16)].

FA composition of plasmalogen subclasses in R. philippinarum *organs*. In marine bivalves, quantities of plasmalogens and of NMI FA vary according to organs (21,22). The FA pattern of GPL classes and subclasses of different organs of *R. philippinarum* was thus examined to assess whether the relationship between *de novo* synthesized FA and plasmalogens exists in all the organs. The specific location of NMI FA and 20:1n-11 in aminoglycerophospholipid plasmalogens was evidenced in all the organs analyzed. However, the proportions of these compounds varied according to the organ. In other words, the greater the plasmalogen content was in the organ, the higher the proportion of the biosynthesized FA was among the total FA of GPL. The highest proportions of plasmalogens, NMI FA, and 20:1n-11 were found in gills, but mantle, foot, and siphon also contained significant quantities of these compounds. The lowest proportion was found in the muscle. A previous study indicated large concentrations of 22:2 NMI FA in polar lipids isolated from gills, mantle, and foot of the hardshell clam *Mercenaria mercenaria* (22). Also, particularly high levels of 20:2 and 22:2 NMI were found in polar lipids of the gills of the mussel *M. edulis* (20). The gills and the mantle of the sea scallop *Placopecten magellanicus* (a pectinidae) exhibited consistently higher 20:1n-11 content than the muscle (35). An earlier review (21) concluded that gills have rather important proportions of plasmalogens, whereas muscle contains the lowest quantities of plasmalogens.

Although not clearly established, a number of functions already have been proposed for NMI FA and plasmalogens in marine organisms. NMI FA were supposed to confer resistance in tissues exposed most often to environmental physicochemical variations (22) or to attack by microbial lipases (37). This could explain the selectivity for NMI FA encountered in the gills, mantle, foot, and siphon of *R. philippinarum*. The high quantities of NMI FA reported in polar lipids of marine organisms also are regularly linked to a structural role in the membrane. They could be important for membrane properties such as phase transition temperature, membrane fluidity, or activity of membrane-bound proteins. However, based on conformational analysis, Rabinovich and Ripatti (38) concluded that the acyl chains with NMI double bonds are principally involved in adjusting membrane fluidity of these poikilothermic animals. The same role was proposed for acyl chains that have one *cis* double bond, as in 20:1n-11. In parallel, Chapelle (21) speculated that plasmalogens in marine animals may be metabolized to maintain cell integrity in response to environmental stresses such as temperature, pH, or salinity. One other function proposed for plasmalogens is that these ether lipids may act as antioxidative components in mammalian cells (2–4,39). In mollusks, in taking into account the asymmetry of their distribution, plasmalogens may function as scavengers of cell reactive oxygen species to protect other components in membranes from oxidative stress.

The present results provide the first evidence that aminoplasmalogens, PSplsm and PEplsm, reflect a higher selectivity for the biosynthesized FA ΣNMI and 20:1n-11 than for dietary PUFA such as 20:5n-3 and 22:6n-3. Moreover, 20:1n-11 can now be considered to be associated with or functionally equivalent to NMI FA in bivalves. The selective incorporation of ΣNMI and 20:1n-11 in PSplsm and PEplsm as well as the parallel variations of NMI FA and 20:1n-11 levels and plasmalogen contents in the different organs of *R. philippinarum* suggests the existence of possible synergistic properties of these compounds that should implicate them in the biological membrane functions of mollusks.

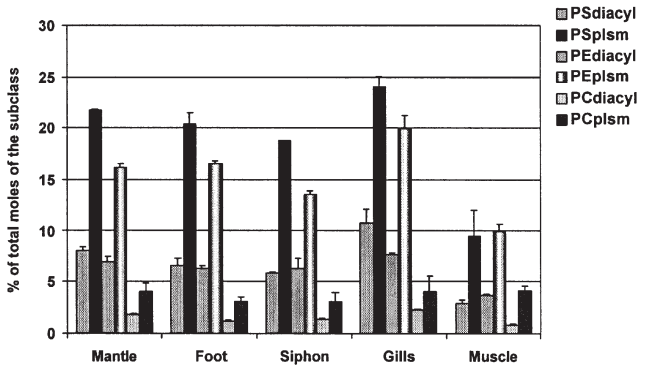

FIG. 3. Percent composition (in mol%, mean ± SD, $n = 3$) of ΣNMI from diacyl and plasmalogen forms of glycerophospholipid PS, PE, and PC of *Ruditapes philippinarum* organs. ΣNMI: sum of all non-methylene-interrupted FA, mainly 22:2NMI(7,15) with minor amounts of 22:2NMI-(7,13), 20:2NMI(5,11), 20:2NMI(5,13), and 22:3NMI(7,13,16).

ACKNOWLEDGMENTS

The authors would like to thank Dr. Aswani K. Volety, Florida Gulf Coast University (Fort Myers, FL), for English revisions. This work was supported by a grant from the Ministère de l'Education Nationale de la Recherche et de la Technologie (MENRT, Paris, France).

REFERENCES

1. Nagan, N., and Zoeller, R.A. (2001) Plasmalogens: Biosynthesis and Functions, *Prog. Lipid Res. 40*, 199–229.
2. Leray, C., Cazenave, J.-P., and Gachet, C. (2002) Platelet Phospholipids Are Differentially Protected Against Oxidative Degradation

by Plasmalogens, *Lipids 37*, 285–290.
3. Maeba, R., Sawada, Y., Shimasaki, H., Takahashi, I., and Ueta, N. (2002) Ethanolamine Plasmalogens Protect Cholesterol-Rich Liposomal Membranes from Oxidation Caused by Free Radicals, *Chem. Phys. Lipids 120*, 145–151.
4. Maeba, R., and Ueta, N. (2003) Ethanolamine Plasmalogen and Cholesterol Reduce the Total Membrane Oxidizability Measured by the Oxygen Uptake Method, *Biochem. Biophys. Commun. Res. 302*, 265–270.
5. Sargent, J.R. (1987) Ether-Linked Glycerides in Marine Animals, in *Marine Biogenic Lipids, Fats, and Oils* (Ackman, R.G., ed.), pp. 176–193, CRC Press, Boca Raton, FL.
6. Joseph, J.D. (1982) Lipid Composition of Marine and Estuarine Invertebrates. Part II: Mollusca, *Prog. Lipid Res. 21*, 109–153.
7. Schrakamp, G., Schutgens, R.B.H., Schalkwijk, C.G., and Van Den Bosch, H. (1991) Comparative Studies on Plasmalogen Biosynthesis in Rat Brain Homogenates and Isolated Oligodendroglial Cells During Development, *Brain Dysfunct. 4*, 217–227.
8. Dembitsky, V.M., and Vaskovsky, V.E. (1976) Distribution of Plasmalogens in Different Classes of Phospholipids of Marine Invertebrates, *Biol. Morya (Kiev) 5*, 68–72.
9. Dembitsky, V.M. (1979) Plasmalogens in Phospholipids of Marine Invertebrates, *Biol. Morya (Kiev) 5*, 86–90.
10. Soudant, P., Marty, Y., Moal, J., and Samain, J.F. (1995) Separation of Major Polar Lipids in *Pecten maximus* by High-Performance Liquid Chromatography and Subsequent Determination of Their Fatty Acids Using Gas Chromatography, *J. Chromatogr. B 673*, 15–26.
11. Soudant, P., Moal, J., Marty, Y., and Samain, J.F. (1996) Impact of the Quality of Dietary Fatty Acids on Metabolism and the Composition of Polar Lipid Classes in Female Gonads of *Pecten maximus* (L.), *J. Exp. Mar. Biol. Ecol. 205*, 149–163.
12. Soudant, P., Moal, J., Marty, Y., and Samain, J.F. (1997) Composition of Polar Lipid Classes in Male Gonads of *Pecten maximus* (L.). Effect of Nutrition, *J. Exp. Mar. Biol. Ecol. 215*, 103–114.
13. Soudant, P., Marty, Y., Moal, J., Masski, H., and Samain, J.F. (1998) Fatty Acid Composition of Polar Lipid Classes During Larval Development of Scallop *Pecten maximus* (L.), *Comp. Biochem. Phys. A 121*, 279–288.
14. Koizumi, C., Jeong, B.Y., and Ohshima, T. (1990) Fatty Chain Composition of Ether and Ester Glycerophospholipids in the Japanese Oyster *Crassostrea gigas, Lipids 25*, 363–370.
15. Jeong, B.Y., Ohshima, T., and Koizumi, C. (1990) Molecular Species of 1-*O*-Alkyl-1′-enyl-2-acyl-, 1-*O*-Alkyl-2-acyl- and 1,2-Diacyl Glycerophospholipids in Japanese Oyster *Crassostrea gigas* (Thunberg), *Lipids 25*, 624–632.
16. Ackman, R.G., and Hooper, S.N. (1973) Non-Methylene-Interrupted Fatty Acids in Lipids of Shallow-Water Marine Invertebrates: A Comparison of Two Molluscs (*Littorina littorea* and *Lunatia triserita*) with the Sand Shrimp (*Crangon septumspinosus*), *Comp. Biochem. Phys. 46B*, 153–165.
17. Dunstan, G.A., Volkman, J.K., and Barrett, S.M. (1993) The Effect of Lyophilization on the Solvent Extraction of Lipid Classes, Fatty Acids and Sterols from the Oyster *Crassostrea Gigas, Lipids 28*, 937–944.
18. Caers, M., Coutteau, P., and Sorgeloos, P. (1999) Dietary Impact of Algal and Artificial Diets, Fed at Different Feeding Rations, on the Growth and Fatty Acid Composition of *Tapes philippinarum* (L.) Spat, *Aquaculture 170*, 307–322.
19. Zhukova, N.V. (1986) Biosynthesis of Non-Methylene-Interrupted Fatty Acids from [^{14}C]Acetate in Molluscs, *Biochim. Biophys. Acta 878*, 131–133.
20. Zhukova, N.V. (1991) The Pathway of the Biosynthesis of Non-Methylene-Interrupted Dienoic Fatty Acids in Molluscs, *Comp. Biochem. Phys. 100B*, 801–804.
21. Chapelle, S. (1987) Plasmalogens and *O*-Alkylglycerophospholipids in Aquatic Animals, *Comp. Biochem. Phys. 88B*, 1–6.
22. Klingensmith, J.S. (1982) Distribution of Methylene and Non-Methylene-Interrupted Dienoic Fatty Acids in Polar Lipids and Triacylglycerols of Selected Tissues of the Hardshell Clam (*Mercenaria mercenaria*), *Lipids 17*, 976–981.
23. Folch, J., Lees, M. and Sloane Stanley, G.H. (1957) A Simple Method for the Isolation and Purification of Total Lipids from Animal Tissues, *J. Biol. Chem. 226*, 497–509.
24. Nelson, G.J. (1993) Isolation and Purification of Lipids from Biological Matrices, in *Analyses of Fats, Oils, and Derivatives* (Perkins, E.G., ed.), pp. 20–59, AOCS Press, Champaign.
25. Marty, Y., Delaunay, F., Moal, J., and Samain, J.F. (1992) Changes in the Fatty Acid Composition of the Scallop *Pecten maximus* (L.) During Larval Development, *J. Exp. Mar. Biol. Ecol. 163*, 221–234.
26. Soudant, P., Chu, F.L.E., and Marty, Y. (2000) Lipid Class Composition of the Protozoan *Perkinsus marinus*, an Oyster Parasite, and Its Metabolism of a Fluorescent Phosphatidylcholine Analog, *Lipids 35*, 1387–1395.
27. Kraffe, E., Soudant, P., Marty, Y., Kervarec, N., and Jehan, P. (2002) Evidence of a Tetradocosahexaenoic Cardiolipin in Some Marine Bivalves, *Lipids 37*, 507–514.
28. Chelomin, V.P., and Zhukova, N.V. (1981) Lipid Composition and Some Aspects of Aminophospholipid Organization in Erythrocyte Membrane of the Marine Bivalve Mollusc *Scapharca broughtoni* (Shrenck), *Comp. Biochem. Phys. 69B*, 599–604.
29. Zhukova, N.V., and Svetashev, V.I. (1986) Non-Methylene-Interrupted Dienoic Fatty Acids in Molluscs from the Sea of Japan, *Comp. Biochem. Phys. 83B*, 643–646.
30. Yorek, M.A. (1993) Biological Distribution, in *Phospholipids Handbook* (Cevc, G., ed.), pp. 745–775, Marcel Dekker, New York.
31. De Moreno, J.E.A., Moreno, V.J., and Brenner, R.R. (1976) Lipid Metabolism of the Yellow Clam, *Mesodesma mactroïdes*: 2–Polyunsaturated Fatty Acid Metabolism, *Lipids 11*, 561–566.
32. Waldock, M.J., and Holland, D.L. (1984) Fatty Acid Metabolism in Young Oysters, *Crassostrea gigas*: Polyunsaturated Fatty Acids, *Lipids 19*, 332–336.
33. Volkman, J.K., Jeffrey, S.W., Nichols, P.D., Rogers, G.I., and Garland, C.D. (1989) Fatty Acid and Lipid Composition of 10 Species of Microalgae Used in Mariculture, *J. Exp. Mar. Biol. Ecol. 128*, 219–240.
34. Stefanov, K., Seizova, K., Brechany, E., and Christie, W.W. (1992) An Unusual Fatty Acid Composition for a Fresh-Water Mussel, *Unio tumidus*, from Bulgaria, *J. Nat. Prod. 55*, 979–981.
35. Napolitano, G.E., and Ackman, R.G. (1993) Fatty Acid Dynamics in Sea Scallops *Placopecten magellanicus* (Gmelin, 1791) from Georges Bank, Nova Scotia, *J. Shellfish Res. 12*, 267–277.
36. Cook, H.W. (1996) Fatty Acid Desaturation and Chain Elongation in Eukaryotes, in *Biochemistry of Lipids, Lipoproteins and Membranes* (Vance, D.E., and Vance, J.E.), pp. 129–152, Elsevier Science, Amsterdam.
37. Paradis, M., and Ackman, R.G. (1977) Potential for Employing the Distribution of Anomalous NMI Dienoic Fatty Acids in Several Marine Invertebrates as Part of Food Web Studies, *Lipids 12*, 170–176.
38. Rabinovich, A.L., and Ripatti, P.O. (1991) The Flexibility of Natural Hydrocarbon Chains with Non-Methylene-Interrupted Double Bonds, *Chem. Phys. Lipids 58*, 185–192.
39. Morand, O.H., Zoeller, R.A., and Raetz, C.R.H. (1988) Disappearance of Plasmalogens from Membranes of Animal Cells Subjected to Photosensitized Oxidation, *J. Biol. Chem. 263*, 11597–11606.

[Received September 18, 2003; accepted November 22, 2003]

Membrane Lipid Profile of an Edible Basidiomycete *Lentinula edodes* During Growth and Cell Differentiation

Hiromichi Sakai and Susumu Kajiwara*

Department of Life Science, Graduate School of Bioscience and Biotechnology, Tokyo Institute of Technology, Yokohama, Kanagawa, 226-8501, Japan

ABSTRACT: The basidiomycetous mushroom *Lentinula edodes* (Shiitake) exhibits a unique process of cell differentiation termed "fruiting-body formation". To clarify the relationship between membrane lipids and fruiting-body formation in this fungus, we investigated variations in levels of phospholipids, cerebrosides, fatty acyl residues in the major phospholipids, and fatty acyl and sphingoid base residues in cerebrosides during vegetative growth and fruiting-body formation. PC, PE, and PS were the primary phospholipids in the cells of *L. edodes*. After a shift in growth temperature of *L. edodes* mycelia has been shifted from 25 to 18°C, the proportion of unsaturated FA (UFA), such as linoleic acid (18:2) and oleic acid (18:1), increased. In contrast, during fruiting-body formation induced by the temperature downshift to 18°C, 18:2 of PC in the primordia and fruiting bodies decreased, and the UFA of PE and 18:1 of PC increased compared with the proportions in mycelia growing at 18°C. These results showed that the proportions of fatty acyl residues in PC and PE differed during fruiting-body formation in *L. edodes*. Moreover, the amount of cerebrosides in primordia increased compared with those in mycelia and fruiting bodies and, in these differentiating tissues, the proportion of 2-hydroxypentadecanoic acid increased whereas that of 2-hydroxyoctadecanoic acid decreased compared with that in the mycelia. However, the proportion of sphingoid base residues in cerebrosides did not change during fruiting-body formation in *L. edodes*.

Paper no. L9334 in *Lipids 39*, 67–73 (January 2004).

The membrane lipids of eukaryotic cells such as animals and fungi generally contain phospholipids, sphingolipids, and sterols. The composition of these membrane lipids is known to change during cell growth and cell differentiation, and upon exposure to exogenous environmental stresses. Therefore, these lipids not only are the basic structural components of biological membranes but also play critical roles in cell physiology.

PC and PE are the most abundant membrane phospholipids in eukaryotes. Perturbation of PC synthesis triggers apoptosis in these cells (1,2), and an absolute level of PE in the membrane is required for cell growth (3). Other phospholipids, such as phosphatidylglycerol (PG) and PA, also play roles in cell growth and cell differentiation (4–8). Moreover, the composition of fatty acyl residues in phospholipids of the cell membrane can be altered by various environmental stresses. In poikilothermic organisms such as fungi, low-temperature stress causes the amount of unsaturated FA (UFA), such as palmitoleic acid, linoleic acid (18:2), and oleic acid (18:1), to increase (9,10). This cellular response is thought to maintain the fluidity of the membrane lipids (11,12). In addition, several studies of filamentous fungi suggest that 18:2 is an important compound for fungal development, especially spore formation (13–16). Psi factors, the 18:2-derived signal molecules, have also been reported to govern the development of cleistothecia and conidiophores (17–19). These results revealed the importance of phospholipid and fatty acyl residue composition of membrane lipids during cell growth and differentiation.

Sphingolipids, such as cerebrosides, are also known to play an important role in cell differentiation of fungi. A cerebroside was shown to strongly induce fruiting-body formation in two basidiomycetous fungi, *Schizophyllum commune* and *Coprinus cinereus* (20,21). Likewise, glucocerebroside, isolated from the fruiting bodies of the edible basidiomycete *Lentinula edodes,* has high fruiting-induction activity in *S. commune* (22). The sphingoid base residue in this cerebroside, 9-methyl 4-*trans*,8-*trans*-sphingadienine, has been identified as essential for induction of fruiting activity in *S. commune* (20,22–24). The other components of cerebroside, 2-hydroxy FA and glucose, had a much weaker effect on fruiting (20,22,25,26). Furthermore, this cerebroside also affected spore germination and hyphal growth in the ascomycetous fungi *Aspergllus nidulans* and *A. fumigatus* (27). Thus, sphingolipids as well as phospholipids are essential structural and functional components of many fungal cells. The other sphingolipids are also detected in these fungi (28,29). However, the variation of sphingoid base and FA in these sphingolipids has not been reported in detail.

Fruiting-body formation of basidiomycetous fungi is the most conspicuous and complex process in cell differentiation, and a temperature downshift (25 to 17–18°C) has been shown to induce fruiting in *L. edodes* (30). The proportion of UFA in both polar and nonpolar lipids increases during fruiting-body formation in *L. edodes* (31). However, specific effects on fatty acyl residues in each membrane lipid during cell growth and differentiation of *L. edodes* have not previously been investigated. In this study, we report the phospholipid content in the

*To whom correspondence should be addressed at 4259 Nagatsuta, Midori-ku, Yokohama, Kanagawa, 226-8501, Japan. E-mail: skajiwar@bio.titech.ac.jp

Abbreviations: 9-Me d18:2^{4t,8t}; 9-methyl 4-*trans*,8-*trans*-sphingadienine; 15:0, pentadecanonic acid; 16:0, palmitic acid; 16h:0, 2-hydroxyhexadecanoic acid; 18:0, stearic acid; 18:1, oleic acid; 18:2, linoleic acid; PG, phosphatidylglycerol; SFA, saturated FA; UFA, unsaturated FA.

cells, the fatty acyl residues in their phospholipids, the sphingolipid content in the cells, and the sphingoid base and fatty acyl composition of sphingolipids during mycelial growth and fruiting-body formation in *L. edodes*.

MATERIALS AND METHODS

Strains and media. The FMC2 strain of *Lentinula* (*Lentinus*) *edodes* (a stock strain of Forestry and Forest Products Research Institute of Japan) is a commercial cell used in our previous studies (32). Potato-dextrose-agar medium (Nissui Co. Ltd., Tokyo, Japan) was used for preculture of *L. edodes* strains on petri dishes. A sawdust-based medium (28% w/w *Fagus crenata* sawdust, 7% w/w corn bran, 65% w/w water) was used for vegetative growth and fruiting of *L. edodes*.

Growth and fruiting-body formation. The dikaryotic mycelium was cultivated in the sawdust-based medium (150 g) at 25°C for 30 d under 1000–1300 lux of light intensity on a 12-h light/12-h dark cycle, and the growth atmosphere was held at 65% RH. After the mycelia had grown in the sawdust-based medium, cultures of the FMC2 strain were transferred into the 18°C incubator. Many primordia appeared on the surface of the medium, and several primordia grew into a fruiting body after about 10 d. Continuous cultivation of the FMC2 strain mycelia at 25°C failed to produce a fruiting body.

Extraction and TLC separation of phospholipids and cerebrosides. Total lipids in the harvested cells of *L. edodes* were extracted by chloroform/methanol (1:2, vol/vol). After these lipids were washed once with water, the organic phase was evaporated to dryness. The residue was dissolved in 50 μL of chloroform/methanol (2:1, vol/vol) and then applied to a TLC plate (silica gel 60, 20 × 20 cm; Merck, Darmstadt, Germany) for chromatographic resolution. 2-D solvent systems were used. The first chromatographic run was performed with chloroform/methanol/7 M ammonia (65:30:4, by vol). The second run was performed with chloroform/methanol/acetic acid/water (170:25:25:4, by vol) at 90° to the original direction. After development, the plate was sprayed with primuline [0.001% wt/vol in acetone/water (4:1)] and viewed under UV light (302 nm) for localization of separated compounds. Each lipid spot on the TLC plate was scraped off by using a razor and then dissolved in chloroform/methanol (2:1 vol/vol). The R_f values of phospholipids and cerebrosides are shown in Table 1.

TABLE 1
R_f Values of Lipids

Lipids	First direction[a]	Second direction[b]
PC	0.26 (0.21–0.31)	0.22 (0.14–0.31)
PE	0.36 (0.31–0.42)	0.54 (0.48–0.61)
PG	0.53 (0.50–0.56)	0.67 (0.65–0.68)
PI	0.11 (0.06–0.17)	0.08 (0.05–0.11)
PS	0.09 (0.03–0.14)	0.15 (0.12–0.19)
PA	0.07 (0.03–0.12)	0.67 (0.62–0.72)
SM	0.06 (0.04–0.08)	0.03 (0.01–0.04)
Cerebrosides	0.53 (0.50–0.56)	0.48 (0.45–0.51)

[a]Chloroform/methanol/7 M ammonia (65:30:4, by vol).
[b]Chloroform/methanol/acetic acid/water (170:25:25:4, by vol). PG, phosphatidylglycerol; SM, sphinomyelin.

Analyses of phospholipids and cerebrosides. Total and individual phospholipids were digested in perchloric acid (70%) for 3 h at 160°C. The inorganic phosphate was quantified colorimetrically (33). The calibration curves were prepared by using potassium dihydrogenphosphate as a standard.

The reagent for acid hydrolysis of cerebrosides was prepared by diluting 8.6 mL of concentrated hydrochloric acid and 9.4 mL of water to 100 mL with methanol, giving 1 N hydrochloric acid (aqueous methanolic HCl). Cerebrosides were hydrolyzed by aqueous methanolic HCl for 18 h at 70°C and then quantified colorimetrically by the methyl orange method using *N*-palmitoyl-D-sphingosine for calibration (34).

Analyses of FA and sphingoid bases. Fatty acyl residues in each phospholipid were methylated with 1% sulfuric acid in methanol for 2 h at 90°C. The FAME obtained were extracted in hexane. FA were analyzed by GLC (GC-18A; Shimadzu, Japan) as described in our previous report (35).

The 2-hydroxy FA in cerebrosides were methylated in aqueous methanolic HCl for 18 h at 70°C. These FAME were extracted in hexane and analyzed by GLC on a DB-5.625 column (J&W Scientific, Folsom, CA). The temperature was programmed from 190°C (2 min hold) to 280°C (35 min hold) at a rate of 4°C/min for very long chain hydroxyl FAME. The injector and detector were maintained at 280°C. Identification was accomplished by comparison of retention times with spectra from a standard.

Sphingoid bases released by aqueous methanolic HCl for 18 h at 70°C were extracted by diethyl ether and reacted with 0.2 M sodium periodate for 2 h to obtain fatty aldehydes. The fatty aldehydes were extracted in dichloromethane, evaporated to dryness, redissolved in 50 μL dichloromethane, and analyzed by GLC (36,37). GLC analysis followed the procedure described above for phospholipids. Sphingoid base fractions were determined by GLC using yeast sphingoid bases as the authentic standard (38).

Statistical analysis. Results are expressed as means ± SD of three experiments. Data were analyzed by one-way ANOVA. After application of one-way ANOVA, the significance of differences in the means among three groups was evaluated by Scheffé's multiple comparison. Differences in FA and sphingoid base content were considered significant at $P < 0.05$, and differences in lipid content by colorimetric assays were considered significant at $P < 0.005$.

RESULTS

The analysis of phospholipids in L. edodes *cells*. To analyze the alteration of membrane lipids during vegetative growth and fruiting-body formation in *L. edodes*, mycelial cells of the FMC2 strain were cultivated on the sawdust-based medium at 25°C for 30 d, and then several of these cultures were transferred from 25 to 18°C to induce formation of fruiting bodies. Lipids were extracted from mycelia cultivated for 30, 40, and 60 d at 25°C, and from mycelia transferred to

TABLE 2
Total Lipids and Total Phospholipids Extracted from the FMC2 Cells During Vegetative Growth at 25°C and Fruiting-Body Formation at 18°C

FMC2 cells	Lipids/cell dry wt (mg/g)[a]	Phospholipids/cell dry wt (μmol/g)[a]	Phospholipids/lipid (mmol/g)
Vegetative growth			
Mycelia (30 d)	31.8 ± 6.1	13.2 ± 1.2	0.42
Mycelia (40 d)	24.3 ± 1.0	10.5 ± 1.3	0.43
Mycelia (60 d)	22.5 ± 1.4	9.1 ± 0.2	0.40
Fruiting-body formation (40 d)			
Mycelia	29.6 ± 1.7	10.7 ± 1.1	0.36
Primordia	58.1 ± 6.8^{*M}	30.3 ± 1.9^{*M}	0.52
Fruiting bodies	38.0 ± 2.4^{*P}	21.8 ± 2.0^{*M,P}	0.57

[a]These values are the means ± SD of three experiments. Significant differences for paired comparisons are: $^*P < 0.005$ (one-way ANOVA and Sheffé's multiple comparison). ^{M}, vs. mycelia; ^{P}, vs. primordia.

18°C after the 25°C incubation. The lipids of mycelia cultivated at 25°C for 30, 40, and 60 d accounted for 3.2, 2.4, and 2.3% (w/w) of the cell weight, respectively (Table 2). The 30-, 40-, and 60-d mycelial cultures yielded 13.2, 10.5, and 9.1 μmol of phospholipids (per 1 g), respectively, whereas mycelia transferred to 18°C on the 30th day contained 3.0% lipids and 10.7 μmol phospholipids. These results showed that the lipid and phospholipid contents in *L. edode*s mycelia were relatively constant during the vegetative growth phase and upon temperature downshift.

In contrast, during fruiting-body formation, the lipid and phospholipid content of *L. edodes* primordia increased drastically (5.8% and 30.3 μmol), although these decreased in the fruiting bodies themselves (3.8% and 21.8 μmol). The ratio of phospholipids to lipids in the fruiting bodies was higher than that of the primordia (Table 2). These data indicated that nonphospholipids, mainly storage lipids such as TAG, in the cells decreased more than the phospholipid levels during the transition from the primordia to the fruiting bodies of *L. edodes*.

In many fungi, membrane phospholipids consist primarily of PC, PE, PI, and PS. To clarify the composition of phospholipids in *L. edodes*, we analyzed the amount of each phospholipid in the FMC2 strain during growth and differentiation. These data are shown in Figure 1. The major phospholipids in *L. edodes* were PC (40.5–49.7%), PE (20.4–28.8%), and PS (10.7–13.7%). Likewise, PA and PI were identified in this fungus, as were trace amounts of PG and sphingomyelin (<1%, not shown). We found few changes in the composition of phospholipids during vegetative growth phase and fruiting-body formation in *L. edodes*.

Variation of fatty acyl residues in the major phospholipids of L. edodes. Previously, the UFA content of both polar and nonpolar lipids was shown to increase during fruiting-body formation in *L. edodes* (31). In the present study, we confirmed that the proportion of UFA in total lipids of this fungus increased during fruiting (data not shown). To detect the alteration of fatty acyl residues in the major phospholipids of *L. edodes*, we analyzed the amount of these residues during vegetative growth and fruiting-body formation. The FAME were prepared from phospholipids isolated from mycelia on the 30th, 40th, and 60th day of cultivation and analyzed by GLC (Table 3). These results showed that FA components of the major *L. edodes* phospholipids primarily induced palmitic acid (16:0) and 18:2, and the amounts of these fatty acyl residues in the three phospholipids did not change during the

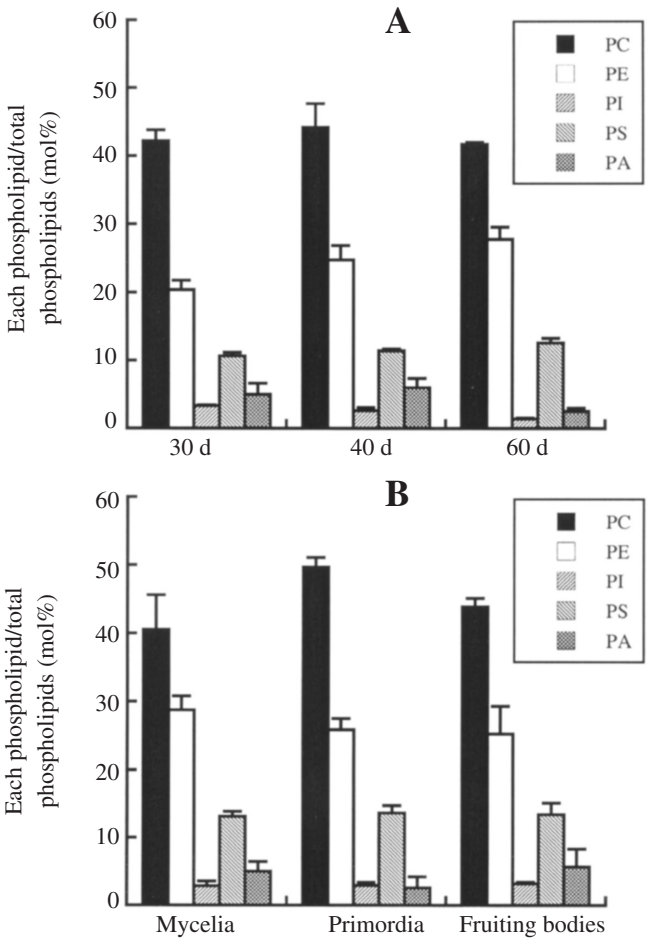

FIG. 1. Phospholipid composition of FMC2 cells during vegetative growth (A) and fruiting-body formation (B). The contribution of PC, PE, PI, PS, and PA is presented as a mean ± SD in mol% of total phospholipids ($n = 3$).

TABLE 3
FA Composition of the Major Phospholipids from the Mycelia Cultivated at 25°C

Phospholipid	Cultivating time (d)	FA content (mol% ± SD)[a]						
		14:0	15:0	16:0	18:0	18:1	18:2	UFA[b]
PC	30	0.1 ± 0.0	0.5 ± 0.1	4.5 ± 0.6	1.9 ± 0.2	0.9 ± 0.1	92.1 ± 0.7	93.0 ± 0.8
	40	Trace[c]	0.6 ± 0.0	4.0 ± 0.2	1.6 ± 0.2	1.3 ± 0.3	92.6 ± 0.3	93.8 ± 0.3
	60	Trace	1.0 ± 0.1^{***M,N}	4.8 ± 0.2	1.2 ± 0.2^{*M}	1.0 ± 0.1	92.0 ± 0.5	93.1 ± 0.5
PE	30	0.3 ± 0.0	1.9 ± 0.0	21.4 ± 1.3	1.0 ± 0.0	2.5 ± 0.2	72.9 ± 1.1	75.4 ± 1.4
	40	0.3 ± 0.0	3.1 ± 0.2^{***M}	21.1 ± 0.8	1.3 ± 0.3	3.6 ± 0.8	70.7 ± 1.3	74.3 ± 1.0
	60	0.2 ± 0.0^{*M}	3.4 ± 0.2^{***M}	20.3 ± 0.9	1.2 ± 0.2	4.6 ± 0.4^{**M}	70.4 ± 1.0	74.9 ± 1.3
PS	30	0.3 ± 0.0	3.0 ± 0.0	46.5 ± 1.5	0.8 ± 0.1	0.8 ± 0.1	48.8 ± 1.4	49.5 ± 1.5
	40	0.3 ± 0.1	4.2 ± 0.2^{***M}	45.2 ± 1.1	1.0 ± 0.1	1.0 ± 0.4	48.4 ± 1.1	49.4 ± 1.0
	60	0.2 ± 0.1	4.8 ± 0.1^{***M,*N}	44.1 ± 3.7	0.8 ± 0.2	0.9 ± 0.2	49.4 ± 3.5	50.2 ± 3.7

[a]Results were determined from the methyl ester peak. These values are the means of three experiments. Significant differences for paired comparisons are: $^{*}P < 0.05$; $^{**}P < 0.01$; $^{***}P < 0.005$ (one-way ANOVA and Sheffé's multiple comparison). ^{M}, vs. mycelia (30 d); ^{N}, vs. mycelia (40 d).
[b]UFA, unsaturated FA.
[c]Trace (less than 0.1%).

the vegetative growth phase of *L. edodes*. On the other hand, in minor FA components, the amounts of pentadecanoic acid (15:0) in the major phospholipids and oleic acid (18:1) in PE increased during vegetative growth, whereas the stearic acid (18:0) levels in PC decreased.

We also investigated the alteration of fatty acyl residues in three phospholipids of the mycelia in response to a temperature downshift. The FMC2 mycelial culture was transferred from 25 to 18°C on day 30 and then cultivated for 10 more days at 18°C. We observed an increase in the proportion of UFA (18:1 and 18:2) in the PC and PE of these mycelia as compared with those from the mycelia cultivated at 25°C for 40 d (two-tailed *t*-test, $P < 0.005$, Tables 3 and 4). These results revealed that the shift to a lower temperature (18°C) increased the proportion of UFA in the most abundant and second-most abundant phospholipids (PC and PE), which represent approximately 70% of the total phospholipids (Fig. 1).

Likewise, we analyzed the fatty acyl residues in PC, PE, and PS at three stages of fruiting-body formation in *L. edodes* (mycelium, primordium, and fruiting body). The three phospholipids were extracted on day 40 from primordia and fruiting bodies of the FMC2 strain cultured at 18°C (Table 4). The proportion of UFA in PE from the primordia and fruiting bodies increased by 8.3 and 6.9%, respectively, over levels in the mycelia. In contrast, the 18:2 levels in PC from the primordia and fruiting bodies were 4.9 and 4.6% lower than that in the mycelia, respectively, although the 18:1 levels in PC of these cells increased. As a result, the UFA levels in PC of the primordia and fruiting bodies were equal to or lower than those in the mycelia at 18°C. Moreover, the percentage of 18:2 in PC from primordia and fruiting bodies (89.4 and 89.7%) was lower than that from mycelia grown at 25°C for 40 d (92.6%) as well as the mycelia moved to the 18°C incubator (94.3%) (Table 3).

Analysis of cerebrosides in L. edodes *cells.* To clarify the alteration of cerebrosides in *L. edodes*, we tried to measure the amount of cerebrosides in the FMC2 strain during growth and differentiation. These data are shown in Figure 2. The

TABLE 4
FA Composition of the Major Phospholipids from *L. edodes* Cells During Fruiting-Body Formation at 18°C

Phospholipid	Stage of fruiting-body formation[a]	FA content (mol% ± SD)[b]						
		14:0	15:0	16:0	18:0	18:1	18:2	UFA
PC	M	Trace	0.7 ± 0.1	3.0 ± 0.2	0.7 ± 0.1	1.4 ± 0.4	94.3 ± 0.6	95.6 ± 0.3
	P	Trace	0.2 ± 0.0	2.8 ± 0.1	1.5 ± 0.2^{*M}	6.1 ± 0.3^{***M}	89.4 ± 0.4^{***M}	95.6 ± 0.2
	F	0.1 ± 0.0	0.6 ± 0.5	3.8 ± 0.4^{*M,***P}	1.9 ± 0.4^{***M}	3.9 ± 1.5^{*M}	89.7 ± 1.1^{***M}	93.5 ± 0.5$^{***M,}_{***P}$
PE	M	0.2 ± 0.0	3.1 ± 0.2	16.0 ± 1.1	1.0 ± 0.1	4.4 ± 0.2	75.4 ± 1.3	79.8 ± 1.2
	P	0.1 ± 0.0^{***M}	0.6 ± 0.0^{**M}	10.5 ± 0.6^{***M}	0.7 ± 0.1^{*M}	7.2 ± 0.3^{***M}	80.9 ± 0.9^{***M}	88.1 ± 0.7^{***M}
	F	0.2 ± 0.0^{*M}	1.2 ± 1.0^{*M}	11.3 ± 1.4^{**M}	0.6 ± 0.1^{**M}	6.5 ± 0.6^{***M}	80.3 ± 1.0^{***M}	86.7 ± 0.4^{***M}
PS	M	0.2 ± 0.0	5.3 ± 0.1	43.9 ± 0.6	0.6 ± 0.0	1.1 ± 0.2	49.1 ± 0.4	50.1 ± 0.6
	P	0.2 ± 0.1	1.7 ± 0.1	43.9 ± 2.6	1.8 ± 0.2^{***M}	2.9 ± 0.1^{***M}	49.6 ± 2.5	52.5 ± 2.5
	F	0.3 ± 0.0	4.3 ± 3.0	44.2 ± 2.8	0.8 ± 0.2	2.2 ± 0.2$^{***M,}_{***P}$	48.2 ± 1.9	50.4 ± 1.9

[a]M, mycelia; P, primordia; F, fruiting bodies.
[b]Results were determined from the methyl ester peak. These values are the means of three experiments. Significant differences for paired comparisons are: $^{*}P < 0.05$; $^{**}P < 0.01$; $^{***}P < 0.005$ (one-way ANOVA and Sheffé's multiple comparison). ^{M}, vs. mycelia; ^{P}, vs. primordia. For other abbreviations, see Table 3.

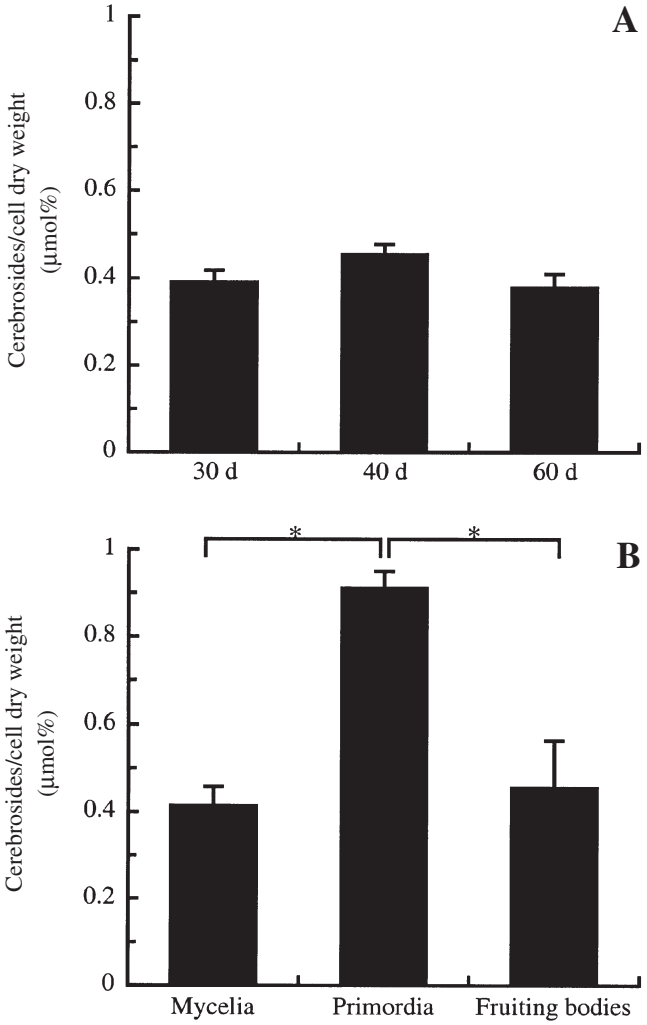

FIG. 2. The cerebroside content of FMC2 cells during vegetative growth (A) and fruiting-body formation (B). The values are the means ± SD of three experiments. Significant differences for paired comparisons are: $^{*}P < 0.005$ (one-way ANOVA and Sheffé's multiple comparison).

mycelia cultivated at 25°C for 30, 40, and 60 d yielded 0.39, 0.45, and 0.38 μmol of the cerebrosides (per 1 g), respectively, and the mycelia transferred to 18°C on the 30th day contained 0.41 μmol of cerebrosides. In contrast, during fruiting-body formation of *L. edodes*, the amount of cerebrosides in the primordia increased drastically (0.91 μmol), and then this amount in the fruiting bodies decreased (0.46 μmol).

Alteration of fatty acyl and sphingoid base residues in cerebrosides of L. edodes. To clarify the profile of fatty acyl and sphingoid base residues in the cerebrosides during fruiting-body formation in *L. edodes*, we analyzed the cerebrosides extracted from mycelia, primordia, and fruiting bodies that had been transferred into the 18°C incubator on day 30 and then cultured for 10 more days. These analyses showed that a 2-hydroxy hexadecanoic acid dominated the fatty acyl residue of the cerebrosides, whereas the sphingoid base included mainly 4-*trans*,8-*trans*-sphingadienine (d18:$2^{4t,8t}$), 9-methyl 4-*trans*,8-*trans*-sphingadienine (9-Me d18:$2^{4t,8t}$), and 4-hydroxy-sphinganine (Table 5). During fruiting-body

TABLE 5
Composition of FA and Sphingoid Bases in Cerebrosides from the Mycelia, Primordia, and Fruiting Bodies

	Percentage ± SD[a]		
Component	Mycelia	Primordia	Fruiting bodies
FA[b]			
14h:0	4.4 ± 0.3	3.3 ± 0.1^{***M}	4.5 ± 0.2^{***P}
15h:0	9.8 ± 0.2	13.3 ± 0.5^{***M}	14.9 ± 0.4^{***M,**P}
16h:0	79.9 ± 0.7	80.1 ± 1.1	77.2 ± 1.1^{*M,*P}
18h:0	3.8 ± 0.2	1.9 ± 0.2^{***M}	1.6 ± 0.1^{***M}
Sphingoid base[c]			
d18:1^{4t}	3.2 ± 0.4	3.1 ± 0.2	3.1 ± 0.2
d18:$2^{4t,8t}$	27.1 ± 0.6	26.6 ± 0.1	27.2 ± 0.2
9-Me d18:$2^{4t,8t}$	36.0 ± 0.6	35.2 ± 0.2	35.8 ± 0.4
t18:0	30.1 ± 1.3	31.4 ± 0.6	30.2 ± 0.7
t20:0	3.5 ± 0.3	3.7 ± 0.1	3.7 ± 0.3

[a]Results were determined from the GLC peaks of FAME and fatty aldehydes. These values are the means of three experiments. Significant differences for paired comparisons are: $^{*}P < 0.05$; $^{**}P < 0.01$; $^{***}P < 0.005$ (one-way ANOVA and Sheffé's multiple comparison). ^{M}, vs. mycelia; ^{P}, vs. primordia.
[b]Hydroxy FA are abbreviated as *X*h:*Y*.
[c]Abbreviations for sphingoid bases are shown as follows: d18:1^{4t}, 4-*trans*-sphingenine; d18:$2^{4t,8t}$, 4-*trans*,8-*trans*-sphingadienine; 9-Me d18:$2^{4t,8t}$, 9-methyl 4-*trans*,8-*trans*-sphingadienine; t18:0, 4-hydroxysphinganine; t20:0, 4-hydroxyeicosasphinganine.

formation in this fungus, the proportion of the 2-hydroxy pentadecanoic acyl residue increased, whereas the proportion of the 2-hydroxy octadecanoic acyl residue decreased. The proportions of these sphingoid base residues remained constant during differentiation as well as after the shift to 18°C (data not shown).

DISCUSSION

We investigated the phospholipid and cerebrosides in *L. edodes* and analyzed the fatty acyl residue profiles of the three major phospholipids and the fatty acyl and sphingoid base residues in the intracellular cerebrosides. PC, PE, and PS were the major phospholipids of the *L. edodes* cells, and no alteration of phospholipid composition was observed during the vegetative growth phase or fruiting-body formation. Few changes were evident in the levels of phospholipids and total lipids in *L. edodes* during the vegetative growth phase. However, the proportion of phospholipids and total lipids increased during the primordial stage, but decreased during the fruiting-body stage. The ratio of phospholipids to total lipids was highest during the fruiting-body stage despite the decrease in total lipids. These results suggest that *L. edodes* cells accumulate their highest lipid levels at the primordial stage, which then degrade mainly to nonpolar storage lipids such as TAG and ergosterol at the fruiting-body stage. For basidomycetes like *L. edodes*, the fruiting-body stage is also a period of basidiospore formation, which occurs when nutrients are exhausted. Thus, a reduction in more available carbon sources such as glucose leads to the degradation of nonpolar lipids during the fruiting-body stage.

Analysis of the fatty acyl residue composition of the phospholipids showed that 18:2 was the major fatty acyl residue

in PC and PE, as was reported previously (31,39). However, saturated FA (SFA), primarily 16:0, accounted for approximately half of the fatty acyl residues in PS. This result suggests that the *sn*-1 or *sn*-2 positions of PS bind only to SFA or 16-carbon FA. In the ascomycetous yeast, *Saccharomyces cerevisaie*, PS is synthesized from CDP-1 and -2-DAG, and the PS synthesis pathway differs from that of PC and PE, which are synthesized from 1,2-DAG (40). Moreover, UFA are associated with more than 54% of the *sn*-1 position and 98% of the *sn*-2 position in PS from *S. cerevisiae* (41). Therefore, the PS of *L. edodes* may be synthesized from the binding of CDP-1,2-DAG to SFA at its *sn*-1 or *sn*-2 position.

When the mycelia of *L. edodes* were cultivated for 60 d at 25°C, the amount of primary fatty acyl residues, 16:0 and 18:2, in the three major phospholipids, PC, PE, and PS, changed little during vegetative growth, although the levels of minor FA residues, 15:0, 18:0, and 18:1, changed slightly. This result suggested that fatty acyl residue composition of phospholipids is not influenced by vegetative growth. However, the fatty acyl residue composition of PC and PE isolated from mycelia that had been transferred into an 18°C incubator appeared to have a higher proportion of UFA than the mycelia growing at 25°C. Low-temperature stress has been shown to alter FA composition in many other organisms (9,10). Moreover, during fruiting-body formation, the proportion of UFA in PE from the primordia and fruiting bodies was higher than that from the mycelia growing at 18°C. Although we observed increases in 18:1 in PC from the primordia and fruiting bodies, 18:2 levels were lower than those in the mycelia growing at 18 or 25°C. Therefore, the change in fatty acyl residues observed during fruiting-body formation in *L. edodes* differs from that which occurs in response to low-temperature stress. This alteration may be specific to cell differentiation in *L. edodes* and may be necessary for induction of FA desaturation, which increases the level of UFA in this fungus. A Δ-12 fatty acid desaturase, which converts 18:1 to 18:2, is known to recognize diacyl-PC as substrate in the yeast *Yarrowia (Candida) lypolytica* (42). Therefore, the activity or the expression of this enzyme may be slightly reduced in the fruiting-body stage. However, neither cloning of the gene encoding Δ-12 FA desaturase nor clarification of FA synthesis in *L. edodes* has been reported. Further studies of the enzymes and genes involved in FA desaturation will clarify the relationship between UFA in phospholipids and fruiting-body formation in *L. edodes*.

Cerebrosides, including 9-Me d18:$2^{4t,8t}$, are known inducers of fruiting-body formation in two species of basidiomycetes. Therefore, we investigated the variation of intercellular cerebrosides of *L. edodes* during vegetative growth and fruiting-body formation and analyzed the alteration of fatty acyl and sphingoid base residues in these cerebrosides during the formation of fruiting bodies. The amount of cerebrosides in *L. edodes* changed little during vegetative growth, whereas the cerebroside level in the primordia was higher than those of the other different stages in the fruiting-body formation. On the other hand, 9-Me d18:$2^{4t,8t}$ is the primary sphingoid base residue in *L. edodes* cerebrosides, and the composition of sphingoid base residues was similar in the mycelia, primordia, and fruiting bodies, although the primordia and fruiting bodies appeared to have a higher proportion of 2-hydroxy fatty acyl residues, especially h16:0, than mycelia. Thus, these data suggest that a change of the components in intracellular cerebrosides, including 9-Me d18:$2^{4t,8t}$, is not essential. Instead, a quantitative accumulation of intracellular cerebrosides acts as an intracellular signal that initiates fruiting-body formation in *L. edodes*.

The present study identified an alteration in membrane lipids of *L. edodes* during growth and cell differentiation and found that these alterations were observed only during fruiting-body formation.

REFERENCES

1. Cui, Z., Houweling, M., Chen, M.H., Record, M., Chap, H., Vance, D.E., and Terce, F. (1996) A Genetic Defect in Phosphatidylcholine Biosynthesis Triggers Apoptosis in Chinese Hamster Ovary Cells, *J. Biol. Chem. 271*, 14668–14671.
2. Cui, Z., and Houweling, M. (2002) Phosphatidylcholine and Cell Death, *Biochim. Biophys. Acta 1585*, 87–96.
3. Storey, M.K., Clay, K.L., Kutateladze, T., Murphy, R.C., Overduin, M., and Voelker, D.R. (2001) Phosphatidylethanolamine Has an Essential Role in *Saccharomyces cerevisiae* That Is Independent of Its Ability to Form Hexagonal Phase Structures, *J. Biol. Chem. 276*, 48539–48548.
4. Kawasaki, K., Kuge, O., Chang, S.C., Heacock, P.N., Rho, M., Suzuki, K., Nishijima, M., and Dowhan, W. (1999) Isolation of a Chinese Hamster Ovary (CHO) cDNA Encoding Phosphatidylglycerophosphate (PGP) Synthase, Expression of Which Corrects the Mitochondrial Abnormalities of a PGP Synthase-Defective Mutant of CHO-K1 Cells, *J. Biol. Chem. 274*, 1828–1834.
5. Hagio, M., Gombos, Z., Varkonyi, Z., Masamoto, K., Sato, N., Tsuzuki, M., and Wada, H. (2000) Direct Evidence for Requirement of Phosphatidylglycerol in Photosystem II of Photosynthesis, *Plant Physiol. 124*, 795–804.
6. Babiychuk, E., Muller, F., Eubel, H., Braun, H.P., Frentzen, M., and Kushnir, S. (2003) *Arabidopsis* Phosphatidylglycerophosphate Synthase 1 Is Essential for Chloroplast Differentiation, but Is Dispensable for Mitochondrial Function, *Plant J. 33*, 899–909.
7. Potocky, M., Elias, M., Profotova, B., Novotna, Z., Valentova, O., and Zarsky, V.V. (2003) Phosphatidic Acid Produced by Phospholipase D Is Required for Tobacco Pollen Tube Growth, *Planta 217*, 122–130.
8. Ritchie, S., and Gilroy, S. (1998) Abscisic Acid Signal Transduction in the Barley Aleurone Is Mediated by Phospholipase D Activity, *Proc. Natl. Acad. Sci. USA 95*, 2697–2702.
9. Walker, G.M. (1998) *Yeast Physiology and Biotechnology*, pp. 101–202, John Wiley & Sons, London.
10. Suutari, M., and Laakso, S. (1994) Microbial Fatty Acids and Thermal Adaptation, *Crit. Rev. Microbiol. 20*, 285–328.
11. Somerville, C. (1995) Direct Tests of the Role of Membrane Lipid Composition in Low-Temperature-Induced Photoinhibition and Chilling Sensitivity in Plants and Cyanobacteria, *Proc. Natl. Acad. Sci. USA 92*, 6215–6218.
12. Hazel, J.R., and Williams, E.E. (1990) The Role of Alterations in Membrane Lipid Composition in Enabling Physiological Adaptation of Organisms to Their Physical Environment, *Prog. Lipid Res. 29*, 167–227.
13. Hyeon, B. (1976) Chemical Studies on the Factors Controlling Sporulation of Fungi, *Chem. Regul. Plants 11*, 69–76.
14. Katayama, M., and Marumo, S. (1978) R(–)-Glycerol Monolinoleate, a Minor Sporogenic Substance of *Sclerotinia fructicola*,

Agric. Biol. Chem. 42, 1431–1433.
15. Nukima, M., Sassa, T., Ikeda, M., and Takahashi, K. (1981) Linoleic Acid Enhances Perithecial Production in *Neurospora crassa, Agric. Biol. Chem. 45*, 2371–2373.
16. Roeder, P.E., Sargent, M.L., and Brody, S. (1982) Circadian Rhythms in *Neurospora crassa*: Oscillations in Fatty Acids, *Biochemistry 21*, 4909–4916.
17. Champe, S.P., Rao, P., and Chang, A. (1987) An Endogenous Inducer of Sexual Development in *Aspergillus nidulans, J. Gen. Microbiol. 133*, 1383–1387.
18. Champe, S.P., and el-Zayat, A.A. (1989) Isolation of a Sexual Sporulation Hormone from *Aspergillus nidulans, J. Bacteriol. 171*, 3982–3988.
19. Calvo, A.M., Gardner, H.W., and Keller, N.P. (2001) Genetic Connection Between Fatty Acid Metabolism and Sporulation in *Aspergillus nidulans, J. Biol. Chem. 276*, 25766–25774.
20. Kawai, G., and Ikeda, Y. (1985) Structure of Biologically Active and Inactive Cerebrosides Prepared from *Schizophyllum commune, J. Lipid Res. 26*, 338–343.
21. Mizushina, Y., Hanashima, L., Yamaguchi, T., Takemura, M., Sugawara, F., Saneyoshi, M., Matsukage, A., Yoshida, S., and Sakaguchi, K. (1998) A Mushroom Fruiting Body-Inducing Substance Inhibits Activities of Replicative DNA Polymerases, *Biochem. Biophys. Res. Commun. 249*, 17–22.
22. Kawai, G. (1989) Molecular Species of Cerebrosides in Fruiting Bodies of *Lentinus edodes* and Their Biological Activity, *Biochim. Biophys. Acta 1001*, 185–190.
23. Kawai, G., and Ikeda, Y. (1982) Fruiting-Inducing Activity of Cerebrosides Observed with *Schizophyllum commune, Biochim. Biophys. Acta 719*, 612–618.
24. Kawai, G., and Ikeda, Y. (1983) Chemistry and Functional Moiety of a Fruiting-Inducing Cerebroside in *Schizophyllum commune, Biochim. Biophys. Acta 754*, 243–248.
25. Kawai, G., Ikeda, Y., and Tubaki, K. (1985) Fruiting of *Schizophyllum commune* Induced by Certain Ceramides and Cerebrosides from *Penicillium funiculosum, Agric. Biol. Chem. 49*, 2137–2146.
26. Kawai, G., Ohnishi, M., Fujino, Y., and Ikeda, Y. (1986) Stimulatory Effect of Certain Plant Sphingolipids on Fruiting of *Schizophyllum commune, J. Biol. Chem. 261*, 779–784.
27. Levery, S.B., Momany, M., Lindsey, R., Toledo, M.S., Shayman, J.A., Fuller, M., Brooks, K., Doong, R.L., Straus, A.H., and Takahashi, H.K. (2002) Disruption of the Glucosylceramide Biosynthetic Pathway in *Aspergillus nidulans* and *Aspergillus fumigatus* by Inhibitors of UDP-Glc:Ceramide Glucosyltransferase Strongly Affects Spore Germination, Cell Cycle, and Hyphal Growth, *FEBS Lett. 525*, 59–64.
28. Dickson, R.C., and Lester, R.L. (1999) Yeast Sphingolipids, *Biochim. Biophys. Acta 1426*, 347–357.
29. Jennemann, R., Geyer, R., Sandhoff, R., Gschwind, R.M., Levery, S.B., Grone, H.J., and Wiegandt, H. (2001) Glycoinositolphosphosphingolipids (basidiolipids) of Higher Mushrooms, *Eur. J. Biochem. 268*, 1190–1205.
30. Matsumoto, T., and Kitamoto, Y. (1987) Induction of Fruit-Body Formation by Water-Flooding Treatment in Sawdust Cultures of *Lentinus edodes, Trans. Mycol. Soc. Jpn. 28*, 437–443.
31. Song, C.H., Cho, K.Y., Nair, N.G., and Vine, J. (1989) Growth Stimulation and Lipid Synthesis in *Lentinus edodes, Mycologia 81*, 514–522.
32. Katayose, Y., Kajiwara, S., and Shishido, K. (1990) The Basidiomycete *Lentinus edodes* Linear Mitochondrial DNA Plasmid Contains a Segment Exhibiting a High Autonomously Replicating Sequence Activity in *Saccharomyces cerevisiae, Nucleic Acid Res. 18*, 1395–1400.
33. Rouser, G., Siakotos, A.N., and Fleischer, S. (1966) Quantitative Analysis of Phospholipid by Thin-Layer Chromatography and Phosphorus Analysis of Spots, *Lipids 1*, 85–88.
34. Lauter, C.J., and Trams, E.G. (1962) A Spectrophotometric Determination of Sphingosine, *J. Lipid Res. 3*, 136–138.
35. Kajiwara, S., Oura, T., and Shishido, K. (2001) Cloning of a Fatty Acid Synthase Component *FAS1* Gene from *Saccharomyces kluyveri* and Its Functional Complementation of *S. cerevisiae fas1* Mutant, *Yeast 18*, 1339–1345.
36. Gaver, R.C., and Sweeley, C.C. (1965) Method for Methanolysis of Sphingolipids and Direct Determination of Long-Chain Bases by Gas–Liquid Chromatography, *J. Am. Oil Chem. Soc. 42*, 294–298.
37. Fujino, Y., and Ohnishi, M. (1977) Structure of Cerebroside in *Aspergillus oryzae, Biochim. Biophys. Acta 486*, 161–171.
38. Takakuwa, N., Kinoshita, M., Oda, Y., and Ohnishi, M. (2002) Existence of Cerebroside in *Saccharomyces kluyveri* and Its Related Species, *FEMS Yeast Res. 1496*, 1–6.
39. Stahl, P.D., and Klug, M.J. (1996) Characterization and Differentiation of Filamentous Fungi Based on Fatty Acid Composition, *Appl. Environ. Microbiol. 62*, 4136–4146.
40. Ratledge, C., and Evans, C.T. (1991) Lipids and Their Metabolism, in *The Yeast*, 2nd edn. (Rose, A.H., and Harrison, J.S., eds.), Vol. 4, pp. 367–455, Academic Press, London.
41. Wagner, S., and Paltauf, F. (1994) Generation of Glycerophospholipid Molecular Species in the Yeast *Saccharomyces cerevisiae*. Fatty Acid Pattern of Phospholipid Classes and Selective Acyl Turnover at *sn*-1 and *sn*-2 Positions, *Yeast 10*, 1429–1437.
42. Ferrante, G., and Kates, M. (1983) Pathways for Desaturation of Oleoyl Chains in *Candida lipolytica, Can. J. Biochem. Cell Biol. 61*, 1191–1196.

[Received June 16, 2003, and in revised form November 5, 2003; revision accepted November 12, 2003]

Incorporation of 1-Chlorooctadecane into FA and β-Hydroxy Acids of *Marinobacter hydrocarbonoclasticus*

Elisabeth Aubert, Pierre Metzger*, and Claude Largeau

Centre Nationale de la Recherche Scientifique, Unité Mixte de Recherche 7573, Ecole Nationale Supérieure de Chimie de Paris, 75231 Paris cedex 05, France

ABSTRACT: The lipids of the gram-negative marine bacterium *Marinobacter hydrocarbonoclasticus*, cultivated in synthetic seawater supplemented with 1-chlorooctadecane as sole source of carbon, were isolated, purified, and their structures determined. Three pools of lipids were isolated according to the sequential procedure used: unbound lipids extracted by organic solvents, ester-bound lipids released under alkaline conditions, and amide-bound lipids released by acid hydrolysis. FA isolated from the unbound lipids included ω-chlorinated (21%, w/w, of this fraction; C_{16} predominant) and nonchlorinated compounds (22%, w/w; C_{18} predominant). These acids were accompanied by a high proportion of ω-chloro-C_{18} alcohols (43%, w/w) and a lower amount of ω-chloro-β-hydroxy-C_{18}, -C_{16}, and -C_{14} acids (5%, w/w). These data, together with the isolation from the culture medium of γ-butyrolactone, suggested a metabolism of 1-chlorooctadecane through oxidation into ω-chloro acid and then the classic β-oxidation pathway. The analysis of the ester-bound and amide-bound lipids revealed that significant amounts of ω-chloro-β-hydroxy C_{10}–C_{12} acids were incorporated into the lipopolysaccharides of the bacterium. Incorporation of these ω-chloro-β-hydroxy acids into the lipopolysaccharides represents a novel route for chloroalkane assimilation in hydrocarbonoclastic gram-negative bacteria. The formation of chlorinated hydroxy acids, like the ω-chloro FA in the cellular lipids, could account for an incomplete mineralization of chloroparaffins in the environment.

Paper no. L9400 in *Lipids 39*, 75–79 (January 2004).

Chloroparaffins are chlorinated, mainly straight-chain, saturated hydrocarbons of the C_{10}–C_{30} range, with a high degree of chlorination (40–70%, w/w) (1). Widely used as plasticizers, flame-proofing agents, and extreme pressure lubricants, their total world production was estimated to be 300,000 tons per year in 1987 (2). The release of such compounds into the environment can occur during production, storage, transportation, and use, potentially causing damage (3), particularly to the fauna (4,5). Considered for a long time as nonbiodegradable, their degradation has been reported, however, in some strains of *Rhodococcus* (6) and *Pseudomonas* (7). By comparison, 1-haloalkanes, which are the simplest compounds of this chemical family, are less recalcitrant to biodegradation. Thus, several strains of fungi, bacteria, and protozoa capable of using hydrocarbons as sole source of carbon are also known to degrade 1-chloroalkanes and to incorporate the resulting FA into their cellular lipids (8–12). In this paper we describe the isolation and the characterization of metabolites formed during the growth of *Marinobacter hydrocarbonoclasticus*, strain SP17, on 1-chlorooctadecane. This microorganism is a ubiquitous aerobic marine gram-negative bacterium, degrading alkanes efficiently (13–15). In addition to chloro FA and chloro fatty alcohols, we report on the formation of chlorinated β-hydroxy acids, not only as free compounds but also covalently bound to the lipopolysaccharides (LPS) of *M. hydrocarbonoclasticus*.

EXPERIMENTAL PROCEDURES

Chemical materials. Silica gel for column chromatography (CC) (silica gel 60, 70–230 mesh) was purchased from Merck Eurolab (Lyon, France). 1-Chlorooctadecane (>98%) was supplied by TCI (Tokyo, Japan); *n*-nonadecane (≥99%) was from Fluka (L'Isle d'Abeau, France); dimethyl disulfide (DMDS) and pyrrolidine were from Merck (Darmstadt, Germany); an etheral solution of diazomethane was prepared from Diazald® (Sigma-Aldrich; l'Isle d'Abeau, France), according to an Aldrich procedure (Technical Information Bulletin number AL-180).

Microorganism and culture conditions. Marinobacter hydrocarbonoclasticus strain SP 17, ATCC 49840 (Rockville, MD), was used. Cells were grown in 3-L Erlenmeyer flasks (×3) containing 1 L of synthetic seawater supplemented with 1-chlorooctadecane (1 g/L). Synthetic seawater was composed of (g/L, in distilled water): Tris, 5; KCl, 0.75; NH_4Cl, 1; $MgSO_4 \cdot 7H_2O$, 3.91; $MgCl_2 \cdot 6H_2O$, 5.08; $CaCl_2$, 1.5; NaCl, 23. The pH was adjusted to 7.8 with 10 M HCl; 2 mL and 4 mL of autoclaved (120°C, 20 min) solutions of $FeSO_4$ (1 g/L) and dipotassium phosphate (18.6 g/L), respectively, were added to 1 L of synthetic seawater immediately before use. The strain was precultured on *n*-nonadecane (1 g/L) and successively inoculated in media progressively enriched in 1-chlorooctadecane (0.25, 0.5, 0.75, and finally 1 g/L) and

*To whom correspondence should be addressed at Laboratoire de Chimie Bioorganique et Organique Physique, CNRS UMR 7573, ENSCP, 11 rue P. et M. Curie, 75231 Paris cedex 05, France.
E-mail: pierre-metzger@enscp.jussieu.fr

Abbreviations: CC, column chromatography; DMDS, dimethyl disulfide; LPS, lipopolysaccharides.

simultaneously impoverished in hydrocarbon in order to maintain a nutrient concentration of 1 g/L. A cell inoculum was finally prepared by cultivating the strain on pure 1-chlorooctadecane. The bacterium was grown aerobically at 22°C with agitation provided by magnetic stirring (100 rpm). The biomass was harvested after 3 wk of growth, when the cells entered the stationary phase of growth, by centrifugation at 7650 × *g*, washed twice with synthetic seawater (200 mL), and freeze-dried.

Extraction and fractionation of lipids. The dry biomass of *M. hydrocarbonoclasticus* (815 mg) was extracted using chloroform/methanol (2:1, vol/vol; 100 mL) with stirring, 18 h at room temperature. After centrifugation of the mixture at 120 × *g*, the pellet was resuspended for 1 h in chloroform/methanol and then centrifuged. The combined supernatants were concentrated under reduced pressure, and the crude extract (287 mg) was fractionated by CC on silica gel (24 g). A chloroalkane fraction was eluted with 90 mL heptane, and then the lipids were recovered by elution with diethyl ether/methanol (3:1, vol/vol; 200 mL). This latter fraction (51 mg) was transesterified in 30 mL of methanol/KOH (0.1 M), at 0°C for 2 h. The reaction mixture was acidified to pH 1 with aqueous HCl 5% (vol/vol) and extracted with diethyl ether, giving the "unbound lipids." The solvent-extracted biomass was then reacted with 40 mL of methanol/KOH (1 M) under reflux for 2 h to cleave ester bonds. The reaction mixture was centrifuged (100 × *g*), and the pellet was rinsed with 50 mL methanol. The combined supernatants were acidified with aqueous HCl (5%) and diluted with water, and the lipids were then extracted with diethyl ether. The concentrated extract (16 mg) constituted the "ester-bound" lipids. The residual biomass was hydrolyzed in 15 mL of aqueous HCl (4 M) for 6 h under reflux to cleave amide bonds. After cooling, the reaction mixture was diluted with distilled water (200 mL) and extracted with diethyl ether. The concentrated extract (17 mg) constituted the "amide-bound" lipids. The two latter extracts were submitted to esterification at room temperature, using an etheral solution of diazomethane (2 mL, 0.12 M). The reaction mixtures were concentrated under reduced pressure.

For the extraction of organic compounds released in the culture medium, 1 L of the supernatant obtained during the recovery of the biomass was continuously extracted with diethyl ether for 72 h. The ether extract was dried with anhydrous Na_2SO_4 and concentrated under reduced pressure.

Derivatization and MS. The three lipid pools and the ether extract of the culture medium were analyzed by GC–MS with a Hewlett-Packard HP 6890 chromatograph coupled with an HP 5973N mass spectrometer (Agilent Technology). The chromatograph was equipped with a J&W Scientific DB-5MS fused-silica column (30 m × 0.25 mm) coated with 95% polydimethylsiloxane and 5% phenylsiloxane (Massy, France). The temperature programs were from 100 to 300°C (4°C/min) for the three lipid pools and from 50 to 300°C (4°C/min) for the ether extract of the culture medium. GC–EI–MS analyses were performed at 70 eV. FAME were identified by coinjection with authentic standards on GC (same conditions as for GC–MS) and comparison of the mass spectra. The position of the double bonds in the FAME was determined by the analysis of the DMDS adducts formed by an I_2-catalyzed reaction (16). The methyl branching on the hydrocarbon chains of the lipids was established by examining the mass spectra of the pyrrolidide derivatives (17). Alcohols and β-hydroxy acids were analyzed as trimethylsilyl ethers (18).

RESULTS AND DISCUSSION

Methodology and quantitative data. To extract the totality of lipids we have used a procedure previously developed for lipid analysis of some gram-negative bacteria such as *Acinetobacter calcoaceticus, Escherichia coli,* and *M. hydrocarbonoclasticus* (15,19), and also some organic materials from a marine environment reworked by bacteria (20). This procedure involves a sequential extraction of the lipids. In a first step, a chloroform/methanol extraction furnishes the main part of the free and membrane lipids of the bacteria. Then the successive alkaline and acid hydrolyses of the extracted biomass liberate FA and hydroxy acids from ester-bound and amide-bound lipid moieties of LPS, respectively.

The crude extract (287 mg) obtained from the dry bacterial biomass (815 mg) by chloroform/methanol extraction accounted for 29% (w/w) of the dry biomass. To remove 1-chlorooctadecane from this mixture, which was adsorbed on the cell surfaces and also ingested by the bacterial cells, the extract was purified by silica gel CC. The recovered purified fraction (the unbound lipids: 51 mg), accounted for 8.8% (w/w) of the biomass free of chloroalkane, whereas the ester-bound and amide-bound lipids corresponded to 2.7 and 2.8% (w/w), respectively. By comparison with the data obtained from the bacterium grown on hydrocarbon (*n*-eicosane), the present results show an increase in lipid concentration in the three pools. On the whole, this corresponds to an absolute increase of about 80% (15).

Identification of lipids. FA were analyzed as FAME; alcohols and hydroxy functions of hydroxy acids were trimethylsilylated, and the three lipid fractions were analyzed by GC and GC–MS. To determine the position of the carbon–carbon double bonds in the monoenoic compounds, DMDS adducts were formed and examined by GC–MS. The presence of a chlorine atom in a molecule was easily established from the mass spectrum, which showed two peaks separated by two mass units for the molecular ion, in relation to the two isotopes ^{35}Cl and ^{37}Cl. These two peaks had heights in a 3:1 ratio, typical of the pattern expected for a compound containing one chlorine atom. The same was observed with chlorine-containing ions. As examples, Figure 1 shows the mass spectra of two derivatives of *M. hydrocarbonoclasticus* chloro lipids: the DMDS adduct of ω-chloro-octadec-9-en-1-ol, as trimethylsilyl derivative (Fig. 1A), and the trimethylsilyl ether of ω-chloro-β-hydroxydodecanoic acid methyl ester (Fig. 1B).

Composition of unbound lipids and metabolism of 1-chlorooctadecane. Lipid distribution by class of compounds in the unbound lipids is listed in Table 1. FA and fatty alcohols, together with their chlorinated analogs, were the major components, with a slight predominance of the latter compounds (45.2%; Table 1). Two C_{18} ω-chloro primary alcohols, together

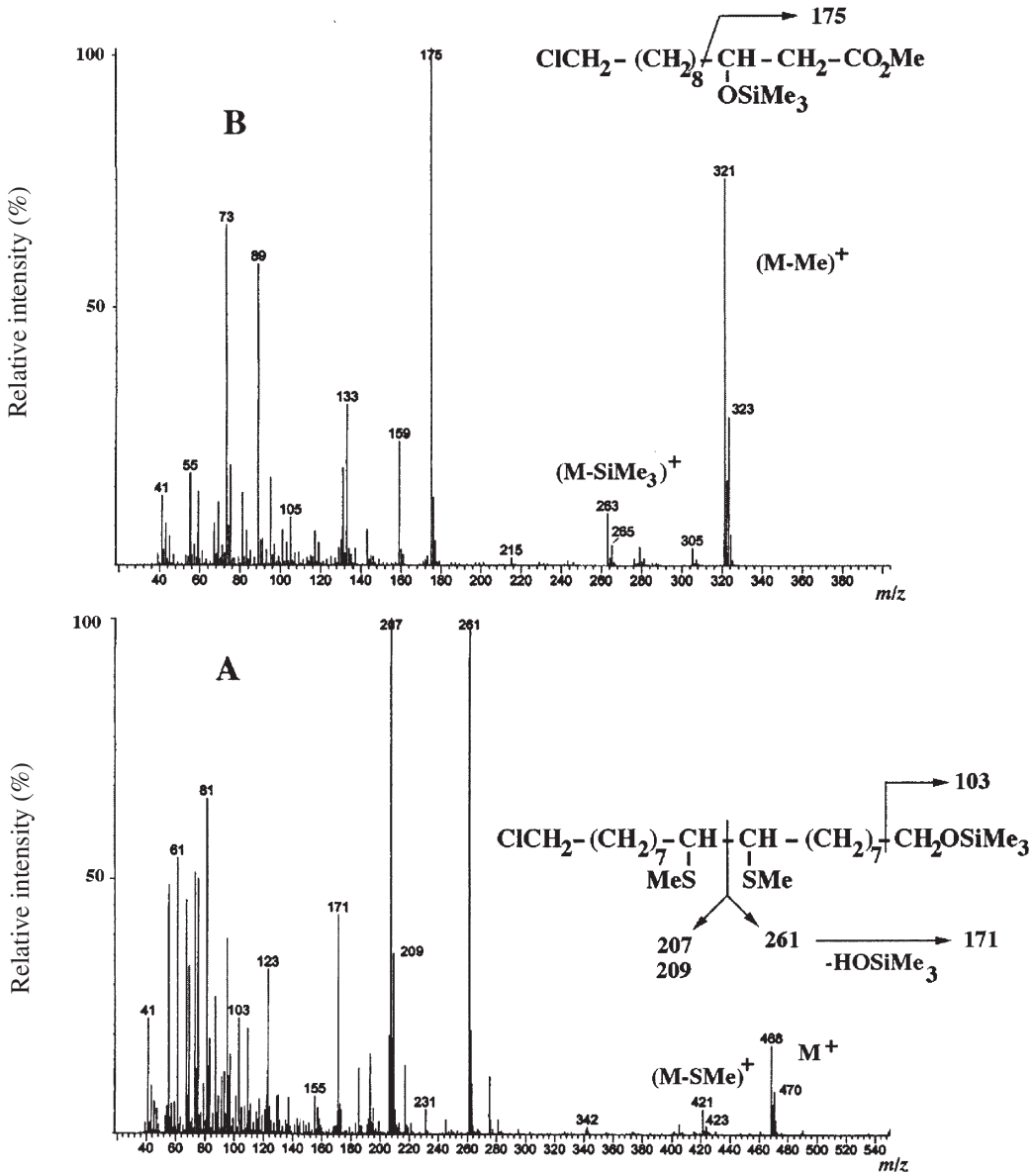

FIG. 1. Mass spectra of trimethylsilyl derivatives of dimethyl disulfide adduct of ω-chlorooctadec-9-en-1-ol (A) and ω-chloro-β-hydroxy-dodecanoic acid methyl ester (B).

representing 94.5% of the fatty alcohols, were the main unbound lipids; a saturated and an ω9 monounsaturated alcohol accounted for 18.1 and 22.4% of the unbound lipids, respectively (Table 2). A lower amount of a C_{18} secondary alcohol, with the hydroxyl group at position 2, was also detected (1.1% of the unbound pool). Stearyl alcohol (18:0) also occurred in significant amount (2% of the unbound lipids). Its presence could argue for the dehalogenation of 1-chlorooctadecane. However, the GC–MS analysis of the commercial chlorohydrocarbon used for this study revealed the presence of *n*-octadecane in low amount (0.2% of the mixture); its oxidation by the bacterium is probably at the origin of the stearyl alcohol. FA and their ω-chlorinated analogs were in almost equal proportion (Table 1). Monounsaturated FA with unsaturation at position ω9 predominated (18:1 dominant) over the ω7 isomers, as previously noted for the bacterium grown on various *n*-alkanes (14,15), whereas in the chlorinated series unsaturation occurred only at position ω9 (ω-Cl-16:1ω9 dominant). Furthermore, ω-chloro-β-hydroxy acids (C_{18}, C_{16}, and C_{14}: 87.3% of the unbound β-hydroxy acids) predominated over the C_{18} and C_{16} nonchlorinated compounds.

TABLE 1
Distribution and Abundance[a] of Lipids in the Three Pools

	Unbound	Ester-bound	Amide-bound
FA	42.1 (48.9)[b]	40.8 (9.3)	7.7 (–)
β-Hydroxy acids	5.5 (87.3)	48.1 (10.8)	78.9 (10.3)
Fatty alcohols	45.2 (94.5)		

[a]Expressed as percent, w/w, of the considered pool.
[b]Values in parentheses represent the proportion (in %) of chloro compounds for a given type of lipids.

TABLE 2
FA, Hydroxy Acid, and Fatty Alcohol Composition of the Three Lipid Pools Isolated from *Marinobacter hydrocarbonoclasticus* Grown on 1-Chlorooctadecane[a]

Lipids	Unbound	Ester-bound	Amide-bound
FA			
10:0	Trace	2.8	—[b]
12:0	Trace	9.8	—
14:0	0.6	Trace	—
Cl-14:0	1.7	0.9	—
14:1n-7	Trace	2.7	—
14:1n-9	2.3	2.7	—
15:0	0.1	—	—
16:0	5.8	11.0	7.7
Cl-16:0	8.5	2.9	—
7Me-16:0	0.5	0.5	—
16:1n-7	0.1	0.4	—
16:1n-9	2.3	0.4	—
Cl-16:1n-9	8.4	—	—
17:0	0.5	0.3	—
18:0	0.1	2.1	—
Cl-18:0	Trace	—	—
18:1n-7	0.1	3.6	—
18:1n-9	9.1	3.6	—
Cl-18:1n-9	2.0	—	—
β-Hydroxy acids			
10:0	—	0.4	0.7
Cl-10:0	—	2.1	1.9
11:0	—	0.2	0.3
Cl-11:0	—	0.2	1.3
12:0	Trace	39.5	69.5
Cl-12:0	Trace	2.9	4.9
12:1	—	0.3	—
Cl-12:1	—	0.3	—
13:0	—	0.5	0.5
14:0	—	—	0.9
Cl-14:0	0.5	—	—
14:1	—	2.0	—
Cl-14:1	0.5	—	—
16:0	0.5	—	—
Cl-16:0	1.5	—	—
Cl-16:1n-9	0.5	—	—
Cl-17:0	Trace	—	—
18:0	0.2	—	—
Cl-18:0	1.4	—	—
Cl-18:1n-9	0.4	—	—
Alcohols			
16:0, 1-OH	0.5	—	—
18:0, 1-OH	2.0	—	—
Cl-18:0, 1-OH	18.1	—	—
Cl-18:0, 2-OH	1.1	—	—
Cl-18:1n-9, 1-OH	22.4	—	—
Cl-18:0, 1,2-diol	1.1	—	—
Other compounds	7.2	10.3	12.3

[a]Expressed as percent of the total lipids for the considered pool.
[b]—, not detected.

From these results, it is likely that *M. hydrocarbonoclasticus* metabolizes 1-chlorooctadecane mainly *via* oxidation of the terminal methyl group to give the primary alcohol (ω-Cl-18:0, 1-OH), which undergoes successive oxidations to the ω-chloro $C_{18:0}$ acid and further degradation *via* the classical β-oxidation cycle involving β-hydroxy acids as intermediates. The desaturation of the ω-chloro alcohol would then give ω-chloro-octadec-9-en-1-ol, which would then be oxidized into the corresponding acid and further metabolized through the β-oxidation pathway. Evidence of metabolism by the β-oxidation route was also provided by the isolation of γ-butyrolactone from the culture medium. The β-oxidation pathway of the even carbon-numbered ω-chloro acids leads to 4-chlorobutyric acid, which can undergo, perhaps in an abiotic reaction, a cyclization to give γ-butyrolactone, as previously observed in the culture of *R. rhodochrous* on 1-chlorohexadecane (11).

Two minor routes also exist for the metabolism of 1-chlorooctadecane in *M. hydrocarbonoclasticus*. Indeed, the detection of a low amount of a secondary alcohol (ω-Cl-18:0, 2-OH) indicated that chlorooctadecane was also oxidized at a subterminal position. Further oxidation of this secondary alcohol would lead, *via* a Bayer–Villiger type reaction (21), to the chlorinated $C_{16:0}$ acid.

Furthermore, the GC–MS analysis of the unbound lipids revealed the unexpected presence of a diol, i.e., ω-chloro-octadecane-1,2-diol (Table 2). Based on the GC–MS analysis of the commercial chlorooctadecane, it appeared that this product contained, in addition to the octadecane already mentioned, low amounts of 1-chlorohexadecane, ω-chloro-octadec-1-ene (for each, about 0.2% of the mixture), and a trace amount of 1-chloroheptadecane. The diol was probably derived from the oxidation of the chlorinated octadecene. In the same way, 1-chloroheptadecane was certainly the basis for the formation of ω-chloro-β-hydroxyheptadecanoic acid.

Composition of the bound lipids. The ester-bound lipids included FA and β-hydroxy acids, the latter compounds being predominant. Contrary to the unbound lipids, nonchlorinated compounds dominated in these two lipid classes (Table 1). FA having short hydrocarbon chains (C_{10} and C_{12}) were more abundant than in the unbound lipids, whereas the proportion of chloro acids with long hydrocarbon chains sharply decreased. β-Hydroxy dodecanoic acid was quite dominant in this lipid pool (39.5% of the ester-bound lipids; Table 2). It was accompanied by low amounts of lower (3-OH-10:0, 3-OH-11:0) and higher (3-OH-13:0, 3-OH-14:1) homologs, along with substantial amounts of the ω-chlorinated derivatives of 3-OH-10:0, 3-OH-11:0, and 3-OH-12:0 (Table 2).

Amide-bound lipids were almost exclusively β-hydroxy acids, as previously observed in the cultures of *M. hydrocarbonoclasticus* on eicosane (15), and some other hydrocarbons (Soltani, M., Metzger, P., and Largeau, C., unpublished results). In the present work, the amide-bound lipids contained β-hydroxy dodecanoic acid as the major compound, together with some chlorinated and nonchlorinated homologous compounds. The distribution pattern of these compounds was rather similar to the one observed in the ester-bound lipids.

From all these results, it appears that *M. hydrocarbonoclasticus* metabolizes 1-chlorooctadecane chiefly *via* oxidation into primary alcohol and acid and further degrades it *via* the β-oxidation cycle. The bacterium is able to incorporate high proportions of chlorinated compounds into the intracellular

lipids. The C_2 units released during the β-oxidation cycle are subsequently used for the *de novo* synthesis of FA and β-hydroxy acids. In gram-negative bacteria, it is well known that β-hydroxy acids exhibit important taxonomic values and are generally the main components of the LPS, whereas nonhydroxy acids are subordinate compounds in these polymers (22). From previous analyses of the lipid composition of *M. hydrocarbonoclasticus*, it was established that β-hydroxy-12:0 acid was the major and sometimes unique hydroxy acid of the LPS, whatever the carbon source may be (15; Soltani, M., Metzger, P., and Largeau, C., unpublished results). In the presence of 1-chlorooctadecane, the LPS of the bacterium still incorporate a high proportion of β-hydroxy-12:0 acid, but also up to 10% of ω-chloro-β-hydroxy acids. This result has environmental and geochemical implications. Indeed, the incorporation of chloro-β-hydroxy acids into LPS diverts a part of the chloroalkane from mineralization and could thus lead to the accumulation of this type of potentially toxic (23) compound in biota. On the other hand, besides anthropogenic inputs of haloalkanes in the environment, two other natural sources have recently been identified: plants from hypersaline environments (24) and some marine sediments (25). Based on the present results, it can be hypothesized that some sedimentary chloro FA and chloro-β-hydroxy acids might be formed through a pathway similar to the one occurring in *M. hydrocarbonoclasticus*.

REFERENCES

1. Schenker, B.A. (1979) Chlorinated Paraffins, in *Encyclopedia of Chemical Technology* (Mark, H.F., Othmer, D.F., Overberger, C.G., and Seaborg, G.T., eds.), Vol. 5, pp. 786–791, John Wiley & Sons, New York.
2. Omori, T., Kimura, T., and Kodama, T. (1987) Bacterial Cometabolic Degradation of Chlorinated Paraffins, *Appl. Microbiol. Biotechnol. 25*, 553–557.
3. National Industrial Chemicals Notification and Assessment Scheme, http://www.nicnas.gov.au/publications/CAR/PEC/PEC16/PEC16index.htm (accessed June 2001).
4. Fisk, A.T., Cymbalisty, C.D., Bergman, Å., and Muir, D.C.G. (1996) Dietary Accumulation of C12 and C16-Chlorinated Alkanes by Juvenile Rainbow Trout (*Oncorhynchus mykiss*), *Environ. Toxicol. Chem. 15*, 1775–1782.
5. Tomy, G.T., Muir, D.C.G., Westmore, J.B., and Stern, G.A. (2000) Levels of C_{10}–C_{13} Polychloro-*n*-alkanes in Marine Mammals from the Arctic and the St. Lawrence River Estuary, *Environ. Sci. Technol. 34*, 1615–1619.
6. Allpress, J.D., and Gowland, P.C. (1999) Biodegradation of Chlorinated Paraffins and Long-Chain Chloroalkanes by *Rhodococcus* sp. S45-1, *Int. Biodegrad. Bioremed. 43*, 173–179.
7. Wischnak, C., Löffler, F.E., Li, J., Urbance, J.W., and Müller, R. (1998) *Pseudomonas* sp. Strain 273, an Aerobic α,ω-Dichloroalkane-Degrading Bacterium, *Appl. Environ. Microbiol. 64*, 3507–3511.
8. Murphy, G.L., and Perry, J.J. (1983) Incorporation of Chlorinated Alkanes into Fatty Acids of Hydrocarbon-Utilizing Mycobacteria, *J. Bacteriol. 156*, 1158–1164.
9. Murphy, G.L., and Perry, J.J. (1984) Assimilation of Chlorinated Alkanes by Hydrocarbon-Utilizing Fungi, *J. Bacteriol. 160*, 1171–1174.
10. Murphy, G.L., and Perry, J.J. (1987) Chlorinated Fatty Acid Distribution in *Mycobacterium convolutum* Phospholipids After Growth on 1-Chlorohexadecane, *Appl. Environ. Microbiol. 53*, 10–13.
11. Curragh, H., Flynn, O., Larkin, M.J., Stafford, T.M., Hamilton, J.T.G., and Harper, D.B. (1994) Haloalkane Degradation and Assimilation by *Rhodococcus rhodochrous* NCIMB 13064, *Microbiology 140*, 1433–1442.
12. Kaska, D.D., Yokota, T., Webb, H.M., Gibor, A., Polne-Fuller, M., and Kaska, W. (1991) Long-Chain Chloroalkane Utilization by a Marine Protozoan, *J. Gen. Microbiol. 137*, 2669–2672.
13. Gauthier, M.J., Lafay, B., Christen, R., Fernandez, L., Acquaviva, L., Bonin, P., and Bertrand, J.-C. (1992) *Marinobacter hydrocarbonoclasticus* gen. nov., sp. nov., a New, Extremely Halotolerant, Hydrocarbon-Degrading Marine Bacterium, *Int. J. Syst. Bacteriol. 42*, 568–576.
14. Doumenq, P., Aries, E., Asia, L., Acquaviva, M., Artaud, J., Gilewicz, M., Mille, G., and Bertrand, J.C. (2001) Influence of *n*-Alkanes and Petroleum on Fatty Acid Composition of a Hydrocarbonoclastic Bacterium: *Marinobacter hydrocarbonoclasticus* Strain 617, *Chemosphere 44*, 519–528.
15. Lattuati, A., Metzger, P., Acquaviva, M., Bertrand, J.-C., and Largeau, C. (2002) *n*-Alkane Degradation by *Marinobacter hydrocarbonoclasticus* Strain SP 17: Long-Chain β-Hydroxy Acids as Indicators of Bacterial Activity, *Org. Geochem. 33*, 37–45.
16. Scribe, P., Pepe, C., Barouxis, A., Fuche, C., Dagaut, J., and Saliot, A. (1990) Détermination de la Position de l'Insaturation des Monoènes par Chromatographie en Phase Gazeuse Capillaire–Spectrométrie de Masse (CGS:SM) des Dérivés Diméthyl-Disulfides: Application à l'Analyse d'un Mélange Complexe d'Alcènes, *Analusis 18*, 284–288.
17. Anderson, B.A., and Holman, R.T. (1974) Pyrrolidides for Mass Spectrometric Determination of the Position of the Double Bond in Monounsaturated Fatty Acids, *Lipids 9*, 185–190.
18. Kates, M. (1986) *Techniques of Lipidology*, 2nd edn., pp. 344–345, Elsevier, Amsterdam.
19. Goossens, H., de Leeuw, J.W., Irene, W., Rijpstra, C., Meyburg, G.J., and Schenk, P.A. (1989) Lipids and Their Mode of Occurrence in Bacteria and Sediments—I. A Methodological Study of the Lipid Composition of *Acinetobacter calcoaceticus* LMD 79-41, *Org. Geochem. 14*, 15–25.
20. Wakeham, S.G. (1999) Monocarboxylic, Dicarboxylic and Hydroxy Acids Released by Sequential Treatments of Suspended Particles and Sediments of the Black Sea, *Org. Geochem. 30*, 1059–1074.
21. Ratledge, C. (1978) Degradation of Aliphatic Hydrocarbons, in *Developments in Biodegradation of Hydrocarbons* (Watkinson, R.J., ed.), Vol. 1, pp. 1–46, Applied Science, London.
22. Wilkinson, S.G. (1988) Gram-Negative Bacteria, in *Microbial Lipids* (Ratledge, C., and Wilkinson, S.G., eds.), Vol. 1, pp. 299–488, Academic Press, London.
23. Ewald, G. (1998) Chlorinated Fatty Acids: Environmental Pollutants with Intriguing Properties, *Chemosphere 37*, 2833–2837.
24. Grossi, V., and Raphel, D. (2003) Long-Chain (C_{19}–C_{29}) 1-Chloro-*n*-alkanes in Leaf Waxes of Halophytes of the Chenopodiaceae, *Phytochemistry 63*, 693–698.
25. Grossi, V., Derenne, S., Raphel, D., and Largeau, C. (2003) Haloalkanes in Polar Geomacromolecules: Towards New Pathways of Organic Matter Diagenesis, in *21st International Meeting on Organic Geochemistry, Book of Abstracts (8–12 September 2003)*, pp. 168–169, EAOG, Kraków, Poland.

[Received October 24, 2003; accepted November 20, 2003]

Impact of *in vivo* Glycation of LDL on Platelet Aggregation and Monocyte Chemotaxis in Diabetic *Psammomys obesus*

Monika Zoltowska[a,b], Edgard Delvin[a,c], Ehud Ziv[d], Noel Peretti[a,b], Manon Chartré[a,b], and Emile Levy[a,b]*

[a]Centre de Recherche Hôpital Sainte-Justine, Départements de [b]Nutritionet [c]Biochemistrie, Université de Montréal, Montréal (Québec), Canada, H3T 1C5, and [d]Diabetes Unit, Division of Internal Medicine, Hadassah University Hospital, Jerusalem 91120, Israel

ABSTRACT: *Psammomys obesus* (sand rat) is an appropriate model to highlight the development of hyperinsulinemia, insulin resistance, obesity, and diabetes. This animal species, with genetically predetermined diabetes, acquires non-insulin dependent diabetes mellitus when exposed to energy-rich diets. In the present study, we explored the possibility that glycation of LDL may occur in diabetes-prone *P. obesus* and affect platelet and macrophage functions. The glycation of LDL, isolated from diabetic animals, was significantly ($P < 0.05$) higher (40%) than that of control animals. The incubation of platelets with glycated LDL enhanced the reactivity of platelets by 32–44% depending on the aggregating agents (thrombin, collagen, ADP). Furthermore, LDL derived from diabetic rats were chemotactic for normal monocytes and stimulated the incorporation of [^{14}C]oleate into cellular cholesteryl esters. The enhancement of platelet aggregation and cholesterol esterification in monocytes may contribute toward the accelerated development of atherosclerotic cardiovascular disease in diabetic *P. obesus* animals. This study also illustrates the relevance of studying atherosclerosis in the *P. obesus* animal model, as it shows an increased tendency to develop diet-induced diabetes, which is associated with cardiovascular disorders.

Paper no. L9380 in *Lipids 39*, 81–85 (January 2004).

Diabetes mellitus is commonly associated with marked alterations in plasma lipoproteins (1,2). Abnormalities of plasma lipids and lipoprotein concentrations and composition contribute to accelerated atherosclerosis (1,2). Several studies have emphasized the involvement of glycation (nonenzymatic glycosylation) in the rapid development of atherosclerosis (3,4). Indeed, the nonenzymatic binding of glucose to reactive amino groups located on lysine side chains of apolipoprotein (apo) B increased its atherogenic potential. Since the pioneering study of Schleicher *et al.* (5), extensive work has been carried out toward understanding the pathophysiologic relevance of glycation and oxidation of LDL. Not only were glycated LDL present in hyperlipidemic and normolipidemic diabetic patients (6,7), but glycation also diminished the high affinity of the LDL receptor, which mediates uptake and degradation of LDL *in vitro* (8). Additionally, glycation promoted internalization by an alternative receptor of monocyte-macrophages that gave rise to foam cells (9), decreased the rate of clearance of LDL *in vivo* (10), and compromised the regulation of HMG-CoA reductase and acyl-CoA:cholesterol acyltransferase activities (11). Furthermore, the presence of nonenzymatically bound glucose on lipoproteins may increase the likelihood of oxidative damage. In this situation, the glycation of apoB may cause the molecule to become chemically unstable, rendering it open to attack by free radicals generated by the peroxidation of lipid components of LDL, or apoB may undergo further direct chemical modifications by oxidation, acetylation, or methylation (3). Finally, the production of autoantibodies directed to glycated proteins occurred *in vivo* (12). These antigen–antibody complexes were found in atherosclerotic lesions and detected in the serum of diabetic rats (13).

Despite major advances in the understanding of the risk factors associated with atherosclerosis, the pathophysiological processes leading toward the development of vascular lesions in diabetes remain obscure. Given the difficulty of exploring the etiology and the time course of lesion development in humans, diabetic animal models may provide excellent opportunities to elucidate mechanisms that may be common to animals and humnas. Recently, we showed that the *Psammomys obesus* (sand rats) developed hyperinsulinemia, hyperglycemia, and obesity when transferred to laboratory diets (14–16). In nature, this animal is an herbivorous rodent, subsisting on a low-energy, electrolyte-rich diet. The diabetic state that develops in captivity can be prevented by feeding the animals a low-energy diet, such as the saltbush diet. Therefore, the *P. obesus* model is particularly well-suited to highlight the development of hyperinsulinemia, insulin resistance, obesity, and diabetes in populations subjected to nutritional abundance and genetically predisposed to diabetes. However, studies are needed to demonstrate that this animal is able to display some of the features associated with the atherosclerotic complications of diabetes. This study was therefore designed to determine whether the glycation of LDL can occur in diabetic *P. obesus* animals, with potential consequences on platelet and macrophage functions.

*To whom correspondence should be addressed at Centre de recherche, Hôpital Sainte-Justine, 3175 Côte Ste-Catherine Rd., Montreal, Quebec, Canada H3T 1C5. E-mail: levye@justine.umontreal.ca

Abbreviations: AGE, advanced glycation end products; apo, apolipoprotein.

MATERIALS AND METHODS

Animals. Psammomys obesus (sand rats; age 2.5–3.5 mon) from Hebrew University (Jerusalem, Israel) were used for this study. After weaning, the animals were maintained on a low-energy diet containing 2.38 kcal/g (Koffolk, Petach Tikva, Israel) until the beginning of the experiments. They were then switched to a high-energy diet (2.93 kcal/g) for 2 wk. Water and food were supplied *ad libitum*. Animals with normoinsulinemia, normoglycemia, hyperglycemia, and hyperinsulinemia were used for the present studies. All experimental procedures performed herein were authorized by the Institutional Animal Care Committee.

Isolation of LDL. Blood was collected on EDTA after an overnight fast. Plasma LDL was isolated by traditional sequential ultracentrifugation, as described previously (17), so the LDL fraction was $1.019 < d < 1.063$ g/mL. Isolated LDL was washed and concentrated by one additional spin and the appropriate KBr density (1.063 g/mL) in a Ti-50 rotor in a Beckman model L5-65 ultracentrifuge for 18 h at 4°C. The LDL fraction was dialyzed exhaustively against 0.15 M NaCl, 0.0001 M EDTA, pH 7.0. Lipoprotein-deficient serum was prepared as reported previously (18).

Glycation. Glycation of LDL, diluted to 1 mg/mL, was measured essentially as described by Lyons *et al*. (19). Briefly, apoprotein of LDL was reduced by tritiated sodium borohydride (360 mCi/mmol; New England Nuclear, Montréal, Canada) so that tritium was incorporated into the ketoamine group formed by the attachment of glucose to protein. After acid hydrolysis for 18 h at 95°C in 12 N HCl, the resultant tritiated glycated amino acids (^{3}H-hexitol amino acids) were eluted through affinity chromatography, and radioactivity was counted. The amount of hydrolyzed apo was applied to chromatography, and the extent of glycation was expressed as dpm/mg protein/min of hydrolyzed protein.

Chemotaxis assay. Chemotaxis was measured by using freshly prepared monocytes as described (20).

Platelet aggregation. Platelets were isolated from citrated blood obtained from normal animals. Platelets were washed, suspended in HEPES-Tyrode's buffer (0.135 M NaCl, 2.7 mM KCl, 11.9 mM $NaHCO_3$, 0.36 mM NaH_2PO_4, 14.7 mM HEPES, pH 7.35), counted, and adjusted to 4×10^8/mL. Platelets were incubated with LDL (1 mg protein/ mL) derived from control or diabetic *P. obesus* at 37°C for 30 min. Platelet aggregation was assessed essentially as described by Watanabe *et al.* (21) except that thrombin, collagen, and ADP also were included as aggregating agents. The final concentrations were 0.5 U/mL thrombin, 2 μg/mL collagen, and 5 mM ADP.

Monocyte isolation and measurement of esterified cholesterol content. Cholesteryl ester synthesis was determined in isolated monocytes after incubation of monocyte-derived macrophages with control or diabetic LDL (100 μg protein/mL) (22). After maturation of macrophages, the cells were extensively washed with PBS and incubated with serum-free medium containing 0.2 mm [^{14}C]oleic acid complexed with 2.4 mg albumin. The cells were then incubated at 37°C for 20 h. After the incubation, the medium was removed and the cells were washed with PBS before being harvested. Lipid extraction of the cells (pelleted by centrifugation) was performed with chloroform/methanol (2:1, vol/vol). Cholesteryl [^{14}C]oleate was isolated by TLC and counted as previously described (23).

Biochemical analyses. Plasma glucose, cholesterol, and TG were determined using Boehringer kits (Mannheim, Germany). Plasma insulin levels were quantified by RIA (Phadesph; Kabi Pharmacia Diagnostics, Uppsala, Sweden).

Statistical analysis. All results were expressed as mean ± SE. Statistical analysis was performed with the paired Student's *t*-test, with $P < 0.05$ accepted as statistically significant.

RESULTS

Plasma parameters. As observed in Table 1, some of the *P. obesus* animals developed diabetes based on glucose and insulin determinations. Concomitantly, they exhibited abnormally high values of TG and cholesterol compared to normal animals.

LDL glycation. For the determination of whether glycation occurred in *P. obesus*, LDL were isolated from both groups of animals and LDL glycation was measured. As shown in Table 2, the glycation of LDL isolated from diabetic *P. obesus* was significantly higher (~40%) than that of LDL particles derived from controls. Changes were also noted in the chemical composition of LDL. TG, cholesteryl ester, and protein enrichment as well as free cholesterol and phospholipid depletion characterized diabetic LDL particles.

Platelet aggregation. The effect of glycated LDL on aggregation of normal platelets was also evaluated. The incubation of platelets with diabetic LDL markedly enhanced the reactivity of platelets with the different aggregating agents (Fig. 1).

Chemotaxis and macrophage cholesterol esterification. LDL derived from diabetic *P. obesus* were found to be chemotactic for monocytes (Table 3). Furthermore, diabetic

TABLE 1
Body Weight and Biochemical Plasma Parameters of Control and Diabetic Animals[a]

Animals	Body weight (g)	Glucose (mg/dL)	Insulin (μU/mL)	TG (mg/dL)	Cholesterol (mg/dL)
Control ($n = 20$)	89.2 ± 3.1	82.0 ± 3.6	68.4 ± 12.7	58.6 ± 8.9	66.0 ± 7.2
Diabetic ($n = 20$)	119.0 ± 4.2	366.1 ± 19.6[b]	205.8 ± 25.3[b]	299.5 ± 13.4[b]	149.4 ± 11.4[b]

[a]Values are means ± SEM.
[b]$P < 0.01$.

TABLE 2
Glycation and Lipid Composition of LDL from Diabetic and Control Animals[a]

Animals	Glycation[b] (dpm/μg protein/min)	TG (%)	CE (%)	PC (%)	PL (%)	PR (%)
Diabetic	72,200 ± 1,000[c]	9.4 ± 0.4[c]	32.4 ± 1.3[c]	7.9 ± 0.7	31.8 ± 1.2	18.4 ± 0.7[c]
Control	51,300 ± 2,300	16.2 ± 0.7	23.7 ± 1.0	9.1 ± 0.5	26.9 ± 1.3	24.2 ± 0.5

[a]Values are means ± SEM of $n = 10$/group of animals.
[b]Measures of [^{3}H]hexitol amino acid.
[c]$P < 0.05$.

LDL stimulated the incorporation of [^{14}C]oleate into cellular cholesteryl esters of monocytes 4.8-fold relative to their plasma LPDS counterpart. On the other hand, only a 2.7-fold stimulation of [^{14}C]oleate incorporation by control LDL was achieved using their plasma LPDS counterpart.

DISCUSSION

Psammomys obesus animals are prone to obesity, hyperglycemia, and hyperinsulinemia when transferred from their desert native saltbush food (*Atriplex halimus*, 1.9 kcal/g) to a laboratory rodent diet, which is higher in energy (3.1 kcal/g) (14–16). However, the abnormalities of lipoprotein metabolism that are intimately related to the development of atherosclerosis have not yet been investigated in this diabetic animal model. In the present study, we explored the possibility that the nonenzymatic glycosylation of LDL, a process occurring in diabetes because of their increased ambient glucose levels, may potentiate certain processes that are relevant to cardiovascular disease. Our data demonstrated that glycated LDL, present in diabetic sand rats, enhanced platelet sensitivity to some aggregating agents. Furthermore, glycated LDL was chemotactic for monocytes and produced much greater stimulation of cholesterol esterification.

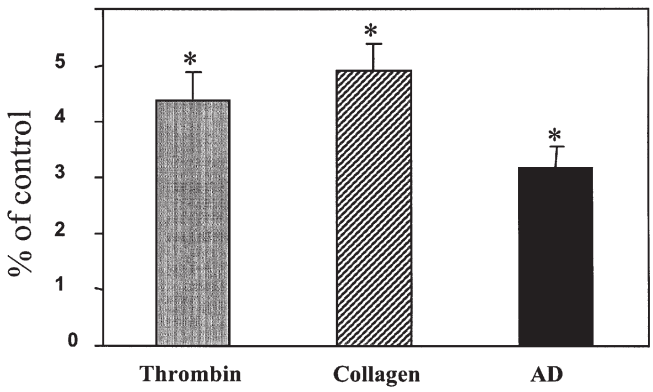

FIG. 1. Aggregation of platelets that were incubated for 5 min with control and glycated LDL. Values are expressed as percentages of aggregation rate of platelets incubated with LDL from normal animals at the maximal amplitude of the aggregation curve (the percentage of platelet-poor plasma being 100%). Platelets were isolated from citrated blood obtained from normal *Psammomys obesus* animals, washed, pooled, suspended in Tyrode's buffer (pH 7.4), and counted. After adjustment to 4×10^8/mL, they were incubated with LDL (1 mg protein/mL) derived from control or diabetic *P. obesus* at 37°C for 30 min. Platelets were then stimulated by either thrombin (0.5 U/mL), collagen (2 mg/mL), or ADP (5 mM) at 37°C for 5 min. Differences with all the aggregating agents were significant (*$P < 0.01$ for $n = 4$ animals/ group).

Increased nonenzymatic glycosylation of proteins has been implicated in the etiology of several complications in diabetes mellitus (24). Advanced glycation end products (AGE) cause numerous abnormal responses in cells that produce serious consequences in macromolecular functions of DNA (25), structural proteins (26), enzymes (27), and growth factors (28). Apart from diabetic microvascular complications (24), AGE also have been implicated in vascular damage, particularly atherosclerosis (29). This is the first study documenting the effect of the nonenzymatic glycosylation of atherogenic LDL particles in *P. obesus* animals. In this context, it has been postulated that abnormal platelet function may be one of the factors contributing to the increased incidence of macrovascular disease in diabetic patients (20). The results presented in this paper show that one of possible mechanisms responsible for the enhancement of platelet aggregation is the glycation of LDL, confirming and extending the data presented previously by Watanabe *et al.* (21). The recognition of glycated LDL by the classic LDL receptor is markedly impaired (8). These biologically modified LDL particles are preferentially recognized by both murine and human macrophages *via* a high-affinity receptor, the scavenger receptor. They may induce a massive intracellular accumulation of cholesteryl ester in these cells (11). Although we have not measured the scavenger receptor activity in the current investigation, our data revealing cholesteryl ester accumulation suggest that monocyte-derived macrophages recognized and degraded glycated LDL in *P. obesus*. Accordingly, Lopes-Virella *et al.* (11) have demonstrated that human monocytes recognize glycated LDL to a greater extent than normal LDL. This probably occurs through a pathway independent of the classic LDL-receptor pathway. As macrophages are thought to be the precursors of most of the lipid-laden foam cells characteristic of the early atheromatous lesion, we suggest that atherosclerosis may be

TABLE 3
Effect of LDL on Chemotaxis and Cholesterol Esterification in *Psammomys obesus* peritoneal Macrophages

LDL source	Chemotatic index[a]	Cholesterol esterification (μmol/mg cell protein/15 h)
Diabetic	5.3 ± 0.7[b]	18.8 ± 3.7[b]
Control	1.6 ± 0.3	2.7 ± 0.3

[a]Number of cells migrating in response to the test substance divided by the number of cells migrating when control medium is present in each chamber. Values for chemotactic index were carried out in triplicate, whereas those of cholesterol esterification are means ± SE for $n = 4$ animals.
[b]$P < 0.05$.

a complication of diabetes characterizing *P. obesus* animals. Importantly, the AGE accumulation in the extracellular matrix of atheromatous arteries might lead to enhanced subintimal protein and lipoprotein deposition with covalent trapping of LDL as well as nitric oxide depletion (30,31). The endothelial migration of monocytes and the uptake of these modified LDL may result in lipid-laden foam cells in the arterial intima and promotion of atherosclerosis.

In view of the chemical abnormalities of LDL isolated from diabetic animals, additional studies are needed to delineate whether glycation *per se* or the other perturbations seen in diabetic LDL are responsible for altered platelet and macrophage function in *P. obesus*. In fact, the development of long-term vascular complications, including atherosclerosis, has been attributed by many investigators to hyperglycemia, the primary clinical manifestation of diabetes (32). The participation of protein glycation in these processes has stimulated considerable interest in recent years. This reaction begins with the spontaneous condensation of a sugar aldehyde with free amino groups and seems responsible for a number of cellular effects despite normal LDL composition in numerous studies. Accordingly, increased platelet aggregation was detected in diabetic patients even when their plasma lipid and lipoprotein levels were normal (20). It is therefore conceivable that glycated LDL could contribute to various monocyte and platelet perturbations, thereby accelerating arterial disease. In other studies, following incubation with glycated LDL, platelets showed deep modifications in the activity of plasma membrane transport enzymes in the cytoplasmic calcium concentrations and in nitric oxide production (33). Therefore, the interaction between glycated LDL and platelets may play a central role in the pathophysiology of the vascular complications of diabetes in *P. obesus*. However, further investigation is required to highlight the separate impact of LDL glycation and lipid composition on platelet and monocyte intracellular events. Nevertheless, it should be noted that LDL composition abnormalities and LDL glycation occur in type 2 diabetes, and these two alterations could result in biological effects similar to those recorded in our studies.

In this study, we examined *in vivo*-occurring, nonenzymatic glycosylation only in LDL. Indeed, increased glycation can affect other lipoprotein classes and apoproteins. Curtiss and Witztum (34) found elevated levels of glycation in VLDL and HDL apoproteins. Further work is necessary to explore the repercussions of these modified particles.

The present work demonstrates abnormal LDL composition and the presence of glycated LDL in diabetic *P. obesus*. Moreover, "diabetic" LDL stimulated monocyte chemotaxis and increased cholesteryl ester formation. Finally, glycated LDL enhanced platelet reactivity. These data suggest that diabetic *P. obesus* animals present various characteristics that are of paramount importance in the initiation of atherosclerotic lesions. Therefore, this animal model of insulin resistance and diet-induced obesity-linked diabetes may be useful to study development of cardiovascular diseases.

ACKNOWLEDGMENTS

This work was supported by the Dairy Farmers of Canada and the Natural Sciences and Engineering Research Council of Canada (NSERC). We thank Schohraya Spahis for skillfully preparing the manuscript.

REFERENCES

1. Timar-Banu, O., Beauregard, H., Tousignant, J., Lassonde, M., Harris, P., Viau, G., Vachon, L., Levy, E., and Abribat, T. (2001) Development of Noninvasive and Quantitative Methodologies for the Assessment of Chronic Ulcers and Scars in Humans, *Wound Repair Regen. 9*, 123–132.
2. Knopp, R.H., Retzlaff, B., Aikawa, K., and Kahn, S.E. (2003) Management of Patients with Diabetic Hyperlipidemia, *Am. J. Cardiol. 91*, 24E–28E.
3. Sakaguchi, T., Yan, S.F., Yan, S.D., Belov, D., Rong, L.L., Sousa, M., Andrassy, M., Marso, S.P., Duda, S., Arnold, B., *et al*. (2003) Central Role of RAGE-Dependent Neointimal Expansion in Arterial Restenosis, *J. Clin. Invest. 111*, 959–972.
4. Vlassara, H., and Palace, M.R. (2002) Diabetes and Advanced Glycation End Products, *J. Intern. Med. 251*, 87–101.
5. Schleicher, E., Deufel, T., and Wieland, O.H. (1981) Nonenzymatic Glycosylation of Human Serum Lipoproteins. Elevated Epsilon-Lysine Glycosylated Low Density Lipoprotein in Diabetic Patients, *FEBS Lett. 129*, 1–4.
6. Mironova, M.A., Klein, R.L., Virella, G.T., and Lopes-Virella, M.F. (2000) Anti-modified LDL Antibodies, LDL-Containing Immune Complexes, and Susceptibility of LDL to *in vitro* Oxidation in Patients with Type 2 Diabetes, *Diabetes 49*, 1033–1041.
7. Klein, R.L., Laimins, M., and Lopes-Virella, M.F. (1995) Isolation, Characterization, and Metabolism of the Glycated and Nonglycated Subfractions of Low-Density Lipoproteins Isolated from Type I Diabetic Patients and Nondiabetic Subjects, *Diabetes 44*, 1093–1098.
8. Wang, X., Bucala, R., and Milne, R. (1998) Epitopes Close to the Apolipoprotein B Low Density Lipoprotein Receptor-Binding Site Are Modified by Advanced Glycation End Products, *Proc. Natl. Acad. Sci. USA 95*, 7643–7647.
9. Zimmermann, R., Panzenbock, U., Wintersperger, A., Levak-Frank, S., Graier, W., Glatter, O., Fritz, G., Kostner, G.M., and Zechner, R. (2001) Lipoprotein Lipase Mediates the Uptake of Glycated LDL in Fibroblasts, Endothelial Cells, and Macrophages, *Diabetes 50*, 1643–1653.
10. Bucala, R., Makita, Z., Vega, G., Grundy, S., Koschinsky, T., Cerami, A., and Vlassara, H. (1994) Modification of Low Density Lipoprotein by Advanced Glycation End Products Contributes to the Dyslipidemia of Diabetes and Renal Insufficiency, *Proc. Natl. Acad. Sci. USA 91*, 9441–9445.
11. Lopes-Virella, M.F., Klein, R.L., Lyons, T.J., Stevenson, H.C., and Witztum, J.L. (1988) Glycosylation of Low-Density Lipoprotein Enhances Cholesteryl Ester Synthesis in Human Monocyte-Derived Macrophages, *Diabetes 37*, 550–557.
12. Bellomo, G., Maggi, E., Poli, M., Agosta, F.G., Bollati, P., and Finardi, G. (1995) Autoantibodies Against Oxidatively Modified Low-Density Lipoproteins in NIDDM, *Diabetes 44*, 60–66.
13. Witztum, J.L., Steinbrecher, U.P., Kesaniemi, Y.A., and Fisher, M. (1984) Autoantibodies to Glucosylated Proteins in the Plasma of Patients with Diabetes Mellitus, *Proc. Natl. Acad. Sci. USA 81*, 3204–3208.
14. Kalderon, B., Adler, J.H., Levy, E., and Gutman, A. (1983) Lipogenesis in the Sand Rat (*Psammomys obesus*), *Am. J. Physiol. 244*, E480–E486.
15. Zoltowska, M., St-Louis, J., Ziv, E., Sicotte, B., Delvin, E., and Levy, E. (2003) Vascular Responses to α-Adrenergic Stimulation and Depolarization Are Enhanced in Insulin Resistant and Diabetic *Psammomys obesus, Can. J. Physiol. Pharmacol. 81*, 704–710.

16. Zoltowska, M., Ziv, E., Delvin, E., Stan, S., Bar-On, H., Kalman, R., and Levy, E. (2001) Circulating Lipoproteins and Hepatic Sterol Metabolism in *Psammomys obesus* Prone to Obesity, Hyperglycemia and Hyperinsulinemia, *Atherosclerosis 157*, 85–96.
17. Suc, I., Brunet, S., Mitchell, G., Rivard, G.E., and Levy, E. (2003) Oxidative Tyrosylation of High Density Lipoproteins Impairs Cholesterol Efflux from Mouse J774 Macrophages: Role of Scavenger Receptors, Classes A and B, *J. Cell Sci. 116*, 89–99.
18. Levy, E., Thibault, L., Roy, C.C., Letarte, J., Lambert, M., and Seidman, E.G. (1990) Mechanisms of Hypercholesterolaemia in Glycogen Storage Disease Type I: Defective Metabolism of Low Density Lipoprotein in Cultured Skin Fibroblasts, *Eur. J. Clin. Invest. 20*, 253–260.
19. Lyons, T.J., Baynes, J.W., Patrick, J.S., Colwell, J.A., and Lopes-Virella, M.F. (1986) Glycosylation of Low Density Lipoprotein in Patients with Type 1 (insulin-dependent) Diabetes: Correlations with Other Parameters of Glycaemic Control, *Diabetologia 29*, 685–689.
20. Keren, P., George, J., Keren, G., and Harats, D. (2001) Non-Obese Diabetic (NOD) Mice Exhibit an Increased Cellular Immune Response to Glycated-LDL but Are Resistant to High Fat Diet Induced Atherosclerosis, *Atherosclerosis 157*, 285–292.
21. Watanabe, J., Wohltmann, H.J., Klein, R.L., Colwell, J.A., and Lopes-Virella, M.F. (1988) Enhancement of Platelet Aggregation by Low-Density Lipoproteins from IDDM Patients, *Diabetes 37*, 1652–1657.
22. Quinn, M.T., Parthasarathy, S., Fong, L.G., and Steinberg, D. (1987) Oxidatively Modified Low Density Lipoproteins: A Potential Role in Recruitment and Retention of Monocyte/Macrophages During Atherogenesis, *Proc. Natl. Acad. Sci. USA 84*, 2995–2998.
23. Marcil, V., Delvin, E., Seidman, E., Poitras, L., Zoltowska, M., Garofalo, C., and Levy, E. (2002) Modulation of Lipid Synthesis, Apolipoprotein Biogenesis, and Lipoprotein Assembly by Butyrate, *Am. J. Physiol. Gastrointest. Liver Physiol. 283*, G340–G346.
24. Stitt, A.W., Jenkins, A.J., and Cooper, M.E. (2002) Advanced Glycation End Products and Diabetic Complications, *Expert. Opin. Investig. Drugs. 11*, 1205–1223.
25. Bucala, R., Model, P., and Cerami, A. (1984) Modification of DNA by Reducing Sugars: A Possible Mechanism for Nucleic Acid Aging and Age-Related Dysfunction in Gene Expression, *Proc. Natl. Acad. Sci. USA 81*, 105–109.
26. Howard, E.W., Benton, R., Ahern-Moore, J., and Tomasek, J.J. (1996) Cellular Contraction of Collagen Lattices Is Inhibited by Nonenzymatic Glycation, *Exp. Cell. Res. 228*, 132–137.
27. Paget, C., Lecomte, M., Ruggiero, D., Wiernsperger, N., and Lagarde, M. (1998) Modification of Enzymatic Antioxidants in Retinal Microvascular Cells by Glucose or Advanced Glycation End Products, *Free Radic. Biol. Med. 25*, 121–129.
28. Giardino, I., Edelstein, D., and Brownlee, M. (1994) Nonenzymatic Glycosylation *in vitro* and in Bovine Endothelial Cells Alters Basic Fibroblast Growth Factor Activity. A Model for Intracellular Glycosylation in Diabetes, *J. Clin. Invest. 94*, 110–117.
29. Stitt, A.W., Li, Y.M., Gardiner, T.A., Bucala, R., Archer, D.B., and Vlassara, H. (1997) Advanced Glycation End Products (AGEs) Co-localize with AGE Receptors in the Retinal Vasculature of Diabetic and of AGE-Infused Rats, *Am. J. Pathol. 150*, 523–531.
30. Stitt, A.W., He, C., Friedman, S., Scher, L., Rossi, P., Ong, L., Founds, H., Li, Y.M., Bucala, R., and Vlassara, H. (1997) Elevated AGE-Modified ApoB in Sera of Euglycemic, Normolipidemic Patients with Atherosclerosis: Relationship to Tissue AGEs, *Mol. Med. 3*, 617–627.
31. Hoff, H.F., Whitaker, T.E., and O'Neil, J. (1992) Oxidation of Low Density Lipoprotein Leads to Particle Aggregation and Altered Macrophage Recognition, *J. Biol. Chem. 267*, 602–609.
32. The Diabetes Control and Complications Trial Research Group (1993) The Effect of Intensive Treatment of Diabetes on the Development and Progression of Long-Term Complications in Insulin-Dependent Diabetes Mellitus, *N. Engl. J. Med. 329*, 977–986.
33. Ferretti, G., Rabini, R.A., Bacchetti, T., Vignini, A., Salvolini, E., Ravaglia, F., Curatola, G., and Mazzanti, L. (2002) Glycated Low Density Lipoproteins Modify Platelet Properties: A Compositional and Functional Study, *J. Clin. Endocrinol. Metab. 87*, 2180–2184.
34. Curtiss, L.K., and Witztum, J.L. (1983) A Novel Method for Generating Region-Specific Monoclonal Antibodies to Modified Proteins. Application to the Identification of Human Glucosylated Low Density Lipoproteins, *J. Clin. Invest. 72*, 1427–1438.

[Received September 10, 2003; accepted December 6, 2003]

Validation of a Single-Isotope-Labeled Cholesterol Tracer Approach for Measuring Human Cholesterol Absorption

Yanwen Wang, Catherine A. Vanstone, William D. Parsons, and Peter J.H. Jones*

School of Dietetics and Human Nutrition, McGill University, Ste-Anne-de-Bellevue, Quebec, Canada, H9X 3V9

ABSTRACT: Cholesterol absorption is frequently determined using the plasma dual stable-isotope ratio method (PDSIRM). However, this method involves intravenous injection of stable-isotope-labeled cholesterol with simultaneous oral administration of differently labeled cholesterol, which results in high study costs and involves additional ethical considerations. The objective of the present study was to validate a simpler single-isotope method for determining cholesterol absorption against PDSIRM by using data from two previous studies. Enrichments of carbon-13 (^{13}C) and deuterium in red blood cells were analyzed by using differential isotope ratio MS. The area under the curve of ^{13}C-enrichment in the plasma free-cholesterol pool was found to be significantly correlated with cholesterol absorption measured by using PDSIRM for study 1 ($r = 0.85$, $P < 0.0001$) and study 2 ($r = 0.81$, $P < 0.0001$). Average ^{13}C-enrichment correlated with the area under the curve of ^{13}C-enrichment in the plasma free cholesterol for both study 1 ($r = 0.98$, $P < 0.0001$) and study 2 ($r = 1.00$, $P < 0.0001$). Study 1 examined the efficacy and mechanisms of unesterified plant sterols and stanols on lipid profiles in hypercholesterolemic men and women, while study 2 investigated the effects of phytosterol vs. phytostanol esters on plasma lipid levels and cholesterol kinetics in hyperlipidemic men. Experimental approaches to determine cholesterol absorption were identical between the two studies. Consequently, in both studies, correlations ($r = 0.88$, $P < 0.0001$ for study 1, and $r = 0.82$, $P < 0.0001$ for study 2) were found between the average ^{13}C-enrichment of plasma free cholesterol and cholesterol absorption measured by PDSIRM. These results suggest that a single-isotope-labeled cholesterol tracer approach can be used as a reliable noninvasive method to replace PDSIRM for examining changes in cholesterol absorption.

Paper no. L9373 in *Lipids 39*, 87–91 (January 2004).

Dietary cholesterol and the large enterohepatic recirculation of endogenous cholesterol readily mix to form a single pool of intestinal cholesterol (1–3). Cholesterol absorption from the gastrointestinal tract is a key component of whole-body cholesterol metabolism. Measurement of cholesterol absorption provides important insights into the relationships among diet and plasma cholesterol levels, cholesterol homeostasis, genetic variations, and drug effects. For this purpose, a variety of different methods have been developed for estimating cholesterol absorption in humans (4,5). Presently, three methods exist for measuring cholesterol absorption: the plasma dual-isotope ratio method (6–8), the fecal dual-isotope ratio method (9), and mass (sterol) balance (10). The simplest of these methods is the plasma dual-isotope ratio method originally introduced by Zilversmit (6).

In 1993, Lutjohann *et al.* (4) introduced the use of stable isotopes into the fecal dual-isotope ratio method for measuring cholesterol absorption. In the same year, Bosner *et al.* (11) developed a plasma dual stable-isotope-ratio method (PDSIRM) to measure cholesterol absorption, based on the plasma dual-isotope ratio method developed by Zilversmit (6). This modified method has been used extensively (12–17). Although this technique can measure cholesterol absorption with good precision and accuracy, it involves intravenous injection of labeled cholesterol. As such, the technique increases study costs dramatically, involves an invasive procedure, and requires additional ethical considerations.

In PDSIRM, the amount of labeled cholesterol absorbed is calculated by the enrichment of orally administered and intravenously injected cholesterol tracers. Isotope enrichment in the cholesterol pool following an oral dose of single-isotope-labeled cholesterol is believed to be indicative of the cholesterol absorption rate (18). However, the relationship between the isotope enrichment of plasma free cholesterol following an oral dose of single-isotope-labeled cholesterol and cholesterol absorption remains to be established as a noninvasive method to compare relative changes in cholesterol absorption. It was hypothesized that the area under the isotope enrichment curve, or the average isotope enrichment, in the plasma free-cholesterol pool following an oral dose of single-isotope-labeled cholesterol tracer correlates with the cholesterol absorption rate. The objective of the current study was to devise a method that would simplify the process of measuring cholesterol absorption in humans.

MATERIALS AND METHODS

Study protocols. Data from two published studies (14,15) were analyzed for the correlations between the area under the curve of a single-isotope enrichment and the cholesterol absorption rate, as measured by PDSIRM. Correlations between the measured cholesterol absorption rate and the average enrichment of the single isotope were also conducted. Experimental approaches to determine cholesterol absorption were identical between the two studies. Study 1 involved 15 otherwise healthy

*To whom correspondence should be addressed at School of Dietetics and Human Nutrition, Macdonald Campus of McGill University, Ste-Anne-de-Bellevue, Quebec, Canada, H9X 3V9. E-mail: jonesp@macdonald.mcgill.ca

Abbreviations: IRMS, isotope ratio MS; PDB, Pee Dee belemnite; PDSIRM, plasma dual stable-isotope ratio method; SMOW, Standard Mean Ocean Water.

hypercholesterolemic subjects (9 male, 6 female; 35–58 yr) who had plasma total cholesterol concentrations in the range of 5.2–9.0 mmol/L and TAG concentrations <3.5 mmol/L. Subjects completed each of four dietary treatments in a randomized crossover double-blind design. The four diets were comprised of solid foods typical of those consumed in North America, and contained 1.8 g/d of cornstarch (control), plant sterols, plant stanols, and a 50:50 mixture of sterols and stanols, respectively. Cholesterol concentrations of the diets were not measured but were calculated to provide approximately 300 mg cholesterol/d, i.e., within the range of typical North American diets. Each treatment phase consisted of a 21-d feeding period and was separated by a 4-wk washout. Ninety-six hours before the end of each phase, a baseline blood sample was drawn prior to subjects receiving an intravenous injection of 15 mg D_7-cholesterol and a 75-mg oral dose of ^{13}C-cholesterol (CDN Isotopes, Pointe-Claire, Quebec, Canada).

Study 2 contained 15 healthy hyperlipidemic males (37–61 yr) who had fasting plasma total cholesterol concentrations in the range of 6.0–10.0 mmol/L and TAG concentrations <3.0 mmol/L. Using a randomized crossover double-blind design, subjects were assigned to one of three typical North American solid-food diets that contained margarine alone, margarine with 8% (w/w based on free sterol content) plant sterol esters, and 8% (w/w based on free stanol content) plant stanol esters, respectively. Cholesterol concentrations of the diets were calculated to provide approximately 300 mg cholesterol/d. Each dietary phase consisted of 21 feeding days followed by a 5-wk washout. Ninety-six hours before the end of each phase, subjects were intravenously injected with 15 mg of D_7-cholesterol and simultaneously ingested 90 mg of ^{13}C-cholesterol.

Determination of cholesterol absorption. Cholesterol absorption was determined in both studies using PDSIRM following the procedure of Bosner *et al.* (11). Briefly, lipids were extracted from red blood cells in duplicate using a modified Folch extraction procedure (19). Free cholesterol was purified by TLC and transferred into combustion tubes each containing 0.5 g cupric oxide, and sealed under vacuum. After combustion at 520°C for 4 h, ^{13}C-enriched CO_2 was vacuum-distilled into sealed tubes; D-enriched water was transferred under vacuum into tubes containing 0.06 g zinc. Tubes containing water and zinc were reduced to D-enriched H_2 gas by combusting at 520°C for 30 min. The ^{13}C-enrichment in CO_2 and D-enrichment in H_2 gas were measured by differential isotope ratio MS (IRMS). Enrichments were expressed relative to the Pee Dee belemnite (PDB) limestone standard of the National Bureau of Standards) (NBS).

The ratio of ingested ^{13}C-cholesterol to injected D_7-cholesterol enrichment relative to baseline samples ($t = 0$) in the plasma free cholesterol after 48 and 72 h was taken as an indicator of the cholesterol absorption rate:

$$\text{absorption (pool/pool)} = \frac{\Delta^{13}\text{C} \times 7 \times 27 \times \text{i.v. dose of D}_7\text{-cholesterol} \times 0.0112}{\Delta\text{D} \times 2 \times 46 \times \text{i.g. dose of } ^{13}\text{C-cholesterol} \times 0.000155} \quad [1]$$

where Δ (‰) for ^{13}C and D is the difference between the enriched sample at 48 or 72 h and the baseline abundance (at $t = 0$) in parts per thousand relative to PDB and Standard Mean Ocean Water (SMOW) standards, respectively. The factors 7:46 and 2:27 reflect the ratios of labeled to unlabeled hydrogen and carbon atoms in the cholesterol tracers, respectively. The constants 0.0112 and 0.000155 represent factors converting the parts-per-thousand units to the equivalent atom percent excess for the PDB and SMOW scales, respectively.

Correlation analysis. The average ^{13}C-enrichment and area under the curve of ^{13}C-enrichment in plasma free cholesterol during a 24–96 h period following the oral dose of ^{13}C-cholesterol were calculated for each subject during each phase. Data from the four treatments in study 1 and the three treatments in study 2 were pooled, respectively. The correlations among cholesterol absorption as measured by PDSIRM, the area under the ^{13}C-enrichment curve, and the average ^{13}C-enrichment were analyzed using Pearson correlations. The same method also was used to analyze the relationship between the area under the ^{13}C-enrichment curve and the average ^{13}C-enrichment in plasma free cholesterol during a 24–96 h period after an oral dose of ^{13}C-cholesterol. Separate analyses were performed for each study.

RESULTS

Study 1. The correlation between the measured cholesterol absorption rate and the area under the curve of ^{13}C-enrichment is presented in Figure 1. The correlation between the measured cholesterol absorption rate and the average ^{13}C-enrichment in the plasma free-cholesterol fraction is presented in Figure 2. We found that the area under the curve of ^{13}C-enrichment in plasma free cholesterol over a 24–96 h period following an oral dose of ^{13}C-cholesterol was correlated ($r = 0.85$, $P < 0.0001$) with the cholesterol absorption rate as measured by PDSIRM. Similarly, the average ^{13}C-enrichment in plasma free cholesterol was also correlated ($r = 0.88$, $P < 0.0001$) with the measured cholesterol absorption rate. A correlation was observed between the area

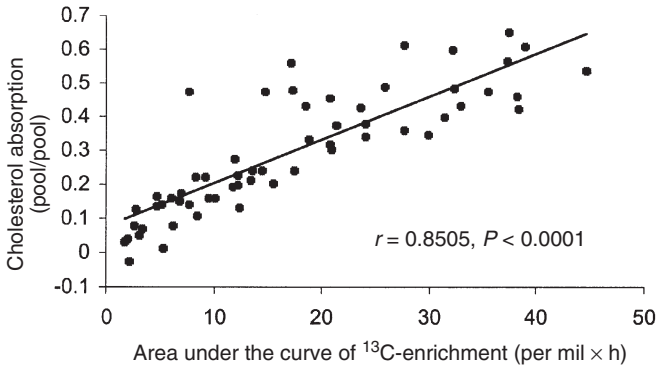

FIG. 1. Relationship between the area under the curve of ^{13}C-enrichment in the cholesterol pool [per thousand atom excess (per mil) × h] and the cholesterol absorption rate (pool/pool) measured using the plasma dual stable-isotope ratio method in study 1. Data were analyzed using a Pearson correlation.

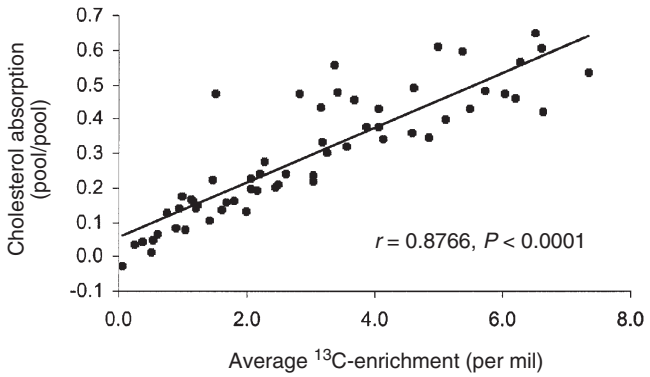

FIG. 2. Relationship between the average ^{13}C-enrichment in the cholesterol pool (per mil) and cholesterol absorption as measured using the plasma dual stable-isotope ratio method in study 1. Data were analyzed using a correlation.

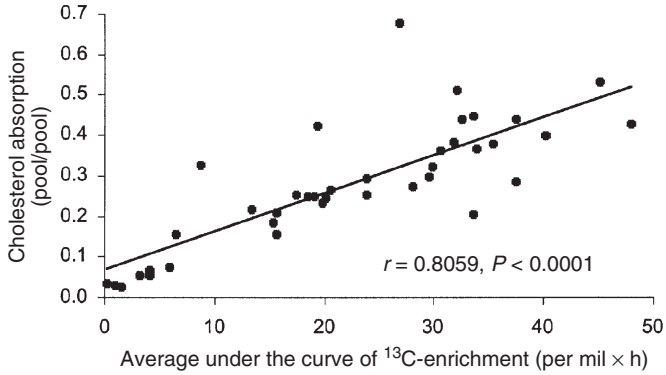

FIG. 4. Relationship between the area under the curve of ^{13}C-enrichment in the plasma cholesterol pool (per mil × h) and the cholesterol absorption rate (pool/pool) as measured using the plasma dual stable-isotope ratio method in study 2. Data were analyzed using a Pearson correlation.

under the curve of ^{13}C-enrichment and the average ^{13}C-enrichment in the plasma free-cholesterol pool after an oral dose of ^{13}C-cholesterol (Fig. 3). The correlation coefficient was 0.99 ($P < 0.0001$).

Study 2. Identical analyses were performed for the data in study 2. As shown in Figure 4, the area under the curve of ^{13}C-enrichment in plasma free cholesterol during a period of 24–96 h following an oral dose of ^{13}C-cholesterol was correlated ($r = 0.82$, $P < 0.0001$) with the cholesterol absorption rate as measured by PDSIRM. The average ^{13}C-enrichment in plasma was also correlated ($r = 0.81$, $P < 0.0001$) with the measured cholesterol absorption rate (Fig. 5). The area under the curve of ^{13}C-enrichment was significantly correlated with the average ^{13}C-enrichment in the plasma free-cholesterol pool after an oral dose of ^{13}C-cholesterol (Fig. 6), with a correlation coefficient of 1.00 ($P < 0.0001$).

DISCUSSION

PDSRIM has been used over the years to measure the cholesterol absorption rate. However, the high cost and ethical considerations of this technique limit its use in human studies. It is very important to devise a less expensive and noninvasive alternative to PDSRIM to compare the changes in cholesterol absorption. Results of the present study suggest that either the area under the ^{13}C-enrichment curve or the average ^{13}C-enrichment during a 24–96-h period following oral ^{13}C-cholesterol administration could be used as a reliable index to compare the differences or changes in cholesterol absorption.

The average ^{13}C-enrichment was found to be correlated with the area under the curve of ^{13}C-enrichment in a 4-d period following the oral dose of ^{13}C-cholesterol, so it was not surprising that the average ^{13}C-enrichment also showed a significant correlation with cholesterol absorption measured by PDSIRM, as did the area under the curve of ^{13}C-enrichment. Integration of the area under the curve of ^{13}C-enrichment is more complicated than calculating the average ^{13}C-enrichment with the use of an integrating program. For example, if statistical software is chosen to integrate the area under the enrichment curve, understanding the integration procedure and the related commands is essential to complete this task. For this reason, calculating the average ^{13}C-enrichment has advantages over calculating the area under the curve of ^{13}C-enrichment for comparing relative changes in the cholesterol absorption rate.

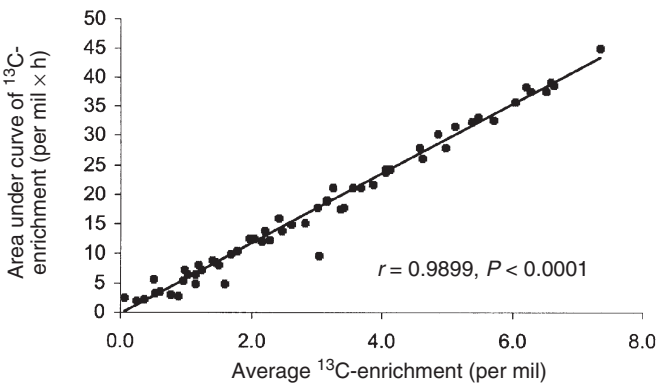

FIG. 3. Correlation between the average ^{13}C-enrichment (per mil) and the area under the curve of ^{13}C-enrichment of plasma free cholesterol (per mil × h) in study 1. Data were analyzed using a Pearson correlation.

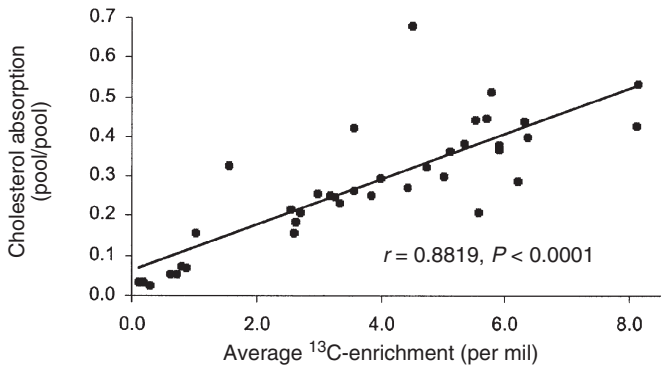

FIG. 5. Relationship between the average ^{13}C-enrichment in the cholesterol pool (per mil) and cholesterol absorption as measured using the plasma dual stable-isotope ratio method in study 2. Data were analyzed using a Pearson correlation.

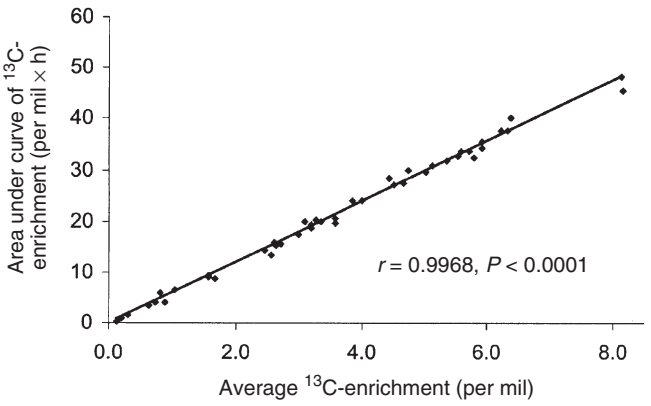

FIG. 6. Correlation between the average ^{13}C-enrichment (per mil) and the area under the curve of ^{13}C-enrichment in the plasma free-cholesterol pool (per mil × h) in study 2. Data were analyzed using a Pearson correlation.

It is well-documented that intestinal cholesterol absorption is a major determinant of whole-body cholesterol homeostasis and plasma LDL cholesterol levels (2,3,20–22), particularly in Western populations that consume significant quantities of cholesterol. Despite the extensive body of literature, important questions remain regarding the measurement of human cholesterol absorption. These shortcomings in our understanding of cholesterol metabolism are, at least in part, due to methodological limitations (11). As such, investigators have developed a wide range of isotope tracer methods to study cholesterol absorption (10,23). However, the methods that were developed initially relied on radioisotope tracers, thus limiting their application in human studies. Bosner *et al.* (11) developed a method that applied stable isotope techniques and MS, and this method was widely used in later studies that investigated the cholesterol absorption rate (14,15,24,25). Although this technique measures cholesterol absorption with good precision and accuracy, it involves both oral administration and intravenous injection of labeled cholesterol. Thus, the use of this technique is limited by the high cost and ethical considerations.

Many studies have measured the cholesterol absorption rate to compare treatment effects on the efficiency of dietary cholesterol absorption in the intestine (11,14,15,24,25). In these studies, the contribution of absorbed cholesterol from dietary sources to the body's cholesterol pool has not been calculated. In fact, most studies have compared the effects of dietary treatment(s) on cholesterol absorption instead of the exact proportion of absorbed cholesterol that contributes to the body's cholesterol pool. In these kinds of investigations, either the average enrichment or the area under the enrichment curve of a single stable isotope in a 4-d period following an oral dose of the single-isotope-labeled cholesterol tracer can be used as a reliable method to achieve the goals of these experiments.

It is evident that the single-isotope-labeled cholesterol tracer method also has limitations in its application. After absorption, the concentration of cholesterol tracer is quickly diluted as it mixes with the body's cholesterol pool. Given an amount of absorbed isotope-labeled cholesterol, the body's cholesterol pool size becomes a key factor that affects the tracer concentration, i.e., a larger cholesterol pool makes the tracer concentration lower, and vice versa. Therefore, the use of a single-stable-isotope cholesterol tracer method to compare cholesterol absorption is based on the assumption that subjects in each treatment have the same cholesterol pool size or baseline. For a crossover design with a washout period, the same subjects go through each treatment. The cholesterol pool size of each subject is assumed to have returned to the initial baseline before commencing the next treatment. Therefore, a single-stable-isotope cholesterol tracer is a reliable indictor to compare the changes caused by different treatments in a crossover design. For a parallel-arm study design, the single-isotope-labeled cholesterol tracer method may be less sensitive because subjects have different body cholesterol pool sizes, although the groups were adjusted by complete randomization of subjects to have no significant difference in their cholesterol pool sizes before receiving different treatments. For this type of study, influence of the body's cholesterol pool size on the accuracy of measurements of the single-stable-isotope cholesterol tracer can be minimized by including the initial cholesterol pool size as a covariant.

If enrichment of the single-isotope cholesterol tracer is used to calculate the percent cholesterol absorption rate, many assumptions have to be made that reduce data reliability and compatibility. These assumptions include the following: (i) that absorbed cholesterol tracers are entirely incorporated into the body's cholesterol pool; (ii) that the absorbed cholesterol tracers are completely equilibrated in the cholesterol pool; (iii) that the cholesterol pool is measured accurately; and (iv) that no significant amount of cholesterol tracers has decayed or cleared out of the cholesterol pool over a period of 24–96 h after oral administration. Therefore, the authors consider it better to use ^{13}C-enrichment to compare differences in cholesterol absorption between treatments or treatment effects relative to a control.

In summary, the area under the ^{13}C-enrichment curve or the average ^{13}C-enrichment is significantly correlated with the cholesterol absorption rate as measured by PDSIRM. It is suggested that either average ^{13}C-enrichment or the area under the curve of ^{13}C-enrichment can be used as an index of cholesterol absorption. The single-stable-isotope cholesterol tracer method has advantages over PDSIRM, as it is simpler, noninvasive, and less expensive. However, this method can be used only to compare the changes in cholesterol absorption. When measurement of the absolute cholesterol absorption rate becomes essential, PDSIRM should be used.

ACKNOWLEDGMENTS

The authors would like to thank Drs. Fady Y. Ntanios, Mahmoud Raeini-Sarjaz, and Jian Y. Feng for their contributions to the data used in this paper.

REFERENCES

1. Grundy, S.M. (1983) Absorption and Metabolism of Dietary Cholesterol, *Annu. Rev. Nutr. 3*, 71–96.
2. Wilson, M.D., and Rudel, L.L. (1994) Review of Cholesterol Absorption with Emphasis on Dietary and Biliary Cholesterol, *J. Lipid Res. 35*, 943–955.
3. Carter, D., Howlett, H.C., Wiernsperger, N.F., and Bailey, C.J. (2003) Differential Effects of Metformin on Bile Salt Absorption from the Jejunum and Ileum, *Diabetes Obes. Metab. 5*, 120–125.
4. Lutjohann, D., Meese, C.O., Crouse, J.R., and von Bergmann, K. (1993) Evaluation of Deuterated Cholesterol and Deuterated Sitostanol for Measurement of Cholesterol Absorption in Humans, *J. Lipid Res. 34*, 1039–1046.
5. Pouteau, E., Piguet-Welsch, C., Berger, A., and Fay, L.B. (2003) Determination of Cholesterol Absorption in Humans: From Radiolabel to Stable Isotope Studies, *Isotopes Environ. Health Stud. 39,* 247–257.
6. Zilversmit, D.B. (1972) A Single Blood Sample Dual Isotope Method for the Measurement of Cholesterol Absorption in Rats, *Proc. Soc. Exp. Biol. Med. 140*, 862–865.
7. Wang, D.Q., Lammert, F., Cohen, D.E., Paigen, B., and Carey, M.C. (1999) Cholic Acid Aids Absorption, Biliary Secretion, and Phase Transitions of Cholesterol in Murine Cholelithogenesis, *Am. J. Physiol. 276*, G751–G760.
8. Wang, D.Q., Paigen, B., and Carey, M.C. (2001) Genetic Factors at the Enterocyte Level Account for Variations in Intestinal Cholesterol Absorption Efficiency Among Inbred Strains of Mice, *J. Lipid Res. 42*, 1820–1830.
9. Borgstrom, B. (1968) Quantitative Aspects of the Intestinal Absorption and Metabolism of Cholesterol and β-Sitosterol in the Rat, *J. Lipid Res. 9*, 473–481.
10. Grundy, S.M., and Ahrens, E.H., Jr. (1969) Measurements of Cholesterol Turnover, Synthesis, and Absorption in Man, Carried Out by Isotope Kinetic and Sterol Balance Methods, *J. Lipid Res. 10*, 91–107.
11. Bosner, M.S., Ostlund, R.E., Jr., Osofisan, O., Grosklos, J., Fritschle, C., and Lange, L.G. (1993) Assessment of Percent Cholesterol Absorption in Humans with Stable Isotopes, *J. Lipid Res. 34*, 1047–1053.
12. Harris, W.S., Windsor, S.L., Newton, F.A., and Gelfand, R.A. (1997) Inhibition of Cholesterol Absorption with CP-148,623 Lowers Serum Cholesterol in Humans, *Clin. Pharmacol. Ther. 61*, 385–389.
13. Ntanios, F.Y., and Jones, P.J. (1999) Dietary Sitostanol Reciprocally Influences Cholesterol Absorption and Biosynthesis in Hamsters and Rabbits, *Atherosclerosis 143*, 341–351.
14. Jones, P.J., Raeini-Sarjaz, M., Ntanios, F.Y., Vanstone, C.A., Feng, J.Y., and Parsons, W.E. (2000) Modulation of Plasma Lipid Levels and Cholesterol Kinetics by Phytosterol Versus Phytostanol Esters, *J. Lipid Res. 41*, 697–705.
15. Vanstone, C.A., Raeini-Sarjaz, M., Parsons, W.E., and Jones, P.J.(2002) Unesterified Plant Sterols and Stanols Lower LDL-Cholesterol Concentrations Equivalently in Hypercholesterolemic Persons, *Am. J. Clin. Nutr. 76*, 1272–1278.
16. Woollett, L.A., Buckley, D.D., Yao, L., Jones, P.J., Granholm, N.A., Tolley, E.A., and Heubi, J.E. (2003) Effect of Ursodeoxycholic Acid on Cholesterol Absorption and Metabolism in Humans, *J. Lipid Res. 44*, 935–942.
17. Pouteau, E.B., Monnard, I.E., Piguet-Welsch, C., Groux, M.J., Sagalowicz, L., and Berger, A. (2003) Non-esterified Plant Sterols Solubilized in Low Fat Milks Inhibit Cholesterol Absorption: A Stable Isotope Double-Blind Crossover Study, *Eur. J. Nutr. 42*, 154–164.
18. Ostlund, R.E., Jr., Spilburg, C.A., and Stenson, W.F. (1999) Sitostanol Administered in Lecithin Micelles Potently Reduces Cholesterol Absorption in Human Subjects, *Am. J. Clin. Nutr. 70*, 826–831.
19. Folch, J., Lees, M., and Sloane Stanley, G.H. (1957) A Simple Method for the Isolation and Purification of Total Lipids from Animal Tissues, *J. Biol. Chem. 226*, 497–509.
20. Dietschy, J.M., Turley, S.D., and Spady, D.K. (1993) Role of Liver in the Maintenance of Cholesterol and Low Density Lipoprotein Homeostasis in Different Animal Species, Including Humans, *J. Lipid Res. 34*, 1637–1659.
21. Rudel, L., Deckelman, C., Wilson, M., Scobey, M., and Anderson, R. (1994) Dietary Cholesterol and Downregulation of Cholesterol 7 α-Hydroxylase and Cholesterol Absorption in African Green Monkeys, *J. Clin. Invest. 93*, 2463–2472.
22. Gylling, H., and Miettinen, T.A. (1995) The Effect of Cholesterol Absorption Inhibition on Low Density Lipoprotein Cholesterol Level, *Atherosclerosis 117*, 305–308.
23. Quarfordt, S.H. (1977) Methods for the *in vivo* Estimation of Human Cholesterol Dynamics, *Am. J. Clin. Nutr. 30*, 967–974.
24. Bosner, M.S., Lange, L.G., Stenson, W.F., and Ostlund, R.E., Jr. (1999) Percent Cholesterol Absorption in Normal Women and Men Quantified with Dual Stable Isotopic Tracers and Negative Ion Mass Spectrometry, *J. Lipid Res. 40*, 302–308.
25. Gremaud, G., Dalan, E., Piguet, C., Baumgartner, M., Ballabeni, P., Decarli, B., Leser, M.E., Berger, A., and Fay, L.B. (2002) Effects of Non-esterified Stanols in a Liquid Emulsion on Cholesterol Absorption and Synthesis in Hypercholesterolemic Men, *Eur. J. Nutr. 41*, 54–60.

[Received August 22, 2003; accepted December 18, 2003]

Phospholipids and Oxophospholipids in Atherosclerotic Plaques at Different Stages of Plaque Development

Amir Ravandi[a,b], Saeid Babaei[b], Ramsey Leung[b], Juan Carlos Monge[b], George Hoppe[c], Henry Hoff[c], Hiroshi Kamido[a], and Arnis Kuksis[a,*]

[a]Banting and Best Department of Medical Research, University of Toronto, Toronto, Canada M5G 1L6, [b]Terrence Donnelly Heart Center, St. Michael's Hospital, University of Toronto, and [c]Department of Cell Biology, Lerner Research Institute, The Cleveland Clinic Foundation, Cleveland, Ohio

ABSTRACT: We identified and quantified the hydroperoxides, hydroxides, epoxides, isoprostanes, and core aldehydes of the major phospholipids as the main components of the oxophospholipids (a total of 5–25 pmol/μmol phosphatidylcholine) in a comparative study of human atheroma from selected stages of lesion development. The developmental stages examined included fatty streak, fibrous plaque, necrotic core, and calcified tissue. The lipid analyses were performed by normal-phase HPLC with on-line electrospray MS using conventional total lipid extracts. There was great variability in the proportions of the various oxidation products and a lack of a general trend. Specifically, the early oxidation products (hydroperoxides and epoxides) of the glycerophosphocholines were found at the advanced stages of the plaques in nearly the same relative abundance as the more advanced oxidation products (core aldehydes and acids). The anticipated linear accumulation of the more stable oxidation products with progressive development of the atherosclerotic plaque was not apparent. It is therefore suggested that lipid infiltration and/or local peroxidation is a continuous process characterized by the formation and destruction of both early and advanced products of lipid oxidation at all times. The process of lipid deposition appears to have been subject to both enzymatic and chemical modification of the normal tissue lipids. Clearly, the appearance of new and disproportionate old lipid species excludes randomness in any accumulation of oxidized LDL lipids in atheroma.

Paper no. L9428 in *Lipids 39*, 97–109 (February 2004).

Oxidative modification of LDL is now recognized as a necessary condition for foam-cell formation. Oxidized LDL, in contrast to native LDL, is taken up avidly by macrophages, which can cause foam-cell formation and eventual development of atherosclerosis. Although a great variety of oxidized LDL components have been identified, only a few have been recovered from atheroma. In most instances, the isolations from atheroma have been confined to the neutral lipids, oxocholesterol and oxidized cholesteryl esters, the concentration of which has been shown to increase dramatically with progressive atherosclerotic disease (1–3). Hoppe *et al.* (4) showed that oxidation products of cholesteryl linoleate are resistant to hydrolysis by macrophages, whereas Huber *et al.* (5) showed that oxidation products of cholesteryl linoleate (cholesteryl [9-oxo]linoleate and hydroperoxylinoleate) stimulate human umbilical vein endothelial cells to specifically bind human peripheral blood mononuclear cells.

Other studies have recognized both isoprostanes (6,7) and hydroxides (8–11) of FA released by saponification from oxidized phospholipids of atherosclerotic plaques. The estimates of the hydroperoxides were found to exceed those of the isoprostanes by more than 20 times.

In parallel, a degradation of the PUFA in the *sn*-2-position of phosphatidylcholine (PtdCho) by oxidation has been recognized as essential for binding oxidized LDL to macrophage scavenger receptors, indicating that oxidized phosholipids are involved in the initial binding process (12–16). The reactive oxidation products derived from phospholipids, such as the core aldehydes, can form covalent adducts with apolipoprotein B. These adducts retain the intact phosphorylcholine headgroup (17,18) and have been demonstrated by immunohistochemical methods to accumulate in atherosclerotic lesions (18). The oxidized PtdCho-containing phospholipid appears to be an immunodominant epitope (19–21). Steinberg (22) has suggested that oxidized phospholipids could be the missing initiating factor(s) in atherosclerosis. Uchida (23) has discussed the role of reactive low-M.W. aldehydes in cardiovascular diseases, although little is known about the effects of oxidative stress on the development of atherosclerosis.

Although the presence of oxo-PtdCho in atherosclerotic lesions has been demonstrated previously (16,24–26), no comparative investigation has been reported on the composition of the native and oxophospholipids at different stages of development of atherosclerosis. By means of normal-phase liquid chromatography/electrospray ionization-mass spectrometry (LC/ESI-MS), we have tentatively identified and quantified the hydroperoxides, hydroxides, epoxides, isoprostanes, and core aldehydes bound to the common phospholipids as the major components of the oxophospholipids. Oxidation prod-

Present address of the seventh author: Midori Health Care Foundation, 3-22-5 Tarumi-cho, Suita, Osaka, 564-0062 Japan

*To whom correspondence should be addressed.
E-mail: arnis.kuksis@utoronto.ca

Abbreviations: DNPH, 2,4-dinitrophenylhydrazones; GroPCho, glycerophosphocholine; GroPEtn, glycerophosphoethanolamine; GroPIns, glycerophosphoinositol; LC/ESI-MS, liquid chromatography/electrospray ionization-mass spectrometry; lysoPtdCho, lysophosphatidylcholine; lysoPtdEtn, lysophosphatidylethanolamine; lysoPtdIns, lysophosphatidylinositol; PAF, platelet-activating factor; PtdCho, phosphatidylcholine; PtdEtn, phosphatidylethanolamine; PtdIns, phosphatidylinositol; PtdSer, phosphatidylserine; SM, sphingomyelin.

ucts from both early and late stages of lipid oxidation were found at all stages of development of the plaque.

MATERIALS AND METHODS

Reference and internal standards. Reference hydroperoxides, epoxides, isoprostanes, and core aldehydes of PtdCho were prepared in the laboratory by treatment of 18:0/20:4 glycerophosphocholine (GroPCho) with *tert*-butyl hydroperoxide as described previously (27). The oxo derivatives of phosphatidylinositol (PtdIns) were prepared by autoxidation as described by Ravandi and Kuksis (24). Other common glycerophospholipid and sphingomyelin (SM) standards were available in the laboratory from previous studies (28).

Source of tissues. Sections of aortic tissue and atheromas were collected from a total of 21 patients undergoing elective aortic grafting or heart transplant surgery. A total of 15 aortic sections were cleaned under a dissection microscope, excised, and placed immediately in cold buffer containing one protease inhibitor tablet/150 mL, 0.008% gentamycin, and 0.008% chloramphenicol (for biochemistry) or buffer containing 4% formaldehyde (for histological classification). These preparations were classified as fatty streaks (three samples), fibrous plaques, necrotic cores, and calcified or ulcerated lesions (four samples each). The other six samples represented mature atheromas (necrotic cores and calcified lesions), which were cleaned of all extraneous fat and were extracted as below.

Preparation of aortic homogenates. The atherosclerotic lesions, including those from postmortem tissues, were thawed, blotted dry, weighed individually, frozen in liquid nitrogen, and powdered in a mortar. The fine tissue powder was suspended in 2 mL of cold buffer, homogenized, and extracted (29) with chloroform/methanol (2:1, vol/vol) following addition (10% of total phospholipid) of an internal standard (15:0/15:0 GroPCho). The extraction utilized 10 mL chloroform/methanol per 0.5 g tissue as described by Piotrowski *et al*. (30). Other samples reconstituted to 10 mL of chloroform/methanol per 0.5 g of tissue were diluted with the internal standard just before LC/ESI-MS analyses.

Another six human coronary artery/aorta samples (0.4 to 0.95 g) were extracted under nitrogen with chloroform/methanol 1:1 (vol/vol) according to Bligh and Dyer (31) or chloroform/methanol 1:1 (vol/vol) containing 2,4-dinitrophenylhydrazine in order to trap any core aldehydes as the dinitrophenylhydrazones (DNPH) (32). The chloroform contained 40 μM BHT. After phospholipase C digestion, the DNPH derivatives were analyzed by HPLC with on-line ESI-MS.

Quantification of total atheroma lipids by high-temperature GLC. Total lipid profiles of mature human atheroma extracts following dephosphorylation with phospholipase C and trimethylsilylation were determined by high-temperature nonpolar capillary GLC using tridecanoylglycerol as internal standard (24,33).

LC-MS. The LC/ESI-MS analysis was performed using a normal-phase silica column (250 × 4.6 mm i.d.; Alltech Associates, Deerfield, IL), in a Hewlett-Packard Model 1060 liquid chromatograph connected to a Hewlett-Packard Model 5989B quadrupole mass spectrometer, equipped with a nebulizer-assisted ESI interface (HP 59987A; Hewlett-Packard, Palo Alto, CA) (24,27,28). The column was eluted with a linear gradient of 100% A (chloroform/methanol/30% ammonium hydroxide 80:19.5:0.5, by vol) for 26 min, followed by 100% B (chloroform/methanol/water/30% ammonium hydroxide, 60:34:5.5:0.5, by vol) for 19 min. The retention time for PtdCho was determined using standard 16:0/20:4 GroPCho. The capillary exit voltage was set at 150 V, with an electron multiplier at 1795 V. For fragmentation the exit voltage was raised to 300 V and the sample was reinjected into the LC/ESI-MS system (pseudo-MS/MS). All the major fragment ions detected in the negative and positive ion mode can be assigned to the plausible cleavage products, including DAG and FA (34). Positive and negative ESI spectra were usually recorded in the mass range 400–1100, but lower mass ranges needed to be used for scanning for FA and nitrogenous bases. The masses given in the figures are nominal masses + 1 $[M + 1]^+$ (positive ion mode), or nominal masses −1 $[M - 1]^-$ (negative ion mode) ions. The molecular species of phospholipid classes, along with their oxidation transformation products, were determined on basis of the HPLC retention time, the molecular mass provided by ESI-MS, and the knowledge of the FA composition of each lipid class and the chemical derivative (DNPH) of molecular species. The ions were identified by reference to the retention times of reference standards analyzed under similar conditions by means of single-ion mass chromatograms. The presence of the major oxolipids was also confirmed by pseudo-MS/MS by increasing the capillary exit voltage from 150 to 300 V and reinjecting the sample.

RESULTS

Total phospholipids. A determination of the total lipid profiles of mature human atherosclerotic lesions showed that the total phospholipids, estimated as the sum of the monoradylglycerols and diradylglycerols derived from lysophosphatidylcholine (lysoPtdCho) and PtdCho, respectively, and the ceramides derived from SM, made up only 10–20% of the total atheroma lipids, the bulk of the lipids being contributed by free cholesterol and cholesteryl esters (33).

Table 1 gives the total and individual lipid class contents of the fatty streaks (three aortas), fibrous plaques (four aortas), necrotic cores (four aortas), and calcified tissues (four aortas). The total PtdCho was estimated by summing the individual molecular species in relation to the internal standard (15:0/15:0 GroPCho). The PtdCho value was related to that of lysoPtdCho, SM, and phosphatidylethanolamine (PtdEtn) using appropriate correction factors in the positive ion mode. The knowledge of PtdEtn content was used as a reference for obtaining the content of PtdIns and phosphatidylserine (PtdSer) in the negative ion mode. Table 1 shows that PtdCho remained as a major lipid component of the atherosclerotic lesion throughout its development and despite a nearly five-

TABLE 1
Phospholipid Class Composition of Human Atherosclerotic Plaques of Different Developmental Stages (mol%)[a]

Lipid class[b]	Normal intima (n = 3)	Fatty streak (n = 3)	Fibrous plaque (n = 4)	Necrotic core (n = 4)	Calcified tissue (n = 4)
PtdCho	43.84 ± 4.56	35.24 ± 6.02	33.75 ± 5.31	34.88 ± 8.09	46.08 ± 1.41
SM	12.41 ± 3.47	16.61 ± 2.12	16.61 ± 2.06	27.93 ± 10.06	32.79 ± 4.59
LysoPtdCho	6.08 ± 2.22	10.74 ± 3.96	16.19 ± 3.69	16.32 ± 3.40	11.80 ± 3.32
PtdEtn	17.77 ± 4.9	13.09 ± 3.54	20.04 ± 6.87	8.99 ± 9.99	4.08 ± 1.72
PtdIns	19.92 ± 5.28	24.32 ± 5.52	11.40 ± 2.90	11.89 ± 2.13	5.25 ± 3.54
PtdSer	Trace	ND	ND	ND	ND
Total[c]	100	100	97.99	100	100

[a]Data are shown as mean ± SD.
[b]PtdCho, phosphatidycholine; SM, sphingomyelin; lysoPtdCho, lysophosphatidylcholine; PtdEtn, phosphatidylethanolamine; PtdIns, phosphatidylinositol. ND, not determined; each sample was analyzed in triplicate.
[c]The total phospholipid contents of the fatty streak, fibrous plaque, necrotic core, and calcified tissue were estimated to average 10–20 mg/g of tissue compared with 4–5 mg/g of normal tissue.

fold increase in total phospholipids. The proportion of PtdCho plus lysoPtdCho remained relatively constant, whereas that of the other glycerophospholipids decreased and that of SM increased two- to threefold. The relative proportion of PtdCho decreased, whereas that of lysoPtdCho increased two- to threefold with the maturation of the plaque. In previous analyses of the plaques, Piotrowski *et al*. (35) estimated the lysoPtdCho as 17% of the PtdCho, but the FA composition of the lysoPtdCho was not determined. Since lysoPtdEtn and lysoPtdIns were not recovered, it was not established whether the relative decreases in PtdEtn and PtdIns were due to simple hydrolysis to the corresponding lyso compounds.

Molecular species of PtdCho. Figure 1 shows the total ion current profile of choline-containing phospholipids of mature atheroma (A) and full mass spectra recorded over the PtdCho (B), SM (C), and lysoPtdCho (D) elution ranges of the chromatogram. The major peaks identified are listed in Tables 2–4. The major PtdCho ions recorded for the necrotic core (14.370–16.353 min, Fig. 1B) ranged in mass from *m/z* 686 to *m/z* 811, with smaller intensities seen at *m/z* 707, 733, 747, 795, 813, and 835. Table 2 lists the molecular species of the diradyl GroPCho corresponding to the major abundances seen in the mass spectra for the different atherosclerotic aorta preparations. In the fatty streak, the major molecular species were: 36:4 (12%), representing mainly 16:0/20:4; 36:2 (10%), mainly 18:0/18:2; 34:1 (10%), mainly 16:0/18:1; 38:4 (9%), mainly 18:0/20:4; 32:0 (9%), mainly 16:0/16:0; and 34:2 (6%), mainly16:0/18:2 GroPCho. About 4% of the total was contributed by 38:4pls (where -pls indicates alkenyl), mainly 1-alkenyl/20:4 GroPCho. There were variable amounts of many minor species, the estimated SD of which approached their means. Only limited changes in the proportions of the major molecular species were found, but some might approach statistical significance when examined in a larger population. The greatest differences were seen between the fatty streak and the calcified tissue. Thus, the proportions of 16:0/18:2, 16:0/18:1, and 18:1/18:3 GroPCho increased from 6, 10, and 3% in the fatty streak to 12, 14, and 6%, respectively, in the calcified tissue, whereas the 16:0/16:0, 16:0/20:0, and 18:0pls/20:4 GroPCho decreased from 9, l2, and 4% in the fatty streak to 6, 9, and 2%, respectively, in the calcified tissue. The molecular species of the GroPCho in the fibrous plaque and necrotic core showed alterations between the just-mentioned extremes. There was a small decrease in some of the polyunsaturated species as samples progressed from the fatty streak to the necrotic core and the calcified tissues, and in comparison with the PtdCho of plasma LDL lipoproteins reported elsewhere (24).

Molecular species of SM. The total mass spectra recorded over the SM elution times for the necrotic core (16.767–19.962 min, Fig. 1C) ranged in mass from *m/z* 676 to 816, with smaller intensities seen at *m/z* 690, 752, 754, and 802, which corresponded rather closely to those of the normal LDL and normal aorta (24). Table 3 gives the composition of the molecular species of the SM, which also changed relatively little over the course of the development of the atherosclerotic plaque. In the fatty streak, the major SM species were 34:1 (41%), representing mainly d18:1/16:0 (where d- indicates that the fatty acid shown by the carbon:double bond number is a sphingosine homolog); 42:2 (9%), mainly d18:1/24:1; 36:1 (7%), mainly d18:1/18:0; 38:1 (5%), mainly d18:1/20:0; 40:1 (5%), mainly d18:1/22:0; and 32:1 (4%), mainly d16:1/16:0. The main differences were seen between the fatty streak and the calcified plaque. Thus, the proportions of d18:1/16:0, d18:1/18:0, d18:1/20:0, and d18:1/24:0 decreased from 41, 7, 3, and 5% in the fatty streak to 38, 4, 3, and 3%, respectively, in the calcified tissue, whereas those of d16:1/16:0 and d18:1/24:1 increased from 4 and 9%, respectively, in the fatty streak to 6 and 13%, respectively, in the calcified tissue. Two masses (*m/z* 689 and 725) making up 0 to 7.5% of the total SM of some of the extracts remained unidentified. A clear trend toward longer or more saturated species therefore was not seen with maturation of the plaque.

Molecular species of lysoPtdCho. The total mass spectra recorded over the lysoPtdCho elution times for the necrotic core (20.304–23.900 min, Fig. 1D) ranged in mass from *m/z* 495 to 569, with smaller intensities seen at *m/z* 483, 503, 507, 509, 525, and 571. The major species corresponded qualitatively to those of the normal LDL (24). Table 4 gives the composition of the molecular species of lysoPtdCho quantified over the course of the development of the plaque. In the fatty streak, the major species were: 16:0 (23%), 20:4 (21%), 18:1 (11%), 18:3 (10%), 18:2 (9%), 18:0 (6%), and 20:3 (4%). The proportions of 16:0, 18:2, 18:0, and 20:3 increased from 23,

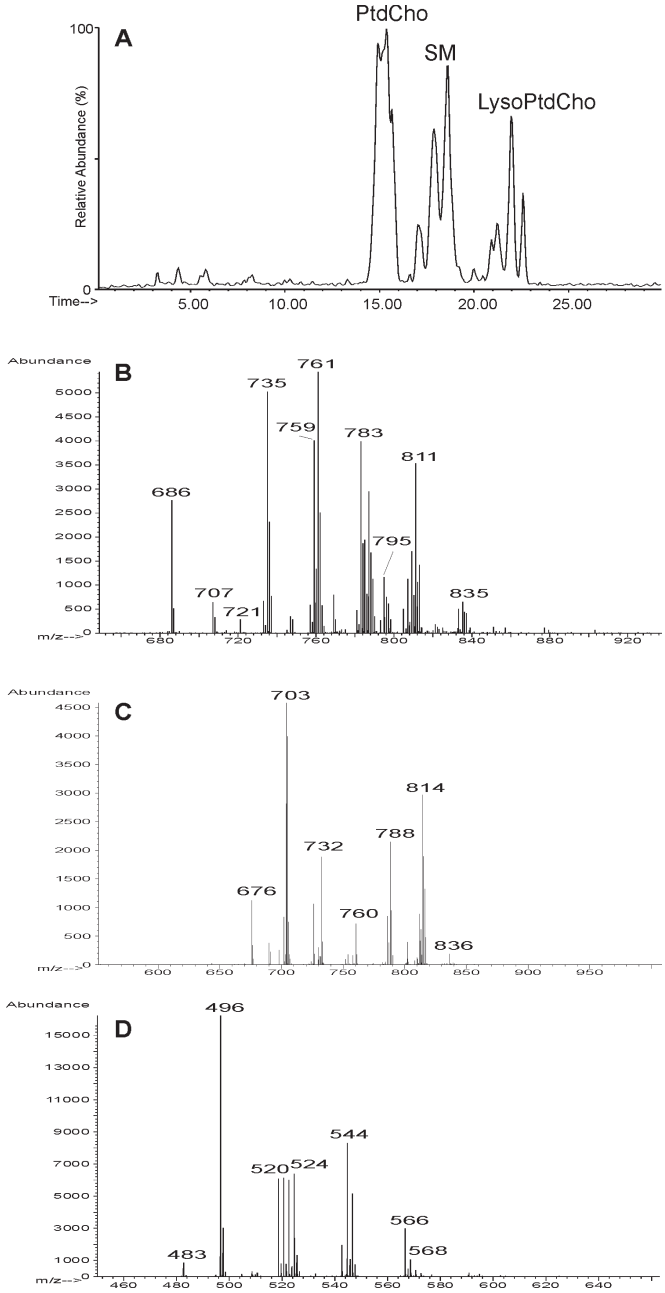

FIG. 1. Total ion current profile of choline-containing phospholipids of mature atheroma (A) and full mass spectra of phosphatidylcholine (PtdCho) (B), sphingomyelin (SM) (C), and lysophosphatidylcholine (lysoPtdCho) (D) as recorded over the elution ranges of the chromatogram. The major peaks identified are shown in Tables 2–4. Liquid chromatography/electrospray ionization-mass spectrometry (LC/ESI-MS) conditions are given in the Materials and Methods section.

9, 6, and 4%, respectively, in the fatty streak to 25, 11, 11, and 6%, respectively, in the calcified tissue. Surprisingly, the lysoPtdCho of all the aortic preparations contained up to 30% polyunsaturated species (e.g., 20:3; 20:4; 20:5; 22:5; 22:6). The content of the polyunsaturated lysoPtdCho decreased with the maturation of the aortic plaque but was still high in the necrotic core and in the calcified plaque. However, neither the alkyl nor the alkenyl lysoPtdCho appeared to have accumulated. An ion at *m/z* 566, corresponding to 1-*O*-stearyl-2-acetoyl-GroPCho (platelet-activating factor, PAF) made up about 6% of the lysoPtdCho fraction of the fatty streak, fibrous plaque, and necrotic core, but decreased to about 3% in the calcified tissue.

Molecular species of PtdCho hydroxides, hydroperoxides, and isoprostanes. The atheroma preparations examined in this study also revealed the presence of ions at *m/z* 790, 822, 818, and 846, corresponding to the hydroperoxide-containing GroPCho as previously reported for the copper-oxidized PtdCho of LDL (24). In most samples, ions at *m/z* 774 (34:2-OH), 790 (34:2-2 × OH), 802 (36:2-OH), 818 (36:2-2 × OH) and 814 (36:4-2 × OH) were found to be eluted with retention times between those of hydroperoxides and the core aldehydes and these were attributed to the hydroxides. Figure 2 shows the single-ion mass chromatograms for the major isoprostanes derived from the arachidonoyl GroPCho isolated from the necrotic core of human atheroma. The ions at *m/z* 828 and 856 were attributed to the 36:4 and 38:4 epoxy isoprostanes. The ions at *m/z* 830 and 858 were attributed to 36:4 and 38:4 E_2/D_2 isoprostanes derived from arachidonoyl GroPCho, whereas those at *m/z* 832 and 860 were attributed to 36:4 and 38:4 F_2 isoprostanes of arachidonoyl GroPCho, as previously described for the isoprostanes accumulated in HDL after oxidation with peroxynitrite (36). Figure 3 gives the isoprostane levels as μg/g of atherosclerotic tissue at different stages of development. Despite marked differences in the degree of progression of the disease and in the overall variability of the estimates, the average quantities and proportions of the various species were quite similar.

PtdCho core aldehydes. Figure 4 shows the single-ion mass chromatograms recorded for the core aldehydes of PtdCho in the necrotic core of mature atheroma. The ions at *m/z* 594 and 622 were attributed to the 16:0/5:0ALD (where ALD is aldehyde) and 18:0/5:0ALD GroPCho, whereas the ions at *m/z* 650 and 678 were attributed to 16:0/9:0ALD and 18:0/9:0ALD GroPCho. The core aldehydes migrated on the HPLC columns with the retention times of synthetic 9:0ALD-containing standards, but these could have been the isobaric 8:1(OH)ALD described by Hoff *et al*. (37). These compounds yielded the same masses for the parent and fragment ions in ESI-MS in the positive and negative ion modes. Figure 5 gives the levels of PtdCho core aldehydes in atherosclerotic tissues at different stages of plaque progression. When expressed as μg/g of tissue, little variation was seen among the lesions. There was no evidence of progressive accumulation with severity of the disease. Since more total PtdCho was found at the later stages of plaque development, the proportion of total aldehydic PtdCho would appear to be decreasing. Among the core aldehydes of GroPCho we had previously recognized small amounts of the alkyl derivatives (33), which were pooled with acyl derivatives in the present study.

Molecular species of acidic phospholipids. Figure 6 shows the total negative ion profile of the acidic phospholipids of the necrotic core of human atheroma (A) and the full mass spectra of PtdEtn (B) and PtdIns (C) as recorded over the

TABLE 2
Molecular Species of PtdCho from Human Atherosclerotic Plaques of Different Developmental Stages (mol%)[a]

Molecular species[b]	$[M + 1]^+$	Fatty streak ($n = 3$)	Fibrous plaque ($n = 4$)	Necrotic core ($n = 4$)	Calcified tissue ($n = 4$)
30:0	706	1.49 ± 0.74	1.33 ± 1.20	1.57 ± 0.88	0.18 ± 0.23
32:0alk	720	0.43 ± 0.66	0.22 ± 0.24	0.76 ± 0.68	0.02 ± 0.03
32:1	732	1.69 ± 0.25	1.93 ± 0.57	1.68 ± 0.71	0.26 ± 0.44
32:0	734	9.08 ± 3.21	10.58 ± 2.79	9.43 ± 3.11	6.26 ± 1.36
34:0pls	748	0.96 ± 1.32	0.59 ± 0.17	1.14 ± 0.77	0.26 ± 0.06
34:3	756	1.85 ± 0.46	2.06 ± 0.35	1.13 ± 0.36	0.87 ± 0.11
34:2	758	6.07 ± 4.32	8.84 ± 1.05	9.39 ± 1.63	12.32 ± 1.61
34:1	760	9.99 ± 2.62	11.46 ± 1.09	11.98 ± 2.69	14.24 ± 1.97
36:4alk	768	0.62 ± 0.99	1.34 ± 0.63	1.53 ± 0.85	0.46 ± 0.45
36:1pls	774	0.22 ± 0.30	0.03 ± 0.05	0.07 ± 0.10	0.13 ± 0.11
36:5	780	2.37 ± 0.71	2.06 ± 1.14	1.25 ± 0.13	0.99 ± 0.86
36:4	782	11.69 ± 2.75	8.20 ± 0.55	8.92 ± 0.65	9.36 ± 0.59
36:3	784	3.38 ± 0.94	5.63 ± 0.88	5.64 ± 0.95	6.02 ± 0.36
36:2	786	10.54 ± 6.60	8.73 ± 1.26	8.28 ± 2.26	8.64 ± 2.46
36:1	788	2.34 ± 1.25	1.70 ± 0.54	2.34 ± 0.52	2.97 ± 0.34
38:4pls	794	4.34 ± 3.48	3.52 ± 1.07	3.10 ± 1.09	1.55 ± 0.35
38:4alk	796	1.99 ± 1.69	2.14 ± 1.11	1.79 ± 0.73	1.69 ± 0.16
38:7	804	1.60 ± 0.23	0.76 ± 0.74	1.00 ± 0.65	0.57 ± 0.51
38:6	806	2.35 ± 0.88	2.35 ± 0.95	1.53 ± 1.00	1.00 ± 1.21
38:5	808	3.45 ± 2.05	2.88 ± 0.22	2.71 ± 0.79	2.03 ± 0.79
38:4	810	9.00 ± 1.67	8.41 ± 0.73	9.41 ± 0.42	8.73 ± 0.41
38:3	812	1.22 ± 0.87	2.19 ± 1.28	2.28 ± 0.83	1.58 ± 1.60
40:6alk	820	0.21 ± 0.34	0.37 ± 0.49	0.22 ± 0.12	0.07 ± 0.06
40:4alk	824	0.21 ± 0.30	0.08 ± 0.14	0.14 ± 0.16	0.14 ± 0.20
40:7	832	0.94 ± 0.55	1.09 ± 0.41	1.08 ± 0.34	0.58 ± 0.04
40:6	834	1.28 ± 0.95	0.84 ± 0.85	0.55 ± 0.64	0.78 ± 0.83
40:5	836	0.81 ± 1.07	0.23 ± 0.12	0.37 ± 0.41	0.27 ± 0.24
40:4	838	0.85 ± 0.90	0.23 ± 0.25	0.22 ± 0.14	0.17 ± 0.12
Other		9.24	10.21	10.49	17.86
Total[c]		100	100	100	100

[a]Data are shown as mean ± SD.
[b]Molecular species are identified by total fatty carbon number:double bond number; each sample analyzed in triplicate. alk, alkyl; pls, alkenyl; for other abbreviation, see Table 1.
[c]PtdCho contents of the fatty streak, fibrous plaque, necrotic core, and calcified tissue are given in Table 1.

TABLE 3
Molecular Species of SM from Human Atherosclerotic Plaques of Different Developmental Stages (mol%)[a]

Molecular species[b]	$[M + 1]^+$	Fatty streak ($n = 3$)	Fibrous plaque ($n = 4$)	Necrotic core ($n = 4$)	Calcified tissue ($n = 4$)
32:1	675	3.76 ± 3.48	6.87 ± 1.20	6.08 ± 2.14	6.04 ± 2.25
X	689	0.54 ± 0.47	1.08 ± 0.91	0.74 ± 0.61	2.52 ± 4.62
34:2	701	5.22 ± 2.48	3.57 ± 0.71	3.72 ± 0.08	5.72 ± 3.17
34:1	703	41.09 ± 10.12	34.96 ± 4.52	36.64 ± 4.58	38.45 ± 8.60
34:0	705	2.81 ± 2.13	2.31 ± 1.00	3.13 ± 2.19	1.31 ± 1.32
XX	725	6.88 ± 2.34	9.09 ± 2.80	6.61 ± 2.03	7.50 ± 0.65
36:2	729	1.31 ± 0.71	1.36 ± 0.76	1.05 ± 0.37	1.69 ± 1.25
36:1	731	6.83 ± 4.54	4.85 ± 2.12	4.83 ± 1.98	4.42 ± 2.85
38:3	756	0.18 ± 0.25	0.00 ± 0.00	0.12 ± 0.17	0.09 ± 0.07
38:2	757	0.43 ± 0.28	0.51 ± 0.46	0.27 ± 0.26	0.18 ± 0.13
38:1	759	5.46 ± 8.10	1.86 ± 1.15	1.85 ± 0.81	2.66 ± 2.37
40:2	785	1.03 ± 1.38	1.84 ± 0.77	2.21 ± 0.69	1.60 ± 0.15
40:1	787	4.72 ± 1.45	4.33 ± 1.54	6.90 ± 2.03	5.00 ± 3.69
41:0	803	0.49 ± 0.43	0.98 ± 0.49	0.93 ± 0.71	1.35 ± 1.57
42:4	809	1.33 ± 0.61	0.38 ± 0.41	0.43 ± 0.50	0.06 ± 0.11
42:3	811	3.66 ± 3.42	7.94 ± 0.86	5.76 ± 1.17	3.87 ± 0.87
42:2	813	9.30 ± 1.27	13.10 ± 2.44	13.39 ± 2.60	12.74 ± 4.04
42:1	815	4.94 ± 0.45	4.98 ± 2.93	5.36 ± 0.65	3.29 ± 2.22
Total[c]		99.98	100.1	100.2	98.49

[a]Data are shown as mean ± SD.
[b]Molecular species are identified by total fatty carbon number:number of double bonds; each sample was analyzed in triplicate. X and XX, unidentified; for other abbreviation see Table 1.
[c]Total SM contents of fatty streak, fibrous plaque, necrotic core, and calcified tissue are given in Table 1.

TABLE 4
Molecular Species of LysoPtdCho from Human Atherosclerotic Plaques of Different Developmental Stages (mol%)[a]

Molecular species[b]	$[M + 1]^+$	Fatty streak ($n = 3$)	Fibrous plaque ($n = 4$)	Necrotic core ($n = 4$)	Calcified tissue ($n = 4$)
15:0	468	0.54 ± 0.78	0.00 ± 0.00	0.06 ± 0.07	0.52 ± 0.64
16:0alk	482	0.50 ± 0.62	0.25 ± 0.24	0.74 ± 0.45	0.59 ± 0.54
16:0	496	23.24 ± 4.95	19.62 ± 1.39	22.72 ± 1.36	25.08 ± 2.55
18:2pls	504	0.27 ± 0.36	0.52 ± 0.11	0.41 ± 0.27	0.38 ± 0.40
18:0pl	508	0.72 ± 0.76	0.71 ± 0.11	1.06 ± 0.78	0.69 ± 0.42
18:0alk	510	0.44 ± 0.57	0.37 ± 0.24	0.37 ± 0.29	0.55 ± 0.51
18:3	518	9.94 ± 2.12	9.82 ± 1.20	8.55 ± 0.60	9.60 ± 1.78
18:2	520	8.76 ± 5.52	11.43 ± 3.57	11.24 ± 2.59	11.44 ± 3.43
18:1	522	11.32 ± 1.68	11.42 ± 3.62	11.32 ± 2.31	11.92 ± 1.60
18:0	524	6.00 ± 1.78	8.52 ± 4.20	10.37 ± 3.40	10.63 ± 3.68
20:5alk	526	0.04 ± 0.07	0.08 ± 0.03	0.14 ± 0.17	0.12 ± 0.12
20:5	542.	3.46 ± 1.24	5.06 ± 1.71	3.99 ± 0.62	3.57 ± 0.9
20:4	544	20.63 ± 5.19	17.05 ± 0.92	14.16 ± 1.20	14.52 ± 3.49
20:3	546	3.56 ± 2.27	5.29 ± 2.26	6.66 ± 0.69	6.14 ± 1.59
18:0paf	566	5.96 ± 1.16	5.00 ± 0.82	4.16 ± 1.57	2.59 ± 1.16
22:6	568	1.28 ± 1.26	2.59 ± 0.88	1.96 ± 1.14	0.49 ± 0.06
22:5	570	1.07 ± 1.80	0.40 ± 0.26	0.43 ± 0.30	0.10 ± 0.09
22:4	572	0.80 ± 0.73	0.68 ± 0.66	0.62 ± 0.59	0.11 ± 0.13
Total[c]		98.53	98.79	98.95	99.05

[a]Data are given as mean ± SD.
[b]Molecular species are identified by total fatty carbon number:number of double bonds each sample analyzed in triplicate. pls, alkenyl; paf, platelet-activating factor; for other abbreviation see Table 2.
[c]Total lysoPtdCho contents of fatty streak, fibrous plaque, necrotic core, and calcified tissue are given in Table 1.

appropriate elution ranges of the chromatogram. The major ions of PtdEtn and PtdIns were identified in Tables 5 and 6, respectively. The large unlabeled peaks following PtdIns are due to the chloride adducts of PtdCho and SM.

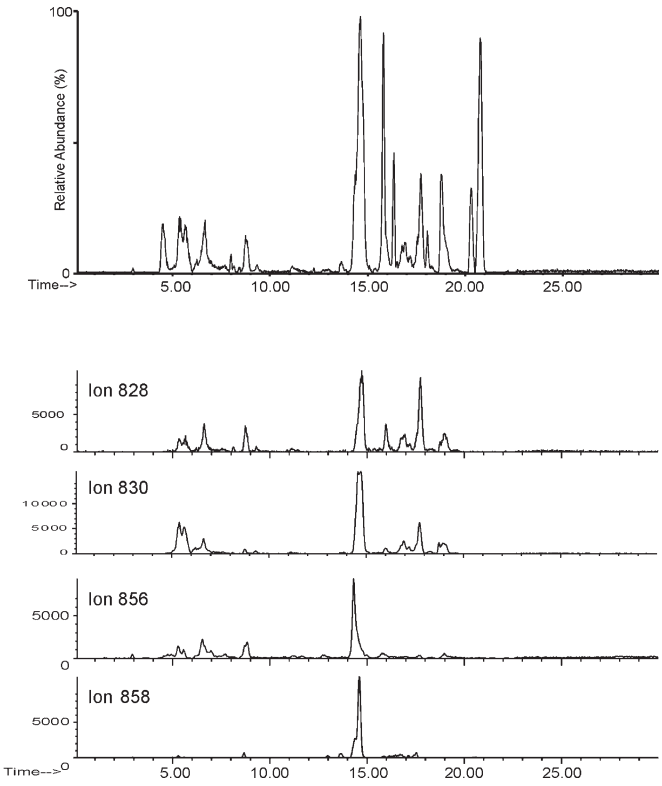

FIG. 2. Single-ion mass chromatograms for the major isoprostane-containing PtdCho of the necrotic core of a human atherosclerotic plaque. Molecular species are identified in the figure. LC/ESI-MS conditions are given in the Materials and Methods section. For abbreviations see Figure 1.

The total mass spectra recorded over the elution range of the ethanolamine phospholipids of the necrotic core (Fig. 6B) ranged in mass from *m/z* 716 to 796, with the major species being due to *m/z* 744, 766, and 794, which correspond to 18:0/18:2, 18:0/20:4, and 18:0/22.4, respectively. The corresponding alkenylacyl glycerophosphoethanolamine (GroPEtn) species (16:0/20:4 and 16:0/20:3) were present in trace amounts only. Table 5 gives the relative composition of the major species of the ethanolamine glycerophospholipids, the proportions of which appeared to be especially variable among the different preparations of atherosclerotic extracts. In the fatty streak, the major PtdEtn species were: 38:4 (55%), corresponding to mainly 18:0/20:4; 40:4 (11%), mainly 18:0/22:4; 40:6 (8%), mainly 18:0/22:6; and 36:1 (7%), mainly 18:0/18:1 GroPEtn. A comparable distribution of these species was seen for the fibrous plaque and the calcified tissue. In contrast, the necrotic core contained only 40% 18:0/20:4 but 21% 18:0/18:1. Both the necrotic core and calcified tissue contained a high proportion of 18:0/22:4 (18–27%). The plasmalogenic species was essentially completely absent. Obviously, the ethanolamine glycerophospholipids of the atherosclerotic lesions had rather limited resemblance to those of LDL (38). No evidence was obtained for the presence of lysophosphatidylethanolamine (lysoPtdEtn) or lysophosphatidylinositol (lysoPtdIns) in any of the lesion preparations. Surprising also was the relative absence of the hydroperoxides, isoprostanes, and core aldehydes from the inositol and ethanolamine-containing phospholipids.

The total mass spectra recorded over the PtdIns elution times of the necrotic core (Fig. 6C) ranged in mass from *m/z* 836 to 944, with the major species being due to *m/z* 885, which corresponded to 18:0/20:4. Table 6 gives the relative composition of the major species of PtdIns, which changed

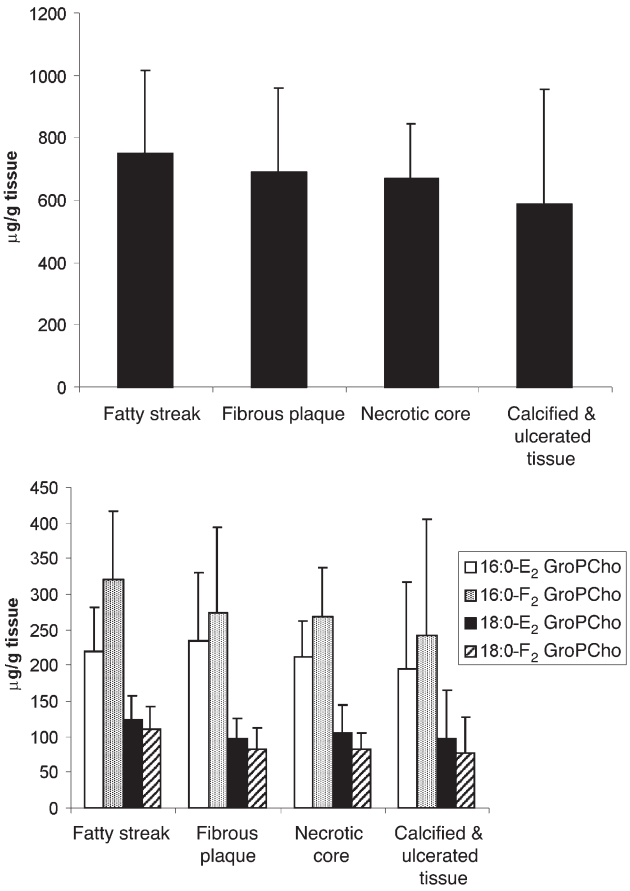

FIG. 3. Isoprostane levels of atherosclerotic tissue at different stages of atheroma development. 16:O/E_2 glycerophosphocholine (GroPCho), palmitoyl GroPCho with an E_2 at the *sn*-2-position; 16:0/F_2 GroPCho, palmitoyl GroPCho with an F_2 at the *sn*-2-position; 18:0/E_2 GroPCho, stearoyl GroPCho with an E_2 at the *sn*-2-position; 18:0/F_2 GroPCho, stearoyl GroPCho with an F_2 at the *sn*-2-position. Isoprostane levels were estimated by LC/ESI-MS in relation to an internal standard; n = 3–4; each sample was analyzed in triplicate. LC/ESI-MS conditions as given in the Materials and Methods section. For other abbreviation see Figure 1.

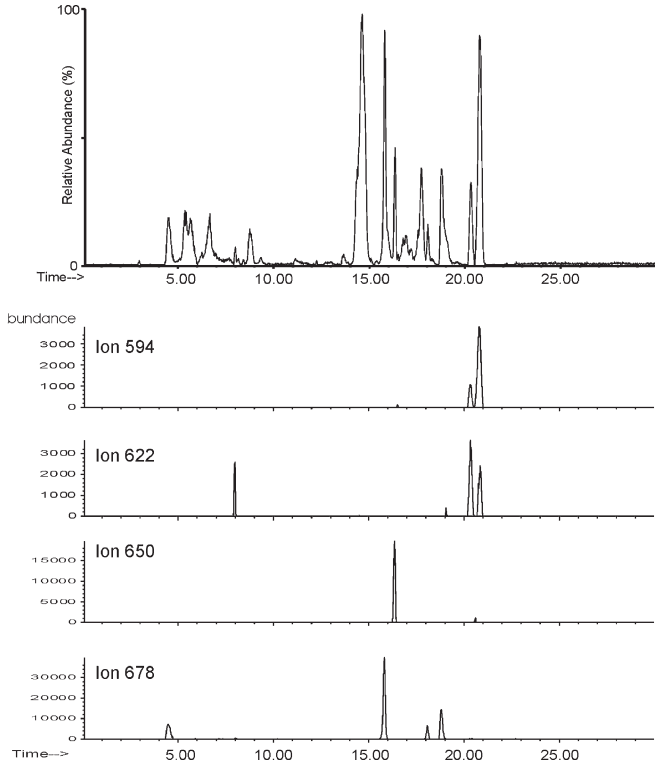

FIG. 4. Single-ion mass chromatograms recorded for the major core aldehydes of PtdCho of the necrotic core of human atheroma. Molecular species are identified in the figure. LC/ESI-MS conditions are given in the Materials and Methods section. For abbreviations see Figure 1.

little with the maturation of the plaques, and corresponded in general to that of plasma LDL (38,39). The major species of PtdIns in the fatty streak, fibrous plaque, necrotic core, and calcified tissue were: 38:4 (75–78%), representing mainly 18:0/20:4; 38:3 (6–8%), mainly 18:0/20:3; 38:5 (3–4%), mainly 18:0/20:5; and 36:2 (3–7%), mainly 18:0/18:2 glycerophosphoinositol (GroPIns). The PtdIns composition of the necrotic core differed markedly from that of the fatty streak, fibrous plaque, and calcified tissue by containing less of the 18:0/20:4 (57%) and more of the 18:0/20:3 (26%) species.

Despite the high polyunsaturation of PtdIns, neither hydroperoxides nor isoprostanes or core aldehydes were found in the present study. Piotrowski *et al.* (30,35) found a linear relationship between total PtdCho and PtdIns and their peroxide content, but the PtdEtn showed no such relationship. Piotrowski *et al*. (30) determined the total phospholipid hydroperoxides in mature atherosclerotic plaques by means of a fluorometric assay.

Among the ethanolamine phospholipids in the atherosclerotic lesions were the glucosylation products, which had been isolated previously from the LDL of normal subjects and diabetics (40,41). Figure 7 shows the elution pattern of the glucosylated and nonglucosylated diradyl GroPEtn recovered from a mature atheroma of a patient with diabetes. Both diacyl and alkenylacyl derivatives of glycated GroPEtn were identified by negative-ion LC/ES-MS. In the present study, a considerable discrepancy existed between the glycated and nonglycated species from lesions at different stages of development. The most abundant glycated PtdEtn species in the plaque was 18:0/20:4 (*m/z* 928). However, the glycated ethanolamine phospholipids also contained high proportions of the 38:5 alkenylacyl (*m/z* 910), mainly 1-*O*-stearyl-2-20:4; 38:4 alkenylacyl (*m/z* 912), mainly 1-*O*-stearyl-2-20:4; and 36:4 alkenylacyl (*m/z* 884), mainly 1-*O*-palmityl-2-20:4 GroPEtn. The high content of the plasmalogens in the glycated ethanolamine phospholipids contrasts with their nearly complete absence from the diacyl GroPEtn homologs. We showed elsewhere (24) that the molecular species of glycated and nonglycated diradyl GroPEtn are quite similar when isolated from the same sample of mature atherosclerotic tissue. In samples from nondiabetic individuals, we found 2.4 nmol glycated diradyl GroPEtn per milligram total lipid, which represented 1.3% of the total atheroma phospholipid. The atherosclerotic tissue from diabetics contained 11.5 nmol glycated diradyl GroPEtn per milligram total lipid, which repre-

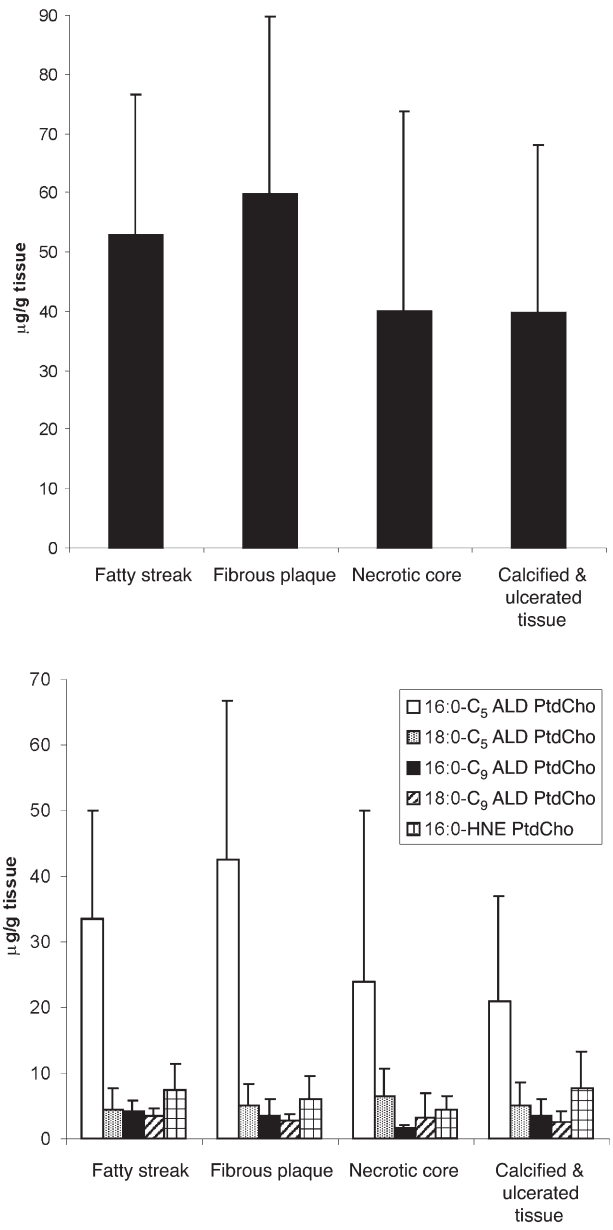

FIG. 5. PtdCho core aldehyde levels at different stages of atheroma development. Core aldehyde levels were estimated by LC-MS in relation to an internal standard; n = 3–4; each sample was analyzed in triplicate. LC/ESI-MS conditions are given in the Materials and Methods section. HNE, 4-hydroxynonenal; C_5 ALD, five-carbon aldehydes; C_9 ALD, nine-carbon aldehydes; for other abbreviations see Figure 1.

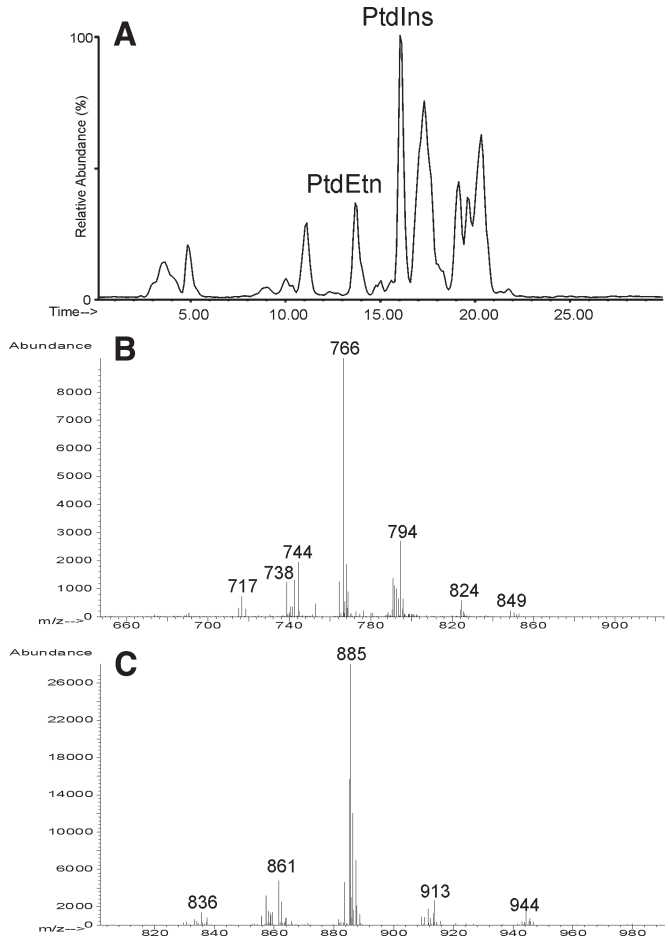

FIG. 6. Total negative ion profile of the inositol and ethanolamine glycerophospholipids of the necrotic core of human atheroma (A) and the full mass spectra of phosphatidylethanolamine (PtdEtn) (B) and phosphatidylinositol (PtdIns) (C) as recorded over the appropriate elution ranges of the chromatogram. The molecular species of the phospholipids are identified as shown in Tables 5 and 6. LC/ESI-MS conditions are given in the Materials and Methods section.

sented 7.3% of the total atheroma phospholipids, whereas the analysis of normal aortic tissue did not show any PtdEtn glycation.

DISCUSSION

Analytical results. There have been no previous detailed analyses of the phospholipids or oxophospholipids of atherosclerotic lesions from different stages of development. Some of our values can be compared, however, to the values extrapolated from the data obtained on mature plaques by Piotrowski *et al*. (30,35). Thus, a fivefold increase in the total phospholipid content of the fibrous plaque found in the present work is of the order reported by Piotrowski *et al*. (30) for the mature plaque when compared with normal intima. The proportions of the PtdCho/PtdIns/PtdEtn (3.4:1:1 by wt) observed for the fibrous plaque were comparable to those extrapolated from the data of Piotrowski *et al*. (35) for mature atherosclerotic plaque (PtdCho/PtdIns/PtdEtn ratio of 6.3:1.5/2.2, by wt). The 19% of lysoPtdCho found in the fibrous plaque in the present study compared to 17% lysoPtdCho extrapolated from the data of Piotrowski *et al*. (35) for the mature plaque. The SM contribution increased from 16 to 32% of total phospholipids during lesion development, whereas a value of about 20% was obtained from the data of Piotrowski *et al*. (35).

The major molecular species of PtdCho resembled those described previously for total plasma (38), whereas the molecular species of SM were similar to those reported earlier for plasma LDL (24,38). The molecular species of lysoPtdCho

TABLE 5
Molecular Species of Ethanolamine Glycerophospholipids from Human Atherosclerotic Plaques of Different Developmental Stages (mol%)[a]

Molecular species[b]	$[M + 1]^+$	Fatty streak ($n = 3$)	Fibrous plaque ($n = 4$)	Necrotic core ($n = 4$)	Calcified tissue ($n = 4$)
34:1	716	0.68 ± 0.71	4.00 ± 1.49	0.21 ± 0.49	2.55 ± 4.41
36:4	738	5.21 ± 5.00	2.12 ± 1.90	0.78 ± 1.80	0.00 ± 0.00
36:2	742	5.19 ± 4.75	3.87 ± 3.35	3.67 ± 7.09	0.85 ± 1.47
36:1	744	6.56 ± 2.62	10.40 ± 2.39	20.94 ± 7.04	3.98 ± 6.29
38:3pls	752	0.12 ± 0.21	1.07 ± 0.94	1.47 ± 3.39	0.00 ± 0.00
38:5	764	5.77 ± 0.52	4.81 ± 6.78	9.11 ± 3.65	0.75 ± 1.29
38:4	766	55.66 ± 12.20	53.03 ± 9.71	39.98 ± 6.38	56.16 ± 12.22
40:6	790	8.23 ± 6.26	8.87 ± 8.31	6.03 ± 8.70	5.50 ± 4.67
40:4	794	10.58 ± 4.64	10.83 ± 2.30	17.79 ± 2.52	27.49 ± 16.78
40:3	796	1.99 ± 1.74	0.99 ± 0.40	0.02 ± 0.05	2.74 ± 0.59
Total[c]		99.99	99.99	99.99	99.99

[a]Data are given as mean ± SD.
[b]Molecular species are identified by total fatty carbon number:number of double bonds; each sample was analyzed in triplicate. pls, alkenyl.
[c]Total ethanolamine glycerophospholipid contents of fatty streak, fibrous plaque, necrotic core, and calcified tissue are given in Table 1.

TABLE 6
Molecular Species of PtdIns from Human Atherosclerotic Plaques of Different Developmental Stages (mol%)[a]

Molecular species[b]	$[M + 1]^+$	Fatty streak ($n = 3$)	Fibrous plaque ($n = 4$)	Necrotic core ($n = 4$)	Calcified tissue ($n = 4$)
36:4	857	1.93 ± 1.77	2.15 ± 1.86	1.30 ± 1.06	2.00 ± 4.00
36:2	861	3.41 ± 2.96	3.43 ± 0.48	6.07 ± 2.96	6.65 ± 5.28
36:1	863	0.25 ± 0.22	2.92 ± 2.79	2.17 ± 1.06	0.00 ± 0.00
38:5	883	4.07 ± 1.38	3.17 ± 2.53	3.82 ± 1.70	2.82 ± 2.26
38:4	885	78.43 ± 9.47	75.09 ± 5.82	57.10 ± 4.75	76.17 ± 10.74
38:3	887	8.15 ± 3.80	11.38 ± 0.53	25.72 ± 3.82	6.54 ± 6.71
40:6	909	0.38 ± 0.66	0.55 ± 0.96	3.56 ± 0.30	0.49 ± 0.99
40:5	911	0.51 ± 0.89	0.30 ± 0.53	0.44 ± 0.89	0.00 ± 0.00
40:4	913	1.65 ± 2.66	0.59 ± 1.02	0.07 ± 0.14	2.03 ± 4.06
Totalb		98.78	99.58	98.95	96.70

[a]Data are given as mean ± SD. For abbreviation see Table 1.
[b]Molecular species are identified by total fatty carbon number:number of double bonds; each sample was analyzed in triplicate.
[c]Total PtdIns contents of fatty streak, fibrous plaque, necrotic core, and calcified tissue are given in Table 1.

were unusual in having a high proportion of the unsaturated species, which are unlikely to have originated from the activity of phospholipase A_2. The finding of a high proportion of PUFA in the *sn*-1-position, as indicated by their chromatographic behavior, may have resulted from isomerization of the *sn*-2-lysophospholipids following prior nonenzymatic (alkenyl group) or enzymatic (acyl group) removal of the *sn*-1-substituent (phospholipase A_1).

The high proportion of total lysoPtdCho may reflect preferential enzymatic destruction of oxo-PtdCho. The present study identifies the major molecular species of the lipid peroxides of atherosclerotic plaques as the mono- and dihydroperoxides of the linoleates of GroPCho, and as the E and F isoprostane derivatives of the arachidonates of GroPCho. The total content of the hydroperoxides measured in the present work exceeds the value reported by Piotrowski *et al*. (35) by twofold, which may have been due to differences in the methodologies used. Our estimates for isoprostanes in the atheroma samples are similar to those of Pratico *et al.* (6), who reported the 8-epi prostaglandin$_{2\alpha}$ (1.310–3.450 pmol/μmol phospholipid) in atherectomy specimens compared with 0.045–0.115 pmol/μmol phospholipid in vascular tissue devoid of atherosclerosis. Corresponding values of IPG$_{2\alpha}$-I were 5.6–13.8 vs. 0.16–0.44 pmol/μmol phospholipid. Assuming a PtdCho level to be 6.3 mg/g of tissue and a total isoprostane level of 630 μg/g tissue, the pmol/μmol concentration estimated in the present study (5–20 pmol/μmol PtdCho) would be in the range reported by Pratico *et al*. (6), which suggests that the plaque isoprostanes are essentially all bound to GroPCho. According to Pratico *et al*. (6), the isoprostane levels remained relatively constant over a range of carotid stenosis of 60 to 95% and an age range of 54 to 76 yr. Taken together, these results suggest the continued production and destruction of hydroperoxides and isoprostanes rather than a linear accumulation. Thomas *et al.* (7) recently showed in lesions from atherosclerotic nonhuman primates that no simple explanation exists as to why F_2-isoprostane accumulation does not depend on the concentration of oxidizable lipids that promote free-radical lipid oxidation. Reilly *et al*. (42) demonstrated, however, an increased formation of distinct F_2 isoprostanes in hypercholesterolemia. Our previous work (40) with oxidized LDL revealed the mono- and dihydroperoxide and isoprostane-containing PtdCho as the major early oxidation products of LDL. Specifically, the monohydroperoxy derivatives of 16:0/18:2 GroPCho (*m/z* 790) and 18:0/18:2 GroPCho (*m/z* 818) were identified, as were the dihydroperoxides of 16:0/20:4 GroPCho (*m/z* 846), and the 16:0/F_2 isoprostane (*m/z* 832) and 16:0/E_2 isoprostane GroPCho (*m/z* 830) arising from the 16:0/20:4 GroPCho.

The lipid hydroxides of atheromas, whatever their origin, have been studied in great detail and quantified by Wadding-

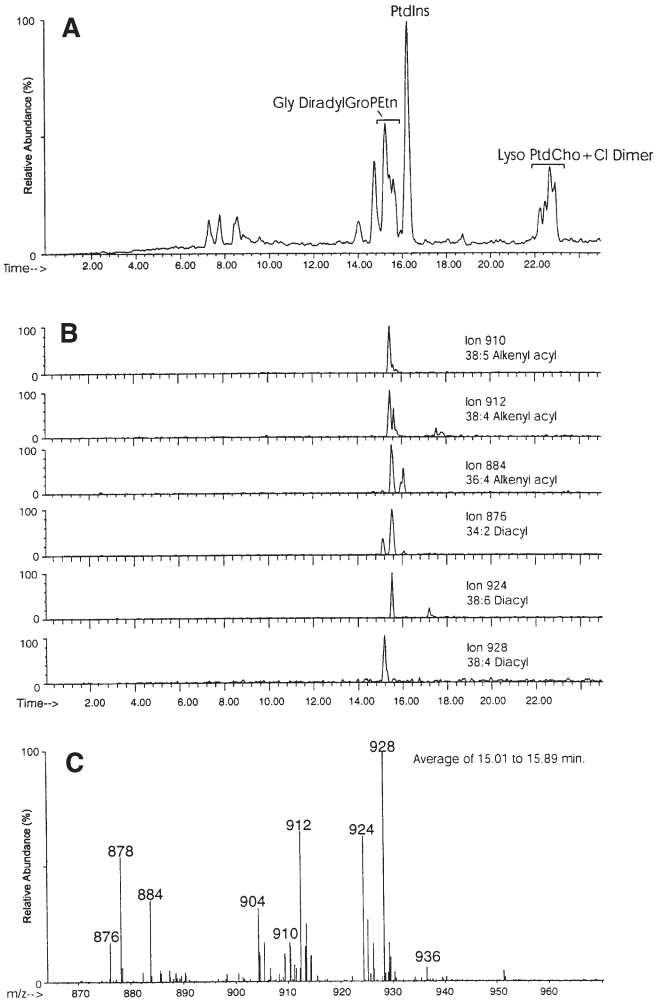

FIG. 7. Elution pattern of the glucosylated and nonglucosylated diradyl glycerophosphoethanolamine (GroPEtn) recovered from a mature atheroma of a diabetic patient. The molecular species have been identified elsewhere (24). LC/ESI-MS conditions are given in the Materials and Methods section. Gly, glycosated; Cl, chloride.

ton *et al.* (11) and earlier by Mallat *et al*. (8). The values of the hydroxides of linoleoyl GroPCho reported by Mallat *et al*. (8) and Waddington and coworkers (10,11) exceeded those of the isoprostanes by more than 20 times. The PtdCho hydroxide values found in the present study barely reached those of the hydroperoxides and isoprostanes. It is possible that the higher recoveries of the hydroxides were facilitated by the saponification and quantification of the hydroxy FAME in the studies of Mallat *et al*. (8) and Waddington *et al*. (11).

The presence of core aldehydes of GroPCho in the atherosclerotic plaques has been recognized only recently (24,25,33). The present levels and composition of molecular species are in the previously reported range, although there may have been some decrease with plaque maturation. Hoff *et al*. (37) anticipated the formation of carboxy-terminal analogs of the 4-hydroxynonenal type during lipid peroxidation in both arachidonate- and linoleate-esterified GroPCho. Kaur *et al*. (43) suggested a likely mechanism of formation of 5-hydroxy-8-oxo-6-octenoic acid ester from arachidonoyl GroPCho and 9-hydroxy-12-oxo-10-dodecenoic acid ester from linoleoyl GroPCho that involved the partitioning of a family of peroxyeicosatetraenoyl radicals generated by nonregioselective hydrogen atom abstraction from arachidonate or linoleate. β-Scission of an alkoxyl radical derived from dihydroperoxide could form two γ-hydroxy-α,β-unsaturated aldehydes such as hydroxynonenal and an analog still esterified to GroPCho. For every molecule of hydroxynonenal formed, a mirror image of esterified hydroxynonenal would also be obtained. Since the γ-hydroxy-α,β-unsaturated terminal aldehyde is characteristic of hydroxynonenal, it was conceived that these compounds would also form Michael adducts with the thiol group of cysteine and amino groups of lysyl derivatives, as recently confirmed experimentally (37).

The major molecular species of the minor plaque glycerophospholipids resembled the composition of the minor phospholipids of LDL, including the high proportion of the 18:0/20:4 species found in PtdIns (38,39). The ethanolamine phospholipids were deficient in plasmalogens, and in this regard differed from the molecular species of those of plasma (38). An anticipated contribution from macrophages, which are known to contain high proportions of both alkenylacyl and alkylacyl GroPEtn species (44,45), could not be verified by the present work. Macrophages appear at a very early stage in the development of atherosclerotic lesions and persist throughout their evolution, indicating a pivotal role of these cells in the disease process. In fact, cholesterol-filled "foam cell" macrophages are a characteristic feature of atherosclerotic lesions (22,46). It is possible that the plasmenylethanolamines were lost from the lesion due to acid-catalyzed decomposition, although the acidity of any potential sites of their degradation is not known. If losses had occurred, they would have been more likely during the sample extraction and workup. Surprisingly, no evidence in this study was obtained for the presence of the core aldehydes of the ethanolamine and inositol glycerophospholipids, which were found to contain over 50–75% of their molecular species in the form of 18:0/20:4 at all stages of atheroma development. It is possible that the absence of these core aldehydes may have been due to their high reactivity and/or polymerization, as suggested by *in vitro* peroxidation studies (21).

The levels of glycated ethanolamine phospholipids found in the atheromas (5% glycated GroPEtn per milligram total phospholipid) are comparable to levels of glycated PtdEtn previously measured in the plasma of diabetic individuals (41). The presence of glycated PtdEtn in atheroma has not been demonstrated previously.

The present experimental results and an examination of the literature show that the accumulated lipid must have multiple precursors, as it does not represent the composition of any of the likely lipid sources. Furthermore, the appearance of new and unusual lipid species appears to exclude the possibility of a simple selectivity in the deposition process. Clearly, the normal transport and biosynthetic processes must have been subject to metabolic intervention, and there is evidence to support this (46). Thus, enzymatic degradation of oxidized phospho-

lipids is likely in the atheromas, as it has been observed in both lipoproteins and in cells. Two enzymes shown to degrade oxidized phospholipids in lipoproteins are paraoxonase (36,47) and PAF acetyl hydrolase (48,49), and these enzymes may have acted on the oxidized glycerolipids in the atherosclerotic plaques. Likewise, the oxidized glycerophospholipids may have been attacked by phospholipases A_1 and A_2, as well as by the secretory group II phospholipase A_2 (50–53). Schissel and coworkers (54,55) have concluded that the LDL retained in atherosclerotic lesions is acted on by an arterial-wall sphingomyelinase, which may participate in LDL aggregation and possibly other sphingomyelinase-mediated processes during atherogenesis. Sphingomyelinase hydrolyzes SM into ceramide and phosphocholine. In turn, ceramide serves as an important stress-signaling molecule. Chatterjee (56) has reviewed the possible involvement of sphingolipids in atherosclerosis and vascular biology. Goyal *et al*. (57) have demonstrated the hydrolysis of oxidized PtdCho by LCAT.

In addition, the composition of the atheroma lipids may undergo changes due to chemical reactivity of some of the lipid classes and molecular species. Thus, the lipid ester core aldehydes are known to form Schiff bases with amino acids, peptides, and proteins and may not be recovered during ordinary lipid extraction (28,32,34). The core aldehydes of PtdCho have been shown to undergo aldol condensation (21) and might not be readily detected under routine LC-MS analysis.

The hydroperoxides may undergo carbon-chain cleavage depending on the availability of divalent metal ions, which may contribute to great variability in the isolation of the hydroperoxides. The hydroperoxides themselves may undergo complexing with other hydroperoxides and hydroxides, which also may result in alterations of the recoverable hydroperoxide content. The core aldehydes may also undergo further oxidation to the core acids and the accumulation of both may depend on the activity of the PAF acetylhydrolase (58).

Significance. The significance of the present findings resides in the documentation of the phospholipid and oxophospholipid composition of the atherosclerotic plaque, which had not been attempted previously. Of special interest is the identification and quantification of several lipid species with potential lipid anchor and signaling properties, yet no specific function has been attributed to the high levels of PtdIns found at all stages of plaque development, which are well-known precursors of lipid-signaling molecules.

Nishi *et al*. (59) have investigated the relationship between clinical features, histopathological characteristics, and lipid peroxidation in patients undergoing carotid endartectomy. The plaque TBARS values of GIII (30% lipid-rich core) were significantly higher than those of other lesion classes. Their results showed that lipid peroxidation in carotid plaques is significantly associated with carotid atherosclerosis, especially plaque instability. In other studies, Loidl *et al*. (60) reported that oxidized phospholipids, such as 1-palmitoyl-2-glutaroyl- and especially 1-palmitoyl-2-(5-oxovaleroyl)-*sn*-glycero-3-phosphocholine, induce signaling cascades *via* activation of acid sphingomyelinase, finally leading to apoptosis of smooth muscle cells, a process contributing to the development of atherosclerosis.

The short-chain core aldehydes of PtdCho, like PAF, are known to activate monocytes *via* the PAF receptor (20,23,48). Furthermore, Tokumura *et al*. (58) showed that the PAF-like lipids regulate DNA synthesis and production of nitric oxide independently of the activation of the PAF receptor in vascular smooth muscle cells.

Ravandi *et al*. (61) showed earlier that the C_5 and C_9 core aldehydes of GroPCho readily form Schiff bases with the amino groups of amino acids, peptides, and myoglobin, as well as PtdEtn, whereas others demonstrated similar Schiff base formation with the core aldehydes derived from cholesteryl linoleate (4) and glyceryl-2-linoleate (34). More recently, Ravandi *et al*. (40) found that glucosylated PtdEtn added to nonglycated LDL promotes the oxidation of PtdCho and cholesteryl esters and the uptake of glucosylated PtdEtn-containing LDL by macrophages. Ravandi *et al*. (27) also demonstrated that glycated PtdEtn promotes macrophage uptake of LDL and accumulation of cholesteryl esters and TAG. Furthermore, glucosylation of PtdEtn promoted its oxidation as well as that of other glycerophospholipids in oxidized LDL.

Zieseniss *et al*. (62) demonstrated that oxidation of unsaturated diacyl GroPEtn promotes thrombin formation and that this effect can be duplicated by PtdEtn modified by a short-chain aldehyde (4-hydroxynonenal) PtdEtn or lysoPtdEtn adduct. Their results suggested that the imino group between the ethanolamine head group and the aldehyde was the major determinant for the stimulation of the prothrombinase activity. A treatment with $NaCNBH_3$ destroyed the activity. In contrast, $NaCNBH_3$ reduction of the Schiff base adduct of glucose (aldehyde form) and PtdEtn did not result in a loss of stimulated uptake of LDL by macrophages.

The dramatic changes in the lipid content and composition of the atheromas demonstrated in the present study and in isolated previous studies, along with the biochemical activity of many oxolipids, clearly exclude their role as innocent bystanders. Although a causal relationship between oxolipid formation and plaque development cannot be established from the present analyses, the demonstration of such a relationship may be possible in the future by correlating the results of sensitive measurements of oxolipid changes with the expression of specific enzyme and receptor activities in the macrophages and in the intimal tissue. Ideally, the findings of the present analyses will encourage such studies and the methodology developed here will help to facilitate their execution.

REFERENCES

1. Carpenter, K.L.H., Taylor, S.E., Ballantine, J.A., Fussell, B., Halliwell, B., and Mitchinson, J. (1993) Lipids and Oxidized Lipids in Human Atheroma and Normal Aorta, *Biochim. Biophys. Acta 1167*, 121–130.
2. Carpenter, K.L.H., Taylor, S.E., van der Veen, C., Williamson, B.K., Ballantine, J.A., and Mitchinson, M.J. (1995) Lipids and Oxidised Lipids in Human Atherosclerotic Lesions at Different Stages of Development, *Biochim. Biophys. Acta 1256*, 141–150.

3. Suarna, C., Dean, R.T., May, J., and Stocker, R. (1995) Human Atherosclerotic Plaque Contains Both Oxidized Lipids and Relatively Large Amounts of α-Tocopherol and Ascorbate, *Arterioscler. Thromb. Vasc. Biol. 15,* 1616–1624.
4. Hoppe, G., Ravandi, A., Herrera, D., Kuksis, A., and Hoff, H.F. (1997) Oxidation Products of Cholesteryl Linoleate Are Resistant to Hydrolysis in Macrophages, Form Complexes with Proteins, and Are Present in Human Atherosclerotic Lesions, *J. Lipid Res. 38*, 1347–1360.
5. Huber, J., Vales, Mitulovic, G., Blumer, M., Schmid, R., Witztum, J.L., Binder, B.R., and Leitinger, N. (2002) Oxidized Membrane Vesicles and Blebs from Apoptotic Cells Contain Biologically Active Oxidized Phospholipids That Induce Monocyte-Endothelial Interactions, *Arterioscler. Thromb. Vasc. Biol. 22,* 101–107.
6. Pratico, D., Juliano, L., Mauriello, A., Spagnoli, L., Lawson, J.A., Maclouf, J., Violi, F., and Fitzgerald, G.A. (1997) Localization of Distinct F_2-Isoprostanes in Human Atherosclerotic Lesion, *J. Clin. Invest. 100,* 2028–2034.
7. Thomas, M.J., Chen, Q., Sorci-Thomas, M.G., and Rudel, L.L. (2001) Isoprostane Levels in Lipids Extracted from Atherosclerotic Arteries of Non-human Primates, *Free Radical Biol. Med. 30*, 1337–1346.
8. Mallat, Z., Nakamura, T., Ohan, J., Leseche, G., Tegui, A., Maclouf, J., and Murphy, R.C. (1999) The Relationship of Hydroxyeicosatetraenoic Acids and F_2-Isoprostanes to Plaque Instability in Human Carotid Atherosclerosis, *J. Clin. Invest. 103,* 421–427.
9. Waddington, E., Sienuarine, K., Puddey, I., and Croft, K. (2001) Identification and Quantification of Unique Fatty Acid Oxidation Products in Human Atherosclerotic Plaque Using High Performance Liquid Chromatography, *Anal. Biochem. 292*, 234–244.
10. Waddington, E., Puddey, I.B., Mori, T.A., and Croft, K.D. (2002) Similarity in the Distribution of F(2)-Isoprostanes in the Lipid Subfractions of Atherosclerotic Plaque and *in vitro* Oxidized Low Density Lipoprotein, *Redox Rep. 7*, 179–184.
11. Waddington, E.I., Croft, K.D., Sienuarine, K., Latham, B., and Puddey, I.B. (2003) Fatty Acid Oxidation Products in Human Atherosclerotic Plaque: An Analysis of Clinical and Histopathological Correlates, *Atherosclerosis 167*, 111–120.
12. Huber, J., Boechzelt, H., Karten, B., Surboeck, M., Bochkov, V.N., Binder, B.R., Sattler, W., and Leitinger, N. (2002) Oxidized Cholesteryl Linoleates Stimulate Endothelial Cells to Bind Monocytes *via* the Extracellular Signal-Regulated Kinase 1/2 Pathway, *Arterioscler. Thromb. Vasc. Biol. 22*, 581–586.
13. Horkko, S., Bird, D.A., Miller, E., Itabe, H., Leitinger, N., Subbanagounder, G., Berliner, J.A., Friedman, P., Dennis, E.A., Curtiss, L.K., *et al.* (1999) Monoclonal Autoantibodies Specific for Oxidized Phospholipids or Oxidized Phospholipid–Protein Adducts Inhibit Uptake of Oxidized Low-Density Lipoproteins, *J. Clin. Invest. 103*, 117–128.
14. Subbanagounder, G., Leitinger, N., Shih, P.T., Faull, K.F., and Berliner, J.A. (1999) Evidence That Phospholipid Oxidation Products and/or Platelet-Activating Factor Play Important Role in Early Atherogenesis. *In vitro* and *in vivo* Inhibition by WEB 2086, *Circ. Res. 85,* 311–318.
15. Bullier, A., Gillotte, K.L., Horkko, S., Friedman, P., Dennis, E.A., Witztum, J.L. Steinberg, D., and Quehenberger, O. (2000) The Binding of Oxidized Low Density Lipoprotein to Mouse CD36 Is Mediated in Part by Oxidized Phospholipids That Are Associated with Both the Lipid and Protein Moieties of the Lipoprotein, *J. Biol. Chem. 275*, 9163–9169.
16. Podrez, E.A., Batyreva, E., Shen, Z., Zang, Z., Deng, Y., Sun, M., Febbraio, M., Hajjar, D.P., Silverstein, R.L., Hoff, H.F., *et al.* (2002) A Novel Family of Atherogenic Oxidized Phospholipids Promotes Foam Cell Formation *via* the Scavenger Receptor CD36 and Is Present in Atherosclerotic Lesion, *J. Biol. Chem. 277*, 38517–38523.
17. Horkko, S., Binder, C.J., Shaw, P.X., Chang, M.K., Silverman, G., Palinski, W., and Witztum, J.L. (2000) Immunological Responses to Oxidized LDL, *Free Radical Biol. Med. 28*, 1771–1779.
18. Itabe, H. (2003) Oxidized Low-Density Lipoproteins: What Is Understood and What Remains to Be Clarified, *Biol. Pharm. Bull. 26*, 1–9.
19. Palinski, W., and Witztum, J.L. (2000) Immune Responses to Oxidative Neoepitopes on LDL and Phospholipids Modulate the Development of Atherosclerosis, *J. Intern. Med. 247*, 371–380.
20. Gillotte, K.L., Horkko, S., Witztum, J.L., and Steinberg, D. (2000) Oxidized Phospholipids, Linked to Apolipoprotein B of Oxidized LDL, Are Ligands for Macrophage Scavenger Receptors, *J. Lipid Res. 41*, 824–833.
21. Friedman, P., Horkko, S., Steinberg, D., Witztum, J.L., and Dennis, E.A. (2002) Correlation of Antiphospholipid Antibody Recognition with the Structure of Synthetic Oxidized Phospholipids. Importance of Schiff Base Formation and Aldol Condensation, *J. Biol. Chem. 277*, 7010–7020.
22. Steinberg, D. (2002) Atherogenesis in Perspective: Hypercholesterolemia and Inflammation as Partners in Crime, *Nature Med. 8*, 1211–1217.
23. Uchida, K. (2000) Role of Reactive Aldehyde in Cardiovascular Diseases, *Free Radical Biol. Med. 28*, 1685–1696.
24. Ravandi, A., and Kuksis, A. (2000) Phospholipids of Plasma Lipoproteins, Red Blood Cells and Atheroma, in *Encyclopedia of Analytical Chemistry* (Meyers, R.A., ed.), pp. 1531–1570, John Wiley & Sons, Chichester, United Kingdom.
25. Kamido, H., Eguchi, H., Ikeda, H., Imaizumi, T., Yamana, K., Hartvigsen, K., Ravandi, A., and Kuksis, A. (2002) Core Aldehydes of Alkyl Glycerophosphocholines in Atheroma Induce Platelet Aggregation and Inhibit Endothelium-Dependent Arterial Relaxation, *J. Lipid Res. 43*, 158–166.
26. Podrez, E.A., Poliakov, E., Shen, Z., Zhang, R., Deng, Y., Sun, M., Finton, P.J., Shan, L., Febbraio, M., Hajjar, D.P., *et al.* (2002) A Novel Family of Atherogenic Oxidized Phospholipids Promotes Macrophage Foam Cell Formation *via* the Scavenger Receptor CD36 and Is Enriched in Atherosclerotic Lesions, *J. Biol. Chem. 277*, 38517–38523.
27. Ravandi, A., Kuksis, A., and Shaikh, N.A. (1999) Glycated Phosphatidylethanolamine Promotes Macrophage Uptake of Low Density Lipoprotein and Accumulation of Cholesteryl Esters and Triacylglycerols, *J. Biol. Chem. 274*, 16494–16500.
28. Ravandi, A., Kuksis, A., Marai, L., and Myher, J.J. (1995) Preparation and Characterization of Glucosylated Aminoglycerophospholipids, *Lipids 30*, 885–891.
29. Folch, J., Lees, M., and Sloane Stanley, G.H. (1957) A Simple Method for the Isolation and Purification of Total Lipids from Animal Tissues, *J. Biol. Chem. 226*, 497–509.
30. Piotrowski, J.J., Hunter, G., Eskelson, C.D., Dubick, M.A., and Bernhard, V.M. (1990) Evidence for Lipid Peroxidation in Atherosclerosis, *Life Sci. 46*, 715–721.
31. Bligh, E.G., and Dyer, W.J. (1959) A Novel Method of Total Lipid Extraction and Purification, *Can. J. Biochem. 37*, 911–917.
32. Kamido, H., Kuksis, A., Marai, L., and Myher, J.J. (1995) Lipid Ester-Bound Aldehydes Among Copper-Catalyzed Peroxidation Products of Human Plasma Lipoproteins, *J. Lipid Res. 36,* 1876–1886.
33. Kamido, H., Nonaka, K., Marai, L., Ravandi, A., and Kuksis, A. (1997) Alkyl Phosphatidylcholine Core Aldehydes Exist in Human Atheromas and Induce Platelet Aggregation Through PAF Receptor, *Atherosclerosis 134*, 183 (abstract).
34. Kurvinen, J.-P., Kuksis, A., Ravandi, A., Sjovall, O., and Kallio, H. (1999) Rapid Complexing of Oxoacylglycerols with Amino Acids, Peptides, and Aminophospholipids, *Lipids 34*, 299–305.
35. Piotrowski, J.J., Shah, S., and Alexander, J.J. (1996) Mature Human Atherosclerotic Plaque Contains Peroxidized Phosphatidylcholine as a Major Lipid Peroxide, *Life Sci. 58,* 735–740.

36. Ahmed, Z., Ravandi, A., Maguire, G.F., Emili, A., Draganov, D., La Du, B.N., Kuksis, A., and Connelly, P.W. (2001) Apolipoprotein A-I Promotes the Formation of Phosphatidylcholine Core Aldehydes That Are Hydrolyzed by Paraoxonase (PON-1) During High Density Lipoprotein Oxidation with a Peroxynitrite Donor, *J. Biol. Chem. 276*, 24473–24481.
37. Hoff, H.F., O'Neil, J., Wu, Z., Hoppe, G., and Salomon, R.L. (2003) Phospholipid Hydroxyalkenals. Biological and Chemical Properties of Specific Oxidized Lipids Present in Atherosclerotic Lesions, *Arterioscler. Thromb. Vasc. Biol. 23,* 275–282.
38. Myher, J.J., Kuksis, A., and Pind, S. (1989) Molecular Species of Glycerophospholipids and Sphingomyelins of Human Plasma: Comparison to Red Blood Cells, *Lipids 24*, 408–418.
39. Breckenridge, W.C., and Palmer, F.B. (1981) Fatty Acid Composition of Human Plasma Lipoprotein Phosphatidylinositols, *Biochim. Biophys. Acta 712,* 707–711.
40. Ravandi, A., Kuksis, A., and Shaikh, N.A. (2000) Glucosylated Glycerophosphoethanolamines Are the Major LDL Glycation Products and Increase LDL Susceptibility to Oxidation. Evidence for Their Presence in Atherosclerotic Lesions, *Arterioscler. Thromb. Vasc. Biol. 20,* 467–477.
41. Ravandi, A., Kuksis, A., Marai, L., Myher, J.J., Steiner, G., Lewis, G., and Kamido, H. (1996) Isolation and Identification of Glycated Aminophospholipids from Red Cells and Plasma of Diabetic Blood, *FEBS Lett. 381,* 77–81.
42. Reilly, M.P., Pratico, D., Delanty, N., DiMinno, G., Tremoli, E., Rader, D., Kapoor, S., Rokach, J., Lawson, J., and FitzGerald, G.A. (1998) Increased Formation of Distinct F2 Isoprostanes in Hypercholesterolemia, *Circulation 98,* 2822–2828.
43. Kaur, K., Salomon, R.G., O'Neil, J., and Hoff, H.F. (1997) (Carboxyalkyl) Pyrroles in Human Plasma and Oxidized Low-Density Lipoproteins, *Chem. Res. Toxicol. 10*, 1387–1396.
44. Sugiura, T., Nakajima, M., Sekiguchi, N., Nakagawa, Y., and Waku, K. (1983) Different Fatty Chain Compositions of Alkenylacyl, Alkylacyl, and Diacyl Phospholipids in Rabbit Alveolar Macrophages: High Amounts of Arachidonic Acid in Ether Phospholipids, *Lipids 18*, 125–129.
45. Gaposchkin, D.P., and Zoeller, R.A. (1999) Plasmalogen Status Influences Docosahexaenoic Acid Levels in Macrophage Cell Line: Insights Using Ether Lipid-Deficient Variants, *J. Lipid Res. 40*, 495–503.
46. Berliner, J. (2002) Lipid Oxidation Products and Atherosclerosis, *Vasc. Pharmacol. 38*, 187–191.
47. Rodrigo, L., Mackness, B., Durrington, P.N., Hernandez, A., and Mackness, M.I. (2001) Hydrolysis of Platelet-Activating Factor by Human Serum Paraoxonase, *Biochem. J. 354*, 1–7.
48. Marathe, G.K., Zimmermann, G.A., and McIntyre, T.M. (2003) Platelet-Activating Factor Acetylhydrolase, and Not Paraoxonase-1, Is the Oxidized Phospholipid Hydrolase of High Density Lipoprotein Particles, *J. Biol. Chem. 278*, 3937–3947.
49. Prescott, S.M., Zimmerman, G.A., Stafforini, D.M., and McIntyre, T.M. (2000) Platelet-Activating Factor and Related Lipid Mediators, *Annu. Rev. Biochem. 69*, 419–445.
50. Menschikowski, M., Kasper, M., Lattke, P., Schiering, A., Schiefer, S., Stockinger, H., and Jaross, W. (1995) Secretory Group II Phospholipase A_2 in Human Atherosclerotic Plaques, *Atherosclerosis 118*, 173–181.
51. Hurt-Camejo, E., Andersen, S., Standal, R., Rosengren, B., Sartipy, P., Stadberg, E., and Johansen, B. (1997) Localization of Nonpancreatic Secretory Phospholipase A2 in Normal and Atherosclerotic Arteries: Activity of the Enzyme on Low-Density Lipoproteins, *Arterioscler. Thromb. Vasc. Biol. 17*, 300–309.
52. Leitinger, N., Tyner, T.R., Oslund, L., Rizza, C., Subbanagounder, G., Lee, H., Shih, P.T., Mackman, N., Tigvi, G., Territo, *et al.* (1999) Structurally Similar Oxidized Phospholipids Differentially Regulate Endothelial Binding of Monocytes and Neutrophils, *Proc. Natl. Acad. Sci. USA 96,* 12010–12015.
53. Kovanen, P.T., and Pentikainen, M.O. (2000) Secretory Group II Phospholipase A_2. A Newly Recognized Acute-Phase Reactant with a Role in Atherogenesis, *Circ. Res. 86*, 610–612.
54. Schissel, S.L., Tweedie-Hardman, J., Rapp, J.H., Graham, G., Williams, K.J., and Tabas, I. (1996) Rabbit Aorta and Human Atherosclerotic Lesions Hydrolyze the Sphingomyelin of Retained Low-Density Lipoproptein. Proposed Role for Arterial-Wall Sphingomyelinase in Subendothelial Retention and Aggregation of Atherogenic Lipoproteins, *J. Clin. Invest. 98*, 1455–1464.
55. Schissel, S.L., Jiang, X.-C., Tweedie-Hardman, J., Jeong, T.-S., Hurt Camejo, E., Najib, J., Rapp, J.H., Williams, K.J., and Tabas, I. (1998) Secretory Sphingomyelinase, a Product of the Acid Sphingomyelinase Gene, Can Hydrolyze Atherogenic Lipoproteins at Neutral pH. Implications for Atherosclerotic Lesion Development, *J. Biol. Chem. 273*, 2738–2746.
56. Chatterjee, S. (1998) Sphingolipids in Atherosclerosis and Vascular Biology, *Arterioscler. Thromb. Vasc. Biol. 18*, 1523–1533.
57. Goyal, J., Wang, K., Liu, M., and Subbaiah, P.V. (1997) Novel Function of Lecithin-Cholesterol Acyltransferase. Hydrolysis of Oxidized Polar Phospholipids Generated During Lipoprotein Oxidation, *J. Biol. Chem. 272,* 16231–16239.
58. Tokumura, A., Sumida, T., Toujima, M., Kogure, K., and Fukuzawa, K. (2000) Platelet-Activating Factor (PAF)-like Oxidized Phospholipids: Relevance to Atherosclerosis, *Biofactors 13*, 29–33.
59. Nishi, K., Uno, M., Fukuzawa, K., Horiguchi, H., Shinno, K., and Nagahiro, S. (2002) Clinicopathological Significance of Lipid Peroxidation in Carotid Plaques, *Atherosclerosis 160*, 289–296.
60. Loidl, A., Sevcsik, E., Riesenhuber, G., Deigner, H.-P., and Hermetter, A. (2003) Oxidized Phospholipids in Minimally Modified Low Density Lipoprotein Induce Apoptotic Signaling *via* Activation of Acid Sphingomyelinase in Arterial Smooth Muscle Cell, *J. Biol. Chem. 278*, 32921–32928.
61. Ravandi, A., Kuksis, A., Shaikh, N., and Jacowski, G. (1997) Preparation of Schiff Base Adducts of Phosphatidylcholine Core Aldehydes and Aminophospholipids, Amino Acids, and Myoglobin, *Lipids 32*, 989–1001.
62. Zieseniss, S., Zahler, S., Muller, I., Hermetter, A., and Engelmann, B. (2001) Modified Phosphatidylethanolamine as the Active Component of Oxidized Low Density Lipoprotein Promoting Platelet Prothrombinase Activity, *J. Biol. Chem. 276*, 19828–19835.

[Received December 21, 2003, and in revised form February 9, 2004; revision accepted February 13, 2004]

Lactational Changes in the Fatty Acid Composition of Human Milk Gangliosides

Samuel Martín-Sosa, María-Jesús Martín, María-Dolores Castro, José A. Cabezas, and Pablo Hueso*

Departamento de Bioquímica y Biología Molecular, Universidad de Salamanca, 37007 Salamanca, Spain

ABSTRACT: The objectives of this work were to study the FA composition of milk gangliosides, as well as to gain further insight into the characterization of human milk gangliosides. The potential capacity of human milk gangliosides to adhere to human enterotoxigenic *Escherichia coli* (ETEC-strains) was also studied. Human milk gangliosides were isolated and identified by high-performance TLC or immunoassay. The latter also was used to assay bacterial adhesion. The FA composition of gangliosides was studied by GC. The presence of *O*-acetyl GD3 (Neu5,9Ac$_2$α2-8 NeuAcα2-3Galβ1-4GlcCer) and trace amounts of GM1 [Galβ1-3GalNAcβ1,-3(NeuAcα2-3)Galβ1-4GlcCer] in human milk was confirmed. Medium-chain FA were almost absent in colostrum, whereas in the subsequent stages they rose to 20%. The levels of long-chain FA decreased after colostrum. With respect to the degree of saturation, gangliosides from colostrum were richer in monounsaturated FA than gangliosides synthesized during the rest of the lactation period, opposite to the pattern for PUFA. A human-ETEC colonization factor antigen II-expressing strain showed binding capacity to human milk GM3 (NeuAcα2-3Galβ1-4GlcCer). New data on human milk gangliosides have been gathered. A thorough knowledge of their composition is needed since they may have important biological implications in regard to newborns' defense against infection.

Paper no. L9354 in *Lipids 39*, 111–116 (February 2004).

Gangliosides are glycosphingolipids consisting of a hydrophobic ceramide and a hydrophilic oligosaccharide chain bearing one or more acidic sugar molecules (sialic acids). They are present in the cell membranes of almost all vertebrate tissues and also in many body fluids (1). In milk, gangliosides are mainly located in milk fat globule membranes. Although the precise role of gangliosides in human milk has not yet been well established, gangliosides could act as analog receptors in the gut, preventing newborns from contracting infections produced by several microorganisms and from their enterotoxins (2). In this sense, gangliosides have been proposed to recognize microorganisms such as *Haemophilus influenzae* or *Pseudomonas* (3,4). They also can block toxins; ganglioside GM1 seems to be the optimal glycolipid receptor for cholera toxin (5), although modifications in the structure of the molecule do not completely abolish its recognition capacity, suggesting a relatively wide spectrum of recognizing molecules, including sialyllactose (6). Besides protective effects, other roles have also been proposed for these molecules: They could be involved in the processes of tissue and organ development in newborns (7).

The composition of milk lipids varies during lactation. The proportions of short- and medium-chain FA increase as lactation progresses; conversely, long-chain PUFA content decreases (8). Several authors have reported variations in bovine milk gangliosides during lactation (9,10). Nevertheless, in humans, there are few studies on composition with regard to the lactational stage, and the data so far available are quite heterogeneous (11–13). Moreover, little attention has been paid to the ceramide moiety and its changes during lactation. To date, its composition has been studied only in bovine milk (10), although the antigenic importance of this part of the ganglioside seems to be greater than previously thought; i.e., it is known that changes in the ceramide composition are responsible for the ability of lactosylceramides to be recognized by *Helicobacter pylori* (14). In this sense, the present study reports new data on the content and distribution of gangliosides in human milk; we also study the FA composition of human milk gangliosides and their changes during lactation. Finally, we suggest an approach to identifying the possible functional role of milk gangliosides by studying their binding capacity to an enterotoxigenic *Escherichia coli* strain (ETEC), which is one of the main causes of diarrhea in infants. Since breast-fed infants appear to undergo fewer or less severe gastrointestinal, respiratory, and urinary infections than formula-fed infants (15,16), we believe that the compositional and functional aspects of human milk should be studied in detail.

EXPERIMENTAL PROCEDURES

Samples. Samples were obtained from 12 healthy Spanish women (Caucasian population) aged between 25 and 35 yr. Donors were primiparous or multiparous women, of a medium-high socioeconomic status, consuming a common Western diet *ad libitum*. Each of them donated three samples, corresponding to each of the three lactational stages considered: colostrum, transitional milk, and mature milk. Colostrum comprised the milk produced between days 1 and 4 of lactation; transitional milk was collected between days 12 and 17 of lactation; and mature milk was collected between days 28 and 32. Milk samples were collected by donors using a hand-operated breast pump or manually throughout the sampling days in plastic containers and was frozen immediately. After collection, the milk was stored at –20°C, lyophilized, and homogenized to ensure uniform distribution of the components.

Extraction of gangliosides. Gangliosides were obtained as previously described (9). Briefly, lyophilized milk was homogenized twice with 10 vol of cold acetone (–20°C) to

*To whom correspondence should be addressed at Departamento de Bioquímica y Biología Molecular, Edificio Departamental (Lab 103) Campus M. Unamuno, 37007 Salamanca, Spain. E-mail: phueso@usal.es

Abbreviations: C, chloroform; CFA/II, colonization factor antigen II; ETEC, enterotoxigenic *Escherichia coli*; HPTLC, high-performance TLC; LCFA, long-chain FA; M, methanol; mAb, monoclonal antibody; MCFA, medium-chain FA; MUFA, monounsaturated FA; SFA, saturated FA; VLCFA, very long chain FA.

The ganglioside nomenclature of Svennerholm (34) is followed.

remove neutral lipids and then filtered. Polar lipids from the acetone powder were then successively extracted with 10 vol chloroform/methanol (C/M) (2:1, 1:1, and 1:2, vol/vol). The extracts were combined and reduced to one-fourth of the original volume by rotary evaporation, and cooled at –20°C overnight; insoluble material was removed by centrifugation. The lipid extract was then evaporated to dryness, taken up in 10 vol C/M (2:1), and subjected to Folch partition (9). The upper phases, containing crude gangliosides, were combined and dialyzed against distilled water at 4°C for 2 d (the water was changed every 6–8 h). The dialysate was then lyophilized, resuspended in C/M 2:1, centrifuged again, and the supernatant was collected. In a preliminary experiment gangliosides were subjected to C18 cartridge (Sep-Pak; Waters, Milford, MA) chromatography instead of dialysis. Gangliosides were adsorbed, and the water-soluble components passed through the column. Gangliosides were then eluted with methanol (17).

Gangliosides were quantified as lipid-bound sialic acids by the resorcinol assay (18). They were separated by high-performance TLC (HPTLC plates; Merck, Darmstadt, Germany) using the following solvent system: C/M/water (50:45:10, by vol) containing 0.02% $CaCl_2$. Individual gangliosides were analyzed with a dual-wavelength TLC densitometer (Shimadzu CS 9000; Kyoto, Japan) after separation by HPTLC and development with the resorcinol reagent. Visualization of gangliosides was also achieved by spraying the plates with the orcinol reagent.

Individual gangliosides for GC analysis were purified by preparative TLC (preparative TLC sheets; Merck) using the following solvent system: methyl acetate/C/M/*n*-propanol/0.25% KCl (25:20:20:20:17, by vol) (19).

Immunostaining assays. Immunostaining on HPTLC plates to identify individual gangliosides was performed as previously reported (20). Different monoclonal antibodies (mAb) against gangliosides were used. Briefly, gangliosides were chromatographed in duplicate on an HPTLC plate. Once dried, half of the plate was developed by orcinol/H_2SO_4. The other half of the plate was soaked with 0.1% polyisobutyl butylmethacrylate (Aldrich Chemical Co., Milwaukee, WI) in *n*-hexane for 75 s and kept overnight at room temperature for drying. The plate was blocked with 1% BSA (Fluka, Buchs, Switzerland) in Tris-0.1 N HCl for 30 min. It was then incubated with the appropriate mAb at room temperature for 2 h. After washing with PBS (10 mM, pH 7.2), the plate was incubated with biotinylated anti-mouse polyvalent immunoglobulins (conjugated biotin, 1:2000 in 1% BSA containing PBS) for 1 h 30 min and then with streptavidin/alkaline phosphatase (1:1000 in the same buffer) for 1 h 30 min before being developed with the substrate.

Methanolysis and GC analysis. After separation, gangliosides were subjected to methanolysis for FA derivatization. The solvent (0.5 M methanol/HCl; Sigma, St. Louis, MO) was added (300 μL) to the gangliosides that had been dried under a nitrogen stream, and sealed tubes were incubated for 20 h at 80°C. Methyl esters were then extracted with hexane, centrifuged, and kept in the organic phase, which was dried under a nitrogen stream. FAME were taken up in isooctane and injected into a GC apparatus (KNK 3000 gas chromatograph equipped with an FID; Konick Instruments, Barcelona, Spain) for their analysis. A SUPELCOWAX 10 semicapillary column (30 m × 0.53 mm) (Supelco, Bellefonte, PA) was used. The injector temperature was 210°C, and the detector temperature was 240°C. The initial temperature was 115°C for 5 min. The temperature was raised to 190°C at 10°C/min, and then to 230°C at 2°C/min. This final temperature was then held for 20 min. Peaks were identified by two procedures: First, sample profiles were compared with those from commercial standards. Second, individual standards were injected together with the sample, and the resulting chromatographic profile was compared with the native sample profile.

Bacterial adhesion to gangliosides on TLC. A strain of ETEC expressing the adhesin colonization factor antigen II (CFA/II) was used. This strain, called 23, was kindly provided by Dr. Jorge Blanco, from the LREC (Laboratorio de Referencia de *Escherichia coli*, Lugo, Spain). Bacteria were grown in Mueller–Hinton broth (Difco, Detroit, MI) and incubated for 5–7 d at 37°C. When grown in this medium, the bacteria lacked fimbriae. For fimbriae expression, the bacteria were incubated on CFA agar plates at 37°C for 16 h, as previously reported by Evans *et al.* (21).

The binding of ETEC to gangliosides on TLC was determined as previously described by Karlsson and Strömberg (22). Total milk gangliosides (3 μg in each lane) were separated in duplicate on HPTLC plates (Merck) using C/M/water (50:45:10, by vol) containing 0.02% $CaCl_2$ as solvent system. Once dried, half of the plate was developed with orcinol/H_2SO_4 for use as a control. The other half of the plate was dipped in 0.1% polyisobutyl methacrylate in *n*-hexane for 75 s and allowed to dry. Once dried, it was soaked in 10 mM PBS pH 7.2, containing 2% BSA (blocking buffer) for 1 h.

Bacteria grown on a Petri dish (approx. 3.2×10^9 colony-forming units) were collected in 1 mL of sterile PBS containing 1% mannose. The plate was covered with the bacterial suspension and incubated for 2 h at 37°C in a humid chamber. Following this, the plate was thoroughly washed four times, 5 min each, with PBS and incubated with the anti-*E. coli* antibody (DAKO, Copenhagen, Denmark) at 1:25 in the blocking buffer for 1 h at room temperature. Biotinylated anti-rabbit immunogloblin G (Sigma) and streptavidin/alkaline phosphatase conjugate (Sigma) were added successively (1:1000 in the blocking buffer) for 1 h at room temperature before development with the substrate.

Statistical assays. To test for statistically significant differences between the three stages of lactation, an ANOVA test was applied in each case.

RESULTS

Ganglioside contents. A marked decrease in ganglioside content was observed during lactation, the values for colostrum being more than double those found in mature milk. The data (mean ± SD, $n = 12$, expressed as mg of lipid-bound sialic acid/kg fresh milk), were as follows: colostrum, 2.3 ± 0.5; transitional milk, 1.38 ± 0.4; and mature milk, 0.8 ± 0.2. Statistically significant differences between colostrum and the other stages

($P < 0.01$) and between transitional and mature milk ($P < 0.05$) were found. Several gangliosides were identified by their chromatographic mobility or by the HPTLC-overlay method, using specific mAb. Up to seven different gangliosides were found in human milk, named from G1 to G7 in order of decreasing chromatographic mobility (Fig. 1, Table 1). The most abundant ganglioside in colostrum was G3, with a chromatographic mobility similar to that of ganglioside GD3. R24, an mAb with a high degree of specificity against this ganglioside, reacted strongly with G3. This ganglioside clearly appeared as a double band. During lactation, the levels of this ganglioside decreased, unlike G1 (with a mobility similar to that of the ganglioside GM3), which appeared to be the most abundant in mature milk. Between G1 and G3 there is another ganglioside (on a TLC plate), G2, which is present in all stages. G2 is sensitive to alkaline hydrolysis; it reacts with the Jones mAb, and the positive staining with the antibody disappears after hydrolysis. G2 was assumed to be *O*-acetyl GD3. G4 was absent from the colostrum. Highly polar gangliosides appeared irregularly during lactation: G5 and G6, with a chromatographic mobility similar to that of GT1b (standard from bovine brain), were present at all stages, whereas G7 appeared only in the colostrum. None of them reacted with the A2B5 mAb, which does not have a high degree of specificity. This antibody has been described to bind GT3, *O*-acetyl GT3, and other gangliosides (23). Finally, despite the absence of ganglioside GM1 on the chemically developed plates, a specific mAb against GM1, called G1, was also used. This more sensitive procedure allowed us to detect a very thin band of GM1 in human milk samples, although it could not be quantified.

Ceramide content. The five gangliosides present during each stage of lactation were isolated by preparative TLC and analyzed by GC. The FA contents of the individual gangliosides were determined. A possible skewing of the FA composition when compared with Sep-Pak methodology instead of dialysis in a preliminary experiment—although not statistically significant—should be mentioned. This could be due to a loss of short-chain compounds (more polar) during dialysis or insufficient elution of long-chain compounds (less polar) from the Sep-Pak cartridge. The results, shown in Table 2, are expressed as mean values ± SD of the FA content of the individual gangliosides from each stage of lactation. The results were grouped according to the length of the chain, and also to the degree of saturation. In the first case, three groups were considered: Medium-chain FA (MCFA), encompassing FA from C_{10} to C_{15}; long-chain FA (LCFA), encompassing FA from C_{16} to C_{21}, and very long chain FA (VLCFA), encompassing FA longer than C_{21}. As seen in Figure 2, whereas in colostrum MCFA were barely present, these FA increased during lactation. At the same time, LCFA diminished after colostrum, whereas VLCFA remained constant in all three stages considered. Regarding the degree of saturation (Fig. 3), we considered saturated FA (SFA), monounsaturated FA (MUFA), and PUFA. Gangliosides from colostrum were richer in MUFA than gangliosides from the rest of the lactation period, unlike PUFA, which increased after colostrum. SFA, however, remained constant during lactation. Taking into consideration the two most abundant gangliosides (GM3 and GD3), we observed a within-group variability of certain FA (Table 3): 16:0 was more abundant in GM3 than in GD3, not only in colostrum (23 and 17%, respectively) but also in mature milk (14% in the former, 10% in the latter). Behenic acid (22:0) was also more abundant in GM3 (5%) than in GD3 (1%) in mature milk, but in colostrum, the inverse situation was observed (3% in GD3, 0.4% in GM3). Curiously, the greatest difference occurred in 20:1 in mature milk, where this FA represented 7% of GD3 but only 0.9% of GM3.

TABLE 1
Relative Amounts[a] (%) of the Ganglioside Sialic Acid Found in Human Milk During the Three Stages Considered

Gangliosides	Colostrum	Transitional milk	Mature milk
G1	8.8 ± 2.2	11.6 ± 2.2	50.2 ± 1.6**‡
G2	2.1 ± 0.9	8.9 ± 2.1*†	2.6 ± 0.5
G3	63.2 ± 3.9	52.4 ± 4.2*	21.3 ± 1.3**‡
G4	ND	6.1 ± 0.1*	7.9 ± 2.2*
G5	13.0 ± 2.0	12.2 ± 1.0	10.3 ± 0.9
G6	9.9 ± 0.7	8.5 ± 2.3	7.5 ± 0.6
G7	2.7 ± 0.1	ND	ND

[a]Values are expressed as means ± SD. Significant difference from colostrum: **($P < 0.01$); *($P < 0.05$). Significant difference from transitional milk: ‡($P < 0.01$). Significant difference from mature milk: †($P < 0.05$). ND, not detected.

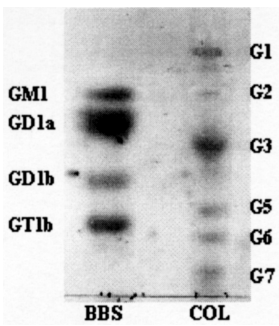

FIG. 1. High-performance TLC separation of human colostrum gangliosides (COL). BBS: Bovine brain standard. Solvent system: chloroform/methanol/water (50:45:10, by vol) containing 0.02% $CaCl_2$. Gangliosides were developed by the resorcinol reagent.

Adhesion to ETEC. As described in the Experimental Procedures section, gangliosides were separated on a HPTLC plate, covered with the bacterial suspension, washed, and incubated with the anti-*E. coli* antibody. As shown in Figure 4, after development with the antibody, only one band was seen on the plates. When compared with the chemical staining, the band corresponded with the ganglioside GM3 from mature milk. No bands corresponding to this ganglioside were found in transitional milk or colostrum. When nonfimbriated bacteria were used, no recognition between gangliosides and bacteria took place.

DISCUSSION

Ganglioside contents followed the trend previously reported for other sialoglycoconjugates in human milk (24), being quite high in colostrum and decreasing markedly with the duration of lactation. However, the available data concerning ganglioside contents are somewhat variable: Whereas some authors have not found differences between the initial and late lactation stages (13), others have reported that the transitional milk

TABLE 2
FA Content[a] (%) of Gangliosides from the Different Stages of Lactation

FA	Colostrum	Transitional milk	Mature milk
10:0	0.12 ± 0.05	8.6 ± 0.56	7.05 ± 1.16
12:0	0.42 ± 0.19	8.69 ± 0.80	7.79 ± 1.45
14:0	4.28 ± 0.62	5.97 ± 1.18	7.84 ± 0.87
15:0	0.80 ± 1.12	0.34 ± 0.32	0.04 ± 0.00
16:0	23.04 ± 5.01	12.22 ± 0.28	10.76 ± 1.42
16:1	3.15 ± 0.84	1.89 ± 0.14	2.33 ± 0.57
17:0	0.68 ± 0.26	0.50 ± 0.13	0.45 ± 0.13
18:0	22.92 ± 2.86	17.25 ± 1.80	12.34 ± 2.63
18:1	19.24 ± 4.33	11.72 ± 2.07	10.40 ± 1.42
18:2	2.82 ± 1.03	3.51 ± 3.01	6.17 ± 5.40
18:3	6.02 ± 2.49	5.19 ± 1.76	5.48 ± 0.79
18:4	3.59 ± 1.01	14.14 ± 1.56	11.85 ± 1.65
20:0	0.82 ± 0.35	0.15 ± 0.10	0.93 ± 0.55
20:1	1.30 ± 0.67	0.38 ± 1.69	4.45 ± 1.93
20:2	0.94 ± 0.24	—	1.81 ± 2.92
21:0	0.78 ± 0.59	0.65 ± 1.64	0.2 ± 0.02
20:4	1.91 ± 0.55	2.17 ± 0.31	1.61 ± 0.78
22:0	1.63 ± 0.81	1.52 ± 0.16	2.38 ± 1.54
23:0	0.7 ± 0.45	0.22 ± 1.03	0.17 ± 0.05
24:0	4.77 ± 1.73	4.80 ± 0.86	4.8 ± 0.8

[a]Values are expressed as means ± SD of the FA contents of the gangliosides from each stage of lactation.

has the highest content of gangliosides (12), or even the lowest (11). Such heterogeneity in the results could be due to differences in the sampling methods used (milk pools of the stage of lactation or individual daily samples) and to differences among authors in defining the stages. Although nutritional aspects should not be overlooked in the case of Oriental diets (13), where fats come mainly from fish, the values obtained by these authors (11–13) were more than triple our own values. The ganglioside content in colostrum was much higher than that previously found in starter infant formulas (0.95–1.3 mg/L) (25); obviously, formula-fed neonates ingest dissimilar ganglioside amounts compared with nursing neonates.

Up to seven different gangliosides were found; we observed a clear reciprocal relationship in the proportion of GD3 and GM3, as already described by other authors (11–13). GM3, the main ganglioside in mature milk, is usually present in mature tissues, whereas GD3 has been described to be present in developing tissues (7). Whether the high concentration of this ganglioside in colostrum contributes to the development of the gut remains unknown. Regarding G2, assigned by us to *O*-acetyl GD3, this does not seem to undergo a regular distribution during lactation. This could be due to the fragility of the *O*-acetyl group; the O-acetylated derivative of GD3 could be subject to modifications during the extraction and purification processes, losing the *O*-acetyl group and being converted to GD3. A ganglioside with similar chromatographic mobility was described in human milk and also named G2; however, it was suggested to be GM2 (26). In bovine milk, *O*-acetyl GD3 has already been described (10). This ganglioside has been described to be present in the nervous system during rat embryonic development (27).

Rueda *et al.* (12) described the presence of several highly polar gangliosides in human milk. The chromatographic mobility of these gangliosides was similar to that of the minor gangliosides we found (G4–G7). Those authors suggested that some of them might be trisialylated gangliosides (GT3 and derivatives). Unfortunately, we were not able to confirm this hypothesis, since none of the above gangliosides (G4–G7) reacted with the A2B5 antibody. In human milk, other authors have found some minor gangliosides with a lower chromatographic mobility than that of GD3 and considered the possibility of these being gangliosides of the c-series (trisialo-, tetrasialo-) (13). Quite complex branched structures have been described

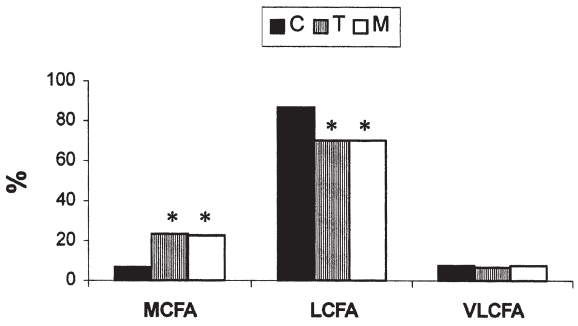

FIG. 2. Distribution of ganglioside FA during lactation, with respect to their chain length. MCFA, medium-chain FA; LCFA, long-chain FA; VLCFA, very long chain FA. *Statistically significant difference from colostrum ($P < 0.01$). C, colostrum; T, transitional milk; M, mature milk.

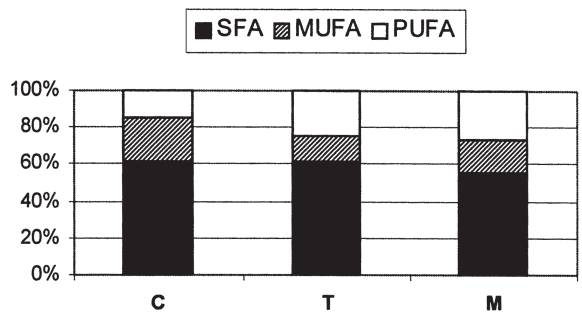

FIG. 3. Distribution of ganglioside FA during lactation, with respect to their degree of saturation. SFA, saturated FA; MUFA, monounsaturated FA. For other abbreviations see Figure 2.

TABLE 3
Individual FA Composition[a] (%) of the Two Main Gangliosides Found in Human Colostrum and Mature Milk

	GD3		GM3	
FA	Colostrum	Mature milk	Colostrum	Mature milk
10:0	0.1 ± 0.03	8.2 ± 0.63	0.2 ± 0.04	6.5 ± 1.4
12:0	0.1 ± 0.01	9.7 ± 0.71	0.5 ± 0.08	7.1 ± 1.2
14:0	3.6 ± 0.41	7.4 ± 0.53	3.8 ± 0.32	5.7 ± 0.83
15:0	2.0 ± 0.62	0.2 ± 0.06	0.5 ± 0.06	1.1 ± 0.04
16:0	17.0 ± 1.94	10.1 ± 1.43	23.0 ± 1.77	13.9 ± 1.84
16:1	3.0 ± 0.58	1.7 ± 0.34	2.3 ± 0.21	3.2 ± 0.23
17:0	2.4 ± 0.49	0.6 ± 0.1	1.0 ± 0.1	1.1 ± 0.47
18:0	21.1 ± 1.74	11.9 ± 1.21	25.1 ± 2.76	17.2 ± 1.93
18:1	20.5 ± 2.0	10.4 ± 1.17	18.1 ± 1.93	12.5 ± 1.13
18:2	3.5 ± 0.83	3.7 ± 0.72	4.0 ± 0.98	3.6 ± 0.54
18:3	5.4 ± 1.1	6.7 ± 0.92	7.1 ± 0.65	5.5 ± 0.84
18:4	4.5 ± 0.74	12.5 ± 1.33	4.2 ± 0.31	10.2 ± 0.62
20:0	1.3 ± 0.1	1.1 ± 0.24	0.4 ± 0.15	0.2 ± 0.05
20:1	1.9 ± 0.34	6.8 ± 0.49	0.4 ± 0.03	0.9 ± 0.1
20:2	1.0 ± 0.06	0.0	0.8 ± 0.2	0.3 ± 0.15
21:0	1.8 ± 0.15	0.0	0.5 ± 0.1	0.5 ± 0.16
20:4	1.9 ± 0.34	2.9 ± 0.39	1.3 ± 0.26	1.1 ± 0.31
22:0	3.0 ± 0.1	1.1 ± 0.25	0.4 ± 0.06	4.8 ± 0.56
23:0	1.0 ± 0.3	0.0	0.2 ± 0.01	0.0
24:0	4.9 ± 0.6	6.0 ± 0.44	6.2 ± 0.9	4.8 ± 0.72

[a]Values are expressed as means ± SD of three different experiments.

in bovine buttermilk (28); their chromatographic mobility was also less than that of GD3. Although the presence of GM1 in human milk has been reported (5), some authors have not succeeded in finding it (13); we found only a trace amount of this ganglioside.

To our knowledge, no data on the FA composition of human milk gangliosides have been reported previously. In our hands, the ganglioside FA composition changed during lactation. With respect to the length of the chain, the situation reflects what takes place at global level with the total FA composition of human milk: an increase in MCFA during lactation as LCFA decrease. MCFA are synthesized exclusively by the mammary gland (29); this organ is not completely mature at the moment of birth and so, at the beginning of lactation, most milk FA, whose origin is in plasma, are LCFA. Since the lactating neonate promotes maturation of the mammary gland (by suckling), this assumes the *de novo* synthesis of FA, increasing the proportion of MCFA (30). The lower band of GD3, corresponding to a ceramide with a higher content in MCFA, increased during lactation. Although the total FA composition of human milk shows a decrease in VLCFA during lactation (31), our values remained constant in all three stages. A similar situation also has been observed in the FA composition of sphingolipids (32), which share a common synthesis pathway with gangliosides. Nevertheless, as regards the degree of saturation, the global ratio between SFA and unsaturated FA remained constant during lactation.

Gangliosides in human milk could play an important defensive role by inhibiting the growth of and preventing infections by enteropathogenic bacteria. Some human ETEC strains expressing CFA/I and some expressing CFA/IV have been described previously as being able to recognize asialo-GM1, and several studies have described the binding of CFA/I adhesins to several sialoglycoconjugates (33). In our study, we observed recognition between GM3 and the ETEC strain expressing CFA/II. However, this only occurred with GM3 from mature milk. Might this be due to a difference in ceramide composition? To determine the biological significance of FA changes, membrane fluidity should be addressed. Changes in the FA content could control the membrane fluidity; unsaturated and short structures suggest a looser membrane than that with long and saturated ceramides. This could also affect the capacity of ceramides to present the oligosaccharidic part of the ganglioside to a possible receptor, i.e., the accessibility of the ganglioside. We are unaware whether any of these aspects might be involved in the recognition capacity of the ETEC strain by GM3 from mature milk. Nevertheless, it is clear that whereas GM3 in mature milk represents more than 50% of total gangliosides, it is not very abundant in the other stages. Furthermore, unlike many animal ETEC, human ETEC fimbriae have only one adhesin molecule at the end of the fimbria, which certainly limits their adhesion ability. Thus, whether human milk gangliosides might play a defensive role in inhibiting bacterial adhesion needs further investigation.

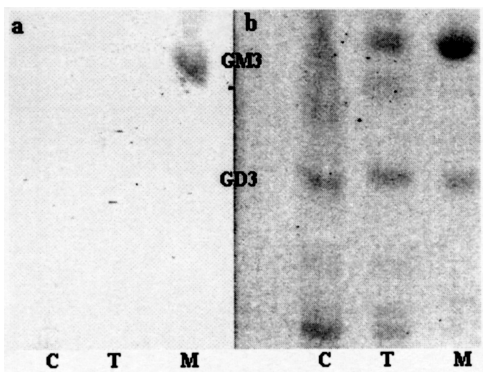

FIG. 4. Adhesion of the CFA/II-adhesin expressing ETEC (enterotoxigenic *Escherichia coli*)-23 strain to human milk gangliosides. (a) Anti-*E. coli* antibody development. (b) Chemical (orcinol reagent) development. No bacteria are present. For solvent system see Figure 1. CFA/II, colonization factor antigen II; for other abbreviations see Figure 2.

ACKNOWLEDGMENTS

This work was supported by grants from the Programa de Apoyo a Proyectos de Investigación de la Consejería de Educación y Cultura de la Junta de Castilla y León, España (SA 093/01) and from the Ministerio de Ciencia y Tecnología (MCYT), España (AGL 2001-2047). We acknowledge the generous collaboration of the private donors, as well as the great help given by Mrs. Esmeralda Gómez, midwife from the Health Center "La Alamedilla" (Salamanca, Spain), who kindly provided us with a large part of the samples. We also thank Mr. Nicholas Skinner (from the Servicio de Idiomas, Universidad de Salamanca) for revising the English version of the manuscript. Dedicated to Prof. Dr. Roland Schauer (Kiel, Germany) on the occassion of his retirement.

REFERENCES

1. Yu, R.K., and Saito, M. (1989) Structure and Localization of Gangliosides, in *Neurobiology of Glycoconjugates* (Margolis, R.U., and Margolis, R.K., eds.), pp. 1–42, Plenum Press, New York.
2. Schroten, H. (1988) The Benefits of Human Milk Fat Globule Against Infection, *Nutrition 14*, 52–53.
3. Fakih, M.G., Murphy, T.F., Pattoly, M.A., and Berenson, C.S. (1997) Specific Binding of *Haemophilus influenzae* to Minor Gangliosides of Human Respiratory Epithelial Cells, *Infect. Immun. 65*, 1695–1700.
4. Baker, N., Hansson, G.C., Leffler, H., Riise, G., and Svanborg-Edén, C. (1990) Glycosphingolipid Receptors for *Pseudomonas aeruginosa, Infect. Immun. 58*, 2361–2366.
5. Laegrid, A., and Otnaess, A.B.K. (1987) Trace Amounts of Ganglioside GM1 in Human Milk Inhibit Enterotoxins from *Vibrio cholerae* and *Escherichia coli, Life Sci. 40*, 55–62.
6. Idota, T., Kawakami, H., Murakawi, Y., and Sugawara, M. (1995) Inhibition of Cholera Toxin by Human Milk Fractions and Sialyllactose, *Biosci. Biotechnol. Biochem. 59*, 417–419.
7. Rueda, R., and Gil, A. (1998) Role of Gangliosides in Infant Nutrition, in *Lipids in Infant Nutrition* (Huang, Y.S., and Sinclair, A.J., eds.), pp. 213–234, AOCS Press, Champaign.
8. Harzer, G., Haug, M., Dieterich, I., and Gentner, P.R. (1983) Changing Patterns of Human Milk Lipids in the Course of Lactation and During the Day, *Am. J. Clin. Nutr. 37*, 612–621.
9. Puente, R., García-Pardo, L.A., and Hueso, P. (1992) Gangliosides in Bovine Milk. Changes in Content and Distribution of Individual Ganglioside Levels During Lactation, *Biol. Chem. Hoppe-Seyler 373*, 283–288.
10. Martín, M.J., Martín-Sosa, S., and Hueso, P. (2001) Bovine Milk Gangliosides: Changes in the Ceramide Moiety with Stage of Lactation, *Lipids 36*, 291–298.
11. Takamizawa, K., Iwamori, M., Mutai, M., and Nagai, Y. (1986) Selective Changes in Gangliosides of Human Milk During Lactation: A Molecular Indicator for the Period of Lactation, *Biochim. Biophys. Acta 879*, 73–77.
12. Rueda, R., Puente, R., Hueso, P., Maldonado, J., and Gil, A. (1995) New Data on Content and Distribution of Gangliosides in Human Milk, *Biol. Chem. Hoppe-Seyler 376*, 723–727.
13. Pan, X.L., and Izumi, T. (2000) Variation of the Ganglioside Composition of Human Milk, Cow's Milk and Infant Formulas, *Early Hum. Dev. 57*, 25–31.
14. Angström, J., Tenneberg, S., Abul Milh, M., Larsson, T., Leonardsson, I., Olsson, B.M., Halvarsson, M.O., Danielsson, D., Näslund, I., Ljungh, A., *et al.* (1998) The Lactosylceramide Binding Specificity of *Helicobacter pylori, Glycobiology 8*, 297–309.
15. Marild, S., Jodal, U., and Hanson, L.A. (1990) Breastfeeding and Urinary-Tract Infection, *Lancet 336*, 942.
16. Kovar, M.G., Sedula, M.K., Marks, J.S., and Frase, D.W. (1984) Review of the Epidemiologic Evidence for an Association Between Infant Feeding and Infant Health, *Pediatrics 74*, 615–638.
17. Williams, M.A., and McCluer, R.H. (1980) The Use of Sep-Pak C18 Cartridges During the Isolation of Gangliosides, *J. Neurochem. 33*, 266–269.
18. Svennerholm, L. (1957) Quantitative Estimation of Sialic Acids. II. A Colorimetric Resorcinol–Hydrochloric Acid Method, *Biochim. Biophys. Acta 24*, 604–611.
19. Zanetta, J.-P., Vitiello, F., and Vincendon, G.F. (1980) Gangliosides from Rat Cerebellum: Demonstration of a Considerable Heterogeneity Using a New Solvent for Thin-Layer Chromatography, *Lipids 15*, 1055–1061.
20. Vazquez, A.M., Alfonso, M., Lanne, B., Karlsson, K.A., Carr, A., Barroso, O., Fernández, L.E., Rengifo, E., Lanio, M.E., Álvarez, C., *et al.* (1995) Generation of a Murine Monoclonal Antibody Specific for *N*-Glycolylneuraminic Acid-Containing Gangliosides That Also Recognizes Sulfated Glycolipids, *Hybridoma 14*, 551–556.
21. Evans, D.G., and Evans, D.J. (1978) New Surface-Associated Heat-Labile Colonization Factor Antigen (CFA/II) Produced by Enterotoxigenic *Escherichia coli* of Serogroups O6 and O8, *Infect. Immun. 21*, 638–647.
22. Karlsson, K.A., and Strömberg, N. (1987) Overlay and Solid-Phase Analysis of Glycolipid Receptors for Bacteria and Viruses, *Methods Enzymol. 138*, 220–231.
23. Dubois, C., Manuguerra, J.C., Hauttecoeur, B., and Maze, J. (1990) Monoclonal Antibody A2B5, Which Detects Cell Surface Antigens, Binds to Ganglioside GT3 [II^3 $(Neu\ Ac)_3LacCer$] and to Its 9-*O*-Acetylated Derivative, *J. Biol. Chem. 265*, 2797–2803.
24. Wang, B., Brand-Miller, J., McVeagh, P., and Petocz, P. (2001) Concentration and Distribution of Sialic Acid in Human Milk and Infant Formulas, *Am. J. Clin. Nutr. 74*, 505–510.
25. Sanchez-Diaz, A., Ruano, M.J., Lorente, F., and Hueso, P. (1997) A Critical Analysis of Total Sialic Acid and Sialoglycoconjugate Contents of Bovine Milk-Based Infant Formulas, *J. Pediatr. Gastroenterol. Nutr. 24*, 405–410.
26. Laegreid, A., and Otnaess, A.B.K. (1986) Purification of Human Milk Gangliosides by Silica Gel Chromatography and Analysis of Trifluoroactate Derivatives by Gas Chromatography, *J. Chromatogr. 377*, 59–67.
27. Birklé, S., Cerato, E., Mezazigh-Hami, A., and Aubry, J. (1999) Les Gangliosides *O*-acétylés, *Regard sur la Biochemie 1*, 15–23.
28. Takamizawa, K., Iwamori, M., Mutai, M., and Nagai, Y. (1986) Gangliosides of Bovine Buttermilk. Isolation and Characterization of a Novel Monosialoganglioside with a New Branching Structure, *J. Biol. Chem. 261*, 5625–5630.
29. Bitman, J., and Wood, L.D. (1990) Changes in Milk Fat Phospholipids During Lactation, *J. Dairy Sci. 73*, 1208–1216.
30. Thompson, B., and Smith, S. (1987) Biosynthesis of Fatty Acids by Lactating Human Breast Epithelial Cells: An Evaluation of the Contribution to the Overall Composition of Human Milk Fat, *Pediatr. Res. 19*, 139–143.
31. Jensen, R.G. (1999) Lipids in Human Milk, *Lipids 34*, 1243–1271.
32. Haug, M., Dieterich, I., Laubach, C., Reinhardt, D., and Harzer, G. (1983) Capillary Gas Chromatography of Fatty Acid Methyl Esters from Human Milk Lipid Subclasses, *J. Chromatogr. 279*, 549–553.
33. Oro, H.S., Kolsto, A.B., Wenneras, C., and Svennerholm, A.M. (1990) Identification of Asialo-GM1 as a Binding Structure for *Escherichia coli* Colonization Factor Antigens, *FEMS Microbiol. Lett. 72*, 289–292.
34. Svennerholm, L. (1963) Chromatographic Separation of Human Brain Gangliosides, *J. Neurochem. 10*, 613–623.

[Received July 24, 2003, and in final revised form and accepted January 13, 2004]

Blood Phospholipid Fatty Acid Analysis of Adults With and Without Attention Deficit/Hyperactivity Disorder

Genevieve S. Young[a], Nicole J. Maharaj[a], and Julie A. Conquer[a,b,*]

[a]Department of Human Biology and Nutritional Sciences and [b]Human Nutraceutical Research Unit, University of Guelph, Guelph, Ontario, N1G 2W1, Canada

ABSTRACT: Several psychiatric disorders, including juvenile Attention Deficit/Hyperactivity Disorder (ADHD), have been associated with abnormalities of certain long-chain PUFA (LCPUFA). Despite this reported association, the FA levels of patients with the adult form of ADHD have not previously been evaluated. In this study we measured the total blood phospholipid FA concentrations in 35 control subjects and 37 adults with ADHD symptoms to determine whether adults with ADHD symptoms would show abnormalities of FA relative to control subjects. In the serum phospholipids, adults with ADHD symptoms had significantly lower levels of total saturated, total polyunsaturated, and total omega-6 (n-6) FA, as well as the omega-3 (n-3) LCPUFA DHA (22:6n-3), and significantly higher levels of total monounsaturated FA and the n-3 LCPUFA docosapentaenoic acid (22:5n-3). In the erythrocyte membrane phospholipids, adults with ADHD symptoms had significantly lower levels of total PUFA, total n-3 FA, and DHA, and significantly higher levels of total saturated FA. Neither serum nor erythrocyte membrane phospholipid DHA was related to ADHD symptom severity (as assessed by the Amen questionnaire) in ADHD subjects. Although the exact cause of these variations is unknown, both environmental and genetic factors may be involved.

Paper no. L9367 in *Lipids 39*, 117–123 (February 2004).

Omega-3 and omega-6 (n-3 and n-6, respectively) FA are considered essential as they cannot be synthesized by mammalian cells and must be obtained from the diet. The essential n-3 FA α-linolenic acid (ALA; 18:3n-3) and the essential n-6 FA linoleic acid (LA; 18:2n-6) can undergo elongation, desaturation, and β-oxidation to form the n-3 long-chain PUFA (LCPUFA) EPA (20:5n-3), docosapentaenoic acid (DPA; 22:5n-3), and DHA (22:6n-3), and the n-6 LCPUFA γ-linolenic acid (GLA; 18:3n-6), dihomo-γ-linolenic acid (DGLA; 20:3n-6), and arachidonic acid (AA; 20:4n-6), respectively (1). As primary constituents of the cell membrane phospholipid bilayer, FA, particularly DHA and AA, make up a large proportion of the brain's lipids (2). The prominent structural role of FA in the brain translates into a functional role, since they affect membrane-associated proteins such as transporters, enzymes, and receptors (3,4).

Attention Deficit/Hyperactivity Disorder (ADHD) is a condition involving "a persistent pattern of inattention and/or hyperactivity-impulsivity that is more frequent and severe than is typically observed in individuals at a comparable level of development" (5). Although originally thought to occur only in children, it is now recognized that in up to 60% of sufferers ADHD persists into adulthood (6). In adults, ADHD is manifested by disorganization, impulsivity, and poor work skills, and sufferers tend to be impatient and easily bored (7). The *Diagnostic and Statistical Manual of Mental Disorders*, 4th edn., requires evidence of hyperactive-impulsive or inattentive symptoms to be present before age 7, although individuals are often diagnosed after the symptoms have been present for several years (5). Since no specific test is diagnostic of ADHD, making an accurate diagnosis is difficult, especially in adults (7).

There is emerging evidence that LCPUFA abnormalities may play a role in a wide range of learning and mood disorders, including ADHD (8–26). Several FA, including AA (9), EPA (9), and DHA (8,10), are present at abnormal levels in children with ADHD. Despite this reported association, the same relationship has not been reported previously in adults. Based on this link, investigation to determine whether there is also an association in adults is warranted. The present study measured erythrocyte membrane and serum phospholipid FA concentrations in control subjects and in adults with ADHD symptoms, and the prospectively defined hypothesis was that adults with ADHD symptoms would show abnormalities of certain LCPUFA, particularly DHA, EPA and AA, relative to control subjects.

MATERIALS AND METHODS

Subjects. Eighty-eight subjects aged 18 to 65 yr were recruited by advertisements and flyers in the local community. Inclusion criteria for adults with ADHD symptoms included a previous diagnosis of ADHD by a physician, based on a comprehensive psychological evaluation, and the ability to give informed consent. Because the physician evaluations were not performed using uniform criteria, these subjects were labeled "adults with ADHD symptoms," although all subjects had in fact been previously diagnosed with ADHD. Both control and ADHD subjects were excluded for one or more of the following

*To whom correspondence should be addressed at Department of Human Biology and Nutritional Science, University of Guelph, Guelph, Ontario N1G 2W1, Canada. E-mail: jconquer@uoguelph.ca

Abbreviations: AA, arachidonic acid; ADHD, Attention Deficit/Hyperactivity Disorder; ALA, α-linolenic acid; DGLA, dihomo-γ-linolenic acid; DPA, docosapentaenoic acid; GLA, γ-linolenic acid; LA, linoleic acid; LCPUFA, long-chain PUFA; LNA, linolenic acid; n-3, omega-3; n-6, omega-6; PLA2, phospholipase A2; RBC, red blood cell.

reasons: (i) diagnosis of another psychiatric disorder (as reported by the subject), (ii) use of dietary supplements (other than vitamins/minerals) within the past month, (iii) use of n-3 FA supplements within the past 6 mon, (iv) history of head injuries or seizures, (v) diagnosis of a lipid metabolism disorder or other serious chronic condition, and (vi) consumption of fish more than once per week. Of the 88 subjects screened, 14 were excluded due to a lack of formal diagnosis of ADHD by a physician, 1 was excluded owing to use of fish oil supplements within the last 6 mon, and 1 was excluded owing to use of flaxseed oil supplements within the last 6 mon. This left 72 subjects, 37 adults with ADHD symptoms and 35 control. ADHD subjects were not excluded on the basis of pharmacological treatment for their condition. ADHD subjects also were not screened for their use of alcohol, tobacco, or recreational drugs. This study was approved by the Research Ethics Board of the University of Guelph.

Behavior assessment. All subjects completed a questionnaire developed by Dr. D. Amen designed to identify and classify ADHD subtypes in adults (27). Questionnaires were graded, with 1 point given for each score of 3 (symptom is experienced frequently) or 4 (symptom is experienced very frequently). The questionnaire has a highest possible score of 71. The Amen questionnaire was not used to diagnose ADHD but rather served to highlight the differences in ADHD symptoms between adults with ADHD symptoms and control subjects. Quantitatively assessing ADHD symptoms also allowed investigation of a correlation between FA levels and symptom severity.

Preparation of sample. All subjects had nonfasting venous blood drawn into heparinized tubes. Whole blood was then centrifuged at room temperature for 10 min at $1000 \times g$, and red blood cells (RBC) were separated from serum. For 30 ADHD subjects, nonfasting blood was also obtained by the finger prick method for serum isolation. Whole blood was centrifuged at room temperature for 10 min at $1250 \times g$ and serum obtained. Serum was stored at –20°C until further analysis. Serum samples were stored for a period of 1–4 mon. Phospholipid FA in serum obtained by venipuncture were analyzed for 42 subjects (7 ADHD and 35 control) and by the finger prick method for the remaining 30 ADHD subjects.

For RBC membrane isolation, cells were washed in cold PBS (pH 7.4) and centrifuged at $1200 \times g$ for 10 min at 4°C (repeated twice). Cells were then lysed in PBS (pH 8) and centrifuged at $20{,}000 \times g$ for 10 min at 4°C (repeated four times). Isolated RBC membranes were stored at –20°C until further analysis. All samples were stored under nitrogen gas to reduce LCPUFA oxidation. RBC membrane samples of ADHD subjects were stored for 1–2 mon, whereas those of control subjects were stored for a period of 2 to 3 mon.

Extraction of lipid. RBC membrane lipids were extracted using chloroform/methanol (2:1), the volume of which was 20 times greater than that of the sample. Serum lipids were extracted using equal volumes of chloroform/methanol (2:1) in the presence of 17:0 internal standard. TLC was used to separate the lipid fraction from both the RBC membranes and serum using hexane/isopropyl ether/acetic acid (60:40:30, by vol) as the solvent system. The samples were spotted on silica gel TLC plates and allowed to develop within 2 cm of the top of the plate, after which the plates were removed and air-dried. The phospholipid bands were scraped, and a methylating agent (6% H_2SO_4 in methanol) was added. Five micrograms of 17:0 internal standard was added to the RBC solution. All samples were heated for 60 min at 80°C, and lipids were extracted with *n*-hexane. The FAME were analyzed by GC at the Lipid Analytical Laboratory (Guelph, Ontario, Canada) with a Varian 3800 gas chromatograph (Palo Alto, CA) equipped with a 30-m DB-23 capillary column (0.32 mm i.d., 0.1 μm film thickness; Varian). The sum of FA from 14:0 to 24:1 was taken as 100, and levels of individual FA were expressed as a percentage of this sum.

Statistical analysis. Statistical analysis was performed using SPSS version 11.5 (SPSS, Inc., Chicago, IL) statistical software. Data were examined for normality of distribution by using frequency distribution plots. Levels of the individual and groups of FA were compared between ADHD and control groups using Mann–Whitney nonparametric tests since the data were not normally distributed. A total of 26 comparisons were made. The Amen questionnaire scores and demographic data also were analyzed using Mann–Whitney tests, again owing to a lack of normal data distribution. Linear regression was used to investigate the relationship between both serum and erythrocyte DHA levels and Amen questionnaire scores. The P value was set at 0.03 because of the increased likelihood of significant results appearing by chance due to the number of comparisons performed.

RESULTS

Thirty-five control and 37 ADHD subjects completed the study. The two groups did not differ with respect to age or sex, as shown in Table 1. There was a statistically significant difference between the scores of the two groups on the Amen

TABLE 1
Subject Characteristics of Control Adults and Adults with ADHD Symptoms[a]

	Control	ADHD	*P* value	*Z* value
Age	29.97 ± 12.99	30.59 ± 13.57	NS	–0.21
Sex (males/females)	16/19	19/18	NA	NA
Amen questionnaire results[b]	4.23 ± 4.24	32.65 ±16.54	<0.001	–7.14

[a]Values are reported as mean ± SD for $n = 35$ (control) and 37 (ADHD).
[b]Score out of a possible score of 71. ADHD, Attention Deficit/Hyperactivity Disorder; NA, not applicable; NS, not significant.

TABLE 2
Total FA Analysis of Serum Phospholipids in Control Adults and Adults with ADHD Symptoms (wt%)[a]

FA	Control	ADHD	*P* value	*Z* value
Saturated	46.24 ± 1.12	43.53 ± 2.03	<0.001	–4.44
Monounsaturated	10.55 ± 1.20	13.33 ± 2.17	<0.001	–5.48
Polyunsaturated	43.21 ± 1.52	40.37 ± 2.43	0.001	–3.47
n-6	38.15 ± 1.83	35.48 ± 2.61	0.007	–2.71
LA	23.30 ± 2.81	21.30 ± 2.98	NS	–1.39
GLA	0.08 ± 0.05	0.11 ± 0.07	NS	–1.94
DGLA	2.29 ± 0.62	2.82 ± 0.69	NS	–0.55
AA	10.79 ± 2.11	10.06 ± 1.51	NS	–1.17
n-3	5.06 ± 1.08	4.89 ± 1.36	NS	–0.83
ALA	0.23 ± 0.09	0.28 ± 0.16	NS	–1.60
EPA	0.66 ± 0.24	0.72 ± 0.33	NS	–0.53
DPA	0.83 ± 0.21	0.99 ± 0.22	0.002	–3.08
DHA	3.23 ± 0.98	2.69 ± 1.10	0.009	–2.62

[a]Values are reported as mean ± SD for $n = 35$ (control) and 36 (ADHD) individuals. LA, linoleic acid; GLA, γ-linolenic acid; DGLA, dihomo-γ-linolenic acid; AA, arachidonic acid; ALA, α-linolenic acid; DPA, docosapentaenoic acid; for other abbreviations see Table 1.

questionnaire, with adults with ADHD symptoms scoring much higher than control subjects.

Table 2 shows the total serum phospholipid FA concentrations of ADHD and control subjects as a percentage of total FA. Serum FA values were not obtained for one subject due to technical difficulties. In the serum phospholipids, adults with ADHD symptoms had significantly lower levels of total saturated, total polyunsaturated, and total n-6 FA, as well as the n-3 LCPUFA DHA, and significantly higher levels of total monounsaturated FA and the n-3 LCPUFA DPA.

Table 3 shows the total RBC membrane phospholipid FA concentrations of ADHD and control subjects as a percentage of total FA. RBC FA values were not obtained from one subject due to difficulty drawing blood by venipuncture. Adults with ADHD symptoms had significantly lower levels of total PUFA, total n-3 FA, and DHA, and significantly higher levels of total saturated FA.

Figure 1 illustrates the relationship between RBC membrane phospholipid DHA and Amen questionnaire scores. There was no significant association between these variables ($r = 0.271$). There was also no significant association between serum phospholipid DHA and Amen questionnaire scores ($r = 0.150$).

DISCUSSION

The objective of this study was to determine whether abnormalities of LCPUFA are present in adults with ADHD symptoms. Our primary finding was a decrease of DHA in both erythrocyte membrane and serum phospholipids. Since FA levels are expressed as a percentage of total weight, the decrease in DHA resulted in decreased levels of total PUFA in both blood fractions, as well as total n-3 FA in erythrocyte membranes. As well, adults with ADHD symptoms showed

TABLE 3
Total FA Analysis of RBC Membrane Phospholipids in Control Adults and Adults with ADHD Symptoms (wt%)[a]

FA	Control	ADHD	*P* value	*Z* value
Saturated	44.59 ± 6.61	44.84 ± 3.32	0.004	–2.87
Monounsaturated	17.74 ± 2.06	18.70 ± 1.99	NS	–0.82
Polyunsaturated	37.67 ± 5.44	36.47 ± 3.91	0.02	–2.29
n-6	30.53 ± 4.47	29.95 ± 3.76	NS	–1.34
LA	10.33 ± 1.58	9.96 ± 1.15	NS	–1.60
GLA	0.07 ± 0.12	0.05 ± 0.06	NS	–1.14
DGLA	1.69 ± 0.65	1.65 ± 0.46	NS	–0.68
AA	13.96 ± 2.52	13.70 ± 2.30	NS	–1.04
n-3	7.14 ± 1.57	6.52 ± 1.29	0.01	–2.49
ALA	0.09 ± 0.07	0.10 ± 0.09	NS	–0.43
EPA	0.46 ± 0.25	0.45 ± 0.21	NS	–0.20
DPA	2.57 ± 0.65	2.64 ± 0.61	NS	–0.09
DHA	3.92 ± 1.03	3.19 ± 0.94	<0.001	–3.49

[a]Values are reported as mean ± SD for $n = 35$ (control) and 36 (ADHD) individuals. RBC, red blood cell; for other abbreviations see Tables 1 and 2.

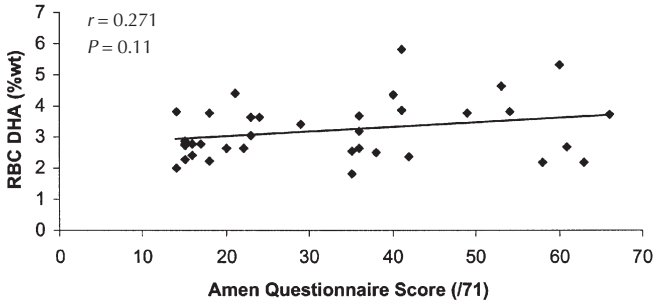

FIG. 1. Correlation between red blood cell (RBC) DHA and Amen questionnaire scores.

decreased levels of total n-6 FA in serum phospholipids, although individual n-6 FA were not significantly affected. Total monounsaturated FA and the n-3 FA DPA were increased in serum phospholipids. Levels of DHA in blood phospholipids were not correlated with symptom severity.

Previous studies have suggested a relationship between LCPUFA abnormalities and ADHD in children. In 1981, it was observed that hyperactive children showed increased thirst relative to children without hyperactivity (28). Increased thirst may be a symptom of EFA deficiency (29). In 1987, Mitchell *et al.* (8) showed that hyperactive children reporting significantly greater thirst did in fact have lower plasma levels of the n-6 FA DGLA and AA and the n-3 FA DHA. Since then, low levels of various LCPUFA have been found in children with ADHD including AA (9), EPA (9), and most commonly, DHA (8,10). Stevens *et al.* (9) also found that a greater number of behavior, learning, and health problems were reported in subjects with lower concentrations of total n-3 FA.

As a result of the observed LCPUFA abnormalities in childhood ADHD, clinical trials have been conducted using a variety of FA to treat the disorder. These trials have yielded mixed results. In 1987, children with marked inattention and hyperactivity were supplemented for a period of 4 wk with a combination of LA and GLA. There was minimal or no improvement in symptoms, depending on the outcome measure used (30). In 2001, Voigt *et al.* (11) treated ADHD children with DHA from an algal source for a period of 4 mon and observed no decrease in symptoms between treated and control subjects, although they did observe an increase in plasma DHA of 260%. And in 2002, Richardson and Puri (31) found that 12 wk of treatment with DHA and evening primrose oil, a source of GLA, improved mean scores for cognitive and general behavior problems on 7 out of 14 scales, vs. no improvement with placebo. Because different treatments, procedures, measures, and selection criteria were used in these trials, it is difficult to make comparisons between them. At this time, there is no clear evidence to suggest that supplementation with any particular LCPUFA or combination thereof is an effective treatment for ADHD in children. There have been no trials investigating the effect of LCPUFA supplementation in adults with ADHD.

ADHD in both children and adults is characterized by difficulties regulating attention and/or monitoring their motor behavior or impulses (32). Dopamine, which acts as a modulator of attention, motivation, and emotion (33), may serve as a link between abnormalities of LCPUFA, particularly DHA, and ADHD. Although very little research has been done on humans, single-emission computed tomography has found that adults with ADHD exhibit increased striatal availability of a dopamine transporter (32), and medications used to treat ADHD commonly exert their effect *via* inhibition of this transporter (34). Animal studies have demonstrated that several aspects of dopamine physiology are affected by levels of FA intake. It has been observed that when piglets are fed a diet deficient in AA and DHA, but adequate in levels of ALA and LA, there is a decrease in dopamine concentration in the frontal cortex (35). Furthermore, when rats are fed a diet deficient in both short- and long-chain n-3 FA, there is inadequate storage of newly synthesized dopamine (36) and an overall reduction in the dopaminergic vesicle pool (37). Alternatively, when rats are fed fish oil containing EPA and DHA, there is a 40% increase in frontal cortex dopamine concentrations as well as a greater binding to dopamine D_2 receptors (38). The low levels of DHA observed in this study could therefore theoretically affect the availability of dopamine, which could subsequently result in impaired attention, motivation, and emotion, which are classical symptoms of ADHD.

As the basic structural components of phospholipids, FA can be found in different locations in the body, including serum and RBC membranes. The levels of both serum (39,40) and RBC (41) phospholipid FA that we observed are similar to those observed in other studies. Phospholipids in different locations contain different proportions of each FA, as is demonstrated in Tables 2 and 3. Phospholipids in different locations also respond differently to dietary FA manipulation. Serum phospholipid FA reflect the dietary intakes of the past few days (42), whereas erythrocyte membrane phospholipid FA reflect the dietary intakes of the past month (43). As compared with the response of serum phospholipids, erythrocytes show less response to dietary change, but their phospholipid FA composition is more stable than that of serum owing to the high turnover rate of FA in the former (44). This likely accounts for the differences that we observed in serum and erythrocyte FA. It has been demonstrated that both serum (45,46) and erythrocyte (47) phospholipid EPA and DHA are correlated with fish consumption, so dietary intake of the n-3 LCPUFA may be accurately reflected in both of these pools of lipids. In this study, we attempted to control for intake of flaxseed and fish oils, which are major contributors of short- and long-chain n-3 FA to the diet, but in the absence of dietary record analysis it is not possible to determine whether differences in dietary intake existed between the two groups of subjects. Therefore, diet may be a contributing cause to the FA abnormalities that we observed.

In addition to differences in dietary intake, it has been suggested that LCPUFA abnormalities may be due to differences in metabolism. As previously mentioned, the EFA must undergo complex biotransformation in order to be converted into their long-chain derivatives, and individuals vary in the efficiency of their conversion mechanisms (1). The hypothe-

sis that the LCPUFA abnormalities observed in ADHD patients may be associated with inefficient conversion of short-chain FA is supported by the fact that serum zinc levels have been found to be significantly associated with low EFA levels in children with ADHD (48), and zinc deficiency inhibits the Δ6-desaturase enzyme (8). Both Δ6-desaturase (49) and Δ5-desaturase (50) enzymes are highly active in the brain, making them candidates for involvement in this disorder. Phospholipase A2 (PLA2), an enzyme that acts to remove highly unsaturated FA from the *sn*-2 position of membrane phospholipids (51), is another possible candidate. PLA2 has been implicated in several neurodevelopmental and psychiatric conditions, including dyslexia (52), depression and bipolar disease (53), schizophrenia (16,17), and Alzheimer's disease (54). ADHD is commonly co-morbid with dyslexia (55), depression (56), and bipolar disease (23).

In fact, it is estimated that 75% of adults with ADHD suffer from other psychiatric disorders (57), and LCPUFA abnormalities have been implicated in many such conditions, including dyslexia (57), depression (12–15), schizophrenia (16–18), autism (58,59), and bipolar disorder (20). In dyslexia, the severity of the disorder has been shown to be related to the degree of clinical signs of deficiency (60). Although one of the exclusion criteria in this study was a diagnosis of another psychiatric condition, since this information was self-reported, it is possible that our ADHD subjects suffered from other psychiatric disorders. Furthermore, we did not control for the use of substances such as alcohol or tobacco. Adults with ADHD show a high frequency of substance abuse disorders (56), and both alcohol (61) and tobacco (62,63) use have been shown to affect levels of LCPUFA adversely. Together, these factors make it difficult to conclude that the observed correlation in this study between LCPUFA abnormalities and ADHD symptoms has not been confounded by other conditions also known to involve variations in FA levels.

LCPUFA in the RBC membranes of autistic subjects exhibit an increased level of degradation relative to control subjects when stored at –20°C (58), and it has been shown that there is a high degree of clinical overlap between autism and ADHD (57). Schizophrenic patients also show an increased rate of LCPUFA degradation at –20°C relative to control subjects, although it may be that this increased degradation is limited to a subset of patients with schizophrenia (64). Conversely, it has been shown that patients with Asperger's syndrome, a condition that shows clinical overlap with autism (65) and is considered by some to be a condition of high-functioning autism (66), show unusually stable RBC membrane LCPUFA when stored at –20°C (58). This variation in stability of membrane LCPUFA at low temperatures has been attributed to variations in phospholipase activity, with low activity increasing the stability at low temperatures and high activity decreasing it (58). Although the degradation of LCPUFA in RBC membranes of ADHD subjects at –20°C has not previously been evaluated, it is possible that they might also show an increased rate relative to control subjects. This is an issue that should be investigated in the future and may be a contributing factor to the low level of DHA observed in this study. However, the similarity between levels of serum and erythrocyte membrane DHA, and the short storage period of all samples, suggests that degradation due to storage temperature was minimal.

It is unclear whether peripheral LCPUFA composition reflects the phospholipid composition of neuronal membranes. Preliminary data in schizophrenic patients do suggest a correlation between RBC membrane phospholipid composition and that of the brain, although such a correlation does not necessarily indicate a causal relationship (67). In this study, we observed low levels of the LCPUFA DHA in both the serum and RBC membrane phospholipids of adults with ADHD symptoms, and although the exact cause of this abnormality is unknown, both environmental and genetic factors may be involved. This observation is complicated by the fact that adult ADHD often co-exists with other psychiatric conditions known to involve alterations of LCPUFA, and by the possibility of enhanced degradation of these FA following storage at –20°C. Regardless, the body of evidence does appear to suggest that abnormalities of LCPUFA can contribute to deficits in concentration, and understanding the precise role of these FA in cognitive processes, as well as the etiology of LCPUFA abnormalities in conditions such as adult ADHD, may prove useful in their management and treatment.

ACKNOWLEDGMENTS

Supported by Adopt-A-Patient Foundation, Methuen, Massachusetts. We would also like to thank all of the student volunteers and University of Guelph laboratory technicians who assisted with this project.

REFERENCES

1. Simopoulos, A.P. (1991) Omega-3 Fatty Acids in Health and Disease and in Growth and Development, *Am. J. Clin. Nutr. 54*, 438–463.
2. Sastry, P.S. (1985) Lipids of Nervous Tissue: Composition and Metabolism, *Prog. Lipid Res. 24*, 69–176.
3. Brenner, R.R. (1984) Effect of Unsaturated Fatty Acids on Membrane Structure and Enzyme Kinetics, *Prog. Lipid Res. 23*, 69–96.
4. Spector, A.A., and Yorek, M.A. (1985) Membrane Lipid Composition and Cellular Function, *J. Lipid Res. 26*, 1015–1035.
5. American Psychiatric Association (1994) *Diagnostic and Statistical Manual of Mental Disorders*, 4th edn., pp. 78–85, American Psychiatric Publishing, Arlington, VA.
6. Spencer, T., Biederman, J., Wilens, T.E., and Faraone, S.V. (1994) Is Attention Deficit Hyperactivity Disorder in Adults a Valid Disorder? *Harv. Rev. Psychiatry 1*, 326–335.
7. Pary, R., Lewis, S., Matuschka, P.R., and Lippmann, S. (2002) Attention-Deficit/Hyperactivity Disorder: An Update, *South. Med. J. 95*, 743–749.
8. Mitchell, E.A., Aman, M.G., Turbott, S.H., and Manku, M. (1987) Clinical Characteristics and Serum Essential Fatty Acid Levels in Hyperactive Children, *Clin. Pediatr. 26*, 406–411.
9. Stevens, L.J., Zentall, S.S., Deck, J.L., Abate, M.L., Watkins, B.A., Lipp, S.R., and Burgess, J.R. (1995) Essential Fatty Acid Metabolism in Boys with Attention-Deficit Hyperactivity Disorder, *Am. J. Clin. Nutr. 62*, 761–768.
10. Stevens, L.J., Zentall, S.S., Abate, M.L., Kuczek, T., and Burgess, J.R. (1996) Omega-3 Fatty Acids in Boys with Behavior, Learning, and Health Problems, *Physiol. Behav. 59*, 915–920.

11. Voigt, R.G., Llorente, A.M., Jensen, C.L., Fraley, J.K., Berretta, M.C., and Heird, W.C. (2001) A Randomized, Double-Blind, Placebo-Controlled Trial of Docosahexaenoic Acid Supplementation in Children with Attention-Deficit/Hyperactivity Disorder, *J. Pediatr. 139*, 189–196.
12. Edwards, R., Peet, M., Shay, J., and Horrobin, D. (1998) Omega-3 Polyunsaturated Fatty Acid Levels in the Diet and in Red Blood Cell Membranes of Depressed Patients, *J. Affect. Disord. 48*, 149–155.
13. Peet, M., Murphy, B., Shay, J., and Horrobin, D. (1998) Depletion of Omega-3 Fatty Acid Levels in Red Blood Cell Membranes of Depressive Patients, *Biol. Psychiatry 43*, 315–319.
14. Maes, M., Smith, R., Christophe, A., Cosyns, P., Desnyder, R., and Meltzer, H. (1996) Fatty Acid Composition in Major Depression: Decreased ω3 Fractions in Cholesteryl Esters and Increased C20:4ω6/C20:5ω3 Ratio in Cholesteryl Esters and Phospholipids, *J. Affect. Disord. 38*, 35–46.
15. Maes, M., Christophe, A., Delanghe, J., Altamura, C., Neels, H., and Meltzer, H.Y. (1999) Lowered ω3 Polyunsaturated Fatty Acids in Serum Phospholipids and Cholesterol Esters of Depressed Patients, *Psychiatry Res. 85*, 275–291.
16. Puri, B.K., Richardson, A.J., Horrobin, D.F., Easton, T., Saeed, N., Oatridge, A., Hajnal, J.V., and Bydder, G.M. (2000) Eicosapentaenoic Acid Treatment in Schizophrenia Associated with Symptom Remission, Normalization of Blood Fatty Acids, Reduced Neuronal Membrane Phospholipid Turnover and Structural Brain Changes, *Int. J. Clin. Pract. 54*, 57–63.
17. Puri, B.K., and Stiner, R. (1998) Sustained Remission of Positive and Negative Symptoms of Schizophrenia Following Treatment with Eicosapentaenoic Acid, *Arch. Gen. Psychiatry 55*, 188–189.
18. Assies, J., Lieverse, R., Vreken, P., Wanders, R.J., Dingemans, P.M., and Linszen, D.H. (2001) Significantly Reduced Docosahexaenoic and Docosapentaenoic Acid Concentrations in Erythrocyte Membranes from Schizophrenic Patients Compared with a Carefully Matched Control Group, *Biol. Psychiatry 49*, 510–522.
19. Hibbeln, J.R., Linnoila, M., Umhau, J.C., Rawlings, R., George, D.T., and Salem, N. (1998) Essential Fatty Acids Predict Metabolites of Serotonin and Dopamine in Cerebrospinal Fluid among Healthy Control Subjects, and Early- and Late-Onset Alcoholics, *Biol. Psychiatry 44*, 235–242.
20. Stoll, A.L., Severus, W.E., Freeman, M.P., Rueter, S., Zboyan, H.A., Diamond, E., Cress, K.K., and Marangell, L.B. (1999) Omega 3 Fatty Acids in Bipolar Disorder: A Preliminary Double-Blind, Placebo-Controlled Trial, *Arch. Gen. Psychiatry 56*, 407–412.
21. Soderberg, M., Edlund, C., Kristensson, K., and Daliner, G. (1991) Fatty Acid Composition of Brain Phospholipids in Aging and Alzheimer's Disease, *Lipids 26*, 421–425.
22. Guan, Z.Z., Soderberg, M., Sindelar, P., and Edlund, C. (1994) Content and Fatty Acid Composition of Cardiolipin in the Brain of Patients with Alzheimer's Disease, *Neurochem. Int. 25*, 295–300.
23. Kyle, D.J., Schaefer, E., Patton, G., and Beiser, A. (1999) Low Serum Docosahexaenoic Acid Is a Significant Risk Factor for Alzheimer's Dementia, *Lipids 34*, S245.
24. Tilvis, R.S., Erkinjuntti, T., Sulkava, R., and Miettinen, T.A. (1987) Fatty Acids of Plasma Lipids, Red Cells and Platelets in Alzheimer's Disease and Vascular Dementia, *Atherosclerosis 65*, 237–245.
25. Montine, T.J., Montine, K.S., and Swift, L.L. (1997) Central Nervous System Lipoproteins in Alzheimer's Disease, *Am. J. Pathol. 151*, 1571–1575.
26. Conquer, J.A., Tierney, M.C., Zecevic, J., Bettger, W.J., and Fisher, R.H. (2000) Fatty Acid Analysis of Blood Plasma of Patients with Alzheimer's Disease, Other Types of Dementia, and Cognitive Impairment, *Lipids 35*, 1305–1312.
27. Amen, D.G. (2002) *Healing ADD: The Breakthrough Program That Allows You to See and Heal the 6 Types of ADD*, pp. 67–76, Berkley Publishing Group, New York.
28. Colquhoun, I., and Bunday, S. (1981) A Lack of Essential Fatty Acids as a Possible Cause of Hyperactivity in Children, *Med. Hypotheses 7*, 673–679.
29. Burr, G.O., and Burr, M.M. (1930) On the Nature and Role of the Fatty Acids Essential in Nutrition, *J. Biol. Chem. 86*, 587–621.
30. Aman, M.G., Mitchell, E.A., and Turbott, S.H. (1987) The Effects of Essential Fatty Acid Supplementation by Efamol in Hyperactive Children, *J. Abnorm. Child Psychol. 15*, 75–90.
31. Richardson, A.J., and Puri, B.K. (2002) A Randomized Double-Blind, Placebo-Controlled Study of the Effects of Supplementation with Highly Unsaturated Fatty Acids on ADHD-Related Symptoms in Children with Specific Learning Difficulties, *Prog. Neuro-Psychopharmacol. Biol. Psychiatry 26*, 233–239.
32. Elliot, H., and Winston-Salem, N.C. (2002) Attention Deficit Hyperactivity Disorder in Adults: A Guide for the Primary Care Physician, *South. Med. J. 95*, 736–742.
33. Le Moal, M., and Simon, H. (1991) Mesocorticolimbic Dopaminergic Networks: Functional and Regulatory Roles, *Physiol. Rev. 71*, 155–234.
34. Cook, E.H., Stein, M.A., Krasowski, M.D., Cox, N.J., Olkon, D.M., Kieffer, J.E., and Leventhal, B.L. (1995) Association of Attention-Deficit Disorder and the Dopamine Transporter Gene, *Am. J. Hum. Genet. 56*, 993–998.
35. De la Presa Owens, S., and Innis, S.M. (1999) Docosahexaenoic Acid and Arachidonic Acid Prevent a Decrease in Dopaminergic and Serotoninergic Neurotransmitters in Frontal Cortex Caused by a Linoleic and α-Linolenic Acid Deficient Diet in Formula-Fed Piglets, *J. Nutr. 129*, 2088–2093.
36. Zimmer, L., Durand, G., Guilloteau, D., and Chalon, S. (1999) n-3 Polyunsaturated Fatty Acid Deficiency and Dopamine Metabolism in the Rat Frontal Cortex, *Lipids 34*, S251.
37. Zimmer, L., Delpal, S., Guilloteau, D., Aioun, J., Durand, G., and Chalon, S. (2000) Chronic n-3 Polyunsaturated Fatty Acid Deficiency Alters Dopamine Vesicle Density in the Rat Frontal Cortex, *Neurosci. Lett. 284*, 25–28.
38. Chalon, S., Delion-Vancassel, S., Belzung, C., Guilloteau, D., Leguisquet, A., Besnard, J.C., and Durand, G. (1998) Dietary Fish Oil Affects Monoaminergic Neurotransmission and Behavior in Rats, *J. Nutr. 128*, 2512–2519.
39. Stark, K.D., Mulvad, G., Pedersen, H.S., Park, E.J., Dewailly, E., and Holub, B.J. (2002) Fatty Acid Composition of Serum Phospholipids of Postmenopausal Women: A Comparison Between Greenland Inuit and Canadians Before and After Supplementation with Fish Oil, *Nutrition 18*, 627–630.
40. Pelikanova, T., Kazdova, L., Chvojkova, S., and Base, J. (2001) Serum Phospholipids Fatty Acid Composition and Insulin Action in Type 2 Diabetic Patients, *Metabolism 50*, 1472–1478.
41. Glatz, J.F., Soffers, A.E., and Katan, M.B. (1989) Fatty Acid Composition of Serum Cholesteryl Esters and Erythrocyte Membranes as Indicators of Linoleic Acid Intake in Man, *Am. J. Clin. Nutr. 49*, 269–276.
42. Kohlmeier, L. (1995) Future of Dietary Exposure Assessment, *Am. J. Clin. Nutr. 61* (Supp.), 702S–709S.
43. Arab, L. (2003) Biomarkers of Fat and Fatty Acid Intake, *J. Nutr. 133*, 925S–932S.
44. Farquhar, J.W., and Ahrens, E.H. (1963) Effects of Dietary Fats on Human Erythrocyte Fatty Acid Patterns, *J. Clin. Invest. 42*, 675–685.
45. Hjartåker, J., Lund, E., and Bjerve, K.S. (1997) Serum Phospholipid Fatty Acid Composition and Habitual Intake of Marine Foods Registered by a Semi-quantitative Food Frequency Questionnaire, *Eur. J. Clin. Nutr. 51*, 736–742.
46. Bjerve, K.S., Brubakk, A.M., Fougner, K.J., Johnsen, H., Midthjell, K. and Vik, T. (1993) Omega-3 Fatty Acids: Essential Fatty

Acids with Important Biological Effects, and Serum Phospholipid Fatty Acids as Markers of Dietary Omega 3-Fatty Acid Intake, *Am. J. Clin. Nutr. 57*, 801S–805S.
47. Godley, P.A., Campbell, M.K., Miller, C., Gallagher, P., Martinson, F.E., Mohler, J.L., and Sandler, R.S. (1996) Correlation Between Biomarkers of Omega-3 Fatty Acid Consumption and Questionnaire Data in African American and Caucasian United States Males With and Without Prostatic Carcinoma, *Cancer Epidemiol. Biomarkers Prev. 5*, 115–119.
48. Bekaroglu, M., Aslan, Y., Gedik, Y., Deger, O., Mocan, H., Erduran, E., and Karahan, C. (1996) Relationships Between Serum Free Fatty Acids and Zinc, and Attention Deficit Hyperactivity Disorder: A Research Note, *J. Child. Psychol. 37*, 225–227.
49. Cho, H.P., Nakamura, M.T., and Clarke, S.D. (1999) Cloning, Expression, and Nutritional Regulation of the Mammalian Δ-6 Desaturase, *J. Biol. Chem. 274*, 471–477.
50. Cho, H.P., Nakamura, M., and Clarke, S.D. (1999) Cloning, Expression, and Fatty Acid Regulation of the Human Δ-5 Desaturase, *J. Biol. Chem. 274*, 37335–37339.
51. Bennett, C.N., and Horrobin, D.F. (2000) Gene Targets Related to Phospholipid and Fatty Acid Metabolism in Schizophrenia and Other Psychiatric Disorders: An Update, *Prostaglandins Leukotrienes Essent. Fatty Acids 63*, 47–59.
52. MacDonell, L.E., Skinner, F.K., Ward, P.E., Glen, A.I., Glen, A.C., Macdonald, D.J., Boyle, R.M., and Horrobin, D.F. (2000) Increased Levels of Cytosolic Phospholipase A2 in Dyslexics, *Prostaglandins Leukotrienes Essent. Fatty Acids 63*, 37–39.
53. Horrobin, D.F., and Bennett, C.N. (1999) Depression and Bipolar Disorder: Relationships to Impaired Fatty Acid and Phospholipid Metabolism and to Diabetes, Cardiovascular Disease, Immunological Abnormalities, Cancer, Ageing and Osteoporosis: Possible Candidate Genes, *Prostaglandins Leukotrienes Essent. Fatty Acids. 60*, 217–234.
54. Gattaz, W.F., Carins, N.J., Levy, R., Forstl, H., Braus, D.F., and Maras, A. (1996) Decreased Phospholipase A2 Activity in the Brain and in Platelets of Patients with Alzheimer's Disease, *Eur. Arch. Psychiatry Clin. Neurosci. 246*, 129–131.
55. Richardson, A.J., and Ross, M.A. (2000) Fatty Acid Metabolism in Neurodevelopmental Disorder: A New Perspective on Associations Between Attention-Deficit/Hyperactivity Disorder, Dyslexia, Dyspraxia and the Autistic Spectrum, *Prostaglandins Leukotrienes Essent. Fatty Acids 63*, 1–9.
56. Spencer, T., Biederman, J., Wilens, T., and Faraone, S.V. (1998) Adults with Attention-Deficit/Hyperactivity Disorder: A Controversial Diagnosis, *J. Clin. Psychiatry 59* (*Suppl. 7*), 59–68.
57. Biederman, J., Faraone, S.V., Spencer, T., Wilens, T., Norman, D., Lapey, K.A., Mick, E., Lehman, B.K., and Doyle, A. (1993) Patterns of Psychiatric Comorbidity, Cognition and Psychosocial Functioning in Adults with Attention Deficit Hyperactivity Disorder, *Am. J. Psychiatry 150*, 1792–1798.
58. Bell, J.G., Sargent, J.R., Tocher, D.R., and Dick J.R. (2000) Red Blood Cell Fatty Acid Composition in a Patient with Autistic Spectrum Disorder: A Characteristic Abnormality in Neurodevelopmental Disorders? *Prostaglandins Leukotrienes Essent. Fatty Acids 63*, 21–25.
59. Vancassel, S., Durand, G., Barthelemy, C., Lejeune, B., Martineau, J., Guilloteau, D., Andres, C., and Chalon, S. (2001) Plasma Fatty Acid Levels in Autistic Children, *Prostaglandins Leukotrienes Essent. Fatty Acids 65*, 1–7.
60. Taylor, K.E., Higgins, C.J., Calvin, C.M., Hall, J.A., Easton, T., McDaid, A.M., and Richardson, A.J. (2000) Dyslexia in Adults Is Associated with Clinical Signs of Fatty Acid Deficiency, *Prostaglandins Leukotrienes Essent. Fatty Acids 63*, 75–78.
61. Pawlosky, R.J., and Salem, N., Jr. (1999) Alcohol Consumption in Rhesus Monkeys Depletes Tissues of Polyunsaturated Fatty Acids and Alters Essential Fatty Acid Metabolism, *Alcohol Clin. Exp. Res. 23*, 311–317.
62. Simon, J.A., Fong, J., Bernert, J.T., and Browner, W.S. (1996) Relation of Smoking and Alcohol Consumption to Serum Fatty Acids, *Am. J. Epidemiol. 144*, 325–334.
63. Kuriki, K., Nagaya, T., Tokudome, Y., Imaeda, N., Fujiwara, N., Sata, J., Goto, C., Ikeda, M., Maki, S., Tajima, K., and Tokudome, S. (2003) Plasma Concentrations of (n-3) Highly Unsaturated Fatty Acids Are Good Biomarkers of Relative Dietary Fatty Acids: A Cross-Sectional Study, *J. Nutr. 133*, 3643–3650.
64. Fox, H., Ross, B.M., Tocher, D., Horrobin, D., Glen, I., and St. Clair, D. (2003) Degradation of Specific Polyunsaturated Fatty Acids in Red Blood Cells Stored at –20°C Proceeds Faster in Patients with Schizophrenia When Compared to Healthy Controls, *Prostaglandins Leukotrienes Essent. Fatty Acids 69*, 291–297.
67. Rinehart, N.J., Bradshaw, J.L., Brereton, A.V., and Tonge, B.J. (2003) A Clinical and Neurobehavioural Review of High-Functioning Autism and Asperger's Disorder, *Aust. N.Z. J. Psychiatry 36*, 762–770.
66. Foster, B., and King, B.H. (2003) Asperger Syndrome: To Be or Not to Be? *Curr. Opin. Pediatr. 15*, 491–494.
67. Yao, J., Stanley, J.A., Reddy, R.D., Keshavan, M.S., and Pettegrew, J.W. (2002) Correlations Between Peripheral Polyunsaturated Fatty Acid Content and *in vivo* Membrane Phospholipid Metabolites, *Biol. Psychiatry 15*, 823–830.

[Received August 18, 2003, and in final form and accepted February 3, 2004]

Dietary Linoleic Acid-Induced Hypercholesterolemia and Accumulation of Very Light HDL in Steers

Valérie Scislowski, Denys Durand*, Dominique Gruffat, and Dominique Bauchart

Institut National de la Recherche Agronomique (INRA), Research Unit on Herbivores, Nutrient and Metabolism Group, 63122 Saint Genès-Champanelle, France

ABSTRACT: This experiment was designed to study the effects in fattening steers of n-6 PUFA supplementation on the plasma distribution and chemical composition of major lipoproteins (TG-rich lipoproteins: $d < 1.006$ g/mL; intermediate density lipoproteins + LDL: $1.019 < d < 1.060$ g/mL; light HDL: $1.060 < d < 1.091$ g/mL; and heavy HDL: $1.091 < d < 1.180$ g/mL). For a period of 70 d, animals [454 ± 20 d; 528 ± 36 kg (mean ± SD)] were given a control diet (diet C, $n = 6$) consisting of hay and concentrate mixture (54 and 46% of diet dry matter, respectively) or the same diet supplemented with sunflower oil (4% of dry matter), given either as crushed seeds (diet S, $n = 6$) or as free oil continuously infused into the duodenum through a chronic canula to avoid ruminal PUFA hydrogenation (diet O, $n = 6$). Plasma lipids increased in steers given diet S (×1.4, $P < 0.05$) and diet O (×2.3, $P < 0.05$), leading to hyperphospholipemia and hypercholesterolemia. With diet S, hypercholesterolemia was associated with higher levels of light (×1.4, $P < 0.05$) and heavy HDL (×1.3, NS). With diet O, it was linked to higher levels of light HDL (×1.8, $P < 0.005$) and to very light HDL accumulation within density limits of 1.019 to 1.060 g/mL, as demonstrated by the apolipoprotein A-I profile. Diet O favored incorporation of 18:2n-6 into polar (×2.2, $P < 0.05$) and neutral lipids (×1.5 to ×8, $P < 0.05$) at the expense of SFA, MUFA, and n-3 PUFA. Thus, protection of dietary PUFA against ruminal hydrogenation allowed them to accumulate in plasma lipoproteins, but the effects of hypercholesterolemia on animal health linked to very light HDL accumulation remain to be elucidated.

Paper no. L9404 in *Lipids 39*, 125–133 (February 2004).

Cardiovascular disease is the main cause of death in humans in industrialized countries. It is closely related to dietary conditions, particularly to the amount and type of FA ingested (1). The PUFA content of human diets is low in comparison with that of saturated FA (SFA), since the quantity of animal fats available is twice that of vegetable oils (2). Unlike feeding monounsaturated FA (MUFA) and PUFA, feeding SFA and *trans*-MUFA increases the LDL cholesterol/HDL cholesterol ratio in plasma, which is one of the main risk factors for cardiovascular disease (3,4). Therefore, dietary lipids, in addition to their contribution to energy needs (33% energy), should provide 8, 20, and 5% of this energy from SFA, MUFA, and PUFA, respectively (1). Moreover, the optimal n-6/n-3 PUFA ratio must be close to 5 for the maximum beneficial effect (1). Therefore, beef in which the PUFA content represents less than 7% of total FA (5) is considered unfavorable for human health.

To make bovine products (meat and milk) more attractive for consumption, many studies have aimed at increasing its PUFA/SFA ratio by nutritional means. Ruminants have been given rations containing high levels of lipids rich in PUFA (6) of plant origin either as crushed or extruded seeds or as free oil (7). In these nutritional studies, the authors have focused mainly on the impact on rumen metabolism and on the digestibility of lipids, animal performance, and the nutritional and organoleptic quality of the meat (7,8). Moreover, numerous data have been obtained from lactating cows concerning the effect of PUFA supplementation on animal metabolism. The main effects are increases in plasma total lipids, cholesterol, TG, phospholipids (PL), and nonesterified FA (7,9). One of the major consequences can be a lipid infiltration of the liver promoted by a higher uptake of nonesterified FA (9–12). This favors the appearance of ketoacidosis, to the detriment to the health and reproductive performance of the animal (9). Other studies have demonstrated that the type of FA influences ovarian structures and reproductive performance (13–15), particularly, that dietary PUFA can inhibit prostaglandin production (16). However, in none of these studies has much notice been taken of the consequences of such PUFA supplementation on lipoprotein metabolism.

In mammals, dietary FA are known to modify lipids and lipoprotein metabolism. The lowering effect of PUFA on plasma LDL cholesterol is well documented in humans and other LDL mammals (1,3,4). By contrast, in the bovine, an HDL mammal (9), the effects of dietary PUFA on lipoprotein metabolism have not been clearly defined since they depend on the composition and degree of protection against biohydrogenation (17).

The present experiment was designed to determine the effects of dietary n-6 PUFA on plasma density distribution and the chemical composition of lipoproteins in fattening steers. Sunflower oil, a source of dietary n-6 PUFA, was given either as crushed seeds incorporated into the ration, favoring partial biohydrogenation of PUFA by rumen bacteria ("unprotected" form), or as free oil continuously infused into the duodenum, avoiding ruminal PUFA hydrogenation ("protected" form).

*To whom correspondence should be addressed.
E-mail: durand@clermont.inra.fr

Abbreviations: apo, apolipoprotein(s); CE, cholesteryl esters; FC, free cholesterol; IDL, intermediate density lipoproteins; MUFA, monounsaturated FA; NS, nonsignificant; PL, phospholipids; SFA, saturated FA, SR-BI, scavenger receptor class B type I; TGRLP, TG-rich lipoproteins; UFA, unsaturated FA.

EXPERIMENTAL PROCEDURES

Animals and diets. Experiments were performed using 18 crossbred Charolais × Salers steers [454 ± 20 d old; live weight: 528 ± 36 kg (mean ± SD)] and covered a 70-d period. Animals were randomly divided into three groups ($n = 6$) on the basis of live weight and daily gain. The control diet (diet C) consisted of 540 g natural-grass hay and 460 g concentrate on a dry matter basis. The average composition of the concentrate mixture was (in g/kg) 575 corn seed, 240 soybean meal, 120 dehydrated alfalfa, 20 cane molasses, 25 urea, and 20 vitamin and mineral mix. The two experimental diets consisted of the same basic diet to which was added 40 g sunflower oil per kilogram DM, given as sunflower seeds incorporated into the feed (diet S) or as sunflower oil continuously infused into the proximal duodenum through a chronic canula (diet O). The three diets were designed to be isoenergetic and isonitrogenous. Ingestion of DM per day was 6.702 (±0.986), 6.797 (±0.965), and 6.730 (±0.967) kg per animal in diet groups C, S, and O, respectively. The FA composition of the three diets is given in Table 1. Crushed sunflower seeds and the corresponding free oil were provided by Vamo Mills Society (Lezoux, France).

Blood samples. Blood samples (300 mL) were collected at the end of the experimental period and just before the morning meal from the jugular vein in Na_2-EDTA, Na-azide, and Merthiolate (final concentration 3 mM, 0.01 and 0.001%, respectively). Plasma was separated by centrifugation at 2700 × *g* for 10 min at 15°C in a Centrikon H-401 ultracentrifuge equipped with an A6-14 fixed-angle rotor (Kontron Analysis Division, Zürich, Switzerland). Five 500-µL fractions of plasma were stored at −20°C until lipid and apolipoprotein (apo) analysis, and 120 mL of plasma was kept at 4°C for 48 h maximum until lipoprotein fractionation.

Lipoprotein isolation. To determine the density distribution of lipoprotein subfractions, separation of plasma lipoproteins was performed in a Centrikon T-2060 ultracentrifuge equipped with a TST 41-14 swinging-bucket rotor (Kontron Analysis Division). TG-rich lipoproteins (TGRLP, $d < 1.018$ g/mL) were first removed from plasma by ultracentrifugal flotation at 205,000 × *g* for 16 h at 15°C (12). From this plasma without TGRLP, lipoprotein fractions were then isolated by ultracentrifugation in a discontinuous density gradient as described by Bauchart *et al.* (18). These gradients were subsequently centrifuged for 46 h at 205,000 × *g* at 15°C and divided into 22 successive fractions ranging in density from 1.006 to 1.180 g/mL. Lipoprotein fractions were then dialyzed at 4°C for 7 h against a buffer (pH 8.6) containing 0.02 M NH_4HCO_3, 1.5 mM NaN_3, and 1 mM Na_2-EDTA in a Gibco BRL Microdialysis System (Bethesda Research Laboratories, Rockville, MD) equipped with membranes with cutoff at 12,000–14,000 Da M.W.

As previously described by Bauchart *et al.* (18), TGRLP were defined as lipoproteins of $d < 1.018$ g/mL, intermediate density lipoproteins (IDL) as lipoproteins of d 1.018 to 1.026 g/mL, LDL as lipoproteins of $d = 1.026$ to 1.060 g/mL, light HDL as lipoproteins of $d = 1.060$ to 1.091 g/mL, and heavy HDL as lipoproteins of $d = 1.091$ to 1.180 g/mL.

To analyze the FA composition of the major lipid classes (neutral and polar lipids) of these main lipoprotein families, lipoproteins were purified from plasma by sequential ultracentrifugal flotation according to Leplaix-Charlat (19) using a Centrikon T-2060 ultracentrifuge equipped with the TFT 38-70 fixed-angle rotor (Kontron Analysis Division). Briefly, the density of plasma without TGRLP was adjusted to 1.060 g/mL by addition of potassium bromide (KBr) salt, and IDL + LDL were isolated after 20 h of centrifugation at 120,000 × *g* at 15°C. The density of the remaining plasma was then adjusted to 1.091 and 1.180 g/mL with KBr salt to isolate light and heavy HDL, respectively, by centrifugation (24 h, 120,000 × *g*, 15°C).

Chemical analysis. Concentrations of the different lipid classes (free cholesterol, FC; cholesteryl esters, CE; TG; PL) in plasma or in lipoprotein subfractions were determined enzymatically as described previously by Leplaix-Charlat *et al.* (12). TG and FC analyses used the reagent Kit Cholesterol Liquide and Cholesterol Libre Enz. Color, respectively, supplied by Biotrol Diagnostic (Chennevières-lès-Louvres, France). TG content was determined using the reagent Kit PAP 150 (ref. 61236) supplied by BioMérieux (Charbonnières-les-Bains, France). PL were determined by the enzymatic method of Trinder using a BioMérieux kit PAP 150 (ref. 61491).

Immunological analysis. Concentrations of apoA-I and apoB in plasma and in lipoprotein fractions were estimated by the technique of Mancini adapted to the bovine by Auboiron

TABLE 1
Composition of Main FA Expressed as the Percentage of Total FA and as g/kg Dry Matter (DM)/d of the Three Diets Given to Steers[a]

	Diet C		Diet S		Diet O	
FA	% of total FA	g/kg DM/d	% of total FA	g/kg DM/d	% of total FA	g/kg DM/d
14:0	1.4	0.3	0.5	0.3	0.6	0.3
16:0	20.8	4.1	11.0	6.0	11.1	5.7
16:1	1.4	0.3	0.5	0.3	0.6	0.3
18:0	2.4	0.5	3.7	2.0	3.4	1.8
18:1	12.8	2.6	20.5	11.2	19.3	10.0
18:2n-6	30.2	6.0	52.2	28.6	52.0	26.8
18:3n-3	21.3	4.2	7.6	4.2	8.3	4.3
Others	9.7	2.0	4.0	2.2	4.7	2.3

[a]Steers were fed either the control diet (diet C, $n = 6$), the same basal diet supplemented with sunflower seeds (diet S, $n = 6$), or the same basal diet with sunflower oil infused into the duodenum (diet O, $n = 6$).

et al. (20). Briefly, this radial immunodiffusion used antiserum to bovine apoA-I (purified from HDL) and to bovine apoB (purified from LDL) raised in rabbits. The diameters of precipitation rings were proportional to the antigen concentration given by a standard range of bovine apoA-I and apoB, respectively.

FA analysis. Total lipids of the three main lipoprotein fractions (IDL + LDL, light HDL, and heavy HDL) were extracted according to the method of Folch *et al.* (21). Their two main components, polar lipids (PL) and neutral lipids (CE and TG), were prepared after isolation of the different lipids by semi-preparative TLC using glass plates covered with lipid-free Kieselgel. FA were extracted from polar and neutral lipids and converted into methyl esters according to a method described earlier (22). The FA composition of polar and neutral lipids was determined by GLC using a DI 200 chromatograph (Perichrom, Saulx les Chartreux, France) with a CP-Sil 88 glass capillary column (100 m length, 0.25 mm i.d.). GLC conditions were as follows: the oven temperature was programmed at 70°C for 30 s, then ramped from 70 to 175°C at 20°C/min, held at 175°C for 25 min, ramped from 175 to 215°C at 10°C/min, and finally held at 215°C for 41 min; injector and detector temperatures were 235 and 250°C, respectively; hydrogen was the carrier gas (H_2 flow: 1.1 mL/min) in conditions of split injection (1:50). FA were identified by comparing their retention times with those of FA standards (Supelco, Bellefonte, PA). Chromatographic signals were analyzed by Winilab II Chromatography Data System software (Perichrom).

Statistical analysis. All data were subjected to analysis by ANOVA using the general linear model procedure of SAS (23). Treatment differences were considered significant at $P < 0.05$. When the diet effect was statistically significant, treatment means of the three groups were compared using Student's *t*-test (24).

RESULTS

Plasma lipids and apolipoproteins. Compared with the control diet, supplementation with 4% sunflower oil led to hyperlipemia, the effect being more marked with diet O (×2.3, $P < 0.05$) than with diet S (×1.4, $P < 0.05$) (Table 2). Hyperlipemia was essentially caused by increases in PL (×1.4, $P < 0.05$, and ×2.1, $P < 0.05$, with diets S and O, respectively) and in cholesterol levels (×1.4, $P < 0.05$, and ×2.5, $P < 0.05$, with diets S and O, respectively), whereas triglyceridemia remained constant (Table 2). The plasma concentration of apoB, specific to TGRLP and LDL, was not modified with the lipid supplements (diets S and O), whereas the concentration of apoA-I, which is characteristic of the HDL subfractions, increased only following oil infusion (×1.8, $P < 0.05$) (Table 2).

Density distribution of plasma lipoproteins. The distribution of lipoprotein particles was determined as a function of their hydrated density. They were fractionated into 22 fractions by isopycnic density gradient ultracentrifugation and subsequently analyzed for their lipid and apo contents. Figure 1A–1D present total lipoproteins, apoB and apoA-I, FC and CE, and TG and PL contents, respectively.

Dietary treatments affected the physicochemical properties of lipoproteins, particularly diet O, which led to a higher concentration of total lipoprotein (×2.0; $P < 0.0001$) and to a shift in the profile to fractions of lower densities (Figs. 1A–1D). From apoA-I and apo B contents (Fig. 1B), five classes of lipoparticles were constituted, and their chemical compositions were determined by regrouping the subfractions as shown in Table 3.

TGRLP (fraction 1, $d < 1.018$ g/mL) represented a minor lipoprotein class (4% of total lipoproteins) in steers receiving diets C and S, and its concentration was higher with diet O (×1.5, $P < 0.05$; Table 3). In control steers, LDL (subfractions 6 to 11: 1.026 to 1.060 g/mL) accounted for 13% of the total lipoproteins (Fig. 1A, Table 3). In animals given diet O, the LDL concentration was 4.6 times higher than those given diet C ($P < 0.05$) (Table 3).

In the control group, HDL (subfractions 12 to 22: 1.060 to 1.180 g/mL) represented the main lipoprotein class (82% of total lipoproteins) (Fig. 1A, Table 3). On the basis of their hydrated density, HDL were divided into light HDL (subfractions 12 to 15) and heavy HDL (subfractions 16 to 22), which represented 66 and 34% of total HDL, respectively (Fig. 1A, Table 3). Compared with diet C, diet S led to higher concentrations

TABLE 2
Total Concentrations of the Major Plasma Lipids[a] and of Plasma Apolipoproteins (apo) B and A-I in Steers Fed One of Three Diets[b]

Component	Diet C	Diet S	Diet O
		mg/dL plasma	
Total lipids	284.3 ± 12.8[a]	396.8 ± 6.3[b]	612.4 ± 46.1[c]
PL	108.6 ± 5.0[a]	152.7 ± 3.7[b]	229.2 ± 14.0[c]
TG	15.3 ± 0.9[a]	15.8 ± 3.1[a]	15.2 ± 2.6[a]
FC	16.9 ± 0.9[a]	24.6 ± 0.8[b]	44.5 ± 3.9[c]
CE	134.3 ± 6.1[a]	191.2 ± 5.0[b]	316.1 ± 26.7[c]
ApoB	19.9 ± 3.5[a]	18.8 ± 2.5[a]	25.7 ± 2.9[a]
ApoA-I	72.1 ± 14.5[a]	86.5 ± 9.5[a]	129.1 ± 12.1[b]

[a]PL, phospholipids; FC, free cholesterol; CE, cholesteryl esters.
[b]Steers were fed either the control diet (diet C, $n = 6$), the same basal diet supplemented with sunflower seeds (diet S, $n = 6$), or the same basal diet, with sunflower oil infused into the duodenum (diet O, $n = 6$) for 70 d. Results are expressed as mean ± SE. [a,b,c] = significant difference between diets for the same lipid class, $P < 0.05$.

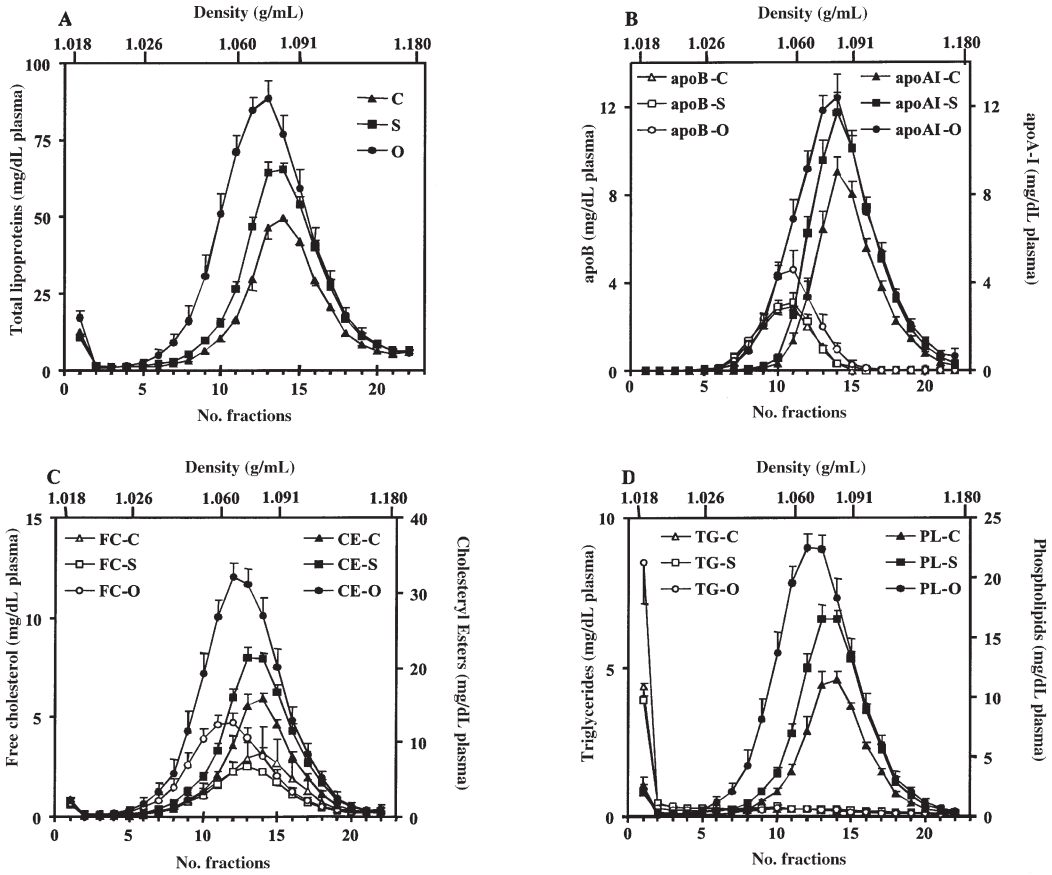

FIG. 1. Plasma concentration and chemical composition of lipoprotein subfractions isolated by density gradient ultracentrifugation from the plasma of steers fed either the control diet (diet C: △, ▲, $n = 6$), the same basal diet supplemented with sunflower seeds (diet S: □, ■, $n = 6$), or the same basal diet with sunflower oil infused into the duodenum (diet O: ○, ●, $n = 6$) for 70 d. (A) Plasma concentration of lipoprotein. (B) Plasma concentration of apolipoprotein (apo) A-I (open symbols) and apoB (solid symbols). (C) Plasma concentration of free cholesterol (FC: open symbols) and esterified cholesterol (CE: solid symbols). (D) Plasma concentration of TG (open symbols) and phospholipids (PL: solid symbols). Results are expressed as mean ± SD.

of plasma light (×1.4, $P < 0.05$) and heavy HDL [×1.3, nonsignificant (NS)] (Table 3). This effect was more pronounced in animals given diet O, especially for the light HDL class (×1.8, $P < 0.05$) (Fig. 1A and Table 3).

From the distribution of apo according to lipoprotein density (Fig. 1B), partially protected (diet S) or totally protected (diet O) dietary PUFA led to higher concentrations of apoA-I in fractions 12 to 18 compared with the control group, corresponding to light HDL (×1.4 and ×1.6 in groups S and O, respectively, $P < 0.05$) and heavy HDL (×1.4 in groups S and O, $P < 0.05$) (Table 3). Furthermore, a shift of the apoA-I profile to HDL fractions of lower densities was observed especially in steers fed diet O (Fig. 1B), leading to higher apoA-I levels in fractions 8 to 11 in the density range of the IDL + LDL family (×7, $P < 0.0005$; Table 3). Concerning the apoB profile, diet O increased apoB concentrations (Fig. 1B), particularly in fractions 6 to 11, corresponding to the LDL fractions (×1.4, $P < 0.05$; Table 3).

Chemical composition of lipoprotein classes. Lipid supplementation led to higher concentrations of CE (Fig. 1C) and PL (Fig. 1D) in the density range of 1.053 to 1.108 g/mL for diet S, and of 1.030 to1.119 g/mL for diet O. Moreover, lipid treatments led to a shift of CE and PL profiles to fractions of lower densities as observed for the apoA-I profile, particularly with diet O (Table 3). Oil infusion led to an enrichment of TGRLP in TG (+40%, $P < 0.005$) to the detriment of CE (–35%, $P < 0.05$) (Table 3). In control steers, CE, which were abundant in light HDL (32% of lipoprotein weight), were increased in steers given diet O (+16%, $P < 0.05$). The same enrichment was noted for IDL (+53%, NS), LDL (+42%, NS), and heavy HDL (+19%, NS) to the detriment of FC, PL, or TG (Table 3).

FA composition of plasma lipoproteins. The FA compositions of neutral and polar lipids are given in Tables 4 and 5, respectively, for the main lipoprotein classes.

For TGRLP, diet S did not modify the FA composition in neutral (Table 4) and polar lipids compared with diet C (Table 5). Diet O led to an increase in the PUFA/SFA ratio in neutral (×5, $P < 0.05$) and polar lipids (×1.3, $P < 0.05$) owing to the enrichment in 18:2n-6 (×8 and ×2.2, respectively, $P < 0.05$), to the detriment of 16:0 in neutral lipids (–38%, $P < 0.05$). By

TABLE 3
Chemical Composition (mean wt%) and Concentration (mg/dL) of the Major Lipoprotein Classes and of ApoB and ApoA-I from the Plasma of Steers Fed One of Three Diets[a]

	Lipoprotein class				
	TGRLP	IDL	LDL	Light HDL	Heavy HDL
Fractions	1	2 to 5	6 to 11	12 to 15	16 to 22
Density limits (g/mL)	<1.018	1.018 to 1.026	1.026 to 1.060	1.060 to 1.091	1.091 to 1.180
Diet C					
FC	5 ± 1	7 ± 3	10 ± 2	9 ± 5	7 ± 4
CE	20 ± 2[a]	15 ± 4	24 ± 5	32 ± 1[a]	26 ± 3
TG	36 ± 2[a]	34 ± 3	16 ± 6	2 ± 1	1 ± 1
PL	19 ± 4	22 ± 2	22 ± 3	22 ± 2	20 ± 1
Proteins	20 ± 1	22 ± 2	28 ± 2	35 ± 2	46 ± 4
Lipoprotein concentration (mg/dL)	12 ± 1[a]	4 ± 1	40 ± 3[a]	168 ± 8[a]	88 ± 6
ApoB concentration (mg/dL)	nd	nd	9 ± 1[a]	3 ± 1	ND
ApoA-I concentration (mg/dL)	ND	ND	2 ± 1[a]	27 ± 3[a]	14 ± 1[a]
Diet S					
FC	5 ± 1	9 ± 3	9 ± 1	5 ± 1	4 ± 1
CE	20 ± 3[a]	14 ± 5	25 ± 5	33 ± 1[a]	28 ± 2
TG	36 ± 3[a]	33 ± 4	13 ± 5	2 ± 1	1 ± 1
PL	19 ± 2	24 ± 2	26 ± 1	25 ± 1	21 ± 1
Proteins	19 ± 1	20 ± 3	27 ± 2	35 ± 1	46 ± 4
Lipoprotein concentration (mg/dL)	11 ± 1[a]	5 ± 1	61 ± 7[a]	230 ± 10[b]	116 ± 10
ApoB concentration (mg/dL)	nd	nd	10 ± 1[a]	4 ± 1	ND
ApoA-I concentration (mg/dL)	ND	ND	3 ± 1[a]	38 ± 4[b]	20 ± 1[b]
Diet O					
FC	4 ± 1	5 ± 1	6 ± 1	6 ± 1	4 ± 1
CE	13 ± 2[b]	23 ± 4	34 ± 2	37 ± 1[b]	31 ± 2
TG	50 ± 3[b]	33 ± 4	10 ± 5	1 ± 1	1 ± 1
PL	14 ± 2	16 ± 4	25 ± 1	25 ± 1	21 ± 1
Proteins	19 ± 1	23 ± 1	25 ± 2	31 ± 2	43 ± 4
Lipoprotein concentration (mg/dL)	17 ± 2[b]	5 ± 2	182 ± 32[b]	309 ± 22[c]	121 ± 17
ApoB concentration (mg/dL)	nd	nd	13 ± 1[b]	7 ± 2	ND
ApoA-I concentration (mg/dL)	ND	ND	14 ± 3[b]	43 ± 3[b]	21 ± 1[b]

[a]Steers were fed either the control diet (diet C, $n = 6$), the same basal diet supplemented with sunflower seeds (diet S, $n = 6$), or the same basal diet with sunflower oil infused into the duodenum (diet O, $n = 6$) for 70 d. Results are expressed as mean ± SE. nd, not detectable, ND, not determined; TGRLP, TG-rich lipoproteins; IDL, intermediate density lipoproteins; for other abbreviations see Table 2. [a,b,c] = significant difference between diets for the same lipoprotein class, $P < 0.05$.

contrast, in polar lipids, the unsaturated FA (UFA)/SFA ratio was not modified with diet O owing to a concomitant lowering effect on MUFA (–31%, $P < 0.05$).

In the IDL + LDL class, diet S did not modify PUFA/SFA and UFA/SFA ratios in polar lipids because the enrichment in n-6 PUFA (×1.3, $P < 0.05$) was at the expense of n-3 PUFA (–58%, $P < 0.05$). In neutral lipids, the enrichment in n-6 PUFA induced by diet S (×1.2, $P < 0.05$) and the simultaneous decrease in SFA (–22%, $P < 0.05$) led to higher PUFA/SFA (×1.5, $P < 0.05$) and UFA/SFA ratios (×1.5, $P < 0.05$). With diet O, changes in the FA composition in polar and neutral lipids of the IDL + LDL concerned the enrichment in 18:2n-6 (×2.1 and ×1.6, respectively, $P < 0.05$), at the expense of MUFA (–57 and –52%, respectively, $P < 0.05$) and n-3 PUFA (–82 and –67%, respectively, $P < 0.05$). In neutral lipids, the SFA content decreased with diet O compared with diet C (–31%, $P < 0.05$).

Concerning the light HDL, the PUFA/SFA and UFA/SFA ratios in polar lipids were not modified by lipid supplements (as in the polar lipids of IDL + LDL) since the enrichment in 18:2n-6 (×1.4, $P < 0.05$) was expressed at the expense of n-3 PUFA (–81%, NS) and 18:1 (–50%, $P < 0.05$) (Table 5). In neutral lipids of light HDL, PUFA/SFA and UFA/SFA ratios increased with diet S (×1.4 and ×1.3, respectively, NS), and particularly with diet O (×2 and ×1.6, respectively, $P < 0.05$), owing to larger incorporation of 18:2n-6 (×1.5, $P < 0.05$) into lipoparticles (Table 4).

In the heavy HDL, diet O led to effects on the FA composition of polar and neutral lipids similar to those observed in the neutral lipids of light HDL.

DISCUSSION

Dietary lipids have been studied in humans and in rodents (3,25,26), mainly with respect to their effects on the pathogenesis of hyperlipidemia and the associated risk for cardiovascular disease, whereas in bovine animals, they have been studied

TABLE 4
FA Composition of Neutral Lipids of the Main Lipoprotein Classes Isolated by Ultracentrifugal Flotation in Steers Fed One of Three Diets[a]

Density limits	TGRLP <1.018				IDL + LDL 1.018 to 1.060				Light HDL 1.060 to 1.091				Heavy HDL 1.091 to 1.180			
(g/mL)	Diet C	Diet S	Diet O	SEM	Diet C	Diet S	Diet O	SEM	Diet C	Diet S	Diet O	SEM	Diet C	Diet S	Diet O	SEM
14:0	3.5^{a}	3.6^{a}	1.7^{b}	0.2	1.4^{a}	1.0^{a}	0.3^{b}	0.1	0.8	0.8	0.5	0.3	1.0	0.5	0.3	0.1
15:0	3.9	2.6	3.2	0.3	1.3	1.0	0.5	0.5	1.2	0.7	0.4	0.5	nd	nd	nd	
16:0	26.9^{a}	24.5^{a}	16.6^{b}	1.3	12.2	9.6	8.9	1.0	11.0	7.9	8.2	1.0	12.9	11.5	10.5	2.0
Sum of 16:1	2.9	2.8	1.0	0.5	2.2	1.5	0.3	0.6	2.3	1.7	0.8	0.7	2.5	1.8	0.8	0.4
17:0	3.2	2.2	2.8	0.4	3.6	2.2	1.8	0.5	2.0	2.2	0.9	0.6	4.1^{a}	2.9^{a,b}	1.3^{b}	0.4
18:0	30.7	33.4	28.5	1.1	14.1	11.6	10.4	1.2	1.9	1.5	1.0	0.2	3.9	2.3	1.9	1.2
Sum of 18:1	15.2	15.0	13.6	0.8	10.4^{a}	11.4^{a}	6.2^{b}	0.4	11.5^{a}	9.9^{a}	2.6^{b}	1.1	12.3	11.6	5.2	1.6
18:2n-6	2.2^{a}	2.6^{a}	17.4^{b}	0.6	41.4^{a}	48.5^{a}	64.6^{b}	1.8	48.0^{a}	58.5^{b}	73.9^{c}	1.8	46.2^{a}	51.8^{a}	71.3^{b}	3.2
18:3n-6	1.6^{a}	3.6^{b}	2.7^{a,b}	0.3	1.9^{a}	2.5^{a}	0.7^{b}	0.2	1.2^{a}	2.1^{b}	0.5^{c}	0.1	1.1^{a}	1.6^{a}	0.3^{b}	0.2
18:3n-3	0.5	0.3	0.7	0.1	3.3^{a}	2.4^{a,b}	0.9^{b}	0.4	5.9^{a}	5.7^{a}	0.6^{b}	0.2	7.1^{a}	5.4^{a}	0.9^{b}	0.5
CLA	0.7	1.2	1.0	0.1	0.3	0.4	0.2	0.1	0.5	0.1	nd	0.1	nd	0.1	nd	
Sum of 20:1	1.4^{a}	2.9^{b}	2.7^{b}	0.2	0.6^{a}	0.6^{a}	0.1^{b}	0.1	0.6	0.4	0.3	0.1	nd	0.1	0.2	0.1
20:2n-6	0.3	0.2	0.3	0.1	0.3	0.3	0.2	0.1	0.4^{a}	0.5^{b}	0.3^{c}	0.1	0.4	0.3	0.2	0.1
20:4n-6	0.3	0.2	0.1	0.1	1.0	1.0	1.1	0.2	1.3^{a}	1.5^{a}	0.7^{b}	0.1	1.3	1.5	1.2	0.3
20:5n 3	0.3	0.6	0.4	0.2	1.1	1.0	0.4	0.2	1.2	0.5	0.5	0.2	1.4	1.4	1.2	0.6
Sum of 22:1	0.5	nd	1.3	0.2	1.2	2.2	0.5	0.6	2.4	2.5	1.7	0.6	0.8	0.6	0.7	0.2
22:5n 3	nd	nd	nd		0.4	0.1	0.1	0.1	0.4	nd	nd		0.3	0.4	0.3	0.3
SFA	70.1^{a}	67.9^{a}	54.9^{b}	3.1	33.3^{a}	26.0^{b}	23.1^{b}	0.7	17.1^{a}	13.5^{a,b}	11.5^{b}	0.9	22.6	17.7	14.2	3.1
MUFA	23.1	22.7	20.2	0.9	15.7^{a}	16.3^{a}	7.6^{b}	1.3	19.8^{a}	15.6^{b}	5.7^{c}	0.7	16.0^{a}	14.4^{a}	7.1^{b}	1.5
PUFA	6.8^{a}	9.5^{b}	24.9^{c}	1.0	51.0^{a}	57.7^{b}	69.3^{c}	1.1	63.1^{a}	70.9^{b}	82.8^{c}	1.1	61.4	67.9	78.7	4.3
n-6 PUFA	4.7^{a}	6.6^{a}	21.4^{b}	0.9	44.9^{a}	52.7^{b}	67.2^{c}	1.6	52.5^{a}	64.2^{b}	81.4^{c}	1.5	51.3^{a}	58.1^{a}	76.0^{b}	3.3
n-3 PUFA	1.4	1.2	2.6	0.2	5.7^{a}	4.5^{a,b}	1.9^{b}	0.7	10.1^{a}	6.6^{b}	1.4^{c}	0.6	10.1	9.7	2.7	2.2
UFA/SFA	0.4^{a}	0.5^{a}	0.8^{b}	0.1	2.0^{a}	2.9^{b}	3.4^{b}	0.1	4.9^{a}	6.5^{a,b}	7.8^{b}	0.5	3.6	5.1	7.3	1.1
PUFA/SFA	0.1^{a}	0.1^{a}	0.5^{b}	0.1	1.5^{a}	2.2^{b}	3.0^{c}	0.1	3.7^{a}	5.3^{a}	7.3^{b}	0.4	2.8	4.3	6.8	1.1

[a]Steers were fed either the control diet (diet C, $n = 6$), the same basal diet supplemented with sunflower seeds (diet S, $n = 6$), or the same basal diet with sunflower oil infused into the duodenum (diet O, $n = 6$) for 70 d. Results are expressed as mean ± SEM. SFA, saturated FA; MUFA, monounsaturated FA; UFA, unsaturated FA; for other abbreviations see Table 3. ^{a,b,c} = significant difference between diets for the same lipoprotein class, $P < 0.05$.

TABLE 5
FA Composition of Polar Lipids of the Main Lipoprotein Classes Isolated by Ultracentrifugal Flotation in Steers Fed One of Three Diets[a]

Density limits	TGRLP <1.018				IDL + LDL 1.018 to 1.060				Light HDL 1.060 to 1.091				Heavy HDL 1.091 to 1.180			
(g/mL)	Diet C	Diet S	Diet O	SEM	Diet C	Diet S	Diet O	SEM	Diet C	Diet S	Diet O	SEM	Diet C	Diet S	Diet O	SEM
14:0	1.7	2.3	1.6	0.4	0.4^{a}	0.3^{b}	0.2^{b}	0.1	0.5^{a}	0.3^{b}	0.3^{b}	0.1	0.4	0.2	0.3	0.1
15:0	1.2	1.7	0.9	0.2	0.2	0.3	0.3	0.2	0.3	0.3	0.3	0.2	nd	nd	0.1	
16:0	12.3	13.9	11.5	1.1	16.8	15.6	13.5	1.1	18.7	14.5	13.5	1.4	18.8^{a}	16.5^{b}	14.4^{c}	0.4
Sum of 16:1	1.8	2.4	1.8	0.6	1.7	0.5	0.3	0.4	1.8	0.5	0.4	0.6	0.6	1.1	0.4	0.3
17:0	1.6	2.3	1.9	0.5	2.5	1.6	2.4	0.3	2.8	2.2	2.4	0.5	3.9^{a}	1.1^{b}	2.1^{b}	0.3
18:0	16.7	14.1	16.3	0.7	23.4	26.6	25.6	0.9	27.6	26.8	24.9	1.4	25.8	25.2	24.1	0.6
Sum of 18:1	25.8^{a}	28.7^{a}	14.5^{b}	0.3	15.5^{a}	17.3^{a}	6.7^{b}	0.4	15.5^{a}	17.0^{b}	7.8^{c}	0.2	16.0^{a}	17.8^{b}	8.9^{c}	0.4
18:2n-6	15.9^{a}	17.3^{a}	34.5^{b}	0.9	19.2^{a}	21.4^{a}	40.9^{b}	0.6	16.6^{a}	21.3^{a}	40.6^{b}	1.7	18.7	20.9	40.1	0.9
18:3n-6	nd	nd	nd		0.4	0.9	0.3	0.2	0.6	0.7	0.5	0.2	0.3^{a}	0.4^{a}	0.1^{b}	0.1
18:3n-3	1.5^{a}	0.8^{b}	0.6^{b}	0.1	1.9^{a}	1.5^{b}	0.4^{c}	0.1	1.5^{a}	1.3^{a}	0.3^{b}	0.2	1.6^{a}	1.2^{b}	0.3^{c}	0.1
CLA	1.2	1.7	1.6	0.1	1.0	0.4	0.1	0.3	0.3	0.5	0.1	0.1	0.1	0.1	0.1	0.1
Sum of 20:1	6.1	6.5	6.1	0.3	0.2	0.6	0.7	0.2	0.4	0.8	0.8	0.2	0.3	0.5	0.3	0.1
20:2n-6	1.8	0.9	0.5	0.2	1.4	3.6	2.0	0.7	2.7	3.9	1.7	0.5	2.9	2.9	1.9	0.3
20:4n-6	4.9^{a}	1.2^{b}	1.5^{b}	0.1	2.3	4.4	3.2	0.7	3.6	4.7	2.8	0.6	3.9	4.2	3.6	0.3
20:5n 3	2.2	2.5	1.6	0.5	3.8	0.8	0.4	0.8	1.4^{a}	0.7^{a,b}	0.3^{b}	0.2	2.2	1.4	1.2	0.5
22:5n 3	0.6	0.5	nd	0.1	2.6^{a}	0.6^{b}	0.7^{b}	0.4	0.7	1.1	0.3	0.3	1.0	0.9	0.7	0.5
SFA	34.5	35.3	33.6	0.6	43.9	45.0	42.7	0.7	50.2	44.8	42.7	2.8	49.3^{a}	43.7^{b}	41.1^{b}	0.9
MUFA	35.6^{a}	39.7^{a}	24.6^{b}	0.5	18.7^{a}	18.8^{a}	8.0^{b}	0.4	18.0^{a}	18.9^{a}	9.5^{b}	0.7	17.5^{a}	19.9^{a}	9.9^{b}	0.6
PUFA	29.8^{a}	24.9^{a}	41.8^{b}	1.2	37.4^{a}	36.2^{a}	49.3^{b}	0.8	31.8	36.4	47.8	3.3	33.2^{a}	36.4^{b}	49.1^{c}	0.7
n-6 PUFA	22.6^{a}	19.5^{a}	36.5^{b}	0.1	24.6^{a}	30.9^{b}	47.1^{c}	1.4	24.0^{a}	31.3^{a}	46.1^{b}	2.7	26.7^{a}	29.3^{a}	45.9^{b}	1.0
n-3 PUFA	4.8	3.8	2.2	0.8	11.7^{a}	4.9^{b}	2.1^{b}	1.2	7.4	4.5	1.4	0.7	6.3	7.0	3.1	1.4
UFA/SFA	1.9	1.8	2.0	0.1	1.3	1.2	1.3	0.1	1.0	1.2	1.4	0.1	1.0^{a}	1.3^{b}	1.4^{b}	0.1
PUFA/SFA	0.9^{a}	0.7^{a}	1.2^{b}	0.1	0.9^{a}	0.8^{a}	1.2^{b}	0.1	0.7	0.8	1.1	0.1	0.7^{a}	0.8^{b}	1.2^{c}	0.1

[a]Steers were fed either the control diet (diet C, $n = 6$), the same basal diet supplemented with sunflower seeds (diet S, $n = 6$), or the same basal diet with sunflower oil infused into the duodenum (diet O, $n = 6$) for 70 d. Results are expressed as mean ± SEM. ^{a,b,c} = significant difference between diets for the same lipoprotein class, $P < 0.05$. For abbreviations see Tables 3 and 4.

mainly for their impact on animal performance and on the nutritional and organoleptic properties of meat (6–8). It is known that the type of fat in the diet can modify lipid profiles as a result of modifications in lipoprotein metabolism (10,12,27), which can finally lead to an alteration of lipid metabolism in tissues (6–8). In this experiment with steers, we determined the consequences of dietary supplementation with sunflower oil rich in linoleic acid (18:2n-6) on the blood transport system of lipids (lipoproteins), a field that is poorly documented.

In the bovine, dietary FA are transported as TG to tissues by TGRLP for fat storage or for oxidation to produce energy (9). We demonstrated that the TGRLP level ($d < 1.018$ g/mL) increased only with the oil infusion, indicating that the effects of fat ingestion depend on the degree of unsaturation of the FA. Similar results were observed previously in adult sheep, where direct infusion of n-6 PUFA in the proximal duodenum increased the intestinal secretion of chylomicrons (28). The enrichment of TGRLP with TG at the expense of CE with the sunflower oil infusion seemed to be specific to ruminant animals, because in preruminant calves receiving soybean oil, the TGRLP level decreased and these lipoparticles were enriched in CE instead of TG (12).

The FA composition of the oil in diets S and O was similarly dominated by linoleic acid (51% of total FA) but affected the FA composition of TGRLP differently. Linoleic acid from the seeds could undergo extensive biohydrogenation in the rumen (60–95%), leading to absorption of less than 20% of dietary linoleic acid by the small intestine (29). Its low bioavailability would explain their low impact on the FA composition of lipids in TGRLP. In steers receiving an oil infusion, in which PUFA ruminal hydrogenation was avoided, linoleic acid was highly incorporated into TGRLP, mainly into TG, the major neutral lipid in these particles. Consequently, large amounts of linoleic acid were transferred into the muscle tissues during lipolysis of TG in the hydrophobic inner core of TGRLP catalyzed by the lipoprotein lipase. This process explains the twofold higher content of linoleic acid found in *rectus abdominis* and *longissimus thoracis* muscles, which elevated the PUFA/SFA ratio by 60% (30).

IDL and LDL are successively generated by the lipolytic cascade of TGRLP catalyzed by the lipoprotein lipase of extrahepatic tissues. This explains why modifications in the FA composition of their lipids were similar to those observed in TGRLP. In the bovine, IDL (1.018 to 1.026 g/mL) represent only 4% of total lipoproteins whatever the diet, probably resulting from the intense captation of these particles by the hepatic and muscle tissues (9). The plasma concentration of LDL (1.026 to 1.060 g/mL) increased only during the sunflower oil infusion, indicating that the degree of unsaturation of dietary FA was more important than the amount of dietary fat in modifying plasma LDL in the bovine. This result did not agree with the common concept accepted in humans of linoleic acid as a "cholesterol-lowering" FA, since its action occurs mainly in the LDL fraction (3), which is poorly represented in the bovine (15% of total lipoproteins).

The hypercholesterolemia observed in steers receiving the sunflower-rich diet was mainly related to their higher plasma concentrations of HDL. The density distribution of apoA-I indicated that supplementation with linoleic acid protected against ruminal hydrogenation induced the formation of very light HDL particles in the density range of LDL (1.026 to 1.060 g/mL). The appearance of very light HDL already has been described in cows fed a diet rich in sunflower oil and protected from ruminal hydrogenation (31), or in preruminant calves given a milk diet rich in soybean oil (12). According to Auboiron *et al.* (11), very light HDL can be generated by the transfer of lipid (PL, CL) and protein (apoC) surface components of TGRLP to the heavy HDL. Moreover, the presence of these very light HDL might be the result of two other mechanisms, one involving the LCAT enzyme and the other involving the catabolism of HDL.

A higher LCAT activity can lead to hypercholesterolemia, as previously shown in humans (32). In steers fed diet O, the high incorporation of linoleic acid into polar lipids of the HDL may facilitate the efflux of cholesterol from tissues and enhance the esterification process by LCAT (33,34). Moreover, accessibility and activity of the LCAT to its substrate on the HDL surface can be improved as a result of the modification of the spatial configuration of apoA-I induced by the changes in FA composition observed in light HDL (35). Cholesteryl linoleate will occupy more space in the inner core of HDL than when the lipids are poor in PUFA (36), favoring generation of very light HDL particles described in the calf as the largest (100 to 190 Å vs. 98 to 145 Å) and the least-dense particles of HDL (9,19). This accumulation of very light HDL would be amplified by the chronic low activity of plasma CETP (37) and of hepatic lipase (38) in the bovine compared to the human.

Yet another mechanism whereby lipid supplementation would favor plasma accumulation of very light HDL particles in steers is through a decrease in their turnover of blood. In steers fed lipid supplements, we can hypothesize that the higher PUFA content of HDL would decrease the recognition of HDL by the scavenger receptor class B type I (SR-BI) and/or the cubilin receptor (39,40), consequently depressing the clearance of HDL, which continue to accumulate CE *via* LCAT activity. In mice with a targeted disruption in the SR-BI gene, plasma cholesterol increased because of the formation of larger HDL (41).

In the bovine, the effects of hypercholesterolemia associated with HDL and with very light HDL accumulation in the blood are still unknown. We previously observed in our laboratory that the enrichment of lipoparticles with PUFA was responsible for a higher susceptibility of these particles to lipid peroxidation (42). In conditions of stress from nutritional, physical, environmental, or infectious origin, lipoperoxidation can affect reproductive functions, animal performance, and the quality of the carcass (43). Moreover, changes in the FA composition in lipoparticles can contribute to chronic disorders (inflammatory and immune disorders, neurological dysfunction, or deteriorations in reproductive and coagulation functions) as observed in humans (1,4). On the other hand, the substitution of PUFA with MUFA (especially oleic acid) noted for bovine lipoparticles seems to be implicated in "homeoviscous adaptation," an event that allows animals to adapt to a PUFA-rich diet by preserving the fluidity of the lipoparticles, thereby preserving

their metabolic functions in the optimal state (44). We believe that new studies should be performed to clarify the consequences on bovine health of long-term modifications in the lipid and lipoprotein profiles induced by the diet.

In conclusion, our study demonstrated that the addition of sunflower oil in the diets of steers increased the content of PUFA carried by plasma lipoparticles, mainly when dietary PUFA were protected against ruminal biohydrogenation. This result was consistent with the nutritional strategy of improving the quality of FA in bovine products (meat and milk). However, the accumulation of PUFA in lipoparticles can become a risk factor for animal health by favoring the peroxidation process. Moreover, the long-term effects of hypercholesterolemia on animal health following very light HDL formation remain to be evaluated to clarify the conditions and the limits of utilizing of such PUFA-rich supplements in ruminants.

ACKNOWLEDGMENTS

The authors wish to thank Sylvie Rudel and Pascal Faure for steer management and Christiane Legay and Marinett Martinaud for their technical assistance.

REFERENCES

1. Legrand, P., Bourre, J.M., Descomps, B., Durand, G., and Renaud, S. (2001) Lipides, in *Apports nutritionnels conseillés pour la population française*, 3rd edn. (TEC and DOC edition), pp. 63–82, Martin A., Lavoisier, Paris.
2. Food and Agriculture Organization/World Health Organization (1998) General Conclusions and Recommendations of the Consultation. Expert Consultation on Fats and Oils in Human Nutrition, FAO, Rome.
3. Grundy, S.M., and Denke, M.A. (1990) Dietary Influences on Serum Lipids and Lipoproteins, *J. Lipid Res. 31*, 1149–1172.
4. Williams, C.M. (2000) Dietary Fatty Acids and Human Health, *Ann. Zootechnol. 49*, 165–180.
5. Badiani, A., Stipa, S., Bitossi, F., Gatta, P.P., Vignola, G., and Chizzolini, R. (2002) Lipid Composition, Retention and Oxidation in Fresh and Completely Trimmed Beef Muscles as Affected by Common Culinary Practices, *Meat Sci. 60*, 169–186.
6. Wood, J.D., Enser, M., Fisher, A.V., Nute, G.R., Richardson, R.I., and Sheard, P.R. (1999) Animal Nutrition and Metabolism Group Symposium on "Improving Meat Production for Future Needs." Manipulating Meat Quality and Composition, *Proc. Nutr. Soc. 58*, 363–370.
7. Clinquart, A., Micol, D., Brundseaux, C., Dufrasne, I., and Istasse, L. (1995) Utilisation des matières grasses chez les bovins à l'engraissement, *INRA Prod. Anim. 8*, 29–42.
8. Demeyer, D., and Doeau, M. (1999) Targets and Procedures for Altering Ruminant Meat and Milk Lipids, *Proc. Nutr. Soc. 58*, 593–607.
9. Bauchart, D. (1993) Lipid Absorption and Transport in Ruminants, *J. Dairy Sci. 76*, 3864–3881.
10. Auboiron, S., Durand, D., and Bauchart, D. (1994) Lipoprotein Metabolism in the Preruminant Calf: Effect of a High Fat Diet Supplemented with L-Methionine, *J. Dairy Sci. 77*, 1870–1881.
11. Auboiron, S., Durand, D., Robert, J.C., Chapman, M.J., and Bauchart, D. (1995) Effects of Dietary Fat and L-Methionine on the Hepatic Metabolism of Very Low Density Lipoproteins in the Preruminant Calf, *Bos* spp., *Reprod. Nutr. Dev. 35*, 167–178.
12. Leplaix-Charlat, L., Bauchart, D., Durand, D., Laplaud, P.M., and Chapman, M.J. (1996) Plasma Lipoproteins in Preruminant Calves Fed Diets Containing Tallow or Soybean Oil With and Without Cholesterol, *J. Dairy Sci. 79*, 1267–1277.
13. Thomas, M.G., Bao, B., and Williams, G.L. (1997) Dietary Fats Varying in Their Fatty Acid Composition Differentially Influence Follicular Growth in Cows Fed Isoenergetic Diets, *J. Anim. Sci. 75*, 2512–2519.
14. Garcia-Bojalil, C.M., Staples, C.R., Risco, C.A., Savio, J.D., and Thatcher, W.W. (1998) Protein Degradability and Calcium Salts of Long-Chain Fatty Acids in the Diets of Lactating Dairy Cows: Reproductive Responses, *J. Dairy Sci. 81*, 1385–1395.
15. Petit, H.V., Dewhurst, R.J., Scollan, N.D., Proulx, J.G., Khalid, M., Haresign, W., Twagiramungu, H., and Mann, G.E. (2002) Milk Production and Composition, Ovarian Function, and Prostaglandin Secretion of Dairy Cows Fed ω-3 Fats, *J. Dairy Sci. 85*, 889–899.
16. Cheng, Z., Robinson, R.S., Pushpakumara, P.G.A., Mansbridge, R.J., and Wathes, D.C. (2001) Effect of Dietary Polyunsaturated Fatty Acids on Uterine Prostaglandin Synthesis in the Cow, *J. Endocrinol. 171*, 463–473.
17. Chilliard, Y., Ferlay, A., Mansbridge, R.M., and Doreau, M. (2000) Ruminant Milk Fat Plasticity: Nutritional Control of Saturated, Polyunsaturated, *trans* and Conjugated Fatty Acids, *Ann. Zootech. 49*, 181–205.
18. Bauchart, D., Durand, D., Laplaud, P.M., Forgez, P., Goulinet, S., and Chapman, M.J. (1989) Plasma Lipoproteins and Apolipoproteins in the Preruminant Calf, *Bos* spp.: Density Distribution, Physicochemical Properties, and the *in vivo* Evaluation of the Contribution of the Liver to Lipoprotein Homeostasis, *J. Lipid Res. 30*, 1499–1514.
19. Leplaix-Charlat, L. (1995) Effets des acides gras et du cholesterol alimentaires sur le métabolisme des lipides et des lipoprotéines aux niveaux plasmatique et hépatique chez le veau préruminant: Conséquences sur la composition lipidique des tissus, Ph.D. Thesis, University of Aix-Marseille, France, pp. 87–93.
20. Auboiron, S., Durand, D., Laplaud, P.M., Levieux, D., Bauchart, D., and Chapman, M.J. (1990) Determination of the Respective Density Distributions of Low- and High-Density Lipoprotein Particles in Bovine Plasma by Immunoassay of Apoproteins A-I and B, *Reprod. Nutr. Dev. 2S*, 227.
21. Folch, J., Lees, M., and Sloane Stanley, G.H. (1957) A Simple Method for the Isolation and Purification of Total Lipids from Animal Tissues, *J. Biol. Chem. 226*, 497–509.
22. Bauchart, D., and Aurousseau, B. (1981) Postprandial Lipids in Blood Plasma of Preruminant Calves, *J. Dairy Sci. 64*, 2033–2042.
23. SAS/STAT (1987) *Guide for Personal Computers*, SAS Institute, Cary, NC.
24. Snedecor, G.W., and Cochran, W.G. (1979) The Comparison of Two Samples, in *Statistical Methods*, 6th edn., The Iowa State University Press, Ames.
25. Harris, W.S. (1997) n-3 Fatty Acids and Serum Lipoproteins: Human Studies, *Am. J. Clin. Nutr. 65S*, 1645–1654.
26. Nicolosi, R.J. (1997) Dietary Fat Saturation Effects on Low-Density-Lipoprotein Concentrations and Metabolism in Various Animal Models, *Am. J. Clin. Nutr. 65S*, 1617–1627.
27. Leplaix-Charlat, L., Durand, D., and Bauchart, D. (1996b) Effects of Diets Containing Tallow and Soybean Oil With and Without Cholesterol on Hepatic Metabolism of Lipids and Lipoproteins in the Preruminant Calf, *J. Dairy Sci. 79*, 1826–1835.
28. Harrisson, F.A., Leat, W.M.F., and Forster, A. (1974) Absorption of Maize Oil Infused into the Duodenum of the Sheep, *Proc. Nutr. Soc. 33*, 101–102.
29. Doreau, M., and Ferlay, A. (1994) Digestion and Utilisation of Fatty Acids by Ruminants, *Anim. Feed Sci. Technol. 45*, 379–396.
30. Bauchart, D., Durand, D., Razavet, S., Dupont, S., Scislowski,

V., and Mouty, D. (2000) Effets comparés de l'apport de graines de tournesol dans la ration à l'infusion duodénale d'huile de tournesol sur la composition en acides gras des muscles et du foie chez le Bouvillon en fin d'engraissement, *Nutr. Clin. Metab. 14* (Suppl. 2), 162 (abstract).
31. Ashes, J.R., Burley, R.W., Sidhu, G.S., and Sleigh, R.W. (1984) Effect of Particle Size and Lipid Composition of Bovine Blood High Density Lipoprotein on Its Function as a Carrier of β-Carotene, *Biochim. Biophys. Acta 797*, 171–177.
32. Albers, J.J., Adolphson, J.L., and Chen, C.H. (1981) Radioimmunoassay of Human Plasma Lecithin-Cholesterol Acyltransferase, *J. Clin. Invest. 67*, 141–148.
33. Dolphin, P. (1992) Lipolytic Enzymes and the Role of Apolipoproteins in the Regulation of Their Activity, in *Structure and Function of Apolipoproteins* (Rosseneu, M., ed.), p. 295, CRC Press, Boca Raton, FL.
34. Frohlich, J., McLeod, R., and Hon, K. (1982) Lecithin:Cholesterol Acyl Transferase (LCAT), *Clin. Biochem. 15*, 269–278.
35. Segrest, J.P., Li, L., Anantharamaiah, G.M., Harvey, S.C., Liadaki K.N., and Zannis, V. (2000) Structure and Function of Apolipoprotein A-I and High-Density Lipoprotein, *Curr. Opin. Lipidol. 11*, 105–115.
36. Ben-Yashar, V., and Barenholz, Y. (1991) Characterization of the Core and Surface of Human Plasma Lipoproteins. A Study Based on the Use of Five Fluorophores, *Chem. Phys. Lipids 60*, 1–14.
37. Ha, Y.C., and Barter, P.J. (1982) Differences in Plasma Cholesteryl Ester Transfer Activity in Sixteen Vertebrate Species, *Comp. Biochem. Physiol. 71B*, 265–269.
38. Cordle, S.R., Yeamen, S.J., and Clegg, R.A. (1983) Salt Resistant (hepatic) Lipase. Evidence of Its Presence in Bovine Liver and Adrenal Cortex, *Biochim. Biophys. Acta 753*, 213–219.
39. Krieger, M. (1999) Charting the Fate of the "Good Cholesterol": Identification and Characterization of the High-Density Lipoprotein Receptor SR-BI, *Annu. Rev. Biochem. 68*, 523–558.
40. Moestrup, S.K., and Kozyraki, R. (2000) Cubilin, a High-Density Lipoprotein Receptor, *Curr. Opin. Lipidol. 11*, 133–140.
41. Rigotti, A., Trigatti, B.L., Penman, M., Rayburn, H., Herz, J., and Krieger, M. (1997) A Targeted Mutation in the Murine Gene Encoding the High Density Lipoprotein (HDL) Receptor Scavenger Receptor Class B Type I Reveals Its Key Role in HDL Metabolism, *Proc. Natl. Acad. Sci. USA 11*, 12610–12615.
42. Scislowski, V., Durand, D., Mouty, D., Laplaud, M., and Bauchart, D. (2000) Fluidité et susceptibilité à la peroxydation des lipoprotéines du bouvillon recevant des rations enrichies en huile de tournesol, *Nutr. Clin. Metab. 14 (*Suppl. 2), 151 (abstract).
43. Aurousseau B. (2002) Les radicaux libres dans l'organisme des animaux d'élevage: Conséquences sur la reproduction, la physiologie et la qualité de leurs produits, *INRA Prod. Anim. 15*, 67–82.
44. Scislowski, V., Durand, D., Gruffat-Mouty, D., Motta, C., and Bauchart, D. (2004) Linoleate Supplementation in Steers Modifies Lipid Composition of Plasma Lipoproteins but Does Not Alter Their Fluidity, *Br. J. Nutr. 91*, 1–11.

[Received October 31, 2003, and in final form and accepted February 10, 2004]

Contrasting Effects of *t*10,*c*12- and *c*9,*t*11-Conjugated Linoleic Acid Isomers on the Fatty Acid Profiles of Mouse Liver Lipids

D.S. Kelley[a,*], G.L. Bartolini[a], J.M. Warren[a], V.A. Simon[a], B.E. Mackey[b], and K.L. Erickson[c]

[a]Western Human Nutrition Research Center, ARS, USDA, and Department of Nutrition, University of California, Davis, California, [b]Western Regional Research Center, Albany, California, and [c]Department of Cell Biology and Human Anatomy, University of California, Davis, California

ABSTRACT: The purpose of this study was to examine the effects of two purified isomers of CLA (*c*9,*t*11-CLA and *t*10,*c*12-CLA) on the weights and FA compositions of hepatic TG, phospholipids, cholesterol esters, and FFA. Eight-week-old female mice (n = 6/group) were fed either a control diet or diets supplemented with 0.5% *c*9,*t*11-CLA or *t*10,*c*12-CLA isomers for 8 wk. Weights of liver total lipids and those of individual lipid fractions did not differ between the control and the *c*9,*t*11-CLA groups. Livers from animals fed the *t*10,*c*12-CLA diet contained four times more lipids than those of the control group; this was mainly due to an increase in the TG fractions (fivefold), but cholesterol (threefold), cholesterol esters (threefold), and FFA (twofold) were also significantly increased. Although *c*9,*t*11-CLA did not significantly alter the weights of liver lipids when compared with the control group, its intake was associated with significant reductions in the weight percentage (wt% of total FAME) of 18:1n-9 and 18:1n-7 in the TG fraction and with significant increases in the weight percentage of 18:2n-6 in the TG, cholesterol ester, and phospholipid fractions. On the other hand, *t*10,*c*12-CLA intake was linked with a significant increase in the weight percentage of 18:1n-9 and a decrease in that of 18:2n-6 in all lipid fractions. These changes may be the result of alterations in the activity of Δ9-desaturase (stearoyl CoA desaturase) and the enzymes involved in the metabolism of 18:2n-6. Thus, the two isomers differed not only in their effects on the weights of total liver lipids and lipid fractions but also on the FA profile of the lipid fractions.

Paper no. L9390 in *Lipids 39,* 135–141 (February 2004).

CLA is a collective term for a group of isomers of linoleic acid that have conjugated double bonds. Depending on the position and geometry of the double bonds, several isomers of CLA have been reported (1). The major dietary sources of *c*9,*t*11-CLA are dairy products and ruminant meat, whereas those of *t*10,*c*12-CLA are partially hydrogenated vegetable oils from margarines and shortenings (2). Most of the published studies have used mixtures of CLA isomers, that were composed of two major forms, *cis*9,*trans*11-CLA (*c*9,*t*11-CLA) and *trans*10, *cis*12-CLA (*t*10,*c*12-CLA), and a number of minor isomers. Feeding a mixture of CLA isomers to animal models has been reported to alter blood lipids, atherogenesis, diabetes, body composition, chemically induced carcinogenesis, and immune cell functions (3). Results from studies in mice (4–7), rats (8–11), chickens (12,13), pigs (14–18), and fish (19) have indicated that supplementing diets with a mixture of CLA isomers causes a reduction in body fat.

Because liver is the major site for FA synthesis, an understanding of the effects of dietary CLA isomers on liver lipids and their FA composition is important in understanding their overall effects on body fat metabolism. Results showing the effects of dietary CLA on liver lipids have been variable. It increased liver lipids in mice (20), increased (12) or decreased (13) them in chickens, decreased them in fish (19), and had no effect in hamsters (21) and rats (22,23). Part of these variations may be due to differences in lipid metabolism among the different species, but they could also be due to differences in the composition of CLA isomers in the mixtures used. Studies conducted with purified isomers have shown that the one responsible for reducing body and adipose tissue weights in mice (5,24–26) and hamsters (21) and for altering mammary lipid metabolism in dairy cows (27) is the *t*10,*c*12-CLA isomer.

Although feeding a mixture of CLA isomers did not alter the concentration of liver lipids in rats (22,23), it altered their FA composition (28). Other studies in rats using purified isomers have shown that the isomer responsible for altering the FA profile of the rat liver lipids was *t*10,*c*12-CLA, whereas the naturally occurring *c*9,*t*11-CLA had no effect (29,30). Thus, the two CLA isomers differ in their effects on the FA profile of rat liver lipids, but the effects of purified isomers on the FA profile of liver lipids in other species have not been studied.

We recently reported that supplementing the diets of mice with purified *c*9,*t*11-CLA and *t*10,*c*12-CLA had similar effects on immune cell functions, but only the *t*10,*c*12-CLA increased the liver lipids (24,31). Which liver lipid fraction is altered by the CLA, and the effects of purified isomers on the FA composition of liver lipid fractions in mice are not known. The purpose of this study was to examine the effects of two purified isomers of CLA (*c*9,*t*11-CLA and *t*10,*c*12-CLA) on the weights and FA compositions of hepatic TG, phospholipids, cholesterol esters, and FFA in mice.

MATERIALS AND METHODS

CLA isomers and diets. Highly enriched *c*9,*t*11-CLA and *t*10, *c*12-CLA isomers in the form of FFA were a kind gift from Natural ASA (Hovdebygda, Norway). The analytical data for

*To whom correspondence should be addressed at USDA/ARS/WHNRC, Dept. of Nutrition, University of California–Davis, One Shields Ave., Davis, CA 95616. E-mail: dkelley@whnrc.usda.gov

Abbreviations: AA, arachidonic acid; MUFA, monounsaturated FA; PPAR, peroxisome proliferator-activated receptor; SREBP-1, sterol regulating element-binding protein-1; SFA, saturated FA.

these isomers was provided by the supplier and confirmed in our laboratory. The preparation enriched in *c*9,*t*11-CLA contained *c*9,*t*11-CLA = 84.6%; *t*10,*c*12-CLA = 7.7%; 18:1n-9 = 3.8%; *t*9,*t*11-CLA + *t*10,*t*12-CLA = 2.0%; and other FA = 1.9%. In the preparation enriched in *t*10,*c*12-CLA, this isomer was 88.1%, with *c*9,*t*11-CLA = 6.6%; *t*9,*t*11-CLA + *t*10,*t*12-CLA = 2.5%; 18:1n-9 = 1.1%; and other FA = 1.7%.

The concentration of CLA used in this study was 0.5 wt% of the diet, comparable to the concentrations used in previous studies with rodent models, which have ranged from 0.1 to 1.5 wt% of a mixture of CLA isomers. AIN-93G, a high-carbohydrate mouse diet, was used as the basal diet. The nutrient and FA composition of this diet has been reported previously (24,31). Briefly, the control diet contained (g/kg): cornstarch 417.5, casein 200, dextrinized cornstarch 132, sucrose 100, corn oil with tocopherol 50 (α-tocopherol 100 mg/kg corn oil), cellulose 50, mineral mixture (AIN-93G) 35, vitamin mixture (AIN-93) 10, L-cysteine 3, and choline bitartrate 2.5. For the two CLA-containing diets, CLA isomer-enriched oils were added by replacing 5 g/kg of corn oil with an equivalent amount of the CLA source. Diets were constantly flushed with nitrogen gas while being gently mixed in a blender. Diets were packaged in 30-g aliquots, flushed with nitrogen gas, and stored at –20°C. Fresh dietary packets were served each day. The animal protocol was approved by the Animal Use Committee at the University of California, Davis.

Animals, feeding, and tissue collection. Eighteen 8-week-old, pathogen-free C57BL/6N female mice were purchased from Charles River (Raleigh, NC). Female mice were chosen because we were also interested in the effects of CLA isomers on immune cell functions, and because male mice fight when caged together, which can affect their immune cell functions. They were maintained in a sterile air curtain isolator at the animal facility of the University of California Medical School, with controlled temperature (25°C) and light and dark cycles (12 h each). They were fed the laboratory chow diet for the first 7 d and experimental diets for the last 56 d. Animals were divided into three groups at the start of the experimental diets (study day 1), with six per group. Details regarding animal handling, sacrifice, tissue collection, and storage have been published previously (24).

Lipid extraction, the isolation of different lipid classes, and FA analysis. Livers were removed, blotted dry with tissue paper, weighed, placed in liquid nitrogen, and stored frozen at –80°C until processed. Lipid extraction and FA analysis were performed according to previously published methods from our laboratory (32).

Briefly, a portion of the frozen liver was weighed and freeze-dried, and a portion of the freeze-dried sample was then weighed and transferred into a 7-mL glass hand homogenizer. The sample was homogenized with 5 mL chloroform/methanol 2:1 (vol/vol) containing 0.005% each BHT and hydroquinone. The homogenate was filtered through prewashed sharkskin paper; the homogenizer and residue on the paper were then washed twice with 1 mL additional solvent, and the combined filtrates were dried under nitrogen. The residue was dissolved in 1 mL chloroform and filtered through prewashed cotton into a 2-mL tared vial. The solvent was removed under dry nitrogen, freeze-dried, and weighed to yield the total lipids extracted (*ca.* 0.01–0.04 g). This was dissolved in a small amount of chloroform and applied as a band to a 20 cm × 20 cm × 250 μm activated silica gel plate. The plate was developed using hexane/ether/acetic acid (85:15:2, by vol), in a chamber flushed with nitrogen and equilibrated with the developing solvent. The plate was dried under a stream of nitrogen at room temperature, then sprayed with 2′,7′-dichlorofluorescein reagent; the bands were then visualized under UV light and scraped into test tubes. Each lipid fraction was extracted with chloroform/methanol (2:1), filtered, and the solvent removed and weighed. Each lipid fraction was transferred into small screw-capped test tubes, to which were added 1 mL dry methanol and one drop toluene. This was followed by the addition of 0.5 mL 0.5 M methanolic sodium methoxide, after which the tubes were flushed with nitrogen and capped. The tubes were then heated at 53–55°C for 10 min and cooled to room temperature. Methanolic HCl, 0.5 mL 3 N, was added to each tube, which was then capped, heated at 53–55°C for 15 min, and cooled to room temperature. Water (4.5 mL) and hexane (2 mL) were then added and mixed. The layers were allowed to separate, and the top hexane layer was transferred to another test tube. The bottom layer was extracted with an additional 2 × 1 mL hexane. The combined hexane extracts were dried over sodium sulfate/sodium bicarbonate (4:1) and filtered through prewashed cotton; the solvent was then removed under a stream of dry nitrogen to yield the transmethylated product. This was dissolved in 5–100 μL isooctane and analyzed on an Agilent 6890 gas–liquid chromatograph equipped with an FID and using a Supelco 2380 column (100 m × 0.25 mm × 0.2 μm film thickness). Oven conditions were as follows: hold at 75°C for 4 min, heat at 13°C/min to 175°C, hold for 27 min, heat at 4°C/min to 215°C, and hold for 20 min. A second 6890 gas–liquid chromatograph equipped with an Agilent 5973 mass selective detector was used to verify the identity of the GLC peaks as necessary.

Statistical analysis. The data were first checked for homogeneity of variance using Levene's test. When heterogeneity was found, either a transformation was used to stabilize the variances among diets or the SAS PROC MIXED was used to incorporate the heterogeneity into the model. The model was a one-way ANOVA, and Dunnett's test was used for diet comparisons with the control group (33).

RESULTS

Effect of CLA isomers on the weights of different classes of liver lipids. Table 1 contains data regarding the total liver lipids and the lipid classes for mice fed the control and CLA-containing diets. Livers from the animals fed the control diet contained an average of 156 mg lipids per liver, which represented 11.3% of the liver weights. Liver lipid contents of the animals fed the *c*9,*t*11-CLA diet did not differ significantly from those in the control group. However, the livers of animals fed diets containing

TABLE 1
Effect of CLA Isomers on Liver Lipid Classes (wt% of total liver lipids or mg/liver)[a]

Lipid fraction	Control	*c*9,*t*11-CLA	*t*10,*c*12-CLA
Lipids (wt% of liver)	11.30 ± 1.30	11.80 ± 0.50	30.30 ± 4.70*
Total lipids (mg/liver)	156.1 ± 18.1	172.2 ± 13.0	641.1 ± 119.1*
TG			
wt% of lipids	63.2 ± 3.40	68.0 ± 2.7	81.9 ± 1.0*
mg/liver	98.7 ± 24.0	117.1 ± 18.0	524.8 ± 63.8*
Phospholipids			
wt%	17.1 ± 2.6	15.9 ± 1.7	4.7 ± 0.4*
mg/liver	26.7 ± 3.1	27.4 ± 4.9	29.5 ± 2.8
Cholesterol			
wt%	6.2 ± 0.7	5.8 ± 0.4	4.8 ± 0.5
mg/liver	9.7 ± 1.2	9.9 ± 2.1	31.4 ± 3.6*
Cholesterol esters			
wt%	9.5 ± 0.9	7.1 ± 0.5*	7.0 ± 0.4*
mg/liver	14.8 ± 2.9	12.3 ± 2.7	44.6 ± 5.5*
FFA			
wt%	4.0 ± 0.6	3.1 ± 0.5	1.7 ± 0.3*
mg/liver	6.2 ± 0.5	5.4 ± 1.6	11.2 ± 2.3

[a]Data are mean ± SEM (n = 6). Numbers marked with an asterisk are significantly ($P < 0.05$) different from corresponding values in the control group.

*t*10,*c*12-CLA contained four times more lipids than the amount found in the control group, and lipids constituted 30% of the liver weight in this group.

TG, phospholipids, cholesterol, cholesterol esters, and FFA, constituted 63.2, 17.1, 6.2, 9.5, and 4.0 wt% of the total liver lipids in animals fed the control diet (Table 1). The percentage distribution of lipids among the different fractions did not differ between the control and the *c*9,*t*11-CLA groups, except that intake of *c*9,*t*11-CLA was associated with a significant reduction in the weight percentage of cholesterol esters. In the animals fed *t*10,*c*12-CLA, the weight percentage of TG was increased ($P < 0.05$), and the weight percentages of phospholipids, cholesterol esters, and FFA were decreased as compared with the corresponding values in the animals fed the control diet. Because not all lipid fractions changed proportionally, these changes did not represent changes in the absolute weights of the different fractions. Based on the total lipids and their percentage distribution among different classes, we calculated the absolute weight (mg/liver) of each lipid class. On the basis of mg/liver, none of the lipid classes differed between the control and the *c*9,*t*11-CLA groups. On this basis, the weights of TG, cholesterol, cholesterol esters, and FFA in the *t*10,*c*12-CLA group were five, three, three, and two times those of the corresponding values in the control group; the absolute weights of phospholipids per liver did not differ among the three groups. These data emphasize that changes in the weight percentage and absolute weight of different lipid fractions can lead to different interpretations, and both should be determined.

FA composition of liver TG, phospholipids, cholesterol esters, and FFA of mice fed the control or CLA-containing diet. The weight percentage (wt% of total FAME) concentrations of CLA and major FA found in the different classes of lipids in the livers of mice fed the control or experimental diet are shown in Table 2. The highest weight percentage of *c*9,*t*11-CLA was found in cholesterol esters (3.1%), followed by TG (1.3%), FFA (1.2%), and phospholipids (0.1%), respectively. The weight percentage of *t*10,*c*12-CLA ranged from 0.3% in TG to 0.1% in cholesterol esters. In animals fed *t*10,*c*12-CLA, the concentrations of *c*9,*t*11-CLA were below the detection limit; however, in animals fed *c*9,*t*11-CLA, the levels of *t*10,*c*12-CLA were detectable in the cholesterol esters and phospholipids. This may be due to impurities in the isomers added to the diets. These data show that both isomers of CLA were incorporated into in all four of the lipid classes investigated; however, the amounts incorporated differed between the two isomers and among the different lipid classes. The relative proportions of *t*10,*c*12-CLA incorporated into all lipid classes except the phospholipids were much smaller than the corresponding proportion of *c*9,*t*11-CLA.

*c*9,*t*11-CLA had only modest effects on the FA profiles of all the lipid fractions when compared with the corresponding values in animals fed the control diet (Table 2). The weight percentages of 18:1n-9 and 18:1n-7 were significantly decreased in the TG fraction, and that of 18:2n-6 was increased in TG, phospholipids, and cholesterol esters in the group fed the *c*9,*t*11-CLA diet. Changes in the proportions of these three FA in other lipid fractions did not attain statistical significance. The sum of monounsaturated FA (MUFA) was significantly decreased in TG, and that of PUFA was increased in the TG, cholesterol ester, and FFA fractions but was unchanged in the phospholipid fraction by the feeding of *c*9,*t*11-CLA compared with the corresponding values in the control group. The weight percentages of all other

TABLE 2
FA Composition (wt%) of Liver TG, Phospholipids, Cholesterol Esters, and FFA of Mice Fed Control or Experimental Diets[a]

	TG			Phospholipids			Cholesterol esters			FFA		
FAME	Control	*c*9,*t*11	*t*10,*c*12	Control	*c*9,*t*11	*t*10,*c*12	Control	*c*9,*t*11	*t*10,*c*12	Control	*c*9,*t*11	*t*10,*c*12
16:0	23.3 ± 0.6	24.0 ± 0.5	25.4 ± 0.7*	16.3 ± 0.5	16.3 ± 0.6	16.1 ± 0.5	22.8 ± 2.3	22.9 ± 2.5	16.0 ± 0.6*	33.7 ± 2.2	32.4 ± 1.4	29.1 ± 1.6
16:1n-7	4.9 ± 0.4	4.7 ± 0.5	4.9 ± 0.3	1.1 ± 0.1	1.0 ± 0.1	1.0 ± 0.0	8.2 ± 0.4	7.5 ± 0.3	8.7 ± 0.2	1.8 ± 0.2	1.4 ± 0.3	1.9 ± 0.2
18:0	2.3 ± 0.1	2.3 ± 0.2	2.1 ± 0.1	18.3 ± 0.5	18.9 ± 0.5	17.7 ± 0.2	4.4 ± 0.1	5.6 ± 0.6*	3.0 ± 0.1*	16.2 ± 1.6	16.9 ± 2.3	10.7 ± 1.9
18:1n-9	46.6 ± 0.9	40.1 ± 1.8*	52.1 ± 0.7*	9.4 ± 0.4	8.3 ± 0.4	12.5 ± 0.2*	41.0 ± 2.4	39.8 ± 3.0	56.1 ± 1.0*	25.1 ± 1.6	21.6 ± 2.7	37.9 ± 3.3*
18:1n-7	3.9 ± 0.4	2.8 ± 0.3*	4.1 ± 0.4	1.9 ± 0.2	1.8 ± 0.1	2.2 ± 0.1	2.2 ± 0.2	2.0 ± 0.2	2.8 ± 0.0*	2.0 ± 0.3	1.5 ± 0.3	3.0 ± 0.4
18:2n-6	13.2 ± 1.2	17.5 ± 1.9*	6.7 ± 0.2*	12.0 ± 0.1	13.9 ± 0.7*	10.5 ± 0.2*	6.6 ± 0.5	9.2 ± 1.1*	4.5 ± 0.2*	5.4 ± 1.2	7.6 ± 1.8	4.5 ± 0.4
*c*9,*t*11-CLA	0.0 ± 0.0	1.3 ± 0.8*	0.0 ± 0.0	0.0 ± 0.0	0.1 ± 0.0*	0.1 ± 0.1*	0.0 ± 0.0	3.1 ± 0.6*	0.2 ± 0.0*	0.0 ± 0.0	1.2 ± 0.3*	0.0 ± 0.0
*t*10,*c*12-CLA	0.0 ± 0.0	0.0 ± 0.0	0.3 ± 0.0*	0.0 ± 0.0	0.0 ± 0.0	0.2 ± 0.0*	0.0 ± 0.0	0.0 ± 0.0	0.1 ± 0.0*	0.0 ± 0.0	0.0 ± 0.0	0.2 ± 0.1*
20:4n-6	0.8 ± 0.1	0.9 ± 0.2	0.2 ± 0.0*	25.0 ± 0.3	23.7 ± 0.4*	24.1 ± 0.3	2.9 ± 0.2	3.1 ± 0.5	1.6 ± 0.1	1.0 ± 0.2	2.6 ± 0.4	3.2 ± 1.0*
22:6n-3	0.1 ± 0.0	0.1 ± 0.0	0.0 ± 0.0	8.2 ± 0.4	7.8 ± 0.6	5.9 ± 0.1*	0.5 ± 0.0	0.6 ± 0.1	0.3 ± 0.1	0.5 ± 0.0	0.5 ± 0.0	0.7 ± 0.0
Sum SFA	26.7 ± 0.6	27.6 ± 0.5	28.4 ± 0.7	35.0 ± 05	35.9 ± 0.7	34.2 ± 0.5	28.1 ± 2.3	30.8 ± 2.7	19.7 ± 0.8*	54.3 ± 2.1	55.1 ± 3.8	41.3 ± 3.2*
Sum MUFA	56.1 ± 1.3	48.7 ± 2.3*	62.4 ± 0.9*	12.7 ± 0.6	11.8 ± 0.4	16.0 ± 0.2*	52.5 ± 2.8	50.0 ± 3.1	69.3 ± 2.2*	29.7 ± 1.9	25.1 ± 3.3	44.2 ± 3.9*
Sum PUFA	15.6 ± 0.7	21.2 ± 2.8*	7.6 ± 0.2*	51.2 ± 0.3	50.5 ± 1.0	47.8 ± 0.5*	10.1 ± 0.5	16.1 ± 1.9*	6.8 ± 0.3	6.3 ± 1.1	11.3 ± 1.7*	7.8 ± 0.8

[a]Data are mean ± SEM ($n = 6$). Numbers marked with an asterisk are significantly different ($P < 0.05$) from corresponding numbers in the control group within the same lipid class. SFA, saturated FA; MUFA, monounsaturated FA.

individual FA and the sum of saturated FA (SFA) did not differ significantly between the control and the *c*9,*t*11-CLA groups.

Feeding the diet containing *t*10,*c*12-CLA was linked with significant increases in the relative proportions of 18:1n-9 and decreases in the proportions of 18:2n-6 in all lipid fractions when compared with the corresponding values in the control group (Table 2). It was associated with significant reductions in the weight percentages of 16:0 and 18:0 in the cholesterol ester fractions and a significant increase in the proportion of 16:0 in the TG fraction. It was also associated with significant reductions in the weight percentage of DHA in phospholipids, arachidonic acid (AA) in TG, and an increase in the proportion of AA in FFA. The proportion of total MUFA increased and that of PUFA decreased in all lipid fractions except for FFA, where total PUFA did not change; the proportion of total SFA decreased in the FFA and cholesterol ester fractions. Thus, the two CLA isomers differed not only in their incorporation into different lipid fractions but also in the changes they caused in the composition of other FA.

DISCUSSION

We compared the effects of two purified isomers of dietary CLA (*c*9,*t*11-CLA and *t*10,*c*12-CLA) on the weights and FA profiles of murine liver TG, phospholipids, cholesterol esters, and FFA with the corresponding fractions in animals fed diets without CLA; we also compared the incorporation of the two CLA isomers into different lipid fractions. Total liver lipids and their distribution among different fractions did not differ between the control and *c*9,*t*11-CLA groups (Table 1). The livers of animals fed diets supplemented with *t*10,*c*12-CLA contained four times more total lipids than the amount found in the livers of animals fed the control diet. Our results showing an increase in liver lipids by feeding *t*10,*c*12-CLA are consistent with those previously reported with a mixture of CLA isomers (0.5–1.5% fed for 6 wk, Ref. 20) or with *t*10, *c*12-CLA (0.4 or 1.0% fed for 4 wk; 25,26) in mice; the increase in liver lipids with the mixture of CLA isomers ranged from 75 to 150% (20), whereas the increase with *t*10,*c*12-CLA (25) was similar to that found in our study. Feeding a mixture of CLA isomers (0.5% for 6 wk) caused a twofold increase in liver lipids in chickens (12), but it did not increase liver lipids in rats fed at 0.5 to 1.5% for 4–6 wk (22,23). Similarly, feeding a mixture of CLA isomers or the purified *c*9,*t*11-CLA or *t*10,*c*12-CLA (0.66% for 8 wk) did not increase liver lipids in hamsters (21). Still others reported a reduction in liver lipids with the feeding of a CLA mixture in fish (19) and chickens (13). These differences may be due to a number factors, including the species, age of the animal, amount and type of CLA, the duration of its feeding, and the composition of the basal diet.

The increase in liver lipids caused by *t*10,*c*12-CLA in our study was largely due to an increase in the weights of liver TG, although cholesterol, cholesterol esters, and FFA also were significantly elevated. These changes in liver lipids most likely resulted from an altered secretion of leptin and insulin. Published reports have indicated that feeding a mixture of CLA isomers

reduces the concentration of circulating leptin and increases that of insulin in mice, rats, and humans (25,34–37). Other reports have indicated that *t*10,*c*12-CLA reduces the mRNA for leptin and adiponectin in the adipose tissue (24) and increases that of sterol regulatory element-binding protein-1 (SREBP-1) in liver (25). Furthermore, leptin infusion was found to reverse the CLA-caused hyperinsulinemia and fat deposition in the liver (34). Together, these results suggest that *t*10,*c*12-CLA reduced the production of leptin by the adipose tissue, which led to increased production of insulin by the pancreas and insulin-activated SREBP-1 in the liver. An increase in SREBP-1 increases both cholesterol and FA synthesis in the liver (25). Thus, the increase in the liver lipid contents of animals fed diets containing *t*10, *c*12-CLA was most likely due to increased lipid synthesis in the liver; however, a reduction in hepatic lipid secretion also may have contributed to this result. The proposed mechanisms are based on the interaction between several organs in the body, and the response of the liver to CLA may be secondary to the response from other organs. In *in vitro* transactivation assays, both CLA isomers were equally effective in activating peroxisome proliferator-activated receptors (PPAR) α, β, and γ (25; Kelley, D.S., and Lee, J.Y., unpublished results). Thus, PPAR activation by *t*10,*c*12-CLA does not seem to be the mechanism by which liver lipids were increased.

The two CLA isomers differed in the proportion of their incorporation into the different lipid fractions and their effects on the FA profiles of the lipid fractions. Overall, incorporation of *c*9,*t*11-CLA was much higher than that of *t*10,*c*12-CLA, and the highest weight percentage of *c*9,*t*11-CLA was found in the cholesterol esters. These results are consistent with those reported in rats (29).

Feeding *c*9,*t*11-CLA in our study was associated with a significant reduction in the weight percentage of 18:1n-9 and an increase in 18:2n-6 (Table 2). A reduction in the proportion of 18:1n-9 may be due to a decrease in the activity of Δ9-desaturase; an increase in the proportion of 18:2n-6 may be due to a reduction in the activity of Δ6-desaturase or other enzymes involved in the metabolism of this FA. Our results in mice showing changes in the proportions of 18:1n-9 and 18:2n-6 contrast with those showing no change in the FA composition of liver lipids isolated from rats fed diets containing *c*9,*t*11-CLA (29,30). These differences may be due to variance in the lipid metabolism between rats and mice.

In contrast to *c*9,*t*11-CLA, feeding the *c*10,*t*12-CLA isomer was associated with an increase in the weight percentage of 18:1n-9, possibly due to an increased activity of Δ9-desaturase (stearoyl CoA desaturase). Pariza's group has published several papers regarding the effects of CLA on the expression and/or activity of this enzyme. They reported a reduction in the mRNA for stearoyl CoA desaturase-1 in the livers of mice fed a diet containing a mixture of CLA isomers (0.5% for 2 wk) (38), and in 3T3-L1 adipocytes *in vitro* by feeding *t*10, *c*12-CLA (25 to 100 μM) but not by feeding *c*9,*t*11-CLA (39). Subsequently, they reported a reduction in the expression or activity of this enzyme by both CLA isomers (45 μM) in two human breast tumor cell lines (40). Their results suggest that, depending on the model used, either *t*10,*c*12-CLA or both the CLA isomers may inhibit the expression or activity of this enzyme. Other reports have indicated that stearoyl CoA desaturase activity is positively associated with hypertriglyceridemia in humans and mice (41), and that disruption of the gene for this enzyme impairs the biosynthesis of cholesterol esters and TG in mice liver (42). Our results concur with the above-mentioned findings that CLA isomers may alter the activity of stearoyl CoA desaturase. However, our results contrast with those from Pariza's laboratory: Our results suggest a stimulation of this enzyme by *t*10,*c*12-CLA and not inhibition, as reported by this group. Since they used a mixture of CLA isomers in their study with mice, it is possible that a reduction in the liver mRNA for this enzyme was caused by *c*9,*t*11-CLA; this would be consistent with our results regarding the effects of this isomer on the liver FA composition. Furthermore, our interpretation of the activity of the enzyme is based on the FA composition, whereas they measured the mRNA for this enzyme; neither measured enzyme activity.

Feeding *t*10,*c*12-CLA was associated with reductions in the weight percentage of 18:2n-6 in all lipid fractions and that of 22:6n-3 in only the phospholipids. A reduction in the proportion of 18:2n-6 may be due to increased activity of Δ6-desaturase or other enzymes involved in the metabolism of this FA. A reduction in 22:6n-3 may be due to decreased activity of Δ5-desaturase or elongases, or to increased activity of enzymes involved in the metabolism of DHA. The reduction in the proportion of 18:2n-6 in the *t*10,*c*12-CLA group in our study is consistent with that reported after feeding a mixture of CLA isomers to mice (20) or rats (23). Our study extends these findings by showing that *t*10,*c*12-CLA is the isomer that caused a reduction in the weight percentage of 18:2n-6; *c*9,*t*11-CLA actually caused an increase in the weight percentage of this FA. Thus, feeding a mixture of the two isomers may increase, decrease, or have no effect on the proportion of 18:2n-6, depending on the ratio between the isomers. A reduction in the weight percentage of DHA in the phospholipids of animals fed *t*10,*c*12-CLA in our study differs from the increase in this FA in rat liver phospholipids caused by the same isomer (29). We did not measure the activities of lipid-metabolizing enzymes. That the enzymes change is one logical explanation for the changes in FA concentrations. It is also possible that changes in the activities of other FA-metabolizing enzymes may have contributed to the altered concentrations of the FA seen in our study.

In summary, our results show that only the *t*10,*c*12-CLA altered the weights of liver lipids, whereas both isomers altered the FA profiles of the lipid fractions. The two isomers differed in the amounts incorporated into liver lipids and the changes they caused in the FA profiles of the lipid fractions. It is important to note that *c*9,*t*11-CLA did not alter the total lipids but altered the FA composition, whereas the *t*10,*c*12-CLA altered both the total lipids and the FA profile.

REFERENCES

1. Eulitz, K., Yurawecz, M.P., Sehat, N., Fritsche, J., Roach, J.A.G., Mossoba, M.M., Kramer, J.K.G., Adlof, R.O., and Ku, Y. (1999) Preparation, Separation, and Confirmation of the Eight Geometrical *cis/trans* Conjugated Linoleic Acid Isomers, 8,10- Through 11,13-18:2, *Lipids 34*, 873–877.

2. McGuire, M.K., McGuire, M.A., Ritzenthaler, K., and Shultz, T.D. (1999) Dietary Sources and Intakes of Conjugated Linoleic Acid Intake in Humans, in *Advances in Conjugated Linoleic Acid* (Yurawecz, M.P., Mossoba, M.M., Kramer, J.K.G., Pariza, M.W., and Nelson, G.J.), Vol. 1, pp. 369–376, AOCS Press, Champaign.
3. Belury, M.A. (2002) Dietary Conjugated Linoleic Acid in Health: Physiological Effects and Mechanisms of Action, *Annu. Rev. Nutr. 22*:505–531.
4. West, D.B., Delaney, J.P., Camet, P.M., Blohm, F., Truett, A.A., and Scimeca, J. (1998) Effects of Conjugated Linoleic Acid on Body Composition and Energy Metabolism in Mice, *Am. J. Physiol. 275*, R667–R672
5. Park, Y., Storkson, J.M., Albright, K.J., Liu, W., and Pariza, M.W. (1999) Evidence That *trans*-10,*cis*-12 Isomer of Conjugated Linoleic Acid Induces Body Composition Changes in Mice, *Lipids 34*, 235–241.
6. Tsuboyama-Kasaoka, N., Takahashi, M., Tanemura, K., Kim, H.J., Tange, T., Okuyama, H., Kasai, M., Shinji, I., and Ezaki, O. (2000) Conjugated Linoleic Acid Supplementation Reduces Adipose Tissue by Apoptosis and Develops Lipodystrophy in Mice, *Diabetes 49*, 1534–1542.
7. Delany, J.P., Blohm, F., Truett, A.A., Scimeca, J.A., and West, D.B. (1999) Conjugated Linoleic Acid Rapidly Reduces Body Fat Content in Mice Without Affecting Energy Intake, *Am. J. Physiol. 276*, R1172–R1179.
8. Azain, M.J., Hausman, D.B., Sisk, M.B., Flatt, W.P., and Jewell, D.E. (2000) Dietary Conjugated Linoleic Acid Reduces Adipose Tissue Cell Size Rather Than Cell Number, *J. Nutr. 130*, 1548–1554.
9. Sisk, M.B., Hausman, D.B., Martin, R.J., and Azain, M.J. (2001) Dietary Conjugated Linoleic Acid Reduces Adiposity in Lean but Not in Obese Zucker Rats, *J. Nutr. 131*, 1668–1674.
10. Stangl, G.I. (2000) Conjugated Linoleic Acids Exhibit a Strong Fat-to-Lean Partitioning Effect, Reduce Serum VLDL Lipids and Redistribute Tissue Lipids in Food-Restricted Rats, *J. Nutr. 130*, 1140–1146.
11. Yamasaki, M., Mansho, K., Mishima, H., Kasai, M., Sugano, M., Tachibana, H., and Yamada, K. (1999) Dietary Effect of Conjugated Linoleic Acid on Lipid Levels in White Adipose Tissue of Sprague-Dawley Rats, *Biosci. Biotechnol. Biochem. 63*, 1104–1106.
12. Cherian, G., Holsonbake, T.B., Goeger, M.P., and Bildfell, R. (2002) Dietary CLA Alters Yolk and Tissue FA Composition and Hepatic Histopathology in Laying Hens, *Lipids 37*, 751–757.
13. Badinga, L., Selberg, K.T., Dinges, A.C., Corner, C.W., and Miles, R.D. (2003) Dietary Conjugated Linoleic Acid Alters Hepatic Lipid Content and Fatty Acid Composition in Broiler Chickens, *Poultry Sci. 82*, 111–116.
14. Bassaganya-Riera, J., Hontecillas-Margarzo, R., Bregendahl, K., Wannemuehler, M.J., and Zimmerman, D.R. (2001) Effects of Dietary Conjugated Linoleic Acid in Nursery Pigs and Clean Environments on Growth, Empty Body Composition, and Immune Competence, *J. Anim. Sci. 79*, 714–721.
15. Dugan, M.E.R., Aalhus, J.L., Schaefer, A.L., and Kramer, J.K.G. (1997) The Effect of Conjugated Linoleic Acid on Fat to Lean Repartitioning and Feed Conversion in Pigs, *Can. J. Anim. Sci. 77*, 723–725.
16. Thiel-Cooper, R.L., Parrish, F.C., Sparks, J.C., Wiegand, B.R., and Ewan, R.C. (2001) Conjugated Linoleic Acid Changes Swine Performance and Carcass Composition, *J. Anim. Sci. 79*, 1821–1828.
17. Ostrowska, E., Muralitharan, M., Cross, R.F., Bauman, D.E., and Dunshea, F.R. (1999) Dietary Conjugated Linoleic Acids Increase Lean Tissue and Decrease Fat Deposition in Growing Pigs, *J. Nutr. 129*, 2037–2042.
18. Wiegand, B.R., Parrish, F.C., Swan, J.E., Larsen, S.T., and Baas, T.J. (2001) Conjugated Linoleic Acid Improves Feed Efficiency, Decreases Subcutaneous Fat, and Improves Certain Aspects of Meat Quality in Stress-Genotype Pigs, *J. Anim. Sci. 79*, 2187–2195.
19. Twibell, R.G., Watkins, B.A., Rogers, L., and Brown, P.B. (2000) Effects of Dietary Conjugated Linoleic Acids on Hepatic and Muscle Lipids in Hybrid Striped Bass, *Lipids 35*, 155–161.
20. Belury, M.A., and Kempa-Steczko, A. (1997) Conjugated Linoleic Acid Modulates Hepatic Lipid Composition in Mice, *Lipids 32*, 199–204.
21. de Deckere, E.A., van Amelsvoort, J.M., McNeil, G.P., and Jones, P. (1999). Effect of Conjugated Linoleic Acid Isomers on Lipid Level and Peroxisome Proliferation in the Hamster, *Br. J. Nutr. 82*, 309–317.
22. Koba, K., Akahoshi, A., Yamasaki, M., Tanaka, K., Yamada, K., Iwata, T., Kamegai, K., Tsutsumi, K., and Sugano, M. (2002) Dietary Conjugated Linolenic Acid in Relation to CLA Differently Modifies Body Fat Mass and Serum and Liver Lipid Levels in Rats, *Lipids 37*, 243–350.
23. Sugano, M., Tsujita, A., Yamasaki, M., Yamada, K., Ikeda, I., and Kritchevsky, D. (1997) Lymphatic Recovery, Tissue Distribution, and Metabolic Effects of Conjugated Linoleic Acid in Rats, *J. Nutr. Biochem. 8*: 38–43.
24. Warren, J.M., Simon, V.A., Bartolini, G., Erickson, K.L., Mackey, B.E., and Kelley, D.S. (2003) *Trans*-10,*cis*-12 CLA Increases Liver and Decreases Adipose Tissue Lipids in Mice: Possible Role of Specific Lipid Metabolism Genes, *Lipids 38*, 497–504.
25. Clément, L., Poirier, H., Noit, I., Bocher, V., Guerre-Milo, M., Knef, S., Staels, B., and Besnard, P. (2002) Dietary *trans*-10,*cis*-12 Conjugated Linoleic Acid Induces Hyperinsulinemia and Fatty Liver in the Mouse, *J. Lipid Res. 43*, 1400–1409.
26. Degrace, P., Demizieux, L., Gresti, J., Chardigny, J.M., Sébédio, J.L., and Clouet P. (2003) Association of Liver Steatosis with Lipid Oversecretion and Hypotriglyceridaemia in C57BL/6J Mice Fed *trans*-10,*cis*-12-Linoleic Acid, *FEBS Lett. 546*, 335–339.
27. Baumgard, L.H., Matitashvili, E., Corl, V.A., Dwyer, D.A., and Bauman, D.E. (2002) *Trans*-10,*cis*-12 CLA Decreases Lipogenic Rates and Expression of Genes Involved in Milk Lipid Synthesis in Dairy Cows, *J. Dairy Sci. 85*, 2155–2163.
28. Li, Y., and Watkins, B.A. (1998) Conjugated Linoleic Acids Alter Bone Fatty Acid Composition and Reduce *ex vivo* Prostaglandins E_2 Biosynthesis in Rats Fed n-6 or n-3 Fatty Acids, *Lipids 33*, 417–425.
29. Sébédio, J.L., Angioni, E., Chardigny, J.M., Gregoire, S., Juaneda, P., and Berdeaux, O. (2001) The Effect of Conjugated Linoleic Acid Isomers on Fatty Acid Profiles of Liver and Adipose Tissues and Their Conversion to Isomers of 16:2 and 18:3 Conjugated Fatty Acids in Rats, *Lipids 36*, 575–582.
30. Banni, S., Carta, G., Angioni, E., Murru, E., Scanu, P., Melis, M.P., Bauman, D.E., Fischer, S.M., and Ip, C. (2001) Distribution of Conjugated Linoleic Acid and Metabolites in Different Lipid Fractions in the Rat Liver, *J. Lipid Res. 42*, 1056–1061.
31. Kelley, D.S., Warren, J.M., Simon, V.A., Bartolini, G., Mackey, B.E., and Erickson, K.L. (2002) Similar Effects of *c*9,*t*11-CLA and *t*10,*c*12-CLA on Immune Cell Functions in Mice, *Lipids 37*, 725–728.
32. Kelley, D.S., Nelson, G.J., Love, J.E., Branch, L., Taylor, P.C., Schmidt, P.C., Mackey, B.E., and Iacono, J.M. (1993) Dietary α-Linolenic Acid Alters Fatty Acid Composition, but Not Blood Lipids, Lipoproteins or Coagulation Status in Humans, *Lipids 28*, 533–537.
33. Littell, R.C., Stroup, W.W., and Freund, R.J. (2002) *SAS for Linear Models*, 4th edn., SAS Institute, Cary, NC.
34. Tsuboyama-Kasaoka, N., Takahashi, M., Tanemura, K., Kim, H.J., Tange, T., Okuyama, H., Kasai, M., Ikemoto, S., and

Ezaki, O. (2000) Conjugated Linoleic Acid Supplementation Reduces Adipose Tissue by Apoptosis and Develops Lipodystrophy in Mice, *Diabetes 49*, 1534–1542.
35. Rahman, S.M., Wang, Y., Yotsumoto, H., Cha, J., Han, S., Inoue, S., and Yanagita, T. (2001) Effects of Conjugated Linoleic Acid on Serum Leptin Concentration, Body-Fat Accumulation, and β-Oxidation of Fatty Acid in OLETF Rats, *Nutrition 17*, 385–390.
36. Medina, E.A., Horn, W.F., Keim, N.L., Havel, P.J., Benito, P., Kelley, D.S., Nelson, G.J., and Erickson, K.L. (2000) Conjugated Linoleic Acid Supplementation in Humans: Effects on Circulating Leptin Concentrations and Appetite, *Lipids 35*, 783–788.
37. Riserus, U., Smedman, A., Basu, S., and Vessby, B. (2003) CLA and Body Weight Regulation in Humans, *Lipids 38*, 133–137.
38. Lee, K.L., Pariza, M.W., and Ntambi, J.M. (1998) Conjugated Linoleic Acid Decreases Hepatic Stearoyl-CoA Desaturase mRNA Expression, *Biochem. Biophys. Res. Commun. 248*, 817–821.
39. Choi, Y., Kim, Y.C., Han, Y.B., Park Y., Pariza, M.W., and Ntambi, J.M. (2000) The *trans*-10,*cis*-12 Isomer of Conjugated Linoleic Acid Downregulates Stearoyl-CoA Desaturase I Gene Expression in 3T3-L1 Adipocytes, *J. Nutr. 130*, 1920–1924.
40. Choi, Y., Park, Y., Storkson, J.M., Pariza, M.W., and Ntambi, J.M. (2002) Inhibition of Stearoyl-CoA Desaturase Activity by *cis*-9,*trans*-11 Isomer and the *trans*-10,*cis*-12 Isomer of Conjugated Linoleic Acid in MDA-MB-231 and MCF-7 Human Breast Cancer Cells, *Biochem. Biophys. Res. Commun. 294*, 785–790.
41. Attie, A.D., Krauss, R.M., Gray-Keller, M.P., Brownlie, A., Miyazaki, M., Kastelein, J.J., Lusis, A.J., Stalenhoef, A.F., Stoehr, J.P., Hayden, M.R., and Ntambi, J.M. (2002) Relationship Between Stearoyl-CoA Desaturase Activity and Plasma Triglycerides in Human and Mouse Hypertriglyceridemia, *J. Lipid Res. 43*, 1899–1907.
42. Miyazaki, M., Kim, Y.-C., Gray-Keller, M.P., Attie, A.D., and Ntambi, J.M. (2000) The Biosynthesis of Hepatic Cholesterol Esters and Triglycerides Is Impaired in Mice with Disruption of the Gene for Stearoyl-CoA Desaturase 1, *J. Biol. Chem. 275*, 30132–30138.

[Received October 3, 2003, and in final form January 30, 2004; revision accepted February 12, 2004]

Modulation of HepG2 Cell Net Apolipoprotein B Secretion by the Citrus Polymethoxyflavone, Tangeretin

Elzbieta M. Kurowska[a,*], John A. Manthey[b], Adele Casaschi[c], and Andre G. Theriault[c]

[a]KGK Synergize Inc., London, Ontario, Canada N6A 5R8, [b]USDA, ARS, South Atlantic Area, Citrus & Subtropical Products Laboratory, Winter Haven, Florida 33881, and [c]Division of Medical Technology, John A. Burns School of Medicine, University of Hawaii at Manoa, Honolulu, Hawaii 96822

ABSTRACT: The purpose of the present study was to examine the role of tangeretin, a polymethoxylated flavone from citrus fruits, on the regulation of apolipoprotein B (apoB) and lipid metabolism in the human hepatoma cell-line HepG2. The marked reduction in apoB secretion observed in cells incubated with 72.8 μM tangeretin was rapid, apoB-specific, and partly reversible. The reduction also was observed under lipid-rich conditions and found to be insensitive to proteasomal degradation of nascent apoB. We followed our study by examining lipid synthesis and mass. A 24-h exposure of cells to 72.8 μM tangeretin decreased intracellular synthesis of cholesteryl esters, free cholesterol, and TAG by 82, 45, and 64%, respectively; tangeretin also reduced the mass of cellular TAG by 37%. The tangeretin-induced suppression of TAG synthesis and mass were associated with decreased activities of DAG acyltransferase (up to –39.0 ± 3.0% vs. control) and microsomal triglyceride transfer protein (up to –35.5 ± 2.5% vs. control). Tangeretin was also found to activate the peroxisome proliferator-activated receptor, a transcription factor with a positive regulatory impact on FA oxidation and TAG availability (up to 36% increase vs. control). The data suggest that tangeretin modulates apoB-containing lipoprotein metabolism through multiple mechanisms.

Paper no. L9415 in *Lipids 39*, 143–151 (February 2004).

Epidemiological studies have yielded evidence that a diet rich in flavonoid-containing foods such as fruits, vegetables, wine, and tea is associated with lower risk of developing chronic diseases such as cardiovascular disease and cancer (1). The cardioprotective action of flavonoids has been attributed to several effects, including an inhibition of LDL oxidation, a decrease in platelet aggregation, an improvement in endothelial function, and recently, a reduction in cholesterol levels (2,3). The role of two common citrus flavonoids, hesperetin and naringenin, in lowering cholesterol levels has been investigated recently. Hesperetin and naringenin, which belong to the class of flavanones, are especially abundant in oranges and grapefruit, respectively, where they occur largely as glycosides called hesperidin and naringin (4). The hypolipidemic effects of citrus flavonoids have been studied extensively in the human hepatoma cell-line HepG2. HepG2 cells are an important *in vitro* model system commonly used to study the regulation of hepatic production and catabolism of apolipoprotein B (apoB)-containing lipoproteins (apoB-Lp) such as VLDL and LDL (5). In this cell-line, hesperetin and naringenin have been shown to dose-dependently reduce the secretion of apoB-Lp and suppress cellular synthesis of a core lipoprotein lipid component, cholesteryl esters (CE) (6). For both flavonoids, these effects were associated with a decreased activity and expression of acyl CoA:cholesterol acyltransferase (ACAT), an enzyme responsible for the synthesis of CE required for lipoprotein assembly (6,7). It was presumed from these studies that ACAT was the enzyme predominantly responsible in the assembly of apoB-Lp in HepG2 cells. However, further studies demonstrated that, for naringenin, the inhibition of ACAT was not the primary mechanism responsible for the reduced lipidation and subsequent secretion of apoB. Instead, naringenin's apoB-lowering effect was largely due to suppression of endoplasmic reticulum (ER) lumenal accumulation of TAG, secondary to microsomal triglyceride transfer protein (MTP) inhibition (8,9). MTP, in addition to catalyzing the transfer of lipids to nascent apoB molecules, has been shown to facilitate the accumulation and attainment of TAG within the ER lumen (10). Under naringenin treatment, insufficient MTP activity was suggested to be the primary reason for the lack of transfer of newly synthesized TAG from the microsomal membrane to the active lumenal pool (9).

In animal studies, dietary supplementation with hesperidin or with hesperidin/naringin mixtures has been shown to reduce blood cholesterol in rats and in ovariectomized mice (11,12). Substantial decreases in serum total and LDL cholesterol also were observed in rabbits with casein-induced hypercholesterolemia given concentrated orange or grapefruit juices (13).

Beneficial changes in lipoprotein metabolism observed in animals and cultured cells exposed to hesperetin, naringenin, and their glycosides prompted us to investigate the hypolipidemic potential of another group of minor components from citrus fruits—highly methoxylated flavones, termed polymethoxyflavones (PMF). PMF, which are known for their anticancer and anti-inflammatory activities (reviewed in Ref. 14), are found in high abundance in tangerines, bitter oranges, and

*To whom correspondence should be addressed at KGK Synergize Inc., Research and Development Division, Ste. 1030, 255 Queens Ave., London, ON Canada N6A 5R8. E-mail: kurowska@kgksynergize.com

Abbreviations: ACAT, acyl CoA:cholesterol acyltransferase, apo B, apolipoprotein B; apoB-Lp, apoB-containing lipoprotein; CE, cholesteryl esters; DGAT, diacylglycerol acyltransferase; EMSA, electrophoretic mobility shift assay; ER, endoplasmic reticulum; HMGR, 3-hydroxy-3-methylglutaryl-CoA reductase; MG-132, carbobenzoxy-L-leucyl-L-leucyl-L-leucinal; MTP, microsomal triglyceride transfer protein; MTT, 3-(4,5-dimethylthiazol-2-yl)-2,5-diphenyltetrazolium bromide; PMF, polymethoxyflavone(s); PPAR, peroxisome proliferator-activated receptor.

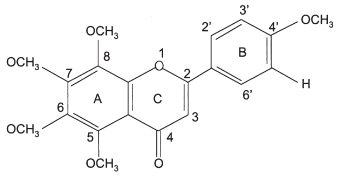

SCHEME 1

orange peel, where they occur as free aglycones (4). Studies on absorption and metabolism demonstrated that the most prevalent PMF, tangeretin (Scheme 1), is well absorbed and extensively metabolized (15). Recently, we showed that several natural and synthetic PMF have the ability to inhibit the net secretion of apoB in HepG2 cells (3). For the two most active PMF, tangeretin and nobiletin, the apoB IC_{50} concentrations (concentrations required to reduce medium apoB by 50% following a 24-h exposure) were much lower than those established for hesperetin and naringenin (7.3 and 13.1 μM vs. 142.2 and 178.1 μM, respectively) (3). This prompted us to speculate that PMF might have greater hypolipidemic potential *in vivo* than hesperidin and naringin. In agreement with this hypothesis, our recent experiments demonstrated that in hypercholesterolemic hamsters, supplementation with 1% tangeretin or with a 1% formulation consisting of tangeretin and other PMF significantly reduced serum total, VLDL + LDL-cholesterol, and TAG by 25, 39, and 48%, respectively. However, when the PMF were replaced with a 1:1 mixture of hesperidin and naringin, a much higher supplementation was required to produce lipid responses comparable to those obtained with 1% PMF (Kurowska, E.M., and Manthey, J.A., unpublished data). The combined content of tangeretin metabolic products in livers from hamsters fed 1% PMF diets was within a range similar to the tangeretin IC_{50} concentration obtained for HepG2 cells. This suggests that tangeretin and nobiletin concentrations that produced apoB-lowering responses in cultured HepG2 cells were physiologically relevant.

The powerful hypolipidemic and apoB-lowering responses induced by PMF *in vitro* and *in vivo* indicate that this particular group of citrus flavonoids might regulate hepatic lipid and apoB metabolism *via* distinct mechanism(s). Hesperetin and naringenin, as well as the principal soy isoflavones genistein and daidzein, have been shown to affect apoB metabolism mainly through inhibition of ACAT and MTP and, to a lesser extent, through enhanced expression and activity of the LDL receptor responsible for lipoprotein reuptake (8,16). On the other hand, two other plant flavonoids, taxifolin and quercetin, were largely associated with suppressed activities of two rate-limiting enzymes in the synthesis of cholesterol and TAG, 3-hydroxy-3-methylglutaryl-coenzyme A reductase (HMGR) and diacylglycerol acyltransferase (DGAT), respectively (17,18). This suggests that flavonoids modulate apoB production *via* multiple pathways and that structural differences may affect the extent by which flavonoids exert their lipid-lowering effects.

Thus far, flavonoids have not been reported to interact with lipid and apoB metabolism through other mechanisms except for those described above. However, recent experiments with natural nonflavonoid compounds have revealed that the hypolipidemic control also might involve enhanced cellular FA β-oxidation (19,20). β-Oxidation of FA *via* increased expression of the two rate-limiting enzymes of the peroxisomal and mitochondrial FA oxidation, acyl CoA oxidase and carnitine palmitoyl-CoA transferase, is known to be activated through peroxisome proliferator-activated receptors (PPAR) (19–21). Increased β-oxidation would thus reduce the availability of FA for incorporation into cellular TAG and limit the production of apoB-Lp. The present study was therefore undertaken to investigate the mechanism(s) by which tangeretin, the most abundant and most active PMF from citrus fruits, regulates apoB protein and lipid metabolism. Using HepG2 cells, we specifically examined the effects of tangeretin on several aspects involved in apoB production and the synthesis of intracellular lipids. Since *in vivo* results demonstrated that tangeretin was a potent serum TAG-reducing agent (Kurowska, E.M., and Manthey, J.A., unpublished data), we also addressed the influence of tangeretin on the activities of MTP, DGAT, and PPAR.

MATERIALS AND METHODS

Materials. Tangeretin (97.4% pure) was isolated from winterized tangerine peel oil precipitate. Tangerine oil precipitate was collected and washed extensively with hexane to remove the volatile oil constituents and other contaminants. The hexane-washed residue was dissolved in chloroform and dried by rotary evaporation. The purified tangeretin was obtained as previously reported (22) and stored at +4°C for up to 1 yr. All tissue culture reagents and plasticware were purchased from Life Technologies (Burlington, Ontario, Canada). MG-132 (carbobenzoxy-L-leucyl-L-leucyl-L-leucinal) was from Calbiochem-Novabiochem (La Jolla, CA). Unless otherwise stated, all other reagents were obtained from Sigma (St. Louis, MO).

Cell culture. HepG2 cells (American Type Culture Collection, Rockville, MD) were grown and maintained as described previously (6). Experimental media consisted of serum-free minimum essential medium containing 1% BSA. Immediately before use, tangeretin was solubilized in DMSO at a concentration of 67.1 mM. Final DMSO concentrations that were added to the cells did not exceed 0.5%. Untreated control cells were incubated with DMSO at corresponding concentrations.

ApoB ELISA and cellular lipid mass. ApoB concentrations in cell culture media were determined by a competitive ELISA essentially as described previously (6,23). Cellular free cholesterol, CE, and TAG contents were measured by enzymatic kits according to the manufacturer's protocol (Boehringer-Mannheim, Montréal, Québec, Canada) after extraction of lipids and their resolubilization (24,25).

Cholesterol and TAG synthesis. Cells were labeled with [1-^{14}C]acetate (0.5 μCi/mL) (Amersham Oakville, Ontario, Canada) to measure the rate of synthesis of cholesterol and CE or with [1-^{14}C]glycerol (0.5 μCi/mL) (Amersham) to determine the rate of TAG synthesis. The incorporation of radioactive tracers into cellular lipids was determined as described previously (6,7). The radioactivity incorporated into free cholesterol, CE,

and TAG was measured after separation of the lipid species by TLC (26). Cell proteins in parallel dishes were digested in 1 mL of 0.1 N NaOH and measured as described below.

DGAT activity assay. Cells were harvested into a Tris buffer (175 mM, pH 7.8) and homogenized with a sonicator. Esterification of DAG was measured by using labeled palmitoyl-CoA as described by Grigor and Bell (27). The assay was performed in a total volume of 250 µL of Tris buffer (175 mM, pH 7.8) containing FA-free BSA (0.14 mg/mL), $MgCl_2$ (4 mM), and 0.25 µCi/mL [palmitoyl 1-^{14}C]palmitoyl-CoA (40–60 mCi/mmol (PerkinElmer Life Science Research Products, Boston, MA). After a 10-min preincubation at 23°C, the reaction was started by adding homogenized cells (400 µg cell protein/mL) and 1,2-DAG (400 µM) for 10 min. The reaction was terminated by the addition of hexane, and the TAG formed was extracted and subjected to TLC in chloroform/acetic acid (96:4). Preliminary experiments indicated that whole-cell DGAT activity correlated with microsomal DGAT activity and that the assay was linear up to 1000 µg/mL of cell protein (data not shown).

MTP activity assay. Cells were harvested into a Tris buffer (10 mM Tris, 150 mM NaCl, 1 mM EDTA, pH 7.4) and homogenized with a sonicator. The MTP activity in the cell extracts was measured by a fluorescent assay according to the manufacturer's protocol (Roar Biomedical, New York, NY). The MTP activity assay uses fluorogenic-labeled donor liposomes and phospholipid acceptor liposomes. Measurements were made within the linear range of the assay.

PPAR activity assay. An electrophoretic mobility shift assay (EMSA) was performed using the PPAR GELSHIFT™ kit according to the manufacturer's protocol (Geneka Biotechnology, Inc., Carlsbad, CA). Nuclear protein extracts (5 µg protein) were prepared essentially as described by Dignam *et al.* (28). The extracts were then incubated in 20 µL of total reaction volume, which contained 3×10^6 cpm ^{32}P-labeled probe and 15 µL of binding buffer containing 4-(2-hydroxyethyl)-1-piperazineethanesulfonic acid. DNA–protein complexes were separated from the unbound DNA probe on a native 5% polyacryl-amide gel by electrophoresis at 200 V for 1 h. The sequence of the double-stranded oligonucleotide probes (labeled with T4 kinase and [γ-^{32}P]ATP and purified using micro-spin columns) containing the PPAR-α, -β, and -γ consensus was as follows: 5′-GGAACTAGGTCAAAGGTCATCCCCT-3′. Unlabeled competitor oligonucleotides were added in a 100-fold excess to confirm the specificity of the binding reactions. The band intensity of the autoradiograph was analyzed and quantified using the Gel Doc™ gel documentation system (Bio-Rad Laboratories, Inc., Hercules, CA).

Other methods. Cell protein content was measured using the Coomassie plus protein assay (Pierce, Rockford, IL) with BSA as the standard. Protein synthesis and secretion were quantitated by TCA precipitation as described previously (29). The MTT [3(4,5-dimethylthiazol-2-yl)-2,5-diphenyltetrazoloum bromide] assay was performed according to the method described by Hansen *et al.* (30) as modified by Kurowska (23).

Statistical analysis. The data are presented as means ± SEM of three independent experiments performed in duplicate. All results with apoB and lipids were normalized to the amount of cellular protein. Statistical analysis was done using Student's *t*-test, and $P < 0.05$ was considered significant.

RESULTS

Tangeretin inhibits apoB secretion time-dependently. To determine the time-course effect of tangeretin-induced decreases in net apoB production, the effect of the most active nontoxic concentration of tangeretin (72.8 µM) on medium accumulation of apoB was analyzed after a 2, 4, and 8 h of exposure to HepG2 cells. Preliminary experiments showed cell viability was not compromised at the 72.8 µM concentration as assessed by the MTT assay (data not shown). At the end of each incubation, culture media were collected and apoB was measured by ELISA. The results demonstrated that different incubation periods with 72.8 µM tangeretin caused very rapid reduction in net apoB secretion in a time-dependent manner. As shown in Figure 1, after a 2-h exposure to tangeretin, medium apoB content was significantly decreased by 52% ($n = 3$, $P < 0.05$ vs. the DMSO control), and the effects were more pronounced as incubation continued.

Tangeretin does not inhibit total protein synthesis and secretion. As a control to determine whether the effect of tangeretin was specific to apoB, cells were incubated with or without 72.8 µM tangeretin in the presence of ^{3}H-leucine (5 dpm/pmol) for 0, 1, 2, 3, and 4 h. The incorporation of label into cell and medium proteins was quantified by TCA precipitation. The results demonstrated that TCA-precipitable radioactivity from media and cells incubated with tangeretin remained unchanged vs. the

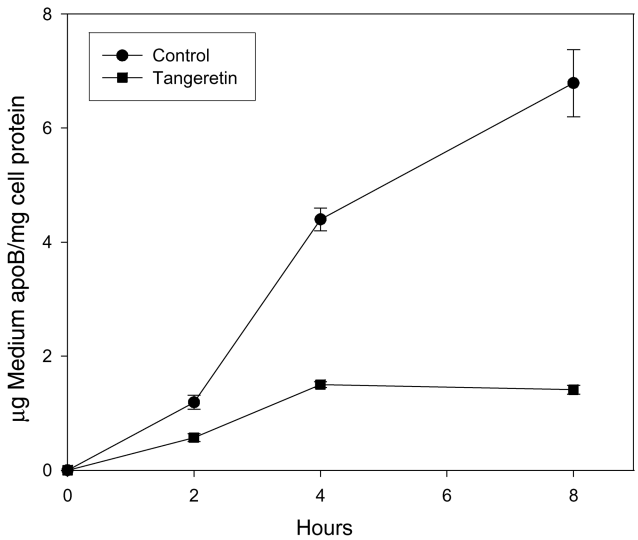

FIG. 1. Time-course effect of tangeretin on apolipoprotein B (apoB) accumulation in the media. Confluent HepG2 cells were incubated for 2 to 8 h in the absence (control) or presence of 72.8 µM of tangeretin. ApoB in the cell culture media was quantified by ELISA and expressed per milligram cell protein. Values are means ± SEM, $n = 3$. All tangeretin-treated values were significantly lower than the control values ($P < 0.05$).

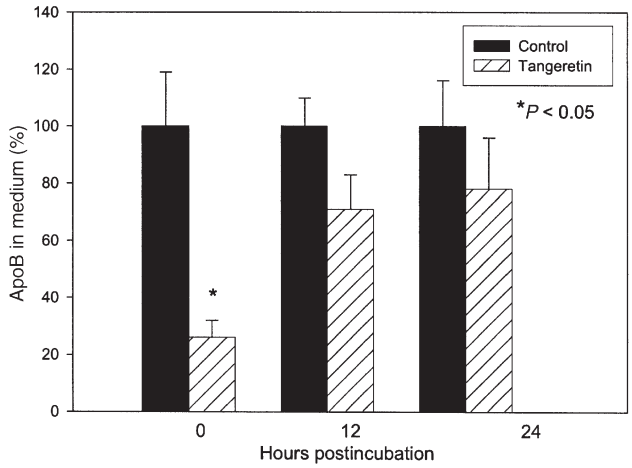

FIG. 2. Reversibility of the tangeretin effect on apoB secretion. Confluent HepG2 cells were incubated for 24 h in the absence or presence of 72.8 μM of tangeretin. The medium was removed and assayed for apoB content by ELISA. Cells were subsequently incubated with tangeretin-free medium for a further 12 or 24 h. The medium was again removed and assayed for apoB content by ELISA. The results are presented as a percentage of the control. Values are means ± SEM, $n = 3$; $^*P < 0.05$ vs. control. For abbreviation see Figure 1.

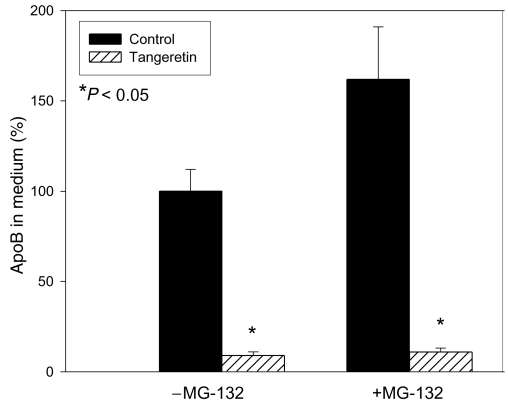

FIG. 3. Effect of tangeretin on net apoB secretion in the presence of carbobenzoy-L-leucyl-L-leucyl-L-leucinal (MG-132). Confluent HepG2 cells were preincubated for 1 h in the absence or presence of 10 μM MG-132 and incubated for a further 4 h in the absence or presence of 72.8 μM tangeretin, with or without MG-132. The medium was collected, and apoB secretion was measured by ELISA. The results are presented as a percentage of the control. Values are means ± SEM, $n = 3$; $^*P < 0.05$ vs. the respective control. For other abbreviations see Figure 1.

untreated control (data not shown, $n = 3$, $P < 0.05$), indicating that the flavonoid did not alter total protein synthesis and secretion. This suggests that the effect of tangeretin on medium apoB content was specific.

Tangeretin-induced inhibition of net apoB secretion is partly reversible. To establish whether the apoB-lowering effect of tangeretin is reversible, HepG2 cells were incubated with 72.8 μM tangeretin for 24 h and then postincubated in a flavonoid-free media for 10 and 24 h. Aliquots of media were collected after the initial 24-h incubation and after the postincubation periods. ApoB secretion was analyzed by ELISA as just described. After both postincubation periods, net apoB secretion returned to within 70–80% of control values (Fig. 2), which suggests that HepG2 cells were, to some degree, able to recover from the apoB-reducing effect of tangeretin.

Tangeretin does not increase the proteasomal degradation of apoB. To determine whether an increase in proteasomal degradation could be responsible for the tangeretin-induced decline in net apoB secretion, HepG2 cells were exposed to tangeretin in the absence and presence of MG-132, a specific inhibitor of the 26S proteasome. HepG2 cells were preincubated for 1 h in the absence or presence of 10 μM MG-132, followed by a 4-h incubation with 72.8 μM tangeretin in the absence or presence of 10 μM MG-132. Aliquots of media were collected at the end of the 5-h treatment, and apoB secretion was analyzed by ELISA. Addition of MG-132 to the untreated control cells raised the medium apoB concentration by 62% (Fig. 3), indicating a protection of apoB from proteasomal degradation. This is consistent with previous data (6,31). In the presence of tangeretin, however, MG-132 failed to block the proteosomal degradation of apoB. After the incubation of cells with tangeretin, an equally marked reduction in apoB secretion was observed in the absence and presence of MG-132 (91 and 93%, respectively) ($n = 3$, $P < 0.05$). Thus, our results indicate that tangeretin does not exert its apoB-lowering effect by increasing proteasomal degradation of the nascent apoB molecule.

Tangeretin inhibits net apoB secretion in oleate-stimulated cells. To assess the effect of oleate-stimulated increases in cellular lipid biosynthesis on a tangeretin-induced decline in medium apoB, cells were incubated with or without oleate-rich medium in the presence and absence of 72.8 μM tangeretin. HepG2 cells were initially incubated for 1 h in the absence or presence of 0.8 mM sodium oleate. This was followed by a 4-h incubation in the presence or absence of 72.8 μM tangeretin, with or without 0.8 mM sodium oleate. ApoB secretion was measured by ELISA. After the 4-h exposure to tangeretin, the inhibition of net apoB secretion was similar for oleate-treated cells and non-oleate-treated cells (74 and 86%, respectively) ($n = 3$, $P < 0.05$ vs. the respective controls) (Fig. 4). In the presence of oleic acid alone, net apoB secretion increased by 32% compared with the untreated control, consistent with earlier data (32). The results suggest that tangeretin also may reduce the net apoB secretion under lipid-rich conditions.

Tangeretin inhibits cellular synthesis and accumulation of lipids. To determine whether exposure to tangeretin altered the biosynthesis of cellular lipids, the effects of tangeretin on the synthesis of cholesterol, CE, and TAG were assessed by measuring the rate of incorporation of [1-^{14}C]acetate and [1-^{14}C]glycerol into cellular lipids. Also, lipid mass was determined as a confirmatory test. Cells were treated for 24 h in the presence and absence of 72.8 μM tangeretin. As shown in Figure 5, tangeretin significantly reduced the rate of incorporation of radiolabeled precursors into cellular cholesterol, CE, and TAG (45, 82, and 64%, respectively) ($n = 3$, $P < 0.05$ vs. the respective controls). The incubation with tangeretin also significantly decreased the mass of cellular TAG by 37% ($n = 3$, $P < 0.05$ vs. the untreated

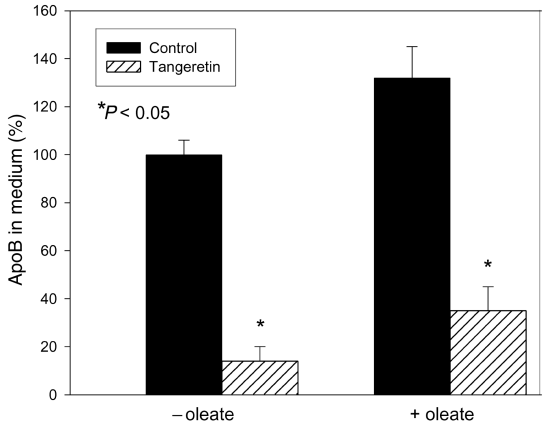

FIG. 4. Effect of tangeretin on net apoB secretion in the presence of exogenous oleate. Confluent HepG2 cells were preincubated for 1 h in the absence or presence of 0.8 mM sodium oleate and incubated for a further 4 h in the absence or presence of 72.8 μM tangeretin, with or without oleate. Medium was collected and apoB secretion was measured by ELISA. The results are presented as a percentage of the control. Values are means ± SEM, $n = 3$; $^*P < 0.05$ vs. the respective control. For abbreviations see Figure 1.

control) but did not alter the mass of cellular cholesterol and CE (Figs. 6A and 6B). The data indicate that the apoB-lowering effect of tangeretin was associated with reduced rates of synthesis of a number of core lipids and with a selective decrease in cellular accumulation of TAG.

Tangeretin decreases DGAT and MTP activities. To determine whether tangeretin-induced decreases in the cellular synthesis and accumulation of TAG were due to an inhibition of DGAT, the rate-limiting enzyme in TAG synthesis, cells were incubated in the presence of various concentrations of tangeretin for 24 h and DGAT activity was measured. As shown in Figure 7A, tangeretin added in various concentrations to the

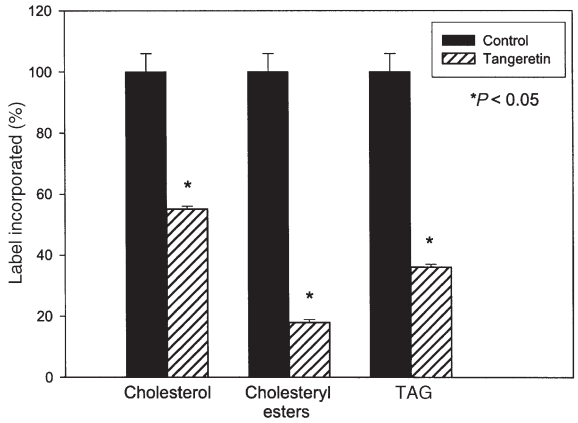

FIG. 5. Effect of tangeretin on cellular lipid synthesis. Confluent HepG2 cells were preincubated for 19 h in the medium with or without 72.8 μM tangeretin and then labeled for 5 h with [1-^{14}C]acetate or [1-^{14}C]glycerol in the presence or absence of 72.8 μM tangeretin. The radioactivity incorporated into cellular lipids was determined by TLC and scintillation counting. The results are presented as a percentage of the control. Values are means ± SEM, $n = 3$; $^*P < 0.05$ vs. control.

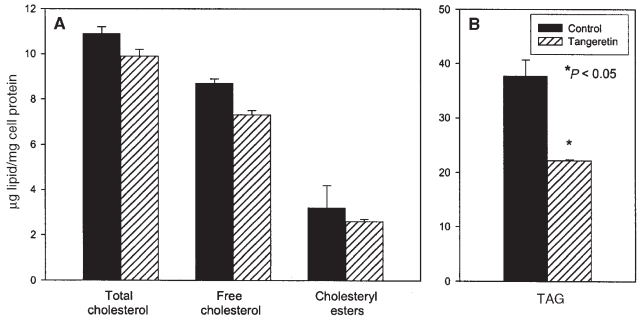

FIG. 6. Effect of tangeretin on the cellular mass of (A) cholesterol and (B) TAG. HepG2 cells were incubated for 24 h in the absence or presence of 72.8 μM tangeretin. Following incubation, cellular lipids were extracted, quantified by spectrophotometric assays, and expressed per milligram of cell protein. Values are means ± SEM, $n = 3$; $^*P < 0.05$ vs. control.

culture medium for 24 h decreased the rate of incorporation of [^{14}C]palmitoyl-CoA into cellular TAG. The percent inhibition of DGAT activity was 35.5 ± 3.5% for a tangeretin concentration of 29.1 μM and 39.0 ± 3.0% for a tangeretin concentration of 72.8 μM ($n = 3$, $P < 0.05$ vs. the DMSO control). Using the same basic protocol, various concentrations of tangeretin were subsequently tested for their effect on the activity of MTP. As shown in Figure 7B, tangeretin decreased MTP activity by 22 ± 1% at a concentration of 29.1 μM and by 35.5 ± 2.5% at a concentration of 72.8 μM ($n = 3$, $P < 0.05$ vs. control). The results of these studies demonstrate that tangeretin dose-dependently inhibited DGAT and MTP activities in HepG2 cells.

Tangeretin increases PPAR activity. To further characterize the decrease in TAG mass, we measured the activity level of PPAR. Activation of PPAR has been shown to enhance β-oxidation (19,20), which may provide an alternative mechanism for the decrease in TAG mass.

Cells were treated with tangeretin at concentrations of 29.1 or 72.8 μM for 24 h and PPAR activity in the homogenates was

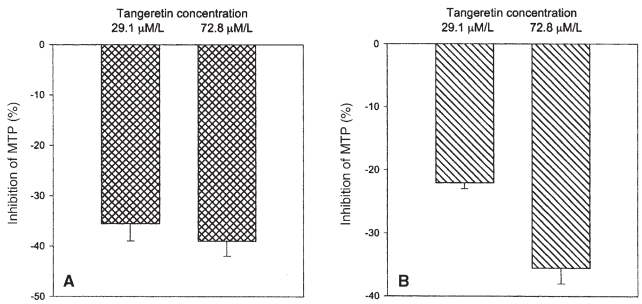

FIG. 7. Effect of tangeretin on (A) diacylglycerol acyltransferase (DGAT) and (B) microsomal triglyceride transfer protein (MTP) activities. HepG2 cells were incubated for 24 h with or without tangeretin at concentrations of 29.1 and 72.8 μM, harvested, and homogenized. DGAT activity was measured using labeled palmitoyl-CoA, and MTP activity was determined by a fluorescent assay. The results are presented as a percentage of the control. Values are means ± SEM, $n = 3$, $^*P < 0.05$ vs. control. DGAT activity in control cells was 260 nmol/min/mg (experiment 1), 350 nmol/min/mg (experiment 2), and 297 nmol/min/mg (experiment 3).

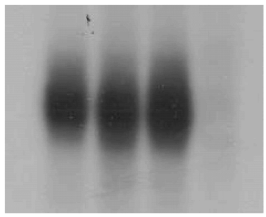

Tangeretin concentration	PPAR activation
29.1 μM/L	+25%
72.8 μM/L	+36%

FIG. 8. Effect of tangeretin on peroxisome proliferator-activated receptor (PPAR) activity. HepG2 cells were incubated for 24 h with or without tangeretin at concentrations of 29.1 and 72.8 μM, and nuclear proteins were isolated. PPAR activity was determined by electrophoretic mobility shift assay and autoradiography. Band intensities were scanned densitometrically. The figure is a representative autoradiograph showing the signals to PPAR with its corresponding table. The results in the bar chart are presented as a percentage of the control.

assessed by EMSA. Figure 8 is the autoradiograph of a typical experiment with a corresponding table. The results demonstrate that incubation with increasing concentrations of tangeretin stimulated HepG2 cell PPAR activation in a dose-dependent manner. Tangeretin increased PPAR activation by 25% at a concentration of 29.1 μM and by 36% at a concentration of 72.8 μM. The results suggested that tangeretin-induced increases in PPAR activity might contribute to the observed decreases in cellular accumulation of TAG *via* β-oxidation. The experiment was repeated twice with similar results.

DISCUSSION

In our initial studies, we examined the time-course effect of tangeretin-induced decreases in net apoB secretion as well as the specificity and reversibility of the tangeretin-mediated apoB-lowering effect. Incubation with the maximum nontoxic concentration of tangeretin decreased net apoB secretion very rapidly, with a 50% reduction in medium apoB mass produced after only 2 h. This early onset was similar to that reported for hesperetin and naringenin except that the decline in medium apoB levels occurred after 4 h (6). Our data suggest that the tangeretin-induced apoB-lowering response was largely mediated by suppressing the assembly and secretion of apoB-Lp. The increased reuptake of apoB-Lp was unlikely to play an important role in the diminished apoB accumulation since the receptor-mediated modulation of apoB-Lp is regulated at the level of gene expression and therefore could not occur as early as 2 h after initiation of the treatment (33). The tangeretin-induced apoB-lowering responses appeared to be apoB-specific, as demonstrated by the lack of difference in intracellular and secreted TCA-precipitable radioactivity between cells incubated with and without tangeretin. This observation was consistent with a similar specificity of apoB modulation reported for hesperetin, naringenin, and quercetin (6,18). Incidentally, hesperetin and naringenin also had little influence on the secretion of HDL-associated apolipoprotein A-I (7), suggesting that the same might hold true for tangeretin. Our experiments further revealed that the effect of tangeretin, similar to that of hesperetin and naringenin, was not completely reversible. The impaired ability of HepG2 cells to recover fully from the apoB-lowering effect caused by the 24-h exposure to tangeretin might be related to the long residency time of flavonoid metabolites inside the cells. It is now well documented that animal and human hepatocytes have the ability to metabolize flavonoids, largely to glucuronides (34–36; Kurowska, E.M., and Manthey, J.A., unpublished data). However, the hepatocyte-mediated conversion of flavonoids into their conjugated derivatives might be relatively slow. It was previously shown that HepG2 cells exposed to the flavonoid chrysin metabolized 50% of the compound after a 6-h incubation and that less than 10% of the unmetabolized chrysin was detected in the medium after 24 h (36).

The results of our subsequent studies were aimed at investigating the mechanisms of action of tangeretin on apoB secretion. That regulation of hepatic apoB secretion occurs at the cotranslational and posttranslational levels is widely accepted, as nascent apoB molecules are either secreted or degraded intracellularly. An ER-localized ubiquitin-proteasome pathway has been primarily implicated in the intracellular degradation of apoB (reviewed in Ref. 37). Davis (37) has proposed that in the presence of lipids, the ubiquinated apoB can be assembled into lipoproteins and be secreted. Our results demonstrate that the tangeretin-induced medium apoB-lowering responses were not reversed in the presence of the specific 26S proteasome inhibitor MG-132, despite an increase in apoB secretion observed in the presence of MG-132 alone. This suggests that tangeretin was unlikely to act by enhancing the proteasome-mediated cotranslational degradation of newly synthesized apoB. Increased proteasomal activity was also unlikely to play a role in the modulation of net apoB secretion by another flavonoid, taxifolin (17). However, evidence for involvement of the proteasomal pathway was recently demonstrated for naringenin (8). The cause for the discrepancy remains unknown.

To determine whether the apoB-lowering effect of tangeretin may be maintained under lipid-rich conditions, HepG2 cells were challenged with oleic acid. The net apoB secretion was increased in the presence of oleate alone, presumably due to a stimulation of TAG synthesis, which is thought to protect fully formed apoB from posttranslational degradation in the ER compartment (32). Addition of tangeretin reversed the stimulatory effect of oleate, and the degree of inhibition was comparable to that observed in the absence of oleate. Thus, our results indicate that tangeretin might induce medium apoB-lowering responses possibly by decreasing the rate of synthesis of TAG and/or other cellular lipids. The inhibition of apoB secretion in oleate-stimulated cells was also previously described for taxifolin, quercetin, hesperetin, and naringenin (7,17,18).

The possibility that tangeretin might inhibit the net apoB secretion by reducing the rates of synthesis of one or more cellular lipids was confirmed in experiments using the radiolabeled lipid substrates [1-^{14}C]acetate and [1-^{14}C]glycerol. The results indicated that exposure of HepG2 cells to tangeretin in serum-free

media significantly decreased the rates of synthesis of cellular CE, free cholesterol, and TAG. The flavonoid-induced inhibition of cellular cholesterol and CE synthesis was also observed earlier for hesperetin, naringenin, genistein, daidzein, and taxifolin, and these effects were associated with suppressed cellular cholesterol esterification, reduced activity and expression of ACAT, and/or suppressed activity of HMGR (6,7,16,17). In contrast, the inhibition of TAG synthesis was thus far demonstrated for only one flavonoid, taxifolin (17). In the presence of hesperetin, naringenin, and soy isoflavones, hepatic TAG synthesis was either unchanged or slightly stimulated (6,16). Again, the cause for the discrepancy remains unknown but suggests that structural differences in these polyphenolic compounds can influence lipid metabolism differently. The methoxy side groups found in tangeretin may have additional lipid-lowering properties in terms of TAG synthesis. Incubation with tangeretin also reduced the mass of intracellular TAG but did not affect the mass of intracellular cholesterol. The absence of the expected cholesterol mass reduction remains unexplained; however, the results suggest that tangeretin might promote cholesterol turnover by inhibiting its synthesis while at the same time enhancing its catabolism.

The question remains as to which lipid and enzyme is predominantly responsible in the assembly of apoB-Lp under flavonoid treatment. Borradaile *et al.* (8) recently made progress in this area by ruling out ACAT activity and CE availability in the regulation of apoB-Lp by the citrus flavonoid naringenin in HepG2 cells. By comparing naringenin to selective HMGR, ACAT, and MTP inhibitors, they concluded that naringenin inhibited apoB secretion by limiting the accumulation of TAG in the active microsomal lumenal pool *via* MTP inhibition (8,9). It is suggested that MTP, in addition to catalyzing the transfer of lipids to nascent apoB molecules, facilitates the transfer of newly synthesized TAG from the microsomal membrane into the lumen (reviewed in Ref. 38). In HepG2 cells, the microsomal lumenal TAG pool is viewed as the regulatory pool responsible for lipoprotein assembly (39). Thus, the suppression of TAG synthesis and the reduction in cellular TAG accumulation with tangeretin were likely to be the primary mechanisms responsible for their apoB-lowering effect.

The observed suppression of cellular TAG synthesis and mass in the tangeretin-treated cells remained in agreement with our *in vivo* results, which demonstrated that dietary supplementation with tangeretin or with mixed PMF decreased the hepatic accumulation of TAG in hypercholesterolemic hamsters (Kurowska, E.M., and Manthey, J.A., unpublished data).

The unique ability of tangeretin to reduce cellular TAG synthesis prompted us to focus on investigating its effect on the activity of DGAT, a microsomal enzyme that plays a central role in the esterification of FA to form TAG. DGAT catalyzes the terminal step in cellular TAG synthesis by using DAG and fatty acyl-CoA. It therefore controls the availability of TAG for the assembly and secretion of lipoproteins (40). Our data indicate that incubation of HepG2 cells with various concentrations of tangeretin inhibited DGAT activity. However, the 39% suppression of the enzyme achieved after a 24-h exposure to 72.8 μM tangeretin was not sufficient to explain the greater 64% inhibition of TAG synthesis, as assessed by the incorporation of [1-^{14}C]glycerol into cellular TAG. It is therefore possible that tangeretin also modulated activities of other enzymes involved in TAG synthesis or that it diminished the availability of FA for TAG synthesis by increasing FA β-oxidation. The involvement of DGAT in the flavonoid-induced control of apoB secretion also has been demonstrated for quercetin incubated with human intestinal CaCo-2 cells (18).

The reduced availability of TAG, *via* inhibition of DGAT activity, partly accounted for the tangeretin-induced decreases in net apoB secretion. Previous evidence has suggested that MTP-dependent modulation in TAG availability within the ER lumen is also an important determining factor in the assembly and secretion of apoB-Lp (8,37). In our study, tangeretin dose-dependently reduced MTP activity by up to 36%. This effect was very similar to that reported for hesperetin and naringenin (7). Taken together, the inhibition of MTP activity combined with the 39% suppression in DGAT activity could contribute to the decrease in medium apoB accumulation observed with tangeretin (72.8 μM, 24 h). The relatively weak dose-dependency of both DGAT and MTP suppression in response to treatment with 29.1 and 72.8 μM tangeretin corresponded to the equally weak dose-dependency of medium apoB reduction observed in HepG2 cells treated with the same concentrations of tangeretin for 24 h (80 and 86%, respectively) (3).

Since DGAT and MTP activity results suggest that other mechanisms may be involved in limiting TAG availability under our conditions, we sought to examine the effect of tangeretin on TAG availability by assessing its impact on activation of cellular PPAR. In the liver, PPARα activation has been shown to reduce the quantity of FA available for synthesis of TAG by enhancing β-oxidation of FA *via* increased expression of the two rate-limiting enzymes of the peroxisomal and mitochondrial FA oxidation, acyl CoA oxidase and carnitine palmitoyl-CoA transferase (21). This mechanism could therefore be responsible for DGAT-independent inhibition of TAG synthesis in tangeretin-treated HepG2 cells. Our results demonstrated that tangeretin dose-dependently activated hepatocellular PPAR by as much as 36%. This suggests that tangeretin may limit the availability of FA and thus reduce the lipid components necessary for lipoprotein assembly. The hypothesis that tangeretin might act as a natural PPAR agonist is interesting since several synthetic PPARα agonists have proven effective in the treatment of dyslipidemia and diabetes (41,42).

In conclusion, our data suggest that tangeretin, a novel hypolipidemic flavonoid from citrus fruits, lowers the secretion of apoB-Lp by decreasing cellular TAG availability *via* at least three major mechanisms: inhibition of DGAT activity and TAG synthesis, inhibition of MTP-mediated accumulation of newly synthesized TAG within the ER lumen, and activation of PPAR. Additionally, the inhibition of net apoB secretion by tangeretin might be partly mediated *via* suppression of the MTP-catalyzed transfer of core lipids to nascent apoB molecules. The fact that tangeretin affects many key factors involved in the regulation of hepatic apoB secretion may have important clinical implications in the treatment of hypertriglyceridemia associated with obesity

and type 2 diabetes. Further studies are therefore needed to examine the potential therapeutic applications of this novel nutraceutical agent.

ACKNOWLEDGMENTS

This work was partly supported by research grants obtained from the Florida Department of Citrus (E.M.K.), American Heart Association, Hawaii Affiliate, grant #0350528Z (A.G.T.), and the Robert C. Perry Fund of the Hawaii Community Foundation, grant #20020609 (A.G.T.).

REFERENCES

1. Hollman, P.C., Hertog, M.G., and Katan, M.B. (1996) Role of Dietary Flavonoids in Protection Against Cancer and Coronary Heart Disease, *Biochem. Soc. Trans. 24*, 785–789.
2. Cook, N.C., and Samman, S. (1996) Flavonoids, Chemistry, Metabolism, Cardioprotective Effects, and Dietary Sources, *J. Nutr. Biochem. 7*, 66–76.
3. Kurowska, E.M., and Manthey, J.A. (2002) Regulation of Lipoprotein Metabolism in HepG2 Cells by Citrus Flavonoids, *Adv. Exp. Med. Biol. 505*, 173–179.
4. Horowitz, R.M., and Gentili, B. (1977) Flavonoid Constituents of Citrus, in *Citrus Science and Technology* (Nagy, S., Shaw, P.E., and Veldhuis, M.K., eds.), Vol. 1, pp. 397–426, AVI Publishing, Westport, CT.
5. Dixon, J.L., and Ginsberg, H.N. (1993) Regulation of Hepatic Secretion of Apolipoprotein B-Containing Lipoproteins: Information Obtained from Cultured Liver Cells, *J. Lipid Res. 34*, 167–179.
6. Borradaile, N.M., Carroll, K.K., and Kurowska, E.M. (1999) Regulation of ApoB Metabolism in HepG2 Cells by the Citrus Flavanones Hesperetin and Naringenin, *Lipids 34*, 591–598.
7. Wilcox, L.J., Borradaile, N.M., de Dreu, L.E., and Huff, M.W. (2001) Secretion of Hepatocyte ApoB Is Inhibited by the Flavonoids, Naringenin and Hesperetin, *via* Reduced Activity and Expression of ACAT2 and MTP, *J. Lipid Res. 42*, 725–734.
8. Borradaile, N.M., de Dreu, L.E., Barrett, P.H., and Huff, M.W. (2002) Inhibition of Hepatocyte ApoB Secretion by Naringenin: Enhanced Rapid Intracellular Degradation Independent of Reduced Microsomal Cholesteryl Esters, *J. Lipid Res. 43*, 1544–1554.
9. Borradaile, N.M., de Dreu, L.E., Barrett, P.H., Behrsin, C.D., and Huff, M.W. (2003) Hepatocyte ApoB-Containing Lipoprotein Secretion Is Decreased by the Grapefruit Flavonoid, Naringenin, *via* Inhibition of MTP-Mediated Microsomal Triglyceride Accumulation, *Biochemistry 11*, 1283–1291.
10. Wang, Y., Tran, K. and Yao, Z. (1999) The Activity of Microsomal Triglyceride Transfer Protein Is Essential for Accumulation of Triglyceride Within Microsomes in McA-RH7777 Cells. A Unified Model for the Assembly of Very Low Density Lipoproteins, *J. Biol. Chem. 274*, 27793–27800.
11. Bok, S.H., Lee, S.H., Park, Y.B., Bae, K.H., Son, K.H., Jeong, T.S., and Choi, M.S. (1999) Plasma and Hepatic Cholesterol and Hepatic Activities of 3-Hydroxy-3-Methyl-Glutaryl-CoA Reductase and Acyl CoA:Cholesterol Transferase Are Lower in Rats Fed Citrus Peel Extract or a Mixture of Citrus Bioflavonoids, *J. Nutr. 129*, 1182–1185.
12. Chiba, H., Uehara, M., Wu, J., Wang, X., Masuyama, R., Suzuki, K., Kanazawa, K., and Ishimi, Y. (2003) Hesperidin, a Citrus Flavonoid, Inhibits Bone Loss and Decreases Serum and Hepatic Lipids in Ovariectomized Mice, *J. Nutr. 133*, 1892–1897.
13. Kurowska, E.M., Borradaile, N.M., Spence, J.D., and Carroll, K.K. (2000) Hypocholesterolemic Effects of Dietary Citrus Juices in Rabbits, *Nutr. Res. 20*, 121–129.
14. Manthey, J.A., Guthrie, N., and Grohmann, K. (2001) Biological Properties of Citrus Flavonoids Pertaining to Cancer and Inflammation, *Curr. Med. Chem. 8*, 135–153.
15. Nielsen, S.E., Breinholt, V., Cornett, C., and Dragsted, L.O. (2000) Biotransformation of the Citrus Flavone Tangeretin in Rats. Identification of Metabolites with Intact Flavane Nucleus, *Food Chem. Toxicol. 38*, 739–746.
16. Borradaile, N.M., de Dreu, L.E., Wilcox, L.J., Edwards, J.Y., and Huff, M.W. (2002) Soya Phytoestrogens, Genistein and Daidzein, Decrease Apolipoprotein B Secretion from HepG2 Cells Through Multiple Mechanisms, *Biochem J. 366*, 531–539.
17. Theriault, A., Wang, Q., Van Iderstine, S.C., Chen, B., Franke, A.A., and Adeli, K. (2000) Modulation of Hepatic Lipoprotein Synthesis and Secretion by Taxifolin, a Plant Flavonoid, *J. Lipid Res. 41*, 1969–1979.
18. Casaschi, A., Wang, Q., Dang, K., Richards, A., and Theriault, A. (2002) Intestinal Apolipoprotein B Secretion Is Inhibited by the Flavonoid Quercetin: Potential Role of Microsomal Triglyceride Transfer Protein and Diacylglycerol Acyltransferase, *Lipids 37*, 647–652.
19. Berge, R.K., Madsen, L., Vaagenes, H., Tronstad, K.J., Gottlicher, M., and Rustan, A.C. (1999) In Contrast with Docosahexaenoic Acid, Eicosapentaenoic Acid and Hypolipidaemic Derivatives Decrease Hepatic Synthesis and Secretion of Triacylglycerol by Decreased Diacylglycerol Acyltransferase Activity and Stimulation of Fatty Acid Oxidation, *Biochem. J. 343*, 191–197.
20. Takahashi, N., Kawada, T., Goto, T., Yamamoto, T., Taimatsu, A., Matsui, N., Kimura, K., Saito, M., Hosokawa, M., Miyashita, K., and Fushiki, T. (2002) Dual Action of Isoprenols from Herbal Medicines on Both PPARγ and PPARα in 3T3-L1 Adipocytes and HepG2 Hepatocytes, *FEBS Lett. 514*, 315–322.
21. Keller, J.M., Collet, P., Bianchi, A., Huin, C., Bouillaud-Kremarik, P., Becuwe, P., Schohn, H., Domenjoud, L., and Dauca, M. (2000) Implications of Peroxisome Proliferator-Activated Receptors (PPARs) in Development, Cell Life Status and Disease, *Int. J. Dev. Biol. 44*, 429–442.
22. Middleton, E., Jr., Drzewiecki, G., and Tatum, J. (1987) The Effects of Citrus Flavonoids on Human Basophil and Neutrophil Function, *Planta. Med. 53*, 325–328.
23. Kurowska, E.M. (2001) Determination of Cholesterol-Lowering Potential of Minor Dietary Components by Measuring Apolipoprotein B Responses in HepG2 Cells, in *Methods in Enzymology, Flavonoids and Polyphenols* (Packer, L., ed.), Vol. 335, pp. 398–404, Academic Press, San Diego, CA.
24. Musanti, R., Giorgini, L., Lovisoli, O., Pirillo, A., Chiari, A., and Ghiselli, G. (1996) Inhibition of Acyl-CoA:Cholesterol Acyltransferase Decreases Apolipoprotein B-100-Containing Lipoprotein from HepG2 Cells, *J. Lipid Res. 37*, 1–14.
25. Carr, T.P., Andersen, C.J., and Rudel, L.L. (1993) Enzymatic Determination of Triglyceride, Free Cholesterol, and Total Cholesterol in Tissue Lipid Extracts, *Clin. Biochem. 26*, 39–42.
26. Zhang, Z., Sniderman, A.D., Kalant, D., Vu, H., Monge, J.C., Tao, Y., and Cianflone, K. (1993) The Role of Amino Acids in ApoB100 Synthesis and Catabolism in Human HepG2 Cells, *J. Biol. Chem. 268*, 26920–26926.
27. Grigor, M.R., and Bell, R.M. (1962) Separate Monoacylglycerol and Diacylglycerol Acyltransferases Function in Intestinal Triacylglycerol Synthesis, *Biochim. Biophys. Acta 712*, 464–472.
28. Dignam, J.D., Lebovitz, R.M., and Roeder, R.G. (1983) Accurate Transcription Initiation by RNA Polymerase II in a Soluble Extract from Isolated Mammalian Nuclei, *Nucleic Acids Res. 11*, 1475–1489.
29. Kurowska, E.M., and Carroll, K.K. (1998) Hypocholesterolemic Properties of Nitric Oxide. *In vivo* and *In vitro* Studies Using Nitric Oxide Donors, *Biochim. Biophys. Acta 1392*, 41–50.

30. Hansen, M.B., Nielsen, S.E., and Berg, K. (1989) Re-examination and Further Development of a Precise and Rapid Dye Method for Measuring Cell Growth/Cell Kill, *J. Immunol. Methods 119*, 203–210.
31. Sakata, N., Wu, X., Dixon, J.L., and Ginsberg, H.N. (1993) Proteolysis and Lipid-Facilitated Translocation Are Distinct but Competitive Processes That Regulate Secretion of Apolipoprotein B in HepG2 Cells, *J. Biol. Chem. 268*, 22967–22970.
32. Arrol, S., Mackness, M.I., and Durrington, P.N. (2000) The Effects of Fatty Acids on Apolipoprotein B Secretion by Human Hepatoma Cells (HepG2), *Atherosclerosis 150*, 255–264.
33. Kraft, H.G., Demosky, S.J., Jr., Schumacher, K., Brewer, H.B., Jr., and Hoeg, J.M. (1992) Regulation of LDL Receptor, ApoB, and ApoE Protein and mRNA in HepG2 cells, *DNA Cell Biol. 11*, 291–300.
34. Senafi, S.B., Clarke, D.J., and Burchell, B. (1994) Investigation of the Substrate Specificity of a Cloned Expressed Human Bilirubin UDP-Glucuronosyltransferase: UDP-Sugar Specificity and Involvement in Steroid and Xenobiotic Glucuronidation, *Biochem. J. 303*, 233–240.
35. O'Leary, K.A., Day, A.J., Needs, P.W., Mellon, F.A., O'Brien, N.M., and Williamson, G. (2003) Metabolism of Quercetin-7- and Quercetin-3-glucuronides by an *in vitro* Hepatic Model: The Role of Human β-Glucuronidase, Sulfotransferase, Catechol-*O*-methyltransferase and Multi-resistant Protein 2 (MRP2) in Flavonoid Metabolism, *Biochem. Pharmacol. 65*, 479–491.
36. Galijatovic, A., Otake, Y., Walle, K., and Walle, T. (1999) Extensive Metabolism of the Flavonoid Chrysin by Human Caco-2 and HepG2 Cells, *Xenobiotica 29*, 1241–1256.
37. Davis, R.A. (1999) Cell and Molecular Biology of the Assembly and Secretion of Apolipoprotein B-Containing Lipoproteins by the Liver, *Biochim. Biophys. Acta 1440*, 1–31.
38. Hussain, M.M., Shi, J., and Dreizen, P. (2003) Microsomal Triglyceride Transfer Protein and Its Role in ApoB-Lipoprotein Assembly, *J. Lipid Res. 44*, 22–32.
39. Wu, X., Shang, A., Jiang, H., and Ginsberg, H.N. (1996) Low Rates of ApoB Secretion from HepG2 Cells Result from Reduced Delivery of Newly Synthesized Triglyceride to a "Secretion-Coupled" Pool, *J. Lipid Res. 37*, 1198–1206.
40. Cases, S., Smith, S.J., Zheng, Y.W., Myers, H.M., Lear, S.R., Sande, E., Novak, S., Collins, C., Welch, C.B., Lusis, A.J., Erickson, S.K., and Farese, R.V., Jr. (1998) Identification of a Gene Encoding an Acyl CoA:Diacylglycerol Acyltransferase, a Key Enzyme in Triacylglycerol Synthesis, *Proc. Natl. Acad. Sci. USA 27*, 13018–13023.
41. Fruchart, J.C., Staels, B., and Duriez, P. (2001) PPARs, Metabolic Disease and Atherosclerosis, *Pharmacol. Res. 44*, 345–352.
42. Berger, J., and Moller, D.E. (2002) The Mechanisms of Action of PPARs, *Annu. Rev. Med. 53*, 409–435.

[Received November 17, 2003, and in final form January 27, 2004; revision accepted February 2, 2004]

β-Oxidation of 18:3n-3 in Atlantic Salmon (*Salmo salar* L.) Hepatocytes Treated with Different Fatty Acids

Bente E. Torstensen* and Ingunn Stubhaug

National Institute of Nutrition and Seafood Research (NIFES), 5804 Bergen, Norway

ABSTRACT: To study whether Atlantic salmon β-oxidation was affected by dietary FA composition, an *in vitro study* with primary hepatocytes was undertaken. Isolated hepatocyte cultures were stimulated with either 16:0, 18:1n-9, 18:2n-6, 18:3n-3, 20:5n-3, or 22:6n-3 in triplicate for 24 h. In addition, a control was included where no FA stimulation was performed, also in triplicate. After stimulation, radiolabeled [1-^{14}C]18:3n-3 was added and the cells were incubated for 2 h at 20°C. The cells were then harvested, and radioactivity was determined in the acid-soluble part of the cells and medium, i.e., the end products of the β-oxidation pathway. Specific β-oxidation activity was significantly higher in hepatocytes stimulated with 18:3n-3. Further, when taking into account the amount of radiolabeled [1-^{14}C]18:3n-3 taken up by the cells—the relative amount of β-oxidized [1-^{14}C]18:3n-3 of the total FA taken up by the hepatocytes—no significant differences were found. Thus, the regulation of β-oxidation activity in the primary Atlantic salmon hepatocytes seems to be at the level of FA uptake and transport into the cell. This *in vitro* study shows that the catabolism processes in salmon hepatocytes are affected by the FA available and probably already regulated at the level of FA uptake.

Paper no. L9384 in *Lipids 39*, 153–160 (February 2004).

In vitro studies done on mitochondrial β-oxidation in fish suggest that there exist substrate preferences for saturated and monounsaturated FA over PUFA (reviewed by Henderson, Ref. 1). Further, 22:1n-11 and 16:0 were found to serve equally well as substrates for mitochondrial β-oxidation in trout (*Onchorhynchus mykiss*) liver (2). Trout liver mitochondria, however, are reported to oxidize 18:0, 18:1, 18:2, and 18:3 at the same rate, 70–80% of pyruvate (3). This was in contrast with red muscle mitochondria, where monounsaturated FA and 22:1 and 22:6n-3 were oxidized at higher rates than 18:2n-6 and 18:3n-3 (3). Further, in developing yolk-sac larvae of Atlantic halibut (*Hippoglossus hippoglossus* L.), 22:6n-3 was reported to be the quantitatively most important FA in energy metabolism (4). Certain vegetable oils contain high levels of FA such as 16:0 and 18:1n-9, possibly preferred for β-oxidation. Potentially, although not previously shown, increased energy production from FA may spare dietary protein used for energy production; thus, higher levels of amino acids may be available for muscle growth in Atlantic salmon.

Generally, the key point in the regulation of mitochondrial β-oxidation is thought to be carnitine palmitoyl transferase I (CPT-I); CPT-I may be inhibited by malonyl-CoA, which is synthesized by the action of acetyl-CoA carboxylase. The inhibition of CPT-I by malonyl-CoA has also been confirmed in Atlantic salmon (5). Both natural factors, such as high-fat diets and PUFA, as well as fibrates can induce mitochondrial and peroxisomal β-oxidation in rodents (6–9). Increased β-oxidation capacities in rat liver may be due to the proliferation of mitochondria and peroxisomes, leading to increased expression of the enzymes involved in β-oxidation (9–11). There are, however, major species differences in the peroxisomal response, and it has been reported that the peroxisomal acyl-CoA oxidase activity in salmon hepatocytes is only mildly increased by fibrates and that the activity is not significantly increased after FA treatment (12).

To increase the β-oxidation capacity in cells and tissues, the number of mitochondria, peroxisomes, and enzymes and/or enzyme activity has to increase (13). Certain FA, such as 20:5n-3, have been found to act as mitochondrial proliferators, thus increasing the capacity for β-oxidation, whereas prolonged feeding of 22:6n-3 increases peroxisomal β-oxidation in rats (6). In an experiment in which Atlantic salmon post-smolt were fed diets with different FA compositions, no changes were found in tissue β-oxidation capacity due to dietary FA composition (14). Thus, to study the effects of dietary FA on Atlantic salmon β-oxidation capacity, *in vitro* studies must first be undertaken. The aim of this study was to investigate whether stimulating primary hepatocytes with saturated, monounsaturated, and n-6 and n-3 FA of different chain lengths and unsaturation would affect the hepatocyte β-oxidation capacity of Atlantic salmon.

MATERIALS AND METHODS

Fish and hepatocyte isolation. Atlantic salmon post-smolt, with weights ranging from 128 to 331 g, were anesthetized with methomidate (7 g L^{-1}) and killed with a blow to the head. Livers were weighed (hepatosomatic index ranged from 1.1 to 1.3%), and hepatocytes were isolated as described by Bell and coworkers (15). Briefly, the liver was removed from the fish immediately after death, and the gall bladder and the main blood

*To whom correspondence should be addressed at National Institute of Nutrition and Seafood Research (NIFES), P.O. Box 176, sentrum, 5804 Bergen, Norway. E-mail: bente.torstensen@nifes.no

Abbreviations: CPT I, carnitine palmitoyl transferase I; CPT II, carnitine palmitoyl transferase II; FAF-BSA, fatty acid-free bovine serum albumin; LDH, lactate dehydrogenase; FABP, fatty acid-binding protein; FATP, fatty acid transport protein; NIFES, National Institute of Nutrition and Seafood Research; PPAR, peroxisome proliferator-activated receptor.

vessels were removed from the liver prior to perfusion *via* the hepatic vein with solution A [calcium- and magnesium-free Hank's solution (HBSS; GIBCO, Invitrogen Co., Grand Island, NY), with 10 mM HEPES and 1 mM EDTA (Sigma, St. Louis, MO)] to clear blood from the tissue. The liver was finely cut with scissors and incubated with solution A containing 0.1% collagenase (Type 2; GIBCO) for 45 min at 20°C in a shaking water bath. The digested liver was then filtered through 100-μm nylon gauze, and the cells were collected by centrifugation at $1000 \times g$ for 5 min. The supernatant was removed, and the cell pellet was washed with 20 mL of solution A containing 1% FA-free BSA (FAF-BSA), followed by another centrifugation at $1000 \times g$ for 5 min at 4°C. The supernatant was removed, and the cells were resuspended in 5 mL of medium L-15 (BioWhittaker, Rockland, ME) containing 10 mM HEPES and 200 mM glutamine (GIBCO). One hundred microliters of the cell suspension was mixed with 100 μL tryptophan blue to investigate the viability and count the amount of hepatocytes using a light microscope. A high viability (92–98%) of unstained cells was routinely observed. The cell suspension was then diluted to a concentration of 2.5 mill cells mL^{-1} prior to dispersion into 25-cm^2 flasks. One hundred microliters was retained for protein determination, which was performed using a Technicon RA-1000 clinical analyzer system (Bayer, Paris, France) according to standard Technicon methods, also described by Sandnes *et al.* (16).

The primary cell cultures were preincubated at 20°C for 24 h prior to initiating the experimental conditions. Each experimental treatment was performed in triplicate, except for stimulation with 18:1n-9, which was performed with four parallels. The study was approved by the local ethics committee at NIFES.

Pilot experiment. Prior to the experiment with FA stimulation, a pilot experiment was performed to test the optimal FA concentration and time of stimulation. Hepatocytes, at a density of *ca.* 5×10^5 cells/cm^2, were incubated with a final concentration of either 60 or 200 μM 18:3n-3 and a control without FA added to medium G [i.e., 1 mL glutamine, 1 mL penicillin/ streptomycin/fungiozone; 10,000 U/10,000 μg/25 μg mL^{-1}, 2 mL 2% Ultroser G (E. Pedersen and Son AS, Oslo, Norway), amounting to 100 mL with L-15 medium]. Stimulation was performed for either 4, 24, or 48 h at 20°C prior to assaying for β-oxidation activity as described below.

Stimulation of hepatocytes with different FA. Hepatocytes, at a density of *ca.* 5×10^5 cells/cm^2, were incubated with 60 μM (final concentration) of either 20:5n-3, 22:6n-3, 18:3n-3, 18:2n-6, 18:1n-9, or 16:0 (Sigma) bound to FAF-BSA and a control with no FA added in 25-m^2 cell culture flasks and with a total volume of 5 mL using medium L-15 (BioWhittaker) mixed with glutamine, penicillin/streptomycin, and Ultroser. The incubation was performed at 20°C for 24 h followed by an assay for β-oxidation activity as described below. Samples for lactate dehydrogenase (LDH) (EC 1.1.1.27) activity and protein were harvested at the start, after 24 h of FA stimulation following the addition of radiolabeled FA. LDH was quantified according to Technicon method No. SM4-0170D91 by RA1000. Total protein measurements were used to calculate specific LDH activity in the medium as units (U)/mg protein, with 1 U defined as 1 μmol NADH consumed min^{-1} (12). An increase in LDH activity in the medium during the cell experiment indicated decreased viability of the cells, causing leakage of LDH from the cells.

Assay of hepatocyte β-oxidation activity. Radioactive acid-soluble products including HCO_3^- were measured in isolated hepatocytes using [1-^{14}C]18:3n-3 (American Radiolabeled Chemicals, Inc., St. Louis, MO) bound to FAF-BSA as substrate essentially as described previously (7,17–19). The hepatocytes, dispensed in 5 mL with medium G (as described previously) in 25-cm^2 cell culture flasks, were treated with 0.925 MBq of [1-^{14}C]18:3n-3 bound to FAF-BSA, prepared as described by Bell *et al.* (15). After the addition of radiolabeled FA, the flasks were incubated for 2 h at 20°C with the screw cap closed to prevent escape of CO_2; thus, CO_2 was dissolved as HCO_3^- in the medium. The incubation was terminated after 2 h by cooling the culture flasks on ice. The cell layer was removed from the flask using a cell scraper, and the cell suspension was transferred into a 10-mL conical plastic tube. The flask was washed with 1 mL of ice-cold HBSS/FAF-BSA (Hank's solution with FAF-BSA, 50 mg mL^{-1}). The cell suspension was centrifuged for 5 min at $1400 \times g$. The supernatant (medium) was then transferred to a clean 10-mL conical plastic tube. For determination of acid-soluble products, 250 μL of the medium was mixed with 100 μL of 6% FAF-BSA and shaken well; 1 μL ice-cold 1 M $HClO_4$ (Merck KGaA, Darmstadt, Germany) was then added to precipitate nonoxidized [1-^{14}C]18:3n-3. The mix was centrifuged at $2400 \times g$ for 10 min, and 500 μL of the supernatant, mixed with 8 mL of scintillation cocktail (Lumasafe™ Plus; Amersham Pharmacia Biotech, Little Chalfont, Buckinghamshire, England), was counted for radioactivity. The cell pellet was washed with 5 mL ice-cold HBSS (GIBCO) containing 1% FAF-BSA and then centrifuged at $1400 \times g$ for 5 min. After discarding the supernatant, the cell pellet was resuspended in 1 mL ddH_2O and analyzed for acid-soluble products and total radioactivity as just described. CO_2 was reported by Frøyland and coworkers (17) to account for less than 10% of total activity; thus, media were precipitated as described above.

Statistical analysis. Significant differences in β-oxidation between treatments were analyzed by breakdown and one-way ANOVA followed by Tukey's honestly significant differences test, using CSS:Statistica (v. 4.5; StatSoft Inc., Tulsa, OK). The significance level was set at $P \leq 0.05$, and data are presented as mean ± SD. The number of experimental units in this study was set as the number of cell culture flasks in each experimental group ($n = 3$, and $n = 4$ for 18:1n-9 stimulation).

RESULTS

In the pilot experiment, the recovery of radiolabeled 18:3n-3 ranged from 86 to 101%, irrespective of the concentration of FA or time of stimulation. Viability of the cells, measured as increased LDH in the medium, was increased by less than 10% during the 48 h of FA stimulation in all groups except the group stimulated with 200 μM for 48 h, where LDH activity increased

by 30%. Further, viability of the cells, measured by staining with tryptophan blue, showed high viability in all groups (92–98% unstained cells). To determine the optimal time of stimulation with the different FA, samples were analyzed after 4, 24, and 48 h of stimulation. There was a decrease in β-oxidation activity of [1-^{14}C]18:3n-3 in the cells with stimulation with 18:3n-3 for 4 to 48 h (Fig. 1). The decrease was highest when the FA concentration was 200 μM, compared with 60 μM, of 18:3n-3. In the following experiment with stimulation using different FA, a 60-μM final concentration of each FA for 24 h was used.

Primary hepatocytes were stimulated in triplicate with 60 μM of either 16:0, 18:1n-9, 18:2n-6, 18:3n-3, 20:5n-3, or 22:6n-3. In addition, one group (in triplicate) was not stimulated with any FA as a negative control. Cell viability was recorded as described above and was satisfactory. The recovery of [1-^{14}C]18:3n-3 was calculated as the amount of radiolabeled FA in the cells and medium. The radiolabeled FA in the medium would then include both FA embedded in lipoproteins and FA bound to albumin, which was not taken up by the hepatocytes and acid-soluble products in the medium. However, we postulated that the amount recovered in lipoproteins was minor compared with the total radioactivity, since the assay lasted for only 2 h, with a low concentration of radiolabeled FA added; thus, the data for recovery represent the total medium and total cell radioactivity. The recovery of [1-^{14}C]18:3n-3 ranged from 75 to 115% in the different groups. Total β-oxidation activity, measured as the total acid-soluble product in medium and cells after 2 h of incubation with [1-^{14}C]18:3n-3, was significantly affected by stimulation of certain FA for 24 h (Fig. 2). Compared with the control, the hepatocytes stimulated with 18:3n-3 showed significantly higher total β-oxidation activity. Further, stimulation with both saturated and monounsaturated FA gave significantly lower β-oxidation activity compared with 18:3n-3. Stimulation with 18:2n-6, 20:5n-3, and 22:6n-3 gave increased hepatic β-oxidation activity compared with the control, although not statistically significant. By adding the radioactivity recovered from [1-^{14}C]18:3n-3 in cells and the acid-soluble metabolites in the medium, an estimate was made of how much added [1-^{14}C]18:3n-3 had been taken up by the cells (Fig. 3). The uptake ranged from 24 to 42%, and the differences in uptake of [1-^{14}C]18:3n-3 were dependent on the FA with which the cells had been stimulated (Fig. 3). Hepatocytes stimulated with 18:3n-3 had a significantly more efficient uptake of [1-^{14}C]18:3n-3 than either the control or hepatocytes stimulated with 16:0. The uptake was also lower compared with 18:3n-3 in the 20:5n-3, 22:6n-3, 18:2n-6, and 18:1n-9 groups, although not statistically significant. Further, when calculating the relative β-oxidation of the total [1-^{14}C]18:3n-3 taken up by the cells, no statistically significant differences between treatments were found (Fig. 4). This was in contrast with the relative β-oxidation of [1-^{14}C]18:3n-3 compared with total [1-^{14}C]18:3n-3 added to the hepatocytes (Fig. 4). Although not statistically significant, the β-oxidized [1-^{14}C]18:3n-3 in cells stimulated with 18:2n-6 was eight percentage points higher compared with 18:1n-9-stimulated cells (Fig. 4). Of the radiolabeled FA taken up by the cells, approximately 50% was β-oxidized, whereas the remaining 50% was either incorporated into phospholipids or TAG, further desaturated and elongated, chain-shortened, or incorporated into lipoproteins and excreted into the medium. These different pathways were not specifically analyzed in this study.

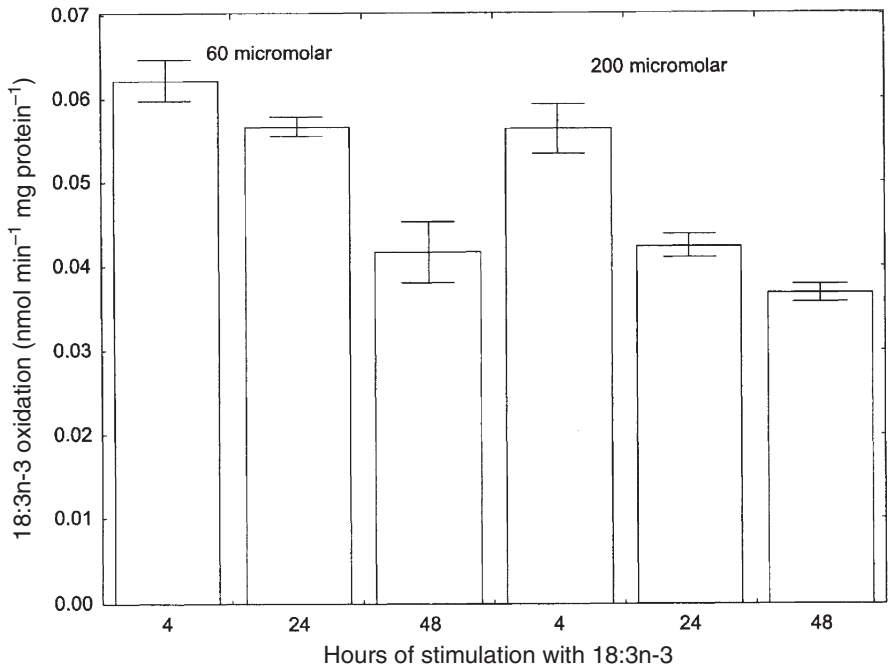

FIG. 1. Total β-oxidation activity of [1-^{14}C]18:3n-3 (nmol min^{-1} mg protein^{-1}) in Atlantic salmon hepatocytes stimulated with 60 and 200 μM 18:3n-3 for 4, 24, and 48 h. Data are presented as mean ± SD (n = 3; n = 4 for 18:1n-9).

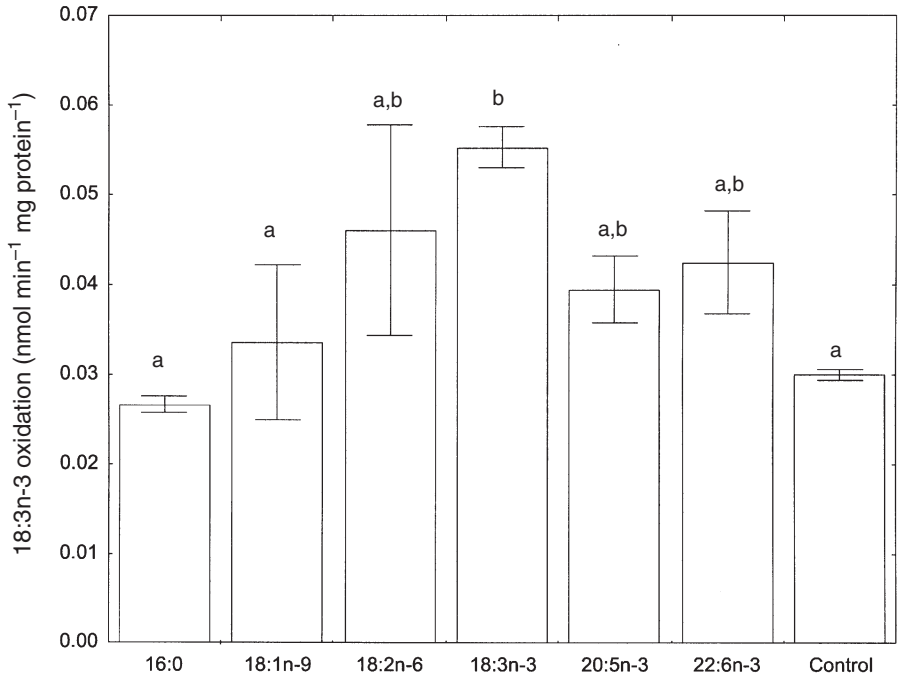

FIG. 2. Total β-oxidation activity of [1-^{14}C]18:3n-3 (nmol min^{-1} mg protein^{-1}) in Atlantic salmon hepatocytes stimulated with 60 μM of different FA for 24 h. Data are presented as mean ± SD (n = 3; n = 4 for 18:1n-9). Different lowercase letters indicate statistical differences ($P \leq 0.01$).

DISCUSSION

Numerous scientific reports are available regarding alternative lipid sources in aquaculture feeds, especially for Atlantic salmon (14,15,20–34). A major concern and challenge with introducing alternative lipid sources into Atlantic salmon diets is that the dietary FA composition must be designed so that a higher proportion of the dietary lipid is used for energy production, thus potentially sparing dietary protein for muscle growth. To achieve this goal, the total capacity of β-oxidation of the salmon tissues has to be increased, possibly by certain dietary FA. However, in dietary studies detailed investigations

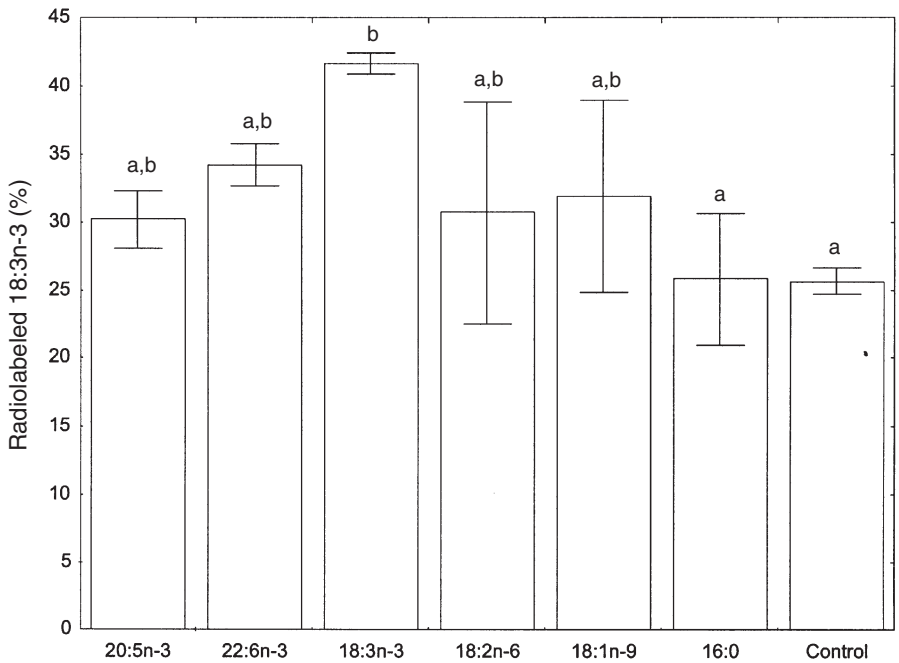

FIG. 3. Relative uptake of [1-^{14}C]18:3n-3 in hepatocytes (total cells + acid-soluble-medium) stimulated with different FA for 24 h. Data are presented as mean ± SD (n = 3; n = 4 for 18:1n-9). Different lowercase letters indicate statistical differences ($P \leq 0.05$).

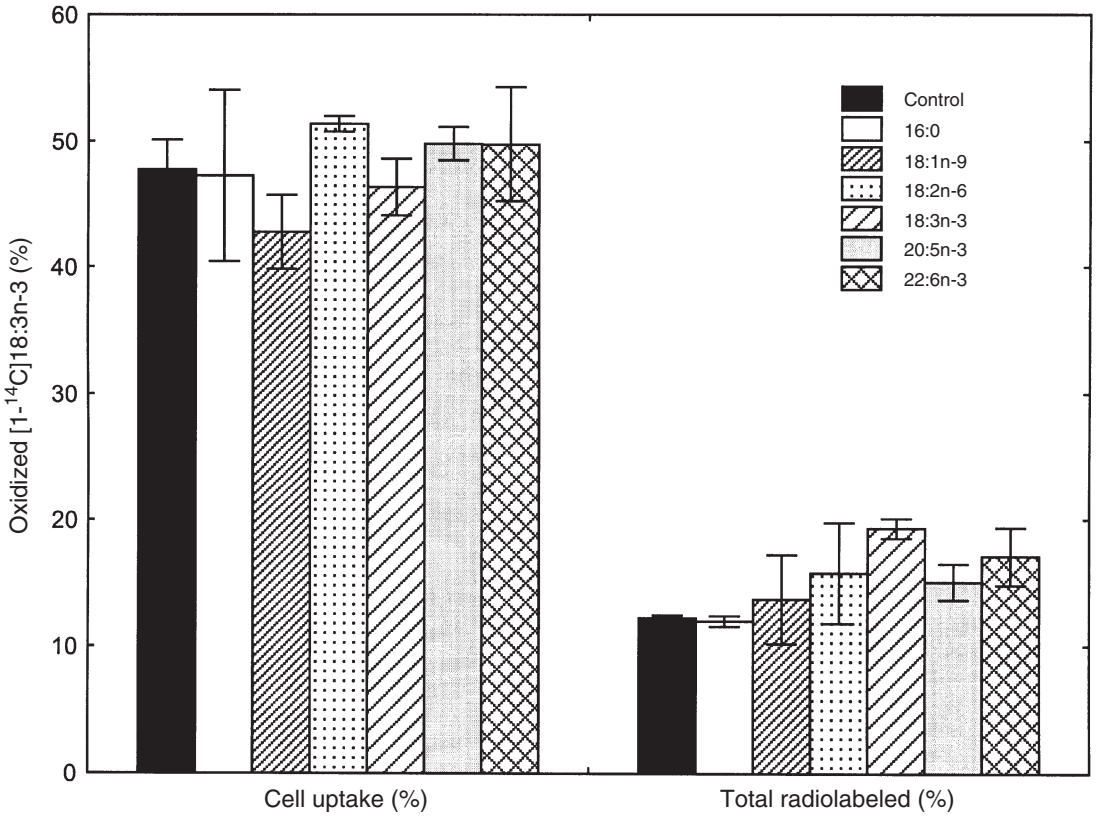

FIG. 4. Relative amount of [1-^{14}C]18:3n-3 oxidized compared with the total amount of radiolabeled FA taken up by the hepatocytes (left columns) and with the total amount added [1-^{14}C]18:3n-3 from hepatocytes stimulated with different FA for 24 h. Data are presented as mean ± SD (n = 3; n = 4 for 18:1n-9).

of individual FA are very difficult, leading to cell studies with a higher degree of control of specific nutrients. In the current *in vitro* study, we demonstrate that Atlantic salmon hepatic β-oxidation is affected by the type of input FA. The total β-oxidation activity of [1-^{14}C]18:3n-3 when the cells had been stimulated with 18:3n-3 for 24 h was higher than in all other groups, especially compared with the control and with saturated and monounsaturated FA stimulation. However, when taking into account the amount of β-oxidized FA relative to the amount taken up by the cell, no major differences were found. Thus, differences in the amount of β-oxidized [1-^{14}C]18:3n-3 seemed to be regulated at the level of FA transport and uptake by the hepatocytes rather than by an actual increased β-oxidation activity of mitochondria and peroxisomes. The uptake and transport of FA are thought to be mediated by FA transport proteins (FATP) and FA-binding proteins (FABP), respectively. FATP have not yet been described in fish; however, studies in rodents have shown that this membrane-bound protein also has very long chain acyl-CoA synthetase activity, suggesting a FA uptake *via* esterification-coupled influx (35,36). The three membrane-bound transporters described in mammals and rodents are all regulated by members of the peroxisome proliferator-activated receptor (PPAR) family of transcription factors (37). These transcription factors also regulate lipid catabolism, suggesting a probable correlation between FA uptake and β-oxidation of FA.

In rat heart and muscle, a correlation between β-oxidation and cytosolic FABP content has been reported (38). Further, a PPARα agonist increased muscle FABP mRNA and β-oxidation enzyme activity in rat skeletal muscle (39). In fish, intracellular FABP concentrations are reported to increase in response to acclimation to the cold (40), which is correlated with increased β-oxidation.

Compared with the control group and hepatocytes stimulated with 16:0, the β-oxidation of [1-^{14}C]18:3n-3 increased 1.8- and 2.1-fold, respectively, in the 18:3n-3-stimulated hepatocytes. Takahashi and coworkers (41) showed that FA β-oxidation increased 2.5-fold with CLA administration in mouse liver. This was concomitant with increased mRNA levels of various FA oxidation enzymes, such as CPT I, carmitine palmitoyl transferase II (CPT II), acyl-CoA oxidase, and long-chain acyl-CoA dehydrogenase. Further, the activity of oxidation enzymes and the mRNA levels were higher in mice fed 18:2n-6 compared with mice fed 16:0 (41), which is in accordance with the current results. Totland and coworkers (11) found that feeding rats EPA generally increased mitochondrial size and CPT II expression, whereas DHA increased peroxisomal fatty acyl-CoA oxidase activity in the liver. To elucidate the mechanism leading to the increased hepatocyte β-oxidation in the current study, further studies of salmon gene transcription regulation should be included. However, the results indicate that regulation was at the FA uptake level and not at the mitochondrial

or peroxisomal enzyme level. An alternative pathway of the radiolabeled [1-^{14}C]18:3n-3 is through cellular uptake and lipoprotein synthesis, followed by excretion again into the medium. These radiolabeled [1-^{14}C]18:3n-3 would be counted in the medium fraction and thus not included in the amount of radioactivity taken up by the cell. In rodents, lipoprotein metabolism is reportedly affected by dietary lipid composition, perhaps through direct regulation by FA of gene expression (42). However, neither apolipoprotein nor lipoprotein synthesis was measured in the current study. Further investigations are necessary to establish the quantitative role of lipoprotein synthesis in this *in vitro* system.

Of the [1-^{14}C]18:3n-3 added to the hepatocyte assay, 11 to 20% was β-oxidized. This is in accordance with results from rodent hepatocytes (7) using a similar assay to measure β-oxidation. A study with hepatocytes from Atlantic salmon fed an EFA-deficient diet, however, reported that only 2–4% of the radiolabeled 18:2n-6 and 18:3n-3 were β-oxidized (19) after 3 h of incubation, although at a 5°C lower incubation temperature compared with the current study.

When stimulating the hepatocytes with different FA, the medium contained no other FA than the experimental FA. This was also the case prior to stimulation when the cells settled in the cell flasks. Thus, the cells in the control group and the hepatocytes stimulated with 16:0 and 18:1n-9 experienced a lower status of EFA 48 h after liver perfusion. Atlantic salmon hepatocytes have the ability to desaturate and elongate [1-^{14}C]18:3n-3 to longer-chain PUFA [19,30,32,43,44]. Ruyter and Thomassen (19) reported increased desaturation and elongation of 18:3n-3 in EFA-deficient Atlantic salmon hepatocytes. However, they also reported very low (2–4%) β-oxidation of 18:3n-3 (19) owing to preferential esterification of the n-3 EFA. Compared with that study, the hepatocytes in the current study were not EFA-deficient enough to affect the β-oxidation results significantly .

Regression feeding studies with Atlantic salmon fed alternative lipid sources (30,32,45,46) have shown that a dietary FA substrate given in great surplus leads to increased catabolism of that specific FA. This is the case in both muscle and liver for saturated FA, monounsaturated FA, 18:2n-6, and 18:3n-3, although not for 22:6n-3 *in vivo* (46). An *in vitro* study with salmon hepatocytes, however, showed an efficient β-oxidation of [1-^{14}C]22:6n-3 when given as the only substrate (45). Thus, *in vivo* studies that support the current results exist, indicating that the FA uptake and catabolism of FA are upregulated when the dietary supply is in surplus (30,32,34,46). The current study indicates that regulation may occur at the levels of cellular uptake, lipoprotein synthesis, and transport, although by which mechanism this is regulated remains to be elucidated.

Previous dietary studies with Atlantic salmon have demonstrated that red and white muscle are quantitatively the most important tissues for FA catabolism (5,45,47–49). Thus, further longer-term studies should be performed with cell cultures, also from muscle cells, to determine the quantitative importance of a stimulation of processes leading to increased β-oxidation.

ACKNOWLEDGMENTS

The National Institute of Nutrition and Seafood Research (NIFES) is thanked for financing the study, and Betty Irgens is acknowledged for excellent technical assistance.

REFERENCES

1. Henderson, R.J. (1996) Fatty Acid Metabolism in Freshwater Fish with Particular Reference to Polyunsaturated Fatty Acids, *Arch. Anim. Nutr. 49*, 5–22.
2. Henderson, R.J., and Sargent, J.R. (1985) Chain-Length Specificities of Mitochondrial and Peroxisomal β-Oxidation of Fatty Acids in Livers of Rainbow Trout, *Comp. Biochem. Physiol. 82B*, 79–85.
3. Kiessling, K.-H., and Kiessling, A. (1993) Selective Utilization of Fatty Acids in Rainbow Trout (*Onchorhynchus mykiss* Walbaum) Red Muscle Mitochondria, *Can. J. Zool. 71*, 248–251.
4. Rønnestad, I., Finn, R.N., Lein, I., and Lie, Ø. (1995) Compartmental Changes in the Contents of Total Lipid, Lipid Classes and Their Associated Fatty Acids in Developing Yolk-Sac Larvae of Atlantic Halibut, *Hippoglossus hippoglossus* (L.), *Aquacult. Nutr. 1*, 119–130.
5. Frøyland, L., Madsen, L., Eckhoff, K.M., Lie, Ø., and Berge, R. (1998) Carnitine Palmitoyltransferase I, Carnitine Palmitoyl Transferase II, and Acyl-CoA Oxidase Activities in Atlantic Salmon (*Salmo salar*), *Lipids 33*, 923–930.
6. Frøyland, L., Madsen, L., Vaagenes, H., Totland, G.K., Auwerx, J., Kryvi, H., Staels, B., and Berge, R.K. (1997) Mitochondrion Is the Principal Target for Nutritional and Pharmacological Control of Triglyceride Metabolism, *J. Lipid Res. 38*, 1851–1858.
7. Madsen, L., Rustan, A.C., Vaagenes, H., Berge, K., Dyrøy, E., and Berge, R.K. (1999) Eicosapentaenoic and Docosahexaenoic Acid Affect Mitochondrial and Peroxisomal Fatty Acid Oxidation in Relation to Substrate Preference, *Lipids 34*, 951–963.
8. Madsen, L., Frøyland, L., Dyrøy, E., Helland, K., and Berge, R.K. (1998) Docosahexaenoic and Eicosapentaenoic Acids Are Differently Metabolized in Rat Liver During Mitochondria and Peroxisome Proliferation, *J. Lipid Res. 39*, 583–593.
9. Willumsen, N., Vaagenes, H., Asiedu, D., Lie, Ø., Rustan, A.C., and Berge, R. (1996) Eicosapentaenoic Acid but Not Docosahexaenoic Acid (both as ethyl esters) Increases Mitochondrial Fatty Acid Oxidation and Upregulates 2,4-Dienoyl-CoA Reductase Gene Expression. A Potential Mechanism for the Hypolipidemic Action of Fish Oil in Rats, *Lipids 31*, 579–592.
10. Willumsen, N., Hexeberg, S., Skorve, J., Lundquist, M., and Berge, R.K. (1993) Docosahexaenoic Acid Shows No Triglyceride-Lowering Effects but Increases the Peroxisomal Fatty Acid Oxidation in Liver of Rats, *J. Lipid Res. 34*, 13–22.
11. Totland, G.K., Madsen, L., Klemetsen, B., Vaagenes, H., Kryvi, H., Frøyland, L., Hexeberg, S., and Berge, R.K. (2000) Proliferation of Mitochondria and Gene Expression of Carnitine Palmitoyl Transferase and Fatty Acyl-CoA Oxidase in Rat Skeletal Muscle, Heart and Liver by Hypolipidemic Fatty Acids, *Biol. Cell 92*, 1–13.
12. Ruyter, B., Andersen, Ø., Dehli, A., Östlund Farrants, A.-K., Gjøen, T., and Thomassen, M.S. (1997) Peroxisome Proliferator Activated Receptors in Atlantic Salmon (*Salmo salar*): Effects on PPAR Transcription and Acyl-CoA Oxidase Activity in Hepatocytes by Peroxisome Proliferators and Fatty acids, *Biochim. Biophys. Acta 1348*, 331–338.
13. Schoonjans, K., Staels, B., and Auwerx, J. (1996) The Peroxisome Proliferator Activated Receptors (PPARs) and Their Effects on Lipid Metabolism and Adipocyte Differentiation, *Biochim. Biophys. Acta 1302*, 92–109.
14. Torstensen, B.E., Lie, Ø., and Frøyland, L. (2000) Lipid Metabolism and Tissue Composition in Atlantic Salmon (*Salmo salar* L.)—Effects of Capelin Oil, Palm Oil, and Oleic Acid-Enriched Sunflower Oil as Dietary Lipid Sources, *Lipids 35*, 653–664.

15. Bell, J.G., Tocher, D., Farndale, B.M., Cox, D.I., McKinney, R.W., and Sargent, J.R. (1997) The Effect of Dietary Lipid on Polyunsaturated Fatty Acid Metabolism in Atlantic Salmon (*Salmo salar*) Undergoing Parr-Smolt Transformation, *Lipids 32*, 515–525.
16. Sandnes, K., Lie, Ø., and Waagbø, R. (1988) Normal Ranges of Some Blood Chemistry Parameters in Adult Farmed Atlantic Salmon, *Salmo salar*, *J. Fish Biol. 32*, 129–136.
17. Frøyland, L., Madsen, L., Sjursen, W., Garras, A., Lie, Ø., Songstad, J., Rustan, A.C., and Berge, R.K. (1997) Effect of 3-Thia Fatty Acids on the Lipid Composition of Rat Liver, Lipoproteins, and Heart, *J. Lipid Res. 38*, 1522–1533.
18. Christiansen, R., Borrebaek, B., and Bremer, J. (1976) The Effect of (–)Carnitine on the Metabolism of Palmitate in Liver Cells Isolated from Fasted and Refed Rats, *FEBS Lett. 62*, 313–317.
19. Ruyter, B., and Thomassen, M.S. (1999) Metabolism of n-3 and n-6 Fatty Acids in Atlantic Salmon Liver: Stimulation by Essential Fatty Acid Deficiency, *Lipids 34*, 1167–1176.
20. Tocher, D.R., Bell, J.G., Dick, J.R., and Sargent, J.R. (1997) Fatty Acyl Desaturation in Isolated Hepatocytes from Atlantic Salmon (*Salmo salar*): Stimulation by Dietary Borage Oil Containing γ-Linolenic Acid, *Lipids 32*, 1237–1247.
21. Bell, J.G., Dick, J.R., McVicar, A.H., Sargent, J.R., and Thompson, K.D. (1993) Dietary Sunflower, Linseed and Fish Oils Affect Phospholipid Fatty Acid Composition, Development of Cardiac Lesions, Phospholipase Activity and Eicosanoid Production in Atlantic Salmon, *Prostagl. Leukotr. Essent. Fatty Acids 49*, 665–673.
22. Bell, J.G., Sargent, J.R., and Raynard, R.S. (1992) Effects of Increasing Dietary Linoleic Acid on Phospholipid Fatty Acid Composition and Eicosanoid Production in Leucocytes and Gill Cells of Atlantic Salmon (*Salmo salar*), *Prostaglandins Leukot. Essent. Fatty Acids 45*, 197–206.
23. Bell, J.G., Raynard, R.S., and Sargent, J.R. (1991) The Effect of Dietary Linoleic Acid on the Fatty Acid Composition of Individual Phospholipids and Lipoxygenase Products from Gills and Leucocytes of Atlantic Salmon (*Salmo salar*), *Lipids 26*, 445–450.
24. Thompson, K.D., Tatner, M.F., and Henderson, R.J. (1996) Effects of Dietary (n-3) and (n-6) Polyunsaturated Fatty Acid Ratio on the Immune Response of Atlantic Salmon, *Salmo salar* L., *Aquacult. Nutr. 2*, 21–31.
25. Rosenlund, G., Obach, A., Sandberg, M.G., Standal, H., and Tveit, K. (2001) Effect of Alternative Lipid Sources on Long-Term Growth Performance and Quality of Atlantic Salmon (*Salmo salar* L.), *Aquacult. Res. 32* (Suppl. 1), 323–328.
26. Rollin, X., Peng, J., Pham, D., Ackman, R.G., and Larondelle, Y. (2003) The Effects of Dietary Lipid and Strain Difference on Polyunsaturated Fatty Acid Composition and Conversion in Anadromous and Landlocked Salmon (*Salmo salar* L.) Parr, *Comp. Biochem. Physiol. B 134*, 349–366.
27. Lie, Ø., Sandvin, A., and Waagbø, R. (1993) Influence of Dietary Fatty Acids on the Lipid Composition of Lipoproteins in Farmed Atlantic Salmon (*Salmo salar*), *Fish Physiol. Biochem. 12*, 249–260.
28. Waagboe, R., Sandnes, K., Lie, Ø., and Nilsen, E.R. (1993) Health Aspects of Dietary Lipid Sources and Vitamin E in Atlantic Salmon (*Salmo sala*). 1. Erythrocyte Total Lipid Fatty Acid Composition, Haematology and Humoral Immune Response, *Fiskeridir. Skr. Ser. Ernaer. 6*, 47–62.
29. Waagboe, R., Sandnes, K., Joergensen, J., Engstad, R., Glette, J., and Lie, Ø. (1993) Health Aspects of Dietary Lipid Sources and Vitamin E in Atlantic Salmon (*Salmo salar*). 2. Spleen and Erythrocyte Phospholipid Fatty Acid Composition, Nonspecific Immunity and Disease Resistance, *Fiskeridir. Skr. Ser. Ernaer. 6*, 63–80.
30. Bell, J.G., Henderson, R.J., Tocher, D.R., McGhee, F., Dick, J.R., Porter, A., Smullen, R.P., and Sargent, J.R. (2002) Substituting Fish Oil with Crude Palm Oil in the Diet of Atlantic Salmon (*Salmo salar*) Affects Muscle Fatty Acid Composition and Hepatic Fatty Acid Metabolism, *J. Nutr. 132*, 222–230.
31. Røsjø, C., Nordrum, S., Olli, J.J., Krogdahl, Å., Ruyter, B., and Holm, H. (2000) Lipid Digestibility and Metabolism in Atlantic Salmon (*Salmo salar*) Fed Medium-Chain Triglycerides, *Aquaculture 190*, 65–76.
32. Bell, J.G., McEvoy, J., Tocher, D.R., McGhee, F., Campbell, P.J., and Sargent, J.R. (2001) Replacement of Fish Oil with Rapeseed Oil in Diets of Atlantic Salmon (*Salmo salar*) Affects Tissue Lipid Compositions and Hepatocyte Fatty Acid Metabolism, *J. Nutr. 31*, 1535–1543.
33. Tocher, D.R., Bell, J.G., Dick, J.R., Henderson, R.J., McGhee, F., Michell, D., and Morris, C. (2000) Polyunsaturated Fatty Acid Metabolism in Atlantic Salmon (*Salmo salar*) Undergoing Parr-Smolt Transformation and the Effects of Dietary Linseed and Rapeseed Oils, *Fish Physiol. Biochem. 23*, 59–73.
34. Bell, J.G., McGee, F., Campbell, P.J., and Sargent, J.R. (2003) Rapeseed Oil as an Alternative to Marine Fish Oil in Diets of Post-Smolt Atlantic Salmon (*Salmo salar*): Changes in Flesh Fatty Acid Composition and Effectiveness of Subsequent Fish Oil "Wash Out," *Aquaculture 218*, 515–528.
35. Coe, N.R., Smith, A.J., Frohnert, B.I., Watkins, P.A., and Bernlohr, D.A. (1999) The Fatty Acid Transport Protein (FATP1) Is a Very Long Chain Acyl-CoA Synthetase, *J. Biol. Chem. 274*, 36300–36304.
36. Herrmann, T., Buchkremer, F., Gosch, I., Hall, A.M., Bernlohr, D.A., and Stremmel, W. (2001) Mouse Fatty Acid Transport Protein 4 (FATP4): Characterization of the Gene and Functional Assessment as a Very Long Chain Acyl-CoA Synthetase, *Gene 270*, 31–40.
37. Frohnert, B.I., and Bernlohr, D.A. (2000) Regulation of Fatty Acid Transporters in Mammalian Cells, *Prog. Lipid Res. 39*, 83–107.
38. Veerkamp, J.H., and van Moerkerk, H.T.B. (1993) Fatty Acid-Binding Protein and Its Relation to Fatty Acid Oxidation, *Mol. Cell. Biochem. 123*, 101–106.
39. Furuhashi, M., Ura, N., Murakami, H., Hyakukoku, M., Yamaguchi, K., Higashiura, K., and Shimamoto, K. (2002) Fenofibrate Improves Insulin Sensitivity in Connection with Intramuscular Lipid Content, Muscle Fatty Acid-Binding Protein, and β-Oxidation in Skeletal Muscle, *J. Endocrinol. 174*, 2, 321–329.
40. Londraville, R.L., and Sidell, B.D. (1996) Cold Acclimation Increase Fatty Acid-Binding Protein Concentration in Aerobic Muscle of Striped Bass, *Morone saxatilis*, *J. Exp. Zool. 175*, 36–44.
41. Takahashi, Y., Kushiro, M., Shinohara, K., and Ide, T. (2003) Activity and mRNA Levels of Enzymes Involved in Hepatic Fatty Acid Synthesis and Oxidation in Mice Fed Conjugated Linoleic Acid, *Biochim. Biophys. Acta 1631*, 265–273.
42. Salter, A.M., Mangiapane, E.H., Bennett, A.J., Bruce, J.S., Billett, M.A., Anderton, K.L., Marenah, C.B., Lawson, N., and White, D.A. (1998) The Effect of Different Dietary Fatty Acids on Lipoprotein Metabolism: Concentration-Dependent Effects of Diets Enriched in Oleic, Myristic, Palmitic and Stearic Acids, *Br. J. Nutr. 79*, 195–202.
43. Tocher, D.R., Bell, J.G., MacGlaughlin, P., McGhee, F., and Dick, J.R. (2001) Hepatocyte Fatty Acid Desaturation and Polyunsaturated Fatty Acid Composition of Liver in Salmonids: Effects of Dietary Vegetable Oil, *Comp. Biochem. Physiol. B 130*, 257–270.
44. Ruyter, B., Roesjoe, C., Maesoeval, K., Einen, O., and Thomassen, M.S. (2000) Influence of Dietary n-3 Fatty Acids on the Desaturation and Elongation of [1-^{14}C]18:2n-6 and [1-^{14}C]18:3n-3 in Atlantic Salmon Hepatocytes, *Fish Physiol. Biochem. 23*, 151–158.
45. Stubhaug, I. (2002) Catabolism of Fatty Acids in Atlantic Salmon (*Salmo salar* L.)—Effects of Dietary Vegetable Oils and an Improved Method for Measuring β-Oxidation Capacity, *Candidata scientiarum* Thesis, University of Bergen, Norway, p. 73.

46. Torstensen, B.E., Frøyland, Ø., and Lie, Ø. (2004) Replacing Dietary Fish Oil with Increasing Levels of Rapeseed Oil and Olive Oil—Effects on Atlantic Salmon (*Salmo salar* L.) Tissue and Lipoprotein Lipid Composition and Lipogenic Enzyme Activities, *Aquacult. Nutr.,* in press.
47. Frøyland, L., Lie, Ø., and Berge, R.K. (2000) Mitochondrial and Peroxisomal β-Oxidation Capacities in Various Tissues from Atlantic Salmon *Salmon salar*, *Aquacult. Nutr. 6*, 85–89.
48. Torstensen, B.E. (2000) Transport and Metabolism of Lipids in Atlantic Salmon (*Salmo salar* L.), *Doctor scientiarum* Thesis, University of Bergen, Norway, pp. 5–43.
49. Henderson, R.J., and Tocher, D.R. (1987) The Lipid Composition and Biochemistry of Freshwater Fish, *Prog. Lipid Res. 26*, 281–347.

[Received September 17, 2003, and in final form and accepted January 30, 2004]

Decreased Production of Inflammatory Mediators in Human Osteoarthritic Chondrocytes by Conjugated Linoleic Acids

Chwan-Li Shen[a,*], Dale M. Dunn[a], Jack H. Henry[b], Yong Li[c], and Bruce A. Watkins[c]

Departments of [a]Pathology and [b]Orthopedic Surgery, Texas Tech University Health Sciences Center, Lubbock, Texas 79430, and [c]Lipid Chemistry and Molecular Biology Laboratory, Department of Food Science, Purdue University, West Lafayette, Indiana 47907

ABSTRACT: Osteoarthritic chondrocytes (OC) produce excessive prostaglandin E_2 (PGE_2) and nitric oxide (NO), which function as inflammation mediators in the pathogenesis of osteoarthritis (OA). This study examined the effect of CLA alone and in combination with other PUFA on the FA composition and the production of PGE_2 and NO in OC cultures isolated from OA patients. Human OC were grown in monolayer and treated with one of the following PUFA treatments: CLA, CLA + arachidonic acid (CLA/AA), CLA + EPA (CLA/EPA), linoleic acid (LA), LA + AA (LA/AA), LA + EPA (LA/EPA), and ethanol (as a vehicle control) at 10 and 20 μM for 6 d. Supplementation of PUFA at 10 μM for 6 d did not introduce any cytotoxic effects or morphological changes in OC, whereas 20 μM resulted in apoptosis. Cultures of OC treated with CLA, CLA/AA, and CLA/EPA had higher concentrations of CLA isomers, and these isomers were not detected in other treatments. Supplementation of CLA or LA alone to the OC led to a lower PGE_2 production compared to the control. Combination of CLA/EPA resulted in the lowest PGE_2 production in cultured OC. OC cultures treated with CLA were lower in NO production than the control, whereas the LA/AA treatment demonstrated the lowest NO production. The fact that CLA alone or in combination with other PUFA modulated PGE_2 and NO production in human OC cultures suggests that these 18:2 isomers may have the potential to influence OA pathogenesis.

Paper no. L9365 in *Lipids 39*, 161–166 (February 2004).

Osteoarthritis (OA) is characterized by progressive destruction of cartilage and secondary inflammation of synovial membranes (1,2). The mechanism of activation and progression of articular cartilage destruction in OA is not fully understood. It was postulated that in OA cartilage, there was an imbalance between (i) anabolic synthesis or repair of matrix by growth factors (3,4) and (ii) catabolic breakdown of matrix by inflammatory cytokines (5), matrix metalloproteinases (5,6), prostaglandin E_2 (PGE_2) (7), and nitric oxide (NO) (8). Among these factors, excessive productions of PGE_2 and NO by cartilage are widely recognized as promoters of cartilage degradation in OA patients and animal models of arthritis (7,8). Therefore, reductions of PGE_2 and NO production are logical targets to evaluate in the management of inflammatory responses associated with the development of OA pathology.

*To whom correspondence should be addressed at Department of Pathology, Texas Tech University Health Sciences Center, 3601 Fourth St., Lubbock, TX 79430. E-mail: Leslie.Shen@ttuhsc.edu.

Abbreviations: AA, arachidonic acid; COX, cyclooxygenase; 5-HETE, 5-hydroxyeicosatetraenoic acid; IL, interleukin; iNOS, inducible nitric oxide synthase; LA, linoleic acid; LnA, α-linolenic acid; LPS, lipopolysaccharides; LT, leukotriene; NO, nitric oxide; OA, osteoarthritis; OC, osteoarthritic chondrocytes; PGE_2, prostaglandin E_2; PPARγ, peroxisome proliferator-activated receptor γ; TNF-α, tumor necrosis factor-α; TX, thromboxane.

A body of recent scientific evidence based on results in cell cultures (9,10) and organ cultures (11) indicates that FA may benefit skeletal health and potentially improve conditions associated with OA. EPA supplementation reduced PGE_2 production, increased collagen synthesis, and modulated interleukin (IL)-1 production in the *in vitro* healing process of medial collateral ligament fibroblasts, whereas arachidonic acid (AA) had opposite effects (9). Cultures of bovine chondrocytes enriched with n-3 PUFA [α-linolenic acid (LnA), EPA, and DHA] resulted in a marked decrease in the cytokine-mediated induction of expression of cyclooxygenase (COX)-2, tumor necrosis factor-α (TNF-α), and IL-1, and inhibited cytokine-mediated upregulation of the expression of aggrecanase-1 and aggrecanase-2 genes, and of aggrecanase activity (10). In addition, Curtis *et al.* (11) reported that supplementation of n-3 PUFA (LnA and EPA) but not n-6 PUFA [linoleic acid (LA) and AA] or any other FA (oleate and palmitate) to cartilage explants from normal bovine and human osteoarthritic cartilage caused a decrease in both cartilage proteoglycan degradation and mRNA expression of inflammation mediators (COX-2, 5-lipoxygenase, 5-lipoxygenase-activating protein, TNF-α, IL-1α, and IL-1β), with no effect on the normal tissue homeostasis. Although there was no direct evidence regarding the effect of n-3 PUFA on NO production in OA, supplementation of LnA, EPA, and DHA suppressed NO production in murine macrophage cells (RAW 264), but those treated with LA or oleic acid showed no effect (12). Studies in animal models of arthritis showed that dietary fish oil (rich in n-3 PUFA) also suppressed inflammation and cartilage degradation (13,14). Compared with corn oil (rich in n-6 PUFA), dietary fish oil delayed the appearance of enlarged lymph nodes in MRL/lpr mice and decreased the concentrations of circulating PGE_2, thromboxane (TX) B_2, leukotriene (LT) B_4, TNF-α, and IL-6, -10, and -12 in a mouse model for rheumatoid arthritis (13). Compared with beef tallow or safflower oil, EPA and DHA both suppressed arthritis in rats, and EPA was more effective than DHA (14).

In addition to specific long-chain n-3 PUFA, CLA have been reported to act as anticancer nutrients (15). CLA are positional and geometric isomers of octadecadienoic acid (18:2) found naturally in ruminant food products, and are especially rich in dairy products and beef (15). Sources of CLA given to rats or supplemented in cell culture were found to increase their presence in tissues, including bone compartments (16) and cellular lipids (17). As CLA isomers are incorporated in various glycerolipids, they may compete with other PUFA, such as LA, in elongation and desaturation steps for the formation of AA

(16). The potential competitive effects of CLA in AA formation and metabolism were reported to be associated with reduced *ex vivo* biosynthesis of PGE_2 in rodent bone organ cultures (16). CLA isomers were also reported to reduce PGE_2 synthesis in mouse keratinocytes (18) and macrophages (19). In a mouse study, CLA inhibited not only the production of PGE_2 but also NO production as well as the gene expression of COX-2 and inducible NO synthase (iNOS) in macrophages (19). The evidence on the actions of CLA in animals and cells suggests that CLA might play an important role in moderating OA by altering inflammation mediators, such as PGE_2 and NO. Therefore, the present study was designed to evaluate the effects of CLA alone or in combination with specific PUFA (AA and EPA) on (i) cell viability, (ii) morphological changes, and (iii) FA composition of human OC. The production of PGE_2 and NO was also measured to determine the effects of the treatments on inflammatory mediators in human OC cultures. The present investigation focused on the effects of CLA alone or in combination with specific PUFA (AA and EPA) on cell viability, FA composition, and the production of inflammatory mediators. In this study no cells were cultured with AA or EPA alone for the following reasons: (i) the primary OC supply was limited and (ii) Hankenson *et al.* (9) have demonstrated that AA increases PGE_2 production, whereas EPA decreases PGE_2 production in medial collateral ligament fibroblasts.

EXPERIMENTAL PROCEDURES

Tissue acquisition. Human osteoarthritic articular cartilage was acquired from patients who received knee arthroplasty surgery performed at the University Medical Center, Texas Tech University Health Sciences Center, Lubbock, Texas. The Texas Tech University Health Sciences Center Internal Review Board approved all protocols, and tissue samples were collected only under patients' consent. Subjects were osteoarthritic patients to receive hip or knee arthroplasty, including both genders, 55 yr of age and older. Their OA status was evaluated by a certified rheumatologist and diagnosed based on the criteria developed by the American College of Rheumatology Diagnostic Subcommittee for OA. Patients with OA resulting from trauma, metabolic bone disease, and rheumatoid arthritis were excluded. After the hip or knee arthroplasty, the articular cartilage was stored in cold PBS (Gibco, Grand Island, NY) with 1% (vol/vol) penicillin-streptomycin-amphotericin B (Gibco) before further processing. All tissues were processed within 2 h after arthroplasty following the chondrocyte isolation procedure.

Isolation and culture of chondrocytes. OC were isolated from articular cartilage following the methods of Shen *et al.* (20). Articular cartilage was first dissected from the connective tissue, muscles, and bone material with a sterile scalpel, washed extensively with PBS containing 1% antibiotics, and then transferred to a sterile Petri dish containing Ham's F-12/DMEM (1:1, vol/vol) (Gibco), 10% FBS (Gibco), and 1% antibiotics. The cartilage tissue was subsequently diced into cubes of 1 to 2 mm. Cartilage fragments were digested with pronase (EC 3.4.24.4; Sigma, St. Louis, MO) at 1.0 mg/mL for 1.5 h at 37°C, followed by collagenase type II (EC 3.4.24.2, Sigma) at 1.0 mg/mL overnight at 37°C. After digestion, the cartilage suspension was filtered sequentially through sterile nylon meshes of 100- and 70-μm pore sizes (Sefar America Inc., Briarcliff Manor, NY), and washed three times with PBS containing 1% antibiotics. The viability of cells after filtration was 95% (trypan blue test). Cells were seeded at a density of 5×10^5 cells/well in six-well culture plates or 1×10^6 cells/plate dishes in 100-mm culture plates, and were allowed to grow in Ham's F-12/DMEM supplemented with 10% FBS and 1% antibiotics. To ensure the chondrocyte phenotype, only primary and first passage cultures were used.

Treatment with PUFA. The PUFA and CLA (99% purity except CLA; Nu-Chek-Prep, Elysian, MN) were dissolved in 100% ethanol (40 mM) (ethanol concentration < 0.01%), flushed with nitrogen gas, kept in glass tubes with Teflon-lined screw caps, and stored at −20°C before use in the cell culture media. When the OC cells reached 60% confluence, they were treated with one of the following PUFA or PUFA combinations (1:1, w/w): CLA, LA, CLA + AA, CLA + EPA, LA + AA, and LA + EPA at 10 and 20 μM in Ham's F-12/DMEM supplemented with 10% FBS and 1% antibiotics for an additional 6 d. The control consisted of no PUFA with ethanol as a vehicle. The media containing different PUFA were changed every other day. The CLA source (18:2) consisted of 39.1% *c*9,*t*11/*t*9,*c*11, 40.7% *t*10,*c*12, 1.8% *c*9,*c*11, 1.3% *c*10,*c*12, 1.9% *t*9,*t*11/*t*10,*t*12, 1.1% *c*9,*c*12, and 14.1% other isomers.

The PUFA-treated cells were examined by commercial Cell Counting Kit-8 (Dojindo Molecular Technologies Inc., Gaithersburg, MD) to determine cell viability. Only a concentration of PUFA that did not affect the cell viability of OC after the 6-d incubation period was used for further experiments. For the experiments measuring PGE_2 and NO production, OC were treated with different PUFA in the presence of lipopolysaccharide (LPS, Sigma) at 10 μg/mL and IL-1β (Sigma) at 5 ng/mL for 6 d. Culture media after treatment with PUFA were collected and stored at −80°C until they were analyzed for PGE_2 and NO.

Morphological cellular changes. To identify morphological changes of cells treated with PUFA, cells were fixed in methanol, stained with Giemsa (Sigma) according to the manufacturer's instruction, and examined using an inverted microscope. Giemsa is a polychromatic stain that produces fine resolution of cellular details. Cells displaying morphological changes including complexity, branching and thinning of cell processes, cytoplasmic vacuolization, and prominence of nucleoli of OC were studied to determine the effects of PUFA on OC (21).

FA composition. After treatment with PUFA for 6 d, OC cells were rinsed with PBS and stored at −20°C before FA analysis. Lipids were extracted with chloroform/methanol (2:1, vol/vol) as previously described (22), and FAME were prepared using sodium methoxide in methanol. FAME were extracted with isooctane and analyzed by GC (Agilent 6890 Plus, autosampler 7683, Chemstation Rev. A.08.03; Agilent Technologies, Inc., Wilmington, DE) equipped with an FID and a DB-23 fused-silica capillary column (30 m, 0.53 mm i.d., 0.5 μm film thickness; Agilent) using helium as the carrier gas. FAME were identified by comparison of their retention times with authentic standards (Nu-Chek-Prep) and FA values expressed as area percentages.

PGE_2 determination. PGE_2 was measured in cell culture medium (in duplicate) by RIA [tracer 5,6,8,11,12,14,15-(n)^{3}H-PGE_2 (Amersham Biosciences, Piscataway, NJ), primary antibody (Sigma), PGE_2 standard (Cayman Chemical Co., Ann Arbor, MI)], and the radioactivity was measured by scintillation counting (Beckman Coulter, Inc.). The sensitivity of the RIA was approximately 3.9 pg/mL PGE_2. Cellular protein of PUFA-treated OC was determined by a bicinchoninic acid protein assay (Pierce; Rockford, IL). PGE_2 values of OC media were expressed as ng per mg of cell protein.

NO determination. A stable product of NO in the culture medium was determined by the Griess reaction (23) with the major procedure described as the following: culture medium of 100 μL was mixed with 100 μL of Griess reagent containing 0.1% (wt/vol) *N*-(1-naphthyl) ethylenediamine dihydrochloride and 1% (wt/vol) sulfanilamide in 5% (vol/vol) concentrated phosphoric acid (Sigma). Absorbance was read at 546 nm using a PerkinElmer HTS 7000 plate reader (PerkinElmer Instruments). Each sample was assayed in duplicate. Sodium nitrite diluted into 0.5% FBS culture medium was used as the standard. NO production of OC cultures was expressed as nmol NO per mg of cell protein.

Statistical analysis. Results were verified in at least three experiments, each performed in triplicate. In most cases, data from a representative experiment were shown. Data were presented as mean ± SEM. Statistical significance was evaluated using one-way ANOVA followed by Fisher's LSD method. A *P*-value less than 0.05 was considered statistically significant.

RESULTS

Effect of PUFA on cytotoxicity and morphology. Supplementation of PUFA at 10 μM for 6 d did not cause any cytotoxic effect or morphological change in OC, and the OC receiving such treatment typically contained a single nucleolus. However, a higher PUFA dose of 20 μM appeared to increase the complexity, branching, and thinning of cell processes, cytoplasmic vacuolization, and prominence of nucleoli of OC (data not shown). Therefore, only the PUFA concentration of 10 μM was used in the subsequent experiments for FA composition and analysis of PGE_2 and NO production. The purity of EPA and AA was approximately 99%, but the CLA was a mixture of several isomers, and the concentration of effective isomer of CLA tested on the production of inflammatory mediators was much less than 10 μM.

Modulation of FA composition by PUFA. OC cultures supplemented with PUFA demonstrated enrichment consistent with the individual treatments (Table 1). Cells treated with CLA, including CLA, CLA/AA, and CLA/EPA, had high levels of CLA isomers [18:2(*c*9,*t*11) and 18:2(*t*10,*c*12)]; and CLA isomers were not detected in the other treatments. Supplementation of media with LA significantly increased the content of 18:2n-6 and 20:2n-6 in the OC compared to the control and CLA-treated groups. The content of 20:5n-3 and other long-chain n-3 PUFA including 22:5n-3 was greatly enriched in OC cultures containing EPA (CLA/EPA and LA/EPA) compared to all other treatment groups. PUFA supplementation modulated the 20:4n-6 levels of OC in the following order: LA/AA = CLA/AA > LA = LA/EPA = CLA > CLA/EPA > control. The treatments of LA and LA/AA showed the highest ratio of n-6 to n-3 PUFA, whereas CLA/EPA had the lowest. There were no significant differences in the values of total saturated FA, total monounsaturated FA, and total PUFA among the PUFA-treated groups. In contrast, supplementation with LA/AA to OC decreased the values for total PUFA compared to the other PUFA treatments.

Effect of PUFA on PGE_2 production. As expected, addition of inducers (LPS and IL-1β) to culture medium without PUFA induced OC PGE_2 production (1733 ng/mg protein) compared to those without inducers (9.2 ng/mg protein). Supplementation of CLA or LA alone to the OC resulted in a lower PGE_2 production compared to that for the control cultures (Fig. 1) ($P < 0.001$). OC incubated with CLA/EPA resulted in the lowest PGE_2 production (1364 ng/mg protein), whereas those incubated with LA/AA, the control, and CLA/AA yielded higher PGE_2 production of 1791, 1733, and 1728 ng/mg protein, respectively. In addition, the LA/EPA group produced lower PGE_2 (statistically the same as CLA and LA groups) compared to the control ($P < 0.001$).

Effect of PUFA on NO production. Similar to the effects of inducers on PGE_2 production in OC cultures without PUFA, use of these compounds significantly increased NO production (198 nmol/mg protein) compared to those without inducers (1.9 nmol/mg protein). The OC cells treated with LA resulted in the highest level of NO production (340 nmol/mg protein), whereas cells treated with LA/AA had the lowest level of NO production (82 nmol/mg protein) (Fig. 2). Compared to the control group, the LA/AA, LA/EPA, and CLA treatments significantly decreased NO production by 70% ($P < 0.001$), 25% ($P < 0.05$), and 23% ($P < 0.05$), respectively. In contrast, OC cultures subjected to the LA and CLA/EPA treatments showed significantly increased NO production by 130% ($P < 0.05$) and 115% ($P < 0.05$), respectively, compared to the control. The CLA/AA treatment was not different from the control. A difference as much as 4.1-fold (Fig. 2; $P < 0.0001$) was observed between the treatments that produced the maximum (LA) and the minimum amount of NO (LA/AA).

DISCUSSION

In the present investigation, a model of human OC culture was successfully used to study the relationships between PUFA treatment and inflammatory agents associated with joint disease. In the study, the FA composition of OC was determined in the control group where OC was not treated with any PUFA and all FA were provided by the 10% FBS in the medium. Compared with the PUFA-treated OC that were also treated with the same 10% FBS, the control group had significantly lower values for 18:2n-6, 20:5n-3, and CLA isomers [18:2(*c*9,*t*11) and 18:2(*t*10, *c*12)]. Therefore, the increased FA in PUFA-treated OC resulted solely from the supplementation of PUFA to the culture medium, and not from FBS. These findings corroborate previous studies where AA and EPA concentrations were increased by the AA and EPA treatments in fibroblasts (9) as well as in primary cultures of chondrocytes (24).

TABLE 1
FA Composition of Human Osteoarthritic Chondrocytes Treated With Different PUFA[a]

	Treatments[b]							Pooled	ANOVA
FA	Control	CLA	CLA/AA	CLA/EPA	LA	LA/AA	LA/EPA	SEM	*P* values
14:0	1.3	0.9	0.8	1.0	0.9	1.8	1.0	0.05	NS
15:0	0.8	0.5	0.6	0.5	0.5	0.7	0.5	0.02	NS
16:0	17.0	16.6	16.9	17.3	17.0	17.1	17.2	0.02	NS
*t*16:1	1.3^{A}	1.1^{B}	1.2^{A}	1.3^{A}	1.2^{A}	1.2^{A}	1.3^{A}	0.0003	0.007
16:1n-7	1.1^{A}	1.0^{B}	1.2^{A}	0.9^{B}	0.8^{C}	1.0^{B}	0.9^{B}	0.01	0.001
17:0	0.9	0.8	0.9	0.8	0.8	0.8	0.8	0.006	NS
18:0	16.1	20.0	17.1	17.4	17.7	17.4	19.3	0.17	NS
18:1n-9	14.0	12.2	13.4	14.2	12.6	12.2	13.1	0.04	NS
18:1n-7	4.6	4.1	4.4	4.5	4.5	4.2	4.5	0.007	NS
18:2n-6	2.2^{D}	$2.7^{C,D}$	$2.7^{C,D}$	3.0^{C}	10.3^{A}	5.6^{B}	6.3^{B}	0.007	0.0001
18:2(*c*9,*t*11)	ND^{C}	2.3^{A}	1.0^{B}	1.6^{B}	ND^{C}	ND^{C}	ND^{C}	0.01	0.003
18:2(*t*10,*c*12)	ND^{C}	2.4^{A}	1.3^{B}	1.6^{B}	ND^{C}	ND^{C}	ND^{C}	0.01	0.005
20:2n-6	ND^{D}	ND^{D}	ND^{D}	ND^{D}	0.9^{A}	0.5^{B}	0.2^{C}	0.009	0.007
20:3n-6	1.3	0.9	1.6	1.5	1.8	1.5	1.8	0.06	NS
20:4n-6	11.9	13.3	15.8	12.4	13.9	15.3	13.6	0.3	NS
20:5n-3	0.3^{C}	0.5^{C}	0.5^{C}	2.0^{A}	0.5^{C}	0.2^{C}	1.3^{B}	0.001	0.0001
22:0	3.5	2.3	1.7	1.0	1.0	3.7	1.7	0.5	NS
22:4n-6	3.1^{C}	4.1^{B}	5.9^{A}	2.8^{C}	3.9^{B}	4.0^{B}	3.4^{C}	0.007	0.001
22:5n-3	3.5^{D}	4.4^{C}	4.2^{C}	7.6^{A}	3.8^{D}	3.4^{D}	5.3^{B}	0.006	0.001
22:6n-3	4.6	5.2	5.1	4.7	4.8	3.8	4.5	0.02	NS
Total CLA	ND^{C}	5.1^{A}	2.3^{B}	3.2^{B}	ND^{C}	ND^{C}	ND^{C}	0.03	0.003
Total n-6	18.5^{D}	$21.1^{C,D}$	26.1^{B}	19.2^{D}	30.9^{A}	$24.0^{B,C}$	25.3^{B}	0.48	0.001
Total n-3	8.4^{D}	$10.1^{B,C}$	$9.7^{B,C}$	14.3^{A}	9.1^{C}	7.3^{D}	11.1^{B}	0.02	0.022
n-6/n-3	2.2^{C}	2.1^{C}	2.7^{B}	1.3^{D}	3.4^{A}	3.3^{A}	2.3^{C}	0.001	0.001
Total SAT[c]	39.7	41.1	38.1	38.3	37.8	41.4	40.5	0.24	NS
Total MONO	21.0	17.9	19.9	20.9	19.2	18.6	19.8	0.08	NS
Total PUFA	29.9	36.3	38.0	36.8	39.9	31.1	36.4	0.64	NS

[a]Mean values for cellular FA ($n = 3$) within a row having different superscripts (A to D) are significantly different by one-way ANOVA followed by Fisher's LSD method ($P \leq 0.05$).
[b]Confluent (60%) human osteoarthritic chondrocytes were treated with the following FA: CLA, CLA/arachidonic acid (AA) (1:1, w/w), CLA/EPA (1:1, w/w), linoleic acid (LA), LA/AA (1:1, w/w), LA/EPA (1:1, w/w), all at 10 μM, and ethanol (as a vehicle control) for 6 d. The medium containing different PUFA was changed every other day.
[c]SAT: saturated FA, MONO: monounsaturated FA, ND: not detected, NS: not significant.

The effects of PUFA on cytokine-induced PGE_2 production were likely mediated by the modulation of cellular FA composition (25). For example, CLA or LA alone reduced PGE_2 production relative to the control; an addition of AA to CLA or LA resulted in the highest PGE_2 production compared with other PUFA-treated cell groups.

Addition of EPA to CLA and to LA treatments resulted in (i) increased concentrations of EPA and its metabolites of desaturation and elongation such as 22:5n-3 in the OC and (ii) decreased levels of PGE_2 compared to the CLA/AA and LA/AA groups. Such an inhibitory effect of EPA on PGE_2 production in the present study agrees with that reported in immune cells of humans (26,27). Suppression of the production of AA-derived prostanoids such as PGE_2 by EPA may be accompanied by an increase in the production of EPA-derived eicosanoids, such as PGE_3. In the present study, CLA/EPA treatment resulted in lower PGE_2 production in OC than the CLA treatment, suggesting that combining EPA with CLA may be additive in inhibiting the production of inflammatory prostanoids.

The results of the present study showed that CLA not only decreased PGE_2 production in OC but also significantly reduced NO production relative to the control group. These findings agree with previous studies where PGE_2 and NO productions in macrophages were decreased by CLA (19,28), a result associated with reduced mRNA expression of COX-2 and iNOS, and transcriptional activity of the COX-2 and iNOS (28). One possible mechanism for the inhibitory effects of CLA on PGE_2 and NO is that CLA may bind to peroxisome proliferator-activated receptor γ (PPARγ) and modulate its action. The CLA–PPARγ complex inhibits activation of the transcription factor, nuclear factor kappa B (NFκB). Expression of COX-2 and iNOS in OC is subsequently inhibited (28,29).

The level of NO production was inversely correlated with the amounts of CLA found in OC. For example, among the CLA-treated groups, the levels of NO production in OC followed the order of CLA/EPA = CLA/AA > CLA. The possible explanation is that supplementing AA or EPA to CLA appeared to diminish the effect of CLA on reducing NO production, because the effective dose of CLA in CLA/EPA and CLA/AA was only 50% of that for CLA alone.

The combination of LA and EPA significantly lowered NO production in OC compared with LA alone. The NO-inhibitory effect may be due to the high concentration of EPA and its metabolites, which is in agreement with previous studies in macrophages (12). In contrast to the response observed with the LA/EPA treatment, the combination of EPA with CLA resulted

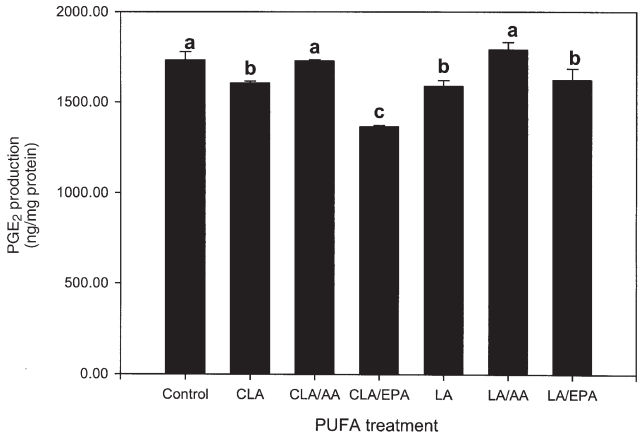

FIG. 1. Prostaglandin E_2 (PGE_2) production by human osteoarthritic chondrocytes. Treatments included no PUFA (control) and supplementation with 10 μM of one of the following: CLA, CLA/arachidonic acid (AA) (1:1, w/w), CLA/EPA (1:1, w/w), linoleic acid (LA), LA/AA (1:1, w/w), and LA/EPA (1:1, w/w) in the presence of lipopolysaccharides (10 μg/mL) and interleukin-1β (5 ng/mL) for 6 d. Values (means ± SEM) represent $n = 3$ per treatment group, and those not sharing a common letter (a–e) are significantly different ($P < 0.05$). PGE_2 concentration was measured in culture supernatant by RIA and cell protein was determined by bicinchoninic acid (BCA).

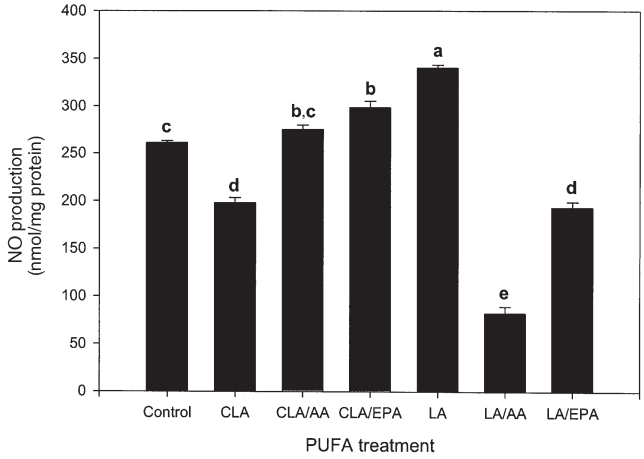

FIG. 2. Nitric oxide (NO) production by human osteoarthritic chondrocytes. Treatments included no PUFA (control) and supplementation with 10 μM of one of the following: CLA, CLA/AA (1:1, w/wt, CLA/EPA (1:1, w/w), LA, LA/AA (1:1, w/w), and LA/EPA (1:1, w/w) in the presence of lipopolysaccharides (10 μg/mL) and interleukin-1β (5 ng/mL) for 6 d. Values (means ± SEM) represent $n = 3$ per treatment group, and those not sharing a common letter (a–e) are significantly different ($P < 0.05$). Production of NO was measured in culture supernatant by Griess reaction, and cell protein was determined by BCA. For abbreviations, see Figure 1.

in higher NO production compared to CLA alone. The lower NO production in the CLA group compared with the CLA/EPA group was due to a higher level of CLA in OC, suggesting that the CLA treatment was more effective in reducing NO production than EPA.

In the present study, we observed a cross-talk and biphasic relationship between PGE_2 and NO: (i) LA-treated OC had higher NO production but lower PGE_2 production compared with the control, (ii) CLA/EPA treatment inhibited PGE_2 production but increased NO production compared to CLA alone, and (iii) the LA/AA treatment resulted in the highest PGE_2 production but the lowest NO production compared to LA. Such a mechanism of cross-talk and biphasic relationships between PGE_2 and NO was found to be involved in the pathophysiology of OA, in which the overproduction of one generally leads to the inhibition of the other, depending on the level of PGE_2 or NO production (20,30,31). Our findings are consistent with those reported in previous studies evaluating antiosteoarthritic drugs in cultures of human OC (20,30) and cartilage (31). Such a relationship was also observed in osteoblastic MC3T3-E1 cells by Kanematsu *et al.* (32): (i) NO produced by iNOS in response to cytokine-activated COX-2 led to an increased production of PGE_2 in the cells and (ii) overproduction of NO in response to proinflammatory cytokines suppressed alkaline phosphatase activity in the cells *via* PGE_2 production by an NO-activated COX-2 pathway.

To our knowledge, the present study is the first to show the effects of CLA isomers on PGE_2 and NO production in human OC cultures. Stimulation of PGE_2 and NO production has been implicated in the pathogenesis of osteoarthritis (7,8). The stimulatory effects of NO production on cartilage metabolism have been linked to increased release of aggrecan by cultures of OC and inhibition of proteoglycans and type II collagen synthesis, thus resulting in OC dysfunction in various animal models of arthritis.

The observation that CLA significantly reduced production of PGE_2 and NO suggests that CLA may have a chondroprotective effect on cartilage metabolism of OA. Benito *et al.* (33) reported that after a 63-d intervention, the supplementation of 3.9 g of CLA per day increased CLA isomer concentration in plasma from 0.28 ± 0.06 to 1.09 ± 0.31% ($n = 10$, $P < 0.05$). In the present study, incubation of OC with media containing 10 μM of CLA, CLA/AA, or CLA/EPA for 6 d resulted in an increase in cellular CLA isomer concentration from 0% (the control) to 1.6% (the CLA/AA and CLA/EPA groups) and to 2.3% (the CLA group). Therefore, the CLA concentration used in the present study was comparable to the physiological dose used for a human intervention study. Future investigations should test the efficacy of individual CLA isomers on the production of inflammatory mediators in human OC and examine their effects on the synthesis of type II collagen and degradation of proteoglycan in OC cell cultures to explore the mechanism of action for CLA isomers in chondrocytes.

ACKNOWLEDGMENT

This work was supported in part by Lubbock Endowed Professorships Earnings.

REFERENCES

1. Hamerman, D. (1993) Aging and Osteoarthritis: Basic Mechanisms, *J. Am. Geriatr. Soc. 41*, 760–770.
2. Moskowitz, R.W. (1999) Bone Remodeling in Osteroarthritis: Subchondral and Osteophytic Responses, *Osteoarthritis Cartilage 7*, 323–324.

3. Martel-Pelletier, J., DiBattista, J.A., Lajeunesse, D., and Pelletier, J.P. (1998) IGF/IGFBP Axis in Cartilage and Bone in Osteoarthritis Pathogenesis, *Inflam. Res. 47*, 90–100.
4. Scharstuhl, A., Glansbeek, H.L., van Beuningen, H.M., Vitters, E.L., van der Kraan, P.M., and van der Berg, W.B. (2002) Inhibition of Endogenous TGF-β During Experimental Osteoarthritis Prevents Osteophyte Formation and Impairs Cartilage Repair, *J. Immunol. 169*, 507–514.
5. Fernades, J.C., Martel-Pelletier, J., and Pelletier, J.P. (2002) The Role of Cytokines in Osteoarthritis Pathophysiology, *Biorheology 39*, 237–246.
6. Nagase, H., and Kashiwagi, M. (2003) Aggrecanases and Cartilage Matrix Degradation, *Arthritis Res. Ther. 5*(2), 94–103.
7. Anderson, G.D., Hauser, S.D., McGarity, K.L., Bremer, M.E., Isakson, P.C., and Gregory, S.A. (1996) Selective Inhibition of Cyclooxygenase (COX)-2 Reverses Inflammation and Expression of COX-2 and Interleukin 6 in Rat Adjuvant Arthritis, *J. Clin. Invest. 97*, 2672–2679.
8. Amin, A.R., Attur, M., and Abramson, S.B. (1999) Nitric Oxide Synthase and Cyclooxygenases: Distribution, Regulation, and Intervention in Arthritis, *Curr. Opin. Rheumatol. 11*, 202–209.
9. Hankenson, K.D., Watkins, B.A., Schoenlein, I.A., Allen, K.G., and Turek, J.J. (2000) Omega-3 Fatty Acids Enhance Ligament Fibroblast Collagen Formation in Association with Changes in Interleukin-6 Production, *Proc. Soc. Exp. Biol. Med. 223*, 88–95.
10. Curtis, C.L., Hughes, C.E., Flannery, C.R., Little, C.B., Harwood, J.L., and Caterson, B. (2000) n-3 Fatty Acids Specifically Modulate Catabolic Factors Involved in Articular Cartilage Degradation, *J. Biol. Chem. 275*, 721–724.
11. Curtis, C.L., Rees, S.G., Little, C.B., Flannery, C.R., Hughes, C.E., Wilson, C., Dent, C.M., Otterness, I.G., Harwood, J.L., and Caterson, B. (2002) Pathologic Indicators of Degradation and Inflammation in Human Osteoarthritic Cartilage Are Abrogated by Exposure to n-3 Fatty Acids, *Arthritis Rheum. 46*, 1544–1553.
12. Ohata, T., Fukuda, K., Takahashi, M., Sugimura, T., and Wakabayashi, K. (1997) Suppression of Nitric Oxide Production in Lipopolysaccharide-Stimulated Macrophage Cells by ω-3 Polyunsaturated Fatty Acids, *Jpn. J. Cancer Res. 88*, 234–237.
13. Venkatraman, J.T., and Chu, W.C. (1999) Effects of Dietary ω-3 and ω-6 Lipids and Vitamin E on Serum Cytokines, Lipid Mediators and Anti-DNA Antibodies in a Mouse Model for Rheumatoid Arthritis, *J. Am. Coll. Nutr. 18*, 602–613.
14. Volker, D.H., Fitzgerald, P.E., and Garg, M.L. (2000) The Eicosapentaenoic to Docosahexaenoic Acid Ratio of Diets Affects the Pathogenesis of Arthritis in Lew/SSN Rats, *J. Nutr. 130*, 559–565.
15. Watkins, B.A., and Li, Y. (2001) Conjugated Linoleic Acid: The Present State of Knowledge, in *Handbook of Nutraceuticals and Functional Foods* (Wildman, R., ed.), pp. 443–474, CRC Press, Boca Raton, FL.
16. Li, Y., and Watkins, B.A. (1998) Conjugated Linoleic Acids Alter Bone Fatty Acid Composition and Reduce *ex vivo* Prostaglandin E_2 Biosynthesis in Rats Fed n-6 or n-3 Fatty Acids, *Lipids 33*, 417–425.
17. Shen, C.-L., Dunn, D.M., Oetama, B., Hong, K.-J., Henry, J., Li, Y., and Watkins, B.A. (2003) Effects of Conjugated Linoleic Acids in Decreasing the Production of Inflammatory Mediators by Human Osteoarthritis Chondrocytes, *FASEB J. 17 (4)*, 688.1 (abstract).
18. Liu, K.L., and Belury, M.A. (1998) Conjugated Linoleic Acid Reduces Arachidonic Acid Content and PGE_2 Synthesis in Murine Keratinocytes, *Cancer Lett. 127*, 15–22.
19. Iwakiri, Y., Sampson, D.A., and Allen, K.G. (2002) Suppression of Cyclooxygenase-2 and Inducible Nitric Oxide Synthase Expression by Conjugated Linoleic Acid in Murine Macrophages, *Prostaglandins Leukot. Essent. Fatty Acids 67*, 435–443.
20. Shen, C.L., Graham, S., Morgan, D.L., Oetama, B., Brewton, L., Marshall, M.P., Lai, T.Y., Chen, Y.S., and Chang, Y.H. (2002) Effects of Chinese Herbal Remedy *Schisandra arisanensis* Hayata on Aggrecans, Morphology, and Production of Inflammatory Mediators by Human Osteoarthritic Chondrocytes and Synoviocytes, *Am. J. Trad. Chin. Med. 3*, 53–63.
21. Cohen, J.J. (1991) Programmed Cell Death in the Immune System, *Adv. Immunol. 50*, 55–85.
22. Li, Y., Seifert, M.F., Ney, D.M., Grahn, M., Grant, A.L., Allen, K.G.D., and Watkins, B.A. (1999) Dietary Conjugated Linoleic Acids Alter Serum IGF-I and IGF Binding Protein Concentrations and Reduce Bone Formation in Rats Fed (n-6) or (n-3) Fatty Acids, *J. Bone Miner. Res. 14*, 1153–1162.
23. Green, L.C., Wagner, D.A., Glogowski, J., Skipper, P.L., Wishnok, J.S., and Tannenbaum, S.R. (1982) Analysis of Nitrate, Nitrite, and [^{15}N]Nitrate in Biological Fluids, *Anal. Biochem. 126*, 131–138.
24. Watkins, B.A., Xu, H., and Turek, J. (1996) Linoleate Impairs Collagen Synthesis in Primary Cultures of Avian Chondrocytes, *Proc. Soc. Exp. Biol. Med. 212*, 153–159.
25. Lippiello, L. (1990) Lipid and Cell Metabolic Changes Associated with Essential Fatty Acid Enrichment of Articular Chondrocytes, *Proc. Soc. Exp. Biol. Med. 195*, 282–287.
26. Calder, P.C. (1998) n-3 Polyunsaturated Fatty Acids and Mononuclear Phagocyte Function, in *Medicinal Fatty Acids in Inflammation* (Kremer, J., ed.), pp. 1–27, Birkhauser Verlag, Basel.
27. Kelley, D.S., Taylor, P.C., Nelson, G.J., Schmidt, P.C., Feretti, A., Erickson, K.L., Yu, R., Chandra, R.K., and Mackey, B.E. (1999) Docosahexaenoic Acid Ingestion Inhibits Natural Killer Cell Activity and Production of Inflammatory Mediators in Young Healthy Men, *Lipids 34*, 317–324.
28. Yu, Y., Correll, P.H., and Vanden Heuvel, J.P. (2002) Conjugated Linoleic Acid Decreases Production of Pro-inflammatory Products in Macrophages: Evidence for a PPARγ-Dependent Mechanism, *Biochim. Biophys. Acta 1581*, 89–99.
29. McCarty, M.F. (2000) Activation of PPARγ May Mediate a Portion of the Anticancer Activity of Conjugated Linoleic Acid, *Med. Hypotheses 55*, 187–188.
30. Pelletier, J.P., Mineau, F., Fernandes, J.C., Duval, N., and Marterl-Pelletier, J. (1998) Diacerhein and Rhein Reduce the Interleukin 1β-Stimulated Inducible Nitric Oxide Synthesis Level and Activity While Stimulating Cyclooxygenase-2 Synthesis in Human Osteoarthritic Chondrocytes, *J. Rheumatol. 25*, 2417–2424.
31. Amin, A.R., Attur, M.G., Patel, R.N., Thakker, G.D., Marshall, P.J., Rediske, J., Stuchin, S.A., Patel, I.R., and Abramson, S.B. (1997) Superinduction of Cyclooxygenase-2 Activity in Human Osteoarthritis-Affected Cartilage: Influence of Nitric Oxide, *J. Clin. Invest. 99*, 1231–1237.
32. Kanematsu, M., Ikeda, K., and Yamada, Y. (2001) Interaction Between Nitric Oxide Synthase and Cyclooxygenase Pathways in Osteoblastic MC3T3-E1 Cells, *J. Bone Miner. Res. 12*, 1789–1796.
33. Benito, P., Nelson, G.J., Kelley, D.S., Bartolini, G., Schmidt, P.C., and Simon, V. (2001) The Effect of Conjugated Linoleic Acid on Plasma Lipoproteins and Tissue Fatty Acid Composition in Humans, *Lipids 36*, 229–236.

[Received August 11, 2003, and in revised form December 18, 2003; revision accepted January 13, 2004]

Synthesis and Anticancer Activities of Fatty Acid Analogs of Podophyllotoxin

Jamal Mustafa[a], Shabana I. Khan[a], Guoyi Ma[a], Larry A. Walker[a,b], and Ikhlas A. Khan[a,c,*]

[a]National Center for Natural Products Research, Research Institute of Pharmaceutical Sciences, Departments of [b]Pharmacology and [c]Pharmacognosy, School of Pharmacy, University of Mississippi, University, Mississippi 38677

ABSTRACT: Derivatives of podophyllotoxin were prepared by coupling 10 FA with the C_4-α-hydroxy function of podophyllotoxin. The coupling reactions between FA and podophyllotoxin were carried out by dicyclohexylcarbodiimide in the presence of a catalytic amount of dimethylaminopyridine to produce quantitative yields of desired products. FA incorporated were the following: 10-hydroxydecanoic, 12-hydroxydodecanoic, 15-hydroxypentadecanoic, 16-hydroxyhexadecanoic, 12-hydroxy-octadec-*Z*-9-enoic, eicosa-*Z*-5,8,11,14-tetraenoic, eicosa-*Z*-8,11, 14-trienoic, eicosa-*Z*-11,14-dienoic, eicosa-*Z*-11-enoic, and eicosanoic acids. Spectroscopic studies confirmed the formation of the desired products. New molecules were investigated for their *in vitro* anticancer activity against a panel of human cancer cell lines including SK-MEL, KB, BT-549, SK-OV-3 (solid tumors), and HL-60 (human leukemia) cells. Most of the analogs were cytotoxic against cancerous cells, whereas no effect was observed against normal cells, unlike the parent compound podophyllotoxin, the use of which is limited due to its severe side effects.

Paper no. L9371 in *Lipids 39*, 167–172 (February 2004).

Podophyllotoxin **1**, a bioactive principle of *Podophyllum pleianthum, P. peltatum,* and *P. emodi*, is known for its antitumor activity (1–4). However, the severe toxicity of **1** has greatly affected its clinical use and resulted in the synthesis of a variety of analogs in search of molecules of improved pharmacological profiles. Etoposide and teniposide are the two semisynthetic podophyllotoxin analogs that are used clinically to treat different types of tumors. The problems of drug resistance, myelosuppression, and low bioavailability, however, have limited their therepeutic use and have necessitated further structural transformation.

A number of investigations have demonstrated that a variety of FA are promising molecules in cancer prevention and have potential in the treatment of cancers (5–7). FA-derived podophyllotoxin analogs have received very little attention despite the fact that such molecules may lead to a new route to potential pharmaceutical molecules (5,8,9). Synthesis and biological studies of short chain-length esters of podophyllotoxin have been reported (10). The preparation of esters of podophyllotoxin and epipodophyllotoxin with a number of unusual medium- and long-chain FA have been described, and some of these derivatives have shown strong activity against P388 lymphocytic leukemia in mice (11,12).

In view of the significance of long-chain FA in the treatment of cancer, we report here the synthesis and spectral studies of new podophyllotoxin analogs containing unusual C_{10} to C_{20} FA along with their *in vitro* evaluation against a panel of human cancer cell lines including SK-MEL, KB, BT-549, SK-OV-3 (solid tumors), and HL-60 (human leukemia). FA incorporated at the C_4 α-hydroxyl group of podophyllotoxin are 10-hydroxydecanoic, 12-hydroxydodecanoic, 15-hydroxypentadecanoic, 16-hydroxyhexadecanoic acids (ω hydroxy FA); 12-hydroxy-octadec-*Z*-9-enoic acid (bifunctional FA); eicosa-*Z*-5,8,11,14-tetraenoic (20:4n-6), eicosa-*Z*-8,11,14-trienoic (20:3n-6), and eicosa-*Z*-11,14-dienoic (20:2n-6) acids; eicosa-*Z*-11-enoic and eicosanoic acids (Scheme 1). This study has investigated the *in vitro* anticancer activity of these semisynthetic podophyllotoxin analogs, derived from unusual FA, and to what extent the formation of these analogs reduces the toxicity of the parent molecule.

EXPERIMENTAL PROCEDURES

TLC was performed on aluminum sheets of silica gel $60F_{254}$ (Merck, KGaA, Darmstadt, Germany), and *n*-hexane/ethyl acetate (1:1, vol/vol) was used as a developing solvent. Reaction products on TLC plates were visualized by UV light and by exposure to iodine vapors. Flash column chromatographic separations were accomplished using 40-μm flash chromatography packing, 60 Å pore diameter (silica gel; J.T.Baker, Phillipsburg, NJ).

^1H and ^{13}C NMR spectra were recorded on a DRX-500 Bruker NMR spectrometer. Molecular weights were determined by electron-spray ionization (ESI) on a Bruker BioApex Fourier transform mass spectrometer. Samples were run in ESI-positive mode by direct injection with a syringe pump mass spectrometer (ESI–MS). FTIR spectra were recorded in $CHCl_3$ on a Genesis Series FTIR™ (Giangarlo Scientific, Pittsburgh, PA) spectrometer. Podophyllotoxin, dimethyl aminopyridine (DMAP), and FA were procured from Aldrich Chemicals (Milwaukee, WI). 12-Hydroxy-octadec-*Z*-9-enoic acid was isolated

*To whom correspondence should be addressed at National Center for Natural Products Research, Research Institute of Pharmaceutical Sciences, School of Pharmacy, University of Mississippi, University, MS 38677. E-mail: ikhan@olemiss.edu

Abbreviations: ATCC, American type culture collection; DCC, dicyclohexylcarbodiimide; DMAP, dimethyl aminopyridine; ESI, electron-spray-ionization; RPMI-1640, Roswell Park Memorial Institute.

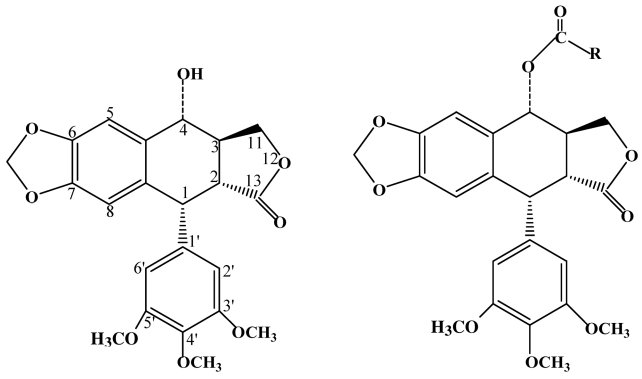

1 **2–11**

R

2. $(CH_2)_9$-OH
3. $(CH_2)_{11}$-OH
4. $(CH_2)_{14}$-OH
5. $(CH_2)_{15}$-OH
6. $(CH_2)_7$-$^{9}CH^{Z}$=$^{}CH$-CH_2-^{12}CH(OH)-$(CH_2)_5CH_3$
7. $(CH_2)_3$-$^{5}CH^{Z}$=$^{}CH$-CH_2-CH^{Z}=$^{}CH$-CH_2-CH^{Z}=$^{}CH$-CH_2-CH^{Z}=$^{}CH$-$(CH_2)_4$-CH_3
8. $(CH_2)_6$-$^{8}CH^{Z}$=$^{}CH$-CH_2-CH^{Z}=$^{}CH$-CH_2-CH^{Z}=$^{}CH$-$(CH_2)_4$-CH_3
9. $(CH_2)_9$-$^{11}CH^{Z}$=$^{}CH$-CH_2-CH^{Z}=$^{}CH$-$(CH_2)_4$-CH_3
10. $(CH_2)_9$-$^{11}CH^{Z}$=$^{}CH$-$(CH_2)_7$-CH_3
11. $(CH_2)_{18}$-CH_3

SCHEME 1

from *Ricinus communis* seed oil (13). The coupling reagent dicyclohexylcarbodiimide (DCC) was purchased from Fluka Chemical Corporation (Hauppage, NY). Methylene chloride was dried by refluxing it with calcium hydride and distilled under nitrogen prior to use.

Chemical procedures. General method for the synthesis of FA analogs of podophyllotoxin. Appropriate amounts of FA (1 mmol) and **1** (1 mmol) were dissolved in dry dichloromethane (5 mL), and DMAP (catalytic amount) was added to this solution. The reaction mixture was stirred at room temperature under nitrogen for 10 min before DCC (1 mmol) was added to it. The reaction mixture was allowed to stir at room temperature. Progress of reaction was monitored on TLC plates. All coupling reactions showed the formation of one product and were completed in 1 h. The reaction mixture was filtered to remove solid dicyclohexylurea, and the filtrate was evaporated under reduced pressure at 20°C. The semisolid mass was subjected to flash column chromatography (*n*-hexane/ethyl acetate, 1:1, vol/vol) on silica gel to purify the desired products.

(i) 4-O-*Podophyllotoxinyl 10-hydroxydecanoate* (***2***). Viscous oil; R_f = 0.5 (*n*-hexane/ethyl acetate, 1:1 vol/vol as developer), isolated yield, 97%. IR ($CHCl_3$, cm^{-1}): 3520.50, 1777.0, 1733.29, 1587.50, 1565.60, 1505.25, 1466.95, 1419.24, 1255.48, 1174.10, 1038.20, 998.82. ^1H NMR ($CDCl_3$, δ_H): 1.31–1.24 (*m*, 12H), 1.55 (*m*, 2H), 1.68 (*m*, 2H), 2.04 (unresolved signal, D_2O exchangeable), 2.83 (*m*, 1H), 2.92 (*dd*, $J_{1,2}$ = 4.5 Hz, $J_{2,3}$ = 14.5 Hz, 1H), 3.62 (*t*, *J* = 6.5 Hz, 2H), 3.76 (*s*, 6H), 3.81 (*s*, 3H), 4.20 (*t*, *J* = 10 Hz, 1H), 4.36 (*dd*, *J* = 9 Hz, *J* = 7.0 Hz, 1H), 4.60 (*d*, $J_{1,2}$ = 4.5 Hz), 5.89 (*d*, $J_{3,4}$ = 9.5 Hz, 1H), 5.98 (*d*, *J* = 3.5 Hz, 1H), 5.99 (*d*, *J* = 3.5 Hz, 1H), 6.39 (*s*, 2H), 6.54 (*s*, 1H), 6.75 (*s*, 1H); ^{13}C NMR ($CDCl_3$, δ_C): 25.33, 26.01, 29.41, 29.44, 29.62, 29.66, 33.02, 34.67, 39.07, 44.00, 45.81, 56.34, 60.89, 63.07, 71.52, 73.51, 101.57, 106.96, 108.13, 109.65, 128.31, 132.19, 134.67, 137.04, 147.377, 147.89, 152.40, 173.33, 173.88. EI–MS found $[M + Na]^+$ 607.2508; $C_{32}H_{40}O_{10}Na$ $[M + Na]^+$ requires 607.2513.

(ii) 4-O-*Podophyllotoxinyl 12-hydroxydodecanoate* (***3***). Viscous oil, R_f = 0.5 (*n*-hexane/ethyl acetate, 1:1 vol/vol as developer), isolated yield, 97.5%. IR ($CHCl_3$, cm^{-1}): 3524.95, 1778.87, 1733.14, 1588.56, 1560.70, 1505.67, 1462.81, 1420.10, 1250.36, 1172.09, 1038.17, 998.97. ^1H NMR ($CDCl_3$, δ_H): 1.30–1.25 (*m*, 16H), 1.52 (*m*, 2H), 1.65 (*m*, 2H), 1.87 (unresolved signal, D_2O exchangeable, 1H), 2.39 (*m*, 2H), 2.81 (*m*, 1H), 2.89 (*dd*, $J_{1,2}$ = 4.4 Hz, $J_{2,3}$ = 14.5 Hz, 1H), 3.59 (*t*, *J* = 6.6 Hz, 2H), 3.73 (*s*, 6H), 3.78 (*s*, 3H), 4.17 (*t*, *J* = 10.1 Hz, 1H), 4.33 (*dd*, *J* = 9.1 Hz, *J* = 7.1 Hz, 1H), 4.57 (*d*, $J_{1,2}$ = 4.3 Hz), 5.86 (*d*, $J_{3,4}$ = 9.1 Hz, 1H), 5.95 (*d*, *J* = 2.5 Hz), 5.96 (*d*, *J* = 2.5 Hz, 1H), 6.37 (*s*, 2H), 6.50 (*s*, 1H), 6.73 (*s*, 1H). ^{13}C NMR ($CDCl_3$, δ_C): 25.36, 26.10, 29.48, 29.55, 29.75, 29.82, 29.88, 33.13, 34.76, 39.15, 44.12, 45.89, 56.50, 61.07, 63.23, 71.76, 73.75, 101.96, 107.37, 108.57, 110.05, 128.85, 132.72, 135.23, 137.58, 147.96, 148.47, 153.00, 174.07, 174.60. EI–MS found $[M + Na]^+$ 635.2822; $C_{34}H_{44}O_{10}Na$ $[M + Na]^+$ requires 635.2834.

(iii) 4-O-*Podophyllotoxinyl 15-hydroxypentadecanoate* (***4***). Viscous oil, R_f = 0.6 (*n*-hexane/ethyl acetate, 1:1 vol/vol as developer), isolated yield, 97%. IR ($CHCl_3$, cm^{-1}): 3430.28, 1778.80, 1732.44, 1588.48, 1505.20, 1462.90, 1420.27, 1331.95, 1238.92, 1128.31, 1038.35, 998.05. ^1H NMR ($CDCl_3$, δ_H): 1.22 (*m*, 22H), 1.51 (*m*, 2H), 1.64 (*m*, 2H), 1.86 (unresolved signal, D_2O exchangeable), 2.39 (*m*, 2H), 2.81 (*m*, 1H), 2.89 (*dd*, $J_{1,2}$ = 4.4 Hz, $J_{2,3}$ = 14.5 Hz, 1H), 3.65 (*t*, *J* = 6.6 Hz, 2H), 3.72 (*s*, 6H), 3.77 (*s*, 3H), 4.16 (*t*, *J* = 10.1 Hz, 1H), 4.32 (*dd*, *J* = 9.1 Hz, *J* = 7.1 Hz, 1H), 4.56 (*d*, $J_{1,2}$ = 4.3 Hz, 1H), 5.86 (*d*, $J_{3,4}$ = 9.1 Hz, 1H), 5.94 (*d*, *J* = 2.5 Hz, 1H), 5.95 (*d*, *J* = 2.5 Hz, 1H), 6.35 (*s*, 2H), 6.49 (*s*, 1H), 6.72 (*s*, 1H). ^{13}C NMR ($CDCl_3$, δ_C): 25.39, 26.13, 29.53, 29.60, 29.80, 29.97, 33.15, 34.78, 39.15, 44.12, 45.92, 56.50, 61.11, 63.32, 71.79, 73.75, 101.97, 107.38, 108.48, 110.07, 128.82, 132.70, 135.25, 137.49, 147.96, 148.47, 152.99, 174.12, 174.66. EI–MS found $[M + H]^+$ 655.3476; $C_{37}H_{51}O_{10}$ $[M + H]^+$ requires 655.3470.

(iv) 4-O-*Podophyllotoxinyl 16-hydroxyhexadecanoate* (***5***). Viscous oil, R_f = 0.6 (*n*-hexane/ethyl acetate, 1:1 vol/vol as developer), isolated yield, 97.5%. IR ($CHCl_3$, cm^{-1}): 3430.25, 1778.78, 1732.34, 1588.76, 1506.98, 1462.88, 1420.17, 1332.81, 1237.73, 1236.32, 1127.36, 1025.48, 998.39. ^1H NMR ($CDCl_3$, δ_H): 1.36 (*m*, 22H), 1.57 (*m*, 2H), 1.68 (*m*, 2H), 2.44 (*m*, 2H), 2.83 (*m*, 1H), 2.93 (*dd*, $J_{1,2}$ = 4.4 Hz, $J_{2,3}$ = 14.5 Hz, 1H), 3.64 (*t*, *J* = 6.6 Hz, 2H), 3.77 (*s*, 6H), 3.82 (*s*, 3H), 4.21 (*t*, *J* = 10 Hz, 1H), 4.37 (*dd*, *J* = 8.9 Hz, *J* = 7.2 Hz, 1H),

4.61 (*d*, $J_{1,2}$ = 4.3 Hz, 1H), 5.90 (*d*, $J_{3,4}$ = 9.1 Hz, 1H), 5.98 (*d*, *J* = 2.5 Hz, 1H), 5.99 (*d*, *J* = 2.5 Hz, 1H), 6.40 (*s*, 2H), 6.54 (*s*, 1H), 6.76 (*s*, 1H). ^{13}C NMR ($CDCl_3$, δ_C): 25.40, 26.13, 29.55, 29.61, 29.81, 29.97, 33.19, 34.80, 39.18, 44.16, 45.98, 56.56, 61.11, 63.41, 71.77, 73.78, 101.96, 107.38, 108.63, 110.11, 128.87, 132.75, 135.22, 137.67, 147.99, 148.51, 153.05, 174.03, 174.63. EI–MS found $[M + Na]^+$ 691.3449; $C_{38}H_{52}O_{10}Na$ $[M + Na]^+$ requires 691.3452.

(v) 4-O-*Podophyllotoxinyl 12-hydroxyl-octadec-Z-9-enoate* (***6***). Viscous oil, R_f = 0.7 (*n*-hexane/ethyl acetate, 1:1 vol/vol as developer), isolated yield, 97.5%. IR ($CHCl_3$, cm^{-1}): 3525, 1779.68, 1734.24, 1588.40, 1505.45, 1484.67, 1419.96, 1239.40, 1127.47, 1038.32, and 999.80. ^{1}H NMR ($CDCl_3$, δ_H): 0.84 (*t*, *J* = 6.40 Hz, 3H), 1.42–1.25 (*m*, 16H), 1.64 (*m*, 2H), 2.02 (*m*, 2H), 2.17 (*m*, 2H), 2.39 (*m*, 2H), 2.83 (*m*, 1H), 2.87 (*dd*, $J_{1,2}$ = 4.5 Hz, $J_{2,3}$ = 14.5 Hz, 1H), 3.56 (*m*, 1H), 3.72 (*s*, 6H), 3.77 (*s*, 3H), 4.17 (*t*, *J* = 10.5 Hz, 1H), 4.32 (*dd*, *J* = 7.0 Hz, *J* = 7.0 Hz, 1H), 4.56 (*d*, $J_{1,2}$ = 4.5 Hz, 1H), 5.34 (*m*, 1H), 5.47 (*m*, 1H), 5.85 (*d*, $J_{3,4}$ = 8.8 Hz, 1H), 5.94 (*d*, *J* = 2.5 Hz, 1H), 5.95 (*d*, *J* = 2.5 Hz, 1H), 6.35 (*s*, 2H), 6.50 (*s*, 1H), 6.72 (*s*, 1H). ^{13}C NMR ($CDCl_3$, δ_C): 14.47, 22.99, 25.36, 26.10, 27.74, 29.48, 29.73, 29.96, 32.22, 34.74, 35.75, 37.24, 39.15, 44.12, 45.94, 56.51, 61.11, 71.84, 73.77, 101.98, 107.38, 108.49, 110.09, 125.76, 128.82, 132.72, 133.51, 135.23, 137.52, 147.97, 148.48, 153.01, 174.07, 174.61. MS–EI found $[M + H]^+$ 695.3769; $C_{40}H_{55}O_{10}$ $[M + H]^+$ requires 695.3789.

(vi) 4-O-Podophyllotoxinyl eicosa-Z-*5,8,11,14-tetraenoate* (***7***). Viscous oil, R_f = 0.9 (*n*-hexane/ethyl acetate, 1:1 vol/vol as developer), isolated yield, 98.5%. IR ($CHCl_3$, cm^{-1}): 1779.15, 1734.62, 1588.11, 1505.04, 1484.55, 1462.84, 1420.29, 1331.78, 1239.20, 1171.51, 1127.49, 1038.39, 999.75. ^{1}H NMR ($CDCl_3$, δ_H): 0.90 (*t*, *J* = 6.6 Hz, 3H), 1.39–1.28 (*m*, 8H), 1.78 (*q*, *J* = 7.2 Hz, 2H), 2.07 (*q*, *J* = 7.0 Hz, 2H), 2.18 (*q*, *J* = 7.0 Hz, 2H), 2.18 (*m*, 2H), 2.88–2.81 (*m*, 7H), 2.94 (*dd*, $J_{1,2}$ = 4.4 Hz, $J_{2,3}$ = 14.5 Hz, 1H), 3.77 (*s*, 6H), 3.83 (*s*, 3H), 4.21 (*t*, *J* = 10 Hz, 1H), 4.37 (*dd*, *J* = 7.1 Hz, *J* = 7.1 Hz, 1H), 4.62 (*d*, $J_{1,2}$ = 4.3 Hz, 1H), 5.46–5.34 (*m*, 8H), 5.91 (*d*, $J_{3,4}$ = 9.2 Hz, 1H), 5.99 (*d*, *J* = 2.5 Hz, 1H), 6.0 (*d*, *J* = 2.5 Hz, 1H), 6.41 (*s*, 2H), 6.55 (*s*, 1H), 6.77 (*s*, 1H). ^{13}C NMR ($CDCl_3$, δ_C): 14.43, 22.94, 25.20, 26.03, 26.92, 27.61, 29.69, 31.90, 34.13, 39.17, 44.16, 46.01, 56.57, 61.12, 71.75, 73.90, 101.97, 107.36, 108.63, 110.13, 127.89, 128.16, 128.32, 128.81, 128.88, 129.05, 129.69, 130.91, 132.76, 135.20, 137.70, 148.01, 148.53, 153.07, 174.01, 174.35. EI–MS found $[M + Na]^+$ 723.3448; $C_{42}H_{52}O_9Na$ $[M + Na]^+$ requires 723.85.

(vii) 4-O-Podophyllotoxinyl eicosa-Z-*8,11,14-trienoate* (***8***). Viscous oil, R_f = 0.9 (*n*-hexane/ethyl acetate, 1:1 vol/vol as developer), isolated yield, 98.5%. IR ($CHCl_3$, cm^{-1}): 1779.05, 1734.52, 1588.21, 1505.44, 1484.48, 1462.90, 1420.20, 1331.69, 1239.20, 1171.59, 1127.39, 1038.30, 998.65. ^{1}H NMR ($CDCl_3$, δ_H): 0.90 (*t*, *J* = 7.0 Hz, 3H), 1.37–1.33 (*m*, 14H), 1.70 (*m*, 2H), 2.0 (*m*, 2H), 2.43 (*m*, 2H), 2.83 (*m*, 5H), 2.94 (*dd*, $J_{1,2}$ = 4.5 Hz, $J_{2,3}$ = 14.5 Hz, 1H), 3.77 (*s*, 6H), 3.82 (*s*, 3H), 4.21 (*t*, *J* = 10.5 Hz, 1H), 4.39 (*dd*, *J* = 7.5 Hz, *J* = 7.5 Hz, 1H), 4.61 (*d*, $J_{1,2}$ = 4.5 Hz, 1H), 5.40–5.35 (*m*, 6H), 5.91 (*d*, $J_{3,4}$ = 9.5 Hz, 1H), 5.99 (*d*, *J* = 2.5 Hz, 1H), 6.0 (*d*, *J* = 2.5 Hz, 1H), 6.40 (*s*, 2H), 6.55 (*s*, 1H), 6.76 (*s*, 1H). ^{13}C NMR ($CDCl_3$, δ_C): 14.45, 22.91, 25.29, 25.97, 27.46, 27.54, 29.21, 29.42, 29.63, 29.74, 31.82, 34.66, 39.05, 44.00, 45.83, 56.35, 60.92, 71.52, 73.54, 101.58, 106.94, 108.12, 109.68, 127.48, 127.84, 128.01, 128.24, 129.85, 130.29, 132.19, 134.68, 137.03, 147.38, 147.90, 152.40, 173.35, 173.85. EI–MS found $[M + H]^+$ 703.3841; $C_{42}H_{55}O_9$ $[M + H]^+$ requires 703.3840.

(viii) 4-O-Podophyllotoxinyl eicosa-Z-*11,14-dienoate* (***9***). Viscous oil, R_f = 0.9 (*n*-hexane/ethyl acetate, 1:1 vol/vol as developer), isolated yield, 99%. IR ($CHCl_3$, cm^{-1}): 1779.0, 1734.59, 1588.09, 1505.53, 1484.59, 1462.90, 1420.28, 1331.72, 1239.27, 1171.69, 1127.30, 1038.30, 998.70. ^{1}H NMR ($CDCl_3$, δ_H): 0.90 (*t*, *J* = 7.0 Hz, 3H), 1.30–1.38 (*m*, 18 H), 1.69 (*m*, 2H), 2.07 (*m*, 2H), 2.45 (*m*, 4H), 2.78 (*t*, *J* = 7.8 Hz, 2H), 2.84 (*m*, 1H), 2.95 (*dd*, $J_{1,2}$ = 4.5 Hz, 1H), 3.77 (*s*, 6H), 3.82 (*s*, 3H), 4.22 (*t*, 10 Hz, 1H), 4.39 (*dd*, *J* = 7.5 Hz, *J* = 7.5 Hz, 1H), 4.61 (*d*, *J* = 4.5 Hz, 1H), 5.40–5.34 (*m*, 4H), 5.99 (*d*, *J* = 1.5 Hz, 1H), 6.00 (*d*, *J* = 1.5 Hz), 6.40 (*s*, 2H), 6.55 (*s*, 1H), 6.76 (*s*, 1H). ^{13}C NMR ($CDCl_3$, δ_C): 14.08, 22.56, 24.97, 25.61, 27.18, 29.15, 29.25, 29.32, 29.52, 29.63, 31.56, 34.36, 38.74, 43.69, 45.49, 56.07, 60.71, 71.41, 73.35, 101.59, 106.99, 107.98, 109.65, 127.90, 127.97, 128.39, 130.06, 130.16, 132.28, 134.87, 136.98, 147.55, 148.07, 152.56, 173.81, 174.28. EI–MS found $[M]^+$ 705.4002; $C_{42}H_{56}O_9$ $[M]^+$ requires 705.3996.

(ix) 4-O-Podophyllotoxinyl eicosa-Z-*11-enoate* (***10***). Viscous oil, R_f = 0.9 (*n*-hexane/ethyl acetate, 1:1 vol/vol as developer), isolated yield, 99%. IR ($CHCl_3$, cm^{-1}): 1780.15, 1735.90, 1586.86, 1515.25, 1486.27, 1465.95, 1423.24, 1331.87, 1238.64, 1172.55, 1127.40, 1038.85, 998.43. ^{1}H NMR ($CDCl_3$, δ_H): 0.89 (*t*, *J* = 7.0 Hz, 3H), 1.28–1.34 (*m*, 24H), 1.69 (*m*, 2H), 2.02 (*m*, 4H), 2.48 (*m*, 2H), 2.84 (*m*, 1H), 2.93 (*dd*, $J_{1,2}$ = 4.5 Hz, *J* = 14.5 Hz, 1H), 3.77 (*s*, 6H), 3.83 (*s*, 3H), 4.21 (*t*, *J* = 9.5 Hz, 1H), 4.37 (*dd*, *J* = 7.0 Hz, *J* = 7.0 Hz, 1H), 4.61 (*d*, $J_{1,2}$ = 4.5 Hz, 1H), 5.35 (*m*, 2H), 5.90 (*d*, $J_{3,4}$ = 9.0 Hz, 1H), 5.98 (*d*, *J* = 2.5 Hz, 1H), 6.0 (*d*, *J* = 2.5 Hz, 1H), 6.55 (*s*, 2H), 6.76 (*s*, 1H), 7.28 (*s*, 1H). ^{13}C NMR ($CDCl_3$, δ_C): 14.48, 23.01, 25.35, 27.52, 27.54, 29.50, 29.58, 29.62, 29.74, 29.83, 30.07, 32.20, 34.69, 39.06, 44.02, 45.83, 56.35, 60.91, 71.51, 73.51, 101.57, 106.96, 108.15, 109.67, 128.35, 129.66, 129.82, 132.20, 134.68, 137.07, 147.38, 147.90, 152.42, 173.31, 173.88; EI–MS found $[M + Na]^+$ 729.3894; $C_{42}H_{58}O_9Na$ $[M + Na]^+$ requires 729.90.

(x) 4-O-*Podophyllotoxinyl eicosanoate* (***11***). Viscous oil, R_f = 0.9 (*n*-hexane/ethyl acetate, 1:1 vol/vol as developer), isolated yield, 99%. IR ($CHCl_3$, cm^{-1}): 1780.0, 1735.60, 1588.68, 1505.87, 1484.57, 1462.86, 1420.28, 1331.77, 1239.27, 1171.69, 1127.45, 1038.47. ^{1}H NMR ($CDCl_3$, δ_H): 0.88 (*t*, *J* = 7.0 Hz, 3H), 1.24 (*m*, 32H), 1.66 (*m*, 2H), 2.49 (*m*, 2H), 2.85 (*m*, 1H), 2.94 (*dd*, $J_{1,2}$ = 4.5 Hz, $J_{2,3}$ = 14.5 Hz, 1H), 3.76 (*s*, 6H), 3.82 (*s*, 3H), 4.20 (*t*, *J* = 9.5 Hz, 1H), 4.36 (*dd*, *J* = 7.0 Hz, *J* = 7.0, 1H), 4.61 (*d*, $J_{1,2}$ = 4.5 Hz, 2H), 5.89 (*d*, $J_{3,4}$ = 9.0 Hz, 1H), 5.97 (*d*, *J* = 2.5 Hz, 1H), 6.0 (*d*, *J* = 2.5 Hz, 1H), 6.55 (*s*, 2H), 6.76 (*s*, 1H), 7.28 (*s*, 1H). ^{13}C NMR ($CDCl_3$, δ_C): 14.50, 23.08, 25.42, 29.57, 29.65, 29.75, 29.85, 30.09, 32.32, 34.80, 39.17, 44.15, 45.97, 56.52, 61.13, 71.79, 73.77, 101.98, 107.39,

108.51, 110.00, 110.10, 128.85, 132.72, 135.23, 137.55, 147.99, 148.49, 153.03, 174.06, 174.64. EI–MS found $[M + Na]^+$ 731.4069, $C_{42}H_{60}O_9Na$ $[M + Na]^+$ 731.91.

Assay for anticancer activity. The compounds **1–11** were tested for their *in vitro* cytotoxicity against a panel of human cancer cell lines including SK-MEL (malignant, melanoma), KB (epidermal carcinoma, oral), BT-549 (ductal carcinoma, breast), SK-OV-3 (ovary carcinoma), and HL-60 (human leukemia). VERO cells (African green monkey kidney fibroblast) were also included in the study as noncancerous mammalian cells (14). All the cell lines were from the American Type Culture Collection (Manassas, VA). The cells were cultured in 75-cm^2 culture flasks in RPMI-1640 medium (GIBCO, Invitrogen Corp., Carlsbad, CA) supplemented with bovine calf serum (10%) and amikacin (60 mg/L), at 37°C, 95% humidity, 5% CO_2 and subcultured every 2–3 d using standard cell culture techniques. For the assay, HL-60 cells (nonadherent) were seeded in 24-well plates at a density of 1×10^5 cells/well and were allowed to grow undisturbed for 24 h before addition of the test samples. After 48 h incubation with samples (diluted in RPMI-1640 medium) at 37°C, cell counts were made by using the Trypan Blue exclusion method to determine cell viability (15). With solid tumor cells (adherent) growing as monolayers, the assay was performed in 96-well microplates. Cells were seeded to the wells of the plate at a density of 25,000 cells/well and grown for 24 h at 37°C. Samples, diluted appropriately in RPMI-1640 medium, were added to the cells and again incubated for 48 h. The number of viable cells was determined using a modified Neutral Red assay procedure (16). Briefly, after incubating with the samples, the cells were washed with saline and incubated for 90 min with the medium containing Neutral Red (166 μg/mL). The cells were washed to remove extracellular dye. A solution of acidified isopropanol (0.33% HCl) was then added to lyse the cells; as a result, the incorporated dye was liberated from the viable cells. The absorbance was read at 540 nm. IC_{50} (the concentration of the test compound that caused a growth inhibition of 50% after 48 h of exposure of the cells) was calculated from the dose curves generated by plotting percent growth vs. the test concentration on a logarithmic scale using Microsoft Excel (Redmond, WA). All assays were performed in triplicate and the mean values are given in Table 1.

RESULTS AND DISCUSSION

The ω hydroxy FA are carcinostatic, prevent cancer metastasis, and prevent the occurrence and reoccurrence of cancer while having few side effects (17). It has been suggested that exogenous unsaturated FA may increase anticancer activity of cancer chemotherapeutic agents (18,19). The present study is based on the synthesis and anticancer activities of podophyllotoxin derivatives derived from ω-FA and FA of different degrees of unsaturation. Ten FA—10-hydroxydecanoic, 12-hydroxydodecanoic, 15-hydroxypentadecanoic, 16-hydroxyhexadecanoic, 12-hydroxyoctadec-*Z*-9-enoic, eicosa-*Z*-5,8,11,14-tetraenoic, eicosa-*Z*-8,11,14-trienoic, eicosa-*Z*-11,14-dienoic, eicosa-*Z*-11-enoic, and eicosanoic—were coupled with the C_4 α-hydroxy group of podophyllotoxin with the help of DCC in the presence of a catalytic amount of DMAP under nitrogen to produce **2–11**, respectively, in quantitative yields (Scheme 1). The products **2–11** were obtained as colorless viscous oils when purified on a silica gel column with *n*-hexane/ethyl acetate (1:1) as eluent. The signals of the FA and podophyllotoxin moieties in the ^1H and ^{13}CNMR spectra of compounds **2–11** were successfully assigned with the help of ^{13}C-^1H COSY correlation, DEPT 135, 90, and 45 techniques. The high-resolution mass (electroionization) spectral studies have further confirmed their structures. A detailed spectral description for compound **6** is discussed below.

Compound **6** has a methylene-interrupted 12-hydroxy and *Z*-9-olefin system in its C_{18} FA moiety. Its IR spectrum revealed three bands at 3525 (OH), 1779.68 (lactone C=O), and 1734.24 cm^{-1} (ester C–O stretching). The presence of the OH group was further confirmed by the chemical shift of 12-H at δ_H 3.56, which was correlated with a carbon signal at δ_C 71.84. The two olefinic protons, 9-H and 10-H, were observed at δ_H 5.34 and 5.47 and correlated with observations at δ_C 125.76 and 132.72, respectively. A few other significant carbon signals for the acyl chain were recorded at δ_C 14.47 (C-18), 22.99 (C-17), 25.36 (C-3), 34.74 (C-2), 174.07 (C-1, ester C=O). Two intense singlets at δ_H 3.72 (6H) and 3.77 (3H) represented three methoxy phenyl groups and correlated with δ_C 56.51 ($2 \times OCH_3$ at 3′-C, 5′-C) and 61.11 (OCH_3 at C-4′). The chemical shifts for the cyclohexyl ring protons were recorded at δ_H 2.83 (*m*, 3-H), 2.87 (*dd*, $J_{1,2}$ = 4.5 Hz, $J_{2,3}$ = 14.5 Hz, 2-H), 4.56 (*d*, $J_{1,2}$ = 4.5 Hz, 1-H), and 5.85 (*d*, $J_{3,4}$ = 8.8 Hz, 4-H), and their respective carbons were observed at δ_C 45.94 (C-3), 39.15 (C-2), 44.12 (C-1), and 73.77 (C-4). Each of the two methylene protons in the lactone ring was resonated separately at δ_H 4.17 (*t*, *J* = 10.5 Hz, 11-H) and 4.32 (*dd*, *J* = 7.0 Hz, *J* = 7.0 Hz, 11-H) and corresponded with δ_C 71.84 (C-11) for their carbon. Two closely spaced doublets were observed for two methylene protons (O–CH_2–O) in the first ring at δ_H 5.94 (*d*, *J* = 2.5 Hz, 1H) and 5.95 (*d*, *J* = 2.5 Hz, 1H), and their carbon has appeared at δ_C 101.98. The chemical shifts for aromatic protons singlets are moved downfield at δ_H 6.35 (2′H, 6′H) 6.50 (8-H), and 6.72 (5-H) and their carbons appeared at δ_C 108.49 (2′C, 6′C), 110.09 (C8), and 107.38 (C-5).

Spectral studies have illustrated that the change in the nature of FA at α-C_4 has not significantly influenced the pattern of proton and carbon signals of the podophyllotoxin moiety. Compounds **7** (20:4n-6) and **8** (20:3n-6) are PUFA with methylene-interrupted *Z*-double bonds. The chemical shifts of olefinic protons and carbons of **7** are present at δ_H 5.46–5.34 and δ_C 127.89, 128.16, 128.32, 128.81, 128.88, 129.05, 129.69, and 130.91. In compound **8**, proton and carbon chemical shifts were recorded at δ_H 5.40–5.35 and δ_C 127.48, 127.84, 128.01, 128.24, 129.85 and 130.29. Product **9** has a methylene-interrupted *Z*-diene system (20:2n-6) in its FA moiety for which proton and carbon signals were observed at δ_H 5.40–5.34 and at δ_C 127.90, 127.97, 130.06, and 130.16. Products **2–5** carry ω-hydroxy FA of different chain lengths. These compounds

TABLE 1
Anticancer Activity of Compounds 1–11

Compounds[a]	Cell lines[b] (IC_{50}, μM)					
	SK-MEL	KB	BT-549	SK-OV-3	HL-60	VERO
1	0.22	0.24	0.36	0.19	0.01	0.55
2	0.21	0.31	0.22	0.26	0.07	NA
3	0.41	1.19	0.29	0.44	0.19	NA
4	0.89	NA	1.19	0.76	0.24	NA
5	0.90	2.39	0.85	0.81	0.18	NA
6	4.0	4.30	2.59	3.75	0.47	NA
7	0.34	0.40	0.27	0.27	0.07	NA
8	1.17	1.35	1.08	1.08	0.24	NA
9	1.42	1.42	0.89	0.79	0.85	NA
10	NA	NA	NA	NA	NA	NA
11	NA	NA	NA	NA	NA	NA

[a]The highest concentration tested was 15 μM.
[b]NA, not active; SK-MEL, human malignant melanoma; KB, human epidermal carcinoma, oral; BT-549, human ductal carcinoma, breast; SK-OV-3, human ovary carcinoma; HL-60, human leukemia; VERO, monkey kidney fibroblasts.

have shown normal FA and podophyllotoxin signals in their NMR spectra with the addition to a two-proton triplet at around δ_H 3.65 and a carbon at around δ_C 63.41. Their IR spectra showed a broad band in the region of 3500 to 3400 cm^{-1}, representing the terminal hydroxyl group.

Our observations show that coupling reactions between FA and podophyllotoxin are stereospecific in nature. The nonexistence of epimerized products (C_4-β isomers) may be explained through the reaction mechanism of the reaction. α-Stereoselectivity of C_4 is retained, as the α-bond between C_4 and the OH group is not involved in the chemical reaction. Spectral studies have further supported stereospecific incorporation of FA molecules (11,12).

Anticancer evaluation. The cytotoxic activity of FA analogs of podophyllotoxin **2–11** was investigated and compared with **1** in an *in vitro* assay against a panel of human solid tumor cells including SK-MEL, KB, BT-549, and SK-OV-3 as well as the leukemia cells (HL-60). Their cytotoxicity was also determined against noncancerous mammalian cells (VERO cells) for comparison. The cytotoxic potencies of these compounds are expressed in terms of IC_{50} values, as shown in Table 1. Compounds **2–9** showed significant cytotoxicity to all cancer cells tested. They did not affect the growth of VERO cells up to the highest concentration of 15 μM in the assay, thus demonstrating a selectivity toward the tumor cells. Compounds **2** and **7** were the most active analogs, with IC_{50} values ranging from 0.07 μM for HL-60 cells to 0.4 μM for KB cells. Compound **2** has the shortest FA carbon chain (C_{10}) of the ω-hydroxy acids tested. The cytotoxicity of the other ω-hydroxy FA analogs, **3–5**, decreased with increasing chain length (C_{11}–C_{15}). The significantly higher activity of **7** may be attributed to the presence of a methylene-interrupted tetra *Z*-unsaturated system on a C_{20} FA side chain in the molecule. The activity of other such molecules was found to decrease with a decrease in the degree of methylene-interrupted *Z*-unsaturation in the FA side chain, as observed for **8** (triene) and **9** (diene). Compounds **6** and **10** carry isolated *Z*-monounsaturation on their respective C_{18} and C_{20} FA side chains. The moderate activity of **6** may be attributed to a 12-hydroxyl group on the side chain, whereas **10** was not active.

The present investigations have indicated that the presence of a hydroxyl group and poly *Z*-unsaturation may be responsible for such activity. This may be why **11** did not show any anticancer activity in any of the cell lines (Table 1). When cells were incubated with equimolar concentrations of the FA used to synthesize **2–11** and podophyllotoxin, the presence of FA did not affect the activity of podophyllotoxin (data not shown), ruling out the possibility that FFA can mitigate the toxicity of podophyllotoxin.

Although the cytotoxic activity of **2–9** is not stronger than the parent compound, **1**, they are not cytotoxic to normal cells, unlike **1**. This observation indicated that these new FA analogs may have some advantages over **1**.

We have demonstrated a facile and quantitative method for the preparation of FA analogs **2–11** of **1** and evaluated their anticancer potential. This is the first report of the reaction of tetra *Z*-unsaturated FA with α-C_4 podophyllotoxin to produce **7.** Analogs **2–9** exhibited cytotoxic activity against a panel of human solid tumor and leukemia cells. Interestingly, none of them showed any cytotoxicity to normal cells.

ACKNOWLEDGMENTS

This work was supported in part by the USDA Research Service Specific Cooperation Agreement no. 58-6408-2-0009. We are also thankful to Frank Wiggers for assistance in NMR spectroscopy and John Trott for assisting in the anticancer assays.

REFERENCES

1. Brewer, C.F., Loike, J.D., Horwitz, S.B., Sternlicht, H., and Gensler,W.J. (1979) Conformational Analysis of Podophyllotoxin and Its Congeners: Structure–Activity Relationship in Microtubule Assembly, *J. Med. Chem. 22*, 215–221.
2. Ward, R.S. (1992) Synthesis of Podophyllotoxin and Related Compounds, *Synthesis*, 719–730.

3. Lear, Y., and Durst, T. (1996) Synthesis and Biological Evaluation of Carbon-Substituted C-4 Derivatives of Podophyllotoxin, *Can. J. Chem. 74*, 1704–1708.
4. Lee, K.H. (1999) Novel Anticancer Agents from Higher Plants, *Med. Res. Rev. 19*, 569–596.
5. Conklin, K.A. (2002) Dietary Polyunsaturated Fatty Acids: Impact on Cancer Chemotherapy and Radiation, *Altern. Med Rev. 7*, 4–21.
6. Bougnoux, P., (1999) n-3 Polyunsaturated Fatty Acids and Cancer, *Curr. Opin. Clin. Nutri. Metab. Care, 2*, 121–126.
7. Berge, R. (2002) Fatty Acid Analogues for the Treatment of Cancer, PCT Int. Application: WO 2001-NO301 20010713, 31 pp.
8. Hardman, W.E., Cameron, I.L., and Moyer, M.P. (2001) Fatty Acids to Minimize Cancer Therapy Side Effects, PCT Int. Application: WO 99-US16666 19990722, 31 pp.
9. Rose, D.P., and Connolly, J.M. (1999) Omega-3 Fatty Acids as Cancer Chemopreventive Agents, *Pharmacol. Ther. 83*, 217–244.
10. Levy, R.K., Hall, I.H., and Lee, K.H., (1983) Synthesis and Biological Evaluation of Podophyllotoxin Esters and Related Derivatives, *J. Pharm. Sci. 72*, 1158–1161.
11. Nagao, Y., Mustafa, J., Sano, S., Ochiai, M., Tazuko, T., and Shigeru, T. (1991) Different Mechanism of Action of Long Chain Fatty Acid Esters of Podophyllotoxin and Esters of Epipodophyllotoxin Against P388 Lymphocytic Leukemia in Mice, *Med. Chem. Res. 1*, 295–299.
12. Lie Ken Jie, M.S.F., Mustafa, J., and Pasha, M.K. (1999) Synthesis and Spectral Characteristics of Some Unusual Fatty Esters of Podophyllotoxin, *Chem. Phys. Lipids 100*, 165–170.
13. Gunstone, F.D. (1954) The Nature of Oxygenated Acid Present in *Vernonia anthelmintica* (Wild.) Seed Oil, *J. Chem. Soc.*, 1611–1616.
14. Queiroz, E.F., Roblot, F., Duret, P., Figadere, B., Gouyette, A., Laprevote, O., Serani, L., and Hocquemiller, R. (2000) Synthesis, Spectroscopy and Cytotoxicity of Glycosylated Acetogenin Derivatives as Promising Molecules for Cancer Therapy, *J. Med. Chem. 43*, 1604–1610.
15. Roper, P.R., and Drewinko, B. (1976) Comparison of *in vitro* methods to Determine Drug-Induced Cell Lethality, *Cancer Res. 36*, 2182–2188.
16. Borenfreund, E., Babich, H., and Martin-Alguacil, N. (1990) Rapid Chemosensitivity Assay with Human Normal and Tumor Cells *in vitro*, *In vitro Dev. Cell. Biol. 26*, 1030–1034.
17. Ito, N., Tsuji, H., and Fukuda, Y. (2002) Anticancer Agents, Perfumes or Foods and Drinks Containing ω-Hydroxy Fatty Acids, PCT Int. Application: WO 0238148 A1 20020516, 41 pp.
18. Menendez, J.A., Ropero, S., Del Mar Barbacid, M., Montero, S., Solanas, M., Escrich, E., Cortes-Funes, H., and Colomer, R. (2002) Synergistic Interaction Between Vinorelbine and γ-Linolenic Acid in Breast Cancer Cells, *Cancer Res. Treat. 72*, 203–219.
19. Miyazawa, A., Igarashi, M., Kameyama, T., and Inoue, Y. (2000) Conjugated Polyunsaturated Fatty Acid Compositions for Killing Cancer Cells, *Jpn. Kokai Tokky Koho*, Application: JP 99-129045 19990330, 10 pp.

[Received August 18, 2003, and in revised form December 10, 2003; revision accepted January 5, 2004]

A Spectroscopic Study of the Interaction of Nigerloxin, a Fungal Metabolite, with Serum Albumin

K.C. Sekhar Rao[a], A.G. Appu Rao[b,*], and A.P. Sattur[a]

[a]Fermemtation Technology and Bioengineering Department and [b]Protein Chemistry and Technology Department, Central Food Technological Research Institute (CFTRI), Mysore 570013, India

ABSTRACT: Nigerloxin [2-amido-3-hydroxy-6-methoxy-5-methyl-4-(prop-1′-enyl) benzoic acid], a fungal metabolite, is an inhibitor of lipoxygenase and aldose reductase with free radical-scavenging properties. The interaction of nigerloxin with bovine serum albumin (BSA) was investigated using fluorescence spectroscopy and circular dichroic measurements. The fluorescence of BSA was quenched following interaction with nigerloxin, and this property was used to generate a binding constant. The estimated association constant was $1.01 \pm 0.2 \times 10^6$ M^{-1}. Job's method of continuous variation indicated that nigerloxin formed a 1:1 ± 0.1 complex with BSA. To understand the nature of the interaction, the variance in the association constant as a function of temperature in the range of 14–45°C was used to calculate the thermodynamic parameters. The thermodynamic parameters at 27°C derived from the mass action plot and van't Hoff's plot were as follows: $\Delta G = -8.2 \pm 0.1$ kcal/mol, $\Delta H \approx 0$ kcal/mol, and $\Delta S = 27.5 \pm 0.4$ cal/mol/K (where ΔG is free energy, ΔH is enthalpy, and ΔS is entropy). Increasing ionic strength did not favor interaction. Circular dichroic measurements revealed that the interaction of nigerloxin with BSA did not lead to changes in the secondary structure of the protein. The reversibility of the interaction verified by the dilution method was found to be reversible. These measurements suggest that partial hydrophobic and partial ionic bonding play a role in the interaction of nigerloxin with BSA.

Paper no. L9403 in *Lipids 39,* 173–177 (February 2004).

During the course of our screening of bioactive molecules from microbial sources (1–3), we reported the discovery of a new metabolite, designated as nigerloxin [2-amido-3-hydroxy-6-methoxy-5-methyl-4-(prop-1′-enyl) benzoic acid; Scheme 1]. Obtained from *Aspergillus niger* CFR-W-105 through solid-state fermentation (4), nigerloxin acts as an inhibitor of lipoxygenase (LOX) and aldose reductase and possesses free radical-scavenging property. Inhibitors against LOX are used as food preservatives or antioxidants in food. In medicine, they are used as anti-asthmatic, anti-inflammatory, anti-angiogenic, anti-cancer, and anti-atherosclerotic agents.

Nigerloxin is a lipophilic molecule with phenolic groups and a conjugated double bond. Many lipophilic molecules, such as long-chain fatty acid (FA), are known to be carried by albumin in the blood (5).

*To whom correspondence should be addressed.
E-mail: appu@cscftri.ren.nic.in

Abbreviations: BSA, bovine serum albumin; CD, circular dichroism; FA, fatty acid; LOX, lipoxygenase; HSA, human serum albumin.

Serum albumin is the most abundant protein in the circulatory system, with a M.W. of 66 kDa [with bovine serum albumin (BSA)]; its principal function is to transport FA, metabolites, and other hydrophobic molecules from the site of injection to the site of their pharmacological action. The crystal structure of BSA was well characterized by Curry *et al.* (6). BSA and human serum albumin (HSA) are frequently used in biophysical and biochemical studies since they have a similar folding, a well-known primary structure, and they have been associated with the binding of many different categories of small molecules. One important difference between BSA and HSA is that BSA has two tryptophan residues, whereas HSA has a unique tryptophan (7). The effectiveness of the compounds from a pharmaceutical standpoint depends on their binding ability with serum albumins. However, whether albumin can function as a carrier molecule for nigerloxin is not known. To assess this, the present investigation was undertaken to study the interaction of nigerloxin with BSA. The interaction was followed by fluorescence quenching and circular dichroism (CD) measurements.

MATERIALS AND METHODS

Nigerloxin was prepared according to the method described in Rao *et al.* (4). *N*-Acetyl tryptophan amide, Trizma® base, and BSA were purchased from Sigma (St. Louis, MO). All other reagents were of analytical reagent grade.

Fluorescence quenching studies. A stock solution of nigerloxin (68 mM) was prepared in DMSO and diluted to 40 μM with 50 mM Tris–HCl buffer (pH 7.4). A working solution of BSA (1.51 μM) was prepared in Tris–HCl buffer (pH 7.4). The intrinsic fluorescence of BSA in the presence and ab-

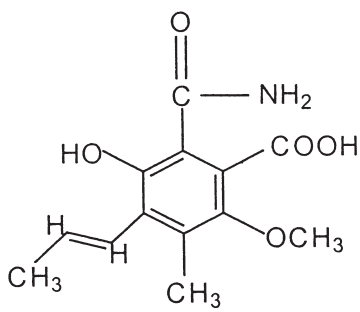

SCHEME 1

sence of nigerloxin at different concentrations was followed at 282 nm excitation and 342 nm emission wavelengths in a Shimadzu RF5000 recording spectrofluorometer (Kyoto, Japan) with a thermostatted cuvette holder attached for constant temperature.

Quenching of the relative fluorescence intensity of BSA by nigerloxin was analyzed in terms of the binding of nigerloxin to protein by using an established method (8), assuming that the binding of each molecule of nigerloxin would cause the same degree of fluorescence quenching. The percentage of quenching of the fluorescence intensity of proteins by nigerloxin was corrected empirically for an inner filter effect by subtracting the percentage of quenching of the fluorescence of *N*-acetyl-tryptophan amide equivalent in absorption to the protein at 282 nm by the same concentration of nigerloxin. The equilibrium constant, K_{eq}, is given by the following equation:

$$K_{eq} = \frac{\beta}{1-\beta} \times \frac{1}{C_f} \qquad [1]$$

where $\beta = Q/Q_{max}$, $C_f = C - n\beta T$, in which Q is the corrected percentage of quenching; Q_{max} is the maximal percentage of quenching; C_f is the molar equilibrium concentration of unbound nigerloxin; C is the molar constituent concentration of nigerloxin; T is the molar constituent concentration of BSA; and n is the binding stoichiometry. The value of K_{eq} is given by the slope of the plot of $\beta/(1-\beta)$ against C_f; Q_{max} was determined by extrapolation of a plot of $1/Q$ against $1/C$ to $1/C = 0$ (9). In both cases, the data were fitted to a straight line by the least squares method. The value of n for the nigerloxin–BSA interaction was obtained by Job's method of continuous variation (10). The total concentration of nigerloxin and BSA was held constant at 2.25 μM, and their relative concentrations were varied. Q was plotted against the mole fraction of BSA, and the linear portions of the curve were extrapolated; the molar ratio of nigerloxin and BSA in the complex were taken from the point of intersection.

The reversibility of the BSA–nigerloxin interaction was verified by dilution measurements.

CD studies CD measurements were made with a JASCO J-810 automatic recording spectropolarimeter (Tokyo, Japan), calibrated with *d*(+)-10-camphor sulfonic acid. Quartz cells of 1 cm pathlength for the 250–500 nm region and 1 mm for the far-UV region were used. Slits were programmed to yield a 10-Å bandwidth at each wavelength (11). Molar ellipticity values, θ_{mrw}, were calculated using a value of 115 for BSA.

RESULTS

Fluorescence spectroscopic studies. Fluorescence emission spectra of BSA, after being excited at 282 nm, were observed at 342 nm. Addition of increasing amounts of nigerloxin quenched the fluorescence of BSA without significantly affecting the fluorescence maxima (data not shown). The relative fluorescence emission intensities at 342 nm were plotted

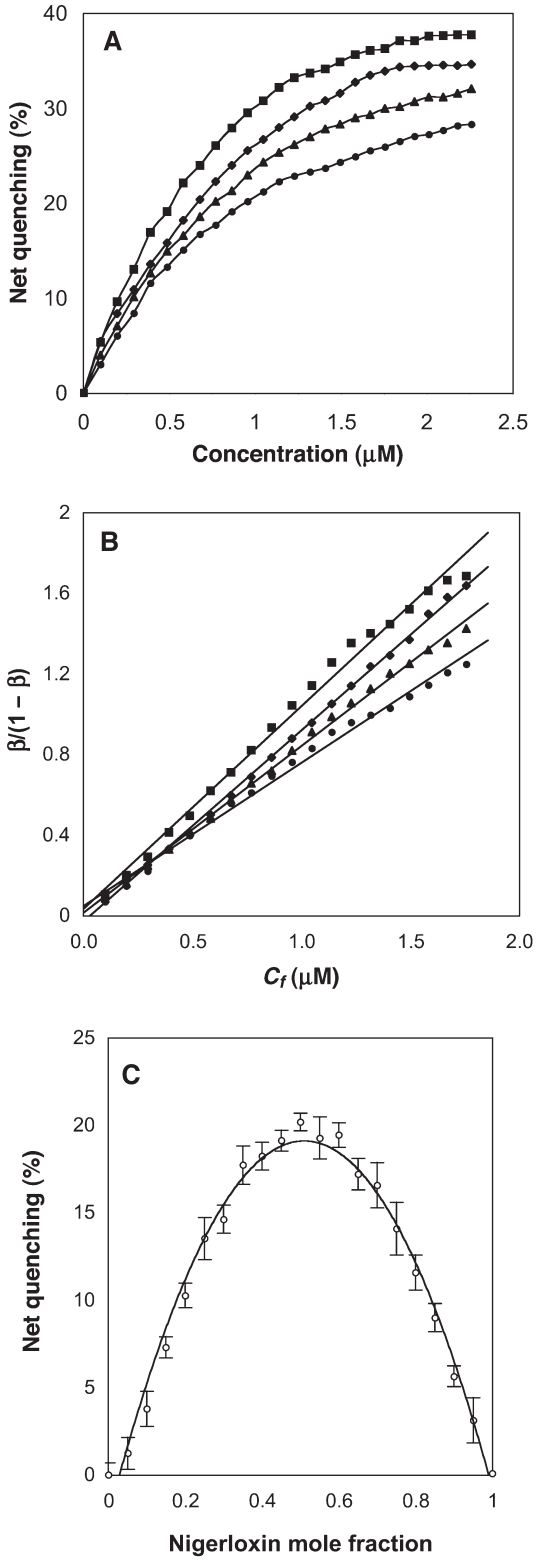

FIG. 1. (A) Fluorescence quenching of BSA by nigerloxin at (◆) 14, (■) 27, (▲) 36, and (●) 45°C. The concentration of BSA was 0.1 mg/mL. Measurements were made in 50 mM Tris–HCl buffer, pH 7.4. (B) Mass action plot of $\beta/(1-\beta)$ against free nigerloxin concentration at (◆) 14, (■) 27, (▲) 36, and (●) 45°C. The slope of the straight line was used to obtain the equilibrium constant (K_{eq}). (C) Job's plot for the interaction of BSA with nigerloxin; [BSA] + [nigerloxin] = 2.25 μM. Error bars represent lower and upper limits of the experimental values.

against the nigerloxin concentrations (Fig. 1A). The fluorescence emission of BSA decreased by 35% at a nigerloxin concentration of 2 μM. From the corresponding double reciprocal plot of fluorescence-quenching data, it is evident that nigerloxin quenches the fluorescence of BSA with a Q_{max} of 57.1 ± 0.2% at 27°C.

The stoichiometry of the binding of nigerloxin to BSA was established using Job's method of continuous variation (Fig. 1C) and was found to be 1:1 ± 0.1. By using the value of n = 1 and the extent of maximal interaction obtained from the double reciprocal plot, a mass action plot was constructed using Equation 1 and is displayed as Figure 1B. From the slope of the mass action plot, the equilibrium constant was found to be $1.01 \pm 0.2 \times 10^6$ M^{-1} at 27°C (Fig. 1B).

The effect of temperature on nigerloxin–BSA interaction. The effect of temperature in the range of 14 to 45°C on nigerloxin–BSA interaction was followed by determining the K_{eq}, which varied over the temperature range studied. The K_{eq} values remained nearly constant from 14 to 36°C, but a further increase in temperature above 36°C showed a decrease in K_{eq} (Table 1).

The change in free energy (ΔG) at various temperatures was also determined (Table 1). The van't Hoff plot was used to determine enthalpy (ΔH) and entropy (ΔS) values for the interaction of nigerloxin with BSA. Thus, van't Hoff's binding enthalpy was $\Delta H° \approx 0$ kcal/mol and the binding reaction was entropy-driven: $\Delta S° = 27.5 \pm 0.4$ cal/mol/K at 27°C with activation free energy of $\Delta G = RT \ln K_{eq} = -8.2 \pm 0.1$ kcal/mol (Table 1).

The effect of ionic strength on nigerloxin–BSA interaction. To determine whether ionic interaction played a role in the binding of nigerloxin with BSA, the ionic strength of the working buffer was increased by adding 0.2 and 0.5 M KCl. We found that as the ionic strength of the buffer was increased to 0.2 M KCl, the Q_{max} dropped to 28%, which was exactly half the maximum quench shown by nigerloxin in the absence of KCl (57%) (Fig. 2). A further increase in the KCl concentration (0.5 M) resulted in the loss of binding efficiency of the nigerloxin with BSA, which was evident from the association constant of $0.07 \pm 0.04 \times 10^6$ M^{-1}, shown in Table 2. Association constants were calculated from the slopes of the curves obtained from the mass action plot of the quenching data in the presence of KCl. It is conceivable that the carboxyl group on the phenyl ring was involved in the ionic bonding that was favored at very low ionic strengths. This suggests that ionic interaction played a role in the interaction of nigerloxin with BSA.

TABLE 1
Changes in the Association Constants and Free Energy (ΔG) at Different Temperatures

Temperature			Association constant	ΔG
°C	K	Q_{max}	($\times 10^6$ M^{-1})	(kcal/mol)
14	287	44.8 ± 0.5	0.95 ± 0.2	−7.8 ± 0.1
27	300	57.1 ± 0.4	1.01 ± 0.2	−8.2 ± 0.1
36	309	49.2 ± 0.6	0.91 ± 0.3	−8.4 ± 0.2
45	318	53.1 ± 0.4	0.50 ± 0.2	−8.3 ± 0.1

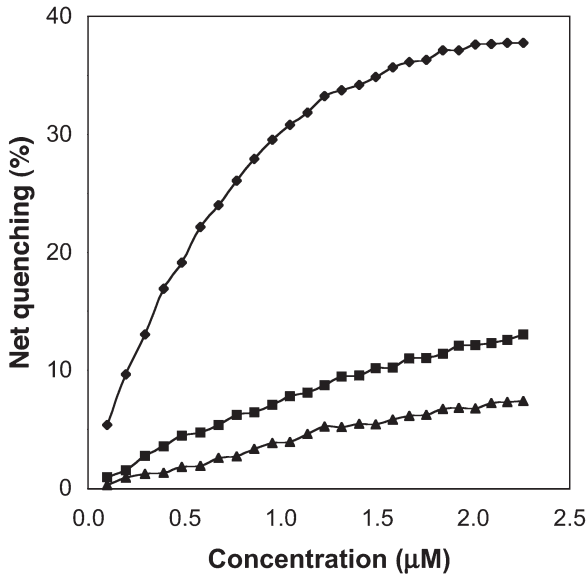

FIG. 2. Fluorescence quenching of BSA by nigerloxin at different concentrations of KCl. Concentration of BSA was 0.1 mg/mL. Measurements were made in (◆) 50 mM Tris–HCl buffer, pH 7.4, and with (■) 0.2 and (▲) 0.5 M KCl.

TABLE 2
Effect of Ionic Strength on the Maximum Fluorescence Quench and Association Constant of Nigerloxin with BSA

Ionic strength	Q_{max}	Association constant ($\times 10^6$ M^{-1})
No KCl	57.1 ± 0.4	1.01 ± 0.2
0.2 M KCl	28.0 ± 0.4	0.12 ± 0.2
0.5 M KCl	<5 ± 1.0	0.07 ± 0.04

The effect of nigerloxin on structural changes of BSA. BSA exhibited broad minima in the near-UV region of 260 to 500 nm. The addition of nigerloxin (up to 125 μM) did not affect the molar ellipticity values in this region (Fig. 3A). Nigerloxin also did not significantly affect the CD bands in the far-UV region (200 to 260 nm) (Fig. 3B). Thus, it did not induce CD bands in any of the regions tested (200 to 500 nm), suggesting that the binding of nigerloxin to BSA does not result in secondary structural changes to the protein.

DISCUSSION

These results indicate that nigerloxin binds to BSA with one binding site, characterized by a K_{eq} of $1.01 \pm 0.2 \times 10^6$ M^{-1}. The binding constant obtained in the present study was the high-affinity binding site (saturated at 2 μM) detected by fluorescence measurements, as no changes were observed in the CD bands in the range of 200 to 500 nm, thus indicating that no other binding sites would lead to structural changes in the BSA molecule.

Nigerloxin has a phenolic structure with conjugated double bonds; proteins and phenols are thought to complex with each other reversibly *via* hydrogen bonding and hydrophobic

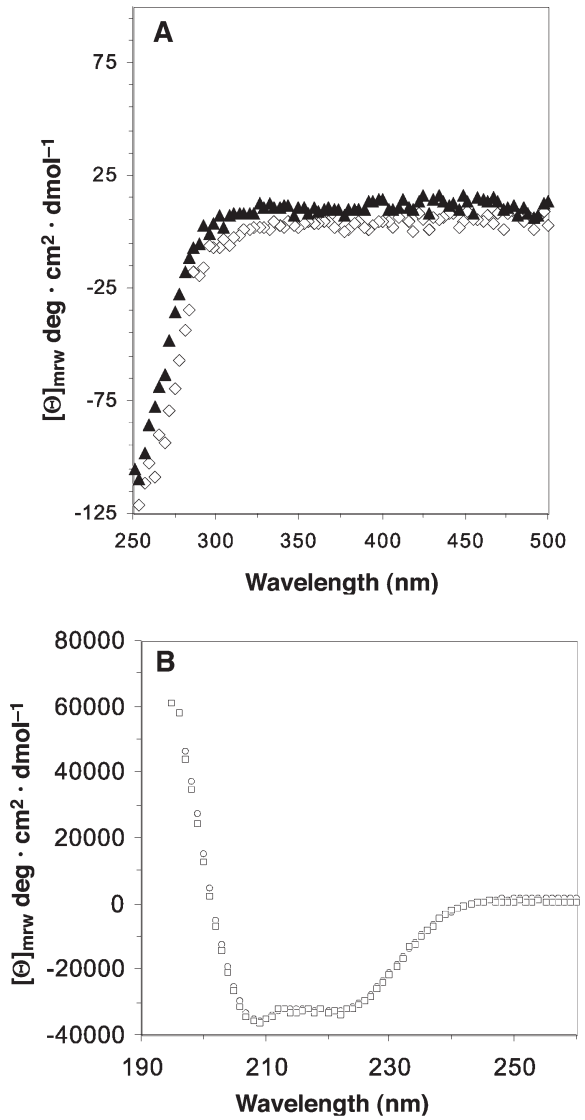

FIG. 3. Circular dichroism (CD) spectra of BSA: (A) near-UV CD (◇) in the absence of nigerloxin and (▲) in the presence of 50 μM nigerloxin. The measurement was made in 1-cm cells, and the BSA concentration was 2 mg/mL. (B) Far-UV CD (○) in the absence of nigerloxin and (□) in the presence of 50 μM nigerloxin. The measurement was made in 1-mm cells, and the BSA concentration was 0.2 mg/mL.

interactions (12). The involvement of hydrophobic groups in the formation and stabilization of phenolic tannins–protein complexes was established in several independent studies (13). Oh *et al*. (13) drew attention to the fact that hydrophobic interactions may dominate ligand–protein interaction.

Earlier workers (14) showed that the capacity of ligands to bind to protein is determined by the chemical and physical nature of the phenolic nucleus itself. Both nigerloxin and BSA contain hydrophobic regions. The propenyl side chain, aromatic methyl, aromatic nucleus, and phenolic groups present in nigerloxin, which are essentially hydrophobic, have an affinity for the aliphatic and aromatic side chains of BSA. The binding stoichiometry of nigerloxin with BSA is indicative of mole-to-mole interaction. Since BSA is known to contain hydrophobic pockets, it is feasible that nigerloxin possibly binds to the hydrophobic pockets of albumin. Our studies on the K_{eq} as a function of temperature favored the concept of hydrophobic bonding as a contributing factor in the binding of nigerloxin to BSA. Changes in the free energy (ΔG) and enthalpy (ΔH) in the temperature range above 27°C support the role of hydrophobic bondings.

The binding stoichiometry of nigerloxin and BSA is indicative of mole-to-mole interaction. The binding constant of nigerloxin with BSA is comparable with that of L-thyroxine (1.7×10^6 M^{-1}) (15) at pH 7.4 and 24°C. L-Tyrosine and L-thyroxine are the only amino acids that bind to albumin. Tryptophan and thyroxine share the same site (16), which will bind short-chain FA as well as numerous organic anions, including diazepines, naproxen, clofibrate, and flufenamic acid. Sudlow *et al*. (17) showed that the cations of these drugs play a major role in binding to serum albumin. Gossypol, a polyphenol present in cottonseed, binds to serum albumin with an association constant of 2.2×10^6 M^{-1} (14). Serum albumin is the carrier of both exogenous and endogenous ligands. These ligands associate with serum albumin in plasma by noncovalent linkages (such as hydrogen bonding, ionic bonding, and hydrophobic bonding), and some of them have very high association constants (18,19).

The effect of KCl on the association constant of the binding was studied to gain insight into the nature of noncovalent interactions. We found that a high ionic strength did not favor the interaction of nigerloxin with BSA. The polar functional groups of nigerloxin, such as the carbonyl, phenolic, and amide groups, might be involved in the ionic interaction with BSA, suggesting that nigerloxin binds to BSA partially by the formation of ionic bonds.

FA in the serum are also carried by albumin, and albumins contain six binding sites for FFA (5). Palmitic acid binds to albumin with an association constant of 5.5×10^6 M^{-1}. An increase in the acyl chain length and degree of acyl chain unsaturation for the same chain length increases the association constant, suggesting that the solubility of FA in an aqueous medium may play a significant role in the equilibrium created by the association of FA with serum albumin and the aqueous phase (20). Because the propenyl side chain of nigerloxin is hydrophobic in nature, it might interact with hydrophobic pockets of BSA. Therefore, partial hydrophobic bonding and partial ionic bonding play major roles in the binding of nigerloxin with BSA, as evidenced from the mass action plot and the effect of KCl concentration, respectively. Furthermore, the K_{eq} obtained for the binding of nigerloxin with BSA was comparable to many of the K_{eq} reported for both exogenous and endogenous ligands with BSA (18).

The reversibility of the interaction of nigerloxin with BSA was verified by the dilution method.

The data generated from this study will be highly valuable to biomedical research, giving more complete insight into the molecular mechanisms of drug activity, detoxification, and general toxicity, which will facilitate the prediction of drug activity and improve rational drug design.

ACKNOWLEDGMENTS

The authors thank Dr. N.G. Karanth, deputy director of CFTRI, for his keen interest and encouragement; and Dr. V. Prakash, director of CFTRI, Mysore, for providing facilities to carry out this work. K.C.S.R. thanks the Council of Scientific and Industrial Research for the award of a senior research fellowship.

REFERENCES

1. Rao, K.C.S., Divakar, S., Rao, A.G.A., Karanth, N.G., and Sattur, A.P. (2002) A Lipoxygenase Inhibitor from *Aspergillus niger, Appl. Microbiol. Biotechnol. 58*, 539–545.
2. Rao, K.C.S., Divakar, S., Rao, A.G.A., Karanth, N.G., and Sattur, A.P. (2002) Lipoxygenase Inhibitor from *Lactobacillus casei*, *Biotechnol. Lett. 24*, 511–513.
3. Rao, K.C.S., Divakar, S., Rao, A.G.A., Karanth, N.G., Suneetha, W.J., Krishnakanth, T.P., and Sattur, A.P. (2002) Asperenone: A Lipoxygenase and Platelet Aggregation Inhibitor from *Aspergillus niger, Biotechnol. Lett. 24*, 1967–1970.
4. Rao, K.C.S., Divakar, S., Babu, K.N., Rao, A.G.A., Karanth, N.G., and Sattur, A.P. (2002) Nigerloxin, a Novel Inhibitor of Aldose Reductase and Lipoxygenase with Free Radical Scavenging Activity from *Aspergillus niger* CFR-W-105*, J. Antibiot. 55*, 789–793.
5. Spector, A.A. (1975) Fatty Acid Binding to Plasma Albumin, *J. Lipid Res. 16,* 165–179.
6. Curry, S., Mandelkow, H., Brick, P., and Franks, N. (1998) Crystal Structure of Human Serum Albumin Complexed with Fatty Acid Reveals an Asymmetric Distribution of Binding Sites, *Nat. Struct. Biol. 5*, 827–835.
7. Gelamo, E.L., and Tabak, M. (2000) Spectroscopic Studies on the Interaction of Bovine and Human Serum Albumins with Ionic Surfactants, *Spectrochim. Acta A 56*, 2255–2271.
8. Lehrer, S.S., and Fasman, G.D. (1966) The Fluorescence of Lysozyme and Lysozyme Substrate Complexes, *Biochem. Biophys. Res. Commun. 23*, 133–138.
9. Rao, A.G.A., and Cann, J.R. (1981) A Comparative Study of the Interaction of Chlorpromazine, Trifluoperazine, and Promethazine with Mouse Brain Tubulin, *Mol. Pharmacol. 19*, 295–301.
10. Jaffe, H.H., and Orchin, M. (1962) *Theory and Applications of Ultraviolet Spectroscopy*, pp. 581–583, John Wiley & Sons, New York.
11. Ikeda, K., and Hamaguchi, K. (1969) The Binding of *N*-Acetylglucose Amine to Lysozyme: Studies on Circular Dichroism, *J. Biochem. 66*, 513–520.
12. Maliwal, B.P., Rao, A.G.A., and Rao, M.S.N. (1985) Spectroscopic Study of the Interaction of Gossypol with Bovine Serum Albumin, *Int. J. Pept. Protein Res. 25*, 382–388.
13. Oh, H.I., Hoff, J.E., Armstrong, G.S., and Haff, L.A. (1980) Hydrophobic Interactions of Tannin–Protein Complexes, *J. Agric. Food. Chem. 28*, 394–398.
14. Rao, A.G.A. (1992) A Stoichiometric Analysis of Bovine Serum Albumin–Gossypol Interactions: A Fluorescence Quenching Study, *Indian J. Biochem. Biophys. 29*, 173–182.
15. Steiner, R.F., Roth, J., and Robbins, J. (1966) The Binding of Thyroxine by Serum Albumin as Measured by Fluorescence Quenching, *J. Biol. Chem. 241*, 560–567.
16. Tritsch, G.L., and Tritsch, N.E. (1963) The Nature of Thyroxine Binding Site of Human Serum Albumin, *J. Biol. Chem. 238*, 138–142.
17. Sudlow, G., Birkett, D.J., and Wade, D.N. (1976) Further Characterization of Specific Drug Binding Sites on Human Serum Albumin, *Mol. Pharmacol. 12*, 1052–1061.
18. Peters, T.J. (1985) Serum Albumin, *Adv. Protein Chem. 37*, 161–245.
19. Seelig, J., and Ganz, P. (1991) Nonclassical Hydrophobic Effect in Membrane Binding Equilibria, *Biochemistry 30*, 9354–9359.
20. Seelig, J. (1997) Titration Calorimetry of Lipid–Peptide Interactions, *Biochim. Biophys. Acta 1331*, 103–116.

[Received October 31, 2003, and in revised form and accepted February 16, 2004]

Characterization of Epoxy Carotenoids by Fast Atom Bombardment Collision-Induced Dissociation MS/MS

Takashi Maoka[a], Yasuhiro Fujiwara[b], Keiji Hashimoto[c], and Naoshige Akimoto[d,*]

[a]Research Institute for Production Development, Kyoto 606-0805, [b]Kyoto Pharmaceutical University, Kyoto 607-8414, Japan, [c]Nagahama Institute of Bio-sciences and Technology, Shiga 526-0829, Japan, and [d]Graduate School of Pharmaceutical Sciences, Kyoto University, Kyoto 606-8501, Japan

ABSTRACT: The characterization and structure of epoxy carotenoids possessing 5,6-epoxy, 5,8-epoxy and 3,6-epoxy end groups conjugated to the polyene chain were investigated using high-energy fast atom bombardment collision-induced dissociation MS/MS methods. In addition to $[M - 80]^{+\cdot}$, a characteristic fragment ion of an epoxy carotenoid, product ions resulting from the cleavage of C–C bonds in the polyene chain from the epoxy end group, such as *m/z* 181 (b ion) and 121 (c ion), were detected. On the other hand, diagnostic ions of *m/z* 286 (e-H ion) and 312 (f-H ion) were observed, not in the 5,6-epoxy or 5,8-epoxy carotenoid but in the 3,6-epoxy carotenoid. These fragmentation patterns can be used to distinguish 3,6-epoxy carotenoids from 5,6-epoxy or 5,8-epoxy carotenoids. The structure of an epoxy carotenoid, 3,6-epoxy-5,6-dihydro-7′,8′-didehydro-β,β-carotene-5,3′-diol (**8**), isolated from oyster, was characterized using FAB CID-MS/MS by comparing fragmentation patterns with those of related known compounds.

Paper no. L9383 in *Lipids 39*, 179–183 (February 2004).

Carotenoids are the pigments responsible for many of the yellow, orange, red, and purple colors distributed throughout nature. More than 600 different, but closely related, structures have been identified from biological sources (1,2), all of which are very labile. Therefore, there is a need to establish a rapid and reliable method for analyzing them (2). Fast atom bombardment collision-induced dissociation (FAB CID)-MS/MS methods have widely been used for the structural analysis of natural products. Van Breemen *et al.* (3) reported the structural analysis of 17 carotenoids by positive ion FAB-MS/MS using a two-sector mass spectrometer with linked scanning at a constant B/E [ratio of magnetic (B) and electric (E) fields held at a constant] and high-energy collisionally activated dissociation. Recently, we reported the relationship between structure and the product ions obtained from molecular ions ($M^{+\cdot}$) by using four-sector tandem MS with high-energy FAB CID-MS/MS spectra of 28 carotenoids (4).

Here, we report the characterization by high-energy FAB CID-MS/MS of epoxy carotenoids possessing 5,6-epoxy, 5,8-epoxy, and 3,6-epoxy end groups conjugated to the polyene chain and the structural analysis of an epoxy carotenoid isolated from the oyster *Crassostrea gigas* by using this method.

EXPERIMENTAL PROCEDURES

FAB CID-MS/MS. MS/MS spectra were recorded using a JEOL JMS-HX/HX 110A four-sector tandem mass spectrometer. A few micrograms of sample dissolved in benzene was placed on a stainless-steel probe tip and added to 1–2 μL of *m*-nitrobenzyl alcohol (NBA) as a matrix. The positive FAB ionization was achieved by bombardment with 6 kV xenon atoms at an atom gun current of 5 mA. The accelerating voltage in the source was 10 kV. The radical cation $M^{+\cdot}$ was selected as a precursor by MS1, and collided with argon in a collision cell located in the third field-free region. Argon gas pressure was adjusted to attenuate the intensity of the precursor ion by 30%. The collision cell potential was 3 kV. The resulting product ions were acquired by accumulating several linked scans on MS2.

Sample preparation. The isolation and purification of epoxy carotenoids were performed by routine procedures. Violaxanthin (5,6,5′,6′-diepoxy-5,6,5′,6′-tetrahydro-β,β-carotene-3,3′-diol; **1**), auroxanthin (5,8,5′,8′-diepoxy-5,8,5′,8′-tetrahydro-β,β-carotene-3,3′-diol; **2**), cycloviolaxanthin (3,6,3′,6′-diepoxy-3,6,3′,6′-tetrahydro-β,β-carotene-5,5′-diol; **3**), antheraxanthin (5,6-epoxy-5,6-dihydro-β,β-carotene-3,3′-diol; **4**), mutatoxanthin (5,8-epoxy-5,8-dihydro-β,β-carotene-3,3′-diol; **5**), and cucurbitaxanthin A (3,6-epoxy-3,6-dihydro-β,β-carotene-5,3′-diol; **7**) were isolated from the pumpkin, *Cucurbita maxima* (5); and diadinochrome (5,8-epoxy-5,8-dihydro-7′,8′-didehydro-β,β-carotene-3,3′-diol; **6**) was isolated from the tunicate, *Amaroucium pliciferum* (6), according to methods previously described. An epoxy carotenoid (**8**) was isolated from the oyster, *C. gigas*, according to routine procedures. The structures of these carotenoids are shown in Scheme 1. The acetone extract of the edible parts (purchased commercially in that form, hence weight of intact animal unknown) of *C. gigas* (10 kg) was partitioned between *n*-hexane/ether (1:1) and aqueous NaCl. The organic layer was dried over Na_2SO_4 and then concentrated to dryness. The residue was subjected to column chromatography on silica gel using an increasing percentage of acetone in *n*-hexane.

*To whom correspondence should be addressed at the Graduate School of Pharmaceutical Sciences, Kyoto University, Sakyo-ku, Kyoto 606-8501, Japan. E-mail: akimoto@pharm.kyoto-u.ac.jp

Abbreviations: FAB CID-MS/MS, fast atom bombardment collision-induced dissociation MS/MS; NBA, nitrobenzyl alcohol.

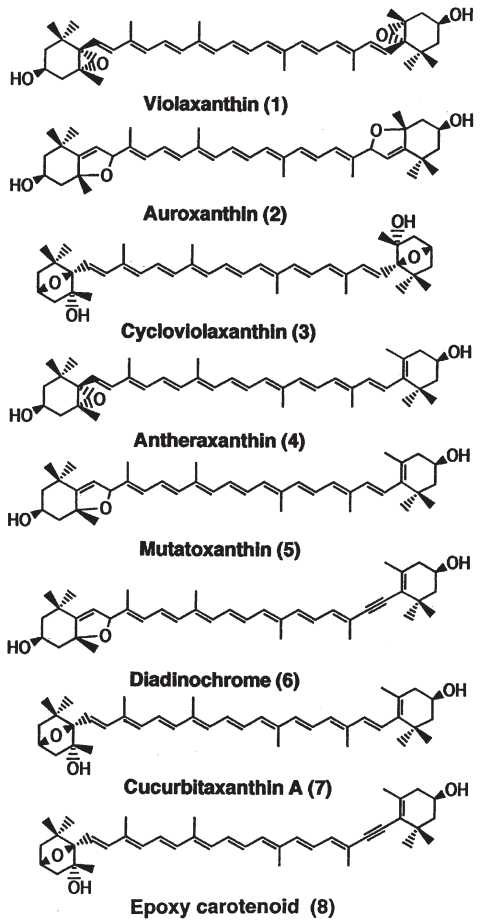

SCHEME 1

The fraction eluted with *n*-hexane/acetone (7:3) was further purified by HPLC on octadecylsilane with chloroform/acetonitrile (1:9) to yield the epoxy carotenoid, **8** (0.5 mg). Details of the isolation and structural elucidation of **8** including an NMR study are reported in the literature (7).

RESULTS AND DISCUSSION

In the positive-ion FAB MS spectra of carotenoids obtained using *m*-NBA as a matrix, the radical cation $[M]^{+\cdot}$ was predominant rather than the protonated molecular ion $[MH]^+$ (4). Therefore, $M^{+\cdot}$ was used as the precursor ion of CID-MS/MS for the epoxy carotenoids investigated in the present study. Characteristic product ions observed in epoxy carotenoids are listed in Table 1. The nomenclature used to denote typical fragments resulting from specific bond cleavages in the polyene chain is shown in Scheme 2.

FAB CID-MS/MS spectra of symmetrical epoxy carotenoids. Violaxanthin (**1**), auroxanthin (**2**), and cycloviolaxanthin (**3**) are symmetrical epoxy carotenoids possessing the same molecular formula, $C_{40}H_{56}O_4$. Violaxanthin (**1**), having a 3-hydroxy-5,6-epoxy end group at both ends of the polyene chain, showed the major product ions *m/z* 582 $[M - 18]^{+\cdot}$ (elimination of water) and 520 $[M - 80]^{+\cdot}$, a characteristic fragment ion observed in the epoxy carotenoids (9,10). Furthermore, a series of product ions resulting from the cleavage of C–C bonds in the polyene chain, from the epoxy end group such as *m/z* 221 (c ion: attributed to cleavage between C10 and C11), 352 (g-H ion: attributed to cleavage between C14′ and C13′ accompanied by a hydrogen transfer to the C13′ side) and 419 (i ion: attributed to cleavage between C9′ and C8′) was detected. However, no loss of toluene $[M - 92]^{+\cdot}$ was observed.

Auroxanthin (**2**), having a 3-hydroxy-5,8-epoxy (furan) end groups on both sides of the polyene chain, showed almost the same product ion patterns as **1**. Furthermore, auroxanthin exhibited additional product ions resulting from the cleavage of single bonds in the polyene chain from the epoxy end group, *m/z* 181 (b ion: attributed to cleavage between C8 and C9), 247 (d ion: attributed to cleavage between C12 and C13), 287 (e ion: attributed to cleavage between C14 and C15), and 379 (h ion: attributed to cleavage between C11′ and C10′).

Cycloviolaxanthin (**3**), possessing a 3-hydroxy-3,6-epoxy end group on both ends of the polyene chain, also showed *m/z*

TABLE 1
Fragment Ions Obtained by FAB CID-MS/MS of Epoxy Carotoids

	1	2	3	4	5	6	7	8
M (*m/z*)	600	600	600	584	584	582	584	582
M – 18	582	582	582	566	566	564	566	564
M – 33	—	—	—	—	—	531	—	531
M – 80	520	520	520	504	504	502	504	502
M – 92	—	—	—	492	492	490	492	490
b	—	181	181	181	181	181	181	181
c	221	221	221	221	221	221	221	221
d	—	247	247	—	—	—	—	—
e	—	287	286 (–H)	—	—	—	286 (–H)	286 (–H)
f	—	—	312 (–H)	—	—	—	312 (–H)	312 (–H)
g	352 (–H)	352 (–H)	—	352 (–H)	352 (–H)	352 (–H)	—	—
h	—	379	379	—	—	—	—	—
i	419	419	419	—	—	—	—	—
j	—	—	445	—	—	—	—	—
b′	—	—	—	404 (–H)	404 (–H)	402 (–H)	—	—
c′	—	—	379	—	—	—	364 (+H)	362 (+H)
x′	—	—	—	—	—	—	416	414

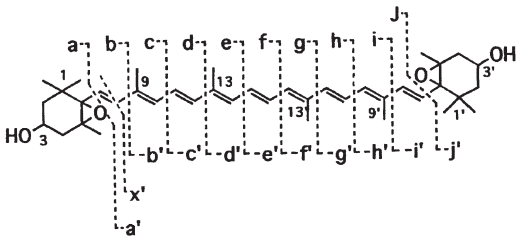

SCHEME 2

520 [M – 80]$^{+\cdot}$. The sequential product ions obtained by cleavage of all single bonds in the polyene chain except for cleavage between C14′ and C13′ (g-H ion; *m/z* 352) were observed in cycloviolaxanthin (**3**). Notably, *m/z* 286 (e-H ion: attributed to cleavage between C14 and C15 and transfer of a hydrogen to the C15 site) was detected, which was not observed in 5,6-epoxy or 5,8-epoxy carotenoids. On the other hand, *m/z* 352 (g-H ion) was not observed for **3**. These fragment patterns characterize the 3,6-epoxy carotenoid. No loss of toluene [M – 92]$^{+\cdot}$ was observed in **2** or **3**.

FAB CID-MS/MS spectra of asymmetrical epoxy carotenoids. Antheraxanthin (**4**), having a 3-hydroxy-5,6-epoxy end group and a 3-hydroxy-β-end group on each side of the polyene chain, showed the major product ions *m/z* 566 [M – 18]$^{+\cdot}$, 504 [M – 80]$^{+\cdot}$, and 492 [M – 92]$^{+\cdot}$ with elimination of a neutral molecule of toluene from the polyene chain (8). Furthermore, a series of product ions resulting from the cleavage of C–C bonds in the polyene chain from the epoxy end group side such as *m/z* 181 (b ion), 221 (c ion), and 352 (g-H ion) were obtained. In addition to these ions, **4** exhibited the diagnostic ion *m/z* 404 (b′ + H ion: loss of the C1 to C8 moiety from the molecule by cleavage between C8 and C9 accompanied by a hydrogen transfer to the C8 site), which could provide structural information on the 3-hydroxy-β-end group side of the molecule.

Mutatoxanthin (**5**), having a 3-hydroxy-5,8-epoxy (furan) end group and a 3-hydroxy-β-end group on both ends of the polyene chain, showed almost the same product ions as that of **4** as shown in Figure 1.

Diadinochrome (**6**), a 7′,8′-didehydro analog of **5**, also showed almost the same fragmentation pattern—*m/z* 580 [M – 18]$^{+\cdot}$, 502 [M – 80]$^{+\cdot}$, 490 [M – 92]$^{+\cdot}$, 181 (b ion), 221 (c ion), and 352 (g-H ion)—as **5**, as shown in Figure 2. On the other hand, **6** showed [M – 33]$^{+}$ (loss of $CH_3^{\cdot}$ and H_2O from $M^{+\cdot}$), a fragment ion characteristic of carotenoids possessing an acetylenic group at 7,8 and/or 7′,8′ in the polyene chain such as alloxanthin, diatoxanthin, and halocynthiaxanthin (4). Moreover, the shift down of b′ + H ion (*m/z* 402) by 2 mass units compared with **5** agreed with the presence of an acetylenic group at the 3-hydroxy-β-end group side (7′,8′ position) in **6**.

Cucurbitaxanthin A (**7**), possessing a 3-hydroxy-3,6-epoxy end group and a 3-hydroxy-β-end group, has the same molecular formula, $C_{40}H_{56}O_3$, as **4** and **5** and also exhibited the product ions *m/z* 582 [M – 18]$^{+\cdot}$, 504 [M – 80]$^{+\cdot}$, 492 [M – 92]$^{+\cdot}$, 181 (b ion), and 221 (c ion) as shown in Figure 3. However, no g-H ion was observed. On the other hand, **7** showed the diagnostic ions *m/z* 416 (x′ ion: cleavage of C=C bond between C7 and C8) and 364 (c′ + H ion). These fragmentation patterns can be used to distinguish a 3,6-epoxy carotenoid from a 5,6-epoxy or 5,8-epoxy carotenoid.

Application of FAB CID-MS/MS to the structural analysis of the epoxy carotenoid isolated from oyster. After characterizing CID-MS/MS fragments of known epoxy carotenoids, we

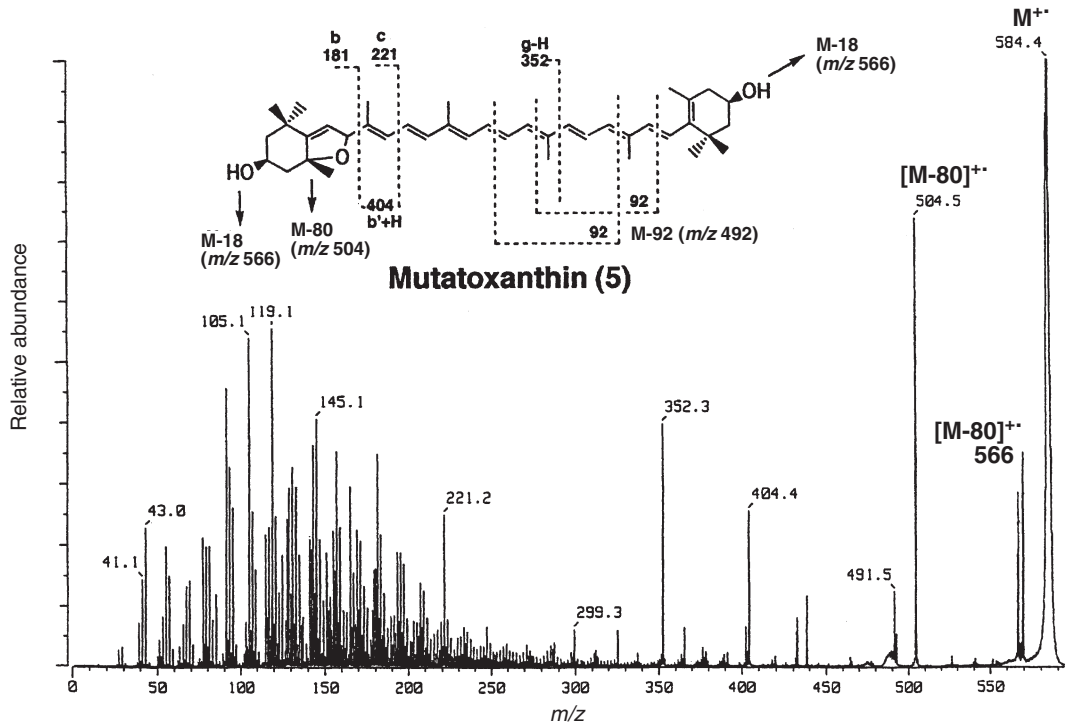

FIG. 1. Fast atom bombardment collision-induced dissociation (FAB CID)-MS/MS spectrum of $M^{+\cdot}$ of mutatoxanthin (**5**).

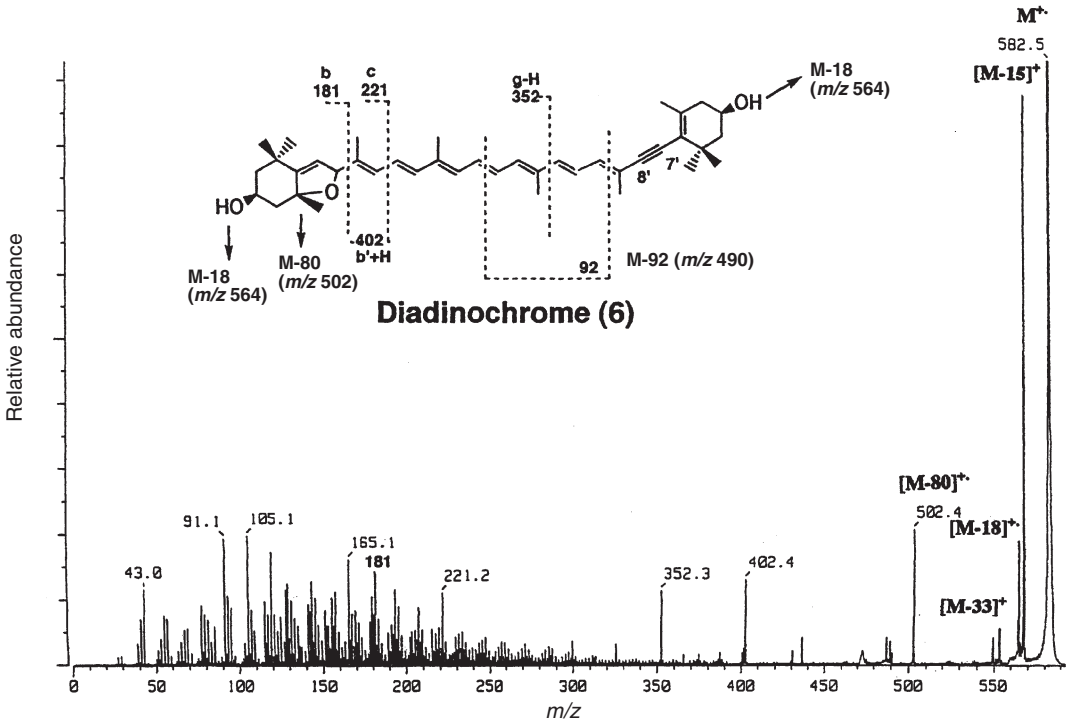

FIG. 2. FAB CID-MS/MS spectrum of $M^{+\cdot}$ of diadinochrome (**6**). For abbreviation see Figure 1.

used this method for the structural analysis of an epoxy carotenoid (**8**) isolated from the oyster, *C. gigas*. Compound **8** was found to have a molecular ion at *m/z* 582.4080, compatible with the formula $C_{40}H_{54}O_3$ by high-resolution EI-MS. The CID spectrum of **8** (Fig. 3) showed product ions typical of a 3,6-epoxy carotenoid, i.e., *m/z* 502 $[M - 80]^{+\cdot}$, 181 (b ion), 221 (c ion), and 286 (e-H ion). Furthermore, **8** showed *m/z* 431 $[M - 33]^{+}$, a product ion characteristic of acetylenic carotenoid (4).

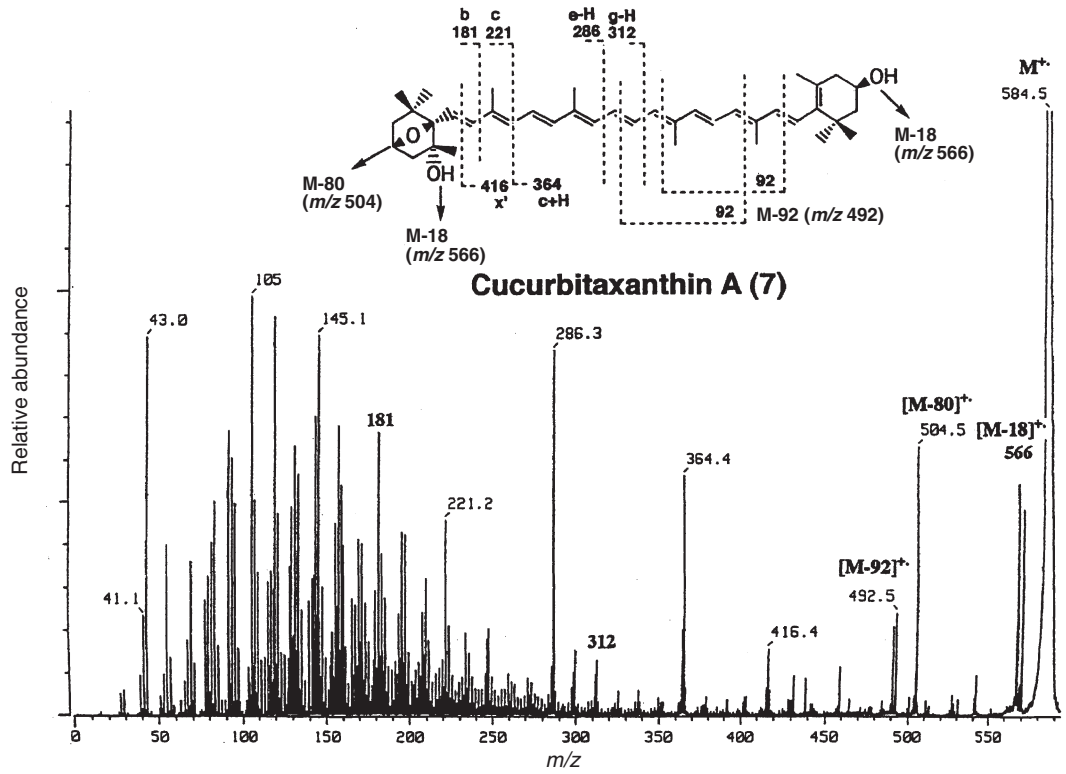

FIG. 3. FAB CID-MS/MS spectrum of $M^{+\cdot}$ of cucurbitaxanthin A (**7**). For abbreviation see Figure 1.

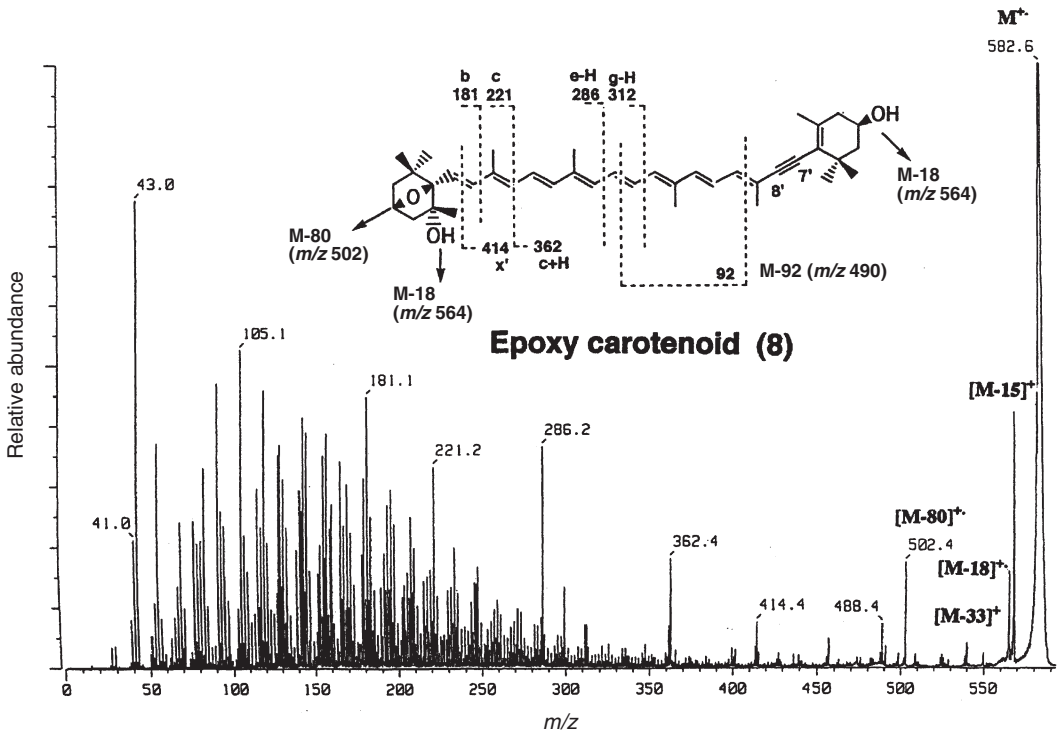

FIG. 4. FAB CID-MS/MS spectrum of $M^{+\cdot}$ of an epoxy carotenoid, 3,6-epoxy-5,6-dihydro-7′,8′-didehydro-β,β-carotene-5,3′-diol (**8**), isolated from oyster. For abbreviation see Figure 1.

Moreover, as well as diadinochrome (**6**), the 2-mass unit shift down of the x′ ion at *m/z* 414 and c′ + H ion at *m/z* 362 compared with **7** clearly indicated the presence of an acetylenic group at the 7′,8′ position in the polyene chain. Therefore, the planar structure of **8** was postulated to be 3,6-epoxy-5,6-dihydro-7′,8′-didehydro-β,β-carotene-5,3′-diol as shown in Figure 4. This finding was supported by NMR analysis (7).

In conclusion, high-energy FAB CID-MS/MS was used to clarify the relationship between the structure and product ions of epoxy carotenoids possessing 5,6-epoxy, 5,8-epoxy, and 3,6-epoxy end groups conjugated to the polyene chain. In addition to $[M - 80]^{+\cdot}$, a fragment ion characteristic of an epoxy carotenoid, product ions resulting from cleavage of C–C bonds in the polyene chain from the epoxy end group such as *m/z* 181 (b ion) and 121 (c ion) were detected. On the other hand, the diagnostic ion *m/z* 286 (e-H ion) was observed, not in the 5,6-epoxy or 5,8-epoxy carotenoid, but in the 3,6-epoxy carotenoid. Furthermore, no g-H ion was detected in 3,6-epoxy carotenoid. These fragmentation patterns can be used to distinguish a 3,6-epoxy carotenoid from a 5,6-epoxy or 5,8-epoxy carotenoid. The structure of an epoxy carotenoid (**8**) isolated from oyster was characterized using FAB CID-MS/MS by comparing fragmentation patterns with those of related known compounds. Therefore, high-energy FAB CID-MS/MS is a useful method for the structural analysis of carotenoids.

REFERENCES

1. Straub, O. (1987) *Key to Carotenoids*, 2nd edn., Birkhauser Verlag, Basel.
2. Pfander, H., and Riesen, R. (1995) Chromatography: Part IV. High-Performance Liquid Chromatography, in *Carotenoids, Vol. 1A* (Britton, G., Liaaen-Jensen, S., and Pfander, H., eds.), pp. 145–190, Birkhauser Verlag, Basel.
3. van Breemen, R.B., Schmitz, H.H., and Schwarz, S.J. (1995) Fast Atom Bombardment Tandem Mass Spectrometry of Carotenoids, *J. Agric. Food. Chem. 43*, 384–389.
4. Akimoto, N., Maoka, T., Fujiwara, Y., and Hashimoto, K. (2000) Analysis of Carotenoids by FAB CID-MS/MS, *J. Mass Spectrom. Soc. Jpn. 48*, 32–41 (in Japanese).
5. Matsuno, T., Tani, Y., Maoka, T., Matsuo, K., and Komori, T. (1986) Isolation and Structural Elucidation of Cucurbitaxanthin A and B from Pumpkin *Cucurbita maxima*, *Phytochemistry 25*, 2837–2840.
6. Matsuno, T., Ookubo, M., and Komori, T. (1985) Carotenoids of Tunicates. III. The Structural Elucidation of Two New Marine Carotenoids Amarouciaxanthin A and B, *J. Nat. Prod. 48*, 606–613.
7. Maoka, T., Akimoto, N., Hashimoto, K., and Fujiwara, Y. (2001) Structures of Five New Carotenoids from the Oyster *Crassostrea gigas*, *J. Nat. Prod. 64*, 578–581.
8. Enzell, C.R., and Bach, S. (1995) Mass Spectrometry in Carotenoids, in *Carotenoids, Vol. 1A* (Britton, G., Liaaen-Jensen, S., and Pfander, H., eds.), pp. 261–320, Birkhauser Verlag, Basel.
9. Johannes, B., Brzezinka, H., and Budzikiewicz, H. (1974) Mass Spectrometric Fragmentation Reactions VII. Degradation of the Polyene Chain of Carotenoids, *Org. Mass Spectrom. 9*, 1095–1113.
10. Budzikiewicz, H. (1983) Mass Spectra of Carotenoids—Labelling Studies, in *Carotenoid Chemistry and Biochemistry* (Britton, G., and Goodwin, T.W., eds.), pp. 155–165, Pergamon Press, Oxford.

[Received September 15, 2003, and in revised form December 24, 2003; revision accepted January 12, 2004]

Synthesis, Isolation, and GC Analysis of All the 6,8- to 13,15-*cis/trans* Conjugated Linoleic Acid Isomers

P. Delmonte[a], J.A.G. Roach[a], M.M. Mossoba[a], G. Losi[b], and M.P. Yurawecz[a,*]

[a]U.S. Food and Drug Administration, Center for Food Safety and Applied Nutrition, College Park, Maryland 20740, and [b]Dipartimento di Protezione e Valorizzazione Agro-Alimentare (DIPROVAL), University of Bologna, Bologna, Italy

ABSTRACT: Octadecadienoic acids with conjugated double bonds are often referred to as conjugated linoleic acid, or CLA. CLA is of considerable interest because of potentially beneficial effects reported from animal studies. Analysis of CLA is usually carried out by GC elution of FAME. If the presence of low-level isomers is of interest, a complementary technique such as silver-ion HPLC is also used. These analyses have been hindered by a lack of well-characterized commercially available reference materials. Described here are the synthesis and isolation of selected 6,8- through 13,15-positional CLA isomers, followed by isomerization of these CLA isomers with iodine to produce all the possible *cis,cis, cis,trans, trans,cis,* and *trans,trans* combinations. Also present are the GC retention times of the CLA FAME relative to γ-linolenic acid (6*c*,9*c*,12*c*-octadecatrienoic acid) FAME using a 100-m CP Sil-88 capillary column (Varian Inc., Lake Forest, CA). These data include all the CLA isomers that have been identified thus far in foods and dietary supplements and should greatly aid in the future analysis of CLA in these products.

Paper no. L9227 in *Lipids 39,* 185–191 (February 2004).

Isomers of octadecadienoic acid with conjugated double bonds are referred to individually or collectively as conjugated linoleic acid (CLA). Fourteen positional isomers of octadecadienoic acid with conjugated double bonds (from 2,4-18:2 to 15,17-18:2) are possible. Positions 2,4 to 14,16 have four geometric isomers (*cis*,*cis*, *cis*,*trans*, *trans*,*cis*, and *trans*,*trans*). Only two isomers with double bonds in the 15- and 17-positions are possible, i.e., the double bond in position 15 can be *cis* or *trans*, whereas the double bond at position 17 is neither *cis* nor *trans*. Thus, a total of 54 CLA isomers are possible. CLA has been of interest because of reported potentially beneficial effects that occur when CLA is added as a dietary component in feeding studies. Most such studies have involved small animals (1). Only five of these CLA isomers (9*c*,11*t*-18:2, 10*t*,12*c*-18:2, 9*c*,11*c*-18:2, 9*t*,11*t*-18:2, and 11*c*,13*t*-18:2) are commercially available. To overcome this problem, the synthesis and chromatographic characterization of all the *cis*/*trans* CLA isomers between the 6,8 and 13,15 double-bond positions were carried out in this study.

*To whom correspondence should be addressed at U.S. Food and Drug Administration, 5100 Paint Branch Parkway, HFS-840, Room IE009, College Park, MD 20740. E-mail: mpy@cfsan.fda.gov

Abbreviations: CLA, conjugated linoleic acid; ALA, α-linolenic acid; DMOX, 4,4′-dimethyl-2-oxazoline; GLA, γ-linolenic acid; MeCN, acetonitrile; RRT, relative retention time.

If one is interested in only total CLA in a properly extracted (2) and methylated sample portion, FAME that elute at the GC retention time of 9*c*,11*t*/7*t*,9*c* will give ~90% accuracy in the analysis of natural products, e.g., milk (3). Analysis of the isomers present at low levels requires procedure(s) that complement GC, such as silver-ion HPLC (Ag^+-HPLC) (4–6). The current interest in CLA isomers other than 9*c*,11*t* has been discussed previously (7). The identification of isomers that occur at low levels in natural products often involves highly intensive analytical chemical confirmations and entails the preparation of 4,4′-dimethyl-2-oxazoline (DMOX) (3) or other derivatives (8) of the FA, followed by mass spectral analysis and interpretation by a skilled analyst.

Previously, we reported the synthesis and isolation of the 7*t*,9*c*-CLA isomer by partial hydrogenation and conjugation of γ-linolenic acid (GLA, 6*c*,9*c*,12*c*-octadecatrienoic acid) (9). In that work we isolated only the 7*t*,9*c*-CLA isomer for further study. In the cleanup reported here, Ag^+-HPLC using new and previously reported elution solvents (4–6,10,11), the isolation of both the 7*t*,9*c*- and the 6*c*,8*t*-CLA isomers are described. In addition, the isolation of the 12*c*,14*t* and 13*t*,15*c* isomers obtained by partial hydrogenation and conjugation of α-linolenic acid (ALA, 9*c*,12*c*,15*c*-octadecatrienoic acid) and the isolation of 8*t*,10*c* from a commercial mixture also are described. CLA isomers (9*c*,11*t*, 10*t*,12*c*, and 11*c*,13*t*), were purchased for this work. In total, eight specific *cis*/*trans*-CLA isomers of known purity were either purchased or isolated from synthetic mixtures. The purchased and isolated CLA isomers were then reacted with I_2 (12) to form all of the geometric (*cis*,*cis*, *cis*,*trans*, *trans*,*cis*, and *trans*,*trans*) isomers.

EXPERIMENTAL PROCEDURES

Mixtures of previously described CLA FFA (4,5) and FAME, as well as ALA and GLA, were purchased from Nu-Chek-Prep, Inc. (Elysian, MN). CLA isomers (9*c*,11*t*-18:2, 10*t*,12*c*-18:2, 9*c*,11*c*-18:2, 9*t*,11*t*-18:2, and 11*c*,13*t*-18:2) were obtained as FFA or FAME from Matreya Inc. (Pleasant Gap, PA). Acetonitrile (MeCN) and hexane were UV grade. Diethyl ether was anhydrous. BF_3 in methanol (No. 3-3021) was obtained from Supelco (Bellefonte, PA), and hydrazine hydrate (No. 10217-52-4) and ethylene glycol (No. 29,323-7) were obtained from Sigma-Aldrich (Milwaukee, WI). Glacial acetic acid (No. 9508-00) was obtained from J.T.Baker (Phillipsburg, NJ). Solvents were glass-distilled grade.

Partial hydrogenation. Partial hydrogenation with hydrazine was carried out for both GLA and ALA as reported for GLA (9,13). Thus, 0.5 g of ALA or GLA was stirred with 100 mL of 10% hydrazine hydrate in methanol for 2.5 h at 45°C. The solution was diluted with 100 mL H_2O and then acidified with 40 mL 6N HCl. Partially hydrogenated FFA were extracted three times with 50 mL (1:1) diethyl ether/petroleum ether. The combined extracts were dried over Na_2SO_4 and concentrated to dryness with argon.

Conjugation. FFA were conjugated (14) by adding 75 mL of 6.6% KOH in ethylene glycol and heated under N_2 purge for 2 h at 150–160°C. The product was acidified with 6 N HCl, and FFA were extracted into diethyl ether/petroleum ether (1:1). Partial hydrogenation was also used to determine the configuration of the 8*t*,10*c* isomer.

Iodine isomerization. The procedure of Eulitz *et al.* (12), the catalytic application of iodine and light, was used to prepare solutions that contained all the geometric isomers of a particular positional CLA isomer. A variable quantity of CLA FAME, 5–20 mg, was dissolved in 2 mL of petroleum ether in a screw-capped glass test tube. A few drops of an I_2 solution (6 mg I_2/100 mL petroleum ether) were added until a light pink color appeared. The tube was exposed for 30 min to ambient laboratory light, then shaken for 10 s with 5 mL of aqueous 0.01 N $Na_2S_2O_3$ to remove the I_2. This step was repeated until a transparent solution was obtained. The organic phase was water-washed and dried over anhydrous Na_2SO_4 prior to chromatographic analysis.

Methylation. The FFA were methylated in 10% BF_3/ methanol (15). Identifications in sample test portions were confirmed by GC-FTIR as described previously (16). Derivatives of DMOX were obtained as described previously (3,17).

Instrumentation. (i) GC-FID. GC was performed by using a Hewlett- Packard 5890A instrument under the following conditions: capillary column, 100 m × 0.25 mm i.d. CP Sil-88 (Varian Inc., Lake Forest, CA); hydrogen carrier gas (1 mL/min); helium makeup gas for the FID; temperatures: injector 222°C, detector 280°C, column 75°C for 2 min, then raised 5°C/min to 175°C and held for 33 min, then raised at 5°C/min to 225°C and held for 8 min. Samples were run in split (20:1) mode.

(ii) GC-EI-MS. The GC-EI-MS was performed using a gas chromatograph (Hewlett-Packard 5890, Series II) coupled to a mass spectrometer (Autospec Q mass spectrometer) and a data system (OPUS 4000; Micromass, Manchester, United Kingdom). The GC-EI-MS system utilized version 2.1 BX software. This system was used with a 50-m CP Sil-88 capillary column as described previously (3). The GC-EI-MS conditions were as follows: splitless injection with helium sweep restored 1 min after injection; injector and transfer line temperatures, 220°C; oven temperature, 75°C for 1 min after injection, then programmed at 20°C/min to 185°C, held there for 15 min, then programmed at 4°C/min to 220°C, and held there for 45 min.

(iii) Analytical HPLC (Ag^+-HPLC I). Ag^+-HPLC separation of the CLA FAME was carried out using a Waters 2960 chromatographic system (Waters Associates, Milford, MA) equipped with a photodiode array detector (Waters 996) operating between 200 and 300 nm, and a Millenium (Waters) 3.20 chromatography manager. Single chromatograms of CLA isomers were measured at 233 nm. Three ChromSpher 5 Lipids analytical silver-impregnated Ag^+-HPLC columns (each 4.6 mm i.d. × 250 mm stainless steel; 5 μm particle size; Varian Inc.) were used in series at room temperature. The columns were conditioned with 1% MeCN/hexane, then equilibrated with the elution solvent for 60 min each day before analysis. The mobile phase, 0.1% acetonitrile and 0.5% diethyl ether in hexane, was prepared fresh daily and introduced isocratically at a flow rate of 1.0 mL/min. Typical injection volumes were 5–15 μL (Ag^+-HPLC I).

(iv) Semipreparative HPLC (Ag^+-HPLC II–IV). A Waters 600E HPLC pump equipped with a Waters 717 autosampler and a Waters 486 UV detector at 250 nm was used. Fractions were collected with a Waters Fraction Collector II. A Millenium (Waters) 3.20 chromatography manager was used to control the system. Different conditions were used to obtain specific separations: three ChromSpher 5 Lipids analytical silver ion-impregnated columns in series and a 2% acetic acid in hexane solution as a mobile phase at 1 mL/min (Ag^+-HPLC II); two ChromSpher 5 Lipids semipreparative Ag^+-HPLC columns (10 mm i.d. × 250 mm stainless steel; 5 μm particle size; Varian Inc.) in series, mobile phase 2% acetic acid/hexane at 3 mL/min (Ag^+-HPLC III); two ChromSpher 5 Lipids semipreparative Ag^+-HPLC columns, with a 0.18% MeCN in hexane mobile phase at 3 mL/min (Ag^+-HPLC IV).

RESULTS AND DISCUSSION

The 9*c*,11*t*-, 10*t*,12*c*-, and 11*c*,13*t*-positional CLA isomers were obtained from commercial sources in sufficient purity for this work. The 9*c*,11*t*-, 10*t*,12*c*-, and 11*c*,13*t*-CLA FAME were isomerized with I_2 to obtain the other possible geometric isomers; their identifications have been reported previously (12). Several milligrams of the *c*/*t*-8,10 FFA isomer that was previously identified in Nu-Chek-Prep CLA (4) were separated from that mixture using Ag^+-HPLC II. After partial hydrogenation, the material was unambiguously identified by GC comparison with reference materials as the 8*t*,10*c* isomer. After a second purification using Ag^+-HPLC II, the 8*t*,10*c* was isolated with a purity greater than 99%. The UV detector was operated at 250 nm wavelength to avoid saturating the signal. The isomer was converted to its FAME before GC and Ag^+-HPLC analysis. The separation obtained for 8*t*,10*c* by Ag^+-HPLC II trapping is shown in Figure 1, where the peak labeled 4 represents the 8*t*,10*c*-CLA. Notably, unlike Ag^+-HPLC elution systems that use MeCN as an eluant component, the use of acetic acid resulted in no significant retention volume drift during isolation, and several milligrams per day of the CLA isomer could be obtained using an unattended system equipped with an autosampler and fraction collector. Catalytic isomerization with I_2 yielded all the other possible geometric isomers (*c*,*t*, *t*,*c*, *c*,*c*, *t*,*t*) of 8,10-CLA, as shown in Figure 2. Figure 2 was obtained using analytical conditions (Ag^+-HPLC I). Before isom-

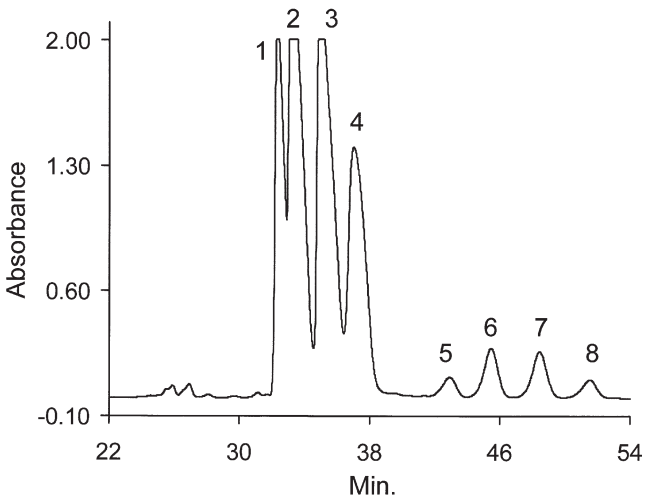

FIG. 1. Partial Ag^+-HPLC chromatogram showing the resolution of peak 4, 8*t*,10*c*-CLA, in a Nu-Chek-Prep (Elysian, MN) CLA FFA mixture using three analytical columns with a 2% acetic acid/hexane mobile phase at 1 mL/min (Ag^+-HPLC II). Other isomers are: peaks 1, 11*c*,13*t*; 2, 10*t*,12*c*; 3, 9*c*,11t; 5–8, *c*,*c*-CLA isomers.

erization with I_2, the 8*t*,10*c* was ~99% pure. After isomerization, the *t*,*t* isomer was predominant (~88%) and each *c*/*t* isomer was ~5.5%, with the *c*,*c* isomer at ~1%.

The 6*c*,8*t*- and 7*t*,9*c*-CLA were synthesized (along with the 9*c*,11*t*- and 10*t*,12*c*-CLA) from the partial hydrogenation and conjugation of GLA, and then purified as indicated in Figure 3. During the partial hydrogenation procedure, the double bonds did not shift position nor did they change the *cis*/*trans* geometry of the remaining unsaturated bonds. The octadecadiene(s) (18:2) that resulted from the partial hydrogenation of GLA were therefore 6*c*,9*c*, 6*c*,12*c*, and 9*c*,12*c*. Of these 18:2 isomers, only the 6*c*,9*c* and 9*c*,12*c* isomers will conjugate under basic conditions (9). The *c*/*t*-18:2 CLA isomers that were formed by conjugating 18:2 from partially hydrogenated GLA with KOH/ethylene glycol at 150–160°C were 6*c*,8*t*-, 7*t*,9*c*-, 9*c*,11*t*-, and 10*t*,12*c*-18:2. Stearate, 6*c*,9*c*, 12*c*-18:3, and fully and partially conjugated 18:3 were also present as products in the final reaction mixture. The 9*c*,11*t* and 10*t*,12*c* reference standards were commercially available, and these compounds were easily identified as reaction products. As for the isolation process indicated in Figure 3 and the chromatogram shown in Figure 4, use of the Ag^+-HPLC III system allowed the trapping of two FFA fractions. The first fraction contained the 9*c*,11*t* and the 10*t*,12*c* isomers, whereas the second fraction contained the 6*c*,8*t* and the 7*t*,9*c* isomers. The two semi-preparative columns were eluted with 2% acetic acid/hexane at 3 mL/min (Ag^+-HPLC III). The isolation shown in Figure 4 differs from that published previously (9) using MeCN with FAME in that the 6*c*,8*t*- and 7*t*,9*c*-FFA isomers eluted together and were sufficiently resolved from the 9*c*,11*t*- and 10*t*,12*c*-FFA. The chromatogram shown in Figure 4 was acquired at 245 nm to avoid overloading the signal while monitoring this separation.

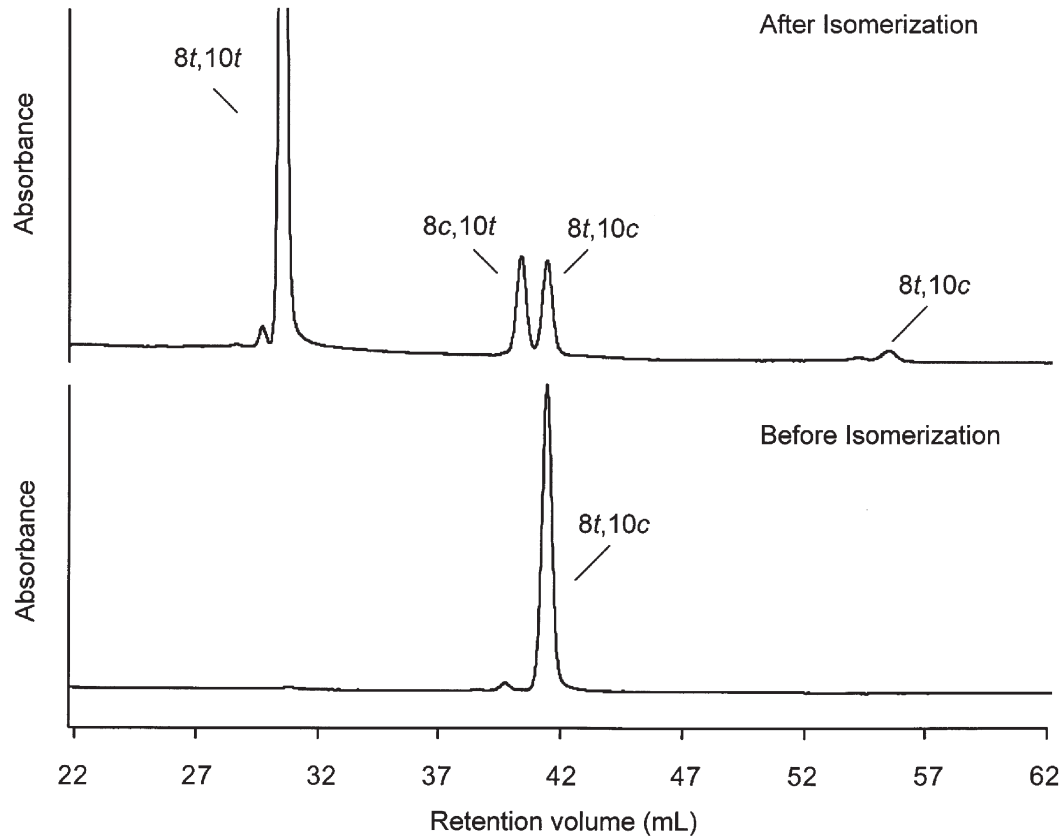

FIG. 2. Partial chromatogram (Ag^+-HPLC I) of 8*t*,10*c*-CLA FAME before and after isomerization with I_2.

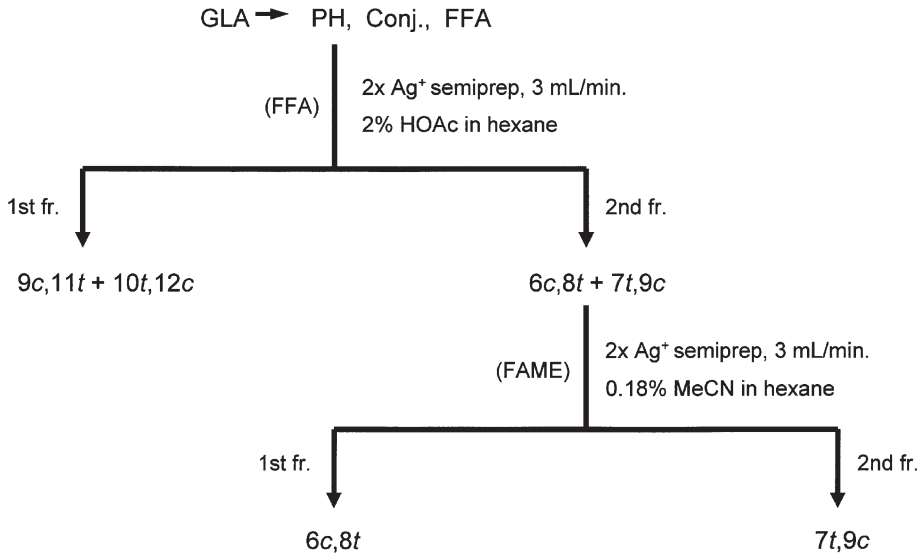

FIG. 3. Isolation of 6*c*,8*t* and 7*t*,9*c*. CLA FFA from GLA after partial hydrazine reduction (PH) and alkali conjugation (Conj.) was separated (Ag^+-HPLC III) into two fractions. The first fraction (1st fr.) contained the 9*c*,11*t*- and 10*t*,12*c*-CLA isomers, and the second fraction (2nd fr.) contained the 6*c*,8*t*- and 7*t*,9*c*-CLA isomers. The separation of 6*c*,8*t* from 7*t*,9*c* (Ag^+-HPLC IV) was accomplished after conversion to FAME.

To separate the 6*c*,8*t* from the 7*t*,9*c* isomer, the mixture of FFA was first converted to FAME using BF_3/methanol (Fig. 3). The separation was accomplished by trapping the individual FAME using two semipreparative columns eluted with 0.18% MeCN/hexane (Ag^+-HPLC IV). This separation is shown in Figure 5. The separated isomers appeared pure when analyzed by Ag^+-HPLC I at 233 nm, but the presence of *cis* monoenes (primarily 6*c*-18:1) was observed by GC-FID.

The 12*c*,14*t* and 13*t*,15*c* isomers were obtained by partial hydrogenation followed by alkali isomerization of the ALA. The partial hydrogenation and the conjugation of ALA were carried out in the same manner as described above for GLA. The reaction product that contained the expected CLA isomers (9*c*,11*t*, 10*t*,12*c*, 12*c*,14*t*, and 13*t*,15*c*) was methylated (BF_3/methanol) prior to the isolation of individual isomers. The isolation scheme for the 12*c*,14*t* and 13*t*,15*c* is outlined in Figure 6. In the first step, a fraction containing the 12*c*,14*t* and 13*t*,15*c* FAME was trapped using two preparative columns and a mobile phase, 2% acetic acid/hexane, at a flow rate of 3 mL/min (Ag^+-HPLC III). The chromatogram in Figure 7 shows the resolution at 250 nm that was found to be reproducible with minimum retention volume drift. The final separation (Fig. 8) of 12*c*,14*t* from 13*t*,15*c* FAME was obtained using three analytical columns in series eluted with 2% acetic acid/hexane to increase the resolution between these isomers with very similar retention volumes. Once again, the solvent system without MeCN showed much less retention volume drift between injections, with little loss of resolution. No other

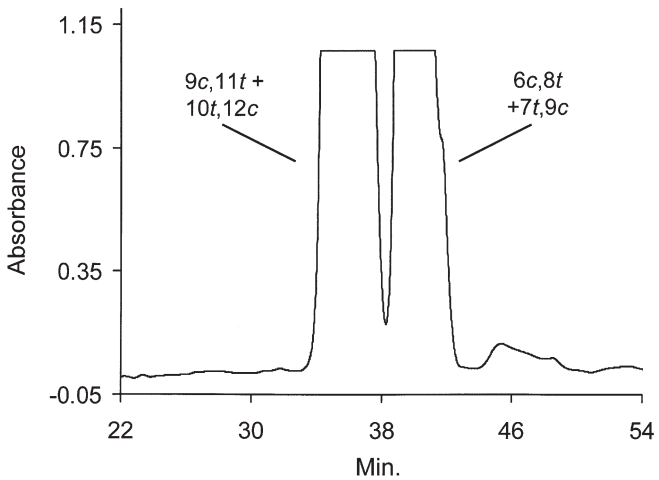

FIG. 4. Partial Ag^+-HPLC chromatogram showing the separation of 6*c*,8*t*- and 7*t*,9*c*-CLA FFA from 9*c*,11*t*- and 10*t*,12*c*-CLA FFA (Ag^+-HPLC III) using two semipreparative columns with a 2% acetic acid/hexane mobile phase.

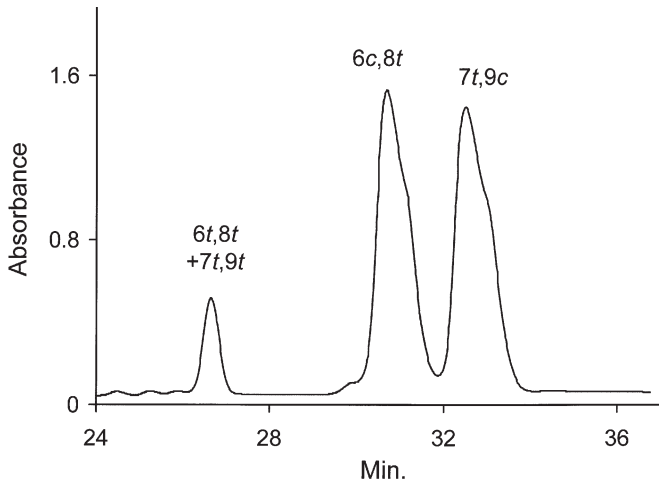

FIG. 5. Partial Ag^+-HPLC chromatogram showing the separation of FAME of 6*c*,8*t* from 7*t*,9*c* (Ag^+-HPLC IV) using two semipreparative columns with 0.18% MeCN/hexane, 3 mL/min.

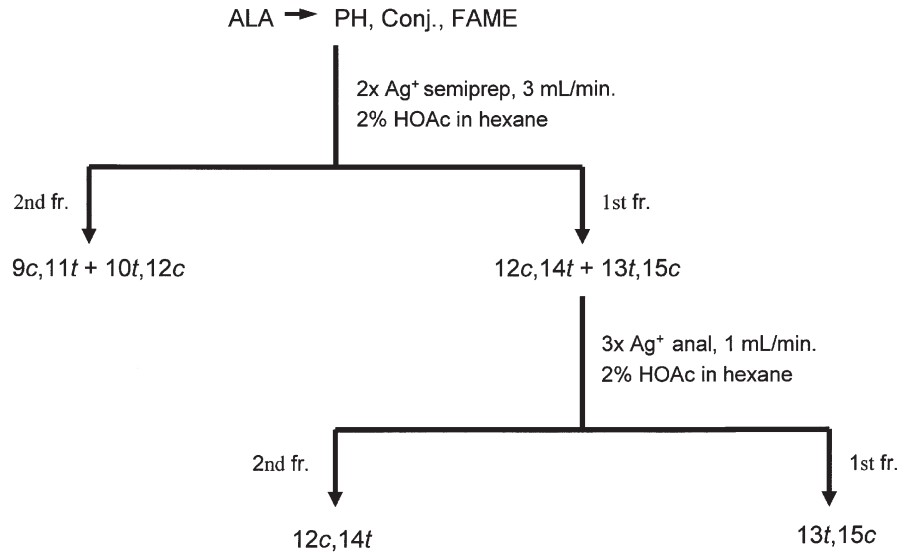

FIG. 6. Isolation of 12*c*,14*t*- and 13*t*,15*c*-CLA. CLA FAME from α-linolenic acid (ALA) after partial hydrazine reduction (PH) and alkali conjugation (Conj.) were separated (Ag^+-HPLC III) into two fractions. The first fraction (1st fr.) contained the 9*c*,11*t*- and 10*t*,12*c*-CLA isomers, and the second fraction (2nd fr.) contained the 12*c*,14*t*- and 13*t*,15*c*-CLA isomers. The separation (Ag^+-HPLC II) of 12*c*,14*t*- from 13*t*,15*c*-CLA was also accomplished as their FAME.

FAME impurities were detected by GC-FID analysis of the isolated fractions of 12*c*,14*t* and 13*t*,15*c* isomers. A summary of the different Ag^+-HPLC isolations described above is presented in Table 1. All of the CLA isolations were monitored at 250 nm. Only the analytical analysis was monitored at 233 nm.

As described above, eight specific *cis*/*trans*-CLA FAME isomers (6*c*,8*t*, 7*t*,*c*9, 8*t*,10*c*, 9*c*,11*t*, 10*t*,12*c*, 11*c*,13*t*, 12*c*,14*t*, and 13*t*,15*c*) representing positions 6,8 through 13,15 were purchased and/or isolated. A portion of each of isomer was reacted with I_2 under laboratory light. After the reaction, the I_2 was destroyed by washing with a solution of sodium thiosulfate as described previously (12). This procedure produced *cis*/*trans* isomerization of the positional isomer used but did not produce new positional isomers. The ratio of *cis*/*trans* isomers produced from a given positional isomer was thermodynamically controlled and were *ca*. *trans*,*trans* (88%), *cis*,*trans* (5.5%), *trans*,*cis* (5.5%), and *cis*,*cis* (1%). We were able to identify the retention times (RT) of all 32 *cis*/*trans* isomers from positions 6,8 to 13,15 by injecting the isolated or purchased *cis*/*trans* isomers and then by injecting the I_2-isomerized mixtures onto the GC. The RT of the non-I_2-isomerized *cis*/*trans* isomers were known from the results of the first injections, and the isomers present at the same quantity in the isomerized mixture were confirmed to be *cis*/*trans* in geometric configuration (FTIR); therefore, they had to be the *cis*/*trans* positional (GC-EI-MS of DMOX) isomers that were complemen-

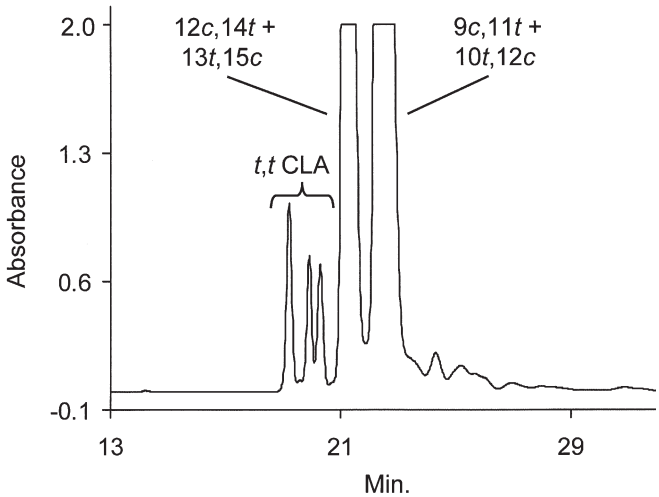

FIG. 7. Partial Ag^+-HPLC chromatogram showing the separation of 12*c*,14*t*- and 13*t*,15*c*-CLA FAME from 9*c*,11*t*- and 10*t*,12*c*-CLA FAME (Ag^+-HPLC III) using two semipreparative columns with a 2% acetic acid/hexane mobile phase at 3 mL/min.

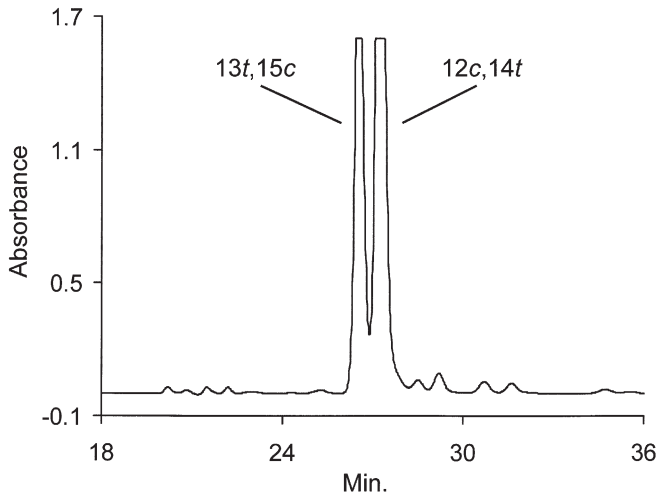

FIG. 8. Partial Ag^+-HPLC chromatogram showing the separation of FAME of 12*c*,14*t*- from 13*t*,15*c*-CLA FAME (Ag^+-HPLC II) using three analytical columns with a 2% acetic acid/hexane mobile phase, 1 mL/min.

TABLE 1
Ag^+-HPLC Used to Isolate CLA Isomers

Technique	Columns	Mobile phase[a] (flow)	Chemical form	Separation
Ag^+-HPLC I	Three analytical	0.1% MeCN/0.5% diethyl ether/ hexane (1 mL/min)	FAME	General analysis
Ag^+-HPLC II	Three analytical	2% acetic acid/hexane (1 mL/min)	FFA FAME	8*t*,10*c* from a commercial mixture 12*c*,14*t* from 13*t*,15*c*
Ag^+-HPLC III	Two semipreparative	2% acetic acid/hexane (3 mL/min)	FFA FAME	(6*c*,8*t* + 7*t*,9*c*) from (9*c*,11*t* + 10*t*,12*c*) (12*c*,14*t* + 13*t*,15*c*) from (9*c*,11*t* + 10*t*,12*c*)
Ag^+-HPLC IV	Two semipreparative	0.18% MeCN/hexane (3 mL/min)	FAME	6*c*,8*t* from 7*t*,9*c*

[a]MeCN, acetonitrile.

tary to the non-I_2-isomerized isomers originally injected. The isomer in each I_2-isomerized mixture that was present in the highest quantity was confirmed to be the *t*,*t* isomer, and the isomer at the lowest quantity was always found to be the *c*,*c* isomer.

The GC relative retention times (RRT) are presented in Table 2. Data were obtained with a 100-m CP Sil-88 capillary column using a temperature program similar to those typically used for FAME analysis, but not optimized specifically for CLA FAME. The RT for each isomer was adjusted for the solvent front and presented relative to GLA FAME as follows: $RRT/GLA = (RT_{isomer} - RT_{solvent})/(RT_{GLA\ FAME} - RT_{solvent})$. With the exception of the 6*c*,8*t* isomer, the RT of the *c*,*t* CLA isomers increased as the *cis* double bonds were located farther away from the carbonyl moiety of the molecule. The 6*c*,8*t* isomer was the exception to this rule because it eluted after the 7*c*,9*t* isomer and the two geometric isomers of *6*,*8* co-eluted. In the cases where two isomers had the same *cis* double-bond location and differ only in the position of the *trans* double bond, the isomer with the *trans* double bond closer to the carbonyl moiety eluted first, e.g., 7*t*,9*c* eluted before 9*c*,11*t*. GC chromatograms of each isomerized mixture are shown in Figure 9.

TABLE 2
GC Relative Retention Times (RRT) for CLA FAME Isomers[a]

Isomer	RRT/GLA	Source
7*c*,9*t*	1.083	I_2 isomerization of 7*t*,9*c*
8*c*,10*t*	1.085	I_2 isomerization of 8*t*,10*c*
6*c*,8*t*	1.086	Conjugation of partially hydrogenated GLA
6*t*,8*c*	1.086	I_2 isomerization of 6*c*,8*t*
7*t*,9*c*	1.091	Conjugation of partially hydrogenated GLA
9*c*,11*t*	1.091	Commercially available
8*t*,10*c*	1.097	Isolated from commercial reference material
10*c*,12*t*	1.104	I_2 isomerization of 10*t*,12*c*
9*t*,11*c*	1.109	I_2 isomerization of 9*c*,11*t*
11*c*,13*t*	1.114	Commercially available
12*c*,14*t*	1.118	Conjugation of partially hydrogenated ALA
10*t*,12*c*	1.122	Commercially available
6*c*,8*c*	1.128	I_2 isomerization of 6*c*,8*t*
8*c*,10*c*	1.131	I_2 isomerization of 8*t*,10*c*
7*c*,9*c*	1.131	I_2 isomerization of 7*t*,9*c*
11*t*,13*c*	1.136	I_2 isomerization of 11*c*,13*t*
9*c*,11*c*	1.137	I_2 isomerization of 9*c*,11*t*
10*c*,12*c*	1.145	I_2 isomerization of 10*t*,12*c*
13*c*,15*t*	1.147	I_2 isomerization of 13*t*,15*c*
12*t*,14*c*	1.149	I_2 isomerization of 12*c*,14*t*
11*c*,13*c*	1.151	I_2 isomerization of 11*c*,13*t*
12*c*,14*c*	1.159	I_2 isomerization of 12*c*,14*t*
13*t*,15*c*	1.166	Conjugation of partially hydrogenated ALA
13*c*,15*c*	1.166	I_2 isomerization of 13*t*,15*c*
12*t*,14*t*	1.171	I_2 isomerization of 12*c*,14*t*
11*t*,13*t*	1.184	I_2 isomerization of 11*c*,13*t*
13*t*,15*t*	1.184	I_2 isomerization of 13*t*,15*c*
9*t*,11*t*	1.191	I_2 isomerization of 9*c*,11*t*
8*t*,10*t*	1.191	I_2 isomerization of 8*t*,10*c*
10*t*,12*t*	1.192	I_2 isomerization of 10*t*,12*c*
6*t*,8*t*	1.192	I_2 isomerization of 6*c*,8*t*
7*t*,9*t*	1.193	I_2 isomerization of 7*t*,9*c*

[a]Entries were obtained as follows: $(RT_{isomer} - RT_{solvent})/(RT_{GLA\ FAME} - RT_{solvent})$. GLA, γ-linolenic acid; ALA, α-linolenic acid; RT, retention time.

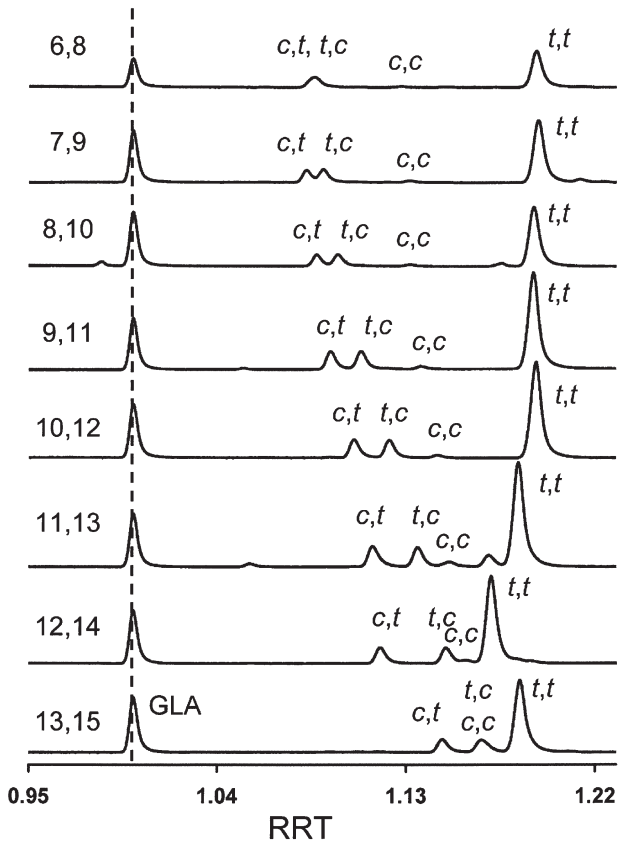

FIG. 9. Gas chromatograms of all the CLA isomers from 6,8- to 13,15-CLA, in relative retention time (RRT)/γ-linolenic acid (GLA) scale. After the elution of GLA FAME, the *c,t* isomer eluted first, followed by the *t,c, c,c,* and *t,t* isomers. The *t,c* and *c,c* isomers co-eluted in the case of the 13,15-positional CLA isomer. The two *c/t* 6,8 geometric isomers also co-eluted. The vertical axis is the response. The horizontal axis is given relative to RRT/GLA units.

The *x* axis in Figure 9 has an RRT scale calculated relative to GLA FAME. The separation between *c*,*t* and *t*,*c* isomers increased as the distance of the carbonyl moiety to the double-bond moiety increased from positions 6,8 to 12,14, where the separation was maximized. The *c*,*t* isomers had a minimum RRT for the 7,9 isomer and a maximum for the 13,15 isomer. The *t*,*t* isomers had a minimum corresponding to the 12,14 isomer and a maximum for the 7,9 isomer. The RRT for the *t*,*c* and *c*,*c* isomers both increased in value, going from the 6,8 through the 13,15 positions, by fitting the second-degree equation with R_2 greater than 0.99.

In conclusion, the identities of the synthesized CLA isomers were confirmed by various combinations of UV spectroscopy, routes of synthesis, GC-EI-MS of DMOX derivatives (3), GC-FTIR of FAME (16), partial hydrogenation, and I_2 isomerization (12). These data were generated to aid in the identification of CLA isomers in foods, dietary supplements, and biological samples, and they were used successfully to test a MeCN chemical-ionization GC-MS-MS technique that produced 32 unique spectra for these 32 synthesized CLA FAME (18). It is of interest that the use of acetic acid/hexane as a mobile phase did not cause any drift in the elution of CLA and allowed for unattended fraction collection for several days when operated with an autosampler and a fraction collector. Limitations of this elution technique are: (i) uncertainty regarding the long-term stability of silver-ion columns under acetic acid elution, and (ii) inability to monitor the presence of nonconjugated FA, e.g., monounsaturated FA and esters, using lower-UV wavelengths because of the UV absorption of acetic acid.

REFERENCES

1. Belury, M.A. (2002) Dietary Conjugated Linoleic Acid in Health: Physiological Effects and Mechanisms of Action, *Annu. Rev. Nutr. 22*, 505–531.
2. Yurawecz, M.P., Hood, J.K., Roach, J.A.G., Mossoba, M.M., Daniels, D.H., Ku, Y., Pariza, M.W., and Chin., S.F. (1994) Conversion of Allylic Hydroxy Oleate to Conjugated Linoleic Acid and Methoxy Oleate by Acid-Catalyzed Methylation Procedures, *J. Am. Oil Chem. Soc. 71*, 1149–1155.
3. Yurawecz, M.P., Roach, J.A.G., Sehat, N., Mossoba, M.M., Kramer, J.K.G., Fritsche, J., and Steinhart, H. (1998) A New Conjugated Linoleic Acid (CLA) Isomer, 7-*trans*,9-*cis*-Octadecadienoic Acid in Cow Milk, Cheese, Beef, and Human Milk and Adipose Tissue, *Lipids 33*, 803–809.
4. Sehat, N., Yurawecz, M.P., Roach, J.A.G., Mossoba, M.M., Kramer, J.K.G., and Ku, Y. (1998) Silver Ion High-Performance Liquid Chromatographic Separation and Identification of Conjugated Linoleic Acid Isomers, *Lipids 33*, 217–221.
5. Sehat, N., Rickert, R., Mossoba, M.M., Kramer, J.K.G., Yurawecz, M.P., Roach, J.A.G., Adlof, R.O., Morehouse, K.M., Fritsche, J., Eulitz, K.D., Steinhart, H., and Ku, Y. (1999) Improved Separation of Conjugated Fatty Acid Methyl Esters by Silver Ion High-Performance Liquid Chromatography, *Lipids 34*, 407–413.
6. Rickert, R., Steinhart H., Fritsche, J., Sehat, N., Yurawecz, M.P., Mossoba, M.M., Roach, J.A.G., Eulitz, K., Ku, Y., and Kramer, J.K.G. (1999) Enhanced Resolution of Conjugated Linoleic Acid Isomers by Tandem-Column Silver-Ion High Performance Liquid Chromatography, *J. High Resol. Chromatogr. 22*, 144–148.
7. Yurawecz, M.P., and Morehouse, K.M. (2001) Silver Ion HPLC of Conjugated Linoleic Acid Isomers, *Eur. J. Lipid Sci. Technol. 103*, 609–613.
8. Spitzer, V. (1999) Gas Chromatography/(Electron Impact) Mass Spectrometry Analysis of Conjugated Linoleic Acid (CLA) Using Different Derivitization Techniques, in *Advances in Conjugated Linoleic Acid Research* (Yurawecz, M.P., Mossoba, M.M., Kramer, J.K.G., Pariza, M.W., and Nelson, G.J., eds.), Vol. 1, pp. 110–125, AOCS Press, Champaign.
9. Delmonte, P., Roach, J.A.G., Mossoba, M.M., Morehouse, K.M., Lehmann, L., and Yurawecz, M.P. (2003) Synthesis and Isolation of *trans*-7,*cis*-9 Octadecadienoic Acid and Other CLA Isomers by Base Conjugation of Partially Hydrogenated γ-Linolenic Acid, *Lipids 38*, 579–583.
10. Ostrowska, E., Dunshea, F.R., Muralitharan, M., and Cross R. (2000) Comparison of Silver Ion High-Performance Liquid Chromatographic Quantification of Free and Methylated Conjugated Linoleic Acids, *Lipids 35*, 1147–1153.
11. Corl, B.A., Baumgard, L.H., Griinari, J.M., Delmonte, P., Morehouse, K.M., Yurawecz, M.P., and Bauman, D.E. (2002) Lactating Dairy Cows Endogenously Synthesize *trans*-7,*cis*-9 CLA, *Lipids 37*, 681–688.
12. Eulitz, K., Yurawecz, M.P., Sehat, N., Fritsche, J., Roach J.A.G., Mossoba, M.M., Kramer, J.K.G., Adlof, R.O., and Ku, Y. (1999) Preparation, Separation, and Confirmation of the Eight Geometrical *cis*/*trans* Conjugated Linoleic Acid Isomers 8,10- Through 11,13-18:2, *Lipids 34*, 873–877.
13. Christie, W.W. (1989) *Gas Chromatography and Lipids: A Practical Guide*, p. 158, The Oily Press, Dundee, Scotland.
14. AOAC (1990) Acids (Polyunsaturated) in Oils and Fats, in *Official Methods of Analysis,* 15th edn. (Helrich, K., ed.), Vol. 2, pp. 960–963, Association of Official Analytical Chemists, Gaithersburg, MD, Sec. 957.13.
15 AOAC (1990) Preparation of Methyl Esters, in *Official Methods of Analysis,* 15th edn. *(*Helrich, K., ed.), Vol. 2, pp. 963–964, Association of Official Analytical Chemists, Gaithersburg, MD, Sec. 969. 33.
16. Mossoba, M.M., McDonald, R.E., Yurawecz, M.P., and Kramer, J.K.G. (2001) Application of On-line Capillary GC-FTIR Spectroscopy to Lipid Analysis, *J. Lipid Sci. Technol. 103*, 826–829.
17. Roach, J.A.G., Mossoba, M.M., Yurawecz, M.P., and Kramer, J.K.G. (2002) Chromatographic Separation and Identification of Conjugated Linoleic Acid Isomers, *Anal. Chim. Acta 465*, 207– 226.
18. Michaud, A.L., Yurawecz, M.P., Delmonte, P., Corl, B.A., Bauman, D.E., and Brenna, J.T. (2003) Identification and Characterization of Conjugated Fatty Acid Methyl Esters of Mixed Double Bond Geometry by Acetonitrile Chemical Ionization Tandem Mass Spectrometry, *Anal. Chem. 75*, 4925–4930.

[Received November 5, 2003; accepted January 15, 2004]

Levels of *N*-Acylethanolamines in Human Tumors: In Search of Reliable Data

Sir:

In a recent study (1) Schmid and coworkers reported the presence of long-chain *N*-acylethanolamines (NAE) in various human tumors and stated that their report was "the first reliable information on the presence of NAE . . . in human cancer." In fact, they claimed that our previous study on this topic (2) "must be accepted with caution because the internal standards were added to aqueous homogenates . . . [and] may have been discarded with the supernatants" (1). In this note we would like to reassure the authors and the readers that our GC–MS analysis of NAE is instead reliable.

First of all, this lipid extraction procedure has been widely used to extract NAE from biological materials (see references cited in 2), and in fact addition of internal standards to aqueous homogenates before lipid extraction is still a common procedure in laboratories with well-established experience in NAE analysis (3,4). In essence, Schmid and coworkers suppose that deuterated anandamide (20:4n-6 NAE; AEAd4), a lipid standard that we and others used to normalize NAE content (2–4), "may have been discarded with the [aqueous] supernatants" (1). This statement does not take into account that we did measure routinely the recovery of our extraction procedure by following the recovery of AEAd4, yielding values of ~60% (2). Quantitative data on NAE were always calculated after correction for this recovery (2), which was determined by comparing the peak areas of AEAd4 in the samples with the peak areas of an external calibration curve of AEAd4. Therefore, "considerable overestimation of the compounds of interest" (1) due to loss of the internal standard was not possible. Additionally, in the process of extracting lipids that innately have a low recovery, we recovered ~2 nmol AEAd4 in the pellet from the second centrifugation step (at $11{,}000 \times g$) from samples containing 5 nmol AEAd4, corresponding to a total recovery of ~40%. Incidentally, ~2.5 nmol AEAd4 (~50% of the initial amount) was recovered in the pellet from the first centrifugation step (at $800 \times g$). Even these low figures would not justify differences of "several orders of magnitude" in NAE quantification (1). In addition, Schmid and coworkers also disregard that in the same paper (2) we reported independent experiments where NAE were extracted from frozen samples, homogenized directly in a mixture of aqueous buffer and ice-cold methanol/chloroform containing AEAd4. This method closely resembles that adopted by Schmid and coworkers (5), as well as by others (6), to extract NAE from biological specimens and was used as a further control of our assay. Interestingly, it yielded the same results as the procedure claimed to be unreliable, mitigating against possible pitfalls in the extraction procedure. Moreover, in a recent paper we used our GC–MS method to measure endogenous levels of anandamide in the striatum of healthy and Parkinsonian rats (7) and found changes superimposable on those reported by others (6). Also this observation speaks in favor of the reliability of our procedure, although we are well aware that discrepancies exist between different studies on the quantification of anandamide. Reported values in rat brain range from pmol/g of fresh tissue (8) to nmol/g (2), but in fresh tissue from rat substantia nigra and globus pallidus (6), from mouse cortex and hippocampus (9), and from mouse uterus (10), concentrations are nmol/g. Incidentally, the latter pioneering study is an elegant investigation by Schmid and coworkers (10). Although we do not have an explanation for the discrepancies in the literature on NAE quantification, we believe that we have already ruled out that artificial increases in endocannabinoid level might occur during our sample preparation and analysis (2,7,9,11). An interesting finding by Schmid and coworkers is that NAE are present in widely differing amounts in human tumors, with anandamide ranging from 1.5 to 48% of total NAE (1). However, no human brain tumors were included in the study. Nonetheless, the authors felt confident to discard as unreliable our data on human meningioma and glioblastoma (1,12).

More generally, any effort aimed at improving our understanding of the ever-growing field of biologically active NAE such as anandamide and related "endocannabinoids" should be appreciated, especially in view of the broad implications of these novel compounds as central and peripheral modulators (13–15). Thus, we believe that advancement of knowledge will benefit from a fair discussion of discrepancies that might be (and often are!) present in the literature.

REFERENCES

1. Schmid, P.C., Wold, L.E., Krebsbach, R.J., Berdyshev, E.V., and Schmid, H.H.O. (2002) Anandamide and the Other *N*-Acylethanolamines in Human Tumors, *Lipids 37*, 907–912.
2. Maccarrone, M., Attinà, M., Cartoni, A., Bari, M., and Finazzi-Agrò, A. (2001) Gas Chromatography–Mass Spectrometry Analysis of Endogenous Cannabinoids in Healthy and Tumoral Human Brain and Human Cells in Culture, *J. Neurochem. 76*, 594–601.
3. Giuffrida, A., Rodriguez de Fonseca, F., and Piomelli, D. (2000) Quantification of Bioactive Acylethanolamides in Rat Plasma by Electrospray Mass Spectrometry, *Anal. Biochem. 280*, 87–93.
4. Wang, L., Liu, J., Harvey-White, J., Zimmer, A., and Kunos, G. (2003) Endocannabinoid Signaling *via* Cannabinoid Receptor 1 Is Involved in Ethanol Preference and Its Age-Dependent Decline in Mice, *Proc. Natl. Acad. Sci. USA 100*, 1393–1398.

Paper no. L9320 in Lipids 39, 193–194 (February 2004).

5. Schmid, P.C., Krebsbach, R.J., Perry, S.R., Dettmer, T.M., Maasson, J.L., and Schmid, H.H. (1995) Occurrence and Postmortem Generation of Anandamide and Other Long-Chain *N*-Acylethanolamines in Mammalian Brain, *FEBS Lett. 375*, 117–120.
6. Di Marzo, V., Hill, M.P., Bisogno, T., Crossman, A.R., and Brotchie, J.M. (2000) Enhanced Levels of Endogenous Cannabinoids in the Globus Pallidus Are Associated with a Reduction in Movement in an Animal Model of Parkinson's Disease, *FASEB J. 14*, 1432–1438.
7. Gubellini, P., Picconi, B., Bari, M., Battista, N., Calabresi, P., Centonze, D., Bernardi, G., Finazzi-Agrò, A., and Maccarrone, M. (2002) Experimental Parkinsonism Alters Endocannabinoid Degradation: Implications for Striatal Glutamatergic Transmission, *J. Neurosci. 22*, 6900–6907.
8. Yang, H.-Y.T., Karoum, F., Felder, C., Badger, H., Wang, T.-C.L., and Markey, S.P. (1999) GC/MS Analysis of Anandamide and Quantification of *N*-Arachidonoyl-phosphatidylethanol-amides in Various Brain Regions, Spinal Cord, Testis, and Spleen of the Rat, *J. Neurochem. 72*, 1959–1968.
9. Maccarrone, M., Valverde, O., Barbaccia, M.L., Castañé, A., Maldonado, R., Ledent, C., Parmentier, M., and Finazzi-Agrò, A. (2002) Age-Related Changes of Anandamide Metabolism in CB_1 Cannabinoid Receptor Knockout Mice: Correlation with Behaviour, *Eur. J. Neurosci. 15*, 1178–1186.
10. Schmid, P.C., Paria, B.C., Krebsbach, R.J., Schmid, H.H.O., and Dey, S.K. (1997) Changes in Anandamide Levels in Mouse Uterus Are Associated with Uterine Receptivity for Embryo Implantation, *Proc. Natl. Acad. Sci. USA 94*, 4188–4192.
11. Maccarrone, M., Bari, M., Di Rienzo, M., Finazzi-Agrò, A., and Rossi, A. (2003) Progesterone Activates Fatty Acid Amide Hydrolase (FAAH) Promoter in Human T Lymphocytes Through the Transcription Factor Ikaros. Evidence for a Synergistic Effect of Leptin, *J. Biol. Chem. 278*, 32726–32732.
12. Schmid, H.H., Schmid, P.C., and Berdyshev, E.V. (2002) Cell Signaling by Endocannabinoids and Their Congeners: Questions of Selectivity and Other Challenges, *Chem. Phys. Lipids 121*, 111–134.
13. Fride, E. (2002) Endocannabinoids in the Central Nervous System—An Overview, *Prostaglandins Leukot. Essent. Fatty Acids 66*, 221–233.
14. Mechoulam, R. (2002) Discovery of Endocannabinoids and Some Random Thoughts on Their Possible Roles in Neuroprotection and Aggression, *Prostaglandins Leukot. Essent. Fatty Acids 66*, 93–99.
15. Maccarrone, M., and Finazzi-Agrò, A. (2002) The Endocannabinoids and Their Actions, *Vitam. Horm. 65*, 225–255.

Mauro Maccarrone[a,b,*], Filomena Fezza[a], and Alessandro Finazzi-Agrò[c]
[a]Department of Biomedical Sciences, University of Teramo, I-64100 Teramo, Italy, [b]IRCCS C. Mondino, Mondino-Tor Vergata-Santa Lucia Center for Experimental Neurobiology, I-00179 Rome, Italy, and [c]Department of Experimental Medicine and Biochemical Sciences, University of Rome "Tor Vergata," I-00133 Rome, Italy

[Received May 15, 2003, and in final form and accepted January 29, 2004]

*To whom correspondence should be addressed at Department of Biomedical Sciences, University of Teramo, Piazza A. Moro 45, I-64100 Teramo, Italy. E-mail: Maccarrone@vet.unite.it

Dedicated to the memory of Prof. Marina Attinà, who developed the GC–MS analysis of NAE and was sorrowfully missed on October 26, 2000.

Abbreviations: AEAd4, deuterated anandamide; NAE, *N*-acylethanolamines.

Maternal Fish Oil Supplementation in Lactation: Effect on Visual Acuity and n-3 Fatty Acid Content of Infant Erythrocytes

Lotte Lauritzen[a,*], Marianne H. Jørgensen[b], Tina B. Mikkelsen[c], Ib M. Skovgaard[d], Ellen-Marie Straarup[e], Sjúrdur F. Olsen[c], Carl-Erik Høy[e], and Kim F. Michaelsen[a]

[a]Centre for Advanced Food Studies, Department of Human Nutrition, The Royal Veterinary and Agricultural University, [b]Department of Pediatrics, Hillerød Hospital, [c]Maternal Nutrition Group, Danish Epidemiology Science Centre, Statens Serum Institut, [d]Department of Mathematics and Physics, The Royal Veterinary and Agricultural University, and [e]BioCentrum-DTU, Biochemistry & Nutrition, Technical University of Denmark, Denmark

ABSTRACT: Studies on formula-fed infants indicate a beneficial effect of dietary DHA on visual acuity. Cross-sectional studies have shown an association between breast-milk DHA levels and visual acuity in breast-fed infants. The objective in this study was to evaluate the biochemical and functional effects of fish oil (FO) supplements in lactating mothers. In this double-blinded randomized trial, Danish mothers with habitual fish intake below the 50th percentile of the Danish National Birth Cohort were randomized to microencapsulated FO [1.3 g/d long-chain n-3 FA (n-3 LCPUFA)] or olive oil (OO). The intervention started within a week after delivery and lasted 4 mon. Mothers with habitual high fish intake and their infants were included as a reference group. Ninety-seven infants completed the trial (44 OO-group, 53 FO-group) and 47 reference infants were followed up. The primary outcome measures were: DHA content of milk samples (0, 2, and 4 mon postnatal) and of infant red blood cell (RBC) membranes (4 mon postnatal), and infant visual acuity (measured by swept visual evoked potential at 2 and 4 mon of age). FO supplementation gave rise to a threefold increase in the DHA content of the 4-mon milk samples ($P < 0.001$). DHA in infant RBC reflected milk contents ($r = 0.564$, $P < 0.001$) and was increased by almost 50% ($P < 0.001$). Infant visual acuity was not significantly different in the randomized groups but was positively associated at 4 mon with infant RBC-DHA ($P = 0.004$, multiple regression). We concluded that maternal FO supplementation during lactation did not enhance visual acuity of the infants who completed the intervention. However, the results showed that infants with higher RBC levels of n-3 LCPUFA had a better visual acuity at 4 mon of age, suggesting that n-3 LCPUFA may influence visual maturation.

Paper no. L9338 in *Lipids 39,* 195–206 (March 2004).

*To whom correspondence should be addressed at Center for Advanced Food Studies, Dept. of Human Nutrition, The Royal Veterinary and Agricultural University, Rolighedsvej 30, 1958 Frederiksberg C, Denmark. E-mail: ll@kvl.dk

Abbreviations BMI, body mass index; DNBC, Danish National Birth Cohort; FA%, percentage of total FA; FFQ, Food Frequency Questionnaire; FO, fish oil; HF-group, reference group, the members of which consumed quantities of fish above the 74th percentile; LCPUFA, long-chain PUFA; logMAR, the logarithm of the minimal angle of resolution; MUFA, monounsaturated FA; OO, olive oil; RBC, red blood cells; SFA, saturated FA; SWEEP-VEP, swept visual evoked potential; VEP, visual evoked potential.

Membranes of the brain and retina contain uniquely high levels of long-chain PUFA (LCPUFA), especially DHA (22:6n-3). Formula-fed infants, who do not receive exogenously preformed LCPUFA, have lower levels of DHA in the membranes of the central nervous system (1,2). A meta-analysis has shown an approximately three-point higher IQ in breast-fed infants compared to formula-fed infants (3). Furthermore, studies on formula-fed infants have indicated beneficial effects of dietary DHA on visual acuity (4–6).

The DHA level of human milk varies by more than a factor of 10 among Danish mothers (7). This variation is caused primarily by differences in maternal fish intake. Intake of fish or marine oils has an acute effect on the DHA content of breast milk (8,9). Fish oil (FO) supplementation of the lactating mother will effectively increase breast-milk DHA levels (10–13).

At present there is insufficient scientific evidence to decide whether the variation in DHA level in breast milk has functional implications for the breast-fed infant. In small cross-sectional studies, associations between milk or blood levels of DHA and visual acuity or cognitive abilities in breast-fed infants have been observed (7,14). However, supplementing lactating mothers with n-3 LCPUFA has, so far, been shown to have no or only limited functional effects on infant visual acuity and mental development (15–17).

The primary aim of the present study was to examine whether FO supplementation of lactating mothers confers an advantage in the acuity performance of breast-fed infants above that provided by the habitual maternal diet. The secondary aim was to investigate how maternal FO supplementation influences the n-3 LCPUFA content of breast milk and how this in turn affects FA composition in infant erythrocytes (RBC). The relationship between infant RBC n-3 LCPUFA and visual acuity was also characterized. The study was designed as a double-blind intervention study, randomizing mothers with habitual fish intakes at levels less than values for the 50th percentile of the Danish National Birth Cohort (DNBC) to microencapsulated FO (1.5 g/d of n-3 LCPUFA) or olive oil (OO), starting in the first week after delivery and

lasting for 4 mon. A reference group of mothers with a high habitual fish intake and their infants was also included.

MATERIALS AND METHODS

Participants. The study protocol was approved by the Scientific-Ethical Committees for Copenhagen and Frederiksberg (KF 01-300/98), and all participants gave written consent to participate after the study had been explained to them.

Participants were selected from among women recruited for the ongoing DNBC (18). Women were recruited for the DNBC at the first antenatal visit to the general practitioner. If they consented to participate, they were interviewed by telephone twice during pregnancy. In the 25th week of gestation they were mailed a comprehensive self-administered, semiquantitative 300-item Food Frequency Questionnaire (FFQ), which questioned them about their diet for the 4 wk prior to completion of the questionnaire. An earlier version of the questionnaire has been validated (19). About 75% of the participants returned the questionnaire. The FFQ contained questions about fish intake for lunch (in Denmark as topping on bread) and dinner. Using assumptions of portion sizes and the nutrient content in foods (determined from the Danish Food tables by The Danish Food Agency, which contained comprehensive information on LCPUFA), we estimated consumption of the average daily intake of n-3 LCPUFA in grams using the program FoodCalc (www.foodcalc.dk). This provided the basis for a sampling of women with an expected low and high habitual consumption of n-3 LCPUFA.

During the December 1998 to November 1999 period, 11,179 women, countrywide, were recruited for DNBC. Only those pregnant Danish women living in the greater Copenhagen area who had a fish intake below the 50th percentile of the DNBC population (<0.4 g n-3 LCPUFA/d; the distribution in the DNBC was positively skewed, the 25th percentile being 0.3 g/d) were eligible to enter the present intervention trial. Women with a fish intake above the 74th percentile (>0.8 n-3 LCPUFA/d) were recruited for the reference group (HF-group). The average fish intake in the two subgroups of women eligible for the present study (<0.4 and >0.8 g n-3 LCPUFA/d) were 12.3 ± 8.2 and 55.2 ± 26.7 g/d, respectively. Over a period of 9 mon, 1473 women were invited in nine rounds (919 and 554 with fish intake <50th percentile and >74th percentile, respectively). Of these, 273 women responded to the invitation, of which 211 fit the other inclusion criteria and were recruited in their 8th month of gestation (147 and 64 with fish intake <50th and >74th percentile, respectively). Based on the previously observed association between milk DHA levels and infant visual acuity (7), the expected change in milk DHA in this intervention should result in a difference in visual acuity at 4 mon of 0.07 times the logarithm of the minimal angle of resolution (logMAR) (equivalent to 0.75 SD). We calculated that we needed 40 infants in each group in order to detect a difference of 0.75 SD in visual acuity (power = 80%, level of significance = 0.05). To allow for exclusions of infants not meeting our inclusion criteria and for dropouts of participants, our aim was to recruit 60 infants for each of the intervention groups.

The other inclusion criteria were that the recruited women had to have an uncomplicated pregnancy, prepregnancy body mass index (BMI) < 30 kg/m^2, and an absence of metabolic disorders. In addition, the participants were included in the study only if they, at the time of recruiting, had the intention to breast-feed for at least 4 mon. The newborns had to be healthy (no admission to a neonatal department), term (37–43 wks of gestation), singleton infants with normal weight for gestation (20) and have an Apgar score >7 at 5 min after delivery. Furthermore, we required that they be started on the supplements within 2 wks after birth. None of the recruited women took any types of oil supplements besides the ones given in the study. The participants were not given any dietary instructions. One hundred twenty-two and 53 women in the low- and high-fish-intake groups, respectively, fulfilled these criteria (see flow diagram of trial in Fig. 1 and characteristics of the participants in Table 1).

After birth, the women with fish intakes below the 50th percentile were randomly assigned to a supplementation group by a randomization schedule prepared by a person uninvolved in the study. Random block-wise allocation to the supplement groups was applied in blocks of two in five strata according to mean parental education (grouped in five categories according to the Official Danish Classification of Educations from 1994). Sixty-two and 60 women were allocated to the experimental group (FO group) and the control group (OO group), respectively. Investigators and families were blinded to the randomization until all data had been analyzed.

Supplements. For the first 4 mon of lactation, the experimental group was given 17 g/d of deodorized microencapsulated FO powder, containing 4.5 g of FO and 1.5 g of n-3 LCPUFA. The supplement dose aimed at making the total n-3 LCPUFA intake in the experimental group equivalent to the habitual intake of the women in the population with the highest fish intake (above the 90th percentile). The control group was given a similar amount of microencapsulated OO. To supply individual n-3 LCPUFA in relative amounts similar to the average Danish fish consumption, we used a 1:2 mixture of two different oils: a standard FO and a tuna oil with a low content of EPA (20:5n-3) (Dry n-3™ 18:12 and Dry n-3™ 5:25, respectively, from BASF Health and Nutrition A/S, Ballerup, Denmark) (see Table 2). The supplied FO and OO were microencapsulated and added to müsli bars (produced by Halo Foods Ltd., Tywyn Gwynedd, Wales, United Kingdom). The participants were instructed to consume two 35-g müsli bars daily, which supplied altogether 285 kcal and the intended doses oil. During the study period we ran out of bars and had to give the supplements in homemade cookies or as capsules; these alternatives were also offered if any of the women disliked the müsli bars. The homemade cookies were made at the department by kitchen personnel not otherwise involved in the study and contained the exact same amounts of microencapsulated oils as the müsli bars. Thus, with respect to formulation as well as blinding of mothers and investigators,

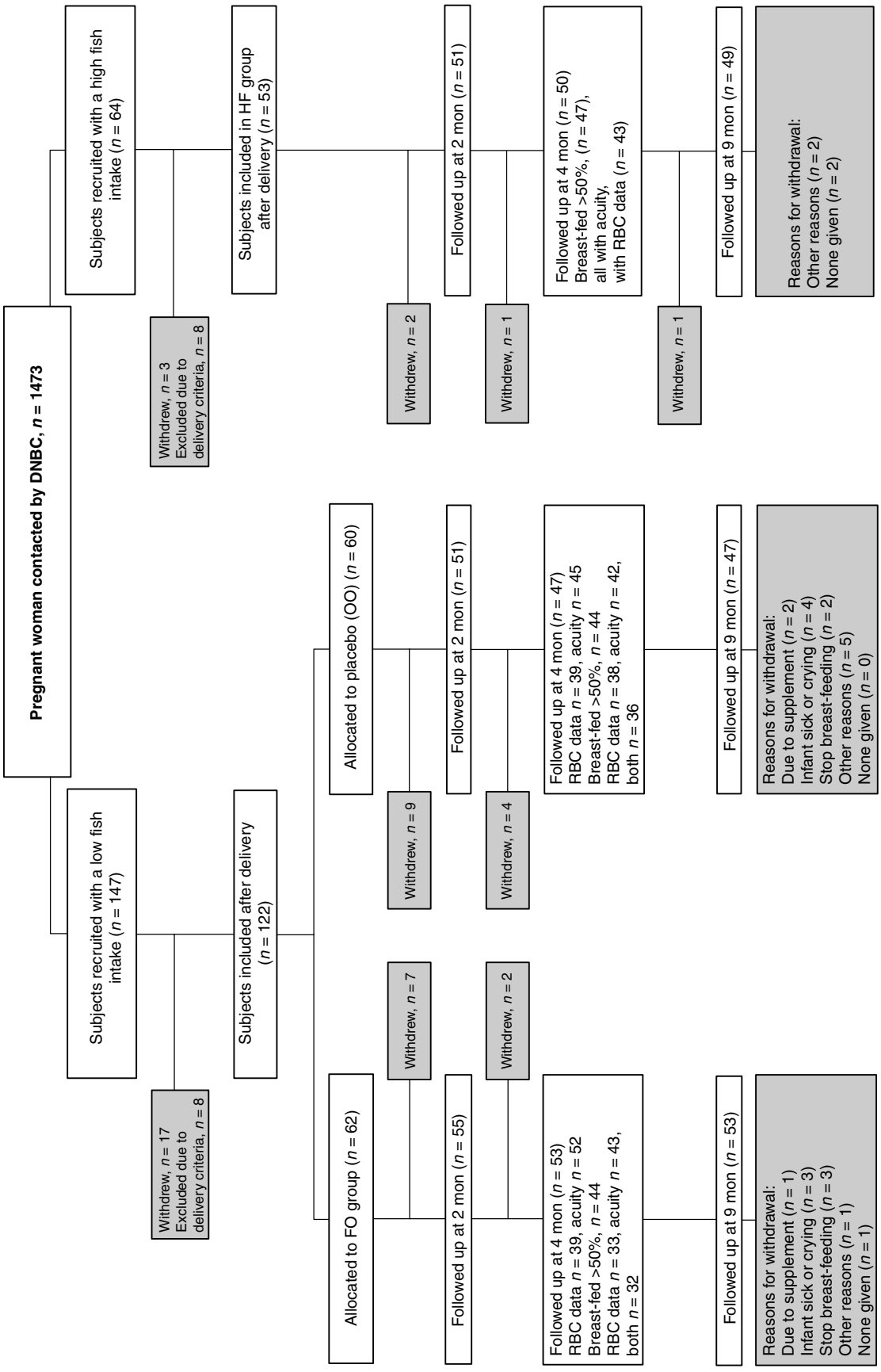

FIG 1. Trial profile summarizing participant flow, numbers of randomization assignments, interventions, and follow-up examinations for all groups. DNBC, Danish National Birth Cohort; FO, fish oil; OO; olive oil; HF group, group eating high amounts of fish; RBC, red blood cell.

TABLE 1
Characteristics of Study Infants and Parents[a]

	Olive oil supplement	Fish oil supplement	High fish
Included subjects (n)	60	62	53
Gender (*n*, male/female)	28:32	37:25	26:27
Cesarian deliveries (%)	10.0	9.7	5.7
Gestational age (wk)	40.1 ± 1.2	40.1 ± 1.1	40.2 ± 1.2
Birth weight (kg)	3.56 ± 0.41	3.60 ± 0.45	3.65 ± 0.44
Birth length (cm)[b]	52 ± 2	52 ± 2	53 ± 2
Head circumference at 1 wk (cm)	35.7 ± 1.5	36.1 ± 1.3	36.2 ± 1.6
Apgar score at 5 min[b]	9.9 ± 0.5	9.9 ± 0.3	10.0 ± 0.1
Siblings (*n*)[b]	0.6 ± 0.8	0.5 ± 0.7	0.7 ± 0.7
Maternal age (yr)	30.2 ± 4.1	29.6 ± 4.3[a]	31.9 ± 4.1
Maternal height (m)[b]	1.69 ± 0.06	1.67 ± 0.05[b,d]	1.71 ± 0.06
Pregravida BMI (kg/m^2)[b]	22.5 ± 2.7	22.5 ± 2.8	22.4 ± 3.0
Weight increase during pregnancy (kg)[c]	13.7 ± 5.1	13.4 ± 5.0	13.2 ± 4.0
Maternal smokers (%)	6.7	11.3	15.1
Maternal education score[b,d]	5.4 ± 1.2	5.3 ± 1.2	5.4 ± 1.3
Paternal height (m)[b]	1.80 ± 0.08[b]	1.82 ± 0.08	1.84 ± 0.06
Paternal smokers (%)	21.7	32.2	35.8
Paternal education score[b,d]	5.3 ± 1.3	5.3 ± 1.2	5.3 ± 1.6
Habitual n-6 PUFA intake (g/d)[b]	9.0 ± 3.3[c]	9.1 ± 3.6[c]	11.2 ± 3.8
Habitual n-3 LCPUFA intake (g/d)[b]	0.3 ± 0.3[c]	0.3 ± 0.3[c]	1.1 ± 0.6
Subjects completing 4 mon (*n*)	47	53	50
n-3 LCPUFA intake in lactation (g/d)[b]	0.3 ± 0.2[c]	1.5 ± 0.3[c,f]	0.9 ± 0.4[f]
Compliance (% taken of intended dose)	87 ± 9	88 ± 9	—
Exclusively breast-fed at 4 mon (%)	74.5	62.3	78.0
Estimated breast-milk intake during the 4 mon (% of total intake)[b,e]	93 ± 19	86 ± 28	93 ± 20
Infants breast-fed <50% (%)	6.4	17.0	6.0

[a]Data given as mean ± SD.
[b]Statistical comparison by nonparametric tests (Kruskal–Wallis and Mann–Whitney U-test). Nominal data tested with χ^2-test and all other data (not indicated by [b]) are compared by ANOVA and Bonferroni post hoc test. Superscript letters indicate the level of significance for statistical comparisons with the high fish group: a, $P < 0.05$; b, $P < 0.01$; or c, $P < 0.001$, or the OO-group: d, $P < 0.05$; e, $P < 0.01$; or f, $P < 0.001$.
[c]Gestational week 36.4 ± 1.54.
[d]Educational scores according to the Official Danish Classification of Educations from 1994. Highest rank (7) is equivalent to >18 yr of education, (6) 17–18 yr, (5) 15–16 yr, (4) 13–14 yr, (3) 11–12 yrs, (2) 10 yr, and (1) <10 yr of education.
[e]Estimated breast-milk intake as a percentage of total dietary intake assessed by their intake of infant formula and solid foods. BMI, body mass index; LCPUFA, long-chain PUFA; OO, olive oil.

cookies were similar to bars. For an approximately similar supplementation with capsules, the control group was given four 1000-mg OO capsules, and the experimental group was given six 500-mg low-EPA FO capsules plus one 1000-mg standard FO capsule (all capsules were a gift from Lupe/ProNova Biocare, Lysaker, Norway). Owing to the nonidentical appearance of the capsules for the two groups, a person who was not otherwise involved in the project handled the capsules in order to avoid breaking the blinding of the investigators. The distribution of müsli bars, cookies, and capsules among participants in the FO and OO groups was identical. Only 10% of the women got their entire supplementation as capsules, whereas 60% of the women only had müsli bars or cookies. The lower oil content in the capsules was taken into account in the calculation of overall supplement compliance. The overall self-reported compliance in both groups was on average 88% of the allocated number of müsli bars (SD = 9%, $n = 99$) during the entire 4 mon supplementation period.

TABLE 2
FA Composition[a] of Microencapsulated Oils Used for the Intervention

	Olive oil	Fish oil
Total SFA	13.6	30.2
Total MUFA	70.9	21.4
18:2n-6	7.4	1.3
20:4n-6	—	1.7
Total n-6 PUFA	7.4	4.0
18:3n-3	0.6	0.5
20:5n-3	—	10.0
22:5n-3	—	1.7
22:6n-3	—	22.8
Total n-3 PUFA	0.6	38.3

[a]FA values are based on GC analysis and are expressed as a percentage of total FA. SFA, saturated FA; MUFA, monounsaturated FA.

Protocol. At the pre-enrollment visit (in week 36.4 ± 1.5 of gestation, 4.0 ± 1.9 wk before birth, $n = 175$), demographic and social information was collected, including parental

education and a 10-mL blood sample for baseline analysis of the RBC FA composition. Within a week following the birth, the parents forwarded to us information about the delivery. Shortly thereafter, we visited the mothers in their homes [(9 ± 3 d after birth (n = 175)], gave them the supplements for the first two months of the intervention period (supplements for the last two months were dispensed at the 2-mon visit), measured the head circumference of the infant, and collected a breast-milk sample for baseline analysis of the milk FA composition.

Mothers and infants were assessed at 2 and 4 mon of age at the Research Department of Human Nutrition. At each assessment the infant was weighed and its length was measured. The mother delivered a breast-milk sample and was interviewed about her fish intake the previous day and for the past month. Fish intake during the intervention period was assessed with a fish frequency questionnaire similar to that used in the DNBC, and intake of n-3 LCPUFA was estimated in the same way as in the DNBC. The visual acuity of the infant was measured by swept visual evoked potential (SWEEP-VEP).

One hundred infant-mother pairs completed the first 4 mon of the intervention trial, and 50 mother-infant pairs from the HF-group were followed up at 4 mon (see Fig. 1). One hundred seven mothers complied with the criterion for exclusive breast-feeding for 4 mon. However, mothers who did not fulfill this criterion were not excluded from the trial or the analysis. Complementary food was introduced in the diet of five of the infants between 3 and 4 mon of age (mean age for complementary food introduction in the entire group of infants was 4.8 ± 1.0 mon). For infants not exclusively breast-fed at the end of the intervention, we estimated to what extent breast-milk covered their energy needs from the amount of formula and complementary food ingested. Thus, for 16 infants, breast-milk covered >90% of the intake, 75–90% for 9 infants, 50–75% for 3 infants, and 15 infants were estimated to be breast-fed <50%. Most of the infants who were breast-fed less than 50% during the 4-mon period were from the FO-group (nine vs. three from both the OO- and HF-group). The degree of breast-feeding was taken into account in the analysis of the outcome. The FA composition of RBC in infants breast-fed <50% is given separately, and visual acuity was analyzed as both intention-to-treat and for the mainly breast-fed alone. At the time of the study there were no LCPUFA-containing infant formulas on the Danish market, and the three most-used formulas had an n-6/n-3 FA ratio of approximately 10.

The mothers were asked to collect milk samples immediately after nursing their baby during the afternoon on the day before the visit at 1 wk and 2 and 4 mon. Milk samples (2–5 mL) were stored in the home at 5°C until they were collected no later than 30 h after expression [previous results had shown that this does not affect the FA composition of the breast-milk as compared to that in immediately frozen samples (Lauritzen, L., unpublished data)]. To 2-mL aliquots of the milk samples were then added 2 drops of 0.01% BHT from Sigma (St. Louis, MO), and aliquots were frozen at –80°C. All milk samples were analyzed within 1 yr after they had been taken.

From 4-mon-old infants, we collected a 500-μL blood sample by heel-prick, and from their mothers a 10-mL blood sample by venipuncture. All blood samples were collected in ice-cold EDTA-conditioned tubes. Immediately after sampling, RBC were separated from plasma and leukocytes and washed thrice in physiological saline. The isolated packed RBC were reconstituted 1:1 in physiological saline with 1 mM EDTA and 0.005% BHT and kept at –80°C until they were analyzed (maximum storage time was 8 mon).

FA analysis. Lipids from 1-mL aliquots of the milk samples were extracted according to Bligh and Dyer (21). Samples of 150 and 500 μL, respectively, of infant and maternal reconstituted RBC were hemolyzed in redistilled water, and the lipids were extracted by the Folch procedure (22). The extracted RBC lipids were methylated with BF_3 in methanolic NaOH, and milk lipids were methylated with KOH in methanol (23). The resulting FAME were extracted with heptane.

FAME from milk as well as from RBC were separated by G-LC on an HP-6890 Series II chromatograph (Hewlett-Packard Inc., Waldbronn, Germany) equipped with an FID and SP2380 capillary columns (30 and 60 m, respectively; i.d. 0.32 and 0.25 mm, respectively; and film thickness 0.2 μm; Supelco Inc., Bellefonte, PA). The milk FAME were injected using split mode (1:49) at 250°C. Initially, the oven temperature was set to 80°C for 3 min and then increased in three steps—to 110°C at 30°C/min, to 208°C at 3°C/min, and to 240°C at 50°C/min—and finally held at 240°C for 10 min before cool-down and injection of a new sample (total run time 46 min). Helium was used as carrier gas at a constant flow of 2 mL/min (pressure 10.7 psi, velocity 35 cm/s). All peaks from lauric acid (12:0) to DHA, except that of BHT, were integrated. RBC FAME-injections were run in split mode with a split ratio of 1:11. Injector and detector temperatures were 270°C. Initial oven temperature was 70°C for 0.5 min, and temperature programming was as follows: 15°C/min to 160°C, 1.5°C/min to 200°C, which was maintained for 15 min followed by a rate of 30°C/min to 225°C, which was maintained for 10 min. The carrier gas was helium at a constant flow of 1.2 mL/min (pressure was 25.0 psi).

The FAME peaks of the resulting chromatograms were tentatively identified from retention times of commercial standards (Nu-Chek-Prep Inc., Elysian, MN) as previously described (8). More than 97 and 99% of the chromatogram areas were identified in the milk- and RBC-FAME analyses, respectively. The FA composition of all samples was determined in duplicate, and in series of 8–18 samples. Each series contained a blank and a reference sample. The whole series was rejected if major FA in the reference sample deviated by more than 2 SD from the previously established mean values. The individual sample was reanalyzed if the relative difference (difference/mean) of major FA in the duplicates was appreciably increased relative to the typical deviation for that particular FA. The interassay variation (CV%) for DHA in milk and RBC was around 5%. The relative amounts of identified FA are given as a percentage of the overall identified FAME area (FA%).

Blood samples were obtained from 147 infants. Eighteen of the infant RBC samples were partly coagulated and thus excluded. An additional eight infant RBC samples had a higher relative content of saturated FA (SFA) and monounsaturated FA (MUFA) and a lower content of PUFA (n-6 and n-3 FA) than in the coagulated samples. All these samples deviated in SFA, MUFA, and PUFA content with >2 SD from the mean of all uncoagulated samples, being on average 58 ± 3, 27 ± 1, and 15 ± 4 (13 ± 3 n-6 PUFA and 1.9 ± 0.9 n-3 PUFA) FA%, respectively. These samples were also excluded, leaving 121 (81%) infants with successful determinations of RBC FA composition. Unfortunately, infants with excluded, coagulated, and missing RBC samples were not balanced between the groups, and the RBC FA analyses resulted in fewer successful determinations in the FO-group (74 vs. 83 and 86% in the OO-group and HF-group, respectively).

SWEEP-VEP visual acuity determination. Binocular visual acuity was assessed by SWEEP-VEP using the NuDiva system (24) equipped with an M2400 high-resolution monochrome monitor (Dotronix, Eau Claire, WI). Infants sitting on their parent's lap were presented with vertical sine-wave gratings at 80% contrast at a mean luminance of 47.6 cd. The gratings were contrast-reversed at a rate of 6.0 Hz, and the spatial frequency of the gratings was increased in 10 linear steps during the 10-s trial. Viewing distance and range of spatial frequencies depended on the age of the subject (for two 1-mon-olds it was 70 cm and 1.70–0.47 times the logMAR; for 4-mon-olds, 100 cm and 1.48–0.27 logMAR) (25). The infant's attention was attracted to the screen by small toys or bells, and trials were interrupted if the infant's gaze moved off the stimuli. Visual evoked potentials (VEP) were recorded with gold EEG electrodes attached to the scalp at five recording points (26). The EEG was amplified (gain 10.000–20.000) and Fourier-transformed to isolate the VEP. Visual acuity was estimated by extrapolating the VEP amplitude at 12 Hz vs. spatial frequency to zero amplitude (27). The signals from the individual trials and averages for each of the five channels were scored automatically by the NuDiva system (27) and checked manually for errors by one trained observer.

We aimed at five trials per session (more if the first five trials did not give 10 successful extrapolations), but in a few cases it was not possible to reach these predefined goals while the infant was attentive. The interassay variation of the SWEEP-VEP assessment of infant visual acuity is 23% (25). Visual acuity is given as the average of all obtained thresholds expressed as logMAR (the lower the logMAR, the better the acuity).

Statistical analysis. Nominal data were compared by χ^2-test for homogeneity. For other types of data, statistical group comparisons were performed with one-way ANOVA and a Bonferroni *post hoc* test or linear regression analysis and Pearson's correlation unless otherwise stated. Alternatively, nonparametric statistics (Kruskall–Wallis test, Mann–Whitney U-test, and Kendall's τ correlation) were applied if data did not agree with a Gaussian distribution (tested by the Kolmogorov–Smirnov test) with equal variances (Levene's test) or if data were in ordinal scale. Parametric statistical methods were used for results on visual acuity and RBC FA composition, whereas nonparametric tests had to be applied for most of the milk FA. All multiple linear regression analyses (milk-DHA vs. maternal n-3 LCPUFA intake, infant RBC-DHA vs. milk-DHA or maternal n-3 LCPUFA intake, and visual acuity vs. infant RBC-DHA or maternal n-3 LCPUFA intake) were performed as parametric analyses with initial inclusion of the explanatory factors maternal BMI, smoking, parity, and infant gestational age. If not significant, these factors were subsequently dropped from the model.

All statistical analyses were performed by SPSS (version 10.0, SPSS Inc., Chicago, IL). Quantitative results from separate groups are generally summarized as a mean ± SD.

RESULTS

The self-reported compliance in the two randomized groups was comparable, as were most of the subject characteristics (Table 1). The intervention resulted in an increase in the estimated total intake of n-3 LCPUFA in the FO-group from 0.3 to 1.5 g/d, equivalent to the highest habitual intakes in the population. Fish intake (expressed as intake of n-3 LCPUFA) in the OO-group remained low during lactation.

FA composition of breast milk. The DHA concentration of a milk sample taken 1 wk after delivery before the start of the intervention was associated with the estimated habitual n-3 LCPUFA intake (from fish) of the mother (r = 0.314, $P < 0.001$, n = 171). The DHA content of milk from women with high fish intake was on average 1.4 times as high as in the milk of those with the lower fish consumption (Table 3).

The FO intervention increased the relative content of DHA in the breast-milk at 2 and 4 mon of lactation (Table 3). The contents of all other n-3 LCPUFA also were increased in the milk of the FO-group, and the overall ratio of n-6 to n-3 FA was approximately 30% lower than that in the OO-group. The content of n-3 FA in the FO-group was similar regardless of supplement form (bars, cookies, or capsules; data not shown). The relative content of individual n-6 FA, including arachidonic acid, in the breast milk from the FO-supplemented women was not significantly lower than in the OO-group. The relatively higher content of n-3 LCPUFA corresponded to a relatively lower content of MUFA, primarily oleic acid. Overall, the differences in the milk FA composition between the FO- and OO-groups reflected the differences in FA composition of the supplements (Table 2). Mead acid (20:3n-9) was not detected in most of the milk, but very low levels (<0.05 FA%) were observed in 2% of the samples. Docosapentaenoic acid of the n-6 family (22:5n-6) was found in approximately half of the samples (47%) with a mean levels of 0.05 ± 0.05 FA%, more often in the FO-group than in the OO-group (data not shown).

The DHA concentration of a breast-milk sample after 4 mon of lactation also was associated with the estimated maternal intake of n-3 LCPUFA from the diet and the

TABLE 3
FA Composition[a] of Breast Milk from Mothers with a High Fish Intake and from Mothers with a Low Fish Intake, Who Were Supplemented with Olive Oil (OO) or Fish Oil (FO) During the First 4 mon of Lactation

	1 wk			2 mon			4 mon		
	OO	FO	High fish	OO	FO	High fish	OO	FO	High fish
n	57	60	52	51	50	48	45	46	47
Total SFA	42.74 ± 4.25	42.50 ± 4.64	43.35 ± 3.13	42.50 ± 4.22	44.80 ± 5.31^{d}	43.17 ± 3.74	42.71 ± 4.13	43.62 ± 4.61	42.51 ± 3.93
Total MUFA	42.58 ± 3.20	42.32 ± 3.14	41.60 ± 3.42	42.51 ± 3.45	39.15 ± 3.91^{a,f}	41.17 ± 3.06	42.38 ± 3.47	39.88 ± 3.96^{b,e}	42.29 ± 3.12
18:2n-6	9.74 ± 1.46	10.04 ± 1.98	9.73 ± 1.55	10.18 ± 1.59	10.06 ± 2.06	10.16 ± 1.42	11.09 ± 2.51	11.26 ± 2.36	10.67 ± 1.89
20:2n-6	0.40 ± 0.10	0.44 ± 0.10^{b,d}	0.39 ± 0.09	0.23 ± 0.04	0.23 ± 0.05	0.21 ± 0.06	0.22 ± 0.05	0.23 ± 0.04	0.22 ± 0.04
20:3n-6	0.46 ± 0.11	0.48 ± 0.14	0.47 ± 0.12	0.40 ± 0.06	0.38 ± 0.08	0.42 ± 0.08	0.33 ± 0.06	0.30 ± 0.07	0.33 ± 0.07
20:4n-6	0.74 ± 0.13	0.76 ± 0.16^{a}	0.70 ± 0.13	0.43 ± 0.09^{a}	0.44 ± 0.09^{a}	0.51 ± 0.20	0.48 ± 0.10	0.51 ± 0.09	0.50 ± 0.07
22:4n-6	0.18 ± 0.08	0.20 ± 0.08	0.17 ± 0.07	0.08 ± 0.07^{a}	0.12 ± 0.09^{e}	0.12 ± 0.09	0.08 ± 0.04	0.08 ± 0.03	0.07 ± 0.04
Total n-6 PUFA	11.71 ± 1.53	12.12 ± 2.10	11.67 ± 1.61	11.39 ± 1.63	11.31 ± 2.14	11.50 ± 1.51	12.36 ± 2.55	12.59 ± 2.46	11.99 ± 1.96
18:3n-3	1.11 ± 0.35	1.09 ± 0.38	1.19 ± 0.35	1.31 ± 0.33	1.29 ± 0.35	1.37 ± 0.35	1.25 ± 0.43^{b}	1.31 ± 0.47	1.50 ± 0.52
20:5n-3	0.17 ± 0.07^{c}	0.17 ± 0.05^{c}	0.23 ± 0.09	0.08 ± 0.08^{c}	0.28 ± 0.13^{c,f}	0.16 ± 0.12	0.13 ± 0.07^{c}	0.30 ± 0.14^{b,f}	0.22 ± 0.09
22:5n-3	0.25 ± 0.10^{c}	0.25 ± 0.08^{b}	0.31 ± 0.09	0.17 ± 0.10^{b}	0.29 ± 0.11^{b,f}	0.23 ± 0.11	0.22 ± 0.06^{c}	0.29 ± 0.10^{f}	0.28 ± 0.08
22:6n-3	0.67 ± 0.28^{c}	0.66 ± 0.23^{c}	0.91 ± 0.31	0.30 ± 0.36^{c}	1.16 ± 0.45^{c,f}	0.60 ± 0.30	0.41 ± 0.20^{c}	1.34 ± 0.67^{c,f}	0.74 ± 0.33
Total n-3 PUFA	2.21 ± 0.55^{c}	2.18 ± 0.51^{c}	2.64 ± 0.60	1.99 ± 0.53^{b}	3.16 ± 0.81^{c,f}	2.47 ± 0.76	2.00 ± 0.56^{c}	3.24 ± 0.95^{b,f}	2.74 ± 0.67
n-6/n-3	5.52 ± 1.21^{c}	5.74 ± 1.22^{c}	4.58 ± 0.99	6.06 ± 1.57^{c}	3.78 ± 1.12^{c,f}	5.00 ± 1.30	6.51 ± 1.77^{c}	4.22 ± 1.80^{a,f}	4.64 ± 1.43

[a]Data are given as mean ± SD. Individual FA are given as a percentage of total FA. Superscript letters indicate the level of significance for statistical comparisons with the high fish group: a, $P < 0.05$; b, $P < 0.01$; or c, $P < 0.001$, and the OO-group; d, $P < 0.05$; e, $P < 0.01$; or f, $P < 0.001$. For other abbreviations see Table 2.

FO-supplement (Kendall's τ; $r = 0.556$, $P < 0.001$, $n = 138$). The n-3 LCPUFA intake from the FO supplement, the estimated mean fish intake during lactation, and the estimated intake of fish within 24 h of milk sampling (all in g/d) were the only factors that were significantly associated with the DHA concentration in the milk sample (dependent variable log-transformed to approximate a Gaussian distribution, all with *P*-values of, at the most, 0.001). Maternal BMI, smoking, parity, and infant gestational age also were included in the analysis, but all were excluded in an automated backward multiple regression analysis, leaving only the estimated n-3 LCPUFA intake factors as significant determinants [with regression coefficients (*b*) of 0.38 ± 0.03, 0.25 ± 0.04, and 0.09 ± 0.02 per gram of n-3 LCPUFA from the FO supplement, habitual fish intake, and acute fish intake, respectively]. The model that included only these three significant factors explained 59% of the overall variance. In the FO-group, maternal BMI had a significant negative effect on the DHA level in milk after control for compliance (data not shown).

Acute influence from dietary n-3 LCPUFA accounted for some of the difference in the DHA content of milk at 2 and 4 mon of lactation between the FO- and HF-groups (Table 3). All milk samples in the FO-group were acutely affected by dietary n-3 LCPUFA as a result of the daily supplements. The DHA content of milk in the HF-group was 1.2 ± 0.4 FA% ($n = 6$) if the mother had eaten >1 g n-3 LCPUFA within 24 h before milk sampling.

FA composition of infant RBC. The FO-intervention exerted a pronounced effect on the FA composition of RBC of the mainly breast-fed infants at 4 mon (Table 4), and the levels of all n-3 FA were similar in all FO-supplement subgroups. The relative content of DHA in RBC membranes in the FO-group compared with the control group equaled an increase of almost 50%. In the FO-group, RBC-DHA and total n-3 PUFA were also significantly higher than in the HF-group. The ratio of n-6 to n-3 PUFA in RBC from infants in the FO-group was lower than that in the OO-groups, not only because of a high content of n-3 PUFA but also because of a low relative content of arachidonic acid and other n-6 LCPUFA. The differences in RBC FA composition between the FO- and OO-groups did not reflect the differences in supplement FA compositions to the same extent as the milk. The n-3 FA content in RBC of infants with an estimated low degree of breast-feeding (<50% of total intake) was significantly lower than that of the other infants, and the level of 20:3n-9 and the 22:5n-6/22:6n-3 and n-6/n-3 PUFA ratios were significantly higher (data not shown). The difference is probably attenuated by the fact that the majority of these infants were from the FO-group (6 out of 7). RBC levels of 20:3n-9 in infants in the FO-group were significantly higher than those in the OO-group when infants breast-fed <50% were excluded from the analysis.

Maternal RBC-DHA was 8.9 ± 1.3 FA% in the FO-group compared with 5.5 ± 1.0 FA% in the control group (t = –14.656, $P < 0.001$, $n = 98$). There was a strong association between maternal and infant RBC-DHA levels at 4 mon given that the degree of breast-feeding was >50% ($r_{(0,0)} = 0.961 \pm 1.550$, $P < 0.001$, $n = 113$). The DHA content of infant RBC was also

TABLE 4
FA Composition of Infant Erythrocytes at 4 mon of Age in the FO- and OO-Supplemented Groups and the Reference Group[a] (high fish)

	OO	FO	High fish
n	39	39	43
Total SFA	42.07 ± 2.79	41.99 ± 2.03	43.02 ± 3.03
Total MUFA	17.67 ± 2.18	17.16 ± 2.15	17.33 ± 1.85
Total PUFA	39.54 ± 4.76	40.19 ± 3.46	38.93 ± 4.59
20:3n-9	0.07 ± 0.06	0.05 ± 0.06	0.06 ± 0.06
18:2n-6	8.55 ± 0.85	8.43 ± 1.10	8.11 ± 0.89
20:3n-6	1.92 ± 0.36	1.73 ± 0.32	1.81 ± 0.33
20:4n-6	16.18 ± 2.38	14.86 ± 1.67[d]	15.40 ± 2.20
22:4n-6	2.92 ± 0.59[c]	2.30 ± 0.45[f]	2.45 ± 0.53
22:5n-6	0.60 ± 0.19[c]	0.52 ± 0.10[a,d]	0.42 ± 0.14
Total n-6 PUFA	30.49 ± 3.01[b]	28.17 ± 2.16[e]	28.51 ± 3.07
20:5n-3	0.54 ± 0.24[b]	1.21 ± 0.58[b,f]	0.88 ± 0.37
22:5n-3	2.06 ± 0.49	1.96 ± 0.36	2.04 ± 0.40
22:6n-3	6.29 ± 1.71[a]	8.72 ± 2.40[b,f]	7.33 ± 1.55
Total n-3 PUFA	8.98 ± 2.31[a]	11.97 ± 3.03[a,f]	10.36 ± 2.14
n-6/n-3	3.64 ± 1.02[b]	2.65 ± 1.31[f]	2.86 ± 0.58
22:5n-6/22:6n-3	0.10 ± 0.04[b]	0.07 ± 0.06[c,f]	0.06 ± 0.02

[a]Individual FA are given as a percentage of total FA in erythrocyte membranes. Data are given as mean ± SD. Superscript letters indicate the level of significance for statistical comparisons with the high fish group: a, $P < 0.05$; b, $P < 0.01$; or c, $P < 0.001$, or the OO-group: d, $P < 0.05$; e, $P < 0.01$; or f, $P < 0.001$.

associated with the DHA content of breast milk (Kendall's τ, $r = 0.416$, $P < 0.001$, $n = 115$), as well as with the estimated maternal n-3 LCPUFA intake during lactation (Kendall's τ, $r = 0.550$, $P < 0.001$, $n = 138$). The association between breast-milk DHA and DHA in infant RBC seemed to follow a saturation curve. Linear regression analysis between the log-transformed DHA concentration of the milk and infant RBC-DHA showed that infant DHA intake as assessed by a single milk sample alone explained approximately 30% of the variation in infant RBC-DHA (Fig. 2). However, more variation was accounted for in a multiple regression analysis with the DHA level of infant RBC vs. the two factors that contribute to the maternal n-3 LCPUFA intake during lactation, that from fish ($b = 1.64 \pm 0.33$ per g/d, $P < 0.001$), and that from the FO-supplement ($b = 2.99 \pm 0.33$ in FO relative to OO, $P < 0.001$), and the extent to which it was transferred to the infant *via* breast milk expressed as the degree of breast-feeding ($b = 0.06 \pm 0.01$ per % increase in estimated breast milk intake, $P < 0.001$). These factors explained 46% of the variation.

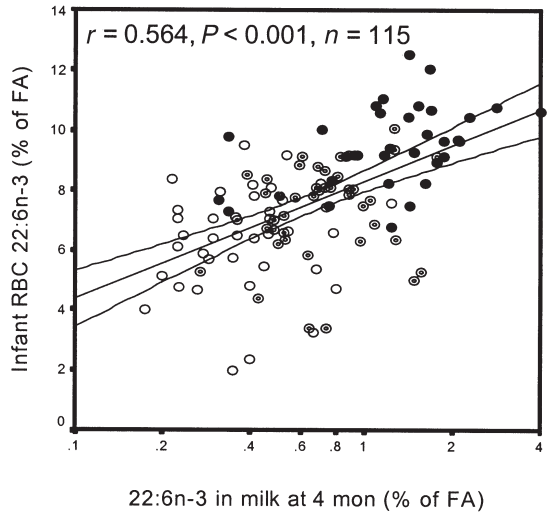

FIG. 2. Association between DHA in infant RBC and a breast-milk sample at 4 mon of age. Symbols indicate whether the mother was supplemented with fish oil (●) or olive oil (○) during the 4 mon of lactation or whether she had a habitual high intake of fish (⊙). The linear regression line is drawn in the plot with 95% confidence intervals. All data were included in the figure. For abbreviation see Figure 1.

Visual acuity of the infants. SWEEP-VEP acuity was determined successfully in 85 and 98% of the 2- and 4-mon-old infants, respectively. Infants with successful SWEEP-VEP acuity determinations were given an average of 5.9 ± 1.9 and 4.8 ± 1.4 trials at the 2- and 4-mon assessment, respectively, which resulted in an average of 12.4 ± 6.8 and 18.1 ± 6.6 scores per session ($n = 133$ and 147), respectively. There was no effect of FO supplementation on visual acuity of the infants at either 2 and 4 mon of age, neither in the intention-to-treat analysis of all infants, those who successfully completed both SWEEP-VEP examinations (Table 5), nor in infants breast-fed more than 50% (data not shown). Furthermore, there was no significant difference between groups in the increase in visual acuity from 2 to 4 mon (data not shown).

TABLE 5
Visual Acuity of the Infants at 2 and 4 mon of Age[a]

	OO	FO	High fish
VEP at 2 mon			
Exact age (wk)	8.27 ± 0.46	8.18 ± 0.48	8.32 ± 0.47
n attempted recorded	50	48	49
n with no implemented trials[b]	1	4	0
n with no extrapolations[c]	3	6	4
n successful	46	42	45
Hereof with 4 mon VEP[d]	40	41	45
Mean acuity	0.84 ± 0.08	0.84 ± 0.09	0.82 ± 0.08
VEP at 4 mon			
Exact age (wk)	17.21 ± 0.50	17.09 ± 0.49	17.35 ± 0.66
n attempted recorded	46	52	50
n with no implemented trials[b]	1	0	0
n with no extrapolations[c]	0	0	0
n successful	45	52	50
Hereof with 2 mon VEP[d]	40	41	45
Mean acuity	0.64 ± 0.09	0.62 ± 0.08	0.63 ± 0.09

[a]Visual acuity was measured by swept visual evoked potential. Individual visual acuities were calculated as the mean of all obtained estimates of visual acuity. Data are based on an intention-to-treat analysis including those who were not exclusively breast-fed. The mean visual acuity in each of the supplement groups is expressed as the logarithim of the minimal angle of resolution and given as mean ± SD. None of the values was significantly different from one another.
[b]Too much noise to complete the 10-s trials.
[c]Signal-to-noise ratio too low to make significant extrapolations to threshold. For abbreviations see Table 3.
[d]Mean activities at 2 and 4 mon are given only for infants with successful VEP determinations at both ages.

We measured a clear improvement in visual acuity with age in all groups (Table 5). At the individual level, there was only a weak tendency toward tracking in visual acuity between the two examinations [i.e., infants with a high (or low) visual acuity at 2 mon tended also to have a high (or low) value at 4 mon, Kendall's τ, $r = 0.11$, $P = 0.14$, $n = 81$]. Furthermore, there was no detectable association between visual acuity and the exact age at testing (at 4 mon Kendall's τ, $r = –0.05$, $P = 0.51$, $n = 97$). Maternal prepregnancy BMI was positively associated with infant visual acuity (at 4 mon Kendall's τ, $r = –0.15$, $P = 0.03$, $n = 97$). The degree of breast-feeding was also associated with infant visual acuity at 4 mon of age (inverse to the expected, and based on a limited number of infants breast-fed <50%) (Kendall's τ, $r = 0.15$, $P = 0.04$, $n = 97$). There was no significant association between visual acuity at 2 or 4 mon and maternal smoking habits, level of education, gestational age, birth weight, head circumference, number of siblings, or gender in this homogeneous group of breast-fed infants. Visual acuity was not univariately associated with the estimated maternal n-3 LCPUFA intake (neither habitual intake from fish, total intake, nor FO supplementation) or with the DHA concentration of breast milk (data not shown). Also, there was no univariate association between infant visual acuity at any age and maternal or infant RBC-DHA at 4 mon (Kendall's τ, $r = –0.09$, $P = 0.20$, $n = 145$ and $r = –0.12$, $P = 0.06$, $n = 119$, respectively, at 4 mon).

Figure 3 shows a plot of bivariate association between infant visual acuity at 4 mon of age and infant RBC-DHA at 4 mon. There was no association between these parameters in the randomized part of the study. In the OO-group there was a near-significant association between visual acuity and infant RBC levels of DHA ($r = –0.309$, $P = 0.059$, $n = 38$). There was no detectable association in the FO-group, which in that respect was similar to the reference group (Fig. 3). However, five of the infants (from the FO- and HF-groups) had visual acuities below that of the average 2-mon-old infants, possibly being erroneous determinations (although we lacked clear exclusion criteria).

The association between infant RBC-DHA and visual acuity was explored by a multiple regression analysis. The degree of breast-feeding was included as a confounding factor in this analysis because it was associated with infant RBC-DHA and has also in previous studies been shown to influence visual acuity (5). Maternal prepregnancy BMI, parity, gestational age, and gender were included as potential confounding factors in the analysis; all but gestational age and parity were excluded in the final model as they did not reach statistical significance in the model. The latter three factors were included because they affected most aspects of infant development: Maternal BMI was significantly associated with visual acuity and breast-milk DHA in the FO-group; gestational age and parity could also in theory influence DHA levels in breast milk and infant RBC; and the sex was unequally distributed between the two randomized groups. This multiple regression analysis showed that infant RBC-DHA was a major determinant of visual acuity in the randomized groups (Table 6). A similar multiple regression analysis was performed with maternal n-3 LCPUFA intake divided in an FO-part and a habitual part, but neither of these was significantly associated with infant visual acuity (data not shown). Simultaneous inclusion of infant RBC-DHA and a group variable (FO vs. OO) in the multiple analyses showed no significant effect of the FO supplement.

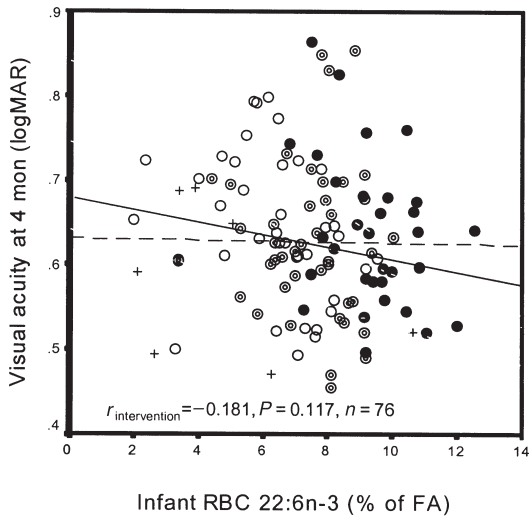

FIG. 3. Association between visual acuity and DHA level in infant RBC at 4 mon of age. Visual acuity, measured as the mean of all thresholds obtained by swept visual evoked potential, is given as the logarithm of the minimal angle of resolution (logMAR). Symbols indicate maternal supplementation with fish oil (●) or olive oil (○) during the 4 mon of lactation, or a habitual high maternal intake of fish (◎) or if the infants had an estimated breast-milk intake of <50% of their diet (+). Regression lines were calculated separately for the high-fish reference (dashed line) and the randomized groups (solid line) (with all infants included irrespective of degree of breast-feeding). For abbreviations see Figure 1.

DISCUSSION

Biochemical outcomes. The FO supplement had a pronounced effect on the DHA content of breast milk, as previously shown (10–13). The effect of FO appeared to be larger (per g) than that caused by the habitual and acute intake of fish. However, this does not necessarily translate into n-3 LCPUFA in FO being more biologically effective than those from fish, as there are some differences to consider. The FO supplement

TABLE 6
Multiple Regression Analysis of Associations with Infant Visual Acuity (logarithm of the minimal angle of resolution)[a]

Factor	Coefficient	*P*
Infant RBC DHA (FA%)	–0.011 ± 0.004	0.008
Degree of breast-feeding (% of nutrition)	0.001 ± 0.000	0.013
Gestational age (wk)	0.024 ± 0.007	0.001
No. of siblings	–0.024 ± 0.011	0.029

[a]The regression was performed on all data for the intervention groups with inclusion of all mentioned factors ($n = 76$). The table gives regression coefficients and *P*-values for significant factors. This model explained 24% (adjusted r^2) of the overall variance in visual acuity.

was taken daily, and in that respect should be considered a habitual as well as an acute dietary factor. Results from our previous study indicated that acute fish intake could exert greater influence than the habitual (8). However, in a study like this, the effects of habitual and acute fish intake are difficult to separate as the probability of obtaining an acutely affected milk sample is higher in women eating more fish owing to the higher frequency of fish intake. Furthermore, calculating the n-3 LCPUFA intake from fish relies on a series of assumptions and uncertainties, whereas the intake of n-3 LCPUFA from FO is known with respect to FA composition as well as dose. We did not determine the total fat intake of the women or their intake of n-6 PUFA, which, *via* dilution and competition, may be an important factor in explaining some of the unaccounted variance observed in the effect of n-3 LCPUFA from fish and FO on milk DHA levels.

Infant RBC-DHA content was also greatly increased by the FO-supplement, in agreement with previous reports (13,15,16). Infant RBC-DHA at 4 mon of age was associated with the current breast-milk DHA content. Owing to fluctuations in milk DHA levels with the acute fish intake of the mother (8), a single milk sample provides only a very rough estimate of infant DHA intake. As in adults (28,29), infant RBC-DHA will reflect the intake of the infant over the past months. This study showed a strong agreement between maternal and infant RBC-DHA levels at 4 mon. This association was stronger than the association between infant RBC-DHA and milk DHA levels. Multiple regression analysis showed that infant RBC-DHA was associated with the estimated maternal n-3 LCPUFA intake during lactation, habitual as well as from the supplement, and the degree of breast-feeding. Thus, infant RBC-DHA at 4 mon seems to reflect infant DHA intake during the lactation period.

Maternal FO-supplementation resulted in a significant decrease in the infant RBC arachidonic acid level. However, the level of arachidonic acid in the RBC of the infants in the FO-group was only about 0.5 SD lower than in the OO-group but was considerably higher than that in infants who were breast-fed less than 50%. In our opinion, this slight decrease in RBC arachidonic acid level should not have any adverse effects on infant development or growth (6).

Functional outcome. We could not show any direct effect of the FO-supplement on infant visual acuity at either 2 or 4 mon of age. However, visual acuity at 4 mon tended to be associated with current infant—as well as maternal—RBC-DHA levels. The association between visual acuity and RBC-DHA was strengthened if controlled for sex, degree of breast-feeding, parity, and maternal BMI, making infant RBC-DHA one of the most significant determinants of infant visual acuity.

Despite the large difference in infant RBC-DHA levels between the OO- and FO-groups, the association between infant RBC-DHA and visual acuity was not reflected in differences in visual acuity between the randomized groups. This could not be explained by accidental differences in other factors (e.g., more primiparous, boys, infants with a low degree of breast-feeding, slightly younger age at testing in the FO-group) nor by possibly erroneously determined low visual acuities (data not shown). Based on the regression line in Figure 3 (or the regression coefficient in Table 6), we estimate that a change in infant RBC-DHA levels from 6.3 to 9.4 FA% should give rise to a difference in visual acuity of roughly around 0.03 logMAR.

However, the SE is about 0.018 logMAR, based on the variations observed in the present study. Therefore, it is not in disagreement with the estimated regression effect of infant RBC-DHA on visual acuity to observe (by chance) no direct intervention effect on visual acuity (i.e., a type II error). The regression has higher power because it also uses the information available in the natural variation in infant RBC-DHA, besides that created by the intervention. The high power of our intervention study for detecting differences in infant RBC-DHA is transformed by the flat regression line to a much lower power for detecting differences in visual acuity (based on post hoc computation). To detect a 0.03 logMAR difference in visual acuity (about 1/3 SD; see Table 5) a study with a power of 80% would require about 140 subjects in each group. The detection of differences in visual acuity of this magnitude is limited by the high CV% of the SWEEP-VEP method (25).

It was not possible to detect an effect of the n-3 LCPUFA of fish oil in multiple regression analyses where this was included in combination with either habitual maternal intake of n-3 LCPUFA, maternal RBC-DHA in pregnancy (as a proxy for the maternal intake of n-3 LCPUFA in the last trimester of pregnancy), or infant RBC-DHA. Infant visual acuity tended to be associated with pre- as well as postintervention RBC levels of DHA of the mothers of the randomized part of the study. This indicates that the association between infant RBC-DHA and visual acuity at 4 mon of age could be secondary to some other association or possibly caused by intrauterine effects of maternal n-3 LCPUFA intake or some dietary or sociocultural factor associated with maternal fish intake. However, the estimated maternal n-3 LCPUFA intake in the OO-group, which contributed most to the association, was not affected by the intervention. Also, there was no significant n-3 LCPUFA-independent effect of fish oil in multiple regression analyses including a group variable (FO vs. OO) and biomarkers of the n-3 LCPUFA intake during lactation (infant or maternal RBC-DHA levels at 4 mon, $P = 0.23$ and $P = 0.068$, respectively). Furthermore, if the observed association had been caused by prenatal factors, we would have expected the regression analysis to give regression coefficients of the same magnitude in the two randomized groups, but with a lower constant in the FO-group. However, the association in the FO-group was like that in the HF-group, indicating that the FO-supplement affected infant visual acuity independent of the RBC level of DHA and that infants in these two groups with respect to visual maturation had optimal levels of RBC-DHA.

The Danish population has a higher fish intake than that in many other countries (30), and this is also reflected in its relatively high RBC DHA content. It is possible that the habitual

fish intake in the randomized trial was close to optimal and that the FO supplementation would have had a larger effect in a population with a lower fish intake. A further limitation of this trial was that not all of the infants were exclusively breast-fed for the entire intervention period. Finally, we aimed at making a perfectly double-blinded trial by adding the supplements in müsli bars and cookies. This was not achieved, however, as some of the subjects were given capsules. Although these subjects were in theory still blinded, it is in most cases possible to taste if one receives FO capsules, which is a limitation in all studies using FO-capsules. This is a potential problem, as one could suspect that the control group might take fish oil if they knew that they were not in the FO-group. However, RBC-DHA and milk DHA (and the SD of these) did not differ between subjects given olive oil as müsli bars and subjects given capsules. Also, RBC-DHA values decreased for all mothers in the OO-group during the intervention.

Two cross-sectional studies have shown an association between visual acuity and breast-milk or infant RBC-DHA levels in subjects with mean milk DHA levels lower than that of the OO-group of this study (both around 0.3 FA%) (7,22). In these studies the observed change in visual acuity at 4 mon of age was between 0 and 0.1 logMAR with changes in milk DHA within the range of 0.1–0.8 FA%. In one of the studies, the association between RBC-DHA and visual acuity was only observed at some of the tested ages (22). Two previous maternal DHA supplementation trials did not show any effects on infant visual acuity in populations with lower baseline levels of milk DHA than the mothers in the present study (16,17). However, one of these trials gave only very small DHA supplements (17) and the other had very few infants with a successful VEP-acuity measure (16). It is therefore our opinion that neither the present nor any of the previous studies provide any solid evidence as to whether the DHA intake of breast-fed infants is of any importance for their visual development.

The estimated maternal n-3 LCPUFA intake during lactation was a strong determinant of the infant RBC-DHA level. Maternal FO supplementation increased the level of DHA and other n-3 LCPUFA in human milk as well as infant RBC. Maternal FO-supplementation during lactation did not enhance visual acuity of those infants who successfully completed the visual assessments. However, the results showed that RBC-DHA was an important determinant of visual acuity. Thus, the results from this study indicate that variation in breast-milk n-3 LCPUFA may have implications for the visual development of breast-fed infants. If this is to be determined conclusively, larger intervention studies in mothers with a very well defined low habitual fish intake are needed.

ACKNOWLEDGMENTS

We gratefully acknowledge dietitian Majken Ege and pediatric nurses Charlotte Mester and Heidi Eismark for collecting the data and technicians Sidsel Abildgaard Jensen, Bettina Sørensen, and Grete Peitersen for performing the FA analyses. This study was financed by FØTEK—The Danish Research and Development Program for Food and Technology and BASF Aktiengesellschaft.

REFERENCES

1. Farquharson, J., Cockburn, F., Patrick, W.A., Jamieson, E.C., and Logan, R.W. (1992) Infant Cerebral Cortex Phospholipid Fatty-Acid Composition and Diet, *Lancet 340,* 810–813.
2. Byard, R.W., Makrides, M., Need, M., Neumann, M.A., and Gibson, R.A. (1995) Sudden Infant Death Syndrome: Effect of Breast and Formula Feeding on Frontal Cortex and Brainstem Lipid Composition, *J. Paediatr. Child Health 31,* 14–16.
3. Anderson, J.W., Johnstone, B.M., and Remley, D.T. (1999) Breast-Feeding and Cognitive Development: A Meta-analysis, *Am. J. Clin. Nutr. 70,* 525–535.
4. SanGiovanni, J.P., Parra-Cabrera, S., Colditz, G.A., Berkey, C.S., and Dwyer, J.T. (2000) Meta-Analysis of Dietary Essential Fatty Acids and Long-Chain Polyunsaturated Fatty Acids as They Relate to Visual Resolution Acuity in Healthy Preterm Infants, *Pediatrics 105,* 1292–1298.
5. SanGiovanni, J.P., Berkey, C.S., Dwyer, J.T., and Colditz, G.A. (2000) Dietary Essential Fatty Acids, Long-Chain Polyunsaturated Fatty Acids, and Visual Resolution Acuity in Healthy Fullterm Infants: A Systematic Review, *Early Hum. Dev. 57,* 165–188.
6. Lauritzen, L., Hansen, H.S., Jørgensen, M.H., and Michaelsen, K.F. (2001) The Essentiality of Long-Chain n-3 Fatty Acids in Relation to Development and Function of the Brain and Retina, *Prog. Lipid Res. 40,* 1–94.
7. Jørgensen, M.H., Hernell, O., Hughes, E., and Michaelsen, K.F. (2001) Is There a Relation Between Docosahexaenoic Acid Concentration in Mother's Milk and Visual Development in Term Infants? *J. Pediat. Gastroenterol. Nutr. 32,* 293–296.
8. Lauritzen, L., Jorgensen, M.H., Hansen, H.S., and Michaelsen, K.F. (2002) Fluctuations in Human Milk Long-Chain PUFA Levels in Relation to Dietary Fish Intake, *Lipids 37,* 237–244.
9. Francois, C.A., Connor, S.L., Wander, R.C., and Connor, W.E. (1998) Acute Effects of Dietary Fatty Acids on the Fatty Acids of Human Milk, *Am. J. Clin. Nutr. 67,* 301–308.
10. Henderson, R.A., Jensen, R.G., Lammi Keefe, C.J., Ferris, A.M., and Dardick, K.R. (1992) Effect of Fish Oil on the Fatty Acid Composition of Human Milk and Maternal and Infant Erythrocytes, *Lipids 27,* 863–869.
11. Makrides, M., Neumann, M.A., and Gibson, R.A. (1996) Effect of Maternal Docosahexaenoic Acid (DHA) Supplementation on Breast-Milk Composition, *Eur. J. Clin. Nutr. 50,* 352–357.
12. Helland, I.B., Saarem, K., Saugstad, O.D., and Drevon, C.A. (1998) Fatty Acid Composition in Maternal Milk and Plasma During Supplementation with Cod Liver Oil, *Eur. J. Clin. Nutr. 52,* 839–845.
13. Jensen, C.L., Maude, M., Anderson, R.E., and Heird, W.C. (2000) Effect of Docosahexaenoic Acid Supplementation of Lactating Women on the Fatty Acid Composition of Breast Milk Lipids and Maternal and Infant Plasma Phospholipids, *Am. J. Clin. Nutr. 71,* 292S–299S.
14. Scott, D.T., Janowsky, J.S., Carroll, R.E., Taylor, J.A., Auestad, N., and Montalto, M.B. (1998) Formula Supplementation with Long-Chain Polyunsaturated Fatty Acids: Are There Developmental Benefits? *Pediatrics 102,* E591–E593.
15. Helland, I.B., Saugstad, O.D., Smith, L., Saarem, K., Solvoll, K., Ganes, T., and Drevon, C.A. (2001) Similar Effects on Infants of n-3 and n-6 Fatty Acids Supplementation to Pregnant and Lactating Women, *Pediatrics 108,* U23–U32.
16. Gibson, R.A., Neumann, M.A., and Makrides, M. (1997) Effect of Increasing Breast Milk Docosahexaenoic Acid on Plasma and Erythrocyte Phospholipid Fatty Acids and Neural Indices of Exclusively Breast Fed Infants, *Eur. J. Clin. Nutr. 51,* 578–584.
17. Jensen, C.L., Prager, T.C., Zou, Y., Fraley, J.K., Maude, M., Anderson, R.E., and Heird, W.C. (1999) Effects of Maternal Docosahexaenoic Acid Supplementation on Visual Function and Growth of Breast-Fed Term Infants, *Lipids 34,* S225.

18. Olsen, J., Melby, M., Olsen, S.F., Sorensen, T.I., Aaby, P., Andersen, A.M., Taxbol, D., Hansen, K.D., Juhl, M., Schow, T.B., *et al.* (2001) The Danish National Birth Cohort—Its Background, Structure and Aim, *Scand. J. Public Health 29,* 300–307.
19. Tjønneland, A., Overvad, K., Haraldsdottir, J., Bang, S., Ewertz, M., and Jensen, O.M. (1991) Validation of a Semiquantitative Food Frequency Questionnaire Developed in Denmark, *Int. J. Epidemiol. 20,* 906–912.
20. Greisen, G., and Michaelsen, K.F. (1989) Perinatal Vækst, *Ugeskr. Læger 151,* 1813–1816.
21. Bligh, E.G., and Dyer, W.J. (1959) A Rapid Method of Total Lipid Extraction and Purification, *Can. J. Biochem. Physiol. 37,* 911–917.
22. Innis, S.M., Gilley, J., and Werker, J. (2001) Are Human Milk Long-Chain Polyunsaturated Fatty Acids Related to Visual and Neural Development in Breast-Fed Term Infants? *J. Pediatr. 139,* 532–538.
23. Christopherson, S.W., and Glass, R.L. (1969) Preparation of Milk Fat Methyl Esters by Alcoholysis in an Essentially Nonalcoholic Solution. *J. Dairy Sci. 52,* 1289–1290.
24. Norcia, A.M., and Tyler, C.W. (1985) Infant VEP Measurements: Analysis of Individual Differences and Measurement Error, *Electroencephalogr. Clin. Neurophysiol. 61,* 359–369.
25. Lauritzen, L., Jørgensen, M.H., and Michaelsen, K.F. (2004) Test–Retest Reliability of Swept Visual Evoked Potential Measurements of Infant Visual Acuity and Constrast Sensitivity, *Pediatr. Res. 55,* 701–708.
26. Jørgensen, M.H., Hølmer, G., Lund, P., Hernell, O., and Michaelsen, K.F. (1998) Effect of Formula Supplemented with Docosahexaenoic Acid and γ-Linolenic Acid on Fatty Acid Status and Visual Acuity in Term Infants, *J. Pediatr. Gastroenterol. Nutr. 26,* 412–421.
27. Norcia, A.M., Clarke, M., and Tyler, C.W. (1985) Digital Filtering and Robust Regression Techniques for Estimating Sensory Thresholds from the Evoked Potential, *IEEE Eng. Med Biol. Mag. 4,* 26–32.
28. Olsen, S.F., Hansen, H.S., Sandstrom, B., and Jensen, B. (1995) Erythrocyte Levels Compared with Reported Dietary Intake of Marine n-3 Fatty Acids in Pregnant Women, *Br. J. Nutr. 73,* 387–395.
29. Prisco, D., Filippini, M., Francalanci, I., Paniccia, R., Gensini, G.F., Abbate, K., and Neri Serneri, G.G. (1996) Effect of n-3 Polyunsaturated Fatty Acid Intake on Phospholipid Fatty Acid Composition in Plasma and Erythrocytes, *Am. J. Clin. Nutr. 63,* 925–932.
30. Welch, A.A., Lund, E., Amiano, P., Dorronsoro, M., Brustad, M., Kumle, M., Rodriguez, M., Lasheras, C., Janzon, L., and Jansson, J. (2002) Variability of Fish Consumption Within the 10 European Countries Participating in the European Investigation into Cancer and Nutrition (EPIC) Study, *Public Health Nutr. 5,* 1273–1285.

[Received June 19, 2003; accepted February 26, 2004]

Modulation of Renal Injury in *pcy* Mice by Dietary Fat Containing n-3 Fatty Acids Depends on the Level and Type of Fat

Deepa Sankaran[a], Jing Lu[b], Neda Bankovic-Calic[a], Malcolm R. Ogborn[a], and Harold M. Aukema[a,*]

[a]University of Manitoba, Winnipeg, Manitoba, R3T 2N2 Canada, and [b]Texas Women's University, Denton, Texas 76383

ABSTRACT: Low-fat diets and diets containing n-3 fatty acids (FA) slow the progression of renal injury in the male Han:Sprague-Dawley (SPRD)-*cy* rat model of polycystic kidney disease. To determine whether these dietary fat effects are similar in females and in another model of renal cystic disease, in this study we used both male and female *pcy* mice to examine the effects of fat level and type on disease progression. Adult *pcy* mice were fed 4, 10, or 20 g soybean oil/100 g diet for 130 d in study 1. In study 2, weanling *pcy* mice were fed high or low levels of fat rich in 18:2n-6 (corn oil, CO), 18:3n-3 (flaxseed oil/CO 4:1 g/g, FO), or 22:6n-3 (algal oil/CO 4:1 g/g, DO) for 8 wk. In adult *pcy* mice, low- compared with high-fat diets lowered kidney weights (2.4 ± 0.2 vs. 3.1 ± 0.2 g/100 g body weight, $P = 0.006$) and serum urea nitrogen (SUN) (9.6 ± 0.6 vs. 11.9 ± 0.6 mmol/L, $P = 0.009$), whereas in young *pcy* mice it reduced renal fibrosis volumes (0.44 ± 0.04 vs. 0.62 ± 0.04 mL/kg body weight, $P < 0.0001$). FO feeding in young *pcy* mice mitigated the detrimental effects of high fat on fibrosis while not altering kidney size, function, and oxidative damage when compared with the CO-fed mice. In contrast, DO- compared with CO-fed mice had higher kidney weights (2.64 ± 0.07 vs. 2.24 ± 0.08 g/100 g body weight, $P = 0.005$), SUN (9.4 ± 0.57 vs. 7.0 ± 0.62 mmol/L, $P < 0.0001$), and cyst volumes (7.9 ± 0.28 vs. 6.2 ± 0.30 mL/kg body weight, $P < 0.0001$) and similar levels of oxidative damage and fibrosis. The FA compositions of the diets were reflected in the kidneys: 18:2n-6, 18:3n-3, and 22:6n-3 were the highest in the CO, FO, and DO diets, respectively. Dietary effects on kidney disease progression were similar in males and females. A low-fat diet slows progression of renal injury in male and female *pcy* mice, consistent with findings in the male Han:SPRD-*cy* rat. Dietary fat type also influenced renal injury, with flaxseed oil diets rich in 18:3n-3 slowing early fibrosis progression compared with diets rich in 18:2n-6 or in 22:6n-3.

Paper no. L9399 in *Lipids 39,* 207–214 (March 2004).

Polycystic kidney disease (PKD) is the fourth most common cause of end-stage renal disease, affecting over 12 million people worldwide, and is primarily caused by mutations in one of two genes, PKD1 and PKD2 (1,2). Treatment of PKD patients involves alleviation of associated secondary disorders, but there currently are no strategies to combat disease progression itself. A number of studies involving dietary interventions using animal models of renal cystic diseases, however, have obtained promising results in retarding disease progression. In these models, disease progression is retarded by the reduction of dietary protein to a low yet growth-maintaining level, substitution of soy protein for casein, supplementation with a saponin-enriched alcohol extract from soy protein isolate, and adding flax or fish oil to the diet, with some of these interventions having been shown to prolong life (3–11).

In male Han:Sprague-Dawley (SPRD)-*cy* rats with PKD, low-fat compared with high-fat feeding is beneficial, resulting in less histological damage, lower serum creatinine, and improved creatinine clearance (11,12). Although the disease progresses at a much slower rate in female Han:SPRD-*cy* rats, dietary fat restriction also is beneficial to a lesser extent (12). The relevance of animal models and of gender to human disease is always an issue, necessitating the use of multiple models of the disease and the inclusion of both genders to examine intervention effects. The *pcy* mouse has a form of renal cystic disease with progressive renal failure and has been used as a model of human autosomal dominant PKD (13–15), although synteny of the *pcy* gene with the NPH3 gene has been observed (16). The NPH3 protein is mutated in adolescent nephronophthisis, another type of renal cystic disease (16). Phenotypically, this model exhibits several characteristics of both of these forms of renal cystic disease (16,17). All renal cystic diseases involve disturbances of regeneration and repair, with different components predominating in different models.

In the *pcy* mouse model, gender differences in response to varying fat type and protein source have been observed (3,18). Therefore, in the first study presented herein, we examined the effects of feeding differing fat levels on the progression of disease in male and female *pcy* mice to determine whether the beneficial effects of fat restriction observed in the Han:SPRD-*cy* rat extend to this model of renal cystic disease. In contrast to previous *pcy* studies in which adult *pcy* mice have been used, in Han:SPRD-*cy* rats the benefits of dietary interventions on renal injury have been observed in young animals (11,12). Therefore, in the second study, we examined whether dietary fat level would have the same effect in weanling *pcy* mice. In this study, the type of fat also was altered to determine whether fat type would influence fat-level effects on disease progression in these mice.

In Han:SPRD-*cy* rats, both fish oil (rich in 20:5n-3 and 22:6n-3) and flax oil (rich in 18:3n-3) slow disease progres-

*To whom correspondence should be addressed at H506 Duff Roblin, University of Manitoba, Winnipeg MB, Canada R3T 2N2.
E-mail: aukema@umanitoba.ca

Abbreviations: CO, corn oil; DO, DHASCO (DHA-rich single-cell oil)/corn oil; FA, fatty acid; FO, flaxseed/corn oil; G, gender; L, level; Ox-LDL, oxidized LDL; PKD, polycystic kidney disease; SPRD, Sprague-Dawley; SUN, serum urea nitrogen; T, type.

sion compared with oils rich in 18:2n-6 (10,11). Furthermore, a fish oil diet mitigates the detrimental effects of a high-fat diet rich in n-6 fatty acids (FA) in weanling Han:SPRD-*cy* rats (11). However, compared with this rat model, the effects of dietary oil rich in n-3 FA are unresolved in studies using adult *pcy* mice given a moderate level of dietary fat. In the long term, fish oil appears to be detrimental (18), whereas in the short term, it appears to be beneficial (19). Therefore, to differentiate between possible effects of oils containing distinct n-3 FA, in the second study weanling *pcy* mice were fed diets containing high and low levels of corn oil (rich in 18:2n-6) compared with flax oil (rich in 18:3n-3) or a novel algal oil (rich in 22:6n-3) to determine whether fat-level effects were influenced by fat type in this model of renal disease.

MATERIALS AND METHODS

Animals. CD1-*pcy/pcy* (*pcy*) mice were obtained from our breeding colony, which was established from mice provided to us by V.H. Gattone II of the University of Kansas Medical Center. The animal experimental protocols were in accordance with the guidelines of the *National Institutes of Health Guide for the Care and Use of Laboratory Animals*. All mice were housed in individual cages under temperature, humidity, and light-controlled conditions. All diet ingredients, with the exception of flax and algal oils, were purchased from Dyets Inc. (Bethlehem, PA) or Harlan Teklad (Madison, WI). Flax oil was a generous gift from Bioriginal Food and Science Corporation (Saskatoon, Saskatchewan), and algal oil (DHASCO, DHA-rich single-cell oil) was from Martek Biosciences Corporation (Winchester, KY).

Diets and experimental protocol . Study 1 had three dietary treatments and two genders in a 3×2 design, with each group having eight mice. Adult male and female mice, at 70 d of age, were randomly assigned to one of three diets containing fat at either a low (4%, 4 g/100 g diet), medium (10%, 10 g/100 g diet), or high level (20%, 20 g/100 g diet). These diets were based on the AIN-93M diet for adult rodents, which uses soybean oil as the lipid source (20), and differed only in fat level. This diet contains 8 g 18:3n-3 and 53 g 18:2n-6 per 100 g of total FA present (11). Energy from fat was substituted for that from carbohydrates and *vice versa*, and other ingredients were adjusted to maintain a constant nutrient-to-energy ratio in these diets. All mice were fed the experimental diets for 130 d.

In study 2, male and female mice were randomly assigned to one of six experimental diets at weaning (4 wk of age, n = 8/diet group). The diets contained three types of dietary oils, namely, corn (rich in 18:2n-6), flaxseed (rich in 18:3n-3), and DHASCO (algal oil rich in 22:6n-3), at high (20%) and low (7%) levels, providing 20 and 7 g of fat/100 g diet, respectively, in a $2 \times 2 \times 3$ design. To compensate for a potential EFA deficiency in the DHASCO oil diet, corn oil was added at a ratio of 4:1 (4 g of DHASCO oil, 1 g of corn oil). The flaxseed oil diet was treated in a similar fashion. Diets are indicated as CO, containing corn oil, DO, containing DHASCO/corn oil (4:1, g/g), and FO, containing flaxseed/corn oil (4:1, g/g). The FA compositions of these diets are shown in Table 1. Since these were growing mice, the level of fat in the low-fat diet was 7 g/100 g diet as prescribed in the AIN-93G diet (compared with 4 g fat/100 g diet in the maintenance diet fed to the adult mice in study 1). Although study 2 was designed as a longer feeding trial, the study was shortened since two males from the high-DO group and one male from the low-DO group died of renal failure after 8 wk of feeding. Mice were added to the study as they became available from the breeding colony and were fed for an 8-wk period. This allowed us to allocate additional mice to the groups in which mice had died along with their littermates placed on the other diets, thus restoring an n = 8 for all groups for analyses at the end of the study. In addition to the three mice that had died of renal failure, some mice did not maintain fluid volume in the last weeks of the study and had to be rehydrated with 0.9% physiologic saline (administered subcutaneously). Weight loss and failure of a portion of the skin raised by "tenting" to resume its normal shape were used to determine whether rehydration was necessary. The average number of treatments per mouse was two, and the volume of saline used was determined based on the extent of weight loss. No animals were dehydrated at termination.

Mice were weighed weekly, and at the end of the feeding period they were killed and the trunk blood was collected to obtain serum. Livers and right kidneys were removed, weighed, and frozen in liquid nitrogen. Left kidneys were removed, weighed, and fixed in 10% buffered formalin for morphological and histological analyses.

Histology and immunohistochemistry. The left kidney was embedded in paraffin and sectioned at 5 μm. Sections for cyst area measurement were stained with hematoxylin and eosin, and those for quantitative analysis of fibrosis were stained with aniline blue (an adaptation of Masson's trichrome stain), which permitted image analysis measurement using a standard incandescent microscope light source. This adaptation demonstrated perfect concordance of staining with an immunofluorescent detection of collagen type III (7,11,21).

TABLE 1
FA Composition of the Experimental Diets[a] (study 2)

FA	CO	DO	FO
10:0	—[b]	0.89 ± 0.02[c]	—
12:0	—	3.36 ± 0.07	—
14:0	—	12.67 ± 0.26	—
16:0	10.91 ± 0.01	14.67 ± 0.16	6.54 ± 0.07
16:1n-7	0.11 ± 0.00	1.15 ± 0.02	—
18:0	2.08 ± 0.03	1.14 ± 0.00	3.21 ± 0.01
18:1n-7	0.54 ± 0.01	0.12 ± 0.00	0.63 ± 0.00
18:1n-9	26.63 ± 0.26	19.92 ± 0.06	19.16 ± 0.00
18:2n-6	57.30 ± 0.29	13.1 ± 0.08	23.48 ± 0.23
18:3n-3	0.94 ± 0.07	0.23 ± 0.00	45.43 ± 0.32
22:5n-3	—	—	—
22:6n-3	—	31.36 ± 0.33	—

[a]CO, corn oil diet; DO, DHASCO (DHA-rich single-cell oil)/corn oil (4:1, g/g) diet; FO, flaxseed/corn oil (4:1, g/g) diet; FA, fatty acid.
[b]<0.1 g/100 g total FA.
[c]Values represent means ± SEM of two determinations of the major FA (≥0.5 g/100 g total FA present in any diet).

As a measure of renal injury, detection of oxidized modifications of LDL (ox-LDL, including Cu^{2+}-ox-LDL and malondialdehyde-LDL) was carried out using a 1:50 dilution of rabbit anti-Cu^{2+}-ox-LDL polyclonal antibody for 30 min (AB3230; Chemicon International, Temecula, CA) (10). Secondary detection was done using a Dako EnVision Plus system (K4008; Dako Corporation, Carpinteria, CA). Sections were counterstained with hematoxylin (Dako Mayer's hematoxylin, S3309; Dako Corporation).

Image analysis. An imaging system comprising a Spot Junior CCD camera mounted on an Olympus BX60 microscope was used for image analysis. After being captured using the SPOT software (version 3.10), images were analyzed as described previously (7,10,11) using the Image Pro Plus software (version 4.10; Media Cybernetics, Silver Spring, MD) for cyst area, renal fibrosis, and ox-LDL. Briefly, the portion of tissue section occupied by the tubular lumen or cyst was measured through a series of images at 10× objective, starting from a random field of tissue section until 25 measurements from 3 to 5 whole-kidney cross-sections were collected. All measurements were carried out in a blinded fashion. Identification of a tubular lumen or cyst was performed by automated measurements using hue and intensity characteristics. The renal fibrosis ratio was determined using a 20× objective and using the proportion of section areas that had taken up aniline blue stain. The cyst area ratio and renal fibrosis ratio were determined in this manner and expressed relative to left kidney and body weight to yield the cyst or fibrosis volume (assuming 1 g = 1 mL) as described previously (7,10,11). Areas positive for fibrosis and ox-LDL were expressed as the fraction of solid tissue area, thereby correcting for the extent of cystic change in each kidney. The cyst and fibrosis volume reflected renal cyst growth and fibrosis, respectively.

Biochemistry. Serum urea nitrogen (SUN) was determined spectrophotometrically using reagents from Sigma kit 640-A (Sigma Chemical Co., St. Louis, MO).

For analyses of dietary fat, 2 g of diet was homogenized in chloroform/methanol (2:1, vol/vol) and filtered. After the addition of water, separation of the organic and aqueous phases was facilitated by letting the mixture sit overnight at room temperature. The organic phase was drawn off, evaporated to dryness at 50–70°C, and resuspended in 1 mL of toluene. The FA were methylated using 3 N methanolic HCl at 80°C for 1 h. FAME were extracted in hexane and analyzed by GC.

For kidney FA analyses, lipids were extracted from the right kidneys of four mice randomly selected from each group. Ten milligrams of lyophilized kidney was homogenized in chloroform/methanol (2:1, vol/vol) containing 0.01% BHT. After centrifugation at 1500 × *g* for 15 min, the supernatant was treated with 0.73% NaCl and was recentrifuged. The aqueous phase was discarded, and the organic phase was washed twice with theoretical upper phase containing chloroform/methanol/water (3:48:47, by vol). The organic layer was transferred to a clean glass tube, dried under nitrogen, and resuspended in 0.6 mL of toluene. The lipid extracts were transmethylated using 3 N methanolic HCl at 80°C for 2 h. After washing twice with water and centrifuging, the organic phase was dried under nitrogen and resuspended in 50 µL of hexane. Both diet and kidney FAME were separated by GLC on a Varian Star 3400 (Varian Inc., Mississauga, Ontario), using a 30-m capillary column, with an i.d. of 0.25 mm and a 0.25-µm film thickness (Agilent Technologies, Mississauga, Ontario).

For conjugated diene analyses, lipids were extracted from livers in the same way as from kidneys, and the conjugated diene concentration was determined spectrophotometrically using AOCS Official Method Ti la-64 (22). The lipid extracts were diluted in isooctane, and the absorbance of samples at 233 nm was measured. By using oxidized oil with a known conjugated diene concentration as a reference, the detection limit was determined to be 17 ng of conjugated dienes.

Statistical analyses. Data were analyzed by two-way (study 1) and three-way (study 2) ANOVA, with litter included as a random effect, using SAS software (SAS Institute, Cary, NC). Normality of the data was tested using a plot of residuals vs. predicted values and Shapiro–Wilk's *W* statistic. Data were normalized by logarithmic transformation when necessary. Differences between means were tested using *post hoc t*-tests (simple contrasts). *Post hoc t*-tests were performed only when the overall main or interaction effect was significant at $P < 0.05$. Main and interaction effects were considered significant at $P < 0.05$. In several cases, interactions of type or level with gender were present; in these cases, male and female data were analyzed separately. In some cases, specific FA were present in trace amounts (<0.1 mol/100 mol total FA); for these FA, only the groups that had >0.1 mol/100 mol of total FA were included in the analyses.

Chi-square analyses were performed on the number of mice requiring rehydration in study 2. Simple effects of fat type, fat level, and gender were compared by this test.

RESULTS

Fat level effects. In adult *pcy* mice, high- compared with low-fat diets resulted in higher kidney weights and SUN concentrations (Table 2). Renal cystic growth and fibrosis were extensive and were not affected by fat level in these animals at 200 d of age. In the early stages of renal disease, as observed in study 2, fat-level effects were observed in renal fibrosis (Table 3), the number of healthy mice (see below), and some renal FA levels (Table 4). Renal fibrosis was reduced in low-fat- compared with high-fat-fed mice in all diets (Table 3), but the detrimental effects of high fat were mitigated by FO, with fibrosis in the high-fat-fed FO group being similar to that in the low-fat CO and DO groups (Table 3).

In addition to the three mice that died of renal failure in study 2 (two on the high-DO and one on the low-DO diet), some mice could not maintain fluid volume in the last weeks of the study and had to be rehydrated with physiologic saline. The number of animals that had to be treated in this way included seven high-DO-fed males, two high-DO-fed females, two high-FO-fed males, one high-CO-fed male, and one low-DO-fed male. Chi-square analyses of fat-level effects (within

TABLE 2
Body and Kidney Weights and Renal Disease Markers in Male and Female *pcy* Mice Fed 4, 10, or 20 g of Soybean Oil per 100 g Diet for 130 d (study 1)[a]

Outcome measurements	Fat level (g/100 g diet)[b] 4%	10%	20%	Pooled SEM	Effects
Body weight (g)					
Male	40.0	38.5	40.5	1.38	G
Female	32.5	32.0	36.9		
Relative kidney weight (g/100 g body weight)					
Male	2.7	3.0	3.5	0.24	G, L[c]
Female	2.2	2.5	2.7		
SUN (mmol/L)					
Male	10.4	12.7	13.4	2.42	G, L[c]
Female	8.9	9.7	10.4		
Cyst volume (mL/kg body weight)[d]	10.8	11.5	13.9	1.02	None
Renal fibrosis (mL/kg body weight)[d,e]	2.39	1.96	1.60	0.39	None

[a]SUN, serum urea nitrogen; G, gender; L, level.
[b]All values in the 4, 10, and 20% columns are least square means (n = 8).
[c]$P < 0.05$, high- compared with low-fat-fed mice.
[d]Data from males only.
[e]Corrected for solid tissue area.

TABLE 3
Body and Kidney Weights and Renal Disease Markers in Male and Female *pcy* Mice Fed Diets Containing CO, DO, and FO Diets at 20 or 7 g of Fat per 100 g Diet for 8 wk (study 2)[a]

Outcome measurements	Fat level (g/100 g diet)[b] CO 7%	CO 20%	DO 7%	DO 20%	FO 7%	FO 20%	Pooled SEM	Effects
Body weight (g)[c]								
Male	30.4	32.2	28.0	24.1	31.3	32.1	0.925	T, L × T[d]
Female	23.8	26.5	24.7	25.4	26.1	27.4	1.320	None
Relative kidney weight (g/100 g body weight)[b]								
Male	2.43	2.74	3.24	3.22	2.85	2.94	0.164	T[e]
Female	2.10	1.70	2.31	1.77	2.06	2.06	0.122	None
SUN (mmol/L)								
Male	7.6	7.9	12.1	10.5	7.7	7.4	1.099	G, T[f]
Female	6.0	6.4	6.8	8.1	6.5	6.5		
Renal fibrosis (mL/kg body weight)[g]								
Male	0.54	0.84	0.51	0.77	0.28	0.48	0.077	G, T[h], L
Female	0.46	0.54	0.58	0.76	0.28	0.35		
Cyst volume (mL/kg body weight)								
Male	6.6	7.7	8.5	8.7	7.1	7.8	0.546	G, T[f]
Female	5.6	4.9	6.2	8.1	5.1	5.4		
Oxidized LDL (cells/high power field)[g]								
Male	0.47	0.59	0.62	0.67	0.41	0.49	0.076	T[i]
Female	0.41	0.40	0.45	0.71	0.35	0.36		

[a]For diet specifications see Table 1. T, type; for other abbreviations see Tables 1 and 2.
[b]All values in the 7 and 20% columns are least square means (n = 8).
[c]Interactions with gender were present; therefore, data were analyzed separately for male and female mice.
[d]Interaction between fat level and type. The only significant effects for simple fat level or type were observed in the high-fat DO males, which had significantly lower body weights than males in all the other groups.
[e]$P < 0.05$, DO > CO.
[f]$P < 0.01$, DO > CO, FO.
[g]Corrected for solid tissue area.
[h]$P < 0.0001$, FO < CO, DO.
[i]$P < 0.005$, DO > FO.

each fat type) revealed that significantly more mice in the high-fat DO group required rehydration than in the low-fat DO group.

Fat type effects. In study 2, after 8 wk of feeding, kidney weights of DO-fed mice were higher than those of CO-fed mice, and SUN concentrations and cyst volumes were higher

TABLE 4
Kidney FA Composition (mol/100 mol of total FA) in Male and Female *pcy* Mice Given CO, DO, and FO Diets at 20 or 7 g of Fat per 100 g Diet[a]

		CO[b]		DO[b]		FO[b]		
FA	Gender	20%	7%	20%	7%	20%	7%	Effect
14:0	Male	0.48 ± 0.06	0.87 ± 0.05	2.57 ± 0.52	1.52 ± 0.18	0.52 ± 0.03	0.89 ± 0.23	T, L × T
	Female	0.42 ± 0.03	0.97 ± 0.05	3.21 ± 0.67	1.82 ± 0.20	0.63 ± 0.10	0.94 ± 0.15	
16:0	Male	20.11 ± 0.31	22.41 ± 0.21	24.00 ± 1.11	25.84 ± 0.86	18.05 ± 0.13	23.57 ± 1.65	G, L, T
	Female	20.61 ± 0.42	25.06 ± 0.25	22.93 ± 0.56	27.58 ± 0.39	19.71 ± 0.22	23.97 ± 0.30	
18:0	Male	14.60 ± 0.28	13.29 ± 0.18	14.82 ± 1.03	15.36 ± 0.47	15.66 ± 0.40	13.76 ± 1.77	L
	Female	15.47 ± 0.50	13.65 ± 0.34	15.44 ± 1.24	13.22 ± 1.00	15.73 ± 1.36	13.82 ± 0.81	
16:1n-7	Male	0.43 ± 0.04	2.05 ± 0.05	0.70 ± 0.11	1.72 ± 0.29	0.46 ± 0.03	2.71 ± 0.70	L
	Female	0.44 ± 0.02	2.32 ± 0.17	0.91 ± 0.19	2.64 ± 0.32	0.91 ± 0.17	3.05 ± 0.64	
18:1n-7[c]	Male	1.34 ± 0.06	2.69 ± 0.11	0.68 ± 0.05	1.23 ± 0.03	1.04 ± 0.03	2.27 ± 0.20	L, T, L × T
	Female	1.36 ± 0.03	2.28 ± 0.11	0.63 ± 0.02	1.76 ± 0.04	1.05 ± 0.04	2.22 ± 0.06	L, T
18:1n-9	Male	9.79 ± 0.63	13.54 ± 1.17	11.44 ± 1.24	12.57 ± 0.76	11.13 ± 0.61	15.23 ± 2.80	G, L
	Female	10.85 ± 0.78	16.61 ± 0.76	12.27 ± 1.56	16.27 ± 1.05	12.85 ± 1.72	16.88 ± 2.44	
18:2n-6[c]	Male	19.56 ± 1.11	11.95 ± 0.42	12.63 ± 0.54	8.47 ± 0.21	16.62 ± 0.37	10.65 ± 0.61	L, T, L × T
	Female	21.11 ± 1.34	13.91 ± 0.38	11.08 ± 0.47	9.27 ± 0.46	17.90 ± 0.55	10.51 ± 0.47	L, T, L × T
18:3n-3[d]	Male	0.14 ± 0.01	—[e]	—	—	6.90 ± 0.78	2.91 ± 0.75	L
	Female	0.20 ± 0.02	0.10 ± 0.01	—	—	7.62 ± 1.69	2.60 ± 0.19	
20:2n-6	Male	1.03 ± 0.04	0.56 ± 0.07	0.25 ± 0.03	0.23 ± 0.01	0.43 ± 0.04	0.40 ± 0.05	G, L, T, L × T
	Female	1.04 ± 0.03	0.53 ± 0.06	0.17 ± 0.01	0.19 ± 0.004	0.35 ± 0.03	0.22 ± 0.01	
20:4n-6[c]	Male	13.95 ± 0.43	13.68 ± 0.84	0.55 ± 0.04	1.09 ± 0.03	6.76 ± 0.38	7.21 ± 1.06	T
	Female	16.64 ± 0.82	15.79 ± 0.47	0.53 ± 0.03	1.43 ± 0.04	8.87 ± 1.09	9.11 ± 0.61	T
20:5n-3[d]	Male	—	—	8.24 ± 0.60	7.23 ± 0.52	2.04 ± 0.07	2.71 ± 0.41	T, L × T
	Female	—	—	9.76 ± 1.06	6.95 ± 0.46	2.71 ± 0.32	3.35 ± 0.48	
22:5n-6[d]	Male	4.44 ± 0.50	6.76 ± 0.31	—	—	—	—	G, L, G × L
	Female	1.48 ± 0.04	1.86 ± 0.11	—	—	—	—	
22:6n-3	Male	9.36 ± 1.16	7.23 ± 0.25	20.54 ± 0.58	20.77 ± 0.91	15.61 ± 0.85	11.60 ± 4.44	T
	Female	5.54 ± 0.23	4.49 ± 0.15	19.47 ± 0.85	14.81 ± 0.73	6.87 ± 0.87	8.19 ± 0.96	

[a]For diet specifications see Table 1. For abbreviations see Tables 1–3.
[b]All values expressed in the 20 and 7% columns are least square means (n = 8). Values expressed as means ± SEM of FA present at a level of >1 mol/100 mol total FA in the kidneys of at least one diet group.
[c]Interactions with gender were present; therefore, data were analyzed separately for male and female mice.
[d]Statistical analyses were performed on only groups having >0.1 mol/100 mol of total FA.
[e]Less than 0.1 mol/100 mol of total FA.

in DO compared with both CO- and FO-fed mice (Table 3). Body weights were lower in high-fat DO-fed male mice compared with other male mice fed high-fat diets (Table 3). There was increased fibrosis in the DO- and CO-fed mice compared with FO-fed mice (Fig. 1), and ox-LDL was higher in DO-compared with FO-fed mice (Table 3). Chi-square analyses of fat-type effects in mice that required rehydration revealed that mice on the high-fat DO diet required rehydration more often those on the high-CO or -FO diets.

To assess whether the higher ox-LDL in DO fed mice was a reflection of systemic oxidative damage due to the higher PUFA content of the diet, conjugated dienes were assessed in the liver, a tissue not affected by cystic injury at this age. There was no evidence of peroxidation in the liver, as the level of conjugated dienes was below the detection limit of 17 ng, which represented less than 0.003% of total lipids (data not shown).

Renal FA levels reflected the FA compositions of the diets and, as a result, 18:2n-6, 18:3n-3, and 22:6n-3 were the highest in the CO, FO, and DO diets, respectively (Table 4). Although the level of 18:2n-6 provided in the FO compared with the DO diet was only twofold higher, the levels of 20:4n-6 in the kidneys of FO-fed mice were 7- to 12-fold higher. Compared to the kidneys of CO-fed mice, the levels of 20:4n-6 were 13- to 15-fold lower in the kidneys of DO-fed mice and twofold lower in the kidneys of FO-fed mice.

Gender effects. Several markers of renal injury and function indicated a lesser degree of renal injury in females. However, the dietary fat level and type effects in females were not different from those in males. A few interactions between gender and fat level and type on body weight and kidney weight, respectively, indicated that dietary effects on these were not as great in females as in males.

DISCUSSION

A high-fat diet worsens renal disease progression in *pcy* mice, with a significant increase in renal fibrosis manifested early in the disease process, and elevated SUN and kidney size were observed in the older animals. There was a threefold increase in renal fibrosis levels in 200-d-old adult *pcy* mice compared with 84-d-old younger mice. This change is similar in magnitude to previously reported renal fibrotic damage in *pcy* mice, which becomes progressively more severe with age (23). The extensive level of renal fibrosis in the older animals may have obscured the changes observed in the younger mice, but the effect on function, as indicated by elevated SUN

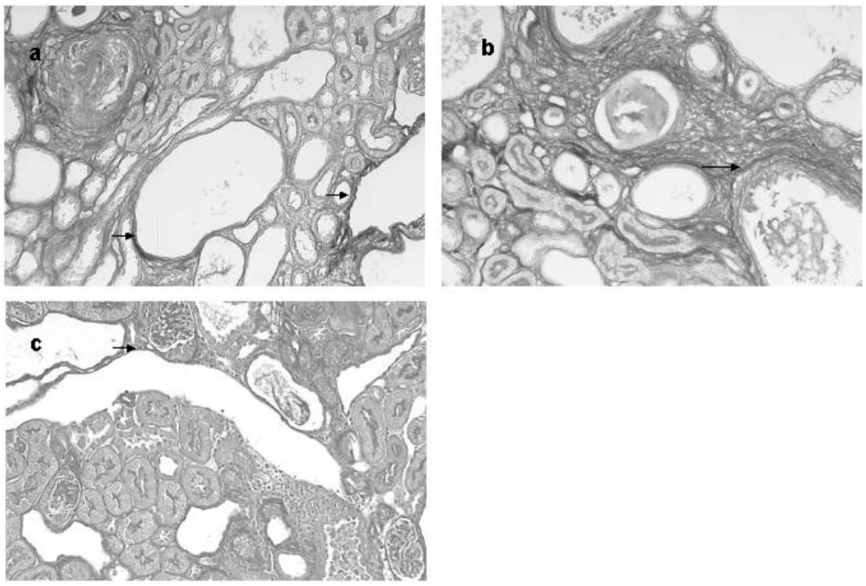

FIG. 1. Renal fibrosis in male *pcy* mice fed high-fat diets (20 g of fat/100 g diet) containing (A) corn oil (CO), (B) DHASCO (DHA-rich single-cell oil)/corn oil (4:1 g/g, DO), or (C) flaxseed/corn oil (4:1 g/g, FO) oil. Aniline blue stain, magnification 40×. Arrows point to areas of increased renal fibrosis identified by darkly stained collagen deposits in interstitial spaces, especially around the periphery of cysts.

levels, suggests that the early changes did have long-term effects. These findings in the *pcy* mouse are consistent with previous studies, which demonstrated that a high-fat diet accelerates renal disease progression in the Han:SPRD-*cy* rat (11,12). It also further extends those studies to demonstrate that the benefits of a low-fat diet are also present in female *pcy* mice. Notably, reducing the dietary fat level slows renal disease progression yet maintains normal body growth.

The most notable fat-type effect on disease progression was observed in the markedly reduced renal fibrosis in the FO- compared to the CO- and DO-fed mice. In addition, the FO diet mitigated the negative effect of high-fat feeding on fibrosis with the high-FO-fed mice having renal fibrosis similar to the low-fat-fed mice on the other diets. The beneficial effect of FO demonstrated herein is consistent with the beneficial effect of oils with n-3 FA on renal injury in the weanling Han:SPRD-*cy* rat (10,11). In contrast to the beneficial effects of FO, mice fed DO, compared with CO, diets failed to thrive, had lower body weights, had increased cystic growth, and exhibited impaired kidney function (higher SUN concentrations). This is reminiscent of previous findings of reduced survival in adult *pcy* mice fed a fish oil diet containing n-3 FA (14). Studies that have exhibited a beneficial effect of dietary n-3 FA on renal injury in the Han:SPRD-*cy* rat model have been short-term supplementation studies in weanling rats, and there is currently no documentation of the long-term effects of dietary n-3 supplementation in this model. Therefore, the possibility that short-term benefits of n-3 FA do not persist in the long term cannot be overlooked. It is therefore imperative to exercise caution in extrapolating the apparent benefits of diets containing n-3 FA in early renal injury to potential benefits in later stages of disease progression.

The greater amount of renal inflammation in the early stages of renal injury in the Han:SPRD-*cy* rat model, compared with the *pcy* mouse, may help explain why n-3 FA are beneficial in early stages of disease progression in the Han:SPRD-*cy* rat while having lesser benefits in the *pcy* mouse. Supplementing the diet with n-3 FA causes a shift in eicosanoid production, with 20:5n-3 inhibiting the metabolism of 20:4n-6 to the more inflammatory eicosanoids, thereby exerting an anti-inflammatory effect in renal disease (24). Thus, the beneficial effects of n-3 FA in early renal disease could be due to a reduction in renal inflammation by altering the renal eicosanoid profile.

Although the DO diet also may have been expected to reduce renal inflammation because of its high n-3 FA content, the reduction in eicosanoid precursors may have been excessive in these mice. Although overproduction of eicosanoids may increase inflammation, normal levels of eicosanoids play an important role in the maintenance of kidney functions, including blood flow, glomerular filtration rate, urine concentration, and renin release (25,26). Although there was increased 20:5n-3 in the kidneys of DO-fed mice, the level of 20:4n-6 was markedly reduced, perhaps resulting in a deficiency of critical eicosanoids in these kidneys. Competition for the Δ6-desaturase enzyme at the 18-carbon FA level by n-6 and n-3 FA has been documented (27), and feeding formulas rich in 22:6n-3 and 20:5n-3 but lacking in 20:4n-6 has resulted in reduced growth of preterm infants (28,29). It is of interest to determine whether the inclusion of 20:4n-6 in the DO diet would have been beneficial, as is the case with infant formulas. In the previous studies in which a diet containing n-3 FA slowed the progression of renal injury, 20:4n-6 levels were maintained at levels similar to those in the FO-fed mice in the current study

(8,11). Thus, the adverse effects of the high-DO diet may have been due to the marked suppression of 20:4n-6, resulting in a greater reduction of critical eicosanoid formation.

The lesser magnitude of renal injury observed in females is consistent with well-documented findings of gender-associated dimorphism in human and animal PKD. The average age of renal failure is about 5 yr earlier in men than in women with PKD (30,31), and disease progression is more aggressive in male Han:SPRD-*cy* rats than in females (32). However, dietary fat effects were similar in female and male *pcy* mice, demonstrating the relevance of dietary fat restriction in females, similar to the previously studied males (11,12).

Renal ox-LDL formation is negligible in normal kidneys of the Han:SPRD-*cy* rat but increases with the extent of injury to the kidneys (10). This is consistent with other studies in which ox-LDL was immunohistochemically demonstrated in the glomeruli of rats, in humans with glomerulosclerosis (33,34), and in various immune- and nonimmune-mediated renal injuries, including PKD, in which oxidized products accumulate (35–37). Compromised resistance to oxidant injury due to the depletion of renal antioxidant enzymes (38) was observed in the Han:SPRD-*cy* rat. We also found the highest levels of ox-LDL in the DO-fed mice, which had the greatest development of renal injury. Although an enrichment of 22:6n-3 in tissue membranes increases their susceptibility to lipid peroxidation (39), the lack of significant accumulation of conjugated dienes in the unaffected livers in our study suggests that the increased renal expression of ox-LDL in mice fed DO is not simply due to an increase in peroxidation of the higher levels of n-3 PUFA. In fact, both DO- and FO-fed mice had similar amounts of renal n-3 PUFA compared with the CO-fed mice, but had differing levels of ox-LDL, as well as other markers of renal injury. However, the possibility that injured kidneys are more susceptible to FA peroxidation cannot be ruled out.

Our results demonstrate that dietary fat alters disease progression in both male and female *pcy* mice. A low-fat diet slows the development of renal injury and flax oil-containing 18:3n-3 reduces early renal disease progression. However, caution is warranted in the use of n-3 FA as potential therapeutic agents in this form of renal injury, as very high levels of 20- and 22-carbon n-3 FA without adequate 20:4n-6 appear to be detrimental.

ACKNOWLEDGMENTS

This work was supported by Natural Sciences and Engineering Research Council of Canada and Manitoba Institute for Child Health. The image analysis unit is supported by an equipment grant from the Children's Hospital Foundation of Manitoba, Inc. D.S. was the recipient of a graduate fellowship from the Kidney Foundation of Canada. This work was presented in part at the 5th Congress of the International Society for the Study of Fatty Acids and Lipids, May 7–11, 2002, Montreal, Canada [D. Sankaran, N. Bankovic-Calic, M.R. Ogborn, H.M. Aukema (2002) Flaxseed Oil Ameliorates Early Renal Disease Progression in pcy Mice (abs.)]. The technical assistance of Marilyn Latta and Mike Darnley is gratefully acknowledged, as is the assistance with conjugated diene analyses from R. Przybylski.

REFERENCES

1. Sutters, M., and Germino, G.G. (2003) Autosomal Dominant Polycystic Kidney Disease: Molecular Genetics and Pathophysiology, *J. Lab. Clin. Med. 141*, 91–101.
2. Igarashi, P., and Somlo, S. (2002) Genetics and Pathogenesis of Polycystic Kidney Disease, *J. Am. Soc. Nephrol. 13*, 2384–2398.
3. Aukema, H.M., Housini, I., and Rawling, J.M. (1999) Dietary Soy Protein Effects on Inherited Polycystic Kidney Disease Are Influenced by Gender and Protein Level, *J. Am. Soc. Nephrol. 10*, 300–308.
4. Keith, D.S., Torres, V.E., Johnson, C.M., and Holley, K.E. (1994) Effect of Sodium Chloride, Enalapril, and Losartan on the Development of Polycystic Kidney Disease in Han:SPRD Rats, *Am. J. Kidney Dis. 24*, 491–498.
5. Tomobe, K., Philbrick, D., Aukema, H.M., Clark, W.F., Ogborn, M.R., Parbtani, A., Takahashi, H., and Holub, B.J. (1994) Early Dietary Protein Restriction Slows Disease Progression and Lengthens Survival in Mice with Polycystic Kidney Disease, *J. Am. Soc. Nephrol. 5*, 1355–1360.
6. Torres, V.E., Mujwid, D.K., Wilson, D.M., and Holley, K.H. (1994) Renal Cystic Disease and Ammoniagenesis in Han:SPRD Rats, *J. Am. Soc. Nephrol. 5*, 1193–1200.
7. Ogborn, M.R., Bankovic-Calic, N., Shoesmith, C., Buist, R., and Peeling, J. (1998) Soy Protein Modification of Rat Polycystic Kidney Disease, *Am. J. Physiol. 274*, F541–F549.
8. Ogborn, M.R., Nitschmann, E., Weiler, H., Leswick, D., and Bankovic-Calic, N. (1999) Flaxseed Ameliorates Interstitial Nephritis in Rat Polycystic Kidney Disease, *Kidney Int. 55*, 417–423.
9. Philbrick, D.J., Bureau, D.P., Collins, F.W., and Holub, B.J. (2003) Evidence That Soyasaponin Bb Retards Disease Progression in a Murine Model of Polycystic Kidney Disease, *Kidney Int. 63*, 1230–1239.
10. Ogborn, M.R., Nitschmann, E., Bankovic-Calic, N., Weiler, H.A., and Aukema, H. (2002) Dietary Flax Oil Reduces Renal Injury, Oxidized LDL Content, and Tissue n-6/n-3 FA Ratio in Experimental Polycystic Kidney Disease, *Lipids 37*, 1059–1065.
11. Lu, J., Bankovic-Calic, N., Ogborn, M., Saboorian, M.H., and Aukema, H.M. (2003) Detrimental Effects of a High Fat Diet in Early Renal Injury Are Ameliorated by Fish Oil in Han:SPRD-*cy* Rats, *J. Nutr. 133*, 180–186.
12. Jayapalan, S., Saboorian, M. H., Edmunds, J.W., and Aukema, H.M. (2000) High Dietary Fat Intake Increases Renal Cyst Disease Progression in Han:SPRD-*cy* Rats, *J. Nutr. 130*, 2356–2360.
13. Takahashi, H., Calvet, J.P., Dittemore-Hoover, D., Yoshida, K., Grantham, J.J., and Gattone, V.H., II (1991) A Hereditary Model of Slowly Progressive Polycystic Kidney Disease in the Mouse, *J. Am. Soc. Nephrol. 1*, 980–989.
14. Aukema, H.M., Ogborn, M.R., Tomobe, K., Takahashi, H., Hibino, T., and Holub, B.J. (1992) Effects of Dietary Protein Restriction and Oil Type on the Early Progression of Murine Polycystic Kidney Disease, *Kidney Int. 42*, 837–842.
15. Gattone, V.H., II, Kuenstler, K.A., Lindemann, G.W., Lu, X., Cowley, B.D., Jr., Rankin, C.A., and Calvet, J.P. (1996) Renal Expression of a Transforming Growth Factor-α Transgene Accelerates the Progression of Inherited, Slowly Progressive Polycystic Kidney Disease in the Mouse, *J. Lab. Clin. Med. 127*, 214–222.
16. Omran, H., Haffner, K., Burth, S., Fernandez, C., Fargier, B., Villaquiran, A., Nothwang, H.G., Schnittger, S., Lehrach, H., Woo, D., Brandis, M., Sudbrak, R., and Hildebrandt, F. (2001) Human Adolescent Nephronophthisis: Gene Locus Synteny with Polycystic Kidney Disease in *pcy* Mice, *J. Am. Soc. Nephrol. 12*, 107–113.
17. Guay-Woodford, L.M. (2003) Murine Models of Polycystic Kidney Disease: Molecular and Therapeutic Insights, *Am. J. Physiol. Renal. Physiol. 285*, F1034–F1049.

18. Aukema, H.M., Yamaguchi, T., Takahashi, H., Philbrick, D.J., and Holub, B.J. (1992) Effects of Dietary Fish Oil on Survival and Renal Fatty Acid Composition in Murine Polycystic Kidney Disease, *Nutr. Res. 12*, 1383–1392.
19. Yamaguchi, T., Valli, V.E., Philbrick, D., Holub, B., Yoshida, K., and Takahashi, H. (1990) Effects of Dietary Supplementation with n-3 Fatty Acids on Kidney Morphology and the Fatty Acid Composition of Phospholipids and Triglycerides from Mice with Polycystic Kidney Disease, *Res. Commun. Chem. Pathol. Pharmacol. 69*, 335–351.
20. Reeves, P.G., Nielsen, F.H., and Fahey, G.C., Jr. (1993) AIN-93 Purified Diets for Laboratory Rodents: Final Report of the American Institute of Nutrition *ad hoc* Writing Committee on the Reformulation of the AIN-76A Rodent Diet, *J. Nutr. 123*, 1939–1951.
21. Cohen, A.H. (1975) Masson's Trichrom Stain in the Evaluation of Renal Biopsies, *Am. J. Clin. Pathol. 65*, 631–643.
22. AOCS (1989) Spectrophotometric Determination of Conjugated Dienoic Acid, in *Official Methods and Recommended Practices of the American Oil Chemists' Society*, 4th edn., American Oil Chemists' Society, Champaign, Official Method Ti-1a-64.
23. Okada, H., Ban, S., Nagao, S., Takahashi, H., Suzuki, H., and Neilson, E.G. (2000) Progressive Renal Fibrosis in Murine Polycystic Kidney Disease: An Immunohistochemical Observation, *Kidney Int. 58*, 587–597.
24. Lefkowith, J.B., and Klahr, S. (1996) Polyunsaturated Fatty Acids and Renal Disease, *Proc. Soc. Exp. Biol. Med. 213*, 13–23.
25. Breyer, M., and Badr, K. (1996) Arachidonic Acid Metabolites and the Kidney, in *The Kidney*, 5th edn. (Brenner, B., ed.), W.B. Saunders, Toronto, Canada.
26. Imig, J.D. (2000) Eicosanoid Regulation of the Renal Vasculature, *Am. J. Physiol. Renal Physiol. 279*, F965–F981.
27. Sprecher, H. (2000) Metabolism of Highly Unsaturated n-3 and n-6 Fatty Acids, *Biochim. Biophys. Acta 1486*, 219–231.
28. Carlson, S.E., and Werkman, S.H. (1996) A Randomized Trial of Visual Attention of Preterm Infants Fed Docosahexaenoic Acid Until Two Months, *Lipids 31*, 85–90.
29. Lapillonne, A., and Carlson, S.E. (2001) Polyunsaturated Fatty Acids and Infant Growth, *Lipids 36*, 901–911.
30. Gabow, P.A., Johnson, A.M., Kaehny, W.D., Kimberling, W.J., Lezotte, D.C., Duley, I.T., and Jones, R.H. (1992) Factors Affecting the Progression of Renal Disease in Autosomal-Dominant Polycystic Kidney Disease, *Kidney Int. 41*, 1311–1319.
31. Choukroun, G., Itakura, Y., Albouze, G., Christophe, J.L., Man, N.K., Grunfeld, J.P., and Jungers, P. (1995) Factors Influencing Progression of Renal Failure in Autosomal Dominant Polycystic Kidney Disease, *J. Am. Soc. Nephrol. 6*, 1634–1642.
32. Cowley, B.D., Jr., Rupp, J.C., Muessel, M.J., and Gattone, V.H., II (1997) Gender and the Effect of Gonadal Hormones on the Progression of Inherited Polycystic Kidney Disease in Rats, *Am. J. Kidney Dis. 29*, 265–272.
33. Lee, H.S., and Kim, Y.S. (1998) Identification of Oxidized Low-Density Lipoprotein in Human Renal Biopsies, *Kidney Int. 54*, 848–856.
34. Magil, A.B., Frohlich, J.J., Innis, S.M., and Steinbrecher, U.P. (1993) Oxidized Low-Density Lipoprotein in Experimental Focal Glomerulosclerosis, *Kidney Int. 43*, 1243–1250.
35. Baud, L., and Ardaillou, R. (1993) Involvement of Reactive Oxygen Species in Kidney Damage, *Br. Med. Bull. 49*, 621–629.
36. Torres, V.E., Bengal, R.J., Litwiller, R.D., and Wilson, D.M. (1997) Aggravation of Polycystic Kidney Disease in Han:SPRD Rats by Buthionine Sulfoximine, *J. Am. Soc. Nephrol. 8*, 1283–1291.
37. Diamond, J.R., and Karnovsky, M.J. (1992) A Putative Role of Hypercholesterolemia in Progressive Glomerular Injury, *Annu. Rev. Med. 43*, 83–92.
38. Maser, R.L., Vassmer, D., Magenheimer, B.S., and Calvet, J.P. (2002) Oxidant Stress and Reduced Antioxidant Enzyme Protection in Polycystic Kidney Disease, *J. Am. Soc. Nephrol. 13*, 991–999.
39. Song, J.H., and Miyazawa, T. (2001) Enhanced Level of n-3 Fatty Acid in Membrane Phospholipids Induces Lipid Peroxidation in Rats Fed Dietary Docosahexaenoic Acid Oil, *Atherosclerosis 155*, 9–18.

[Received October 23, 2003; and in revised form and accepted February 24, 2004]

Influences of Dietary n-3 Long-Chain PUFA on Body Concentrations of 20:5n-3, 22:5n-3, and 22:6n-3 in the Larvae of a Marine Teleost Fish from Australian Waters, the Striped Trumpeter (*Latris lineata*)

M.P. Bransden[a,*], G.A. Dunstan[b], S.C. Battaglene[a], J.M. Cobcroft[a], D.T. Morehead[a], S. Kolkovski[c], and P.D. Nichols[b]

[a]Marine Research Laboratories, Tasmanian Aquaculture and Fisheries Institute and Aquafin Cooperative Research Centre (CRC), University of Tasmania, Hobart, Tasmania, 7001, Australia, [b]Commonwealth Scientific & Industrial Research Organisation (CSIRO) Marine Research and Aquafin Cooperative Research Centre (CRC), Hobart, Tasmania, 7001, Australia, and [c]Department of Fisheries, Fremantle, Western Australia, 6160, Australia

ABSTRACT: We determined the effect of dietary long-chain ($\geq C_{20}$) PUFA (LC-PUFA), 20:5n-3 and 22:6n-3, on larval striped trumpeter (*Latris lineata*) biochemistry through early development and during live feeding with rotifers (*Brachionus plicatilis*). Rotifers were enriched using seven experimental emulsions formulated with increasing concentrations of n-3 LC-PUFA, mainly 20:5n-3 and 22:6n-3. Enriched rotifer n-3 LC-PUFA concentrations ranged from 10–30 mg/g dry matter. Enriched rotifers were fed to striped trumpeter larvae from 5 to 18 d post-hatch (dph) in a short-term experiment to minimize gross deficiency symptoms such as poor survival that could confound results. No relationships were observed between larval growth or survival with dietary n-3 LC-PUFA at 18 dph. The larval FA profiles generally reflected those of the rotifer diet, and significant positive regressions were observed between most dietary and larval FA at 10, 14, and 18 dph. The major exception observed was an inverse relationship between dietary and larval 22:5n-3. The presence of 22:5n-3 in elevated amounts when dietary 22:6n-3 was depressed suggests that elongation of 20:5n-3 may be occurring in an attempt to raise body concentrations of 22:6n-3. We hypothesize that accumulation of 22:5n-3 might be an early indicator of 22:6n-3 deficiency in larval fish that precedes a reduction in growth or survival. A possible role of 22:5n-3 as a biochemical surrogate for 22:6n-3 is discussed.

Paper no. L9372 in *Lipids 39*, 215–222 (March 2004).

Unlike freshwater fish, the marine fish studied thus far have a limited ability to convert 18:3n-3 and 18:2n-6 to long-chain ($\geq C_{20}$) PUFA (LC-PUFA) owing to limited expression of genes coding for enzymes required in the biosynthesis (1,2). Subsequently, marine fish have an essential dietary requirement for preformed 20:4n-6, 20:5n-3, and 22:6n-3 (1). Marine fish larvae hatch with sufficient stores of FA derived from the egg to support development up to the first feeding. Even during times of starvation, body concentrations of 22:6n-3 and 20:4n-6 are highly conserved in marine larvae (summarized by Izquierdo, see Ref. 3). Consequently, feeding diets devoid of these long-chain EFA during the early stages of larval life can often have little effect on development compared with diets apparently sufficient in nutrients (4–6). Longer-term feeding of EFA-deficient diets ultimately results in reduced growth and survival, particularly at key developmental stages such as metamorphosis, a major physiological event in larval fish requiring increased levels of LC-PUFA to accommodate tissue structural changes (4).

Although marine fish are limited in their ability to convert 18:3n-3 to 20:5n-3, they have some capacity to convert 20:5n-3 to 22:6n-3, albeit only at low rates (7,8). The conversion of 20:5n-3 to 22:5n-3 generally proceeds quickly *via* elongase enzymes; however, final conversion of 22:5n-3 to 22:6n-3 is far more complicated, with elongation, desaturation, and chain-shortening steps all being required, and is a rate-limiting process. Hence, marine fish fed diets deficient in 22:6n-3 are unable to completely elongate and desaturate 20:5n-3 to 22:6n-3 rapidly enough to meet requirements, and the intermediate product, 22:5n-3, accumulates. For example, Bell *et al.* (9) found that juvenile herring (*Clupea harengus*) fed a live food, *Artemia*, that was low in 22:6n-3 and 20:5n-3 and completely void of 22:5n-3, had significant increases of 22:5n-3 in the eyes. Conversely, herring fed *Artemia* with sufficient 22:6n-3 and some 22:5n-3 resulted in eyes with markedly higher 22:6n-3, but only half of the 22:5n-3 of their 22:6n-3-deprived counterparts. Growth was unaffected during the 102-d study, although the ability of the 22:6n-3-deficient herring to feed was significantly reduced under low light intensities owing to visual problems, which were attributed to the importance of 22:6n-3 in light-sensitive tissues. Although indicators such as growth and survival are most often used for quantifying nutrient requirements in the longer term, the work with herring demonstrated important nutritional effects occurring at a subclinical level. Further, the research by Bell *et al.* (9) suggests

*To whom all correspondence should be addressed at TAFI-MRL, University of Tasmania, Private Bag 49, Hobart, Tasmania, 7001, Australia. E-mail: Matthew.Bransden@utas.edu.au

Abbreviations: DM, dry matter; dph, days post-hatch; MUFA, monounsaturated FA; LC-PUFA, long-chain PUFA; SFA, saturated FA; TFA, total FA; TO, tuna oil.

that assessing biochemical status by looking at relationships between dietary levels and tissue FA accumulation and depletion may be useful in assessing nutritional deficiencies in marine fish larvae. To examine relationships between dietary FA and tissue FA, dose–response studies with multiple, graduated treatments are able to provide better insights than often-used "low" or "high" concentrations of a particular FA. However, dose–response studies with nutrients are seldom used in larval fish studies owing to the complexities and costs of enriching and delivering multiple batches of live feed.

Like most other marine fish larvae (3), the striped trumpeter (*Latris lineata*) strongly conserves tissue proportions of 22:6n-3 and 20:4n-6 when feeding is delayed beyond yolk-sac absorption (5 d post-hatch, dph; Bransden, M.P., unpublished data), suggesting the essentiality of these FA (3). Our study therefore aimed to determine the effect of feeding striped trumpeter larvae on a live feed (rotifers, *Brachionus plicatilis*) enriched with seven graduated concentrations of n-3 LC-PUFA, mainly 20:5n-3 and 22:6n-3. Larvae grow quickly, and tissues respond rapidly to dietary changes during early development. A short feeding period from 5 to 18 dph was chosen to minimize possible gross deficiency symptoms such as poor larval survival that could confound results. The overall aim was to assess trends in larval body biochemistry, particularly body levels of 20:5n-3, 22:5n-3, and 22:6n-3, to determine if any of these parameters could be helpful as early indicators of n-3 LC-PUFA deficiency.

MATERIALS AND METHODS

Live feed enrichment. Seven experimental emulsions were prepared (Nutra-Kol, Western Australia, Australia) by mixing tuna body oil (TO) and coconut oil to provide incremental concentrations of n-3 LC-PUFA (Table 1). A 20:4n-6-rich oil (Vevodar®; DSM Food Specialties, Delft, The Netherlands) was gradually included as coconut oil replaced TO to ensure that the dietary concentration of 20:4n-6 remained constant. Final emulsions contained 0 (0% TO), 90 (9% TO), 182 (18% TO), 274 (27% TO), 366 (37% TO), 458 (46% TO), or 550 (55% TO) mg TO/g of emulsion. Emulsions were stored at 4°C under nitrogen prior to use. Rotifers at a density of 500/mL were enriched on the emulsions (0.1 g/L) in 20-L plastic containers with gentle aeration and oxygenation. All enrichments were conducted for 12 h at 22°C. Samples of rotifers fed each of the emulsions were collected during the experiment for biochemical analysis ($n = 3$). Where appropriate, enriched rotifers are hereafter referred to as the larval "diet."

Larval rearing and the experimental system. Striped trumpeter broodstock were held under controlled light and ambient temperatures at the Tasmanian Aquaculture and Fisheries Institute–Marine Research Laboratories, Hobart (10). Eggs were stripped from one female and fertilized with the milt of four males. Eggs were incubated at 14°C in 250-L cylindro-conical tanks with seawater recirculating at ~150 L/h. Eggs were disinfected with 1.0 ppm ozone for 60 s at 3 d post-fertilization. Eggs hatched after 5 d at 14°C, and the temperature was gradually increased to 16°C.

Larvae were transferred at 2 dph to an experimental unit that consisted of twenty-four 300-L black hemispherical fiberglass tanks, on a photoperiod of an 18:6-h light-dark cycle and a water surface light intensity of ~15 μmol/s/m^2. Larvae were randomly stocked at 4500 larvae/tank. All tanks remained static until 5 dph, when filtered seawater was exchanged at a rate of 100%/d and recirculated at 900%/d. Recirculated water was screened to remove uneaten rotifers. Triplicate tanks of larvae received rotifers enriched with one of seven enrichments for the first time at 1700 h, 5 dph, and thereafter at 0900 and 1700 h each day up to and including 17 dph. Rotifers were fed to larvae at a density of 5 rotifers/mL. Surface skimmers were used from 7–18 dph to remove surface oil and promote swim bladder inflation (11). The antibiotic oxytetracycline (active form, oxytetracycline hydrochloride) was added daily at 25 ppm from 6 dph until the conclusion of the experiment. Water quality was measured daily with an average (± SD) temperature of 15.8 ± 0.4°C, salinity 33.4 ± 0.2 ppt, dissolved oxygen 7.6 ± 0.3 mg O_2/L, and pH 8.0 ± 0.2. At 10, 14, and 18 dph, 150 larvae/tank were removed by siphon for visual assessment of larval quality ($n = 20$ larvae) or for biochemical analysis. The larvae were sampled in the dark prior to feeding to ensure that no residual gut contents remained, and gut evacuation was confirmed during microscopic assessment.

All aspects of the trial were conducted in accordance with University of Tasmania Animal Ethics guidelines in relation to research on experimental animals (UTas Animal Ethics Approval: A0005845).

Biochemical analysis. Samples of rotifers were collected on a 63-μm mesh screen, washed with 0.5 M ammonium formate to remove residual sea water (12), transferred to vials, and immediately frozen in liquid nitrogen before being transferred to a freezer at –80°C. A known number (30–50) of anesthetized striped trumpeter larvae were collected on a preweighed glass microfiber filter, washed with ammonium formate, immediately frozen in liquid nitrogen, and subsequently stored at –80°C. Samples were freeze-dried to a constant weight immediately prior to biochemical analysis.

FAME were formed by a direct transesterification process, which had been validated for a microheterotroph (13) and for striped trumpeter larvae and rotifers (Bransden, M.P., and Dunstan, G.A., unpublished data) against a conventional extraction (14), followed by transesterification. Freeze-dried samples were directly transesterified with a solution of methanol/chloroform/hydrochloric acid (10:1:1, by vol) at 80°C for 2 h. FAME were extracted using three washes of hexane/chloroform (4:1, vol/vol), concentrated under a stream of nitrogen gas, and an internal standard (methyl tricosanoate) was added. FAME were analyzed by GC using a Hewlett-Packard 5890A gas chromatograph fitted with a split/splitless injector, an HP 7673 autosampler, an FID, and an HP-5 cross-linked methyl silicone fused-silica capillary column (50 m × 0.32 mm i.d.; Hewlett-Packard, Palo Alto, CA). Helium was the carrier gas. Oven temperature was held at 50°C for 1 min before being raised to 150°C at 30°C/min, then to 250°C at 2°C/min, and finally to 300°C at 5°C/min. FA were quantified using Waters Millenium software

TABLE 1
Formulation (mg/g) of Experimental Emulsions Used to Enrich Rotifers, and the Resultant FA Profile of Rotifers (mg/g DM)

Enrichment	0% TO	9% TO	18% TO	27% TO	37% TO	46% TO	55% TO
Composition							
TO[a]	0.0	90.0	182.0	274.0	366.0	458.0	550.0
Coconut oil	530.0	443.0	354.5	266.0	177.0	88.5	0.0
Vevodar®[b]	20.0	17.0	13.5	10.0	7.0	3.5	0.0
Ascorbic acid[c]	30.0	30.0	30.0	30.0	30.0	30.0	30.0
Mixed tocopherols[d]	30.0	30.0	30.0	30.0	30.0	30.0	30.0
Other[e]	390.0	390.0	390.0	390.0	390.0	390.0	390.0
Rotifer FA							
12:0	27.75	16.75	12.65	8.96	4.23	1.51	0.11
14:0	16.83	13.42	11.64	10.11	6.57	4.20	2.59
16:0	13.86	13.77	14.83	16.35	15.57	15.88	16.57
18:0	3.99	3.86	3.89	4.20	3.88	3.87	3.88
Total SFA[f]	63.55	49.15	44.66	41.55	32.23	27.59	25.43
16:1n-7	7.07	5.97	6.94	7.64	7.23	7.36	7.57
18:1n-9[g]	16.38	16.57	17.43	18.95	17.79	18.09	17.88
18:1n-7	1.97	1.95	2.18	2.49	2.49	2.57	2.72
20:1n-9	2.67	2.35	2.43	2.50	2.34	2.38	2.33
22:1n-9	0.66	0.63	0.63	0.63	0.60	0.61	0.62
Total MUFA[h]	32.38	31.49	34.08	37.30	35.55	36.47	36.74
18:2n-6	12.42	10.85	10.13	10.05	9.05	8.80	8.40
20:2n-6	0.87	0.77	0.74	0.75	0.63	0.64	0.62
20:3n-6	0.71	0.62	0.60	0.63	0.56	0.55	0.57
20:4n-6	3.97	3.29	3.27	3.26	2.92	2.89	2.85
22:5n-6	0.09	0.24	0.40	0.55	0.65	0.76	0.86
Total n-6[i]	18.68	16.37	15.74	15.90	14.42	14.63	13.96
18:4n-3	0.06	0.14	0.31	0.45	0.52	0.65	0.73
20:4n-3	0.64	0.76	0.89	1.06	1.03	1.14	1.18
20:5n-3	4.54	4.62	5.75	6.92	7.05	7.90	8.36
22:5n-3	2.60	2.80	3.01	3.33	3.26	3.51	3.66
22:6n-3	1.91	5.05	8.25	11.20	12.72	14.99	16.42
24:6n-3	0.04	0.06	0.09	0.10	0.11	0.11	0.12
Total n-3 LC-PUFA	10.03	13.58	18.24	22.94	24.51	28.00	30.16
Total n-3[j]	10.09	13.73	18.55	23.39	25.03	28.66	30.88
Total PUFA[k]	30.42	31.76	35.93	41.12	41.16	44.98	46.63
Total FA	126.39	112.47	114.75	120.05	109.03	109.15	108.91
n-3/n-6	0.54	0.83	1.17	1.48	1.75	1.99	2.25

[a]Clover Corporation, Victoria, Australia.
[b]DSM Food Specialties, Delft, The Netherlands.
[c]Cognis Australia Pty. Ltd., Victoria, Australia.
[d]Hoffman-La Roche, NSW, Australia.
[e]Other components not contributing to vitamins or lipid profile (commercial in confidence, Nutra-Kol, Western Australia).
[f]Total SFA also includes 15:0, 17:0, 20:0, 22:0, and 24:0.
[g]Includes 18:3n-3 as a minor component.
[h]Total MUFA also includes 15:1, 16:1, 16:1n-7*t*, 16:1n-5, 17:1, 18:1, 18:1n-7*t*, 18:1n-5, 19:1n-10, 19:1n-8, 20:1n-11, 20:1n-7, 22:1n-11, 22:1n-7, 24:1n-9, and 24:1n-7.
[i]Total n-6 also includes 18:3n-6, 22:4n-6, and 22:3n-6.
[j]Total n-3 also includes 21:5n-3 and 22:4n-3.
[k]Total PUFA also includes 18:3n-6, 18:2, 21:5n-3, 22:4n-6, 22:3n-6, and 22:4n-3.
TO, tuna oil; SFA, saturated FA; MUFA, monounsaturated FA; LC, long chain ($\geq C_{20}$); DM, dry matter.

(Milford, MA), with the percentage of individual components expressed as the uncorrected percentage of the total area. Individual components were identified by comparing retention times and mass spectral data [Finnigan ThermoQuest GCQ gas chromatograph–mass spectrometer (Austin, TX) fitted with an on-column injector, configured as above] with data obtained for authentic and laboratory standards.

Statistics. Significant differences between larval FA concentrations at 18 dph were determined by performing one-way ANOVA followed by a Tukey–Kramer honestly significant differences multiple comparison of means. Assumptions of ANOVA were assessed by the Shapiro–Wilk test to determine whether residuals were normally distributed, and Bartlett's test was used to determine the homogeneity of variance. Regression analysis was performed using a second-order polynomial. Statistical significance was accepted at $P < 0.05$. Statistical analyses were performed using JMP® version 5.1 (SAS Institute Inc., Cary, NC) statistical software and Microsoft® Excel 2000.

TABLE 2
Concentration of FA (mg/g DM, mean ± SD, n = 3) in Larvae at 1 and 5 Days Post-hatch (dph), or at 18 dph After Being Fed Rotifers Enriched on Experimental Emulsions[a]

Day post-hatch	1	5	18						
Enrichment			0% TO	9% TO	18% TO	27% TO	37% TO	46% TO	55% TO
12:0	0.0 ± 0.0	0.0 ± 0.0	5.6 ± 1.8^{a}	3.0 ± 0.6^{b}	3.4 ± 0.8^{a,b}	2.2 ± 0.2^{b,c}	1.6 ± 0.3^{b,c}	0.6 ± 0.2^{c}	0.1 ± 0.1^{c}
14:0	4.4 ± 0.3	1.4 ± 0.3	8.9 ± 0.8^{a}	6.9 ± 0.3^{b}	6.7 ± 0.4^{b}	5.2 ± 0.2^{c}	4.4 ± 0.1^{c}	3.0 ± 0.3^{d}	1.8 ± 0.2^{e}
16:0	28.1 ± 1.2	17.0 ± 0.6	14.1 ± 0.5^{b}	14.3 ± 0.1^{b}	16.2 ± 1.3^{a,b}	15.5 ± 0.6^{a,b}	16.6 ± 0.3^{a,b}	17.1 ± 0.7^{a}	16.9 ± 1.7^{a}
18:0	6.9 ± 0.3	6.7 ± 0.0	7.9 ± 0.4	7.9 ± 0.1	8.5 ± 0.5	8.2 ± 0.2	8.5 ± 0.2	8.5 ± 0.2	8.6 ± 0.5
Total SFA[b]	41.7 ± 1.9	26.6 ± 1.2	38.6 ± 2.7^{a}	34.1 ± 1.2^{a,b,c}	37.0 ± 2.1^{a,b}	33.5 ± 1.0^{b,c}	33.6 ± 0.9^{a,b,c}	31.9 ± 1.7^{c}	29.9 ± 2.3^{c}
16:1n-7	8.5 ± 0.4	2.3 ± 0.4	4.1 ± 0.3^{b,c}	4.0 ± 0.2^{c}	4.7 ± 0.2^{a,b}	4.7 ± 0.1^{a}	5.1 ± 0.1^{a}	5.1 ± 0.1^{a}	4.7 ± 0.4^{a}
18:1n-9[c]	20.4 ± 0.8	7.5 ± 1.6	14.5 ± 0.9	14.0 ± 0.6	16.1 ± 1.6	14.9 ± 0.4	16.0 ± 0.3	15.9 ± 0.6	15.6 ± 1.7
18:1n-7	5.7 ± 0.2	2.3 ± 0.7	2.6 ± 0.2^{d}	2.7 ± 0.1^{c,d}	3.0 ± 0.2^{b,c}	3.0 ± 0.1^{b,c,d}	3.3 ± 0.1^{a,b}	3.4 ± 0.1^{a}	3.5 ± 0.2^{a}
20:1n-9	1.3 ± 0.1	0.7 ± 1.0	1.7 ± 0.1	1.5 ± 0.1	1.6 ± 0.0	1.5 ± 0.1	1.6 ± 0.1	1.6 ± 0.1	1.7 ± 0.1
22:1n-9	0.2 ± 0.0	2.1 ± 2.8	0.3 ± 0.1	0.3 ± 0.0	0.3 ± 0.0	0.3 ± 0.1	0.3 ± 0.0	0.4 ± 0.0	0.4 ± 0.0
Total MUFA[d]	40.7 ± 1.6	17.4 ± 0.4	27.9 ± 1.6^{b,c}	27.0 ± 1.3^{c}	30.8 ± 2.0^{a,b,c}	29.9 ± 0.8^{a,b,c}	32.1 ± 0.3^{a,b}	32.5 ± 0.9^{a}	32.1 ± 2.7^{a,b}
18:2n-6	5.1 ± 0.2	1.9 ± 0.3	12.4 ± 0.9^{a}	11.1 ± 0.5^{a,b}	11.0 ± 0.5^{a,b}	9.8 ± 0.2^{b,c}	9.9 ± 0.2^{b,c}	9.5 ± 0.2^{c}	8.6 ± 0.6^{c}
20:2n-6	0.4 ± 0.0	0.2 ± 0.0	1.2 ± 0.1^{a}	1.1 ± 0.0^{b,c}	1.1 ± 0.1^{b}	0.9 ± 0.1^{c,d}	1.0 ± 0.0^{b,c,d}	0.9 ± 0.0^{d}	0.9 ± 0.1^{d}
20:3n-6	0.2 ± 0.0	0.1 ± 0.0	0.9 ± 0.1^{a}	0.7 ± 0.0^{b}	0.7 ± 0.0^{b,c}	0.6 ± 0.0^{c,d}	0.6 ± 0.0^{d,e}	0.6 ± 0.0^{d,e}	0.6 ± 0.0^{e}
20:4n-6	2.8 ± 0.1	2.1 ± 0.3	6.5 ± 0.3^{a}	5.7 ± 0.1^{b}	5.6 ± 0.2^{b,c}	5.2 ± 0.1^{b,c,d}	5.3 ± 0.1^{c,d}	5.0 ± 0.1^{d}	4.8 ± 0.2^{d}
22:5n-6	0.5 ± 0.0	0.3 ± 0.0	0.3 ± 0.0^{e}	0.5 ± 0.0^{d}	0.8 ± 0.0^{c}	0.9 ± 0.0^{b,c}	1.0 ± 0.1^{a,b}	1.1 ± 0.1^{a}	1.1 ± 0.1^{a}
Total n-6[e]	9.6 ± 0.4	5.1 ± 0.6	22.5 ± 1.4^{a}	20.2 ± 0.9^{a,b}	19.7 ± 0.8^{b,c}	18.1 ± 0.6^{b,c,d}	18.3 ± 0.3^{b,c,d}	17.8 ± 0.8^{c,d}	16.4 ± 0.5^{d}
18:4n-3	1.7 ± 0.1	0.5 ± 0.0	0.1 ± 0.0^{e}	0.2 ± 0.0^{e}	0.3 ± 0.0^{d}	0.4 ± 0.0^{c}	0.5 ± 0.0^{b}	0.6 ± 0.0^{a,b}	0.7 ± 0.0^{a}
20:4n-3	1.1 ± 0.1	0.4 ± 0.0	0.9 ± 0.1^{d}	0.9 ± 0.1^{c,d}	1.0 ± 0.1^{b,c}	1.1 ± 0.0^{a,b}	1.1 ± 0.0^{a,b}	1.2 ± 0.0^{a}	1.2 ± 0.0^{a}
20:5n-3	16.6 ± 0.5	6.9 ± 1.0	5.6 ± 0.3^{e}	5.9 ± 0.2^{d}	6.9 ± 0.1^{c}	7.3 ± 0.2^{b}	8.2 ± 0.0^{a}	8.6 ± 0.1^{a}	8.5 ± 0.2^{a}
22:5n-3	4.8 ± 0.1	2.5 ± 0.0	6.5 ± 0.3^{a}	6.0 ± 0.3^{a,b}	5.7 ± 0.2^{b,c}	5.5 ± 0.2^{b,c}	5.2 ± 0.1^{c}	5.6 ± 0.2^{b,c}	5.5 ± 0.1^{b,c}
22:6n-3	31.4 ± 0.8	19.6 ± 3.3	9.8 ± 0.5^{f}	15.2 ± 0.2^{e}	21.0 ± 1.1^{d}	24.0 ± 0.9^{c}	27.1 ± 1.0^{b}	28.2 ± 0.8^{a,b}	30.3 ± 1.3^{a}
24:6n-3	0.1 ± 0.0	0.3 ± 0.3	0.1 ± 0.0^{b}	0.1 ± 0.0^{a,b}	0.1 ± 0.0^{a,b}	0.1 ± 0.0^{a,b}	0.1 ± 0.0^{a}	0.1 ± 0.0^{a,b}	0.1 ± 0.0^{a,b}
Total n-3 LC-PUFA	54.3 ± 1.4	29.7 ± 3.9	23.3 ± 0.6^{f}	28.6 ± 0.6^{e}	35.3 ± 1.4^{d}	38.5 ± 1.2^{c}	42.2 ± 0.9^{b}	44.1 ± 0.8^{a,b}	46.1 ± 1.7^{a}
Total n-3[f]	56.0 ± 1.5	30.2 ± 3.9	23.4 ± 0.8^{f}	28.8 ± 0.6^{e}	35.6 ± 1.4^{d}	38.9 ± 1.2^{c}	42.7 ± 0.9^{b}	44.7 ± 0.8^{a,b}	46.8 ± 1.7^{a}
Total PUFA[g]	66.3 ± 1.8	35.6 ± 4.2	47.3 ± 2.0^{d}	50.3 ± 1.3^{d}	56.9 ± 2.3^{c}	58.3 ± 1.5^{b,c}	62.2 ± 1.0^{a,b}	63.8 ± 1.3^{a}	64.5 ± 2.4^{a}
Total FA	148.7 ± 5.3	79.6 ± 2.6	113.9 ± 6.0^{b,c}	111.6 ± 3.6^{c}	124.8 ± 6.3^{a,b,c}	121.9 ± 2.0^{a,b,c}	128.1 ± 2.1^{a}	128.4 ± 3.8^{a}	126.7 ± 7.4^{a,b}
n-3/n-6	5.8 ± 0.1	6.0 ± 0.1	1.0 ± 0.0^{g}	1.4 ± 0.0^{f}	1.8 ± 0.0^{e}	2.1 ± 0.1^{d}	2.3 ± 0.0^{c}	2.5 ± 0.1^{b}	2.9 ± 0.0^{a}
µg TFA/larva	10.7 ± 0.4	4.7 ± 0.4	36.1 ± 5.2	35.0 ± 5.0	38.8 ± 4.3	37.8 ± 3.7	40.7 ± 4.1	40.1 ± 0.9	38.5 ± 2.7

[a]18 dph values in the same row but not sharing a common roman superscript letter (a–f) are significantly different ($P < 0.05$). For abbreviations see Table 1.
[b]Total SFA also includes 15:0, 17:0, 20:0, 22:0, and 24:0.
[c]Includes 18:3n-3 as a minor component.
[d]Total MUFA also includes 15:1, 16:1, 16:1n-7*t*, 16:1n-5, 17:1, 18:1, 18:1n 7*t*, 18:1n-5, 19:1n-10, 19:1n-8, 20:1n-11, 20:1n-7, 22:1n-11, 22:1n-7, 24:1n-9, and 24:1n-7.
[e]Total n-6 also includes 18:3n-6, 22:4n-6, and 22:3n-6.
[f]Total n-3 also includes 21:5n-3 and 22:4n-3.
[g]Total PUFA also includes 18:3n-6, 18:2, 21:5n-3, 22:4n-6, 22:3n-6, and 22:4n 3.

RESULTS

Rotifer FA profile. The FA profiles of rotifers changed considerably depending on the relative amounts of the three oils (tuna, coconut, or Vevodar) that were contributing to the FA composition of the emulsions. Approximately half of the total FA (TFA) in rotifers consisted of saturated FA (SFA) when coconut was the primary component of the emulsion, and this was gradually replaced with monounsaturated FA (MUFA) and n-3 LC-PUFA as more was included (Table 1). Despite limited n-3 LC-PUFA in the ingredients used to produce the 0% TO emulsion, some n-3 LC-PUFA [10 mg/g dry matter (DM)] were still found in rotifers enriched in this product, whereas the 55% TO emulsion produced a rotifer with 30 mg/g DM of n-3 LC-PUFA. The 22:6n-3 content in the rotifers ranged between 2 and 16 mg/g DM, whereas the 22:5n-3 concentration ranged from 2.6 to 3.7 mg/g DM, with increasing amounts as more TO was included in the emulsion.

Larval performance and FA profiles. There was no significant relationship ($P > 0.05$) between dietary n-3 LC-PUFA to dry weight of larvae (overall mean ± SD, 314.4 ± 24.3 μg) and larval survival (61.3 ± 6.4%) at 18 dph.

The FA profile of larvae at 1, 5, and 18 dph is provided in Table 2. Significant differences (ANOVA) were detected for most FA at 18 dph, with larvae fed the experimental diets having FA profiles that generally reflected the feeds. The ranges of 20:4n-6, 20:5n-3, and 22:6n-3 concentrations (0–55% TO) were 6.5–4.8, 5.6–8.5, and 9.8–30.3 mg/g DM, respectively.

In general, significantly positive regressions were identified at all sampling points for most larval FA and their corresponding dietary FA on an absolute (mg/g DM) or relative (g/100 g total FA) basis, although only regressions for 20:5n-3, 22:5n-3, and 22:6n-3 are shown here (Figs. 1A–I). The concentration of larval 20:5n-3 was generally similar, between 10 (Fig. 1A) and 14 dph (Fig. 1B), and then increased at 18 dph (Fig. 1C). The range of larval 22:6n-3 concentrations increased over the duration of the experiment, ranging from 14–27 mg/g DM (0–55% TO) at 10 dph, and increasing to 9–30 mg/g DM (0–55% TO) at 18 dph. In contrast to what was observed for all other FA, an inverse relationship between larval and dietary 22:5n-3 was recorded. Although no significant relationship was detected for 22:5n-3 at 10 dph (Fig. 1G), significant polynomial regressions were found at 14 (Fig. 1H) and 18 dph (Fig. 1I).

DISCUSSION

Significant relationships were found between dietary FA and the FA composition of the larvae throughout the present trial, which is consistent with other studies on larval marine fish (15–17). Notably, the deposition of 20:5n-3 and 22:6n-3 in larval tissues relative to the diet was generally linear at 10, 14, and 18 dph. At 10 dph, no relationship was found between dietary and larval 22:5n-3. However, at 14 and 18 dph an inverse relationship was observed that did not occur with any other FA. Accumulation of 22:5n-3 has been recorded in other larval marine fish when dietary 22:6n-3 is low, although these experiments have often investigated "high" and "low" dietary 22:6n-3 treatments rather than the graded approach used here. Thus, Furuita *et al.* (18) used three 22:6n-3 concentrations in the live food *Artemia* fed to Japanese flounder (*Paralichthys olivaceus*) and found an inverse relationship between larval body 22:5n-3 and dietary 22:6n-3, despite very low dietary (*Artemia*) levels of 22:5*n*-3, suggesting that conversion of 20:5n-3 to 22:5n-3 was increased in the larvae as dietary 22:6n-3 was decreased. Similarly, Izquierdo *et al.* (19) observed increased levels of 22:5n-3 in Japanese flounder when dietary 22:6n-3 was low. An increase in 22:5n-3 in the combined brain and eyes of white bass (*Morone chrysops*) that was inversely related to dietary (*Artemia*) 22:5n-3 and 22:6n-3 also has been reported (20), as has an accumulation of 22:5n-3 in 22:6n-3-deficient herring, as described previously (9).

In the present trial, the highest concentration of 22:5n-3 was found in the larvae at 18 dph when the concentration of dietary 22:6n-3 was at it lowest (0% TO diet). In the larvae fed higher dietary levels of 22:6n-3, the accumulation of 22:5n-3 was reduced. The inverse trend in 22:5n-3 accumulation became more evident as the larvae developed. This temporal variation in larval 22:5n-3 concentration suggests either that larvae are less efficient in the elongation of 20:5n-3 early in their development, or that critical points in tissue 22:6n-3 concentration are reached, triggering the need for *in vivo* 22:6n-3 production. Ruyter and Thomassen (21) showed that the conversion of 18:3n-3 to 20:5n-3 and 22:6n-3 increases in livers of Atlantic salmon (*Salmo salar*) under conditions of dietary and presumably tissue deprivation of 22:6n-3. This enhanced conversion of 20:5n-3 to 22:5n-3 under conditions of 22:6n-3 deficiency would explain the temporal trends in body FA composition in the present experiment. The increase in body 22:5n-3 in larvae fed 46 and 55% TO that results in an inflexion of the polynomial curve (Fig. 1I) probably represents deposition of 22:5n-3-from the diet under normal dietary 22:6n-3-sufficient conditions.

All of the 11 species of marine fish studied thus far have a strict dietary requirement for 20:5n-3 and 22:6n-3, and probably also 20:4n-6 (1). However, *in vivo* studies and *in vitro* cell culture studies using radioactive precursors, particularly with turbot (*Scopthalmus maximus*) and sea bream (*Sparus aurata*), have shown very low but significant rates of conversion of 18:3n-3 to 20:5n-3, and especially of 20:5n-3 to 22:5n-3 and 22:6n-3, and also the presence of very low Δ6- and Δ5-desaturase and PUFA elongase activities (1). However, the rates of conversion of C_{18} to C_{20} and of C_{20} to C_{22} n-3 PUFA by marine fish are far below those necessary to meet the dietary requirements of the fish for 20:5n-3 and 22:6n-3. Although such detailed studies have not been conducted in the striped trumpeter, there is no reason to suggest that this species is fundamentally different from those marine species studied thus far. Indeed, the accumulation of 22:5n-3 under conditions of 22:6n-3 deprivation in the striped trumpeter is to be expected on the basis of current knowledge of the nutritional biochemistry of fish and the various feeding studies with marine fish referred to earlier. It is interesting to note that although there was an accumulation of tissue 22:5n-3, subsequent elongation and desaturation products were generally

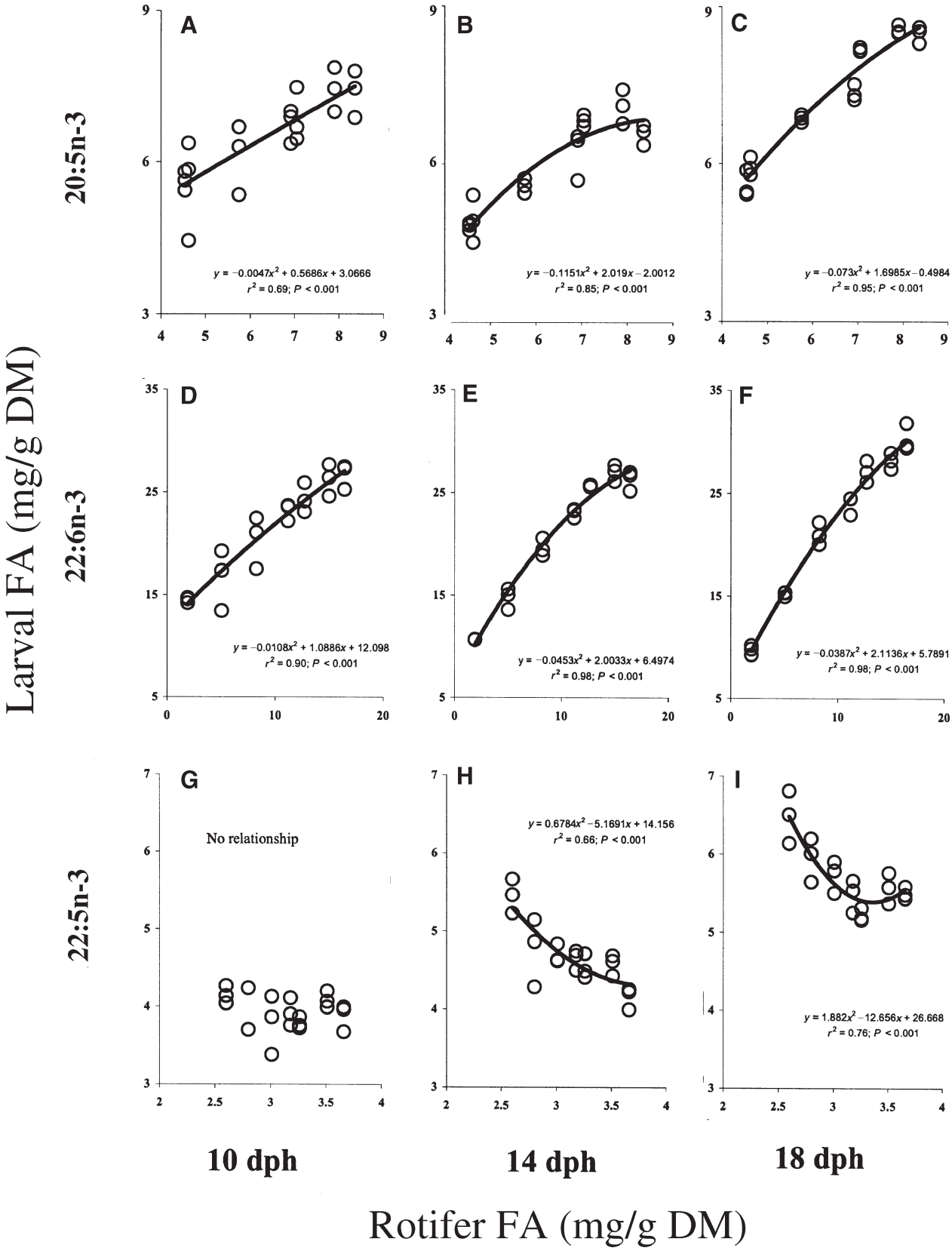

FIG. 1. The relationship between rotifer FA [mg/g dry matter (DM), *x*-axis] and larval FA (mg/g DM, *y*-axis) for 20:5n-3 (A–C), 22:6n-3 (D–F), and 22:5n-3 (G–I) at 10, 14, and 18 d post-hatch (dph). Each value (○) represents a replicate from a treatment. Second-order polynomials were fitted to the data. The *x*- and *y*-axes do not necessarily begin at zero.

found in only trace amounts. It has been established that the 22:5n-3 accumulating in juvenile herring fed diets deficient in 22:6n-3 is present in tissue (eye) phospholipids (9), so it is possible that 22:5n-3 may be used as a temporary or best-available surrogate for 22:6n-3 in tissue phospholipids when the diet is deficient in the latter. Indeed, 22:5n-3 may exhibit biochemical characteristics more similar to 22:6n-3 than to C_{24} n-3 PUFA or its precursor 20:5n-3. Alternatively, accumulation of 22:5n-3 also may be related to the conversion of 20:5n-3 to 22:5n-3, occurring more readily than the further conversion of 22:5n-3 to 22:6n-3 *via* 24:5n-3 and 24:6n-3. Regardless, we hypothesize that the accumulation of 22:5n-3 with constant or reduced 22:6n-3 in larval fish tissues may be an early indicator of n-3 PUFA deficiency.

To our knowledge, this is the first experiment in marine fish larvae to use multiple (seven) dietary n-3 PUFA concentrations to demonstrate a direct, inverse relationship between dietary 22:6n-3 and the deposition of 22:5n-3 in the tissues. Although other studies have demonstrated an accumulation of 22:5n-3 when dietary 22:6n-3 is low, this is usually in response to a single deficient treatment, rather than the graded dose–response technique described herein. Consequently, in those studies a clear pattern of dose and response is not available. In the present trial, combined totals of tissue 20:5n-3 and 22:5n-3 were almost constant regardless of diet, with actual proportions seemingly associated with dietary 22:6n-3. Therefore, we propose that the inverse relationship between tissue 22:5n-3 and dietary 22:6n-3 indicates elongation of 20:5n-3 when dietary 22:6n-3 is insufficient, as well as a cessation in the elongation of 20:5n-3 when the dietary 22:6n-3 requirement is met. Additionally, we hypothesize that the accumulation of 22:5n-3 in tissues might be used as an early indicator of 22:6n-3 deficiency in larval fish. The lowest point in the polynomial relationship (Fig. 1I) occurs in larvae fed the 37% TO diet, which contained 12.7 mg 22:6n-3/g DM, and may provide some indication of the minimum dietary requirement of 22:6n-3 for 18-dph striped trumpeter larvae. This value is in the range normally recorded for dietary 22:6n-3 requirements of other larval marine fish, although these studies have generally used growth or survival as the requirement criterion (3). Gross clinical signs such as growth and survival, or subclinical signs such as visual capability and stress resistance, during longer studies on striped trumpeter larvae subjected to similar treatments are required to substantiate our hypothesis that 22:5n-3 accumulation may be an indication of actual or incipient 22:6n-3 deficiency. Further, *in vitro* or *in vivo* studies to elucidate why the striped trumpeter accumulates 22:5n-3 in preference to further elongated and desaturated n-3 LC-PUFA, and indeed to determine if 22:6n-3 can be produced at all from 20:5n-3, are required. Such studies are important in future EFA nutritional research on larvae and post-larvae of the striped trumpeter and marine teleost fish in general.

ACKNOWLEDGMENTS

The authors appreciate the invaluable comments made on the manuscript by Professors John Sargent, Robert Ackman, and Howard Knapp, and two anonymous referees. We also gratefully acknowledge the technical assistance of Anna Overweter, Andrew Trotter, Malcolm Brown, Mina Brock, Ross Goldsmid, Bill Wilkinson, Allan Beech, and Danny Holdsworth. The Clover Corporation kindly provided the refined 22:6n-3-containing TO used in this study; we thank the company for their ongoing interest in and support of Australian marine oil research. Experimental emulsions were kindly prepared by Judith Kolkovski (Nutra-Kol, Western Australia). Malcolm Haddon kindly advised us on statistical analysis. This work formed part of a project for Aquafin CRC, and received funds from the Australian Government's CRC Program, the Fisheries Research and Development Corporation, and other CRC participants.

REFERENCES

1. Sargent, J.R., Tocher, D.R., and Bell, J.G. (2002) The Lipids, in *Fish Nutrition* (Halver, J.E., and Hardy, R.W., eds.), pp. 181–257, Academic Press, San Diego.
2. Tocher, D.R. (2003) Metabolism and Functions of Lipids and Fatty Acids in Teleost Fish, *Rev. Fish. Sci. 2*, 107–184.
3. Izquierdo, M.S. (1996) Essential Fatty Acid Requirements of Cultured Marine Fish Larvae, *Aquacult. Nutr. 2*, 183–191.
4. Tuncer, H., and Harrell, R.M. (1992) Essential Fatty Acid Nutrition of Larval Striped Bass (*Morone saxatilis*) and Palmetto Bass (*M. saxatilis* × *M. chrysops*), *Aquaculture 101*, 105–121.
5. Salhi, M., Izquierdo, M.S., Hernández-Cruz, C.M., González, M., and Fernández-Palacios, H. (1994). Effect of Lipid and n-3 HUFA Levels in Microdiets on Growth, Survival, and Fatty Acid Composition of Larval Gilthead Sea Bream (*Sparus aurata*), *Aquaculture 124*, 275–282.
6. Dhert, P., Lavens, P., Duray, M., and Sorgeloos, P. (1990) Improved Larval Survival at Metamorphosis of Asian Seabass (*Lates calcarifer*) Using ω-3-HUFA-Enriched Live Food, *Aquaculture 90*, 63–74.
7. Sargent, J.R., Bell, J.G., Bell, M.V., Henderson, R.J., and Tocher, D.R. (1995) Requirement Criteria for Essential Fatty Acids, *J. Appl. Ichthyol. 11*, 183–198.
8. Sargent, J., Henderson, R.J., and Tocher, D.R. (1989) The Lipids, in *Fish Nutrition* (Halver, J.E., ed.), pp. 153–218, Academic Press, San Diego.
9. Bell, M.V., Batty, R.S., Dick, J.R., Fretwell, K., Navarro, J.C., and Sargent, J.R. (1995) Dietary Deficiency of Docosahexaenoic Acid Impairs Vision at Low Light Intensities in Juvenile Herring (*Clupea harengus* L.), *Lipids 30*, 443–449.
10. Morehead, D.T., Ritar, A.J., and Pankhurst, N.W. (2000) Effect of Consecutive 9- or 12-Month Photothermal Cycles and Handling on Sex Steroid Levels, Oocyte Development, and Reproductive Performance in Female Striped Trumpeter *Latris lineata* (Latrididae), *Aquaculture 189*, 293–305.
11. Trotter, A.J., Battaglene, S.C., and Pankhurst, P.M. (2003) Effects of Photoperiod and Light Intensity on Initial Swim Bladder Inflation, Growth, and Post-inflation Viability in Cultured Striped Trumpeter (*Latris lineata*) Larvae, *Aquaculture 224*, 141–158.
12. Brown, M.R., Skabo, S., and Wilkinson, B. (1998) The Enrichment and Retention of Ascorbic Acid in Rotifers Fed Microalgal Diets, *Aquacult. Nutr. 4*, 151–156.
13. Lewis, T., Nichols, P.D., and McMeekin, T.A. (2000) Evaluation of Extraction Methods for Recovery of Fatty Acids from Lipid-Producing Microheterotrophs, *J. Microbiol. Methods 43*, 107–116.
14. Bligh, E.G., and Dyer, W.G. (1959) A Rapid Method of Total Lipid Extraction and Purification, *Can. J. Biochem. Physiol. 37*, 911–917.
15. Koven, W., Barr, Y., Lutzky, S., Ben-Atia, I., Weiss, R., Harel, M., Behrens, P., and Tandler, A. (2001) The Effect of Dietary Arachidonic Acid (20:4n-6) on Growth, Survival and Resistance

to Handling Stress in Gilthead Seabream (*Sparus aurata*) Larvae, *Aquaculture 193*, 107–122.
16. Mourente, G., Rodriguez, A., Tocher, D.R., and Sargent, J.R. (1993) Effects of Dietary Docosahexaenoic Acid (DHA, 22:6n-3) on Lipid and Fatty Acid Compositions and Growth in Gilthead Sea Bream (*Sparus aurata* L.) Larvae During First Feeding, *Aquaculture 112*, 79–98.
17. Rodriguez, C., Perez, J.A., Izquierdo, M.S., Mora, J., Lorenzo, A., Fernandez-Palacios, H. (1994) Essential Fatty Acid Requirements of Larval Gilthead Sea Bream, *Sparus aurata* (L.), *Aquacult. Fish. Manage. 25*, 295–304.
18. Furuita, H., Konishi, K., and Takeuchi, T. (1999) Effect of Different Levels of Eicosapentaenoic Acid and Docosahexaenoic Acid in *Artemia nauplii* on Growth, Survival, and Salinity Tolerance of Larvae of the Japanese Flounder, *Paralichthys olivaceus, Aquaculture 170*, 59–69.
19. Izquierdo, M.S., Arakawa, T., Takeuchi, T., Haroun, R., and Watanabe, T. (1992) Effect of n-3 HUFA Levels in *Artemia* on Growth of Larval Japanese Flounder (*Paralichthys olivaceus*), *Aquaculture 105*, 73–82.
20. Harel, M., Lund, E., Gavasso, S., Herbert, R., and Place, A.R. (2000) Modulation of Arachidonate and Docosahexaenoate in *Morone chrysops* Larval Tissues and the Effect on Growth and Survival, *Lipids 35*, 1269–1280.
21. Ruyter, B., and Thomassen, M.S. (1999) Metabolism of n-3 and n-6 Fatty Acids in Atlantic Salmon Liver: Stimulation by Essential Fatty Acid Deficiency, *Lipids 34*, 1167–1176.

[Received August 7, 2003, and in final form and accepted April 20, 2004]

Replacement of Dietary Fish Oil with Increasing Levels of Linseed Oil: Modification of Flesh Fatty Acid Compositions in Atlantic Salmon (*Salmo salar*) Using a Fish Oil Finishing Diet

J. Gordon Bell*, R. James Henderson, Douglas R. Tocher, and John R. Sargent

Lipid Nutrition Group, Institute of Aquaculture, University of Stirling, FK9 4LA, Scotland, United Kingdom

ABSTRACT: Five groups of salmon, of initial mean weight 127 ± 3 g, were fed increasing levels of dietary linseed oil (LO) in a regression design. The control diet contained capelin oil (FO) only, and the same oil was blended with LO to provide the experimental diets. After an initial period of 40 wk, all groups were switched to a finishing diet containing only FO for a further 24 wk. Growth and flesh lipid contents were not affected by dietary treatment. The FA compositions of flesh total lipids were linearly correlated with dietary FA compositions (r^2 = 0.88–1.00, $P < 0.0001$). LO included at 50% of added dietary lipids reduced flesh DHA and EPA (20:5n-3) concentrations to 65 and 58%, respectively, of the concentrations in fish fed FO. Feeding 100% LO reduced flesh DHA and EPA concentrations to 38 and 30%, respectively, of the values in fish fed FO. Differences between diet and flesh FA concentrations showed that 16:0, 18:1n-9, and especially DHA were preferentially retained in flesh, whereas 18:2n-6, 18:3n-3, and 22:1n-11 were selected against and presumably utilized for energy. In fish previously fed 50 and 100% LO, feeding a finishing diet containing FO for 16 wk restored flesh DHA and EPA concentrations, to ~80% of the values in fish fed FO throughout. Flesh DHA and EPA concentrations in fish fed up to 50% LO were above recommended intake values for humans for these EFA. This study suggests that LO can be used as a substitute for FO in seawater salmon feeds and that any reductions in DHA and EPA can be largely overcome with a finishing diet high in FO before harvest.

Paper no. L9420 in *Lipids 39*, 223–232 (March 2004).

The importance of the n-3 PUFA, and specifically the n-3 highly unsaturated FA (HUFA) DHA (22:6n-3) and EPA (20:5n-3), in human nutrition is now widely recognized (1,2). There is also increasing evidence that a range of conditions currently prevalent in the developed world, including cardiovascular disease, diabetes, rheumatoid arthritis, neurological disorders, and metabolic disorders such as diabetes and obesity, are influenced by changes in dietary FA intake (3).

Fish, particularly those with high levels of body fat, such as salmon, herring, and sardines, represent a rich source of EPA and DHA for the human consumer. Owing to increased population pressure, worldwide demand for seafood is increasing, yet traditional food-grade fisheries are unable to match demand with supply (4). Increased demand has resulted in rapid expansion of aquaculture production to alleviate this potential seafood deficit (5,6). However, the feed-grade fisheries that have supplied the raw materials for aquaculture feeds have reached sustainable limits, and it is estimated that by the year 2010 more than 85% of world fish oil (FO) supplies will be used for aquaculture production (7). Consequently, continued expansion of the aquaculture industry can occur only if sustainable alternatives to FO, derived from terrestrial plants, are researched and implemented.

The lipids in feeds for Atlantic salmon must meet both energy and EFA requirements to allow for the rapid growth and development required in modern aquaculture production (8,9). Earlier studies on β-oxidation activity suggest that salmonid fish have a preference for 16:0, 16:1, 18:1n-9, and 22:1n-11, as well as 18:2n-6 (10,11), although more recent studies with salmon and rainbow trout suggest that 18:3n-3 and 20:5n-3 may also be utilized for energy production when present at higher concentrations (12–14). The high-latitude FO that are currently favored in salmon production are very rich in 20:1n-9 and 22:1n-11, whereas different vegetable oils are rich in 16:0, 18:1n-9, 18:2n-6, and 18:3n-3. Several recent studies have shown that salmon can be cultured for up to 30 wk using diets formulated with up to 100% replacement of added FO by vegetable oils (15–18). The ability to convert C_{18} PUFA to their long-chain HUFA products has been confirmed in Atlantic salmon, as has the up-regulation of these pathways in hepatocytes and enterocytes of fish fed vegetable oil-containing diets (19,20). However, the increased flux through the FA desaturation and elongation pathway is unlikely to compensate fully for reduced dietary EPA, DHA, and possibly arachidonic acid requirements; thus, a sufficient dietary supply of these HUFA will need to be provided (12,13).

Atlantic salmon fed diets containing raw materials of predominantly marine origin are of high nutritional quality, being rich in EPA and DHA and with an n-3/n-6 ratio of around 4:1 (21,22). Recent studies have shown that salmon cultured using diets in which >50% of added FO has been replaced with vegetable oil show significant reductions in flesh EPA and DHA concentrations (14–17). Obviously, from a

*To whom correspondence should be addressed. E-mail:g.j.bell@stir.ac.uk

Abbreviations: FO, fish oil; HUFA, highly unsaturated FA; LO, linseed oil.

human health perspective, any changes to n-3 HUFA content should be kept to a minimum, and any FO replacement should provide sufficient energy alternatives to long-chain monoenes, maximize conversion of dietary 18:3n-3, and preserve endogenous n-3 HUFA levels. In this regard, linseed oil (LO) is an important candidate for FO replacement, not only because it is rich in 18:3n-3, the precursor for n-3 HUFA, but also because 18:3n-3 is a favored substrate for β-oxidation both in salmonid fish and in mammals (12–14,23). Furthermore, increasing salmon flesh concentrations of 18:3n-3 should not be perceived as detrimental, from a human nutrition perspective, as 18:3n-3 has been shown to be beneficial in cardiovascular disease and some forms of cancer (24), possibly due to inhibition of the conversion of 18:2n-6 to 20:4n-6 and the inhibition of cyclooxygenase (25,26). The aim of this study was to determine the effects of replacing FO with LO, in a graded fashion, in terms of growth performance and, more importantly, to assess the changes in flesh FA composition that arise from LO inclusion. The relevance of reducing EPA and DHA concentrations, as well as increasing 18:2n-6 and 18:3n-3 concentrations, is discussed in the context of human nutrition. In addition, the successful restoration of EPA and DHA levels by feeding a FO finishing diet are relevant to human nutrition and to future production protocols for cultured Atlantic salmon.

In the present study, Atlantic salmon post-smolt were stocked into five seawater pens and fed one of four diets containing 25, 50, 75, or 100% LO, or a control diet containing only FO. The fish were grown for 40 wk before sampling, and thereafter fish on all treatments were switched to a diet containing only FO for a further 24 wk to follow the accumulation of DHA and EPA and the dilution of 18:3n-3 and 18:2n-6 from LO.

MATERIALS AND METHODS

Fish and diets. Atlantic salmon post-smolt (n = 3000) of initial mean weight 127 ± 3 g (individual weights of 50 fish/pen) were distributed into five net pens (5 × 5 m; 600 fish/pen) in Loch Duich, Lochalsh, Scotland, in June 2001. The temperature over the experimental period (June 2001–December 2002) ranged from 5.0 to 16.8°C, with a mean temperature of 10.8 ± 2.2°C. The fish were fed one of four experimental diets in which the FO component was replaced by LO or a control diet containing only FO (capelin oil). Specifically, the five diets were 100% FO (FO); FO/LO, 3:1 w/w (25% LO); FO/LO, 1:1 w/w (50% LO); FO/LO, 1:3 w/w (75% LO); and 100% LO. Feeds were fed to satiation by hand twice a day for a period of 40 wk and all feed fed was recorded. After this time, samples of fish were collected for analysis, and the remaining fish were all switched to the FO diet for a further 24 wk. The 24-wk time frame was chosen to allow as long as possible for the restoration of a marine FA profile and also so that fish did not exceed the normal market weight (5 kg). We were aware that the regression experimental design, with only one replicate per treatment, had statistical limitations. However, this compromise was made to allow growth from 150 g to 2 kg over a period of 40 wk on a commercial scale at reasonable cost. The data obtained are still highly relevant to both the aquaculture industry and to human nutrition. The five practical diet types (Nutreco Aquaculture Research Centre, Stavanger, Norway) were formulated to fully satisfy the nutritional requirements of salmonid fish and differed only in their oil composition (27). The main dietary components (in g kg^{-1}) were fishmeal, 338; capelin oil, 0–258, and/or linseed oil 0–258; maize gluten, 200; soy meal, 100; and micronutrients, 25. The diets were produced in 3-, 6- and 9-mm sizes and had average proximate compositions of 44.1 ± 0.3% crude protein, 29.4 ± 0.6% crude lipids, 7.1 ± 0.45% ash, and 5.9 ± 0.3% moisture. The FA compositions of the experimental diets are shown in Table 1. The FO diet containing capelin oil contained about 20% saturates, mainly 16:0, and almost 60% monoenes, of which 50% were the long-chain 20:1n-9 and 22:n-11. The FO diet contained 5% n-6 FA, mostly 18:2n-6, and 16% n-3 FA, dominated by EPA and DHA in almost equal amounts and with 18:3n-3 less than 1%. Addition of increasing levels of dietary LO resulted in increasing levels of 18:3n-3, 18:2n-6, and 18:1n-9 and decreasing levels of EPA, DHA, 16:0, total saturates, 20:1n-9, 22:1n-11, and total monoenes. Thus, the 100% LO diet contained 10% total saturates, 21% total monoenes, 15% 18:2n-6, and 50% 18:3n-3, with EPA and DHA accounting for only 2.5% of total dietary FA.

TABLE 1
FA Compositions (g FA/100 g total FA) and Astaxanthin Concentrations (mg/kg) in Experimental Diets

FA	FO	25% LO	50% LO	75% LO	100% LO
14:0	6.3	4.7	3.4	2.0	0.4
16:0	12.1	10.6	9.3	8.1	6.1
18:0	1.1	1.7	2.1	2.7	3.1
Total saturates[a]	19.9	17.2	15.1	13.0	10.5
16:1n-7	8.1	6.1	4.2	2.3	0.5
18:1n-9	11.9	13.6	15.1	16.0	17.0
18:1n-7	3.3	2.6	2.2	1.6	1.0
20:1n-9	17.9	13.1	9.0	5.0	1.1
22:1n-11	13.3	10.1	7.1	4.3	1.1
22:1n-9	2.1	1.5	1.0	0.5	0.1
Total monoenes[b]	58.4	48.4	39.6	30.5	21.1
18:2n-6	4.2	7.4	9.8	12.3	15.1
20:4n-6	0.2	0.2	0.1	0.1	0.1
Total n-6[c]	5.0	8.0	10.2	12.6	15.2
18:3n-3	0.9	14.0	25.6	37.8	50.4
18:4n-3	2.9	2.1	1.6	0.9	0.2
20:3n-3	0.1	0.1	0.1	0.1	0.1
20:4n-3	0.4	0.3	0.2	0.2	0.1
20:5n-3	5.9	4.6	3.5	2.2	1.0
22:6n-3	5.0	4.0	3.4	2.4	1.5
Total n-3[d]	15.7	25.6	34.6	43.7	53.3
Total PUFA	21.7	34.4	45.3	56.5	68.5
n-3/n-6	3.1	3.2	3.4	3.5	3.5
Astaxanthin (mg/kg)	56.9	61.8	66.6	72.2	68.7

[a]Includes 15:0, 17:0, 20:0, and 22:0.
[b]Includes 16:1n-9, 20:1n-11, 20:1n-7, 22:1n-13, and 24:1.
[c]Includes 20:2n-6, 20:3n-6, and 22:5n-6.
[d]Includes 20:3n-3, 20:4n-3, and 22:5n-3. FO, fish oil; LO, linseed oil.

Sampling procedures. After 40 wk, 18 fish were selected from each treatment and killed by a blow to the head after anesthetizing them with MS222 (Sigma-Aldrich, Poole, England). A sample of flesh, representative of the edible portion, was obtained by cutting a steak between the leading and trailing edges of the dorsal fin. The samples were combined as six pools of three steaks in each pool. The steaks were frozen on dry ice and stored at –40°C until processed. The steaks were thawed, skinned, and deboned, and the flesh was homogenized in a food processor after removal of the dorsal fat body. The homogenate was frozen immediately and stored at –40°C prior to analysis. During the period in which fish from all treatments were returned to a FO diet, samples were collected after 4, 8, 16, and 24 wk following reintroduction of the FO diet. At each time point, nine fish were sampled from each treatment group and were combined as three pools of three steaks in each pool. The steaks were processed and stored as described above.

Lipid extraction and FA analysis. Total lipids were extracted from 2 g of homogenized muscle by homogenizing in 20 vol of chloroform/methanol (2:1, vol/vol) in an Ultra-Turrax tissue disrupter (Fisher Scientific, Loughborough, United Kingdom). Total lipids were prepared according to the method of Folch *et al*. (28), and nonlipid impurities were removed by washing with 0.88% (wt/vol) KCl. The weight of lipids was determined gravimetrically after evaporation of the solvent and overnight desiccation *in vacuo*. FAME were prepared by acid-catalyzed transesterification of total lipids according to the method of Christie (29). Extraction and purification of FAME were performed as described by Ghioni *et al*. (30). FAME were separated and quantified by GLC (Vega 8160; Carlo Erba, Milan, Italy) using a 30 m × 0.32 mm i.d. capillary column (CP Wax 52CB; Chrompak, London, United Kingdom) and on-column injection. Hydrogen was used as the carrier gas, and temperature programming was from 50 to 150°C at 40°C min^{-1} and then to 230°C at 2.0°C min^{-1}. Individual methyl esters were identified by comparison with known standards and by reference to published data (30,31). Data were collected and processed using the Chromcard for Windows (version 1.19) computer package (Thermoquest Italia S.p.A., Milan, Italy).

Statistical analysis. The significance of differences ($P < 0.05$) between dietary treatments was determined by one-way ANOVA. Differences between means were determined by Tukey's test. Data identified as nonhomogeneous, using Bartlett's test, were subjected to log or arcsin transformation before applying the ANOVA. A regression analysis was used to obtain correlation coefficients and slopes from plots of dietary vs. flesh FA concentrations. ANOVA and the regression analysis were performed using a Graphpad Prism™ (version 3.0) statistical package (Graphpad Software, San Diego, CA).

RESULTS

After feeding the five diets for 40 wk, the final weights of the fish were 1.79 ± 0.40 (FO), 1.89 ± 0.34 (25% LO), 1.90 ± 0.33 (50% LO), 1.87 ± 0.35 (75% LO), and 1.87 ± 0.33 kg (100% LO); there were no significant differences between dietary treatments ($P = 0.156$, $n = 87$). Specific growth rates were very similar (% weight gain d^{-1}), varying from 0.94 (FO) to 0.98 (25% LO), and feed conversion ratios (dry feed consumed/wet weight gain) varied from 1.29 (25 and 75% LO) to 1.41 (50% LO). Flesh lipid contents varied from 7.4 ± 1.4% (FO) to 8.8 ± 1.7% (25% LO), and flesh astaxanthin contents varied from 3.31 ± 0.58 (FO) to 3.60 ± 0.49 mg kg^{-1} (50% LO). These values showed no significant differences between dietary treatments. After feeding the finishing diet for 24 wk, the final weights of the fish were 4.50 ± 0.71 (FO), 4.68 ± 0.62 (25% LO), 4.72 ± 0.79 (50% LO), 4.48 ± 0.80 (75% LO), and 4.58 ± 0.67 kg (100% LO); and there were no significant differences between dietary treatments ($P = 0.783$, $n = 20$). Specific growth rates were very similar (% weight gain d^{-1}), varying from 0.51 (75% LO) to 0.55 (100% LO), and feed conversion ratios (dry feed consumed/wet weight gain) varied from 1.05 (75% LO) to 1.14 (50% LO). Flesh lipid contents varied from 9.6 ± 1.1% (100% LO) to 13.0 ± 2.3% (50% LO). These values showed no significant differences between dietary treatments.

Flesh FA compositions: 40 wk feeding LO-containing diets. The FA compositions of flesh total lipids reflected the changes in dietary FA attributable to increasing inclusion of LO (Table 2). Total saturated FA decreased significantly with increasing LO inclusion, largely because of significant reductions in both 14:0 and 16:0, although 18:0 was increased with the addition of LO. Total monoene FA were reduced by more than half in fish fed 100% LO compared with those fed FO owing to significant reductions in 16:1n-7, 20:1n-9, and 22:1n-11 with each addition of dietary LO. Total n-6 FA were increased by more than twofold, largely due to 18:2n-6 increasing from 3.9 g/100 g of FA in flesh from fish fed FO to 13.1 g/100 g in fish fed 100% LO. Flesh 20:4n-6 concentrations were significantly lower in fish fed 75 and 100% LO compared with those fed FO. Total n-3 FA were increased significantly with each addition of LO, largely because of increased flesh deposition of 18:3n-3, although the elongation and desaturation products, 20:3n-3 and 20:4n-3, were also increased significantly. However, both EPA and DHA were significantly reduced in the flesh from fish fed LO, with values for EPA and DHA in fish fed 100% LO being reduced to 30 and 38% of values in fish fed FO. The n-3/n-6 ratios were similar for all treatments, being in the range of 3.2–3.6.

Plotting the FA concentration (g/100 g) in flesh lipids (Table 2) against the FA concentration in dietary lipids (Table 1) resulted in linear regressions, as shown in Figures 1 and 2. These graphs demonstrate that concentrations of dietary FA were linearly correlated with flesh FA concentrations, with r^2 values in the range of 0.966–0.999; different slope values indicate that the relationship between dietary and flesh FA concentrations was different for each FA (Table 3). This is shown more clearly in Table 3 by comparing the differences (Δ values) between the concentrations of individual FA in dietary and flesh lipids for fish fed the FO, 50% LO, and 100% LO

TABLE 2
Total Lipid FA Compositions[a] (g FA/100 g total FA) of Flesh from Atlantic Salmon Fed the LO Experimental Diets for 40 wk

FA	FO	25% LO	50% LO	75% LO	100% LO
14:0	4.7 ± 0.2[a]	3.9 ± 0.1[b]	2.9 ± 0.1[c]	0.8 ± 0.1[d]	0.7 ± 0.1[d]
16:0	12.9 ± 0.2[a]	11.7 ± 0.2[b]	10.7 ± 0.3[c]	9.6 ± 0.2[d]	8.3 ± 0.2[e]
18:0	1.9 ± 0.1[e]	2.3 ± 0.0[d]	2.8 ± 0.1[c]	3.1 ± 0.0[b]	3.6 ± 0.1[a]
Total saturates[b]	19.9 ± 0.3[a]	18.1 ± 0.2[b]	16.5 ± 0.4[c]	14.7 ± 0.2[d]	12.7 ± 0.3[e]
16:1n-7	7.5 ± 0.2[a]	5.5 ± 0.1[b]	4.0 ± 0.1[c]	2.3 ± 0.1[d]	0.8 ± 0.0[e]
18:1n-9	16.0 ± 0.4[c]	17.4 ± 0.3[b]	17.6 ± 0.3[b]	17.6 ± 0.3[b]	18.6 ± 0.3[a]
18:1n-7	3.8 ± 0.0[a]	3.4 ± 0.3[b]	2.5 ± 0.1[c]	2.2 ± 0.1[d]	1.3 ± 0.1[e]
20:1n-9	16.6 ± 0.3[a]	11.9 ± 0.2[b]	8.7 ± 0.1[c]	4.8 ± 0.0[d]	1.6 ± 0.1[e]
22:1n-11	9.9 ± 0.1[a]	7.3 ± 0.3[b]	5.4 ± 0.1[c]	3.0 ± 0.0[d]	1.1 ± 0.1[e]
Total monoenes[c]	57.1 ± 0.6[a]	48.4 ± 0.6[b]	40.3 ± 0.4[c]	31.5 ± 0.3[d]	24.2 ± 0.4[e]
18:2n-6	3.9 ± 0.1[e]	6.8 ± 0.1[d]	8.6 ± 0.1[c]	11.0 ± 0.1[b]	13.1 ± 0.2[a]
20:2n-6	0.4 ± 0.0[d]	0.5 ± 0.0[c]	0.6 ± 0.0[b]	0.6 ± 0.0[b]	0.7 ± 0.0[a]
20:4n-6	0.3 ± 0.1[a]	0.2 ± 0.0[a,b]	0.2 ± 0.0[a,b]	0.1 ± 0.1[b]	0.1 ± 0.0[b]
Total n-6[d]	4.9 ± 0.2[e]	7.8 ± 0.1[d]	9.8 ± 0.2[c]	11.8 ± 0.1[b]	14.0 ± 0.1[a]
18:3n-3	0.8 ± 0.2[e]	11.5 ± 0.3[d]	20.1 ± 0.3[c]	30.1 ± 0.4[b]	38.7 ± 0.8[a]
18:4n-3	1.5 ± 0.1[a]	1.3 ± 0.1[b]	1.3 ± 0.1[b]	1.2 ± 0.1[b]	1.2 ± 0.1[b]
20:3n-3	0.1 ± 0.0[e]	0.7 ± 0.0[d]	1.4 ± 0.1[c]	2.1 ± 0.1[b]	2.7 ± 0.1[a]
20:4n-3	1.2 ± 0.0[d]	1.4 ± 0.0[c]	1.5 ± 0.0[b,c]	1.6 ± 0.0[b]	1.8 ± 0.1[a]
20:5n-3	4.3 ± 0.2[a]	3.0 ± 0.1[b]	2.5 ± 0.1[c]	1.8 ± 0.1[d]	1.3 ± 0.1[e]
22:5n-3	1.5 ± 0.0[a]	1.1 ± 0.1[b]	1.0 ± 0.0[b]	0.6 ± 0.1[c]	0.4 ± 0.1[d]
22:6n-3	8.1 ± 0.7[a]	6.1 ± 0.7[b]	5.3 ± 0.4[b,c]	4.3 ± 0.5[c]	3.1 ± 0.2[d]
Total n-3	17.5 ± 0.7[e]	25.2 ± 0.7[d]	33.1 ± 0.6[c]	41.7 ± 0.3[b]	49.1 ± 0.6[a]
Total PUFA	22.9 ± 0.8[e]	33.4 ± 0.7[d]	43.1 ± 0.7[c]	53.7 ± 0.3[b]	66.1 ± 0.7[a]
n-3/n-6	3.6 ± 0.4	3.2 ± 0.3	3.4 ± 0.3	3.5 ± 0.2	3.5 ± 0.3

[a]Values are mean ± SD, $n = 6$.
[b]Includes 15:0, 17:0, 20:0, and 22:0.
[c]Includes 16:1n-9, 20:1n-11, 20:1n-7, 22:1n-13, and 24:1.
[d]Includes 18:3n-6, 20:3n-6, and 22:5n-6. SD values <0.05 are shown as 0.0. Values in the same row with a different superscript roman letter are significantly different ($P < 0.05$). For abbreviations see Table 1.

diets. For all the PUFA and HUFA listed in Table 3, only DHA was present in flesh at a greater concentration than in the diet for all three treatments. This situation is in contrast with both 18:3n-3, which was always present in flesh at a lower concentration than in the diet, and 20:5n-3, which had a higher value in flesh than in the diet only when diet concentrations were low. Palmitic acid (16:0), total saturates, and 18:1n-9 all showed positive Δ values for each of the three diets, suggesting that both saturated FA and 18:1n-9 were being preferentially retained by the fish. In contrast, 18:2n-6, 18:3n-3, 20:1n-9, and 22:1n-11 were generally discriminated against in terms of flesh deposition, particularly when present at high concentrations in the diet.

Flesh FA compositions: 24 wk feeding a FO finishing diet in all dietary treatments. By returning all experimental treatments to a FO-containing diet for 24 wk, following the initial 40 wk feeding phase, the differences between flesh FA compositions were reduced (Table 4). The concentrations of 16:0 and total saturates were significantly higher only in fish fed FO throughout compared with those previously fed 75 and 100% LO. A similar result was seen for 16:1n-7; 20:1n-9 and 22:1n-11 were significantly different for all treatment groups, although fish previously fed 75% LO were not different from those fed 50 or 100% LO. Concentrations of total monoenes showed similar differences, but the concentration in fish previously fed 100% LO was restored to 80% of the value in fish fed FO throughout. The 18:2n-6 and total n-6 FA concentrations were not different between fish fed either FO or 25% LO, and these two treatments were significantly lower than fish previously fed 75 and 100% LO. Concentrations of flesh 20:4n-6 were restored to similar values for all dietary treatments. The flesh concentrations of 18:3n-3 were significantly higher in fish previously fed 75 and 100% LO compared with fish previously fed 50% or 25% LO or FO. The concentration of EPA was significantly higher in fish fed FO throughout compared with those previously fed 50, 75, and 100% LO. In addition concentrations of 22:5n-3 were significantly higher in fish fed FO throughout compared with all other treatments, which had similar concentrations. The concentration of flesh DHA was significantly higher in fish fed FO throughout compared with fish previously fed 50 and 100% LO. Concentrations of total n-3 FA were significantly higher in fish previously fed 75 and 100% LO compared with fish fed the other three diets.

After feeding the experimental diets for 40 wk, the flesh 18:2n-6 concentrations were significantly different among fish fed FO, 50% LO, and 100% LO (Fig. 3A), with the highest values in fish fed 100% LO being 236% higher than those in fish fed FO. After feeding the FO-containing finishing diet in all treatments, the 18:2n-6 concentrations were still significantly different between treatments after 56 and 64 wk. However, after 64 wk the 18:2n-6 concentrations in fish previously

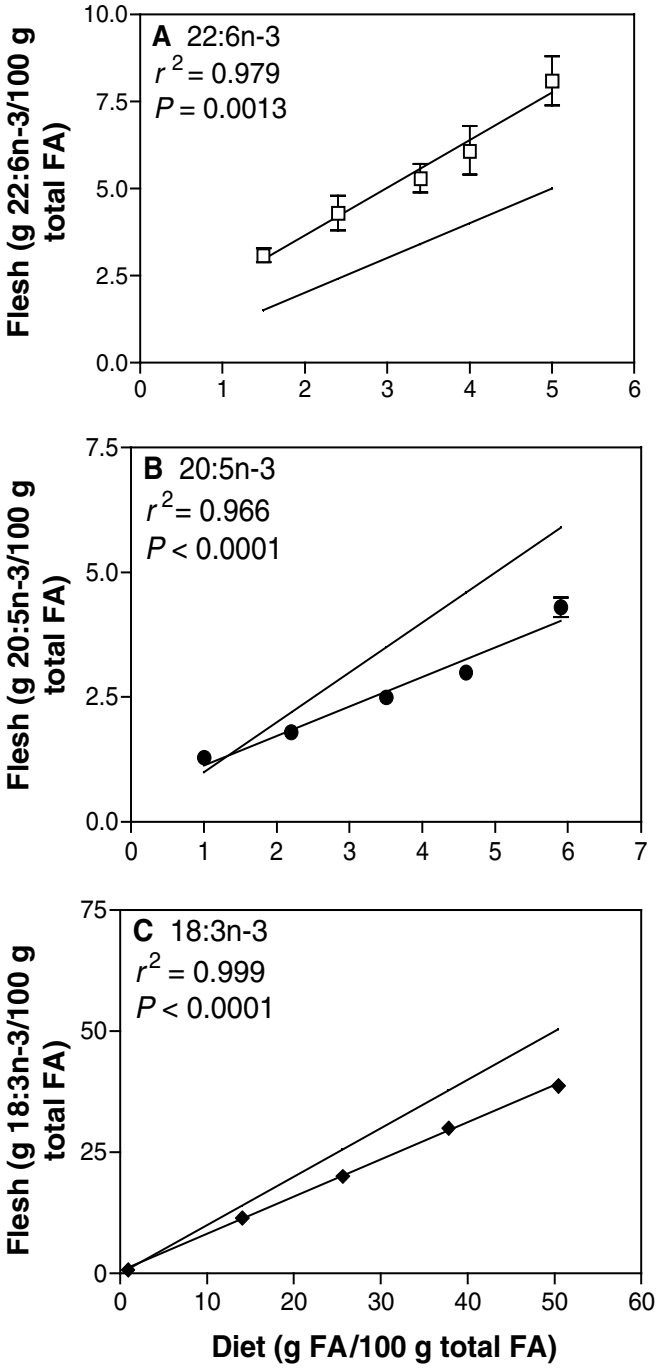

FIG. 1. Relationship between dietary FA concentration and muscle FA concentration for 22:6n-3 (A), 20:5n-3 (B), and 18:3n-3 (C) in total lipids of Atlantic salmon fed diets containing blends of fish oil (FO) and linseed oil (LO). The additional line represents the line of equality. Error bars represent mean ± SD.

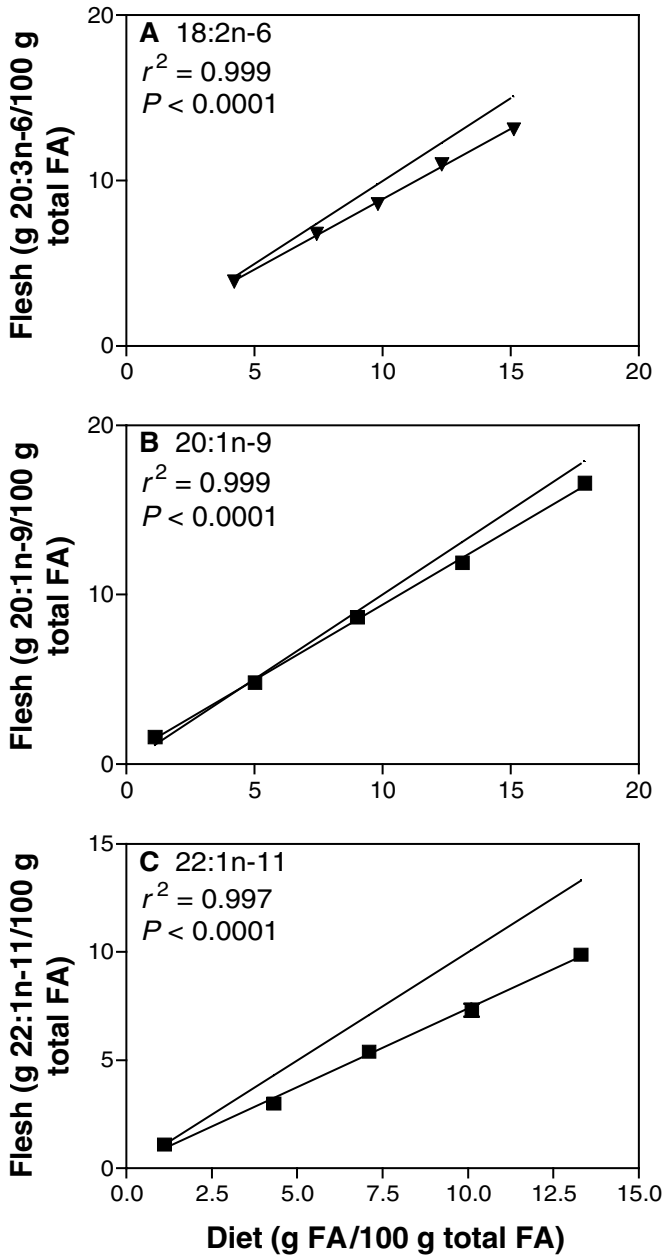

FIG. 2. Relationship between dietary FA concentration and muscle FA concentration for 18:2n-6 (A), 20:1n-9 (B), and 22:1n-11 (C) in total lipids of Atlantic salmon fed diets containing blends of FO and LO. The additional line represents the line of equality. For abbreviations see Figure 1.

fed the 50 and 100% LO diets were reduced by 31 and 44%, respectively, following the 24-wk FO refeeding period (Fig. 3A). A similar result was observed for 18:3n-3 such that the concentrations in fish previously fed the 50 and 100% LO diets were still significantly different, both from each other and from fish fed FO, after 16 and 24 wk on an FO diet (Fig. 3B). However, the concentrations of 18:3n-3 in fish previously fed 50 and 100% LO were reduced by 64 and 66%, respectively, following the 24-wk FO refeeding period.

After the initial 40-wk feeding period, the flesh concentration of EPA was significantly lower in fish fed 50 and 100% LO compared with those fed FO (Fig. 4A). After refeeding FO for 16 and 24 wk, the flesh EPA concentration increased such that fish previously fed the 50 and 100% LO diets had similar EPA concentrations, but they were still significantly lower than fish fed FO throughout. However, the flesh concentrations of EPA in fish previously fed 50 and

TABLE 3
Correlation Coefficients and Slopes from Plots of Dietary FA Concentrations vs. Flesh FA Concentrations Including the Differences (Δ) Between Diet and Flesh FA Values for Salmon Fed 100% FO, 50% LO, and 100% LO Diets[a]

FA	Correlation coefficient (r^2)	Slope	Δ100% FO	Δ50% LO	Δ100% LO
16:0	0.997	0.78 ± 0.02	0.8	1.4	2.2
Total saturates	0.998	0.77 ± 0.02	0.0	1.4	2.2
18:1n-9	0.876	0.43 ± 0.09	4.1	2.5	1.6
20:1n-9	0.999	0.89 ± 0.02	–1.3	–0.3	0.5
22:1n-11	0.997	0.73 ± 0.02	–3.4	–1.7	0.0
18:2n-6	0.999	0.85 ± 0.02	–0.3	–1.2	–2.0
18:3n-3	0.999	0.77 ± 0.01	–0.1	–5.5	–11.7
20:5n-3	0.966	0.59 ± 0.06	–1.6	–1.0	0.3
22:6n-3	0.979	1.37 ± 0.12	3.1	1.9	1.6

[a]FA concentrations are g FA/100 g total FA in muscle and diets. Negative Δ values indicate lower values in muscle compared with diet, whereas positive values indicate accumulation in muscle relative to diet.

100% LO were restored to 88 and 83%, respectively, of the concentration in fish fed FO throughout, following the 24-wk FO refeeding period. A very similar result was seen with flesh DHA concentrations in fish previously fed 50 and 100% LO, whereby DHA concentrations were restored to 80 and 83%, respectively, of the concentration in fish fed FO throughout following the 24-wk refeeding period. Interestingly, the flesh EPA and DHA concentrations were restored to 81 and 74% and to 85 and 79%, respectively, for fish previously fed 50 and 100% LO diets, after feeding the FO finishing diet for only 16 wk.

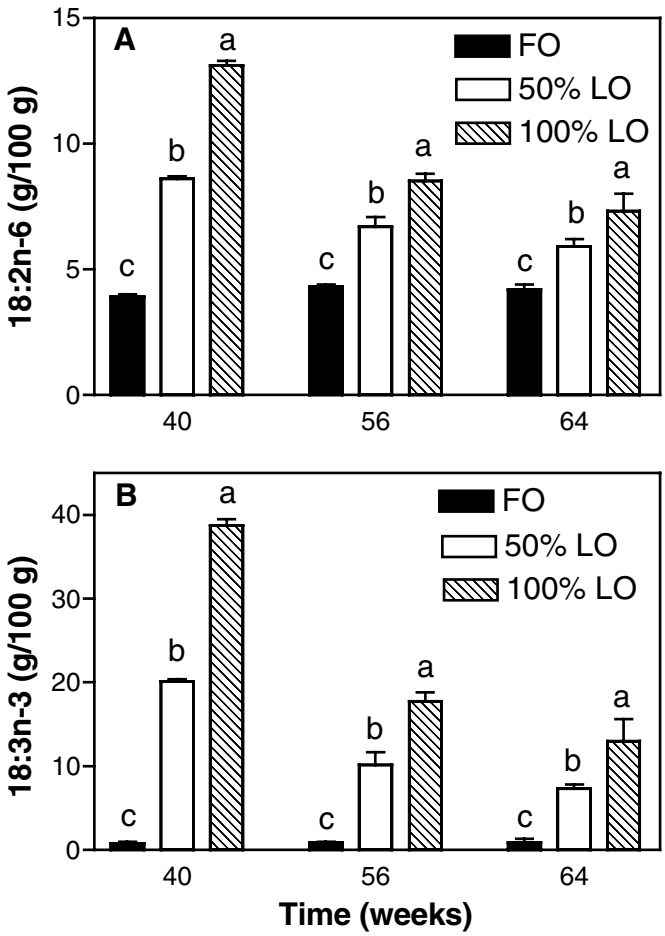

FIG. 3. (A) Linoleic acid (18:2n-6) and (B) linolenic acid (18:3n-3) concentrations in total lipids from salmon flesh after feeding diets containing 100% FO, 50% LO, or 100% LO for 40 wk and after feeding a 100% FO diet for a further 16 and 24 wk to all treatment groups. Columns assigned a different letter within each time point are significantly different ($P < 0.05$). Error bars represent mean ± SD.

DISCUSSION

Salmon produced using diets containing raw materials with high levels of marine FO currently provide a rich source of the n-3 HUFA, EPA, and DHA that are relatively cheap and highly nutritious (21,22). However, the growth in aquaculture required to augment dwindling seafood stocks can be sustained only if alternatives to marine FO can be found (5,7). In the present study, graded levels of LO were used to replace FO in the culture of Atlantic salmon to market size with no obvious detriment in terms of the growth and health of the fish. Although a number of previous studies have looked at FO substitution in salmon, most have used smaller fish or ones that were cultured on the experimental feeds for relatively short periods (16,17,32–34). However, the growth results obtained with the present study using LO compare favorably with studies utilizing soy and rapeseed oils as FO replacements and suggest that the energy requirements of Atlantic salmon can be satisfied by vegetable oils with variable FA compositions (18,35). A few studies have investigated LO alone or LO blended with other oils in salmon feeds, and these also have confirmed no obvious effects on growth parameters (14,33,34).

Atlantic salmon store high amounts of lipids in their flesh, and in market-size salmon (2–5 kg) lipid levels would normally be in the range of 10–20% of wet weight (21,22). Changing the FA composition of salmon diets can affect the composition and quantity of flesh lipid stores, and previous studies using rapeseed and palm oils to replace FO have indicated reduced flesh lipids at replacement levels above 50% (16,17). In the present study, fish of ~2 kg had lipid levels of

TABLE 4
Total Lipid FA Compositions (g/100 g total FA) of Flesh from Atlantic Salmon Fed the LO Experimental Diets for 40 wk, Followed by Refeeding a 100% FO Diet for 24 wk[a]

FA	FO	25% LO	50% LO	75% LO	100% LO
14:0	4.8 ± 0.1[a]	4.5 ± 0.1[b]	3.9 ± 0.1[c]	3.8 ± 0.1[c]	3.6 ± 0.3[c]
16:0	12.6 ± 0.2[a]	12.1 ± 0.0[a,c]	12.3 ± 0.3[a]	11.3 ± 0.3[b,c]	11.2 ± 0.5[b]
18:0	2.1 ± 0.1[b]	2.2 ± 0.1[b]	2.3 ± 0.0[b,c]	2.5 ± 0.1[a,c]	2.6 ± 0.1[a]
Total saturates[b]	9.9 ± 0.2[a]	19.0 ± 0.1[a,c]	18.7 ± 0.5[a,b]	17.8 ± 0.5[b,c]	17.5 ± 0.8[b]
16:1n-7	7.5 ± 0.1[a]	7.0 ± 0.1[a,b]	6.5 ± 0.3[b]	5.8 ± 0.1[c]	5.3 ± 0.4[c]
18:1n-9	16.2 ± 0.2[b]	16.6 ± 0.1[a,b]	16.9 ± 0.1[a]	16.7 ± 0.2[a]	16.9 ± 0.3[a]
18:1n-7	3.9 ± 0.1[b]	4.1 ± 0.1[a,b]	4.3 ± 0.2[a]	3.4 ± 0.1[c]	3.1 ± 0.2[c]
20:1n-9	16.7 ± 0.0[a]	14.9 ± 0.1[b]	13.2 ± 0.4[c]	12.1 ± 0.2[c,d]	11.1 ± 0.8[d]
22:1n-11	10.3 ± 0.1[a]	9.2 ± 0.3[b]	8.2 ± 0.3[c]	7.7 ± 0.3[c,d]	7.2 ± 0.6[d]
Total monoenes[c]	57.9 ± 0.3[a]	55.7 ± 0.7[a]	53.0 ± 0.7[b]	48.8 ± 0.6[c]	46.4 ± 1.9[c]
18:2n-6	4.2 ± 0.2[d]	5.1 ± 0.1[c,d]	5.9 ± 0.3[b,c]	6.7 ± 0.2[a,b]	7.3 ± 0.7[a]
20:2n-6	0.4 ± 0.0[b]	0.5 ± 0.1[a,b]	0.5 ± 0.0[a,b]	0.5 ± 0.0[a,b]	0.6 ± 0.1[a]
20:4n-6	0.2 ± 0.0	0.2 ± 0.0	0.2 ± 0.0	0.2 ± 0.0	0.2 ± 0.1
Total n-6[d]	5.2 ± 0.1[d]	6.2 ± 0.2[c,d]	6.9 ± 0.4[b,c]	7.7 ± 0.3[a,b]	8.4 ± 0.7[a]
18:3n-3	0.9 ± 0.4[c]	4.0 ± 0.4[b,c]	7.3 ± 0.5[b]	10.9 ± 0.7[a]	13.0 ± 2.6[a]
18:4n-3	1.4 ± 0.0	1.4 ± 0.0	1.4 ± 0.1	1.4 ± 0.1	1.4 ± 0.0
20:3n-3	0.1 ± 0.0[d]	0.3 ± 0.1[c,d]	0.5 ± 0.1[b,c]	0.8 ± 0.1[a,b]	1.0 ± 0.2[a]
20:4n-3	1.3 ± 0.0	1.3 ± 0.0	1.3 ± 0.1	1.5 ± 0.1	1.5 ± 0.1
20:5n-3	4.1 ± 0.1[a]	3.8 ± 0.1[a,b]	3.6 ± 0.1[b,c]	3.4 ± 0.1[c]	3.4 ± 0.2[c]
22:5n-3	1.9 ± 0.1[a]	1.6 ± 0.0[b]	1.4 ± 0.1[b]	1.4 ± 0.1[b]	1.4 ± 0.1[b]
22:6n-3	6.6 ± 0.1[a]	6.1 ± 0.1[a,b]	5.3 ± 0.6[b]	5.7 ± 0.1[a,b]	5.5 ± 0.6[b]
Total n-3	16.3 ± 0.3[c]	18.6 ± 0.6[b,c]	20.9 ± 0.8[b]	25.1 ± 0.9[a]	27.2 ± 2.0[a]
Total PUFA	22.0 ± 0.4[c]	25.1 ± 0.7[b,c]	28.1 ± 1.1[b]	33.1 ± 1.1[a]	35.9 ± 2.7[a]
n-3/n-6	3.1 ± 0.3	3.0 ± 0.2	3.0 ± 0.3	3.3 ± 0.2	3.2 ± 0.4

[a]Values are mean ± SD, $n = 3$.
[b]Includes 15:0, 17:0, 20:0, and 22:0.
[c]Includes 16:1n-9, 20:1n-11, 20:1n-7, 22:1n-13, and 24:1.
[d]Includes 18:3n-6, 20:3n-6, and 22:5n-6. SD values <0.05 are shown as 0.0. Values in the same row with a different superscript roman letters are significantly different ($P < 0.05$).

7.4–8.8%, and there were no significant differences between treatments. In a previous study with salmon harvested at a similar size and fed diets with varying levels of FO, LO, and rapeseed oil, no differences in flesh lipid contents were observed (14). However, lipid concentrations in the livers of fish from the present dietary trial, reported in a recent publication (19), showed significantly increased lipid deposition in fish fed diets with >50% LO, suggesting that changes in the dietary FA composition can affect adiposity in specific tissues.

It is well documented that the tissue FA composition in salmonid fish is closely related to the dietary FA composition and that feeding high levels of vegetable oils will strongly influence the flesh FA composition (14–18). The results from the present study confirm this relationship in which linear correlations between dietary FA concentrations and flesh FA concentrations are clearly demonstrated. Similar linear relationships have been observed in previous studies in which rapeseed, palm, and blends of rapeseed and LO were used, along with FO, in salmon feed formulations (14,16,17). The present study confirms that individual FA, within a blend of dietary FA, are selectively retained or metabolized, depending on their concentration in the diet and the biological function of the specific FA. In practical terms, these linear correlations (Figs. 1 and 2) can be used to predict the flesh concentration of a particular FA, when present in a mixture of FA, derived from blends of LO and FO fed to salmon in seawater.

Additional information on the selective retention or metabolism of different dietary FA present in different oil blends can be obtained from Figures 1 and 2 and from Tables 2 and 3. One of the most striking effects is the preferential deposition and retention of DHA in flesh lipids, regardless of the concentration present in the diet. The Δ values in Table 3 show positive values in the range 1.6–3.1 for 100% LO, 50% LO, and FO treatments, indicating that, regardless of dietary concentration, DHA was selectively deposited and retained in salmon flesh. This selectivity presumably reflects the specificity of the fatty acyl transferase enzymes that incorporate the FA into flesh TAG and phospholipids, a phenomenon that has been observed in previous studies with salmon fed different combinations of vegetable oils (14,16,17).

By comparison, the other PUFA and HUFA tended to be directed toward metabolism, presumably largely for energy production rather than deposition, especially when present at high concentrations. When present at low concentrations, only EPA showed a positive Δ value. In contrast, both 18:2n-6 and especially 18:3n-3 were selected against in terms of flesh deposition. The tendency toward preferential metabolism of C_{18} PUFA by β-oxidation has been observed not only in salmonid fish (12,13) but also in humans, in whom 18:3n-3 was preferred over 18:2n-6 as an oxidative substrate (23). However, it also should be noted that both 18:2n-6 and 18:3n-3 are substrates

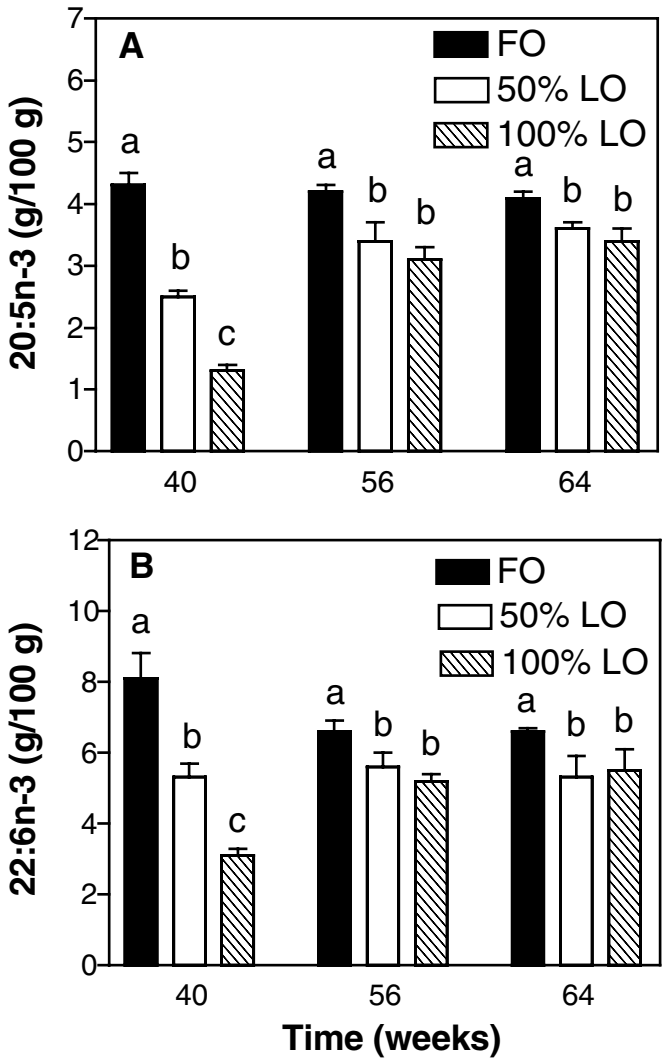

FIG. 4. (A) EPA (20:5n-3) and (B) DHA (22:6n-3) concentrations in total lipids from salmon flesh after feeding diets containing 100% FO, 50% LO, or 100% LO for 40 wk and after feeding a 100% FO diet for a further 16 and 24 wk to all treatment groups. Columns assigned a different letter within each time point are significantly different ($P < 0.05$). Error bars represent mean ± SD.

for Δ6-desaturase, and Atlantic salmon hepatocytes reportedly tend to favor desaturation and elongation of 18:3n-3 over 18:2n-6 (20,34). In addition to PUFA, the long-chain monoene FA that are characteristic of high-latitude FO (9) are thought to be important catabolic substrates. This appeared to be confirmed in the present study, in which 22:1n-11 appeared to be preferred over 20:1n-9 even though the former was less abundant in the diets than the latter.

The literature suggests that 22:1n-11 and 18:2n-6 are preferred substrates for β-oxidation, along with 16:0, 16:1, and 18:1n-9 (11,36,37). However, in the present study 16:0, and especially 18:1n-9, had positive Δ values (Table 3), indicating that these two FA were being selectively retained in flesh lipids rather than being metabolized for energy production. This is in contrast to two previous studies, which showed that 18:1n-9 was used for energy production by the β-oxidation pathway in salmon fed diets containing blends of LO and rapeseed oil, although both 18:2n-6 and 18:3n-3 appeared to be preferred over 18:1n-9 (14,35). Perhaps these differences can be explained in part by genetic differences in the salmon stock used in the different trials. The selection of 18:1n-9 and 16:0 for deposition, rather than mobilization, in flesh may reflect the structural function of these FA in membrane phospholipids, where they are often located in the *sn*-1 position of phospholipids, especially of PC and PE, with HUFA being favored in the *sn*-2 position (9,38).

The diet of early humans pursuing a hunter/gatherer lifestyle was probably considerably lower in fat and had an n-6/n-3 ratio of around 1:1, in comparison with the current diet in the developed world with an n-6/n-3 ratio of 10–20:1 (39). The health benefits of diets rich in EPA and DHA, which can reduce this high n-6/n-3 ratio, are well documented, and the outcome of a number of conditions prevalent in the developed world, including cardiovascular disease, immune dysfunction, diabetes, and other inflammatory disorders, can be improved as a result (40–42). Although outcomes of clinical trials with 18:3n-3 have been less clear than those with n-3 HUFA, evidence exists that diets promoting increased tissue levels of 18:3n-3 also can be beneficial to health (24). The benefits of increased 18:3n-3 for cardiovascular disorders, including rhythm disorders, myocardial infarctions, sudden cardiac death, and coronary thrombosis, have been reported (43–45). In addition, some studies have reported low tissue levels of 18:3n-3 as a risk factor for both breast and prostate cancers (46,47).

Atlantic salmon presently cultured using only marine FO are rich in n-3 HUFA and, as such, represent a valuable source of EPA and DHA for the human consumer (21,22). The present study suggests that when salmon are cultured with LO replacing up to 50% of FO, a moderate reduction of n-3 HUFA but increased deposition of 18:3n-3 and only moderate deposition of 18:2n-6 can be observed, meaning that flesh n-3/n-6 ratios of >3 are maintained. Furthermore, even salmon fed 100% LO provide n-3 HUFA levels of 0.12 g EPA and 0.28 g DHA, as well as 3.48 g 18:3n-3 and 1.12 g 18:2n-6 per 100 g of salmon flesh. These values are close to the recommended 0.22 g/d each for EPA and DHA, 2.22 g/d for 18:3n-3, and are well below the maximum recommended intake of 18:2n-6 of 6.67 g/d (39). However, increasing the dietary n-3/n-6 ratio is also recommended, especially the level of n-3 HUFA of marine origin (39,40).

This study has demonstrated mechanisms by which the ratio of DHA/EPA/18:3n-3/18:2n-6 can be manipulated in salmon flesh so that precise "tailored" EFA compositions can be delivered to human consumers. This can be achieved *via* the initial dietary input, for the majority of the ongrowing phase, and by the use of a FO finishing diet to restore the values of the aforementioned EFA to the desired concentrations. The latter procedure restored both EPA and DHA concentrations in flesh to >80% of the value in fish fed FO throughout

the 24 wk, whereas18:2n-6 and 18:3n-3 concentrations were 74% and 1344% higher than in fish fed FO. These results are similar to previous studies with Atlantic salmon and gilthead seabream, which showed that restoration of the flesh EPA and DHA concentrations can be achieved relatively easily with finishing diets but that C_{18} PUFA concentrations still remain elevated (14,48,49). A recent study of Atlantic salmon described a dilution model that allowed changes in flesh FA to be accurately predicted following a switch from vegetable oil to FO diets (50). The model described by Jobling (50) supports the results of the present study, which showed that relatively constant concentrations for DHA and EPA were found after feeding the FO finishing diet for 16 or 24 wk.

In conclusion, this study suggests that Atlantic salmon can be cultured, during the marine phase of their life cycle, by using diets in which the FO is replaced by LO without any apparent reduction in the growth rates or health of the fish. In addition, culturing salmon with diets containing up to 50% LO, or up to 100% LO followed by a period of 16–24 wk on an FO finishing diet, can provide a carcass EFA composition that is highly beneficial for human health. Although the goal of minimizing reliance on marine raw materials cannot be achieved overnight, this study suggests that salmon can be cultured on diets with minimal FO input yet still retain a high functional nutritional value that cannot be replicated in terrestrial farmed foodstuffs.

ACKNOWLEDGMENTS

This work was supported by the European Union Framework V program [Researching Alternatives to Fish Oils in Aquaculture (RAFOA), QLRT-2000-30058]. We would like to acknowledge Bill Gordon and Iain Martin for their assistance with fish husbandry.

REFERENCES

1. Simopoulos, A.P. (1999) Essential Fatty Acids in Health and Chronic Disease, *Am. J. Nutr. 70*, 560S–569S.
2. Connor, W.E. (2000) Importance of n-3 Fatty Acids in Health and Disease, *Am. J. Clin. Nutr. 71*, 171S–175S.
3. WHO (2002) Reducing Risks, Promoting a Healthy Life, World Health Organization, Geneva, Switzerland.
4. Williams, N. (1998) Overfishing Disrupts Entire Ecosystems, *Science 279*, 809–810.
5. Tidwell, J.H., and Allan, G.L. (2002) Fish as Food: Aquaculture's Contribution, *World Aquacult. 33*, 44–48.
6. Sargent, J.R., and Tacon, A.G.J. (1999) Development of Farmed Fish: A Nutritionally Necessary Alternative to Meat, *Proc. Nutr. Soc. 58*, 377–383.
7. Barlow, S. (2000) Fishmeal and Fish Oil: Sustainable Ingredients for Aquafeeds, *Global Aquacult. Advocate 4*, 85–88.
8. Frøyland, L., Madsen, L., Eckhoff, K.M., Lie, Ø., and Berge, R. (1998) Carnitine Palmitoyltransferase I, Carnitine Palmitoyltransferase II, and Acyl-CoA Oxidase Activities in Atlantic Salmon (*Salmo salar*), *Lipids 33*, 923–930.
9. Sargent, J.R., Tocher, D.R., and Bell, J.G. (2002) The Lipids, in *Fish Nutrition*, 3rd edn. (Halver, J.E., and Hardy, R.W., eds.), pp. 181–257, Elsevier Science, New York.
10. Henderson, R.J., and Sargent, J.R. (1985) Chain Length Specificities of Mitochondrial and Peroxisomal β-Oxidation of Fatty Acids in Rainbow Trout (*Salmo gairdneri*), *Comp. Biochem. Physiol. 82B*, 79–85.
11. Henderson, R.J. (1996) Fatty Acid Metabolism in Freshwater Fish with Particular Reference to Polyunsaturated Fatty Acids, *Arch. Anim. Nutr. 49*, 5–22.
12. Bell, M.V., Dick, J.R., and Porter, A.E.A. (2001) Biosynthesis and Tissue Deposition of Docosahexaenoic Acid (22:6n-3) in Rainbow Trout (*Oncorhynchus mykiss*), *Lipids 36*, 1153–1159.
13. Bell, M.V., Dick, J.R., and Porter, A.E.A. (2003) Pyloric Ceca Are a Major Site of 22:6n-3 Synthesis in Rainbow Trout (*Oncorhynchus mykiss*), *Lipids 39*, 39–44.
14. Bell, J.G., Tocher, D.R., Henderson, R.J., Dick, J.R., and Crampton, V.O. (2003) Altered Fatty Acid Compositions in Atlantic Salmon (*Salmo salar*) Fed Diets Containing Linseed and Rapeseed Oils Can Be Partially Restored by a Subsequent Fish Oil Finishing Diet, *J. Nutr. 133*, 2793–2801.
15. Torstensen, B.E., Lie, Ø., and Frøyland, L. (2000) Lipid Metabolism and Tissue Composition in Atlantic Salmon (*Salmo salar* L.)—Effects of Capelin Oil, Palm Oil, and Oleic Acid-Enriched Sunflower Oil as Dietary Lipid Sources, *Lipids 35*, 653–664.
16. Bell, J.G., McEvoy, J., Tocher, D.R., McGhee, F., Campbell, P.J., and Sargent, J.R. (2001) Replacement of Fish Oil with Rapeseed Oil in Diets of Atlantic Salmon (*Salmo salar*) Affects Tissue Lipid Compositions and Hepatocyte Fatty Acid Metabolism, *J. Nutr. 131*, 1535–1543.
17. Bell, J.G., Henderson, R.J., Tocher, D.R., McGhee, F., Dick, J.R., Porter, A., Smullen, R.P., and Sargent, J.R. (2002) Substituting Fish Oil with Crude Palm Oil in the Diet of Atlantic Salmon (*Salmo salar*) Affects Muscle Fatty Acid Composition and Hepatic Fatty Acid Metabolism, *J. Nutr. 132*, 222–230.
18. Rosenlund, G., Obach, A., Sandberg, M.G., Standal, H., and Tveit, K. (2001) Effect of Alternative Lipid Sources on Long-Term Growth Performance and Quality of Atlantic Salmon (*Salmo salar* L.), *Aquacult. Res. 32*, 323–328.
19. Tocher, D.R., Fonseca-Madrigal, J., Bell, J.G., Dick, J.R., Henderson, R.J., and Sargent, J.R. (2002) Effects of Diets Containing Linseed Oil on Fatty Acid Desaturation and Oxidation in Hepatocytes and Intestinal Enterocytes in Atlantic Salmon (*Salmo salar*), *Fish Physiol. Biochem. 26*, 157–170.
20. Ruyter, B., Røsjø, C., Grisdale-Helland, B., Rosenlund, G., Obach, A., and Thomassen, M.S. (2003) Influence of Temperature and High Dietary Linoleic Acid Content on Esterification, Elongation, and Desaturation of PUFA in Atlantic Salmon Hepatocytes, *Lipids 38*, 833–840.
21. Bell, J.G., McEvoy, J., Webster, J.L., McGhee, F., Millar, R.M., and Sargent, J.R. (1998) Flesh Lipid and Carotenoid Composition of Scottish Farmed Atlantic Salmon (*Salmo salar*), *J. Agric. Food Chem. 46*, 119–127.
22. Aursand, M., Mabon, F., and Martin, G.J. (2000) Characterization of Farmed and Wild Salmon (*Salmo salar*) by a Combined Use of Compositional and Isotopic Analyses, *J. Am. Oil Chem. Soc. 77*, 659–666.
23. DeLany, J.P., Windhauser, M.M., Champagne, C.M., and Bray, G.A. (2000) Differential Oxidation of Individual Dietary Fatty Acids in Humans, *Am. J. Clin. Nutr. 79*, 905–911.
24. Sinclair, A.J., Attar-Bashi, N.M., and Li, D. (2002) What is the Role of α-Linolenic Acid for Mammals? *Lipids 37*, 1113–1123.
25. Garg, M.L., Thomson, A.B.R., and Clandinin, M.T. (1990) Interactions of Saturated, n-6 and n-3 Polyunsaturated Fatty Acids to Modulate Arachidonic Acid Metabolism, *J. Lipid Res. 31*, 271–277.
26. Huang, Y.S., Smith, R.S., Redden, P.R., Cantrill, R.C., and Horrobin, D.F. (1991) Modification of Liver Fatty Acid Metabolism in Mice by n-3 and n-6 Δ6-Desaturase Substrates and Products, *Biochim. Biophys. Acta 1082*, 319–327.

27. National Research Council (1993) *Nutrient Requirements of Fish*, National Academy Press, Washington, DC.
28. Folch, J., Lees, M., and Sloane Stanley, G.H. (1957) A Simple Method for the Isolation and Purification of Total Lipids from Animal Tissues, *J. Biol. Chem. 226*, 497–509.
29. Christie, W.W. (1982) *Lipid Analyses*, 2nd edn., pp. 52–56, Pergamon Press, Oxford, United Kingdom.
30. Ghioni, C., Bell, J.G., and Sargent, J.R. (1996) Polyunsaturated Fatty Acids in Neutral Lipids and Phospholipids of Some Freshwater Insects, *Comp. Biochem. Physiol. 114B*, 161–170.
31. Ackman, R.G. (1980) Fish Lipids, Part 1, in *Advances in Fish Sciences and Technology* (Connell, J.J., ed.), pp. 86–103, Fishing News Books, Farnham, United Kingdom.
32. Dosanjh, B.S., Higgs, D.A., McKenzie, D.J., Randall, D.J., Eales, J.G., Rowshandeli, N., Rowshandeli, M., and Deacon, G. (1998) Influence of Dietary Blends of Menhaden Oil and Canola Oil on Growth, Muscle Lipid Composition, and Thyroidal Status of Atlantic Salmon (*Salmo salar*) in Sea Water, *Fish Physiol. Biochem. 19*, 123–134.
33. Tocher, D.R., Bell, J.G., Dick, J.R., Henderson, R.J., McGhee, F., Mitchell, D.F., and Morris, P.C. (2000) Polyunsaturated Fatty Acid Metabolism in Atlantic Salmon (*Salmo salar*) Undergoing Parr-Smolt Transformation and the Effects of Dietary Linseed and Rapeseed Oils, *Fish Physiol. Biochem. 23*, 59–73.
34. Bell, J.G., Tocher, D.R., Farndale, B.M., Cox, D.I., McKinney, R.W., and Sargent, J.R. (1997) The Effect of Dietary Lipid on Polyunsaturated Fatty Acid Metabolism in Atlantic Salmon (*Salmo salar*) Undergoing Parr-Smolt Transformation, *Lipids 32*, 515–525.
35. Torstensen, B.E., Frøyland, L., and Lie, Ø. (2003) Replacing Dietary Fish Oil with Increasing Levels of Rapeseed Oil and Olive Oil—Effects on Atlantic Salmon (*Salmo salar* L.) Tissue and Lipoprotein Lipid Composition and Lipogenic Enzyme Activities, *Aquacult. Nutr. 10*, 1–18.
36. Kiessling, K.-H., and Keissling, A. (1993) Selective Utilisation of Fatty Acids in Rainbow Trout (*Oncorhynchus mykiss*, Walbaum) Red Muscle Mitochondria, *Can. J. Zool. 71*, 248–251.
37. Frøyland, L., Lie, Ø., and Berge, R.K. (2000) Mitochondrial and Peroxisomal β-Oxidation Capacities in Various Tissues from Atlantic Salmon, *Salmo salar*, *Aquacult. Nutr. 6*, 85–89.
38. Bell, M.V., and Dick, J.R. (1991) Molecular Species Composition of the Major Diacyl Glycerophospholipids from Muscle, Liver, Retina, and Brain of Cod (*Gadus morhua*), *Lipids 26*, 565–573.
39. Simopoulos, A.P. (2001) n-3 Fatty Acids and Human Health: Defining Strategies for Public Policy, *Lipids 36*, S83–S89.
40. de Deckere, E.A.M., Korver, O., Verschuren, P.M., and Katan, M.B. (1998) Health Aspects of Fish and n-3 Polyunsaturated Fatty Acids from Plant and Marine Origin, *Eur. J. Clin. Nutr. 52*, 749–753.
41. Bechoua, S., Dubois, M., Vericel, E., Chapuy, P., Lagarde, M., and Prigent, A.-F. (2003) Influence of Very Low Dietary Intake of Marine Oil on Some Functional Aspects of Immune Cells in Healthy Elderly People, *Br. J. Nutr. 89*, 523–531.
42. Sanderson, P., Finnegan, Y.E., Williams, C.M., Calder, P.C., Burdge, G.C., Wootton, S.A., Griffin, B.A., Millward, D.J., Pegge, N.C., and Bemelmans, W.J.E. (2002) UK Food Standards Agency α-Linolenic Acid Workshop Report, *Br. J. Nutr. 88*, 573–579.
43. Billman, G.E., Kang, J.X., and Leaf, A. (1999) Prevention of Sudden Cardiac Death by Dietary Pure Omega-3 Polyunsaturated Fatty Acids in Dogs, *Circulation 99*, 2452–2457.
44. Singh, R.B., Niaz, M.A., Sharma, J.P., Kumar, R., Rastogi, V., and Moshiri, M. (1997) Randomized Double-Blind, Placebo-Controlled Trial of Marine Omega-3 Oil and Mustard Oil in Patients with Suspected Acute Myocardial Infarction: The Indian Experiment of Infarct Survival—4, *Cardiovasc. Drugs Ther. 11*, 485–491.
45. Ferreti, A., and Flanagan, V.P. (1996) Antithromboxane Activity of Dietary α-Linolenic Acid: A Pilot Study, *Prostaglandins Leukot. Essent. Fatty Acids 54*, 451–455.
46. Maillard, V., Bougnoux, P., Ferrari, P., Jourdan, M.L., Pinault, M., Lavillonniere, F., Body, G., Le Floch, O., and Chajes, V. (2002) n-3 and n-6 Fatty Acids in Breast Cancer in a Case-Control Study in Tours, France, *Int. J. Cancer 98*, 78–93.
47. Newcomer, L.M., King, I.B., Wicklund, K.G., and Stanford, J.L. (2001) The Association of Fatty Acids with Prostate Cancer, *Prostate 47*, 262–268.
48. Mourente, G., Good, J.E., and Bell, J.G. (2004) Partial Substitution of Fish Oil with Rapeseed Oil, Linseed Oil and Olive Oil in Diets for European Sea Bass (*Dicentrarchus labrax* L.): Effects on Flesh Fatty Acid Composition, Plasma Prostaglandins E_2 and $F_{2\alpha}$ Production, and Effectiveness of Subsequent Fish Oil "Wash Out," *Aquacult. Nutr.*, in press.
49. Mourente, G., and Dick, J.R. (2002) Influence of Partial Substitution of Dietary Fish Oil by Vegetable Oils on the Metabolism of [1-C^{14}]18:3n-3 in Isolated Hepatocytes of European Sea Bass (*Dicentrarchus labrax* L.), *Fish Physiol. Biochem. 26*, 297–308.
50. Jobling, M. (2003). Do Changes in Atlantic Salmon, *Salmo salar* L., Fillet Fatty Acids Following a Dietary Switch Represent Wash Out or Dilution? Test of a Dilution Model and Its Application, *Aquacult. Res. 34*, 1215–1221.

[Received December 9, 2003; accepted April 10, 2004]

The Up-Regulation of Hepatic Acyl-CoA Oxidase and Cytochrome P_{450} 4A1 mRNA Expression by Dietary Oxidized Frying Oil Is Comparable Between Male and Female Rats

Pei-Min Chao[a], Shan-Ching Hsu[c], Fu-Jung Lin[c], Yi-Jen Li[c], and Ching-jang Huang[b,c,*]

[a]Department of Nutrition, China Medical University, Taichung 404, Taiwan, [b]Laboratory of Nutritional Biochemistry, Department of Biochemical Science and Technology, and [c]Institute of Microbiology and Biochemistry, National Taiwan University, Taipei 106, Taiwan

ABSTRACT: We previously demonstrated that oxidized frying oil (OFO) activates peroxisome proliferator-activated receptor α (PPARα) and up-regulates hepatic acyl-CoA oxidase (ACO) and cytochrome P_{450} 4A1 (CYP4A1) genes in male rats. As female rats were shown to be less responsive to some peroxisome proliferators (PP), this study compared the expression of a few PPARα target genes in male and female rats fed diets containing OFO. Male and female rats were fed a diet containing 20 g/100 g OFO (O diet) or fresh soybean oil (F diet) for 6 wk. Both male and female rats fed the O diet showed significantly higher liver weight, hepatic ACO and catalase activities, CYP4A protein, and expression of ACO and CYP4A1 mRNA ($P < 0.05$) compared with their control groups. The mRNA expression of two other PPARα target genes, FA-binding protein and HMG-CoA synthase, were marginally increased by dietary OFO ($P = 0.0669$ and 0.0521, respectively). Female rats fed the O diet had significantly lower CYP4A protein than male rats fed the same diet. The remaining OFO-induced effects were not significantly different between male and female rats fed the O diet. These results indicate that dietary OFO, unlike clofibrate or other PP, had minimal sexual dimorphic effect on the induction of hepatic PPARα target gene expression.

Paper no. L9402 in *Lipids 39*, 233–238 (March 2004).

Peroxisome proliferator-activated receptor α (PPARα), a ligand-dependent transcription factor that belongs to the steroid hormone receptor family, plays a pivotal role in regulating liver lipid homeostasis (1–5). Peroxisome proliferators (PP), including the fibrate class of hypolipidemic drugs, FA, and eicosanoids are known ligands of PPARα (1,6). Upon activation by a ligand, PPAR heterodimerizes with retinoid X receptor and promotes the transcription of its target genes. The target genes of PPARα are mainly a homogeneous group of genes that participate in aspects of lipid catabolism such as FA uptake and binding; FA oxidation in microsomes, mitochondria, and peroxisomes; and lipoprotein assembly and transport. Studies in PPARα gene knockout mice clearly demonstrate that the pleiotropic response and enhanced FA oxidation in the liver of mice treated with PP are mediated by PPARα (7).

*To whom correspondence should be addressed at Laboratory of Nutritional Biochemistry, Department of Biochemical Science and Technology, National Taiwan University, Taipei 106, Taiwan.
E-mail: cjjhuang@ntu.edu.tw

Abbreviations: ACO, acyl-CoA oxidase; CFAM, cyclic FA monomer; CYP4A1, cytochrome P_{450} 4A1; FABP, fatty acid-binding protein; HS, HMG-CoA synthase; NEFA, nonesterified FA; OFO, oxidized frying oil; PFOA, perfluoro-octanoic acid; PL, phospholipids; PNS, post-nuclear supernatant; PP, peroxisome proliferators; PPARα, peroxisome proliferator-activated receptor α; RT, reverse transcription; TC, total cholesterol; TG, triacylglycerol.

A number of studies showed that there were sex-related differences in the response level to the treatment of some PP. When rodents were treated, females showed lower induction of hepatic peroxisome proliferation (8), peroxisomal β-oxidation (9,10), cytochrome P_{450} 4A (CYP4A) activity (11), protein and mRNA (11,12), acyl-CoA oxidase (ACO) activity (12), and protein levels of several PPARα target genes (8) compared with males. The difference has been attributed to the inhibition effect of estradiol and the enhancing effect of testosterone (9–11,13).

Recently, we reported that dietary oxidized frying oil (OFO) up-regulated the expression of hepatic PPARα target genes including ACO and CYP4A1 in male rats (14). In addition, we demonstrated that hydrolyzed OFO displayed a higher potency for PPARα transactivation than hydrolyzed fresh soybean oil. The results indicated that dietary OFO contained PPARα activators that exhibited a higher activating potency than the original FA such as linoleic acid or linolenic acid in fresh soybean oil.

To examine whether there is a gender difference in the response of PPARα target genes to dietary OFO, male and female rats were fed diets containing 20 g/100 g OFO or fresh soybean oil for 6 wk, and the expression of PPARα target genes including ACO and CYP4A1 in liver, was detected in this study.

MATERIALS AND METHODS

Animals and diets. Male and female weanling Sprague-Dawley rats weighing 60–80 g were purchased from the laboratory animal center of the National Science Council (Taipei, Taiwan). Based on a 2×2 factorial design, two groups of male and two groups of female rats were respectively fed the two test diets (F or O diet). The O diet contained 20 g/100 g OFO, and the F diet (the control) contained a similar amount of fresh soybean oil. All rats were housed individually in stainless steel wire cages in a room maintained at 23 ± 2°C, with a controlled 12-h light/dark cycle and free access to food and tap water. Body weight and food intake were recorded weekly. Animal care and handling conformed to accepted guidelines (15).

The OFO was prepared by frying wheat dough sheets in soybean oil (President, Tainan, Taiwan) at 205 ± 5°C for 24 h, as described previously (14). The composition of the test diets is shown in Table 1; the ratios of casein, vitamin, and mineral mixtures to energy were comparable to the AIN-76 diet.

Biochemical analyses. After 6 wk of feeding, rats were killed by carbon dioxide asphyxiation after overnight fasting. Blood was collected from the abdominal vena cava with EDTA-containing tubes. Liver and kidney were excised and

weighed, and a small portion of each was immediately frozen in liquid nitrogen and stored at –80°C for the analysis of mRNA expression. A second portion of liver was frozen at –20°C for the analysis of liver lipids. Remaining portions of liver were freshly homogenized for the preparation of post-nuclear supernatant (PNS) and microsome, respectively, as described (14). Plasma samples were obtained by centrifugation of blood and stored at –20°C for the analysis of lipids. For the analysis of liver lipids, frozen liver samples were thawed and extracted by the method of Folch *et al*. (16). Total lipids, triacylglycerol (TG), total cholesterol (TC), nonesterified FA (NEFA), and phospholipids (PL) in plasma and liver lipid extract were measured enzymatically by a commercial kit (Randox Lab, Crumlin, Northland, United Kingdom). The peroxisomal ACO and catalase activities in the PNS of liver were determined by the method of Lazarow (17) and Luck (18), respectively. The CYP4A protein in liver microsomal suspension was detected by Western blot analysis as previously described (14). Briefly, 5 μg liver microsomal protein was subjected to 10% SDS-PAGE, then transferred to a polyvinylidene fluoride-plus transfer membrane (NEN Life Science, Boston, MA). The blot was immunodetected with an enhanced chemiluminescence Western blotting kit (Amersham International, Amersham, United Kingdom) in which sheep anti-rat CYP4A was used as the primary antibody and a biotinylated donkey anti-sheep immunoglobulin G was used as the secondary antibody.

RNA purification and Northern blot analyses. Total RNA was extracted from the liver and kidney with trizol reagent (Life Technologies, Rockville, MD). Total RNA (20 μg) was separated by electrophoresis in denaturing formaldehyde agarose gel and then transferred to nylon membrane. The blots were prehybridized at 42°C for 3 h in the hybridization buffer containing salmon sperm DNA (20 μg/mL), then hybridized at 42°C for 12–15 h with ^{32}P-labeled cDNA probes of ACO, CYP4A1, FA binding protein (FABP), HMG-CoA synthase (HS), or β-actin sequentially after deprobing previous probe remained on membrane. All the cDNA probes were synthesized by reverse transcription (RT)-PCR to amplify encoding base pairs 74–2059 for ACO (according accession number J02752), 13–2040 for CYP4A1 (M14972), 33–405 for FABP (M35991), 385–1374 for HS (M33648), and 103–642 for β-actin (55574). To correct for possible differences in transfer and loading, β-actin was used as an internal control. After washing at the appropriate stringency, the blots were exposed to X-OMAT AR film (Kodak). Signals were quantified using the microcomputer imaging device image analysis system (Fuji, Tokyo, Japan). PPARα mRNA content was semiquantified by RT-PCR as previously described (14).

Statistical analysis. Data were expressed as mean ± SD. To test the significance of the effects of dietary fat quality (fresh soybean oil vs. OFO), gender, and their interaction, data of the four groups were analyzed by two-way ANOVA. When a significant interaction ($P < 0.05$) existed between fat quality and gender, the significance of differences among the four groups was further analyzed statistically by one-way ANOVA and Duncan's multiple range test. Data were transformed to log values for the statistical analysis if the variances were not homogeneous. The SAS System (SAS Institute, Cary, NC) was employed for the statistical analysis, and differences were considered significant at $P < 0.05$.

TABLE 1
Composition of Test Diets Used in the Feeding Experiment[a,b]

	F diet	O diet
	(g/kg diet)	
Casein	235	235
Cornstarch	448	448
Fresh soybean oil	200	—
Oxidized frying oil[c]	—	200
Cellulose	59	59
Mineral mixture	41	41
Vitamin mixture	12	12
DL-Methionine	3	3
Choline	2	2

[a]Two test diets containing 20% fresh soybean oil (F diet) or oxidized frying oil (O diet) were given to male and female rats.
[b]Sources of ingredients: casein, AIN-76 mineral mixture, and AIN-76 vitamin mixture ICN (Aurora, OH); cornstarch, Samyang (Seoul, Korea); cellulose, J. Rettenmaier & Söhne (Holzmühle, Germany); soybean oil, President Co. (Tainan, Taiwan); methionine and choline chloride, Sigma Chemical (St. Louis, MO).
[c]Prepared by frying sheets of dough in soybean oil at 205 ± 5°C for 24 h.

RESULTS

Effect of OFO on growth and tissue weight of female vs. male rats. As shown in Table 2, there were significant effects of diet fat quality, gender, and the interactions of these two factors on body weight gain and feed efficiency. Both male and female rats fed the O diet showed significantly lower body weight gain and feed efficiency than rats fed the F diet ($P < 0.05$), but the differences between the O and F groups were to a greater extent in male rats than in females. Diet fat quality ($P = 0.0001$) and gender ($P = 0.0001$) significantly affected food intake without a significant interaction. Relative kidney weight was also significantly affected by the interaction between gender and fat quality ($P < 0.01$). Male rats fed the O diet showed significantly higher relative kidney weight than those fed the F diet. In contrast, there was no difference in the relative kidney weight between the F and O diet group in female rats. Both male and female rats fed the O diet showed significantly higher relative liver weight ($P = 0.0001$) than those fed the F diet, and there was neither a gender effect nor interaction ($P > 0.05$). The extent of liver enlargement induced by dietary OFO observed in female rats was comparable to males (1.68-fold in both male and female rats).

Effect of OFO on liver and plasma lipids of female vs. male rats. Not only gender and fat quality but also the interaction of these two factors had significant effects on liver total lipid, TG, and TC ($P = 0.0001$, Table 3). Rats fed the O diet showed significantly lower liver lipids except for PL than those fed the F diet. Female rats fed the F diet had significantly lower liver total lipid, TG, and TC than male rats fed the same diet. In contrast, liver total lipid, TG, and TC of female rats fed the O diet were comparable to those of male rats fed the O diet. This indi-

TABLE 2
Body Weight Gain, Food Intake, Feed Efficiency, and Relative Liver and Kidney Weight of Male and Female Rats Fed Diets Containing 20 g/100 g Fresh Soybean Oil (F diet) or Oxidized Frying Oil (O diet) for 6 wk[a]

	Body weight gain	Food intake	Feed efficiency	Relative liver weight	Relative kidney weight
	(g/d)		(g gain/g feed)	(g/100 g body)	
Male					
F diet	8.1 ± 0.9[a]	16.1 ± 1.3	0.51 ± 0.03[a]	3.5 ± 0.2	0.73 ± 0.05[b]
O diet	4.8 ± 0.6[b]	11.2 ± 1.1	0.42 ± 0.04[b]	5.9 ± 0.4	0.91 ± 0.08[a]
Female					
F diet	4.8 ± 0.8[b]	13.1 ± 1.5	0.36 ± 0.03[c]	3.4 ± 0.3	0.87 ± 0.13[a]
O diet	3.1 ± 0.4[c]	9.3 ± 1.3	0.33 ± 0.02[d]	5.7 ± 0.5	0.88 ± 0.06[a]
			P-value		
Gender	0.0001	0.0001	0.0001	0.3162	0.0613
Fat quality	0.0001	0.0001	0.0001	0.0001	0.0032
Gender × quality	0.0020	0.2587	0.0377	0.6089	0.0066

[a]Values are means ± SD, $n = 8$. *P* values for gender, fat quality, and their interaction were analyzed by two-way ANOVA. When there was a significant interaction between gender and fat quality, the significance of differences among four groups was analyzed by Duncan's multiple range test. Values not sharing a superscript letter within a column are significantly different, $P < 0.05$.

cated that the lowering effect of dietary OFO on liver lipids was greater in male than in female rats.

Rats fed the O diet had significantly lower plasma total lipid than those fed the F diet ($P < 0.05$, Table 3). The difference in plasma total lipid between rats fed O diet and F diet was similar in male and female rats. The plasma NEFA concentration was affected by gender and not by dietary fat quality. Female rats showed significantly higher plasma NEFA than male rats ($P < 0.005$). Neither gender nor fat quality significantly affected plasma TG, TC, and PL ($P > 0.05$).

Effect of OFO on enzyme activities and protein content of female vs. male rats. In Figure 1 are shown the specific activities of ACO and catalase in the liver of four groups of tested rats. These two enzymes were markers of peroxisomal β-oxidation and peroxisome proliferation, respectively. Feeding OFO resulted in significant ($P = 0.0001$) increases of ACO and catalase activities in both male and female rats. There were neither significant gender effects nor interactions with fat quality on ACO and catalase activities. In female rats, the specific activities of ACO and catalase induced by dietary OFO were about 5.5-fold and 3.7-fold higher, respectively, which were almost equivalent to the responses observed in males (6.0-fold and 2.3-fold induction, respectively).

Western blot analysis demonstrated that the protein content of CYP4A in liver microsomes was significantly increased by the feeding of O diet (Fig. 2A). Results of two-way ANOVA showed that gender, fat quality, and the interaction exerted significant effects on the liver CYP4A protein ($P < 0.05$, Fig. 2B). In rats fed the F diet, there was no significant difference between males and females ($P > 0.05$). In contrast, male rats fed the O diet had a significantly higher CYP4A protein than female rats fed the same diet ($P < 0.05$). The induction of CYP 4A by feeding the O diet was greater in male rats (75-fold) than in females (24-fold).

Effect of OFO on mRNA content of female vs. male rats. In Figure 3 is shown the result of Northern blot analysis of the mRNA content of PPARα target genes including ACO, CYP4A1, FABP, and HS in the liver of four groups rats. Both male and female rats fed the O diet had significantly higher mRNA of ACO ($P < 0.05$), CYP4A1 ($P < 0.005$), FABP ($P =$

TABLE 3
Plasma and Liver Lipids of Male and Female Rats Fed Diets Containing 20 g/100 g Fresh Soybean Oil (F diet) or Oxidized Frying Oil (O diet) for 6 wk[a]

	Plasma lipids					Liver lipids				
	Total lipid	TG	TC	PL	NEFA	Total lipid	TG	TC	PL	NEFA
	(g/L)		(mmol/L)			(mg/g)		(μmol/g)		
Male										
F diet	4.8 ± 2.0	1.1 ± 0.4	2.8 ± 0.8	2.0 ± 0.4	0.6 ± 0.1	75 ± 9[a]	98 ± 14[a]	12.4 ± 2.1[a]	16 ± 2	25 ± 10
O diet	3.3 ± 0.9	0.8 ± 0.3	2.4 ± 0.5	2.1 ± 0.3	0.6 ± 0.1	25 ± 3[c]	28 ± 6[c]	5.6 ± 0.4[c]	16 ± 2	10 ± 4
Female										
F diet	4.4 ± 2.0	1.1 ± 0.4	2.3 ± 0.7	2.0 ± 0.5	0.8 ± 0.2	40 ± 16[b]	54 ± 19[b]	7.3 ± 1.2[b]	15 ± 2	16 ± 7
O diet	3.1 ± 0.7	1.0 ± 0.2	2.1 ± 0.4	1.8 ± 0.2	0.7 ± 0.2	24 ± 2[c]	31 ± 7[c]	5.7 ± 2[c]	18 ± 3	10 ± 3
					P-value					
Gender	0.5499	0.5486	0.0813	0.4105	0.0011	0.0001	0.0001	0.0001	0.2327	0.0349
Fat quality	0.0191	0.1352	0.2535	0.8995	0.5162	0.0001	0.0001	0.0001	0.0403	0.0001
Gender × quality	0.9013	0.4542	0.6319	0.3189	0.3141	0.0001	0.0001	0.0001	0.2042	0.0524

[a]Values are means ± SD, $n = 8$. *P*-values for gender, fat quality, and their interaction were analyzed by two-way ANOVA. When there was a significant interaction between gender and fat quality, the significance of differences among four groups was analyzed by Duncan's multiple-range test. Values not sharing a superscript letter within a column are significantly different, $P < 0.05$. TG, triacylglycerol; TC, total cholesterol; PL, phospholipids; NEFA, nonesterified FA.

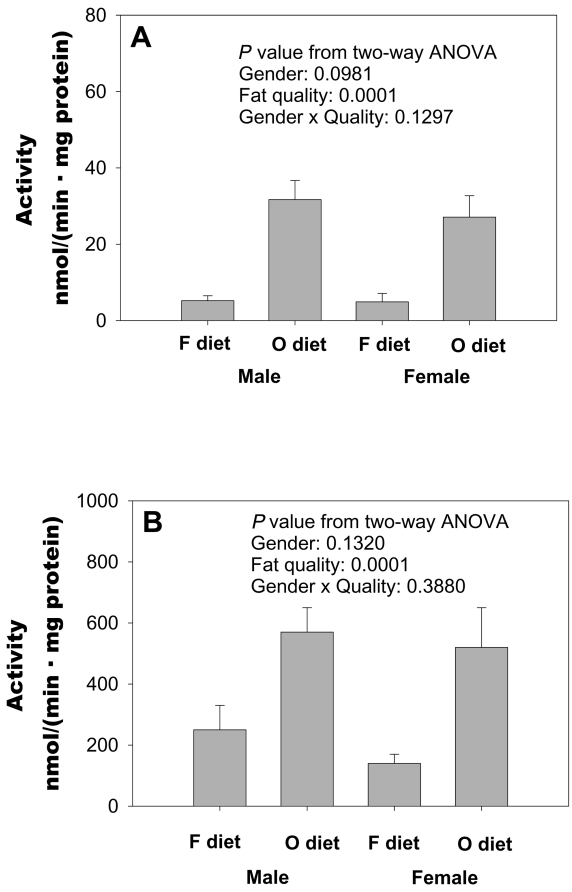

FIG. 1. The specific activities of acyl-CoA oxidase (ACO) (A) and catalase (B) in liver postnuclear supernatant (PNS) of male and female rats fed diets containing 20 g/100 g fresh soybean oil (F diet) or oxidized frying oil (O diet) for 6 wk. Values are means ± SD, $n = 8$. Two-way ANOVA was conducted for the four groups.

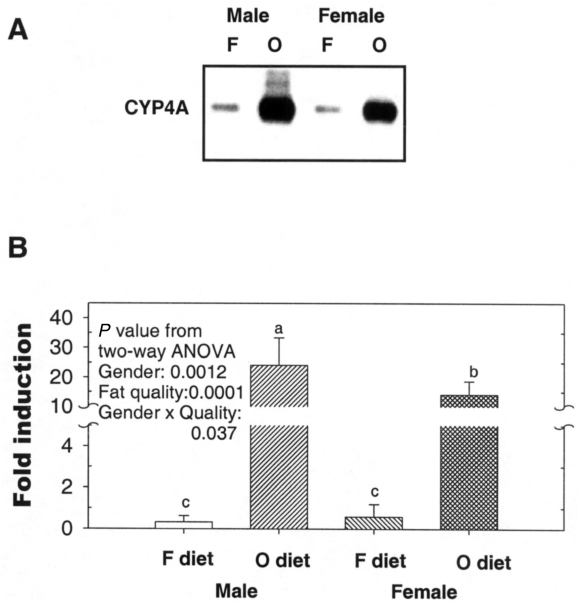

FIG. 2. Western blot analysis (A) for cytochrome P_{450} 4A (CYP4A) protein content in liver microsomes of male and female rats fed diets containing 20 g/100 g fresh soybean oil (F diet; F) or oxidized frying oil (O diet; O) for 6 wk. Signals were quantified by image analysis (B). Values are means ± SD, $n = 8$. Two-way ANOVA was conducted for the four groups. Where there was a significant interaction ($P < 0.05$), the significance of the difference was further analyzed by Duncan's multiple-range test. Values not sharing a common letter are significantly different ($P < 0.05$).

0.067), and HS ($P = 0.052$) than those fed the F diet. There were neither significant gender effects nor interactions of the two factors. In other words, a comparable induction by OFO feeding between male and female rats was observed. The liver ACO and CYP4A1 mRNA of rats fed the O diet were 1.5- and 3.1-fold those fed the F diet in males, and were 2.6- and 2.2-fold, respectively, in females. There was no significant effect of gender, fat quality, or their interaction on PPARα mRNA expression in liver, analyzed by semi-quantitative RT-PCR (data not shown).

The CYP4A1 mRNA expression in kidney was also measured by Northern blot analysis. The CYP4A1 mRNA in kidney was significantly lower in female than in male rats (gender effect, $P < 0.05$). There was neither a significant effect of fat quality nor an interaction with gender on kidney CYP4A1 mRNA expression (data not shown).

DISCUSSION

A 2 × 2 factorial design was used in the present study to observe the effects of OFO and gender on the expression of some PPARα target genes in rats. A significant interaction between OFO (fat quality) and gender, shown in the results of the two-way ANOVA statistical analysis, indicated that the response to OFO was different between male and female rats, or the gender difference was not similar between rats fed the O diet and the control F diet. Without a significant interaction, a significant gender effect indicated that the gender difference in rats fed the F diet was similar to those in rats fed the O diet.

Data from this study indicated that in female rats, dietary OFO also induced liver enlargement and up-regulated the expression of hepatic PPARα target genes ACO and CYP4A1, as in male rats. There were no significant interactions between gender and fat quality on relative liver weight, enzyme activities of ACO and catalase, and mRNA content of ACO, CYP4A1, FABP, and HS. However, there was a significant interaction ($P < 0.05$) in the hepatic CYP4A protein expression between gender and quality (Fig. 2). Female rats fed the O diet had significantly lower CYP4A protein than male rats fed the same diet.

It has been reported that hepatic responses to the treatment of several PP were less pronounced in female than in male rodents. For example, feeding a 0.02% perfluoro-octanoic acid (PFOA) diet for 1 wk increases peroxisomal β-oxidation and liver weight in male rats, but not in females (9). On intraperitoneal administration of 40 mg/kg clofibrate (ethyl ester) for 3 d, Sundseth and Waxman (12) found a 26-fold vs. 6-fold increase in ACO activity and 39-fold vs. 3-fold increase in CYP4A1 mRNA in male vs. female rats. Sugiyama *et al.* (10) also reported a significantly higher increase in ACO activity in male rats (12-fold) than in females (4-fold) after they had been

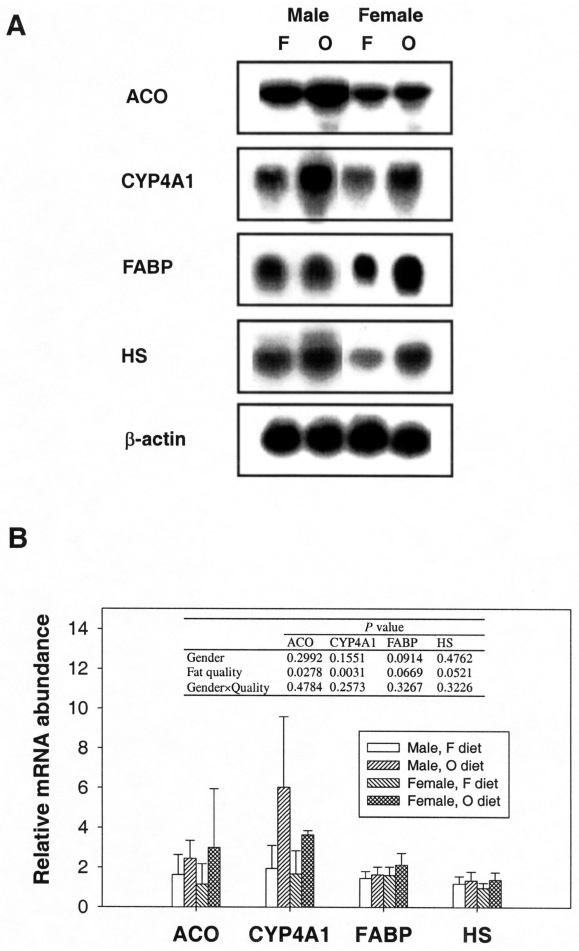

FIG. 3. Northern blot analysis (A) for mRNA of liver ACO, CYP4A1, FA-binding protein (FABP), and HMG-CoA synthase (HS) of male and female rats fed diets containing 20 g/100 g fresh soybean oil (F diet; F) or oxidized frying oil (O diet; O) for 6 wk. Signals were quantified by image analysis (B). Each value was normalized by β-actin. Values are means ± SD, n = 6. Two-way ANOVA was conducted for the four groups and results were shown in the inset table. For other abbreviations see Figures 1 and 2.

orally administered with 300 mg/kg of clofibric acid for 3 d. Hiratsuka *et al*. (11) showed that the increased activity, protein, and mRNA content of lauric acid ω-hydroxylase (CYP4A) in rats intraperitoneally treated with 250 mg/kg clofibrate for 3 d were to a significantly lower extent in female than in male rats.

A few underlying mechanisms for the lower responsiveness to PP induction in female rats have been proposed. In using hormone manipulations *in vivo* (9,10) or *in vitro* (19), it was observed that the PP responses induced by clofibrate or PFOA were stimulated by testosterone and inhibited by estradiol. In addition to a sex hormone, a pituitary-dependent factor such as a growth hormone, which has a characteristic continuous profile in adult female rats, played a suppressive role (10,12,19). An alteration in the pharmacokinetics of PP elimination by the sex hormone was also suggested. Since the serum clofibrate level was found to be lower in castrated rats than intact or testosterone-treated castrated rats (13), the metabolism of clofibrate may be accelerated by androgen deficiency.

In this study, however, we did not observe sex-related differences in mRNA expression of PPARα target genes and ACO activity in response to dietary OFO. It appears unlikely that the longer treatment period (6 wk) in this study than in the above-mentioned studies (a few days or weeks) could account for the difference. It is more likely that, unlike clofibrate, there may not be a sex-related difference in the catabolism or elimination of OFO. The sex-dependent regulation by trichloroethylene through PPARα also has been attributed to a difference in the ability to produce the metabolite trichloroacetic acid, which is the ultimate PPARα activator (8). Similar to our results, no sex differences in the extent of induction by WY-14643, a potent activator of PPARα, were mentioned in the paper of Nakajima *et al*. (8) in which the unpublished data of Aoyama *et al*. were cited.

In this study, the OFO-induced CYP4A protein in liver is significantly lower in female rats than in males. Since the anti-CYP4A antibody we used can detect CYP4A1, -4A2, and -4A3, the CYP4A protein immuno-detected in this study was the sum of three isoforms. It had been reported that CYP4A2 is not expressed in female liver (12,20,21). Hence, the significantly lower liver CYP4A protein levels in OFO-fed female rats could be due to the absence of male-specific CYP4A2 expression and induction. Although the mRNA detected by full-length CYP4A1 cDNA probe in liver tended to be lower in female than male rats, the difference did not reach statistical significance. Because the cDNA of CYP4A2 and -4A3 has 60–65% nucleotide sequence homology to that of CYP4A1, the full-length CYP4A1 cDNA probe we used may have detected the mRNA of CYP4A2 and -4A3 as well.

The ACO, CYP4A1, FABP, and HS mRNA measured in this study were all target genes regulated by PPARα (22–24). We have observed that the mRNA expression of all four of these genes was significantly induced in the liver of male rats fed a diet containing 0.5% clofibrate for 1 wk (data not shown). In contrast, the OFO-induced ACO and CYP4A1 mRNA expressions were significant, but those of FABP and HS were marginal. It seemed that FABP and HS were less responsive to OFO up-regulation than to a typical PP, such as clofibrate.

Hydroxy FA produced presumably by lipoxygenase reaction (such as 9- and 13-hydroxyoctadecadienoate, isolated from oxidized LDL) and CLA have been reported to activate PPAR (25–28). Results of a rat study showed that cyclic FA monomer (CFAM) significantly increased the activities of enzymes that were PPARα target gene products, hence implying the CFAM that may exist in frying oil in minute amounts may also activate PPARα (29). Kamal-Eldin *et al.* (30) fractionated and analyzed commercial frying oils after saponification and found the major altered FA were oxidized monomers, representing complex mixture of monomeric FA with at least one oxygenated function, e.g., epoxy, keto, or hydroxy. It is speculated that these monomeric FA with an oxygenated function may be responsible for PPARα activation.

In conclusion, results of this study showed that PPARα activators in dietary OFO, unlike clofibrate or other PP, induced ACO and CYP4A1 mRNA expression to a similar extent in female and male rats.

ACKNOWLEDGMENTS

This work was supported by grants NSC89-2320-B-002-184 from the National Science Council, Taipei, Taiwan, and CMC90-NT-07 from China Medical University, Taichung, Taiwan.

REFERENCES

1. Issemann, I., and Green, S. (1990) Activation of a Member of the Steroid Hormone Receptor Superfamily by Peroxisome Proliferators, *Nature 347*, 645–650.
2. Schoonjans, K., Staels, B., and Auwerx, J. (1996) The PPARs and Their Effects on Lipid Metabolism and Adipocyte Differentiation, *Biochim. Biophys. Acta 1302*, 93–109.
3. Kroetz, D.L., Yook, P., Costet, P., Bianchi, P., and Pineau, T. (1998) Peroxisome Proliferator-Activated Receptor α Controls the Hepatic *CYP4A* Induction Adaptive Response to Starvation and Diabetes, *J. Biol. Chem. 273*, 31581–31589.
4. Kersten, S., Seydoux, J., Peters, J.M., Gonzalez, F.J., Desvergne, B., and Wahli, W. (1999) Peroxisome Proliferator-Activated Receptor α Mediates the Adaptive Response to Fasting, *J. Clin. Invest. 103*, 1489–1498.
5. Hashimoto, T., Cook, W.S., Qi, C., Yeldandi, A.V., Reddy, J.K., and Rao, M.S. (2000) Defect in Peroxisome Proliferator-Activated Receptor α-Inducible Fatty Acid Oxidation Determines the Severity of Hepatic Steatosis in Response to Fasting, *J. Biol. Chem. 275*, 28918–28928.
6. Kliewer, S.A., Sundseth, S.S., Jones, S.A., Brown, P.J., Wisely, G.B., Koble, C.S., Devchand, P., Wahli, W., Willson, T.M., Lenhard, J.M., and Lehmann, J.M. (1997) Fatty Acids and Eicosanoids Regulate Gene Expression Through Direct Interactions with Peroxisome Proliferator-Activated Receptors α and γ, *Proc. Natl. Acad. Sci. USA 94*, 4318–4323.
7. Lee, S.S., Pineau, T., Drago, J., Lee, E.J., Owens, J.W., Kroetz, D.L., Fernandez-Salguero, P.M., Westphal, H., and Gonzalez, F.J. (1995) Targeted Disruption of the α Isoform of the Peroxisome Proliferator-Activated Receptor Gene in Mice Results in Abolishment of the Pleiotropic Effects of Peroxisome Proliferators, *Mol. Cell. Biol. 15*, 3012–3022.
8. Nakajima, T., Kamijo, Y., Usuda, N., Liang, Y., Fukushima, Y., Kametani, K., Gonzalez, F.J., and Aoyama, T. (2000) Sex-Dependent Regulation of Hepatic Peroxisome Proliferation in Mice by Trichloroethylene *via* Peroxisome Proliferator-Activated Receptor α, *Carcinogenesis 21*, 677–682.
9. Kawashima, Y., Uy-Yu, N., and Kozuka, H. (1989) Sex-Related Difference in the Inductions by Perfluoro-octanoic Acid of Peroxisomal β-Oxidation, Microsomal 1-Acylglycerophosphocholine Acyl Transferase and Cytosolic Long-Chain Acyl-CoA Hydrolase in Rat Liver, *Biochem. J. 261*, 595–600.
10. Sugiyama, H., Yamada, J., and Suga, T. (1994) Effects of Testosterone, Hypophysectomy and Growth Hormone Treatment on Clofibrate Induction of Peroxisomal β-Oxidation in Female Rat Liver, *Biochem. Pharmacol. 47*, 918–921.
11. Hiratsuka, M., Matsuura, T., Sato, M., and Suzuki, Y. (1996) Effects of Gonadectomy and Sex Hormones on the Induction of Hepatic CYP4A by Clofibrate in Rats, *Biol. Pharm. Bull. 19*, 34–38.
12. Sundseth, S.S., and Waxman, D.J. (1992) Sex-Dependent Expression and Clofibrate Inducibility of Cytochrome P_{450} 4A Fatty Acid ω-Hydroxylases: Male Specificity of Liver and Kidney CYP4A2 mRNA and Tissue-Specific Regulation by Growth Hormone and Testosterone, *J. Biol. Chem. 267*, 3915–3921.
13. Paul, H.S., Sekas, G., and Winters, S.J. (1994) Role of Testosterone in the Induction of Hepatic Peroxisome Proliferation by Clofibrate, *Metabolism 43*, 168–173.
14. Chao, P.M., Chao, C.Y., Lin, F.J., and Huang, C.J. (2001) Oxidized Frying Oil Up-Regulates Hepatic Acyl-CoA Oxidase and Cytochrome P_{450} 4A1 Genes in Rats and Activates PPARα, *J. Nutr. 131*, 3166–3174.
15. National Research Council, *Guide for the Care and Use of Laboratory Animals*, Publication No. 85-23 (rev.), National Institutes of Health, Bethesda, MD.
16. Folch, J., Lees, M., and Sloane Stanley, G.H. (1957) A Simple Method for the Isolation and Purification of Total Lipids from Animal Tissues, *J. Biol. Chem. 226*, 497–509.
17. Lazarow, P.B. (1981) Assay of Peroxisomal β-Oxidation of Fatty Acids, *Methods Enzymol. 72*, 315–319.
18. Luck, H. (1963) Catalase, in *Methods of Enzymatic Analysis* (Bergmeyer, H.U., ed.), pp. 885, Academic Press, New York.
19. Yamada, J., Sugiyama, H., Tamura, H., and Suga, T. (1994) Hormonal Modulation of Peroxisomal Enzyme Induction Caused by Peroxisome Proliferators: Suppression by Growth and Thyroid Hormones in Cultured Rat Hepatocytes, *Arch. Biochem. Biophys. 315*, 555–557.
20. Helvig, C., Dishman, E., and Capdevila, J.H. (1998) Molecular, Enzymatic, and Regulatory Characterization of Rat Kidney Cytochromes P450 4A2 and 4A3, *Biochemistry 37*, 12546–12558.
21. Ito, O., Alonso-Galicia, M., Hopp, K.A., and Roman, R.J. (1998) Localization of Cytochrome P-450 4A Isoforms Along the Rat Nephron, *Am. J. Physiol. 274*, F395–F404.
22. Issemann, I., Prince, R., Tugwood, J., and Green, S. (1992) A Role for Fatty Acids and Liver Fatty Acid Binding Protein in Peroxisome Proliferation, *Biochem. Soc. Trans. 20*, 824–827.
23. Juge-Aubry, C., Pernin, A., Favez, T., Burger, A.G., Wahli, W., Meier, C.A., and Desvergne, B. (1997) DNA Binding Properties of Peroxisome Proliferator-Activated Receptor Subtypes on Various Natural Peroxisome Proliferator Response Elements. Importance of the 5′-Flanking Region, *J. Biol. Chem. 272*, 25252–25259.
24. Hegardt, F.G. (1998) Transcriptional Regulation of Mitochondrial HMG-CoA Synthase in the Control of Ketogenesis, *Biochimie 80*, 803–806.
25. Nagy, L., Tontonoz, P., Alvarez, J.G., Chen, H., and Evans, R.M. (1998) Oxidized LDL Regulates Macrophage Gene Expression Through Ligand Activation of PPARγ, *Cell 93*, 229–240.
26. Sethi, S., Ziouzenkova, O., Ni, H., Wagner, D.D., Plutzky, J., and Mayadas, T.N. (2002) Oxidized Omega-3 Fatty Acids in Fish Oil Inhibit Leukocyte-Endothelial Interactions Through Activation of PPARα, *Blood 100*, 1340–1346.
27. Rong, R., Ramachandran, S., Penumetcha, M., Khan, N., and Parthasarathy, S. (2002) Dietary Oxidized Fatty Acids May Enhance Intestinal Apolipoprotein A-I Production, *J. Lipid Res. 43*, 557–564.
28. Moya-Camarena, S.Y., Van den Heuvel, J.P., and Belury, M.A. (1999) Conjugated Linoleic Acid Activates Peroxisome Proliferator-Activated Receptor α and β Subtypes but Does Not Induce Hepatic Peroxisome Proliferation in Sprague-Dawley Rats, *Biochim. Biophys. Acta 1436*, 331–342.
29. Martin, J.C., Joffre, F., Siess, M.H., Vernevaut, M.F., Collenot, P., Genty, M., and Sebedio, J.L. (2000) Cyclic Fatty Acid Monomers from Heated Oil Modify the Activities of Lipid Synthesizing and Oxidizing Enzymes in Rat Liver, *J. Nutr. 130*, 1524–1530.
30. Kamal-Eldin, A., Marquez-Ruiz, G., Dobarganes, C., and Appelqvist, L.A. (1997) Characterization of Aldehydic Acids in Used and Unused Frying Oils, *J. Chromatogr. A 776*, 245–254.

[Received October 27, 2003, and in final form February 26, 2004; accepted March 8, 2004]

8302A/C and (TTA)n Polymorphisms in the HMG-CoA Reductase Gene May Be Associated with Some Plasma Lipid Metabolic Phenotypes in Patients with Coronary Heart Disease

Yu Tong[a], Sizhong Zhang[a,*], Hai Li[b], Zhiguang Su[a], Xiangdong Kong[a], Hekun Liu[a], Cuiying Xiao[a], Yan Sun[a], and Jia Jun Shi[a]

[a]Department of Medical Genetics, West China Hospital, and [b]Department of Advanced Mathematics, College of Mathematics, Sichuan University, Sichuan, Chengdu 610041, China

ABSTRACT: HMG-CoA reductase (HMGCR) is a rate-limiting enzyme that participates in cholesterol metabolism. Here we analyzed the 8302A/C and the (TTA)n polymorphisms in the *HMGCR* gene in 169 Chinese patients with coronary heart disease (CHD) and 161 age-matched controls. Results indicated that the levels of plasma VLDL and TG in patients with the AA genotype of the 8302A/C locus were significantly higher than in patients with other genotypes ($P < 0.05$). In addition, the frequency of allele A4 of the (TTA)n locus was higher ($P < 0.05$) and the frequency of allele A5 was lower ($P = 0.002$) in CHD patients than in the controls. This suggests that both polymorphisms in the *HMGCR* gene may be associated with lipid and lipoprotein abnormalities in CHD in the Chinese.

Paper no. L9455 in *Lipids 39,* 239–241 (March 2004).

Coronary heart disease (CHD) is a common and complex multifactorial disease (1). Numerous factors, including genetic and environmental ones, increase the risk of CHD (2). Plasma cholesterol, as an important component of plasma lipoproteins (3), has an apparent relationship with the development of and mortality from CHD (4).

HMG-CoA reductase (HMGCR) is one of the most important enzymes that participate in cholesterol metabolism (5). It plays a rate-limiting role in cholesterol biosynthesis (6). The statins, which are widely prescribed in cholesterol-lowering therapy, are inhibitors of this enzyme (7) that decrease the biosynthesis of intrahepatic cholesterol and hence prevent or stabilize the atherosclerotic plaque (8). Therefore, it is reasonable to postulate that HMGCR, coded by the *HMGCR* gene, may be related to the development of CHD. At present, this has not been studied.

Several polymorphisms, including the 8302A/C and (TTA)n trinucleotide repeats, in the *HMGCR* gene are known, but their possible association with CHD and its clinical–biochemical phenotypes have not been studied. Here we report the results of our investigation of these polymorphisms and their possible association with CHD in the Chinese.

*To whom correspondence should be addressed.
E-mail: szzhang@mcwcums.com

Abbreviations: CE, cholesterol ester; CHD, coronary heart disease; HMGCR, HMG-CoA reductase.

MATERIALS AND METHODS

Subjects. One hundred sixty-nine unrelated patients with CHD were selected by coronary angiography using the Judkins technique. All were from the West China Hospital, Sichuan University, in Chengdu. Individuals with at least one stenosis of >60% in any major coronary artery branch (left anterior descending, left circumflex artery, right coronary artery) were qualified as "CHD patients" in the study. In addition, 161 unrelated age-matched subjects, who were free of any clinical and biochemical signs of CHD, were selected *via* health screening at the same hospital and used as controls.

Genotyping of the 8302A/C and the (TTA)n trinucleotide repeats. Genomic DNA isolated from peripheral blood leukocytes using the "salting-out" procedure (9) was then stored at 4°C for use. Genotypes of the 8302A/C and (TTA)n trinucleotide repeats were isolated as described previously by Leitersdorf *et al.* (10) and Zuliani and Hobbs (11), respectively.

Statistical analysis. Frequencies of the alleles and genotypes were calculated by counting. The assumption of the Hardy–Weinberg equilibrium was tested by means of gene counting and χ^2 analysis. Lipid phenotypic data among different genotypes were then analyzed statistically using the SPSS, version 10.0, software.

RESULTS

8302A/C polymorphism. The distribution of the alleles and genotypes of the 8302A/C polymorphism in CHD patients and the control group is shown in Table 1. Genotypes followed the Hardy–Weinberg equilibrium in both the control and CHD patient groups (data not shown). There was no significant difference between the CHD and control groups ($P > 0.05$) in the frequency of alleles and genotypes of the 8302A/C polymorphism (Table 1). However, CHD patients with the AA genotype had significantly higher TG and VLDL levels than the other genotype

TABLE 1
Genotype and Allele Frequencies of *HMGCR* Gene in Coronary Heart Disease (CHD) Patients and in the Control Group[a]

		Genotype (%)			Allele (%)	
Group	Case	AA	AC	CC	A	C
CHD	169	42 (24.9)	92 (54.4)	35 (20.7)	52.1	47.9
Controls	161	30 (18.6)	83 (51.6)	48 (29.8)	44.4	55.6

[a]All *P* values >0.05 ($P > 0.05$).

TABLE 2
Plasma Lipids in CHD Patients with Different Genotypes[a]

	Genotype			*P* value		
Item	AA	AC	CC	AA vs. AC	AA vs. CC	AC vs.CC
		(mmol/L)				
TC	4.010 ± 0.358	4.251 ± 0.193	4.089 ± 0.158	0.528	0.855	0.610
TG	2.448 ± 0.484	1.816 ± 0.170	1.561 ± 0.161	0.048*	0.037*	0.052
HDL-C	0.988 ± 0.070	1.173 ± 0.085	1.136 ± 0.083	0.239	0.417	0.791
LDL-C	1.912 ± 0.403	2.401 ± 0.148	2.226 ± 0.240	0.161	0.435	0.572
VLDL	1.318 ± 0.284	0.826 ± 0.081	0.782 ± 0.021	0.018*	0.011*	0.062

[a]TC, total cholesterol; HDL-C, HDL cholesterol; LDL-C, LDL cholesterol; for other abbreviation see Table 1. *, $P < 0.05$.

subgroups ($P < 0.05$) (Table 2), a result not found in the control group (data not shown).

(TTA)n trinucleotide repeats. As in other populations (11), seven distinct alleles, namely A1–A7, with the copy numbers of 10–16 in intron 10 of the *HMGCR* gene, were detected in both CHD patients and the control group, and no significant deviations from the Hardy–Weinberg equilibrium were found in the genotype frequency of either group (data not shown). The frequency of alleles in both groups is summarized in Table 3.

As one can observe from Table 3, allele A4 was present at a significantly higher frequency in CHD patients than that in the controls ($P < 0.05$), whereas allele A5 was present at a significantly lower frequency in CHD patients than in the controls ($P = 0.002$).

The distribution of plasma lipids in control and CHD patients with the various alleles is shown in Table 4. There was no significant difference in the levels of plasma lipids of CHD patient and control subgroups with various alleles ($P > 0.05$).

DISCUSSION

1.8302A/C restriction polymorphism. Although there was no significant difference between the CHD and control groups in the frequency of alleles and genotypes in the 8302A/C polymorphism, association studies showed that the levels of plasma VLDL and TG in patients with the AA genotype were significantly higher than those with other genotypes ($P < 0.05$). Since the cholesterol ester (CE) is an essential component in the normal formation of VLDL (12), an increase in CE content leads to an increase in the formation and secretion of VLDL in the liver (13). We speculated that allele A may be associated with the esterification of cholesterol. Also, VLDL is the main lipoprotein with the highest component of TG (14), and it plays an important role in TG transportation (15). The level of plasma TG is known to be positively associated with the level of plasma VLDL (16). This means that the AA genotype also may be related to the level of plasma VLDL.

TABLE 3
Frequency of Alleles of the TTA Polymorphism of the *HMGCR* Gene in CHD Patients and in the Control Group

Alleles	Amplified product (bp)	CHD (%) ($n = 338$)[a]	Control (%) ($n = 322$)[a]	*P* value
A1	88	33 (9.76)	34 (10.56)	>0.05
A2	91	43 (12.72)	59 (18.32)	>0.05
A3	94	62 (18.34)	52 (16.15)	>0.05
A4	97	65 (19.23)	42 (13.04)	<0.05
A5	100	41 (12.13)	68 (21.12)	0.002
A6	103	61 (18.05)	40 (12.42)	>0.05
A7	106	33 (9.76)	27 (8.39)	>0.05

[a]*n*, number of chromosomes; bp, base pairs; for other abbreviation see Table 1.

TABLE 4
Distribution of Plasma Lipids in the Control Group and in CHD Patients[a]

Group	Allele	TG	TC	HDL-C	LDL-C	VLDL
				(mmol/L)		
CHD	A1	1.952 ± 0.626	4.300 ± 0.506	0.935 ± 0.159	2.345 ± 0.803	0.888 ± 0.285
	A2	2.172 ± 0.657	4.106 ± 0.215	1.204 ± 0.149	2.470 ± 0.303	1.178 ± 0.324
	A3	1.860 ± 0.371	4.090 ± 0.311	1.130 ± 0.181	2.255 ± 0.258	0.827 ± 0.214
	A4	2.125 ± 0.294	4.209 ± 0.215	1.132 ± 0.079	2.286 ± 0.258	1.062 ± 0.154
	A5	2.006 ± 0.104	4.216 ± 0.459	0.920 ± 0.070	2.413 ± 0.578	1.204 ± 0.365
	A6	1.816 ± 0.186	4.324 ± 0.449	0.890 ± 0.264	2.207 ± 0.771	0.728 ± 0.107
	A7	1.830 ± 0.230	4.120 ± 0.130	1.149 ± 0.043	2.293 ± 0.078	0.972 ± 0.083
Control	A1	2.138 ± 0.401	4.216 ± 0.203	1.448 ± 0.096	2.345 ± 0.803	0.752 ± 0.122
	A2	1.961 ± 0.186	4.260 ± 0.142	1.410 ± 0.074	2.207 ± 0.123	1.178 ± 0.324
	A3	1.706 ± 0.301	4.127 ± 0.152	1.424 ± 0.066	2.057 ± 0.140	0.827 ± 0.214
	A4	2.014 ± 0.267	4.328 ± 0.338	1.523 ± 0.126	2.317 ± 0.318	0.806 ± 0.093
	A5	2.389 ± 0.984	4.109 ± 0.230	1.299 ± 0.075	2.174 ± 0.167	1.037 ± 0.268
	A6	1.885 ± 0.500	4.340 ± 0.282	1.428 ± 0.156	2.285 ± 0.252	0.743 ± 0.108
	A7	1.790 ± 0.130	4.155 ± 0.055	1.385 ± 0.115	2.115 ± 0.475	0.919 ± 0.172

[a]All P values >0.05 ($P > 0.05$). For abbreviations see Tables 1 and 2.

(TTA)n trinucleotide repeats. Our study also showed that allele A4 was present at a significantly higher frequency in CHD patients than that in the controls ($P < 0.05$), whereas allele A5 was present at a lower frequency in CHD patients than that in the controls ($P = 0.002$). This caused us to speculate that the TTA trinucleotide locus in intron 10 of the *HMGCR* gene also may be associated with CHD.

In summary, the present study is the first to evaluate the possible association between polymorphisms of the *HMGCR* gene and the development of CHD. Since the polymorphisms studied are in the introns, they usually do not affect the activity of the enzyme directly. Therefore, the observed associations between the polymorphisms and some biochemical phenotypes may be explained by their linkage disequilibrium with other functional sites. Additional studies are needed to elucidate the role of the polymorphic loci in enzyme activity as well as in the development of CHD.

ACKNOWLEDGMENTS

This work was supported by grants 2001AA224021-03 and 2002BA711A08 from the National High Technology Research and Development Program, and by grant 39993240 from the National Natural Science Foundation of China and the China Medical Board Foundation.

REFERENCES

1. Robinson, S.M., and Barker, D.J. (2002) Coronary Heart Disease: A Disorder of Growth, *Proc. Nutr. Soc. 61*, 537–542.
2. Stephens, J.W., and Humphries, S.E. (2003) The Molecular Genetics of Cardiovascular Disease: Clinical Implications, *J. Intern. Med. 253*, 120–127.
3. Campos, E., Kotite, L., Blanche, P., Mitsugi, Y., Frost, P.H., Masharani, U., Krauss, R.M., and Havel, R.J. (2002) Properties of Triglyceride-rich and Cholesterol-rich Lipoproteins in the Remnant-like Particle Fraction of Human Blood Plasma, *J. Lipid Res. 43*, 365–374.
4. Mantel-Teeuwisse, A.K., Verschuren, W.M., Klungel, O.H., Kromhout, D., Lindemans, A.D., Avorn, J., Porsius, A.J., and de Boer, A. (2003) Undertreatment of Hypercholesterolaemia: A Population-Based Study, *Br. J. Clin. Pharmacol. 55*, 389–397.
5. Gotto, A.M., Jr. (2003) Treating Hypercholesterolemia: Looking Forward, *Clin Cardiol. 26* (Suppl. 1), 121–128.
6. Eisenberg, D.A. (1998) Cholesterol Lowering in the Management of Coronary Artery Disease: The Clinical Implications of Recent Trials, *Am. J. Med. 28*, 53–64.
7. Istvan, E. (2003) Statin Inhibition of HMG-CoA Reductase: A 3-Dimensional View, *Atherosclerosis* (Suppl.) *4*, 3–8.
8. Xydakis, A.M., and Jones, P.H. (2003) Use of Statins for Secondary Prevention, *Curr. Treat. Options Cardiovasc. Med. 5*, 63–73.
9. Miller, S.A., Dykes, D.D., and Polesky, H.F. (1988) A Simple Salting Out Procedure for Extracting DNA from Human Nucleated Cells, *Nucleic Acids Res. 16*, 1215.
10. Leitersdorf, E., Hwang, M., and Luskey, K.L. (1990) ScrF1 Polymorphism in the 2nd Intron of the HMGCR Gene, *Nucleic Acids Res. 8*, 5584.
11. Zuliani, G., and Hobbs, H.H. (1990) A High Frequency of Length Polymorphisms in Repeated Sequences Adjacent to Alu Sequences, *Am. J. Hum. Gent. 46*, 963–969.
12. Musanti, R., Giorgini, L., Lovisolo, P.P., Pirillo, A., Chiari, A., and Ghiselli, G. (1996) Inhibition of Acyl-CoA:Cholesterol Acyltransferase Decreases Apolipoprotein B-100-Containing Lipoprotein Secretion from HepG2 Cells, *J. Lipid Res. 37*, 1–14.
13. Miyazaki, A., and Koga, T. (2002) Pravastatin Sodium, an Inhibitor of 3-Hydroxy-3-methylglutaryl Coenzyme A Reductase, Decreases Serum Total Cholesterol in Japanese White Rabbits by Two Different Mechanisms, *Atherosclerosis 162*, 299–306.
14. Maldonado, E.N., Romero, J.R., Ochoa, B., and Aveldano, M.I. (2001) Lipid and Fatty Acid Composition of Canine Lipoproteins, *Comp. Biochem. Physiol. B 128*, 719–729.
15. Hammad, S.M., Siegel, H.S., and Marks, H.L. (1998) Total Cholesterol, Total Triglycerides, and Cholesterol Distribution Among Lipoproteins as Predictors of Atherosclerosis in Selected Lines of Japanese Quail, *Comp. Biochem. Physiol A Integr. Physiol. 119*, 485–492.
16. Karpe, F., Hellenius, M.L., and Hamsten, A. (1999) Differences in Postprandial Concentrations of Very-Low-Density Lipoprotein and Chylomicron Remnants Between Normotriglyceridemic and Hypertriglyceridemic Men With and Without Coronary Heart Disease, *Metabolism 48*, 301–307.

[Received February 23, 2004; accepted April 15, 2004]

Fatty Acids Induce Increased Granulocyte Macrophage-Colony Stimulating Factor Secretion Through Protein Kinase C-Activation in THP-1 Macrophages

Nahid Bahramian, Gunnel Östergren-Lundén, Göran Bondjers, and Urban Olsson*

Wallenberg Laboratory for Cardiovascular Research, Sahlgrenska Academy at Göteborg University, Göteborg, Sweden

ABSTRACT: Insulin resistance and type 2 diabetes are associated with elevated circulating levels of nonesterified FA (NEFA) and lipoprotein remnants. The dyslipidemia is an important contributor to the excess arterial disease associated with insulin resistance and type 2 diabetes, but the mechanisms involved are elusive. In the present study we examined the effect of NEFA on macrophages. For this purpose, we utilized human macrophages, prepared by treating THP-1 monocytes with phorbol ester. We found that albumin-bound NEFA at physiological levels increase the secretion of granulocyte macrophage-colony stimulating factor (GM-CSF) by the THP-1 macrophages in a dose-dependent manner. The effect was registered as an increase in mRNA, and the amount of GM-CSF secreted correlated with the accumulation of TAG and DAG in the cell. The NEFA-induced rise in GM-CSF appeared to be mediated by activation of protein kinase C, probably acting on extracellular signal-regulated kinases 1 and 2 and being calcium dependent. We speculate that increased secretion of GM-CSF by resident macrophages in the intima exposed chronically to high levels of NEFA, such as those present in insulin resistance, may contribute to a proatherogenic response of arterial cells.

Paper no. L9460 in *Lipids 39*, 243–249 (March 2004).

Atherosclerotic vascular disease is the main cause of type 2 diabetes mortality, these patients being exposed to a 2–4 times higher risk than nondiabetic subjects with a comparable profile of other risk factors (1). Prospective and cross-sectional studies indicate that the dyslipidemia of insulin resistance and type 2 diabetes is an important contributor to atherosclerotic disease and a better predictor of its associated mortality than hyperglycemia (2). However, why a relatively mild dyslipidemia characterized by modest elevations of TAG, near-normal LDL cholesterol levels, and modest reduction of HDL cholesterol can cause such an impact in vascular disease is not well understood. An important component of the dyslipidemia of insulin resistance and type 2 diabetes, the chronic elevation of nonesterified FA (NEFA), is not usually included in prospective and cross-sectional studies. NEFA originate in the postabsorptive period from the partial failure of insulin in inhibiting the hormone-sensitive lipase of adipose tissue in insulin resistance. During the postprandial period, albumin-bound NEFA come mainly from hydrolysis of TAG-rich lipoproteins of intestinal origin by the lipoprotein lipase (3,4). In the last few years, the roles of FA as hormones in signaling between organs, in intercellular signaling, and intracellularly have been identified (5).

In vitro studies point to direct, potentially atherogenic, effects of NEFA on arterial cells. Albumin-bound NEFA can change the basement membrane structure of arterial endothelial cells, altering the function of the basement membrane as macromolecular permeability barrier and inducing proinflammatory activation (6,7). In human arterial smooth muscle cells, NEFA can induce the production of extracellular matrix proteoglycans with high affinity for LDL (8).

Macrophages have important functions during atherogenesis, mainly as originators of foam cells by uptake of modified apolipoprotein B-containing lipoproteins trapped in the extracellular matrix of the intima (9). For monocytic cells invading the intima to become functional resident macrophages, they require the autocrine action of essential growth factors such as macrophage colony-stimulating factor (M-CSF) and granulocyte macrophage colony-stimulating factor (GM-CSF) (10,11). Both proteins and their receptors are present in foam cell-rich atherosclerotic lesions. Furthermore, macrophages, when exposed to oxidized LDL, respond with elevation of GM-CSF mRNA, sustained at the protein level (12). It should be stressed that each modified LDL molecule entrapped in the intima extracellular matrix that becomes internalized by a macrophage carries with it more than 2,600 molecules of esterified FA together with approximately 2,200 molecules of esterified and nonesterified cholesterol (13). In insulin resistance and type 2 diabetes, the arterial cells are exposed in addition to chronically high levels of circulating albumin-bound NEFA complexes (3). In the present experiments we explored the effects of NEFA on GM-CSF secretion by macrophages. The results indicate that albumin-bound NEFA, in a dose-related manner, increase the secretion of GM-CSF. We speculate that increased GM-CSF secretion may be part of the proatherogenic effects of high circulating levels of FFA on arterial cells.

*To whom correspondence should be addressed at Amersham Biosciences, Björkgatan 30, 751 84 Uppsala, Sweden. E-mail: urban.olsson@amersham.com

Abbreviations: Anti-phospho-JNK, anti-phospho-Jun Amino-terminal activated kinase; BIM, bisindolylmaleimide 1; ECL, enhanced chemiluminescence; ERK, extracellular signal-regulated kinase; G3PDH, glyceraldehyde-3-phosphate dehydrogenase; GM-CSF, granulocyte macrophage-colony stimulating factor; HRP, horseradish peroxidase; JNK, Jun amino-terminal activated kinase; MAP kinase, mitogen-activated protein kinase; M-CSF, macrophage-colony stimulating factor; MEK, MAP kinase/ERK kinase; MEK 1/2, MAP kinase kinase; NEFA, nonesterified fatty acids; nifedipine, 1,4-dihydro-2,6-dimethyl-4-(2-nitrophenyl)-3,5-pyridinedicarboxylic acid dimethyl ester; PD 098059, 2-(2-amino-3-methoxyphenyl)-4H-1-benzopyran-4-one; PKC, protein kinase C; PMA, phorbol myristate acetate; RT, reverse transcriptase; SAPK, stress-activated protein kinase; TBS-T, 5% nonfat dried milk in 20 mM Tris, pH 7.6, 138 mM NaCl, and 0.1% Tween-20.

EXPERIMENTAL PROCEDURES

Materials. Sodium salts of linoleic acid, linolenic acid, palmitic acid, oleic acid, BSA (FA-free), and phorbol myristate acetate (PMA) were from Sigma-Aldrich (St. Louis, MO). Bisindolylmaleimide 1 (BIM), PD 098059 (2-(2-amino-3-methoxyphenyl)-4H-1-benzopyran-4-one), and nifedipine (1,4-dihydro-2,6-dimethyl-4-(2-nitrophenyl)-3,5-pyridinedicarboxylic acid dimethyl ester) were purchased from Calbiochem (San Diego, CA), and stored at −20°C as stock solutions in dimethyl sulfoxide (Me_2SO). The final concentrations of Me_2SO were ≤0.1% in the culture medium, which did not affect cell viability when estimated by lactate dehydrogenase release and gross morphology. Cell culture media were from BioWhittaker (Verviers, Belgium). FBS was from Biochrom KG (Berlin, Germany). Primers for reverse transcriptase (RT)-PCR were obtained from Life Technologies (Gaithersburg, MD). Reagents and fluorescently labeled probes for real-time PCR were purchased from Applied Biosystems (Foster City, CA). ELISA for determination of GM-CSF was purchased from R&D Systems (Minneapolis, MN). Polyclonal antibodies against protein kinase C (PKC) isoforms and monoclonal antibody against extracellular signal-regulated kinase (ERK) 2 were purchased from Santa Cruz Biotechnology (Santa Cruz, CA). Polyclonal anti-phospho-p38 mitogen-activated protein kinase (MAP kinase), anti-phospho-Jun amino-terminal activated kinase (anti-phospho-JNK) and anti-phospho-ERK antibodies, anti-rabbit horseradish peroxidase (HRP)-conjugated secondary antibody, monoclonal antibody against ERK 1/2 and p44/42 MAP Kinase Assay Kit were purchased from New England Biolabs (Beverly, MA). Anti-goat, -mouse, and -rabbit HRP-conjugated secondary antibodies were purchased from Dako (Cambridge, United Kingdom). The enhanced chemiluminesence (ECL) kit was from Amersham Biosciences (Uppsala, Sweden). ^{14}C Linoleic acid (40–60 mCi/mmol, 1.85 MBq) was from NEN (Boston, MA). All other chemicals were of the highest purity commercially available.

Cell culture. THP-1 cells were obtained from the American Type Culture Collection (ATCC number TIB-202; Manassas, VA). Cells were maintained in RPMI 1640 medium supplemented with 10% (v/v) FBS, 25 μM β-mercaptoethanol, 50 μg/mL gentamicin, glutamine, and sodium pyruvate at 37°C in a 5% CO_2 atmosphere. The medium was changed every seventh day. THP-1 cells were plated at a cell density of $0.3 \times 10^6/cm^2$ dish in RPMI with 10% FBS, 100 U/mL penicillin, 100 μg/mL streptomycin, glutamine, and sodium pyruvate (medium A), and 50 ng/mL PMA for 3–4 d to become fully differentiated macrophages. Differentiated THP-1 macrophages were washed two times with PBS with Ca^{2+} and Mg^{2+} to remove PMA and incubated for another 24 h without PMA. The cells were then washed twice with PBS to remove nonadherent cells, and incubated with the respective stimuli in medium A.

All kinase inhibitors used were added to the cells 1 h before addition of the media containing NEFA and PMA. For inhibition of MAP kinase kinase (MEK 1/2), PD 098059 was added to a final concentration of 10 μM. BIM at a concentration of 1 μM was used for inhibition of PKC.

Likewise, calcium channel blockage was achieved by adding 100 μM of nifedipine to the cells 1 h before addition of the media containing NEFA and PMA.

Albumin–FA complex. Media containing NEFA were prepared according to Montell *et al.* (14) with minor modifications. In brief, sodium salts of NEFA (100–1000 μM) were dissolved in warm deionoized water and were added dropwise to medium A containing 300 μM FA-free BSA. The pH values of the media were adjusted to 7.4 with NaOH, and they were filtered through a 0.22-μm filter before addition to the cells. In the present studies the molar ratio of FA to BSA did not exceed 4. In evaluating the extent of NEFA binding to albumin, a trace amount of ^{14}C-labeled linoleic acid (0.005 mCi) was added together with the nonlabeled species. Agarose electrophoresis and subsequent autoradiography showed that more than 99% of the NEFA was albumin-bound. There was no reduction of cell viability or indication of cell damage as judged by lactate dehydrogenase production even at a high concentration (800 μM) of BSA-linoleic acid (18:2). We have not previously been able to find evidence of NEFA free radical-mediated oxidation under the incubation conditions used (8). FA concentrations in the media were confirmed by a colorimetric kit from Wako (Neuss, Germany).

RT-PCR. After incubation in medium with or without NEFA, cells were detached by a brief (5-min) incubation with trypsin, collected in cold PBS with Ca^{2+} and Mg^{2+}, and immediately put on ice. Cells were pelleted, and a kit was used to prepare total RNA (Invitrogen, Leek, The Netherlands). After converting mRNA to cDNA by incubation with RT and the appropriate additions, the samples were divided. The fluorogenic 5′ nuclease (TaqMan®) assay (real-time PCR) (15) and the ABI Prism® 7700 sequence detector system (Applied Biosystems) were used to estimate mRNA content. Primers for human GM-SCF were sense CCTGAAGGACTTTCTGCTTGTCA (position 386–408) and antisense TGGCCGGTCTCACTCCTG (position 435–452), defining a fragment of 67 nucleotides. FAM (6-carboxy-fluorescein)-labeled probe CCCCTTTGA CTGCTGGGAGCCAGT (position 410–433) was used. Predeveloped primer/probe for control glyceraldehyde-3-phosphate-dehydrogenase (G3PDH) was purchased from Applied Biosystems.

ELISA for GM-CSF. The THP-1 macrophage cells were incubated with different concentrations of linoleic acid (18:2) (0 to 1000 μM) in six-well plates (3.5 cm in diameter) with 2 mL of medium. After 24 h, the supernatant was collected and centrifuged at 10,000 rpm for 1 min to remove any particulate material and analyzed directly. The concentration of GM-CSF protein was determined following the instructions in the ELISA kit. Total cell protein was measured according to the method of Bradford (16) using a colorimetric assay kit from Bio-Rad (Hercules, CA). Cell viability and cell damage were evaluated visually and by lactate dehydrogenase release.

Cell total lipid analysis. Quantitative evaluation of total cell lipids was performed on chloroform/methanol (2:1, vol/vol) extracts of washed cells detached from the plates and suspended in phosphate buffer (17). The chloroform phase con-

taining the lipids was dried under nitrogen and dissolved in the initial phase of the HPLC system used (Gynkotec, Münich, Germany). The lipids were separated on a Spherisorb 5 µm column (Waters, Sollentuna, Sweden), and peaks were evaluated using a Gynkotec M480 ternary system with the aid of an ELSD, PL-ELS 1000 (Polymer Laboratories, Shropshire, United Kingdom). The chromatographic conditions were essentially those described by Homan and Anderson (18). Standard mixtures were purchased from Larodan Laboratories (Malmö, Sweden).

Western blot of PKC isoforms. THP-1 macrophages ($1–2 \times 10^7$ cells/plate, 10 cm in diameter) were incubated for different times in 10 mL of RPMI 1640 medium with NEFA-bound albumin. The cells were washed three times with ice-cold PBS and detached from the plate using a rubber policeman in 1 mL of cold lysis buffer (20 mM Tris-HCL, pH 7.5, 150 mM NaCl, 1 mM EDTA, 1% Triton X-100, 2.5 mM sodium pyrophosphate, 1 mM β-Na_3VO_4, 1 µg/mL leupeptin), and sonicated four times for 5 s on ice. Cell extracts were centrifuged for 10 min at 4°C, and the supernatant was aliquoted and stored at –80°C. Protein concentrations were determined as described above. Total cytosolic protein (50–60 µg) was solubilized in SDS sample buffer (62.5 mM Tris-HCl pH 6.8, 2% wt/vol SDS, 10% glycerol, 50 mM DTT, 0.1% wt/vol bromphenol blue) and then separated on a 10% polyacrylamide gel. The separated proteins were transferred to a nitrocellulose membrane (BioRad) at a constant voltage of 100 V for 30 min. Membrane blockage was achieved with TBS-T (5% nonfat dried milk in 20 mM Tris, pH 7.6, 138 mM NaCl, 0.1% Tween-20) for 1–3 h at room temperature and probed with anti-PKC isoform (1:1000) overnight at 4°C. Membranes were washed three times in TBS-T and incubated with appropriate HRP-conjugated secondary antibody (1:2000) for another 1.5 h at room temperature. The membrane was washed as above, and bound secondary antibodies were visualized by using an ECL Western blot detection system according to the manufacturer's instructions. The membranes were stripped up to five times for 30 min at 50°C in 100 mM 2-mercaptoethanol, 2% SDS, 62.5 mM Tris-HCl, pH 6.7, and used again to label with different antibodies against PKC isoforms.

Analysis of MAP kinase activation. Activation of MAPK (ERK 1/2) was detected using a p44/42 MAP Kinase Assay Kit, following the manufacturer's instructions. Briefly, whole cell extracts were incubated with an immobilized phospho-p44/42 MAP kinase (Thr202/Tyr204) monoclonal antibody overnight at 4°C with gentle rocking. The immunocomplex was washed and incubated in kinase buffer (25 mM Tris, pH 7.5, 5 mM β-glycerol phosphate, 2 mM DTT, 0.1 mM Na_3VO_4, 10 mM $MgCl_2$) at 30°C for 30 min in the presence of ATP and Elk-1 fusion protein, which allows immunoprecipitated actine MAP kinase to phosphorylate Elk-1. The kinase reaction was terminated by addition of SDS sample buffer. Proteins were separated and transferred as described above, with exchange of suitable antibodies (phosphor-Elk-1, Ser383) and visualized with an ECL detection system.

Data analysis. Densitometric evaluations were done with ImageQuant program software (Amersham Biosciences). Graph Pad Prism software (San Diego, CA) was used to fit binding curves and correlation to the data. The difference between the two groups was identified with a Student's *t*-test. For multiple groups, one-way ANOVA and the Newman–Keuls test were used to identify differences. $P > 0.05$ was considered nonsignificant. Significance was defined as $P < 0.05$ (*), $P < 0.01$ (**), and $P < 0.001$ (***).

RESULTS

FA affect GM-CSF expression and secretion and cell lipids. In the study of the effects of NEFA on macrophages, THP-1 macrophages were exposed to different albumin-bound NEFA. We were particularly interested in the expression of M-CSF and GM-CSF by the macrophages. Initial studies did not detect an effect on M-CSF (not shown), whereas GM-CSF appeared to be markedly increased by FA exposure. At 300 µM albumin-bound linoleic acid, the expression of GM-CSF by the macrophages appeared to be in the order of three times that of macrophages exposed to medium supplemented with BSA alone (Fig. 1). GM-CSF secretion increased dose-dependently after incubation for 24 h with BSA-linoleic acid (18:2) (Fig. 2). Albumin-bound oleic (18:1) and linolenic acids (18:3) induced similar increases in GM-CSF secretion (not shown). Palmitic acid (16:0) induced at 300–400 µM a fourfold increase in the secretion of the growth factor but led to cell detachment above these concentrations. Based on these results and the fact that linoleic acid is a prominent FA in human plasma, we selected this complex to explore the mechanism behind the phenomenon further. The largest effect on GM-CSF secretion was observed at 800 µM linoleic acid (Fig. 2). Eight hundred micromolar is within the physiologic range of NEFA concentration in circulation, and in type 2 diabetes this elevated level can be found for extended time periods (3). Therefore, we chose this concentration as an accentuated model of high circulating levels of albumin-bound NEFA. The

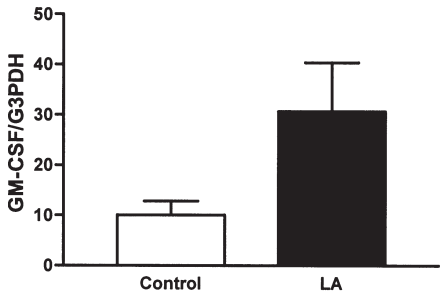

FIG. 1. Effect of linoleic acid on mRNA for granulocyte macrophage-colony stimulating factor (GM-CSF) in THP-1 macrophages. Messenger RNA for GM-CSF was evaluated by real-time PCR, as described in the Experimental Procedures section, in total RNA preparations from THP-1 macrophages. The cells were exposed for 24 h to 300 µM BSA in medium A with (LA) or without (Control) 300 µM linoleic acid. Data are presented as mean copy number normalized to glyceraldehyde-3-phosphate dehydrogenase (G3PDH) mRNA with SD ($n = 3$). Data analysis (Student's *t*-test) did not indicate a significant difference between the two groups ($P = 0.075$).

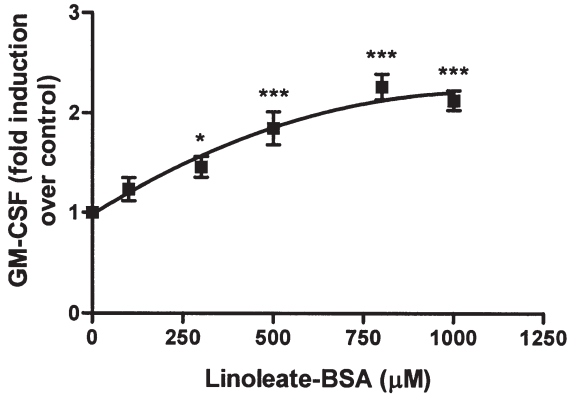

FIG. 2. BSA-linoleic acid stimulates secretion of GM-CSF dose-dependently in THP-macrophages. THP-1 macrophages were incubated with different concentrations (0–1000 μM) of albumin-bound linoleate (BSA-18:2) for 24 h. GM-SCF in the supernatant was determined with an ELISA method as described in the Experimental Procedures section. The points in the curve represent the mean ± SEM of six measurements in individual cell cultures using the mean value of control dishes (exposed to 300 μM BSA alone) as 1. Bars judged statistically different from the control (one-way ANOVA and Newman–Keuls test) are indicated by * ($P < 0.05$) and *** ($P < 0.001$). For abbreviation see Figure 1.

time course of induction of increased GM-CSF secretion was investigated by exposing THP-1 macrophages to 500 μM albumin-bound linoleic acid for different lengths of time (Fig. 3). The maximal effect appeared to be reached somewhere between 8 and 24 h and sustained for 48 h.

Incubation with BSA-linoleic acid caused a concentration-dependent increase of total cell TAG that correlated with an increase in DAG (Fig. 4). There was no detectable effect of NEFA on the content of cholesteryl esters or the main phospholipids (data not shown).

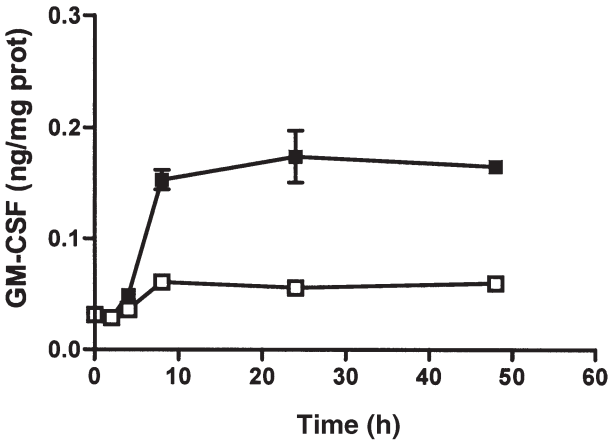

FIG. 3. Time course of stimulation of GM-CSF secretion. THP-1 macrophages were incubated with 500 μM albumin-bound linoleate (BSA-18:2, closed symbols) or BSA (300 μM) alone (control, open symbols) for the periods of time indicated. GM-SCF in the supernatant was determined with an ELISA method as described in the Experimental Procedures section. The points in the curve represent the mean ± SEM of three dishes. For abbreviation see Figure 1.

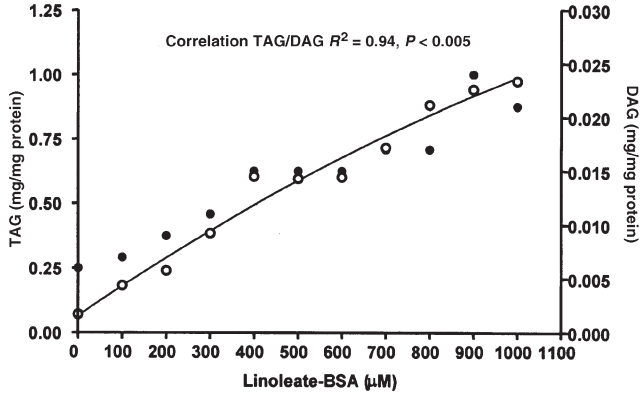

FIG. 4. BSA-linoleic acid produces a concentration-dependent increase in total cell TAG (●) and DAG (○). Cells were incubated for 24 h with different concentrations (0–1000 μM) of BSA-linoleic acid (18:2). Total cell lipid extracts were used to separate the lipids by HPLC as described in the Experimental Procedures section. In all dishes, including the control (0 μM), the culture medium was supplemented with 300 μM BSA.

Involvement of protein kinases and calcium in the NEFA induction of GM-CSF. DAG and phorbol esters, like PMA, activate PKC isoforms by serving as hydrophobic ligands that anchor the conventional and novel PKC in the plasma membrane (19). We found that the actions of PMA and NEFA on GM-CSF secretion were additive. Incubation for 24 h with 800 μM linoleic acid further increased growth factor secretion caused by 5 nM PMA, added after washing out the amount used as the initiator of differentiation (Fig. 5A).

The above observations suggested that interactions between DAG and PKC may be mediators of the effects of NEFA on GM-CSF production in THP-1 macrophages. BIM, a selective and cell-permeable inhibitor of PKC, decreased linoleic acid and PMA stimulated GM-CSF secretion by ~20% (not statistically significant) and ~40% (not statistically significant), respectively (Fig. 5A). The additive stimulation of GM-CSF secretion by combination of NEFA and PMA was decreased by 46% ($P < 0.001$) by PKC inhibition.

Western blot analysis of total cell lysates indicated the presence in the differentiated THP-1 cells of the classical PKC isotypes (α, β1, β11, and γ) and of the novel isoforms δ and ε but not of the atypical PKC (ζ) (data not shown). This indicates that PKC susceptible to BIM inhibition were present in the differentiated THP-1 cells.

FA can increase the intracellular levels of calcium, either through mobilization of internal stores or by acting as calcium ionophores. Calcium and PMA have been described to induce synergistic effects. To estimate the role of calcium, stimulation of GM-CSF secretion was performed in the presence of a calcium channel blocker, nifedipine. This agent appeared to completely abolish the stimulation of GM-CSF secretion achieved by linoleic acid ($P < 0.05$) or PMA alone ($P < 0.05$), to the level of secretion in cells incubated with BSA addition only (control). At the concentration used (100 μM), nifedipine reduced the stimulation of GM-CSF secretion induced by the combination of linoleic acid and PMA by 47% ($P < 0.001$), but not all

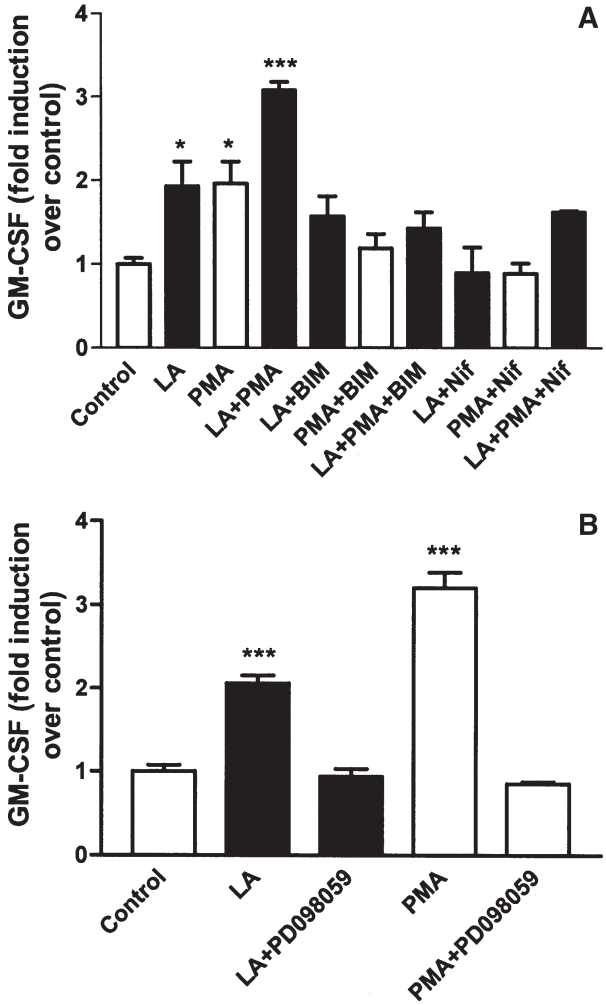

FIG. 5. Effects of kinase modulators and calcium channel blockage on BSA-linoleic acid and phorbol myristate acetate (PMA)-induced secretion of GM-CSF. Protein kinase C inhibition and calcium channel blockage (panel A) or inhibition of mitrogen-activated protein kinase/extracellular signal-regulated kinase (panel B) modulate GM-CSF secretion. THP-1 macrophage cells were incubated with bisindolylmaleimide 1 (BIM, 1 μM), nifedipine (Nif, 100 μM), or PD 098059 (10 μM) for 1 h and then treated with 800 μM BSA-linoleic acid (LA), PMA (5 nM), or 800 μM linoleic acid plus 5 nM PMA (LA + PMA) in the presence of the modulators as indicated for 24 h. ELISA was used for measurement of GM-CSF in the supernatant as described in the Experimental Procedures section. The bars represent average ± SD of three or four individual determinations. Bars that were judged statistically different from the control (one-way ANOVA and Newman–Keuls test) are indicated by * ($P < 0.05$) and *** ($P < 0.001$). In all dishes, including the control, the culture medium was supplemented with 300 μM BSA. Nifedipine, 1,4-dihydro-2,6-dimethyl-4-(2-nitrophenyl)-3,5-pyridinedicarboxylic acid dimethyl ester; PD 098059, 2-(2-amino-3-methoxyphenyl)-4H-1-benzopyran-4-one; for other abbreviation see Figure 1.

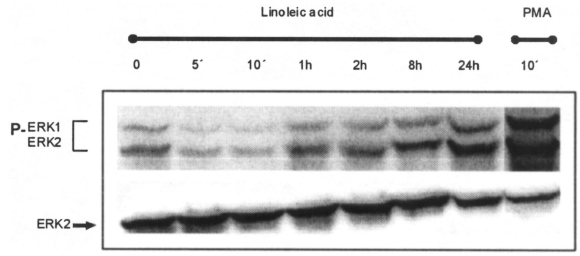

FIG. 6. BSA-linoleic acid and PMA induce phosphorylation of extracellular signal-regulated kinase (ERK) 1 and 2. Lysates from THP-1 macrophage cells treated with BSA-linoleic acid (800 μM) or PMA (80 nM) for the indicated times were used for SDS-PAGE. Immunoblots were obtained using anti-ERK 2 (bottom panel) or the phosphospecific anti-ERK 1/2 (top panel) antibodies. For other abbreviation see Figure 5.

the way down to the basal level of secretion in control cells (Fig. 5A). Thus, the stimulation of GM-CSF secretion by linoleic acid and by PMA appeared to be calcium dependent.

PKC activation of the ERK-kinase cascade. PKC and the downstream MAP kinase pathway are activated by DAG and PMA and are part of a phosphorylation cascade that has cytosolic and nuclear targets in macrophages (20,21). To examine whether ERK participates in the linoleic acid-induced production of GM-CSF, THP-1-differentiated cells were pretreated with PD 098059, an inhibitor of MAP kinase/ERK kinase (MEK), an upstream kinase of ERK (22). At 10 μM, PD 098059 inhibited the linoleic acid- and PMA-increased production of GM-CSF by ~60 and ~70%, respectively (to basal level, $P < 0.001$) (Fig. 5B). To determine the effect of inhibition of both PKC and ERK MAP kinase on linoleic acid-dependent GM-CSF production, the macrophages were pretreated with both 1 μM BIM and 10 μM PD098059 for 1 h, and experiments corresponding to Figures 5A and 5B were performed. The decrease in GM-CSF production in response to both inhibitors did not reach beyond that of PD 098059 alone (not shown). The variation in stimulation of GM-CSF reached with BSA-linoleic acid or PMA in panels A and B of Figure 5 represents variation between experiments (different THP-1 macrophage preparations).

The participation of downstream components of the MAPK cascade triggered by linoleic acid was confirmed by analysis of phosphorylation of the ERK/MAP kinase. Two approaches were used. By the ERK substrate method, we detected a twofold rise in phosphorylated Elk-1 (transcription factor), independent of the amount of ERK protein, after 24 h incubation with BSA-linoleic acid (not shown). The phosphorylation of ERK 1 and 2 also increased with incubation time in the presence of BSA-linoleic acid, independently of the amount of ERK protein (Fig. 6). Growth factors and stress-induced cytokine production mediated by the MAP kinases cascade can also use the stress-activated protein kinases (SAPK) p38 and JNK as downstream signals. To determine whether other ERK-related kinases such as SAPK/JNK and p38 MAP kinase are involved in the production of GM-CSF, we measured phosphorylation of SAPK/JNK and p38 by using antibodies specific for activated SAPK/JNK and p38. We detected phosphorylation of SAPK/JNK only at 1 and 2 h after start of incubation with BSA-linoleic acid but similar amounts of SAPK/JNK were detected at all time points (data not shown). We found phosphorylation of p38 only at 0 and 1 h, whereas the amounts of p38 protein were similar at all time points (data not shown).

DISCUSSION

Searching for potential mechanisms by which elevated circulating NEFA may contribute to atherosclerosis, we exposed a human macrophage model, THP-1 macrophages, to NEFA *in vitro*. We found that NEFA induced increased secretion of an important cytokine, GM-CSF; the effect was calcium dependent, and we found indications of downstream mechanisms.

In the experiments shown in Figures 5 and 6, the THP-1 macrophages were challenged with 800 μM of albumin (300 μM)-bound linoleic acid in combination with various modulators. The choice of NEFA concentration and type can be challenged. As mentioned in the Results section, linoleic acid (18:2) was chosen because it is a prominent component in human plasma and because oleic (18:1) and linolenic acids (18:3) induced similar increases in GM-CSF secretion. An alternative approach would have been to use a mixture of FA that mimics a more physiological situation. The use of mixtures with several physiologically relevant compositions is an important question that should be addressed in depth in a separate set of studies. The concentration of NEFA, 800 μM, was chosen not only because we observed the greatest increase in GM-CSF secretion at that level (Fig. 2) but also because it may represent a physiologically relevant high level of circulating NEFA in type 2 diabetes. Disparate figures on circulating levels of NEFA in type 2 diabetes have been reported. Although fairly high levels of NEFA can be found in uncompensated diabetes, most diagnosed type 2 diabetes patients receive some kind of treatment and medication. Reaven *et al.* (3) reported a variation of 400–800 μM NEFA over 24 h in nonobese type 2 diabetics and 150–500 μM NEFA over 24 h in healthy control subjects. In another paper, 1400 μM was claimed to be a representative level of NEFA found in type 2 diabetes (23). Carlsson *et al.* (24) found that (type 2) diabetic subjects had higher NEFA concentrations than nondiabetic subjects, that diabetic women (averaging 900 μM fasting NEFA) had higher NEFA concentrations than men, and that obese diabetics displayed the highest levels of circulating NEFA. Mingrone *et al.* (25) reported an average of 1517 μM NEFA in obese diabetic patients (all receiving treatment).

Our results indicate that the human THP-1 macrophage cells, differentiated by pretreatment with phorbol esters, increase their GM-CSF secretion in response to albumin-bound NEFA (Fig. 2). The effect was also seen on a transcriptional level (Fig. 1). Secretion of GM-CSF by macrophages in growing atherosclerotic lesions is thought to enhance macrophage accretion and smooth muscle cell migration from the media into the intima (26). GM-CSF also has been proposed to have a tissue remodeling role in atherosclerosis by inducing the secretion of specific extracellular matrix components by smooth muscle cells (27). Moreover, in human lesions GM-CSF was found to be a mediator of myeloperoxidase secretion by macrophages, an effect that may contribute to plaque rupture at terminal stages of cardiovascular events (28).

Chronic exposure to high circulating levels of NEFA appears to be causal for insulin resistance in muscle, adipose tissue, and probably liver. Some of these actions seem mediated by an intracellular increase of DAG and subsequent activation of PKC, which in turn interfere with normal insulin signaling (29–31). Our results suggest that NEFA increased GM-CSF by raising intracellular DAG, which results in activation of a PKC-MAPK phosphorylation cascade. The THP-1 macrophages appeared to incorporate the FA rapidly and avidly and to synthesize and store them in the form of DAG and TAG (Fig. 4). Visual inspection revealed lipid droplets incorporated in the macrophages, and this was more pronounced in the dishes where the cells were exposed to higher amounts of NEFA. The observation that inhibition of PKC by BIM partially inhibited the production of GM-CSF induced by NEFA and PMA (Fig. 5A) suggests that conventional and novel PKC isoforms that are sensitive to DAG activation participate in the chain of events leading to increased secretion. The effect also appeared to be calcium dependent, as the blockade of calcium channels with nifedipine abolished GM-CSF induction (Fig. 5A). PMA is a potent DAG analog that induces PKC activation, which in turn provokes many cellular responses in monocytic cells, apparently by similar mechanisms as those used by the natural lipid mediator (32). Whether it is the FA *per se,* or the resulting DAG, or both that activate PKC is difficult to determine, but we can conclude that NEFA increased GM-CSF secretion and that the effect could be decreased by PKC inhibition.

The activation of PKC in THP-1 macrophages and the ability of PKC to activate components of the downstream MAPK cascade suggest that one or more of these MAPK cascade elements are involved in GM-CSF production. These activation events may occur *via* parallel pathways (20). We found that PD 098059, which inhibits MEK, decreased the production of GM-CSF by linoleic acid and PMA-exposed THP-1 macrophages (Fig. 5B). Furthermore, Western blot results showed that in the THP-1 cells, activation of the ERK MAP kinase by linoleic acid was persistent (Fig. 6), as has been described for DAG in other monocytic cell lines (33). The rather slow kinetics of ERK activation may indicate an autocrine regulatory loop induced by GM-CSF. Activation detected by phospho-specific antibodies of other MAP kinase family downstream members, such as p38 MAP kinase and JNK/SAPK, by NEFA and PMA was found to last for only 1 to 2 h, although increased protein levels were sustained for up to 24 h.

Taken together, our observations indicate that high levels of albumin-bound FA, probably by increasing intracellular concentrations of DAG and subsequent activation of PKC and the MAPK/ERK pathway, can augment the secretion of GM-CSF from macrophages. We speculate that a similar phenomenon in arteries of individuals with insulin resistance may add to the atherogenic response triggered by the dyslipidemia associated with this condition.

ACKNOWLEDGMENTS

We thank Doctor David Buckley for help. This work was supported by grants from the Swedish Medical Research Council, the Swedish Heart-Lung foundation, Strategic Funds National Network for Cardiovascular

Research, the Foundations of the National Board of Health and Welfare, the Medical Faculty at Göteborg University, Magnus Bergvalls Foundation, and AstraZeneca.

REFERENCES

1. von Eckardstein, A., and Assman, G. (2000) Prevention of Coronary Heart Disease by Raising High-Density Lipoprotein Cholesterol, *Curr. Opin. Lipidol. 11*, 627–637.
2. Lehto, S., Rönnema, T., Haffner, S., Pyörälä, K., Kallio, V., and Laakso, M. (1997) Dyslipidemia and Hyperglycemia Predict Coronary Heart Disease Events in Middle-Aged Patients with NIDDM, *Diabetes 46*, 1354–1359.
3. Reaven, G.M., Hollenbeck, C., Jeng, C.Y., Wu, M.S., and Chen, Y.D. (1988) Measurement of Plasma Glucose, Free Fatty Acid, Lactate, and Insulin for 24 h in Patients with NIDDM, *Diabetes 37*, 1020–1024.
4. Camejo, G., Olsson, U., Hurt-Camejo, E., Bahramian, N., and Bondjers, G. (2002) The Extracellular Matrix on Atherogenesis and Diabetes-Associated Vascular Disease. *Atheroscler. Suppl. 3*, 3–9.
5. Willson, T.M., Brown, P.J., Sternbach, D.D., and Henke, B.R. (2000) The PPARs: From Orphan Receptors to Drug Discovery, *J. Med. Chem. 43*, 527–550.
6. Hennig, B., Lipke, D.W., Biossonneault, G.A., and Ramasamy, S. (1995) Role of Fatty Acids and Eicosanoids in Modulating Proteoglycan Metabolism in Endothelial Cells, *Prostaglandins Leukot. Essent. Fatty Acids 53*, 315–324.
7. Hennig, B., Meerarani, P., Ramadass, P., Watkins, B.A., and Toborek, M. (2000) Fatty Acid-Mediated Activation of Vascular Endothelial Cells, *Metabolism 49*, 1006–1013.
8. Olsson, U., Bondjers, G., and Camejo, G. (1999) Fatty Acids Modulate the Composition of Extracellular Matrix in Cultured Human Arterial Smooth Muscle Cells by Altering the Expression of Genes for Proteoglycan Core Proteins, *Diabetes 48*, 616–622.
9. Steinberg, D., and Witztum, J. (1999) Lipoproteins, Lipoprotein Oxidation and Atherogenesis, in *Molecular Basis of Cardiovascular Disease* (Breslow, J., Leiden, J., Rosenberg, R., and Seidman, C., eds.), pp. 458–475, W.B. Saunders, Philadelphia.
10. Langstein, J., Michel, J., and Schwarz, H. (1999) CD137 Induces Proliferation and Endomitosis in Monocytes, *Blood 94*, 3161–3168.
11. Ross, R. (1999) Atherosclerosis—An Inflammatory Disease, *N. Engl. J. Med. 340*, 115–126.
12. Biwa, T., Sakai, M., Matsumura, T., Kobori, S., Kaneko, K., Miyazaki, A., Hakamata, H., Horiuchi, S., and Shichiri, M. (2000) Sites of Action of Protein Kinase C and Phosphatidylinositol 3-Kinase Are Distinct in Oxidized Low Density Lipoprotein-Induced Macrophage Proliferation, *J. Biol. Chem. 275*, 5810–5816.
13. Esterbauer, H. (1995) The Chemistry of Oxidation of Lipoproteins, in *Oxidative Stress, Lipoproteins and Cardiovascular Dysfunction* (Rice-Evans, C., and Bruckdorfer, K., eds.), pp. 55–79, Portland Press, London.
14. Montell, E., Turini, M., Marotta, M., Roberts, M., Noe, V., Ciudad, C.J., Mace, K., and Gomez-Foix, A.M. (2001). DAG Accumulation from Saturated Fatty Acids Desensitizes Insulin Stimulation of Glucose Uptake in Muscle Cells, *Am. J. Physiol. Endocrinol. Metab. 280*, E229–E237.
15. Lie, Y.S., and Petropoulos, C.J. (1998) Advances in Quantitative PCR Technology: 5′ Nuclease Assays, *Curr. Opin. Biotechnol. 9*, 43–48.
16. Bradford, M.M. (1976) A Rapid and Sensitive Method for the Quantitation of Microgram Quantities of Protein Utilizing the Principle of Protein-Dye Binding, *Anal. Biochem. 72*, 248–254.
17. Hurt-Camejo, E., Camejo, G., Rosengren, B., Lopez, F., Wiklund, O., and Bondjers, G. (1990) Differential Uptake of Proteoglycan-Selected Subfractions of Low Density Lipoprotein by Human Macrophages, *J. Lipid Res. 31*, 1387–1398.
18. Homan, R., and Anderson, M.K. (1998) Rapid Separation and Quantitation of Combined Neutral and Polar Lipid Classes by High-Performance Liquid Chromatography and Evaporative Light-Scattering Mass Detection, *J. Chromatogr. B Biomed. Sci. Appl. 708*, 21–26.
19. Newton, A.C. (1995) Protein Kinase C: Structure, Function, and Regulation, *J. Biol. Chem. 270*, 28495–28498.
20. Garrington, T., and Johnson, G. (1999) Organization and Regulation of Mitogen-Activated Protein Kinase Signaling Pathways, *Cur. Opin. Cell Biol. 11*, 211–218.
21. Rao, M.K. (2001) MAP Kinase Activation in Macrophages, *J. Leukoc. Biol. 69*, 3–10.
22. Alessi, D.R., Cuenda, A., Cohen, P., Dudley, D.T., and Saltei, A.R. (1995) PD 098059 Is a Specific Inhibitor of the Activation of Mitogen-Activated Protein Kinase Kinase *in vitro* and *in vivo, J. Biol. Chem. 270*, 27489–27494.
23. Bergman, R.N., and Ader, M. (2000) Free Fatty Acids and Pathogenesis of Type 2 Diabetes Mellitus, *Trends Endocrinol. Metab. 11*, 351–356.
24. Carlsson, M., Wessman, Y., Almgren, P., and Groop, L. (2000) High Levels of Nonesterified Fatty Acids Are Associated with Increased Familial Risk of Cardiovascular Disease, *Arterioscler. Thromb. Vasc. Biol. 20*, 1588–1594.
25. Mingrone, G., DeGaetano, A., Greco, A.V., Capristo, E., Benedetti, G., Castagneto, M., and Gasbarrini, G. (1997) Reversibility of Insulin Resistance in Obese Diabetic Patients: Role of Plasma Lipids, *Diabetologia 40*, 599–605.
26. Sakai, M., Kobori, S., Miyazaki, A., and Horiuchi, S. (2000) Macrophage Proliferation in Atherosclerosis, *Curr. Opin. Lipidol. 11*, 503–509.
27. Plenz, G., Reichenberg, S., Koenig, C., Rauterberg, J., Deng, M.C., Baba, H.A., and Robenek, H. (1999) Granulocyte-Macrophage Colony-Stimulating Factor (GM-CSF) Modulates the Expression of Type VIII Collagen mRNA in Vascular Smooth Muscle Cells and Both Are Codistributed During Atherogenesis, *Arterioscler. Thromb. Vasc. Biol. 19*, 1658–1668.
28. Sugiyama, S., Okada, Y., Sukhova, G.K., Virmani, R., Heinecke, J.W., and Libby, P. (2001) Macrophage Myeloperoxidase Regulation by Granulocyte Macrophage Colony-Stimulating Factor in Human Atherosclerosis and Implications in Acute Coronary Syndromes, *Am. J. Pathol. 158*, 879–891.
29. Griffin, M.E., Marcucci, M.J., Cline, G.W., Bell, K., Barucci, N., Lee, D., Goodyear, L.J., Kraegen, E.W., White, M.F., and Shulman, G.I. (1999) Free Fatty Acid-Induced Insulin Resistance Is Associated with Activation of Protein Kinase C θ and Alterations in the Insulin Signaling Cascade, *Diabetes 48*, 1270–1274.
30. Kraegen, E.W., Cooney, G.J., Ye, J., and Thompson, A.L. (2001) Triglycerides, Fatty Acids and Insulin Resistance—Hyperinsulinemia, *Experim. Clin. Endocrin. Diabetes 109*, S516–S526.
31. McGarry, J.D. (2002) Banting Lecture 2001: Dysregulation of Fatty Acid Metabolism in the Etiology of Type 2 Diabetes, *Diabetes 51*, 7–18.
32. Liu, W.S., and Heckman, C.A. (1998) The Sevenfold Way of PKC Regulation, *Cell Signal. 10*, 529–542.
33. Nishizuka, Y. (1995) Protein Kinase C and Lipid Signaling for Sustained Cellular Responses, *FASEB J. 9*, 484–496.

[Received March 3, 2004; accepted April 30, 2004]

Purification and Characterization of an Extracellular Lipase from *Geotrichum marinum*

Youliang Huang*, Robert Locy, and John D. Weete

Department of Biological Sciences, Auburn University, Auburn, Alabama 36849

ABSTRACT: An extracellular lipase (EC 3.1.1.3) from *Geotrichum marinum* was purified 76-fold with 46% recovery using Octyl Sepharose 4 Fast Flow and Bio-Gel A 1.5 m chromatography. The purified enzyme showed a prominent band on SDS-PAGE and a single band on native PAGE based on the activity staining. The molecular mass of the lipase was estimated to be 62 kDa using SDS-PAGE and Bio-Gel A chromatography, indicating that the lipase likely functions as a monomer. The pI of the lipase was determined to be 4.54. The apparent V_{max} and K_m were 1000 μmol/min/mg protein and 11.5 mM, respectively, using olive oil emulsified with taurocholic acid as substrate. The lipase demonstrated a pH optimum at pH 8.0 and a temperature optimum at 40°C. At 6 mM, Na^+, K^+, Ca^{2+}, and Mg^{2+} stimulated activity, but Na^+ and K^+ at 500 mM and Fe^{2+} and Mn^{2+} at 6 mM reduced lipase activity. The anionic surfactant, taurocholic acid, and the zwitterionic surfactant, 3-[(3-cholamidopropyl)dimethylammonio]-1-propanesulfonate, enhanced the activity at 0.1 mM. Other anionic surfactants such as SDS and sodium dioctyl sulfosuccinate, the cationic surfactants methylbenzethonium bromide and cetyltriethylammonium bromide, and the nonionic surfactants Tween-20 and Triton X-100 inhibited the lipase activity to different extents. The lipase was found to have a preference for TG containing *cis* double bonds in their FA side chains, and the reaction rate increased with an increasing number of double bonds in the side chain. The lipase had a preference for ester bonds at the *sn*-1 and *sn*-3 positions over the ester bond at the *sn*-2 position.

Paper no. L9339 in *Lipids 39,* 251–257 (March 2004).

Lipases [EC 3.1.1.3, triacylglycerol (TG) acylhydrolase] are versatile enzymes that catalyze both the hydrolysis and the synthesis of esters formed from glycerol and long-chain FA (1). Numerous potential uses have been explored in various fields in the last decade (2,3). Lipases occur in animals, plants, and microorganisms. Among the different biological sources of the lipases studied, filamentous fungi are thought to be the best source for industrially useful lipases because these lipases are usually extracellular and soluble. Fungal lipases from the genera *Geotrichum, Penicillium, Aspergillus, Rhizopus,* and *Rhizomucor* (4) have been the most widely studied and consequently are the most widely used in industrial applications. The selectivity of lipases for saturated or unsaturated FA has brought about an increasing interest in using lipases as potential catalysts to selectively enrich certain FA (5–7). Most *Geotrichum* lipases are from the species *G. candidum* (8–10). Lipases from different fungi, different species, or even different strains of the same species may differ in their molecular or catalytic properties (11). In this paper, we describe the production, purification, and characterization of an extracellular lipase from the marine fungus *G. marinum,* which requires the salt concentration of seawater for optimal growth.

MATERIALS AND METHODS

Materials. Trizma maleate, olive oil, triolein, trilinolein, trilinolenin, trielaidin, tristearin, taurocholic acid, 3-[(cholamidopropyl)dimethylammonio]-1-propanesulfonate (CHAPS), FFA (oleic acid), 1,2(2,3)-dioleoyl-*sn*-glycerol [1,2(2,3)-DG], 1,3-diacylglycerol (1,3-DG: 1,3-diolein), monoacylglycerol (2-monoolein), Fast Blue RR Salt, bovine IgG, BSA ovalbumin, carbonic anhydrase, glyceraldehyde-3-phosphate dehydrogenase, α-lactalbumin, Tween-20, Triton X-100, SDS, sodium dioctyl sulfosuccinate, methylbenzethonium bromide, cetyltriethylammonium bromide, polyoxyethlene 10-tridecyl ether, and reagents for PAGE were all purchased from Sigma Chemical Company (St. Louis, MO). Octyl Sepharose 4 Fast Flow was purchased from Pharmacia Biotech (Uppsala, Sweden). Bio-Gel A 1.5 m was obtained from Bio-Rad Laboratories (Hercules, CA). Bicinchoninic acid (BCA) was from Pierce Chemical Co. (Rockford, IL). Instant Ocean synthetic sea salt was purchased from Aquarium Systems Inc. (Mentor, OH).

Fungus. Geotrichum marinum (ATCC 20614) was maintained in a medium containing 2% (wt/vol) glucose and 1% (wt/vol) yeast extract in seawater at 23°C with rotary shaking at 120 rpm. The fungus was transferred to a new medium at 6-d intervals. The seawater used in the medium was made by dissolving 38 g Instant Ocean synthetic sea salt in 1 L distilled water.

Lipase production. Eighty milliliters of 6-d subculture, grown as described in the preceding paragraph, was inoculated into 800 mL YO medium containing 0.5% (wt/vol) yeast extract and 2% (vol/vol) olive oil in seawater (as defined in the preceding paragraph) in a 4-L flask. The fungus was then incubated at 23°C in

*To whom correspondence should be addressed at 209 Upchurch Hall, Department of Animal Sciences, Auburn University, Auburn, AL 36849.
E-mail: huangyo@mail.auburn.edu
Present address of third author: Research Office, West Virginia University, 886 Chestnut Ridge Rd., Suite 201, P.O. Box 6216, Morgantown, WV 26506.

Abbreviations: 1,2(2,3)-DG, 1,2(2,3)-dioleoyl-*sn*-glycerol; 1,3-DG, 1,3-diacylglycerol (1,3-diolein); BCA, bicinchoninic acid; CHAPS, 3-[(3-cholamidopropyl)dimethylammonio]-1-propanesulfonate; IEF, isoelectric focusing; TG, triacylglycerol.

a Lab-Line rotary incubator (Melrose Park, IL) at 200 rpm for 4 d. The culture medium was filtered through Whatman #2 filter paper, and the filtrate was stored at –20°C for further use.

Lipase purification. Two hundred milliliters of Octyl Sepharose 4 Fast Flow, pre-equilibrated with 10 mM imidazole buffer, pH 6.8, was added to 2000 mL of culture filtrate, and the mixture was gently agitated at room temperature for 2 h. The resin was collected by passing the mixture through a Buchner funnel fitted with a fritted glass disk. The collected resin was resuspended and loaded into a 3.0 × 50 cm column. The packed column was washed with 1800 mL of 10-mM imidazole buffer, pH 6.8, and a certain amount of water at a flow rate of 1 mL/min, and the enzyme was eluted from the column using 0.5% polyoxyethylene 10-tridecyl ether in 10 mM imidazole buffer at a flow rate of 0.5 mL/min. Fractions of 5 mL each were collected. The protein concentration in each fraction was determined by the BCA method (12), and the activity in each fraction was assayed using the emulsion assay method described in the following section (13).

Fractions containing significant enzyme activity were pooled and concentrated to 4 mL using an Amicon centriflo membrane cone (Amicon, Beverly, MA) under vacuum. The concentrated enzyme was applied onto a 2.0 × 80 cm Bio-Gel A 1.5 m column (Bio-Rad Laboratories) pre-equilibrated with 50 mM potassium phosphate buffer, pH 7.5, containing 10% glycerol. The proteins were eluted from the Bio-Gel column with the same buffer at a flow rate of 0.3 mL/min, and 3 mL fractions were collected. The protein concentration in each fraction was measured by absorbance at 280 nm ($O.D._{280}$), and the lipase activity in each fraction was measured using the emulsion assay (13). The active fractions were pooled, and the protein concentration was determined by the BCA method.

Assay of lipase activity. Lipase activity was measured with the emulsion assay method described by Mozaffar and Weete (13). Briefly, the reaction mixture was made by combining 2 mL 0.2 M Tris maleate–NaOH buffer, pH 7.5, 1 mL 0.06 M $CaCl_2$, 1 mL olive oil emulsion (50%, vol/vol, olive oil and 2 mM taurocholic acid), and appropriate amounts of distilled water and lipase preparation to make up 10 mL of the final volume of reaction mixture. The reaction mixture was mixed well and incubated at 40°C on a reciprocal shaker at 60 rpm for 60 min. After incubation, the mixture was shaken vigorously with 20 mL of acetone/ethanol (1:1, vol/vol) to stop the enzyme reaction and break down the emulsion. The amount of FFA liberated during the reaction was titrated with 0.1 M NaOH on an autotitrator system (ABU901 and PHM290; Radiometer America, Inc., Westlake, OH). One unit of lipase activity was defined as the amount of enzyme required to liberate 1 μM equivalent of FFA per minute. Specific activity was defined as units of lipase activity per milligram protein.

Protein assay. Protein concentrations in the culture medium and fractions collected from the Octyl Sepharose column were determined with the BCA method. Proteins in the fractions collected from the Bio-Gel A column were measured by $O.D._{280}$. Proteins in the culture medium and fractions collected from both hydrophobic chromatography and gel filtration chromatography were determined with the BCA method. Bovine IgG was used as the standard.

Molecular mass, isoelectric point, and kinetic parameters. Molecular mass of the *G. marinum* lipase was determined by SDS-PAGE (11) using a 10% slab gel and gel filtration on a Bio-Gel A 1.5 m column (2.0 × 80 cm). For SDS-PAGE, BSA (66 kDa), ovalbumin (45 kDa), glyceraldehyde-3-phosphate dehydrogenase (36 kDa), and carbonic anhydrase (29 kDa) were used as M.W. markers, and the gel was stained using Coomassie brilliant blue R-250 (14). For gel filtration chromatography, cytochrome C (12.4 kDa), carbonic anhydrase (29 kDa), alcohol dehydrogenase (150 kDa), and blue dextran (2000 kDa) were used as standards to calibrate the column.

Isoelectric focusing (IEF) was performed on a precast IEF agarose gel (Hypure Gel FS-5080, pH 4–6; EG&G Wallac, Akron, OH) at 40 W for 60 min at 12–15°C after loading an 8.5-μL purified sample into the well. The gel was stained using Coomassie brilliant blue R-250 as just described. The pH gradient was determined by cutting the gel into 1-cm pieces and soaking the individual pieces in 10 mM KCl for 30 min. The pH of each KCl extract was then determined using a pH meter.

Values for the apparent K_m and V_{max} were determined from double reciprocal plots of substrate concentration vs. initial reaction rates (15). Eleven concentrations, from 1 to 150 mM, of triolein and 30 μL of enzyme preparation were chosen for measuring enzyme activity by the emulsion assay method just described. Initial rates for all triolein concentrations were determined by decreasing the amount of enzyme preparation to a proper level and standardizing it to the same protein concentration.

Active staining. The purified lipase was analyzed on a 7.5% polyacrylamide gel under nondenaturing conditions, and the lipolytic active zone was identified by staining the gel with 0.03% Fast Blue RR salt, 0.05% α-naphthyl acetate, and 1% acetone in 25 mM Tris–HCl buffer at pH 7.4 (16). The substrate α-naphthyl acetate used in this experiment can also be used to detect nonlipase-type ester hydrolase (EC 3.1.1.1) activity.

Effect of temperature and pH on lipase activity. The effect of temperature on lipase stability was determined by measuring the activity remaining (emulsion assay) after incubation of the purified lipase at 20, 40, 60, and 80°C for different times. The incubations were started sequentially at the scheduled times to make different incubation times such that 5-, 10-, and 15-min time points were taken for 60 and 80°C only, whereas 0-, 20-, 40-, 60-, 120-, 180-, and 240-min incubation times were taken for all temperature treatments.

The optimal temperature for activity was measured from 20 to 60°C at 10°C intervals using the emulsion assay just described.

The optimal pH for the lipase reaction was analyzed by the emulsion assay method at different pH values. Different pH values of the reaction mixture were made by adjusting 0.2 M Tris maleate buffer to different pH values, from pH 4.0 through 10.0, with either 1 M HCl or 1 M NaOH. The emulsion assay was performed as just described except for changes in the pH value of the buffer.

Effect of metal ions on lipase activity. The effect of metal ions on lipase activity was measured using the aforementioned emulsion assay method except that $CaCl_2$ was omitted from the base reaction and replaced with distilled water. Reaction rates with added metal ions (6 mM final concentration for both monovalent and divalent ions, and 500 mM final concentration for NaCl and KCl) were then compared with the ion-free blank reaction.

Effect of surfactant on lipase activity. To determine the effect of various surfactants on lipase activity, the emulsion assay described earlier was used with 1 mL olive oil emulsion from Sigma (50%, vol/vol) as the substrate. Each selected surfactant was added to the reaction mixture at a final concentration of 0.1 and 1 mM, and the reaction mixture was mixed well by vigorous shaking. The surfactants tested were anionic (taurocholic acid/Na, SDS, and sodium dioctyl sulfosuccinate), cationic (methylbenzethonium bromide and cetyltriethylammonium bromide), zwitterionic (CHAPS), and nonionic (Tween-20 and Triton X-100).

Substrate specificity determination. To determine the preference of the purified lipase for specific substrates, various TG with differing degrees of unsaturation in the side-chain FA were used as substrates in the emulsion assay. The substrates tested were tristearin (18:0), triolein (18:1*cis*-9), trielaidin (18:1*trans*-9), trilinolein (18:2*cis*-9,12) and trilinolenin (18:3*cis*-9,12,15). An emulsion of each of these substrates was made by sonicating 5 mL of 100-mM selected substrate in 1 mM taurocholic acid for 1 min on ice. One milliliter of each emulsion was then used in a standard 10-mL reaction mixture as described in the aforementioned emulsion activity assay. The final concentration of each substrate in the reaction mixture was 10 mM.

Position preference determination. To prevent acyl migration, the triolein hydrolysis reaction was carried out at 20°C. At 0, 5, 15, and 30 min during the course of triolein hydrolysis, 2-mL aliquots were removed and mixed with 10 mL diethyl ether by vortexing to stop the reaction and to extract the products. The organic layer was removed and concentrated under a stream of nitrogen gas. The extracted product was dissolved in diethyl ether to a concentration of about a 50-µg equivalent of triolein. The products were analyzed by TLC on 250-µm Silica gel 60 on a 10×20 cm glass plate. Four hundred micrograms of each sample was applied to the TLC plate, and the plate was developed in a chamber with hexane/diethyl ether/acetic acid (79:20:4, by vol) as the solvent system. Before development, the chamber was saturated for 4 h with the same developing solvent system. The components of the products were visualized with iodine vapor and identified by comparison of their R_f values with those of known standards. The visualized spots on the TLC plates were quantified with a scanner (Quick Scan R & D; Helena Laboratories, Beaumont, TX).

RESULTS

Lipase purification. The lipase from *G. marinum* was purified by affinity and gel-filtration chromatographies. Significant initial purification was obtained by affinity chromatography on an Octyl Sepharose column using a low ionic strength buffer (10 mM imidazole buffer, pH 6.8). Under these conditions, lipase binds strongly to the Octyl Sepharose resin, whereas most other proteins in the culture filtrate do not bind to the resin (data not shown). Following the binding of lipases to the resin and packing of the resin in a column, the column was washed with water until the $O.D._{280}$ was reduced to nearly zero. The column was then washed with 0.5% detergent, and the main lipase activity was eluted in a single sharp peak (Fig. 1A). Fractions 35–44 were pooled and concentrated to a small volume. Although slightly more than 1% of the protein in the crude culture filtrate was recovered in the Octyl Sepharose purified fraction, 66% of the enzyme activity applied to the resin was recovered, and the specific activity increased 56-fold, as shown in Table 1. The pooled fractions were enriched in a 62-kDa protein, as shown by SDS-PAGE (Fig. 2A).

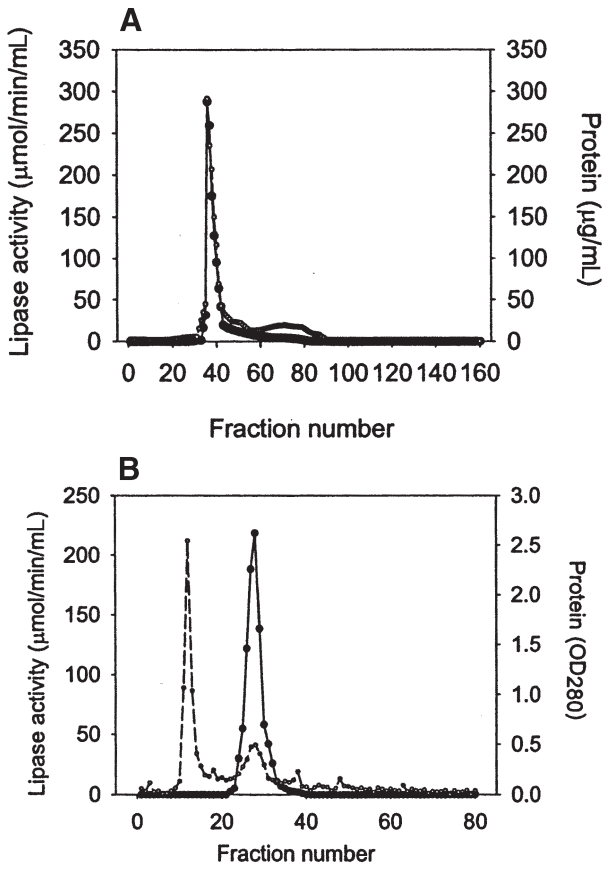

FIG. 1. Chromatographies of the lipase from *Geotrichum marinum* ATCC 20614. (A) Column chromatography on Octyl Sepharose 4 Fast Flow (Pharmacia Biotech, Uppsala, Sweden). Lipase was eluted with 0.5% polyoxyethylene 10-tridecyl ether. The volume for each fraction was 5 mL. Protein concentration (--○--) was determined by the bicinchoninic acid (BCA) method. Lipase activity (—●—) was measured with the emulsion assay method. (B) Gel filtration chromatography on Bio-Gel A (Bio-Rad Laboratories, Hercules, CA). Lipase was eluted with 50 mM phosphate buffer, pH 7.5, starting at fraction 1. Protein concentration (--○--) was determined by absorbance at 280 nm ($O.D._{280}$). Lipase activity (—●—) was measured by the emulsion assay method.

TABLE 1
Purification of an Extracellular Lipase from *Geotrichum marinum*

Steps	Volume (mL)	Protein (mg)	Specific activity (μmol/min/mg protein)	Yield (%)	Purification factor
Culture	2000	1134	10.23	100	1
Octyl Sepharose[a]	55.7	13.35	575	66	56
Bio-Gel A[b]	55.7	6.96	773	46	76

[a]Octyl Sepharose 4 Fast Flow (Pharmacia Biotech, Uppsala, Sweden).
[b]Bio-Gel A 1.5 m (Bio-Rad Laboratories, Hercules, CA).

The pooled, concentrated sample from the Octyl Sepharose column was subsequently applied to a Bio-Gel A column; the peaks of lipase activity eluted from this column are shown in Figure 1B. A single, relatively symmetrical peak of enzyme activity eluted from the Bio-Gel A column, whereas two main peaks of protein were observed based on the absorbance of the fractions at 280 nm. The initial large protein peak contained a high amount of contaminating protein (not demonstrating lipase activity), whereas a smaller protein peak eluting in fractions 22–41 (Fig. 1B) corresponded to the lipase activity eluting from the column. The pooled, lipase-containing fractions from the Bio-Gel A column contained slightly more than 50% of the protein and 70% of the enzyme activity applied to the column, yielding 46% of the total lipase activity in the crude culture filtrate and 76-fold purification (Table 1). The pooled fractions showed a single clear band in SDS-PAGE (Fig. 2A) and a single active band in native PAGE gel (Fig. 2B).

Molecular mass, isoelectric point, and kinetic parameters. The molecular mass of 62 kDa for the purified *G. marinum* lipase was obtained by both SDS-PAGE (Fig. 2A) and gel-filtration chromatography. The isoelectric point for the purified lipase was pH 4.54 based on its focusing on the IEF gel. Kinetic constants for the purified lipase from *G. marinum* were obtained using the emulsion assay method with triolein as the substrate. The apparent K_m and V_{max} values obtained from the Lineweaver–Burk plot using a linear regression analysis were 11.5 mM and 1000 μmol/min/mg protein, respectively.

Effect of temperature and pH on lipase activity. To analyze the stability of the purified lipase against temperature, lipase activity was determined after incubation at different temperatures for various time periods, as outlined in the Materials and Methods section. The lipase was stable at 20 and 40°C for at least 1 h. However, after 1 h the lipase activity began to decrease. When the lipase was incubated at 20 and 40°C for 4 h, it retained 52 and 49% of its full activity. Lipase activity was significantly more sensitive to higher temperatures. Incubation at 60 and 80°C for 5 min resulted in losses of 92 and 98% activity, respectively.

The optimal temperature for activity determination was examined within a range of 20 to 60°C. The rate of catalysis, as demonstrated by specific activity, increased slightly between 20 and 40°C. The highest activity was obtained at 40°C under the conditions described in the Materials and Methods section. However, the activity decreased dramatically at 50 and 60°C.

The effect of pH on lipase activity was studied in a range from pH 4 to 10. The lipase was found to be most active at pH 8 and 40°C using a 60-min reaction, as shown in Figure 3. The lower pH obviously decreased the lipase activity. At pH 4.0, no lipase activity was obtained, and only 20% of the total activity was obtained at pH 5.0.

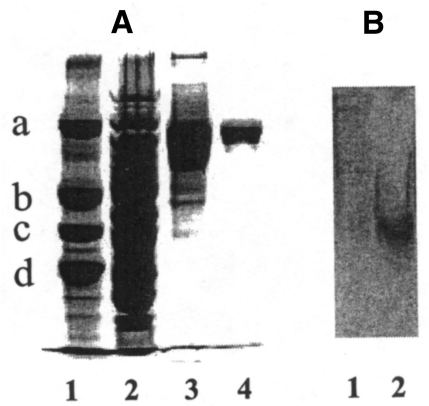

FIG. 2. Analysis of proteins at different stages during purification of the lipase from *G. marinum* by PAGE. (A) Analysis of proteins from each purification step by 10% SDS-PAGE. The gel was stained with Coomassie brilliant blue R-250. Lane 1, standard proteins: (a) BSA (66 kDa); (b) ovalbumin (45 kDa); (c) glyceraldehyde-3-phosphate dehydrogenase (36 kDa); (d) carbonic anhydrase (29 kDa); lane 2, crude preparation; lane 3, after Octyl Sepharose column chromatography; lane 4, after Bio-Gel A gel filtration chromatography. (B) Analysis of the lipase from *G. marinum* by 7.5% native PAGE. Lane 1, sample from the culture broth; lane 2, lipase preparation from Bio-Gel A. The active zone was identified by staining the gel with 0.03% Fast Blue RR salt, 0.05% α-naphthyl acetate, and 1% acetone in 25 mM Tris–HCl buffer at pH 7.4. For column suppliers and abbreviation, see Figure 1.

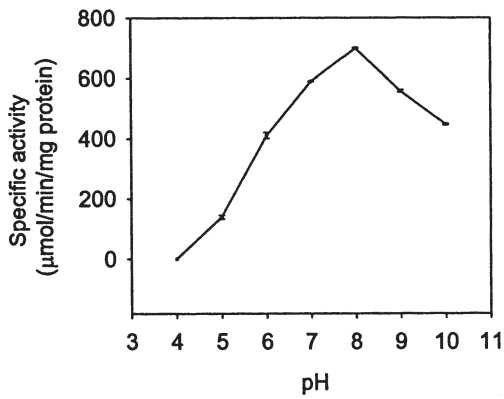

FIG. 3. Effect of pH on *G. marinum* lipase activity. Lipase activities were measured by the emulsion assay method. See Figure 1 for abbreviation.

TABLE 2
Effect of Metal Ions on *G. marinum* Lipase Activity

Treatment	Specific activity[a] (μmol/min/mg protein)	Relative activity (%)[b]
Control (no metal ions)	380.9 ± 9.4	100
NaCl (6 mM)	445.1 ± 8.0	117
NaCl (500 mM)	158.4 ± 7.3	42
KCl (6 mM)	440.6 ± 9.1	116
KCl (500 mM)	123.9 ± 1.5	33
$CaCl_2$ (6 mM)	395.0 ± 1.5	104
$MgCl_2$ (6 mM)	475.4 ± 4.8	125
$FeCl_2$ (6 mM)	192.5 ± 3.8	51
$MnCl_2$ (6 mM)	199.9 ± 2.0	52
$CoCl_2$ (6 mM)	377.4 ± 6.3	99

[a]The activities were assayed by the emulsion method described in the Materials and Methods section and represent the arithmetic mean ± SD of three determinations.
[b]The activities are expressed relative to the activity obtained without adding metal ions. See Table 1 for abbreviation.

Effect of metal ions on lipase activity. Two monovalent (Na^+ and K^+) and five divalent ions (Ca^{2+}, Co^{2+}, Fe^{2+}, Mg^{2+}, and Mn^{2+}) were tested for their effects on the activity of the *G. marinum* lipase. As shown in Table 2, different metal ions had different effects on the activity of the lipase from *G. marinum*. The monovalent ions, Na^+ and K^+, enhanced the activity by 17 and 16% at 6 mM, but Na^+ and K^+ decreased the activity by 58 and 67% when the concentration was increased to 500 mM. Divalent ions affected the activity differently at 6 mM. Ca^{2+} and Mg^{2+} increased the activity by 4 and 25%, whereas Co^{2+} had no effect on the activity. $Fe^{2+}$and Mn^{2+} inhibited the activity by 49 and 48%.

Effect of surfactant on lipase activity. The effects of two concentrations (0.1 and 1.0 mM) of eight selected surfactants on *G. marinum* lipase activity were determined. As shown in Table 3, at 0.1 mM, taurocholic acid and CHAPS enhanced the lipase activity by 239 and 263%, respectively, but at 1 mM, only taurocholic acid increased the activity (by 50%) and CHAPS inhibited the activity by 33%. All other surfactants tested inhibited the lipase activity to different extents. SDS, cetyltriethylammonium bromide, Tween-20, and Triton X-100 totally inhibited the lipase activity at 0.1 and 1 mM. Sodium dioctyl sulfosuccinate and methylbenzethonium bromide inhibited the lipase activity by 45 and 14% at 0.1 mM, and by 47 and 98% at 1 mM, respectively.

TABLE 3
Effect of Surfactant on *G. marinum* Lipase Activity

Surfactant[a]	Relative activity (% ± SD)[b] 0.1 mM	1 mM
None	100 ± 7	100 ± 6
Taurocholic acid	339 ± 23	150 ± 13
SDS	0 ± 0	0 ± 0
Sodium dioctyl sulfosuccinate	55 ± 21	53 ± 3
Methylbenzethonium bromide	86 ± 27	2 ± 1.5
Cetyltriethylammonium bromide	0 ± 0	0 ± 0
CHAPS	363 ± 21	67 ± 22
Tween-20	0 ± 0	0 ± 0
Triton X-100	0 ± 0	0 ± 0

[a]CHAPS, 3-[(3-cholamidopropyl)dimethylammonio]-1-propanesulfonate; see Table 1 for other abbreviation.
[b]Each value is the arithmetic mean ± SD of three determinations. The relative activities were calculated relative to the control (without additives) using mean values.

TABLE 4
Substrate Specificity of *G. marinum* Lipase Activity

Substrate	Specific activity[a] (μmol/min/mg protein ± SD)	Relative activity (%)[b]
Triolein (18:1*cis*-9)	448.3 ± 3.5	100
Trilinolein (18:2*cis*-9,12)	489.8 ± 2.4	109
Trilinolenin (18:3*cis*-9,12,15)	520.8 ± 5.6	116
Trielaidin (18:1*trans*-9)	205.9 ± 1.9	46
Tristearin (18:0)	0	0

[a]The activities were assayed by the emulsion method described in the Materials and Methods section and represent the arithmetic mean ± SD of at least three determinations.
[b]The relative activities are expressed relative to the activity obtained using triolein as substrate.

Substrate specificity. Geotrichum marinum lipase activity, as a function of the degree of unsaturation of the FA substituents in TG substrates, was determined to evaluate the substrate specificity. The lipase was found to have a strong preference for substrates containing *cis*-unsaturated FA substituents (Table 4). Upon setting the activity using triolein (18:1*cis*-9) as a substrate at 100%, the activity toward trielaidin (18:1*trans*-9) was only 46%. For the substrates containing exclusively saturated FA side chains, e.g., tristearin (18:0), no hydrolysis was observed. However, activities toward trilinolein (18:2*cis*-9,12) and trilinolenin (18:3*cis*-9,12,15) were 109 and 116% of that obtained using triolein (18:1*cis*-9).

Position preference. TLC analysis of the products from the triolein hydrolysis by *G. marinum* lipase showed that 1,2- and 2,3-DG were readily released, along with a small amount of 1,3-DG (Fig. 4). Quantification by scanning the spots showed that the amount of 1,2(2,3)-DG was more than 10 times that of

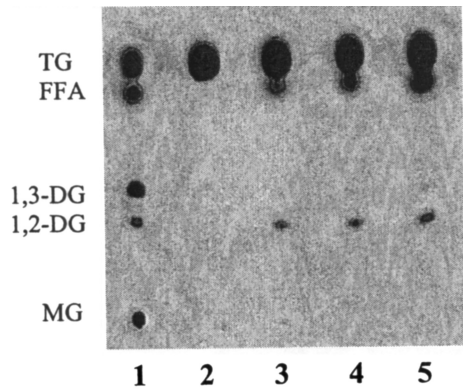

FIG. 4. TLC of products of triolein hydrolysis by *G. marinum* lipase. The reaction conditions are given in the Materials and Methods section. TG, triolein; FFA (oleic acid); 1,3-DG, 1,3-diacylglycerol (diolein); 1,2(2,3)-DG, 1,2(2,3)-diacylglycerol (1,2(2,3)-dioleoyl-*sn*-glycerol); MG, monoacylglycerol (2-monoolein). Lane 1, standards; lane 2, sample from the reaction mixture (0 min); lane 3, products from the hydrolysis after a 5-min reaction; lane 4, products from the hydrolysis after a 15-min reaction; lane 5, products from the hydrolysis after a 30-min reaction. See Figure 1 for abbreviation.

1,3-DG, indicating that *G. marinum* lipase had a preference for ester bonds at the *sn*-1 and *sn*-3 positions over the ester bond at the *sn*-2 position.

DISCUSSION

Purification of the lipase from *G. marinum* in this study involved removal of fungal mycelium by filtration, followed by affinity chromatography using Octyl Sepharose at a low salt concentration and gel-filtration chromatography on a Bio-Gel A column, which gave a 76-fold purification and 46 recovery of the total lipase activity. The purification presented here was similar to the purification of lipases from *G. candidum* NRRL Y-553 (17) in that Octyl Sepharose chromatography was used, but the procedure differed in other steps. The purification of the lipase from *G. marinum* demonstrated here also differed from other *G. candidum* lipase purification procedures (10,18,19). Most *G. candidum* lipase purifications contain either ammonia sulfate or ethanol precipitation steps and an ion-exchange chromatography step. Our initial attempts to purify the lipase from *G. marinum* included both ammonium sulfate precipitation and ion-exchange chromatography steps, but only 10% of the lipase activity was precipitated when up to 90% saturation of ammonium sulfate was used. Using ion-exchange chromatography on an AG MP-1 column (9), a single protein was purified that appeared as a single protein band by SDS-PAGE, but this protein fraction lost all lipase activity during purification (data not shown). These results suggest that the lipase from *G. marinum* has a number of different properties from the lipases from *G. candidum* (10,17,19).

Other studies have demonstrated that *G. candidum* produces multiple lipases that differ in molecular mass within the range of 45 to 66 kDa, in pI within the range of pH 4.0 to 5.0, and in substrate specificity according to the strain from which they come (9,17,20–22). Unlike the multiple lipases with different specificities demonstrated in *G. candidum* strains, a single lipase with molecular mass of 62 kDa and pI of 4.54 was purified from *G. marinum* in this study. However, it cannot be concluded that *G. marinum* produces only one lipase, since we found very low lipase activity in the Octyl Sepharose chromatography fractions 45 to 70, and the possibility that these or other fractions could exhibit significant activity when assayed using other conditions or substrates cannot be ruled out. However, the prominent lipase activity in *G. marinum* was observed in fractions 35 to 44, which was purified and further characterized in this study.

The lipase from *G. marinum* had a preference for substrates containing *cis*-unsaturated FA. The hydrolysis reaction against TG increased with increasing numbers of double bonds in the FA substituents. This result is consistent with the reports for lipases from *Pythium ultimum* (13), the extracellular lipase from *G. candidum* (23), and lipase I from *G. candidum* (24). In contrast, the lipase purified from *G. marinum* is different from the lipase from *Candida deformans* (25) and *Humicola lanuginosa* No. 3 (26), whose activities were inhibited with increasing unsaturation of the substrate. In this study, no activity against tristearin (18:0) was detected. We reason that the poor emulsification of tristearin occurred because the *G. marinum* lipase showed almost the same activity against trioctanoin (8:0) as against triolein (18:1) in a separate experiment.

The divalent ions Ca^{2+} and Mg^{2+} stimulated the hydrolysis activity of the lipase from *G. marinum*, which is in agreement with observations of other lipases from *P. ultimum* (13) and *A. terreus* (27). Others have also reported the positive effect of Ca^{2+} for lipases from *P. candidum* (28), *R. delemar* (29), and *P. expansum* (30). In contrast, Ca^{2+} strongly inhibited the activity of lipases from *G. candidum* (10) and *P. citrinum* (31). Mg^{2+} had a negative effect on lipases from *A. niger* (32) and *G. candidum* (10). However, Ca^{2+} and Mg^{2+} had neither a positive nor a negative effect on the activity of the lipase from *Botrytis cinerea* (33).

Calcium may stimulate lipase activity by such mechanisms as binding to the enzyme, resulting in conformational change and facilitating the process through which the lipase moves into the substrate–water interface, and/or by removing FA products released by hydrolysis from the interface, possibly reducing end-product inhibition of the reaction (34). For example, the binding of calcium is known to be important for the structural stabilization of *Staphylococcus hyicus* lipase and for catalytic activity at high temperatures (35). However, stimulation of *C. rugosa* lipase activity by calcium in a normal-phase emulsion with olive oil as substrate was ascribed to the formation of calcium salts in the FA reaction products (36), and the influence of calcium ions on the titration efficiency of the liberated FA was attributed to a reduction in end-product inhibition by long-chain FA (37). Further explanation of the role of calcium ions in *G. marinum* lipase cannot be inferred without determining in some manner the calcium-binding properties of the enzyme. This could be accomplished if calcium binding sites were apparent, based on amino acid sequence similarity to other known calcium-binding lipases.

The *G. marinum* lipase described here differs in detail from those reported from other species in the genus *Geotrichum* in one or more of the following aspects: molecular mass, pI, chemical properties, effect of Ca^{2+}, and substrate specificity. The two major differences are the responses to Ca^{2+} and Mg^{2+}. These properties in particular apparently make the *G. marinum* lipase different from those lipases of other *Geotrichum* species. Additionally, the preference of *G. marinum* lipase for unsaturated substrates demonstrates the potential usefulness of this enzyme for splitting and restructuring the unsaturated FA found in TG.

ACKNOWLEDGMENT

This work is supported by the Mississippi–Alabama Sea Grant Consortium.

REFERENCES

1. Jaeger, K.E., and Reetz, M.T. (1998) Microbial Lipases Form Versatile Tools for Biotechnology, *Trends Biotechnol. 16*, 396–403.

2. Vulfson, E.N. (1994) Industrial Applications of Lipases, in *Lipases* (Woolley, P., and Peterson, S.B., eds.), pp. 271–288, Cambridge University Press, New York.
3. Bjorkling, F., Godtfredsen, S.E., and Kirk, O. (1991) The Future Impact of Industrial Lipases, *Trends Biotechnol. 9*, 360–363.
4. Persson, M., Svensson, I., and Adlercreutz, P. (2000) Enzymatic Fatty Acid Exchange in Digalactosyldiacylglycerol, *Chem. Phys. Lipids 104*, 13–21.
5. Rice, K.E., Watkins, J., and Hill, C.G., Jr. (1999) Hydrolysis of Menhaden Oil by a *Candida cylindracea* Lipase Immobilized in a Hollow-Fiber Reactor, *Biotechnol. Bioeng. 63*, 33–45.
6. Jonzo, M.D., Hiol, A., Zagol, I.I., Druet, D., and Comeau, L. (2000) Concentrates of DHA from Fish Oil by Selective Esterification of Cholesterol by Immobilized Isoforms of Lipase from *Candida Rugosa, Enzyme Microb. Technol. 27*, 443–450.
7. Garcia, H.S., Arcos, J.A., Ward, D.J., and Hill, C.G., Jr. (2000) Synthesis of Glycerides Containing n-3 Fatty Acids and Conjugated Linoleic Acid by Solvent-Free Acidolysis of Fish Oil, *Biotechnol. Bioeng. 70*, 587–591.
8. Litthauer, D., Louw, C.H., and Du Toit, P.J. (1996) *Geotrichum Candidum* P-5 Produces an Intracellular Serine Protease Resembling Chymotrypsin, *Int. J. Biochem. Cell Biol. 28*, 1123–1130.
9. Sugihara, A., Hata, S., Shimada, Y., Goto, K., Tsunasawa, S., and Tominaga, Y. (1993) Characterization of *Geotrichum Candidum* Lipase III with Some Preference for the Inside Ester Bond of Triglyceride, *Appl. Microbiol Biotechnol. 40*, 279–283.
10. Veeraragavan, K., Colpitts, T., and Gibbs, B.F. (1990) Purification and Characterization of Two Distinct Lipases from *Geotrichum candidum, Biochim. Biophys. Acta 1044*, 26–33.
11. Jacobsen, T., and Poulsen, O.M. (1995) Comparison of Lipases from Different Strains of the Fungus *Geotrichum candidum*, *Biochim. Biophys. Acta 1257*, 96–102.
12. Smith, P.K., Krohn, R.I., Hermanson, G.T., Mallia, A.K., Gartner, F.H., Provenzano, M.D., Fujimoto, E.K., Goeke, N.M., Olson, B.J., and Klenk, D.C. (1985) Measurement of Protein Using Bicinchoninic Acid, *Anal. Biochem. 150*, 76–85.
13. Mozaffar, Z., and Weete, J.D. (1993) Purification and Properties of an Extracellular Lipase from *Pythium Ultimum, Lipids 28*, 377–382.
14. Bollag, D.M., and Edelstein, S.J. (1991) Staining a Gel with Coomassie Blue, in *Protein Methods* (Bollag, D.M., and Edelstein, S.J., eds.), pp. 114 –116, Wiley-Liss, New York.
15. Lineweaver, H., and Burk, D. (1934) The Determination of Enzyme Dissociation Constants, *J. Am. Chem. Soc. 56*, 658–666.
16. Torossian, K., and Bell, A.W. (1991) Purification and Characterization of an Acid-Resistant Triacylglycerol Lipase from *Aspergillus niger, Biotechnol. Appl. Biochem. 13*, 205–211.
17. Baillargeon, M.W., and McCarthy, S.G. (1991) *Geotrichum candidum* NRRL Y 553 Lipase: Purification, Characterization and Fatty Acid Specificity, *Lipids 26*, 831–836.
18. Baillargeon, M.W. (1990) Purification and Specificity of Lipase from *Geotrichum candidum, Lipids 25*, 841–848.
19. Sugihara, A., Shimada, Y., and Tominaga, Y. (1990) Separation and Characterization of Two Molecular Forms of *Geotrichum candidum* Lipase, *J. Biochem.* (Tokyo) *107*, 426–430.
20. Jacobsen, T., and Poulsen, O.M. (1992) Separation and Characterization of 61- and 57-kDa Lipases from *Geotrichum Candidum* ATCC 66592, *Can. J. Microbiol. 38*, 75–80.
21. Sidebottom, C.M., Charton, E., Dunn, P.P., Mycock, G., Davies, C., Sutton, J.L., Macrae, A.R., and Slabas, A.R. (1991) *Geotrichum candidum* Produces Several Lipases with Markedly Different Substrate Specificities, *Eur. J. Biochem. 202*, 485–491.
22. Sugihara, A., Shimada, Y., Nakamura, M., Nagao, T., and Tominaga, Y. (1994) Positional and Fatty Acid Specificities of *Geotrichum candidum* Lipases, *Protein Eng. 7*, 565–588.
23. Jensen, R.G. (1974) Characteristics of the Lipase from the Mold, *Geotrichum candidum*: A Review, *Lipids 9*, 149–157.
24. Bertolini, M.C., Schrag, J.D., Cygler, M., Ziomek, E., Thomas, D.Y., and Vernet, T. (1995) Expression and Characterization of *Geotrichum candidum* Lipase I Gene. Comparison of Specificity Profile with Lipase II, *Eur. J. Biochem. 228*, 863–869.
25. Muderhwa, J.M., and Ratomahenina, R. (1985) Purification and Properties of the Lipase from *Candida deformans* (Zach) Langeron and Guerra, *J. Am. Oil Chem. Soc. 62*, 1031–1036.
26. Omar, I.C., Hayashi, M., and Nagai, S. (1987) Purification and Some Properties of a Thermostable Lipase from *Humicola lanuginosa* No. 3, *Agric. Biol. Chem. 51*, 37–45.
27. Yadav, R.P., Saxeena, R.K., Gupta, R., and Davidson, S. (1998) Lipase Production by *Aspergillus* and *Penicillium* species, *Folia Microbiol.* (Praha) *43*, 373–378.
28. Ruiz, B., Farres, A., Langley, E., Masso, F., and Sanchez, S. (2001) Purification and Characterization of an Extracellular Lipase from *Penicillium candidum, Lipids 36*, 283–289.
29. Haas, M.J., Cichowicz, D.J., and Bailey, D.G. (1992) Purification and Characterization of an Extracellular Lipase from the Fungus *Rhizopus delemar, Lipids 27*, 571–576.
30. Stocklein, W., Sztajer, H., Menge, U., and Schmid, R.D. (1993) Purification and Properties of a Lipase from *Penicillium expansum, Biochim. Biophys. Acta 1168*, 181–189.
31. Krieger, K., Taipa, M.A., Melo, E.H.M., Lima-Filho, J.L., Aires-Barros, M.R., and Carbral, J.M.S. (1999) Purification of a *Penicillium citrinum* Lipase by Chromatographic Processes, *Bioprocess Eng. 20,* 59–65.
32. Olama, Z.A., and el-Sabaeny, A.H. (1993) Lipase Production by *Aspergillus niger* Under Various Growth Conditions Using Solid State Fermentation, *Microbiologia 9*, 134–141.
33. Commenil, P., Belingheri, L., Sancholle, M., and Dehorter, B. (1995) Purification and Properties of an Extracellular Lipase from the Fungus *Botrytis cinerea, Lipids 30*, 351–356.
34. Weete, J.D. (1998) Microbial Lipases, in *Food Lipids* (Akoh, C.C., and Min, D.B., eds.), pp. 641–664, Marcel Dekker, New York.
35. Simons, J.W.F.A., Van Kampen, M.D., Ubarretxena-Belandia, I., Cox, R.C., Alves Dos Santos, C.M., Egmond, M.R., and Verheij, H.M. (1999) Identification of a Calcium Binding Site in *Staphylococcus hyicus* Lipase: Generation of Calcium-Independent Variants, *Biochemistry 38*, 2–10.
36. Wang, Y.J., Sheu, J.Y., Wang, F.F., and Shaw, J.F. (1988) Lipase-Catalyzed Oil Hydrolysis in the Absence of Added Emulsifier, *Biotechnol. Bioeng. 31*, 628–633.
37. Benzonana, G., and Desnuelle, P. (1968) Action of Some Effectors on the Hydrolysis of Long-Chain Triglycerides by Pancreatic Lipase, *Biochim. Biophys. Acta 164*, 47–58.

[Received June 23, 2004, and in revised form February 12, 2004; revision accepted February 20, 2004]

Notes to Author
L9339

1.manuscript page (msp.) 2, Abbreviations footnote: Note that *Lipids* now uses a list of standard abbreviations (please visit our web site). To avoid confusion, I have maintained the abbreviations as you have listed them, although I would like to clarify one point. Here, TG is defined as "triacylglycerol (triolein)." However, on msp. 10 (*Substrate specificity determination* subsection, first sentence), it discusses the use of "various triglycerides with differing degrees of unsaturation . . . tristearin (18:0), triolein (18:1*cis*-9), trielaidin (18:1*trans*-9), trilinolein (18:2*cis*-9,12), and trilinolenin (18:3*cis*-9,12,15)." Generally, we use either TG or TAG consistently within a paper, and our standard abbreviation for "triglycerides" is TG. Could you clarify whether your abbreviation in the footnote includes all these or only triolein? Please note that I have eliminated the abbreviation MG because it is used only once in the paper (excluding Tables and figures, which are treated separately).
2.msp. 3, Abstract, sentence, ninth sentence; msp. 9, *Effect of surfactant on lipase activity* subsection, third sentence; msp. 13, *Effect of surfactant on lipase activity* subsection, fifth sentence; and msp. 32, Table 3: Two different spellings were shown for methylben**ze**thonium bromide or methylben**e**thonium bromide. Which is correct?
3.msp. 5, Materials and Methods section, *Materials* subsection, first sentence: The Abbreviations footnote gives "1,2-DG, 1,2-dioleoyl-*sn*-glycerol"; should this be changed to "1,2(2,3)-DG, 1,2(2,3)-dioleoyl-*sn*-glycerol" for consistency with this sentence (as well as the Figure 4 legend)? Please check other additions to this list of items for correctness as well.
4.msp. 5, *Lipase production* subsection, second sentence: May I include the location of this supplier, for the benefit of readers?
5.msp. 7, *Assay of lipase activity* subsection, fifth sentence: Please verify the supplier as Radiometer America, Inc. (rather than "American") and the location as Westlake, Ohio.
6.msp. 11, *Position preference determination* subsection, ninth sentence: Please verify the location of Helena Laboratories as Beaumont, Texas.
7.msp. 11, *Lipase purification* subsection, second paragraph, first sentence: Please check edits.
8.msp. 13, *Effect of temperature and pH on lipase activity* subsection, seventh sentence: Ok to delete the sentence "Figure 6 shows . . . for various periods of time," as we have no Figure 6 in the manuscript, and Figures 1-4 do not seem to include this information.
9.msp. 13, *Effect of metal ions on lipase activity* subsection, first sentence: May I use *G. marinum* in place of GM?
10.msp. 13, *Effect of surfactant on lipase activity* subsection, first sentence: See note 9above.
11.msp. 14, *Substrate specificity* subsection, first sentence: See note 9.
12.msp. 14, *Position preference* subsection, first sentence: See note 9.
13.msp. 14, *Position preference* subsection, first sentence: Should the Abbreviations footnote read "1,2(2,3)-DG," as shown in the next sentence?
14.
1.msp. 14, *Position preference* subsection, second sentence: See note 9.
2.msp. 16, Discussion section, third paragraph, first sentence: Would it change your meaning to use the standard abbreviation TG here? (See note 1 above.)
3.msp. 16, *Discussion* section, third paragraph, sixth sentence: See note 9.
4.msp. 19, Ref. 2: Please verify the location of Cambridge University Press as New York.
5.msp. 20, Ref. 14: Please verify the location of Wiley-Liss as New York.
6.msp. 23, Ref. 34: Please verify the location of Marcel Dekker as New York.
7.msp. 24, Figure 2 legend: Manuscript page 7 (*Molecular mass, isoelectric pont, and kinetic parameters* subsection, second sentence) shows this as "Coumassie **brilliant** blue R"; here it is "Coumassie blue R**-250**." Should both appear as "Coumassie brilliant blue R-250"?
8.msp. 30, Table 1: Please check that the supplier information added in footnotes a and b is ok.
9. Typesetter could not open the table file so they were keyed in. Please proof tables carefully.
Thank you for your contribution to *Lipids*.

Sincerely,

Susan Krusemark
Copy editor

Ozonation of Cholesterol in the Presence of Ethanol: Identification of a Cytotoxic Ethoxyhydroperoxide Molecule

Misako Tagiri-Endo[a,b], Kiyotaka Nakagawa[a], Tatsuya Sugawara[a], Kaori Ono[a], and Teruo Miyazawa[a,*]

[a]Food & Biodynamic Chemistry Laboratory, Graduate School of Life Science and Agriculture, Tohoku University, Sendai, Japan, and [b]Industrial Technology Institute, Miyagi Prefectural Government, Sendai, Japan

ABSTRACT: Cholesterol ozonation was carried out in ethanol-containing aqueous or nonaqueous solvent, and the ozonized products were analyzed by chemiluminescence detection-HPLC with on-line electrospray MS (HPLC-CL-MS) and characterized on the basis of NMR and FABMS. After the ozonolysis of cholesterol in water/ethanol (aqueous system) as well as in chloroform/ethanol (nonaqueous system), a unique ethoxyhydroperoxide molecule (7α-ethoxy-3β-hydroxy-5α-B-homo-6-oxacholestane-5-hydroperoxide, termed "7α-ethoxy-5-OOH") appeared as main ozonation product. In addition to structural analysis, we confirmed the remarkable cytotoxicity of 7α-ethoxy-5-OOH toward human lung adenocarcinoma A549 cells and found that its cytotoxicity is superior to that of the commonly known autoxidized cholesterol (3β-hydroxycholest-5-ene-7-one). Hence, 7α-ethoxy-5-OOH is a toxic molecule of primary importance, arising during cholesterol ozonation in the presence of ethanol.

Paper no. L9370 in *Lipids 39,* 259–264 (March 2004)

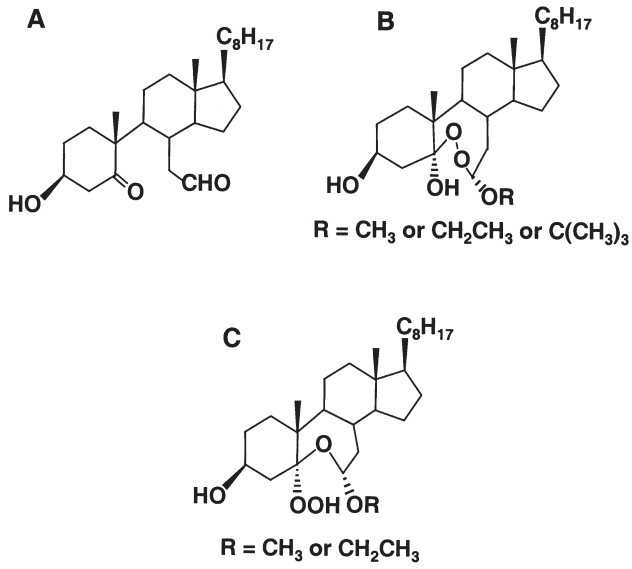

SCHEME 1

Ozone, a very powerful oxidant, is frequently used for disinfection, deodorization, and bleaching of wastewater and polluted air as well as foodstuffs (1). Since the primary targets of ozone are unsaturated lipids in cell membranes and foods, the chemistry of ozone reactions with lipids has been studied in detail (2–6). In particular, studies have focused on the ozonolysis of cholesterol that yields various oxygenated cholesterol derivatives (7–9).

In the case of ozonation of cholesterol in organic solvents, the reaction gave the expected ozonide, which was easily reduced to 3β-hydroxy-5-oxo-5,6-secocholestan-6-al as a major product (Scheme 1A) (8,10). The same compound also was formed in aqueous environments (7,9). By contrast, the ozonation of cholesterol in alcohol-containing solvent proceeded *via* a unique pathway that yielded a unique solvent-participated product (7). In 1988, Jaworski and Smith (11) investigated the reaction product of cholesterol with ozone in the presence of alcohol, and they proposed its structure to be an epidioxide, 7a-alkoxy-B-dihomo-6,7-dioxacholestan-3β,5-diol (Scheme 1B). This epidioxide structure was corrected to "alkoxy-hydroperoxide" (Scheme 1C; 7α-alkoxy-3β-hydroxy-5α-B-homo-6-oxacholestane-5-hydroperoxide) on the basis of recent NMR and X-ray studies (12–14).

Despite recent progress in the structural elucidation of ozonized cholesterol, information on its formation and accumulation in food and biological samples has never been sought. In addition, little is known about the biological role of cholesterol ozonation products, and whether ozonized cholesterol is biologically more active than the commonly known oxysterols (e.g., 3β-hydroxycholest-5-ene-7-one, a major product of cholesterol autoxidation) has not been evaluated. The causes of such uncertainty are many, but foremost among them might be the lack of a suitable analytical method for measuring ozonized cholesterol directly. Hence, in this study, we report on an assay of cholesterol ozonation products and

Present address of third author: Graduate School of Agriculture, Kyoto University, Kyoto, Japan.

*To whom correspondence should be addressed at Food & Biodynamic Chemistry Laboratory, Graduate School of Life Science and Agriculture, Tohoku University, 1-1 Tsutsumidori Amamiyamachi, Sendai 981-8555, Japan. E-mail: miyazawa@biochem.tohoku.ac.jp

Abbreviations: CL, chemiluminescence; ESI, electrospray ionization; 7α-ethoxy-5-OOH, 7α-ethoxy-3β-hydroxy-5α-B-homo-6-oxacholestane-5-hydroperoxide; FAB, fast-atom bombardment mode; 7-OOH, 3β-hydroxycholest-5-ene-7-hydroperoxide; NBA, *m*-nitrobenzyl alcohol; TIC, total ion current.

its use as a tool to gain insight into the role of these compounds. Using a chemiluminescence detection-HPLC system with on-line MS (HPLC-CL-MS), which we previously developed to measure ozonized phospholipids sensitively and selectively (15), we found that 7α-ethoxy-3β-hydroxy-5α-B-homo-6-oxacholestane-5-hydroperoxide (termed "7α-ethoxy-5-OOH") is a major product of cholesterol ozonolysis carried out in an ethanol-containing aqueous or nonaqueous solvent. In addition, we confirmed that 7α-ethoxy-5-OOH is highly toxic for human lung tumor cells.

EXPERIMENTAL PROCEDURES

Materials. Cholesterol and FBS were purchased from ICN Biomedicals Inc. (Aurora, OH). The 3β-hydroxycholest-5-ene-7-one and RPMI-1640 medium were obtained from Sigma (St. Louis, MO). Human lung adenocarcinoma A549 cells (TKG0184) were from the Cell Resource Center for Biomedical Research at Tohoku University School of Medicine (Sendai, Japan). All other reagents were of analytical grade.

Generation of ozone. An EO-301 ozonator (Okano Works, Osaka, Japan) was used for generating a 1.3% ozone-in-oxygen stream. Cholesterol sample solutions were bubbled at a flow rate of 100 mL/min under various conditions as described below.

Ozonation of cholesterol in chloroform/ethanol. Cholesterol (460 mg) was dissolved in 100 mL of chloroform/ethanol (1:1, vol/vol) and treated with ozone gas for 20 min under ice-cold conditions (7). After ozonation, the reaction mixture was dried and redissolved in 10 mL of chloroform. An aliquot portion (10 μL) was subjected to HPLC-CL-MS (detailed conditions as described below) for monitoring the yields of ozonized lipids.

Ozonation of cholesterol in water. Cholesterol (100 mg) was dissolved in 50 mL of acetone and then mixed with water (120 mL). The resultant mixture (170 mL) was concentrated to nearly 100 mL in a rotary evaporator. A 50-mL portion of the concentrated aqueous dispersion (containing 50 mg of cholesterol) was treated with ozone gas for 1 h at room temperature. After that, 50 mL of chloroform was added to the reaction mixture, shaken vigorously, and centrifuged at $1000 \times g$ for 10 min. The organic layer was collected, evaporated, and redissolved in 10 mL of chloroform. A 10-μL sample of the chloroform solution was subjected to HPLC-CL-MS.

Ozonation of cholesterol in water/ethanol. Cholesterol (50 mg) in 100 mL of water/ethanol (1:1) was ozonized for 1 h at room temperature. The ozonation products were extracted with chloroform and analyzed by HPLC-CL-MS.

HPLC analysis. For the HPLC-CL-MS system (15), an ODS column (TSK-gel 80Ts, 5 μm, 4.6 × 250 mm; Tosoh, Tokyo, Japan) was used. The column was eluted using a binary gradient, consisting of the following HPLC solvents: A (water) and B (methanol). Ammonium acetate (0.1 mM) was added to both mobile phases A and B. The gradient profile was as follows: 0–10 min, 90% B; 10–15 min, 90–100% B linear; 15–30 min, 100% B. The flow rate was adjusted to 1 mL/min, and the column temperature was maintained at 40°C. At the postcolumn, the eluent was split. One of the eluents (flow rate, 0.95 mL/min) was mixed with the hydroperoxide-specific CL reagent (a mixture of cytochrome *c* and luminol in 50 mM borate buffer, pH 10) (16,17) and sent to a JASCO 825-CL detector (Japan Spectroscopic Co., Tokyo, Japan). The flow rate of CL reagent was 0.9 mL/min. The other column eluent (flow rate, 0.05 mL/min) was sent to a Mariner electrospray ionization (ESI)/time-of-flight mass spectrometer (Applied Biosystems, Farmington, MA). Parameters for MS were positive-ion measurement mode, a spray voltage of 1900 V, a nozzle potential of 150 V, and a nozzle temperature of 150°C. The flow rate of nebulizer gas was 0.3 mL/min. Full scan spectra were obtained by scanning ions between *m/z* 300 and 900 at 4 s/scan.

Identification procedures. By using the HPLC technique, ozonized cholesterol was isolated and purified from the sample reaction mixture, and its chemical structure was characterized by the following spectroscopic procedures. The mass of the purified ozonation product was determined using a JEOL-JMS-700 mass station (JEOL, Tokyo, Japan) in fast-atom bombardment mode (FAB). FAB-MS measurement was performed in the positive and negative mode with *m*-nitrobenzyl alcohol (NBA) as a matrix. ^{1}H and ^{13}C NMR spectra were recorded on a Varian Unity 600 spectrometer (Varian, Palo Alto, CA) at 600 MHz for ^{1}H NMR and at 150 MHz for ^{13}C NMR using $CDCl_3$ as a solvent. The IR spectrum was assayed using JEOL JIR-5500.

Cytotoxicity of ozonide. Lung adenocarcinoma A549 cells were seeded on 96-well culture plates at densities of 1×10^4 cells/well in 100 μL of RPMI-1640 medium containing 10% FBS, penicillin G (100 units/mL), and streptomycin (100 μg/mL). After incubation at 37°C in a 5% CO_2 incubator for 24 h, the culture medium was replaced with 100 μL of FBS-free medium containing test samples at various concentrations. Twenty-four hours later, 50 μL of 3-(4,5-dimethylthiazol-2-yl)-2,5-diphenyl tetrazolium bromide solution was added to each well for evaluating cell viability (18). After 3 h of incubation, cells were washed with 0.2 mL of PBS, resuspended in 200 μL of 2-propanol containing 0.04 N HCl, and left in the dark for 10 min. The plates were measured by a microplate reader (Elx 800; Bio-Tek Instruments Inc., Winoski, Vermont) with a wavelength of 570 nm and a reference wavelength of 630 nm.

Statistical analysis. The data were expressed as the mean ± SD. Statistical comparisons were made with Student's *t*-test.

RESULTS AND DISCUSSION

Among three different reaction conditions, we first tested the chloroform/ethanol system. Figure 1A shows the typical total ion current (TIC) chromatogram, when ozone gas-exposed cholesterol in chloroform/ethanol (1:1) was subjected to HPLC-CL-MS. After ozonation, cholesterol itself was completely decomposed, and two large peak components ***1*** and ***2*** appeared as the main ozonation products in the TIC chromatogram (Fig. 1A). Peaks ***1*** (retention time = 18 min) and ***2*** (25

min) gave clear ESI/MS spectra (ions at *m/z* 497 for ***1*** and 434, 416 for ***2***) (Figs. 1B and 1C). In the CL chromatogram, both ***1*** and ***2*** gave intense chemiluminescence peaks (retention time of 18 min for ***1*** and 25 min for ***2***) (Fig. 1D), indicating that both peak components might possess hydroperoxide groups.

To determine the chemical structures of compounds ***1*** and ***2***, these components were isolated by HPLC, and their structures were determined using FAB-MS and NMR. Peak ***2*** was identified as the ethoxy-hydroperoxide, 7α-ethoxy-3β-hydroxy-5α-B-homo-6-oxacholestane-5-hydroperoxide (7α-ethoxy-5-OOH, Scheme 2): (–) FAB-MS (70 eV, NBA) $[M - H]^-$ *m/z* 479; (+) FAB-MS (70 eV, NBA) $[M - CH_3CH_2OH - H_2O + H]^+$ *m/z* 417; ESI-MS *m/z* 434, 416; m.p. 133–135°C; IR (KBr) 3275, 1169, 1142, 1068, 1041, 1016, 987, 953 cm^{-1}. ^1H NMR ($CDCl_3$:δ): 2.00 (2H, *m*, 7a-H), 2.65 (1H, *d*, 4α-H), 3.99 and 3.58 (2H, AB *x* 3 *m*, $O\underline{C}H_2CH_3$), 3.89 (1H, *m*, 3α-H), 4.74 (1H, *t*, 7-H), 10.26 ppm (1H, *s*, 5-OOH). ^{13}C NMR ($CDCl_3$:δ): 15.1 ($OCH_2\underline{C}H_3$), 63.9 ($O\underline{C}H_2CH_3$), 66.8 (C-3), 100.7 (C-7), 111.8 ppm (C-5). In the ^1H NMR measurement, an important signal at δ10.26, characteristic of the hydroperoxide group, was clearly confirmed (Fig. 2). Considering the structure of 7α-ethoxy-5-OOH, the unknown ESI/MS spectrum of peak 2 from the HPLC-CL-MS analysis (Fig. 1C) would correspond to the fragment ions of 7α-ethoxy-5-OOH: $[M - CH_3CH_2OH]^+$ *m/z* 434 and $[M - CH_3CH_2OH - H_2O]^+$ *m/z* 416. On the other hand, peak component ***1*** (*m/z* 497 in the ESI/MS analysis) was speculated to be a novel ozonized cholesterol. The amount of component ***1*** available in the present study was not sufficient to carry out NMR and other identification procedures. Therefore, the structure of component ***1*** could not be determined.

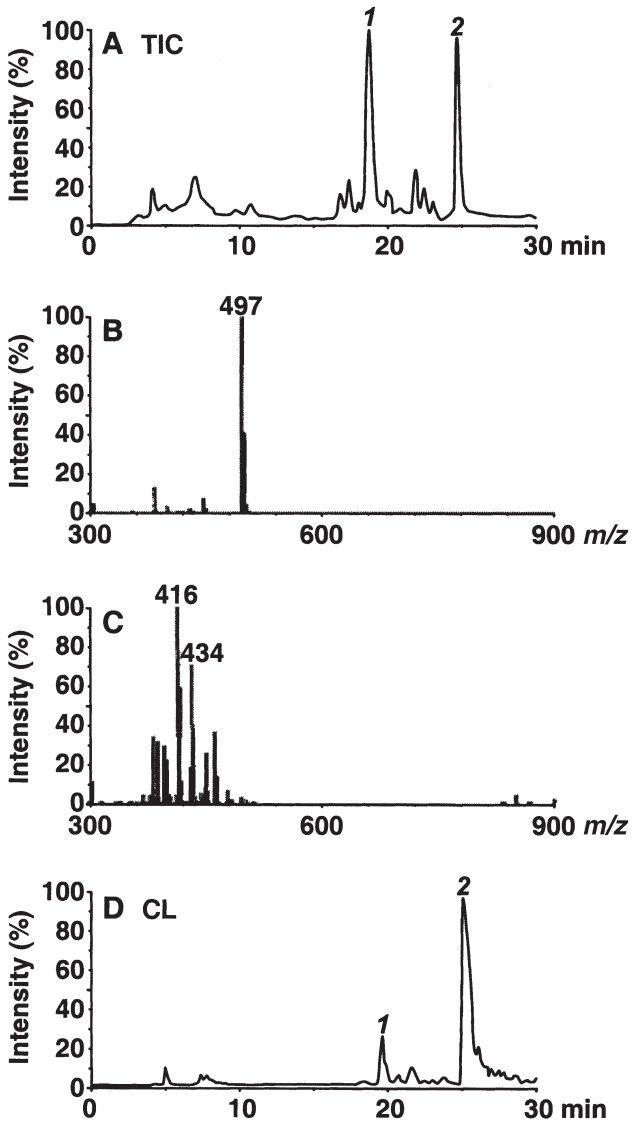

FIG. 1. Ozonation products of cholesterol in chloroform/ethanol system. Cholesterol (460 mg) in chloroform/ethanol (1:1) was exposed to ozone gas for 20 min and analyzed by HPLC-CL-MS. (A) Total ion current (TIC) chromatogram; (B) mass spectrum of peak ***1*** (18 min) detected in chromatogram A; (C) mass spectrum of peak ***2*** (25 min) in chromatogram A; (D) chemiluminescence (CL) chromatogram.

In our opinion, the ozonation that takes place in aqueous environments (rather than in organic solvent) better reflects the reaction of lipids with ozone gas that actually occurs in food and biological samples. However, little is known about cholesterol ozonation in aqueous systems, except for the study by Gumulka and Smith (7). Thus, we then investigated the reaction of cholesterol with ozone in water/ethanol or in water alone. Figure 3 shows the typical TIC and CL chromatograms of the ozonized cholesterol in water/ethanol (1:1). Peaks ascribed to component ***1*** (retention time = 18 min) and 7α-ethoxy-5-OOH (25 min) were clearly detected in TIC and CL chromatograms, together with another peak component ***3*** (20 min) that produces strong chemiluminescence (Fig. 3). Peak ***3*** showed the molecular ion $[M - H_2O]^+$ *m/z* 400, and the same retention time as the synthetic reference 3β-hydroxycholest-5-ene-7α-hydroperoxide (7α-OOH) and 3β-hydroxycholest-5-ene-7β-hydroperoxide (7β-OOH) (19). Hence, Peak ***3*** was tentatively identified as a mixture of isomers of 7α-OOH and 7β-OOH, which are the well-known oxidized cholesterol. However, the formation of 7α-OOH and 7β-OOH during ozonation has not been reported in the past. Therefore, if such epimeric 7-hydroperoxides are actually formed, this mechanism is interesting. Further study would be needed to elucidate whether 7α-OOH and 7β-OOH arise from ozone action on cholesterol. In the case of cholesterol ozonation in water, component ***1*** and 7α-ethoxy-5-OOH were absent entirely (data not shown). Thus, component ***1*** and 7α-ethoxy-5-OOH would appear to be principal products during ozonation in the presence of alcohol (ethanol).

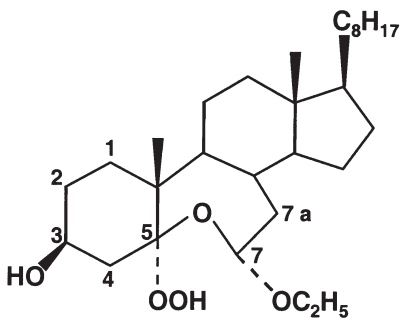

SCHEME 2

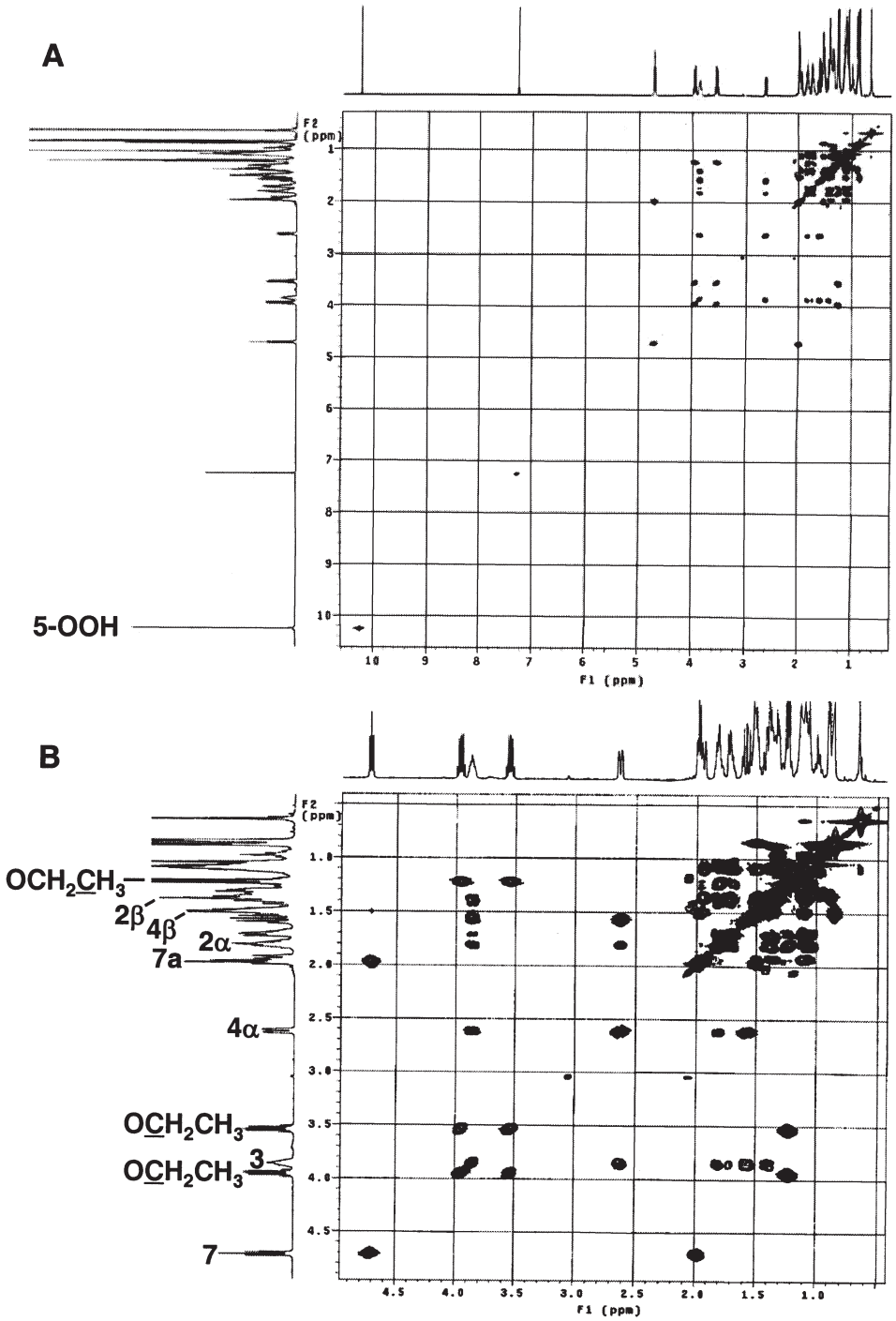

FIG. 2. (A) ^{1}H-^{1}H correlation spectroscopy 2-D NMR spectrum of 7α-ethoxy-3β-hydroxy-5α-B-homo-6-oxacholestane-5-hydroperoxide (7α-ethoxy-5-OOH). (B) An expanded spectrum between 0 and 5.0 ppm.

In considering the present results, it could be rationalized that 7α-ethoxy-5-OOH are formed by the Criegee mechanism (14) during cholesterol ozonation in the presence of ethanol. A possible 7α-ethoxy-5-OOH formation pathway is shown in Scheme 3. The ozonation of cholesterol gives a primary ozonide ***4***, and the ozonide is converted into carbonyl oxide intermediate ***5***. The intramolecular partial capture of ***5*** by the 6-carbonyl oxygen yields the dipolar intermediate ***6***. Ethanol can readily react with the intermediate ***6*** to form 7α-ethoxy-5-OOH. In the presence of water, the intermediate ***6*** reacts with H_2O, which gives secoaldehyde ***7***.

It is generally difficult to characterize the structure of ozonized cholesterol, and caution is required when judging whether ozonized cholesterol possesses a hydroperoxide group. Consequently, a simple and reliable method for characterizing ozonized cholesterol has been highly desired. As

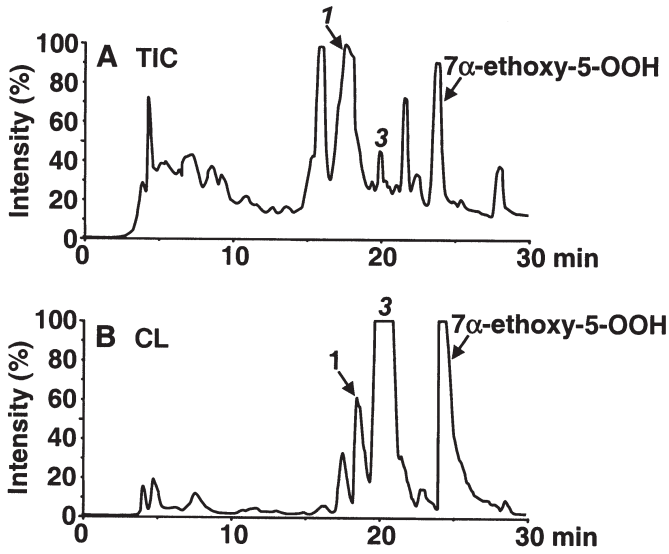

FIG. 3. Ozonation products of cholesterol in water/ethanol system. Cholesterol (50 mg) in water/ethanol (1:1) was exposed to ozone gas for 1 h and then analyzed by HPLC-CL-MS. (A) TIC chromatogram; (B) CL chromatogram. For abbreviations see Figure 1.

shown in Figures 1 and 3, we succeeded in detecting 7α-ethoxy-5-OOH by using the HPLC-CL-MS system. This analytical system can easily identify the cholesterol ozonides bearing a hydroperoxide moiety, because detection by CL is highly specific for the hydroperoxide group (15–17,19–23).

Next, the cytotoxic effect of 7α-ethoxy-5-OOH on human lung adenocarcinoma A549 cells was investigated because the biological role of the cholesterol ozonation products has never been evaluated. We used 3β-hydroxycholest-5-ene-7-one as a reference compound. Treating A549 cells with 7α-ethoxy-5-OOH (1–20 μg/mL), we confirmed that the compound significantly reduced the number of viable cells (Fig. 4). Especially, 20 μg/mL of 7α-ethoxy-5-OOH resulted in an approximately 70% reduction in the viability of lung tumor cells. In contrast, 3β-hydroxycholest-5-ene-7-one was less toxic, even at 20 μg/mL. These results clearly indicated that ethoxyhydroperoxide (7α-ethoxy-5-OOH) arising during cholesterol ozonation is a cytotoxic molecule and that its cytotoxicity is greater than that of 3β-hydroxycholest-5-ene-7-one. This implies that ozonized cholesterol may be more toxic than autoxidized cholesterol.

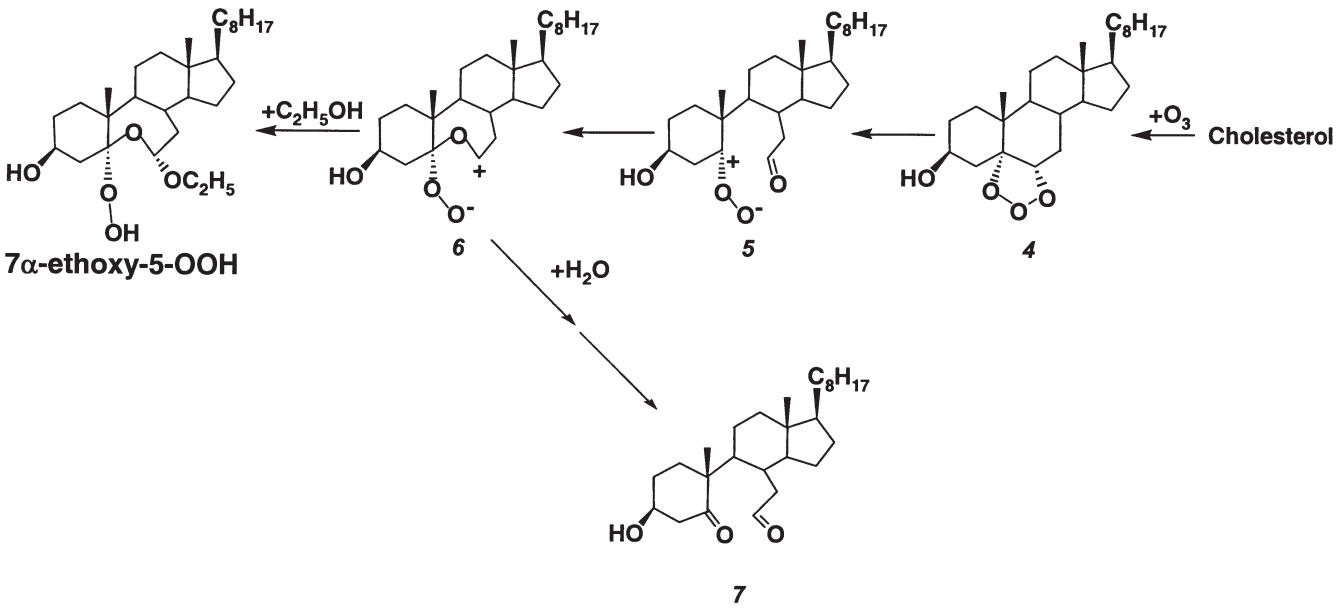

SCHEME 3

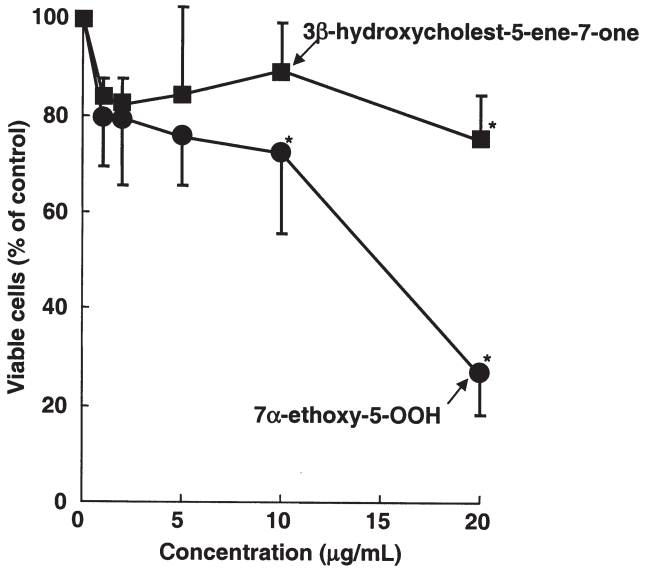

FIG. 4. Effects of increasing concentrations of 7α-ethoxy-3β-hydroxy-5α-B-homo-6-oxacholestane-5-hydroperoxide (7α-ethoxy-5-OOH) and 3β-hydroxycholest-5-ene-7-one on the viability of human lung adenocarcinoma A549 cells. Cells were incubated in medium containing 7α-ethoxy-5-OOH (●) or 3β-hydroxycholest-5-ene-7-one (■) at concentrations from 0 (control) to 20 μg/mL for 24 h. The viable cells were then assessed by the 3-(4,5-dimethylthiazol-2-yl)-2,5-diphenyltetrazolium bromide assay. Data are expressed as mean ± SD; $n = 6$. $^*P < 0.05$ as compared to control cells.

As for the sterilization of foods, the use of a combination of different disinfection procedures (i.e., treatment with ozone together with alcohol or UV light) was recently recommended to enhance bactericidal effect (24,25). If one is applying ozone/ethanol treatment for food disinfection, 7α-ethoxy-5-OOH may be formed from food cholesterol. This compound would be toxic due to its highly reactive hydroperoxide group, thereby influencing the quality and flavor of food. Our HPLC-CL-MS system might be used to elucidate compounds formed by ozone-sterilization of foods, since CL detection enables easy identification of the hydroperoxide structure.

REFERENCES

1. Moore, G., Griffith, C., and Peters, A. (2000) Bactericidal Properties of Ozone and Its Potential Application as a Terminal Disinfectant, *J. Food Prot. 63*, 1100–1106.
2. Pryor, W.A., Wang, K., and Bremudez, E. (1991) The Ozonation of Unsaturated Fatty Acids: Aldehydes and Hydrogen Peroxide as Products and Possible Mediators of Ozone Toxicity, *Chem. Res. Toxicol. 4*, 341–348.
3. Santrock, J., Gorski, R.A., and O'Gara, J.F. (1992) Products and Mechanism of the Reaction of Ozone with Phospholipids in Unilamellar Phospholipid Vesicles, *Chem. Res. Toxicol. 5*, 134–141.
4. Pryor, W.A., and Wu, M. (1992) Ozonation of Methyl Oleate in Hexane, in a Thin Film, in SDS Micelles, and in Distearoylphosphatidylcholine Liposomes: Yields and Properties of the Criegee Ozonide, *Chem. Res. Toxicol. 5*, 505–511.
5. Squandrito, G.L., Uppu, R.M., Cueto, R., and Pryor, W.A. (1992) Production of the Criegee Ozonide During the Ozonation of 1-Palmitoyl-2-oleoyl-*sn*-glycero-3-phosphocholine Liposomes, *Lipids 27,* 955–958.
6. Mudd, J.B., Dawson, P.J., and Santrock, J. (1997) Ozone Does Not React with Erythrocyte Membrane Lipids, *Arch. Biochem. Biophys. 341,* 251–266.
7. Gumulka, J., and Smith, L.L. (1983) Ozonization of Cholesterol, *J. Am. Chem. Soc. 105,* 1972–1979.
8. Jaworski, K., and Smith, L.L. (1988) Ozonization of Cholesterol in Nonparticipating Solvents, *J. Org. Chem. 53,* 545–554.
9. Pryor, W.A., Wang, K., and Bremudez, E. (1992) Cholesterol Ozonation Products as Biomarkers for Ozone Exposure in Rats, *Biochem. Biophys. Res. Commun. 188,* 618–623.
10. Wang, K., Bremudez, E., and Pryor, W.A. (1993) The Ozonation of Cholesterol: Separation and Identification of 2,4-Dinitrophenylhydrazine Derivatization Products of 3β-Hydroxy-5-oxo-5,6-secocholestan-6-al, *Steroids 58,* 225–228.
11. Jaworski, K., and Smith, L.L. (1988) Nuclear Magnetic Resonance and Infrared Spectral Characterization of Some Peroxysterols, *Magn. Reson. Chem. 26,* 104–107.
12. Paryzek, Z., Martynow, J., and Swoboda, W. (1990) The Reaction of Cholesterol with Ozone and Alcohols: A Revised Mechanism and Structure of the Principal Product, *J. Chem. Soc., Perkin Trans. 1,* 1222–1223.
13. Smith, L.L., Ezell, E.L., and Jaworski, K. (1996) On the Ozonization of Cholesterol 3-Acyl Esters in Protic Media, *Steroids 61,* 401–406.
14. Paryzek, Z., and Urszula, R. (1997) Ozonolysis of Cholesterol and Other 5-Steroids in the Presence of Alcohols: A Revised Mechanism and Hydroperoxide Structure of the Solvent-Participated Product, Confirmed by X-Ray Analysis, *J. Chem. Soc., Perkin Trans. 2,* 2313–2318.
15. Tagiri-Endo, M., Ono, K., Nakagawa, K., Yotsu-Yamashita, M., and Miyazawa, T. (2002) Ozonation of PC in Ethanol: Separation and Identification of a Novel Ethoxyhydroperoxide, *Lipids 37,* 1007–1012.
16. Miyazawa, T., Suzuki, T., Fujimoto, K., and Yasuda, K. (1992) Chemiluminescent Simultaneous Determination of Phosphatidylcholine Hydroperoxide and Phosphatidylethanolamine Hydroperoxide in the Liver and Brain of the Rat, *J. Lipid Res. 33,* 1151–1159.
17. Miyazawa, T., Fujimoto, K., Suzuki, T., and Yasuda, K. (1994) Determination of Phospholipid Hydroperoxides Using Luminol Chemiluminescence–High-Performance Liquid Chromatography, *Methods Enzymol. 233,* 324–332.
18. Sladowski, D., Steer, S.J., Clothier, R.H., and Balls, M. (1993) An Improved MTT Assay, *J. Immunol. Methods 157,* 203–207.
19. Adachi, J., Asano, M., Naito, T., Ueno, Y., and Tatsuno, Y. (1998) Chemiluminescence Detection of Cholesterol Hydroperoxide in Human Erythrocyte Membrane, *Lipids 33,* 1235–1240.
20. Miyazawa, T. (1989) Determination of Phospholipid Hydroperoxides in Human Blood Plasma by a Chemiluminescence– HPLC Assay, *Free Radic. Biol. Med. 7,* 209–217.
21. Miyazawa, T., Yamashita, T., Fujimoto, K., and Yasuda, K. (1992) Chemiluminescence Detection of 8α-Hydroperoxy-tocopherone in Photooxidized α-Tocopherol, *Lipids 27,* 289–294.
22. Khono, T., Sakamoto, O., Nakamura, T., and Miyazawa, T. (1993) Determination of Human Skin Surface Lipid Peroxides by Chemiluminescence–HPLC, *J. Jpn. Oil Chem. Soc. 42,* 204–209.
23. Miyazawa, T., Kunika, H., Fujimoto, K., Endo, Y., and Kaneda, T. (1995) Chemiluminescence Detection of Mono-, Bis-, and Tris-hydroperoxy Triacylglycerols Present in Vegetable Oils, *Lipids 30,* 1001–1006.
24 Naito, S. (1989) Effect of Ozone Treatment on Elongation of Hypocotyls and Microbial Counts of Bean Sprouts (in Japanese), *Nippon Shokuhin Kogyo Gakkaishi 36,* 181–188.
25. Naito, S. (1990) Effect of Ozone Treatment on the Rheological Properties of Wheat Flour (in Japanese), *Nippon Shokuhin Kogyo Gakkaishi 37,* 810–813.

[Received August 18, 2003, and in final form February 20, 2004; revision accepted February 27, 2004]

Identification of Minor Fatty Acids and Various Non-methylene-interrupted Diene Isomers in Mantle, Muscle, and Viscera of the Marine Bivalve *Megangulus zyonoensis*

H. Kawashima[a,*] and M. Ohnishi[b]

[a]Bioscience Laboratory, Miyako College Division, Iwate Prefectural University, Iwate 027-0039, Japan, and
[b]Department of Bioresource Science, Obihiro University of Agriculture and Veterinary Medicine, Hokkaido 080-8555, Japan

ABSTRACT: To clarify the occurrence of nonmethylene-interrupted (NMI) FA in the marine bivalve *Megangulus zyonoensis,* methyl esters of unsaturated FA were fractionated according to the degree of their unsaturation by using argentation TLC. Their structures were elucidated by using GC–MS of their FAME and 2-alkenyl-4,4-dimethyloxazoline derivatives. Seventy-two unsaturated FA, including the novel 7,15-21 and 20:4n-1, were identified. The unusual tetraenoic acids 20:4n-4, 20:4n-1, 21:4n-6, and 21:4n-5 were found in *M. zyonoensis.* This bivalve was extremely rich in the positional isomers of 19:1, 20:2, and 20:3. The distribution of NMI and positional isomers of unusual FA in the bivalve tissues was also discussed.

Paper no. L9427 in *Lipids 39,* 265–271 (March 2004).

Nonmethylene-interrupted (NMI) FA and particularly C_{20} and C_{22} dienoic acids have frequently been found in lipids of many marine invertebrates (1,2), but their physiological function is not fully understood. NMI FA in the phospholipid membranes of marine bivalves may act as inhibitors of lipid peroxidation processes (3), and a competitive incorporation rate into lipids may exist between NMI dienoic acids and n-3 PUFA in marine organisms (4). Of great importance to physiological and biochemical studies of marine mollusks may be the accurate determination of both NMI FA and PUFA (5,6).

In Japan the marine bivalve *Megangulus* is a valuable food resource because of its soft flesh texture, rich sweetness, and good taste. However, the FA composition and distribution in *Megangulus* have not been investigated except for our studies. We had previously analyzed various tissue lipids from the marine bivalves *M. venulosus* and *M. zyonoensis* to compare the occurrence and distribution of their FA (7). Typical NMI dienoic acids, 7,13-22:2 and 7,15-22:2, were identified in mainly the mantle and muscle, but not in the viscera. Thus, this study focused on the identification and distribution of minor unsaturated FA in *M. zyonoensis,* especially in relation to the possible biosynthesis of NMI unsaturated FA and the positional isomer distribution of unusual unsaturated FA in various tissue lipids. We have also identified minor polyenoic FA with even- and odd-numbered carbon chains that have not previously been reported.

*To whom correspondence should be addressed at Bioscience Laboratory, Miyako College Division, Iwate Prefectural University, Iwate 027-0039, Japan. E-mail: ajoe@iwate-pu.ac.jp

Abbreviations: DMOX, 4,4-dimethyloxazoline; ECL, equivalent chain length; NMI FA, nonmethylene-interrupted fatty acids.

EXPERIMENTAL PROCEDURES

Materials, lipid extraction, and preparation of FAME. Megangulus zyonoensis was harvested wild from the sea and was obtained from a local fish market (Tomakomai Fishermen's Cooperative Association, Hokkaido, Japan) in April 2002. Dissected tissues were suspended in a chloroform/methanol mixture (2:1, vol/vol), and were then homogenized for 30 s at $861 \times g$ by using an IKA Ultra-Turrax® T25 Basic (IKA Japan KK, Nara, Japan) for cell disruption. Lipids were then extracted by using the method of Bligh and Dyer (8). The extracted total lipids were converted to FAME by direct transesterification with 14% BF_3/methanol for 1 h at 100°C in a screw-capped tube (9). FAME were purified by using TLC on Kieselgel 60G plates (Merck Co., Darmstadt, Germany) with *n*-hexane/diethyl ester (80:20, vol/vol) for development.

Argentation TLC. FAME were fractionated according to the degree of unsaturation by argentation TLC on 5% (w/w) silver nitrate-impregnated layers of Kieselgel 60G with development in *n*-hexane/diethyl ester (80:20, vol/vol). The plates were sprayed with a solution of 2′,7′-dichlorofluorescein and viewed under UV light. Bands corresponding to saturated, monoenoic, dienoic, trienoic, tetraenoic, and pentaenoic acids were separately scraped off and transferred to test tubes; and methanol (1 mL), *n*-hexane (2 mL), and a solution of NaCl (6% wt/vol, 1 mL) were successively added with thorough mixing after each addition. The nonpolar phase was evaporated under a stream of N_2, and the residue was dissolved in chloroform to prepare 4,4-dimethyloxazoline (DMOX) derivatives.

Analysis of DMOX. DMOX derivatives were prepared by adding 200 μL of 2-amino-2-methyl-1-propanol to the fractionated methyl esters in screw-capped tubes. The tubes were flushed for 1 min with N_2, capped, and heated at 185°C overnight (10). The reaction mixture was cooled and then was dissolved in 2 mL of dichloromethane, which was washed

three times with 2 mL of distilled water. After drying the organic phase with anhydrous Na_2SO_4, the dichloromethane phase was removed under a stream of N_2. The samples were dissolved in *n*-hexane for analysis by GC–MS. Most of the unsaturated FA in the present work coincide with those of commercial standards and other known FA using DMOX and picolinyl derivatives (11).

Hydrogenation of FAME. FAME were hydrogenated by stirring for 1 h at 20°C in *n*-hexane with catalytic amounts of palladium black (Wako Pure Chemical Industries, Ltd., Osaka, Japan).

GLC and GC–MS. FAME were analyzed by using GLC with a Shimadzu GC-8A instrument (Shimadzu Seisakusho Co., Kyoto, Japan) equipped with an FID and a SUPELCOWAX™-10 capillary column (30 m × 0.25 mm i.d., 0.25 μm film thickness; Supelco Inc., Bellefonte, PA). The column temperature was either isothermal at 220°C or programmed from 150 to 220°C (2°C/min). The injector and detector temperatures were 250 and 260°C, respectively. The carrier gas was helium at a flow rate of 1.5 mL/min. FAME and DMOX derivatives were analyzed by using GC–MS with a Hewlett-Packard Agilent 5973N MSD and an Agilent 6890N GC (Hewlett-Packard, Palo Alto, CA) equipped with an Omegawax™-320 capillary column (30 m × 0.32 mm i.d., 0.25 μm film thickness; Supelco Inc.). The column temperature was programmed as follows: isothermal at 150°C for 3 min, increased from 150 to 190°C (5°C/min), and then from 190 to 210°C (1°C/min), where the temperature was maintained for 30 min. All spectra were recorded at an ionization energy of 70 eV (electron impact ionization). FAME and DMOX derivatives were identified by comparing their retention times with those of authentic standards and other known FA and were confirmed by GC–MS. The proportion of each component was calculated from the total isomers and total FA. Analyses in all cases were done in duplicate with the results expressed as mean values. Most standard reagents used in this study were purchased from Sigma Chemical Co. (St. Louis, MO).

RESULTS

GLC analysis of typical FAME from *M. zyonoensis* is shown in Figure 1. Table 1 lists 72 unsaturated FA of *M. zyonoensis* that were identified by their FAME and DMOX derivatives. *Megangulus zyonoensis* was rich in the positional isomers of heptadecenoic (17:1), octadecenoic (18:1), nonadecenoic (19:1), eicosadienoic (20:2), eicosatrienoic (20:3), and eicosatetraenoic (20:4) acids. The most interesting characteristic was the presence of long-chain (C_{18}, C_{20}) n-7, n-4, and n-1 PUFA in *M. zyonoensis.* Table 2 lists the characteristic mass spectrometric fragments of DMOX derivatives of unsaturated FA.

In the diene fraction, 8 NMI dienoic acids, 5,11-18:2, 5,11-20:2, 5,13-20:2, 7,13-20:2, 7,13-21:2, 7,15-21:2, 7,13-22:2,

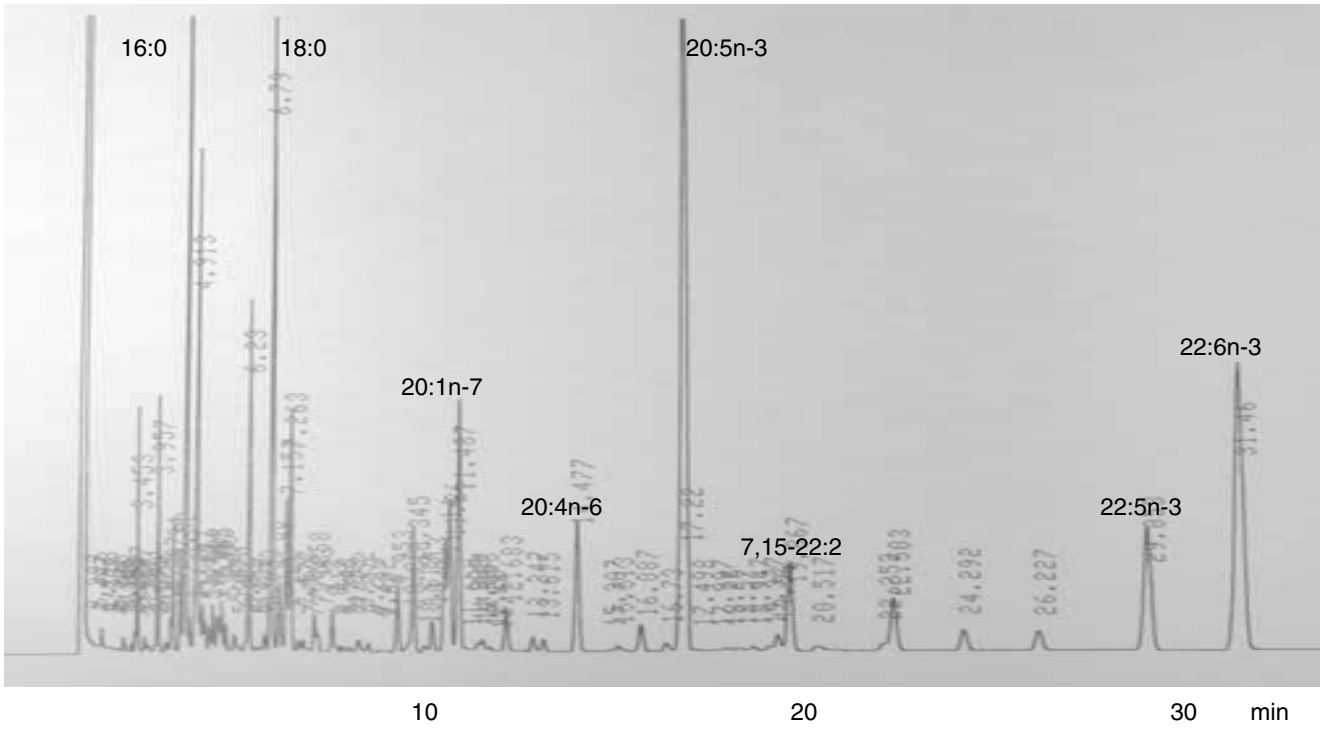

FIG. 1. Gas chromatogram of FAME from the total lipids of *Megangulus zyonoensis* (SUPELCOWAX™-10; Supelco, Bellefonte, PA; column temperature of 220°C).

TABLE 1
Identification of 4,4-Dimethyloxazoline Derivatives in Different Fractions of PUFA in the Lipids from Whole *Megangulus zyonoensis*

FA	RT (min)[a]	Molecular ion (*m/z*)	FA	RT (min)	Molecular ion (*m/z*)
Monoene			Diene (cont.)		
14:1n-5	2.72	279	7,13-21:2	13.42	375
15:1n-8	3.26	293	7,15-21:2	13.68	375
15:1n-6	3.30	293	7,13-22:2	16.87	389
16:1n-10	3.99	307	7,15-22:2	17.25	389
16:1n-7	4.04	307	22:2n-7	18.05	389
16:1n-5	4.16	307	22:2n-6	18.45	389
17:1n-8	5.04	321			
17:1n-7	5.12	321	Triene		
17:1n-6	5.19	321	16:3n-4	4.95	303
17:1n-3	5.37	321	18:3n-6	7.54	331
18:1n-13	6.22	335	18:3n-4	8.02	331
18:1n-9	6.36	335	18:3n-3	8.29	331
18:1n-7	6.50	335	20:3n-9	11.41	359
18:1n-4	6.85	335	5,11,14-20: 3	11.77	359
19:1n-11	7.91	349	20:3n-6	12.10	359
19:1n-8	8.17	349	20:3n-4	12.85	359
19:1n-7	8.26	349	20:3n-3	13.31	359
19:1n-6	8.41	349	7,13,16-22:3	18.90	387
19:1n-4	8.73	349			
20:1n-13	10.03	363	Tetraene		
20:1n-9	10.28	363	16:4n-1	5.63	301
20:1n-7	10.53	363	18:4n-4	8.49	329
22:1n-9	16.40	391	18:4n-3	8.76	329
			18:4n-1	9.18	329
Diene			19:4n-5	10.02	343
16:2n-7	4.34	305	20:4n-6	12.67	357
16:2n-6	4.39	305	20:4n-4	13.45	357
16:2n-4	4.63	305	20:4n-3	14.04	357
17:2n-5	5.72	319	20:4n-1	14.67	357
5,11-18:2	6.69	333	21:4n-6	16.02	371
18:2n-7	6.99	333	21:4n-5	16.44	371
18:2n-6	7.11	333	22:4n-6	20.36	385
18:2n-4	7.48	333			
19:2n-6	9.37	347	Pentaene		
19:2n-4	9.57	347	20:5n-3	14.71	355
5,11-20:2	10.54	361	21:5n-3	18.77	369
5,13-20:2	10.70	361	22:5n-6	21.57	383
7,13-20:2	10.80	361	22:5n-3	23.36	383
20:2n-7	11.24	361			
20:2n-6	11.48	361	Hexaene		
20:2n-4	12.10	361	22:6n-3	24.81	381

[a]Retention times.

and 7,15-22:2, were identified from *Megangulus*. Among them, 5,11-18:2, 7,13-21:2, and 7,15-21:2 were identified from bivalves for the first time, and 7,15-21:2 probably has not been reported previously from living organisms. However, 5,11-18:2 and 7,13-21:2 have been found, respectively, in the seaweed *Cladophora rupestris* (12) and the white shrimp *Penaeus setiferus* (13). The DMOX derivatives 7,13-21:2 and 7,15-21:2 had a molecular ion at *m/z* = 375, and their double bonds were definitely assigned by the gaps of 12 amu between 168–180 and 250–262, and 168–180 and 278–290, respectively. The structure of 7,15-21:2 was confirmed by the disappearance of the corresponding GC peak upon catalytic hydrogenation and by a molecular ion at *m/z* = 340 and 379 for the corresponding methyl ester and DMOX derivatives. Furthermore, the mass spectrum of the picolinyl ester of 7,15-21:2 had diagnostic peaks at *m/z* = 413 $[M]^+$ (16%) and 206 (8.8%), 232 (2%), 316 (3%), and 342 (11%) for double bonds at positions 7 and 15. In the triene fraction, the DMOX derivatives 5,11,14-20:3 and 7,13,16-22:3 had the characteristic fragments shown in Table 2, and these spectra agreed with their data from other studies (14–16). The presence of both these FA in *Megangulus* is reported here for the first time. In the tetraene fraction, four isomers of 20:4, including 20:4n-6 and 20:4n-3, were detected in our sample. The DMOX derivatives of 20:4n-4 and 20:4n-1 had a molecular ion at *m/z* = 357, and the double bonds of 20:4n-4 were identified individually by ions that differed by 12 amu from *m/z* = 168 to 180, 208 to 220, 248 to 260, and 288 to 300 (16). A double bond at positions 10, 13, and 16 of 20:4n-1 was located by the gaps of 12 amu from *m/z* = 210 to 222, 250 to 262, and 290 to 302 but could only be inferred at position 19. Similar results were obtained for the DMOX and picolinyl ester derivatives of

TABLE 2
Characteristic Mass Spectrometric Fragments of 4,4-Dimethyloxazoline Derivatives of Dienoic, Trienoic, and Tetraenoic Fractions of PUFA in the Lipids from Whole *Megangulus zyonoensis*

FA	Characteristic fragments (*m/z*, relative intensity)
Diene	
16:2n-7	126 (100), 152 (11), 167 (32), 194 (7), 206 (8), 305 (4)
16:2n-6	126 (100), 168 (8), 180 (23), 208 (10), 220 (9), 305 (6)
16:2n-4	126 (100), 196 (8), 208 (3), 236 (11), 248 (4), 305 (18)
17:2n-5	126 (100), 196 (9), 208 (6), 236 (15), 248 (8), 319 (17)
5,11-18:2	113 (100), 153 (10), 222 (2), 262 (2), 333 (1)
18:2n-7	126 (100), 182 (7), 194 (4), 222 (13), 234 (7), 333 (15)
18:2n-6	126 (100), 196 (6), 222 (3), 236 (16), 248 (6), 333 (18)
18:2n-4	113 (100), 224 (5), 236 (5), 264 (17), 276 (6), 333 (28)
19:2n-6	126 (100), 210 (15), 222 (9), 250 (12), 262 (6), 347 (19)
19:2n-4	113 (100), 238 (6), 250 (2), 278 (12), 290 (5), 347 (25)
5,11-20:2	113 (100), 153 (11), 222 (3), 234 (2), 361 (2)
5,13-20:2	113 (100), 153 (11), 250 (1), 262 (1), 361 (5)
7,13-20:2	126 (100), 168 (9), 180 (50), 250 (5), 262 (5), 361 (6)
20:2n-7	113 (100), 210 (7), 222 (7), 250 (23), 262 (5), 361 (23)
20:2n-6	113 (100), 224 (5), 236 (8), 264 (19), 276 (8), 361 (27)
20:2n-4	113 (100), 252 (4), 264 (3), 292 (16), 304 (6), 361 (33)
7,13-21:2	126 (100), 168 (8), 180 (55), 250 (3), 262 (4), 375 (5)
7,15-21:2	126 (100), 168 (7), 180 (26), 278 (4), 290 (2), 375 (9)
7,13-22:2	126 (100), 168 (10), 180 (65), 250 (3), 262 (5), 389 (8)
7,15-22:2	126 (100), 168 (10), 180 (30), 278 (3), 290 (4), 389 (16)
22:2n-7	126 (100), 238 (6), 250 (8), 278 (13), 290 (10), 389 (28)
22:2n-6	126 (100), 252 (5), 264 (3), 292 (21), 304 (8), 389 (24)
Triene	
16:3n-4	126 (100), 152 (11), 167 (18), 194 (9), 206 (6), 234 (4), 246 (3), 303 (4)
18:3n-6	126 (100), 152 (9), 167 (17), 194 (10), 206 (6), 234 (6), 246 (4), 331 (6)
18:3n-4	126 (100), 182 (10), 194 (4), 222 (10), 234 (6), 262 (9), 274 (5), 331 (13)
18:3n-3	126 (100), 196 (6), 208 (3), 236 (12), 248 (7), 276 (13), 288 (6), 331 (22)
20:3n-9	113 (100), 153 (20), 180 (7), 192 (6), 220 (7), 232 (4), 359 (7)
5,11,14-20:3	126 (100), 153 (14), 222 (2), 234 (6), 262 (2), 274 (3), 359 (4)
20:3n-6	126 (100), 182 (11), 194 (4), 222 (13), 234 (7), 262 (13), 274 (6), 359 (20)
20:3n-4	126 (100), 210 (6), 222 (6), 250 (14), 262 (6), 290 (16), 302 (6), 359 (29)
20:3n-3	126 (100), 224 (5), 236 (4), 264 (13), 276 (7), 304 (16), 316 (9), 359 (33)
7,13,16-22:3	126 (100), 168 (9), 180 (36), 250 (3), 262 (7), 290 (11), 302 (6), 387 (14)
Tetraene	
16:4n-1	126 (100), 152 (8), 167 (17), 194 (9), 206 (11), 234 (5), 246 (4), 301 (3)
18:4n-4	113 (100), 153 (21), 180 (4), 192 (4), 220 (3), 232 (3), 260 (1), 272 (1), 329 (3)
18:4n-3	126 (100), 152 (9), 167 (17), 194 (9), 206 (7), 234 (8), 246 (5), 274 (3), 286 (3), 329 (5)
18:4n-1	126 (100), 182 (10), 194 (5), 222 (8), 234 (7), 262 (6), 274 (6), 329 (6)
19:4n-5	113 (100), 153 (23), 180 (5), 192 (4), 220 (6), 232 (2), 260 (2), 272 (1), 343 (4)
20:4n-6	113 (100), 153 (24), 180 (5), 192 (4), 220 (6), 232 (3), 260 (2), 272 (1), 357 (4)
20:4n-4	126 (100), 168 (8), 180 (33), 208 (15), 220 (10), 248 (15), 260 (7), 288 (4), 300 (6), 357 (11)
20:4n-3	126 (100), 182 (11), 194 (4), 222 (11), 234 (5), 262 (16), 274 (6), 302 (5), 314 (5), 357 (11)
20:4n-1	126 (100), 210 (4), 222 (5), 250 (9), 262 (7), 290 (15), 302 (6), 357 (14)
21:4n-6	126 (100), 152 (11), 167 (20), 194 (10), 206 (22), 234 (11), 246 (7), 274 (3), 286 (2), 371 (7)
21:4n-5	126 (100), 168 (8), 180 (23), 208 (11), 220 (8), 248 (16), 260 (9), 288 (7), 300 (4), 371 (8)
22:4n-6	126 (100), 168 (9), 180 (38), 208 (9), 220 (3), 248 (20), 260 (7), 302 (4), 314 (7), 385 (10)

16:4n-1 and 18:4n-1, which had double bonds at terminal positions 15 and 17, respectively. The position of a terminal double bond in n-1 PUFA was further confirmed by analysis of its methyl ester spectra. The methyl ester spectrum of 20:4n-1 had a molecular ion at *m/z* =318 $[M]^+$ (0.9%) and a typical characteristic ion at *m/z* = 277 $[M - 41]^+$ (4.2%), indicating the presence of a terminal double bond. The mass spectrum of the picolinyl ester of 20:4n-1 {395 $[M]^+$ (15%) and 248 (4%), 274 (12%), 288 (5%), 314 (24%), 328 (5%), and 354 (13%)} was similar to the result obtained with the DMOX derivative. Equivalent chain length (ECL) values for methyl esters of 18:4n-4, 18:4n-1, 20:4n-4, and 20:4n-1 were 19.50, 19.84, 21.52, and 21.83 on SUPELCOWAX-10 at 220°C, respectively. The difference in ECL values (Δ ECL) for 20:4n-4 and 20:4n-1 can be compared with the Δ ECL of the only other n-4/n-1 FAME pair (18:4n-4 and 18:4n-1). The Δ ECL for 20:4n-4/20:4n-1 and 18:4n-4/18:4n-1 was 0.31 and 0.34, respectively. From these data, the terminal double bond at

position 19 was finally identified (20:4n-1). As far as we know, 20:4n-1 has been identified from living organisms for the first time in this study. In addition, the two isomers of heneicosatetraenoic acid (21:4), 21:4n-6 and 21:4n-5, were also identified.

To show how the distribution of NMI FA components of *M. zyonoensis* is related to their possible biosynthesis in the bivalve, the FA and isomers of *M. zyonoensis* in various tissues were analyzed for comparison among tissue lipids (Table 3). The major monoene acids 17:1n-8 and 18:1n-7 were most abundant in the muscle. The positional isomers of C_{17} and C_{19} monoene acids had high proportions of n-6 and n-8 FA, which were predominantly found in the muscle. Among monoene acids, the isomer composition of 19:1 in the mantle differed considerably from that of other tissues. Among even-chain monoene acids, both 18:1n-7 and 20:1n-7 were most abundant in all tissues, and their proportions were more than about 60 and 50%, respectively, of the total isomers. The main isomers of 17:1 and 19:1 differed from those of even-chain monoenes according to the tissue of *M. zyonoensis.* A high proportion of the unique FA 16:2n-4 was found in the mantle and muscle, but it was much lower in the viscera. In addition, two other isomers of 16:2, 16:2n-7 and 16:2n-6, were also detected. In particular, *M. zyonoensis* was extremely rich in the positional isomers 20:2 and 20:3, even though they were considerably less than for eicosenoic acid (20:1).

In this study, positional isomers of C_{18}, C_{20}, C_{21}, and C_{22} NMI dienoic acids were widely present in lipids of various tissues. Among the isomers of 18:2, the proportion of 5,11-18:2 detected was relatively low in all tissues examined, even though the proportions of 18:2n-4 and 18:2n-6 were much more than for other isomers. The proportions of 20:2n-6 and 20:2n-4 totaled 75–82% of total 20:2 isomers in lipids of each tissue. The proportion of 7,13-21:2 was much more than that for 7,15-21:2. However, among isomers of docosadienoic acid (22:2), 7,15-22:2 is most abundant in bivalves and other marine invertebrates (7,17,18). Thus, marked differences between tissue lipids and isomer compositions are typical of C_{20}, C_{21}, and C_{22} NMI FA detected in bivalves, but the reason remains unclear.

The proportion of 20:4n-6 was much higher in the mantle and muscle than in the viscera. In contrast, the highest proportions of 20:4n-3 and 20:4n-1 were determined in the

TABLE 3
Distribution of Positional Isomers of Unsaturated FA in Lipids of Various Tissues of *Megangulus zyonoensis*

FA	Mantle	Muscle	Viscera	FA	Mantle	Muscle	Viscera	FA	Mantle	Muscle	Viscera
17:1n-8	61.4	74.0	40.9	5,11-18:2	<0.1	<0.1	2.8	20:3n-9	<0.1	<0.1	<0.1
17:1n-7	<0.1	<0.1	7.6	18:2n-7	<0.1	1.5	2.9	5,11,14-20:3	7.5	6.8	6.4
17:1n-6	13.3	26.0	22.7	18:2n-6	51.4	32.8	31.4	20:3n-6	71.3	51.9	47.3
17:1n-3	25.3	<0.1	28.8	18:2n-4	48.6	65.7	62.9	20:3n-4	15.0	35.1	<0.1
Total[a] 17:1	0.6	0.4	<0.1	Total 18:2	1.1	1.6	1.7	20:3n-3	6.2	6.2	46.3
								Total 20:3	0.4	<0.1	<0.1
18:1n-13	4.3	<0.1	5.0	5,11-20:2	0.9	2.1	4.3				
18:1n-9	32.8	27.3	18.6	5,13-20:2	15.4	5.8	14.9	7,13,16-22:3	100	100	100
18:1n-7	60.8	65.8	66.0	7,13-20:2	5.4	11.0	<0.1	Total 22:3	0.7	0.4	0.5
18:1n-4	2.1	6.9	10.4	20:2n-7	3.0	2.5	1.8				
Total 18:1	5.1	4.2	5.3	20:2n-6	53.3	59.9	64.3	16:4n-1	100	ND[c]	100
				20:2n-4	22.0	18.7	14.7	Total 16:4	<0.1	ND	1.8
19:1n-11	22.1	<0.1	<0.1	Total 20:2	1.5	1.1	1.3				
19:1n-8	26.0	52.0	47.6					18:4n-4	<0.1	6.9	3.5
19:1n-7	34.8	<0.1	<0.1	7,13-21:2	83.1	80.3	79.5	18:4n-3	100	93.1	90.6
19:1n-6	11.6	30.7	21.4	7,15-21:2	16.9	19.7	20.5	18:4n-1	<0.1	<0.1	5.9
19:1n-4	5.5	17.3	31.0	Total 21:2	<0.1	<0.1	<0.1	Total 18:4	0.8	0.8	3.7
Total 19:1	<0.1	<0.1	<0.1								
				7,13-22:2	15.7	3.9	9.1	20:4n-6	87.3	75.9	43.1
20:1n-13	26.4	20.3	17.0	7,15-22:2	84.3	96.1	90.9	20:4n-4	3.5	4.1	2.1
20:1n-9	24.2	31.6	27.7	22:2n-7	<0.1	<0.1	<0.1	20:4n-3	8.3	16.1	44.0
20:1n-7	49.4	48.1	55.3	22:2n-6	<0.1	<0.1	<0.1	20:4n-1	0.9	3.9	10.8
Total 20:1	9.1	7.9	3.7	Total 22:2	5.1	2.4	1.0	Total 20:4	5.3	3.5	3.2
16:2n-7	12.1	<0.1	<0.1	16:3n-4	100	100	100	21:4n-6	59.3	43.2	55.6
16:2n-6	<0.1	23.7	66.9	Total 16:3	<0.1	<0.1	0.8	21:4n-5	40.7	56.8	45.3
16:2n-4	87.9	76.3	33.1					Total 21:4	<0.1	<0.1	<0.1
Total 16:2[b]	0.7	0.4	1.1	18:3n-6	6.4	14.7	10.3				
				18:3n-4	47.6	51.8	74.0	22:4n-6	100	100	100
				18:3n-3	46.0	33.5	15.7	Total 22:4	1.0	0.7	<0.1
				Total 18:3	<0.1	<0.1	0.8				

[a]Percentage of total FA.
[b]Including phytanic acid.
[c]Not detected.

viscera, at 54.8% of total isomers of 20:4 in this study. The unusual isomers 20:4n-4 and 20:4n-1 were found in bivalves for the first time. The unusual isomer 20:4n-4 has been detected only in the diatom *Stauroneis amphioxys* (19) and the shrimp *Rimicaris exculpate* (20) together with 20:4n-6 and 20:4n-3, but 20:4n-1 probably has not been reported previously from living organisms. Among the isomers of 21:4, the proportion of 21:4n-6 in the mantle and viscera was higher than in muscle, at 55.6 to 59.3%. In contrast, the proportion of 21:4n-5 in the muscle was higher than in other tissues.

DISCUSSION

The occurrence and biosynthetic pathway of NMI FA in *M. zyonoensis* is reported here for the first time, although the FA composition of marine bivalves has been examined in many works (1,2,14,17). Eight NMI dienoic acids were detected in all tissues examined, but not in high amounts. The identification of 5,11-20:2, 5,13-20:2, 7,13-22:2, and 7,15-22:2 in this study supports a possible biosynthetic pathway of NMI dienoic acids (Fig. 2). Direct evidence exists of the ability of the bivalve *Scapharca broughtonii* to biosynthesize 7,13-22:2 and 7,15-22:2 from acetate (21). From these results, we speculate that a biosynthetic pathway for NMI dienoic acids 7,13-22:2 and 7,15-22:2, as previously reported for other mollusks, is also present in the marine bivalve *M. zyonoensis.* In *Ginkgo* seeds, 5,11-18:2 was present in predominant occurrence (22), and also found in various marine macrophytes. Therefore, the presence of 5,11-18:2 as 18:2 in *M. zyonoensis* in this study suggests that this FA is probably derived from the diet or is the result of food web effects.

The most interesting series of monoene FA was a family of four heptadecenoic and five nonadecenoic acids with double bonds at delta-9, delta-10, delta-11, or delta-14, and at delta-8, delta-11, delta-12, delta-13, or delta-15, respectively. Among the total isomers of 17:1 and 19:1, the n-8 monoene isomers were present in high proportions and predominated in the muscle and viscera. Odd-chain NMI dienes 7,13-21:2 and 7,15-21:2 and monoenes were detected in *M. zyonoensis*. From these results, we speculate that 7,13-21:2 and 7,15-21:2 are biosynthesized by conversion of 19:1n-8 and 19:1n-6 by Δ-5 desaturation and chain elongation steps, respectively. The putative desaturation products 5,11-19:2 and 5,13-19:2 were not detected in *M. zyonoensis* owing to their very low amounts. That both products were formed suggests the existence of Δ-5 desaturation in bivalves that produce NMI dienoic FA from related monoene FA. The occurrence of 5,13-19:2, together with 5,9,23-nonacosatrienoic and 5,9,23-tricosatrienoic acids as major components, has been reported in the Caribbean sponge *Amphimedon viridis* (23), but not in other organisms. The identification of 5,11-19:2 and 5,13-19:2 in marine bivalves needs to be investigated. However, our results suggest that a novel biosynthetic pathway of odd-chain NMI dienoic FA exists in marine bivalves together with pathways of even-chain NMI dienoic FA 7,13-22:2 and 7,15-22:2, as already reported by Zhukova (21,24). In contrast, the odd-chain NMI FA identified in *M. zyonoensis* may also be of dietary origin because these FA are present in very low concentrations, compared with even-chain NMI dienoic FA. The detection of 5,11,14-20:3 and 7,13,16-22:3 suggests that 7,13,16-22:3 can be biosynthesized in *M. zyonoensis* by Δ-5 desaturation and then by elongation of 20:2n-6. The fact that some isomers of NMI FA have not been reported previously from marine mollusks may be because they are present in amounts that are too small or that analytical studies have not sought them. Therefore, other NMI FA may exist in *M. zyonoensis* that we could not detect. The role of NMI FA in marine bivalves is not well understood. This study should promote research on the distribution and physiological role of odd- and even-chain NMI dienoic acids in mollusks.

I. NMI dienoic acids
(1) 18:1n-9→20:1n-9→5,11-20:2→7,13-22:2
(2) 18:1n-7→20:1n-7→5,13-20:2→7,15-22:2

II. NMI trienoic acids
(3) 9,12-18:2→11,14-20:2→5,11,14-20:3→7,13,16-22:3

FIG. 2. Possible biosynthetic pathways of nonmethylene-interrupted (NMI) dienoic and trienoic acids in *Megangulus zyonoensis.*

In this study, the well-known C_{16} PUFA, 16:2n-4, 16:3n-4, and 16:4n-1, together with 16:2n-7 and 16:2n-6, were detected in the tissues examined, but in very low concentrations. However, 16:3n-4 and 16:4n-1, together with 16:3n-3 and 16:4n-3, were found in *Patella* spp. soft bodies and gonads. These FA were present in very low amounts (below 1%) and were probably linked with the limpet's diet (25).

Although 20:4n-6, 20:4n-4, and 20:4n-3 have been reported from marine invertebrates (19,20), 20:4n-1 probably has not been observed in any living organisms. *Megangulus zyonoensis* was rich in 20:4n-1, at about 11% of the total isomers of 20:4, in viscera lipids. Bivalves have little or no ability to synthesize C_{20} and C_{22} PUFA with more than three double bonds. However, the oyster protozoan parasite *Perkinsus marinus* can synthesize 20:4n-6 from acetate (26), which indicates that isomers of 20:4 may be associated with some symbiotic organisms. In this study, n-4 and n-1 FA from C_{16} to C_{20} were identified as unusual FA components. Future study will be necessary to find out whether the occurrence of 20:4n-4 and 20:4n-1 reflects the consequences of intake from the marine food chain web or *de novo* synthesis. Further studies should include the occurrence and distribution of 20:4n-4 and 20:4n-1 in marine invertebrates.

Although 21:5n-3 is present in small amounts (below 1%) in some bivalves, 21:4n-6 and 21:4n-5 are little known as FA components in marine bivalves and other invertebrates (7,17,21,27). The C_{21} PUFA tend to accumulate in long-lived animals, especially in seals and their fat (1). An entire population of the genus *Megangulus* takes about 10 yr to become sexually mature (28). As 21:5n-3 may be formed from 22:5n-3 by the α-oxidation route, the formation of 21:4n-6 from 22:4n-6 by the same route is also possible. Therefore, our results suggest that 21:4n-6 and 21:5n-3 may be derived from 22:4n-6 and 22:5n-3, respectively, by α-oxidation.

The unusual groups n-7, n-4, and n-1 FA, and the odd-chain isomers C_{17}, C_{19}, and C_{21} as unique components of FA compositions were widely distributed in *M. zyonoensis*. The unusual FA identified in this study should provide a clue to the formation of a novel biosynthetic pathway of polyenoic FA, including NMI FA. Therefore, the identification of a minor NMI FA will give a better understanding of the biological role and function of these FA in marine invertebrates.

ACKNOWLEDGMENTS

This study was supported in part by a Grant-in-Aid for Scientific Research of the Iwate Prefectural Foundation of Academic Research Promotion. We thank Professor S. Ogawa, Iwate University, for his helpful suggestions of the identification of FA, and Professor N. Miyazaki, The University of Tokyo, for encouragement throughout this work. This study was done as a cooperative research program with the International Coastal Research Center, Ocean Research Institute, The University of Tokyo.

REFERENCES

1. Ackman, R.G. (1989) Fatty Acids, in *Marine Biogenic Lipids, Fats, and Oils* (Ackman, R.G., ed.), Vol. 1, pp. 103–137, CRC Press, Boca Raton.
2. Joseph, J.D. (1989) Distribution and Composition of Lipids in Marine Invertebrates, in *Marine Biogenic Lipids, Fats, and Oils* (Ackman, R.G., ed.), Vol. 2, pp. 51–143, CRC Press, Boca Raton.
3. Zakhartsev, M.V., Naumenko, N.V., and Chelomin, V.P. (1998) Non-methylene-Interrupted Fatty Acids in Phospholipids of the Membranes of the Mussel *Crenomytilus grayanus, Russ. J. Mar. Biol. 24*, 183–186.
4. Klingensmith, J.S. (1982) Distribution of Methylene and Non-methylene-Interrupted Dienoic Fatty Acids in Polar Lipids and Triacylglycerols of Selected Tissues of the Hardshell Clam (*Mercenaria mercenaria*). *Lipids 12*, 976–981.
5. Abad, M., Ruiz, C., Martinez, D., Mosquera, G., and Sánchez, J.L. (1995) Seasonal Variations of Lipid Classes and Fatty Acids in Flat Oyster, *Ostrea edulis,* from San Cibran (Galicia, Spain), *Comp. Biochem. Physiol. C 110*,109–118.
6. Labarta, U., Fernández-Reiriz, M.J., and Pére-Camacho, A. (1999) Dynamics of Fatty Acids in the Larval Development, Metamorpohsis and Post-metamorphosis of *Ostrea edulis* (L), *Comp. Biochem. Physiol. A 123*, 249–254.
7. Kawashima, H., and Ohnishi, M. (2003) Fatty Acid Compositions of Various Tissue Lipids in the Marine Bivalves, *Megangulus venulosus* and *Megangulus zyonoensis,* from Coastal Waters of Hokkaido, Northern Japan, *J. Oleo Sci. 52,* 309–315.
8. Bligh, E.G., and Dyer, W.J.. (1959) A Rapid Method of Total Lipid Extraction and Purification, *Can. J. Biochem. Physiol. 37*, 911–917.
9. Morrison, W.R., and Smith, L.M. (1964) Preparation of Fatty Acid Methyl Esters and Dimethylacetals from Lipids with Boron Fluoride-Methanol, *J. Lipid Res. 5*, 600–608.
10. Garrido, J.L., and Medina, I. (1994) One-Step Conversion of Fatty Acids into Their 2-Alkenyl-4,4-dimethyloxazoline Derivatives Directly from Total Lipids, *J. Chromatogr. 673*, 101–105.
11. Destaillats, F., Wolff, R.L., and Angers, P. (2002) Saturated and Unsaturated Anteiso-C_{19} Acids in the Seed Lipids from *Hesperopeuce mertensiana* (Pinaceae), *Lipids 37*, 325–328.
12. Ratnayake, W.M.N., and Ackman, R.G. (1979) Identification of Novel Octadecenoic Fatty Acids in the Seaweed *Cladophora rupestris* Through Oxidative Ozonolysis of the Alcohols Prepared from the Acids, *Lipids 14*, 580–584.
13. Robert, E.P., and Lewis, W.S. (1977) Non-methylene Interrupted and ω-4 Dienoic Acids of the White Shrimp *Penaeus setiferus, Lipids 12*, 544–549.
14. Garrido, J.L., and Medina, I. (2002) Identification of Minor Fatty Acids in Mussels (*Mytilus galloprovincialis*) by GC–MS of Their 2-Alkenyl-4,4-dimethyloxazoline Derivatives, *Anal. Chim. Acta. 465*, 409–416.
15. Scottish Crop Research Institute, http://www.lipid.co.uk/infores/masspec.html (accessed December 2003).
16. Luthria, D.L., and Specher, H. (1993) 2-Alkenyl-4,4-dimethyloxazolines as Derivatives for the Structural Elucidation of Isomeric Unsaturated Fatty Acids, *Lipids 28*, 561–564.
17. Dunstan, G.A., Volkman, J.K., and Barrett, S.M. (1993) The Effect of Lyophilization on the Solvent Extraction of Lipid Classes, Fatty Acids and Sterols from the Oyster *Crassostrea gigas, Lipids 28*, 937–944.
18. Stefanov, K., Seizova, K., Brechny, E.Y., and Christie, W.W. (1992) An Unusual Fatty Acid Composition for a Fresh-water Mussel, *Unio tumidus,* from Bulgaria, *J. Nat. Prod. 55*, 979–981.
19. Cillan, F.T., McFadden, G.I., Wetherbee, R., and Johns, R.B. (1981) Sterols and Fatty Acids of an Antarctic Sea Ice Diatom, *Stauroneis amphioxys, Phytochemistry 20*, 1935–1937.
20. Allen, C.E., Copley, J.T., and Tyler, P.A. (2001) Lipid Partitioning in the Hydrothermal Vent Shrimp *Rimicaris exoculata, Mar. Ecol. 22*, 241–253.
21. Zhukova, N.V. (1986) Biosynthesis of Non-methylene-interrupted Dienoic Fatty Acids from [^{14}C]Acetate in Molluscs, *Biochim. Biophys. Acta 878*, 131–133.
22. Takagi, T., and Itabashi, Y (1982) *cis*-5-Olefinic Unusual Fatty Acids in Seed Lipids of Gymnospermae and Their Distribution in Triglycerols, *Lipids 17*, 716–723.
23. Caraballeira, N.M., and Shalabi, F. (1994) Unusual Lipids in the Caribbean Sponges *Amphimedon viridis* and *Desmapsamma anchorata*, *J. Nat. Prod. 57*, 1152–1159.
24. Zhukova, N.V. (1991) The Pathway of the Biosynthesis of Non-methylene-interrupted Dienoic Fatty Acids in Molluscs, *Comp. Biochem. Physiol. 100B,* 801–804.
25. Brazão, S., Morais, S., Boaventura, D., Ré, P., Narciso, L., and Hawkins, S.J. (2003) Spatial and Temporal Variation of the Fatty Acid Composition of *Patella* spp. (Gastropoda: Prosobranchia) Soft Bodies and Gonads, *Comp. Biochem. Physiol. B 136*, 425–441.
26. Chu, F.-L.E., Lund, E., Soudant, P., and Harvey, E. (2002) *De novo* Arachidonic Acid Synthesis in *Perkinsus marinus*, a Protozoan Parasite of the Eastern Oyster *Crassostrea virginica*, *Mol. Biochem. Parasitol. 119*, 179–190.
27. Murphy, K.J., Mooney, B.D., Mann, N.J., Nichols, P.D., and Sinclair, A.J. (2002) Lipid, FA, and Sterol Composition of New Zealand Green Lipped Mussel (*Perna canaliculus*) and Tasmanian Blue Mussel (*Mytilus edulis*), *Lipids 37*, 587–595.
28. Goshima, S., Nagamoto, K., Kawai, K., and Nakao, S. (1991) Reproductive Cycle and Growth of the Northern Great Tellin, *Megangulus venulosus*, in Shiriuchi, Hokkaido, *Benthos Res. 40*, 23–33.

[Received December 18, 2003; accepted April 4, 2004]

Determining the Relative Amounts of Positional Isomers in Complex Mixtures of Triglycerides Using Reversed-Phase High-Performance Liquid Chromatography–Tandem Mass Spectrometry

Michael Malone and Jason J. Evans*

University of Massachusetts Boston, Boston, Massachusetts 02125

ABSTRACT: A reversed-phase HPLC–tandem mass spectrometry (RP-HPLC-MS-MS) method was refined for the positional analysis of complex mixtures of TAG. This method has the advantages of speed, ease of automation, and specificity over traditional digestion-based methods for the positional analysis of TAG. Collision-induced dissociation (CID) of ammoniated TAG in an ion-trap mass spectrometer produced spectra that were dependent on the FA position. Dominant DAG fragments were formed from the loss of a FA moiety from the ammoniated TAG species. The loss of FA in the outer positions was favored over their loss in the central position. The combination of RP-HPLC and CID produced spectra that were free of the isotope effects that can complicate spectral interpretation in existing methods. The combination also provided selectivity based on the chromatographic fractionation of TAG, in addition to the selectivity inherent in the CID process. Proof-of-concept experiments were performed with binary mixtures of TAG from the SOS/SSO, OSO/OOS, and the PSO/POS/SPO positional isomer systems (where S is 18:0, stearic acid; O is 18:1 (*cis*-9), oleic acid; and P is 16:0, palmitic acid). Plots of fractional DAG fragment intensities vs. fractional composition of the binary mixtures were linear. These plots were used to determine the fractional composition of each of these isomeric systems in a variety of vegetable oils and animal fats. Current limitations, future developments, and applications of this method are discussed.

Paper no. L9417 in *Lipids 39*, 273–284 (March 2004).

TAG consist of three FA moieties attached to a glycerol backbone. The main biological function of TAG is to serve as an energy source. Dietary TAG are digested, reconstituted, and packaged as chylomicrons prior to entering the blood stream. Ultimately, the TAG are delivered to cells in need of energy or stored as reserves in adipose tissue. Evidence is mounting that suggests TAG absorption (1–5), metabolism (1,6–12), and atherogenic potential (2,3,13–23) (tendency for deposition of lipoproteins on the artery walls) may be influenced by FA position. Additional work is needed in these areas to obtain a more complete understanding of the relationship between dietary lipids and heart disease. The development of efficient methods for the positional analysis of individual TAG species will facilitate the advancement of these studies.

The positional analysis of TAG species has traditionally been performed through digestion of the outer two FA and subsequent HPLC analysis of the resulting 2-MAG and FFA (2,8,24–27). Commonly, complex mixtures of TAG are digested in a single step, and the overall FA composition is compared with the position-specific FA composition. These data have revealed general patterns, namely, that monounsaturated FA are overwhelmingly favored in the central position and saturated FA are favored in the outer positions for most animal and vegetable oils, suggesting that FA are selectively attached to the glycerol backbone. Extensive work on the details of TAG biosynthesis (28–33) has explained the positional dependence of the FA composition. These studies have established that unique enzymes catalyze the attachment of FA onto each of the positions, and that these enzymes possess different FA selectivities (34–42).

The digestion-based methods of positional analysis just discussed have been plagued with problems associated with FA migration during digestion (43,44). In addition, these methods are cumbersome and time-consuming for investigations focusing on individual TAG species, since the mixtures must be fractionated prior to hydrolysis. Furthermore, the analysis of the hydrolysis products of co-eluting TAG species often produces ambiguous results.

MS methods have recently been developed that are less labor intensive, more conducive to performing positional analyses on individual TAG species, and more easily automated. HPLC atmospheric pressure chemical ionization (APCI) MS (HPLC-APCI-MS) has been shown to be useful for this purpose (45–48). The protonated TAG formed during the APCI process acquire sufficient energy to fragment in the source. The major ions formed in the APCI process are the DAG fragments, in which one of the FA groups leaves the protonated TAG as a neutral FA. The data of Evershed and colleagues (45–47) show that fragmentation is less likely to occur in the central position than in the outer positions. The authors were able to predict which positional isomer was most abundant based on the DAG fragment of lowest relative abundance.

*To whom correspondence should be addressed at University of Massachusetts Boston, Chemistry Department, 100 Morrissey Blvd., Boston, MA 02125. E-mail: jason.evans@umb.edu

Abbreviations: A, 20:0, eicosanic acid; A_1, 20:1 (*cis*-11), eicosenoic acid; A_2, 20:2 (*cis,cis*-11,14), eicosadienoic acid; APCI, atmospheric pressure chemical ionization; B, 22:0, behenic acid; CID, collision-induced dissociation; ESI, electrospray ionization; L, 18:2 (*cis,cis*-9,12), linoleic acid; Lg, 24:0, lignoceric acid; Ln, 18:3 (*cis,cis,cis*-9,12,15), linolenic acid; MTBE, methyl *t*-butyl ether; NICI, negative-ion chemical ionization; O, 18:1 (*cis*-9), oleic acid; P, 16:0, palmitic acid; P_1, 16:1 (*cis*-9), palmitoleic acid; RP-HPLC-MS-MS, reversed-phase HPLC tandem MS; S, 18:0, stearic acid.

The drawback of the APCI method is that many co-eluting TAG produce common DAG fragments. As a result, it is often difficult to assign peaks to specific TAG. In addition, it is not possible to deconvolute peak intensities, which would be necessary for the quantification of positional isomers. These difficulties are overcome to a great extent by combining RP-HPLC with the use of tandem MS (MS-MS).

Kallio and coworkers (49,50) have used ammonia negative-ion CI (NICI) in conjunction with MS-MS (NICI-MS-MS) for their analysis. The TAG sample is directly inserted into an ammonia CI source of a triple-quadrupole mass spectrometer *via* a probe, and all of the TAG are ionized under ammonia NICI conditions simultaneously. Deprotonated TAG are formed in the source and mass-selected by the first quadrupole. These ions are transmitted to the second quadrupole for collision-induced dissociation (CID). The product ions are analyzed by a third quadrupole to produce a mass spectrum of the CID products. The most abundant fragment ions are deprotonated FA fragments, but DAG-containing fragments (the information-rich fragments) are fairly abundant. CID affords a high level of selectivity, since ions of a particular mass-to-charge ratio are selected by the mass analyzer and subjected to CID. As a result, the analysis can be targeted to TAG of a particular M.W. Direct analysis by MS-MS without any chromatography to fractionate the TAG can provide a wealth of information in a relatively short period of time (15–20 min), even for very complex extracts. In this time, a series of CID mass spectra can be acquired on several $[M - H]^-$ peaks of interest. However, this method has two main limitations. First of all, ^{13}C isotope contributions from TAG that are lower in M.W. by two mass units must be meticulously subtracted from the measured intensities, limiting the precision of the method. The DAG ions of interest in the CID spectra are often overwhelmed by other ^{13}C isotope-containing DAG fragments. Second, TAG with the same M.W. and one of the three FA in common, such as OOS and POA_1 [where O is 18:1 (*cis*-9), oleic acid; S is 18:0, stearic acid; P is 16:0, palmitic acid; and A_1 is 20:1 (*cis*-11), eicosenoic acid] will yield common DAG CID fragments, interfering with quantification of positional isomers. Nevertheless, Kallio *et al.* (49,50) were able to construct plots for some positional isomers that correlated the relative abundances of the DAG ions with their composition. By contrast, the use of RP-HPLC prior to CID analysis completely eliminates the problems associated with ^{13}C isotope peaks because TAG that differ by two mass units are generally completely separated chromatographically. The second limitation is also avoided in many cases by adequate separation of the interfering species. Data highlighting these advantages are presented in this work.

The analysis of TAG by electrospray ionization (ESI)-MS was first reported by Duffin *et al.* (51). They showed that the addition of ammonium acetate to the TAG sample could produce intense $[M + NH_4]^+$ ions that are efficiently dissociated in CID experiments to form dominant DAG fragments, indicative of the loss of the FA moieties. Using an ESI double-focusing sector instrument, Cheng *et al.* (52) observed that the CID spectra of $[M + NH_4]^+$ from positional isomers were indistinguishable (PPO and POP produced the same CID spectra). Han and Gross (53) obtained similar results with a triple-quadrupole instrument analyzing the CID products of lithium adducts. However, in an HPLC-ESI-MS-MS study with a triple-quadrupole instrument, Hvattum (54) observed that the relative abundances of DAG fragments from ammoniated TAG were dependent on the FA position, similar to the NICI experiments of Kallio *et al*. Our experiments using an ion-trap mass spectrometer also showed that in the CID spectra, ammoniated TAG were dependent on the FA position.

We report the use of RP-HPLC-ESI-MS-MS for the fractional composition analysis of TAG positional isomers. This method combines the advantages of efficient fractionation of the TAG *via* RP-HPLC and enhanced selectivity provided by the CID process (DAG fragments derived from TAG of only the selected M.W.). This added degree of selectivity enables the quantification of many systems of positional isomers that would otherwise be difficult. The relative intensities of the DAG fragments in the CID spectrum of mixtures of positional isomers can be used to measure their relative abundances. Standard mixtures of positional isomers were analyzed, and calibration plots of fractional DAG fragment intensities vs. the fractional composition of three sets of positional isomers were constructed and used to determine the fraction composition of positional isomers in various vegetable oils and animal fats.

EXPERIMENTAL PROCEDURES

The TAG designations used throughout this paper consist of three letters, each indicating the presence of a particular FA. The middle letter designates which FA is in the central position. No distinction is made between the outer two positions. (The standard symbols and one-letter abbreviations used throughout the paper are also listed in a footnote at the beginning of the paper.)

HPLC-grade methanol, *n*-propanol, *n*-butanol, and methyl *t*-butyl ether (MTBE) were purchased from Acros Organics (Fairlawn, NJ). Ammonium formate (99%) also was purchased from Acros Organics. Purified TAG [LnLnLn, LLL, OOO, PPO, POP, SOS, SSO, POS, PSO, SPO, SSO, SOS, APO, POA, and PAO, where Ln is 18:3 (*cis,cis,cis*-9,12,15), linolenic acid; L is 18:2 (*cis,cis*-9,12), linoleic acid; and A is 20:0, eicosanic acid] were purchased from Larodan (Malmo, Sweden). The unsaturated FA contained in purchased TAG were all in the *cis* configuration. The current study did not investigate possible differences in the relative intensities of DAG fragments between TAG containing *cis* vs. *trans* FA. Various vegetable oils were purchased at the local supermarket, and fats from pork, chicken, and beef were carved from meat products purchased at the local supermarket.

Standards solutions of each of the pure TAG were prepared in *n*-propanol at concentrations of 100 ± 2 μM. Diluted standards (10.00 μM) for each were prepared in methanol/ammonium formate. These diluted standards were used to prepare standard solutions for a variety of different experiments that were performed in this work.

Extracts from various vegetable oils were prepared in 20-mL vials by dissolving a drop of oil in 15 mL *n*-propanol. The extract was subsequently diluted to 1:100 with methanol. A mixed extract was also prepared in this manner from one drop each of peanut oil and corn oil. The fats were extracted into MTBE at 120°C for 1 h using the 20-mL vials and a variable-temperature heating manifold. One drop of the extract was completely dissolved in 15 mL *n*-butanol and the resulting solution was diluted 1:100 in methanol in preparation for analysis.

Mass spectrometer parameters. A ThermoFinnigan LCQ Advantage ion-trap mass spectrometer (Sunnyvale, CA) was used to detect and characterize the TAG. The connection from the syringe pump (direct-injection experiments) or the HPLC column to the ESI source was made through a 1/16″ stainless-steel zero-dead volume union and a 30 cm long, 50 μm i.d., 185 μm o.d., segment of fused-silica capillary. The end of the fused-silica capillary was fed into the ESI interface through a metal sheath. The tip of the capillary was carefully cut to provide a uniformly shaped tip. The tip of the capillary was then positioned so that it was at the edge of the metal sheath. The electrospray cone was formed by applying a potential difference between the metal sheath and the ion-transfer tube that focused the ions into the mass analyzer. The operating parameters of the ion-trap mass spectrometer were as follows: capillary temperature, 280°C; spray voltage, 4.00 kV; sheath gas, 30 cm^3/min. CID was performed at a relative collision energy of 28 (unitless quantity) unless otherwise stated. This value should be applicable to other LCQ systems, assuming that the instrument calibration procedures described by the manufacturer are carefully followed.

HPLC parameters. A low-flow Shimadzu (Kyoto, Japan) HPLC system, which included an SCL-10A vp controller, two LC-10AD vp pumps, an SIL-10AD vp auto injector, and a 10 cm, 1 mm i.d., 3 μm particle-size, C_{18} BetaBasic column (ThermoElectron Corporation, Sunnyvale, CA), was used to separate the TAG. The high-performance liquid chromatograph was operated at a flow rate of 35 μL/min (low-flow pumps/no splitting necessary). A gradient elution was utilized, consisting of mobile phase A [methanol/*n*-propanol (80:20, vol/vol), saturated ammonium formate (*ca.* 1 mM), pH 7] and mobile phase B [methanol/*n*-propanol (20:80, vol/vol), saturated ammonium formate, pH 7]. The binary gradient was as follows: 0 min/0% B, 4 min/10% B, 36 min/60% B, 38–40 min/85% B. The injection volume was 5 μL for all samples (0.5–5.0 pmol of TAG on-column).

CID spectra of the standards by direct infusion. The 10-μM diluted standards were each analyzed by direct-infusion ESI-MS-MS (no HPLC column) using a syringe pump with a 500-μL syringe. The flow rate was 5 μL/min. The CID spectra were acquired under the conditions described above.

Analysis of a standard mixture and an oil extract by RP-HPLC-ESI-MS-MS. A mixture containing each of the standard TAG at concentrations of about 0.7 μM was prepared in methanol using the diluted standards described above. This mixture was analyzed by RP-HPLC-MS in the MS-only mode and in a targeted RP-HPLC-MS-MS mode. In the MS-only mode, a mass spectrum of the ions formed in the ESI process was produced at a rate of about one spectrum per second throughout the course of the chromatographic run. The targeted MS-MS analysis was developed based on the retention times determined from the experiment performed in the MS-only mode. In this targeted mode, the mass spectrometer was programmed to select the appropriate *m/z* ratio for CID analysis during a 2–3-min chromatographic time window corresponding to the eluting TAG. The mixed extract of peanut oil/corn oil also was analyzed in the MS-only targeted MS-MS modes.

Experiments performed to construct calibration plots. The 10-μM standards SOS, SSO, OSO, OOS, PSO, SPO, and POS were used to prepare known binary mixtures of positional isomers. Standard mixtures of the following pairs of positional isomers were prepared: SOS/SSO, OSO/OOS, POS/SPO, PSO/POS, and SPO/PSO. The sum of the concentrations of the pair of positional isomers for each of the standard mixtures was 1 μM. The fractions of a positional isomer in the binary mixtures ranged from 0.00 to 1.00 in increments of 0.10. Each of the standard mixtures was analyzed by a targeted RP-HPLC-MS-MS method designed specifically for these three systems of positional isomers. The oil and fat extracts described above also were analyzed by this method in an effort to perform a positional analysis of various oils and fats for these three systems of positional isomers.

Data analysis. The spectra used in this work to define the intensities of the DAG fragments were the composite average of 50 spectra, unless otherwise stated. Regression parameters for the calibration plots were used to calculate the fractional composition of various vegetable-based oils and animal fats. For the SSO/SOS and OOS/OSO systems, the linear regression data from the calibration plots were used directly. Repeated measurements of samples over the course of several months suggested that this method measures the ratio of DAG fragment ions and is reproducible to within ± 5%. The average relative SE of the OOS/OSO and SSO/SOS calibration plots were 0.005 and 0.007, respectively, giving relative errors in the predicted fractions of *ca.* 2–5% (*ca.* standard error/slope). For the POS/SPO/PSO system, the linear regression data from the three calibration plots were used to construct three simultaneous equations that were used to solve for the fractional composition data on each of the three positional isomers in each of the samples. The errors in the fractions were found through the application of a Monte Carlo analysis. Our Monte Carlo approach used repeated iterations (N = 10,000) to solve the equations simultaneously while randomly modulating the error in the input ion ratios obtained from the analysis of the oil and fat samples within a 5% tolerance. The results gave Gaussian distributions for each of the fractions. The SD of these distributions were reported as reasonable estimates of the errors. This Monte Carlo analysis was performed using Mathematica 4.2 (Wolfram Research, Champaign, IL).

RESULTS

Direct-infusion CID spectra of each of the standard TAG. The CID spectra for each of the standard TAG were acquired *via*

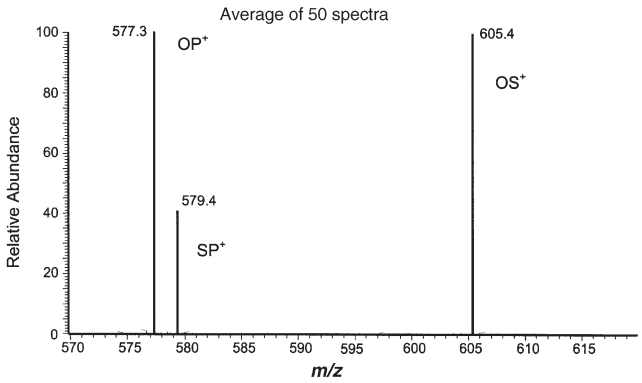

FIG. 1. Collision-induced dissociation (CID) spectrum of POS. The SP^+ that formed from the loss of the oleate moiety from the central position was the DAG fragment of lowest abundance. Abbreviations: P, 16:0, palmitic acid; O, 18:1 (*cis*-9), oleic acid; S, 18:0, stearic acid.

direct-infusion ESI-MS-MS. Figure 1 shows the CID spectrum of POS. This spectrum zoomed in on the DAG fragments ($[M + NH_4 - FA + NH_3]^+$), which were the most intense fragment ions under these experimental conditions. These ions were presumably formed *via* the loss of a neutral FA and ammonia. The fragment ions resulting from the loss of the oleate moiety were of significantly lower abundance than the fragment ions resulting from the loss of the palmitate and stearate moieties. We speculated that fragmentation initiates at the ammoniated FA group and that adduct formation at the central FA position is less probable, perhaps as a consequence of steric hindrance. The relative intensities of DAG fragments in the CID spectra of all of the TAG standards studied in this work are listed in Table 1. The less favorable loss of the FA from the central position appears to be universal for all TAG. Other trends that can be observed from careful inspection of Table 1 are that fragmentation at a particular position increases with an increasing degree of unsaturation and, although to a lesser extent, with increasing chain length. Assuming that the mechanism for fragmentation given above is correct (fragmentation occurs at the ammoniated FA), these trends can be rationalized on the basis of ammonium ion affinities, which are likely to increase with an increasing degree of unsaturation and FA chain length (55).

Chromatography. Figure 2A shows a chromatogram of the standard mixture of TAG. Figure 2B shows a chromatogram of the peanut oil/corn oil extract. Data were collected in the MS-only mode. Our data showed that retention increased for TAG with FA of longer chain lengths and lower degrees of unsaturation. These observations agree with previously reported data illustrating that the retention of TAG species in RP-HPLC can be predicted reasonably well based on the sum of empirically derived retention factors for the constituent FA groups (56). The major TAG species present in the standard mixture are labeled on the chromatogram shown in Figure 2A.

In addition, targeted CID experiments were performed on the standard mixture and the peanut oil/corn oil extract. For the standard mixture, the CID spectra of the *m/z* 878 and 904 peaks, which corresponded to the positional isomer systems of POS/PSO/SPO and SOO/OSO, respectively, were examined to investigate the extent at which positional isomers co-eluted. In both cases, the ratios of the relative intensities of the DAG fragments did not vary as one moved across a chromatographic peak. This indicates that little to no fractionation of the positional isomers of TAG occurred in our RP-HPLC method.

The masses and relative intensities of the DAG fragments from the targeted MS-MS experiments were used to identify the major and minor TAG species in the peanut oil/corn oil extract. Labels indicating these identified species are noted above the chromatographic peaks in Figure 2B. Each labeled species is the most abundant positional isomer of its system. The dominance of the unsaturated FA in the central position is apparent. Figure 3A also provides data from the targeted CID experiment on the peanut oil/corn oil extract. It shows

TABLE 1
Relative Intensities of the DAG Collision-Induced Dissociation (CID) Fragments $[M + NH_4 - FA + NH_3]^+$ for the Standard TAG Analyzed in this Work[a]

TAG	Parent ion	PP^+	PO^+	SP^+	OO^+	SO^+	SS^+/AP^+	AO^+	TO^+	TT^+
POP	850.8	16.2	100.0	—	—	—	—	—	—	—
PPO	850.8	100.0	92.8	—	—	—	—	—	—	—
SPO	878.6	—	66.5	100.0	—	22.4	—	—	—	—
POS	878.6	—	100.0	40.7	—	99.0	—	—	—	—
PSO	878.6	—	25.4	100.0	—	67.9	—	—	—	—
OOS	904.8	—	—	—	55.0	100.0	—	—	—	—
OSO	904.8	—	—	—	17.0	100.0	—	—	—	—
SSO	906.6	—	—	—	—	90.0	100.0	—	—	—
SOS	906.6	—	—	—	—	100.0	17.1	—	—	—
APO	906.6	—	69.3	—	—	—	100.0	25.0	—	—
AOP	906.6	—	100.0	—	—	—	41.4	89.9	—	—
PAO	906.6	—	32.6	—	—	—	100.0	63.1	—	—
LgOLg	1075.0	—	—	—	—	—	—	—	100.0	22.3

[a]These data support the general rule that cleavage of the FA in the central position is unfavorable. Data for the LnLnLn, LLL, and OOO are not shown here, because the CID spectra for these simple TAG were trivial. $LnLn^+$, LL^+, and OO^+, respectively, were the only DAG fragments present in the spectra. Abbreviations: A, 20:0, eicosanic acid; L, 18:2 (*cis,cis*-9,12), linoleic acid; Ln, 18:3 (*cis,cis,cis*-9,12,15), linolenic acid; O 18:1 (*cis*-9), oleic acid; P, 16:0, palmitic acid; S, 18:0, stearic acid; T, Lg, 24:0, lignoceric acid.

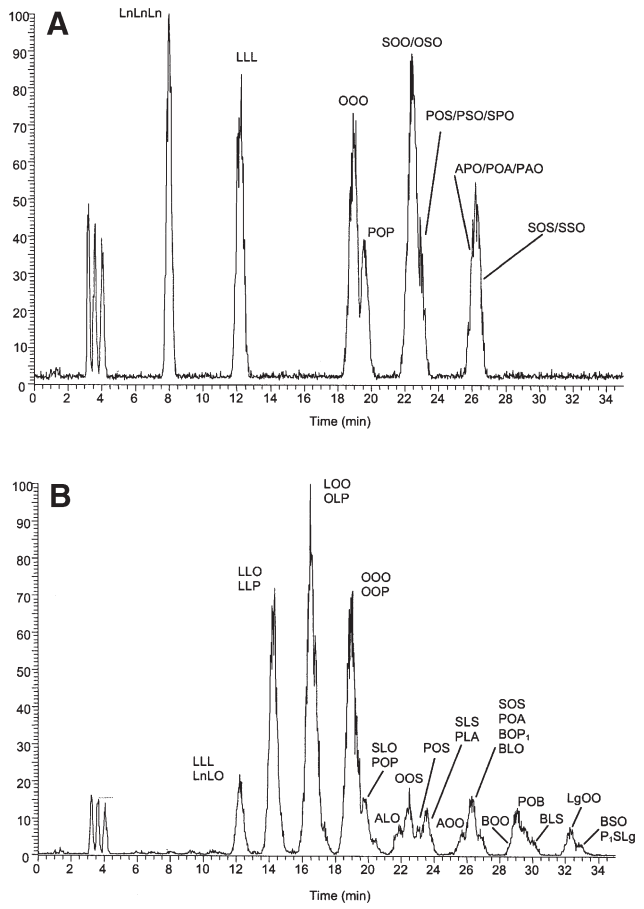

FIG. 2. Ion chromatograms from *m/z* 800–1000 for the standard TAG mixture (A) and an extract of a mixture of peanut and corn oils (B). The masses and intensities of the DAG fragments in the CID spectra were used to identify the major TAG species. Abbreviations: Ln, 18:3 (*cis,cis,cis*-9,12,15); linolenic acid; L, 18:2 (*cis,cis*-9,12); A, 20:0, eicosanic acid; B, 22:0, behenic acid; P_1, 16:1 (*cis*-9), palmitoleic acid; Lg, 24:0, lignoceric acid; for other abbreviations see Figure 1.

the total ion chromatogram of the CID products of TAG with a M.W. of 884.5 amu ($[M + NH_4]^+$ ion at *m/z* 902.6). The chromatogram indicates that TAG of the same M.W. were partially fractionated by the RP-HPLC method. Figure 3B shows the average CID spectrum across these fractionated chromatographic peaks. The intense peak at *m/z* 603.3 corresponds to OO^+ or LS^+, and the peaks at *m/z* 601.3 and *m/z* 605.4 correspond to LO^+ and SO^+, respectively. These DAG fragments indicate the dominant presence of OOO and LOS/LSO/SLO in the oil mixture.

Advantages of using HPLC in conjunction with CID analysis. To highlight the advantages of combining HPLC and CID, experiments were designed to compare RP-HPLC-MS-MS data directly with direct-infusion MS-MS data. The sample used for this comparison was the peanut oil/corn oil mixture. Figure 4A is the CID of the *m/z* 900.5 peak acquired under direct-infusion analysis. Figure 4B is the CID spectrum of the *m/z* 900.5 peak (TAG of M.W. 882.5 amu) acquired during a targeted RP-HPLC-MS-MS analysis. The key DAG peaks in these spectra consisted of *m/z* 599.3 (LL^+), 601.3 (OL^+), and 603.3 (OO^+ and LS^+), indicating the presence of the OOL/OLO and SLL/LSL systems at *m/z* 900.5. The intensities of the peaks in the targeted MS-MS data suggest that OOL and SLL were the dominant positional isomers. In comparison, the direct-infusion analysis was difficult to interpret because DAG fragments from the corresponding ^{13}C isotope peaks of ammoniated TAG of M.W. 880.5 amu had a dominant presence in the spectrum, as evident from the peaks at *m/z* 600 and 602. TAG species that contain two ^{13}C can produce DAG fragments containing two, one, or no ^{13}C isotopes, and as a result, some of the intensity at the *m/z* 599, 601, and 603 peaks also resulted from these ^{13}C-containing fragment ions. Another factor contributing to the complexity of the spectra resulted from the limited trapping resolution of the ion trap. It is possible that some ^{13}C-containing ions at *m/z* 899.5 also may have been trapped and fragmented. These complications are not present in the HPLC-MS-MS analyses. The TAG that produced ammoniated ions at *m/z* 898 and 900 were completely separated, thus removing these isotope effects. In addition, through a direct comparison of the two spectra it was evident that the ratios among the *m/z* 599.3, 601.3, and 603.3 ions were altered by these isotope effects. As a result, quantification of positional isomers using the direct-infusion method yielded erroneous results.

Partial fractionation of isomeric TAG species by HPLC-MS-MS can be useful in some cases in the quantification of positional isomers. As mentioned previously, it is evident from Figure 3 that our RP-HPLC analysis partially resolved TAG that formed $[M + NH_4]^+$ ions at *m/z* 902.6. The CID spectrum obtained from averaging 18 scans from 17.9 to 18.5 min is shown in Figure 5A, and the CID spectrum of the later-eluting TAG are shown in Figure 5B, which was obtained by carefully subtracting the contribution from the earlier eluting peak. Analysis of Figure 5A shows only one DAG peak at *m/z* 603.3. This ion corresponds to OO^+, confirming the identity of the earlier-eluting TAG as OOO. Analysis of Figure 5B shows DAG peaks at *m/z* 601.3, 603.3, and 605.3, as well as ions of lower intensity at *m/z* 575.3 and 629.4. These ions correspond to OL^+, SL^+, OS^+/PA_1^+, PL^+, and A_1L^+, respectively, confirming the identities of the later-eluting TAG as LOS/LSO/SLO and $A_1LP/LA_1P/A_1PL$ positional isomers. The intensities of these DAG peaks suggest that LOS is likely to be the dominant positional isomer of the LOS/LSO/SLO system in these oils. The minor presence of $A_1LP/LA_1P/A_1PL$ positional isomers would not interfere to any great extent with the relative quantification of the LOS/LSO/SLO system. Figure 5C illustrates the average CID spectrum of the *m/z* 902.5 ion acquired *via* direct-infusion ESI-MS-MS. Interpretation of this spectrum was difficult, as already discussed. Quantitative analysis of the LOS/LSO/SLO system was not possible from this spectrum. Furthermore, the DAG peaks indicating the presence of the $A_1LP/LA_1P/A_1PL$ positional isomers were lost in the background noise. The enhanced signal-to-noise ratio was yet another advantage of combining the HPLC and CID analysis.

Quantification of positional isomers. The CID spectrum of $[M + NH_4]^+$ for a given mixture of positional isomers corresponded

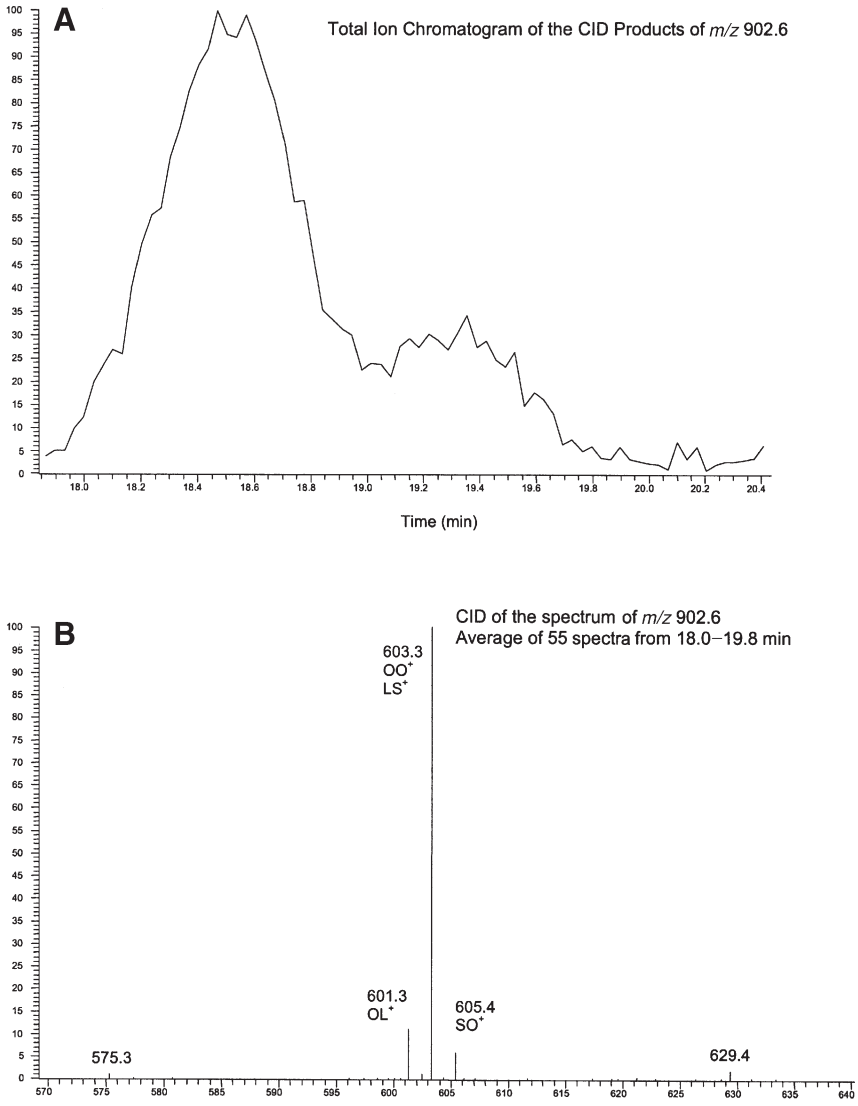

FIG. 3. (A) The total ion chromatogram of the CID products of the *m/z* 902.6 ion from a targeted MS-MS analysis. The chromatogram shows clear signs of TAG that have been partially fractionated by the RP-HPLC method. (B) The average CID spectrum across the fractionated chromatographic peaks. The masses of the DAG peaks suggest the presence of OOO and LOS/LSO/SLO. For abbreviations see Figures 1 and 2.

to a weighted average of each the positional isomers in the mixture. Since positional isomers co-eluted, as highlighted in the preceeding paragraphs, the CID spectra from targeted RP-HPLC-MS-MS analyses contained fractional composition information. To obtain this fractional composition information, calibration curves were useful. To illustrate the utility of such calibration plots, binary mixtures of the SOP/SPO/PSO, OSO/OOS, and SOS/SSO positional isomer systems were analyzed by targeted RP-HPLC-MS-MS. Figure 6 presents these calibration plots for the five sets of binary mixtures analyzed in these experiments. The fractional peak intensities of the DAG fragments are plotted against the mole fraction of the positional isomers. A linear relationship is apparent from the data.

These calibration plots were applied to the positional analysis of these systems of positional isomers in several vegetable oils and animal fats. Table 2 shows the results of these experiments, which were in agreement with previous data from the traditional digestion methods (7,8,57,58) and MS data (45,46,50). For the vegetable-based oils and beef and chicken fat, the oleate moiety was placed in the central position of the TAG almost exclusively for the systems examined in this study. In contrast, but consistent with the results of others, the palmitate moiety was favored in the central position for the POS/SPO/PSO system in pork fat (essentially 100% of this positional isomer was in the SPO form). Also, the stearate moiety was favored in the central position (90%) for the SSO/SOS system in pork fat.

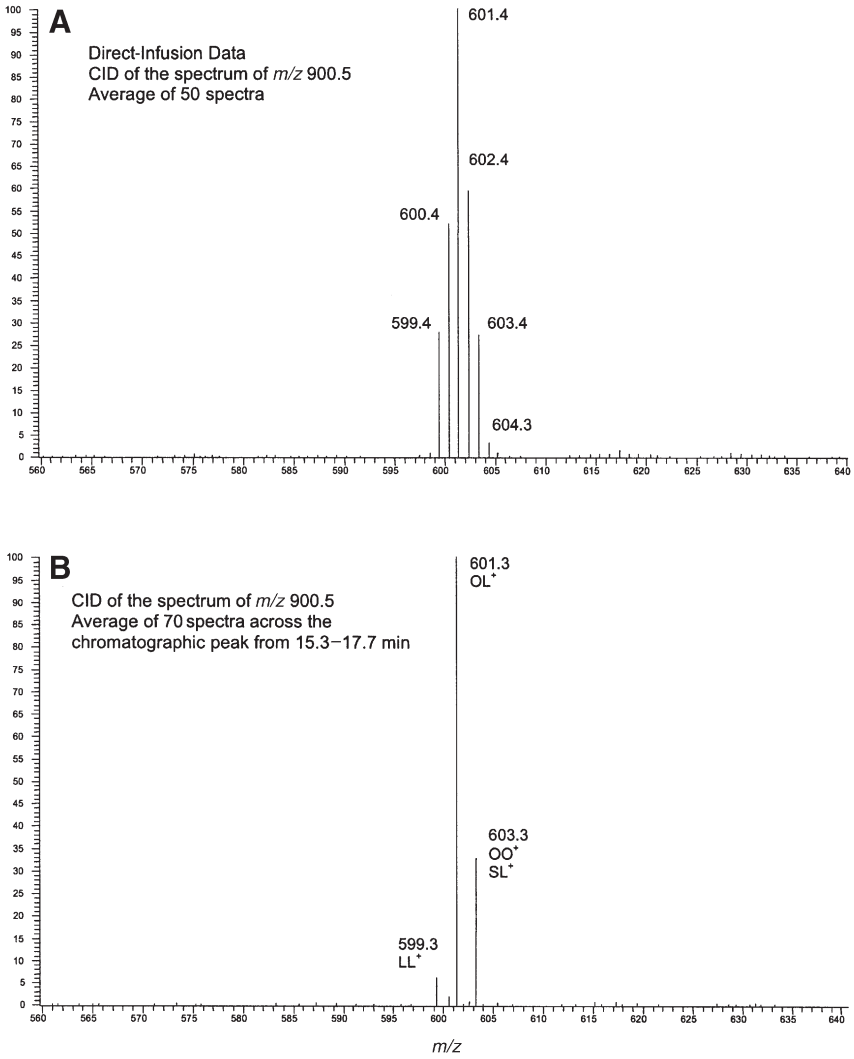

FIG. 4. (A) The average CID spectrum of the *m/z* 900.6 ion acquired *via* direct-infusion MS-MS of the peanut oil/corn oil mixture. (B) The average CID spectrum of the *m/z* 900.6 ion acquired *via* RP-HPLC-MS-MS of the peanut oil/corn oil mixture. The major advantage of using HPLC to fractionate the TAG prior to CID analysis is the removal of interfering ^{13}C isotope effects present in the direct-infusion spectra. For abbreviations see Figures 1 and 2.

The errors associated with the POS/PSO/SPO system were greater than those associated with the SSO/SOS and OSO/OOS systems owing to a propagation of errors from the regression parameters of the three calibration plots. This propagation was inherent in the Monte Carlo simulations. Nevertheless, fractional compositions for the POS/SPO/PSO systems were determined to within ± 0.1.

Determining reliable fractional composition data for a given system, such as the POS/SPO/PSO, SSO/SOS, and OSO/OOS systems examined in this study, can be complicated by the presence of other isomeric species with different FA compositions that happen to co-elute. For example, with the analysis of the SSO/SOS system in peanut oil, the CID of the *m/z* 906.5 ion (the mass of the ammoniated parent from SSO/SOS) produced intense DAG fragments at *m/z* 577 and 631, corresponding to PO^+ and AO^+, respectively. This indicates a significant presence of the co-eluting POA/OPA/PAO TAG system in peanut oil. The loss of the oleate moiety from these TAG produced a peak at *m/z* 607 (PA^+), as did the loss of oleate from SSO and SOS (SS^+). We could not differentiate the portion of the *m/z* 607 peak that was attributable to the SOS/SSO system from the portion attributable to the POA/OPA/PAO TAG system, and, as a result, fractional composition data were unattainable. Owing to the abundant presence of POA/OPA/PAO TAG, reliable data for the SSO/SOS system could not be obtained for many of the oils. The $A_1PO/A_1OP/OA_1P$ system of positional isomers co-eluted with the OSO/OOS system and therefore interfered with its quantitative positional analysis. The $A_1PO/A_1OP/OA_1P$ TAG were only very minor components in the oils that we investigated and did

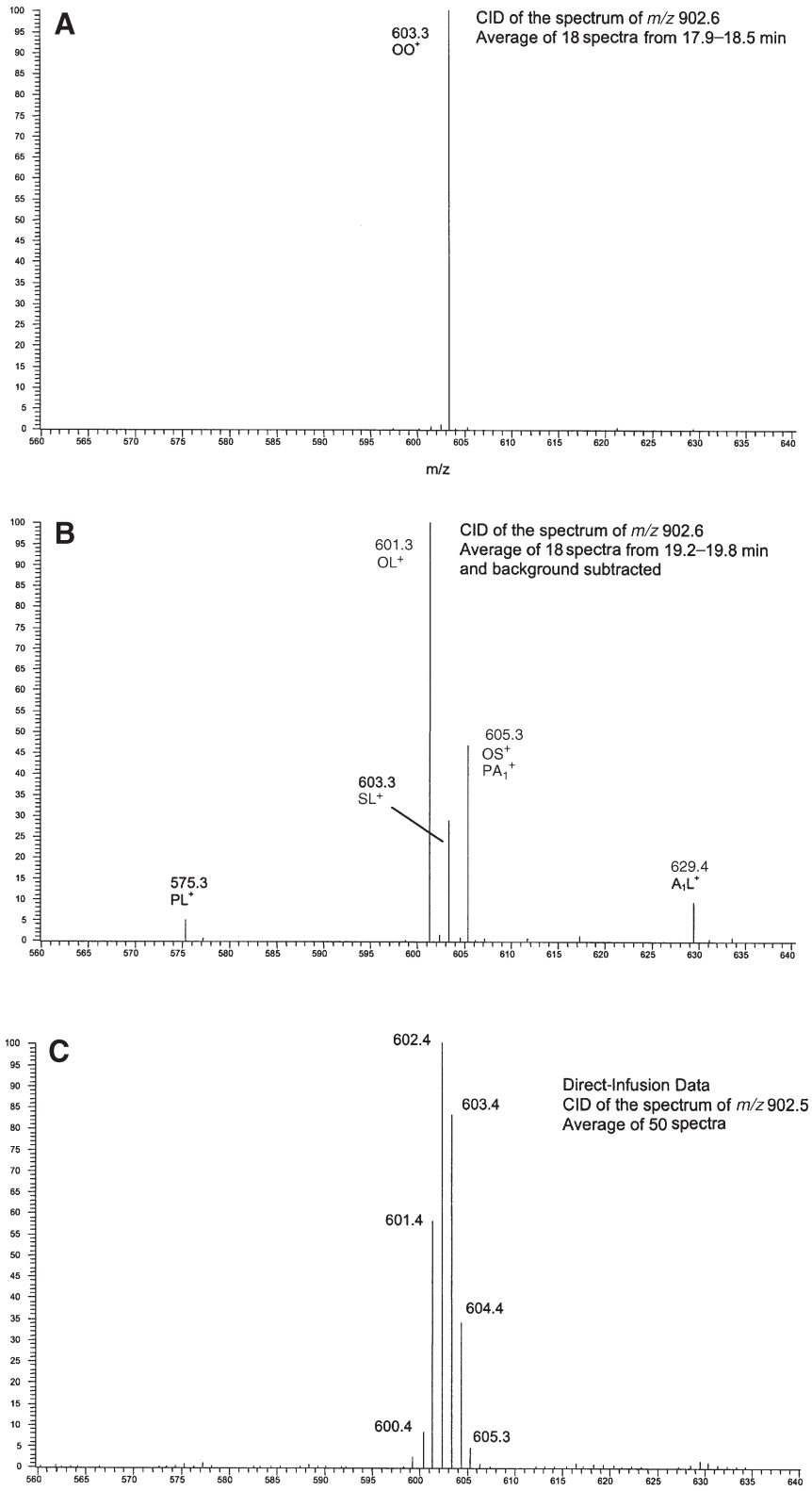

FIG. 5. Deconvoluted CID spectra of the first (A) and second (B) fractions shown in Figure 3A. Through subtraction, a representative spectrum of the LOS/LSO/SLO system was obtained that could be used for the quantification of this system of positional isomers. (C) CID spectra of the 902.6 ion acquired *via* direct-infusion electrospray ionization MS-MS. A_1, 20:1 (*cis*-11), eicosenoic acid; for other abbreviations see Figures 1 and 2.

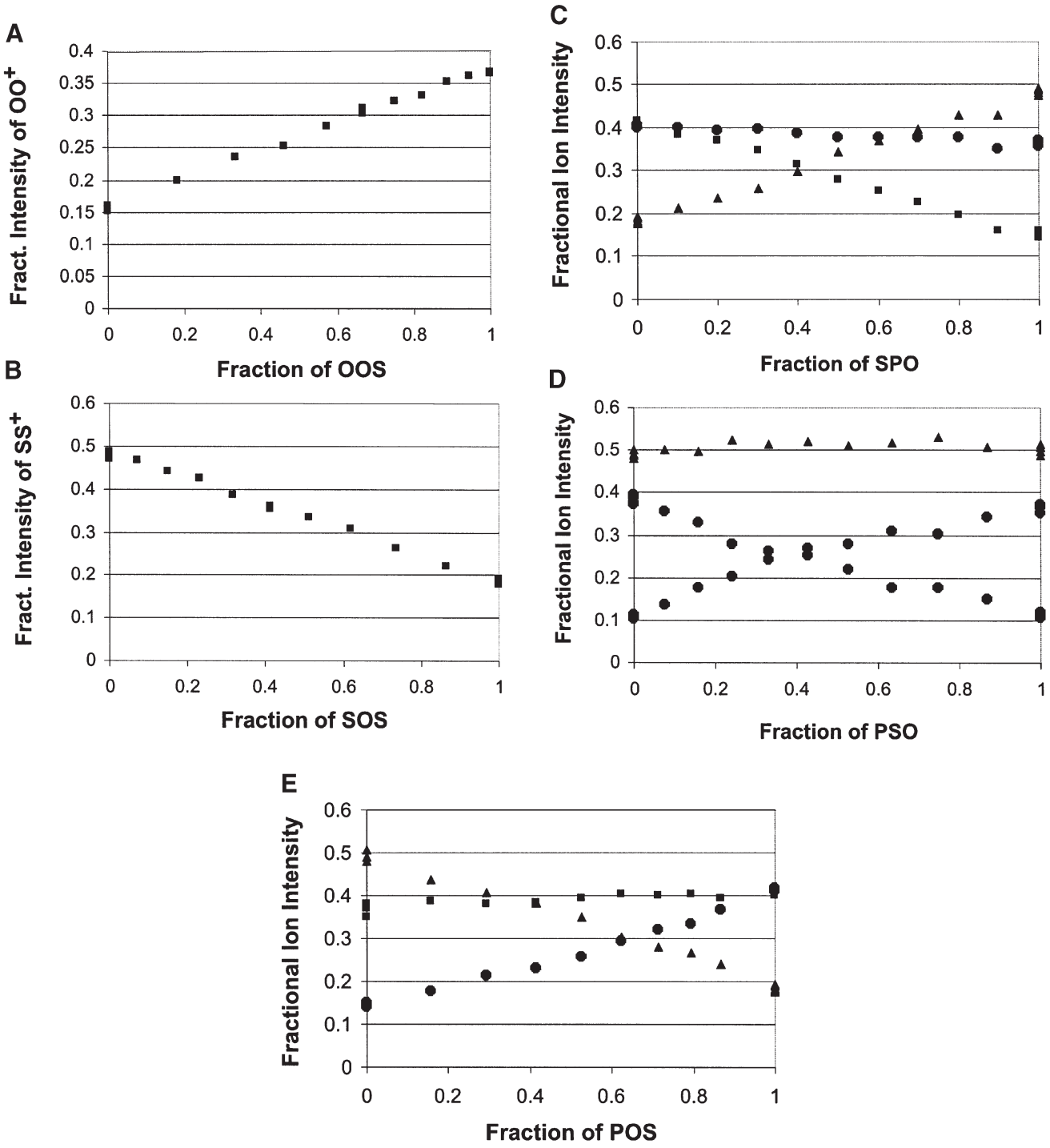

FIG. 6. Calibration plots for binary mixtures of positional isomers. All fractional intensities are relative to the sum of all DAG fragments. (A) Fractional intensities of the OO^+ ion as a function of the fractional composition of binary mixtures of OOS and OSO. (B) Fractional intensities of the SS^+ ion as a function of the fractional composition of binary mixtures of SSO and SOS. (C) Fractional intensities of the DAG fragments as a function of the fractional composition of binary mixtures of POS and SPO. (D) Fractional intensities of the DAG fragments as a function of the fractional composition of binary mixtures of PSO and SPO. (E) Fractional intensities of the DAG fragments as a function of the fractional composition of binary mixtures of PSO and POS. (C–E) ■ represents the fractional intensity of SO^+, ▲ represents the fractional intensity of SP^+, and ● represents the fractional intensity of PO^+.

not greatly affect quantification of the SOS/SSO system. However, the $A_1PO/A_1OP/OA_1P$ TAGs were present in significant amounts in pig fat, making reliable data for the OSO/OOS system unattainable. Further research is in progress that attempts to address the limitations that some co-eluting isomeric TAG species place on the current methodology.

TABLE 2
Fractional Composition Data for the Three Isomeric Systems Analyzed for Various Oils and Fats[a]

Oil/fat	POS	PSO	SPO	SOS	SSO	OOS	OSO
Corn	0.99 ± 0.09	–0.02 ± 0.10	0.16 ± 0.09	Int	Int	0.99 ± 0.05	0.01 ± 0.05
Vegetable	1.02 ± 0.09	0.00 ± 0.10	0.00 ± 0.10	Int	Int	1.07 ± 0.10	–0.07 ± 0.10
Safflower	0.97 ± 0.09	0.03 ± 0.10	0.04 ± 0.09	Int	Int	1.01 ± 0.04	–0.01 ± 0.04
Olive	1.05 ± 0.09	–0.06 ± 0.11	0.08 ± 0.09	Int	Int	1.05 ± 0.06	–0.05 ± 0.06
Peanut	1.06 ± 0.09	–0.08 ± 0.12	0.00 ± 0.09	Int	Int	0.98 ± 0.08	0.02 ± 0.08
Tanning	1.01 ± 0.09	0.05 ± 0.12	0.01 ± 0.09	0.96 ± .04	0.04 ± 0.04	0.95 ± 0.04	0.05 ± 0.04
Cocoa	1.04 ± 0.09	0.04 ± 0.12	0.00 ± 0.10	0.94 ± .04	0.06 ± 0.04	1.02 ± 0.04	–0.02 ± 0.04
Crisco®	0.66 ± 0.10	0.33 ± 0.12	0.00 ± 0.08	0.55 ± .04	0.45 ± 0.04	0.89 ± 0.04	0.11 ± 0.04
Chicken	0.62 ± 0.09	0.29 ± 0.12	0.10 ± 0.08	0.56 ± .06	0.44 ± 0.06	0.76 ± 0.04	0.24 ± 0.04
Beef	0.64 ± 0.09	0.13 ± 0.12	0.23 ± 0.07	0.79 ± .04	0.21 ± 0.06	1.00 ± 0.04	0.00 ± 0.04
Pork	0.08 ± 0.15	–0.12 ± 0.15	1.03 ± 0.05	0.1 ± 0.1	0.9 ± 0.1	Int	Int

[a]The first three columns consist of fractional composition data for the POS/PSO/SPO system. The next two columns give fractional composition data for the SOS/SSO system. The final two columns give fractional composition data for the OOS/OSO system. The designation "Int" indicates that accurate data could not be obtained due to a co-eluting TAG that interfered with quantification. For abbreviations see Table 1.

DISCUSSION

This paper illustrates that calibration plots for systems of positional isomers can be constructed and used to measure the fractional compositions of positional isomers in complex mixtures. Further work is being performed to extend this work to other isomeric systems, including the development of a model that can predict the relative intensities of the DAG fragments in the CID spectrum of any ammoniated TAG. Additional investigations are also focusing on evaluating the chromatographic and CID characteristics of TAG containing *cis* vs. *trans* FA.

The method described in this paper has the advantages of providing CID spectra that are easier to interpret and that give more precise quantitative information. The spectra are easier to interpret as a result of the elimination of ^{13}C isotope effects. The added precision results from both the removal of the ^{13}C isotope effects and the added selectivity obtained by combining HPLC with CID. Only co-eluting TAG of the same M.W. that yielded a common CID product interfered with the quantitative positional analysis. Thus, the possible interferences were significantly reduced. However, interferences do still occur when analyzing certain TAG species, and overcoming these difficulties is a challenge that lies ahead.

Improvements in the chromatographic resolution of the TAG may help to separate some of the interfering species. The RP-HPLC method used in this work was optimized for the methanol/*n*-propanol (ammonium formate) mobile phase system. However, better separations have been reported in the literature (56,59,60), and it may be possible to improve on our current HPLC method. Future work will include an investigation of different mobile phase systems that may be compatible with the formation of $[M + NH_4]^+$ ions.

MS-MS-MS experiments have proven to be very powerful for some applications and may be a useful approach for dealing with these interferences. Byrdwell and Neff (61) reported that the key MS-MS-MS products were the acylium ions (RCO^+), which revealed the identities of individual FA chains. In this approach, DAG fragments of a certain *m/z* ratio formed in the first CID event were isolated in the ion trap and subjected to another round of CID. The following example for the SOS/SSO system is offered as an illustration of the potential application of MS-MS-MS experiments in a quantitative positional analysis of TAG. As mentioned above, the DAG peak at *m/z* 607 could be formed *via* CID of the ammoniated TAG from both the SOS/SSO (SS^+) and PAO/APO/AOP (AP^+) systems. Once formed, if these fragments were isolated in the ion trap and subsequently dissociated in another round of CID, the acylium fragments produced would correspond to S, O, A, and P. The relative abundances of the O and S acylium fragments would likely be indicative of the fractional composition of the SOS/SSO, and the relative abundances of the intensities for the A and P acylium fragments would likely be indicative of the fractional composition of the PAO/APO/AOP. These MS-MS-MS experiments are currently under investigation. Initial work has proven to be challenging because the intensities of the MAG fragments are very low. However, we are attempting to fine-tune the conditions necessary to produce useful MS-MS-MS data.

Upon further development we plan to utilize this method to investigate the influence of FA position on the metabolism, absorption, transport, biosynthesis, and mobilization of essentially any set of positional TAG isomers in biological systems. The kinetics of these processes is under investigation for systems of positional isomers using stable isotope incorporation in conjunction with this methodology.

ACKNOWLEDGMENT

The liquid chromatograph/mass spectrometer used in this work was acquired through partial support from the National Science Foundation.

REFERENCES

1. Kubow, S. (1996) The Influence of Positional Distribution of Fatty Acids in Native, Interestified, and Structure-Specific Lipids on Lipoprotein Metabolism and Atherogenesis, *J. Nutr. Biochem. 7*, 530–541 (1996).
2. Filer, L.J., Jr., Mattson, F.H., and Fomon, S.J. (1969) Triglyceride Configuration and Fat Absorption by the Human Infant, *J. Nutr. 99*, 293–298.

3. Lien, E.L., Boyle, F.G., Yuhas, R., Tomarelli, R.M., and Quinlan, P. (1997) The Effect of Triglyceride Positional Distribution on Fatty Acid Absorption in Rats, *J. Pediatr. Gastroenterol. Nutr. 25*, 167–174.
4. Renaud, S.C., Ruf, J.C., and Petithory, D. (1995) The Positional Distribution of Fatty Acids in Palm Oil and Lard Influences Their Biologic Effects in Rats, *J. Nutr. 125*, 229–237.
5. Summers, L.K., Fielding, B.A., Herd, S.L., Ilic, V., Clark, M.L., Quinlan, P.T., and Frayn, K.N. (1999) Use of Structured Triacylglycerols Containing Predominantly Stearic and Oleic Acids to Probe Early Events in Metabolic Processing of Dietary Fat, *J. Lipid Res. 40*, 1890–1898.
6. Decker, E.A. (1996) The Role of Stereospecific Saturated Fatty Acid Positions on Lipid Metabolism, *Nutr. Rev. 54*, 108–110.
7. Brockerhoff, H., Hoyle, R.J., and Wolmark, N. (1966) Positional Distribution of Fatty Acids in Triglycerides of Animal Depot Fats, *Biochim. Biophys. Acta 116*, 67–72.
8. Brockerhoff, H., and Yurkowski, M. (1966) Stereospecific Analyses of Several Vegetable Fats, *J. Lipid Res. 7*, 62–64.
9. Nawar, W.W. (1996) *Lipids*, 3rd edn., Marcel Dekker, New York.
10. Small, D.M. (1991) The Effects of Glyceride Structure on Absorption and Metabolism, *Annu. Rev. Nutr. 11*, 413–434 (1991).
11. Padley, F.B., Gunstone, F.D., and Harwood, J.L. (1994) *Occurrence and Characteristics of Oils and Fats*, 2nd edn., Chapman & Hall, London.
12. Kritchevsky, D. (1988) Effects of Triglyceride Structure on Lipid Metabolism, *Nutr. Rev. 46*, 177–181.
13. Hunter, J.E. (2001) Studies on Effects of Dietary Fatty Acids as Related to Their Position on Triglycerides, *Lipids 36*, 655–668.
14. Kritchevsky, D., Tepper, S.A., Chen, S.C., Meijer, G.W., and Krauss, R.M. (2000) Cholesterol Vehicle in Experimental Atherosclerosis. 23. Effects of Specific Synthetic Triglycerides, *Lipids 35*, 621–625.
15. Kritchevsky, D., Tepper, S.A., Kuksis, A., Wright, S., and Czarnecki, S.K. (2000) Cholesterol Vehicle in Experimental Atherosclerosis. 22. Refined, Bleached, Deodorized (RBD) Palm Oil, Randomized Palm Oil and Red Palm Oil, *Nutr. Res. 20*, 887–892.
16. Summers, L.K., Fielding, B.A., Ilic, V., Quinlan, P.T., and Frayn, K.N. (1998) The Effect of Triacylglycerol-Fatty Acid Positional Distribution on Postprandial Metabolism in Subcutaneous Adipose Tissue, *Br. J. Nutr. 79*, 141–147.
17. Kritchevsky, D., Tepper, S.A., and Klurfeld, D.M. (1998) Lectin May Contribute to the Atherogenicity of Peanut Oil, *Lipids 33*, 821–823.
18. Kritchevsky, D., Tepper, S.A., Kuksis, A., Eghtedary, K., and Klurfeld, D.M. (1998) Cholesterol Vehicle in Experimental Atherosclerosis. 21. Native and Randomized Lard and Tallow, *J. Nutr. Biochem. 9*, 582–585.
19. Kritchevsky, D., Tepper, S.A., Wright, S., Kuksis, A., and Hughes, T.A. (1998) Cholesterol Vehicle in Experimental Atherosclerosis. 20. Cottonseed Oil and Randomized Cottonseed Oil, *Nutr. Res. 18*, 259–264.
20. Aoyama, T., Fukui, K., Taniguchi, K., Nagaoka, S. Yamaoto, T., and Hashimoto, Y. (1996) Absorption and Metabolism of Lipids in Rats Depend on Fatty Acid Isomeric Position, *J. Nutr. 126*, 225–231.
21. Pufal, D.A., Quinlan, P.T., and Salter, A.M. (1995) Effect of Dietary Triacylglycerol Structure on Lipoprotein Metabolism: A Comparison of the Effects of Dioleoylpalmitoylglycerol in Which Palmitate Is Esterified to the 2- or 1(3)-Position of the Glycerol, *Biochim. Biophys. Act. 1258*, 41–48.
22. Lien, E.L., Yuhas, R.J., Boyle, F.G., and Tomarelli, R.M. (1993) Corandomization of Fats Improves Absorption in Rats, *J. Nutr. 123*, 1859–1867.
23. Kritchevsky, D., Tepper, S.A., Vesselinovitch, D., and Wissler, R.W. (1973) Cholesterol Vehicle in Experimental Atherosclerosis. 13. Randomized Peanut Oil, *Atherosclerosis 17*, 225–243.
24. Brockerhoff, H. (1967) Stereospecific Analysis of Triglycerides: An Alternative Method, *J. Lipid Res. 8*, 167–169.
25. Brockerhoff, H., and Ackman, R.G. (1967) Positional Distribution of Isomers of Monoenoic Fatty Acids in Animal Glycerolipids, *J. Lipid Res. 8*, 661–666.
26. Slakey, P.M., and Lands, W.E.M. (1967) The Structure of Rat Liver Triglycerides, *Lipids 3*, 30–36.
27. Akesson, B. (1969) Composition of Rat Liver Triacylglycerols and Diacylglycerols, *Eur. J. Biochem. 9*, 463–477.
28. Brown, J.L., and Johnston, J.M. (1964) The Utilization of 1- and 2-Monoglycerides for Intestinal Triglyceride Biosynthesis, *Biochim. Biophys. Acta. 84*, 448–457.
29. Pieringer, R.A., Bonner, H., Jr., and Kunnes, R.S. (1967) Biosynthesis of Phosphatidic Acid, Lysophosphatidic Acid, Diglyceride, and Triglyceride by Fatty Acyltransferase Pathways in *Escherichia coli, J. Biol. Chem. 242*, 2719–2724.
30. Polheim, D., David, J.S., Schultz, F.M., Wylie, M.B., and Johnston, J.M. (1973) Regulation of Triglyceride Biosynthesis in Adipose and Intestinal Tissue, *J. Lipid Res. 14*, 415–421.
31. Lehner, R., and Kuksis, A. (1996) Biosynthesis of Triacylglycerols, *Prog. Lipid Res. 35*, 169–201.
32. Sorger, D., and Daum, G. (2002) Synthesis of Triacylglycerols by the Acyl-Coenzyme A:Diacylglycerol Acyltransferase Dga1p in Lipid Particles of the Yeast *Saccharomyces cerevisiae*, *J. Bacteriol. 184*, 519–524.
33. Sorger, D., and Daum, G. (2003) Triacylglycerol Biosynthesis in Yeast, *Appl. Microbiol Biotechnol. 61*, 289–299.
34. Brown, A.P., Slabas, A.R., and Denton, H. (2002) Substrate Selectivity of Plant and Microbial Lysophosphatidic Acid Acyltransferases, *Phytochemistry 61*, 493–501.
35. Reeves, C.D., Murli, S., Ashley, G.W., Piagentini, M., Hutchinson, C.R., and McDaniel, R. (2001) Alteration of the Substrate Specificity of a Modular Polyketide Synthase Acyltransferase Domain Through Site-Specific Mutations, *Biochemistry 40*, 15464–15470.
36. Holub, B.J. (1981) The Suitability of Different Acyl Acceptors as Substrates for the Acyl-CoA:2-Acyl-*sn*-glycero-3-phosphorylcholine Acyltransferase in Rat Liver Microsomes, *Biochim. Biophys Acta 664*, 221–228.
37. Holub, B.J., and Piekarski, J. (1977) The Relative Utilization of Different Molecular Species of Unsaturated 1,2-Diacyglycerols by the Acyl-CoA:1,2-Diacyl-*sn*-glycerol Acyltransferase in Rat Liver Microsomes, *Can. J. Biochem. 55*, 1186–1190.
38. Ichihara, K., Takahashi, T., and Fujii, S. (1988) Diacylglycerol Acyltransferase in Maturing Safflower Seeds: Its Influences on the Fatty Acid Composition of Triacylglycerol and on the Rate of Triacylglycerol Synthesis, *Biochim. Biophys. Acta 958*, 125–129.
39. Ichihara, K., Asahi, T., and Fujii, S. (1987) 1-Acyl-*sn*-glycerol-3-phosphate Acyltransferase in Maturing Safflower Seeds and Its Contribution to the Non-random Fatty Acid Distribution of Triacylglycerol, *Eur. J. Biochem. 167*, 339–347.
40. Okuyama, H., Yamada, K., Ikezawa, H., and Wakil, S.J. (1976) Factors Affecting the Acyl Selectivities of Acyltransferases in *Escherichia coli, J. Biol. Chem. 251*, 2487–2492.
41. Okuyama, H., Yamada, K., and Ikezawa, H. (1975) Accepton Concentration Effect in the Selectivity of Acyl Coenzyme A:U Aclglycerylphosphorylcholine[sic] Acyltransferase System in Rat Liver, *J. Biol. Chem. 250*, 1710–1713.
42. Yamada, K., and Okuyama, H. (1978) Selectivity of Diacylglycerophosphate Synthesis in Subcellular Fractions of Rat Liver, *Arch. Biochem. Biophys. 190*, 409–420.
43. Brockerhoff, H. (1965) A Stereospecific Analysis of Triglycerides, *J. Lipid Res. 79*, 10–15.
44. Jensen, R.G., Sampugna, J., Carpenter, D.L., and Pitas, R.E.

(1967) Structural Analysis of Triglyceride Classes Obtained from Cow's Milk Fat by Fractional Crystallization, *J. Dairy Sci. 50*, 231–234.
45. Mottram, H.R., Woodbury, S.E., and Evershed, R.P. (1997) Identification of Triacylgylcerol Positional Isomers Present in Vegetable Oils by High Performance Liquid Chromatography/Atmospheric Pressure Chemical Ionization Mass Spectrometry, *Rapid Commun. Mass Spectrom. 11*, 1240–1252.
46. Mottram, H.R., Crossman, Z.M., and Evershed, R.P. (2001) Regiospecific Characterisation of the Triacylglycerols in Animal Fats Using High Performance Liquid Chromatography–Atmospheric Pressure Chemical Ionisation Mass Spectrometry, *Analyst 126*, 1018–1024.
47. Mottram, H.R., and Evershed, R.P. (2001) Elucidation of the Composition of Bovine Milk Fat Triacylglycerols Using High-Performance Liquid Chromatography–Atmospheric Pressure Chemical Ionisation Mass Spectrometry, *J. Chromatogr. A 926*, 239–253.
48. Byrdwell, W.C. (2001) Atmospheric Pressure Chemical Ionization Mass Spectrometry for Analysis of Lipids, *Lipids 36*, 327–346.
49. Kallio, H., Yli-Jokipii, K., Kurvinen, J.P., Sjovall, O., and Tahvonen, R. (2001) Regioisomerism of Triacylglycerols in Lard, Tallow, Yolk, Chicken Skin, Palm Oil, Palm Olein, Palm Stearin, and a Transesterified Blend of Palm Stearin and Coconut Oil Analyzed by Tandem Mass Spectrometry, *J. Agric. Food Chem. 49*, 3363–3369.
50. Currie, G.J., and Kallio, H. (1993) Triacylglycerols of Human Milk: Rapid Analysis by Ammonia Negative Ion Tandem Mass Spectrometry, *Lipids 28*, 217–222.
51. Duffin, K.L., Henion, J.D., and Shieh, J.J. (1991) Electrospray and Tandem Mass Spectrometric Characterization of Acylglycerol Mixtures That Are Dissolved in Nonpolar Solvents, *Anal. Chem. 63*, 1781–1788.
52. Cheng, C., Gross, M.L., and Pittenauer, E. (1998) Complete Structural Elucidation of Triacylglycerols by Tandem Sector Mass Spectrometry, *Anal. Chem. 70*, 4417–4426.
53. Han, X., and Gross, R.W. (2001) Quantitative Analysis and Molecular Species Fingerprinting of Triacylglyceride Molecular Species Directly from Lipid Extracts of Biological Samples by Electrospray Ionization Tandem Mass Spectrometry, *Anal. Biochem. 295*, 88–100.
54. Hvattum, E. (2001) Analysis of Triacylglycerols with Non-aqueous Reversed-Phase Liquid Chromatography and Positive Ion Electrospray Tandem Mass Spectrometry, *Rapid Commun. Mass Spectrom. 15*, 187–190.
55. Evans, J., Nicol, G., and Munson, B. (2000) Proton Affinities of Saturated Aliphatic Methyl Esters, *J. Am. Soc. Mass Spectrom. 11*, 789–796.
56. Sjovall, O., Kuksis, A., Marai, L., and Myher, J.J. (1997) Elution Factors of Synthetic Oxotriacylglycerols as an Aid in Identification of Peroxidized Natural Triacylglycerols by Reversed-Phase High-Performance Liquid Chromatography with Electrospray Mass Spectrometry, *Lipids 32*, 1211–1218.
57. Christie, W.W., and Moore, J.H. (1970) A Comparison of the Structures of Triglycerides from Various Pig Tissues, *Biochim. Biophys. Acta 210*, 46–56.
58. Christie, W.W., and Moore, J.H., (1970) The Structure of Egg Yolk Triglycerides, *Biochim. Biophys. Acta 218*, 83–88.
59. Byrdwell, W.C., Neff, W.E., and List, G.R. (2001) Triacylglycerol Analysis of Potential Margarine Base Stocks by High-Performance Liquid Chromatography with Atmospheric Pressure Chemical Ionization Mass Spectrometry and Flame Ionization Detection, *J. Agric. Food Chem. 49*, 446–457.
60. Jham, G.N., Nikolova-Damyavova, B., Viera, M., Natalino, R., and Rodrigues, A.C. (2003) Determination of the Triacylglycerol Composition of Coffee Beans by Reversed-Phase High-Performance Liquid Chromatography, *Phytochem. Anal. 14*, 310–314.
61. Byrdwell, W.C., and Neff, W.E. (2002) Dual Parallel Electrospray Ionization and Atmospheric Pressure Chemical Ionization Mass Spectrometry (MS), MS/MS, and MS/MS/MS for the Analysis of Triacylglycerols and Triacylglycerol Oxidation Products, *Rapid Commun. Mass Spectrom. 16*, 300–319.

[Received November 20, 2003, and in revised form and accepted April 22, 2004]

An Efficient and Novel Method for the Synthesis of Cardiolipin and Its Analogs

Zhen Lin, Moghis U. Ahmad, Shoukath M. Ali, and Imran Ahmad*

NeoPharm, Inc., Waukegan, Illinois 60085

ABSTRACT: A novel synthetic method has been developed for cardiolipin and its analog *via* a chlorophosphoramidite coupling reaction followed by oxidation. The reagent, *N,N*-diisopropylmethylphosphoramidic chloride, couples effectively with 1,2-*O*-dimyristoyl-*sn*-glycerol in the presence of an amidite activator to form a phosphoamidite intermediate, which then reacts with 2-*O*-benzylglycerol in the presence of a basic catalyst followed by *in situ* oxidation to give the corresponding protected cardiolipin. Deprotection of the protecting groups provides tetramyristoyl cardiolipin in good overall yield of 60%. The synthetic method is applicable to large-scale synthesis of cardiolipin and various analogs with or without unsaturation for liposomal drug delivery.

Paper no. L9411 in *Lipids 39,* 285–290 (March 2004).

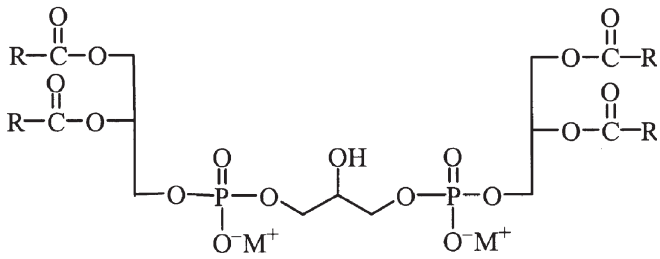

1 R = fatty acid chain, M = H, cardiolipin

1a R = $C_{13}H_{27}$, M = NH_4, tetramyristoyl cardiolipin ammonium salt

SCHEME 1

We report herein a simple, efficient method for the synthesis of cardiolipin **1** (Scheme 1) and its ether anolog **7**. Cardiolipin, also referred as to diphosphatidylglycerols, constitutes a class of complex phospholipids that occur mainly in the heart and skeletal muscles and that usually are associated with membranes of subcellular fractions showing high metabolic activity, for example, the mitochondria (1–3). Cardiolipin plays an important role in many biological processes as well as in many areas of biochemical and biomedical studies (4–7). During the past decade, more attention has been focused on the use of cardiolipin in drug delivery, therapeutic imaging, diagnostic imaging, and as contrast agents (8–10). In one of the most challenging areas, liposomes formed by cardiolipin were found to be a unique way to deliver drugs to tumor cells (11). Encapsulating anticancer drugs such as doxorubicin in liposomes using synthetic tetramyristoyl cardiolipin not only enhances their antitumor activities but also may provide the ability to modulate multidrug resistance and reduce toxicities (12,13). The synthetic approaches described to date for the synthesis of cardiolipin have involved multi-steps along with difficulties in purification that resulted in poor yields (14–20). We describe here the development of a practical and efficient method for the synthesis of cardiolipins and their ether analogs using a chlorophosphoramidite approach.

The literature on the synthesis of cardiolipin is divided mainly into two types of reactions, either by the simultaneous coupling at both the C-1 and C-3 hydroxy groups of 2-*O*-protected glycerol with DAG *via* a phosphodiester or phosphotriester linkage using a phosphorylating agent (14–16), or by the condensation of both the C-1 and C-3 hydroxy groups of 2-*O*-protected glycerol with PA in the presence of 2,4,6-triisopropylbenzenesulfonyl chloride (TPSCl) (17,18). Saunders and Schwarz (14) described the preparation of cardiolipin by using phosphorus oxychloride ($POCl_3$) as phosphorylating reagent, but this method was later found to be unreproducible (15). The method using di(1,2-dimethylethylene)pyrophosphate as phosphorylating agent suffers from a significant transesterification reaction that generates a number of side products in addition to the desired cardiolipin (15). The traditional method using TPSCl as a condensation reagent is impractical owing to the lower stability of PA and the difficulties in removing large amounts of pyridine in the scaleup synthesis (17,18). Another approach to the synthesis of cardiolipin claimed in literature is the condensation of the silver salt of diacylglycerophosphoric acid benzyl ester with 1,3-diiodopropanol benzyl ether (19,20). This method is not feasible for the routine preparation of large quantities owing to the many steps involved, the use of highly photosensitive silver salt intermediates, and unstable iodo intermediates.

EXPERIMENTAL PROCEDURES

NMR spectra were recorded on a Varian Inova (500 MHz) NMR spectrometer or a Varian VXR (300 MHz) NMR spectrometer from solutions in deuteriochloroform with tetramethylsilane

*To whom correspondence should be addressed at NeoPharm, Inc., 1850 Lakeside Dr., Waukegan, IL 60085. E-mail: Imran@neophrm.com

Presented at the 94th AOCS Annual Meeting & Expo, Kansas City, Missouri, May 4–7, 2003.

Abbreviations: ATR, attenuated total reflectance; DIEA, *N,N*-diisopropylethylamine; ESI, electron spray ionization; MCPBA, *m*-chloroperoxybenzoic acid; rt, room temperature; TMS, tetramethylsilane; TPSCl, 2,4,6-triisopropylbenzenesulfonyl chloride.

(TMS) as the internal reference standard. Chemical shifts are given in ppm (δ) downfield from TMS (δ_{TMS} = 0 ppm). Mass spectral analyses [electron spray ionization (ESI)] were carried out on Triple Quadrupole LC/MS/MS mass spectrometer API 4000 (Applied Biosystems). IR spectra were recorded on a Nicolet Nexus 470 FT-IR. Samples were prepared by the attenuated total reflectance (ATR) method. Optical rotations were measured on a model 341 Perkin-Elmer polarimeter. Bovine heart cardiolipin was purchased from Sigma Chemical Co. (St. Louis, MO). *N,N*-Diisopropylmethylphosphonamidic chloride and 2-*O*-benzylglycerol were purchased from Aldrich Chemical Co. (Milwaukee, WI). 1,2-*O*-Dimyristoyl-*sn*-glycerol was purchased from Genzyme Pharmaceuticals (Cambridge, MA). 1,2-*O*-Dimyristyl-*sn*-glycerol was prepared in this laboratory starting from (*R*)-(+)-1-*O*-benzylglycerol and 1-bromotetradecane; both are available from Aldrich Chemical Co. 1,2-*O*-Dioleoyl-*sn*-glycerol was purchased from Avanti Polar Lipids (Alabaster, AL). All reactions requiring anhydrous conditions were performed under a positive pressure of dry argon. All anhydrous solvents such as dichloromethane and THF were purchased from Aldrich Chemical Co. and were used as such. Chromatographic purifications were done using Silica gel 60 (230–400 mesh, Whatman) and the indicated solvent systems. TLC was done on Silica gel 60 F_{254} plates (250 μm; EM Science, Gibbstown, NJ), and spots were visualized either by spraying with phosphomolybdate reagent followed by heating or spraying with molybdenum blue (Sigma Chemical Co.).

Synthesis of 2-O-*benzyl-1,3-bis[(1,2*-O-*dimyristoyl*-sn-*glycero-3)phosphoryl]glycerol dimethyl ester **5a***. To a solution of *N,N*-diisopropylmethylphosphonamidic chloride **3** (1.92 g, 9.22 mmol) and dry *N,N*-diisopropylethylamine (DIEA; 1.92 mL, 11.1 mmol) in CH_2Cl_2 (10 mL) was added dropwise a solution of 1,2-*O*-dimyristoyl-*sn*-glycerol **2a** (4.61 g, 9.0 mmol) in CH_2Cl_2 (45 mL) at room temperature over 30 min. After addition, the reaction mixture was stirred at room temperature for 1.5 h and then 1*H*-tetrazole of 3 wt% solution in acetonitrile (71.8 mL, 24.3 mmol) was added. To this reaction mixture, a solution of 2-*O*-benzylglycerol **4** (0.66 g, 3.60 mmol) in CH_2Cl_2 (10 mL) was added dropwise. The reaction mixture was stirred at room temperature for 3 h. The reaction mixture was then cooled to –40°C, and a solution of 77% *m*-chloroperoxybenzoic acid (MCPBA; 2.64 g, 11.80 mmol) in CH_2Cl_2 (10 mL) was added such that the temperature of the reaction mixture was kept below 0°C. The mixture was warmed to 25°C before it was transferred to a separatory funnel and washed with 5% $Na_2S_2O_3$ (2 × 30 mL), 5% $NaHCO_3$ (2 × 50 mL), cold 1 N HCl (2 × 15 mL), water, and brine. The organic phase was dried over anhydrous Na_2SO_4 and concentrated *in vacuo* to yield an oil residue. The residue was purified by flash chromatography on silica gel, eluting with hexane/ethyl acetate (2:1 to 1:1, vol/vol) to afford **5a** as a colorless oil. Yield 4.38 g (90%). TLC (hexane/EtOAc 1:1, vol/vol), R_f = 0.16; ^{1}H NMR (300 MHz, $CDCl_3$) δ: 7.35 (*m*, 5H, Ar*H*), 5.22 (*m*, 2H, RCOOC*H*), 4.67 (*s*, 2H, CH_2Ph), 4.34–4.06 (*m*, 12H, RCOOCH_2, POCH_2), 3.83 (*m*, 1H, BnOC*H*), 3.75 (*dt, J* = 11.4, 3.0 Hz, 6H, POCH_3), 2.31 (*m*, 8H, –CH_2COO–), 1.59 (*m*, 8H, –CH_2CH$_2$COO–), 1.25 (*br s*, 80H, CH_2), 0.88 (*t, J* = 6.6 Hz, 12H, CH_3).

Synthesis of 2-O-*benzyl-1,3-bis[(1,2*-O-*dimyristoyl*-sn-*glycero-3)phosphoryl]glycerol diammonium salt **6a***. To a stirred solution of compound **5a** (1.80 g, 1.32 mmol) in 2-butanone (85 mL) was added NaI (0.59 g, 3.96 mmol), and the reaction mixture was refluxed for 1.5 h and then cooled to 25°C. The resulting white precipitate was filtered and washed with cold 2-butanone to yield 1.71 g of 2-*O*-benzyl-1,3-bis(1,2-*O*-dimyristoyl-*sn*-glycero-3-phosphoryl)glycerol disodium salt as a white solid. The disodium salt was dissolved in a cold mixture of $CHCl_3$ (80 mL), MeOH (160 mL), and 0.1 N HCl (80 mL) and stirred at room temperature for 40 min. After addition of H_2O (80 mL) and $CHCl_3$ (80 mL), the $CHCl_3$ layer was isolated and washed with H_2O (50 mL). The organic layer was neutralized by addition of 15 mL of 10% NH_4OH. The organic layer was separated and concentrated *in vacuo* to give a residue, which was further purified through a short silica gel column using $CHCl_3$/MeOH/NH_4OH (65:15:1, by vol) to afford 2-*O*-benzyl-1,3-bis[(1,2-*O*-dimyristoyl-*sn*-glycero-3)phosphoryl]glycerol diammonium salt **6a** as a white solid. Yield 1.42 g (79%). TLC ($CHCl_3$/MeOH/NH_4OH 65:25:5, by vol), R_f = 0.64; ^{1}H NMR (300 MHz, $CDCl_3$) δ: 7.55 (*br s*, 8H, NH_4), 7.33–7.31 (*m*, 5H, Ar*H*), 5.20 (*m*, 2H, RCOOC*H*), 4.60 (*s*, 2H, CH_2Ph), 4.29–3.89 (*m*, 12H, RCOOCH_2, POCH_2), 3.69 (*m*, 1H, BnOC*H*), 2.27 (*m*, 8H, –CH_2COO–), 1.56 (*m*, 8H, –CH_2CH$_2$COO–), 1.25 (*br s*, 80H, CH_2), 0.88 (*t, J* = 6.5 Hz, 12H, CH_3); ESI–MS, *m/z* $(M - 2NH_4)^{2-}$ 664.9, $(M - 2NH_4 - RCOO)^-$ 1102.0, $(M - 2NH_4 + H)^-$ 1330.3.

Synthesis of 1,3-bis[(1,2-O-*dimyristoyl*-sn-*glycero-3)phosphoryl]glycerol diammonium salt **1a** (tetramyristoyl cardiolipin)*. A sample of 2-*O*-benzyl-1,3-bis[(1,2-*O*-dimyristoyl-*sn*-glycero-3)phosphoryl]glycerol diammonium salt **6a** (1.52 g, 1.10 mmol) was dissolved in THF (40 mL) and hydrogenated with 10% Pd-C (1.16 g) at a pressure of 50 psi for 9 h. After filtration on Celite to remove the catalyst, the solution was evaporated to dryness. The residue was dissolved in chloroform (8 mL) and precipitated using acetone (60 mL). The mixture was kept in a freezer overnight, and the white solid was filtered and washed with a small amount of cold acetone. After drying in a vacuum desiccator under Drierite for 3 h and then over phosphorus pentoxide (P_2O_5) overnight, 1,3-bis[(1,2-*O*-dimyristoyl-*sn*-glycero-3)phosphoryl]glycerol diammonium salt **1a** (tetramyristoyl cardiolipin) was obtained. Yield 1.21 g (85%). TLC ($CHCl_3$/MeOH/NH_4OH 65:25:5, by vol), R_f = 0.29; ($[\alpha]_D^{25}$ = +4.5 c = 1.5 in $CHCl_3$); ^{1}H NMR (500 MHz, $CDCl_3$) δ: 7.32 (*br s*, 8H, NH_4), 5.26 (*m*, 2H, RCOOC*H*), 4.34–3.92 (*m*, 13H, RCOOCH_2, POCH_2, HOC*H*), 2.33 (*m*, 8H, –CH_2COO–), 2.29 (*t, J* = 7.5 Hz, 1H, CHO*H*), 1.58 (*m*, 8H, –CH_2CH$_2$COO–), 1.30 (*br s*, 80H, CH_2), 0.88 (*t, J* = 6.5 Hz, 12H, CH_3); FTIR (ATR) 3231s, 2918s, 2850s, 1738s, 1467w, 1378w, 1203ms, 1067s cm^{-1}; ESI–MS, *m/z* $(M - 2NH_4)^{2-}$ 619.9, $(M - 2NH_4 - RCOO)^-$ 1011.9, $(M - 2NH_4 + H)^-$ 1240.2.

Synthesis of 2-O-*benzyl-1,3-bis[(1,2*-O-*dimyristyl*-sn-*glycero-3)phosphoryl]glycerol dimethyl ester **5b***. This compound was prepared following the procedure described for the

preparation of **5a**, substituting 1,2-*O*-dimyristyl-*sn*-glycerol **2b** in place of 1,2-*O*-dimyristoyl-*sn*-glycerol **2a**. The crude product was purified by flash chromatography on silica gel, eluting with a gradient of hexane/ethyl acetate (1:0 to 1:1, vol/vol) to give 2-*O*-benzyl-1,3-bis[(1,2-*O*-dimyristyl-*sn*-glycero-3)phosphoryl]glycerol dimethyl ester **5b** in the yield of 79%. TLC (hexane/EtOAc 1:1, vol/vol), R_f = 0.24. ^{1}H NMR (300 MHz, $CDCl_3$): δ: 7.35–7.29 (*m*, 5H, Ar*H*), 4.68 (*s*, 2H, CH_2Ph), 4.26–4.02 (*m*, 8H, POCH_2), 3.86 (*m*, 2H, ROC*H*), 3.75 (*d, J* = 12.0, 6H, POCH_3), 3.61–3.38 (*m*, 13H, –CH_2OCH_2–, –CH_2-OCH–, BnOC*H*), 1.54 (*m*, 8H, –CH_2CH_2O–), 1.29 (*m*, 88H, CH_2), 0.88 (*t, J* = 6.7, 12H, CH_3).

*Synthesis of 2-*O*-benzyl-1,3-bis[(1,2-*O*-dimyristyl-*sn*-glycero-3)phosphoryl]glycerol diammonium salt **6b***. Following the procedure described for the preparation of **6a**, 2-*O*-benzyl-1,3-bis[(1,2-*O*-dimyristyl-*sn*-glycero-3)phosphoryl]glycerol dimethyl ester **5b** was treated with NaI in 2-butanone. The resulting disodium salt was converted to its free acid, then neutralized with concentrated aqueous NH_4OH to afford 2-*O*-benzyl-1,3-bis[(1,2-*O*-dimyristyl-*sn*-glycero-3)phosphoryl] glycerol diammonium salt **6b** in the yield of 60%. TLC ($CHCl_3$/MeOH/NH_4OH, 65:25:5, by vol), R_f = 0.50; ^{1}H NMR (500 MHz, $CDCl_3$): δ: 7.29–7.21 (*m*, 5H, Ar*H*), 4.57 (*s*, 2H, CH_2Ph), 4.21–3.38 (*m*, 23H, POCH_2, –CH_2OCH_2–; –CH_2OC*H*–, BnOC*H*), 1.50 (*m*, 8H, CH_2CH_2O–), 1.25 (*m*, 88H, CH_2), 0.89 (*t*, 12H, *J* = 6.54 Hz, CH_3); ESI–MS, *m/z* $(M - 2NH_4 + H)^-$ 1274.1, $(M - 2NH_4)^{2-}$ 636.9.

*Synthesis of 1,3-bis[(1,2-*O*-dimyristyl-*sn*-glycero-3)phosphoryl]glycerol diammonium salt **7** (tetramyristyl cardiolipin ether analog).* Following the procedure described for the preparation of **1a**, 2-*O*-benzyl-1,3-bis[(1,2-*O*-dimyristyl-*sn*-glycero-3)phosphoryl]glycerol diammonium salt **6b** was hydrogenated in THF with 10% Pd-C at 50 psi for 16 h to afford 1,3-bis[(1,2-*O*-dimyristyl-*sn*-glycero-3)phosphoryl]glycerol diammonium salt **7** in the yield of 56%. TLC ($CHCl_3$/ MeOH/ NH_4OH, 65:25:5, by vol), R_f = 0.28; ^{1}H NMR (500 MHz, $CDCl_3$): δ: 7.29 (*br s*, 8H, NH_4), 4.20–3.80 (m, 8H, POCH_2), 3.57–3.41 (*m*, 15H, CH_2OCH_2, CH_2OC*H*–, HOC*H*), 2.3 (*br*, 1H, O*H*), 1.53 (*m*, 8H, CH_2CH_2O–), 1.25 (*m*, 88H, CH_2), 0.87 (*t*, 12H, *J* = 6.9 Hz, CH_3); ESI–MS, *m/z* 1184.7 $(M - 2NH_4 + H)^-$, 591.3 $(M - 2NH_4)^{2-}$.

*Synthesis of 2-*O*-benzyl-1,3-bis[(1,2-*O*-dioleoyl-*sn*-glycero-3)phosphoryl]glycerol dimethyl ester **9***. To a solution of *N,N*-diisopropylmethylphosphoramidic chloride **3** (0.48 g, 2.31 mmol) and dry DIEA (0.48 mL, 2.78 mmol) in CH_2Cl_2 (2.5 mL) was added dropwise a solution of 1,2-*O*-dioleoyl-*sn*-glycerol **8** (1.38 g, 2.22 mmol) in CH_2Cl_2 (10 mL) at room temperature. After the reaction mixture was stirred at room temperature (rt) for 1.5 h, 1*H*-tetrazole of 3 wt% solution in acetonitrile (17.6 mL, 5.97 mmol) was added. To this reaction mixture, a solution of 2-*O*-benzylglycerol **4** (147 mg, 0.81 mmol) in CH_2Cl_2 (10 mL) was added dropwise. The reaction mixture was stirred at room temperature for 2.5 h, then cooled to –40°C, and 0.70 mL of *t*-butylperoxide (*t*-BuOOH) (5.0–6.0 M solution in nonane) was added with stirring. The reaction was warmed to 25°C and was transferred to a separatory funnel, diluted with CH_2Cl_2, and washed with 5% $Na_2S_2O_3$ (2 × 20 mL), 5% $NaHCO_3$ (2 × 20 mL), cold 1 N HCl (15 mL), water, and brine. The organic phase was dried over anhydrous Na_2SO_4 and concentrated *in vacuo* to yield an oil residue. The residue was purified by flash chromatography on silica gel eluting with hexane/ethyl acetate (2:1 to 1:1, vol/vol) to afford 2-*O*-benzyl-1,3-bis[(1,2-*O*-dioleoyl-*sn*-glycero-3)phosphoryl]glycerol dimethyl ester **9** as a colorless oil. Yield 0.90 g (71%). TLC (hexane/EtOAc 1:1, vol/vol), R_f = 0.29; ^{1}H NMR (300 MHz, $CDCl_3$) δ: 7.35 (*m*, 5H, Ar*H*), 5.34 (*m*, 8H, C*H*=C*H*), 5.22 (*m*, 2H, RCOOC*H*), 4.67 (*s*, 2H, CH_2Ph), 4.33–4.06 (*m*, 12H, RCOOCH_2, POCH_2), 3.83 (*m*, 1H, BnOC*H*), 3.75 (*dt, J* = 11.2, 3.0 Hz, 6H, POCH_3), 2.32 (*m*, 8H, –CH_2COO–), 2.00 (*m*, 16H, allylic CH_2), 1.59 (*m*, 8H, –CH_2CH_2COO–), 1.28 (*br s*, 80H, CH_2), 0.88 (*t, J* = 6.6 Hz, 12H, CH_3).

*Synthesis of 2-*O*-benzyl-1,3-bis[(1,2-*O*-dioleoyl-*sn*-glycero-3)phosphoryl]glycerol diammonium salt **10***. This compound was prepared as described for the preparation of **6a**, substituting **9** in place of **5a**. The free form of 2-*O*-benzyl-1,3-bis[(1,2-*O*-dioleoyl-*sn*-glycero-3)phosphoryl]glycerol in $CHCl_3$ was neutralized by addition of concentrated aqueous NH_4OH at 0°C. The mixture was stirred at room temperature for a few minutes and concentrated *in vacuo* to give a residue, which was further taken in hexanes and evaporated twice and dried under high vacuum overnight. 2-*O*-Benzyl-1,3-bis[(1,2-*O*-dioleoyl-*sn*-glycero-3)phosphoryl]glycerol diammonium salt **10** was obtained as a white gummy solid in the yield of 91%. TLC ($CHCl_3$/MeOH/NH_4OH 65:25:5, by vol), R_f = 0.67; ^{1}H NMR (500 MHz, $CDCl_3$) δ: 7.57 (*br* s, 8H, NH_4), 7.33 (*m*, 5H, Ar*H*), 5.34 (*m*, 8H, C*H*=C*H*), 5.21 (*m*, 2H, RCOOC*H*), 4.61 (*s*, 2H, CH_2Ph), 4.35–3.89 (*m*, 12H, RCOOCH_2, POCH_2), 3.73 (*m*, 1H, BnOC*H*), 2.29 (*m*, 8H, –CH_2COO–), 2.00 (*m*, 16H, allylic CH_2), 1.58 (*m*, 8H, –CH_2 CH_2COO–), 1.28 (*br s*, 80H, CH_2), 0.88 (*t, J* = 6.6 Hz, 12H, CH_3); ESI–MS, *m/z* $(M - 2NH_4)^{2-}$ 772.5, $(M - 2NH_4 + H)^-$ 1545.9.

*Synthesis of 1,3-bis[(1,2-*O*-dioleoyl-*sn*-glycero-3)phosphoryl]glycerol diammonium salt **11** (tetraoleoyl cardiolipin).* To a solution of 2-*O*-benzyl-1,3-bis[(1,2-*O*-dioleoyl-*sn*-glycero-3)phosphoryl]glycerol diammonium salt **10** (357.6 mg, 0.23 mmol) in CH_2Cl_2 (40 mL) was added dropwise a 1.0-M solution of boron trichloride in CH_2Cl_2 (1.25 mL, 1.25 mmol) at –78°C over 5 min. The reaction mixture was stirred at –78 to 0°C for 1.5 h. To this, crushed ice was added to quench the reaction at –10°C, then 1 mL of concentrated aqueous NH_4OH was added dropwise. The mixture was concentrated *in vacuo* until a small amount of water remained. Hexane was added, and the water layer was separated. The organic layer was concentrated *in vacuo*. The residue was purified by flash chromatography on silica gel by eluting with $CHCl_3$/MeOH/NH_4OH (65:15:1 to 65:25:2.5, by vol) to afford 1,3-bis[(1,2-*O*-dioleoyl-*sn*-glycero-3)phosphoryl]glycerol diammonium salt **11** (tetraoleoyl cardiolipin) as a white gummy solid. Yield 250 mg (74%). TLC ($CHCl_3$/MeOH/NH_4OH 65:25:5), R_f = 0.40; $[\alpha]_D^{25}$ = +3.1 (c = 1.5 in $CHCl_3$); ^{1}H NMR (500 MHz, $CDCl_3$): δ: 7.43 (*br s*, 8H, NH_4), 5.34 (*m*, 8H, olefinic protons), 5.19

(*m*, 2H, RCOOC*H*), 4.38–3.91 (*m*, 13H, RCOOCH_2, POCH_2, HOC*H*), 2.29 (*m*, 8H, –CH_2COO–), 2.17 (*br s*, 1H, O*H*), 2.01 (*m*, 16H, allylic CH_2), 1.58 (*m*, 8H, –CH_2CH_2COO–), 1.29 (*br s*, 80H, CH_2), 0.88 (*t, J* = 6.5 Hz, 12H, CH_3). ESI–MS, *m/z* $(M - 2NH_4)^{2-}$ 727.6, $(M - 2NH_4 - RCOO)^-$ 1174.2, $(M - 2NH_4 + H)^-$ 1456.6.

RESULTS AND DISCUSSION

The synthetic methodology that we have developed involves the application of chlorophosphoramidite **3** (Scheme 2) as a phosphorating agent to build a cardiolipin core structure through a phosphotriester approach. The phosphoramidite chemistry is well known in oligonucleotide synthesis (21,22). The method is attractive because phosphorus(III) reagents are generally more reactive than phosphorus(V) reagents and usually offer higher yield. The *N,N*-diiospropylmethylphosphoramidic chloride **3** has the advantage of reacting with two different alcohols in a stepwise manner to form an unsymmetric phosphite triester. This reagent has been reported in the synthesis of PI 3-phosphates (23). To our knowledge, it has not been used for cardiolipin synthesis. As illustrated in Scheme 2, 1,2-*O*-dimyristoyl-*sn*-glycerol **2a** is subsequently reacted with reagent **3** in an inert solvent such as dichloromethane in the presence of DIEA, then with 2-*O*-benzylglycerol **4** in the presence of 1*H*-tetrazole followed by oxidation with MCPBA to form the symmetrically substituted cardiolipin precursor **5a**. To minimize side product formation, the chlorophosphoramidite **3** was first coupled with the bulkier of the two alcohol reactants, and the proton acceptor, DIEA, was introduced at the same time to avoid the possibility of a migration of the acyl group from the 1,2-position into the 1,3-position. The resulting phosphoramidite intermediate was subsequently reacted with 2-*O*-benzylglycerol **4** in the same flask. The second phosphorylation is promoted by 1*H*-tetrazole, which activates the amidite and acts as a scavenger of the generated amine. In the routine oxidation of phosphite triester to phosphate triester, it is necessary to remove the excess DIEA and its hydrochloride salt prior to oxidation (24). To simplify the reaction procedure, we used excess 1*H*-tetrazole in the subsequent alcohol phosphorylation, which allowed us to oxidize the phosphite triester intermediate with MCPBA to the desired phosphate triester **5a** without isolation of excess DIEA and its hydrochloride salt. After oxidation, the product was purified on silica gel chromatography. The coupling and oxidation reaction sequence was accomplished in a simple one-pot manner under mild conditions to provide the fully protected cardiolipin **5a** in high yield (90%).

The deprotection of the methyl group of the cardiolipin precursor **5a** was carried out by refluxing with NaI in 2-butanone to quantitatively produce a disodium salt, which was then converted to its ammonium salt **6a** by treatment with 0.1 N HCl followed by 10% ammonium hydroxide. Use of a methyl group as a protecting group gives the advantage of facile deprotection, and the resulting disodium salt generated from the reaction precipitates out easily in 2-butanone and can be converted to its ammonium salt by simple acid–base transformation. In the final step, deprotection of benzyl group of **6a** was accomplished by

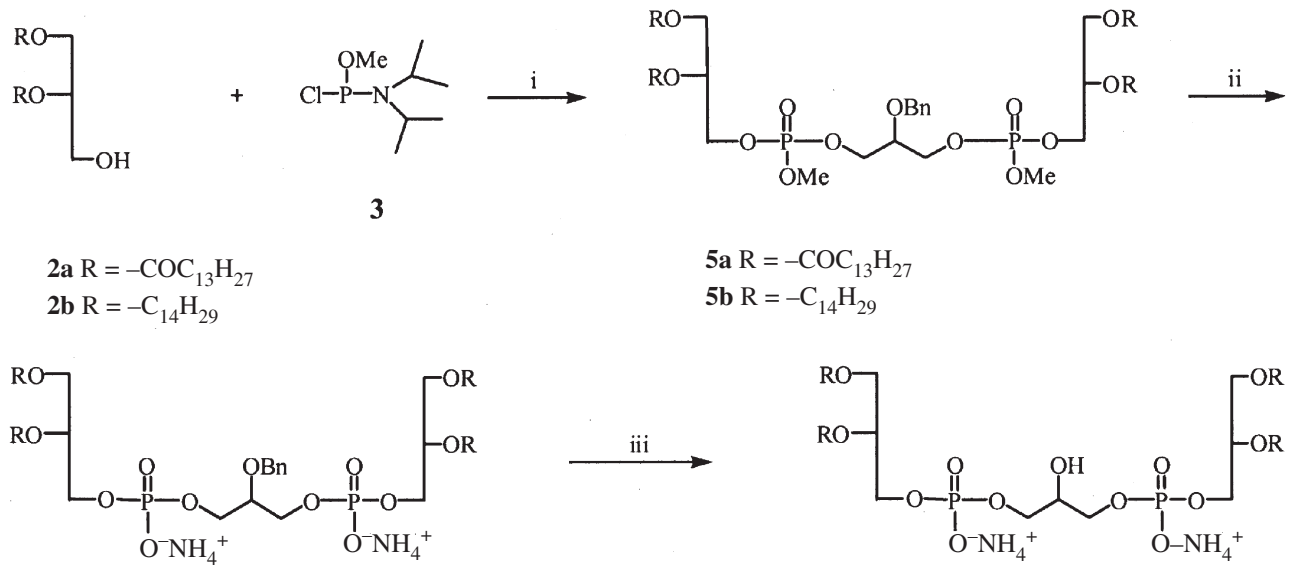

Reagents and conditions: (i) (a) *N,N*-diisopropylethylamine, CH_2Cl_2, room temperature (rt), 1.5 h; (b) 2-*O*-benzylglycerol **4**, 1*H*-tetrazole, rt, 3 h; (c) *m*-chloroperoxybenzoic acid, –40°C to rt; (ii) (a) NaI, 2-butanone, reflux, 1.5 h; (b) dil. HCl, then aq. NH_4OH; (iii) H_2, THF, 10% Pd/C.

SCHEME 2

catalytic hydrogenation to yield pure cardiolipin as its ammonium salt **1a** in 85% yield. The final product was purified by the precipitation from chloroform/acetone (1:7.5) at –20°C.

The generality of the method was further exemplified by the synthesis of ether analog 7 of cardiolipin. As depicted in Scheme 2, 1,2-*O*-dimyristyl-*sn*-glycerol **2b** is reacted to couple it with 2-*O*-benzylglycerol in the presence of chlorophosphoramidite **3** to provide an intermediate **5b**. Demethylation of this intermediate **5b** with NaI in 2-butanone yielded the protected cardiolipin analog **6b**, which on deprotection yielded ether analog **7** of cardiolipin.

Synthetic substitutes of naturally occurring cardiolipin containing unsaturated acyl chains are not fully investigated. Methods for the synthesis of these series of compounds have been somewhat restricted because of the lack of an efficient method for removal of the protecting group, such as the benzyl group, without affecting the double bonds as well as their propensity to undergo facile oxidation. The *t*-butyldimethylsilyl group was commonly employed as the protecting group for the hydroxyl functionality of the central glycerol unit in the synthesis of unsaturated cardiolipin (15,16). To extend the scope of chlorophosphoramidite application, we further established a versatile procedure to synthesize cardiolipin bearing unsaturated acyl side chains. In Scheme 3, 1,2-*O*-dioleoyl-*sn*-glycerol **8** is subsequently reacted with the reagent **3** in dichloromethane in the presence of DIEA, then with 2-*O*-benzylglycerol **4** in the presence of 1*H*-tetrazole followed by *in situ* oxidation to form tetraoleoyl cardiolipin precursor **9** in good overall yield of 71%. Although olefin can be epoxidized with any peracids, it is unreactive with an alkylperoxide in the absence of a catalyst of a transition metal complex (25). Therefore, oxidation of phosphite triester generated from the coupling reaction by using *t*-butylperoxide proceeds smoothly to give the corresponding phosphate triester **9**. Compound **9** was easily demethylated to afford cardiolipin precursor **10** in high yield of 91%. Boron trichloride has been reported to deprotect the benzyl group of 1-*O*-benzyl-2,3-*O*-diacylglycerol at low temperature without affecting double bonds (26). This reagent was successfully utilized in the deprotection of benzyl-protected cardiolipin **10** to produce tetraoleoyl cardiolipin **11** in good yield of 74%.

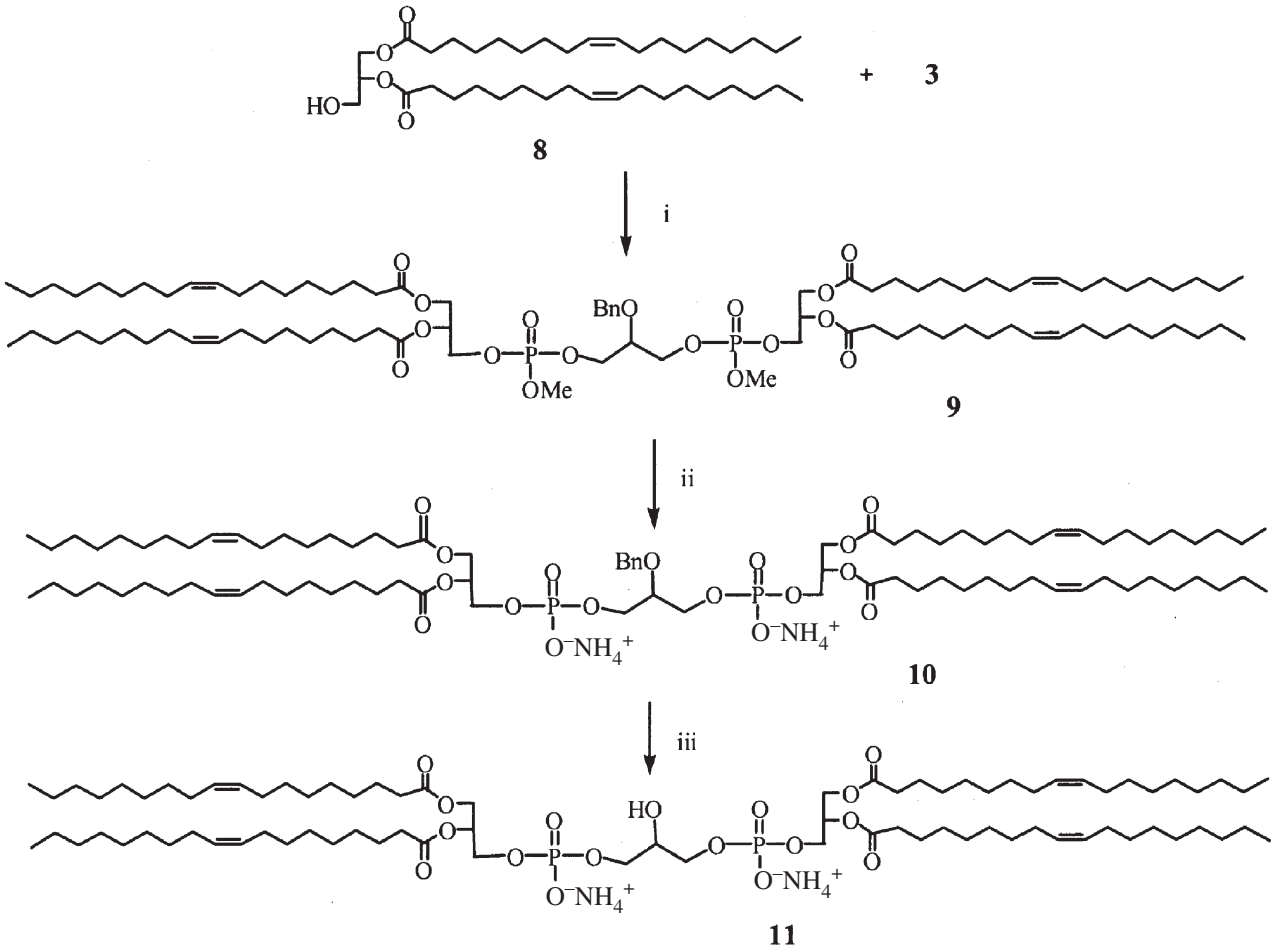

Reagents and conditions: (i) (a) *N*,*N*-diisopropylethylamine, CH_2Cl_2, room temperature (rt), 1.5 h; (b) 2-*O*-benzylglycerol **4**, 1*H*-tetrazole, rt, 2.5 h; (c) *t*-BuOOH, –40°C to rt; (ii) (a) NaI, 2-butanone, reflux, 1 h; (b) dil. HCl, then aq. NH_4OH; (iii) BCl_3, CH_2Cl_2, –78 to 0°C.

SCHEME 3

The synthetic cardiolipins were compared to the natural cardiolipin by NMR and optical rotation. The highly characteristic 500 MHz ^{1}H NMR spectra of **1a** and **11** were essentially identical with natural cardiolipin from bovine heart (Sigma Chemical Co.) except for the additional resonances seen in the latter due to vinyl and allylic protons. Both **1a** and **11** are *dextro* isomers (**1a**, $[\alpha]_D^{25} = +4.5$, c = 1.5 in $CHCl_3$; **11**, $[\alpha]_D^{25} = +3.1$, c = 1.5 in $CHCl_3$) that are consistent with cardiolipin sodium salt from bovine heart ($[\alpha]_D^{25} = +4.8$, c = 1.5 in $CHCl_3$). As anticipated, the optical rotations are not exactly identical because the natural cardiolipin from bovine heart is a mixture of cardiolipin derivatives.

In conclusion, the experiments outlined herein convincingly establish the utility of chlorophosphoramidite coupling and oxidation protocol for the efficient synthesis of cardiolipin and its analogs. There are three distinctive features of the method: (i) It is a simple and straightforward approach to synthesize cardiolipin. The synthesis involves three steps, with 60% overall yield to produce tetramyristoyl cardiolipin and about 50% overall yield for the synthesis of tetraoleoyl cardiolipion; (ii) the one-pot coupling/oxidation procedure as well as the easy deprotection and purification procedure is suitable for large-scale production of tetramyristoyl cardiolipin; and (iii) the synthetic methodology can be applied to prepare symmetrical cardiolipin species and analogs bearing a variety of different glyceryl units. This flexibility provides a general method to synthesize various cardiolipins and analogs.

REFERENCES

1. Ioannou, P., and Golding, B.T. (1979) Cardiolipins: Their Chemistry and Biochemistry, *Prog. Lipid Res. 17*, 279–318.
2. Semin, B.K., Saraste, M., and Wikstrom, M. (1984) Calorimetric Studies of Cytochrome Oxidase–Phospholipid Interactions, *Biochim. Biophys. Acta 769*, 15–22.
3. Thompson, D.A., and Ferguson-Miller, S. (1983) Lipid and Subunit III Depleted Cytochrome *c* Oxidase Purified by Horse Cytochrome *c* Affinity Chromatography in Lauryl Maltoside, *Biochemistry 22*, 3178–3187.
4. Chen, Q.P., and Li, Q.T. (2001) Effect of Cardiolipin on Proton Permeability of Phospholipid Liposomes: The Role of Hydration at the Lipid–Water Interface, *Arch. Biochem. Biophys. 389*, 201–206.
5. Chauhan, A., Ray, I., and Chauhan, V.P. (2000) Interaction of Amyloid β-Protein with Anionic Phospholipids: Possible Involvement of Lys28 and C-Terminus Aliphatic Amino Acids, *Neurochem. Res. 25*, 423–429.
6. Weissig, V., and Torchilin, V. P. (2000) Mitochondriotropic Cationic Vesicles: A Strategy Towards Mitochondrial Gene Therapy, *Curr. Pharm. Biotechnol. 1*, 325–346.
7. Fernandez, J.A., Kojima, K., Petäjäa, J., Hackeng, T.M., and Griffin, J.H. (2000) Cardiolipin Enhances Protein C Pathway Anticoagulant Activity, *Blood Cells, Mol. Dis. 26*, 115–123.
8. Guilmin, T., Goormaghtigh, E., Brasseur, R., Caspers, J., and Ruysschaert, J.M. (1982) Evaluation of the Anesthetic–Lipid Association Constant. A Monolayer Approach, *Biochim. Biophys. Acta 685*, 169–176.
9. Mestres, C., Ortiz, A., Haro, I., Reig, F., and Alsina, M.A. (1997) Influence of Phospholipidic Charge on the Interaction of a Multiple Antigenic Peptide from Hepatitis A Virus with Monolayers and Bilayers, *Langmuir 13*, 5669–5673.
10. Tavitian, B., Marzabal, S., Boutet, V., Kuhnast, B., Terrazzino, S., Moynier, M., Dolle, F., Deverre, J.R., and Thierry, A.R. (2002) Characterization of a Synthetic Anionic Vector for Oligonucleotide Delivery Using *in vivo* Whole Body Dynamic Imaging, *Pharm. Res. 19*, 367–376.
11. Deborah, J. (2002) Encapsulating the Science of Liposomes, *Drug Discov. Devel. 5(5)*, 28–32 (www.dddmag.com).
12. Gokhale, P.C., Radhakrishnan, B., Husain, S.R., Abernethy, D. R., Sacher, R., Dritschilo, A., and Rahman, A. (1996) An Improved Method of Encapsulation of Doxorubicin in Liposomes: Pharmacological, Toxicological and Therapeutic Evaluation, *Br. J. Cancer 74*, 43–48.
13. Thierry, A.R., Rahman, A., and Dritschilo, A. (1994) A New Procedure for the Preparation of Liposomal Doxorubicin: Biological Activity in Multidrug-Resistant Tumor Cells, *Cancer Chemother. Pharmacol. 35*, 84–88.
14. Saunders, R.M., and Schwarz, H.P. (1966) Synthesis of Phosphatidylglycerol and Diphosphatidylglycerol, *J. Am. Chem Soc. 88*, 3844–3847.
15. Ramirez, F., Ioannou, P.V., Marecek, J.F., Dodd, G.H., and Golding, B.T. (1977) Synthesis of Phospholipids by Means of Cyclic Enediol Pyrophosphates Optically Active Monovalent and Divalent Cation Salts of Diphosphatidylglycerol (cardiolipin), *Tetrahedron 33*, 599–608.
16. Duralski, A.A., Spooner, P.J.R., Rankin, S.E., and Watts, A. (1998) Synthesis of Isotopically Labelled Cardiolipins, *Tetrahedron Lett. 39*, 1607–1610.
17. Mishina, I.M., Vasilenko, I.A., Stepanov, A.E., and Shvets, V.I. (1987) Studies on Complex Lipids. Synthesis of Diphosphatidylglycerol (cardiolipin) with Unsaturated Fatty Acids, *Bioorg. Khim. 13*, 1110–1115.
18. Mishina, I.M., Vasilenko, I.A., Stepanov, A.E., and Shvets, V.I. (1984) Study of Lipids. Synthesis of Phosphatidylglycerol and Diphosphatidylglycerol, *Zh. Org. Khim. 20*, 985–988.
19. Inoue, K., and Nojima, S. (1968) Immunochemical Studies of Phospholipids. II. Syntheses of Cardiolipin and Analogues, *Chem. Pharm. Bull. 16*, 76–81.
20. De Haas, G.H., Bonsen, P.P.M., and Van Deenen, L.L.M. (1966) Studies on Cardiolipin III. Structural Identity of Ox-Heart Cardiolipin and Synthetic Diphosphatidyl Glycerol, *Biochim. Biophys. Acta 116*, 114–124.
21. Atkinson, T., and Smith, M. (1984) *Oligonucletide Synthesis—A Practical Approach* (Gait, M.J., ed.), IRL, Oxford.
22. Beaucage, S.L., and Radhakrishnan, P.I. (1993) The Synthesis of Specific Ribonucleotides and Unrelated Phosphorylated Biomolecules by the Phosphoramidite Method, *Tetrahedron 49*, 10441–10488.
23. Bruzik, K.S., and Kubiak, R.J. (1995) General Synthesis of Phosphatidylinositol 3-Phosphates, *Tetrahedron Lett. 36*, 2415–2418.
24. Martin, S.F., Josey, J.A., Wong, Y.-L., and Dean, D.W. (1994) General Method for the Synthesis of Phospholipid Derivatives of 1,2-*O*-Diacyl-*sn*-glycerols, *J. Org. Chem. 59*, 4805–4820.
25. March, J. (1992) *Advanced Organic Chemistry*: *Reactions, Mechanisms, and Structure,* 4th edn., pp. 826–828, John Wiley & Sons, New York.
26. Xia, J., and Hui, Y.Z. (1999) Synthesis of a Small Library of Mixed-Acid Phospholipids from D-Mannitol as a Homochiral Starting Material, *Chem. Pharm. Bull. 47*, 1659–1663.

[Received November 14, 2003; accepted February 23, 2004]

Diets Play a Major Role in Heart Diseases in China

Sir:

I wish to echo Dr. Lands' plea that diets could prevent many diseases (1). That diets could prevent coronary artery disease and hypertension is certainly supported by data emanating from China.

Coronary artery disease used to be extremely rare in old China (2). But it has increased considerably in prevalence in the past several decades, rising from the fifth-most common form of heart disease in 1948–1957 (6%) to the second-most common in 1958–1968 (16%) and 1969–1979 (26%), and to the most common in 1980–1989 (27%), where it remains until this date (3). The main culprit is the changing dietary habits. The modern-day Chinese love atherogenic fast foods and devour them at an ever faster rate. The huge success of two of the world's best-known fast-food giants, McDonald's and Kentucky Fried Chicken, is the result of a change of Chinese lifestyles, disposable income, and eating habits, which are becoming more geared to speed, convenience, and fashion. There are more than 800 Kentucky Fried Chicken and 430 McDonald's restaurants in China (3); the numbers continue to grow. Every child in China knows the name and can sing the song of McDonald's, although completely unaware of the frightening fact that a Big Mac contains 34 grams of fat (4). More than one-third of all adults in China and over half of the adults in China's urban areas consume over 30% of their energy from fat (5).

As a consequence of the recent change of dietary habits in China, the normal plasma cholesterol values in modern (especially urban) China have shown a steady increase. In 2002, the upper limit of normal was 6.0 mmol/L or 232 mg/dL, and the mean value was 5.06 mmol/L or 196 mg/dL (6). These "normal" values were considerably higher than the normal values in China published in 1958 (155 mg/dL) (7), in 1981 (191 mg/dL) (7), and in 1997 (200 mg/dL) (8). In 1998 mean serum cholesterol levels in adults from rural China were still reported to be 127 mg/dL, compared with 203 mg/dL in residents of the United States (9).

Hypertension in China is another diet-induced disease caused by excessive salt intake in the diet. The fast foods sold by convenience restaurants are high not only in fat but also in sodium. There is a linear relation between salt intake as measured by daily urinary sodium excretion and levels of blood pressure in people from different cities in China (Fig. 1; Ref. 10). In general, blood pressure and urinary sodium excretion tend to be higher in northern China, e.g., Beijing, Altai, and Shijiazhuang, than in southern China, e.g., Guangzhou. Of particular interest was the finding that a 1989 study in Guangzhou had shown a gradual rise of both systolic and diastolic blood pressures as compared with a 1985 study, associated with a corresponding increase in urinary sodium excretion. The increase in sodium intake between these two surveys coincided with the rise in the number of American fast-food restaurants, such as McDonald's, Kentucky Fried Chicken, and Pizza Hut, that had opened in Guangzhou during that period (11).

Whereas too much fat and salt intake can cause coronary artery disease and hypertension, respectively, too little selenium can result in Keshan disease and Kashin–Beck disease in China. Keshan disease is an endemic type of dilated cardiomyopathy, first discovered in Keshan County in Heilongjiang Province, China, but it has largely disappeared now owing to progressive economic development, improved living conditions, and adequate selenium intake in the diet in modern China (12). Besides Keshan disease, chronic selenium deficiency can also cause Kashin–Beck disease (12,13), the most frequent rheumatological problem of children in

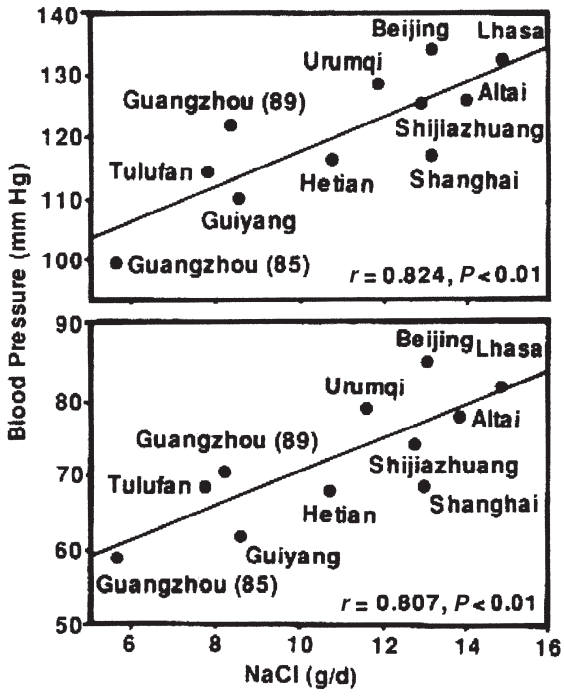

FIG. 1. Linear relation between sodium intake as expressed in daily urinary sodium chloride excretion (NaCl g/d) on the abscissa and systolic (top) and diastolic (bottom) blood pressures on the ordinate in people from different cities in China. The numbers in parentheses after the city of Guangzhou denote the different years, i.e., 85 for 1985 and 89 for 1989. From Reference 10.

Paper no. L9392 in *Lipids 39*, 291–292 (March 2004).

China (14); it is endemic in Tibet, affecting 9% of its population (15).

Therefore, dietary indiscretions play a major role in the rising prevalence of heart diseases in China, and their correction should be able to reverse this trend. Neither diseases of affluence nor diseases of poverty should exist in any part of the world in the 21st century.

REFERENCES

1. Lands, W.E.M. (2003) Diets Could Prevent Many Diseases, *Lipids 38*, 317–321.
2. Snapper, I. (1941) *Chinese Lessons to Western Medicine*, p. 160, Interscience, New York.
3. Cheng, T.O. The Current State of Cardiology in China, *Int. J. Cardiol.,* in press.
4. Leung, S. (2003) Experts Differ on Healthiness of 'Fast' Salad, *Wall Street Journal* (May 8, 2003), p. B1.
5. Du, S., Lu, B., Zhai, F., and Popkin, B.M. (2002) A New Stage of the Nutrition Transition in China, *Public Health Nutr. 5(1A)*, 169–174.
6. Wang, X., Fan, Z., Huang, J., Su, S., Yu, Q., Zhao, J., Hui, R., Yao, Z., Shen, Y., *et al.* (2003) Extensive Association Analysis Between Polymorphisms of PON Gene Cluster with Coronary Heart Disease in Chinese Han Population, *Arterioscler. Thromb. Vasc. Biol. 23*, 328–334.
7. Cheng, T.O. (1987) *The International Textbook of Cardiology*, p. 12, Pergamon, New York.
8. Chen, G.W., and Cheng, T.O. (2002) *The Textbook of Modern Cardiology*, 2nd edn., p. 1546, Hunan Science & Technology Press, Changsha, China.
9. Campbell, T.C., Parpia, B., and Chen, J. (1998) Diet, Lifestyle, and the Etiology of Coronary Artery Disease: The Cornell China Study, *Am. J. Cardiol. 82*(10B), 18T–21T.
10. Cheng, T.O. (2000) Systolic and Diastolic Blood Pressures and Urinary Sodium Excretion in Mainland China, *Q.J. Med. 93,* 557–558.
11. Cheng, T.O. (1998) Cardiovascular Disease in China, *Nat. Med. 4*, 1209–1210.
12. Gu, B.-Q., and Cheng, T.O. (1987) Keshan Disease, in *The International Textbook of Cardiology* (Cheng, T.O., ed.), pp. 752–765, Pergamon Press, New York.
13. Cheng, T.O. (1989) Kashin–Beck Disease, *N.Y. State J. Med. 89*, 585–586.
14. Sokoloff, L. (1987) Kashin-Beck Disease, *Rheum. Dis. Clin. North Am. 13*, 101–104.
15. Yardley, J. (2003) Stunted by Illness, Tibetan Villagers Ponder Flight, *New York Times* (September 29, 2003), p. A7.

Tsung O. Cheng
George Washington University Medical Center
Washington, DC 20037

[Received October 9, 2003; accepted April 10, 2004]

REVIEW

Isoprenoids: Remarkable Diversity of Form and Function

Sarah A. Holstein and Raymond J. Hohl*

Departments of Internal Medicine and Pharmacology, University of Iowa, Iowa City, Iowa 52242

ABSTRACT: The isoprenoid biosynthetic pathway is the source of a wide array of products. The pathway has been highly conserved throughout evolution, and isoprenoids are some of the most ancient biomolecules ever identified, playing key roles in many life forms. In this review we focus on C-10 mono-, C-15 sesqui-, and C-20 diterpenes. Evidence for interconversion between the pathway intermediates farnesyl pyrophosphate and geranylgeranyl pyrophosphate and their respective metabolites is examined. The diverse functions of these molecules are discussed in detail, including their ability to regulate expression of the β-HMG-CoA reductase and Ras-related proteins. Additional topics include the mechanisms underlying the apoptotic effects of select isoprenoids, antiulcer activities, and the disposition and degradation of isoprenoids in the environment. Finally, the significance of pharmacological manipulation of the isoprenoid pathway and clinical correlations are discussed.

Paper no. L9488 in *Lipids 39,* 293–309 (April 2004).

The isoprenoid biosynthetic pathway (Fig. 1) is the source of a very diverse family of compounds. Over 23,000 naturally occurring isoprenoids have been identified, and new compounds continue to be discovered (1). Isoprenoids, in the form of hopanoids, have been identified in sediments dating back 2.5 billion years (2). Isoprenoids and their derivatives play key roles in all aspects of life, e.g., as regulators of gene expression, constituents of membranes, vitamins, antimicrobial agents, mating pheromones, reproductive hormones, components of signal transduction pathways, and constituents of electron transport and photosynthetic machinery. In this review we discuss the isoprenoid biosynthetic pathway and its products, in particular the monoterpenes, sesquiterpenes, and diterpenes. Special attention is paid to the regulatory properties of these isoprenoids. The diverse functions of farnesyl pyrophosphate (FPP) and its derivative farnesol (FOH) are examined in detail. Pharmacological manipulation of the isoprenoid biosynthetic pathway as well as associated clinical correlations are discussed.

*To whom correspondence should be addressed at Department of Internal Medicine, C32 GH, University of Iowa, Iowa City, IA 52242.
E-mail: raymond-hohl@uiowa.edu

Abbreviations: CPT, cholinephosphotransferase; DMAPP, dimethylallyl pyrophosphate; DOXP, deoxy-D-xylulose 5-phosphate; DXPS, deoxyxylulose 5-phosphate synthase; FOH, farnesol; FPP, farnesyl pyrophosphate; FPPase, farnesyl pyrophosphatase; FPTase, farnesyl protein transferase; FXR, farnesoid X receptor; GGA, geranylgeranylacetone; GGOH, geranylgeraniol; GGPP, geranylgeranyl pyrophosphate; GGPTase, geranylgeranyl protein transferase; GOH, geraniol; GPP, geranyl pyrophosphate; HIDS, hyper-IgD and periodic fever syndrome; HMGR, HMG-CoA reductase; IDS, isoprenyl diphosphate synthases; IPP, isopentenyl pyrophosphate; JH, juvenile hormone; LXR, liver X receptor; MA, mevalonic aciduria; MK, mevalonate kinase; PKC, protein kinase C; PPAR, peroxisome proliferator-activated receptor; RAR, retinoic acid receptor; ROS, reactive oxygen species; RXR, retinoid X receptor.

ISOPRENOID BIOSYNTHETIC PATHWAY

The isoprenoid pathway and its products are shown in Figure 1. β-Hydroxymethylglutaryl coenzyme A (HMG-CoA), ultimately derived from acetyl-CoA, is converted to mevalonate (3) *via* the NADPH-requiring enzyme HMG-CoA reductase (HMGR) in the rate-limiting step of the pathway. Mevalonate kinase (MK) phosphorylates mevalonate to yield 5-phosphomevalonate (4). The five-carbon compound isopentenyl pyrophosphate (IPP) is formed following additional phosphorylation and decarboxylation (5). IPP may be isomerized to dimethylallyl pyrophosphate (DMAPP) *via* the enzyme isopentenyl pyrophosphate isomerase (6). DMAPP serves as the isoprene donor in the production of isopentenyl adenine used for tRNA (7) and in the synthesis of cytokinins in plants (8). The five-carbon compounds IPP and DMAPP are condensed to form the 10-carbon geranyl pyrophosphate (GPP). GPP serves as the precursor for the synthesis of all monoterpenes. The addition of another IPP unit to GPP yields the 15-carbon farnesyl pyrophosphate (FPP). The enzyme FPP synthase catalyzes the synthesis of both GPP and FPP in mammals (9), whereas in plants a separate GPP synthase has been identified (10). FPP sits at the branch-point between sterol and longer-chain nonsterol synthesis. The enzyme squalene synthase catalyzes the head-to-head condensation of two FPP molecules to form the sterol precursor squalene (11). Subsequent cyclization steps lead to sterol synthesis. Plants also use FPP as a substrate for sesquiterpene synthesis. In insects, FPP is the precursor for juvenile hormone (JH) production (12). Geranylgeranyl pyrophosphate (GGPP) synthase catalyzes the addition of IPP to FPP to form the 20-carbon product GGPP (13). In plants, GGPP serves as the precursor for carotenoids, diterpenes, and chlorophylls, and in some instances, is used to make longer-chain products. Analogous to the condensation of two FPP molecules to form squalene, carotenoids are derived from the head-to-head condensation of GGPP. FPP and GGPP also serve as isoprene donors in the isoprenylation of proteins catalyzed by the enzymes farnesyl protein transferase (FPTase) and geranylgeranyl protein transferase (GGPTase) I and II (14–17).

In addition to FPP synthase and GGPP synthase, there are two other isoprenyl diphosphate enzyme systems in mammals (18). Long *E*-isoprenyl diphosphate synthase (IDS) and dehydrodolichyl diphosphate synthase catalyze the consecutive condensations of IPP, starting with FPP. Long *E*-IDS produces the

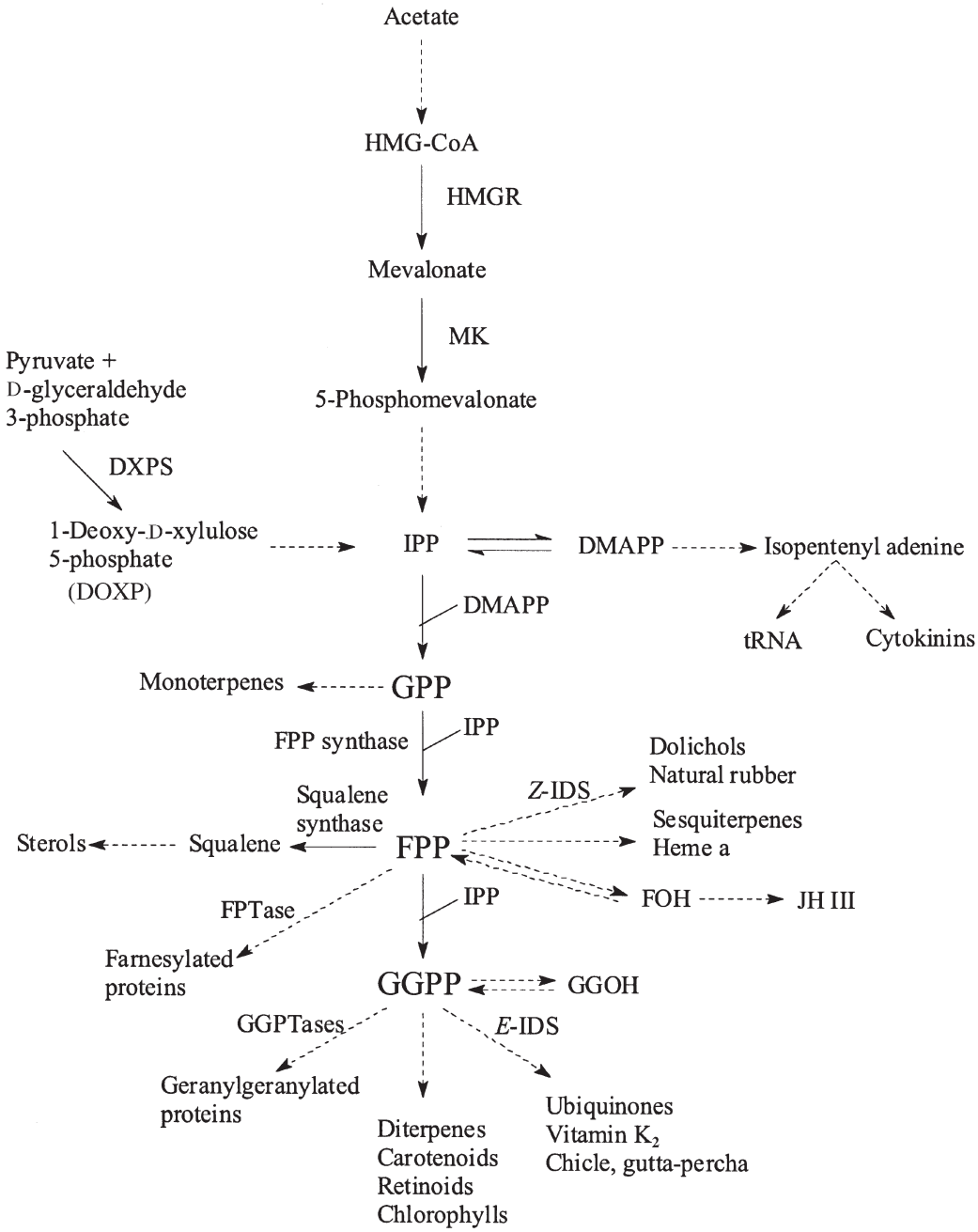

FIG. 1. The isoprenoid biosynthetic pathway and its products.

side chains of ubiquinone, the chain length of which varies among organisms: A C_{50} synthase is found in humans (19). In plants, the ultimate products of *E*-IDS activity include chicle and gutta-percha, composed of approximately 100 and 700 isoprene units, respectively (18). Dehydrodolichyl diphosphate synthase, the only *Z*-IDS found in mammals, is responsible for the synthesis of the sugar carriers dolichol and dolichyl phosphate (20). Plants have additional *Z*-IDS, which can catalyze the production of very long isoprene species, including natural rubber, composed of over 1000 isoprene units (21). Most bacteria have FPP synthase as well as both long *E*- and *Z*-IDS (22–24). In addition, some bacterial species produce carotenoids *via* GGPP (25).

In plants, a newly discovered mevalonate-independent deoxy-D-xylulose 5-phosphate (DOXP) pathway exists. The first step in this pathway involves the condensation of pyruvate and D-glyceraldehyde-3-phosphate to form 1-deoxy-D-xylulose 5-phosphate, catalyzed by deoxyxylulose 5-phosphate synthase (DXPS) (26–28). Subsequent reactions lead to the synthesis of IPP (29,30). The compartmentalization of isoprenoid biosynthesis in higher plants is such that sterols, sesquiterpenes, triterpenes, and polyterpenes are synthesized in

the cytosol through the mevalonate pathway, whereas monoterpenes, diterpenes, carotenoids, plastoquinones, and the prenyl side chain of chlorophyll are synthesized in the plastid through the DOXP pathway (31). Genomic analyses have indicated that the mevalonate-dependent pathway is the ancestral pathway in archaebacteria, and the DOXP pathway is the ancestral source of IPP in eubacteria (32). Phylogenetic studies in bacteria suggest that the DOXP pathway is the more ancient pathway and that it is much more common in bacteria than is the mevalonate-dependent pathway (33). Although the DOXP pathway has been identified in a variety of bacteria, mycobacteria, and algae (34–38), it has not been found in fungi or yeasts (39).

GPP DERIVATIVES

Monoterpenes and monoterpenoids are formed predominantly by plants and, to a lesser extent, by insects and fungi. It has been estimated that there are nearly 1,000 monoterpenes (40). The function of monoterpenes in plants is not completely understood; however, there is evidence that monoterpenes play roles in attracting seed-dispersing animals or pollinating insects, repelling browsing animals or insect pests, resisting microbial attack, and inhibiting the growth of competitors (41). Although once viewed as inert waste products, the finding that monoterpenes are rapidly synthesized and catabolized suggests critical biological functions.

From a historical perspective, monoterpenes, as components of essential oils, herbs, and spices, were early items of commerce and of interest to alchemists. Plant extracts containing monoterpenes have been used in the treatment of a wide variety of human diseases dating back to dynastic Egypt (3000 BC) (42). Today, monoterpenes are used as ingredients in products such as food flavorings, cosmetics, and cleaning products. Additionally, monoterpenes such as limonene and perillyl alcohol are of interest because of their chemopreventative and chemotherapeutic activities. Limonene has been shown to inhibit the development of spontaneous neoplasms as well as chemically induced tumors in rodents (43). Dietary limonene inhibits the development of *ras* oncogene-induced mammary tumors in rats (44). In addition, perillyl alcohol (Scheme 1), carvone, carveol, menthol, and geraniol may also have chemopreventative activities (43). Limonene and perillyl alcohol cause the complete regression of chemically induced rat mammary tumors (45,46). Perillyl alcohol inhibits the growth and induces complete regression of transplanted hamster pancreatic tumors (47). Perillyl alcohol also induces apoptosis in a variety of cell culture lines (48–51). Several phase I clinical trials for limonene and perillyl alcohol have been completed (52–57). These trials have shown that the two monoterpenes are fairly well tolerated, and one study reported a patient with metastatic colon cancer treated with perillyl alcohol who had a near-complete response of greater than 2 yr (55).

Previous investigation had suggested an interaction between monoterpenes and isoprenylated proteins. Studies utilizing radiolabeled mevalonate showed that incorporation of radiolabel into small GTPases was decreased in the presence of limonene metabolites (58). At the time, the results of these studies were interpreted to indicate monoterpene inhibition of isoprenyl transferases (58). However, it has subsequently been demonstrated that the decrease in farnesylated Ras levels by perillyl alcohol is a consequence of decreased *de novo* synthesis of Ras protein (59). Furthermore, analysis of a number of monoterpenes revealed that select monoterpenes inhibit upregulation of Ras and the Ras-related protein; and a structure–activity relationship model for these effects was defined (60). These studies reveal that plant-derived isoprenoids influence expression of mammalian Ras superfamily proteins. Further studies are required to clarify the consequences of these induced changes in the expression of Ras proteins and to define the relationship between these changes and the ascribed biological effects of monoterpenes.

FPP DERIVATIVES

FPP is the precursor for all sesquiterpenes. These volatile molecules are primarily products of plants, insects, and fungi. Interestingly, unlike the monoterpenes, some sesquiterpenes may also be produced by certain vertebrates (61–63). Novel sesquiterpenes continue to be isolated, and the functions of the majority of the compounds are unknown. Many plant-derived sesquiterpenes have anitibacterial, antimalarial, and antifungal properties. Fungi also produce a wide variety of sesquiterpenes with antibacterial activities. Juvenile hormones (JH), which are derivatives of farnesoic acid, play key roles in regulating growth and development in insects. Myriad other biological activities have been reported including sex-attractant pheromones (64), insect feeding stimulants (65), defensive secretions in insects (66), inducers of superficial scald in apples (67), inhibitors of γ-aminobutyric acid receptors (68), inhibitors of nuclear factor kappaB (69), inhibitors of cytokine production (70), phytoestrogens (71), antitumor agents (72), inhibitors of angiogenesis (73), and anti-HIV agents (74). Discussion of these highly derivatized sesquiterpenes is outside the scope of this review. Here we will focus primarily on the activities of FPP and FOH (Scheme 1).

Interconversion of FPP and its metabolites. There is increasing evidence to support the hypothesis that there is an interconversion between FPP and FOH in cells. Over 40 yr ago, Christophe and Popják (75) documented the metabolism of allyl pyrophosphates into acids following the dephosphorylation to free alcohols by a rat liver microsomal phosphatase. More recently, enzyme activity mediating conversion of FPP to FOH (farnesyl pyrophosphatase; FPPase) has been described in rat liver microsomes (76). FPPase activity in CHO cell microsomes was found to be enhanced under conditions of deficient squalene synthase activity or high exogenous mevalonate levels but diminished in cells treated with an HMGR inhibitor (77).

Evidence for the utilization of FOH by the isoprenoid biosynthetic pathway has come from a number of sources. Radiolabeled FOH is incorporated into the triterpenes of the microalga *Botryococcus braunii* (78). Radioactivity from labeled

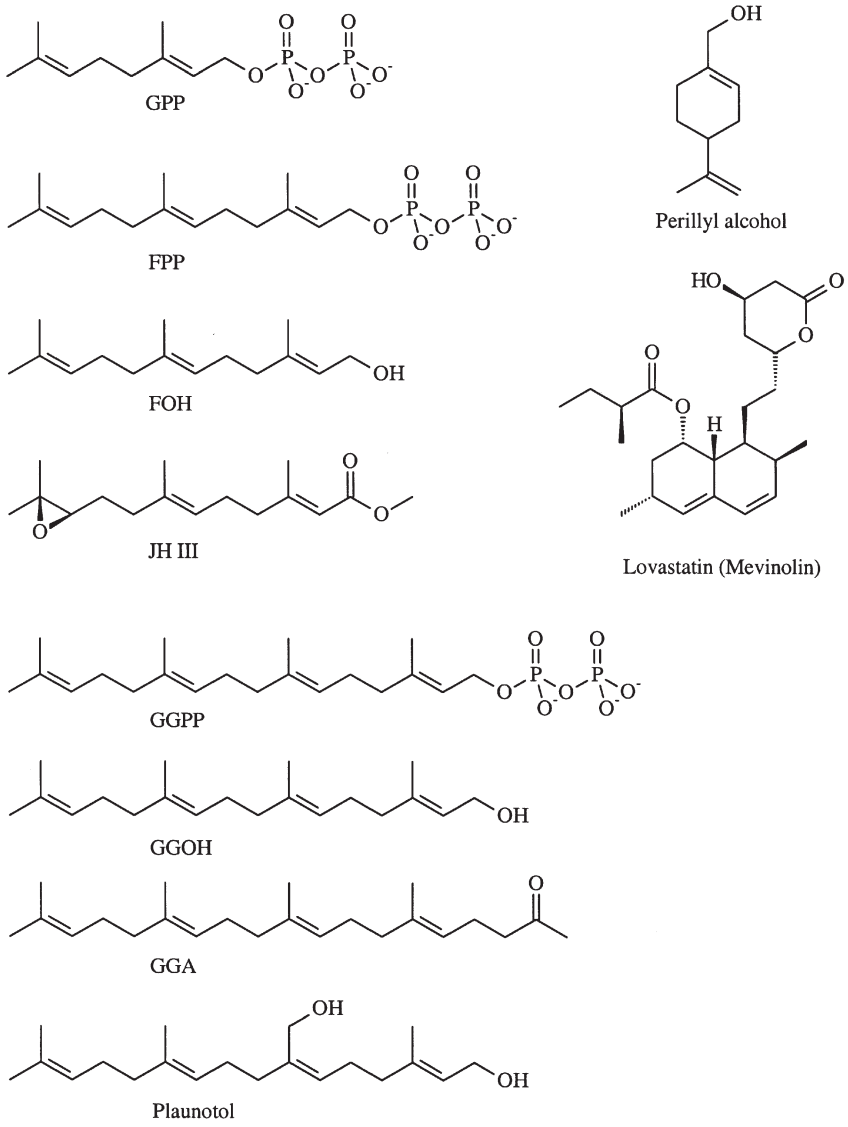

SCHEME 1

FOH is incorporated into cholesterol, ubiquinone, and isoprenylated proteins in mammalian cell lines (79,80). Conversion of FOH to FPP has been demonstrated in rat liver microsomal and peroxisomal fractions (81) as well as in cell-free extracts from the archaeon *Haloferax volcanii* (82). Farnesol kinase and farnesyl phosphate kinase activities, dependent on ATP and CTP, respectively, have been identified in rat liver microsomes (83). In plants, FOH kinase, farnesyl monophosphate kinase, geranylgeraniol (GGOH) kinase, and geranylgeranyl monophosphate kinase activities have been found in tobacco microsomes (84). The gene(s) encoding these putative FOH kinases have not yet been identified. The generation of geranyl and farnesyl triphosphates by nucleoside diphosphate kinases has been reported (85), but the physiological relevance of these triphosphates is unknown.

Conversion of FOH to farnesoic acid has been demonstrated in *Drosophila* cells, rat liver homogenate, and bovine retina homogenate (86,87). This conversion likely involves the initial oxidation of FOH to the aldehyde farnesal. FOH, as well as geraniol, can serve as substrates for several human liver alcohol dehydrogenase isozymes (88). Generation of farnesal in cells also occurs through the action of prenylcysteine lyase, which cleaves the thioether bond of the farnesylcysteine or geranylgeranylcysteine moieties derived from isoprenylated proteins, releasing free cysteine/cysteine methyl ester and farnesal and geranylgeranial (89). Studies utilizing squalene synthase inhibitors *in vivo* have revealed that excess FPP is metabolized to farnesoic acid and FOH-derived dicarboxylic acids in the liver and excreted in the urine (90,91). In insects the initial steps in the synthesis of JH III involve sequential oxidation of FOH to farnesal and then to farnesoic acid (92).

Quantification of nonsterol isoprenoids has proven challenging; however, some preliminary reports have estimated their concentrations. Under normal conditions, the concentration

of FOH in rat liver cells is ~0.1 μg/g wet weight (~0.45 nmol/g) (93). This level increased 10-fold after treatment of rats with a squalene synthase inhibitor (93). Unexpectedly, treatment with lovastatin, an HMGR inhibitor, did not lower FOH levels (93). The presence of FOH concentrations in the range of 0.1–0.8 nmol/g wet weight in mouse, rat, and human brains has been demonstrated (94). Dog and human plasma levels of FPP have been estimated to be in the range of 5–7 ng/mL (~15 nM), whereas FOH levels were below the detection limit of 0.5 ng/mL (~2 nM) (95). Levels of IPP and FPP in rat and mouse liver have been measured as 0.36–1.27 nmol/g wet tissue (96). Although a diet supplemented with cholesterol led to a decrease in both IPP and FPP, fasting resulted in lowered IPP, but not FPP, levels (96). In aggregate, these data support the likelihood for strict maintenance of FPP levels, presumably because of the centralized location of FPP in the isoprenoid pathway (Fig. 1).

Some evidence suggests an interaction between FPP derivatives and the cytochrome P450 system. Raner *et al.* (97) reported that FOH inhibits rabbit liver microsomal P450 2E1 activity and suggested that FOH might serve as a substrate for other P450 isozymes. In insects, epoxidation of methyl farnesoate, a step in the biosynthesis of JH, is linked to cytochrome P450 activity (98). Specifically, cytochrome P450 6A1 has been shown to epoxidize methyl farnesoate, JH I, JH III, and farnesal, but not FOH or farnesoic acid (99). In addition, P450 proteins related to CYP4 are linked to ω-hydroxylation of farnesol, JH III, and other JH-like sesquiterpenoids (100).

Regulation of HMGR. HMGR has been the focus of research for more than four decades since the synthesis of mevalonate was found to be the rate-limiting step in the isoprenoid biosynthetic pathway (101,102). An early observation was the marked upregulation of HMGR protein following treatment of cells with inhibitors of HMGR (103). Since inhibition of mevalonate synthesis leads to the depletion of both sterol and nonsterol species, it was possible that either one was responsible for the autoregulation. In fact, both sterols and nonsterols have been shown to regulate the expression of HMGR through distinct mechanisms. Furthermore, this regulation is multifaceted and involves transcriptional, translational, and posttranslational elements.

The transcriptional regulation of HMGR is mediated through sterol regulatory element-binding proteins. Activation of transcription from sterol response elements found in the promoters of target genes occurs in serum-deprived states, whereas the presence of sterols represses transcription. The genes of many of the enzymes in the cholesterol biosynthetic pathway are regulated in this manner including HMG-CoA synthase, IPP isomerase, FPP synthase, GGPP synthase, and squalene synthase (104).

Sterols also have been shown to regulate HMGR posttranscriptionally. The sterol 24(*S*), 25-oxidolanosterol downregulates the synthesis of HMGR protein independent of any transcriptional effects (105). In mutant Chinese hamster fibroblasts that lack sterol-dependent repression of gene transcription, treatment with an HMGR inhibitor results in a sevenfold decrease in the rate of degradation of HMGR (106). The addition of sterols (25-hydroxysterol and cholesterol) reverses this effect, indicating that the sterols regulate HMGR posttranslationally by accelerating the rate of protein degradation (106).

The first evidence to suggest that sterols are not the only regulatory species was obtained through experiments with HMGR inhibitor-treated cells. In these cells it was observed that, whereas addition of exogenous mevalonate could reverse the upregulation of HMGR, addition of exogenous sterols was only partially effective (107–109). This suggested that nonsterol species might also regulate the expression of HMGR. Subsequent studies, which employed inhibitors of more distal steps in the isoprenoid pathway or FPP analogs, revealed that the regulatory nonsterol species was derived from FPP (108,110–112). *In vivo* experiments in rats showed that treatment with high levels of FOH did not alter HMGR activity, protein level, or half-life (93). The conclusion drawn by the authors of that study was that FOH is not the key regulatory species and that the responsible nonsterol lies beyond FPP (93). This interpretation requires that HMGR expression not already be maximally inhibited by endogenous FOH levels. There has been some controversy over whether FOH or FPP is responsible for regulating HMGR. Evidence for a direct role by FOH was suggested through studies in CHO cells utilizing an FPP analog that inhibits FPP. The analog prevented the mevalonate-dependent, sterol-induced degradation of HMGR, and this effect was reversed by the addition of exogenous FOH (77). Studies in yeast have supported a more direct role for FPP, as a mutant strain lacking the farnesyl pyrophosphatases LPP1 and DPP1 displayed similar responses to FPP as wild-type strains in regulating HMGR degradation (113). Recent studies examining the ubiquitin-mediated degradation of HMGR demonstrated enhanced degradation of HMGR by addition of GGOH (Scheme 1), but not FOH, and only in the presence of sterols (114). HMGR also has been reported to be regulated by the monoterpenes. Plant-derived limonene, perillyl alcohol, and geraniol have been shown to downregulate HMGR protein synthesis, and geraniol also decreases HMGR mRNA levels in hamster kidney cells (115).

Nonsterol-mediated regulation of HMGR also has been demonstrated in insects. Although insects lack squalene synthase and thus sterol synthesis, they produce a diverse array of hemiterpenoids, monoterpenoids, and sesquiterpenoids, which serve as pheromones, as well as ubiquinones and dolichols (116). In the pine bark beetle, the production of the sesquiterpenoid JH III is stimulated following feeding. This in turn leads to *de novo* synthesis of monoterpenoid pheromones (117). The increased activity of the isoprenoid pathway coincides with the upregulation of expression of the HMGR gene induced by JH III (118). The precise mechanism by which JH III induces an increase in HMGR mRNA levels has not yet been described.

The regulation of HMGR in plants appears to be even more complex than in animals. There are multiple genes that encode HMGR in higher plants, and these genes have different expression patterns depending on the stimulus (119). HMGR activity in plants varies during development, in response to red light, and with exposure to pathogens (119). There is increasing evidence

for both sterol- and non-sterol-mediated regulation as well. In tobacco cells, inhibition of squalene synthase or squalene epoxidase resulted in an increase in HMGR activity level (120). In the case of squalene synthase inhibition, the authors demonstrated an increase in HMGR mRNA levels (120). In contrast to studies performed in animal cells, treatment of tobacco cells with FOH stimulated HMGR activity (121). The increase in activity correlated with an increase in steady-state HMGR mRNA levels (121).

Regulation of Ras-related protein expression. With the exception of RhoB, little work has been done with regard to the transcriptional and posttranscriptional regulatory determinants of Ras and Ras-related proteins. The extent to which these proteins are regulated by their isoprenylation status or by specific isoprenoid species has only recently been elucidated. The discovery of the HMGR inhibitors (122) enabled understanding of the importance of the roles of isoprene moieties in posttranslational modification of many signaling proteins. HMGR inhibitors, through their ability to deplete cells of the mevalonate-derived products FPP and GGPP (Fig. 1), have long been known to result in the inhibition of isoprenylation (123,124). An observation made nearly 10 yr ago was that treatment of cells with lovastatin, an HMGR inhibitor, in addition to inhibiting Ras farnesylation, appeared to increase the total amount of Ras protein (59). More recently, studies have demonstrated that mevalonate depletion results in the upregulation of Ras and the Ras-related proteins Rap1a, RhoA, and RhoB through multiple mechanisms including modulation at the transcriptional, translational, and posttranslational levels (125). Inhibition of HMGR also has been shown to upregulate expression of Rab5 and Rab7 (126). Interestingly, in yeast, mevalonate depletion leads to a decrease in Ras1p and Ras2p levels (127).

The observed upregulation of the Ras-related proteins in response to mevalonate depletion in mammalian cells could be a result of global inhibition of isoprenylation or of depletion of key regulatory isoprenoid species. That the upregulation was not due to inhibition of isoprenylation was shown in experiments utilizing specific inhibitors of the isoprenyl transferases (128). Furthermore, studies using intermediates of the isoprenoid pathway as well as inhibitors of enzymes in the pathway demonstrated that the nonsterol species FPP and GGPP were the critical regulatory isoprenoids (128). The use of analogs of FPP and GGPP allowed identification of compounds that have activity as either functional antagonists or agonists with respect to the endogenous isoprenoid pyrophosphates and suggested the existence of specific isoprenoid binding factors that are involved in the regulation of Ras-related protein expression (129).

Interaction with transcription factors. FOH, along with JH III, has been shown to modulate the activity of the farnesoid X receptor (FXR), a transcription factor (130). Subsequent studies have suggested that bile acids may be the physiological activators of FXR and that FXR represses the transcription of the gene encoding the rate-limiting enzyme in bile acid synthesis (cholesterol 7α-hydroxylase) as well as activates a gene encoding a bile acid transporter (131–133). Both FOH and JH induce differentiation in epidermal keratinocytes through activation of the related transcription factor peroxisome proliferator-activated receptor (PPARα) (134). Treatment with FOH increased PPARα mRNA levels and the activity of a PPAR response element (134). Direct binding of FOH or JH to FXR or PPARα has not been demonstrated. However, the structurally related retinoids all-*trans* retinoic acid and 9-*cis* retinoic acid are well-known for their ability to modulate gene expression through direct interaction with the retinoic acid receptor (RAR) and retinoid X receptor (RXR) transcription factors (135). Furthermore, methoprene, methoprene acid, and hydroprene acid, all analogs of JH, activate RXR in insect and mammalian cell systems, and methoprene acid has been shown to directly bind RXR (136). GGPP has recently been shown to decrease the expression of the ATP-binding cassette transporter A1 (137). This effect appears to be due to the ability of GGPP to act as an antagonist of LXR by reducing the interaction of liver X receptor (LXR) with its nuclear coactivator (137).

Apoptotic effects. FOH (10–80 μM) has been reported to inhibit cell proliferation and induce apoptosis in a wide variety of cells including human leukemia cell lines (138–140), human lung cancer cells (141), human pancreatic tumor cells (142), *Saccharomyces cerevisiae* (143), and tobacco cells (121). Initial work suggested that FOH decreases cholinephosphotransferase (CPT) activity and therefore inhibits PC synthesis (144). Miquel *et al.* (141) demonstrated that both FOH and GGOH are competitive inhibitors of CPT with respect to DAG. Induction of apoptosis by FOH or GGOH could be prevented by treatment with either DAG or PC (141). The assertion that the ability of FOH to induce apoptosis is a consequence of inhibition of CPT has been questioned. Overexpression of human choline/ethanolamine-phosphotransferase 1, a ubiquitous CPT, reverses FOH-induced inhibition of PC synthesis but does not rescue cells from FOH-induced apoptosis (145). Furthermore, use of a mixed-micelle assay demonstrated that FOH does not directly inhibit CPT (145). The mixed-micelle assay system solubilizes the membrane containing the enzyme such that adding exogenous lipids will not disrupt the physical properties of the membrane (145). Wright *et al.* (145) also showed that whereas exogenous DAG does prevent FOH-induced apoptosis, it does not restore PC synthesis; thus, FOH-induced apoptosis may be due to inhibition of a DAG-mediated process that is distinct from PC synthesis. Of note is the finding that FOH causes inactivation of protein kinase C (PKC), an enzyme activated by DAG, by causing translocation of PKC from the membrane to the cytosol (146).

In yeast, a connection between FOH and generation of reactive oxygen species (ROS) has been made. Studies performed in *S. cerevisiae* demonstrated that treatment of cells with FOH, but not geraniol (GOH), GGOH, or squalene, leads to an increase in ROS production (143). Investigations into the underlying mechanism revealed that FOH does not inhibit reactions catalyzed by NADPH oxidase, succinate oxidase, or cytochrome c oxidase (143). Subsequently, FOH was shown to promote hyperpolarization of the mitochondrial transmembrane potential mediated by the proton pump F_0F_1-ATPase (147). Interestingly,

12,13-dehydrogeranylgeraniol, isolated from the aquatic plant *Saururus cernuus,* has been found to scavenge ROS in HL-60 cells (148).

FOH and calcium channels. FOH, but not GOH or GGOH, can prevent norepinephrine-induced vasoconstriction of vascular smooth muscle cells (149). This effect appears to be due to the ability of FOH to inhibit calcium channels reversibly (150). Micromolar concentrations of FOH have been shown to block high-voltage activated calcium channels rather nonspecifically (94). In contrast, FOH at submicromolar concentrations is a selective, high-affinity inhibitor of N-type calcium channels (94). These studies suggest that FOH serves as an endogenous high-affinity ligand of N-type calcium channels and thus participates in the regulation of vascular tone.

FPP derivatives and Candida. There is increasing evidence for the role of FPP metabolites in regulating *Candida albicans* growth. This dimorphic fungus is capable of switching between a budding yeast form and an invasive filamentous form. Recently, Oh *et al.* (151) identified farnesoic acid as the autoregulatory substance that is excreted by *C. albicans* during the filamentous-to-budding yeast transition. Addition of purified farnesoic acid (3.12 μg/mL) led to the inhibition of the yeast-to-hypha transition and inhibited filamentous cell growth but not yeast cell growth (151). Subsequently, FOH was found to be an even more potent inhibitor of the yeast-to-hypha transition (152). The effect of FOH was less selective than farnesoic acid, as FOH was also shown to inhibit yeast cell growth at higher concentrations (152). Shortly thereafter, Hornby *et al.* (153) identified FOH as the extracellular quorum-sensing molecule that controls the inoculum size effect, and thus the transition from mycelia to budding yeast, in *C. albicans*. Studies using radiolabeled FPP demonstrated that *C. albicans* cell homogenate can convert FPP to FOH (154). FOH also inhibits *C. albicans* biofilm formation at high concentrations and alters the composition of the biofilms at lower concentrations (155). Treatment of *C. albicans* cultures with zaragozic acid, a squalene synthase inhibitor, was shown to lead to an increase in intracellular and extracellular FOH levels (154). An intriguing hypothesis is that the antifungal activity of zaragozic acid and other compounds that are used to block ergosterol synthesis (e.g., azoles) is due in part to the accumulation of FOH and subsequent inhibition of the yeast-to-hypha transition (154).

GGPP DERIVATIVES

Over 1,000 diterpenes have been identified, predominantly through isolation from plants, although insects and mammals can also produce some diterpenes (41). Although the function of the majority of the diterpenes is not known, a wide variety of activities have been described including antibacterial (156), antifungal (157), antiparasitic (158), 15-lipoxygenase inhibition (159), insect antifeedant (160), antihyperglycemic (161), and antitumor (162), just to name a few. A detailed discussion of these diterpenes is outside the scope of this review. Here we focus on GGPP and several of its acyclic derivatives. A discussion of the regulatory properties of GGPP with respect to HMGR and Ras-related proteins can be found above.

Interconversion of GGPP and its metabolites. As with FPP and FOH, there is evidence for interconversion between GGPP and GGOH. Enzyme activity controlling conversion of GGPP to GGOH (geranylgeranyl pyrophosphatase) has been described in rat liver microsomes (76). Evidence that GGOH may be phosphorylated to GGPP comes from studies demonstrating that radiolabeled GGOH can become incorporated into isoprenylated proteins (79). Interestingly, in one report, radioactivity from C1-labeled GGOH was also found in cholesterol fractions; however the mechanism by which this occurs is unknown (163). GGOH kinase and geranylgeranyl monophosphate kinase activities have been found in tobacco microsomes and in the archaebacterium *Sulfolobus acidocaldarius* (84,164). Estimates of levels of GGPP and GGOH in tissues have yet to be reported. Excess levels of GGOH, like FOH, are likely to be oxidized, as studies using radiolabeled GGOH or geranylgeranial in rat thymocytes found incorporation of the radiolabel into geranylgeranoic acid and 2,3-dihydrogeranylgeranoic acid (165). Interestingly, geranylgeranoic acid has been shown to inhibit osteoclast formation *in vitro* and to increase bone mineral density *in vivo* (166). Studies using radiolabeled geranylgeranylacetone (GGA) have shown that the radiolabel becomes incorporated into nonessential amino acids and FA, suggesting that metabolism of GGA can occur (167). Further studies demonstrated that metabolism of GGA involves ω-oxidation followed by β-oxidation steps (168). Similar studies have yet to be performed with GGPP or GGOH.

Apoptotic effects. GGOH, at concentrations ranging from 20 to 80 μM, has been found to induce apoptosis in a variety of cell lines including human leukemia (169), lung cancer (141), and hepatoma (170). Geranylgeranoic acid also has been found to induce apoptosis in human hepatoma and prostate cancer lines (171,172). Although, as mentioned earlier, it has been suggested that GGOH, like FOH, is a competitive inhibitor of CPT (141), the precise mechanism by which GGOH induces apoptosis is not known. GGOH-induced apoptosis in HL-60 cells has been associated with a preceding decrease in expression of calreticulin, a calcium-binding protein (173). GGOH, but not geraniol or GGA, also has been shown to induce activation of caspase-3 and c-Jun N-terminal kinase (174,175). The induction of apoptosis in a human hepatoma line by 4,5-didehydrogeranylgeranoic acid is associated with downregulation of transforming growth factor α expression (176).

Antiulcer activities. GGA was first developed in Japan, where it was found to have antiulcer activity in rats (177) and is now used clinically in Asia as a gastric cytoprotective agent (teprenone). A number of effects have been reported, including stimulation of mucus production by gastric epithelium (178), suppression of *Helicobacter pylori*-induced interleukin-8 production (179), suppression of spontaneous apoptosis of gastric pit cells (180), and induction of expression of heat shock proteins in gastric mucosa (181). Heat shock proteins belong to a highly conserved family that mediates cellular response to acute stress. GGA also has been shown to induce expression of heat shock proteins in the liver, small intestine, heart, kidney, lung, and brain (182,183) and is being investigated as a potential therapeutic intervention in glaucoma

(184) and in ischemia-reperfusion injury in the liver and heart (185,186).

Plaunotol (Scheme 1), a product of a Thai plant called "plau-noi" (*Croton sublyratus*) has also been used as an antiulcer agent. Plaunotol has antibacterial activity against *H. pylori,* a causative agent for gastritis and gastric ulcers (156). In addition, administration of plaunotol decreases the number of *H. pylori* in the stomachs of mice with gastritis (156). This bactericidal effect is believed to be due to the ability of plaunotol to interact with the *H. pylori* cell membrane and consequently alter the membrane fluidity, leading to lysis of the bacteria (187). A number of other gastric-protective effects have been reported including stimulation of prostaglandin synthesis (188), increased secretin release (189), suppressed superoxide production (190), and inhibition of neutrophil activation (191).

DISPOSITION AND DEGRADATION OF ISOPRENOIDS

Isoprenoids account for a significant fraction of the nonmethane carbon pool. Worldwide, trees are estimated to emit terpenes at a rate of 4.8×10^{14} g/yr (192). Acyclic isoprenoid species (≤20 carbons) are a common component of marine sediments (193). For many years it has been recognized that branched alkanes are more resistant to biodegradation than are linear alkanes (194). In fact, it is for this reason that isoprenoids such as phytane and pristine have been used as biomarkers for petroleum contamination (195). It is becoming increasingly clear, however, that biotransformation of isoprenoids does take place. In many cases, denitrifying bacteria have been identified as organisms capable of anaerobically degrading a diverse array of isoprenoids, including monoterpenes, squalene, phytol, and cholesterol (193,196–198). The denitrifying bacteria have the enzymes necessary to catalyze alternating β-decarboxymethylation and β-oxidation reaction sequences, thereby avoiding the problem of β-methyl-branched blockages associated with molecular oxygen-mediated reactions (193). Aerobic biodegradation of monoterpenes and squalene has also been reported (197,199). *Alcanivorax* has been found to degrade pristane and phytane readily, thus allowing it to flourish in oil-contaminated seawater (200). Several actinomycetes are capable of utilizing either natural or synthetic rubber as their sole carbon source, indicating that extremely long-chain isoprenoids are also biodegraded (201).

PHARMACOLOGICAL MANIPULATION

Statins. In 1976 the first HMGR inhibitor, mevastatin (compactin), was isolated from a culture of *Penicillium citrinum* by Endo *et al.* (122). During that same year, researchers at Beecham Laboratories isolated mevastatin from *P. brevecompactum* (202). Mevastatin was found to be a potent inhibitor of HMGR *in vitro* (203), to inhibit cholesterol synthesis in tissue culture cells (204,205), and to reduce plasma cholesterol levels in dogs (206), monkeys (207), and humans (208) following chronic administration. In 1980 lovastatin (mevinolin) (Scheme 1) was isolated from a strain of *Aspergillus terreus* (209). Subsequently, HMGR inhibitors have been isolated from *Pleurotus, Monascus, Paecilomyces, Trichoderma, Scopulariopsis,* and *Doratomyces* fungal genera as well as several yeast including *C. cariosilignicola* and *Pichia labacensis* (210–213).

Lovastatin is even more potent than mevastatin with a K_i of 0.6 nM (compared with 1.4 nM for mevastatin) (209). Treatment of dogs for 3 wk with lovastatin resulted in a 30% lowering of plasma cholesterol. Since then, a number of derivatives of lovastatin have been investigated and used clinically. HMGR inhibitors ("statins"), used in the treatment of hypercholesterolemia, are now some of the most widely prescribed drugs in the United States (~11 million patients) (214). In addition, there has been increasing interest in the use of statins in other clinical settings because of the influence of statins on a variety of physiological and pathophysiological processes including anticancer activity (215), Alzheimer's disease (216), osteoporosis (217), acute coronary syndrome (218), pro- and antiangiogenic activities (219), cardiac hypertrophy (220), immunomodulatory effects (221), endothelial function (222), coagulation (223), and thrombosis (224). The molecular mechanisms underlying these effects have yet to be fully elucidated.

Lovastatin and mevastatin are synthesized *via* polyketide pathways. Polyketides encompass a large group of structurally diverse molecules that are secondary metabolites produced by bacteria, fungi, and plants. Examples of polyketides include rapamycin, erythromycin A, aflatoxin B1, and amphotericin B (225). In the case of compactin, a biosynthetic gene cluster in *P. citrinum* that includes genes encoding polyketide synthases, enzymes responsible for postpolyketide modification, and regulators of polyketide synthesis, has been identified (226). Interestingly, two genes have been identified that may play roles in conferring resistance to compactin. One encodes a protein with significant homology to HMGR, whereas the other appears to be an efflux pump (226). A similar mechanism of self-resistance is found in *A. terreus* where the *lvrA* gene encodes a protein related to HMGR (227). The factors influencing production of lovastatin or mevastatin are not well understood. Studies of *A. terreus* grown in chemically defined media indicate that lovastatin synthesis is initiated after glucose exhaustion and after lactose consumption had ceased (228). The authors of this study concluded that synthesis of lovastatin is elicited under starvation conditions (228). However, Shindia (229) reported that the production of lovastatin by *A. terreus* was highest when glucose was used as the sole carbon source.

The nature of the advantage for producing HMGR inhibitors is unclear, although it could be hypothesized that the statins either enhance the growth of the fungi that produce them or inhibit the growth of their environmental competitors. Since mevinolin production reaches its peak only after the dry weight of *A. terreus* has plateaued, it does not seem likely that mevinolin provides a growth advantage (213). In addition, whereas *A. terreus* grows on all experimental media tested, production of mevinolin is dependent on the composition of the medium (229). Although mevastatin was initially detected by its antifungal activity (202), the magnitude of this effect is not published. Only four out of

over 300 strains of yeast were found to be growth-inhibited by compactin analogs (230). Since bacteria predominantly utilize the mevalonate-independent pathway, they are not likely to be affected by HMGR inhibitors. Finally, it has been suggested that lovastatin may serve as an herbicide, because treatment of radish seedlings resulted in inhibition of root elongation growth (231) and inhibited the growth of seedlings and cell cultures of *Solanum xanthocarpum* (232). However, the applicability of these findings to other plants is unknown. Thus, the reason for HMGR inhibitor production by fungi remains to be determined.

Bisphosphonates. Recently, bisphosphonates, a class of drugs used to inhibit bone resorption in a variety of diseases, including osteoporosis, tumor-associated bone disease, and Paget's disease, were shown to target FPP synthase (233–235). Aminobisphosphonates (e.g., pamidronate, zoledronic acid), but not bisphosphonates lacking nitrogen (e.g., clodronate), inhibit the mevalonate pathway and prevent both farnesylation and geranylgeranylation of small GTPases (236–238). It has been suggested that the loss of activity of geranylgeranylated proteins, such as cdc42, Rac, and Rho in osteoclasts, is directly related to the antiresorptive effects, because restoration of geranylgeranylation blocks the effects of the aminobisphosphonates on osteoclasts (237,239,240). The bisphosphonates may have additional therapeutic uses: It was recently demonstrated that alendronate inhibits the invasion of both prostate and breast cancer cells (241). This effect appears to be related to the inhibition of the isoprenoid pathway. In addition to inhibiting FPP synthase, several of the bisphosphonates also have been reported to inhibit GGPP synthase, although much less effectively (242). Selective GGPP synthase inhibitors have not yet been identified but are of interest because of their potential to affect a more specific population of isoprenoid products.

CLINICAL CORRELATIONS

Although a number of genetic disorders associated with isoprenoid biosynthesis have been identified, the great majority involve enzymes necessary for sterol synthesis. HMGR knockout mice are embryonic lethal (243), and there have not been any reported cases of FPP or GGPP synthase deficiency. However, two disorders, mevalonic aciduria (MA) and hyper-IgD and periodic fever syndrome (HIDS) are caused by deficient MK activity. Although initially identified as two different autosomal recessive disorders, genetic analysis has revealed that the two diseases represent the same disorder with differing degrees of severity. MA, first identified in 1985 (244), is characterized by severe developmental delay, hepatosplenomegaly, lymphadenopathy, anemia, cataracts, malabsorption, and dysmorphic features (245). These patients often die during infancy. HIDS, first identified in 1984 (246), is a less severe disease and involves recurrent fever episodes. These episodes, lasting 3–7 d and occurring every 2–6 wk, are associated with lymphadenopathy, abdominal pain, diarrhea, headache, arthralgias, and hepatosplenomegaly (245). Patients with MA also experience recurrent fever episodes (245).

Many mutations in the MK gene, including missense, nonsense, and insertions, have been identified as disease-causing (247–251). The most common mutation in HIDS is V377I, and most patients are compound heterozygotes (252). When MK proteins with these mutations are expressed in *Escherichia coli*, they are found to have markedly decreased enzymatic activity (247,250,251). MK enzyme activity cannot be detected in the fibroblasts of MA patients, but in HIDS patients, activity levels of 1–7% of the control can be found in fibroblasts and leukocytes (248,249,253). With regard to the V377I mutation, although the mutant protein has enzymatic activity when expressed in *E. coli*, protein levels in patients fibroblasts are very low (248). Further studies have shown temperature-dependent instability of the mutant protein, indicating that the V377I mutation alters MK protein folding (254).

The effect of deficient MK activity on the rest of the isoprenoid biosynthetic pathway has been examined. Despite the nondetectable MK activity in MA fibroblasts, studies have shown that these cells can synthesize cholesterol from radiolabeled acetate (255,256). In addition, near-normal plasma levels of cholesterol have been found in MA patients (253). Synthesis of ubiquinone-10 in these patients appears to be decreased as does N-glycosylated products (253,257,258). Evidence for increased HMGR and LDL receptor pathway activity has been demonstrated in fibroblasts (256,258). Initial studies suggest levels of isoprenylated Ras and RhoA proteins in MA and HIDS fibroblasts are similar to those in control fibroblasts under control conditions (259). However, there appears to be increased sensitivity to simvastatin such that accumulation of cytosolic Ras and RhoA occurs at lower concentrations of the HMGR inhibitor in the patient cells than in the control cells, consistent with the reduced ability of these cells to synthesize FPP and GGPP (259). The use of lovastatin in two patients with MA has provided additional insight into the pathophysiology of this disease. Lovastatin was given with the idea that a decrease in the concentration of mevalonate might improve the clinical picture in two patients with MA. However, treatment with lovastatin had to be discontinued because the two children became more ill with fever, acute myopathic changes, worsening ataxia, and diarrhea (253). In aggregate, these studies suggest that excessive levels of mevalonate may not be the cause of the clinical phenotype and that high HMGR activity and mevalonate levels are required for these cells to maintain nonsterol synthesis. Furthermore, Houten *et al.* (254) have raised the hypothesis that fever episodes in HIDS occur as a result of impairment in the residual activity of MK (e.g., through changes in temperature secondary to infection or exercise) with a subsequent decrease in the production of nonsterols that play roles in modulating inflammation. A greater understanding of these roles may yield novel treatment strategies.

SUMMARY

Isoprenoids represent a large number and variety of natural products. Recognition of the significance of these compounds as mediators of biological processes is far from complete. Whereas the sequential condensations of isoprene units beyond

IPP are relatively simple reactions, the products derived from GPP, FPP, and GGPP are a consequence of complex and diverse chemistry. Although there is a significant body of knowledge related to FPP, GGPP, and their respective alcohols, there is obviously much more to be learned as evidenced by recent findings of their novel regulatory functions. Better understanding of isoprenoids will undoubtedly lead to the development of new pharmaceutics, herbicides, and insecticides as well as novel approaches to the management of petroleum-related environmental contamination.

ACKNOWLEDGMENTS

This project was supported by the Roy J. Carver Charitable Trust as a Research Program of Excellence and the Roland W. Holden Family Program for Experimental Cancer Therapeutics.

REFERENCES

1. Sacchettini, J.C., and Poulter, C.D. (1997) Creating Isoprenoid Diversity, *Science 277*, 1788–1789.
2. Summons, R.E., Jahnke, L.L., Hope, J.M., and Logan, G.A. (1999) 2-Methylhopanoids as Biomarkers for Cyanobacterial Oxygenic Photosynthesis, *Nature 400*, 554–557.
3. Ferguson, J.J., Durr, I.F., and Rudney, H. (1959) The Biosynthesis of Mevalonic Acid, *Proc. Nat. Acad. Sci. USA 45*, 499–504.
4. Tchen, T.T. (1958) Mevalonic Kinase: Purification and Properties, *J. Biol. Chem. 233*, 1100–1103.
5. Tada, M., and Lynen, F. (1961) On the Biosynthesis of Terpenes. XIV. On the Determination of Phosphomevalonic Acid Kinase and Pyrophosphomevalonic Acid Decarboxylase in Cell Extracts, *J. Biochem. 49*, 758–764.
6. Agranoff, B.W., Eggerer, H., Henning, U., and Lynen, F. (1960) Biosynthesis of Terpenes. VII. Isopentenyl Pyrophosphate Isomerase, *J. Biol. Chem. 235*, 326–332.
7. Milstone, D.S., Vold, B.S., Glitz, D.G., and Shutt, N. (1978) Antibodies to N^6-(Δ^2-isopentenyl) Adenosine and Its Nucleotide: Interaction with Purified tRNAs and with Bases, Nucleosides and Nucleotides of the Isopentenyladenosine Family, *Nucleic Acids Res. 5*, 3439–3455.
8. Taya, Y., Tanaka, Y., and Nishimura, S. (1978) 5′-AMP Is a Direct Precursor of Cytokinin in *Dictyostelium discoideum, Nature 271*, 545–547.
9. Poulter, C.D., and Rilling, H.C. (1978) The Prenyl Transfer Reaction: Enzymic and Mechanistic Studies on the 1′-4 Coupling Reaction in the Terpene Biosynthetic Pathway, *Acc. Chem. Res. 11*, 307–313.
10. Croteau, R., and Purkett, P.T. (1989) Geranyl Pyrophosphate Synthase: Characterization of the Enzyme and Evidence That This Chain-Length-Specific Prenyltransferase Is Associated with Monoterpene Biosynthesis in Sage (*Salvia officinalis*), *Arch. Biochem. Biophys. 271*, 524–535.
11. Beytia, E., Qureshi, A.A., and Porter, J.W. (1973) Squalene Synthetase. 3. Mechanism of the Reaction, *J. Biol. Chem. 248*, 1856–1867.
12. Koyama, T., Matsubara, M., and Ogura, K. (1985) Isoprenoid Enzyme Systems of Silkworm. II. Formation of the Juvenile Hormone Skeletons by Farnesyl Pyrophosphate Synthetase II, *J. Biochem. 98 (Tokyo)*, 457–463.
13. Kandutsch, A.A., Paulus, H., Levin, E., and Bloch, K. (1964) Purification of Geranylgeranyl Pyrophosphate Synthetase from *Micrococcus lysodeikticus, J. Biol. Chem. 239*, 2507–2515.
14. Reiss, Y., Goldstein, J.L., Seabra, M.C., Casey, P.J., and Brown, M.S. (1990) Inhibition of Purified p21ras Farnesyl:Protein Transferase by Cys-AAX Tetrapeptides, *Cell 62*, 81–88.
15. Moomaw, J.F., and Casey, P.J. (1992) Mammalian Protein Geranylgeranyltransferase. Subunit Composition and Metal Requirements, *J. Biol. Chem. 267*, 17438–17443.
16. Yokoyama, K., and Gelb, M.H. (1993) Purification of a Mammalian Protein Geranylgeranyltransferase. Formation and Catalytic Properties of an Enzyme–Geranylgeranyl Pyrophosphate Complex, *J. Biol. Chem. 268*, 4055–4060.
17. Armstrong, S.A., Seabra, M.C., Sudhof, T.C., Goldstein, J.L., and Brown, M.S. (1993) cDNA Cloning and Expression of the Alpha and Beta Subunits of Rat Rab Geranylgeranyl Transferase, *J. Biol. Chem. 268*, 12221–12229.
18. Wang, K.C., and Ohnuma, S. (2000) Isoprenyl Diphosphate Synthases, *Biochim. Biophys. Acta 1529*, 33–48.
19. Teclebrhan, H., Olsson, J., Swiezewska, E., and Dallner, G. (1993) Biosynthesis of the Side Chain of Ubiquinone:*trans*-Prenyltransferase in Rat Liver Microsomes, *J. Biol. Chem. 268*, 23081–23086.
20. Matsuoka, S., Sagami, H., Kurisaki, A., and Ogura, K. (1991) Variable Product Specificity of Microsomal Dehydrodolichyl Diphosphate Synthase from Rat Liver, *J. Biol. Chem. 266*, 3464–3468.
21. Ibata, K., Mizuno, M., Takigawa, T., and Tanaka, Y. (1983) Long-Chain Betulaprenol-Type Polyprenols from the Leaves of *Ginkgo biloba, Biochem. J. 213*, 305–311.
22. Fujisaki, S., Hara, H., Nishimura, Y., Horiuchi, K., and Nishino, T. (1990) Cloning and Nucleotide Sequence of the ispA Gene Responsible for Farnesyl Diphosphate Synthase Activity in *Escherichia coli, J. Biochem. (Tokyo) 108*, 995–1000.
23. Apfel, C.M., Takacs, B., Fountoulakis, M., Stieger, M., and Keck, W. (1999) Use of Genomics to Identify Bacterial Undecaprenyl Pyrophosphate Synthetase: Cloning, Expression, and Characterization of the Essential uppS Gene, *J. Bacteriol. 181*, 483–492.
24. Ogura, K., Koyama, T., and Sagami, H. (1997) Polyprenyl Diphosphate Synthases, *Subcell. Biochem. 28*, 57–87.
25. Kuntz, M., Romer, S., Suire, C., Hugueney, P., Weil, J.H., Schantz, R., and Camara, B. (1992) Identification of a cDNA for the Plastid-Located Geranylgeranyl Pyrophosphate Synthase from *Capsicum annuum*: Correlative Increase in Enzyme Activity and Transcript Level During Fruit Ripening, *Plant J. 2*, 25–34.
26. Sprenger, G.A., Schorken, U., Wiegert, T., Grolle, S., de Graaf, A.A., Taylor, S.V., Begley, T.P., Bringer-Meyer, S., and Sahm, H. (1997) Identification of a Thiamin-Dependent Synthase in *Escherichia coli* Required for the Formation of the 1-Deoxy-D-xylulose 5-phosphate Precursor to Isoprenoids, Thiamin, and Pyridoxol, *Proc. Nat. Acad. Sci. USA 94*, 12857–12862.
27. Lange, B.M., Wildung, M.R., McCaskill, D., and Croteau, R. (1998) A Family of Transketolases That Directs Isoprenoid Biosynthesis *via* a Mevalonate-Independent Pathway, *Proc. Nat. Acad. Sci. USA 95*, 2100–2104.
28. Eisenreich, W., Schwarz, M., Cartayrade, A., Arigoni, D., Zenk, M.H., and Bacher, A. (1998) The Deoxyxylulose Phosphate Pathway of Terpenoid Biosynthesis in Plants and Microorganisms, *Chem. Biol. 5*, R221–R233.
29. Flesch, G., and Rohmer, M. (1988) Prokaryotic Hopanoids: The Biosynthesis of the Bacteriohopane Skeleton. Formation of Isoprenic Units from Two Distinct Acetate Pools and a Novel Type of Carbon/Carbon Linkage Between a Triterpene and D-Ribose, *Eur. J. Biochem. 175*, 405–411.
30. Lange, B.M., and Croteau, R. (1999) Isopentenyl Diphosphate Biosynthesis *via* a Mevalonate-Independent Pathway: Isopentenyl Monophosphate Kinase Catalyzes the Terminal Enzymatic Step, *Proc. Nat. Acad. Sci. USA 96*, 13714–13719.
31. Lichtenthaler, H.K., Rohmer, M., and Schwender, J. (1997)

Two Independent Biochemical Pathways for Isopentenyl Diphosphate and Isoprenoid Biosynthesis in Higher Plants, *Physiol. Plant. 101*, 643–652.
32. Lange, B.M., Rujan, T., Martin, W., and Croteau, R. (2000) Isoprenoid Biosynthesis: The Evolution of Two Ancient and Distinct Pathways Across Genomes, *Proc. Nat. Acad. Sci. USA 97*, 13172–13177.
33. Boucher, Y., and Doolittle, W.F. (2000) The Role of Lateral Gene Transfer in the Evolution of Isoprenoid Biosynthesis Pathways, *Mol. Microbiol. 37*, 703–716.
34. Flesch, G., and Rohmer, M. (1989) Prokaryotic Triterpenoids. A Novel Hopanoid from the Ethanol-Producing Bacterium *Zymomonas mobilis, Biochem. J. 262*, 673–675.
35. Rohmer, M., Knani, M., Simonin, P., Sutter, B., and Sahm, H. (1993) Isoprenoid Biosynthesis in Bacteria: A Novel Pathway for the Early Steps Leading to Isopentenyl Diphosphate, *Biochem. J. 295*, 517–524.
36. Putra, S.R., Disch, A., Bravo, J.M., and Rohmer, M. (1998) Distribution of Mevalonate and Glyceraldehyde 3-Phosphate/Pyruvate Routes for Isoprenoid Biosynthesis in Some Gram-Negative Bacteria and Mycobacteria, *FEMS Microbiol. Lett. 164*, 169–175.
37. Knöss, W., Reuter, B., and Zapp, J. (1997) Biosynthesis of the Labdane Diterpene Marrubiin in *Marrubium vulgare via* a Non-mevalonate Pathway, *Biochem. J. 326*, 449–454.
38. Schwender, J., Seemann, M., Lichtenthaler, H.K., and Rohmer, M. (1996) Biosynthesis of Isoprenoids (carotenoids, sterols, prenyl side-chains of chlorophylls and plastoquinone) *via* a Novel Pyruvate/Glyceraldehyde 3-Phosphate Non-mevalonate Pathway in the Green Alga *Scenedesmus obliquus, Biochem. J. 316*, 73–80.
39. Disch, A., and Rohmer, M. (1998) On the Absence of the Glyceraldehyde 3-Phosphate/Pyruvate Pathway for Isoprenoid Biosynthesis in Fungi and Yeasts, *FEMS Microbiol. Lett. 168*, 201–208.
40. Mahmoud, S.S., and Croteau, R.B. (2002) Strategies for Transgenic Manipulation of Monoterpene Biosynthesis in Plants, *Trends Plant Sci. 7*, 366–373.
41. Porter, J.W., and Spurgeon, S.L. (1981) *Biosynthesis of Isoprenoid Compounds*, Vol. 1, John Wiley & Sons, New York.
42. Harrewijn, P., van Oosten, A.M., and Piron, P.G.M. (2001) *Natural Terpenoids as Messengers: A Multidisciplinary Study of Their Production, Biological Functions and Practical Applications*, pp. 1–9, Kluwer Academic, Dordrecht.
43. Crowell, P.L. (1999) Prevention and Therapy of Cancer by Dietary Monoterpenes, *J. Nutr. 129*, 775S–778S.
44. Gould, M.N., Moore, C.J., Zhang, R., Wang, B., Kennan, W.S., and Haag, J.D. (1994) Limonene Chemoprevention of Mammary Carcinoma Induction Following Direct *in situ* Transfer of v-Ha-ras, *Cancer Res. 54*, 3540–3543.
45. Elegbede, J.A., Elson, C.E., Tanner, M.A., Qureshi, A., and Gould, M.N. (1986) Regression of Rat Primary Mammary Tumors Following Dietary D-Limonene, *J. Natl. Cancer Inst. 76*, 323–325.
46. Haag, J.D., and Gould, M.N. (1994) Mammary Carcinoma Regression Induced by Perillyl Alcohol, a Hydroxylated Analog of Limonene, *Cancer Chemother. Pharmacol. 34*, 477–483.
47. Stark, M.J., Burke, Y.D., McKinzie, J.H., Ayoubi, A.S., and Crowell, P.L. (1995) Chemotherapy of Pancreatic Cancer with the Monoterpene Perillyl Alcohol, *Cancer Lett. 96*, 15–21.
48. Elegbede, J.A., Flores, R., and Wang, R.C. (2003) Perillyl Alcohol and Perillaldehyde Induced Cell Cycle Arrest and Cell Death in BroTo and A549 Cells Cultured *in vitro, Life Sci. 73*, 2831–2840.
49. Ahn, K.J., Lee, C.K., Choi, E.K., Griffin, R., Song, C.W., and Park, H.J. (2003) Cytotoxicity of Perillyl Alcohol Against Cancer Cells Is Potentiated by Hyperthermia, *Int. J. Radiat. Oncol. Biol. Phys. 57*, 813–819.
50. Unlu, S., Mason, C.D., Schachter, M., and Hughes, A.D. (2000) Perillyl Alcohol, an Inhibitor of Geranylgeranyl Transferase, Induces Apoptosis of Immortalized Human Vascular Smooth Muscle Cells *in vitro*, *J. Cardiovasc. Pharmacol. 35*, 341–344.
51. Sahin, M.B., Perman, S.M., Jenkins, G., and Clark, S.S. (1999) Perillyl Alcohol Selectively Induces G0/G1 Arrest and Apoptosis in Bcr/Abl-Transformed Myeloid Cell Lines, *Leukemia. 13*, 1581–1591.
52. Ripple, G.H., Gould, M.N., Stewart, J.A., Tutsch, K.D., Arzoomanian, R.Z., Alberti, D., Feierabend, C., Pomplun, M., Wilding, G., and Bailey, H.H. (1998) Phase I Clinical Trial of Perillyl Alcohol Administered Daily, *Clin. Cancer Res. 4*, 1159–1164.
53. Vigushin, D.M., Poon, G.K., Boddy, A., English, J., Halbert, G.W., Pagonis, C., Jarman, M., and Coombes, R.C. (1998) Phase I and Pharmacokinetic Study of D-Limonene in Patients with Advanced Cancer. Cancer Research Campaign Phase I/II Clinical Trials Committee, *Cancer Chemother. Pharmacol. 42*, 111–117.
54. Hudes, G.R., Szarka, C.E., Adams, A., Ranganathan, S., McCauley, R.A., Weiner, L.M., Langer, C.J., Litwin, S., Yeslow, G., Halberr, T., *et al.* (2000) Phase I Pharmacokinetic Trial of Perillyl Alcohol (NSC 641066) in Patients with Refractory Solid Malignancies, *Clin. Cancer Res. 6*, 3071–3080.
55. Ripple, G.H., Gould, M.N., Arzoomanian, R.Z., Alberti, D., Feierabend, C., Simon, K., Binger, K., Tutsch, K.D., Pomplun, M., Wahamaki, A., *et al.* (2000) Phase I Clinical and Pharmacokinetic Study of Perillyl Alcohol Administered Four Times a Day, *Clin. Cancer Res. 6*, 390–396.
56. Murren, J.R., Pizzorno, G., DiStasio, S.A., McKeon, A., Peccerillo, K., Gollerkari, A., McMurray, W., Burtness, B.A., Rutherford, T., Li, X., *et al.* (2002) Phase I Study of Perillyl Alcohol in Patients with Refractory Malignancies, *Cancer Biol. Ther. 1*, 130–135.
57. Bailey, H.H., Wilding, G., Tutsch, K.D., Arzoomanian, R.Z., Alberti, D., Feierabend, K.S., Marnocha, R., Holstein, S.A., Stewart, J., Lewis, K.A., and Hohl, R.J. (2004) A Phase I Trial of Perillyl Alcohol Administered 4 Times Daily for 14 Days out of 28 Days, *Cancer Chemother. Pharmacol.*, in press.
58. Crowell, P.L., Chang, R.R., Ren, Z.B., Elson, C.E., and Gould, M.N. (1991) Selective Inhibition of Isoprenylation of 21–26 kDa Proteins by the Anticarcinogen D-Limonene and Its Metabolites, *J. Biol. Chem. 266*, 17679–17685.
59. Hohl, R.J., and Lewis, K. (1995) Differential Effects of Monoterpenes and Lovastatin on RAS Processing, *J. Biol. Chem. 270*, 17508–17512.
60. Holstein, S.A., and Hohl, R.J. (2003) Monoterpene Regulation of Ras and Ras-Related Protein Expression, *J. Lipid Res. 44*, 1209–1215.
61. Goodwin, T.E., Rasmussen, E.L., Guinn, A.C., McKelvey, S.S., Gunawardena, R., Riddle, S.W., and Riddle, H.S. (1999) African Elephant Sesquiterpenes, *J. Nat. Prod. 62*, 1570–1572.
62. Schulz, S., Kruckert, K., and Weldon, P.J. (2003) New Terpene Hydrocarbons from the Alligatoridae (Crocodylia, Reptilia), *J. Nat. Prod. 66*, 34–38.
63. Novotny, M., Harvey, S., and Jemiolo, B. (1990) Chemistry of Male Dominance in the House Mouse, *Mus domesticus, Experientia 46*, 109–113.
64. McBrien, H.L., Millar, J.G., Rice, R.E., McElfresh, J.S., Cullen, E., and Zalom, F.G. (2002) Sex Attractant Pheromone of the Red-Shouldered Stink Bug *Thyanta pallidovirens*: A Pheromone Blend with Multiple Redundant Components, *J. Chem. Ecol. 28*, 1797–1818.
65. Tesh, R.B., Guzman, H., and Wilson, M.L. (1992) *Trans*-Beta-Farnesene as a Feeding Stimulant for the Sand Fly *Lutzomyia longipalpis* (Diptera: Psychodidae), *J. Med. Entomol. 29*, 226–231.
66. Quintana, A., Reinhard, J., Faure, R., Uva, P., Bagnères, A.G., Massiot, G., and Clément, J.L. (2003) Interspecific Variation in

Terpenoid Composition of Defensive Secretions of European *Reticulitermes* Termites, *J. Chem. Ecol. 29*, 639–652.
67. Rowan, D.D., Hunt, M.B., Fielder, S., Norris, J., and Sherburn, M.S. (2001) Conjugated Triene Oxidation Products of α-Farnesene Induce Symptoms of Superficial Scald on Stored Apples, *J. Agric. Food. Chem. 49*, 2780–2787.
68. Kuriyama, T., Schmidt, T.J., Okuyama, E., and Ozoe, Y. (2002) Structure–Activity Relationships of *seco*-Prezizaane Terpenoids in γ-Aminobutyric Acid Receptors of Houseflies and Rats, *Bioorg. Med. Chem. 10*, 1873–1881.
69. Castro, V., Murillo, R., Klaas, C.A., Meunier, C., Mora, G., Pahl, H.L., and Merfort, I. (2000) Inhibition of the Transcription Factor NF-κB by Sesquiterpene Lactones from *Podachaenium eminens, Planta Med. 66*, 591–595.
70. Duan, H., Takaishi, Y., Momota, H., Ohmoto, Y., Taki, T., Jia, Y., and Li, D. (2001) Immunosuppressive Sesquiterpene Alkaloids from *Tripterygium wilfordii, J. Nat. Prod. 64*, 582–587.
71. Appendino, G., Spagliardi, P., Cravotto, G., Pocock, V., and Milligan, S. (2002) Daucane Phytoestrogens: A Structure–Activity Study, *J. Nat. Prod. 65*, 1612–1615.
72. Chang, F.R., Hayashi, K., Chen, I.H., Liaw, C.C., Bastow, K.F., Nakanishi, Y., Nozaki, H., Cragg, G.M., Wu, Y.C., and Lee, K.H. (2003) Antitumor Agents. 228. Five New Agarofurans, Reissantins A–E, and Cytotoxic Principles from *Reissantia buchananii, J. Nat. Prod. 66*, 1416–1420.
73. Jeong, S.J., Itokawa, T., Shibuya, M., Kuwano, M., Ono, M., Higuchi, R., and Miyamoto, T. (2002) Costunolide, a Sesquiterpene Lactone from *Saussurea lappa*, Inhibits the VEGFR KDR/Flk-1 Signaling Pathway, *Cancer Lett. 187*, 129–133.
74. Duan, H., Takaishi, Y., Imakura, Y., Jia, Y., Li, D., Cosentino, L.M., and Lee, K.H. (2000) Sesquiterpene Alkaloids from *Tripterygium hypoglaucum* and *Tripterygium wilfordii*: A New Class of Potent Anti-HIV Agents, *J. Nat. Prod. 63*, 357–361.
75. Christophe, J., and Popják, G. (1961) Studies on the Biosynthesis of Cholesterol: XIV. The Origin of Prenoic Acids from Allyl Pyrophosphates in Liver Enzyme Systems, *J. Lipid Res. 2*, 244–257.
76. Bansal, V.S., and Vaidya, S. (1994) Characterization of Two Distinct Allyl Pyrophosphatase Activities from Rat Liver Microsomes, *Arch. Biochem. Biophys. 315*, 393–399.
77. Meigs, T.E., and Simoni, R.D. (1997) Farnesol as a Regulator of HMG-CoA Reductase Degradation: Characterization and Role of Farnesyl Pyrophosphatase, *Arch. Biochem. Biophys. 345*, 1–9.
78. Huang, Z., and Poulter, C.D. (1989) Stereochemical Studies of Botryococcene Biosynthesis: Analogies Between 1′-1 and 1′-3 Condensations in the Isoprenoid Pathway, *J. Am. Chem. Soc. 111*, 2713–2715.
79. Crick, D.C., Andres, D.A., and Waechter, C.J. (1995) Farnesol Is Utilized for Protein Isoprenylation and the Biosynthesis of Cholesterol in Mammalian Cells, *Biochem. Biophys. Res. Commun. 211*, 590–599.
80. Fliesler, S.J., and Keller, R.K. (1995) Metabolism of [^{3}H]Farnesol to Cholesterol and Cholesterogenic Intermediates in the Living Rat Eye, *Biochem. Biophys. Res. Commun. 210*, 695–702.
81. Westfall, D., Aboushadi, N., Shackelford, J.E., and Krisans, S.K. (1997) Metabolism of Farnesol: Phosphorylation of Farnesol by Rat Liver Microsomal and Peroxisomal Fractions, *Biochem. Biophys. Res. Commun. 230*, 562–568.
82. Tachibana, A., Tanaka, T., Taniguchi, M., and Oi, S. (1996) Evidence for Farnesol-Mediated Isoprenoid Synthesis Regulation in a Halophilic Archaeon, *Haloferax volcanii, FEBS Lett. 379*, 43–46.
83. Bentinger, M., Grunler, J., Peterson, E., Swiezewska, E., and Dallner, G. (1998) Phosphorylation of Farnesol in Rat Liver Microsomes: Properties of Farnesol Kinase and Farnesyl Phosphate Kinase, *Arch. Biochem. Biophys. 353*, 191–198.
84. Thai, L., Rush, J.S., Maul, J.E., Devarenne, T., Rodgers, D.L., Chappell, J., and Waechter, C.J. (1999) Farnesol Is Utilized for Isoprenoid Biosynthesis in Plant Cells *via* Farnesyl Pyrophosphate Formed by Successive Monophosphorylation Reactions, *Proc. Natl. Acad. Sci. USA 96*, 13080–13085.
85. Wagner, P.D., and Vu, N.D. (2000) Phosphorylation of Geranyl and Farnesyl Pyrophosphates by Nm23 Proteins/Nucleoside Diphosphate Kinases, *J. Biol. Chem. 275*, 35570–35576.
86. Gonzalez-Pacanowska, D., Arison, B., Havel, C.M., and Watson, J.A. (1988) Isopentenoid Synthesis in Isolated Embryonic *Drosophila* Cells. Farnesol Catabolism and Omega-Oxidation, *J. Biol. Chem. 263*, 1301–1306.
87. Fliesler, S.J., and Schroepfer, G.J., Jr. (1983) Metabolism of Mevalonic Acid in Cell-Free Homogenates of Bovine Retinas. Formation of Novel Isoprenoid Acids, *J. Biol. Chem. 258*, 15062–15070.
88. Keung, W.M. (1991) Human Liver Alcohol Dehydrogenases Catalyze the Oxidation of the Intermediary Alcohols of the Shunt Pathway of Mevalonate Metabolism, *Biochem. Biophys. Res. Commun. 174*, 701–707.
89. Zhang, L., Tschantz, W.R., and Casey, P.J. (1997) Isolation and Characterization of a Prenylcysteine Lyase from Bovine Brain, *J. Biol. Chem. 272*, 23354–23359.
90. Bostedor, R.G., Karkas, J.D., Arison, B.H., Bansal, V.S., Vaidya, S., Germershausen, J.I., Kurtz, M.M., and Bergstrom, J.D. (1997) Farnesol-Derived Dicarboxylic Acids in the Urine of Animals Treated with Zaragozic Acid A or with Farnesol, *J. Biol. Chem. 272*, 9197–9203.
91. Vaidya, S., Bostedor, R., Kurtz, M.M., Bergstrom, J.D., and Bansal, V.S. (1998) Massive Production of Farnesol-Derived Dicarboxylic Acids in Mice Treated with the Squalene Synthase Inhibitor Zaragozic Acid A, *Arch. Biochem. Biophys. 355*, 84–92.
92. Baker, F.C., Mauchamp, B., Tsai, L.W., and Schooley, D.A. (1983) Farnesol and Farnesal Dehydrogenase(s) in Corpora Allata of the Tobacco Hornworm Moth, *Manduca sexta, J. Lipid Res. 24*,1586–1594.
93. Keller, R.K., Zhao, Z., Chambers, C., and Ness, G.C. (1996) Farnesol Is Not the Nonsterol Regulator Mediating Degradation of HMG-CoA Reductase in Rat Liver, *Arch. Biochem. Biophys. 328*, 324–330.
94. Roullet, J.B., Spaetgens, R.L., Burlingame, T., Feng, Z.P., and Zamponi, G.W. (1999) Modulation of Neuronal Voltage-Gated Calcium Channels by Farnesol, *J. Biol. Chem. 274*, 25439–25446.
95. Saisho, Y., Morimoto, A., and Umeda, T. (1997) Determination of Farnesyl Pyrophosphate in Dog and Human Plasma by High-Performance Liquid Chromatography with Fluorescence Detection, *Anal. Biochem. 252*, 89–95.
96. Bruenger, E., and Rilling, H.C. (1988) Determination of Isopentenyl Diphosphate and Farnesyl Diphosphate in Tissue Samples with a Comment on Secondary Regulation of Polyisoprenoid Biosynthesis, *Anal. Biochem. 173*, 321–327.
97. Raner, G.M., Muir, A.Q., Lowry, C.W., and Davis, B.A. (2002) Farnesol as an Inhibitor and Substrate for Rabbit Liver Microsomal P450 Enzymes, *Biochem. Biophys. Res. Commun. 293*,1–6.
98. Feyereisen, R., Pratt, G.E., and Hamnett, A.F. (1981) Enzymic Synthesis of Juvenile Hormone in Locust Corpora Allata: Evidence for a Microsomal Cytochrome P-450 Linked Methyl Farnesoate Epoxidase, *Eur. J. Biochem. 118*, 231–238.
99. Andersen, J.F., Walding, J.K., Evans, P.H., Bowers, W.S., and Feyereisen, R. (1997) Substrate Specificity for the Epoxidation of Terpenoids and Active Site Topology of House Fly Cytochrome P450 6A1, *Chem. Res. Toxicol. 10*, 156–164.
100. Sutherland, T.D., Unnithan, G.C., Andersen, J.F., Evans, P.H., Murataliev, M.B., Szabo, L.Z., Mash, E.A., Bowers, W.S., and Feyereisen, R. (1998) A Cytochrome P450 Terpenoid Hydroxylase Linked to the Suppression of Insect Juvenile Hormone Synthesis, *Proc. Nat. Acad. Sci. USA 95*, 12884–12889.

101. Bucher, N.L.R., McGarrahan, K., Gould, E., and Loud, A.V. (1959) Cholesterol Biosynthesis in Preparations of Liver from Normal, Fasting, X-Irradiated, Cholesterol-Fed, Triton, or Δ^4-Cholesten-3-one-Treated Rats, *J. Biol. Chem. 234*, 262–267.
102. Siperstein, M.D., and Fagan, V.M. (1966) Feedback Control of Mevalonate Synthesis by Dietary Cholesterol, *J. Biol. Chem. 241*, 602–609.
103. Brown, M.S., Faust, J.R., and Goldstein, J.L. (1978) Induction of 3-Hydroxy-3-methylglutaryl Coenzyme A Reductase Activity in Human Fibroblasts Incubated with Compactin (ML-236B), a Competitive Inhibitor of the Reductase, *J. Biol. Chem. 253*, 1121–1128.
104. Sakakura, Y., Shimano, H., Sone, H., Takahashi, A., Inoue, N., Toyoshima, H., Suzuki, S., Yamada, N., and Inoue, K. (2001) Sterol Regulatory Element-Binding Proteins Induce an Entire Pathway of Cholesterol Synthesis, *Biochem. Biophys. Res. Commun. 286*, 176–183.
105. Panini, S.R., Delate, T.A., and Sinensky, M. (1992) Post-transcriptional Regulation of 3-Hydroxy-3-methylglutaryl Coenzyme A Reductase by 24(*S*),25-Oxidolanosterol, *J. Biol. Chem. 267*, 12647–12654.
106. Dawson, P.A., Metherall, J.E., Ridgway, N.D., Brown, M.S., and Goldstein, J.L. (1991) Genetic Distinction Between Sterol-Mediated Transcriptional and Posttranscriptional Control of 3-Hydroxy-3-methylglutaryl-Coenzyme A Reductase, *J. Biol. Chem. 266*, 9128–9134.
107. Nakanishi, M., Goldstein, J.L., and Brown, M.S. (1988) Multivalent Control of 3-Hydroxy-3-methylglutaryl Coenzyme A Reductase. Mevalonate-Derived Product Inhibits Translation of mRNA and Accelerates Degradation of Enzyme, *J. Biol. Chem. 263*, 8929–8937.
108. Roitelman, J., and Simoni, R.D. (1992) Distinct Sterol and Nonsterol Signals for the Regulated Degradation of 3-Hydroxy-3-methylglutaryl-CoA Reductase, *J. Biol. Chem. 267*, 25264–25273.
109. Correll, C.C., and Edwards, P.A. (1994) Mevalonic Acid-Dependent Degradation of 3-Hydroxy-3-methylglutaryl-coenzyme A Reductase *in vivo* and *in vitro*, *J. Biol. Chem. 269*, 633–638.
110. Correll, C.C., Ng, L., and Edwards, P.A. (1994) Identification of Farnesol as the Non-sterol Derivative of Mevalonic Acid Required for the Accelerated Degradation of 3-Hydroxy-3-methylglutaryl-coenzyme A Reductase, *J. Biol. Chem. 269*, 17390–17393.
111. Bradfute, D.L., and Simoni, R.D. (1994) Non-sterol Compounds That Regulate Cholesterogenesis. Analogues of Farnesyl Pyrophosphate Reduce 3-Hydroxy-3-methylglutaryl-coenzyme A Reductase Levels, *J. Biol. Chem. 269*, 6645–6650.
112. Parker, R.A., Pearce, B.C., Clark, R.W., Gordon, D.A., and Wright, J.J. (1993) Tocotrienols Regulate Cholesterol Production in Mammalian Cells by Post-transcriptional Suppression of 3-Hydroxy-3-methylglutaryl-coenzyme A Reductase, *J. Biol. Chem. 268*, 11230–11238.
113. Gardner, R.G., and Hampton, R.Y. (1999) A Highly Conserved Signal Controls Degradation of 3-Hydroxy-3-methylglutaryl-Coenzyme A (HMG-CoA) Reductase in Eukaryotes, *J. Biol. Chem. 274*, 31671–31678.
114. Sever, N., Song, B.L., Yabe, D., Goldstein, J.L., Brown, M.S., and DeBose-Boyd, R.A. (2003) Insig-Dependent Ubiquitination and Degradation of Mammalian 3-Hydroxy-3-methylglutaryl-CoA Reductase Stimulated by Sterols and Geranylgeraniol, *J. Biol. Chem. 278*, 52479–52490.
115. Peffley, D.M., and Gayen, A.K. (2003) Plant-Derived Monoterpenes Suppress Hamster Kidney Cell 3-Hydroxy-3-methylglutaryl Coenzyme A Reductase Synthesis at the Post-transcriptional Level, *J. Nutr. 133*, 38–44.
116. Seybold, S.J., and Tittiger, C. (2003) Biochemistry and Molecular Biology of *de novo* Isoprenoid Pheromone Production in the Scolytidae, *Annu. Rev. Entomol. 48*, 425–453.
117. Hall, G.M., Tittiger, C., Blomquist, G.J., Andrews, G.L., Mastick, G.S., Barkawi, L.S., Bengoa, C., and Seybold, S.J. (2002) Male Jeffrey Pine Beetle, *Dendroctonus jeffreyi*, Synthesizes the Pheromone Component Frontalin in Anterior Midgut Tissue, *Insect Biochem. Mol. Biol. 32*, 1525–1532.
118. Tittiger, C., Barkawi, L.S., Bengoa, C.S., Blomquist, G.J., and Seybold, S.J. (2003) Structure and Juvenile Hormone-Mediated Regulation of the HMG-CoA Reductase Gene from the Jeffrey Pine Beetle, *Dendroctonus jeffreyi, Mol. Cell. Endocrinol. 199*, 11–21.
119. Stermer, B.A., Bianchini, G.M., and Korth, K.L. (1994) Regulation of HMG-CoA Reductase Activity in Plants, *J. Lipid Res. 35*, 1133–1140.
120. Wentzinger, L.F., Bach, T.J., and Hartmann, M.A. (2002) Inhibition of Squalene Synthase and Squalene Epoxidase in Tobacco Cells Triggers an Up-regulation of 3-Hydroxy-3-methylglutaryl Coenzyme A Reductase, *Plant Physiol. 130*, 334–346.
121. Hemmerlin, A., and Bach, T.J. (2000) Farnesol-Induced Cell Death and Stimulation of 3-Hydroxy-3-methylglutaryl-coenzyme A Reductase Activity in Tobacco cv Bright Yellow-2 Cells, *Plant Physiol. 123*, 1257–1268.
122. Endo, A., Kuroda, M., and Tsujita, Y. (1976) ML-236A, ML-236B, and ML-236C, New Inhibitors of Cholesterogenesis Produced by *Penicillium citrinium*, *J. Antibiot. (Tokyo) 29*, 1346–1348.
123. Schafer, W.R., Kim, R., Sterne, R., Thorner, J., Kim, S.H., and Rine, J. (1989) Genetic and Pharmacological Suppression of Oncogenic Mutations in RAS Genes of Yeast and Humans, *Science 245*, 379–385.
124. Leonard, S., Beck, L., and Sinensky, M. (1990) Inhibition of Isoprenoid Biosynthesis and the Post-translational Modification of pro-p21, *J. Biol. Chem. 265*, 5157–5160.
125. Holstein, S.A., Wohlford-Lenane, C.L., and Hohl, R.J. (2002) Consequences of Mevalonate Depletion. Differential Transcriptional, Translational, and Post-translational Up-regulation of Ras, Rap1a, RhoA, and RhoB, *J. Biol. Chem. 277*, 10678–10682.
126. Laezza, C., Bucci, C., Santillo, M., Bruni, C.B., and Bifulco, M. (1998) Control of Rab5 and Rab7 Expression by the Isoprenoid Pathway, *Biochem. Biophys. Res. Commun. 248*, 469–472.
127. Dimster-Denk, D., Schafer, W.R., and Rine, J. (1995) Control of RAS mRNA Level by the Mevalonate Pathway, *Mol. Biol. Cell. 6*, 59–70.
128. Holstein, S.A., Wohlford-Lenane, C.L., and Hohl, R.J. (2002) Isoprenoids Influence the Expression of Ras and Ras-Related Proteins, *Biochemistry 41*, 13698–13704.
129. Holstein, S.A., Wohlford-Lenane, C.L., Wiemer, D.F., and Hohl, R.J. (2003) Isoprenoid Pyrophosphate Analogues Regulate Expression of Ras-Related Proteins, *Biochemistry 42*, 4384–4391.
130. Forman, B.M., Goode, E., Chen, J., Oro, A.E., Bradley, D.J., Perlmann, T., Noonan, D.J., Burka, L.T., McMorris, T., Lamph, W.W., *et al.* (1995) Identification of a Nuclear Receptor That Is Activated by Farnesol Metabolites, *Cell 81*, 687–693.
131. Wang, H., Chen, J., Hollister, K., Sowers, L.C., and Forman, B.M. (1999) Endogenous Bile Acids Are Ligands for the Nuclear Receptor FXR/BAR, *Mol. Cell. 3*, 543–553.
132. Parks, D.J., Blanchard, S.G., Bledsoe, R.K., Chandra, G., Consler, T.G., Kliewer, S.A., Stimmel, J.B., Willson, T.M., Zavacki, A.M., Moore, D.D., and Lehmann, J.M. (1999) Bile Acids: Natural Ligands for an Orphan Nuclear Receptor, *Science 284*, 1365–1368.
133. Makishima, M., Okamoto, A.Y., Repa, J.J., Tu, H., Learned, R.M., Luk, A., Hull, M.V., Lustig, K.D., Mangelsdorf, D.J., and Shan, B. (1999) Identification of a Nuclear Receptor for Bile Acids, *Science 284*, 1362–1365.
134. Hanley, K., Komuves, L.G., Ng, D.C., Schoonjans, K., He, S.S., Lau, P., Bikle, D.D., Williams, M.L., Elias, P.M., Auwerx, J., and Feingold, K.R. (2000) Farnesol Stimulates Differentiation in Epidermal Keratinocytes *via* PPARα, *J. Biol. Chem. 275*, 11484–11491.

135. Mangelsdorf, D.J., Kliewer, S.A., Kakizuka, A., Umesono, K., and Evans, R.M. (1993) Retinoid Receptors, *Recent Prog. Horm. Res. 48*, 99–121.
136. Harmon, M.A., Boehm, M.F., Heyman, R.A., and Mangelsdorf, D.J. (1995) Activation of Mammalian Retinoid X Receptors by the Insect Growth Regulator Methoprene, *Proc. Natl. Acad. Sci. USA 92*, 6157–6160.
137. Gan, X., Kaplan, R., Menke, J.G., MacNaul, K., Chen, Y., Sparrow, C.P., Zhou, G., Wright, S.D., and Cai, T.Q. (2001) Dual Mechanisms of ABCA1 Regulation by Geranylgeranyl Pyrophosphate, *J. Biol. Chem. 276*, 48702–48708.
138. Rioja, A., Pizzey, A.R., Marson, C.M., and Thomas, N.S. (2000) Preferential Induction of Apoptosis of Leukaemic Cells by Farnesol, *FEBS. Lett. 467*, 291–295.
139. Voziyan, P.A., Haug, J.S., and Melnykovych, G. (1995) Mechanism of Farnesol Cytotoxicity: Further Evidence for the Role of PKC-Dependent Signal Transduction in Farnesol-Induced Apoptotic Cell Death, *Biochem. Biophys. Res. Commun. 212*, 479–486.
140. Yasugi, E., Nakata, K., Yokoyama, Y., Kano, K., Dohi, T., and Oshima, M. (1998) Dihydroheptaprenyl and Dihydrodecaprenyl Monophosphates Induce Apoptosis Mediated by Activation of Caspase-3-like Protease, *Biochim. Biophys. Acta 1389*, 132–140.
141. Miquel, K., Pradines, A., Terce, F., Selmi, S., and Favre, G. (1998) Competitive Inhibition of Choline Phosphotransferase by Geranylgeraniol and Farnesol Inhibits Phosphatidylcholine Synthesis and Induces Apoptosis in Human Lung Adenocarcinoma A549 Cells, *J. Biol. Chem. 273*, 26179–26186.
142. Burke, Y.D., Stark, M.J., Roach, S.L., Sen, S.E., and Crowell, P.L. (1997) Inhibition of Pancreatic Cancer Growth by the Dietary Isoprenoids Farnesol and Geraniol, *Lipids 32*, 151–156.
143. Machida, K., Tanaka, T., Fujita, K., and Taniguchi, M. (1998) Farnesol-Induced Generation of Reactive Oxygen Species *via* Indirect Inhibition of the Mitochondrial Electron Transport Chain in the Yeast *Saccharomyces cerevisiae, J. Bacteriol. 180*, 4460–4465.
144. Voziyan, P.A., Goldner, C.M., and Melnykovych, G. (1993) Farnesol Inhibits Phosphatidylcholine Biosynthesis in Cultured Cells by Decreasing Cholinephosphotransferase Activity, *Biochem. J. 295*, 757–762.
145. Wright, M.M., Henneberry, A.L., Lagace, T.A., Ridgway, N.D., and McMaster, C.R. (2001) Uncoupling Farnesol-Induced Apoptosis from Its Inhibition of Phosphatidylcholine Synthesis, *J. Biol. Chem. 276*, 25254–25261.
146. Yazlovitskaya, E.M., and Melnykovych, G. (1995) Selective Farnesol Toxicity and Translocation of Protein Kinase C in Neoplastic HeLa-S3K and Non-neoplastic CF-3 Cells, *Cancer Lett. 88*, 179–183.
147. Machida, K., and Tanaka, T. (1999) Farnesol-Induced Generation of Reactive Oxygen Species Dependent on Mitochondrial Transmembrane Potential Hyperpolarization Mediated by F(0)F(1)-ATPase in Yeast, *FEBS Lett. 462*, 108–112.
148. Rajbhandari, I., Takamatsu, S., and Nagle, D.G. (2001) A New Dehydrogeranylgeraniol Antioxidant from *Saururus cernuus* That Inhibits Intracellular Reactive Oxygen Species (ROS)-Catalyzed Oxidation Within HL-60 Cells, *J. Nat. Prod. 64*, 693–695.
149. Roullet, J.B., Xue, H., Chapman, J., McDougal, P., Roullet, C.M., and McCarron, D.A. (1996) Farnesyl Analogues Inhibit Vasoconstriction in Animal and Human Arteries, *J. Clin. Invest. 97*, 2384–2390.
150. Roullet, J.B., Luft, U.C., Xue, H., Chapman, J., Bychkov, R., Roullet, C.M., Luft, F.C., Haller, H., and McCarron, D.A. (1997) Farnesol Inhibits L-Type Ca^{2+} Channels in Vascular Smooth Muscle Cells, *J. Biol. Chem. 272*, 32240–32246.
151. Oh, K.B., Miyazawa, H., Naito, T., and Matsuoka, H. (2001) Purification and Characterization of an Autoregulatory Substance Capable of Regulating the Morphological Transition in *Candida albicans, Proc. Natl. Acad. Sci. USA 98*, 4664–4668.
152. Kim, S., Kim, E., Shin, D.S., Kang, H., and Oh, K.B. (2002) Evaluation of Morphogenic Regulatory Activity of Farnesoic Acid and Its Derivatives Against *Candida albicans* Dimorphism, *Bioorg. Med. Chem. Lett. 12*, 895–898.
153. Hornby, J.M., Jensen, E.C., Lisec, A.D., Tasto, J.J., Jahnke, B., Shoemaker, R., Dussault, P., and Nickerson, K.W. (2001) Quorum Sensing in the Dimorphic Fungus *Candida albicans* Is Mediated by Farnesol, *Appl. Environ. Microbiol. 67*, 2982–2992.
154. Hornby, J.M., Kebaara, B.W., and Nickerson, K.W. (2003) Farnesol Biosynthesis in *Candida albicans*: Cellular Response to Sterol Inhibition by Zaragozic Acid B, *Antimicrob. Agents Chemother. 47*, 2366–2369.
155. Ramage, G., Saville, S.P., Wickes, B.L., and Lopez-Ribot, J.L. (2002) Inhibition of *Candida albicans* Biofilm Formation by Farnesol, a Quorum-Sensing Molecule, *Appl. Environ. Microbiol. 68*, 5459–5463.
156. Koga, T., Kawada, H., Utsui, Y., Domon, H., Ishii, C., and Yasuda, H. (1996) *In-vitro* and *in-vivo* Antibacterial Activity of Plaunotol, a Cytoprotective Antiulcer Agent, Against *Helicobacter pylori, J. Antimicrob. Chemother. 37*, 919–929.
157. Rasoamiaranjanahary, L., Marston, A., Guilet, D., Schenk, K., Randimbivololona, F., and Hostettmann, K. (2003) Antifungal Diterpenes from *Hypoestes serpens* (Acanthaceae), *Phytochemistry 62*, 333–337.
158. Habtemariam, S. (2003) *In vitro* Antileishmanial Effects of Antibacterial Diterpenes from Two Ethiopian *Premna* Species: *P. schimperi* and *P. oligotricha, BMC Pharmacol. 3*, 6.
159. Carroll, J., Jonsson, E.N., Ebel, R., Hartman, M.S., Holman, T.R., and Crews, P. (2001) Probing Sponge-Derived Terpenoids for Human 15-Lipoxygenase Inhibitors, *J. Org. Chem. 66*, 6847–6851.
160. Klein Gebbinck, E.A., Jansen, B.J., and de Groot, A. (2002) Insect Antifeedant Activity of Clerodane Diterpenes and Related Model Compounds, *Phytochemistry 61*,737–770.
161. Silva, R.M., Santos, F.A., Rao, V.S., Maciel, M.A., and Pinto, A.C. (2001) Blood Glucose- and Triglyceride-Lowering Effect of *trans*-Dehydrocrotonin, a Diterpene from *Croton cajucara* Benth., in Rats, *Diabetes Obes. Metab. 3*, 452–456.
162. Iwamoto, M., Ohtsu, H., Tokuda, H., Nishino, H., Matsunaga, S., and Tanaka, R. (2001) Anti-tumor Promoting Diterpenes from the Stem Bark of *Thuja standishii* (Cupressaceae), *Bioorg. Med. Chem. 9*, 1911–1921.
163. Ownby, S.E., and Hohl, R.J. (2002) Farnesol and Geranylgeraniol: Prevention and Reversion of Lovastatin-Induced Effects in NIH3T3 Cells, *Lipids 37*, 185–192.
164. Ohnuma, S., Watanabe, M., and Nishino, T. (1996) Identification and Characterization of Geranylgeraniol Kinase and Geranylgeranyl Phosphate Kinase from the Archaebacterium *Sulfolobus acidocaldarius, J. Biochem. (Tokyo) 119*, 541–547.
165. Kodaira, Y., Usui, K., Kon, I., and Sagami, H. (2002) Formation of (*R*)-2,3-Dihydrogeranylgeranoic Acid from Geranylgeraniol in Rat Thymocytes, *J. Biochem. (Tokyo) 132*, 327–334.
166. Wang, X., Wu, J., Shidoji, Y., Muto, Y., Ohishi, N., Yagi, K., Ikegami, S., Shinki, T., Udagawa, N., Suda, T., and Ishimi, Y. (2002) Effects of Geranylgeranoic Acid in Bone: Induction of Osteoblast Differentiation and Inhibition of Osteoclast Formation, *J. Bone Miner. Res. 17*, 91–100.
167. Nishizawa, Y., Tanaka, H., and Kinoshita, K. (1987) Incorporation of Radioactivity into Amino Acids and Fatty Acids After Administration of ^{14}C-Geranylgeranylacetone to Rats, *Xenobiotica 17*, 469–476.
168. Nishizawa, Y., Abe, S., Yamada, K., Nakamura, T., Yamatsu, I., and Kinoshita, K. (1987) Identification of Urinary and Microsomal Metabolites of Geranylgeranylacetone in Rats, *Xenobiotica 17*, 575–584.
169. Ohizumi, H., Masuda, Y., Nakajo, S., Sakai, I., Ohsawa, S., and

Nakaya, K. (1995) Geranylgeraniol Is a Potent Inducer of Apoptosis in Tumor Cells, *J. Biochem. (Tokyo) 117*, 11–13.
170. Takeda, Y., Nakao, K., Nakata, K., Kawakami, A., Ida, H., Ichikawa, T., Shigeno, M., Kajiya, Y., Hamasaki, K., Kato, Y., and Eguchi, K. (2001) Geranylgeraniol, an Intermediate Product in Mevalonate Pathway, Induces Apoptotic Cell Death in Human Hepatoma Cells: Death Receptor-Independent Activation of Caspase-8 with Down-Regulation of Bcl-xL Expression, *Jpn. J. Cancer Res. 92*, 918–925.
171. Shidoji, Y., Nakamura, N., Moriwaki, H., and Muto, Y. (1997) Rapid Loss in the Mitochondrial Membrane Potential During Geranylgeranoic Acid-Induced Apoptosis, *Biochem. Biophys. Res. Commun. 230*, 58–63.
172. Kotake-Nara, E., Kim, S.J., Kobori, M., Miyashita, K., and Nagao, A. (2002) Acyclo-Retinoic Acid Induces Apoptosis in Human Prostate Cancer Cells, *Anticancer Res. 22*, 689–695.
173. Nakajo, S., Okamoto, M., Masuda, Y., Sakai, I., Ohsawa, S., and Nakaya, K. (1996) Geranylgeraniol Causes a Decrease in Levels of Calreticulin and Tyrosine Phosphorylation of a 36-kDa Protein Prior to the Appearance of Apoptotic Features in HL-60 Cells, *Biochem. Biophys. Res. Commun. 226*, 741–745.
174. Masuda, Y., Nakaya, M., Nakajo, S., and Nakaya, K. (1997) Geranylgeraniol Potently Induces Caspase-3-Like Activity During Apoptosis in Human Leukemia U937 Cells, *Biochem. Biophys. Res. Commun. 234*, 641–645.
175. Masuda, Y., Nakaya, M., Aiuchi, T., Hashimoto, S., Nakajo, S., and Nakaya, K. (2000) The Mechanism of Geranylgeraniol-Induced Apoptosis Involves Activation, by a Caspase-3-like Protease, of a c-jun N-Terminal Kinase Signaling Cascade and Differs from Mechanisms of Apoptosis Induced by Conventional Chemotherapeutic Drugs, *Leuk. Res. 24*, 937–950.
176. Nakamura, N., Shidoji, Y., Moriwaki, H., and Muto, Y. (1996) Apoptosis in Human Hepatoma Cell Line Induced by 4,5-Didehydro Geranylgeranoic Acid (acyclic retinoid) *via* Down-Regulation of Transforming Growth Factor-α, *Biochem. Biophys. Res. Commun. 219*, 100–104.
177. Murakami, M., Oketani, K., Fujisaki, H., Wakabayashi, T., and Ohgo, T. (1981) Antiulcer Effect of Geranylgeranylacetone, a New Acyclic Polyisoprenoid, on Experimentally Induced Gastric and Duodenal Ulcers in Rats, *Arzneimittelforschung. 31*, 799–804.
178. Terano, A., Hiraishi, H., Ota, S., and Sugimoto, T. (1986) Geranylgeranylacetone, a Novel Anti-ulcer Drug, Stimulates Mucus Synthesis and Secretion in Rat Gastric Cultured Cells, *Digestion 33*, 206–210.
179. Yoshimura, N., Suzuki, Y., and Saito, Y. (2002) Suppression of *Helicobacter pylori*-Induced Interleukin-8 Production in Gastric Cancer Cell Lines by an Anti-ulcer Drug, Geranylgeranylacetone, *J. Gastroenterol. Hepatol. 17*, 1153–1160.
180. Tsutsumi, S., Rokutan, K., Tsuchiya, T., and Mizushima, T. (1999) Geranylgeranylacetone Suppresses Spontaneous Apoptotic DNA Fragmentation in Cultured Guinea Pig Gastric Pit Cells, *Biol. Pharm. Bull. 22*, 886–887.
181. Hirakawa, T., Rokutan, K., Nikawa, T., and Kishi, K. (1996) Geranylgeranylacetone Induces Heat Shock Proteins in Cultured Guinea Pig Gastric Mucosal Cells and Rat Gastric Mucosa, *Gastroenterology 111*, 345–357.
182. Tsuruma, T., Yagihashi, A., Hirata, K., Araya, J., Katsuramaki, T., Tarumi, K., Yanai, Y., and Watanabe, N. (2000) Induction of Heat Shock Protein-70 (hsp-70) by Intraarterial Administration of Geranylgeranylacetone, *Transplant. Proc. 32*, 1631–1633.
183. Fujiki, M., Kobayashi, H., Abe, T., and Ishii, K. (2003) Astroglial Activation Accompanies Heat Shock Protein Upregulation in Rat Brain Following Single Oral Dose of Geranylgeranylacetone, *Brain Res. 991*, 254–257.
184. Caprioli, J., Ishii, Y., and Kwong, J.M. (2003) Retinal Ganglion Cell Protection with Geranylgeranylacetone, a Heat Shock Protein Inducer, in a Rat Glaucoma Model, *Trans. Am. Ophthalmol. Soc. 101*, 39–50.
185. Fudaba, Y., Ohdan, H., Tashiro, H., Ito, H., Fukuda, Y., Dohi, K., and Asahara, T. (2001) Geranylgeranylacetone, a Heat Shock Protein Inducer, Prevents Primary Graft Nonfunction in Rat Liver Transplantation, *Transplantation 72*, 184–189.
186. Yamanaka, K., Takahashi, N., Ooie, T., Kaneda, K., Yoshimatsu, H., and Saikawa, T. (2003) Role of Protein Kinase C in Geranylgeranylacetone-Induced Expression of Heat-Shock Protein 72 and Cardioprotection in the Rat Heart, *J. Mol. Cell. Cardiol. 35*, 785–794.
187. Koga, T., Watanabe, H., Kawada, H., Takahashi, K., Utsui, Y., Domon, H., Ishii, C., Narita, T., and Yasuda, H. (1998) Interactions of Plaunotol with Bacterial Membranes, *J. Antimicrob. Chemother. 42*, 133–140.
188. Ushiyama, S., Matsuda, K., Asai, F., and Yamazaki, M. (1987) Stimulation of Prostaglandin Production by (2*E*,6*Z*,10*E*)-7-Hydroxymethyl-3,11,15-trimethyl-2,6,10,14-hexadecatetraen-1-ol (plaunotol), a New Anti-Ulcer Drug, *in vitro* and *in vivo*, *Biochem. Pharmacol. 36*, 369–375.
189. Chang, J.H., Watanabe, S., Shiratori, K., Moriyoshi, Y., and Takeuchi, T. (1989) Plaunotol Stimulates Endogenous Secretin Release and Exocrine Pancreatic Secretion in Rats, *Digestion 44*, 142–147.
190. Okabe, N., Okada, M., Sakai, T., and Kuroiwa, A. (1995) Effect of Plaunotol on Superoxide Production Activity *in vivo*, *Dig. Dis. Sci. 40*, 2321–2322.
191. Murakami, K., Okajima, K., Harada, N., Isobe, H., Liu, W., Johno, M., and Okabe, H. (1999) Plaunotol Prevents Indomethacin-Induced Gastric Mucosal Injury in Rats by Inhibiting Neutrophil Activation, *Aliment. Pharmacol. Ther. 13*, 521–530.
192. Zimmermann, P.R., Chatfield, R.B., Fishman, J., Crutzen, P.J., and Hanst, P.L. (1978) Estimates of the Production of CO and H_2 from the Oxidation of Hydrocarbon Emissions from Vegetation, *Geophys. Res. Lett. 5*, 679–682.
193. Rontani, J.F., Bonin, P.C., and Volkman, J.K. (1999) Biodegradation of Free Phytol by Bacterial Communities Isolated from Marine Sediments Under Aerobic and Denitrifying Conditions, *Appl. Environ. Microbiol. 65*, 5484–5492.
194. Pirnik, M.P., Atlas, R.M., and Bartha, R. (1974) Hydrocarbon Metabolism by *Brevibacterium erythrogenes*: Normal and Branched Alkanes, *J. Bacteriol. 119*, 868–878.
195. Berthou, F., and Friovourt, M.P. (1981) Gas Chromatographic Separation of Diastereomeric Isoprenoids as Molecular Markers of Oil Pollution, *J. Chromatogr. A. 219*, 393–402.
196. Harder, J., and Probian, C. (1995) Microbial Degradation of Monoterpenes in the Absence of Molecular Oxygen, *Appl. Environ. Microbiol. 61*, 3804–3808.
197. Rontani, J.F., Mouzdahir, A., Michotey, V., and Bonin, P. (2002) Aerobic and Anaerobic Metabolism of Squalene by a Denitrifying Bacterium Isolated from Marine Sediment, *Arch. Microbiol. 178*, 279–287.
198. Harder, J., and Probian, C. (1997) Anaerobic Mineralization of Cholesterol by a Novel Type of Denitrifying Bacterium, *Arch. Microbiol. 167*, 269–274.
199. Misra, G., Pavlostathis, S.G., Perdue, E.M., and Araujo, R. (1996) Aerobic Biodegradation of Selected Monoterpenes, *Appl. Microbiol. Biotechnol. 45*, 831–838.
200. Hara, A., Syutsubo, K., and Harayama, S. (2003) *Alcanivorax* Which Prevails in Oil-Contaminated Seawater Exhibits Broad Substrate Specificity for Alkane Degradation, *Environ. Microbiol. 5*, 746–753.
201. Linos, A., Berekaa, M.M., Reichelt, R., Keller, U., Schmitt, J., Flemming, H.C., Kroppenstedt, R.M., and Steinbuchel, A. (2000) Biodegradation of *cis*-1,4-Polyisoprene Rubbers by Distinct Actinomycetes: Microbial Strategies and Detailed Surface Analysis, *Appl. Environ. Microbiol. 66*, 1639–1645.
202. Brown, A.G., Smale, T.C., King, T.J., Hasenkamp, R., and Thompson, R.H. (1976) Crystal and Molecular Structure of

Compactin, a New Antifungal Metabolite from *Penicillium brevicompactum, J. Chem. Soc. Perkin I*, 1165–1170.
203. Tanzawa, K., and Endo, A. (1979) Kinetic Analysis of the Reaction Catalyzed by Rat-Liver 3-Hydroxy-3-methylglutaryl-Coenzyme-A Reductase Using Two Specific Inhibitors, *Eur. J. Biochem. 98*, 195–201.
204. Kaneko, I., Hazama-Shimada, Y., and Endo, A. (1978) Inhibitory Effects on Lipid Metabolism in Cultured Cells of ML-236B, a Potent Inhibitor of 3-Hydroxy-3-methylglutaryl-Coenzyme-A Reductase, *Eur. J. Biochem. 87*, 313–321.
205. Doi, O., and Endo, A. (1978) Specific Inhibition of Desmosterol Synthesis by ML-236B in Mouse LM Cells Grown in Suspension in a Lipid-Free Medium, *Jpn. J. Med. Sci. Biol. 31*, 225–233.
206. Tsujita, Y., Kuroda, M., Tanzawa, K., Kitano, N., and Endo, A. (1979) Hypolipidemic Effects in Dogs of ML-236B, a Competitive Inhibitor of 3-Hydroxy-3-methylglutaryl Coenzyme A Reductase, *Atherosclerosis 32*, 307–313.
207. Kuroda, M., Tsujita, Y., Tanzawa, K., and Endo, A. (1979) Hypolipidemic Effects in Monkeys of ML-236B, a Competitive Inhibitor of 3-Hydroxy-3-methylglutaryl Coenzyme A Reductase, *Lipids 14*, 585–589.
208. Yamamoto, A., Sudo, H., and Endo, A. (1980) Therapeutic Effects of ML-236B in Primary Hypercholesterolemia, *Atherosclerosis 35*, 259–266.
209. Alberts, A.W., Chen, J., Kuron, G., Hunt, V., Huff, J., Hoffman, C., Rothrock, J., Lopez, M., Joshua, H., Harris, E. *et al.* (1980) Mevinolin: A Highly Potent Competitive Inhibitor of Hydroxymethylglutaryl-Coenzyme A Reductase and a Cholesterol-Lowering Agent, *Proc. Natl. Acad. Sci. USA 77*, 3957–3961.
210. Gunde-Cimerman, N., Plemenitas, A., and Cimerman, A. (1993) *Pleurotus* Fungi Produce Mevinolin, an Inhibitor of HMG CoA Reductase, *FEMS Microbiol. Lett. 113*, 333–337.
211. Gunde-Cimerman, N., Plemenitas, A., and Cimerman, A. (1995) A Hydroxymethylglutaryl-CoA Reductase Inhibitor Synthesized by Yeasts, *FEMS Microbiol. Lett. 132*, 39–43.
212. Endo, A. (1979) Monacolin K, a New Hypocholesterolemic Agent Produced by a *Monascus* Species, *J. Antibiot. (Tokyo) 32*, 852–854.
213. Shindia, A.A. (2000) Studies on Mevinolin Production by Some Fungi, *Microbios 102*, 53–61.
214. Topol, E.J. (2004) Intensive Statin Therapy—A Sea Change in Cardiovascular Prevention, *New Engl. J. Med. 350*, 1562–1564.
215. Chan, K.K., Oza, A.M., and Siu, L.L. (2003) The Statins as Anticancer Agents, *Clin. Cancer Res. 9*, 10–19.
216. Meske, V., Albert, F., Richter, D., Schwarze, J., and Ohm, T.G. (2003) Blockade of HMG-CoA Reductase Activity Causes Changes in Microtubule-Stabilizing Protein Tau *via* Suppression of Geranylgeranylpyrophosphate Formation: Implications for Alzheimer's Disease, *Eur. J. Neurosci. 17*, 93–102.
217. Bauer, D.C., Mundy, G.R., Jamal, S.A., Black, D.M., Cauley, J.A., Ensrud, K.E., van der Klift, M., and Pols, H.A. (2004) Use of Statins and Fracture: Results of 4 Prospective Studies and Cumulative Meta-analysis of Observational Studies and Controlled Trials, *Arch. Intern. Med. 164*, 146–152.
218. Spin, J.M., and Vagelos, R.H. (2003) Early Use of Statins in Acute Coronary Syndromes, *Curr. Atheroscler. Rep. 5*, 44–51.
219. Weis, M., Heeschen, C., Glassford, A.J., and Cooke, J.P. (2002) Statins Have Biphasic Effects on Angiogenesis, *Circulation 105*, 739–745.
220. Patel, R., Nagueh, S.F., Tsybouleva, N., Abdellatif, M., Lutucuta, S., Kopelen, H.A., Quinones, M.A., Zoghbi, W.A., Entman, M.L., Roberts, R., and Marian, A.J. (2001) Simvastatin Induces Regression of Cardiac Hypertrophy and Fibrosis and Improves Cardiac Function in a Transgenic Rabbit Model of Human Hypertrophic Cardiomyopathy, *Circulation 104*, 317–324.
221. Blanco-Colio, L.M., Tunon, J., Martin-Ventura, J.L., and Egido, J. (2003) Anti-inflammatory and Immunomodulatory Effects of Statins, *Kidney Int. 63*, 12–23.
222. Wolfrum, S., Jensen, K.S., and Liao, J.K. (2003) Endothelium-Dependent Effects of Statins, *Arterioscler. Thromb. Vasc. Biol. 23*, 729–736.
223. Krysiak, R., Okopien, B., and Herman, Z. (2003) Effects of HMG-CoA Reductase Inhibitors on Coagulation and Fibrinolysis Processes, *Drugs. 63*, 1821–1854.
224. Fenton, J.W., Jr., and Shen, G.X. (1999) Statins as Cellular Antithrombotics, *Haemostasis 29*, 166–169.
225. Staunton, J., and Weissman, K.J. (2001) Polyketide Biosynthesis: A Millennium Review, *Nat. Prod. Rep. 18*, 380–416.
226. Abe, Y., Suzuki, T., Ono, C., Iwamoto, K., Hosobuchi, M., and Yoshikawa, H. (2002) Molecular Cloning and Characterization of an ML-236B (compactin) Biosynthetic Gene Cluster in *Penicillium citrinum, Mol. Genet. Genomics 267*, 636–646.
227. Hutchinson, C.R., Kennedy, J., Park, C., Kendrew, S., Auclair, K., and Vederas, J. (2000) Aspects of the Biosynthesis of Non-aromatic Fungal Polyketides by Iterative Polyketide Synthases, *Antonie van Leeuwenhoek 78*, 287–295.
228. Hajjaj, H., Niederberger, P., and Duboc, P. (2001) Lovastatin Biosynthesis by *Aspergillus terreus* in a Chemically Defined Medium, *Appl. Environ. Microbiol. 67*, 2596–2602.
229. Shindia, A.A. (2001) Some Nutritional Factors Influencing Mevinolin Production by *Aspergillus terreus* Strain, *Folia Microbiol. (Praha) 46*, 413–416.
230. Ikeura, R., Murakawa, S., and Endo, A. (1988) Growth Inhibition of Yeast by Compactin (ML-236B) Analogues, *J. Antibiot. (Tokyo) 41*, 1148–1150.
231. Bach, T.J., and Lichtenthaler, H.K. (1982) Mevinolin: A Highly Specific Inhibitor of Microsomal 3-Hydroxy-3-methylglutaryl-Coenzyme A Reductase of Radish Plants, *Z. Naturforsch. [C] 37*, 46–50.
232. Josekutty, P.C. (1998) Inhibition of Plant Growth by Mevinolin and Reversal of This Inhibition by Isoprenoids, *S. Afr. J. Bot. 64*, 18–24.
233. van Beek, E., Pieterman, E., Cohen, L., Lowik, C., and Papapoulos, S. (1999) Farnesyl Pyrophosphate Synthase Is the Molecular Target of Nitrogen-Containing Bisphosphonates, *Biochem. Biophys. Res. Commun. 264*, 108–111.
234. Keller, R.K., and Fliesler, S.J. (1999) Mechanism of Aminobisphosphonate Action: Characterization of Alendronate Inhibition of the Isoprenoid Pathway, *Biochem. Biophys. Res. Commun. 266*, 560–563.
235. Bergstrom, J.D., Bostedor, R.G., Masarachia, P.J., Reszka, A.A., and Rodan, G. (2000) Alendronate Is a Specific, Nanomolar Inhibitor of Farnesyl Diphosphate Synthase, *Arch. Biochem. Biophys. 373*, 231–241.
236. Luckman, S.P., Hughes, D.E., Coxon, F.P., Graham, R., Russell, G., and Rogers, M.J. (1998) Nitrogen-Containing Bisphosphonates Inhibit the Mevalonate Pathway and Prevent Post-translational Prenylation of GTP-Binding Proteins, Including Ras, *J. Bone Miner. Res. 13*, 581–589.
237. Reszka, A.A., Halasy-Nagy, J.M., Masarachia, P.J., and Rodan, G.A. (1999) Bisphosphonates Act Directly on the Osteoclast to Induce Caspase Cleavage of Mst1 Kinase During Apoptosis. A Link Between Inhibition of the Mevalonate Pathway and Regulation of an Apoptosis-Promoting Kinase, *J. Biol. Chem. 274*, 34967–34973.
238. Benford, H.L., Frith, J.C., Auriola, S., Monkkonen, J., and Rogers, M.J. (1999) Farnesol and Geranylgeraniol Prevent Activation of Caspases by Aminobisphosphonates: Biochemical Evidence for Two Distinct Pharmacological Classes of Bisphosphonate Drugs, *Mol. Pharmacol. 56*, 131–140.
239. Fisher, J.E., Rogers, M.J., Halasy, J.M., Luckman, S.P., Hughes, D.E., Masarachia, P.J., Wesolowski, G., Russell, R.G., Rodan, G.A., and Reszka, A.A. (1999) Alendronate Mechanism of Action: Geranylgeraniol, an Intermediate in the Mevalonate Pathway, Prevents Inhibition of Osteoclast Formation,

Bone Resorption, and Kinase Activation *in vitro*, *Proc. Natl. Acad. Sci. USA 96*, 133–138.
240. van beek, E., Lowik, C., van der Pluijm, G., and Papapoulos, S. (1999) The Role of Geranylgeranylation in Bone Resorption and Its Suppression by Bisphosphonates in Fetal Bone Explants *in vitro*: A Clue to the Mechanism of Action of Nitrogen-Containing Bisphosphonates, *J. Bone Miner. Res. 14*, 722–729.
241. Virtanen, S.S., Vaananen, H.K., Harkonen, P.L., and Lakkakorpi, P.T. (2002) Alendronate Inhibits Invasion of PC-3 Prostate Cancer Cells by Affecting the Mevalonate Pathway, *Cancer Res. 62*, 2708–2714.
242. Szabo, C.M., Matsumura, Y., Fukura, S., Martin, M.B., Sanders, J.M., Sengupta, S., Cieslak, J.A., Loftus, T.C., Lea, C.R., Lee, H.J., *et al.* (2002) Inhibition of Geranylgeranyl Diphosphate Synthase by Bisphosphonates and Diphosphates: A Potential Route to New Bone Antiresorption and Antiparasitic Agents, *J. Med. Chem. 45*, 2185–2196.
243. Ohashi, K., Osuga, J., Tozawa, R., Kitamine, T., Yagyu, H., Sekiya, M., Tomita, S., Okazaki, H., Tamura, Y., Yahagi, N., *et al.* (2003) Early Embryonic Lethality Caused by Targeted Disruption of the 3-Hydroxy-3-methylglutaryl-CoA Reductase Gene, *J. Biol. Chem. 278*, 42936–42941.
244. Berger, R., Smit, G.P., Schierbeek, H., Bijsterveld, K., and le Coultre, R. (1985) Mevalonic Aciduria: An Inborn Error of Cholesterol Biosynthesis? *Clin. Chim. Acta 152*, 219–222.
245. Houten, S.M., Frenkel, J., and Waterham, H.R. (2003) Isoprenoid Biosynthesis in Hereditary Periodic Fever Syndromes and Inflammation, *Cell. Mol. Life Sci. 60*, 1118–1134.
246. van der Meer, J.W., Vossen, J.M., Radl, J., van Nieuwkoop, J.A., Meyer, C.J., Lobatto, S., and van Furth, R. (1984) Hyperimmunoglobulinaemia D and Periodic Fever: A New Syndrome, *Lancet 1*, 1087–1090.
247. Houten, S.M., Romeijn, G.J., Koster, J., Gray, R.G., Darbyshire, P., Smit, G.P., de Klerk, J.B., Duran, M., Gibson, K.M., Wanders, R.J., and Waterham, H.R. (1999) Identification and Characterization of Three Novel Missense Mutations in Mevalonate Kinase cDNA Causing Mevalonic Aciduria, a Disorder of Isoprene Biosynthesis, *Hum. Mol. Genet. 8*, 1523–1528.
248. Houten, S.M., Kuis, W., Duran, M., de Koning, T.J., van Royen-Kerkhof, A., Romeijn, G.J., Frenkel, J., Dorland, L., de Barse, M.M., Huijbers, W.A., *et al.* (1999) Mutations in MVK, Encoding Mevalonate Kinase, Cause Hyperimmunoglobulinaemia D and Periodic Fever Syndrome, *Nat. Genet. 22*, 175–177.
249. Houten, S.M., Koster, J., Romeijn, G.J., Frenkel, J., Di Rocco, M., Caruso, U., Landrieu, P., Kelley, R.I., Kuis, W., Poll-The, B.T., *et al.* (2001) Organization of the Mevalonate Kinase (MVK) Gene and Identification of Novel Mutations Causing Mevalonic Aciduria and Hyperimmunoglobulinaemia D and Periodic Fever Syndrome, *Eur. J. Hum. Genet. 9*, 253–259.
250. Hinson, D.D., Ross, R.M., Krisans, S., Shaw, J.L., Kozich, V., Rolland, M.O., Divry, P., Mancini, J., Hoffmann, G.F., and Gibson, K.M. (1999) Identification of a Mutation Cluster in Mevalonate Kinase Deficiency, Including a New Mutation in a Patient of Mennonite Ancestry, *Am. J. Hum. Genet. 65*, 327–335.
251. Hinson, D.D., Chambliss, K.L., Hoffmann, G.F., Krisans, S., Keller, R.K., and Gibson, K.M. (1997) Identification of an Active Site Alanine in Mevalonate Kinase Through Characterization of a Novel Mutation in Mevalonate Kinase Deficiency, *J. Biol. Chem. 272*, 26756–26760.
252. Frenkel, J., Houten, S.M., Waterham, H.R., Wanders, R.J., Rijkers, G.T., Duran, M., Kuijpers, T.W., van Luijk, W., Poll-The, B.T., and Kuis, W. (2001) Clinical and Molecular Variability in Childhood Periodic Fever with Hyperimmunoglobulinaemia D, *Rheumatology 40*, 579–584.
253. Hoffmann, G.F., Charpentier, C., Mayatepek, E., Mancini, J., Leichsenring, M., Gibson, K.M., Divry, P., Hrebicek, M., Lehnert, W., Sartor, K., *et al.* (1993) Clinical and Biochemical Phenotype in 11 Patients with Mevalonic Aciduria, *Pediatrics 91*, 915–921.
254. Houten, S.M., Frenkel, J., Rijkers, G.T., Wanders, R.J., Kuis, W., and Waterham, H.R. (2002) Temperature Dependence of Mutant Mevalonate Kinase Activity as a Pathogenic Factor in Hyper-IgD and Periodic Fever Syndrome, *Hum. Mol. Genet. 11*, 3115–3124.
255. Hoffmann, G., Gibson, K.M., Nyhan, W.L., and Sweetman, L. (1988) Mevalonic Aciduria: Pathobiochemical Effects of Mevalonate Kinase Deficiency on Cholesterol Metabolism in Intact Fibroblasts, *J. Inherit. Metab. Dis. 11*, 229–232.
256. Gibson, K.M., Hoffmann, G., Schwall, A., Broock, R.L., Aramaki, S., Sweetman, L., Nyhan, W.L., Brandt, I.K., Wappner, R.S., Lehnert, W., and Trefz, F.H. (1990) 3-Hydroxy-3-methylglutaryl Coenzyme A Reductase Activity in Cultured Fibroblasts from Patients with Mevalonate Kinase Deficiency: Differential Response to Lipid Supplied by Fetal Bovine Serum in Tissue Culture Medium, *J. Lipid Res. 31*, 515–521.
257. Hubner, C., Hoffmann, G.F., Charpentier, C., Gibson, K.M., Finckh, B., Puhl, H., Lehr, H.A., and Kohlschutter, A. (1993) Decreased Plasma Ubiquinone-10 Concentration in Patients with Mevalonate Kinase Deficiency, *Pediatr. Res. 34*, 129–133.
258. Hoffmann, G.F., Wiesmann, U.N., Brendel, S., Keller, R.K., and Gibson, K.M. (1997) Regulatory Adaptation of Isoprenoid Biosynthesis and the LDL Receptor Pathway in Fibroblasts from Patients with Mevalonate Kinase Deficiency, *Pediatr. Res. 41*, 541–546.
259. Houten, S.M., Schneiders, M.S., Wanders, R.J., and Waterham, H.R. (2003) Regulation of Isoprenoid/Cholesterol Biosynthesis in Cells from Mevalonate Kinase-Deficient Patients, *J. Biol. Chem. 278*, 5736–5743.

[Received April 19, 2004; accepted May 21, 2004]

Cloning and Characterization of a cDNA Encoding Diacylglycerol Acyltransferase from Castor Bean

Xiaohua He, Charlotta Turner, Grace Q. Chen, Jiann-Tsyh Lin, and Thomas A. McKeon*

Western Regional Research Center, USDA, Albany, California 94710

ABSTRACT: The oil from castor seed (*Ricinus communis*) contains 90% ricinoleate, a hydroxy FA that is used in producing numerous industrial products. Castor diacylglycerol acyltransferase (RcDGAT) is a critical enzyme, as it catalyzes the terminal step in castor oil biosynthesis in which the products contain two or three ricinoleoyl moieties. We have isolated a cDNA encoding RcDGAT from developing castor seeds. Analysis of the sequence reveals that this cDNA encodes a protein of 521 amino acids with a molecular mass of 59.9 kDa. Although there are regions of high similarity to other plant DGAT coding sequences, there are sequences that distinguish it as well. Southern blot analysis suggests that the castor genome contains a single copy of RcDGAT. Analysis by reverse transcription-PCR reveals that the accumulation of the mRNA reaches its highest level at 19 d after pollination and declines thereafter. Expression of the full-length cDNA for RcDGAT in the yeast *Saccharomyces cerevisiae*, strain INVSc1 results in sevenfold higher DGAT activity compared with controls. When different molecular species of DAG were provided as substrates to the microsomal mixture, the RcDGAT showed a greater preference to catalyze the transfer of oleate from [^{14}C]oleoyl-CoA to diricinolein than to diolein and dipalmitolein. With the addition of 0.25 mM substrates, diricinolein gave 318 pmol/mg/min diricinoleoyloleoylglycerol (RRO), while diolein and dipalmitolein gave only about 195 pmol/mg/min of triolein (OOO) and 120 pmol/mg/min dipalmitoyleoylglycerol (PoPoO), respectively. This work will facilitate investigation of the role of RcDGAT in castor oil biosynthesis.

Paper no. L9414 in *Lipids 39*, 311–318 (April 2004).

In some plants, the principal seed storage material is TAG, located in oil bodies of seeds. Acyl CoA:diacylglycerol acyltransferase (DGAT), a transmembrane enzyme that catalyzes the final step in the Kennedy pathway for TAG biosynthesis (1), has been proposed to be the rate-limiting enzyme in plant storage lipid accumulation (2,3). Because of its role in TAG biosynthesis, DGAT is implicated in diverse cellular processes (4–6). An *Arabidopsis* mutant deficient in DGAT activity resulted in a reduced TAG content, delayed seed development, and altered seed FA composition (7), whereas overexpression of DGAT in *Arabidopsis* seeds enhanced oil deposition and seed weight (8). Genes encoding DGAT from several plant species have been cloned and characterized (9–11). The DGAT of any particular crop may have structural features that enable them to efficiently acylate with the FA that predominate in that crop. Acylation activity in microsomes from *Ricinus communis* endosperm clearly demonstrated a preference for inserting ricinoleate into TAG (12), but the same substrate was not efficiently used by other plant species. Lin *et al*. (13) also have demonstrated that castor endosperm microsomes have a strong preference for incorporating ricinoleate into TAG in comparison with oleate and other FA.

Ricinoleic acid is a hydroxy FA that constitutes 90% of the FA in castor oil. This unusual FA is used in making lubricants for heavy equipment and is also for coatings, paints, plastics, antifungal compounds, shampoo, thermopolymers, and cosmetics (14). However, production of castor is seriously hindered by the presence of the toxic protein ricin and of allergenic 2S albumins. One approach used to overcome these obstacles has been to produce ricinoleate in plants lacking these noxious components. Expression of a cDNA encoding fatty acyl hydroxylase (FAH), an enzyme catalyzing the hydroxylation of oleate to ricinoleate in castor, resulted in the accumulation of low levels of hydroxy FA in tobacco and *Arabidopsis* (15,16). These results suggest that the FAH gene itself is not sufficient to produce the high level of ricinoleate that is characteristic of castor.

The metabolic pathway of castor oil biosynthesis has been elucidated (17), and enzymatic steps that appear critical to high ricinoleate content have been identified (18). Discovery and characterization of genes provide an unparalleled method for gaining insight into the molecular basis of any biological process. In plant lipid metabolism, isolated genes have been used directly to manipulate plant lipid biosynthesis for the purpose of altering FA composition (19). Application of additional genes involved in castor oil biosynthesis underlies future progress in developing crops containing high levels of hydroxylated FA. In this study, we report the identification of a cDNA encoding castor diacylglycerol acyltransferase (RcDGAT), one of the key enzymes involved in castor oil biosynthesis (18), and demonstrate that the expression of RcDGAT in yeast cells confers high levels of membrane-associated DGAT activity. We also provide information for the specificity of RcDGAT for DAG substrates.

EXPERIMENTAL PROCEDURES

Cloning of RcDGAT cDNA. A 378 base pair (bp) fragment of RcDGAT cDNA was amplified from RNA samples extracted

*To whom correspondence should be addressed at U.S. Department of Agriculture, 800 Buchanan St., Albany, CA 94710.
E-mail: tmckeon@pw.usda.gov

Abbreviations: bp, base pair; DAP, days after pollination; DGAT, diacylglycerol acyltransferase; DIG, digoxigenin; FAH, fatty acyl hydroxylase; O, oleate; P, palmitate; Po, palmitoleate; R, ricinoleate; RACE, rapid amplification of cDNA ends; RcDGAT, DGAT from *Ricinus communis*; RT, reverse transcription.

from castor seeds by reverse transcription (RT)-PCR using degenerate primers: 5′-GCKCCMACAYTRTGTTAT-3′ and 5′-CCAYTTRTGAACAGGCATATTCCA-3′. These two primers were designed based on the highly conserved amino acid sequence regions, APTLCY and WNMPVHKW, of DGAT. The sequence information obtained from the 378 bp cDNA fragment was then used to generate gene-specific primers for 3′- and 5′-RACE (rapid amplification of cDNA ends) (20). By using the known sequence information obtained from 3′- and 5′-RACE, primers were designed for end-to-end amplification of the complete gene from the RACE-ready cDNA template following the manufacturer's instruction (Invitrogen, Carlsbad, CA). The full-length cDNA was completely sequenced in both directions using ABI PRISM Big Dye Terminators v3.0 Cycle Sequencing Kit (Applied Biosystems, Foster City, CA). Sequence alignment and similarity among species were determined using the Clustal W program available at http://pbil.ibcp.fr/NPSA/npsa_prosite.html. The protein motifs were identified using ScanProsite at http://www.expasy.ch/tools/scnpsit1.html.

Southern blot analysis. Castor genomic DNA was isolated from leaves using the CTAB (*N*-cetyl-*N*,*N*,*N*-trimethylammonium bromide) procedure (21). Southern analysis was carried out according to the digoxigenin (DIG) application manual for hybridization of DNA probes to a Southern blot (Roche, Indianapolis, IN). DNA samples (3 μg) were separated on a 1% Tris-acetate agarose gel, then transferred to a positively charged nylon membrane (Roche). The filter was hybridized to a DIG-labeled DNA probe amplified from RcDGAT cDNA by PCR using primers, 5′-AAGACCCCATGGCGATTCT GAAACG-CCAGAA-3′ (HE-15F) and 5′-CTGGAGCTTCAGAACC-CTCTCAA-3′ (HE-6R).

RNA extraction and RT-PCR. RNA samples were extracted from castor seeds at different development stages using the method of Gu *et al*. (22). RT-PCR was carried out using the Gibco BRL SuperScript First-Strand Synthesis System for RT-PCR (Grand Island, NY). Briefly, 5 μg of total RNA was used to synthesize the first-strand cDNA using oligo(dT) primers, then 10% of the first-strand cDNA was used to amplify the target cDNA, RcDGAT, *FAH*, and actin, using gene-specific primers. The primers for RcDGAT gene were HE-15F and HE-6R. The primers for the *FAH* gene were 5′-CGCCGCACAC-GAAGCCTCCT-3′ and 5′-AGGCTACATGACACTTTTT-TAATACTTGTTCCGG-3′. The primers for the actin gene were 5′-AGGGGATAACCACCCCATGAATCCA-3′ and 5′-TGCATGGTCTCCTGATACGGCCAAG-3′. PCR was performed for 30 cycles with an annealing temperature of 65°C. One-tenth of the PCR product was analyzed on 1% agarose gel.

Expression of RcDGAT in yeast cells. The RcDGAT coding region was subcloned into a pYES2.1/V5-His-TOPO vector (Invitrogen) and transformed into *Saccharomyces cerevisiae* strain INVSc1 according to the manufacturer's instruction (Invitrogen). The primers used were 5′-GACCATGGGGAT-TCTCGAAACGCCAGAAAC-3′ and 5′- GTTCCCATCGC-GATTCATTAGGTC-3′. To ensure that the insertion contained a yeast consensus sequence for initiation of translation, (G/A)N-NATGG, the second amino acid codon was changed from acg (threonine) to ggg (glycine). The translation stop site (5′-TGA-3′) was removed to fuse RcDGAT in frame with the V5 epitope and polyhistidine tag for detection and purification of the protein. The expression of proteins in yeast cells was carried out according to manufacturer's instructions. Briefly, a single colony containing the pYES2.1/V5-His/RcDGAT or pYES2.1/V5-His/*LacZ* construct was inoculated into medium containing 2% glucose and grown overnight at 30°C with shaking. Galactose (2%) was added to the medium to induce expression of the recombinant proteins from the *GAL1* promoter. Cells were harvested at 14 h after induction, and the cell pellets were stored at –80°C until ready to use.

Western blot analysis. Microsomal samples (30 μg of total protein) from RcDGAT- or *LacZ*-transformed yeast were separated by SDS-PAGE and electrotransferred onto PVDF membranes. The membranes were incubated with the anti-V5 antibodies (Invitrogen) at 1:5000 dilution and horseradish peroxidase-conjugated goat-anti-mouse secondary antibodies (Roche) at 1:1000 dilution. Horseradish peroxidase activity was visualized by chemiluminescence using the ECL kit (Amersham, Arlington Heights, IL).

Assay for DGAT activity. Microsomes were isolated from harvested yeast cells as described by Urban *et al.* (23) and resuspended in 0.1 M Tris-HCl, pH 7.0, containing 20% glycerol (5 mg protein/mL) and kept frozen at –80°C. Protein concentration was determined using a bicinchoninic acid protein assay kit (Pierce, Rockford, IL). DGAT assays were performed as in Cases *et al*. (24) with small modifications. [^{14}C]Oleoyl-CoA was synthesized according to McKeon *et al.* (25). The reaction mixture (100 μL) consisted of 0.1 M Tris-HCl, pH 7.0, containing 20% glycerol, microsomes (100 μg of protein), and [^{14}C]oleoyl-CoA (20 μM, 200,000 cpm) and was incubated for 15 min at 30°C. In assays for substrate specificity of RcDGAT, different molecular species of DAG dissolved in 5 μL of methanol were added to the above reaction mixture (concentration from 0 to 1.0 mM). 1,2-Diolein and 1,2-dipalmitolein were purchased from Larodan Fine Chemicals AB (Malmo, Sweden); 1,2-diricinolein was prepared in our laboratory (26). The reactions were stopped and lipids were extracted using chloroform/methanol as previously described (27). Different molecular species of TAG products were separated from FFA using C_{18} HPLC (25 × 0.46 cm, 5 μm, Ultrasphere C18; Beckman Instruments Inc., Fullerton, CA) (28). DGAT activity (pmol TAG formed/mg protein/min) was determined based on the [^{14}C]-label incorporated into the TAG products from [^{14}C]oleoyl-CoA.

RESULTS AND DISCUSSION

Cloning of a cDNA encoding DGAT from R. communis. Conserved regions of DGAT were identified by sequence alignment of deduced amino acid sequences from different organisms, and degenerate primers were generated based on corresponding DNA sequences of these conserved regions. By using degenerate primers, a DNA fragment of 378 bp was amplified

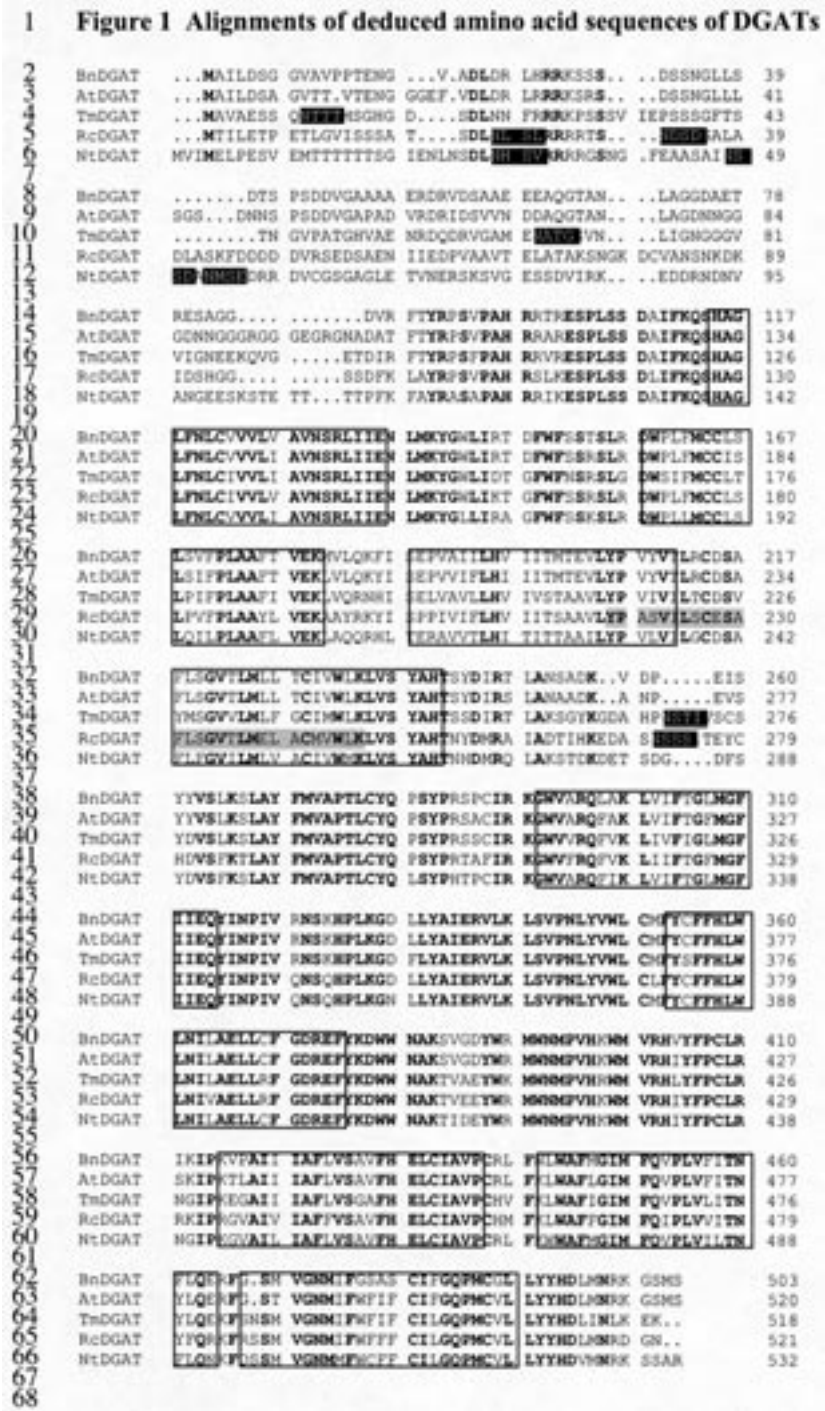

FIG. 1. Alignments of deduced amino acid sequences of diacylglycerol acyltransferases (DGAT). Alignments were generated by using the Clustal W program in GCG output format freely available at http://pbil.ibcp.fr/NPSA/npsa_prosite.html. The GeneBank accession numbers for the listing DGAT are: AtDGAT from *Arabidopsis thaliana*, AF 051849; BnDGAT from *Brassica napus*, AF 164434; NtDGAT from *Nicotiana tobacum*, AF 129003; RcDGAT from *Ricinus communis*, AY366496; TmDGAT from *Tropaeolum majus*, AY 084052. The identical residues among the five proteins are in bold and the transmembrane segments are boxed. N-Glycosylation sites are highlighted. The binding-protein-dependent transport systems' inner membrane component signature is shaded in gray. The potential protein kinase phosphorylation sites are as follows: (i) cAMP- and cGMP-dependent protein kinase phosphorylation site, amino acid residues 27–30; 28–31; (ii) protein kinase C phosphorylation site, amino acid residues 24–26, 73–75, 85–87, 112–114, 165–167, 168–170, 283–285; (iii) casein kinase II phosphorylation site, amino acid residues 2–5, 30–33, 43–46, 85–88, 112–115, 168–171, 236–239, 254–257, 274–277, 403–406; (iv) tyrosine kinase phosphorylation site, amino acid residues 388–395.

from castor seeds by RT-PCR and sequenced. Based on the sequence information, gene-specific primers for 3′- and 5′-RACE were designed, yielding a full-length cDNA. Sequence analysis indicates that the castor DGAT cDNA is 2067 bp long with 266 bp 5′- and 235 bp 3′-end untranslated regions (GenBank accession number AY366496). This cDNA is predicted to encode a protein of 521 amino acids with a molecular mass of 59.9 kDa. The deduced amino acid sequence of RcDGAT shares 65–67% identity with other cloned plant DGAT. When all five DGAT are aligned, their identity reaches 50.18%, with the most conserved regions in the C terminus (63.27% identity within 422 amino acids), whereas the first 119 N-terminal amino acid residues share only 5.88% identity (Fig. 1).

Identification of putative functional motifs in RcDGAT. Searches of the protein databases indicate that the predicted RcDGAT protein has an isoelectric point of 8.39 (predicted by Protparam at http://www.expasy.ch) and thus is positively charged at neutral pH. The deduced amino acid sequence of RcDGAT contains three potential N-linked glycosylation sites (N-X-S/T), which are also present in the TmDGAT and Nt-DGAT, but not in the AtDGAT and BnDGAT (Fig. 1). Since the RcDGAT protein expressed in yeast cells matches the predicted molecular size (see later *Functional expression* section) and treatment with glycosidase had no effect on electrophoretic migration (data not shown), it appears that RcDGAT is not glycosylated. In addition, RcDGAT contains a unique site, that is, the binding-protein-dependent transport system's inner membrane component signature, residing in residues 219–247 (Fig. 1). The significance of the presence of this signature *in vivo* is unknown. In bacteria, such sites often interact with a binding protein, allowing transmembrane transport (29). We speculate that this site in RcDGAT would interact with the acyl-CoA substrates bound to acyl-CoA binding proteins. The most notable structures that RcDGAT shares in common with other plant DGAT cloned to date are the multiple transmembrane domains in the C terminal conserved regions (Fig. 1), consistent with an integral membrane enzyme.

RcDGAT is a single-copy gene in the castor plant. To determine the copy number of RcDGAT gene in castor plants, we performed Southern blot analysis of genomic DNA under high-stringency hybridization conditions. The results from the restriction enzyme digestion patterns of HindIII, SmaI, XhoI, and PvuII suggest that RcDGAT is a single-copy gene in castor. A single band was detected with restriction enzymes HindIII, SmaI and XhoI, and two bands were detected with PvuII owing to the presence of an internal cutting site (Fig. 2). However, two bands were detected with PstI, although there is no cutting site in the cDNA sequence (Fig. 2). This may be due to the presence of a PstI site in intron regions. Six randomly selected RcDGAT cDNA were sequenced and found to be identical, supporting that RcDGAT may be a single-copy gene in the castor genome.

Expression of RcDGAT mRNA during seed development. For the purpose of monitoring the gene expression pattern of RcDGAT, an equal amount of total RNA from each time point was used, and RT-PCR reactions were performed. It is well-known that actin is a plant housekeeping gene and its expression level correlates well with total RNA during different development stages. The results from actin RT-PCR (Fig. 3) suggest that the efficiencies of RT-PCR among samples are uniform in this system. The results in Figure 3 reveal that the accumulation patterns of RcDGAT and FAH mRNA are very different, although both of them encode enzymes for castor oil biosynthesis. The amount of RcDGAT mRNA is maximal at an early stage of seed development [19 d after pollination (DAP)], and declined thereafter, whereas the FAH mRNA was maximal at a later stage (33 DAP) of seed development and continued until 47 DAP. Ample evidence indicates that genes involved in storage product synthesis are concomitantly expressed, and it has been reported that the *in vitro* activities of DGAT peak during the active period of

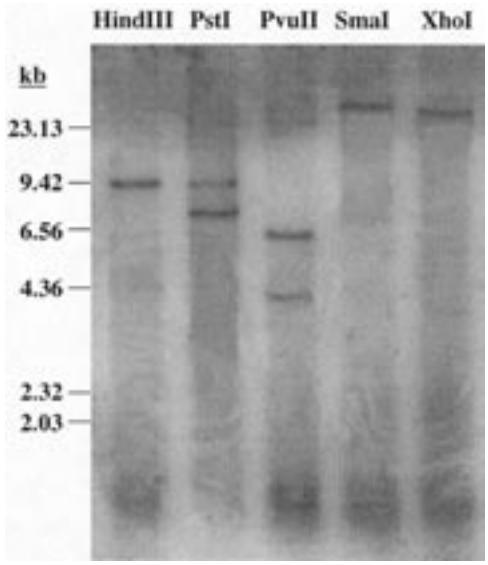

FIG. 2. DNA gel blot analysis of castor genomic DNA. Castor genomic DNA (3 μg/lane) was digested with the indicated restriction enzymes, and the DNA blot was hybridized to a dioxigenin-labeled DGAT cDNA probe. For other abbreviation see Figure 1.

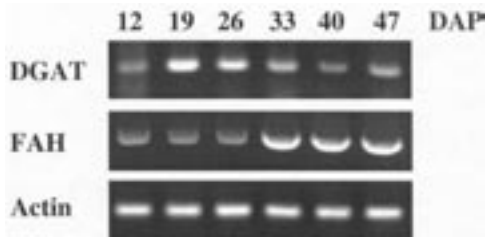

FIG. 3. Expression patterns of *FAH*, RcDGAT, and actin genes in castor plants. Shown is an agarose gel of reverse transcription-PCR products. RNA samples were extracted from castor seeds at different development stages including 12, 19, 26, 33, 40, and 47 d after pollination (DAP). Five micrograms of total RNA was used from each time course to synthesize the first-strand cDNA using oligo(dT) primers, then 10% of the first-strand cDNA was used to amplify target genes using gene-specific primers. One-tenth of the PCR product was analyzed on a 1% agarose gel. FAH, fatty acyl hydroxylase; RcDGAT, diacylglycerol transferase from *Ricinus communis*.

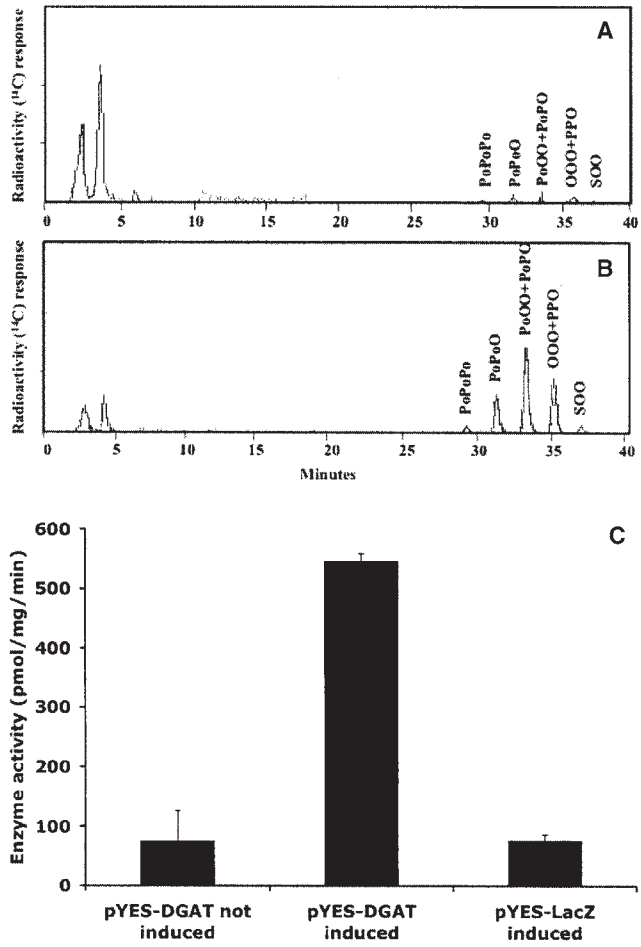

FIG. 4. DGAT activities in yeast microsomes. Batches of microsomes (100 μg of total protein) extracted from yeast cells carrying the indicated plasmids with or without induction by galactose were incubated with [^{14}C]oleoyl-CoA in 100 μL of 0.1 M Tris-HCl, pH 7.0 containing 20% glycerol for 15 min at 30°C. Assays were terminated by addition of $CHCl_3/CH_3OH$ (1:2, vol/vol) and lipids were extracted. The C_{18} HPLC radiochromatograms show the separation of molecular species of TAG from incubations of yeast microsomes expressing β-galactosidase (A) and RcDGAT (B). The molecular species of TAG are given as the abbreviations of their FA constituents: Po, palmitoleate; P, palmitate; O, oleate; and S, stearate. DGAT activities were measured based on the [^{14}C]label incorporated into the TAG products (C). Values are means of three replicate experiments with SD. For other abbreviations see Figures 1 and 3.

TAG accumulation (around 30 DAP) (30–32). Thus, the mRNA for RcDGAT may encode a stable protein and, accordingly, its level would not correlate with RcDGAT protein level and enzyme activity, or the enzyme activity may be posttranscriptionally controlled. Indeed, there are multiple potential phosphorylation sites based on functional motifs and critical amino acid residues in the deduced amino acid sequence of RcDGAT (see Fig. 1 legend). Enzyme activity could be regulated by some specific protein kinases. As well, a second DGAT may exist and play a role in oil formation at later stages of seed formation. Alternatively, RcDGAT may be involved in some other processes in the early stages of seed development. In mammalian systems, DGAT can remove DAG, a signaling molecule in the phospholipase C-inositol phospholipid cascade by converting it to TAG (33). It is possible that DGAT in plants serves additional roles beyond oil biosynthesis and that the expression pattern of RcDGAT could reflect one such role. We also detected RcDGAT mRNA in vegetative tissues such as roots, stems, cotyledons, and true leaves (data not shown); the importance of RcDGAT in these tissues is unknown.

Functional expression of RcDGAT in yeast. To determine whether the cloned RcDGAT cDNA codes for an active DGAT, we cloned RcDGAT cDNA into the pYES2.1/V5-His-TOPO vector and transformed it into yeast *S. cerevisiae*, INVSc-1 strain. Microsomes were extracted from cells after 14 h induction with 2% galactose, and DGAT activity was determined by measuring the incorporation of [^{14}C]oleoyl-CoA into TAG. As negative controls, DGAT activities in cells with pYES2.1/V5-His/RcDGAT grown under the repression (2% glucose) condition and with pYES2.1/V5-His/*LacZ* grown under the induction (2% galactose) condition were measured. Figures 4A and 4B show the separation of the molecular species of [^{14}C]TAG extracted from yeast microsomal incubation on C_{18} HPLC. The five [^{14}C] peaks labeled were identified by matching the retention times of the TAG identified previously (34) based on FA compositions of the yeast microsomes examined by GC analyses of FAME (data not shown). The major molecular species of TAG predicted in the yeast cells are PoPoPo, PoPoO, PoOO, PoPO, OOO, PPO, and SOO (Po- palmitoleate, P- palmitate, O- oleate, S- stearate). We found that cells expressing RcDGAT exhibited more than sevenfold higher DGAT activity than the controls (Fig. 4C). Wild-type yeast cells had low DGAT activity in our system (Figs. 4A, 4C). Bouvier-Nave *et al.* (10) observed that expression of the *Arabidopsis* DGAT in yeast resulted in the formation of a floating layer on top of the 100,000 × *g* supernatant during the preparation of microsomes that displayed extremely high DGAT activity. We also observed a thin floating layer on top of the 100,000 × *g* supernatant during the RcDGAT-transformed yeast microsomal isolation that exhibited some DGAT activity, but the activity was much lower than that of the microsomal fraction.

Cells transformed with the plasmid carrying RcDGAT cDNA expressed a ~65 kDa protein (V5 epitope and the polyhistidine tag from the vector add approximately 5 kDa to the size of the protein) when induced with 2% galactose, but this protein was not detected in the same cells grown under 2% glucose (Fig. 5).

Specificity of RcDGAT for molecular species of DAG. We next examined the effectiveness of RcDGAT on using different molecular species of DAG for TAG. The substrates 1,2-diolein, 1,2-dipalmitolein, and 1,2-diricinolein were incubated with yeast microsomes and [^{14}C]oleoyl-CoA. RcDGAT activities were then determined. The addition of different molecular species of DAG up to 1 mM to the microsomal mixture had little effect on the amount of total TAG formed in the assay. However, the RcDGAT clearly demonstrated a preference for diricinoleins. With the addition of 0.25 mM DAG, the amount of RRO from diricinolein increased 318 pmol/mg/min (Fig. 6A), whereas the amount of OOO from diolein and PoPoO

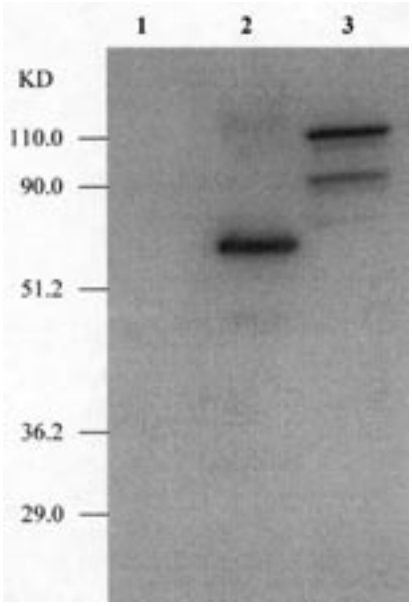

FIG. 5. Western blot of microsomal protein (30 μg/lane) probed with anti-V5 antibodies. Overnight cultures were harvested at 14 h of growth: lane 1, under repression condition (2% glucose); lanes 2 and 3, under induction condition (2% galactose). Microsomes were extracted from yeast cells transformed with RcDGAT (lanes 1 and 2) and *LacZ* (lane 3).

from dipalmitolein increased only 34 and 10 pmol/mg/min compared with that without exogenous DAG (Figs. 6B, 6C). Although complicated by the presence of endogenous diolein and dipalmitolein in the yeast cells, the absolute incorporation of oleate into RRO still was much higher than OOO and PoPoO (456 vs. 278 and 204 pmol/mg/min, with 1 mM of DAG). We also measured DGAT activity using microsomes extracted from yeast cells carrying RcDGAT gene but grown under the repression condition. The absolute incorporation of [^{14}C]oleate into RRO was less than 20 pmol/mg/min in the presence of 1 mM diricinolein. This result suggests that the RRO detected in RcDGAT-containing microsomes was mostly generated by RcDGAT, instead of yeast endogenous DGAT. Our previous results from isolated castor microsomes suggest that the final acylation step in castor oil biosynthesis displays a strong preference for diricinolein vs. other DAG (13, 35). In future studies we hope to further elucidate differential interactions resulting from DAG and acyl-CoA.

An important role for DGAT in oil biosynthesis has been established by the cloning of DGAT genes from different organisms. However, the gene for DGAT in castor bean has never been cloned. In this study, we identified a cDNA encoding a protein that shares high sequence similarity with the acyl-CoA-dependent DGAT and possesses DGAT activity. This cloned RcDGAT was found to be a single copy gene, although it is possible that there exists a second DGAT with different nucleic acid sequence (36) or an acyl-CoA-independent phospholipid:DGAT gene (37) in the castor genome. Currently, one of the major issues in plant lipid biochemistry and biotechnology is the understanding of how plants assemble TAG and, specifically, how a plant such as castor can accumulate seed oil for

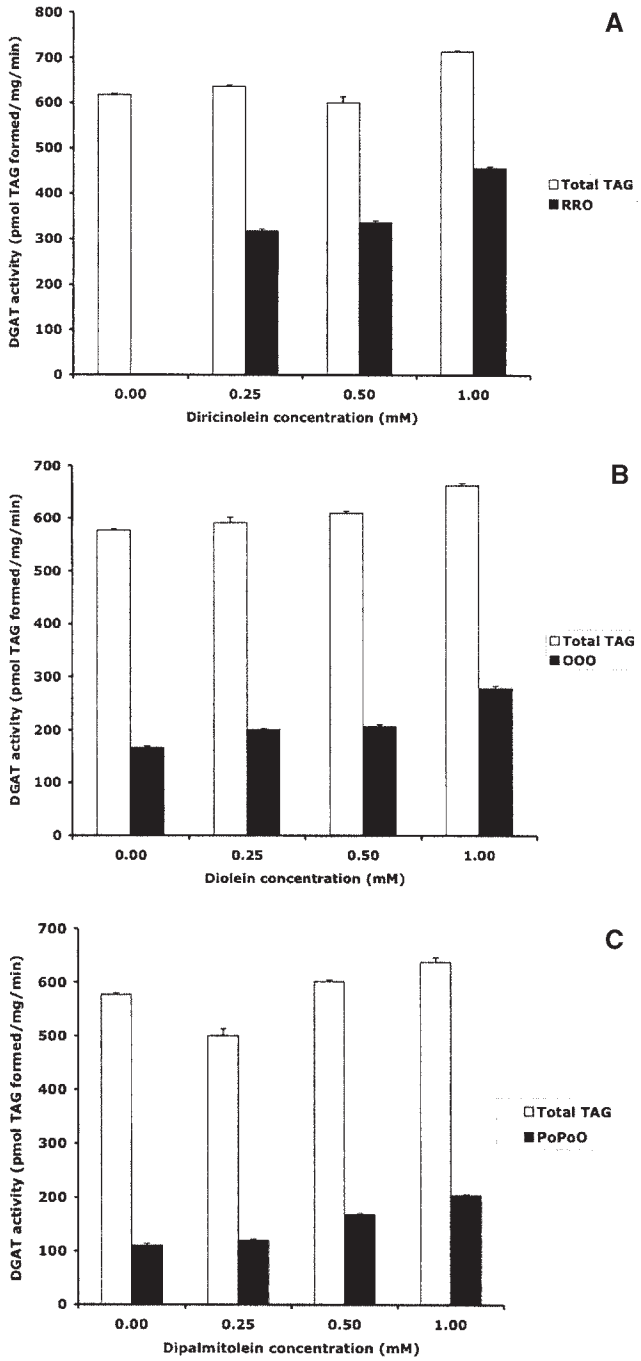

FIG. 6. Specificity of RcDGAT for molecular species of DAG. Batches of microsomes (100 μg of total microsomal protein) extracted from yeast cells expressing RcDGAT were used in the assay. The microsomes were supplied with diricinolein (A), diolein (B), and dipalmitolein (C) and incubated with [^{14}C]oleoyl-CoA in 100 μL of 0.1 M Tris-HCl, pH 7.0, containing 20% glycerol for 15 min at 30°C. Assays were then terminated by addition of $CHCl_3/CH_3OH$ (1:2, vol/vol). DGAT activities were determined based on the ^{14}C-label incorporated into the TAG products. The abbreviations of TAG are RRO, diricinoleoyloleoylglycerol; OOO, triolein; PoPoO, dipalmitoyloleoylglycerol. Values are means of three replicate experiments with SD.

which the FA composition exceeds 90% in a single FA, ricinoleate. The cloning of RcDGAT makes it possible to elucidate the individual role of this particular enzyme in castor oil

biosynthesis. Several reports in the literature, all of which used castor microsomes, describe castor DGAT substrate specificity (12,13,38). It is difficult to conclude that the substrate specificity is solely due to a single enzyme in the castor microsomes, since a number of activities are present that can contribute to the end product. We investigated the substrate specificity of this enzyme in a yeast cell system, which has the benefit of low fat content and biosynthetic capacity. We synthesized the diricinolein (26) and purchased the other DAG substrates. By applying these DAG substrates in the assay, we discovered that the RcDGAT exhibited much higher activity with diricinolein than with diolein and dipalmitolein. The information presented here is important for better understanding of the regulation of triricinolein biosynthesis in castor plants and provides a valuable means for engineering crops containing high levels of hydroxylated FA.

ACKNOWLEDGMENTS

This work was supported in part by ARS CRIS Project 5325-21000-006-00D, ARS Research Associate Program, and a cooperative agreement with Dow Chemical Company, Midland, Michigan. We would also like to thank Jennifer Chen and Pei Chen for technical assistance.

REFERENCES

1. Kennedy, E. (1961) Biosynthesis of Complex Lipids, *Fed. Proc. 20*, 934–940.
2. Ichihara, K., Takahashi, T., and Fujii, S. (1988) Diacylglycerol Acyltransferase in Maturing Safflower Seed: Its Influences on the Fatty Acid Composition and on the Rate of Triacylglycerol Synthesis, *Biochim. Biophys. Acta 958*, 125–129.
3. Perry, H.J., and Harwood, J.L. (1993) Changes in the Lipid Content of Developing Seeds of *Brassica napus*, *Phytochemistry. 32*, 1411–1415.
4. Zou, J.T., Wei, Y.D., Jako, C., Kumar, A., Selvaraj, G., and Taylor, D.C. (1999) The *Arabidopsis thaliana* TAG1 Mutant Has a Mutation in a Diacylglycerol Acyltransferase Gene, *Plant J. 19*, 645–653.
5. Lu, C., and Hill, M.J. (2002) *Arabidopsis* Mutants Deficient in Diacylglycerol Acyltransferase Display Increased Sensitivity to Abscisic Acid, Sugars, and Osmotic Stress During Germination and Seedling Development, *Plant Physiol. 129*, 1352–1358.
6. Kaup, M.T., Froese, C.D., and Thompson, J.E. (2002) A Role for Diacylglycerol Acyltransferase During Leaf Senescence, *Plant Physiol. 129*, 1616–1626.
7. Katavic, V., Reed, D.W., Taylor, D.C., Giblin, E.M., Barton, D.L., Zou, J.T., MacKenzie, S.L., Covello, P.S., and Kunst, L. (1995) Alteration of Seed Fatty Acid Composition by an Ethyl Methanesulfonate-Induced Mutation in *Arabidopsis thaliana* Affecting Diacylglycerol Acyltransferase Activity, *Plant Physiol. 108*, 399–409.
8. Jako, C., Kumar, A., Wei, Y.D., Zuo, J.T., Barton, D.L., Giblin, E.M., Covello, P.S., and Taylor, D.C. (2001) Seed-Specific Over-expression of an *Arabidopsis* cDNA Encoding a Diacylglycerol Acyltransferase Enhances Seed Oil Content and Seed Weight, *Plant Physiol. 126*, 861–874.
9. Hobbs, D.H., Lu, C.F., and Hill, M.J. (1999) Cloning of a cDNA Encoding Diacylglycerol Acyltransferase from *Arabidopsis thaliana* and Its Functional Expression, *FEBS Lett. 452*, 145–149.
10. Bouvier-Nave, P., Benveniste, P., Oelkers, P., Sturley, S.L., and Schaller, H. (2000) Expression in Yeast and Tobacco of Plant cDNAs Encoding Acyl CoA:Diacylglycerol Acyltransferase, *Eur. J. Biochem. 267*, 85–96.
11. Nykiforuk, C.L., Furukawa-Stoffer, T.L., Huff, P.W., Sarna, M., Laroche, A., Moloney, M.M., and Weselake, R.J. (2002) Characterization of cDNAs Encoding Diacylglycerol Acyltransferase from Cultures of *Brassica napus* and Sucrose-Mediated Induction of Enzyme Biosynthesis, *Biochim. Biophys. Acta 1580*, 95–109.
12. Vogel, G., and Browse, J. (1996) Cholinephosphotransferase and Diacylglycerol Acyltransferase, *Plant Physiol. 110*, 923–931.
13. Lin, T.A., Chen, J.M., Liao, L.P., and McKeon, T.A. (2002) Molecular Species of Acylglycerols Incorporating Radiolabeled Fatty Acids from Castor (*Ricinus communis* L.) Microsomal Incubations, *J. Agric. Food Chem. 50*, 5077–5081.
14. Caupin, H-J. (1997) Products from Castor Oil: Past, Present, and Future, in *Lipid Technologies and Applications* (Gunstone, F.D., and Padley, F.B., eds.), pp. 787–795, Marcel Dekker, New York.
15. Van De Loo, F.J., Broun, P., Turner, S., and Somerville, C. (1995) An Oleate 12-Hydroxylase from *Ricinus communis* L. Is a Fatty Acyl Desaturase Homolog, *Proc. Natl. Acad. Sci. USA. 92*, 6743–6747.
16. Broun, P., and Somerville, C. (1997) Accumulation of Ricinoleic, Lesquerolic, and Densipolic Acids in Seeds of Transgenic *Arabidopsis* Plants That Express a Fatty Acyl Hydroxylase cDNA from Castor Bean, *Plant Physiol. 113*, 933–942.
17. Bafor, M., Smith, M.A., Jonsson, L., Stobart, K., and Stymne, S. (1991) Ricinoleic Acid Biosynthesis and Triacylglycerol Assembly in Microsomal Preparations from Developing Castor Bean (*Ricinus communis*) Endosperm, *Biochem. J. 280*, 507–514.
18. Lin, J.T., Woodruff, C.L., Lagouche, O.J., McKeon, T.A., Stafford, A.E., Goodrich-Tanrikulu, M., Singleton, J.A., and Haney, C.A. (1998) Biosynthesis of Triacylglycerols Containing Ricinoleate in Castor Microsomes Using 1-Acyl-2-oleoyl-*sn*-glycero-3-phosphocholine as the Substrate of Oleoyl-12-hydroxylase, *Lipids 33*, 59–69.
19. Kinney, A.J., Cahoon, E.B., and Hitz, W.D. (2002) Manipulating Desaturase Activities in Transgenic Crop Plants, *Biochem. Soc. Trans. 30*, 1099–1103.
20. Schaefer, B.C. (1995) Revolutions in Rapid Amplification of cDNA Ends: New Strategies for Polymerase Chain Reaction Cloning of Full-Length cDNA Ends, *Anal. Biochem. 227*, 255–273.
21. Doyle, J.J., and Doyle, J.L. (1987) A Rapid DNA Isolation Procedure for Small Quantities of Fresh Leaf Tissue, *Phytochem. Bull. 19*, 11.
22. Gu, Y.Q., Yang, C., Thara, V.K., Zhou, J., and Martin, G.B. (2000) *Pti4* Is Induced by Ethylene and Salicylic Acid, and Its Product Is Phosphorylated by the Pto Kinase, *Plant Cell 12*, 771–785.
23. Urban, P., Werck-Reichhart, D., Teutsch, H.G., Durst, F., Regnier, S., Kazmaier, M., and Pompon, D. (1994) Characterization of Recombinant Plant Cinnamate 4-Hydroxylase Produced in Yeast. Kinetic and Spectral Properties of the Major Plant P450 of the Phenylpropanoid Pathway, *Eur. J. Biochem. 222*, 843–850.
24. Cases, S., Smith, S.J., Zheng, Y.W., Myers, H.M., Lear, S.R., Sande, E., Novak, S., Collins, C., Welch, C.B., Lusis, A.J., *et al.* (1998) Identification of a Gene Encoding an Acyl CoA:Diacylglycerol Acyltransferase, a Key Enzyme in Triacylglycerol Synthesis, *Proc. Natl. Acad. Sci. USA 95*, 13018–13023.
25. McKeon, T.A., Lin, J.T., Goodrich-Tanrikulu, M., and Stafford, A.E. (1997) Ricinoleate Biosynthesis in Castor Microsomes, *Ind. Crops Prod. 6*, 383–389.
26. Turner, C., He, X., Nguyen, T., Lin, J.T., Wong, R.Y., Lundin,

R.E., Harden, L., and McKeon, T.A. (2003) Synthesis of 1,2(2,3)-Diricinolein by Lipase-Catalyzed Methanolysis in Organic Solvent, *Lipids 38*, in press.
27. Lin, J.T., McKeon, T.A., Goodrich-Tanrikulu, M., and Stafford, A.E. (1996) Characterization of Oleoyl-12-hydroxylase in Castor Microsomes Using the Putative Substrate, 1-Acyl-2-oleoyl-*sn*-glycero-3-phosphocholine, *Lipids 31*, 571–577.
28. Lin, J.T., Woodruff, C.L., and McKeon, T.A. (1997) Nonaqueous Reversed-Phase High-Performance Liquid Chromatography of Synthetic Triacylglycerols and Diacylglycerols, *J. Chromatogr. A 782*, 41–48.
29. Higgins, C.F., Hyde, S.C., Mimmack, M.M., Gileadi, U., Gill, D.R., and Gallagher, M.P. (1990) Binding Protein-Dependent Transport Systems, *J. Bioenerg. Biomembr. 22*, 571–592.
30. Tzen, J.T.C., Cao, Y.Z., Laurent, P., Ratnayake, C., and Huang, A.H.C. (1993) Lipids, Proteins, and Structure of Seed Oil Bodies from Diverse Species, *Plant Physiol. 101*, 267–276.
31. Weselake, R.J., Pomeroy, M.K., Furukawa, T.L., Golden, J.L., Little, D.B., and Laroche, A. (1993) Developmental Profile of Diacylglycerol Acyltransferase in Maturing Seeds of Oilseed Rape and Safflower and Microspore-Derived Cultures of Oilseed Rape, *Plant Physiol. 102*, 565–571.
32. Giroux, M., Boyce, C., Feix, G., and Hannah L.C. (1994) Coordinated Transcriptional Regulation of Storage Product Genes in the Maize Endosperm, *Plant Physiol. 106*, 713–722.
33. Irvine, R.F. (2002) Nuclear Lipid Signaling, *Sci. STKE. 150*, RE13.
34. Lin, J.T., and McKeon, T.A. (2003) Relative Retention Times of Molecular Species of Acylglycerols, Phosphatidylcholines, and Phosphatidylethanolamines Containing Ricinoleate in Reversed-Phase HPLC, *J. Liq. Chromatogr. Rel. Tech. 26*, 1051–1058.
35. Lin, J.T., Turner, C., Liao, L.P., and McKeon, T.A. (2003) Identification and Quantification of the Molecular Species of Acylglycerols in Castor Oil by HPLC Using ELSD, *J. Liq. Chromatogr. Rel. Tech. 26*, 773–780.
36. Cases, S., Stone, S.J., Zhou, P., Yen, E., Tow, B., Lardizabal, K.D., Voelker, T., and Farese, R.V., Jr. (2001) Cloning of DGAT2, a Second Mammalian Diacylglycerol Acyltransferase, and Related Family Members, *J. Biol. Chem. 276*, 38870–38876.
37. Dahlqvist, A., Stahl, U., Lenman, M., Banas, A., Lee, M., Sandager, L., Ronne, H., and Stymne, S. (2000) Phospholipid:Diacylglycerol Acyltransferase: An Enzyme That Catalyzes the Acyl-CoA-Independent Formation of Triacylglycerol in Yeast and Plants, *Proc. Natl. Acad. Sci. USA 97*, 6487–6492.
38. Wiberg, E., Tillberg, E., and Stymne, S. (1994) Substrates of Diacylglycerol Acyltransferase in Microsomes from Developing Oil Seeds, *Phytochemistry 36*, 573–577.

[Received November 17, 2003, and in revised form January 19, 2004; revision accepted January 21, 2004]

Biosynthesis and Isomerization of 11-Hydroperoxylinoleates by Manganese- and Iron-Dependent Lipoxygenases

Ernst H. Oliw[a,*], Mirela Cristea[a], and Mats Hamberg[b]

[a]Department of Pharmaceutical Biosciences, Uppsala University, Uppsala Biomedical Center, SE-751 24 Uppsala, Sweden, and [b]Division of Physiological Chemistry II, Department of Medical Biochemistry and Biophysics, Karolinska Institutet, SE-171 77 Stockholm, Sweden

ABSTRACT: Manganese lipoxygenase (Mn-LO) oxygenates linoleic acid (LA) to a mixture of the hydroperoxides—11(*S*)-hydroperoxy-9*Z*,12*Z*-octadecadienoic acid [11(*S*)-HPODE] and 13(*R*)-hydroperoxy-9*Z*,11*E*-octadecadienoic acid [13(*R*)-HPODE]—and also catalyzes the conversion of 11(*S*)-HPODE to 13(*R*)-HPODE *via* oxygen-centered (LOO•) and carbon-centered (L•) radicals [Hamberg, M., Su, C., and Oliw, E. (1998) Manganese Lipoxygenase. Discovery of a Bis-allylic Hydroperoxide as Product and Intermediate in a Lipoxygenase Reaction, *J. Biol. Chem. 273*, 13080–13088]. The aims of the present work were to investigate whether 11-HPODE can also be produced by iron-dependent lipoxygenases and to determine the enzymatic transformations of stereoisomers of 11-HPODE by lipoxygenases. Rice leaf pathogen-inducible lipoxygenase, but not soybean lipoxygenase-1 (sLO-1), generated a low level of 11-HPODE (0.4%) besides its main hydroperoxide, 13(*S*)-HPODE, on incubation with LA. Steric analysis revealed that 11-HPODE was enriched with respect to the *R* enantiomer [74% 11(*R*)]. In agreement with previous results, 11(*S*)-HPODE incubated with Mn-LO provided 13(*R*)-HPODE, and the same conversion also took place with the methyl ester of 11(*S*)-HPODE. 11(*R,S*)-HPODE was metabolized biphasically in the presence of Mn-LO, i.e., by a rapid phase during which the 11(*S*)-enantiomer was converted into 13(*R*)-HPODE and a slow phase during which the 11(*R*)-enantiomer was converted into 9(*R*)-HPODE. sLO-1 catalyzed a slow conversion of 11(*S*)-HPODE into a mixture of 13(*R*)-HPODE (75%), 9(*S*)-HPODE (10%), and 13(*S*)-HPODE (10%), whereas 11(*R,S*)-HPODE produced a mixture of nearly racemic 13-HPODE (≈70%) and 9-HPODE (≈30%). The results showed that 11-HPODE can also be produced by an iron-dependent LO and suggested that the previously established mechanism of isomerization of 11(*S*)-HPODE involving suprafacial migration of O_2 is valid also for the isomerizations of 11(*R*)-HPODE by Mn-LO and of 11(*S*)-HPODE by sLO-1.

Paper no. L9484 in *Lipids 39,* 319–323 (April 2004).

Widely distributed in plants and mammals, lipoxygenases (LO) oxygenate PUFA to *cis-trans* conjugated hydroperoxides (1,2). Plant and mammalian LO studied so far contain iron and belong to the same gene family. These enzymes have important biological functions. Their products may act as precursors of biological mediators such as 12-oxophytodienoic acid and jasmonic acid in plants (3) and leukotrienes in animals (4). LO also catalyze the transformation of hydroperoxides to epoxy alcohols and other products (5), and some enzymes are involved in the chemical warfare of hosts and pathogens, e.g., the defensive rice leaf pathogen-inducible lipoxygenase (RLI-LO) and supposedly harmful manganese-LO (Mn-LO) secreted by the take-all fungus (6,7). The reaction mechanisms of LO have been investigated thoroughly with soybean LO-1 (sLO-1) as the prototype enzyme (1).

The take-all fungus, *Gaeumannomyces graminis*, is a devastating root pathogen of wheat worldwide. *Gaeumannomyces graminis* secretes a unique LO, which contains manganese as the catalytic metal (8). Mn-LO belongs to the LO gene family (9). Its amino acid sequence can be aligned with 26–27% identity and 40–46% similarity with mammalian and plant LO, and site-directed mutagenesis suggests that several metal ligands are conserved in Mn-LO and other LO (Cristea, M., Engström, Å, Su, C., Hörnsten, L., and Oliw, E.H., unpublished observation). The catalytic properties of Mn-LO are similar in many aspects to those of other LO (8,10,11) .

The metal center of sLO-1 (and other iron LO) redox cycles between Fe^{2+} (inactive state) and Fe^{3+} (active state), and the mononuclear metal center of Mn-LO seems to redox-cycle between Mn^{2+} and Mn^{3+} in the same way (1,11,12). The active states of both enzymes likely contain the catalytic base M^{3+}–OH (*cf.* Refs. 13,14), which abstracts stereospecifically a bisallylic hydrogen from linoleic acid (LA) and forms a carbon-centered radical, L•. This process involves hydrogen tunneling as judged by the occurrence of unusually large kinetic isotope effects (10,15). L• reacts with molecular oxygen and forms a peroxyl radical (LOO•). Antarafacial oxygen insertion is catalyzed by sLO-1 and suprafacial oxygen insertion by Mn-LO (1,10). sLO-1 oxidizes LA to 13(*S*)-hydroperoxy-9*Z*,11*E*-octadecadienoic acid [13(*S*)-HPODE], whereas Mn-LO forms 13(*R*)-hydroperoxy-9*Z*,11*E*-octadecadienoic acid [13(*R*)-HPODE]. In addition, Mn-LO oxygenates LA to ~35% 11(*S*)-hydroperoxy-9*Z*,12*Z*-octadecadienoic acid [11(*S*)-HPODE] and also isomerizes this compound to the end product, 13(*R*)-HPODE (10,16).

Hamberg *et al.* (10) investigated the mechanism of the isomerization of 11(*S*)-HPODE to 13(*R*)-HPODE by Mn-LO in detail. The results were consistent with hydrogen abstraction from

*To whom correspondence should be addressed at Division of Biochemical Pharmacology, Department of Pharmaceutical Biosciences, Uppsala University, P.O. Box 591, SE-751 24 Uppsala, Sweden.
E-mail: Ernst.Oliw@farmbio.uu.se

Abbreviations: CP-HPLC, chiral phase HPLC; HODE, hydroxyoctadecadienoic acid; HPODE, hydroperoxyoctadecadienoic acid; L•, carbon-centered radical; LA, linoleic acid; LO, lipoxygenase; LOO•, oxygen-centered radical; Mn-LO, manganese lipoxygenase; RLI-LO, rice leaf-inducible lipoxygenase; sLO-1, soybean lipoxygenase-1; SP-HPLC, straight phase-HPLC.

11(*S*)-HPODE, leading to the peroxyl radical, LOO•. Experiments under ^{18}O showed that LOO• was in equilibrium with L• plus O_2, and that molecular oxygen may react with L• either at C-11 or at C-13. Mn-LO is the only known LO that forms 11(*S*)-HPODE and can metabolize it further.

3-D structures are available for sLO-1, sLO-3, and rabbit reticulocyte arachidonic acid 15-LO (17,18). The substrate FA align in a relatively narrow substrate channel. The catalytic sites also can accommodate the formed hydroperoxy FA. 13(*S*)-HPODE, for example, is formed by sLO-1 and can oxidize other sLO-1 molecules into the active state. It therefore seemed worth investigating whether 11(*S*)-HPODE, 11(*R*)-HPODE, and their methyl ester derivatives might bind at the active site of Mn-LO and sLO-1 in the vicinity of the catalytic metal. If this is the case, hydrogen abstraction by the LO might lead to formation of LOO• in equilibrium with L• and O_2, and conversion to 13- or 9-HPODE by oxygen rebound at C-13 or C-9.

MATERIALS AND METHODS

Materials. LA (99%) and α-linolenic acids (99%) were from Merck (Darmstadt, Germany). Racemic 9-, 11-, and 13-HPODE were obtained by vitamin E-controlled autoxidation of LA essentially as described (19), purified by silicic acid chromatography (Silicar CC-4; Mallinckrodt Laboratory Chemicals, Phillipsburg, NJ; eluted with 7 and 25% diethyl ether in hexane, respectively) and by RP-HPLC, and characterized by UV and LC–MS analysis; 13(*R*)-HPODE, 13(*S*)-HPODE, and 9(*S*)-HPODE were obtained enzymatically by Mn-LO, sLO-1, and potato 5-LO (Cayman, Ann Arbor, MI) as described (8,20). Samples of authentic 11(*S*)- and 11(*R,S*)-hydroxy-9(*Z*),12(*Z*)-octadecadienoates were prepared as previously described (10,21). sLO-1 was from Sigma (Lipoxidase type IV; Sigma, St. Louis, MO). Recombinant Mn-LO was prepared by expression in *Pichia pastoris* (Cristea, M., Engström, Å, Su, C., Hörnsten, L., and Oliw, E.H., unpublished data) and purified by hydrophobic interaction chromatography as described (8). Recombinant (RLI-LO) (6) was expressed in *Escherichia coli* as previously described (22).

Spectroscopy. Light absorption was measured with a dual beam spectrophotometer (Shimadzu UV-2101PC). The *cis-trans* conjugated hydro(pero)xy FA were assumed to have a molar extinction coefficient of 25,000.

Isomerization of 11-HPODE. Mn-LO and sLO-1 with substrates (added in ethanol, final concentration ~1%) were assayed in 0.1 M sodium borate buffer (pH 9.0) under ambient atmosphere at 23°C. sLO-1 was used at a concentration of 36,000 units (0.25 mg) per mL, and recombinant Mn-LO in a concentration of 2–3 μg per mL. The reaction was terminated by addition of 1 vol of water containing ~10 mg $NaBH_4$/mL (prepared fresh), and placed on ice for 15 min, diluted with 0.1 M potassium phosphate buffer (pH 7.0), extracted on cartridge with octadecyl silica (SepPak/C_{18}; Waters, Milford, MA), methylated with diazomethane as required, and analyzed by HPLC.

HPLC analysis. 9-, 11-, and 13-HPODE were purified by RP-HPLC (octadecyl silica, 5-μm; 200 × 8 mm) using methanol/water/acetic acid, 80:20:0.01, and detected by UV absorbance at 235 and 210 nm (19). Fractions with 11-HPODE were diluted with water and extracted on a cartridge of octadecyl silica (Sep-Pak/C_{18}). Separation of methyl 13- and 9-hydroxylinoleates was performed by straight phase-HPLC (SP-HPLC; Nucleosil 50-5, 250 × 4.6 mm; eluted with 2 mL/min) or by chiral phase-HPLC (CP-HPLC; (*R*)-(−)-*N*-3,5-dinitrobenzoyl-α-phenylglycine, 250 × 4.1 mm; eluted with 0.8 mL/min) with 0.5% isopropanol in hexane (vol/vol) as eluent (23). To confirm the order of elution of stereoisomers, mixtures of methyl 13- and 9-HODE were added to the samples. The HPLC system consisted of a diode array detector (Waters 996 PDA) and pump (CM-4000; Milton Roy, Oaklands Park, Berkshire, United Kingdom). For LC-MS analysis, the column contained octadecyl silica (5-μm, 250 × 2 mm; Kromasil 5 C_{18} 100 Å; Phenomenex, Macclesfield, United Kingdom) and it was eluted with methanol/water/acetic acid, 80:20:0.01, at 0.4 mL/min (SpectraSystem P2000 pump; Spectra Physics, San Jose, CA), and the products were analyzed as acids. The effluent was subject to electrospray ionization in an ion trap mass spectrometer (LCQ; ThermoFinnigan, San Jose, CA) as described (16).

Biosynthesis of 11-HPODE by RLI-LO. RLI-LO was incubated for 20 min with linoleic acid (400 μM) at 23°C in potassium phosphate buffer pH 6.7 under oxygen gas. Material extracted with diethyl ether was analyzed by RP-HPLC using a solvent system of acetonitrile/water/acetic acid (60:40:0.02, by vol). Methods for structure determination (10) and steric analysis of partially hydrogenated material (24) were as indicated.

RESULTS

Generation of 11-HPODE in RLI-LO-catalyzed oxygenation. Analysis by RP-HPLC of products generated from linoleic acid upon incubation with RLI-LO demonstrated a main compound (>95%; effluent volume, 16.8 mL) as well as a less abundant compound (0.4%; effluent volume, 13.9 mL). The first-mentioned material was identified as 13(*S*)-HPODE, in agreement with previous work (22). The identity of the latter material with 11-HPODE was suggested by the appearance of strong UV absorptions at λ_{max} 259, 268, and 279 upon treatment with perchloric acid. This spectrum was indicative of a conjugated triene structure, which is produced from 11-HPODE upon acidification. Further structural support came from analysis of the $NaBH_4$-reduced material, which behaved identically with authentic 11-hydroxy-9(*Z*),12(*Z*)-octadecadienoic acid on analysis by GLC [equivalent chain length (C-value) 19.41 (8)] and GC–MS [mass spectrum showing prominent ions at *m/z* 382 (38%, M^+), 311 (32%, $M^+ - C_5H_{11}$), 253 (9%), and 225 (44%, $[CH{=}CH{-}CH(OSiMe_3){-}CH{=}CH{-}C_5H_{11}]^+$)]. Steric analysis of the reduced and partially hydrogenated hydroperoxide identified 2-hydroxynonanoic acid (73% *R*) as well as 2-hydroxydodecane-1,12-dioic acid (75% *S*). Based on these results, the minor hydroperoxide generated from linoleic acid in the presence of RLI-LO was identified as 11-hydroperoxy-9(*Z*),12(*Z*)-octadecadienoic acid [74% 11(*R*)].

Search for 11-HPODE in soybean lipoxygenase-catalyzed oxygenation. Linoleic acid (1.1 M; 5 mg) was stirred for 15 min at 0°C under O_2 with 5,000–25,000 units of sLO-1. Analysis of the products by RP-HPLC showed the presence of 13-HPODE (>95%). 11-HPODE or 11-HODE could not be detected.

Isomerization of 11-HPODE by Mn-LO. As previously reported, 11(*S*)-HPODE was efficiently isomerized to 13(*R*)-HPODE at 30% of the rate of oxygenation of linoleic acid to 13(*R*)-HPODE (k_{cat} = 9 and 26 s^{-1}, respectively) (10,11). With the exception of 11(*S*)-HPODE, the substrates discussed below were metabolized much less efficiently by Mn-LO (presumably due to high K_m and low V_{max} values).

UV analysis showed that 11(*R,S*)-HPODE was swiftly transformed by Mn-LO to 13(*R*)-HPODE as the main product within 6–7 min (Fig. 1A). This occurred with a kinetic lag time (insert in Fig. 1A). The biosynthesis of *cis-trans*-conjugated products reached its maximal rate after a few minutes during which the concentration of *cis-trans*-conjugated products increased 12 μM min^{-1}. The biosynthesis then declined, but it did not cease completely. The 11(*R*) stereoisomer was apparently also transformed to a *cis-trans* conjugated chromophore, as judged from the steady increase in concentration of *cis-trans*-conjugated products (0.2 μM min^{-1}) for up to 1 h. After reduction with $NaBH_4$, this metabolite was identified by UV analysis, LC–MS, SP-HPLC, and CP-HPLC as 9(*R*)-HPODE. LC–MS analysis after reduction with $NaBH_4$ showed that only a fraction of the 11-HODE remained (Fig. 1B). MS/MS analysis (*m/z* 295 → full scan) of the major product showed strong signals, *inter alia*, at *m/z* 277 (A^- – 18, loss of water; relative intensity 100%), *m/z* 252 (A^- – 44, loss of CO_2; 10%), and characteristic ions of 13-HODE [*m/z* 195, loss of O=CH–$(CH_2)_4CH_3$; 70%] and 9-HODE [*m/z* 171, loss of O=CH–$(CH=CH)_2$–$(CH_2)_4CH_3$; 60%]. The 9-HPODE/13-HODE ratios increased from 0.07 after 6 min incubation to 0.3 after 45 min as judged by SP-HPLC analysis. CP-HPLC showed that the 9*R* stereoisomer was mainly formed (Fig. 1C).

The low conversion of 11(*R*)-HPODE was not due to product inhibition by 13(*R*)-HPODE. 11-HPODE enriched in 11(*R*)-HPODE was obtained by treatment of 11(*R,S*)-HPODE with Mn-LO as in Figure 1A. The reaction was stopped after 10 min. The remaining 11-HPODE was purified by RP-HPLC, and it was only slowly oxidized by Mn-LO.

Mn-LO does not metabolize methyl linoleate; however, the methyl ester of 11(*S*)-HPODE was partly converted to *cis-trans*-conjugated chromophores, and biosynthesis ceased when only a fraction of the substrate was converted (data not shown). CP-HPLC analysis showed that the main metabolite of 11(*S*)-HPODE methyl ester was 13(*R*)-HPODE methyl ester. In addition, small amounts of 13(*S*)-HPODE methyl ester [~5% of 13(*R*)-HPODE methyl ester] and 9(*S*)-HPODE methyl ester [~5% of 13(*R*)-HPODE] were detected along with traces of 9(*R*)-HPODE methyl ester [about 1% of 13(*R*)-HPODE]. The steric analysis of the 9-HPODE metabolites is shown in Figure 1C. The low accumulation of 9(*R*)-HPODE suggested that the isomerization was mainly enzymatic, and not due to nonenzymatic breakdown of 11(*S*)-HPODE. The products were analyzed without methylation, and formation of metabolites due to incomplete methylation of 11(*S*)-HPODE could also be excluded.

The methyl ester of 11(*R*)-HPODE was not isomerized to methyl 9(*R*)-HPODE or other products to any significant extent, as the CP-HPLC analysis yielded the same amounts of metabolites from methyl 11(*S*)-HPODE as from methyl 11(*R,S*)-HPODE.

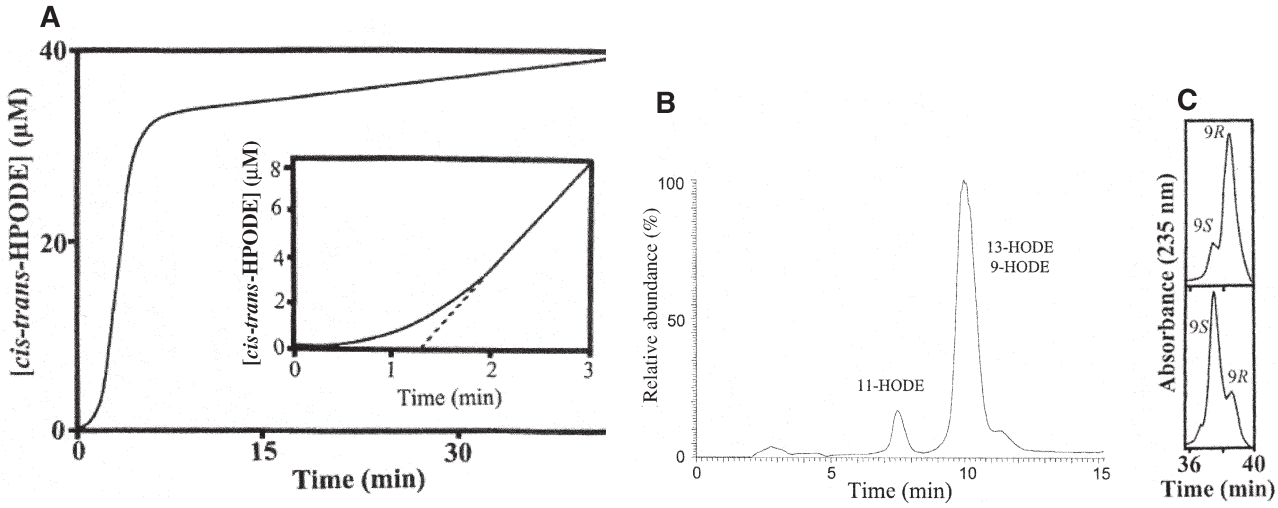

FIG. 1. Isomerization of 11(*R,S*)-HPODE by Mn-LO to 13(*R*)-HPODE and 9(*R*)-HPODE. (A) Time curve for formation of UV-absorbing material at 235 nm from an incubation of 11(*R,S*)-HPODE with Mn-LO. The insert shows the kinetic time lag during the first minutes, as highlighted by the dotted line. (B) Reconstructed ion chromatogram (*m/z* 295) from LC-MS analysis of products with the molecular mass of the singly charged carboxylate anion of HODE. The metabolites were identified by MS/MS analysis (*m/z* 295 → full scan) as indicated in the chromatogram (13- and 9-HODE co-elute on RP-HPLC). (C) Steric analysis of 9-HPODE by chiral phase-HPLC after $NaBH_4$ reduction and methylation. Top, products formed from 11(*R,S*)-HPODE; bottom, products formed from methyl 11(*R,S*)-HPODE. HPODE, hydroperoxyoctadecadienoic acid; Mn-LO, manganese lipoxygenase; HODE, hydroxyoctadecadienoic acid; MS/MS, tandem MS.

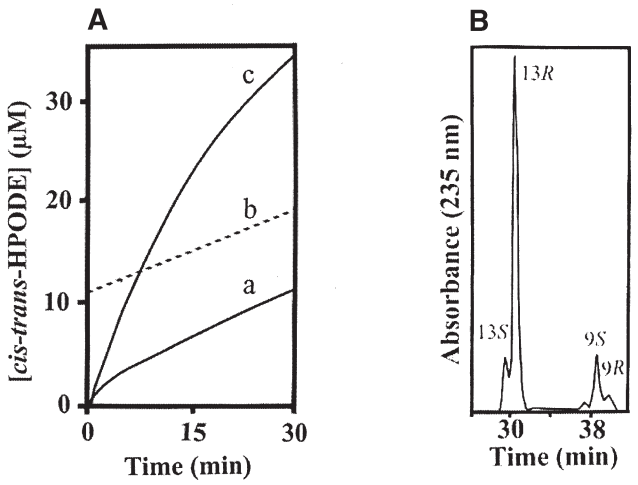

FIG. 2. Isomerization of 11(*S*)-HPODE by sLO-1 to 13(*R*)-HPODE, 13(*S*)-HPODE and 9(*S*)-HPODE. (A) Increase in UV absorbance at 235 nm during incubation of sLO-1 with 11(*S*)-HPODE (trace a, and restarted for an additional 30 min, trace b, dotted line) and methyl 11(*S*)-HPODE (trace c). (B) Chiral analysis of the metabolites of 11(*S*)-HPODE after $NaBH_4$ reduction and methylation. sLO-1, soybean lipoxygenase-1; for other abbreviations see Figure 1.

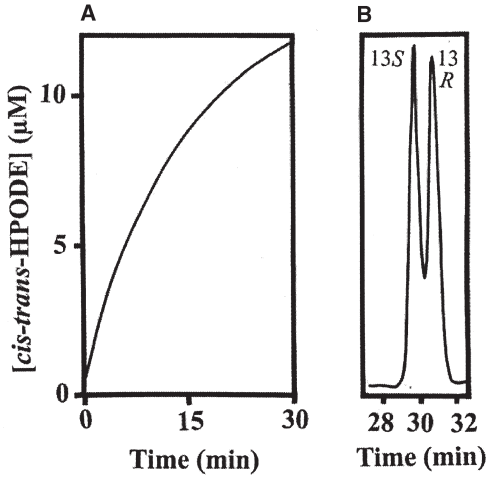

FIG. 3. Isomerization of 11(*R,S*)-HPODE by sLO-1. (A) Increase in UV absorbance at 235 nm during incubation of sLO-1 with 11(*R,S*)-HPODE. (B) Separation of the two formed 13-HPODE stereoisomers by CP-HPLC. 9-HPODE was also formed in a nearly racemic mixture (data not shown). CP-HPLC, chiral phase HPL; for other abbreviations see Figures 1 and 2.

We conclude that 11(*R*)-HPODE is slowly converted to 9(*R*)-HPODE, and that methyl 11(*S*)-HPODE can be isomerized to methyl 13(*R*)-HPODE, but both transformations occur much less efficiently than the isomerization of 11(*S*)-HPODE to 13(*R*)-HPODE.

Isomerization of 11-HPODE by sLO-1. 11(*S*)-HPODE is a poor substrate of sLO-1, as previously reported (10). Long incubation times and large amounts of sLO were needed to identify the products, which accumulated only slowly (Fig. 2A). 11(*S*)-HPODE was isomerized to 13(*R*)-HPODE as the main product (Fig. 2B), but significant amounts of 13(*S*)-HPODE and 9(*S*)-HPODE [about 15% of 13(*R*)-HPODE each] were also formed along with 9(*R*)-HPODE [5% of 13(*R*)-HPODE]. The 9(*S*)-HPODE/13(*R*)-HPODE ratio was 0.15.

Methyl 11(*S*)-HPODE was metabolized more efficiently by sLO-1 than 11(*S*)-HPODE (Fig. 2A). The two main products were methyl 13(*R*)-HPODE (62%) and 9(*S*)-HPODE (38%), but there was a relatively large formation of 13(*S*)-HPODE [about 30% of 13(*R*)-HPODE] and 9(*R*)-HPODE (about 30% of 9*S*).

11(*R,S*)-HPODE was slowly isomerized to *cis-trans* conjugated products by sLO-1 as shown in Figure 3A. The main product was 13(*R,S*)-HPODE (Fig. 3B), but an almost racemic mixture of 9(*R*)- and 9(S)-HPODE was also formed (30%). This suggested that the main product of 11(*R*)-HPODE was 13(*S*)-HPODE, as the main product of 11(*S*)-HPODE was 13(*R*)-HPODE. As regards 11(*R,S*)-HPODE methyl ester, it was also converted to 13(*S*)-HPODE and 13(*R*)-HPODE as main products (in a 2:3 ratio) and to 9(*R,S*)-HPODE.

In conclusion, 11(*S*)-HPODE was isomerized to 13(*R*)-HPODE as the main product by sLO-1, and the isomerization of 11(*R,S*)-HPODE suggested that 11(*R*)-HPODE was converted to 13(*S*)-HPODE.

DISCUSSION

The reaction mechanism of LO has been studied in considerable detail (1). Only Mn-LO can oxidize linoleic acid to 11(*S*)-HPODE as a major product as far as is known, but the present work shows that RLI-LO also can form 11-HPODE [74% 11(*R*)], albeit as a very minor enzymatic product. The isomerization of 11-HPODE and its methyl esters by Mn-LO and sLO-1 to other hydroperoxylinoleates has not been investigated previously. This is likely due to difficulties in preparing 11-HPODE. Our study was made possible by Brash (19), who reported that 11(*R,S*)-HPODE was formed in small amounts (~5%) relative to 13- and 9-HPODE during vitamin E-controlled autoxidation of linoleic acid, and by the biosynthesis of 11(*S*)-HPODE by Mn-LO (10).

The positional specificity of Mn-LO was investigated with 11(*R,S*)-HPODE as a substrate. As expected, the 11(*S*) stereoisomer was converted to 13(*R*)-HPODE. In addition, 9(*R*)-HPODE was identified. Since the hydroperoxydiene moieties of the 9(*R*)- and (13*R*)-hydroperoxides are spatially identical when the molecules are arranged head to tail in opposite orientations, this suggests that 11(*S*)-HPODE and 11(*R*)-HPODE aligned in opposite orientations at the active site. The results also suggest that 11(*R*)-HPODE is transformed to a peroxyl radical, LOO•, in equilibrium with L• and O_2. Oxygen rebound is then likely controlled by steric factors and the orientation of L•. The free carboxyl group of 11(*S*)-HPODE was not absolutely required, as methyl 11(*S*)-HPODE could be transformed into methyl 13(*R*)-HPODE in detectable amounts. Methyl 11(*R*)-HPODE, however, did not appear to be a substrate.

The isomerization of 11-HPODE by sLO-1 occurred with less regio- and stereospecificity in comparison with Mn-LO.

Mn-LO and sLO-1 both abstract the *pro-S* hydrogen at C-11 and form L•, but L• reacts with oxygen at C-13 so that 13(*R*)-HPODE is formed by Mn-LO and 13(*S*)-HPODE by LO-1 (10). It seemed likely that sLO-1 should isomerize 11(*R*)-HPODE to 13(*S*)-HPODE as a major product, as both hydroperoxide groups can be visualized as formed by oxygen insertion from the one side of a plane containing the two double bonds of linoleic acid and C-11 with the *pro-R* hydrogen. This also appeared to be the case, as 11(*S*)-HPODE was transformed to 13(*R*)-HPODE as the main product, whereas 11(*R*)-HPODE appeared to be transformed to 13(*S*)-HPODE. In addition, 11(*S*)- and methyl 11(*S*)-HPODE were transformed to 9(*S*)- as well as 13(*R*)-HPODE; these show that the stereospecificity is reduced. Clearly, L• formed by sLO-1-catalyzed oxidation of linoleic acid and by the sLO-1-catalyzed isomerization reaction of 11-HPODE align differently in the active site of sLO-1, as judged from the products formed.

A detailed analysis of the isomerization of 11-HPODE by sLO-1 will need optimization of substrate and enzyme concentrations and other reaction conditions based on V_{max}, K_m, kinetic lag phase, the oxidation state of sLO-1 by EPR spectroscopy, and experiments under oxygen-18. These studies were far beyond the scope of our investigation and will require large amounts of 11(*R,S*)-HPODE and 11(*S*)-HPODE. It is also possible that other LO may handle 11-HPODE more efficiently than sLO-1 and can be a better tool for these studies.

In conclusion, sLO-1 can metabolize 11-HPODE only slowly with some degree of stereo- and regiospecificity, whereas Mn-LO can isomerize 11(*R*)-HPODE to 9(*R*)-HPODE. 11-HPODE is also formed by RLI-LO in small amounts. A postulated intermediate in these transformations and in the oxidation of linoleic acid is the carbon-centered radical, L•. This radical likely adopts different conformations in the active site depending on its route of biosynthesis, as judged from the products formed by Mn-LO, sLO-1 and RLI-LO.

ACKNOWLEDGMENTS

Supported by the Swedish Medical Research Council (03X-06523), Magn. Bergvalls Stiftelse, and by the Swedish Council for Forestry and Agricultural Research (proj. 980.0897/00).

REFERENCES

1. Brash, A.R. (1999) Lipoxygenases: Occurrence, Functions, Catalysis, and Acquisition of Substrate, *J. Biol. Chem. 274*, 23679–23682.
2. Lütteke, T., Krieg, P., Fürstenberger, G., and von der Lieth, C.W. (2003) LOX-DB—A Database on Lipoxygenases, *Bioinformatics 19*, 2482–2483. Also available at netlink www.dkfz-heidelberg.de/spec/lox-db/
3. Schaller, F. (2001) Enzymes of the Biosynthesis of Octadecanoid-Derived Signalling Molecules, *J. Exp. Bot. 52*, 11–23.
4. Samuelsson, B. (2000) The Discovery of Leukotrienes, *Am. J. Respir. Crit. Care Med. 161*, S2–S6.
5. Yu, Z., Schneider, C., Boeglin, W.E., Marnett, L.J., and Brash, A.R. (2003) The Lipoxygenase Gene ALOXE3 Implicated in Skin Differentiation Encodes a Hydroperoxide Isomerase, *Proc. Natl. Acad. Sci. USA 100*, 9162–9167.
6. Peng, Y.L., Shirano, Y., Ohta, H., Hibino, T., Tanaka, K., and Shibata, D. (1994) A Novel Lipoxygenase from Rice. Primary Structure and Specific Expression upon Incompatible Infection with Rice Blast Fungus, *J. Biol. Chem. 269*, 3755–3761.
7. Oliw, E.H. (2002) Plant and Fungal Lipoxygenases, *Prostaglandins Other Lipid Mediat. 68–69*, 313–323.
8. Su, C., and Oliw, E.H. (1998) Manganese Lipoxygenase. Purification and Characterization, *J. Biol. Chem. 273*, 13072–13079.
9. Hörnsten, L., Su, C., Osbourn, A.E., Hellman, U., and Oliw, E.H. (2002) Cloning of the Manganese Lipoxygenase Gene Reveals Homology with the Lipoxygenase Gene Family, *Eur. J. Biochem. 269*, 2690–2697.
10. Hamberg, M., Su, C., and Oliw, E. (1998) Manganese Lipoxygenase. Discovery of a Bis-allylic Hydroperoxide as Product and Intermediate in a Lipoxygenase Reaction, *J. Biol. Chem. 273*, 13080–13088.
11. Su, C., Sahlin, M., and Oliw, E.H. (2000) Kinetics of Manganese Lipoxygenase with a Catalytic Mononuclear Redox Center, *J. Biol. Chem. 275*, 18830–18835.
12. Ruddat, V.C., Whitman, S., Holman, T.R., and Bernasconi, C.F. (2003) Stopped-flow Kinetic Investigations of the Activation of Soybean Lipoxygenase-1 and the Influence of Inhibitors on the Allosteric Site, *Biochemistry 42*, 4172–4178.
13. Tomchick, D.R., Phan, P., Cymborowski, M., Minor, W., and Holman, T.R. (2001) Structural and Functional Characterization of Second-Coordination Sphere Mutants of Soybean Lipoxygenase-1, *Biochemistry 40*, 7509–7517.
14. Segraves, E.N., and Holman, T.R. (2003) Kinetic Investigations of the Rate-Limiting Step in Human 12- and 15-Lipoxygenase, *Biochemistry 42*, 5236–5243.
15. Rickert, K.W., and Klinman, J.P. (1999) Nature of Hydrogen Transfer in Soybean Lipoxygenase 1: Separation of Primary and Secondary Isotope Effects, *Biochemistry 38*, 12218–12228.
16. Oliw, E.H., Su, C., Skogström, T., and Benthin, G. (1998) Analysis of Novel Hydroperoxides and Other Metabolites of Oleic, Linoleic, and Linolenic Acids by Liquid Chromatography–Mass Spectrometry with Ion Trap MS^n, *Lipids 33*, 843–852.
17. Skrzypczak-Jankun, E., Amzel, L.M., Kroa, B.A., and Funk, M.O., Jr. (1997) Structure of Soybean Lipoxygenase L3 and a Comparison with Its L1 Isoenzyme, *Proteins 29*, 15–31.
18. Gillmor, S.A., Villasenor, A., Fletterick, R., Sigal, E., and Browner, M.F. (1997) The Structure of Mammalian 15-Lipoxygenase Reveals Similarity to the Lipases and the Determinants of Substrate Specificity, *Nat. Struct. Biol. 4*, 1003–1009.
19. Brash, A.R. (2000) Autoxidation of Methyl Linoleate: Identification of the Bis-Allylic 11-Hydroperoxide, *Lipids 35*, 947–952.
20. Reddanna, P., Whelan, J., Maddipati, K.R., and Reddy, C.C. (1990) Purification of Arachidonate 5-Lipoxygenase from Potato Tubers, *Methods Enzymol. 187*, 268–277.
21. Hamberg, M. (1997) Myoglobin-Catalyzed Bis-Allylic Hydroxylation and Epoxidation of Linoleic Acid, *Arch. Biochem. Biophys. 344*, 194–199.
22. Zhang, L.Y., and Hamberg, M. (1996) Specificity of Two Lipoxygenases from Rice: Unusual Regiospecificity of a Lipoxygenase Isoenzyme, *Lipids 31*, 803–809.
23. Kühn, H., Wiesner, R., Lankin, V.Z., Nekrasov, A., Alder, L., and Schewe, T. (1987) Analysis of the Stereochemistry of Lipoxygenase-Derived Hydroxypolyenoic Fatty Acids by Means of Chiral Phase High-Pressure Liquid Chromatography, *Anal. Biochem. 160*, 24–34.
24. Hamberg, M., Gerwick, W.H., and Åsén, P.A. (1992) Linoleic Acid Metabolism in the Red Alga *Lithothamnion corallioides*: Biosynthesis of 11(*R*)-Hydroxy-9(*Z*),12(*Z*)-octadecadienoic Acid, *Lipids 27*, 487–493.

[Received April 14, 2004; accepted May 19, 2004]

Dose Effect of α-Linolenic Acid on PUFA Conversion, Bioavailability, and Storage in the Hamster

Anne Morise[a,*], Nicole Combe[b], Carole Boué[b], Philippe Legrand[c], Daniel Catheline[c], Bernadette Delplanque[a], Evelyne Fénart[d], Pierre Weill[e], and Dominique Hermier[a]

[a]Laboratoire de Physiologie de la Nutrition, Université Paris Sud, 91405 Orsay cedex, [b]Département de Biochimie-Nutrition/Institut des Techniques d'Etude et de Recherche des Corps Gras (ITERG), Unité de Nutrition et Signalisation Cellulaire, Université Bordeaux 1, 33405 Talence cedex, [c]Laboratoire de Biochimie, Ecole Nationale Supérieure d'Agronomie de Rennes-Institut National de la Recherche Agronomique, 35042 Rennes cedex, [d]Organisation, Nationale Interprofessionnelle des Oléagineux (ONIDOL), 75008 Paris, and [e]La Messayais, 35210 Combourtillé, France

ABSTRACT: If an increased consumption of α-linolenic acid (ALA) is to be promoted in parallel with that of n-3 long-chain-rich food, it is necessary to consider to what extent dietary ALA can be absorbed, transported, stored, and converted into long-chain derivatives. We investigated these processes in male hamsters, over a broad range of supply as linseed oil (0.37, 3.5, 6.9, and 14.6% energy). Linoleic acid (LA) was kept constant (8.5% energy), and the LA/ALA ratio was varied from 22.5 to 0.6. The apparent absorption of individual FA was very high (>96%), and that of ALA remained almost maximum even at the largest supply (99.5%). The capacity for ALA transport and storage had no limitation over the chosen range of dietary intake. Indeed, ALA intake was significantly correlated with ALA level not only in cholesteryl esters (from 0.3 to 9.7% of total FA) but also in plasma phospholipids and red blood cells (RBC), which makes blood components extremely reliable as biomarkers of ALA consumption. Similarly, ALA storage in adipose tissue increased from 0.85 to 14% of total FA and was highly correlated with ALA intake. As for bioconversion, dietary ALA failed to increase 22:6n-3, decreased 20:4n-6, and efficiently increased 20:5n-3 (EPA) in RBC and cardiomyocytes. EPA accumulation did not tend to plateau, in accordance with identical activities of Δ5- and Δ6-desaturases in all groups. Dietary supply of ALA was therefore a very efficient means of improving the 20:4n-6 to 20:5n-3 balance.

Paper no. L9432 in *Lipids 39*, 325–334 (April 2004).

n-3 PUFA play multiple roles in growth and development (1), in the modulation of inflammatory and immune processes (2), and in the prevention of diseases, particularly of cardiovascular diseases (3–5). Among n-3 PUFA, the precursor α-linolenic acid (ALA, 18:3n-3) must be distinguished from its main long-chain (LC) derivatives, such as EPA (20:5n-3) and DHA (22:6n-3). Indeed, only the precursor ALA is strictly essential, since it cannot be synthesized and must be provided by the diet. ALA is found in all plants but is especially abundant in seeds, nuts, and beans such as linseed, perilla, and, to a lesser extent, rapeseed, walnuts, and soybeans. By contrast, LC-PUFA are not only of dietary origin (fish essentially) but can also be formed *in vivo* alternately by desaturation and elongation of ALA. According to nutritional enquiries, ALA is the main dietary n-3 PUFA in individuals on a typical Western diet (6); thus, it may represent a major contributor to the long-term maintenance of the n-3 LC-PUFA supply to the body.

When compared with the recommendations of the most recent guidelines (7,8), the dietary intake of n-3 PUFA, ALA as well as EPA and DHA, is very insufficient in many Western countries (9–11). In U.S. adolescents, the total intake of n-3 PUFA represents only 30% of the recommended daily allowance (10). Similarly, in France women consume less than half of the French recommended intake of ALA (9). In light of this difficulty in reaching these dietary recommendations, it seems to be beneficial to promote consumption of all sources of n-3 PUFA, including vegetable oils rich in ALA.

Seminal studies on the dose–effect of dietary ALA were performed by Holman and colleagues on rats made PUFA deficient and then fed low levels of ALA (12,13). However, very little is known about the ability of the body to absorb, store, and convert large amounts of ALA. If the dietary intake of ALA is to be promoted, it is necessary to consider a possible limitation of these biological processes. Indeed, some of the most recent human studies suggest that increasing ALA intake results (i) in a decrease of its conversion, due presumably to accumulation of its LC products, and (ii) in an increased partitioning of ALA toward oxidation to the detriment of conversion (14). Furthermore, not only dietary ALA but also linoleic acid (18:2n-6, LA) have to be taken into account, since ALA conversion would be efficient only when the dietary supply of LA is low (15). Nevertheless, most studies modify both ALA and LA dietary content to attain a broad range of LA/ALA ratios, which blurs the specific effects of ALA.

The purpose of this study was therefore to investigate the dose–response effects of dietary ALA, provided as linseed oil, over a broad range of ALA intakes while keeping the LA intakes constant, and thus varying dramatically the LA/ALA ratios. We chose the hamster as a validated model for assessing the effects of dietary fats on lipid metabolism (16–18), and the following tissues and compartments as valuable indicators of the bioavailability of n-3 PUFA: feces for intestinal absorption; plasma cholesteryl esters (CE) and epididymal adipose tissue

*To whom correspondence should be addressed at Laboratoire d'Endocrinologie de la Nutrition, Bâtiment 447, Université Paris Sud, 91405 Orsay Cedex, France. E-mail: anne.morise@ibaic.u-psud.fr

Abbreviations: AA, arachidonic acid; ALA, α-linolenic acid; CE, cholesteryl ester; DPA, docosapentaenoic acid; EAT, epididymal adipose tissue; LA, linoleic acid; LC, long chain; MUFA, monounsaturated FA; PL, phospholipid; RBC, red blood cell; SFA, saturated FA; TFA, *trans* FA.

(EAT) for ALA transport and storage, respectively; and plasma phospholipids (PL) on the one hand, and red blood cell (RBC) membranes and heart PL on the other hand, for the transport and storage of LC derivatives, respectively. The primary end point was to determine whether there was a biological limitation to the processes of absorption, transport, and storage of dietary ALA and to the synthesis, transport, and storage of its LC derivatives. A secondary aim was to assess the value of some blood lipids, in plasma or RBC, as biomarkers of ALA intake and bioconversion.

MATERIALS AND METHODS

Animals. Twenty-four male golden Syrian hamsters were obtained from Janvier (Centre d'élevage Janvier, Le Genest-St Isle, France) at 4 wk of age. They were housed in colony cages with wood litter (6/cage) in a controlled environment (22°C, 14:10 h light/dark cycle) and received *ad libitum* distilled water and a ground commercial diet (containing, by weight, 72.0% cereals, 17.8% soy meal, 6.0% fish meal, 4.2% vitamin and mineral mix; and providing 5.1% lipids and 19.3% proteins) (UAR113, Villemoisson, France). At 8 wk of age, the hamsters were housed in colony cages with wire floors, weighed weekly, and fed experimental diets. The present work was carried out in agreement with the French legislation on animal experimentation and with the authorization of the French Ministry of Agriculture (Animal Health and Protection Directorate).

Diets. The four experimental diets consisted by weight of 84.4% of the above commercial ground pellets, 3% water, 0.03% cholesterol (5-cholesten-3β-ol; Sigma, St. Louis, MO), and 12.5% vegetable oil mix. The calculated composition (in wt%) of the four diets was 16.3% protein, 52.6% carbohydrate, 16.6% lipid, 11.8% water, and 4.6% minerals. Lipids provided about one-third (35.3%) of the total energy intake. The vegetable oil mix consisted of linseed oil [53.6% ALA, 15.7% LA, 20% oleic acid, and 10% saturated FA (SFA)] (Valorex, Javené, France), and high-oleic sunflower oil (0.1% ALA, 14.6% LA, 74.9% oleic acid, and 10% SFA) added in different proportions to increase ALA concentration and to keep the levels of LA and SFA constant. As a consequence, ALA and oleic acid (18:1n-9) varied in opposite proportions. The calculated proportions of linseed oil and high-oleic sunflower oil were 0:100, 22:78, 47:53, and 97:3, providing theoretically 1, 10, 20, and 40% ALA (as % of total FA) in the L1, L10, L20, and L40 diets, respectively. The contribution of ALA to total energy intake varied from less than 1% (L1 diet) to 14.6% (L40 diet). The FA profile of the experimental diets was determined as described below and is shown in Table 1.

Experimental procedure. After 5 wk on experimental diets, hamsters were housed in individual cages with wire floors to measure their dietary consumption and to collect the feces during the seventh week. To assess the body weight gain during the last week, hamsters were weighed after an overnight fast (18 h) at the end of the sixth week. At 15 wk of age, after having been on the experimental diets for 7 wk, all hamsters were fasted overnight, then weighed and anesthetized by intramuscular injection of Zoletil 50 (Virbac, Carros, France) at a dose of 4 mg/100 g of body weight. Blood was taken by intracardiac puncture using a heparinized syringe (10 units heparin/mL blood). Plasma was separated from blood by centrifugation for 20 min at 4°C and 1700 × *g*, then stored at −20°C. RBC were washed with physiological serum and stored at −80°C. After

TABLE 1
Lipid Composition of the Experimental Diets[a]

	Unit	L1	L10	L20	L40
Total lipids	g/100 g diet	15.7	16.0	14.9	15.6
Cholesterol	g/100 g diet	0.072	0.075	0.075	0.072
FA					
4:0	% of total FA	0.52	0.09	0.12	0.08
8:0		0.06	0.07	0.08	0.04
10:0		0.04	0.02	0.02	0.02
14:0		0.11	0.12	0.13	0.15
16:0		6.49	6.6	7.36	7.84
18:0		3.74	3.5	3.83	3.52
18:1n-9		63.74	55.47	43.95	21.79
18:2n-6		23.65	23.48	24.28	24.55
18:3n-3		1.05	9.95	19.50	41.30
20:1n-9		0.33	0.36	0.34	0.39
20:5n-3		0.04	0.10	0.11	0.12
22:6n-3		0.21	0.23	0.30	0.25
ΣSFA	% of total FA	10.96	10.4	11.54	11.65
ΣMUFA		64.07	55.83	44.29	22.18
ΣPUFA		24.95	33.77	44.19	66.22
Σn-6		23.65	23.48	24.28	24.55
Σn-3		1.30	10.29	19.91	41.67
18:2n-6/18:3n-3		22.52	2.36	1.25	0.59

[a]ΣSFA, sum of saturated FA; ΣMUFA, sum of monounsaturated FA; ΣPUFA, sum of PUFA; Σn-6, sum of n-6 FA; Σn-3, sum of n-3 FA.

blood sampling, the abdominal cavity was opened surgically, and the hamsters were killed by section of the jugular vein. The liver was carefully removed, and a sample of about 200 mg was kept on ice for preparation of a postmitochondrial supernatant that was used for the measurement of Δ6- and Δ5-desaturase activities. Heart tissues and EAT were taken, weighed, and stored at −80°C.

FA analyses. (i) Diet. Lipids were extracted according to the method of Folch *et al.* (19), dried under N_2, and transmethylated with BF_3 in methanol (14%) according to the method of Morisson and Smith (20). After completion of the reaction (100°C for 1 h), FAME were extracted with hexane, briefly dried under a N_2 stream, diluted in hexane, and analyzed by GLC with a Fisons 8000 chromatograph (Thermo Products, Les Ulis, France) equipped with an on-column injector and an FID. Separation of FAME was realized with a BPX70 fused-silica capillary column (60 m length × 0.32 mm i.d., 0.25 μm film thickness; SGE, Villeneuve St Georges, France). The hydrogen flow rate was 1.5 mL·min^{-1}. The oven was programmed from 60 to 220°C with four temperature steps (60°C for 1 min, rise of 20°C·min^{-1}, 170°C for 30 min, rise of 10°C·min^{-1}, 200°C for 15 min, rise of 10°C·min^{-1}, 220°C for 10 min).

(ii) Feces. Feces were hydrated and homogenized in distilled water with diatomaceous earth (Sigma) before being hydrolyzed in HCl (6 N) for 1 h. The mixture was filtered, washed to reach pH 5.0, and dried under vacuum. Lipids were then extracted according to the method of Folch *et al.* (19) using heptadecanoic acid (17:0) as an internal standard (Sigma). Lipids were then dried and weighed. After transmethylation, in the same conditions as described above, FAME were purified by TLC on a silica plate (silica gel 60A; SDS, Peypin, France). Elution solvents were hexane/diethyl ether/acetic acid (70:30:1, by vol). FAME were extracted from the gel by a biphasic solvent system made of ethanol (2 mL), hexane/diethyl ether (2:1, vol/vol; 2 mL), distilled water (2 mL), and a few drops of concentrated ammonia. The upper organic phase was withdrawn and evaporated under a stream of N_2 after removing residual water by passage through Na_2SO_4. The dry residue was used for analysis by GLC under the same conditions as in dietary FAME. For total lipids and each FA, the following determination was made:

$$\text{apparent absorption (in \%)} = (\text{amount ingested} - \text{amount excreted})/\text{amount ingested} \quad [1]$$

(iii) Plasma. Plasma (1.5 mL) was treated according to the method of Folch *et al.* (19). Total lipids were separated by TLC on 0.3-mm thick silica gel (Kieselgel H 60; Merck, Darmstadt, Germany) laboratory-coated plates using the solvent mixture hexane/diethyl ether/acetic acid (90:10:1, by vol). FAME from CE and PL were prepared by transmethylation of individually isolated fractions in the presence of silica gel and under the same conditions as already discussed. FAME were analyzed according to Boué *et al.* (21) on a Fisons 8000 (Thermo Products) equipped with a split injector and an FID kept at 250°C. The split ratio was 1:80. Separation of FAME was performed on the same column as above. The hydrogen flow rate was 1 mL·min^{-1}. The oven temperature was programmed from 150 to 200°C at 1.5°C·min^{-1}, then to 230°C at 2.5°C·min^{-1}, and held at 230°C for 30 min.

(iv) RBC and heart. RBC (1.5 mL) and hearts were treated according to the method of Folch *et al.* (19). PL from hearts were prepared like those from plasma. Total lipids from RBC and PL from hearts were then transmethylated as described for dietary FA. FAME analysis was performed as in plasma.

(v) EAT. Total lipids were transesterified directly from the tissue, without prior extraction, according to the method of Lepage and Roy (22), with 2 mL of methanol/benzene (4:1, vol/vol) containing 0.02% BHT (wt/vol) as an antioxidant and 200 μL acetyl chloride (22). GLC analyses of FAME were the same as in plasma. This fast protocol provides FA compositions of total lipids not significantly different from those obtained by the procedure of Morisson and Smith (20) described above.

Measurement of hepatic Δ6- and Δ5-desaturase activities. Enzymatic activities were determined as described by Guillou *et al.* (23). Briefly, after isolation by centrifugation, a postmitochondrial supernatant was incubated with [1-^{14}C] α-linolenic or [1-^{14}C]eicosatrienoic acids, used as substrate for the Δ6- and the Δ5-desaturases, respectively. FA were then extracted, converted to fatty acid naphthacyl esters according to the method of Wood and Lee (24), and separated on HPLC (Alliance Integrated System; Waters, St Quentin en Yvelines, France) using a Novapack C_{18} column (4 μm, 4.6·250 mm; Waters) and a guard column (Novapack C_{18}; 4 μm, 3.9·20 mm; Waters). The column temperature was maintained at 30°C. Elution was performed at a programmed flow rate of 1 mL/min with a gradient of methanol/acetonitrile/water starting at 80:10:10 (by vol), increasing first linearly to 86:10:4 (by vol) in 30 min, then increasing linearly to 90:10:0 (by vol) in 10 min, holding at 90:10:0 (by vol) for 5 min and returning to the initial conditions in 5 min (25). Radiolabeled substrates and products of each desaturase assay were collected and subjected to liquid scintillation counting. From the amount of radioactivity incubated, the enzyme activity could be calculated with this formula:

$$A_e = \frac{\text{radioactivity of product}}{(\text{radioactivity of product}) + (\text{radioactivity of substrate})} \times \frac{\text{moles of substrate incubated}}{(\text{protein wt})\,(\text{time})} \quad [2]$$

where A_e is expressed as pmol substrate converted to product per min per mg of protein.

Statistical analyses. The data were analyzed by using the Statview 4.5 program (Abacus Concepts, Berkeley, CA). Statistical differences between means were determined by ANOVA and Fisher's test and considered to be significant at $P < 0.05$. Correlations between dietary ALA intake and FA profile were determined by linear regression.

TABLE 2
Weight Parameters, Dietary Intake, and Apparent Absorption[a]

	Unit	L1[b]	L10[b]	L20[b]	L40[b]
Final body weight	g	120 ± 2[a]	115 ± 1[a,b]	110 ± 2[b]	110 ± 3[b]
Weight gain	g/d	0.09 ± 0.09[a,b]	0.27 ± 0.11[a]	–0.07 ± 0.15[b]	0.23 ± 0.06[a,b]
Food intake		6.05 ± 0.11[a,b]	6.29 ± 0.19[a]	5.77 ± 0.25[b]	6.02 ± 0.11[a,b]
Lipid intake		1.02 ± 0.02[a,b]	1.06 ± 0.03[a]	0.97 ± 0.04[b]	1.01 ± 0.02[a,b]
FA intake	mg/d				
SFA		112 ± 2	110 ± 3	110 ± 5	118 ± 2
18:3n-3		11 ± 0.2[d]	105 ± 3[c]	189 ± 8[b]	417 ± 7[a]
18:2n-6		241 ± 4	248 ± 8	236 ± 10	249 ± 4
18:1n-9		648 ± 12[a]	586 ± 18[b]	427 ± 18[c]	220 ± 4[d]
Cholesterol intake	mg/d	4.2 ± 0.1[a,b]	4.4 ± 0.14[a]	4.0 ± 0.2[b]	4.2 ± 0.1[a,b]
Apparent absorption	%				
Lipids		95.5 ± 0.1[a]	95.1 ± 0.3[a,b]	95.7 ± 0.4[a]	94.6 ± 0.1[b]
ΣSFA		96.4 ± 0.2	96.5 ± 0.2	96.9 ± 0.2	96.5 ± 0.1
18:1n-9		99.1 ± 0.1[a]	99.0 ± 0.1[a]	99.0 ± 0.1[a]	98.4 ± 0.1[b]
18:2n-6		98.6 ± 0.1	98.4 ± 0.2	98.7 ± 0.1	98.6 ± 0.1
18:3n-3		97.6 ± 0.9[b]	99.5 ± 0.1[a]	99.5 ± 0.1[a]	99.5 ± 0.0[a]

[a]The dietary intakes, body weight gain, and apparent absorptions were measured during the last week of experimentation.
[b]Results are mean ± SEM of six hamsters in each group. Values with different roman superscripts are considered significantly different by Fisher's test ($P < 0.05$). ΣSFA, sum of saturated FA.

RESULTS

Body weight, dietary consumption, and apparent absorption of lipids (Table 2). Final body weight differed slightly but significantly between the four groups, being highest with the L1 diet and lowest with the L20 and L40 diets. This did not result from parallel differences in food intake and weight gain during the last week, which were the highest in the L10 group and the lowest in the L20 groups. Consequently, lipid intake paralleled that of food intake and was slightly lower in the L20 group. However, the consumption of LA was the same in all groups, and that of ALA almost doubled between the L10 and L20 groups, as well as between the L20 and L40 groups. Apparent lipid absorption was very high among the four groups (about 95%). However, animals from the L1 and L20 groups absorbed 1% more lipids than those from the L40 group. FA absorption was also very high for all groups. The absorption of ALA and oleic acid, the only FA whose dietary proportions varied, were lower in the animals fed the L1 and the L40 diets, respectively. By contrast, the absorption of LA and SFA did not differ among groups.

FA composition of lipids from blood, adipose tissue, and heart. (i) Plasma PL (Table 3). Plasma PL contained a majority of PUFA (45%), most of them belonging to the n-6 family. The proportion of ALA was very low; however, it reflected the increased dietary intake from L1 to L40 (Fig. 1). In parallel,

TABLE 3
FA Composition[a] of Plasma Phospholipids (PL) and Cholesteryl Esters (CE) (as % of total FA)

	L1		L10		L20		L40	
	PL	CE	PL	CE	PL	CE	PL	CE
ΣSFA	41.11 ± 0.39	9.85 ± 0.19	41.45 ± 0.35	10.11 ± 0.17	41.98 ± 0.56	10.52 ± 0.43	42.66 ± 0.80	10.19 ± 0.53
ΣMUFA	14.99 ± 0.66[a]	34.80 ± 0.51[a]	13.80 ± 0.34[a,b]	32.45 ± 0.40[b]	13.33 ± 0.47[b]	31.36 ± 0.79[b]	10.46 ± 0.63[c]	19.44 ± 0.52[c]
18:1n-9	11.91 ± 0.62[a]	32.48 ± 0.45[a]	10.94 ± 0.34[a,b]	30.18 ± 0.37[b]	10.29 ± 0.38[b]	28.76 ± 0.76[b]	7.65 ± 0.54[c]	16.87 ± 0.39[c]
ΣPUFA	43.63 ± 0.69[b]	55.17 ± 0.70[c]	44.44 ± 0.39[b]	57.30 ± 0.41[b,c]	44.37 ± 0.86[b]	57.91 ± 1.19[b]	46.50 ± 0.45[a]	70.18 ± 0.92[a]
Σn-6	32.98 ± 0.11[b]	54.15 ± 0.78[b]	33.11 ± 0.19[b]	54.69 ± 0.42[b]	33.17 ± 0.35[b]	53.40 ± 0.95[b]	35.33 ± 0.32[a]	59.59 ± 1.21[a]
18:2n-6	22.28 ± 0.37[c]	51.25 ± 0.82[b]	24.41 ± 0.16[c]	52.40 ± 0.44[b]	24.48 ± 0.64[b]	51.59 ± 0.82[b]	27.47 ± 0.25[a]	57.67 ± 1.17[a]
20:4n-6	8.74 ± 0.32[a]	2.60 ± 0.12[a]	7.10 ± 0.11[b]	2.04 ± 0.05[b]	7.12 ± 0.34[b]	1.59 ± 0.15[c]	6.28 ± 0.13[c]	1.70 ± 0.09[b,c]
Σn-3	10.65 ± 0.71	1.02 ± 0.10[d]	11.32 ± 0.29	2.60 ± 0.05[c]	11.20 ± 0.78	4.51 ± 0.45[b]	11.17 ± 0.19	10.59 ± 0.51[a]
18:3n-3	0.09 ± 0.01[d]	0.29 ± 0.02[d]	0.44 ± 0.03[c]	1.81 ± 0.05[c]	0.74 ± 0.04[b]	4.00 ± 0.40[b]	1.55 ± 0.07[a]	9.66 ± 0.51[a]
20:5n-3	0.27 ± 0.02[d]	0.11 ± 0.02[c]	0.55 ± 0.02[c]	0.20 ± 0.02[b]	0.73 ± 0.06[b]	0.18 ± 0.02[b,c]	1.24 ± 0.05[a]	0.41 ± 0.04[a]
22:5n-3	0.41 ± 0.02[b]	ND	0.60 ± 0.03[a]	ND	0.61 ± 0.05[a]	ND	0.69 ± 0.01[a]	ND
22:6n-3	9.88 ± 0.69[a]	0.62 ± 0.08[a]	9.73 ± 0.27[a]	0.59 ± 0.03[a]	9.13 ± 0.71[a,b]	0.33 ± 0.04[b]	7.69 ± 0.19[b]	0.52 ± 0.05[a]
18:3n-3/ 18:2n-6	248.4 ± 13.5[a]	178.9 ± 13.1[a]	56.1 ± 3.9[b]	29.0 ± 1.0[b]	33.7 ± 2.1	13.6 ± 1.4[b,c]	17.9 ± 0.7	6.1 ± 0.4[c]

[a]Results are mean ± SEM of six hamsters in each group. Only FA that are quantitatively or physiologically important are mentioned. Values on the same line and in the same tissue with different roman superscripts are considered significantly different by Fisher's test ($P < 0.05$). 18:2n-6/18:3n-3, ratio of 18:2n-6 to 18:3n-3 FA; for other abbreviations see Table 1.

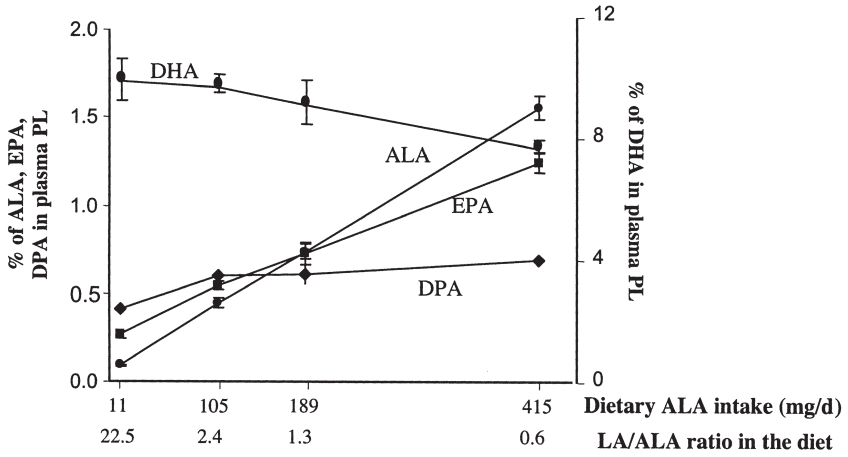

FIG. 1. Proportion of n-3 PUFA in plasma phospholipids (PL) of hamsters fed increasing intakes of α-linolenic acid (ALA) varying from 1% total FA (L1 diet) to 40% (L40 diet). Values are mean ± SEM (n = 6). LA, linoleic acid; DPA, docosapentaenoic acid.

there was a proportional enrichment in EPA and DPA but not in DHA, the percentage of which decreased in the group fed the highest ALA dose (L40). Since DHA was the major n-3 PUFA, the percentage of total n-3 PUFA was not increased by dietary ALA. Coefficients of linear regressions between dietary intake of ALA and percentage of ALA and EPA in plasma PL were very high (0.97 and 0.93, respectively, $P < 0.0001$) which indicated that the dose of dietary ALA was decisive for the incorporation of ALA and EPA into plasma PL. Conversely, the ingestion of increasing doses of ALA and decreasing doses of oleic acid decreased the proportion of n-6 LC-PUFA and oleic acid. Although the proportion of LA did not differ in the four experimental diets, there was a slight increase in the proportion of LA in PL, from the L1 to the L40 diet, that paralleled that of ALA.

(ii) Plasma CE (Table 3). As usual in CE, the main FA was LA (51–58% of total FA). Plasma CE carried more ALA than plasma PL, which carried mainly n-3 LC-PUFA (Fig. 2). Dietary ALA intake and ALA content of plasma CE were highly correlated (r^2 = 0.97, $P < 0.0001$). The enrichment of CE in ALA reached about 10% in response to the L40 diet. EPA and DHA were minor components, and their proportions did not vary linearly with the dietary intake of their precursor, ALA. As in plasma PL, LA increased and oleic acid decreased when dietary ALA increased at the expense of oleic acid.

(iii) RBC (Table 4). The FA profile of RBC was characteristic of membrane PL with a high PUFA content (40%), most of them from the n-6 family. The percentages of ALA, EPA, and DPA were proportional to dietary ALA (coefficients of linear regression were, respectively, 0.99, 0.97, and 0.91, $P < 0.0001$), contrary to those of DHA, which were significantly lower in response to the highest ALA intake (Fig. 3). As in plasma

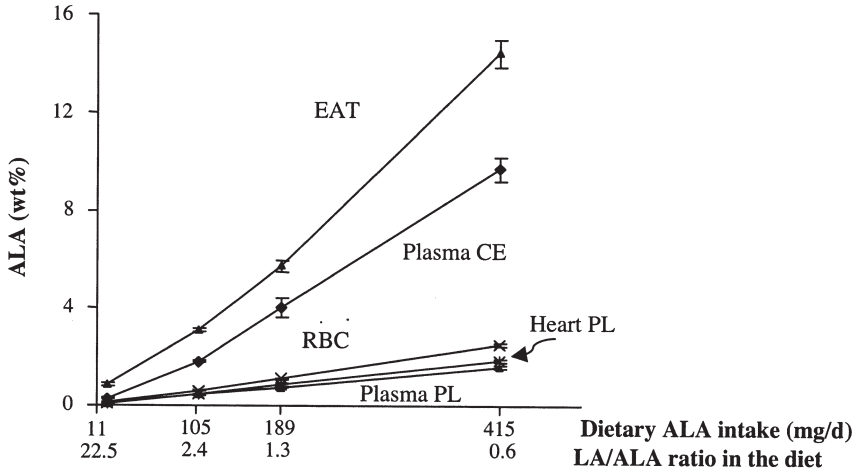

FIG. 2. Proportion of ALA in different tissues of hamsters fed increasing intakes of ALA varying from 1% total FA (L1 diet) to 40% (L40 diet). Values are mean ± SEM (n = 6). RBC, red blood cell; EAT, epididymal adipose tissue; CE, cholesteryl ester; for other abbreviations see Figure 1.

TABLE 4
FA Composition[a] of Red Blood Cells (RBC) and Heart PL (as % of Total FA)

	L1		L10		L20		L40	
	RBC	Heart	RBC	Heart	RBC	Heart	RBC	Heart
ΣSFA	35.62 ± 0.40^{b}	37.44 ± 0.43^{b}	35.73 ± 0.36^{b}	36.60 ± 0.38^{b}	36.80 ± 0.55^{b}	36.39 ± 1.02^{a,b}	38.06 ± 0.32^{a}	39.08 ± 0.28^{a}
ΣMUFA	26.71 ± 0.35^{a}	13.77 ± 0.31^{a}	25.41 ± 0.13^{b}	12.83 ± 0.19^{b}	24.10 ± 0.15^{c}	12.32 ± 0.51^{b}	19.61 ± 0.27^{d}	9.19 ± 0.09^{c}
18:1n-9	20.59 ± 0.33^{a}	11.09 ± 0.29^{a}	19.59 ± 0.14^{b}	10.17 ± 0.18^{b}	18.10 ± 0.18^{c}	9.73 ± 0.38^{b}	14.21 ± 0.24^{d}	6.72 ± 0.06^{c}
ΣPUFA	37.40 ± 0.67^{b}	48.43 ± 0.49^{b}	38.58 ± 0.39^{b}	50.19 ± 0.35^{a}	38.83 ± 0.65^{b}	50.85 ± 0.54^{a}	42.03 ± 0.32^{a}	51.26 ± 0.27^{a}
Σn-6	32.29 ± 0.49^{a}	35.92 ± 0.30^{a,b}	31.69 ± 0.37^{a,b}	36.02 ± 0.20^{a,b}	31.01 ± 0.43^{b}	36.63 ± 0.59^{a}	31.23 ± 0.20^{a,b}	35.05 ± 0.47^{a}
18:2n-6	14.69 ± 0.24^{c}	26.57 ± 0.36^{b}	15.24 ± 0.11^{b}	27.40 ± 0.14^{a,b}	15.64 ± 0.17^{b}	28.07 ± 0.48^{a}	16.96 ± 0.16^{a}	27.40 ± 0.45^{a,b}
20:4n-6	13.10 ± 0.32^{a}	7.74 ± 0.17^{a}	12.68 ± 0.26^{a,b}	7.10 ± 0.08^{b}	12.19 ± 0.34^{b,c}	7.21 ± 0.12^{b}	11.51 ± 0.15^{c}	6.36 ± 0.05^{c}
Σn-3	5.11 ± 0.24^{d}	12.45 ± 0.53^{c}	6.90 ± 0.23^{c}	14.14 ± 0.25^{b}	7.81 ± 0.27^{b}	14.15 ± 0.29^{b}	10.80 ± 0.23^{a}	16.14 ± 0.30^{a}
18:3n-3	0.11 ± 0.01^{d}	0.064 ± 0.003^{d}	0.59 ± 0.01^{c}	0.43 ± 0.01^{c}	1.11 ± 0.03^{b}	0.86 ± 0.04^{b}	2.51 ± 0.06^{a}	1.86 ± 0.06^{a}
20:5n-3	0.26 ± 0.01^{d}	0.16 ± 0.01^{d}	0.55 ± 0.02^{c}	0.28 ± 0.01^{c}	0.81 ± 0.03^{b}	0.36 ± 0.02^{b}	1.51 ± 0.05^{a}	0.55 ± 0.02^{a}
22:5n-3	0.84 ± 0.05^{d}	0.61 ± 0.04^{c}	1.83 ± 0.04^{c}	0.91 ± 0.03^{b}	2.43 ± 0.09^{b}	1.00 ± 0.02^{b}	3.35 ± 0.08^{a}	1.29 ± 0.03^{a}
22:6n-3	3.91 ± 0.19^{a}	11.6 ± 0.5	3.93 ± 0.18^{a}	12.5 ± 0.2	3.47 ± 0.15^{a,b}	11.9 ± 0.3	3.44 ± 0.11^{b}	12.4 ± 0.3
18:3n-3/ 18:2n-6	139.7 ± 6.5^{a}	417.8 ± 18.8^{a}	25.7 ± 0.3^{b}	64.1 ± 2.0^{b}	14.2 ± 0.3^{c}	33.0 ± 1.5^{c}	6.8 ± 0.1^{c}	14.8 ± 0.2^{c}

[a]Results are mean ± SEM of six hamsters in each group. Only FA that are quantitatively or physiologically important are mentioned. Values on the same line and in the same tissue with different roman superscripts are considered significantly different by Fisher's test ($P < 0.05$). For other abbreviations see Tables 1 and 3.

lipids, LA content increased and that of AA and oleic acid decreased when dietary oleic acid was substituted by ALA. In addition, the SFA content was higher in the L40 group than in the other groups.

(iv) Heart (Table 4). As in RBC and plasma, PL of cardiomyocytes contained a majority of PUFA (44%), essentially LA (26–28%), DHA (12–13%), and AA (7%). The percentages of ALA and docosapentaenoic acid (DPA) were proportional to dietary ALA (coefficients of linear regression were, respectively, 0.98 and 0.95, $P < 0.0001$). By contrast, the proportion of DPA seemed to reach a plateau, and that of DHA did not vary with the diets (Fig. 4). LA did not increase but oleic acid decreased when dietary ALA increased at the expense of oleic acid. As in RBC, SFA content was highest in the L40 group.

(v) Epididymal adipose tissue (Table 5). The weight of EAT was the same in all groups (2.46 ± 0.09 g). The main FA in this tissue were oleic acid (35–54%), LA (21–24%), and palmitic acid (15%). ALA was proportional to dietary intake of ALA (the coefficient of linear regression was 0.98, $P < 0.0001$), reaching 14% of total FA in response to the L40 diet (Fig. 2). As usual in TG, the amount of LC-PUFA was very weak for the n-6 family, and null for the n-3 family. As described in the other tissues, LA increased with dietary ALA.

Δ5- and Δ6-desaturase activities. Increased dietary intakes of ALA did not influence the hepatic Δ6-desaturase of which activity was 358 ± 39, 423 ± 62, 363 ± 41, and 383 ± 52 pmol substrate/min/mg in the L1, L10, L20, and L40 groups, respectively (mean ± SEM of six hamsters in each group). The Δ5-desaturase activity was lower than that of the Δ6-desaturase and was also identical in all groups: 206 ± 7, 203 ± 27, 209 ± 22, and 215 ± 28 pmol substrate/min/mg in the L1, L10, L20, and L40 groups, respectively (mean ± SEM of six hamsters in each group).

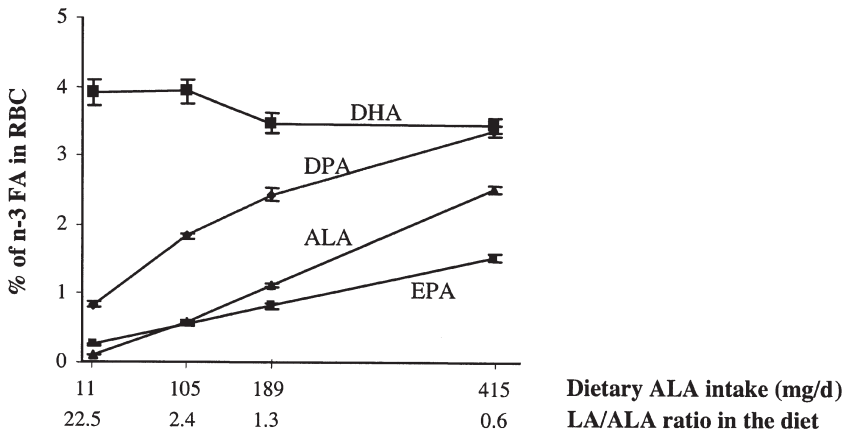

FIG. 3. Proportion of n-3 PUFA in RBC of hamsters fed increasing amounts of ALA, varying from 1% total FA (L1 diet) to 40% (L40 diet). Values are mean ± SEM ($n = 6$). For abbreviations see Figures 1 and 2.

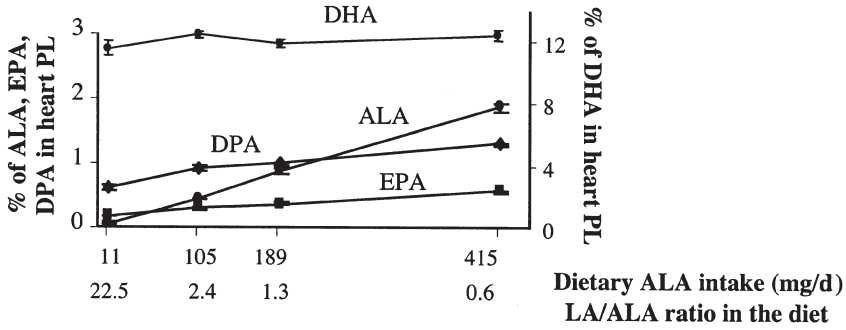

FIG. 4. Proportion of n-3 PUFA in heart PL of hamsters fed increasing intakes of ALA, varying from 1% total FA (L1 diet) to 40% (L40 diet). Values are mean ± SEM (n = 6). For abbreviations see Figure 1.

DISCUSSION

Absorption, transport, and storage of ALA. The ALA content of the experimental diets varied from 1 to 40% of total FA at the expense of oleic acid, resulting in LA/ALA ratios between 22.5 and 0.6. As a consequence, the range of dietary ALA intake was very broad, from 11 to 417 mg/d (Table 2). However, even for the highest supply, there was no apparent saturation of ALA absorption, which was almost maximal. There was also no apparent limitation to its transport, at least in the range of dietary ALA used. Indeed, plasma CE, the main form of transport of ALA, and also plasma PL were enriched in ALA proportionally to its dietary supply (Fig. 2). Epidemiological studies prefer to use biological indicators of consumption rather than nutritional surveys, and the present data confirm the reliability of ALA content in plasma CE as a marker of ALA consumption (9) over a broad range of dietary supplies and LA/ALA ratios. Because the response of the proportion of ALA in RBC was even more linear that in plasma CE, and because RBC are easily available, the percentage of ALA in these cells could be a good marker of ALA consumption. However, the level of incorporation of ALA in RBC was clearly lower than in plasma CE, and the reliability of this marker has to be tested in the human. The partitioning of ALA toward oxidation also has to be considered as a variable in the use of the composition of blood lipid pools as markers of ALA intake. Indeed, the proportion of oxidized ALA differs markedly among species, being less pronounced in the human (14,26) than in the rat (27). Moreover, in the human, oxidation is also influenced by gender, ALA being more oxidized and less converted into LC-PUFA in women than in men (26,28).

ALA storage in the EAT was also parallel to the dietary intake, and in our broad range of ALA intakes, we found no limits to this storage, which accounted for up to 14% of total FA (Table 5). This is of particular interest, since adipose tissue represents one of the most important pools of ALA (29) that is available to the body when needed.

Synthesis, transport, and storage of LC derivatives. Transport and storage of EPA, which is the first significant derivative of ALA, were highly responsive to dietary ALA. Indeed, in PL from plasma, RBC, and cardiomyocytes, EPA content was strictly linear and proportional to dietary ALA intake (Tables 3, 4; Figs. 1, 3, 4). This suggests that partitioning of ALA between oxidation and conversion into "LC-PUFA" was not affected by dietary ALA intake. Even if the FA composition of a given tissue is not directly related to hepatic desaturase activity, the lack of effect of dietary ALA on its own conversion into EPA is in accordance with the observation that, in the liver, maximal activities of Δ5- and Δ6-desaturases were similar in all groups. The effects of dietary ALA on the regulation of these enzymes are controversial. In the human, data on Δ6- and Δ5-desaturase activities are not available, but indirect measurements can be

TABLE 5
FA Composition[a] of Epididymal Adipose Tissue (as % of total FA)

	L1	L10	L20	L40
ΣSFA	18.84 ± 0.27^{c}	19.31 ± 0.21^{b,c}	19.89 ± 0.38^{a,b}	20.27 ± 0.27^{a}
ΣMUFA	58.92 ± 0.53^{a}	56.15 ± 0.31^{b}	51.47 ± 0.10^{c}	40.44 ± 0.43^{d}
18:1n-9	54.16 ± 0.59^{a}	51.57 ± 0.43^{b}	46.18 ± 0.26^{c}	35.26 ± 0.38^{d}
ΣPUFA	21.95 ± 0.27^{d}	24.27 ± 0.25^{c}	28.34 ± 0.45^{b}	38.93 ± 0.44^{a}
18:2n-6	20.90 ± 0.25^{c}	20.98 ± 0.19^{c}	22.43 ± 0.26^{b}	24.29 ± 0.32^{a}
20:4n-6	0.02 ± 0.00	0.02 ± 0.00	0.02 ± 0.00	0.03 ± 0.01
18:3n-3	0.86 ± 0.05^{d}	3.10 ± 0.07^{c}	5.70 ± 0.24^{b}	14.40 ± 0.54^{a}
18:3n-3/ 18:2n-6	24.70 ± 1.26^{a}	6.79 ± 0.14^{b}	3.70 ± 0.16^{c}	1.70 ± 0.08^{d}

[a]Results are mean ± SEM of six hamsters in each group. Only FA that are quantitatively or physiologically important are mentioned. Values on the same line with different roman superscripts are considered significantly different by Fisher's test ($P < 0.05$). For abbreviations see Table 1.

obtained *via* the use of ALA labeled with stable isotopes (14,30–34). In some studies, dietary ALA was found to inhibit its own conversion, thus favoring its oxidation (14), whereas other studies showed no effects (30). The present study supports the hypothesis that dietary ALA, even in the very large amounts used, does not regulate its own Δ6- and Δ5-desaturation, at least in the hamster liver.

The proportion of DPA in PL from plasma, RBC, and cardiomyocytes also increased with dietary ALA supply (Figs. 1, 3, 4). However, in contrast to EPA, this response was not linear, but rather followed a Michaelis curve and tended to plateau, especially in plasma (Table 3). This reflects the complex equilibrium between EPA storage and elongation into DPA, further metabolism of DPA to form DHA, and retroconversion of DHA into DPA and EPA (35). The present study did not allow drawing a clear-cut explanation.

In parallel with the enrichment of plasma and membrane PL in EPA and DPA, there was a decrease in the proportions of n-6 LC-PUFA, and especially of arachidonic acid (AA) (Tables 3 and 4). Therefore, the proportion of AA in PL fell when that of ALA rose. At the same time, the proportion of LA in PL increased together with dietary ALA, whereas the proportion of dietary LA was constant in all groups. This complex balance of n-6 PUFA may be due to two simultaneous mechanisms. First, an increase in the availability of n-3 LC-PUFA can lead to a decrease in n-6 LC-PUFA in order to respect the physicochemical constraints of membranes and lipoprotein particles in terms of fluidity and curvature. Second, we could hypothesize a competition between ALA and LA for the Δ6-desaturases, ALA being the preferential substrate of the Δ6-desaturase (36). Thus, as the ALA/LA ratio increased, less LA was converted into AA and less LA was accumulated. This concomitant increase in EPA and decrease in AA in response to dietary ALA should favor the generation of anti-inflammatory and antiaggregant molecules (from EPA) to the detriment of proinflammatory and proaggregant ones (from AA) (37).

In contrast to EPA and DPA, DHA had a paradoxical response to dietary ALA. In plasma PL and CE as well as in RBC, the DHA content did not change between L1 and L10 (LA/ALA ratios of 22.5 and 2.4, respectively), but decreased linearly from L10 to L40 when the LA/ALA ratio decreased from 2.4 to 0.6 (Figs. 1, 3, 4). Since the plasma PL concentration increases and that of CE does not change with dietary ALA intake (data not shown), the decrease in DHA in these compartments reflects not only relative but also absolute variations in the amounts of this FA. This is consistent with many animal and human studies that showed that the DHA content of most tissues does not respond linearly to dietary ALA (38). A recent study in piglets showed that the DHA content of plasma PL and RBC increased with a dietary proportion of ALA up to 6.3% of total FA with a LA/ALA ratio equal to 2.0, then decreased (39). The conversion of EPA into DHA necessitates the elongation of EPA into 24:5n-3 followed by peroxisomal Δ6-desaturation and partial β-oxidation (40). Because the same Δ6-desaturase is thought to act on both 18:3n-3 and 24:5n-3 (41), these two FA would therefore compete for the same enzyme (42). Since ALA appears to be a better substrate than 24:5n-3 (43), an increase in ALA availability would result in a paradoxically negative response of DHA level to dietary ALA, at least with high doses. Besides, the final step of DHA synthesis necessitates a peroxisomal β-oxidation (40). In this respect, and because high ALA intake stimulates β-oxidation (44), the possibility that ALA in our conditions enhances β-oxidation more intensively in mitochondria than in peroxisomes has to be considered as well as a greater sensitivity to oxidation for DHA than for EPA. This would allow regulation of DHA synthesis independently from that of EPA and DPA.

The slight but significant DHA decrease in PL from plasma and RBC in response to high ALA supplies needs to be considered in terms of cellular functionality and possible adverse side effects. In this respect, it is noticeable that cardiomyocytes responded differently from plasma lipids or RBC. Indeed, their DHA content, which was the highest of all the studied tissues, did not decrease with the highest ALA supplies (Table 4). These results contrast with previous studies in the rat showing that, when compared with other dietary fats, dietary ALA resulted in a higher DHA content of myocardial cells (45,46). In view of the relative resistance of cardiac cell membranes to dietary changes in our hamster model, it is questionable whether these animals would be protected from arrhythmia and sudden cardiac death by n-3 PUFA, as demonstrated in other animal species and suggested in the human (47). Because of these species differences in the response of cardiomyocytes membrane composition to dietary ALA, the relevance of the rodent models to human cardiopathies should be considered carefully.

In conclusion, these data show that in the hamster (i) ALA absorption, storage, and conversion into EPA did not seem to be overwhelmed even by the highest dietary intake of ALA. (ii) Important quantities of ALA have been efficiently stored in EAT, constituting a pool that could be released, then metabolized. (iii) ALA and/or EPA content of adipose tissue, plasma (CE, PL), and RBC were extremely reliable as biomarkers of ALA consumption and/or bioconversion over a broad range of dietary supplies and LA/ALA ratio. (iv) Dietary ALA failed to increase DHA, but it increased EPA efficiently and, to a lesser extent, DPA and decreased AA. EPA accumulation in cell membranes paralleled dietary ALA intake, without a tendency to plateau. This is of particular interest in the prevention of cardiovascular diseases, since EPA is the precursor of prostaglandins of the 3-series, known to protect against these pathologies. In this context, the dietary supply of vegetable sources of ALA improves the AA to EPA balance in various compartments and could be promoted in parallel to the consumption of n-3 LC-PUFA-rich foods. However, an adverse effect of very high ALA intake on DHA content of some tissues has to be considered in the human.

ACKNOWLEDGMENTS

The authors gratefully acknowledge the financial support work of ONIDOL and ONIOL (Office National Interprofessionnel des

Oléagineux, protéagineux et cultures textiles). They also sincerely thank the Valorex Company (La Messayais, 35210 Combourtillé, France) for providing linseed oil, Laurence Fonseca and Sabrina Serrano (ITERG) for their valuable contribution to FA analyses, Jean-Marc Hallouis (INRA) for his invaluable technical advice, and Nathalie Samson (Université Paris-Sud) for animal care.

REFERENCES

1. Simopoulos, A.P. (2001) n-3 Fatty Acids and Human Health: Defining Strategies for Public Policy, *Lipids 36* (Suppl.), S83–S89.
2. Gil, A. (2002) Polyunsaturated Fatty Acids and Inflammatory Diseases, *Biomed. Pharmacother. 56*, 388–396.
3. Renaud, S., de Lorgeril, M., Delaye, J., Guidollet, J., Jacquard, F., Mamelle, N., Martin, J.L., Monjaud, I., Salen, P., and Toubol, P. (1995) Cretan Mediterranean Diet for Prevention of Coronary Heart Disease, *Am. J. Clin. Nutr. 61*, 1360S–1367S.
4. Nordoy, A., Marchioli, R., Arnesen, H., and Videbaek, J. (2001) n-3 Polyunsaturated Fatty Acids and Cardiovascular Diseases, *Lipids 36* (Suppl.), S127–S129.
5. de Lorgeril, M., Renaud, S., Mamelle, N., Salen, P., Martin, J.L., Monjaud, I., Guidollet, J., Touboul, P., and Delaye, J. (1994) Mediterranean alpha-Linolenic Acid-rich Diet in Secondary Prevention of Coronary Heart Disease, *Lancet 343*, 1454–1459.
6. Ministry of Agriculture, Fisheries and Food (1997) *Dietary Intake of Iodine and Fatty Acids*, Food Information Surveillance Sheet No. 127, Ministry of Agriculture, Fisheries and Food, London.
7. Simopoulos, A.P. (2000) Human Requirement for n-3 Polyunsaturated Fatty Acids, *Poult. Sci. 79*, 961–970.
8. Legrand, P., Bourre, J.M., Descomps, B., Durand, G., and Renaud, S. (2001) Lipides, in *Apports Nutritionnels Conseillés pour la Population Française* (Martin, A., ed.), Vol. 1, pp. 63–82, Lavoisier, Paris.
9. Combe, N., and Boué, C. (2001) Apports Alimentaires en Acide Linoleique et α-Linolénique d'une Population d'Aquitaine, *Oléagineux Corps Gras Lipides 8*, 118–121.
10. Harel, Z., Riggs, S., Vaz, R., White, L., and Menzies, G. (2001) Omega-3 Polyunsaturated Fatty Acids in Adolescents: Knowledge and Consumption, *J. Adolesc. Health 28*, 10–15.
11. Kris-Etherton, P.M., Taylor, D.S., Yu-Poth, S., Huth, P., Moriarty, K., Fishell, V., Hargrove, R.L., Zhao, G., and Etherton, T.D. (2000) Polyunsaturated Fatty Acids in the Food Chain in the United States, *Am. J. Clin. Nutr. 71*, 179S–188S.
12. Mohrhauer, H., and Holman, R.T. (1963) The Effect of Dose Level of Essential Fatty Acids upon Fatty Acid Composition of the Rat Liver, *J. Lipid Res. 58*, 151–159.
13. Pudelkewicz, C., Seufert, J., and Holman, R.T. (1968) Requirements of the Female Rat for Linoleic and Linolenic Acids, *J. Nutr. 94*, 138–146.
14. Vermunt, S.H., Mensink, R.P., Simonis, M.M., and Hornstra, G. (2000) Effects of Dietary α-Linolenic Acid on the Conversion and Oxidation of ^{13}C-α-Linolenic Acid, *Lipids 35*, 137–142.
15. Sinclair, A.J., Attar-Bashi, N.M., and Li, D. (2002) What Is the Role of α-Linolenic Acid for Mammals? *Lipids 37*, 1113–1123.
16. Surette, M.E., Whelan, J., Lu, G.P., Broughton, K.S., and Kinsella, J.E. (1992) Dependence on Dietary Cholesterol for n-3 Polyunsaturated Fatty Acid-Induced Changes in Plasma Cholesterol in the Syrian Hamster, *J. Lipid. Res. 33*, 263–271.
17. Surette, M.E., Whelan, J., Lu, G., Hardard'ottir, I., and Kinsella, J.E. (1995) Dietary n-3 Polyunsaturated Fatty Acids Modify Syrian Hamster Platelet and Macrophage Phospholipid Fatty Acyl Composition and Eicosanoid Synthesis: A Controlled Study, *Biochim. Biophys. Acta 1255*, 185–191.
18. Spady, D.K., Kearney, D.M., and Hobbs, H.H. (1999) Polyunsaturated Fatty Acids Up-Regulate Hepatic Scavenger Receptor B1 (SR-BI) Expression and HDL Cholesteryl Ester Uptake in the Hamster, *J. Lipid Res. 40*, 1384–1394.
19. Folch, J., Lees, M., and Sloane Stanley, G.H. (1957) A Simple Method for the Isolation and Purification of Total Lipids from Animal Tissues, *J. Biol. Chem. 226*, 497–509.
20. Morisson, W., and Smith, L. (1964) Preparation of Fatty Acid Methyl Esters and Dimethylacetals from Lipids with Boron Fluoride Methanol, *J. Lipid Res. 5*, 600–608.
21. Boué, C., Combe, N., Billeaud, C., Mignerot, C., Entressangles, B., Thery, G., Geoffrion, H., Brun, J.L., Dallay, D., and Leng, J.J. (2000) *Trans* Fatty Acids in Adipose Tissue of French Women in Relation to Their Dietary Sources, *Lipids 35*, 561–566.
22. Lepage, G., and Roy, C.C. (1986) Direct Transesterification of All Classes of Lipids in a One-Step Reaction, *J. Lipid Res. 27*, 114–120.
23. Guillou, H., Martin, P., Jan, S., D'Andrea, S., Roulet, A., Catheline, D., Rioux, V., Pineau, T., and Legrand, P. (2002) Comparative Effect of Fenofibrate on Hepatic Desaturases in Wild-Type and Peroxisome Proliferator-Activated Receptor α-Deficient Mice, *Lipids 37*, 981–989.
24. Wood, R., and Lee, T. (1983) High-Performance Liquid Chromatography of Fatty Acids: Quantitative Analysis of Saturated, Monoenoic, Polyenoic and Geometrical Isomers, *J. Chromatogr. A 254*, 237–246.
25. Rioux, V., Catheline, D., Bouriel, M., and Legrand, P. (1999) High Performance Liquid Chromatography of Fatty Acids as Naphthacyl Derivatives, *Analusis 27*, 186–193.
26. Burdge, G.C., Jones, A.E., and Wootton, S.A. (2002) Eicosapentaenoic and Docosapentaenoic Acids Are the Principal Products of α-Linolenic Acid Metabolism in Young Men, *Br. J. Nutr. 88*, 355–363.
27. Leyton, J., Drury, P.J., and Crawford, M.A. (1987) Differential Oxidation of Saturated and Unsaturated Fatty Acids *in vivo* in the Rat, *Br. J. Nutr. 57*, 383–393.
28. Burdge, G.C., and Wootton, S.A. (2002) Conversion of α-Linolenic Acid to Eicosapentaenoic, Docosapentaenoic and Docosahexaenoic Acids in Young Women, *Br. J. Nutr. 88*, 411–420.
29. Fu, Z., and Sinclair, A.J. (2000) Increased α-Linolenic Acid Intake Increases Tissue α-Linolenic Acid Content and Apparent Oxidation with Little Effect on Tissue Docosahexaenoic Acid in the Guinea Pig, *Lipids 35*, 395–400.
30. Burdge, G.C., Finnegan, Y.E., Minihane, A.M., Williams, C.M., and Wootton, S.A. (2003) Effect of Altered Dietary n-3 Fatty Acid Intake upon Plasma Lipid Fatty Acid Composition, Conversion of [^{13}C]α-Linolenic Acid to Longer-Chain Fatty Acids and Partitioning Towards β-Oxidation in Older Men, *Br. J. Nutr. 90*, 311–321.
31. Emken, E.A., Adlof, R.O., and Gulley, R.M. (1994) Dietary Linoleic Acid Influences Desaturation and Acylation of Deuterium-Labeled Linoleic and Linolenic Acids in Young Adult Males, *Biochim. Biophys. Acta 1213*, 277–288.
32. Salem, N., Jr., Pawlosky, R., Wegher, B., and Hibbeln, J. (1999) *In vivo* Conversion of Linoleic Acid to Arachidonic Acid in Human Adults, *Prostaglandins Leukot. Essent. Fatty Acids 60*, 407–410.
33. Pawlosky, R.J., Hibbeln, J.R., Lin, Y., Goodson, S., Riggs, P., Sebring, N., Brown, G.L., and Salem, N., Jr. (2003) Effects of Beef- and Fish-Based Diets on the Kinetics of n-3 Fatty Acid Metabolism in Human Subjects, *Am. J. Clin. Nutr. 77*, 565–572.
34. Pawlosky, R.J., Hibbeln, J.R., Novotny, J.A., and Salem, N., Jr. (2001) Physiological Compartmental Analysis of α-Linolenic Acid Metabolism in Adult Humans, *J. Lipid Res. 42*, 1257–1265.
35. Sprecher, H. (2002) The Roles of Anabolic and Catabolic Reactions in the Synthesis and Recycling of Polyunsaturated Fatty Acids, *Prostaglandins Leukot. Essent. Fatty Acids 67*, 79–83.
36. Brenner, R.R., and Peluffo, R.O. (1966) Effect of Saturated and Unsaturated Fatty Acids on the Desaturation *in vitro* of Palmitic,

Stearic, Oleic, Linoleic, and Linolenic Acids, *J. Biol. Chem. 241*, 5213–5219.
37. Simopoulos, A.P., Kifer, R.R., and Wykes, A.A. (1991) Omega 3 Fatty Acids: Research Advances and Support in the Field Since June 1985 (worldwide), *World Rev. Nutr. Diet 66*, 51–71.
38. Gerster, H. (1998) Can Adults Adequately Convert α-Linolenic Acid (18:3n-3) to Eicosapentaenoic Acid (20:5n-3) and Docosahexaenoic Acid (22:6n-3)? *Int. J. Vitam. Nutr. Res. 68*, 159–173.
39. Blank, C., Neumann, M.A., Makrides, M., and Gibson, R.A. (2002) Optimizing DHA Levels in Piglets by Lowering the Linoleic Acid to α-Linolenic Acid Ratio, *J. Lipid Res. 43*, 1537–1543.
40. Sprecher, H. (2000) Metabolism of Highly Unsaturated n-3 and n-6 Fatty Acids, *Biochim. Biophys. Acta 1486*, 219–231.
41. D'Andrea, S., Guillou, H., Jan, S., Catheline, D., Thibault, J.N., Bouriel, M., Rioux, V., and Legrand, P. (2002). The Same Rat Δ6-Desaturase Not Only Acts on 18- but Also on 24-Carbon Fatty Acids in Very-Long-Chain Polyunsaturated Fatty Acid Biosynthesis, *Biochem. J. 364*, 49–55.
42. Voss, A., Reinhart, M., Sankarappa, S., and Sprecher, H. (1991) The Metabolism of 7,10,13,16,19-Docosapentaenoic Acid to 4,7,10,13,16,19-Docosahexaenoic Acid in Rat Liver Is Independent of a 4-Desaturase, *J. Biol. Chem. 266*, 19995–20000.
43. Geiger, M., Mohammed, B.S., Sankarappa, S., and Sprecher, H. (1993) Studies to Determine If Rat Liver Contains Chain-Length-Specific Acyl-CoA 6-Desaturases, *Biochim. Biophys. Acta 1170*, 137–142.
44. Ide, T., Murata, M., and Sugano, M. (1996) Stimulation of the Activities of Hepatic Fatty Acid Oxidation Enzymes by Dietary Fat Rich in α-Linolenic Acid in Rats, *J. Lipid Res. 37*, 448–463.
45. Liautaud, S., Grynberg, A., Mourot, J., and Athias, P. (1991) Fatty Acids of Hearts from Rats Fed Linseed or Sunflower Oil and of Cultured Cardiomyocytes Grown on Their Sera, *Cardioscience 2*, 55–61.
46. McLennan, P.L., and Dallimore, J.A. (1995) Dietary Canola Oil Modifies Myocardial Fatty Acids and Inhibits Cardiac Arrhythmias in Rats, *J. Nutr. 125*, 1003–1009.
47. Leaf, A., Xiao, Y.F., Kang, J.X., and Billman, G.E. (2003) Prevention of Sudden Cardiac Death by n-3 Polyunsaturated Fatty Acids, *Pharmacol. Ther. 98*, 355–377.

[Received January 12, 2004; accepted May 17, 2004]

Type 1 Diabetes Compromises Plasma Arachidonic and Docosahexaenoic Acids in Newborn Babies

Kebreab Ghebremeskel[a,*], Beverley Thomas[a], Clara Lowy[b], Yoeju Min[a], and Michael A. Crawford[a]

[a]Institute of Brain Chemistry and Human Nutrition, London Metropolitan University, London, N7 8DB, United Kingdom, and [b]Endocrine and Diabetic Day Centre, Guy's, King's and St. Thomas' Hospitals Medical School, London, SE1 7EH, United Kingdom

ABSTRACT: The activity of Δ6- and Δ5-desaturase, enzymes required for the synthesis of AA and DHA, are impaired in human and experimental diabetes. We have investigated whether neonates of type 1 diabetic women have compromised plasma AA and DHA at birth. Cord blood was obtained from healthy babies born to mothers with (n = 31) and without (n = 59) type 1 diabetes. FA composition of plasma choline phosphoglycerides (CPG), TG, and cholesterol esters (CE) was assayed. The neonates of the diabetics had lower levels of AA (20:4n-6, $P < 0.0001$), adrenic acid (22:4n-6, $P < 0.01$), Σn-6 metabolites ($P < 0.0001$), docosapentaenoic acid (22:5n-3, $P < 0.0001$), DHA (22:6n-3, $P < 0.0001$), Σn-3 ($P < 0.0001$), and Σn-3 metabolites ($P < 0.0001$) in CPG compared with the corresponding babies of the nondiabetic mothers. Similarly, they had lower levels of AA ($P < 0.05$), Σn-6 metabolites ($P < 0.05$), DHA ($P < 0.0001$), and Σn-3 metabolites ($P < 0.01$) in plasma CE. There was also a nonsignificant reduction of AA and DHA in TG in the babies of the diabetic group. The current investigation indicates that healthy neonates born to mothers with type 1 diabetes have highly compromised levels of AA and DHA. These nutrients are of critical importance for neurovisual and vascular system development. In poorly controlled maternal diabetes, it is conceivable that the relative "insufficiency" of AA and DHA may exacerbate speech and reading impairments, behavioral disorders, suboptimal performance on developmental tests, and lower IQ, which have been reported in some children born to mothers with type 1 diabetes mellitus. Further studies are needed to understand the underlying mechanism for this biochemical abnormality and its implications for fetal and infant development.

Paper no. L9441 in *Lipids 39*, 335–342 (April 2004).

The developing fetus and the neonate can synthesize arachidonic (AA) and docosahexaenoic (DHA) acids from their respective parent compounds linoleic (LA) and α-linolenic (ALA) acids (1–5). However, the rate of synthesis is not fast enough to meet the high fetal and neonatal requirements (6–10), and they have to rely on the mother for an optimal supply of these vital nutrients both *in utero* and postnatally.

It is estimated that the fetus accumulates about 70 mg/d of n-3 long-chain PUFA (LCPUFA), mainly DHA, during the third trimester (11,12). The accumulation of AA is thought to be substantially higher since it is omnipresent in most tissues in significant amounts. There is evidence that women of childbearing age have a greater capacity for synthesizing DHA (13,14). Because both FA share the same synthetic pathway (15), it is possible that the effect on AA is similar.

The activity of Δ6- and Δ5-desaturase, enzymes required for the synthesis of AA and DHA, is impaired in human (types 1 and 2) and experimental diabetes (16–18). In addition, levels of membrane LCPUFA are reduced (19–21). Consequently, expectant and nursing mothers with type 1 diabetes may not be able to provide sufficient AA and DHA for optimal fetal and neonatal growth and development. Indeed, Jackson *et al.* (22) and Thomas *et al.* (23) have shown that the breast milk of women with type 1 diabetes has reduced levels of AA and DHA. Similarly, Ghebremeskel *et al.* (24), in a pilot study, found lower levels of both FA in plasma choline phosphoglycerides (CPG) of neonates of type 1 diabetic women. Because the latter study was based on only six subjects, it was not possible to establish with confidence whether type 1 diabetes imposed a significant constraint on the supply of LCPUFA, specifically AA and DHA, to the fetus. Moreover, it was not clear whether a similar adverse effect was also manifested in the other major plasma lipid fractions, *viz.*, TG and cholesterol esters (CE). The aim of the current study was to establish whether the nondiabetic neonates born to mothers with type 1 diabetes had diminished levels of plasma n-6 and n-3 LCPUFA at birth.

MATERIALS AND METHODS

Recruitment. Type 1 diabetic (n = 31) and healthy nondiabetic (n = 59) women, aged 16 yr and over, with uncomplicated singleton pregnancy were recruited during the first trimester (before week 15) from St. Thomas' Hospital (London, United Kingdom). The nondiabetic women did not have a family history of diabetes, were normotensive, and were free of other chronic disorders. The control women were screened for gestational diabetes mellitus (GDM) by monitoring their blood glucose at 60 and 120 min following an oral administration of 75 g of glucose (25). If the concentration was less than or equal to

*To whom correspondence should be addressed at Institute of Brain Chemistry and Human Nutrition, London Metropolitan University, 166-220 Holloway Rd., London, N7 8DB, United Kingdom.
E-mail: keb@kebgm.demon.co.uk

Abbreviations: AA, arachidonic acid; ALA, α-linolenic acid; CE, cholesterol esters; CPG, choline phosphoglycerides; DHGLA, dihomo-γ-linolenic acid; FABP, FA binding proteins; GDM, gestational diabetes mellitus; GLA, γ-linolenic acid; LA, linoleic acid; LCPUFA, long-chain PUFA.

8 mmol/L at 60 min, they were considered normal. From those with glucose concentrations greater than 8 mmol/L, a second blood sample was taken at 120 min. GDM was diagnosed if the concentration of the second sample was equal to or greater than 9 mmol/L. The type 1 diabetics were treated with one of two basic insulin regimes. The first was a twice-daily combination of short- and intermediate-acting insulin injected before breakfast and the evening meal, and the second was short-acting insulin injected before each main meal and intermediate-acting insulin injected at bedtime. Insulin doses were adjusted by the women themselves or at the biweekly consultation with a diabetologist in the combined antenatal and diabetic clinic.

Neonates and collection of cord blood. At delivery, detailed anthropometric and clinical information was obtained from the babies born to the type 1 diabetic ($n = 31$) and nondiabetic ($n = 59$) mothers. Blood glucose was routinely measured 2 h after birth, and hypoglycemia was diagnosed if the concentration was <2 mmol/L. The hypoglycemic infants were treated with milk feeds (bottle) every 1–2 h. If the blood glucose remained low after 3 h, the babies were transferred to the Neonatal Unit and treated with either intravenous dextrose or nasogastrically delivered feed. About 5 mL of cord venous blood was collected in heparinized tubes using a double-clamp procedure for FA analysis. Ethical approval from the Ethics Committee of the Lambeth & Southwark Health Authority and informed written consent from the mothers were obtained for the study.

Sample processing and FA analysis. Plasma was separated from the whole blood by cold centrifugation and stored at –20°C. The samples were subsequently transported to the Institute of Brain Chemistry and Human Nutrition, where they were stored at –70°C until analysis. Total lipids were extracted by the method of Folch *et al.* (26) by homogenizing the plasma samples in chloroform and methanol (2:1 vol/vol) containing BHT (0.01% wt/vol) under nitrogen. The plasma lipid fraction CPG, TG, and CE were separated by TLC on silica gel plates by using the developing solvents petroleum spirit/ether/formic acid/methanol (85:15:2.5:1 by vol) containing BHT. The plasma lipid fraction bands were detected by spraying the TLC plate with a methanolic solution of 2,7-dichlorofluorescein (0.01% wt/vol) and then identified by using authentic standards. FAME were prepared by heating the plasma lipid fractions scraped from the silica plate with 15% acetyl chloride in methanol in a sealed tube at 70°C for 3 h under nitrogen. FAME were separated on a gas chromatograph (HRGC MEGA 2 series; Fisons Instruments, Milan, Italy) fitted with a capillary column (25 m × 0.32 mm i.d., 0.25 μm film, BP20). Hydrogen was used as a carrier gas, and the injector, oven, and detector temperatures were maintained at 235, 210, and 260°C, respectively. FAME were identified by comparison of the retention times with authentic standards (Sigma-Aldrich Co. Ltd., Gillingham, United Kingdom) and interpretation of the ECL values. Peak areas were quantified by an EZChrom Chromatography data system (Scientific Software Inc., San Ramon, CA).

Data analyses. Data were analyzed for gestational age, parity, and maternal diabetes with an unpaired *t*-test. The results are expressed as mean ± SD. The effect of the severity of maternal diabetes (retinopathy, nephropathy, and neuropathy) on the FA levels of the neonates was tested with one-way ANOVA. The chi square test was used to examine statistical differences in the number of caesarean deliveries between the diabetic and nondiabetic women. *P*-values of less than 0.05 were taken to be statistically significant. All calculations were undertaken by the use of SPSS for Windows, release 9 (SPSS Inc., Chicago, IL).

RESULTS

Anthropometric, demographic, and clinical variables. *(i) Mothers*. Anthropometric, clinical, and demographic data on the two groups of mothers are given in Tables 1 and 2. The mean age ($P < 0.05$), prepregnancy weight ($P < 0.05$), weight at the third trimester ($P < 0.01$), and the third-trimester systolic and diastolic blood pressure ($P < 0.0001$) of the type 1 diabetic women were significantly higher than those of the nondiabetics.

(ii) Neonates. Anthropometric and clinical data of the babies at birth are given in Table 3. Elective caesarean accounted for 28.8 and 90.3% of the deliveries in the nondiabetic and type 1 diabetic babies, respectively ($P < 0.0001$). Neonates in the latter group had a lower mean gestational age ($P < 0.0001$) and a higher incidence of hypoglycemia ($P < 0.0001$) compared with those of the nondiabetics. There was no difference in mean birthweight, length, or head circumference between the two groups of babies.

FA. There was no difference in the levels of the FA in plasma CPG, TG, or CE between the preterm and term babies, and those of low- (0 and 1) and high- (≥2) parity mothers ($P > 0.05$). Similarly, the babies of the diabetics with and without complications

TABLE 1
Anthropometric and Demographic Variables of Pregnant Women With and Without Type 1 Diabetes

Characteristics	Nondiabetics ($n = 59$)	Type 1 diabetics ($n = 31$)
Age (yr)	28.23 ± 5.54	31.16 ± 5.05
Height (m)	1.63 ± 0.07	1.65 ± 0.06
Prepregnancy weight (kg)	63.72 ± 13.32	70.90 ± 14.16
Prepregnancy BMI	24.05 ± 5.17	26.25 ± 5.50
Weight (third trimester) (kg)	74.71 ± 12.23	85.95 ± 15.13
BMI (third trimester)	28.28 ± 4.5	31.85 ± 5.7
Ethnicity		
Caucasian	30	28
Afro-Caribbean/African	18	2
Indo-Pakistani	6	—
Others	5	1
Parity		
0	33	16
1	18	8
≥2	8	7
Smoking		
Never	37	20
In the past	9	8
Current	13	3

[a]BMI, body mass index.

TABLE 2
Clinical Data on Pregnant Women With and Without Type 1 Diabetes

Clinical variables	Nondiabetics (n = 59)	Type 1 diabetics (n = 31)
Systolic blood pressure	113.9 ± 13.7	129.5 ± 17.0
Diastolic blood pressure	67.5 ± 9.22	82.9 ± 9.57
Pregestational treatment		
Insulin + diet	—	31
Insulin injections/day		
≤2	—	13
3	—	12
4	—	5
≥5	—	1
No. units/d		
20–39	—	10
40–59	—	17
60–80	—	4
No. units/d in third trimester		
20–39	—	—
40–59	—	11
60–80	—	12
>80		6
Pregestational retinopathy	—	8
Pregestational neuropathy		1
Pregestational nephropathy		1
Retinopathy + nephropathy	—	3
Retinopathy + neuropathy	—	1
Retinopathy + neuropathy + nephropathy	—	2
No complications	—	15

had comparable percentages of FA in the three plasma lipid classes ($P > 0.05$). Hence, the data were not stratified by gestational age, parity, or the severity of maternal diabetes.

Plasma CPG. The mean FA composition of plasma CPG is given in Table 4. The plasma of babies of the type 1 diabetic women at birth had lower levels of stearic acid (18:0, $P < 0.0001$), AA (20:4n-6, $P < 0.0001$), adrenic acid (22:4n-6, $P < 0.01$), Σn-6 metabolites ($P < 0.0001$), docosapentaenoic acid (22:5n-3, $P < 0.0001$), DHA (22:6n-3, $P < 0.0001$), Σn-3 ($P < 0.0001$), and Σn-3 metabolites ($P < 0.0001$) compared with the corresponding cord plasma of the nondiabetic mothers. However, they had higher levels of myristic acid (14:0, $P < 0.05$), palmitic acid (16:0, $P < 0.001$), palmitoleic acid (16:1n-7, $P < 0.0001$), oleic acid (18:1n-9, $P < 0.0001$), Σmonoenes ($P < 0.0001$), LA (18:2n-6, $P < 0.05$), γ-linolenic acid (GLA, 18:3n-6, $P < 0.05$), ALA (18:3n-3, $P < 0.01$), and Mead acid (20:3n-9, $P < 0.05$).

Plasma TG. Table 5 shows the FA composition of cord plasma TG. The percentages of arachidic acid (20:0; $P < 0.05$), palmitoleic acid ($P < 0.05$), and Σmonoenes ($P < 0.05$) were higher, and those of LA ($P < 0.01$), GLA ($P < 0.05$), dihomo-γ-linolenic acid (DHGLA, 20:3n-6, $P < 0.01$), Σn-6 ($P < 0.0001$), and ALA ($P < 0.01$) were lower in the cord plasma of the type 1 diabetic mothers. There was no difference in the proportions of AA, DHA, and Mead acid between the two groups ($P > 0.05$).

Plasma CE. The mean FA composition of plasma CE is given in Table 6. The cord plasma of the type 1 diabetic group had higher levels of palmitoleic acid ($P < 0.01$) and lower levels of AA ($P < 0.05$), Σn-6 metabolites ($P < 0.05$), DHA ($P < 0.0001$), and Σn-3 metabolites ($P < 0.01$) than those of babies of the nondiabetics. The two groups of babies had comparable proportions of LA, ALA, and Mead acid.

DISCUSSION

Consistent with our pilot study (24), the results of the current investigation reveal that the cord plasma AA and DHA obtained from type 1 diabetic women were significantly reduced. The

TABLE 3
Anthropometric Data on the Neonates of Women With and Without Type 1 Diabetes

Anthropometric variables	Nondiabetics (n = 59)	Type 1 diabetics (n = 31)	Level of significance
Gestational age (wk)	39.36 ± 1.59	37.10 ± 1.79	<0.0001
No. of term deliveries (≥ 37 wk)	57	22	
No. of preterm deliveries (34–36 wk)	2	9	
Gender			
Male	38	15	
Female	21	16	
Birthweight (kg)			
Male + female	3.33 ± 0.53	3.35 ± 0.70	NS[a]
Male	3.36 ± 0.57	3.54 ± 0.66	NS
Female	3.26 ± 0.48	3.17 ± 0.70	NS
Length (cm)			
Male + female	50.77 ± 3.01	50.87 ± 3.68	NS
Male	51.16 ± 3.10	52.50 ± 2.86	NS
Female	50.09 ± 2.78	49.55 ± 3.81	NS
Head circumference (cm)			
Male + female	34.73 ± 2.41	34.09 ± 1.75	NS
Male	35.04 ± 2.78	34.56 ± 1.57	NS
Female	34.19 ± 1.43	33.68 ± 1.85	NS
No. with hypoglycemia	2	18	<0.0001
Mode of delivery			
Vaginal	41	3	<0.0001
Caesarean	17	28	<0.0001

[a]NS, nonsignificant.

TABLE 4
Mean (± SD) FA Composition (%) of Plasma Choline Phosphoglycerides of Neonates Born to Women With and Without Type 1 Diabetes[a]

FA	Nondiabetics (n = 59)	Type 1 diabetics (n = 31)	Level of significance
14:0	0.17 ± 0.10	0.23 ± 0.16	<0.05
16:0	28.97 ± 2.71	30.87 ± 2.50	<0.001
18:0	15.06 ± 1.36	13.54 ± 1.78	<0.0001
20:0	0.07 ± 0.03	0.07 ± 0.04	NS
22:0	0.26 ± 0.49	0.45 ± 0.66	NS
24:0	0.09 ± 0.12	0.06 ± 0.03	NS
ΣSaturates	44.54 ± 3.13	45.08 ± 2.85	NS
16:1n-7	0.91 ± 0.31	1.28 ± 0.40	<0.0001
18:1n-9	10.07 ± 1.71	11.56 ± 1.70	<0.0001
20:1n-9	0.11 ± 0.06	0.16 ± 0.10	<0.05
22:1n-9	0.05 ± 0.04	0.11 ± 0.09	<0.05
24:1n-9	0.17 ± 0.44	0.09 ± 0.09	NS
ΣMonoenes	11.26 ± 1.93	13.09 ± 2.00	<0.0001
18:2n-6	8.47 ± 2.71	9.96 ± 3.50	<0.05
18:3n-6	0.10 ± 0.03	0.12 ± 0.05	<0.05
20:2n-6	0.52 ± 0.39	0.76 ± 0.62	<0.05
20:3n-6	5.15 ± 1.16	5.09 ± 0.94	NS
20:4n-6	17.27 ± 2.43	14.67 ± 2.52	<0.0001
22:4n-6	0.63 ± 0.17	0.51 ± 0.22	<0.01
22:5n-6	0.94 ± 0.58	0.98 ± 0.52	NS
Σn-6	33.05 ± 2.73	32.08 ± 2.05	NS
Σn-6 metabolites	24.59 ± 2.86	22.12 ± 3.05	<0.0001
AA/LA ratio	2.16 ± 0.53	1.63 ± 0.52	<0.0001
Σn-6 metabolite/LA ratio	3.08 ± 0.74	2.45 ± 0.74	<0.0001
22:4n-6/22:5n-6	0.82 ± 0.35	0.71 ± 0.53	NS
18:3n-3	0.06 ± 0.04	0.11 ± 0.11	<0.01
20:5n-3	0.45 ± 0.22	0.43 ± 0.25	NS
22:5n-3	0.51 ± 0.25	0.34 ± 0.15	<0.0001
22:6n-3	6.32 ± 1.88	4.64 ± 1.52	<0.0001
Σn-3	7.33 ± 2.18	5.51 ± 1.67	<0.0001
Σn-3 metabolites	7.28 ± 2.18	5.41 ± 1.68	<0.0001
20:3n-9	0.45 ± 0.31	0.64 ± 0.55	<0.05

[a]ΣSaturates = 12:0 + 14:0 + 16:0 + 18:0 + 20:0 + 22:0 + 24:0; Σmonoenes = 14:1 + 16:1 + 18:1 + 20:1 + 22:1 + 24:1; Σn-6 = 18:2 + 18:3 + 20:2 + 20:3 + 20:4 + 22:4 + 22:5; Σn-6 metabolites = 18:3 + 20:2 + 20:3 + 20:4 + 22:4 + 22:5; n-3 = 18:3 + 20:5 + 22:5 + 22:6 ; Σn-3 metabolites = 20:5 + 22:5 + 22:6. For other abbreviation see Table 3.

levels of AA and DHA, relative to the cord values of babies of the nondiabetics, were reduced by 15.1 and 26.6% and by 20 and 41.9% in plasma CPG and CE, respectively. The TG values showed the same trend. With the exception of two pilot studies based on small sample sizes (24,27), no comprehensive published data are available on the effect of type 1 diabetes in pregnancy on maternal and/or cord FA. However, it has been reported that babies of gestational diabetic women have reduced levels of AA and DHA in red-cell phospholipids (28), red-cell CPG (29), and plasma CPG (30) at birth. The aforementioned studies on GDM suggest that metabolic perturbation during pregnancy has a discernible adverse effect on fetal AA and DHA status.

Our findings were rather intriguing, since the type 1 diabetic women had acceptable glycemic control, with a mean HbA_{1c} value of 6.6 ± 0.8, range 5.5–8.1, and their babies were born with no malformations. The mother is the primary source of fetal LA, ALA, AA, and DHA, and the latter two FA are selectively transferred from maternal to fetal circulation (31–33). Hence, it is likely that the lower cord plasma AA and DHA in the babies of the diabetic group were a reflection of a low maternal status, impaired placental transfer, or both. The activity of Δ6- and Δ5-desaturase, enzymes that are vital for the synthesis of AA and DHA, is impaired by diabetes (16–18). In addition, type 1 diabetic patients (17,34) and experimental diabetic animals (35) have reduced levels of n-6 LCPUFA. There is evidence that insulin treatment fully restores the inhibition of Δ6- and Δ5-desaturase activity induced by diabetes (36). The type 1 diabetic women were on insulin therapy throughout their pregnancy, and their n-6 and n-3 FA intake was no different from that of the control subjects (37). Yet the cord plasma of the babies of the diabetic group had reduced levels of AA and DHA. It is plausible that the combination of diabetes- and pregnancy-induced metabolic changes (38) and the consumption of a high-saturated-fat "Western diet" may have depressed the AA and DHA levels in the pregnant type 1 diabetic women and consequently the fetus. We have found that the levels of AA and DHA in plasma CPG of pregnant type 1 diabetic women were 14 and 38.9% lower

TABLE 5
Mean (± SD) FA Composition (%) of Plasma TG of Neonates Born to Women With and Without Type 1 Diabetes[a]

FA	Nondiabetics (n = 59)	Type 1 diabetics (n = 31)	Level of significance
14:0	1.60 ± 0.44	1.42 ± 0.55	NS
16:0	27.46 ± 2.99	28.45 ± 2.50	NS
18:0	4.67 ± 1.63	5.23 ± 1.29	NS
20:0	0.09 ± 0.06	0.15 ± 0.18	<0.05
22:0	0.54 ± 0.82	0.27 ± 0.31	NS
24:0	0.11 ± 0.15	0.10 ± 0.11	NS
ΣSaturates	34.34 ± 4.04	35.59 ± 3.48	NS
16:1n-7	6.03 ± 1.42	6.93 ± 2.07	<0.05
18:1n-9	29.90 ± 4.82	31.46 ± 4.54	NS
20:1n-9	0.33 ± 0.15	0.34 ± 0.19	NS
22:1n-9	0.26 ± 0.23	0.39 ± 0.31	NS
24:1n-9	0.11 ± 0.01	0.09 ± 0.05	NS
ΣMonoenes	36.42 ± 5.02	39.05 ± 5.34	<0.05
18:2n-6	12.47 ± 3.87	9.80 ± 2.76	<0.01
18:3n-6	0.31 ± 0.13	0.23 ± 0.17	<0.05
20:2n-6	0.49 ± 0.26	0.43 ± 0.33	NS
20:3n-6	0.52 ± 0.22	0.45 ± 0.24	<0.01
20:4n-6	2.48 ± 1.17	2.15 ± 1.21	NS
22:4n-6	1.08 ± 1.07	1.03 ± 1.06	NS
22:5n-6	1.97 ± 1.90	2.01 ± 2.09	NS
Σn-6	19.60 ± 4.23	16.00 ± 3.57	<0.0001
Σn-6 metabolites	7.13 ± 2.96	6.20 ± 2.40	NS
AA/LA ratio	0.23 ± 0.11	0.22 ± 0.10	NS
Σn-6 metabolite/LA ratio	0.68 ± 0.38	0.75 ± 0.37	NS
22:4n-6/22:5n-6	1.04 ± 1.27	1.90 ± 4.74	NS
18:3n-3	0.49 ± 0.25	0.33 ± 0.17	<0.01
20:5n-3	0.34 ± 0.33	0.25 ± 0.13	NS
22:5n-3	0.30 ± 0.19	0.30 ± 0.33	NS
22:6n-3	1.65 ± 1.13	1.32 ± 1.03	NS
Σn-3	2.76 ± 1.54	2.15 ± 1.26	NS
Σn-3 metabolites	2.27 ± 1.48	1.81 ± 1.24	NS
20:3n-9	0.46 ± 0.33	0.55 ± 0.32	NS

[a]For abbreviations see Tables 3 and 4.

than those of healthy nondiabetics (24). Similarly, Lakin *et al.* (27) have reported a significant reduction in n-6 and n-3 LCPUFA in the erythrocytes of pregnant women with type 1 diabetes.

The uptake of the LCPUFA by the placenta is thought to be mediated by membrane-bound cytosolic FA-binding proteins (FABP) (39). Moreover, the rate of flux is primarily dependent on the abundance of the available binding sites and on the fact that placental FABP polymorphisms may affect the processes involved in the selective transfer of LCPUFA (40). Recent evidence demonstrates that the membrane protein CD36 (FA translocase), a facilitator in the uptake of long-chain FA (41), is deficient in a rat model of human metabolic syndrome X (42). It is conceivable that type 1 diabetes may have an adverse effect on the binding capacity of FABP and the activity of FA translocase.

Prenatal LCPUFA. The LCPUFA AA and DHA are structural components of cell and subcellular membranes. They are vital for the function of neurovisual, vascular, and immune systems (43–46). It has been shown that intrauterine growth-restricted neonates (47) and those with low birth weight and a small head circumference (6) have reduced levels of AA and DHA at birth. Zhang (48) demonstrated that treatment with LA and ALA increases biparietal diameter and weight in the intrauterine-restricted fetus. There is evidence that maternal supplementation with n-3 FA during pregnancy, and during pregnancy and lactation is associated with cerebral maturation of the newborn (49) and enhanced mental development at age 4 (50), respectively. In addition, a relationship has been reported between infant DHA status and maturation of the retina at birth (51), and between enhanced stereoacuity at age of 3.5 yr and maternal intake of a DHA-rich diet during pregnancy (52).

Because of the critical importance of AA and DHA, the relative "insufficiency" of these nutrients in neonates of the type 1 diabetic group may have had a subclinically adverse impact on prenatal development of the neurovisual and vascular systems. In poorly controlled diabetes, this insufficiency may be severe enough to be a risk for congenital malformation. Indeed, Reece *et al.* (53) have reported that diabetic embryopathy in rats is associated with a state of EFA deficiency and that it can be significantly reduced by supplementation with dietary PUFA.

Postnatal LCPUFA. Speech and reading impairments, behavioral disorders, suboptimal performance on developmental

TABLE 6
Mean (± SD) FA Composition (%) of Plasma Cholesterol Esters of Neonates Born to Women With and Without Type 1 Diabetes

FA	Nondiabetics (n = 59)	Type 1 diabetics (n = 31)	Level of significance
14:0	0.66 ± 0.26	0.71 ± 0.34	NS
16:0	20.69 ± 3.77	21.32 ± 3.13	NS
18:0	3.31 ± 1.22	3.33 ± 1.11	NS
20:0	0.15 ± 0.17	0.10 ± 0.08	NS
22:0	0.73 ± 1.31	0.56 ± 0.75	NS
24:0	0.11 ± 0.13	0.08 ± 0.11	NS
ΣSaturates	25.49 ± 4.54	26.03 ± 4.19	NS
16:1n-7	7.82 ± 1.83	9.52 ± 2.65	<0.01
18:1n-9	28.27 ± 4.91	29.04 ± 4.82	NS
20:1n-9	0.14 ± 0.08	0.14 ± 0.12	NS
22:1n-9	0.16 ± 0.17	0.30 ± 0.49	NS
24:1n-9	0.14 ± 0.13	0.11 ± 0.14	NS
ΣMonoenes	36.31 ± 5.96	38.80 ± 6.46	NS
18:2n-6	20.78 ± 7.20	20.32 ± 7.57	NS
18:3n-6	0.54 ± 0.18	0.49 ± 0.20	NS
20:2n-6	0.30 ± 0.35	0.25 ± 0.24	NS
20:3n-6	1.18 ± 0.34	1.06 ± 0.28	NS
20:4n-6	9.00 ± 3.40	7.20 ± 3.11	<0.05
22:4n-6	0.12 ± 0.11	0.09 ± 0.08	NS
22:5n-6	0.43 ± 0.44	0.61 ± 0.55	NS
Σn-6	32.17 ± 7.81	29.80 ± 7.74	NS
Σn-6 metabolites	11.39 ± 3.69	9.48 ± 3.35	<0.05
AA/LA ratio	0.46 ± 0.19	0.38 ± 0.16	<0.05
Σn-6 metabolite/LA ratio	0.59 ± 0.21	0.50 ± 0.18	NS
22:4n-6/22:5n-6	1.05 ± 2.64	0.55 ± 0.60	NS
18:3n-3	0.68 ± 1.02	0.65 ± 0.72	NS
20:5n-3	0.30 ± 0.23	0.23 ± 0.24	NS
22:5n-3	0.05 ± 0.06	0.07 ± 0.07	NS
22:6n-3	0.62 ± 0.34	0.36 ± 0.26	<0.0001
Σn-3	1.51 ± 1.01	1.23 ± 0.96	NS
Σn-3 metabolites	0.90 ± 0.49	0.60 ± 0.38	<0.01
20:3n-9	0.39 ± 0.33	0.40 ± 0.26	NS

[a]For abbreviations see Tables 3 and 4.

tests, and lower IQ have been reported in infants and children of diabetic mothers (54–56). These problems have been attributed to poor maternal diabetic control, elevated β-hydroxybutyrate, and lipid metabolic perturbation during pregnancy (54,55). Epidemiological (57) and experimental (58–61) studies indicate that a nutritional constraint or imbalance *in utero* may precipitate physiological or biochemical dysfunction in postnatal life. Bjerve *et al.* (62) reported that low levels of plasma DHA at birth are associated with lower psychomotor performance scores at 1 yr of age. Similarly, there is evidence that a suboptimal provision of DHA or of DHA and AA postnatally is associated with lower neurovisual development in experimental animals and in preterm and term infants (63–69). Hence, it is tenable to assume that prenatal (22) and postnatal (23) insufficiency of these FA may contribute to cognitive impairment and/or behavioral disorders in children of diabetic mothers.

The current investigation indicates that nondiabetic neonates born to mothers with type 1 diabetes have highly compromised plasma AA and DHA. Further studies are needed to understand the underlying mechanism for this biochemical abnormality and its implications for fetal and infant development.

ACKNOWLEDGMENTS

The authors gratefully acknowledge the financial support of Diabetes UK, the March of Dimes Birth Defect Foundation, the Mother and Child Foundation, and Shida Kanzume Co. Ltd. In addition, we thank Bridget Offley-Shore for her competent assistance in recruiting and collecting demographic information, and the mothers for participating in the study.

REFERENCES

1. Chambaz, J., Ravel, D., Manier, M.C., Pepin, D., Mulliez, N., and Bereziat, G. (1985) Essential Fatty Acids Interconversion in the Human Fetal Liver, *Biol. Neonate 47*, 136–140.
2. Poisson, J.P., Dupuy, R.P., Sarda, P., Descomps, B., Narce, M., Rieu, D., and Crastes de Paulet, A. (1993) Evidence That Liver Microsomes of Human Neonates Desaturate Essential Fatty Acids, *Biochim. Biophys. Acta 1167*, 109–113.

3. Descomps, B., and Rodriguez, A. (1995) Essential Fatty Acids and Prematurity: A Triple Experimental Approach, *C R Seances Soc. Biol. Fil. 189*, 781–796.
4. Carnielli, V.P., Wattimena, D.J.L., Luijendijk, I.H.T., Boerlage, A., Degenhart, H.J., and Sauer, P.J. (1996) The Very Low Birth Weight Premature Infant Is Capable of Synthesizing Arachidonic and Docosahexaenoic Acids from Linoleic and Linolenic Acids, *Pediatr. Res. 40*, 169–174.
5. Sauerwald, T.U., Hachey, D.L., Jensen, C.L., Chen, H., Anderson, R.E., and Heird, W.C. (1997) Intermediates in Endogenous Synthesis of C22:6 Omega-3 and 20:4 Omega-6 by Term and Preterm Infants, *Pediatr. Res. 41*, 183–187.
6. Leaf, A., Leighfield, M.J., Costeloe, K., and Crawford, M.A., (1992) Factors Affecting Long-Chain Polyunsaturated Fatty Acid Composition of Plasma Choline Phosphoglycerides in Preterm Infants, *J. Pediatr. Gastroenterol. Nutr. 14*, 300–308.
7. Makrides, M., Neumann, M.A., Byard, R.W., Simmer, K., and Gibson, R.A. (1994) Fatty Acid Composition of Brain, Retina, and Erythrocytes in Breast- and Formula-fed Infants, *Am. J. Clin. Nutr. 60*, 189–194.
8. Farquharson, J., Jamieson, E.C., Abbasi, K.A., Patrick, W.J.A., Logan, R.W., and Cockburn, F. (1995) Effect of Diet on the Fatty Acid Composition of the Major Phospholipids of Infant Cerebral Cortex, *Arch. Dis. Child 72*, 198–203.
9. Salem, N., Jr., Wegher, B., Mena, P., and Uauy, R. (1996) Arachidonic and Docosahexaenoic Acids Are Biosynthesized from Their 18-Carbon Precursors in Human Infants, *Proc. Natl. Acad. Sci. USA 93*, 49–54.
10. Koletzko, B.B., Decsi, T., and Demmelmair, H. (1996) Arachidonic Acid Supply and Metabolism in Human Infants Born at Full Term, *Lipids 31*, 79–83.
11. Clandinin, M.T., Chappell, J.E., Leong, S., Heim, T., Swyer, P.R., and Chance, G.W. (1980) Intrauterine Fatty Acid Accretion in Human Brain: Implications for Fatty Acid Requirements, *Early Hum. Dev. 4*, 131–138.
12. Martinez, M. (1992) Tissue Levels of Polyunsaturated Fatty Acids During Early Human Development, *J. Pediatr. 120*, S129–S134.
13. Burdge, G.C., and Wootton, S.A. (2002) Conversion of α-Linolenic Acid to Eicosapentaenoic, Docosapentaenoic, and Docosahexaenoic Acids in Young Women, *Br. J. Nutr. 88*, 411–420.
14. Pawlosky, R., Hibbeln, J., Lin, Y., and Salem, N., Jr. (2003) n-3 Fatty Acid Metabolism in Women, *Br. J. Nutr. 90*, 993–994.
15. Voss, A.M., Reinhart, S., Sankarappa, S., and Sprecher, H. (1991) The Metabolism of 7,10,13,16,19-Docosahexapentaenoic Acid to 4,7,10,13,16,19-Docosahexaenoic Acid in Rat Liver Is Independent of a 4-Desaturase, *J. Biol. Chem. 266*, 19995–20000.
16. el Boustani, S., Causse, J.E., Descomps, B., Monnier, L., Mendy, F., and De Poulet, A.C. (1989) Direct *in vivo* Characterization of Δ5-Desaturase Activity in Humans by Deuterium Labeling: Effect of Insulin, *Metabolism 38*, 315–321.
17. Arisaka, M., Arisaka, O., and Yamashiro, Y. (1991) Fatty Acid and Prostaglandin Metabolism in Children with Diabetes Mellitus. II. The Effect of Evening Primrose Oil Supplementation on Serum Fatty Acid and Plasma Prostaglandin Levels, *Prostaglandins Leukot. Essential. Fatty Acids 43*, 197–201.
18. Brenner, R.R., Bernasconi, A.M., and Garda, H.A. (2000) Effect of Experimental Diabetes on the Fatty Acid Composition, Molecular Species of Phosphatidylcholine and Physical Properties of Hepatic Microsomal Membranes, *Prostaglandins Leukot. Essent. Fatty Acids 63*, 167–176.
19. Tilvis, R.S., and Miettinen, T.A. (l985) Fatty Acid Composition of Serum Lipids, Erythrocytes and Platelets in Insulin Dependent Diabetic Women, *J. Clin. Endocrinol. Metab. 61*, 741–745.
20. Mikhailidis, D.P., Kirtland, S.J., Barradas, M.A., Mahadeviah, S., and Dandona, P. (1986) The Effect of Dihomogammalinolenic Acid on Platelet Aggregation and Prostaglandin Release, Erythrocyte Membrane Fatty Acids and Serum Lipids: Evidence for Defects in PGE1 Synthesis and Δ5-Desaturase Activity in Insulin-Dependent Diabetics, *Diabetes Res. 3*, 7–12.
21. Igal, R.A., Mandon, E.C., and de Gomez Dumm, I.N. (1991) Abnormal Metabolism of Polyunsaturated Fatty Acids in Adrenal Glands of Diabetic Rats, *Mol. Cell Endocrinol. 77*, 217–227.
22. Jackson, M.B., Lammi-Keefe, C.J., Jensen, R.G., Couch, S.C., and Ferris, A.M. (1994) Total Lipid and Fatty Acid Composition of Milk from Women With and Without Insulin-Dependent Diabetes Mellitus, *Am. J. Clin. Nutr. 60*, 353–61.
23. Thomas, B., Ghebremeskel, K., Offley-Shore, B., Lowy, C., and Crawford, M.A. (2000) Fatty Acid Composition of Maternal Milk from Insulin-Dependent Diabetic, Gestational Diabetic and Healthy Women, *Proc. Nutr. Soc. 59*, 59A.
24. Ghebremeskel, K., Thomas, B., Min, Y., Stacy, F., Koukkou, E., Lowy, C., Erskine, K., Crawford, M.A., and Offley-Shore, B. (l998) Fatty Acid in Pregnant Diabetic Women and Neonates: Implications for Growth and Development, in *Essential Fatty Acids and Eicosanoids: Invited Papers from the 4th International Congress*, (Riemersma, R.A., Armstrong, R., Kelly, R.W., and Wilson, R., eds.), pp. 104–107, AOCS Press, Champaign.
25. National Diabetes Data Group (1979) Classification and Diagnosis of Diabetes Mellitus and Other Categories of Glucose Intolerance, *Diabetes 28*, 1039–1057.
26. Folch, J., Lees, M., and Sloane Stanley, G.H. (1957) A Simple Method for the Isolation and Purification of Total Lipids from Animal Tissues, *J. Biol. Chem. 226*, 497–509.
27. Lakin, V., Haggarty, P., Abramovich, D.R., Ashton, J., Moffat, C.F., McNeill, G., Danielian, P.J., and Grubb, D. (1998) Dietary Intake and Tissue Concentration of Fatty Acids in Omnivore, Vegetarian and Diabetic Pregnancy, *Prostaglandins Leukot. Essent. Fatty Acids 59*, 209–220.
28. Wijendran, V., Bendel, R.B., Couch, S.C., Philipson, E.H., Cheruku, S., and Lammi-Keefe, C.J. (2000) Fetal Erythrocyte Phospholipids Polyunsaturated Fatty Acids Are Altered in Pregnancy Complicated with Gestational Diabetes Mellitus, *Lipids 35*, 927–931.
29. Min, Y., Ghebremeskel, K., Lowy, C., Thomas, B., and Crawford, M.A. (2004) Adverse Effect of Obesity on Red Cell Membrane Arachidonic and Docosahexaenoic Acids in Gestational Diabetes, *Diabetologia 49*, 75–81.
30. Thomas, B., Ghebremeskel, K., Lowy, C., and Crawford, M.A. (2004) Comparative Plasma Fatty Acid Status of Neonates Born to Mothers With and Without Pregnancy-Induced Diabetes—A Specific Focus on n-6 and n-3 Families, *Acta Paediatr.* (in press).
31. Haggarty, P., Ashton, J., Joynson, M., Abramovich, D.R., and Page, K. (1999) Effect of Maternal Polyunsaturated Fatty Acid Concentration on Transport by the Human Placenta, *Biol. Neonate 75*, 350–359.
32. Crawford, M.A. (2000) Placental Delivery of Arachidonic and Docosahexaenoic Acids: Implications for the Lipid Nutrition of Preterm Infants, *Am. J. Clin. Nutr. 71* (Suppl.), 275S–284S.
33. Herrera, E. (2002) Implications of Dietary Fatty Acids During Pregnancy on Placental, Fetal and Postnatal Development—A Review, *Placenta 23* (Suppl. A), S9–19.
34. Horrobin, D.F. (1988) The Role of Essential Fatty Acids in the Development of Diabetic Neuropathy and Other Complications of Diabetes Mellitus, *Prostaglandins Leukotr. Essent. Fatty Acids 31*, 181–197.
35. Holman, R.T., Johnson, S.B., Gerard, J.M., Mauer, S.M., Kupcho-Sandberg, S., and Brown, D.M. (1983) Arachidonic Acid Deficiency in Streptozotocin-Induced Diabetes, *Proc. Natl. Acad. Sci. USA 80*, 2375–2379.
36. Offley-Shore, B., Thomas, B., Ghebremeskel, K., Crawford, M.A., and Lowy, C. (1999) Does Maternal Diabetes Impair Long-Chain Essential Fatty Acid Synthesis in Mother, Fetus and

Breast Milk? 35th Annual Meeting: European Association for the Study of Diabetes, Brussels, Abstract OP11:76.
37. Poisson, J.-P. (1989) Essential Fatty Acid Metabolism in Diabetes, *Nutrition 5,* 263–266.
38. Montelongo, A., Lasuncion, M.A., Pallardo, L.F., and Herrera, E. (1992) Longitudinal Study of Plasma Lipoproteins and Hormones During Pregnancy in Normal and Diabetic Women, *Diabetes 41*, 1651–1659.
39. Dutta-Roy, A.K. (2000) Transport Mechanisms for Long-Chain Polyunsaturated Fatty Acids in the Human Placenta, *Am. J. Clin. Nutr. 71* (Suppl. 1), 315S–322S.
40. Haggarty, P. (2002) Placental Regulation of Fatty Acid Delivery and Its Effect on Fetal Growth, *Placenta 23* (Suppl. A), S28–S38.
41. Coburn, C.T., Knapp, F.F., Jr., Febbraio, M., Beets, A.L., Silverstein, R.L., and Abumrad, N.A. (2000) Defective Uptake and Utilization of Long Chain Fatty Acids in Muscle and Adipose Tissues of CD36 Knockout Mice, *J. Biol. Chem. 275*, 32523–32529.
42. Aitman, T.J., Glazier, A.M., Wallace, C.A., Cooper, L.D., Norsworthy, P.J., Wahid, F.N., Al-Majali, K.M., Trembling, P.M., Mann, C.J., Shoulders, C.C. *et al.* (1999) Identification of CD36 (fat) as an Insulin-Resistance Gene Causing Defective Fatty Acid and Glucose Metabolism in Hypertensive Rats, *Nat. Genet. 21*, 76–83.
43. Svennerholm, L. (1968) Distribution and Fatty Acid Composition of Phosphoglycerides in Normal Human Brain, *J. Lipid Res 9*, 570–579.
44. Fliesler, S.J., and Anderson, R.E. (1983) Chemistry and Metabolism of Lipids in the Vertebrate Retina, *Prog. Lipid Res. 22*, 79–131.
45. Sastry, P.S. (1985) Lipids of Nervous Tissue: Composition and Metabolism, *Prog. Lipid Res. 24*, 69–176.
46. Stulnig, T.M. (2003) Immunomodulation by Polyunsaturated Fatty Acids: Mechanisms and Effects, *Int. Arch. Allergy Immunol. 132*, 310–321.
47. Vilbergsson, G., Wennergren, M., Samsioe, G., Percy, P., Percy, A., Mansson, J.E., and Svennerholm, L. (1994) Essential Fatty Acid Status Is Altered in Pregnancies Complicated by Intrauterine Growth Retardation, *World Rev. Nutr. Diet 76*, 105–109.
48. Zhang, L. (1997) The Effects of Essential Fatty Acids Preparation in the Treatment of Intrauterine Growth Retardation, *Am. J. Perinatology 14*, 535–537.
49. Helland, I.B., Saugstad, O.D., Smith, L., Saarem, K., Solvoll K., Ganes, T., and Drevon, C.A. (2001) Similar Effects on Infants of n-3 and n-6 Fatty Acids Supplementation to Pregnant and Lactating Women, *Pediatrics. 108*, E82–92.
50. Helland, I.B., Smith, L., Saarem, K., Saugstad, O.D., and Drevon, C.A. (2003) Maternal Supplementation with Very-Long-Chain n-3 FA During Pregnancy and Lactation Augments Children's IQ at 4 Years of Age, *Pediatrics 111*, 1–10.
51. Malcolm, C.A., Hamilton, R., McCulloch, D.L., Montgomery, C., and Weaver, L.T. (2003) Scotopic Electroretinogram in Term Infants Born of Mothers Supplemented with Docosahexaenoic Acid During Pregnancy, *Invest. Ophthalmol. Vis. Sci. 44*, 3685–3691.
52. Williams, C., Birch, E.E., Emmett, P.M., and Northstone, K. (2001) Stereoacuity at Age 3.5 y in Children Born Full-Term Is Associated with Prenatal and Postnatal Dietary Factors: A Report from a Population-Based Cohort Study, *Am. J. Clin. Nutr. 73*:316–22.
53. Reece, E.A., Wu, Y.K., Wiznitzer, A., Homko, C., Yao, J., Borenstein, M., and Sloskey, G. (1996) Dietary Polyunsaturated Fatty Acid Prevents Malformations in Offspring of Diabetic Rats, *Am. J. Obstet. Gynecol. 175*, 818–823.
54. Rizzo, T., Metzger, B.E., Burns, W.J., and Burns, K. (1991) Correlations Between Antepartum Maternal Metabolism and Child Intelligence, *N. Engl. J. Med. 325*, 911–916.
55. Rizzo, T.A., Metzger, B.E., Dooley, S.L., and Cho, N.H. (1997) Early Malnutrition and Child Neurobehavioral Development: Insights from the Study of Children of Diabetic Mothers, *Child Dev. 68*, 26–38.
56. Yamashita, Y., Kawano, Y., Kuriya, N., Murakami, Y., Matsuishi, T., Yoshimatsu, K., and Kato, H. (1996) Intellectual Development of Offspring of Diabetic Mothers, *Acta Paediatr. 85*, 1192–1196.
57. Barker, D.J. (1997) Maternal Nutrition, Fetal Nutrition, and Disease in Later Life, *Nutrition 13*, 807–813.
58. Langley S.C., and Jackson, A.A. (1994) Increased Systolic Blood Pressure in Adult Rats Induced by Fetal Exposure to Maternal Low Protein Diets, *Clin. Sci.* (London) *86*, 217–222.
59. Ozanne, S.E., Martensz, N.D., Petry, C.J., Loizou, C.L., and Hales, C.N. (1998) Maternal Low Protein Diet in Rats Programmes Fatty Acid Desaturase Activities in the Offspring, *Diabetologia 41*, 1337–1342.
60. Ozaki, T., Nishina, H., Hanson, M.A., and Poston, L. (2001) Dietary Restriction in Pregnant Rats Causes Gender-Related Hypertension and Vascular Dysfunction in Offspring, *J. Physiol. 530*, 141–152.
61. Ghosh, P., Bitsanis, D., Ghebremeskel, K., Crawford, M.A., and Poston, L. (2001) Abnormal Aortic Fatty Acid Composition and Small Artery Function in Offspring of Rats Fed a High Fat Diet in Pregnancy, *J. Physiol. 15*, 533, 815–822.
62. Bjerve, K.S., Thoresen, L., Bonaa, K., Vik, T., Johnsen, H., and Brubakk, A.M. (1992) Clinical Studies with α-Linolenic Acid and Long-Chain n-3 Fatty Acids, *Nutrition 8*, 130–132.
63. Neuringer, M., Connor, W.E., Lin, D.S., Barstad, L., and Luck, S. (1986) Biochemical and Functional Effects of Prenatal and Postnatal Omega-3 Fatty Acid Deficiency on Retina and Brain in Rhesus Monkeys, *Proc. Natl. Acad. Sci. USA 83*, 4021–4025.
64. Weisinger, H.S., Vingrys, A.J., and Sinclair, A.J. (1996) Effect of Dietary n-3 Deficiency on the Electroretinogram in the Guinea Pig, *Ann. Nutr. Metab. 40*, 91–98.
65. Carlson, S.E., Ford, A.J., Werkman, S.H., Peeples, J.M., and Koo, W.W. (1996) Visual Acuity and Fatty Acid Status of Term Infants Fed Human Milk and Formulas With and Without Docosahexaenoate and Arachidonate from Egg Yolk Lecithin, *Pediatr. Res. 39*, 882–888.
66. Willatts, P., Forsyth, J.S., DiModugno, M.K., Varma, S., and Colvin, M. (1998) Effect of Long-Chain Polyunsaturated Fatty Acids in Infant Formula on Problem Solving at 10 Months of Age, *Lancet 352*, 688–691.
67. Agostoni, C., and Giovannini, M. (2001) Cognitive and Visual Development: Influence of Differences in Breast and Formula Fed Infants, *Nutr. Health 15*, 183–188.
68. O'Connor, D.L., Hall, R., Adamkin, D., Auestad, N., Castillo, M., Connor, W.E., Connor, S.L., Fitzgerald, K., Groh-Wargo, S., Hartmann, E.E., *et al.* (2001) Growth and Development in Preterm Infants Fed Long-Chain Polyunsaturated Fatty Acids: A Prospective, Randomized Controlled Trial, *Pediatrics 108*, 359–371.
69. Uauy, R., Hoffman, D.R., Mena, P., Llanos, A., and Birch, E.E. (2003) Term Infant Studies of DHA and ARA Supplementation on Neurodevelopment: Results of Randomized Controlled Trials, *J. Pediatr. 143* (Suppl. 4), S17–S25.

[Received January 27, 2004; accepted June 8, 2004]

An Isocaloric PUFA Diet Enhances Lipid Uptake and Weight Gain in Aging Rats

Trudy D. Woudstra[a], Laurie A. Drozdowski[a], Gary E. Wild[b], M.T. Clandinin[a], Luis B. Agellon[c], and Alan B.R. Thomson[a,*]

[a]Nutrition and Metabolism Group, Division of Gastroenterology, Department of Medicine, University of Alberta, Edmonton, Alberta, Canada, [b]Department of Anatomy and Cell Biology, McGill University, Montréal, Québec, Canada and [c]Department of Biochemistry, University of Alberta, Edmonton, Alberta, Canada

ABSTRACT: Aging is associated with a change in the morphology and absorptive capacity of the small intestine. In young rats, feeding a semisynthetic diet containing saturated FA (SFA) increases nutrient uptake, as compared with an isocaloric diet containing polyunsaturated FA (PUFA). We tested the hypotheses that (i) aging is associated with a decline in lipid absorption in the Fischer 344 rat; (ii) this decline can be corrected by manipulating the fat composition of the diet; and (iii) the age- and diet-associated variations in lipid uptake are associated with changes in the ileal lipid-binding protein (ILBP) or the intestinal or liver FA-binding proteins (I- or L-FABP, respectively) in the cytosol of the enterocyte. In rats fed SFA or PUFA, aging was associated with a decline in the *in vitro* uptake of stearic acid (18:0) when expressed on the basis of intestinal or mucosal weight. In contrast, age had no effect on lipid uptake when expressed on the basis of serosal surface area, whereas lipid uptake increased with age when expressed on the basis of mucosal surface area. The age-associated variations in lipid uptake were not associated with changes in protein abundance and/or expression of ILBP, I-FABP, or L-FABP. In 24-mon-old rats, when uptake of lipids was expressed on the basis of mucosal surface area, feeding PUFA enhanced lipid uptake and body weight gain as compared with rats fed SFA. Future studies must determine whether the enhanced lipid uptake and body weight gain observed in older animals fed PUFA have any therapeutic benefit.

Paper no. L9270 in *Lipids 39,* 343–354 (April 2004).

Developed nations are faced with the demographics of an aging population. In Canada, over 12% of the population is older than 64 yr, and this value is expected to grow by 2% within 11 yr (1). Aging is associated with an increased prevalence of many conditions such as diabetes, heart disease, and malnutrition (2,3). Some of these age-associated conditions may benefit from dietary modification. However, little is known about the influence of age on the effect of dietary lipid modification on lipid nutrient absorption.

*To whom correspondence should be addressed at 205 College Plaza, University of Alberta, Edmonton, AB T6G 2C8, Canada.
E-mail: alan.thomson@ualberta.ca

Abbreviations: BBM, brush border membrane, DIG, digoxigenin; F344 rat, Fischer 344 rat; FABPpm, FA-binding protein in the plasma membranes; FAT, FA translocase; FATP, FA transport protein; ILBP, ileal lipid-binding protein; I-FABP, intestinal FA-binding protein; L-FABP, liver FA-binding protein; mRNA, messenger ribonucleic acid; MTP, microsomal triglyceride transport protein; PPAR, peroxisome proliferator-activated receptors; SFA, saturated FA; UWL, intestinal unstirred water layer.

Aging is associated with a decline in the absorptive capacity of the small intestine for carbohydrates (4), amino acids (5), calcium (6), and lipids (7–9). Alterations in the dietary content of carbohydrates (10) and lipids (11) influence the absorptive function of the intestine. For example, young animals fed diets rich in saturated FA (SFA) have increased intestinal uptake of sugars and lipids when compared with animals fed a PUFA-rich diet (11).

The complexity of lipid absorption may make it highly susceptible to the effects of aging (12). Such factors as the pH of the microenvironment adjacent to the intestinal brush border membrane (BBM) (13), BBM fluidity (14), the effective resistance of the unstirred water layer (UWL), and the contribution of FA-binding proteins (FABP) may be subject to age-associated alterations and affect the response of the intestine to changes in dietary lipids.

Several BBM-associated proteins (17) may also contribute to lipid absorption in the intestine, such as the FABP in the plasma membrane (FABPpm), the FA translocase (FAT) (15), and FA transport protein-4 (FATP-4) (16). Cytosolic-lipid binding proteins found in the intestinal epithelium include the liver-FABP (L-FABP), the intestinal FA-binding protein (I-FABP), and the ileal lipid-binding protein (ILBP) (17). L-FABP is a 14.1-kDa protein located in the duodenum and jejunum, with maximal expression in the proximal jejunum (17). I-FABP is a 15.1-kDa protein that is expressed throughout the small intestine, with maximal expression in the distal jejunum (18). It is likely that L-FABP and I-FABP play different roles in the absorption of lipids. For example, the FA transfer from I-FABP occurs by direct collisional interaction with the phospholipid bilayer, and I-FABP may play a role in the uptake or subcellular targeting of FA (19). In contrast, L-FABP may transfer FA in an aqueous diffusion-mediated process, and may act as a cytosolic buffer for FA (19). Both I-FABP and L-FABP have a high affinity for binding long-chain FA. Rats treated with clofibrate (a hypolipidemic drug) have increased expression of L-FABP protein and messenger RNA (mRNA), with no change in the expression of the I-FABP counterparts (20). The mRNA expression of I-FABP and L-FABP is increased in rats fed a diet rich in polyunsaturated fats (21). ILBP is a 14-kDa cytoplasmic protein that binds bile acids (22), is structurally related to the FABP family, and is located predominantly in the distal ileum (23).

TABLE 1
FA Composition of the Semisynthetic Diets

FA (% of total)	Diet enriched with saturated FA (SFA)	Diet enriched with PUFA
14:0	1.8	0.1
14:1n-9	0.0	0.0
15:0	0.2	0.0
16:0	21.8	5.5
16:1n-7	0.0	0.1
18:0	61.1	5.2
18:1n-9	2.8	16.3
18:1n-7	0.1	0.2
18:2n-6	9.6	69.2
18:3n-3	0.0	0.8
18:3n-6	0.0	0.1
18:4n-3	0.0	0.0
19:0	0.2	0.0
20:0	1.5	0.2
20:1n-9	0.0	0.3
20:1n-7	0.1	0.3
20:2n-6	0.1	0.2
20:3n-9	0.1	0.2
20:3n-6	0.0	0.0
20:4n-6	0.0	0.0
20:5n-3	0.0	0.3
22:0	0.0	0.4
22:1n-9	0.0	0.0
22:1n-7	0.3	0.3
22:4n-6	0.0	0.1
22:5n-6	0.0	0.0
22:5n-3	0.1	0.1
24:0	0.1	0.1
22:6n-3	0.1	0.0

The Fischer 344 (F344) rat is an established and widely recognized rat model of aging; 64% of rat studies published in U.S. aging journals have used this strain (24). It has been described as a "healthy" model of aging, as it has a relatively low incidence of spontaneous malignant tumors (25). This reduced mortality allows animals to have a lifespan of greater than 24 mon, and helps to minimize the compounding effect of diseases of the aging process.

This study was undertaken to test the hypotheses that (i) aging is associated with a decrease in the absorption of lipids in F344 rats; (ii) the decreased absorption of lipid is due to a decline in the abundance of selected lipid-binding proteins and/or the expression of their respective mRNA in the intestine; and (iii) the age-associated decrease in lipid uptake can be reversed by feeding a saturate-enriched rather than a polyunsaturate-enriched diet.

MATERIALS AND METHODS

Animals. The principles for the care and use of laboratory animals, approved by the Canadian Council on Animal Care and the Council of the American Physiological Society, were observed in the conduct of this study. Male F344 rats, aged 1, 9, and 24 mon, were obtained from the National Institute on Aging (Bethesda, MD) colony and Harlan Laboratories (Madison, WI). Pairs of rats were housed at a temperature of 21°C, with 12 h of light and 12 h of darkness. Water and food were supplied *ad libitum*. There were 8 animals in each group.

Animals were fed standard Purina® rat chow (St. Louis, MO) for 1 wk and then were fed for 2 wk a semipurified diet containing 20% (w/w) fat and enriched with either SFA or PUFA (Tables 1, 2). The isocaloric semipurified diets were nutritionally adequate, providing for all known essential nutrient requirements. Animal weights were recorded weekly during the study period.

Uptake studies. (i) Probe and marker compounds. The [^{14}C]-labeled probes included cholesterol (0.05 mM) and FA 12:0, 16:0, 18:0, 18:1, 18:2, and 18:3 (0.1 mM). The labeled and unlabeled probes were supplied by Amersham Biosciences Inc. (Baie d'Urfe, Québec, Canada) and Sigma Co. (St. Louis, MO), respectively. The probes were prepared by solubilizing them in 10 mM of taurodeoxycholic acid (Sigma Co.) in Krebs-bicarbonate buffer, with the exception of 12:0, which was solubilized in only Krebs-bicarbonate buffer. [^{3}H]Inulin was used as a nonabsorbable marker to correct for the adherent mucosal fluid volume.

(ii) Tissue preparation. Eight animals per treatment group were sacrificed by an intraperitoneal injection of Euthanyl® (sodium pentobarbitol, 240 mg/100 g body weight). The whole length of the intestine was rapidly removed and rinsed with 150 mL cold saline. The proximal third of the small intestine, beginning at the ligament of Treitz, was termed the jejunum, and the distal third was termed the ileum; the middle third was discarded. The intestine was opened along its mesenteric border, and pieces of the segment were cut and mounted as flat sheets in the transport chambers. A 5-cm piece of each segment of jejunum and ileum was gently scraped with a glass slide to determine the percentage of the

TABLE 2
Macronutrient Composition of the Semisynthetic Diets

Ingredient	Concentration (g/kg diet)
Fat[a,b]	200.00
Cornstarch	378.00
Casein	270.50
Nonnutritive fiber	80.00
Vitamin mix[c]	10.00
Mineral mix[d]	50.00
L-Methionine	2.50
Choline	2.75
Inositol	6.25

[a]Beef tallow was obtained from Canamera Foods (Edmonton, Alberta, Canada).
[b]Safflo® sunflower oil was obtained from Unico (Concord, Ontario, Canada).
[c]AOAC vitamin mix (Teklad Test Diets, Madison, WI) provided the following per kilogram of complete diet: 20,000 IU of vitamin A; 2,000 IU of vitamin D; 100 mg of vitamin E; 5 mg of menadione; 5 mg of thiamine-HCl; 8 mg of riboflavin; 40 mg of pyridoxine-HCl; 40 mg of niacin; 40 mg of pantothenic acid; 2000 mg of choline; 100 mg of myoinositol; 100 mg of *p*-aminobenzoic acid; 0.4 mg of biotin; 2 mg of folic acid; and 30 mg of vitamin B_{12}.
[d]The Bernhart Tomarelli mineral mix (General Biochemicals, Chagrin Falls, OH) was modified to provide 77.5 mg of Mn and 0.06 mg Se per kilogram of complete diet.

intestinal wall composed of mucosa. The chambers were placed in preincubation beakers containing oxygenated Krebs-bicarbonate buffer (pH 7.2) at 37°C, and the tissue disks were preincubated for 15 min to allow the tissue to equilibrate at this temperature. The rate of uptake of lipids was determined from the timed transfer of the transport chambers to the incubation beakers containing [^{3}H]inulin and ^{14}C-labeled probe molecules in oxygenated Krebs-bicarbonate (pH 7.2, 37°C). Preincubation and incubation chambers were mixed with circular magnetic bars at identical stirring rates, which were precisely adjusted using a strobe light. Stirring rates were reported as rpm. A stirring rate of 600 rpm was selected to achieve low effective resistance of the intestinal UWL (26,27).

(iii) Determination of uptake rates. After incubation of the disks in labeled solutions for 6 min, each experiment was terminated by removing the chamber and rinsing the tissue in cold saline for approximately 5 s. The exposed mucosal tissue was then cut out of the chamber with a circular steel punch, placed on a glass slide, and dried overnight in an oven at 55°C. The dry weight of the tissue was determined, and the tissue was transferred to a scintillation counting vial. The samples were saponified with 0.75 M NaOH, scintillation fluid was added, and radioactivity was determined by means of an external standardization technique to correct for variable quenching of the two isotopes (26).

The rates of uptake were determined as nmol·(100 mg mucosal tissue^{-1})·min^{-1}, nmol·(cm^{-2} serosal surface area)·min^{-1}, and nmol·(cm^{-2} mucosal surface area)·min^{-1}.

Morphology, protein, and messenger RNA analysis. (i) Tissue preparation. For Northern blotting, morphological analysis, and immunohistochemistry, a second group of animals was raised and sacrificed similarly as for the uptake studies. A 5-cm portion of proximal jejunum and distal ileum was quickly harvested following rinsing, snap-frozen in liquid nitrogen, and stored at –80°C for later mRNA isolation. The remaining intestine was opened along the mesenteric border. Two 1-cm pieces of each section were mounted on a styrofoam block and were preserved in 10% formalin for later paraffin block mounting to be used in the morphological and immunohistochemical analyses.

(ii) Morphological analysis. To determine the surface area of the intestine based on its 3-D architecture, a transverse and a vertical section were prepared for the jejunum and ileum. Hematoxylin-stained slides were prepared from paraffin blocks. Crypt depth and villous height, as well as villous width, depth, and density were measured. The measurements of villous height, villous width at half height, villous width at base, and crypt depth were obtained from vertical sections. The measurement of villous depth was obtained from transverse tissue sections. Group means were obtained based on 10 villi and 20 crypts per slide, with a minimum of 4 animals in each group. A published method was used to calculate the mucosal surface area (28,29). Mean values and SE of the mean were used for statistical analyses.

(iii) Immunohistochemistry. Jejunal and ileal tissues were embedded in paraffin, and 4–5-μm sections were mounted on glass slides. The sections were heated and placed immediately in the following solutions: xylene (3 × for 5 min each), absolute ethanol (3 × for 2 min each), 90% ethanol (1 min), and 70% ethanol (1 min), followed by a tap water rinse. Slides were incubated in hydrogen peroxide/methanol solution, rinsed, and counterstained with Harris hematoxylin (7.5%; Sigma Diagnostics, St. Louis, MO). Slides were then air-dried, and the tissue was encircled with hydrophobic slide marker (PAP pen; BioGenex, San Ramon, CA). Slides were rehydrated and then incubated for 15 min in blocking reagent (20% normal goat serum) followed by primary antibody to ILBP or I-FABP for 30 min. Slides were incubated in LINK® and LABEL® and working DAB® solution. Slides were washed, restained in hematoxylin, dehydrated in absolute ethanol, and cleared in xylene.

The slides were photographed, and the antibody density along the crypt-villous axis was determined by densitometry. The results were expressed as a ratio of density of the antibody-positive preparation vs. antibody-negative preparation. Statistical analyses were based on a minimum of 4 villi per animal and 3 animals per group.

(iv) RNA isolation. The intestinal pieces (minimum of 6 animals per group) were homogenized in a denaturing solution containing guanidinium thiocyanate, using a Fast Prep cell disruptor (Savant Instruments Inc., Holbrook, NY). After addition of 2 M sodium acetate, a phenol chloroform extraction was performed. The upper aqueous phase containing the RNA was collected. RNA was precipitated with isopropanol overnight at –80°C, with a final wash with 70% ethanol. The concentration and purity of RNA were determined by spectrophotometry at 260 and 280 nm. Samples were stored at –80°C.

(v) Preparation of probes for Northern blotting. DH5α bacteria were transformed and plasmid isolation was carried out using a Boehringer Mannheim High Pure Plasmid Isolation Kit. To make cDNA probes, the DNA insert was cut by two specific restriction enzymes (Life Technologies, Grand Island, NY). A digoxigenin (DIG)-labeled nucleotide (Roche Diagnostics, Québec, Canada) was incorporated during the *in vitro* DNA synthesis using the Klenow fragment of a DNA polymerase (Roche Diagnostics, Québec, Canada).

Fifteen (15) micrograms of total RNA was loaded and electrophoresed for 5 h at 100 V (HLB12 Complete Horizontal Long Bed Gel System; Tyler, Edmonton, Canada) in a denaturing agarose gel (1% agarose, 0.66 M formaldehyde gel). Capillary diffusion was used to transfer the RNA to a nylon membrane (Roche Molecular Biochemicals, Mannheim, Germany), and RNA was fixed to the membrane by baking at 80°C for 2 h. Membranes were hybridized with the DIG-labeled probe according to the manufacturer's protocol (Roche Diagnostics, Québec, Canada). Detection of the bound antibody was performed using CDP-STAR chemiluminescent substrate (Roche Diagnostics, Québec, Canada), and membranes were exposed to X-ray films (X-Omat; Kodak, Rochester, NY).

The density of the mRNA bands was determined by transmittance densitometry (model GS-670, imaging densitometer; Biorad Laboratory, Mississauga, Canada). Quantification of the 28 S ribosomal units from the membranes was used to account for possible loading discrepancies.

Expression of results. The results were expressed as mean ± SE of the mean, as determined using Lotus 1-2-3. To determine the effects of age, diet, and age × diet interactions, the data were analyzed using a two-way ANOVA ($P < 0.05$). Individual differences between ages were determined using a Student–Neuman–Keuls multiple range test. Statistical significance was accepted for values of $P \leq 0.05$.

RESULTS

Animal characteristics. In rats fed SFA or PUFA, the rate of body weight change fell between 1 and 9 and between 1 and 24 mon (Fig. 1). When examining body weight changes over the course of the study, 9- and 24-mon-old rats maintained their weights, whereas 1-mon-old rats gained weight over the 2-wk period, as expected (Fig. 2). At each age the PUFA diet was associated with greater weight gain than the SFA diet. Food intake was not influenced by the age of the rats, regardless of whether they were fed SFA or PUFA (data not shown). When food intake was expressed per gram body weight, 1-mon-old rats had significantly higher food intakes than did 9- or 24-mon-old rats (Fig. 3). In addition, 1-mon-old rats fed PUFA ate significantly more per gram body weight than did 1-mon-old animals fed SFA.

In the jejunum, neither age nor diet had an effect on the weight of the intestine, the weight of the intestinal mucosa, or the percentage of the intestinal wall comprised of mucosa (Table 3). In rats fed SFA, the ileal weight was higher at 9 and 24 mon when compared with 1 mon. In rats fed PUFA, the ileal weight was lower at 9 and 24 mon when compared with 1 mon. Therefore, the weight of the mucosa had to be taken into account when expressing the rate of uptake of the lipids.

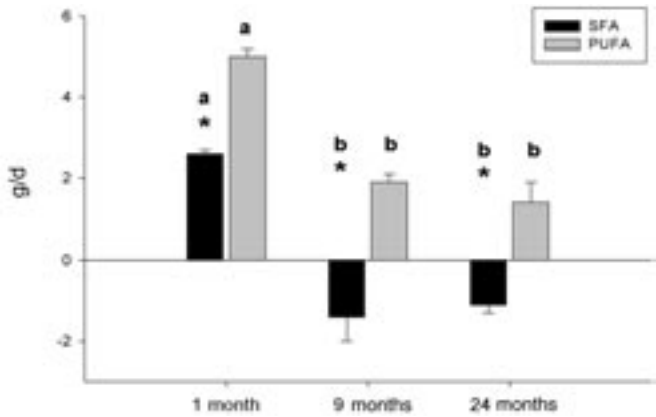

FIG. 1. Effect of age and dietary lipids on body weight change in Fischer 344 (F344) rats. Values are mean ± SEM. The data were analyzed using a two-way ANOVA. Different letters denote a significant age effect, and an asterisk (*) denotes a significant diet effect [saturated FA (SFA) vs. PUFA] ($P \leq 0.05$; $n = 14$). There was no significant age × diet interaction.

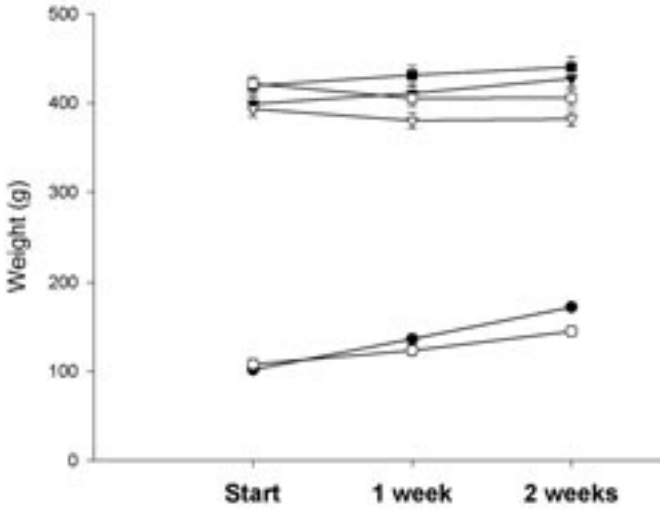

FIG. 2. Effect of age and diet on F344 rat body weights over time. (●, ▼, ■) PUFA-fed animals; (○, ▽, □) SFA-fed animals. Animals fed for 1 (●, ○), 9 (▼, ▽), and 24 mon (■, □). For abbreviations see Figure 1.

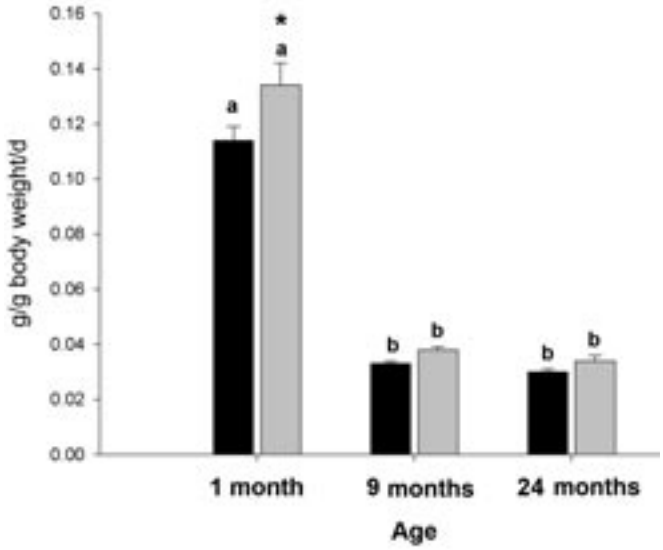

FIG. 3. Effect of age and dietary lipids on daily food intake per gram of body weight in F344 rats. Values are mean ± SEM. The data were analyzed using a two-way ANOVA. Different letters denote a significant age effect, and an asterisk (*) denotes a significant diet effect [SFA (solid bar) vs. PUFA (shaded bar)] ($P \leq 0.05$; $n = 14$). There was no significant age × diet interaction. For abbreviations see Figure 1.

There were no differences in the heights of the villi of the jejunum or ileum of rats aged 1, 9, or 24 mon (data not shown). In animals fed SFA, the jejunal and ileal mucosal surface areas were lower at 9 and 24 mon as compared with 1 mon (Fig. 4). In those fed PUFA, the jejunal surface area was lower at 24 as compared with 1 and 9 mon, and the ileal mucosal surface area was lower at 24 and 9 mon as compared with 1 mon. In the jejunum, diet had no effect on the mucosal surface area at 1, 9, or 24 mon. In contrast, in the ileum the surface area was lower in 1-mon-old animals fed PUFA as compared with SFA.

TABLE 3
Effect of Age[a] and Diet[b] on Intestinal Weights

	Tissue weight (mg/cm)	Mucosal weight (mg/cm)	% Mucosa
Jejunum			
1 mon			
SFA	8.8 ± 0.9	4.6 ± 0.7	51.7 ± 3.7
PUFA	10.1 ± 1.4	5.5 ± 0.9	55.0 ± 6.2
9 mon			
SFA	12.5 ± 0.5	6.3 ± 0.6	50.6 ± 3.7
PUFA	11.2 ± 0.8	5.9 ± 1.0	51.8 ± 6.2
24 mon			
SFA	13.6 ± 2.1	7.2 ± 1.5	51.4 ± 3.6
PUFA	10.5 ± 1.1	5.6 ± 0.8	51.2 ± 3.4
Ileum			
1 mon			
SFA	6.8 ± 0.6 a*	3.1 ± 0.5	45.6 ± 5.0
PUFA	9.4 ± 0.8 a	4.7 ± 0.7	49.9 ± 5.3
9 mon			
SFA	10.4 ± 1.9 b	5.6 ± 1.1	51.4 ± 3.6
PUFA	7.6 ± 1.1 b	3.9 ± 1.0	48.8 ± 5.4
24 mon			
SFA	8.5 ± 0.9 a	4.2 ± 0.7	49.3 ± 4.0
PUFA	5.4 ± 1.1 b	2.9 ± 0.7	42.8 ± 8.9

[a]Different letters denote a significant age effect ($P < 0.05$).
[b]An asterisk (*) denotes a significant diet effect (SFA vs. PUFA) ($P < 0.05$) ($n = 8$). For abbreviation see Table 1.

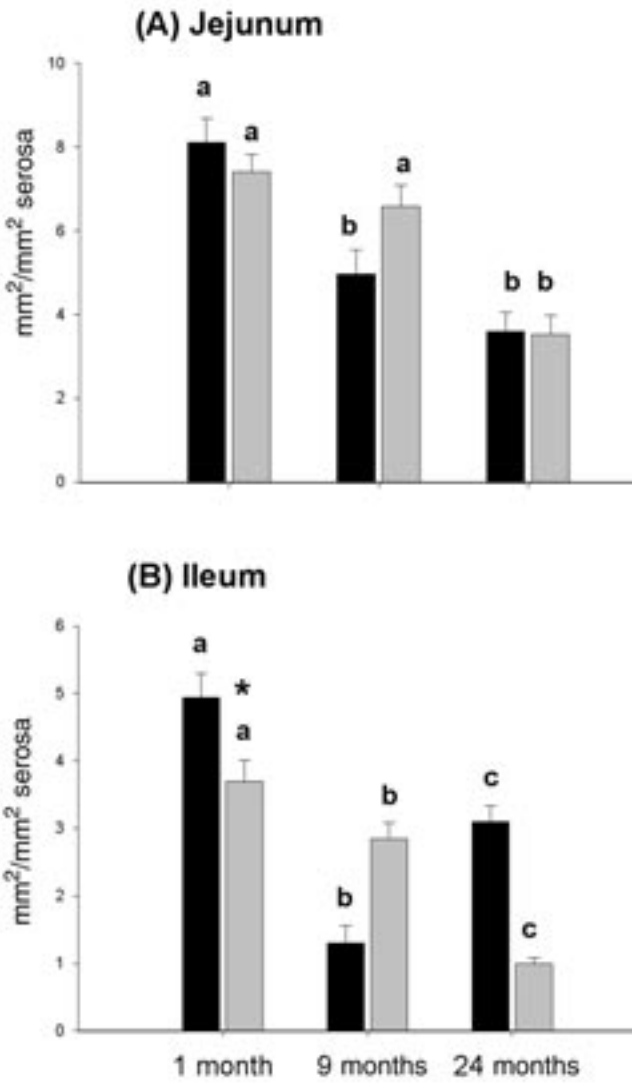

FIG. 4. Mucosal surface area of the small intestine in SFA- and PUFA-fed F344 rats. Values are mean ± SEM. The data were analyzed using a two-way ANOVA. Different letters denote a significant age effect, and an asterisk (*) denotes a significant diet effect [SFA (solid bar) vs. PUFA (shaded bar)] ($P \leq 0.05$; $n = 14$). There was no significant age × diet interaction. For abbreviations see Figure 1.

The rate of uptake was initially expressed on the basis of the weight of the mucosa (nmol·100 mg mucosal tissue^{-1}·min^{-1}) (Figs. 5, 6). In animals fed SFA, there was reduced jejunal uptake of 18:0 between 1 and 9 mon (Fig. 5). Feeding SFA was associated with reduced ileal uptake of 18:0 between 1 and 24 mon (Fig. 6). Feeding PUFA increased the ileal uptake of 18:3 between 1 and 24 mon. The ileal uptake of 18:3 was higher in PUFA than in SFA in 24-mon-old animals.

In rats fed SFA, the jejunal uptake of lauric acid (12:0) was not affected by age, whereas the ileal uptake of 12:0 was lower at 9 vs. 1 or 24 mon (data not shown). In animals fed PUFA, there was an increase in jejunal and ileal uptake of 12:0 between 24 and 1 or 9 mon.

Aging had no effect on lipid uptake in animals fed SFA or PUFA when expressed on the basis of serosal surface area (data not shown). Because the mucosal surface area of the intestine fell with age in animals fed SFA and PUFA (Fig. 4), the rate of uptake was also expressed on the basis of the mucosal surface area (nmol·cm^{-2}·min^{-1}). In animals fed SFA, there was increased jejunal uptake of 18:1 and cholesterol between 1 and 24 mon. In animals fed PUFA there was increased jejunal uptake of 18:2 at 24 mon when compared with 1 or 9 mon (Fig. 7). In the ileum of rats fed SFA, there was increased uptake of 18:0, 18:2, and cholesterol between 1 and 9 mon. In animals fed PUFA, there was increased ileal uptake of 16:0, 18:3, and cholesterol (Fig. 8). Only at 9 mon was the ileal uptake of cholesterol higher with SFA as compared with PUFA. Otherwise, at 24 mon the ileal uptake of 16:0, 18:3, and cholesterol was higher in PUFA than in SFA.

Intestinal lipid-binding proteins. In rats fed SFA, the expression of L-FABP mRNA in the jejunum was higher at 24 mon than at 1 or 9 mon (data not shown). ILBP mRNA expression in the ileum was not significantly affected by age in animals fed SFA or PUFA (data not shown). The abundance of ILBP protein was unaffected by age or by diet, and the abundance of I-FABP protein also was unaffected by age or by diet when measured by Western blot (data not shown). When the I-FABP protein abundance was examined using immunohistochemistry, jejunal I-FABP protein was not significantly affected by age or diet (Figs. 9, 11). In the ileum of SFA-fed animals, I-FABP protein increased at 24 mon compared with 9 mon.

The abundance of ILBP protein in the ileum as determined by immunohistochemistry was not affected by age or diet in SFA-fed animals but increased at 9 and 24 mon as compared with 1 mon in PUFA-fed animals. In 1-mon animals the

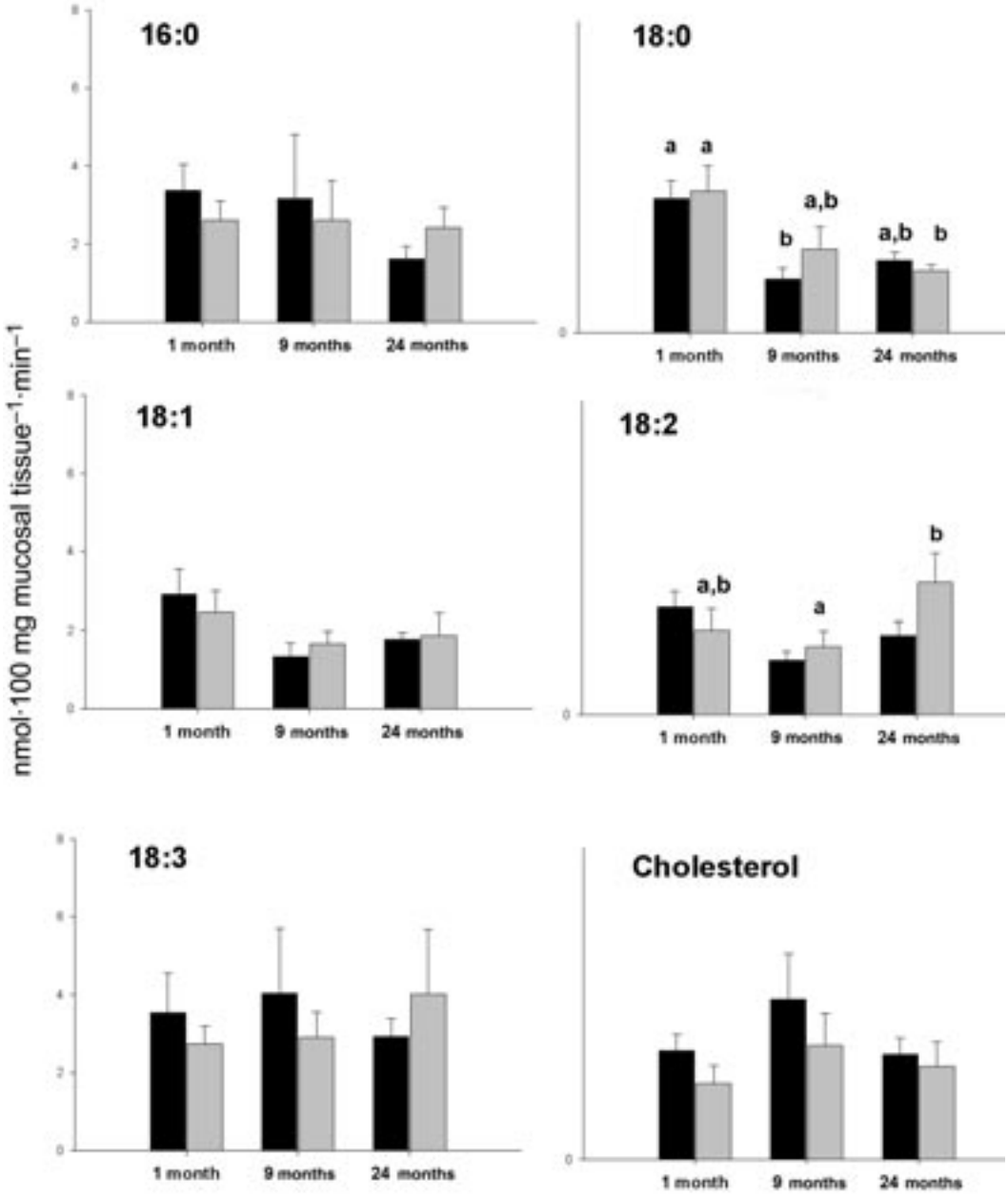

FIG. 5. Jejunal uptake of FA and cholesterol expressed as nmol·100 mg mucosal tissue^{-1}·min^{-1}. Values are mean ± SEM. The data were analyzed using a two-way ANOVA. Different letters denote a significant age effect ($P \leq 0.05$) ($n = 8$). There was no significant age × diet interaction. SFA, solid bars; PUFA, shaded bars. For abbreviation see Figure 1.

PUFA diet decreased the abundance of ILBP as compared with those fed SFA (Fig. 10).

DISCUSSION

Throughout the course of the 2-wk feeding period, 1-mon-old animals gained weight, as expected. Animals fed SFA, however, gained less weight than did animals fed PUFA (Fig. 1). The 9- and 24-mon-old animals fed SFA lost weight. The decline in body weight that typically begins at 18 mon in the F344 rat may represent a period of functional decline for the animal, marked by the onset of pathologies such as leukemia and pituitary adenoma (30). The PUFA diet influenced this period by preventing weight loss in older animals (Fig. 3). In senescence-accelerated mice a safflower-enriched diet (low n-3/n-6 ratio) increased mean life span from 357 to 426 d over perilla oil (high n-3/n-6 ratio)-fed animals. However, in the safflower-fed group, the incidence of tumors was higher, as were the serum total cholesterol, HDL cholesterol, TAG, and phospholipids levels (31). The short- and long-term effects of feeding a PUFA-enriched diet compared with a SFA-enriched diet on disease and life span in the F344 rat are not known.

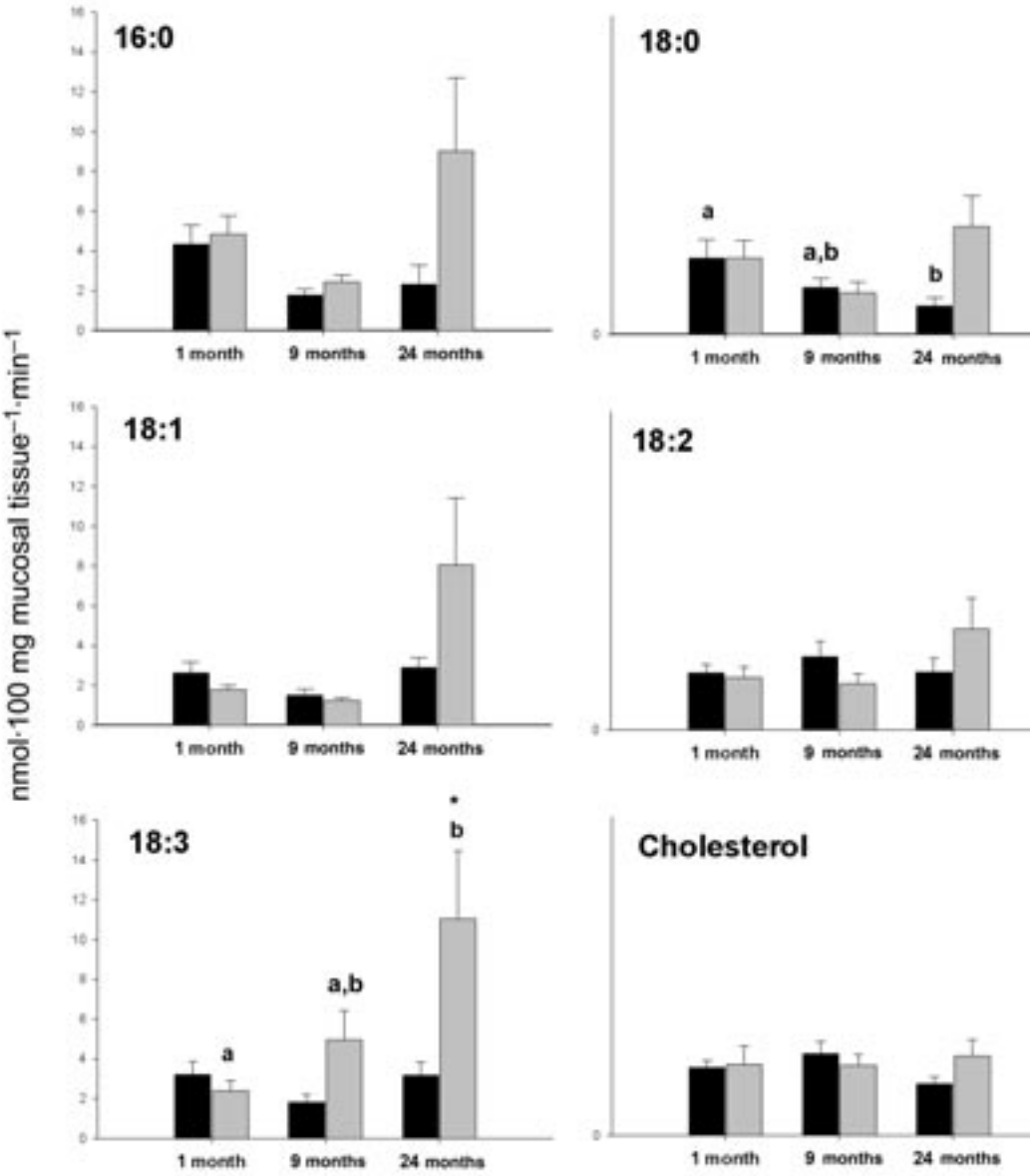

FIG. 6. Ileal uptake of FA and cholesterol expressed as nmol·100 mg mucosal tissue^{-1}·min^{-1}. Values are mean ± SEM. The data were analyzed using a two-way ANOVA. Different letters denote a significant age effect, and an asterisk (*) denotes a significant diet effect (SFA vs. PUFA) ($P \leq 0.05$) ($n = 8$). There was no significant age × diet interaction. SFA, solid bars; PUFA, shaded bars. For abbreviation see Figure 1.

However, the short-term feeding of a PUFA diet may provide a therapeutic option to mitigate weight loss associated with aging.

The simplest way of expressing the rate of *in vitro* uptake of nutrients is on the basis of the weight of the full thickness of the intestine. However, if a treatment alters the weight of the intestine (Table 3) or surface area of the intestine (Fig. 4), then there may be variations in the rate of nutrient uptake that are understandable in the light of there simply being more mucosal tissue or more surface area. For this reason, it is also appropriate to express uptake on the basis of these factors, rather than simply the weight of the intestinal wall. It is still possible, of course, that nutrient uptake may change without an alteration in the mucosal mass or villous surface area, with uptake adapting to a modification in the distribution of transporters along the villus or a variation in the BBM permeability. For example, aging is associated with a decline in the jejunal uptake of 18:0 when expressed on the basis of mucosal weight (Fig. 5), but is increased when expressed on the basis of mucosal surface area (Fig. 7). Thus, the interpretation of the influence of age on intestinal uptake of lipids depends on the method used to express the results.

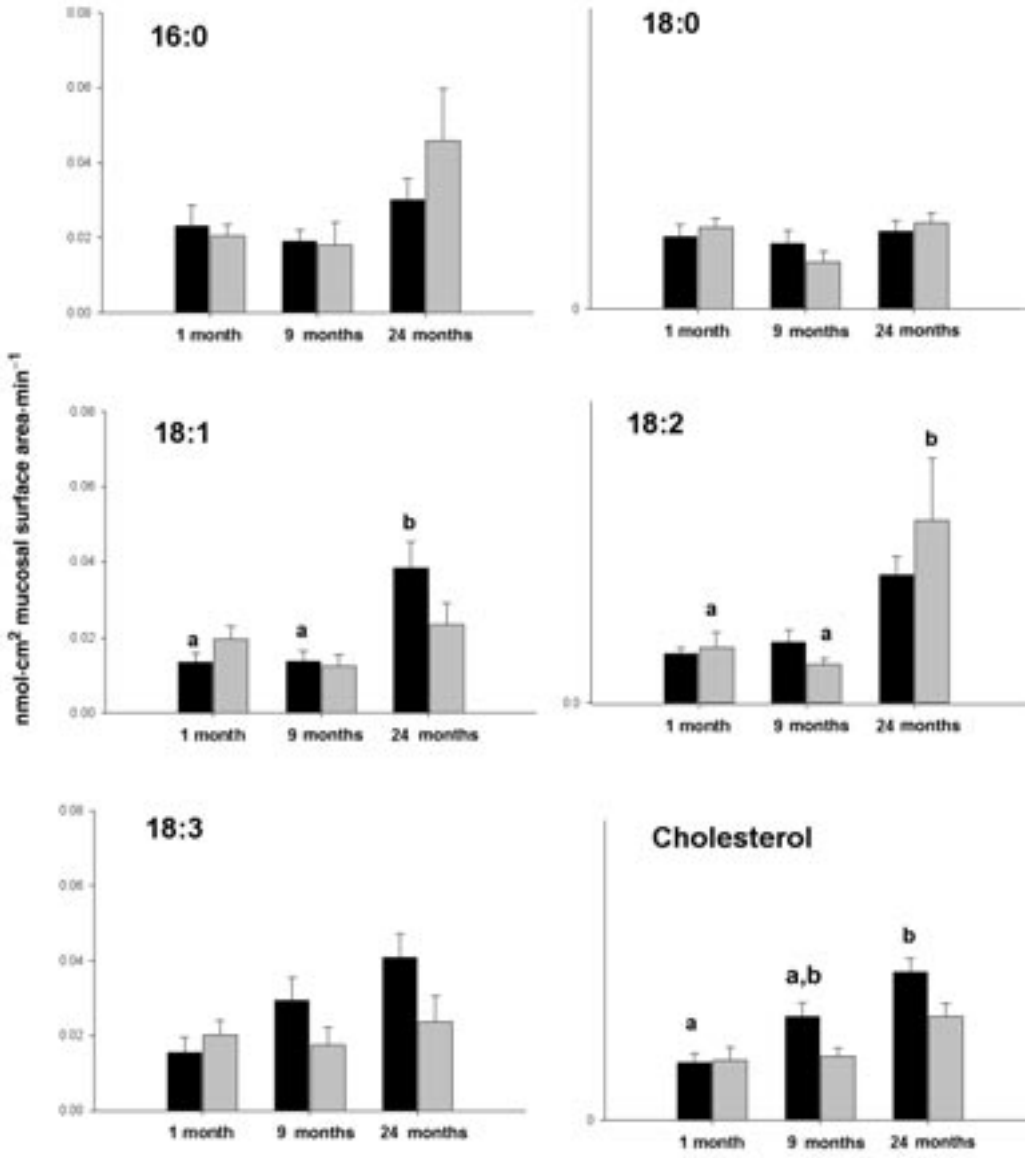

FIG. 7. Jejunal uptake of FA and cholesterol expressed on the basis of mucosal surface area. Values are mean ± SEM. The data were analyzed using a two-way ANOVA. Different letters denote a significant age effect ($P \leq 0.05$) ($n = 8$). There was no significant age × diet interaction. SFA, solid bars; PUFA, shaded bars. For abbreviation see Figure 1.

The passive uptake of lipids across the BBM may be affected by membrane fluidity and by the pH microenvironment adjacent to the BBM (13,32). Previous work suggests that the lipid composition of the BBM may contribute to alterations in lipid uptake (33). There is an age-associated decrease in BBM fluidity (14), which could contribute to the altered lipid absorption with aging. The low pH of the microenvironment adjacent to the BBM increases the bile acid critical-micellar concentration, resulting in a dissociation of lipids from bile acid micelles (13). In aging there is an increase in the pH of the microenvironment, which would contribute to reduced absorption in aging (34). Measurements of the pH of the microenvironment and the BBM composition were not analyzed in this study.

The uptake of 12:0 is a reflection of the effective resistance of the UWL, with higher uptake reflecting lower resistance (7,26). In PUFA-fed animals the uptake of 12:0 at 24 mon in the jejunum and ileum was higher than at 9 or 1 mon (data not shown), indicating lower UWL, and yet the uptake of most lipids except 18:0 was unchanged (Figs. 5, 6). This suggests that the age-associated alterations in lipid uptake could not be explained by alterations in UWL.

The reduced lipid absorption in aging (when expressed on the basis of mucosal weight) could not be explained by alterations in the protein abundance or mRNA expression of the lipid binding proteins. In I-FABP knockout mice, FA uptake is maintained, demonstrating that the I-FABP protein is not required for intestinal lipid uptake (35). In the jejunum of rats

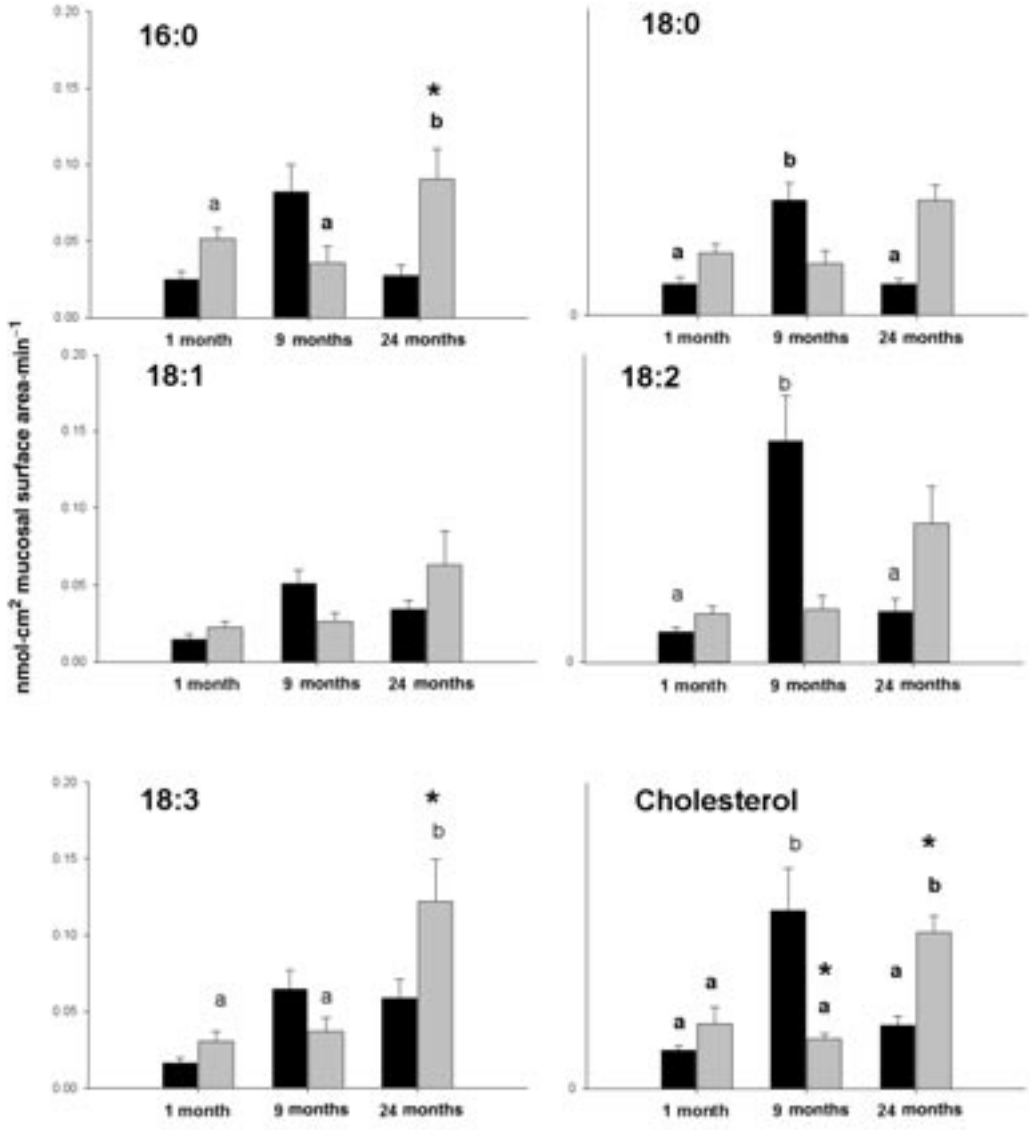

FIG. 8. Ileal uptake of FA and cholesterol expressed on the basis of mucosal surface area. Values are mean ± SEM. Different letters denote a significant age effect ($P \leq 0.05$), and an asterisk (*) denotes a significant diet effect (SFA vs. PUFA) ($P \leq 0.05$) ($n = 8$). There were significant age × diet interactions for 16:0, 18:0, 18:2, and cholesterol ($P < 0.05$). SFA, solid bars; PUFA, shaded bars. For abbreviation see Figure 1.

fed SFA or PUFA, the rate of uptake of 18:0 was reduced in the 24-mon group as compared with the 1-mon group (Fig. 5), yet the expression of L-FABP mRNA was increased in SFA but not in PUFA (data not shown), ILBP protein was increased in PUFA but not SFA (Fig. 10), and ILBP mRNA was unchanged (data not shown). Although we do not have data on I-FABP mRNA, in SFA jejunal I-FABP protein was unchanged (Fig. 9), whereas reductions in lipid uptake were observed in both the 9- and the 24-mon group as compared with the 1-mon group (Fig. 5). In the ileum, I-FABP protein was increased in SFA and was unchanged in PUFA and did not reflect changes in uptake. However, it is possible that dietary fat may influence the abundance of other lipid-binding proteins in the enterocyte, which may play a role in lipid uptake. Other proteins may also be key regulators of lipid absorption, such as the FATP-4 (16) or the FAT in the BBM of enterocytes (15). The mRNA expression of I-FABP and L-FABP is increased in rats fed a diet rich in polyunsaturated fats (21). The mechanism by which dietary lipids modulate lipid uptake may involve their effect on peroxisome proliferator-activated receptors (PPAR). PPAR can be activated by FA or FA derivatives (36). PUFA metabolites, such as eicosanoids, have a high affinity for PPARα, making them particularly potent activators of PPAR-dependent genes (37).

Once activated, PPAR regulate many genes involved in lipid metabolism and transport. FAT and FATP are regulated by PPAR agonists (38–40), and both I-FABP and L-FABP mRNA expression may be regulated by the PPARα activator

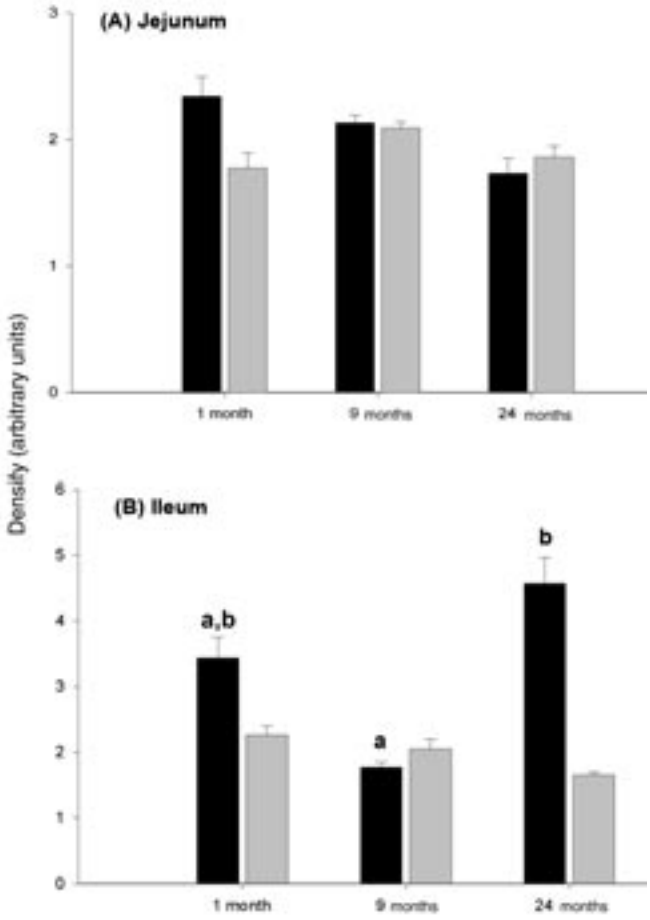

FIG. 9. Abundance of intestinal FA-binding protein (I-FABP) as determined by immunohistochemistry. Values are mean ± SEM. The data were analyzed using a two-way ANOVA. Different letters denote a significant age effect ($P \leq 0.05$) ($n = 3$). There was no significant age × diet interaction. SFA, solid bars; PUFA, shaded bars. For abbreviation see Figure 1.

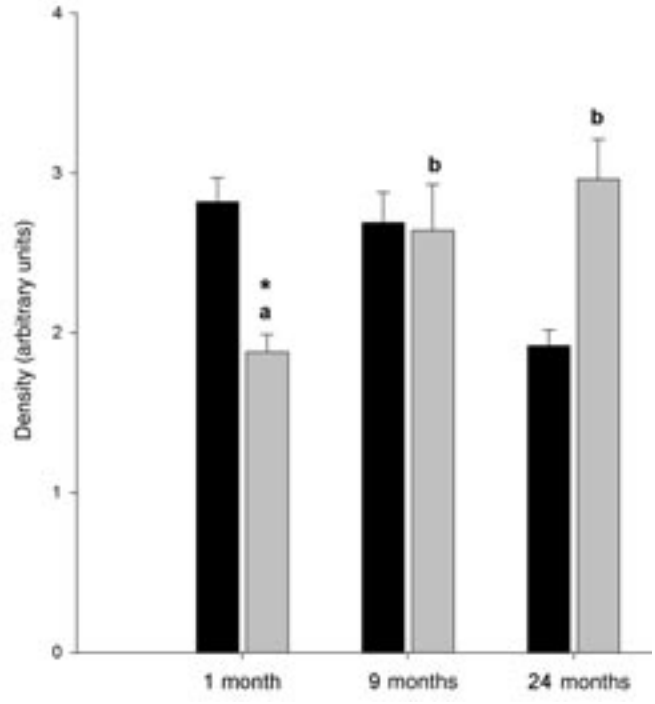

FIG. 10. Abundance of ileal lipid-binding protein as determined by immunohistochemistry. Values are mean ± SEM. The data were analyzed using a two-way ANOVA. Different letters denote a significant age effect, and an asterisk (*) denotes a significant diet effect (SFA vs. PUFA) ($P \leq 0.05$) ($n = 3$). There was no significant age × diet interaction. SFA, solid bars; PUFA, shaded bars. For abbreviation see Figure 1.

Wy14,643 (41). In this study we have not demonstrated differences in L-FABP mRNA levels in PUFA- when compared with SFA-fed rats. We may speculate that PUFA-induced changes in other lipid-binding proteins, such as I-FABP, FAT, or FATP, may explain the differences in uptake observed between PUFA- and SFA-fed animals.

It has also been suggested that the rate-limiting step in lipid absorption is the formation of a prechylomicron transport vesicle in the endoplasmic reticulum (42). Thus, we cannot dismiss the possibility that some lipid-binding proteins not assessed in this study may play some role in the control of lipid uptake in aging and in association with variations in dietary lipids.

Others have also suggested that the intestine of the older animal may be less capable of adapting in response to changes in the composition of the diet. (4,43,44). Previous work in young rats has shown an increase in the rate of uptake of lipids, cholesterol, and carbohydrates in animals fed an SFA-enriched diet (11,45). When uptake was expressed on the basis of mucosal weight, the uptake of lipids in 24-mon-old rats was similar in SFA- and PUFA-fed animals (Figs. 5, 6). When the rates of uptake were expressed on the basis of mucosal surface area, the ileal uptakes of 16:0, 18:3, and cholesterol were higher with PUFA than with SFA (Fig. 8). Thus, the older animals maintain the ability to modify lipid uptake in response to variations in the lipids in the diet. This may partially explain the lower weight loss in rats fed PUFA as compared with SFA (Fig. 1). Thus, the possible use of PUFA diets to reduce lipid uptake in younger animals may have the opposite effect on older rats. Clearly, the nature of intestinal adaptation observed in young rats does not necessarily apply in older animals. Future studies must determine whether the enhanced lipid uptake and body weight gain observed in older animals fed PUFA has any therapeutic benefit.

Aging is associated with changes in lipid uptake in the jejunum and ileum. However, the direction of these changes is dependent on the method used to calculate the uptake. Although the ileum does not compensate for the loss of function of the jejunum in aging, the ileum of old rats does demonstrate a higher degree of adaptive response to alterations in dietary fat than the jejunum. Old animals adapt differently to alterations in dietary fat compared with young animals, with a PUFA diet resulting in increased absorptive function in old animals and an SFA diet in increased absorption in younger animals. Changes in lipid uptake were not explained by the mRNA expression of L-FABP or ILBP. In aging, the reduced uptake of some dietary fats is associated with a concomitant

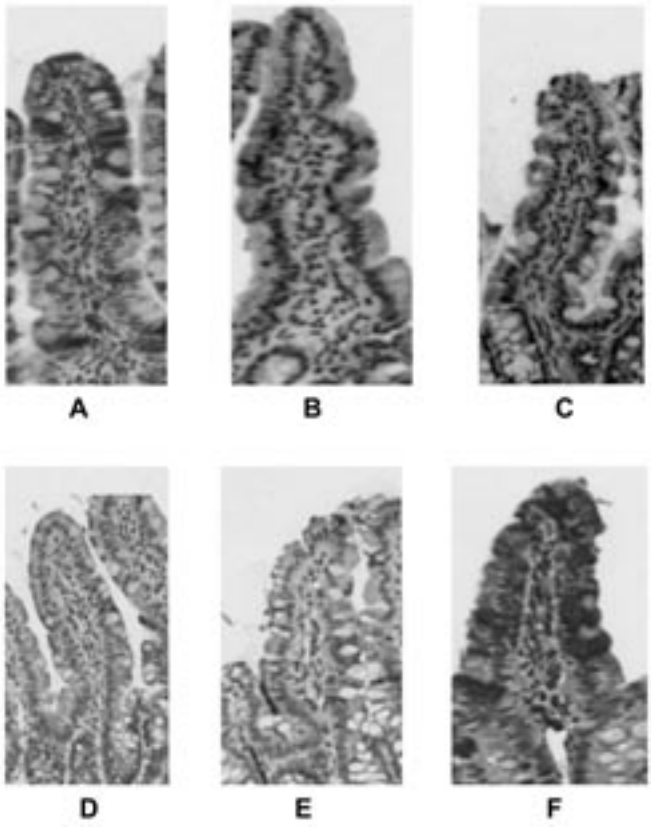

FIG. 11. Representative I-FABP immunohistochemistry. Ileal sections from PUFA-fed rats: (A) 1-mon-old, (B) 9-mon-old, and (C) 24-mon-old. Ileal sections from SFA-fed rats: (D) 1-mon-old, (E) 9-mon-old, and (F) 24-mon-old. For abbreviations see Figures 1 and 9.

decline in the abundance in ILBP. However, dietary fat influences the abundance of I-FABP and ILBP differently, without a clear correlation with changes in lipid uptake. It is speculated that aging and dietary fat may alter lipid uptake *via* alternative mechanisms.

REFERENCES

1. *Canada's Aging Population* (2002) Division of Aging and Seniors, Health Canada, Ottawa, Canada.
2. Halter, J.B. (1999) *Principles of Geriatric Medicine and Gerontology*, pp. 991–1011, McGraw-Hill, New York.
3. Morley, J.E. (1999) An Overview of Diabetes Mellitus in Older Persons, *Clin. Geriatr. Med. 15*, 211–223.
4. Ferraris, R.P., and Vinnakota, R.R. (1993) Regulation of Intestinal Nutrient Transport Is Impaired in Aged Mice, *J. Nutr. 123*, 502–511.
5. Chen, T.S., Currier, G.J., and Wabner, C.L. (1990) Intestinal Transport During the Life Span of the Mouse, *J. Gerontol. 45(4)*, B129–B133.
6. Scopasa, F., Wishart, J.M., Horowitz, M., Morris, H.A., and Need, A.G. (2004) Relation Between Calcium Absorption and Serum Calcitriol in Normal Men: Evidence for Age-Related Intestinal Resistance to Calcitriol, *Eur. J. Clin. Nutr. 58*, 264–269.
7. Thomson, A.B.R. (1980) Effect of Age on a Homologous Series of Saturated Fatty Acid into Rabbit Jejunum, *Am. J. Physiol. 239*, G363–G371.
8. Peachey, S.E., Dawson, J.M., and Harper, E.J. (1999) The Effect of Ageing on Nutrient Digestibility by Cats Fed Beef Tallow-, Sunflower Oil- or Olive Oil-Enriched Diets, *Growth Dev. Aging 63*, 61–70.
9. Woudstra, T. (2002) Aging and Intestinal Adaptation, M.Sc. Thesis, 119 pp., University of Alberta, Edmonton, Canada.
10. Ferraris, R.P., and Diamond, J.M. (1989) Specific Regulation of Intestinal Nutrient Transporters by Their Dietary Substrates, *Annu. Rev. Physiol. 51*, 125–141.
11. Thomson, A.B.R., Keelan, M., Clandinin, M.T., and Walker, K. (1986) Dietary Fat Selectively Alters Transport Proteins of Rat Jejunum, *J. Clin. Invest. 77*, 279–288.
12. Keelan, M., and Thomson, A.B.R. (2001) *Handbook of Nutrition in the Aged*, 3rd edn., pp. 275–295, CRC Press, Boca Raton, FL.
13. Shiau, Y.F. (1990) Mechanism of Intestinal Fatty Acid Uptake in the Rat: The Role of an Acidic Microclimate, *J. Physiol. 421*, 463–474.
14. Wahnon, R., Mokady, S., and Cogan, U. (1989) Age and Membrane Fluidity, *Mech. Ageing Dev. 50*, 249–255.
15. Abumrad, N.A., Park, J.H., and Park, C.R. (1984) Permeation of Long Chain Fatty Acid into Adipocytes, *J. Biol. Chem. 259*, 8945–8953.
16. Stahl, A., Hirsch, D.J., Gimeno, R.E., Punreddy, S., Ge, P., Watson, N., Patel, S., Kotler, M., Raimondi, A., Tartaglia, L.A., and Lodish, H.F. (1999) Identification of the Major Intestinal Fatty Acid Transport Protein, *Mol. Cell 4*, 299–308.
17. Agellon, L.B., Toth, M.J., and Thomson, A.B. (2002) Intracellular Lipid Binding Proteins of the Small Intestine, *Mol. Cell Biochem. 239*, 79–82.
18. Hallden, G., and Aponte, G.W. (1997) Evidence for a Role of the Gut Hormone PYY in the Regulation of Intestinal Fatty Acid-Binding Protein Transcripts in Differentiated Subpopulations of Intestinal Epithelial Cell Hybrids, *J. Biol. Chem. 272*, 12591–12600.
19. Hsu, K.T., and Storch, J. (1996) Fatty Acid Transfer from Liver and Intestinal Fatty Acid-Binding Proteins to Membranes Occurs by Different Mechanisms, *J. Biol. Chem. 271*, 13317–13323.
20. Bass, N.M., Manning, J.A., Ockner, R.K., Gordon, J.I., Seetharam, S., and Alpers, D.H. (1985) Regulation of the Biosynthesis of Two Distinct Fatty Acid-Binding Proteins in Rat Liver and Intestine. Influences of Sex Difference and of Clofibrate, *J. Biol. Chem. 260*, 1432–1436.
21. Poirier, H., Degrace, P., Noit, I., Benard, A., and Besnard, P. (1996) Localization and Regulation of the Putative Membrane Fatty Acid-Transporter (FAT) in the Small Intestine. Comparison with Fatty Acid-Binding Proteins (FABP), *Eur. J. Biochem. 238*, 368–373.
22. Lin, M.C., Gong, Y.Z., Geoghegan, K.F., and Wilson, F.A. (1991) Characterization of a Novel 14 kDa Bile Acid-Binding Protein from Rat Ileal Cytosol, *Biochim. Biophys. Acta 1078*, 329–335.
23. Kramer, W., Corsiero, D., Friedrich, M., Girbig, F., Stengelin, S., and Weyland, C. (1998) Intestinal Absorption of Bile Acids: Paradoxical Behaviour of the 14 kDa Ileal Lipid-Binding Protein in Differential Photoaffinity Labeling, *Biochem. J. 333 (Pt. 2)*, 335–341.
24. Sprott, R.L., and Ramirez, I. (1997) Current Inbred and Hybrid Rat and Mouse Models, *ILAR J. 38*, 104–109.
25. Coleman, G.L., Barthold, S.W., Osbaldiston, G.W., Foster, S.J., and Jonas, A.M. (1977) Pathological Changes During Aging in Barrier-Reared Fischer 344 Male Rats, *J. Gerontol. 32*, 258–278.
26. Lukie, B.E., Westergaard, H., and Dietschy, J.M. (1974) Validation of a Chamber That Allows Measurement of Both Tissue Uptake Rates and Unstirred Layer Thicknesses in the Intestine Under Conditions of Controlled Stirring, *Gastroenterology 67*, 652–661.
27. Westergaard, H., and Dietschy, J.M. (1976) The Mechanism

Whereby Bile Acid Micelles Increase the Rate of Fatty Acid and Cholesterol Uptake into the Intestinal Mucosal Cell, *J. Clin. Invest. 58*, 97–108.
28. Ecknauer, R., Vadakel, T., and Welper, T. (1982) Intestinal Morphology and Cell Production Rate in Aging Rats, *J. Gerontol. 37*, 151–155.
29. Keelan, M., Walker, K., and Thomson, A.B.R. (1985) Effect of Chronic Ethanol and Food Deprivation on Intestinal Villus Morphology and Brush Border Membrane Content of Lipid and Marker Enzymes, *Can. J. Physiol. Pharmacol. 63*, 1312–1320.
30. Turturro, A., Witt, W.W., Lewis, S., Hass, B.S., Lipman, R.D., and Hart, R.W. (1999) Growth Curves and Survival Characteristics of the Animals Used in the Biomarkers of Aging Program, *J. Gerontol. A Biol. Sci. Med. Sci. 54*, B492–B501.
31. Umezawa, M., Takeda, T., Kogishi, K., Higuchi, K., Matushita, T., Wang, J., Chiba, T., and Hosokawa, M. (2000) Serum Lipid Concentrations and Mean Life Span are Modulated by Dietary Polyunsaturated Fatty Acids in the Senescence-Accelerated Mouse, *J. Nutr. 130*, 221–227.
32. Higgins, C.F. (1994) Flip-flop. The Transmembrane Translocation of Lipids, *Cell 79*, 393–395.
33. Ikuma, M., Hanai, H., Kaneko, E., Hayashi, H., and Hoshi, T. (1996) Effects of Aging on the Microclimate pH of the Rat Jejunum, *Biochim. Biophys. Acta 1280*, 19–26.
34. Keelan, M., Cheeseman, C., Walker, K., and Thomson, A.B. (1986) Effect of External Abdominal Irradiation on Intestinal Morphology and Brush Border Membrane Enzyme and Lipid Composition, *Radiat. Res. 105*, 84–96.
35. Vassileva, G., Huwyler, L., Poirier, K., Agellon, L.B., and Toth, M.J. (2000) The Intestinal Fatty Acid Protein Is Not Essential for Dietary Fat Absorption in Mice, *FASEB J. 14*, 2040–2046.
36. Chinetti, G., Fruchart, J.C., and Staels, B. (2000) Peroxisome Proliferator-Activated Receptors (PPARs): Nuclear Receptors at the Crossroads Between Lipid Metabolism and Inflammation, *Inflamm. Res. 49*, 497–505.
37. Krey, G., Braissant, O., L'Horset, F., Kalkoven, E., Perroud, M., Parker, M.G., and Wahli, W. (1997) Fatty Acids, Eicosanoids, and Hypolipidemic Agents Identified as Ligands of Peroxisome Proliferator-Activated Receptors by Coactivator-Dependent Receptor Ligand Assay, *Mol. Endocrin. 11*, 779–791.
38. Martin, G., Schoonjans, K., Lefebvre, A.M., Staels, B., and Auwerx, J. (1997) Coordinate Regulation of the Expression of the Fatty Acid Transport Protein and Acyl-CoA Synthetase Genes by PPARα and PPARγ Activators, *J. Biol. Chem. 272*, 28210–28217.
39. Teboul, L., Febbraio, M., Gaillard, D., Amri, E.Z., Silverstein, R., and Grimaldi, P.A. (2001) Structural and Functional Characterization of the Mouse Fatty Acid Translocase Promoter: Activation During Adipose Differentiation, *Biochem. J. 360 (Pt. 2)*, 305–312.
40. Motojima, K., Passilly, P., Peters, J.M., Gonzalez, F.J., and Latruffe, N. (1998) Expression of Putative Fatty Acid Transporter Genes Are Regulated by Peroxisome Proliferator-Activated Receptor α and γ Activators in a Tissue- and Inducer-Specific Manner, *J. Biol. Chem. 273*, 16710–16714.
41. Motojima, K. (2000) Differential Effects of PPARα Activators on Induction of Ectopic Expression of Tissue-Specific Fatty Acid Binding Protein Genes in the Mouse Liver, *Int. J. Biochem. Cell Biol. 32*, 1085–1092.
42. Holt, P.R., and Balint, J.A. (1993) Effect of Aging on Intestinal Lipid Absorption, *Am. J. Physiol. 264*, G1–G6.
43. Mansbach, C.M., and Dowell, R. (2000) Effect of Increasing Lipid Loads on the Ability of the Endoplasmic Reticulum to Transport Lipid to the Golgi, *J. Lipid Res. 41*, 605–612.
44. Ferraris, R.P. (1997) Effect of Aging and Caloric Restriction on Intestinal Sugar and Amino Acid Transport, *Front. Biosci. 2*, 108–115.
45. Thomson, A.B.R., Keelan, M., Clandinin, M.T., Rajotte, R.V., Cheeseman, C.I., and Walker, K. (1987) Treatment of the Enhanced Intestinal Uptake of Glucose in Diabetic Rats with a Polyunsaturated Fatty Acid Diet, *Biochim. Biophys. Acta 905*, 426–434.

[Received February 21, 2003; accepted June 8, 2004]

CLA Isomers in Milk Fat from Cows Fed Diets with High Levels of Unsaturated Fatty Acids

Marius Collomb*, Robert Sieber, and Ueli Bütikofer

Agroscope Liebefeld-Posieux, Swiss Federal Research Station for Animal Production and Dairy Products (ALP), CH-3003 Berne, Switzerland

ABSTRACT: The concentrations of CLA isomers were determined by Ag^+-HPLC in the milk fat of cows fed a control diet consisting of hay *ad libitum* and 15 kg of fodder beets or this diet supplemented with oilseeds containing either high levels of oleic acid (rapeseed), linoleic acid (sunflower seed), or α-linolenic acid (linseed). Highly significant ($P \leq 0.001$) correlations were found between the daily intakes of oleic acid and the concentration of the CLA isomer *trans*-7,*cis*-9 in milk fat; of linoleic acid and the CLA isomers *trans*-10,*trans*-12, *trans*-9,*trans*-11, *trans*-8,*trans*-10, *trans*-7,*trans*-9, *trans*-10,*cis*-12, *cis*-9,*trans*-11, *trans*-8,*cis*-10, and *trans*-7,*cis*-9; and of α-linolenic acid and the CLA isomers *trans*-12,*trans*-14, *trans*-11,*trans*-13, *cis,trans*/*trans,cis*-12,14, *trans*-11,*cis*-13, and *cis*-11,*trans*-13. CLA concentrations were also determined in the milk fat of cows grazing in the lowlands (600–650 m), the mountains (900–1210 m), and the highlands (1275–2120 m). The concentrations of many isomers were highest in milk fat from the highlands, but only three CLA isomers (*cis*-9,*trans*-11, *trans*-11,*cis*-13, and *trans*-8,*cis*-10) showed a nearly linear increase with elevation. Therefore, these three CLA isomers, and particularly the CLA isomer *trans*-11,*cis*-13, the second-most important CLA in milk fat from cows grazing at the three altitudes, could be useful indicators of milk products of Alpine origin.

Paper no. L9439 in *Lipids 39,* 355–364 (April 2004).

Unsaturated FA (UFA) are generally converted in the rumen of the cow to saturated FA within a short time through ruminal biohydrogenation, but the extent of lipolysis and biohydrogenation in the rumen decreases with increasing amounts of substrate (1). Many *trans*-FA are found in the ruminal fluid (2) and milk fat (3), and these are believed to originate from double-bond migration or alternative pathways of biohydrogenation (4). These *trans* FA are precursors of CLA, a collective term for several conjugated isomers of linoleic acid (5–7).

CLA consists of a collection of positional and geometrical isomers of octadecadienoic acid, with conjugated double bonds ranging from 6,8 to 12,14. For every positional isomer, four geometric pairs of isomers are possible (i.e., *cis*,*trans*; *trans*,*cis*; *cis*,*cis*; and *trans*,*trans*). CLA therefore includes 28 positional and geometrical isomers, of which only *cis*-9, *trans*-11, *trans*-10,*cis*-12, and *trans*-9,*trans*-11 have thus far been proven to have biological activities (8–12). Individual CLA isomers have exhibited different biological activities in animal and cancer cell studies. For example, Corl *et al.* (9) showed that the *cis*-9,*trans*-11 CLA isomer can reduce cancer risk in rats, and Park *et al.* (10) reported that the *trans*-10,*cis*-12 isomer was more effective for the reduction of mouse body fat than the *cis*-9,*trans*-11 CLA isomer. The *trans*-10,*cis*-12 CLA isomer was also found to inhibit cell growth and secretion of insulin-like growth factor-II in Caco-2 cells (11). In addition, current studies show that a mixture of *trans,trans* CLA isomers, mainly composed of *trans*-10,*cis*-12 and *trans*-9,*trans*-11 isomers, exhibited stronger cytotoxicity against NCI-N87 gastric cancer cells than *cis,trans/trans,cis* CLA isomers by inhibiting proliferation and modulating arachidonic acid metabolism (12). These suggest that the biological activities of all individual CLA isomers must be evaluated.

The content of CLA in milk fat can vary widely (about 3 to 25 mg g^{-1} fat) (8,13–15). The underlying factors resulting in this variation are predominantly related to the diet, to the methods of raising ruminants (16), and also to animal variation (17,18). Feeding of rapeseed, soybean, or linseed oils (19,20); rapeseed press cake; full-fat rapeseed or oil-rich rapeseed cake (21); extruded soybeans and fish oil, fed alone or in combination (22); marine oils (23); or a patented high-fat diet (24) has been shown to increase the concentration of CLA in milk fat. Also, the milk fat of cows grazing in the Alps is extraordinarily rich in total CLA (19.20 to 28.70 mg g^{-1} fat) (13), which is also true for Alpine cheese (25). Collomb *et al*. (26) correlated the FA in milk fat with botanical families and individual plant species. The percentage of three species [*Leontodon hispidus, Lotus corniculatus (*and *alpina),* and *Trifolium pratense*] correlated positively with the concentrations of CLA and monounsaturated *trans* 18:1 FA in milk fat. In the majority of studies, only the *cis*-9,*trans*-11 and *trans*-10,*cis*-12 CLA isomers have been used, and only a few publications have dealt with the occurrence of other CLA isomers in milk (27–29). Our knowledge of the variation of isomer distribution in ruminant fat is therefore limited.

The aim of the present experiments was to evaluate variations in the distribution of CLA isomers in milk fat from cows fed either a control diet (CD) consisting of hay *ad libitum* and 15 kg of fodder beets or the CD supplemented with ground

*To whom correspondence should be addressed at Agroscope Liebefeld-Posieux, Swiss Federal Research Station for Animal Production and Dairy Products (ALP), Schwarzenburgstrasse 161, CH-3003 Berne, Switzerland. E-mail: marius.collomb@alp.admin.ch

Abbreviations: Ag^+-HPLC, silver-ion HPLC; CD, control diet (hay *ad libitum* and 15 kg fodder beets); DM, dry matter; LIN1 diet, CD supplemented with 1.0 kg of ground linseed; LIN1.4 diet, CD supplemented with 1.4 kg of ground linseed; RAP1 diet, CD supplemented with 1.0 kg of ground rapeseed; SFA, saturated FA; SUN1 diet, CD supplemented with 1.0 kg of ground sunflower seed; SUN1.4 diet, CD supplemented with 1.4 kg of ground sunflower seed; *t*VA, *trans* vaccenic acid; UFA, unsaturated FA.

oilseeds containing a high concentration of either oleic (rapeseed), linoleic (sunflower seed), or α-linolenic acid (linseed). In a second study, we analyzed the CLA isomer distribution in milk fat from cows grazing at three altitudes. Comparisons were made between the results obtained from the two studies.

MATERIALS AND METHODS

Aim and approach. The composition of the CLA isomers in deep-frozen milk fats (–20°C) originating from two previous studies (13,14,30,31) was analyzed using silver-ion HPLC (Ag^+-HPLC). GC results of the FA composition of these milk fats has already been published (13,14).

Briefly, the first study (14) dealt with the impact of a CD consisting of hay fed *ad libitum* and 15 kg of fodder beets supplemented with each of three ground oilseeds on the FA composition of the milk fat. Thirty-three cows of the breeds Red Holstein, Holstein, and Brown Swiss were included. All animals were fed the CD for 2 wk. From week 3 to 4, the cows were divided into three groups, and the CD was supplemented daily with either 1.0 kg of ground rapeseed (RAP1 diet) [0.92 kg dry matter (DM)], sunflower seed (SUN1 diet) (0.95 kg DM), or linseed (LIN1 diet) (0.87 kg DM). From week 5 to 6, the amount of either sunflower seed or linseed oil increased by 0.4 kg to 1.27 (SUN1.4 diet) or 1.24 kg DM d^{-1} (LIN1.4 diet), respectively. The diets were supplemented with a cereal mix and a protein concentrate based on the average milk yield, milk content, animal body weight, and feed intake of the previous week. Table 1 presents the concentrations of fat, the predominant UFA in the three oilseeds, and the daily intake of UFA in the diets of cows.

The second study (13,30,31) dealt with the impact on the FA composition of milk fat of the fodder plants on which cows grazed in the lowlands (600–650 m), mountains (900–1210 m), and highlands (1275–2120 m) of Switzerland (13). In this investigation, Simmental × Red Holstein cows (45 to 50 cows in the lowlands, four to six herds of 10 to 30 cows in the mountains, and 57 to 88 cows in the highlands) were included. Twelve observations per site were carried out on the three vegetation sites: two sites in the highlands (pooled into a single zone, since their FA compositions did not differ significantly), one site in the mountains, and one site in the lowlands over a period of 3.5 mon (from June to mid-September).

Sample selection. From the first study, we analyzed 10 milk fats from individual cows fed the CD and 10 milk fats from individual cows fed the CD supplemented with oilseeds (five variants) by Ag^+-HPLC. From the second study, 10 summer mixed milk fats from each of three altitudes were analyzed by the same method. In total, 90 milk fats were analyzed.

Sample treatment. The milk samples were centrifuged, and the resulting creams were churned at *ca.* 5°C (32). After the resulting molten butter had been filtered through a hydrophobic filter (Schleicher Schuell no. 597 HY 1/2), the pure milk fat was collected. Fat from cheese samples was extracted in accordance with an IDF standard. All milk fats were frozen and stored at −20°C until analysis.

Methods of analysis. (i) Methylation. The milk fat was dissolved in hexane, and the glycerides were transesterified to the corresponding FAME by a solution of potassium hydroxide in methanol in accordance with an ISO standard (33).

(ii) GC analysis. FAME were analyzed according to Collomb and Bühler (34) using an Agilent 6890 gas chromatograph equipped with an on-column injector and an FID. The FA were separated on a CP-Sil 88 capillary column (100 m × 0.25 mm i.d. × 0.20 μm; Varian BV, Middelburg, The Netherlands) and quantified using nonanoic acid as an internal standard. The results were expressed in absolute values, as milligrams of FA (and not as esters) per gram of fat.

(iii) Ag^+-HPLC analysis. The methyl esters of *cis*-9,*trans*-11 (98%), *trans*-10,*cis*-12 (98%), and technical-grade *cis*-9, *trans*-11 (75–78%) were obtained from Matreya Inc. (Pleasant Gap, PA). Other CLA isomers were synthesized by isomerization of the commercially available reference (technical grade) with I_2 (35). Identification of the CLA isomers was based on co-injection with a commercial reference material and synthesized CLA as well as by comparing the elution order of CLA isomers with the existing literature (27,35). CLA were analyzed by Ag^+-HPLC according to Rickert *et al.*

TABLE 1
Concentrations of Fat and of the Predominant Unsaturated FA of the Three Oilseeds, and Daily Intake in the Diets of Cows

	Ground rapeseed	Ground sunflower seed		Ground linseed	
FA	1.0 kg (RAP1)	1.0 kg (SUN1)	1.4 kg (SUN1.4)	1.0 kg (LIN1)	1.4 kg (LIN1.4)
Fat in oilseeds (g kg^{-1} DM)	513	551		388	
Predominant FA in oilseeds (g kg^{-1} fat)					
Oleic acid	**546.7**[a]	152.0		175.5	
Linoleic acid	179.5	**536.2**		142.1	
α-Linolenic acid	88.8	1.4		**466.3**	
Daily intake (g day^{-1} cow^{-1})					
Oleic acid	**258**	80	106	59	84
Linoleic acid	85	**281**	**375**	48	68
α-Linolenic acid	42	1	1	**157**	**224**

[a]Boldface type indicates the most important FA. RAP1, control diet (hay fed *ad libitum* and 15 kg of fodder beets) supplemented with 1.0 kg of ground rapeseed; SUN1, control diet supplemented with 1.0 kg of ground sunflower seed; SUN1.4, control diet supplemented with 1.4 kg of ground sunflower seed; LIN1, control diet supplemented with 1.0 kg of ground linseed; LIN1.4, control diet supplemented with 1.4 kg of ground linseed; DM, dry matter.

(36), as modified by Kraft *et al.* (27). The analysis was performed on an Agilent LC series 1100 equipped with a photodiode array detector using three ChromSpher 5 Lipids columns in series (stainless steel, 250 × 4.6 mm, 5 μm particle size; Chrompack, Middleburg, The Netherlands). The solvent consisted of UV-grade hexane with 0.1% acetonitrile and 0.5% ethyl ether (flow rate, 1 mL min^{-1}), prepared fresh daily. Ethyl ether was used to reduce the analysis time and minimize retention volume drift, which is a well-known problem encountered in working with Ag^+-HPLC. The column was pretreated daily by eluting it with 1% acetonitrile/hexane for 30–60 min prior to sample analysis. The usual injection volumes were 10–20 μL, representing <250 μg of lipids. The HPLC areas for *trans*-7,*cis*-9 + *trans*-8,*cis*-10 + *cis*-9,*trans*-11 were added and used for comparison with the peak area of the three isomers from the GC chromatogram. The results were expressed as absolute values in mg g^{-1} fat. The Ag^+-HPLC chromatogram is presented in Figure 1.

Statistical analysis. Principal component analysis, ANOVA, and pairwise comparisons of mean values with Fisher's LSD test were performed with Systat for Windows, version 9.0 (37).

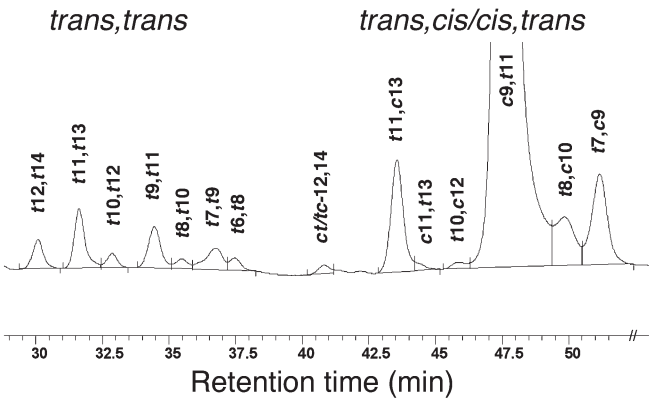

FIG. 1. Silver-ion-HPLC (Ag^+-HPLC) separation of CLA methyl esters of a milk fat using three columns in series.

RESULTS

Oleic, linoleic, α-linolenic and trans *FA in milk fat from cows fed CD or the CD supplemented with oilseeds.* The concentrations of oleic, linoleic, and α-linolenic acids and *trans*-FA in milk depended on the fat source fed (Table 2). The concentrations of most of the *trans*-FA generally increased in parallel with the daily intake of oleic, linoleic, or α-linolenic acid in the LIN1, RAP1, SUN1, LIN1.4, or SUN1.4 diet. At oilseed intakes of 1 kg, the highest concentration of *trans* 6–8 18:1 FA (3.00 mg g^{-1} fat) was found in milk fat from cows fed the oleic acid-rich RAP1 diet. Among the *trans* 18:1 isomers, the highest concentration was found for the combined *trans*-10/*trans*-11 FA (41.91 mg g^{-1} fat) in milk fat from cows fed the linoleic acid-rich SUN1.4 diet. Among the *trans* 18:2 isomers, the highest concentration was found for the combined *trans*-11,*cis*-15/*trans*-9,*cis*-12 18:2 FA (5.00 mg g^{-1} fat) in milk fat from cows fed the α-linolenic acid-rich LIN1.4 diet.

CLA isomers in milk fat from cows fed the CD or the CD supplemented with oilseeds. In milk fat from cows fed the α-linolenic acid-rich LIN1.4 diet, the highest concentrations (Table 3, bold) were found for the CLA isomers *trans*-12, *trans*-14 (0.31 mg g^{-1} fat), *trans*-11,*trans*-13 (0.48 mg g^{-1} fat), *cis,trans*/*trans,cis*-12,14 (0.34 mg g^{-1} fat), *trans*-11, *cis*-13 (0.47 mg g^{-1} fat), and *cis*-11,*trans*-13 (0.03 mg g^{-1} fat). From the LIN1 to the LIN1.4 diet, the concentrations of all these CLA isomers increased significantly ($P \leq 0.05$). The concentrations of the CLA isomers *trans*-12,*trans*-14, *cis,trans*/*trans,cis*-12,14 and *cis*-11,*trans*-13 did not change when the CD was supplemented with each of the other oilseeds rich in either oleic acid (RAP1) or linoleic acid (SUN1 or SUN1.4); no increases in the concentrations of the CLA isomers *trans*-11,*trans*-13 and *trans*-11,*cis*-13 were found when the RAP1 and SUN1 diets were fed.

In milk fat from cows fed the linoleic acid-rich SUN1.4 diet, the highest concentrations of CLA (Table 3, bold) were found for the isomers *trans*-10,*trans*-12 (0.17 mg g^{-1} fat), *trans*-9,*trans*-11 (0.17 mg g^{-1} fat), *trans*-8,*trans*-10 (0.05 mg g^{-1} fat), *trans*-7,*trans*-9 (0.08 mg g^{-1} fat), *trans*-10,*cis*-12

TABLE 2
Oleic, Linoleic, and α-Linolenic Acids and the Most Important *trans* FA in Milk Fat from Cows Fed the Control Diet (CD) or CD Supplemented with Oilseeds[a]

FA	CD	RAP1	SUN1	SUN1.4	LIN1	LIN1.4
18:1 *cis*-9	110.13 ± 16.25^{c}	**166.12** ± 18.79^{a}	160.62 ± 31.85^{a,b}	**175.80** ± 32.24^{a}	143.47 ± 12.73^{b}	**173.13** ± 26.64^{a}
18:2 *cis*-9,*cis*-12	16.19 ± 3.37^{b}	16.08 ± 3.17^{b}	**22.42** ± 4.23^{a}	**25.54** ± 3.98^{a}	14.61 ± 2.83^{b}	15.47 ± 1.83^{b}
18:3 *cis*-9,*cis*-12,*cis*-15	7.02 ± 1.06^{c}	7.29 ± 1.14^{c}	7.04 ± 1.06^{c}	7.19 ± 1.29^{c}	11.80 ± 2.09^{b}	**15.93** ± 2.45^{a}
18:1 *trans*-6–8	0.53 ± 0.14^{e}	3.00 ± 0.49^{b}	2.34 ± 0.55^{c}	**3.66** ± 0.53^{a}	1.45 ± 0.38^{d}	2.14 ± 0.39^{c}
18:1 *trans*-9	1.42 ± 0.14^{d}	3.42 ± 0.40^{b}	3.03 ± 0.53^{b}	**4.40** ± 0.73^{a}	2.24 ± 0.25^{c}	2.93 ± 0.35^{b}
18:1 *trans*-10–11	8.70 ± 1.55^{c}	16.00 ± 3.04^{c}	20.81 ± 4.01^{b}	**41.91** ± 7.71^{a}	13.57 ± 3.63^{c}	21.10 ± 3.40^{b}
18:1 *trans*-12	0.96 ± 0.15^{d}	2.95 ± 0.35^{c}	4.00 ± 1.01^{b}	**5.72** ± 0.83^{a}	2.54 ± 0.59^{c}	3.83 ± 0.61^{b}
18:1 *trans*-13–14 + *cis*-6–8	2.72 ± 0.33^{d}	6.63 ± 0.73^{c}	7.93 ± 1.72^{c}	10.48 ± 1.44^{b}	8.24 ± 1.85^{c}	**13.19** ± 2.25^{a}
18:1 *trans*-16+ *cis*-14	1.26 ± 0.22^{d}	3.06 ± 0.42^{c}	3.77 ± 0.82^{b}	**4.93** ± 0.83^{a}	3.65 ± 0.78^{b,c}	**5.29** ± 0.73^{a}
18:2 *cis*-9,*trans*-12 + *trans*-8,*cis*-13	1.78 ± 0.29^{d}	2.67 ± 0.18^{c}	3.09 ± 0.41^{b,c}	3.45 ± 0.53^{a,b}	2.90 ± 0.45^{c}	**3.75** ± 0.51^{a}
18:2 *cis*-9,*trans*-13 + *trans*-8,*cis*-12	0.98 ± 0.24^{c}	2.13 ± 0.30^{b}	2.48 ± 0.59^{b}	3.19 ± 0.79^{a}	2.39 ± 0.52^{b}	**3.77** ± 0.79^{a}
18:2 *trans*-11,*cis*-15 + *trans*-9,*cis*-12	0.87 ± 0.19^{c}	1.18 ± 0.18^{c}	1.25 ± 0.34^{c}	1.59 ± 0.26^{c}	2.47 ± 0.73^{b}	**5.00** ± 0.81^{a}

[a]Mean ± SD; n = 10 per treatment (values in mg g^{-1} fat). For diet descriptions, see Table 1. Boldface type indicates the highest mean values. $^{a–d}$Values in a row not sharing a common superscript roman letter differ significantly ($P \leq 0.05$).

TABLE 3
CLA Isomer Composition in Milk Fat from Cows Fed the Control Diet (CD) Supplemented with Rapeseed, Linseed, or Sunflower Seed[a]

18:2 CLA	CD	RAP1	SUN1	SUN1.4	LIN1	LIN1.4
Σ*trans/trans*	0.28 ± 0.04^{c}	0.35 ± 0.05^{c}	0.40 ± 0.06^{c}	0.65 ± 0.16^{b}	0.58 ± 0.11^{b}	**1.09** ± 0.21^{a}
12,14	0.03 ± 0.01^{c}	0.04 ± 0.01^{c}	0.03 ± 0.01^{c}	0.05 ± 0.02^{c}	0.13 ± 0.04^{b}	**0.31** ± 0.08^{a}
11,13	0.05 ± 0.01^{d}	0.09 ± 0.02^{c,d}	0.07 ± 0.02^{c,d}	0.12 ± 0.04^{c}	0.23 ± 0.06^{b}	**0.48** ± 0.11^{a}
10,12	0.05 ± 0.01^{c}	0.05 ± 0.01^{c}	0.09 ± 0.02^{b}	**0.17** ± 0.07^{a}	0.05 ± 0.02^{c}	0.06 ± 0.02^{c}
9,11	0.05 ± 0.01^{e}	0.07 ± 0.01^{d,e}	0.09 ± 0.02^{c}	**0.17** ± 0.05^{a}	0.08 ± 0.02^{c,d}	0.13 ± 0.03^{b}
8,10	0.03 ± 0.01^{b,c}	0.03 ± 0.01^{b,c}	0.04 ± 0.01^{b}	**0.05** ± 0.01^{a}	0.02 ± 0.01^{c}	0.03 ± 0.01^{b,c}
7,9	0.06 ± 0.01^{b}	0.06 ± 0.01^{b}	0.06 ± 0.01^{b}	**0.08** ± 0.02^{a}	0.06 ± 0.01^{b}	0.06 ± 0.01^{b}
6,8	0.02 ± 0.01	0.02 ± 0.01	0.01 ± 0.00	0.02 ± 0.01	0.01 ± 0.01	0.02 ± 0.01
Σ*cis,trans/trans,cis*	4.44 ± 1.16^{d}	6.41 ± 1.08^{c}	8.45 ± 1.65^{b}	**16.98** ± 3.10^{a}	5.68 ± 1.57^{c,d}	8.83 ± 1.99^{b}
12,14	0.02 ± 0.01^{c}	0.03 ± 0.01^{c}	0.03 ± 0.00^{c}	0.04 ± 0.01^{c}	0.12 ± 0.04^{b}	**0.34** ± 0.09^{a}
trans-11,*cis*-13	0.09 ± 0.03^{c}	0.11 ± 0.04^{c}	0.12 ± 0.06^{c}	0.21 ± 0.07^{b}	0.23 ± 0.11^{b}	**0.47** ± 0.11^{a}
cis-11,*trans*-13	0.01 ± 0.00^{c}	0.01 ± 0.00^{c}	0.01 ± 0.01^{c}	0.01 ± 0.01^{c}	0.02 ± 0.01^{b}	**0.03** ± 0.01^{a}
trans-10,*cis*-12	0.02 ± 0.01^{c}	0.03 ± 0.01^{c}	0.06 ± 0.01^{b}	**0.10** ± 0.03^{a}	0.02 ± 0.00^{c}	0.02 ± 0.01^{c}
cis-9,*trans*-11	4.07 ± 1.09^{c}	5.47 ± 0.98^{c}	7.46 ± 1.47^{b}	**15.46** ± 2.84^{a}	4.85 ± 1.35^{c}	7.37 ± 1.77^{b}
trans-8,*cis*-10	0.08 ± 0.02^{c}	0.11 ± 0.02^{c}	0.22 ± 0.06^{b}	**0.29** ± 0.08^{a}	0.12 ± 0.04^{c}	0.13 ± 0.04^{c}
trans-7,*cis*-9	0.16 ± 0.03^{e}	0.66 ± 0.10^{b}	0.56 ± 0.12^{c}	**0.88** ± 0.17^{a}	0.33 ± 0.08^{d}	0.49 ± 0.11^{c}
ΣCLA	4.72 ± 1.16^{d}	6.77 ± 1.10^{c}	8.84 ± 1.69^{b}	**17.63** ± 3.22^{a}	6.26 ± 1.62^{c,d}	9.92 ± 2.06^{b}

[a]Mean ± SD; n = 10 per treatment (values in mg g^{-1} milk fat). CLA are ordered according to increasing retention time. Boldface type indicates the highest mean values. [a–e]Values in a row not sharing a common superscript roman letter differ significantly ($P \leq 0.05$). For diet abbreviations see Table 1.

(0.10 mg g^{-1} fat), *cis*-9,*trans*-11 (15.46 mg g^{-1} fat), *trans*-8, *cis*-10 (0.29 mg g^{-1} fat), and *trans*-7,*cis*-9 (0.88 mg g^{-1} fat). From the SUN1 to the SUN1.4 diet, the concentrations of all these CLA isomers increased significantly ($P \leq 0.05$). Compared with the CD, no significant increases in the concentrations of the CLA isomers *trans*-10,*trans*-12, *trans*-8,*trans*-10, *trans*-10,*cis*-12, and *trans*-8,*cis*-10 were found in milk fat from cows fed each of the other oilseeds.

At oilseed intakes of 1 kg, the concentration of *trans*-7,*cis*-9 CLA was highest (0.66 mg g^{-1} fat) when the oleic acid-rich RAP1 diet was fed.

Compared with the CD, the concentration of the main CLA isomer in milk fat, *cis*-9,*trans*-11, increased significantly by 34% on the RAP1 diet, by 19% on the LIN1 diet, by 81% on the LIN1.4 diet, by 83% on the SUN1 diet, and by 280% on the SUN1.4 diet. When the diet was changed from SUN1 to SUN1.4, a 33% increase in the daily intake of linoleic acid (from 281 to 375 g; α-linolenic acid, 1 g) increased the total CLA content by 107% (from 7.5 to 15.5 mg g^{-1} fat).

Table 4 illustrates the significant, positive Pearson correlation coefficients ($P \leq 0.001$) found between the daily intake of oleic, linoleic, or α-linolenic acid from oilseeds and the concentrations of CLA isomers in milk fat. There were significant positive correlations ($P \leq 0.001$) between the daily intake of linoleic acid and the concentrations of the *trans*,*trans* CLA (*trans*-10,*trans*-12, *trans*-9,*trans*-11, *trans*-8, *trans*-10, and *trans*-7,*trans*-9) (Table 4, Fig. 2) and between the daily intakes of α-linolenic acid and the concentrations of the *trans*-12,*trans*-14 and *trans*-11,*trans*-13 CLA. By contrast, the correlations between the daily intake of oleic acid and the *trans,trans* CLA isomers were not significant.

For the *cis,trans*/*trans,cis* CLA, significant positive correlations ($P \leq 0.001$) were also found between the daily intake of linoleic acid and the concentrations of the *trans*-10,*cis*-12, *cis*-9,*trans*-11, *trans*-8,*cis*-10, and *trans*-7,*cis*-9 isomers in milk fat (Table 4, Fig. 3) and between the daily intake of α-linolenic acid and the concentrations of the *cis,trans*/*trans*, *cis*-12,14, *trans*-11,*cis*-13, and *cis*-11,*trans*-13 isomers in milk fat. Only the correlation between the daily intake of oleic acid and the *trans-7,cis-9* CLA isomer was significant.

The two biplots (Figs. 2 and 3) also show excellent discrimination between the *trans,trans* or *cis,trans*/*trans,cis* CLA in the milk fat of the different diets.

Oleic, linoleic, and α-linolenic acids and trans *FA in the milk fat from cows grazing at three altitudes*. The concentrations of oleic, linoleic, and α-linolenic acids and of most *trans* 18:1 FA were highest in the milk fat from cows grazing in the mountains or the highlands (Table 5). Among the *trans* 18:1 isomers, the *trans*-10–11 were the most abundant FA (50.12

TABLE 4
Significant Positive Pearson Correlation Coefficients ($P \leq 0.001$) Between the Daily Intake of Oleic, Linoleic, or α-Linolenic Acid (values in g day^{-1} cow^{-1}) from an Oilseed and the Concentration of CLA in Milk Fat (values in mg g^{-1} fat)

18:2 CLA	Oleic acid	Linoleic acid	α-Linolenic acid
trans/trans	—	—	—
12,14	—	—	0.88
11,13	—	—	0.89
10,12	—	0.78	—
9,11	—	0.58	—
8,10	—	0.60	—
7,9	—	0.47	—
6,8	—	—	—
cis,trans/trans,cis	—	—	—
12,14	—	—	0.88
trans-11,*cis*-13	—	—	0.76
cis-11,*trans*-13	—	—	0.74
trans-10,*cis*-12	—	0.89	—
cis-9,*trans*-11	—	0.81	—
trans-8,*cis*-10	—	0.85	—
trans-7,*cis*-9	0.57	0.74	—

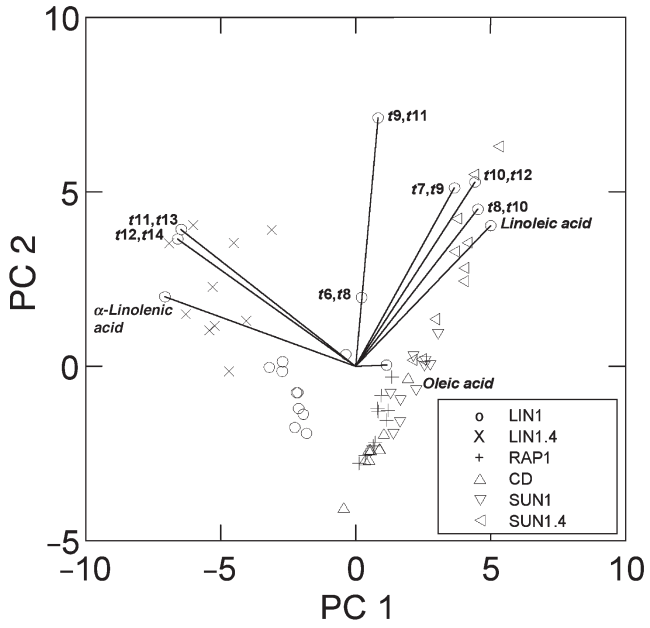

FIG. 2. Correlations between the daily intake of oleic acid, linoleic acid, and α-linolenic acid and the *trans,trans* CLA isomers in milk fat. The first principal component (PC 1) explained 39% of the total variance, and the second principal component (PC 2) explained 28%.

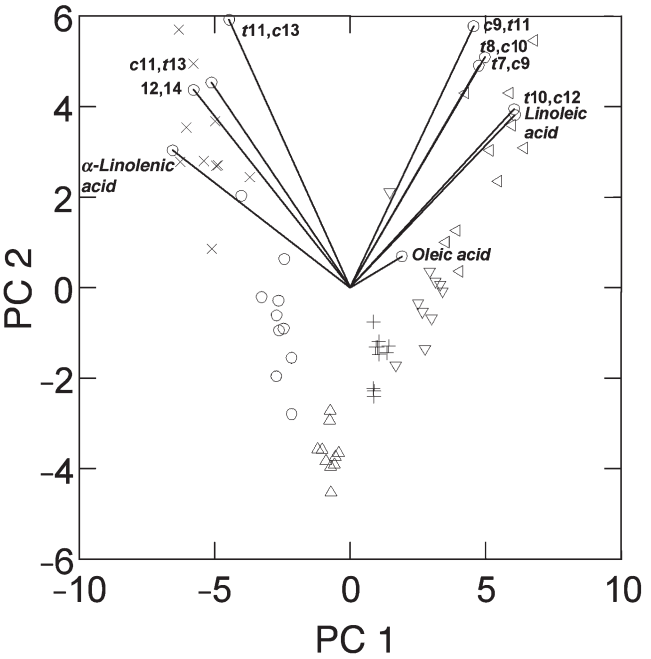

FIG. 3. Correlations between the daily intake of oleic acid, linoleic acid, and α-linolenic acid and the *cis,trans/trans,cis* CLA isomers in milk fat. The first principal component (PC 1) explained 46% of the total variance and the second principal component (PC 2) explained 35%. For symbols see Figure 2.

mg g^{-1} fat) in milk fat from the highlands. The concentrations of all the *trans* 18:2 FA were also highest in milk fat from the highlands. Among the *trans* 18:2 isomers, *trans*-11,*cis*-15/*trans*-9,*cis*-12 was the most abundant (7.32 mg g^{-1} fat) in milk fat from the highlands.

CLA isomers in the milk fat from cows fed grass at different altitudes. The milk fat of cattle at three different altitudes showed many significant differences in the concentrations of CLA isomers. In the milk fat from cows grazing in the mountains, the highest concentrations (Table 6, bold) were found for the CLA isomers *trans*-10,*trans*-12 (0.07 mg g^{-1} fat), *trans*-8,*trans*-10 (0.04 mg g^{-1} fat), *trans*-7,*trans*-9 (0.09 mg g^{-1} fat), *trans*-6,*trans*-8 (0.04 mg g^{-1} fat), *trans*-10,*cis*-12 (0.03 mg g^{-1} fat), and *trans*-7,*cis*-9 (0.51 mg g^{-1} fat). In milk fat from the highlands, the predominant CLA isomers were *trans*-12,*trans*-14 (0.23 mg g^{-1} fat), *trans*-11,*trans*-13 (0.46 mg g^{-1} fat), *trans*-9,*trans*-11 (0.13 mg g^{-1} fat), *trans*-7,*trans*-9 (0.09 mg g^{-1} fat), *cis,trans*/*trans,cis*-12,14 (0.07 mg g^{-1} fat), *trans*-11,*cis*-13 (1.75 mg g^{-1} fat), *cis*-11,*trans*-13 (0.04 mg g^{-1} fat), *cis*-9,*trans*-11 (21.33 mg g^{-1} fat), *trans*-8,*cis*-10 (0.31 mg g^{-1} fat), and *trans*-7,*cis*-9 (0.49 mg g^{-1} fat) (Table 6). The concentrations of the CLA isomers *trans*-7,*trans*-9 and *trans*-7,*cis*-9 were similar in milk fat from the mountains and the highlands and significantly higher than in milk fat from the lowlands. In the milk fat from cows grazing at the three altitudes, the *cis*-9,*trans*-11 and *trans*-11,*cis*-13 CLA isomers were the most abundant among the *cis,trans*/*trans,cis* isomers, and the *trans*-11,*trans*-13 isomer was the most abundant isomer among the *trans,trans* CLA. For the SD of the mean, the values obtained in mixed milks from this study (Table 6) were generally lower than those found in individual milks from the first study (Table 3).

The concentrations of many CLA isomers were highest in milk fat from the mountains or highlands. However, three of these isomers (*cis*-9,*trans*-11, *trans*-11,*cis*-13, and *trans*-8, *cis*-10) exhibited a nearly linear increase in concentration from the lowlands to the highlands as a function of altitude. Compared with the lowlands, the concentration of the *cis*-9, *trans*-11 CLA in milk fat from cows grazing in the mountains increased by 81%; in milk fat from cows grazing in the highlands it increased by 175%. The concentration of the *trans*-11, *cis*-13 CLA (the second-most important CLA isomer in milk fat from cows grazing at different altitudes) increased by 88% in milk fat from the mountains and by 310% in milk fat from the highlands.

DISCUSSION

Different studies have shown the influence of fodder on the concentration of CLA in milk, but only a few have analyzed the different isomers using Ag^+-HPLC (27–29).

Oleic acid in the fodder and CLA in the milk fat. In the first study, with oilseed intakes of 1 kg, the high concentration of the combined *trans*-6–8 18:1 FA (3.00 mg g^{-1} fat) (Table 2) in milk fat from cows fed the oleic acid-rich RAP1 diet (Table 1) was probably due to the increase in the concentration of *trans*-7 18:1 FA. Indeed, the daily intake of oleic acid correlated significantly with the concentration of the CLA isomer *trans*-7,*cis*-9 in milk (Table 4). It is also well known that oleic acid from fodder in the rumen is either not hydrogenated (38), is isomerized to *trans* 18:1 FA with double bonds at positions

TABLE 5
Oleic, Linoleic, and α-Linolenic Acids and the Most Important *trans* FA in Milk Fat from Cows Grazing at Different Altitudes

FA	Lowlands	Mountains	Highlands
18:1 *cis*-9	168.60 ± 15.49[b]	**193.60** ± 9.01[a]	175.34 ± 15.14[b]
18:2 *cis*-9,*cis*-12	11.78 ± 1.39[b]	**13.70** ± 0.88[a]	**13.75** ± 1.23[a]
18:3 *cis*-9,*cis*-12,*cis*-15	8.29 ± 1.63[b]	8.34 ± 0.44[b]	**12.34** ± 1.32[a]
18:1 *trans*-6–8	1.26 ± 0.22[c]	**2.05** ± 0.33[a]	1.85 ± 0.28[b]
18:1 *trans*-9	2.37 ± 0.26[c]	**3.46** ± 0.66[a]	2.92 ± 0.36[b]
18:1 *trans*-10–11	21.50 ± 2.44[c]	36.00 ± 3.08[b]	**50.12** ± 4.94[a]
18:1 *trans*-12	2.27 ± 0.26	2.26 ± 0.24	2.28 ± 0.38
18:1 *trans*-13–14 + *cis*-6–8	**7.51** ± 0.77[a]	5.98 ± 0.67[b]	**6.69** ± 0.96[a]
18:1 *trans*-16 + *cis*-14	3.79 ± 0.46[b]	3.61 ± 0.25[b]	**4.04** ± 0.44[a]
18:2 *cis*-9,*trans*-12 + *trans*-8,*cis*-13	2.75 ± 0.25[b]	2.75 ± 0.11[b]	**3.09** ± 0.21[a]
18:2 *cis*-9,*trans*-13 + *trans*-8,*cis*-12	2.49 ± 0.30[b]	2.35 ± 0.16[b]	**3.01** ± 0.40[a]
18:2 *trans*-11,*cis*-15 + *trans*-9,*cis*-12	3.38 ± 0.36[c]	4.29 ± 0.42[b]	**7.32** ± 1.56[a]

[a]Mean ± SD; $n = 10$ per altitude (values in mg g^{-1} fat). [a–c]Values in a row not sharing a common superscript roman letter differ significantly ($P \leq 0.05$). Boldface type indicates the highest mean values. Lowlands, 600–650 m; mountains, 900–1210 m; highlands, 1275–2120 m.

6–16 of the carbon chain, or is hydrogenated directly to stearic acid (39). Through the use of two different inhibitors of Δ^9-desaturase, Corl *et al.* (5) demonstrated that the *trans*-7, *cis*-9 CLA in milk fat originated almost exclusively *via* endogenous synthesis by Δ^9-desaturase with ruminally derived *trans*-FA; consistent with this result, the CLA isomer *trans*-7, *cis*-9 was not present in the ruminal fluid and was present in only small quantities in the duodenal flow (28). However, Secchiari *et al.* (29) found practically the same high concentrations (1.10 and 1.13 mg g^{-1} fat, respectively) of this CLA isomer when feeding either an olive oil soap that was rich in oleic acid (oleic acid: 38.7 g 100 g^{-1}; linoleic acid: 19.6 g 100 g^{-1} FA) or full-fat extruded soybeans that contained less oleic acid (oleic acid: 22.0 g 100 g^{-1} FA; linoleic acid: 48.9 g 100 g^{-1} FA). The biohydrogenation of linoleic acid in the soybeans into oleic acid in the rumen is certainly the cause of the nondifferentiated concentration of the CLA isomer *trans*-7, *cis*-9. Figure 4 illustrates the metabolic pathway for the formation of the *trans*-7,*cis*-9 CLA and for other CLA.

TABLE 6
CLA Isomer Composition of Milk Fat from Cows Fed Grass at Different Altitudes[a]

18:2 CLA	Lowlands	Mountains	Highlands
Σ *trans/trans*	0.82 ± 0.08[b]	0.83 ± 0.04[b]	**1.03** ± 0.09[a]
12,14	0.15 ± 0.02[b]	0.15 ± 0.01[b]	**0.23** ± 0.04[a]
11,13	0.38 ± 0.06[b]	0.32 ± 0.03[c]	**0.46** ± 0.05[a]
10,12	0.07 ± 0.01[b]	**0.07** ± 0.01[a]	0.06 ± 0.01[c]
9,11	0.11 ± 0.01[b]	0.11 ± 0.08[b]	**0.13** ± 0.01[a]
8,10	0.02 ± 0.00[c]	**0.04** ± 0.00[a]	0.03 ± 0.01[b]
7,9	0.07 ± 0.01[b]	**0.09** ± 0.01[a]	**0.09** ± 0.01[a]
6,8	0.02 ± 0.01[c]	**0.04** ± 0.01[a]	0.03 ± 0.01[b]
Σ *cis,trans/trans,cis*	8.74 ± 1.14[c]	15.68 ± 1.93[b]	**24.01** ± 2.76[a]
12,14	0.07 ± 0.01[a]	0.05 ± 0.01[b]	**0.07** ± 0.01[a]
trans-11,*cis*-13	0.43 ± 0.08[c]	0.80 ± 0.08[b]	**1.75** ± 0.42[a]
cis-11,*trans*-13	0.02 ± 0.00[b]	0.02 ± 0.00[b]	**0.04** ± 0.00[a]
trans-10,*cis*-12	0.03 ± 0.01[b]	**0.03** ± 0.00[a]	0.02 ± 0.01[c]
cis-9,*trans*-11	7.77 ± 1.05[c]	14.06 ± 1.79[b]	**21.33** ± 2.35[a]
trans-8,*cis*-10	0.13 ± 0.02[c]	0.21 ± 0.02[b]	**0.31** ± 0.05[a]
trans-7,*cis*-9	0.31 ± 0.05[b]	**0.51** ± 0.06[a]	**0.49** ± 0.05[a]
Σ CLA	9.57 ± 1.19[c]	16.50 ± 1.94[b]	**25.05** ± 2.78[a]

[a]Mean ± SD; $n = 10$ per altitude (values in mg g^{-1} milk fat). Boldface type indicates the highest mean values. [a–c]Values in a row not sharing a common superscript roman letter differ significantly ($P \leq 0.05$). For description of altitudes, see Table 5.

In the second study, the concentration of the *trans*-6–8 18:1 FA (Table 5) was significantly higher in milk fat from the mountains and highlands (2.05 and 1.85 mg g^{-1} fat, respectively) than in the lowlands (1.26 mg g^{-1} fat), in accordance with a similar increase in the concentration of the CLA isomer *trans*-7,*cis*-9 (Table 6).

Linoleic acid in the fodder and CLA in the milk fat. In the first study, the concentration of the *trans*-10–11 FA was highest in milk fat from cows fed the linoleic acid-rich SUN diets (SUN1 diet: 20.81; SUN1.4 diet: 41.91 mg g^{-1} fat) (Table 2), whereas in the second study, it was highest in milk fat from cows grazing in the highlands (50.12 mg g^{-1} fat) (Table 5). A strong positive correlation between the *trans* isomers of 18:1 [*trans* vaccenic acid (*t*VA), *trans*-13–14, *trans*-15, and *trans*-16] in milk fat and the level of linoleic acid in the diet was first found by Loor *et al.* (40). The latter compound is first isomerized to the CLA *cis*-9,*trans*-11 by *cis*-9,*trans*-11 isomerase and then hydrogenated by *Butyrivibrio fibrisolvens* to *t*VA in the rumen (41) (Fig. 4). These initial steps occur rapidly. The hydrogenation of *t*VA to stearic acid appears to involve a different group of organisms and occurs at a slow rate (42). For this reason, *t*VA typically accumulates in the rumen. This FA is also mainly present in the duodenal flow of lactating cows (28). It is well known that this main *trans* FA is responsible for the formation of the CLA isomer *cis*-9, *trans*-11, which occurs by desaturation of the ruminally derived *t*VA in the mammary gland (7,28). The notable increase in the concentration of the *cis*-9,*trans*-11 isomer when the diet was changed from SUN1 to SUN1.4 (Table 3) was also observed by Secchiari *et al.* (29) and Dhiman *et al.* (19) in milk from cows fed full-fat extruded soybeans or a soybean oil supplement. The latter authors concluded that it may be caused by incomplete biohydrogenation in the rumen and in-

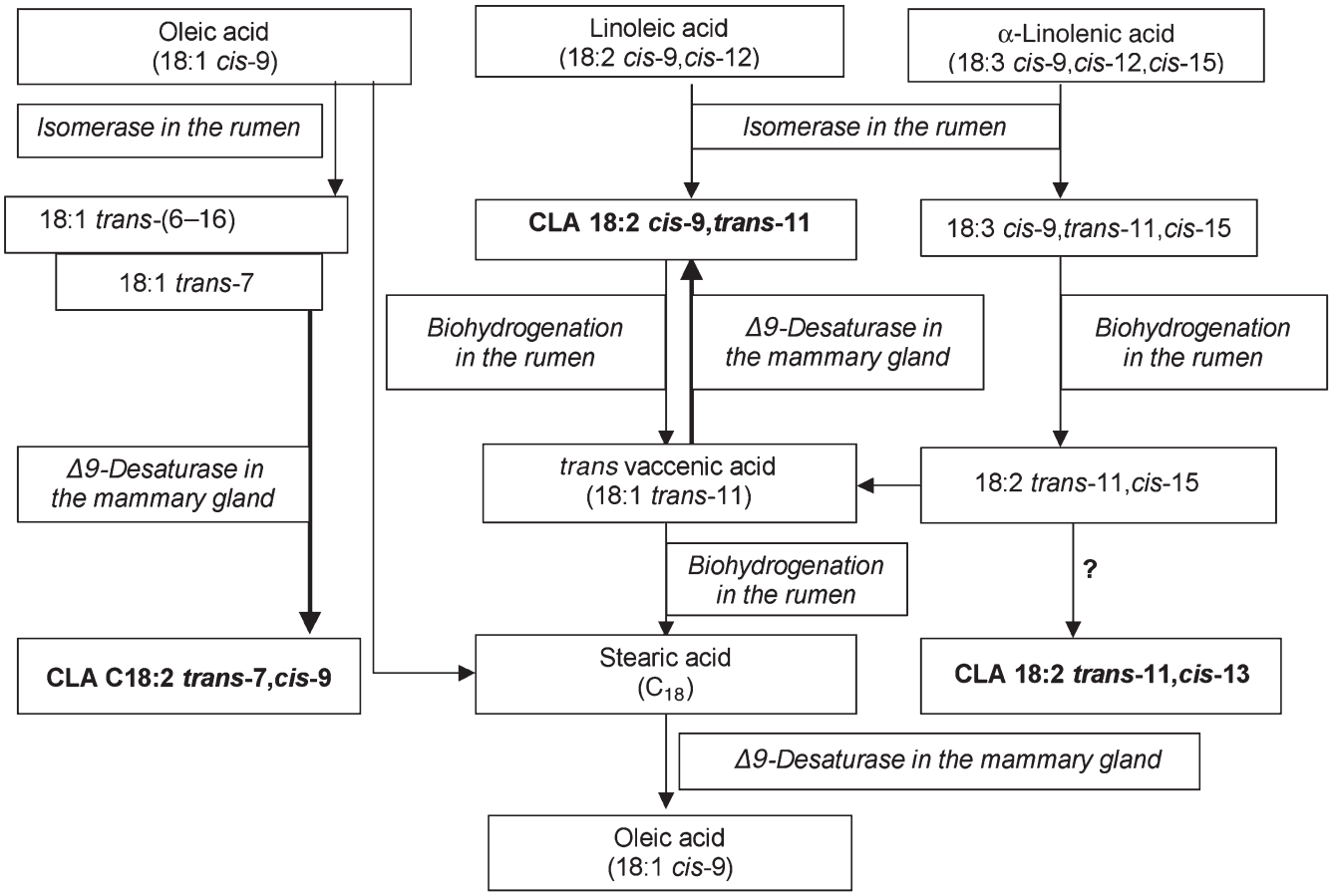

FIG. 4. Known metabolic pathways for the formation of CLA isomers and their precursors.

creased escape of the CLA from the rumen to the lower digestive tract. Piperova *et al.* (28) found much lower CLA concentrations in the duodenal flow of lactating cows fed diets with high (8.6 or 9.1 g d^{-1}) compared with low (1.1 or 1.8 g d^{-1}) proportions of forage than in milk fat. They concluded that the main CLA isomers, excluding *cis*-9,*trans*-11 and *trans*-7,*cis*-9, were essentially formed in the rumen. In the second study, the highest concentration of the *cis*-9,*trans*-11 CLA was found in milk fat from cows grazing in the highlands (21.3 mg g^{-1} fat). French *et al.* (43) also found increased CLA contents in the intramuscular fat from steers grazing on grass compared with grass silage or ingesting concentrate-based diets. It therefore seems that grass provides protection against biohydrogenation in the rumen.

In the first study, the concentration of the CLA isomer *trans*-10,*cis*-12 also correlated strongly with the daily intake of linoleic acid (Table 4). This CLA isomer is a product of ruminal biohydrogenation in which the initial isomerization takes place at the *cis*-9 position of linoleic acid rather than at the *cis*-12 position, as in the more typical pathway (4). Kraft *et al.* (44) found a 40% decrease in milk fat 5 d after an intraduodenal infusion of a CLA mixture, indicating that the *trans*-10,*cis*-12 isomer is responsible for the inhibition of milk fat synthesis. According to Viswanadha *et al.* (45), an intravenous administration of 6 g d^{-1} of this isomer decreased the milk fat percentage from 4.17 to 2.92% on day 5. In a dose–response experiment, Baumgard *et al.* (46,47) confirmed these results when they fed the pure *trans*-10,*cis*-12 isomer. The milk fat from cows supplemented with the highest dose (14 g d^{-1}) contained more *trans*-10,*cis*-12 compared with *cis*-9,*trans*-11, resulting in a dramatically curvilinear reduction in milk fat yield.

α-Linolenic acid in the fodder and CLA in the milk fat. In the first study, the highest concentration of the combined *trans*-11,*cis*-15/*trans*-9,*cis*-12 18:2 FA was found in milk fat from cows fed LIN1 (2.47 mg g^{-1} fat) or LIN1.4 (5.00 mg g^{-1} fat); it was attributed to the high level of *trans*-11,*cis*-15 18:2 with the increase in α-linolenic acid. The correlation coefficient between the concentrations of the combined *trans*-11, *cis*-15/*trans*-9,*cis*-12 18:2 FA in the milk fat and the *trans*-11, *cis*-13 CLA was very high (0.94; $P \leq 0.001$). It is well known that the pathway for the hydrogenation of *cis*-9,*cis*-12,*cis*-15 18:3 FA in the rumen involves an initial isomerization to a conjugated triene (*cis*-9,*trans*-11,*cis*-15 18:3), followed by reduction of double bonds at carbons 9, 15, and 11 to yield the *trans*-11,*cis*-15 18:2, *trans*-11 18:1, and 18:0 FA, respectively, but not *cis*-9,*trans*-11 CLA, as intermediates (48). Kraft *et al.* (27) hypothesized that α-linolenic acid is the indirect precursor of *trans*-11,*cis*-13 CLA. The highest levels of this CLA isomer found in milk fat from cows fed the

α-linolenic acid-rich LIN diets (LIN 1, 0.23 mg g^{-1} fat; LIN1.4, 0.47 mg g^{-1} fat) (Table 3) confirmed that α-linolenic acid was the main indirect precursor of the CLA isomer *trans*-11,*cis*-13 in milk fat. Nevertheless, the increase in the concentration of this CLA isomer in milk fat when the diet was changed from SUN1 (0.12 mg g^{-1}) to SUN1.4 (0.21 mg g^{-1}) (daily intake of α-linolenic acid, 1 g; Table 1) indicated that linoleic acid was the second-most important precursor of this CLA.

Normally, after the overwhelmingly predominant CLA isomer *cis*-9,*trans*-11, the *trans*-7,*cis*-9 is the second-most predominant CLA isomer in ruminant fat (5,28,29,49–51). Piperova *et al.* (52) reported that this isomer represents as much as 40% of the total CLA under special conditions. According to these authors (28), when cows were fed a high- or low-forage diet with or without buffer, most of this isomer may have been produced by the action of Δ^9-desaturase on *trans*-7 18:1 in bovine tissues. By contrast, in milk fat from cows grazing at the three altitudes, the second-most important CLA isomer was the *trans*-11,*cis*-13 CLA (Table 6). The concentration of this CLA in milk fat from cows grazing in the highlands was much higher (about a factor of 4) than in milk fat from cows fed the LIN1.4 diet. Although linseed (14) and fresh grass (53) both contain a high proportion of α-linolenic acid, Wachira *et al.* (54) speculated that the biohydrogenation rate of α-linolenic acid differs depending on the source. α-Linolenic acid is predominantly bound to TAG, whereas in grass the predominant form is glycolipids. The increase in the concentration of this CLA isomer with elevation also could be related to the higher percentage of α-linolenic acid in plants living at lower environmental temperatures, such as in the Alps (53). The pathway from *trans*-11,*cis*-15 FA to the second-most important CLA isomer, *trans*-11,*cis*-13, is as yet unclear (Fig. 4).

CLA are highly correlated with either oleic, linoleic, or α-linolenic acid. The strong positive correlations (Table 4) between the daily intakes of (i) oleic acid or linoleic acid and the concentration of the CLA isomer *trans*-7,*cis*-9 in milk fat; (ii) linoleic acid and the CLA isomers *trans*-10,*trans*-12, *trans*-9,*trans*-11, *trans*-8,*trans*-10, *trans*-7,*trans*-9, *trans*-10, *cis*-12, *cis*-9,*trans*-11, *trans*-8,*cis*-10, and *trans*-7,*cis*-9; and (iii) α-linolenic acid and the CLA isomers *trans*-12,*trans*-14, *trans*-11,*trans*-13, *cis,trans*/*trans*,*cis*-12,14, *trans*-11,*cis*-13, and *cis*-11,*trans*-13 (Table 4) indicated that these FA (oleic, linoleic, and α-linolenic acids) are probably the main indirect precursors of the above-mentioned CLA. Nevertheless, it is well known, for example, that linoleic and α-linolenic acid are both indirect precursors of the CLA isomer *cis*-9,*trans*-11 (55), but the highest concentration of this CLA isomer is generally obtained with linoleic acid-rich diets (14,19).

CLA are potential indicators of Alpine milk products. In the second study, the concentrations of many isomers were the highest in milk fat from the highlands (Table 6), but only three CLA isomers (*cis*-9,*trans*-11, *trans*-11,*cis*-13, and *trans*-8,*cis*-10) showed a nearly linear increase with elevation. The concentration of the isomer *trans*-11,*cis*-13 in milk fat from the highlands (Table 6) was about four times higher than in milk fat from cows fed LIN1.4 (Table 3), which was rich in α-linolenic acid (Table 1). These three CLA isomers, and particularly the CLA isomer *trans*-11,*cis*-13, could therefore be useful indicators of milk products of Alpine origin. Recently, Karoui *et al.* (56) showed that CLA may help to differentiate Alpine from lowlands milk products by using fluorescence spectrometry.

ACKNOWLEDGMENT

The authors would like to thank their colleague Patrick Malke for his careful technical assistance.

REFERENCES

1. Jenkins, T.C. (1993) Lipid Metabolism in the Rumen, *J. Dairy Sci. 76*, 3851–3863.
2. Katz, I., and Keeney, M. (1966) Characterization of the Octadecenoic Acids in Rumen Digesta and Rumen Bacteria, *J. Dairy Sci. 49*, 962–966.
3. Parodi, P.W. (1976) Distribution of Isomeric Octadecenoic Fatty Acids in Milk Fat, *J. Dairy Sci. 59,* 1870–1873.
4. Griinari, J.M., and Bauman, D.E. (1999) Biosynthesis of Conjugated Linoleic Acid and Its Incorporation into Milk and Meat in Ruminants, in *Advances in Conjugated Linoleic Acid Research*, *Volume 1* (Yurawecz, M.P., Mossoba, M.M., Kramer, J.K.G., Pariza, M.W., and Nelson, G.J., eds.), pp. 180–200, AOCS Press, Champaign.
5. Corl, B.A., Baumgard, L.H., Griinari, J.M., Delmonte, P., Morehouse, K.M., Yurawecz, M.P., and Bauman, D.E. (2002) *Trans*-7,*cis*-9 CLA Is Synthesized Endogenously by Δ^9-Desaturase in Dairy Cows, *Lipids 37*, 681–688.
6. Dhiman, T.R., Arnand, G.R., Satter, L.D., and Pariza, M.W. (1999) Conjugated Linoleic Acid Content of Milk from Cows Fed Different Diets, *J. Dairy Sci. 82*, 2146–2156.
7. Griinari, J.M., Corl, B.A., Lacy, S.H., Chouinard, P.Y., Nurmela, K.V.V., and Bauman, D.E. (2000) Conjugated Linoleic Acid Is Synthesized Endogenously in Lactating Dairy Cows by Δ^9-Desaturase, *J. Nutr. 130*, 2285–2291.
8. Banni, S., and Martin, J.C. (1998) Conjugated Linoleic Acid and Metabolites, in Trans *Fatty Acids in Human Nutrition* (Sébédio J.L., and Christie, W.W., eds.), pp. 261–302, The Oily Press, Dundee, Scotland.
9. Corl, B.A., Barbano, D.M., Bauman, D.E., and Ip, C. (2003) *Cis*-9,*trans*-11 CLA Derived Endogenously from *trans*-11 18:1 Reduces Cancer Risk in Rats, *J. Nutr. 133*, 2893–2900.
10. Park, Y., Storkson, J.M., Albright, K.J., Liu, W., Cook, M.E., and Pariza, M.W. (1999) Evidence That the *trans*-10,*cis*-12 Isomer of Conjugated Linoleic Acid Induces Composition Changes in Mice, *Lipids 34*, 235–241.
11. Kim, E.J., Holthuizen, P.E., Park, H.S., Ha, Y.L., Jung, K.C., and Park, J.H.Y. (2002) *Trans*-10,*cis*-12 Conjugated Linoleic Acid Inhibits Caco-2 Colon Cancer Cell Growth, *Am. J. Physiol. Gastrointest. Liver Physiol. 283*, G357–G367.
12. Park, S.J., Park, C.W., Kim, S.J., Kim, J.K., Kim, Y.R., Kim, Y.S., and Ha, Y.L. (2003) Divergent Cytotoxic Effects of Conjugated Linoleic Acid Isomers on NCI-N87 Cells, *ACS Symp. Series 851*, 113–118.
13. Collomb, M., Bütikofer, U., Sieber, R., Jeangros, B., and Bosset, J.O. (2002) Composition of Fatty Acids in Cow's Milk Fat Produced in the Lowlands, Mountains and Highlands of Switzerland Using High Resolution Gas Chromatography, *Int. Dairy J. 12*, 649–659.
14. Collomb, M., Sollberger, H., Bütikofer, U., Sieber, R., Stoll, W.,

and Schaeren, W. (2004) Impact of a Basal Diet of Hay and Fodder Beet Supplemented with Rapeseed, Linseed and Sunflowerseed on the Fatty Acid Composition of Milk Fat, *Int. Dairy J. 14*, 549–559.
15. Fritsche, J., and Steinhart, H. (1998) Analysis, Occurrence, and Physiological Properties of *trans* Fatty Acids (TFA) with Particular Emphasis on Conjugated Linoleic Acid Isomers (CLA)—A Review, *Fett/Lipid 100,* 190–210.
16. Jahreis, G., Fritsche, J., Möckel, P., Schöne, F., Möller, U., and Steinhart, H. (1999) The Potential Anticarcinogenic Conjugated Linoleic Acid, *cis*-9,*trans*-11 C18:2, in Milk of Different Species: Cow, Goat, Ewe, Sow, Mare, Woman, *Nutr. Res. 19*, 1541–1549.
17. Peterson, D.G., Kelsey, J.A., and Bauman, D.E. (2002) Analysis of Variation in *cis*-9,*trans*-11 Conjugated Linoleic Acid (CLA) in Milk Fat of Dairy Cows, *J. Dairy Sci. 85*, 2164–2172.
18. Kelsey, J.A., Corl, B.A., Collier, R.C., and Bauman, D.E. (2002) Effect of Breed, Parity and Stage of Lactation on Milk Fat Content of CLA in the Dairy Cow, *J. Dairy Sci. 85* (Suppl. 1), 298–299.
19. Dhiman, T.R., Satter, L.D., Pariza, M.W., Galli, M.P., Albright, K., and Tolosa, M.X. (2000) Conjugated Linoleic Acid (CLA) Content of Milk from Cows Offered Diets Rich in Linoleic and Linolenic Acid, *J. Dairy Sci. 83*, 1016–1027.
20. Reklewska, B., Oprzadek, A., Reklewski, Z., Panicke, L., Kuczynska, B., and Oprzadek, J. (2002) Alternative for Modifying the Fatty Acid Composition and Decreasing the Cholesterol Level in the Milk of Cows, *Livestock Prod. Sci. 76*, 235–243.
21. Jahreis, G., Steinhart, H., Pfalzgraf, A., Flachowsky, G., and Schöne, F. (1996) Zur Wirkung von Rapsölfütterung an Milchkühe auf das Fettsäurespektrum des Butterfettes, *Z. Ernährungswiss. 35*, 185–190.
22. AbuGhazaleh, A.A., Schingoethe, D.J., Hippen, A.R., Kalscheur, K.F., and Whitlock, L.A. (2002) Fatty Acid Profiles of Milk and Rumen Digesta from Cows Fed Fish Oil, Extruded Soybeans or Their Blend, *J. Dairy Sci. 85*, 2266–2276.
23. Chilliard, Y., Ferlay, A., and Doreau, M. (2001) Effect of Different Types of Forages, Animal Fat and Marine Oils in Cow's Diet on Milk Fat Secretion and Composition, Especially Conjugated Linoleic Acid (CLA) and Polyunsaturated Fatty Acids, *Livestock Prod. Sci. 70*, 31–48.
24. Bell, J.A., and Kennelly, J.J. (2002) The Potential of Nutrition to Modify the Fat Composition of Dairy Products, in *Proceedings of the Eastern Nutrition Conference,* University of Guelph, Guelph, Ontario, pp. 94–110.
25. Hauswirth, C.B., Scheeder, M.R.L., and Beer, J.H. (2004) High ω-3 Fatty Acid Content in Alpine Cheese. The Basis for an Alpine Paradox, *Circulation 109*, 103–107.
26. Collomb, M., Bütikofer, U., Sieber, R., Jeangros, B., and Bosset, J.O. (2002) Correlation Between Fatty Acids in Cow's Milk Fat Produced in the Lowlands, Mountains and Highlands of Switzerland and Botanical Composition of the Fodder, *Int. Dairy J. 12*, 661–666.
27. Kraft, J., Collomb, M., Möckel, P., Sieber, R., and Jahreis, G. (2003) Differences in CLA Isomer Distribution of Cow's Milk Lipids, *Lipids 38,* 657–664.
28. Piperova, L.S., Sampugna, J., Teter, B.B., Kalscheur, K.F., Yurawecz, M.P., Ku, Y., Morehouse, K.M., and Erdman, R.A. (2002) Duodenal and Milk *trans* Octadecenoic Acid and Conjugated Linoleic Acid (CLA) Isomers Indicate That Postabsorptive Synthesis Is the Predominant Source of *cis*-9-Containing CLA in Lactating Dairy Cows, *J. Nutr. 132*, 1235–1241.
29. Secchiari, P., Antongiovanni, M., Mele, M., Serra, A., Buccioni, A., Ferruzzi, G., Paoletti, F., and Petacchi, F. (2003) Effect of Kind of Dietary Fat on the Quality of Milk Fat from Italian Friesian Cows, *Livest. Prod. Sci. 83*, 43–52.
30. Jeangros, B., Troxler, J., Conod, D., Scehovic, J., Bosset, J.O., Bütikofer, U., Gauch, R., Mariaca, R., Pauchard, J.P., and Sieber, R. (1997) Etude des Relations Entre les Caractéristiques des Herbages et celles du Lait, de la Crème et du Fromage de Type l'Etivaz ou Gruyère, I. Présentation du Projet, *Rev. Suisse Agricult. 29*, 23–34.
31. Bosset, J.O., Jeangros, B., Berger, T., Bütikofer, U., Collomb, M., Gauch, R., Lavanchy, P., Scehovic, J., Troxler, J., and Sieber, R. (1999) Comparaison de Fromages à Pâte Dure de Type Gruyère Produits en Région de Montagne et de Plaine, *Rev. Suisse Agricult. 31*, 17–22.
32. International Dairy Federation (IDF) (1995*)* Milk and Milkproducts, Extraction Methods for Lipids and Liposoluble Compounds, IDF/ISO Standard 172.
33. International Organization for Standardization (ISO) (1997) Milkfat, Determination of the Fatty Acid Composition by Gas Liquid Chromatography, ISO Standard 15885.
34. Collomb, M., and Bühler, T. (2000) Analyse de la Composition en Acides Gras de la Graisse de Lait, Optimisation et Validation d'une Méthode Générale à Haute Résolution, *Trav. Chim. Alim. Hyg*. *91*, 306–332.
35. Eulitz, K., Yurawecz, M.P., Sehat, N., Fritsche, J., Roach, J.A.G., Mossoba, M., Kramer, J.K.G., Adolf, R.O., and Ku, Y. (1999) Preparation, Separation, and Confirmation of the Eight Geometrical *cis/trans* Conjugated Linoleic Acid Isomers 8,10-Through 11,13-18:2, *Lipids 34*, 873–877.
36. Rickert, R., Steinhart, H., Fritsche, J., Sehat, N., Yurawecz, M.P., Mossoba, M.M., Roach, J.A.G., Eulitz, K., Ku, Y., and Kramer, J.K.G. (1999) Enhanced Resolution of Conjugated Linoleic Acid Isomers by Tandem-Column Silver-Ion High Performance Liquid Chromatography, *J. High Res. Chromatogr. 22*, 144–148.
37. Systat Software Inc. (1999) *Systat for Windows, version 9.0,* Systat Software, Chicago.
38 Morris, L.J. (1970) Mechanisms and Stereochemistry in Fatty Acid Metabolism, *Biochem. J. 118*, 681–693.
39. Mosley, E.E., Powell, G.L., Riley, M.B., and Jenkins, T.C. (2002) Microbial Biohydrogenation of Oleic Acid to *trans* Isomers *in vitro, J. Lipid Res. 43*, 290–296.
40. Loor, J.J., Bandara, A.B.P.A., and Herbein, J.H., (2002) Characterization of C18:1 and C18:2 Isomers Produced During Microbial Biohydrogenation of Unsaturated Fatty Acids from Canola and Soya Bean Oil in the Rumen of Lactating Cows, *J. Anim. Physiol. Anim. Nutr. 86,* 422–432.
41. Kepler, C.R., Hirons, K.P., McNeill, J.J., and Tove, S.B. (1966) Intermediates and Products of the Biohydrogenation of Linoleic Acid by *Butyrivibrio fibrisolvens*, *J. Biol. Chem. 241*, 1350–1354.
42. Griinari, J.M., Chouinard, P.Y., and Bauman, D.E. (1997) *Trans* Fatty Acid Hypothesis of Milk Fat Depression Revised, *Proceedings of the Cornell Nutrition Conference for Feed Manufacturers*, Cornell University, Ithaca, New York, pp. 208–216.
43. French, P., Stanton, C., Lawless, F., O'Riordan, E.G., Monahan, F.J., Caffrey, P.J., and Moloney, A.P. (2000) Fatty Acid Composition, Including Conjugated Linoleic Acid, of Intramuscular Fat from Steers Offered Grazed Grass, Grass Silage, or Concentrate-Based Diets, *J. Anim. Sci. 78*, 2849–2855.
44. Kraft, J., Lebzien, P., Flachowsky, G., Möckel, P., and Jahreis, G. (2000) Duodenal Infusion of Conjugated Linoleic Acid Mixture Influences Milk Fat Synthesis and Milk CLA Content in Dairy Cows, in *Milk Composition* (Agnew, R.E., Agnew, A.K., and Fearon, A.M., eds.), Occasional Publication No. 25, British Society of Animal Science, pp. 143–147.
45. Viswanadha, S., Giesy, J.G., Hanson, T.W., and McGuire, M.A. (2003) Dose–Response of Milk Fat to Intravenous Administration of the *trans*-10,*cis*-12 Isomer of Conjugated Linoleic Acid, *J. Dairy Sci. 86*, 3229–3236.
46. Baumgard, L.H., Corl, B.A., Dwyer, D.A., Saebo, A., and Bauman, D.E. (2000) Identification of Conjugated Linoleic Acid Isomer That Inhibits Milk Fat Synthesis, *Am. J. Physiol. 278*, R179–R184.

47. Baumgard, L.H., Sangster, J.K., and Bauman, D.E. (2000) Milk Fat Synthesis in Dairy Cows Is Progressively Reduced by Increasing Supplemental Amounts of *trans*-10,*cis*-12 Conjugated Linoleic Acid (CLA), *J. Nutr. 131*, 1764–1769.
48. Wilde, P.F., and Dawson, R.M. (1966) The Biohydrogenation of α-Linolenic Acid and Oleic Acid by Rumen Microorganisms, *Biochem. J. 98*, 469–475.
49. Sehat, N., Kramer, J.K.G., Mossoba, M.M., Yurawecz, M.P., Roach, J.A.G., Eulitz, K., Morehouse, K.M., and Ku, Y. (1998) Identification of Conjugated Linoleic Acid Isomers in Cheese by Gas Chromatography, Silver Ion High Performance Liquid Chromatography, and Mass Spectral Reconstructed Ion Profiles. Comparison of Chromatographic Elution Sequences, *Lipids 33*, 963–971.
50. Yurawecz, M.P., Roach, J.A.G., Sehat, N., Mossoba, M.M., Kramer, J.K.G., Fritsche, J., Steinhart, H., and Ku, Y. (1998) A New Conjugated Linoleic Acid Isomer, 7-*trans*,9-*cis*-Octadecadienoic Acid, in Cow Milk, Cheese, Beef, and Human Milk and Adipose Tissue, *Lipids 33*, 803–809.
51. Fritsche, J., Rickert, R., Steinhart, H., Yurawecz, M.P., Mossoba, M.M., Sehat, N., Roach, J.A.G., Kramer, J.K.G., and Ku, Y. (1999) Conjugated Linoleic Acid (CLA) Isomers: Formation, Analysis, Amounts in Foods and Dietary Intake, *Fett/Lipid 101*, 272–276.
52. Piperova, L.S., Teter, B.B., Bruckental, I., Sampugna, J., Mills, S.E., Yurawecz, M.P., Fritsche, J., Ku, K., and Erdman, R.A. (2000) Mammary Lipogenic Enzyme Activity, *trans* Fatty Acids and Conjugated Linoleic Acids Are Altered in Lactating Cows Fed a Milk Fat-Depressing Diet, *J. Nutr. 130*, 2568–2574.
53. Hawke, J.C. (1973) Lipids, in *Chemistry and Biochemistry of Herbage* (Butler, G.W., and Baily, R.W., eds.), Vol. 1, pp. 213–263, Academic Press, London.
54. Wachira, A.M., Sinclair, L.A., Wilkinson, R.G., Hallet, K., Enser, M., and Wood, J.D. (2000) Rumen Biohydrogenation of n-3 Polyunsaturated Fatty Acids and Their Effects on Microbial Efficiency and Nutrient Digestibility in Sheep, *J. Agric. Sci. 135*, 419–428.
55. Aii, T., Tamaki, M., Shimabukuro, H., Hayasawa, H., Shimizu, T., and Ishida, S. (1999) Conjugated Linoleic Acid Content in Milk Fat of the Cows Fed a Large Amount of Linseed, *Anim. Sci. J. 70*, 535–541.
56. Karoui, R., Bosset, J.O., and Dufour, E. (2003) Monitoring the Geographic Origin of Swiss Gruyère and l'Etivaz PDO Cheese Using Fluorescence Spectrometry, *Proceedings of the 5th International Meeting on Mountain Cheese* (Arêches-Beaufort, France; September 11–12, 2003), pp. 23, INRA, Theix, France.

[Received January 22, 2004; and in final revised form May 12, 2004; revision accepted May 20, 2004]

Effect of CLA on Milk Fat Synthesis in Dairy Cows: Comparison of Inhibition by Methyl Esters and Free Fatty Acids, and Relationships Among Studies

Michael J. de Veth[a], J. Mikko Griinari[b], Angelika-Maria Pfeiffer[c], and Dale E. Bauman[a,*]

[a]Department of Animal Science, Cornell University, Ithaca, New York 14853, [b]Clanet Ltd., 02660 Espoo, Finland, and [c]BASF-AG, Nutrition Research Station, Offenbach, Germany

ABSTRACT: CLA is a potent inhibitor of milk fat synthesis, as shown by investigations using mixtures of CLA isomers in FFA form. However, methyl esters of CLA can be initially formed in commercial synthesis, and their use in a supplement has certain manufacturing and cost advantages. Our objective was to compare abomasal infusion of methyl esters of CLA (ME-CLA) and FFA of CLA (FFA-CLA) on milk fat synthesis. Data were also combined with previous investigations to examine broader relationships between *trans*-10,*cis*-12 CLA and the reduction in milk fat. Three mid-lactation, rumen-fistulated Holstein cows were used in a 3 × 3 Latin square design. Treatments were (i) control, (ii) ME-CLA, and (iii) FFA-CLA. The ME-CLA and FFA-CLA treatments (4.2 g/d *trans*-10,*cis*-12 CLA) resulted in a comparable reduction in milk fat yield (38 and 39%, respectively) and pattern of reduction in individual FA. In contrast, milk yield, milk protein, and feed intake were unaltered by CLA treatment. Combining data across studies revealed strong correlations relating the reduction in milk fat yield to abomasal dose of *trans*-10,*cis*-12 CLA (R^2 = 0.86), milk fat content of *trans*-10,*cis*-12 CLA (R^2 = 0.93), and milk fat secretion of *trans*-10,*cis*-12 CLA (R^2 = 0.82). Across studies, transfer efficiency of abomasally infused *trans*-10,*cis*-12 CLA into milk fat was relatively constant (22%; R^2 = 0.94). Overall, ME-CLA and FFA-CLA were equally potent in reducing milk fat, and either form could be used to formulate a dietary supplement that would induce milk fat depression.

Paper no. L9407 in *Lipids 39*, 365–372 (April 2004).

CLA is a generic term for octadecadienoic acid isomers with conjugated double bonds. Two of the isomers, *cis*-9,*trans*-11 and *trans*-10,*cis*-12 CLA, are known to confer a number of beneficial biological effects. These effects have been identified in a range of animal species and include anticarcinogenesis, immunomodulation, antiatherosclerosis, and alteration in body composition (1,2). The *trans*-10,*cis*-12 CLA isomer is also a potent inhibitor of milk fat synthesis (3–5) and has been implicated in diet-induced milk fat depression (MFD) in dairy cows. This isomer is formed by rumen biohydrogenation, existing in trace levels in the rumen of cows under most diets, with elevated levels occurring in certain diets associated with MFD (6,7).

*To whom correspondence should be addressed at 262 Morrison Hall, Department of Animal Science, Cornell University, Ithaca, NY 14853-4801. E-mail: deb6@cornell.edu

Abbreviations: DMI, dry matter intake; FFA-CLA, free fatty acid CLA supplement; ME-CLA, methyl ester CLA supplement; MFD, milk fat depression; SCC, somatic cell count; TMR, total mixed ration.

The extent to which the lipid form of *trans*-10,*cis*-12 CLA influences the effect of the isomer on milk fat synthesis is unknown. The majority of studies that have investigated *trans*-10,*cis*-12 CLA have used commercial mixtures of CLA in a FFA form (see review by Bauman *et al.,* Ref. 7). This is an important consideration from a production standpoint, as the chemical synthesis of a methyl ester CLA has a number of benefits over that of FFA of CLA. These include reductions in manufacturing time and costs, and the production of a high-purity CLA product (8). However, it is not known what influence the methyl ester may have on intestinal absorption of the *trans*-10,*cis*-12 CLA isomer and its subsequent regulation of milk fat synthesis. Previous studies that have described intestinal absorption of ethyl and methyl esters of FA have involved rodents and given inconsistent results (9–11). It is also unclear to what extent results from rodent studies can be applied to the lactating dairy cow when fed CLA in the methyl ester form.

Abomasal infusion has been used as a convenient experimental method of providing CLA isomer supplements to avoid biohydrogenation and alterations by rumen bacteria. The nature and extent of the milk fat synthesis response to abomasal infusion of various doses of *trans*-10,*cis*-12 CLA to lactating dairy cows has been described previously (4,5). Peterson *et al.* (5) found a strong curvilinear relationship between the content of *trans*-10,*cis*-12 CLA in milk and changes in milk fat yield, and recent studies (12–14) provide additional data. However, the dose–response relationship between the amounts of *trans*-10,*cis*-12 CLA abomasally infused and the quantity that is secreted into the milk has not been examined across studies.

The primary objective of the present study was to compare the effects of abomasal infusion of CLA supplements based on methyl esters of CLA (ME-CLA) or FFA of CLA (FFA-CLA) on milk fat synthesis in dairy cows. A secondary objective was to combine data from the present study in which lactating dairy cows were abomasally infused with *trans*-10,*cis*-12 CLA with those from previous investigations to examine the relationship between the extent of MFD and milk fat *trans*-10,*cis*-12 CLA, as well as the efficiency of transfer of this CLA isomer into milk fat.

EXPERIMENTAL PROCEDURES

In vivo study. Three lactating Holstein cows (168 ± 49 d in milk; mean ± SE) fitted with rumen fistula were used in a 3 × 3 Latin square experiment. Cows were housed in metabolic tie

TABLE 1
Ingredient and Chemical Composition of the Diet and Estimated Net Energy of Lactation (NE_L)

Composition	
Ingredient (% of dry matter)[a]	
Chopped alfalfa hay	55.0
Ground corn	29.2
Soybean meal	3.7
Whole cottonseed	7.5
Mineral and vitamin mix[b]	1.4
Urea	0.3
Dicalcium phosphate	0.4
Sodium bicarbonate	0.6
Chemical analysis (% of dry matter)	
Crude protein	15.7
Soluble crude protein	4.7
Neutral detergent fiber	44.9
Acid detergent fiber	29.9
Crude fat	5.6
NE_L (Mcal/kg dry matter)	1.43

[a]Dietary dry matter averaged 91.1%.
[b]Contained 20.0% Cl, 12.3% Ca, 17.7% Na, 8.0% S, 7.5% Mg, 1.0% K, 0.62 Zn, 0.54% Mn, 0.20% Fe, 0.08% Cu, 0.01% P, 0.009% I, 0.006% Co, 0.0002% Se, 113 IU/g vitamin A, 27 IU/g vitamin D, and 612 IU/g vitamin E.

TABLE 2
FA Profiles of the CLA Supplements and Amounts of FA They Provided

	Treatment[a]	
FA	ME-CLA	FFA-CLA
Composition (wt%)		
16:0	5.0	5.1
18:0	4.2	4.3
cis-9 18:1	25.6	25.4
cis-9,*cis*-12 18:2	0.3	0.4
cis-9,*trans*-11 18:2	30.1	29.7
trans-10,*cis*-12 18:2	30.0	29.6
Others	4.8	5.5
Abomasal infusion (g/d)		
16:0	0.70	0.72
18:0	0.59	0.61
cis-9 18:1	3.58	3.60
cis-9,*cis*-12 18:2	0.04	0.06
cis-9,*trans*-11 18:2	4.21	4.21
trans-10,*cis*-12 18:2	4.20	4.20
Others	0.67	0.78

[a]CLA supplements represented methyl esters of CLA (ME-CLA) and FFA of CLA (FFA-CLA).

stalls at the Large Animal Research and Teaching Unit at Cornell University. The diet was a total mixed ration (TMR) formulated to meet or exceed nutrient requirements using the Cornell Net Carbohydrate and Protein System (15). Cows were fed *ad libitum* with equal portions of fresh feed offered at 0600 and 1800 daily (Table 1). Water was available at all times. Orts were weighed and recorded on a daily basis. Daily feed samples were composited by treatment period and analyzed by wet chemistry (Dairy One Cooperative, Inc., Ithaca, NY). The Cornell University Institutional Animal Care and Use Committee approved all procedures involving animals.

Treatments were abomasal infusion of (i) ethanol (control), (ii) ME-CLA, or (iii) FFA-CLA. We chose a daily infusion rate of 4.2 g of *trans*-10,*cis*-12 CLA, designed to achieve a decrease in milk fat yield of about one-half of the maximum (4,5). The amounts of supplement administered to provide this dose of *trans*-10,*cis*-12 CLA were 14.19 and 14.70 g/d for the ME-CLA and FFA-CLA treatments, respectively. The composition of CLA supplements (Natural ASA, Hovdebygda, Norway) and amounts infused are presented in Table 2.

The forms of CLA were solubilized in 95% ethanol at a ratio of 5:1 (ethanol/CLA) and flushed with O_2-free N_2 before being stored at 4°C until use (maximum of 4 d). The solubilized supplements were infused directly into the abomasum to avoid any potential alterations by rumen bacteria. This was accomplished by infusing them into a 0.5-cm (i.d.) polyvinyl chloride tube that passed through the rumen fistula and sulcus omasi into the abomasum as described previously (16). Each treatment was infused for 5 d, with a 7-d interval between infusion periods. One-fourth of the daily dose was administered every 6 h over the infusion period.

Cows were milked at 0600 and 1800 daily. Milk was sampled, and the yield was determined at each milking. One aliquot was stored at 4°C with a preservative (bronopol tablet; D&F Control Systems, San Ramon, CA) until analysis for fat and protein content by IR (Ref. 17: method 972.160) and somatic cell count (SCC) by an optical fluorescence method (Ref. 17: method 978.26) (Dairy One Cooperative, Inc.). A second aliquot of milk was stored at –20°C until analysis for FA composition by GC as detailed by Perfield *et al.* (18), with the only modification being the use of a CP-Sil 88 fused-silica capillary column [100 m × 0.25 mm (i.d.) with 0.2-μm film thickness; Varian, Inc., Walnut Creek, CA]. Glycerol content of the milk fat was calculated as described by Schauff *et al.* (19) and used to determine FA yields.

Data were analyzed as a 3 × 3 Latin square design using the PROC MIXED procedure of SAS (20), with period and cow considered random effects and treatment a fixed effect. All data are presented as least square means. Orthogonal contrasts comparing (i) control vs. CLA (combined ME-CLA and FFA-CLA) and (ii) ME-CLA vs. FFA-CLA were conducted using the ESTIMATE statement of SAS.

Multiple study analysis. Data from the present study and six other studies in which lactating dairy cows were abomasally infused with *trans*-10,*cis*-12 CLA (3–5,12–14) were combined to describe the relationships between (i) abomasal dose of *trans*-10, *cis*-12 CLA and change in milk fat yield, (ii) milk fat content of *trans*-10,*cis*-12 CLA and change in milk fat yield, (iii) secretion of *trans*-10,*cis*-12 CLA in milk fat and change in milk fat yield, and (iv) dose of *trans*-10,*cis*-12 CLA and secretion of *trans*-10,*cis*-12 CLA in milk fat. These studies all had 4–5-d periods of a CLA infusion that was predominately *trans*-10,*cis*-12 CLA (3–5,12) or a mixture consisting mainly of *trans*-10,*cis*-12 and one other isomer (13,14, and present study). All cows were in mid or late lactation and fed a TMR. Milk yields of individual FA were not reported in the six studies outside the current study. Therefore, a milk glycerol concentration of 11.8% was assumed (based on the average of the current study) and used to calculate the amount of *trans*-10,*cis*-12 CLA secreted in the milk fat.

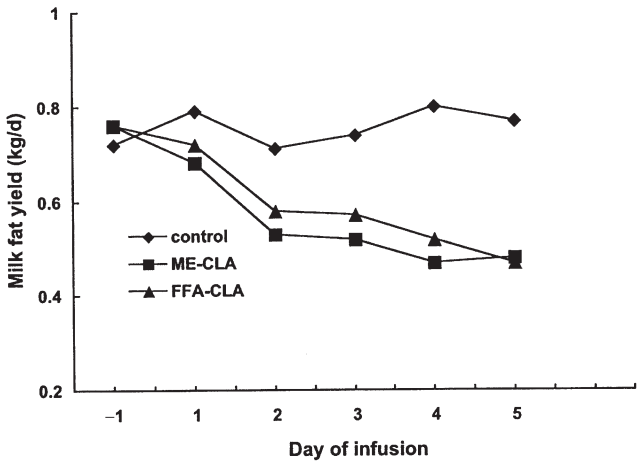

FIG. 1. Temporal pattern of milk fat yield in cows ($n = 3$) during abomasal infusion of different forms of CLA. Treatments were control (excipient only), methyl esters of CLA (ME-CLA), and FFA of CLA (FFA-CLA). The SEM averaged 0.127 kg/d for milk fat yield across days –1 to 5.

The relationships between the change in milk fat yield and (i) dose, (ii) milk fat content, and (iii) milk fat yield of *trans*-10,*cis*-12 CLA were analyzed using PROC NLIN in SAS (20) with an exponential decay model. Parameter estimation was conducted using the Marquardt nonlinear algorithm. Model adequacy was diagnosed based on mean square error, residuals against both fitted and predicted values, and a normal probability plot.

The relationship between abomasal dose of *trans*-10,*cis*-12 CLA and its secretion in milk fat was analyzed by regression analysis with PROC REG in SAS (20). Data relating to doses of *trans*-10,*cis*-12 CLA greater than 10 g/d were omitted from this analysis because they lay at a point at which the depression in milk fat synthesis had reached a plateau in the exponential decay model developed for milk fat content of *trans*-10,*cis*-12 CLA vs. change in milk fat yield. Diagnostic plots showed no serious departures from model assumptions.

RESULTS

In vivo *study.* All treatments were abomasally infused for 5 d, with the temporal pattern in milk fat yield indicating that CLA treatments resulted in a progressive decrease (Fig. 1). As the nadir was not reached until days 4–5, all subsequent performance and milk FA data are reported for day 5 of each treatment period.

CLA treatments reduced the milk fat yield compared with the control, but there were no differences between ME-CLA and FFA-CLA (Table 3). The milk fat content was similarly decreased by CLA treatments, but again no difference was observed between CLA forms. Milk yield, milk protein yield and content, milk SCC, and dry matter intake (DMI) were unaltered ($P > 0.1$) by CLA treatment or CLA form.

The FA composition of the milk fat is presented in Table 4. The proportion of *trans*-10,*cis*-12 CLA increased from undetectable levels (<0.01%) in the control period to 0.17 and 0.18% of total milk FA for ME-CLA and FFA-CLA, respectively. The concentrations of few other long-chain FA were altered by CLA treatment. Similarly, the concentrations of only 6:0, 8:0, and 10:0 were decreased ($P < 0.05$) by CLA treatment. The form of CLA had no effect on the FA composition of the milk fat. Four pairs of milk FA serve as a proxy for Δ^9-desaturase activity in the mammary gland (7). The ratios of these pairs were unaltered by CLA treatment and CLA form, except for an increase in the ratio of *cis*-9,*trans*-11 CLA to *trans*-11 18:1 in response to CLA treatment (Table 4). This presumably reflects the transfer of the *cis*-9,*trans*-11 CLA present in the infused supplements to milk fat, as *trans*-11 18:1 was unaltered.

The yields of all milk FA were decreased by CLA treatment, except for *cis*-9,*trans*-11 and *trans*-10,*cis*-12 CLA, the two CLA isomers that were present in the CLA treatments (Table 5). Milk fat secretion of *cis*-9,*trans*-11 was maintained, whereas the yield of *trans*-10,*cis*-12 was increased by the CLA treatments. However, there were no differences between the CLA forms in the yield of individual FA, except for a slightly higher yield of 12:0 for the ME-CLA treatment. Based on the

TABLE 3
Intake and Milk Production Results During Abomasal Infusion of CLA Supplements

	Treatment[a]				*P*	
	Control	ME-CLA	FFA-CLA	SEM	CLA[b]	Form[c]
DMI[d] (kg)	20.9	21.4	20.0	2.28	0.88	0.41
Milk yield (kg)	21.6	22.0	20.6	3.77	0.78	0.28
Milk fat						
Content (wt%)	3.55	2.18	2.27	0.12	0.01	0.64
Yield (kg)	0.77	0.48	0.47	0.12	0.02	0.92
Milk protein						
Content (wt%)	2.97	3.02	3.17	0.18	0.14	0.14
Yield (kg)	0.63	0.65	0.64	0.09	0.53	0.53
SCC[e] (×1000)	58	75	101	45.00	0.19	0.28

[a]Values represent day 5 of abomasal infusion for control (excipient only), ME-CLA, and FFA-CLA. For abbreviations see Table 2.
[b]Contrast between the control and the combined CLA treatments.
[c]Contrast between the ME-CLA and FFA-CLA treatments.
[d]DMI, dry matter intake.
[e]SCC, somatic cell count.

TABLE 4
Composition of Milk Fat During Abomasal Infusion of CLA

FA (g/100 g)	Treatment[a]			SEM	*P*	
	Control	ME-CLA	FFA-CLA		CLA[b]	Form[c]
4:0	3.96	3.64	3.54	0.62	0.26	0.75
6:0	1.55	1.14	1.08	0.14	<0.01	0.38
8:0	0.71	0.50	0.47	0.05	<0.01	0.26
10:0	1.41	1.04	0.97	0.12	0.03	0.50
12:0	1.72	1.61	1.49	0.19	0.20	0.37
14:0	8.19	7.76	7.35	0.47	0.28	0.50
14:1	0.69	0.65	0.63	0.14	0.64	0.82
15:0	0.86	0.87	0.95	0.05	0.51	0.41
16:0	25.76	24.01	24.48	0.83	0.07	0.43
16:1	1.31	1.36	1.43	0.26	0.78	0.81
17:0	0.53	0.56	0.57	0.03	0.22	0.63
18:0	12.99	13.95	14.67	0.85	0.13	0.35
18:1						
cis-9	30.40	31.81	31.50	0.77	0.13	0.65
trans-6–8	0.36	0.44	0.46	0.01	0.03	0.47
trans-9	0.33	0.36	0.37	0.02	0.03	0.26
trans-10	0.47	0.45	0.45	0.03	0.35	0.88
trans-11	1.56	1.65	1.58	0.07	0.54	0.56
trans-12	0.60	0.62	0.63	0.03	0.53	0.70
18:2						
cis-9,*cis*-12	2.72	3.29	3.12	0.21	0.05	0.32
cis-9,*trans*-11[d]	0.63	0.95	0.90	0.03	0.01	0.38
trans-10,*cis*-12	<0.01	0.17	0.18	0.03	0.01	0.71
18:3	0.39	0.44	0.39	0.06	0.35	0.27
20:0	0.11	0.11	0.11	<0.01	0.08	0.20
Other	2.75	2.65	2.70	0.09	0.13	0.36
Desaturase ratio[e]						
14:1/14:0	0.08	0.08	0.09	0.02	0.94	0.92
16:1/16:0	0.05	0.06	0.06	0.01	0.58	0.88
18:1/18:0	2.34	2.33	2.18	0.17	0.45	0.31
*c*9,*t*11/18:1*t*11	0.41	0.58	0.57	0.01	0.01	0.82

[a]Values represent day 5 of abomasal infusion for control (excipient only), ME-CLA, and FFA-CLA. For abbreviations see Table 2.
[b]Contrast between the control and the combined CLA treatments.
[c]Contrast between the ME-CLA and FFA-CLA treatments.
[d]Includes *trans*-7,*cis*-9 CLA that co-eluted owing to the GC method used. In milk fat from dairy cows, the *trans*-7,*cis*-9 CLA isomer is generally about 10% of the *cis*-9,*trans*-11 CLA isomer (7).
[e]Ratio for FA pairs that represent product/substrate for Δ^9-desaturase.

amount of *trans*-10,*cis*-12 CLA abomasally infused and its secretion in milk, the transfer efficiency of *trans*-10,*cis*-12 CLA into milk fat was calculated as 17.8% for ME-CLA and 18.8% for FFA-CLA. When milk FA were grouped based on their source (6), decreases in the response to CLA treatment were obtained in the secretion of the *de novo* synthesized FA (<16-carbon FA), preformed FA taken up from circulation (>16-carbon FA), and FA derived from both sources (16-carbon FA).

Multiple study analysis. When data from the present study and six other studies in which lactating dairy cows were abomasally infused with *trans*-10,*cis*-12 CLA (3–5,12–14) were combined, the exponential decay model accurately described the relationships between the change in milk fat yield and (i) abomasal dose of *trans*-10,*cis*-12 CLA (Fig. 2; $R^2 = 0.86$), (ii) milk fat content of *trans*-10,*cis*-12 CLA (Fig. 3; $R^2 = 0.93$), and (iii) secretion of *trans*-10,*cis*-12 CLA in milk fat (Fig. 4; $R^2 = 0.82$). The relationship between the dose of *trans*-10,*cis*-12 CLA and the secretion of *trans*-10,*cis*-12 CLA in milk fat was also of interest, as there was a strong positive linear relationship across studies; the slope indicates the efficiency of transfer of *trans*-10,*cis*-12 CLA into milk fat, and this value was 22% (Fig. 5).

DISCUSSION

A major objective was to investigate the effect of different forms of CLA on milk fat synthesis. A substantial reduction in milk fat synthesis occurred when CLA was supplied either as a methyl ester or as a FFA, with no difference between the two forms (Table 3). The only previous study to compare the effect of forms of CLA on milk fat synthesis is the abstract by Hanson *et al.* (21), who found no difference in the extent of MFD with abomasal infusion of FFA-CLA and TG of CLA. The dose of *trans*-10,*cis*-12 CLA in that study (~10 g/d) was near the upper range at which *trans*-10,*cis*-12 CLA produced its maximal level of MFD (Fig. 2; Refs. 4,5) and had the potential to

TABLE 5
Secretion of FA in Milk Fat During Abomasal Infusion of CLA

	Treatment[a]				*P*	
FA (g/d)	Control	ME-CLA	FFA-CLA	SEM	CLA[b]	Form[c]
4:0	24.62	13.99	14.14	5.43	0.04	0.96
6:0	10.06	4.54	4.41	1.81	0.02	0.91
8:0	4.67	1.99	1.88	0.74	0.01	0.80
10:0	9.22	4.21	3.94	1.26	<0.01	0.57
12:0	11.17	6.53	5.96	1.39	<0.001	0.02
14:0	55.29	32.56	30.59	7.95	<0.001	0.11
14:1	4.62	2.59	2.33	0.69	0.05	0.70
15:0	5.78	3.69	3.73	0.71	<0.01	0.87
16:0	179.42	102.10	103.12	28.26	0.02	0.94
16:1	9.16	5.44	5.42	1.37	0.08	0.99
17:0	3.59	2.40	2.44	0.56	0.04	0.90
18:0	89.64	60.61	63.80	15.56	0.04	0.75
18:1						
cis-9	208.27	135.63	131.41	28.94	0.02	0.78
trans-6–8	2.43	1.90	1.96	0.41	0.07	0.75
trans-9	2.19	1.51	1.51	0.26	0.03	0.97
trans-10	3.19	1.94	1.89	0.43	0.01	0.82
trans-11	10.65	7.10	6.82	1.67	0.03	0.75
trans-12	4.06	2.64	2.67	0.53	0.03	0.92
18:2						
cis-9,*cis*-12	18.34	14.01	13.06	2.59	0.03	0.41
cis-9,*trans*-11[d]	4.29	4.10	3.86	0.81	0.38	0.52
trans-10,*cis*-12	<0.01	0.75	0.79	0.20	0.05	0.86
18:3	2.64	1.77	1.72	0.45	0.04	0.85
20:0	0.73	0.47	0.48	0.11	0.02	0.87
Other	18.86	11.31	11.25	2.46	0.02	0.97
Summation[e]						
<16	125.44	70.09	66.98	19.27	<0.01	0.62
16:0 and 16:1	188.58	107.54	108.54	19.40	0.02	0.94
>16	350.01	234.83	232.41	51.80	0.03	0.93

[a]Values represent day 5 of abomasal infusion for control (excipient only), ME-CLA, and FFA-CLA. For abbreviations see Table 2.
[b]Contrast between the control and the combined CLA treatments.
[c]Contrast between the ME-CLA and FFA-CLA treatments.
[d]Includes *trans*-7,*cis*-9 CLA that co-eluted owing to the GC method used. In milk fat from dairy cows, the *trans*-7,*cis*-9 CLA isomer is generally about 10% of the *cis*-9,*trans*-11 CLA isomer (7).
[e]Grouping is by the source of milk FA. FA <16 carbons were derived from *de novo* synthesis in the mammary gland; those >16 carbons were taken up preformed from circulation, and 16-carbon FA were derived from both sources.

conceal differences between the forms of CLA. The present experiment indicates that the reduction in milk fat synthesis for both ME-CLA and FFA-CLA was comparable at a dose of *trans*-10,*cis*-12 CLA below that which induced maximum levels of MFD.

Previous studies have investigated the digestion of FAME using rodent models. Mead *et al*. (11) found that intestinal absorption of methyl esters of 9,11-octadecadienoic acid was normal in mice, provided some TG or MG was present to promote emulsification. More recent studies with rats indicated that the intestinal hydrolysis and absorption rates of methyl esters of FA from menhaden and rapeseed oils were severalfold slower than the corresponding TG (9,10). In the present study, the similarity between ME-CLA and FFA-CLA in the reduction in milk fat secretion (38 vs. 39%) and the proportion of the abomasal dose of *trans*-10,*cis*-12 CLA transferred to milk fat (18 vs. 19%) clearly indicated that the two forms of CLA were digested with equal efficiency. The commercial manufacture of the methyl esters of CLA utilizes lower levels of catalyst and solvents at lower reaction temperatures as compared with the manufacture of the FFA form, thereby reducing production costs and affording a product of higher purity (8,22). Thus, the methyl ester form of CLA has several potential advantages when applied as an animal supplement. The use of CLA in ruminants will still require it to be protected from rumen metabolism, and several methods of rumen protection have been developed, including Ca salts of FA, amides of FA, formaldehyde treatment, and encapsulation (23,24). The former two methods require the CLA be as a FFA, whereas the latter two methods could use the methyl ester form of CLA to produce a supplement.

The temporal pattern of milk fat secretion showed a decline after the first day of CLA infusion, with the nadir achieved by days 4–5. Further, CLA treatment had no effect on milk yield, yield and content of milk protein, SCC, or feed intake. The temporal pattern and the specificity of the response for milk fat

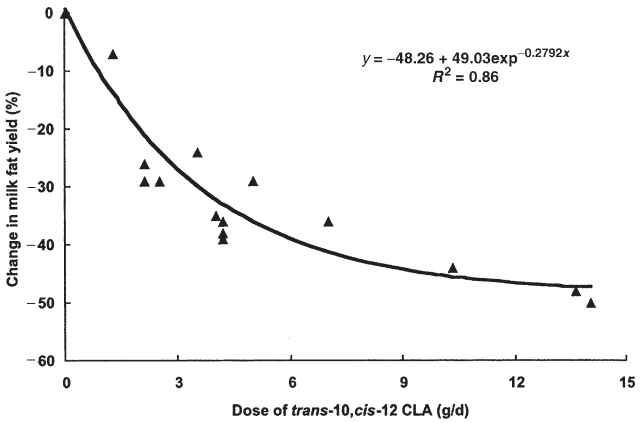

FIG. 2. Decay model of the relationship between the change in milk fat yield and the dose of *trans*-10,*cis*-12 CLA abomasally infused in lactating cows. Points were derived from the present investigation and six other studies (3–5,12–14). For the exponential decay equation fitting the data, y = % change in milk fat yield and x = dose of *trans*-10,*cis*-12 CLA (g/d); $P < 0.001$; SD = 5.74% change in milk fat.

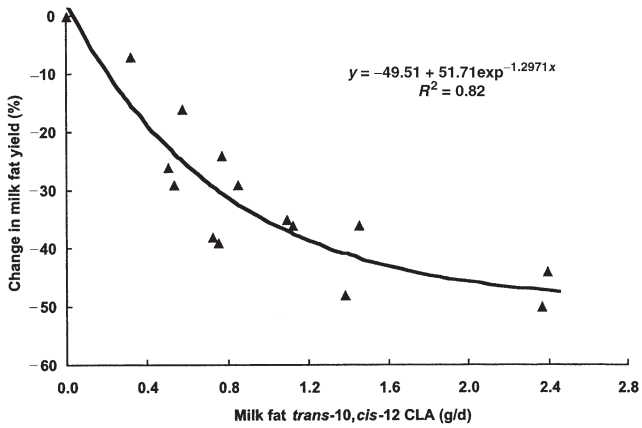

FIG. 4. Decay model of the relationship between the change in milk fat yield and the secretion of *trans*-10,*cis*-12 CLA in milk fat during abomasal infusion of *trans*-10,*cis*-12 CLA in lactating cows. Points were derived from the present investigation and six other studies (3–6,12–14). For the exponential decay equation fitting the data, y = % change in milk fat yield and x = milk fat *trans*-10,*cis*-12 CLA (g/d); $P < 0.001$; SD = 6.55% change in milk fat.

are consistent with results from previous studies in which *trans*-10,*cis*-12 CLA was abomasally infused to mid- and late-lactation dairy cows (3–5,12–14). The milk fat content returned to pretreatment levels by day 5 after the CLA treatment ceased (data not shown), which is also consistent with results from other CLA abomasal infusion studies.

Although a greater decline (116 vs. 57 g/d) occurred in the incorporation of preformed FA ($>C_{16}$) into milk fat than in that of the *de novo* synthesized FA ($<C_{16}$), there was a relatively similar decrease in the proportion of milk FA derived from these two sources (45 and 33% for $<C_{16}$ and $>C_{16}$, respectively). This also has been observed in previous studies in which cows received low doses of *trans*-10,*cis*-12 CLA (<5 g/d) but where, at higher doses, the effects on *de novo* synthesized FA were more pronounced (3–5). Similarly, the lack of effect of CLA treatment on the desaturase ratio, as seen in the current study, has been observed by others at low CLA doses (4,5). *Trans*-10,*cis*-12 CLA has been shown to inhibit both gene expression and activity of Δ^9-desaturase (12,25–27) and to have effects on the desaturase ratio in lactating cows at higher abomasal doses (3,4). However, in considering mechanisms, the results of the present study show that alterations in the desaturase ratio are not essential to obtain a marked reduction in milk fat secretion. The pattern of changes in milk FA suggests that the mechanism through which *trans*-10,*cis*-12 CLA inhibits milk fat synthesis probably involves the coordinated regulation of key lipogenic enzymes. Indeed, Baumgard

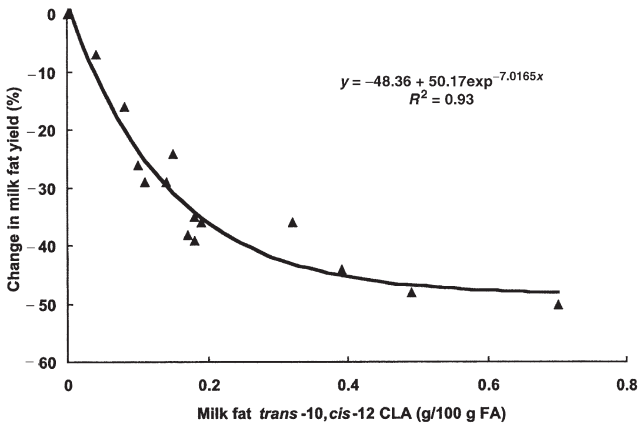

FIG. 3. Decay model of the relationship between the change in milk fat yield and the milk fat content of *trans*-10,*cis*-12 CLA during abomasal infusion of *trans*-10,*cis*-12 CLA in lactating cows. Points were derived from the present investigation and six other studies (3–5,12–14). For the exponential decay equation fitting the data, y = % change in milk fat yield and x = milk fat *trans*-10,*cis*-12 CLA (g/100 g FA); $P < 0.001$; SD = 4.11% change in milk fat.

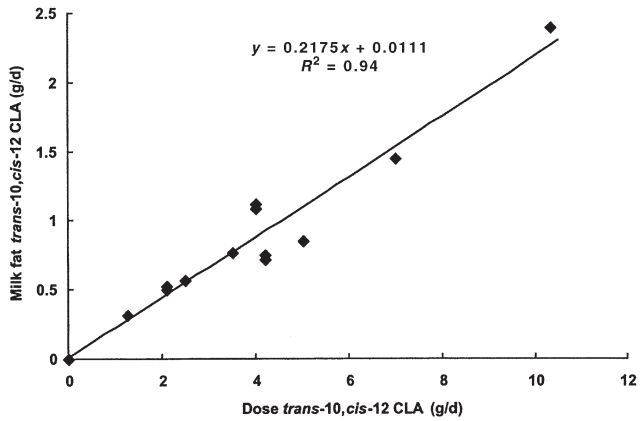

FIG. 5. Relationship between secretion of *trans*-10,*cis*-12 CLA in milk fat and the abomasal infusion dose of *trans*-10,*cis*-12 CLA in lactating cows. Points were derived from the present investigation and five other studies (3–5,13,14). For the linear equation fitting the data, y = milk fat *trans*-10,*cis*-12 CLA (g/d) and x = dose of *trans*-10,*cis*-12 CLA (g/d); $P < 0.001$; SE = 0.043 g/d of *trans*-10,*cis*-12 CLA secreted in milk fat.

et al. (12) demonstrated that mammary tissue from cows abomasally infused with *trans*-10,*cis*-12 CLA had reductions in mRNA abundance for lipogenic genes involved in the uptake and transport, *de novo* synthesis, desaturation, and TG synthesis. Consistent with the coordinated pattern of regulation by *trans*-10,*cis*-12 CLA, recent investigations using bovine mammary cell cultures indicate that the signaling involves the sterol response element-binding protein regulatory pathway (28).

A second objective of the present study was to develop generalized relationships between *trans*-10,*cis*-12 CLA and milk fat across studies. The data set included the present study plus six other studies in which *trans*-10,*cis*-12 CLA had been abomasally infused (3–5,12–14). The exponential decay model that describes the relationship between abomasal dose and milk fat yield (Fig. 1) indicates that, at a low dose of *trans*-10,*cis*-12 CLA, substantial decreases in milk fat yield occur, but beyond a dose of 6 g/d, little additional decrease in milk fat synthesis is observed. Although Bell and Kennelly (29) induced negative effects on milk synthesis (reduction in milk yield and yields of protein and lactose), they found that when *trans*-10,*cis*-12 CLA was abomasally infused at a dose *ca.* eightfold greater (46 g/d), the extent of MFD was limited to 57%, confirming that little or no further reduction in milk fat synthesis occurs at doses of *trans*-10,*cis*-12 CLA greater than 10 g/d.

The exponential decay models for the relationships between the change in milk fat yield and the *trans*-10,*cis*-12 CLA content and yield were appropriate models from a biological basis, as small increases in milk fat content and yield of *trans*-10,*cis*-12 CLA below 0.2% and 1.2 g/d, respectively, were associated with relatively large decreases in milk fat yield (Figs. 3 and 4). In contrast, a milk fat *trans*-10,*cis*-12 CLA content and yield greater than 0.2% and 1.2 g/d, respectively, were associated with a nadir in the reduction in milk fat yield ranging from 40 to 50%.

We also observed a linear relationship between CLA dose and milk yield of *trans*-10,*cis*-12 CLA. Thus, across studies the mammary uptake and use of *trans*-10,*cis*-12 CLA for milk fat synthesis was constant, with a 22% transfer efficiency of the abomasal supply over the range of doses (0 to 10 g/d *trans*-10,*cis*-12 CLA) and milk yields (20 to 37 kg/d). This is particularly impressive given the concomitant decrease in milk fat yield that occurred as the abomasal dose of *trans*-10,*cis*-12 CLA increased (Fig. 2). This suggests that the mechanisms coordinating the CLA-induced decrease in the use of preformed FA for milk fat synthesis had a less pronounced effect on the mammary uptake and incorporation of *trans*-10,*cis*-12 CLA into milk fat, but the basis for this difference is not evident.

Overall, our results demonstrate that *trans*-10,*cis*-12 CLA supplied as a methyl ester or a FFA were equally potent in reducing milk fat synthesis. Thus, rumen-protected forms that utilize either methyl esters or FFA of *trans*-10,*cis*-12 CLA would be effective dietary supplements of CLA to induce MFD. Finally, when data were combined from a range of studies with differing doses of *trans*-10,*cis*-12 CLA, response curves were developed that showed high correlations relating the reduction in milk fat yield to dose, milk fat content, and milk fat secretion of *trans*-10,*cis*-12 CLA. Likewise, across studies the transfer efficiency of abomasally infused *trans*-10,*cis*-12 CLA into milk fat was relatively constant at 22%.

ACKNOWLEDGMENTS

The authors gratefully acknowledge Dr. Luis Tedeschi for his statistical advice and the assistance of Dr. Benjamin Corl, Debbie Dwyer, Dr. Daniel Peterson, Euridice Castaneda-Gutierrez, James Perfield, Sarah Beam, Joseph McFadden, Stephen Tucker, William English, and Gladys Birdsall in implementing the study. This study was supported in part by the U.S. Department of Agriculture's Cooperative State Research, Education, and Extension Service, National Research Initiative Competitive Grants Program (USDA-CSREES-NRICGP, grant 2003-35206-12819), BASF AG (Ludwigshafen, Germany), and the Cornell Agriculture Experimental Station.

REFERENCES

1. Belury, M.A. (2002) Dietary Conjugated Linoleic Acid in Health: Physiological Effects and Mechanisms of Action, *Annu. Rev. Nutr. 22*, 505–531.
2. Pariza, M.W., Park, Y., and Cook, M.E. (2001) The Biologically Active Isomers of Conjugated Linoleic Acid, *Prog. Lipid Res. 40*, 283–298.
3. Baumgard, L.H., Corl, B.A., Dywer, D.A., Sæbø, A., and Bauman, D.E. (2000) Identification of the Conjugated Linoleic Acid Isomer That Inhibits Milk Fat Synthesis, *Am. J. Physiol. 278*, R179–R184.
4. Baumgard, L.H., Sangster, J.K., and Bauman, D.E. (2001) Milk Fat Synthesis in Dairy Cows Is Progressively Reduced by Increasing Supplemental Amounts of *trans*-10,*cis*-12 Conjugated Linoleic Acid (CLA), *J. Nutr. 131*, 1764–1769.
5. Peterson, D.G., Baumgard, L.H., and Bauman, D.E. (2002) Short Communication: Milk Fat Response to Low Doses of *trans*-10,*cis*-12 Conjugated Linoleic Acid (CLA), *J. Dairy Sci. 85*, 1764–1766.
6. Bauman, D.E., and Griinari, J.M. (2003) Nutritional Regulation of Milk Fat Synthesis, *Annu. Rev. Nutr. 23*, 203–227.
7. Bauman, D.E., Corl, B.A., and Peterson, D.G. (2003) The Biology of Conjugated Linoleic Acid in Ruminants, in *Advances in Conjugated Linoleic Acid Research* (Sébédio, J., Christie, W.W., and Adlof, R.O., eds.), Vol. 2, pp. 146–173, AOCS Press, Champaign.
8. Sæbø, A. (2003) Commercial Synthesis of Conjugated Linoleate, in *Advances in Conjugated Linoleic Acid Research* (Sébédio, J.L., Christie, W.W., and Adlof, R., eds.), Vol. 2, pp. 71–81, AOCS Press, Champaign.
9. Yang, L.Y., Kuksis, A., and Myher, J.J. (1989) Lumenal Hydrolysis of Menhaden and Rapeseed Oils and Their Fatty Acid Methyl and Ethyl Esters in the Rat, *Biochem. Cell Biol. 67*, 192–204.
10. Yang, L.Y., Kuksis, A., and Myher, J.J. (1990) Intestinal Absorption of Menhaden and Rapeseed Oils and Their Fatty Acid Methyl and Ethyl Esters in the Rat, *Biochem. Cell Biol. 68*, 480–491.
11. Mead, J.F., Bennett, L.R., Decker, A.B., and Schoenberg, M.D. (1951) The Absorption of Fatty Esters in the Mouse Intestine, *J. Nutr. 43*, 477–484.
12. Baumgard, L.H., Matitashvili, E., Corl, B.A., Dywer, D.A., and Bauman, D.E. (2002) *Trans*-10,*cis*-12 Conjugated Linoleic Acid Decreases Lipogenic Rates and Expression of Genes Involved in Milk Lipid Synthesis in Dairy Cows, *J. Dairy Sci. 85*, 2155–2163.
13. Perfield, J.W., II, Sæbø, A., and Bauman, D.E. (2004) Use of Conjugated Linoleic Acid (CLA) Enrichments to Examine the Effects of *trans*-8,*cis*-10 CLA and *cis*-11,*trans*-13 CLA on Milk Fat Synthesis, *J. Dairy Sci. 85*, 1196–1202.

14. Sæbø, A., Perfield, J.W., II, and Bauman, D.E. (2003) Abomasal Infusion of a Mixture of Conjugated Linolenic Acid ($C_{18:3}$) Isomers Had No Effect on Milk Fat Synthesis, *J. Dairy Sci. 86* (Suppl 1), 245 (abstract).
15. Fox, D.G., Sniffen, C.J., O'Connor, J., Russell, J.B., and Van Soest, P.J. (1992) A Net Carbohydrate and Protein System for Evaluating Cattle Diets. III. Cattle Requirements and Diet Adequacy, *J. Anim. Sci. 70*, 3578–3596.
16. Spires, H.R., Clark, J.H., Derrig, R.G., and Davis, C.L. (1975) Milk Production and Nitrogen Utilization in Response to Postruminal Infusion of Sodium Caseinate in Lactating Cows, *J. Nutr. 105*, 1111–1121.
17. Association of Official Analytical Chemists International (2000) *Official Methods of Analysis*, 17th edn., AOAC, Arlington, VA.
18. Perfield, J.W., II, Bernal-Santos, G., Overton, T.R., and Bauman, D.E. (2002) Effects of Dietary Supplementation of Rumen-Protected Conjugated Linoleic Acid in Dairy Cows During Established Lactation, *J. Dairy Sci. 85*, 2609–2617.
19. Schauff, D.J., Clark, J.H., and Drackley, J.K. (1992) Effects of Feeding Lactating Dairy Cows Diets Containing Extruded Soybeans and Calcium Salts of Long-Chain Fatty Acids, *J. Dairy Sci. 75*, 3003–3019.
20. SAS (2001) *SAS/STAT Users Guide* (release 8.0), SAS Institute, Inc., Cary, NC.
21. Hanson, T.W., Giesy, J.G., McGuire, M.A., Annen, E.L., Bauman, D.E., Sæbø, A., and McGuire, M.K. (2000) Conjugated Linoleic Acids as Free Fatty Acids or Triglycerides Cause Milk Fat Depression, *J. Dairy Sci. 83* (Suppl. 1), 692 (abstract).
22. Fimreite, D., and Sæbø, A. (2003) Conjugated Linoleic Acid Compositions, U.S. Patent 6,524,527.
23. Doreau, M., Demeyer, D.I., and Van Nevel, C.J. (1997) Transformation and Effects of Unsaturated Fatty Acids in the Rumen: Consequences on Milk Fat Secretion, in *Milk Composition, Production and Biotechnology* (Welch, R.A.S., Burns, D.J.W., Davis, S.R., Popay, A.I., and Prosser, C.G., eds.), pp. 73–92, CAB International, Wallinford, Oxfordshire, United Kingdom.
24. Wu, S.H.W., and Papas, A. (1997) Rumen-Stable Delivery Systems, *Adv. Drug Delivery Rev. 28*, 323–334.
25. Lee, K.N., Pariza, M.W., and Ntambi, J.M. (1998) Conjugated Linoleic Acid Decreases Hepatic Stearoyl-CoA Desaturase mRNA Expression, *Biochem. Biophys. Res. Comm. 248*, 817–821.
26. Bretillon, L., Chardigny, J.M., Grégoire, S., Berdeaux, O., and Sébédio, J.L. (1999) Effects of Conjugated Linoleic Acid Isomers on the Hepatic Microsomal Desaturation Activities *in vitro*, *Lipids 34*, 965–969.
27. Park, Y., Storkson, J.M., Ntambi, J.M., Cook, M.E., Sih, C.J., and Pariza, M.W. (2000) Inhibition of Hepatic Stearoyl-CoA Desaturase Activity by *trans*-10,*cis*-12 Conjugated Linoleic Acid and Its Derivatives, *Biochem. Biophys. Acta 1486*, 285–292.
28. Peterson, D.G., Matitashvili, E., and Bauman, D.E. (2003) The Inhibitory Effect of *t*10,*c*12 CLA on Lipid Synthesis in Bovine Mammary Epithelial Cells Involves Reduced Proteolytic Activation of the Transcription Factor SREBP-1, *Exp. Biol. 2003*, 686.6 (abstract).
29. Bell, J.A., and Kennelly, J.J. (2003) Short Communication: Postruminal Infusion of Conjugated Linoleic Acid Negatively Impacts Milk Synthesis in Holstein Cows, *J. Dairy Sci. 86*:1321–1324.

[Received November 12, 2003; accepted May 14, 2004]

Positional Distribution of Decanoic Acid: Effect on Chylomicron and VLDL TAG Structures and Postprandial Lipemia

Kaisa M. Yli-Jokipii[a,*], Ursula S. Schwab[b], Raija L. Tahvonen[a], Xuebing Xu[c], Huiling Mu[c], and Heikki P.T. Kallio[a,d]

[a]Department of Biochemistry and Food Chemistry, University of Turku, Turku, Finland, [b]Department of Clinical Nutrition, University of Kuopio and Kuopio University Hospital, Kuopio, Finland, [c]BioCentrum-DTU, Center for Advanced Food Studies, Technical University of Denmark, Lyngby, Denmark, and [d]Functional Foods Forum, University of Turku, Turku, Finland

ABSTRACT: Although medium-chain FA (MCFA) are mainly absorbed *via* the portal venous system, they are also incorporated into chylomicron TAG; therefore, the positional distribution of MCFA in TAG is likely to affect their metabolic fate. We studied chylomicron and VLDL TAG structures, as well as the magnitude of postprandial lipemia, after two oral fat loads containing decanoic acid (10:0) predominantly at the *sn*-1(3),2 (MML) or at the *sn*-1,3 positions (MLM) of TAG in a randomized, double-blind, crossover clinical trial with 10 healthy, normal-weight volunteers. An MS-MS method was used to analyze TAG regioisomers. The position of decanoic acid in chylomicron TAG reflected its position in the TAG ingested, and TAG with none, one, two, or three decanoic acid residues were detected after ingestion of both fats. More ($P < 0.05$) 30:0 and 38:1 TAG (acyl carbons:double bonds) and fewer 46:5, 54:5, and 54:4 TAG were found in chylomicrons after ingestion of MML than after MLM. The VLDL TAG composition did not differ between the fat loads but did change ($P < 0.05$) 2 to 6 h after ingestion of both fats. No statistical differences were seen between the fat loads in areas under the plasma, chylomicron, or VLDL TAG response curves or in FFA concentrations. Thus, the positional distribution of MCFA in TAG affects their metabolic fate, but the magnitude of postprandial lipemia does not seem to be dependent on the positional distribution of MCFA in the ingested fat.

Paper no. L9454 in *Lipids 39*, 373–381 (April 2004).

TAG with medium-chain FA (MCFA, C_6–C_{10}) and long-chain FA (LCFA, $>C_{10}$), attached to specific locations on the glycerol backbone, were first developed to deliver both energy and EFA to infants and patients suffering from pancreatic insufficiency. Unlike LCFA, which are transported in chylomicrons, MCFA are transported predominantly in the portal blood. MCFA enter mitochondria without carnitine and are preferentially oxidized. TAG containing MCFA are ideal ingredients for functional foods, since, in the long run, they may increase energy expenditure, result in faster satiety, and facilitate weight control when included in the diet as a replacement for fats containing LCFA (1).

The methodology for producing structured TAG with MCFA predominantly in the *sn*-1/3 positions and LCFA in the *sn*-2 position has been studied extensively. However, molecular-level effects of TAG with similar FA compositions but different positional distributions of FA have previously been compared in the rat model only. In these studies MCFA have been absorbed *via* the portal venous system as well as incorporated into chylomicron TAG (2–5). The proportion of MCFA incorporated into chylomicrons has depended on the position of the MCFA in the TAG molecule (2,6), and the overall lymph flow or TAG output has (7) or has not (5) been affected by the location of the MCFA.

The metabolic fate of MCFA of different structures has been difficult to study at the molecular level in humans because of the lack of sensitive methods of analysis. In this study, the MS-MS method previously applied to regioisomer analysis of various physiological samples containing TAG with LCFA (8–10) and edible oils containing MCFA (11,12) was applied to the analysis of chylomicron and VLDL TAG. The postprandial effects of two fats containing decanoic acid residues predominantly at the *sn*-1(3),2 or the *sn*-1,3 positions (MML and MLM, respectively) were compared.

MATERIALS AND METHODS

Study design. The study used a randomized, double-blind crossover design. Postprandial responses to two oral fat loads predominantly containing decanoic acid at either the *sn*-1(3),2 or the *sn*-1,3 positions were measured over 6 h on two occasions 4 wk apart. The study plan was approved by the Ethics Committee of the Hospital District of Northern Savo.

Subjects. Seven female and three male volunteers were recruited from the student population of the University of Kuopio, Finland. Each subject had normal liver, kidney, and thyroid functions and had no chronic illnesses. Each subject gave written informed consent, and the subjects were free to discontinue participation at any point in the study without explanation.

The volunteers [aged 24 ± 3 yr (mean ± SD), body mass index 22.0 ± 2.4 kg/m^2] exhibited the following characteristics

*To whom correspondence should be addressed at Department of Biochemistry and Food Chemistry, University of Turku, FIN-20014 TURKU, Finland. E-mail: kaisa.yli-jokipii@utu.fi

Abbreviations: ACN, acyl carbon number; DB, double bond; LCFA, long-chain FA; LLM, structured TAG with MCFA predominantly in the *sn*-1/3 position; LML, structured TAG with MCFA predominantly in the *sn*-2 position; MCFA, medium-chain FA; MLM, structured TAG with MCFA predominantly at the *sn*-1,3 positions; MML, structured TAG with MCFA predominantly at the *sn*-1(3),2 positions.

at the fasting state: total cholesterol 4.5 ± 0.7 mmol/L, LDL cholesterol 2.5 ± 0.5 mmol/L, HDL cholesterol 1.6 ± 0.3 mmol/L, TAG 1.0 ± 0.5 mmol/L, and plasma glucose 5.1 ± 0.3 mmol/L. There were no differences in any fasting values between the oral fat loads. Female volunteers were at the same stage of their menstrual cycle on both test days.

The subjects were asked to fast overnight (14 h) and advised not to consume alcohol or engage in strenuous exercise for 5 d before the fat load. The subjects were advised to eat as usual but to avoid fatty foods the evening before the fat load. The subjects kept food records from Wednesday to Saturday the week prior to the test week and the day preceding the test day. The food diaries were calculated with Micronutrica software (version 2.5), and no statistical differences were found between the fat loads in the intake of energy nutrients (fat, protein, or carbohydrate), FA (saturated, monounsaturated, or polyunsaturated), or total energy.

Oral fat load. Fat of the MML type was made from tridecanoin (Grünau GmbH, Illertissen, Germany) and rapeseed oil FA (Henkel KGaA, Düsseldorf, Germany), and fat of the MLM type was made from rapeseed oil (Aarhus Olie, Aarhus, Denmark) and decanoic acid (Grünau GmbH). Both were produced by acidolysis [in either a continuous (MML) or batch (MLM) reactor] with Lipozyme RM IM (Novozymes A/S, Bagsværd, Denmark) as the active enzyme (13). The two resulting fats had different positional distributions of FA but quite similar FA compositions (Table 1) when measured as described previously (14). Both fats were liquid at room temperature.

The amount of fat in the test meal was 35 g per body square meter area according to the Dubois body surface chart. The fat was blended with ultra-high-temperature-treated skim milk low in lactose so that the percentage of fat in the resulting mixture was 30. Chocolate aroma (0.1 g) (Chocolate Flav-o-lok, Givaudan, Barneveld, The Netherlands) and 0.5 g of sweetener containing 3% aspartame and 97% maltodextrin (G.D. Searle and Co., Paris, France) were added, and the blend was served. Five minutes prior to ingestion of the test meal, a rice cake (8.2 g) topped with low-fat cheese [10 g cheese (12% fat, 7% saturated fat)/70 kg body weight; Valio Ltd., Helsinki, Finland] was served. Water (0.1 L) was provided with the meal. After 2 h, subjects were provided water *ad libitum*.

TABLE 1
Total and *sn*-2 Position FA Composition of Test Fats (mol%), 1,2(2,3)-Didecanoyl-3(1)-Long-Chain FA-*sn*-Glycerol Type Fat (MML) and 1,3-Didecanoyl-2-Long-Chain FA-*sn*-Glycerol Type Fat (MLM)

	MML		MLM	
FA	Total	*sn*-2	Total	*sn*-2
8:0	3.2	4.6	0.8	0.0
10:0	63.6	91.3	59.3	13.7
16:0	1.7	0.1	1.0	0.6
18:0	0.5	0.0	0.3	0.2
18:1	20.9	1.5	20.9	41.3
18:2n-6	6.3	0.5	11.7	28.3
18:3n-3	1.8	0.1	5.1	12.5
Others	2.0	1.8	0.9	3.6

Laboratory methods. Blood was drawn from an antecubital vein at the fasting state and postprandially: at 20-min intervals during the first hour; at 30-min intervals during the second hour; and at 3, 4, 5, and 6 h.

The isolation of chylomicron- (Svedberg flotation > 400) and VLDL- (Svedberg floation 20 to 400) rich fractions was performed as described previously (15). Plasma TAG and serum FFA concentrations were determined by enzymatic colorimetric methods (Monotest Triglyceride GPO-PAP, Boehringer Mannheim, Mannheim, Germany; NEFA C, ACS-ACOD method, Wako Chemicals GmbH, Neuss, Germany). Serum insulin was measured by a radioimmunoassay method (Phadeseph Insulin RIA 100; Pharmacia Diagnostics, Uppsala, Sweden). Plasma glucose was analyzed with a glucose dehydrogenase method (Granutest 250; Diagnostica Merck, Darmstadt, Germany). Incremental areas under the TAG response curves were calculated by the trapezoidal rule with Canvas™ software (version 6, Deneba Software Inc., Miami, FL).

Lipids from the chylomicron and VLDL samples collected at 90 min to 6 h postprandially were extracted, and TAG were separated from the extracted lipid mixture (16,17).

The M.W. distributions of TAG extracted from the chylomicron and VLDL samples were determined with a triple-quadrupole tandem mass spectrometer (TSQ-700; Finnigan MAT, San Jose, CA) in quadruplicate (18,19). TAG regioisomers of chylomicron samples at 1.5 to 6 h and VLDL samples at 2, 4, and 6 h postprandially were determined in quadruplicate by an MS-MS analysis based on negative-ion CI and collision-induced dissociation with argon with the same instrument as in the M.W. determination (18,20,21).

Results were calculated with an MSPECTRA program (Nutrifen, Turku, Finland) (22). The M.W. fractions corresponding to the acyl carbon number:number of double bonds (ACN:DB) 46:3, 46:2, 52:3, and 52:2 were analyzed from chylomicron TAG, and the 50:2, 52:3, and 52:2 fractions were analyzed from VLDL TAG.

Mixtures of 1,2-dioleoyl-3-decanoyl-*rac*-glycerols and 1,3-dioleoyl-2-decanoyl-*sn*-glycerols (99% pure; Larodan, Malmö, Sweden) were used to optimize the MS-MS method for TAG containing decanoic acid. The method was found to be less regioselective in the analysis of TAG containing decanoic acid than in that of TAG containing LCFA only, and to overestimate the proportion of decanoic acid in the *sn*-2 position. Regioisomerism results of TAG containing decanoic acid were corrected according to second-order curves of real vs. measured results. Despite this correction, the method was unable to detect less than 5.7% TAG containing decanoic acid in the *sn*-1/3 position from TAG containing decanoic acid in the *sn*-2 position (LLM and LML, respectively); these cases (12 of 960 analyses) were assumed to contain 5.7% LLM and 94.3% LML.

Statistical methods. Normal distribution of the data was tested with the Shapiro–Wilk test. Paired-samples *t*-tests or Wilcoxon matched-pairs signed ranks tests, depending on the normality of the distribution, were used to compare dietary records, chylomicron, and VLDL TAG M.W. fractions, regioisomers, incremental areas, and individual time points of

plasma, chylomicrons, or VLDL TAG between the oral fat loads. ANOVA for repeated measures (general linear model test) was used to compare differences between chylomicron and VLDL attributes within treatment. SPSS for Windows (version 10; SPSS Inc., Chicago, IL) was used to analyze data.

RESULTS

No statistical differences were found between the fat loads in areas under the plasma, chylomicron, of VLDL TAG response curves or in the TAG, FFA, glucose, or insulin concentrations at individual time points, except for a higher concentration of chylomicron TAG after ingestion of MLM than after ingestion of MML at the 6-h time point (0.17 ± 0.13 mmol/L and 0.07 ± 0.05 mmol/L, $P = 0.01$) (Fig. 1).

Chylomicron TAG that were more abundant than 1.5% at any measured time point, and the capric acid-containing TAG 38:3 and 44:3 are presented in Figures 2A and B. Major proportions (54–72% after ingestion of MML and 62–76% after ingestion of MLM) were likely to contain no decanoic acid residues (ACN 48–54). The proportion of TAG with predominantly one decanoic acid residue (ACN 42–46) was 15–27% after ingestion of MML and 15–26% after MLM, and that of two decanoic acid residues (ACN 32–38) was 8.3–13% after MML and 5.0–7.8% after MLM. Tricaprin (ACN 30) accounted for 1.5–2.6% after ingestion of MML and 0.3–0.8% after MLM. There were proportionally more M.W. fractions of 30:0 and 38:1 and fewer of 46:5, 54:5, and 54:4 ($P < 0.05$ in five or six of the six measured time points) in chylomicrons after ingestion of MML than after MLM.

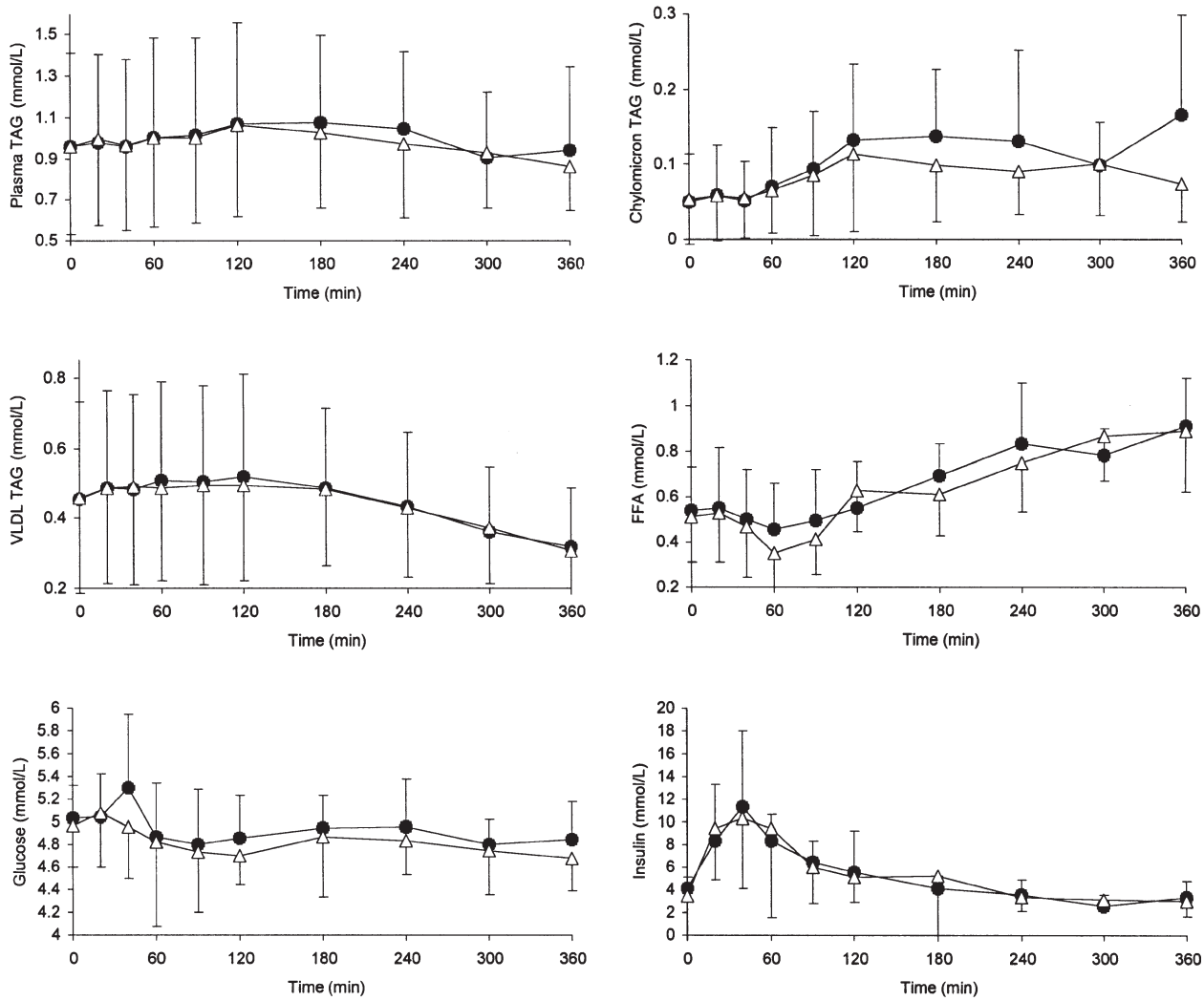

FIG. 1. Postprandial responses of plasma TAG, chylomicron TAG, VLDL TAG, FFA, insulin, and glucose after oral fat loads containing fats of 1,2(2,3)-didecanoyl-3(1)-long-chain FA-*sn*-glycerol type (MML) (△) and 1,3-didecanoyl-2-long-chain FA-*sn*-glycerol type (MLM) (●). Values are means ± SD ($n = 10$). No statistical differences were seen between fat loads in areas under the plasma or chylomicron of VLDL TAG response curves, or in TAG, FFA, glucose, or insulin concentrations at individual time points, except for a higher concentration of TAG after ingestion of MLM than after MML at the 6-h time point (0.17 ± 0.13 mmol/L and 0.07 ± 0.05 mmol/L, $P = 0.01$).

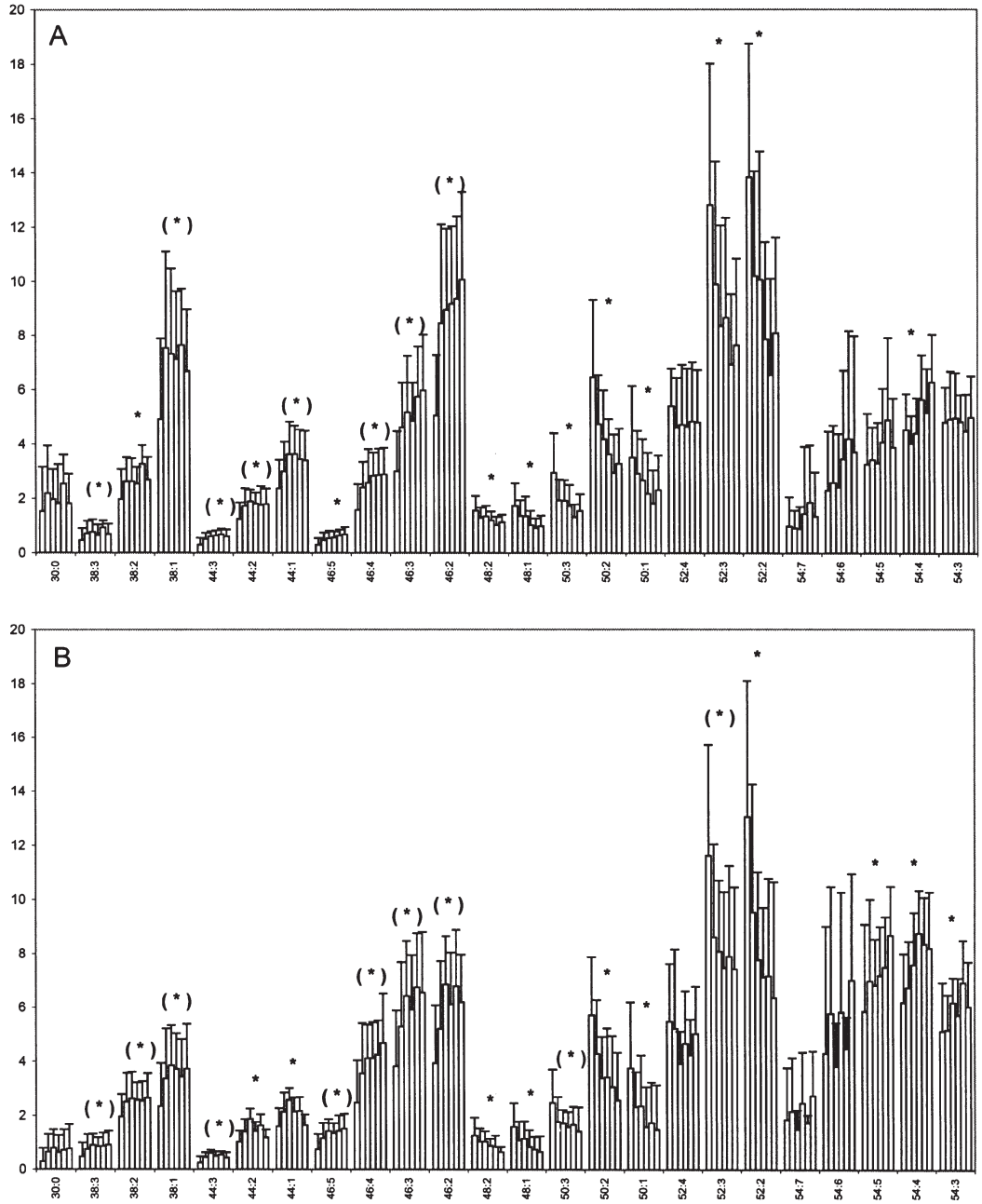

FIG. 2. Chylomicron TAG M.W. distribution. Molar percentages of chylomicron TAG according to M.W. (acyl carbon number:number of double bonds, ACN:DB) during postprandial lipemia in subjects receiving an oral fat load containing structured fats of MML type (A) or MLM type (B). Values are means ± SD (n = 10). Times of blood draw (1.5, 2, 3, 4, 5, and 6 h from left to right, respectively) are represented by the bars. An asterisk, *, and asterisk in parentheses, (*), indicate a difference from the linear trend ($P < 0.05$) between time points 2–6 h and 1.5–6 h, and 1.5–6 h only, respectively, in the general linear model test for the corresponding ACN:DB fractions within a fat load. The following ACN:DB fractions differ ($P < 0.05$) in five or six of the six measured time points between fat loads: 30:0, 38:1, 46:5, 54:5, and 54:4. For other abbreviations see Figure 1.

The proportions of several chylomicron TAG M.W. fractions changed during the postprandial response ($P < 0.05$) after both fat loads (Figs. 2A and 2B). In many cases, only the 1.5-h time point differed from the other time points. The proportion of decanoic acid-containing TAG remained constant for 2 to 6 h after ingestion of both fats. The 48:2, 48:1, 50:2, 50:1, and 52:2 TAG decreased and the 54:4 increased ($P < 0.05$) in chylomicrons 2 to 6 h after ingestion of both fat loads. Twelve TAG regioisomers were quantified from M.W. fractions of 46:3, 46:2, 52:3, and 52:2 (Figs. 3A and 3B). The position of dec-anoic acid in chylomicron TAG reflected its position in the ingested fat, and the proportion of each decanoic acid-containing TAG differed ($P < 0.05$) after ingestion of fats of the MML and MLM type at all measured time points. The proportion of

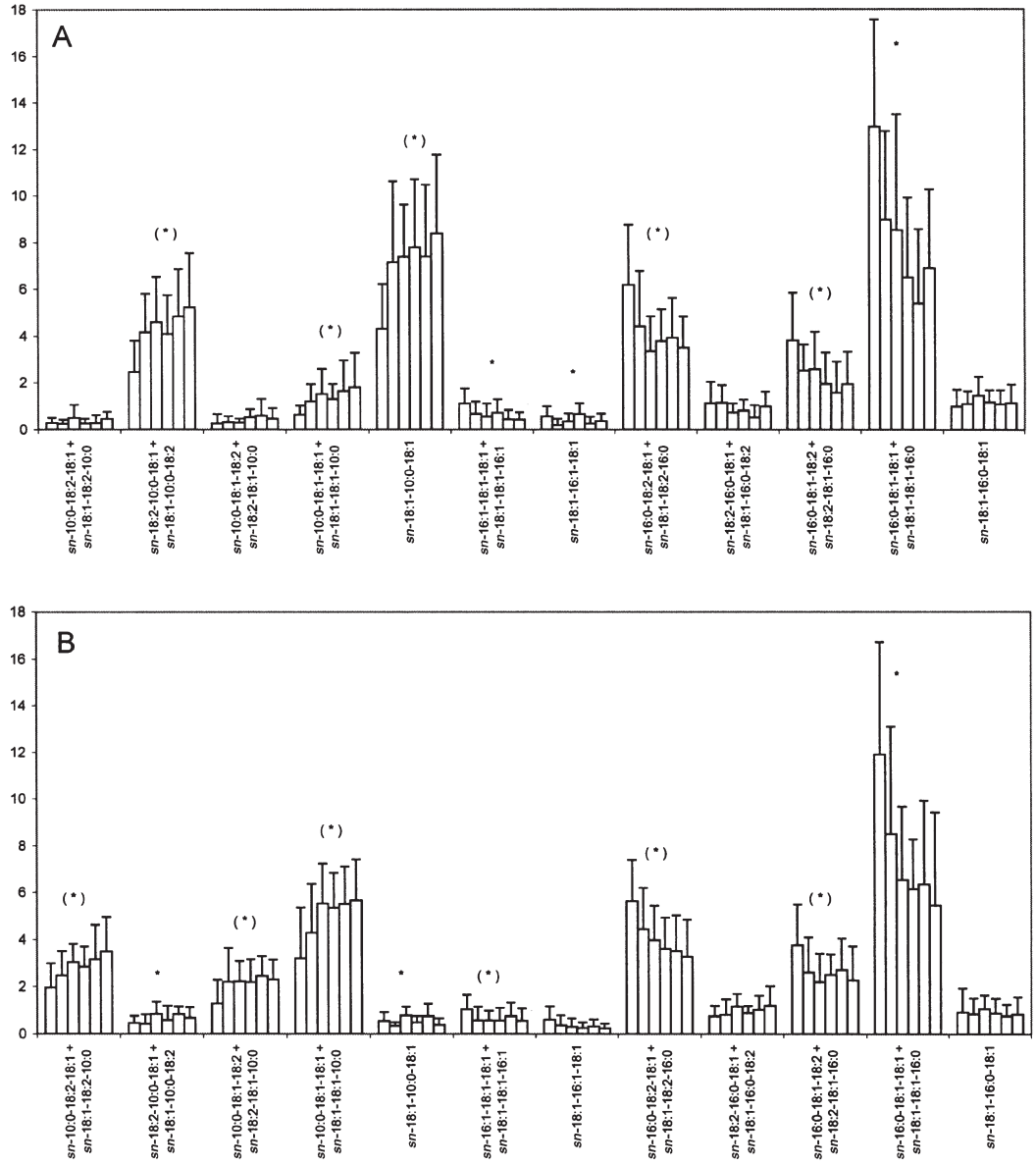

FIG. 3. Positional distribution of FA in chylomicron TAG. Positional distribution of chylomicron TAG with ACN:DB 46:3, 46:2, 52:3, and 52:2 during postprandial lipemia in subjects receiving an oral fat load containing structured fats of MML type (A) or MLM type (B). Values are molar percentages (means ± SD) of chylomicron TAG (n = 10). Times of blood draw (1.5, 2, 3, 4, 5, and 6 h from left to right, respectively) are represented by the bars. An asterisk, *, and an asterisk in parentheses, (*), indicate a difference from the linear trend ($P < 0.05$) between time points 2–6 h and 1.5–6 h, and 1.5–6 h only, respectively, in the general linear model test for the corresponding regioisomer within a treatment. The following regioisomers differ between fat loads: TAG containing decanoic acid at all time points, *sn*-18:1-16:1-18:1 at 4 h, and *sn*-18:1-16:0-18:1 at 4 h. For abbreviations see Figures 1 and 2.

TAG without decanoic acid did not differ between fat loads. Only two regioisomers were present at significantly different proportions after ingestion of the two fats (*sn*-18:1-16:1-18:1 at 4 h and *sn*-18:1-16:0-18:1 at 4 h). Proportionally nonlinear ($P < 0.05$) behavior was often seen between the 1.5- and 6-h time points, but not between the 2- and 6-h time points. *sn*-16:0-18:1-18:1 + *sn*-18:1-18:1-16:0 decreased ($P < 0.05$) after both meals.

The VLDL TAG M.W. fractions that were more abundant than 1.5% at any measured time point are presented in Figures 4A and 4B. Most VLDL TAG contained three LCFA residues, but some TAG that were likely to contain one decanoic acid residue were present in the VLDL fraction. Many VLDL TAG showed significant ($P < 0.05$) nonlinear behavior after ingestion of the MLM fat load only, but similar nonsignificant ($P > 0.05$) behavior was also noticeable after ingestion of MML. In general, at 1.5 to 6 h postprandially, TAG with ACN of 44–46 fluctuated, whereas TAG with ACN of 48–52 had a tendency to decrease, and TAG with ACN of 54 had a tendency to increase.

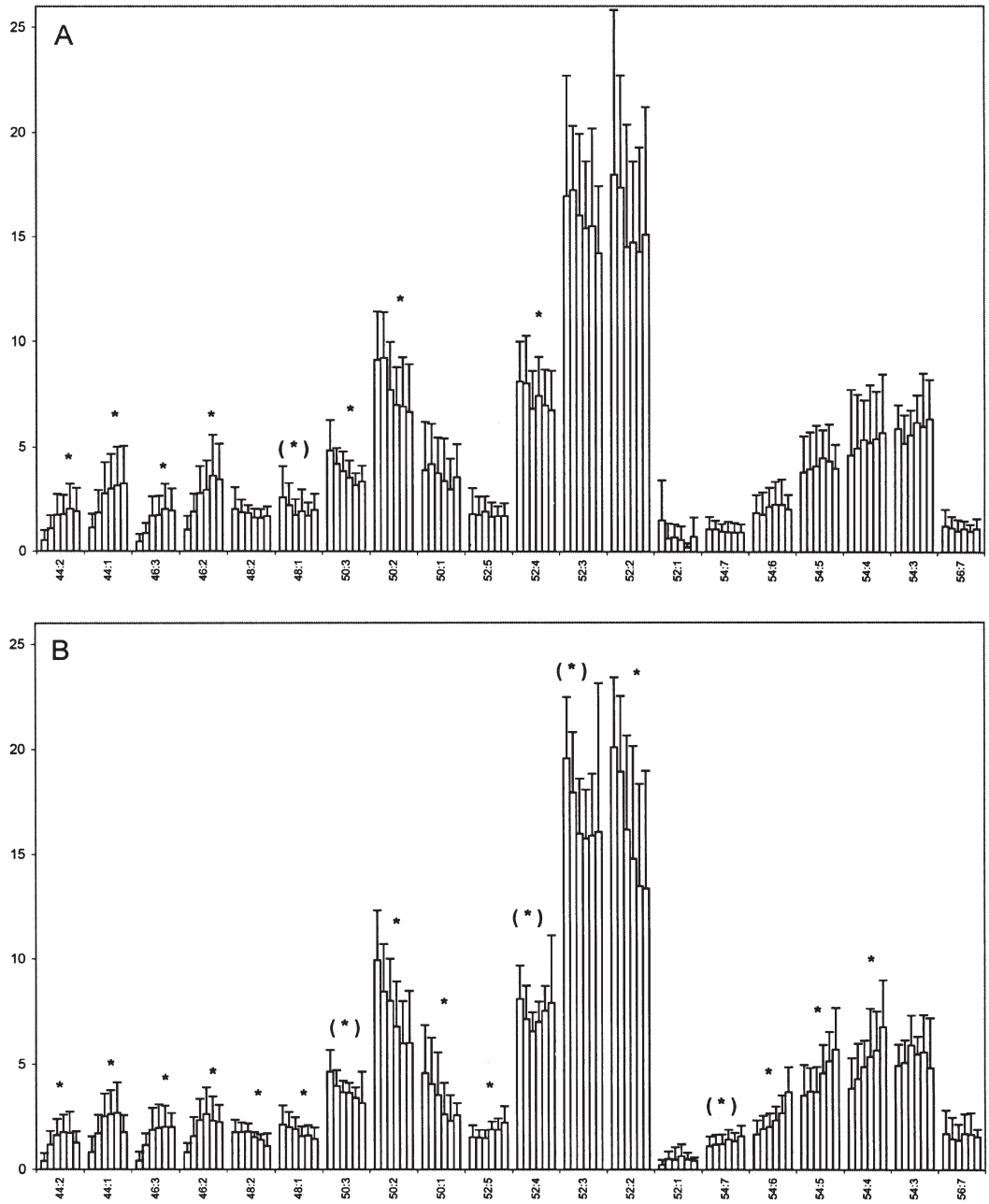

FIG. 4. VLDL TAG M.W. distribution. Molar percentages of VLDL TAG according to M.W. (ACN:DB) during postprandial lipemia in subjects receiving an oral fat load containing structured fats of MML type (A) or MLM type (B). Values are means ± SD (n = 10). Times of blood draw (1.5, 2, 3, 4, 5, and 6 h from left to right, respectively) are represented by the bars. An asterisk, *, and asterisk in parentheses, (*), indicate a difference from the linear trend ($P < 0.05$) between time points 2–6 h and 1.5–6 h, and 1.5–6 h only, respectively, in the general linear model test for the corresponding ACN:DB fractions within treatment. The following ACN:DB fractions differ ($P < 0.05$) between fat loads: 44:2, 6 h; 44:1, 6 h; 46:3, 2 h; 46:2, 5 h, 6 h, 48:2, 6 h; 52:5 6 h; 52:1, 1.5 h; 54:7, 4 h, 5 h, 6 h, 54:6 6 h, 54:5 6 h, 54:4 4 h, 56:7 4 h, 5 h, 6 h. For abbreviations see Figures 1 and 2.

Fourteen regioisomers were quantified from the M.W. fractions of 50:2, 52:3, and 52:2 (Figs. 5A and 5B). *sn*-16:0-18:1-18:1 + *sn*-18:1-18:1-16:0 was the most abundant (12–18 %) of all the VLDL TAG. Between-treatment differences were minimal: Only the 4-h time point of *sn*-18:2-16:0-18:1 + *sn*-18:1-16:0-18:2 and the 6-h time point of *sn*-18:1-16:0-18:1 differed ($P < 0.05$) between treatments. *sn*-16:0-18:1-18:1 + *sn*-18:1-18:1-16:0, *sn*-14:0-18:1-18:1 + *sn*-18:1-18:1-14:0, *sn*-16:0-16:1-18:1 + *sn*-18:1-16:1-16:0, and *sn*-16:0-16:0-18:2 + *sn*-18:2-16:0-16:0 decreased ($P < 0.05$) after ingestion of both fat loads.

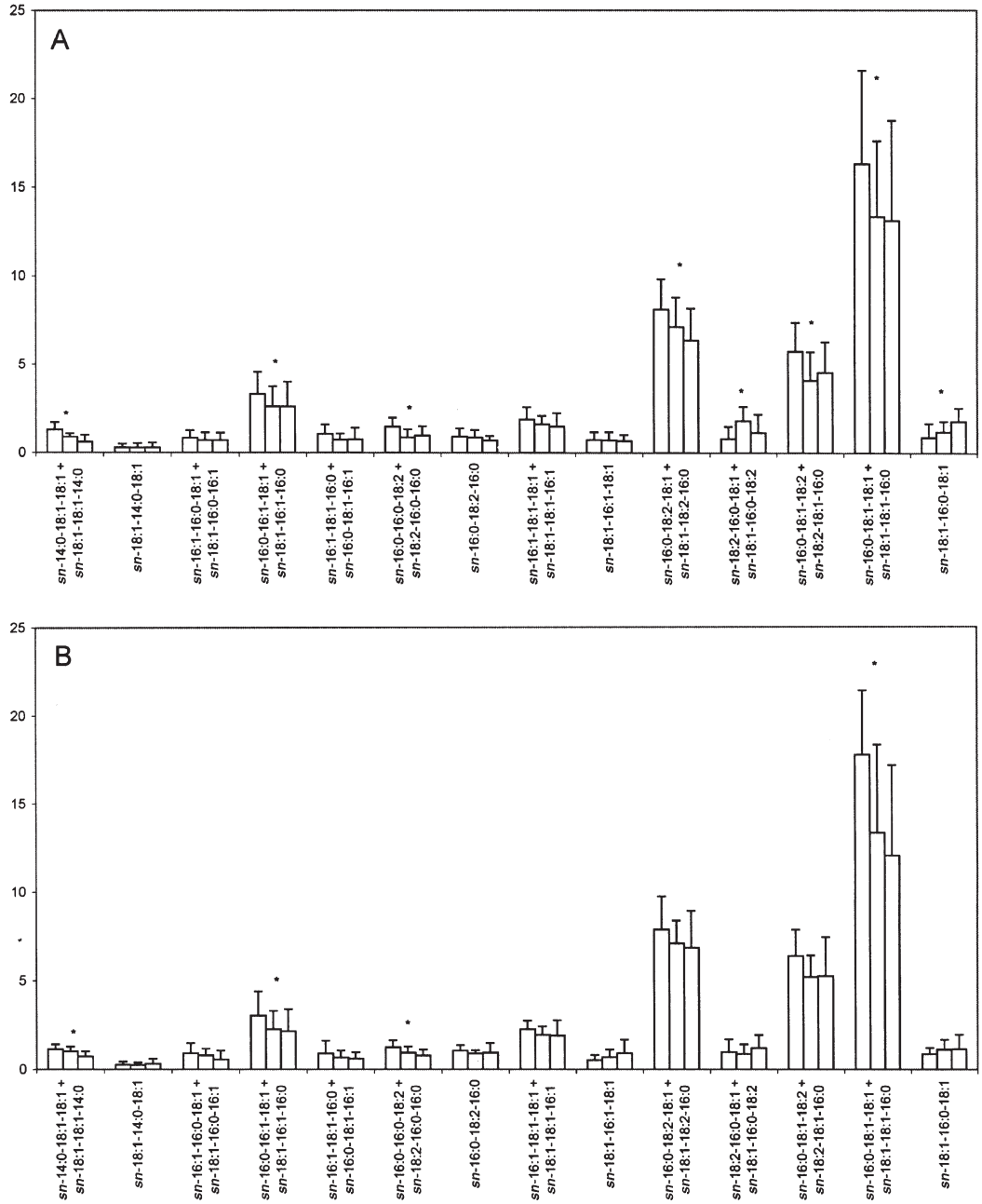

FIG. 5. Positional distribution of FA in VLDL TAG. Positional distribution of VLDL TAG with ACN:DB 50:2, 52:3, and 52:2 during postprandial lipemia in subjects receiving an oral fat load containing structured fats of MML type (A) or MLM type (B). Values are molar percentages (means ± SD) of VLDL TAG (n = 10). Times of blood draw (2, 4, and 6 h from left to right, respectively) are represented by the bars. An asterisk, *, indicates a difference from the linear trend ($P < 0.05$) between time points in the general linear model test for the corresponding regioisomer within a fat load. The following regioisomers differ between fat loads: *sn*-18:2-16:0-18:1 + *sn*-18:1-16:0-18:2 at 4 h and *sn*-18:1-16:0-18:1 at 6 h. For abbreviations see Figures 1 and 2.

DISCUSSION

As previously observed in rats (3), decanoic acid was transported both *via* the portal venous route and in chylomicrons. Large individual variations in plasma and chylomicon TAG concentrations and chylomicron TAG M.W. compositions were likely to result from individual differences in the magnitude of the two transport routes. Decanoic acid was transported in chylomicrons predominantly in the same position as in the fat ingested, indicating that decanoic acid had entered the same pathway as chylomicron LCFA.

The larger proportions of decanoic acid-containing 30:0 and

38:1 TAG after ingestion of MML in chylomicrons was compensated for by larger proportions of non-decanoic acid-containing 54:5 and 54:4 TAG after ingestion of MLM, possibly causing the areas under the chylomicron TAG response curves to be undifferentiated. In rats, the lymphatic absorption of MCFA located in the *sn*-2 position has been more efficient than of those located in the *sn*-1/3 positions in some (2,6) but not all (23) studies. Neither the lymphatic output rate nor the accumulated lymphatic transport has previously been related to the position of MCFA in the TAG (5,23). However, Straarup and Høy (23) concluded that higher recovery of exogenous α-linolenic acid after ingestion of structured MLM-type fat than after ingestion of a randomized oil or a physical mixture, and a similar quantity of decanoic acid in the lymph after ingestion of the three oils were indications of better hydrolysis and absorption of the structured MLM fat than of the other oils tested. Our present results indicate that structured TAG do not necessarily provide any extra benefit to healthy adults compared with randomized TAG with the same FA composition where the magnitude of postprandial lipemia is concerned. In this aspect, our study supports a recent study in which no differences in energy expenditure or substrate oxidation were found in a crossover trial with 11 healthy volunteers who consumed three meals with modified fats containing octanoic acid and LCFA in the same proportions but in different *sn*-positions (structured MLM, randomized fats, and physically mixed fats) (24). Although structured lipids have, to date, not proven to reduce the postprandial lipid response or increase satiety in healthy adults compared with randomized fats with the same FA composition, structured lipids of MLM are important in the nutritional support of patients suffering from malabsorption (23,25,26).

Changes in the chylomicron TAG M.W. composition, and variations between subjects, were of greater magnitude in the current study than in our previous trials with palm oil (9) or lard (10). However, some of the results obtained in these three trials are surprisingly similar: Of the M.W. fractions followed after six meals (palm oil, transesterified palm oil, lard, modified lard, MLM, and MML), 48:2 has decreased (1.5 to 6 h postprandially, $P < 0.05$) on five of six occasions, 48:1 on four of six occasions, 50:3 on all six occasions, and 50:2 on five of six occasions. However, comparison of these studies is problematic, since the FA compositions of palm oil, lard, and structured TAG are very different.

In the current study, the nonlinear behavior of M.W. fractions is believed to result from at least three factors. First, the fact that significantly less decanoic acid-containing TAG (38:3, 38:1, 44:3, 46:4, 46:3, and 46:2) were present at the 1.5-h time point than at the 2- to 6-h time points could have resulted from greater transport of decanoic acid in the portal venous blood up to 1.5 h or from the greater contribution of endogenous FA up to this point. Second, LCFA could have been preferentially incorporated into chylomicron TAG in the enterocytes until the storage capacity of the cell was full. However, the difference between chylomicron TAG at the 1.5-h time point and at the 2- to 6-h time points also was noticeable after ingestion of palm oil (9). Third, the physical properties of chylomicrons depend on the FA composition (27) and structure of TAG, and decanoic acid might have altered chylomicron susceptibility to the stereoselective behavior of lipoprotein lipase. However, action of the lipoprotein lipase did not seem to be affected by the positional distribution of decanoic acid, since all non-decanoic acid-containing TAG behaved similarly after ingestion of both meals.

Some low-molecular-weight TAG (ACN 44–46) were found in the VLDL-rich fraction. It is theoretically possible that these TAG were not in VLDL but in chylomicron remnants, since the chylomicron- and VLDL-rich fractions were isolated based on density of the lipoproteins. However, we think this is unlikely, because these low-molecular-weight of TAG were not present in VLDL in the same proportions as in the chylomicrons and because differences in the VLDL TAG structure have been modest in our previous trials (8,10), despite clear differences in TAG structure in the chylomicron fraction.

The behavior of VLDL TAG was similar after ingestion of both fats, despite the fact that some changes were significant after only one of the fat loads. The TAG 50:3 and 50:2 decreased in the current study and in the lard-based study, but 52:3 and 52:2 behaved differently in the two studies (10). The behavior of many VLDL TAG regioisomers was dissimilar in the current study compared with the lard-based study (10), but *sn*-16:0-18:1-18:1 + *sn*-18:1-18:1-16:0 was the most abundant VLDL TAG in all three of the studies (8,10).

Our studies confirm that decanoic acid is transported both *via* the portal venous route and in chylomicrons in healthy adults, and that the positional distribution of the fat ingested is well preserved in chylomicrons. The positional distribution of MCFA affected their metabolic fate, but the magnitude of postprandial lipemia did not seem to be dependent on the positional distribution of MCFA in the ingested fat.

ACKNOWLEDGMENTS

We are grateful for the volunteers who participated in this study. Erja Kinnunen, Kaisa Vartio, Antti Järvinen, Vesa Puoskari, and Eveline Kole are thanked for excellent assistance. The Applied Bioscience Graduate School, Raisio Group Foundation, Raisio plc, and Atria plc as well as European MRI program via LMC, Denmark, are acknowledged for financial support.

REFERENCES

1. St-Onge, M.-P., and Jones, P.J.H. (2002) Physiological Effects of Medium Chain Triglycerides: Potential Agents in the Prevention of Obesity, *J. Nutr. 132*, 329–332.
2. Ikeda, I., Tomari, Y., Sugano, M., Watanabe, S., and Nagata, J. (1991) Lymphatic Absorption of Structured Glycerolipids Containing Medium-Chain Fatty Acids and Linoleic Acid, and Their Effect on Cholesterol Absorption in Rats, *Lipids 26*, 369–373.
3. Mu, H., and Høy, C.-E. (2001) Intestinal Absorption of Specific Structured Triacylglycerols, *J. Lipid Res. 42*, 792–798.
4. Swift, L.L., Hill, J.O., Peters, J.C., and Greene, H.L. (1990) Medium-Chain Fatty Acids: Evidence for Incorporation into Chylomicron Triglycerides in Humans, *Am. J. Clin. Nutr. 52*, 834–836.
5. Carvajal, O., Nakayma, M., Kishi, T., Sato, M., Ikeda, I., Sugano, M., and Imaizumi, K. (2000) Effect of Medium-Chain

Fatty Acid Positional Distribution in Dietary Triacylglycerol on Lymphatic Lipid Transport and Chylomicron Composition in Rats, *Lipids 35*, 1345–1351.
6. Jensen, M.M., Christensen, M.S., and Høy, C.-E. (1994) Intestinal Absorption of Octanoic, Decanoic, and Linoleic Acids: Effects of Triglyceride Structure, *Ann. Nutr. Metab. 38*, 104–116.
7. Carvajal, O., Sakono, M., Sonoki, H., Nakayama, M., Kishi, T., Sato, M., Ikeda, I., Sugano, M., and Imaizumi, K. (2000) Structured Triacylglycerol Containing Medium-Chain Fatty Acids in *sn*-1(3) Facilitates the Absorption of Dietary Long-Chain Fatty Acids in Rats, *Biosci. Biotechnol. Biochem. 64*, 793–798.
8. Yli-Jokipii, K., Kallio, H., Schwab, U., Mykkänen, H., Kurvinen, J.-P., Savolainen, M.J., and Tahvonen, R. (2001) Effects of Palm Oil and Transesterified Palm Oil on Chylomicron and VLDL Triacylglycerol Structures and Postprandial Lipid Response, *J. Lipid. Res. 42*, 1618–1625.
9. Yli-Jokipii, K.M., Schwab, U.S., Tahvonen, R.L., Kurvinen, J.-P., Mykkänen, H.M., and Kallio, H.P.T. (2002) Triacylglycerol Molecular Weight and, to a Lesser Extent, Fatty Acid Positional Distribution, Affect Chylomicron Triacylglycerol Composition in Women, *J. Nutr. 132*, 924–929.
10. Yli-Jokipii, K.M., Schwab, U.S., Tahvonen, R.L., Kurvinen, J.-P., Mykkänen, H.M., and Kallio, H.P.T. (2003) Chylomicron and VLDL Triacylglycerol Structures and Postprandial Lipid Response Induced by Lard and Modified Lard, *Lipids 38*, 693–703.
11. Kurvinen, J.-P., Mu, H., Kallio, H., Xu, H., and Høy, C.E. (2001) Regioisomers of Octanoic Acid-Containing Structured Triacylglycerols Analyzed by Tandem Mass Spectrometry Using Ammonia Negative Ion Chemical Ionization, *Lipids 36*, 1377–1382.
12. Mu, H., Kurvinen, J.-P., Kallio, H., Xu, X., and Høy, C.-E. (2001) Quantitation of Acyl Migration During Lipase-Catalyzed Acidolysis, and of the Regioisomers of Structured Triacylglycerols Formed, *J. Am. Oil Chem. Soc. 78*, 959–964.
13. Xu, X., Balchen, S., Høy, C.-E., and Adler-Nissen, J. (1998) Production of Specific-Structured Lipids by Enzymatic Interesterification in a Pilot Continuous Enzyme Bed Reactor, *J. Am. Oil Chem. Soc. 75*, 1573–1579.
14. Mu, H., and Høy, C.-E. (2000) Effects of Different Medium-Chain Fatty Acids on Intestinal Absorption of Structured Triacylglycerols, *Lipids 35*, 83–89.
15. Ågren, J.J., Valve, R., Vidgren, H., Laakso, M., and Uusitupa, M. (1998) Postprandial Lipemic Response Is Modified by the Polymorphism at Codon 54 of the Fatty Acid-Binding Protein 2 Gene, *Arterioscler. Thromb. Vasc. Biol. 18*, 1606–1610.
16. Folch, J., Lees, M., and Sloane Stanley, G.H. (1957) A Simple Method for the Isolation and Purification of Total Lipides from Animal Tissues, *J. Biol. Chem. 226*, 497–509.
17. Hamilton, J.G., and Comai, K. (1988) Rapid Separation of Neutral Lipids, Free Fatty Acids and Polar Lipids Using Prepacked Silica Sep-Pak Columns, *Lipids 23*, 1146–1149.
18. Kallio, H., and Currie, G. (1993) Analysis of Low Erucic Acid Turnip Rapeseed Oil (*Brassica campestris*) by Negative Ion Chemical Ionization Tandem Mass Spectrometry. A Method Giving Information on the Fatty Acid Composition in Positions *sn*-2 and *sn*-1/3 of Triacylglycerols, *Lipids 28*, 207–215.
19. Laakso, P., and Kallio, H. (1996) Optimization of the Mass Spectrometric Analysis of Triacylglycerols Using Negative-Ion Chemical Ionization with Ammonia, *Lipids 31*, 33–42.
20. Kallio, H., and Rua, P. (1994) Distribution of the Major Fatty Acids of Human Milk Between *sn*-2 and *sn*-1/3 Positions of Triacylglycerols, *J. Am. Oil Chem. Soc. 71*, 985–992.
21. Kallio, H., and Currie, G. (1997) A Method of Analysis, European Patent 0,566,599.
22. Kurvinen, J.-P., Rua, P., Sjövall, O., and Kallio, H. (2001) Software (MSPECTRA) for Automatic Interpretation of Triacylglycerol Molecular Mass Distribution Spectra and Collision Induced Dissociation Product Ion Spectra Obtained by Ammonia Negative Ion Chemical Ionization Mass Spectrometry, *Rapid Commun. Mass Spectrom. 15*, 1084–1091.
23. Straarup, E.M., and Høy, C.-E. (2000) Structured Lipids Improve Fat Absorption in Normal and Malabsorbing Rats, *J. Nutr. 130*, 2802–2808.
24. Bendixen, H., Flint, A., Raben, A., Høy, C.-E., Mu, H., Xu, X., Bartels, E.M., and Astrup, A. (2002) Effect of 3 Modified Fats and a Conventional Fat on Appetite, Energy Intake, Energy Expenditure, and Substrate Oxidation in Healthy Men, *Am. J. Clin. Nutr. 75*, 47–56.
25. Pscheidl, E., Hedwig-Geissing, M., Winzer, C., Richter, S., and Rügheimer, E. (1995) Effects of Chemically Defined Structured Lipid Emulsions on Reticuloendothelial System Function and Morphology of Liver and Lung in a Continous Low-Dose Endotoxin Rat Model, *J. Parent. Enter. Nutr. 19*, 33–40.
26. Christensen, M.S., Müllertz, A., and Høy, C.-E. (1995) Absorption of Triglycerides with Defined or Random Structure by Rats with Biliary and Pancreatic Diversion, *Lipids 30*, 521–526.
27. Sato, K., Takahashi, T., Takahashi, Y., Shiono, H., Katoh, N., and Akiba, Y. (1999) Preparation of Chylomicrons and VLDL with Monoacid-Rich Triacylglycerol and Characterization of Kinetic Parameters in Lipopotein-Lipase-Mediated Hydrolysis in Chickens, *J. Nutr. 129*, 126–131.

[Received February 2, 2004; accepted June 3, 2004]

Selective Increase in Pinolenic Acid (all-*cis*-5,9,12-18:3) in Korean Pine Nut Oil by Crystallization and Its Effect on LDL-Receptor Activity

Jin-Won Lee[a], Kwang-Won Lee[b,*], Seog-Won Lee[c], In-Hwan Kim[d], and Chul Rhee[b]

[a]Department of Agricultural Chemistry, [b]Division of Food Science, and [c]Institute of Life Science and Natural Resources, College of Life & Environmental Sciences, and [d]Department of Food & Nutrition, College of Health Sciences, Korea University, Seoul 136-703, Korea

ABSTRACT: The aims of this study were to obtain concentrated pinolenic acid (5,9,12-18:3) from dietary Korean pine (*Pinus koraiensis*) nut oil by urea complexation and to investigate its cholesterol-lowering effect on the LDL-receptor activity of human hepatoma HepG2 cells. Pine nut oil was hydrolyzed to provide a low-pinolenic acid-containing FA extract (LPAFAE), followed by crystallization with different ratios of urea in ethanol (EtOH) or methanol (MeOH) as a solvent to produce a high-pinolenic acid-containing FA extract (HPAFAE). The profiles of HPAFAE obtained by urea complexation showed different FA compositions compared with LPAFAE. The long-chain saturated FA palmitic acid (16:0) and stearic acid (18:0) were decreased with urea/FA ratios (UFR) of 1:1 (UFR1), 2:1 (UFR2), and 3:1 (UFR3). Linoleic acid (9,12-18:2) was increased 1.3 times with UFR2 in EtOH, and linolenic acid (9,12,15-18:3) was increased 1.5 times with UFR3 in MeOH after crystallization. The crystallization with UFR3 in EtOH provided the highest concentration of pinolenic acid, which was elevated by 3.2-fold from 14.1 to 45.1%, whereas that of linoleic acid (9,12-18:2) was not changed, and that of oleic acid (9-18:1) was decreased 7.2-fold. Treatment of HepG2 cells with HPAFE resulted in significantly higher internalization of 3,3′-dioctadecylindocarbocyanine-LDL (47.0 ± 0.15) as compared with treatment with LPAFAE (25.6 ± 0.36) ($P < 0.05$). Thus, we demonstrate a method for the concentration of pinolenic acid and suggest that this concentrate may have LDL-lowering properties by enhancing hepatic LDL uptake.

Paper no. L9464 in *Lipids 39,* 383–387 (April 2004).

Many people are becoming more aware of the relationship between diet and disease and believe that foods can be designed to help prevent various diseases (1). Functional and nutraceutical foods are food components that provide demonstrated physiological benefits or reduce the risk of chronic disease above and beyond their basic nutritional functions (2,3). Thus, dietary modification is a potential strategy for the prevention of chronic diseases such as arthritis, coronary heart disease, and osteoporosis. It has been reported that dietary fat clearly affects plasma lipoprotein levels, and that FA have unequal lipid-lowering properties (4). PUFA have been shown to reduce plasma lipid levels, but their plasma lipid-lowering effects differ depending on the type of PUFA (5). Because PUFA have hypocholesterolemic activity but are not converted to biologically active eicosanoids, they are assumed to be desirable. In this regard, the nuts of a certain class of plant, Pinaceae, have been investigated for the past 10 yr. The conifer nuts contain unusual unsaturated polymethylene-interrupted FA (UPIFA) with a *cis*-5 ethylenic bond, designated Δ-UPIFA (6). Among them, dietary pine (*Pinus koraiensis*) nuts are traditionally consumed in Asia as a condiment for various dishes. The pine nut oil is known as the only conifer nut oil rich in pinolenic acid (5,9,12-18:3), a UPIFA that is available commercially (6,7). The main FA of pine nut oil are linoleic acid (9,12-18:2, 48.4%), oleic acid (9-18:1, 25.5%), and Δ-UPIFA (17.7%), of which pinolenic acid (14.9%) is a major component (8).

Many studies have shown that pine nut oil has hypocholesterolemic activity in animals. For example, it reduces blood pressure and attenuates serum VLDL-TAG and VLDL cholesterol (8,9). However, it is difficult to investigate the effect of pinolenic acid on cholesterol metabolism, because the FA composition of dietary fat in several studies has been shown to contain a significant amount of other PUFA, such as linoleic acid, which has been reported to have hypocholesterolemic effects (10,11). The main objective of this work was to produce concentrated pinolenic acid from pine nut oil by urea crystallization because pinoleic acid content is the main variable in compositions of PUFA. A higher concentration of natural pinolenic acid would make it possible to study the positive effects of any particular pinolenic acid on lipid metabolism. We also compared the cholesterol-lowering effects of high-pinolenic acid-containing FA extract (HPAFAE) with the control—low-pinolenic acid-containing FA extract (LPAFAE)—by measuring the hepatic LDL receptor.

MATERIALS AND METHODS

Reagents and materials. All chemicals and solvents were of analytical grade. Potassium hydroxide and FA standards were from Sigma Chemical Co. (St. Louis, MO).

Preparation of pine nut oil. For the preparations of pine nut oil, *P. koraiensis* seeds collected in Korea were purchased locally

*To whom correspondence should be addressed at Division of Food Science, College of Life & Environmental Sciences, Korea University, 1,5-ka, Anam-dong, Sungbuk-ku, Seoul 136-701, Republic of Korea.
E-mail: kwangwon@korea.ac.kr

Abbreviations: DiI, 3,3′-dioctadecylindocarbocyanine; DiI-LDL, DiI-labeled LDL; HPAFAE, high-pinolenic acid-containing FA extract; LPAFAE, low-pinolenic acid-containing FA; MEM, minimum essential medium; UFR, urea/FA ratio; UPIFA, unsaturated polymethylene-interrupted FA.

(Agricultural Marketing Center, Seoul, Korea). The oil from the dehulled seeds was extracted by a modification of the procedure of Gomes and Caponio (12). A volume (1 L) of *n*-hexane was added to 0.2 kg of pine nuts, which were macerated for 2 min in a Waring blender. The suspension was thoroughly mixed for 12 h. A solvent-and-oil solution was then separated from the pine nut residue. The process was repeated twice with 1 L of *n*-hexane. Finally, the combined hexane solution was passed through filter paper in a separatory funnel, and the solvent was removed in a rotary evaporator at 40°C to yield pine nut oil.

Preparation of FA of pine nut oil. The pine nut oil sample (5 g) was hydrolyzed by refluxing it with 500 mL of 1.25 N NaOH solution in 95% ethanol for 30 min. The solution was cooled, and 2 N HCl was then added and mixed. The mixture was extracted twice with 500 mL of hexane and washed with water until the pH was neutralized. The hexane layer was dried over anhydrous sodium sulfate. LPAFAE were recovered with a rotary evaporator, followed by N_2-gas purging.

Crystallization. The LPAFAE sample (5 g) was dissolved in 60 mL of two different solvents, ethanol (EtOH) or methanol (MeOH). Then 10 g of urea [urea/FA ratio 1:1 (UFR1), 2:1 (UFR2), or 3:1 (UFR3)] was added to each alcoholic solution, which was then refluxed for 20 min and cooled. The solution was allowed to crystallize at 4°C for 24 h. The crystals were shaken and then removed by filtration on a Büchner funnel. The filtrate was vacuum-evaporated at 40°C, and 125 mL of 6 N hot HCl was added for its acidification. To recover the HPAFAE, the acidified solution was extracted three times with 125 mL of hexane. The hexane extract was neutralized with water, dried over Na_2SO_4, and evaporated to dryness in a rotary evaporator followed by N_2-gas purging. The dried FA were weighed to determine crystallization yield.

GC analysis. Derivatizations of the pine nut oil and isolated FA were performed as described by Ko *et al.* (13). Methyl esters of FA were extracted with *n*-hexane. Then 1-μL aliquots of the extracts were injected into a gas chromatograph (Varian 3800; Varian Inc., Walnut Creek, CA) equipped with an FID. The column used was a SUPELCOWAX 10 fused-silica capillary column (30 m × 0.32 mm i.d.; Supelco, Bellefonte, PA). The injector, oven, and detector temperatures were 240, 190, and 260°C, respectively. Pinolenic acid was identified by GC–MS, and other FA were identified by comparison with the retention times of standards. FA analysis was conducted in triplicate for each sample collected at different time points.

GC–MS spectroscopy analysis. To identify pinolenic acid in the pine nut oil, a GC-mass analysis was performed on a gas chromatograph (Agilent 6890 plus; Agilent, Palo Alto, CA) equipped with a SUPELCOWAX 10 fused-silica capillary column (30 m × 0.32 mm i.d.; Supelco) and coupled to a mass spectrometer (Agilent 5973 MSD) with a Mass Lab data system. Helium was used as a carrier gas at a flow rate of 1 mL/min. The injector temperature was 250°C, and the samples were injected under the same conditions as reported earlier for GC analyses. The mass spectra were recorded at an electron energy of 70 eV, and the ion source temperature was 270°C. Mass spectra were compared with those of mass spectra libraries.

Subfraction of LDL. Blood samples were provided from the Hanyang University College of Medicine (Seoul, Korea). The blood sample was added to 0.1% EDTA, and plasma was prepared by centrifugation (1000 × *g* for 20 min). The LDL fraction was isolated as described by Graham *et al.* (14). Briefly, 50% (wt/vol) iodixanol solution was prepared by diluting 5 vol of Optiprep™ (Axis-Shield PoC AS, Oslo, Norway) with 1 vol of 0.8% (wt/vol) NaCl and 0.2 mM of PBS, pH 7.4. Plasma (3 mL) was mixed with 50% iodixanol (1 mL) to give a final concentration of iodixanol of 12.5% (wt/vol), and 0.5 mL was transferred to tubes (Beckman Coulter, Fullerton, CA) for a VTi 65.1 vertical rotor (Beckman Coulter). The samples were underlain with a cushion of 20% (wt/vol) iodixanol (0.5 mL) before the tubes were filled by overlaying them with PBS. The tubes were ultracentrifuged at 33,000 × *g* at 16°C for 3 h in an ultracentrifuge, and the gradient of LDL was collected.

LDL labeling. The LDL label was prepared with the fluorescent probe 3,3′-dioctadecylindocarbo-cyanine (DiI; Molecular Probes, Eugene, OR) by a modification of the method described by Stephan and Yurachek (15). Briefly, a stock solution of DiI was made by dissolving 30 mg of DiI in 1 mL of DMSO, and an appropriate volume was added to the LDL solution, with adjustment to 1 mg of LDL per mL to yield a final concentration of 300 μg of DiI per mg of LDL protein. The mixture was incubated at 37°C for 18 h under dark conditions to produce DiI-labeled LDL (DiI-LDL), to which was subsequently added 50% iodixanol solution as described in the *Subfraction of LDL* section. DiI-LDL was reisolated by ultracentrifugation (33,000 × *g* at 16°C for 3 h), dialyzed (Spectrapor MWCO 3500; Serva, Heidelberg, Germany) against PBS (18 h, 4°C), and sterilized by filtration (0.4 μm; Sigma, St. Louis, MO). The final protein concentration was determined by the method of Lowry *et al.* (16). The DiI-LDL was stored at 4°C in the dark and used within 7 d.

DiI and DiL-LDL standard curve. A standard solution of DiI (0–200 ng/mL) was prepared in isopropanol, and its fluorescence was measured in a fluorometer (Model SFM-25; Kontron, Zürich, Switzerland) with excitation/emission wavelengths of 522/564 nm. Standard solutions of DiI-LDL (100–1000 ng of protein per mL) were prepared from a stock solution of 2.3 mg of LDL protein per mL in isopropanol, and their fluorescence was measured as already described. The specific activity of DiI-LDL samples was calculated as the amount of DiI (μg) incorporated into 1 mg of LDL protein.

Cell culture and LDL-uptake assay. HepG2 cells were obtained from the American Type Culture Collection (Rockville, MD). The cells were routinely cultured in minimum essential medium (MEM) containing 10% FBS and penicillin G (100 IU/mL; Sigma, St. Louis, MO) and were maintained at 37°C in equilibrium with 5% CO_2–95% air in T-75 cell-culture tubes (Nunclon™; Nunc A/S, Roskilde, Denmark). For experiments, cells (2.5×10^5 cells/well) were seeded into six-well plates in MEM supplemented with 10% FBS, grown until the culture was 70–80% confluent, and switched to MEM containing 7.5% FA-free BSA for an additional 24 h.

Afterward, to determine the dose–response of cell-bound or

cell-associated LDL, the HepG2 cells were incubated with DiI-LDL (10–90 μg protein/mL) for 2 h at 4 and 37°C, respectively; to perform experiments with FA, cells were treated with serum-free MEM containing 1.0 mM of a respective FA extract/albumin complex or 0.25 mM of albumin alone as a control at 37°C for 2 h. The cells were then incubated with 10 μg protein/mL of DiI-LDL in MEM containing 7.5% FA-free BSA for an additional 2 h at 4 and 37°C, respectively. Stock solutions of FA extract/albumin mixture were prepared as described by Cho *et al.* (17). Briefly, 20 μmol of the appropriate FA extract prepared from pine nut oil or its concentrate were dissolved in 1.0 mL of sterilized water at temperatures between 25 and 75°C. Five micromoles (300 mg) of FA-free BSA were dissolved in 4.0 mL of MEM culture medium (pH 7.4). The FA extract solution was complexed to FA-free BSA (4:1 molar ratio) by dropwise addition of FA dissolved in ethanol to a solution of BSA with continuous stirring and mixed with MEM containing 10% FBS in a final concentration of 1 mM.

At the end of each incubation period, the cells were washed extensively with PBS, and 2 mL of isopropanol was added to each well, with gentle shaking of the plates for 15 min. The extracts were collected into 15-mL centrifuge tubes and centrifuged at 1500 × *g* for 15 min at 4°C, after which the fluorescence was determined as described above. DiI content in the extracts was determined according to the DiI standard curve. The cells were dissolved in 2 N NaOH for protein determination. The dose–response of internalized LDL was calculated as the difference between cell-associated (37°C) and membrane-bound (4°C) LDL.

RESULTS AND DISCUSSION

Enrichment in pinolenic acid by crystallization and the FA profile. The crystallization of pine nut oil was performed with UFR1, UFR2, and UFR3 to provide the highest possible yield of pinolenic acid. The yields of total FA with the urea/FA ratios of UFR1, UFR2, and UFR3 in EtOH as a solvent were 77, 58, and 23%, respectively, and in MeOH as a solvent they were 65, 65, and 27%, respectively (Table 1).

Urea forms a complex with high-carbon-number alkanes compared with unsaturated FA (17). The saturated FA, palmitic acid (16:0) and stearic acid (18:0), were decreased with an increased UFR and were efficiently eliminated from pine nut oil after crystallization (Table 1). The monounsaturated FA oleic acid (18:1) was also decreased 7.2-fold with UFR3 in EtOH and 5.4-fold with UFR3 in MeOH. Conversely, of the PUFA, linoleic acid (9,12-18:2) was increased 1.3 times with UFR2 in EtOH, and linolenic acid (9,12,15-18:3) was increased 1.5 times with UFR3 in MeOH after crystallization.

Enrichment of pinolenic acid in pine nut oil also depends on the UFR. The level of pinolenic acid was increased from 14.1 to 16.8, 23.0, and 45.1% with UFR1, UFR2, and UFR3 in EtOH, respectively, and to 15.1, 20.4, and 33.6% with UFR1, UFR2, and UFR3 in MeOH, respectively. The highest concentration of pinolenic acid (a 3.2-fold elevation) was achieved by crystallization with UFR3 in EtOH.

Considering that the oleic acid concentration was decreased to a large extent and that the linolenic acid level was not changed with this condition, the crystallization with UFR3 in EtOH provided an optimal condition for the selective increase in pinolenic acid enhancement in LPAFAE. In comparing the HPAFAE with UFR3 in EtOH with the LPAFAE as a control, the difference in PUFA composition between LPAFAE and HPAFAE was mainly attributed to the pinolenic acid concentration. We investigated the LDL-uptake assay with these two FA extracts in the next experiment.

LDL receptor activity with DiI-LDL. In dose–response studies, the cell-associated, -bound, and -internalized DiI-LDL appeared to reach a plateau by 60 μg/mL (Fig. 1). Because the internalization of LDL by receptor-mediated endocytosis is inhibited at 4°C, the total LDL binding at this temperature exclusively represents cell surface binding.

The cell association, surface binding, and internalization of DiI-LDL (60 μg/mL) in cells treated with LPAFAE or

TABLE 1
Urea Crystallization of FA Prepared from Korean Pine Nut Oil[a]

FA	Control (LPAFAE)	Solvents[b] UFR-EtOH 1:1	UFR-EtOH 2:1	UFR-EtOH 3:1	UFR-MeOH 1:1	UFR-MeOH 2:1	UFR-MeOH 3:1
Yield (wt%)[c]	100	77	58	23	65	65	27
16:0	3.88	1.17	0.34	0.27	1.26	0.48	0.17
18:0	2.01	0.32	0.14	0.12	0.35	0.24	ND
18:1	28.9	23.8	10.8	4.11	27.3	14.4	5.05
5,9-18:2	2.27	2.60	3.10	1.88	2.50	2.90	2.76
9,12-18:2	48.7	55.2	62.3	48.2	53.2	61.4	58.2
5,9,12-18:3	14.1	16.8	23.0	45.1	15.2	20.4	33.6
9,12,15-18:3	0.19	0.21	0.25	0.25	0.20	0.23	0.28
Recovery of pinolenic acid (wt%)[d]	100	91.8	95.4	74.0	40.4	94.0	64.5

[a]For the urea crytallization procedure, see the Materials and Methods section. LPAFAE, low-pinolenic acid-containing FA extract; EtOH, ethanol; MeOH, methanol.
[b]UFR-EtOH, urea/FA ratio (UFR) in EtOH as a solvent; UFR-MeOH, UFR in MeOH as a solvent.
[c]Weight% based on the original FA.
[d]Recovery of pinolenic acid based on the initial contents in FA. ND, not detected.

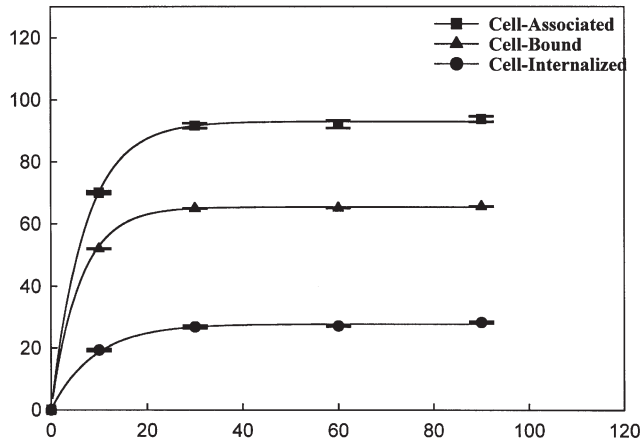

FIG. 1. Dose–response measurement of cell-associated, -bound, and -internalized 3,3′-dioctadecylindocarbocyanine-labeled LDL (DiI-LDL) in HepG2 cells. The cells were grown in minimum essential medium (MEM) containing 10% BSA at 37°C until the culture was 70–80% confluent and then switched to MEM containing 7.5% FA-free BSA for an additional 24 h. Afterward, cells were incubated with 30, 60, and 90 μg/mL of DiI-LDL in MEM for 2 h at 4 or 37°C. The values are mean ± SD (n = 3) and expressed as ng of LDL/mg of cell protein.

HPAFAE at 37 and 4°C are shown in Table 2. The treatment of cells with 1 mM of HPAFAE or LPAFAE for 2 h resulted in a significant increase in the cell-associated DiI-LDL compared with the nontreated control (92.2 ± 1.25) ($P < 0.05$). However, the bound DiL-LDL was lower in cells exposed to HPAFAE (66.3 ± 0.43) than to LPAFAE (74.8 ± 0.74). The internalization of DiI-LDL was significantly higher in cells exposed to HPAFAE (47.0 ± 0.15) than to LPAFAE (25.6 ± 0.36) ($P < 0.05$). These results may be related to the findings of Cho *et al.* (17) in which HepG2 cells treated with 18:0 showed significantly decreased LDL uptake compared with 18:1, 18:2, and 18:3. In our study, the levels of the saturated FA 16:0 and 18:0 contained in HPAFAE were 14 and 17 times lower, respectively, than those in LPAFAE (Table 1). Our study cannot directly answer whether the observed effect on LDL-receptor activity was due to pinolenic acid since we did not use purified FA. In the preliminary study, however, we treated HepG2 cells with mixtures of 16:0, 18:0, and 18:1 corresponding to the molar amounts of each of these FA present in LPAFAE and HPAFAE. The mixtures of the three FA corresponding to the molar amounts in LPAFAE showed the lowest LDL uptake value; the mixtures having the molar amounts in HPAFAE showed a higher LDL uptake value than the control, and the value was the highest in cells exposed to HPAFAE (data not shown), suggesting that pinolenic acid in HPAFAE is likely to have contributed to the effect of LDL uptake.

From these results, we demonstrated that urea complex formation is a promising method for fractionating pinolenic acid from pine nut oils. This method involves ecologically friendly reagents and reagent recycling (18). The mild conditions would not affect the molecular structures of the highly unsaturated FA (19). Pinolenic acid content was the main variable that differed between HPAFAE and LPAFAE in compositions of PUFA, and it increased 3.2-fold, to 45.1% of the total FA in HPAFAE. In this study, HPAFAE had the potential to lower LDL *via* hepatic uptake *in vitro*. Thus, the beneficial effects of this particular acid on various lipid variables in animal studies can be investigated effectively and precisely with this high-pinolenic acid extract and with further purified pinolenic acid.

TABLE 2
Cell-Associated, -Bound, and -Internalized DiI-LDL in HepG2 Cells Treated with HPAFAE and LPAFAE[a]

DiI-LDL (μg/mL)	None	LPAFAE	HPAFAE
Cell-associated	92.2 ± 1.25^c	100 ± 0.08^b	113.3 ± 1.55^a
Cell-bound	65.1 ± 0.03^c	74.8 ± 0.74^a	66.3 ± 0.43^b
Cell-internalized	27.1 ± 0.45^b	25.6 ± 0.36^c	47.0 ± 0.15^a

[a]Values presented as mean ± SD (n = 3). Letters sharing different superscript letters in the same row are significantly different ($P < 0.05$). DiI-LDL; 3,3′-dioctadecylindocarbocyanine-labeled LDL; HPAFAE, high-pinolenic acid-containing FA extract; for other abbreviation see Table 1.

ACKNOWLEDGMENT

This work was supported by grant No. R01-2002-000-00447-0 from the Basic Research Program of the Korea Science & Engineering Foundation.

REFERENCES

1. Hollingsworth, P. (1997) Mainstreaming Healthy Foods, *Food Technol. 51*, 55–58.
2. Bloch, A., and Thomson, C.A. (1995) Position of the American Dietetic Association: Phytochemicals and Functional Foods, *J. Am. Diet. Assoc. 95*, 493–496.
3. Hardy, G. (2000) Nutraceuticals and Functional Foods: Introduction and Meaning, *Nutrition 16*, 688–689.
4. Lichtenstein, A.H. (1996) Dietary Fatty Acids and Lipoprotein Metabolism, *Curr. Opin. Lipidol. 7*, 155–161.
5. Phillipson, B.E., Rothrock, D.W., Connor, W.E., Harris, W.S., and Illingworth, D.R. (1985) Reduction of Plasma Lipids, Lipoproteins, and Apoproteins by Dietary Fish Oils in Patients with Hypertriglyceridemia, *N. Engl. J. Med. 312*, 1210–1216.
6. Imbs, A.B., Nevshupova, N.V., and Pham, L.Q. (1998) Triacylglycerol Composition of *Pinus koraiensis* Seed Oil, *J. Am. Oil Chem. Soc. 75*, 865–870.
7. Robert, L.W., Eric, D., and Jean-Charles, M. (1997) Positional Distribution of Δ5 Olefinic Acids in Triacylglycerols from Conifer Seed Oils: General and Specific Enrichment in the *sn*-3 Position, *J. Am. Oil Chem. Soc. 74*, 515–523.
8. Asset, G., Staels, B., Wolff, R.L., Bauge, E., Madj, Z., Fruchart, J.C., and Dallongeville, J. (1999) Effects of *Pinus pinaster* and *Pinus koraiensis* Seed Oil Supplementation on Lipoprotein Metabolism in the Rat, *Lipids 34*, 39–44.
9. Sugano, M., Ikeda, I., Wakamatsu, K., and Oka, T. (1994) Influence of Korean Pine (*Pinus koraiensis*)-Seed Oil Containing *cis*-5,*cis*-9,*cis*-12-Octadecatrienoic Acid on Polyunsaturated Fatty Acid Metabolism, Eicosanoid Production and Blood Pressure of Rats, *Br. J. Nutr. 72*, 775–783.
10. Kurushima, H., Hayashi, K., Toyota, Y., Kambe, M., and Kajiyama, G. (1995) Comparison of Hypocholesterolemic Effects Induced by Dietary Linoleic Acid and Oleic Acid in Hamsters, *Atherosclerosis 114*, 213–221.

11. Ibrahim, J.B., and McNamara, D.J. (1988) Cholesterol Homeostasis in Guinea Pigs Fed Saturated and Polyunsaturated Fat Diets, *Biochim. Biophys. Acta 963*, 109–118.
12. Gomes, T., and Caponio, F. (1997) Evaluation of the State of Oxidation of Crude Olive-Pomace Oils. Influence of Olive-Pomace Drying and Oil Extraction with Solvent, *J. Agric. Food Chem. 45*, 1381–1384
13. Ko, S.N., Kim, H., Lee, K.T., Ha, T.Y., Chung, S.H., Lee, S.M., and Kim, I.H. (2003) Optimization of Enzymatic Synthesis of Structured Lipid with Perilla Oil and Medium Chain Fatty Acid, *Food Sci. Biotechnol. 12*, 253–256.
14. Graham, J.M., Higgins, J.A., Gillott, T., Taylor, T., Wilkinson, J., Ford, T., and Billington D. (1996) A Novel Method for the Rapid Separation of Plasma Lipoproteins Using Self-Generating Gradients of Iodixanol, *Atherosclerosis 124*, 125–135.
15. Stephan, Z.F., and Yurachek, E.C. (1993) Rapid Fluorometric Assay of LDL Receptor Activity by DiI-Labeled LDL, *J. Lipid Res. 34*, 325–330.
16. Lowry, O.H., Rosebrough, N.J., Farr, A.L., and Randall, R.J. (1951) Protein Measurement with Folin Phenol Reagent, *J. Biol. Chem. 193*, 265–275.
17. Cho, B.H., Dokko, R.C., and Chung, B.H. (2002) Oleic, Linoleic and Linolenic Acids Enhance Receptor-Mediated Uptake of Low Density Lipoproteins in Hep-G2 Cells, *J. Nutr. Biochem. 13*, 330–336.
18. Hayes, D.G., Bengtsson, Y.C., Van Alstine, J.M., and Setterwall, F. (1998) Urea Complexation for the Rapid, Ecologically Responsible Fraction of Fatty Acids from Seed Oil, *J. Am. Oil Chem. Soc. 75*, 1403–1409.
19. Grompone, M.A. (1992) Enrichment of Omega-3 PUFAs from Fur Seal Oil, *Fat Sci. Technol. 94*, 388–394.

[Received March 9, 2004; accepted June 3, 2004]

Fenitrothion-Induced Structural and Functional Perturbations in the Yolk Lipoproteins of the Shrimp *Macrobrachium borellii*

Fernando García, María R. Gonzalez-Baró*, Horacio Garda, Monica Cunningham, and Ricardo Pollero

Instituto de Investigaciones Bioquímicas de La Plata (INIBIOLP), Consejo Nacional de Investigaciones Científicas y Técnicas (CONICET)–Universidad Nacional de La Plata (UNLP), (1900) La Plata, Argentina

ABSTRACT: Two lipovitellin (LV) forms containing the same apoproteins but differing in their lipid composition were isolated from *Macrobrachium borelii* eggs at early (LVe) and late (LVl) embryogenic stages and characterized. These two forms of LV, as well as liposomes prepared with lipids extracted from them, were used as simpler models to study the effect of the pesticide fenitrothion (FS) on their structures and functions. Rotational diffusion and fluorescence lifetime of two fluorescent probes [1,6-diphenyl-1,3,5-hexatriene (DPH) and 3-(*p*-(6-phenyl)-1,3,5-hexatrienal)phenylpropionic acid (DPH-PA)] were used to obtain information on structural changes induced by FS in the inner and outer regions of the LV, respectively. Comparison of the rotational behavior of these probes in native LV and liposomes (LP) from extracted LV lipids suggests that apoprotein–lipid interactions result in an ordered neutral lipid core. FS increased the lipid phase polarity of both LV and LP forms. The rotation of these probes in LP was not affected, suggesting a dependence of FS action on lipid–protein interactions. DPH-PA steady-state anisotropy showed that, unlike the LVe form, the LVl form was sensitive to extremely low FS concentrations. The ability of both LV to transfer palmitic acid to albumin was increased, but in a dissimilar manner, by the presence of FS. Such differences in the sensitivity of the LV at different steps of embryogenesis to FS influence the toxic action of this insecticide.

Paper no. L9429 in *Lipids 39*, 389–396 (April 2004).

Pesticides frequently have toxic effects on nontarget organisms. In this regard, some lipophilic insecticides tend to accumulate in cellular membranes, modifying their physicochemical properties and physiological functions (1–3). Small amounts of organophosphate insecticides alter several properties of artificial phospholipid bilayers and natural vertebrate or invertebrate membranes, such as permeability, lipid order, and dynamics (4–12). We have demonstrated that the organophosphate insecticide fenitrothion (FS; *O,O*-dimethyl *O*-4-nitro-*m*-tolyl phosphorothioate) also incorporates into several circulating invertebrate lipoproteins, altering their lipid dynamics, the penetration of water into the lipid phase, and their ability to exchange FA. Differential alterations in these physical properties were found in shrimp lipoproteins with different lipid and apoprotein compositions (13). These changes were also found in spider lipoproteins, e.g., a different basal lipid order as well as lipid/apoprotein ratio (14). Use of lipoprotein systems with fewer variables should be suitable for carrying out studies of liposomes (LP) or lipoproteins that exhibit either a different lipid or apoprotein composition.

Crustacean lipovitellins (LV), the main energy and carbon source in the vitellus, are necessary for embryogenesis. They are likely to be exposed to insecticides, either by direct water–egg contact or when transported to the ovary by a plasma vitellogenin (15). The shrimp *Macrobrachium borellii* contains only one LV, which is consumed during embryo development (16). In the present work two forms of this LV, one obtained from eggs at early embryonic stages (LVe) and the other at late stages (LVl), were characterized with respect to their lipid and protein compositions. These two forms of LV, as well as LP prepared with lipids extracted from them, were used as simpler models to study the effect of the pesticide FS on their structures and functions.

The structural organization of LV as related to the presence of FS was studied by measuring the lipid-phase dynamics and polarity. The rotational behavior and fluorescent lifetime of two lipid-soluble fluorescent probes, 1,6-diphenyl-1,3,5-hexatriene (DPH) and its propionic acid derivative 3-(*p*-(6-phenyl)-1,3,5-hexatrienyl)phenylpropionic acid (DPH-PA), were determined. Although these probes contain the same fluorescent moiety, they are expected to locate in different regions of the lipoprotein lipid phase. The neutral DPH senses the deep hydrophobic region of lipid bilayers and the neutral lipid core in spherical lipoproteins (17), whereas the amphipathic DPH-PA aligns its carboxylate group with the phospholipid polar head and thus senses the surface lipid monolayer of spherical lipoproteins or the most external regions of lipid bilayers. The same measurements were made in LP prepared with extracted LV lipids to elucidate the role of LV lipids and apolipoproteins.

*To whom correspondence should be addressed at INIBIOLP, Facultad de Cs. Médicas, UNLP, Calle 60 y 120, La Plata (1900), Argentina.
E-mail: mgbaro@atlas.med.unlp.edu.ar

Abbreviations: CHO, cholesterol; △, polarized phase shift; DPH, 1,6-diphenyl-3,5-hexatriene; DPH-PA, 3-(*p*-(6-phenyl)-1,3,5-hexatrienyl)phenylpropionic acid; FS, fenitrothion (*O,O*-dimethyl *O*-4-nitro-*m*-tolyl phosphorothioate); LP, liposome; LPe, liposome at early embryogenic stage; LPl, liposome at late embryogenic stage; LV, lipovitellin; LVe, lipovitellin at early embryogenic stage; LVl, lipovitellin at late embryogenic stage; r_s, steady-state anisotropy; r_∞, limiting anisotropy; SM, sphingomyelin; τ, fluorescence lifetime; τ_m, modulation lifetime; τ_p, phase-shift measured lifetime; τ_r, rotational correlation time.

The importance of FS–lipoprotein interactions can be considered in two ways: (i) Lipoproteins may carry FS to target organs (13), and (ii) FS may alter the transfer of other lipids by the lipoprotein. The latter mechanism was explored in this work by studying the effect of FS on the palmitic acid transfer capacity of LV by using albumin as the acceptor.

EXPERIMENTAL PROCEDURES

Samples. Wild animals were captured in a water course close to Rio de la Plata, Argentina, immediately before the experiment. Eggs from females (150 eggs each) at early (<26 d) and late (>40 d) embryonic development stages were collected. The different stages were identified according to previous reports dealing with the whole embryogenesis (18). Eggs were homogenized in 3 mL of phosphate buffer, 50 mM, pH 7.4, and sequentially ultracentrifuged at 10,000 × *g* for 20 min and then at 100,000 × *g* for 60 min. LV were isolated from the final supernatant (cytosolic fraction).

LV isolation. Yolk lipoproteins were isolated by density gradient ultracentrifugation. Cytosolic fraction (1 mL) was overlayered on 3 mL NaBr solution (density 1.26 g/mL) containing 0.01% sodium azide and centrifuged at 178,000 × *g* for 24 h at 10°C in a Beckman L8 70 M centrifuge, using a SW 60 Ti rotor. Saline solution of the same density as that of samples was centrifuged in parallel to determine relative densities and to check the appropriate gradient formation. Density was determined in a Bausch & Lomb refractometer. The total volume of the tubes was fractionated from top to bottom into 0.2-mL aliquots, and the protein content of each fraction was monitored spectrophotometrically at 280 nm. The zone in the gradient containing LV (aliquots 9–11) was separated as a whole fraction. Thus, LVe and LVl were obtained from eggs at the early and late embryogenesis stages, respectively.

Lipid and protein analysis. Lipids were extracted following the method of Folch *et al.* (19). Lipid classes were quantified by TLC coupled with an FID in an Iatroscan apparatus Model TH-10, after separation on Chromarods SIII (Iatron, Tokyo, Japan), using a triple development solvent system as described previously (20). MAG was used as internal standard. FA were analyzed by GLC under the conditions described previously (21).

Total protein concentration in each fraction isolated from the density gradient was measured colorimetrically by the method of Lowry *et al.* (22). LVe and LVl apoproteins were analyzed by native and dissociating electrophoresis. Analyses in nondissociating conditions were performed by using a 4–23% PAGE. Protein subunits were analyzed by SDS-PAGE using a gradient of 4–23% acrylamide (23). The gels were stained with Coomassie Brilliant Blue R-250 (Sigma Chemical Co., St. Louis, MO). M.W. were calculated as previously described (24).

LP preparation. Total lipids of LVe and LVl were extracted and used for LP preparation (LPe and LPl, respectively). Extracts containing 1 mg lipids were evaporated to dryness, hydrated with 3 mL of 50-mM potassium phosphate buffer, pH 7.4, vortexed, and then sonicated using a tip sonicator for 5 min. After centrifugation for 2 h at 80,000 × *g*, lipid analysis of the supernatant confirmed that all lipids originally present in the sample had been dispersed and incorporated into LP.

Sample labeling with fluorescent probes. For labeling, 3 mL of 50-mM potassium phosphate buffer, pH 7.4, with LV (0.1 mg/mL in protein) or LP (0.09 mg/mL in lipid) were mixed with a few microliters of concentrated DMSO solutions of DPH or DPH-PA to reach a final concentration of 2 μM. Blanks without the fluorescent probes and with the same volume of DMSO were used to correct the measurements for nonspecific fluorescence and light scattering. Samples were gently swirled at 20°C for at least 2 h in darkness to allow a complete equilibration of the probes with the LV or LP. FS from a concentrated ethanolic solution was added to samples prior to equilibration at concentrations of 1, 10, or 20 ppm.

Fluorescence measurement. All fluorescence measurements were carried out in an SLM 4800 C phase-modulation spectrofluorometer (SLM Instruments Inc., Urbana, IL). Steady-state anisotropy (r_s) was measured within a temperature range of 10–30°C for LV, and 10–45°C for LP. Fluorescence lifetime (τ) and differential polarized phase shift (△) were measured only at 10 and 30°C.

Measurements of r_s, τ, and △ were made as described (12) by using an excitation wavelength of 361 nm and a cutoff filter (Schott KV 389) to isolate the emitted light. For τ measurements, exciting light was amplitude-modulated at 18 and 30 MHz by a Debye–Sears modulator and vertically polarized by a Glan–Thompson polarizer. Emitted light passed through the filter and then through a Glan–Thompson polarizer oriented 55° to the vertical to eliminate effects of Brownian motion (25). Phase shift and demodulation of emitted light relative to a reference of known τ were determined and used to compute phase-shift measured lifetime (τ_p) and modulation lifetime (τ_m), respectively (25). 1,4-Bis(5-phenyloxazol-2-yl) benzene in ethanol, which has a τ of 1.35 ns (26,27), was used as reference. △ was determined according to Lakowicz (28,29) by excitation with light modulated at 18 and 30 MHz and vertically polarized, and the phase difference between the parallel and perpendicular components of the emitted light was measured.

The obtained values for r_s, τ, and △ were used to calculate the limiting anisotropy (r_∞) and the rotation rate as previously described (26,27) in accordance with the theory developed by Weber (30). Calculation of τ_r and r_∞ from measurements at discrete frequencies requires homogeneity in the rotamer fluorescence lifetime (25,26).

Release of FA from LV. Proteins from LVe and LVl (30 mg) were incubated with 3 μCi [1-^{14}C]palmitic acid (57.0 mCi/mmol, 99% radiochemically pure; NEN, Boston, MA) as the ammonium salt for 30 min and dialyzed for 24 h using 0.1 M Tris-HCl, pH 8.0, to remove the nonbound FA. The labeled LVe and LVl were exposed to 0, 1, and 20 ppm of FS for 1 h. Samples were then incubated with 20 mg/mL of albumin as FA acceptor for 30 min. After incubation, samples were analyzed under native conditions by preparative gel filtration fast-flow protein LC on a Superdex 200 HR 10/30 column (Amersham-Pharmacia, Uppsala, Sweden) using 0.1 M Tris-HCl, pH 8.0,

at a flow rate of 0.4 mL/min. Protein was detected spectrophotometrically at 280 nm. The column was calibrated with thyroglobulin, ferritin, BSA, and ribonuclease A (Amersham-Pharmacia) as M.W. protein markers. LV and albumin fractions were separately collected on the basis of their retention times and relative mass ratios. The radioactivity of palmitic acid bound to each protein peak was quantified by liquid scintillation counting. The amount of protein in each peak was colorimetrically quantified using the method of Lowry *et al.* (22).

RESULTS

Isolation and characterization of LV. LV were isolated from the cytosol of eggs at different embryonic development stages by density gradient ultracentrifugation. Measurements of absorbance at 280 nm performed on each fraction from the gradients showed similar protein profiles for both LV forms (Fig. 1). Fractions containing the maxima, corresponding to LVe and LVl, respectively, were characterized separately. Hydrated density, and lipid and FA compositions of both forms of LV are shown in Table 1. PC was the most abundant lipid in LVe, followed by other phospholipids and TAG. A marked decrease in PC, a minor decrease in TAG, and a concomitant increase in FFA, cholesterol (CHO), and sphingomyelin (SM) contents were observed throughout development. Also, palmitic acid (16:0) declined as the percentage of 20-carbon PUFA (20:4 and 20:5) increased. Lipid/protein ratios in LVe and LVl were found to be similar and consistent with their densities.

Figure 2 shows the results obtained from the electrophoretic analysis of LVe and LVl performed under native (A) and dissociating (B) conditions. Electrophoretic mobility of the proteins revealed, under native conditions, a predominant band of 440 kDa in both LV (Fig. 2A). In dissociating conditions, two bands of 94 and 112 kDa were observed (Fig. 2B).

Effect of FS on the rotational behavior of DPH and DPH-PA in LV and LP built up with LV lipids. Steady-state anisotropy of DPH (Figs. 3 and 5) and DPH-PA (Figs. 4 and 6) were measured over temperature ranges of 10–30°C in LV (Figs. 3 and 4) and 10–45°C in LP (Figs. 5 and 6) in the absence or the presence of 1, 10, and 20 ppm of FS. Although r_s is often used as a mobility parameter, it is highly dependent on τ. Then measurements of τ are essential to interpret r_s variations correctly and to determine the environment polarity. Time-resolved or phase-modulation-resolved anisotropy as limiting anisotropy (r_∞) and rotational correlation time (τ_r) were used for a thorough interpretation of the rotational motion of a fluorescent probe (DPH or DPH-PA) and the environment properties. r_∞ is inversely related to the extent of wobbling motion of the probe

TABLE 1
Lipid Composition[a] of Lipovitellins Isolated from Vitellus of Egg Yolk of *Macrobrachium borellii*

	Fraction	
Lipid classes	LVe	LVl
TAG (%)	20.5 ± 1.8	16.7 ± 1.5
FFA (%)	5.9 ± 0.6	10.4 ± 0.7
Cholesterol (%)	7.9 ± 0.5	13.7 ± 1.0
PE (%)	15.8 ± 1.2	19.5 ± 3.6
PC (%)	41.9 ± 3.6	24.9 ± 4.4
Sphingomyelin (%)	7.6 ± 0.5	14.1 ± 1.5
Major FA (%)		
14:0	3.7	2.4
16:0	22.3	17.6
16:1n-7	14.0	10.9
18:0	9.0	8.9
18:1n-9	20.1	20.5
18:1n-7	10.6	11.9
18:2n-6	7.0	7.7
20:4n-6	4.1	7.0
20:5n-3	7.8	11.9
Total lipids (mg/150 eggs)	14.1 ± 4.3	3.5 ± 2.6
Total proteins (mg/150 eggs)	47.2 ± 8.0	14.1 ± 7.0
Lipid/protein ratio	0.29	0.25
Hydrated density (g/mL)	1.18–1.19	1.18–1.19

[a]Data are expressed as weight percentage of lipids as determined by TLC-FID. Values represent the mean ± SD of three analyses. LVe, lipovitellin at an early embryogenic stage; LVl, lipovitellin at a late embryogenic stage.

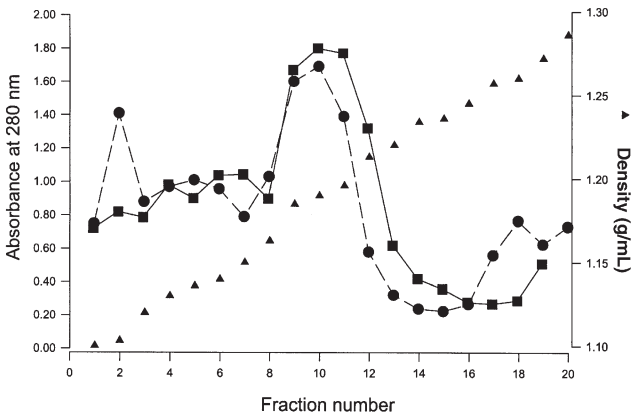

FIG. 1. Total protein (absorbance at 280 nm) and density distribution (▲) in egg cytosol fractions after gradient ultracentrifugation. Samples of egg cytosol were obtained at early (LVe) (●) and late (LVl) (■) stages of embryonic development. LVe, lipovitellin at an early embryogenic stage; LVl, lipovitellin at a late embryonic stages.

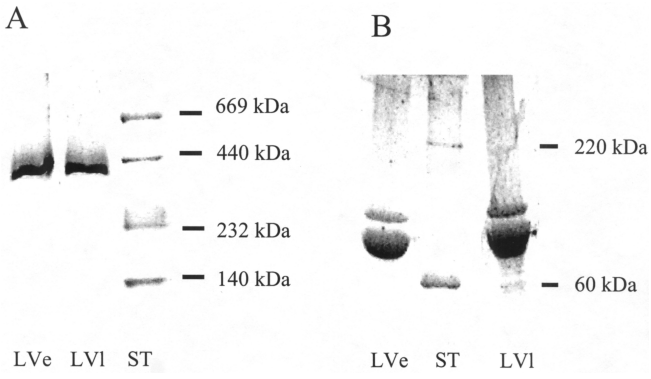

FIG. 2. Native (A) and dissociating (B) gel electrophoresis of LVe and LVl. Both gels were done using polyacrylamide gradients of 4–23% wt/vol. Proteins were revealed by Coomassie Blue staining. ST, standard; for other abbreviations see Figure 1.

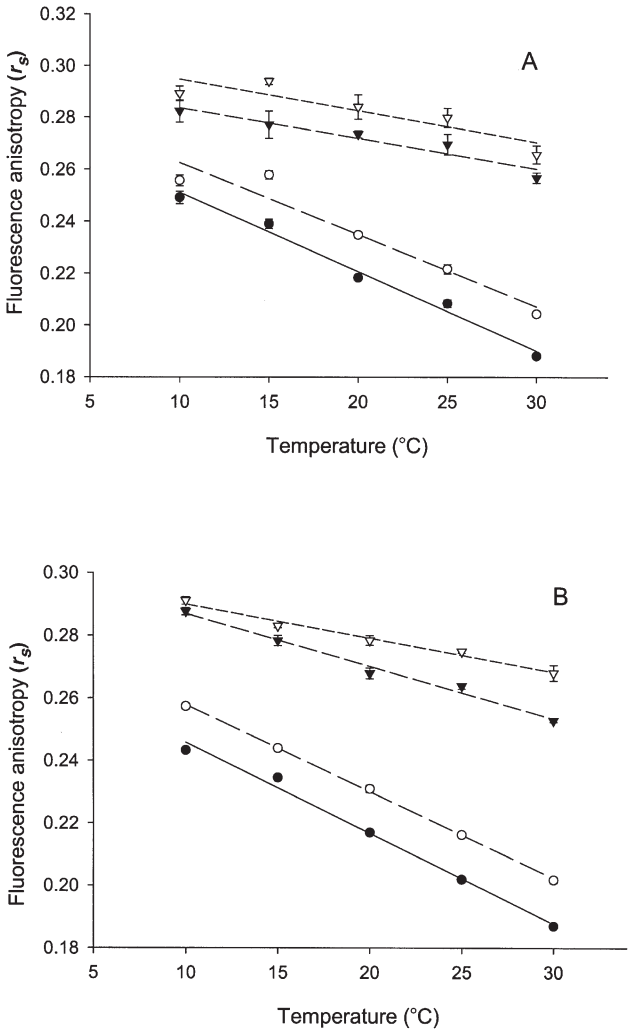

FIG. 3. Effect of fenitrothion (FS) on the 1,6-diphenyl-1,3,5-hexatriene (DPH) fluorescence anisotropy (r_s) in LVe (A) and LVl (B). r_s is plotted vs. temperature in the absence (●) or in the presence of 1 (○), 10 (▼), and 20 ppm (▽) of FS. Values represent the average of five different determinations ± SD. For other abbreviations see Figure 1.

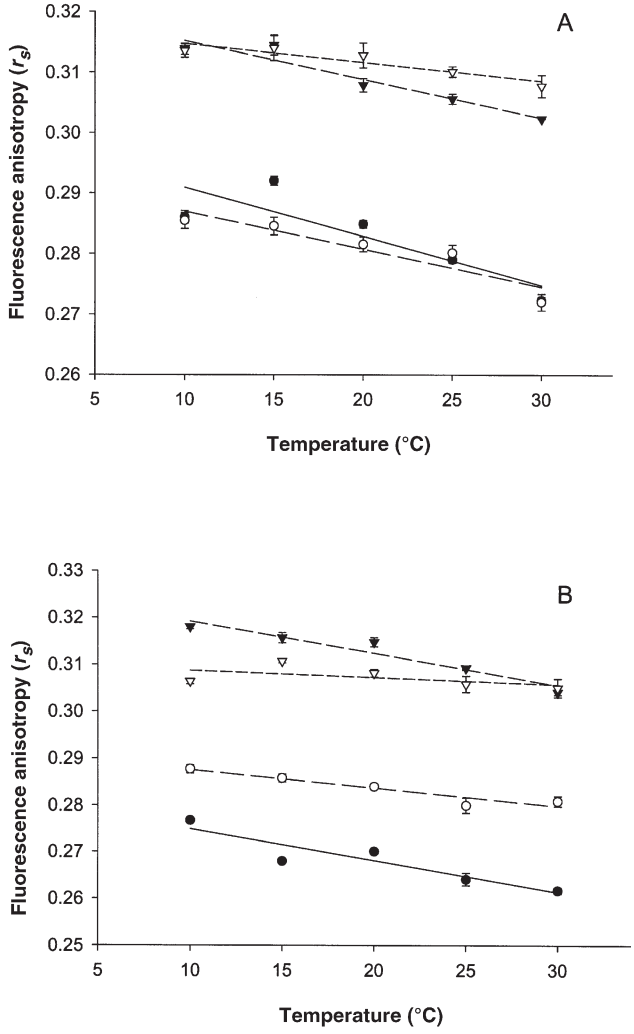

FIG. 4. Effect of FS on the 3-(*p*-(6-phenyl)-1,3,5-hexatrienyl)phenylpropionic acid (DPH-PA) r_s in LVe (A) and LVl (B). (r_s) is plotted vs. temperature in the absence (●) or in the presence of 1 (○), 10 (▼), and 20 ppm (▽) of FS. Values represent the average of five different determinations ± SD. For other abbreviations see Figures 1 and 3.

and indicates the ordering of the environment; τ_r is the inverse of the rotational rate and provides data on the environmental viscosity. For both probes, but especially for DPH, τ_m were somewhat higher than phase lifetimes, τ_P, indicating some heterogeneity in the fluorophore population. However, the fact that the values obtained for τ_r and r_∞ were relatively independent of the frequency indicated that they were essentially correct average values of the rotamer populations.

(*i) Influence of apolipoproteins and different lipid composition on LVe and LVl.* All samples showed a linear decrease of r_s with temperature, but DPH r_s showed a greater temperature dependence than did DPH-PA r_s (Figs. 3–6). Comparison of LV with their corresponding LP indicated that the presence of apolipoproteins increased the r_s in both probes, this effect being more conspicuous for DPH r_s. This particular effect was also observed on τ values, since apolipoproteins increased the lifetimes of DPH without altering DPH-PA lifetimes (Fig. 7). r_∞ was increased by apolipoproteins in the environment of DPH-PA (up to 2.5-fold higher at 30°C), and to an even greater extent in the environment of DPH (up to 12-fold higher in LV than in LP) (Table 2). Moreover, the time τ_r of DPH was increased by the presence of apolipoproteins, but DPH-PA τ_r was not affected (Table 2). Altogether, these data indicate a particular effect of apolipoproteins on the neutral lipid core, decreasing the DPH environment polarity as well as hindering and slowing the DPH rotational motion. In the absence of apolipoproteins, DPH rotation became nearly isotropic (with a very low r_∞) at 30°C.

Similar DPH r_s values were observed when comparing both LV, whereas DPH-PA r_s was higher in LVe than in LVl (Fig. 4). A similar difference was observed when comparing LPe with LPl (Fig. 6); a somewhat higher DPH-PA r_∞ was observed in

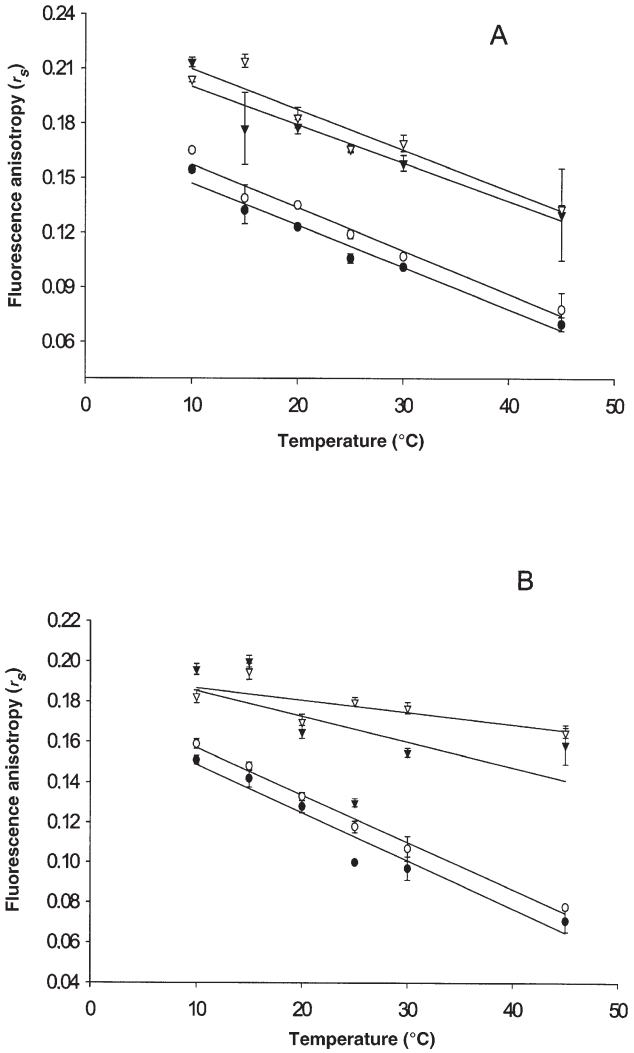

FIG. 5. Effect of FS on the DPH r_s in LPe (A) and LPl (B). r_s is plotted vs. temperature in the absence (●) or in the presence of 1 (○), 10 (▼), and 20 ppm (▽) of FS. Values represent the average of five different determinations ± SD. For abbreviations see Figures 1 and 3.

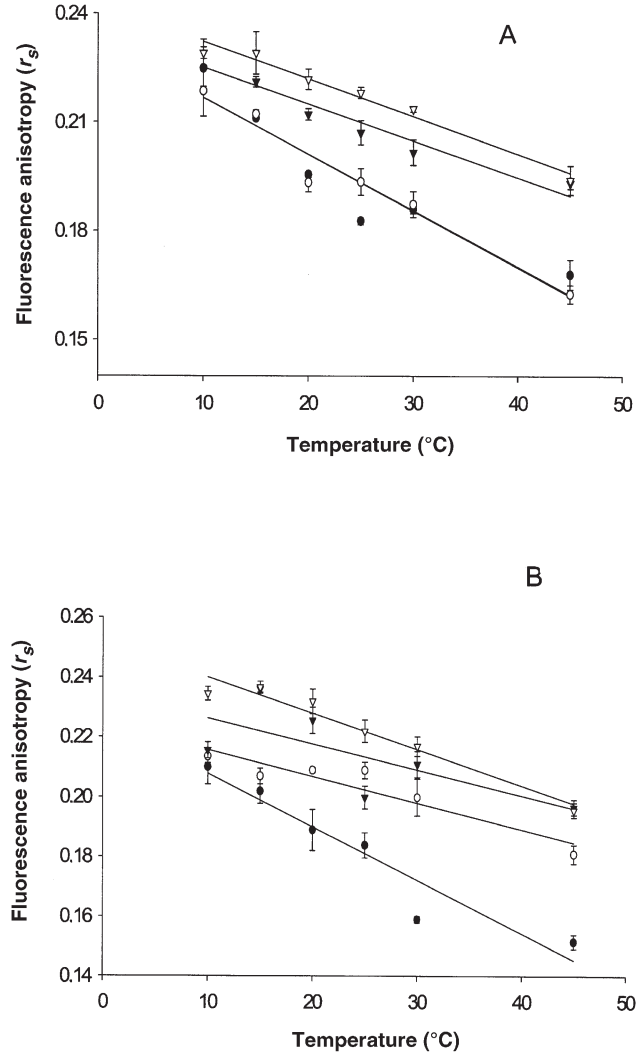

FIG. 6. Effect of FS on the DPH-PA r_s in LPe (A) and LPl (B). r_s is plotted vs. temperature in the absence (●), or in the presence of 1 (○), 10 (▼), and 20 ppm (▽) of FS. Values represent the average of five different determinations ± SD. For abbreviations see Figures 1, 3, and 4.

LVe with respect to LVl (see Table 2), and the same trend was observed when comparing LPe with LPl. However, no differences could be found in r_∞ of DPH nor in the τ_r of DPH and DPH-PA in both LV forms. These facts suggest that the different lipid compositions of the LV affected the lipid ordering in the surface monolayer but not in the neutral lipid core. A slightly increased τ for both probes also was observed in LVe with respect to LVl (Fig. 7). However, differences in τ values were not noticeable when comparing LPe with LPl in the absence of apolipoproteins (Fig. 7); they could be attributed to a different interaction of apolipoproteins with the lipids in each LV.

(ii) Influence of FS. The presence of high concentrations of FS resulted in a strong increase of r_s for both probes in both types of LV and LP. The major effect of the insecticide was observed at higher temperatures, resulting in a decreased temperature dependence of r_s in FS-containing samples. FS also produced a large decrease in τ of both probes, an effect that was greater with DPH (Fig. 7). No detectable effect of FS on the rotational behavior of DPH and DPH-PA in the LP samples could be observed. Thus, the increase in DPH and DPH-PA r_s that was noted in samples containing FS was exclusively due to the reduction of τ. The same effect was observed in LVe for DPH-PA, whose rotational behavior was not affected by FS (Table 2). But an increase in lipid ordering, as reflected by measurements of r_∞ values, was detected for both LV with the core-sensing probe DPH, and only for LVl with the surface probe DPH-PA (see Table 2). A decrease in τ_r of DPH and DPH-PA was also observed for LVl, but not for LVe. Thus, these data indicated that FS was incorporated into all these systems, decreasing the polarity of the regions sensed by DPH and DPH-PA. However, FS altered the lipid dynamics only in the neutral lipid core sensed by DPH in LVe, whereas both

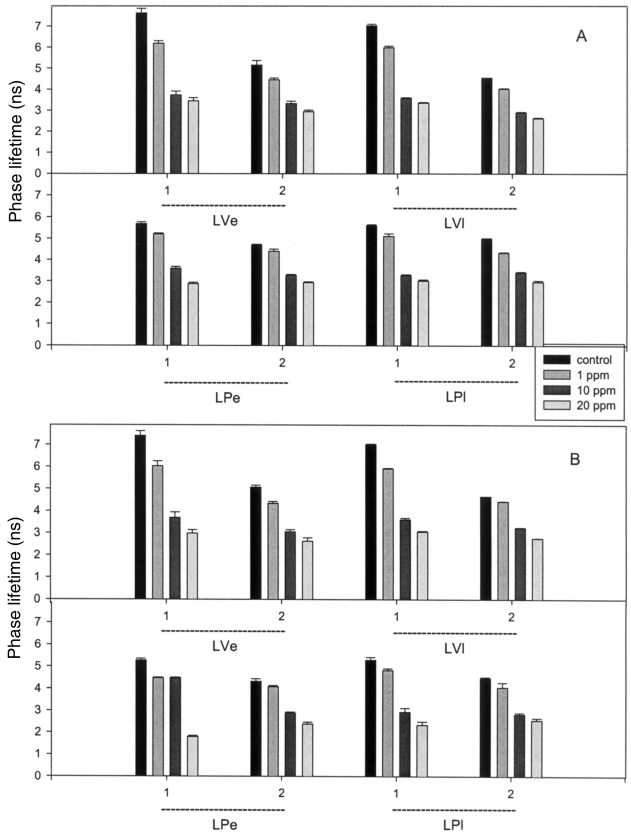

FIG. 7. Phase lifetime (τ_P) of DPH (1) and DPH-PA (2) in LVe, LVl, LPe, and LPl of *Macrobrachium borellii*, measured at 18 MHz in the absence or presence of 1, 10, and 20 ppm FS at 10 (A) and 30°C (B). Student's *t*-test was used to compare the significance of the differences with respect to the sample without FS: $P < 0.0001$. For abbreviations see Figures 1, 3, and 4.

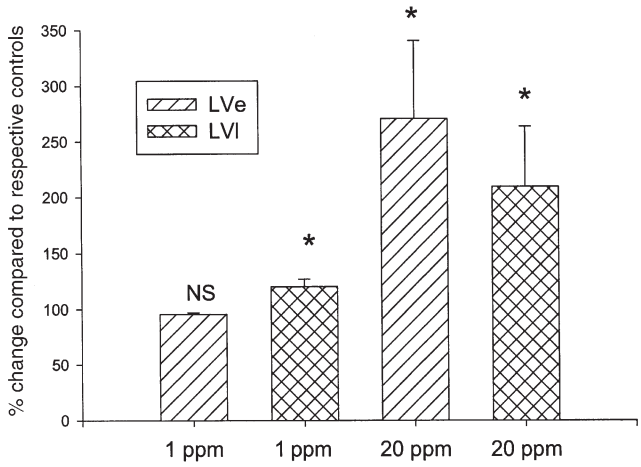

FIG. 8. Release of palmitic acid from LVe and LVl. Releasing capacity of palmitic acid from LV of *M. borellii* was checked in the presence of 1 and 20 ppm of FS. Purification of LV was done by FPLC, and radioactivity was quantitated by liquid scintillation. *P* was calculated by Student's *t*-test by comparison of treated and untreated samples: $P < 0.05$(*); NS, not significant.

regions (neutral core and surface monolayer) were affected in LVl. These effects of FS on the lipid dynamics were dependent on the presence of apolipoproteins, since they were not evident in the protein-free LP systems.

At low FS concentrations, r_s measurements for LV and LP showed different degrees of sensitivity to the insecticide. On one hand, the lipid region sensed by DPH was more sensitive to 1 ppm FS in whole LV (Fig. 3) than in LP (Fig. 5), also pointing out the importance of apolipoproteins on the FS action in the neutral lipid core. On the other hand, DPH-PA r_s was sensitive to 1 ppm FS in LVl but not in LVe (Fig. 4), and the same was observed for the corresponding LP (Fig. 6), suggesting that the different lipid compositions of these lipoproteins can modulate the effect of FS on the surface lipid monolayer properties.

Effect of FS on the transfer of [^{14}C]palmitic acid from LV to albumin. Figure 8 shows the percentage of [^{14}C]palmitic acid transferred from LV to albumin either in the absence or in the presence of 1 and 20 ppm of FS. The addition of 20 ppm FS produced an increment of around 170 and 109% in palmitic acid transfer from LVe and LVl, respectively. However, at low FS concentrations, LVl was more sensitive than LVe, since 1 ppm FS did not alter palmitate transfer from LVe but increased it around 20% from LVl.

TABLE 2
Rotation Correlation Time (τ_r) and Limiting Anisotropy (r_∞) of DPH and DPH-PA at 30°C in Liposomes (LP) and LV[a]

		τ_r	r_∞			τ_r	r_∞
DPH							
LVe	Control	2.40 ± 0.6	0.12 ± 0.02	LVl	Control	2.20 ± 0.26	0.12 ± 0.001
	+20 ppm	1.60 ± 1.0	0.21 ± 0.05*		+20 ppm	1.30 ± 0.70 *	0.22 ± 0.02*
LPe	Control	1.38 ± 0.4	0.02 ± 0.03	LPl	Control	1.50 ± 0.60	0.01 ± 0.04
	+20 ppm	2.24 ± 2.0	0.01 ± 0.05		+20 ppm	1.40 ± 0.69	0.08 ± 0.05
DPH-PA							
LVe	Control	1.80 ± 1.0	0.23 ± 0.02	LVl	Control	1.87 ± 0.24	0.2 ± 0.008
	+20 ppm	1.88 ± 1.0	0.25 ± 0.06		+20 ppm	0.94 ± 0.50*	0.28 ± 0.01*
LPe	Control	1.63 ± 0.8	0.10 ± 0.04	LPl	Control	1.60 ± 0.57	0.08 ± 0.04
	+20 ppm	0.90 ± 0.4	0.16 ± 0.02		+20 ppm	1.20 ± 1.0	0.14 ± 0.07

[a]Values represent the average of five determinations ± SD. *P* was calculated by two-way Student's *t*-test, comparing samples with their respective controls. Asterisk (*), $P < 0.001$. DPH, 1,6-diphenyl-3,5-hexatriene; DPH-PA, 3-(*p*-(6-phenyl)-1,3,5-hexatrienyl)-phenylpropionic acid; for other abbreviations see Table 1.

DISCUSSION

Structural organization of lipids in LV. Neutral and amphipathic probes like DPH and DPH-PA have been used to obtain information on the structural organization of natural (17) or reconstituted (31) lipoproteins. In lipoproteins with a high content of neutral lipids such as TAG, these lipids build up a central core surrounded by a superficial monolayer of amphipathic lipids. Certain lipids such as DAG (17) and CHO (32) can be distributed between the core and surface. On the other hand, lipoproteins lacking neutral lipids have a discoidal morphology with a bilayer of amphipathic lipids (33). LV lack cholesteryl esters but have about 20% of TAG that are, in principle, a somewhat high amount to be easily accommodated within a phospholipid bilayer. It is expected that a neutral molecule such as DPH will display less hindered rotation in a disordered neutral lipid core than in a lipid bilayer. Although r_∞ of DPH in LV is lower than that of DPH-PA, it is relatively high for a disordered lipid core and compatible with values obtained in lipid bilayers. However, it should be taken into account that DPH should partition between the core and superficial monolayer (17), and a relatively small core has to be expected with only 20% of neutral lipids. Another fact to be taken into account is the influence of apolipoproteins. In this respect, the results obtained here with LP of LV lipids are enlightening. DPH r_∞ is extremely low in these protein-free systems, indicating nearly isotropic rotation, which is incompatible with a bilayer organization. This fact suggests that, in the absence of apolipoproteins, LV lipids are organized as small emulsions with a highly disordered core and a surface monolayer of amphipathic lipids. Comparison of the rotational behavior of DPH and DPH-PA in LV and LP systems indicates that apoproteins preferentially hinder DPH rotation. It is possible that apolipoproteins force the incorporation of neutral lipids of LV into the bilayer of a discoidal lipoprotein. However, recent evidence obtained from negative staining electron microscopy (Garcia, C.F., unpublished results) indicates that LVe does not form the "rolls" of stacked structures characteristic of discoidal lipoproteins. Thus, TAG in LV likely form a core with relatively high ordering owing to interaction with one or both apolipoproteins. This interaction of apolipoproteins with the neutral lipid core of LV is also suggested by the selective increase in DPH τ, when comparing LV with LP systems.

LV modification during embryogenesis. During embryogenesis in *M. borellii*, the lipid composition of LV was modified without changes in apolipoprotein composition and lipid/protein ratio. The major changes were an increase in SM, CHO, and FFA with a corresponding decrease in PC contents. A replacement of saturated FA by PUFA was also observed. One of the aims of this work was to study how these changes in lipid composition affect the lipid dynamics and apolipoprotein–lipid interaction in LV. In spite of the large changes in lipid composition in LVe and LVl, no difference in the rotational mobility of DPH was observed, and only a small decrease in lipid ordering was sensed by DPH-PA in LVl compared with LVe. The environmental polarity of both probes was somewhat higher in LVl than in LVe. Moreover, these differences between LVe and LVl were not evident when the apolipoprotein-free systems LPe and LPl were compared, indicating that they depended on apolipoprotein–lipid interactions or some other structural characteristic that was disrupted in the procedure of lipid extraction and LP preparation. These results indicated that the condensing effect expected as a result of the increase in CHO and SM content in LVl was counterbalanced by other changes such as replacement of saturated FA by PUFA or the increase in FFA content.

Effect of FS on LV lipid phase properties. FS at high concentrations decreased the τ of DPH by more than 50% and of DPH-PA by about 30% in both LV and LP. This effect was observed in other lipoprotein and lipid systems (13,14) and was attributed to an increased amount of water penetration in the lipid phase owing to packing defects produced by the insecticide. FS also produced an increase in r_∞ of DPH in LVe and LVl, indicating that this insecticide increased the ordering of the neutral lipid core in both LV. The rotational behavior of DPH-PA, however, was affected by FS in LVl but not in LVe, a difference that should be attributed to the different compositions in amphipathic lipids evoked by these forms of LV. FS affected the properties of the superficial monolayer of LVl in such a way that DPH-PA seemed to wobble in a more restricted angle but at a higher rate, as indicated by the increase in r_∞ and the decrease in τ_r. No appreciable influence of FS on the rotational behavior of DPH or DPH-PA was observed in LP of the extracted LV lipids, a fact that indicates that apolipoprotein–lipid or apolipoprotein–FS interactions play an important role in the effect of this insecticide. A higher sensitivity of LVl to FS in comparison with that of LVe is evidenced by measurements of DPH-PA r_s at low FS concentrations (1 ppm).

Effect of FS on the transfer of palmitic acid to albumin. The ability of LV to transfer palmitic acid to albumin is increased by FS in a concentration-dependent way. It was shown that FS decreased FA uptake by other lipoproteins (13). These facts suggest that FS decreases the capacity and/or affinity of lipoprotein to bind FA, which in turn might be due to a competition between FS and FA for the same binding site or to the alteration of the lipid phase properties produced by FS. Further experimentation will be necessary to distinguish among these possibilities and to identify the molecular basis of FS action on the ability of LV to transfer FA. At a low FS concentration (1 ppm), palmitic acid transfer to albumin was not affected in LVe, but it was increased about 20% in LVl; this fact correlates with a higher sensitivity of LVl to the changes produced by FS in the lipid phase properties.

In short, these results indicate that the modification in lipid composition during embryogenesis in *M. borellii* LV plays an important role in the structural changes and alterations in FA transfer produced by FS. Such differences in sensitivity to FS of the LV at different steps of embryogenesis affect the toxic action of this insecticide. Additional research will be required to learn whether FS can alter the transference of FA or other lipids to physiological acceptors.

ACKNOWLEDGMENTS

M.R.G.B. and H.G. are members of Carrera del Investigador CONICET, Argentina. R.P. is member of Carrera del Investigador CICBA, Argentina. This work was partially funded by CONICET grant PEI 791/98 (M.R.G.B.) and by Agencia Nacional de Promoción Cientifica y Technológica (FONCyT) grant PICT 1970 (R.J.P.).

REFERENCES

1. Omann, G.M., and Lakowicz, J.R. (1982) Interactions of Chlorinated Hydrocarbon Insecticides with Membranes, *Biochim. Biophys. Acta 684*, 83–95.
2. Perez-Albarsanz, M.A., Lopez-Aparicio, P., Senar, S., and Recio, M.N. (1991) Effects of Lindane on Fluidity and Lipid Composition in Rat Renal Cortex Membranes, *Biochim. Biophys. Acta 1066*, 124–130.
3. Lopez-Aparicio, P., Recio, M.N., Prieto, J.C., Carmena, M.J., and Perez-Albarsanz, M.A. (1991) Effect of Lindane upon the β-Adrenergic Stimulation of Cyclic AMP Accumulation in Rat Renal Cortical Tubules Caused by Alterations in Membrane Fluidity, *Life Sci. 49*, 1141–1154.
4. Stelzer, K.J., and Gordon, M.A. (1985) Interactions of Pyrethroids with Phosphatidylcholine Liposomal Membranes, *Biochim. Biophys. Acta 812*, 361–368.
5. Antunes-Madeira, M.C., Videira, R.A., and Madeira, V.M. (1994) Effects of Parathion on Membrane Organization and Its Implications for the Mechanisms of Toxicity, *Biochim. Biophys. Acta 1190*, 149–154.
6. Antunes-Madeira, M.C., Almeida, L.M., and Madeira, V.M. (1993) Depth-Dependent Effects of DDT and Lindane on the Fluidity of Native Membranes and Extracted Lipids. Implications for Mechanisms of Toxicity, *Bull. Environ. Contam. Toxicol. 51*, 787–794.
7. Antunes-Madeira, M.C., and Madeira, V.M. (1993) Effects of DDE on the Fluidity of Model and Native Membranes: Implications for the Mechanisms of Toxicity, *Biochim. Biophys. Acta 1149*, 86–92.
8. Antunes-Madeira, M.A., and Madeira, V.M. (1990) Membrane Fluidity as Affected by the Organochlorine Insecticide DDT, *Biochim. Biophys. Acta 1023*, 469–474.
9. Videira, R.A., Antunes-Madeira, M.C., Custodio, J.B., and Madeira, V.M. (1995) Partition of DDE in Synthetic and Native Membranes Determined by Ultraviolet Derivative Spectroscopy, *Biochim. Biophys. Acta 1238*, 22–28.
10. González-Baró, M.R., Garda, H., and Pollero, R.J. (1997) Effect of Fenitrothion on Hepatopancreas Microsomal Membrane Fluidity in *Macrobrachium borellii*, *Pest. Biochem. Physiol. 58*, 133–143.
11. Blasiak, J. (1993) Changes in the Fluidity of Model Lipid Membranes Evoked by the Organophosphorus Insecticide Methylbromfenvinfos, *Acta Biochim. Pol. 40*, 39–41.
12. González-Baró, M.R., Garda, H., and Pollero, R.J. (2000) Effect of Fenitrothion on Dipalmitoyl and 1-Palmitoyl-2-oleoylphosphatidylcholine Bilayers, *Biochim. Biophys. Acta 1468*, 304–310.
13. Garcia, C.F., Cunningham, M.L., González-Baró, M.R., Garda, H., and Pollero, R. (2002) Effect of Fenithothion on the Physical Properties of Crustacean Lipoproteins, *Lipids 37*, 673–678.
14. Cunningham, M.L., Garcia, C.F., González-Baró, M.R., Garda, H., and Pollero, R. (2002) Organophosphorous Insecticide Fenitrothion Alters the Lipid Dynamics in the Spider *Polybetes pythagoricus* High Density Lipoproteins, *Pest. Biochem. Physiol. 73*, 37–47.
15. Okuno, A., Yang, W.J., Jayasankar, V., Saido-Sakanaka, H., Huong, D., Jasmani, S., Atmomarsono, M., Subramoniam, T., Tsutsui, N., Ohira, T., *et al.* (2002) Deduced Primary Structure of Vitellogenin in the Giant Freshwater Prawn, *Macrobrachium rosenbergii*, and Yolk Processing During Ovarian Maturation, *J. Exp. Zool. 292*, 417–429.
16. Heras, H., Gonzalez Baró, M.R., and Pollero, R.J. (2000) Lipid and Fatty Acid Composition and Energy Partitioning During Embryo Development in the Shrimp *Macrobrachium borellii*, *Lipids 35*, 645–651.
17. Rimoldi, O.J., Garda, H.A., and Brenner, R.R. (1996) Effect of Phospholipids on the Structure of *Triatoma infestans* Lipophorin Studied by Fluorescence Methods, *J. Lipid Res. 37*, 2125–2135.
18. Lavarias, S., Heras, H., Demichelis, S., Portiansky, E., and Pollero, R. (2002) Morphometric Study of Embryonic Development of *Macrobrachium borellii* (Arthropoda: Crustacea), *Invert. Reprod. Devel. 41* 157–163.
19. Folch, J., Lees, M., and Sloane Stanley, G.H. (1957) A Simple Method for the Isolation and Purification of Total Lipids from Animal Tissues, *J. Biol. Chem. 226*, 497–509.
20. Cunningham, M., and Pollero, R.J. (1996) Characterization of Lipoprotein Fractions with High Content of Hemocyanin in the Hemolymphatic Plasma of *Polybetes pythagoricus*, *J. Exp. Zool. 274*, 275–280.
21. Gaspar, M.L., Cabello, M.N., Pollero, R., and Aon, M.A. (2001) Fluorescein Diacetate Hydrolysis as a Measure of Fungal Biomass in Soil, *Curr. Microbiol. 42*, 339–344.
22. Lowry, O.H., Rosebrough, N.J., Farr, A.R., and Randall, R.J. (1951) Protein Measurement with the Folin Phenol Reagent, *J. Biol. Chem. 193*, 265–275.
23. Laemmli, U.K. (1970) Cleavage of Structural Proteins During the Assembly of the Head of Bacteriophage T4, *Nature 227*, 680–685.
24. Garin, C.F., Heras, H., and Pollero, R.J. (1996) Lipoproteins of the Egg Perivitelline Fluid of *Pomacea canaliculata* Snails (Mollusca: Gastropoda), *J. Exp. Zool. 276*, 307–314.
25. Spencer, R.D., and Weber, G. (1970) Influence of Brownian Rotations and Energy Transfer upon the Measurements of Fluorescence Lifetime, *J. Chem. Phys. 52*, 1654–1663.
26. Tricerri, M.A., Garda, H.A., and Brenner, R.R. (1994) Lipid Chain Order and Dynamics at Different Bilayer Depths in Liposomes of Several Phosphatidylcholines Studied by Differential Polarized Phase Fluorescence, *Chem. Phys. Lipids 71*, 61–72.
27. Garda, H.A., Bernasconi, A.M., and Brenner, R.R. (1994) Possible Compensation of Structural and Viscotropic Properties in Hepatic Microsomes and Erythrocyte Membranes of Rats with Essential Fatty Acid Deficiency, *J. Lipid Res. 35*, 1367–1377.
28. Lakowicz, J.R., Prendergast, F.G., and Hogen, D. (1979) Differential Polarized Phase Fluorometric Investigations of Diphenylhexatriene in Lipid Bilayers. Quantitation of Hindered Depolarizing Rotations, *Biochemistry 18*, 508–519.
29. Lakowicz, J.R. (1983) *Principles of Fluorescence Spectroscopy*, 1st edn., Chapters 3 and 6, Plenum Press, New York.
30. Weber, G. (1978) Limited Rotational Motion: Recognition by Differential Phase Fluorometry, *Acta Phys. Pol. A 54*, 173–179.
31. Rye, K.A., Garrety, K.H., and Barter, P.J. (1993) Preparation and Characterization of Spheroidal, Reconstituted High-Density Lipoproteins with Apolipoprotein A-1 Only or with Apolipoprotein A-1 and A-2, *Biochim. Biophys. Acta 1167*, 316–325.
32. Ekman, S., Derksen, A., and Small, D.M. (1988) The Partitioning of Fatty Acid and Cholesterol Between Core and Surfaces of Phosphatidylcholine-Triolein Emulsions at pH 7.4, *Biochim. Biophys. Acta 959*, 343–348.
33. Brouillette, C.G., Anantharamaia, G.M., Engler, J.A., and Borhani, D.W. (2001) Structural Models of Human Apolipoprotein A-1: A Critical Analysis and Review, *Biochim. Biophys. Acta 1531*, 4–46.

[Received December 31, 2003; accepted May 14, 2004]

Synthesis of Deuterated Fatty Acids to Investigate the Biosynthetic Pathway of Disparlure, the Sex Pheromone of the Gypsy Moth, *Lymantria dispar*

José-Luis Abad*, Gemma Fabriàs, and Francisco Camps

Departamento de Química Orgánica Biológica, Instituto de Investigaciones Químicas y Ambientales de Barcelona (IIQAB), Consejo Superior de Investigaciones Científicas (CSIC), 08034-Barcelona, Spain

ABSTRACT: The preparation and characterization of a series of deuterium-labeled intermediates used in the study of the biosynthetic pathway for disparlure, the sex pheromone of *Lymantria dispar,* is reported. The synthetic route starts with propargyl alcohol, and the deuterium atoms are introduced by deuteration of an alkyne precursor in the presence of Wilkinson's catalyst. The olefinic bond was created by the Wittig reaction of a suitable aldehyde with a common tetradeuterated phosphonium ylide intermediate. The presence of the expected label and its correct location were confirmed by both MS and ^{13}C NMR. These compounds were successfully used to elucidate the disparlure biosynthetic pathway.

Paper no. L9472 in *Lipids 39,* 397–401 (April 2004).

Many female insects produce and release their sex pheromones into the environment to attract their conspecific males for mating. These sex pheromones usually consist of complex blends of chemical components that the male can detect. In this context, considerable research on the sex pheromone communication system has been conducted in the past 25 yr. However, how females biosynthesize the species-specific pheromone components is known for only a few species that utilize alcohols, aldehydes, or acetates. So far, very little research has been conducted on the biosynthetic pathways leading to hydrocarbon sex pheromone components in moths, cockroaches, and flies (1–4). That has been the case for disparlure, (7*R*,8*S*)-2-methyl-7,8-epoxyoctadecane, the main component of the gypsy moth sex pheromone blend (5). This compound is an epoxide pheromone that is produced by oxidation of (*Z*)-2-methyl-7-octadecene (6).

Recently, we have studied the sex pheromone biosynthetic pathway for disparlure in the gypsy moth, *Lymantria dispar* (6). This biosynthetic pathway has been elucidated by means of deuterium-labeled precursors (see Scheme 1), although a brief description of their synthesis was given in a previous article. In this work we present a full account of the preparation of these deuterated probes as well as the structural characterization of the different synthetic intermediates.

*To whom correspondence should be addressed at Departamento de Química Orgánica Biológica (IIQAB, CSIC), Jordi Girona 18-26, 08034-Barcelona, Spain. E-mail: jlaqob@iiqab.csic.es

Abbreviations: DMF, dimethylformamide; DMM, dimethoxymethane; HMPA, hexamethylphosphoramide; MTBE, *tert*-butyl methyl ether; NBS, *N*-bromosuccinimide; PDC, pyridinium dichromate; PPh_3, triphenylphosphine; *p*-TSOH, *p*-toluenesulfonic acid.

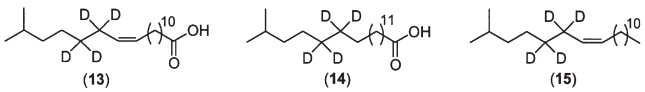

SCHEME 1

EXPERIMENTAL PROCEDURES

General methods. Commercial-grade reagents and solvents were used directly as supplied with the following exceptions: Acetonitrile (CH_3CN) and THF were distilled over CaH_2 and Na/benzophenone, respectively, under an argon atmosphere. Dimethylformamide (DMF) and hexamethylphosphoramide (HMPA) were distilled and kept over molecular sieves (3Å). Unless otherwise noted, all reactions sensitive to oxygen and moisture were performed in flame-dried septum-sealed flasks under either an argon or nitrogen atmosphere. Melting points (m.p.) were determined in soft glass capillary tubes on a Stuart Scientific SMP 10 apparatus and are uncorrected. Unless otherwise stated, organic solutions obtained from the workup of crude reaction mixtures were dried over $MgSO_4$, and the purification procedures were carried out by flash chromatography on silica gel (230–400 mesh); products were obtained mostly as oils. Visualization of UV-inactive materials was accomplished by soaking the TLC plates in an ethanolic solution of anisaldehyde and sulfuric acid (96:2:2, by vol) or in an ethanolic solution of phosphomolybdic acid (5%). Unless otherwise noted, all ^1H NMR spectra were acquired at 300 MHz, and ^{13}C NMR spectra were obtained at 75 MHz in freshly neutralized $CDCl_3$ solutions. Chemical shifts are given in ppm downfield from $Si(CH_3)_4$ for ^1H and downfield from $CDCl_3$ for ^{13}C. Assignment of critical signals in the ^{13}C NMR spectra was carried out on the basis of distortionless enhancement by polarization transfer. GC–MS was performed by electron impact at 30 eV on a Fisons gas chromatograph (8000 series) coupled to a Fisons MD-800 mass detector. All IR spectra were run on a Michelson Bomem MB-120 spectrometer. Elemental analyses were obtained from the Microanalysis Service of IIQAB–CSIC; these were conventional combustion analyses without discrimination between the hydrogen and deuterium contents. Deuterium gas (deuterium content 99.8%) was obtained from Aldrich Chemical Co. (Milwaukee, WI). The contents of the labeled substrates were determined by GC–MS analysis and were found to be higher than 99%. For this purpose, acids **13** and **14** were derivatized to the respective methyl esters.

*12-Bromo-1-dodecanol (**1**).* To a solution of 1,12-dodecandiol (4.04 g, 20 mmol) in 50 mL of toluene cooled to 0°C was added 28 mL of HBr (48%, 240 mmol), and the mixture was refluxed in the dark for 5 h (TLC monitoring). The reaction was allowed to cool to room temperature, and 50 mL of brine was then added. The mixture was extracted with hexane, dried, filtered, and concentrated at reduced pressure. The residue was purified by flash chromatography on silica gel using hexane/MTBE (*tert*-butyl methyl ether) 5:1 to afford 4.88 g (92% yield) of the expected product. IR: 3330 (OH), 2935, 2860, 1465, 1440, 1245, 1055 cm^{-1}; ^1H NMR: δ 3.63 (*t*, *J* = 6.5 Hz, 2H, CH_2OH), 3.41 (*t*, *J* = 7 Hz, 2H, CH_2Br), 1.85 (*quint*, *J* = 7 Hz, 2H, CH_2CH_2Br), 1.65 (*s*, 1H, OH), 1.56 (*m*, 2H, CH_2–CH_2OH), 1.50–1.24 (16H, CH_2); ^{13}C NMR: δ 62.9 (CH_2OH), 34.0 (CH_2CH_2Br), 32.8 (CH_2Br), 32.7 (CH_2CH_2OH), 29.5 (CH_2), 29.4 (CH_2), 29.4 (CH_2), 29.4 (CH_2), 28.7 (CH_2), 28.1 (CH_2), 25.7 (CH_2).

*1-Bromo-13,15-dioxahexadecane (**2**).* This compound was prepared following the procedure reported by Gras *et al.* (7). To a stirred solution of bromoalcohol **1** (3.98 g, 15 mmol) in 60 mL of dimethoxymethane (DMM) were added LiBr (435 mg, 5 mmol) and *p*-toluenesulfonic acid (*p*-TSOH; 190 mg, 1 mmol) at room temperature, and stirring was continued overnight. Brine was added (50 mL), and the crude residue was extracted with hexane, dried, and concentrated at reduced pressure. The resulting oil was purified by flash chromatography on silica gel using hexane/MTBE 85:15 to afford 4.37 g of the expected product **2** (94% yield). IR: 2925, 2855, 1465, 1440, 1215, 1150, 1110, 1045, 920 cm^{-1}; ^1H NMR: δ 4.62 (*s*, 2H, OCH_2O), 3.52 (*t*, *J* = 6.5 Hz, 2H, CH_2O), 3.41 (*t*, *J* = 7 Hz, 2H, CH_2Br), 3.36 (*s*, 3H, OCH_3), 1.85 (*quint*, *J* = 7 Hz, 2H, CH_2CH_2Br), 1.59 (*m*, 2H, CH_2CH_2O), 1.50–1.22 (16H, CH_2); ^{13}C NMR: δ 96.3 (OCH_2O), 67.8 (CH_2O), 55.1 (OCH_3), 34.0 (CH_2CH_2Br), 32.8 (CH_2Br), 29.7 (CH_2), 29.5 (CH_2), 29.5 (CH_2), 29.5 (CH_2), 29.4 (CH_2), 28.7 (CH_2), 28.1 (CH_2), 26.2; MS: *m/z* 309 ($M^{\cdot+}$, 1), 277 (2), 162 (12), 148 (20), 123 (25), 109 (40), 97 (90), 83 (100), 69 (98).

*13,15-dioxahexadecanal (**3**).* This compound was prepared using the procedure reported by Stowell (8). A mixture of **2** (3.10 g, 10 mmol), pyridine oxide (20 mmol), and sodium bicarbonate (20 mmol) in 50 mL of toluene was heated with vigorous stirring under a nitrogen atmosphere at 80°C for 24 h. The reaction mixture was allowed to cool, and 10 mL of water was then added. The organic layer was separated, and the water layer was extracted with hexane (2 × 4 mL). The combined organic fractions were dried, concentrated to dryness, and purified by flash chromatography on silica gel (0–10% MTBE/hexane) to give 1.84 g (75% yield) of the pure aldehyde. IR: 2930, 2855, 2715, 1725 (CO), 1465, 1145, 1110, 1045, 920 cm^{-1}; ^1H NMR: δ 9.77 (*t*, *J* = 2 Hz, 1H, CHO), 4.62 (*s*, 2H, OCH_2O), 3.52 (*t*, *J* = 6.5 Hz, 2H, CH_2O), 3.36 (*s*, 3H, OCH_3), 2.42 (*dt*, J_1 = 2 Hz, J_2 = 7.5 Hz, 2H, CH_2CHO), 1.60 (*m*, 2H, CH_2CH_2O), 1.44–1.20 (16H, CH_2); ^{13}C NMR: δ 203.0 (CHO), 96.3 (OCH_2O), 67.8 (CH_2O), 55.1 (OCH_3), 43.9 (CH_2CHO), 29.7 (CH_2), 29.5 (CH_2), 29.5 (CH_2), 29.4 (CH_2), 29.4 (CH_2), 29.3 (CH_2), 29.1 (CH_2), 26.2 (CH_2), 22.0 (CH_2); MS: *m/z* 213 ($M^{\cdot+}$ – OCH_3, 5), 199 (15), 182 (10), 163 (12), 135 (25), 121 (40), 109 (55), 95 (100), 81 (98), 67 (88).

*5,5,5-Triphenyl-4-oxa-1-pentyne (**4**).* To a solution of 1.12 g (20 mmol) of propargyl alcohol in 50 mL of dry pyridine was added 5.86 g (21 mmol) of trityl chloride ($ClCPh_3$). The reaction mixture was stirred at room temperature for 36 h, and 25 mL of water was then added. The mixture was extracted with CH_2Cl_2, and the organic layer was concentrated to dryness and purified by flash chromatography on silica gel (0–10% MTBE/hexane) to give 5.66 g of a white solid (95% yield), m.p. 115–116°C. IR: 3290, 3275, 1490, 1445, 1370, 1065, 1055 cm^{-1}; ^1H NMR: δ 7.50–7.43 (6H, Ar H), 7.34–7.18 (9H, Ar H), 3.75 (*d*, *J* = 2.5 Hz, 2H, CH_2CCH), 2.38 (*t*, *J* = 2.5 Hz, 1H, CCH); ^{13}C NMR: δ 143.3 (Ar C), 128.5 (Ar CH), 127.9 (Ar CH), 127.2 (Ar CH), 87.5 (C), 80.3 (*C*CH), 73.5 (C*CH*), 52.9 (CH_2); MS: *m/z* 298 ($M^{\cdot+}$, 2), 243 (45), 165, (90), 105 (100), 77 (40); Anal. Calcd. for $C_{22}H_{18}O$: C, 88.56; H, 6.08. Found: C, 88.52; H, 6.02.

*8-Methyl-2-oxa-1,1,1-triphenyl-4-nonyne (**5**).* To a stirred solution of 2.98 g (10 mmol) of **4**, 15 mL of anhydrous THF and 10 mL of dry HMPA was added 8 mL of a solution of butyllithium in hexane (1.5 M) at 0°C. The resulting dark red mixture was stirred for 10 min, and 2.38 g (12 mmol) of 1-iodo-3-methylbutane dissolved in 4 mL of THF was added dropwise while holding the temperature at 0°C. The reaction mixture was worked up within 2 h by pouring it into ice water and extracting with hexane. The organic layer was dried, concentrated to dryness, and purified by flash chromatography on silica gel (0–3% MTBE/hexane) to give 3.39 g (92% yield) of product **5**. IR: 3060, 3040, 2955, 2930, 2865, 1490, 1450, 2370, 1055 cm^{-1}; ^1H NMR: δ 7.50–7.43 (6H, Ar H), 7.34–7.18 (9H, Ar H), 3.72 (*t*, *J* = 2 Hz, 2H, OCH_2CC), 2.22 (*tt*, J_1 = 2 Hz, J_2 = 7.5 Hz, 2H, $CCCH_2$), 1.68 (*hept*, *J* = 6.5 Hz, 1H, $(CH_3)_2CH$), 1.40 (*q*, *J* = 7 Hz, 2H, $CHCH_2$), 0.89 (*d*, *J* = 6.5 Hz, 6H, CH_3); ^{13}C NMR: δ 143.3 (Ar C), 128.6 (Ar CH), 127.8 (Ar CH), 127.0 (Ar CH), 87.3 (C), 86.2 ($CCCH_2$), 76.3 (OCH_2CC), 53.5 (OCH_2C), 37.5 (CH_2), 27.2 (CH), 22.2 (CH_3), 16.9 ($CCCH_2$); MS: *m/z* 368 ($M^{\cdot+}$, 0.5), 338 (1), 298 (40), 243 (65), 165 (100). Anal. Calcd. for $C_{27}H_{28}O$: C, 88.00; H, 7.66. Found: C, 88.12; H, 7.65.

Preparation of Wilkinson's catalyst. This compound was prepared using the procedure reported by Osborn *et al.* (9) with minor modifications. A mixture of 2.1 g (8 mmol) of triphenylphosphine and 0.25 g (1.2 mmol) of $RhCl_3$ in 60 mL of ethanol was refluxed under an argon atmosphere. Heating was continued for 5 d until red crystals precipitated, and then the solution was allowed to cool to room temperature. The precipitate was filtered out, washed with methanol and ether, and dried at reduced pressure to afford 1.08 g (1.16 mmol, 98% yield) of Wilkinson's catalyst, which was stored at 4°C in the dark under an argon atmosphere. The product prepared under these conditions was active after 1 yr of storage.

*[5,5,6,6-$^2H_4$]-2-Methyl-8-oxa-9,9,9-triphenylnonane (**6**).* To a mixture of 1.84 g (5 mmol) of **5** and 275 mg (0.3 mmol) of $RhCl(PPh_3)_3$ was added 28 mL of degassed benzene under an argon atmosphere to obtain a reddish solution. The system was purged by passing a stream of D_2 through, and then the D_2

atmosphere was kept using a common rubber balloon filled with D_2, and the solution was stirred for 36 h. The mixture was filtered through a bed of Celite©, and the solvent was evaporated. The residue was then purified by flash chromatography on silica gel (0–3% MTBE/hexane) to give 1.86 g of product **6** (99% yield). IR: 3070, 3050, 3030, 2945, 2915, 2890, 2195, 2105, 1595, 1480, 1555, 1075, 755, 700 cm^{-1}; ^1H NMR: δ 7.48–7.38 (6H, Ar H), 7.34–7.16 (9H, Ar H), 3.02 (*bs*, 2H, OCH_2CD_2), 1.49 (*hept*, *J* = 6.5 Hz, 1H, $(CH_3)_2CH$), 1.30–1.05 (4H, CH_2), 0.84 (*d*, *J* = 6.5 Hz, 6H, CH_3); ^{13}C NMR: δ 144.5 (Ar C), 128.7 (Ar CH), 127.7 (Ar CH), 126.8 (Ar CH), 86.2 (C), 63.5 (OCH_2CD_2), 38.9 (CH_2CH), 29.1 (*quint*, *J* = 15 Hz, CD_2), 27.9 (CH), 27.0 (CD_2CH_2), 25.5 (*quint*, *J* = 15 Hz, CD_2), 22.6 (CH_3); MS: *m/z* 376 ($M^{\cdot+}$, 7), 299 (12), 243 (100), 165 (80), 105 (30); Anal. Calcd. for $C_{27}H_{28}{}^2H_4O_2$: C, 86.12; H, 8.57. Found: C, 86.03; H, 8.49.

*[2,2,3,3-$^2H_4$]-6-Methyl-1-heptanol (**7**).* Product **6** (1.13 g, 3 mmol) was trityl-deprotected to the corresponding alcohol by treatment with 60 mL of a MeOH/$CHCl_2COOH$ solution (6%) for 48 h at room temperature. The acid solution was neutralized with saturated $NaHCO_3$, extracted with CH_2Cl_2, dried, and carefully concentrated. The residue was then purified by flash chromatography on silica gel (0–10% AcOEt/pentane) to give 362 mg (90% yield) of the corresponding pure alcohol **7**. IR: 3340 (OH), 2955, 2915, 2870, 1470, 1045 cm^{-1}; ^1H NMR: δ 3.62 (*bs*, 2H, CH_2OH), 1.70 (*bs*, 1H, OH), 1.53 (*hept*, *J* = 6.5 Hz, 1H, CH), 1.30–1.05 (4H, CH_2), 0.87 (*d*, *J* = 6.5 Hz, 6H, CH_3); ^{13}C NMR: δ 62.9 (CH_2), 38.9 (CH_2), 31.8 (*quint*, *J* = 19 Hz, CD_2), 27.9 (CH), 26.9 (CH_2), 25.0 (*quint*, *J* = 15 Hz, CD_2), 22.6 (CH_3); MS: *m/z* 133 ($M^{\cdot+}$ – 1, 1), 101 (42), 86 (33), 72 (75), 56 (100); Anal. Calcd. for $C_8H_{14}{}^2H_4O$: C, 71.57; H, 13.52. Found: C, 71.61; H, 13.48.

*[2,2,3,3-$^2H_4$]-1-Bromo-6-methylheptane (**8**).* This reaction was accomplished with minor modifications according to the procedure described by Bates *et al.* (10). A solution of *N*-bromosuccinimide (NBS) (4.5 mmol, 0.8 g in 4 mL) was slowly added at room temperature to a stirred DMF solution (4.5 mL) containing 335 mg (2.5 mmol) of alcohol **7** and 1.05 g (4 mmol) of PPh_3. Stirring was continued for 1 h, and 250 µL of methanol was added to the brown mixture to quench the reagent excess. After 5 min, ethyl ether was added, and the organic layer washed with saturated NaCl and carefully evaporated to dryness. The residue was purified by flash chromatography on silica gel using pentane as the eluent to afford 350 mg (75% yield) of product **8**. IR: 2935, 2915, 2850 cm^{-1}; ^1H NMR: δ 3.39 (*bs*, 2H, CH_2Br), 1.53 (*sept*, *J* = 6.5 Hz, 1H, CH), 1.34–1.10 (4H, CH_2), 0.86 (*d*, *J* = 6.5 Hz, 6H, CH_3); ^{13}C NMR: δ 38.7 (CH_2), 33.8 (CH_2), 31.9 (*quint*, *J* = 19.5 Hz, CD_2), 27.9 (CH), 27.4 (*quint*, *J* = 15 Hz, CD_2), 26.3 (CH_2), 22.6 (CH_3); MS: *m/z* 155 ($M^{\cdot+} - C_3H_7$, 74), 153 ($M^{\cdot+} - C_3H_7$, 76), 139 (20), 109 (10), 101 (25), 73 (100), 57 (80).

*(Z)-[5,5,6,6-$^2H_4$]-2-Methyl-20,22-dioxa-7-tricosene (**9**).* A mixture of 188 mg (1 mmol) of bromoderivative **8** and 328 mg (1.25 mmol) of PPh_3 was refluxed in 20 mL of anhydrous CH_3CN under argon atmosphere for 24 h. The solvent was evaporated, and the residue was suspended in pentane (3 × 20 mL), decanted, and dried at reduced pressure.

To the solution of triphenylphosphonium bromide previously obtained, 5 mL of anhydrous THF and 1 mL of dry HMPA, a butyllithium solution in hexane (1.8 equivalents, 1.6 M) was added dropwise at –50°C under a nitrogen atmosphere to afford a dark red suspension. The reaction mixture was stirred at that temperature for 30 min and then cooled at –78°C. Protected aldehyde **3** dissolved in 2 mL of anhydrous THF was added dropwise and stirred for 1 h at –78°C and for 3 h at room temperature. The reaction mixture was poured into water and extracted with hexane. The combined organic fractions were dried, concentrated to dryness, and purified by flash chromatography on silica gel (0–1% MTBE/hexane) to give 208 mg of a 94:6 mixture of *Z/E* isomers (60% yield from **8**). IR: 2925, 2855, 1465, 1440, 1150, 1110, 1045, 920 cm^{-1}; ^1H NMR: δ 5.35 (*m*, 1H, CH), 5.34 (*t*, *J* = 4.5 Hz, 1H, CH), 4.62 (*s*, 2H, OCH_2O), 3.52 (*t*, *J* = 6.5 Hz, 2H, CH_2O), 3.36 (*s*, 3H, OCH_3), 2.01 (*m*, 2H, CH_2CH), 1.56 (*m*, 2H, CH_2CH_2O), 1.52 (*sept*, *J* = 6.5 Hz, 1H, $(CH_3)_2CH$), 1.44–1.21 (18H, CH_2), 1.17 (*m*, 2H, CH_2), 0.86 (*d*, *J* = 6.5 Hz, 6H, CH_3); ^{13}C NMR: δ 129.9 (CH), 129.8 (CH), 96.4 (OCH_2O), 67.9 (CH_2O), 55.1 (OCH_3), 38.8 (CH_2), 29.8 (CH_2), 29.7 (CH_2), 29.6 (CH_2), 29.5 (CH_2), 29.4 (CH_2), 29.3 (CH_2), 28.0 ($(CH_3)_2CH$), 27.2 (CH_2), 26.8 (CH_2), 26.2 (CH_2), 22.6 (CH_3); MS: *m/z* 344 ($M^{\cdot+}$, 0.5), 312 (5), 199 (12), 184 (10), 126 (12), 112 (25), 97 (43), 83 (55), 69 (50), 57 (40), 45 (100); Anal. Calcd. for $C_{22}H_{40}{}^2H_4O_2$: C, 76.68; H, 12.88. Found: C, 76.65; H, 12.80.

*(Z)-[5,5,6,6-$^2H_4$]-2-Methyl-7-octadecene (**15**)* (6). In this case, undecanal (208 mg, 1.2 mmol) was allowed to couple with the triphenylphosphonium salt of **8** (460 mg, 1 mmol). Purification by flash chromatography on silica gel (hexane) gave a 94:6 mixture of *Z/E* isomers. Repurification by flash chromatography on silica gel impregnated with $AgNO_3$ (10%) using hexane as the eluent afforded 216 mg (80% yield) of pure (*Z*)-olefin.

*Reduction to [14,14,15,15-$^2H_4$]-22-Methyl-2,3-dioxatricosane (**10**).* A mixture of 22 mg (0.064 mmol) of **9** and 4 mg of Pd/C (10%) in 4 mL of degassed MeOH was purged by passing a stream of H_2 through. The H_2 atmosphere was kept using a common rubber balloon filled with D_2, and the reaction mixture was stirred vigorously for 48 h, then filtered through a bed of Celite and the solvent evaporated. The residue was purified by flash chromatography on silica gel (0–1% MTBE/hexane) to give 20 mg of product **10** (90% yield). IR: 2930, 2855, 1465, 1440, 1150, 1110, 1050, 920 cm^{-1}; ^1H NMR: δ 4.62 (*s*, 2H, OCH_2O), 3.52 (*t*, *J* = 6.5 Hz, 2H, CH_2O), 3.36 (*s*, 3H, OCH_3), 1.58 (*m*, 2H, CH_2CH_2O), 1.52 (*sept*, *J* = 6.5 Hz, 1H, $((CH_3)_2CH)$, 1.42–1.20 (26H), 1.15 (*m*, 2H, CH_2), 0.86 (*d*, *J* = 6.5 Hz, 6H, CH_3); ^{13}C NMR: δ 96.4 (OCH_2O), 67.9 (CH_2O), 55.1 (OCH_3), 39.0 (CH_2), 29.7 (CH_2), 29.6 (CH_2), 29.4 (CH_2), 28.0 ($(CH_3)_2CH$), 27.2 (CH_2), 26.2 (CH_2), 22.7 (CH_3); MS: *m/z* 345 ($M^{\cdot+}$–1, 0.5), 313 (8), 282 (10), 253 (15), 226 (10), 212 (10), 198 (8), 169 (9), 155 (10), 139 (20), 124 (25), 111 (30), 96 (60), 82 (70), 71 (60), 57 (45), 45 (100); Anal. Calcd. for $C_{22}H_{42}{}^2H_4O_2$: C, 76.23; H, 13.38. Found: C, 76.25; H, 13.22.

Methoxymethane deprotection. General procedure. Products **9** and **10** were deprotected to the corresponding alcohols by treatment with a MeOH/HCl solution (0.5 M) for 24 h at

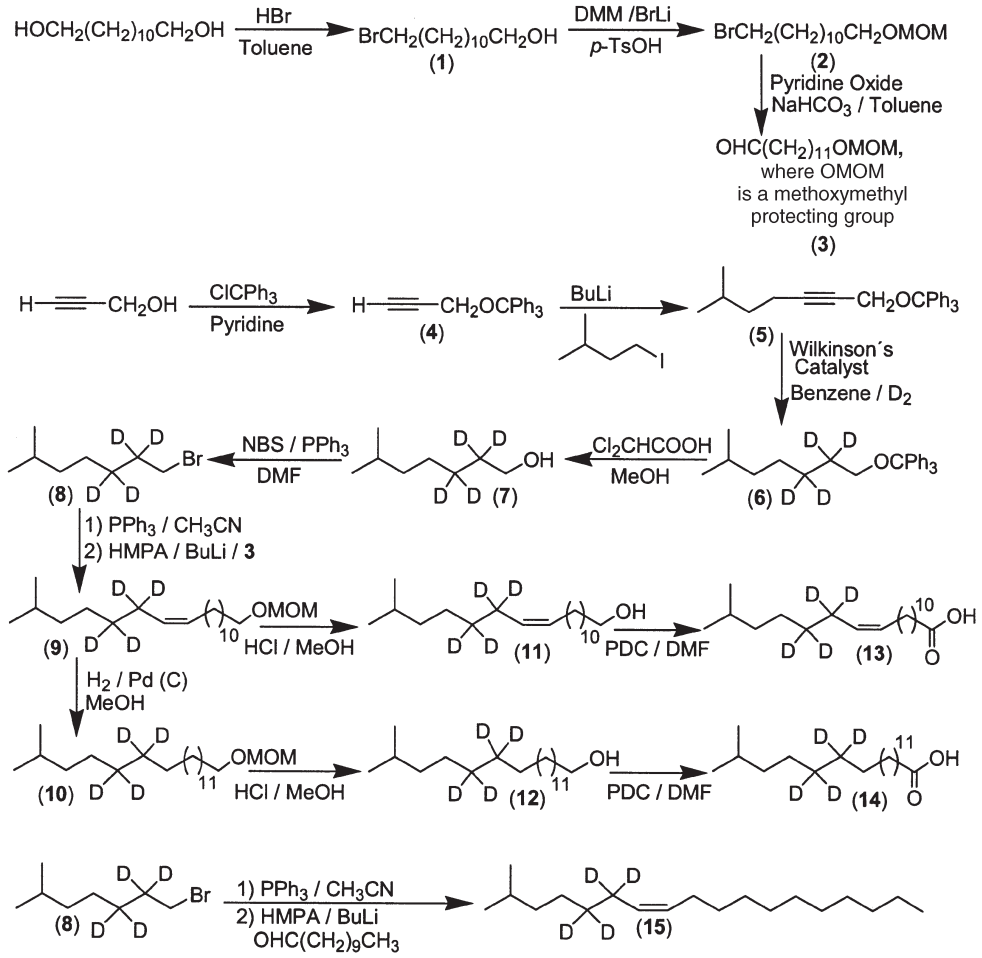

SCHEME 2

room temperature. The solvent was evaporated, and the crude residue was treated with 2 mL of water, extracted with CH_2Cl_2, dried, and concentrated to a residue, which was then purified by flash chromatography on silica gel (10–15% AcOEt/hexane).

*(Z)-[14,14,15,15-$^2H_4$]-18-Methyl-12-nonadecen-1-ol (**11**).* This product (27 mg, 89%) was isolated from 35 mg of **9**. IR: 3355 (OH), 2925, 2855, 1465, 1055 cm^{-1}; ^{1}H NMR: δ 5.37 (*m*, 1H, CH), 5.35 (*t*, *J* = 4.5 Hz, 1H, CH), 3.63 (*t*, *J* = 6.5 Hz, 2H, C*H*$_2$OH), 2.01 (*m*, 2H, C*H*$_2$CH), 1.55 (*m*, 2H, C*H*$_2$CH$_2$OH), 1.52 (*sept*, *J* = 6.5 Hz, 1H, (CH$_3$)$_2$C*H*), 1.44–1.21 (20H, CH$_2$), 1.16 (*m*, 2H, CH$_2$), 0.86 (*d*, *J* = 6.5 Hz, 6H, CH$_3$); ^{13}C NMR: (125.7 MHz) δ 129.9 (CH), 129.7 (CH), 63.0 (CH$_2$OH), 38.8 (CH$_2$), 32.8 (CH$_2$), 29.8 (CH$_2$), 29.6 (CH$_2$), 29.6 (CH$_2$), 29.5 (CH$_2$), 29.4 (CH$_2$), 29.3 (CH$_2$), 29.0 (*quint*, *J* = 19 Hz, CD$_2$), 27.9 ((CH$_3$)$_2$*C*H), 27.2 (CH$_2$), 26.8 (CH$_2$), 26.3 (*quint*, *J* = 19 Hz, CD$_2$), 25.7 (CH$_2$), 22.6 (CH$_3$); MS: *m/z* 300 (M$^{\cdot+}$, 0.5), 282 (5), 138 (12), 124 (24), 110 (30), 96 (80), 82 (100), 69 (85), 57 (78).

*[14,14,15,15-$^2H_4$]-18-Methyl-1-nonadecanol (**12**).* This product (27 mg, 90%) was isolated from 34 mg of **10**. IR: 3285 (OH), 2920, 2850, 1470 cm^{-1}; ^{1}H NMR: δ 3.64 (*t*, *J* = 6.5 Hz, 2H, C*H*$_2$OH), 1.58 (*m*, 2H, C*H*$_2$CH$_2$OH), 1.51 (*sept*, *J* = 6.5 Hz, 1H, (CH$_3$)$_2$C*H*), 1.42–1.20 (24H), 1.15 (*m*, 2H), 0.86 (*d*, *J* = 6.5 Hz, 6H, CH$_3$); ^{13}C NMR: δ 63.1 (*C*H$_2$OH), 39.0 (CH$_2$), 32.8 (CH$_2$), 29.7 (CH$_2$), 29.6 (CH$_2$), 29.4 (CH$_2$), 28.0 ((CH$_3$)$_2$*C*H), 27.2 (CH$_2$), 25.7 (CH$_2$), 22.7 (CH$_3$); MS: *m/z* 302 (M$^{\cdot+}$, 2), 284 (10), 256 (30), 226 (20), 141 (25), 126 (24), 111 (35), 98 (45), 83 (95), 69 (85), 57 (100).

Preparation of carboxylic acids. These compounds were prepared using the procedure reported by Corey and Schmidt (11). Alcohols were treated with a 0.2 M (6 equiv) solution of pyridinium dichromate (PDC) in DMF at room temperature for 48 h; 2 mL of HCl (1 M) was then added; the solution was extracted with CH_2Cl_2, dried, and concentrated to a residue that was purified by flash chromatography on silica gel using hexane/MTBE 85:15 to give the corresponding acids in 67% yield.

*(Z)-[14,14,15,15-$^2H_4$]-18-Methyl-12-nonadecenoic acid (**13**) (6).* This product (11 mg, 67%) was isolated from 19 mg of **11**. MS: *m/z* (–OMe ester) 328 (M$^{\cdot+}$, 5), 254 (15), 212 (10), 153 (10), 141 (15), 123 (24), 110 (38), 87 (100), 74 (98), 57 (95).

*[14,14,15,15-$^2H_4$]-18-Methyl-nonadecanoic acid (**14**) (6).* This compound was isolated as a white solid (11 mg, 67%) and obtained from 19 mg of **12**. MS: *m/z* (–OMe ester) 330 (M$^{\cdot+}$,

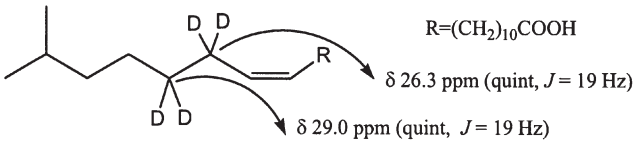

SCHEME 3

26), 287 (22), 231 (10), 199 (15), 185 (10), 143 (58), 129 (22), 111 (10), 87 (98), 74 (100), 57 (35).

RESULTS AND DISCUSSION

The synthesis of the required tracers was carried out as depicted in Scheme 2. In this synthesis, the key synthon for these three compounds was tetradeuderated bromide **8**. Thus, coupling of trityl-protected alcohol **4** with 1-iodo-3-methylbutane afforded alkyne **5**, which could be reduced to the deuterated product **6** with D_2 using Wilkinson's catalyst. Use of this catalyst and alkynol protection avoided the occurrence of scrambling and ensured the correct positioning of the mass labels (12). Once the alkyne functionality was deuterated, deprotection of the trityl group with dichloroacetic acid using methanol as solvent gave rise to the corresponding alcohol **7**. To produce the brominated intermediate **8** from alcohol **7**, it was neccesary to perform the reaction with NBS in the presence of PPh_3 in DMF as solvent, since the reaction with HBr in toluene led to benzylbromide as the only product. The Wittig reaction of the triphenylphosphorane generated from the phosphonium salt of **8** with the proper aldehyde furnished the *cis*-olefin **9** (*Z*/*E*: 94:6) as the main product. Acid treatment of **9** released the methoxymethane protecting group to afford the corresponding olefinic alcohol **11**, which was transformed into the unsaturated acid **13** by Corey oxidation with PDC (11). On the other hand, hydrogenation of **9** using Pd/C as catalyst gave the tetradeuterated protected alcohol **10**, which was hydrolyzed and further oxidized to obtain the labeled saturated acid **14**. Finally, the reaction of undecanal with the phosphorane formed by treatment of the triphenylphosphonium salt of **8** with *n*-BuLi afforded the deuterated olefin **15**.

In all the deuterated intermediates, the presence of the expected labels was assessed by GC–MS, whereas the isotope positions were unambiguously confirmed by both chemical shift and multiplicity of the deuterium-substituted carbon atoms. As exemplified for the final tracers **13** and **15** in Scheme 3, the ^{13}C NMR (125 MHz) chemical shifts of the deuterated carbon atoms in the allylic and homoallylic positions gave very low intensive quintuplets (J = 19 Hz) at 26.3 and 29.0 ppm, respectively. In the case of the saturated product **14**, it was very difficult to distinguish these signals from the rest of the chemical shifts of the CH_2 groups (29 ppm).

ACKNOWLEDGMENTS

Financial support for this work from Comisión Interministerial de Ciencia y Tecnología (CICYT) and Fondo Europeo de Desarrollo Regional (FEDER) (grant AGL-2001-0585), the Comissionat per a Universitats i Recerca from the Generalitat de Catalunya (grant 2001SGR-00342), and Sociedad Española de Desarrollos Químicos (SEDQ) is gratefully acknowledged. J.-L.A. thanks the Spanish Ministry of Science and Technology for a Ramon y Cajal contract.

REFERENCES

1. Rule, G.S., and Roeloks, W.L. (1989) Biosynthesis of Sex Pheromone Components from Linolenic Acid in Arctiid Moths, *Arch. Insect Biochem. Physiol. 12*, 89–97.
2. Reed, J.R., Vanderwel, D., Choi, S., Pomonis, J.G., Reitz, R.C., and Blomquist, G.J. (1994) Unusual Mechanism of Hydrocarbon Formation in the Housefly: Cytochrome P450 Converts Aldehyde to the Sex Pheromone Component (*Z*)-9-Tricosene and CO_2, *Proc. Natl. Acad. Sci. USA 91*, 10000–10004.
3. Schal, C., Gu, X., Burns, E.L., and Blomquist, G.J. (1994) Patterns of Biosynthesis and Accumulation of Hydrocarbons and Contact Sex Pheromone in the Female German Cockroach, *Blattella germanica, Arch. Insect Biochem. Physiol. 25*, 375–391.
4. Charlton, R.E., and Roelofs, W.L. (1991) Biosynthesis of a Volatile Methyl-Branched Hydrocarbon Sex Pheromone from Leucine by Arctiid Moths (*Holomelina* spp.), *Arch. Insect Biochem. Physiol. 18*, 81–97.
5. Bierl, B.A., Beroza, M., and Collier, C.W. (1970) Potent Sex Attractant of the Gypsy Moth: Its Isolation, Identification, and Synthesis, *Science 170*, 87–89.
6. Jurenka, R.A., Subchev, M., Abad, J.-L., Choi, M.Y., and Fabriàs, G. (2003) Sex Pheromone Biosynthetic Pathway for Disparlure in the Gypsy Moth, *Lymantria dispar, Proc. Natl. Acad. Sci. USA 100*, 800–814.
7. Gras, J.-L., Kong, Y.-Y., Chang, W., and Guerin, A. (1985) Lithium-Bromide-Assisted Protection of Primary and Secondary Alcohols as Methoxymethyl Ethers Using Dimethoxymethane, *Synthesis*, 74–75.
8. Stowell, J.C. (1970) A Short Synthesis of the Sex Pheromone of the Bollworm Moth, *J. Org. Chem. 35*, 244–245.
9. Osborn, J.A., Jardine, F.H., Young, J.F., and Wilkinson, G. (1966) The Preparation and Properties of Tris(triphenylphosphine)halogenorhodium (i) and Some Reactions Thereof Including Catalytic Homogeneous Hydrogenation of Olefins and Acetylenes and Their Derivatives, *J. Chem. Soc. A*, 1711–1732.
10. Bates, H.A., Farina, J., and Tong, M. (1986) An Approach to Pseudomonic Acids from Acetylenic Precursors: Synthesis of 2-(hydroxymethyl)-3-Butyn-1-ol, *J. Org. Chem. 51*, 2637–2641.
11. Corey, E.J., and Schmidt, G. (1979) Useful Procedures for the Oxidation of Alcohols Involving Pyridinium Dichromate in Aprotic Media, *Tetrahedron Lett.*, 399–402.
12. Rakoff, H., and Rohwedder, W.K., (1992) Catalytic Deuteration of Alkynols and Their Tetrahydropyranyl Ethers, *Lipids 27*, 567–569.
13. Abad, J.-L., Fabriàs, G., and Camps, F. (2000) Synthesis of Dideuterated and Enantiomers of Monodeuterated Tridecanoic Acids at C-9 and C-10 Positions, *J. Org. Chem. 65*, 8582–8588.

[Received March 17, 2004; accepted May 27, 2004]

A Critical Evaluation of Raman Spectroscopy for the Analysis of Lipids: Fatty Acid Methyl Esters

J. Renwick Beattie[a], Steven E.J. Bell[a,*], and Bruce W. Moss[b]

Schools of [a]Chemistry, and [b]Agriculture and Food Science,
Queen's University, Belfast BT9 5AG, Northern Ireland

ABSTRACT: The work presented here is aimed at determining the potential and limitations of Raman spectroscopy for fat analysis by carrying out a systematic investigation of C_4–C_{24} FAME. These provide a simple, well-characterized set of compounds in which the effect of making incremental changes can be studied over a wide range of chain lengths and degrees of unsaturation. The effect of temperature on the spectra was investigated over much larger ranges than would normally be encountered in real analytical measurements. It was found that for liquid FAME the best internal standard band was the carbonyl stretching vibration ν(C=O), whose position is affected by changes in sample chain length and physical state; in the samples studied here, it was found to lie between 1729 and 1748 cm^{-1}. Further, molar unsaturation could be correlated with the ratio of the ν(C=O) to either ν(C=C) or δ(H–C=) with $R^2 > 0.995$. Chain length was correlated with the $\delta(CH_2)_{tw}/\nu(C{=}O)$ ratio, (where "tw" indicates twisting) but separate plots for odd- and even-numbered carbon chains were necessary to obtain $R^2 > 0.99$ for liquid samples. Combining the odd- and even-numbered carbon chain data in a single plot reduced the correlation to $R^2 = 0.94$–0.96, depending on the band ratios used. For molal unsaturation the band ratio that correlated linearly with unsaturation ($R^2 > 0.99$) was $\nu(C{=}C)/\delta(CH_2)_{sc}$ (where "sc" indicates scissoring). Other band ratios show much more complex behavior with changes in chemical and physical structure. This complex behavior results from the fact that the bands do not arise from simple vibrations of small, discrete regions of the molecules but are due to complex motions of large sections of the FAME so that making incremental changes in structure does not necessarily lead to simple incremental changes in spectra.

Paper no. L9437 in *Lipids 39*, 407–419 (May 2004).

The potential of Raman spectroscopy for the analysis of fats and oils has been recognized for some decades (1,2). The main advantages of the technique are that no sample preparation is required (allowing *in situ* or on-line studies) and that it can be applied to samples in any physical state including gases, liquids, gels, amorphous solids, and crystals. However, until recently, adoption of Raman methods for routine analysis of fats and oils has been hindered by the high cost and complexity of the instrumentation required. This situation is now changing rapidly; a number of technological advances, such as holographic notch filters for rejection of elastically scattered light, the availability of long-wavelength (750–1064 nm) excitation lasers (which reduce background fluorescence problems), high-throughput, single-stage monochromators, and highly sensitive charge-coupled detectors (CCD, which have a high quantum efficiency allowing detection of ultra-low levels of light) are making the technique more accessible than ever before, and the introduction of simple-to-use commercial instruments means that it is now straightforward for nonspecialists to record good-quality Raman data.

Because technical problems no longer dominate the field, there are clear opportunities for routine analysis by Raman spectroscopy. Indeed, it has already been successfully used to determine important composition/physical structure parameters in a wide range of sample types. These include the following: *cis/trans* isomer ratio (3), molar unsaturation (C=C per molecule) (4), mass unsaturation (C=C per unit mass, which is also known as degree of unsaturation, a molal unit) (5), conjugated double-bond content (6), and chain length (7). Given that there is a relatively large body of published data on various aspects of fat/oil characterization by Raman spectroscopy, it is surprising that have few studies have attempted to bring together these disparate strands of research systematically and comprehensively.

The work presented here is an attempt to determine the limits and potential of Raman spectroscopy for fat analysis by carrying out a systematic investigation of well-defined series of FAME as model lipid compounds under different experimental conditions. It is hoped that this investigation will identify the significant variables for the analysis of FA-based lipid systems, highlight the factors that need to be controlled in the experiments, and give guidance on the degree of accuracy that can be expected. Such data are vital in underpinning future analytical methodologies for "real-life" fats and oils.

Of particular interest is the extent to which the Raman signal from a particular lipid can be approximated as simply the sum of signals arising from distinct units within the molecule. The tacit assumption underlying much of the analytical methodology already developed or proposed is that this *aufbau* approach is generally valid. However, the consensus in the vibrational spectroscopy of a wide range of disparate systems is that treating molecules simply as a collection of small independent constituent units can lead to problems when dealing with vibrational motions, which are typically complex motions of large numbers of atoms within the molecular framework.

The data reported here are developed entirely from FAME because these provide a simple, well-characterized set of

*To whom correspondence should be addressed. E-mail: S.Bell@QUB.ac.uk

Abbreviations: CCD, charge-coupled detector; ip, in-plane; IV, iodine value; op, out-of-lane; sc, scissoring; tw, twisting.

compounds in which the effect of making incremental changes can be studied over a wide range of chain lengths and degrees of unsaturation.

EXPERIMENTAL PROCEDURES

The nomenclature of the model lipids used here is the comprehensive system described by Stauffer (8). The general format is C:U*c*/*t* Δ*x* where C is the number of carbons on the FA chain (i.e., all carbons except the one added in forming the methyl ester), U is the number of olefinic double bonds, and *c* or *t* is used to distinguish *cis* from *trans* isomers. Δ*x* is the position of the olefinic bond within the FA chain, in terms of number of carbons counted from the ester end of the chain. All the monounsaturated FA had the olefinic bond placed centrally in the chain.

The samples investigated were: all the members of the series of saturated FAME from 4:0 (butyric) to 24:0 (lignoceric) methyl esters; a series of monounsaturated methyl esters from 14:1*c* Δ7 (myristoleic) to 22:1*c* Δ11 (erucic) in steps of 2 CH_2; and a series of 18-carbon methyl esters with increasing unsaturation from 18:0 (stearic) to 18:3*c* Δ6,9,12 (linolenic). These samples were GC grade (>99% purity; Sigma-Aldrich Inc., Milwaukee, WI), and their purity was checked by using GC prior to Raman analyses and by using TLC afterward.

All the Raman data were collected using a home-built Raman spectrometer using 785-nm excitation (100 mW at sample) from a Spectra Physics (St. Albans, United Kingdom) model 2020 Ar^+ laser pumping a Spectra Physics 3900 Ti/Sapphire laser. The Raman scattering was collected using a 180° backscattering geometry (50 mm f2 lens) and passed through a Jobin Yvon HR640 spectrometer to a Princeton Instruments LN liquid-nitrogen-cooled CCD. The Raman signal was recorded from 270 to 1900 cm^{-1}, the region containing the C–C, C=C, C–O, and C=O stretches and bends as well as the C–H bends at a resolution of 10 cm^{-1}. The Raman shift was calibrated using the American Society for Testing and Materials frequency standards for 50:50 (vol/vol) acetonitrile/toluene (ASTM E 1840). Apart from the contribution from the Raman scattering, the raw data also contain a broad background from several unrelated optical processes, which must be removed (9); so the experimental data were automatically processed by macros written in the SpectraCalc™ (Galactic Industries, Salem, NH) spectral manipulation package, which removed cosmic ray signals and carried out a 16-point baseline correction. Peak deconvolution and relative peak height analysis were carried out in Microsoft Excel (10). Partial least squares (PLS) regression was performed in The Unscrambler™ V7.5 (Camo, Trondheim, Norway) with the spectra initially normalized about the carbonyl band and then mean-centered, and validation was by full cross-validation. The "jack-knife" tool was used to select the wavenumber positions that were most nearly correlated with the parameter of interest with the uncorrelated positions excluded from the subsequent analysis.

For all work on the model lipids, the samples were placed in holes (0.8 mm diameter, ~5 mm depth giving a sample mass of *ca.* 10 mg) in an aluminum block. All three series of FAME were run in the liquid state, and in addition, a solid-state series was recorded for the saturated FAME. In the liquid-state studies, any samples that were liquid at ambient temperature were simply recorded at room temperature, whereas for those that were solid at room temperature (saturated FAME > 12 carbons), the samples were heated to about 10°C above their m.p. (see Table 1 for temperatures; only heated FAME are listed, others were at ambient temperature). For the solid state, the block was cooled to 77 K using liquid nitrogen.

TABLE 1
Temperatures at Which Raman Spectra Were Recorded for the FAME That Were Solid at, or near, Ambient Temperature (21°C)

FAME	Temperature (°C)	FAME	Temperature (°C)
14:0	30	19:0	50
15:0	30	20:0	55
16:0	40	21:0	55
16:1*t* Δ8	40	22:0	60
17:0	40	23:0	60
18:0	50	24:0	65
18:1 Δ9	55		

Several samples were recorded over a range of temperatures to investigate the sensitivity of their Raman bands to temperature. For these experiments, all the solid lipids were loaded into the sample container first, heated to 80°C, and then cooled to room temperature, at which point the liquid lipids were added and the block was then cooled by a flow of liquid nitrogen to −180°C and held at that temperature for 15 min. Spectra were then recorded as the samples were heated from –180 to 80°C. Because the sample warmed at a rate of *ca.* 5°C/min, the spectra were recorded from a dynamic system, not a series of equilibrated states, and so a short accumulation time was used (~20 s, temperature ±1°C/spectrum) to collect data every 10°C. Spectra were recorded during the heating stage of the cycle to avoid potential problems with supercooling and metastable phases.

In investigating the effect of the polarity of the local solvent environment on the spectra, 10:0 (capric acid methyl ester) was mixed with 1,2-dichloroethane, dichloromethane, trichloromethane, tetrachloromethane, THF, acetone, toluene, acetonitrile, and methanol (50:50 vol/vol in each case). This gave a range of polarities from ε = 2.2 (tetrachloromethane) to 37.5 (acetonitrile).

RESULTS AND DISCUSSION

The Raman spectra of the liquid and crystalline forms of the methyl esters of stearic acid, 18:0 (one of the most common FA present in food), and oleic acid, 18:1*c* Δ9, are shown for reference in Figure 1. The assignments of the major bands in the spectra are well-established in the literature and are given in Table 2; more complete, rigorous assignments of the solid-state spectra obtained from density functional calculations are also now available (11,12). Although the number of studies using Raman spectroscopy to predict FA-based lipid properties has grown considerably since the early 1990s, there have been few

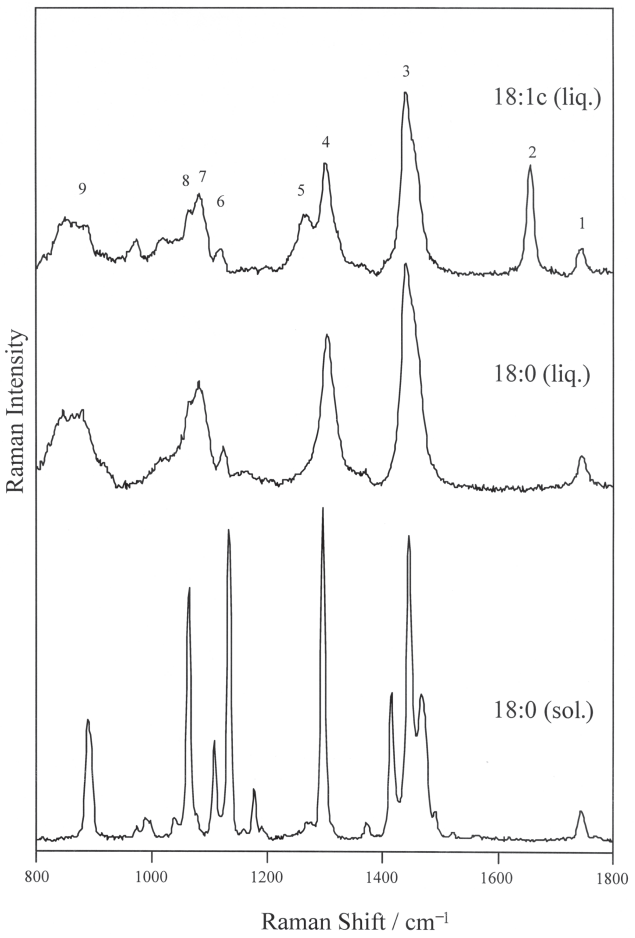

FIG. 1. Typical Raman spectra of unsaturated (oleic acid, 18:1*c* Δ9) and saturated (stearic, 18:0) FAME as solids (sol.) or liquids (liq.). The peak numbers refer to assignments shown in Table 2.

studies on the fundamental aspects of the relationship between the Raman spectroscopy and FA lipids since Spiro and Tu published chapters reviewing the subject (1,2). At first sight, it might appear that quantitative analysis of lipids would be straightforward since their spectra are rich in well-resolved bands, some of which are characteristic of particular functional groups, such as the ester carbonyl or olefinic C=C bonds. However, these bands are subject to a range of external and internal perturbations that can change both their intensities and positions. For example, there are very marked changes in the Raman spectra of FAME on melting/crystallization where many of the peaks narrow and change wavenumber position. These changes are most marked in the regions 1000–1100 and 1400–1500 cm^{-1}, which are dominated by C–C stretching and CH_2 scissor vibrations, respectively, but, as Figure 1 shows, the changes in band position are not confined solely to this region. In most off-line quality control applications, it should be possible to choose the most appropriate temperature to carry out the analysis so the data can be recorded either at high temperatures, where all fats are liquid, or at low temperatures, where complete solidification occurs. However, since in a mixed fat at a given temperature there will always be some components closer to their normal melting temperatures than others in the sample, the effect on Raman features at temperatures away from the phase boundaries needs to be considered if a general methodology is to be established. Moreover, although the temperature of the sample is normally the dominant factor in determining the nature and extent of inter- and intramolecular interactions of the lipids, these interactions are also affected by the composition of the sample, the matrix/environment in which it is placed, and, in enantiomeric systems such as TG, the positional isomerization of the individual molecules (13).

Choice of the internal molar standard. The absolute Raman signal intensity from a given sample depends not only on the composition of the sample but also on a number of trivial, hard-to-control experimental factors. These include laser power, sample transparency/light absorbance, and optical alignment (including the exact position of the sample with respect to the focus position of the spectrometer's collection optics). For all of these reasons it is extremely difficult to obtain Raman signals with low variation (±2%) in absolute signal levels, even over the course of 1 d, so quantitative analysis of Raman data generally depends on measurements of relative peak heights or areas rather than on absolute signals. When it is possible to add a known amount of an internal standard material to the sample, the spectra can be normalized to the band(s) of the added standard. However, in systems where addition of a foreign ma-

TABLE 2
Assignments of Raman Modes in FAME, Taken from References as Indicated

Band	Band position (cm^{-1})	Assignment
1	1730–1750	ν(C=O) Carbonyl stretch (5)
2	1640–1680	ν(C=C) Olefinic stretch (5)
3	1400–1500	$\delta(CH_2)_{sc}$ Methylene scissor deformations (5)
4	1295–1305	$\delta(CH_2)_{tw}$ Methylene twisting deformations (5)
5	1250–1280	$\delta(=CH)_{ip}$ In-plane olefinic hydrogen bend (5)
6	1100–1135	$\nu(C–C)_{ip}$ In-phase aliphatic C–C stretch all-*trans* (36)
7	1080–1110	$\nu(C–C)_g$ Liquid: aliphatic C–C stretch in *gauche* (39) and ν(C–C) Solid: aliphatic C–C stretch all-*trans* (38)
8	1060–1065	$\nu(C–C)_{op}$ Out-of-phase aliphatic C–C stretch all-*trans* (37)
9	800–920	$\nu(C_1–C_2)$, $CH_{3,rk}$, ν(C–O) Solid: mixture of stretches and rocks at acyl and methyl terminals. Complex broad plateau in liquid state (28)

terial to act as an internal standard is undesirable (such as in process control), the effects of spectrometer alignment, sample position, and the like must be compensated by measuring the intensities (or areas) of the bands of interest relative to other Raman bands of the sample. For lipids based on FA esters, the most obvious choice for an internal standard would be the ester end group, since there will normally be one and only one carbonyl moiety per chain. Moreover, the carbonyl gives a distinct, isolated stretching peak around 1745 cm^{-1}, which is in a spectral region clear of other potentially interfering bands. A second candidate for the internal standard would be the peak associated with the C_1–C_2 stretching vibration (i.e., the carbonyl carbon and the first carbon in the chain), which lies in the 880–920 cm^{-1} range. Because establishing a reliable internal standard is a critical first step in carrying out quantitative analysis, we have examined the behavior of both these peaks under a wide range of experimental conditions to determine the degree of trust that can be placed in them.

The carbonyl band has been utilized extensively as a reference peak in studies of molar unsaturation (4,5,14–16) and chain length (16). Ideally, if it is to be used as an internal standard it should be barely affected by chemical and physical factors. Unfortunately, this is not the case because the position is affected by changes in sample chain length and physical state; in the samples studied here, under a variety of physical conditions, it was found to lie between 1729 and 1748 cm^{-1}.

Figure 2 illustrates the effect of chain length on the position of the carbonyl stretching band and shows there is a systematic shift to higher wavenumber with increasing chain length. These changes could be due either to differences in the vibrational mode itself, which are brought about directly by changing the structure, or to changes in polarity of the environment in which the carbonyl sits (longer-chain FAME are less polar). That we cannot reproduce the shift by dissolving FAME samples in solvents with different polarities (ranging from tetrachloromethane to acetonitrile) must mean that solvent polarity is not an important factor, and therefore the source of the changes must be in the vibrations themselves, i.e., the vibration of the carbonyl moiety is not completely divorced from the structure of the FAME to which it is attached. This observation challenges the assumption that Raman bands in FAME can be regarded as arising from effectively independent characteristic groups; this is particularly striking because, of all the bands in the spectra, the carbonyl would be expected to be the one least likely to couple with other modes. Although we have no good model for the source of the shift, its effect is that for this extended series of FAME, the peak height at a fixed wavenumber cannot be used as an internal standard. This will also be true for edible lipids if the samples have significant differences in average chain length. What constitutes a significant difference will vary with the mean of the range—longer chain lengths show smaller changes per CH_2 than shorter chain lengths. Typically, FA in most foods (palm oil, coconut butter) have 16–22 carbons, and fortunately at these relatively long (>12) chain lengths, changes in carbonyl band position with chain length are minimal, so the carbonyl band remains at essentially the same position between

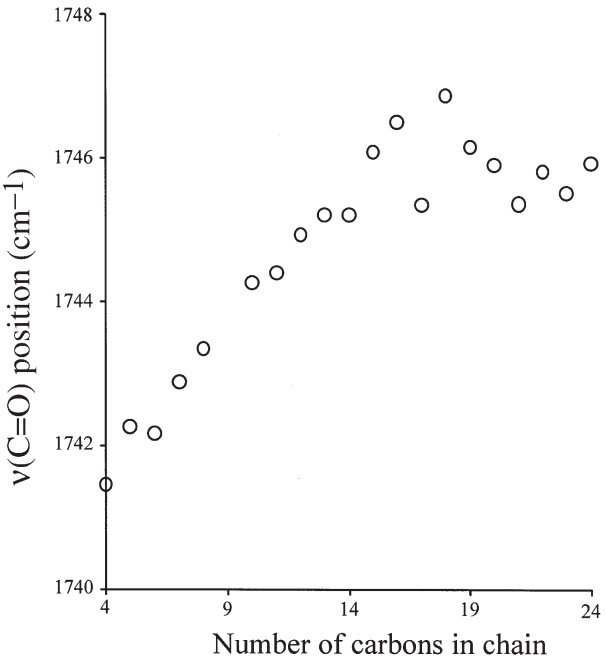

FIG. 2. Effect of chain length (4 to 24 carbons) on the position of the carbonyl stretching mode for liquid-state saturated FAME. Wavenumber calibration error was ±0.8 cm^{-1}.

samples. It is only with other specialty oils that the chain lengths are much shorter, e.g., 12 or 14, and the shifts in ν(C=O) with chain length will become more problematic.

Similarly, although the position and width of the carbonyl band are not significantly affected by temperature within a given state, they are changed on phase transitions (including solid–solid transitions) or by very large temperature changes [150°C gives a 1-pixel shift (1.5 cm^{-1}) for 18:0 in the solid state]. Again, this can be minimized by studying all samples in the same state and, as experimental data will typically be recorded at similar temperatures, the effects due to large temperature excursions will normally not arise.

In the solid state, it is known that altering the conformations about the C_1–C_2 bond gives significant changes in the carbonyl position. Two predominant torsion angles are typically observed: In the noneclipsed conformation [T_1 = 180° (11), previously described as *trans* (17)], the band lies in the 1730–1750 cm^{-1} range, whereas in the eclipsed conformation (T_1 = ±60°, previously described as *cis*), it lies at <1730 cm^{-1}. The T_1 = 180° conformation is the most common and is observed where the FA chains are free to rotate. However, in solid TG, rotation is restricted so that in β′ crystals, for example, one FA chain adopts the eclipsed conformation in order to pack efficiently and this gives rise to a second peak *ca.* 10 cm^{-1} below the usual position (18). In these cases, the heights of both bands will need to be combined for use as a molar standard. This is not a major problem because either melting the samples or simply combining the area of both peaks can easily nullify the effect of crystal packing on the carbonyl band.

The final possibly complicating factor in adoption of the

carbonyl band as a standard is that any FFA or their salts that are present will give a carbonyl stretching vibration that is shifted from the ester position, typically appearing in the same region as olefinic stretching at *ca.* 1660 cm^{-1} [1640–1670 cm^{-1} (19) in free acids or 1590–1600 cm^{-1} in salts (20)]. In addition to this transfer of carbonyl intensity on forming the acid or salt, any FFA in the sample can also hydrogen-bond to the ester carbonyls, which causes them to shift to a lower wavenumber and broaden (21). However, the level of FFA in most edible fats and oils is low, and a separate calibration could, in any case, be established specifically for samples with a high FFA content. A recent study has been able to predict the FFA content using the Raman spectrum of FA-based lipids (22).

All the data just discussed suggest that the carbonyl band is appropriate as an internal standard, provided that suitable care is taken in establishing appropriate experimental conditions and that factors such as FFA content are considered. The only factor not considered up this point is the effect of adding unsaturation, which makes a much larger difference in position of the carbonyl band (up to 13 cm^{-1}) than either changing chain length or altering the sample temperature, although the width is not affected significantly by the addition of C=C bonds in the chain. In general, the effect of unsaturation is larger in the solid state than in liquids so that changes of one *cis* olefinic bond/chain will not have a great effect with the liquid state (<1 cm^{-1}) but will give larger changes in the solid state (≤13 cm^{-1}). This means that for liquid samples with only moderate differences in unsaturation levels, measuring the intensity of the carbonyl band at a single position for all samples is appropriate (assuming chain length and the like also remains suitably consistent), but for samples spanning a larger range of unsaturation, it will be necessary to allow for shifts in the band between samples.

In the FAME model systems studied here, quantitative peak fitting with unrestricted central wavenumber was necessary because the samples spanned large chain-length, temperature, and unsaturation ranges. For measurements on sample sets with much more similar composition, e.g., for process control or quality assurance/quality control on edible fats and oils, the degree of variation is much smaller, which is presumably why previous work using simple measurements of the carbonyl band as an internal standard were successful, despite the fact that the band does change with sample composition and temperature.

If the carbonyl band is to be used as the internal standard, it would generally be better to work with fully melted samples because of the complications that arise with solid samples. However, since it may sometimes be necessary to investigate solid samples, we have also investigated the possibility of using the C–C stretching band that lies in the region 850–920 cm^{-1} as an alternative standard for use with solid samples. This band is not useful for liquids because the region becomes swamped by a broad mass of bands that are chain-length dependent and that possibly arise from C–C stretching modes for the *gauche* conformations, but since the carbonyl band works well in liquids, this is not a problem. There has been some dispute in the literature concerning the origin of the C–C stretching band at *ca*. 900 cm^{-1} in the solid state. It has been assigned either as a stretching mode of the C_1–C_2 bond [i.e., the bond between the carbonyl carbon and the terminal C of the chain (23)] or to the $C_{\omega-1}$–C_ω bond [i.e., the bond between the terminal methyl C atom and the next C in the chain (24–26)]. Either of these modes would be expected to be independent of chain length, and even in the absence of detailed calculations, the more convincing argument was for the band to be attributed to a combination of both modes (27,28). Recently, density functional calculations have shown that there are both terminal methyl and C_1–C_2 bands in this region and that their relative intensities vary quite considerably with chain length in a complex manner (12). For convenience, this band is referred to it as $\nu(C_1–C_2)$ in this work.

The effect of temperature on the intensity and position of the bands in the 820–920 cm^{-1} region is small, as is the case for the carbonyl band. However, over extended temperature ranges it is possible to detect changes in, for example, the relative intensity of this $\nu(C_1–C_2)$ band to one of the main scissoring vibrations of the chain [$\delta(CH_2)_{sc}$sym, see Fig. 3], whereas in the plot using the carbonyl band as the internal standard, any change with respect to $\delta(CH_2)_{sc}$sym is of the same order as experimental uncertainty. Of course, because these are ratios, the

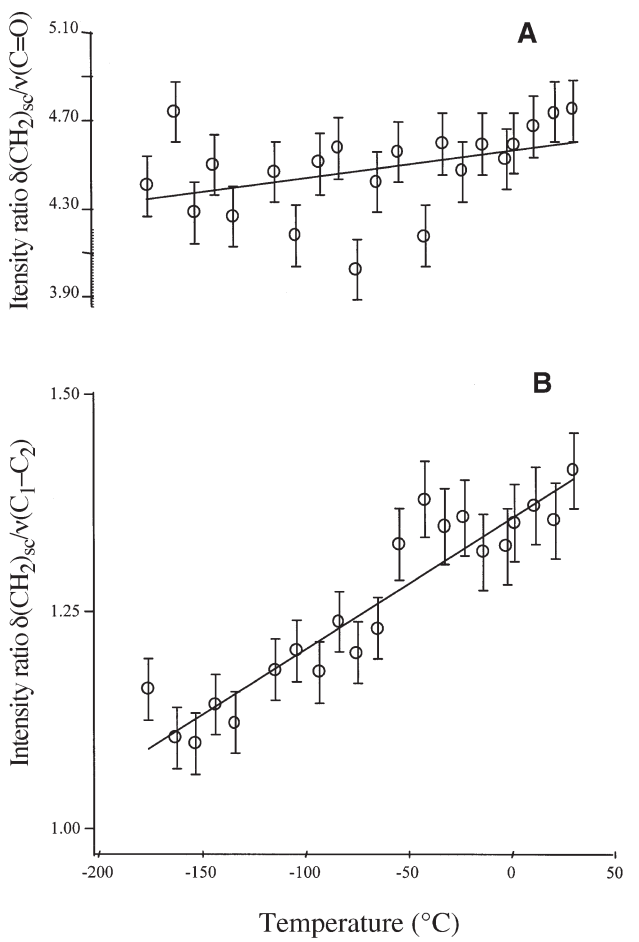

FIG. 3. Effect of temperature on the ratio of the 1450 cm^{-1} CH_2 scissoring band in 18:0 to two different potential internal standard bands. (A) The carbonyl stretching mode at *ca.* 1740 cm^{-1}. (B) The acyl stretching mode at *ca.* 890 cm^{-1}.

change could be due either to differences in the "standard" or the other band that is being measured. In many cases, we have found that only one of the two peak ratios obtained from using either one of the two "standard" bands is unchanged with temperature whereas the other does show a detectable effect (although only over extended temperature ranges). Presumably, this arises because the effects of temperature on both standards are different, so that if the band that is measured against them also changes, the effects will cancel for only one of them.

In general, the low sensitivity to temperature makes the $\nu(C_1–C_2)$ band at *ca.* 900 cm^{-1} potentially useful as a standard in solids. Unfortunately, its position changes erratically with chain length, varying from 884 to 914 cm^{-1}, which makes it less attractive than the simple carbonyl band as an internal standard (although, as just discussed, even the carbonyl band is not without problems). This, combined with the fact that it is completely unsuitable for liquid samples, means that the overall balance lies in favor of the carbonyl band as the internal standard, and in the remainder of this paper the carbonyl is used exclusively as the internal molar standard.

Measurement of molar unsaturation. Several studies have used bands associated with the olefinic bonds to determine unsaturation within the samples; indeed, determining unsaturation is one of the most common objectives of Raman studies on fats and oils (4,5,7,29–31). The most obvious Raman bands to use for detection of olefinic bonds are the C=C stretch at *ca.* 1650–1670 cm^{-1} and the δ(H–C=) bend at *ca.* 1260 cm^{-1}. The positions of these bands are sensitive to both *cis/trans* isomerization and the conformations of the bonds on either side of the olefinic group.

Typically, using either one of these two peaks in a univariate correlation to determine unsaturation parameters gives reasonably high correlations (>0.95) (4,32). The olefinic stretch occurs at 1640–1665 cm^{-1} for *cis* and 1670–1680 cm^{-1} for *trans* isomers of isolated olefinic bonds, shifting to <1630 cm^{-1} for conjugated olefinic bonds. The difference in wavenumber of the C=C stretch in *cis* and *trans* olefins allows measurement of *cis/trans* ratios (3).

The position of the olefinic stretch is also affected by the conformation of the adjacent bonds (33) and can be shifted quite considerably when conformations are highly strained, e.g., in crystalline 20:3*c* Δ7,10,13, bands appear at 1600 and 1634 cm^{-1} as well as the more usual 1660 cm^{-1}. Generally, the *cis* isomer will adopt one of two main conformers about the olefinic bonds, which occur at ~1660 (most common form) and ~1640 cm^{-1} (in some lattice types). Slight deformations of these conformations can shift the position by a few wavenumbers. For *trans* isomers, the two main conformers are spectroscopically similar.

The position of the olefinic hydrogen in-plane bend, like the stretching vibration, is sensitive to conformation. In the *cis* isomer, the shifts in position of the bend with changes in conformation are *ca.* half the magnitude of those of the stretching vibration. However, the intensities are more problematic, since the intensity of bending vibration is very sensitive to conformation, not even appearing in some crystal types (conformations). In contrast, the intensity of the stretching mode is relatively insensitive to conformation. The bending mode in *trans* isomers is weak, although it has been assigned to 1320 cm^{-1} (31) by one author.

To test the extent to which the ratio of the ν(C=O) to either ν(C=C) or δ(H–C=) could be used as a direct measure of molar unsaturation, we measured these ratios in the spectra of a series 18-carbon FAME from 18:0 to 18:3*c* Δ6,9,12 (Fig. 4). This set spans a very large iodine value range and was chosen specifically to allow detection of any small deviation from linearity over a range much larger than would normally be encountered in analysis of edible fats and oils.

We found that, for liquid samples, plotting the intensities of the 1660 and 1260 cm^{-1} bands relative to those of the ν(C=O) (at *ca.* 1745 cm^{-1}) against molar unsaturation (number of double bonds per chain) gave straight lines with correlation coefficients of 0.995 and 0.996, respectively. This good correlation shows that the sequential addition of isolated double bonds in the chain does indeed have the expected effect of giving simple additive changes in spectral bands, and it is therefore straightforward to determine molar unsaturation from either of these Raman band ratios.

The single *trans* olefin plotted on the data lies slightly off the trend lines established for the *cis* series; in the plots using

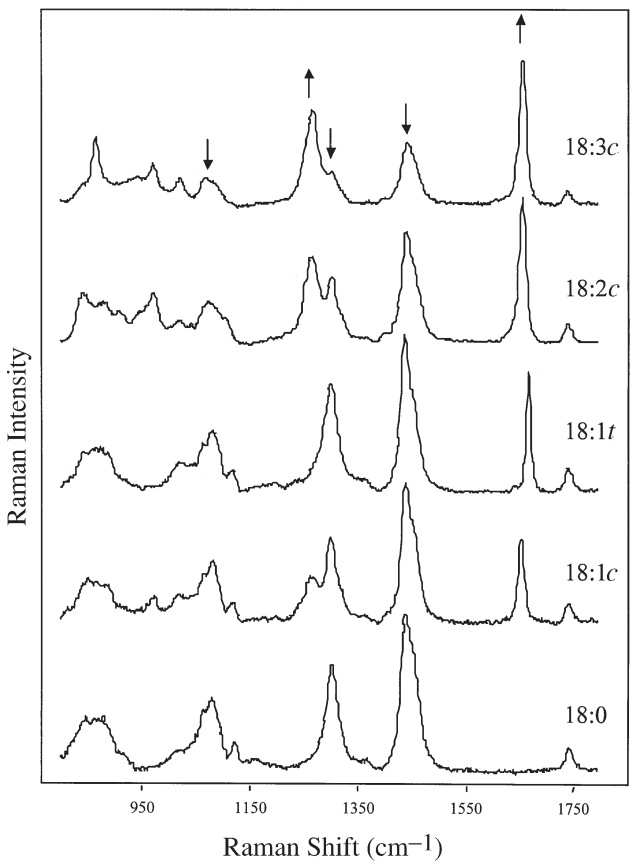

FIG. 4. The Raman spectra of the 18:n series of FAME in the liquid state. The peaks discussed in the text are indicated by arrows.

the ν(C=C) band, it lies consistently above the trend line, whereas in those involving ν(H–C=) it lies below. This slight deviation is to be expected since the slopes of the trend lines depend on the relative Raman scattering cross-sections of the olefin vibrations vs. those of the reference peaks. Differences in the Raman scattering cross-sections for *cis* and *trans* olefinic groups would lead to deviations above or below the trend lines, the sign of the deviation depending on whether the *cis* or *trans* form gives the larger Raman signal. This means that separate calibrations have to be carried out for *cis* and *trans* isomers.

In the solid state, the olefinic hydrogen bend region shows complex behavior (34), but since the preferred method would be to measure liquid samples (to reduce complications associated with the carbonyl internal standard), this is unlikely to constitute a serious problem.

Chain length determination. The second molecular parameter that would be expected to be readily accessible through Raman methods is the chain length (7). Surprisingly, to our knowledge, there are no other examples of the determination of FA chain length directly from Raman data, although there is an example in which the chain length was calculated by combining molar and mass unsaturation determinations (16). The scissoring and twist vibrations of the chain are the two most promising candidates for chain length determination.

(i) Scissoring region. The scissoring region is complex, with between two and six apparently resolved observed bands (Fig. 5). In fact, these bands are themselves not composed of pure CH_2 scissoring modes but contain contributions from vibrations of all the CH_x units present in the FAME (11). Because of this complexity, in this paper we will confine discussion to the most intense band in the scissoring region (which lies at *ca.* 1440 cm^{-1} in both the solid and liquid states), the 1460 cm^{-1} band in the liquid, and the 1410 cm^{-1} band in the solid.

In the liquid state, the scissoring region (1400–1500 cm^{-1}) shows one dominant band at around 1440 cm^{-1} with a strong shoulder at 1460 cm^{-1}. The relative intensity of these bands to each other does not change with chain length, but their positions (like that of the C=O stretch) do change. The overall shift is large, *ca.* 15 cm^{-1}, but unlike ν(C=O) the majority of the shift occurs in the short-chain (<10:0) FAME (1470–1460 and 1455–1443 cm^{-1}, respectively, for the two bands). The gradual nature of the shift for lipids with longer average chain lengths, around 14–18, means that the change in position of these bands with even significant changes in chain length would be negligible and a peak height at fixed wavenumber would adequately describe the band. However, because we have chosen to study a very wide range of chain lengths, we have been forced to use values for peak heights obtained by curve-fitting each spectrum separately and taking the band heights from the fitted data in which the band centers were allowed to move with chain length.

The fitted data were used to calculate the ratios of the heights of either of these two $\delta(CH_2)_{sc}$ observed bands (*ca.* 1440 and 1460 cm^{-1}) against the intensity of the ν(C=O) at *ca.* 1750 cm^{-1}. Both of these ratios would be expected to be directly proportional to the number of CH_2 groups in the chain,

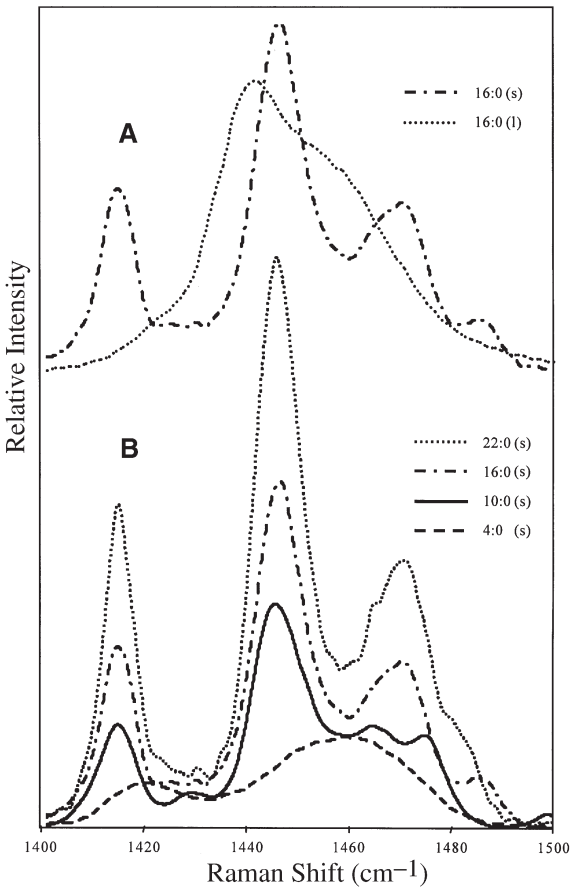

FIG. 5. The scissoring region of the Raman spectra of (A) solid (s) and liquid (l) 16:0 and (B) selected solid saturated FAME. All spectra were normalized to the carbonyl stretching mode at *ca.* 1740 cm^{-1}.

but plots of $\delta(CH_2)_{sc}/\nu TCO$) vs. chain length (plot for the 1440 cm^{-1}) band is shown in Fig. 6), although approximately linear, had least squares regression coefficients of only 0.94 and 0.95 for the full range, which is very poor for a model system expected to be linear. However, there is evidence for odd/even alternation in the 1440/ν(C=O) plot in the region of the plot corresponding to medium (14–20) chain length, with the odd-numbered chains sitting above the best fit trend line and the even-numbered chains below it. Separating this plot into odd- and even-numbered chains improves the regression coefficients to 0.98. Combining the total intensity of all the bands in the scissoring region for these liquid samples in the same way as is discussed for the solids (discussed shortly) does not improve the correlation, and the odd/even pattern is again observed.

The origin of the odd/even alternation is difficult to establish with certainty since odd/even changes in either the C=O or CH_2 vibrations could give the effect. It does not appear to have the same source as the odd/even alternation found in m.p. of FAME since that is known to be due to crystal packing effects, whereas the effect observed here is more clearly discernible in the melted FAME than in the solid forms. There is no evidence of any odd/even alternation in the carbonyl stretching mode in terms of width or position, nor in ratios with unsaturated bands

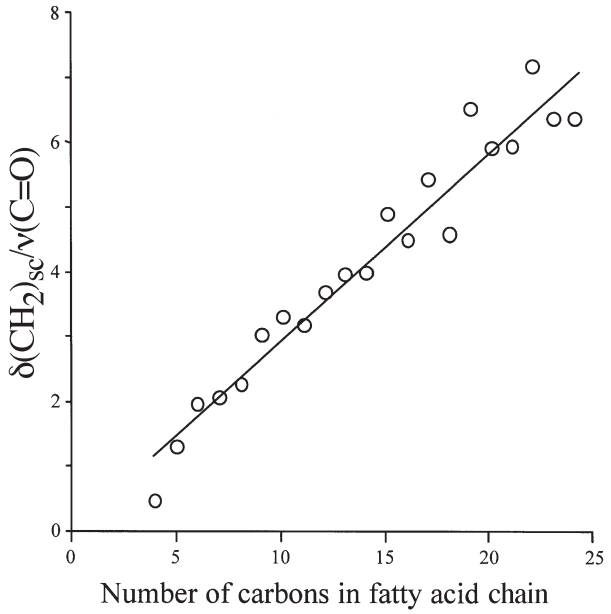

FIG. 6. Plot of the intensity of the 1440 cm^{-1} scissor band (normalized to the carbonyl stretch at *ca.* 1740 cm^{-1}) against chain length in liquid-state saturated FAME.

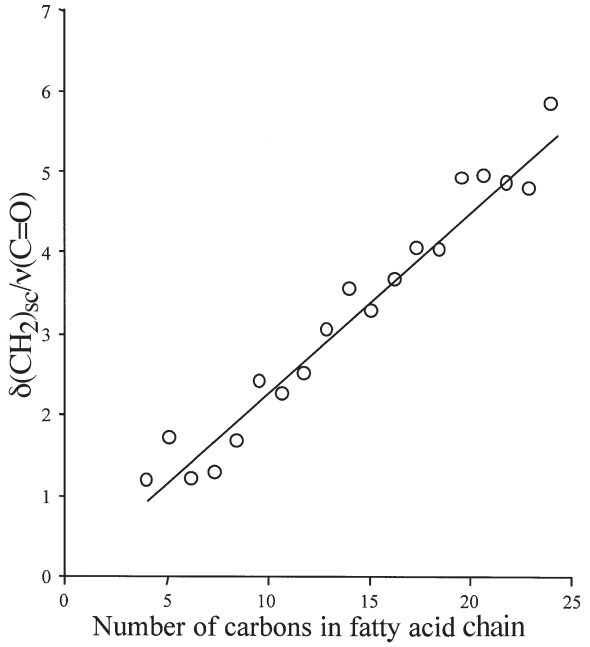

FIG. 7. Plot of the intensity of the 1410 cm^{-1} scissor band (normalized to the carbonyl stretch) against chain length in solid saturated FAME.

and some other saturated bands. A more likely candidate for odd/even alternation is therefore the second band used in the ratio, which is notionally described as a CH_2 mode.

In practice, the need to split the data for odd- and even-numbered chain lengths is unlikely to cause significant errors in Raman-based chain length calculations for natural fats and oils, since these are principally composed of TG with medium-length (14–20), even-numbered chains. However, for some natural and processed fats and oils, such as lamb and beef fats, it may be necessary to establish calibrations allowing for significant amounts of odd-chain FA.

In the solid state the situation is more complex, with up to six main bands present in the CH_2 scissoring region of the spectrum (Fig. 5). Curve-fitting can deconvolve the bands, but the individual components that are obtained by the process do not show the smooth trends observed in the liquid. For example, the position of the strongest band in the solid state does not show the continuous shift to lower wavenumber with increasing chain length that is found for the strongest band in the liquid; instead, it oscillates erratically. Conversely, the low-frequency component shifts up to about 13:0 and then remains constant up to 24:0. The high-frequency components also shift around unpredictably.

In view of the degree of complexity of the Raman spectra of the solid FAME in this spectral region, it was not clear whether any of the scissoring bands could be used as reliable indicators of chain length. When the ratios of the heights of the two strongest scissoring vibrations (ratioed against the carbonyl stretch) were calculated and plotted against chain length, the results were similar to the data for the liquid FAME, giving low R^2 values of 0.96 and 0.93 for the two main peaks at 1410 (Fig. 7) and 1440 cm^{-1}, respectively. However, unlike the liquid FAME, there was no evidence for odd/even alternation in the plots, so that separating the plot into odd- and even-numbered chains did not improve the regression coefficients. However, although the individual peak parameters did not correlate well with chain length, a similar plot using the sum of the peak heights for all the scissoring vibrations ratioed to the carbonyl stretching vibration did give partial cancellation of the errors associated with the individual peaks and yielded a plot with a more satisfactory 0.98 correlation coefficient.

(ii) Twisting region. The other potentially useful band is the CH_2 twist peak at 1300 cm^{-1}, which has been determined to arise almost exclusively from CH_2 twisting motions and is affected by the conformation of the polymethylene backbone, shifting from 1294 to 1306 cm^{-1} with width increase/height decrease upon melting. In the solid state, small bands due to mixing of twisting-rocking modes have been observed at 1255–1275 cm^{-1} (35). Indeed, density functional calculations (11) show numerous other minor bands in this region close to, or underlying, the main CH_2 twist band.

There is a striking similarity between the behavior of the $\delta(CH_2)_{tw}$ and $\delta(CH_2)_{sc}$ vibrations. The $\delta(CH_2)_{tw}$ spectral region is considerably less complex than that of $\delta(CH_2)_{sc}$ vibrations, which makes observation of the effects more straightforward. Again, erratic behavior is observed in the short chains, presumably arising from differences in crystal packing that are reflected in both the scissoring and twisting vibrations; of course, this behavior is not observed in the liquid state.

To test whether this band could be used for determination of average chain length, the $\delta(CH_2)_{tw}/\nu TC{=}O)$ ratios were plotted against chain length. As was the case for the $\delta(CH_2)_{sc}$, for

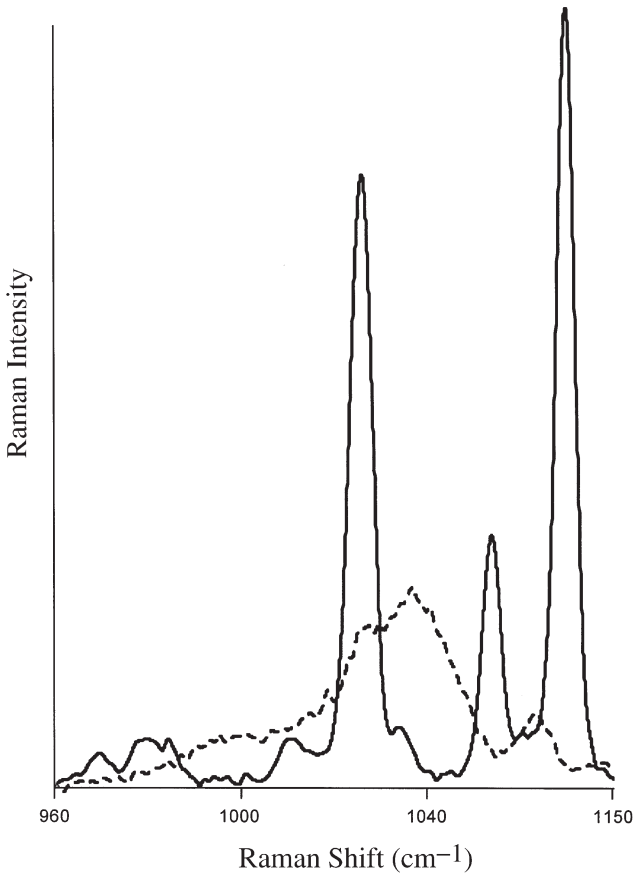

FIG. 8. The C–C stretching region of 18:0 in the solid and liquid states, normalized about the carbonyl stretching mode at *ca.* 1750 cm^{-1}. The solid line is from the solid state; the dashed spectrum is from the liquid state.

liquid samples there is a distinct odd/even alternation in the region of the plots corresponding to medium (11–20)-chain-lengths, with the odd-numbered chains sitting above the best fit trend line and the even-numbered chains below. The correlation coefficient for this plot was only 0.95, but separating the calibration curves into even- and odd-numbered carbon chains gave coefficients of 0.99 for each of the two sets. Conversely, the low-temperature data showed that the band position displayed an erratic dependence on chain length; hence, we might not expect to obtain a good correlation between chain length and band intensity for the solid samples, since packing effects will change absolute Raman intensities as well as positions. In the solid state, the calibration plot has a correlation coefficient of only 0.97, which does not improve on dividing the data into odd/even sets because there is no detectable odd/even variation. Summing the whole region (from 1265 to 1320 cm^{-1}) marginally improves the correlation.

(iii) C–C stretching region. Another possible candidate for the determination of chain length is the C–C stretching region, as this region contains a series of bands that arise from single bonds between carbon atoms. The ν(C–C) region of the spectrum is affected by the conformation of the chain, i.e., the intramolecular interactions. This region consists of four main peaks, the in-plane (ip; 1100–1130 cm^{-1}) (36) and out-of-plane (op; 1060 cm^{-1}) (37) all-*trans* C–C stretch, another C–C stretch (1080–1100 cm^{-1}) with a phase angle between 0 and π (38), and a broad band for *gauche* C–C stretch (1090 cm^{-1}) (39). On solid–liquid phase transition, the region changes dramatically, as can be seen in Figure 8, with the sharp peaks characteristic of the solid state becoming a series of overlapping broad bands dominated by a central band at 1080 cm^{-1}. A problem identified in the literature is the inability to obtain absolute values for each conformation from the band intensities/positions and the fact that the changes are not linear (40). This problem led to a considerable number of papers devoted to correlating various peak ratios to the conformation of the acyl chain in the solid state (41–44).

The C–C stretching region is unreliable for chain length prediction in the liquid state because a broad mass of peaks is found in this region, which makes deconvolution tricky. The broad *gauche* band is the easiest to deconvolve and yields a correlation of just 0.94, with evidence of odd/even alternation as seen in the CH_2 modes. The $\nu(C–C)_{ip}$ height declined in a stepwise manner corresponding to short-, medium-, and long-chain FA, whereas the area showed a linear decrease ($R^2 = 0.52$). The $\nu(C–C)_{op}$ band showed a nonlinear increase in both height and area. There is also a broad band on the lower wavenumber side of the region, which is very tricky to deconvolve and gave a weak correlation with area ($R^2 = 0.77$). The total area of the C–C region in the liquid state gives a correlation of 0.90. Not surprisingly, the well-separated peaks of the solid state give better predictions of the chain length. $\nu(C–C)_{ip}$, ν(C–C), and $\nu(C–C)_{op}$ give correlations of 0.99, 0.96, and 0.97, respectively, with the combined heights giving a correlation of 0.99.

Thus, the overall picture is that for liquid FAME, no perfect calibration is possible for both odd- and even-numbered FA together (the best correlation had an R^2 of 0.97). However, better calibrations are obtained on splitting the calibration in odd- and even-numbered FA measuring $\delta(CH_2)_{tw}/\nu(C{=}O)$ to give R^2= 0.99. Moreover, this is not a big problem in practice, as most natural fats and oils contain predominantly even-numbered FA. The best ratio for the determination of chain length in the solid state is straightforward, 1060/1750 cm^{-1} $[\nu(C–C)_{ip}/\nu(C{=}O)]$ which also gives $R^2 = 0.99$.

An alternative to simple univariate analysis is the use of multivariate analyses, which use multiple data points from the Raman spectra and in this case dramatically reduce the amount of preprocessing of the data because it can be carried out without the need first to curve-fit the Raman bands of interest. PLS regressions against chain length for both the solid and liquid states (see Fig. 9, one factor) looked very similar to the univariate determinations. The regression validation coefficient for the full range of samples (even and odd) in the liquid state was 0.976. However, the prediction error is large (±0.33 C/chain) due to the inherent nonlinearities within the calibration. Analyzing the samples in the solid state again improved the correlation ($R^2 = 0.984$, two factors), and it reduced the error of prediction to ±0.28 C/chain. There were not enough samples to carry out calibrations of the unsaturated series of FAME.

Mass unsaturation. Given the success in predicting both chain length and number of double bonds per chain, it would

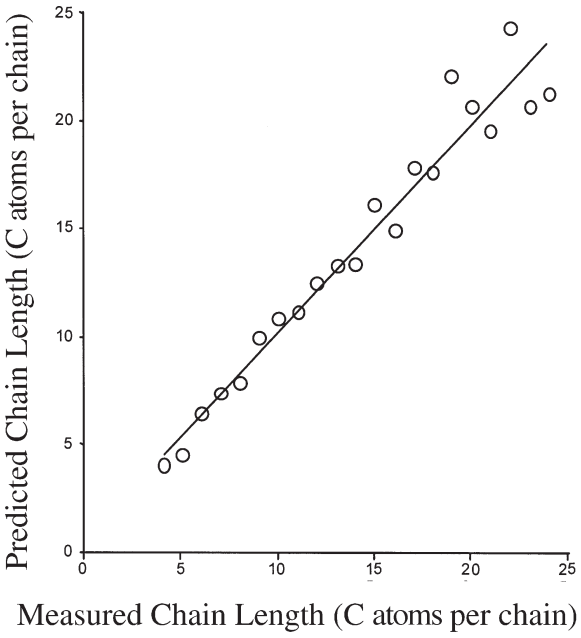

FIG. 9. Partial least squares regression for the prediction of chain length in saturated FAME.

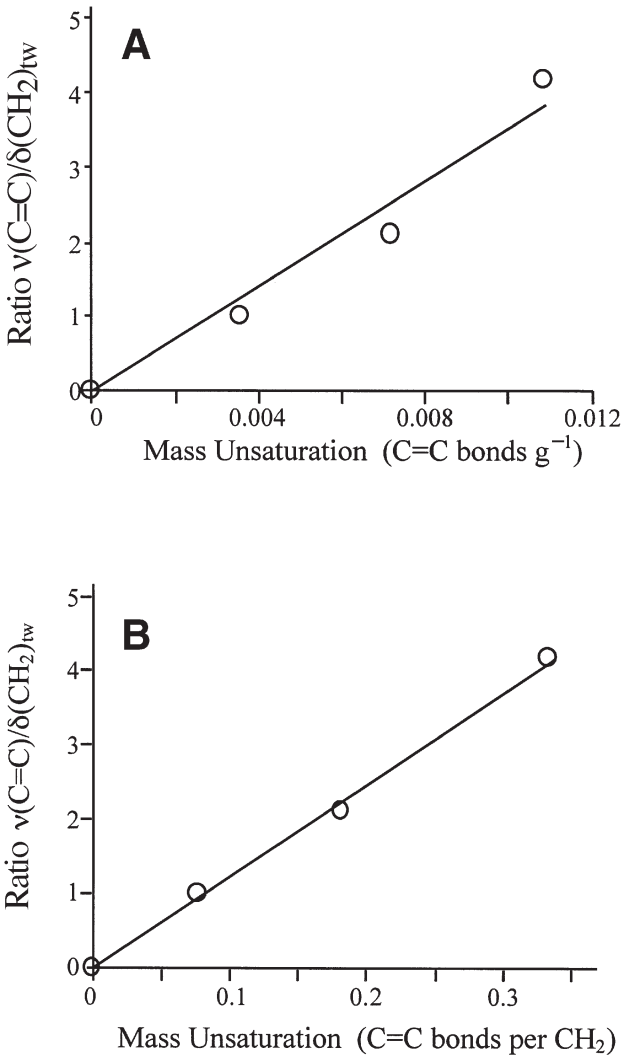

FIG. 10. Plots of the intensity ratio $\nu(C=C)/\delta(CH_2)_{tw}$ against two different measurements of mass unsaturation for 18:0–18:3*c*. (A) Against the number of C=C bonds per gram, which shows a small deviation from linearity (R^2= 0.955). (B) Against the calculated (known) $C=C/CH_2$ ratio, which gives the expected straight line (R^2 = 0.993).

appear that extracting mass unsaturation values would be straightforward, but this is not the case because of two separate issues, one trivial and one more fundamental.

The first (trivial) difficulty is that if relative sample band intensities are used, it is necessary to exercise some care in interpretation of the data because altering the composition of the sample may change the absolute intensity of many of the bands in the spectrum, including those that appear to be the best candidates for the "internal" standards. As illustrated above, the molar unsaturation (C=C/C=O) can be measured directly from the ratio of the appropriate C=C and C=O Raman bands, since any increase in molar unsaturation will be directly reflected in this ratio. Unfortunately, this ratio cannot give mass unsaturation values (double bonds per gram of sample) because the mass unsaturation depends on both the number of double bonds per chain and the number of chains per gram, i.e, there are more olefinic bonds in a gram of short-chain monoene than in a long-chain monoene. In studies where the samples have different mass unsaturation values but where the average chain length remains approximately constant (for example, in studies comparing oils with successively higher degrees of hydrogenation), the correction would be expected to be small, and spectroscopic C=C/C=O ratios will be proportional to molal measurements of unsaturation, such as iodine values (IV). However, in studies where there is significant variation in chain lengths, as well as unsaturation, the simple Raman C=C/C=O ratio will not be directly related to IV.

The obvious choice of bands to use when determining mass unsaturation from Raman spectra is $\nu(C=C)/\delta(CH_2)$ since this includes a component dependent on chain length, and indeed this ratio previously has been correlated with mass unsaturation (typically as IV) (5,29–31). However, with this approach the addition of double bonds will reduce the number of CH_2 groups in the chain, so increasing unsaturation reduces the apparent chain length as determined from the intensities of CH_2 bands. This means that the $\nu(C=C)/\delta(CH_2)$ ratio will not increase linearly with the number of double bonds in the samples. To use a simple example, in looking at two FAME with the same chain length (and therefore near-identical molecular mass), one of which is a monoene and one a triene, the IV of the triene will be three times that of the monoene. However, the ratio of C=C to CH_2 groups in each of the samples (which is the parameter measured in the Raman data) will not differ by a factor of three because each C=C bond introduced also removes two CH_2 groups. For example, in 18:1 Δ9 the $C=C/CH_2$ value is 1:16, whereas that of 18:3 Δ6,9,12 is 3:12; this means that the spectroscopically measured $C=C/CH_2$ values differ by a factor of 4 even though the IV will differ by a factor of only *ca.* 3. Figure 10A shows a plot of the

TABLE 3
Least Squared Correlation Coefficients for the Peak Ratios Used to Predict Composition Parameters in FAME

Parameter	Band ratio	Conditions	R^2
Molar unsaturation	ν(C=C)/ν(C=O)	Liquid	>0.99
	δ(=C–H)/ν(C=O)	Liquid	>0.99
Chain length	$\delta(CH_2)_{sc}$ 1440/ν(C=O)	Liquid: Total (Odd/even separated)	0.94 (0.98)
	$\delta(CH_2)_{sc}$ 1460/ν(C=O)	Liquid	0.95
	Total $\delta(CH_2)_{sc}$/ν(C=O)	Liquid: Total (Odd/even)	0.96 (0.97)
	$\delta(CH_2)_{tw}$/ν(C=O)	Liquid: Total (Odd/even)	0.95 (0.99)
	$\delta(CH_2)_{sc}$ 1440/ν(C=O)	Solid	0.93
	$\delta(CH_2)_{sc}$ 1410/ν(C=O)	Solid	0.96
	Total $\delta(CH_2)_{sc}$/ν(C=O)	Solid	0.98
	$\delta(CH_2)_{tw}$/ν(C=O)	Solid	0.97
	$\nu(C–C)_{ip}$/ ν(C=O)	Solid	0.98
	ν(C–C)/ν(C=O)	Solid	0.95
	$\nu(C–C)_{g}$/ν(C=O)	Liquid	0.94
	$\nu(C–C)_{op}$/ν(C=O)	Solid	0.99
	Full-spectra PLS	Liquid	0.98[a]
	Full-spectra PLS	Solid	0.98[a]
	$\delta(CH_2)_{sc}$ 1440/ν(C=O)	Liquid–monounsaturated	0.50
	$\delta(CH_2)_{sc}$ 1460/ν(C=O)	Liquid–monounsaturated	0.85
	$\delta(CH_2)_{tw}$/ν(C=O)	Liquid–Monounsaturated	>0.99
Mass unsaturation	ν(C=C)/$\delta(CH_2)_{sc}$ 1440	Liquid–18-carbon series	>0.99
	ν(C=C)/$\delta(CH_2)_{sc}$ 1460	Liquid–18-carbon series	>0.99
	δ(=C–H)/$\delta(CH_2)_{tw}$	Liquid–18-carbon series	0.98

[a]Partial least squares (PLS) validation correlation coefficient. For other abbreviations see Table 2.

ratios of the 1660 cm^{-1}/1300 cm^{-1} Raman bands [ν(C=C)/δ–$(CH_2)_{tw}$) against mass unsaturation for 18:0–18:3*c* Δ6,9,12, which shows the expected small deviation from linearity and gives an R^2 value of 0.955. This curvature is not due to experimental error since plotting the same ν(C=C)/$\delta(CH_2)_{tw}$ ratio against the calculated (known) C=C/CH_2 ratio gives the expected straight line (R^2 = 0.993, Fig. 10B).

The second region of the Raman spectra that can be used to determine chain length is the scissoring region (*ca.* 1440 cm^{-1}). Unlike the twist region, in the scissoring region there is evidence that olefinic bonds with detectable intensity do appear. Although these olefinic bands are not resolved under our experimental conditions, it is possible to deduce their existence by plotting the measured $\delta(CH_2)_{sc}$/ν(C=O) ratio against the calculated CH_2/C=O ratio for a series of monounsaturated FAME with increasing chain length. This plot has a very small slope and does not extrapolate to zero relative intensity at zero CH_2 units. The net result of the serendipitous effect is that use of the $\delta(CH_2)_{sc}$ band partially self-corrects for the problem of increasing unsaturation reducing the number of CH_2 groups. For example, plotting the ratios of the ν(C=C)/$\delta(CH_2)_{sc}$ (1660 cm^{-1}/1440 cm^{-1}) Raman bands against mass unsaturation for the 18:0–18:3*c* Δ6,9,12 series gives a line for which R^2 = 0.982, which is much better than the 0.955 value observed when the twist peak (R^2 = 0.955) was used. This improved linearity arises because the olefinic groups that are introduced actually have bands in the same region as the main scissor band, so that the loss of CH_2 intensity in this region is at least partly compensated by the appearance of new bands in the same region.

Table 3 brings together all the correlation coefficients of the various band ratios measured against compositional parameters such as mass unsaturation and chain length.

The data we have obtained clearly show that although Raman spectra can be used to determine compositional parameters for FAME and that good correlations can be obtained, the choice of which ratios to use depends on the nature of the samples. For example, the carbonyl stretching mode is a suitable molar internal standard for both solid and liquid samples, whereas the terminal C–C stretching mode at *ca.* 890 cm^{-1} is only suitable for use in the solid state. For molal determinations, such as the degree of unsaturation, the $\delta(CH_2)_{sc}$ band was found to be the most suitable owing to the combination of both saturated and unsaturated modes within that band. Thus, molar unsaturation is best determined by measuring the ν(C=C)/ ν(C=O) ratio, and for molal unsaturation the ratio ν(C–C)$\delta(CH_2)_{sc}$ is best. In addition, calibrations established for a particular range of samples will not necessarily transfer to other samples, for example, if there is a change in the proportion of odd-numbered carbon chain FA or average chain length. These effects are the direct result of the fact that the *aufbau* approach rapidly breaks down in the Raman spectroscopic analyses of FA, and incremental changes in structure do not necessarily lead to incremental changes in Raman bands. However, the FA lipids in many foodstuffs are restricted to even numbers of carbons per chain and have relatively long chain lengths (>12 carbons), and for these systems a simple approach based on the bands just discussed is appropriate.

ACKNOWLEDGMENTS

The authors would like to thank Alan Beattie and Ann Fearon for supplying the FAME used in this work. J.R.B. wishes to thank the Department of Agriculture and Rural Development for Northern Ireland for the provision of a postgraduate studentship to undertake this work and for the facilities provided at the Agriculture and Food Science Centre, Belfast.

REFERENCES

1. Spiro, T.G. (1986) *Biological Applications of Raman Spectroscopy*, Vol. 1, John Wiley & Sons, New York.
2. Tu, A.T. (1982) *Raman Spectroscopy in Biology: Principles and Applications*, John Wiley & Sons, New York.
3. Bailey, G.F., and Horvat, R.J. (1972) Raman Spectroscopy Analysis of the *cis/trans* Isomer Composition of Edible Vegetable Oils, *J. Am. Oil Chem. Soc. 49*, 494–498.
4. Sadeghi-Jorabchi, H., Wilson, R.H., Belton, P.S., Edwards-Webb, J.D., and Coxon, D.T. (1991) Quantitative Analysis of Oils and Fats by Fourier Transform Raman Spectroscopy, *Spectrochim. Acta A 47*, 1449–1458.
5. Sadeghi-Jorabchi, H., Hendra, P.J., Wilson, R.H., and Belton, P.S. (1990) Determination of the Total Unsaturation in Oils and Fats by Fourier Transform Raman Spectroscopy, *J. Am. Oil Chkem. Soc. 67*, 483–486.
6. Chmielarz, B., Bajdor, K., Labudzinska, A., and Klukowskamajewska, Z. (1995) Studies on the Double-Bond Positional Isomerization Process in Linseed Oil by UV, IR and Raman-Spectroscopy, *J. Mol. Struct. 348*, 313–316.
7. Beattie, J.R., Bell, S.E.J., and Moss, B.W. (2000) Raman Studies of Lipid Structure and Composition in Proceedings of the XIIth *International Conference on Raman Spectroscopy*, Beijing, China (Zhang, S.L., and Zhu, B.F., eds.), John Wiley & Sons, New York, p. 708.
8. Stauffer, C.E. (1996) *Fats And Oils*, 1st edn., Eagan Press, St. Paul, MN.
9. Beattie, J.R., Bell, S.E.J., Farmer, L.J., Moss, B.W., and Patterson, D. (2004) Preliminary Investigation of the Application of Raman Spectroscopy to the Prediction of the Sensory Quality of Beef Silverside, *Meat Sci. 66*, 903–913.
10. Diamond, D., & Hanratty, V.C.A. (1997) *Spreadsheet Applications in Chemistry Using Microsoft Excel*, Wiley-Interscience, New York.
11. Oakes, R.E., Beattie, J.R., Moss, B., and Bell, S.E.J. (2002) Conformations, Vibrational Frequencies and Raman Intensities of Short Chain Fatty Acid Methyl Esters Using DFT with 6-31 G(d) and Sadlej pVTZ Basis Sets, *J. Mol. Struct. 586*(1–3), 91–110.
12. Oakes, R.E., Beattie, J.R., Moss, B., and Bell, S.E.J. (2003) DFT Studies of Long-Chain FAMEs: Theoretical Justification for Determining Chain Length and Unsaturation from Experimental Raman Spectra, *J. Mol. Struct. 626*, 27–45.
13. Love, J.A. (1996) Animal Fats, in *Bailey's Industrial Oil and Fat Products*, 5th edn. (Yui, Y.H., ed.), Vol. 1. pp. 1–18, John Wiley & Sons, New York.
14. Baraga, J.J., Feld, M.S., and Rava, R.P. (1992) *In-situ* Optical Histochemistry of Human Artery Using Near Infrared Fourier Transform Raman Spectroscopy, *Proc. Natl. Acad. Sci. USA, 89*, 3473–3477.
15. Frank, C.J., Redd, D.C.B., Gansler, T.S., and Mccreery, R.L. (1994) Characterization of Human Breast Biopsy Specimens with Near-IR Raman-Spectroscopy, *Anal Chem. 66*(3), 319–326.
16. Takai, Y., Masuko, T., and Takeuchi, H. (1997) Lipid Structure of Cytotoxic Granules in Living Human Killer T Lymphocytes Studied by Raman Microspectroscopy, *Biochim. Biophys. Acta 1335*, 199–208.
17. Levin, I.W., Mushayakarara, E., and Bittman, R. (1982) Vibrational Assignment of the *sn*-1 and *sn*-2 Chain Carbonyl Stretching Modes of Membrane Phospholipids, *J. Raman Spectrosc. 13*, 231–234.
18. Simpson, T.D., and Hagemann, J.W. (1982) Evidence of Two β′ Phases in Tristearin, *J. Am. Oil Chem. Soc. 59*, 169–171.
19. Tandon, P., Forster, G., Neubert, R., and Wartewig, S. (2000) Phase Transitions in Oleic Acid as Studied by X-ray Diffraction and FT-Raman Spectroscopy, *J. Mol. Struct. 524*, 201–215.
20. Tandon, P., Neubert, R., and Wartewig, S. (2000) Thermotropic Phase Behavior of Sodium Oleate as Studied by FT-Raman Spectroscopy and X-ray Diffraction, *J. Mol. Struct. 526*, 49–57.
21. Mushayakarara, E., and Levin, I.W. (1982) Determination of Acyl Chain Conformation at the Lipid Interface Region: Raman Spectropscopic Study of the Carbonyl Stretching Mode Region of Dipalmitoyl Phosphatidylcholine and Structurally Related Compounds, *J. Phys. Chem. 86*, 2324–2327.
22. Muik, B., Lendl, B., Molina-Díaz, A., and Ayora-Cañada, M.J. (2003) Direct, Reagent-Free Determination of Free Fatty Acid Content in Olive Oil and Olives by Fourier Transform Raman Spectrometry, *Anal. Chim. Acta 487*, 211–210.
23. Bicknell-Brown, E., Brown, K.G., and Person, W.B. (1981) Configuration-Dependent Raman Bands of Phospholipid Surfaces II. Head Group and Acyl Stretching Modes in the 800–900 cm^{-1} Region, *J. Raman Spectrosc. 11*, 356–362.
24. Kim, Y., Strauss, H.L., and Snyder, R.G. (1989) Conformational Disorder in the Binary Mixture n-$C_{50}H_{102}$/n-$C_{46}H_{94}$: A Vibrational Spectroscopic Study, *J. Phys. Chem. 93*, 485–490.
25. Maissara, M., and Devaure, J. (1987) Raman Study of Odd-Numbered C_{11}–C_{23} n-Alkanes in Their High-Temperature Solid Phases, *J. Raman Spectrosc. 18*, 177–179.
26. Vogel, H., and Jähnig, F. (1981) Conformational Order of the Hydrocarbon Chains in Lipid Bilayers. A Raman Spectroscopic Study, *Chem. Phys. Lipids 29*, 83–101.
27. Brown, K.G. (1987) Raman Active Bands Sensitive to Motion and Conformation at the Chain Termini and Backbones of Alkanes and Lipids, *J. Phys. Chem. 91*, 3436–3442.
28. Kint, S., Wermer, P.H., and Scherer, J.R. (1992) Raman-Spectra of Hydrated Phospholipid-Bilayers. 2. Water and Headgroup Interactions, *J. Phys. Chem. 96*, 446–452.
29. Butler, M., Salem, N., Hoss, W., and Spoonhower, J. (1979) Raman Spectral Analysis of the 1300 cm^{-1} Region for Lipid and Membrane Studies, *Chem. Phys. Lipids. 29*, 99–102.
30. da Silva, M.I.P., Nery, M.P., and Tellez, C.A. (2000) Castor Oil Catalytic Hydrogenation Reaction Monitored by Raman Spectroscopy, *Mater. Lett. 45*, 197–202.
31. Lerner, B., Garry, M., and Walder, F. (1992) Characterisation of Polyunsaturation in Cooking Oils by the 910 FT-Raman, paper presented at the 2nd International Workshop on FT-IR, University of Antwerp, Antwerp, Belgium, pp. 75–82.
32. Weng, Y.M., Weng, R.H., Tzeng, C.Y., and Chen, W.L. (2003). Structural Analysis of Triacylglycerols and Edible Oils by Near-Infrared Fourier Transform Raman Spectroscopy, *Appl. Spectrosc. 57*, 413–418.
33. Koyama, Y., and Ikeda, K.I. (1980) Raman Spectra and Conformation of the *cis*-Unsaturated Fatty-Acid Chains, *Chem. Phys. Lipids 26*, 149–172.
34. Kaneko, F., Yamazaki, K., and Kobayashi, M. (1994) Vibrational Spectroscopic Study on Polymorphism of Erucic Acid and Palmitoleic Acid: γ1–α1 and γ–α Reversible Solid State Phase Transitions, *Spectrochim. Acta A 50*, 1589–1603.
35. Sprunt, J.C., Jayasooriya, U.A., and Wilson, R.H. (2000) A Simultaneous FT-Raman-DSC (SRD) Study of Polymorphism in *sn*-1,3-Distearoyl-2-oleoylglycerol (SOS), *Phys. Chem. Chem. Phys. 2*, 4299–4305.
36. Snyder, R.G., Cameron, D.G., Casal, H.L., Compton, D.A.C., and Mantsch, H.H. (1982) Studies on Determining Conformational Order in n-Alkanes and Phospholipids from the 1130 cm^{-1} Raman Band, *Biochim. Biophys. Acta 684*, 111–116.
37. Susi, H., Sampugna, J., Hampson, J.W., and Ard, J.S. (1979) Laser-Raman Investigation of Phospholipid-Polypeptide Interactions in Model Membranes, *Biochemistry 18*, 297–301.
38. Zerbi, G., Conti, G., Minoni, G., Pison, S., and Bigotto, A. (1987) Premelting Phenomena in Fatty Acids: An Infrared and Raman Study, *J. Phys. Chem. 91*, 2386–2393.
39. Lawson, E.E., Anigbogu, A.N.C., Williams, A.C., Barry, B.W.,

and Edwards, H.G.M. (1998) Thermally Induced Molecular Disorder in Human Stratum Corneum Lipids Compared with a Model Phospholipid System; FT-Raman Spectroscopy, *Spectrochim. Acta A* 54, 543–558.
40. Pink, D.A., Green, T.J., and Chapman, D. (1980) Raman Scattering in Bilayers of Saturated Phosphatidylcholines. Experiment and Theory, *Biochemistry 19*, 349–356.
41. Bertoluzza, A., Bonora, S., Fini, G., Morelli, M.A., and Simoni, R. (1983) Phospholipid–Protein Molecular Interactions in Relation to Immunological Processes: 1. Raman Spectroscopic and Calorimetric Studies of Phospholipid–Polyglycine Molecular Interactions in Model Membranes, *J. Raman Spectrosc. 14*, 395–400.
42. Bush, S.F., Adams, R.G., and Levin, I.W. (1980) Structural Reorganizations in Lipid Bilayer Systems: Effect of Hydration and Sterol Addition on Raman Spectra of Dipalmitoylphosphatidylcholine Multilayers, *Biochemistry 19*, 4429–4436.
43. Carrier, D., and Pézolet, M. (1981) Raman Spectroscopic Study of the Interaction of Poly-L-lysine with Dipalmitoylphosphatidylcholine Bilayers, *Biophys. J. 46*, 497–506.
44. Gaber, P.G., and W.L. Peticolas (1978) Interpretation of Biomembrane Structure by Raman Difference Spectroscopy: Nature of the Endothermic Transitions in Phosphatidylcholines, *Biophys. J. 21*, 161–176.

[Received January 16, 2004; accepted June 2, 2004]

Dietary Intake of Essential and Long-Chain Polyunsaturated Fatty Acids in Pregnancy

Elizabeth D. Loosemore, Michelle P. Judge, and Carol J. Lammi-Keefe*

University of Connecticut, Department of Nutritional Sciences, Storrs, CT 06269-4017

ABSTRACT: The dietary intake of EFA and long-chain PUFA (LCPUFA) by women with (n = 14) and without (n = 31) gestational diabetes mellitus (GDM) was determined by repeated 24-h recalls. Women with GDM consumed significantly more energy as fat compared with women who had uncomplicated pregnancies; absolute dietary fat did not differ. Dietary n-3 LCPUFA was substantially lower than the current recommendation for pregnancy, whereas intake of saturated FA (SFA) exceeded it. We conclude that replacing dietary sources of SFA with those of EFA and LCPUFA, especially n-3 LCPUFA, would benefit the dietary fat profiles of all pregnant women.

Paper no. L9438 in *Lipids 39,* 421–424 (May 2004).

The importance of EFA and their long-chain PUFA (LCPUFA) products in humans has seen a renewed interest in recent years. The roles of EFA and LCPUFA as precursors of the prostaglandins in growth and in the development of the retina and brain are well documented (1–6). Recent reports support the notion that deficiencies of EFA and PUFA, particularly LCPUFA, play a role in the development of cardiovascular disease (7–10), type 2 diabetes mellitus (1,3,9), osteoporosis (3,9), and brain-related diseases such as Parkinson's, dementia, and attention-deficit disorders (3,9). Because LCPUFA must be synthesized from EFA or ingested as preformed lipids (6,11,12), the role of diet is very important, particularly for pregnant women. Although there is evidence that the fetus and neonate can elongate and desaturate EFA to form LCPUFA, the capacity to do this is extremely limited, making the developing fetus dependent on maternal sources for an adequate supply of LCPUFA (6,11,12). Further, the importance of nutrients during pregnancy vis-à-vis adaptations to prenatal nutrition has been highlighted by the recent report of Waterland and Jirtle (13).

Previous work from our laboratory (14) demonstrated that women with gestational diabetes mellitus (GDM) do not preferentially transfer LCPUFA to the developing fetus in the manner that women with uncomplicated pregnancies do, thereby creating a relative LCPUFA deficiency for their infants. The mechanism for the compromised transfer in GDM has not been elucidated, but we propose that increased dietary LCPUFA, especially docosahexaenoic acid (DHA), for pregnant women, and particularly for women with GDM, may be beneficial to the developing fetus. In the earlier study (14), we reported that pregnant women were consuming 60 mg DHA on average. In the current study we have assessed dietary intake of EFA and LCPUFA in pregnant women with and without GDM to determine whether diets have changed in the last decade with respect to DHA intake.

*To whom correspondence should be addressed at University of Connecticut, Dept. of Nutritional Sciences, 3624 Horsebarn Hill Rd., Unit 4017, Storrs, CT 06269-4017. E-mail: Carol.LammiKeefe@uconn.edu

Abbreviations: CHO, carbohydrate; DHA, docosahexaenoic acid; GDM, gestational diabetes mellitus; HbA_{lc}, hemoglobin A_{lc}; LCPUFA, long-chain polyunsaturated FA; OGTT, oral glucose tolerance test; PL, phospholipid; SFA, saturated FA.

METHODS

Subjects. Women with GDM (n = 14) and healthy pregnant women (controls, n = 31) were recruited from Diabetes Life Care Center, Women's Ambulatory Health Department, and Childbirth Education Classes offered by the Department of Obstetrics and Gynecology at Hartford Hospital (Hartford, CT). The protocol was approved by the Hartford Hospital and University of Connecticut Human Subject Approval Committees. Written informed consent was obtained from all subjects. As described previously (15), a screening test for GDM was typically administered between 24 and 30 wk of gestation. Women with a positive screening test were given an oral glucose tolerance test (OGTT). Pregnancies with GDM were defined by the OGTT criteria of Coustan and Carpenter (16). Women with GDM and healthy pregnant women with negative screening tests were enrolled in the study between 26 and 30 wk of gestation.

Study design. The study was longitudinal in design. As in the study by Wijendran *et al.* (14), women with GDM were prescribed diets based on individual needs, generally with approximately 45% of energy/d from carbohydrate (CHO), approximately 22% from protein, and approximately 35% from fat, divided among three meals and three snacks per day. Subjects were scheduled for diet interviews and venous blood draws at the time of recruitment (26 to <30 wk gestation), at 30 to <34 wk gestation, and at 34 to <38 wk gestation. Twenty-four-hour recalls were obtained from all subjects to determine the intake of macronutrients, micronutrients, and FA during the third trimester.

A registered phlebotomist, nurse, or physician collected 7- and 2-mL blood samples in tubes containing EDTA and a 7-mL blood sample in a tube with no additives. The 7-mL samples were centrifuged at 700 × g for 10 min, and serum and plasma were separated. Serum and the 2-mL sample containing EDTA were sent to an outside laboratory (Quest Diagnostics, Wallingford, CT) for analysis of fructosamine and hemoglobin A_{1c} (HbA_{1c}) concentrations, respectively. Plasma was stored at –80°C until subsequent analyses.

Sample analysis. Maternal plasma phospholipid (PL) FA were determined using methods that are routine in our laboratory (15). The separated PL FA were identified by comparison with external standards and quantified as relative wt%.

Dietary analysis. The repeated 24-h recalls were coded and analyzed using the University of Minnesota Nutrition Data System (NDS 4.04_32).

Statistical analyses. Statistical analyses were primarily conducted using SPSS, version 11.0. Nutrients analyzed included energy (kcal), CHO (g and as % energy), protein (g and as % energy), fat (g and as % energy), saturated FA (SFA; g and as % energy), monounsaturated FA (g and as % energy), 18:2n-6 (g and as % energy), 18:3n-3 (g), 20:4n-6, 20:5n-3 (mg), 22:6n-3 (mg) and PUFA/SFA ratio. Total n-3 PUFA (g/d), total n-6 PUFA (g/d), total n-3 LCPUFA (mg/d), total EFA (as % energy), and total PUFA (as % energy) were calculated. There were no intraindividual significant differences across time for the nutrients being examined (SAS, version 8, PROC MIXED; SAS Institute, Cary, NC); thus, the mean intake of each nutrient for each subject was estimated using a minimum of two 24-h recalls. Means by number of recalls for total energy, CHO, fat, and protein intake (g and % energy) and for classifications of fats and FA reported in this study were determined using ANOVA. There were no significant differences between those individuals who had two 24-h recalls and those who had three recalls. Therefore, those women with two and three recalls were combined for the final analyses. Group (GDM vs. controls) differences were determined using ANOVA.

RESULTS

Subject characteristics are provided in Table 1. HbA_{1c} (GDM, 5.40% ± .62, range 4.9 to 6.1; controls, 5.07% ± .38, range 4.4 to 5.9) and fructosamine (GDM, 182.33 μmol/L ± 29.96, range 149 to 207; controls, 181.59 μmol/L ± 19.62, range 126 to 222) values indicated that women with GDM were in clinical control (normal HbA_{1c}: 4.0–7.0%; normal fructosamine: <285 μmol/L). There were no significant differences between groups with either measure (HbA_{1c}: $F_{23} = 1.774$, $P = .196$; fructosamine, $F_{23} = .003$, $P = .954$). As shown in Table 2, significant differences between groups were noted for CHO intake, both in g/d and as a percentage of energy, total fat as a percentage of energy, and MUFA as a percentage of energy. As shown in Table 3, significant differences existed between groups in both plasma PL total n-6 FA and n-6 LCPUFA, but not in the n-3 FA.

DISCUSSION

The distribution of macronutrients generally recommended for healthy individuals is 30% or less total kcal from fat, of which <10% are from SFA, approximately 15% of total kcal are from protein, and the remaining 55% of kcal are from CHO. In pregnancy complicated by GDM, it is generally recommended that CHO constitute 42 to 45% of energy intake, distributed among six to eight meals and snacks throughout the day, with smaller amounts of CHO (15 to 45 g) at breakfast and snacks. The sources should be complex CHO, such as unrefined whole-grain

TABLE 1
Characteristics of the Maternal Study Population

Characteristic	Control subjects ($n = 31$)	Women with GDM[a] ($n = 14$)
Age (y)	25 ± 5.7[b]	29.6 ± 5.1[c]
Race (*n*)		
Asian/Indian	0	2
Black—United States	1	1
Black—other	1	1
Caucasian	7	7
Latino—Caribbean	17	2
Latino—non-Caribbean	2	0
Parity (*n*)		
0	10	7
1	13	3
2	4	2
3	1	0
≥4	0	1
Height (m)	1.63 ± .07	1.63 ± .10
Weight (kg, prepregnancy)	67.5 ± 16.8	78.2 ± 26.0
Weight (kg, at delivery)	84.8 ± 16.4	89.0 ± 26.6
Pregravid BMI (kg/m^2)	25.3 ± 5.1	29.1 ± 7.0[d]
≤19.8	1	0
>19.8 to ≤25.5	17	6
>25.5 to <30	5	1
≥30	5	6
Weight gain (kg, prepregnancy wt to delivery)	17.2 ± 7.1	10.8 ± 6.3[c]

[a]GDM, gestational diabetes mellitus; BMI, body mass index.
[b]Mean ± SD.
[c]Significant difference ($P < 0.05$).
[d]Trend for a difference between groups ($P < 0.10$).

TABLE 2
Mean Estimated Dietary Intakes in Control Subjects and in Women with GDM During the Third Trimester[a]

Nutrient	Unit	Control subjects (n = 31)	Women with GDM (n = 14)
Energy	kcal	2168 ± 585	1957 ± 332
Carbohydrate	g/d	290.54 ± 82.54	228.15 ± 46.89[b]
	% of energy	54.03 ± 8.13	46.74 ± 6.84[b]
Protein	g/d	84.17 ± 29.44	84.35 ± 18.21
	% of energy	15.05 ± 4.5	17.31 ± 2.81
Fat	g/d	74.03 ± 28.71	81.32 ± 22.88
	% of energy	31.86 ± 6.83	37.25 ± 6.54[b]
Total SFA	g/d	29.86 ± 11.53	28.68 ± 8.70
	% of energy	12.23 ± 3.30	13.86 ± 3.38
Total MUFA	g/d	27.76 ± 10.34	30.04 ± 8.39
	% of energy	11.42 ± 2.72	14.36 ± 6.59[b]
18:2n-6	g/d	11.56 ± 5.44	14.36 ± 6.56
	% of energy	4.74 ± 1.82	6.44 ± 2.00
20:4n-6	mg/d	155.38 ± 86.49	133.93 ± 69.72
18:3n-3	g/d	1.34 ± .66	1.52 ± .88
20:5n-3	mg/d	15.81 ± 20.57	12.26 ± 9.07
22:6n-3	mg/d	67.69 ± 99.58	34.05 ± 18.92
Total n-6 PUFA[c]	g/d	11.71 ± 5.49	14.49 ± 6.59
Total n-6 LCPUFA[d]	g/d	.16 ± .086	.13 ± .07
Total n-3 PUFA[e]	g/d	1.46 ± .71	1.57 ± .89
Total n-3 LCPUFA[f]	g/d	.12 ± .20	.050 ± .033
Total EFA[g]	% of energy	5.29 ± 2.01	7.11 ± 2.22
Total PUFA[h]	% of energy	5.40 ± 2.02	7.20 ± 2.21
EFA n-6/EFA n-3 ratio		9.04 ± 2.68	9.77 ± 1.77
Total n-6/total n-3 ratio		4.53 ± 4.66	3.96 ± 4.03
LCPUFA n-6/n-3 ratio		3.80 ± 4.77	3.06 ± 2.12
PUFA/SFA ratio		.51 ± .19	.59 ± .22

[a]Mean ± SD. SFA, saturated FA; MUFA, monounsaturated FA; LCPUFA, long-chain PUFA; P/S, ratio of PUFA to SFA. For other abbreviation see Table 1.
[b]Significantly different from control subjects ($P \leq 0.05$).
[c]Σ18:2 and 20:4.
[d]20:4 was the only n-6 LCPUFA identified.
[e]Σ18:3, 20:5, 22:5, and 22:6.
[f]Σ20:5, 22:5, and 22:6.
[g]Σ18:2n-6 and 18:3n-3.
[h]Σn-6 and n-3 FA.

breads, old-fashioned oatmeal, nuts, legumes, and lentils. Additionally, protein should comprise 20–25% of calories, which is enough to meet the Recommended Dietary Allowance for pregnancy. Fat is recommended to range from 30 to 40% of total calories to maintain adequate caloric intake while reducing CHO intake (17). The women in this study were consuming diets compatible with the macronutrient recommendations for their particular group, i.e., control or GDM.

The women with GDM had a significantly higher percentage of energy from fat intake than controls, whereas absolute dietary fat intake did not differ. Dietary EFA and LCPUFA did not differ between the groups. However, with the exception of four controls, n-3 LCPUFA was substantially lower than the current LCPUFA recommendation of 200 to 300 mg/d (18). Those women whose LCPUFA intake met the recommendation consumed at least one serving of fish per recall, plus eggs, chicken, or turkey. The n-6/n-3 ratio for all subjects was higher than the recommended n-6/n-3 ratio of 1:1 to 2:1 (19). Although the limited number of repeated 24-h recalls for our subjects may be viewed as a limitation of the study, our finding regarding intake of the n-3 FA is in good agreement with other reports (15,20). Based on our data and given the potential implications for long-term health, as well as the more immediate effects on fetal development, we suggest that strategies to increase EFA and LCPUFA in the diets of pregnant women should be considered. The percentage of energy from SFA exceeded the recommendations in both groups. Replacing dietary sources of SFA with those containing EFA and LCPUFA would benefit pregnant women by improving both the diet EFA/LCPUFA and SFA profiles of these women. Protein and fat sources for these women were generally beef or pork, usually the higher-fat cuts, or chicken, usually fried. Rarely did women describe consuming protein sources that provided low to moderate levels of fat and higher levels of n-3 LCPUFA, such as tuna, salmon, and other cold-, deep-water marine fish.

The current work parallels previous work reported by Wijendran *et al.* (15), who reported on the nutrient intake of pregnant women studied in the early 1990s. These parallels indicate that the message regarding the importance of n-3 FA has not yet resulted in dietary changes in this population.

ACKNOWLEDGMENTS

Supported in part by the Donaghue Medical Research Foundation, the University of Connecticut Research Foundation, and the United States Department of Agriculture. Special thanks to Charlotte de Maré, Melissa Keplinger, Gisella Mutungi, and Brunella Ibarolla for

TABLE 3
Mean Estimated Plasma Phospholipid FA (wt%) in Control Subjects and in Women with GDM at Time of Delivery[a]

FA	Control subjects (n = 27)	Women with GDM (n = 13)
18:2n-6 (linoleic acid)	22.1 ± 3.7	19.8 ± 3.3
	(11.1 to 28.2)	(12.3 to 23.6)
18:3n-3 (α-linolenic acid)	0.20 ± 0.12	0.17 ± 0.26
	(0.00 to 0.45)	(0.00 to .093)[b]
20:4n-6 (AA)	9.8 ± 2.0	7.9 ± 3.1
	(5.3 to 13.2)	(3.0 to 11.8)
22:6n-3 (DHA)	3.4 ± 1.1	3.1 ± 1.6
	(1.5 to 5.5)	(0.00 to 5.2)
Total n-3 FA[c]	4.7 ± 2.3	3.6 ± 1.6
	(2.2 to 13.42)	(0.00 to 5.8)
Total n-6 FA[d]	35.9 ± 4.7	30.3 ± 6.5
	(22.6 to 42.4)	(18.8 to 38.2)[e]
Total n-6 LCPUFA[f]	13.7 ± 2.5	10.5 ± 4.2
	(7.1 to 10.9)	(4.1 to 16.3)[e]
Total n-3 LCPUFA[g]	4.5 ± 2.3	3.4 ± 1.6
	(1.9 to 13.2)	(0.00 to 5.53)
Ratio n-6/n-3 plasma FA	8.9 ± 3.8	8.9 ± 4.2
	(2.7 to 17.5)	(4.5 to 20.7)
Ratio n-6/n3 plasma LCPUFA	3.5 ± 1.3	3.3 ± 1.8
	(1.0 to 6.2)	(1.6 to 8.1)

[a]Mean ± SD (minimum to maximum) AA, anachidonic acid; DHA, docosahexaenoic acid.
[b]Significantly different from control subjects ($P \leq 0.05$).
[c]Σ18:3n-3, 20:5n-3, 22:5n-3, and 22:6n-3.
[d]Σ18:2n-6, 18:3n-6, 20:2n-6, 20:3n-6, and 20:4n-6.
[e]Significantly different from control subjects ($P \leq 0.005$).
[f]Σ20:5n-3, 22:5n-3, and 22:6n-3
[g]Σ20:2n-6, 20:3n-6, and 20:4n-6

their help with recruiting subjects and to Sally Cote and Meredith Ryan for their help with data entry of the dietary data.

REFERENCES

1. Bhathena, S.J. (2000) Relationship Between Fatty Acids and the Endocrine System, *Biofactors. 13*, 35–39.
2. Carlson, S., Werkman, S., Peeples, J., Cooke, R., and Tolley, E. (1993) Arachidonic Acid Status Correlates with First Growth in Preterm Infants, *Proc. Natl. Acad. Sci. USA 90*, 1073–1077.
3. Connor, W.E. (2000) Importance of n-3 Fatty Acids in Health and Disease, *Am. J. Clin. Nutr. 71* (Suppl.), 171S–175S.
4. Leaf, A., Leighfield, M., Costeloe, K., and Crawford, M. (1992) Long-Chain Polyunsaturated Fatty Acids and Fetal Growth, *Early Hum. Dev. 30*, 183–191.
5. Neuringer, M., Connor, W., Lin, D., Barstad, L., and Luck, S. (1986) Biochemical and Functional Effects of Prenatal and Postnatal n-3 Fatty Acid Deficiency on Retina and Brain in Rhesus Monkeys, *Proc. Natl. Acad. Sci. USA 83*, 4021–4025.
6. Innis, S. (1991) Essential Fatty Acids in Growth and Development, *Prog. Lipid Res. 30*, 39–103.
7. Harper, C.R., and Jacobson, T.A. (2001) The Fats of Life: The Role of Omega-3 Fatty Acids in the Prevention of Coronary Heart Disease, *Arch. Int. Med. 161*, 2185–2192.
8. Harris, W.S. (1999) n-3 Fatty Acids and Human Lipoprotein Metabolism: An Update, *Lipids 34*, S257–S258.
9. Horrocks, L.A., and Yeo, Y.K. (1999) Health Benefits of Docosahexaenoic Acid (DHA), *Pharmacol. Res. 40*, 211–225.
10. Hu, F.B., Bronner, L., Willett, W.C., Stampfer, M.J., Rexrode, K.M., Albert, C.M., Hunter, D., and Manson, J.E. (2002) Fish and Omega-3 Fatty Acid Intake and Risk of Coronary Heart Disease in Women, *J. Am. Med. Assoc. 287*, 1815–1822.
11. Brody, T. (1994) *Nutritional Biochemistry*, Academic Press, San Diego.
12. Salem, N.J., Wegher, B., Mena, P., and Uauy, R. (1996) Arachidonic and Docosahexaenoic Acids Are Biosynthesized from Their 1-Carbon Precursors in Human Infants, *Proc. Natl. Acad. Sci. USA 93*, 49–54.
13. Waterland, R.A., and Jirtle, R.L. (2003) Transposable Elements: Targets for Early Nutritional Effects on Epigenetic Gene Regulation, *Mol. Cell Biol.* 5293–5300.
14. Wijendran, V., Bendel, R.B., Couch, S.C., Philipson, E.H., Cheruku, S.R., and Lammi-Keefe, C.J. (2000) Fetal Erythrocyte Phospholipid Polyunsaturated Fatty Acids Are Altered in Pregnancy Complicated with Gestational Diabetes Mellitus, *Lipids 35*, 927–931.
15. Wijendran, V., Bendel, R.B., and Couch, S.C. (1999) Maternal Plasma Phospholipid Polyunsaturated Fatty Acids in Pregnancy With and Without Gestational Diabetes Mellitus: Relations with Maternal Factors, *Am. J. Clin. Nutr. 70*, 53–61.
16. Coustan, D.R., and Carpenter, M.W. (1998) The Diagnosis of Gestational Diabetes, *Diab. Care 21* (Suppl. 2), B5–B8.
17. ADA (2001) American Dietetic Association Medical Nutrition Therapy Evidence-Based Guides for Practice: Nutrition Practice Guidelines for Gestational Diabetes Mellitus, American Dietetic Association, Chicago.
18. Collected Recommendations for Long-Chain Polyunsaturated Fatty Acid Intake (2003) *inform 14*, 762–763 (table reprinted from the *PUFA Newsletter*, September 2003, www.pufanewsletter.com/article.asp?i-a&d-142).
19. Simopoulos, A.P. (2001) The Mediterranean Diets: What Is So Special About the Diet of Greece? The Scientific Evidence, *J. Nutr. 131*, 3065S–3073S.
20. Lewis, N.M., Widga, A.C., Buck, J.S., and Frederick, A.M. (1995) Survey of Omega-3 FA in Diets of Midwest Low-Income Pregnant Women, *J. Agromed. 2*, 49–57.

[Received January 21, 2004; accepted June 25, 2004]

Fatty Acid Profile and Affective Dysregulation in Irritable Bowel Syndrome

Tessa O.C. Kilkens[a,b,*], Adriaan Honig[a], Michael Maes[a], Richel Lousberg[a], and Robert-Jan M. Brummer[b]

Departments of [a]Psychiatry and [b]Gastroenterology, University Hospital Maastricht, 6202 AZ, Maastricht, The Netherlands

ABSTRACT: Irritable bowel syndrome (IBS) is a functional gastrointestinal disorder with a high co-occurrence with affective dysregulation. Affective disorders have been associated with specific changes in the PUFA and cholesterol profile. In IBS, similar changes may be present as have been reported in patients with affective disorders. This exploratory study investigates (i) the level of affective dysregulation (AD) in IBS patients and healthy controls; (ii) PUFA and cholesterol profiles in IBS patients compared with controls; and (iii) associations between PUFA and cholesterol parameters with the level of AD. Blood samples were obtained for determination of the FA composition of plasma phospholipids and serum cholesterol in 23 diarrhea-predominant IBS patients and 23 healthy matched controls. AD was scored using the Symptom Check List depression scale, the Hospital Anxiety and Depression Scale, and the Hamilton Depression Rating Scale. The level of AD was higher in IBS patients compared with controls. PUFA and cholesterol profiles did not differ significantly between groups. Total n-3 PUFA and cholesterol were significantly negatively associated and the ratio of n-6 to n-3 PUFA and the ratio of arachidonic acid to EPA were significantly positively associated with the level of AD. The findings of the present study reveal that AD was higher in IBS patients compared with healthy controls and that changes in PUFA and cholesterol profiles were significantly associated with the level of AD. These results warrant further studies regarding the role of PUFA and cholesterol status in the co-occurrence of AD and functional gastrointestinal disorders.

Paper no. L9478 in *Lipids 39,* 425–431 (May 2004).

Irritable bowel syndrome (IBS) is a functional gastrointestinal disorder characterized by abdominal pain or discomfort associated with alteration in defecation, in the absence of structural or biochemical abnormalities that can be identified with currently available tests (1). About 10–20% of the Western population has symptoms consistent with a diagnosis of IBS (2). The quality of life of individuals with IBS is lower than that of individuals with congestive heart failure; health care and employer costs of IBS are high (3,4). IBS can be classified into diarrhea-predominant (d-IBS), constipation-predominant, and mixed type of IBS. The pathophysiology of IBS is poorly understood. A multicomponent conceptual model of IBS has been postulated, involving physiological, affective, cognitive, and behavioral factors (5). Within this model the "brain–gut axis" has gained interest. The brain–gut axis is a theoretical model describing the bidirectional neural pathways linking cognitive and emotional centers in the brain to neuroendocrine centers, the enteric nervous system, and the immune system. This brain–gut axis plays a major role in the concept of IBS (6).

The prevalence of affective dysregulation in IBS patients seen in a gastroenterologic setting is estimated between 40 and 90% (7–10). Chronic modulation of serotonergic activity has been widely applied in the treatment of both affective disorders and IBS. Treatment using serotonergic modulators has been reported to influence both gastrointestinal and psychiatric symptoms in IBS (11). Disturbed serotonergic metabolism seems especially prevalent in the d-IBS type of IBS (12–14). The high rates of affective dysregulation in IBS patients may be a specific and integral part of IBS, rather than a nonspecific co-morbid syndrome related to a chronic intestinal disease (11,15,16).

In patients with affective disorders, such as major depression, specific changes in the composition of PUFA and cholesterol profiles have been observed. Specifically, affective disorders are associated with diminished levels of plasma total n-3 PUFA, a higher ratio of n-6 to n-3 PUFA, a higher ratio of arachidonic acid (AA) to EPA, and lower serum total cholesterol levels (17–21).

The role of PUFA and cholesterol in the pathophysiology of affective disorders has been related to alterations in central nervous system (CNS) serotonergic neurotransmitter systems, membrane-bound receptor function, and enzymatic activity caused by disruption of neuronal membrane composition and structure (22–24). In addition, the immune system may play a role in the mechanism of action of PUFA in affective disorders (25,26).

Consequently, more knowledge of PUFA composition in d-IBS patients may have both pathophysiological and therapeutic implications. As IBS is associated with a high co-occurrence of affective dysregulation, and as affective disorders have been associated with specific changes in the PUFA and cholesterol profile, we hypothesized that in d-IBS similar changes may be present as have been reported in patients with affective disorders.

*To whom correspondence should be addressed at Maastricht University, Dept of Psychiatry and Neuropsychology (P&N), Dr. Tanslaan 10, Nivo 3, 6229 ET, Maastricht, The Netherlands.
E-mail: T.Kilkens@pn.unimaas.nl

Abbreviations: AA, arachidonic acid; ALA, α-linolenic acid; BMI, body mass index; CNS, central nervous system; d-IBS, diarrhea-predominant irritable bowel syndrome (IBS); DPA, docosapentaenoic acid; HADS, Hospital Anxiety and Depression Rating Scale; HAM-D17, 17-item Hamilton Depression Rating Scale; IBD, inflammatory bowel disease; IBS, irritable bowel syndrome; LA, linoleic acid; MINI, Mini International Neuropsychiatric Interview; MUFA, monounsaturated fatty acids; Oba, Osbond acid; SAFA, saturated FA; SCL, Symptom Check List.

This exploratory study investigates: (i) the level of affective dysregulation in d-IBS patients and healthy controls; (ii) PUFA and cholesterol profiles in d-IBS patients compared with controls; and (iii) associations between PUFA and cholesterol parameters, respectively, and the level of affective dysregulation.

MATERIALS AND METHODS

Subjects. Patients were recruited from the outpatient Department of Gastroenterology of University Hospital Maastricht (Maastricht, The Netherlands). Healthy control subjects were enrolled *via* advertising in local papers. The Medical Ethics Committee of the University Hospital Maastricht approved the study protocol, and all subjects gave their written informed consent before the start of the study. The required number of subjects was based on results of other ongoing studies at our department and an estimated effect size of 0.9 (based on the standardized mean difference between postmyocardial infarction patients with co-morbid depression and postmyocardial infarction patients without co-morbid depression with respect to the AA/EPA ratio), with $\beta = 0.2$ and $\alpha = 0.05$ resulting in $n = 21$ per group. Patients fulfilled the diagnosis of d-IBS according to the ROME II criteria, as diagnosed by an experienced gastroenterologist (27). These diagnostic criteria for IBS are abdominal discomfort or pain for at least 12 wk, which need not be consecutive, in the preceding 12 mon that has two out of three features: (i) relieved with defecation; and/or (ii) onset associated with a change in frequency of stool; and/or (iii) onset associated with a change in form of stool in absence of structural or metabolic abnormalities to explain symptoms. Additional criteria for d-IBS are more than three bowel movements a day or loose/watery stools or urgency. Before participating in the study, all subjects were screened by a standardized psychiatric examination comprising the Mini International Neuropsychiatric Interview (MINI) to determine the present psychiatric state (28). The level of affective dysregulation was assessed by using the depression scale of the Symptom Check List (SCL-depression) (29), the Hospital Anxiety and Depression Rating Scale (HADS) (30), and the 17-item Hamilton Depression Rating Scale (HAM-D17) (31). Physical health was assessed by means of a standard physical examination and urine test. A pregnancy test was performed on all female subjects. Exclusion criteria were abdominal surgery, use of medications other than oral contraceptives within 14 d before testing, lactose malabsorption (using the H_2-breath test) (32,33), a positive first-degree psychiatric family history (34), any history of psychiatric disease or use of psychoactive medication, premenstrual syndrome, dieting, pregnancy or lactation, excessive alcohol intake (>20 alcoholic consumptions a week), and hypertension (diastolic >100 mm Hg, systolic >170 mm Hg), respectively. For the control subjects, the same exclusion criteria applied as those for the patients. Additional exclusion criteria for the control subjects were current or history of gastrointestinal disorder, current psychiatric or psychological symptomatology defined as: a diagnosis on the MINI, SCL-depression score for females equal to or above 28 and for males equal to or above 23, HADS scores equal to or above 8, and HAM-D17 scores above 18.

Design. To eliminate possible bias, all women were evaluated in the follicular phase of the menstrual cycle or while taking oral contraception. To exclude possible seasonal variation, the patient and corresponding matched control subject were evaluated within 3 mon time. They were asked to abstain from heavy physical exercise and consumption of alcoholic beverages the day before their visit. Subjects attended the laboratory after an overnight fast (after 10:00 PM, no eating, drinking, or smoking allowed) at 8:00 AM for blood collection.

Biochemical parameters. Blood for plasma PUFA determination was sampled in Vacutainer (K2E) tubes and was immediately placed on ice. Blood for serum cholesterol was sampled in Vacutainer (SST) tubes. All samples were centrifuged within 30 min (10 min, $900 \times g$, 4°C) and stored at −80°C until analysis. PUFA samples were preserved from oxidation by blanketing them with nitrogen (35). Samples were analyzed blind as to subject status in a single run. Plasma phospholipid concentrations were determined, after isolation from plasma, as FAME. To 100 μL of plasma, 300 μL of 1% EDTA and 50 μL of internal standard were added (620 mg/L 1,2-dinonadecanoyl-*sn*-glycero-3-phosphocholine (Avanti Polar, Alabaster, AL); to all solutions BHT was added as an antioxidant. Total lipids were extracted from plasma with a modified extraction according to Folch *et al.* (36). The phospholipid fraction was isolated by multiple solid-phase extraction (Bond Elut aminopropyl bonded silica columns 3 mL, 500 mg; Varian, Palo Alto, CA) as described previously (37). Phospholipids were hydrolyzed, and the resulting FA converted to methyl esters with boron trifluoride/methanol (14%). The FAME were determined by a gas chromatograph with FID (HP5890 series II; Hewlett-Packard, Palo Alto, CA) with a dual capillary column technique for optimal separation of *cis*- and *trans*-FAME (BP1 50 m × 0.22 mm, i.d. 0.1 μm, BPX70 50 m × 0.22 mm, i.d. 0.25 μm; SGE, Melbourne, Australia). Serum total cholesterol, HDL cholesterol (HDL-C), and LDL cholesterol (LDL-C) were measured by a commercially available colorimetric assay (Beckman Synchron LX20 systems, Fullerton, CA).

Statistical analyses. Group differences (IBS vs. control) in demographic data were analyzed using independent *t*-tests. PUFA profile was the primary outcome parameter consisting of three FA outcome parameters (total n-3 PUFA, ratio of n-6 to n-3 PUFA, and ratio of AA to EPA). The secondary outcome parameter was cholesterol profile (serum total cholesterol, HDL-C, and LDL-C). Group differences in outcome parameters were assessed by means of two multivariate ANOVA (one for FA parameters, one for cholesterol parameters). Associations between outcome parameters with level of affective dysregulation as indicated by SCL-depression, HADS, and HAM-D17 scores, respectively, were analyzed by linear regression. Cook's distance was used to identify possible influential cases according to the lines described by Hair (38). Data are presented as mean ± SEM. Two-tailed *P*-values ≤ 0.05 were considered statistically significant. Statistical analyses were performed

TABLE 1
Demographic Data of Patients with Irritable Bowel Syndrome (IBS) and Healthy Matched Controls (mean ± SEM)

	IBS (n = 23)	Controls (n = 23)	Patients vs. controls[a] P value
Females (n)	14/23	14/23	
Oral contraceptives (n)	11/14	11/14	
Males (n)	9/23	9/23	
Age	32.9 ± 2.3	28.6 ± 3.3	0.3
Body mass index	23.1 ± 0.9	22.7 ± 0.5	0.7
Alcohol units/d	1.12 ± 0.6	0.53 ± 0.1	0.4
Cigarettes/d	2.10 ± 0.8	1.27 ± 0.7	0.4
Diagnosis on MINI	7[b]	0	—
SCL-depression	20.5 ± 1.2	17.3 ± 0.5	0.02
HADS	6.22 ± 0.7	3.17 ± 0.6	0.002
HAM-D17	4.2 ± 0.8	0.83 ± 0.2	<0.001

[a]Independent samples t-test comparing IBS patients vs. control subjects.
[b]Seven subjects had a psychiatric diagnosis: depression (n = 2), agoraphobia (n = 3), social phobia (n = 2), and anxiety disorder (n = 2), respectively. MINI, Mini International Neuropsychiatric Interview; HAM-D17, 17-item Hamilton Depression Rating Scale; SCL, Symptom Check List; HADS, Hospital Anxiety and Depression Rating Scale.

using the SPSS 10.0 for Windows software package (Chicago, IL).

RESULTS

Sample description. Table 1 summarizes characteristics of the 46 participants (23 patients and 23 healthy controls). No significant differences were found between the two groups with respect to sex, age, body mass index (BMI), contraceptive use, or alcohol and cigarette consumption ($P \geq 0.3$). Severity of affective dysregulation, as indicated by the SCL-depression, HADS, and HAM-D17 scores, was significantly higher in IBS patients than in healthy controls for all three parameters ($P \leq 0.02$).

FA profile of plasma phospholipids. The amounts of the various FA were expressed as weight percentages (wt%) of total FA as well as absolute concentrations (mg/L). In total, 35 FA were identified, but FA percentages <0.1% were not recorded; therefore, 26 FA were listed in Table 2. The following FA combinations were calculated: ΣSAFA (sum of all saturated FA),

TABLE 2
Descriptive (wt% of total FA[a] and absolute levels in mg/L) as Well as Outcome Parameters of FA Profile of Plasma Phospholipids in IBS Patients and Healthy Controls (mean ± SE)

	IBS (n = 23)		Controls (n = 23)	
	wt%	mg/L	wt%	mg/L
Total FA	—	1421 ± 46.4	—	1364 ± 47.5
14:0	0.33 ± 0.02	4.77 ± 0.33	0.31 ± 0.01	4.24 ± 0.29
15:0	0.18 ± 0.01	2.56 ± 0.16	0.19 ± 0.10	2.64 ± 0.13
16:0	29.3 ± 0.38	417 ± 15.1	29.3 ± 0.36	400 ± 16.2
17:0	0.32 ± 0.01	4.49 ± 0.19	0.34 ± 0.01	4.59 ± 0.14
18:0	12.4 ± 0.41	176 ± 8.49	12.0 ± 0.32	163 ± 5.65
20:0	0.47 ± 0.02	6.64 ± 0.23	0.50 ± 0.01	6.80 ± 0.29
22:0	1.47 ± 0.06	20.6 ± 0.83	1.54 ± 0.03	20.9 ± 0.68
23:0	0.59 ± 0.02	8.31 ± 0.26	0.67 ± 0.01	9.14 ± 0.34
24:0	1.26 ± 0.05	17.8 ± 0.73	1.36 ± 0.03	18.5 ± 0.66
16:1n-7	0.45 ± 0.03	6.45 ± 0.58	0.38 ± 0.04	5.33 ± 0.65
18:1n-7	1.69 ± 0.06	23.9 ± 1.13	1.63 ± 0.03	22.2 ± 0.92
18:1n-9	8.16 ± 0.26	117 ± 6.12	8.36 ± 0.24	114 ± 5.26
20:1n-9	0.15 ± 0.01	2.15 ± 0.13	0.16 ± 0.01	2.20 ± 0.15
20:3n-9	0.12 ± 0.01	1.67 ± 0.17	0.11 ± 0.01	1.53 ± 0.12
24:1n-9	2.06 ± 0.11	28.8 ± 1.12	2.09 ± 0.10	28.5 ± 1.44
18:2n-6 (LA)	21.0 ± 0.54	297 ± 11.0	22.0 ± 0.53	292 ± 9.92
20:2n-6	0.36 ± 0.02	5.13 ± 0.27	0.37 ± 0.01	5.12 ± 0.29
20:3n-6	3.04 ± 0.13	43.9 ± 2.77	3.03 ± 0.14	41.8 ± 2.70
20:4n-6 (AA)	8.93 ± 0.35	127 ± 6.52	8.43 ± 0.28	116 ± 6.55
22:4n-6	0.32 ± 0.02	4.48 ± 0.32	0.30 ± 0.01	4.01 ± 0.17
22:5n-6 (Oba)	0.19 ± 0.01	2.77 ± 0.22	0.20 ± 0.02	2.71 ± 0.27
24:2n-6	0.24 ± 0.01	3.34 ± 0.19	0.24 ± 0.01	3.34 ± 0.18
18:3n-3 (ALA)	0.23 ± 0.02	3.23 ± 0.26	0.21 ± 0.01	2.91 ± 0.18
20:5n-3 (EPA)	0.79 ± 0.13	11.4 ± 2.00	0.64 ± 0.06	8.78 ± 0.90
22:5n-3 (DPA)	0.77 ± 0.06	11.0 ± 1.00	0.72 ± 0.05	10.0 ± 0.60
22:6n-3 (DHA)	3.10 ± 0.15	43.4 ± 2.43	3.13 ± 0.13	43.2 ± 2.94
ΣSAFA	46.3 ± 0.26	659 ± 21.9	46.2 ± 0.21	631 ± 21.4
ΣMUFA	12.5 ± 0.29	178 ± 7.60	12.7 ± 0.27	173 ± 7.42
ΣPUFA	39.0 ± 0.32	554 ± 17.8	38.9 ± 0.36	531 ± 19.3
Σn-6	34.1 ± 0.41	483 ± 15.5	34.2 ± 0.42	465 ± 16.4
Outcome parameters				
Σn-3	4.92 ± 0.24	69.0 ± 4.29	4.77 ± 0.19	64.5 ± 3.91
Σn-6/Σn-3	7.35 ± 0.43	7.48 ± 0.43	7.42 ± 0.33	7.56 ± 0.34
AA/EPA	16.8 ± 2.18	16.8 ± 2.17	16.3 ± 2.00	16.3 ± 2.02

[a]AA, arachidonic acid; ALA, α-linolenic acid; DPA, docosapentaenoic acid; LA, linoleic acid; Oba, Osbond acid; ΣSAFA, sum of all saturated FA; ΣMUFA, sum of all monounsaturated FA; ΣPUFA, sum of all PUFA; Σn-6, sum of all n-6 PUFA; Σn-3, sum of all n-3 PUFA; for other abbreviation see Table 1.

TABLE 3
Serum Total Cholesterol, HDL Cholesterol (HDL-C) and LDL Cholesterol (LDL-C) in IBS[a] Patients and Healthy Controls (mean ± SE)

	IBS (n = 23)	Controls (n = 23)
Total cholesterol (mmol/L)	5.13 ± 0.18	5.09 ± 0.19
HDL-C (mmol/L)	1.09 ± 0.07	1.22 ± 0.08
LDL-C (mmol/L)	3.31 ± 0.17	3.39 ± 0.18

[a]For abbreviation see Table 1.

ΣMUFA (sum of all monounsaturated FA), ΣPUFA (sum of all PUFA), Σn-6 PUFA, Σn-3 PUFA, ratio of n-6 to n-3 PUFA, and ratio of AA to EPA (20:4n-6/20:5-n3).

PUFA and cholesterol profile. In Table 2 the FA outcome parameters and in Table 3 the cholesterol parameters are listed. As can be seen in these tables, there was no difference in outcome parameters between subject groups. Multivariate analyses did not show a significant difference in total n-3 PUFA, ratio of n-6 to n-3 PUFA, and ratio of AA to EPA ($F_{(HOT)} = 0.4$, DF = 3.42, $P = 0.8$) nor in total cholesterol, HDL-C, and LDL-C between IBS patients and controls ($F_{(HOT)} = 1.8$, DF = 3.42, $P = 0.2$), with no univariate significance.

Associations between PUFA and total cholesterol with level of affective dysregulation. Total n-3 PUFA tended to be significantly negatively associated with SCL-depression scores ($F = 3.5$, $P = 0.07$, $R^2 = 0.07$). Cook's distance analyses showed that the regression model was unstable as indicated by two large Cook's measures; subsequently, these two cases (2 patients) were excluded. After removal of these two cases, total n-3 PUFA was significantly negatively associated with SCL-depression scores ($F = 8.6$, $P = 0.006$, $R^2 = 0.18$). Total n-3 PUFA tended to be negatively associated with HADS scores ($F = 3.5$, $P = 0.06$, $R^2 = 0.08$). The ratio n-6 to n-3 PUFA was significantly positively associated with SCL-depression scores ($F = 11.9$, $P = 0.002$, $R^2 = 0.22$) and HADS scores ($F = 4.8$, $P = 0.03$, $R^2 = 0.11$). The ratio of AA to EPA was significantly positively associated with SCL-depression scores ($F = 12.9$, $P = 0.002$, $R^2 = 0.24$). Total serum cholesterol was significantly negatively associated with SCL-depression scores ($F = 7.6$, $P = 0.005$, $R^2 = 0.15$). PUFA and cholesterol profile were not significantly associated with Hamilton scores ($P > 0.2$). As an example, Figure 1 illustrates the associations between total n-3 PUFA and ratio of AA to EPA with SCL-depression scores.

DISCUSSION

The patient group demonstrated a higher level of affective dysregulation compared with the control group but did not differ in PUFA and cholesterol profiles. However, total n-3 PUFA and cholesterol were significantly negatively associated and the ratio of n-6 to n-3 PUFA as well as the ratio of AA to EPA were significantly positively associated with level of affective dysregulation, respectively.

To our knowledge no previous studies have determined possible changes in PUFA profile in IBS patients compared with healthy matched controls. IBS patients had increased levels of affective dysregulation, and PUFA and cholesterol profiles were significantly associated with affective dysregulation. However, we did not show differences in PUFA and cholesterol indices between IBS patients and controls, as have been reported in patients with affective disorders. This may be explained by the fact that the level of affective dysregulation in our IBS patients was attenuated compared with that of patients primarily presenting with affective disorders. In addition, we chose to study the d-IBS type of IBS, because classification into subtypes appears to reflect physiological differences between each type (39,40); and we excluded patients with a previous psychiatric diagnosis or first-degree family history of affective disorders (41). As a result, failure to identify group differences may be due to inclusion bias and a type II error. Future studies could include a larger cohort of IBS patients that are followed over time.

At present, it is unclear whether changes in PUFA profile are state markers, i.e., only present during an illness episode,

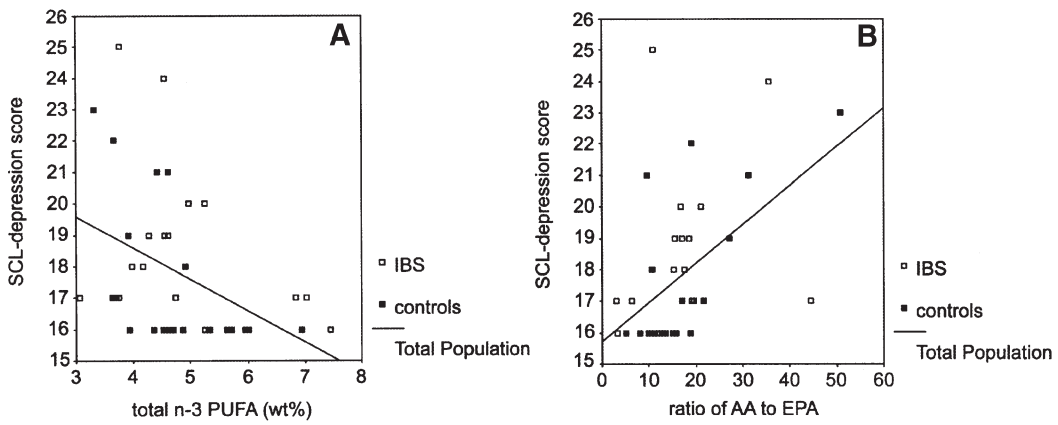

FIG. 1. Associations between (A) total percentage n-3 PUFA in phospholipids (wt% of total FA) and (B) ratio of arachidonic acid (AA) to EPA with level of affective dysregulation as indicated by the Symptom Check List (SCL) depression score. IBS, irritable bowel syndrome.

or trait markers, i.e., also present in symptom-free episodes and in those subjects at risk of affective dysregulation. Alterations in PUFA profile have been reported in symptom-free first-degree relatives of patients with affective disorders who did not have a previous or current psychiatric diagnosis (41). Our findings indicate that an association between PUFA profile and affective dysregulation is also present in a population with a low level of affective dysregulation and without a previous psychiatric diagnosis or first-degree family history of affective disorders. Serotonergic modulators are used in the treatment of both affective disorders and IBS, and it has been shown that serotonin is a mediator of brain–gut responses (11,42,43). In addition, changes in PUFA are associated with parameters of central serotonergic activity (23,41,44). Whether these findings indicate a role for PUFA profile as a metabolic mediator in the brain–gut interaction remains to be elucidated.

In addition to the role of PUFA in serotonergic neurotransmitter systems, PUFA are the precursors of eicosanoids (prostaglandins, thromboxanes, prostacyclines, and leukotrienes), which participate in the regulation of immunological and inflammatory responses (45). Supplementation with n-3 PUFA leads to the production of eicosanoids with attenuated inflammatory effects in comparison with those produced from n-6 PUFA (46). Interestingly, co-administration of n-3 PUFA has been reported to improve affective dysregulation in major depressive disorder (47–49).

IBS has always been considered a functional gastrointestinal disorder without any signs of structural or metabolic abnormalities, such as inflammation of the gut wall. However, the observations that d-IBS may be precipitated by an acute enteric infection and that some d-IBS patients have an increased number of inflammatory cells in the intestinal mucosa have recently prompted consideration of inflammation as a putative basis for symptom generation in d-IBS (50–52). In this regard, d-IBS may follow a pattern of pathogenesis similar to other chronic relapsing inflammatory disorders such as rheumatoid arthritis and chronic obstructive pulmonary disease. Dietary supplements of n-3 PUFA have been reported as beneficial in the treatment of many inflammatory conditions, i.e., inflammatory bowel disease (IBD: Crohn's disease and ulcerative colitis), eczema, psoriasis, and rheumatoid arthritis (53,54).

Although not the aim of our study, comparison of the functional bowel disorder IBS with IBD with respect to the influence of PUFA on the pathophysiological processes and course of the diseases is challenging. In both disorders the brain–gut axis seems to play an important role in the pathophysiology (55,56). The role of the brain–gut axis, however, has been far better established in IBS than IBD. On the other hand, the role of inflammation, even at a systemic level, is much more pronounced in IBD with regard to the pathophysiology and generation of symptoms. Regarding future research, it would be interesting to obtain intestinal biopsies in IBS patients in order to subdivide IBS patients into groups with and without signs of intestinal inflammation and to study the relation with PUFA profile and affective dysregulation (57).

Examination of the data concerning an association between n-3 PUFA and SCL-depression scores revealed two outliers. Because of the relatively small number of subjects and the strong influence of these two patients' scores on the regression model, we considered the model without the two outliers to be a better estimation of the association between total n-3 PUFA and SCL-depression scores (58). Potential confounders are not expected to explain our findings. IBS patients were successfully matched to controls with respect to age, gender, BMI, alcohol consumption, smoking behavior, menstrual cycle phase, and contraception. As we did not assess dietary fat intake, we cannot exclude that the quantitative and qualitative intake in IBS patients differed from that in the controls (59). However, we screened all subjects for cholesterol-restricted or weight-reducing diets. In addition, patients were screened for the presence of possible lactose malabsorption, which has been associated with symptoms identical to d-IBS as well as with signs of mental depression and could be associated with malabsorption of relevant nutrients (33). Furthermore, the absolute FA concentrations as well as the percentages of linoleic acid and α-linolenic acid, the precursors of the n-6 and n-3 PUFA series, did not significantly differ between patients and controls, which suggests no difference in intake, intestinal absorption, or synthesis between patients and controls.

In conclusion, the findings of the present study revealed that affective dysregulation was higher in IBS patients compared with healthy controls and that changes in PUFA and cholesterol profile were significantly associated with affective dysregulation. These results warrant further studies regarding the role of PUFA and cholesterol status in the co-occurrence of affective dysregulation and functional gastrointestinal disorders.

ACKNOWLEDGMENT

We thank the University Hospital Maastricht for a support grant.

REFERENCES

1. Talley, N.J., and Spiller, R. (2002) Irritable Bowel Syndrome: A Little Understood Organic Bowel Disease? *Lancet 360*, 555–564.
2. Thompson, W.G., Longstreth, G.F., Drossman, D.A., Heaton, K.W., Irvine, E.J., and Muller-Lissner, S.A. (1999) Functional Bowel Disorders and Functional Abdominal Pain, *Gut 45* (Suppl. 2), II43–II47.
3. El-Serag, H.B., Olden, K., and Bjorkman, D. (2002) Health-Related Quality of Life Among Persons with Irritable Bowel Syndrome: A Systematic Review, *Aliment. Pharmacol. Ther. 16*, 1171–1185.
4. Sandler, R.S., Everhart, J.E., Donowitz, M., Adams, E., Cronin, K., Goodman, C., Gemmen, E., Shah, S., Avdic, A., and Rubin, R. (2002) The Burden of Selected Digestive Diseases in the United States, *Gastroenterology 122*, 1500–1511.
5. Mayer, E.A. (1999) Emerging Disease Model for Functional Gastrointestinal Disorders, *Am. J. Med. 107*, 12S–19S.
6. Mayer, E.A., and Gebhart, G.F. (1994) Basic and Clinical Aspects of Visceral Hyperalgesia [see Comments], *Gastroenterology 107*, 271–293.
7. Noyes, R., Jr., Cook, B., Garvey, M., and Summers, R. (1990)

Reduction of Gastrointestinal Symptoms Following Treatment for Panic Disorder, *Psychosomatics 31*, 75–79.
8. Ford, M.J., Miller, P.M., Eastwood, J., and Eastwood, M.A. (1987) Life Events, Psychiatric Illness and the Irritable Bowel Syndrome, *Gut 28*, 160–165.
9. Walker, E.A., Roy-Byrne, P.P., and Katon, W.J. (1990) Irritable Bowel Syndrome and Psychiatric Illness, *Am. J. Psychiatry 147*, 565–572.
10. Lydiard, R.B., Fossey, M.D., Marsh, W., and Ballenger, J.C. (1993) Prevalence of Psychiatric Disorders in Patients with Irritable Bowel Syndrome, *Psychosomatics 34*, 229–234.
11. Kilkens, T.O., Honig, A., Rozendaal, N., Van Nieuwenhoven, M.A., and Brummer, R.J. (2003) Serotonergic Modulators in the Treatment of Irritable Bowel Syndrome—Influence on Psychiatric and Gastrointestinal Symptoms, *Aliment. Pharmacol. Ther. 17*, 43–51.
12. Houghton, L.A., Atkinson, W., Whitaker, R.P., Whorwell, P.J., and Rimmer, M.J. (2003) Increased Platelet Depleted Plasma 5-Hydroxytryptamine Concentration Following Meal Ingestion in Symptomatic Female Subjects with Diarrhœa Predominant Irritable Bowel Syndrome, *Gut 52*, 663–670.
13. Singh, R.K., Pandey, H.P., and Singh, R.H. (2003) Correlation of Serotonin and Monoamine Oxidase Levels with Anxiety Level in Diarrhea-Predominant Irritable Bowel Syndrome, *Indian J. Gastroenterol. 22*, 88–90.
14. Camilleri, M., Northcutt, A.R., Kong, S., Dukes, G.E., McSorley, D., and Mangel, A.W. (2000) Efficacy and Safety of Alosetron in Women with Irritable Bowel Syndrome: A Randomised, Placebo-Controlled Trial [see Comments], *Lancet 355*, 1035–1040.
15. Walker, E.A., Roy-Byrne, P.P., Katon, W.J., Li, L., Amos, D., and Jiranek, G. (1990) Psychiatric Illness and Irritable Bowel Syndrome: A Comparison with Inflammatory Bowel Disease, *Am. J. Psychiatry 147*, 1656–1661.
16. Fock, K.M., Chew, C.N., Tay, L.K., Peh, L.H., Chan, S., and Pang, E.P. (2001) Psychiatric Illness, Personality Traits and the Irritable Bowel Syndrome, *Ann. Acad. Med. Singapore 30*, 611–614.
17. Maes, M., Smith, R., Christophe, A., Cosyns, P., Desnyder, R., and Meltzer, H. (1996) Fatty Acid Composition in Major Depression: Decreased ω3 Fractions in Cholesteryl Esters and Increased C20:4ω6/C20:5ω3 Ratio in Cholesteryl Esters and Phospholipids, *J. Affect. Disord. 38*, 35–46.
18. Hibbeln, J.R., Umhau, J.C., Linnoila, M., George, D.T., Ragan, P.W., Shoaf, S.E., Vaughan, M.R., Rawlings, R., and Salem, N., Jr. (1998) A Replication Study of Violent and Nonviolent Subjects: Cerebrospinal Fluid Metabolites of Serotonin and Dopamine Are Predicted by Plasma Essential Fatty Acids, *Biol. Psychiatry 44*, 243–249.
19. Adams, P.B., Lawson, S., Sanigorski, A., and Sinclair, A.J. (1996) Arachidonic Acid to Eicosapentaenoic Acid Ratio in Blood Correlates Positively with Clinical Symptoms of Depression, *Lipids 31* (Suppl.), S157–S161.
20. Freeman, M.P. (2000) Omega-3 Fatty Acids in Psychiatry: A Review, *Ann. Clin. Psychiatry 12*, 159–165.
21. Morgan, R.E., Palinkas, L.A., Barrett-Connor, E.L., and Wingard, D.L. (1993) Plasma Cholesterol and Depressive Symptoms in Older Men, *Lancet 341*, 75–79.
22. Hibbeln, J.R., and Salem, N., Jr. (1995) Dietary Polyunsaturated Fatty Acids and Depression: When Cholesterol Does Not Satisfy, *Am. J. Clin. Nutr. 62*, 1–9.
23. Hibbeln, J.R., Linnoila, M., Umhau, J.C., Rawlings, R., George, D.T., and Salem, N., Jr. (1998) Essential Fatty Acids Predict Metabolites of Serotonin and Dopamine in Cerebrospinal Fluid Among Healthy Control Subjects, and Early- and Late-Onset Alcoholics, *Biol. Psychiatry 44*, 235–242.
24. Chalon, S., Vancassel, S., Zimmer, L., Guilloteau, D., and Durand, G. (2001) Polyunsaturated Fatty Acids and Cerebral Function: Focus on Monoaminergic Neurotransmission, *Lipids 36*, 937–944.
25. Horrobin, D.F., and Bennett, C.N. (1999) Depression and Bipolar Disorder: Relationships to Impaired Fatty Acid and Phospholipid Metabolism and to Diabetes, Cardiovascular Disease, Immunological Abnormalities, Cancer, Ageing and Osteoporosis. Possible Candidate Genes, *Prostaglandins Leukot. Essent. Fatty Acids 60*, 217–234.
26. Maes, M., Christophe, A., Delanghe, J., Altamura, C., Neels, H., and Meltzer, H.Y. (1999) Lowered ω3 Polyunsaturated Fatty Acids in Serum Phospholipids and Cholesteryl Esters of Depressed Patients, *Psychiatry Res. 85*, 275–291.
27. Drossman, D.A., Heaton, K., Irvine, E.J., and Muller-Lissner, S. (2000) Functional Bowel Disorders and Functional Abdominal Pain, in *The Functional Gastrointestinal Disorders. Diagnosis, Pathophysiology, and Treatment: A Multinational Consensus* (Drossman, D.A., Corazziari, E., Talley, N., Thompson, W.G., and Whitehead, W.E., eds.), pp. 351–398, Degnon Associates, McLean, VA.
28. Sheehan, D. (1994) *MINI International Neuropsychiatric Interview*, University of South Florida, Tampa.
29. Arrindell, W.A., and Ettema, J.H.M. (1986) *SCL-90. Een multidimensionale psychopathologie indicator [SCL-90. A Multidimensional Indicator of Psychopathology]*, Swets & Zeitlinger, Lisse, The Netherlands.
30. Mykletun, A., Stordal, E., and Dahl, A.A. (2001) Hospital Anxiety and Depression (HAD) Scale: Factor Structure, Item Analyses and Internal Consistency in a Large Population, *Br. J. Psychiatry 179*, 540–544.
31. Hamilton, M. (1967) Development of a Rating Scale for Primary Depressive Illness, *Br. J. Soc. Clin. Psychol. 6*, 278–296.
32. Hermans, M.M., Brummer, R.J., Ruijgers, A.M., and Stockbrugger, R.W. (1997) The Relationship Between Lactose Tolerance Test Results and Symptoms of Lactose Intolerance, *Am. J. Gastroenterol. 92*, 981–984.
33. Ledochowski, M., Sperner-Unterweger, B., and Fuchs, D. (1998) Lactose Malabsorption Is Associated with Early Signs of Mental Depression in Females: A Preliminary Report, *Dig. Dis. Sci. 43*, 2513–2517.
34. Sobczak, S., Riedel, W.J., Booij, I., Aan Het Rot, M., Deutz, N.E., and Honig, A. (2002) Cognition Following Acute Tryptophan Depletion: Difference Between First-Degree Relatives of Bipolar Disorder Patients and Matched Healthy Control Volunteers, *Psychol. Med. 32*, 503–515.
35. Zeleniuch-Jacquotte, A., Chajes, V., Van Kappel, A.L., Riboli, E., and Toniolo, P. (2000) Reliability of Fatty Acid Composition in Human Serum Phospholipids, *Eur. J. Clin. Nutr. 54*, 367–372.
36. Folch, J., Lees, M., and Sloane Stanley, G.H. (1957) A Simple Method for the Isolation and Purification of Total Lipides from Animal Tissues, *J. Biol. Chem. 226*, 497–509.
37. Kaluzny, M.A., Duncan, L.A., Merritt, M.V., and Epps, D.E. (1985) Rapid Separation of Lipid Classes in High Yield and Purity Using Bonded Phase Columns, *J. Lipid Res. 26*, 135–140.
38. Hair, J.F. (1998) *Multivariate Data Analysis*, Prentice Hall, Upper Saddle River, NJ.
39. Prior, A., Maxton, D.G., and Whorwell, P.J. (1990) Anorectal Manometry in Irritable Bowel Syndrome: Differences Between Diarrhœa and Constipation Predominant Subjects, *Gut 31*, 458–462.
40. Elsenbruch, S., and Orr, W.C. (2001) Diarrhea- and Constipation-Predominant IBS Patients Differ in Postprandial Autonomic and Cortisol Responses, *Am. J. Gastroenterol. 96*, 460–466.
41. Sobczak, S., Honig, A., Christophe, A., Maes, M., Helsdingen, R.W., De Vriese, S.A., and Riedel, W.J. (2004) Lower High-Density Lipoprotein Cholesterol and Increased Omega-6

Polyunsaturated Fatty Acids in First-Degree Relatives of Bipolar Patients, *Psychol. Med. 34*, 103–112.
42. Kilkens, T.O.C., Honig, A., Van Nieuwenhoven, M.A., Riedel, W.J., and Brummer, R.-J.M. Acute Tryptophan Depletion Affects Brain–Gut Responses in IBS and Controls, *Gut*, in press.
43. Kim, D.Y., and Camilleri, M. (2000) Serotonin: A Mediator of the Brain–Gut Connection, *Am. J. Gastroenterol. 95*, 2698–2709.
44. Kodas, E., Galineau, L., Bodard, S., Vancassel, S., Guilloteau, D., Besnard, J.C., and Chalon, S. (2004) Serotoninergic Neurotransmission Is Affected by n-3 Polyunsaturated Fatty Acids in the Rat, *J. Neurochem. 89*, 695–702.
45. Calder, P.C. (2001) Polyunsaturated Fatty Acids, Inflammation, and Immunity, *Lipids 36*, 1007–1024.
46. Calder, P.C. (2003) n-3 Polyunsaturated Fatty Acids and Inflammation: From Molecular Biology to the Clinic, *Lipids 38*, 343–352.
47. Su, K.P., Huang, S.Y., Chiu, C.C., and Shen, W.W. (2003) Omega-3 Fatty Acids in Major Depressive Disorder. A Preliminary Double-Blind, Placebo-Controlled Trial, *Eur. Neuropsychopharmacol. 13*, 267–271.
48. Puri, B.K., Counsell, S.J., Richardson, A.J., and Horrobin, D.F. (2002) Eicosapentaenoic Acid in Treatment-Resistant Depression, *Arch. Gen. Psychiatry 59*, 91–92.
49. Peet, M., and Horrobin, D.F. (2002) A Dose-Ranging Exploratory Study of the Effects of Ethyl-Eicosapentaenoate in Patients with Persistent Schizophrenic Symptoms, *J. Psychiatr. Res. 36*, 7–18.
50. Collins, S.M., Piche, T., and Rampal, P. (2001) The Putative Role of Inflammation in the Irritable Bowel Syndrome, *Gut 49*, 743–745.
51. Barbara, G., De Giorgio, R., Stanghellini, V., Cremon, C., and Corinaldesi, R. (2002) A Role for Inflammation in Irritable Bowel Syndrome? *Gut 51* (Suppl. 1), i41–i44.
52. Spiller, R.C. (2003) Postinfectious Irritable Bowel Syndrome, *Gastroenterology 124*, 1662–1671.
53. Gil, A. (2002) Polyunsaturated Fatty Acids and Inflammatory Diseases, *Biomed. Pharmacother. 56*, 388–396.
54. Geerling, B.J., v Houwelingen, A.C., Badart-Smook, A., Stockbrugger, R.W., and Brummer, R.J. (1999) Fat Intake and Fatty Acid Profile in Plasma Phospholipids and Adipose Tissue in Patients with Crohn's Disease, Compared with Controls, *Am. J. Gastroenterol. 94*, 410–417.
55. Hollander, D. (2003) Inflammatory Bowel Diseases and Brain–Gut Axis, *J. Physiol. Pharmacol. 54* (Suppl. 4), 183–190.
56. Mertz, H.R. (2003) Overview of Functional Gastrointestinal Disorders: Dysfunction of the Brain–Gut Axis, *Gastroenterol. Clin. North Am. 32*, 463–476.
57. Dunlop, S.P., Jenkins, D., Neal, K.R., and Spiller, R.C. (2003) Relative Importance of Enterochromaffin Cell Hyperplasia, Anxiety, and Depression in Postinfectious IBS, *Gastroenterology 125*, 1651–1659.
58. Cohen, J., and Cohen, P. (1983) *Applied Multiple Regression/Correlation Analyses for the Behavioral Sciences*, Erlbaum, Hillsdale, NJ.
59. Arab, L. (2003) Biomarkers of Fat and Fatty Acid Intake, *J. Nutr. 133* (Suppl. 3), 925S–932S.

[Received March 31, 2004; accepted June 18, 2004]

Low Concentration of Oxidized Low Density Lipoprotein Suppresses Platelet Reactivity *in vitro*: An Intracellular Study

Duen-Suey Chou[a,b], George Hsiao[b], Ming-Yi Shen[a], Tsorng-Harn Fong[a], Chien-Huang Lin[a], Tzeng-Fu Chen[b], and Joen-Rong Sheu[a,b,*]

Graduate Institutes of [a]Medical Sciences and [b]Pharmacology, Taipei Medical University, Taipei 110, Taiwan

ABSTRACT: The intracellular mechanisms underlying oxidized low density lipoprotein (oxLDL)-signaling pathways in platelets remain obscure and findings have been controversial. Therefore, we examined the influence of oxLDL in washed human platelets. In this study, oxLDL concentration-dependently (20–100 μg/mL) inhibited platelet aggregation in human platelets stimulated by collagen (1 μg/mL) and arachidonic acid (60 μM), but not by thrombin (0.02 U/mL). The activity of oxLDL was greater at 24 h in inhibiting platelet aggregation than at 12 h. At 24 h, oxLDL concentration-dependently inhibited intracellular Ca^{2+} mobilization and thromboxane B_2 formation in human platelets stimulated by collagen. In addition, at 24 h oxLDL (40 and 80 μg/mL) significantly increased the formation of cyclic AMP, but not cyclic GMP or nitrate. In an ESR study, 24 h-oxLDL (40 μg/mL) markedly reduced the ESR signal intensity of hydroxyl radicals ($OH^{\cdot-}$) in both collagen (2 μg/mL)-activated platelets and Fenton reaction (H_2O_2 + Fe^{2+}). The inhibitory effect of oxLDL may induce radical–radical termination reactions by oxLDL-derived lipid radical interactions with free radicals (such as hydroxyl radicals) released from activated platelets, with a resultant lowering of intracellular Ca^{2+} mobilization, followed by inhibition of thromboxane A_2 formation, thereby leading to increased cyclic AMP formation and finally inhibited platelet aggregation. This study provides new insights concerning the effect of oxLDL in platelet aggregation.

Paper no. L9421 in *Lipids 39,* 433–440 (May 2004).

The oxidation theory of atherosclerosis proposes that formation of oxidized LDL (oxLDL) in the subendothelial space of artery walls represents a causative event for atherogenesis. Evidence from oxidized lipoproteins has been detected in atherosclerotic lesions (1), and oxLDL exhibits various proatherogenic activities (2). Macrophage cholesterol accumulation and foam cell formation is a hallmark of atherogenesis (3). Platelets interact with plasma lipoprotein as well as with arterial wall macrophages that play an important role in atherogenesis (4). Plasma lipoproteins have been shown to affect platelet activity *in vitro* and *in vivo*. The susceptibility of platelets to aggregation *in vitro* on stimulation by aggregating agents, such as ADP and collagen, has been shown to increase in most, but not all, studies of platelet-rich plasma (PRP) from hypercholesterolemic individuals (5).

Oxidation of LDL may be one of the main factors involved in the initial development of atherosclerotic lesions (1). LDL can be oxidized within the arterial wall by macrophages; this process, which favors the accumulation of LDL in the intima of the arterial wall, is thought to be a possible explanation for the progression of arteriosclerotic lesions. Endothelial cells also induce oxLDL formation, but in turn may be damaged by oxLDL (1). LDL has been suggested to have platelet-activating properties such as decreasing the threshold for stimulation by aggregation agents and inducing platelet aggregation (6,7). However, evidence regarding the induction of platelet activation by LDL is controversial. Several studies have reported the inhibition of agonist-induced platelet aggregation by native LDL (nLDL) (8,9). In others, platelet-activating effects of either lower nLDL (10–50 μg/mL) (10) or higher concentrations of LDL (more than 1–2 mg/mL) have been described (7). Furthermore, platelet-activating activity was found to reside in oxLDL rather than in nLDL (11). oxLDL plays an important role in the pathogenesis of atherosclerosis; it also has been reported to enhance platelet activation in some (6,12), but not all, studies (13,14). Vlasova *et al.* (14) found that highly oxidized LDL not only failed to activate platelet aggregation but also inhibited ADP-induced aggregation. However, they also found that mildly oxidized LDL diminished the time-dependent decrease in platelet aggregability in PRP (15). Such discrepancies among reported oxLDL–platelet interactions may depend on methodological variations in the isolation, oxidization, and dosage of lipoproteins employed, which might result in nonhomogeneous oxidation (8).

In this study, we found that oxLDL (LDL oxidized with copper), at lower concentrations (40–80 μg/mL), significantly inhibited agonist-induced platelet aggregation. However, the detailed intracellular mechanisms underlying oxLDL–platelet interaction still remain obscure. We therefore systemically examined the influence of oxLDL in washed human platelets and utilized the findings to characterize the mechanisms involved in this influence.

MATERIALS AND METHODS

Materials. Collagen (Type I, bovine achilles tendon), arachidonic acid (AA), sodium citrate, luciferin-luciferase,

*To whom correspondence should be addressed at Graduate Institute of Medical Sciences, Taipei Medical University, No. 250, Wu-Hsing St., Taipei 110, Taiwan. E-mail: sheujr@tmu.edu.tw

Abbreviations: 12h-oxLDL, 12-h oxidized LDL; 24h-oxLDL, 24-h oxidized LDL; AA, arachidonic acid; $[Ca^{2+}]i$, concentration of inorganic calcium ion; DEPMPO, 5-diethoxyphosphoryl-5-methyl-1-pyrroline-*N*-oxide; DTS, dense tubular system; EIA, enzyme immunoassay; nLDL, native LDL; oxLDL, oxidized LDL; PGE_1, prostaglandin E_1; PLA_2, phospholipase A_2; PRP, platelet-rich plasma; TxA_2 and TxB_2, thromboxanes A_2 and B_2.

indomethacin, prostaglandin E_1 (PGE_1), nitroglycerin, apyrase, catalase, thrombin, BSA, and heparin were purchased from Sigma Chemical (St. Louis, MO). Fura 2-AM was purchased from Molecular Probe (Eugene, OR). DEPMPO (5-diethoxyphosphoryl-5-methyl-1-pyrroline-*N*-oxide) was purchased from OXIS (Portland, OR). Cyclic AMP, cyclic GMP, and thromboxane B_2 (TxB_2) enzyme immunoassay (EIA) kits were purchased from Cayman (Ann Arbor, MI).

Preparation of human platelet suspensions. Human platelet suspensions were prepared as previously described (16). In this study, human volunteers gave informed consent. In brief, blood was collected from healthy human volunteers who had taken no medicine during the preceding 2 wk and then mixed with an acid/citrate/glucose anticoagulant (9:1 blood/anticoagulant, vol/vol). After centrifugation at $120 \times g$ for 10 min at room temperature, the supernatant (PRP) was supplemented with PGE_1 (0.5 μM) and heparin (6.4 IU/mL), then incubated for 10 min at 30°C, and centrifuged at $500 \times g$ for 10 min. The washed platelets were finally suspended in Tyrode's solution containing BSA (3.5 mg/mL) and adjusted to a concentration of 4.5×10^8 platelets/mL. The final concentration of Ca^{2+} in Tyrode's solution was 1 mM.

Isolation of human plasma LDL. Human LDL (at a density of 1.109–1.063) was isolated from fresh plasma of fasted normolipidemic human volunteers collected in EDTA (2 mM) by sequential density gradient ultracentrifugation as described by Dousset *et al.* (17). In brief, plasma density was adjusted to 1.02 g/mL using a NaCl/KBr solution for immediate separation of VLDL and intermediate density lipoproteins, and then adjusted to 1.063 g/mL for the separation of LDL. The LDL was further purified by resuspension in the appropriate NaCl/KBr solution (1.063 g/mL) and ultracentrifuged. The LDL was then dialyzed for 24 h at 4°C against three changes of nitrogen-gassed 0.02 M Tris buffer to remove the EDTA and KBr. After dialysis, LDL was stored for not more than 7 d under nitrogen at 4°C in the dark. Total protein concentration was measured by the Lowry method using BSA as the standard (18).

Oxidation of LDL. After adjustment of the LDL concentration to 0.5 mg/mL (expressed as total LDL concentration), lipoprotein preparations were dialyzed against 100 vol of 10 mM sodium phosphate buffer (containing 150 mM NaCl, pH 7.4) for 18 h, at 4°C in the dark. Oxidation was initiated by addition of $CuSO_4$ (5 μM) for 12 and 24 h at 37°C, respectively, and was stopped after the addition of EDTA (20 μM). Before the functional studies, oxLDL was filtered through a Sephadex PD-10 column (Pharmacia, Uppsala, Sweden) to remove EDTA and copper and was reconcentrated at 4°C using Centricon 3000 filters (Amicon, Bedford, MA) according to the manufacturer's instructions. Oxidation was confirmed by the TBARS assay (19). Tetramethoxypropane was used as a standard, and the results were expressed as nanomoles of malondialdehyde equivalents per milligram protein of LDL. The extent of aldehyde-modified lysine in oxidized LDL (adjusted to 0.1 mg LDL protein/mL) was monitored by determining the fluorescence intensity (excitation at 350 nm, emission at 420 nm) (20). The 12-h (12h-oxLDL) and 24-h (24h-oxLDL) lipoproteins were used in all of the functional studies within 48 h of preparation.

Platelet aggregation. The turbidimetric method was applied to measure platelet aggregation (19), using a Lumi-Aggregometer (Payton, Ontario, Canada). Platelet suspensions (4.5×10^8 platelets/mL, 0.4 mL) were prewarmed to 37°C for 2 min (stirring at 1200 rpm) in a silicone-treated glass cuvette. oxLDL (20–100 μg/mL) was added 3 min before the addition of platelet-aggregation inducers. The reaction was allowed to proceed for at least 6 min, and the extent of aggregation was expressed in light-transmission units. When measuring ATP release, 20 μL of the luciferin/luciferase mixture was added 1 min before the addition of the agonists, and ATP release was compared with that of the control.

Measurement of platelet [Ca^{2+}]i mobilization by Fura 2-AM fluorescence. Citrated whole blood was centrifuged at $120 \times g$ for 10 min. The supernatant was protected from light and incubated with Fura 2-AM (5 μM) at 37°C for 1 h. Human platelets were then prepared as described above. Finally, the external Ca^{2+} concentration of the platelet suspensions was adjusted to 1 mM. The rise in [Ca^{2+}]i was measured using a fluorescence spectrophotometer (CAF 110; JASCO, Tokyo, Japan) at excitation wavelengths of 340 and 380 nm, and an emission wavelength of 500 nm. [Ca^{2+}]i was calculated from the fluorescence, using 224 nM as the Ca^{2+}-Fura 2 dissociation constant (21).

Measurement of TxB_2 formation. Washed human platelet suspensions (4.5×10^8/mL) were preincubated for 3 min in the absence or presence of oxLDL (40 and 80 μg/mL) before the addition of collagen (1 μg/mL). Six minutes after the addition of the agonist, 2 mM EDTA and 50 μM indomethacin were added to the reaction suspensions. The vials were then centrifuged for 3 min at $15{,}000 \times g$. The TxB_2 levels of the supernatants were measured using an EIA kit (Cayman) according to the instructions of the manufacturer.

Estimation of platelet cyclic AMP and cyclic GMP formations. The method of Karniguian *et al.* (22) was followed. In brief, platelet suspensions were warmed to 37°C for 1 min, then either PGE_1 (10 μM), nitroglycerin (10 μM), or oxLDL (40 and 80 μg/mL) was added and incubated for 6 min. The incubation was stopped, and the solution was immediately boiled for 5 min. After cooling to 4°C, the precipitated protein was collected as sediment after centrifugation. Fifty microliters of supernatant was used to determine the cyclic AMP and cyclic GMP contents by EIA kits (Cayman) following acetylation of the samples as described by the manufacturer.

Estimation of nitrate in human platelet suspensions. Platelet suspensions (1×10^9/mL) were preincubated with collagen (1 μg/mL) or oxLDL (40 and 80 μg/mL) for 6 min followed by centrifugation ($17{,}500 \times g$) for 5 min. The supernatants were deproteinized by incubation with 95% ethanol at 4°C for 30 min. Samples were then centrifuged for a further 7 min at $15{,}000 \times g$. It should be noted that the nitrate concentrations in the platelet suspensions reported in this study actu-

ally represent the total of both nitrite and nitrate concentrations in the platelet suspensions. The amount of nitrate in the platelet suspensions (10 μL) was measured by adding a reducing agent (0.8% VCl_3 in 1 M HCl) to the purge vessel to convert nitrate to NO, which was stripped from the platelet suspensions by a helium purge gas. The NO was then drawn into a Sievers Nitric Oxide Analyzer (280 NOA; Sievers Instruments, Boulder, CO). Nitrate concentrations were calculated by comparison with standard solutions of sodium nitrate.

Measurement of free radicals in platelet suspensions by ESR spectrometry. The ESR method used a Bruker EMX ESR spectrometer as described previously (23). In brief, platelet suspensions (4.5×10^8 platelets/mL, 0.4 mL) were prewarmed to 37°C for 2 min, and then oxLDL (40 μg/mL) or catalase (1000 U/mL) was added 3 min before the addition of collagen (2 μg/mL). The reaction was allowed to proceed for 1 min, followed by the addition of 100 mM DEPMPO for the ESR study. In addition, Fe^{2+} (1 μM) was preincubated with H_2O_2 (10 μM) in Tyrode's solution, followed by the addition of 24h-oxLDL (40 and 80 μg/mL) and further incubated with 50 mM DEPMPO for the Fenton reaction. ESR spectra were recorded on a Bruker EMX ESR spectrometer using a flat quartz cell designed for aqueous solutions. Conditions of ESR spectrometry were as follows: 20 mW power at 9.78 GHz, 1 G modulation, and 100 G scanning for 42 s, with 10 scans accumulated.

Statistical analysis. The experimental results are expressed as the means ± SEM and are accompanied by the number of observations. Data were assessed using ANOVA. If this analysis indicated significant differences among the group means, then each group was compared using the Newman–Keuls method. A P value <0.05 was considered statistically significant.

RESULTS

Effect of oxLDL on platelet aggregation in human platelet suspensions. The 12h- and 24h-oxLDL preparations were oxidized under identical conditions. Under these conditions, the concentrations of 12h- and 24h-oxLDL after incubation were 50.3 ± 0.6 and 51.4 ± 1.8 nmol of MDA/mg protein, respectively. The extents of aldehyde-modified lysine in 12h- and 24h-oxLDL were about 11.0 ± 1.1 and 13.1 ± 1.4, respectively. In this study, we found that the 12h- and 24h-oxLDL, but not nLDL, concentration-dependently (20–100 μg/mL) inhibited platelet aggregation stimulated by collagen (1 μg/mL) (Figs. 1, 2) and AA (60 μM) (Fig. 3) in human platelet suspensions. Furthermore, both types of oxLDL inhibited the ATP-release reaction when stimulated by agonists (i.e., collagen) (Fig. 1). The IC_{50} values of the 12h- and 24h-oxLDL for platelet aggregation induced by collagen were estimated to be about 46.3 ± 1.1 and 55.2 ± 1.0 μg/mL, respectively (Fig. 2). The 24h-oxLDL exhibited more potent activity than 12h-oxLDL in inhibiting platelet aggregation stimulated by agonists. On the other hand, neither type of oxLDL significantly inhibited thrombin (60 μM)-induced platelet aggregation (Fig. 3). Additionally, neither 12h- nor

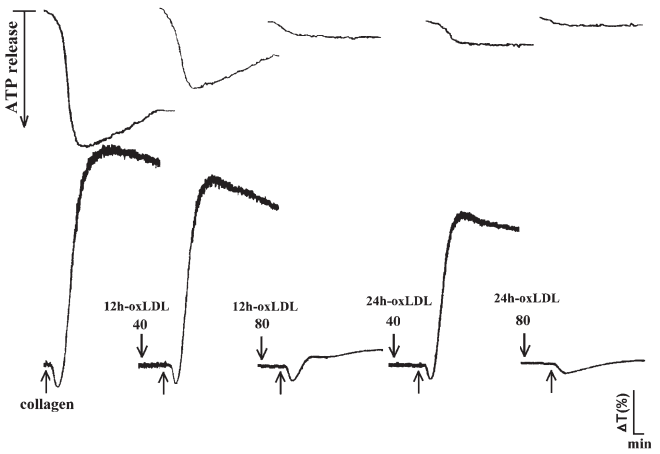

FIG. 1. Tracing curves of oxidized LDL (oxLDL) on collagen (1 μg/mL)-induced platelet aggregation in washed human platelets. Platelets were preincubated with 12h- and 24h-oxLDL (40 and 80 μg/mL) for 3 min. Collagen was then added to trigger aggregation (lower tracings) and ATP release (upper tracings). Profiles are representative examples of five similar experiments. ΔT(%), percent change in transmission.

24h-oxLDL significantly induced spontaneous platelet aggregation in the absence of agonists (data not shown). In the following studies, we used 24h-oxLDL as a tool to further explore the mechanisms of oxLDL in platelet aggregation.

Effect of 24h-oxLDL on [Ca^{2+}]i mobilization. Free cytoplasmic Ca^{2+} concentrations in human platelets were measured by the Fura 2-AM loading method. As shown in Figure 4, collagen (1 μg/mL) evoked a marked increase in [Ca^{2+}]i mobilization. 24h-oxLDL (40 and 80 μg/mL) concentration-dependently inhibited the collagen-evoked increase in [Ca^{2+}]i by about 91 and 96%, respectively. This suggests that oxLDL exerts an inhibitory effect on [Ca^{2+}]i mobilization in human platelets stimulated by collagen.

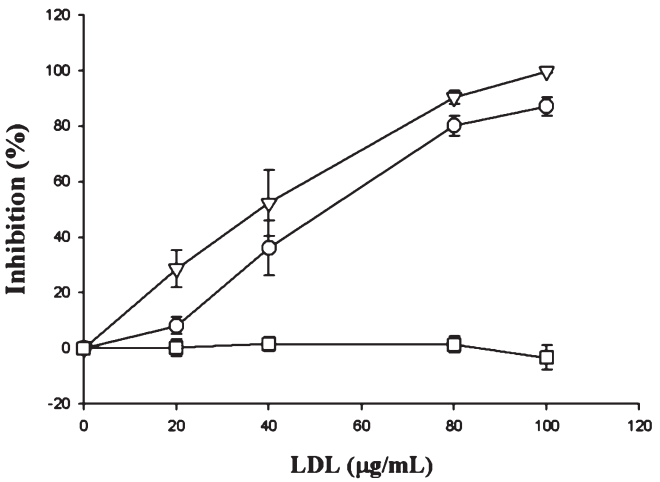

FIG. 2. Concentration-inhibition curves of LDL on collagen (1 μg/mL)-induced platelet aggregation in washed human platelets. Platelets were preincubated with various concentrations (20–100 μg/mL) of 12h-oxLDL (○), 24h-oxLDL (▽), and native LDL (nLDL) (□) for 3 min, followed by the addition of collagen to trigger platelet aggregation. Data are presented as a percentage of the control (means ± SEM, n = 5). For other abbreviation see Figure 1.

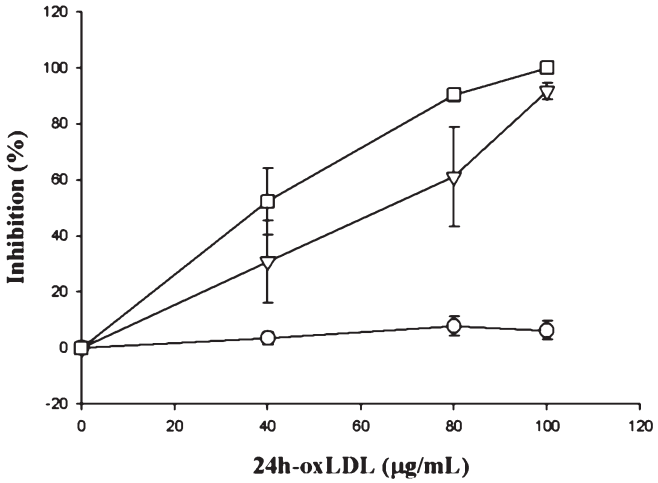

FIG. 3. Concentration-inhibition curves of 24h-oxLDL on thrombin (0.02 U/mL, ○)-, arachidonic acid (60 μM, ▽)-, and collagen (1 μg/mL, □)-induced platelet aggregation in washed human platelets. Platelets were preincubated with 24h-oxLDL (40–100 μg/mL) for 3 min. Agonists were then added to trigger platelet aggregation. Data are presented as a percentage of the control (means ± SEM, $n = 5$).

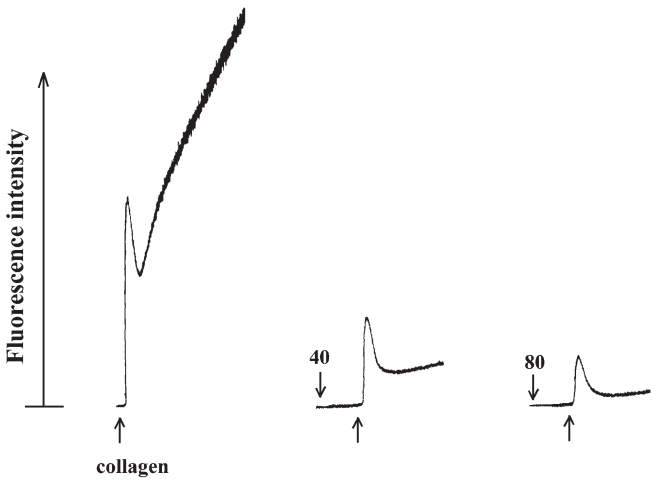

FIG. 4. Effect of 24h-oxLDL on collagen-induced intracellular Ca^{2+} mobilization in Fura 2-AM-loaded human platelets. Platelet suspensions were preincubated with Fura 2-AM (5 μM), followed by the addition of collagen (1 μg/mL) in the absence or presence of 24h-oxLDL (40 and 80 μg/mL), which was added 3 min prior to the addition of collagen. Profiles are representative examples of four similar experiments. For abbreviation see Figure 1.

Effect of 24h-oxLDL on TxB_2 formation. As shown in Table 1, resting platelets produced relatively little TxB_2 compared with collagen-activated platelets. PGE_1 (10 μM) inhibited TxB_2 formation in collagen-activated platelets by 82% (data not shown). Furthermore, results obtained using various concentrations of 24h-oxLDL indicated that 24h-oxLDL markedly inhibited TxB_2 formations in platelets stimulated by collagen (1 μg/mL). At 80 μg/mL, 24h-oxLDL almost completely inhibited TxB_2 formation (Table 1). These results suggest that oxLDL exerts an inhibitory effect on TxA_2 formation.

TABLE 1
Effect of Oxidized LDL (oxLDL) on Thromboxane B_2 Formation in Washed Human Platelets[a]

	Concentration	Thromboxane B_2[b] (ng/mL)
Resting		10.8 ± 5.3
Collagen (μg/mL)	1	80.5 ± 17.2**
24h-oxLDL (μg/mL)	40	47.9 ± 11.2#
	80	9.5 ± 3.0##

[a]Platelet suspensions were preincubated with 24h-oxLDL (40 and 80 μg/mL) for 3 min at 37°C and then collagen (1 μg/mL) was added to trigger thromboxane B_2 formation.
[b]Data are presented as the means ± SEM ($n = 4$). **$P < 0.01$ as compared with the resting group; #$P < 0.05$ and ##$P < 0.01$ as compared with the collagen group.

Effect of 24h-oxLDL on cyclic AMP, cyclic GMP, and nitrate formations in washed human platelets. The level of cyclic AMP in unstimulated platelets was low (2.1 ± 0.5 pmol/10^9 platelets, $n = 4$). Addition of PGE_1 (10 μM) increased the cyclic AMP level to 18.9 ± 3.9 pmol/10^9 platelets ($n = 4$). When platelet suspensions were preincubated with various concentrations of 24h-oxLDL (40 and 80 μg/mL) for 3 min at 37°C, we found that 24h-oxLDL increased cyclic AMP levels to 4.9 ± 0.2 and 5.4 ± 0.8 pmol/10^9 platelets, respectively (Table 2). We also performed similar studies measuring the cyclic GMP response. The level of cyclic GMP in unstimulated platelets was very low, but when nitroglycerin (10 μM) was added to the platelet suspensions, the cyclic GMP level increased from the resting level to 3.6 ± 0.4 pmol/10^9 platelet (Table 2). However, addition of 24h-oxLDL (40 and 80 μg/mL) resulted in no significant increase in platelet cyclic GMP levels (0.9 ± 0.2 and 0.8 ± 0.1 pmol/10^9 platelets, $n = 4$).

On the other hand, NO was quantified using a sensitive and specific ozone redox–chemiluminescence detector. As shown in Table 2, collagen (1 μg/mL) caused about a 2.6-fold rise in nitrate formation, compared with that in resting platelets. In the presence of 24h-oxLDL (40 and 80 μg/mL), nitrate production did not significantly increase after incubation with platelets for 6 min (Table 2). Furthermore, nitrate production did not increase even after prolongation of the incubation time to 30 min (data not shown). These results imply that the antiplatelet activity of oxLDL may act partially through stimulation of cyclic AMP formation in human platelets.

Free radical-scavenging activity of 24h-oxLDL in collagen-activated platelets. The rate of free radical-scavenging activity is defined by the following equation: inhibition rate = 1 – signal height (24h-oxLDL)/signal height (control) (20). In this study, a typical ESR signal of the hydroxyl radical (OH^-) was induced by collagen (2 μg/mL) in human platelets (Fig. 5B). 24h-oxLDL (40 μg/mL) and catalase (1000 U/mL) suppressed hydroxyl radical formation by about 43 and 76% ($n = 4$), respectively (Figs. 5C, 5D). On the other hand, 24h-oxLDL (40 and 80 μg/mL) also concentration-dependently inhibited the nonenzymatic hydroxyl radical generation in the Fenton reaction ($H_2O_2 + Fe^{2+}$) by about 71 and 91% (Figs. 5F, 5G) compared with the control group (Fig. 5E). This observation provides *in vitro* evidence of the free radical-scavenging activity of oxLDL in both activated platelets and the Fenton reaction.

TABLE 2
Effect of 24-h Oxidized LDL (24h-oxLDL) on Cyclic AMP, Cyclic GMP, and Nitrate Formation in Washed Human Platelets[a]

	Concentration	Cyclic AMP[b] (pmol/10^9 platelets)	Cyclic GMP[b] (pmol/10^9 platelets)	Nitrate[b] (μM)
Resting		2.1 ± 0.5	0.6 ± 0.1	3.2 ± 0.6
PGE_1 (μM)	10	18.9 ± 3.9**	—	—
NTG (μM)	10	—	3.6 ± 0.4***	—
Collagen (μg/mL)	2	—	—	8.3 ± 1.1**
24h-oxLDL (μg/mL)	40	4.9 ± 0.2**	0.9 ± 0.2	4.3 ± 0.2
	80	5.4 ± 0.8*	0.8 ± 0.1	4.9 ± 0.7

[a]Platelet suspensions were preincubated with 24h-oxLDL (40 and 80 μg/mL) at 37°C. Addition of prostaglandin E_1 (PGE_1), nitroglycerin (NTG), and collagen in platelet suspensions served as positive controls of cyclic AMP, cyclic GMP, and nitrate, respectively.
[b]Data are presented as the means ± SEM (n = 4). *P < 0.05, **P < 0.01, and ***P < 0.001 as compared with the resting groups.

FIG. 5. ESR spectra of 24h-oxLDL in the inhibition of hydroxyl radical ($OH^{\cdot}$) formation in collagen-activated platelets and Fenton reaction. Platelet suspensions (4.5×10^8 platelets/mL, 0.4 mL) were preincubated with (A) PBS without activation (resting) or with (B) PBS, (C) 24h-oxLDL (40 μg/mL), and (D) catalase (1000 U/mL) for 3 min; then collagen (2 μg/mL) was added to trigger platelet aggregation as described in the Materials and Methods section. Furthermore, hydroxyl radical was generated in the Fenton reaction (H_2O_2 + Fe^{2+}) incubation with (E) PBS, (F) 24h-oxLDL (40 μg/mL), and (G) 24h-oxLDL (80 μg/mL) for 3 min, followed by the addition of 50 mM DEPMPO (5-diethoxyphosphoryl-5-methyl-1-pyrroline-*N*-oxide) for ESR. The reaction was allowed to proceed for 5 min, followed by the addition of DEPMPO (100 mM) for ESR experiments. The spectrum is a representative example of four similar experiments.

DISCUSSION

The principal objective of this study was to describe the intracellular mechanisms involved in the inhibition of agonist-induced human platelet aggregation by oxLDL. This inhibitory effect of oxLDL was demonstrable with the use of the agonists collagen and AA but not with thrombin. The inhibition was directly proportional to the concentrations of oxLDL used. In this study, both platelet aggregation and the ATP-release reaction induced by agonists (i.e., collagen) appeared to be affected by the presence of oxLDL. Therefore, this implies that oxLDL may partially affect Ca^{2+} release from intracellular Ca^{2+} storage sites [i.e., the dense tubular system (DTS) or dense bodies] (Fig. 4), and this is in accord with the concept that intracellular Ca^{2+} release is responsible for the ATP-release reaction (21).

TxA_2 is an important mediator of the release reaction and aggregation of platelets (Fig. 6) (24). Collagen-induced formation of TxB_2, a stable metabolite of TxA_2, was concentration-dependently inhibited by oxLDL (40 and 80 μg/mL) (Table 1). It has been demonstrated that phosphoinositide breakdown can induce TxA_2 formation *via* free AA release by DG lipase or by endogenous phospholipase A_2 (PLA_2) from membrane phospholipids (Fig. 6) (25). Thus, it seems likely that TxB_2 formation plays a role in mediating the inhibitory effect of oxLDL on human platelets.

Activation of human platelets is inhibited by two intracellular pathways regulated by either cyclic AMP or cyclic GMP (26). The importance of cyclic AMP in modulating platelet reactivity is well established (22). In addition to inhibiting most platelet responses, elevated levels of cyclic AMP decrease intracellular Ca^{2+} concentrations by the uptake of Ca^{2+} into the DTS, which negatively affects the action of protein kinase C (Fig. 6) (26). Elevated platelet TxA_2 levels reportedly inhibited platelet membrane-associated adenylate cyclase, which lowers cyclic AMP levels in platelets (27). On the other hand, signaling by cyclic GMP somehow interferes with the agonist-stimulated phosphoinositide turnover that creates Ca^{2+}-mobilizing second messengers (28). In this study, we found that oxLDL did not induce NO formation in human platelets. This result is in accord with results of the cyclic GMP study, because the NO being produced is biologically active, since most cellular actions of NO occur *via* stimulation of intracellular guanylate cyclase, leading to an increase in cyclic GMP (28). Therefore, the inhibitory effects of oxLDL on collagen-induced platelet aggregation seem to

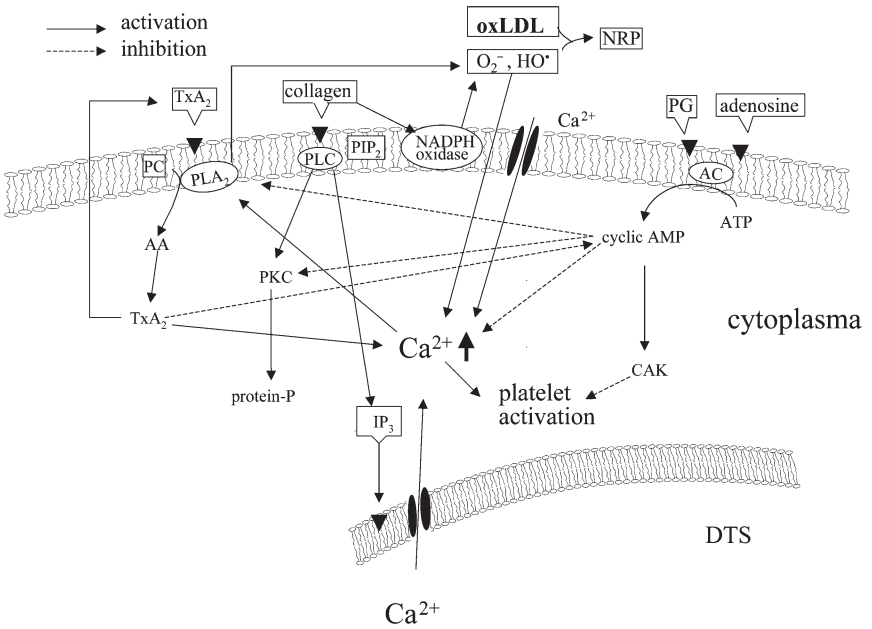

FIG. 6. Schematic hypothesis of the intracellular mechanisms of oxLDL on platelet aggregation. Agonists can activate several phospholipases, including phospholipase C (PLC) and phospholipase A_2 (PLA_2). Collagen or arachidonic acid (AA) stimulates the release of O_2^- and OH^- from platelets. oxLDL can react with O_2^- and OH^- to form nonradical products (NRP). Products of the action of PLC on phosphatidylinositol 4,5-bisphosphate (PIP_2) include 1,2-DAG and inositol 1,4,5-trisphosphate (IP_3). DAG stimulates protein kinase C (PKC), followed by phosphorylation of a 47-kDa protein (protein-P). IP_3 induces the release of Ca^{2+} from dense tubular systems (DTS). The major metabolite of AA in platelets is thromboxane A_2 (TxA_2). Cyclic AMP, cyclic 3′,5′-adenosine monophosphate; AC, adenylate cyclase; CAK, cyclic AMP-activated cyclic AMP-dependent protein kinase; for other abbreviation see Figure 1.

be mediated, at least partially, by an increase in cyclic AMP levels in human platelets.

Modification of LDL *in vitro* is usually performed by incubation of LDL with traces of transition metals (copper or iron). Kalyanaraman *et al.* (29) showed direct evidence for the formation of the α-tocopheroxyl radical and lipid radicals during the oxidation of LDL using the spin trap technique. Schneider *et al.* (30) also detected lipid radical formation in the Cu^{2+}-induced oxidation of LDL. Thus, it has been suggested that the oxidation of lipid present in LDL particles proceeds *via* a radical mechanism (30,31).

Lipid peroxidation is initiated by abstraction of bisallylic hydrogen (LH) from lipids by the peroxyl radical (ROO^-), thereby generating a lipid radical (L^-) and a peroxide (ROOH). In the presence of O_2, lipid peroxyl radicals (LOO^-) are formed, which stimulate lipid peroxidation (LOOH) *via* a chain reaction that produces many molecules of LOOH per ROO^- (32). Thomas and Stocker (32) found that these lipid radicals react with other radical oxidants, including the α-tocopheroxyl radical, Cu^{2+}, or the hydroxyl radical (OH^-), to form nonradical products (by the radical–radical termination reaction) (32). Furthermore, reactive oxygen species act as second messengers during the initial phase of platelet activation processes (33). Mirabelli *et al.* (34) showed an increase in cytosolic Ca^{2+} concentration upon platelet exposure to oxidative stress (Fig. 6). Platelets primed by exposure to subthreshold concentrations of AA or collagen are known to be activated by nanomolar levels of hydrogen peroxide, and this effect is mediated by hydroxyl radicals formed in an extracellular Fenton-like reaction (35). It is also evident that some of the hydrogen peroxide produced by platelets is converted into hydroxyl radicals, as platelet aggregation can be inhibited by hydroxyl radical scavengers (36). A recent study demonstrated that collagen-induced platelet aggregation is associated with O_2^- and OH^- formation, which is dependent on AA release and metabolism (Fig. 6) (37). In addition, the study also found that AA, but not ADP or thrombin, stimulates the release of O_2^- and OH^- from platelets (37). Our findings are also consistent with this observation, because the release of hydroxyl radicals by collagen-stimulated platelets was reduced to the resting level by oxLDL (Fig. 5).

In conclusion, the observations of this study suggest that oxLDL inhibits collagen- and AA-induced human platelet aggregation. The inhibitory effect of oxLDL may induce the radical–radical termination reaction by the interaction of oxLDL-derived lipid radicals with the free radicals (such as hydroxyl radicals) released from activated platelets, with a resultant lowering of intracellular Ca^{2+} mobilization, followed by inhibition of PLA_2 activation and of TxA_2 formation, thereby leading to increased cyclic AMP formation, and finally to further inhibition of $[Ca^{2+}]i$ mobilization and platelet aggregation. This study provides new insights concerning the effects of oxLDL on platelet aggregation.

ACKNOWLEDGMENT

This work was supported by a grant from the National Science Council of Taiwan (NSC 92-2320-B-038-026).

REFERENCES

1. Leeuwenburgh, C., Hardy, M.M., Hazen, S.L., Wagner, P., Ohishi, S., Steinbrecher, U.P., and Heinecke, J.W. (1997) Reactive Nitrogen Intermediates PromoteLow-Density Lipoprotein Oxidation in Human Atherosclerotic Intima, *J. Biol. Chem. 272*, 1433–1436.
2. Berliner, J.A., and Heinecke, J.W. (1996) The Role of Oxidized Lipoproteins in Atherogenesis, *Free Radic. Biol. Med. 20*, 707–727.
3. Gerrity, R.G. (1981) The Role of the Monocyte in Atherogenesis. I. Transition of Bloom-Borne Monocyte into Foam Cells in Fatty Lesions, *Am. J. Pathol. 103*, 181–185.
4. Weksler, B.B., and Nachman, R.L. (1981) Platelets and Atherosclerosis, *Am. J. Med. 71*, 331–333.
5. Tremoli, E., Colli, S., Maderna, P., Baldassarre, D., and Di Minno, G. (1993) Hypercholesterolemia and Platelets, *Semin. Thromb. Hemost. 19*, 115–121.
6. Ardlie, N.G., Selley, M.L., and Simons, L.A. (1989) Platelet Activation by Oxidatively Modified Low-Density Lipoproteins, *Atherosclerosis 76*, 117–124.
7. Andrews, H.E., Aitken, J.W., Hassall, D.G., Skinner, V.O., and Bruckdorfer, K.R. (1987) Intracellular Mechanisms in the Activation of Human Platelets by Low-Density Lipoproteins, *Biochem. J. 242*, 559–564.
8. Takahashi, Y., Chiba, H., Matsuno, K., Akita, H., Hui, S.P., Nagasaka, H., Nakamura, H., Kobayashi, K., Tandon, N.N., and Jamieson, G.A. (1996) Native Lipoproteins Inhibit Platelet Activation Induced by Oxidized Lipoproteins, *Biochem. Biophys. Res. Commun. 222*, 453–458.
9. Katzman, P.L., Bose, R., Walker, S., Perry, Y., and Bolli, P. (1991) Temperature-Dependence of LDL Binding and Activation of Human Platelets, *Thromb. Res. 64*, 503–508.
10. Block, L.H., Knorr, M., Vogt, E., Locher, R., Vetter, W., Groscurth, P., Qiao, B.Y., Pometta, D., James, R., Regenass, M., *et al.* (1988) Low-Density Lipoprotein Causes General Cellular Activation with Increased Phosphatidyl Inositol Turnover and Lipoprotein Catabolism, *Proc. Natl. Acad. Sci. USA 85*, 885–889.
11. Weidtmann, A., Scheithe, R., Hrboticky, N., Pietsch, A., Lorenz, R., and Siess, W. (1995) Mildly Oxidized LDL Induces Platelet Aggregation Through Activation of Phospholipase A_2, *Arterioscler. Thromb. Vasc. Biol. 15*, 1131–1138.
12. Katzman, P.L., Bose, R., Henry, S., McLean, D.L., Walker, S., Fyfe, C., Perry, Y., Mymin, D., and Bolli, P. (1994) Serum Lipid Profile Determines Platelet Reactivity to Native and Modified LDL-Cholesterol in Humans, *Thromb. Haemost. 71*, 627–632.
13. Pedreno, J., de Castellarnau, C., Cullare, C., Ortin, R., Sanchez, J.L., Llopart, R., and Gonzalez-Sastre, F. (1994) Platelet Receptor Recognizes with Same Apparent Affinity Both Oxidative and Native LDL, *Arterioscler. Thromb. Vasc. Biol. 14*, 401–408.
14. Vlasova, I.I., Azizova, O.A., and Lopukhin, Y.M. (1997) Inhibitor Analysis of LDL Induced Platelet Aggregation, *Biochemistry (Moscow) 62*, 307–311.
15. Vlasova, I.I. (2000) The Effect of Oxidatively Modified Low-Density Lipoproteins on Platelet Aggregability and Membrane Fluidity, *Platelets 11,* 406–414.
16. Sheu, J.R., Lee, C.R., Lin, C.C., Kan, Y.C., Lin, C.H., Hung, W.C., Lee, Y.M., and Yen, M.H. (1999) The Antiplatelet Activity of PMC, a Potent α-Tocopherol Analogue, Is Mediated Through Inhibition of Cyclooxygenase, *Br. J. Pharmacol. 127*, 1206–1212.
17. Dousset, N., Ferretti, G., Taus, M., Valdiguie, P., and Curatola, G. (1994) Fluorescence Analysis of Lipoprotein Peroxidation, *Methods Enzymol. 233*, 459–469.
18. Lowry, O.H., Rosebrough, N.J., Farr, A.L., and Randall, R.J. (1951) Protein Measurement with the Folin Phenol Reagent, *J. Biol. Chem. 193,* 265–275.
19. Sheu, J.R., Lee, C.R., Hsiao, G., Hung, W.C., Lee, Y.M., Chen, Y.C., and Yen, M.H. (1999) Comparison of the Relative Activities of α-Tocopherol and PMC on Platelet Aggregation and Antioxidative Activity, *Life Sci. 65*, 197–206.
20. Steinbrecher, U.P. (1987) Oxidation of Human Low-Density Lipoprotein Results in Derivatization of Lysine Residues of Apolipoprotein B by Lipid Peroxide Decomposition Products, *J. Biol. Chem. 262*, 3603–3608.
21. Sheu, J.R., Lee, C.R., Lin, C.H., Hsiao, G., Ko, W.C., Chen, Y.C., and Yen, M.H. (2000) Mechanisms Involved in the Antiplatelet Activity of *Staphylococcus aureus* Lipoteichoic Acid in Human Platelets, *Thromb. Haemost. 83*, 777–784.
22. Karniguian, A., Legrand, Y.J., and Caen, J.P. (1982) Prostaglandins: Specific Inhibition of Platelet Adhesion to Collagen and Relationship with Cyclic AMP Level, *Prostaglandins 23*, 437–457.
23. Hsiao, G., Shen, M.Y., Lin, K.H., Chou, C.Y., Tzu, N.H., Lin, C.H., Chou, D.S., Chen, T.F., and Sheu, J.R. (2003) Inhibitory Activity of Kinetin on Free Radical Formation of Activated Platelets *in vitro* and on Thrombus Formation *in vivo*, *Eur. J. Pharmacol. 465*, 281–287.
24. Hornby, E.J. (1982) Evidence That Prostaglandin Endoperoxides Can Induce Platelet Aggregation in the Absence of Thromboxane A_2 Production, *Biochem. Pharmacol. 31*, 1158–1160.
25. McKean, M.L., Smith, J.B., and Silver, W.J. (1981) Formation of Lysophosphatidylcholine in Human Platelets in Response to Thrombin, *J. Biol. Chem. 256*, 1522–1524.
26. Walter, U., Eigenthaler, M., Geiger, J., and Reinhard, M. (1993) Role of Cyclic Nucleotide-Dependent Protein Kinases and Their Common Substrate VASP in the Regulation of Human Platelets, *Adv. Exp. Med. Biol. 344*, 237–249.
27. Chen, S.Y., Yu, B.J., Liang, Y.Q., and Lin, W.D. (1990) Platelet Aggregation, Platelet cAMP Levels and Thromboxane B_2 Synthesis in Patients with Diabetes Mellitus, *Clin. Med. J. 103*, 312–318.
28. McDonald, L.J., and Murad, F. (1996) Nitric Oxide and Cyclic GMP Signaling, *Proc. Soc. Exp. Biol. Med. 211*, 1–6.
29. Kalyanaraman, B., Antholine, W.E., and Parthasarathy, S. (1990) Oxidation of Low-Density Lipoprotein by Cu^{2+} and Lipoxygenase: An Electron Spin Resonance Study, *Biochim. Biophys. Acta 1035*, 286–292.
30. Schneider, M., Jentzsch, A.M., Trommer, W.E., and Biesalski, H.K. (1998) EPR Kinetic Studies of the LDL Oxidation Process Driven by Free Radicals, *Free Radic. Res. 28*, 451–458.
31. Witting, P.K., Willhite, C.A., Davies, M.J., and Stocker, R. (1999) Lipid Oxidation in Human Low-Density Lipoprotein Induced by Metmyoglobin/H_2O_2: Involvement of α-Tocopheroxyl and Phosphatidylcholine Alkoxyl Radicals, *Chem. Res. Toxicol. 12*, 1173–1181.
32. Thomas, S.R., and Stocker, R. (2000) Molecular Action of Vitamin E in Lipoprotein Oxidation: Implications for Atherosclerosis, *Free Radic. Biol. Med. 28*, 1795–1805.
33. Iuliano, L., Colavita, A.R., Leo, R., Pratico, D., and Violi, F. (1997) Oxygen Free Radicals and Platelet Activation, *Free Radic. Biol. Med. 22*, 999–1006.
34. Mirabelli, F., Salis, A., Vairetti, M., Bellomo, G., Thor, H., and Orrenius, S. (1989) Cytoskeletal Alterations in Human Platelets Exposed to Oxidative Stress Are Mediated by Oxidative and Ca^{2+} Dependent Mechanism, *Arch. Biochem. Biophys. 270*, 478–488.
35. Pietraforte, D., Turco, L., Azzini, E., and Minetti, M. (2002) Online EPR Study of Free Radicals Induced by Peroxidase/H_2O_2

in Human Low-Density Lipoprotein, *Biochim. Biophys. Acta 1583*, 176–184.
36. Leo, R., Ghiselli, A., Iuliano, L., and Violi, F. (1995) Detection of Hydroxyl Radicals by the Salicylate *Bis*-Hydroxylation During Arachidonic Acid-Dependent Platelet Activation, *Thromb. Haemost. 73*, A347.
37. Caccese, D., Pratico, D., Ghiselli, A., Natoli, S., Pignatelli, P., Sanguigni, V., Iuliano, L., and Violi, F. (2000) Superoxide Anion and Hydroxyl Radical Release by Collagen-Induced Platelet Aggregation—Role of Arachidonic Acid Metabolism, *Thromb. Haemost. 83*, 485–490.

[Received December 12, 2003; accepted July 13, 2004]

Effect of a Modified Milk Fat and Calcium in Purified Diets on Cholesterol Metabolism in Hamsters

Michael Pellizzon, John Santa Ana, Edgar Buison, Jennifer Martin, Anne Buison, and K.-L. Catherine Jen*

Department of Nutrition and Food Science, Wayne State University, Detroit, Michigan 48202

ABSTRACT: Modification of milk fat both by partially replacing saturated FA with oleic acid (18:1) and by increasing calcium intake independently reduces plasma cholesterol. Whether modification of both factors together would synergistically reduce plasma cholesterol is unknown. Seventy-two male golden Syrian hamsters were separated into four diet treatment groups (n = 18/group) and fed *ad libitum* for 7 wk. Diets contained either modified milk fat (MMF) or regular milk fat (RMF) with either 0.5% (MMF and RMF) or 1.3% calcium (w/w) (MMFC and RMFC). All diets contained 11% test fat, 4% soybean oil, and 0.15% cholesterol (w/w). During the last week, feces were collected for three consecutive days for analysis of fecal FA, cholesterol, and calcium excretion. Overnight-fasted animals were sacrificed, and plasma and livers were collected for lipid analysis. Neither MMF nor additional calcium significantly affected plasma lipids. However, significant interactions existed between MMF and additional calcium for the ratio of LDL cholesterol to HDL cholesterol (LDL/HDL), indicating that increased calcium intake reduced this ratio only in RMF animals. In addition, MMF reduced LDL/HDL relative to RMF. MMF significantly increased hepatic total and esterified cholesterol. Additional calcium significantly increased fecal calcium and saturated FA (SFA) excretion, whereas MMF significantly reduced SFA excretion. RMFC induced the highest excretion of 16:0 among all groups. Replacement of SFA with 18:1 in the MMF reduced the impact of high calcium on LDL/HDL. Additional calcium reduced LDL/HDL only in the presence of RMF, which may be achieved through an increased excretion of 16:0.

Paper no. L9442 in *Lipids 39,* 441–448 (May 2004).

A high intake of dairy products has been associated with an increase in plasma total and LDL cholesterol (LDL-C) levels (1–3). These associations are thought to be due to high concentrations of lauric (12:0), myristic (14:0), and palmitic acids (16:0) in milk fat (4), which have been shown to elevate total cholesterol and LDL-C levels in humans (5–8) and in animal models such as the hamster (9–11) and nonhuman primates (12,13).

Modification of milk fat by replacing hypercholesterolemic saturated FA (SFA) with oleic (18:1) and linoleic acids (18:2) has been shown to reduce plasma total and LDL-C levels while maintaining HDL cholesterol (HDL-C) levels in humans (14–17). However, findings from studies examining the effect of replacing SFA with 18:1 alone have been inconsistent. In one study, a butter/olive oil blend reduced total and LDL-C concentrations of normocholesterolemic healthy male subjects relative to unmodified butter (3). However, another study involving healthy male subjects with normal cholesterol levels showed that a modified butter containing a higher concentration of 18:1 than conventional butter had no effect on plasma total or LDL-C levels (18). Therefore, the effect of replacing SFA in milk fat with oleic acid on plasma lipids deserves further attention. This is of importance to the food industry since the potential hypocholesterolemic effect of such a modification would improve marketability of dairy products high in fat content.

Although dairy products have lipid-elevating factors, they also contain a high amount of calcium, which has been shown to reduce plasma total cholesterol levels in humans (19–21), rats (22–25), rabbits (26), and pigs (27). A few studies in humans have shown that the hypocholesterolemic potential of dietary calcium is attributable to the lowering of LDL-C levels (19–21). This reduction in LDL-C levels is thought to be due to increased intestinal binding of hypercholesterolemic SFA to calcium and the excretion of this complex as calcium soaps (20–24). This effect is greater with diets high in SFA compared with those high in PUFA (23,28). Therefore, the hypocholesterolemic potential of calcium is reduced in the presence of low concentrations of SFA. However, neither one of these previous studies examined the effect of calcium intake when there was only a partial replacement of SFA by monounsaturated FA. In addition, there are no reports regarding the impact of calcium in the presence of varying FA profiles on lipoprotein cholesterol levels.

Therefore, the present study was designed to determine whether a modified milk fat (MMF), in which SFA are partially replaced by 18:1, would reduce plasma cholesterol levels in hamsters. In addition, because SFA were still present in the MMF, the present study was performed to address whether additional calcium would improve the cholesterol reduction potential of an MMF diet fed to hamsters.

EXPERIMENTAL PROCEDURES

Animals. Seventy-two male golden Syrian hamsters (Harlan Corp., Indianapolis, IN) were 8 wk old and weighed 98 ± 1 g

*To whom correspondence should be addressed at Department of Nutrition and Food Science, Wayne State University, 3003 Science Hall, Detroit, MI 48202. E-mail: cjen@sun.science.wayne.edu

Abbreviations: FPLC, fast protein liquid chromatography; HDL-C, HDL cholesterol; LDL-C, LDL cholesterol; MMF, modified milk fat; MMFC, MMF diet with additional calcium and phosphorus; RMF, regular milk fat; RMFC, RMF diet with additional calcium and phosphorus; SFA, saturated FA.

TABLE 1
Mean FA Profiles of Regular Milk Fat (RMF) and Modified Milk Fat (MMF) in Fat Sources Alone and When Combined with 4% Soybean Oil

	Fat sources		Fat sources + soybean oil	
FA	RMF	MMF	RMF	MMF
	g/100 g total FA			
Butyric (4:0)	4.7	2.1	—	—
Caproic (6:0)	2.4	1.2	—	—
Caprylic (8:0)	1.4	0.7	—	—
Capric (10:0)	2.8	1.6	—	—
Lauric (12:0)	3.2	1.8	2.6 (0.8)[a]	1.8 (0.6)
Myristic (14:0)	11.1	6.5	9.6 (3.1)	6.1 (2.0)
Palmitic (16:0)	30.3	21.7	32.1 (10.4)	25.7 (8.4)
Stearic (18:0)	13.2	8.8	8.1 (2.6)	5.8 (1.9)
Palmitoleic (16:1)	1.9	1.8	0.7 (0.2)	0.5 (0.2)
Oleic (18:1)	26.3	47.7	27.0 (8.8)	41.1 (13.4)
Linoleic (18:2)	2.4	4.9	15.9 (5.2)	15.9 (5.2)
Linolenic (18:3)	0.3	1.2	1.2 (0.4)	1.1 (0.4)
Total SFA	69.2	44.5	52.4 (16.7)	39.4 (12.9)
Total MUFA	28.2	49.5	27.7 (9.0)	41.6 (13.6)
Total PUFA	2.7	6.0	17.1 (5.6)	17.0 (5.6)
Unidentified	—	—	3.0 (1.0)	2.0 (0.5)
MUFA/SFA ratio	0.5	1.3	0.5	1.1
PUFA/SFA ratio	0.05	0.15	0.3	0.4

[a]Values in parentheses represent percentage of energy contributed by each FA. SFA, saturated FA; MUFA, monounsaturated FA.

at baseline. Hamsters were housed in polycarbonate cages (3 to 5 animals in each cage) with a 12-h light/dark cycle (lights on at 0600h). The room temperature was maintained at 22 ± 1°C.

Diets. Hamsters were fed AIN-93M formulated diets with some modifications (29). All diets were commercially prepared in pelleted form by Dyets, Inc. (Bethlehem, PA) and contained (w/w): 20% casein, 12.5% dextrinized cornstarch, 7.5% sucrose, 9.9% cellulose, 3.5% mineral mix, 1.0% vitamin mix, 0.18% L-cystine, 0.25% choline bitartrate, 0.0008% TBHQ, and 0.15% cholesterol. The addition of cholesterol was necessary because previous data demonstrated the importance of the presence of dietary cholesterol for examining the impact of dietary FA profile on plasma cholesterol levels (30). The cholesterol level chosen was similar to that of other previous studies examining the effect of FA profile on plasma cholesterol levels in hamsters (31). Table 1 presents the FA profile of the MMF and regular milk fat (RMF) alone (columns 1 and 2) and in combination with soybean oil (columns 3 and 4). The data in columns 3 and 4 represent the final FA profile of the dietary treatments fed to the hamsters. Milk fat modification was performed by the addition of β-cyclodextrin to remove SFA and cholesterol out of regular milk fat (32). As shown in columns 1 and 2 of Table 1, the MMF contained a lower concentration of all SFA and a higher concentration of 18:1 than the RMF. Therefore, the MMF diet had a higher ratio of 18:1 to SFA (18:1/SFA) relative to RMF (Table 1). Because the method of milk fat modification removed cholesterol as well as SFA and we were interested only in how the MMF FA profile would influence plasma lipoprotein cholesterol levels, we added more cholesterol to the MMF diet in order to match the cholesterol content of the RMF diet. Both MMF and RMF made up 11% of the total weight in each diet with the remaining 4% contributed by soybean oil to provide EFA (29). Two diets contained additional calcium as calcium carbonate (2% w/w) and potassium phosphate (0.55% w/w), which replaced an equal weight of cornstarch. The addition of calcium carbonate increased the calcium content from 0.5% (w/w), as provided by the AIN-93M mineral mix, to 1.3% (w/w). Therefore, the four diet treatments were as follows: RMF, RMF diet with additional calcium and phosphorus (RMFC), MMF diet, and MMF diet with additional calcium and phosphorus (MMFC).

Procedure. After a 1-wk adaptation period, all hamsters were separated into four treatment groups (n = 18/group) and were fed MMFC, RMFC, MMF, or RMF throughout the entire

study. Body weight and food intake data were recorded weekly. After 6 wk of feeding, 12 animals per group were transferred to metabolic cages for the collection of feces and urine for 3 consecutive days after a 1-d adaptation period. At the end of the collection period, all animals were fasted for ~15 h, sedated by CO_2 exposure, and sacrificed by decapitation. Trunk blood was immediately collected in a tube containing 0.15% EDTA, vortexed, and centrifuged at $1000 \times g$ for 20 min at 4°C. Plasma supernatant was stored in a −20°C freezer for future assays. Livers were harvested, immediately frozen in liquid nitrogen, and then stored in a −70°C freezer for future analyses. This protocol was approved by the Animal Investigation Committee at Wayne State University.

Plasma lipoprotein cholesterol determination by fast performance liquid chromatography (FPLC). Plasma total cholesterol (Sigma kit no. 352; Sigma Chemicals, St. Louis, MO) and TAG (Sigma kit no. 336) levels from all animals were determined. In addition, lipoprotein cholesterol levels were determined by FPLC fractions. In brief, 100 µL of plasma was injected into an FPLC system. The FPLC system was equipped with a Superose 6 HR10/30 column (Amersham Pharmacia Biotech, Piscataway, NJ), which separated lipoprotein particles into 0.5-mL fractions. The lipoprotein particles were eluted with a saline solution containing sodium chloride (0.15 M), EDTA (0.1%), sodium azide (0.1%), and phenylmethylsulfonyl fluoride (2 mM) (adjusted to pH 7.3) at a flow rate of 0.5 mL/min. This saline solution was degassed and filtered prior to use. Cholesterol was determined from 100 µL of each fraction using Sigma kit no. 352. The fraction number for VLDL, LDL, and HDL was determined by chromatographing hamster lipoproteins, which were isolated by sequential ultracentrifugation using a Sorvall ultracentrifuge (DuPont, Wilmington, DE). For the isolation of VLDL [density (d) < 1.006 g/mL], 500 µL of plasma was centrifuged with sodium chloride (0.15 M) in a Ti 50.4 rotor at 12°C and $121{,}000 \times g$ for 18 h. The top 1 mL fraction removed was considered VLDL and was kept at 4°C until cholesterol analysis. The remaining volume was used for LDL isolation. For separation of LDL ($1.006 < d < 1.063$), sodium bromide was added to increase the density of plasma to 1.063 g/mL and tubes were spun for 18 h at 12°C and $121{,}000 \times g$. The top 1 mL fraction was removed and dialyzed for approximately 36 h. The remaining plasma was taken for HDL isolation ($1.063 < d < 1.21$). The plasma density was increased to 1.21 g/mL with sodium bromide and the plasma was centrifuged at 12°C and $150{,}000 \times g$ for 24 h. Recovered HDL was dialyzed for approximately 48 h.

Liver cholesterol determination. Total and unesterified cholesterol contents were determined as performed by Trautwein *et al.* (33). In brief, homogenized livers were extracted with chloroform/methanol (2:1, vol/vol) and shaken in a water bath overnight. After samples had been centrifuged, the supernatant was evaporated under nitrogen and the remainder was then dissolved in chloroform. A small aliquot was dried under nitrogen and then redissolved in isopropanol. Total cholesterol was determined by using Sigma kit no. 352. Unesterified cholesterol was analyzed by the Wako free cholesterol C kit (Wako Chemicals, Richmond, VA). Esterified cholesterol was determined by subtracting unesterified cholesterol from total cholesterol.

Dietary FA determination. Lipid extractions were performed by the method of Folch *et al.* (34). Lipid classes were separated by TLC and identified using a standard containing cholesterol, cholesteryl ester, triolein, oleic acid, and lecithin (20% w/w each; Nu-Chek-Prep, Elysian, MN). TAG isolated from TLC were methylated using the alkaline methanolysis method of Sun and Horrocks (35) along with heptadecanoic acid as an internal standard (Nu-Chek-Prep). After methylation, FAME were separated with a GC system (Hewlett-Packard 6890, Wilmington, DE) using a 30 m, 0.25 mm i.d. Stabilwax^{TM} column (Alltech, Deerfield, IL). GC parameters were set as follows: split ratio, 2:1; average velocity, 32 cm/s; flow rate, 1.5 mL/min; FID, 300°C; front inlet temperature, 220°C; and oven temperature, initial 40°C, hold for 2 min; ramp 1, 30°C/min to 145°C, hold for 5 min; ramp 2, 1°C/min to 187°C, hold for 1 min. The following certified FAME standards (Sigma Chemicals) were injected to determine their retention times: lauric acid, myristic acid, myristoleic acid, pentadecanoic acid, pentadecenoic acid, palmitic acid, palmitoleic acid, heptadecanoic acid, stearic acid, oleic acid, linoleic acid, linolenic acid, and arachidic acid.

Fecal calcium. Fecal samples were dried in an oven at 100°C for 24 h and then ashed in a furnace at 600°C for 24 h. In an acid-washed flask, ashed fecal samples were gently boiled with 10 mL of concentrated nitric acid until almost dry. After cooling the samples, they were boiled gently in 10 mL of 30% hydrogen peroxide until completely dry. The dried samples were redissolved into 50 mL of 0.01% nitric acid, and samples were subsequently diluted 1:10 with 0.1% nitric acid and measured for calcium content with a PerkinElmer Model 5000 atomic absorption spectrophotometer (PerkinElmer, Norwalk, CT) at a wavelength of 422.7 nm. Certified calcium standards were obtained from Fisher Scientific (Fair Lawn, NJ).

Fecal FA. FA from collected feces were extracted according to the method of Van de Kamer *et al.* (36). The samples were then methylated with 2% sulfuric acid in methanol. After methylation, 1 mL of potassium carbonate (6%) was added and HPLC-grade hexane was used to extract the FAME. Extracted samples were dried under nitrogen and then stored in a −20°C freezer until later analysis by GC. The GC protocol used was the same as that used for dietary FAME analysis.

Data analysis. All statistics were performed using SPSS, version 10.0 (Chicago, IL). Simple two-factor ANOVA models involving the two dietary calcium levels, the two different FA profiles, and the interaction of these two dietary factors were performed on all plasma, liver, and fecal parameters. Significance was set at $P < 0.05$. *Post hoc* tests were performed using the least significant difference *t*-test.

RESULTS

Plasma and liver cholesterol concentrations. All groups weighed similarly at both baseline and sacrifice and had similar daily caloric intake throughout the study (data not shown). At sacrifice, neither MMF nor dietary calcium level had any

TABLE 2
Plasma and Hepatic Lipid Concentrations[a] for All Groups at Sacrifice

	MMFC	RMFC	MMF	RMF	Fat[b]	Ca[c]	Fat × Ca
Plasma							
Total cholesterol (mg/dL)	183 ± 5	187 ± 5	181 ± 6	176 ± 5	0.864	0.213	0.404
TAG (mg/dL)	63.5 ± 2.0	68.5 ± 4.7	68.0 ± 1.7	75.2 ± 4.8	0.079	0.106	0.752
VLDL-C (mg/dL)	11.2 ± 2.3	13.7 ± 1.9	12.2 ± 2.0	15.7 ± 2.6	0.220	0.518	0.844
LDL-C (mg/dL)	15.0 ± 1.6	12.2 ± 1.6	14.1 ± 1.4	17.4 ± 1.7	0.879	0.224	0.082
HDL-C (mg/dL)	163 ± 9	168 ± 8	168 ± 14	147 ± 10	0.521	0.538	0.277
VLDL/HDL ratio	.071 ± .016	.082 ± .013	.078 ± .014	.114 ± .034	0.229	0.317	0.530
LDL/HDL ratio	.093 ± .009[a,b]	.073 ± .010[a]	.086 ± .009[a]	.123 ± .024[b]	0.498	0.108	<0.05
Liver							
Total cholesterol (mg/g)	38.1 ± 2.0[a]	29.1 ± 5.1[b]	37.5 ± 9.6[a]	25.9 ± 3.7[b]	<0.001	0.317	0.487
Esterified cholesterol (mg/g)	29.2 ± 2.2[a]	22.3 ± 1.4[b,c]	27.2 ± 2.6[a,b]	17.0 ± 1.8[c]	<0.001	0.091	0.441
Free cholesterol (mg/g)	9.9 ± 1.6	6.8 ± 1.8	10.4 ± 2.6	8.9 ± 2.5	0.141	0.414	0.604

[a]Data are expressed as means ± SEM. Mean values within a row not sharing a common superscript letter are significantly different ($P < 0.05$).
[b]Fat: effect of modification of milk fat.
[c]Ca: effect of varying levels of calcium. MMFC, MMF diet with additional calcium and phosphorus; RMFC, RMF diet with additional calcium and phosphorus. For other abbreviations see Table 1.

significant effect on the plasma lipid parameters measured (Table 2). However, a significant interaction existed between dietary fat source and calcium level for the ratio of LDL/HDL ($P < 0.05$). *Post hoc* analysis revealed that the MMF and RMFC groups had significantly lower ratios of LDL/HDL than the RMF group. MMFC had similar ratios compared with the rest of the groups.

All groups had similar liver weights and percentages of liver weight relative to body weight (data not shown). Hepatic cholesterol data also are presented in Table 2. Overall, MMF increased the concentration of total and esterified cholesterol, but not free cholesterol. High calcium level had no significant effect on total, esterified, or free cholesterol levels.

Fecal calcium and total FA concentrations. Fecal calcium and lipid data are presented in Table 3. Fecal dry weight and calcium (both concentration and total) were significantly increased by additional calcium. However, MMF had no significant effect on these parameters. Animals fed the RMFC diet excreted significantly more feces than the MMF and RMF animals, but had similar levels compared with MMFC. The MMFC, MMF, and RMF groups excreted similar levels. The MMFC and RMFC groups excreted similar amounts of calcium (concentration and total), and both groups excreted significantly higher amounts than the MMF and RMF groups. Additional calcium significantly increased FA excretion (both concentration and total). Modification of milk fat significantly reduced total FA excretion, but not the concentration. The RMFC group excreted the highest level of total FA over the 3-d collection among all groups, whereas the other three groups excreted similar levels. The FA concentration for RMFC was similar to that of MMFC and RMF and significantly higher than that of MMF. The MMFC, MMF, and RMF groups all had similar concentrations.

Fecal FA profile. Table 4 presents data regarding the fecal FA profile (concentration and total) over the 3-d fecal collection period. Modification of milk fat reduced total myristic acid excretion but had no effect on the concentration. Calcium supplementation had no effect on either the total amount or concentration of myristic acid excreted. Total myristic acid excretion was significantly higher for RMFC-fed animals relative to that of MMF, but was similar to that of MMFC and RMF. MMF animals excreted lower total amounts compared with RMF. The concentration of 14:0 excreted was similar for all groups. In regards to palmitic acid excretion, modification of milk fat reduced the concentration and total excretion of palmitic acid. On the other hand, calcium supplementation increased the concentration and total amount of palmitic acid excreted. Both MMFC and RMF animals excreted significantly higher concentrations of 16:0 relative to MMF. RMFC animals excreted the highest total amount of 16:0 relative to all groups. MMFC, MMF, and RMF all excreted similar amounts of 16:0. The hamsters' concentration and total excretion of stearic acid was reduced by modification of milk fat. However, stearic acid excretion was significantly increased by calcium. RMFC hamsters

TABLE 3
Fecal Calcium and FA Data[a] for All Groups During the 3-d Fecal Collection Period

	MMFC	RMFC	MMF	RMF	Fat[b]	Ca[c]	Fat × Ca
Dry weight (g/3 d)	1.4 ± 0.1[a,b]	1.7 ± 0.1[a]	1.3 ± 0.1[b]	1.4 ± 0.1[b]	0.098	<0.05	0.399
Calcium (mg/g)	131 ± 4[a]	136 ± 3[a]	102 ± 3[b]	110 ± 3[b]	0.059	<0.01	0.626
Calcium (mg/3 d)	26.4 ± 1.9[a]	31.0 ± 1.6[a]	10.2 ± 1.8[b]	11.1 ± 1.8[b]	0.137	<0.001	0.304
Total FA (mg/g)	20.9 ± 1.7[a,b]	23.9 ± 2.3[a]	15.4 ± 1.5[b]	20.2 ± 2.1[a,b]	0.056	<0.05	0.658
Total FA (mg/3 d)	28.2 ± 4.2[a]	41.9 ± 3.8[b]	19.2 ± 4.0[a]	27.5 ± 4.4[a]	<0.05	<0.01	0.519

[a]Data expressed as means ± SEM. Mean values within a row not sharing a common superscript letter are significantly different ($P < 0.05$).
[b]Fat: effect of modification of milk fat.
[c]Ca: effect of varying levels of calcium. For abbreviations see Tables 1 and 2.

TABLE 4
Fecal FA Concentration (mg/g) and Total Excretion (mg/3 d) for All Groups During the 3-d Fecal Collection Period[a]

	MMFC	RMFC	MMF	RMF	Fat[b]	Ca[c]	Fat × Ca
Myristic acid (14:0)							
mg/g	0.80 ± 0.2	1.2 ± 0.2	0.83 ± 0.2	1.1 ± 0.2	0.077	0.773	0.800
mg/3 d	1.3 ± 0.3[a,b]	2.3 ± 0.5[b]	1.0 ± 0.2[a]	1.7 ± 0.4[b]	<0.05	0.276	0.740
Palmitic acid (16:0)							
mg/g	7.1 ± 0.9[a]	9.7 ± 0.9[b]	4.5 ± 0.9[c]	7.8 ± 1.0[a,b]	<0.01	<0.05	0.718
mg/3 d	10.7 ± 1.8[a]	16.9 ± 1.8[b]	5.7 ± 1.9[a]	9.4 ± 2.2[a]	<0.05	<0.01	0.518
Stearic acid (18:0)							
mg/g	3.9 ± 0.4[a]	5.6 ± 0.4[b]	2.0 ± 0.4[c]	4.3 ± 0.5 [a]	<0.001	<0.001	0.496
mg/3 d	5.9 ± 1.0[a]	10.7 ± 1.0[b]	2.5 ± 1.0[c]	5.7 ± 1.3[a,c]	<0.01	<0.001	0.471
14:0 + 16:0 + 18:0							
mg/g	12.1 ± 1.5[a]	17.2 ± 1.5[b]	7.4 ± 1.6[c]	13.4 ± 1.7[a,b]	<0.001	<0.01	0.775
mg/3 d	18.3 ± 3.8[a]	29.9 ± 3.1[b]	9.2 ± 3.2[c]	17.2 ± 4.1[a]	<0.01	<0.01	0.602
Oleic acid (18:1)							
mg/g	3.3 ± 0.4	2.5 ± 0.4	2.8 ± 0.4	2.8 ± 0.5	0.335	0.879	0.336
mg/3 d	4.4 ± 0.7	3.9 ± 0.7	3.8 ± 0.7	3.3 ± 0.8	0.484	0.422	0.964

[a]Data are expressed as means ± SEM. Mean values within a row not sharing a common superscript letter are significantly different ($P < 0.05$).
[b]Fat: effect of modification of milk fat.
[c]Ca: effect of varying levels of calcium.

excreted the highest concentration and total amount of 18:0 relative to the rest of the groups. MMFC animals excreted significantly more 18:0 (both concentration and total) relative to MMF, but excreted similar levels relative to RMF. Both MMF- and RMF-fed animals had similar total amounts of 18:0. However, RMF animals excreted a higher concentration of 18:0 relative to MMF and MMFC. When combining all SFA measured (14:0, 16:0, and 18:0), the modification of milk fat reduced the excretion of total SFA. In contrast, calcium supplementation increased the concentration and total amount excreted. The RMFC group excreted a significantly higher total amount relative to all groups. The concentration of total SFA excreted was significantly increased in RMFC hamsters relative to that of MMFC and MMF, but was similar to that of RMF. Both MMFC- and RMF-fed animals excreted significantly more total SFA (both concentration and total) relative to MMF. MMFC and RMF hamsters excreted similar levels (both concentration and total). Neither modification of milk fat nor additional calcium significantly influenced the concentration or 3-d excretion of 18:1.

DISCUSSION

The present study demonstrated that modification of milk fat by partial replacement of SFA with oleic acid (18:1) did not significantly influence plasma lipoprotein cholesterol concentrations in male golden Syrian hamsters. In addition, the presence of higher levels of calcium in either MMF or RMF diets did not significantly affect plasma lipoprotein cholesterol concentrations.

Previous hamster studies showed that chow-based diets high in oleic acid reduced plasma total cholesterol and LDL-C levels relative to those diets higher in SFA (particularly 12:0, 14:0, and 16:0) (9–11,30,37). This hypocholesterolemic effect of oleic acid on plasma cholesterol levels has been shown only when cholesterol is present in the diet (38). Therefore, to improve the hypocholesterolemic potential of MMF, cholesterol was added to the diets at a level similar to those of the above-mentioned studies. However, these studies used chow-based diets, which affect plasma cholesterol levels differently from purified diets (31). More specifically, the non-HDL-C levels of hamsters fed chow-based diets are higher than those fed purified diets. The current study used purified diets. Nevertheless, the expected reductions in plasma total and non-HDL-C levels by diets high in oleic acid relative to those high in SFA would still be expected. Trautwein *et al.* (39) showed that plasma total cholesterol and VLDL cholesterol levels were reduced by purified diets high in oleic acid relative to those high in palmitic acid. Therefore, the lack of a change in plasma non-HDL-C and total cholesterol levels in the current study suggested that the modification to regular milk fat was not dramatic enough to produce any strong effect on these lipid parameters. Trautwein *et al.* (39) showed that hamsters fed purified diets containing olive oil (high in 18:1), rapeseed oil (high in 18:1), sunflower oil (high in 18:2), or palm stearin (high in 16:0) had similar concentrations of LDL-C. All hamsters in the study of Trautwein *et al.* (39) had low levels of LDL-C, which probably reduced the potential for any influence of dietary FA on this parameter. Similarly, hamsters in our study had low LDL-C levels. Therefore, as in the study by Trautwein *et al.* (39), any potential for MMF to reduce LDL-C levels in the current study may have been compromised by the existing low levels of LDL-C in these hamsters. Other studies with hamsters fed a purified diet have reported that both total and non-HDL-C levels were not influenced by diets containing olive oil relative to those containing palm oil (high in 16:0) (40), palm stearin (high in 16:0), butter (high in 14:0 and 16:0), or coconut oil (high in 12:0 and 14:0) (41). Therefore, the results from the current study are consistent with other studies comparing the effect of diets high in SFA relative to those high in 18:1 on lipoprotein cholesterol levels.

Another factor that may have influenced the results of the current study was that all diets contained a relatively high percentage of energy from linoleic acid, which was contributed by soybean oil. The soybean oil was added at a level of 4% (w/w)

to stay in line with AIN-93M dietary guidelines. In a previous study, it was observed that normally hypercholesterolemic SFA such as 12:0 or 16:0 had no effect on plasma cholesterol levels of hamsters when 18:2 was in the range of 5–6% of energy (42). Because the level of linoleic acid in the current study was in this range (5.2%), this may have blunted the differences in plasma cholesterol levels between MMF and RMF.

Although there were no changes in plasma cholesterol levels, MMF significantly increased the concentration of hepatic total and esterified cholesterol. The replacement of SFA (especially 16:0 and 18:0) with 18:1 has been shown in other hamster studies to increase hepatic total and esterified cholesterol levels (12,31,39,41). This is most likely due to the fact that 18:1 is a better substrate than SFA for ACAT, an enzyme that converts free cholesterol to cholesteryl esters (43). Although some of these studies indicated that an increase in hepatic cholesterol esters is associated with reductions in plasma cholesterol levels (31), this was not true in other studies (39,41). Therefore, the current results are in agreement with those studies by Trautwein *et al.* (39), who also used purified diets and found that increases in hepatic cholesterol levels in hamsters fed higher levels of 18:1 may occur independently of changes in plasma cholesterol levels. Regarding free cholesterol levels, MMF had no effect on this parameter, which is consistent with results of other studies feeding hamsters with high levels of 18:1 or SFA (31, 39).

To our knowledge, the present study is the first to report the effect of calcium intake on plasma cholesterol levels in hamsters. The results demonstrated that calcium at levels over two times that in the AIN-93M formula did not significantly influence plasma total cholesterol, LDL-C, or HDL-C levels when in the presence of either MMF or RMF. This is in contrast to results in studies that showed that additional calcium reduced plasma total cholesterol levels in animals such as rats (22–25), rabbits (26), and pigs (27). Although it may be difficult to compare results from the current study with those of other studies using different animal models, the hypocholesterolemic potential of dietary calcium is not demonstrated by all animal studies and may depend on several factors. For example, this may depend on the levels of calcium used in the experimental and control groups. In the current study, the control diet contained recommended levels of calcium as provided by the AIN-93M formula (0.5% w/w), and the experimental diet contained 1.3% (w/w). Some studies with rats (22) have observed that additional dietary calcium (1.2%) significantly reduces plasma total cholesterol concentrations only relative to suboptimal levels (0.08%) and not when compared with those fed more adequate levels (0.2%). This idea was also demonstrated in a study performed with rabbits, which showed that those fed 0.8 and 1.6% calcium had similar plasma cholesterol levels, but both had significantly lower levels than those fed <0.02% (44). Nevertheless, Vaskonen *et al.* (25) demonstrated that increasing dietary calcium content from 0.8 to 2.1% significantly reduced plasma total cholesterol levels in obese Zucker rats. However, LDL-C and HDL-C were not significantly influenced, which is in agreement with the results of the current study.

Although calcium did not have any significant impact on plasma lipids, the current study demonstrated that high levels of calcium increased the excretion of both 16:0 and 18:0, but not 18:1. As reported previously, SFA are highly susceptible to complexing with calcium and forming calcium soaps (45,46). Nevertheless, the ability of calcium to bind SFA is dependent on their positional distribution on the TAG molecule. The FA in the *sn*-2 position are not susceptible to pancreatic lipase, are retained on the glycerol backbone, and are not available to complexing with calcium. In addition, Brink *et al.* (47) showed that excretion of 18:0 was more pronounced in the presence of high levels of calcium when the 18:0 was located in the *sn*-1 and *sn*-3 positions compared with when it was located in the *sn*-1 and *sn*-2 positions. A high concentration of 16:0 in bovine milk fat is located in the *sn*-1 (~47%) and *sn*-2 positions (~45%) (48); the large concentration of 16:0 in *sn*-2 may have compromised the ability of calcium to complex these FA. Since 16:0 is considered hypercholesterolemic, the large percentage of 16:0 in the *sn*-2 position may have reduced the hypocholesterolemic potential of calcium.

Dietary calcium did not significantly increase hepatic total, esterified, or free cholesterol. These results are similar to those of others, which indicated that additional calcium intake beyond an adequate level did not significantly influence liver cholesterol concentrations in rats fed beef tallow (22), cocoa butter, or corn oil (23), and rabbits fed beef tallow (26). There was a tendency for increased calcium intake to increase the concentration of esterified cholesterol ($P = 0.091$). This shift in esterified cholesterol concentration by calcium reduced the differences between the RMF and MMF groups.

The current study is the first (to our knowledge) that has reported the effect of additional calcium on lipoprotein cholesterol levels in the presence of varying FA profiles. Although plasma lipoprotein cholesterol levels were not significantly influenced by any of the dietary manipulations, a significant interaction existed between calcium level and fat modification for the LDL/HDL ratio. The results indicated that increased dietary calcium significantly reduced this ratio in the presence of the RMF diet, but not in the presence of MMF. In addition, the results indicated that MMF reduced this ratio relative to RMF, but that MMFC did not further reduce this ratio. The effect of calcium intake on the LDL/HDL ratio may be partially explained by its ability to increase the excretion of SFA. As indicated above, calcium significantly enhanced SFA excretion in both diets. However, the excretion of 16:0 and 18:0 (both concentration and total excretion) was significantly higher in animals fed RMFC relative to those fed MMFC. This was most likely explained by the higher availability of these FA in the RMF diet compared with the MMF diet. The reduced concentration of SFA in the MMF diet may explain why additional calcium in this diet did not further reduce the LDL/HDL ratio. A previous study in young, healthy male subjects fed diets containing high or low

levels of calcium in the presence of either palm oil (high in 16:0) or safflower oil (high in 18:2) showed that calcium significantly increased excretion of SFA and reduced plasma total cholesterol levels of subjects consuming palm oil, but did not significantly affect the excretion of SFA and levels of plasma total cholesterol in subjects consuming safflower oil (28). Another study performed in rats indicated that additional calcium increased the excretion of SFA and reduced plasma total cholesterol levels in the presence of cocoa butter (high in 18:0) compared with a cocoa butter and corn oil combination (high in 18:2) (23). Although these previous studies assessed only total cholesterol and not lipoprotein cholesterol concentrations, they do emphasize the importance of the FA profile and may help to explain the results in the current study.

In conclusion, neither modification of milk fat *via* partial replacement of SFA with 18:1 nor addition of calcium at over two times the level of the AIN-93M formula had a significant impact on plasma lipoprotein cholesterol levels. However, there were reductions in the ratio of LDL/HDL when calcium was fed in the presence of the RMF. This may be important because the ratio of LDL/HDL has been shown to be an important predictor for coronary heart disease risk and may actually be a better predictor than LDL-C levels alone (49). The MMF diet also reduced the ratio of LDL/HDL relative to RMF, but additional calcium produced no further reductions. Therefore, the increased excretion of palmitic acid when additional calcium was added to the RMF diet relative to addition to the MMF diet may offset the adverse influence of a high intake of SFA on this ratio. This may explain why increased consumption of full-fat, calcium-rich dairy products is not associated with elevation of plasma total cholesterol and LDL-C and the ratio of LDL/HDL in humans (50). On the other hand, when subjects increase their intake of dairy products low in calcium (i.e., butter), plasma LDL-C concentrations are elevated (3). As a consequence of the beneficial effect of calcium supplementation on the ratio of LDL/HDL in a recent 12-mon study involving postmenopausal women (51) and data from the current study, future studies evaluating the effect of the dietary FA profiles and varying levels of calcium on plasma lipoprotein cholesterol levels in humans may be warranted.

ACKNOWLEDGMENTS

Both MMF and RMF were provided by Aziz Awad from Michigan State University. Michael Pellizzon was supported by a Dissertation Fellowship provided by the Graduate School of Wayne State University.

REFERENCES

1. Kris-Etherton, P.M., Derr, J., Mitchell, D.C., Mustad, V.A., Russel, M.E., McDonnell, E.T., Salabsky, D., and Pearson, T.A. (1993) The Role of Fatty Acid Saturation on Plasma Lipids, Lipoproteins, and Apolipoproteins: I. Effects of Whole Food Diets High in Cocoa Butter, Olive Oil, Soybean Oil, Dairy Butter, and Milk Chocolate on the Plasma Lipids of Young Men, *Metabolism 42*, 121–129.
2. Baudet, M.F., Lasserre, D., Esteva, O., and Jacotot, B. (1984) Modification in the Composition and Metabolic Properties of Human Low Density and High Density Lipoproteins by Different Dietary Fats, *J. Lipid Res. 25*, 456–468.
3. Wood, R., Kubena, K., O'Brien, B., Tseng, S., and Martin, G. (1993). Effect of Butter, Mono- and Polyunsaturated Fatty Acid-Enriched Butter, *trans* Fatty Acid Margarine, and Zero *trans* Fatty Acid Margarine on Serum Lipids and Lipoproteins in Healthy Men, *J. Lipid Res. 34*, 1–11.
4. Posati, L.P., and Orr, M.L. (1976) Composition of Foods, Dairy and Egg Products, *Agriculture Handbook 8-1*, Agricultural Research Service, USDA, U.S. Government Printing Office, Washington, DC.
5. Mensink, R.P., and Katan, M.B. (1992) Effect of Dietary Fatty Acids on Serum Lipids and Lipoproteins. A Meta-analysis of 27 Trials, *Arterioscler. and Thromb. 12*, 911–919.
6. Yu, S., Derr, J., Etherton, T.D., and Kris-Etherton, P.M. (1995) Plasma Cholesterol-Predictive Equations Demonstrate That Stearic Acid Is Neutral and Monounsaturated Fatty Acids Are Hypocholesterolemic, *Am. J. Clin. Nutr. 61*, 1129–1139.
7. Hegsted, D.M., Ausman, L.M., Johnson, J.A., and Dallal, G.E. (1993) Dietary Fat and Serum Lipids: An Evaluation of the Experimental Data, *Am. J. Clin. Nutr. 57,* 875–883.
8. Hegsted, D.M., McGandy, R.B., Myers, M.L. and Stare, F.J. (1965) Quantitative Effects of Dietary Fat on Serum Cholesterol in Man, *Am. J. Clin. Nutr. 17*, 281–295.
9. Bennett, A.J., Billett, M.A., Salter, A.M., Mangiapane, E.H., Bruce, J.S., Anderton, K.L., Marenah, C.B., Lawson, N., and White, D.A. (1995) Modulation of Hepatic Apolipoprotein B, 3-Hydroxy-3-methylglutaryl-CoA Reductase and Low-Density Lipoprotein Receptor mRNA and Plasma Lipoprotein Concentrations by Defined Dietary Fats, *Biochem J. 311*, 167–173.
10. Kurushima, H., Hayashi, K., Shingu, T., Kuga, Y., Ohtani, H., Okura, Y., Tanaka, K., Yasunobu, Y., Nomura, K., and Kajiyama, G. (1995) Opposite Effects on Cholesterol Metabolism and Their Mechanisms Induced by Dietary Oleic Acid and Palmitic Acid in Hamsters, *Biochim. Biophys. Acta 1258*, 251–256.
11. Sessions, V.A., and Salter, A.M. (1994) The Effects of Different Dietary Fats and Cholesterol on Serum Lipoprotein Concentrations in Hamsters, *Biochim. Biophysi. Acta 1211*, 207–214.
12. Rudel, L.L., Haines, J.L., and Sawyer, J.K. (1990) Effects on Plasma Lipoproteins of Monounsaturated, Saturated, and Polyunsaturated Fatty Acids in the Diet of African Green Monkeys, *J. Lipid. Res. 31*, 1873–1882.
13. Hayes, K.C., Pronczuk, A., Lindsey, S., and Diersen-Schade, D. (1991) Dietary Saturated Fatty Acids (12:0, 14:0, 16:0) Differ in Their Impact on Plasma Cholesterol and Lipoproteins in Nonhuman Primates, *Am. J. Clin. Nutr. 53*, 491–498.
14. Labat, J.B., Martini, M.C., Carr, T.P., Elhard, B.M., Olson, B.A., Bergmann, S.D., Slavin, J.L., Hayes, K.C., and Hassel, C.A. (1997) Cholesterol-Lowering Effects of Modified Animal Fats to Postmenopausal Women, *J. Am. Coll. Nutr. 16*, 570–577.
15. Noakes, M., Nestel, P.J., and Clifton, P.M. (1996) Modifying the Fatty Acid Profile of Dairy Products Through Feedlot Technology Lowers Plasma Cholesterol of Humans Consuming the Products, *Am. J. Clin. Nutr. 63*, 42–46.
16. Estevez-Gonzalez, M.D., Saavedra-Santana, P., and Betancor-Leon, P. (1998) Reduction of Serum Cholesterol and Low-Density Lipoprotein Cholesterol Levels in a Juvenile Population After Isocaloric Substitution of Whole Milk with a Milk Preparation (skimmed milk enriched with oleic acid), *J. Pediatr. 132*, 85–89.
17. Davis, P.A., Platon, J.-F., Gershwin, M.E., Halpern, G.M., Keen, C.L., DiPaolo, D., Alexander, J., and Ziboh, V.A. (1993) A Linoleate-Enriched Cheese Product Reduces Low-Density Lipoprotein in Moderately Hypercholesterolemic Adults, *Ann. Intern. Med. 119*, 555–559.

18. Tholstrup, T., Sandstrom, B., Hermansen, J.E, and Holmer, G. (1998) Effect of Modified Dairy Fat on Postprandial and Fasting Plasma Lipids and Lipoproteins in Healthy Young Men, *Lipids 33*, 11–21.
19. Bell, L., Halstenson, C.E., Halstenson, C.J., Macres, M., and Keane, W.F. (1992) Cholesterol-Lowering Effects of Calcium Carbonate in Patients with Mild to Moderate Hypercholesterolemia, *Arch. Intern. Med. 152*, 2441–2444.
20. Denke, M.A., Fox, M.M., and Schulte, M.C. (1993) Short-Term Dietary Calcium Fortification Increases Fecal Saturated Fat Content and Reduces Serum Lipids in Men, *J. Nutr. 123*, 1047–1053.
21. Shahkhalili, Y., Murset, C., Meirim, I., Duruz, E., Guinchard, S., Cavadini, C., and Acheson, K. (2001) Calcium Supplementation of Chocolate: Effect on Cocoa Butter Digestibility and Blood Lipids in Humans, *Am. J. Clin. Nutr. 73*, 246–252.
22. Fleischman, A.I., Yacowitz, H., Hayton, T., and Bierenbaum, M.L. (1966) Effects of Dietary Calcium upon Lipid Metabolism in Mature Male Rats Fed Beef Tallow, *J. Nutr. 88*, 255–260.
23. Yacowitz, H., Fleischman, A.I., Amsden, R.T., and Bierenbaum, M.L. (1967) Effects of Dietary Calcium upon Lipid Metabolism in Rats Fed Saturated or Unsaturated Fat, *J. Nutr. 92*, 389–392.
24. Fleischman, A.I., Yacowitz, H., Hayton, T., and Bierenbaum, M.L. (1967) Long-Term Studies on the Hypolipiemic Effect of Dietary Calcium in Mature Male Rats Fed Cocoa Butter, *J. Nutr. 91*, 151–157.
25. Vaskonen, T., Mervaala, E., Sumuvuori, V., Seppanen-Laakso, T., and Karppanen, H. (2002) Effects of Calcium and Plant Sterols on Serum Lipids in Obese Zucker Rats on a Low-Fat Diet, *Br. J. Nutr. 87*, 239–245.
26. Dougherty, R.M., and Iacono, J.M. (1979) Effects of Dietary Calcium on Blood and Tissue Lipids, Tissue Phospholipids, Calcium and Magnesium Levels in Rabbits Fed Diets Containing Beef Tallow, *J. Nutr. 109*, 1934–1945.
27. De Rodas, B.Z., Gilliland, S.E., and Maxwell, C.V. (1996) Hypocholesterolemic Action of *Lactobacillus acidophilus* ATCC 43121 and Calcium in Swine with Hypercholesterolemia Induced by Diet, *J. Dairy Sci. 79*, 2121–2128.
28. Bhattacharyya, A.K., Thera, C., Anderson, J.T., Grande, F., and Keys, A. (1969) Dietary Calcium and Fat: Effect on Serum Lipids and Fecal Excretion of Cholesterol and Its Degradation Products in Man, *Am. J. Clin. Nutr. 22*, 1161–1174.
29. Reeves, P.G., Nielsen, F., and Fahey, G.C., Jr. (1993) AIN-93 Purified Diets for Laboratory Rodents: Final Report of the American Institute of Nutrition Ad Hoc Writing Committee on the Reformulation of the AIN-76A Rodent Diet, *J. Nutr. 123*, 1939–1951.
30. Spady, D.K., and Dietschy, J.M. (1988) Interaction of Dietary Cholesterol and Triglycerides in the Regulation of Hepatic Low Density Lipoprotein Transport in the Hamster, *J. Clin. Invest. 81*, 300–309.
31. Nicolosi, R.J., Wilson, T.A., Lawton, C., Rogers, E.J., Wiseman, S.A., Tijburg, L.B.M., and Kritchevsky, D. (1998) The Greater Atherogenicity of Non-purified Diets Versus Semipurified Diets in Hamsters Is Mediated *via* Differences in Plasma Lipoprotein Cholesterol Distribution, LDL Oxidative Susceptibility, and Plasma α-Tocopherol Concentration, *J. Nutr. Biochem. 9*, 591–597.
32. Awad, A.C., and Gray, J.I. (2000) Methods to Reduce Free Fatty Acids and Cholesterol in Anhydrous Animal Fat, U.S. Patent No. 6,129,945.
33. Trautwein, E.A., Liang, J., and Hayes, K.C. (1993) Plasma Lipoproteins, Biliary Lipids and Bile Acid Profile Differ in Various Strains of Syrian Hamsters *Mesocricetus auratus, Comp. Biochem. Physiol. Comp. Physiol. 104A*, 829–835.
34. Folch, J., Lees, M., and Sloane Stanley, G.H. (1957) A Simple Method for the Isolation and Purification of Total Lipids from Animal Tissues, *J. Biol. Chem. 226*, 497–509.
35. Sun, G., and Horrocks, L.A. (1967) The Fatty Acid and Aldehyde Composition of the Major Phospholipids of Mouse Brain, *Lipids 3*, 79–83.
36. van de Kamer, J.H., ten Bokkel Huinink, H., and Weyers, H.A. (1949) Rapid Method for the Determination of Fat in Feces, *J. Biol. Chem. 177*, 347–355.
37. Salter, A., Mangiapane, E., Bennett, A.J, Bruce, J.S, Billett, M.A., Anderton, K.L., Marenah, C.B., Lawson, N., and White, D.A. (1998) The Effect of Different Dietary Fatty Acids on Lipoprotein Metabolism: Concentration-Dependent Effects of Diets Enriched in Oleic, Myristic, Palmitic and Stearic Acids, *Br. J. Nutr. 79*, 195–202.
38. Kris-Etherton, P.M., Dietschy, J. (1997) Design Criteria for Studies Examining Individual Fatty Acid Effects on Cardiovascular Disease Risk Factors: Human and Animal Studies, *Am. J. Clin. Nutr. 65(5* Suppl.), 1590S–1596S.
39. Trautwein, E.A., Rieckhoff, D., Kunath-Rau, A., and Erbersdobler, H.F. (1999) Replacing Saturated Fat with PUFA-rich (sunflower oil) or MUFA-rich (rapeseed, olive and high-oleic sunflower oil) Fats Resulted in Comparable Hypocholesterolemic Effects in Cholesterol-Fed Hamsters, *Ann. Nutr. Metab. 43*, 159–172.
40. Terpstra, A.H., van den Berg, P., Jansen, H., Beynen, A.C., and van Tol, A. (2000) Decreasing Dietary Fat Saturation Lowers HDL-Cholesterol and Increases Hepatic HDL Binding in Hamsters, *Brit. J. Nutr. 83*, 151–159.
41. Trautwein, E.A., Kunath-Rau, A., Dietrich, J., Drusch, S., and Erbersdobler, H.F. (1997) Effect of Dietary Fats Rich in Lauric, Myristic, Palmitic, Oleic or Linoleic Acid on Plasma, Hepatic and Biliary Lipids in Cholesterol-Fed Hamsters, *Br. J. Nutr. 77*, 605–620.
42. Hayes, K.C., and Khosla, P. (1992) Dietary Fatty Acid Thresholds and Cholesterolemia, *FASEB J 6*, 2600–2607.
43. Goodman, D.S., Deykin, D., and Shiratori, T. (1964) The Formation of Cholesterol Esters with Rat Liver Enzymes, *J. Biol. Chem. 239*, 1335–1345.
44. Iacono, J.M. (1974) Effect of Varying the Dietary Level of Calcium on Plasma and Tissue Lipids of Rabbits, *J. Nutr. 104*, 1165–1171.
45. Carroll, K.K., and Richards, J.F. (1957) Factors Affecting Digestability of Fatty Acids in the Rat, *J. Nutr. 64*, 411–424.
46. Ockner, R.K., Pittman, J.P., and Yager, J.L. (1972) Differences in the Intestinal Absorption of Saturated and Unsaturated Long Chain Fatty Acids, *Gastroenterology 62*, 981–992.
47. Brink, E.J., Haddeman, E., de Fouw, N.J., and Weststrate, J.A. (1995) Positional Distribution of Stearic Acid and Oleic Acid in a Triacylglycerol and Dietary Calcium Concentration Determines the Apparent Absorption of These Fatty Acids in Rats, *J. Nutr. 125*, 2379–2387.
48. Jensen, R.G., Ferris, A.M., and Lammi-Keefe, C.J. (1991) Symposium: Milk Fat-Composition, Function and Potential for Change: The Composition of Milk Fat, *J. Dairy Sci. 74*, 3228–3243.
49. Kinosian, B., Glick, H., Preiss, L., and Puder, K.L. (1995) Cholesterol and Coronary Heart Disease: Predicting Risks in Men by Changes in Levels and Ratios, *J. Investig. Med. 43*, 443–450.
50. Steinmetz, K.A., Childs, M.T., Stimson, C., Kushi, L.H., McGovern, P.G., Potter, J.D., and Yamanaka, W.K. (1994) Effect of Consumption of Whole Milk and Skim Milk on Blood Lipid Profiles in Healthy Men, *Am. J. Clin. Nutr. 59*, 612–618.
51. Reid, I.R., Mason, B., Horne, A., Ames, R., Clearwater, J., Bava, U., Orr-Walker, B., Wu, F., Evans, M.C., and Gamble, G.D. (2003) Effects of Calcium Supplementation on Serum Lipid Concentrations in Normal Older Women: A Randomized Controlled Trial, *Am. J. Med. 112*, 343–347.

[Received January 27, 2004; accepted July 6, 2004]

Dietary TAG Source and Level Affect Performance and Lipase Expression in Larval Sea Bass (*Dicentrarchus labrax*)

S. Morais[a,]*, C. Cahu[b], J.L. Zambonino-Infante[b], J. Robin[b], I. Rønnestad[c], M.T. Dinis[a], and L.E.C. Conceição[a]

[a]Centro de Ciências do Mar (CCMAR), Universidade do Algarve, Campus de Gambelas, 8005-139 Faro, Portugal, [b]Institut Français de Recherche pour l'Exploration de la Mer (IFREMER), 29280 Plouzané, France, and [c]Department of Zoology, University of Bergen, N-5007 Bergen, Norway

ABSTRACT: The influence of dietary TAG source (fish oil, triolein, and coconut oil) and level (7.5 and 15% of the diet) on growth, lipase activity, and mRNA level was studied in sea bass larvae, from mouth opening until day 24 and from day 37 to 52. Fish oil and triolein induced better growth in both experiments, this being significant at a higher dietary level. Coconut oil significantly decreased growth at the higher level, possibly as the result of an excessive supply of medium-chain TAG. Growth was not related to lipase specific activity, suggesting a production in excess to dietary needs. Body lipid content was positively related to dietary lipid level and was affected by lipid quality. In addition, larval FA composition generally reflected that of the diet. The source of dietary lipid, but not the quantity, was shown to affect lipase activity significantly. Coconut oil diets induced the highest lipase activity, whereas the effect of fish oil was age dependent—it was similar to coconut oil at day 24 but induced the lowest lipase activity in 52-d-old larvae. The differential lipase response was probably caused by differences in the FA composition of the diet, related to the specificity of lipase toward FA differing in chain length and degree of saturation. No significant differences were found in lipase/glyceraldehyde-3-phosphate dehydrogenase mRNA, which suggests the existence of a posttranscriptional regulation mechanism.

Paper no. L9445 in *Lipids 39,* 449–458 (May 2004).

In spite of the considerable progress achieved in marine larval nutrition in the last decades, larval rearing of many commercially important marine species is still far from optimal. Marine larval rearing is mostly dependent on the production of live feeds and on the manipulation of their nutritional profile, although relatively good results have been achieved recently with the exclusive use of inert diets (1). Some of the earlier studies conducted with fish larvae associated the simple morphological structure of the digestive system with a low production of proteolytic enzymes and explained the failure of rearing fish larvae with formulated diets by a lower digestion efficiency (e.g., 2,3). Nonetheless, in general, measurements of the digestive enzyme content of larvae reveal significant levels of pancreatic and intestinal enzymes (4–6). Therefore, the problems encountered in rearing marine larvae on formulated diets may be more a question of an inadequacy of the diet composition and physical properties in relation to the digestive characteristics of the larval stages, leading to an inadequate stimulation of enzyme release, rather than a low digestive capacity (5,7).

Relatively few studies have examined the influence of dietary composition on the regulation of gastrointestinal tract function and development in fish, even though diet quality appears to have a direct effect on the onset of the maturation processes of the digestive tract (5,8,9). Studies looking at the quantitative lipid requirements of marine fish larvae have described a stimulation of the lipolytic activities of pancreatic lipase and phospholipase A_2 by an increase in their substrate level in the diet (8). However, the quality of the dietary lipid source is also an important parameter and has been little investigated. TAG are generally the quantitatively most important lipid class in fish diets, and their physical nature, namely, the carbon chain length and the degree of saturation of their FA, has been shown to affect digestion and absorption (10–13). Having this in mind, the present study was conducted to study the effect of dietary TAG quality and quantity in larval development and lipase expression in European sea bass (*Dicentrarchus labrax* L.).

MATERIALS AND METHODS

Rearing and experimental diets. Eggs of European sea bass (*D. labrax* L.) were obtained from the marine hatchery of Aquanord (Gravelines, France). Two experiments were conducted at IFREMER–Station de Brest, using the same batch of eggs (January 2003), and in both larvae were fed only formulated diets from mouth opening (day 5). The first experiment was carried out from day 5 until day 24. Rearing of the experimental animals was conducted in 18 black cylindrical-conical tanks (35 L). Initial stocking density in the first experiment was 80 larvae/L. The tanks were supplied with running filtered and thermoregulated seawater (sand filter, tungsten heater, degassing column, UV lamp, and, finally, 10 μm cartridge filter). The temperature was regulated at 14°C for the 5-d-old larvae and gradually increased during 4 d, finally being stabilized at 18–19°C. Salinity was lowered from 35–38 to 25 ppL at day 5. Light intensity was progressively increased until reaching full light at day 16, with a maximum intensity of 9 W/m^2 at the water surface. The oxygen level was maintained above 6 mg/L by setting the water exchange

*To whom correspondence should be addressed. E-mail: smorais@ualg.pt

Abbreviations: CCK, cholecystokinin; DM, dry matter; GAPDH, glyceraldehyde-3-phosphate dehydrogenase; HUFA, highly unsaturated FA; IFREMER, Institut Français de Recherche pour l'Exploration de la Mer; MCFA, medium-chain FA; MCT, medium-chain TAG; MUFA, monounsaturated FA; PCR, polymerase chain reaction; RT, reverse-transcripted; SFA, saturated FA.

to 30% per hour (0.18 L/min). The second experiment lasted from day 37 (average wet weight = 35.4 mg) to day 52. During the first 36 days larvae were reared in the same conditions as in the first experiment, except for the diet fed (Gemma Micro 150, followed by Gemma Micro 300; Trouw, Fontaine-les-vervins, France). Larvae were stocked in the experimental tanks on day 36 at a density of 19 larvae/L.

Six microparticulate diets were formulated to contain three different neutral lipid sources, differing in the carbon chain length and degree of saturation of their FA—fish oil (cod liver oil), purified (>99%) triolein (a TAG composed of a glycerol backbone and three 18:1n-9 acids), and coconut oil—at two inclusion levels (7.5 and 15%), and were designated as F7.5, T7.5, C7.5, F15, T15 and C15 (Table 1). The two lipid levels were achieved by balancing the level of carbohydrate (starch), while protein was maintained constant. The dietary ingredients were mechanically mixed with 10% water using a Hobart mixer (Bernstein Schaltsysteme, Offenberg, Germany), pelleted, and dried at 60°C for 30 min. The pellets were ground and sieved to obtain particles of size <400 μm. Fish were continuously fed in excess (2 g/d/tank on days 6–10, 4 g/d/tank until day 15, 6 g/d/tank until day 25, and 8 g/d/tank from day 26 onward) with belt feeders, during 18 h per day. Food ingestion was monitored by observing the larval digestive tract under a binocular microscope, and diet acceptability was found to be good from the start of feeding. Each diet was tested in triplicate randomized tanks.

Sampling. All sampling procedures were conducted in the morning, after cleaning the tanks and before food distribution, to ensure that larvae had an empty digestive tract. To monitor growth, 15 larvae were removed weekly from each tank in the first experiment (days 11, 18, and 24) and at the start and end of the second experiment, rinsed in fresh water, and immediately weighed. Survival was only determined at the end of the second experiment by individually counting the larvae (individuals removed during sampling were added to the number of surviving animals). For the biochemical assays larvae were collected straight into ice, without rinsing in fresh water. Collection of larvae for lipase activity assays was conducted on day 18 (n = 100 larvae per tank) and day 24 (n variable—all surviving larvae) in the first experiment, and at the end of the second experiment (day 52, n = 12 larvae per tank). Larvae were immediately stored at −80°C, pending dissection of the pancreatic segment and assays. In the first experiment

TABLE 1
Experimental Diet Formulation and Proximate Composition[a]

	F7.5	T7.5	C7.5	F15	T15	C15
Diet ingredients (g/kg dry diet)						
Constant ingredients						
Fish meal[b]	540	540	540	540	540	540
Hydrolyzed fish meal[c]	130	130	130	130	130	130
Soybean lecithin[d]	50	50	50	50	50	50
Vitamin mixture[e]	80	80	80	80	80	80
Mineral mixture[f]	40	40	40	40	40	40
Betaine[g]	10	10	10	10	10	10
Variable ingredients						
Fish oil (cod liver oil)[h]	75	0	0	150	0	0
Triolein (purified)[i]	0	75	0	0	150	0
Coconut oil[j]	0	0	75	0	0	150
Starch[k]	75	75	75	0	0	0
Proximate composition						
Dry matter (DM, %)	97.8 ± 0.0	97.6 ± 0.0	97.6 ± 0.1	97.1 ± 0.0	97.4 ± 0.2	97.5 ± 0.0
Protein (N × 6.25) (% DM)	58.3 ± 0.2	58.7 ± 0.4	58.8 ± 0.2	58.5 ± 0.0	57.7 ± 0.0	58.4 ± 0.4
Lipid (% DM)	17.0 ± 0.6	16.9 ± 0.7	16.0 ± 0.1	24.2 ± 0.5	24.4 ± 0.6	23.9 ± 0.7
Ash (% DM)	12.0 ± 0.1	12.0 ± 0.0	12.2 ± 0.1	12.0 ± 0.0	13.5 ± 0.1	12.0 ± 0.0
Protein energy/lipid energy[l]	1.5	1.5	1.6	1.1	1.0	1.1

[a]Values are means ± SD (n = 2). DM, dry matter.
[b]La Lorientaise, Sopropêche, Lorient, France.
[c]CPSP 90, Sopropêche, Boulogne sur mer, France.
[d]Louis François, St. Maur, France.
[e]Composé Vitaminique 762, INRA, Jouy-en-Josas, France. Per kg of vitamin mix: retinyl acetate, 1 g; cholecalciferol, 2.5 mg; all-*rac*-α-tocopherol acetate, 10 g; menadione, 1 g; thiamin, 1 g; riboflavin, 0.4 g; D-calcium pantothenate, 2 g; pyridoxine HCl, 0.3 g; cyanocobalamin, 1 g; niacin, 1 g; choline chloride, 200 g; ascorbic acid, 20 g; folic acid, 0.1 g; biotine, 1 g; *meso*-inositol, 30 g.
[f]Composé Minéral 763, INRA, Jouy-en-Josas, France. Per kg of mineral mix: KCl, 90 g; KI, 40 mg; $CaHPO_4 \cdot 2H_2O$, 500 g; NaCl, 40 g; $CuSO_4 \cdot 5H_2O$, 3 g; $ZnSO_4 \cdot 7H_2O$, 4 g; $CoSO_4 \cdot 7H_2O$, 20 mg; $FeSO_4 \cdot 7H_2O$, 20 g; $MnSO_4 \cdot H_2O$, 3 g; $CaCO_3$, 215 g; $MgSO_4 \cdot 7H_2O$, 124 g; NaF, 1 g.
[g]Betaine (min. 99%), Sigma, France.
[h]La Lorientaise, Sopropêche, Lorient, France (14:0, 6.3%; 15:0, 1.0%; 16:0, 14.0%; 16:1, 6.0%; 18:0, 1.7%; 18:1, 16.7%; 18:2, 2.0%; 18:3, 1.2%; 18:4, 3.0%; 20:1, 11.3%; 20:5, 9.8%; 22:1, 12.4%; 22:5, 0.6%; 22:6, 8.0%).
[i]VWR Prolabo, Fontenay-sous-Bois, France. $C_{57}H_{104}O_6$; *d.* 0.91; M = 885.46 g/mol.
[j]Coconut Oil Supreme™, Mid-American Marketing Corp., Eaton, Ohio (8:0, 8.86%; 10:0, 6.17%; 12:0, 48.83%; 14:0, 19.97%; 16:0, 7.84%; 18:0, 3.06%; 18:2, 0.76%; 18:1, 4.44%; 20:0, 0.05%).
[k]Pregelatinised Starch, Pregeflo® P100, Roquette, Lille, France.
[l]Calculated as: lipid × 37.7 J kg^{-1}; protein × 16.7 J kg^{-1}.

whole larvae were assayed. Larvae were also collected for mRNA quantification but, in this case, total RNA extraction (of whole larvae in the first experiment and of dissected pancreatic segments in the second) was carried out immediately. This was performed on day 16 (n variable—approximately 250–300 mg wet weight) in the first experiment and on day 51 (n = 5 larvae per tank) in the second experiment. Dissections were performed on a glass maintained on ice; a segment containing the pancreatic section was cut from just behind the head to the middle of the digestive tract. Samples for biochemical composition and FA analysis were also collected at the start (day 36; n = 100 larvae per triplicate) and at the end (day 52; n = 60 larvae per tank) of the second experiment. Larvae were immediately stored at −20°C until analysis.

Proximate composition and FA analysis. The diets were ground, and whole larvae (day 36 and 52) were ground frozen, freeze-dried, and homogenized before analysis. Duplicate aliquots were analyzed for dry matter (DM) after desiccation in an oven (105°C, 24 h) and ash (incineration at 550°C, 12 h), following standard laboratory procedures (14). Total protein content was determined according to Dumas (15) (N × 6.25) in a Nitrogen Analyzer NA2000 (Fison instrument), using DL-methionine as an internal standard. Total lipid was extracted using the method of Folch *et al*. (16), with chloroform being replaced by dichloromethane. Total FA were saponified by a 2 M KOH/methanol solution and then esterified in a 0.7 M HCl/methanol solution. FAME were separated by GC in a PerkinElmer Auto-system with a FID, BPX 70 capillary column (25 m × 0.22 mm i.d. × 0.25 μm film thickness; SGE, Melbourne, Australia), split-splitless injector, with helium as carrier gas. The injector and detector temperatures were 220 and 260°C, respectively. Initial temperature of the oven was 50°C, increased to 180°C by increments of 15°C/min, maintained for 5 min, and finally increased to 220°C by increments of 3°C/min. Data acquisition and handling were carried out by connecting the gas chromatograph to a PE Nelson computer. The individual FAME were identified by comparing the retention time of standard methyl ester mixtures—68A (Interchim, Montluçon, France), ME64 (Larodan, Malmo, Sweden), AOCS no. 5 (Sigma, St. Louis, MO); and the results of individual FA are expressed as percentages of total identified FAME. Proximate composition of the diets and larvae is shown in Tables 1 and 3, respectively, while the FA composition of the experimental diets and larvae can be seen in Table 2.

Lipase enzymatic determination. Pancreatic segments were homogenized in 1.5 mL (first experiment) or 3 mL (second experiment) of cold (4°C) distilled water. Lipase activity was assayed according to a spectrophotometric method slightly modified from Iijima *et al*. (17), using as substrate *p*-nitrophenyl myristate (Sigma) dissolved in 65.8 mM DMSO (Merck-Schuchardt; Hohenbrunn, Germany), as this was found to aid substrate solubilization. Protein was determined according to Bradford (18), and enzymatic activity was expressed as specific activity, U/mg protein (U = μmol of substrate hydrolyzed per min at 30°C).

mRNA quantification. Lipase mRNA was quantified through reverse transcriptase–PCR analysis. Total RNA extraction was performed using TRIzol® (Gibco BRL, Gaithersburg, MD). After RNA quantification by spectrophotometry reading, 5.5 μg of total RNA was collected and reverse-transcripted (RT) to cDNA, using the Ready To Go T-Primed First Strand Kit (Pharmacia Biotech, Uppsala, Sweden). The quantification of mRNA coding for lipase was normalized relative to the mRNA-specific housekeeping gene glyceraldehyde-3-phosphate dehydrogenase (GAPDH), i.e., results are presented as lipase mRNA/GAPDH mRNA. GAPDH was chosen as the housekeeping gene since its expression did not significantly vary during sea bass larval development (1). PCR of a 50-μL solution containing 1–3 μL of cDNA, 5 μL of a 10× buffer solution (Qbiogene, Illkirch, France), 2 μL of 20 mM dNTPs (Eurogentec, Seraing, Belgium), 0.5 μL of 5 U/μL Taq polymerase (Qbiogene), 50 pmol of each primer, and sterilized distilled water to complete the 50 μL volume was carried out in a thermocycler (Robocycler® Gradient 96; Stratagene, LaJolla, CA). PCR conditions were as follows: initial denaturation at 94°C for 30 s followed by 30 cycles including denaturation at 94°C for 1 min, annealing at specific temperatures (50°C for lipase and 56°C for GAPDH) for 1.5 min, and 2 min elongation at 72°C. A final extension cycle was performed at 72°C for 7 min. Primer sequences were: 5′–TGT GGC TTC AAC AGC–3′ and 5′–CGC TCC AAG RCT GTA–3′ (Cybergene, Ivry, France) for lipase; and 5′–CAC CAC GCT CAC CAT CGC–3′ and 5′–CAT CTT GGG GAA CAT GTG–3′ (Eurogentec) for GAPDH. Quantification of RT-PCR products coding for lipase and GAPDH was achieved by applying 10 μL of each PCR product on a 1.2% agarose (0.8% agarose plus 0.4% low-melting-temperature agarose)–ethidium bromide (1 mg/L) gel, followed by image capture in a multi-imager (Bio-Rad Multi-Analyst™) and quantification using the software Image Master™ TotalLab (Amersham Pharmacia Biotech, Uppsala, Sweden). The limits of the exponential phase and the beginning of the saturation phase of the amplification reaction were determined for each gene (by a calibration curve plotting the product of a 30-cycle PCR against the known start concentration of the cDNA) to ensure the linear relationship between start RNA and final RT-PCR product.

Statistical analyses. Results are given as mean values ± SD of triplicate or duplicate (diet biochemical composition) samples. Data from larval weight, survival rate, body composition, lipase activity, and mRNA levels were compared by a two-way ANOVA followed by the Tukey HSD multiple range test when significant differences were found at the $P < 0.05$ level, using the software Statistica 6 (StatSoft Inc., Tulsa, OK). The two analyzed factors were "lipid quantity" (two levels—7.5 and 15%) and "lipid quality" (three levels—fish oil, triolein, and coconut oil). The assumption of homogeneity of variance was previously checked using the Bartlett's test and survival rates were $\arcsin(x^{1/2})$ transformed (19). In the cases where a significant interaction was found between the two factors, a one-way ANOVA was performed to analyze the results.

TABLE 2
FA Composition of the Experimental Diets and of the Larvae at the Start (day 36) and at the End of the Second Experiment (day 52)[a]

	Experimental diets						Larvae						
FA (%)	F7.5	T7.5	C7.5	F15	T15	C15	Start	F7.5	T7.5	C7.5	F15	T15	C15
8:0	0.0	0.0	1.9	0.0	0.0	2.5	0.0	0.0	0.0	0.0	0.0	0.0	0.0
10:0	0.0	0.0	3.0	0.0	0.0	4.0	0.0	0.0	0.0	0.3	0.0	0.0	0.5
12:0	0.2	0.0	26.9	0.1	0.0	36.8	0.0	0.0	0.0	7.1	0.0	0.0	11.5
14:0	5.5	1.8	12.4	5.8	1.2	15.3	1.5	3.4	1.2	7.2	3.2	0.9	9.5
16:0	16.4	10.2	12.6	16.1	7.9	11.0	17.5	18.2	11.9	17.2	16.0	9.3	16.3
18:0	3.3	3.7	3.3	3.3	3.6	3.0	5.4	5.2	4.9	5.7	4.5	4.6	5.6
20:0	0.2	0.2	0.1	0.3	0.3	0.1	0.2	0.2	0.2	0.2	0.2	0.2	0.2
22:0	0.2	0.6	0.1	0.2	0.7	0.1	0.1	0.0	0.2	0.0	0.0	0.3	0.0
14:1	0.3	0.2	0.2	0.3	0.1	0.0	0.2	0.1	0.0	0.0	0.2	0.0	0.0
16:1n-7	5.3	1.8	1.8	5.9	1.3	1.2	2.5	4.7	1.8	2.3	5.2	1.3	2.1
18:1n-7	1.0	0.0	0.0	1.1	0.0	0.0	2.9	3.2	2.0	1.9	3.3	1.8	1.6
20:1n-7	0.3	0.0	0.1	0.3	0.0	0.0	0.2	0.4	0.0	0.0	0.4	0.0	0.0
18:1n-9	10.8	45.2	7.0	11.7	56.5	6.3	12.0	12.3	37.8	10.6	12.3	48.5	10.9
20:1n-9	5.6	2.9	2.5	5.9	2.3	1.9	4.5	5.4	3.7	3.6	5.5	3.6	3.0
22:1n-9	0.7	0.3	0.3	0.8	0.3	0.2	0.5	0.5	0.3	0.3	0.5	0.2	0.2
24:1n-9	0.6	0.3	0.3	0.6	0.2	0.2	0.2	0.3	0.3	0.3	0.2	0.2	0.2
18:1n-11	2.8	1.6	1.1	3.0	1.4	0.8	0.5	1.3	0.0	1.0	1.3	0.0	0.5
20:1n-11	0.8	0.3	0.3	0.8	0.0	0.0	0.7	1.0	0.4	0.7	1.0	0.0	0.6
22:1n-11	6.4	3.2	3.0	6.6	2.1	1.8	2.9	3.9	2.1	2.2	3.7	1.4	1.5
18:2n-6	12.4	15.4	11.0	9.1	13.6	7.3	23.2	12.1	14.6	13.5	9.6	13.8	12.2
18:3n-6	0.2	0.1	0.1	0.2	0.1	0.0	0.1	0.2	0.2	0.2	0.2	0.2	0.2
20:2n-6	0.3	0.1	0.1	0.3	0.1	0.0	1.4	1.0	0.8	1.6	0.9	0.6	1.5
20:3n-6	0.2	0.0	0.0	0.2	0.0	0.0	0.0	0.1	0.1	0.1	0.2	0.0	0.1
20:4n-6	0.6	0.3	0.3	0.6	0.2	0.2	0.8	1.0	0.7	0.8	0.9	0.4	0.8
22:5n-6	0.3	0.4	0.1	0.3	0.3	0.1	0.1	0.3	0.2	0.2	0.3	0.2	0.3
18:3n-3	2.4	1.8	1.9	2.0	1.2	1.2	2.9	1.8	1.6	2.0	1.7	1.2	1.8
18:4n-3	2.3	1.0	1.0	2.3	0.7	0.7	0.7	1.3	0.6	1.0	1.5	0.4	0.9
20:3n-3	0.1	0.0	0.0	0.1	0.0	0.0	0.1	0.0	0.0	0.1	0.0	0.0	0.0
20:4n-3	0.8	0.2	0.2	1.0	0.2	0.1	0.3	0.6	0.3	0.4	0.9	0.2	0.3
20:5n-3	8.5	3.0	3.1	9.0	2.1	1.9	6.1	7.4	4.3	6.1	9.4	3.3	5.6
22:5n-3	1.5	0.4	0.3	1.9	0.2	0.2	0.8	1.5	0.6	0.8	2.0	0.5	0.7
22:6n-3	10.1	4.9	4.9	10.3	3.3	2.9	11.9	12.7	9.4	12.5	14.6	6.9	11.3
∑ SFA	25.7	16.5	60.3	25.7	13.7	72.9	24.6	27.0	18.4	37.6	23.9	15.3	43.5
∑ MUFA	34.6	55.9	16.8	37.1	64.2	12.4	27.1	32.9	48.4	23.0	33.7	57.0	20.7
∑ PUFA	39.7	27.6	22.9	37.3	22.1	14.7	48.3	40.1	33.3	39.4	42.3	27.8	35.8
∑ HUFA	21.0	8.5	8.5	22.2	5.8	5.1	19.0	22.2	14.5	19.8	27.0	10.8	18.0

[a]Values are means (diets, $n = 2$; larvae, $n = 3$, except F15, where $n = 1$); SD was below 0.004 in diets and 0.05 in larvae. SFA, saturated FA; MUFA, monounsaturated FA; HUFA, highly unsaturated FA. For diet descriptions and other abbreviation see Table 1.

TABLE 3
Survival and Biochemical Composition of the Larvae at the Start (day 36) and at the End of the Second Experiment (day 52)[a]

	Start	F7.5	T7.5	C7.5	F15	T15	C15
Survival (%)		89.1 ± 3.1	85.7 ± 3.0	88.4 ± 2.9	92.8 ± 3.1	90.4 ± 3.0	87.9 ± 2.4
Biochemical composition							
Moisture (%)	91.6 ± 1.2	87.7 ± 0.6	86.2 ± 1.4	86.4 ± 1.4	87.0 ± 1.3	86.2 ± 1.6	88.7 ± 1.8
Ash (% DM)	22.0 ± 0.0	16.3 ± 0.9	15.1 ± 0.3	16.2 ± 0.6	14.3 ± 0.8	15.0 ± 2.3	17.7 ± 2.2
Lipid (% DM)	20.3 ± 1.3	19.9 ± 1.1^{a,b}	20.9 ± 0.2^{b}	17.2 ± 1.0^{c}	24.6 ± 0.5^{d}	26.5 ± 0.5^{d}	18.7 ± 0.2^{a,c}
Total FA (% DM)	14.6 ± 0.1	14.6 ± 1.1^{a,b}	16.6 ± 0.2^{a,b}	13.2 ± 0.9^{a}	17.2 ± 2.7^{b}	21.7 ± 1.0^{c}	13.9 ± 0.3^{a,b}
Protein (N × 6.25) (% DM)	61.1 ± 2.4	62.2 ± 0.9	64.0 ± 3.3	64.6 ± 1.2	59.1 ± 0.3	58.3 ± 0.6	62.6 ± 0.4

[a]Values are means ± SD ($n = 3$). Values on the same line with different superscript roman letters are significantly different ($P < 0.05$, one-way ANOVA), but only results at the end of the experiment (day 52) were compared. For diet descriptions see Table 1. For abbreviations see Tables 1 and 2.

RESULTS

Larval performance. No significant differences in survival were found in the second experiment (Table 3). On the assumption that the sampling of larvae would not result in further mortality (sampling times were concentrated at the end of the experiment), survival varied between 86 and 93%. In the first experiment, due to reduced growth, all surviving larvae were required for lipase assays and survival was not quantified, as it would extend sampling time and potentially lead to enzyme degradation. In terms of growth, statistically significant differences were found in the first experiment, on

all sampling dates (Fig. 1), and at the end of the second experiment (Fig. 2). A significant effect of lipid quantity was found at all sampling dates except for day 11 of the first experiment, and the factor lipid quality had a significant effect at all times. However, a significant interaction was found between the two analyzed factors on days 17 and 24 of the first experiment and in the second experiment, most probably as the result of the effect of coconut oil on larval growth. In both experiments, an increase in the dietary lipid level resulted in a significantly higher growth of larvae fed the fish oil and triolein diets, whereas for coconut oil a higher dietary level was responsible for a significantly lower growth. In terms of lipid quality, fish oil induced a significantly higher growth at day 11 of the first experiment, whereas no significant differences were found between triolein and coconut oil at this time. At days 17 and 24 of the first experiment, significant differences were found between all lipid sources, with triolein and coconut oil inducing the significantly highest and lowest growth, respectively. At the end of the second experiment, the diet containing fish oil at a higher inclusion level gave a significantly higher growth (although not statistically different from diet T15).

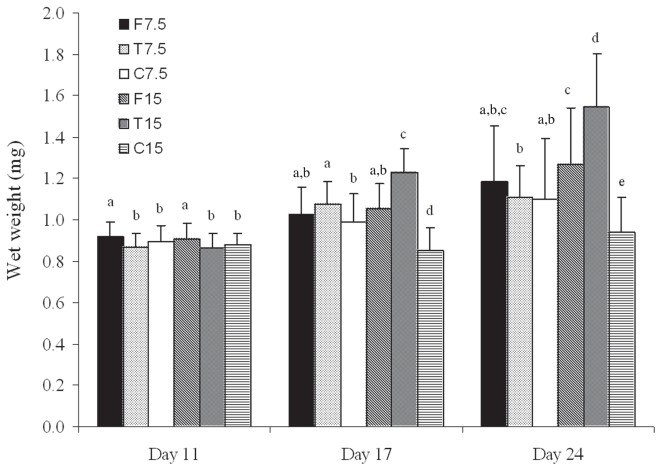

FIG. 1. Wet weight (mg) on days 11, 17, and 24 of the first experiment. Data are means ± SD (n = 3). Columns with different superscript letters on each day are significantly different ($P < 0.05$; one-way ANOVA). Diet contents are enumerated in Table 1.

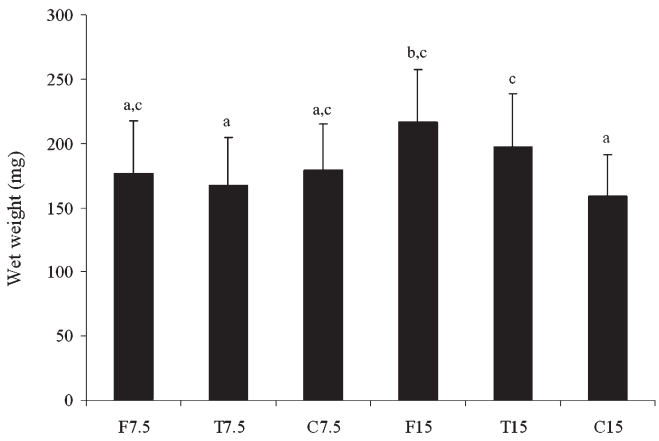

FIG. 2. Wet weight (mg) at the end of the second experiment (day 52). Data are means ± SD (n = 3). Columns with different superscript letters are significantly different ($P < 0.05$; one-way ANOVA). Diet contents are enumerated in Table 1.

Larval biochemical composition. No significant differences were found in the moisture and ash content of the larvae at the end of the second experiment (Table 3). As for the total lipid and FA content, significant differences were found for both factors. A higher dietary lipid level gave a significantly higher larval lipid and FA content. There was also a significant effect of lipid quality, with the triolein diet giving a significantly higher lipid and FA content, followed by the fish oil diet, and the coconut oil diet gave a significantly lower body incorporation of lipid and FA. For protein content, an inverse trend was noted, but it was not statistically significant. The results of the sea bass FA analysis (Table 2) revealed an increase in the relative amount of the FA predominant in the diet over the course of the experiment. The fish oil diets gave the highest larval PUFA content, mainly as a result of the high HUFA (highly unsaturated FA; ≥20 carbon atoms, ≥4 double bonds) level. The larvae fed these diets presented intermediate levels of saturated FA (SFA) and monounsaturated FA (MUFA), as a result of the high levels of 14:0 and 16:0 and of most MUFA, except 18:1n-9. The triolein diets gave the highest MUFA (mainly 18:1n-9) level and the lowest total SFA and PUFA contents. The larvae fed coconut oil diets had the highest level of SFA, particularly of 10:0, 12:0 and 14:0; only in these larvae were 10:0 and 12:0 detected. In addition, larvae fed the C7.5 and C15 diets obtained relative levels of PUFA and HUFA similar to those of larvae fed fish oil diets, particularly F7.5, and to those measured at the start of the experiment. When the dietary oil inclusion level was increased, the general effect on the larvae was an increase in the relative level of the predominant FA, accompanied by a concomitant decrease in the remaining FA.

Lipase specific activity and mRNA level. In the first experiment, no significant differences were found in lipase specific activity on day 18 (Fig. 3A), whereas some differences were found on day 24 for both lipid quantity and quality (Fig. 3B). At this age, a lower lipid inclusion level was responsible for a significantly higher lipase activity, independent of lipid source. The analysis of the factor lipid quality revealed that triolein was responsible for a significantly lower lipase activity, whereas no significant differences were found between fish oil and coconut oil. At the end of the second experiment, only the factor lipid quality was found to give significant differences in lipase specific activity, with all dietary lipid sources being statistically different from each other (Fig. 4A). Diets containing coconut oil induced a significantly higher lipase activity at day 52, and those having fish oil were responsible for the lowest lipase activity. No significant changes occurred when the lipid inclusion level was increased from 7.5 to 15%. No significant differences were found in the lipase/GAPDH mRNA values, during both the first (Fig. 3C) and second (Fig. 4B) experiments.

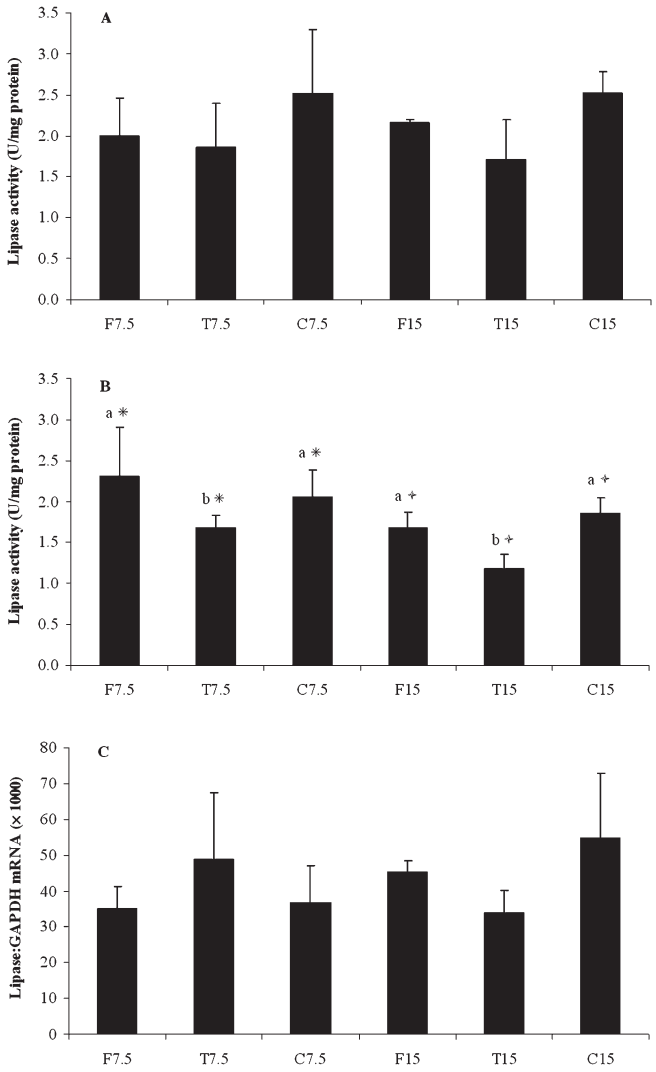

FIG. 3. Lipase specific activity (U/mg protein) and lipase/glyceraldehyde-3-phosphate dehydrogenase (GAPDH) mRNA values assayed in the first experiment. (A) Day 18; (B) day 24; (C) day 16. Data are means ± SD (n = 3). Columns with different symbols ("lipid quantity" factor) or different letters ("lipid quality" factor) are significantly different ($P < 0.05$; two-way ANOVA). Diet contents are enumerated in Table 1.

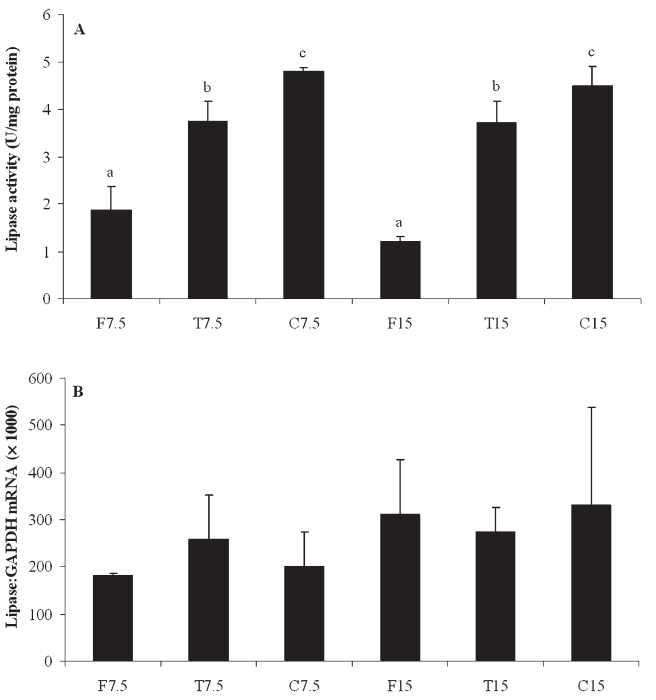

FIG. 4. Lipase specific activity (U/mg protein) and lipase/GAPDH mRNA values assayed at the end of the second experiment. (A) Day 52; (B) day 51. Data are means ± SD (n = 3). Columns with different letters ("lipid quality" factor) are significantly different ($P < 0.05$; two-way ANOVA). Diet contents are enumerated in Table 1. For abbreviation see Figure 3.

DISCUSSION

The long-term adaptation of larval fish lipolytic enzymes to the qualitative lipid content of the diet has not, to our knowledge, been addressed previously. Hence, the objectives of this study were to investigate the effect not only of TAG quantity but also of TAG quality on performance, body composition, lipase activity, and mRNA levels in sea bass larvae.

Larval performance in relation to lipid source. Fish oil is generally considered as a reference oil for fish nutrition. The use of triolein as the neutral lipid source in the diet of larval sea bass produced growth results close to those obtained with fish oil, particularly at the high inclusion level. Larval growth obtained with coconut oil at a low dietary inclusion level was comparable to other TAG sources, whereas at a higher level it had a growth-depressing effect. Coconut oil is one of the few natural sources of medium-chain TAG (MCT), which are composed of SFA with a carbon chain length between 6 and 12 carbon atoms. Medium-chain FA (MCFA) are water soluble, which facilitates their emulsification, hydrolysis, and uptake by the intestinal mucosa. They are not re-esterified by the enterocyte, being transported directly to the liver as FFA (bound to albumin) in the portal circulation (11,20). Coconut oil has been used previously with good growth results in larval carp (21,22) and in juvenile red drum (23). In the present study, however, the C15 diet contained a higher amount of coconut oil than has been tested before. Fontagné *et al*. (21,22) found that coconut oil can be fed to common carp larvae without adverse effects up to 10% in the diet. However, the MCFA caprylic acid (8:0), one of the components of the coconut oil diet, gave reduced growth in common carp at levels above 2% of the diet (or around 10% of total FA), but lower levels were well utilized (22). In our study, the C15 diet included 2.5% caprylic acid. Craig and Gatlin (23) also noted that juvenile red drum were generally not able to utilize 8:0 efficiently, although at a low level, weight gain was not significantly different from a control diet. The negative effects of MCFA have been explained by the high ketogenic properties of these FA, particularly of 8:0 (21,23). The intensive β-oxidation of MCFA leads to the production of ketone bodies, which may be well or poorly utilized as an energy source depending on the amount of MCT used, type of MCFA, quantities of other dietary ingredients (e.g., carbohydrates), species-specific dif-

ferences, size (i.e., "dilution" of dietary FA by endogenous FA), stage of development, and energetic needs (21,22,24,25). In the present study, total FA levels of 2.5% of caprylic acid (8:0), 4.0% of capric acid (10:0), and 36.8% of lauric acid (12:0) were associated with a significantly decreased growth of sea bass larvae, indicating that they may be at least as vulnerable to dietary MCT as carp or red drum. However, the experimental design of the present study does not allow clarifying whether the growth depression was a consequence of an excessive dietary supply of coconut oil or of the higher relative level of a specific MCFA. In addition, the higher lipid level in the C15 diet was achieved through the elimination of dietary starch, and this might have exacerbated the metabolic effects of MCFA (24). Younger larvae appeared more sensitive to coconut oil, given that in 52-d-old fish, diet C15 resulted in a significantly lower growth than diets F15 and T15, but, contrary to the first experiment, growth was not significantly different from the diets F7.5, T7.5, and C7.5. Finally, it should be noted that the lower growth obtained with the C15 diet was not associated with a lower survival of 52-d-old sea bass, as obtained with other fish larvae fed high levels of MCFA (21–23). However, just as with the detrimental effects on growth, mortality has been related to high levels of 8:0 in the diet and not to dietary coconut oil.

Larval performance in relation to lipid level. It has been suggested that young sea bass larvae do not tolerate high dietary neutral lipid levels (1). The generally poor growth obtained in the first experiment also indicated this, but growth in the second experiment starting at 37 d appeared not to be affected by the inclusion of neutral lipids, even at higher levels. In general, higher growth was achieved when a larger amount of total energy was supplied in the lipid form, as previously observed (8,9). This indicates a potential effect of lipid in sparing protein for growth, as also found in juvenile fish (26,27). On the other hand, a higher total energy intake might also explain the results if larval fish do not regulate food intake according to dietary energy content, as previously described for juvenile and adult fish (26,27). Coconut oil was an exception in terms of potentially having a protein-sparing effect, even though MCFA have been shown to enhance nutrient absorption and decrease amino acid oxidation (28). However, alterations of FA metabolism, as just discussed, might have obscured any potential protein-sparing effect of coconut oil.

Effect of dietary TAG level and source on body composition. Increasing the lipid level in the diets resulted in an overall rise in the sea bass body lipid content. Differences in adiposity were also found depending on the source of lipid. The triolein diets were responsible for the highest body lipid accumulation, whereas reduced lipid deposition was noted in larvae fed the coconut oil diets. The same has been found by researchers testing the beneficial effects of dietary MCT in improving carcass quality in several fish species (21,28–30). The FA composition of sea bass larvae generally reflected that of their diet, as is commonly found in fish (21,29). The fish oil diets that had the highest PUFA levels gave the highest PUFA and HUFA contents in the larvae. Unusually high amounts of 14:0 were found in larvae fed the coconut oil diets, as well as of 12:0 and 10:0, which were not detected in any of the other larvae. Therefore, as previously observed in larval sea bass, carp, and juvenile red drum (21,25,29), MCFA were incorporated into body lipid stores, although at a low level. Despite the relatively low level of PUFA in the coconut oil diets compared with the fish oil diets, the larvae fed these diets had a similar PUFA and HUFA content, and the relative content of HUFA did not change substantially from the start of the experiment. This might be explained by the presence of MCFA in the coconut oil diets, which are preferentially catabolized for energy production (24), potentially "sparing" the essential PUFA. Furthermore, a likely consequence of the lower total lipid content of larvae fed coconut oil diets is a higher proportion of polar lipids, which are richer in PUFA, particularly 22:6n-3 (DHA) and 20:5n-3 (EPA). Finally, the triolein diets produced very high levels of 18:1n-9 in the larvae, which directly reflect the composition of the diet. This was not previously seen in larval sea bass fed a diet containing triolein, where a low deposition of 18:1n-9 in body lipids was explained by its degradation for energetic purposes (25).

Effect of dietary TAG source on lipase activity. In the present study, the source of dietary TAG significantly affected lipase enzymatic activity, most likely as a consequence of their substantially different FA composition. The FA specificity of lipolytic enzymes has been relatively well studied, and the effects of FA on the activity of pancreatic lipase are related to both the acyl chain length and degree of saturation (11,31). In fish, the digestibility of FA has been shown to decrease with increasing chain length and to increase with unsaturation (10,13). Fish lipases have a preference for PUFA as substrates, followed by MUFA, with SFA being more resistant to lipolysis (12,13,17,32,33). Therefore, fish oils commonly have a good digestibility, whereas vegetable oils containing MUFA and particularly SFA are less digestible. In general, when coconut oil was used as the lipid source, sea bass had a higher lipase specific activity (although not significantly different from fish oil in the first experiment). The present results suggest therefore that lipolytic activity may be stimulated by the MCFA and/or SFA (mainly 12:0 and 14:0) present in coconut oil. More than half of the coconut oil SFA are of the MCFA type, which have the advantage of being rapidly and completely digested, even in the absence of bile salts, requiring minimal pancreatic lipase activity (24). In fact, TAG containing FA having <12 carbons can even be absorbed directly, without hydrolysis (24). MCT replacing fish oil in the diets of adult Atlantic salmon improved lipid digestibility by 3% and increased pancreatic proteolytic activity of the chyme; lipolytic activity was also slightly enhanced, although not significantly (28). Saraux *et al*. (34) noted that in rat lipase, activity was maximally stimulated by coconut oil, but not significantly differently from lard (99% C>12:0). In addition, the digestibility of coconut oil was analyzed in Artic charr and 12:0 was found to be a good substrate for intestinal lipase, the lipolysis of 14:0 being intermediate (13).

A surprising finding was the marked decrease in enzymatic activity caused by the fish oil diet in the second experiment, particularly at the higher inclusion level. This difference in lipase activity (nearly four times lower in the group fed the F15 diet, compared with the group fed C7.5) is unlikely to be caused by the difference in weight among the fish groups, which was about 17%. The fish oil diet is characterized by a high level of PUFA, for which lipase has maximal specificity (13). Nevertheless, it also contained the highest levels of several long-chain MUFA and of the SFA 16:0, which have been reported to be resistant to hydrolysis and absorption (12,32). Austreng *et al*. (10) noted that in spite of the high digestibility of long-chain (C_{20}–C_{22}) FA characteristic of marine oils, the C_{16}–C_{18} FA also present in these oils were less well digested than those in soybean oil. On the other hand, the physiological digestive response to the fish oil-based diet was age-dependent, as the same diet gave relatively high levels of lipase specific activity (comparable to coconut oil) in the first experiment.

The chemical nature of the FA, particularly their carbon chain length, has been shown to influence the release of cholecystokinin (CCK) and secretin, hormones that are implicated in the stimulation of pancreatic enzyme secretion (31,35,36). However, results obtained with different species reveal that MCT or long-chain TAG may cause distinct effects in humans and other mammals (37–39). Additionally, ketones have been implicated as mediators of pancreatic adaptation to dietary lipids, as blood ketone levels are strongly correlated with pancreatic lipase content (31). This may partially explain the results obtained with the coconut oil diets, which are more ketogenic that the other diets tested. Except for preliminary work on the CCK-mediated stimulation of pancreatic secretion by proteins and amino acids (40,41), the adaptation of pancreatic secretion to dietary components in fish remains completely unknown. However, having in mind the present results, it may be hypothesized that if a CCK-mediated mechanism exists, CCK release is probably also sensitive to the chemical nature of the FA. In addition, it can be hypothesized that the long-term feeding of sea bass larvae with more digestible diets containing long-chain FA, such as those using fish oil, causes an adaptative response leading to a lower secretion of pancreatic lipolytic enzymes. On the contrary, in a dietary regime containing less-digestible oils, an elevated lipolytic activity would be maintained. However, there are many confounding effects in the diets of the present study, and definite conclusions cannot be drawn at this time.

Effect of dietary TAG level on lipase activity. A stimulating effect of dietary lipid content on lipolytic enzymes has been reported both in mammals (31,36,42) and in fish, including sea bass (8,43). In rats, lipase activity was correlated with lipid intake, but the range of adaptative variation was narrow (approximately twofold) (34). In the present study, the increase in dietary lipid level was generally not found to affect lipase specific activity and, on day 24, a lower lipid level even appeared to induce a higher lipase activity. However, differences in the lipid level (17 vs. 24% total lipid) were not as marked as in the previous work conducted with sea bass, in which significant differences were found only between the dietary groups containing 10% lipids and >20% lipids (8). Moreover, the low lipid level (17%) was close to the plateau of 20% dietary lipids reported by Zambonino Infante and Cahu (8), over which there was no further stimulation of lipase activity. Additionally, the pancreatic enzyme response to intestinal stimulants has been related to the load (amount per unit of time) rather than to concentration. Thus, it has been suggested that the intestinal receptors for these intraluminal stimulants require only a very low concentration for activation, the length of the intestine exposed to these products being the main determinant of the total pancreatic secretory response (35). If this is the case in marine fish larvae, the ingestion rate of the diet may also play a major role in determining lipase activity. In accordance with this theory, Hoehne-Reitan *et al*. (44) showed that the bile salt-dependent lipase content of turbot larvae appeared to be a function of the ingestion rate, whereas the lipid level of the prey had no effect.

Lipase activity and growth. Growth was not related to lipase enzymatic activity, indicating that these two factors might be independent. In fact, a large excess of pancreatic lipase secretion in relation to dietary needs has been reported in humans (31). If this is also the case in young fish, a diminished lipase specific activity might not necessarily affect growth. Results obtained so far by studying lipid digestion and transport in fish larvae seem to indicate that the transport of lipid from the enterocytes into the peripheral tissues may be more of a problem in small larvae than lipid digestion (45). In larval red drum fed a microparticulate diet, live prey, or both, enzyme activity was not the limiting factor for growth (46). Furthermore, measurements of bile salt-dependent lipase in turbot larvae suggest that it is present in ample quantity for the lipid digestion of all ingested prey (47). The physiological significance of pancreatic adaptation to the diet therefore remains puzzling.

Regulation of lipase activity. Both transcriptional and translational regulation has been detected in rat pancreatic lipase in response to high-fat diets (31,42). In the present study no significant differences were found in the lipase/GAPDH mRNA values, confirming the previous hypothesis of an involvement of a posttranscriptional or translational mechanism, with a hormonal modulation (eventually through CCK or secretin action) of the efficiency of mRNA translation (1,8). However, it was additionally postulated that the regulation of lipase activity occurs also at the transcriptional level in sea bass larvae (1,8). No evidence of this was found in the present study, although the high variability associated with the determination of mRNA synthesis may have obscured potential dietary effects.

In conclusion, the data presented here suggest the existence of a regulatory mechanism of neutral lipolytic enzyme secretion and activity according to the dietary FA composition operating in marine fish larvae. However, an understanding of the underlying mechanisms controlling such an adaptation as well as of the physiological importance of such a regulation is still incomplete.

ACKNOWLEDGMENTS

Sofia Morais acknowledges support from the "Fundação para a Ciência e a Tecnologia," Portugal (grant SFRH/BD/4902/2001) and from the European Commission (ASEFAF, EEC HPRI–CT–2001 –0014; IFREMER ref. no. 01/1214121/TF). The authors would like to express their gratitude to Patrick Quazuguel for assistance during diet formulation, Magali Hervy for helping with larval rearing and sampling, Marie Le Gall for technical assistance in the laboratory, and Hervé Le Delliou for diet and larval composition analysis.

REFERENCES

1. Cahu, C.L., Zambonino Infante, J.L., and Barbosa, V. (2003) Effect of Dietary Phospholipid Level and Phospholipid:Neutral Lipid Value on the Development of Sea Bass (*Dicentrarchus labrax*) Larvae Fed a Compound Diet, *Br. J. Nutr. 90*, 21–28.
2. Lauff, M., and Hofer, R. (1984) Proteolytic Enzymes in Fish Development and the Importance of Dietary Enzymes, *Aquaculture 37*, 335–346.
3. Person Le Ruyet, J., Alexandre, J.C., Thébaud, L., and Mugnier, C. (1993) Marine Fish Larvae Feeding: Formulated Diets or Live Prey? *J. World Aquacult. Soc. 24*, 211–224.
4. Pedersen, B.H., Nilssen, E.M., and Hjelmeland, K. (1987) Variations in the Content of Trypsin and Trypsinogen in Larval Herring (*Clupea harengus*) Digesting Copepod Nauplii, *Mar. Biol. 94*, 171–181.
5. Cahu, C.L., Zambonino Infante, J.L., Le Gall, M.M., and Quazuguel, P. (1995) Early Weaning of Seabass: Are Digestive Enzymes Limiting? in *LARVI '95—Fish & Shellfish Larviculture Symposium* (Lavens, P., Jaspers, E., and Roelants, I., eds.), European Aquaculture Society Special Publication No. 24, pp. 268–271, Ghent, Belgium.
6. Ribeiro, L., Zambonino Infante, J.L., Cahu, C., and Dinis, M.T. (1999) Development of Digestive Enzymes in Larvae of *Solea senegalensis*, Kaup 1858, *Aquaculture 179*, 465–473.
7. Hjelmeland, K., Pedersen, B.H., and Nilssen, E.M. (1988) Trypsin Content in Intestines of Herring Larvae, *Clupea harengus*, Ingesting Inert Polystyrene Spheres or Live Crustacea Prey, *Mar. Biol. 98*, 331–335.
8. Zambonino Infante, J.L., and Cahu, C.L. (1999) High Dietary Lipid Levels Enhance Digestive Tract Maturation and Improve *Dicentrarchus labrax* Larval Development, *J. Nutr. 129*, 1195–1200.
9. Buchet, V., Zambonino Infante, J.L., and Cahu, C.L (2000) Effect of Lipid Level in a Compound Diet on the Development of Red Drum (*Sciaenops ocellatus*) Larvae, *Aquaculture 184*, 339–347.
10. Austreng, E., Skrede, A., and Eldegard, Å. (1979) Effect of Dietary Fat Source on the Digestibility of Fat and Fatty Acids in Rainbow Trout and Mink, *Acta Agric. Scand. 29*, 119–126.
11. Linscheer, W.G., and Vergroesen, A.J. (1994) Lipids, in *Modern Nutrition in Health and Disease* (Shils, M.E., Olson, J.A., and Shike, M., eds.), pp. 47–88, Williams & Wilkins, Baltimore.
12. Koven, W.M., Henderson, R.J., and Sargent, J.R. (1994) Lipid Digestion in Turbot (*Scophthalmus maximus*). I: Lipid Class and Fatty Acid Composition of Digesta from Different Segments of the Digestive Tract, *Fish Physiol. Biochem. 13*, 69–79.
13. Olsen, R.E., Henderson, R.J., and Ringø, E. (1998) The Digestion and Selective Absorption of Dietary Fatty Acids in Arctic Charr, *Salvelinus alpinus*, *Aquacult. Nutr. 4*, 13–21.
14. AOAC (Association of Official Analytical Chemists) (1984) *Official Methods of Analysis*, 12th edn., AOAC, Washington, DC.
15. Dumas, J.-B. (1831) Proćedés de l'analyse organique, *Ann. Chim. Phys. 47*, 198.
16. Folch, J., Lees, M., and Sloane Stanley, G.H. (1957) A Simple Method for the Isolation and Purification of Total Lipids from Animal Tissues, *J. Biol. Chem. 226*, 497–509.
17. Iijima, N., Tanaka, S., and Ota, Y. (1998) Purification and Characterization of Bile Salt-Activated Lipase from the Hepatopancreas of Red Sea Bream, *Pagrus major*, *Fish Physiol. Biochem. 18*, 59–69.
18. Bradford, M.M. (1976) A Rapid and Sensitive Method for the Quantitation of Microgram Quantities of Protein Utilizing the Principle of Protein-Dye Binding, *Anal. Biochem. 72*, 248–254.
19. Zar, J.H. (1996) *Biostatistical Analysis,* Prentice Hall International, Englewood Cliffs, NJ.
20. Jenkins, D.J.A., Wolever, T.M.S., and Jenkins, A.L. (1994) Diet Factors Affecting Nutrient Absorption and Metabolism, in *Modern Nutrition in Health and Disease* (Shils, M.E., Olson, J.A., and Shike, M., eds.), pp. 583–602, Williams & Wilkins, Baltimore.
21. Fontagné, S., Pruszynski, T., Corraze, G., and Bergot, P. (1999) Effect of Coconut Oil and Tricaprylin vs. Triolein on Survival, Growth and Fatty Acid Composition of Common Carp (*Cyprinus carpio* L.) Larvae, *Aquaculture 179*, 241–251.
22. Fontagné, S., Corraze, G., and Bergot, P. (2000) Response of Common Carp (*Cyprinus carpio*) Larvae to Different Dietary Levels and Forms of Supply of Medium-Chain Fatty Acids, *Aquat. Liv. Resour. 13*, 429–437.
23. Craig, S.R., and Gatlin, D.M. (1995) Coconut Oil and Beef Tallow, but Not Tricaprylin, Can Replace Menhaden Oil in the Diet of Red Drum (*Sciaenops ocellatus*) Without Adversely Affecting Growth or Fatty Acid Composition, *J. Nutr. 125*, 3041–3048.
24. Bach, A.C., and Babayan, V.K. (1982) Medium-Chain Triglycerides: An Update, *Am. J. Clin. Nutr. 36*, 950–962.
25. Fontagné, S., Robin, J., Corraze, G., and Bergot, P. (2000) Growth and Survival of European Sea Bass (*Dicentrarchus labrax*) Larvae Fed from First Feeding on Compound Diets Containing Medium-Chain Triacylglycerols, *Aquaculture 190*, 261–271.
26. Boujard, T., and Médale, F. (1994) Regulation of Voluntary Feed Intake in Juvenile Rainbow Trout Fed by Hand or by Self Feeders with Diets Containing Two Different Protein/Energy Ratios, *Aquat. Liv. Resour. 7*, 211–215.
27. Sæther, B.-S., and Jobling, M. (2001) Fat Content in Turbot Feed: Influence on Feed Intake, Growth and Body Composition, *Aquacult. Res. 32*, 451–458.
28. Nordrum, S., Krogdahl, Å., Røsjø, C., Olli, J.J., and Holm, H. (2000) Effects of Methionine, Cysteine and Medium Chain Triglycerides on Nutrient Digestibility, Absorption of Amino Acids Along the Intestinal Tract and Nutrient Retention in Atlantic Salmon (*Salmo salar* L.) Under Pair-Feeding Regime, *Aquaculture 186*, 341–360.
29. Davis, D.A., Lazo, J.P., and Arnold, C.R. (1999) Response of Juvenile Red Drum (*Sciaenops ocellatus*) to Practical Diets Supplemented with Medium Chain Triglycerides, *Fish Physiol. Biochem. 21*, 235–247.
30. Røsjø, C., Nordrum, S., Olli, J.J., Krogdahl, Å., Ruyter, B., and Holm, H. (2000) Lipid Digestibility and Metabolism in Atlantic Salmon (*Salmo salar*) Fed Medium-Chain Triglycerides, *Aquaculture 190*, 65–76.
31. Brannon, P.M. (1990) Adaptation of the Exocrine Pancreas to Diet, *Annu. Rev. Nutr. 10*, 85–105.
32. Lie, Ø., and Lambertsen, G. (1985) Digestive Lipolytic Enzymes in Cod (*Gadus morhua*): Fatty Acid Specificity, *Comp. Biochem. Physiol. 80B*, 447–450.
33. Gjellesvik, D.R. (1991) Fatty Acid Specificity of Bile Salt-Dependent Lipase: Enzyme Recognition and Super-Substrate Effects, *Biochim. Biophys. Acta 1086*, 167–172.
34. Saraux, B., Girard-Globa, A., Ouagued, M., and Vacher, D. (1982) Response of the Exocrine Pancreas to Quantitative and Qualitative Variations in Dietary Lipids, *Am. J. Physiol. 243*, G10–G15.
35. Singer, M.V. (1987) Pancreatic Secretory Response to Intestinal Stimulants: A Review, *Scand. J. Gastroent. 22* (Suppl. 139), 1–13.

36. Spannagel, A.W., Nakano, I., Tawil, T., Chey, W.Y., Liddle, R.A., and Green, G.M. (1996) Adaptation to Fat Markedly Increases Pancreatic Secretory Response to Intraduodenal Fat in Rats, *Am. J. Physiol. 33*, G128–G135.
37. Hopman, W.P.M., Jansen, J.B.M.J., Rosenbusch, G., and Lamers, C.B.H.W. (1984) Effect of Equimolar Amounts of Long-Chain Triglycerides and Medium-Chain Triglycerides on Plasma Cholecystokinin and Gallbladder Contraction, *Am. J. Clin. Nutr. 39*, 356–359.
38. Matzinger, D., Degen, L., Drewe, J., Meuli, J., Duebendorfer, R., Ruckstuhl, N., D'Amato, M., Rovati, L., and Beglinger, C. (2000) The Role of Long Chain Fatty Acids in Regulating Food Intake and Cholecystokinin Release in Humans, *Gut 46*, 688–693.
39. Douglas, B.R., Jansen, J.B.M.J., De Jong, A.J.L., and Lamers, C.B.H.W. (1990) Effect of Various Triglycerides on Plasma Cholecystokinin Levels in Rats, *J. Nutr. 120*, 686–690.
40. Koven, W., Rojas-Garcia, C.R., Finn, R.N., Tandler, A., and Rønnestad, I. (2002) Stimulatory Effect of Ingested Protein and/or Free Amino Acids on the Secretion of the Gastroendocrine Hormone Cholecystokinin and on Tryptic Activity, in Early-Feeding Herring Larvae, *Clupea harengus*, *Mar. Biol. 140*, 1241–1247.
41. Rojas-García, C.R., and Rønnestad, I. (2002) Cholecystokinin and Tryptic Activity in the Gut and Body of Developing Atlantic Halibut (*Hippoglossus hippoglossus*): Evidence for Participation in the Regulation of Protein Digestion, *J. Fish Biol. 61*, 973–986.
42. Wicker, C., and Puigserver, A. (1989) Changes in mRNA Levels of Rat Pancreatic Lipase in the Early Days of Consumption of a High-Lipid Diet, *Eur. J. Biochem. 180*, 563–567.
43. Borlongan, I.G. (1990) Studies on the Digestive Lipases of Milkfish, *Chanos chanos*, *Aquaculture 89*, 315–325.
44. Hoehne-Reitan, K., Kjørsvik, E., and Reitan, K.I. (2001) Bile Salt-Dependent Lipase in Larval Turbot, as Influenced by Density and Lipid Content of Fed Prey, *J. Fish Biol. 58*, 746–754.
45. Izquierdo, M.S., Socorro, J., Arantzamendi, L., and Hernández-Cruz, C.M. (2000) Recent Advances in Lipid Nutrition in Fish Larvae, *Fish Physiol. Biochem. 22*, 97–107.
46. Lazo, J.P., Holt, G.J., and Arnold, C.R. (2000) Ontogeny of Pancreatic Enzymes in Larval Red Drum *Sciaenops ocellatus*, *Aquacult. Nutr. 6*, 183–192.
47. Hoehne-Reitan, K., Kjørsvik, E., and Gjellesvik, D.R. (2001) Development of Bile Salt-Dependent Lipase in Larval Turbot, *J. Fish Biol. 58*, 737–745.

[Received February 10, 2004; accepted June 17, 2004]

Tocotrienol-Rich Fraction from Palm Oil Affects Gene Expression in Tumors Resulting from MCF-7 Cell Inoculation in Athymic Mice

Kalanithi Nesaretnam[a,*], Roberto Ambra[b], Kanga Rani Selvaduray[a], Ammu Radhakrishnan[c], Karin Reimann[a], Ghazali Razak[a], and Fabio Virgili[b]

[a]Malaysian Palm Oil Board, Bandar Baru Bangi, 4300 Selangor, Malaysia, [b]National Institute for Food and Nutrition Research, Rome, Italy, and [c]International Medical University, Kuala Lumpur, Malaysia

ABSTRACT: It has recently been shown that tocotrienols are the components of vitamin E responsible for inhibiting the growth of human breast cancer cells *in vitro*, through an estrogen-independent mechanism. Although tocotrienols act on cell proliferation in a dose-dependent manner and can induce programmed cell death, no specific gene regulation has yet been identified. To investigate the molecular basis of the effect of tocotrienols, we injected MCF-7 breast cancer cells into athymic nude mice. Mice were fed orally with 1 mg/d of tocotrienol-rich fraction (TRF) for 20 wk. At end of the 20 wk, there was a significant delay in the onset, incidence, and size of the tumors in nude mice supplemented with TRF compared with the controls. At autopsy, the tumor tissue was excised and analyzed for gene expression by means of a cDNA array technique. Thirty out of 1176 genes were significantly affected. Ten genes were down-regulated and 20 genes up-regulated with respect to untreated animals, and some genes in particular were involved in regulating the immune system and its function. The expression of the interferon-inducible transmembrane protein-1 gene was significantly up-regulated in tumors excised from TRF-treated animals compared with control mice. Within the group of genes related to the immune system, we also found that the CD59 glycoprotein precursor gene was up-regulated. Among the functional class of intracellular transducers/effectors/modulators, the c-myc gene was significantly down-regulated in tumors by TRF treatment. Our observations indicate that TRF supplementation significantly and specifically affects MCF-7 cell response after tumor formation *in vivo* and therefore the host immune function. The observed effect on gene expression is possibly exerted independently from the antioxidant activity typical of this family of molecules.

Paper no. L9459 in *Lipids 39*, 459–467 (May 2004).

Vitamin E is a generic term referring to an entire class of compounds that is further divided into two subgroups called tocopherols and tocotrienols. Just as there are several forms of tocopherols (α, β, γ, and δ), there are also α-, β-, γ-, and δ-tocotrienols. Although tocopherols are found abundantly in oils extracted from soybean, olive, cottonseed, and sunflower seed, tocotrienols are found only in the oil fractions of some cereal grains such as wheat, barley, rice, and, most abundantly, the fruit of palm (1). Commercial quantities of tocotrienols are, in fact, extracted from palm oil and rice bran oil. A standardized tocotrienol-rich fraction (TRF) composed of 32% α-tocopherol and 68% tocotrienols can be obtained from palm oil after esterification and following distillation, crystallization, and chromatography (2).

Recent work has shown that tocotrienols, but not tocopherols, can exert direct inhibitory effects on cell growth in human breast cancer cell lines *in vitro* (3–5) and also induce cells to undergo apoptosis (6). The inhibitory effect, however, occurs irrespective of the estrogen receptor status of the cells (7). The inhibitory effect on cell growth is more pronounced with γ- and δ-tocotrienols (5,7). The mechanism of action is not yet completely understood, with previous data suggesting that the action is independent from an antagonism with estrogen activity (7). However, it has been reported that α-tocopherol itself has no inhibitory activity on breast cancer cell growth (3,4,7,8). Tocotrienols are also reported to have a pro-apoptotic effect on several lines of tumor cells (6,9,10). McIntyre and coworkers (10) have also shown that highly malignant cells are more sensitive to the antiproliferative and apoptotic effects of tocotrienols in comparison with preneoplastic cells.

Although vitamin E (both tocopherols and tocotrienols) is a potent antioxidant, the antitumor activity of vitamin E may not be associated with its antioxidant activity (11). It is thought that vitamin E exerts its antitumor activity by modulating a number of intracellular signaling pathways involved in mitogenesis (12–14) and apoptosis (10,12,15). Oral administration of tocopherols and tocotrienols also reportedly affects the immune system and the proliferation of spleen and mesenteric lymph node lymphocytes (16). We have preliminary evidence suggesting that the number of natural killer (NK) cells increases in nude mice supplemented with tocotrienols and challenged with MCF-7 human breast cancer cells (Nesaretnam, K., unpublished data). Other researchers also have reported that oral administration of tocopherols and

*To whom correspondence should be addressed at Malaysian Palm Oil Board, 6 Persiaran Institusi, Bandar Baru Bangi, 43000 Kajang.
E-mail: sarnesar@mpob.gov.my

*K.N. and R.A. contributed equally to this paper.

Abbreviations: APC, antigen-presenting cell; FcRn, IgG Fe receptor large subunit P51 precursor; IFITM-1, interferon-inducible transmembrane protein-1; IFN-γ, interferon-γ; MHC, major histocompatibility; NK, natural killer; TRF, tocotrienol-rich fraction.

tocotrienols can affect the immune system and the proliferation of spleen and mesenteric lymph node lymphocytes (16). However, the mechanism by which vitamin E helps to boost the immune system to fight tumor growth and spread is not known.

The *in vivo* study reported herein was designed on the basis of a heterogeneic model (human breast cancer cells implanted into a rodent host) in order to (i) specifically focus on the effect of TRF on the growth of cancer cells rather than on the host, and (ii) assess whether implantation into the host results in a different pattern of gene expression and sensitivity to tocotrienols in the tumor mass. Even though the second issue might appear quite obvious, no current studies are able to provide a reliable database to either support or discard this hypothesis.

To investigate the molecular basis of the effect of tocotrienols on tumor growth, we administered a standardized mixture of tocotrienols extracted from palm oil and performed an array analysis of cancer-related gene expression on tumors resulting from the inoculation of MCF-7 cells in control and TRF-supplemented athymic nude mice.

MATERIALS AND METHODS

Isolation of the TRF. The TRF was obtained from Golden Hope Plantation (Ipoh, Malaysia). TRF has a standardized composition of 32% α-tocopherol, 25% α-tocotrienol, 29% γ-tocotrienol, and 14% δ-tocotrienol. The chemical structure of tocotrienols present in TRF is shown in Figure 1. Extraction of TRF from palm oil has been described by Sundram and Gapor (2). Briefly, palm oil fatty acid distillate was converted into methyl esters by esterification. The methyl esters were then removed by distillation, leaving a vitamin E concentrate. This was further concentrated by crystallization and passed through an ion-exchange column to give 60–70% pure vitamin E. Further purification was achieved by washing and then drying the concentrate, followed by a second molecular distillation stage. The final purity of the vitamin E preparation, TRF, was 95–99%.

Analysis of tocotrienols and tocopherols. The tocopherols and tocotrienols were analyzed by HPLC. The system used was a Shimadzu LC-10AT high-performance liquid chromatograph coupled with a Shimadzu RF-10AXL fluorescence spectrophotometer, Shimadzu Class VP data acquisition software, and a silica column (YMC A-012, 150 × 6 mm i.d., 5 μm; YMC Co., Ltd., Kyoto, Japan). The eluting solvent was hexane/isopropyl alcohol (99.5:0.5 vol/vol) at a flow rate of 2.0 mL/min. The detector was set at an excitation wavelength of 295 nm and an emission wavelength of 325 nm. A 500-mg sample of tissue was homogenized with a 4:1:1 mixture of hexane/ethanol and 0.9% sodium chloride at 11,000 rpm for 5 min. The homogenate was then centrifuged at 800 × *g* for 5 min. The resulting supernatant was filtered and evaporated using a rotary evaporator. A known amount of lipid sample was dissolved in a 10-mL volumetric flask using the eluting solvent, and 10 μL of the solution was injected into the HPLC system. A standard solution of a mixture of α-tocopherol and α-, γ-, and δ-tocotrienols was also injected using the same procedure. Quantification of the major components of vitamin E was carried out by comparing the peak areas of the components with those of the standards.

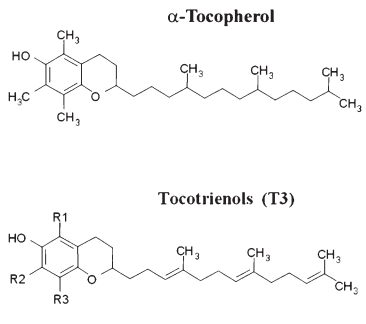

	R1	R2	R3
α-T3	CH_3	CH_3	CH_3
γ-T3	H	CH_3	CH_3
δ-T3	H	H	CH_3

FIG. 1. Structure of vitamin E (tocopherol and tocotrienol) components in the tocotrienol-rich fraction (TRF) from palm oil.

Culture of stock cells. MCF-7 human breast cancer cells were kindly provided by Dr. Kent C. Osborne at passage number 390 (17). Stock cells were grown as monolayer cultures in DMEM supplemented with 5% FCS (Gibco, BRL Life Technologies Incorporated, Grand Island, NY) and 10^{-8} M estradiol in a humidified atmosphere of 5% carbon dioxide in 95% air at 37°C. Cells were subcultured at weekly intervals by suspension with 0.06% trypsin/0.02% EDTA (pH 7.3). Tumor cells were harvested for inoculation by incubating briefly with 0.06% trypsin and 0.02% EDTA. The tissue culture flask was tapped to dislodge the cells, which were then resuspended in DMEM supplemented with 5% FCS. Tumor cells intended for inoculation were washed by centrifugation and resuspended in DMEM.

Animals. Forty female athymic nude mice (NCR nu/nu), 3 to 4 wk old, were obtained from the Animal Breeding Unit, Institute for Medical Research, Kuala Lumpur, Malaysia. The animals were housed under specific pathogen-free conditions in micro-isolator cages. The care and treatment of the experimental animals conformed to the guidelines of the Institute for Medical Research for the ethical treatment of laboratory animals. Animals were randomly divided into an experimental and a control group. Both the control and the experimental groups were treated topically with 10^{-5} M estradiol and fed a commercial mouse pellet diet for 20 wk and then sacrificed before excising the tumor mass. The experimental group was supplemented with 1 mg/d of TRF (dissolved in palm oil) by gavage on the same day as tumor cell inoculation (see next paragraph), whereas control animals were treated with the carrier only.

Tumor inoculation. Animals were anesthetized with phentobarbital, and tumor cells injected into a right-sided thoracic mammary fat pad that had been exposed by a small incision (5 mm). The mammary fat pad was exposed, and a 50-μL volume of inoculum containing 10^6 cells was injected into the tissue through a 27-gauge needle. By exposing the fat pad, we were able to ensure that the cells were injected into the tissue

and not into the subcutaneous space. The incision was then closed with a skin clip. Mice were weighed, and the inoculation site was palpated at weekly intervals by an investigator who was blinded to the treatments in order to evaluate tumor surface area. TRF treatment was not associated with any significant changes in growth rate and final body weight in comparison with the group of control animals (data not shown). The experiment was terminated 20 wk after injection of the tumor cells, and the mice were killed by CO_2 euthanasia. At necropsy, body and tumor weights were determined.

RNA isolation and purification. Total RNA was extracted from pooled tumor tissues from three randomly selected animals using a Trizol solution (BRL Life Technologies) according to the manufacturer's instructions, with some minor modifications, in order to obtain sufficient RNA for the array analysis. Tissues and cells were homogenized in the Trizol solution and incubated for 15 min at room temperature. After the addition of a 20% volume of chloroform, homogenates were vortexed for 2 min and centrifuged at 12,000 × *g* for 20 min at 4°C. The resulting inorganic phase was subjected to three extractions with acid phenol/chloroform/isoamyl alcohol (125:24:1; Ambion, Austin, TX) and one extraction with chloroform. RNA was precipitated overnight at 4°C with 0.75 vol of 7.5 M LiCl and then centrifuged at 12,000 × *g* for 10 min at 4°C. The pellet was resuspended in 400 μL of distilled water, reprecipitated with 40 μL of 3 M Na acetate (pH 5.2) and 1 mL of ethanol, and washed with 70% ethanol. RNA integrity was checked by denaturing gel electrophoresis. Before labeling, total RNA was treated with 25 units of DNase I to remove any contaminating DNA.

cDNA labeling and Atlas™ Cancer Array membrane hybridization, exposure, and analysis. Atlas™ Human Cancer cDNA Expression Arrays (Cat. #7851-1) were purchased from Clontech Laboratories Inc. (Palo Alto, CA). Array membranes contained 10 ng of each gene-specific cDNA from 1176 known genes and 9 housekeeping genes (see http://www.clontech.com for the complete list of genes). Poly A^+ RNA enrichment, cDNA Probe Synthesis, and purification were performed using the Atlas Pure RNA Labeling system (Clontech) following the manufacturer's instructions, starting from 50 μg total RNA and using [α-^{32}P]dATP (NEN, Boston, MA). Membrane arrays were hybridized for 18 h at 68°C into rolling bottles with 5 mL ExpressHyb hybridization solution (Clontech) containing the denatured probes (10×10^6 cpm) and 5 μg Cot-1 DNA. The membranes were then washed in bottles for 2 h at 68°C in 2× SSC, 1% SDS with three changes of solutions, and then for 30 min at 68°C in 0.1× SSC, and 0.5% SDS. Membranes were finally rinsed in 2× SSC at room temperature and exposed to X-ray films (Kodak Biomax from Kodak, Rochester, NY, or Amersham MP from Amersham, Piscataway, NJ) at −70°C for 1 to 6 d. Films were acquired with a scanner for transparencies, and images were analyzed with AtlasImage software (Version 2.01, Clontech). The software analysis results were confirmed by visual inspection of hybridization signals to ensure reliability. Since tocotrienols were found to modulate the expression of one of the housekeeping genes included in the array (see the Results section), a global gene-normalization method was preferred. In such a method, the normalization coefficient is calculated using the average value of all genes in the array instead of using only the housekeeping genes.

Reproducibility and precision limits. Previous studies addressing the application of a cDNA array have indicated that the CV for differential gene expression in cultured cells is 10–15% (18). Studies on the reproducibility and variability of array results have indicated that a difference of twofold or greater in the expression of a particular gene is to be considered a real difference in transcript abundance (19,20). Data are reported according to the suggested standardization of microarray experiments (minimal information about a microarray experiment) (21). A difference in gene expression between the TRF-treated samples and controls was therefore considered significant at a ratio of twofold or more and when both readings had a signal intensity above 1000 units. Data discussed herein were confirmed by a Northern blot hybridization technique (see next paragraph).

Northern blot hybridization. Ten micrograms of total RNA separated through electrophoresis in 1.2% agarose gels was blotted onto Genescreen-N nylon membranes (DuPont, Wilmington, DE) and hybridized according to the manufacturer's instructions. Gene transcripts of MIC-1, CD74/Ii, and the interferon-inducible transmembrane protein-1 (IFITM-1) were detected using [α-^{32}P]dATP (NEN) random primed DNA ampliclones (Boehringer Ingelheim, Ingelheim, Germany) obtained by PCR using sequence-specific primers (see Table 1 for sequences). Normalization of gene expression was achieved by hybridization of the same membranes with a labeled PCR fragment of the GAPDH gene.

Statistical analysis and data presentation. Statistical analysis was performed using the SPSS program (SPSS Inc., Chicago, IL). Fisher's exact test was used to test for a significant difference in the incidence and size of tumors between experimental and control mice. Scion Image® software was used for quantification of the transcripts' relative abundance in Northern blot experiments. The figures present one out of at least three separate experiments providing similar results.

TABLE 1
Nucleotide Sequences (from 5′ to 3′) of Primers Used for the Preparation of Probes in Northern Blot Hybridizations

Genes	Forward	Reverse
MIC-1	CGC GCA ACG GGG ACC ACT	TGA GCA CCA TGG GAT TGT AGC
CD74/Ii	ACC TCA TCC CAT GAG ACC TG	TCC AAA ACA TTG GCT CTT CC
IFITM-1	TGC ACA AGG AGG AAC ATG AG	TGA ATC CAA TGG TCA TGA GG
GAPDH	TGA AGG TCG GAG TCA ACG GAT TTG G	CAT GTG GGC CAT GAG GTC CAC CAC

TABLE 2
Tocopherol and Tocotrienol Concentrations in Plasma, Liver, and Adipose Tissue in Control Animals and in Animals Fed 1 mg/d of a Tocotrienol-Rich Fraction (TRF) by Gavage[a]

Tissue	Total tocopherols	Total tocotrienols
Plasma		
Control	1.88 ± 0.34	1.03 ± 0.66
TRF treatment	3.89 ± .64	6.72 ± 1.79
Liver		
Control	2.36 ± 0.89	0.30 ± 0.06
TRF treatment	7.73 ± 3.90	6.35 ± 4.79
Adipose tissue		
Control	7.46 ± 3.12	1.57 ± 0.54
TRF treatment	20.21 ± 6.48	74.16 ± 23.91

[a]Data are presented as the mean ± SD of 10 animals per group and expressed as μg/mL (plasma) and μg/g tissue (liver and adipose tissue).

RESULTS

We previously reported the effect of TRF on MCF-7 cell proliferation *in vitro* (6,7,9,10). In the present study, we found TRF supplementation to be associated with a significant inhibition of tumor growth *in vivo*.

Effect of TRF on plasma and tissue levels of tocopherols and tocotrienols. The administration of TRF resulted in a significant increase in tocopherol and tocotrienol concentrations in the plasma and tissues of animals in comparison with the control group (see Table 2). The levels of tocopherol increased in all tissues by about threefold. As expected, the increase in tocotrienol levels associated with TRF administration was much more evident than that of tocopherol levels: In plasma we observed levels sevenfold higher than in control animals, and an even more dramatic increase was observed in the liver and adipose tissue (more than 20-fold and about 50-fold, respectively), confirming that selected tissues are able to accumulate and store tocotrienols available in the diet (22).

Effect of TRF on tumor development in nude mice after MCF-7 cell inoculation. The cumulative incidence of mammary fat pad tumors in the two groups of animals over a period of 20 wk is shown in Figure 2A. Tumor growth was detected in the control group (i.e., mice not supplemented with TRF) 2 wk after inoculation of the MCF-7 cells. In addition, by week 7 the incidence of mammary fat pad tumors was 100% (i.e., detected in all mice in the control group). On the other hand, TRF-supplemented mice started to develop palpable tumors only from the seventh week of inoculation and, more importantly, only 50% of the mice in this group had tumors at week 14. TRF supplementation also affected tumor size. Tumor surface area was in fact significantly reduced in treated animals, being on the average about one-third that of control animals at the end of the experimental period (see Figure 2B).

Effect of TRF supplementation on gene expression in tumors resulting from inoculating nude mice with MCF-7 cells: cDNA array data. Two hundred and forty-six genes were significantly hybridized, with a total of 1185 cDNA spotted onto the membrane. The expression of 30 genes (i.e., 12% of the total number of hybridized genes) was significantly affected by the supplementation of TRF from palm oil *in vivo* in the tumor mass that resulted after 20 wk of inoculation of MCF-7 into nude mice. Among these 30 genes, 20 genes were up-regulated and 10 were down-regulated (see Table 2). The complete list of genes whose expression was affected following TRF supplementation in the tumor tissue is presented in Table 3. Genes have been classified into functional groups according to the putative function of the encoded proteins. However, the data discussed hereafter focus on only a selected subsample of genes involved in specific groups.

In tumors excised from nude mice, the expression of the CD74/Ii gene displayed the highest up-regulation (11-fold), whereas the IgG Fc receptor large subunit P51 precursor (FcRn) displayed a significant down-regulation (3.3-fold). The expression of the IFITM-1 gene was significantly up-regulated in tumor cells following TRF treatment with respect to control mice. Within the group of genes related to the immune system, we also found that the CD59 glycoprotein precursor gene was also up-regulated by TRF. Among the 30 genes modulated by TRF supplementation in MCF-7-induced tumors, nine genes could be functionally classified as intracellular transducers/effectors/modulators (see Table 2). This category includes the c-myc gene, which is a gene that was significantly down-regulated in tumors after TRF treatment.

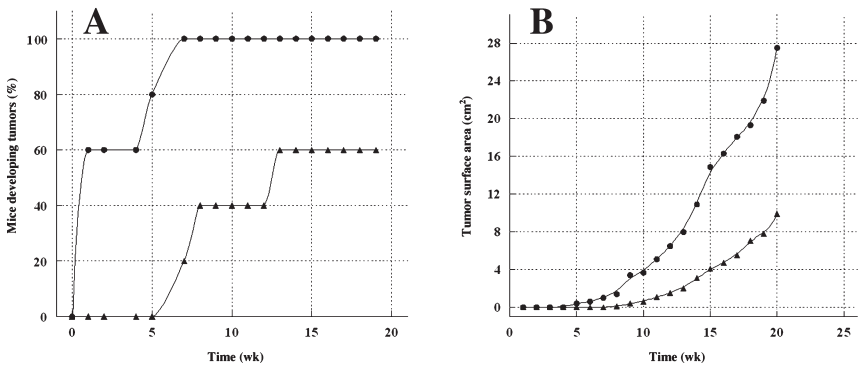

FIG. 2. Cumulative tumor incidence (A) and tumor surface area (B) in control and TRF-supplemented nude mice inoculated with MCF-7 cells. There were 20 animals in each group. -●- = Control animals; -▲- = TRF treatment. For abbreviation see Figure 1.

TABLE 3
Fold Changes in Gene Expression in MCF-7-Induced Tumors in Nude vs. Control Mice[a]

Genes	Gene bank no.	Treated vs. control
Oncogenes and tumor suppressors		
IFITM-1 (interferon-inducible protein 9-27)	J04164	2.2
c-myc oncogene	V00568	0.5
Prohibitin (PHB)	S85655; U17179	0.4
Metalloproteinase inhibitor 3 precursor; tissue inhibitor of metalloproteinases 3 (TIMP3); mitogen-inducible gene 5 (MIG5)	Z30183	5.1
Synapse-associated protein 102 (SAP102); neuroendocrine-DLG [NE-DLG; DLG3; human homolog of Drosophila discs large (DLG)]	U49089	3.1
p33ING1	AF001954	3.5
Apoptosis-associated proteins and DNA-binding and -damage signaling/repair proteins		
BCL-2 binding athanogene-1 (BAG-1); glucocorticoid receptor-associated protein (RAP46)	S83171; Z35491	2.4
Induced myeloid leukemia cell differentiation protein (MCL-1)	L08246	2.4
Fas-activated serine/threonine (FAST) kinase	X86779	2.2
DNA-repair protein XRCC1	M36089	0.5
Immune system proteins		
IgG receptor FC large subunit P51 precursor (FCRN); neonatal FC receptor; IgG FC fragment receptor transporter alpha chain	U12255	0.3
HLA-DR antigen-associated invariant subunit (CD74/Ii ANTIGEN)	X00497	11.5
CD59 glycoprotein precursor; membrane attack complex inhibition factor (MACIF); MACIP; MEM43; MIRL; HRF20; 1F5	M34671	2.9
Extracellular cell-signaling and cell receptors		
Macrophage inhibitory cytokine 1 (MIC1)	AF019770	2.9
Intracellular transducers/effectors/modulators		
Serine/threonine-protein kinase PCTAIRE 1 (PCTK1)	X66363	0.4
Placental calcium-binding protein; calvasculin; S100 calcium-binding protein A4; MTS1 protein	M80563	2.4
Zyxin + zyxin-2	X94991; X95735	2.1
PTPCAAX1 nuclear tyrosine phosphatase (PRL-1)	U48296	2.1
Transcription activators/repressors		
TAX1-binding protein 151 (TXBP151)	U33821	2.6
Transcription factor erf-1; AP2 gamma transcription factor	U85658	2.5
Metabolism		
Methylenetetrahydrofolate dehydrogenase-methylenetetrahydrofolate cyclohydrolase-formyltetrahydrofolate synthetase	J04031	0.4
Purine nucleoside phosphorylase (PNP); inosine phosphorylase	X00737	0.4
L-Lactate dehydrogenase M subunit (LDHA)	X02152	0.4
Cell adhesion proteins		
40S ribosomal protein SA (RPSA); 34/67-kDa laminin receptor (LAMR1); colon carcinoma laminin-binding protein; NEM/1CHD4	U43901	0.4
Integrin alpha 3 (ITGA3); galactoprotein B3 (GAPB3); VLA3 alpha subunit; CD49C antigen	M59911	5.2
Membrane channels and transporters		
PKU-alpha	AB004884	2.2
Trafficking and extracellular matrix proteins		
Fibronectin precursor (FN)	X02761; K00799; K02273; X00307; X00739	3.6
TRAM protein	X63679	2.2
Type I cytoskeletal 10 keratin; cytokeratin 10 (K10)	M19156	0.4
Type I cytoskeletal 14 keratin; cytokeratin 14 (K14; CK14)	J00124	3.5

[a]Changes greater than twofold or less than 0.5-fold were considered significant and included in the table.

Northern blot hybridization. RNA extracted from tumors that grew in TRF-supplemented mice and control mice was subjected to Northern blot hybridization to confirm data obtained by means of cDNA array analysis. We performed Northern blot analyses on only a selected number of genes, i.e., MIC-1, CD74, IFITM-1, and GAPDH. Their hybridization signals, together with the quantification obtained after normalization to the expression of GAPDH, are shown in Figure 3. Northern blotting confirmed the up-regulation of MIC-1 (about tenfold), CD74/Ii (about fourfold), and IFITM-1 (about twofold) gene expression in MCF-7-induced tumors in nude mice fed TRF in comparison with control animals.

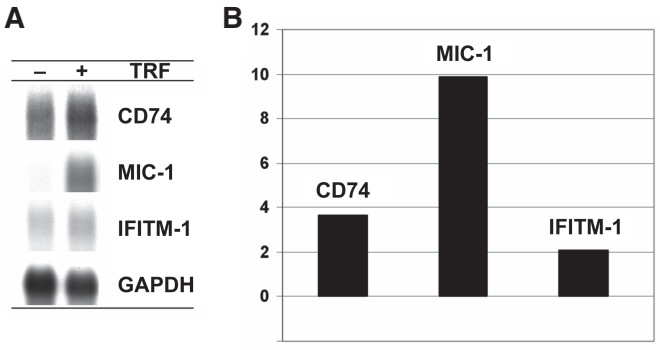

FIG. 3. (A) Northern blot analyses of TRF effects on the expression of MIC-1, CD74, and IFITM-1 genes in the tumor mass resulting from MCF-7 inoculation in nude mice. (B) Fold changes in gene expression calculated using Scion software and normalized by hybridization signals of the GAPDH gene. For abbreviation see Figure 1.

DISCUSSION

We have previously reported that TRF inhibits proliferation of estrogen receptor-positive and estrogen receptor-negative human breast tumor cell lines *in vitro* (4,7,23). Moreover, several studies have shown that high dietary intake of tocotrienols can suppress carcinogen-induced mammary tumorigenesis in experimental animals (24,25).

This study reports the effect of the administration of TRF, a standardized tocotrienol-rich extract from palm oil, on tumor incidence resulting from inoculation of MCF-7 breast cancer cells into athymic nude mice. Our data show that at the end of the experimental period of 20 wk, there was a significant delay in the onset, incidence, and size of tumor growth in nude mice supplemented with TRF compared with the controls, which did not receive any TRF. As expected, TRF supplementation was associated with a significant increase in both tocopherol and tocotrienol concentrations in plasma, liver, and adipose tissue, the concentration of tocotrienols being much more dramatic than that of tocopherols, particularly in the adipose tissue (about 50-fold with respect to the unsupplemented animals).

Differential gene expression in the tumor mass was assessed by means of a macroarray analysis, which allowed the identification of a number of genes modulated by the supplementation of TRF in the tumor mass. In this paper, we included a complete list of genes affected by TRF treatment in tumors excised from TRF-treated and -untreated animals. However, we focus our discussion herein on some of the genes involved in the regulation of the immune system and its function. In fact, some preliminary data suggest that TRF from palm oil is able to exert an immunomodulatory role in nude mice (unpublished data), possibly due at least in part to a response to signals secreted from tumor cells. In accordance with this hypothesis, lines of evidence indicate that the likelihood of tumor growth is a consequence of a balance between the host immune response and tumor growth kinetics. The initiation of a host immune response toward the tumor is dependent on the activation of T-lymphocytes that can recognize tumor cells as abnormal. The activation of naïve T-lymphocytes requires two distinct signals (26,27). The first one is delivered following the engagement of the T-cell receptor with the major histocompatibility (MHC)-peptide complex on an antigen-presenting cell (APC). The second signal, which is a costimulatory signal (28), is delivered following the binding of coreceptors on the T-cell with its respective ligands on the APC. Although tumors may be able to deliver antigen-specific signals to T-cells, they are generally unable to deliver the necessary costimulatory signals required for the full activation of naïve T-lymphocytes (26,29,30). Antigen recognition in the absence of the second signal will render T-cells nonreactive or anergic (31), or it may cause these cells to be deleted from the host T-cell repertoire.

Recent evidence (32) indicates that peripheral solid tumors usually evade the host immune response. Hence, one of the therapeutic approaches to curbing the growth and spread of tumors would be to find a more effective way of inducing a cell-mediated immune response where both NK cells and cytotoxic T-lymphocytes can be appropriately activated (33).

The MHC-class Ii-associated invariant chain (CD74/Ii) reportedly plays a central role in the biological function of the MHC class Ii molecules (34). The invariant chain plays a critical role in the presentation of processed peptides to the $CD4^+$ T-lymphocytes by influencing the expression and peptide loading of the MHC class II molecules (35). We have observed that TRF supplementation causes the expression of the CD74/Ii gene to be strongly up-regulated in MCF-7-induced tumors of animals fed TRF (see Fig. 3). This observation suggests that the antitumor effect of tocotrienols may be the result of increasing the host immune functions. Several indications support this hypothesis. It has been reported that the treatment of normal human monocytes and macrophages with interferon-γ (IFN-γ) markedly enhances the expression of the CD74/Ii protein in these cells (36). Moreover, Balkwill and collaborators (37) showed that the expression of the CD74/Ii gene on solid tumors of nude mice can be modulated in a dose-dependent fashion and reversibly by IFN-γ administration. Such regulation involves a signal transduction pathway activated in lymphoma and normal mouse B cells by protein kinase C and in controlling the stability of CD74/Ii messenger RNA (38). Therefore, the antineoplastic activity of TRF could be mimicking the effects of an IFN-γ treatment, which in turn can cause an increased expression of the CD74/Ii gene by macrophages and T-lymphocytes.

In agreement with the expression of CD74/Ii, we also observed the up-regulation of the interferon-inducible protein-1 (IFITM-1, IFI17, or 9-27) in MCF-7-induced tumors. Gutterman (39) suggested that expression of this membrane protein, which was identified for its inducibility by interferons, is necessary for the antiproliferative effect of interferons. IFITM-1 has been shown to be a component of a multimeric complex involved in the transduction of antiproliferative and adhesion signals (40). The up-regulation of this gene in tumors from tocotrienol-treated nude mice injected with MCF-7 parallels the up-regulation of CD74/Ii and reinforces the idea of

tocotrienols being able to mimic an interferon-like activation of immune functions through the IFITM-1 and CD74/Ii molecules.

Interferons are also known to exert their inhibitory effect on cell growth by acting at many levels, such as directly affecting the function of proteins (c-myc and Rb) involved in the cell cycle (39). In our array analysis, we detected a significant down-regulation of c-myc gene expression in tocotrienol-treated MCF-7-induced tumors (see Table 2). The c-myc down-regulation by tocotrienols is in agreement with the *in vivo* inhibition in growth by tocotrienols and tocopherols reported by Gu and coworkers (16). This is a very promising finding as the expression of the c-myc oncogene has been implicated in malignant progression in a variety of human tumors (41,42).

Both the array analysis and Northern blot hybridization indicated that TRF up-regulated the expression of MIC-1, a member of the transforming growth factor-β superfamily (43) in tumors resulting from MCF-7 cell injection (see Fig. 2). Although MIC-1 is not expressed in monocytes/macrophages or undifferentiated resting cells, it is progressively up-regulated upon differentiation of these cells by a number of activation agents (44). It has been suggested that MIC-1 could be an autocrine inhibitor of macrophage activation (45,46). Albertoni and collaborators (47), reporting on the antitumorigenic properties of MIC-1 in nude mice, identified this cytokine as a prominent target gene of p53 in the glioblastoma cell line and as a mediator of cellular stress signaling. Moreover, large amounts of MIC-1 are also present in the amniotic fluids and placental extracts, increasing in the sera of pregnant women. It has been suggested that MIC-1 may promote fetal survival by suppressing the production of maternally derived proinflammatory cytokines within the uterus (48,49). Our finding suggests that one of the mechanisms by which tumor cells can escape host immune surveillance may involve the expression of the MIC-1 gene. The role of MIC-1 in inflammatory processes and as a possible means of escape from host immune surveillance requires more investigation.

cDNA array analyses identified two other TRF-sensitive genes coding for immune system proteins: the FcRn (neonatal Fc receptor) and the glycoprotein CD59. FcRn is an MHC complex class I-related receptor that plays a role both in the passive delivery of immunoglobulin from the mother to the fetus during colostrum formation and in the regulation of serum IgG transport to tissues (50). CD59 is a potent complementary inhibitor protein. Durrant and Spendlove (51) reported that CD59 binding to the membrane is able to inhibit the formation of the membrane attack complex (MAC) on the surface of tumor cells, thus inhibiting the direct cytolytic activity of the MAC against tumor cells. Even though more studies are warranted to understand the role of these immune-related genes, TRF appears to have the potential to modulate host immune function in our breast cancer model.

Our study suggests that TRF from palm oil is able to support the host in fighting tumor growth and spread, possibly by modulating the immune response. Even though TRF also provides a significant proportion of tocopherols, previous studies carried out *in vitro* have indicated that tocotrienols, but not tocopherols, significantly affect breast cancer cell growth (3,4). In a recent study (52) conducted on nude mice supplemented with tocopherol succinate, the authors showed reduced tumor incidence when tocopherol succinate was given intraperitoneally. However, when tocopherol succinate was given orally, the effect was lost. The authors speculate that the oral administration failed because, once ingested, vitamin E succinate was hydrolyzed to vitamin E.

These reports suggest that the effect on gene expression we observed in the present study is to be ascribed to tocotrienols. This could be due to the induction of protein expression involved in cell growth inhibition, such as IFITM-1. More studies are needed to test the possibility that tocotrienols are able to induce the production of interferon in the host. Tocotrienols may also exert their antitumor effects by inhibiting the ability of the breast tumor cells to escape from the host immune system by inhibiting the expression of CD74/Ii in tumor cells.

REFERENCES

1. Ong, A.S.H. (1993) Natural Sources of Tocotrienols, in *Vitamin E in Health and Disease* (Packer, L., and Fuchs, J., eds.), pp. 3–8, Marcel Dekker, New York.
2. Sundram, K., and Gapor, A. (1992) Vitamin E from Palm Oil. Its Extraction and Nutritional Properties, *Lipid Technol. 4*, 137–141.
3. Nesaretnam, K., Dorasamy, S., and Darbre, P.D. (2000) Tocotrienols Inhibit Growth of ZR-75-1 Mammary Cancer Cells, *Int. J. Food Sci. Nutr. 51*, 95–105.
4. Nesaretnam, K., Guthrie, N., Chambers, A.F., and Carroll, K.K. (1995) Effect of Tocotrienols on the Growth of a Human Breast Cancer Cell Line in Culture, *Lipids 30*, 1139–1143.
5. Carroll, K.K., Guthrie, N., Nesaretnam, K., Gapor, A., and Chambers, A.F. (1995) Anti-cancer Properties of Tocotrienols from Palm Oil, in *Nutrition, Lipids, Health, and Disease* (Ong, A.S.H., Niki, E., and Packer, L., eds.), pp. 117–121, AOCS Press, Champaign.
6. Yu, W., Simmons-Menchaca, M., Gapor, A., Sander, B.G., and Kline, K. (1999) Induction of Apoptosis in Human Breast Cancer Cells by Tocopherols and Tocotrienols, *Nutr. Cancer 33*, 26–32.
7. Nesaretnam, K., Stephen, R., Dils, R., and Darbre, P. (1998) Tocotrienols Inhibit the Growth of Human Breast Cancer Cells Irrespective of Estrogen Receptor Status, *Lipids 33*, 461–469.
8. Djuric, Z., Heilbrun, L.K., Lababidi, S., Everett-Bauer, C.K., and Fariss, M.W. (1997) Growth Inhibition of MCF-7 and MCF-10A Human Breast Cells by α-Tocopheryl Hemisuccinate, Cholesteryl Hemisuccinate and Their Ether Analogs, *Cancer Lett. 111*, 133–139.
9. Mo, H., and Elson, C.E. (1999) Apoptosis and Cell-Cycle Arrest in Human and Murine Tumor Cells Are Initiated by Isoprenoids, *J. Nutr. 129*, 804–813.
10. McIntyre, B.S., Briski, K.P., Gapor, A., and Sylvester, P.W. (2000) Antiproliferative and Apoptotic Effects of Tocopherols and Tocotrienols on Preneoplastic and Neoplastic Mouse Mammary Epithelial Cells, *Proc. Soc. Exp. Biol. Med. 2224*, 292–301.
11. Packer, L. (1991) Protective Role of Vitamin E in Biological Systems, *Am. J. Clin. Nutr. 53*, 1050S–1055S.

12. Schwenke, D.C. (2002) Does Lack of Tocopherols and Tocotrienols Put Women at Increased Risk of Breast Cancer? *J. Nutr. Biochem. 13*, 2–20.
13. Ricciarelli, R., Zingg, J.M., and Azzi, A. (2001) Vitamin E: Protective Role of a Janus Molecule, *FASEB J. 15*, 2314–2325.
14. Chatelain, E., Boscoboinik, D.O., Bartoli, G.M., Kagan, V.E., Gey, F.K., Packer, L., and Azzi, A. (1993) Inhibition of Smooth Muscle Cell Proliferation and Protein Kinase C Activity by Tocopherols and Tocotrienols, *Biochim. Biophys. Acta 1176*, 83–89.
15. Kline, K., Yu, W., and Sanders, B.G. (2001) Vitamin E: Mechanisms of Action as Tumour Cell Growth Inhibitors, *J. Nutr. 131*, 161–163.
16. Gu, J.Y., Wakizono, Y., Sunada, Y., Hung, P., Nonaka, M., Sugano, M., and Yamada, K. (1999) Dietary Effect of Tocopherols and Tocotrienols on the Immune Function of Spleen and Mesenteric Lymph Node Lymphocytes in Brown Norway Rats, *Biosci. Biotechnol. Biochem. 63*, 1697–1702.
17. Osborne, C.K., Hobbs, K., and Trent, J.M. (1987) Biological Differences Among MCF-7 Human Breast Cancer Cell Lines from Different Laboratories, *Breast Cancer Res. Treat. 9*, 111–121.
18. Yue, H., Eastman, P.S., Wang, B.B., Minor, J., Doctolero, M.H., Nuttall, R.L., Stack, R., Becker, J.W., Montgomery, J.R., Vainer, M., and Johnston, R. (2001) An Evaluation of the Performance of cDNA Microarrays for Detecting Changes in Global mRNA Expression, *Nucleic Acids Res. 29*, E41–41 (on-line).
19. Fischer, A., Pallauf, J., Gohil, K., Weber, S.U., Packer, L., and Rimbach, G. (2001) Effect of Selenium and Vitamin E Deficiency on Differential Gene Expression in Rat Liver, *Biochem. Biophys. Res. Commun. 285*, 470–475.
20. Hellmann, G.M., Fields, W.R., and Doolittle, D.J. (2001) Gene Expression Profiling of Cultured Human Bronchial Epithelial and Lung Carcinoma Cells, *Toxicol. Sci. 61*, 154–163.
21. Brazma, A., Hingamp, P., Quackenbush, J., Sherlock, G., Spellman, P., Stoeckert, C., Aach, J., Ansorge, W., Ball, C.A., Causton, H.C., *et al.* (2001) Minimum Information About a Microarray Experiment (MIAME)—Toward Standards for Microarray Data, *Nature Genet. 29*, 365–371.
22. Okabe, M., Oji, M., Ikeda, I., Tachibana, H., and Yamada, K. (2002) Tocotrienol Level in Various Tissues of Sprague-Dawley Rats after Intragastric Administration of Tocotrienols, *Biosci. Biotechnol. Biochem. 66*, 1768–1771.
23. Guthrie, N., Gapor, A., Chambers, A.F., and Carroll, K.K. (1997) Inhibition of Proliferation of Estrogen Receptor-Negative MDA-MB-435 and -Positive MCF-7 Human Breast Cancer Cells by Palm Oil Tocotrienols and Tamoxifen, Alone and in Combination, *J. Nutr. 127*, 544S–548S.
24. Gould, M.N., Haag, J.D., Kennan, W.S., Tanner, M.A., and Elson, C.E. (1991) A Comparison of Tocopherol and Tocotrienol for the Chemoprevention of Chemically Induced Rat Mammary Tumors, *Am. J. Clin. Nutr. 53*, 1068S–1070S.
25. Nesaretnam, K., Khor, H.T., Ganeson, J., Chong, Y.H., Sundram, K., and Gapor, A. (1992) The Effect of Vitamin E Tocotrienols from Palm Oil on Chemically Induced Mammary Carcinogenesis in Female Rats, *Nutr. Res. 12*, 879–892.
26. Gill, R.G., Coulombe, M., and Lafferty, K.J. (1996) Pancreatic Islet Allograft Immunity and Tolerance: The Two-Signal Hypothesis Revisited, *Immunol. Rev. 149*, 75–96.
27. Matzinger, P. (1994) Tolerance, Danger, and the Extended Family, *Annu. Rev. Immunol. 12*, 991–1045.
28. Allison, J.P., Hurwitz, A.A., and Leach, D.R. (1995) Manipulation of Costimulatory Signals to Enhance Antitumor T-Cell Responses, *Curr. Opin. Immunol. 7*, 682–686.
29. Chen, L., Ashe, S., Brady, W.A., Hellstrom, I., Hellstrom, K.E., Ledbetter, J.A., McGowan, P., and Linsley, P.S. (1992) Costimulation of Antitumor Immunity by the B7 Counterreceptor for the T Lymphocyte Molecules CD28 and CTLA-4, *Cell 71*, 1093–1102.
30. Townsend, S.E., and Allison, J.P. (1993) Tumour Rejection After Direct Costimulation of CD8+ T Cells by B7-Transfected Melanoma Cells, *Science 259*, 368–370.
31. Schwartz, R.H. (1990) A Cell Culture Model for T Lymphocyte Clonal Anergy, *Science 248*, 1349–1356.
32. Ochsenbein, A.F., Klenerman, P., Karrer, U., Ludewig, B., Pericin, M., Hengartner, H., and Zinkernagel, R.M. (1999) Immune Surveillance Against a Solid Tumour Fails Because of Immunological Ignorance, *Proc. Natl. Acad. Sci. USA 96*, 2233–2238.
33. Ohashi, P.S., Oehen, S., Aichele, P., Pircher, H., Odermatt, B., Herrera, P., Higuchi, Y., Buerki, K., Hengartner, H., and Zinkernagel, R.M. (1993) Induction of Diabetes Is Influenced by the Infectious Virus and Local Expression of MHC Class I and Tumour Necrosis Factor-α, *J. Immunol. 150*, 5185–5194.
34. Eynon, E.E., Schlax, C., and Pieters, J. (1999) A Secreted Form of the Major Histocompatibility Complex Class II-Associated Invariant Chain Inhibiting T Cell Activation, *J. Biol. Chem. 274*, 26266–26271.
35. Topilski, I., Harmelin, A., Flavell, R.A., Levo, Y., and Shachar, I. (2002) Preferential Th1 Immune Response in Invariant Chain-Deficient Mice, *J. Immunol. 168*, 1610–1617.
36. Koeffler, H.P., Ranyard, J., Yelton, L., Billing, R., and Bohman, R. (1984) γ-Interferon Induces Expression of the HLA-D Antigens on Normal and Leukemic Human Myeloid Cells, *Proc. Natl. Acad. Sci. USA 81*, 4080–4084.
37. Balkwill, F.R., Stevens, M.H., Griffin, D.B., Thomas, J.A., and Bodmer, J.G. (1987) Interferon γ Regulates HLA-D Expression on Solid Tumors *in vivo*, *Eur. J. Cancer Clin. Oncol. 23*, 101–106.
38. Shih, N.Y., Soesilo, I., and Floyd-Smith, G. (1997) Stabilization of Invariant Chain mRNA by 12-*O*-Tetradecanoylphorbol-13-Acetate Is Blocked by IFN-γ in a Murine B Lymphoma Cell Line, *J. Interferon Cytokine Res. 17*, 747–755.
39. Gutterman, J.U. (1994) Cytokine Therapeutics: Lessons from Interferon α, *Proc. Natl. Acad. Sci. USA 91*, 1198–1205.
40. Deblandre, G.A., Marinx, O.P., Evans, S.S., Majjaj, S., Leo, O., Caput, D., Huez, G.A., and Wathelet, M.G. (1995) Expression Cloning of an Interferon-Inducible 17-kDa Membrane Protein Implicated in the Control of Cell Growth, *J. Biol. Chem. 270*, 23860–23866.
41. Shiina, H., Igawa, M., Shigeno, K., Terashima, M., Deguchi, M., Yamanaka, M., Ribeiro-Filho, L., Kane, C.J., and Dahiya, R. (2002) β-Catenin Mutations Correlate with Over-expression of c-myc and Cyclin D1 Genes in Bladder Cancer, *J. Urol. 168*, 2220–2226.
42. Orr, M.S., Fornari, F.A., Randolph, J.K., and Gewirtz, D.A. (1995) Transcriptional Down-regulation of c-myc Expression in the MCF-7 Breast Tumour Cell Line by the Topoisomerase II Inhibitor, VM-26, *Biochim. Biophys. Acta 1262*, 139–145.
43. Bauskin, A.R., Zhang, H.P., Fairlie, W.D., He, X.Y., Russell, P.K., Moore, A.G., Brown, D.A., Stanley, K.K., and Breit, S.N. (2000) The Propeptide of Macrophage Inhibitory Cytokine (MIC-1), a TGF-β Superfamily Member, Acts as a Quality Control Determinant for Correctly Folded MIC-1, *EMBO J. 19*, 2212–2220.
44. Bootcov, M.R., Bauskin, A.R., Valenzuela, S.M., Moore, A.G., Bansal, M., He, X.Y., Zhang H.P., Donnellan, M., Mahler S., Pryor, K., *et al.* (1997) MIC-1, a Novel Macrophage Inhibitory Cytokine, Is a Divergent Member of the TGF-β Superfamily, *Proc. Natl. Acad. Sci. USA 94*, 11514–11519.
45. Fairlie, W.D., Moore, A.G., Bauskin, A.R., Russell, P.K., Zhang, H.P., and Breit, S.N. (1999) MIC-1 Is a Novel TGF-β Superfamily Cytokine Associated with Macrophage Activation, *J. Leukocyte Biol. 64*, 2–5.

46. Fairlie, W.D., Zhang, H.P., Wu, W.M., Pankhurst, S.L., Bauskin, A.R., Russell, P.K., Brown, P.K., and Breit, S.N. (2001) The Propeptide of the Transforming Growth Factor-β Superfamily Member, Macrophage Inhibitory Cytokine-1 (MIC-1), Is a Multifunctional Domain That Can Facilitate Protein Folding and Secretion, *J. Biol. Chem. 276*, 16911–16918.
47. Albertoni, M., Shaw, P.H., Nozaki, M., Godard, S., Tenan, M., Hamou, M.F., Fairlie, D.W., Breit, S.N., Paralkar, V.M., de Tribolet, N., *et al.* (2002) Anoxia Induces Macrophage Inhibitory Cytokine-1 (MIC-1) in Glioblastoma Cells Independently of p53 and HIF-1, *Oncogene 21*, 4212–4219.
48. Moore, A.G., Brown, D.A., Fairlie, W.D., Bauskin, A.R., Brown, P.K., Munier, M.L.C., Russell, P.K., Salamonsen, L.A., Wallace, E.M., and Breit, S.N. (2000) The Transforming Growth Factor-β Superfamily Cytokine Macrophage Inhibitory Cytokine-1 Is Present in High Concentrations in the Serum of Pregnant Women, *J. Clin. Endocrinol. Metabol. 85*, 4781–4788.
49. Yokoyama-Kobayashi, M., Saeki, M., Sekine, S., and Kato, S. (1997) Human cDNA Encoding a Novel TGF-β Superfamily Protein Highly Expressed in Placenta, *J. Biochem. 122*, 622–626.
50. Ghetie, V., and Ward, E.S. (2000) Multiple Roles for the Major Histocompatibility Complex Class I-Related Receptor FcRn, *Annu. Rev. Immunol. 18*, 739–766.
51. Durrant, L.G., and Spendlove, I. (2001) Immunization Against Tumor Cell Surface Complement-Regulatory Proteins, *Curr. Opin. Investig. Drugs 2*, 959–966.
52. Malafa, M.P., and Neitzel, L.T. (2000) Vitamin E Succinate Promotes Breast Cancer Tumor Dormancy, *J. Surgical Res. 93*, 163–170.

[Received February 25, 2004; accepted July 15, 2004]

Distribution of Tocopherols and Tocotrienols to Rat Ocular Tissues After Topical Ophthalmic Administration

Masaki Tanito[a], Nanako Itoh[b], Yasukazu Yoshida[b,*], Mieko Hayakawa[b], Akihiro Ohira[a], and Etsuo Niki[b]

[a]Department of Ophthalmology, Shimane University School of Medicine, Shimane, 693-8501, Japan, and [b]Human Stress Signal Research Center, National Institute of Advanced Industrial Science and Technology (AIST)

ABSTRACT: With increasing evidence suggesting the involvement of oxidative stress in various disorders and diseases, the role of antioxidants *in vivo* has received much attention. Chemically, tocopherols and tocotrienols are closely related; however, it has been observed that they have widely varying degrees of biological effectiveness. The present study has been carried out in an attempt to deepen our understanding of whether there is a significant difference in distribution between tocopherol and tocotrienol homologs to rat eye tissues. Rats were administered 5 μL of pure tocopherol or tocotrienol to each eye once a day for 4 d. Various tissues of the eyes were separated and analyzed for tocopherol and tocotrienol concentrations. The concentration of α-tocotrienol increased markedly in every tissue to which it was administered; however, no significant increase was observed in the case of α-tocopherol. The intraocular penetration of γ-tocopherol and γ-tocotrienol did not differ significantly. Additionally, a significant increase in total vitamin E concentration was observed in ocular tissues, including crystalline lens, neural retina, and eye cup, with topical administration using a relatively small amount (5 μL) of vitamin E, whereas no significant increase was observed when the same amount of vitamin E was administered orally. Topical administration of tocotrienols is thus an effective way to increase ocular tissue vitamin E concentration.

Paper no. L9449 in Lipids 39, 469–474 (May 2004).

Increasing experimental and clinical evidence suggests the involvement of oxidative stress induced by active oxygen and nitrogen species in the pathogenesis of various diseases, cancer, and aging (1). As a consequence, the role of antioxidants has received much attention (2–4). Protection against oxidative stress in ocular tissues is mediated by several antioxidant systems such as vitamins C and E (5), superoxide dismutases (6), the glutathione system (7), and the thioredoxin system (8). The preventive and therapeutic effects of the administration of vitamin E, an antioxidant, have been suggested in various types of ocular diseases in animal models (9–11) and in humans (12–16).

Vitamin E is a generic description for all tocopherol (Toc) and tocotrienol (Toc-3) derivatives. Toc have a phytyl chain, whereas Toc-3 have a similar chain but with three double bonds at positions 3′, 7′, and 11′. Both Toc and Toc-3 have four isomers, designated as α-, β-, γ-, and δ-, which differ by the number and position of methyl groups on the chroman ring (17). α-Tocopherol (α-Toc) is the major vitamin E *in vivo* and exerts the highest biological activity. Toc are present in polyunsaturated vegetable oils and in the germ of cereal seeds, whereas Toc-3 are found in the aleurone and subaleurone layers of cereal seeds and in palm oils. Although Toc and Toc-3 are closely related chemically, they have widely varying degrees of biological effectiveness (18–29). Whereas there are numerous reports on the antioxidant properties of Toc, fewer studies are available for Toc-3.

The present study has been carried out to deepen our understanding of whether there is a significant difference between the distribution of Toc and Toc-3 homologs to rat ocular tissues.

MATERIALS AND METHODS

Materials. Natural 2*R*-, 4*R*′-, 8*R*′-α-, and γ-tocopherol and 2*R*-α- and -γ-tocotrienol were kindly supplied by Eisai Co. Ltd. (Tokyo, Japan). Other chemicals were of the highest grade available commercially.

Animals. Male Wistar rats [specific pathogen-free, young adult (7–9 wk), weighing 200–220 g] were purchased from Japan SLC, Inc. (Shizuoka, Japan). Rats were housed in groups and fed a standard laboratory diet (CE-2, containing 0.007 wt% α-Toc; Nippon Clea Co., Tokyo, Japan), and maintained under standardized conditions of temperature 22°C and RH (70%). The light intensity in the colony room of Japan SLC or our laboratory was 300 lux, and that within the cages in our laboratory was 20–40 lux. All rats were kept under a 12-h light/dark cycle (8:00 AM to 8:00 PM in the colony room of Japan SLC, and 7:00 AM to 7:00 PM in our laboratory). Before the experiments, all animals were checked, and no rat showed ocular pathology, including corneal ulcer and conjunctivitis.

Preparation of eye tissues. Rats were administrated Toc, Toc-3, or stripped corn oil topically or orally. In topical administration, 5 μL of pure Toc or pure Toc-3 (2.23 ± 0.14 mg) was applied to each eye once a day for 4 consecutive days. Twenty-four hours after the last administration, rats were sacrificed under anesthesia with sodium pentobarbital (30 mg/kg, ip). After the blood was collected from the inferior vena cava using

*To whom correspondence should be addressed at AIST, 1-8-31 Midorigaoka Ikeda, Osaka 563-8577, Japan. E-mail: yoshida-ya@aist.go.jp

Abbreviations: RPE, retinal pigment epithelium; Toc, tocopherol; α-Toc, α-tocopherol; Toc-3, tocotrienol; Total T, sum of Toc + Toc-3.

a heparinized syringe, ice-cold PBS was irrigated from the left ventricle to wash out the blood, and then both eyes as well as the total brain were rapidly removed. Blood was separated into erythrocytes and plasma by centrifugation (2400 × *g* for 10 min). Under a microscope, removed eyes were separated into cornea, crystalline lens, iris, neural retina, and eye cup, which consisted of retinal pigment epithelium (RPE), choroid, and sclera. All of these tissues were weighed immediately as wet weight. Both eyes from each rat were analyzed for vitamin E concentrations separately, and mean values from both eyes were used for the value of each rat. Four animals (8 eyes) were used for one experimental group. Experimental protocols were approved by the Animal Welfare, Care and Use Committee of AIST Kansai.

Analysis of antioxidants. Plasma antioxidants were extracted by chloroform/methanol (2:1, vol/vol). Ocular tissues were homogenized with 100 μL PBS (pH 7.4) with pestles and tubes (Bel-Art Products, Pequannock, NJ) for 4 min. Chloroform/methanol (450 μL, 2:1, vol/vol) was added to the homogenized suspension, and lipids and vitamin E were extracted by centrifugation (20,000 × *g* at 4°C for 20 min) after mixing vigorously with a vortex mixer. Brain was also homogenized with an equal volume of PBS (pH 7.4) by Polytron (PT3100; Kinematica AG, Lucerne, Switzerland).Then an aliquot of the solution was extracted with chloroform/methanol (2:1, vol/vol) using a volume twice that of the sample. α- and γ-Toc and α- and γ-Toc-3 were detected using HPLC by an amperometric electrochemical detector (Nanospace SI-1; Shiseido, Tokyo, Japan) set at 800 mV, with an ODS column (5 μm, 250 × 4.6 mm; LC-18; Supelco, Tokyo, Japan) and methanol/*tert*-butyl alcohol (95:5, vol/vol) containing 50 mM sodium perchlorate as eluent at 1 mL/min.

Analyses of lipids. Ocular tissues were homogenized in PBS (pH 7.4) and extracted by chloroform/methanol (2:1, vol/vol) as mentioned above and PC, PEA, PI, PS, sphingomyelin (SM), triacylglycerol (TG), and cholesterol (FC) in the chloroform layer were measured by using a TLC system equipped with FID (MK-5; Iatron Laboratories, Tokyo, Japan). Samples in chloroform solution (2 μL) were spotted onto sintered silicagel rods (Chromarod-SIII; Iatron Laboratories) with a Drummond micro dispenser. For the analyses of PC, PE, PI, SM, and PS, the spotted Chromarods were developed in chloroform/methanol/water/formic acid (45:25:2.5:1, by vol) at 25°C and then dried with a blower. The Chromarods were developed again in hexane/diethyl ether (63:7) at 25°C and then dried at 120°C for 10 min. For the analyses of TG and FC, the spotted Chromarods were developed in three different eluents, chloroform/methanol (1:1, vol/vol), benzene/chloroform/acetic acid (50:20:0.7, by vol), and hexane/benzene (1:1, vol/vol) at 25°C and then dried with a blower. The Chromarods were scanned by FID with a constant hydrogen flow rate of 160 mL/min.

Statistical analyses. All statistical analyses were performed on a Microsoft personal computer by ANOVA using the Dunnett test for multiple comparisons, and $P < 0.05$ was determined to be significant. Data were expressed as mean values ± SD.

RESULTS AND DISCUSSION

Table 1 shows the α-Toc and α-Toc-3 distributions to ocular tissues, blood, and brain following topical administration of α-Toc or α-Toc-3. The intact rat ocular tissues contain different concentrations of α-Toc depending on the tissues. It is known that only α-Toc is selectively and preferentially transferred into plasma lipoproteins by α-Toc transfer protein (30). The concentrations of α-Toc in avascular transparent tissues such as the cornea and crystalline lens were much lower than those in the iris, neural retina, and eye cup, which are enriched with blood vessels. Previous investigators also reported a higher concentration of α-Toc in the neural retina and RPE in humans (31) as well as in rats (32), and the concentrations of α-Toc within these tissues in rats are very sensitive to dietary intake of vitamin E (32). Accordingly, the difference in vitamin E uptake from the bloodstream may explain the different vitamin E concentrations among ocular tissues.

It can be seen from Table 1 that administration of α-Toc-3 increased its concentrations remarkably in every tissue examined, although little increase was observed in the case of α-Toc. Those results suggest that topically applied α-Toc-3 was incorporated into the ocular tissues, and that there was a difference in incorporation between Toc and Toc-3 into ocular tissues after topical administration. The drug applied as a drop large enough in size for the conjunctival sac was absorbed into the blood system across the conjunctiva or in the nasolacrimal duct or digestive system, and it could penetrate the ocular tissues of both eyes (33). In Table 1, one can see a slight increase of α-Toc-3 in the plasma (0.61 μM) and brain (0.68 nmol/g-wet tissue) by its administration, suggesting the possible transfer of α-Toc-3 *via* the blood system to ocular tissues by means other than direct penetration.

To clarify the difference in incorporation between Toc and Toc-3 into ocular tissues and to elucidate the involvement of the systemic transfer of drugs into ocular tissues, we carried out additional experiments. The same volume of both γ-Toc and γ-Toc-3 was simultaneously applied to rats topically or orally, and vitamin E concentrations in ocular tissues were assessed (Table 2). The concentrations of γ-Toc and γ-Toc-3 in topically and orally treated rats were increased for almost all samples analyzed, compared with the controls. Additionally, the concentrations of both γ-Toc and γ-Toc-3 by topical treatment were much higher in all ocular tissues than those by oral treatment. In contrast, no difference in concentrations was observed in plasma and brain between topical and oral treatments. These observations suggest that topically applied γ-Toc and γ-Toc-3 were absorbed by the blood and that systemic transfer contributed in part to their incorporation into ocular tissues, whereas direct penetration contributed mainly to the increase of vitamin E concentration in the ocular tissues. Compared with oral treatment with γ-Toc and γ-Toc-3, the increase of γ-Toc-3 in ocular tissues following topical treatment was greater than that of γ-Toc. For example, the ratio of γ-Toc-3 concentration for topical/oral administration (0.87 nmol/0.12 nmol = 7.3) in

TABLE 1
Tissue and Plasma Levels[a] of Vitamin E in Rat Eyes by Topical Administration[b]

Administration	Tissue	α-Toc	γ-Toc	α-Toc-3	[Total T]a/[Total T]c
α-Toc-3	Cornea	3.45 ± 0.31	0.06 ± 0.05	2.42 ± 2.50	1.31
	Crystalline lens	0.54 ± 0.21	0.02 ± 0.02	0.13 ± 0.07	1.31
	Iris	36.12 ± 24.06	0.36 ± 0.41	3.86 ± 1.93	1.23
	Neural retina	44.39 ± 8.97	0.66 ± 0.16	2.61 ± 1.14	1.09
	Eye cup	17.56 ± 4.04	0.19 ± 0.22	4.54 ± 1.47	1.17
	Plasma[b]	7.38 ± 0.46	0.26 ± 0.14	0.61 ± 0.15	0.83
	Brain	26.45 ± 9.23	0.32 ± 0.29	0.68 ± 0.36	1.02
α-Toc	Cornea	4.58 ± 1.30	0.06 ± 0.05	0.02 ± 0.03	1.03
	Crystalline lens	0.56 ± 0.19	0.03 ± 0.04	0.01 ± 0.02	1.15
	Iris	28.85 ± 9.60	0.23 ± 0.27	0.01 ± 0.01	0.92
	Neural retina	35.28 ± 2.42	0.36 ± 0.25	0.05 ± 0.06	0.82
	Eye cup	20.38 ± 0.62	0.22 ± 0.29	0.04 ± 0.05	1.08
	Plasma[b]	12.18 ± 1.95	0.19 ± 0.08	ND	1.25
	Brain	29.04 ± 9.17	0.32 ± 0.19	0.01 ± 0.01	1.09
None	Cornea	4.42 ± 1.47	0.12 ± 0.15	ND	
(stripped corn oil)	Crystalline lens	0.47 ± 0.09	0.05 ± 0.10	ND	
	Iris	32.19 ± 6.75	0.61 ± 0.77	ND	
	Neural retina	43.05 ± 6.95	0.64 ± 0.12	0.06 ± 0.07	
	Eye cup	18.57 ± 2.92	0.36 ± 0.41	0.13 ± 0.17	
	Plasma[b]	9.52 ± 0.71	0.41 ± 0.14	ND	
	Brain	26.51 ± 11.64	0.38 ± 0.34	0.10 ± 0.06	

[a]Plasma: in μM (n = 4); others: in nmol/g-wet tissue [n = 4 (8 eyes)]. α- and γ-Toc, α- and γ-tocopherol; α-Toc-3, α-tocotrienol; [Total T]a/[Total T]c, the ratio of the total of Toc plus Toc-3 concentrations [Total T] by administration to that without any administration; ND, not detected.
[b]Pure α-Toc, α-Toc-3, or stripped corn oil (5 μL/eye/d) was administered by drop for 4 d.

TABLE 2
Tissue and Plasma Levels[a] of Vitamin E in Rat Eyes Either by Topical Administration or by Mouth

Administration	Tissue	α-Toc	γ-Toc	γ-Toc-3	[Total T]a/[Total T]c
γ-Toc + γ-Toc-3	Cornea	3.99 ± 1.02	0.68 ± 0.41	1.03 ± 0.51	1.25
(to eye)	Crystalline lens	0.51 ± 0.16	0.24 ± 0.35	0.27 ± 0.31	1.94
	Iris	22.47 ± 3.52	2.69 ± 2.06	1.33 ± 1.75	0.81
	Neural retina	39.43 ± 5.65	1.36 ± 1.19	0.87 ± 0.75	0.95
	Eye cup	17.48 ± 2.54	2.02 ± 0.61	0.80 ± 0.20	1.06
	Plasma	7.14 ± 1.06	0.44 ± 0.07	0.06 ± 0.01	0.77
	Brain	33.40 ± 4.29	0.64 ± 0.20	0.08 ± 0.05	1.26
γ-Toc + γ-Toc-3	Cornea	3.02 ± 1.09	0.12 ± 0.14	0.05 ± 0.07	0.70
(po)	Crystalline lens	0.37 ± 0.03	0.01 ± 0.01	0.01 ± 0.01	0.65
	Iris	17.31 ± 3.15	1.39 ± 0.40	0.13 ± 0.16	0.65
	Neural retina	23.28 ± 12.59	0.87 ± 1.19	0.12 ± 0.09	0.69
	Eye cup	14.54 ± 1.45	0.99 ± 0.37	0.18 ± 0.15	1.49
	Plasma	5.27 ± 0.59	0.39 ± 0.12	0.05 ± 0.02	0.83
	Brain	26.69 ± 6.21	0.45 ± 0.16	ND	1.35
Stripped corn oil	Cornea	4.52 ± 1.36	ND	ND	
(po)	Crystalline lens	0.59 ± 0.35	ND	ND	
	Iris	29.18 ± 12.68	ND	ND	
	Neural retina	35.45 ± 4.79	ND	ND	
	Eye cup	10.55 ± 1.87	ND	ND	
	Plasma	6.68 ± 0.43	0.20 ± 0.08	ND	
	Brain	19.81 ± 1.50	0.36 ± 0.23	ND	

[a]Plasma: in μM (n = 4); others: in nmol/g-wet tissue [n = 4 (8 eyes)].
[b]Pure γ-Toc and γ-Toc-3 (2.5 + 2.5 μL eye/d) were administered by drop for 4 d. Pure γ-Toc and γ-Toc-3 (5 + 5 μL) were diluted with 2 mL stripped corn oil and administered by mouth for 4 d; po, per os (by mouth); for other abbreviations see Table 1.

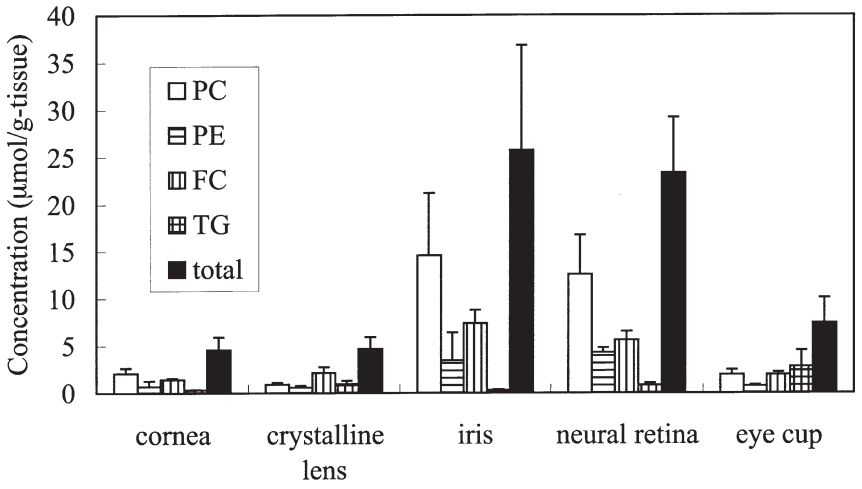

FIG. 1. Concentrations of lipids in ocular tissues after topical administration of corn oil for 4 d (5 μL for both eyes). For experimental protocol see the Materials and Methods section. Data are shown as mean ± SD [$n = 4$ (8 eyes)]. FC, cholesterol; TG, triacylglycerol; total, PC+PEA+FC+TG.

neural retina was much higher than that of γ-Toc (1.36 nmol/0.87 nmol = 1.6). These tendencies of a higher ratio of Toc-3 than Toc after topical administration were observed in other ocular tissues as shown in Tables 1 and 2. The results suggest that the ways by which Toc and Toc-3 were incorporated into ocular tissue differ and that direct distribution makes a greater contribution in Toc-3 than in Toc after topical administration. It has been pointed out that α-Toc-3 is more readily incorporated into lipid particles (34) and cultured cells (26–28) than α-Toc. Thus, the difference in cellular membrane penetration may explain the difference of incorporation between Toc-3 and Toc just described.

Two main routes of direct penetration of topically applied drug into the ocular tissues already have been reported; one is the corneal route formed by the cornea, anterior chamber, lens, and uveal tissues, and the other is the conjunctival route formed by the conjunctiva, sclera, choroid, retinal pigment epithelial layer, and neural retina (33). With the topical administration of α-Toc-3 (Table 1) and simultaneous administration of γ-Toc and γ-Toc-3 (Table 2), the increases of α-Toc-3 and γ-Toc-3, respectively, were relatively small in the lens compared with other ocular tissues. This may suggest that both the corneal and conjunctival routes can contribute to the incorporation of Toc-3 into ocular tissues, whereas the conjunctival route may contribute predominantly to the incorporation of Toc-3 into the posterior segment of ocular tissues.

To elucidate the effect of lipid concentrations on the penetrations of Toc and Toc-3, the lipids of ocular tissues after the topical treatment with corn oil also were analyzed. As shown in Figure 1, higher concentrations of total lipids in the iris and neural retina were observed than in the cornea, crystalline lens, and eye cup. Interestingly, the concentrations of vitamin E incorporated into ocular tissues after topical administration were not necessarily dependent on the total lipid concentrations. High concentrations of Toc and Toc-3 in the eye cup, which contains lower concentrations of lipids than the iris and neural retina, may explain the conjunctival route mentioned above. The lipids of ocular tissues after the topical treatment of Toc and/or Toc-3 also were assessed; however, there was little difference between kinds of administration and vitamin E properties (data not shown). Further study is needed on the roles of Toc and Toc-3 and their effects on lipid distribution in ocular tissues.

In monkeys and in rats, vitamin E deficiency results in retinal degeneration (35,36). In the rhesus monkey, the concentration of vitamin E in retina-RPE-choroid declines to a minimum near the foveal crest (37), and it has been postulated that this minimum results in the vulnerability in this area (38). In rat models of cataract (an opacity of crystalline lens), an increment of vitamin E concentration in lens tissue was related to the prevention of cataract genesis. In any event, the concentration of vitamin E in ocular tissues is closely related to their integrity. As shown in Table 1, the increase of total Toc and Toc-3 concentrations, [Total T], in ocular tissues was more remarkable in topical administration of α-Toc-3 (1.09- to 1.31-fold compared with topically stripped corn oil-treated rats) than those in topical administration of α-Toc (0.82- to 1.15-fold). As shown in Table 2, increases of Total T in ocular tissues were much higher in rats that were topically treated with γ-Toc and γ-Toc-3 (0.77- to 1.94-fold compared with topically stripped corn oil-treated rats) than rats that were orally treated with γ-Toc and γ-Toc-3 (0.65- to 1.49-fold compared with orally stripped corn oil-treated rats). These results suggest that the topical administration of Toc-3 may be effective for the prevention of ocular pathology such as retinal degeneration induced by vitamin E deficiency and experimental cataract in rats.

ACKNOWLEDGMENTS

A generous gift of natural forms of α- and γ-Toc and α- and γ-Toc-3 from Eisai Co. Ltd. is gratefully acknowledged.

REFERENCES

1. Halliwell, B., and Gutteridge, J.M.C. (1999) *Free Radicals in Biology and Medicine*, 3rd edn., Oxford University Press, Oxford.
2. Papas, A.M. (ed.) (1999) *Antioxidant Status, Diet, Nutrition, and Health*, CRC Press, Boca Raton.
3. Frei, B. (ed.) (1994) *Natural Antioxidants in Human Health and Disease*, Academic Press, San Diego.
4. Packer, L., and Cadenas, E. (eds.) (1997) *Handbook of Synthetic Antioxidants*, Marcel Dekker, New York.
5. Penn, J.S., Naash, M.I., and Anderson, R.E. (1987) Effect of Light History on Retinal Antioxidants and Light Damage Susceptibility in the Rat, *Exp. Eye Res. 44*, 779–788.
6. Yamamoto, M., Lidia, K., Gong, H., Onitsuka, S., Kotani, T., and Ohira, A. (1999) Changes in Manganese Superoxide Dismutase Expression After Exposure of the Retina to Intense Light, *Histochem. J. 31*, 81–87.
7. Ohira, A., Tanito, M., Kaidzu, S., and Kondo, T. (2003) Glutathione Peroxidase Induced in Rat Retinas to Counteract Photic Injury, *Invest. Ophthalmol. Vis. Sci. 44*,1230–1236.
8. Tanito, M., Masutani, H., Nakamura, H., Ohira, A., and Yodoi, J. (2002) Cytoprotective Effect of Thioredoxin Against Retinal Photic Injury in Mice, *Invest. Ophthalmol. Vis. Sci. 43*, 1162–1167.
9. Kowluru, R.A., Tang, J., and Kern, T.S. (2001) Abnormalities of Retinal Metabolism in Diabetes and Experimental Galactosemia. VII. Effect of Long-Term Administration of Antioxidants on the Development of Retinopathy, *Diabetes 50,* 1938–1942.
10. Cid, L., Pararajasegaram, G., Sevanian, A., Gauderman, W., Romero, J.L., Marak, G.E., and Rao, N.A., Jr., (1992) Anti-Inflammatory Effects of Vitamin E on Experimental Lens-Induced Uveitis, *Int. Ophthalmol. 16*, 27–32.
11. Ohta, Y., Yamasaki, T., Niwa, T., Majima, Y., and Ishiguro, I. (1999) Preventive Effect of Topical Vitamin E-Containing Liposome Instillation on the Progression of Galactose Cataract. Comparison Between 5-Week- and 12-Week-Old Rats Fed a 25% Galactose Diet, *Exp. Eye Res. 68*, 747–755.
12. Bursell, S.E., Clermont, A.C., Aiello, L.P., Aiello, L.M., Schlossman, D.K., Feener, E.P., Laffel, L., and King, G.L. (1999) High-Dose Vitamin E Supplementation Normalizes Retinal Blood Flow and Creatinine Clearance in Patients with Type 1 Diabetes, *Diabetes Care 22*, 1245–1251.
13. Johnson, L., Quinn, G.E., Abbasi, S., Gerdes, J., Bowen, F.W., and Bhutani, V. (1995) Severe Retinopathy of Prematurity in Infants with Birth Weights Less Than 1250 Grams: Incidence and Outcome of Treatment with Pharmacologic Serum Levels of Vitamin E in Addition to Cryotherapy from 1985 to 1991, *J. Pediatr. 127*, 632–639.
14. Pasantes-Morales, H., Quiroz, H., and Quesada, O. (2002) Treatment with Taurine, Diltiazem, and Vitamin E Retards the Progressive Visual Field Reduction in Retinitis Pigmentosa: A 3-Year Follow-up Study, *Metab. Brain Dis. 17*, 183–197.
15. van Rooij, J., Schwartzenberg, S.G., Mulder, P.G., and Baarsma, S.G. (1999) Oral Vitamins C and E as Additional Treatment in Patients with Acute Anterior Uveitis: A Randomised Double Masked Study in 145 Patients, *Br. J. Ophthalmol. 83*, 1277–1282.
16. Age Related Eye Disease Study Research Group (2002) A Randomized, Placebo-Controlled, Clinical Trial of High-Dose Supplementation with Vitamins C and E, Beta Carotene, and Zinc for Age-Related Macular Degeneration and Vision Loss: AREDS Report No. 8, *Arch. Ophthalmol. 119*, 1417–1436.
17. Packer, L., Weber, S.U., and Rimbach, G. (2001) Molecular Aspects of α-Tocotrienol Antioxidant Action and Cell Signalling, *J. Nutr. 131*, 369S–373S.
18. Nakano, M., Sugioka, K., Nakamura, T., and Ogi, T. (1980) Interaction Between an Organic Hydroperoxide and an Unsaturated Phospholipid and α-Tocopherol in Model Membranes, *Biochim. Biophys. Acta 619*, 274–286.
19. Kato, A., Yamaoka, M., Tanaka, A., and Umezawa, I.J. (1985) Physiological Effects of Tocotrienol, *Jpn. Oil Chem. Soc. 34*, 375–376.
20. Komiyama, K., Iizuka, K., Yamaoka, M., Watanabe, H., Tsuchiya, N., and Umezawa, I. (1989) Studies on the Biological Activity of Tocotrienols, *Chem. Pharm. Bull. 37*, 1369–1371.
21. Servinova, E., Kagan, V., Han, D., and Packer, L. (1991) Free Radical Recycling and Intramembrane Mobility in the Antioxidant Properties of α-Tocopherol and α-Tocotrienol, *Free Radic. Biol. Med. 10*, 263–275.
22. Suarna, C., Hood, R.L., Dean, R.T., and Stocker, R. (1993) Comparative Antioxidant Activity of Tocotrienols and Other Natural Lipid-Soluble Antioxidants in a Homogeneous System, and in Rat and Human Lipoproteins, *Biochim. Biophys. Acta 1166*, 163–170.
23. Suzuki, Y.J., Tsuchiya, M., Wassall, S.R., Choo, Y.M., Govil, G., Kagan, V.E., and Packer, L. (1993) Structural and Dynamic Membrane Properties of α-Tocopherol and α-Tocotrienol: Implication to the Molecular Mechanism of Their Antioxidant Potency, *Biochemistry 32*, 10692–10699.
24. Black, T.M., Wang, R., Maeda, N., and Coleman, R.A. (2000) Palm Tocotrienols Protect ApoE+/−Mice from Diet-Induced Atheroma Formation, *J. Nutr. 130*, 2420–2426.
25. O'Byrne, D., Grundy, S., Packer, L., Devaraj, S., Baldenius, K., Hoppe, P.P., Kraemer, K., Jialal, I., and Traber, M.G. (2000) Studies of LDL Oxidation Following α-, γ-, or δ-Tocotrienyl Acetate Supplementation of Hypercholesterolemic Humans, *Free Radic. Biol. Med. 29*, 834–845.
26. Sen, C.K., Khanna, S., Roy, S., and Packer, L.J. (2000) Tocotrienol Potently Inhibits Glutamate-Induced $pp60^{c\text{-}Src}$ Kinase Activation and Death of HT4 Neuronal Cells, *J. Biol. Chem. 275*, 13049–13055.
27. Noguchi, N., Hanyu, R., Nonaka, A., Okimoto, Y., and Kodama, T. (2003) Inhibition of THP-1 Cell Adhesion to Endothelial Cells by α-Tocopherol and α-Tocotrienol Is Dependent on Intracellular Concentration of the Antioxidants, *Free Radic. Biol. Med. 34*, 1614–1620.
28. Saito, Y., Yoshida, Y., Akazawa, T., Takahashi, K., and Niki, E. (2003) Cell Death Caused by Selenium Deficiency and Protective Effect of Antioxidants, *J. Biol. Chem. 278*, 39428–39434.
29. Kamat, J.P., and Devasagayam, T.P. (1995) Tocotrienols from Palm Oil as Potent Inhibitors of Lipid Peroxidation and Protein Oxidation in Rat Brain Mitochondria, *Neurosci. Lett. 195*, 179–182.
30. Arita, M., Sato, Y., Miyata, A., Tanabe, T., Takahashi, E., Kayden, H.J., Arai, H., and Inoue, K. (1995) Human α-Tocopherol Transfer Protein: cDNA Cloning, Expression and Chromosomal Localization, *Biochem. J. 306*, 437–443.
31. Friedrichson, T., Kalbach, H.L., Buck, P., and Van Kuijk, F.J. (1995) Vitamin E in Macular and Peripheral Tissues of the Human Eye, *Curr. Eye Res. 14*, 693–701.
32. Stephens, R.J., Negi, D.S., Short, S.M., Van Kuijk, F.J., Dratz, E.A., and Thomas, D.W. (1988) Vitamin E Distribution in Ocular Tissues Following Long-Term Dietary Depletion and Supplementation as Determined by Microdissection and Gas Chromatography–Mass Spectrometry, *Eye Res. 47*, 237–245.
33. Maurice, D.M. (2002) Drug Delivery to the Posterior Segment from Drops, *Surv. Ophthalmol. 47* (Suppl. 1), S41–S52.
34. Sarks, J.P., Sarks, S.H., and Killingsworth, M.C. (1988) Evolution of Geographic Atrophy of the Retinal Pigment Epithelium, *Eye 2* (Part 5), 552–577.

35. Hayes, K.C. (1974) Retinal Degeneration in Monkeys Induced by Deficiencies of Vitamin E or A, *Invest. Ophthalmol. 13*, 499–510.
36. Farnsworth, C.C., Stone, W.L., and Dratz, E.A. (1979) Effects of Vitamin E and Selenium Deficiency on the Fatty Acid Composition of Rat Retinal Tissues, *Biochim. Biophys. Acta. 552*, 281–293.
37. Crabtree, D.V., Adler, A.J., and Snodderly, D.M. (1996) Radial Distribution of Tocopherols in Rhesus Monkey Retina and Retinal Pigment Epithelium Choroid, *Invest. Ophthalmol. Vis. Sci. 37*, 61–76.
38. Yoshida, Y., Niki, E., and Noguchi, N. (2003) Comparative Study on the Action of Tocopherols and Tocotrienols as Antioxidant: Chemical and Physical Effects, *Chem. Phys. Lipids 123*, 63–75.

[Received February 17, 2004; accepted July 15, 2004]

Oxidation Rate of Conjugated Linoleic Acid and Conjugated Linolenic Acid Is Slowed by Triacylglycerol Esterification and α-Tocopherol

Tsuyoshi Tsuzuki[a], Miki Igarashi[a], Toshio Iwata[b], Yoshie Yamauchi-Sato[b], Takaya Yamamoto[b], Kanehide Ogita[b], Toshihide Suzuki[a], and Teruo Miyazawa[a,*]

[a]Food & Biodynamic Chemistry Laboratory, Graduate School of Agricultural Science, Tohoku University, Sendai 981-8555, Japan, and [b]Rinoru Oil Mills Co., Ltd., Tokyo, 104-0033, Japan

ABSTRACT: We have recently shown that α-eleostearic acid (α-ESA), a conjugated linolenic acid, has a stronger antitumor effect than conjugated linoleic acid (CLA), both *in vitro* and *in vivo*. In this study, the oxidative stability of α-ESA was examined compared with linoleic acid (LA), α-linolenic acid (LnA), and CLA. Thin layers of the FA (LA, 9*Z*,11*E*-CLA, 10*E*,12*Z*-CLA, LnA, and α-ESA) were auto-oxidized at 37°C, and the FA remaining, the absorbed oxygen volume, the lipid hydroperoxide content, and the TBARS content were determined. The oxidation rate of α-ESA was faster than that of the unconjugated FA and CLA (9*Z*,11*E*-CLA and 10*E*,12*Z*-CLA). However, the lipid hydroperoxide and TBARS contents following α-ESA oxidation were low, suggesting production of only small amounts of rapid-reacting secondary oxidation products. Furthermore, the oxidative stability of conjugated FA (CLA and CLnA) in which the carboxylic acid group was esterified with triacylglycerol was greater than that of the FFA. Addition of an antioxidant (α-tocopherol) also increased the stability of the conjugated FA to a level similar to that of the unconjugated FA.

Paper no. L9394 in *Lipids 39*, 475–480 (May 2004).

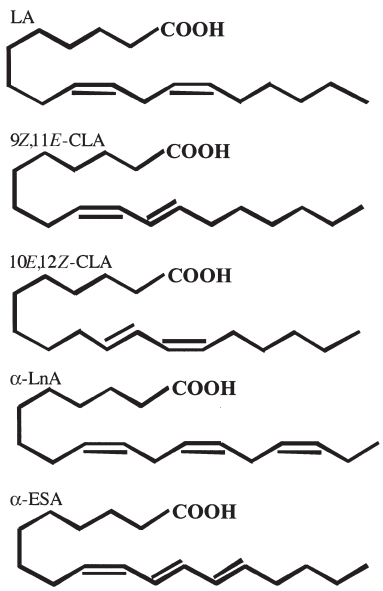

FIG. 1. Chemical structures of LA, 9*Z*,11*E*-CLA, 10*E*,12*Z*-CLA, α-LnA, and α-ESA. LA, Linoleic acid: 9*Z*,12*Z*-18:2; 9*Z*,11*E*-CLA, 9*Z*,11*E*-18:2; 10*E*,12*Z*-CLA, 10*E*,12*Z*-18:2; α-LnA, α-linolenic acid: 9*Z*,12*Z*, 15*Z*-18:3; α-ESA, α-eleostearic acid: 9*Z*,11*E*,13*E*-18:3.

FA with conjugated double bonds exist in nature, but they occur only in small quantities. A conjugated linoleic acid (CLA; 18:2) (Fig. 1), a geometrical and positional isomer of linoleic acid (LA; 9*Z*,12*Z*-18:2), is found in dairy products such as milk and cheese and is also present in beef (1,2). It has been reported that CLA has very useful bioactive properties, including anticancer and anti-obesity activity (1,3–5). The bioactivity of CLA was initially considered to be associated with antioxidant action, and Ha *et al.* (1) described the antioxidant properties of CLA in an animal study. However, from an *in vitro* study, Van Den Berg *et al.* (6) suggested that CLA is a pro-oxidant. Subsequently, the oxidative stability of CLA was examined under various conditions (7–11). CLA in the FFA form was found to be extremely unstable; its stability is similar to that of DHA and its oxidation rate is considerably greater than that of LA, linolenic acid (LnA), and arachidonic acid (8,10).

Many conjugated FA other than CLA exist in nature. The seeds of some plants include conjugated triene and tetraene FA such as α-eleostearic acid (α-ESA; 9*Z*,11*E*,13*E*-18:3), calendic acid (8*E*,10*E*,12*Z*-18:3), and parinaric acid (9*Z*,11*E*,13*E*,15*Z*-18:4) (12,13) (Fig. 1), and seaweeds such as red and green algae include highly unsaturated conjugated FA, i.e., bosseopentaenoic acid (5*Z*,8*Z*,10*E*,12*E*,14*Z*-20:5) and stellaheptaenoic acid (4*Z*,7*Z*,9*E*,11*E*,13*Z*,16*Z*,19*Z*-22:7) (14–16). These conjugated FA have not been investigated in detail, compared with CLA. Hence, we have an interest in the potential bioactivity of these conjugated FA, and we anticipate that they may show a higher bioactivity than CLA (17–21). A FA mixture containing a large amount of conjugated triene FA that were prepared from alkali isomerization

*To whom correspondence should be addressed at Food and Biodynamic Chemistry Laboratory, Graduate School of Agricultural Science, Tohoku University, Tsutsumidori-Amamiyamachi 1-1, Sendai 981-8555, Japan.
E-mail: miyazawa@biochem.tohoku.ac.jp
Present address of seventh author: Forensic Chemistry, Faculty of Pharmaceutical Sciences, Teikyo University, Kanagawa 220-0200, Japan.

Abbreviations: CLnA, conjugated linolenic acid; α-ESA, α-eleostearic acid; FOX, ferrous oxidation in xylenol orange; LA, linoleic acid; LnA, linolenic acid; LOOH, lipid hydroperoxide; TBARS, thiobarbituric acid reactive substances; TG, triacylglycerol; α-Toc, α-tocopherol.

of LnA (18:3), EPA (20:5), and DHA (22:6) had a stronger cytocidal effect on human cultured tumor cells than that of CLA, with the proposed mechanism being apoptosis induction *via* lipoperoxidation (17,18,20). In contrast, the tumoricidal effect of CLA does not occur *via* lipoperoxidation (22). Recently, we found in both *in vivo* and *in vitro* studies that α-ESA, which is found in tung (*Aleurites fordii*) and bitter gourd (*Momordica charantia*) seeds in large amounts, had a stronger antitumor effect than CLA (21). Furthermore, lipoperoxidation was significantly involved in this bioactivity. These results suggested that the bioactivities of conjugated FA may be related to oxidation, and evaluating the oxidative stability of such conjugated FA is therefore important.

In this study, the oxidative stabilities of conjugated linolenic acid (CLnA), CLA, LA, and α-LnA were compared. These FA were prepared in a tube and auto-oxidized at 37°C. To evaluate the oxidative stability, the following items were determined: the remaining FA content, to evaluate the stability of the FA themselves; the absorbed oxygen volume, to evaluate the reactivity with oxygen; the lipid hydroperoxide (the first oxide of a PUFA) content, using a ferrous oxidation in xylenol orange (FOX) assay; and the secondary oxide content, using a thiobarbituric acid (TBA) test. On the assumption that CLnA may be used in foods, we investigated the oxidative stability of the triacylglycerol (TG) ester form of CLnA, and we also examined the oxidative stability in the presence of α-tocopherol (α-Toc), an antioxidant.

EXPERIMENTAL PROCEDURES

Materials. Margaric acid (17:0), LA (18:2n-6), α-LnA (18:3n-3), BHT, and DL-α-Toc were obtained from Sigma Chemical Co. (St. Louis, MO). 9*Z*,11*E*-CLA (98% purity) and 10*E*,12*Z*-CLA (98% purity) were obtained from Cayman Chemical Co. (Ann Arbor, MI). α-ESA (98% purity) was obtained from Larodan Fine Chemicals AB (Malmö, Sweden). Safflower oil, perilla oil, and TG-containing CLA (CLA-TG: approximately 80% of the acyl groups of TG were associated with the CLA) were provided by Rinoru Oil Mills Co. Ltd. (Nagoya, Japan). Tung oil was provided by Nippon Oil and Fats Co. Ltd. (Tokyo, Japan).

Oxidation study of FFA. One-half milligram of a given FA (LA, 9*Z*,11*E*-CLA, 10*E*,12*Z*-CLA, LnA, α-ESA) and 0.25 mg of margaric acid (internal standard) were spread thinly onto the bottom of a 10-mL opaque glass tube by blowing nitrogen gas over the FA. The tube was kept at room temperature for 10 min, then sealed with a rubber stopper and incubated in a dark room at 37°C for 0 to 24 h. After incubation, the oxidative reaction was terminated by the addition of 0.5 mL of BHT solution (1 mM in hexane). The following items were determined: volume of oxygen absorbed from the air in the tube, using a headspace gas assay; the remaining FA content, using GC analysis; the lipid hydroperoxide content, using a FOX assay; and the secondary oxide content, using a TBA test.

Headspace gas assay. Using the headspace gas in the tube, we determined the oxygen volume absorbed by the FA by using a GC-4C gas chromatograph (Shimadzu, Kyoto, Japan). A thermal conductivity detector, a 5 Å molecular sieve stainless steel column (200 × 0.3 cm i.d.), and helium as carrier gas were used. The temperatures of the injector and detector were set at 100 and 90°C, respectively, and the temperature of the oven was raised from 80 to 90°C at 5°C/min and then held at 90°C. The absorbed oxygen volume was calculated from the ratio of oxygen to nitrogen.

GC analysis. The remaining FA content was determined using a 353B gas chromatograph (GL Sciences Inc., Tokyo, Japan), using a previously reported method (19,23). In the FAME preparation, trimethylsilyldiazomethane solution (23,24) and $NaOCH_3$/MeOH (23,25) were used for FFA and TG, respectively.

FOX assay. The lipid hydroperoxide content in 100 μL of solution was determined using the FOX assay (26).

TBA test. The secondary oxide content in a 100-μL solution was determined using the TBA test (19,27).

Preparation of TG samples. For the TG samples, safflower oil (LA-TG), perilla oil (LnA-TG), CLA-TG, and tung oil (CLnA-TG) were used as the TG-protected forms of LA, LnA, CLA, and CLnA, respectively. The composition of the FA was determined using GC analysis (Table 1). Before use, tocopherol was removed from the oils using an alumina column to adjust the tocopherol content in the samples (28). The tocopherol content was determined using HPLC with a fluorescence detector (29), and was found to be 6.7, 6.7, 6.5, and 6.9 mg/100 g in safflower oil, CLA-TG, perilla oil, and tung oil, respectively.

Oxidation study of TG samples. For each TG sample, (LA-TG, CLA-TG, LnA-TG, and CLnA-TG), 0.5 mg of TG and 0.25 mg of margaric acid (internal standard) were spread thinly onto the bottom of a 10-mL opaque glass tube by blowing nitrogen gas over the sample plus standard. The tube was kept at room temperature for 10 min, and then sealed with a rubber stopper and incubated in a dark room at 37°C for 0 to 14 d. After incubation, 0.5 mL of BHT solution (1 mM in hexane) was added to terminate the oxidative reaction. The remaining FA content was determined using GC analysis, and the degraded secondary product content was determined using a TBA test.

Antioxidant study. For each TG sample (LA-TG, CLA-TG, LnA-TG and CLnA-TG), 0.5 mg of TG, 0.5 μg of α-Toc, and 0.25 mg of margaric acid (internal standard) were spread thinly onto the bottom of a 10-mL opaque glass tube by blowing nitrogen gas over the mixture. By using the same procedures as above, the remaining FA content was determined using GC analysis, and the degraded secondary product content was determined using a TBA test.

Statistics. Statistical analysis was performed using one-way ANOVA, followed by the Newman–Keuls test for multiple comparisons among several groups. A difference was considered to be significant at $P < 0.05$.

TABLE 1
FA Composition of Sample Oils[a]

FA	LA-TG (safflower oil) (%)	CLA-TG (%)	LnA-TG (perilla oil) (%)	CLnA-TG (tung oil) (%)
16:0	7.7	4.4	5.9	4.6
18:0	2.2	2.2	1.4	4.5
18:1n-9	11.7	14.4	13.9	9.9
18:2n-6	78.4	1.1	16.0	6.1
9*Z*,11*E*-CLA	—[b]	34.2	—	—
10*E*,12*Z*-CLA	—	38.5	—	—
Other CLA	—	5.2	—	—
18:3n-3	—	—	62.8	—
α-ESA	—	—	—	72.1
β-ESA	—	—	—	2.8

[a]The FAME, prepared from TG samples, were analyzed by GC.
[b]—, not detected (below 0.1%). LA, linoleic acid; TG, triacylglycerol; LnA, linolenic acid; CLnA, conjugated linolenic acid; ESA, eleostearic acid.

RESULTS

Oxidation of FFA. Use of α-ESA in foods requires it to be stable. Hence, the oxidative stability of α-ESA was examined in comparison with unconjugated FA (LA and LnA), and whether α-ESA is converted to CLA was also considered. The CLA isomers 9*Z*,11*E*-CLA and 10*E*,12*Z*-CLA, the main compounds produced in the preparation of CLA from LA using an alkali isomerization procedure, and the CLnA isomer α-ESA (9*Z*,11*E*,13*E*-18:3), which is a component of tung oil, were used. To evaluate the oxidative stability of the FA (LA, 9*Z*,11*E*-CLA, 10*E*,12*Z*-CLA, LnA, α-ESA), the following items were determined: the remaining FA content, to evaluate the stability of the FA themselves; the oxygen volume absorbed, to evaluate the reactivity of the FA with oxygen; the lipid hydroperoxide (the first oxide formed from a PUFA) content; and the secondary oxide content. The contents of remaining 10*E*,12*Z*-CLA, 9*Z*,11*E*-CLA, LnA, and LA after 24 h were 20, 40, 45, and 65%, respectively (Fig. 2A). α-ESA was not detected after 24 h. A comparison between conjugated and unconjugated FA with the same number of double bonds showed that the conjugated FA content declined more rapidly, and FA with more double bonds also degraded faster. The FA content following oxidation of 9*Z*,11*E*-CLA decreased more slowly than for 10*E*,12*Z*-CLA oxidation. After α-ESA incubation for 24 h at 37°C, CLA was not detected. The oxygen volume absorbed by each FA followed a trend very similar to that of the remaining FA content (Figs. 2A, 2B). However, the oxygen volume absorbed per molecule of conjugated FA seemed to be less than that for unconjugated FA (Fig. 2B). There was no great difference in the oxygen volume absorbed following LnA and α-ESA incubation for 24 h. The lipid hydroperoxide content and the TBARS content were largest for LnA, followed by LA (Figs. 2C, 2D). Little or none of these substances was produced by conjugated FA oxidation. These results show that the oxidative stability of α-ESA was inferior to that of CLA, LA, and LnA. Oxidation products of α-ESA included small amounts of lipid hydroperoxides and highly reactive aldehydes.

Oxidation of TG samples. Using α-ESA in its FFA form may be impractical because of its low oxidative stability. To overcome this problem, α-ESA in its TG ester form may be more suitable, and therefore the oxidative stability of the TG-form of α-ESA was compared with that of unconjugated FA and CLA by means of the remaining FA and TBARS content. A safflower oil containing LA as 78.4% of the total FA content was esterified with TG, yielding LA-TG. Similarly, perilla oil

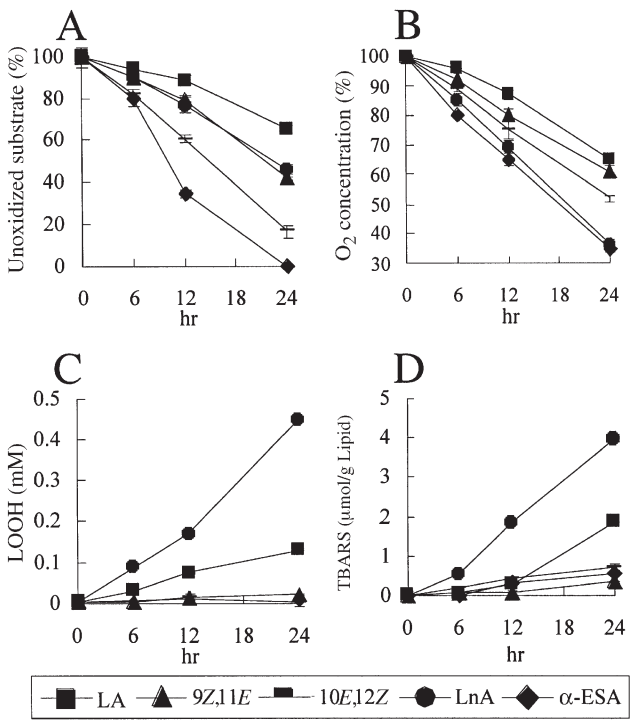

FIG. 2. Thin-film oxidation of FA (LA, 9*Z*,11*E*-CLA, 10*E*,12*Z*-CLA, LnA, and α-ESA) in an air atmosphere (0.5 mg/10 mL test tube) at 37°C for 0–24 h. Changes in unoxidized FA (A), oxygen absorption (B), lipid hydroperoxide (LOOH) formation (C), and TBARS (D) are shown. Values are means ± SD (n = 6). For abbreviations see Figure 1.

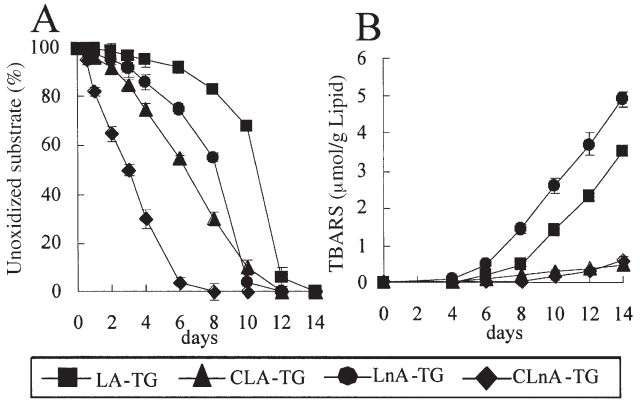

FIG. 3. Oxidation of triacylglycerol (TG) samples (LA-TG, CLA-TG, LnA-TG, and CLnA-TG) in an air atmosphere (0.5 mg/10-mL test tube) at 37°C for 0–14 d. Changes in unoxidized fatty acids (A) and TBARS (B) are shown. Values are means ± SD (n = 6). For abbreviations see Figure 1.

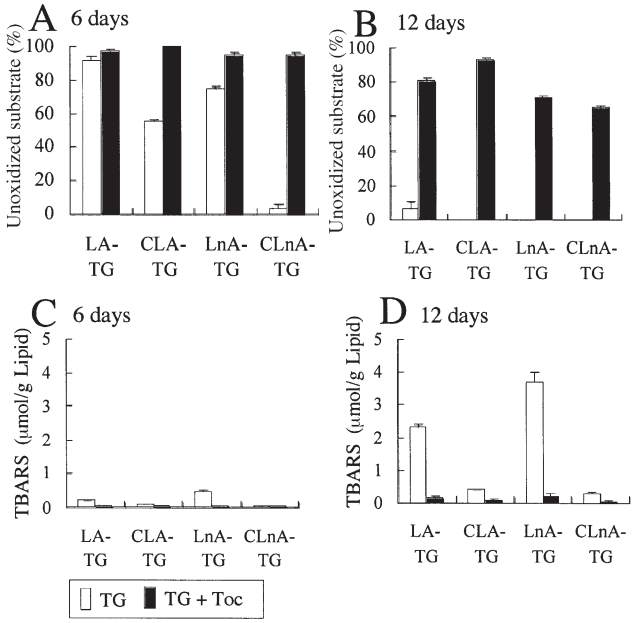

FIG. 4. Oxidation of TG samples (0.5 mg/10-mL test tube) in the presence of α-tocopherol (Toc). α-Toc (0.1%) was added to the TG samples, and the mixtures were left to stand in an air atmosphere at 37°C for 6 d and for 12 d. The changes in unoxidized FA after 6 d (A) and 12 d (B), and TBARS after 6 d (C) and 12 d (D), are given. Values are means ± SD (n = 6). For abbreviations see Figures 1 and 3.

with an LnA content of 62.8% (LA + LnA = 78.8%), CLA-TG with a CLA content of 77.9% (LA + CLA = 79.0%), and tung oil with a CLnA content of 74.9% (LA + ESA = 81.0%) were esterified and used as samples that are referred to as LnA-TG, CLA-TG, and CLnA-TG, respectively (Table 1). TG ester samples in which the amount of FA with two double bonds or more was close to 80% were selected. The oxidative stability of the FA following TG esterification of the carboxyl group was greatly increased (Figs. 2, 3). The remaining FA content was reduced to 80% of the initial content approximately 10-, 8-, 10-, and 10-fold more slowly than in the oxidation of the unprotected FA LA, CLA, LnA, and CLnA, respectively (Figs. 2A, 3A). However, the oxidative stabilities of the TG-protected conjugated FA were inferior to those of the TG-protected unconjugated FA (Fig. 3A). For the unconjugated FA LA-TG and LnA-TG, the oxidation rate rapidly increased around day 6, but the conjugated FA CLA-TG and CLnA-TG were oxidized continuously at a constant rate. After incubation of CLnA-TG that included a large amount of α-ESA for 14 d at 37°C, CLA was not detected. After oxidation of the TG-protected conjugated FA, the TBARS content, a measure of the secondary oxide content, was less than that for the TG-protected unconjugated FA (Fig. 3B), following a trend similar to that seen for the FFA.

Addition of an antioxidant. Compared with unconjugated FA, the oxidative stability of conjugated FA is insufficient for their use in foods. Therefore, α-Toc, an antioxidant, is typically added to improve the oxidative stability of conjugated FA. Safflower and perilla oils available from retail sources contain approximately 0.1% tocopherol, and therefore α-Toc was added to each TG sample (LA-TG, CLA-TG, LnA-TG, and CLnA-TG) at 0.1% of the sample weight. The samples were then auto-oxidized at 37°C, as described above, and the oxidative stability was evaluated from the remaining FA content and the TBARS content. Addition of α-Toc markedly improved the oxidative stability of the TG-protected FA (Fig. 4), and these samples had barely undergone oxidation on day 6 (Figs. 4A, 4C). On day 12, CLA-TG showed the highest oxidative stability of the four TG-protected FA (Figs. 4B, 4D). In particular, CLA-TG showed superior oxidative stability to LA-TG. The oxidative stability of CLnA-TG was similar to that of LnA-TG.

DISCUSSION

We have recently found in both *in vivo* and *in vitro* studies that α-ESA, a CLnA, has a stronger antitumor effect than CLA (21). In this study, the oxidative stability of α-ESA was examined using LA, LnA, and CLA as controls. On the basis of the remaining FA content and the volume of absorbed oxygen, conjugated FA (CLA and α-ESA) appear to be oxidized extremely easily (Fig. 2). However, they are still oxidized less than the equivalent unconjugated FA, based on the lipid hydroperoxide and TBARS content after oxidation (Fig. 2). The oxidative stability of CLA was similar to that previously reported (9,11). In comparing the two CLA isomers, 9*Z*,11*E*-CLA had a better oxidative stability than 10*E*,12*Z*-CLA (Fig. 2). This result suggests that the oxidation rate of CLA depends on the position of the double bond. Similarly to CLA, oxidation of α-ESA did not increase the lipid hydroperoxide and TBARS contents, suggesting that α-ESA causes little oxidative stress to organisms, again similarly to CLA. In this context, we note that there were no significant differences in the lipid hydroperoxide and TBARS levels in the liver and plasma of rats that were given feed containing 1% LA, CLA, LnA, or CLnA for 4 wk (19).

The oxidation rate of α-ESA was much faster than that of the two CLA isomers. For the use of α-ESA in foods, the TG

form of α-ESA may be more suitable; therefore, the oxidative stability of the TG-form of α-ESA was compared with that of unconjugated FA and CLA. For both the conjugated and unconjugated FA, the oxidation rate of the TG samples was slower by approximately 10-fold compared with that of the FFA samples (Fig. 3). The oxidative stability of CLnA-TG was not higher than that of LnA-TG, but the results generally suggest that the oxidative stability of conjugated FA is improved by protecting the carboxylic acid group through esterification. To increase the oxidative stability of CLnA still further, α-Toc, a fat-soluble antioxidant, was added at 0.1% of sample weight. As a result, the oxidative stability of CLnA-TG was increased to that of LnA-TG (Fig. 4).

In our previous study, CLA was detected in rats after 4 wk of α-ESA administration, and we found that α-ESA was saturated to CLA (19). This metabolic mechanism is under investigation, and in this study we have confirmed that α-ESA cannot be converted to CLA without the presence of an enzyme.

We previously found in both *in vivo* and *in vitro* studies that α-ESA had a much stronger antitumor effect than CLA (21). The mechanism of this antitumor effect involved α-ESA induction of apoptosis *via* lipoperoxidation. Furthermore, α-ESA induced lipoperoxidation only in tumor cells and had no effect on normal cells; it was concluded that either α-ESA itself or an oxidative product was specifically involved with lipoperoxidation in tumor cells. Results of detailed studies on CLA oxides have produced interesting results, such as their conversion into furan FA (11,30). We have shown that the antitumor effect of CLA is not correlated with lipoperoxidation (21,22). The results of the present study suggest that α-ESA oxidation may occur through a process similar to that of oxidation of CLA but that the α-ESA oxides may differ from the CLA oxidation products. Further studies of α-ESA oxidation are required to clarify this issue.

The results of this study showed that α-ESA in its FFA form was easily oxidized, suggesting that use of the FFA form of α-ESA in foods or medicines would result in oxidation before absorption, and would not allow for beneficial bioactivity. Using α-ESA in its TG ester form and in the presence of an antioxidant significantly improved its stability, and such a formulation of α-ESA may allow the retention of stability prior to absorption.

REFERENCES

1. Ha, Y.L., Grimm, M.W., and Pariza, M.W. (1987) Anticarcinogens from Fried Ground Beef: Heat-Altered Derivatives of Linoleic Acid, *Carcinogenesis 8*, 1881–1887.
2. Lin, H., Boylston, T.D., Chang, M.J., Luedecke, L.O., and Shultz, T.D. (1995) Survey of the Conjugated Linoleic Acid Contents of Dairy Products, *J. Dairy Sci. 78*, 2358–2365.
3. Park, Y., Albright, K.J., Storkson, J.M., Liu, W., Cook, M.E., and Pariza, M.W. (1999) Changes in Body Composition in Mice During Feeding and Withdrawal of Conjugated Linoleic Acid, *Lipids 34*, 243–248.
4. Lee, K.N., Kritchevsky, D., and Pariza, M.W. (1994) Conjugated Linoleic Acid and Atherosclerosis in Rabbits, *Atherosclerosis 108*, 19–25.
5. Chin, S.F., Liu, W., Storkson, J.M., Ha, Y.L., and Pariza, M.W. (1992) Dietary Sources of Conjugated Dienoic Isomers of Linoleic Acid, a Newly Recognized Class of Anticarcinogens, *J. Food Comp. Anal. 5*, 185–197.
6. Van den Berg, J.J.M., Cook, N.E., and Tribble, D.L. (1995) Reinvestigation of the Antioxidant Properties of Conjugated Linoleic Acid, *Lipids 30*, 599–605.
7. Hämäläinen, T.I., Sundberg, S., Mäkinen, M., Kaltia, S., Hase, T., and Hopia, A. (2001) Hydroperoxide Formation During Autoxidation of Conjugated Linoleic Acid Methyl Ester, *Eur. J. Lipid Sci. Technol. 103*, 588–593.
8. Chen, J.F., Tai, C.-Y., Chen, Y.C., and Chen, B.H. (2001) Effects of Conjugated Linoleic Acid on the Degradation and Oxidation Stability of Model Lipids During Heating and Illumination, *Food Chem. 72*, 199–206.
9. Yang, L., Leung, L.K., Huang, Y., and Chen, Z.Y. (2000) Oxidative Stability of Conjugated Linoleic Acid Isomers, *J. Agric. Food Chem. 48*, 3072–3076.
10. Zhang, A., and Chen, Z.Y. (1997) Oxidative Stability of Conjugated Linoleic Acids Relative to Other Polyunsaturated Fatty Acids, *J. Am. Oil Chem. Soc. 74*, 1611–1613.
11. Yurawecz, M.P., Delmonte, P., Vogel, T., and Kramer, J.K.G. (2002) Oxidation of Conjugated Linoleic Acid: Initiators and Simultaneous Reactions: Theory and Practice, in *Advances in Conjugated Linoleic Acid Research, Vol. 2* (Sebedio, J.L., Christie, W.W., and Adlof, R.O., eds.), pp. 56–70, AOCS Press, Champaign.
12. Hopkins, C.Y. (1972) Fatty Acids with Conjugated Unsaturation, in *Topics in Lipid Chemistry* (Gunstone, F.D., ed.), pp. 37–87, ELEK Science, London.
13. Badami, R.C., and Patil, K.B. (1981) Structure and Occurrence of Unusual Fatty Acids in Minor Seed Oils, *Prog. Lipid Res. 19*, 119–153.
14. Lopez, A., and Gerwick, W.H. (1987) Two New Icosapentaenoic Acids from the Temperate Red Seaweed *Ptilota filicina* J. Agardh, *Lipids 22*, 190–194.
15. Burgess, J.R., de la Rosa, R.I., Jacobs, R.S., and Butler, A. (1991) A New Eicosapentaenoic Acid Formed from Arachidonic Acid in the Coralline Red Algae *Bossiella orbigniana*, *Lipids 26*, 162–165.
16. Mikhailova, M.V., Bemis, D.L., Wise, M.L., Gerwick, W.H., Norris, J.N., and Jacobs, R.S. (1995) Structure and Synthesis of Novel Conjugated Polyene Fatty Acids from the Marine Green Alga *Anadyomene stellate*, *Lipids 30*, 583–589.
17. Igarashi, M., and Miyazawa, T. (2000) Do Conjugated Eicosapentaenoic Acid and Conjugated Docosahexaenoic Acid Induce Apoptosis *via* Lipid Peroxidation in Cultured Human Tumor Cells? *Biochem. Biophys. Res. Commun. 270*, 649–656.
18. Igarashi, M., and Miyazawa, T. (2000) Newly Recognized Cytotoxic Effect of Conjugated Trienoic Fatty Acids on Cultured Human Tumor Cells, *Cancer Lett. 148*, 173–179.
19. Tsuzuki, T., Igarashi, M., Komai, M., and Miyazawa, T. (2003) A Metabolic Conversion of 9,11,13-Eleostearic Acid (18:3) to 9,11-Conjugated Linoleic Acid (18:2) in the Rat, *J. Nutr. Sci. Vitaminol. 49*, 195–200.
20. Tsuzuki, T., Igarashi, M., and Miyazawa, T. (2004) Conjugated Eicosapentaenoic Acid Inhibits Transplanted Tumor Growth *via* Membrane Lipid Peroxidation in Nude Mice, *J. Nutr. 134*, 1162–1166.
21. Tsuzuki, T., Tokuyama, Y., Igarashi, M., and Miyazawa, T. (2004) Tumor Growth Suppression by α-Eleostearic Acid, a Linolenic Acid Isomer with a Conjugated Triene System, *via* Lipid Peroxidation, *Carcinogenesis 25*, 1417–1425.
22. Igarashi, M., and Miyazawa, T. (2001) The Growth Inhibitory Effect of Conjugated Linoleic Acid on a Human Hepatoma Cell Line, HepG2, Is Induced by a Change in Fatty Acid Metabolism, but Not the Facilitation of Lipid Peroxidation in the Cells, *Biochim. Biophys. Acta 1530*, 162–171.
23. Igarashi, M., Tsuzuki, T., Kambe, T., and Miyazawa, T. (2004)

Recommended Methods of Fatty Acid Methylester Preparation for Conjugated Dienes and Trienes in Food and Biological Samples, *J. Nutr. Sci. Vitaminol. 50*, 121–128.
24. Hashimoto, N., Aoyama, T., and Shioiri, T. (1981) New Methods and Reagents in Organic Synthesis. 14. A Simple Efficient Preparation of Methyl Esters with Trimethylsilyldiazomethane ($TMSCHN_2$) and Its Application to Gas Chromatographic Analysis of Fatty Acids, *Chem. Pharm. Bull. 29*, 1475–1478.
25. Christie, W.W. (1982) A Simple Procedure for Rapid Transmethylation of Glycerolipids and Cholesteryl Ester, *J. Lipid Res. 23*, 1072–1075.
26. Zadeh, J.N. (1999) Ferrous Ion Oxidation in the Presence of Xylenol Orange for Detection of Lipid Hydroperoxides in Plasma, *Methods Enzymol. 300*, 58–62.
27. Ohkawa, H., Ohnishi, N., and Yagi, K. (1979) Assay for Lipid Peroxides in Animal Tissues by Thiobarbituric Acid Reaction, *Anal. Biochem. 95*, 351–358.
28. Kazimoto, G., Hiromi, H., and Shibahara, A. (1975) *Oil Chemistry 24*, 511 (in Japanese).
29. Igarashi, O. (1982) Vitamin E, in *Vitamin Handbook, Vol. 3* (The Vitamin Society of Japan, ed.) pp. 27–35, Kagakudojin, Kyoto (in Japanese).
30. Yurawecz, M.P., Hood, J.K., Mossoba, M.M., Roach, J.A., and Ku, Y. (1995) Furan Fatty Acids Determined as Oxidation Products of Conjugated Octadecadienoic Acid, *Lipids 30*, 595–598.

[Received October 14, 2003, and in revised form June 11, 2004; revision accepted July 9, 2004]

Formation of Genotoxic Dicarbonyl Compounds in Dietary Oils upon Oxidation

Kazutoshi Fujioka and Takayuki Shibamoto*

Department of Environmental Toxicology, University of California–Davis, Davis, California 95616

ABSTRACT: Dietary oils—tuna, salmon, cod liver, soybean, olive, and corn oils—were treated with accelerated storage conditions (60°C for 3 and 7 d) and a cooking condition (200°C for 1 h). Genotoxic malonaldehyde (MA), glyoxal, and methylglyoxal formed in the oils were analyzed by GC. Salmon oil produced the greatest amount of MA (1070 ± 77.0 ppm of oil) when it was heated at 60°C for 7 d. The highest formation of glyoxal was obtained from salmon oil heated at 60°C for 3 d. More glyoxal was found from salmon and cod liver oils when they were heated for 3 d (12.8 ± 1.10 and 7.07 ± 0.19 ppm, respectively) than for 7 d (6.70 ± 0.08 and 5.94 ± 0.38 ppm, respectively), suggesting that glyoxal underwent secondary reactions during a prolonged time. The amount of methyglyoxal formed ranged from 2.03 ± 0.13 (cod liver oil) to 2.89 ± 0.11 ppm (tuna oil) in the fish oils heated at 60°C for 7 d. Among vegetable oils, only olive oil yielded methylglyoxal (0.61 ± 0.03 ppm) under accelerated storage conditions. When oils were treated under cooking conditions, the aldehydes formed were comparable to those formed under accelerated storage conditions. Fish oils produced more MA, glyoxal, and methylglyoxal than did vegetable oils because the fish oils contained higher levels of long-chain PUFA, such as EPA and DHA, than did the vegetable oils. A statistically significant correlation ($P < 0.05$) between the α-tocopherol content and the oxidation parameters was obtained from only MA and fish oils heated at 60°C for 3 d.

Paper no. L9465 in *Lipids 39,* 481–486 (May 2004).

It is well known that oxidative damage, in particular, lipid peroxidation, is strongly associated with various diseases (1). Also, the effects of lipid peroxidation on food quality and food safety have been reported (2,3). In addition, many reports have appeared on the toxicity of oxidized fats and the formation of toxic compounds from oxidized oils (4–6). For example, oxidized methyl linoleate, containing 4-hydroxy-2-nonenal as the major component, caused lymphocyte necrosis in the thymus and Peyer's patches in mice (7). Palm oil oxidized by heat caused reduced rates of pregnancy (by 55%) in rats (8). Lipid peroxidation yields reactive oxygen species (ROS) such as the hydroxyl radical, which leads to the formation of toxic chemicals from lipids, including malonaldehyde (MA). The toxicity of lipid peroxidative products is caused by the interaction of these secondary products, such as MA, rather than ROS directly, because ROS are not readily absorbed by the intestines (9).

Among the many products of lipid peroxidation, dicarbonyl compounds, such as MA, glyoxal, and methylglyoxal, have received much attention because they are implicated in various diseases (10,11). Pancreatic lesions consisting primarily of atrophied exocrine cells with loss of zymogen granulation occurred in 8-wk-old female Swiss mice that received 500 μg MA/g body weight (12). Methylglyoxal is also reported to have biological implications (13). Development of stomach neoplasms was observed in 6% of experimental animals (mice) that were administered 10 μg MA/g body weight (14). Methylglyoxal inhibited protein, DNA, and RNA synthesis in villus and crypt cells as well as colonocytes (15). A study using outbred male Wistar rats indicated that glyoxal exerts tumor-promoting activity on rat glandular stomach carcinogenesis (16). These reports clearly indicate that some dicarbonyl compounds produced from lipids by oxidation caused genotoxicities in experimental animals.

In the present study, genotoxic MA, glyoxal, and methylglyoxal formed in oxidized dietary oils were analyzed by GC to assess the role of these compounds in food safety.

MATERIALS AND METHODS

Chemicals and reagents. BHT, MA tetrabutylammonium salt, α-tocopherol, SDS, 1,2-phenylenediamine, and methylhydrazine were purchased from Sigma Chemical Co. (St. Louis, MO). Starch solution (1%) and 0.01 N sodium thiosulfate solution were bought from LabChem, Inc. (Pittsburgh, PA). Standard quinoxaline and 2-methylquinoxaline were synthesized by a previously reported method (17).

Dietary oils. Olive oil, soybean oil, corn oil, tuna oil, cod liver oil, and salmon oil were provided by Arista Industries, Inc. (Wilton, CT).

Oxidation of oils. An oil (1 g) was heated in an 8-mL amber vial at 60°C for 3 and 7 d using a thermostatic oven (Precision, Jouan, Inc., Winchester, VA). A tightly Teflon-sealed cap was used in an 8-mL amber vial to prevent the escape of volatile MA, glyoxal, and methylglyoxal during storage. The same oil was also heated to 200°C for 1 h under aerobic conditions. The oxidized samples were kept in a freezer (–5°C) until analysis.

Measurement of PV of oxidized oils. PV were measured according to AOAC method 965.33 with minor modifications

*To whom correspondence should be addressed at Department of Environmental Toxicology, University of California–Davis, One Shields Ave., Davis, CA 95616. E-mail: tshibamoto@ucdavis.edu

Abbreviations: MA, malonaldehyde; 1-MP, 1-methylpyrazole; NPD, nitrogen phosphorus detector; ROS, reactive oxygen species; SPE, solid-phase extraction.

(18). An oil (100 μL) was mixed with 10 mL of chloroform/acetic acid (2:3, vol/vol) and 0.5 mL of aqueous saturated potassium iodide in a 25-mL Erlenmeyer flask. After the mixture was shaken for 1 min, deionized water (10 mL) and 0.5 mL of a 1% starch solution were added. The solution was titrated with 0.01 N sodium thiosulfate solution. A blank determination was conducted daily and was subtracted from a sample titration. The PV was calculated as

$$\text{milliequivalents to moles of } O_2 \text{ (mequiv } O_2\text{/kg)} = S \times N \times 1000\text{/g of sample} \quad [1]$$

where S = amount of sodium thiosulfate solution used (mL), and N = normality of thiosulfate solution.

Analysis of α-tocopherol in oils. An oil (100 μL) was dissolved into 0.5 mL of 2-propanol. The solution was placed in a C_{18} solid-phase extraction (SPE) cartridge (Varian, Harbor City, CA) and then eluted with 5 mL of methanol under reduced pressure using a vacuum manifold (Alltech Associates, Inc., Deerfield, IL). The SPE cartridge was preconditioned by rinsing with 1 vol each of ethyl acetate and methanol, in a series, prior to use. The eluent was concentrated under a purified nitrogen stream to 0.5 mL in volume. α-Tocopherol was analyzed by a Waters Model 501 HPLC equipped with a Capcell Pak C_{18} reversed-phase column (Shiseido Inc., Tokyo, Japan) and a UV detector (set at 290 nm). The flow rate of the methanol mobile phase was 1.0 mL/min with an isocratic mode. The sample injection volume was 20 μL.

Analysis of MA. MA was analyzed after it was derivatized into 1-methylpyrazole (1-MP) by a method slightly modified from previous reports (19–21). An aqueous solution (5 mL) containing 100 μL of an oxidized or nonoxidized oil (blank), 0.5 mL of 1% SDS, and 30 μL of methylhydrazine was stirred with a magnetic stirrer at room temperature for 1 h. The reaction solution was placed in a C_{18} SPE cartridge and then eluted with 5 mL of ethyl acetate under reduced pressure. The SPE cartridge was preconditioned by rinsing with 1 vol each of ethyl acetate, methanol, and deionized water, in series, prior to use. The eluent was concentrated under a purified nitrogen stream to 0.5 mL. The volume of the ethyl acetate eluent was brought to 5 mL with ethyl acetate, and then 10 μL of 2-methylpyrazine solution (10 mg/mL ethyl acetate) was added as a GC internal standard. MA was analyzed as 1-MP by GC with a nitrogen phosphorus detector (NPD) (refer to the subsequent *Instrumentation* section for the detailed GC conditions). A typical gas chromatogram of ethyl acetate extract obtained from salmon oil stored at 60°C for 7 d is shown in Figure 1. A gas chromatograph/mass spectrometer (GC/MS) was used to confirm the identity of the 1-MP. The mass spectral data of 1-MP are as follows: *m/z* (relative intensity) = 82 [M^+, 100], 54 [31], 53 [14], and 41 [14].

Analysis of glyoxal and methylglyoxal. Glyoxal and methylglyoxal were analyzed after they had been derivatized into quinoxaline and 2-methylquinoxaline, respectively, by a method slightly modified from previous reports (17). An aqueous solution (5 mL) containing 100 μL of an oil, 0.5 mL

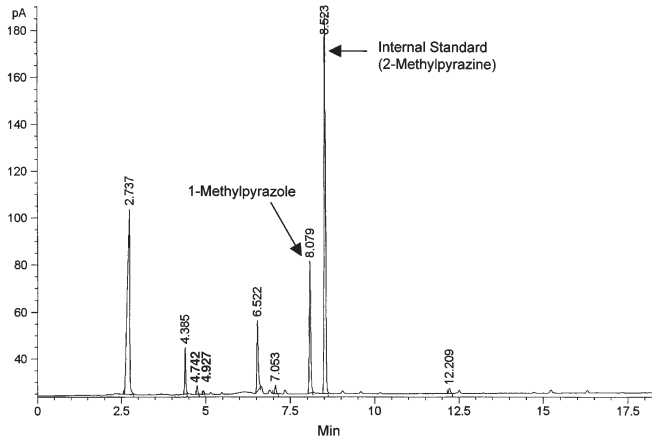

FIG. 1. A typical gas chromatogram of the ethyl acetate extract obtained from salmon oil heated at 60°C for 7 d (see Materials and Methods section for GC conditions). Malonaldehyde was determined as 1-methylpyrazole (retention time of 8.079 min).

of aqueous 1% SDS solution, and 100 μL of 1,2-phenylenediamine solution (10 mg/mL), in which the pH was adjusted to 7.0 with 0.1 N sodium hydroxide solution, was stirred with a magnetic stirrer at room temperature for 2 h. The reaction solution was loaded onto a C_{18} SPE cartridge and then eluted with 5 mL of ethyl acetate under reduced pressure. The SPE cartridge was preconditioned by rinsing with 1 vol each of ethyl acetate, methanol, and deionized water, in series, prior to use. The eluent was condensed to 1.5 mL in volume with a purified nitrogen stream. After 20 μL of 2-methylpyrazine solution (0.2 mg/mL ethyl acetate) was added as a GC internal standard, the solution was brought to 2 mL in volume with ethyl acetate. Glyoxal and methylglyoxal were analyzed as quinoxaline and 2-methylquinoxaline by GC with an NPD (refer to the subsequent *Instrumentation* section for detailed GC conditions). A typical gas chromatogram of ethyl acetate extract obtained from salmon oil stored at 60°C for 3 d is shown in Figure 2. A GC/MS was used to confirm the identity of quinoxaline and 2-methyl quinoxaline. The mass spectral data of quinoxaline are as follows: *m/z* (relative intensity) = 130 [M^+, 100], 103 [61], 76 [49], and 50 [21]. The mass spectral data of 2-methylquinoxaline are as follows: 144 [M^+, 100], 117 [81], 76 [41], and 50 [23].

Recovery efficiency test of MA from SPE. An aqueous solution (5 mL) containing 100 mM of MA tetrabutylammonium salt, 2 mL of phosphate buffer (pH 7.4), and 10 μL of methylhydrazine was stirred for 1 h at room temperature using a magnetic stirrer. The reaction solution was loaded onto a C_{18} SPE cartridge and then eluted with 5 mL of ethyl acetate under reduced pressure. The SPE cartridge was preconditioned by rinsing with 1 vol each of ethyl acetate, methanol, and deionized water, in series, prior to use. After 10 μL of 2-methylpyrazine solution (10 mg/mL ethyl acetate) was added as a GC internal standard, the solution was brought to 5.0 mL in volume with ethyl acetate. Glyoxal and methylglyoxal were analyzed as quinoxaline and 2-methylquinoxaline by GC with an NPD.

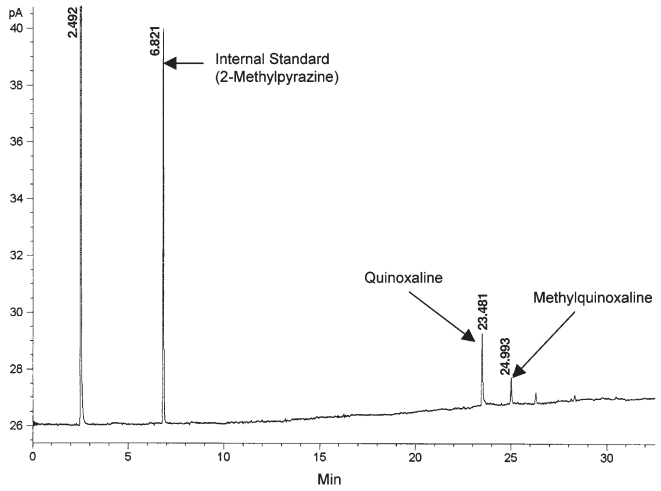

FIG. 2. A typical gas chromatogram of the ethyl acetate extract obtained from salmon oil heated at 60°C for 3 d (see Materials and Methods section for GC conditions). Glyoxal and methylglyoxal were determined as quinoxaline (retention time of 23.481 min) and methylquinoxaline (retention time at 24.993 min), respectively.

Recovery efficiency test of glyoxal and methylglyoxal from SPE. An aqueous solution (5 mL) containing 100 μL of corn oil, 10 μL of glyoxal, 10 μL of methylglyoxal, 0.5 mL of 1% SDS, and 100 μL of 1,2-phenylenediamine solution (10 mg/mL water) was stirred for 2 h at room temperature using a magnetic stirrer. The solution was neutralized with 110 mL of 0.1 N sodium hydroxide solution prior to stirring. The reaction solution was loaded onto a C_{18} SPE cartridge and then eluted with 5 mL of ethyl acetate under reduced pressure. The SPE cartridge was preconditioned by rinsing with 1 vol each of ethyl acetate, methanol, and deionized water, in series, prior to use. The eluent was condensed to 1.5 mL with a purified nitrogen stream. After 20 μL of 2-methylpyrazine solution (0.2 mg/mL ethyl acetate) had been added as a GC internal standard, the solution was brought to 2.0 mL with ethyl acetate. Glyoxal and methylglyoxal were analyzed as quinoxaline and 2-methylquinoxaline by GC with an NPD.

Instrumentation. An Agilent Technologies Model 6980N gas chromatograph equipped with a 30 m × 0.25 mm (d_f = 0.25 μm) ZB-WAX fused-silica capillary column (Phenomenex, Torrance, CA) and an NPD were used for quantitative analysis of 1-MP, quinoxaline, and 2-methylquinoxaline. The GC oven temperature was programmed from 60 to 130°C at 3°C/min for 1-MP analysis. The GC oven temperature was held at 80°C for 3 min and then programmed to 180°C at 4°C/min for quinoxaline and 2-methylquinoxaline analysis.

A Hewlett-Packard model 5890 series II gas chromatograph interfaced to an HP 5971 mass spectrometer was used to confirm 1-MP, quinoxaline, and 2-methylquinoxaline. The GC conditions were the same as those just described. The mass spectra were obtained by EI ionization at 70 eV at an ion source temperature of 250°C.

Data analysis. All measurements were in triplicate, and results were expressed as mean ± SD (n = 3). Linear correlation coefficients (R) between α-tocopherol content and oxidation parameters (PV, amount of MA, amount of glyoxal, and amount of methylglyoxal) were calculated using JMP IN software (version 4.0) (SAS Institute Inc., Cary, NC).

RESULTS AND DISCUSSION

Prior to the present study, 1-MP derived from MA was recovered using a liquid–liquid continuous extractor with dichloromethane (20–22). Liquid–liquid continuous extraction provides satisfactory recovery efficiency (82–91%) (23), but the process is somewhat tedious. Moreover, because halogenated solvents such as dichloromethane damage the NPD, the solvent must be changed to a nonhalogenated one such as ethyl acetate before the sample is injected into the gas chromatograph. Therefore, SPE was used to recover 1-MP in the present study. The result of the recovery efficiency test of MA as 1-MP was 111.3 ± 2.0%. The recovery efficiencies of glyoxal and methylglyoxal were 45.8 ± 1.7 and 82.0 ± 2.7%, respectively. The recovery of glyoxal was rather low. However, the values of SD were relatively low, indicating that the reproducibility of the recovery is satisfactory.

Using elevated temperatures is a common practice to examine the storage stability of foods. For example, changes in the chemical compositions and properties of Australian honeys was investigated at 50°C (24,25). Antioxidative activity of TBHQ was investigated using canola oil heated at 65°C (26). The oxidative status of high-heat (45°C) and medium-heat (25°C) whole milk powder was investigated by measuring the formation of TBARS (27). Therefore, the formation of MA, glyoxal, and methylglyoxal was investigated at accelerated storage conditions of 60°C. Also, the investigation was conducted at a cooking temperature of 200°C.

Figure 3 shows the PV of thermally oxidized dietary oils. When the oils were heated at 60°C for 3 d, soybean oil had the highest value (110 ± 4.30 mEq O_2/kg sample). The PV of soybean oil (260 ± 7.50 mEq O_2/kg sample) was higher than that of olive oil (200 ± 1.00 mEq O_2/kg sample), even though

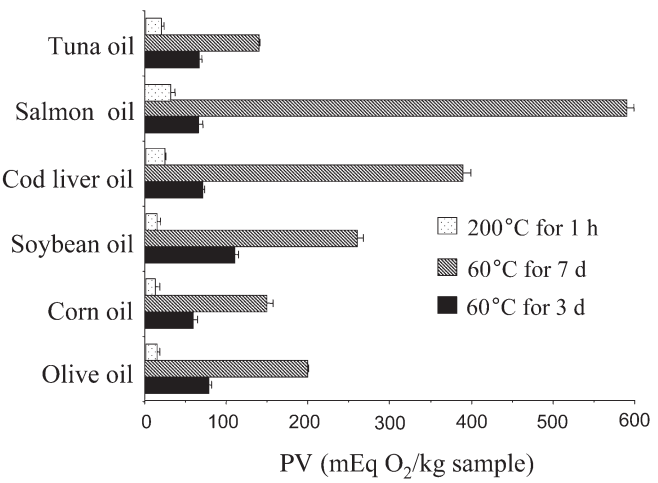

FIG. 3. PV of thermally oxidized dietary oils. Data are expressed as mean ± SD (n = 3).

the α-tocopherol content was higher in soybean oil (21.0 ± 2.80 ppm) than in olive oil (12.0 ± 1.60 ppm). It is interesting that the PV of oils heated at 200°C for a short time (1 h) were much lower than those heated at 60°C for a prolonged time (3 and 7 d). This may be due to the degradation of peroxides at a higher temperature (200°C).

Figure 4 shows the MA formed from thermally oxidized dietary oils. The MA content of natural oils ranged from 1.88 ± 0.530 (soybean oil) to 33.8 ± 11.7 ppm (salmon oil). Salmon oil seems to be most susceptible to oxidation. Salmon oil produced MA at a level of 1070 ± 77.0 ppm when it was heated at 60°C for 7 d, whereas corn oil produced only 6.65 ± 0.640 ppm under the same conditions. Fish oils produced more MA. MA formed from fish oils and vegetable oils ranged from 35.3 ± 2.80 (tuna oil) to 95.6 ± 2.30 ppm (salmon oil) and from 2.33 ± 0.25 (corn oil) to 9.56 ± 0.320 ppm (soybean oil), respectively, when they were heated at 60°C for 3 d. Also, MA formed from fish oils ranged from 157 ± 15.0 (tuna oil) to 1070 ppm ± 77.0 (salmon oil), whereas MA formed from vegetable oils ranged from 6.65 ± 0.640 (corn oil) to 35.9 ± 5.20 ppm (soybean oil) when they were heated at 60°C for 3 or 7 d. Much more MA formed from the vegetable oils heated at 200°C for 1 h than at 60°C for a prolonged time. On the other hand, the formation of MA from fish oils heated at 200°C for 1 h was somewhere between MA from fish oils heated at 60°C for 3 and 7 d. The results suggest that, in general, vegetable oils are oxidized more quickly at a high temperature.

Figure 5 shows the amount of glyoxal formed from thermally oxidized dietary oils. More glyoxal was formed from fish oils than from vegetable oils. The highest formation of glyoxal was obtained from salmon oil heated at 60°C for 3 d. It is interesting that more glyoxal was recovered from salmon and cod liver oils when they were heated for 3 d (12.8 ± 1.10 and 7.07 ± 0.19 ppm, respectively) than for 7 d (6.70 ± 0.080 and 5.94 ± 0.380 ppm, respectively). The results suggest that glyoxal underwent secondary reactions during the 7-d period and yielded secondary products, such as glyoxylic acid, CO_2 (34). In a previous study, 27 ppm of glyoxal was formed from cod liver oil irradiated with UV light for 10 h (17). Glyoxal was analyzed to examine the effects of antioxidants, including α-tocopherol, in cod liver oil oxidized by Fenton's reagent (35). Therefore, it is obvious that genotoxic glyoxal is formed in oxidized oils in ppm levels.

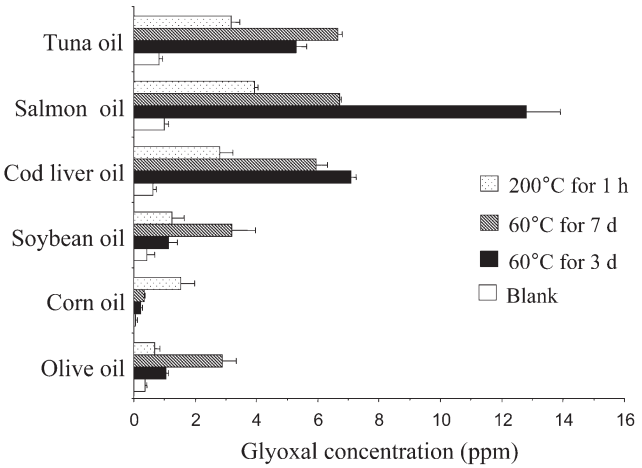

FIG. 5. Results of glyoxal analysis in thermally oxidized dietary oils. Data are expressed as mean ± SD (n = 3).

Figure 6 shows the amount of methylglyoxal formed from thermally oxidized dietary oils. Fish oils also produced much more methylglyoxal than did vegetable oils. For example, the level of methylglyoxal ranged from 2.03 ± 0.130 (cod liver oil) to 2.89 ± 0.110 ppm (tuna oil) in the fish oils heated at 60°C for 7 d. On the other hand, only 0.61 ± 0.030 ppm methylglyoxal formed in olive oil heated at the same conditions. Soybean and corn oils did not produce a detectable amount of methylglyoxal under accelerated storage conditions (heated at 60°C for 3 and 7 d). However, vegetable oils produced an appreciable amount of methylglyoxal (e.g., 0.38 ± 0.160 ppm from corn oil) when they were heated at a cooking condition (200°C for 1 h). Cod liver oil also produced 5.7 ppm of methylglyoxal with 10 h of UV irradiation (17). Therefore, genotoxic methylglyoxal is also formed in dietary oils upon oxidation.

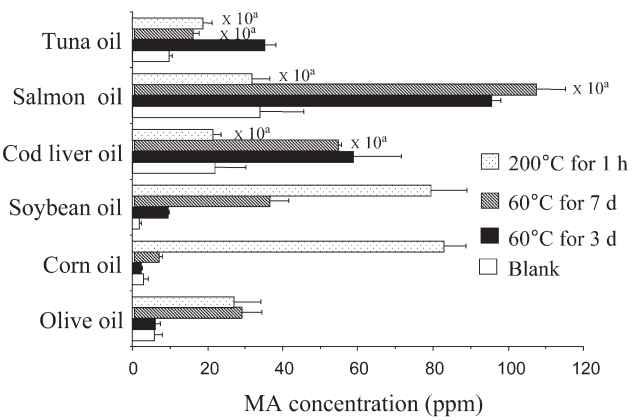

FIG. 4. Results of MA analysis in thermally oxidized dietary oils. [a]Actual values are the values in the figure × 10. Data are expressed as mean ± SD (n = 3).

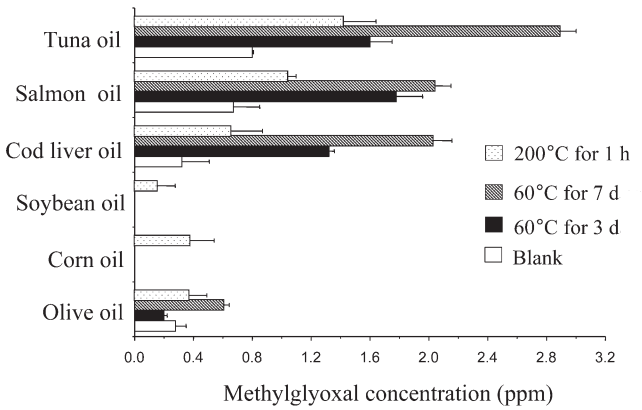

FIG. 6. Results of methylglyoxal analysis in thermally oxidized dietary oils.

Figure 7 shows the α-tocopherol content in dietary oils. α-Tocopherol content ranged from 12.0 ± 1.60 (olive oil) to 700 ± 66.0 ppm (tuna oil) in the dietary oils used in the present study. α-Tocopherol is a well-known, naturally occurring antioxidant that has been used as a standard antioxidant in numerous lipid peroxidation studies (28–30). Therefore, it is important to know the α-tocopherol content in dietary oils to evaluate their oxidative damages caused by heat.

The α-tocopherol content did not correlate with the PV among the six dietary oil samples heated at 60°C either for 3 ($R = -0.53$, $P = 0.27$) or 7 d ($R = -0.26$, $P = 0.62$). When the three fish oils were heated at 60°C for 7 d, the α-tocopherol content seemed to correspond, although not significantly, to the PV ($R = -0.98$, $P = 0.11$). The statistically significant correlation ($P < 0.05$) between the α-tocopherol content and the oxidation parameters was obtained only from MA and fish oils heated at 60°C for 3 d ($R = -0.99$, $P = 0.02$). All other correlations between the α-tocopherol content and the oxidation parameters were not statistically significant, although there was borderline significance between the α-tocopherol content and MA in the fish oils heated at 60°C for 7 d ($R = -0.99$, $P = 0.06$). A decrease of α-tocopherol was reportedly accompanied by an increase of MA when rapeseed oil was thermally oxidized at 170°C (32). Vitamin E (α-tocopherol) significantly influenced the antioxidant capacity of virgin olive, olive, and sunflower oils after frying (33).

Overall, the α-tocopherol content in the original oils did not significantly correspond to the oxidation parameters of the oxidized oils except in the case of MA. Perhaps the α-tocopherol was rapidly consumed and therefore ineffective. In addition to α-tocopherol, these oils also contain natural antioxidants, such as flavonoids, ascorbic acid, and carotenes (31), which may play a more significant role than α-tocopherol in the PV of oxidized oils. More detailed experiments are necessary to examine the role of antioxidants in the oxidation of lipids.

The formation mechanisms of these compounds are rather complex. There are many hypotheses about the mechanisms of MA formation in oxidized oils. For example, it has been proposed that MA forms from the decomposition of prostaglandin-like endoperoxide intermediates (36). This mechanism requires at least three methylene-interrupted double bonds in a molecule. However, it was later found that MA also formed from a FA with one or two double bonds (33). Glyoxal and methylglyoxal were formed from low-M.W. carbonyl compounds, including acetaldehyde, acrolein, propanal, and acetone on 6 h of UV irradiation (17).

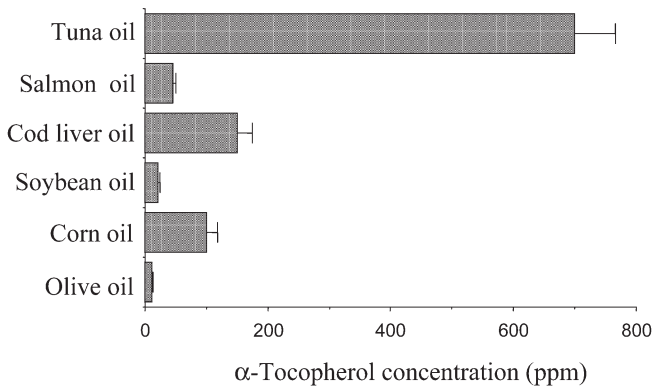

FIG. 7. Results of α-tocopherol analysis in dietary oils. Data are expressed as mean ± SD ($n = 3$).

It is well known that numerous carbonyl compounds are produced from long-chain PUFA (38,39). Therefore, the formation of MA, glyoxal, and methylglyoxal may be influenced by the content of long-chain PUFA, EPA, and DHA, rather than the TG content. A previous report showed a positive correlation between the rate of oxidation and the numbers of double bonds in the FA of a TG (40). PUFA are present in greater amounts in fish oils than in vegetable oils. Cod liver oil consists of 12.6% EPA and 10.6% DHA. Salmon oil contains 4.5% EPA and 17% DHA. Tuna oil has 6.7% EPA and 28.8% DHA. On the other hand, vegetable oils (soybean, corn, and olive) contain neither EPA nor DHA (41).

The results of the present study indicate that the formation of genotoxic dicarbonyl compounds is influenced by storage and cooking conditions. The kind of dietary oils also plays an important role in the production of these chemicals. The oils containing higher levels of long-chain PUFA, such as fish oils, produced more genotoxic dicarbonyl compounds. Further investigation to clarify formation mechanisms of these compounds is in order. However, the investigation of these genotoxic dicarbonyl compounds from dietary oils performed in the present study is one avenue to assess food safety.

REFERENCES

1. Yoshikawa, T. (1985) Diseases, in *Peroxide Lipid in Biological Systems* (Uchiyama, M., Matsuo, M., and Sagai, M., eds.), pp. 289–313, Japan Scientific Society Press, Tokyo.
2. St. Angelo, A.J. (1996) Lipid Oxidation in Foods, *Crit. Rev. Food Sci. Nutr. 36,* 175–224.
3. Vercelotti, J.R., St. Angelo, A.J., and Spanier, A.M. (1992) Lipid Oxidation in Foods: An Overview, in *Lipid Oxidation in Foods* (St. Angelo, A.J., ed.), pp. 1–11, American Chemical Society Symposium Series 500, American Chemical Society, Washington, DC.
4. Kubow, S. (1990) Toxicity of Dietary Lipid Peroxidation Products, *Trends Food Sci. Technol. 1*, 67–71.
5. Ohta, S. (1985) Toxicity of Oxidized Oils and Fats, *Shoku no Kagaku 91,* 43–48.
6. Edem, D.O. (2002) Palm Oil. Biochemical, Physiological, Nutritional, Hematological and Toxicological Aspects: A Review, *Plant Foods Hum. Nutr. 57,* 319–341.
7. Oarada, M., Miyazawa, T., Fujimoto, K., Ito, E., Terao, K., and Kaneda, T. (1988) Degeneration of Lymphoid Tissues in Mice with the Oral Intake of Low Molecular Weight Compounds Formed During Oil Autoxidation, *Agric. Biol. Chem. 52,* 2101–2102.
8. Isong, E.U., Ebong, P.E., Ifon, E.T., Umoh, I.B., and Eka, O.U. (1997) Thermoxidized Palm Oil Induces Reproductive Toxicity in Healthy and Malnourished Rats, *Plant Foods Hum. Nutr. 51*, 159–166.
9. Frankel, E.N., and Neff, W.E. (1983) Formation of Malonaldehyde from Lipid Oxidation Products, *Biochim. Biophys. Acta 754,* 264–270.

10. Yin, D., and Brunk, U.T. (1995) Carbonyl Toxification Hypothesis of Biological Aging, in *Molecular Basis of Aging* (Macieira-Coelh, A., ed.), pp. 421–436, CRC, Boca Raton, FL.
11. Okado-Matsumoto, A., and Fridovich, I. (2000) The Role of α,β-Dicarbonyl Compounds in the Toxicity of Short Chain Sugars, *J. Biol. Chem. 275,* 34853–34857.
12. Siu, G.M., Draper, H.H., and Valli, V.E. (1983) Oral Toxicity of Malonaldehyde: A 90-Day Study on Mice, *J. Toxicol. Environ. Health 11,* 105–119.
13. Kalapos, M.P. (1999) Methylglyoxal in Living Organisms. Chemistry, Biochemistry, Toxicology and Biological Implications, *Toxicol. Lett. 110,* 145–175.
14. Bird, R.P., Draper, H.H., and Valli, V.E.O. (1982) Toxicological Evaluation of Malonaldehyde: A 12-Month Study of Mice, *J. Toxicol. Environ. Health 10,* 897–905.
15. Baskaran, S., and Balasubramanian, K.A. (1990) Toxicity of Methylglyoxal Towards Rat Enterocytes and Colonocytes, *Biochem. Int. 21,* 165–174.
16. Takahashi, M., Okamiya, H., Furukawa, F., Toyoda, K., Sato, H., Imaida, K., and Hayashi, Y. (1989) Effect of Glyoxal and Methyl Glyoxal Administration on Gastric Carcinogenesis in Wistar Rats After Initiation with *N*-Methyl-*N*′-nitro-*N*-nitrosoguanidine, *Carcinogenesis 10,* 1925–1927.
17. Niyati-Shirkhodaee, F., and Shibamoto, T. (1993) Gas Chromatographic Analysis of Glyoxal and Methylglyoxal Formed from Lipids and Related Compounds upon Ultraviolet Irradiation, *J. Agric. Food Chem. 41*, 227–230.
18. Eder, K., Keller, U., Hirche, F., and Brandsch, C. (2003) Thermally Oxidized Dietary Fats Increase the Susceptibility of Rat LDL to Lipid Peroxidation but Not Their Uptake by Macrophages, *J. Nutr. 133,* 2830–2837.
19. Umano, K., Dennis, K.J., and Shibamoto, T. (1988) Analysis of Free Malondialdehyde in Photoirradiated Corn Oil and Beef Fat *via* a Pyrazole Derivative, *Lipids 23*, 811–814.
20. Dennis, K.J., and Shibamoto, T. (1990) Gas Chromatographic Analysis of Reactive Carbonyl Compounds Formed from Lipids upon UV Irradiation, *Lipids 25,* 460–464.
21. Tamura, H., and Shibamoto, T. (1991) Gas Chromatographic Analysis of Malonaldehyde and 4-Hydroxy-2-(*E*)-nonenal Produced from Arachidonic Acid and Linoleic Acid in a Lipid Peroxidation Model System, *Lipids 26*, 170–173.
22. Miyake, T., and Shibamoto, T. (1998) Inhibition of Malonaldehyde and Acetaldehyde Formation from Blood Plasma Oxidation by Naturally Occurring Antioxidants, *J. Agric. Food Chem. 46,* 3694–3697.
23. Ichinose, T., Miller, M.G., and Shibamoto, T. (1989) Gas Chromatographic Analysis of Free and Bound Malonaldehyde in Rat Liver Homogenates, *Lipids 24,* 895–898.
24. Wootton, M., Edwards, R.A., Faraji-Haremi, R., and Johnson, A.T. (1976) Effect of Accelerated Storage Conditions on the Chemical Composition and Properties of Australian Honeys. 1. Color, Acidity and Total Nitrogen Content, *J. Apicul. Res. 15,* 23–28.
25. Wootton, M., Edwards, R.A., Faraji-Haremi, R., and Williams, P.J. (1978) Effect of Accelerated Storage Conditions on the Chemical Composition and Properties of Australian Honeys. 3. Changes in Volatile Components, *J. Apicul. Res. 17,* 167–172.
26. Hawrysh, A.J., Shand, P.J., Tokarska, B., and Lin, C. (1988) Effects of Tertiary Butylhydroquinone on the Stability of Canola Oil. I. Accelerated Storage, *Can. Inst. Food Sci. Technol. J. 21,* 549–554.
27. Stapelfeldt, H., Nielsen, B.R., and Skibsted, L.H. (1997) Effect of Heat Treatment, Water Activity and Storage Temperature on the Oxidative Stability of Whole Milk Powder, *Int. Dairy J. 7,* 331–339.
28. Ogata, J., Hagiwara, Y., Hagiwara, H., and Shibamoto, T. (1996) Inhibition of Malonaldehyde Formation by Antioxidants from ω-3 Polyunsaturated Fatty Acids, *J. Am. Oil Chem. Soc. 73,* 653–656.
29. Lee, K.-G., Mitchell, A.E., and Shibamoto, T. (2000) Determination of Antioxidant Properties of Aroma Extracts from Various Beans, *J. Agric. Food Chem. 48,* 4817–4820.
30. Lee, K.-G., and Shibamoto, T. (2002) Determination of Antioxidant Potential of Volatile Extracts Isolated from Various Herbs and Spices, *J. Agric. Food Chem. 50,* 4947–4952.
31. Yanishilieva, N.V., and Marinova, E. M. (2001) Stabilization of Edible Oils with Natural Antioxidants, *Eur. J. Lipid Sci. Technol. 103*, 752–767.
32. Kishida, E., Oribe, M., and Kojo, S. (1990) Relationship Among Malondialdehyde, TBA-Reactive Substances, and Tocopherols in the Oxidation of Rapeseed Oil, *J. Nutr. Sci. Vitaminol. 35,* 619–623.
33. Quiles, J.L., Ramirez-Tortosa, M.C., Gomez, J.A., Huertas, J.R., and Mataix, J. (2002) Role of Vitamin E and Phenolic Compounds in the Antioxidant Capacity, Measured by ESR, of Virgin Olive, Olive and Sunflower Oils After Frying, *Food Chem. 76,* 461–468.
34. Moree-Testa, P., and Saint-Jalm, Y. (1981) Determination of α-Dicarbonyl Compounds in Cigarette Smoke, *J. Chromatogr. 217,* 197–208.
35. Nishiyama, T., Hagiwara, Y., Hagiwara, H., and Shibamoto, T. (1994) Formation and Inhibition of Genotoxic Glyoxal and Malonaldehyde from Phospholipids and Fish Liver Oil upon Lipid Peroxidation, *J. Agric. Food Chem. 42,* 1728–1731.
36. Pryor, W. A., Stanley, J.P., and Blair, E. (1976) Autoxidation of Polyunsaturated Fatty Acids: II. A Suggested Mechanism for the Formation of TBA-Reactive Materials from Prostaglandin-like Endoperoxides, *Lipids 11*, 370-379.
37. Tamura, H., Kitta, K., and Shibamoto. T. (1991) Formation of Reactive Aldehydes from Fatty Acids in a Fe^{2+}/H_2O_2 Oxidation System, *J. Agric. Food Chem. 39,* 439–442.
38. Frankel, E.N. (1993) Formation of Headspace Volatiles by Thermal Decomposition of Oxidized Fish Oils vs. Oxidized Vegetable Oils, *J. Am. Oil Chem. Soc. 70*, 767–772.
39. Esterbauer, H. (1982) Aldehydic Products of Lipid Peroxidation, in *Free Radicals, Lipid Peroxidation, Cancer* (McBrien, D.C.H., and Slater, T.F., eds.), pp. 101–128, Academic Press, London.
40. Neff, W.E., Selke, E., Mounts, T.L., Rinsch, W., Frankel, E.N., and Zeitoun, M. (1992) Effect of Triacylglycerol Composition and Structures on Oxidative Stability of Oils from Selected Soybean Germplasm, *J. Am. Oil Chem. Soc. 69,* 111–118.
41. Gunstone, F.D., Harwood, J.L., and Padley, F.B. (1986) *The Lipid Handbook,* Chapman & Hall, New York.

[Received March 9, 2004; accepted July 15, 2004]

Fatty Acids of the Seeds of *Origanum onites* L. and *O. vulgare* L.

Nezihe Azcan,[a,*] Mustafa Kara[a], Betül Demirci[b], and K. Hüsnü Can Başer[b]

Anadolu University, Faculties of [a]Engineering and Architecture, Department of Chemical Engineering, and [b]Pharmacy, Department of Pharmacognosy, 26470 Eskişehir, Turkey

ABSTRACT: Seed oils of *Origanum onites* L. from the Antalya and Mugla regions and *O. vulgare* L. from the Kirklareli region of Turkey were extracted with hexane in a Soxhlet apparatus. The oil yields were 14.1–20.0 and 18.5%, respectively. FA compositions of the seed oils were determined by GC and GC/MS. Twenty FA were identified in both *O. onites* and *O. vulgare* seeds. The major FA of both species were linolenic (56.3–57.0%; 61.8%), linoleic (21.5–21.7%; 18.8%), oleic (8.7–8.9%; 5.9%), palmitic (5.9–6.5%; 5.5%), stearic (2.1–2.4%; 2.1%), and (*Z*)-11-octadecenoic (0.6–0.8%; 0.5%), respectively.

Paper no. L9389 in *Lipids 39,* 487–489 (May 2004).

"Oregano" is a general term applied to plants with a specific aroma arising from carvacrol in the essential oil. Turkey is the principal supplier of oregano. Oregano exports from Turkey amounted to 7,400 tons in 2000, for earnings of U.S.$15,400,000. The commercial *Origanum* species include *O. onites*, *O. vulgare* subsp. *hirtum*, *O. majorana*, *O. minutiflorum* (endemic), and *O. syriacum* var. *bevanii*. In addition, *Thymbra, Coridothymus,* and *Satureja* species are also collected and exported under the name oregano (Kekik in Turkish). They are widely used as industrial raw material for producing essential oil, as a tea, or as a culinary herb. Among them, *O. onites* is economically the most important species. It is the principal oregano plant cultivated in areas exceeding 600 hectares (2500 acres) in western Turkey (1). Data on the FA composition of the aerial parts of *O. onites* (2), *O. dictamnus* (3), *O. majorana* (4), *O. tytthanthum* (5) and of the seed oils of *O. tytthanthum* (6), and *O. vulgare* (7) have been reported. There has been only one report (7) giving the seed oil composition of *O. vulgare* (4.2% palmitic, 1.3% stearic, 6.1% oleic, 23.8% linoleic, and 64.6% linolenic acids); no data have been reported yet on the FA composition of *O. onites* seed oil.

Here we report on the FA compositions of the seed oils of *O. onites*, collected from two different regions of Turkey (Antalya and Mugla), and *O. vulgare* (Kirklareli).

EXPERIMENTAL PROCEDURES

Seeds were supplied by the seed bank at the Aegean Agricultural Research Institute (AARI) in Menemen, Izmir. Passport records (record number, accession number, collection site, altitude) of the materials are shown in Table 1.

The purity of the seeds was checked under a stereomicroscope. Seeds were then crushed in a mortar. The amount of seeds from each species was 0.92–0.95 g. Seed oils were extracted by *n*-hexane for 6 h using a 25-mL capacity Soxhlet apparatus. The solvent was then evaporated under reduced pressure using a rotary evaporator at 40°C, and the residue was refluxed with 5 mL of 0.5 N sodium hydroxide solution in methanol for 10 min. Then 5 mL of 14% BF_3 in methanol solution was added through the condenser and the mixture was boiled for 2 min. *n*-Heptane (5 mL) was then added through the condenser, and the mixture was boiled for 1 min longer. The solution was cooled, 5 mL of saturated NaCl solution was added, and the flask was rotated very gently several times. Additional saturated NaCl solution was added to float the *n*-heptane solution into the neck of the flask. One milliliter upper *n*-heptane solution was transferred into a test tube and dried with anhydrous Na_2SO_4. The FAME were recovered after the solvent was removed using nitrogen gas (8). The FA compositions were determined by GC/MS. Separated constituents were characterized by using the in-house Başer GC/MS Library containing data based on genuine FAME standards. The mass spectra were also compared with those of reference compounds and confirmed with the aid of retention indices from published data and our own sources. Relative percentage amounts of the separated compounds were calculated by GC-FID.

The GC/MS analysis was carried out using a Hewlett-Packard GCD system (SEM Ltd., Istanbul, Turkey). HP-Innowax fused-silica capillary column (60 m × 0.25 i.d., 0.25 μm) was used with helium as carrier gas (flow rate: 1 mL/min). MS were taken at 70 eV. The injection temperature was 250°C and oven temperature was kept at 60°C for 10 min and programmed to 220°C at a rate of 4°C/min, then kept constant at 220°C for 10 min and then programmed to 240°C at a rate of 1°C/min then kept at 240°C for 20 min. The split ratio was adjusted to 50:1, and the injection volume was 1 μL.

GC analysis was carried out using a Hewlett-Packard 6890 system. An HP-Innowax FSC column (60 m × 0.25 i.d., 0.25 μm film thickness) was used with nitrogen as carrier gas (1 mL/min). GC oven temperature programming was as described above. The injector temperature was at 250°C. The percentage compositions were obtained from electronic integration measurements using FID (250°C). The relative percentages of the characterized components appear in Table 2.

*To whom correspondence should be addressed.
E-mail: nazcan@anadolu.edu.tr

Abbreviation: U/S, unsaturated FA/saturated FA (%/%).

TABLE 1
Passport Records of Study Material

Record no.	Botanical name	Accession no.	Collection site	Altitude (m)
TR 54467	*Origanum onites*	HO AA NB 290890 0303	Antalya	60–70
TR 54488	*Origanum onites*	HO AOS EB 090891 0101	Mugla	150–200
TR 67149	*Origanum vulgare*	AT AK 180998 0601	Kirklareli	534

TABLE 2
FA Compositions of Seed Oil of *Origanum onites* and *O. vulgare*

	Seed		
	O. onites[a]	*O. onites*[b]	*O.vulgare*[c]
Oil yield (%)	20.0	14.1	18.5
FA	%	%	%
Caprylic (8:0)	Trace	Trace	0.1
Pelargonic (9:0)	Trace	Trace	Trace
Capric (10:0)	Trace	Trace	0.1
Lauric (12:0)	Trace	Trace	Trace
Myristic (14:0)	0.1	0.1	0.1
Pentadecanoic (15:0)	0.1	0.1	0.1
Palmitic (16:0)	6.5	5.9	5.5
(*Z*)-9-Hexadecenoic (16:1)	0.1	0.1	0.2
(*Z*)-7-Hexadecenoic (16:1)	0.1	0.1	0.1
Margaric (17:0)	Trace	Trace	Trace
Stearic (18:0)	2.4	2.1	2.1
(*Z*)-9-Octadecenoic (18:1)—Oleic	8.7	8.9	5.9
(*Z*)-11-Octadecenoic (18:1)	0.6	0.8	0.5
Linoleic (18:2)	21.7	21.5	18.8
α-Linolenic (18:3)	56.3	57.0	61.8
Arachidic (20:0)	0.2	0.2	0.2
11-Eicosenoic (20:1)	0.2	0.2	0.2
Behenic (22:0)	0.1	0.1	0.1
Tricosanoic (23:0)	0.4	0.6	0.4
Lignoceric (24:0)	—	Trace	—
Σ Saturated	9.8	9.1	8.7
Σ Unsaturated	87.7	88.6	87.5
Total	97.5	97.7	96.2
Unsaturated/saturated	8.9	9.7	10.1
18:3/18:2	2.6	2.7	3.3

[a]From Mugla, Turkey.
[b]From Antalya, Turkey.
[c]From Kirklareli, Turkey. Trace <0.1%

RESULTS AND DISCUSSION

Seed oil yields of *O. onites* (from Mugla and Antalya) and *O. vulgare* (from Kirklareli) were found to be 20.0–14.1 and 18.5%, respectively. *Origanum onites* from the Mugla region yielded the highest oil content.

The oils were analyzed by GC-FID (Table 2). Twenty FA representing about 97.5% of the total FA were characterized. The dominant FA in both species was α-linolenic acid. Its content ranged from 56.3 to 61.8%. Major FA components characterized in the oils of *O.onites* from two different regions of Turkey were palmitic (5.9–6.5%), stearic (2.1–2.4%), oleic (8.7–8.9%), (*Z*)-11-octadecenoic (0.6–0.8%), linoleic (21.5–21.7%), and α-linolenic (56.3–57.0%). Those in the seed oil of *O. vulgare* were palmitic (5.5%), stearic (2.1%), oleic (5.9%), (*Z*)-11-octadecenoic (0.5%), linoleic (18.8%), and α-linolenic (61.8%). FA compositions of seed oil of *O. onites* from two different regions were similar, and no significant difference between the seed oil of *O. onites* and *O. vulgare* was found.

Genera under the subfamily Nepetoidae have been reported to contain unsaturated FA as predominant constituents, and the content of α-linolenic acid was reported as usually over 40% (9). Our results conform to these criteria since *Origanum* is included in Nepetoideae.

The U/S (unsaturated/saturated) index, which is considered a taxonomic marker (7), is presented in Table 2. U/S ratios were 8.9 and 9.7 in *O. onites*, and 10.1 in *O. vulgare*. The U/S ratio 10.1 of *O. vulgare* did not agree with the 17.2 reported earlier for the same species (7). This discrepancy is possibly due to the fact that more FA were characterized in the present study

than in Reference 7, altering hence the calculated values. However, the 18:3/18:2 ratio (3.3) of this study is close to the previously reported ratio of 2.7.

The high content of PUFA in *Origanum* seed oils suggests their possible use as a food additive. Such acids have been reported to help lower the blood cholesterol. They also have antioxidant activity (10).

Origanum seeds are obtained as a by-product during oregano herb processing by being trapped in cyclones (11). Large amounts of the so-called cyclone powder are produced during processing. Therefore, access to a steady supply of seeds may not cause any problem.

ACKNOWLEDGMENT

We would like to thank Seed Bank of Aegean Agricultural Institute, Menemen, Izmir, for supplying the seeds.

REFERENCES

1. Başer, K.H.C. (2002) The Turkish *Origanum* Species, in *Oregano—The Genera* Origanum *and* Lippia (Kintzios, S.E., ed.), pp. 109–126, Taylor & Francis, London.
2. Azcan, N., Kara, M., Asilbekova, D.T., Özek, T., and Başer, K.H.C. (2000) Lipids and Essential Oil of *Origanum onites, Khim. Prir. Soedin 2*, 106–109.
3. Revinthi, M.K., Komaitis, M.E., Evangelatos, G., and Kapoulas, V.V. (1985) Identification and Quantitative Determination of the Lipids of Dried *Origanum dictamnus* Leaves, *Food Drug Cosmet. Law J. 16*, 15–24.
4. Taskinen, J. (1974) Composition of the Essential Oil of Sweet Marjoram Obtained by Distillation with Steam and by Extraction and Distillation with Alcohol–Water Mixture, *Acta Chem. Scand. B 28*, 1121–1128.
5. Gusakova, S.D. Kholmatov, Kh.K., and Umarov, A.U. (1976) Seed Oil Compositions of *Origanum tytthanthum* and *Mentha asiatica, Khim. Prir. Soedin. 2*, 149–155.
6. Asilbekova, D.T., Glushenkova, A.I., Azcan, N., Özek, T., and Baser, K.H.C. (2000) Lipids of *Origanum tytthanthum, Khim. Prir. Soedin. 2*, 100–102.
7. Marin, P.D., Sajdl, V., Kapor, S., Tatic, B., and Petkovic, B. (1991) Fatty Acids of the Saturejoideae, Ajugoideae and Scutellarioideae (Lamiaceae), *Phytochemistry 30*, 2979–2982.
8. Williams, S. (ed.) (1984) *Official Methods of Analysis of the Association of Official Analytical Chemists*, 14th edn., pp. 513–514, AOAC Publications, Arlington, VA.
9. Cantino, P.D. and Sanders, R.W. (1986) Subfamilial Classification of Labiatae, *Systematic Bot. 11*, 163–185.
10. Castro-Martinez, R., Pratt, D.E., and Miller, E.E. (1986) Natural Antioxidants of Chia Seeds, in *Proceedings of the World Conference on Emerging Technologies in the Fats and Oils Industry* (Baldwin, A.R., ed.) American Oil Chemists' Society, Champaign.
11. Azcan, N., Kara, M., Özek, T., and Başer, K.H.C. (2000) Utilization of Industrial Waste Material of *Origanum* (Kekik) Cyclone Powder, in *Proceedings of the IV National Chemical Engineering Symposium* (4–7 September, Istanbul) (Boz, I., Hasdemir, M., and Gürkaynak, eds.), pp. 720–725, Istanbul University Press, Istanbul.

[Received September 29, 2003; accepted June 16, 2004]

Effects of Hydrocarbon Structure on Fatty Acid, Fatty Alcohol, and β-Hydroxy Acid Composition in the Hydrocarbon-Degrading Bacterium *Marinobacter hydrocarbonoclasticus*

Mohamed Soltani, Pierre Metzger*, and Claude Largeau

Centre Nationale de la Recherche Scientifique (CNRS) UMR 7573,
Ecole Nationale Supérieure de Chimie de Paris, 75231 Paris cedex 05, France

ABSTRACT: The lipids of the gram-negative bacterium *Marinobacter hydrocarbonoclasticus* grown in a synthetic seawater medium supplemented with various hydrocarbons as the sole carbon source were isolated, purified, and their structures determined. The hydrocarbons were normal, *iso, anteiso,* and mid-chain branched alkanes, phenylalkanes, cyclohexylalkanes, and a terminal olefin. According to the sequential procedure used for lipid extraction, three pools were isolated: unbound lipids extracted with organic solvents (corresponding to metabolic lipids and to the main part of membrane lipids), OH^- labile lipids [mainly ester-bound in the lipopolysaccharides (LPS)], and H^+ labile lipids (mainly amide-bound in the LPS). Each pool contained FA, fatty alcohols, and β-hydroxy acids. The proportions of these lipids in the unbound lipid pools were 84–98%, 1.1–11.6%, and 0.1–3.6% (w/w), respectively. The chemical structures of the lipids were strongly correlated with those of the hydrocarbons fed; analytical data suggested a metabolism essentially through oxidation into primary alcohol, then into FA and degradation *via* the β-oxidation pathway. Subterminal oxidation of the hydrocarbon chains, α-oxidation of FA or double-bond oxidation in the case of the terminal olefin, were minor, although sometimes substantial, routes of hydrocarbon degradation. Cyclohexyldodecane did not support growth, likely because of the toxicity of cyclohexylacetic acid formed in the oxidation of the alkyl side chain. In the OH^- and H^+ labile lipid pools, β-hydroxy acids, the lipophilic moiety of LPS, generally dominated (28–72% and 64–98%, w/w, respectively). The most remarkable feature of these cultures on hydrocarbons was the incorporation in LPS of β-hydroxy acids with C_{odd}, ω-unsaturated, *iso*, or *anteiso* alkyl chains in addition to the specific β-hydroxy acid of *M. hydrocarbonoclasticus*, 3-OH-*n*-12:0. These β-hydroxy acids were tolerated insofar as their geometry and steric hindrance were close to those of the 3-OH-*n*-12:0 acid.

Paper no. L9470 in *Lipids 39*, 491–505 (May 2004).

Hydrocarbon biodegradation has drawn attention for many years in relation to its importance in removing petroleum hydrocarbons, oily wastes, or some pesticides from marine and freshwater environments (1,2). The microbial degradation of alkanes, alkenes, alkylcycloalkanes, and alkylbenzenes under aerobic conditions has been thoroughly reviewed (3–6). The primary oxidation step of hydrocarbons comprising aliphatic long chains generally leads to primary (predominantly) or secondary alcohols, which undergo oxidation to FA and further degradation *via* the classical α- or β-oxidation pathways (3). Although the effect of hydrocarbons on the FA composition of several microorganisms has been widely investigated (7–12), little is known about their influence on the distribution of other lipids. Numerous gram-negative bacteria have been adapted to degrade hydrocarbons (6,11), one of which is the marine species *Marinobacter hydrocarbonoclasticus* (13). This ubiquitous bacterium is able to use straight-chain hydrocarbons as the sole carbon source (12–14). Analytical data have suggested a metabolism of these compounds through oxidation into acids, and then through the classical β-oxidation pathway *via* β-hydroxy acids (14,15). In *M. hydrocarbonoclasticus* grown on *n*-eicosane, long-chain β-hydroxy acids (C_{16}–C_{20}) were identified in the lipids extracted with solvents. By contrast, shorter-chain β-hydroxy acids (C_{10}, C_{12} maximum) occurred as ester-bound and amide-bound lipids in the lipopolysaccharides (LPS).

The major aim of the present work was to determine the influence of various hydrocarbons on the lipid composition of *M. hydrocarbonoclasticus*, particularly on the different pools of β-hydroxy acids. The tested hydrocarbons were normal, *iso*, *anteiso*, and mid-chain methyl-branched alkanes, cyclohexyl- and phenylalkanes, and a terminal olefin. This work also has the geochemical prospect of evaluating the impact of hydrocarbon pollution on organic matter in sediments, in particular that of prokaryotic origin. To apply the analytical procedure to sediments, which are often recalcitrant to the extraction of total lipids, a sequential extraction was used (14,16–20). A first extraction with organic solvents was performed to isolate neutral lipids and the major part of glyco- and phospholipids, referred to here as "unbound" lipids. Basic and acid hydrolyses of the extracted cells then furnished the

*To whom correspondence should be addressed at Laboratoire de Chimie Bioorganique et Organique Physique, CNRS UMR 7573, ENSCP, 11 Rue P. et M. Curie, 75231 Paris cedex 05, France.

E-mail: pierre-metzger@enscp.jussieu.fr

Abbreviations: CC, column chromatography; Ch-C_{12}, cyclohexyldodecane; Ch-C_{13}, cyclohexyltridecane; DMDS, dimethyl disulfide; LPS, lipopolysaccharides; Ph-C_{12}, 1-phenyldodecane; Ph-C_{13}, 1-phenyltridecane; THF, tetrahydrofuran; TMSi, trimethylsilyl.

ester-bound ("OH^- labile") and amide-bound ("H^+ labile") lipids present in lipoconjugates not extractable with organic solvents, i.e., mainly LPS. In this paper we report on the influence of hydrocarbon structure on the composition of FA, fatty alcohol, and β-hydroxy acid of *M. hydrocarbonoclasticus* and describe their metabolic pathways. Analytical data showed that some structural variations were tolerated by the bacterium for incorporating hydrocarbon chains into the β-hydroxy acids of LPS.

EXPERIMENTAL PROCEDURES

Chemicals. Silica gel and alumina (both 70–230 mesh) were from Merck Eurolab (Lyon, France). TLC was performed on commercial plates (silica gel 60 F_{254}; Merck Eurolab). FA standards were purchased from Sigma Aldrich (L'Isle d'Abeau, France) and Larodan (Malmö, Sweden). An etheral solution of diazomethane was prepared from Diazald® (Sigma Aldrich) according to an Aldrich procedure (Technical Information Bulletin AL-180). Dimethyldisulfide (DMDS) and pyrrolidine were from Merck (Darmstadt, Germany).

Some hydrocarbons were from commercial sources: *n*-$C_{19:0}$ (purity ≥99%) and *n*-nonadec-1-ene (purity ≥99%) were from Fluka (L'Isle d'Abeau, France), and 1-phenyldodecane (Ph-C_{12}; purity 96%) and 1-phenyltridecane (Ph-C_{13}; purity 99%) were from Sigma Aldrich.

Anteiso-nonadecane, *iso*- and *anteiso*-eicosanes, and 10-methylnonadecane were synthesized *via* Wittig reactions and catalytic hydrogenation of the olefins formed. Thus, 10-methylnonadecane was prepared *via* the following process. Methyltriphenylphosphonium bromide (11.22 g, 31.5 mmol; Acros, Noisy-le Grand, France) dissolved in THF (50 mL) was added to a THF solution (60 mL) of *n*-butyl lithium (1.5 M in hexane, 32.4 mmol; Lancaster, Bischleim, France). After 2 h at room temperature, a THF solution (10 mL) of nonadecan-10-one (3 g, 10.5 mmol; Lancaster) was added, and the mixture was refluxed for 72 h. The cooled reaction mixture was centrifuged ($120 \times g$) for 10 min, and the supernatant was diluted with 200 mL diethyl ether and washed with distilled water (2×200 mL). The organic phase was concentrated under reduced pressure, and the crude product was chromatographed using alumina (60 g, activity II) column chromatography (CC). Elution with heptane (660 mL) gave 10-methylene-nonadecane. Hydrogenation of this olefin dissolved in heptane (15 mL) was performed in the presence of a catalytic amount of Rh/C 5% (Acros) at 70°C under 20 atm hydrogen for 12 h. The catalyst was separated by centrifugation, and the purification of the product using alumina (60 g, activity II) CC by elution with heptane (660 mL) afforded pure 10-methylnonadecane (2.37 g). *a*-C_{19} and *a*-C_{20} alkanes were similarly prepared *via* reaction of ethylidene triphenylphosphorane, prepared by reaction of ethyltriphenylphosphonium bromide (Fluka) with *n*-butyl lithium, with *n*-heptadecan-2-one (Fluka, purity ≥99%), and with *n*-octadecan-2-one (Fluka, purity ≥99%), respectively, followed by catalytic hydrogenation of the isolated olefins. *iso*-Eicosane issued from the coupling of *n*-nonadecan-2-one (Fluka) with methylidene trimethylphosphorane, prepared by reaction of methyltriphenylphosphonium bromide with *n*-butyl lithium and subsequent hydrogenation of the formed olefin.

iso-Nonadecane was prepared by catalytic hydrogenation (conditions as just discussed) of *cis*-2-methyl-octadec-7-ene (Lancaster, purity 98%), cyclohexyltridecane (Ch-C_{13}), and cyclohexyldodecane (Ch-C_{12}) in a similar manner from the corresponding phenylalkanes.

GC–mass spectra of the synthesized hydrocarbons indicated molecular masses at *m/z* 268 for *i*-C_{19} and *a*-C_{19}; *m/z* 282 for *i*-C_{20}, *a*-C_{20}, and 10-methyl-nonadecane; and *m/z* 252 and 266 for Ch-C_{12} and Ch-C_{13}, respectively; purity: *i*-C_{19} 96%, *a*-C_{19} 98%, *i*-C_{20} 97%, *a*-C_{20} 99%, 10-methyl-nonadecane 97%, Ch-C_{12} 99%, and Ch-C_{13} 99%.

Cultures. The type strain of *M. hydrocarbonoclasticus* (strain SP17, ATCC 49840; Rockville, MD) was used. Cells were grown in 3-L Erlenmeyer flasks containing 750 mL of synthetic seawater medium (14) supplemented with the tested hydrocarbon. *Marinobacter hydrocarbonoclasticus* was cultured at 25°C under aerobic conditions (aeration was provided by agitation with magnetic stirring at 400 rpm). Growth was monitored by measuring the optical density at 450 nm with a Varian DMS 90 UV-vis spectrophotometer. At the late exponential growth phase, the biomass was harvested by centrifugation at $12{,}000 \times g$ for 15 min at 4°C, washed twice with 30 mL of synthetic medium, and freeze-dried.

Isolation of lipids. For each culture, the dry biomass was extracted overnight with 100 mL of chloroform/methanol (2:1, vol/vol), with stirring at room temperature. The residue was removed by filtration over a 0.5-μm FH-type membrane (Millipore; Saint-Quentin en Yvelines, France), and the solid was rinsed with methanol. The combined extract and washings were evaporated to dryness under reduced pressure. This lipid extract was then transesterified in 70 mL of methanol/KOH (0.1 M) at 0°C for 2 h. The reaction mixture was acidified to pH 1 with aqueous HCl 5% (vol/vol) and extracted with 250 mL diethyl ether/heptane (3:1, vol/vol). The product was then purified using silica gel CC. A first elution with heptane furnished the nonmetabolized hydrocarbons, and elution with diethyl ether/methanol (4:1, vol/vol) then furnished the unbound lipids. The solvent-extracted biomass was saponified by refluxing for 2 h in 20 mL of methanol/1 M KOH. After cooling, the residue was separated by filtration and thoroughly rinsed with 20 mL of methanol. The combined filtrates were acidified with aqueous HCl (5%), diluted with distilled water, and extracted with diethyl ether. The concentrated extract was submitted to esterification by addition of an etheral solution of diazomethane at room temperature; the recovered products constituted the OH^- labile lipids. The residual biomass was finally hydrolyzed in 12 mL of aqueous 4 M HCl under reflux for 6 h, and the reaction mixture was treated as already described. These recovered lipids constituted the H^+ labile lipids.

Separation of unbound lipids. Lyophilized cells of a microbial culture on *i*-C_{19} (833 mg) were extracted with 100 mL

of chloroform/methanol as described in the preceding paragraphs. The lipid extract (208 mg) was impregnated with 3 g of silica and placed at the top of a glass column containing 12 g of silica. Neutral lipids (81 mg) were eluted first with 300 mL of chloroform, glycolipids (8 mg) with 1200 mL of acetone, and phospholipids (96 mg) with 300 mL of methanol (21). Neutral lipids were separated using silica gel (12 g) CC by elution with heptane (45 mL; 37 mg), heptane/diethyl ether (19:1, vol/vol; 60 mL; 3 mg), and then diethyl ether/methanol (4:1, vol/vol; 50 mL; 40 mg). The diethyl ether/methanol fraction was investigated by silica gel TLC for the presence of TAG by elution with heptane/diethyl ether (9:1, vol/vol), with TAG from olive oil (Larodan) as the reference; spots were revealed by Rhodamine B and visualized under UV light. The three fractions were analyzed by GC and GC–MS as described next. The former two fractions corresponded to the nonmetabolized hydrocarbon. The third fraction was reacted with diazomethane before GC and GC–MS analyses. The phospholipid fraction was transesterified in 20 mL methanol/KOH (0.1 M) at 0°C for 2 h, then acidified and extracted with diethyl ether as just described.

Derivatization and GC–MS. Lipids were analyzed by GC–MS (70 eV) with a Hewlett-Packard HP 6890 gas chromatograph coupled with a HP 5973N mass spectrometer (Agilent Technology). The chromatograph was equipped with a J&W Scientific (Massy, France) DB-5MS fused-silica column (30 m × 0.25 mm) coated with 95% polydimethylsiloxane and 5% phenylsiloxane (film thickness 0.25 μm). The temperature program was from 100 to 300°C (4°C/min). FAME were identified by co-injection with authentic standards on GC (using the same conditions as for GC–MS) and comparison of the mass spectra. Alcohols and β-hydroxy acids were analyzed as trimethylsilyl (TMSi) ethers (22). Standards of primary *iso* and *anteiso* fatty alcohols were prepared by reduction of the corresponding FAME (5 mg in 10 mL anhydrous diethyl ether) with $AlLiH_4$ (10 mg) (Fluka) under a nitrogen atmosphere and refluxing for 1 h, followed by careful addition of a few drops of aqueous HCl 5% and extraction with diethyl ether. DMDS adducts were prepared by an I_2 reaction (23), and *N*-acyl pyrrolidides were prepared by direct treatment of methyl esters with pyrrolidine/acetic acid (24).

RESULTS

Methodology and quantitative data. The dry biomass of each culture was submitted to a sequential extraction procedure to extract the totality of lipids (14,15). In brief, the main part of the free and membrane lipids was recovered by extraction with chloroform/methanol. This lipid mixture was further purified by silica gel CC to remove the hydrocarbons adsorbed on the cell surfaces and ingested by the cells, and then transesterified to give the unbound lipids. Thereafter, the successive alkaline and acid hydrolyses of the solvent-extracted biomass released FA and hydroxy acids from ester-bound (OH^- labile) and amide-bound (H^+ labile) lipid moieties occurring in some lipoconjugates. These lipoconjugates were LPS, lipoproteins, and ornithine lipids (25). In gram-negative bacteria, amide-bound hydroxy acids are known to occur in LPS (mainly) and in ornithine lipids, whereas ester-bound hydroxy acids occur only in LPS. These considerations, in combination with analytical data, indicate that bound hydroxy acids come mainly from LPS (14,26). In sharp contrast, the origin of FA present in these hydrolysates is less clear: They can derive from ester-linked acyl moieties in LPS, ornithine lipids, and lipoproteins and from amide-linked acyl moieties in lipoproteins (25).

The foregoing procedure is the one classically used for studies of lipids in sediments; it was therefore used in the present study to allow for comparison with geochemical data. However, this procedure may exhibit two drawbacks compared with some more classical extraction procedures followed by CC separation into neutral, glyco-, and phospholipids: (i) TAG, if present in the extract, would be unnoticed, and (ii) poor extraction of phospholipids may occur. To test this, a parallel control experiment was performed on the culture grown on *i*-C_{19}. Extraction with chloroform/methanol was performed in the same manner, and the lipid extract was separated into neutral, glyco-, and phospholipids. Analysis of the neutral lipid fraction showed the presence of the nonmetabolized *i*-C_{19} (49%), *i*-C_{19} fatty alcohols (26%), and *i*-$C_{17:0}$ and *i*-$C_{19:0}$ β-hydroxy acids (7%). In addition, analysis of the neutral lipids showed a low content (about 3% of neutral lipids) of FA, thus indicating that only limited hydrolytic activity had taken place upon extraction and processing. Like numerous bacterial species, *M. hydrocarbonoclasticus* does not produce TAG. Quantification of the phospholipids showed a content of about 5% of dry cells, i.e., in the range commonly observed for gram-negative bacteria (25), thus indicating that the bulk of the phospholipids was recovered by chloroform/methanol extraction. Moreover, GC–MS analysis of the derived methyl esters showed a FA distribution of phospholipids rather similar to that observed for the unbound lipids (see later paragraphs and Table 3).

When the bacterium reached the stationary phase of growth, the cell yield (Table 1) was higher when the culture was performed on a hydrocarbon liquid at room temperature, i.e., C_{19} and C_{20} methyl-branched hydrocarbons and olefin (about 300 mg/L of dry cells in the case of 10-MeC_{19}), than that obtained with cultures on dispersed solids such as *n*-C_{19}, cyclohexyl-, and phenylalkanes (about 160 mg/L of dry cells). The purified fractions of unbound lipids accounted for 5.5 (culture on *i*-C_{20}) up to 14.4% (culture on *n*-$C_{19:1}$) of the dry cells free of hydrocarbons, whereas the OH^- labile lipids varied between 1.1 (cultures on *i*-C_{20} and *a*-C_{19}) and 3.1% (culture on *n*-C_{19}), and the H^+ labile lipids varied between 0.5 (culture on *i*-C_{19}) and 0.9% (cultures on *n*-C_{19} and Ch-C_{13}) of the dry cells (Table 1). On the whole, total lipids accounted for 7.3 (culture on *i*-C_{20}) up to 17.1% (culture on *n*-$C_{19:1}$) of the dry cells.

Identification of lipids. The FA, hydroxy acid, and fatty alcohol distributions in the unbound, OH^- labile, and H^+ labile lipids are listed in Tables 2–8. FA were analyzed as FAME;

TABLE 1
Abundance of Lipid Pools Isolated from *Marinobacter hydrocarbonoclasticus* Cultivated on Different Carbon Sources

Carbon source	Cell yield[a] (mg/L)	Lipid contents (as % of dry cells)			
		Total	Unbound	OH^- labile	H^+ labile
Ammonium acetate[b]	ND[c]	5.2	3.5	1.1	0.6
n-$C_{19:0}$	155	12.7	8.7	3.1	0.9
n-$C_{20:0}$[b]	ND	7.8	5.6	1.5	0.7
i-$C_{19:0}$	266	12.3	10.2	1.6	0.5
i-$C_{20:0}$	ND	7.3	5.5	1.1	0.7
a-$C_{19:0}$	240	11.0	9.2	1.1	0.7
a-$C_{20:0}$	245	10.3	8.0	1.6	0.7
10-Me-$C_{19:0}$	302	10.2	7.9	1.5	0.8
n-$C_{19:1}$	205	17.1	14.4	1.9	0.8
Ch-$C_{13:0}$	165	8.7	6.1	1.7	0.9
Ph-$C_{12:0}$	152	8.1	5.9	1.6	0.6
Ph-$C_{13:0}$	172	8.8	6.3	1.8	0.7

[a]Dry weight (free of nonmetabolized hydrocarbons).
[b]Data taken from a previous study (15).
[c]ND, not determined. Ch-$C_{13:0}$, cyclohexyltridecane; Ph-$C_{12:0}$, 1-phenyldodecane; Ph-$C_{13:0}$, 1-phenyltridecane.

alcohols and hydroxyl functions of hydroxy acids were trimethylsilylated, and each lipid fraction was analyzed by GC and GC–MS. The locations of the carbon–carbon double bonds and branching in the aliphatic chains were determined by means of GC–MS analyses of DMDS adducts and *N*-pyrrolidide derivatives, respectively. As examples, Figure 1 shows the mass spectra of two acid derivatives: the pyrrolidide derivative of 8-methyl-heptadecanoic acid (Fig. 1A), and the 12,13-DMDS adduct of the TMSi ether derivative of 3-hydroxy-tridec-12-enoic acid methyl ester (Fig. 1B), identified in the cultures on 10-Me-C_{19} (Table 5) and *n*-$C_{19:1}$ (Table 6), respectively. In the pyrrolidide derivative, the methyl substitution caused a 28-mass-unit gap between 182 and 210 in the series of fragments separated by 14 mass units, allowing the methyl group to locate at position 8 in the chain. Similarly, the mass spectra of *iso*- and *anteiso*-FA pyrrolidides (not shown) lacked M – 29 and M – 43 ions, respectively. β-Hydroxy acids were identified by the presence in their mass spectra of an intense peak at *m/z* 175, originating from the cleavage of the Cβ–Cγ bond. Moreover, in the case of the DMDS adduct of β-hydroxy tridecenoic acid methyl ester (Fig. 1B), the presence on the spectrum of intense ions at *m/z* 61 and 347 established that the initial double bond was at the terminal position.

Figure 2 shows the mass spectra of the TMSi derivatives of methyl-branched primary (Figs. 2A and 2B) and secondary (Figs. 2C and 2D) fatty alcohols derived from the oxidation of *anteiso*-nonadecane and *anteiso*-eicosane, respectively (Table 4). The mass spectra of the two isomeric primary alcohols (Figs. 2A and 2B) were rather similar, with abundant ions at *m/z* 341 $[M - Me]^+$, and peaks of lower intensity at *m/z* 103, $[CH_2OSiMe_3]^+$, and *m/z* 75, $[Me_2Si = OH]^+$. As a result, the TMSi-derivatized *anteiso*-nonadecan-1-ol could be identified only by means of a co-injection on GC with an authentic standard and comparison of the mass spectra. The mass spectra of the TMSi-derivatized secondary alcohols were more informative for structural determination. Indeed, as illustrated in Figure 2C, the spectra of *anteiso*-alkan-2-ols displayed a small peak at *m/z* M – 29 indicative of an *anteiso*-methyl-branching, whereas it lacked in the spectra of the 3-Me-alkan-2-ols (Fig. 2D).

ω-Phenyl- and ω-cyclohexyl-alkanoic acids were identified in the lipids of *M. hydrocarbonoclasticus* grown on 1-phenylalkanes and 1-cyclohexyltridecane, respectively (Tables 7 and 8). Mass spectra of phenylalkanoic methyl esters displayed a base peak at *m/z* 91 for the tropylium ion, abundant ions at *m/z* 74 and *m/z* M – MeOH, and distinct molecular ions. The spectra of cyclohexylalkanoic methyl esters showed a base peak at *m/z* 74, prominent peaks at *m/z* 55 and 87, and abundant ions at *m/z* M and *m/z* 83 for cyclohexyl fragments. All these spectra match those reported for some natural cyclo-alkanoic acids well (27,28). The mass spectra of the TMSi-derivatized phenyl and cyclohexyl alkanols exhibited prominent fragment ions typical of primary or secondary (subterminal) alcohols at *m/z* 75 and 117, respectively, and the characteristic fragments of the cyclic moiety. Moreover, the spectra of the TMSi-derivatized β-hydroxy methyl esters exhibited major ions at *m/z* M – 15, 175, $[CH(OSiMe_3)CH_2CO_2Me]^+$, and 83 (cyclohexyl ion) or 91 (tropylium ion).

To keep the data as clear as possible, only FA accounting for at least 2% of a given lipid pool are quoted in Tables 2–8.

Culture on n*-nonadecane.* The distribution of the lipids extracted from the culture on *n*-nonadecane is listed in Table 2, together with previous data obtained from a culture on *n*-eicosane (14). FA were the major components of the unbound lipids, accounting for 90.4 and 85.4% of the pools recovered from *n*-C_{19} and *n*-C_{20} cultures (Table 9), respectively. Culture on *n*-C_{19} principally led to C_{odd} FA (mainly 17:0 and 17:1), whereas the culture on *n*-C_{20} mainly furnished C_{even} FA (essentially 16:0, 16:1, and 18:1). Three *n*-C_{19} fatty alcohols were identified in the unbound lipids of the *n*-C_{19} culture (Table 2): two primary (a saturated and an unsaturated) and a secondary with the hydroxyl group at the subterminal position. The oddness/evenness of the hydrocarbon chain length of β-hydroxy acids depended on the alkane fed, with C_{19} and

TABLE 2
FA, Hydroxy Acid, and Fatty Alcohol Composition of the Three Lipid Pools[a] Isolated from *M. hydrocarbonoclasticus* Grown on *n*-C_{19} and *n*-C_{20}[b] Alkanes

	Unbound		OH^- labile		H^+ labile	
Lipids	*n*-C_{19}	*n*-C_{20}	*n*-C_{19}	*n*-C_{20}	*n*-C_{19}	*n*-C_{20}
Saturated FA						
n-10:0	—[c]	—	—	17.6	—	—
n-12:0	—	—	+[d]	37.8	—	+
n-13:0	—	+	+	—	5.2	—
n-14:0	+	+	+	+	4.6	+
n-15:0	7.2	+	5.8	+	—	—
n-16:0	3.4	25.3	5.6	2.5	7.9	+
n-17:0	25.8	+	15.4	—	+	—
n-18:0	2.0	+	+	—	3.8	+
n-19:0	2.5	—	+	—	+	—
Unsaturated FA[e]						
n-14:1(5)	—	+	+	9.3	—	—
n-15:1(6;7;9)	2.1 (6)	—	4.6 (7;9)	—	—	—
n-16:1(7;9*c*)	2.1 (7)	25.1 (7)	+	+	—	—
n-17:1(7;9)	28.9 (9)	—	16.2 (9)	—	—	—
n-18:1(9*c*;11*c*)	10.3 (9*c*)	26.6 (9*c*)	5.9 (9*c*)	+	+	—
n-19:1(9;11)	2.9 (9)	—	5.6 (9)	—	—	—
n-20:1(11)	—	4.2	—	—	—	—
β-Hydroxy acids						
n-10:0	—	—	—	0.2	—	0.5
n-11:0	—	—	4.8	—	2.7	—
n-12:0	—	0.2	16.0	28.1	38.8	97.6
n-13:0	—	—	6.3	—	22.7	—
n-13:1(5)	—	—	0.5	—	—	—
n-14:0	—	0.1	—	Trace	—	0.2
n-17:0	0.3	—	Trace	—	—	—
n-18:0	—	0.4	—	—	—	—
n-18:1(9)	—	0.3	—	—	—	—
n-19:0	0.6	—	—	—	—	—
n-20:0	—	0.6	—	—	—	—
n-20:1(11)	—	0.3	—	—	—	—
Alcohols						
n-17:0,1-OH	0.9	—	—	—	—	—
n-19:0,1-OH	3.8	—	—	—	—	—
n-19:1,1-OH	0.1	—	—	—	—	—
n-19:0,2-OH	0.6	—	—	—	—	—
n-20:0,1-OH	—	1.3	—	—	—	—
n-20:1(11),1-OH	—	10.3	—	—	—	—
Other lipids	6.5	5.3	13.3	4.5	14.3	1.7

[a]Expressed as the percentage of total lipids for the considered pool.
[b]Data taken from Reference 15.
[c]—, not detected.
[d]+, FA accounting for less than 2% of a considered pool.
[e]When several isomers are present, the percentages correspond to the total of the considered series; the position of the unsaturation for the dominant unsaturated FA is given in parentheses.

C_{17} compounds in the culture on *n*-C_{19} and even-carbon-numbered C_{12}–C_{20} β-hydroxy acids in the case of the *n*-C_{20} culture. By contrast, short-chain β-hydroxy acids dominated in the OH^- and H^+ labile lipid pools, with high proportions of both *n*-12:0 and *n*-13:0 compounds in the case of the culture on *n*-C_{19}, whereas only minor amounts of the latter were detected in the culture on *n*-C_{20} (Tables 2, 10, and 11).

Cultures on iso- *and* anteiso-*alkanes.* The lipid distributions of the cultures on *iso*- and *anteiso*-C_{19} and C_{20} alkanes are listed in Tables 3 and 4. The FA, β-hydroxy acids, and fatty alcohols present in the unbound lipids appeared to relate rather well to the structure of the hydrocarbons fed, with *iso* or *anteiso* and even or odd predominating. For instance, FA of the *iso*-eicosane culture mainly comprised *i*-18:0, *i*-16:0, and *i*-14:0. The predominant unsaturated FA were, however, the *n*-18:1 acids, accompanied by *n*-16:1 FA and some branched (*i*-18:1, *i*-16:1) acids. On the whole, cultures on *iso*- and *anteiso*-alkanes led to predominant saturated FA series, whereas those on *n*-alkanes furnished preferably unsaturated FA series (Table 9). In bacteria grown on *anteiso*-alkanes, two primary and two secondary alcohols

TABLE 3
FA, Hydroxy Acid, and Fatty Alcohol Composition of the Three Lipid Pools[a] Isolated from *M. hydrocarbonoclasticus* Grown on *iso*-C_{19} and -C_{20} Alkanes

	Unbound		OH^- labile		H^+ labile	
Lipids	*i*-C_{19}	*i*-C_{20}	*i*-C_{19}	*i*-C_{20}	*i*-C_{19}	*i*-C_{20}
Saturated FA						
n-12:0	—[b]	+[c]	2.4	3.0	—	+
n-14:0	+	+	+	+	2.3	+
i-14:0	+	13.5	—	2.4	—	+
i-15:0	16.2	2.5	6.5	—	—	—
n-16:0	2.3	+	2.6	2.1	—	3.7
i-16:0	+	32.7	+	8.3	—	+
i-17:0	27.1	+	10.6	+	+	+
i-18:0	+	9.2	—	+	—	+
Unsaturated FA[d]						
n-14:1(5;7)	—	—	5.1 (5)	5.6 (5)	—	—
n-16:1(7;9*c*;11)	4.2 (9*c*;7)	2.8 (9*c*)	2.4 (7;9*c*)	+	—	+
i-16:1(5;7;9)	—	3.1 (7;9)	—	+	—	—
i-17:1(7;9)	8.1 (7)	+	2.3 (9)	—	—	—
n-18:1(9*c*;11*c*;13)	17.9 (9*c*)	11.4 (9*c*)	6.5 (9*c*)	3.9 (9*c*)	—	5.7 (11*c*)
i-18:1(7;9)	—	6.9 (7)	—	+	—	—
i-19:1(9)	2.4	+	—	+	—	—
β-Hydroxy acids						
n-10:0	—	—	0.2	0.7	0.5	1.0
n-11:0	—	0.2	0.4	3.5	0.7	4.3
n-12:0	—	0.2	50.6	44.5	87.8	68.5
n-12:1(5)	—	—	1.7	5.5	0.4	—
i-12:0	—	—	—	0.1	—	1.1
n-13:0	—	—	0.3	2.1	0.7	5.0
n-13:1(5)	—	—	0.3	3.2	—	—
i-13:0	—	—	0.6	Trace	1.9	0.2
n-14:0	—	—	—	Trace	1.0	1.7
n-14:1(5)	—	—	1.5	3.3	0.4	—
i-14:0	—	—	—	Trace		0.1
i-17:0	3.5	—	Trace	—	—	—
i-18:0	—	1.0	—	—	—	—
i-19:0	0.6	0.1	Trace	—	Trace	—
i-20:0	—	0.2	—	—	—	Trace
Alcohols						
i-18:0,1-OH	—	0.1	—	—	—	—
i-19:0,1-OH	5.9	—	0.3	—	—	—
i-19:1(9),1-OH	1.7	—	—	—	—	—
i-19:0,2-OH	0.2	—	—	—	—	—
2-Me-18:0,1-OH	Trace	—	—	—	—	—
i-20:0,1-OH	—	2.1	—	0.1	—	0.2
i-20:0,2-OH	—	0.4	—	—	—	—
2-Me-19:0,1-OH	—	0.9	—	—	—	0.1
Other lipids	9.9	12.7	5.7	11.7	4.3	8.4

[a]Expressed as the percentage of total lipids for the considered pool.
[b]—, not detected.
[c]+, FA accounting for less than 2% of a considered pool.
[d]When several isomers are present, the percentages correspond to the total of the considered series; the position of the unsaturation for the dominant unsaturated FA is given in parentheses.

were identified, with the less sterically hindered predominating (Table 4). In addition, a lower homolog, *a*-19:0,1-OH, was identified in the culture on *a*-C_{20}. By contrast, *iso*-alkanes led to only one secondary fatty alcohol (Table 3).

Iso and *anteiso* series dominated the saturated FA in the OH^- labile lipids (Tables 3 and 4), whereas unsaturated FA mainly comprised straight-chain acids. β-Hydroxy acids were abundant in this pool, ranging from 54 up to 66%, with *n*-12:0 predominating (Table 10), but low amounts of higher (*n*-13:0 and *n*-14:0) and lower (*n*-10:0 and *n*-11:0) homologs were also detected, together with an unsaturated series (12:1, 13:1, and 14:1). *Iso*- and *anteiso*-β-hydroxy acids ranged from 0.1 up to 1.6% of the OH^- labile lipids. Rather similar profiles of β-hydroxy acids were observed in the H^+ labile lipids (Tables 3, 4, and 11).

TABLE 4
FA, Hydroxy Acid, and Fatty Alcohol Composition of the Three Lipid Pools[a] Isolated from *M. hydrocarbonoclasticus* Grown on *anteiso*-C_{19} and -C_{20} Alkanes

	Unbound		OH^- labile		H^+ labile	
Lipids	*a*-C_{19}	*a*-C_{20}	*a*-C_{19}	*a*-C_{20}	*a*-C_{19}	*a*-C_{20}
Saturated FA						
n-12:0	+[b]	—[c]	4.0	+	+	5.4
a-14:0	+	5.9	·	6.3	—	3.0
a-15:0	20.1	+	7.2	+	+	—
n-16:0	2.9	2.4	2.8	2.4	2.4	+
a-16:0	—	20.4	—	2.9	—	+
a-17:0	35.1	10.3	13.6	2.7	+	+
n-18:0	+	+	+	+	2.2	+
a-18:0	+	16.2	—	2.8	—	+
a-19:0	2.8	+	+	+	Trace	+
Unsaturated FA[d]						
n-14:1(5;7)	—	—	4.3 (5)	+	—	+
n-16:1(7;9*c*;11)	2.3 (7;9*c*)	3.4 (9*c*)	+	+	—	+
n-18:1(7;9*c*;11*c*)	10.4 (9*c*)	16.5 (9*c*)	4.7 (9*c*)	5.2 (9*c*)	—	+
a-18:1(8;9;11)	—	3.6 (9)	—	+	—	+
β-Hydroxy acids						
n-10:0	—	—	1.2	0.2	0.2	0.6
n-11:0	—	—	2.3	1.3	1.7	2.8
a-11:0	—	—	Trace	—	0.2	—
n-12:0	Trace	—	36.5	53.7	65.5	62.6
n-12:1(5)	—	—	5.6	2.4	Trace	3.6
a-12:0	—	—	—	0.6	0.2	0.7
n-13:0	—	—	1.4	1.8	4.6	2.0
n-13:1(5)	—	—	2.0	1.7	Trace	2.0
i-13:0	—	—	0.7	Trace	3.0	Trace
a-13:0	—	—	1.6	Trace	11.9	Trace
n-14:0	—	—	0.3	0.5	2.2	0.4
n-14:1(5)	—	—	2.1	2.7	0.1	2.8
a-14:0	—	—	Trace	0.7	0.2	0.6
a-15:0	0.4	—	0.1	—	0.2	—
a-17:0	0.7	Trace	—	—	Trace	—
a-18:0	0.1	Trace	—	—	—	—
a-19:0	0.5	Trace	Trace	—	Trace	—
Alcohols						
a-19:0,1-OH	7.8	0.2	—	—	—	—
a-19:0,2-OH	0.1	—	—	—	—	—
3-Me-18:0,1-OH	1.3	—	—	—	—	—
3-Me-18:0,2-OH	0.1	—	—	—	—	—
a-20:0,1-OH	—	1.9	—	1.3	—	Trace
a-20:0,2-OH	—	0.1	—	—	—	—
3-Me-19:0,1-OH	—	1.0	—	—	—	—
3-Me-19:0,2-OH	—	0.1	—	—	—	—
Other lipids	15.4	18.0	9.6	10.8	5.4	13.5

[a]Expressed as the percentage of total lipids for the considered pool.
[b]+, FA accounting for less than 2% of a considered pool.
[c]—, not detected.
[d]When several isomers are present, the percentages correspond to the total of the considered series; the position of the unsaturation for the dominant unsaturated FA is given in parentheses.

Culture on 10-methyl-nonadecane. Data concerning the culture on the mid-chain branched alkane are listed in Table 5 and summarized in Tables 9–11. In the unbound lipids, *n*-acids were predominant (Tables 5 and 9), whereas a series deriving from the oxidation of the alkane (10-Me-19:0, 8-Me-17:0, 6-Me-15:0, and 4-Me-13:0 FA; Table 5) constituted 35.4%. On the whole, the *n*-17-carbon FA series dominated the straight-chain acids, accounting for 21.8% of the unbound lipids. Two 10-Me-19:0 alcohols were identified: a primary (0.9%) and a secondary (in trace amount). Three methyl-branched β-hydroxy acids were also detected: 3-OH,6-Me-15:0, 3-OH,8-Me-17:0, and 3-OH,10-Me-19:0.

OH^- labile lipids contained straight-chain compounds, with the exception of 10-Me-19:0, 8-Me-17:0, 6-Me-15:0,

TABLE 5
FA, Hydroxy Acid, and Fatty Alcohol Composition of the Three Lipid Pools[a] Isolated from *M. hydrocarbonoclasticus* Grown on 10-Me-C_{19} Alkane

Lipids	Unbound	OH^- labile	H^+ labile
Saturated FA			
3-Me-12:0	—[b]	2.0	—
4-Me-13:0	2.8	—	—
n-15:0	2.6	+[c]	+
n-16:0	9.7	3.4	+
6-Me-15:0	6.9	3.4	—
n-17:0	10.4	4.9	+
8-Me-17:0	23.5	13.0	—
10-Me-19:0	2.2	+	—
Unsaturated FA[d]			
n-14:1(5;7)	+	2.5 (5)	—
n-16:1(7;9*c*;11)	3.5 (7)	+	—
n-17:1(7;9)	11.4 (7)	5.9 (9)	—
n-18:1(9c;11c;13)	18.0 (9*c*)	9.2 (9*c*)	+
β-Hydroxy acids			
n-10:0	—	0.1	—
n-11:0	Trace	7.1	7.3
n-12:0	Trace	31.8	71.0
n-12:1(5)	—	0.4	—
n-13:0	Trace	5.6	12.4
n-13:1(5;7)	—	2.3 (5)	—
a-13:0	—	Trace	Trace
n-14:0	0.1	0.1	0.5
n-14:1(5)	—	0.5	—
6-Me-15:0	0.2	—	—
8-Me-17:0	0.1	—	—
10-Me-19:0	0.2	—	—
Alcohols			
10-Me-19:0,1-OH	0.9	—	—
10-Me-19:0,2-OH	Trace	—	—
Other lipids	7.5	7.8	8.8

[a]Expressed as the percentage of total lipids for the considered pool.
[b]—, not detected.
[c]+, FA accounting for less than 2% of a considered pool.
[d]When several isomers are present, the percentages correspond to the total of the considered series; the position of the unsaturation for the dominant unsaturated FA is given in parentheses.

TABLE 6
FA, Hydroxy Acid, and Fatty Alcohol Composition of the Three Lipid Pools[a] Isolated from *M. hydrocarbonoclasticus* Grown on *n*-Nonadec-1-ene

Lipids	Unbound	OH^- labile	H^+ labile
Saturated FA			
n-12:0	+[b]	4.8	—[c]
n-15:0	2.0	—	—
n-16:0	11.3	4.5	0.8
n-17:0	3.3	+	+
Monounsaturated FA[d]			
n-13:1(11;12)	+	2.0 (11)	—
n-14:1(5)	+	3.3	—
n-15:1(6;9;14)	10.1 (14)	Trace	—
n-16:1(7;9c;11)	6.7 (7;9*c*)	+	—
n-17:1(9;16)	20.6 (16)	3.7 (16)	—
n-18:1(9*c*)	13.9 (9*c*)	3.8 (9*c*)	—
Diunsaturated FA[d]			
n-17:2(7;16)	3.7	+	—
n-17:2(8;16)	3.9	—	—
n-17:2(9;16)	6.3	+	—
n-19:2(9;18)	2.4	—	—
α-Hydroxy acid			
n-19:0	Trace	—	—
β-Hydroxy acids			
n-10:0	—	0.2	0.8
n-11:0	—	2.1	2.6
n-12:0	—	50.6	85.7
n-13:0	—	1.1	3.1
n-14:0	—	0.2	—
n-18:0	0.2	—	—
n-19:0	0.1	—	—
n-12:1(4;11)	—	1.2 (4;11)	—
n-13:1(5;11;12)	—	14.8 (12)	0.2 (12)
n-13:2	—	0.6	—
n-17:1(16)	0.2	0.3	—
n-19:1(18)	0.2	—	—
Alcohols			
n-16:1(15),1-OH	0.1	—	—
n-17:1(16),1-OH	0.1	—	—
n-18:1(17),1-OH	0.1	—	—
n-19:1(18),1-OH	1.1	—	—
n-19:1(18),2-OH	Trace	—	—
n-19:2,1-OH	0.4	—	—
n-19:0,1,2-dihydroxy	1.8	1.1	0.3
Other lipids	11.5	5.7	6.5

[a]Expressed as the percentage of total lipids for the considered pool.
[b]+, FA accounting for less than 2% of a considered pool.
[c]—, not detected.
[d]When several isomers are present, the percentages correspond to the total of the considered series; the position of the unsaturation for the dominant unsaturated FA is given in parentheses.

and 3-Me-12:0 FA (Table 5). As in the previous cultures, β-hydroxy acids were abundant in this pool (47.9%; Table 10) and highly dominant in the H^+ labile lipids (91.2%; Table 11). In both cases, 3-OH-*n*-12:0 was predominant, and the proportions of its higher (13:0 and 14:0) and lower (10:0 and 11:0) homologs were similar to those observed with the cultures on *iso*- and *anteiso*-alkanes.

Culture on n-*nonadec-1-ene.* Unusual lipids exhibiting an ω-unsaturation were detected for each class of unbound lipids (Table 6). Diunsaturated FA exhibiting an odd carbon number and a terminal unsaturation accounted for a substantial percentage of this pool. Three monounsaturated FA from *n*-13:1 to *n*-17:1 (Table 6), showing the features just described, were also identified, but in lower proportions. Furthermore, we detected six ω-unsaturated fatty alcohols, a diol (*n*-nonadecane-1,2-diol), and two ω-unsaturated β-hydroxy acids—3-OH-*n*-19:1(18) and 3-OH-*n*-17:1(16) (Table 6). In addition, 2-hydroxy-nonadecanoic acid was present at a trace level. Among the usual FA, palmitic and oleic acids were the predominant compounds.

The proportions of the ω-unsaturated lipids decreased considerably in the OH^- labile lipids and disappeared almost totally in the H^+ labile lipids. In the OH^- labile lipid pool, the β-hydroxy acids (71.9% of this pool) included 3-OH-*n*-12:0 (70% of the β-hydroxy acids; Table 10), 3-OH-*n*-13:1(12)

TABLE 7
FA, Hydroxy Acid, and Fatty Alcohol Composition of the Three Lipid Pools[a] Isolated from *M. hydrocarbonoclasticus* Grown on Phenyl-C_{12} and Phenyl-C_{13} Hydrocarbons

	Unbound		OH^- labile		H^+ labile	
Lipids	Ph-C_{12}	Ph-C_{13}	Ph-C_{12}	Ph-C_{13}	Ph-C_{12}	Ph-C_{13}
Saturated FA						
n-10:0	—[b]	—	3.4	+[c]	—	—
n-12:0	—	+	15.9	12.6	+	+
n-14:0	+	+	+	5.1	+	+
n-16:0	16.4	16.6	6.8	4.3	2.6	6.5
n-18:0	5.6	6.1	+	2.3	+	4.9
Unsaturated FA[d]						
n-14:1(5)	—	—	7.5 (5)	6.8 (5)	—	—
n-16:1(7;9*c*;11)	3.4 (7)	4.2 (7)	+	+	+	2.5 (7)
n-18:1(9*c*;11*c*;13)	36.6 (9*c*)	34.4 (9*c*)	6.3 (9*c*)	6.3 (9*c*)	+	6.2 (9*c*)
Phenyl-*n*-alkanoic and -alkenoic acids						
Ph-*n*-9:0[e]	—	+	—	4.3	—	—
Ph-*n*-10:0	6.5	+	+	—	—	—
Ph-*n*-11:0	—	9.3	—	+	—	—
Ph-*n*-12:0	17.1	—	3.0	+	+	—
Ph-*n*-13:0	+	12.9	—	+	—	2.9
Ph-*n*-13:1	—	+	—	—	—	—
β-Hydroxy acids						
n-10:0	—	—	—	0.5	0.4	0.1
n-11:0	—	—	—	0.2	1.8	0.1
n-12:0	—	—	48.1	46.5	84.7	58.4
n-12:1	—	—	—	0.2	—	—
n-13:0	—	—	—	0.4	0.4	0.1
n-14:0	—	—	—	—	—	0.3
Ph-*n*-8:0[e]	0.3	—	0.2	—	—	—
Ph-*n*-10:0	0.1	—	0.1	—	—	—
Ph-*n*-11:0	—	0.2	—	—	—	—
Ph-*n*-12:0	0.1	—	Trace	—	—	—
Ph-*n*-13:0	—	0.5	—	Trace	—	—
Alcohols						
Ph-*n*-12:0,1-OH[e]	6.7	—	0.2	—	—	—
Ph-*n*-12:0,2-OH	1.0	—	—	—	—	—
Ph-*n*-13:0,1-OH	—	6.6	—	Trace	—	1.3
Ph-*n*-13:0,2-OH	—	Trace	—	—	—	—
Other lipids	6.2	9.2	8.5	10.5	10.1	16.7

[a]Expressed as the percentage of total lipids for the considered pool. For abbreviations see Table 1.
[b]—, not detected.
[c]+, FA accounting for less than 2% of a considered pool.
[d]When several isomers are present, the percentages correspond to the total of the considered series; the position of the unsaturation for the dominant unsaturated FA is given in parentheses.
[e]The shorthand designation used for the lipids deriving from phenyl(Ph)alkanes gives the total number of carbon atoms in the aliphatic straight chain before the colon, and after the colon, the number of double bonds in this chain.

(14%), and 3-OH-*n*-12:1(11) (1.1%). β-Hydroxy acids accounted for 92.4% of the H^+ labile lipids, with 3-OH-*n*-12:0 predominating (93%; Table 11).

Cultures on phenylalkanes. The compositions of the three lipid pools isolated from the cultures on Ph-C_{12} and Ph-C_{13} are shown in Table 7 and summarized in Tables 9–11. In the unbound lipids from the two cultures, straight-chain FA were highly predominant. Oleic acid was the predominant FA (Table 7). The oddness/evenness of the phenylalkanoic acids was closely related to the length of the aliphatic chain of the hydrocarbon fed. The same trends were observed with the ω-phenyl β-hydroxy acids and the ω-phenyl alkanols (Table 7). Primary (predominant) and secondary alcohols were identified.

β-Hydroxy acids constituted near the half part of the OH^- labile lipids and showed the predominance of 3-OH-*n*-12:0 (Table 10), whereas the ω-phenyl β-hydroxy acids showed only a very low abundance. By comparison, the proportions of β-hydroxy acids increased in the H^+ labile lipids, with 3-OH-*n*-12:0 still predominating (Table 11), and no ω-phenyl β-hydroxy acid was detected.

Cultures on cyclohexylalkanes. Marinobacter hydrocarbonoclasticus did not grow on cyclohexyldodecane but was successfully cultured on cyclohexyltridecane. Analytical data

TABLE 8
FA, Hydroxy Acid, and Fatty Alcohol Composition of the Three Lipid Pools[a] Isolated from *M. hydrocarbonoclasticus* Grown on Cyclohexyltridecane

Lipids	Unbound	OH^- labile	H^+ labile
Saturated FA			
n-12:0	—[b]	12.8	—
n-16:0	6.5	2.7	2.3
n-18:0	3.8	+[c]	+
Unsaturated FA[d]			
n-14:1(5)	—	10.4	—
n-16:1(7;9*c*;11)	5.2 (9*c*)	+	—
n-18:1(9*c*;11*c*;13)	35.3 (9*c*)	+	+
Cyclohexyl-alkanoic and -alkenoic acids			
Ch-*n*-9:0[e]	2.2	+	—
Ch-*n*-11:0	35.3	3.1	—
Ch-*n*-13:0	6.6	+	—
Ch-*n*-13:1	+	—	—
β-Hydroxy acids			
n-10:0	—	0.2	—
n-11:0	—	0.1	—
n-12:0	0.1	62.0	88.0
n-12:1(5)	—	1.1	—
n-13:0	—	0.1	0.5
n-14:0	—	—	1.3
n-14:1(5)	—	1.2	—
Ch-*n*-11:0[e]	0.2	—	—
Ch-*n*-13:0	Trace	—	—
Alcohol			
Ch-*n*-13:0,1-OH[e]	0.8	0.1	—
Other lipids	4.0	6.2	7.9

[a]Expressed as the percentage of total lipids for the considered pool.
[b]—, not detected.
[c]+, FA accounting for less than 2% of a considered pool.
[d]When several isomers are present, the percentages correspond to the total of the considered series; the position of the unsaturation for the dominant unsaturated FA is given in parentheses.
[e]The shorthand designation used for the lipids deriving from cyclohexyl (Ch)tridecane gives the total number of carbon atoms in the aliphatic straight chain before the colon, and after the colon, the number of double bonds in this chain.

on the lipids extracted from this latter culture are listed in Tables 8–11. FA distribution in the unbound lipids was rather similar to that noted with the culture on Ph-C_{13}, with palmitic and oleic acids being predominant in the saturated and unsaturated lipids, respectively. Cyclohexylalkanoic acids accounted for 44.1% of this lipid pool, with cyclohexylundecanoic acid (Ch-*n*-11:0) being predominant (35.3% of the lipids). In addition to minute amounts of 3-OH-*n*-12:0, two β-hydroxy acids derived from Ch-C_{13} occurred: 3-hydroxy-cyclohexyltridecanoic acid (3-OH-Ch-*n*-13:0, at a trace level), and 3-hydroxy-cyclohexylundecanoic acid (3-OH-Ch-*n*-11:0, 0.2%) (Table 8). The main alcohol was cyclohexyltridecan-1-ol (Ch-*n*-13:0,1-OH); no secondary alcohol was observed. β-Hydroxy acids constituted 64.4 and 89.8% of the OH^- and H^+ labile lipids, respectively. 3-OH-*n*-12:0 dominated in both cases (Tables 10 and 11); no ω-cyclohexyl β-hydroxy acid was detected.

DISCUSSION

FA composition. This study shows that *M. hydrocarbonoclasticus* is able to use a wide range of hydrocarbons and that its FA profile changes markedly with the chemical structure of the hydrocarbon fed. For instance, the growth on *n*-eicosane induced an almost exclusive production of C_{even} FA, as in most gram-negative bacteria grown on complex media (25). By contrast, on *iso*- or *anteiso*-alkanes, FA profiles became typical of gram-positive bacteria, with high proportions of branched FA (29,30). Such variations in lipid composition emphasize the need for caution when FA are used as taxonomic markers.

Numerous acids identified in the unbound lipids clearly derived from the oxidation of the hydrocarbons fed. Their parity was directed by the hydrocarbon chain length, as has been generally observed in alkane biodegradation under aerobic conditions (6,9,12,31). However, the relationship between *anteiso*-FA and *anteiso*-alkanes was not so clear: The proportion of *anteiso*-C_{odd} FA (mainly *anteiso*-17:0) was 22% of the total *anteiso*-FA in the unbound lipids of the culture on *anteiso*-20:0. Such a discrepancy could result from a regulation process consisting of adapting the FA chain length to the requirement of the bacterium.

The results of this study also show that, in most cases, FA not arising from the direct biodegradation of hydrocarbons are in descending order: *n*-18:1(9*c*) > *n*-16:0 > *n*-16:1(7) + *n*-16:1(9*c*), a distribution similar to that previously reported for the bacterium grown on acetate or on a rich medium (12,14,32). This means that neither the *de novo* synthesis nor the subsequent desaturation of FA were affected by the nature of the carbon source.

Biodegradation pathways. Marinobacter hydrocarbonoclasticus metabolizes hydrocarbons exhibiting aliphatic chains, mainly *via* oxidation of the less hindered terminal methyl group. The primary alcohols arising from oxidation of the *iso* group undergo oxidation and further degradation *via* the β-oxidation pathway, whereas those arising from the oxidation of the *anteiso* group [$HOCH_2CH_2CH(CH_3)$–R] can be degraded only *via* the α-oxidation pathway.

Evidence for metabolism *via* the β-oxidation pathway was provided by the detection of high proportions of saturated and unsaturated *n*-17 FA in the culture on 10-methyl-nonadecane (Table 5). The successive steps of β-oxidation would result in the formation of 2-methyl-undecanoic acid, which in turn is oxidized into *n*-9:0 acid. This acid or a C_{odd} lower homolog could then be taken in the *de novo* synthesis and lead to *n*-17 FA. The inability of the bacterium to grow on Ch-C_{12} could be related to the formation of 2-cyclohexane-acetic acid from a C_{even} cyclohexylalkane during the β-oxidation cycle, an acid generally toxic for bacteria (4).

Subterminal oxidation is a minor route for the biodegradation of the tested hydrocarbons. The derived C_n secondary alcohols were likely oxidized *via* a Bayer–Villiger-type reaction to the corresponding C_{n-2} acids (3), according to the detection of intermediates such as *n*-17:0,1-OH, *i*-18:0,1-OH, and *n*-17:1,1-OH in the cultures on *n*-$C_{19:0}$, *i*-$C_{20:0}$, and *n*-$C_{19:1}$, respectively.

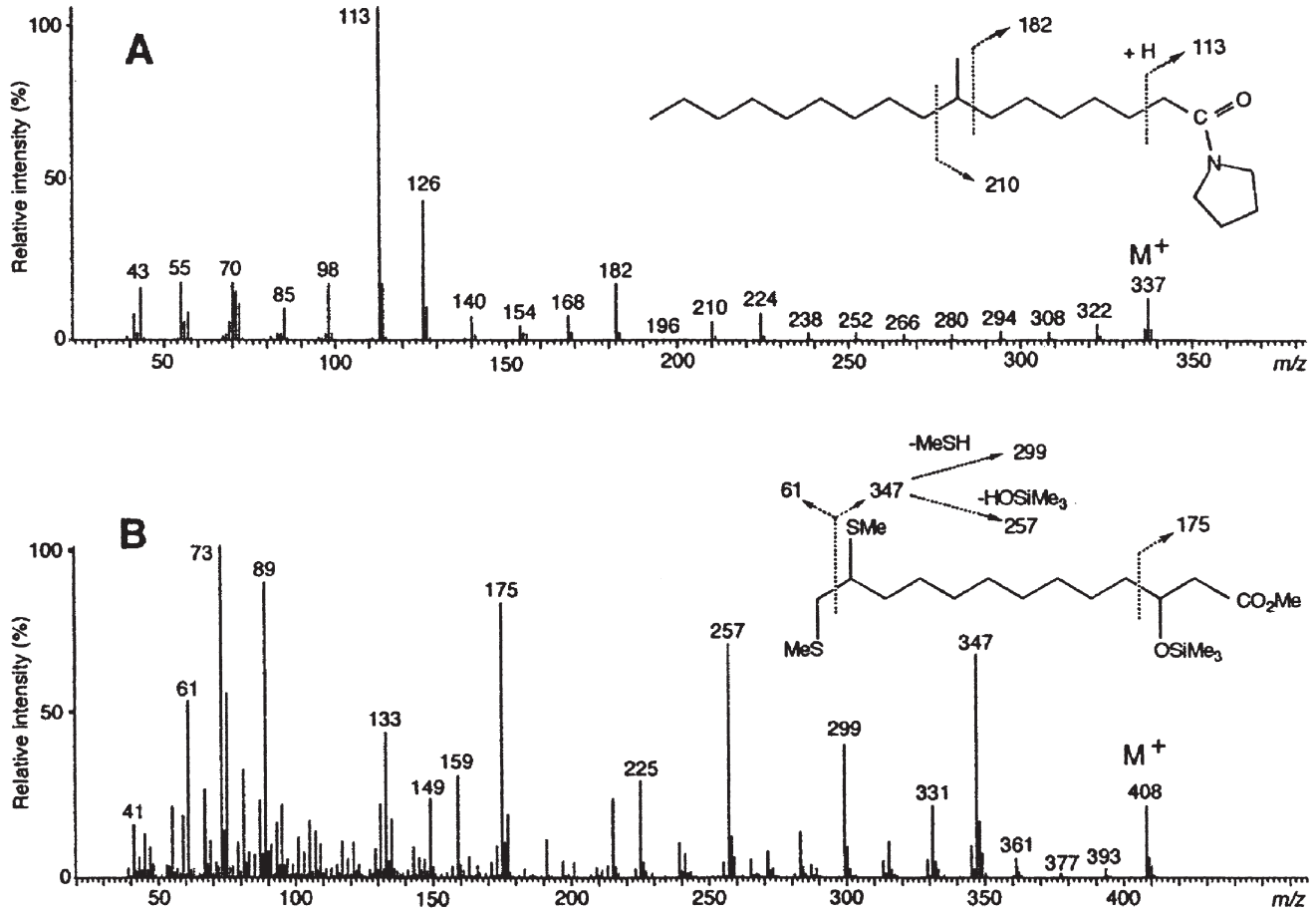

FIG. 1. Mass spectra of the pyrrolidide derivative of 8-methyl-heptadecanoic acid (A) and the 12,13-dimethyl disulfide adduct of the trimethylsilyl ether derivative of 3-hydroxy-tridec-12-enoic acid methyl ester (B).

In the degradation of the terminal olefin *n*-nonadec-1-ene, the identification of *n*-nonadecan-1,2-diol, likely arising from the corresponding epoxide (3), indicated that oxidation of the unsaturation had also occurred (Fig. 3). Oxidation of the diol into 2-hydroxy-*n*-19:0 acid would lead to stearic acid (*n*-18:0 FA) *via* subsequent decarboxylation.

In the present study, α-oxidation of FA appears to be a minor route, with the exception of *anteiso*-eicosane. In this case, the presence of the high amount of *anteiso*-17:0 FA can be explained only by α-oxidation of *anteiso*-18:0 FA.

β-Hydroxy acids. In the unbound lipids, a wide range of β-hydroxy acids was found. They exhibit carbon atom numbers in the range of C_{14}–C_{20}, resulting from the metabolism of the hydrocarbons, and their chemical structures are closely related to those of the hydrocarbons fed. By contrast, the bound β-hydroxy acids have carbon atom numbers in the range of C_{10}–C_{14}, with a maximum at *n*-12:0, as previously observed in cultures on *n*-eicosane, ammonium acetate, 1-chlorooctadecane, or a complex medium (12,14,15). Comparison of the profiles of the bound β-hydroxy acids shows some differences, however. LPS incorporate (i) a high proportion of 3-OH-*n*-13:0 acid in the presence of a C_{odd} *n*-alkane (24 and 35% of the ester- and amide-bound hydroxy acids, respectively), (ii) a similar proportion of ω-unsaturated 3-OH-*n*-13:1(12) acid, as an ester-bound hydroxy acid, in the presence of a terminal *n*-olefin (21%) but not in the amide-bound lipids, and (iii) low amounts of short-chain *iso*- or *anteiso*-β-hydroxy acids (1 to 2% of the ester- and amide-bound hydroxy acids) in the presence of *iso*- and *anteiso*-alkanes. The parities of these β-hydroxy *iso*- and *anteiso*-acids are identical to those of the parent hydrocarbons. The growth on methyl-branched alkanes induces the production of a series of Δ5-unsaturated β-hydroxy acids, *n*-12:1, *n*-13:1, and *n*-14:1, accounting on the whole for 1–2% (*iso*-alkanes) up to 10% (*anteiso*- and mid-chain branched alkanes) of the total β-hydroxy acids. By contrast, β-hydroxy acids from cultures on cyclohexyl- and phenylalkanes exhibited mainly normal saturated hydrocarbon chains. In addition, in a recent work on the degradation of 1-chlorooctadecane by *M. hydrocarbonoclasticus,* we observed that *ca.* 10% of the hydroxy acids in LPS were ω-chlorinated (15). Together, these data suggest that LPS can incorporate nonspecific β-hydroxy acids insofar as their steric hindrance and geometry do not markedly differ from those of the specific β-hydroxy acids synthesized by the bacterium in complex media. Their level of incorporation decreases with the following substituents in the order: CH_3 (ω) > –CH=CH_2 (ω) > Cl (ω) > CH_3 (*iso* or *anteiso*), for ester-bound β-hydroxy acids, and CH_3 (ω) > Cl (ω) > CH_3 (*iso* or

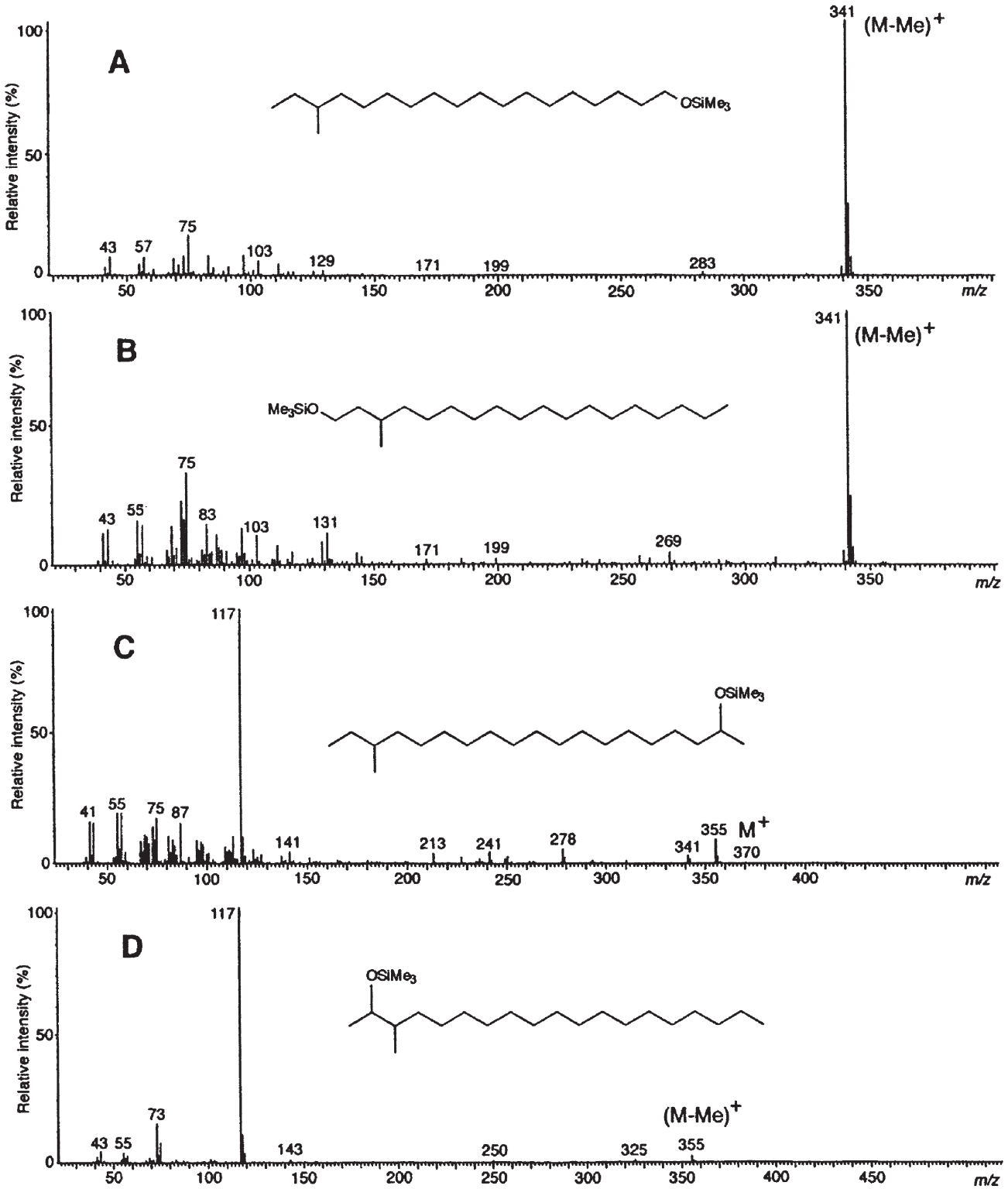

FIG. 2. Mass spectra of trimethylsilyl ether derivatives of *anteiso*-nonadecan-1-ol (A), 3-methyl-octadecan-1-ol (B), *anteiso*-eicosan-2-ol (C), and 3-methyl-nonadecan-2-ol (D).

anteiso), for amide-bound β-hydroxy acids. On the other hand, β-hydroxy acids comprising mid-chain branching or large groups, such as phenyl or cyclohexyl, as well as terminal unsaturation in amide-bound β-hydroxy acids, are prohibited in LPS of *M. hydrocarbonoclasticus*.

β-Hydroxy acids in LPS are attached to a phosphorylated *N*-acetyl glucosamine dimer, forming the lipid A moiety. Most modifications of lipid A are relatively moderate. For instance, from strain to strain they concern the fatty acyl chain length and the number of secondary acyl chains bound to the

TABLE 9
Proportions (wt%) of Unbound Lipids According to the Hydrocarbon Source

	n-19	*n*-20	*i*-19	*i*-20	*a*-19	*a*-20	10-Me-19	*n*-19:1	Ph-C_{12}	Ph-C_{13}
Total FA	90.4	85.4	87.4	92.0	84.1	94.1	96.7	94.1	89.4	90.5
n-FA	86.8	85.4	27.8	20.3	20.9	27.0	58.8	93.7	64.1	64.2
Other FA	3.6	—[a]	59.6	71.6	63.2	67.1	37.9	0.4	25.3	26.3
Total saturated[c]	44.1	29.0	53.9	64.3	68.2	64.7	61.4	19.7	51.4	51.2
Total unsaturated	46.3	56.4	33.5	27.6	15.9	29.4	35.3	74.4	38.0	39.3
Total *n*-16	5.5	50.4	6.5	3.9	5.2	4.4	13.2	18.0	19.8	20.8
Total *n*-17	54.7	0.4	1.4	2.9	2.3	2.3	21.8	39.2	1.1	0.2
Total *n*-18	11.8	28.1	19.2	12.5	12.1	17.8	19.6	14.9	42.2	40.5
Total hydroxy acids	0.9	2.2	4.1	1.8	1.7	0.1	0.6	0.7	0.5	0.7
Total fatty alcohols	6.5	11.6	8.2	3.9	10.4	3.5	1.4	4.0	8.0	7.5
n-Fatty alcohols	6.5	11.6	0.4	0.4	1.1	0.2	Trace	4.0	0.3	0.9
Other fatty alcohols	—	—	7.8	3.5	9.3	3.3	0.9	—	7.7	6.6

[a]—, not detected.
[b]Including some branched FA.
[c]Compounds comprising a saturated aliphatic hydrocarbon chain. For abbreviations see Table 1.

TABLE 10
Proportions (wt%) of OH^- Labile Lipids According to the Hydrocarbon Source

	n-19	*n*-20	*i*-19	*i*-20	*a*-19	*a*-20	10-Me-19	*n*-19:1	Ph-C_{12}	Ph-C_{13}
Total FA	70.8	71.3	42.4	32.4	42.0	30.0	48.5	25.8	48.2	47.5
n-FA	69.0	71.3	21.9	18.1	19.3	13.0	27.5	25.8	43.6	41.3
Other FA	1.8	—[a]	20.5	14.3	22.7	17.0	21.0	—	4.6	6.2
Total hydroxy acids	27.6	28.3	55.6	62.9	53.9	65.6	47.9	71.9	48.4	47.8
% of β-OH *n*-12:0	58	99	91	71	68	82	66	70	99	97
Total fatty alcohols	0.6	—	0.5	0.6	0.7	1.8	0.2	1.5	0.5	0.7

[a]—, not detected. For abbreviations see Table 1.

TABLE 11
Proportions (wt%) of H^+ Labile Lipids According to the Hydrocarbon Source

	n-19	*n*-20	*i*-19	*i*-20	*a*-19	*a*-20	10-Me-19	*n*-19:1	Ph-C12	Ph-C13
Total FA	24.5	1.0	3.3	13.2	7.0	18.1	4.6	4.6	8.0	28.3
n-FA	24.5	1.0	2.9	12.5	5.7	10.0	4.6	4.6	7.9	25.2
Other FA	—[a]	—	0.4	0.7	1.3	8.1	—	—	0.1	3.1
Total hydroxy acids	64.3	98.3	97.7	81.9	90.0	78.1	91.2	92.4	87.3	59.0
% of β-OH *n*-12:0	60	99	90	84	73	80	78	93	97	99
Total fatty alcohols	6.1	—	1.0	1.6	0.8	1.8	1.6	2.2	0.4	5.0

[a]—, not detected. For abbreviations see Table 1.

3-hydroxy acid (25). During the last decade, it was shown that the nature of hydroxy acids is determined by the very high specificity of the acyl-carrier protein enzymes responsible for the *O*-acyl and *N*-acyl transfers in lipid A biosynthesis (33–35). The present study provides new insight into the incorporation of some nonspecific β-hydroxy acids into LPS of a hydrocarbonoclastic bacterium.

ACKNOWLEDGMENTS

The authors thank Dr. M. Acquaviva and Pr. J.-C. Bertrand, Centre d'Océanographie de Marseille, for their valuable advice on the culture of bacteria on hydrocarbons.

REFERENCES

1. Klug, M.J., and Markovetz, A.J. (1971) Utilization of Aliphatic Hydrocarbons by Micro-organisms, *Adv. Microbial Physiol. 5,* 1–43.
2. The National Academies (2003) *Oil in the Sea. III. Input, Fates, and Effects*, The National Academies Press, Washington, DC.
3. Ratledge, C. (1978) Degradation of Aliphatic Hydrocarbons, in *Developments in Biodegradation of Hydrocarbons* (Watkinson, R.J., ed.), Vol. 1, pp. 1–46, Applied Science, London.
4. Trudgill, P.W. (1978) Microbial Degradation of Alicyclic Hydrocarbons, in *Developments in Biodegradation of Hydrocarbons* (Watkinson, R.J., ed.), Vol. 1, pp. 47–84, Applied Science, London.
5. Hopper, D.J. (1978) Microbial Degradation of Aromatic Hydrocarbons, in *Developments in Biodegradation of Hydrocarbons*

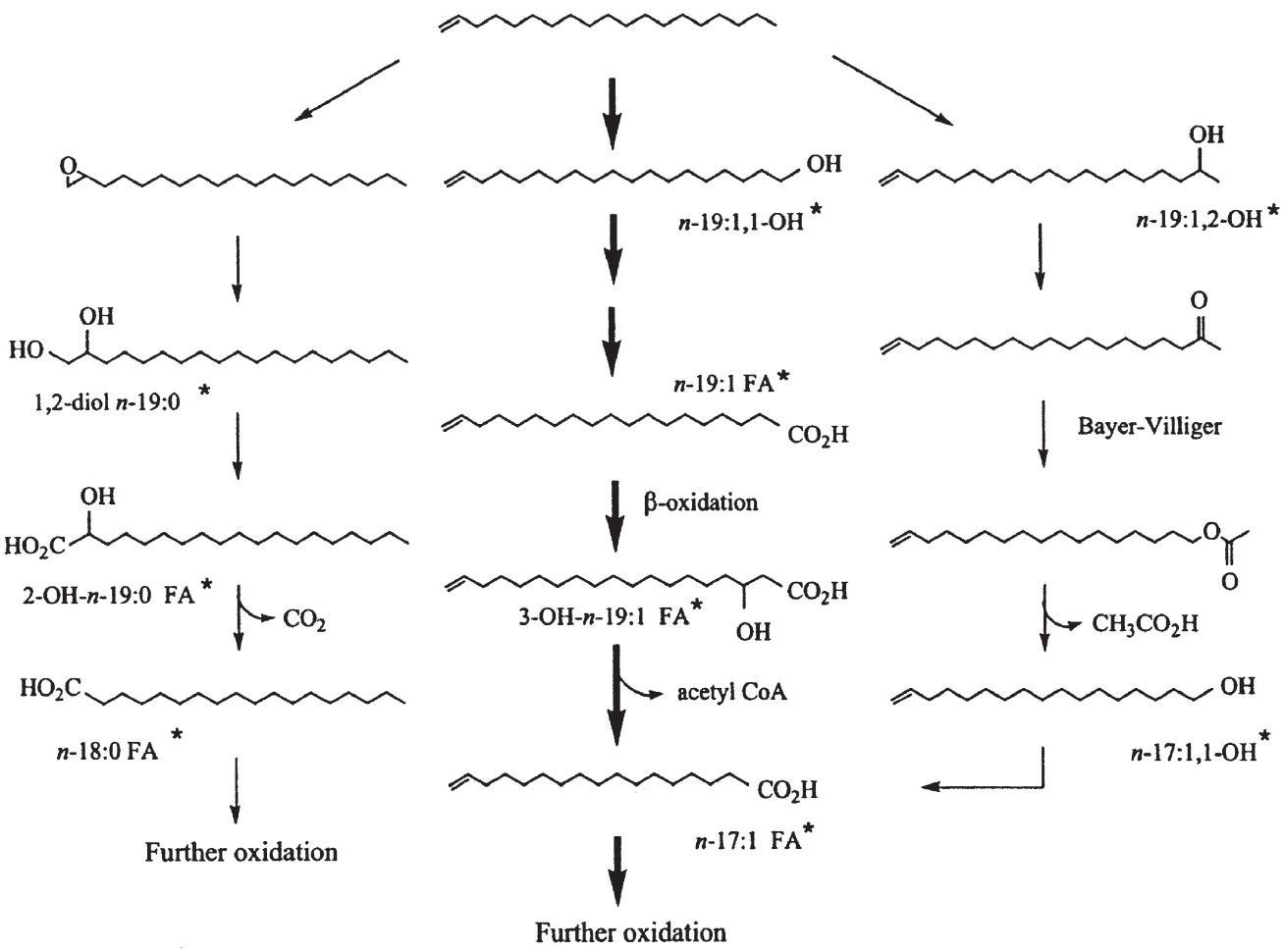

FIG. 3. Metabolic pathways of *n*-nonadec-1-ene in *Marinobacter hydrocarbonoclasticus.* Compounds identified in the lipid extracts are indicated by an asterisk (*). The predominant pathway is shown by arrows in bold.

(Watkinson, R.J., ed.), Vol. 1, pp. 85–112, Applied Science, London.
6. Rehm, H.J., and Reiff, I. (1981) Mechanism and Occurrence of Microbial Oxidation of Long-Chain Alkanes, *Adv. Biochem. Eng. 19,* 173–215.
7. Makula, R., and Finnerty, W.R. (1968) Microbial Assimilation of Hydrocarbons. I. Fatty Acids Derived from Normal Alkanes, *J. Bacteriol. 95,* 2102–2107.
8. Makula, R., and Finnerty, W.R. (1968) Microbial Assimilation of Hydrocarbons. II. Fatty Acids Derived from 1-Alkenes, *J. Bacteriol. 95,* 2108–2111.
9. King, D.H., and Perry, J.J. (1975) The Origin of Fatty Acids in the Hydrocarbon Utilizing Microorganism *Mycobacterium vaccae, Can. J. Microbiol. 21,* 85–89.
10. Doumenq, P., Acquaviva, M., Asia, L., Durbec, J.C., Le Dréau, Y., Mille, G., and Bertrand, J.-C. (1999) Changes in Fatty Acids of *Pseudomonas nautica*, a Marine Denitrifying Bacterium, in Response to *n*-Eicosane as Carbon Source and Various Culture Conditions, *FEMS Microbiol. Ecol. 28,* 151–161.
11. Aries, E., Doumenq, P., Artaud, J., Acquaviva, M., and Bertrand, J.-C. (2001) Effects of Petroleum Hydrocarbons on the Phospholipid Fatty Acid Composition of a Consortium Composed of Marine Hydrocarbon-Degrading Bacteria, *Org. Geochem. 32,* 891–903.
12. Doumenq, P., Aries, E., Asia, L., Acquaviva, M., Artaud, J., Gilewicz, M., Mille, G., and Bertrand, J.-C. (2001) Influence of *n*-Alkanes and Petroleum on the Fatty Acid Composition of a Hydrocarbonoclastic Bacterium: *Marinobacter hydrocarbonoclasticus* Strain 617, *Chemosphere 44,* 519–528.
13. Gauthier, M.J., Lafay, B., Christen, R., Fernandez, L., Aquaviva, M., Bonin, P., and Bertrand, J.-C. (1992) *Marinobacter hydrocarbonoclasticus* gen. nov., sp. nov., a New, Extremely Halotolerant, Hydrocarbon-Degrading Marine Bacterium, *Int. J. Syst. Bacteriol. 42,* 568–576.
14. Lattuati, A., Metzger, P., Acquaviva, M., Bertrand, J.-C., and Largeau, C. (2002) *n*-Alkane Degradation by *Marinobacter hydrocarbonoclasticus* SP 17: Long Chain β-Hydroxy Acids as Indicators of Bacterial Activity, *Org. Geochem. 33,* 37–45.
15. Aubert, E., Metzger, P., and Largeau, C. (2004) Incorporation of 1-Chlorooctadecane into FA and β-Hydroxy Acids of *Marinobacter hydrocarbonoclasticus, Lipids 39,* 81–85.
16. Mendoza, Y.A., Gülçar, F.O., and Buchs, A. (1987) Comparison of Extraction Techniques for Bound Carboxylic Acids in Recent Sediments. 2. β-Hydroxy Acids, *Chem. Geol. 62,* 321–330.
17. Goossens, H., Düren, R.R., de Leeuw, J.W., and Schenck, P.A. (1989) Lipids and Their Mode of Occurrence in Bacteria and Sediments—II. Lipids in the Sediment of a Stratified, Freshwater Lake, *Org. Geochem. 14,* 27–41.
18. Zegouagh, Y., Derenne, S., Largeau, C., and Saliot, A. (1996) Organic Matter Sources and Early Diagenetic Alterations in Arctic Surface Sediments (Lena River Delta and Laptev Sea, Eastern Siberia)—I. Analysis of the Carboxylic Acids Released *via* Sequential Treatments, *Org. Geochem. 24,* 841–857.
19. Wakeham, S.G. (1999) Monocarboxylic, Dicarboxylic and Hydroxy

Acids Released by Sequential Treatments of Suspended Particles and Sediments of the Black Sea, *Org. Geochem. 30,* 1059–1074.
20. Wakeham, S.G., Pease, T.K., and Benner, R. (2003) Hydroxy Fatty Acids in Marine Dissolved Organic Matter as Indicators of Bacterial Membrane Material, *Org. Geochem. 34,* 857–868.
21. Kates, M. (1986) *Techniques of Lipidology,* 2nd edn., p. 192, Elsevier, Amsterdam.
22. Kates, M. (1986) *Techniques of Lipidology*, 2nd edn., pp. 344–345, Elsevier, Amsterdam.
23. Scribe, P., Pepe, C., Barouxis, A., Fuche, C., Dugant, J., and Saliot, A. (1990) Détermination de la Position de l'Insaturation des Monoènes par Chromatographie en Phase Gazeuse Capillaire–Spectrometrie de Masse des Dérivés Dimethyl-Disulfures: Application à l'Analyse d'un Mélange Complexe d'Alcènes, *Analusis 18,* 284–288.
24. Anderson, B.A., and Holman, R.T. (1974) Pyrrolidides for Mass Spectrometric Determination of the Position of the Double Bond in Monounsaturated Fatty Acids, *Lipids 9,* 185–190.
25. Wilkinson, S.G. (1988) Gram-Negative Bacteria, in *Microbial Lipids* (Ratledge, C., and Wilkinson, S.G., eds.), Vol. 1, pp. 299–488, Academic Press, London.
26. Goossens, H., de Leeuw, J.W., Rijpstra, W.I.C., Meyburg, G.J., and Schenk, P.A. (1989) Lipids and Their Mode of Occurrence in Bacteria and Sediments: I. A Methodological Study of the Lipid Composition of *Acinetobacter calcoaceticus* LMD 79-41, *Org. Geochem. 14,* 15–25.
27. Schmid, P.C., Holman, R.T., and Soukup, V.G. (1997) 13-Phenyltridecanoic Acid in Seed Lipids of Some Aroids, *Phytochemistry 45,* 1173–1175.
28. Lipid Analysis Unit, http://www.lipid.co.uk/infoes/masspec.html (accessed January 2004).
29. O'Leary, W.M., and Wilkinson, S.G. (1988) Gram-Positive Bacteria, in *Microbial Lipids* (Ratledge, C., and Wilkinson, S.G., eds.), Vol. 1, pp. 117–201, Academic Press, London.
30. Kaneda, T. (1991) *Iso-* and *anteiso*-Fatty Acids in Bacteria: Biosynthesis, Function, and Taxonomic Significance, *Microbiol. Rev. 55,* 288–302.
31. Alvarez, H.M. (2003) Relationship Between β-Oxidation Pathway and the Hydrocarbon-Degrading Profile in Actinomycetes Bacteria, *Int. Biodeterior. Biodegrad. 52,* 35–42.
32. Huu, N.B., Denner, E.B.M., Ha, D.T.C., Wanner, G., and Stan-Lotter, H. (1999) *Marinobacter aquaeolei* sp. nov., a Halophilic Bacterium Isolated from a Vietnamese Oil-Producing Well, *Int. J. Syst. Bacteriol. 49,* 367–375.
33. Williamson, J.M., Anderson, M.S., and Raetz, R.H. (1991) Acyl–Acyl Carrier Protein Specificity of UPD-GlcNAc Acyltransferases from Gram-Negative Bacteria: Relationship to Lipid A Structure, *J. Bacteriol. 173,* 3591–3596.
34. Wyckohh, T.J.O., Lin, S., Cotter, R.J., Dotson, G.D., and Raetz, C.R.H. (1998) Hydrocarbon Rulers in UDP-*N*-acetylglucosamine Acyltransferases, *J. Biol. Chem. 273,* 32369–32372.
35. Sweet, C.R., Preston, A., Tolands, E., Ramirez, S.M., Cotter, R.J., Maskell, D.J., and Raetz, C.R.H. (2002) Relaxed Acyl Chain Specificity of *Bordetella* UDP-*N*-acetylglucosamine Acyltransferases, *J. Biol. Chem. 277,* 18281–18290.

[Received March 16, 2004; accepted July 30, 2004]

METHOD

New Approach to the Analysis of Oxidized Triacylglycerols in Lipoproteins

Jukka-Pekka Suomela[a,*], Markku Ahotupa[b], Olli Sjövall[a], Juha-Pekka Kurvinen[a], and Heikki Kallio[a]

[a]Department of Biochemistry and Food Chemistry and [b]MCA Research Laboratory, Department of Physiology, University of Turku, FIN-20014 Turku, Finland

ABSTRACT: The oxidation of human LDL lipids and the structures of oxidized TAG molecules found in LDL were investigated. Pooled samples of 10 normolipidemic and 10 hyperlipidemic subjects were analyzed. For determination of the oxidation levels, the LDL baseline diene conjugation (LDL-BDC) method was used. A method based on HPLC and electrospray ionization-MS was optimized and applied to the analysis of molecular structures of oxidized TAG in LDL. Differences were found between the oxidation levels of the samples. The LDL-BDC value was 22.2 μmol/L serum in the normolipidemic group, and 88.1 μmol/L serum in the hyperlipidemic group. The amounts of oxidized TAG molecules were small. However, several species of oxidized TAG were identified. These included TAG molecules with a keto or an epoxy group attached to a FA, and TAG molecules with a FA core aldehyde. In some TAG, the keto/epoxy ratio was greater in the hyperlipidemic group compared to the normolipidemic group. The results show that our approach is applicable to research on lipid oxidation in lipoproteins.

Paper no. L9352 in *Lipids 39*, 507–512 (May 2004).

During the last decade, evidence has accumulated on the role of LDL in the development of atherosclerosis. Studies suggest that the ultimate atherogenic agents are the modified, mainly oxidized, forms of LDL (1–5). Most of the theories and speculations concerning LDL oxidation and its role in atherosclerosis have been based on the assumption that oxidation of LDL is exclusively of endogenous origin. However, some studies have shown that the oxidation of dietary lipids is reflected in the degree of oxidation of chylomicrons and VLDL (6,7).

At present, there are few methods for direct measurement of the lipoprotein oxidation level. Estimation of *in vivo* LDL oxidation has been based largely on the determination of autoantibodies to oxidized LDL (8). A novel method, LDL baseline diene conjugation (LDL-BDC), has been developed for fast measurement of oxidized LDL in human blood samples (8–10). Implications of LDL-BDC in human atherosclerosis, as well as relationships between LDL-BDC and various risk factors, have been investigated in recent studies (10–12).

Because the diet may contribute to the burden of oxidized lipids in plasma lipoproteins, it is worthwhile to investigate the link between oxidized dietary lipids and the oxidation of lipoproteins. However, only a few species of oxidized lipids in lipoproteins have been studied. These are mainly cholesteryl esters and glycerophospholipids (13–15). To our knowledge, the structures of oxidized TAG molecules of lipoproteins have not been identified earlier, although they also may have an important role in lipoprotein oxidation (16) and are thus an interesting object of investigation.

Nonvolatile autoxidation products of TAG have a hydroperoxy, hydroxy, epoxy, or oxo (aldehyde or ketone) group(s) or a combination of these groups attached to the TAG molecule. Some studies have been performed on the structures of oxidized TAG. The research group of Steenhorst-Slikkerveer (17) has used normal-phase HPLC to analyze oxidation products of vegetable oils. Byrdwell and Neff (18–20) have investigated nonvolatile autoxidation products of TAG using RP-HPLC combined with atmospheric-pressure chemical ionization-MS (APCI-MS) or electrospray ionization-MS (ESI-MS). These researchers have detected several hydroperoxide, epoxide, and ketone structures. Sjövall *et al.* (21) determined elution factors of synthetic, oxidized TAG for RP-HPLC. For the detection of molecular ions, the researchers used ESI-MS. The elution factors of oxidized TAG were obtained by plotting the retention times of the compounds against the theoretical carbon number. With the help of the elution factors, a curve-fitting procedure could be applied to different compounds to identify them (21).

The current study is partly based on the results of Sjövall *et al*. (21). The HPLC-ESI-MS method used by the group was optimized and applied to the analysis of oxidized TAG molecular structures of human LDL samples. The LDL-BDC method was used to evaluate the oxidation levels of the samples.

MATERIALS AND METHODS

Chemicals and reagents. 3-Chloroperoxybenzoic acid, triphenyl phosphine (TPP), and activated manganese dioxide (MnO_2) were obtained from Aldrich Chemical Co. (Milwaukee, WI) and 2,4-dinitrophenylhydrazine (DNPH) from Sigma Chemical Co. (St. Louis, MO). Reagents were of reagent grade quality or better. All solvents were of chromatography or reagent grade and were purchased from local suppliers. Synthetic saturated monoacid TAG were included in the HPLC standard (G-1) obtained from Nu-Chek-Prep, Inc. (Elysian, MN). Synthetic 1,3-distearoyl-2-oleoyl-*sn*-glycerol was obtained from Sigma Chemical Co. 1,3-Didocosanoyl-2-oleoyl-

*To whom correspondence should be addressed. E-mail: jusuom@utu.fi

Abbreviations: BDC, baseline diene conjugation; DNPH, dinitrophenyl hydrazine; ESI, electrospray ionization; TPP, triphenyl phosphine.

sn-glycerol and 1-linoleoyl-2-oleoyl-3-palmitoyl-*sn*-glycerol were obtained from Larodan Fine Chemicals AB (Malmö, Sweden).

Preparation of reference compounds. The synthetic TAG, along with their oxidized derivatives prepared in this study, are listed in Table 1. Core aldehyde standards (IIa, IIb, IVa, Vc, Vd, VIc, VId) were obtained by TPP reduction of ozonides (22). TAG (5–40 mg) was dissolved in 4 mL of hexane and ozonized for 40 min in an ice bath. After the solvent was removed by blowing N_2 across the solution, the ozonides were dissolved in 4 mL of chloroform and reduced to aldehydes by reacting with 25–50 mg of TPP for 1 h at room temperature. The aldehydes were purified by TLC as described below, and part of them were converted into DNPH derivatives (IIb, IVa, Vd, VId) by treating with 1–4 mL of DNPH reagent (1 mg DNPH in 2 mL of 1 M HCl) at 60°C for 30 min (23). The DNPH derivatives were extracted from the solution with chloroform/methanol (2:1, vol/vol).

Epoxides (Ia, IIIa, Va, VIa) were prepared by the method of Deffense (24). A sample of 2–5 mg of TAG was oxidized with 4–10 mg of 3-chloroperoxybenzoic acid in 400 μL of dichloromethane at room temperature for 1–2 h followed by purification using TLC as described below.

Hydroperoxides (Ib, IIIb, IIIc, Vb, VIb) were prepared by photo-oxidation (25). TAG (10–20) was added to 3 mL of methylene blue solution (0.1 mM of methylene blue in dichloromethane) in a test tube that was placed in an ice bath under a 250-W photographer's lamp. The distance between the sample solution and the lamp was 20 cm. Hydroperoxides were purified by TLC as described below.

For the preparation of hydroxides (Ic, VIe), 1 mg of hydroperoxide was dissolved in 2 mL of chloroform and reduced to hydroxide by reacting with 15–20 mg of TPP for 1 h at room temperature (26). The hydroxy compounds were purified by TLC as described below.

Ketone standards (Id, VIf) were prepared by oxidizing the corresponding hydroxides with activated manganese dioxide (27). The hydroxide (0.3 mg) was dissolved in 0.5 mL of chloroform. The solution and 50 mg manganese dioxide were transferred to a test tube, which was placed in a shaker. Reaction was allowed to take place for 6 d at 37°C (Id) or for 3.25 h at 60°C (VIf) .

Purification of TAG and their oxidation products. Normal-phase TLC was used to purify TAG and their derivatives (28). Heptane/di-isopropyl ether/acetic acid (60:40:4, by vol) solution was used as the mobile eluent. Samples were applied to silica G-plates. Resolved components were scraped off the plates and were recovered from the silica gel by extraction with chloroform/methanol (2:1, vol/vol). When TLC was used to separate the LDL lipid samples, the fraction below the TAG band, which contained the oxidized TAG molecules, was scraped from the plate (21). The extracts were washed with distilled water. TAG and their hydroxy, hydroperoxy, keto, and epoxy derivatives were detected in UV light after spraying with 2,7-dichlorofluorescein. Core aldehydes showed a purple color with a Schiff base reagent (28).

Derivatization of LDL-TAG core aldehydes. To derivatize the TAG core aldehydes of LDL, part of the oxidized TAG of the LDL samples was allowed to react with DNPH as described for the reference compounds, the exception being that the reaction took place at 6°C overnight.

Samples. Two pooled serum samples each from 10 subjects of various ages were collected. In regard to total cholesterol level, one of the groups (group 1) consisted of normolipidemic subjects (close to the lower limit of normal range) and the other (group 2) of hyperlipidemic subjects. Blood samples were obtained by venipuncture after an overnight fast. Serum was separated from cells by centrifugation at $3000 \times g$ for 15 min. LDL was precipitated by buffered heparin as described earlier (11). LDL was suspended in 1.15% sodium chloride solution, and total lipids were extracted from LDL using chloroform/methanol (2:1, vol/vol). Lipid classes were separated from each other using the TLC system described above.

Determination of the oxidation level of LDL. For estimation of LDL oxidation by the baseline level of diene conjugation in LDL, part of the total lipid extract was dissolved in cyclohexane and analyzed spectrophotometrically at 234 nm. Absorbance units were converted to molar units using the molar extinction coefficient $2.95 \times 10^4\ M^{-1}\ cm^{-1}$ (11).

FA analysis of sample TAG. The FAME of TAG were prepared by sodium methoxide-catalyzed transesterification (29). Methyl esters were dissolved in hexane and analyzed by GC (Perkin-Elmer AutoSystem, Norwalk, CT) using a DB-23 column (30 m

TABLE 1
Reference Compounds Used in the Study[a]

Number	TAG[b]	Number	Derivatized TAG[b]
I	18:0-18:1-18:0	Ia	18:0-18:1 epoxy[c]-18:0
		Ib	18:0-18:1 OOH-18:0
		Ic	18:0-18:1 OH-18:0
		Id	18:0-18:1 keto-18:0
II	18:1-18:0-18:0	IIa	9:0 ALD-18:0-18:0
		IIb	9:0 ALD-18:0-18:0 DNPH
III	18:1-18:1-18:0	IIIa	18:1-18:1-18:0 diepoxy[c]
		IIIb	18:1 OOH-18:1-18:0
		IIIc	18:1 OOH-18:1 OOH-18:0
IV	18:2-18:1-16:0	IVa	9:0 ALD-9:0 ALD-16:0 di-DNPH
V	18:0-18:2-18:0	Va	18:0-18:2 diepoxy[c]-18:0
		Vb	18:0-18:2 OOH-18:0
		Vc	18:0-9:0 ALD-18:0
		Vd	18:0-9:0 ALD-18:0 DNPH
VI	22:0-18:1-22:0	VIa	22:0-18:1 epoxy[c]-22:0
		VIb	22:0-18:1 OOH-22:0
		VIc	22:0-9:0 ALD-22:0
		VId	22:0-9:0 ALD-22:0 DNPH
		VIe	22:0-18:1 OH-22:0
		VIf	22:0-18:1 keto-22:0
VII	Series of saturated TAG (24:0–54:0)		

[a]ALD, aldehyde; DNPH, 2,4-dinitrophenylhydrazone.
[b]Regioisomers (*sn*-1 and *sn*-3 positions not distinguished from each other).
[c]Position of an epoxy group has been marked as an underlined double bond.

× 0.32 mm i.d., 0.25 μm film thickness; Agilent Technologies, Palo Alto, CA). The instrument was equipped with an FID.

Analysis of samples by HPLC-UV/ELSD and HPLC-ESI-MS. TAG and their oxidation products were separated by RP-HPLC. The HPLC system consisted of a Hitachi (Tokyo, Japan) L-6200 Intelligent Pump with a Discovery® HS C18 column (250 × 4.6 mm i.d.; Supelco Inc., Bellefonte, PA). The column was eluted at 0.85 mL/min, and a linear gradient was used: 20% 2-propanol in methanol was changed to 80% 2-propanol in 20 min. The final composition was held for 10 min. Eighty-five percent of the effluent (0.72 mL/min) was led to a Sedex 75 (S.E.D.E.R.E., Alfortville, France) ELSD through a Shimadzu (Kyoto, Japan) SPD-6AV UV/vis detector that was used for the analysis of DNPH derivatives of core aldehydes at 358 nm. An evaporation temperature of 70°C and nebulizer gas (air) pressure of 2.7 bar were used in the ELSD. Fifteen percent of the effluent (0.13 mL/min) was led to a Finnigan MAT TSQ 700 triple quadrupole mass spectrometer (Finnigan, San Jose, CA) equipped with a nebulizer-assisted electrospray interface. As a sheath liquid, 1% ammonia in methanol was added at a flow rate of 3 μL/min to improve ionization. Full-scan MS spectra were collected in negative (*m/z* 600–1200) and positive (*m/z* 450–1100) ionization mode.

Statistical analysis. SPSS 10.0 for Windows (Chicago, IL) was used for data analysis. The comparison of FA compositions was carried out with independent samples *t*-tests.

RESULTS AND DISCUSSION

LDL-BDC values of the samples were 22.2 and 88.1 μmol/L for groups 1 and 2, respectively. Thus, the serum of group 2 contained more conjugated dienes in LDL lipids than the serum of group 1. It is important to notice that the lipid content of LDL of group 2 was over twice that of group 1 (7.1 vs. 3.1 mg/mL serum). The molar proportion of conjugated dienes in the LDL lipids of group 2 was therefore 1.7 times higher than in the LDL lipids of group 1. Physiologically this is probably not particularly important, yet it is noteworthy during sample preparation and analysis.

FA compositions of the TAG of LDL of the two groups are listed in Table 2. Normolipidemic subjects had more 18:1n-9 (oleic acid), 18:2n-6 (linoleic acid), 18:3n-3 (α-linolenic acid) and 18:3n-6 (γ-linolenic acid) and less 14:0 (myristic acid), 16:0 (palmitic acid), and 16:1n-7 (palmitoleic acid) in their LDL-TAG than did hyperlipidemic subjects. The results were anticipated owing to generally poorer dietary habits of hyperlipidemic subjects.

The retention times obtained with the present HPLC column were longer than those with the column used by Sjövall *et al.* (21). This is why the linear gradient was changed from the original 30 min to 20 min. Despite the change, the standard curve made with a series of saturated TAG (G-1) was linear between 10 and 30 min. The validity of the elution factors determined by Sjövall *et al.* for the present column and gradient program was tested with TAG of different molecular species and with core aldehyde, hydroperoxide, hydroxide, and epoxide reference compounds (Table 1). Based on these results, the conclusion was drawn that the elution factors could be applied to the present column as such.

TABLE 2
FA Composition of LDL TAG of Groups 1 (normolipidemic) and 2 (hyperlipidemic)[a]

FA	Group 1	Group 2
14:0	2.0 ± 0.14[b]	3.5 ± 0.02[c]
14:1n-5	0.2 ± 0.0	0.4 ± 0.0
15:0	0.3 ± 0.00[b]	0.4 ± 0.00[c]
16:0	25.7 ± 0.32[b]	30.5 ± 0.04[c]
16:1n-7	3.8 ± 0.02[b]	5.9 ± 0.04[c]
17:0	0.3 ± 0.02[b]	0.5 ± 0.00[c]
18:0	3.6 ± 0.1	4.0 ± 0.0
18:1n-9	41.7 ± 0.4	39.8 ± 0.0
18:1n-7	3.1 ± 0.02[b]	2.6 ± 0.02[c]
18:2n-6	14.2 ± 0.23[b]	9.3 ± 0.03[c]
18:3n-6	0.3 ± 0.00[b]	0.2 ± 0.00[c]
18:3n-3	1.6 ± 0.02[b]	1.1 ± 0.01[c]
20:1n-9	0.6 ± 0.2	0.3 ± 0.0
20:4n-6	1.2 ± 0.1	0.7 ± 0.0
20:5n-3	0.6 ± 0.2	0.3 ± 0.0
22:6n-3	1.0 ± 0.2	0.6 ± 0.0

[a]Results are expressed as percentage of total FA, mean ± SD ($n = 2$; same samples analyzed twice). Different superscript roman letters indicate significant differences between groups ($P < 0.05$).

Some oxidation products of TAG could be detected from the TLC fraction below the TAG band. The oxidized structures were found by extracting peaks of a specific *m/z* value from MS chromatograms (Fig. 1). Only $[M + Na]^+$ ions were formed from molecules other than DNPH derivatives, which were seen as $[M - H]^-$ ions. This simplified identification. If the retention time for a peak of an *m/z* value suggested a certain type of oxidation product and a particular FA composition, and a homologous series of ions was found in the chromatogram, this was regarded as strong evidence of a specific molecular structure. Our HPLC method makes it possible to distinguish between oxidized FA that are in the *sn*-1/3 position and those that are in the *sn*-2 position (21). However, this was not possible in the present study owing to the low intensity of the peaks in the MS chromatograms. Thus, the molecular structures of oxidized TAG described below do not denote regioisomers.

Because of the small amounts of oxidation products, no quantification could be made. In ELSD chromatograms, no proper peaks were found for oxidized TAG molecules. Likewise, no quantification could be made based on UV or MS chromatograms. In an ELSD chromatogram, a peak became visible when approximately 40 ng oxidized TAG reference compound was injected into the column. Based on this, it was estimated that, on the average, at most 20 ng/mL of nonvolatile oxidation products of LDL-TAG occurred in the serum of the subjects.

Oxidation had occurred in only one of the FA of a TAG molecule in those oxidation products that were detected. These products consisted of TAG molecules with a hydroxy (uncertain), keto, or epoxy group attached to a FA, or of TAG molecules with a FA core aldehyde. The postulated molecular

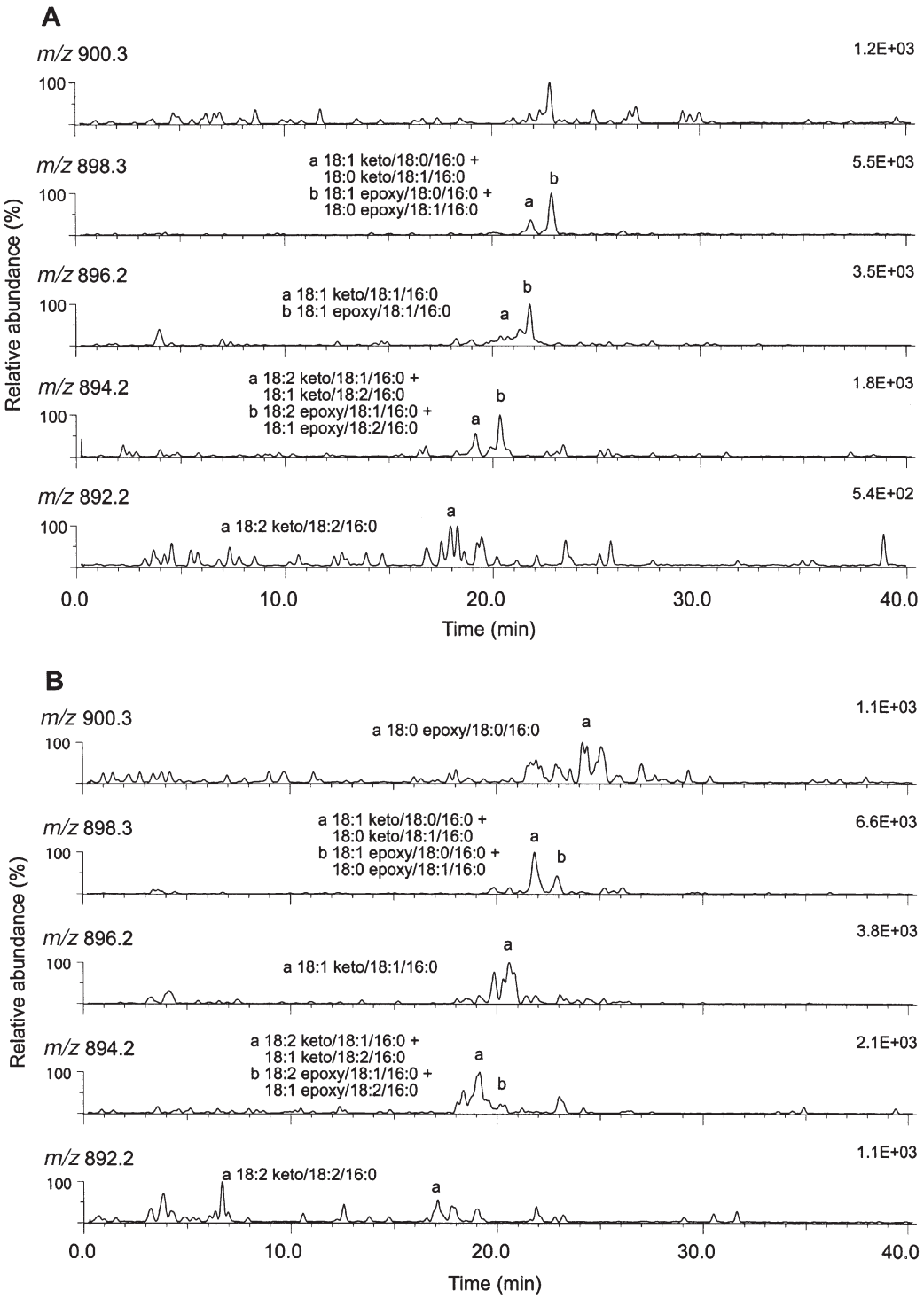

FIG 1. Ion chromatograms showing the oxidized TAG molecules of 52 acyl carbons with a ketone or an epoxy group attached to a FA. Postulated molecular structures (not regioisomers) are included in the chromatograms. The mass calibration of the instrument was made using *m/z* values 0.5 units higher than the calculated isotopic masses; the ions have been detected accordingly. (A) Normolipidemic subjects. (B) Hyperlipidemic subjects.

structures of these products are listed in Table 3. No retention factors were determined earlier for ketone compounds. Thus, the postulated presence of ketones based on the extracted peaks in the MS chromatograms (Fig. 1) had to be confirmed. For this purpose we prepared reference compounds (Table 1). The retention times of the postulated ketone peaks were compared to the retention times of the reference compounds. Based on the results, the presence of TAG molecules with a ketone group in

TABLE 3
Postulated Structures of the Oxidized TAG Molecules Found in the LDL Samples[a]

ACN[b]	Ketones	Epoxides	Aldehydes	Hydroxides
48	16:1 keto/16:1/16:0			
	16:1 keto/16:0/16:0			
	16:0 keto/16:0/16:0			
50	18:2 keto/16:0/16:0	18:0 epoxy/16:0/16:0	9:0 ALD/16:0/16:0	
	18:1 keto/16:0/16:0			
	18:0 keto/16:0/16:0			
52	18:2 keto/18:2/16:0	18:2 epoxy/18:1/16:0	9:0 ALD/18:2/16:0	18:1 OH/18:1/16:0[d]
	18:2 keto/18:1/16:0	18:1 epoxy/18:2/16:0	9:0 ALD/18:1/16:0	
	18:1 keto/18:2/16:0	18:1 epoxy/18:1/16:0[c]		
	18:1 keto/18:1/16:0	18:1 epoxy/18:0/16:0		
	18:1 keto/18:0/16:0	18:0 epoxy/18:1/16:0		
	18:0 keto/18:1/16:0	18:0 epoxy/18:0/16:0[c]		
54	18:2 keto/18:1/18:1	18:1 epoxy/18:0/18:1	9:0 ALD/18:1/18:1	
	18:1 keto/18:2/18:1	18:0 epoxy/18:1/18:1		
	18:1 keto/18:1/18:1			
	18:1 keto/18:1/18:0			

[a]The most probable molecular structures, presented here, are on *m/z* values, TAG FA compositions, and the assumption that the most unsaturated FA is oxidized; regioisomers are not distinguished.
[b]Acyl carbon number of the original TAG molecule.
[c]Only in group 1 (normolipidemic subjects).
[d]Uncertain.

one of the FA became evident. The ketone structures may have formed in either of two ways: Either the number of double bonds between FA carbons had not changed (e.g., conversion of a hydroperoxide to a ketone by dehydration), or there was one less double bond (formation of a ketone at a site of unsaturation).

Autoxidation of TAG may also produce two distinct classes of epoxides (20), those in which the oxygen atom is added at the site where a double bond has been, and those in which the epoxide is added near a double bond so that no double bonds are lost.

No major differences were found between the oxidation products of the samples. Noticeable differences were found only in the molecules of 52 acyl carbons, 52 being was the most common and abundant acyl carbon number for the oxidized TAG molecules. The structures 18:1 keto/18:1/16:0 and 18:1 keto/18:0/16:0 + 18:0 keto/18:1/16:0 seemed to be more abundant in group 2, and the structure 18:1 epoxy/18:1/16:0 was found only in group 1 (Fig. 1). Otherwise, the same oxidation products were found in both samples.

An interesting detail is that no hydroperoxides were found in the TAG. This is surprising, but is in accordance with the hypothesis that only traces of unmodified hydroperoxy lipids are found in tissue and blood samples (30). According to the studies of Yamamoto (31), cholesteryl ester hydroperoxides are present in rat and human plasma, whereas PC hydroperoxides are undetectable because of enzymatic and non-enzymatic reduction and conversion. Modification of hydroperoxide structures could also take place in the TAG molecules of LDL. TAG hydroperoxides of dietary origin may, to a large degree, be reduced and decomposed to secondary oxidation products already in the gastrointestinal tract (32,33).

Also, the presence of hydroxides in our samples remains uncertain, although some weak peaks that could represent the molecular structure 18:1 OH/18:1/16:0 were found in the samples (Table 3). The possibility that some decomposition of hydroperoxy and hydroxy structures had occurred during sample preparation and analysis cannot be excluded. However, our reference compounds were observed to be relatively stable during storage and during TLC and HPLC-MS runs. Therefore, sample preparation probably does not explain the absence of hydroperoxides in the samples. What may cause some distortion to the seeming proportions of oxidized TAG molecules is that most core aldehydes may not be detected as such, because they form easily covalent bonds with amino acids, peptides, and proteins (34,35). Also, minor amounts of artificially formed oxidized lipids could be present in the samples (36).

In conclusion, our approach seems to be applicable to research on physiological LDL samples. The LDL-BDC method already has been shown to be a sensitive method for the determination of LDL lipid oxidation. The method based on HPLC-ESI-MS enables identification of individual molecular structures of oxidized TAG, but it has not been used for the analysis of physiological samples before now. The results of the present study show that even small amounts of oxidized TAG structures can be detected and identified in lipoprotein samples.

ACKNOWLEDGMENTS

This work was supported by funds from the Applied Bioscience Graduate School, Raisio Nutrition Ltd., and Wäinö Edward Miettinen Foundation.

REFERENCES

1. Steinbrecher, U.P., Zhang, H., and Lougheed, M. (1990) Role of Oxidatively Modified LDL in Atherosclerosis, *Free Radic. Biol. Med. 9*, 155–168.
2. Esterbauer, H., Gebicki, J., Puhl, H., and Jurgens, G. (1992) The Role of Lipid Peroxidation and Antioxidants in Oxidative Modifications of LDL, *Free Radic. Biol. Med. 13*, 241–290.
3. Witztum, J.L. (1994) The Oxidation Hypothesis of Atherosclerosis, *Lancet 344*, 793–795.
4. Berliner, J.A., and Heinecke, J.W. (1996) The Role of Oxidized Lipoproteins in Atherogenesis, *Free Radic. Biol. Med. 20*, 707–727.
5. Jialal, I., and Devaraj, S. (1996) Low-Density Lipoprotein Oxidation, Antioxidants, and Atherosclerosis: A Clinical Biochemistry Perspective, *Clin. Chem. 42*, 498–506.
6. Staprans, I., Rapp, J.H., Pan, X.-M., Kim, K.Y., and Feingold, K.R. (1994) Oxidized Lipids in the Diet Are a Source of Oxidized Lipid in Chylomicrons of Human Serum, *Arterioscler. Thromb. 14*, 1900–1905.
7. Staprans, I., Rapp, J.H., Pan, X.-M., and Feingold, K.R. (1996) Oxidized Lipids in the Diet Are Incorporated by the Liver into Very Low Density Lipoprotein in Rats, *J. Lipid Res. 37*, 420–430.
8. Ahotupa, M., Marniemi, J., Lehtimäki, T., Talvinen, K., Raitakari, O.T., Vasankari, T., Viikari, J., Luoma, J., and Ylä-Herttuala, S. (1998) Baseline Diene Conjugation in LDL Lipids as a Direct Measure of *in vivo* LDL Oxidation, *Clin. Biochem. 31*, 257–261.
9. Ahotupa, M., Ruutu, M., and Mäntylä, E. (1996) Simple Methods of Quantifying Oxidation Products and Antioxidant Potential of Low Density Lipoproteins, *Clin. Biochem. 29*, 139–144.
10. Ahotupa, M., and Vasankari, T.J. (1999) Baseline Diene Conjugation in LDL Lipids: An Indicator of Circulating Oxidized LDL, *Free Radic. Biol. Med. 27*, 1141–1150.
11. Gavella, M., Lipovac, V., Car, A., and Vucic, M. (2002) Baseline Diene Conjugation in LDL Lipids from Newly Diagnosed Type 2 Diabetic Patients, *Diabetes Metab. 28*, 391–396.
12. Vasankari, T., Fogelholm, M., Kukkonen-Harjula, K., Nenonen, A., Kujala, U., Oja, P., Vuori, I., Pasanen, P., Neuvonen, K., and Ahotupa, M. (2001) Reduced Oxidized Low-Density Lipoprotein After Weight Reduction in Obese Premenopausal Women, *Int. J. Obes. 25*, 205–211.
13. Kamido, H., Kuksis, A., Marai, L., and Myher, J.J. (1995) Lipid Ester-Bound Aldehydes Among Copper-Catalyzed Peroxidation Products of Human Plasma Lipoproteins, *J. Lipid Res. 36*, 1876–1886.
14. Karten, B., Boechzelt, H., Abuja, P.M., Mittelbach, M., and Sattler, W. (1999) Macrophage-Enhanced Formation of Cholesteryl Ester-Core Aldehydes During Oxidation of Low Density Lipoprotein, *J. Lipid Res. 40*, 1240–1253.
15. Niu, X., Zammit, V., Upston, J.M., Dean, R.T., and Stocker, R. (1999) Coexistence of Oxidized Lipids and α-Tocopherol in All Lipoprotein Density Fractions Isolated from Advanced Human Atherosclerotic Plaques, *Arterioscler. Thromb. Vasc. Biol. 19*, 1708–1718.
16. Hamsten, A. (1993) Lipids as Coronary Risk Factors: Analysis of Hyperlipidaemias, *Postgrad. Med. J. 69*, S8–S11.
17. Steenhorst-Slikkerveer, L., Louter, A., Janssen, H.-G., and Bauer-Plank, C. (2000) Analysis of Nonvolatile Lipid Oxidation Products in Vegetable Oils by Normal-Phase High-Performance Liquid Chromatography with Mass Spectrometric Detection, *J. Am. Oil Chem. Soc. 77*, 837–845.
18. Byrdwell, W.C., and Neff, W.E. (1999) Non-volatile Products of Triolein Produced at Frying Temperatures Characterized Using Liquid Chromatography with Online Mass Spectrometric Detection, *J. Chromatogr. A 852*, 417–432.
19. Byrdwell, W.C., and Neff, W.E. (2001) Autoxidation Products of Normal and Genetically Modified Canola Oil Varieties Determined Using Liquid Chromatography with Mass Spectrometric Detection, *J. Chromatogr. A 905*, 85–102.
20. Neff, W.E., and Byrdwell, W.C. (1998) Characterization of Model Triacylglycerol (triolein, trilinolein and trilinolenin) Autoxidation Products *via* High-Performance Liquid Chromatography Coupled with Atmospheric Pressure Chemical Ionization Mass Spectrometry, *J. Chromatogr. A 818*, 169–186.
21. Sjövall, O., Kuksis, A., Marai, L., and Myher, J.J. (1997) Elution Factors of Synthetic Oxotriacylglycerols as an Aid in Identification of Peroxidized Natural Triacylglycerols by Reverse-Phase High-Performance Liquid Chromatography with Electrospray Mass Spectrometry, *Lipids 32*, 1211–1218.
22. Ravandi, A., Kuksis, A., Myher, J.J., and Marai, L. (1995) Determination of Lipid Ester Ozonides and Core Aldehydes by High-Performance Liquid Chromatography with On-line Mass Spectrometry, *J. Biochem. Biophys. Methods 30*, 271–285.
23. Esterbauer, H., and Cheeseman, K.H. (1990) Determination of Aldehydic Peroxidation Products: Malonaldehyde and 4-Hydroxynonenal, *Methods Enzymol. 186*, 407–421.
24. Deffense, E. (1993) Nouvelle Méthode d'Analyse pour Séparer, *via* HPLC, les Isomères de Position 1-2 et 1-3 des Triglycérides Mono-insaturés des Graisses Végétales, *Rev. Fr. Corps Gras 40*, 33–39.
25. Neff, W.E., Frankel, E.N., and Weisleder, D. (1982) Photosensitized Oxidation of Methyl Linolenate. Secondary Products, *Lipids 17*, 780–790.
26. Chiba, T., Takazawa, M., and Fujimoto, K. (1989) A Simple Method for Estimating Carbonyl Content in Peroxide-Containing Oils, *J. Am. Oil Chem. Soc. 66*, 1588–1592.
27. Gritter, R.J., and Wallace, T.J. (1959) The Manganese Dioxide Oxidation of Allylic Alcohols, *J. Org. Chem. 24*, 1051–1056.
28. Skipski, V.P., and Barclay, M. (1969) Thin-Layer Chromatography, *Methods Enzymol. 14*, 542–548.
29. Christie, W.W. (1982) A Simple Procedure for Rapid Transmethylation of Glycerolipids and Cholesteryl Esters, *J. Lipid Res. 23*, 1072–1075.
30. Spiteller, G. (1998) Linoleic Acid Peroxidation—The Dominant Lipid Peroxidation Process in Low Density Lipoprotein—and Its Relationship to Chronic Diseases, *Chem. Phys. Lipids 95*, 105–162.
31. Yamamoto, Y. (2000) Fate of Lipid Hydroperoxides in Blood Plasma, *Free Radic. Res. 33*, 795–800.
32. Aw, T.Y., Williams, M.W., and Gray, L. (1992) Absorption and Lymphatic Transport of Peroxidized Lipids by Rat Small Intestine *in vivo*: Role of Mucosal GSH, *Am. J. Physiol. 262*, G99–G106.
33. Kanazawa, K., and Ashida, H. (1998) Dietary Hydroperoxides of Linoleic Acid Decompose to Aldehydes in Stomach Before Being Absorbed into the Body, *Biochim. Biophys. Acta 1393*, 349–361.
34. Karten, B., Boechzelt, H., Abuja, P.M., Mittelbach, M., Oettl, K., and Sattler, W. (1998) Femtomole Analysis of 9-Oxononanoyl Cholesterol by High-Performance Liquid Chromatography, *J. Lipid Res. 39*, 1508–1519.
35. Kurvinen, J.-P., Kuksis, A., Ravandi, A., Sjövall, O., and Kallio, H. (1999) Rapid Complexing of Oxoacylglycerols with Amino Acids, Peptides and Aminophospholipids, *Lipids 34*, 299–305.
36. Podrez, E.A., Poliakov, E., Shen, Z., Zhang, R., Deng, Y., Sun, M., Finton, P.J., Shan, L., Gugiu, B., Fox, P.L., *et al.* (2002) Identification of a Novel Family of Oxidized Phospholipids That Serve as Ligands for the Macrophage Scavenger Receptor CD36, *J. Biol. Chem. 277*, 38503–38516.

[Received July 18, 2003; accepted June 10, 2004]

REVIEW

Protein Engineering and Applications of *Candida rugosa* Lipase Isoforms

Casimir C. Akoh[a,b], Guan-Chiun Lee[b], and Jei-Fu Shaw[b,*]

[a]Department of Food Science and Technology, University of Georgia, Athens, Georgia 30602-7610, and
[b]Institute of Botany, Academia Sinica, Nankang, Taipei, 11529, Taiwan

ABSTRACT: Commercial preparations of *Candida rugosa* lipase (CRL) are mixtures of lipase isoforms used for the hydrolysis and synthesis of various esters. The presence of variable isoforms and the amount of lipolytic protein in the crude lipase preparations lead to a lack of reproducibility of biocatalytic reactions. Purification of crude CRL improve their substrate specificity, enantioselectivity, stability, and specific activities. The expression of the isoforms is governed by culture or fermentation conditions. Unfortunately, the nonsporogenic yeast *C. rugosa* does not utilize the universal codon CTG for leucine; therefore, most of the CTG codons were converted to universal serine triplets by site-directed mutagenesis to gain expression of functional lipase in heterologous hosts. Recombinant expressions by multiple-site mutagenesis or complete synthesis of the lipase gene are other possible ways of obtaining pure and different CRL isoforms, in addition to culture engineering. Protein engineering of purified CRL isoforms allows the tailoring of enzyme function. This involves computer modeling based on available 3-D structures of lipase isoforms. Lid swapping and DNA shuffling techniques can be used to improve the enantioselectivity, thermostability, and substrate specificity of CRL isoforms and increase their biotechnological applications. Lid swapping can result in chimera proteins with new functions. The sequence of the lid can affect the activity and specificity of recombinant CRL isoforms. *Candida rugosa* lipase is toxicologically safe for food applications. Protein engineering through lid swapping and rationally designed site-directed mutagenesis will continue to lead to the production of CRL isoforms with improved catalytic power, thermostability, enantioselectivity, and substrate specificity, while providing evidence for the mechanisms of actions of the various isoforms.

Paper no. L9534 in *Lipids 39,* 513–526 (June 2004).

Candida rugosa (formerly *C. cylindracea*) is a nonsporogenic, unicellular, nonpathogenic yeast. It has the GRAS (generally regarded as safe) status, and no adverse effect on human or other forms of life has been reported as a result of traditional or open fermentation when both purified and crude preparations are used for the production of food and flavor materials. Strain ATCC 14830 and Type VII are the wild-type strains most widely used to produce lipases. Other commercial sources of crude *C. rugosa* lipases (CRL) are Amano, Biocatalysts, Roche, Meyto-Sangyo, BDH, Fluka, and Genzyme. Extracellular lipases (TAG acylhydrolase, EC 3.1.1.3) are versatile enzymes used to catalyze both the hydrolysis and synthesis of ester compounds. Crude CRL is a widely used enzyme for biotransformations and biocatalysis (acylation and deacylation) reactions to produce useful materials for food, flavor, fragrance, cosmetics, pharmaceutical, and other industrial applications. The wild-type lipase is a mixture of many lipases and esterases acting often in direct competition or in concert with each other to affect a process. Because the individual lipases (isomers, isozymes, or isoforms) are not isolated and purified before most applications, the native or wild-type enzyme exhibits a wide range of substrate specificity, acyl chain length specificity, and stereoselectivity.

Lipases, in general, have broad specificities (substrate, FA chain length, position, and enantioselectivity). However, various preparations of CRL are classified as nonpositional specific lipases. That is, they can catalyze hydrolysis or esterification at the *sn*-1, -2, and -3 positions of the glycerol molecule and other nonglycerol moieties such as phospholipids, sugars, and polyhydric alcohols (polyols). Substrate specificity is important in the purification, hydrolysis, and synthesis of important compounds. This factor greatly limits the application of crude CRL (mixed isoforms) in the production of specific compounds with high purity and reproducibility. This lack of reproducibility of reactions was attributed to the variable proportion of isoforms, amount of water in the crude lyophilized lipase, and the amount of lipolytic protein present in the powdered enzyme (1). It is important therefore that the different isoforms of crude CRL be separated and purified to homogeneity, if possible, to enable us to understand the mechanism of lipase catalysis and to find ways to engineer the lipases to utilize new substrates; increase their substrate specificity, enantioselectivity, stability (temperature, pH, organic solvent, etc.), and specific activities; act in concert with other enzymes; and find new applications. Therefore, manipulating culture conditions and using recombinant DNA technology are means of obtaining different CRL isoforms. Many applications of crude CRL have been reviewed (2,3). These include use in flavor development of cheese, fermented products, and ice cream; production of bioactive pharmaceuticals; stereoselective synthesis of desired enantiomers of racemic compounds through hydrolysis or esterification; carbohydrate FA ester

*To whom correspondence should be addressed.
E-mail: boplshaw@gate.sinica.edu.tw

Abbreviations: CRL, *Candida rugosa* lipase; GRAS, generally regarded as safe; RT-PCR, reverse transcription-polymerase chain reaction; Trx, thioredoxin.

synthesis for use as emulsifiers and biosurfactants, glycero-glycolipids, MAG, DAG, and TAG, amides, biocides or pesticides; bioremediation in waste disposal; the tanning process; as possible biosensors for determination of TAG in clinical, food, and chemical diagnosis; and in cosmetics and perfumery (Table 1). The current review does not cover the function of lipases during digestion and absorption. Specifically, this review will highlight the problems of using commercial lipases in biotransformations and biocatalysis; highlight what has been done so far to isolate and purify the multiple forms of CRL, to improve their catalytic power, substrate specificity, and enantioselectivity using the tools of molecular biology; and indicate their potential applications.

PURIFICATION OF *C. RUGOSA* LIPASE AND ISOFORMS

When enzyme proteins contain other proteins and enzymes, the specific activity of the enzyme in question is suppressed. Purification by various methods increases the enzyme's specific activity while reducing the effect of other contaminants. Crude CRL is no exception. Indeed, studies have shown that there are up to seven isoforms of the same lipase (4). The expression of these isoforms is governed by culture or fermentation conditions. Fermentation processes in submerged batch, and continuous cultures are available for *C. rugosa* lipase production (5–7). Usually, a carbon source to support growth, a lipid source to induce lipase production, nitrogen, dissolved oxygen, and a pH value of 5.5–7.0 are required to produce lipases (7). FA with higher solubilities tend to support higher cell growth but reduced or no lipase production (6). Oleic acid is one of the best inducers of lipase production. For example, oleic acid is known to greatly induce the preferential expression of the Lip1 isoform, possibly at the level of transcription.

CRL purification can be carried out using available protein/enzyme purification techniques such as ammonium sulfate precipitation at different concentrations, precipitation with acetone, sodium cholate and ethanol/ether precipitation, anion exchange chromatography on DEAE-Sephacel or Sepharose CL-6B, a gel filtration technique on Sephacryl S-100 HR, and SDS-PAGE gel electrophoresis (with appropriate stain for protein and enzyme activity).

ASSAY

Different assay methods are available for lipase activity, depending on the application of the enzyme and substrates involved (i.e., whether hydrolysis, esterification, etc.). Lipase activity is usually determined titrimetrically by a pH-Stat method using tributyrin, triolein, olive oil, or other emulsified TAG substrates, which may include mixed TAG. One unit of enzyme activity is defined as the amount of lipase that releases 1 μmol of FA per min under the defined assay condition. Spectrophotometric assays are available using chromogenic substrates such as *p*-nitrophenyl esters. The change in absorbance is measured at 348 nm (isosbestic point of the *p*-nitrophenol/*p*-nitrophenoxide couple) to avoid the absorbance change due to the pH effect on the *p*-nitrophenol/*p*-nitrophenoxide ratio. One lipase activity unit is defined as the amount of lipase required to release 1 μmol of product per min under a defined assay condition. An alternative colorimetric assay uses 1,2-*O*-dilauryl-*rac*-glycero-3-glutaric-resorufin ester (Roche) as a specific lipase chromogenic substrate (8). Sometimes, esterase activity is measured because most of the lipases contain esterase activity. In this case, a spectrophotometer is used and *p*-nitrophenyl ester of different acyl chain length becomes the test substrate, and the absorbance of released *p*-nitrophenol is measured at 410 nm where *p*-nitrophenoxide has a maximal molar extinction coefficient at alkaline pH.

TABLE 1
Selected Applications of Crude Commercial Mixtures of *Candida rugosa* Lipase[a]

Application	Reaction type	Reference
Preparation of alkyl esters of FA	Esterification	62
Monoestolides	Esterification	63
FA production	Hydrolysis	64–70
Discrimination against DHA, GLA, and DHGLA	Kinetic resolution, transesterification	71–73
Enrichment of erucic acid up to 80%	Selective hydrolysis	74,75
Optically active ibuprofen	Resolution of racemates by hydrolysis	76
Naproxen	Esterification of racemic mixture	77
Ketoprofen	Hydrolysis	78
Synthesis of acylglycerols containing PUFA and CLA	Interesterification	79
Purification of CLA isomers	Selective esterification	80
Steryl, stanyl, and steroid ester synthesis	Esterification, transesterification	81
Bioremediation	Hydrolysis	82
Enantioselective production of anti-inflammatory drug	Hydrolysis	83
Resolution of DL-menthol	Esterification	84,85
Polymer degradation	Hydrolysis of side chain	86
Synthesis of structured lipids	Interesterification	87
Synthesis of terpene or flavor esters	Esterification	88
Synthesis of alkyl glucoside FA esters	Esterification	89

[a]GLA, γ-linoleic acid; DHGLA, dihomo-γ-linoleic acid; CLA, conjugated linoleic acid.

EXPRESSION OF DIFFERENT ISOFORMS

Crude commercial CRL obtained from various sources show remarkable variations in catalytic efficiency, substrate specificity, and enantioselectivity. They lack reproducibility when used in food processing and biocatalysis; thus, it is difficult to compare and interpret results from various applications and from the literature. Native or wild-type CRL obtained by conventional fermentation techniques are a mixture of various isoforms (isozymes) owing to the differential response of the different genes, in both the wild-type and mutant strains, to the varied fermentation conditions employed by different enzyme suppliers (9–11). The importance and the difficulty of separating these isoforms by normal chromatographic techniques cannot be overemphasized. This problem is accentuated by a high similarity and sequence homology in their structure, leading to similar physical properties that make isolation an uphill task. Depending on the purification scheme employed, the property of the different isoforms may be altered (12). Up to seven lipase genes (*LIP1–LIP7*) have been described in *C. rugosa*, and only three (*LIP1*, *LIP2*, and *LIP3*) have been successfully identified (4,6,13–16) in commercial crude CRL preparations.

Cloning seems to be a viable and reasonable approach to the isolation, purification, production, characterization, and optimization of the biocatalytic properties of the different pure isoforms in an industrial scale. Unfortunately, despite the general availability of the cloned genes, the nonsporogenic yeast *C. rugosa* does not utilize the universal codon CTG for leucine. Indeed, *C. rugosa* utilizes nonuniversal codons by reading CTG as serine (17,18). The CTG triplet encodes most of the serine residues in five *C. rugosa* lipases, including the catalytic Ser-209 (Fig. 1). Attempts to express such genes heterologously (in other hosts) may lead to the production of inactive lipases. Therefore, there is a great need to convert most of the CTG codons to universal serine triplets for the expression of a functional lipase protein in heterologous hosts such as *Escherichia coli* or *Pichia pastoris*. We have amended *LIP4* and *LIP2* genes by site-directed mutagenesis and successfully expressed the amended genes in *E. coli* and *P. pastoris* (17,19,20). An alternative approach is to perform complete synthesis of the gene as in the case of *LIP1* (21).

We have previously identified multiple forms and functions of CRL in three commercial *C. rugosa* lipase preparations (9). The purified isoforms have different catalytic efficiency, substrate specificities, and thermal stabilities. Surfactants are known to induce lipase production. Tweens 20 and 80 were able to promote lipase production as well as change the expression of lipase isoforms in cultured *C. rugosa*. These suggest that the specificity and stability of lipase preparations can be changed by engineering the culture conditions, which in turn result in change of the isoform compositions.

Five lipase-encoding genomic sequences from *C. rugosa* have been characterized (22,23). LIP1–LIP5 genes (lipase-encoding genes) were isolated from a *Sac* I genomic library

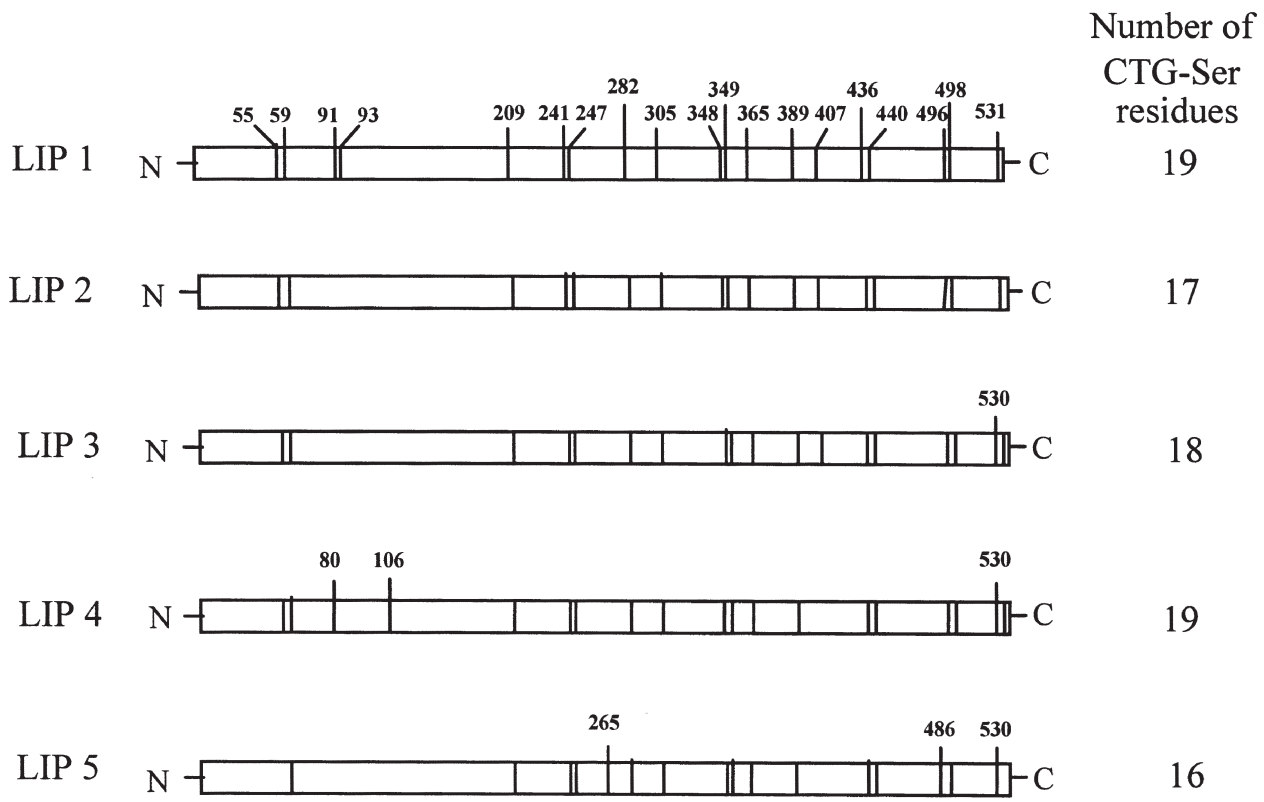

FIG. 1. Distribution of codon triplets, CTG, encoding the serine residues including the active site Ser 209, in five *Candida rugosa* lipase isoforms.

of *C. rugosa* by colony hybridization. These genes encode for mature proteins of 534 amino acid residues with putative signal peptides of 15 amino acids in (LIP1, LIP3, LIP4, and LIP5) and 14 in LIP2, respectively. The deduced amino acid sequences of the five genes share an overall identity of 66% and similarity of 84%. Because of the high sequence homology among the five sequences and the differential expression level of the five lipase genes, it is very difficult to purify each isoform directly from the cultures of *C. rugosa* on an industrial scale. Therefore, for highly related genes, the conventional methods of mRNA analysis are not specific and sensitive enough to distinguish and quantify individual mRNA. The transcription pattern of such genes is difficult to distinguish by the usual Northern blot analysis. The nuclease protection assay can discriminate among closely related genes. However, this method, like the Northern blot, is not sensitive enough to detect low levels of mRNA and allow their quantification. Hence, the competitive reverse transcription polymerase chain reaction (RT-PCR) technique was developed to circumvent this problem and obtain quantitative information on highly related *C. rugosa LIP* genes at the transcriptional level owing to the high specificity and sensitivity of the technique (10). In using the RT-PCR technique, the relative abundance of *LIP* mRNA was found to be *LIP1*, *LIP3*, *LIP2*, *LIP5*, and *LIP4* (in decreasing order). High expression of *LIP1* and *LIP3* was achieved, whereas the expression of *LIP4* and *LIP5* was only 0.1–0.5% of the expression of the *LIP1* transcript using YM (0.3% yeast extract, 0.3% malt extract, 0.5% peptone, and 1% dextrose) culture conditions. The expression profiles were consistent with the findings that LIP1 and LIP3 are the major lipase proteins obtained by purification methods (14,24). The five *LIP* genes are transcriptionally active. However, the presence of different inducers may change the expression profile of the individual genes. *LIP1* and *LIP3* genes were constitutively expressed and showed minor changes at the transcriptional level in various culture media. On the other hand, the *LIP1* gene was found to be suppressed by oleic acid whereas *LIP3* expression was induced by oleic acid. Both olive oil and oleic acid promoted the expression of inducible *LIP2*, *LIP4*, and *LIP5* even in the presence of glucose—a reported repressing carbon source (25). Tween 20 significantly induced the expression of *LIP4* only. This demonstrates that the expression profiles of *C. rugosa LIP* genes can be altered by different culture conditions and batch-to-batch differences in culture. Thus, the ability to produce different CRL isoforms by engineering the culture conditions is physiologically important for the nonsporogenic yeast *C. rugosa*, enabling the organism to grow on different environments and substrates. The aim of traditional fermentation is to optimize the culture conditions for maximal production and enzyme activity. We believe and have shown that the quality of enzyme produced is as important as the quantity since the different culture conditions produce heterogeneous mixtures of lipase isoforms that display different catalytic ability and substrate specificity. CRL preparations enriched in the desired lipase isoforms for specific applications can be obtained by engineering the culture conditions. Studies are needed to fully understand the mechanism of differential regulation of *LIP* genes by various inducers because it is possible that the expression profile of these genes may be accompanied by different regulation of the *LIP* promoter activities. We cloned and sequenced the five CRL gene promoters and showed they were different and contained different nutrient-related transcriptional controlling elements (Lee, G.-C., and Shaw, J.-F., unpublished data).

RECOMBINANT TECHNOLOGY

One way to overcome the problem of lack of reproducibility of reactions while using mixed crude *C. rugosa* lipase isoforms from commercial preparations is to work with pure isolated enzymes. The individual pure isoforms of the lipase can be purified by chromatography, culture engineering, or a recombinant DNA technique. However, the unusual codon usage problem has hindered the use of recombinant CRL isoenzymes (isoforms). The conversion of all CTG genes is required for the expression of functional lipase proteins in heterologous hosts. Heterologous expression of the cloned genes is useful as a basis for the study of structure–function relationships in CRL. Great progress has been made with the conversion of all the 19 CTG and 17 CUG codons in LIP4 and LIP2, respectively, to universal serine codons using site-directed mutagenesis and achievement of the expression of active LIP4 in the methylotrophic yeast *P. pastoris* and in *E. coli* (17,19), and LIP2 in *P. pastoris* (20), which were successfully secreted into the culture medium. We used a more efficient overlap extension PCR-based multiple mutagenesis to convert the 17 nonuniversal serine codons (CTG) in the *C. rugosa LIP2* gene into universal serine codons (TCT) (20). The recombinant LIP1 isoform was functionally expressed in both *Saccharomyces cerevisiae* and *P. pastoris* by complete synthesis of the *LIP1* gene with an optimized nucleotide sequence (21). Multiple-site mutagenesis was also used to produce highly active LIP1, LIP3, and two other newly identified isoforms, LIP8 and LIP9 (26).

The LIP1, LIP2, and LIP4 CRL isoforms have been characterized. LIP1 and LIP3 were purified from commercial preparations or cultures of *C. rugosa* by complex procedures (15,16,27,28). The properties of recombinant LIP1 were compared with those of a commercial CRL preparation. The physicochemical properties were found to be similar, whereas their substrate specificities toward FAME differed significantly, indicating clear differences between the commercial and recombinant lipases (21,29). In comparison to recombinant LIP1, commercial CRL exhibits a marked preference for longer (C_{14}–C_{18}) acyl chains. These characteristics may be due to the presence of one or several isoforms in the commercial CRL with a preference for long-chain acyl esters. However, recombinant LIP1 catalytic activity was similar to that of commercial lipase, suggesting that the major component of the commercial lipase is LIP1 (21). In contrast, recombinant LIP4 prefers longer acyl chain substrates (C_{16} and C_{18})

whereas LIP1 prefers C_8 and C_{10} acyl chains as substrates. These results confirm that individual CRL isoforms do possess distinctive enzyme activities even though sequence similarity (81% identity in LIP1 and LIP4) exists and that the variations in substrate specificities in commercial lipase preparations may be due to the different combinations of catalytic activities of the individual CRL isoforms (8).

Glycosylation and other posttranslational modifications of lipases may be partly responsible for the heterogeneity, thermal stability, and activities of the different CRL isoforms. The commercial lipase and recombinant glycosylated LIP4 from *P. pastoris* have higher M.W. than recombinant LIP4 from *E. coli* due to glycosylation (19). It has been proposed that LIP1, LIP3, and LIP5 have three glycosylation (a posttranslational event) sites based on DNA sequence data and that LIP2 and LIP4 have only one such site (30). We used a computer program to analyze the DNA sequence of LIP4 and found that only one potential N-glycosylation motif (Asn-Val-Thr) existed and that the Asn residue involved in the glycosylation was Asn 351. We believe that Asn 351 may be the major glycosylation site in CRL isoforms. However, Asn 291 and Asn 314 were also considered potential sites, but they may not undergo glycosylation in LIP1, LIP3, and LIP5. Carbohydrates appear to play an important role in the activation of CRL by providing an additional stabilization to the open conformation of the flap (31). Glycoslation was not detected in the LIP4 expressed in *E. coli*. However, its catalytic activity was not different from the LIP4 expressed in *P. pastoris*. This means that glycosylation may not significantly affect LIP4 enzyme activity. One important observation was the increase in the thermal stability of glycosylated LIP4 compared with the nonglycosylated LIP4. There is a possibility that glycosylation level among CRL isoforms may affect their structure, thermal stability, and secretion into the culture medium. This was demonstrated to be the case for the activation of LIP1 by replacing the three N-linked glycosylation sites in Asn 291, 314, and 351 of recombinant LIP1 with Gln using site-directed mutagenesis (32). When the authors compared the activity of the mutants Asn314Gln and Asn351Gln with that of the wild-type lipase, they found that substitution with Gln influenced the hydrolysis and esterification activity of LIP1 to a different extent, but it did not alter the enzyme water activity profiles in organic solvents or temperature stability. Replacing Asn 351 with Gln probably disrupted the stabilizing interaction between the sugar chain and residues of the inner side of the lid in the enzyme active conformation. The effect of deglycosylation at position 314 suggests a more general role of the sugar moiety for the structural stability of LIP1. Conversely, Asn351Gln substitution did not affect the lipolytic or the esterase activity of the mutant LIP1 that behaved essentially as a wild-type enzyme. This observation supports the hypothesis that changes in activity of Asn314Gln and Asn351Gln mutants are specifically due to deglycosylation (32).

Recombinant LIP2 overexpressed in *P. pastoris* has a M.W. similar to the native LIP2 isoform purified from *C. rugosa* fermentation (20,33). The native LIP2 and LIP3 were prepared by ammonium sulfate precipitation, sodium cholate treatment, ethanol/ether precipitation, and anion exchange chromatography (DEAE-Sephacel). Pure and monomeric enzymes were characterized with respect to glycosylation, substrate specificity, pI, and activity. The recombinant and native LIP2 lipases had similar substrate specificities for the hydrolysis of long-chain *p*-nitrophenyl esters. However, the recombinant lipases displayed higher specific activity toward the *p*-nitrophenyl esters compared with the native lipase. The chain length preference for the TAG substrates was significant and different for the two enzymes. Recombinant LIP2 showed preference for the hydrolysis of short-chain TAG (tributyrin) whereas the native LIP2 preferred the long-chain triolein. The differences may be attributed to glycosylation, the additional N-terminal peptide, or amino acid substitutions between the recombinant and native LIP2.

3-D STRUCTURAL ANALYSIS AND MECHANISTIC CONSIDERATIONS

The 3-D structure of three (LIP1, LIP2, and LIP3) of the five native CRL isoforms purified from the commercial crude enzyme mixtures have been elucidated (13,31,34–38). The structure of *C. rugosa* lipase and conformational flexibility was reviewed (39). The 3-D structural analysis is very important in our understanding of lipase functions. Often, enzyme inhibitors (substrate-like molecules) are used to study and understand lipase structure. Lipases from different organisms vary widely in size from 20 to 65 kDa. The CRL genes code for 534 amino acids with M.W. of the proteins of approximately 60 kDa. The sequence homology of the isoforms is 85–90% amino acids. All lipases share a common structural motif called lipase fold (40), a subset of the α/β-hydrolase fold. The lipase/esterase enzymes also possess this fold, which is comprised of a central, mostly parallel β-sheet with several helices on both sides of the sheet (40).

CRL have a catalytic triad of Ser 209, Glu 341, and His 449 residues at the active site with a well-conserved hydrogen bonding pattern stabilizing the triads in three isoforms (LIP1, LIP2, and LIP3), similar to the catalytic triad found in serine proteases. One important difference between the proteases and lipases is that the active sites have opposite handedness. Therefore, the nucleophiles in lipases approach the plane of the acyl group of the substrate from the side opposite to that of the proteases, to the plane of the equivalent peptide bond (39). In addition, CRL have Glu instead of Asp at the active site for most serine lipases and proteases. Studies conducted with complexes of CRL with substrate-like inhibitors show that the oxyanion hole, whose role is to stabilize the oxyanion developing on the carbonyl group of the substrates, is an important part of the active site in *C. rugosa* lipases as well as all other lipases. The oxyanion hole in CRL that is predicted to be formed by the backbone NH groups of residues Gly 124 and Ala 210 is also conserved among the LIP1, LIP2, and LIP3 isoforms.

Every CRL isoform has an amphipathic α-helix that serves as a lid (or flap) covering the active site. In the closed lipase

structure, the hydrophilic side of the lid faces the solvent, and the hydrophobic side is directed toward the protein core. When the lipase shifts to open conformation, the hydrophobic side becomes exposed and subsequently contributes to the substrate-binding site and substrate recognition. Both the amphipathic nature of the lid and the specific amino acid sequence may be important for lipase specificity and activity. The flap regions are quite different among the CRL isoforms. For example, the LIP2 has 11 different amino acid residues compared with LIP1, and 9 different residues compared with LIP3 in the 30 amino acid-flap region (31). The differences in the hinge point presumably affect the opening of the flap of different isoforms, and the hydrophobicity differences of these residues in the internal side were suggested to affect substrate binding. The amino acid residues at the hinge point are Glu 66, Met 66, and Glu 66 for LIP1, LIP2, and LIP3, respectively. The flap of LIP2 is more hydrophobic than the LIP1 or LIP3 flaps. Flap interaction with the substrate binding pocket is important in understanding the different catalytic properties found among CRL isoforms (35).

All lipases have essentially two binding sites, one for the substrate or acyl group and the other for alcohol binding. A comparison of the substrate-binding sites of the three CRL isoforms revealed amino acid variations that may affect substrate specificity and catalytic properties (35). It was hypothesized that the Phe content at the mouth of the hydrophobic tunnel (i.e., acyl binding site) greatly affected the substrate-recognition properties of the CRL isoforms. The Phe content of this region for LIP1, LIP2, and LIP3 is 5, 3, and 4, respectively. Amino acid residues 296 and 344 for LIP1, LIP2, and LIP3 are Phe-Phe, Val-Leu, and Phe-Ile, respectively. The lipase/esterase activity ratio toward triacetin substrate for LIP1, LIP2, and LIP3 is 43.7, 7.3, and 7.6, respectively. In contrast, the cholesterol esterase activity decreases from LIP2 >> LIP3 > LIP1. It appears that the Phe content in the mouth of the hydrophobic tunnel significantly affects the environment of the catalytic triad, the lipase/esterase catalytic properties, and substrate specificities. However, it is important that this be confirmed by site-directed mutagenesis.

To understand the molecular basis of substrate specificity, we compared the geometry and properties of the CRL isoforms. The 3-D structures of the LIP4 and LIP5 isoforms were obtained from the Web-based SWISS-MODEL server (Version 3.5; Glaxo Smith Kline S.A., Geneva, Switzerland; www.expasy.org/swissmod/SWISS-MODEL.html), which utilizes the comparative modeling approach (41). The structures of molecular complexes of LIP1 with hexadecanesulfonyl chloride inhibitor (36), LIP2 (35), and LIP3 with cholesteryl linoleate (34) were obtained from the Research Collaboratory for Structural Bioinformatics (Rutgers University, Piscataway, NJ) protein data bank (42) under the entry numbers 1LPO, 1GZ7, and 1CLE, respectively. These structures were used as the corresponding templates for comparative protein modeling. Display and analysis of modeled structures were performed using a Swiss-Pdb Viewer (Glaxo Smith Kline S.A.). Figure 2 illustrates the comparative 3-D topography of substrate-binding sites for CRL isoforms. The results allowed analysis of the cholesterol linoleate-binding site and the acyl-binding tunnel. Amino acid changes in these regions may determine changes in the interactions affecting the stability and specificity of the CRL isoforms. Most of the residues located in close proximity to the cholesterol linoleate molecule and in place of the acyl chain (within the 4-Å cutoff distance) were identical and shared the same conformations as those of the template residues. Some of the substrate-binding residues showed differences between LIP isoforms (Table 2). Four definite differences were found at the 20 amino acids of the acyl-binding sites. The alcohol-binding sites showed more variations in that five of the eight amino acids were not conserved. The hydrophobic face of the flap, which also plays an important role when the enzyme is in contact with the substrate, had five variations in the eleven residues.

Lipase catalysis mostly occurs *via* an interfacial activation process. The presence of a water–lipid interface is required for efficient catalysis (43). The basic reactions, kinetics, and mechanisms of lipase-catalyzed reactions (hydrolysis, esterification, acidolysis, alcoholysis, ester exchange) have been discussed (3,44–46). In the presence of a suitable lipase as the biocatalyst, the following reactions are possible (the reactions are also reversible under appropriate conditions):

Hydrolysis:

$$R_1\text{–CO–OR} + H_2O \longrightarrow R_1\text{–COOH} + \text{R–OH} \quad [1]$$

Direct esterification:

$$R_1\text{–CO–OH} + \text{R–OH} \longrightarrow R_1\text{–CO–OR} + H_2O \quad [2]$$

Acidolysis:

$$R_1\text{–CO–OR} + R_2\text{–CO–OH} \longrightarrow R_2\text{–CO–OR} + R_1\text{–CO–OH} \quad [3]$$

Alcoholysis:

$$\text{R–CO–OR}_1 + R_2\text{–OH} \longrightarrow \text{R–CO–OR}_2 + R_1\text{–OH} \quad [4]$$

Ester-interchange:

$$R_1\text{–CO–OR}_2 + R_3\text{–CO–OR}_4 \longrightarrow R_1\text{–CO–OR}_4 + R_3\text{–CO–OR}_2 \quad [5]$$

Glycerolysis:

$$R_1\text{–CO–OR} + R_2\text{–OH} \longrightarrow R_1\text{–CO–OR}_2 + \text{R–OH} \quad [6]$$

where R_1, R_2, R_3, and R_4 represent the alkyl chain of the acyl group or alcohol. Lipases catalyze the reactions of water-insoluble substrates, whereas esterases mainly catalyze the reactions of water-soluble substrates. Lipases occur widely in nature and are active at the oil–water interface in heterogeneous reaction systems. Lipases hydrolyze TAG to MAG, DAG, FFA, and glycerol.

Lipase-catalyzed reactions are a combination of esterification and hydrolysis (reverse reaction) reactions. The degree to which hydrolysis occurs relative to esterification is governed by the concentration of water present. When excess water is present, hydrolysis predominates, resulting in the accumulation of FFA, MAG, and DAG. On the other hand, esterification predominates under water-limiting conditions or in organic solvents (i.e., acidolysis, alcoholysis, or glycerolysis). However, some water is essential for enzymatic catalysis because it maintains enzyme dynamics during noncovalent

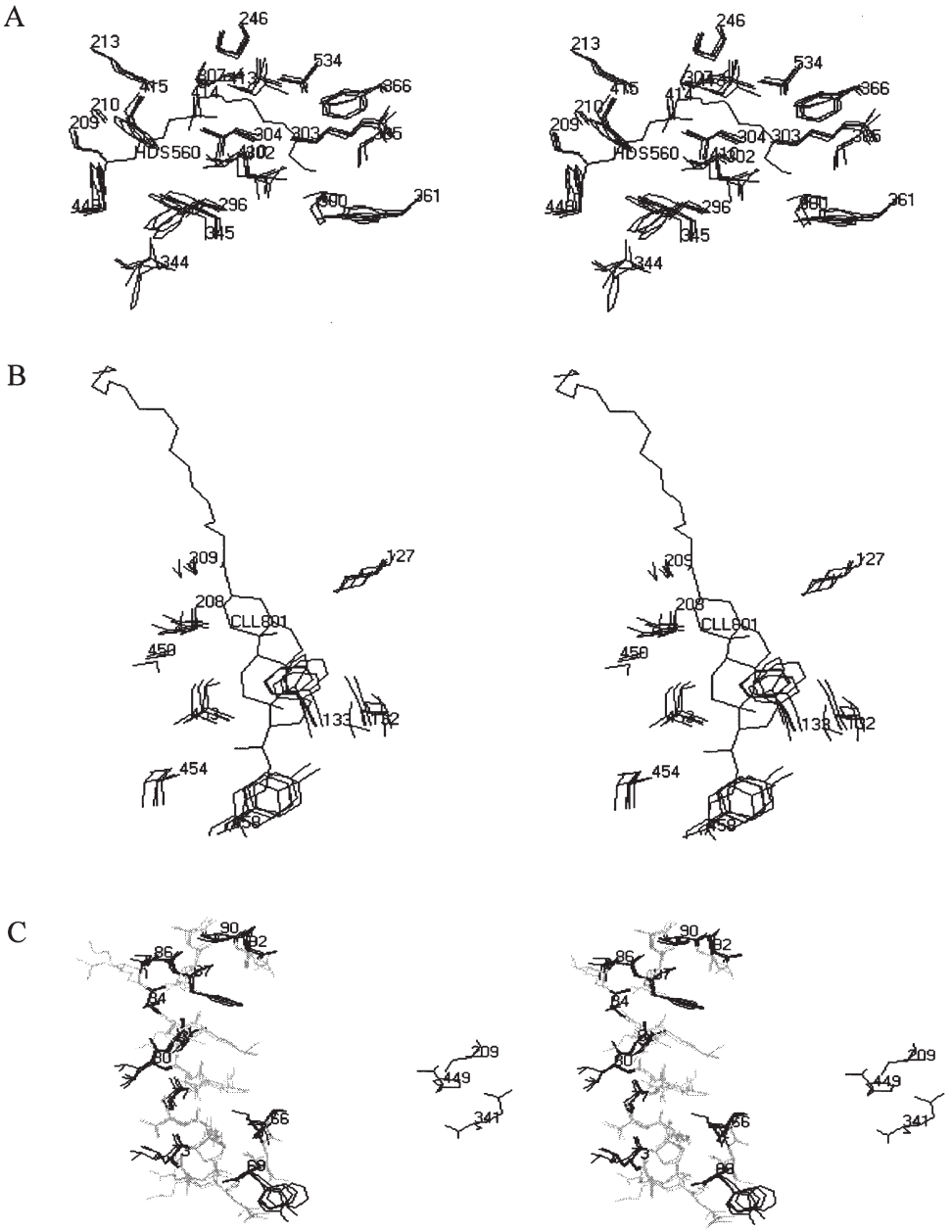

FIG. 2. Substrate-binding regions of *Candida rugosa* lipase (CRL) isoforms depicting the structural differences resulting from amino acid changes in these regions. (A) Superposition of the FA-binding tunnels of the CRL LIP1, LIP2, LIP3, LIP4, and LIP5. The same residue numbers among the five isoforms are indicated. The inhibitor hexadecane sulfonate is labeled in HDS560. (B) Superposition of the alcohol-binding sites of CRL isoforms. The cholesteryl linoleate molecule is labeled in CLL801. (C) Superposition of the flaps (residues 66–92) of CRL isoforms. The amino acid residues facing the substrate pocket are indicated in residue number and most of them are nonpolar (black). The amino acid residues in the opposite side of the flap facing the outside were mostly basic, acidic, and polar (gray). The catalytic triad residues (Ser 209, GLu 341, and His 449) are also shown. The images were produced using Swiss-Pdb Viewer (Glaxo Smith Kline S.A.).

interactions. To optimize one-step lipase-catalyzed reactions, it is necessary to strike a balance between hydrolysis and esterification. Lipase-catalyzed interesterification reactions offer the advantage of greater control over the positional distribution of FA in the final product, owing to the lipases' FA selectivity and regiospecificity. One great advantage is that these lipase reactions have no cofactor requirement.

Many lipases undergo conformational changes with the binding of substrates. The active site may be exposed to the solvent or inaccessible to the solvent in cases where the active site is protected by one or more polypeptides. The conformational changes correlate with interfacial activation. Multiple conformation states that show interfacial activation were observed for CRL (31). CRL undergoes a conformational

TABLE 2
Important Amino Acid Changes Producing Structural Differences Among *C. rugosa* Lipases[a]

Residue	LIP1	LIP2	LIP3	LIP4	LIP5
FA-binding site					
210	Ala	Ala	Ala	Ala	Ala
213	Met	Met	Met	Met	Met
246	Pro	Pro	Pro	Pro	Pro
296	**Phe**	**Val**	**Phe**	**Ala**	**Phe**
300	**Ser**	**Pro**	**Ser**	**Pro**	**Thr**
302	Leu	Leu	Leu	Leu	Leu
303	Arg	Arg	Arg	Arg	Arg
304	Leu	Leu	Leu	Leu	Leu
307	Leu	Leu	Leu	Leu	Leu
344	**Phe**	**Leu**	**Ile**	**Val**	**Leu**
345	Phe	Phe	Phe	Phe	Phe
361	Tyr	Tyr	Tyr	Tyr	Tyr
365	Ser	Ser	Ser	Ser	Ser
366	Phe	Phe	Phe	Phe	Phe
410	Leu	Leu	Leu	Leu	Leu
413	Leu	Leu	Leu	Leu	Leu
414	**Gly**	**Ala**	**Ala**	**Ala**	**Thr**
415	Phe	Phe	Phe	Phe	Phe
449	His	His	His	His	His
534	Val	Val	Val	Val	Val
Alcohol-binding site					
127	**Val**	**Leu**	**Ile**	**Val**	**Ile**
132	**Thr**	**Leu**	**Ile**	**Leu**	**Ile**
133	Phe	Phe	Phe	Phe	Phe
208	Glu	Glu	Glu	Glu	Glu
450	**Ser**	**Gly**	**Ala**	**Ala**	**Ala**
453	Ile	Ile	Ile	Ile	Ile
454	**Val**	**Ile**	**Val**	**Val**	**Val**
458	**Tyr**	**Tyr**	**Tyr**	**Phe**	**Phe**
Hydrophobic face of the flap					
66	**Glu**	**Met**	**Glu**	**Leu**	**Glu**
69	**Tyr**	**Phe**	**Phe**	**Trp**	**Tyr**
73	Leu	Leu	Leu	Leu	Leu
77	Ala	Ala	Ala	Ala	Ala
80	**Leu**	**Leu**	**Leu**	**Ser**	**Leu**
81	**Val**	**Val**	**Val**	**Leu**	**Val**
84	Ser	Ser	Ser	Ser	Ser
86	**Val**	**Ile**	**Val**	**Leu**	**Val**
87	Phe	Phe	Phe	Phe	Phe
90	Val	Val	Val	Val	Val
92	Pro	Pro	Pro	Pro	Pro

[a]The nonconserved positions are shown in bold.

rearrangement that involves a single 26-residue long surface loop (lid). In the presence of substrates, inhibitors, or less polar solvents, the loop swings to the side, leading to open state conformation. The loop does not move as a rigid body but undergoes an internal rearrangement, with the α-helix unwinding at one end and extending at the other end (39). In the open state, the nucleophilic serine is positioned in the center of a hydrophobic patch on the enzyme's surface and is easily accessible. The closed state has a tunnel that starts near Ser 209. The presence of a large tunnel is unique in *C. rugosa* and *Geotrichum candidum* lipases. The mouth of the tunnel is close to the active site and the conserved Glu 208, which confers negative potential on the vicinity of the active site (39). Recent studies from our laboratory indicate that the recombinant LIP4 from *C. rugosa* does not show interfacial activation in the presence of tributyrin and triolein as substrates when compared with LIP1 (19). Other yeast lipases such as *C. antarctica* B showed no interfacial activation and no conformational rearrangement upon inhibitor binding (47). The recombinant LIP4 obeys the Michaelis–Menten kinetics at all substrate concentrations. However, *Pseudomonas* lipases (48), pancreatic lipase (49), and certain isoforms of *C. rugosa* lipase undergo interfacial activation during catalysis (31) and do not obey the Michaelis–Menten kinetics or give sigmoidal curves against substrate concentration. These observations clearly indicate that despite the high level of sequence homology among CRL, the catalytic properties of the individual isoforms may differ.

PROTEIN ENGINEERING OF CRL ISOFORMS—TAILORING ENZYME FUNCTION

Site-directed mutagenesis has been very useful for the production of pure lipase isoforms of *C. rugosa* and is expected to continue to provide insight into lipase catalysis and specificity. Since the 3-D structure of some of the isoforms (LIP4 and LIP5) is not available yet, computer models based on the available 3-D structures of LIP1, LIP2, and LIP3 were used to help us understand the apparent differences in the biocatalytic properties of various isoforms. These known 3-D structures will definitely help scientists improve on the catalytic activity, substrate specificity, enantioselectivity, lid structures, chain length specificity, and enzyme stability of CRL isoforms for possible industrial applications, by applying gene shuffling (directed evolution) or rational design protein engineering. A tailor-made enzyme to modify the molecular recognition of 2-arylpropionic esters by recombinant LIP1 using site-directed mutagenesis of Phe 344 and Phe 345 was reported (50). Enzyme activity and selectivity were significantly decreased by Phe345Val (substituting Phe with Val at position 345) mutation and Phe344,345Val double mutation. The result suggested that Phe plays an important role in the S-enantiomer preference of (±)-2-(3-benzoylphenyl) propionic acid (ketoprofen) and (±)-2-(6-methoxy-2-naphthyl) propionic acid (naproxen), which are nonsteroidal anti-inflammatory drugs.

CRL was modified by engineering the amino acids at the substrate binding site (tunnel) of *C. rugosa* lipase mutants using computer modeling in an attempt to understand the substrate specificity and enantioselectivity of the enzyme for ketoprofen methyl ester (50). Manetti *et al.* (50) proposed that Phe 344 and Phe 345, in addition to the residues constituting the catalytic triad and the oxyanion hole, were the amino acids mainly involved in the enzyme–ligand (i.e., enzyme–substrate) interactions. Site-directed mutagenesis was then used to evaluate the importance of these amino acid residues in catalysis and selectivity toward different substrates. Phe 344 and especially Phe 345 influenced CRL activity, supporting

the theoretical computer model. In another study, both molecular modeling and site-directed mutagenesis were used to study the synthetic *LIP1* gene and the lipase mutants expressed in *P. pastoris* and assayed for chain length specificity in single and competitive substrates. Mutation of amino acids at different locations inside the tunnel (P246F, L413F, L410W, L410F/S300E, L410F/S365L) resulted in mutants with different chain length specificity (51). The lipase activity for a FA sharply decreased as the chain became long enough to reach the mutated site. Increasing the bulkiness of the amino acid at position 410 led to mutants that showed a strong discrimination of chain lengths longer than C_{14}. Different chain length specificity of the enzyme was achieved by mutating different amino acid residues of CRL inside the tunnel (51). Computer modeling helped to reveal that P246 and L413 were located near atom C6/C8 of the bound FA. P246F and L413F blocked chains longer than C6/C8, and the mutant enzymes strongly favored the hydrolysis of short-chain TAG. The P246F mutant enzyme had a 67- and 14-fold relative activity toward C_4 and C_6 chains, respectively, compared with the activity toward C_8 chains. In contrast, the corresponding activity of the wild-type CRL was 0.78 and 0.16, respectively. It is interesting to note that mutant L304F, which blocked the tunnel entrance, did not accept C_4 and C_6 short-chain TAG but hydrolyzed TAG with chains ≥8. An alternative binding site outside the tunnel for medium- and long-chain FA was proposed (51). Short-chain FA preferably bind to the tunnel, whereas medium- and long-chain FA can bind to either the tunnel or the alternative site, which has no specificity.

LID SWAPPING AND DNA SHUFFLING

Lid swapping/changing is a form of protein engineering used to provide clues to enzyme mechanisms by studying chain-length specificity, enantioselectivity or enantiopreference for substrates, and substrate specificity. Lid swapping may result in chimera proteins with new functions. The diversities in enzyme activity of CRL isozymes may be related to variations in the protein sequence, since the lid, a substrate-interacting domain, is not conserved in the isozymes. A strategy of fusing the thioredoxin (Trx) gene with the LIP4 gene was used to express the recombinant lipases in *E. coli*. The effect of lid region on the recombinant *C. rugosa* LIP4 lipase activity and specificity was studied by exchanging the lid regions from the other four *C. rugosa* isoforms (LIP1, LIP2, LIP3, and LIP5; and corresponding lids 1, 2, 3, and 5) with that of LIP4 and expressed as chimera proteins, Trx-LIP4/lid1, Trx-LIP4/lid2, Trx-LIP4/lid3, and Trx-LIP4/lid5, respectively (26,52). Lid swapping resulted in increased hydrolytic activities of the chimeric Trx-LIP4/lid2 and Trx-LIP4/lid3 by 14 and 32%, respectively, with tributyrin as substrate, whereas chimeric Trx-LIP4/lid1 and Trx-LIP4/lid5 activities decreased by 85 and 20%, respectively, compared with the native nonchimeric Trx-LIP4 with an unmodified lid. Cholesteryl caprate was the best substrate for Trx-LIP4, Trx-LIP4/lid2, and Trx-LIP4/lid3, but Trx-LIP4/lid1 and Trx-LIP4/lid5 showed a preference for cholesteryl stearate. In contrast, when *p*-nitrophenyl esters were the hydrolysis substrates, both *p*-nitrophenyl caprate and stearate were preferred by Trx-LIP4/lid2 and Trx-LIP4. The lid change affected the substrate specificity of the enzymes toward selectivity of various unsaturated FA with cholesteryl oleate (18:1) being the best substrate for Trx-LIP4, followed by cholesteryl linoleate (18:2, relative activity 68%); cholesteryl stearate (18:0) was a poor substrate (relative activity 7%). Both Trx-LIP4/lid2 and Trx-LIP4/lid3 had a similar substrate preference pattern toward Trx-LIP4. The lid domain also affected the enantioselectivity of CRL preferring the hydrolysis of *l*-menthyl acetate (desired isomer) over the *d*-menthyl acetate. *l*-Menthol is used as a flavor compound in beverages, toothpaste, cosmetic products, and local anesthetics because of its cool sensation. Interestingly, the recombinant Trx-LIP4 and all chimera LIP4 showed much better enantiopreference than the commercially available *C. rugosa* lipase (Lipase Type VII, Sigma). Among the chimeric LIP4, only Trx-LIP4/lid3 and Trx-LIP4 had similar enantioselectivity or enantiopreference. The other chimera proteins (Trx-LIP4/lid1, Trx-LIP4/lid2, and Trx-LIP4/lid5) showed significant decreases in enantioselectivity toward menthyl acetate. What is not known is how the enantioselectivity of the chimera proteins will be affected if other chiral or racemic substrates are used. This is still a potential area of research—to find ways to tailor the lipases to accept new substrates by lid swapping.

Recently, it was reported that the sequence of the lid affected the activity and specificity of recombinant CRL LIP1 isoform by similar lid-swapping engineering (53). Brocca *et al.* (53) demonstrated that swapping the LIP3 lid, which has high activity toward cholesterol esters, with the LIP1 isoform conferred cholesterol esterase activity to LIP1, which had no cholesterol esterase activity in its native form. No change in chain length specificity was observed. In another study, Secundo *et al.* (54) swapped the LIP1 lid with the lid of LIP3, and the chimera enzyme obtained was used for reactions in organic solvent. The chimera enzyme was less active and enantioselective than the wild-type in all the conditions tested. They postulate that the decrease in activity may be due to the chimera enzyme having a lower proportion of enzyme molecule in the open form, thereby hindering access to the enzyme active site during the alcoholysis of chloroethyl-2-hydroxy hexanoate with methanol and of vinyl acetate with 6-methyl-5-hepten-2-ol.

DNA shuffling is another potentially useful method (55) to design lipases to catalyze new reactions, to confer thermostability, and to improve on the enantioselectivity and substrate specificity of CRL lipases with potential applications in the production of useful materials, including foods, to benefit humankind. This technology has been successfully used to improve enantioselectivity (56), thermostability (57), and substrate specificity (58). More research effort is definitely needed to understand the chemistry and molecular biology of CRL isoforms.

RECENT APPLICATIONS OF PURIFIED AND RECOMBINANT CRL

Crude commercial CRL have been widely used in various biotransformations and biocatalysis (Table 1). The use of cross-linked enzyme crystals of CRL provided significant improvement in the enantioselective resolution of ketoprofen and other chiral esters compared with the crude CRL, and this was attributed to the selective removal of one isoenzyme during the crystallization (59). Very few lipases accept tertiary alcohols as substrates. However, CRL and a few other lipases accept tertiary alcohols as substrates owing to the presence of the amino acid motif (GGGX motif) in the oxyanion hole, and this further broadens the possible areas of application for CRL (60). There have been few reports on the use of purified and recombinant CRL and isoforms because of the difficulties of isolating and purifying the various isoforms, as mentioned previously. Progress is being made, and some of the new and potential applications of purified and recombinant isoforms are shown in Table 3. These involve mainly hydrolysis and synthetic reactions for the resolution of racemic mixtures, drug design, acylglycerols, and flavor and fragrances.

A comparison of pure recombinant LIP2 and LIP4 lipases with a crude preparation revealed that recombinant LIP2 possesses unique and remarkable catalytic properties different from those of LIP4 and crude CRL. LIP2 had a high specific activity toward cholesteryl esters, and this property may be useful for the determination of cholesterol in both clinical and food analyses. Since 70–80% of serum cholesterol is esterified with FA, it is possible to couple LIP2 to cholesterol oxidase and peroxidase, and then use it as a biosensor (enzyme sensor) for the determination of serum cholesterol. LIP2 also showed a high activity toward long-chain alcohols in the esterification of myristic acid. This enzyme could be used for the industrial production of wax esters, such as hexadecyl myristate and octadecyl myristate, for use in lubricants and cosmetics. LIP2 showed a preference for short-chain FA such as butyric acid in the esterification of propanol with various acyl chain lengths. Therefore, LIP2 could be useful in the production of important flavor compounds for food and fragrance use.

REGULATORY AND SAFETY CONSIDERATIONS

Any enzyme intended for use in the processing of foods or synthesis of compounds or ingredients for food use must have a GRAS status or undergo the regulatory process of approval. The Food Chemical Codex lists *C. rugosa* lipase as an enzyme used in dairy products, in confectionery, and for flavor development in processed foods. The enzyme has been used over the past 20 yr in Japan and the United States for the hydrolysis of milk fat to produce flavor compounds. Site-directed mutagenesis and lid swapping have led to the improvement of CRL isoform substrate selectivity and enantioselectivity. However, the controversy over genetically modified organisms should be taken into consideration by molecular biotechnologists and applied lipid biotechnologists as they design new lipases for new uses. The new lipases must be cloned into food-grade organisms for consumer acceptance of the products made with them, and for regulatory approval.

The safety and toxicity of *C. rugosa* lipase was studied using Sprague-Dawley rats who consumed the enzyme, at various concentrations, in the feed for 13 wk. *Candida rugosa* was found to possess no genotoxic potential when subjected to a battery of tests including bacterial mutation in *Salmonella typhimurium* strains TA98, TA100, TA1535, and TA1537 and in *E. coli* strain WP2 *uvr*A, *in vitro* chromosome aberration, and forward mutation in L5178Y mouse lymphoma cells (61). The yeast producing CRL was nonpathogenic to mice at doses up to 1.5×10^7 CFU/body. Flood and Kondo (61) concluded that

TABLE 3
New and Potential Applications of Purified Recombinant *C. rugosa* Lipases[a] (isoforms)

Application	Lipase/isoform	Reference
Ketoprofen (desired isomer)	LIP1, site-directed mutagenesis	50
Naproxen (desired isomer)	LIP1, site-directed mutagenesis	50
Hydrolysis of short-chain FA	LIP1, amino acid change at tunnel	51
Cholesteryl esterase activity	Swapping LIP3 lid with LIP1 lid	53
Increased hydrolysis of short-chain FA	Chimeras Trx-LIP4/lid2, Trx-LIP4/lid3	52
Enantioselectivity by alcoholysis	Swapping LIP1 lid with LIP3 lid	54
Esterase activity toward long-chain esters	Recombinant LIP4 in *Escherichia coli*	17
Short-chain flavor ester production	LIP2	20
Substrate specificity for cholesteryl esters, long-chain alcohols, and tributyrin	LIP2, multiple site-directed mutagenesis	20
Preferential hydrolysis of acylglycerol of different chain lengths	LIP1, LIP2, and LIP3 in organic media	90
Resolution of ibuprofen	LIP1 and LIP3	90
Enzyme sensor for cholesterol analysis	LIP2 coupled to cholesterol oxidase and peroxidase	Possibility
Synthesis of acylglycerols and structured lipids	Any of the isoforms	Possibility
Separation of conjugated linoleic isomers	To be determined	Possibility
Paper and pulp industry	To be determined	Possibility
Laundry detergents	Isoforms stable at alkaline pH	Possibility
Synthesis of surfactants and emulsifiers	To be determined	Possibility
Concentration of physiologically important FA such as CLA, EPA, DHA, and GLA	To be determined	Possibility

[a]TRX, thioredoxin; see Table 1 for other abbreviations.

the commercial crude enzyme preparation satisfied the basic requirements for safety testing established by the U.S. Food and Drug Administration for substances that will be present in the diet at low levels. Neither the enzyme preparation nor the production organism has any health-related hazard, and both lack any oral toxicity and genotoxicity. More studies are needed to prove the safety of recombinant CRL isoforms.

POTENTIAL FOR RESEARCH AND USE

CRL was identified over 40 yr ago and has been used in various applications, as stated earlier, but mainly in the crude form. The specific activities varied with the commercial suppliers and the source of the enzyme. The result was inconsistencies in the literature reports and in reproducibility of experimental and application data. Purifications, expressions in heterologous hosts, and characterizations of several CRL isoforms have clearly demonstrated that commercial crude CRL are mixtures of multiple isoforms that have significantly varied biochemical and application properties. The compositions of the various isoforms in the crude enzyme vary greatly owing to differential expression of isoforms in response to culture conditions and posttranslational modifications, such as glycosylation. However, the cloning and sequence analysis of five genes revealed a high sequence identity (77–88%), encoding 534 amino acid residues with predicted M.W. ranging from 56 to 58 kDa. The 3-D data for LIP1, LIP2, and LIP3 provided insights into the structure–function relationship of various CRL isoforms.

The breakthrough in overcoming the unusual serine codon usage by *C. rugosa* was an important milestone. This was achieved by either total synthesis or site-directed mutagenesis followed by successful expression of various functional recombinant isoforms in conventional heterologous hosts such as *P. pastoris* and *E. coli*. Ultimately, this achievement paved the way to high-level purification and possible industrial production of individual isoforms for biotransformations and biotechnological applications. Protein engineering through lid swapping and rationally designed site-directed mutagenesis have led and will continue to lead to CRL isoforms with improved catalytic power, thermostability, enantioselectivity, and substrate specificity, while allowing a better understanding of the mechanisms of actions of the various isoforms. We strongly believe that tailor-made lipases for specific applications will be possible in the near future.

Areas that would require further studies include the following: improvement of the stability of various CRL isoforms or selective improvement of the thermostability of a particular isoform by the use of lid swapping or other directed evolution techniques; new substrate specificity so that the enzyme will catalyze new reactions or multistep reactions; fusion of lipase genes to other enzymes or *vice versa* for industrial processes such as detergents, the tanning process, bioremediations, and as enzyme sensors; mechanistic studies on individual isoforms; use of protein engineering to produce novel true *sn*-2 specific lipases (which has been the desire of many lipid biotechnologists, food scientists, and research pharmacologists) for nutritional and nutraceutical lipid synthesis; multiple mutagenesis and selection of functional proteins with desired functional properties; chiral resolution of racemates of compounds with food, flavor, and pharmaceutical applications; and finally the production of food-grade recombinant/transgenic CRL. These enzymes must be produced and sold commercially at reasonable costs to benefit the consumer and industry. Subtle amino acid changes within a highly conserved protein fold may produce enzyme protein variants or isoforms enriched with new lipase properties, and this possibility needs to be explored and understood. Ultimately, the result, if accomplished, will be better biotechnological processes for the production of healthful foods, consumer necessities, better ingredients, active drugs, cheaper flavors and fragrances, cosmetics, a cleaner environment, and many more applications yet to be discovered. There is no limit to protein engineering capabilities and the application of pure CRL in the fats and oils and related industries.

Protein engineering will lead to changes in chain length specificity, enantioselectivity, substrate specificity, specific activity, thermal stability, and catalytic properties, and will provide mechanistic evidence for the different CRL isoforms.

ACKNOWLEDGMENTS

We acknowledge financial support by grant NSC-92-2313-B-001-025 from the National Science Council, Republic of China. We thank the University of Georgia, Athens, Georgia, for granting Professor Akoh a leave of absence to Academia Sinica, Taipei, Taiwan.

REFERENCES

1. Dominguez de Maria, P., and Sinisterra Gago, J. (1999) Causes of Unreproducibility of *C. rugosa* Lipase-Catalyzed Reactions in Slightly Hydrated Organic Media, *Tetrahedron 55*, 8555–8566.
2. Ghosh, P.K., Saxena, R.K., Gupta, R., Yadav, R.P., and Davidson, S. (1996) Microbial Lipases: Production and Applications, *Sci. Prog. 79 (Pt. 2)*, 119–157.
3. Benjamin, S., and Pandey, A. (1998) *Candida rugosa* Lipases: Molecular Biology and Versatility in Biotechnology, *Yeast 14*, 1069–1087.
4. Hube, B., Stehr, F., Bossenz, M., Mazur, A., Kretschmar, M., and Schafer, W. (2000) Secreted Lipases of *Candida albicans*: Cloning, Characterisation and Expression Analysis of a New Gene Family with at Least Ten Members, *Arch. Microbiol. 174*, 362–374.
5. Valero, F., del Rio, J.L., Poch, M., and Sola, C. (1991) Fermentation Behaviour of Lipase Production by *Candida rugosa* Growing on Different Mixtures of Glucose and Olive Oil, *J. Ferment. Bioeng. 72*, 399–401.
6. Ferrer, P., Montesinos, J.L., Valero, F., and Sola, C. (2001) Production of Native and Recombinant Lipases by *Candida rugosa*: A Review, *Appl. Biochem. Biotechnol. 95*, 221–255.
7. Gordillo, M.A., Obradors, N., Montesinos, J.L., Valero, F., Lafuente, J., and Sola, C. (1995) Stability Studies and Effect of the Initial Oleic Acid Concentration on Lipase Production by *Candida rugosa, Appl. Microbiol. Biotechnol. 43*, 38–41.
8. Thomson, C.A., Delaquis, P.J., and Mazza, G. (1999) Detection and Measurement of Microbial Lipase Activity: A Review, *Crit. Rev. Food Sci. Nutr. 39*, 165–187.
9. Chang, R.C., Chou, S.J., and Shaw, J.F. (1994) Multiple Forms and Functions of *Candida rugosa* Lipase, *Biotechnol. Appl. Biochem. 19*, 93–97.

10. Lee, G.C., Tang, S.J., Sun, K.H., and Shaw, J.F. (1999) Analysis of the Gene Family Encoding Lipases in *Candida rugosa* by Competitive Reverse Transcription-PCR, *Appl. Environ. Microbiol. 65*, 3888–3895.
11. Shaw, J.F., Chang, C.H., and Wang, Y.J. (1989) Characterization of Three Distinct Forms of Lipolytic Enzyme in a Commercial *Candida* Lipase Preparation, *Biotechnol. Lett. Surrey Sci. Technol. Lett. (11)*, 779–784.
12. Hernaiz, M.J., Rua, M., Celda, B., Medina, P., Sinisterra, J.V., and Sanchez-Montero, J.M. (1994) Contribution to the Study of the Alteration of Lipase Activity of *Candida rugosa* by Ions and Buffers, *Appl. Biochem. Biotechnol. 44*, 213–229.
13. Grochulski, P., Li, Y., Schrag, J.D., Bouthillier, F., Smith, P., Harrison, D., Rubin, B., and Cygler, M. (1993) Insights into Interfacial Activation from an Open Structure of *Candida rugosa* Lipase, *J. Biol. Chem. 268*, 12843–12847.
14. Rua, L., Diaz-Maurino, T., Fernandez, V.M., Otero, C., and Ballesteros, A. (1993) Purification and Characterization of Two Distinct Lipases from Candida cylindracea, *Biochim. Biophys. Acta 1156*, 181–189.
15. Kaiser, R., Erman, M., Duax, W.L., Ghosh, D., and Jornvall, H. (1994) Monomeric and Dimeric Forms of Cholesterol Esterase from *Candida cylindracea*. Primary Structure, Identity in Peptide Patterns, and Additional Microheterogeneity, *FEBS Lett. 337*, 123–127.
16. Diczfalusy, M.A., Hellman, U., and Alexson, S.E. (1997) Isolation of Carboxylester Lipase (Cel) Isoenzymes from *Candida rugosa* and Identification of the Corresponding Genes, *Arch. Biochem. Biophys. 348*, 1–8.
17. Tang, S.-J., Sun, K.-H., Sun, G.-H., Chang, T.-Y., and Lee, G.-C. (2000) Recombinant Expression of the *Candida rugosa* Lip4 Lipase in *Escherichia coli, Protein Express. Purification 20*, 308–313.
18. Kawaguchi, Y., Honda, H., Taniguchi-Morimura, J., and Iwasaki, S. (1989) The Codon CUG Is Read as Serine in an Asporogenic Yeast *Candida cylindracea, Nature 341*, 164–166.
19. Tang, S.-J., Shaw, J.-F., Sun, K.-H., Sun, G.-H., Chang, T.-Y., Lin, C.-K., Lo, Y.-C., and Lee, G.-C. (2001) Recombinant Expression and Characterization of the *Candida rugosa* Lip4 Lipase in *Pichia pastoris*: Comparison of Glycosylation, Activity, and Stability, *Arch. Biochem. Biophys. 387*, 93–98.
20. Lee, G.C., Lee, L.C., Sava, V., and Shaw, J.F. (2002) Multiple Mutagenesis of Non-universal Serine Codons of the *Candida rugosa* Lip2 Gene and Biochemical Characterization of Purified Recombinant Lip2 Lipase Overexpressed in *Pichia pastoris, Biochem. J. 366*, 603–611.
21. Brocca, S., Schmidt-Dannert, C., Lotti, M., Alberghina, L., and Schmid, R.D. (1998) Design, Total Synthesis, and Functional Overexpression of the *Candida rugosa* Lip1 Gene Coding for a Major Industrial Lipase, *Protein Sci. 7*, 1415–1422.
22. Longhi, S., Fusetti, F., Grandori, R., Lotti, M., Vanoni, M., and Alberghina, L. (1992) Cloning and Nucleotide Sequences of Two Lipase Genes from *Candida cylindracea, Biochim. Biophys. Acta 1131*, 227–232.
23. Lotti, M., Grandori, R., Fusetti, F., Longhi, S., Brocca, S., Tramontano, A., and Alberghina, L. (1993) Cloning and Analysis of *Candida cylindracea* Lipase Sequences, *Gene 124*, 45–55.
24. Diczfalusy, M.A., and Alexson, S.E.H. (1996) Isolation and Characterization of Novel Long-Chain Acyl-CoA Thioesterase/Carboxylesterase Isoenzymes from *Candida rugosa, Arch. Biochem. Biophys. 334,* 104–112.
25. Lotti, M., Monticelli, S., Luis Montesinos, J., Brocca, S., Valero, F., and Lafuente, J. (1998) Physiological Control on the Expression and Secretion of *Candida rugosa* Lipase, *Chem. Phys. Lipids 93*, 143–148.
26. Shaw, J.F., Lee, G.C., and Tang, S.J. (2002) Recombinant *Candida rugosa* Lipases, *EPC* European Patent Application 02009616. 02009610.
27. Rua, M.L., Diaz-Maurino, T., Fernandez, V.M., Otero, C., and Ballesteros, A. (1993) Purification and Characterization of Two Distinct Lipases from *Candida cylindracea*, *Biochim. Biophys. Acta (BBA) 1156*, 181–189.
28. Brahimi-Horn, M.C., Guglielmino, M.L., Elling, L., and Sparrow, L.G. (1990) The Esterase Profile of a Lipase from *Candida cylindracea, Biochim. Biophys. Acta 1042*, 51–54.
29. Schmidt-Dannert, C., Pleiss, J., and Schmid, R.D. (1998) A Toolbox of Recombinant Lipases for Industrial Applications, *Ann. N.Y. Acad. Sci. 864*, 14–22.
30. Lotti, M., Tramontano, A., Longhi, S., Fusetti, F., Brocca, S., Pizzi, E., and Alberghina, L. (1994) Variability Within the *Candida rugosa* Lipases Family, *Protein Eng. 7*, 531–535.
31. Grochulski, P., Li, Y., Schrag, J.D., and Cygler, M. (1994) Two Conformational States of *Candida rugosa* Lipase, *Protein Sci. 3*, 82–91.
32. Brocca, S., Persson, M., Wehtje, E., Adlercreutz, P., Alberghina, L., and Lotti, M. (2000) Mutants Provide Evidence of the Importance of Glycosydic Chains in the Activation of Lipase 1 from *Candida rugosa, Protein Sci. 9*, 985–990.
33. Pernas, M.A., Lopez, C., Pastrana, L., and Rua, M.L. (2000) Purification and Characterization of Lip2 and Lip3 Isoenzymes from a *Candida rugosa* Pilot-Plant Scale Fed-Batch Fermentation, *J. Biotechnol. 84*, 163–174.
34. Ghosh, D., Wawrzak, Z., Pletnev, V.Z., Li, N., Kaiser, R., Pangborn, W., Jornvall, H., Erman, M., and Duax, W.L. (1995) Structure of Uncomplexed and Linoleate-Bound *Candida cylindracea* Cholesterol Esterase, *Structure 3*, 279–288.
35. Mancheño, J.M., Pernas, M.A., Martínez, M.J., Ochoa, B., Rúa, M.L., and Hermoso, J.A. (2003) Structural Insights into the Lipase/Esterase Behavior in the *Candida rugosa* Lipases Family: Crystal Structure of the Lipase 2 Isoenzyme at 1.97 Å Resolution, *J. Mol. Biol. 332*, 1059–1069.
36. Grochulski, P., Bouthillier, F., Kazlauskas, R.J., Serreqi, A.N., Schrag, J.D., Ziomek, E., and Cygler, M. (1994) Analogs of Reaction Intermediates Identify a Unique Substrate Binding Site in *Candida rugosa* Lipase, *Biochemistry 33*, 3494–3500.
37. Cygler, M., Grochulski, P., Kazlauskas, R.J., Schrag, J.D., Bouthillier, F., Rubin, B., Serreqi, A.N., and Gupta, A.K. (1994) A Structural Basis for the Chiral Preferences of Lipases, *J. Am. Chem. Soc. 116*, 3180–3186.
38. Pletnev, V., Addlagatta, A., Wawrzak, Z., and Duax, W. (2003) Three-Dimensional Structure of Homodimeric Cholesterol Esterase-Ligand Complex at 1.4 Å Resolution, *Acta Crystallogr. D. Biol. Crystallogr. 59*, 50–56.
39. Cygler, M., and Schrag, J.D. (1999) Structure and Conformational Flexibility of *Candida rugosa* Lipase, *Biochim. Biophys. Acta 1441*, 205–214.
40. Ollis, D.L., Cheah, E., Cygler, M., Dijkstra, B., Frolow, F., Franken, S.M., Harel, M., Remington, S.J., Silman, I., Schrag, J., *et al.* (1992) The Alpha/Beta Hydrolase Fold, *Protein Eng. 5*, 197–211.
41. Schwede, T., Kopp, J., Guex, N., and Peitsch, M.C. (2003) SWISS-MODEL: An Automated Protein Homology-Modeling Server, *Nucleic Acids Res. 31*, 3381–3385.
42. Berman, H.M., Westbrook, J., Feng, Z., Gilliland, G., Bhat, T.N., Weissig, H., Shindyalov, I.N., and Bourne, P.E. (2000) The Protein Data Bank, *Nucleic Acids Res. 28,* 235–242.
43. Verger, R. (1997) "Interfacial Activation" of Lipases: Facts and Artifacts, *Trends Biotechnol. 15*, 32–38.
44. Malcata, F.X., Reyes, H.R., Garcia, H.S., Hill, C.G., Jr., and Amundson, C.H. (1992) Kinetics and Mechanisms of Reactions Catalysed by Immobilized Lipases, *Enzyme Microb. Technol. 14*, 426–446.
45. Marangoni, A.G. (1994) Enzyme Kinetics of Lipolysis Revisited: The Role of Lipase Interfacial Binding, *Biochem. Biophys. Res. Commun. 200*, 1321–1328.

46. Janssen, A.E.M., Vaidya, A.M., and Halling, P.J. (1996) Substrate Specificity and Kinetics of *Candida rugosa* Lipase in Organic Media, *Enzyme Microb. Technol. 18*, 340–346.
47. Uppenberg, J., Ohrner, N., Norin, M., Hult, K., Kleywegt, G.J., Patkar, S., Waagen, V., Anthonsen, T., and Jones, T.A. (1995) Crystallographic and Molecular-Modeling Studies of Lipase B from *Candida antarctica* Reveal a Stereospecificity Pocket for Secondary Alcohols, *Biochemistry 34*, 16838–16851.
48. Schrag, J.D., Li, Y., Cygler, M., Lang, D., Burgdorf, T., Hecht, H.J., Schmid, R., Schomburg, D., Rydel, T.J., Oliver, J.D., *et al*. (1997) The Open Conformation of a *Pseudomonas* Lipase, *Structure 5*, 187–202.
49. van Tilbeurgh, H., Egloff, M.P., Martinez, C., Rugani, N., Verger, R., and Cambillau, C. (1993) Interfacial Activation of the Lipase–Procolipase Complex by Mixed Micelles Revealed by X-ray Crystallography, *Nature 362*, 814–820.
50. Manetti, F., Mileto, D., Corelli, F., Soro, S., Palocci, C., Cernia, E., D'Acquarica, I., Lotti, M., Alberghina, L., and Botta, M. (2000) Design and Realization of a Tailor-Made Enzyme to Modify the Molecular Recognition of 2-Arylpropionic Esters by *Candida rugosa* Lipase, *Biochim. Biophys. Acta 1543*, 146–158.
51. Schmitt, J., Brocca, S., Schmid, R.D., and Pleiss, J. (2002) Blocking the Tunnel: Engineering of *Candida rugosa* Lipase Mutants with Short Chain Length Specificity, *Protein Eng. 15*, 595–601.
52. Lee, G.C., Tang, S.J., and Shaw, J.F. (1999) Structure and Function of *Candida rugosa* Lipase, presented at the 90th Annual Meeting of the American Oil Chemists' Society, May 9–13, Orlando.
53. Brocca, S., Secundo, F., Ossola, M., Alberghina, L., Carrea, G., and Lotti, M. (2003) Sequence of the Lid Affects Activity and Specificity of *Candida rugosa* Lipase Isoenzymes, *Protein Sci. 12*, 2312–2319.
54. Secundo, F., Carrea, G., Tarabiono, C., Brocca, S., and Lotti, M. (2004) Activity and Enantioselectivity of Wildtype and Lid-Mutated *Candida rugosa* Lipase Isoform 1 in Organic Solvents, *Biotechnol. Bioeng. 86*, 236–240.
55. Stemmer, W.P. (1994) DNA Shuffling by Random Fragmentation and Reassembly: *In vitro* Recombination for Molecular Evolution, *Proc. Natl. Acad. Sci. USA 91*, 10747–10751.
56. Reetz, M.T. (2004) Controlling the Enantioselectivity of Enzymes by Directed Evolution: Practical and Theoretical Ramifications, *Proc. Natl. Acad. Sci. USA 101*, 5716–5722.
57. Arnold, F.H., Giver, L., Gershenson, A., Zhao, H., and Miyazaki, K. (1999) Directed Evolution of Mesophilic Enzymes into Their Thermophilic Counterparts, *Ann. N.Y. Acad. Sci. 870*, 400–403.
58. Song, J.K., Chung, B., Oh, Y.H., and Rhee, J.S. (2002) Construction of DNA-Shuffled and Incrementally Truncated Libraries by a Mutagenic and Unidirectional Reassembly Method: Changing from a Substrate Specificity of Phospholipase to That of Lipase, *Appl. Environ. Microbiol. 68*, 6146–6151.
59. Lalonde, J.J., Govardhan, C., Khalaf, N., Martinez, A.G., Visuri, K., and Margolin, A.L. (1995) Cross-Linked Crystals of *Candida rugosa* Lipase: Highly Efficient Catalysts for the Resolution of Chiral Esters, *J. Am. Chem. Soc. 117*, 6845–6852.
60. Henke, E., Pleiss, J., and Bornscheuer, U.T. (2002) Activity of Lipases and Esterases Towards Tertiary Alcohols: Insights into Structure–Function Relationships, *Angew. Chem. Int. Ed. Engl. 41*, 3211–3213.
61. Flood, M.T., and Kondo, M. (2001) Safety Evaluation of Lipase Produced from *Candida rugosa*: Summary of Toxicological Data, *Regul. Toxicol. Pharmacol. 33*, 157–164.
62. Basri, M., Ampon, K., Yunus, W., Razak, C.N.A., and Salleh, A.B. (1995) Enzymatic Synthesis of Fatty Esters by Hydrophobic Lipase Derivatives Immobilized on Organic Polymer Beads, *J. Am. Oil Chem. Soc. 72*, 407–411.
63. Hayes, D.G., and Kleiman, R. (1995) Lipase-Catalyzed Synthesis and Properties of Estolides and Their Esters, *J. Am. Oil Chem. Soc. 72*, 1309–1316.
64. Hoq, M.M., Yamane, T., Shimizu, S., Funada, T., and Ishida, S. (1984) Continuous Synthesis of Glycerides by Lipase in a Microporous Membrane Bioreactor, *J. Am. Oil Chem. Soc. 61*, 776–781.
65. Linfield, W.M., O'Brien, D.J., Serota, S., and Barauskas, R.A. (1984) Lipid–Lipase Interactions. 1. Fat Splitting with Lipase from *Candida rugosa, J. Am. Oil Chem. Soc. 61*, 1067–1071.
66. Marangoni, A.G. (1994) *Candida* and *Pseudomonas* Lipase-Catalyzed Hydrolysis of Butteroil in the Absence of Organic Solvents, *J. Food Sci. 59*, 1096–1099.
67. Virto, M.D., Agud, I., Montero, S., Blanco, A., Solozabal, R., Lascaray, J.M., Llama, M.J., Serra, J.L., Landeta, L.C., and Derenobales, M. (1994) Hydrolysis of Animal Fats by Immobilized *Candida rugosa* Lipase, *Enzyme Microb. Technol. 16*, 61– 65.
68. Wang, Y.J., Sheu, J.Y., Wang, F.F., and Shaw, J.F. (1988) Lipase-Catalyzed Oil Hydrolysis in the Absence of Added Emulsifier, *Biotechnol. Bioeng. 31*, 628–633.
69. Watanabe, T., Suzuki, Y., Sagesaka, Y., and Kohashi, M. (1995) Immobilization of Lipases on Polyethylene and Application to Perilla Oil Hydrolysis for Production of Alpha-Linolenic Acid, *J. Nutr. Sci. Vitaminol. 41*, 307–312.
70. Murty, V.R., Bhat, J., and Muniswaran, P.K. (2004) Hydrolysis of Rice Bran Oil Using an Immobilized Lipase from *Candida rugosa* in Isooctane, *Biotechnol. Lett. 26*, 563–567.
71. Mukherjee, K.D., Kiewitt, I., and Hills, M.J. (1993) Substrate Specificities of Lipases in View of Kinetic Resolution of Unsaturated Fatty Acids, *Appl. Microbiol. Biotechnol. 40*, 489–493.
72. Osterberg, E., Blomstrom, A.C., and Holmberg, K. (1989) Lipase Catalyzed Transesterification of Unsaturated Lipids in a Microemulsion, *J. Am. Oil Chem. Soc. 66*, 1330–1333.
73. Rangheard, M.S., Langrand, G., Triantaphylides, C., and Baratti, J. (1989) Multi-competitive Enzymatic Reactions in Organic Media: A Simple Test for the Determination of Lipase Fatty Acid Specificity, *Biochim. Biophys. Acta 1004*, 20–28.
74. McNeill, G.P., and Sonnet, P.E. (1995) Isolation of Erucic Acid from Rapeseed Oil by Lipase-Catalyzed Hydrolysis, *J. Am. Oil Chem. Soc. 72*, 213–218.
75. Kaimal, T.N.B., Prasad, R.B.N., and Rao, T.C. (1993) A Novel Lipase Hydrolysis Method to Concentrate Erucic Acid Glycerides in Cruciferae Oils, *Biotechnol. Lett. 15*, 353–356.
76. Kim, M.G., and Lee, S.B. (1996) Enzymatic Resolution of Racemic Ibuprofen by Lipase-Catalyzed Esterification Reaction: Effects of Water Content and Solid Supports, *J. Ferment. Bioeng. 81*, 269–271.
77. Tsai, S.W., Lu, C.C., and Chang, C.S. (1996) Surfactant Enhancement of (S)-Naproxen Ester Productivity from Racemic Naproxen by Lipase in Isooctane, *Biotechnol. Bioeng. 51*, 148–156.
78. Lalonde, J. (1995) The Preparation of Homochiral Drugs and Peptides Using Cross-Linked Enzyme Crystals, *Chim. Oggi–Chem. Today 13*, 31–35.
79. Garcia, H.S., Arcos, J.A., Ward, D.J., and Hill, C.G. (2000) Synthesis of Glycerides Containing n-3 Fatty Acids and Conjugated Linoleic Acid by Solvent-Free Acidolysis of Fish Oil, *Biotechnol. Bioeng. 70*, 587–591.
80. Nagao, T., Yamauchi-Sato, Y., Sugihara, A., Iwata, T., Nagao, K., Yanagita, T., Adachi, S., and Shimada, Y. (2003) Purification of Conjugated Linoleic Acid Isomers Through a Process Including Lipase-Catalyzed Selective Esterification, *Biosci. Biotechnol. Biochem. 67*, 1429–1433.
81. Weber, N., Weitkamp, P., and Mukherjee, K.D. (2001) Fatty Acid Steryl, Stanyl, and Steroid Esters by Esterification and Transesterification *in vacuo* Using *Candida rugosa* Lipase as Catalyst, *J. Agric. Food Chem. 49*, 67–71.
82. Benjamin, S., and Pandey, A. (1998) *Candida rugosa* and Its Lipases—A Retrospect, *J. Sci. Ind. Res. 57*, 1–9.
83. Calleri, E., Temporini, C., Furlanetto, S., Loiodice, F., Fracchiolla, G., and Massolini, G. (2003) Lipases for Biocatalysis: Development of a Chromatographic Bioreactor, *J. Pharmaceut. Biomed. Anal. 32*, 715–724.
84. Wang, D.L., Nag, A., Lee, G.C., and Shaw, J.F. (2002) Factors

Affecting the Resolution of DL-Menthol by Immobilized Lipase-Catalyzed Esterification in Organic Solvent, *J. Agric. Food Chem. 50*, 262–265.
85. Wu, W.H., Akoh, C.C., and Phillips, R.S. (1996) Lipase-Catalyzed Stereoselective Esterification of DL-Menthol in Organic Solvents Using Acid Anhydrides as Acylating Agents, *Enzyme Microb. Technol. 18*, 536–539.
86. Chattopadhyay, S., Sivalingam, G., and Madras, G. (2003) Lipase Specificity for the Hydrolysis of Poly(vinyl acetate), *Polymer Degrad. Stability 80*, 477–483.
87. Lee, K.T., and Akoh, C.C. (1998) Immobilization of Lipases on Clay, Celite 545, Diethylaminoethyl-, and Carboxymethyl-Sephadex and Their Interesterification Activity, *Biotechnol. Techn. 12*, 381–384.
88. Shieh, C.J., Akoh, C.C., and Yee, L.N. (1996) Optimized Enzymatic Synthesis of Geranyl Butyrate with Lipase AY from *Candida rugosa, Biotechnol. Bioeng. 51*, 371–374.
89. Mutua, L.N., and Akoh, C.C. (1993) Synthesis of Alkyl Glycoside Fatty Acid Esters in Nonaqueous Media by *Candida* sp. Lipase, *J. Am. Oil Chem. Soc. 70*, 43–46.
90. Lopez, N., Pernas, M.A., Pastrana, L.M., Sanchez, A., Valero, F., and Rua, M.L. (2004) Reactivity of Pure *Candida rugosa* Lipase Isoenzymes (Lip1, Lip2, and Lip3) in Aqueous and Organic Media. Influence of the Isoenzymatic Profile on the Lipase Performance in Organic Media, *Biotechnol. Prog. 20*, 65–73.

[Received June 28, 2004; accepted August 9, 2004]

Dietary Intakes and Food Sources of n-6 and n-3 PUFA in French Adult Men and Women

Pierre Astorg*, Nathalie Arnault, Sébastien Czernichow, Nathalie Noisette, Pilar Galan, and Serge Hercberg

UMR INSERM 557/INRA/CNAM Epidémiologie Nutritionnelle, Institut Scientifique et Technique de la Nutrition et de l'Alimentation (ISTNA), Conservatoire National des Arts et Métiers (CNAM), Paris, France

ABSTRACT: The intake of individual n-6 and n-3 PUFA has been estimated in 4,884 adult subjects (2,099 men and 2,785 women), volunteers from the French SU.VI.MAX intervention trial. The food intakes of each subject were recorded in at least ten 24-h record questionnaires completed over a period of 2.5 yr, allowing the estimation of the daily intake of energy; total fat; and linoleic, α-linolenic, arachidonic, eicosapentaenoic (EPA), n-3 docosapentaenoic (DPA), and docosahexaenoic (DHA) acids. The mean total fat intake corresponded to 94.1 g/d (36.3% of total energy intake) in men and 73.4 g/d (38.1% of energy) in women. The intake of linoleic acid was 10.6 g/d in men and 8.1 g/d in women, representing 4.2% of energy intake; that of α-linolenic acid was 0.94 g/d in men and 0.74 g/d in women, representing 0.37% of energy intake, with a mean linoleic/α-linolenic acid ratio of 11.3. The mean intakes of long-chain PUFA were: arachidonic acid, 204 mg/d in men and 152 mg/d in women; EPA, 150 mg/d in men and 118 mg/d in women; DPA, 75 mg/d in men and 56 mg/d in women; DHA, 273 mg/d in men and 226 mg/d in women; long-chain n-3 PUFA, 497 mg/d in men and 400 mg/d in women. Ninety-five percent of the sample consumed less than 0.5% of energy as α-linolenic acid, which is well below the current French recommendation for adults (0.8% of energy). In contrast, the mean intakes of long-chain n-6 and n-3 PUFA appear fairly high and fit the current French recommendations (total long-chain PUFA: 500 mg/d in men and 400 mg/d in women; DHA: 120 mg/d in men and 100 mg/d in women). The intakes of α-linolenic acid, and to a lesser extent of linoleic acid, were highly correlated with that of lipids. Whereas the main source of linoleic acid was vegetable oils, all food types contributed to α-linolenic acid intake, the main ones being animal products (meat, poultry, and dairy products). The main source of EPA and DHA (and of total long-chain n-3 PUFA) was fish and seafood, but the major source of DPA was meat, poultry, and eggs. Fish and seafood consumption showed very large interindividual variations, the low consumers being at risk of insufficient n-3 PUFA intake.

Paper no. L9468 in *Lipids 39,* 527–535 (June 2004).

EFA are nutrients of primary importance for health, and research in the last 15 yr has demonstrated the potential role of an adequate intake of n-3 PUFA in the prevention of several diseases, cardiovascular diseases in particular (1). As linoleic and α-linolenic acids compete for the same enzymes in their metabolism to longer-chain PUFA, their optimal intakes are mutually dependent (2). In Western countries, the increasing use in the last 50 yr of vegetable oils rich in linoleic acid and poor in α-linolenic acid in farm animal feed and human food has resulted in a high n-6/n-3 PUFA (or linoleic/α-linolenic acid) ratio in the diet, above the values considered as optimal (2–4). In addition, the conversion of linoleic and α-linolenic acids to long-chain PUFA occurs in humans with only a low yield, and the intake of even small amounts of long-chain n-6 and n-3 PUFA contributes significantly to the EFA status (2). Therefore, the evaluation of the adequacy of EFA intakes in a population needs to estimate individual intakes of both precursor FA (linoleic and α-linolenic acids) and long-chain PUFA of the n-6 and n-3 series. In recent years, recommended dietary allowances have been published in several countries, including France, not only for linoleic and α-linolenic acids but also for long-chain n-3 PUFA, especially for DHA (5,6). However, insufficient data are available on the real intake of individual PUFA in human populations. In particular, studies reporting the intake of individual long-chain n-6 or n-3 PUFA are not common, as they depend on the availability and completeness of PUFA food composition tables. The few existing studies concerning the French population deal only with the intakes of linoleic and α-linolenic acids (7). Recent population-based studies have considered long-chain PUFA consumption in countries from Europe and North America and in Australia and Japan (8–15). This study is based on the SU.VI.MAX study, an interventional prospective study on a sample of French adults of both sexes, during which the food habits of participants were recorded, and on a food composition table that we developed to allow the estimation of the intake of n-6 and n-3 PUFA of interest.

MATERIALS AND METHODS

Population sample. The SU.VI.MAX study is a randomized, double-blind, placebo-controlled primary prevention trial designed to test the effects of daily supplementation with a mixture of vitamin C, vitamin E, β-carotene, zinc, and selenium on the incidence of cardiovascular diseases and of cancers in a population of adult men and women in France (16). Other objectives of the study were to evaluate food consumption in

* To whom correspondence should be addressed at ISTNA/CNAM, 5 rue du Vertbois, 75003, Paris, France. E-mail: pierre.astorg@cnam.fr

Abbreviations: DHA, docosahexaenoic acid; DPA, n-3 docosapentaenoic acid; EFA, essential fatty acids; EPA, eicosapentaenoic acid; PUFA, polyunsaturated FA.

the French general population and to contribute to a better understanding of the relation between nutrition and health. The population sample consisted of 12,741 subjects (5,028 men and 7,713 women) from all regions of France, who were included in 1994–1995 with a planned follow-up of 8 yr. Men were aged 45–63 and women 35–63 at inclusion. A larger age range with younger ages was chosen for women to take into account the younger onset of breast cancer in women (from 40 yr old) than of all cancers in men. Other details on study design, recruitment, and baseline characteristics of the subjects have been reported previously (16). All subjects gave their informed written consent to the study. The study was approved by *ad hoc* ethical committees, i.e., the "Comité consultatif de protection des personnes dans la recherche biomédicale" (CCPPRB no. 706, Cochin Hospital, Paris, France), and the "Commission nationale de l'informatique et des libertés" (CNIL no. 334641).

Dietary assessment. At inclusion and every 2 mon until the end of the study, subjects were asked to complete a 24-h dietary record questionnaire, i.e., a total of six questionnaires per year. The days of record were fixed for each subject and randomized to assess 4 weekdays and 2 weekend days each year. The 24-h record data were transmitted with the Minitel, a small terminal coupled to a telephone line, widely used in France in the 1990s. At the beginning of the study, the participants received a small processing unit, to be coupled with the Minitel, that was especially developed for the study. This unit was loaded with specialized software allowing the participants to fill out their dietary records directly on their Minitel and to transmit the data during brief telephone connections. The software allowed completion of a 24-h record questionnaire according to a detailed pattern. A large choice of foods and drinks (about 900 items) was displayed for each of three meals (breakfast, lunch, and dinner) and of four other food intake occurrences (during the morning, during the afternoon, during late evening, and during the night). The list included both simple food items (for example, mutton chop, lettuce, banana, or orange juice) and complex dishes (for example, couscous, cassoulet, or paella). Foods not included in the list could also be mentioned by the subjects. For each food or drink mentioned, the subjects were asked to indicate the portion size consumed. They were helped by an instruction manual given to them at the start of the study, including photographs of portions sizes of 236 foods and drinks. Three portion sizes were shown for each food or drink, with possibilities of intermediate or out-of-scale choices (for example, between the first and the second, or more than the third). The use of these portion photographs was previously validated on 687 subjects in a pilot study (17). The questionnaire also included questions on the cooking methods, and on the type of oil or fat used for seasoning or cooking. For this study, we selected participants who had completed at least 10 questionnaires within a period of 2.5 yr between the inclusion and 1998. A previous study showed that 10 records were sufficient to estimate the individual intakes of the main FA classes (saturated, monounsaturated, and PUFA) with a good accuracy (18). For each of these subjects, the data produced were drawn from all completed questionnaires obtained in the required period.

Food composition table. A food composition table adapted to the analysis of the dietary data collected in the SU.VI.MAX study was developed on the basis of existing data (19). The contents of foods with respect to energy, total fat, linoleic acid, α-linolenic acid, arachidonic acid, and the long-chain n-3 EPA, n-3 docosapentaenoic acid (DPA), and DHA were compiled from existing tables: the French food composition table (20) and its recent additions (21); the USDA National Nutrient Database (22); and the British McCance & Widdowson's food composition table (23), as well as from original publications. In particular, many data on the contents of meat, poultry, eggs, fish, and seafood with respect to n-6 and n-3 long-chain PUFA were drawn principally from original publications, as the existing tables were incomplete.

Statistical analyses. Data were compiled on an Alpha-VMS system, and statistical analyses were performed using SAS software (SAS Institute, Cary, NC). Correlations between variables were calculated using the Spearman's correlation coefficient. Means of quintiles of FA intakes were compared with the Bonferroni test and with the test of linear trend.

RESULTS

Complete dietary data from at least ten 24-h record questionnaires were obtained from 4,884 subjects (2,099 men and 2,785 women), who formed the population sample used for this study and who represented 38.3% of the whole cohort (41.7% of men and 36.1% of women). The intakes of total fat and of individual n-6 and n-3 PUFA by men and women are given in Tables 1 and 2. When total fat and FA intakes are expressed as the percentage of energy intake (Table 2), women appear to have consumed slightly more total fat than men (38.1 vs. 36.3% of energy), as well as slightly more linoleic and α-linolenic acids; there are no or only minute differences between sexes concerning long-chain PUFA consumption on an energy basis. The mean linoleic acid intakes amounted to *ca.* 4.2% of energy intake in both men and women, and less than 5% of the population consumed less than 2.7% of energy as linoleic acid (Table 2). The mean α-linolenic acid intakes were *ca.* 0.38% of energy, and 95% of the population sample did not reach 0.5% of energy intake as α-linolenic acid. As a consequence, the linoleic acid/α-linolenic acid ratio was fairly high: 11.3 on average, with 50% of the population having a ratio over 10.8. One-half of the population sample (56.8% of men and 45.6% of women) had both an α-linolenic acid intake of less than 0.4% of energy and a linoleic acid/α-linolenic acid ratio greater than 10. Whereas the arachidonic acid mean intakes amounted to 204 mg/d in men and 152 mg/d in women (0.08% of energy for both), long-chain n-3 PUFA mean intakes were 497 mg/d in men and 400 mg/d in women, representing 0.21% of energy, and consisted of 55% DHA, 30% EPA, and 15% DPA. In contrast to the other PUFA, intakes of long-chain n-3 PUFA, and especially those

TABLE 1
Intakes of Total Fat and of n-6 and n-3 PUFA (g or mg/d)

	Total fat (g/d)	18:2n-6 (g/d)	18:3n-3 (g/d)	18:2n-6/ 18:3n-3	20:4n-6 (mg/d)	20:5n-3 (mg/d)	22:5n-3 (mg/d)	22:6n-3 (mg/d)	LC n-3[a] (mg/d)
Men									
(*n* = 2099)									
Mean	94.06	10.64	0.94	11.5	203.9	149.9	74.8	272.6	497.3
SD	22.42	3.28	0.25	3.0	66.0	112.1	33.0	191.3	325.1
Minimum	32.11	2.74	0.37	4.8	55.1	4.5	12.9	10.0	39.9
5th percentile	59.97	6.13	0.59	7.7	111.1	27.5	33.5	66.0	139.3
Median	93.32	10.12	0.92	11.0	197.0	119.6	68.2	221.3	408.3
95th percentile	134.42	16.74	1.37	16.9	323.2	375.1	138.4	668.4	1159.3
Maximum	187.53	27.85	2.62	39.3	558.2	768.5	275.7	1472.8	2617.0
Women									
(*n* = 2785)									
Mean	73.55	8.10	0.74	11.1	151.9	117.8	55.9	225.9	399.6
SD	19.17	2.60	0.20	2.7	49.2	94.2	27.8	170.9	286.0
Minimum	19.46	2.10	0.21	4.8	14.5	2.0	2.3	6.5	10.8
5th percentile	44.29	4.29	0.45	7.6	79.2	19.2	22.9	50.0	101.3
Median	72.00	7.80	0.71	10.7	147.8	91.4	50.2	177.0	320.6
95th percentile	106.88	12.75	1.10	16.3	238.6	308.5	109.1	574.2	980.2
Maximum	172.15	21.11	1.98	32.1	347.4	853.3	269.5	1770.2	2893.0

[a]Long-chain (LC) n-3 PUFA: sum of 20:5n-3, 22:5n-3, and 22:6n-3.

TABLE 2
Intakes of Total Fat and of n-6 and n-3 PUFA (% of total energy intake)

	Total fat	18:2n-6	18:3n-3	20:4n-6	20:5n-3	22:5n-3	22:6n-3	LC n-3[a]
Men								
(*n* = 2099)								
Mean	36.29	4.13	0.36	0.08	0.06	0.03	0.11	0.21
SD	4.58	1.08	0.07	0.02	0.05	0.01	0.08	0.13
Minimum	18.87	1.45	0.20	0.02	0.00	0.01	0.01	0.02
5th percentile	28.41	2.71	0.28	0.05	0.01	0.01	0.03	0.06
Median	36.30	3.95	0.35	0.08	0.05	0.03	0.09	0.16
95th percentile	43.65	6.13	0.48	0.12	0.15	0.05	0.26	0.45
Maximum	56.11	11.04	1.11	0.19	0.48	0.10	0.54	0.97
Women								
(*n* = 2785)								
Mean	38.12	4.22	0.38	0.08	0.06	0.03	0.12	0.21
SD	4.44	1.06	0.07	0.02	0.05	0.01	0.09	0.16
Minimum	18.41	1.68	0.18	0.01	0.00	0.00	0.01	0.01
5th percentile	30.73	2.75	0.30	0.05	0.01	0.01	0.03	0.06
Median	38.33	4.08	0.38	0.08	0.05	0.03	0.09	0.17
95th percentile	44.60	6.14	0.50	0.12	0.17	0.06	0.30	0.52
Maximum	53.65	10.20	1.04	0.22	0.53	0.17	1.11	1.81
P (*t*-test), men vs. women	<0.0001	0.002	<0.0001	0.42	0.40	0.37	<0.0001	0.01

[a]Long-chain (LC) n-3 PUFA: sum of 20:5n-3, 22:5n-3, and 22:6n-3.

of EPA and DHA, had a skewed distribution (mean/median = 1.27), with an SD reaching more than 70% of the mean. The ratio between the 95th and the 5th percentiles reached 10–12 for EPA and 13–16 for DHA, but only 2–3 for linoleic, α-linolenic, and arachidonic acids. This reflects much larger interindividual variations in the intakes of n-3 long-chain PUFA, especially EPA and DHA, than for the other PUFA.

Both linoleic and α-linolenic acid intakes were highly correlated to total energy and total fat intakes (Table 3), the correlation coefficients being the highest for α-linolenic acid. Correlations with total energy and total fat intakes were quite significant, though of lesser intensity, with arachidonic acid and DPA intakes, whereas they were much weaker with EPA and DHA intakes (Table 3). Both linoleic and α-linolenic acid intakes were correlated with the intakes of animal products (meat, processed meat, offal, poultry, game, and eggs), whereas only linoleic acid intake was strongly correlated with the intake of vegetable oils. α-Linolenic acid intake was very poorly correlated with the intake of α-linolenic acid-rich vegetable oils present on the French market (rapeseed, soybean, and walnut oils). Arachidonic acid intake was highly correlated with the intake of animal products, whereas EPA and

TABLE 3
Intakes of n-6 and n-3 PUFA: Correlations with the Intakes of Energy, Total Fat, and Some Food Groups (Spearman's correlation coefficients)

	18:2n-6	18:3n-3	20:4n-6	20:5n-3	22:5n-3	22:6n-3	LC n-3[a]
18:3n-3	0.73[b]						
20:4n-6	0.54	0.53					
20:5n-3	0.18	0.20	0.36				
22:5n-3	0.39	0.39	0.70	0.80			
22:6n-3	0.20	0.21	0.40	0.93	0.81		
LC n-3	0.22	0.23	0.44	0.97	0.86	0.99	
Total energy	0.69	0.83	0.57	0.20	0.42	0.21	0.24
Total fat	0.74	0.85	0.63	0.19	0.44	0.21	0.24
Fatty and half-fatty fish[c]	0.11	0.12	0.24	0.83	0.67	0.85	0.85
Fish and seafood[d]	0.17	0.18	0.27	0.75	0.54	0.73	0.74
Meat, poultry, and eggs[e]	0.48	0.45	0.75	0.11	0.50	0.10	0.16
Dairy foods	0.04	0.16	–0.01	0.01	–0.02	0.02	0.01
	$P = 0.006$		$P > 0.1$	$P > 0.1$	$P > 0.1$	$P > 0.1$	$P > 0.1$
Vegetable oils	0.53	0.29	0.26	0.11	0.22	0.10	0.12
Rapeseed, soybean, and walnut oils	0.05	0.11	0.00	0.05	0.03	0.05	0.05
			$P > 0.1$		$P = 0.04$		

[a]Long-chain (LC) n-3 PUFA: sum of 20:5n-3, 22:5n-3, and 22:6n-3.
[b]All correlation coefficients are significant for $P < 0.001$, except those for which a P value is indicated.
[c]Fatty fish (more than 1.5 g of n-3 LC PUFA/100 g): fish roe, herring, mackerel, salmon, fresh sardines, fresh tuna; half-fatty fish (between 0.5 g and 1.5 g of n-3 LC PUFA/100 g): anchovies, eel, sea bass, carp, halibut, mullet, dogfish, canned sardines, trout; lean fish: the other fish items described (less than 0.5 g of n-3 LC PUFA/100 g).
[d]Includes fatty fish, half-fatty fish, lean fish, and seafood.
[e]Includes meat, processed meat, offal, poultry, game, and eggs.

DHA intakes were highly correlated with fish and seafood intakes, especially that of fatty fish. The intake of DPA was correlated both with the intake of fish and seafood and with that of meat, poultry, and eggs.

The percentages of each FA provided by the different food types were calculated separately in men and in women and were quite similar in both sexes; the results are therefore presented in the whole population sample (Table 4). The main source of linoleic acid was fats and oils, which contributed to one-third of the intake. Within fats and oils, vegetable oils (including those present in fatty sauces) were by far the main source, margarines being only a minor contributor to linoleic acid intake. Animal products other than dairy products were also an important source of linoleic acid. Almost all types of food, except fish and seafood, contributed significantly to the intake of α-linolenic acid. Both dairy products and other animal products (other than fish and seafood) were major sources of α-linolenic acid, together providing more than 41% of the intake. Fruits and vegetables (including vegetable-based preparations) were also a significant source of α-linolenic acid, in spite of their low lipid contents. Fats and oils contributed only to *ca*. 10% of the α-linolenic acid intake, as a consequence of the very low consumption of α-linolenic acid-rich oils (rapeseed, soybean, walnut) in France. In fact, the vegetable oils consumed by the sample studied were: sunflower oil (38.5% of the total intake of vegetable oils), olive oil (35.2%), peanut oil (13.3%), blended oil (8.0%), grapeseed oil (1.6%), corn oil (1.6%), rapeseed oil (0.9%), walnut oil (0.6%), and soybean oil (0.3%). Meats, poultry, and eggs were by far the main source of arachidonic acid, contributing more than two-thirds of the intake. The main sources of n-3 long-chain PUFA were fish, seafood, and animal products other than dairy products. Fish and seafood were the major source of EPA and DHA: They contributed 72 and 65%, respectively, of the intake of these FA. At variance, DPA was principally obtained from meat, poultry, and eggs, which contributed 55% of its intake, fish and seafood being the source second in importance. The small amounts of long-chain PUFA found in pasta and rice, vegetables, potatoes, and soups are due to the fact that these items include preparations containing some animal products. Globally, 60% of the n-3 long-chain PUFA intake was provided by fish and seafood and 25% by terrestrial animal products, which therefore represent a significant contribution. Although it could be of major importance in some individuals, the contribution of fish oil supplements to the intake of n-3 long-chain PUFA was on average very low (less than 1%).

To obtain additional information on the foods associated with different levels of n-3 FA intake in the population sample, we calculated some characteristics of the quintiles of the sample according to α-linolenic acid intake or to long-chain n-3 FA intake (expressed as the percentage of energy intake); these are shown in Tables 5 and 6, respectively. The total fat intake level (expressed as the percentage of energy intake) was increased through successive quintiles of α-linolenic acid intake, but total energy intake did not increase at the same time. In contrast, it slightly decreased in men (Table 5). The intakes of animal products followed different patterns across quintiles of α-linolenic acid intakes: Meat, poultry, and eggs remained unchanged or were increased, whereas dairy products were decreased between the 1st and the 5th quintile (Table 5). Vegetable oil consumption was increased in successive quintiles of α-linolenic acid intakes; the intake of oils rich in α-linolenic acid was strongly increased, but at very

TABLE 4
Food Sources of Total Fat and of n-6 and n-3 PUFA (% of the total intake of total fat or of each FA brought by each food group: means of the whole population sample)

Food groups	Total fat	18:2n-6	20:4n-6	18:3n-3	20:5n-3	22:5n-3	22:6n-3	LC n-3[a]
Meats and meat dishes	9.63	6.00	14.60	7.73	8.25	18.84	2.07	6.75
Processed meats	8.00	8.29	16.22	5.45	4.50	17.08	2.83	5.88
Poultry and game	2.24	3.35	14.99	2.44	2.22	7.90	1.90	2.99
Offal	0.42	0.33	4.44	0.24	1.92	5.17	1.34	2.27
Eggs	2.71	3.33	16.92	1.32	0.64	6.27	10.28	6.88
Total meat, poultry, and eggs	23.00	21.30	67.17	17.18	17.53	55.26	18.42	24.77
Milk	2.23	0.40	0.00	1.37	0.00	0.00	0.00	0.00
Butter and cream	11.57	1.91	0.00	9.24	0.00	0.00	0.00	0.00
Cheeses	11.94	2.14	1.06	11.83	0.00	0.00	0.00	0.00
Fresh cheese	1.15	0.23	0.00	0.86	0.00	0.00	0.00	0.00
Yogurts	1.50	0.37	0.00	1.34	0.00	0.00	0.00	0.00
Total dairy products	28.39	5.05	1.06	24.64	0.00	0.00	0.00	0.00
Fatty fish[b]	1.13	0.30	4.66	0.99	32.93	19.99	33.00	30.87
Half-fatty fish[c]	0.33	0.25	1.62	0.36	11.15	3.90	8.14	8.50
Lean fish[d]	0.61	0.54	2.04	0.28	14.39	4.55	15.03	12.73
Molluscs and crustaceans	0.27	0.12	2.74	0.12	13.51	3.96	8.51	9.06
Total fish and seafood	2.34	1.21	11.06	1.75	71.98	32.40	64.68	61.16
Vegetable oils	5.26	16.98	0.00	3.74	0.00	0.00	0.00	0.00
Margarines	2.43	3.81	0.00	2.79	0.00	0.00	0.00	0.00
Animal fats	0.21	0.19	0.20	0.21	0.05	0.28	0.05	0.09
Fatty sauces	4.73	12.56	0.84	3.24	0.03	0.33	0.48	0.31
Total fats and oils	12.64	33.54	1.04	9.98	0.08	0.61	0.53	0.40
Breakfast cereals	0.48	1.15	0.00	0.52	0.00	0.00	0.00	0.00
Bread	1.99	6.44	0.01	5.86	0.00	0.00	0.01	0.00
Yeast-raised rolls	2.70	1.61	1.99	2.93	0.06	0.72	1.24	0.81
Pasta and rice[e]	1.10	1.11	0.40	0.47	0.42	0.43	0.17	0.27
Total cereal products	6.27	10.31	2.40	9.78	0.48	1.15	1.41	1.08
Fruits	0.77	1.88	0.00	6.36	0.00	0.00	0.00	0.00
Nuts	1.39	3.16	0.00	3.12	0.00	0.00	0.00	0.00
Vegetables[f]	1.88	4.12	0.16	8.29	0.23	0.08	0.17	0.16
Legumes	0.09	0.26	0.00	1.16	0.00	0.00	0.00	0.00
Potatoes[g]	1.55	3.33	0.16	1.47	0.00	0.04	0.08	0.05
Soups	1.25	0.31	0.21	0.73	0.89	0.51	0.60	0.65
Total fruits and vegetables	6.93	13.06	0.53	21.13	1.12	0.63	0.85	0.86
Biscuits	0.69	0.76	0.35	0.91	0.01	0.12	0.21	0.14
Chocolate	1.41	0.64	0.00	0.28	0.00	0.00	0.00	0.00
Pastry, desserts	10.20	6.74	11.21	7.43	0.31	3.87	7.06	4.53
Sugar and sweets	0.04	0.07	0.00	0.35	0.00	0.00	0.00	0.00
Total sweet products	12.34	8.21	11.55	8.97	0.32	3.99	7.27	4.67
Spices and dressings[h]	0.28	0.22	0.04	0.45	0.02	0.04	0.01	0.01
Hot drinks	1.07	0.33	0.00	0.58	0.00	0.00	0.00	0.00
Dietetetic products	0.09	0.09	0.02	0.17	1.97	1.06	1.09	1.40
Snacks	5.93	5.23	4.11	4.49	4.36	3.98	4.36	4.18
Miscellaneous	0.71	1.42	1.03	0.85	2.13	0.87	1.37	1.45
Total miscellaneous	8.08	7.29	5.20	6.54	8.48	5.95	6.83	7.04

[a]Long-chain (LC) n-3 PUFA: sum of 20:5n-3, 22:5n-3, and 22:6n-3.
[b]More than 1.5 g of LC n-3 PUFA/100 g: fish roe, herring, mackerel, salmon, fresh sardines, fresh tuna.
[c]Between 0.5 and 1.5 g of LC n-3 PUFA/100 g: anchovies, sea bass, carp, eel, halibut, mullet, dogfish, canned sardines, trout.
[d]Less than 0.5 g of n-3 PUFA/100 g: all other fish items described.
[e]Including pasta- or rice-based dishes.
[f]Including vegetable-based dishes.
[g]Including potato-based dishes.
[h]Except fatty sauces, which are classed in the fats and oils group.

low levels (Table 5). The consumption of fruits and vegetables was increased by *ca*. 45% between the first and the 5th quintile of α-linolenic acid intake (Table 5). Subjects in the 5th quintile of long-chain n-3 PUFA intake consumed 24 times more fatty fish, 7 times more half-fatty fish, 2 times more lean fish, and 4 times more molluscs and crustaceans than subjects in the 1st quintile (Table 6). In contrast, the intake of energy decreased, and that of total fat (% of energy) and of meat, poultry, and eggs did not vary much across the quintiles of long-chain n-3 PUFA intake.

TABLE 5
Characteristics of Quintiles of 18:3n-3 Intake in Men and Women (means ± SEM)[a]

Quintiles of 18:3n-3 intake (% of energy)		< 0.32 / < 0.33	[0.33–0.34] / [0.33–0.36]	[0.34–0.37] / [0.36–0.39]	[0.37–0.40] / [0.39–0.42]	>0.40 / >0.42	*P* for Fisher's test	*P* for linear trend
No. of subjects	Men	419	420	420	420	420	—	—
	Women	557	557	557	557	557		
Total energy intake (kcal/d)	Men	2363 ± 24	2352 ± 24	2351 ± 24	2307 ± 21	2285 ± 22	0.075	0.006
	Women	1719 ± 16	1755 ± 16	1744 ± 17	1726 ± 16	1708 ± 16	0.240	0.314
Total fat (% of energy)	Men	32.4 ± 0.2^{a}	35.5 ± 0.2^{b}	36.6 ± 0.2^{c}	38.4 ± 0.2^{d}	38.6 ± 0.2^{d}	<0.001	<0.001
	Women	34.9 ± 0.2^{a}	37.5 ± 0.2^{b}	38.5 ± 0.2^{c}	39.5 ± 0.2^{d}	40.2 ± 0.2^{e}	<0.001	<0.001
18:2n-6 (% of energy)	Men	3.64 ± 0.05^{a}	3.95 ± 0.05^{b}	4.04 ± 0.05^{b}	4.35 ± 0.05^{c}	4.65 ± 0.05^{d}	<0.001	<0.001
	Women	3.70 ± 0.04^{a}	4.04 ± 0.04^{b}	4.18 ± 0.04^{b}	4.39 ± 0.04^{c}	4.81 ± 0.04^{d}	<0.001	<0.001
18:2n-6/18:3n-3	Men	12.6 ± 0.2^{a}	12.0 ± 0.2^{b}	11.4 ± 0.1^{c}	11.3 ± 0.1^{c}	10.2 ± 0.1^{d}	<0.001	<0.001
	Women	12.0 ± 0.1^{a}	11.6 ± 0.1^{b}	11.1 ± 0.1^{b,c}	10.9 ± 0.1^{c}	10.1 ± 0.1^{d}	<0.001	<0.001
Meats, poultry, and eggs[b] (g/d)	Men	186 ± 4	188 ± 3	186 ± 3	191 ± 4	185 ± 4	0.609	0.481
	Women	119 ± 2^{a}	129 ± 2^{a,b}	133 ± 2^{b,c}	136 ± 2^{c}	132 ± 2^{b,c}	<0.001	<0.001
Dairy products (g/d)	Men	270 ± 8	268 ± 8	281 ± 7	259 ± 8	253 ± 7	0.262	0.698
	Women	266 ± 7	253 ± 6	249 ± 6	255 ± 6	235 ± 6	0.201	0.193
Vegetable oils and fatty sauces (g/d)	Men	9.7 ± 0.3^{a}	10.9 ± 0.3^{a,b}	11.0 ± 0.3^{b,c}	11.6 ± 0.3^{b,c}	12.4 ± 0.3^{c}	<0.001	<0.001
	Women	7.4 ± 0.2^{a}	8.4 ± 0.2^{b}	9.1 ± 0.2^{b,c}	9.8 ± 0.2^{c}	10.5 ± 0.2^{d}	<0.001	<0.001
Rapeseed, soybean, and walnut oils (g/d)	Men	0.01 ± 0.00^{a}	0.02 ± 0.00^{a,b}	0.04 ± 0.01^{a,b}	0.08 ± 0.01^{b}	0.19 ± 0.03^{c}	<0.001	<0.001
	Women	0.01 ± 0.00^{a}	0.02 ± 0.00^{a}	0.02 ± 0.01^{a}	0.04 ± 0.01^{a}	0.15 ± 0.02^{b}	<0.001	<0.001
Fruits and vegetables (g/d)	Men	291 ± 7^{a}	333 ± 7^{b}	365 ± 8^{c}	373 ± 8^{c,d}	426 ± 9^{d}	<0.001	<0.001
	Women	274 ± 7^{a}	294 ± 5^{b}	326 ± 6^{b}	357 ± 6^{c}	386 ± 6^{d}	<0.001	<0.001

[a]Within each line, means followed by a common letter are not significantly different according to the Bonferroni test ($P < 0.05$).
[b]Includes meats and meat products, processed meats, offal, poultry, game, and eggs.

DISCUSSION

The quality of the estimation of nutrient intakes of populations depends on the method used to measure the intakes of foods. A good estimation of the intakes of energy, total fat, and FA requires a detailed measure of the intake of all foods, since a large number of foods contribute to the intake of these nutrients. One strength of this study is the method used to record food intake: The repeated 24-h record with indication of portion sizes allows accurate and detailed food recording, as does inclusion of enough days of record over a sufficiently long period to estimate without major bias the individual mean intakes of most food types. Other strengths of our study are the national recruitment of subjects and the significant cohort size. Its main limit resides in the recruitment of volunteers implied by an interventional trial such as SU.VI.MAX: People willing to take a nutritional supplement daily and to answer many questionnaires over 8 yr cannot be considered as representative of the population but are likely to be more health-conscious and nutritionally aware than the average French citizen.

In spite of large differences in dietary habits, linoleic acid intake does not show great variations between population samples from diverse countries (Canada, the United States, Japan, Norway, Germany, Belgium, The Netherlands, Australia, and France): Most estimations of linoleic acid mean intake comprise between 4 and 6% of total energy intake (7–9,11–15,24–27). Higher values have been found in Germany (12) and The Netherlands (27,28) (about 5–6%), and lower values in France (3.9–4.4%) (7,28). Remarkably, the latter estimations, obtained from small samples and by different methods, are close to ours. The Japanese consume on average less total fat than people from Western countries: 20–29% of energy compared with 33–45% (9,26,29,30), but their linoleic acid intake is as high (9,10,26,31). At variance with linoleic acid, the intake of α-linolenic acid appears to vary significantly between populations: from 0.3 to 1% of energy intake. The highest mean intakes are found in Japanese samples: 1.7–2.2 g/d or 0.7–1% of energy, with a linoleic/α-linolenic acid ratio varying between 4 and 8 (9,10,26,31,32), as a consequence of the widespread use of rapeseed and soybean oils in Japan (29,30). In samples from Western countries (the United States, Canada, Norway, Germany, Belgium, the Netherlands, Australia), most values of α-linolenic acid intake are in the range of 1.3–1.8 g/d for men and 1.2–1.7 g/d for women, or 0.5–0.6% of energy, and the linoleic/α-linolenic acid ratio is generally between 6 and 10 (8,11–15,25,27). In a small sample of French women (7), the intake of α-linolenic acid was estimated as 0.6–0.8 g/d, or 0.30–0.36% of energy, in good agreement with our estimate (0.7 g/d in women, or 0.38% of energy). The mean linoleic/α-linolenic acid ratio found in Combe and Boué's study (7) and in our study are consistently higher than in other studies (11–14 vs. 6–10). The TRANSFAIR study has compared the intakes of FA of population samples from 14 countries in Europe (28). In the French sample of that study, the α-linolenic acid intake was estimated as 0.6 g/d in men and 0.5 g/d in women, about 30% lower than our estimation, and the lowest among the countries studied, in which the intake ranged from 0.6 to 2.2 g/d in both sexes (28). Other countries from southern Europe (Greece,

TABLE 6
Characteristics of Quintiles of Long-Chain n-3 PUFA[a] Intake in Men and Women (means ± SEM)[b]

Quintiles of long-chain n-3 PUFA intake (% of energy)							*P* for Fisher's test	*P* for linear trend
	Men	<0.09	[0.09–0.14]	[0.14–0.19]	[0.20–0.28]	>0.28		
	Women	<0.09	[0.09–0.14]	[0.14–0.20]	[0.20–0.32]	>0.32		
No. of subjects	Men	419	420	420	420	420	—	—
	Women	557	557	557	557	557		
Total energy intake (kcal/J)	Men	2404 ± 23[a]	2355 ± 22[a]b	2356 ± 23[a,b]	2299 ± 22[b,c]	2245 ± 23[c]	<0.001	<0.001
	Women	1784 ± 17[a]	1755 ± 17[a]	1754 ± 16[a]	1721 ± 16[a]	1639 ± 15[b]	<0.001	<0.001
Total fat (% of energy)	Men	35.4 ± 0.2[a]	36.0 ± 0.2[a,b]	36.7 ± 0.2[b]	36.6 ± 0.2[b]	36.8 ± 0.2[b]	<0.001	<0.001
	Women	38.0 ± 0.2	37.8 ± 0.2	38.4 ± 0.2	38.3 ± 0.2	38.2 ± 0.2	0.129	0.150
Meats, poultry, and eggs[c] (g/d)	Men	189 ± 3	192 ± 3	193 ± 4	180 ± 3	182 ± 3	0.044	0.012
	Women	127 ± 2[a,b]	134 ± 2[a]	133 ± 2[a,b]	131 ± 2[a,b]	124 ± 2[b]	0.003	0.167
Fatty fish[d] (g/d)	Men	0.6 ± 0.1[a]	2.4 ± 0.1[b]	5.8 ± 0.3[c]	11.1 ± 0.3[d]	26.5 ± 0.7[e]	<0.001	<0.001
	Women	0.4 ± 0.0[a]	1.5 ± 0.1[b]	4.6 ± 0.2[c]	10.3 ± 0.3[d]	23.4 ± 0.5[e]	<0.001	<0.001
Half-fatty fish[e] (g/d)	Men	1.1 ± 0.1[a]	3.4 ± 0.3[b]	5.2 ± 0.3[b,c]	7.0 ± 0.5[c,d]	9.7 ± 0.7[d]	<0.001	<0.001
	Women	0.5 ± 0.1[a]	2.7 ± 0.2[b]	4.0 ± 0.3[c]	5.0 ± 0.3[c,d]	6.7 ± 0.5[d]	<0.001	<0.001
Lean fish[f] (g/d)	Men	13.8 ± 0.7[a]	21.6 ± 0.9[b]	24.6 ± 1.2[b]	27.4 ± 1.2[b]	27.6 ± 1.2[b]	<0.001	<0.001
	Women	11.1 ± 0.5[a]	18.3 ± 0.6[b]	18.7 ± 0.7[b]	20.3 ± 0.8[b]	22.3 ± 0.8[c]	<0.001	<0.001
Molluscs and crustaceans (g/d)	Men	3.8 ± 0.3[a]	8.2 ± 0.5[b]	11.5 ± 0.7[b]	15.1 ± 0.8[c]	16.7 ± 0.9[c]	<0.001	<0.001
	Women	2.8 ± 0.2[a]	6.8 ± 0.4[b]	9.9 ± 0.5[c]	10.7 ± 0.6[c]	12.6 ± 0.6[c]	<0.001	<0.001
Total fish and seafood (g/d)	Men	19.3 ± 0.7[a]	35.6 ± 0.9[b]	47.0 ± 1.3[c]	60.6 ± 1.4[d]	80.4 ± 1.7[e]	<0.001	<0.001
	Women	14.7 ± 0.5[a]	29.3 ± 0.7[b]	37.1 ± 0.8[c]	46.4 ± 1.0[d]	64.8 ± 1.2[e]	<0.001	<0.001

[a]Long-chain n-3 PUFA: sum of 20:5n-3, 22:5n-3, and 22:6n-3.
[b]Within each line, means followed by a common letter are not significantly different according to the Bonferroni test ($P < 0.05$).
[c]Includes meats and meat products, processed meats, offal, poultry, game, and eggs.
[d]Contains more than 1.5 g of n-3 PUFA/100 g: fish roe, herring, mackerel, salmon, fresh sardines, fresh tuna.
[e]Contains between 0.5 and 1.5 g of n-3 PUFA/100 g: anchovies, sea bass, carp, eel, halibut, mullet, dogfish, canned sardines, trout.
[f]Contains less than 0.5 g of n-3 PUFA/100 g: includes all other fish items described.

Italy, Portugal, Spain) also had low values of α-linolenic acid intake (0.6–0.8 g/d in men) and high linoleic/α-linolenic acid ratios (>13), whereas values closer to recommendations were found in countries of northwestern Europe (Belgium, Denmark, Finland, Iceland, The Netherlands, Sweden, and United Kingdom) (28). Among the food habits accounting for this difference, the much lower consumption of margarines in France and in southern Europe than in northwestern Europe (33) is likely to be of importance. Our finding that animal products are the main sources of α-linolenic acid is in accordance with the study by Combe and Boué (7). Remarkably, the variation in linolenic acid intake within the population sample of our study is not related to the consumption of these animal products, but mainly to total fat intake and also to the intake of relatively minor sources such as fruits and vegetables.

Our estimates of arachidonic intake (on average, 204 mg/d in men and 152 mg/d in women) are in the range of values found in other countries (Canada, Germany, Japan, The Netherlands, Sweden): 160–230 mg/d in men and 120–200 mg/d in women (9–14,26,32). Higher values have been found in a study from northern Spain (about 250 mg/d on average, pooled men and women) (34). Lower values were found in Australian studies: 130 mg/d in men and 96 mg/d in women (35), 68 mg/d in men and 41 mg/d in women aged 19–64 (15). Since meat and egg consumption appears about the same or even higher in white Australians (36) than in French adults, the lower values found by Australian studies might be due to lower values of arachidonic acid contents in foods. However, the arachidonic acid contents of lean red meats, poultry, liver, and eggs in our table (Table 19) are quite comparable to those published in one of these studies (35). We have taken into account in our table that meat fat, especially pork fat, can significantly contribute to dietary arachidonic acid intake (37), but this does not seem to be able to explain the large difference between the study by Meyer *et al.* (15) and this and other studies. The single 24-h recall used in the study by Meyer *et al.* has perhaps underestimated the intake of some foods. For example, the very low contribution of eggs to arachidonic acid intake in that study (0.16%) appears surprising: It would correspond to an unlikely average intake of less than 0.1 g egg/d, compared with an 18 g/d estimate in an Australian study using a food-frequency questionnaire (36).

The published estimations of long-chain n-3 PUFA intakes show great variations between studies and countries. The highest intakes are found in Japan, with EPA + DHA intakes amounting to 1–1.5 g/d in men and 0.7–1.1 g/d in women (9,10,26,31,32), but high values also have been found in Norway (1 g/d in men and 0.7 g/d in women) (14) and in Spain (about 0.7 g/d in pooled men and women) (34,37), likely due to the higher consumption of fish in Scandinavian countries and in Spain than in the rest of Europe (38). Lower values of EPA + DHA intake have been found in the United States (210 mg/d in men and 240 mg/d in women) (24), in Germany (*ca.* 315 mg/d in men and 215 mg/d in women) (12), and in Australia

(190 mg/d in men and 135 mg/d in women) (15), but the single 24-h recall method used in the two latter studies has possibly underestimated fish consumption. The mean fish and seafood consumption in France ranks among high values in Europe (after Spain and Scandinavian countries) (38). DPA intake has been estimated less frequently. Higher values have been found in Japan (85–105 mg/d) (10,32); our values are similar to those of a Swedish study (80 mg/d in men and 60 mg/d in women). Again, lower values were found in Australia (33 mg/d in men and 21 mg/d in women) (15). We agree with Australian studies that meat, poultry, and eggs contribute largely (50% or more) to and correlate with DPA intake (15,36).

In summary, it appears from our work that the mean α-linolenic acid intake in the French adult population is low: 0.38% of energy intake, with 95% of the population having an intake below 0.5%. This is lower than values found in North America, Australia, and Japan, and among the lowest values found in Europe. On the other hand, the level of linoleic acid intake is comparable to that of many other countries (4.2% of energy intake), although in the lower range of values. This results in a rather high linoleic/α-linolenic ratio: 11.3 on average. In terms of nutritional adequacy, the adult French population is far from the current recommendations, which are of 0.8–1% of energy for α-linolenic acid intake (5,6), with a linoleic/α-linolenic ratio of 5 (5) or even less (6). This situation is for the most part the consequence of both the high intake of linoleic acid-rich oils (sunflower oil) and the low intake of some good sources of α-linolenic acid: rapeseed, soybean, and walnut oils, as well as margarines, which often incorporate rapeseed or soybean oils.

In contrast, the mean intake of long-chain n-3 PUFA reaches 400–500 mg/d or 0.21% of energy intake, of which 0.11% is DHA, which is well over the current recommendations for adult subjects (0.2% of energy for all long-chain PUFA, of which 0.05% of energy as DHA) (5). However, there are very large individual differences owing to the great variation in fish and seafood consumption. People in the lowest quintile of n-3 long-chain PUFA consumption have an intake of less than 0.09% of their energy intake as n-3 long-chain PUFA and consume on average only 15 g fish and seafood/d, of which less than 1 g/d is fatty fish (Table 6). However, the population sample studied is likely to be more health-conscious than the average French person, and to eat more fish. Therefore, the n-3 long-chain PUFA consumption of the lower quintile of the whole French population is most likely lower than our estimate. Encouraging fish consumption to reach at least two fish portions/wk, of which one portion is fatty fish, would raise the intake of n-3 long-chain PUFA to 0.2% of calories or more.

At variance with other animal species, the biosynthesis of n-3 long-chain PUFA from α-linolenic acid occurs in humans with a low yield: less than 5% in most studies (39), and perhaps even much lower, at 0.2%, published recently (40). If one considers that α-linolenic acid exerts its effect through its conversion to long-chain n-3 PUFA, this means that 50 mg of the latter, perhaps much less, is nutritionally equivalent to 1 g of α-linolenic acid. However, the question of the biological role of α-linolenic acid *per se* is still a matter of debate (41). Awaiting new advances in the field, adjusting the linoleic/α-linolenic acid intake ratio by favoring the consumption of linolenic acid-rich oils and fats at the expense of linoleic acid-rich sources and by promoting the consumption of fish are both possible means to improve the EFA intake of the French population.

REFERENCES

1. Carroll, D.N., and Roth, M.T. (2002) Evidence for Cardioprotective Effects of Omega-3 Fatty Acids, *Ann. Pharmacother. 36*, 1950–1956.
2. Simopoulos, A.P. (2002) The Importance of the Ratio of Omega-6/Omega-3 Essential Fatty Acids, *Biomed. Pharmacother. 56*, 365–379.
3. Kris-Etherton, P.M., Shaffer Taylor, D., and Yu-Poth, S. (2000) Polyunsaturated Fatty Acids in the Food Chain in the United States, *Am. J. Clin. Nutr. 71*, 179S–189S.
4. Sanders, T.A.B. (2000) Polyunsaturated Fatty Acids in the Food Chain in Europe, *Am. J. Clin. Nutr. 71*, 176S–178S.
5. Legrand, P., Bourre, J.M., Descomps, B., Durand, G., and Renaud, S. (2001) Lipides, in *Apports nutritionnels conseillés pour la population française,* 3rd edn. (Martin, A., ed.), pp. 63–82, Tec & Doc, Paris.
6. Simopoulos, A.P., Leaf, A., and Salem, N., Jr. (1999) Workshop on the Essentiality of and Recommended Dietary Intakes for Omega-6 and Omega-3 Fatty Acids, *J. Am. Coll. Nutr. 18*, 487–489.
7. Combe, N., and Boué, C. (2001) Apports alimentaires en acides linoléique et alpha-linolénique d'une population d'Aquitaine, *Oléag. Corps Gras Lipides 8*, 118–121.
8. Knutsen, S.F., Fraser, G.E., Beeson, W.L., Lindsted, K.D., and Shavlik, D.J. (2003) Comparison of Adipose Tissue Fatty Acids with Dietary Fatty Acids as Measured by 24-Hour Recall and Food Frequency Questionnaire in Black and White Adventists: the Adventist Health Study, *Ann. Epidemiol. 13*, 119–127.
9. Okita, M., Yoshida, S., Yamamoto, J., Suzuki, K., Kaneyuki, T., Kubota, M., and Sasagawa, T. (1995) n-3 and n-6 Fatty Acid Intake and Serum Phospholipid Fatty Acid Composition in Middle-Aged Women Living in Rural and Urban Areas in Okayama Prefecture, *J. Nutr. Sci. Vitaminol. (Tokyo) 41*, 313–323.
10. Kobayashi, M., Sasaki, S., Kawabata, T., Hasegawa, K., and Tsugane, S. (2003) Validity of a Self-Administered Food Frequency Questionnaire Used in the 5-Year Follow-up Survey of the JPHC Study Cohort I to Assess Fatty Acid Intake: Comparison with Dietary Records and Serum Phospholipid Level, *J. Epidemiol. 13*, S64–S81.
11. De Vriese, S.R., De Henauw, S., De Backer, G., Dhont, M., and Christophe, A.B. (2001) Estimation of Dietary Fat Intake of Belgian Pregnant Women. Comparison of Two Methods, *Ann. Nutr. Metab. 45*, 273–278.
12. Linseisen, J., Schulze, M.B., Saadatian-Elahi, M., Kroke, A., Miller, A.B., and Boeing, H. (2003) Quantity and Quality of Dietary Fat, Carbohydrate, and Fiber Intake in the German EPIC Cohorts, *Ann. Nutr. Metab. 47*, 37–46.
13. Innis, S.M., and Elias, S.L. (2003) Intakes of Essential n-6 and n-3 Polyunsaturated Fatty Acids Among Pregnant Canadian Women, *Am. J. Clin. Nutr. 77*, 473–478.
14. Johansson, L.R., Solvoll, K., Bjorneboe, G.E., and Drevon, C.A. (1998) Intake of Very-Long-Chain n-3 Fatty Acids Related to Social Status and Lifestyle, *Eur. J. Clin. Nutr. 52*, 716–721.
15. Meyer, B.J., Mann, N.J., Lewis, J.L., Milligan, G.C., Sinclair, A.J., and Howe, P.R. (2003) Dietary Intakes and Food Sources

of Omega-6 and Omega-3 Polyunsaturated Fatty Acids, *Lipids 38*, 391–398.
16. Hercberg, S., Preziosi, P., Briancon, S., Galan, P., Triol, I., Malvy, D., Roussel, A.M., and Favier, A. (1998) A Primary Prevention Trial Using Nutritional Doses of Antioxidant Vitamins and Minerals in Cardiovascular Diseases and Cancers in a General Population: The SU.VI.MAX Study—Design, Methods, and Participant Characteristics. SUpplementation en VItamines et Mineraux AntioXydants, *Control Clin. Trials 19*, 336–351.
17. Le Moullec, N., Deheeger, M., Preziosi, P., Monteiro, P., Valeix, P., Rolland-Cachera, M.-F., Potier de Courcy, G., Christidès, J.-P., Cherouvrier, F., Galan, P., and Hercberg, S. (1996) Validation du manuel-photos utilisé pour l'enquête alimentaire de l'étude SU.VI.MAX, *Cah. Nutr. Diét. 31*, 158–164.
18. Mennen, L.I., Bertrais, S., Galan, P., Arnault, N., Potier de Courcy, G., and Hercberg, S. (2004) The Use of Computerised 24 h Dietary Recalls in the French SU.VI.MAX Study: Number of Recalls Required, *Eur. J. Clin. Nutr. 56*, 659–665.
19. Hercberg, S. (2004) *Table de composition des aliments SUVIMAX,* Editions INSERM, Paris, in press (the part of the table dealing with total fat and n-6 and n-3 PUFA can be obtained from P. Astorg on request, in the form of an Excel file).
20. Favier, J.C., Ireland-Ripert, J., Toque, C., and Feinberg, M. (1995) *Répertoire général des aliments, table de composition,* 2nd edn., Tec & Doc, Paris.
21. Ireland, J., Favier, J.C., and Feinberg, M. (2002) *Répertoire général des aliments. Tome 2: Produits laitiers,* Tec & Doc, Paris.
22. U.S. Department of Agriculture (USDA), Agricultural Research Service, USDA National Nutrient Database for Standard Reference, Release 16, 2003. Netlink: http://www.nal.usda.gov/fnic/foodcomp (accessed March–June 2003).
23. Ministry of Agriculture, Fisheries and Food, (2004) *Fatty Acids. Supplement to McCance & Widdowson's The Composition of Foods,* Royal Society of Chemistry, Cambridge.
24. Ma, J., Folsom, A.R., Shahar, E., and Eckfeldt, J.H., and the Atherosclerosis Risk in Communities (ARIC) Study Investigators (1995) Plasma Fatty Acid Composition as an Indicator of Habitual Dietary Fat Intake in Middle-Aged Adults. The Atherosclerosis Risk in Communities (ARIC) Study Investigators, *Am. J. Clin. Nutr. 62*, 564–571.
25. Ollis, T.E., Meyer, B.J., and Howe, P.R. (1999) Australian Food Sources and Intakes of Omega-6 and Omega-3 Polyunsaturated Fatty Acids, *Ann. Nutr. Metab 43*, 346–355.
26. Tokudome, Y., Imaeda, N., Ikeda, M., Kitagawa, I., Fujiwara, N., and Tokudome, S. (1999) Foods Contributing to Absolute Intake and Variance in Intake of Fat, Fatty Acids and Cholesterol in Middle-Aged Japanese, *J. Epidemiol. 9*, 78–90.
27. Voskuil, D.W., Feskens, E.J., Katan, M.B., and Kromhout, D. (1996) Intake and Sources of α-Linolenic Acid in Dutch Elderly Men, *Eur. J. Clin. Nutr. 50*, 784–787.
28. Hulshof, K.F.A.M., van Erp-Baart, M.A., Anttolainen, M., Becker, W., Church, S.M., Couet, C., Herrmann-Kunz, E., Kesteloot, H., Leth, T., and Martins, I. (1999) Intake of Fatty Acids in Western Europe with Emphasis on *trans* Fatty Acids: The TRANSFAIR Study, *Eur. J. Clin. Nutr. 53*, 143–157.
29. Sugano, M. (1996) Characteristics of Fats in Japanese Diets and Current Recommendations, *Lipids 31*, S283–S286.
30. Sugano, M., and Hirahara, F. (2000) Polyunsaturated Fatty Acids in the Food Chain in Japan, *Am. J. Clin. Nutr. 71*, 189S–196S.
31. Tokudome, Y., Kuriki, K., Imaeda, N., Ikeda, M., Nagaya, T., Fujiwara, N., Sato, J., Goto, C., Kikuchi, S., Maki, S., and Tokudome, S. (2003) Seasonal Variation in Consumption and Plasma Concentrations of Fatty Acids in Japanese Female Dietitians, *Eur. J. Epidemiol. 18*, 945–953.
32. Kuriki, K., Nagaya, T., Topkudome, Y., Imaeda, N., Fujiwara, N., Sato, J., Goto, C., Ikeda, M., Maki, S., Tajima, K., and Tokudome, S. (2003) Plasma Concentrations of (n-3) Highly Unsaturated Fatty Acids Are Good Biomarkers of Relative Dietary Fatty Acid Intakes: A Cross-Sectional Study, *J. Nutr. 133*, 3643–3650.
33. Linseisen, J., Bergstrom, E., Gafa, L., Gonzalez, C.A., Thiebaut, A., Trichopoulou, A., Tumino, R., Navarro, S.C., Martinez, G.C., Mattisson, I., *et al.* (2002) Consumption of Added Fats and Oils in the European Prospective Investigation into Cancer and Nutrition (EPIC) Centres Across 10 European Countries as Assessed by 24-Hour Dietary Recalls, *Public Health Nutr. 5*, 1227–1242.
34. Amiano, P., Dorronsoro, M., de Renobales, M., Ruiz de Gordoa, J.C., Irigoyen, I., and and the EPIC Group of Spain (2001) Very-Long-Chain Omega-3 Fatty Acids as Markers for Habitual Fish Intake in a Population Consuming Mainly Lean Fish: The EPIC Cohort of Gipuzkoa, *Eur. J. Clin. Nutr. 55*, 827–832.
35. Mann, N.J., Johnson, L.G., Warrick, G.E., and Sinclair, A.J. (1995) The Arachidonic Acid Content of the Australian Diet Is Lower than Previously Estimated, *J. Nutr. 125*, 2528–2535.
36. Li, D., Zhang, H., Hsu-Hage, B.H., Wahlqvist, M.L., and Sinclair, A.J. (2001) The Influence of Fish, Meat and Polyunsaturated Fat Intakes on Platelet Phospholipid Polyunsaturated Fatty Acids in Male Melbourne Chinese and Caucasian, *Eur. J. Clin. Nutr. 55*, 1036–1042.
37. Li, D., Ng, A., Mann, N.J., and Sinclair, A.J. (1998) Contribution of Meat Fat to Dietary Arachidonic Acid, *Lipids 33*, 437–440.
38. Welch, A., Lund, E., Amiano, P., Dorronsoro, M., Brustad, M., Kumle, M., Rodriguez, M., Lasheras, C., Janzon, N., Jansson, J., and Luben, R. (2002) Variability of Fish Consumption Within the 10 European Countries Participating in the European Investigation into Cancer and Nutrition (EPIC) Study, *Public Health Nutr. 5*, 1273–1285.
39. Brenna, J.T. (2002) Efficiency of Conversion of α-Linolenic to Long-Chain n-3 Fatty Acids in Man, *Curr. Opin. Clin. Nutr. Metab. Care 5*, 127–132.
40. Pawlosky, R.J., Hibbeln, J.R., Lin, Y., Goodson, S., Riggs, P., Sebring, N., Brown, G.L., and Salem, N., Jr. (2003) Effects of Beef- and Fish-Based Diets on the Kinetics of n-3 Fatty Acid Metabolism in Human Subjects, *Am. J. Clin. Nutr. 77*, 565–572.
41. Sinclair, A.J., Attar-Bashi, A.M., and Li, D. (2002) What Is the Role of α-Linolenic Acid for Mammals? *Lipids 37*, 1113–1123.

[Received March 15, 2004; accepted August 10, 2004]

Effects of Specific Conjugated Linoleic Acid Isomers on Growth Characteristics in Obese Zucker Rats

Sara R. Sanders[a], Mary K. Teachey[b], Arne Ptock[c], Klaus Kraemer[c], Oliver Hasselwander[c], Erik J. Henriksen[b], and Lance H. Baumgard[a,*]

Departments of Animal Sciences[a], and [b]Physiology, University of Arizona, Tucson, Arizona, and [c]BASF AG, Ludwigshafen, Germany

ABSTRACT: Growing female obese Zucker (fa/fa) rats were treated (*via* intragastric gavage) for 21 d with either a (i) vehicle [corn oil; 0.9 g/kg body weight (BW)], (ii) CLA mixture [50:50; *trans*-10,*cis*-12 and *cis*-9,*trans*-11 CLA], (iii) *cis*-9,*trans*-11 CLA, or (iv) *trans*-10,*cis*-12 CLA (CLA treatments at 1.5 g CLA/kg BW). Compared with controls, average daily gain (g/d) was reduced 24 and 44% by the CLA mixture and *trans*-10,*cis*-12 CLA, respectively. There was no treatment effect on average whole-body (minus heart and liver) composition (dry matter basis): fat (70.2%), protein (21.0%), and ash (4.3%). Compared with animals treated with *cis*-9,*trans*-11 CLA, obese Zucker rats treated with *trans*-10,*cis*-12 and the CLA mixture had 7.8% more carcass water. Treatment had no effect on heart or liver weights or on heart or liver weights as a percentage of body weight, but compared with the other treatments *trans*-10,*cis*-12 CLA increased liver lipid content by 33%. Hepatic lipid ratios of 16:1/16:0 and 18:1/18:0 (a proxy for Δ^9-desaturase capability) were not affected by treatment (0.1 and 0.6, respectively). Similar to previous reports, CLA increased hepatic lipid content and altered both liver and carcass FA composition (i.e., reduced arachidonic acid content), but the ability of CLA to manipulate body composition in obese Zucker rats remains questionable.

Paper no. L9434 in *Lipids 39*, 537–543 (June 2004).

CLA represent a mixture of geometric and positional isomers of octadecadienoic acid without a methylene group between double bonds. CLA are found naturally in dairy products and ruminant meat as a result of PUFA biohydrogenation by rumen bacteria (1). Several CLA isomers that differ in the position of the double bond pairs have been identified, each having a potentially different and unique biological or biochemical effect. Dietary CLA is associated with a number of potential human health benefits, including a decrease in the incidence and severity of mutagenesis, carcinogenesis, atherosclerosis, cachexia, and obesity (2,3). Identifying the specific CLA isomer responsible for the aforementioned biological effects has been difficult, as most investigations have utilized a supplement containing a variety of isomers. However, anticancer properties are associated with the *cis*-9,*trans*-11 CLA isomer (4), whereas the *trans*-10,*cis*-12 isomer markedly alters adipocyte and mammary lipid metabolism in a number of species (5–9).

Although dietary CLA has been shown to affect glucose parameters adversely in some animal models (10), CLA supplements actually improve metabolic parameters of type 2 diabetes (11,12) in the Zucker diabetic fatty rat. Based on differences in CLA isomer composition between treatments, it was speculated that the *trans*-10,*cis*-12 isomer was responsible for improving type 2 diabetes (13), and this has now been confirmed, as *trans*-10,*cis*-12 CLA dramatically improved whole-body and skeletal muscle insulin action, whereas *cis*-9,*trans*-11 CLA was ineffective at altering these metabolic variables (14). It is unclear whether these improvements are a direct result of CLA mediating a specific aspect of glucose homeostasis or an indirect result of altered body composition. High body fat content or obesity has long been tightly linked with adult-onset type 2 diabetes (15). The mechanism by which obesity either causes or contributes to this disorder is not clear but may include adipocyte-derived cytokines (16) and dyslipidemia (17).

As stated earlier, dietary CLA has been demonstrated to be extremely effective at decreasing the fat content (≥60%) in a number of rodent models (3) and pigs (8). However, a CLA supplement was ineffective at decreasing the fat content of lean Sprague-Dawley rats (18) and genetically lean pigs (19), and CLA actually increased fat pad weight in the obese Zucker rat (20). Inconsistent effects on carcass composition studies may be due to differences in CLA isomer composition, CLA dose, feeding duration, physiological age and state of experimental animals, and animal genotype.

The objectives of this study were to compare two specific CLA isomers (*cis*-9,*trans*-11 and *trans*-10,*cis*-12) on growth characteristics, whole body composition, organ weight, and FA profiles in the obese Zucker (fa/fa) rat. Furthermore, we were interested in determining whether the improvements in defective metabolic parameters observed in the obese Zucker rat were associated with decreases in carcass fat content.

EXPERIMENTAL PROCEDURES

All protocols and procedures were approved by The University of Arizona Institutional Animal Care and Use Committee. Female obese Zucker rats (Hsd/Ola: ZUCKER-fa; Harlan, Indianapolis, IN) were used to determine the effects of a CLA supplement and specific CLA isomers (relatively pure *cis*-9,

*To whom correspondence should be addressed at the University of Arizona, 1200 E. South Campus Dr., P.O. Box 210038 RM 228, Tucson, AZ 85721. E-mail: baumgard@Ag.arizona.edu

Abbreviations: ADG, average daily body weight gain; BW, body weight; N, nitrogen.

trans-11 and *trans*-10,*cis*-12) on glucose homeostasis parameters (glucose tolerance tests, skeletal muscle glucose transport activity, muscle glucose transporter-4 (GLUT-4) protein level, muscle citrate synthase activity, muscle carbonyl levels, and muscular TG concentration), and these results have been presented elsewhere (14).

Animals and experimental design. The study protocol has been described in detail previously (14). Briefly, growing female obese Zucker (fa/fa) rats [n = 19; mean initial body weight (BW) was 279 ± 11 g, mean ± SD] were fed a standard common diet (Table 1) and treated, *via* intragastric gavage, for 21 d with either a (i) control/carrier (n = 5; corn oil; 0.9 g/kg BW), (ii) CLA mixture (n = 4; 45% *trans*-10,*cis*-12; 45% *cis*-9,*trans*-11 CLA; 8% 18:1; <1% 18:0 + 16:0; 1.5 g/kg BW), (iii) *cis*-9,*trans*-11 CLA (n = 5; 53% *cis*-9,*trans*-11; 27% 18:1; 17% *trans*-10,*cis*-12 CLA; 3.3% 18:2; <0.5% 16:0 + 18:0; 1.5 g/kg BW), or (iv) *trans*-10,*cis*-12 CLA (n = 5; 72% *trans*-10,*cis*-12; 9% 18:1; 8% *cis*-9,*trans*-11 CLA; 7% 16:0; 2% 18:0; 1.5 g/kg BW). All CLA were kindly provided by BASF (Ludwigshafen, Germany) and were delivered as ethyl esters.

Following an overnight fast, animals were anesthetized with pentobarbital sodium (50 mg/kg BW ip), and final carcass weights were determined. The heart, kidney, liver, and soleus and plantaris muscles were dissected out and weighed. Kidneys were added back to the carcass for whole-body composition analysis, but livers were kept separate for additional analyses. Hearts and aforementioned muscles (~100–200 mg) were used as previously described (14) and were not included in the body composition analyses. Animals were quartered and freeze-dried (Virtis, Gardiner, NY) for 7 d to ensure complete removal of water. Freeze-dried carcasses were homogenized, along with dry ice, using a commercial food processor (Robot Coupe, Jackson, MS), and the homogenate was used to determine dry matter, ash, protein, and fat percentage.

TABLE 1
Diet Chemical Composition[a]

Nutrient[b]	Units	Composition[b]
Water[c]	%	10.00
Protein[c]	%	25.03
Fat[c,d]	%	4.25
Fiber[c]	%	4.67
Ash[c]	%	10.09
Nitrogen-free extract	%	46.16
Gross energy	kcal/g	3.82
Digestible energy	kcal/g	3.23
Metabolizable energy	kcal/g	2.94

[a]Teklad 7001 4% Mouse/Rat Diet; Harlan Teklad (Madison, WI).
[b]Ingredients include: soybean meal, ground corn, meat and bone meal, ground wheat, ground barley, ground oats, dehydrated alfalfa meal, ground limestone, dried skim milk, animal fat (lard), iodized salt, dicalcium phosphate, choline chloride, vitamin A acetate, vitamin D-activated animal sterol, vitamin E supplement, niacin, calcium pantothenate, riboflavin, thiamine mononitrate, pyridoxine hydrochloride, menadione sodium bisulfite complex, folic acid, biotin, vitamin B_{12} supplement, calcium carbonate, manganous oxide, ferrous sulfate, copper sulfate, zinc oxide, calcium iodate, and cobalt carbonate.
[c]On an as-fed basis.
[d]FA composition is as follows: 14:0 2%, 16:0 23%, 18:0 9%, 18:1 37%, 18:2 26%, 18:3 3%, 20:4 0.5%.

Body composition analysis. For ashing, tissue (2 g) was dried overnight in a 100°C oven, weighed, placed in a muffle furnace for 6 h at 550°C, and then reweighed. Protein analysis was performed using a FP-528 Nitrogen Determinator (LECO Corp., St. Joseph, MI) using 0.2 g of tissue. Total N content was multiplied by a correction factor of 6.25 to obtain protein concentration. Both ash and protein analyses were performed in triplicate. Percent fat was determined using a modified Folch *et al.* method (21). Briefly, a 2:1 chloroform/methanol solution was added to tissue (2 g), vortexed for 5 min, and centrifuged (400 × g). Supernatant was filtered through a Buchner funnel using #1 Whatman paper. To the filtrate, 0.58% NaCl solution was added; this mixture was mixed, recentrifuged (400 × g), and the top layer was removed and discarded. The lower layer was dried under N_2 until less than 8 mL remained and then transferred to a preweighed extraction tube and dried completely. Fat extractions were performed in duplicate. A separate extraction was performed for FA analyses.

FA analysis. FAME from carcass and liver lipids were prepared by the transmethylation procedure described by Christie (22) with modifications (23). Briefly, hexane (2 mL, HPLC grade) was added to 40 mg of lipid followed by 40 μL of methyl acetate. After vortexing, 40 μL of methylation reagent (1.75 mL methanol and 0.4 mL of 5.4 mol/L sodium methylate) was added, the mixture was revortexed and then allowed to react for 10 min and then 60 μL of termination reagent (1 g oxalic acid in 30 mL diethyl ether) and ~200 mg of calcium chloride were added and allowed to stand for 60 min. Samples were centrifuged at 2,400 × g at 4°C for 5 min. Following centrifugation, the liquid portion was transferred to a labeled GC vial and stored at –20°C. FAME were quantified using a gas chromatograph (Hewlett-Packard GC system 6890; Wilmington, DE) equipped with an FID and a CP-7420 fused-silica capillary column (100 m × 0.25 mm i.d. with 0.2-μm film thickness; Varian, Walnut Creek, CA). Initial oven temperature (160°C) was held for 28 min then ramped at 5°C/min to 220°C, where it was held for 10 min. Inlet and detector temperatures were maintained at 250°C, and the split ratio was 100:1. Hydrogen carrier gas flow rate through the column was 1 mL/min. Hydrogen flow to the detector was 30 mL/min, air flow was 400 mL/min, and the nitrogen makeup gas flow was 25 mL/min. Peaks in the chromatogram were identified and quantified using pure methyl ester standards (GLC60; Nu-Chek-Prep, Elysian, MN; GLC60, Matreya, Inc., Pleasant Gap, PA; *cis*-9,*trans*-11 and *trans*-10,*cis*-12 CLA; Nu-Chek-Prep).

Statistical analyses. Data were statistically analyzed using the 1992 PROC-MIXED procedure of SAS (Cary, NC). Data are presented as least square means ± SEM and considered significant when main effects were less than $P < 0.05$.

RESULTS

Average daily body weight gain (ADG) was reduced ($P <$ 0.01) 24 and 44% by the CLA mixture and *trans*-10,*cis*-12 CLA, respectively (Table 2). Compared to control and *cis*-9, *trans*-11 CLA treated animals, obese Zucker rats treated with

TABLE 2
Growth Rates and Body Composition of Obese Zucker Rats Treated with Isomers of CLA

	Treatment[a]					
Variable	Control	CLA mix[b]	*c*9,*t*11 CLA	*t*10,*c*12 CLA	SEM	*P*
ADG[c] (g/d)	2.5[b,c]	1.9[a,b]	2.7[c]	1.4[a]	0.2	<0.01
Body composition						
Water %	38.0[a,b]	40.8[c]	37.0[a]	39.0[b,c]	0.7	<0.01
Protein[d] %	20.4	22.2	20.3	20.9	0.7	0.32
Fat[d] %	70.9	68.6	71.4	70.2	1.1	0.36
Ash[d] %	4.1	4.5	4.5	4.1	0.4	0.76

[a]Rows with different roman superscripts indicate difference, $P < 0.05$.
[b]Contains 50:50 *trans*-10,*cis*-12 and *cis*-9,*trans*-11 CLA.
[c]Average daily body weight gain.
[d]Values are on a dry matter basis.

trans-10,*cis*-12 CLA and the CLA mixture had 7.8% more ($P < 0.01$) carcass water (Table 2). There was no treatment effect on whole-body composition (average dry matter basis): fat (70.2%), protein (21.0%), and ash (4.3%). There was no treatment effect on soleus and plantaris muscle weights (13) or on wet heart, kidney, or liver weights (Table 3). Compared with the other treatments, Zucker rats treated with *trans*-10,*cis*-12 CLA had increased (33%; $P < 0.01$) liver lipid content (Table 3). There was no treatment effect on hepatic moisture content (29.2%; data not shown).

Analysis of carcass FA indicated *cis*-9,*trans*-11 CLA content was increased ($P < 0.01$) more than 10-fold in both the *cis*-9,*trans*-11- and CLA mix-treated animals (Table 4). Similarly, *trans*-10,*cis*-12 CLA content was increased (>ninefold; $P < 0.01$) in both the *trans*-10,*cis*-12- and mixed CLA-treated animals (Table 4). Similar to carcass FA composition, hepatic FA analysis indicated higher ($P < 0.01$) levels of both *cis*-9,*trans*-11 CLA and *trans*-10,*cis*-12 CLA due to specific CLA treatments and the CLA mix administration (Table 5). Ratios of 16:1/16:0 and 18:1/18:0 (a proxy for Δ^9-desaturase capability) were unaffected in hepatic lipids (0.10 and 0.60, respectively). Both *cis*-9,*trans*-11 and *trans*-10,*cis*-12 CLA and the CLA mixture decreased ($P < 0.01$) the arachidonic acid (20:4n-6) concentration in liver lipids by ~15% (Table 5).

DISCUSSION

Although dietary CLA have been demonstrated to have a wide range of beneficial effects in animal models (2), it has been shown to cause mild insulin resistance in nondiabetic rodent models and human individuals susceptible to type 2 diabetes (10,24). However, dietary CLA improves defective metabolic parameters associated with type 2 diabetes (10) in some species, and it is thought that *trans*-10,*cis*-12 CLA is an isomer responsible for this phenomenon (13). Henriksen and colleagues (14) recently directly demonstrated that *trans*-10,*cis*-12 CLA improves glucose disposal and reduces the insulin resistance of skeletal muscle glucose transport in obese Zucker rats. The *cis*-9,*trans*-11 CLA isomer had little or no effect on the aforementioned glucose homeostatic parameters (14).

Animals receiving both the CLA mixture and the purified *trans*-10,*cis*-12 CLA had reduced ADG compared with controls and the *cis*-9,*trans*-11 CLA-treated groups (Table 2), and we assume that a reduction in caloric intake can at least partially explain this (unfortunately, feed intake was not measured). Although reduced weight gain cannot be ruled out as a partial mechanism by which CLA improves type 2 diabetes, the ability of CLA to improve glucose metabolic parameters in the obese Zucker diabetic rat model is not due to improved body composition because we demonstrated that neither *trans*-10,*cis*-12 nor *cis*-9,*trans*-11 CLA reduced carcass fat percentage or increased body protein content (Table 2). Although these findings are in agreement with previous work using the obese Zucker model (20), the lack of effect on tissue composition in the current investigation is surprising as CLA, specifically, *trans*-10,*cis*-12 CLA, has been shown to be very effective at reducing body fat (i.e., >50%) in a number of rodent models (25–27). A small sample size (n = 4–5/treatment) may have limited our ability to detect statistical differences, but there were no numerical trends even hinting

TABLE 3
Wet Organ Weights of Obese Zucker Rats Treated with Isomers of CLA

	Treatment[a]					
Organ (g)	Control	CLA mix[b]	*c*9,*t*11 CLA	*t*10,*c*12 CLA	SEM	*P*
Heart	0.7	0.6	0.7	0.7	<0.1	0.37
Kidney	1.8	1.7	1.8	1.7	<0.1	0.85
Liver	10.1	10.2	9.9	9.6	0.5	0.80
Lipid[c] %	23.6[a]	22.0[a]	24.4[a]	31.0[b]	1.1	<0.01

[a]Rows with different roman superscripts indicate difference, $P < 0.05$.
[b]Contains 50:50 *trans*-10,*cis*-12 and *cis*-9,*trans*-11 CLA.
[c]On a dry matter basis.

TABLE 4
Carcass FA Profile of Obese Zucker Rats Treated with Isomers of CLA

FA	Treatment[a]				SEM	*P*
	Control	CLA mix[b]	*c*9,*t*11 CLA	*t*10,*c*12 CLA		
			g/100 g FA			
12:0	0.29	0.28	0.23	0.38	0.08	0.58
14:0	1.80[a]	1.71[a]	2.08[b]	2.07[b]	0.07	<0.01
14:1	0.14	0.13	0.15	0.13	0.01	0.37
16:0	29.95[a]	25.27[b]	30.66[a]	31.19[a]	1.06	<0.01
16:1	6.68	6.61	7.34	6.53	0.23	0.19
18:0	4.81[a]	3.96[b]	4.70[b]	5.18[a]	0.18	<0.01
18:1*c*9	33.39	32.14	34.39	31.95	0.79	0.21
18:1*c*11	2.29	2.27	2.29	2.30	0.09	0.99
18:2*c*9,*c*12	15.56[a,b]	18.99[a]	11.66[b]	12.81[b]	1.39	0.01
18:2*c*9,*t*11	0.16[a]	2.15[b]	1.96[b]	0.46[a]	0.24	<0.01
18:2*t*10,*c*12	0.14[a]	1.35[b]	0.49[a]	1.37[b]	0.26	0.02
18:3	0.93[a]	1.52[b]	1.07[a,b]	0.97[a]	0.14	0.03
20:0	0.10	0.13	0.20	0.24	0.09	0.66
20:1n-9	0.34	0.37	0.55	0.36	0.05	0.16
20:2n-6	0.23	0.32	0.29	0.21	0.06	0.49
20:4n-6	0.60[a,b]	0.82[a]	0.66[a,b]	0.42[b]	0.09	0.04
Unknown	2.73	1.98	1.27	3.62	1.13	0.53
Totals						
Saturated	36.92[a]	31.35[b]	37.87[a]	38.96[a]	1.30	<0.01
MUFA[c]	42.84	41.52	44.72	41.27	1.03	0.19
PUFA	20.23[a]	27.13[b]	17.41[a]	19.77[a]	1.79	<0.01
16:1/16:0	0.22[b]	0.26[a]	0.24[a,b]	0.21[b]	0.01	0.04
18:1/18:0	6.98[a]	8.12[b]	7.33[a,b]	6.22[a]	0.36	0.01

[a]Rows with different roman superscripts indicate difference, $P < 0.05$.
[b]Contains 50:50 *trans*-10,*cis*-12 and *cis*-9,*trans*-11 CLA.
[c]Monounsaturated FA.

at treatment effects. In addition, others have demonstrated effects with a similar sample size (6). An insufficient CLA dose can likely be ruled out, as the animals utilized in this study were fed relatively purified CLA isomers at ~1.5% of the diet or ~1,100 mg pure CLA/kg $BW^{0.75}$ [based on feed intake of obese Zucker rats at a similar stage and weight (28)]. The percentage of CLA both in the diet and on a metabolic BW basis are higher than typically utilized in experiments in which marked improvements in body composition are observed (29, 30), and this is especially pertinent as we utilized semipurified (>70%) CLA isomers (*cis*-9,*trans*-11 and *trans*-10,*cis*-12).

The length of time (3 wk) that rats were treated with purified CLA isomers may not have been long enough to elicit changes in nutrient partitioning. Previous CLA rodent trials generally supplied dietary CLA for 4–5 wk or longer (6,18). Rats used in this study were at the approximate age (9 wk) when obese Zucker rats are typically depositing a large amount of adipose tissue (28) *via* hepatic-derived preformed FA (31). There are many reports that suggest that one mechanism by which CLA, and specifically the *trans*-10,*cis*-12 isomer, reduces adiposity is *via* reducing lipoprotein lipase expression and activity (32,33), thus reducing cellular FA uptake. Therefore, because these obese Zucker rats were depositing large amounts of adipose tissue at the time of CLA treatment, it is likely that 3 wk should have been adequate to detect differences in body fatness.

A more likely explanation for the lack of an effect of CLA on body fat content in this study is species or genotypic variation. For example, CLA appears to be more effective in mice than in rats (6,7,18). Furthermore, CLA has been less effective or ineffective at decreasing the fat content of Sprague-Dawley rats [generally a lean rodent model (18)], fish (34), genetically lean pigs (19,35), and humans (36,37). In fact, even in the same species there are large differences in CLA effect on lipid metabolism as CLA decreased the adiposity of lean Zucker rats but actually increased fat pad weights in the obese Zucker rats (20). Similar inconsistencies have been demonstrated in different strains of mice (38). The mechanism by which these species differences exist is not clear, but the rate of intracellular adipocyte TG turnover (26) and basal metabolic rate (30) have been identified as probable causes.

Neither the CLA mixture nor specific isomers changed the carcass percentage of protein or ash (Table 2). Dietary CLA has been demonstrated to modestly increase carcass protein percentage in a number of rodent models (6,26,39), although there appears to be little or no effect of CLA on yield or amount of carcass protein in these rodent trials.

A more consistent observation made in CLA-treated animals is the increase in carcass moisture, and this was confirmed in the current study (Table 2). Obese Zucker rats treated with the CLA mixture and *trans*-10,*cis*-12 CLA had enhanced carcass water compared with controls and *cis*-9,*trans*-

TABLE 5
Liver FA Profile of Obese Zucker Rats Treated with Isomers of CLA

FA	Treatment[a]				SEM	*P*
	Control	CLA mix[b]	*c*9,*t*11 CLA	*t*10,*c*12 CLA		
	g/100 g FA					
14:0	0.32	0.50	0.41	0.41	0.04	0.09
15:0	0.08	0.10	0.08	0.09	0.01	0.32
16:0	17.72[a]	18.54[a,b]	19.76[b]	20.16[b]	0.62	0.04
16:1	1.74	2.12	2.08	1.90	0.18	0.46
17:0	0.28	0.27	0.26	0.24	0.02	0.40
18:0	23.52	21.93	22.62	21.55	1.04	0.56
18:1*c*9	13.33	12.49	13.47	13.47	0.70	0.75
18:1*c*11	1.70	1.76	1.69	1.71	0.03	0.56
18:2*c*9,*c*12	9.62	10.39	8.49	10.53	0.58	0.08
18:2*c*9,*t*11	0.05[a]	1.06[b]	1.11[b]	0.37[c]	0.09	<0.01
18:2*t*10,*c*12	0.05[a,b]	0.57[b]	0.16[a]	1.06[c]	0.14	<0.01
18:3	0.27	0.39	0.31	0.48	0.06	0.07
20:0	0.26	0.19	0.18	0.17	0.03	0.17
20:1n-9	0.12	0.11	0.11	0.12	0.16	0.87
20:2n-6	0.21[b,c]	0.25[a]	0.19[c]	0.22[b]	0.01	<0.01
20:4n-6	19.61[a]	17.09[b]	17.36[b]	15.87[b]	0.70	0.01
22:0	0.72[a]	0.67[a]	0.66[a]	0.51[b]	0.04	0.01
22:5n-3	0.77[a]	1.21[b]	1.01[c]	1.00[c]	0.05	<0.01
22:6n-3	7.00	7.45	7.22	7.06	0.37	0.84
Unknown	2.70	2.91	2.82	3.08	0.15	0.36
Totals						
Saturated	42.89	42.19	43.98	43.13	0.59	0.26
MUFA[c]	16.90	16.47	17.36	17.20	0.89	0.91
PUFA	37.51	38.42	35.84	36.58	0.72	0.12
16:1/16:0	0.10	0.11	0.10	0.10	0.01	0.43
18:1/18:0	0.57	0.57	0.60	0.64	0.06	0.77

[a]Rows with different roman superscripts indicate difference, $P < 0.05$.
[b]Contains 50:50 *trans*-10,*cis*-12 and *cis*-9,*trans*-11 CLA.
[c]Monounsaturated FA.

11 CLA-supplemented animals, respectively (Table 2). The increase in carcass water content is in agreement with other rodent trials (6,40) and finishing pig experiments (8,41). It is unknown why CLA, specifically the *trans*-10,*cis*-12 isomer, increases carcass moisture. A large portion of body fluid is associated with lean tissue, which is composed of water and protein, and CLA has been demonstrated to increase water accretion rates while having very little effect on protein deposition in pigs (8,42). It is possible, because water represents such a large proportion of muscle (>70%), that minor increases in muscle synthesis would be more easily detected in water content changes rather than protein. This may explain the enhanced carcass water content in the CLA mixture and *trans*-10,*cis*-12-treated Zucker rats without an effect on whole-body protein levels (Table 2).

There was no effect of either CLA isomer on heart or kidney weight (Table 3), which is in agreement with other rodent models (7,40,43). Likewise there was no effect of CLA on liver wet weight (g or percentage of BW), which is consistent with previous studies using rat models (18,39,44). However, this is in contrast to several studies using mice and hamster models that indicate CLA, and specifically *trans*-10,*cis*-12, induces marked hepatomegaly (7,30,45). CLA effect on hepatic lipid metabolism is clearly species dependent, as dietary CLA actually decreased liver weight in the obese and lean Zucker rats (20) and fish (34). Although actual liver weight did not differ between treatments, hepatic lipid content increased (31% compared to controls) in obese Zucker rats supplemented with *trans*-10,*cis*-12 CLA (Table 3). The increase in hepatic steatosis without an increase in liver weight agrees with another study using a rat model (46), and the increased liver lipid content agrees with other rodent (mainly mice) trials (5,38,43,47). The mechanism by which *trans*-10,*cis*-12 CLA mediates hepatocyte lipid filling is not clear, but reduced VLDL export *via* decreasing apoprotein B secretion has been demonstrated (48). In addition, the CLA-induced increase in plasma insulin that is sometimes observed (2) is thought to increase hepatic fat synthesis *via* up-regulating FA synthetase and acetyl CoA carboxylase, resulting in liver fat accumulation (38) Our results do not support this hypothesis, as the *trans*-10,*cis*-12 CLA-treated animals had reduced insulin levels (14) but had enhanced liver lipid content (Table 3), thus suggesting the increase in hepatic fat content is insulin-independent. Furthermore, contrary to previous suggestions (38,49), enhanced liver lipid is not necessarily adverse, as there are some physiological circumstances that will naturally cause fatty liver (i.e., liver regeneration) and not impair hepat-ocyte function (50). To our knowledge, there is no evidence suggesting

CLA or CLA-induced liver steatosis is cytotoxic to healthy hepatocytes.

As anticipated, the incorporation of specific CLA isomers into whole carcass lipids (Table 4) and total liver lipids (Table 5) reflected the CLA profile of specific treatments. The increase in liver and carcass *cis*-9,*trans*-11 and *trans*-10,*cis*-12 content in the CLA-treated groups corresponds to the proportionate impurities of the CLA supplements. In addition to the increase in respective CLA isomers, both CLA isomers and the CLA mixture decreased the content of hepatic arachidonic acid (Table 5). This is not surprising, as both *cis*-9,*trans*-11 and *trans*-10,*cis*-12 CLA have been shown to decrease Δ^5-desaturase (51) and Δ^6-desaturase (the rate-limiting step of arachidonic acid synthesis) systems (52), and CLA is thought to displace arachidonic acid in phospholipids (2). A decrease in arachidonic acid and thus arachidonate-derived eicosanoids (prostaglandins E_2 and $F_{2\alpha}$ etc.) has been suggested to be a mediator of many, if not most, of CLA' s biological effects (2,27).

In addition, although hepatic nonesterified FA (NEFA) uptake is proportionate to plasma NEFA levels (53), *trans*-10,*cis*-12 CLA enhanced liver lipid content (Table 3), even though plasma NEFA concentrations were actually decreased by this specific CLA isomer (14).

In conclusion, although dietary *trans*-10,*cis*-12 CLA improves defective glucose homeostatic parameters in the obese Zucker rat, neither this specific isomer nor *cis*-9,*trans*-11 CLA altered whole body composition. This suggests that the mechanism by which CLA alleviates insulin resistance is independent of changes in body protein and lipid content.

ACKNOWLEDGMENTS

The technical assistance of Henry Hafliger, Octavio Mendivil, Clay Bailey, Jane Kay, and Chel Moore, and the personal communication with Drs. Mark McGuire, Mike Pariza, and Dale Bauman are greatly appreciated. This work was partially supported by the University of Arizona Experimental Station, #ARZT-136339-H-24-130.

REFERENCES

1. Bauman, D.E., Baumgard, L.H., Corl, B.A., and Griinari, J.M. (2000) Biosynthesis of Conjugated Linoleic Acid in Ruminants, *Proc. Am. Soc. Anim. Sci.* (1999) Available at: http://www. asas. org/jas/symposia/proceedings/0937.pdf (accessed December 2000).
2. Belury, M.A. (2002) Dietary Conjugated Linoleic Acid in Health: Physiological Effects and Mechanisms of Action, *Annu. Rev. Nutr. 22*, 505–531.
3. Pariza, M.W., Park, Y., and Cook, M.E. (2000) Mechanisms of Action of Conjugated Linoleic Acid: Evidence and Speculation, *Proc. Soc. Exp. Biol. Med. 223*, 8–13.
4. Ip, C., Banni, S., Angioni, E., Carta, G., McGinley, J., Thompson, H.J., Barbano, D., and Bauman, D.E. (1999) Conjugated Linoleic Acid-Enriched Butter Fat Alters Mammary Gland Morphogenesis and Reduces Cancer Risk in Rats, *J. Nutr. 129*, 2135–2142.
5. Delany, J.P., Blohm, F., Truett, A.A., Scimeca, J.A., and West, D.B. (1999) Conjugated Linoleic Acid Rapidly Reduces Body Fat Content in Mice Without Affecting Energy Intake, *Am. J. Physiol. 276*, R1172–R1179.
6. Park, Y., Albright, K.J., Liu, W., Storkson, J.M., Cook, M.E., and Pariza, M.W. (1997) Effect of Conjugated Linoleic Acid on Body Composition in Mice, *Lipids 32*, 853–858.
7. West, D.B., DeLany, J.P., Camet, P.M., Blohm, F., Truett, A.A., and Scimeca, J. (1998) Effects of Conjugated Linoleic Acid on Body Fat and Energy Metabolism in the Mouse, *Am. J. Physiol. 275*, R667–R672.
8. Ostrowska, E., Muralitharan, M., Cross, R.F., Bauman, D.E., and Dunshea, F.R. (1999) Dietary Conjugated Linoleic Acids Increase Lean Tissue and Decrease Fat Deposition in Growing Pigs, *J. Nutr. 129*, 2037–2042.
9. Baumgard, L.H., Corl, B.A., Dwyer, D.A., Saebo, A., and Bauman, D.E. (2000) Identification of the Conjugated Linoleic Acid Isomer That Inhibits Milk Fat Synthesis, *Am. J. Physiol. 278*, R179–R184.
10. Larsen, T.M., Toubro, S., and Astrup, A. (2003) Efficacy and Safety of Dietary Supplements Containing CLA for the Treatment of Obesity: Evidence from Animal and Human Studies, *J. Lipid Res. 44*, 2234–2241.
11. Houseknecht, K.L., Vanden Heuvel, J.P., Moya-Camarena, S.Y., Portocarrero, C.P., Peck, L.W., Nickel, K.P., and Belury, M.A. (1998) Dietary Conjugated Linoleic Acid Normalizes Impaired Glucose Tolerance in the Zucker Diabetic Fatty *fa/fa* Rat, *Biochem. Biophys. Res. Commun. 244*, 678–682.
12. Belury, M., and Vanden Heuvel, J.P. (1999) Modulation of Diabetes by Conjugated Linoleic Acid, in *Advances in Conjugated Linoleic Acid Research*, *Vol. 1* (Yurawecz, M.P., Mossoba, M.M., Kramer, J.K.G., Pariza, M.W., and Nelson, G., eds.), pp. 404–411, AOCS Press, Champaign, IL.
13. Ryder, J.W., Portocarrero, C.P., Song, X.M., Cui, L., Yu, M., Combatsiaris, T., Galuska, D., Bauman, D.E., Barbano, D.M., Charron, M.J., *et al.* (2001) Isomer-Specific Antidiabetic Properties of Conjugated Linoleic Acid: Improved Glucose Tolerance, Skeletal Muscle Insulin Action, and UCP-2 Gene Expression, *Diabetes 50*, 1149–1157.
14. Henriksen, E.J., Teachey, M.K., Taylor, Z.C., Jacob, S., Ptock, A., Kramer, K., and Hasselwander, O. (2003) Isomer-Specific Actions of Conjugated Linoleic Acid on Muscle Glucose Transport in the Obese Zucker Rat, *Am. J. Physiol. 285*, E98–E105.
15. Vague, J. (1956) The Degree of Masculine Differentiation of Obesities: A Factor Determining Predisposition to Diabetes, Atherosclerosis, Gout and Uric Calculous Disease, *Am. J. Clin. Nutr. 4*, 20–34.
16. Grimble, R.F. (2002) Inflammatory Status and Insulin Resistance, *Curr. Opin. Clin. Nutr. Metab. Care 5*, 551–559.
17. Frayn, F.N. (2000) Visceral Fat and Insulin Resistance—Causative or Correlative, *Br. J. Nutr. Suppl. 1*, S71–S77.
18. Azain, M.J., Hausman, D.B., Sisk, M.B., Flatt, W.P., and Jewell, D.E. (2000) Dietary Conjugated Linoleic Acid Reduces Rat Adipose Tissue Cell Size Rather Than Cell Number, *J. Nutr. 130*, 1548–1554.
19. Eggert, J.M., Belury, M.A., Kempa-Steczko, A., Mills, S.E., and Schinckel, A.P. (2001) Effects of Conjugated Linoleic Acid (CLA) on the Belly Firmness and Fatty Acid Composition of Genetically Lean Pigs, *J. Anim. Sci. 79*, 2866–2872.
20. Sisk, M.B., Hausman, D.B., Martin, R.J., and Azain, M.J. (2001) Dietary Conjugated Linoleic Acid Reduces Adiposity in Lean but Not Obese Zucker Rats, *J. Nutr. 131*, 1668–1674.
21. Folch, J., Lees, M., and Sloane Stanley, M.H. (1956) A Simple Method for the Isolation and Purification of Total Lipids from Animal Tissues, *J. Biol. Chem. 226*, 497–509.
22. Christie, W.W. (1982) A Simple Procedure for Rapid Transmethylation of Glycerolipids and Cholesteryl Esters, *J. Lipid Res. 23*, 1072–1075.
23. Chouinard, P.Y., Corneau, L., Barbano, D.M., Metzger, L.E., and Bauman, D.E. (1999) Conjugated Linoleic Acids Alter Milk Fatty Acid Composition and Inhibit Milk Fat Secretion in Dairy Cows, *J. Nutr. 129*, 1579–1584.
24. Riserus, U., Arner, P., Brismar, K., and Vessby, B. (2002) Treatment with Dietary *trans*-10,*cis*-12 Conjugated Linoleic Acid

Causes Isomer-Specific Insulin Resistance in Obese Men with the Metabolic Syndrome, *Diabetes Care 25*, 1516–1521.
25. Jahreis, G., Kraft, J., Tischendorf, F., Schone, F., and von Loeffelholz, C. (2000) Conjugated Linoleic Acids: Physiological Effects in Animal and Man with Special Regard to Body Composition, *Eur. J. Lipid Sci. Technol. 102*, 695–703.
26. Pariza, M.W., Park, Y., and Cook, M.E. (2001) The Biologically Active Isomers of Conjugated Linoleic Acid, *Progr. Lipid Res. 40*, 283–298.
27. Whigham, L.D., Cook, M.E., and Atkinson, R.L. (2000) Conjugated Linoleic Acid: Implications for Human Health, *Pharmacol. Res. 42*, 503–510.
28. Liu, R.H., Mizuta, M., Kurose, T., and Matsukura, S. (2002) Early Events Involved in the Development of Insulin Resistance in the Zucker Fatty Rat, *Int. J. Obes. 26*, 318–326.
29. Evans, M.E., Brown, J.M., and McIntosh, M.K. (2002) Isomer-Specific Effects of Conjugated Linoleic Acid (CLA) on Adiposity and Lipid Metabolism, *J. Nutr. Biochem. 13*, 508–516.
30. Terpstra, A.H.M. (2001) Differences Between Humans and Mice in Efficacy of the Body Fat Lowering Effect of Conjugated Linoleic Acid: Role of Metabolic Rate, *J. Nutr. 131*, 2067–2068.
31. Azain, M.J., Hausman, D.B., Kasser, T.R., and Martin, R.J. (1995) Effect of Somatotropin and Feed Restriction on Body Composition and Adipose Metabolism in Obese Zucker Rats, *Am. J. Physiol. 269*, E137–E144.
32. Park, Y., Storkson, J.M., Albright, K.J., Liu, W., and Pariza, M.W. (1999) Evidence That the *trans*-10,*cis*-12 Isomer of Conjugated Linoleic Acid Induces Body Composition Changes in Mice, *Lipids 34*, 235–241.
33. Baumgard, L.H., Matitashvili, E., Corl, B.A., Dwyer, D.A., and Bauman, D.E. (2002) *Trans*-10,*cis*-12 CLA Decreases mRNA Expression of Key Mammary Lipogenic Enzymes in Lactating Dairy Cattle, *J. Dairy Sci. 85*, 2155–2163.
34. Twibell, R.G., Watkins, B.A., Rogers, L., and Brown, P.B. (2000) Effects of Dietary Conjugated Linoleic Acids on Hepatic and Muscle Lipids in Hybrid Striped Bass, *Lipids 35*, 155–161.
35. Averette Gatlin, L., See, M.T., Hansen, J.A., Sutton, D., and Odle, J. (2002) The Effects of Dietary Fat Sources, Levels, and Feeding Intervals on Pork Fatty Acid Composition, *J. Anim. Sci. 80*, 1606–1615.
36. Zambell, K.L., Keim, N.L., Van Loan, M.D., Gale, B., Benito, P., Kelley, D.S., and Nelson, G.J. (2000) Conjugated Linoleic Acid Supplementation in Humans: Effects on Body Composition and Energy Expenditure, *Lipids 35*, 777–782.
37. Berven, G., Bye, A., Hals, O., Blankson, H., Fagertun, H., Thom, E., Wadstein, J., and Gudmundsen, O. (2000) Safety of Conjugated Linoleic Acid (CLA) in Overweight or Obese Human Volunteers, *Eur. J. Lipid Sci. Technol. 102*, 455–462.
38. Clement, L., Poirier, H., Niot, I., Bocher, V., Guerre-Millo, M., Krief, S., Staels, B., and Besnard, P. (2002) Dietary *trans*-10, *cis*-12 Conjugated Linoleic Acid Induces Hyperinsulinemia and Fatty Liver in the Mouse, *J. Lipid Res. 43*, 1400–1409.
39. Stangl, G.I. (2000) Conjugated Linoleic Acids Exhibit a Strong Fat-to-Lean Partitioning Effect, Reduce Serum VLDL Lipids and Redistribute Tissue Lipids in Food-Restricted Rats, *J. Nutr. 130*, 1140–1146.
40. Peters, J.M., Park, Y., Gonzalez, F.J., and Pariza, M.W. (2001) Influence of Conjugated Linoleic Acid on Body Composition and Target Gene Expression in Peroxisome Proliferator-Activated Receptor Alpha-Null Mice, *Biochim. Biophys, Acta. 1533*, 233–242.
41. Bassaganya-Riera, J., Hontecillas-Magarzo, R., Bregendahl, K., Wannemuehler, M.J., and Zimmerman, D.R. (2001) Effects of Dietary Conjugated Linoleic Acid in Nursery Pigs of Dirty and Clean Environments on Growth, Empty Body Composition, and Immune Competence, *J. Anim. Sci. 79*, 714–721.
42. Ostrowska, E., Suster, D., Muralitharan, M., Cross, R.F., Leury, B.J., Bauman, D.E., and Dunshea, F.R. (2003) Conjugated Linoleic Acid Decreases Fat Accretion in Pigs: Evaluation by Dual-Energy X-ray Absorptiometry, *Br. J. Nutr. 89*, 219–229.
43. Tsuboyama-Kasaoka, N., Takahashi, M., Tanemura, K., Kim, H.J., Tange, T., Okuyama, H., Kasai, M., Ikemoto, S., and Ezaki, O. (2000) Conjugated Linoleic Acid Supplementation Reduces Adipose Tissue by Apoptosis and Develops Lipodystrophy in Mice, *Diabetes 49*, 1534–1542.
44. Poulos, S.P., Sisk, M., Hausman, D.B., Azain, M.J., and Hausman, G.J. (2001) Pre- and Postnatal Dietary Conjugated Linoleic Acid Alters Adipose Development, Body Weight Gain and Body Composition in Sprague-Dawley Rats, *J. Nutr. 131*, 2722–2731.
45. de Deckere, E.A., van Amelsvoort, J.M., McNeill, G.P., and Jones, P. (1999) Effects of Conjugated Linoleic Acid (CLA) Isomers on Lipid Levels and Peroxisome Proliferation in the Hamster, *Br. J. Nutr. 82*, 309–317.
46. Yamasaki, M., Mansho, K., Mishima, H., Kimura, G., Sasaki, M., Kasai, M., Tachibana, H., and Yamada, K. (2000) Effect of Conjugated Linoleic Acid on Lipid Peroxidation and Histological Change in Rat Liver Tissues, *J. Agric. Food Chem. 48*, 6367–6371.
47. Warren, J.M., Simon, V.A., Bartolini, G., Erickson, K.L., Mackey, B.E., and Kelley, D.S. (2003) *Trans*-10,*cis*-12 CLA Increases Liver and Decreases Adipose Tissue Lipids in Mice: Possible Roles of Specific Lipid Metabolism Genes, *Lipids 38*, 497–504.
48. Yotsumoto, H., Hara, E., Naka, S., Adlof, R.O., Emken, E.A., and Yanagita, T. (1999) *Trans*-10,*cis*-12 Conjugated Linoleic Acid Reduces Apolipoprotein B Secretion in HepG2 Cells, *Food Res. Int. 31*, 403–409.
49. Kelley, D.S., and Erickson, K.L. (2003) Modulation of Body Composition and Immune Cell Functions by Conjugated Linoleic Acid in Humans and Animal Models: Benefits vs. Risks, *Lipids 38*, 377–386.
50. Plaa, G.L. (1986) Toxic Responses of the Liver, in *Toxicology, the Basic Science of Poisons* (Klassen, C.D., Amdur, M.O., and Doull, J., eds.), pp. 292–293, Macmillan, New York.
51. Eder, K., Slomma, N., and Becker, K. (2002) *Trans*-10,*cis*-12 Conjugated Linoleic Acid Suppresses the Desaturation of Linoleic and Alpha-Linolenic Acids in HepG2 Cells, *J. Nutr. 132*, 1115–1121.
52. Bretillon, L., Chardigny, J.M., Gregoire, S., Berdeaux, O., and Sébédio, J.L. (1999) Effects of Conjugated Linoleic Acid Isomers on the Hepatic Microsomal Desaturation Activities *in Vitro*, *Lipids 34*, 965–969.
53. Bell, A.W. (1995) Regulation of Organic Nutrient Metabolism During the Transition from Late Pregnancy to Early Lactation, *J. Anim. Sci. 73*, 2804–2819.

[Received January 13, 2004; accepted August 9, 2004]

Incorporation of n-3 Fatty Acids into Plasma and Liver Lipids of Rats: Importance of Background Dietary Fat

Lesley K. MacDonald-Wicks and Manohar L. Garg*

Nutrition & Dietetics, University of Newcastle, New South Wales, Australia

ABSTRACT: The health benefits of long-chain n-3 PUFA (20:5n-3 and 22:6n-3) depend on the extent of incorporation of these FA into plasma and tissue lipids. This study aimed to investigate the effect of the background dietary fat (saturated, monounsaturated, or n-6 polyunsaturated) on the quantitative incorporation of dietary 18:3n-3 and its elongated and desaturated products into the plasma and the liver lipids of rats. Female weanling Wistar rats ($n = 54$) were randomly assigned to six diet groups ($n = 9$). The fat added to the semipurified diets was tallow (SFA), tallow plus linseed oil (SFA-LNA), sunola oil (MUFA), sunola oil plus linseed oil (MUFA-LNA), sunflower oil (PUFA), or sunflower oil plus linseed oil (PUFA-LNA). At the completion of the 4-wk feeding period, quantitative FA analysis of the liver and plasma was undertaken by GC. The inclusion of linseed oil in the rat diets increased the level of 18:3n-3, 20:5n-3, and, to a smaller degree, 22:6n-3 in plasma and liver lipids regardless of the background dietary fat. The extent of incorporation of 18:3n-3, 20:5n-3, and 22:5n-3 followed the order SFA-LNA > MUFA-LNA > PUFA-LNA. Levels of 22:6n-3 were increased to a similar extent regardless of the type of major fat in the rat diets. This indicates that the background diet affects the incorporation in liver and plasma FA pools of the n-3 PUFA with the exception of 22:6n-3 and therefore the background diet has the potential to influence the already established health benefits of long-chain n-3 fatty acids.

Paper no. L9458 in *Lipids 39,* 545–551 (June 2004).

Dietary intake of long-chain n-3 FA (EPA, 20:5n-3; and DHA, 22:6n-3) has been shown to affect the progression of chronic diseases such as coronary heart disease and atherosclerosis, hypertension, mature-onset diabetes, and inflammatory and autoimmune diseases such as rheumatoid arthritis and psoriasis (1). This impact occurs largely through the role of n-3 PUFA in eicosanoid and cytokine production, gene expression, and cell membrane stability. This is accompanied by effects on TAG and cholesterol fractions, on aggregation and thrombotic events, and on inflammation (1–3). Several reports have indicated that n-3 PUFA reduce plasma TAG, with more equivocal effects on total cholesterol and the LDL and HDL cholesterol fractions (3). These effects of n-3 PUFA are dose dependent and relate to the extent of incorporation into plasma and tissue lipids. Vegetarians depend largely on plant sources of n-3 PUFA (α-linolenic acid, LNA; 18:3n-3), which is then desaturated and chain-elongated to 20:5n-3 and 22:6n-3 in the human body. It has been demonstrated that humans, unlike rats, have a limited capacity to convert linoleic acid (LA; 18:2n-6) and 18:3n-3 to the longer, desaturated 20- and 22-carbon chains (4); therefore, dietary 18:3n-3 is thought to have limited health benefits. n-3 PUFA make up only a small proportion of the total fat intake, and therefore it is likely that the background dietary fat composition influences the metabolism of 18:3n-3 in humans, thus masking any potential health effects.

The typical Western diet has adequate n-6 PUFA in the form of vegetable oils (sunflower, safflower, corn, and cottonseed oil) but a limited intake of the n-3 PUFA (flaxseed, canola, or soybean oils) (5,6). The effect of n-3 FA on chronic disease may be obscured by the concomitant intake of other types of dietary fats (6). It is recognized that there is competition between n-6 and n-3 PUFA for elongation and desaturation; this competition for the Δ-6 desaturase enzyme affects the incorporation of longer-chain n-3 PUFA metabolites in tissue, which will affect the impact of these FA on chronic disease (6). Intake of the n-6 PUFA promotes the role of arachidonic acid (20:4n-6) as a precursor for the 2-series prostanoids and the 4-series leukotrienes in eicosanoid metabolism. This creates a proinflammatory, proaggregatory environment, which may affect the development or progression of chronic disease states. Intake from the n-3 PUFA (from linseed oil or the long-chain desaturated products found in marine oils) partially replaces the 20:4n-6 in eicosanoid metabolism, favoring the less inflammatory and aggregatory 3-series prostanoids and 5-series leukotrienes (6). This competition between n-6 and n-3 PUFA extends to the preferential incorporation of n-3 PUFA into the *sn*-2 position of phospholipids by the acyltransferases, and possibly there is also competition for absorption in the small bowel (7). Competition between n-6 and n-3 PUFA may be clinically important and may affect the development or progression of disease (5).

This study aimed to examine for the first time the effect of background diet fat (saturated, monounsaturated, or n-6 polyunsaturated) on the quantitative incorporation of n-3 PUFA into the plasma and the liver lipids of rats. The results presented suggest that background dietary fat influences the degree of incorporation of 18:3n-3 and its longer-chain metabolites, 20:5n-3 and 22:5n-3, but not that of 22:6n-3; the

*To whom correspondence should be addressed at Nutrition and Dietetics, School of Health Science, Faculty of Health, Level 3, Medical Sciences Bldg., University of Newcastle, Callaghan, NSW-2308, Australia.
E-mail: Manohar.Garg@newcastle.edu.au

Abbreviations: AA, arachidonic acid; LA, linoleic acid; LNA, α-linolenic acid; MUFA, monounsaturated FA; SFA, saturated FA.

clinical studies involving 18:3n-3 merit revisiting to evaluate health effects with special considerations given to the background diet fat.

MATERIALS AND METHODS

Study design. Fifty-four female weanling Wistar rats (Animal Resource Centre, Murdoch, WA, Australia) weighing between 69 and 119 g (99 ± 1.6) (mean ± SEM) were randomly assigned to six diet groups of nine rats in each group. The diets consisted of commercially supplied, semipurified, nutritionally adequate diets (Glen Forrest Stockfeeders, Perth, WA, Australia) with 20% (w/w) added fat. The powdered food contained sucrose (44 g/100 g), maize starch (18 g/100 g), cellulose (7 g/100 g), casein (25 g/100 g), methionine (0.38 g/100 g), AIN 93G mineral mix (4.2 g/100 g), and AIN 93G vitamin mix (1.2 g/100 g). The added fat was saturated (tallow) or monounsaturated (sunola oil; Meadow Lea Foods, Port Melbourne, Australia) or n-6 polyunsaturated (sunflower oil: Meadow Lea Foods) as the background diets and flaxseed oil as the source of n-3 FA. To the powdered diet (800 g), six different fat types were added: 180 g tallow and 20 g sunflower oil (SFA); 200 g sunola oil (MUFA); 200 g sunflower oil (PUFA): These were the control diets. Tallow 135 g, sunflower oil 15 g, and flaxseed oil 50 g (SFA-LNA); sunola oil 150 g and flaxseed oil 50 g (MUFA-LNA); and sunflower oil 150 g and flaxseed oil 50 g (PUFA-LNA) were added to the semisynthetic diets to provide n-3 PUFA-enriched diets. Details of the proportion and type of fat in the diets are available in Table 1. Vitamin E levels were standardized with the addition of α-tocopherol acetate (to 55 mg α-tocopherol equivalents/200 g oil), to account for variation in the vitamin E level in different oils.

The rats were individually caged in polycarbonate cages with high-topped wire lids and housed in a temperature-controlled facility with alternating 12-h light/dark cycles. The rats were fed the diets *ad libitum,* and any uneaten food was collected and weighed daily. After 4 wk these animals were anesthetized with isoflurane (Veterinary Medical Supplies, Newcastle, New South Wales, Australia), a heart puncture was performed for the purpose of collecting the blood sample, and the animals were then euthanized with CO_2. This study was approved by The University of Newcastle's Animal Care and Ethics Committee.

FA analysis. After sacrifice, whole blood was collected into EDTA tubes pretreated with reduced glutathione. The sample was centrifuged at 3000 × *g* at 4°C for 10 min, and the plasma and erythrocyte fractions were stored separately in a −70°C freezer. Analysis of the sample occurred within 6 mon of collection.

(i) Tissue preparation. A known weight of liver tissue was diced and suspended in 15 mL of Folch solution (2:1 chloroform/methanol) as outlined in the method by Folch *et al.* (8). Briefly, the tissue was mixed with the solution for more than 24 h, and then filtered through Whatman Grade 1 filter paper (W&R Balston Ltd., Maidstone, England). The chloroform fraction containing the FA was then separated from the methanol by the addition of sodium chloride solution (0.29% NaCl solution) and collected for FA analysis. The chloroform was evaporated under N_2, and lipids were stored at −80°C until further analysis.

(ii) FA determination. Liver and plasma total FA were determined by the method of Lepage and Roy (9). One milliliter of the suspended tissue (described above) or 200 μL of plasma sample was added to a methanol/toluene (4:1 vol/vol)

TABLE 1
Fat Content and FA Composition[a] of the Experimental Diets (%w/w)

	Diet					
Oil	SFA	SFA-LNA	MUFA	MUFA-LNA	PUFA	PUFA-LNA
	g/kg diet					
Tallow	180	135				
Sunflower	20	15			200	150
Sunola			200	150		
Flaxseed		50		50		50
FA						
	%w/w					
14:0	3.1	2.6	0.1	0.1	0.1	0.1
16:0	25.5	21.9	4.2	4.7	6.2	6.1
16:1n-7	2.1	1.8		0.1		
18:0	21.9	19.0	4.9	4.9	5.8	5.6
18:1n-9	34.4	31.0	74.4	60.1	21.6	20.2
18:1n-7	3.0	2.8	1.4	1.4	0.9	1.0
18:2n-6	8.5	5.8	11.8	12.7	63.4	51.6
18:3n-6			0.2			
18:3n-3	0.8	14.2	0.4	14.1	0.1	14.2
20:0	0.3	0.2	0.4	0.3	0.3	0.3
20:1n-9	0.3	0.3	0.3	0.3	0.2	0.2
22:0			1.1	0.9	0.9	0.7
24:0			0.9	0.5	0.5	

[a]SFA, saturated FA (tallow); LNA, α-linolenic acid; MUFA, monounsaturated FA.

mixture containing 21:0 as an internal standard (0.02 mg/mL) and BHT (0.12 g/L). The FA were methylated by the dropwise addition of 200 µL of acetyl chloride while vortexing, followed by incubation at 100°C for 1 h. Potassium carbonate (6% K_2CO_3) was added to halt the reaction, and the mixture was centrifuged at 3000 × *g* at 4°C for 10 min to facilitate the separation of layers; the upper toluene phase containing the FAME was collected and stored in a −20°C freezer for subsequent analysis. FAME in the toluene phase were analyzed by GC using a 30 m × 0.25 mm (DB-225) fused carbon-silica column, coated with cyanopropylphenyl as previously described (10). The injector and detector port temperatures were 250°C. The oven temperature began at 170°C for 2 min, then increased 10°C/min to 220°C; this temperature was maintained throughout the run time of 30 min. The sample FA peaks were identified by comparison with a mixture of authentic standards. The addition of the internal standard 21:0 in a known level enabled the quantification of FA in µg/mL amounts.

(iii) Determination of unsaturated index. The unsaturated index (or double-bond index) was calculated by multiplying the amount (µg/mL) of unsaturated FA by the number of double bonds in the FA; the values were then summed to provide a number that represented the FA unsaturated index (11).

Statistical analysis. Data were analyzed using Minitab version 12 for Windows (Minitab Inc., State College, PA). Normally distributed data are presented as mean ± SEM. Data were tested for normality by using the Anderson–Darling normality test and for homogeneity of variance. If normally distributed or homogeneous, statistical comparisons were performed using ANOVA with a significance level of 0.05. If a nonparametric comparison was needed, data were expressed as median (interquartile range), statistical comparisons were performed using the Kruskal–Wallace single-factor analysis by ranks, and then a Tukey multiple comparison test, the nonparametric version, was carried out. The data are valid only for equal replicates in each treatment with no tied ranks (12,13); differences were considered significant when $P < 0.05$.

RESULTS

The lipid and FA contents of the diets are presented in Table 1. The SFA diet was made up predominantly of saturated FA for which the sum of myristic (14:0), palmitic (16:0), and stearic acids (18:0) totaled greater than 50% of the FA present (50.5%) with sufficient 18:2n-6 (8.5%) to prevent EFA deficiency. The MUFA diet had the largest amount of 18:1n-9 (74.4%), with an adequate amount of 18:2n-6 (11.8%). The PUFA diet had the highest amount of 18:2n-6 (63.4%). The addition of flaxseed oil to the diets increased the proportion of 18:3n-3 from 0.8, 0.4, and 0.1% (SFA, MUFA, and PUFA diets, respectively) to 14.2, 14.1, and 14.2% (SFA-LNA, MUFA-LNA, and PUFA-LNA diets, respectively) (Table 1). The average weight gain for the rats in each of the diet groups did not differ significantly ($P = 0.53$). There was also no difference in the average liver weights ($P = 0.82$) and liver weight/body weight ratio between the diet groups ($P = 0.5$), despite there being significantly less of the SFA diet consumed compared with the PUFA-LNA and the MUFA-LNA diets ($P < 0.04$) (Table 2).

The quantitative analysis of the plasma FA is presented in Table 3. The MUFA group and the MUFA-LNA group had the highest level of plasma 18:1n-9 ($P < 0.001$) in comparison with the PUFA groups. The PUFA and the PUFA-LNA groups had the highest level of plasma 18:2n-6. There were equivalent amounts of 20:4n-6 and 20:5n-3 in the SFA, MUFA, and PUFA groups. The addition of flaxseed oil to the background diets uniformly increased the level of plasma 18:3n-3 (1.2 ± 0.1 to 16.75 ± 1.1 µg/mL in SFA groups; trace amounts to 13.7 ± 1.3 µg/mL in MUFA groups; trace amounts to 12.7 ± 1.2 µg/mL in PUFA groups) and increased the level of 20:5n-3 (6.4 ± 0.4 to 122.5 ± 12.4 µg/mL in the SFA groups, $P < 0.001$; 6.0 ± 0.1 to 82.5 ± 9.7 µg/mL in the MUFA groups, $P < 0.001$; and 6.1 ± 0.3 to 18.3 ± 2.3 µg/mL in the PUFA groups, $P < 0.001$). There was a concomitant decrease in the 20:4n-6 levels [291.6 ± 24.3 to 118.6 ± 4.5 µg/mL in the SFA group, $P < 0.001$; 282.1 ± 15.4 to 182.1 ± 10.2 µg/mL in the MUFA group, $P < 0.001$; 335.5 ± 24.4 to 308.1 ± 23.4 µg/mL in the PUFA group (not significant)]. The addition of 18:3n-3 to the diets also brought about a significant but similar increase in 22:6n-3, regardless of the background dietary fat (Table 3).

The liver FA analysis is presented in Table 4. The MUFA group had levels of 18:1n-9 similar to those of the SFA group, but higher levels of 18:1n-9 than the PUFA group ($P < 0.001$). The PUFA group and the PUFA-LNA group had the highest levels of 18:2n-6 ($P < 0.001$), and the PUFA group had the highest level of 20:4n-6 ($P < 0.001$). The addition of flaxseed oil to these background diets increased the level of 18:3n-3 in

TABLE 2
Dietary Consumption, Growth, Body and Liver Weight Measurements for All Experimental Diet Groups[a,b]

	Diet group						
Parameter	SFA	SFA-LNA	MUFA	MUFA-LNA	PUFA	PUFA-LNA	*P* value
Diet consumption (g/d)	15.7 ± 0.4[a]	16.8 ± 1.1[a,b]	18.2 ± 0.6[a,b]	20.0 ± 1.0[b]	18.9 ± 0.9[a,b]	19.8 ± 0.9[b]	<0.005
Weight gain (g/4 wk)	118 ± 12	104 ± 5	101 ± 5	114 ± 7	107 ± 5	110 ± 5	
Liver weight (g)	7.7 ± 0.4	7.7 ± 0.3	7.2 ± 0.3	8.0 ± 0.6	7.8 ± 0.4	8.0 ± 0.4	
Liver/body weight ratio	15.3 ± 1.2	13.5 ± 0.3	14.2 ± 0.4	14.5 ± 0.7	13.7 ± 0.6	13.8 ± 0.3	

[a]Values are presented as mean ± SEM, $n = 9$.
[b]Values without a common superscript in a row are significantly different. For abbreviations see Table 1.

TABLE 3
Plasma FA Composition[a] for All Experimental Diets (μg/mL)

	Diet (μg/mL)						
FA	SFA	SFA-LNA	MUFA	MUFA-LNA	PUFA	PUFA-LNA	*P* value
14:0	4.8 ± 0.4[a]	3.5 ± 0.2[a,b]	2.9 ± 0.2[b]	3.0 ± 0.1[b]	2.8 ± 0.1[b]	3.2 ± 0.2[b]	<0.001
16:0	129.7 ± 8.2[a]	106.1 ± 4.5[a,b]	95.5 ± 4.0[b]	111.0 ± 5.5[a,b]	110.9 ± 6.9[a,b]	122.2 ± 7.4[a]	<0.05
16:1n-7	10.0 ± 0.7[a]	7.4 ± 0.5[b]	4.7 ± 0.5[c]	6.1 ± 0.5[b,c]	4.3 ± 0.4[c]	6.1 ± 0.6[b,c]	<0.001
18:0	215.6 ± 15.1	170.8 ± 9.2	186.5 ± 6.9	194.2 ± 12.1	204.6 ± 15.3	209.3 ± 13.6	
18:1n-9	175.3 ± 16.4[a]	137.1 ± 10.3[a]	146.6 ± 4.7[a]	146.6 ± 9.9[a]	77.3 ± 9.4[b]	75.8 ± 5.0[b]	<0.001
18:1n-7	19.3 ± 1.7[a]	12.5 ± 0.8[b]	12.0 ± 0.5[b]	11.6 ± 0.8[b]	10.5 ± 0.8[b]	10.8 ± 0.7[b]	<0.001
18:2n-6	95.9 ± 8.1[a]	92.5 ± 5.5[a]	56.5 ± 2.7[b]	98.5 ± 5.1[a]	143.8 ± 10.6[c]	154.5 ± 10.9[c]	<0.001
18:3n-6	2.7 ± 0.2[a]	1.3 ± 0.1[b]	2.1 ± 0.1[a]	1.8 ± 0.2[a,b]	5.2 ± 0.5[c]	2.9 ± 0.3[a]	<0.001
18:3n-3	1.2 ± 0.1	16.75 ± 1.1	ND	13.7 ± 1.3	ND	12.7 ± 1.2	
20:0	1.8 ± 0.1	1.5 ± 0.1	1.5 ± 0.03	1.5 ± 0.03	1.6 ± 0.1	1.5 ± 0.1	
20:2n-6	2.7 ± 2.2[a]	1.3 ± 0.1[b]	2.2 ± 0.1[a]	ND	1.9 ± 0.2[b]	1.6 ± 0.1[b]	<0.001
20:3n-6	4.4 ± 0.5[a,b]	5.1 ± 0.4[a]	2.5 ± 0.2[b]	5.7 ± 0.8[a]	3.3 ± 0.5[a,b]	4.0 ± 0.4[a,b]	<0.005
20:4n-6	291.6 ± 24.3[a]	118.6 ± 4.5[b]	282.1 ± 15.4[a]	182.1 ± 10.2[b]	335.5 ± 24.4[a]	308.1 ± 23.4[a]	<0.001
20:5n-3	6.4 ± 0.4[a]	122.5 ± 12.4[b]	6.0 ± 0.1[a]	82.5 ± 9.7[c]	6.1 ± 0.3[a]	18.3 ± 2.3[a]	<0.001
22:0	5.7 ± 0.3[a]	6.1 ± 0.3[a]	7.8 ± 0.4[b]	7.9 ± 0.2[b]	8.0 ± 0.5[b]	8.0 ± 0.4[b]	<0.001
22:5n-3	2.2 ± 0.2[a]	11.7 ± 0.6[b]	2.3 ± 0.2[a]	8.6 ± 0.8[c]	ND	7.4 ± 0.5[c]	<0.001
22:6n-3	15.5 ± 1.3[a]	22.21 ± 1.4[b]	15.1 ± 1.2[a]	23.3 ± 1.7[b]	8.5 ± 0.5[c]	26.6 ± 2.0[b]	<0.001
Total FA	1,011.8 ± 71.1	859.7 ± 46.1	862.4 ± 31.7	930.6 ± 54.5	973.2 ± 71.1	1,006.2 ± 63.7	
∑SFA	371.9 ± 24.5	304.0 ± 14.2	314.2 ± 10.6	339.9 ± 17.7	351.2 ± 23.1	370.7 ± 21.8	
∑MUFA	212.2 ± 18.0[a]	164.2 ± 11.3[a]	172.7 ± 5.8[a]	174.3 ± 11.3[a]	96.9 ± 10.4[b]	100.0 ± 5.8[b]	<0.001
∑n-6 PUFA	397.1 ± 31.4[a]	218.4 ± 9.6[b]	345.5 ± 16.4[a]	288.4 ± 15.3[b]	489.7 ± 36.0[c]	470.5 ± 33.6[c]	<0.001
∑n-3 PUFA	30.5 ± 2.3[a]	173.2 ± 14.3[b]	30.0 ± 2.1[a]	128.1 ± 12.9[c]	35.4 ± 4.0[a]	64.9 ± 4.6[a]	<0.001
Unsaturated index	1,752.1 ± 135.5	1,698.9 ± 104.3	1,582.3 ± 74.9	1,758.9 ± 119.8	1,900.6 ± 140.9	1,990.0 ± 139.8	

[a]ND = not detected. Values are reported as average ± SEM; *n* = 9. Values without a common superscript in a row are significantly different. For abbreviations see Table 1.

TABLE 4
Liver FA Composition[a] for All Experimental Diets (μg/g tissue)

	Diet (μg/g tissue)						
FA	SFA	SFA-LNA	MUFA	MUFA-LNA	PUFA	PUFA-LNA	*P* value
14:0	351 ± 42[a]	204 ± 21[b]	182 ± 26[b]	135 ± 12[b]	135 ± 17[b]	118 ± 16[b]	<0.001
16:0	10,631 ± 681[a]	8,282 ± 654[a,b]	7,551 ± 806[b]	6,869 ± 672[b]	7,085 ± 820[b]	6,627 ± 604[b]	<0.005
16:1n-7	878 ± 74[a]	529 ± 55[b]	388 ± 76[b]	368 ± 33[b]	244 ± 30[b]	285 ± 38[b]	<0.001
18:0	7,740 ± 384	7,209 ± 326	7,611 ± 312	7,331 ± 393	7,633 ± 304	7,433 ± 248	
18:1n-9	16,047 ± 1,460[a]	10,580 ± 1,078[a]	15,563 ± 1,953[a]	11,151 ± 1,271[a]	4,464 ± 544[b]	4,181 ± 518[b]	<0.001
18:1n-7	1,814 ± 132[a]	1,172 ± 91[b]	1,133 ± 85[b]	840 ± 46[b,c]	784 ± 52[b,c]	696 ± 55[c]	<0.001
18:2n-6	4,841 ± 250[a]	4,054 ± 272[a]	3,086 ± 327[a]	4,337 ± 464[a]	10,809 ± 1,623[b]	9,706 ± 1,257[b]	<0.001
18:3n-6	221 ± 15[a]	92 ± 5[a]	175 ± 16[a]	103 ± 10[a]	503 ± 67[b]	208 ± 21[a]	<0.001
18:3n-3	115 ± 7[a]	2,498 ± 280[b]	71 ± 9[a]	1,413 ± 231[c]	58 ± 10[a]	1,343 ± 219[c,b]	<0.001
20:0	26 ± 2[a,b]	21 ± 1[a]	27 ± 1[a,b]	23 ± 2[a]	29 ± 1[b]	24 ± 1[a,b]	<0.005
20:1n-9	74 ± 8[a]	60 ± 7[b]	98 ± 6[a]	62 ± 4[a,b]	38 ± 4[c]	34 ± 4[c]	<0.001
20:2n-6	164 ± 9[a]	66 ± 11[b]	141 ± 9[a]	48 ± 7[c]	178 ± 13[a]	115 ± 11[a]	<0.001
20:3n-6	205 ± 16[a,b]	245 ± 12[a]	162 ± 17[b]	250 ± 12[a]	253 ± 28[a]	221 ± 17[a,b]	<0.01
20:4n-6	6,526 ± 309[a]	3,219 ± 165[b]	7,051 ± 287[a]	4,307 ± 308[c]	8,424 ± 488[d]	6,154 ± 157[a,d]	<0.001
20:5n-3	112 ± 7[a]	4,298 ± 356[b]	57 ± 9[a]	2,348 ± 124[c]	49 ± 8[a]	788 ± 101[d]	<0.001
22:0	94 ± 8[a]	52 ± 5[b]	98 ± 10[a]	68 ± 6[a,b]	93 ± 8[a]	78 ± 6[a,b]	<0.005
22:2n-6	23 ± 4	16 ± 2	21 ± 2	ND	ND	16 ± 1	
22:5n-3	135 ± 6[a]	983 ± 102[b]	75 ± 5[c]	591 ± 57[b]	69 ± 7[c]	497 ± 50[b]	<0.001
22:6n-3	1,042 ± 56[a]	1,702 ± 138[b]	949 ± 46[a]	1,515 ± 112[b]	497 ± 35[c]	1,564 ± 76[b]	<0.001
Total FA	51,791 ± 2,887	45,640 ± 3,066	45,375 ± 3,698	42,205 ± 3,457	43,041 ± 3,844	40,553 ± 3,079	
∑SFA	19,141 ± 917[a]	15,993 ± 924[a,b]	15,793 ± 1,097[a,b]	14,765 ± 1,016[b]	15,339 ± 1,047[a,b]	14,674 ± 704[b]	<0.05
∑MUFA	18,938 ± 1,657[a]	12,425 ± 1,212[a,c]	17,277 ± 2,090[a,c]	12,509 ± 1,347[c]	5,577 ± 623[b]	5,255 ± 605[b]	<0.001
∑n-6 PUFA	11,979 ± 444[a]	7,688 ± 401[b]	10,632 ± 593[a]	9,049 ± 760[a,b]	20,176 ± 2,165[c]	16,414 ± 1,402[a,c]	<0.001
∑n-3 PUFA	1,734 ± 94[a]	9,534 ± 781[b]	1,672 ± 79[a]	5,883 ± 481[c]	1,949 ± 111[a]	4,210 ± 405[c]	<0.001
Unsaturated index	65,197 ± 2,867	78,845 ± 5,298	61,181 ± 3,810	67,643 ± 5,288	71,074 ± 6,174	70,712 ± 5,286	

[a]Values are reported as average ± SEM; values without common superscripts in a row are significantly different. For abbreviations see Tables 1 and 3.

the liver of all the diet groups (SFA groups 115 ± 7 to 2498 ± 280 μg/g; MUFA groups 71 ± 9 to 1413 ± 231 μg/g; PUFA groups 58 ± 10 μg/g to 1343 ± 219 μg/g). The increase in 18:3n-3 resulted in an increase of 20:5n-3 (SFA groups 112 ± 7 to 4298 ± 356 μg/g; MUFA groups 57 ± 9 to 2348 ± 124 μg/g; PUFA groups 49 ± 8 to 788 ± 101 μg/g, $P < 0.001$) and a concomitant decrease in 20:4n-6 (SFA groups 6526 ± 309 to 3219 ± 165 μg/g; MUFA groups 7051 ± 287 to 4307 ± 308 μg/g; PUFA groups 8424 ± 488 to 6154 ± 157 μg/g). Also, there was a significant increase in 22:6n-3 ($P < 0.001$) across all the flaxseed oil groups to a similar extent regardless of the background dietary fat type (Table 4).

DISCUSSION

This study aimed to investigate the effect of adding plant n-3 PUFA to a background diet of saturated, monounsaturated, or n-6 polyunsaturated fats on the quantitative incorporation of n-3 PUFA into plasma and liver lipid pools in rats. The type of major dietary fat had no effect on the weight gain, liver weight, or liver weight/body weight ratio of the animals in all the diet groups, which is supported by the literature (14). This indicated that all the diets were reasonably well tolerated by the rats, although it is clear from the diet consumption data that the SFA diet was not consumed at the same rate as some of the other diets. The FA analysis of the plasma and liver reflected the dietary fat intake. The SFA group had predominantly saturated FA, the MUFA group had the highest level of 18:1n-9, and the PUFA group had the highest level of 18:2n-6 in the plasma and liver lipids. In general, the effect of dietary fat manipulation was to increase the n-3 PUFA and decrease the n-6 PUFA following supplementation with LNA in both the plasma and the liver samples. However, some differences were noticeable; in particular, the greater accumulation of 18:3n-3 in the liver following the SFA-LNA diet was not apparent in the plasma. In plasma, 18:3n-3 contents were increased to a similar extent regardless of the background diet.

The addition of 18:3n-3 increased the amount of n-3 PUFA (18:3n-3, 20:5n-3, 22:5n-3, and 22:6n-3) regardless of the background dietary fat. The concomitant reduction in 20:4n-6 content following dietary 18:3n-3 supplementation is well documented in the scientific literature (15–17). This reduction can be attributed to the well-known competition between 18:2n-6 and 18:3n-3 at the Δ-6 desaturation step as well as to the preferential incorporation of desaturated/elongated n-3 PUFA (20:5n-3 and 22:6n-3) into the *sn*-2 position of the phospholipids (18). Limited substrate (18:2n-6) availability for 20:4 synthesis combined with presence of the competitor 18:3n-3 resulted in the greatest reduction in 20:4n-6 levels in the SFA-LNA when compared with the MUFA-LNA and PUFA-LNA diet groups. Substrate level competition was also responsible for a greater conversion of 18:3n-3 to 20:5n-3 and 22:5n-3 and their incorporation into plasma and liver lipids in the SFA-LNA diet compared with the MUFA-LNA and PUFA-LNA diet groups. The conversion of 18:3n-3 to 20:5n-3 and 22:5n-3 in rats and humans is well documented. Consistent with the results presented, several studies have demonstrated that some 18:3n-3 is converted to the longer-chain n-3 PUFA (20:5n-3, 22:5n-3, and 22:6n-3); the extent of this conversion is modest and controversial. Emken *et al.* (18) found a 15% conversion, whereas Pawlosky *et al.* (19) reported 0.2%; both reported that the conversion to 22:6n-3 was much less than to 20:5n-3 and 22:5n-3. The extent of conversion and incorporation of 18:3n-3 to 22:6n-3 into plasma and liver lipids appears to be independent of the 18:2n-6/18:3n-3 ratio and specific to the tissue type examined (20–22). Controversy exists for conversion of 20:5n-3 to 22:6n-3, whereas evidence is available to suggest retroconversion of 22:6n-3 to 20:5n-3. The controversy surrounds whether 20:5n-3 is first converted to 24:5n-3 by two successive chain elongation steps followed by conversion to 24:6n-3 by Δ-6 desaturase and then β-oxidation to 22:6n-3 or *via* the traditional pathway involving a single elongation step to form 22:5n-3 followed by a Δ-4 desaturase step to synthesize 22:6n-3 (23). Regardless of the pathway by which 20:5n-3 is converted into 22:6n-3, it is apparent from the results that the rats do have the capacity to synthesize 22:6n-3. It is likely that the Δ-4 and/or Δ-6 desaturase enzymes involved in the conversion of 20:5n-3 to 22:6n-3 are saturated by low levels of substrate (22:5n-3 or 24:5n-3); therefore, despite the large difference in the amount of 20:5n-3 and 22:5n-3, 22:6n-3 levels are increased to a similar degree in all the diet groups supplemented with linseed oil. In agreement with our results, Jeffery *et al.* (24) demonstrated that consumption of a diet reduced in n-6 PUFA by substituting 16:0 for 18:2n-6 enhanced the efficacy of the n-3 PUFA to modulate lipid and inflammatory biomarkers. In the presence of 16:0, there was an increased cholesterol-lowering effect and decreased *ex vivo* proliferation of spleen lymphocytes; however, when 16:0 was not present (in the high n-6 PUFA diet), n-3 PUFA did not have the same efficacy. Undoubtedly, the incorporation of n-3 PUFA into plasma and tissue pools can be improved by reducing the dietary n-6/n-3 ratio. There are three possible ways to achieve this: (i) simply increasing n-3 PUFA consumption in the diet; (ii) keeping SFA, MUFA, and n-3 PUFA content constant and decreasing n-6 PUFA in the diet. However, taking a whole-diet approach and in light of general dietary advice to decrease SFA content in the diet, to concomitantly decrease n-6 PUFA will encourage a low fat intake, which has the potential to reduce the level of circulating HDL (25,26); (iii) maintaining the level of n-3 PUFA, decreasing total n-6 PUFA, and making up the shortfall in dietary fat intake with MUFA and/or SFA. This will improve the n-6/n-3 ratio without reducing the fat content in the diet and therefore avoid the detrimental effects of a reduction in circulating HDL. Which one of the last two options is ideal to optimize n-3 PUFA incorporation in plasma and tissue lipids without adversely affecting the plasma lipid profile remains to be established. We have previously shown that the lipid-lowering effects of marine n-3 PUFA were maximized when the 18:2n-6 to SFA ratio in the background diet was low (27,28). Similarly, it was found that n-3 PUFA supplementation had the greatest TG-lowering effect in conjunc-

tion with a background diet of SFA (29). If this is the case, then for the health benefits of n-3 PUFA to be maximized, the corresponding background diet of the patient needs to be paid special consideration.

It is not likely that n-3 PUFA, whether of plant or marine origin, will become a major component of the human diet. Even after making drastic alterations to the diet, the contribution by n-3 PUFA to the total FA pool is minor (30). If it is true that health effects of n-3 PUFA are dose dependent, then it behooves us to optimize the health effects of n-3 by ensuring the maximal incorporation of this class of FA into the tissue pools. This study demonstrates that one way of optimizing the n-3 PUFA incorporation into the tissue pools is in conjunction with a background diet with a low 18:2n-6/SFA ratio. One concern of supplementing n-3 PUFA with a high level of saturated fat in the background diet may be the cholesterol-raising effects of SFA. Whereas it is well established that diets rich in SFA increase plasma cholesterol, the concomitant addition of n-3 PUFA may ameliorate this effect. In this respect, we have previously demonstrated that a diet high in 18:2n-6 redistributes plasma cholesterol to the liver pools and that this redistribution is not apparent when 18:3n-3 is present in the same diet (31). Therefore, it would appear that addition of n-3 PUFA to a high-saturated fat diet may mitigate the cholesterol-raising potential of SFA. Furthermore, the TG-lowering potential of n-3 PUFA has been shown to be maximized when n-3 PUFA are supplemented with saturated fat in comparison with an n-6 PUFA fat in the background diet (29). Further studies are warranted to establish whether diets high in saturated fat but containing adequate levels of n-3 PUFA can ameliorate lipid buildup in the circulation.

In conclusion, in this study n-3 PUFA supplementation in the form of 18:3n-3 is most effective in modulating the incorporation of n-6 and n-3 PUFA in conjunction with a background diet of predominantly SFA. In the light of these results, the health effects of dietary 18:3n-3 and marine n-3 PUFA in general on hypertension, arthritis, arteriosclerosis, depression, and thrombosis merit reconsideration with special emphasis on background dietary fat.

ACKNOWLEDGMENTS

This research was supported by a joint grant from Grain Research and Development Council (GRDC), Meadow Lea, Australia, and the University of Newcastle. The authors would like to acknowledge Robert Blake for his assistance in FA analysis by GC.

REFERENCES

1. Simopoulos, A.P. (1991) Omega-3 Fatty Acids in Health and Disease and in Growth and Development, *Am. J. Clin. Nutr. 54,* 438–463.
2. Leigh-Firbank, E.C., Minihabne, A.M., Leake, D.S., Wright, J.W., Murphy, M.C., Griffin, B.A., and Williams, C.M. (2002) Eicosapentaenoic Acid and Docosahexaenoic Acid from Fish Oils: Differential Associations with Lipid Responses, *Br. J. Nutr. 87,* 435–445.
3. Mori, T.A., Burke, V., Puddey, I.B., Watts, G.F., O'Neal, D.N., Best, J.D., and Beilin, L.J. (2000) Purified Eicosapentaenoic Acid and Docosahexaenoic Acids Have Differential Effects on Serum Lipids and Lipoproteins, LDL Particle Size, Glucose, and Insulin in Mildly Hyperlipidemic Men, *Am. J. Clin. Nutr. 71,* 1085–1094.
4. Singer, P., Berger, I., Wirth, M., Godicke, W., Jaeger, W., and Voigt, S. (1986) Slow Desaturation and Elongation of Linoleic and α-Linolenic Acids as a Rationale of Eicosapentaenoic Acid-Rich Diet to Lower Blood Pressure and Serum Lipids in Normal, Hypertensive and Hyperlipemic Subjects, *Prostaglandins Leukot. Med. 24,* 173–193.
5. Volker, D., and Garg, M. (1996) Dietary n-3 Fatty Acid Supplementation in Rheumatoid Arthritis—Mechanisms, Clinical Outcomes, Controversies and Future Directions, *J. Clin. Biochem. Nutr. 20,* 83–97.
6. James, M., Gibson, R., and Cleland, L. (2000) Dietary Polyunsaturated Fatty Acids and Inflammatory Mediator Production, *Am. J. Clin. Nutr. 72* (Suppl.), 343S–348S.
7. Thomson, A.B.R., Keelan, M., Garg, M.L., and Clandinin, M.T. (1989) Influence of Dietary Fat Composition on Intestinal Absorption in the Rat, *Lipids 24,* 494–501.
8. Folch, J., Lees, M., and Sloane Stanley, G.H. (1957) A Simple Method for the Isolation and Purification of Total Lipids from Animal Tissues, *J. Biol. Chem. 226,* 497–509.
9. Lepage, G., and Roy, C.C. (1986) Direct Transesterification of All Classes of Lipids in a One-Step Reaction, *J. Lipid Res. 27,* 114–120.
10. Garg, M.L., and Blake, R. (1997) Cholesterol Dynamics in Rats Fed Diets Containing Either Canola Oil or Sunflower Oil, *Nutr. Res. 17,* 485–492.
11. Cabre, E., Nunez, M., Gonzalez-Huix, F., Fernandez-Banares, F., Abad, A., Gil, A., Esteve, M., Planas, R., Moreno, J., Morillas, R., and Gassull, M.A. (1993) Clinical and Nutritional Factors Predictive of Plasma Lipid Unsaturation Deficiency in Advanced Liver Cirrhosis: A Logistic Regression Analysis, *Am. J. Gastroenterol. 88,* 1738–1743.
12. Fowler, J., Cohen, L., and Jarvis, P. (1998) *Practical Statistics for Field Biology,* John Wiley & Sons, Brisbane.
13. Zar, J.H. (1999) *Biostatistical Analysis,* Prentice Hall, Upper Saddle River, NJ.
14. Garg, M.L., Snoswell, A.M., and Sabine, J.R. (1986) Influence of Dietary Cholesterol on Desaturase Enzymes of Rat Liver Microsomes, *Prog. Lipid Res. 25,* 639–644.
15. Rambjor, G.S., Walen, A.I., Windsor, S.L., and Harris, W.S. (1996) Eicosapentaenoic Acid Is Primarily Responsible for Hypotriglyceridemic Effect of Fish Oil in Humans, *Lipids 31,* S45–S49.
16. Alsted, A., and Høy, C. (1992) Fatty Acid Profiles of Brain Phospholipid Subclasses of Rats Fed n-3 Polyunsaturated Fatty Acids of Marine or Vegetable Origin. A Two Generation Study, *Biochim. Biophys. Acta 1125,* 237–244.
17. Marshal, L., and Johnston, P. (1982) Modulation of Tissue Prostaglandin Synthesizing Capacity by Increased Ratios of Dietary α-Linolenic Acid to Linoleic Acid, *Lipids 17,* 905–913.
18. Emken, E.A., Adlof, R.O., and Gulley, R.M. (1994) Dietary Linoleic Acid Influences Desaturation and Elongation of Deuterium Labelled Linoleic and Linolenic Acids in Young Adult Males, *Biochim. Biophys. Acta 1213,* 277–288.
19. Pawlosky, R.J., Hibbelin, J.R., Novotny, J.A., and Salem, N., Jr. (2001) Physiological Compartmental Analysis of α-Linolenic Acid Metabolism in Adult Humans, *J. Lipid Res. 42,* 1257–1265.
20. Tahin, Q.S., Blum, M., and Carafoli, E. (1981) The Fatty Acid Composition of Subcellular Membranes of Rat Liver, Heart, and Brain: Diet-Induced Modifications, *Eur. J. Biochem. 121,* 5–13.
21. Bowen, R.A., and Clandinin, M.T. (2000) High Dietary 18:3n-3 Increases 18:3n-3 but Not the 22:6n-3 Content in the Whole Body, Brain, Skin, Epididymal Fat Pad and Muscles of Suckling Rat Pups, *Lipids 35,* 389–394.

22. Abedin, L., Lien, E.L., Vingrys, A.J., and Sinclair, A.J. (1999) The Effects of Dietary α-Linolenic Acid Compared with Docosahexaenoic Acid on Brain, Retina, Liver and Heart in Guinea Pig, *Lipids 34,* 475–482.
23. Qiu, X. (2003) Biosynthesis of Docosahexaenoic Acid (DHA, 22:6-4,7,10,13,16,19): Two Distinct Pathways, *Prostaglandins, Leukotrienes Essent. Fatty Acids 68,* 181–186.
24. Jeffery, N., Newsholme, E., and Calder, P. (1997) Level of Polyunsaturated Fatty Acids and the n-6 to n-3 Polyunsaturated Fatty Acid Ratio in the Rat Diet Alter Serum Lipid Levels and Lymphocyte Functions, *Prostaglandins, Leukotrienes Essent. Fatty Acids 57,* 149–160.
25. Katan, M.B. (1998) Effect of Low Fat Diets on Plasma High Density Lipoprotein Concentrations, *Am. J. Clin. Nutr. 67,* 573S–576S.
26. Terpstra, A.H.M., van den Berg, P., Jansen, H., Beynen, A.C., and van Tol, A. (2000) Decreasing Dietary Fat Saturation Lowers HDL-Cholesterol and Increases Hepatic HDL Binding in Hamsters, *Br. J. Nutr. 83,* 151–159.
27. Garg, M., Wierzbicki, A.A., Thomson, A.B.R., and Clandinin, M.T. (1988) Fish Oil Reduces Cholesterol and Arachidonic Acid Content More Efficiently in Rats Fed Diets Containing Low Linoleic Acid to Saturated Fatty Acid Ratios, *Biochim. Biophys. Acta 962,* 337–344.
28. Garg, M., Thomson, A.B.R., and Clandinin, M.T. (1990) Interactions of Saturated, n-6 and n-3 Polyunsaturated Fatty Acids to Modulate Arachidonic Acid Metabolism, *J. Lipid Res. 31,* 271–277.
29. Garg, M.L., Thomson, A.B.R., and Clandinin, M.T. (1989) Hypotriglyceridemic Effect of Dietary ω-3 Fatty Acids in Rats Fed Fats from Vegetable or Animal Origin, *Biochim. Biophys. Acta 1006,* 127–130.
30. Mantzioris, E., Cleland, L., Gibson, R., Newmann, M., Demasi, M., and James, M. (2000) Biochemical Effects of a Diet Containing Foods Enriched with n-3 Fatty Acids, *Am. J. Clin. Nutr. 72,* 42–48.
31. Garg, M.L., Sebokova, E., Wierzbicki, A., Thomson, A.B.R., and Clandinin, M.T. (1988) Differential Effects of Dietary Linoleic and α-Linolenic Acid on Lipid Metabolism in Rat Tissue, *Lipids 23,* 847–852.

[Received March 2, 2004; accepted August 4, 2004]

Phospholipase D and Phosphatidate Phosphohydrolase Activities in Rat Cerebellum During Aging

S.J. Pasquaré, G.A. Salvador, and N.M. Giusto*

Instituto de Investigaciones Bioquímicas de Bahía Blanca, Universidad Nacional del Sur and Consejo Nacional de Investigaciones Científicas y Técnicas (CONICET), B8000FWB Bahía Blanca, Argentina

ABSTRACT: Aging is a process that affects different organs, of which the brain is particularly susceptible. PA and DAG are central intermediates in the phosphoglyceride as well as in the neutral lipid biosynthetic pathway, and they have also been implicated in signal transduction. Phospholipase D (PLD) and phosphatidate phosphohydrolase (PAP) are the enzymes that generate PA and DAG. The latter can be transformed into MAG by diacylglycerol lipase (DGL). In the present study, we examine how aging modulates the PLD, PAP, and DGL isoforms in cerebellar subcellular fractions from 4- (adult), 28-, and 33-mon-old (aged) rats. PI-4,5-bisphosphonate (PIP_2)-dependent PLD, PAP1, and DGL1 were distributed in different percentages in all cerebellum subcellular fractions. On the other hand, PAP2 and DGL2 activities were observed in all subcellular fractions except in the cytosolic fraction. Aging modified the enzyme distribution pattern. In addition, aging decreased nuclear (45%), mitochondrial-synaptosomal (55%), and cytosolic (71%) PAP1 activity and increased (28%) microsomal PAP1 activity. DGL1 activity was decreased in nuclear (85%) and mitochondrial-synaptosomal (63%) fractions by aging. On the other hand, PIP_2-dependent PLD activities were increased in the mitochondrial-synaptosomal fraction. PAP2 and DGL2 were increased in the microsomal fraction by 87 and 114%, respectively, and they were decreased in the nuclear fraction. The changes observed in cerebellum PAP1 and DGL1 activities from aged rats with respect to adult rats could be related to modifications in lipid metabolism. Differential PA metabolization during aging through PIP_2-dependent PLD/PAP2/DGL2 activities could be related to alterations in the neural signal transduction mechanisms.

Paper no. L9467 in *Lipids 39,* 553–560 (June 2004).

The aging brain is characterized by a measurable decline of physiological functions resulting from a series of causes that remain largely unknown. One intriguing feature of the aging process is the modification of cellular membrane properties. As phospholipids are an integral part of membranes, they undoubtedly play an important role in the regulation of the cell membrane function; therefore, any modification in their metabolism and/or in the enzymatic activities metabolizing them may influence the cellular function.

The cerebellum (CRBL) in particular plays a crucial role in the control of very rapid muscular activities; it helps plan the motor activities and monitors and makes corrective adjustments in the motor activities elicited by other parts of the brain. Our previous studies on different brain areas from aged rats document changes in the lipid profile and lipid metabolism in the CRBL. Such changes consisted of (i) an increase in the total cholesterol/phospholipid molar ratio (1), (ii) an increase in the proportion of monounsaturated acyl chains, and (iii) a decrease in the proportion of polyunsaturated acyl chains esterified to phospholipids. In addition, the phospholipid FA composition is markedly affected by aging, and serine base exchange activity is selectively increased by aging (2).

PA and DAG are central intermediates in phosphoglyceride and neutral lipid biosynthetic pathways, and they also have been implicated in signal transduction (3,4). PA is generated by a *de novo* pathway (5), by phosphorylation of DAG by diacylglycerolkinase (6), and/or by phospholipase D (PLD) action on PC (7,8). In addition, DAG is produced by the phosphatidate phosphohydrolase (PAP) on PA produced by PLD (9,10).

There are at least three distinct PLD isoforms in the central nervous system, namely, an oleic acid-dependent isoform and two PI-4,5-bisphosphate (PIP_2)-dependent isoforms (PLD1 and PLD2, respectively) (11–13). However, it has been recently reported that PLD2 is activated by oleic acid in the presence of PIP_2. These data may lead to the conclusion that oleate-activated PLD is PLD2 (14). Two types of mammalian PAP hydrolyze PA to yield DAG. One is the cytosolic/microsomal Mg^{2+}-dependent enzyme (PAP1), which is selectively inactivated by the thioreactive *N*-ethylmaleimide (NEM) (15), which has not been purified and for which the cDNA has not been cloned (16). The other one is the Mg^{2+}-independent, NEM-insensitive PAP (PAP2) (15), which is mainly, although not exclusively, located in the plasma membrane as well as in the endoplasmic reticulum associated with PLD (17,18). Several PAP2 isoforms have been cloned to date (19). The PAP2 family has been proposed to be renamed as lipid phosphate phosphohydrolases because they hydrolyze a variety of lipid phosphates (20).

We reported that PAP1 and PAP2 hydrolyze PA in the brain of adult rats and that their activities are significantly modified in aged rats (21). We have also observed that the DAG produced

*To whom correspondence should be addressed at Instituto de Investigaciones Bioquímicas de Bahía Blanca, Universidad Nacional del Sur and CONICET, C.C. 857, B8000FWB Bahía Blanca, Argentina.
E-mail: ngiusto@criba.edu.ar

Abbreviations: CRBL, cerebellum; Cyto, cytosolic fraction; DGL, diacylglycerol lipase; DPPC, 1,2-dipalmitoyl-*sn*-glycero-3-phosphocholine; MAM, endoplasmic reticulum-like membranes associated with mitochondria; MS, microsomal fraction; MT-Syn, mitochondrial- synaptosomal fraction; NEM, *N*-ethylmaleimide; PAP, phosphatidate phosphohydrolase; PAP1, NEM-sensitive phosphatidate phosphohydrolase; PAP2, NEM-insensitive phosphatidate phosphohydrolase; PIP_2, phosphatidylinositol-4,5-bisphosphate; PKC, protein kinase C; PLD, phospholipase D.

by the different PAP activities were metabolized to MAG by diacylglycerol lipases (DGL) (21). In addition, we observed that the process of aging modified PIP_2-dependent PLD, PAP2, and DGL activities in cerebral cortical synaptosomes and that these enzymatic activities were modulated by cytosolic factors in senescent rat synaptosomal membranes (22).

Alterations in glycerolipid composition and modification of glycerophospholipid-degrading enzymes have been reported in different models of neurodegeneration (23); however, no evidence has been reported about the modulation of CRBL lipid-metabolizing enzymes nor about the modulation of enzymes that generate lipid second messengers during aging. The aim of the present paper was therefore to determine PLD, PAP, and DGL activities in CRBL subcellular fractions of adult rats and to observe whether aging modifies them.

MATERIALS AND METHODS

[2-^{3}H]Glycerol (200 mCi/mmol), 1,2-dipalmitoyl-*sn*-glycero-3-phospho[methyl-^{3}H]choline (DPPC; 43 Ci/mmol), and Omnifluor were obtained from NEN Life Science Products Inc. (Boston, MA). All other chemicals were of the highest purity available. Monoclonal anti-PLD1 and anti-PAP 2b were obtained from Upstate Biotechnology (Lake Placid, NY).

Preparation of subcellular fractions. Wistar-strain rats were kept under constant environmental conditions and fed on a standard pellet diet. Rats were killed by decapitation. The CRBL was immediately dissected and stored at −80°C before use.

Homogenates were prepared from the CRBL of 4-mon-old (adult) and 28- or 33-mon-old rats (aged), which were killed by decapitation. All animal handling was performed in agreement with the standards stated in the *Guide to the Care and Use of Experimental Animals* published by the Canadian Council on Animal Care. CRBL homogenates (20% wt/vol) were prepared in a medium containing 0.32 M sucrose, 1 mM EDTA, and 5 mM HEPES buffer (pH 7.4). The homogenate was centrifuged at 1,300 × *g* for 3 min, and the supernatant was poured into another tube. The nuclear pellet was resuspended with the isolation medium and was subsequently spun at 1,300 × *g* for 3 min. The combined supernatant was subsequently centrifuged at 17,000 × *g* for 10 min to obtain the crude mitochondrial pellet. For the purpose of washing the mitochondrial pellet, it was resuspended with the isolation medium and centrifuged at 17,000 × *g* for 10 min. The combined postmitochondrial supernatant was centrifuged at 130,000 × *g* for 45 min to obtain the microsomal and cytosolic fractions.

Determination of PLD activity. For the determination of PIP_2-dependent PLD activity, PC hydrolysis was determined by using an assay described by Brown *et al.* (24) with slight modifications. Briefly, 50 µL of mixed lipid vesicles (PE/ PIP_2/dipalmitoylphosphatidylcholine, molar ratio 16:1.4:1) with choline-methyl-^{3}H]DPPC to yield 200,000 cpm per assay was added to 100 µL of either the membrane or the cytosolic fraction (100 µg of protein) in a total volume of 200 µL containing 50 mM HEPES (pH 7.5), 3 mM EGTA, 80 mM KCl, and 2.5 mM $MgCl_2$. The reaction was incubated at 37°C for 30 min and stopped by the addition of 1 mL of chloroform/methanol/concentrated HCl (50:50:0.3, by vol) and 0.35 mL of 1 M HCl/5 mM EGTA. The aqueous phase was obtained after centrifugation for 5 min at 1,300 × *g*, and choline was separated from the other water-soluble products by using TLC on silica gel G plates (Merck, Darmstadt, Germany) and a mobile phase made of methanol/0.5% NaCl/NH_3 (50:50:1, by vol) (25). Choline was scraped off the plate and quantified by liquid scintillation spectroscopy.

Determination of PAP activities. PAP activities were differentiated on the basis of NEM-sensitivity (26,27). For the determination of NEM-insensitive PAP activity (PAP2), each assay contained 50 mM Tris-maleate buffer, pH 6.5, 1 mM DTT, 1 mM EDTA plus 1 mM EGTA, 4.2 mM NEM, and 100 µg of either the membrane or the cytosolic protein in a volume of 0.200 mL. The reaction was started by adding 0.6 mM of [2-^{3}H]phosphatidate.

NEM-sensitive PAP activity (PAP 1) was determined in an assay containing 50 mM Tris-maleate buffer, pH 6.5, 1 mM DTT, 1 mM EDTA and 1 mM EGTA, 0.2 mM Mg^{2+}, and 100 µg of either the membrane or the cytosolic protein in a volume of 0.200 mL. The reaction was started by adding 0.6 mM of [2-^{3}H]phosphatidate plus 0.4 mM PC. Parallel incubations were carried out after preincubating either the membrane or the cytosolic fraction with 4.2 mM NEM for 10 min. The difference between the two types of activity was labeled as PAP1.

All the assays for the determination of PAP1 or PAP2 activities were conducted at 37°C for 30 min. The enzyme assays were stopped by adding chloroform/methanol (2:1, vol/vol). Blanks were prepared identically, except that either the membrane or the cytosolic fraction was boiled for 5 min before being used.

PAP activity products diacyl [2-^{3}H]glycerol and monoacyl [2-^{3}H]glycerol were isolated and measured as described below. PAP activity was expressed as the sum of nmol of (diacyl [2-^{3}H]glycerol and monoacyl [2-^{3}H]glycerol) × (hour × mg protein)$^{-1}$.

Determination of DGL activity. DGL activity was determined by monitoring the formation rate of MAG, using PAP1- or PAP2-generated DAG as substrate. Standard assays contained approximately 80 nM DAG, and pH conditions, protein concentration, time, and final volume of incubation were the same as those described for PAP assay (28).

Preparation of radioactive 1,2-diacyl-sn-*glycero-3-phosphate.* Radioactive PA was obtained from [2-^{3}H glycerol]PC, which was synthesized from bovine retinas incubated with [2-^{3}H]glycerol (200 mCi/mmol) as previously described (29). Lipids were extracted from the tissue as described in Folch *et al.* (30). [2-^{3}H glycerol]PC was isolated by one-dimensional TLC and eluted therefrom (31). Then [2-^{3}H glycerol]PC was hydrolyzed with PLD (32), and PA, the hydrolysis product, was purified by one-dimensional TLC on silica gel H (Merck) developed with chloroform/methanol/acetic acid/acetone/water (9:3:3:12:1.5, by vol). The substrate was eluted from silica gel with neutral solvents to avoid the formation of lyso-PA and was subsequently converted into free acid by washing it twice using an upper phase containing 0.1 M sulfuric acid and then an upper phase containing water. Radioactivity and phosphorus content were measured to determine specific radioactivity (33).

[2-^{3}H]PA had a specific radioactivity of 0.1–0.2 μCi/μmol. To determine NEM-sensitive PAP activity, the substrate was prepared by sonicating 3.33 mM [2-^{3}H]phosphatidate (0.1–0.2 μCi/μmol) and 2.22 mM 1,2-dipalmitoyl-*sn*-glycero-3-phosphocholine in 5.56 mM EGTA and 5.56 mM EDTA. For the determination of NEM-insensitive PAP activity, an identical emulsion was prepared as indicated previously except that PC was omitted (26,27).

Extraction and isolation of lipids. Lipids were extracted with chloroform/methanol (2:1, vol/vol) and washed with a 0.2 vol of $CaCl_2$ (0.05%) (30). Neutral lipids were separated by gradient-thickness TLC on silica gel G (34) and developed with hexane/diethyl ether/acetic acid (35:65:1, by vol). To separate MAG from phospholipids, the chromatogram was rechromatographed up to the middle of the plate by using hexane/diethyl ether/acetic acid (20:80:2.3, by vol) as developing solvent. Once the chromatogram was developed, [2-^{3}H]PA and phospholipids were retained at the spotting site. Lipids were visualized by exposure of the chromatograms to iodine vapors and scraped off for counting by liquid scintillation after the addition of 0.4 mL water and 10 mL 5% Omnifluor in toluene/Triton X-100 (4:1, vol/vol).

Western blot analysis. Subcellular fractions were lysed with buffer containing 1% Nonident P-40, 0.25% sodium deoxycholate, 50 mM Tris-HCl, 150 mM NaCl, 1 mM EGTA, 1 mM NaF, 1 mM Na_3VO_4, 1 μg/mL aprotinin, 2 μg/mL leupeptin, 1 μg/mL pepstatin, and 0.1 mM phenylmethylsulfonylfluoride, pH 7.5. Proteins obtained from equivalent amounts of either adult or aged subcellular fraction lysates were resolved by SDS-PAGE (35) using 7.5 or 10% gels. Resolved proteins were transferred to Immobilon P membranes using a Mini Trans-Blot cell electroblotter (Bio-Rad Life Science Group, Hercules, CA) for 1 h. Membranes were blocked overnight with Tris-buffered saline (20 mM Tris-HCl, 300 mM NaCl), pH 7.5, containing 0.1% Tween 20 and 5% crystalline-grade BSA. Incubations with primary antisera (anti-PLD1 or anti-PAP2b) were performed for 2–3 h at room temperature. Immunoreactions were detected either with horseradish peroxidase conjugated to goat anti-rabbit or goat anti-mouse IG, followed by enhanced chemiluminescence substrates (Amersham Biosciences, Inc., Buenes Aires, Argentina).

Other methods. Protein and lipid phosphorus were determined according to Bradford (36) and Rouser *et al.* (33), respectively.

Statistical analysis. Statistical analysis was performed using Student's *t*-test, with the values representing the mean ± SD corresponding to six individual samples per condition. Each sample was obtained from a different adult or aged animal.

RESULTS

PAP1 and DGL1 activities in CRBL subcellular fractions from adult (4-mon) and aged (28-mon) rats. PAP activities were differentiated on the basis of NEM-sensitivity, since NEM inhibits PAP1 activity but does not affect PAP2 activity. PAP1 was assayed using [2-^{3}H]PA plus DPPC. DAG produced by PAP1 were additionally metabolized to MAG by DGL. In this work, DGL activity coupled to PAP1 was named as DGL1. A differential distribution of PAP1 and DGL1 activities was observed in adult CRBL subcellular fractions. PAP1 activity distribution was as follows: crude nuclear fraction (35.7%), mitochondrial-synaptosomal fraction (MT-Syn) (33.2%), cytosolic fraction (Cyto) (26.5%), and microsomal fraction (MS) (4.9%). DGL1 activity was highest in the nuclear fraction and MT-Syn (45%) with a minor distribution in MS (9%) and Cyto (6%). A different PAP1 and DGL1 distribution was observed in aged animals. PAP1 was 39.3, 30.8, 14.4, and 15.5%, and DGL1 was 13.1, 45.6, 26.1, and 15.2% in the nuclear fraction, the MT-Syn, the MS, and the Cyto, respectively (Table 1).

Figure 1 shows the effect of aging on PAP1 and DGL1 activities in the subcellular fractions of CRBL from adult and aged rats. PAP1 was observed to decrease in the nuclear fraction, the MT-Syn, and Cyto (45, 55, and 71%, respectively) from aged rats. In contrast, microsomal PAP1 activity from aged rats was increased by 28% with respect to the PAP1 activity found in adult animals.

DGL1 activity from aged rats was decreased in the nuclear fraction and the MT-Syn by 85 and 63%, respectively. Microsomal and cytosolic DGL1 activities were not modified by aging.

PLD isoforms in subcellular fractions of CRBL from adult (4-mon) and aged (28-mon) rats. PLD activity was measured by quantification of choline generation from [^{3}H]DPPC by adding PIP_2 as cofactor (PIP_2-dependent PLD) as specified in the Materials and Methods section. The results obtained with

TABLE 1
Percentage Distribution of PLD, PAP, and DGL Isoforms in Subcellular Fractions from Adult and Aged Cerebellum[a]

	Nuclear fraction		Mitochondrial-synaptosomal fraction		Microsomal fraction		Cytosolic fraction	
Enzyme	Adult	Aged	Adult	Aged	Adult	Aged	Adult	Aged
PAP1	35.7 ± 0.2	39.3 ± 0.2	33.2 ± 0.1	30.8 ± 0.2	4.9 ± 0.1	14.4 ± 0.1	26.5 ± 0.1	15.5 ± 0.1
DGL1	41.2 ± 0.4	13.1 ± 0.6	45.6 ± 3.6	45.7 ± 1.1	9.1 ± 1.1	26.1 ± 0.5	6.1 ± 0.4	15.2 ± 1.8
PIP_2-PLD	19.4 ± 0.2	19.6 ± 1.0	29.4 ± 2.2	36.5 ± 12.6	48.7 ± 0.7	40.4 ± 8.2	2.9 ± 0.64	3.3 ± 0.3
PAP2	34.1 ± 0.4	25.9 ± 0.4	56.5 ± 0.2	54.7 ± 0.4	9.5 ± 0.2	19.3 ± 0.3	ND	ND
DGL2	33.2 ± 1.2	23.0 ± 1.3	58.2 ± 1.7	54.1 ± 1.8	8.7 ± 0.5	23.0 ± 0.6	ND	ND

[a]100% represents the sum of each one of the enzymatic activities determined in nuclear, mitochondrial-synaptosomal, microsomal, and cytosolic fractions. Each value is the mean ± SD, corresponding to six individual samples per condition. Each sample was obtained from a different adult or aged animal. NEM, *N*-ethylmaleimide; PAP1, NEM-sensitive phosphatidate phosphohydrolase (PAP); DGL1, DAG lipase 1; PIP_2, PI-4,5-bisphosphate; PLD, phospholipase D; PAP2, NEM-insensitive PAP; DGL2, DAG lipase 2; ND, not detected.

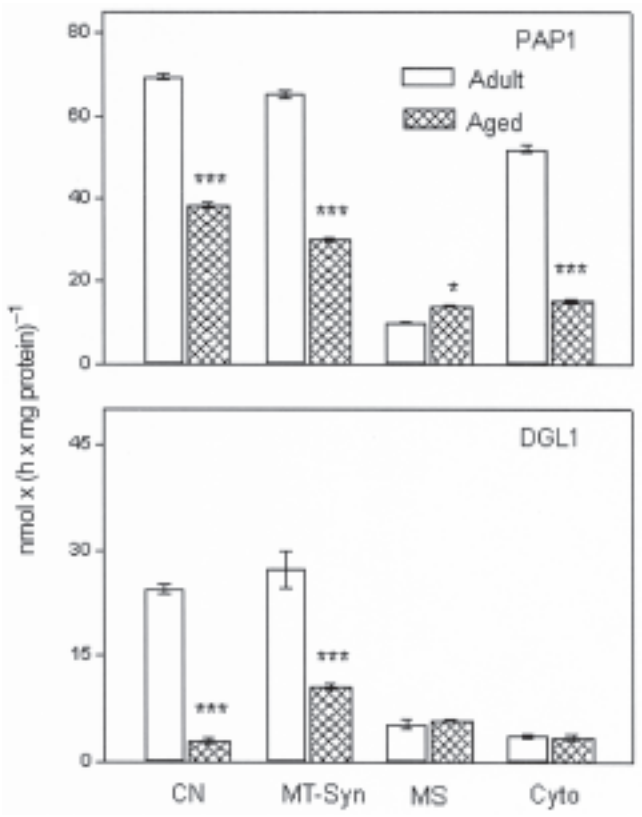

FIG. 1. PAP1 and DGL1 activities in CRBL subcellular fractions from adult and aged rats. PAP1 activity was determined using [2-^{3}H]PA (0.6 mM) plus dipalmitoyl PC (0.4 mM); total activity was measured with Mg^{2+} (3 mM) and NEM (4.2 mM); parallel incubations were carried out after preincubating the membranes with 4.2 mM NEM for 10 min. The difference between these two activities was taken as PAP1. DGL1 activity was determined using DAG generated from PAP1 as substrate. The enzymatic activities were expressed as nmol × (h × mg protein)$^{-1}$ of [2-^{3}H]DAG plus [2-^{3}H]MAG and [2-^{3}H]MAG for PAP1 and DGL1, respectively. Each value is the mean ± SD corresponding to six individual samples per condition. Each sample was obtained from a different adult or aged animal. (***$P < 0.001$, *$P < 0.05$). NEM, *N*-ethylmaleimide; PAP1, NEM-sensitive phosphatidate phosphohydrolase (PAP); DGL1, DAG lipase 1; CRBL, cerebellum; CN, nuclear fraction; MT-Syn, mitochondrial-synaptosomal fraction; MS, microsomal fraction; Cyto, cytosolic fraction.

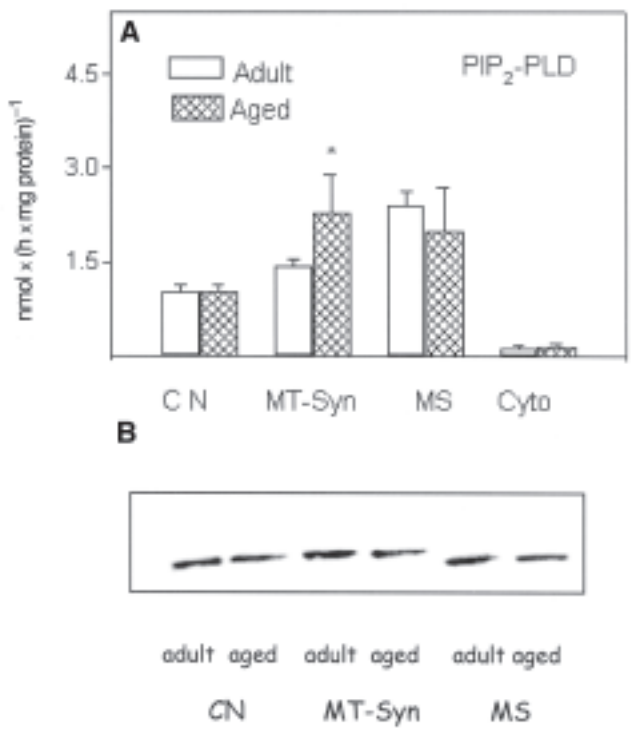

FIG. 2. (A) PLD activity in CRBL subcellular fractions. PLD activity was determined using a mixed lipid vesicle formed by PE/PIP$_2$/DPPC as substrate in a molar ratio of 16:1.4:1 with [^{3}H]DPPC (200,000 cpm). The enzymatic activity was expressed as nmol × (hour × mg protein)$^{-1}$ of [^{3}H]choline. Each value is the mean ± SD corresponding to six individual samples per condition. Each sample was obtained from a different adult or aged animal. (**$P < 0.05$; *$P < 0.005$). (B) Immunoblot of subcellular fractions from adult and aged animals with anti-PLD1 (1:500). Each line contains 30 μg of protein. PLD, phospholipase D; PIP$_2$, PI-4,5-bisphosphate; DPPC, 1,2-dipalmitoyl-*sn*-glycero-3-phosphocholine; for other abbreviations see Figure 1.

[^{3}H]DPPC were confirmed by measuring the specific PLD product, PE, using 1-stearoyl 2-[^{14}C]arachidonoyl-*sn*-glycero-3-phosphocholine and ethanol as substrates. Two PIP$_2$-dependent PLD isoforms (PLD1 and PLD2) have been characterized in the central nervous system (37). To determine PLD1/PLD2 activities in the CRBL, we used liposomes constructed with PIP$_2$/PE/DPPC (1.4:16:1, molar ratio). Under these experimental conditions, the distribution pattern of PLD activity in adult animals was as follows: MS (48.7%), MT-Syn (29.4%), nuclear fraction (19.4%), and Cyto (2.9%). Aging did not modify significantly the distribution pattern of PIP$_2$-dependent PLD (Table 1). Aging only modified mitochondrial-synaptosomal PLD activity (Fig. 2). To test whether the aging effect observed on PLD activity was due to an enhancement of enzyme activity or an increase in expression levels, Western blot analysis was performed with anti-PLD1 antibody. PLD was present in the nuclear fraction, the MT-Syn, and the MS. No differences in expression levels were observed between adult and aged animals, except in MT-Syn, where aged animals presented lower PLD1 expression levels with respect to adult animals. It has been reported that PLD1 activity is barely detected in the absence of small G proteins such as ARF (adenosine diphosphate ribosylation factor, a member of the RAS GTPase superfamily involved in vesicular trafficking) and RHoA (Rho, a subfamily of GTPases involved in cytoskeleton regulation), whereas PLD2 has a high basal activity (37). For this reason we can assume that, under our experimental conditions, in the presence of PIP$_2$ with no other activators, the principal PLD activity measured corresponds to the PLD2 isoform.

PAP2 and DGL2 activities in subcellular fractions of CRBL homogenates from adult (4-mon) and aged (28-mon) rats. PAP2 activity is mainly coupled to PIP$_2$-dependent PLD activity because the main product of the hydrolytic PLD activity, PA, is the substrate for PAP2 to yield DAG. PAP2 activity was determined in the presence of NEM by using [^{3}H]PA as substrate. DGL activity was assayed using DAG, which is produced by PAP2 activity, as substrate. The DGL activity measured under these experimental conditions was named DGL2.

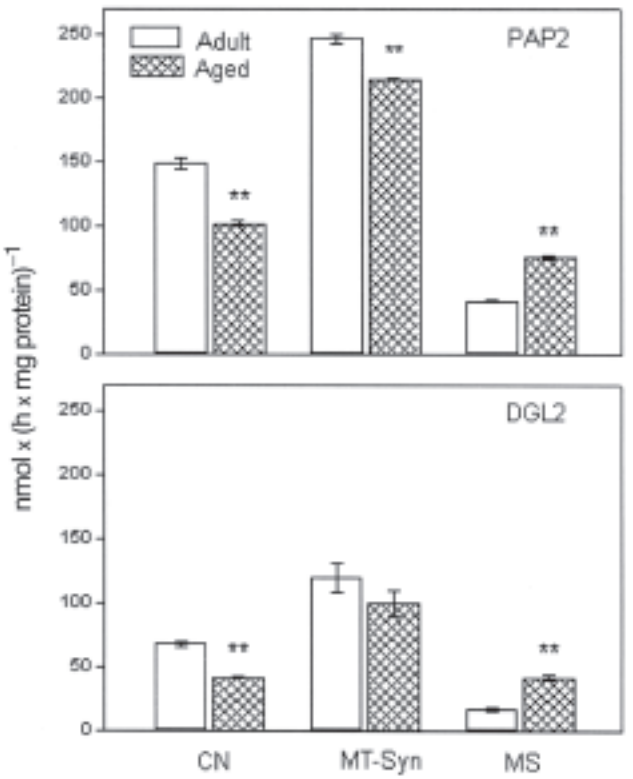

FIG. 3. PAP2 and DGL2 activities in CRBL subcellular fractions from adult and aged rats. For the determination of PAP2 activity, the assay was carried out by preincubating the membranes with 4.2 mM NEM for 10 min. The reaction was started by adding 0.6 mM [2-^{3}H]PA. DGL2 activity was determined using DAG generated from PAP2 as substrate. The enzymatic activities were expressed as nmol × (h × mg protein)$^{-1}$ of [2-^{3}H]DAG plus [2-^{3}H]MAG and [2-^{3}H]MAG for PAP2 and DGL2, respectively. Each value is the mean ± SD corresponding to six individual samples per condition. Each sample was obtained from a different adult or aged animal. (**$P < 0.005$). PAP2, NEM-insensitive phosphatidate phosphohydrolase; DGL2, DAG lipase 2; for other abbreviations see Figure 1.

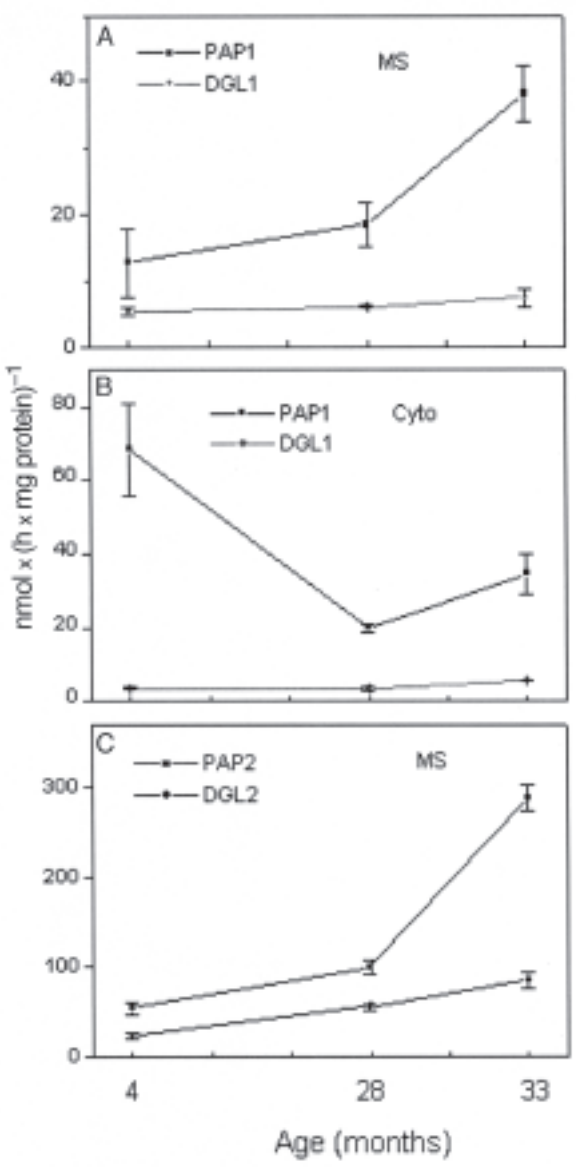

FIG. 4. PAP and DGL activities in CRBL MS (A and C) and Cyto (B) as a function of aging. The subcellular fractions were obtained from adult (4-mon-old) and aged (28- and 33-mon-old) CRBL rats as described in the Materials and Methods section. The enzymatic activities were assayed as specified in Figure 1. Each value is the mean ± SD corresponding to six individual samples per condition. Each sample was obtained from a different adult or aged animal. For abbreviations see Figures 1 and 3.

In adult rats, PAP2 and DGL2 activities were distributed in a similar pattern, namely, MT-Syn (56.5%), nuclear fraction (34%), and MS (9%), and they were not detected in the Cyto. The PAP2 distribution profile in aged animals was the same as that for DGL2, showing an increase in the MS (111%) and a decrease in the nuclear fraction (24%) (Table 1) with respect to adult animals.

Figure 3 shows PAP2 and DGL2 activities in the CRBL subcellular fractions from adult and aged rats. PAP2 and DGL2 activities were modified by aging and were increased in the MS by 87 and 114%, respectively. PAP2 activity was decreased in the nuclear fraction and MT-Syn, whereas DGL2 activity was only decreased in the nuclear fraction from aged rats. No immunodetection with anti-PAP2b was observed in our studies. This could be indicative of the presence of either PAP2a or PAP2c isoforms.

PAP and DGL activities in the CRBL MS and Cyto from adult (4-mon-old) and aged (28- and 33-mon-old) rats. Figure 4A shows PAP1 and DGL1 activities in the CRBL MS and Cyto from adult and aged (28- and 33-mon-old) rats. It can be observed that the microsomal PAP1 increased, whereas DGL1 was not modified as an age function, the increase in microsomal PAP1 activity in 33-mon-old rats being 194% higher than in 4-mon-old rats. A decrease of 70 and 50% in cytosolic PAP1 activity was observed in 28- and 33-mon-old rats, respectively (Fig. 4B).

PAP2 and DGL2 activities were increased as a function of age. The greatest effect was observed in the 33-mon-old animals (400%) (Fig. 4C).

Effect of aging on the distribution of PAP1 activity between CRBL MS and Cyto. Figure 5 shows the distribution changes of the CRBL PAP1 between MS and Cyto in aged rats with respect

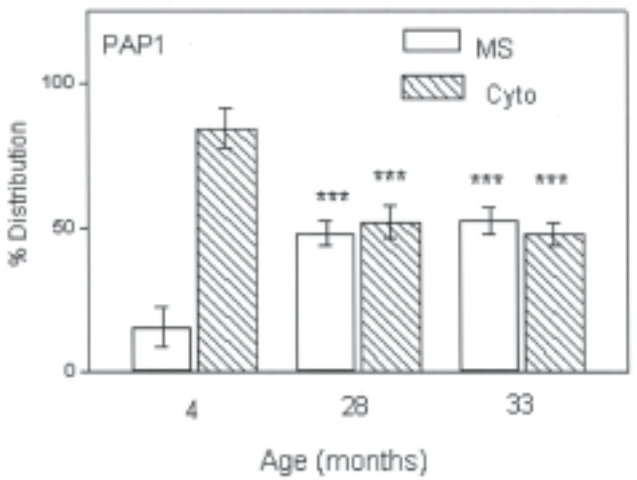

FIG. 5. Percentage distribution of PAP1 activity in MS and Cyto from CRBL as a function of aging. The value 100% represents the sum of the enzymatic activities determined in microsomal and cytosolic fractions. Each value is the mean ± SD corresponding to six individual samples per condition. Each sample was obtained from a different adult or aged animal. (***$P < 0.001$, for comparison of adult vs. aged). For abbreviations see Figures 1 and 3.

to adult rats, showing an increase in MS of 206 (28-mon-old) and 233% (33-mon-old) and a decrease in the Cyto of 38% (28-mon-old) and 43% (33-mon-old), respectively. No differences were observed in the distribution of DGL1 and PLD between the MS and Cyto (data not shown).

DISCUSSION

Aging is a complex process throughout which the brain undergoes a pattern of changes that include enhanced glycerophospholipid metabolism in specific brain areas (23). In this paper we analyzed the activities of different PLD, PAP, and DGL isoforms in nuclear, mitochondrial-synaptosomal, microsomal, and cytosolic cerebellar fractions and the way in which aging affects these activities.

Cerebellar PAP1 shows a similar percentage of distribution in nuclear fractions, MT-Syn, and Cyto with minor activity in the MS. Maximal DGL1 activity was observed in the nuclear fractions and MT-Syn with a minor and similar distribution pattern in the other subcellular fractions. DGL1 was coupled to PAP1 in subcellular fractions, as has been previously reported for other tissues (21,28), and it could participate in the regulation of DAG availability for *de novo* biosynthesis of zwitterionic phospholipids. It has been described that the nucleus presents its own lipid metabolism (38–40). Another potential role of nuclear PAP1 could be related to its participation in signal transduction, changing the balance from PA to DAG; PAP1 is involved in cyclo-oxygenase expression through PKC activation (41) and it co-immunoprecipitates with activated epidermal growth factor-receptor (42). PAP1 and DGL1 activities observed in MT-Syn could be due to either mitochondrial original activities [which are absent in synaptosomes (22)] or a translocation from the cytosol (43), or else they could be native to endoplasmic reticulum-like membranes associated with mitochondria (MAM). It has been previously reported that MAM contain other enzymes involved in *de novo* biosynthesis of lipids (44).

The physiological role of PAP1 in microsomal and cytosolic fractions has been extensively analyzed, and the most characterized function is its participation in the Kennedy pathway (5,16).

Aging decreases PAP1 activity in the nuclear fraction, MT-Syn, and Cyto; increases the microsomal PAP1 activity; exerts an additional inhibitory effect on nuclear and mitochondrial-synaptosomal DGL1 activities (independently of the effect on PAP1 activity); and differentially modifies microsomal and cytosolic DGL1 activities compared with those observed in PAP1. Aging translocates PAP1 activity from the Cyto to the MS place of zwitterionic phospholipid biosynthesis. The translocation of PAP1 could be a mechanism to reach the appropriate DAG levels for PC and PE synthesis in aged microsomes.

PLD activity was present in all CRBL subcellular fractions and exhibited the maximal activity in the microsomal fraction. The presence of PLD has been described in purified nuclei from different tissues (45) and in all subcellular liver fractions except mitochondria (46). PLD activity levels in the cerebellar mitochondrial fraction are undoubtedly due to the presence of synaptosomes in neural tissues where PLD has been previously detected at one of the highest specific activities (11,22). The PLD activity found in the MS and related membranes has been involved in vesicular traffic events, and its function in cytosol has not been completely elucidated (47,48).

To date, two PIP_2-dependent PLD isoforms, PLD1 and PLD 2, have been cloned. They differ in their regulatory mechanism although both are stimulated by the presence of PIP_2 (48). Whereas PLD2 has a high basal activity, PLD1 needs stimulation factors such as ARF and RhoA to be detected (13,47,49). PLD showed the maximal activity in the MS followed by the MT-Syn, the nuclear fraction, and the Cyto fractions. PLD activity was increased in the MT-Syn fraction by aging. Interestingly, Western blot analyses with anti-PLD1 showed lower expression levels in MT-Syn fractions in aged animals than adult animals. Under our experimental conditions, in the presence of PIP_2 with no other activators, it can be assumed that the major PLD activity measured corresponds to the PLD2 isoform. The presence of an increased level of PLD in the MT-Syn from aged rats could be due to an attempt to increase choline generation for acetylcholine synthesis (50). This finding is in agreement with the cholinergic hypothesis, according to which acetylcholine dysfunction is the cause of the cognitive decline observed in senescence (51).

PAP2 and DGL2 evidenced the maximal activities in MT-Syn, with an important activity in the nuclear fraction. It has been reported that PAP2 dephosphorylates PA, produced by PIP_2-dependent PLD, and a variety of lipid phosphates such as lysophosphatidic acid, sphingosine-1-phosphate ceramide-1-phosphate, and diacylglycerolphosphate (52). The presence of PAP2 coupled to PIP_2-dependent PLD in the nuclear fraction could be mainly generating lipid-signaling molecules as previously reported by Tamiya-Koizumi (38). The presence of these enzymes in MT-Syn may be mainly due to the presence of

synaptosomal membranes, as previously reported (22). No PAP2 and DGL2 activities were found in the Cyto. These results are in agreement with previous findings indicating that PAP2 is associated with particulate fractions with low or no activity present in the cytosol (16,21). As PAP2 is an integral membrane protein always present in an active state, it is likely that this form of the enzyme is involved both in the metabolism of membrane phospholipids and in the signal transduction mechanisms mediated by PLD (53). PAP2 activity was diminished in the nuclear fraction and in the MT-Syn by aging. As to the effect of aging on cerebellar PIP_2-dependent PLD from the MT-Syn, we can assume that the higher PA levels produced by the increased PLD activity are not further metabolized to DAG by PAP2. This could indicate that in this fraction aging promotes a partial PA availability. Microsomal PAP2 and DGL2 activities were increased by the effect of aging, whereas PIP_2-dependent PLD was not modified. Taking into account that PIP_2-dependent PLD, PAP2, and DGL2 may act in a concerted manner, one can assume that PA provided by PLD action could be quickly removed by the increased action of PAP2 and DGL2. Higher production of MAG has been associated with neurodegenerative diseases (23).

The calcium hypothesis of aging suggests that basal intracellular calcium is increased in aged animals, altering Ca^{2+}-dependent processes (54). These changes are primarily attributable to a metabolic dysfunction in which mitochondrial impairment plays an important role because, in nerve cells, mitochondria serve as a dynamic store involved in the regulation of calcium homeostasis (55). Several lines of evidence suggest that mitochondria are affected by aging and that they are progressively more damaged in senescent tissue (56). It has been reported that in the rat CRBL there is a significant age-dependent decrease in the expression of the voltage-gated calcium channels (57). As PLD and PAP are indirectly regulated by protein kinase Cs and as typical protein kinase C isoforms are modulated by calcium, alterations in the homeostasis of this ion as a consequence of senescent mitochondria could modify PLD and PAP enzymatic activities in the aging process (14,58).

A logical explanation for the different subcellular locations of PAP, PLD, and DGL activities in the aged CRBL is that they can provide independent pools of PA, DAG, and MAG for specific cellular functions (59). The behavior of different types of PLD, PAP, and DGL activities and their distribution during aging open an important field of study aimed at elucidating the physiological role of these enzymes in the cerebellar lipid metabolism and signal transduction and their implications in the cerebellar cognitive and motor function.

ACKNOWLEDGMENTS

This research was supported by CONICET, the Secretaría General de Ciencia y Tecnología, Universidad Nacional del Sur, and the Carrillo-Oñativia grant (Ministerio de Salud) Argentina. Norma M. Giusto and Gabriela A. Salvador are research members of the CONICET.

REFERENCES

1. López, G.H., Ilincheta de Boschero, M.G., Castagnet, P.I., and Giusto, N.M. (1995) Age-Associated Changes in the Content and Fatty Acid Composition of Brain Glycerophospholipids, *Comp. Biochem. Physiol. 112B*, 331–343.
2. Ilincheta de Boschero, M.G., Roque, M.E., Salvador, G.A., and Giusto, N.M. (2000) Alternative Pathways for Phospholipid Synthesis in Different Brain Areas During Aging, *Exp. Gerontol. 35*, 653–668.
3. Brindley, D.N., Abousalham, A., Kikuchi, Y., and Wang, C.N. (1996) "Cross-talk" Between the Bioactive Glycerolipids and Sphingolipids in Signal Transduction, *Biochem. Cell Biol. 71*, 469–476.
4. English, D., Martin, M., Harvey, K., Akard, L., Allen, R., Widlanski, T.S., García, J., and Siddiqui, R.A. (1997) Characterization and Purification of Neutrophil Ecto-phosphatidic Phosphohydrolase, *Biochem. J. 324*, 941–950.
5. Kennedy, E.P. (1961) Biosynthesis of Complex Lipids, *Fed. Proc. 20*, 934–940.
6. Topham, M.K., and Prescott, S.M. (1999) Mammalian Diacylglycerol Kinases with Signaling Functions, *J. Biol. Chem. 274*, 11447–11450.
7. Kanfer, J.N. (1980) The Base Exchange Enzymes and Phospholipase D of Mammalian Tissue, *Can. J. Biochem. 58*, 1370–1380.
8. Exton, J.H. (1997) New Developments in Phospholipase D, *J. Biol. Chem. 272*, 15579–15582.
9. Smith, M.E., Sedgwick, B., Brindley, D.N., and Hubscher, G. (1967) The Role of Phosphatidate Phosphohydrolase in Glyceride Biosynthesis, *Eur. J. Biochem. 3*, 70–77.
10. Jamal, Z., Martin, A., Gomez-Muñoz, A., Hales, P., Chang, E., Russell, J.C., and Brindley, D.N. (1992) Phosphatidate Phosphohydrolases in Liver, Heart and Adipose Tissue of the JCR:LA Corpulent Rat and Lean Genotypes: Implications for Glycerolipid Synthesis and Signal Transduction, *Int. J. Obes. Relat. Metab. Disord 16*, 789–799.
11. Kobayashi, M., and Kanfer, J.N. (1987) Phosphatidylethanol Formation *via* Transphosphatidylation by Rat Brain Synaptosomal Phospholipase D, *J. Neurochem. 48*, 1597–1603.
12. Massenburg, D., Han, J.S., Liyanage, M., Patton, W.A., Rhee, S.G., Moss, J., and Vaughan, M. (1994) Activation of Rat Brain Phospholipase D by ADP-Ribosylation Factors 1, 5, and 6: Separation of ADP Ribosylation Factor-Dependent and Oleate-Dependent Enzymes, *Proc. Natl. Acad. Sci. USA 91*, 11718–11722.
13. Liscovitch, M., Czarny, M., Fiucci, G., Lavie, Y., and Tang, X. (1999) Localization and Possible Functions of Phospholipase D Isozymes, *Biochim. Biophys. Acta 1439*, 245–263.
14. Sarri, E., Pardo, R., Fensome-Green, A., and Cockcroft, S. (2003) Endogenous Phospholipase D2 Localizes to the Plasma Membrane of RBL-2H3 Mast Cells and Can Be Distinguished from ADP Ribosylation Factor-Stimulated Phospholipase D1 Activity by Its Specific Sensitivity to Oleic Acid, *Biochem. J. 369*, 319–329.
15. Martin, A., Gomez-Muñoz, A., Jamal, Z., and Brindley, D.N. (1991) Characterization and Assay of Phosphatidate Phosphohydrolase, *Methods Enzymol. 197*, 553–563.
16. Nanjundan, M., and Possmayer, F. (2003) Pulmonary Phosphatidic Acid Phosphatase and Lipid Phosphate Phosphohydrolase, *Am. J. Physiol. Lung Cell Mol. Physiol. 284*, 1–23.
17. Sciorra, V.A., and Morris, A.J. (1999) Sequential Actions of Phospholipase D and Phosphatidic Acid Phosphohydrolase 2 b Generate Diglyceride in Mammalian Cells, *Mol. Biol. Cell 1*, 3863–3876.
18. Fleming, I.N., and Yeaman, S.J. (1995) Subcellular Distribution of *N*-Ethylmaleimide-Sensitive and -Insensitive Phosphatidic Acid Phosphohydrolase in Rat Brain, *Biochim. Biophys. Acta 1254*, 161–168.
19. Sciorra, R.R., and Morris, A.J. (1998) Human Type 2 Phosphatidic Acid Phosphohydrolases. Substrate Specificity of the Type 2a, 2b, and 2c Enzymes and Cell Surface Activity of the 2a Isoform, *J. Biol. Chem. 273*, 22059–22067.

20. Brindley, D.N., and Waggoner, W. (1998) Mammalian Lipid Phosphate Phosphohydrolases, *J. Biol. Chem. 273*, 24281–24284.
21. Pasquaré, S.J., Ilincheta de Boschero, M.G., and Giusto, N.M. (2001) Aging Promotes a Different Phosphatidic Acid Utilization in Cytosolic and Microsomal Fractions from Brain and Liver, *Exp. Gerontol. 36*, 1387–1401.
22. Salvador, G.A., Pasquaré, S.J., Ilincheta de Boschero, M.G., and Giusto, N.M. (2002) Differential Modulation of Phospholipase D and Phosphatidate Phosphohydrolase During Aging in Rat Cerebral Cortex Synaptosomes, *Exp. Gerontol. 37*, 543–552.
23. Farooqui, A.A., Horrocks, L.A., and Farooqui, T. (2000) Glycerophospholipids in Brain: Their Metabolism, Incorporation into Membranes, Functions, and Involvement in Neurological Disorders, *Chem. Phys. Lipids 106*, 1–29.
24. Brown, H.A., Gutowski, S., Moomaw, C.R., Slaughter, C., and Sternways, P.C. (1993) ADP-Ribosylation Factor, a Small GTP-Regulatory Protein, Stimulates Phospholipase D Activity, *Cell 75*, 1137–1144.
25. Yavin, E. (1976) Regulation of Phospholipid Metabolism in Differentiating Cells from Rat Brain Cerebral Hemispheres in Culture, Patterns of Acetylcholine Phosphocholine, and Choline Phosphoglycerides Labeling from (methyl-^{14}C) Choline, *J. Biol. Chem. 251*, 1392–1397.
26. Jamal, Z., Martin, A., Gomez-Muñoz, A., and Brindley, D.N. (1991) Plasma Membrane Fractions from Rat Liver Contain a Phosphatidate Phosphohydrolase Distinct from That in the Endoplasmic Reticulum and Cytosol, *J. Biol. Chem. 266*, 2988–2996.
27. Hooks, S.B., Ragan, S.P., and Lynch, K.R. (1998) Identification of a Novel Human Phosphatidic Acid Phosphatase Type 2 Isoform, *FEBS Lett. 427*, 188–193.
28. Pasquaré, S.J., and Giusto, N.M. (1993) Differential Properties of Phosphatidate Phosphohydrolase and Diacylglyceride Lipase Activities in Retinal Subcellular Fractions and Rod Outer Segments, *Comp. Biochem. Physiol. 104*, 141–148.
29. Pasquaré de García, S.J., and Giusto, N.M. (1986) Phosphatidate Phosphatase Activity in Isolated Rod Outer Segment from Bovine Retina, *Biochim. Biophys. Acta 875*, 195–202.
30. Folch, J., Lees, M., and Sloane Stanley, G.H. (1957) A Simple Method for the Isolation and Purification of Total Lipides from Animal Tissues, *J. Biol. Chem. 226*, 497–509.
31. Arvidson, G.A.E. (1968) Structural and Metabolic Heterogeneity of Rat Liver Glycerophosphatides, *Eur. J. Biochem. 4*, 478–486.
32. Kates, M., and Sastry, P.S. (1969) Phospholipase D, *Methods Enzymol. 14*, 197–203.
33. Rouser, G., Fleischer, S., and Yamamoto, A. (1970) Two-Dimensional Thin-Layer Chromatographic Separation of Polar Lipids and Determination of Phospholipids by Phosphorus Analysis of Spots, *Lipids 5*, 494–496.
34. Giusto, N.M., and Bazán, N.G. (1979) Phospholipids and Acylglycerols Biosynthesis and ^{14}C Production from [^{14}C]Glycerol in the Bovine Retina: The Effects of Incubation Time, Oxygen and Glucose, *Exp. Eye Res. 29*, 155–168.
35. Laemli, U.K. (1970) Cleavage of Structural Proteins During the Assembly of the Head of Bacteriophage T4, *Nature 227*, 680–685.
36. Bradford, M.M. (1976) A Rapid and Sensitive Method for the Quantitation of Microgram Quantities of Protein Utilizing the Principle of Protein–Dye Binding, *Anal. Biochem. 72*, 248–254.
37. Liscovitch, M., and Chalifa-Caspi, V. (1996) Enzymology of Mammalian Phospholipase D: *In Vitro* Studies, *Chem. Phys. Lipids 80*, 320–344.
38. Tamiya-Koizumi, K. (2002) Nuclear Lipid Metabolism and Signaling, *J. Biochem. (Tokyo) 132*, 13–22.
39. Lykidis, A., Murti, K.G., and Jackowski, S. (1998) Cloning and Characterization of a Second Human CTP:phosphocholine Cytidylyltransferase, *J. Biol. Chem. 273*, 14022–14029.
40. Lykidis, A., Baburina, I., and Jackowski, S. (1999) Distribution of CTP:Phosphocholine Cytidylyltransferase (CCT) Isoforms. Identification of a New CCTβ Splice Variant, *J. Biol. Chem. 274*, 26992–27001.
41. Johnson, C.A., Balboa, M.A., Balsinde, J., and Dennis, E.A. (1999) Regulation of Cyclooxygenase-2 Expression by Phosphatidate Phosphohydrolase in Human Amnionic WISH Cells, *J. Biol. Chem. 274*, 27689–27693.
42. Jiang, Y., Lu, Z., Zang, Q., and Foster, D.A. (1996) Regulation of Phosphatidic Acid Phosphohydrolase by Epidermal Growth Factor. Reduced Association with the EGF Receptor Followed by Increased Association with Protein Kinase Cε, *J. Biol. Chem. 271*, 29529–29532.
43. Freeman, M., and Mangiapane, E.H. (1989) Translocation to Rat Liver Mitochondria of Phosphatidate Phosphohydrolase, *Biochem. J. 263*, 589–595.
44. Vance, J.E., Stone, S.J., and Faust, J.R. (1997) Abnormalities in Mitochondria-Associated Membranes and Phospholipid Biosynthetic Enzymes in the mnd/mnd Mouse Model of Neuronal Ceroid Lipofuscinosis, *Biochim. Biophys. Acta 1344*, 286–299.
45. Kanfer, J.N., McCartney, D., Singh, I., and Freysz, L. (1996) Phospholipase D Activity of Rat Brain Neuronal Nuclei, *J. Neurochem. 67*, 760–766.
46. Provost, J.P., Fudge, J., Israelist, S., Siddiqui, A.R., and Exton, J.H. (1996) Tissue-Specific Distribution and Subcellular Distribution of Phospholipase D in Rat: Evidence for Distinct RhoA- and ADP-Ribosylation (ARF)-Regulated Isoenzymes, *Biochem. J. 319*, 285–291.
47. Liscovitch, M., Czarny, M., Fiucci, G., Lavie, Y., and Tang, X. (2000) Phospholipase D: Molecular and Cell Biology of a Novel Gene Family, *Biochem. J. 345*, 401–415.
48. Exton, J.H. (2002) Regulation of Phospholipase D, *FEBS Lett. 531*, 58–61.
49. Cockcroft, S., Thomas, G.M., Fensome, A., Geny, B., Cunningham, E., Gout, I., Hiles, I., Totty, N.F., Truong, O., and Hsuan, J.J. (1994) Phospholipase D: A Downstream Effector of ARF in Granulocytes, *Science 263*, 523–526.
50. Zhao, D., Frohman, M.A., and Blusztajn, J.K. (2001) Generation of Choline for Acetylcholine Synthesis by Phospholipase D Isoforms, *BMC Neurosci. 2*, 16–26.
51. Terry, A.V., Jr., and Buccafusco, J.J. (2003) The Cholinergic Hypothesis of Age and Alzheimer's Disease-Related Cognitive Deficits: Recent Challenges and Their Implications for Novel Drug Development, *J. Pharmacol. Exp. Ther. 306*, 821–827.
52. Waggoner, D.W., Xu, J., Singh, I., Jasinska, R., Zhang, Q.X., and Brindley, D.N. (1999) Structural Organization of Mammalian Lipid Phosphate Phosphatase: Implications for Signal Transduction, *Biochim. Biophys. Acta 1439*, 299–316.
53. Martin, A., Gomez-Muñoz, A., Waggoner, D.W., Stone, J.C., and Brindley, D.N. (1993) Decreased Activities of Phosphatidate Phosphohydrolase and Phospholipase D in ras and Tyrosine Kinase (fps) Transformed Fibroblast, *J. Biol. Chem. 268*, 23924–23032.
54. Verkhratsky, A., and Toescu, E.C. (1998) Calcium and Neuronal Ageing, *Trends Neurosci. 21*, 2–7.
55. Nicholls, D., and Budd, S. (2000) Mitochondria and Neuronal Survival, *Physiol. Rev. 80*, 315–360.
56. Cortopasi, G., and Wong, A. (1999) Mitochondria in Organismal Aging and Degeneration, *Biochim. Biophys. Acta 1410*, 183–193.
57. Chung, Y.H., Shin, C.M., Kim, M.J., Shin, D.H., Yoo, Y.B. and Cha, C.I. (2001) Differential Alterations in the Distribution of Voltage-Gated Calcium Channels in Aged Rat Cerebellum, *Brain Res. 903*, 247–252.
58. Roque, M.E., Pasquaré, S.J., Castagnet, P.I., and Giusto, N.M. (1998) Can Phosphorylation and Dephosphorylation of Rod Outer Segment Membranes Affect Phosphatidate Phosphohydrolase and Diacylglycerol Lipase Activities? *Comp. Biochem. Physiol. B Biochem. Mol. Biol. 119*, 85–93.
59. Vance, J.E. (1998) Eukaryotic Lipid-Biosynthetic Enzymes: The Same but Not the Same, *Trends Biochem. Sci. 23*, 423–428.

[Received March 15, 2004, and in revised form and accepted August 9, 2004]

Isolation and Structures of Two Divinyl Ether Fatty Acids from *Clematis vitalba*

Mats Hamberg*

Department of Medical Biochemistry and Biophysics, Division of Physiological Chemistry II, Karolinska Institutet, S-171 77 Stockholm, Sweden

ABSTRACT: [1-^{14}C]Linolenic acid was incubated with a homogenate of leaves of *Clematis vitalba*, a plant belonging to the *Ranunculaceae* family. Analysis of the reaction product by reversed-phase high-performance liquid radiochromatography demonstrated the presence of the following labeled oxylipins: 12-oxo-10,15(*Z*)-phytodienoic acid, 9(*S*)-hydroxy-10(*E*),12(*Z*),15(*Z*)-octadecatrienoic acid, ω5(*Z*)-etherolenic acid, and 9-[1´(*E*),3´(*Z*),6´(*Z*)-nonatrienyloxy]-8(*Z*)-nonenoic acid [8(*Z*)-colnelenic acid]. The last compound was a new divinyl ether FA, and an analogous compound, i.e., 9-[1´(*E*),3´(*Z*)-nonadienyloxy]-8(*Z*)-nonenoic acid [8(*Z*)-colneleic acid], was obtained following incubation of linoleic acid with the *Clematis* homogenate. Structures of the two divinyl ethers were assigned by spectral and chromatographic comparison with authentic compounds prepared synthetically using previously described methodology. Separate incubation of the 9- and 13-hydroperoxides of linolenic acid demonstrated that the first hydroperoxide served as the precursor of 8(*Z*)-colnelenic acid and indicated the presence in *C. vitalba* of a new divinyl ether synthase acting on 9-lipoxygenase-generated hydroperoxides. A close structural relationship between this enzyme and the well-studied divinyl ether synthase in the potato and tomato seems likely.

Paper no. L9532 in *Lipids 39,* 565–569 (June 2004).

Enzymes catalyzing the formation of hydroperoxides from FA occur widely in nature. In plants, lipoxygenases (1) and α-dioxygenases (2) have important roles in generating FA hydroperoxides, which in turn serve as substrates for secondary enzymes producing allene oxides, alcohols, aldehydes, epoxy alcohols, or divinyl ethers (1). The discovery of the last class of compounds dates back to 1972, when Galliard and Phillips described the structures of two divinyl ether FA generated from linoleic and linolenic acids in homogenates of the potato tuber (3). These compounds, named "colneleic acid" [9-[1´(*E*),3´(*Z*)-nonadienyloxy]-8(*E*)-nonenoic acid] and "colnelenic" acid [9-[1´(*E*),3´(*Z*),6´(*Z*)-nonatrienyloxy]-8(*E*)-nonenoic acid], respectively, were produced from the FA by sequential action of the enzymes 9-lipoxygenase and divinyl ether synthase. The latter is a membrane-bound cytochrome P-450 protein occurring not only in the tubers of potato but also in potato leaves (4) and tomato roots (5). Genes encoding for divinyl ether synthases have been cloned (6,7). Also, 13-lipoxygenase-generated hydroperoxides serve as precursors of divinyl ether FA in higher plants, i.e., etheroleic acid [12-[1´(*E*)-hexenyloxy]-9(*Z*),11(*E*)-dodecadienoic acid] and etherolenic acid [12-[1´(*E*),3´(*Z*)-hexadienyloxy]-9(*Z*),11(*E*)-dodecadienoic acid] in bulbs of garlic (8) as well as ω5(*Z*)-etherole(n)ic acids (9) and 11(*Z*)-etherole(n)ic acids (10) in *Ranunculus* plants.

The fact that infection of potato leaves with pathogenic fungi leads to the accumulation of colneleic and colnelenic acids (4,11) and to increased levels of divinyl ether synthase (7), coupled with the inhibitory effect of the divinyl ethers mentioned on mycelial growth and spore germination of the potato pathogen *Phytophthora infestans* (4), indicates that the lipoxygenase-divinyl ether synthase pathway is of functional importance in the defense of plants against attacking pathogens. In an ongoing survey of FA hydroperoxide metabolism in plant leaves, we recently detected two new isomers of colneleic and colnelenic acids; the structures of these compounds are described in the present paper.

EXPERIMENTAL PROCEDURES

Plant materials. Specimens of *Clematis vitalba* L. ("Traveller's Joy") were obtained from three different suppliers and grown in a local garden. Leaves were either used directly or shock-frozen in liquid nitrogen and stored at –80°C until use.

FA, FA hydroperoxides, and divinyl ethers. Linoleic and linolenic acids were purchased from Nu-Chek-Prep (Elysian, MN). With the exception of 9(*E*)-etheroleic acid, which was prepared as described previously (12), all unlabeled oxylipins used in the present work, i.e., 9(*S*)-hydroperoxy-10(*E*),12(*Z*),15(*Z*)-octadecatrienoic acid [9(*S*)-HPOT], 13(*S*)-hydroperoxy-9(*Z*),11(*E*),15(*Z*)-octadecatrienoic acid [13(*S*)-HPOT], 9(*S*)-hydroperoxy-10(*E*),12(*Z*)-octadecadienoic acid [9(*S*)-HPOD], 13(*S*)-hydroperoxy-9(*Z*),11(*E*)-octadecadienoic acid [13(*S*)-HPOD], 12-oxo-10,15(*Z*)-phytodienoic

*E-mail: Mats.Hamberg@mbb.ki.se

The results of this study were presented in preliminary form at the symposium "Plant Oxylipins" held in Göttingen, Germany, June 12–14, 2003.

Abbreviations and trivial names: 9(*S*)-H(P)OD, 9(*S*)-hydro(pero)xy-10(*E*),12(*Z*)-octadecadienoic acid; 9(*S*)-H(P)OT, 9(*S*)-hydro(pero)xy-10(*E*),12(*Z*),15(*Z*)-octadecatrienoic acid; 12-oxo-PDA, 12-oxo-10,15(*Z*)-phytodienoic acid; 13(*S*)-H(P)OD, 13(*S*)-hydro(pero)xy-9(*Z*),11(*E*)-octadecadienoic acid; 13(*S*)-H(P)OT, 13(*S*)-hydro(pero)xy-9(*Z*),11(*E*),15(*Z*)-octadecatrienoic acid; colneleic acid, 9-[1´(*E*),3´(*Z*)-nonadienyloxy]-8(*E*)-nonenoic acid; colnelenic acid, 9-[1´(*E*),3´(*Z*),6´(*Z*)-nonatrienyloxy]-8(*E*)-nonenoic acid; etheroleic acid, 12-[1´(*E*)-hexenyloxy]-9(*Z*),11(*E*)-dodecadienoic acid; etherolenic acid, 12-[1´(*E*),3´(*Z*)-hexadienyloxy]-9(*Z*),11(*E*)-dodecadienoic acid; RP-HPLC, reversed-phase HPLC; SP-HPLC, straight-phase HPLC.

TABLE 1
UV Data and Chromatographic Properties of Divinyl Ethers

Compound	λ_{max}[a] (nm)	ε[a]	Retention vol[b] (mL)	C-value[c]
Compound **3**	252	32,100	26.8	18.80
8(*Z*)-Colnelenic acid	252		26.8	18.80
Colnelenic acid	253		30.2	19.45[d]
Compound **6**	250		22.6	18.76
8(*Z*)-Colneleic acid	250		22.6	18.76
Colneleic acid	250		25.5	19.41
Etherolenic acid	268		25.8	19.74[d]
ω5(*Z*)-Etherolenic acid	267	41,200	27.2	19.74
11(*Z*)-Etherolenic acid	267	41,600	30.9	19.96
Etheroleic acid	250		21.4	19.33
ω5(*Z*)-Etheroleic acid	250		20.8	18.83
11(*Z*)-Etheroleic acid	253		23.0	19.60
9(*E*)-Etheroleic acid	250		21.9	19.81

[a]UV spectra were recorded on the free acids dissolved in 99.5% ethanol.
[b]SP-HPLC was performed on the methyl esters using a Nucleosil 50-5 column and a solvent system of ethyl acetate/hexane (8:992, vol/vol) at a flow rate of 1.0 mL/min. The detector was set at 250 nm.
[c]GLC was performed on the methyl esters using a methyl silicone capillary column (25 m) at 230°C.
[d]Partial degradation on the capillary column. Colnelenic acid, 9-[1′(*E*),3′(*Z*),6′(*Z*)-nonatrienyloxyl]-8(*E*)-nonenoic acid; colneleic acid, 9-[1′(*E*),3′(*Z*)-nonadienyloxy]-8(*E*)-nonenoic acid; etherolenic acid, 12-[1′(*E*),3′(*Z*)-hexadienyloxy]-9(*Z*),11(*E*)-dodecadienoic acid; etheroleic acid, 12-[1′(*E*)-hexenyloxy]-9(*Z*),11(*E*)-dodecadienoic acid.

acid (12-oxo-PDA), as well as colnele(n)ic acids, etherole(n)ic acids, ω5(*Z*)-etherole(n)ic acids, and 11(*Z*)-etherole(n)ic acids, were purchased from Larodan Fine Chemicals (Malmö, Sweden).

[1-^{14}C]Linolenic acid (PerkinElmer Life and Analytical Sciences, Boston, MA) was mixed with unlabeled material and purified by SiO_2 chromatography to afford a specimen having a specific radioactivity of 5.3 kBq/μmol. Aliquots of this preparation were incubated with soybean lipoxygenase or tomato lipoxygenase to generate [1-^{14}C]13(*S*)-HPOT and [1-^{14}C]9(*S*)-HPOT, respectively.

Enzyme preparation. Leaves of *C. vitalba* were minced and homogenized at 0°C in 0.1 M potassium phosphate buffer, pH 6.7 (5:1, vol/wt), using an UltraTurrax. The homogenate was filtered through gauze, and the filtrate was used directly in the incubations.

Incubations and treatments. Filtered homogenates (5–50 mL) were stirred at 23°C for 20 min in the presence of 300 μM linolenic or linoleic acid or hydroperoxide. Material obtained after extraction with diethyl ether was subjected to solid-phase extraction using aminopropyl columns (0.5 g; Supelco, Bellefonte, PA) (9) and analyzed by reversed-phase high-performance liquid radiochromatography. The effluent was led to a Bischoff model DAD-100 diode-array detector (Bischoff Chromatography, Leonberg, Germany) serially connected to a liquid scintillation counter (IN/US Systems, Tampa, FL).

*8(*Z*)-Colneleic acid [9-[1′(*E*),3′(*Z*)-nonadienyloxy]-8(*Z*)-nonenoic acid]*. The methyl ester of 8(*Z*)-colneleic acid was synthesized from the methyl ester of 9(*S*)-HPOD (51 mg) as described previously (13). The product, consisting of a mixture of the methyl esters of 8(*Z*)-colneleic acid and colneleic acid in proportions of 1:4, was subjected to straight-phase HPLC (SP-HPLC) using a Nucleosil 50-5 column (Macherey-Nagel, Düren, Germany) and a solvent system of ethyl acetate/hexane (0.8:99.2, vol/vol) to provide pure methyl 8(*Z*)-colneleate (retention volume, 22.6 mL). Analysis by GC–MS showed a single peak having a C-value of C-18.76 (reference, methyl colneleate, C-19.41). The mass spectrum of methyl 8(*Z*)-colneleate was similar to that of methyl colneleate and showed prominent ions at *m/z* (% relative intensity; ion) 308 (36; M^+), 279 (2; $M^+ - 29$; loss of $\cdot C_2H_5$), 277 (2; $M^+ - 31$; loss of $\cdot OCH_3$), 251 [9; $M^+ - 57$; loss of $\cdot(CH_2)_3–CH_3$], 237 [3; $M^+ - 71$; loss of $\cdot(CH_2)_4–CH_3$], 165 (10), 123 (28), 95 (43), 81 (71), and 67 (100). An aliquot of the methyl 8(*Z*)-colneleate thus prepared was treated with 0.2 M NaOH at 37°C for 2 h under argon to provide 8(*Z*)-colneleic acid. The UV spectrum of this material showed an absorption band with λ_{max} = 250 nm (Table 1).

*8(*Z*)-Colnelenic acid [9-[1′(*E*),3′(*Z*),6′(*Z*)-nonatrienyloxy]-8(*Z*)-nonenoic acid]*. The methyl ester of 8(*Z*)-colnelenic acid was prepared from the methyl ester of 9(*S*)-HPOT (51 mg) using the same protocol as that used to prepare the methyl ester of 8(*Z*)-colneleate (13). The product, consisting of methyl 8(*Z*)-colnelenate and methyl colnelenate in proportions of 1:3, was separated by SP-HPLC to provide pure methyl 8(*Z*)-colnelenate (retention volume, 26.8 mL; C-value, 18.80). The mass spectrum showed prominent ions at *m/z* (% relative intensity; ion) 306 (47; M^+), 277 (3; $M^+ - 29$; loss of $\cdot C_2H_5$), 275 (2; $M^+ - 31$; loss of $\cdot OCH_3$), 245 (2), 163 [6; $M^+ - 143$; loss of $\cdot(CH_2)_6–COOCH_3$], 137 (11), 121 (57), 93 (72), 79 (100), and 55 (74). Saponification, as described for methyl 8(*Z*)-colneleate, provided 8(*Z*)-colnelenic acid, which showed a UV absorption band with λ_{max} = 252 nm (Table 1).

Methyl nonyloxy-9-nonanoate. The methyl ester of colneleic acid (3 mg) was dissolved in 0.5 mL of methanol containing 2 mg of platinum catalyst and stirred under hydrogen gas for 15 min. A main peak was observed on GC–MS, and the mass spectrum showed prominent ions at *m/z* (%

relative intensity; ion) 314 (1; M^+), 283 (3; $M^+ - 31$; loss of $\cdot OCH_3$), 241 (1; $M^+ - 73$), 187 [33; $M^+ - 127$; loss of $\cdot(CH_2)_8–CH_3$], 172 [23; $M^+ - 142$; loss of OHC–$(CH_2)_7–CH_3$], 155 [85; $M^+ - (127 + 32)$], 138 (67), 74 [64; $CH_2=C(OH)–OCH_3)^{+\cdot}$], and 55 (100).

Chemical, chromatographic, and instrumental methods. A detailed description of the methodology used for isolation and structural analysis is given or referred to in a previous study on hydroperoxide metabolism in *Ranunculus* plants (9). Reversed-phase HPLC (RP-HPLC) was carried out with a Nucleosil 100-5 C_{18} column (250 × 4.6 mm; Macherey-Nagel). For analysis of the oxidation products of linoleic acid, a solvent system of acetonitrile/water/acetic acid in proportions of 60:40:0.02 (by vol) was used, whereas the oxidation products of linolenic acid were chromatographed using the proportions 50:50:0.02 (by vol) for the initial period of the run (0–25 min), followed by 70:30:0.02 (by vol) for the second period (25–45 min). C-values recorded during GC were calculated from diagrams constructed by plotting the retention times of standard saturated FAME on a logarithmic scale vs. the number of carbon atoms of the carbon chains on a linear scale.

RESULTS

Isolation of oxidation products of linolenic acid and its hydroperoxides. [1-^{14}C]Linolenic acid (300 μM) was stirred at 23°C for 20 min with a whole homogenate preparation (10 mL) of *C. vitalba*. Material obtained by extraction with diethyl ether and solid-phase extraction was subjected to reversed-phase high-performance liquid radiochromatography. In addition to unconverted linolenic acid (80% of the recovered radioactivity), four labeled products were observed, i.e., compounds **1** (23.6 mL effluent; 32% of the oxidation product), **2** (25.8 mL; 36%), **3** (55.4 mL; 22%), and **4** (57.3 mL; 10%) (Scheme 1). Compound **1** was identified as 12-oxo-PDA by UV spectroscopy and GC–MS using the authentic compound as reference (*cf.* Ref. 9). Using the same criteria, compound **2** was identified as 9(*S*)-HOT [9(*S*)-hydroxy-10(*E*),12(*Z*),15(*Z*)-octadecatrienoic acid], and compound **4** was identified as the divinyl ether FA ω5(*Z*)-etherolenic acid (9). Compound **3** was a new oxylipin, and its structure was determined as described in the following section. Incubation of [1-^{14}C]9(*S*)-HPOT (300 μM) using the same protocol produced labeled compound **3** in a higher yield (40% of the recovered radioactivity) accompanied by 9(*S*)-HOT (20%), whereas incubation of 13(*S*)-HPOT generated 12-oxo-PDA (60%) accompanied by 13(*S*)-HOT [13(*S*)-hydroxy-9(*Z*),11(*E*),15(*Z*)-octadecatrienoic acid] (12%) and ω5(*Z*)-etherolenic acid (20%).

Structure of compound 3. Compound **3** showed strong UV absorption with λ_{max} (EtOH) = 252 nm, ε = 32,100, suggesting a divinyl ether structure (Table 1). The mass spectrum of the methyl ester of compound **3** showed prominent ions at *m/z* (% relative intensity; ion) 306 (47; M^+), 277 (3; $M^+ - 29$; loss of $\cdot C_2H_5$), 275 (2; $M^+ - 31$; loss of $\cdot OCH_3$), 245 (4), 163 [6; $M^+ - 143$; loss of $\cdot(CH_2)_6–COOCH_3$], 137 (11), 121 (57), 93 (72), 79 (100), and 55 (74). Catalytic hydrogenation of the methyl ester of compound **3** provided an octahydro derivative, the mass spectrum of which was identical to that recorded on authentic methyl nonyloxy-9-nonanoate. Oxidative ozonolysis performed on the methyl ester of compound **3** produced monomethyl suberate as the major nonvolatile fragment.

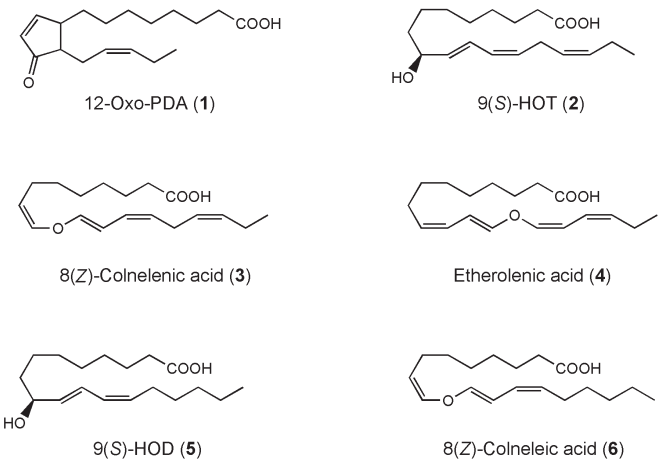

SCHEME 1

The results mentioned showed that compound **3** had the same skeletal structure as that of colnelenic acid but differed from this compound with respect to the geometrical configuration. Because of the relatively weak enzyme activities detected and the limited amount of plant material available, large-scale preparation of compound **3** for NMR analysis was not possible. Instead, double-bond configurations were assigned by chromatographic comparison with authentic reference compounds of known stereochemistry. The chromatographic properties of four isomeric divinyl ether FA derived from 13(*S*)-HPOD, i.e., etheroleic acid (**8**), ω5(*Z*)-etheroleic acid (**9**), 11(*Z*)-etheroleic acid (**10**), and 9(*E*)-etheroleic acid (**11**), were determined in previous work (9,10,12), and these data (Table 2) could be used to evaluate the stereochemistry of compound **3**. As seen in Table 2, a change in the geometrical configuration of the isolated vinyl ether double bond of etheroleic acid from *E* to *Z* (**8**→**9**) resulted in a lowered C-value as determined by GC and a shortened retention time as determined by SP-HPLC, whereas the opposite was true for an *E* to *Z* isomerization of the conjugated vinyl ether double bond (**8**→**10**) or a *Z* to *E* isomerization of the conjugated nonvinylic double bond (**8**→**11**). The chromatographic properties of compound **3** (Table 1), coupled with the data in Table 2, suggest that the isolated vinyl ether bond of this compound had the *Z* configuration. The required 8(*Z*) isomer of colnelenic acid was prepared from the methyl ester of 9(*S*)-HPOT using a well-established procedure (13) and was found to give results identical to compound **3** regarding C-value, retention volume, and UV spectrum (Table 1). Furthermore, the mass spectra recorded for the methyl ester of compound **3** and for methyl 8(*Z*)-colnelenate were identical. On the basis of these data, compound **3** could be identified as 8(*Z*)-colnelenic acid. Notably, formation of colnelenic acid from linolenic acid or 9(*S*)-HPOT was not observed.

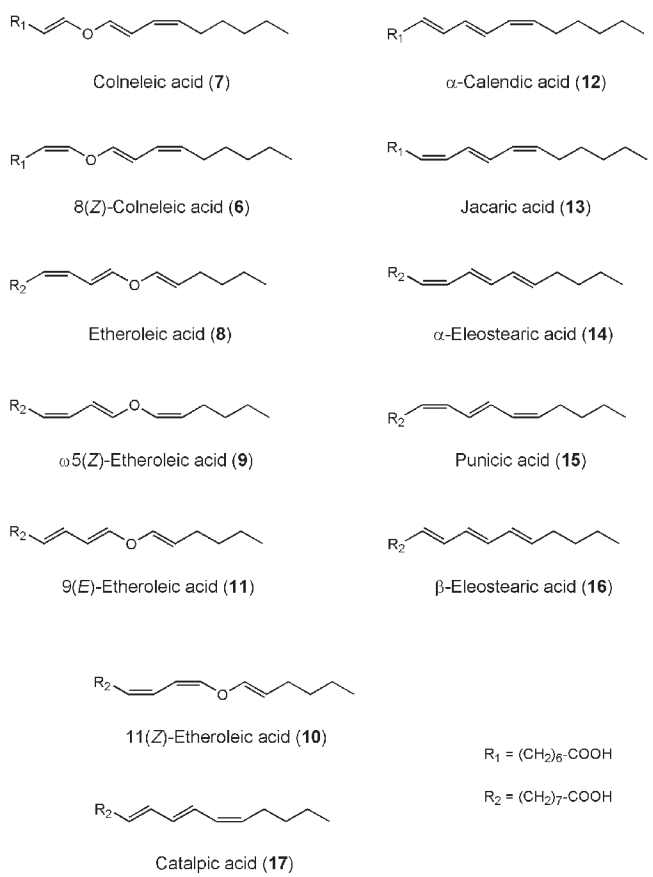

SCHEME 2

Isolation of oxidation products of linoleic acid and its hydroperoxides. Incubation of linoleic acid (300 μM) as described in the foregoing discussion, followed by analysis by RP-HPLC, led to the formation of compound **5** (18 mL effluent; 5% of the recovered radioactivity) and a new oxylipin designated as compound **6** (44 mL; 1%). Compound **5** was identified as 9(*S*)-HOD [9(*S*)-hydroxy-10(*E*),12(*Z*)-octadecadienoic acid] by chromatographic and spectral comparison with authentic material. Incubation of 9(*S*)-HPOD, but not 13(*S*)-HPOD, produced compounds **5** and **6**, demonstrating that both were 9-lipoxygenase products.

*Structure of compound **6***. The UV spectrum of compound **6** showed a strong absorption band with λ_{max} = 250 nm (Table 1), suggesting a divinyl ether partial structure. The mass spectrum of the methyl ester of compound **6** showed prominent ions at *m/z* (% relative intensity; ion) 308 (36; M^+), 279 (2; $M^+ - 29$; loss of $\cdot C_2H_5$), 277 (2; $M^+ - 31$; loss of $\cdot OCH_3$), 251 [9; $M^+ - 57$; loss of $\cdot(CH_2)_3–CH_3$], 237 [3; $M^+ - 71$; loss of $\cdot(CH_2)_4–CH_3$], 165 (10), 123 (28), 95 (43), 81 (71), and 67 (100). Catalytic hydrogenation of the methyl ester of **6** provided a hexahydro derivative, the mass spectrum of which was identical to that of methyl nonyloxy-9-nonanoate. Oxidative ozonolysis performed on the methyl ester of **6** yielded methyl hydrogen suberate as the nonvolatile product, thus localizing the divinyl ether structure to the C-8 to C-13 segment of the carbon chain.

The shifts in C-value and retention volume noted for compound **6** relative to colneleic acid were both negative (Table 1); together with the data in Table 2, this indicated that the nonconjugated vinylic double bond in compound **6** had the *Z* configuration. The required reference, 8(*Z*)-colneleic acid, was synthesized from the methyl ester of 9(*S*)-HPOD and was found to have chromatographic and UV spectrophotometric properties identical to those of compound **6** (Table 1). Furthermore, identical mass spectra were recorded on the methyl esters of compound **6** and 8(*Z*)-colneleic acid, thus confirming the identity of the two compounds.

DISCUSSION

Etherolenic and etheroleic acids are divinyl ether FA produced from the 13(*S*)-hydroperoxides of linolenic and linoleic acids, respectively, and previous studies have demonstrated the existence in plant tissues of geometrical isomers of these compounds. Whereas etherole(n)ic acids are produced in bulbs of garlic (8), many terrestrial *Ranunculus* plants possess a divinyl ether synthase that produces the ω5(*Z*) isomers of etherole(n)ic acids (9). Futhermore, *R. lingua* and *R. peltatus*, two aquatic *Ranunculus* plants, produce the 11(*Z*) isomers of etherole(n)ic acids (10). The present work extends the family of divinyl ether FA by identifying the 8(*Z*) isomers of colnelenic and colneleic acids as products of the 9-hydroperoxides of linolenic and

TABLE 2
Correlation of Geometrical Configurations and Chromatographical Properties of Etheroleic Acid Isomers[a]

Compound	Partial structure	Configuration	ΔRetention volume[b] (mL)	ΔC-value[c] (units)
Etheroleic acid (**8**)	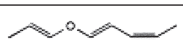	*E,E,Z*	0	0
ω5(*Z*)-Etheroleic acid (**9**)		*Z,E,Z*	–0.6	–0.50
11(*Z*)-Etheroleic acid (**10**)		*E,Z,Z*	+1.6	+0.27
9(*E*)-Etheroleic acid (**11**)		*E,E,E*	+0.5	+0.48

[a]Data taken from References 9, 10, and 12. See Table 1 for abbreviations.
[b]See Table 1 for conditions used for SP-HPLC.
[c]See Table 1 for conditions used for GLC.

linoleic acids. The new divinyl ether synthase responsible for this transformation was detected in the leaves of *C. vitalba*, a common garden plant belonging to the *Ranunculaceae* family.

The multiple occurrence of divinyl ether synthases in the *Ranunculaceae* family is intriguing and may point to a specific function of divinyl ethers in these plants. From a biochemical standpoint, it seems likely that only subtle differences in the structures of the various divinyl ether synthases, such as mutation of even a single amino acid residue, could suffice to produce a change in the geometrical configuration of divinyl ether FA. One can anticipate that the divinyl ether synthases producing etherole(n)ic acid isomers present in garlic and *Ranunculus* plants will be closely related in structure, and that this will also be the case with the divinyl ether synthases present in potato or tomato and in *Clematis*, which produce colnele(n)ic acid isomers.

Formally, divinyl ether FA can be regarded as oxa analogs of the various conjugated trienoic FA, which are well-known constituents of certain seed oils. This family of compounds is formed from linoleic acid by a non-lipoxygenase pathway involving so-called "conjugases" or "(1,4)-desaturases." Conjugases generating α-eleostearic acid **14** (14,15), α-calendic acid **12** (16,17), and punicic acid **15** (18,19) have been described thus far, and it seems likely that other conjugated trienoic acid isomers are also formed by the action of specific but closely related conjugases. It is interesting to note that five of the six divinyl ethers derived from linoleic acid can be paired structurally with conjugated trienoic acids (Scheme 2). However, because of the distinct biosynthetic mechanisms in the formation of the two classes of compounds, it is unlikely that this pairing mirrors any structural relationship between the enzymes involved (divinyl ether synthase/conjugase).

ACKNOWLEDGMENTS

Gunvor Hamberg is thanked for expert technical assistance and for the collection and identification of the plant materials used. This work was supported by a generous grant given by Prof. Sune Bergström, Stockholm, and by the European Union (Project No. QLK5-CT-2001-02445).

REFERENCES

1. Feussner, I., and Wasternack, C. (2002) The Lipoxygenase Pathway, *Annu. Rev. Plant Biol. 53*, 275–297.
2. Hamberg, M., Ponce de Léon, I., Sanz, A., and Castresana, C. (2002) Fatty Acid α-Dioxygenases, *Prostaglandins Other Lipid Mediat. 68–69*, 363–374.
3. Galliard, T., and Phillips, D.R. (1972) The Enzymic Conversion of Linoleic Acid into 9-(nona-1´,3´-dienoxy)Non-8-enoic Acid, a Novel Unsaturated Ether Derivative Isolated from Homogenates of *Solanum tuberosum* Tubers, *Biochem. J. 129*, 743–753.
4. Weber, H., Chételat, A., Caldelari, D., and Farmer, E.E. (1999) Divinyl Ether Fatty Acid Synthesis in Late Blight-Diseased Potato Leaves, *The Plant Cell 11*, 485–493.
5. Caldelari, D., and Farmer, E.E. (1998) A Rapid Assay for the Coupled Cell Free Generation of Oxylipins, *Phytochemistry 47*, 599–604.
6. Itoh, A., and Howe, G.A. (2001) Molecular Cloning of a Divinyl Ether Synthase. Identification as a CYP74 Cytochrome P-450, *J. Biol. Chem. 276*, 3620–3627.
7. Stumpe, M., Kandzia, R., Göbel, C., Rosahl, S., and Feussner, I. (2001) A Pathogen-Inducible Divinyl Ether Synthase (*CYP74D*) from Elicitor-Treated Potato Suspension Cells, *FEBS Lett. 507*, 371–376.
8. Grechkin, A.N., Fazliev, F.N., and Mukhtarova, L.S. (1995) The Lipoxygenase Pathway in Garlic (*Allium sativum* L.) Bulbs: Detection of the Novel Divinyl Ether Oxylipins, *FEBS Lett. 371*, 159–162.
9. Hamberg, M. (1998) A Pathway for Biosynthesis of Divinyl Ether Fatty Acids in Green Leaves, *Lipids 33*, 1061–1071.
10. Hamberg, M. (2002) Biosynthesis of New Divinyl Ether Oxylipins in *Ranunculus* Plants, *Lipids 37*, 427–433.
11. Göbel, C., Feussner, I., Hamberg, M., and Rosahl, S. (2002) Oxylipin Profiling in Pathogen-Infected Potato Leaves, *Biochim. Biophys. Acta 1584*, 55–64.
12. Grechkin, A.N., Ilyasov, A.V., and Hamberg, M. (1997) On the Mechanism of Biosynthesis of Divinyl Ether Oxylipins by Enzyme from Garlic Bulbs, *Eur. J. Biochem. 245*, 137–142.
13. Corey, E.J., Nagata, R., and Wright, S.W. (1987) Biomimetic Total Synthesis of Colneleic Acid and Its Function as a Lipoxygenase Inhibitor, *Tetrahedron Lett. 28*, 4917–4920.
14. Cahoon, E.B., Carlson, T.J., Ripp, K.G., Schweiger, B.J., Cook, G.A., Hall, S.E., and Kinney, A.J. (1999) Biosynthetic Origin of Conjugated Double Bonds: Production of Fatty Acid Components of High-Value Drying Oils in Transgenic Soybean Embryos, *Proc. Natl. Acad. Sci. USA 96*, 12935–12940.
15. Dyer, J.M., Chapital, D.C., Kuan, J.C., Mullen, R.T., Turner, C., McKeon, T.A., and Pepperman, A.B. (2002) Molecular Analysis of a Bifunctional Fatty Acid Conjugase/Desaturase from Tung. Implications for the Evolution of Plant Fatty Acid Diversity, *Plant Physiol. 130*, 2027–2038.
16. Cahoon, E.B., Ripp, K.G., Hall, S.E., and Kinney, A.J. (2001) Formation of Conjugated Δ8,Δ10-Double Bonds by Δ12-Oleic Acid Desaturase-Related Enzymes: Biosynthetic Origin of Calendic Acid, *J. Biol. Chem. 276*, 2637–2643.
17. Qiu, X., Reed, D.W., Hong, H., MacKenzie, S.L., and Covello, P. (2001) Identification and Analysis of a Gene from *Calendula officinalis* Encoding a Fatty Acid Conjugase, *Plant Physiol. 125*, 847–855.
18. Hornung, E., Pernstich, C., and Feussner, I. (2002) Formation of Conjugated Δ11,Δ13-Double Bonds by Δ12-Linoleic Acid (1,4)-Acyl-Lipid-Desaturase in Pomegranate Seeds, *Eur. J. Biochem. 269*, 4852–4859.
19. Iwabuchi, M., Kohno-Murase, J., and Imamura, J. (2003) Δ12-Oleate Desaturase-Related Enzymes Associated with Formation of Conjugated *trans*-Δ11,*cis*-Δ13 Double Bonds, *J. Biol. Chem. 278*, 4603–4610.

[Received June 28, 2004; accepted August 3, 2004]

Geranium sanguineum (Geraniaceae) Seed Oil: A New Source of Petroselinic and Vernolic Acid

N. Tsevegsuren[a], K. Aitzetmuller[b,*], and K. Vosmann[c]

[a]Department of Organic & Food Chemistry, Faculty of Chemistry, National University of Mongolia, Ulaanbaatar, Mongolia, and [b]Institute for Chemistry and Physics of Lipids and [c]Institute for Lipid Research, BAGKF, D-48147 Münster, Germany

ABSTRACT: The occurrence of petroselinic acid (18:1Δ6*cis*) in seed oils was believed to be limited to the Umbelliferae or Apiaceae, and a few other members of the Umbelliflorae. A major occurrence of petroselinic acid outside the Umbelliflorae must therefore be regarded as highly unusual and surprising. The seed oil of *Geranium sanguineum*, a member of the family Geraniaceae, has now been found to contain petroselinic and vernolic acids as major FA in its seed oil TAG. These unusual FA have not been reported previously as constituents of Geraniaceae seed oils. The structure and composition of the seed oil FA from *G. sanguineum* were determined by combined use of chromatographic (TLC, capillary GLC) and spectroscopic (IR, GC–MS) techniques. The double-bond position in petroselinic acid was located unambiguously by the characteristic mass fragmentation of its dimethyldisulfide (DMDS) adduct. The epoxy FA was identified as vernolic acid by co-chromatography and by the mass fragments formed during GC–MS of the products of the epoxy ring-opening reaction with BF_3 in methanol.

Paper no. L9499 in *Lipids 39*, 571–576 (June 2004).

Petroselinic acid (18:1Δ6*cis*) is known to be a major FA in the seed oils of most of the members of the Umbelliflorae plant families (1). Placek (2) mentions only a few rare occurrences outside these families.

The genus *Geranium,* with about 300 species, is the principal genus of the plant family Geraniaceae (3). About 28 *Geranium* species can be found growing in Europe. Most of the *Geranium* species are annual or perennial herbs, sometimes pachycaul shrublets, and many of these are cultivated as ornamentals, especially for ground cover. A number of species from this genus are cultivated as medical plants, and extracts from the roots of some *Geranium* spp. are used in traditional medicine, tanning, and dyeing.

The genus *Geranium* is well studied with regard to its chemical constituents other than lipids (4,5). However, only a few studies on seed oils or FA of genus *Geranium* appear in the published literature. The seed oil of *G. carolinianum* was previously studied by IR and UV and was reported to have the usual FA composition ("normal" FA only) (6). An exhaustive survey of the literature yielded no other work on the seed oil of *Geranium* species, but a few data, without further comment, can be found in the NCAUR database (7). None of these data, however, show the presence of either petroselinic or vernolic acid.

The present report describes for the first time the unique occurrence of petroselinic acid and vernolic acid along with normal FA in the seed oil of *G. sanguineum.* This extends the list of natural sources of these two unusual FA (2,8) by inclusion of the Geraniaceae plant family. As a part of our screening program of lesser-known seed oils, the seed oil of *G. sanguineum* was analyzed for its FA composition. The present paper describes the separation, identification, and structure elucidation of its two unusual components—petroselinic and vernolic acids.

MATERIALS AND METHODS

Seed materials. Seeds of *G. sanguineum* sample no. 1 were collected by the second author from a plant of Austrian origin cultivated in a local garden in 1995. Sample no. 2 was supplied by Professor F. Albers, Department of Botany, University of Münster, Germany, in 1995. Seeds of *G. sanguineum* sample no. 3 were collected by the first author in the Botanical Garden of Münster University in the first week of August 1996. *Euphorbia lagascae* seed oil, used for comparison purposes as a reference oil that contains vernolic acid, was available in this laboratory from previous investigations.

Oil extraction and preparation of FA derivatives. The ground seeds were extracted with *n*-hexane in a flow-through extractor. FAME of the seed oils were prepared by saponification in 1.0 N KOH/ethanol followed by reaction with 20% BF_3/methanol, or by transesterification with 2.0 M sodium methoxide in methanol as described in our previous papers (9–12). The dimethyldisulfide (DMDS) adducts of FA were prepared as described in Reference 13.

TLC, GC–MS, and *IR*. TLC was carried out, and GC–MS and IR spectra were recorded as described (14–16).

Capillary GLC. Capillary GLC of FAME was performed on three gas chromatographs (two Hewlett-Packard HP 5890 and a PerkinElmer F22) equipped with FID and with fused-silica WCOT capillary columns (length 50 m, i.d. 0.25 and 0.22 mm) packed with stationary phases of different polarity (Silar 5 CP, CP Sil 88, and BPX 70; Chrompack, Middelburg, The Netherlands). Chromatographic data were evaluated with integrators (Chromato-Integrator D2000, HP 3396 Series II Integrator, and Shimadzu Chromatopac C-R3A). The identification of individ-

* To whom correspondence should be addressed at Feldbehnstr. 64 a, D-25451 Quickborn, Germany. E-mail: aitzetm@freenet.de or aitzetm@web.de

Abbreviations: DMDS, dimethyldisulfide adducts; ECL, equivalent chain length; PRV, peak recognition value; SOFA, seed oil FA (for SOFA database, go to netlink: www.bagkf.de/SOFA).

ual FAME was by chromatographic comparison with authentic standards, by co-chromatography, and by calculation of relative retention times and peak recognition values (PRV), similar to equivalent chain length (ECL) values (17).

GLC conditions, Silar 5 CP. The temperature was held at 165°C for 1 min, then programmed from 165 to 205°C at 1°C/min, then held at 205°C for *ca.* 60 min before cooling the column to 165°C. The injector and detector temperatures were 230 and 260°C, respectively. For improved separation of 18:1Δ6*cis* from 18:1Δ9*cis* methyl esters, the following conditions were used on Silar 5 CP: The temperature program was run isothermally for 48 min at 165°C, then the column was cleaned by heating at 205°C for *ca.* 60 min before cooling the column to 165°C. The injector and detector temperatures were as above for Silar 5 CP.

BPX 70. The temperature was programmed from 100 to 240°C at 2°C/min and maintained at 240°C for 32 min. The injector temperature was 260°C and the detector temperature was 240°C.

CP Sil 88. The temperature was programmed from 100 to 220°C at 1.5°C/min and maintained at 220°C for 20 min. The injector temperature was 270°C and the detector temperature was 240°C.

Nitrogen (for Silar 5 CP and BPX 70) and helium (for CP Sil 88) were used as carrier gases. Flow rates were 1.13 mL N_2/min for the Silar 5 CP column, 0.69 mL N_2/min for BPX 70, and 1.0 mL He/min for CP Sil 88.

Capillary GC–MS. GC–MS analysis was carried out using the electron ionization mode (70 eV) on a Hewlett-Packard instrument model 5890 series II/5989A, equipped with a Permabond OV-1 fused-silica capillary column (Macherey-Nagel, Düren, Germany), 25 m × 0.32 mm i.d., film thickness 0.23 µm. The carrier gas was helium at a flow rate of 1.5 mL/min.

GC–MS conditions. For DMDS adducts the column temperature was initially kept at 100°C, then programmed from 100 to 280°C at 10°C/min. The final temperature was held for 10 min. In the case of the FAME, the column temperature was initially kept at 180°C, then programmed from 180 to 260°C at 1.5°C/min. The final temperature was held for 5 min. In both cases, the other operating conditions were: split/splitless injector in split mode (split ratio = 1:20) at a temperature of 300°C, an interface temperature of 280°C, and an ion source temperature of 200°C.

RESULTS

Data for the oil content of the three samples of seeds and the FA composition of the *G. sanguineum* seed oil obtained from them are presented in Table 1. The range of oil contents was 18.8 to 23.7% in the seeds from the *G. sanguineum* accessions investigated here. TLC of the seed oil and of the FAME showed the presence of oxygenated TAG in *G. sanguineum* seed oil and the presence of oxygenated FAME that had the same R_F value as did vernolic acid methyl ester from *E. lagascae* seed oil. The IR spectra did not show any absorption for *trans* double bonds. By GLC, the seed oil of *G. sanguineum* was found to contain two unusual FA in a rather large proportion in addition to common FA (Table 1). These unusual FA were later identified as petroselinic acid (48.4%) and vernolic acid (7.1%) (see below).

TABLE 1
FA Composition of Three *Geranium sanguineum* Samples (FA data shown are GLC area% of total FA; fat content is shown in weight%)

FA (GLC area%)	PRV	Sample 1	Sample 2	Sample 3
14:0	14.00	0.1	0.1	0.1
16:0	16.00	5.3	4.5	4.4
16:1Δ7*c*	16.24	1.1	0.8	0.7
16:1Δ9*c*	16.30	Trace	—	Trace
17:0	16.91	0.1	0.1	0.1
18:0	18.00	3.0	3.5	3.5
18:1Δ6*c*	18.26	48.4	43.2	34.4
18:1Δ9*c*	18.30	9.9	9.8	11.2
18:1Δ11*c*	18.35	0.3	0.2	0.3
18:2Δ9*c*,12*c*	18.77	21.4	28.6	32.6
18:3Δ9*c*,12*c*,15*c*	19.40	0.4	0.6	2.3
20:0	20.00	0.5	0.4	0.4
20:1Δ9*c*	20.14	0.3	0.5	0.3
20:1Δ11*c*	20.27	0.5	0.5	0.5
22:0	22.00	0.4	0.3	0.2
12,13-*O*-18:1Δ9*c* (vernolic)	23.04	7.1	5.2	8.4
24:0	24.00	0.2	0.2	0.1
Σ of 18:1 + 18:2 + vernolic		87.1	87.0	86.9
Fat content (weight%)		23.7	20.8	18.8

Capillary GLC analysis of the FAME of *G. sanguineum* seed oil on columns of Silar 5 CP and BPX 70 revealed the presence of two unusual FA along with the normal FA. The first unusual FAME had a PRV (similar to ECL) of 18.26, using our normal conditions for seed oil fatty acid (SOFA) fingerprints on Silar 5 CP and led to a split peak because of considerable overlap with methyl oleate, which elutes slightly later at a PRV of 18.30. It was not separated from methyl oleate at all on the BPX 70 column under the given conditions. The PRV values suggest that this ester was derived from petroselinic acid, a *cis*-6-octadecenoic acid (18:1Δ6*cis* or 18:1n-12).

The second unusual FAME had a PRV of 23.04 on Silar 5 CP, which pointed to the possibility that this peak was derived from vernolic acid. Additional proof for this was the fact that the peak at this PRV was found only when alkaline transesterification was used to produce the FAME required for the GC separation (peak **9** in Fig. 1). With BF_3 in methanol, two later-eluting peaks (at PRV 24.67 and 24.93) were found (peaks **11** and **12** in Fig. 1), which consisted of the corresponding hydroxy-methoxy products formed by the ring-opening addition of methanol to the epoxy ring system in vernolic acid.

Vernolic acid is known as a constituent of seed oils from a number of unrelated plant families such as Euphorbiaceae and Asteraceae (8,18). It has been used as a stabilizer for plastics formulations and as a raw material for oleochemical synthesis. The typical GLC separation of FAME of seed oils from *G. sanguineum* is shown in Figure 1, by way of the standardized "Seed Oil Fatty Acid Fingerprints" or "SOFA-Fingerprints" (11) used frequently in plant chemotaxonomy (9,19,20).

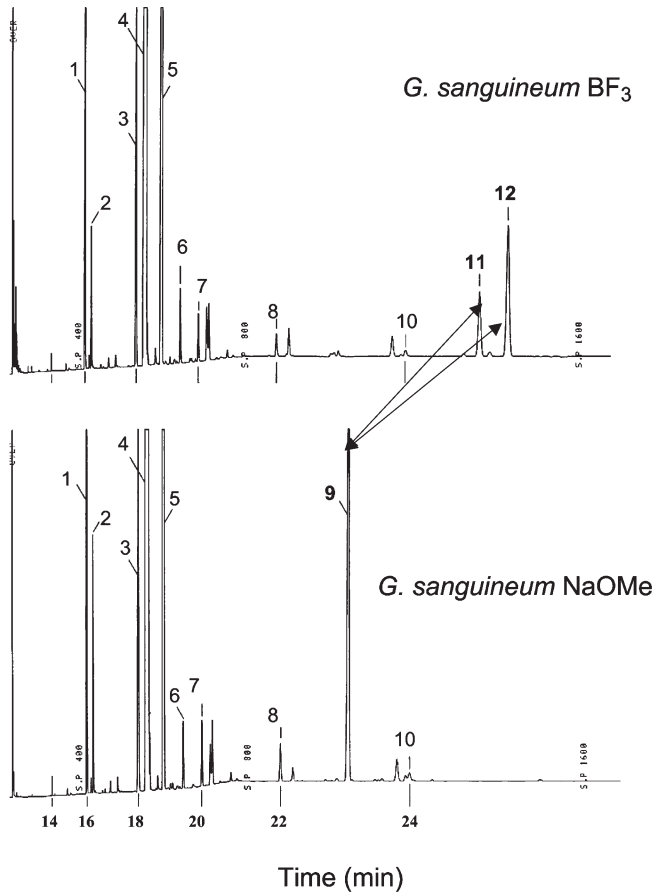

FIG. 1. Typical standardized Seed Oil Fatty Acids (SOFA)-Fingerprints (11) of two *Geranium sanguineum* samples. Top: FAME prepared as described in Reference 11 with BF_3/methanol after saponification and removal of the unsaponifiables. Bottom: Second sample, where the FAME were prepared as described (9,11) without removal of the unsaponifiables by transesterification with sodium methoxide in methanol. The first (BF_3–) procedure causes the ring-opening of vernolic acid (peak **9**) to produce two isomers of hydroxy-methoxy-octadecenoic acid, peaks **11** and **12**. Peak numbers: Δ-Notations are used as in the SOFA database (26,27); see these references for a more detailed explanation. **1** = 16:0; **2** = 16:1Δ9*c*; **3** = 18:0; **4** = 18:1Δ6*c* + 18:1Δ9*c* (petroselinic + oleic acid overlapping); **5** = 18:2Δ9*c*,12*c*; **6** = 18:3Δ9*c*,12*c*,15*c*; **7** = 20:0; **8** = 22:0; **9** = 12,13-*O*-18:1Δ9*c* (vernolic acid); **10** = 24:0; **11** = 13-OH-12-MeO-18:1Δ9*c* (ring-opening derivative of vernolic acid); **12** = 12-OH-13-MeO-18:1Δ9*c* (ring-opening derivative of vernolic acid).

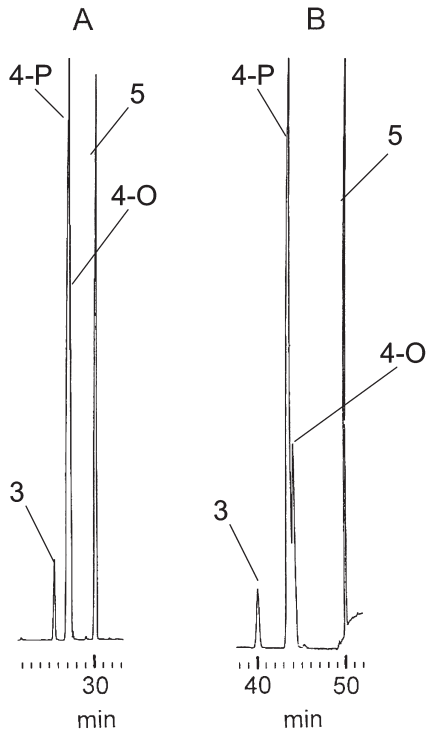

FIG. 2. GLC of *G. sanguineum* seed oil FAME under special conditions, showing partial separation of petroselinic and oleic acid methyl esters in an initially isothermal run on a Silar 5 CP column. (A still better separation can be achieved on CP Sil 88.) Peaks: 4-P = petroselinic acid; 4-O = oleic acid; other peaks as in Figure 1. For abbreviation see Figure 1.

Under special conditions, on both the CP Sil 88 and on the Silar 5 CP columns, a better partial separation of the isomeric 18:1Δ6*c* and 18:1Δ9*c* FAME is achieved (Fig. 2). Figure 2A is an excerpt of an original fingerprint chromatogram (where peak **5** elutes after 30 min), and Figure 2B shows the somewhat better separation effect, when an initially isothermal run on the Silar 5 CP column is used (so that peak **5** appears later, after *ca.* 50 min, when heating sets in). On a CP Sil 88 column, an even better separation can be achieved. Although these are not baseline separations, they permit one to estimate the amounts present of each of the two isomeric FA esters.

To confirm the postulated structures further, the DMDS adducts of the FAME obtained by the reaction of the corresponding FA with DMDS were analyzed by GC–MS. Figure 3 shows the mass spectrum of the DMDS adducts of the 18:1 FAME fraction, including the fragmentation pattern of the methyl petroselinate adduct. The two positional isomers of octadecenoic acid (18:1Δ6*c* and 18:1Δ9*c*) are not separated on the OV-1 column used for GC–MS. Besides the molecular ion at *m/z* 390, which is obtained from both isomers, the typical fragments of DMDS adducts of methyl petroselinate and methyl oleate can be observed. The signals at *m/z* 215 and 175 indicate the key fragment ions formed by the cleavage between the carbon atoms C-6 and C-7 of the DMDS adduct of petroselinic acid. Together with the ion at *m/z* 143, which is created from the signal at *m/z* 175 by the loss of methanol, they clearly establish the structure of methyl petroselinate. Besides this, the much weaker signals at *m/z* 217 and 173 corresponding to the typical fragmentation pattern of the DMDS adduct of methyl oleate (13,21,22) also can be found. Clearly, the oleate DMDS fragments are much less prominent, again confirming the predominance of petroselinic acid as found by GLC under special conditions (Table 1).

Vernolic acid is identified by the two methoxy-hydroxy derivatives formed because quantitative ring opening occurs during the treatment of epoxy FA with BF_3/methanol (23). Figure 4 shows the mass spectra of both derivatives and illustrates their fragmentation patterns. Unlike Kleiman and Spencer (23), it was possible for us to separate the two positional isomers on a nonpolar OV 1 column. The structures of the earlier-eluting 12-methoxy-13-hydroxy derivative, and

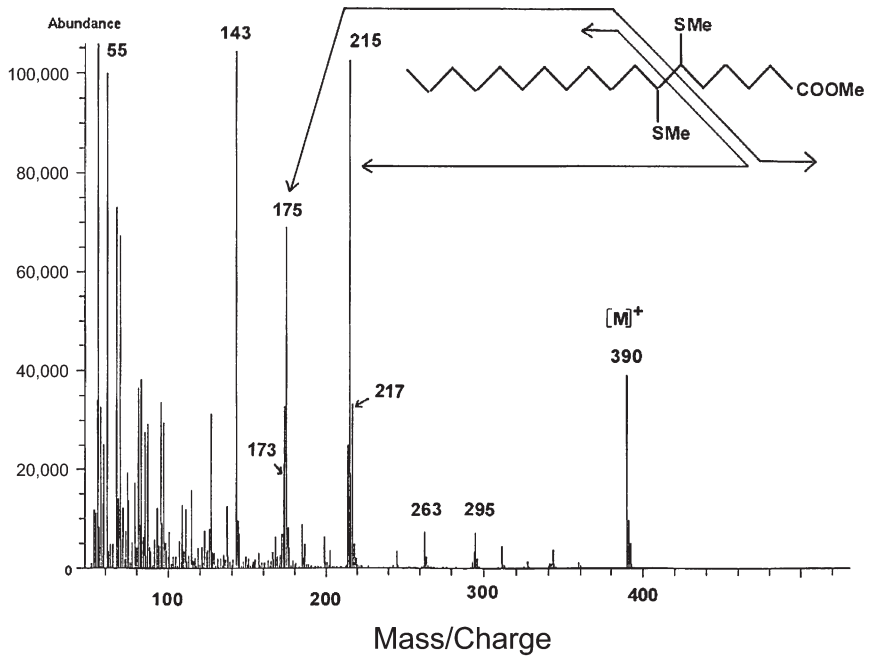

FIG. 3. Mass spectrum of the dimethyldisulfide (DMDS) adduct of the mixture of methyl petroselinate and methyl oleate as obtained from *G. sanguineum* seed oil. (The DMDS adducts of petroselinic and oleic acid cannot be separated by GLC under these conditions on the OV-1 column used for GC–MS.) For abbreviation see Figure 1.

that of the later-eluting 12-hydroxy-13-methoxy derivative, are clearly established by the fragments that are formed by the cleavage between the carbon atoms C-12 and C-13, and the base peak at *m/z* 145 is common for both isomers.

DISCUSSION

Until now, petroselinic acid was believed to be a chemotaxonomic marker for a number of closely related plant families within the Umbelliflorae, with very few exceptions (1,4). It is the major FA in seeds of the Umbelliferae (or Apiaceae) and Araliaceae. This is the first observation of an occurrence of petroselinic acid—as the main component of a seed oil—in a member of a plant family that does not belong to the Umbelliflorae group of families. However, it should also be noted that the position of the Geraniaceae family in relation to other plant families is still very much in discussion (24), and the presence of petroselinic acid in some members of this plant family could perhaps indicate a closer relation to Umbelliflorae.

On account of the unusual Δ6-position of the double bond, petroselinic acid is a valuable raw material for the production of lauric and adipic acids, which in turn are intermediates for detergents and for one type of nylon, and for the synthesis of other bioactive compounds, e.g., pheromones. Petroselinic acid is the characteristic FA for seed oils of the plant order Umbelliflorae, where it occurs in high amounts. Levels of up to 85% have been reported in only three plant families (Umbelliferae, Araliaceae, and Garryaceae) (1,2). This acid has not been previously reported as a main component of seed oils from other than these three plant families, and this work extends the list of natural sources of petroselinic acid by the plant family Geraniaceae.

Vernolic acid has also been found for the first time as a component of the seed oil of a *Geranium* species. Although this epoxy FA is known to occur in seed oils of many other unrelated plant families (4,18), this FA also has never before been reported to occur within the family Geraniaceae. Indeed, vernolic acid seems to have evolved separately, and independently, several times during Angiosperm evolution (25), and its presence or absence in a seed oil is therefore of lesser chemotaxonomic value if compared with petroselinic acid. It is of particular interest, however, that in all three samples the sum of vernolic acid + 18:1 + 18:2 was highly constant at 87.0 ± 0.1% (see Table 1). In sample 3, where the petroselinic acid content was notably lower than in the other two samples, the linoleic and vernolic acid contents were correspondingly higher (Table 1). This is what is expected if there is a direct biosynthetic link between these acids, and the individual differences found may be related to climatic factors (i.e., a temperature influence on desaturase activity) or to degree of seed maturity.

A more detailed study on the FA composition data of members of the Geraniaceae will be reported separately (Aitzetmuller, K., Tsevegsuren, N., and Albers, F., unpublished data). Preliminary results show that the presence or absence of petroselinic (and, to a lesser extent, vernolic) acid appears to be a useful chemotaxonomic marker for the differentiation between sections of species within genus *Geranium*, where some sections apparently do contain petroselinic acid, whereas other sections do not. Petroselinic acid is apparently

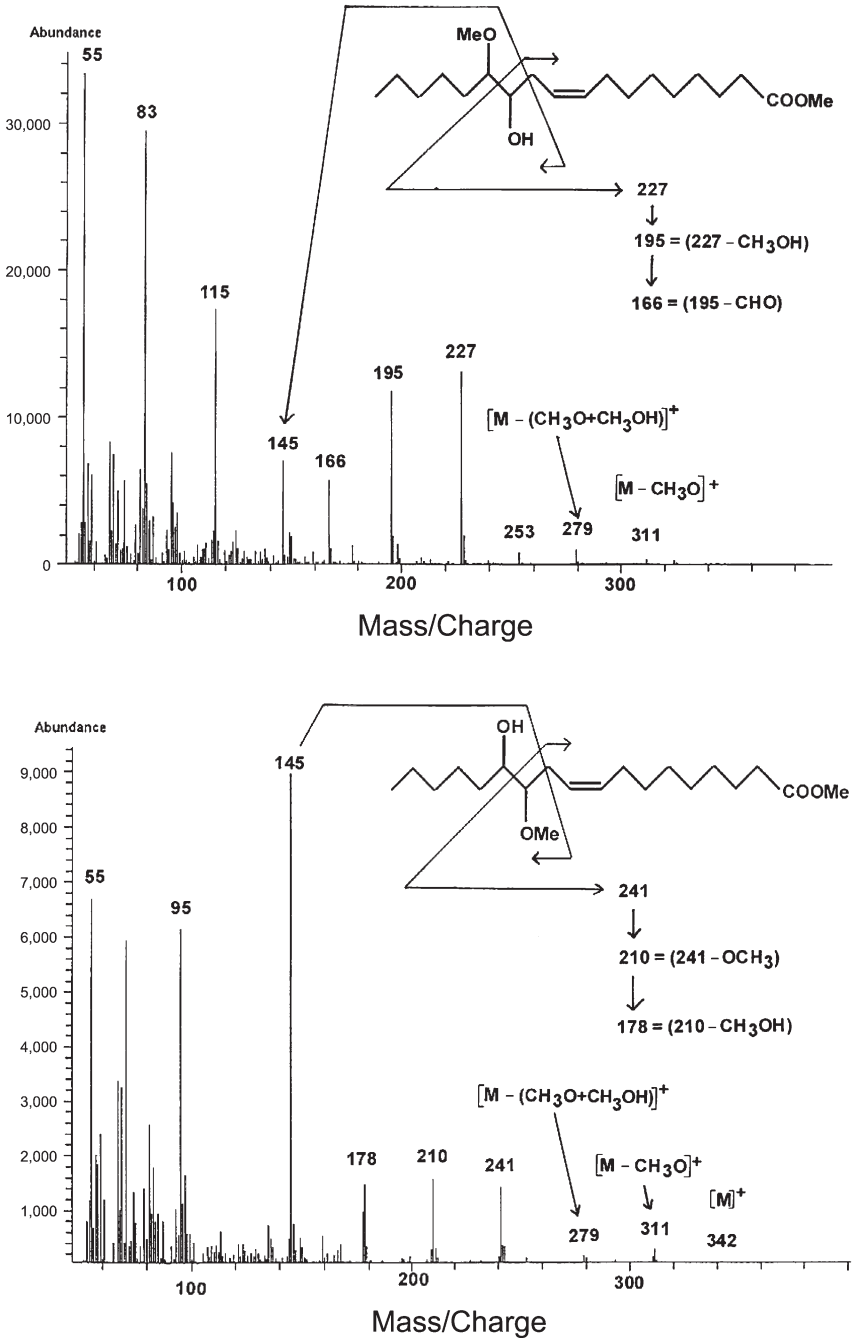

FIG. 4. Mass spectra of the ring-opening methoxy derivatives of vernolic acid methyl ester obtained by derivatization of *G. sanguineum* seed oil with BF_3/methanol. Top: Mass spectrum of 12-OH-13-MeO-18:1Δ9*c*. Bottom: Mass spectrum of 13-OH-12-MeO-18:1Δ9*c*. The two isomers obtained could be separated on the OV-1 column in the GC–MS system. For abbreviation see Figure 1.

not present in other genera (*Pelargonium* and *Erodium*) of the plant family Geraniaceae.

ACKNOWLEDGMENTS

One of us (N.T.) is indebted to the Alexander von Humboldt Foundation, Bonn, for a two-year fellowship in Germany. The authors are indebted to Prof. F. Albers, head of the Botanical Garden, University of Münster, and his co-workers for the collection of *G. sanguineum* seed samples nos. 2 and 3, as well as for other samples of Geraniaceae seeds. We wish to thank Gisela Werner and Dr. L. Brühl for the GLC analysis on Silar 5 CP and CP Sil 88 columns, Barbara Engel for the preparation of DMDS derivatives of FA, Gisela Werner and Miriam Schmitz-Peters for the maintenance of the Institute's SOFA Data Collection and database, and Stefanie Enste for her assistance in the preparation of the electronic manuscript (all Institute for Chemistry and Physics of Lipids, BAGKF, Münster, Germany, which has since been renamed Institute for Lipid

Research). This work and the SOFA database of this Institute (http://www.bagkf.de/SOFA) were partially supported by Fachagentur Nachwachsende Rohstoffe, Gülzow, Germany (grant no. FNR FKZ 97NR193).

REFERENCES

1. Kleiman, R., and Spencer, G.F. (1982) Search for New Industrial Oils: XVI. Umbelliflorae—Seed Oils Rich in Petroselinic Acid, *J. Am. Oil Chem. Soc. 59,* 29–38.
2. Placek, L.L. (1963) A Review on Petroselinic Acid and Its Derivatives, *J. Am. Oil Chem. Soc. 40,* 319–329.
3. Mabberley, D.J. (1987) *The Plant-Book*, Cambridge University Press, Cambridge.
4. Hegnauer, R. (1990) *Chemotaxonomie der Pflanzen*, Birkhäuser, Basel.
5. Saleh, N.A.M., El-Kamery, Z.A.R., Mansour, R.M.A., and Fayed, A.-A.A. (1983) A Chemosystematic Study of Some Geraniaceae, *Phytochemistry 22,* 2501–2505.
6. Barclay, A.S., and Earle, F.R. (1974) Chemical Analyses of Seeds. III. Oil and Protein Content of 1253 Species, *Econ. Bot. 28,* 178–236.
7. Abbott, T.P., Phillips, B.S., Butterfield, R.O., Isbell, T.A., and Kleiman, R. (1997) On-line Chemical Database for New Crop Seeds, *J. Am. Oil Chem. Soc. 74,* 723–726.
8. Badami, R.C., and Patil, K.B. (1981) Structure and Occurrence of Unusual Fatty Acids in Minor Seed Oils, *Progr. Lipid Res. 19,* 119–153.
9. Aitzetmuller, K., Werner, G., and Tsevegsuren, N. (1993) Screening of Seed Lipids for γ-Linolenic Acid: Capillary Gas–Liquid Chromatographic Separation of 18:3 Fatty Acids with Δ-5 and Δ-6 Double Bonds, *Phytochem. Anal. 4,* 249–255.
10. Tsevegsuren, N., and Aitzetmuller, K. (1993) γ-Linolenic Acid in *Anemone* spp. Seed Lipids, *Lipids 28,* 841–846.
11. Aitzetmuller, K. (1993) Capillary GLC Fatty Acid Fingerprints of Seed Lipids—A Tool in Plant Chemotaxonomy? *J. High Resolut. Chromatogr. 16,* 488–490.
12. Tsevegsuren, N., and Aitzetmuller, K. (1996) Gamma-Linolenic and Stearidonic Acid in Mongolian Boraginaceae, *J. Am. Oil Chem. Soc. 73,* 1681–1684.
13. Francis, G.W. (1981) Alkylthiolation for the Determination of Double-Bond Position in Unsaturated Fatty Acid Esters, *Chem. Phys. Lipids 29,* 369–374.
14. Aitzetmuller, K., Tsevegsuren, N., and Vosmann, K. (1997) A New Allenic Fatty Acid in *Phlomis* (Lamiaceae) Seed Oil, *Fett–Lipid 99,* 74–78.
15. Tsevegsuren, N., Aitzetmuller, K., Brühl, L., and Werner, G. (2000) Seed Oil Fatty Acids of Mongolian Compositae: The *trans*-Fatty Acids of *Heteropappus hispidus*, *Asterothamnus centrali-asiaticus* and *Artemisia palustris*, *J. High Resolut. Chromatogr. 23,* 360–366.
16. Aitzetmuller, K., and Guaraldo Goncalves, L.A. (1990) Dynamic Impregnation of Silica Stationary Phases for the Argentation Chromatography of Lipids, *J. Chromatogr. 519,* 349–358.
17. Tsevegsuren, N., Aitzetmuller, K., and Vosmann, K. (2003) Isomers of 16:1 and 16:2 Fatty Acids in *Androsace septentrionalis* (Primulaceae) Seed Oil, *Lipids 38,* 1173–1178.
18. Gunstone, F.D. (1980) Natural Oxygenated Acids, in *Fats and Oils: Chemistry and Technology* (Hamilton, R.J., and Bhati, A., eds.), pp. 47–58, Applied Science, London.
19. Aitzetmuller, K., Wolff, R.L., and Pasquier, E. (2000) Gymnosperm Seed Oils: Capillary Gas Chromatographic Fatty Acid Fingerprints in Chemotaxonomic Classification of Gymnosperm Genera, in *Proceedings of the 23rd International Symposium on Capillary Chromatography* (Riva, Italy, 05.-10.06.2000). Paper No. M-08; on CD-Rom only, 9 pp.
20. Aitzetmuller, K. (1995) Fatty Acid Patterns of Ranunculaceae Seed Oils: Phylogenetic Relationships, *Plant Syst. Evol. (Suppl.) 9,* 229–240.
21. Shibahara, A., Yamamoto, K., Nakayama, T., and Kajimoto, G. (1986) *cis*-Vaccenic Acid in Mango Pulp Lipids, *Lipids 21,* 388–394.
22. Shibahara, A., Yamamoto, K., Nakayama, T., and Kajimoto, G. (1987) *Cis*-Vaccenic Acid in Pulp Lipids of Commonly Available Fruits, *J. Am. Oil Chem. Soc. 64,* 397–401.
23. Kleiman, R., and Spencer, G.F. (1973) Gas Chromatography–Mass Spectrometry of Methyl Esters of Unsaturated Oxygenated Fatty Acids, *J. Am. Oil Chem. Soc. 50,* 31–38.
24. Price, R.A., and Palmer, J.D. (1993) Phylogenetic Relationships of the Geraniaceae and Geraniales from rbcL Sequence Comparisons, *Ann. Missouri Bot. Gard. 80,* 661–671.
25. Aitzetmuller, K. (1996) Seed Fatty Acids, Chemotaxonomy and Renewable Resources, in *Oils—Fats—Lipids 1995: Proceedings of the 21st World Congress of the International Society for Fat Research, The Hague, 1995*, pp. 117–120, P.J. Barnes & Associates, Bridgewater.
26. Aitzetmuller, K., Matthäus, B., and Friedrich, H. (2003) A New Database for Seed Oil Fatty Acids—The Database SOFA, *Eur. J. Lipid Sci. Technol. 105,* 92–103.
27. Aitzetmuller, K., and Matthaus, B. (2003) Potential Uses of the Seed Oil Fatty Acids Database 'SOFA,' *Lipid Technol. Newsletter 9,* 123–127.

[Received May 3, 2004; accepted July 9, 2004]

Photochemical Production of Conjugated Linoleic Acid from Soybean Oil

R.R. Gangidi and A. Proctor*

Department of Food Science, University of Arkansas, Fayetteville, Arkansas 72704

ABSTRACT: Conjugated linoleic acid (CLA), an anticarcinogenic compound with numerous other health benefits, is present mainly in dairy and beef lipids. The main CLA isomer present in dairy and beef lipids is *cis* 9,*trans* 11 CLA at a 0.5% concentration. The typical minimum human dietary intake of CLA is 10 times less than the 3 g/d suggested requirement that has been extrapolated from animal and cell-line studies. The objectives of this study were to produce CLA isomers from soybean oil by photoisomerization of soybean oil linoleic acid and to study the oxidation status of the oil. Refined, bleached, and deodorized soybean oil with added iodine concentrations of 0, 0.1, 0.25, and 0.5% was exposed to a 100-W mercury lamp for 0 to 120 h. An SP-2560 fused-silica capillary GC column with FID was used to analyze the esterified CLA isomers in the photoisomerized oil. The CLA content of the individual isomers was optimized by response surface methodology. Attenuated total reflectance (ATR)-FTIR spectra in the 3400 to 3600 cm^{-1} range and ^1H NMR spectra in the 8 to 12 ppm range of the photoisomerized soybean oil were obtained to follow hydroperoxide formation. The largest amount of *cis* 9,*trans* 11 CLA isomer in soybean oil was 0.6%, obtained with 0.25% iodine and 84 h of photoisomerization. Lipid hydroperoxide peaks in the ATR-FTIR spectra and aldehyde peaks in the ^1H NMR spectra were not observed in the photoisomerized soybean oil, and the spectra were similar to that of fresh soybean oil. This study shows that CLA isomers can be produced simply and inexpensively from soybean oil by photoisomerization.

Paper no. L9450 in *Lipids 39,* 577–582 (June 2004).

CLA refers to the group of positional isomers of linoleic acid (octadecadienoic acid) having a conjugated double-bond system starting at carbons 7 to 13 and including all possible geometric configurations of *cis-trans*, *cis-cis*, and *trans-trans* isomers (1). Dietary sources of CLA include beef (0.43% of total beef lipids) and dairy products (0.40 to 0.55% of total dairy lipids) (2). *Cis* 9,*trans* 11 CLA, also called rumenic acid, is the main isomer, constituting 90% of the total CLA found in dairy and beef lipids.

CLA is well recognized as an anticarcinogenic (1,3) and antiatherogenic (4) compound. Other health benefits of CLA identified in animal and cell-line studies include the ability to reduce body fat, increase lean body mass (5), and protect against immune-induced muscle wasting (6). However, the current human intake of CLA is 10 times less than the 3 g/d minimum value extrapolated from animal studies for optimal beneficial effects (3,7). By diversifying dietary sources of CLA to include vegetable oils, the human intake of CLA could be increased. Lee *et al.* (8) attempted to incorporate CLA FFA into soybean oil by lipase-catalyzed interesterification, but this procedure resulted in high levels of oxidation of the oil. However, isomers of CLA could be produced from vegetable oils by photoisomerization. In the photoisomerization studies conducted by Seki *et al.* (9), Canaguier *et al.* (10,11), and Julliard *et al.* (12), an 80% yield of CLA methyl esters was produced from linoleic acid methyl esters, but specific CLA isomer compositions were not reported. In these methods, linoleic acid methyl esters (5–10%) were dissolved in petroleum ether, benzene, or carbon disulfide and then exposed to a strong light source in the presence of iodine as a sensitizer (9–12). However, there are no reports on the effect of direct photoisomerization of linoleic acid in vegetable oils esterified in the absence of solvents. Soybean oil contains *ca.* 50% linoleic acid that could be photoisomerized to CLA (13). Thus, the goal of this study was to investigate the extent to which CLA isomers could be produced directly from a readily available, commercial linoleic acid-rich vegetable oil such as soybean oil in the absence of solvents. The specific objectives were (i) to determine the presence and concentration of CLA isomers in soybean oil upon photoisomerization; (ii) to optimize the iodine content and time of photoisomerization; and (iii) to determine the oxidation status of the photoisomerized soybean oil by FTIR and ^1H NMR spectroscopy.

EXPERIMENTAL PROCEDURES

Processing. Soybean oil (Wesson; ConAgra, Irvine, CA) was obtained from a local grocery store (Fayetteville, AR). Iodine (crystals, resublimed; EM Science, Cherry Hill, NJ) at levels of 0.5, 0.25, 0.1, and 0% (w/w) was added to 200 g of soybean oil in a 250-mL beaker, and then heated for 3 to 5 min at 80°C or until the iodine was completely dissolved. The beaker was flushed with nitrogen during heating. The beaker was wrapped with aluminum foil to prevent the oil from being exposed to outside light, but the oil was not stirred during photoisomerization. The oil was then exposed to a 100-W mercury lamp. The lamp was a Model B 100-YP Black Ray long-wave UV lamp with a 100-W Sylvania Par 38-R spot bulb (Osram Sylvania Inc., Winchester, KY). The spot bulb was constructed with an outer glass bulb and an internal arc tube made of quartz. The mercury arc tube operated under

*To whom correspondence should be addressed at 2650 N. Young Ave., Department of Food Science, University of Arkansas, Fayetteville, AR 72704. E-mail: aproctor@uark.edu

pressures of up to 50 psi and at high temperatures. The lamp had a yellow filter that allowed strong mercury lines at 543, 574, and 576 nm; however, the yellow filter was removed for this study. In addition to the spot bulb, the lamp assembly consisted of a transformer, a lamp funnel that held the spot bulb, and a lamp visor that directed the light onto the sample (UVP Inc., Upland, CA). The output of the lamp was in the visible range of 380 to 700 nm, with strong emissions in the range of 426, 450, 543, 574, and 576 nm. The outer glass on the spot bulb absorbed the UV light. Hence, the spectral characteristics of the light were in the visible range. The photosensitizer iodine maximum absoptivity was at 520 nm (λ_{max}) (12). Hence, the lamp emitted the required wavelength. The power supply required for the lamp was 115 V/60 Hz/2.5 A.

The lamp was suspended 45 cm above the beaker. Every 12 h, for 120 h, approximately 7 mL of soybean oil was collected from the beaker in a 7-mL glass vial wrapped with aluminum foil, purged and capped, and then immediately refrigerated at 4°C. The temperature of the oil during photoisomerization was between 35 and 40°C.

Methyl ester preparation. Methyl esters were prepared by base catalysis as described by Christie *et al.* (14). A base-catalyzed method was chosen for methyl ester preparation to reduce the formation of conjugated *trans*,*trans* isomers during analysis. One hundred milligrams of photoisomerized soybean oil, 500 μL of 1% heptadecanoic acid methyl ester (17:0, internal standard), 2 mL of toluene, and 4 mL of 0.5 M sodium methoxide (EM Science, Darmstadt, Germany) in methanol were placed in a 25-mL centrifuge tube and then purged with nitrogen gas. The centrifuge tube was heated to 50°C for 10 to 12 min and then cooled for 5 min. Glacial acetic acid (200 μL) was added to the centrifuge tube to inhibit the formation of sodium hydroxide, which could hydrolyze the methyl esters to FFA. Five milliliters of distilled water was added to the centrifuge tube followed by 5 mL of hexane. The tube was then vortexed for 2 min, and the top hexane layer was extracted and dried over anhydrous sodium sulfate (EM Science). Another 5 mL of hexane was added to the centrifuge tube, the tube was vortexed for 2 more min, and the hexane layer was dried over anhydrous sodium sulfate prior to methyl ester analysis.

CLA methyl ester analysis by GC. Methyl esters were analyzed by GC as described by Ma *et al.* (7) using an SP 2560 fused-silica capillary column (100 m × 0.25 mm i.d. × 0.2 μm film thickness; Supelco Inc., Bellefonte, PA) with an FID (model 3800, Varian, Walton Creek, CA). The samples were injected in duplicate by an autosampler (AS 300; HTA s.r.1, Brescia, Italy), and gas chromatograms were printed by the data module printer (Waters, Milford, MA). Commercial CLA methyl ester samples (Sigma) were used as standards. The standards contained equal proportions of the *cis* 9,*trans* 11 CLA isomer and the *trans* 10,*cis* 12 CLA isomer, and trace amounts of *trans*,*trans* CLA isomers. The standard CLA concentrations in hexane used for calibration were 0.005, 0.01, 0.03, 0.05, 0.07, and 0.1%. CLA concentrations were calculated by the following equation: internal standard concentration (5 mg)/internal standard peak area × peak area × relative response factor. Plots of the *cis* 9,*trans* 11 and *trans* 10,*cis* 12 CLA isomers with photoisomerization time were produced.

ATR-FTIR analysis of the photoisomerized soy oil. ATR-FTIR spectra of soybean oil containing 0, 0.1, 0.25, and 0.50% iodine and photoisomerized for 0 to 120 h and a control spectrum of fresh soybean oil were obtained. Spectra were collected by placing samples on a horizontal ATR 45° ZnSe trough plate (Spectra-Tech Inc., Shelton, CT). The trough plate was placed in a slide-mounted horizontal ATR with prealigned fixed mirrors (Spectra-Tech Inc.), and absorbance spectra were obtained using a Nicolet Impact 410 spectrophotometer (Nicolet Analytical Instruments, Madison, WI) in the range of 700 to 4000 cm^{-1}. One hundred scans were co-added to obtain a spectrum with 8 cm^{-1} resolution, 4 cm^{-1} data spacing, and 0.63 cm/s mirror velocity throughout. Triplicate spectra were obtained for each sample. Differences between the spectra were evaluated for hydroperoxides in the range of 3400 to 3600 cm^{-1}.

^{1}H NMR analysis of the photoisomerized soy oil. The samples were analyzed with an ^{1}H NMR spectrometer (Avance 300; Bruker, Rheinstetten, Germany) operating at 300 MHz. The acquisition parameters were as follows: spectral width, 6172.839 Hz; relaxation delay, 1 s; number of scans, 24; acquisition time, 2 min 37 s; pulse width, 12.20 μs. The experiments were carried out at 45°C. Samples were dissolved in 30% $CDCl_3$ (w/w). Free induction decay data were Fourier transformed and then phase corrected with MestRe-C software (Beta version 3.8.9.0; MestRe-C, A Coruña, Spain) to obtain the NMR spectra. Spectra were obtained for soybean oil, soybean oil containing 100 ppm hexanal, and 120-h photoisomerized soybean oil containing 0.25% iodine. The spectra were observed for proton peaks of aldehyde carbonyl and of hydroperoxides in the range of 8–12 ppm.

Optimization of iodine and photoisomerization time by response surface modeling. Iodine content and photoisomerization time were optimized by the maximum desirability function of the response surface prediction profiler (JMP IN; SAS, Cary, NC) for the maximum yield of *cis* 9,*trans* 11 CLA and *trans* 10,*cis* 12 CLA.

RESULTS AND DISCUSSION

CLA methyl ester analysis by GC. Figure 1 shows the *cis* 9,*trans* 11 CLA isomer concentrations in soybean oil with various concentrations of iodine and photoisomerization times. The maximum yield of *cis* 9,*trans* 11 CLA of almost 0.6%, which is slightly more than that found in the dairy and beef lipids, was formed in the soybean oil containing 0.25% iodine after approximately 48 h of photoisomerization. The 0.25% iodine concentration produced more isomers than the larger and smaller iodine doses, but in each case the optimal amount of CLA was produced after about 48 h. Larger LSD values were observed with CLA isomers from 0.25% iodine-containing soybean oil than with the other isomers, a result that could be due to the greater CLA levels. However, no sig-

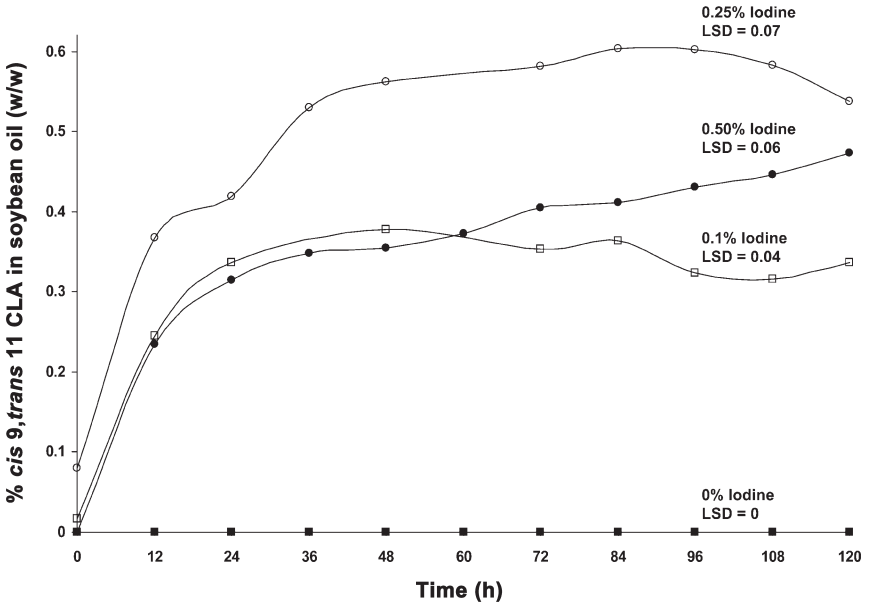

FIG. 1. *Cis* 9,*trans* 11 CLA isomer content (%) in photoisomerized soybean oil with iodine as a photosensitizer. The CLA isomer content in soybean oil was calculated on a soybean oil weight basis, i.e., iodine content was subtracted.

nificant increase in the CLA content was observed after 60 h of photoisomerization at all iodine concentrations. There was no significant difference in the CLA contents of the oils with 0.1 and 0.5% iodine concentrations until 60 h of photoisomerization, but with 0.5% iodine, CLA isomer formation increased after 60 h.

No CLA isomer was formed with the 0% iodine control, even when exposed to light for up to 120 h, suggesting that the iodine photosensitizer was important for CLA formation. However, experimental samples that contained iodine produced CLA at 0 time, likely due to accidental light exposure prior to photoisomerization.

Figure 2 shows the amount of *trans* 10,*cis* 12 isomer formed during photoisomerization. This isomer formed in amounts almost equal to the *cis* 9,*trans* 11 CLA isomer for the same iodine concentration and photoisomerization time (Fig. 1).

Figure 3A shows the SP-2560 gas chromatogram of the CLA standard (Sigma). The CLA standard contained 42% of the *cis*-9,*trans*-11 CLA isomer and 44% of the *trans*-10,*cis*-12 CLA isomer, and the peak retention times of the isomers

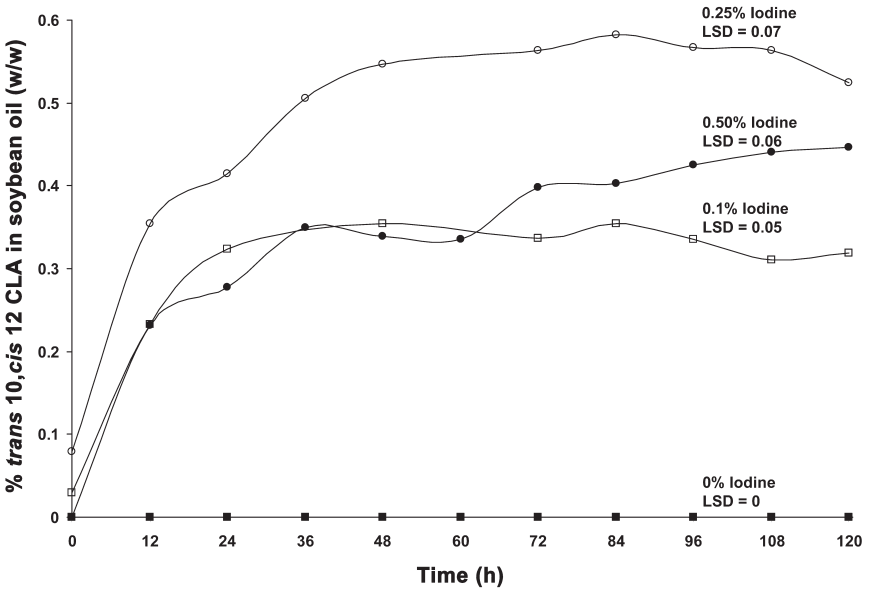

FIG. 2. *Trans* 10,*cis* 12 CLA isomer content (%) in photoisomerized soybean oil with iodine as a photosensitizer. The CLA isomer content in soybean oil was calculated on a soybean oil weight basis, i.e., iodine content was subtracted.

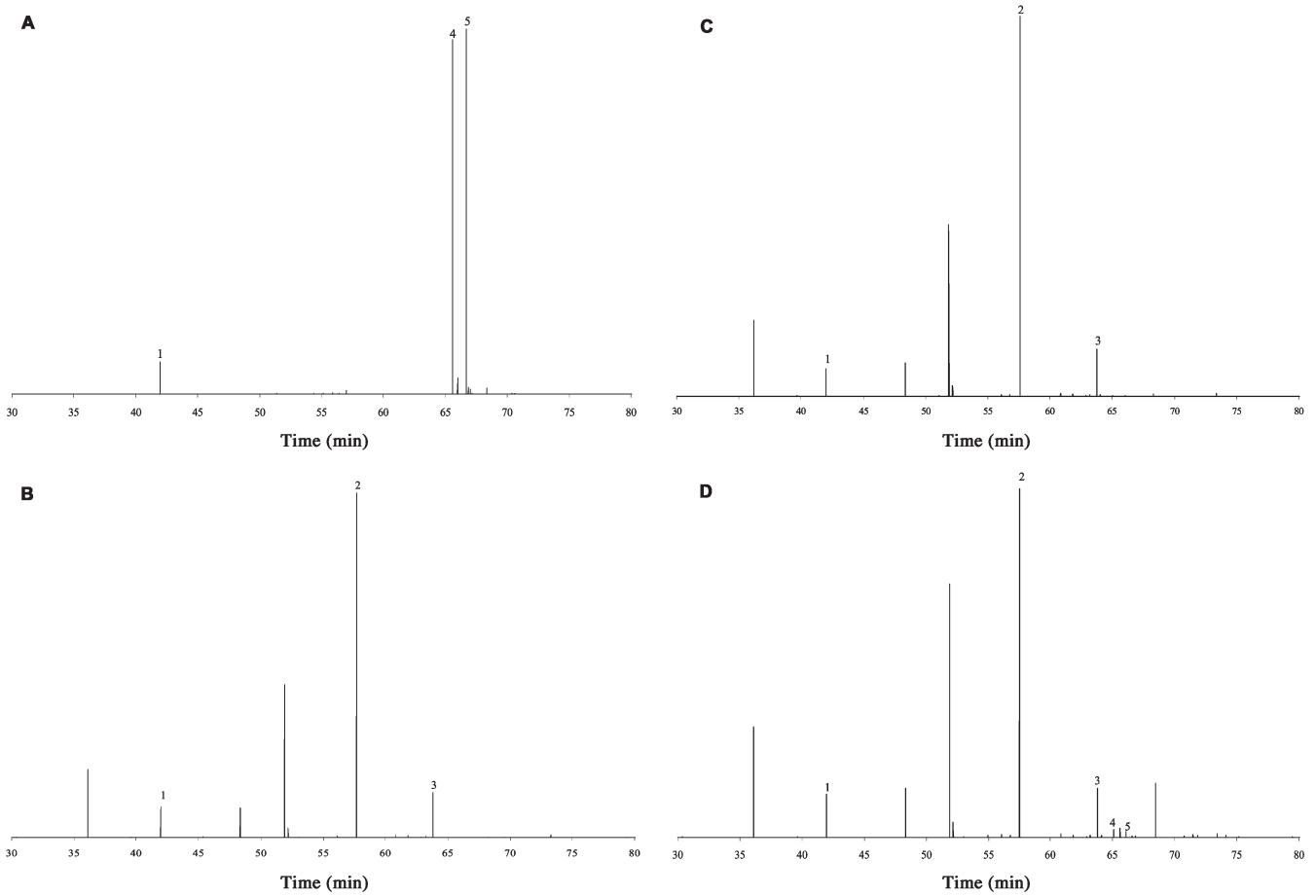

FIG. 3. Partial gas chromatograms of the methyl esters of (A) the CLA standard, (B) soybean oil, (C) soybean oil containing 0.25% iodine and 0 h of photoisomerization, (D) soybean oil containing 0.25% of iodine and 120 h of photoisomerization. Gas chromatograms were obtained with an SP-2560 100-m fused-silica capillary column (Supelco, Bellefonte, PA) and FID (Varian, Walton Creek, CA). Peaks: 1, heptadecanoic acid methyl ester; 2, linoleic acid methyl ester; 3, linolenic acid methyl ester; 4, *cis* 9,*trans* 11 CLA isomer; and 5, *trans* 10,*cis* 12 CLA isomer.

were 65.6 and 66.5 min, respectively. The soybean oil gas chromatogram had a linoleic acid methyl ester peak at 57.6 min and a linolenic acid methyl ester peak at 63.8 min (Fig. 3B). In this chromatogram, peaks at retention times of 65.6 and 66.5 min were absent. The soybean oil gas chromatogram was similar to that of the oil containing 0.25% iodine (Fig. 3C).

Figure 3D shows the oil containing 0.25% iodine and photoisomerized for 120 h. The soybean oil chromatogram had the *cis* 9,*trans* 11 CLA isomer peak at a retention time of 65.6 min and the *trans* 10,*cis* 12 CLA isomer at 66.5 min. The peak at 66.0 min could have been due to a *cis*,*trans* CLA isomer.

Optimization of iodine and photoisomerization time by response surface modeling. Table 1 shows the optimal iodine concentration and photoisomerization time for individual isomers and the total *cis*,*trans* CLA isomers as determined by response surface methodology. The maximum amount of *cis* 9,*trans* 11 CLA isomer in soybean oil was 0.61% and required an optimal iodine concentration of 0.3% and 90 h of photoisomerization. This concentration of *cis* 9,*trans* 11 isomer was slightly greater than that present in beef and dairy lipids (0.5%), the main dietary sources of CLA.

The concentration of *cis*,*trans* CLA formed in the present study was found to be lower than that obtained from earlier studies with methyl esters (9–12). In those studies, linoleic acid methyl esters (5 to 10%) were dissolved in petroleum ether or carbon disulfide and photoisomerized with light in the presence of iodine. Seventy to 80% of the total methyl esters were converted to conjugated isomers, and 25% of the conjugated species were *cis*,*trans* isomers. The higher concentrations of *cis*,*trans* CLA isomers in earlier studies (9–12) could have been caused by linoleic acid methyl esters being

TABLE 1
CLA Isomer Concentration and the Optimal Iodine Concentration and Photoisomerization Time as Obtained with Response Surface Methodology[a]

	Optimal conditions		
Isomer	Isomer concentration (%)	Iodine (%)	Photoisomerization time (h)
Cis 9,*trans* 11 CLA	0.61	0.33	90
Trans 10,*cis* 12 CLA	0.59	0.33	91

[a]JMP IN (SAS, Cary, NC).

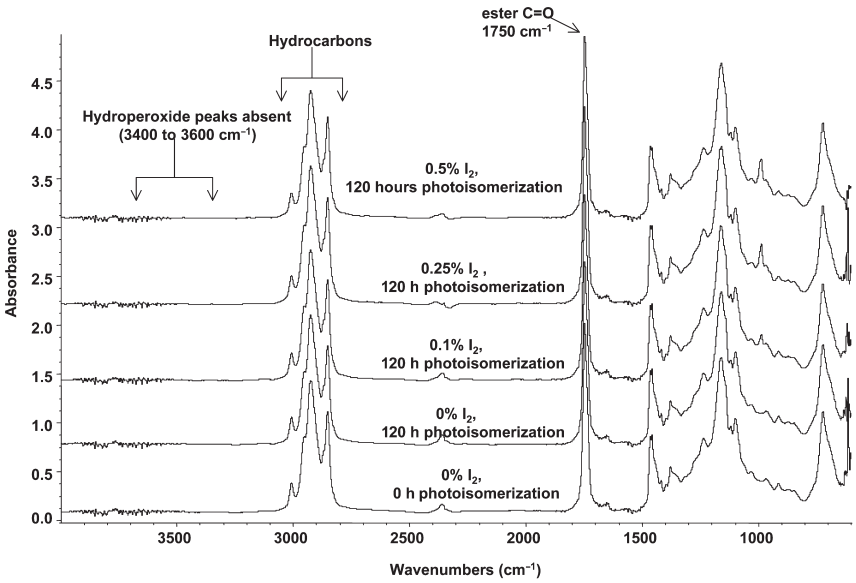

FIG. 4. FTIR spectra (4000 to 700 cm^{-1}) of photoisomerized soybean oil samples. Iodine was used as the photosensitizer. An attenuated total reflectance accessory with a ZnSe trough plate was used to collect the FTIR spectra.

present in a diluted form (5–10%) in the solvent, which may have allowed greater light exposure. In our study, lower yields of *cis*,*trans* CLA isomers in soybean oil could have been due to the absence of solvent, the low surface area-to-volume ratio of the oil in the beaker, and the lack of stirring.

ATR-FTIR analysis of photoisomerized soybean oil. Figure 4 shows the ATR-FTIR spectra of soybean oil containing 0.5, 0.25, 0.1, and 0% iodine and photoisomerized for 120 h. No major peroxide peaks were observed in the range of 3400 to 3600 cm^{-1}, suggesting no formation of peroxides even after photoisomerization with a high-intensity mercury lamp for 120 h. In the 3400 to 3600 cm^{-1} range, the ATR-FTIR spectra of fresh soybean oil (0 h photoisomerized; 0% iodine) was similar to that of soybean oil photoisomerized for 12 to 108 h (data not shown).

^{1}H NMR analysis of photoisomerized soy oil. The ^{1}H NMR spectra of soybean oil containing hexanal (100 ppm) showed a peak at 9.4 ppm (Fig. 5B). Peaks were not observed in the 8–12 ppm range of the NMR spectra of soybean oil (Fig. 5A), nor of oil containing 0.25% iodine and photoisomerized for 120 h (Fig. 5C). The absence of peaks indicates the absence of aldehydes and hydroperoxides in the samples. The protons of aldehyde carbonyl and hydroperoxide show peaks in the 8–12 ppm range of the ^{1}H NMR spectra. This confirms the results of the ATR-FTIR analysis of photoisomerized soybean oil (Fig. 4). The characteristics of the remaining portions of the NMR spectra for the three samples were similar (data not shown).

In an earlier study conducted by Lee *et al.* (8), CLA FFA were first synthesized from linoleic acid FFA, and CLA isomers were then introduced into the soybean oil by lipase-catalyzed interesterfication. However, they reported high oxidation of the soybean oil and suggested adding rosemary extract to inhibit oxidation. In our study no oxidation was found, as determined by FTIR and NMR, and iodine could easily be removed from the soybean oil by adsorption on activated carbon (15,16).

This study shows that CLA can be generated from soybean oil by photoisomerization in the absence of a solvent. Although CLA yields were low compared with an earlier study with methyl esters, this difference may have been due to the dilution of methyl esters (10%), whereas in our study the oil was undiluted. Light penetration into the beaker may have limited production of the CLA mainly to the surface of the oil, so by varying the intensity of the mercury lamp and maximizing the exposure of the oil to light, higher yields of CLA isomers may be produced.

ACKNOWLEDGMENTS

We thank the Arkansas Biosciences Institute, Little Rock, for the funding of this project. We thank Mr. Marvin Leister (Department of Chemistry and Biochemistry, University of Arkansas, Fayetteville) for his assistance with the NMR studies.

REFERENCES

1. Ha, Y.L., Grimm, N.K., and Pariza, M.W. (1987) Anticarcinogens from Fried Ground Beef: Heat-Altered Derivatives of Linoleic Acid, *Carcinogenesis 8*, 1881–1887.
2. Chin, S.F., Liu, W., Storkson, J.M., Ha, Y.L., and Pariza, M.W. (1992) Dietary Sources of Conjugated Dienoic Isomers of Linoleic Acid, a Newly Recognized Class of Anticarcinogens, *J. Food Compos. Anal. 5*, 39–42.
3. Ip, C., Singh, M., Thompson, H.J., and Scimeca, J.A. (1994) Conjugated Linoleic Acid Suppresses Mammary Carcinogenesis and Proliferation Activity of the Mammary Gland in the Rat, *Cancer Res. 54*, 1212–1215.
4. Lee, K.N., Kritchevsky, D., and Pariza, M.W. (1994) Conju-

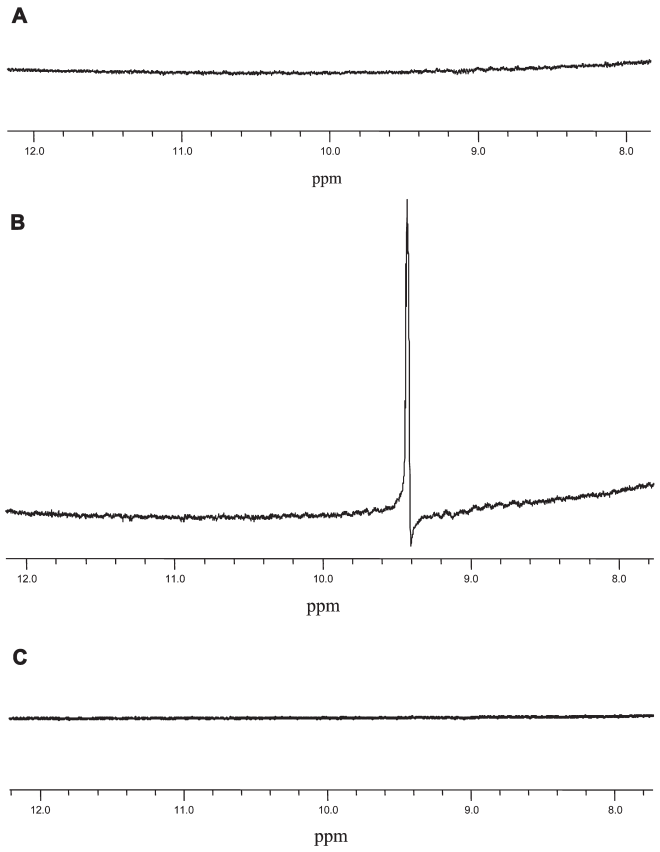

FIG. 5. Partial 300-MHz ^{1}H NMR spectra in the 8 to 12 ppm range of (A) soybean oil, (B) 100 ppm of hexanal in soybean oil, and (C) soybean oil containing 0.25% iodine and photoisomerized for 120 h. Samples were dissolved in 30% $CDCl_3$ (w/w).

gated Linoleic Acid and Atherosclerosis in Rabbits, *Atherosclerosis 108*, 19–25.

5. Park, Y., Storkson, J.M., Albright, K.J., Liu, W., and Pariza, M.W. (1999) Evidence That the *trans*-10,*cis*-12 Isomer of Conjugated Linoleic Acid Induces Body Composition Changes in Mice, *Lipids 34*, 235–241.
6. Miller, C.C., Park, Y., Pariza, M.W., and Cook, M.E. (1994) Feeding Conjugated Linoleic Acid to Animals Partially Overcomes Catabolic Responses Due to Endotoxin Injection, *Biochem. Biophys. Res. Commun. 198*, 1107–1112.
7. Ma, D.W.L., Wierzbicki, A.A., Field, C.J., and Clandinin, M.T. (1999) Conjugated Linoleic Acid in Canadian Dairy and Beef Products, *J. Agric. Food Chem. 47*, 1956–1960.
8. Lee, J.H., Kim, M.R., Kim, H.R., Kim, L.H., and Lee, K.T. (2003) Characterization of Lipase-Catalyzed Structured Lipids from Selected Vegetable Oils with Conjugated Linoleic Acid: Their Oxidative Stability with Rosemary Extracts, *J. Food Sci. 68*, 1653–1658.
9. Seki, K., Kaneko, R., and Kobayashi, K. (1998) Photoconjugation of Methyl Linoleate in the Presence of Iodine as Sensitizer, *Yukagaku 38*, 949–954.
10. Canaguier, R., Chevalier, J.L., Cecchi, G., and Ucciani, E. (1986). Photoisomerization Solaire des Huiles Vegetales Catalysee par l'Iode, *Rev. Fr. Corps Gras 33*, 157–162.
11. Canaguier, R., Cecchi, G., Ucciani, E., and Chevalier, J.L. (1984) Isomerisation Photochimique des Acides Gras Polyinsatures Catalysee par l'Iode, *Rev. Fr. Corps Gras 31*, 401–409.
12. Julliard, M., Luciani, A., Chevalier, J.L., Cecchi, G., and Ucciani, E. (1987) Photosensitized Conjugation of Methyl 9,12-Octadecadienoate, *J. PhotoChem. 38*, 345–355.
13. Liu, K. (1997) *Soybeans—Chemistry, Technology, and Utilization*, p. 29, Chapman & Hall, New York.
14. Christie, W.W., Sébédio, J.L., and Juaneda, P. (2001) A Practical Guide to the Analysis of Conjugated Linoleic Acid, *inform 12*, 147–152.
15. Juhola, A.J. (1975) Iodine Adsorption and Structure of Activated Carbon, *Carbon 13*, 437–442.
16. Bhatia, S.K., Liu, F., and Arvind, G. (2000) Effect of Pore Blockage on Adsorption Isotherms and Dynamics: Anomalous Adsorption of Iodine on Activated Carbon, *Langmuir 16*, 4001–4008.

[Received February 19, 2004, and in revised form July 27, 2004; revision accepted August 5, 2004]

Reaction of Mono-epoxidized Conjugated Linoleic Acid Ester with Boron Trifluoride Etherate Complex

Marcel S.F. Lie Ken Jie* and Corey N.W. Lam

Department of Chemistry, The University of Hong Kong, Hong Kong, SAR, People's Republic of China

ABSTRACT: The reaction of methyl 11,12-*E*-epoxy-9*Z*-octadecenoate (**1**) with boron trifluoride etherate furnished a mixture of methyl 12-oxo-10*E*-octadecenoate (**3a**) and methyl 11-oxo-9*E*-octadecenoate (**3b**) in 66% yield. Methyl 9,10-*Z*-epoxy-11*E*-octadecenoate (**2**) with boron trifluoride etherate furnished a mixture of methyl 9-oxo-10*E*-octadecenoate (**4a**, 45%) and methyl 10-oxo-11*E*-octadecenoate (**4b**, 19%). A plausible mechanism is proposed for these reactions, which involves the attack on the epoxy ring system by BF_3, followed by deprotonation, oxo formation, and double bond migration to give a mixture of two positional α,β-unsaturated C_{18} enone ester derivatives (**3a**/**3b**, **4a**/**4b**). The structures of these C_{18} enone ester derivatives (**3a**/**3b**, **4a**/**4b**) were identified by a combination of NMR spectroscopic and mass spectrometric analyses.

Paper no. L9490 in *Lipids 39,* 583–587 (June 2004).

CLA are found in the fat of many herbivores, with levels as high as 4.3% in beef tallow (1). In lamb and pork the levels are about 1.2 and 0.12%, respectively, whereas in fish CLA are found in trace amounts (0.01–0.09%) (2). Cow's milk contains about 2 to 37 mg/g of CLA (3). The CLA content of human milk ranges from 1.9 to 5.8 mg/g fat (4–6).

The major isomers of CLA found in nature are 9*Z*,11*E*-octadecadienoic acid [18:2(9*Z*,11*E*)] and 10*E*,12*Z*-octadecadienoic acid [18:2(10*E*,12*Z*)], which are likely produced endogenously from 11*E*-octadecenoic acid by Δ^9-desaturase (7,8).

CLA have been found to be responsible for various bioactivities in various animal models. These effects include anticarcinogen and antitumor properties (9–11), enhancement of the production of whole-body protein accompanied by reduction of fat mass in mice (12–14), and an antiatherogenic effect in hamsters (15).

Two important books on CLA have been published that review many of the nutritional and biological aspects of CLA including the oxidation, synthesis, and some of the spectroscopic properties of this unusual class of FA (16,17).

Except for the work on the oxidation of CLA (16), little has been done on the chemistry of CLA. We have recently reported the reactions of 18:2(9*Z*,11*E*) with various epoxidizing agents (18), which yield two mono-epoxy derivatives, namely, methyl 11,12-*E*-epoxy-9*Z*-octadecenoate (**1**) and methyl 9,10-*Z*-epoxy-11*E*-octadecenoate (**2**). This paper describes the reaction of these mono-epoxy derivatives with boron trifluoride etherate complex, which leads to the production of conjugated C_{18}-enone (or keto-ene) fatty ester derivatives. Several nonconjugated C_{18}-enone FA from seed oils have been reported: 7-oxo-11*Z*-octadecenoic acid (19–21), 9-oxo-11*Z*-octadecenoic acid (22), 9-oxo-12*Z*-octadecenoic acid (23,24), and 9-oxo-13*Z*-octadecenoic acid (25). To our knowledge, no conjugated C_{18}-enone FA has been found in seed oils. However, methyl 12-oxo-10*E*-octadecenoate has been prepared from methyl ricinoleate (methyl 12-hydroxy-9*Z*-octadecenoate) (26,27).

MATERIALS AND METHODS

Instrumentation. Column chromatographic separation was performed on silica gel (Kieselgel 60, particle size 0.040–0.063 mm, 230–400 mesh ASTM, E. Merck No. 1.09385; Merck, Darmstadt, Germany) as the adsorbent using gradient elution with a mixture of *n*-hexane/diethyl ether as the mobile phase. IR spectra were recorded on a Bio-Rad FTS-165 FT-IR spectrometer (Biorad Inc., Hercules, CA). Samples were run as neat films on KBr plates. UV spectra were recorded on a diode array spectrophotometer (model 8452A; Hewlett-Packard, Palo Alto, CA). All samples were dissolved in dichloromethane. GC analysis was conducted on a Hewlett-Packard gas chromatograph model 5890 equipped with an FID and a Hewlett-Packard model HP3394A electronic integrator. The stationary phases of the columns were cross-linked polyethylene glycol (30 m × 0.32 mm, 0.25 μm film thickness) or cross-linked methyl silicone gum (30 m × 0.32 mm, 0.25 μm film thickness). The column oven temperature was maintained at 220°C. Helium was used as the mobile phase at 2 mL/min. NMR spectra were recorded on a Bruker Avance DPX_{300} (300 MHz) Fourier Transform NMR spectrometer (Bruker, Fallanden, Switzerland) from solutions in deuteriochloroform ($CDCl_3$) (0.2–0.3 mM) with tetramethylsilane (TMS) as the internal reference standard. Chemical shifts are given in δ-values in ppm downfield from TMS (δ_{TMS} = 0 ppm). Mass spectral analyses were carried out on a Finnigan MAT-95 (Finnigan Corp., San Jose, CA) under electron impact ionization at 20 eV. Compounds **1** and **2** were synthesized by epoxidation of methyl 9*Z*,11*E*-octadecadienoate with *m*-chloroperoxybenzoic acid as described elsewhere (18).

To whom correspondence should be addressed at Department of Chemistry, The University of Hong Kong, Pokfulam Rd., Hong Kong, SAR, China. E-mail: hrsclkj@hkucc.hku.hk

Abbreviations: TMS, tetramethylsilane.

EXPERIMENTAL PROCEDURE

*Reaction of **1** with boron trifluoride etherate*. A mixture of **1** (180 mg, 0.58 mmol), boron trifluoride etherate (0.1 mL, 0.8 mmol), and chloroform (5 mL) was stirred for 2 h at room temperature. Aqueous sodium hydrogen carbonate solution (10% w/w, 10 mL) was added, and the reaction mixture was extracted with diethyl ether (3 × 20 mL). The ethereal extract was washed successively with water (2 × 10 mL) and brine (20 mL), and then it was dried over anhydrous magnesium sulfate. The filtrate was evaporated under reduced pressure, and the residue was column chromatographed on silica gel (15 g) using a mixture of *n*-hexane/diethyl ether (90:10, vol/vol) as eluent to furnish a mixture of methyl 12-oxo-10*E*-octadecenoate (**3a**) and methyl 11-oxo-9*E*-octadecenoate (**3b**) (143 mg, 66%). Physical state: colorless oil. Spectral analysis was conducted on the mixture of compounds **3a** and **3b**. IR (neat): 1741 (*s*, ester C=O, str.), 1698 (*s*, oxo C=O, str.), 1630 (*s*, olefin CH=CHCO, str.), and 1172 (*s*, C=O, str.) cm^{-1}; ^1H NMR ($CDCl_3$, δ_H) 0.88 (*t*, *J* = 6.5 Hz, 3H, C*H*$_3$), 1.30–1.31 (*m*, 14H, C*H*$_2$), 1.42–1.48 (*m*, 2H, 8-*H*$_2$ of **3a** and 7-*H*$_2$ of **3b**), 1.55–1.62 (*m*, 4H, 3-*H*$_2$/14-*H*$_2$ of **3a** and 3-*H*$_2$/13-*H*$_2$ of **3b**), 2.20 (*q*, *J* = 7.2 Hz, 2H, 9-*H*$_2$ of **3a** and 8-*H*$_2$ of **3b**), 2.30 (*t*, *J* = 7.5 Hz, 2H, 2-*H*$_2$), 2.52 (*t*, *J* = 7.4 Hz, 2H, 13-*H*$_2$ of **3a** and 12-*H*$_2$ of **3b**), 3.66 (*s*, 3H, COOC*H*$_3$), 6.08 (*d*, *J* = 15.9 Hz, 1H, 11-*H* of **3a** and 10-*H* of **3b**), and 6.82 (*m*, 1H, 10-*H* of **3a** and 9-*H* of **3b**); ^{13}C NMR ($CDCl_3$, δ_C) 14.07 (C-18 of **3a**), 14.10 (C-18 of **3b**), 22.55 (C-17 of **3a**), 22.66 (C-17 of **3b**), 24.23/24.91 (C-3/C-13 of **3b**), 24.34/24.93 (C-3/C-14 of **3a**), 28.13 (C-8 of **3a**), 28.16 (C-7 of **3b**), 28.99, 29.03, 29.09, 29.13, 29.19, 29.20, 31.68 (C-16 of **3a**), 31.77 (C-16 of **3b**), 32.45 (C-9 of **3a**), 32.49 (C-8 of **3b**), 34.08 (C-2), 40.02 (C-12 of **3b**), 40.15 (C-13 of **3a**), 51.45 (COO*C*H$_3$), 130.35 (C-10 of **3b**), 130.39 (C-11 of **3a**), 147.22 (C-10 of **3a**), 147.40 (C-9 of **3b**), 174.26 (C-1), 200.83 (C-11 of **3b**), and 200.96 (C-12 of **3a**).

EI-MS of saturated (hydrogenated) **3a/3b**, *m/z* (%): 313 (6) ($M^+ + 1$), 312 (10) (M^+), 281 (42) ($M^+ - OCH_3$), 242 (54) (**3a**, McLafferty rearrangement ion), 227 (23) (**3a**, $M^+ - CH_3(CH_2)_5$), 213 (15) (**3b**, $M^+ - CH_3(CH_2)_6$), 210 (23) (**3a**, McLafferty rearrangement ion), 142 (31) (**3b**, McLafferty rearrangement ion), 128 (100) (**3a**, McLafferty rearrangement ion), 127 (18) (**3b**, $M^+ - (CH_2)_9COOCH_3$), 113 (45) (**3a**, $M^+ - (CH_2)_{10}COOCH_3$); high-resolution mass spectral analysis: found, M^+, 312.2664; $C_{19}H_{34}O_3$ requires 312.2664.

*Reaction of **2** with boron trifluoride etherate*. A mixture of **2** (140 mg, 0.45 mmol), boron trifluoride etherate (0.1 mL, 0.8 mmol), and chloroform (5 mL) was stirred for 2 h at room temperature. Aqueous sodium hydrogen carbonate solution (10% w/w, 10 mL) was added, and the reaction mixture was extracted with diethyl ether (3 × 20 mL). The ethereal extract was successively washed with water (2 × 10 mL) and brine (20 mL), and then it was dried over anhydrous magnesium sulfate. The filtrate was evaporated under reduced pressure, and the residue was column chromatographed on silica gel (15 g) using a mixture of *n*-hexane/diethyl ether (90:10, vol/vol) as eluent to give a mixture of methyl 9-oxo-10*E*-octadecenoate (**4a**) and methyl 10-oxo-11*E*-octadecenoate (**4b**) (89 mg, 64%). Physical state: colorless oil. Spectral analysis was conducted on the mixture of compounds **4a** and **4b**. IR (neat): 1741 (*s*, ester C=O, str.), 1698 (*s*, oxo C=O, str.), 1630 (*s*, olefin CH=CHCO, str.), and 1172 (*s*, C=O, str.) cm^{-1}; ^1H NMR ($CDCl_3$, δ_H) 0.88 (*t*, *J* = 6.2 Hz, 3H, C*H*$_3$), 1.26–1.40 (*m*, 14H, C*H*$_2$), 1.43–1.49 (*m*, 2H, 13-*H*$_2$ of **4a** and 14-*H*$_2$ of **4b**), 1.51–1.60 (*m*, 4H, 3-*H*$_2$/7-*H*$_2$ of **4a** and 3-*H*$_2$/8-*H*$_2$ of **4b**), 2.21 (*q*, *J* = 6.8 Hz, 2H, 12-*H*$_2$ of **4a** and 13-*H*$_2$ of **4b**), 2.30 (*t*, *J* = 7.5 Hz, 2H, 2-*H*$_2$), 2.52 (*t*, *J* = 7.4 Hz, 2H, 8-*H*$_2$ of **4a** and 9-*H*$_2$ of **4b**), 3.66 (*s*, 3H, COOC*H*$_3$), 6.08 (*d*, *J* = 15.9 Hz, 1H, 10-*H* of **4a** and 11-*H* of **4b**), and 6.77–6.87 (*dt*, *J* = 9.9, 15.9 Hz, 1H, 11-*H* of **4a** and 12-*H* of **4b**); ^{13}C NMR ($CDCl_3$, δ_C) 14.10 (C-18), 22.55 (C-17 of **4b**), 22.66 (C-17 of **4a**), 24.24 (C-3), 24.35 (C-8 of **4b**), 24.91 (C-7 of **4a**), 28.16 (C-13 of **4a** and C-14 of **4b**), 28.89, 29.00, 29.04, 29.09, 29.13, 29.19, 31.68 (C-16 of **4b**), 31.77 (C-16 of **4a**), 32.46 (C-13 of **4b**), 32.49 (C-12 of **4a**), 34.08 (C-2), 40.03 (C-8 of **4a**), 40.16 (C-9 of **4b**), 51.46 (COO*C*H$_3$), 130.35 (C-10 of **4a**), 130.39 (C-11 of **4b**), 147.24 (C-12 of **4b**), 147.42 (C-11 of **4a**), 174.27 (C-1), and 200.87 (C-9 of **4a** and C-10 of **4b**).

RESULTS AND DISCUSSION

Epoxidation of methyl 9*Z*,11*E*-octadecadienoate with *m*-chloroperoxybenzoic acid gave a mixture of mono-epoxy derivatives (namely, **1**, **2**) and a diepoxy derivative (methyl 9,10-*Z*;11,12-*E*-diepoxy-stearate) (18). These epoxy derivatives could be separated by silica column chromatography into pure components.

Reaction of **1** with BF_3-Et_2O furnished a main fraction (**3a/3b**, R_f = 0.4, *n*-hexane/diethyl ether, 4:1 vol/vol, as developer, 66% yield) by silica column chromatographic separation. GC analysis gave a single peak of an ECL (28) value of 27.6 on cross-linked polyethylene glycol and an ECL value of 20.6 on cross-linked methyl silicone gum.

The IR spectrum provided proof of the presence of a conjugated enone system from the absorption bands at 1630 (olefin CH=CHCO, str.) and 1698 (oxo C=O, str.) cm^{-1}. The UV spectrum confirmed the α,β-unsaturated oxo system from the absorption band at λ_{max} of 237 nm (ε = 14,100).

To determine the positions of the oxo groups in the product mixture of **3a/3b**, a portion of this mixture was hydrogenated over palladium on charcoal to give a mixture of oxo-stearate

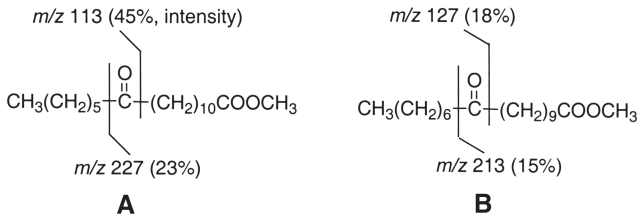

FIG. 1. Mass spectral fragmentation of (A) methyl 12-oxo-octadecanoate and (B) methyl 11-oxo-octadecanoate.

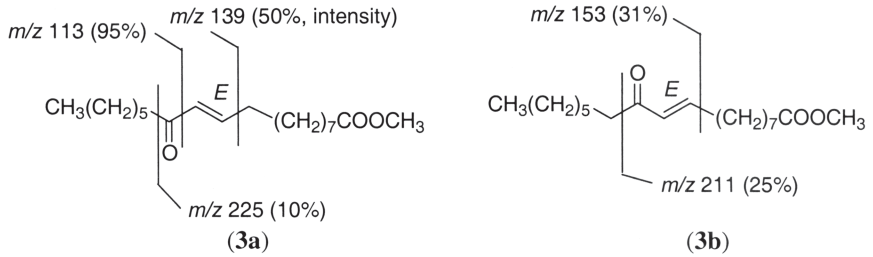

FIG. 2. Mass spectral fragmentation of methyl 12-oxo-10*E*-octadecenoate (**3a**) and methyl 11-oxo-9*E*-octadecenoate (**3b**).

isomers. Mass spectral analysis showed the oxo group to be either at the C-11 (methyl 11-oxo-octadecanoate) [from the fragment ions at *m/z* = 127 (18%), 213 (15%), and 142 (McLafferty rearrangement ion, 31%)] or at the C-12 (methyl 12-oxo-octadecanoate) [from *m/z* = 113 (45%), 227 (23%), and 242 (McLafferty rearrangement ion, 54%)] position (Fig. 1). From the intensity of the peaks, it could be ascertained that the ratio of compounds **3a/3b** was about 3:2.

When the mixture of **3a/3b** (conjugated enones as confirmed by IR and UV spectral data as described above) was subjected to mass spectral analysis, it could be rationalized from the fragmentation pattern that the fragment ions at *m/z* = 113 (95%), 139 (50%), and 225 (10%) arose from the fragmentation of **3a** (methyl 12-oxo-10*E*-octadecenoate), whereas the less intense fragment ions at *m/z* = 153 (31%) and 211 (25%) arose from the fragmentation of compound **3b** (methyl 11-oxo-9*E*-octadecenoate) (Fig. 2).

The high-resolution mass spectral analysis of **3a/3b** gave a molecular ion M^+ = 310.2512, which agreed with the calculated mass of 310.2508 for a C_{18} enone methyl ester of molecular formula $C_{19}H_{34}O_3$.

The ^1H NMR spectrum showed the presence of an olefinic system from the signals at δ_H 6.08 (*d*, 1H, *J* = 15.9 Hz) and 6.82 (*m*, 1H), which were coupled to the carbon shifts at δ_C 130.35/130.39 and 147.22/147.40 in the ^{13}C-^1H COSY NMR spectrum, respectively. The characteristic coupling constant (*J*) of 15.9 Hz of the olefinic protons and the appearance of carbon signals at δ_C 32.45/32.49 in the ^{13}C NMR spectrum showed the olefinic system in the *E*-configuration. The carbon shifts at δ_C 200.83/200.96 were indicative of the presence of an oxo group. The methylene groups adjacent to the oxo group appeared at δ_C 40.02 and 40.15, and were coupled to the protons signals at δ_H 2.52 (*t*, 2H *J* = 7.4 Hz) in the ^{13}C-^1H COSY NMR spectrum. The spectral properties were in agreement with data reported by Pasha and Ahmad (26). The observation of close pairs of signals in the ^{13}C NMR spectrum for the allylic methylene carbon nuclei adjacent to the *E*-olefinic system (at δ_C 32.45/32.49) and for oxo carbon atoms (at δ_C 200.83/200.96) and for the olefinic carbons (at δ_C 130.35/130.39 and δ_C 147.22/147.40) was a firm indication of the presence of two positional isomers in the reaction product. The ratio of **3a/3b** was in the order of 3:2, based on the relative intensities of the olefinic carbon atom signals (130.39/130.35 = 3:2 and δ_C 147.22/147.40 = 3:2) in the ^{13}C NMR spectrum.

In view of the fact that the mixture of **3a/3b** was composed of methyl 12-oxo-10*E*-octadecenoate and methyl 11-oxo-9*E*-octadecenoate, it was necessary to confirm at least one of these two isomers by an authentic sample. Hence, a pure sample of methyl 12-oxo-10*E*-octadecenoate was prepared from methyl ricinoleate (methyl 12-hydroxy-9*Z*–octadecenoate) (29). With reference to the proton and carbon shifts of the pure sample of methyl 12-oxo-10*E*-octadecenoate, the proton and carbon signals arising from compound **3a** in the mixture of **3a/3b** could be readily identified (by assigning the more intense signals to compound **3a**, as the ratio of **3a/3b** was found to be 3:2 as described above). This allowed the signals for compound **3b** also to be identified as shown in the Experimental Procedures section.

Gunstone and his coworkers (30) studied the reactions of nonconjugated epoxyoctadecenoate and diepoxyoctadecanoate with BF_3-Et_2O to yield furanoid esters, dioxo-stearate, bicyclic ketals, and hydroxy cyclic ethers. However, the mechanism leading to these products was not discussed. We propose a plausible mechanism for the reaction between compound **1** and boron trifluoride as outlined in Scheme 1. Boron trifluoride, acting as a Lewis acid, attacks the oxygen atom of the epoxy system and causes the ring to open at either the C-11 or C-12 position of the alkyl chain. When ring opening occurs at C-12, an allylic carbocation is formed. Deprotonation at C-12 occurs, which gives rise to a conjugated diene intermediate. The oxo group is formed at the C-12 position with the double bond migrating to the C-10/C-11 position. Compound **3a** is formed as the dominant product. When the epoxy ring opens at the C-11 position of the alkyl chain instead, a less stable carbocation is formed as compared with the allylic carbocation. A 1,2-hydride transfer from C-11 to C-12 follows to give rise to an initial *cis*-enone intermediate, which isomerizes to yield compound **3b**. This mechanism is supported by the acid-catalyzed reaction of epoxides as described by Fujimoto *et al.* (31), Pocker and Ronald (32), and Bach and Domagala (33).

Reaction of **2** with BF_3-Et_2O gave a major fraction (R_f = 0.4, *n*-hexane/diethyl ether, 4:1 vol/vol, as developer; 64% yield) by silica column chromatography. Following a similar interpretation of the spectroscopic and spectrometric results

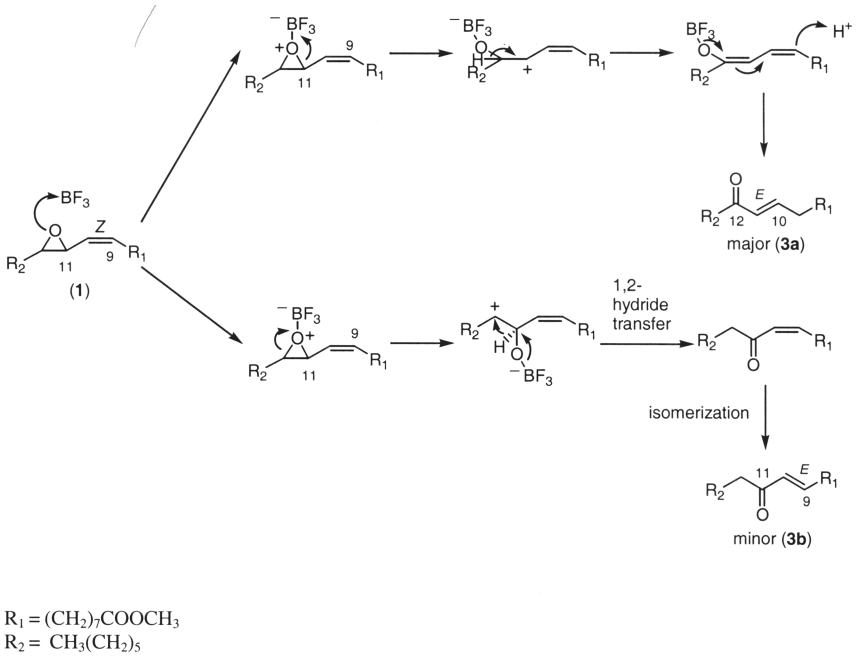

$R_1 = (CH_2)_7COOCH_3$
$R_2 = CH_3(CH_2)_5$

SCHEME 1

as described above for the identification of compounds **3a** and **3b**, the products from the reaction of **2** with BF_3-Et_2O were identified as **4a** and **4b** in a ratio of *ca*. 7:3. The formation of these products would follow the same proposed reaction mechanism as described for compound **1** (Scheme 1).

In summary, fatty esters with an allylically positioned epoxy system, such as compounds **1** and **2**, are readily converted to a mixture of α,β-unsaturated *trans*-enone fatty ester isomers by boron trifluoride etherate.

ACKNOWLEDGMENT

The authors thank the Science Faculty Collaborative Seed Grant, 2002, Lipid Research Fund (Hong Kong University), the Research Grants Council of Hong Kong, the Committee on Research and Conference Grants of the University of Hong Kong, for financial assistance.

REFERENCES

1. Fritsche, S., and Fritsche, J. (1998) Occurrence of Conjugated Linoleic Acid Isomers in Beef, *J. Am. Oil Chem. Soc. 75*, 1449–1451.
2. Fritsche, J., and Steinhart, H. (1998) Amounts of Conjugated Linoleic Acid (CLA) in German Foods and Evaluation of Daily Intake, *Z. Lebensm. Unters. Forsch. A. 206*, 77–82.
3. Parodi, P.W. (1999) Conjugated Linoleic Acid: The Early Years, in *Advances in Conjugated Linoleic Acid Research, Volume 1* (Yurawecz, M.P., Mossoba, M.M., Kramer, J.K.G., Pariza, M.W., and Nelson, G.J., eds.), pp. 1–11, AOCS Press, Champaign.
4. Jensen, R.G., Lammi-Keefe, C.J., Hill, D.W., Kind, A.J., and Henderson, R. (1998) The Anticarcinogenic Conjugated Fatty Acid, 9*c*,11*t*-18:2, in Human Milk: Confirmation of Its Presence, *J. Human Lact. 14*, 23–27.
5. Fogerty, A.C., Ford, G.L., and Svoronos, D. (1998) Octadec-9,11-dienoic Acid in Foodstuffs and in the Lipids of Human Blood and Breast Milk, *Nutr. Rep. Int. 38*, 937–944.
6. McGuire, M.K., Park, Y., Behre, R.A., Harrison, L.Y., Shultz, T.D., and McGuire, M.A. (1997) Conjugated Linoleic Acid Concentrations of Human Milk and Infant Formula, *Nutr. Res. 17*, 1277–1283.
7. Griinari, J.M., Corl, B.A., Lacy, S.H., Chouinard, P.Y., Nurmela, K.V., and Bauman, D.E. (2000) Conjugated Linoleic Acid Is Synthesized Endogenously in Lactating Daily Cows by Δ^9-Desaturase, *J. Nutr. 130*, 2285–2291.
8. Griinari, J.M., Chouinard, P.Y., and Bauman, D.E. (1997) *Trans* Fatty Acid Hypothesis of Milk Fat Depression Revised, *Proc. Cornell Nutr. Conf. Feed Manuf.,* 208–216.
9. Chin, S.F., Storkson, J.M., and Pariza, M.W. (1993) Conjugated Dienoic Derivatives of Linoleic Acid—A New Class of Food Derived Anticarcinogens, *Am. Chem. Soc. Symp. Ser. 528*, 262–271.
10. Ha, Y.L., Grimm, N.K., and Pariza, M.W. (1987) Anticarcinogens from Fried Ground Beef: Heat Altered Derivatives of Linoleic Acid, *Carcinogenesis 8*, 1881–1887.
11. Ha, Y.L., Storkson, J.M., and Pariza, M.W. (1990) Inhibition of Benzo(α)pyrene-Induced Mouse Forestomach Neoplasia by Conjugated Dienoic Derivatives of Linoleic Acid, *Cancer Res. 50*, 1097–1101.
12. Park, Y., Albright, K.J., Liu, W., Storkson, J.M., Cook, M.E., and Pariza, M.W. (1997) Effect of Conjugated Linoleic Acid on Body Composition in Mice, *Lipids 32*, 853–858.
13. Park, Y., Albright, K.J., Storkson, J.M., Liu, W., Cook, M.E., and Pariza, M.W. (1999) Changes in Body Composition in Mice During Feeding and Withdrawal of Conjugated Linoleic Acid, *Lipids 34*, 243–248.
14. Park, Y., Storkson, J.M., Albright, K.J., Liu, W., and Pariza, M.W. (1999) Evidence That the *trans*-10,*cis*-12 Isomer of Conjugated Linoleic Acid Induces Body Composition Changes in Mice, *Lipids 34*, 235–241.
15. Nicolosi, R.J., Rogers, E.J., Kritchevsky, D., Scimeca, J.A., and Huth, P.J. (1997) Dietary Conjugated Linoleic Acid Reduces

Plasma Lipoproteins and Early Aortic Atherosclerosis in Hypercholesterolemic Hamsters, *Artery 22*, 266–277.
16. Yurawecz, M.P., Mossoba, M.M., Kramer, J.K.G., Pariza, M.W., and Nelson, G.J. (eds.) (1999) *Advances in Conjugated Linoleic Acid Research, Volume 1*, AOCS Press, Champaign.
17. Sébédio, J.-L., Christie, W.W., and Adlof, R. (eds.) (2003) *Advances in Conjugated Linoleic Acid Research, Volume 2*, AOCS Press, Champaign.
18. Lie Ken Jie, M.S.F., Lam, C.N.W., Ho, J.C.M., and Lau, M.M.L. (2003) Epoxidation of a Conjugated Linoleic Acid Isomer, *Eur. J. Lipid Sci. Technol. 105*, 391–396.
19. Mahmood, C., Daulatabad, J.D., Mulla, G.M.M., Mirajkar, A.M., and Hosamani, K.M. (1991) 7-Keto-octadec-*cis*-11-enoic Acid from *Gardenia lucida* Seed Oil, *Phytochemistry 30*, 2399–2400.
20. Daulatabad, C.D., Bhat, G.G., and Jamkhandi, A.M. (1996) A Novel Keto Fatty Acid from *Cassia occidentalis* Seed Oil, *Fett-Lipid 98*, 176–177.
21. Daulatabad, C.D., and Jamkhandi, A.M. (1997) A Keto Fatty Acid from *Amoora rohituka* Seed Oil, *Phytochemistry 46*, 155–156.
22. Jehan, C.M., Daulatabad, D., and Mirajkar, A.M. (1990) A Keto Fatty Acid from *Lagerstroemia speciosa* Seed Oil, *Phytochemistry 29*, 2323–2324.
23. Jamal, S., Ahmad, I., Agarwal, R., Ahmad, M., and Osman, S.M. (1987) A Novel Oxo Fatty Acid in *Plantago ovata* Seed Oil, *Phytochemistry 26*, 3067–3069.
24. Daulatabad, C.D., and Bhat, G.G. (1997) Occurrence of Keto Fatty Acid in *Hibiscus ficulneus* Seed Oil, *J. Food Sci. Technol. Mysore 34*, 240–241.
25. Daulatabad, C.D., Bhat, G.G., and Jamkhandi, A.M. (1996) A Keto Fatty Acid from *Smilax macrophylla* Seed Oil, *Phytochemistry 42*, 889–890.
26. Pasha, M.K., and Ahmad, F. (1993) Synthesis of Oxygenated Fatty Acid Esters from Santalbic Acid Ester, *Lipids 28*, 1027–1031.
27. Wong, K.P. (1991) Derivatives of 2,5-Disubstituted C_{18} Furanoid Fatty Esters, M. Phil. Thesis, The University of Hong Kong, pp. 118–121.
28. Miwa, T.K., Mikolajczak, K.L., Earle, F.R., and Wolff, I.A. (1960) Gas Chromatographic Characterization of Fatty Acids. Identification Constants for Mono- and Dicarboxylic Methyl Esters, *Anal. Chem. 32*, 1739–1742.
29. Syed-Rahmatullah, M.S.K. (1991) Synthesis and Physical Properties of C_{18} Azido-Oxygenated and *N*-Heterocyclic Fatty Acid Derivatives, Ph.D. Thesis, The University of Hong Kong, pp. 141–144.
30. Gunstone, F.D., and Schuler, H.R. (1975) Fatty Acids. 45. Epoxyoctadecenoates, Dihydroxyoctadecenoates, and Diepoxyoctadecanoates—Preparation, Chromatographic Properties, and Reaction with Boron-Trifluoride Etherate, *Chem. Phys. Lipids 15*, 174–188.
31. Fujimoto, Y., Kanzawa, Y., Ikuina, Y., Kakinuma, K., and Ikekawa, N. (1989) Mechanism of the Boron Trifluoride Etherate-Catalysed Rearrangement of an Acyclic Trisubstituted Epoxide to a Carbonyl Compound, *J. Chem. Soc., Chem. Commun. (16)*, 1107–1109.
32. Pocker, Y., and Ronald, B.P. (1978) A Nuclear Magnetic Resonance Kinetic Study of the Acid-Catalyzed Epoxide Ring Opening of Tetramethylethylene Oxide, *J. Am. Chem. Soc. 100*, 3122–3127.
33. Bach, R.D., and Domagala, J.M. (1984) The Effect of Lewis Acid and Solvent on Concerted 1,2-Acyl Migration, *J. Org. Chem. 49*, 4181–4188.

[Received April 21, 2004; accepted August 7, 2004]

Successful Utilization of Lyophilized Lipoprotein(a) as a Biological Reagent

Angelo M. Scanu[a,b,*], Janet Hinman[a], Ditta Pfaffinger[a], and Celina Edelstein[a]

Departments of [a]Medicine and [b]Biochemistry and Molecular Biology, University of Chicago, Chicago, Illinois 60637

ABSTRACT: Lipoprotein(a) [Lp(a)] represents a class of lipoprotein particles having as a protein moiety apoB-100 linked by a single disulfide bond to apolipoprotein(a) [apo(a)], a multikringle structure with a high degree of homology with plasminogen. A recognized feature of Lp(a) is its instability on storage caused by attendant protein and lipid modifications that affect the structural, functional, and immunological properties of this lipoprotein. Here we present data showing that, under appropriate conditions of cryopreservation, Lp(a) retains the properties of the freshly isolated product, and we provide examples supporting the stability of this cryopreserved product as a primary standard in immunoassay settings and in cell culture systems.

Paper no. L9510 in *Lipids 39,* 589–593 (June 2004).

Lipoprotein(a) [Lp(a)] is known to be unstable on storage, either in the plasma or after isolation (1,2). This problem, which is common to apolipoprotein B-100 (apoB-100)-containing lipoproteins, is heightened in the case of Lp(a) by the fact that apoB-100 is linked covalently to apolipoprotein(a) [apo(a)], a multikringle structure that itself is prone to modifications (3). Like apoB-100, apo(a) can be modified by oxidative and proteolytic events, particularly by the action of enzymes of the elastase and metalloproteinase families (4). Moreover, like LDL, Lp(a) may be modified by oxidative and lipolytic events (4). Given this ready proclivity to degradation, the preservation of Lp(a) stability on storage is an important issue when studying this lipoprotein, both from a structural and from a biological standpoint. We reported previously that Lp(a), stored in a lyophilized state in the presence, but not in the absence, of an appropriate cryopreservative (sucrose), retains the properties of the nonlyophilized product upon reconstitution in aqueous buffers (5). Those observations prompted us to investigate whether lyophilized Lp(a) [lyo-Lp(a)] can serve as an all-around reagent and be an effective substitute for a freshly isolated product. In the current study we focused our attention on the use of lyo-Lp(a) in three areas: (i) as a primary standard in immunochemical analyses; (ii) its reactivity to a monoclonal antibody known to react against phosphorylcholine (6) and functionally identical to autoantibody EO6, which reacts against lysine-oxidized (ox) phospholipid adducts (7); and (iii) its ability to stimulate interleukin 8 (IL-8) production in cultured human macrophages (8). The results of these studies, acknowledged in the Official Report of the Lp(a) Study Group (9), are the subject of this report.

*To whom correspondence should be addressed at Department of Medicine, MC5041, University of Chicago, 5841 S. Maryland Ave., Chicago, IL 60637. E-mail: ascanu@medicine.bsd.uchicago.edu

Abbreviations: APMSF, (4-amidinophenyl)-methanesulfonyl fluoride; apo(a), apolipoprotein(a); apoB-100, apolipoprotein B-100; G3PDH, glyceraldehyde-3-phosphate-dehydrogenase; KI, kallikrein inactivator; IL-8, interleukin 8; Lp(a), lipoprotein(a); lyo-Lp(a), lyophilized Lp(a); ox, oxidized.

EXPERIMENTAL PROCEDURES

Chemicals and reagents. Materials were purchased from the following sources: Cyanogen bromide-Sepharose 4B, ε-aminocaproic acid, (4-amidinophenyl)-methanesulfonyl fluoride (APMSF), PMA, EDTA, L-lysine, β-mercaptoethanol, BHT formamide, and formaldehyde were from Sigma Chemical Company (St. Louis, MO). Kallikrein inactivator (KI) was purchased from Calbiochem Co. (San Diego, CA). M.W. standards were from Pharmacia-LKB (Alameda, CA). Immobilon-P membranes were from Millipore (Bedford, MA), and an enhanced chemiluminescence kit (ECL Western Blotting Detection kit) was from Amersham (Arlington Heights, IL). All the tissue culture reagents were obtained from Life Technologies, Inc. (Grand Island, NY) and were of low endotoxin grade. Nuclease-free water and the RNAse-free plasticware were from Ambion, Inc. (Austin, TX). All other chemicals were of reagent grade.

Polyclonal antisera. Rabbit affinity-purified antibodies to Lp(a), apo(a), and LDL were prepared as described previously (10). Anti-Lp(a) and anti-apo(a) did not react against LDL or plasminogen, and anti-LDL was unreactive to apo(a).

T-15 monoclonal antibody. The mouse myeloma B cell line AB1-2 was obtained from the American Type Culture Collection (ATCC number HB-33) and propagated in the Immunology Core Laboratory of the University of Chicago, which also attended to the purification of the monoclonal antibody and isotyped it as IgG1. This monoclonal antibody is identical in specificity to the monoclonal idiotype EO6 (11), which we have recently shown to react with the ox-phospholipid–lysine adducts present both in freshly prepared Lp(a) and in free apo(a) isolated from it (7).

Isolation of Lp(a) from plasma. We used healthy male donors with levels of Lp(a) expressed as protein [apoB-100 plus apo(a)] of 10–30 mg/dL having a single apo(a) size isoform. To prevent lipoprotein degradation, the plasma obtained by plasmapheresis was adjusted with 0.15% EDTA, 0.01% NaN_3, 10,000 U/L KI, and 1 mM APMSF. Lp(a) was isolated by sequential ultracentrifugation and lysine-Sepharose chromatography as described previously (12). The purity of the product was assessed by mobility on precast 1% agarose gels (Ciba-Corning, Palo Alto, CA) and Western blots of SDS-PAGE using anti-Lp(a) and anti-apoB-100. Blood donors signed an informed consent form approved by the Institutional Review Board of the University of Chicago.

Phenotyping of apo(a). Apo(a) phenotyping was performed on either reduced plasma, isolated apo(a), or Lp(a) samples by SDS-PAGE, followed by immunoblotting using anti-Lp(a). The mobility of the individual apo(a) bands was compared with isolated apo(a) isoforms of known M.W. Some of the standards consisting of number-based recombinant apo(a) kringle IV were a gift from Dr. Eduardo Angles-Cano (INSERM U.143, Paris, France).

Storage studies. The freshly isolated Lp(a) was dialyzed against 10 mM phosphate buffer, pH 7.2, containing 1 mM EDTA and 0.02% NaN_3. Each preparation was stored at 4°C in 1-mL airtight vials.

Lyophilization step. Before lyophilization, fresh Lp(a) was dialyzed against 8 L of 5 mM NH_4HCO_3, after which sucrose (5% final) was added as described previously (5), lyophilized, and then stored at –20°C, both in 500-µL vials containing 1 mg Lp(a) protein/mL (destined for small-scale studies) and 1.5 mL vials having the same Lp(a) protein concentration (destined for large-scale studies).

Reconstitution step. Prior to use, the lyophilized samples were reconstituted using the desired buffer, sterile filtered, and either studied immediately or stored at 4°C in airtight sterile vials. For the purpose of quantification by ELISA, we saw no need to remove the sucrose from the sample because of the high dilutions (>100-fold) required for the assay. The reconstitution buffer was 10 mM PO_4, pH 7.4, containing 1 mM EDTA, 0.02% NaN_3, and 1 mM APMSF. For other purposes, where sucrose could have represented a confounding factor, the cryopreservative was removed by dialysis against a total volume of 8 L of the desired buffer. In every instance, the reconstituted samples were sterile filtered before use.

Lp(a) quantification. Lp(a) was quantified in terms of protein, i.e., apoB plus apo(a), by a sandwich ELISA essentially as described previously (10), except that affinity-purified polyclonal antibodies from rabbit were used for capture [anti-Lp(a) IgG] and anti-apoB-100 IgG was conjugated to alkaline phosphatase for detection. The values were expressed in mg/dL. In the initial studies, as a primary standard, we used a freshly purified Lp(a) in which the total protein mass was determined using the Bio-Rad DC Protein assay (Bio-Rad, Hercules, CA). The freshly reconstituted lyo-Lp(a) was calibrated against the primary standard and an internal reference plasma sample with a known Lp(a) protein concentration that favorably matched the internal standard sample kindly provided by Dr. Santica Marcovina of the Department of Medicine of the University of Washington, Seattle (see the Results section for more details). In our format, the assay was unaffected by apo(a) size.

Electrophoretic methods. SDS-PAGE (4% polyacrylamide) was performed on a Novex system (Novex, San Diego, CA) for 1.5 h at constant voltage (120 V) at 22°C as described previously (5). Immediately after electrophoresis, the gels were placed onto Immobilon-P sheets (Millipore Corp.) that were previously wetted with a buffer containing 48 mM Tris and 39 mM glycine, pH 8.9. Blotting was performed on a horizontal semidry electroblot apparatus (Pharmacia-LKB) at 0.8–1 mA/cm^2 for 45 min at room temperature.

Agarose gel electrophoresis was carried out on Agarose Universal Electrophoresis film (Ciba Corning Diagnostics Corp., Alameda, CA). After electrophoresis, the lipoproteins were fixed and stained with Fat Red 7B.

Immunoblotting. After electroblotting, the Immobilon-P blots were blocked in PBS containing 5% nonfat dry powdered milk and 0.3% Tween 20, followed by incubation with anti-Lp(a) or anti-apoB antibody. The blots were washed and incubated with anti-rabbit horseradish peroxidase-labeled IgG. Subsequently, the blots were developed with the ECL Western Detection Reagent according to the manufacturer's instructions.

Detection of ox-products with the IgG1 monoclonal antibody T-15 was performed by first blocking the Immobilon-P sheets with SuperBlock (Pierce, Rockford, IL) for 1 h at 23°C, followed by incubation for 18 h at 4°C with T-15 in 10% SuperBlock after washing (three times at 15 min each) (7). The membranes were visualized as described except that goat anti-mouse IgG peroxidase-conjugated antibodies were used.

Cell culture studies. We used THP-1 monocytes transformed into macrophages by PMA as described in our previous studies (8). After 72 h, the cells were washed once with RPMI 1640 serum-free medium and incubated with a new aliquot of the serum-free medium for 16 h. At this point, the medium was replaced with a fresh serum-free medium containing indicated amounts of either fresh or lyophilized samples for the indicated period of time. At the end of the incubation period, the cells were immediately processed for the isolation of RNA as described next. The supernatants from each well were collected, centrifuged to eliminate debris, and either used for determination of the concentration of IL-8 by ELISA or frozen at –20°C until further analysis. All the experiments were conducted in duplicate and were repeated at least twice.

Analysis of RNA. Total cellular RNA was isolated using the Trizol reagent (Life Technologies). Quality of the RNA preparations was verified by 1% denatured formaldehyde agarose gel electrophoresis as described by Sambrook *et al.* (13).

For Northern blot analysis, 10 µg of total RNA as fractionated by 1% denatured formaldehyde agarose gel electrophoresis and blotted onto a Zeta Probe Nylon membrane (Bio-Rad) by

capillary transfer according to the manufacturer's instructions. After cross-linking with UV irradiation (Stratalinker model 2400; Stratagene, La Jolla, CA), the membranes were hybridized with a human radiolabeled IL-8 probe (289 bp), stripped, and subsequently hybridized with a human radiolabeled glyceraldehyde-3-phosphate-dehydrogenase (G3PDH) probe (983 bp). For preparation of the hybridization probes, total RNA isolated from THP-1 cells was subjected to reverse transcriptase-PCR by using the Super Script One-Step kit from Life Technologies under the conditions described previously (8) and the corresponding PCR primers from Clontech (Palo Alto, CA) as described previously (8).

Hybridization and washes were performed as recommended by the manufacturer of the membrane (Bio-Rad). After autoradiography, the signals were quantified by densitometric analysis (ImageQuant software, version 3.3; Molecular Dynamics, Sunnyvale, CA), and the relative mRNA level of IL-8 was normalized against that of G3PDH.

Determination of the IL-8 concentration in culture media. The amount of IL-8 released in the media was assessed by ELISA (Biosource International, Camarillo, CA) according to the manufacturer's instructions. All of the measurements were conducted in triplicate.

RESULTS

Lyo-Lp(a) as a primary standard. Lyo-Lp(a) was reconstituted with 10 mM PO_4 buffer, pH 7.4, containing 1 mM EDTA, 0.02% NaN_3, and 1 mM APMSF. Once sterile filtered, the sample was diluted so that the final protein concentration was in the range of the fresh Lp(a) preparation, as determined by the Bio-Rad assay. The ELISA used fresh Lp(a) as a primary standard and a plasma reference sample of a known Lp(a) protein concentration. These studies showed an equivalent performance between fresh and lyo-Lp(a) and an excellent agreement between the expected theoretical and ELISA values (5). Therefore, the subsequent studies were carried out using lyo-Lp(a) as the sole primary standard. The results in Figure 1 show that the Lp(a) concentrations of three internal plasma reference samples remained within two SD of the mean for 30 mon, the limit of our observation.

Reactivity of lyo-Lp(a) to monoclonal T-15. We previously reported that Lp(a) reacts with EO6, the natural monoclonal autoantibody that recognizes the oxidized PC group linked as a Schiff base to apo(a) (7). In this study we used monoclonal autoantibody T-15, which has been shown to have immunological properties similar to that of EO6. The results in Figure 2 provide evidence that both fresh Lp(a) (lane 3) and its lyophilized counterpart (lane 1) reacted against T-15. Moreover, this reactivity was retained even after storage of reconstituted Lp(a) for 6 mon (lane 2). No later studies were conducted.

Stimulation of IL-8 production in THP-1 macrophages by lyo-Lp(a). THP-1 macrophages were incubated separately with fresh Lp(a) and reconstituted lyo-Lp(a) and then evaluated for the level of IL-8 expression by both Northern blot analysis and IL-8 protein concentration in the medium by

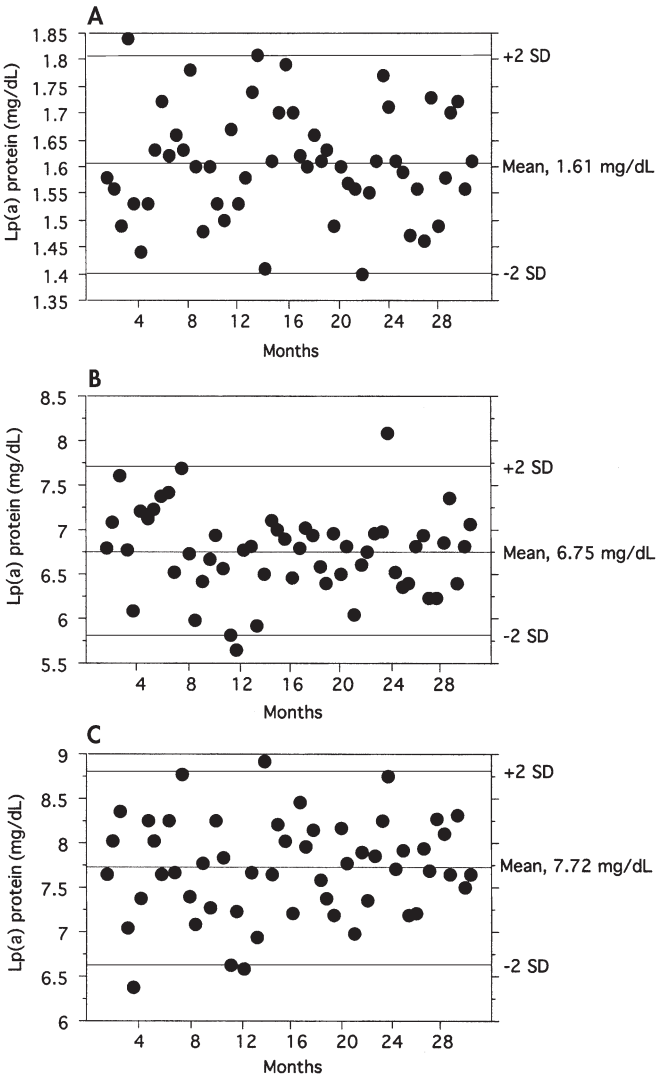

FIG. 1. Lipoprotein(a) [Lp(a)] protein concentrations of the plasma samples used as internal standards determined as a function of time using the ELISA as described in the Experimental Procedures section. Lyophilized Lp(a) [lyo-Lp(a)] was reconstituted in 10 mM PO_4, pH 7.4, containing 1 mM EDTA, 0.02% NaN_3, and 1 mM (4-amidinophenyl)-methanesulfonyl fluoride (APMSF), sterile filtered, stored at 4°C, and used as a primary standard. The three plasma samples used as internal standards were obtained from normal healthy donors and stored at –80°C in small aliquots. Panels A, B, and C refer to the three different donors and give mean Lp(a) protein levels of 1.61, 6.75, and 7.72 mg/dL, respectively.

ELISA. As shown in Figure 3, treatment of the THP-1 macrophages with either Lp(a) preparation resulted in a comparable stimulation of both IL-8 mRNA and the secretion of IL-8 into the culture medium, namely, about a twofold increase over the control cells that were incubated with only medium.

DISCUSSION

The present studies provide evidence that lyo-Lp(a), when reconstituted in appropriate aqueous buffers, behaves as its

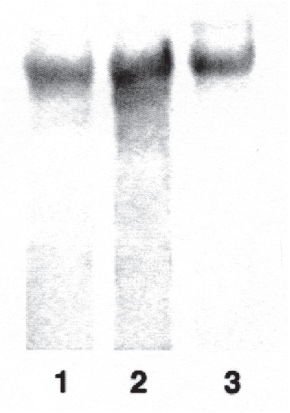

FIG. 2. Western blot analyses of Lp(a) before and after lyophilization carried out in the presence of 5% sucrose. The lyo-Lp(a) was reconstituted in 10 mM PO_4, pH 7.4, containing 1 mM EDTA, 0.02% NaN_3, and 1 mM APMSF and either analyzed immediately or stored at 4°C for 6 mon. The analyses were carried out on 4% SDS-PAGE under reduced conditions and were Western blotted. Monoclonal antibody T-15 was used to probe the blot. Lane 1, lyo-Lp(a) reconstituted and applied immediately; lane 2, lyo-Lp(a) reconstituted and stored for 6 mon; lane 3, Lp(a) untreated, freshly prepared. For abbreviations see Figure 1.

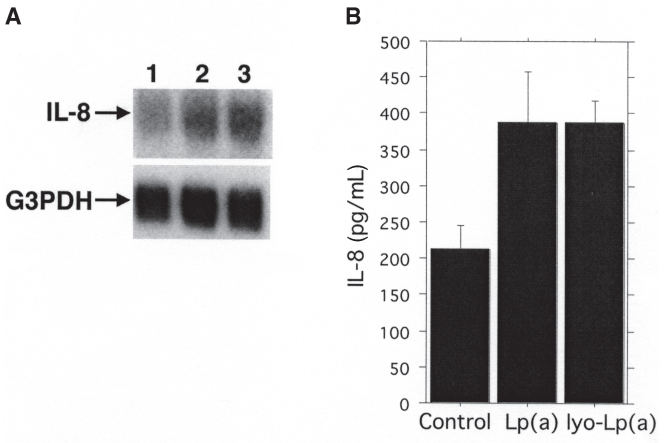

FIG. 3. Effect of lyo-Lp(a) on the production of interleukin 8 (IL-8) by THP-1 macrophages. The cells were incubated with either Lp(a) or lyophilized and reconstituted Lp(a) each at 220 nM for 24 h at 37°C. (A) Northern blot analysis of total cellular RNA extracted at the end of the incubation: lane 1, medium from unstimulated cells; lane 2, fresh, untreated Lp(a); lane 3, lyo-Lp(a), reconstituted. (B) Concentration of IL-8 released into the cell culture medium as determined by ELISA. The data are representative of two independent experiments, each conducted in duplicate. G3PDH, glyceraldehyde-3-phosphate-dehydrogenase; for other abbreviations see Figure 1.

nonlyophilized counterpart in the immunological and biological systems examined. As shown in Figure 1, lyo-Lp(a) effectively served as a primary standard in immunoassays directed at the quantification of Lp(a) over a 2-yr period. This documentation of stability is of particular importance since the lack of a stable primary standard has been among the limiting factors in Lp(a) assay performance and reproducibility (9). The theoretically indefinite shelf life of lyo-Lp(a) also offers the advantage that it reduces the bleeding frequency of human Lp(a) donors and ensures the availability of a viable Lp(a) from subjects not available for long-term follow-up. Moreover, the storage flexibility of lyo-Lp(a), including at room temperature, markedly facilitates sample handling and shipping options.

In a previous study we showed parallel behavior between lyo-Lp(a) and its nonlyophilized counterpart in terms of ultracentrifugal, electrophoretic, lysine-binding, and immunochemical behavior as well as the ability to generate free apo(a) (5). Those data, coupled with the current findings, support the conclusion that lyophilization, in the presence of a cryopreservative such as sucrose, does not significantly affect the structural and functional properties of Lp(a). This conclusion is corroborated by the current observation that lyo-Lp(a), like the nonlyophilized product, reacts with T-15, a monoclonal antibody shown previously to be identical in immunological properties to monoclonal EO6 (11), which, in turn, specifically recognizes ox-phospholipid–lysine adducts in apo(a) kringle V (7). These observations provide an exquisite example of epitope preservation in apo(a) made possible by the lyophilization procedure used in this study. They are of biological importance in that lyo-Lp(a), like untreated Lp(a), in cultured THP-1 macrophages stimulates the production of IL-8, a process that, according to our previous studies (7), involves kringle V, likely *via* ox-phospholipid adducts.

Variability in results within and outside laboratories has been a recognized problem for those working in the Lp(a) field (9). This variability may be attributable to differences in the structural properties of the Lp(a) preparations used. However, other factors might play a role, including inadequate storage and inadequate knowledge of the properties of Lp(a), both preventable issues, as indicated by the results of the current study.

ACKNOWLEDGMENTS

This work was supported by National Institutes of Health Grants HL 63209, HL 63115, and NHLBI-NIH Contract N01 HV88175.

REFERENCES

1. Fless, G.M., ZumMallen, M.E., and Scanu, A.M. (1986) Physicochemical Properties of Apolipoprotein(a) and Lipoprotein(a) Derived from the Dissociation of Human Plasma Lipoprotein(a), *J. Biol. Chem. 261,* 8712–8718.
2. Marcovina, S.M., Albers, J.J., Scanu, A.M., Kennedy, H., Giaculli, F., Berg, K., Couderc, R., Dati, F., Rifai, N., Sakurabayashi, I., *et al.* (2000) Use of a Reference Material Proposed by the International Federation of Clinical Chemistry and Laboratory Medicine to Evaluate Analytical Methods for the Determination of Plasma Lipoprotein(a), *Clin. Chem. 46,* 1956–1967.
3. Scanu, A.M. (2003) Lipoprotein(a) and the Atherothrombotic Process: Mechanistic Insights and Clinical Implications, *Curr. Atheroscler. Rep. 5,* 106–113.
4. Edelstein, C., Italia, J.A., Klezovitch, O., and Scanu, A.M. (1996) Functional and Metabolic Differences Between Elastase-Generated Fragments of Human Lipoprotein(a) and Apolipoprotein(a), *J. Lipid Res. 37,* 1786–1801.
5. Edelstein, C., Hinman, J., Marcovina, S.M., and Scanu, A.M. (2001) Preservation of the Properties of Free- and Lipoprotein-Bound Apolipoprotein(a) After Lyophilization in the Presence of Cryopreservatives, *Anal. Biochem. 288,* 201–208.

6. Kearney, J.F., Barletta, R., Quan, Z.S., and Quintans, J. (1981) Monoclonal vs. Heterogeneous Anti-H-8 Antibodies in the Analysis of the Antiphosphorylcholine Response in BALB/c Mice, *Eur. J. Immunol. 11,* 877–883.
7. Edelstein, C., Pfaffinger, D., Hinman, J., Miller, E., Lipkind, G., Tsimikas, S., Bergmark, C., Getz, G.S., Witztum, J.L., and Scanu, A.M. (2003) Lysine–Phosphatidylcholine Adducts in Kringle V Impart Unique Immunological and Potential Proinflammatory Properties to Human Apolipoprotein(a), *J. Biol. Chem. 278,* 52841–52847.
8. Klezovitch, O., Edelstein, C., and Scanu, A.M. (2001) Stimulation of Interleukin-8 Production in Human THP-1 Macrophages by Apolipoprotein(a): Evidence for a Critical Involvement of Elements of Its C-Terminal Domain, *J. Biol. Chem. 276,* 46864–46869.
9. Marcovina, S.M., Koschinsky, M.L., Albers, J.J., and Skarlatos, S. (2003) Report of the National Heart, Lung, and Blood Institute Workshop on Lipoprotein(a) and Cardiovascular Disease: Recent Advances and Future Directions, *Clin. Chem. 49,* 1785–1796.
10. Fless, G.M., Snyder, M.L., and Scanu, A.M. (1989) Enzyme-Linked Immunoassay for Lp(a), *J. Lipid Res. 30,* 651–662.
11. Shaw, P. X., Hörkkö, S., Chang-Kyung, M., Curtiss, L.K., Palinski, W., Silverman, G.J., and Witztum, J.L. (2000) Natural Antibodies with the T15 Idiotype May Act in Atherosclerosis, Apopotic Clearance, and Protective Immunity, *J. Clin. Invest. 105,* 1731–1740.
12. Fless, G.M., ZumMallen, M.E., and Scanu, A.M. (1985) Isolation of Apolipoprotein(a) from Lipoprotein(a), *J. Lipid Res. 26,* 1224-1229.
13. Sambrook, J., Fritsch, E.F., and Maniatis, T. (1989) *Molecular Cloning: A Laboratory Manual,* 2nd edn., Cold Spring Harbor Laboratory, Cold Spring Harbor, NY.

[Received May 27, 2004; accepted August 3, 2004]

A Short, Concise Route to Diphosphatidylglycerol (cardiolipin) and Its Variants

U. Murali Krishna, Moghis U. Ahmad, Shoukath M. Ali, and Imran Ahmad*

NeoPharm, Inc., Waukegan, Illinois 60085

ABSTRACT: A new approach is described for the synthesis of the cardiolipin family of phospholipids that uses phosphonium salt methodology. The method involves the reaction of 2-O-protected glycerol with a trialkyl phosphite derived from 1,2-diacyl-*sn*-glycerol in the presence of pyridinium bromide perbromide and triethylamine to afford the phosphoric triesters. The synthesis involves three steps and allows the preparation of a wide range of cardiolipins with different substitution patterns and chain lengths, including unsaturated derivatives. The use of inexpensive protecting groups and the ease of purification facilitate this synthetic route and allow its scale-up in a higher overall yield (72%) than the literature methods.

Paper no. L9491 in *Lipids 39,* 595–600 (June 2004).

The ready availability of chemically well-defined complex lipids is important to many areas of biomedical research. Phospholipids are involved in a wide range of physiological and bioregulatory processes (1,2). Some of the most potent lipid compounds occur in very low concentrations in the cell such that the preparation of synthetic derivatives represents a clear prerequisite to the elucidation of their biochemical mechanism of action. These compounds are required for both structural and dynamic studies of biomembranes, with particular emphasis on establishing structure–activity relationships with respect to phospholipid–protein interactions. Cardiolipin (CL), also known as diphosphatidylglycerol (Scheme 1), constitutes a class of complex anionic phospholipids characterized by the type and distribution of FA; CL is typically purified from cell membranes of tissues associated with high metabolic activity, including the mitochondria of heart and skeletal muscles (3,4). CL is integral to the normal functioning of mitochondrial electron transport and energy metabolism. The presence of CL in mitochondrial inner membranes suggests that it is involved in site-directed structure–function relationships with mitochondrial transporters and electron transfer complexes (5–8). Modification of the FA composition of CL would exert a major impact on phospholipid packing and interaction with proteins in the bilayer. CL present in mitochondrial membranes mediates the targeting of tBid to mitochondria through a three-helix domain in tBid, implicating CL in the pathway for the release of cytochrome *c* (9). CL

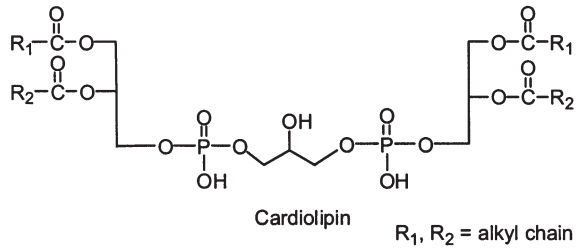

SCHEME 1

is utilized in drug delivery systems in the form of liposomes (10) to enhance the therapeutic efficacy of antitumor drugs. The encapsulation of chemotherapeutic agents (11) in a macromolecular carrier, such as liposomes, significantly reduces the distribution volume and thereby increases the concentration of drug in the tumor. This results in a decrease in the amount and types of nonspecific toxicities and in an increase in the amount of drug that can be effectively delivered to the tumor. Under optimal conditions, the drug is carried within the liposomal aqueous space while in circulation but leaks at a sufficient rate to become bioavailable on arrival at the tumor. The liposome protects the drug from metabolism and inactivation in the plasma and, because of size limitations in the transport of large molecules or carriers across the healthy endothelium, the drug accumulates to a reduced extent in healthy tissues. The potential effects of the length and nature of CL FA chains (i.e., saturated or unsaturated) on liposome aggregation have not been elucidated. We are developing CL-containing liposome-based formulations of a broad spectrum of therapeutic agents ranging from difficult-to-formulate, water-insoluble drugs to delivery of molecules to intracellular targets. Although long-chain CL is available from natural resources and through semisynthetic methods, CL with short-chain FA is as yet unknown.

The most general methods used for the chemical synthesis of CL involve phosphatidic acids (PA) (**1**) and phosphatidylglycerols (PG) (**2**) (Scheme 2). Selective phosphorylation of the primary alcohol group of PG with PA either by a semisynthetic method (by enzymes) (12) or by condensation of PG or 2-O-protected glycerols with PA in the presence of 2,4,6-triisopropylbenzenesulfonyl chloride (13–16) will result in protected CL. Other synthetic approaches describe the use of phosphorylating agents such as cyclic enediol pyrophosphates (17–19), silver salts of PA (20–22), phosphorus oxychloride (23), and 2-chlorophenyl phosphorodi-(1,2,4-triazolide) (24).

*To whom correspondence should be addressed at NeoPharm, Inc., 1850 Lakeside Dr., Waukegan, IL 60085. E-mail: Imran@neophrm.com

Abbreviations: ATR, attenuated total reflectance; CL, cardiolipin; ESI, electron spray ionization; PBP, pyridinium bromide perbromide; PG, phosphatidylglycerol(s).

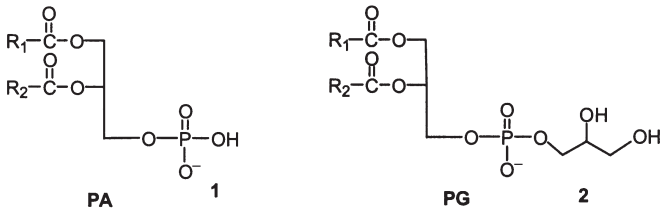

SCHEME 2

Although these methods are suitable for the preparation of small quantities of CL, those are unattractive for the routine preparation of larger quantities because of the many steps involved, the requirement for careful purification of intermediates, and the use of highly photosensitive silver salt derivatives and unstable iodo intermediates. The phosphotriester approach, which involves reactive phosphoryl [O=P(V)] species and the phosphoramidite method (25–27) involving [P(III)] derivatives, has been used widely in the synthesis of oligonucleotides and phospholipids. However, the use of phosphate triesters in preparing phospholipids such as CL having varying FA chain lengths is not well established. As part of our ongoing research toward the synthesis of CL and its analogs (28,29), we have developed a concise and convenient alternate synthetic methodology for CL synthesis based on phosphite chemistry. Herein we report the versatility of this method as exemplified by the synthesis of saturated (lauroyl) CL (Scheme 3) and unsaturated (oleoyl) CL (Scheme 4) as well as ether analogs having FA chains ranging from C_6 to C_{18}.

EXPERIMENTAL PROCEDURES

Melting points were determined at atmospheric pressure and were uncorrected. ^1H, ^{13}C, and ^{31}P NMR spectra were recorded using a Varian Inova (500 MHz) NMR spectrometer at 500, 125, and 100 MHz, respectively. ^1H chemical shifts are in ppm from internal tetramethylsilane. ^{13}C chemical shifts are reported in ppm relative to $CDCl_3$ (77.0 ppm). For ^{31}P the external standard was 85% H_3PO_4 calibrated to 0 ppm. Mass spectral analyses (electron spray ionization, ESI) were carried out on an API 4000 Triple Quadruple LC-MS-MS mass spectrometer (Applied Biosystems). IR spectra were recorded on a Nicolet Nexus 470 FTIR spectrophotometer. Samples were prepared by the attenuated total reflectance (ATR) method. TLC was carried out on Merck silica gel 60 F_{254} plates (250 μm; Merck, Darmstadt, Germany) and developed with the appropriate solvents. The TLC spots were visualized with either UV light or by heating plates stained with a solution of phosphomolybdic acid (5% ethanolic solution) or spraying with molybdenum blue (Sigma Chemical Co., St. Louis, MO). Flash column chromatography was carried out on silica gel (230–400 mesh). All chemicals were purchased from Aldrich Chemical Co. (Milwaukee, WI) except for 1,2-dilauroyl-*sn*-glycerol (Genzyme Pharmaceuticals, Cambridge, MA) and 1,2-*O*-dioleoyl-*sn*-glycerol (Avanti Polar Lipids, Alabaster, AL). All of the extracts were dried over anhydrous Na_2SO_4. Dichloromethane and THF were used without drying.

*2-Benzyl-1,3-bis[(1,2-dilauroyl-*sn*-glycero-3)-phosphoryl] glycerol dibenzyl ester (**6**).* To a solution of 1,2-dilauroyl-*sn*-

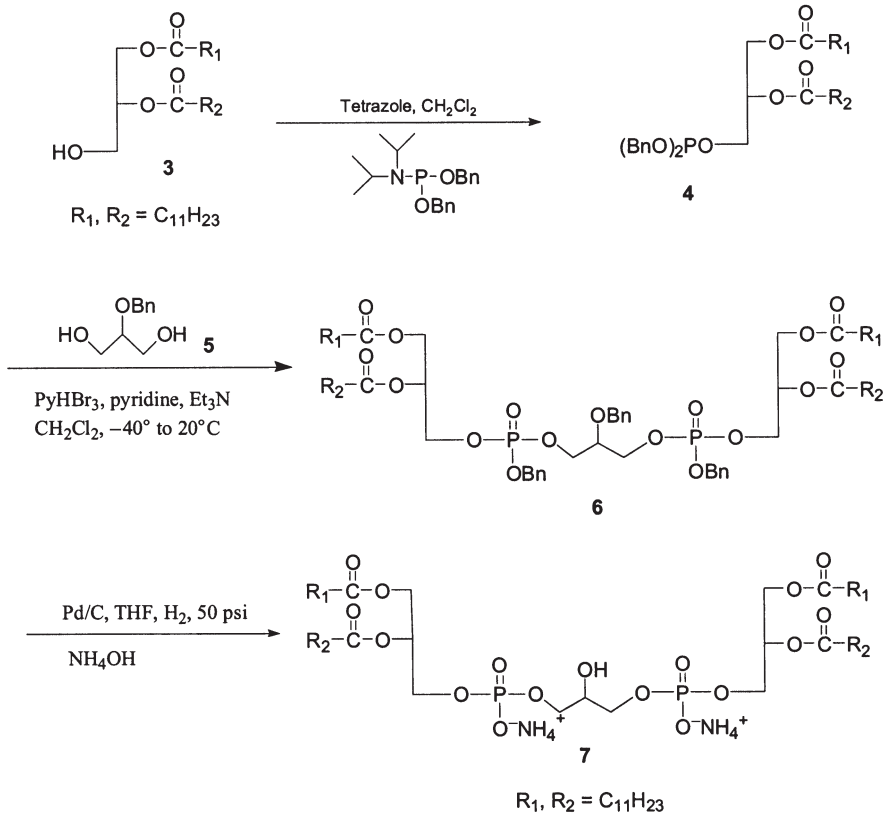

SCHEME 3

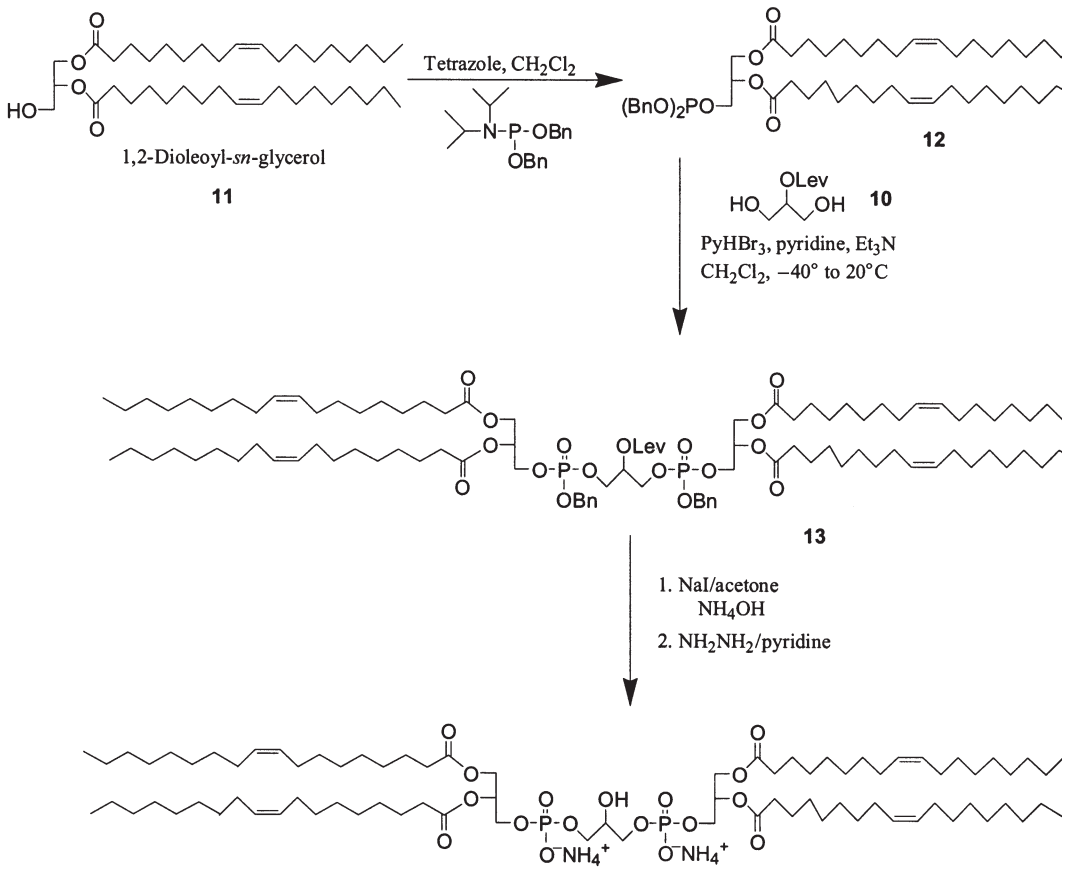

SCHEME 4

glycerol **3** (10.0 g, 21.92 mmol) and tetrazole (58.4 mL of 0.45 M solution in acetonitrile, 26.3 mmol) in 80 mL anhydrous CH_2Cl_2, dibenzyl diisopropyl phosphoramidite (8.32 g, 24.12 mmol) was added and stirred at room temperature for 1 h. The contents were diluted with 200 mL of CH_2Cl_2, washed with 5% aqueous $NaHCO_3$ (2 × 50 mL) and then with brine (2 × 50 mL), dried over Na_2SO_4, and concentrated *in vacuo*. The oily residue **4** (7.68 g) was then dried in a desiccator for 8 h and used as such in the next reaction.

A solution of the aformentioned phosphite **4**, 2-benzyloxy-1,3-propanediol **5** (1.6 g, 8.77 mmol), pyridine (10.62 mL, 131.52 mmol), and Et_3N (9.1 mL, 65.76 mmol) in CH_2Cl_2 (140 mL) was cooled to –40°C, and pyridinium tribromide (10.52 g, 32.88 mmol) was added at once. The mixture was stirred at the same temperature for 1 h, gradually allowed to attain room temperature over a period of 2 h, and then treated with water (30 mL). The contents were diluted with EtOAc (250 mL), and the organic layer was washed successively with aqueous 5% $NaHCO_3$ (2 × 50 mL), water (50 mL), and brine (50 mL), after which it was dried (Na_2SO_4) and concentrated. The residue was purified on SiO_2 (8% acetone in CH_2Cl_2) to give 9.84 g (80%) of **6** as a colorless syrup. TLC (SiO_2) hexane/EtOAc (3:2) R_f ~ 0.44. ^{1}H NMR ($CDCl_3$, 500 MHz): δ 0.88 (*t, J* = 7.0 Hz, 12H), 1.22–1.34 (*m,* 64H), 1.52–1.66 (*m,* 8H), 2.22–2.29 (*m,* 8H), 3.70–3.78 (*m,* 1H), 4.01–4.16 (*m,* 10H), 4.22–4.28 (*m,* 2H), 4.60 (*d, J* = 7.8 Hz, 2H), 5.01–5.05 (*m,* 4H), 5.15–5.18 (*m,* 2H), 7.28–7.36 (*m,* 15H).

*1,3-Bis[(1,2-dilauroyl-*sn*-glycero-3)-phosphoryl] glycerol diammonium salt (**7**).* A solution of protected CL **6** (6.0 g, 4.28 mmol) in THF (50 mL) was hydrogenated at 50 psi over 10% Pd/C (800 mg) for 10 h. The catalyst was filtered off over a bed of Celite, treated with 5 mL of 30% ammonia solution, and concentrated. The residue was dissolved in $CHCl_3$, filtered through a 0.25-μm filter, and precipitated with acetone to give tetralauroyl CL **7** (4.48 g, 90%), as a white solid. TLC (SiO_2) $CHCl_3$/MeOH/NH_4OH (6.5:2.5:0.5) R_f ~ 0.48. m.p. 182–184°C. $[\alpha]^{25}_D$ = +6.77 (*c* 2.0, $CHCl_3$). FTIR (ATR): 3207, 3041, 2956, 2918, 2850, 1737, 1467, 1378, 1327, 1206, 1092, 1065 cm^{-1}. ^{1}H NMR ($CDCl_3$, 500 MHz): δ 0.88 (*t, J* = 7.0 Hz, 12H), 1.22–1.34 (*br s,* 64H), 1.52–1.66 (*m,* 8H), 2.26–2.34 (*m,* 8H), 2.94 (*br s,* 1H), 3.82–3.98 (*m,* 9H), 4.12–4.18 (*m,* 2H), 4.35–4.42 (*m,* 2H), 5.14–5.24 (*m,* 2H), 7.41 (*br s,* 8H). ^{13}C NMR ($CDCl_3$, 125 MHz): δ 14.07, 22.67, 24.87, 24.93, 29.18, 29.22, 29.36, 29.37, 29.40, 29.57, 29.60, 29.66, 29.67, 29.69, 29.72, 31.91, 34.09, 34.28, 62.62, 63.57, 66.77, 69.47, 70.29, 173.25, 173.56. ^{31}P NMR (10% CD_3OD in $CDCl_3$, 100 MHz): δ –2.40. ESI-MS (negative) *m/z*: 1150.1 (M – $2NH_4^+$ + Na^+), 1127 (M – $2NH_4^+$), 1128.0 (M – $2NH_4^+$ + H^+), 928.0 (M – $2NH_4^+$ –

RCOO$^-$), 563.6 (M – 2NH$_4^+$)$^{2-}$. Anal. calcd. for $C_{57}H_{116}N_2O_{17}P_2$: C, 58.84; H, 10.05; N, 2.41; P, 5.32. Found: C, 57.75; H, 9.83; N, 2.34; P, 5.28.

Cis-*5-levulinoyl-2-phenyl-1,3-dioxane (**9**).* To a solution of *cis*-1,3-*O*-benzylideneglycerol **8** (5.0 g, 27.74 mmol) in CH_2Cl_2 (80 mL) at 0°C, 1,3-dicyclohexylcarbodiimide (8.58 g, 41.61 mmol), 4-(dimethylamino)pyridine (3.38 g, 27.74 mmol), and levulinic acid (4.0 g, 34.68 mmol) were added sequentially. The mixture was stirred for 24 h at room temperature. The separated urea was filtered, and the filtrate was then concentrated and purified by flash chromatography with 80% EtOAc/hexane as eluent to afford product **9** (5.86 g, 76%). TLC (SiO_2) hexane/EtOAc (1:1) R_f ~ 0.51. ^{1}H NMR ($CDCl_3$, 500 MHz): δ 2.19 (*s,* 3H), 2.58–2.89 (*m,* 4H), 4.18 (*dd, J* = 12.0, 1.5 Hz, 2H), 4.25 (*dd, J* = 12.0, 1.5 Hz, 2H), 4.71 (*dd, J* = 1.5, 1.5 Hz, 1H), 5.55 (*s,* 1H), 7.24–7.53 (*m,* 5H).

*2-Levulinoyl-1,3-propanediol (**10**).* A solution of **9** (5.8 g, 20.86 mmol) in EtOH/EtOAc (1:1, 100 mL) was hydrogenated at 50 psi over 10% Pd/C (800 mg, 10%) for 8 h. The catalyst was filtered off over a bed of Celite and concentrated; the resulting 2-levulinoyl glycerol was then purified by flash chromatography with 6% MeOH/CH_2Cl_2 as eluent to afford product **10** as a low-melting white solid (2.82 g, 70%). TLC (SiO_2) MeOH/CH_2Cl_2 (1:9) R_f ~ 0.31. ^{1}H NMR ($CDCl_3$, 500 MHz): δ 2.19 (*s,* 3H), 2.58 (*dd, J* = 6.0, 6.0 Hz, 2H), 2.80 (*dd, J* = 6.0, 6.0 Hz, 2H), 3.09 (*br s,* 2H), 3.72–3.87 (*m,* 4H), 4.90 (*q, J* = 5.1 Hz, 1H).

*2-Levulinoyl-1,3-bis[(1,2-oleoyl-*sn*-glycero-3)phosphoryl] glycerol dibenzyl ester (**13**).* Compound **13** was made in a manner similar to **6** in 76% yield. TLC (SiO_2) hexane/EtOAc (1:2) R_f ~ 0.64. Yield 68%. ^{1}H NMR ($CDCl_3$, 300 MHz): δ 0.88 (*t, J* = 7.0 Hz, 12H), 1.22–1.34 (*m,* 80H), 1.52–1.66 (*m,* 8H), 1.96–2.07 (*m,* 16H), 2.15 (*s,* 3H), 2.22–2.31 (*m,* 8H), 2.52–2.57 (*m,* 2H), 2.66–2.74 (*m,* 2H), 4.01–4.32 (*m,* 12H), 5.01–5.10 (*m,* 5H), 5.15–5.18 (*m,* 2H), 5.28–5.39 (*m,* 8H), 7.28–7.39 (*m,* 10H).

*1,3-Bis[(1,2-dioleoyl-*sn*-glycero-3)-phosphoryl] glycerol diammonium salt (**14**).* A solution of protected CL **13** (3.15 g, 1.81 mmol) in acetone (20 mL) and sodium iodide (816 mg, 5.44 mmol) was refluxed for 3 h. The volatiles were evaporated, and the residue was purified on SiO_2 (10% methanol in CH_2Cl_2 containing 1% of ammonia) to give 2.16 g (75%) of the product as a colorless semisolid. TLC (SiO_2) $CHCl_3$/MeOH/NH_4OH (6.5:2.5:0.5) R_f ~ 0.63. ^{1}H NMR ($CDCl_3$, 500 MHz): δ 0.88 (*t, J* = 7.0 Hz, 12H), 1.22–1.39 (*m,* 80H), 1.52–1.65 (*m,* 8H), 1.96–2.07 (*m,* 16H), 2.18 (*s,* 3H), 2.23–2.35 (*m,* 8H), 2.52–2.59 (*m,* 2H), 2.71–2.79 (*m,* 2H), 3.83–4.04 (*m,* 6H), 4.12–4.23 (*m,* 4H), 4.31–4.39 (*m,* 2H), 5.01–5.09 (*m,* 1H), 5.17–5.26 (*m,* 2H), 5.28–5.39 (*m,* 8H), 7.41–7.59 (*br s,* 8H). ESI-MS (negative) *m/z*: 1576.5 (M – 2NH$_4^+$ + Na$^+$)$^-$, 1554 (M – 2NH$_4^+$), 1272.2 (M – 2NH$_4^+$ – RCOO$^-$), 776 (M – 2NH$_4^+$)$^{2-}$.

To a solution of the aforementioned lev-protected CL (1.8 g, 1.13 mmol) in pyridine (3 mL) was added hydrazine (90 mg, 2.83 mmol), and the mixture was stirred for 30 min. The volatiles were removed in a rotary evaporator, and the residue was purified on SiO_2 (10% methanol in CH_2Cl_2 containing 1% of ammonia) to give 1.19 g (71%) of **14** as a white semisolid. TLC (SiO_2) (6.5:2.5:0.5) R_f ~ 0.55. $[\alpha]^{25}_D$ = +4.09 (*c* 1.74, $CHCl_3$). ^{1}H NMR ($CDCl_3$, 500 MHz): δ 0.88 (*t, J* = 7.0 Hz, 12H), 1.22–1.39 (*m,* 80H), 1.52–1.65 (*m,* 8H), 1.82 (*br s,* 1H), 1.96–2.07 (*m,* 16H), 2.23–2.35 (*m,* 8H), 3.83–3.94 (*m,* 7H), 4.12–4.23 (*m,* 4H), 4.33–4.39 (*m,* 2H), 5.17–5.23 (*m,* 2H), 5.28–5.39 (*m,* 8H), 7.41–7.59 (*br s,* 8H). ^{31}P NMR (10% CD_3OD in $CDCl_3$, 100 MHz): δ 0.51. ESI-MS (negative) *m/z*: 1478.4 (M – 2NH$_4^+$ + Na$^+$)$^-$, 1456 (M – 2NH$_4^+$), 1174.1 (M – 2NH$_4^+$ – RCOO$^-$), 727.6 (M – 2NH$_4^+$)^2. Anal. calcd. for $C_{81}H_{156}N_2O_{17}P_2$: C, 65.20; H, 10.54; N, 1.88; P, 4.15. Found: C, 64.99; H, 10.51; N, 1.81; P, 4.11.

RESULTS AND DISCUSSION

The method based on the phosphonium salt methodology (30–32) involves treatment of 2-O-protected glycerol with 1,2-diacyl-*sn*-glyceryl phosphite in the presence of pyridinium bromide perbromide (PBP) and triethylamine in dichloromethane to afford phosphoric triester. Removal of the protecting groups will furnish CL. Saturated analogs can be prepared much more easily than the unsaturated version since the former synthetic procedures allow the use of common benzyl protecting groups that are removed by hydrogenolysis. However, the choice of protecting groups for alcohol and phosphate functionalities is most crucial in unsaturated CL synthesis. We illustrate that benzyl and levulinoyl groups (33,34) can be efficiently utilized as protecting groups for the hydroxyl functionality of the central core. The levulinyl group is stable to both acidic as well as basic conditions and can be deprotected under mild conditions by hydrazinolysis.

Accordingly, treatment of 2-*O*-benzylglycerol (**5**) with dibenzyl 1,2-dilauroyl-*sn*-glyceryl phosphite (**4**) [prepared by a 1H-tetrazole-mediated reaction of 1,2-dilauroyl-*sn*-glycerol (**3**) with dibenzyl *N,N*-diisopropyl phosphoramidite] in the presence of PBP and triethylamine afforded benzyl-protected CL (**6**) in 80% yield. The global deprotection of benzyl groups was achieved by hydrogenolysis with 10% Pd/C at 50 psi in THF at room temperature to obtain tetralauroyl CL (**7**) (90%), which was immediately converted to ammonium salt with the addition of ammonia (Scheme 3).

For the synthesis of unsaturated CL (tetraoleoyl CL **14**), 2-*O*-levulinoyl glycerol (**10**) was used. The 2-*O*-levulinoyl glycerol was synthesized starting from commercially available *cis*-1,3-*O*-benzylideneglycerol (**8**) by 1,3-dicyclohexylcarbodiimide-mediated levulinoylation followed by hydrogenolysis (Scheme 5).

The synthesis of **14** was initiated by treating **10** with dibenzyl 1,2-dioleoyl-*sn*-glyceryl phosphite (**12**) [prepared by a 1H-tetrazole-mediated reaction of 1,2-dioleoyl-*sn*-glycerol (**11**) with dibenzyl *N,N*-diisopropyl phosphoramidite] in the presence of PBP and triethylamine to afford protected CL (**6**) in 76% yield. Deprotection of the phosphate function was carried out prior to the removal of the levulinoyl group to avoid migration of the phosphate. The benzyl groups of the phosphate moiety in **13** were cleaved with sodium iodide in refluxing acetone and converted into ammonium

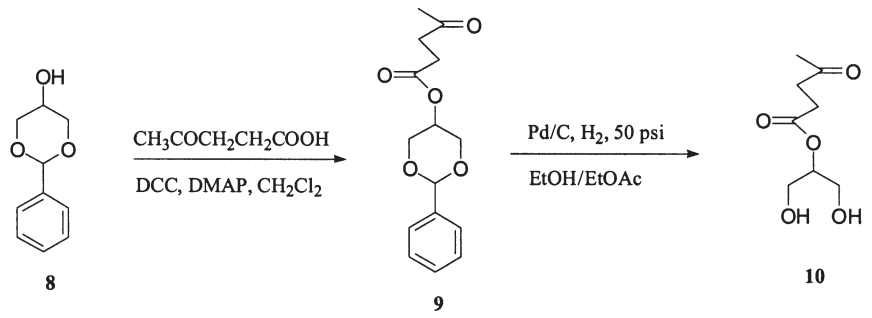

SCHEME 5

salt. The hydrazinolysis was accomplished smoothly by treatment with hydrazine to obtain the tetraoleoyl CL **14** (Scheme 4). The products **7** and **14** were soluble in $CHCl_3$ and showed relatively clear ^1H NMR signals. The structures of the final products were characterized by NMR (^1H, ^{13}C, and ^{31}P) and ESI-MS, and their homogeneity by TLC and HPLC and were identical to the CL from bovine heart. Similarly, the method was extended to synthesize a broad range of short-chain (C_6–C_{12}) and long-chain (C_{14}–C_{18}) CL and their ether analogs.

In summary, the route outlined here to make CL derivatives offers several advantages over the other strategies used. The synthesis begins with readily available 1,2-DAG and dibenzyl phosphoramidites. Installation of the polar head group has been made easy by using phosphite chemistry instead of phosphorus oxychloride (which is difficult to handle) as well as cyclic enediol pyrophosphates (17–19) and relatively labile PA. The use of labile protecting groups such as silyl (14,15,17,18,24) was avoided. In addition, our method can be carried out on a gram scale and can be applied to the synthesis of similar compounds such as PE, PG, and platelet-activating factors.

ACKNOWLEDGMENTS

We thank the Bioanalytical group of the Pharmacokinetics, Safety and Efficacy (PSE) Department at NeoPharm for the mass spectral analyses.

REFERENCES

1. Paltauf, F., and Hermetter, A. (1994) Strategies for the Synthesis of Glycerophospholipids, *Prog. Lipid Res. 33,* 239–328.
2. Eibl, H. (1980) Synthesis of Glycerophospholipids, *Chem. Phys. Lipids 26,* 405–429.
3. Ioannou, P., and Golding, B.T. (1979) Cardiolipins: Their Chemistry and Biochemistry, *Prog. Lipid Res. 17,* 279–318.
4. Semin, B.K., Saraste, M., and Wikstrom, M. (1984) Calorimetric Studies of Cytochrome Oxidase–Phospholipid Interactions, *Biochim. Biophys. Acta 769,* 15–22.
5. Thompson, D.A., and Ferguson-Miller, S. (1983) Lipid and Subunit III Depleted Cytochrome *c* Oxidase Purified by Horse Cytochrome *c* Affinity Chromatography in Lauryl Maltoside, *Biochemistry 22,* 3178–3187.
6. Schlame, M., Rua, D., and Greenberg, M.L. (2000) The Biosynthesis and Functional Role of Cardiolipin, *Prog. Lipid Res. 39,* 257–288.
7. McMillin, J.B., and Dowhan, W. (2002) Cardiolipin and Apoptosis, *Biochim. Biophys. Acta 1585,* 97–107.
8. Haines, T.H., and Dencher, N.A. (2002) Cardiolipin: A Proton Trap for Oxidative Phosphorylation, *FEBS Lett. 528,* 35–39.
9. Lutter, M., Fang, M., Luo, X., Nishijima, M., Xie, X.S., and Wang, X. (2000) Cardiolipin Provides Specificity for Targeting of tBid to Mitochondria, *Nature Cell Biol. 2,* 754–756.
10. Gokhale, P.C., Zhang, C., Newsome, J.T., Pei, J., Ahmad, I., Rahman, A., Dritschilo, A., and Kasid, U.N. (2002) Pharmacokinetics, Toxicity, and Efficacy of Ends-Modified *raf* Antisense Oligodeoxyribonucleotide Encapsulated in a Novel Cationic Liposome, *Clin. Cancer Res. 8,* 3611–3621.
11. Drummond, D.C., Meyer, O., Hong, K., Kirpotin, D.B., and Papahadjopoulos, D. (1999) Optimizing Liposomes for Delivery of Chemotherapeutic Agents to Solid Tumors, *Pharmacol. Rev. 51,* 691–744.
12. Arrigo, P.D., Ferra, L.D., Fantoni, G.P., Scarcelli, D., Servi, S., and Strini, A. (1996) Enzyme-Mediated Synthesis of Two Diastereoisomeric Forms of Phosphatidylglycerol and of Diphosphatidylglycerol (cardiolipin), *J. Chem. Soc., Perkin Trans. 1, 21,* 2657–2660.
13. Keana, J.F.W., Shimiju, M., and Jernstedt, K.K. (1986) A Short, Flexible Route to Symmetrically and Unsymmetrically Substituted Diphosphatidylglycerols (cardiolipin), *J. Org. Chem. 51,* 2297–2299.
14. Mishina, I.M., Vasilenko, A.E., Stepanov, A.E., and Shvets, V.I. (1987) Studies on Complex Lipids. Synthesis of Diphosphatidylglycerol (cardiolipin) with Unsaturated Fatty Acids, *Bioorg. Khim. 13,* 1110–1115.
15. Mishina, I.M., Vasilenko, A.E., Stepanov, A.E., and Shvets, V.I. (1985) Synthesis of Diphosphatidylglycerol (cardiolipin) with Unsaturated Fatty Acids, *Bioorg. Khim. 11,* 992–994.
16. Mishina, I.M., Vasilenko, A.E., Stepanov, A.E., and Shvets, V.I. (1984) Study of Lipids. Synthesis of Phosphatidylglycerol and Diphosphatidylglycerol, *Zh. Org. Khim. 20,* 985–988.
17. Ramirez, F., Ioannou, P.V., Marecek, J.F., Dodd, G.H., and Golding, B.T. (1977) Synthesis of Phospholipids by Means of Cyclic Enediol Pyrophosphates, *Tetrahedron 33,* 599–608.
18. Ramirez, F., Ioannou, P.V., Marecek, J.F., Golding, B.T., and Dodd, G.H. (1976) Application of Cyclic Enediol Pyrophosphates to the Synthesis of Phospholipids. Diphosphatidylglycerol (cardiolipin), *Synthesis,* 769–770.
19. Ioannou, P.V., and Marecek, J.F. (1986) Studies on the Chemical Synthesis and Stability of Cardiolipins and Related Compounds, *Chem. Chron. 15,* 205–220.
20. Inoue, K., and Nojima, S. (1968) Immunochemical Studies of Phospholipids. II. Syntheses of Cardiolipin and Its Analogues, *Chem. Pharm. Bull. 16,* 76–81.
21. Inoue, K., and Nojima, S. (1963) On the Cardiolipin Analogues. Syntheses of Dipalmitoyl-D,L-α-glycerylphosphoryl-propanol Sodium Salt and Bis(dipalmitoyl-D,L-α-glycerylphosphoryl)-1,3-propanediol Disodium Salt, *Chem. Pharm. Bull. 11,* 1150–1156.
22. De Hass, G.H., Bonsen, P.P.M., and Van Deenen, L.L.M. (1966) Studies on Cardiolipin. Structural Identity of Ox-Heart Cardiolipin and Synthetic Diphosphatidylglycerol, *Biochim. Biophys. Acta 116,* 114–124.

23. Saunders, R.M., and Schwarz, H.P. (1966) Synthesis of Phosphatidylglycerol and Diphosphatidylglycerol, *J. Am. Chem. Soc. 88,* 3844–3847.
24. Duralski, A.A., Spooner, P.J.R., Rankin, S.E., and Watts, A. (1998) Synthesis of Isotopically Labelled Cardiolipins, *Tetrahedron Lett. 39,* 1607–1610.
25. Browne, J.E., Driver, M.J., Russel, J.C., and Sammes, P.G. (2000) Preparation of Phospholipid Analogues Using the Phosphoramidite Route, *J. Chem. Soc., Perkin Trans. 1, 5,* 653–657.
26. Dreef, C.E., Elie, C.J.J., Hoogerhout, P., van der Marel, G.A., and Van Boom, J.H. (1988) Synthesis of 1-*O*-(1,2-di-*O*-palmitoyl-*sn*-glycero-3-phospho)-*d*-myo-inositol 4,5-*bis*phosphate: An Analogue of Naturally Occurring (ptd)Ins(4,5)P_2, *Tetrahedron Lett. 29,* 6513–6516.
27. Beaucage, S.L., and Iyer, R.P. (1993) The Synthesis of Specific Ribonucleotides and Unrelated Phosphorylated Biomolecules by the Phosphoramidite Method, *Tetrahedron 49,* 10441–10488.
28. Krishna, U.M., Ahmad, M.U., and Ahmad, I. (2004) Phosphoramidite Approach for the Synthesis of Cardiolipin, *Tetrahedron Lett. 45,* 2077–2079.
29. Lin, Z., Ahmad, M.U., Ali, S.M., and Ahmad, I. (2004) An Efficient and Novel Method for the Synthesis of Cardiolipin and Its Analogs, *Lipids 39,* 285–290.
30. Watanabe, Y., Hirofuji, H., and Ozaki, S. (1994) Synthesis of a Phosphatidylinositol 3,4,5-Triphosphate, *Tetrahedron Lett. 35,* 123–124.
31. Watanabe, Y., Nakamura, T., and Mitsumoto, H. (1997) Protection of Phosphate with the 9-Fluorenylmethyl Group. Synthesis of Unsaturated-Acyl Phosphatidylinositol 4,5-Bisphosphate, *Tetrahedron Lett. 38,* 7407–7410.
32. Watanabe, Y., and Nakatomi, M. (1998) Synthesis of Natural PI(3,4,5)P_3, *Tetrahedron Lett. 39,* 1583–1586.
33. Hassner, A., Strand, G., Rubinstein, M., Patchornik, A. (1975) Levulinic Esters. Alcohol Protecting Group Applicable to Some Nucleosides, *J. Am. Chem. Soc. 97,* 1614–1615.
34. Van Boom, J.H., and Burgers, P.M.J. (1976) Use of Levulinic Acid in the Protection of Oligonucleotides *via* the Modified Phosphotriester Method: Synthesis of Decaribonucleotide u-a-u-a-u-a-u-a-u-a, *Tetrahedron Lett. 17,* 4875–4878.

[Received April 24, 2004; accepted August 3, 2004]

LETTERS TO THE EDITOR

Re: Effect of Dietary Protein and CLA Interaction on Lipid Metabolism in Rats

Sir:

We read with great interest the paper of Akahoshi *et al.* (1) in which they reported the effect of the interaction of CLA and source of dietary protein (casein vs. soy protein) on lipid metabolism in young (4-wk-old) rats. They also suggested that the source of dietary protein may modify the antiobesity activity of CLA.

Unfortunately, Akahoshi *et al.* (1) did not provide enough information about diet composition, which is essential if other researchers are to be able to confirm their findings. Akahoshi *et al.* (1) mention that the experimental diets used in their study were prepared according to the AIN-93G specifications (2). Since the AIN-93G control diet includes supplementation of casein with L-cystine (3 g/kg diet) (2), it could be assumed that the soy protein diet was also supplemented with the same amount of L-cystine. If this was the case, then the soy protein diet would be deficient in methionine for rat growth. Unlike casein, soy protein contains a significant amount of cystine (about 1:1 methionine/cystine ratio), and the addition of supplemental cystine to soy protein would exacerbate the imbalance. Therefore, the possible deficiency of methionine in the soy protein diet may have been responsible for the significantly lower weight gain and food efficiency ratio for rats fed the soy protein diets compared with those fed the casein diets, as noted in Table 1 of Akahoshi *et al.* (1).

The lower growth of rats fed the soy protein diets compared with those fed the casein diets may be partly responsible for the observed beneficial effect of the soy protein diets on total blood cholesterol and antiobesity parameters reported by Akahoshi *et al.* (1). It is well known that soy protein is limiting in methionine for rat growth (3), and that dietary cystine is negatively correlated with levels of blood cholesterol in rats (4,5). Therefore, Akahoshi *et al.* (1) are requested to clarify the details of the diet formulations and to discuss the impact of cystine supplementation of soy protein diet on lipid metabolism in rats. It would also be useful to provide data on protein and amino acid composition (especially sulfur amino acids) of the soy protein used in their study, as amino acid profiles of soy protein products may vary considerably based on their methods of preparation. This information would enable researchers in other laboratories to confirm and potentially enhance the findings of Akahoshi *et al.* (1).

REFERENCES

1. Akahoshi, A., Koba, K., Ichinose, F., Kaneko, M., Shimoda, A., Nonaka, K., Yamasaki, M., Iwata, T., Yamauchi, Y., Tsutsumi, K., and Sugano, M. (2004) Dietray protein modulates the effect of CLA on Lipid Metabolism in Rats, *Lipids 39*, 25–30.
2. Reeves, P.G., Nielsen, F.H., and Fahey, G.C. (1993) AIN-93 Purified Diets for Laboratory Rodents: Final Report of the American Institute of Nutrition *ad hoc* Writing Committee on the Reformulation of the AIN-76A Rodent Diet, *J. Nutr. 123*, 1939–1951.
3. Sarwar, G., Botting, H.G., Peace, R.W., and Noel, F.J. (1981) Effect of Methionine Supplemented Legume Protein Products on Liver Fat in Rats, *Nutr. Rep. Int. 24*, 267–276.
4. Sautier, C., Dieng, K., Flament, C., Doucet, C., Suquet, J.P., and Lemonnier, D. (1983) Effect of Wheat Protein, Casein, Soybean, and Sunflower Protein on the Serum, Tissue and Faecal Steroids in Rats, *Br. J. Nutr. 49*, 313–319.
5. Sautier, C., Flament, C., Doucet, C., and Suquet, J.P. (1986) Effects of Eight Dietary Proteins and Their Amino Acid Content on Serum, Hepatic and Faecal Steroids in the Rat, *Nutr. Rep. Int. 34*, 1051–1061.

[Received June 24, 2004; accepted August 17, 2004]

G. Sarwar Gilani
W.M. Nimal Ratnayake*
Nutrition Research Division, Food Directorate
Health Canada, Government of Canada,
Ottawa, Ontario, Canada K1A OL2

*To whom correspondence should be addressed at Nutrition Research Division, Food Directorate, Health Canada, Government of Canada, Banting Building (2203C), Tunney's Pasture, Ottawa, Ontario, Canada K1A OL2.
E-mail: nimal_ratnayake@hc-sc.gc.ca

Sir:

Thank you for your constructive criticism of our paper published in *Lipids* (1). Cystine was added not only to casein but also to soy protein diets in our study. As you suggest, it is possible that methionine deficiency may have been exacerbated by the excess cystine in the soy protein diets and may have caused the growth retardation and lowering of feed efficiency. However, it is also possible that added cystine saves methionine. In addition, soy protein stimulates FA β-oxidation in relation to casein (1,2), and in our paper the energy expenditure seems to be increased as the weight of brown adipose tissue increased in rats fed soy protein (1). It is thus likely that the methionine deficiency is not the sole factor responsible for the growth retardation, but instead is just one of the factors. The amino acid composition of soy protein preparations may differ from sample to sample, and in fact in our preceding trials with rats there was no apparent difference in growth parameters between casein and soy protein (2). We always use soy protein from the same company, we do not know whether the amino acid composition is kept constant.

A number of mechanisms have been proposed to explain the serum cholesterol-lowering effects of dietary soy protein in relation to casein. The amino acid composition is one such factor, and cystine is said to be negatively correlated with the cholesterol concentration (3). However, the change attributable to added cystine seems to be within the normal range, and in humans serum cholesterol is not lowered excessively even when large quantities of soy protein are consumed (4).

We surmise that dietary cystine levels do not have a large influence on serum cholesterol.

In this context, it is necessary to confirm the influence of the content and balance of sulfur amino acids in our experimental diets on weight gain and serum cholesterol level.

REFERENCES

1. Akahoshi, A., Koba, K., Ichinose, F., Kaneko, M., Shimoda, A., Nonaka, K., Yamasaki, M., Iwata, T., Yamauchi, Y., Tsutsumi, K., and Sugano, M. (2004) Dietary Protein Modulates the Effect of CLA on Lipid Metabolism in Rats, *Lipids 39*, 25–30.
2. Sugano, M., Akahoshi, A., Koba, K., Tanaka, K., Okumura, T., Matsuyama, H., Goto, Y., Miyazaki, T., Murao, K., Yamamsaki, M., Nonaka, M., and Yamada, K. (2001) Dietary Manipulation of Body Fat-Reducing Potential of Conjugated Linoleic Acid in Rats, *Biosci. Biotechnol. Biochem. 65*, 2535–2541.
3. Sautier, C., Dieng, K., Flament, C., Doucet, C., Sequet, J.P., and Lemonnier, D. (1983) Effects of Whey Protein, Casein, Soybean and Sunflower Protein on the Serum, Tissue and Fecal Steroids in Rats, *Br. J. Nutr. 49*, 313–319.
4. Anderson, J.W., Johnstone, B.M., and Cook-Newell, M.E. (1995) Meta-analysis of the Effects of Soy Protein Intake on Serum Lipids, *N. Engl. J. Med. 333*, 276–282.

[Received August 18, 2004; accepted August 27, 2004]

A. Akahoshi* and M. Sugano
Prefectural University of Kumamoto
Faculty of Environmental and Symbiotic Sciences
Kumamoto 862-8502, Japan

*To whom correspondence should be addressed at Prefectural University of Kumamoto, Faculty of Environmental and Symbiotic Sciences, Tsukide 3-1-100, Kumamoto 862-8502, Japan. E-mail: a-asuka@pu-kumumoto.as.jp

LETTERS TO THE EDITOR

Re: Effect of Dietary Protein and CLA Interaction on Lipid Metabolism in Rats

Sir:

We read with great interest the paper of Akahoshi *et al.* (1) in which they reported the effect of the interaction of CLA and source of dietary protein (casein vs. soy protein) on lipid metabolism in young (4-wk-old) rats. They also suggested that the source of dietary protein may modify the antiobesity activity of CLA.

Unfortunately, Akahoshi *et al.* (1) did not provide enough information about diet composition, which is essential if other researchers are to be able to confirm their findings. Akahoshi *et al.* (1) mention that the experimental diets used in their study were prepared according to the AIN-93G specifications (2). Since the AIN-93G control diet includes supplementation of casein with L-cystine (3 g/kg diet) (2), it could be assumed that the soy protein diet was also supplemented with the same amount of L-cystine. If this was the case, then the soy protein diet would be deficient in methionine for rat growth. Unlike casein, soy protein contains a significant amount of cystine (about 1:1 methionine/cystine ratio), and the addition of supplemental cystine to soy protein would exacerbate the imbalance. Therefore, the possible deficiency of methionine in the soy protein diet may have been responsible for the significantly lower weight gain and food efficiency ratio for rats fed the soy protein diets compared with those fed the casein diets, as noted in Table 1 of Akahoshi *et al.* (1).

The lower growth of rats fed the soy protein diets compared with those fed the casein diets may be partly responsible for the observed beneficial effect of the soy protein diets on total blood cholesterol and antiobesity parameters reported by Akahoshi *et al.* (1). It is well known that soy protein is limiting in methionine for rat growth (3), and that dietary cystine is negatively correlated with levels of blood cholesterol in rats (4,5). Therefore, Akahoshi *et al.* (1) are requested to clarify the details of the diet formulations and to discuss the impact of cystine supplementation of soy protein diet on lipid metabolism in rats. It would also be useful to provide data on protein and amino acid composition (especially sulfur amino acids) of the soy protein used in their study, as amino acid profiles of soy protein products may vary considerably based on their methods of preparation. This information would enable researchers in other laboratories to confirm and potentially enhance the findings of Akahoshi *et al.* (1).

REFERENCES

1. Akahoshi, A., Koba, K., Ichinose, F., Kaneko, M., Shimoda, A., Nonaka, K., Yamasaki, M., Iwata, T., Yamauchi, Y., Tsutsumi, K., and Sugano, M. (2004) Dietray protein modulates the effect of CLA on Lipid Metabolism in Rats, *Lipids 39*, 25–30.
2. Reeves, P.G., Nielsen, F.H., and Fahey, G.C. (1993) AIN-93 Purified Diets for Laboratory Rodents: Final Report of the American Institute of Nutrition *ad hoc* Writing Committee on the Reformulation of the AIN-76A Rodent Diet, *J. Nutr. 123*, 1939–1951.
3. Sarwar, G., Botting, H.G., Peace, R.W., and Noel, F.J. (1981) Effect of Methionine Supplemented Legume Protein Products on Liver Fat in Rats, *Nutr. Rep. Int. 24*, 267–276.
4. Sautier, C., Dieng, K., Flament, C., Doucet, C., Suquet, J.P., and Lemonnier, D. (1983) Effect of Wheat Protein, Casein, Soybean, and Sunflower Protein on the Serum, Tissue and Faecal Steroids in Rats, *Br. J. Nutr. 49*, 313–319.
5. Sautier, C., Flament, C., Doucet, C., and Suquet, J.P. (1986) Effects of Eight Dietary Proteins and Their Amino Acid Content on Serum, Hepatic and Faecal Steroids in the Rat, *Nutr. Rep. Int. 34*, 1051–1061.

[Received June 24, 2004; accepted August 17, 2004]

G. Sarwar Gilani
W.M. Nimal Ratnayake*
Nutrition Research Division, Food Directorate
Health Canada, Government of Canada,
Ottawa, Ontario, Canada K1A OL2

*To whom correspondence should be addressed at Nutrition Research Division, Food Directorate, Health Canada, Government of Canada, Banting Building (2203C), Tunney's Pasture, Ottawa, Ontario, Canada K1A OL2.
E-mail: nimal_ratnayake@hc-sc.gc.ca

Sir:

Thank you for your constructive criticism of our paper published in *Lipids* (1). Cystine was added not only to casein but also to soy protein diets in our study. As you suggest, it is possible that methionine deficiency may have been exacerbated by the excess cystine in the soy protein diets and may have caused the growth retardation and lowering of feed efficiency. However, it is also possible that added cystine saves methionine. In addition, soy protein stimulates FA β-oxidation in relation to casein (1,2), and in our paper the energy expenditure seems to be increased as the weight of brown adipose tissue increased in rats fed soy protein (1). It is thus likely that the methionine deficiency is not the sole factor responsible for the growth retardation, but instead is just one of the factors. The amino acid composition of soy protein preparations may differ from sample to sample, and in fact in our preceding trials with rats there was no apparent difference in growth parameters between casein and soy protein (2). We always use soy protein from the same company, we do not know whether the amino acid composition is kept constant.

A number of mechanisms have been proposed to explain the serum cholesterol-lowering effects of dietary soy protein in relation to casein. The amino acid composition is one such factor, and cystine is said to be negatively correlated with the cholesterol concentration (3). However, the change attributable to added cystine seems to be within the normal range, and in humans serum cholesterol is not lowered excessively even when large quantities of soy protein are consumed (4).

The Age-Related Decline in Intestinal Lipid Uptake Is Associated with a Reduced Abundance of Fatty Acid-Binding Protein

Trudy D. Woudstra[a], Laurie A. Drozdowski[a], Gary E. Wild[b], M.T. Clandinin[a], Luis B. Agellon[c], and Alan B.R. Thomson[a,*]

[a]Nutrition and Metabolism Group, Division of Gastroenterology, Department of Medicine, University of Alberta, Edmonton, Alberta, [b]Department of Anatomy and Cell Biology, McGill University, Montreal, Quebec, and [c]Department of Biochemistry, University of Alberta, Edmonton, Alberta

ABSTRACT: Aging is associated with changes in the absorptive capacity of the small intestine. We tested the hypotheses that (i) aging is associated with a decline in lipid absorption, and that (ii) this decreased lipid absorption is due to a decline in the abundance of mRNA and/or the enterocyte cytosolic intestinal FA-binding protein (I-FABP), the liver FA-binding protein (L-FABP), and the ileal lipid-binding protein (ILBP). *In vitro* uptake studies were performed on Fischer 344 rats at ages 1, 9, and 24 mon. Northern blotting (L-FABP, ILBP) and immunohistochemistry (I-FABP, ILBP) were performed. Aging was associated with decreased animal weights, but the surface area of the intestine was not significantly altered with age. The rates of ileal uptake of 16:0, 18:0, 18:1, and 18:2 were reduced by greater than 50% with aging when expressed on the basis of mucosal weight. This decline was not associated with reduced expression of mRNA for L-FABP or ILBP but was associated with a 50% decrease in the abundance of I-FABP and a 40% decrease in the abundance of ILBP. Thus, the decrease with aging in the ileal uptake of some FA when rates were expressed on the basis of mucosal weight was associated with a reduced abundance of I-FABP and ILBP.

Paper no. L9519 in *Lipids 39*, 603–610 (July 2004).

Developed nations are faced with the demographics of an aging population. In Canada, more than 12% of the population is older than 64 yr, and this percentage is expected to grow to 14% within 11 yr (1). Aging is associated with an increased prevalence of many conditions such as diabetes, heart disease, and malnutrition (2,3). Aging is also associated with a decline in the absorptive capacity of the small intestine for carbohydrates (4), amino acids (5), calcium (6), and lipids (7,8). The complexity of lipid absorption may make it susceptible to the effects of aging (9). Such factors as the pH of the microclimate adjacent to the intestinal brush border membrane (BBM) (10), BBM fluidity (11), the effective resistance of the unstirred water layer (UWL), and the contribution of lipid-binding proteins may be subject to age-associated alterations.

*To whom correspondence should be addressed at 205 College Plaza, University of Alberta, Edmonton, AB T6G 2C8, Canada.
E-mail: alan.thomson@ualberta.ca

Abbreviations: BBM, brush border membrane; F344 rats, Fischer 344 rats; ILBP, ileal lipid-binding protein; FAT, FA translocase; I-FABP, intestinal FA-binding protein; LCFA, long-chain FA; L-FABP, liver FA-binding protein; UWL, effective resistance of the intestinal unstirred water layer.

Numerous lipid-binding proteins are found in the BBM and cytosol of enterocytes (12). Several BBM-associated proteins also may contribute to lipid absorption in the intestine, such as the FA-binding protein in the plasma membrane (13,14), FA translocase (FAT) (15), and FA transport protein-4 (FATP4) (16). Enterocyte cytosolic lipid-binding proteins include the liver FA-binding protein (L-FABP), the intestinal FA-binding protein (I-FABP), and the ileal lipid-binding protein (ILBP) (reviewed in Ref. 17). L-FABP is a 14.1-kDa protein located in the duodenum and jejunum, with maximal expression in the proximal jejunum. The distribution along the intestine is influenced by the species studied; for example, in contrast to mice, L-FABP is expressed in the ileum of rats and humans. I-FABP is a 15.1-kDa protein that is expressed throughout the small intestine, with maximal expression in the distal jejunum (18). L-FABP and I-FABP likely play different roles in the absorption of lipids. For example, FA transfer from I-FABP occurs by direct collisional interaction with the phospholipid bilayer. In contrast, L-FABP may transfer FA in an aqueous diffusion-mediated process and may act as a cytosolic buffer for FA (19). Both I-FABP and L-FABP have a high affinity for binding long-chain FA (LCFA) (20). Rats treated with clofibrate (a hypolipidemic drug) have increased expression of L-FABP protein and mRNA, with no change in the expression of I-FABP (21). The mRNA expression of I-FABP and L-FABP is increased in rats fed a diet rich in polyunsaturated fats (22). The ILBP is a 14-kDa cytoplasmic protein that binds bile acids (23). ILBP is structurally related to the FABP family and is located predominantly in the distal ileum (24).

This study was undertaken to test the hypotheses that (i) aging is associated with a decrease in the absorption of lipids in Fischer 344 (F344) rats, and that (ii) the decreased lipid uptake is due to a decline in the abundance of mRNA and/or selected lipid-binding proteins in the intestine.

MATERIALS AND METHODS

Animals. The principles for the care and use of laboratory animals approved by the Canadian Council on Animal Care and the Council of the American Physiological Society were observed in the conduct of this study. Male F344 rats aged 1, 9, and 24 mon were obtained from the National Institute of

Aging colony and Harlan Laboratories (Indianapolis, IN). Pairs of rats were housed at a temperature of 21°C, with 12 h of light and 12 h of darkness. Water and a standard laboratory PMI #5001 chow diet were supplied *ad libitum*. Eight rats were placed in each of the three age groups.

Uptake studies. (i) Probe and marker compounds. The [^{14}C]-labeled probes included cholesterol (0.05 mM) and the following FA (0.1 mM): lauric (12:0), palmitic (16:0), stearic (18:0), oleic (18:1n-9), linoleic (18:2n-6), and linolenic (18:3n-3) acids. The labeled and unlabeled probes were supplied by Amersham (Piscataway, NJ) and Sigma Co. (St. Louis, MO), respectively. The specific activity of the probes ranged from 40 to 60 mCi/mmol. The probes were prepared by solubilizing them in 10 mM of taurodeoxycholic acid (Sigma Co.) in Krebs-bicarbonate buffer, with the exception of 12:0, which was solubilized in only Krebs-bicarbonate buffer. [^{3}H]Inulin was used as a nonabsorbable marker to correct for adherent mucosal fluid volume.

(ii) Tissue preparation. Eight animals per age group were sacrificed by an intraperitoneal injection of Euthanyl® (sodium pentobarbitol, 240 mg/100 g body weight). The whole length of the intestine was rapidly removed and rinsed with 150 mL of cold saline. The proximal third, beginning at the ligament of Treitz, was termed the jejunum, and the distal third was termed the ileum; the middle third of the small intestine was discarded. The intestine was opened along its mesenteric border, and pieces of the segment were cut and mounted as flat sheets in transport chambers. A 5-cm piece of each segment of jejunum and ileum was gently scraped with a glass slide to determine the percentage of the intestinal wall composed of mucosa. The chambers were placed in preincubation beakers containing oxygenated Krebs-bicarbonate buffer (pH 7.2) at 37°C, and the tissue disks were preincubated for 15 min to allow the tissue to equilibrate at this temperature. The rate of uptake of lipids was determined from the timed transfer of the transport chambers to the incubation beakers containing [^{3}H]inulin and ^{14}C-labeled probe molecules in oxygenated Krebs-bicarbonate (pH 7.2, 37°C). The preincubation and incubation chambers were mixed with circular magnetic bars at identical stirring rates, which were precisely adjusted using a strobe light. Stirring rates were reported as revolutions per minute (rpm). A stirring rate of 600 rpm was selected to achieve a low UWL, thereby allowing for better assessment of the lipid uptake properties of the BBM (25,26).

(iii) Determination of uptake rates. After incubation of the disks in labeled solutions for 6 min, each experiment was terminated by removing the chamber and rinsing the tissue in cold saline for approximately 5 s. The exposed mucosal tissue was then cut out of the chamber with a circular steel punch, placed on a glass slide, and dried overnight in an oven at 55°C. The dry weight of the tissue was determined, and the tissue was transferred to scintillation-counting vials. The samples were saponified with 0.75 M NaOH, scintillation fluid was added, and radioactivity was determined by means of an external standardization technique to correct for variable quenching of the two isotopes (25).

The rates of uptake in the mucosa and in the mucosal surface area were determined as Jm = nmol · 100 mg mucosal tissue^{-1} · min^{-1} and Jsam = nmol · cm^{-2} mucosal surface area · min^{-1}, respectively.

Morphology, protein, and mRNA analysis. (i) Tissue preparation. For Northern blotting, morphological analysis, and immunohistochemistry, a second group of animals was raised and sacrificed in a manner similar to those in the uptake studies. Five-centimeter portions of proximal jejunum and distal ileum were quickly harvested following rinsing, snap-frozen in liquid nitrogen, and stored at −80°C for later mRNA isolation. The remaining intestine was opened along the mesenteric border. Two 1-cm pieces of each section were mounted on a styrofoam block and preserved in 10% formalin for later paraffin block mounting, to be used in the morphological and immunohistochemical analyses.

(ii) Morphological analysis. To determine the surface area of the intestine based on its 3-D architecture, a transverse and a vertical section were prepared for the jejunum and ileum. Hematoxylin-stained slides were prepared from the paraffin blocks. Crypt depth and villous height, as well as villous width, depth, and density were measured. The measurements of villous height, villous width at half height, villous width at the base, and crypt depth were obtained from the vertical sections. The measurement of villous depth was obtained from the transverse tissue sections. Group means were obtained based on 10 villi and 20 crypts per slide, with a minimum of 4 animals in each group. A published method was used to calculate the mucosal surface area (27,28). Mean values and SEM were used for statistical analyses.

(iii) Immunohistochemistry. Jejunal and ileal tissue were embedded in paraffin and 4- to 5-μm sections were mounted on glass slides. The sections were heated and placed immediately in the following solutions: xylene (3× for 5 min each), absolute ethanol (3× for 2 min each), 90% ethanol (1 min), and 70% ethanol (1 min); the sections were then rinsed with tap water. Slides were incubated in a hydrogen peroxide/methanol solution, rinsed, and counterstained with Harris hematoxylin. Slides were then air-dried, and the tissue was encircled with hydrophobic slide marker (PAP pen; BioGenex, San Ramon, CA). Slides were rehydrated and incubated for 15 min in blocking reagent (20% normal goat serum) followed by primary antibody to ILBP or I-FABP for 30 min. Slides were incubated in LINK®, LABEL®, and working DAB® solutions (BioGenex). Slides were washed, restained in hematoxylin, dehydrated in absolute ethanol, and cleared in xylene.

The slides were photographed, and the antibody density along the crypt-villous axis was determined by densitometry. The results were expressed as a ratio of the density of the antibody-positive preparation vs. the antibody-negative preparation. Statistical analyses were based on a minimum of 4 villi per animal and 3 animals per group.

(iv) RNA isolation. The intestinal pieces (minimum of 6 animals per group) were homogenized in a denaturing solution containing guanidinium thiocyanate, using a Fast Prep cell disruptor (Savant Instruments Inc., Holbrook, NY). Following addition of

2 M sodium acetate, a phenol chloroform extraction was performed. The upper aqueous phase containing the RNA was collected, and RNA was precipitated with isopropanol overnight at –80°C, with a final wash with 70% ethanol. The concentration and purity of RNA were determined by spectrophotometry at 260 and 280 nm. Samples were stored at –80°C until use for Northern blot or reverse-transcriptase PCR.

(v) Preparation of probes for Northern blotting. DH5α bacteria were transformed, and plasmid isolation was carried out using a Boehringer Mannheim High Pure Plasmid Isolation Kit (Mannheim, Germany). To make cDNA probes, the DNA insert was cut by EcoR1 and HindIII restriction enzymes (Gibco BRL, Life Technologies, Carlsbad, CA). A DIG-labeled nucleotide (Roche Diagnostics, Quebec, CA) was incorporated during the *in vitro* DNA synthesis using the Klenow fragment of a DNA polymerase (Roche Diagnostics).

Fifteen (15) µg of total RNA was loaded in a denaturing agarose gel (1% agarose, 0.66 M formaldehyde gel) and electrophoresed for 5 h at 100 V (HLB12 Complete Horizontal Long Bed Gel System, Tyler, Edmonton, Alberta, Canada). Capillary diffusion was used to transfer the RNA to a nylon membrane (Roche Molecular Biochemicals, Mannheim, Germany), and RNA was fixed to the membrane by baking at 80°C for 2 h. Membranes were hybridized with the DIG-labeled probe according to the manufacturer's protocol (Roche Diagnostics). Detection of the bound antibody was performed using a CDP-STAR chemiluminescence substrate (Roche Diagnostics), and membranes were exposed to X-ray films (X-Omat; Kodak, Rochester, NY).

The density of the mRNA bands was determined by transmittance densitometry (Model GS-670 Imaging Densitometer; Bio-Rad Laboratory, Mississauga, Ontario, Canada). Quantification of the 28S ribosomal units from the membranes was used to account for possible loading discrepancies.

Expression of results. Results were expressed as mean ± SEM. The statistical significance of the differences between the three age groups was determined by ANOVA ($P < 0.05$). Individual differences between ages were determined using a Student–Neuman–Keuls multiple range test.

RESULTS

Animal characteristics. The rate of body weight change did not differ between the 1- and 9-mon-old animals, but it decreased between 9 and 24 mon (Fig. 1). In the jejunum, age had no effect on the weight of the intestine, the weight of the mucosa, or the percentage of the intestinal wall comprised of mucosa (Table 1). In the ileum, the weight of the intestine and the weight of the intestinal mucosa were approximately twice as high at 24 mon than at 1 mon (Table 1).

No differences were observed in the heights of the villi, or in either the jejunal or the ileal mucosal surface area at 1, 9, or 24 mon (data not shown).

Uptake of lipids. Because the weight of the mucosa is influenced by the age of the animals (Table 1), the rate of uptake was expressed on the basis of the weight of the mucosa (Jm = nmol · 100 mg mucosal tissue^{-1} · min^{-1}) (Fig. 2). There was reduced jejunal uptake of 18:0 between 1 and 9 mon; reduced ileal uptake of 16:0, 18:0, and 18:1 between 1 and 9, and between 1 and 24 mon; and reduced ileal uptake of 18:2 between 1 and 24 mon (Fig. 2). The rate of jejunal uptake of 12:0 increased between 9 and 24 mon, whereas in the ileum, the rate of uptake decreased between 1 and 9 mon (data not shown).

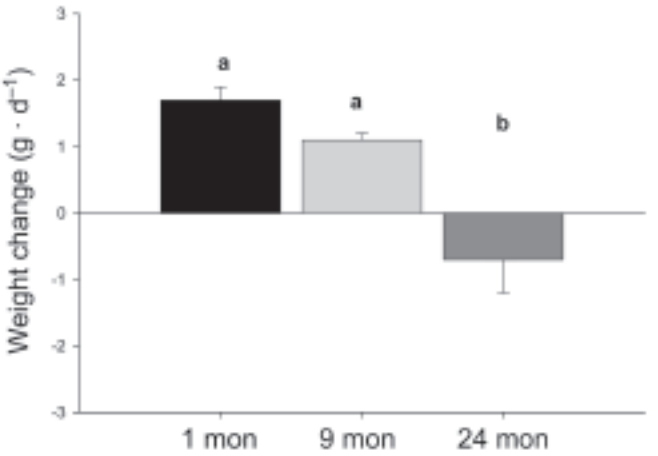

FIG. 1. Effect of age on the body weight change of Fischer 344 rats fed chow. Values are mean ± SEM. Different letters denote a significant age effect ($P < 0.05$).

TABLE 1
Effect of Age on Intestinal Weight[a]

	Tissue weight (mg/cm)	Mucosal weight (mg/cm)	Intestinal wall composed of mucosa (%)
Jejunum			
1 mon	9.0 ± 0.7	4.0 ± 0.5	44.5 ± 2.9
9 mon	12.3 ± 1.3	6.3 ± 1.2	48.8 ± 5.2
24 mon	10.7 ± 1.5	5.6 ± 1.1	48.7 ± 4.0
Ileum			
1 mon	6.4 ± 0.7[a]	2.9 ± 0.6[a]	38.3 ± 4.7
9 mon	7.8 ± 0.8[a]	3.5 ± 0.6[a]	43.9 ± 3.1
24 mon	11.1 ± 1.7[b]	6.0 ± 1.1[b]	50.1 ± 6.4

[a]Values are mean ± SEM. Different letters denote a significant age effect ($P < 0.05$).

When uptake was expressed on the basis of mucosal surface area (Jsam = nmol · cm^{-2} mucosal surface area · min^{-1}), jejunal uptake of 18:2 was increased between 1 and 9 or 1 and 24 mon, and 18:3 uptake was increased between 1 and 9 mon. The ileal uptake of cholesterol was increased between 1 and 9 mon (Fig. 3).

Intestinal lipid-binding proteins. The expression of ILBP mRNA in the ileum was higher at 24 than at 9 mon, but was similar to the value at 1 mon (Figure 4A). The expression of L-FABP mRNA in the jejunum and ileum did not change significantly with the age of the animals (Figs. 4B, 4C). The abundance of ILBP, as measured by immunohistochemistry, was reduced in the ileum at 9 or 24 mon as compared with 1 mon (Figs 5A, 6A–C). The abundance of I-FABP protein examined using

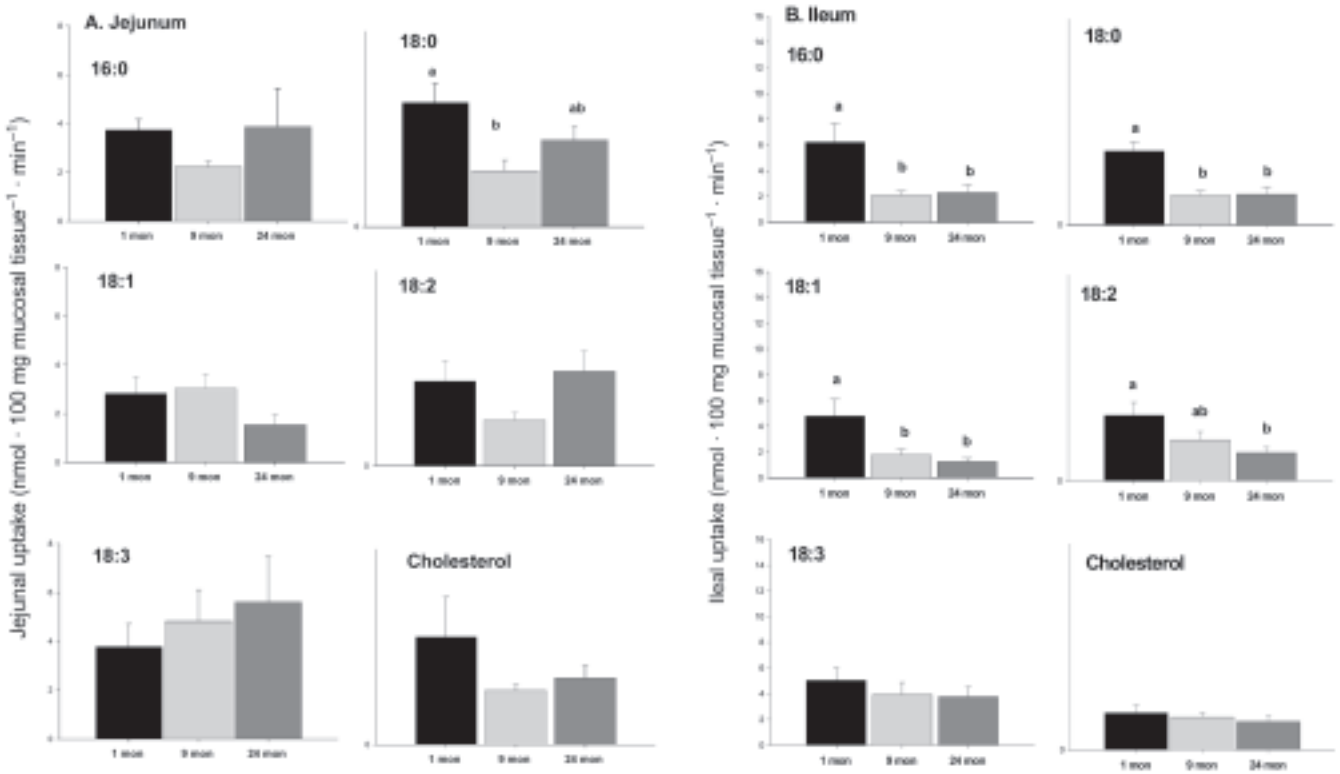

FIG. 2. (A) Jejunal and (B) ileal uptake of FA and cholesterol expressed as nmol · 100 mg mucosal tissue^{-1} · min^{-1}. Values are mean ± SEM. Different letters denote a significant age effect ($P < 0.05$).

immunohistochemistry was lower in the jejunum at 24 mon than at 1 mon, and higher in the ileum at 9 mon than at 1 or 24 mon (Figs. 5B, 6D–F).

DISCUSSION

Body weight change. The F344 rat is expected to gain weight from birth to approximately 18 mon, after which the weight plateaus and then gradually declines (29). The 24-mon-old animals lost body weight with aging (Fig. 1). We did not determine food intake in this study, but it is possible that the reduced uptake of FA (Fig. 2) may have contributed to this body weight loss.

Although the weight of the jejunal wall and mucosa did not change with aging, the weight of the ileum and ileal mucosa almost doubled (Table 1). The explanation for this is not clear; we speculate that the jejunal malabsorption of sugars and amino acids that occurs with aging (4,5) may result in the delivery of a greater nutrient load to the ileum, thereby resulting in greater mucosal weight. To account for these changes, our data were expressed on the basis of mucosal weight (Jm) to determine whether specific changes in lipid uptake occurred that were not simply explainable by increases in mucosal mass.

Methods of expressing uptake rates. The usual way of expressing the rate of *in vitro* uptake of nutrients is on the basis of the weight of the full thickness of the intestine. However, if a treatment alters the weight of the intestine, then there may be variations in the rate of nutrient uptake that are understandable simply because there would be different amounts of mucosal tissue. For this reason, since there were treatment-associated variations in mucosal weight (Table 1), it was appropriate to express uptake on the basis of the mass of the transporting mucosal tissue. It is still possible, of course, that nutrient uptake may alter without a change in mucosal mass or villous surface area, with uptake either responding to a change in the distribution of transporters along the villus or adapting to an alteration in BBM permeability. Thus, although aging is associated with a decline in the uptake of some lipids, when expressed on the basis of mucosal weight (Fig. 2) and when age-associated alterations in surface area are taken into account, there is actually an increased rather than a decreased uptake of some lipids (Fig. 3). When using an *in vivo* perfusion technique and expressing lipid uptake on the basis of the length of the intestine, the uptake of cholesterol and FA has been shown to increase in aging rats (30,31). In an *in vivo* perfusion study, Holt and Dominguez (32) found a decrease in lipid uptake in 21-mon-old as compared with 4-mon-old rats when uptake was expressed on the basis of intestinal weight. Thus, the qualitative aspect of the effect of aging on lipid uptake depends on the method used to express the results.

Passive uptake of lipids across the BBM may be affected by BBM fluidity and by the pH microclimate adjacent to the BBM (10,33). Previous work suggests that the lipid composition of the BBM may contribute to alterations in lipid uptake

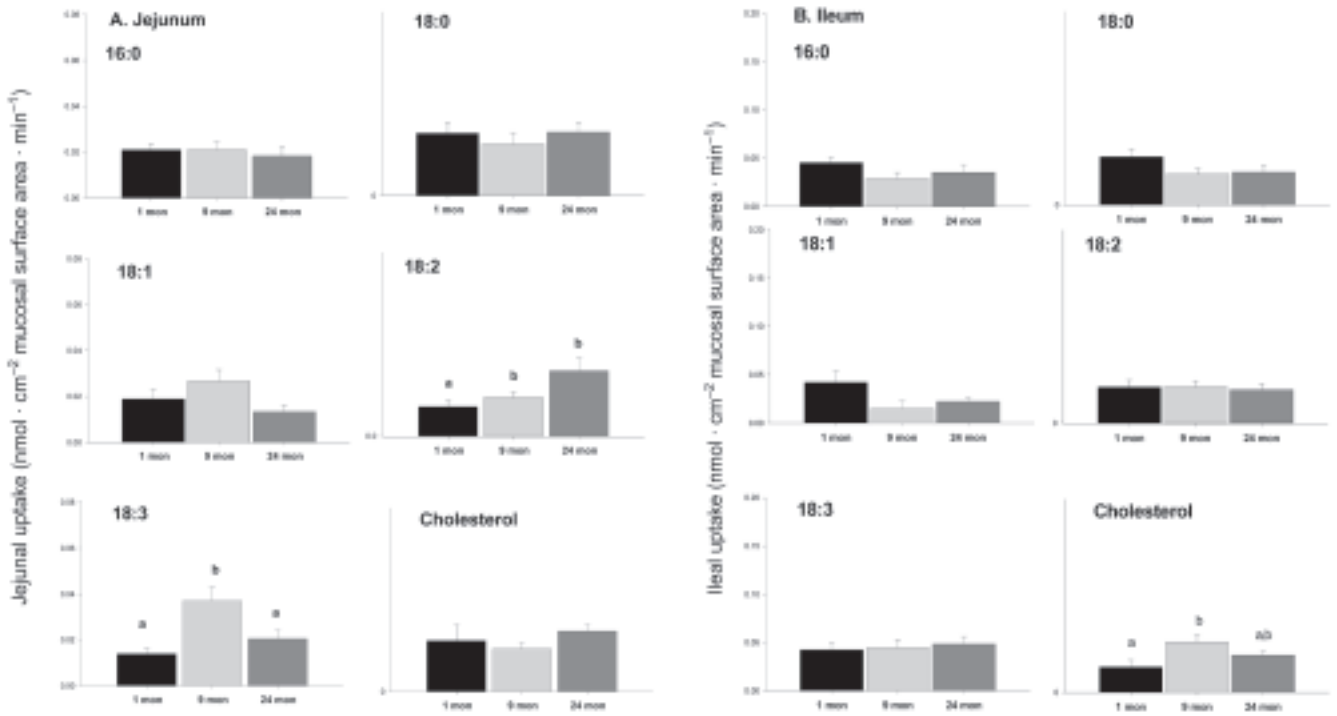

FIG. 3. (A) Jejunal and (B) ileal uptake of FA and cholesterol expressed on the basis of mucosal surface area. Values are mean ± SEM (n = 8). Different letters denote a significant age effect ($P < 0.05$).

(34). An age-associated decrease occurs in BBM fluidity (11), which could contribute to altered lipid absorption with aging. The low pH of the microclimate adjacent to the BBM increases the bile acid critical micellar concentration, resulting in a dissociation of lipids from bile acid micelles (10). In aging, there is an increase in the pH of the microclimate, which would potentially contribute to reduced absorption (35). Measurements of the pH of the microclimate and the BBM lipid composition were not performed in this study. Although this study shows an effect of aging on lipid uptake, i.e., the rate-limiting step, it is possible that other factors may change with aging and thereby alter the absorptive process. These factors include alterations in motility, blood or lymph flow, and enterocyte metabolism of lipids. It is also important to stress that lipid uptake did not change in the jejunum, the site at which most of the lipid uptake is thought to occur. The nutritional impact of the reduced FA uptake observed in the ileum is unclear.

The effect of UWL. The uptake of 12:0 is a reflection of the UWL, with higher uptake reflecting lower resistance (7). In 24-mon-old animals, the jejunal uptake of 12:0 was increased, suggesting lower UWL (data not shown). This lower resistance would help to increase the uptake of diffusion-limited probes, such as LCFA (26). However, at 24 mon the jejunal uptake of most lipids was unchanged when expressed on the basis of mucosal weight, and the ileal uptake of FA fell. Thus, the age-associated alterations in lipid uptake could not be explained by variations in the UWL.

Lipid-binding proteins. Numerous lipid-binding proteins are found in the BBM and the cytosol of the enterocyte (reviewed in Ref. 12). For example, the FATP4 (16), and the FAT are in the BBM of enterocytes (36). Furthermore, it has also been suggested that the rate-limiting step in lipid absorption is the formation of a prechylomicron transport vesicle in the endoplasmic reticulum (37). These were not measured in this study. The reduced ileal lipid absorption in aging (expressed on the basis of intestinal or mucosal weight) was associated with reduced abundance of I-FABP (Figs. 5B, 6D–G) and ILBP (Figs. 5A, 6A–C). However, it is not certain whether the age-associated alterations in lipid uptake were causally related to variations in the abundance of I-FABP and ILBP. ILBP does not bind LCFA, and in I-FABP knockout mice, FA uptake is maintained, suggesting that the I-FABP protein is not required for intestinal lipid uptake (38). The association between the decline in lipid uptake and the fall in I-FABP and ILBP does not prove they are causally related. It is possible, of course, that changes in some of the other lipid-binding proteins not measured in these studies may have contributed to changes in lipid absorption that occur with aging.

Finally, it is not apparent why age had varying effects on the uptake of each of the individual FA. For example, in contrast to 16:0, 18:0, 18:1, and 18:2, ileal 18:3 uptake was not reduced with aging (Fig. 2B). One may speculate that this may reflect the varying affinities of the lipid-binding proteins. Although both L-FABP and I-FABP preferentially bind LCFA, L-FABP has a higher affinity for polyunsaturated LCFA (39). Furthermore, Hanhoff *et al.* (40) demonstrated that several factors influence the binding affinity of FABP, including the solubility of the FA in the aqueous phase, the conformation of the FA, the degree of unsaturation, and the position of the double bond.

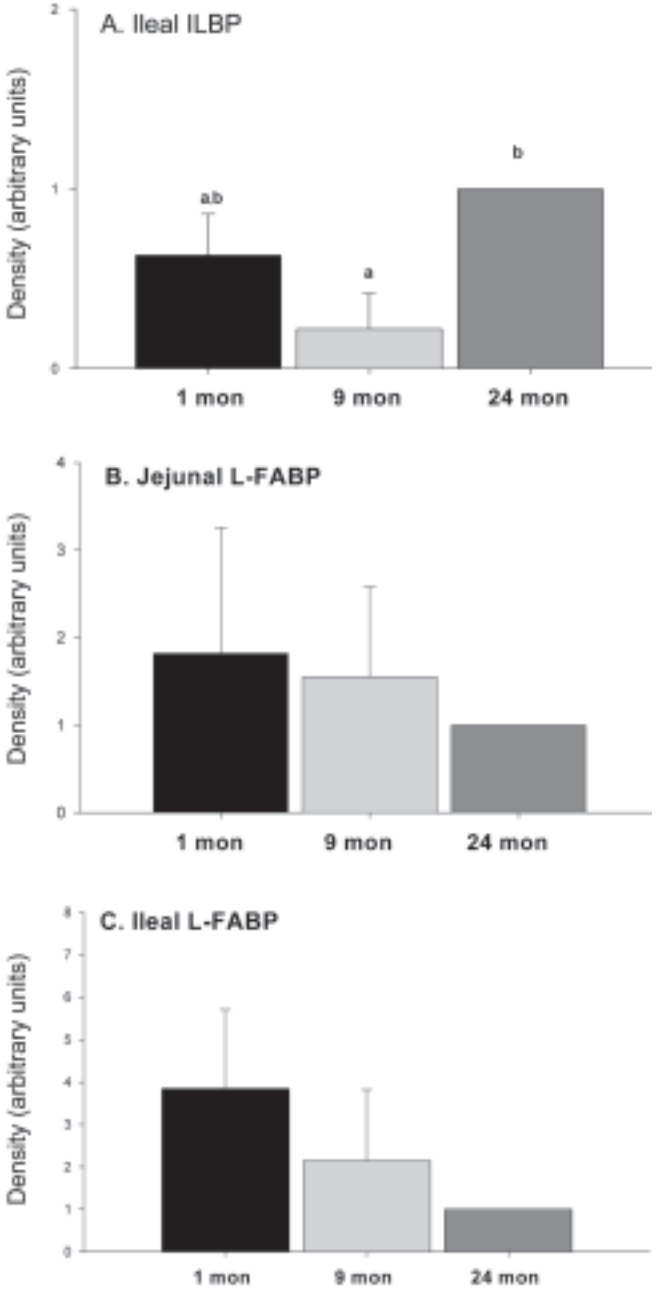

FIG. 4. Expression of (A) ileal lipid-binding protein (ILBP), (B) jejunal liver FA-binding protein (L-FABP), and (C) ileal L-FABP mRNA as determined by Northern blotting, with values normalized to the 24-mon group. Values are mean ± SEM (n = 4). Different letters denote a significant age effect ($P < 0.05$).

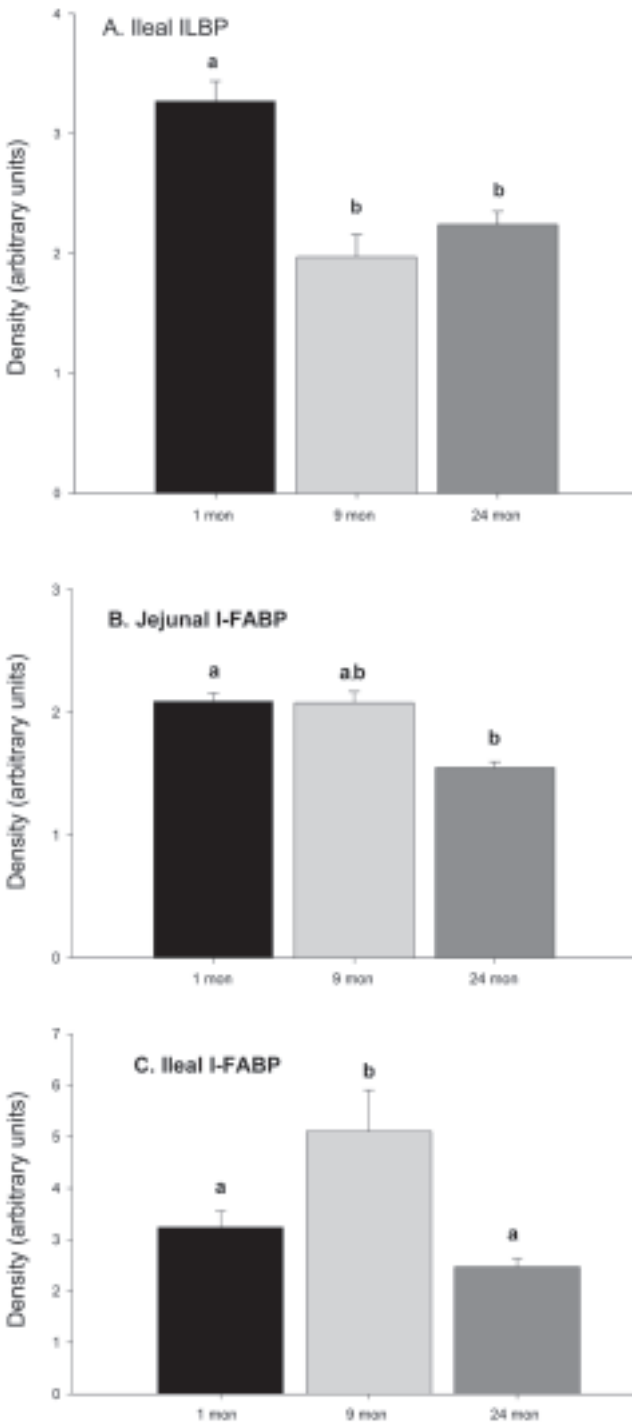

FIG. 5. Abundance of (A) ILBP, (b) jejunal intestinal FA-binding protein (I-FABP), and (c) ileal I-FABP as determined by immunohistochemistry. Values are mean ± SEM. Different letters denote a significant age effect ($P < 0.05$). For other abbreviation see Figure 4.

Similarly, cholesterol uptake was not reduced with aging (Fig. 2B), despite decreases in some of the lipid-binding proteins (Figs. 5A, 5B). This result may be explained by the presence of the recently identified Niemann–Pick C1 Like 1 protein, which is essential for the transport of cholesterol across the BBM of the enterocyte (41). The expression of this protein with aging has not been studied, but our data suggest that its activity may be maintained with age, as we did not see age-related reductions in intestinal cholesterol uptake.

REFERENCES

1. Health Canada (2002) *Canada's Aging Population*, Division of Aging and Seniors, Health Canada, Ottawa, Ontario, Canada, http://www.hc-sc.gc.ca/seniors-aines/_pubs/fed_paper/pdfs/fedpager_e.pdf (accessed June 2004).

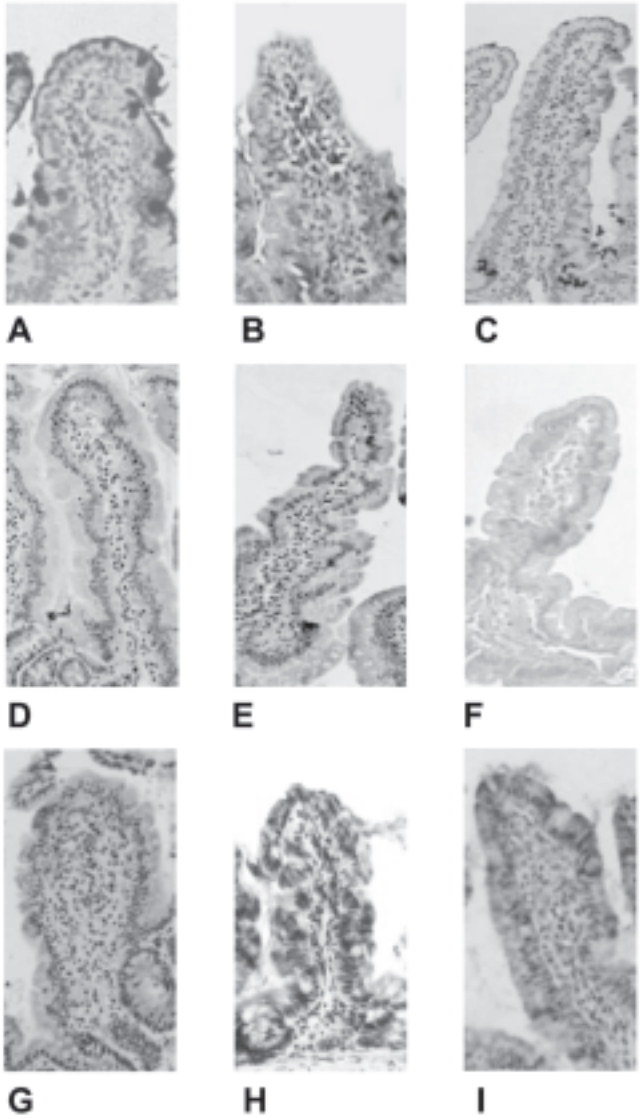

FIG. 6. Representative ILBP and I-FABP immunohistochemistry. Ileal ILBP: (A) 1-; (B) 9-; and (C) 24-mon-old rats. Jejunal I-FABP: (D) 1-; (E) 9-; and (F) 24-mon-old rats. Ileal I-FABP: (G) 1-; (H) 9-; and (I) 24-mon-old rats. For abbreviations see Figures 4 and 5.

2. Halter, J.B. (1999) Diabetes Mellitus, in *Principles of Geriatric Medicine and Gerontology* (Hazzard, W.M., Blass, J.P., Ettinger, W.H., Jr., Halter, J.B., and Ouslander, J.G., eds.), pp. 991–1011, McGraw-Hill, New York.
3. Morley, J.E. (1999) An Overview of Diabetes Mellitus in Older Persons, *Clin. Geriatr. Med. 15,* 211–223.
4. Ferraris, R.P., and Vinnekota, R.R. (1993) Regulation of Intestinal Nutrient Transport Is Impaired in Aged Mice, *J. Nutr. 123,* 502–511.
5. Chen, T.S., Currier, G.J., and Wabner, C.L. (1990) Intestinal Transport During the Life Span of the Mouse, *J. Gerontol. 45(4),* B129–133.
6. Morris, H.A., Nordin, B.E.C., Fraser, V., Hartley, T.F., Need, A.G., and Horowitz, M. (1985) Calcium Absorption and Serum 1,25-Dihydroxy Vitamin D Levels in Normal and Osteoporotic Women, *Gastroenterology 88(5)*, A1508.
7. Thomson, A.B.R. (1980) Effect of Age on a Homologous Series of Saturated Fatty Acids into Rabbit Jejunum, *Am. J. Physiol. 239,* G363–G371.
8. Peachey, S.E., Dawson, J.M., and Harper, E.J. (1999) The Effect of Ageing on Nutrient Digestibility by Cats Fed Beef Tallow-, Sunflower Oil-, or Olive Oil-Enriched Diets, *Growth Dev. Aging 63*, 61–70.
9. Keelan, M., and Thomson, A.B.R. (2001) Effect of Aging on Intestinal Lipid Absorption, in *Handbook of Nutrition in the Aged* (Wolinsky, I., and Hickson, J.F., Jr., eds.), 3rd edn., pp. 275–295, CRC Press, Boca Raton, FL.
10. Shiau, Y.F. (1990) Mechanism of Intestinal Fatty Acid Uptake in the Rat: The Role of an Acidic Microclimate, *J. Physiol. 421*, 463–474.
11. Wahnon, R., Mokady, S., and Cogan, U. (1989) Age and Membrane Fluidity, *Mech. Ageing Dev. 50*, 249–255.
12. Besnard, P., Niot, I., Poirier, H., Clement, L., and Bernard, A. (2002) New Insights into the Fatty Acid-Binding Protein (FABP) Family in the Small Intestine, *Mol. Cell Biochem. 239*, 139–147.
13. Stremmel, W., Lotz, G., Strohmeyer, G., and Berk, P.D. (1985) Identification, Isolation, and Partial Characterization of a Fatty Acid Binding Protein from Rat Jejunal Microvillous Membranes, *J. Clin. Invest. 75*, 1068–1076.
14. Stremmel, W. (1988) Uptake of Fatty Acids by Jejunal Mucosal Cells Is Mediated by a Fatty Acid Binding Membrane Protein, *J. Clin. Invest. 82*, 2001–2010.
15. Abumrad, N.A., El-Maghrabi, M.R., Amri, E.-Z., Lopez, E., and Grimaldi, P.A. (1993) Cloning of Rat Adipocyte Membrane Protein Implicated in Binding or Transport of Long-Chain Fatty Acids That Is Induced During Preadipocyte Differentiation, *J. Biol. Chem. 268*, 17665–17668.
16. Stahl, A., Hirsch, D.J., Gimeno, R.E., Punreddy, S., Ge, P., Watson, N., Patel, S., Kotler, M., Raimondi, A., Tartaglia, L.A., and Lodish, H.F. (1999) Identification of the Major Intestinal Fatty Acid Transport Protein, *Molecular Cell 4*, 299–308.
17. Agellon, L.B., Toth, M.J., and Thomson, A.B. (2002) Intracellular Lipid Binding Proteins of the Small Intestine, *Mol. Cell Biochem. 239,* 79–82.
18. Poirier, H., Niot, I., Degrace, P., Monnot, M.C., Bernard, A., and Besnard, P. (1997) Fatty Acid Regulation of Fatty-Acid Binding Protein Expression in the Small Intestine, *Am. J. Physiol. 273,* G289–G295.
19. Hsu, K.T., and Storch, J. (1996) Fatty Acid Transfer from Liver and Intestinal Fatty Acid-Binding Proteins to Membranes Occurs by Different Mechanisms, *J. Biol. Chem. 271*, 13317–13323.
20. Richieri, G.V., Ogata, R.T., and Kleinfeld, A.M. (1999) Fatty Acid Interactions with Native and Mutant Fatty Acid Binding Proteins, *Mol. Cell Biochem. 192*, 77–85.
21. Bass, N.M., Manning, J.A., Ockner, R.K., Gordon, J.I., Seetharam, S., and Alpers, D.H. (1985) Regulation of the Biosynthesis of Two Distinct Fatty Acid-Binding Proteins in Rat Liver and Intestine. Influences of Sex Difference and of Clofibrate, *J. Biol. Chem. 260*, 1432–1436.
22. Poirier, H., Degrace, P., Noit, I., Benard, A., and Besnard, P. (1996) Localization and Regulation of the Putative Membrane Fatty Acid-Transporter (FAT) in the Small Intestine. Comparison with Fatty Acid-Binding Proteins (FABP), *Eur. J. Biochem. 238*, 368–373.
23. Lin, M.C., Gong, Y.Z., Geoghegan, K.F., and Wilson, F.A. (1991) Characterization of a Novel 14 kDa Bile Acid-Binding Protein from Rat Ileal Cytosol, *Biochim. Biophys. Acta 1078*, 329–335.
24. Kramer, W., Corsiero, D., Friedrich, M., Girbig, F., Stengelin, S., and Weyland, C. (1998) Intestinal Absorption of Bile Acids: Paradoxical Behaviour of the 14 kDa Ileal Lipid-Binding Protein in Differential Photoaffinity Labeling, *Biochem. J. 333,* 335–341.
25. Lukie, B.E., Westergaard, H., and Dietschy, J.M. (1974) Validation of a Chamber That Allows Measurement of Both Tissue Uptake Rates and Unstirred Layer Thicknesses in the Intestine

Under Conditions of Controlled Stirring, *Gastroenterology 67*, 652–61.
26. Westergaard, H., and Dietschy, J.M. (1976) The Mechanism Whereby Bile Acid Micelles Increase the Rate of Fatty Acid and Cholesterol Uptake into the Intestinal Mucosal Cell, *J. Clin. Invest. 58*, 97–108.
27. Ecknauer, R., Vadakel, T., and Welper, T. (1982) Intestinal Morphology and Cell Production Rate in Aging Rats, *J. Gerontol. 37*, 151–155.
28. Keelan, M., Walker, K., and Thomson, A.B.R. (1985) Effect of Chronic Ethanol and Food Deprivation on Intestinal Villus Morphology and Brush Border Membrane Content of Lipid and Marker Enzymes, *Can. J. Physiol. Pharmacol. 63*, 1312–1320.
29. Masoro, E.J. (1980) Mortality and Growth Characteristics of Rat Strains Commonly Used in Aging Research, *Exp. Aging Res. 6*, 219–233.
30. Hollander, D., and Morgan, D. (1979) Aging: Its Influence on Vitamin A Intestinal Absorption *in vivo* by the Rat, *Exp. Gerontol. 14*, 301–305.
31. Hollander, D., and Dadufalza, V.D. (1983) Increased Intestinal Absorption of Oleic Acid with Aging in the Rat, *Exp. Gerontol. 18*, 287–292.
32. Holt, P.R., and Dominguez, A.A. (1981) Intestinal Absorption of Triglyceride and Vitamin D3 in Aged and Young Rats, *Dig. Dis. Sci. 26*, 1109–1115.
33. Higgins, C.F. (1994) Flip-Flop. The Transmembrane Translocation of Lipids, *Cell 79*, 393–395.
34. Keelan, M., Cheeseman, C., Walker, K., and Thomson, A.B. (1986) Effect of External Abdominal Irradiation on Intestinal Morphology and Brush Border Membrane Enzyme and Lipid Composition, *Radiat. Res. 105*, 84–96.
35. Ikuma, M., Hanai, H., Kaneko, E., Hayashi, H., and Hoshi, T. (1996) Effects of Aging on the Microclimate pH of the Rat Jejunum, *Biochim. Biophys. Acta 1280*, 19–26.
36. Chen, M., Yang, Y., Braunstein, E., Georgeson, K.E., and Harmon, C.M. (2001) Gut Expression and Regulation of FAT/CD36: Possible Role in Fatty Acid Transport in Rat Enterocytes, *Am. J. Physiol. 281(5)*, E916–E923.
37. Mansbach, C.M., and Dowell, R. (2000) Effect of Increasing Lipid Loads on the Ability of the Endoplasmic Reticulum to Transport Lipid to the Golgi, *J. Lipid Res. 41*, 605–612.
38. Vassileva, G., Huwyler, L., Poirier, K., Agellon, L.B., and Toth, M.J. (2000) The Intestinal Fatty Acid Protein Is Not Essential for Dietary Fat Absorption in Mice, *FASEB J. 14,* 2040–2046.
39. Richieri, G.V., Ogata, R.T., and Kleinfeld, A.M. (1994) Equilibrium Constants for the Binding of Fatty Acids with Fatty Acid-Binding Proteins from Adipocyte, Intestine, Heart, and Liver Measured with the Fluorescent Probe ADIFAB, *J. Biol. Chem. 269*, 23918–23930.
40. Hanhoff, T., Lucke, C., and Spener, F. (2002) Insights into Binding of Fatty Acids by Fatty Acid Binding Proteins, *Mol. Cell Biochem. 239*, 45–54.
41. Altmann, S.W., Davis, H.R. Jr., Zhu, L.J., Yao, X., Hoos, L.M., Tetzloff, G., Iyer, S.P., Maguire, M., Golovko, A., Zeng, M., *et al.* (2004) Niemann-Pick C1 Like 1 protein Is Critical for Intestinal Cholesterol Absorption, *Science 303 (5661)*, 1201–1204.

[Received June 3, 2004; accepted September 15, 2004]

Conjugated Linoleic Acid Isomer Effects in Atherosclerosis: Growth and Regression of Lesions

David Kritchevsky[a,*], Shirley A. Tepper[a], Scott Wright[a], Susanne K. Czarnecki[b], Thomas A. Wilson[c], and Robert J. Nicolosi[c]

[a]The Wistar Institute, Philadelphia, Pennsylvania 19104, [b]Department of Chemistry, Chestnut Hill College, Philadelphia, Pennsylvania 19118, and [c]Department of Health and Clinical Sciences, University of Massachusetts–Lowell, Lowell, Massachusetts 01854

ABSTRACT: Conjugated linoleic acid (CLA), a mixture of positional and geometric isomers of octadecadienoic acid, has been shown to inhibit experimentally induced atherosclerosis in rabbits and also to cause significant regression of pre-established atheromatous lesions in rabbits. The two major CLA isomers (*cis*9,*trans*11 and *trans*10,*cis*12), now available at 90% purity, have been tested individually for their anti-atherogenic or lesion regression potency. The two major isomers and the mixture were fed for 90 d to rabbits fed 0.2% cholesterol. Atherosclerosis was inhibited significantly by all three preparations. The two CLA isomers and the isomer mix were also fed (1.0%) as part of a cholesterol-free diet for 90 d to rabbits bearing atheromatous lesions produced by feeding an atherogenic diet. A fourth group was maintained on a cholesterol-free diet. On the CLA-free diet atherosclerosis was exacerbated by 35%. Reduction of severity of atheromatous lesions was observed to the same extent in all three CLA-fed groups. The average reduction of severity in the three CLA-fed groups was 26 ± 2% compared with the first control (atherogenic diet) and 46 ± 1% compared with the regression diet. Insofar as individual effects on atherosclerosis were concerned, there was no difference between the CLA mix and the *cis*9,*trans*11 and *trans*10,*cis*12 isomers. They inhibit atherogenesis by 50% when fed as a component of a semipurified diet containing 0.2% cholesterol; and when fed as part of a cholesterol-free diet, they reduce established lesions by 26%. Reduction of atheromata to the observed extent by dietary means alone is noteworthy.

Paper no. L9457 in *Lipids 39*, 611–616 (July 2004).

CLA is a collective term describing positional and geometric isomers of octadecadienoic acid. It is produced in the rumen of ruminant animals and occurs naturally in the meat of ruminant animals as well as in products prepared from their milk, e.g., cheese and butter. The major naturally occurring modification of CLA is the *cis*9,*trans*11 (*c*9,*t*11) isomer (1). The original studies with CLA were carried out using a commercially available synthetic product that contained 40–45% each of the *c*9,*t*11 and the *trans*10,*cis*12 (*t*10,*c*12) modifications.

Most of the early CLA literature describes the inhibitory effects of the CLA mixture on experimental carcinogenesis (2). This mixture has also been shown to inhibit atherosclerosis in rabbits (3–5) and hamsters (6,7) even when fed at relatively low concentrations. Munday *et al*. (8) reported that CLA promoted fatty streak formation in C57BL/6 mice despite lowering the total/HDL cholesterol ratio. The mice were fed 0.25 or 0.50% CLA and 1% cholesterol. In our experiments with hamsters (6,7), we found that increasing the level of dietary CLA led to greater inhibition of aortic fatty streak formation. This may be the case in Munday's study. It is possible that the level of dietary CLA required to suppress aortic fatty streaking and atherosclerosis is a function of the species being studied as well as the level of dietary cholesterol.

Park *et al*. (9) reported in 1997 that accretion of body fat was significantly reduced in mice fed CLA. It was shown later (10) that the effect was due specifically to the *t*10,*c*12 isomer. The availability of the two major CLA isomers at >90% purity has afforded the opportunity to test them individually, and there are now a number of instances in which isomer-specific effects have been reported (11). Thus, only *t*10,*c*12 CLA increases insulin resistance (12) and circulating C-reactive protein (13) in obese men. It also causes hyperinsulinemia in mice (14,15), reduces leptin secretion (16) and lipogenesis (17) in cells in culture, and increases lipoprotein lipase activity in adipocytes (18).

In this communication we describe the individual effects of *c*9,t11 and *t*10,*c*12 CLA on the development of cholesterol-induced atherosclerosis in rabbits as well as their effects on regression of pre-established atherosclerotic lesions.

EXPERIMENTAL PROCEDURES

Atherogenesis studies. Forty male New Zealand White rabbits were randomized into four groups of 10 rabbits each. The starting average body weight of the four groups was the same (2600 g). The rabbits were housed in individual stainless steel cages in a temperature-controlled, humidified room maintained on a 12 h on/off light cycle and were provided free access to food and water. The rabbits were fed a semipurified, atherogenic diet (Table 1) to which we added 0.5% of either CLA isomer or the mixture. All CLA preparations were purchased from Natural ASA (Hovdebygda, Norway). The composition of the CLA preparations is given in Table 2.

After 90 d, the rabbits were bled under light anesthesia and euthanized with ketamine/xylazine 10:3. Blood was taken for cholesterol analysis using a commercial kit (Sigma, St. Louis,

*To whom correspondence should be addressed at The Wistar Institute, 3601 Spruce St., Philadelphia, PA 19104. E-mail: kritchevsky@wistar.upenn.edu

Abbreviations: *c*9,*t*11, *cis*9,*trans*11 CLA; ICAM, intercellular adhesion molecule; PGE_2, prostaglandin E_2; *t*10,*c*12, *trans*10,*cis*12 CLA.

TABLE 1
Semipurified, Atherogenic Diet[a]

Ingredient	%	% Calories
Casein	25.00	25.8
DL-Methionine	0.20	
Sucrose	20.48	21.1
Starch	20.00	20.6
Cholesterol	0.20	
Coconut oil	13.00	30.1
Corn oil	1.00	2.3
Cellulose	15.00	
Mineral mix	4.00	
Vitamin mix	1.00	
Choline bitartrate	0.12	
Total	100.00	100.00

[a]CLA (0.5%) was added at the expense of sucrose. This addition increased total caloric content of the diet by 2 kcal (388 to 390). Calories from fat were increased by 3%.

TABLE 2
Composition (%) of CLA Preparations Used in Atherogenesis Study[a]

	CLA preparation		
FA	>90% *c*9,*t*11	>90% *t*10,*c*12	Mixture
*c*9,*t*11 CLA	91.6	2.9	42.8
*t*10,*c*12 CLA	1.8	93.2	44.6
Oleic (18:1)	4.4	0.8	5.7
Other	2.2	3.1	6.9

[a]Analytical data provided by Natural ASA (Hovdebygda, Norway). *c*9,*t*11 CLA, *cis*9,*trans*11 CLA; *t*10,*c*12 CLA, *trans*10,*cis*12 CLA.

MO); livers were removed and weighed; and 1-g aliquots were taken for determination of free and total cholesterol. The liver aliquots were extracted with chloroform/methanol 2:1 (19). The extracts were taken to dryness, and the residual lipid was solubilized with an appropriate surface-active agent (20), in this case 1% Triton in chloroform. The Triton/lipid solution was taken to dryness under N_2 and reconstituted in 200 μL of distilled water. Aliquots (25 μL) of the lipid solution were analyzed enzymatically for total and free cholesterol using reagent kits (Wako Chemical, Richmond, VA). Analyses were carried out in triplicate. This assay has been used successfully for analysis of tissue lipids of hamsters (21).

At necropsy, aortas were removed and cleaned of adhering tissue; and the severity of atherosclerotic lesions was graded visually using a 0–4 scale (22). In previous studies, when visual grading was compared with morphometric methodology under double-blind conditions, excellent correlation ($r > 0.90$) was observed (23; Kritchevsky, D., and Klurfeld, D.M., unpublished data).

Regression studies. Forty male New Zealand White rabbits (average weight 2865 g) were housed under the conditions described above and maintained on the atherogenic regimen (Table 1) for 90 d. At this time each rabbit's serum cholesterol level was determined. The rabbits were randomized into five groups of eight rabbits each having the same average serum cholesterol level (678 ± 82 mg/dL). One group (C1) was necropsied; the serum lipids were analyzed using commercial kits (Wako Chemical), the liver lipids analyzed as described (20,21), and the aortas graded visually on a 0–4 scale (22). This group served as the initial control against which subsequent findings were compared. The other four groups were fed a cholesterol-free regimen containing 6% corn oil (C2) (Table 3) or the same diet in which 1% of the corn oil was replaced by 1% CLA (*c*9,*t*11; *t*10,*c*12; or the mixture). The composition of the CLA mixtures is given in Table 4. To forestall difficulties that have been encountered internationally when using some commercial preparations of choline bitartrate (24), choline chloride was used in the preparation of the regression diet.

After 90 d the rabbits were bled after an overnight fast, and sera, livers, and aortas were subjected to the same analytical procedures as described above. All diets were prepared to our specifications and pelleted by Dyets, Inc. (Bethlehem, PA). All experimental procedures were approved by the Wistar Institute Animal Care and Use Committee (IUCAC).

Statistical methods. ANOVA was determined using a general linear models procedure (SAS PROC GLM-SAS Software, Carey, NC). The Student–Newman–Keuls multiple comparison test was used to determine which of the treatments significantly affected the dependent variables. Analysis of the severity of aortic atherosclerosis was carried out using the Kruskal–Wallis one-way analysis on ranks.

RESULTS

Atherogenesis. Our findings are summarized in Table 5. The rabbits showed minimal change in body weight. Liver weights (actual) and relative liver weights (as % body weight) were in the same range for all groups. Serum cholesterol levels in the control group were slightly higher than those in the

TABLE 3
Cholesterol-Free "Regression" Diet

Ingredient	%	% Calories
Casein	24.0	27.4
DL-Methionine	0.3	
Sucrose	30.0	34.3
Cornstarch	20.0	22.9
Corn oil[a]	6.0	15.4
Cellulose	14.0	
Mineral mix	4.0	
Vitamin mix	1.0	
Choline chloride	0.7	
Total	100.0	100.0

[a]CLA preparations (1%) added at expense of corn oil.

TABLE 4
Composition (%) of CLA Preparations Used in Regression Study[a]

	CLA preparation		
FA	>90% *c*9,*t*11	>90% *t*10,*c*12	Mixture
*c*9,*t*11 CLA	88.6	5.7	44.3
*t*10,*c*12 CLA	3.0	89.5	43.9
Oleic acid (18:1)	3.7	1.6	5.5
Other	4.7	3.2	6.3

[a]Analytical data provided by Natural ASA (Hovdebygda, Norway).

TABLE 5
Necropsy Data[a]: Rabbits Fed Atherogenic Diet Plus 0.5% CLA for 90 d (mean ± SEM)

	Group			
	Control	*c*9,*t*11-CLA	*t*10,*c*12-CLA	CLA-mix
No.	9	9	10	10
Wt gain (g)	6 ± 29	–1 ± 12	–17 ± 12	–10 ± 10
Liver wt (g)	70.6 ± 5.04	59.8 ± 2.68[a]	69.1 ± 2.04[a]	69.8 ± 4.19
Liver % body wt	2.78 ± 0.21	2.29 ± 0.10[a,b]	2.67 ± 0.06[a]	2.67 ± 0.15[b]
Serum lipids (mg/dL)				
Cholesterol	647 ± 66	556 ± 57	582 ± 46	511 ± 52
TG	198 ± 28	167 ± 32	186 ± 25	191 ± 24
Liver cholesterol (mg/g)				
Total	3.10 ± 0.29	2.57 ± 0.26	3.17 ± 0.14	3.03 ± 0.18
Esterified	1.91 ± 0.22	1.53 ± 0.19	1.89 ± 0.15	1.87 ± 0.13
% Esterified	61.3 ± 2.13	59.0 ± 1.37	59.0 ± 1.85	61.4 ± 1.44
Atherosclerosis[b]				
Aortic arch[c]	2.39 ± 0.3[a,b,c]	1.56 ± 0.3[a]	1.10 ± 0.4[b]	1.10 ± 0.2[c]
Thoracic aorta[d]	1.17 ± 0.4[a,b]	0.28 ± 0.1[a]	0.50 ± 0.2	0.25 ± 0.1[b]

[a]Values in horizontal row bearing same superscript roman letter are significantly different ($P < 0.05$) by *t*-test.
[b]Significant by Kruskal–Willis one-way ANOVA on ranks.
[c]$P = 0.010$.
[d]$P = 0.009$.

three test groups, but the differences were not significant. Serum TG levels were lowest in rabbits fed the *c*9,*t*11 isomer but were not significantly different from the other groups. The rabbits fed the diet rich in *c*9,*t*11 CLA also had the lowest levels of liver cholesterol (by 15–18%) but again none of the differences were statistically significant.

The rabbits fed the control diet exhibited significantly more severe atherosclerosis than did those fed CLA. The differences in both the aortic arch and thoracic aorta were significant, being $P = 0.010$ and $P = 0.009$, respectively. There were no differences among the three CLA preparations. In general they reduced severity of lesions by 62% (mixed CLA), 48% (*c*9,*t*11 CLA), and 55% (*t*10,*c*12 CLA) compared with the control group.

Regression study. Our findings are summarized in Table 6. Replacement of the atherogenic diet by a cholesterol-free regimen significantly lowered actual and relative liver weights compared with the first control group (C1), but there were no differences among the four surviving groups. Liver weight was reduced by about 24% and liver cholesterol by about 29%. Serum cholesterol levels fell significantly in all the test groups. The serum cholesterol levels in the second control group fell most steeply and were significantly lower than those in the three groups on CLA.

There were no significant differences in serum cholesterol among the three CLA groups, but rabbits fed the CLA mix had higher levels than those fed *c*9,*t*11 CLA (by 53%) or *t*10,*c*12 CLA (by 31%). In this study we also determined serum HDL-cholesterol levels. The sera of group C1 were lost, but among the four other groups the second control group exhibited the highest % HDL cholesterol levels. The differences in % HDL cholesterol between group C2 and the

TABLE 6
Influence of CLA Isomers and CLA Mix on Regression of Pre-established Atherosclerosis in Rabbits[a]

	C1	C2	*c*9,*t*11	*t*10,*c*12	Mix	ANOVA
No.	8	8	8	8	8	
Δ wt (g)	175 ± 88[a]	121 ± 51[b]	110 ± 60[a,b]	114 ± 162[a,b]	106 ± 85	NS
Liver wt (g)	83.9 ± 3.46[a,b,c]	60.4 ± 2.54[a]	62.4 ± 3.93[b]	63.4 ± 3.94[c]	69.4 ± 8.30	S
L% BWT	3.04 ± 0.10[a,b,c,d]	2.01 ± 0.08[a]	2.25 ± 0.11[b]	2.12 ± 0.11[c]	2.30 ± 0.23[d]	S
Serum (mg/dL)						
Cholesterol	677 ± 74[a,b,c,d]	116 ± 31[a,f,g,h]	262 ± 43[b,f]	307 ± 33[c,g]	401 ± 67[d,h]	S
% HDL C	—	17.3 ± 3.33[a,b]	10.8 ± 1.44	7.6 ± 1.22[a]	6.2 ± 1.08[b]	S
TG	170 ± 9[a,b,c,d]	35 ± 4[a,e,f,g]	63 ± 7[b,d]	70 ± 10[c,f]	104 ± 20[d,g]	S
Liver (g/liver)						
Total C	1.16 ± 0.14[a]	0.79 ± 0.13	0.81 ± 0.12	0.69 ± 0.07[a]	0.91 ± 0.11	NS
Ester C	1.03 ± 0.13[a]	0.70 ± 0.12	0.72 ± 0.07	0.63 ± 0.06[d]	0.82 ± 0.10	NS
% ester	89.9 ± 1.34[a]	89.3 ± 1.38[b]	89.6 ± 0.78[c]	91.0 ± 1.17[d]	70.4 ± 1.28[a,b,c,d]	NS
Aorta (0–4)						Kruskal–Wallis[b]
Arch	2.3 ± 0.2	2.9 ± 0.4[a]	1.9 ± 0.3	2.1 ± 0.3	1.9 ± 0.2[a]	NS
Thoracic	1.5 ± 0.1[a,b]	2.1 ± 0.4[c,d,e]	0.9 ± 0.28[c]	0.8 ± 0.2[a,d]	0.8 ± 0.2[b,e]	$P = 0.01$

[a]Values in horizontal row bearing same superscript roman letter are significantly different ($P < 0.05$) by *t*-test. S = significant; NS = not significant.
[b]By Kruskal–Wallis one-way ANOVA on ranks.

groups fed *c*9,*t*11 CLA, *t*10,*c*12 CLA, or the CLA mix were significant by Student's *t*-test.

Serum TG were reduced significantly in all four surviving groups. The lowest serum TG levels were seen in the second control, and the pattern of TG levels was similar to that seen for serum cholesterol, namely, *c*9,*t*11 < *t*10,*c*12 < mix. Total liver cholesterol was reduced by 22–40% in the four surviving groups (not significant), but the percentage of liver cholesteryl ester was significantly lower in the rabbits fed the CLA mix.

As is often observed in regression studies, the rabbits placed on the second control (cholesterol-free) diet actually exhibited increased severity of lesions, by 31% in the aortic arch and by 42% in the thoracic aorta. Severity of aortic lesions fell in all three CLA-fed groups. The severity of lesions in the aortic arch was 16, 5, and 16% lower than the initial control in the groups fed *c*9,*t*11 CLA, *t*10,*c*12 CLA, and the CLA mix, respectively. The severity of lesions in the aortic arch in the three CLA groups was 36, 28, and 36% lower than that seen in the second control. Lesions of the thoracic aorta were 42% more severe in the second control (C2) than in the first (C1). Compared with the first and second controls, aortic lesions in rabbits fed the cholesterol-free regression diet were reduced by 41 and 59% (*c*9,*t*11 CLA), 50 and 65% (*t*10,*c*12 CLA), and 50 and 65% (CLA mixed isomers). Differences of severity of lesions in the thoracic aorta were significant, $P = 0.011$. These findings confirm our earlier observations (4).

DISCUSSION

We have confirmed our earlier findings that mixed CLA isomers (0.5%) inhibit atherogenesis significantly in cholesterol-fed rabbits and effect significant regression of established lesions when fed (1.0%) as part of a cholesterol-free regimen. We have also shown that the major isomers of CLA (*c*9,*t*11 and *t*10,*c*12) exert similar effects. There were no significant differences in effect among rabbits fed either isomer (about 90% pure) or the mixture of isomers (about 45% of each).

The extent to which severity of atherosclerosis has been inhibited or diminished is in the same range for all of our studies. Thus, atherogenesis was inhibited by about 60% in this study as well as in our previous studies (4,5), and regression of lesions was in the 35–45% range. These calculations were based on total severity of atherosclerosis, i.e., aortic arch plus thoracic aorta.

Inhibition of experimental atherogenesis has been accomplished by a number of dietary or pharmacologic means, and our findings are one more example of an effective agent. The effect of CLA on regression of pre-established lesions is noteworthy, however. In an earlier publication (4) we reviewed the literature pertaining to attempted regression of atheromata and found most of the efforts involving dietary [no fat (25), corn oil (26), peanut oil (27)] or pharmacological [sitosterol (28), dihydrocholesterol (29), clofibrate (30), thyroxine (31), fluvastatin (32)] treatment had no effect on regression and often led to exacerbation of lesions. Intravenous injection of HDL protein (33), subcutaneous injection of diethylstilbesterol estradiol (34), and dietary cholestyramine (35) has been reported to cause regression of lesions.

The mechanism(s) by which CLA affects carcinogenesis and atherogenesis are unresolved. In the case of effects on atherosclerosis we must first examine CLA effects on lipid metabolism. In the present study CLA feeding (mix or individual isomers) had no significant effects on either serum or liver lipids. Serum cholesterol levels in the CLA-fed groups were 10–21% higher than those in the control group. Liver cholesterol levels were lowest in rabbits fed the *c*9,*t*11 isomer. In our initial study (3), rabbits were maintained on the atherogenic diet for 22 wk and serum lipid levels determined every week. At week 12 the cholesterol levels of the test and control groups were the same. By week 22 serum lipid levels of the CLA-fed rabbits had become significantly lower than the control levels. However, subsequent CLA studies have been terminated at 12 week (4,5) and, as in the original experiment, there have been no differences in serum lipids between any of the dietary groups at that point in time. A review of effects of CLA on lipid metabolism by Khosla and Fungwe (36) shows that CLA effects may be erratic.

CLA has been reported to exhibit antioxidant activity *in vivo* (37) as well as *in vitro* (38). Since oxidized LDL may affect atherogenicity, CLA may exert its anti-atherogenic effects in this manner. Assay for TBARS in plasma of control and CLA-fed rabbits in our first study showed no differences, but Kim *et al*. (39) suggest that the TBARS assay does not always correlate with the progression of atherosclerosis. Sugano *et al*. (40) found no significant differences in TBARS values in serum and liver of CLA-fed or control rats. CLA appears to have minimal antioxidant activity (41,42).

In rats CLA is incorporated into phospholipids (40,43) and is also metabolized to arachidonic acid homologs. By sequentially undergoing Δ6 desaturation, elongation, and Δ5 desaturation, the *c*9,*t*11 isomer is converted to a *cis*5,*cis*8,*cis*11,*trans*13 arachidonic acid isomer, which still retains the conjugated double bonds. The *t*10,*c*12 isomer is converted to the *cis*5,*cis*8,*trans*12,*cis*14 arachidonic acid isomer (44). These structural changes decrease availability of arachidonic acid for prostaglandin (PG) formation and/or provide different substrates, which would, in turn, give different PG. Liu and Belury (45) showed that CLA reduced arachidonate content and prostaglandin E_2 (PGE_2) synthesis in murine keratinocytes. Kavanaugh *et al.* (46) reported that CLA reduced phorbol ester-induced PGE_2 production in mouse epidermis. Sugano *et al*. (40) found that CLA significantly lowered PGE_2 levels in serum and spleen of rats.

CLA has been shown to inhibit (by 50%) production of intracellular adhesion molecules ICAM-1 and E-selectin in human umbilical vein endothelial cells (47). Dietary CLA (1%) causes a significant reduction of ICAM levels in mice bearing human tumors (48).

The findings reported here confirm our earlier observations (3–5) that a dietary CLA mixture inhibits atherosclerosis in rabbits and also leads to significant regression of pre-estab-

lished lesions. We now show that the *c*9,*t*11 and *t*10,*c*12 isomers of CLA are identical to each other and to the CLA mixture with regard to both atherogenesis and regression of lesions. The mechanism of CLA action remains moot but does not appear to involve effects on serum lipids or lipid oxidation. Future efforts should be directed at eicosanoid and cytokine effects. Lusis (49) and Libby (50) have reviewed the array of complex inflammatory and other factors that play a role in atherogenesis.

ACKNOWLEDGMENTS

Supported, in part, by a Research Career Award from the National Institutes of Health (HL00734 to D.K.), and by grants from the National Cattlemen's Beef Association (Englewood, CO), the Eugene Garfield Foundation (Philadelphia, PA), and the Commonwealth Universal Research Enhancement Program, Pennsylvania Department of Health.

REFERENCES

1. Chin, S.F., Liu, W., Storkson, J.M., Ha, Y.L., and Pariza, M.W. (1992) Dietary Sources of Conjugated Dienoic Isomers of Linoleic Acid, a Newly Recognized Class of Anticarcinogens, *J. Food Comp. Anal. 5*, 185–197.
2. Kritchevsky, D. (2000) Antimutagenic and Some Other Effects of Conjugated Linoleic Acid, *Br. J. Nutr. 83*, 459–465.
3. Lee, K.N., Kritchevsky, D., and Pariza, M.W. (1994) Conjugated Linoleic Acid and Atherosclerosis in Rabbits, *Atherosclerosis 108*, 19–25.
4. Kritchevsky, D., Tepper, S.A., Wright, S., Tso, P., and Czarnecki, S.K. (2000) Influence of Conjugated Linoleic Acid (CLA) on Establishment and Progression of Atherosclerosis in Rabbits, *J. Am. Coll. Nutr. 19*, 472S–477S.
5. Kritchevsky, D., Tepper, S.A., Wright, S., and Czarnecki, S.K. (2002) Influence of Graded Levels of Conjugated Linoleic Acid (CLA) on Experimental Atherosclerosis in Rabbits, *Nutr. Res. 22*, 1275–1279.
6. Nicolosi, R.J., Rogers, E.J., Kritchevsky, D., Scimeca, J.A., and Huth, P.J. (1997) Dietary Conjugated Linoleic Reduces Plasma Lipoproteins and Early Aortic Atherosclerosis in Hypercholesterolemic Hamsters, *Artery 22*, 266–277.
7. Wilson, T.A., Nicolosi, R.J., Chrysam, M., and Kritchevsky, D. (2000) Conjugated Linoleic Acid Reduces Early Atherosclerosis Greater Than Linoleic Acid in Hypercholesterolemic Hamsters, *Nutr. Res. 20*, 1795–1805.
8. Munday, J.S., Thompson, K.G., and James, K.A.C. (1999) Dietary Conjugated Linoleic Acids Promote Fatty Streak Formation in the C57BL/6 Mouse Atherosclerosis Model, *Br. J. Nutr. 81*, 251–255.
9. Park, Y., Albright, K.J., Liu, W., Storkson, J.M., Cook, M.E., and Pariza, M.W. (1997) Effect of Conjugated Linoleic Acid on Body Composition in Mice, *Lipids 32*, 853–858.
10. Park, Y., Storkson, J.M., Albright, K.J., Liu, W., and Pariza, M.W. (1999) Evidence That the *trans*-10,*cis*-12 Isomer of Conjugated Linoleic Acid Induces Body Composition Changes in Mice, *Lipids 34*, 235–241.
11. Evans, M.E., Brown, J.M., and McIntosh, M.K. (2002) Isomer Specific Effects of Conjugated Linoleic Acid (CLA) on Adiposity and Lipid Metabolism, *J. Nutr. Biochem. 13*, 508–516.
12. Risérus, U., Arner, P., Brismar, K., and Vessby, B. (2002) Treatment with Dietary *trans*10,*cis*12 Conjugated Linoleic Acid Causes Isomer-Specific Insulin Resistance in Obese Men with Metabolic Syndrome, *Diabetes Care 25*, 1516–1521.
13. Risérus, V., Basu, S., Jovinge, S., Fredrikson, G.N., Ärnlöv, J., and Vessby, B. (2002) Supplementation with Conjugated Linoleic Acid Causes Isomer-Dependent Oxidative Stress and Elevated C-Reactive Protein. A Potential Link to Fatty Acid-Induced Insulin Resistance, *Circulation 106*, 1925–1929.
14. Clément, L., Porrier, H., Niot, I., Bocher, V., Guerre-Milo, M., Krief, S., Staels, B., and Besnard, P. (2002) Dietary *trans*10,*cis*12 Conjugated Linoleic Acid Induces Hyperinsulinemia and Fatty Liver in the Mouse, *J. Lipid Res. 43*, 1400–1409.
15. Roche, H.M., Noone, E., Sewter, C., McBennett, S., Savage, D., Gibney, M.J., O'Rahilly, S.O., and Vidal-Piug, J. (2002) Isomer-Dependent Metabolic Effects of Conjugated Linoleic Acid: Insights from Molecular Markers Sterol Regulatory Element-Binding Protein-1c and LXRα, *Diabetes 51*, 2037–2044.
16. Kang, K., and Pariza, M.W. (2001) *Trans*10,*cis*12-Conjugated Linoleic Acid Reduces Leptin Secretion from 3T3-L1 Adipocytes, *Biochem. Biophys. Res. Commun. 287*, 377–382.
17. Brown, J.M., Halvorsen, Y.D., Lea-Currie, Y.R., Geigerman, C., and McIntosh, M. (2001) *Trans*10,*cis*12 but Not *cis*9,*trans*11, Conjugated Linoleic Acid Attenuates Lipogenesis in Primary Cultures of Stromal Vascular Cells from Human Adipose Tissue, *J. Nutr. 131*, 2316–2321.
18. Lin, Y., Kreeft, A., Schuurbiers, A.E., and Draijer, R. (2001) Different Effects of Conjugated Linoleic Isomers on Lipoprotein Lipase Activity in 3T3-L1 Adipocytes, *J. Nutr. Biochem. 12*, 183–189.
19. Folch, J., Lees, M., and Sloane-Stanley, G.H. (1957) A Simple Method for the Isolation and Purification of Total Lipids from Animal Tissue, *J. Biol. Chem. 226*, 497–509.
20. DeHoff, J.L., Davidson, L.M., and Kritchevsky, D. (1978) An Enzymatic Assay for Determinations of Free and Total Cholesterol in Tissue, *Clin. Chem. 24*, 433–435.
21. Wilson, T.A., Nicolosi, R.J., Rogers, E.J., Sacchiero, R., and Goldberg, D.J. (1998) Studies of Cholesterol and Bile Acid Metabolism, and Early Atherogenesis in Hamsters Fed GT16-239, a Novel Bile Acid Sequestrant, *Atherosclerosis 140*, 315–324.
22. Duff, G.L., and McMillan, G.C. (1949) The Effect of Alloxan Diabetes on Experimental Atherosclerosis in Rabbits, *J. Exp. Med. 89*, 611–630.
23. Wei, W., Li, C., Wang, Y., Su, H., Zhu, J., and Kritchevsky, D. (2003) Hypolipidemic and Anti-atherogenic Effects of Long-Term Cholestin (*Monascus purpureus*-fermented rice, red yeast rice) in Cholesterol-Fed Rabbits, *J. Nutr. Biochem. 14*, 314–318.
24. Klurfeld, D.M. (2002) Kidney and Bladder Stones in Rodents Fed Purified Diets, *J. Nutr. 132*, 3784.
25. McMillan, G.C., Horlick, L., and Duff, G.L. (1955) Cholesterol Content of Aorta in Relation to Severity of Atherosclerosis. Studies During Progression and Retrogression of Experimental Lesions, *Arch. Pathol. 59*, 285–290.
26. Kritchevsky, D., and Tepper, S.A. (1962) Cholesterol Vehicle in Experimental Atherosclerosis. 5. Influence of Fats and Fatty Acids on Pre-established Atheromata, *J. Atheroscler. Res. 2*, 471–477.
27. Kritchevsky, D., Tepper, S.A., and Story, J.A. (1978) Cholesterol Vehicle in Experimental Atherosclerosis. 16. Effect of Peanut Oil on Pre-established Lesions, *Atherosclerosis 31*, 365–370.
28. Beher, W.T., Anthony, W.L., and Baker, G.D. (1956) Effects of Beta Sitosterol on Regression of Cholesterol Atherosclerosis in Rabbits, *Circulation Res. 4*, 485–487.
29. Beher, W.T., Baker, G.D., and Anthony, W.L. (1957) Effect of Dehydrocholesterol and Beta-Sitosterol on Cholesterol Atherosclerosis in Rabbits, *Circulation Res. 5*, 202–206.
30. Kritchevsky, D., Sallata, P., and Tepper, S.A. (1968) Influence of Ethyl *p*-Chlorophenoxyisobutyrate (CPIB) upon Establishment and Progression of Experimental Atherosclerosis in Rabbits, *J. Atheroscler. Res. 8*, 755–761.

31. Kritchevsky, D., Moynihan, J.L., Langan, J., Tepper, S.A., and Sachs, M.L. (1961) Effects of D- and L-Thyroxine and D- and L-3,5,3′-Tricodothyronine on Development and Regression of Experimental Atherosclerosis in Rabbits, *J. Atheroscler. Res. 1*, 211–221.
32. Kano, H., Hayashi, T., Sumi, D., Esaki, T., Asai, Y., Thankur, N.K., Jayachandran, M., and Iguchi, A. (1999) A HMG-CoA Reductase Inhibitor Improved Regression of Atherosclerosis in the Rabbit Aorta Without Affecting Serum Lipid Levels: Possible Relevance to Up-Regulation of Endothelial NO Synthetase mRNA, *Biochem. Biophys. Res. Commun. 259*, 414–419.
33. Badimon, J.J., Badimon, L., and Fuster, V. (1990) Regression of Atherosclerotic Lesions by High Density Lipoprotein Plasma Fraction in the Cholesterol-Fed Rabbit, *J. Clin. Invest. 85*, 1234–1241.
34. Constantinides, P., and Gutmann-Auersperg, N. (1960) Inhibition of Progress of Pre-established Atherosclerosis by Diethylstilbesterol in Rabbits, *Arch. Pathol. 70*, 35–42.
35. Vesselinovitch, D., Wissler, R.W., Fisher-Dzoga, K., Hughes, R., and Dubien, L. (1974) Regression of Atherosclerosis in Rabbits. 1. Treatment with Low-Fat Diet, Hyperoxia and Hypolipidemic Agents, *Atherosclerosis 19*, 259–275.
36. Khosla, P., and Fungwe, T.V. (2001) Conjugated Linoleic Acid: Effects on Plasma Lipids and Cardiovascular Function, *Curr. Opin. Lipidol. 12*, 31–34.
37. Ip, C., Chin, S.F., Scimeca, J.A., and Pariza, M.W. (1991) Mammary Cancer Prevention by Conjugated Dienoic Derivatives of Linoleic Acid, *Cancer Res. 51*, 6118–6124.
38. Ha, Y.L., Storkson, J., and Pariza, M.W. (1990) Inhibition of Benzo(a)pyrene-Induced Mouse Forestomach Neoplasia by Conjugated Dienoic Derivatives of Linoleic Acid, *Cancer Res. 50*, 1097–1101.
39. Kim, D.N., Ho, H.T., Lawrence, D.A., Schmee, J., and Thomas, W.A. (1989) Modification of Lipoprotein Patterns and Retardation of Atherosclerosis by a Fish Oil Supplement to a Hyperlipidemic Diet for Swine, *Atherosclerosis 76*, 35–54.
40. Sugano, M., Tsujita, A., Yamasaki, M., Yamada, K., Ikeda, I., and Kritchevsky, D. (1997) Lymphatic Recovery, Tissue Distribution, and Metabolic Effects of Conjugated Linoleic Acid in Rats, *J. Nutr. Biochem. 8*, 34–43.
41. van den Berg, J.J., Cook, N.E., and Tribble, D.L. (1995) Reinvestigation of the Antioxidant Properties of Conjugated Linoleic Acid, *Lipids 30*, 599–605.
42. Banni, S., Angioni, E., Contini, M.S., Carta, G., Casu, V., Iengo, G.A., Melis, M.P., Deiana, M., Dessi, M.A., and Corongiu, F.P. (1998) Conjugated Linoleic Acid and Oxidative Stress, *J. Am. Oil Chem. Soc. 75*, 261–267.
43. Stangl, G.I. (2000) High Dietary Levels of a Conjugated Linoleic Acid Mixture After Hepatic Glycerophospholipid Class Profile and Cholesterol-Carrying Serum Lipoproteins in Rats, *J. Nutr. Biochem. 11*, 184–191.
44. Banni, S. (2002) Conjugated Linoleic Acid Metabolism, *Curr. Opin. Lipidol. 13*, 261–266.
45. Liu, K.L., and Belury, M.A. (1998) Conjugated Linoleic Acid Reduces Arachidonic Acid Content and PGE_2 Synthesis in Murine Keratinocytes, *Cancer Lett. 127*, 15–22.
46. Kavanaugh, C.J., Liu, K.L., and Belury, M.A. (1999) Effect of Dietary Conjugated Linoleic Acid on Phorbol Ester-Induced PGE_2 Production and Hyperplasia in Mouse Epidermis, *Nutr. Cancer 33*, 132–138.
47. Crosby, A.J., Wahle, K.W.J., and Duthie, G.G. (1996) Modulation of Glutathione Peroxidase Activity in Human Vascular Endothelial Cells by Fatty Acids and the Cytokine, Interleukin 1β, *Biochim. Biophys. Acta 1303*, 187–192.
48. Cesano, A., Visonneau, S., Scimeca, J.A., Kritchevsky, D., and Santoli, D. (1998) Opposite Effects of Linoleic Acid and Conjugated Linoleic Acid on Human Prostatic Cancer in SCID Mice, *Anticancer Res. 18*, 833–838.
49. Lusis, A.J. (2000) Atherosclerosis, *Nature 407*, 233–241.
50. Libby, P. (2002) Inflammation in Atherosclerosis, *Nature 420,* 868–874.

[Received February 25, 2004, and in revised form September 14, 2004; revision accepted September 25, 2004]

Gestational Age and Birth Weight in Relation to n-3 Fatty Acids Among Inuit (Canada)

Michel Lucas[a], Éric Dewailly[a,b,*], Gina Muckle[a], Pierre Ayotte[a], Suzanne Bruneau[a], Suzanne Gingras[a], Marc Rhainds[a], and Bruce J. Holub[c]

[a]Public Health Research Unit, Laval University Medical Research Centre, Centre Hospitalier Universitaire de Québec (CHUQ), Québec G1V 5B3, Canada, [b]Department of Social and Preventive Medicine, Laval University, Québec G1K 7P4, Canada, and [c]Department of Human Biology and Nutritional Sciences, University of Guelph, Guelph N1G 2W1, Canada

ABSTRACT: Seafood consumption during pregnancy carries both benefits (high n-3 FA intake) and risks (exposure to environmental contaminants) for the developing fetus. We determined the impacts of marine n-3 FA and environmental contaminants on gestational age (GA) of Nunavik women and the anthropometric characteristics of their newborns. FA and contaminant (polychlorinated biphenyls and mercury) concentrations were measured in cord plasma of Nunavik newborns (n = 454) and compared with those of a group of newborns (n = 29) from southern Québec. Data were collected from hospital records and birth certificates. In Nunavik newborns, arachidonic acid (AA) was two times lower ($P < 0.0001$), whereas DHA concentration, the Σn-3/Σn-6 ratio, and the percentage of n-3 highly unsaturated FA (HUFA) (of the total HUFA) were three times higher ($P < 0.0001$) compared with southern Québec newborns. After controlling for confounders, GA and birth weight were higher by 5.4 d [95% confidence interval (CI): 0.7–10.1] and 77 g (95% CI: −64 to 217) in the third tertile of percentage of n-3 HUFA (of the total HUFA) as compared with the first tertile. There was no evidence that contaminants had negative effects on GA or birth weight. In this seafood-eating population, an increase in the proportion of n-3 HUFA (of the total HUFA), measured in umbilical cord plasma phospholipids, was associated with a significantly longer GA.

Paper no. L9444 in *Lipids 39*, 617–626 (July 2004).

Maternal diet is known to be associated with gestational age (GA) as well as with birth weight (1). Furthermore, GA and birth weight are important predictors of the survival and health status of newborns (2,3). In our industrialized societies, prematurity (<37 wk), which is strongly associated with a low birth weight (LBW) (<2500 g), is the second-highest cause of infant death after birth defects (4). Furthermore, preterm LBW babies who survive are more likely to suffer from severe and permanent disabilities (5). A shortened GA predisposes to a deficiency in nutrients that are needed for organ and tissue development (6). Therefore, premature children are more likely to be susceptible to various illnesses during their adult life than those born full term (6,7).

Prostaglandins (PG) are potent myometrial contractile agents that play an important role in the physiology of cervical ripening, and are essential for parturition (8,9). Arachidonic acid (AA) is the precursor of PGE_2 and $PGF_{2\alpha}$, which stimulate contractions in the gravid human uterus (8,10). A high intake of n-3 highly unsaturated FA (HUFA) competitively decreases the endogenous production of AA-derived PG, such as $PGF_{2\alpha}$ and PGE_2 that promote parturition (11–16).

Epidemiological and clinical studies have suggested that marine n-3 HUFA can reduce or at least prevent prematurity and its complications (17,18). Marine n-3 HUFA also have been associated with increased birth weight and longer GA (17,19–25). Results from two double-blind randomized trials have shown that the gestational duration and birth weight could be improved with fish oil supplementation during pregnancy as compared with a placebo group (26,27). In a recent case–control study, the risk of premature delivery and LBW was reported as 3.6 times higher among women who did not eat any fish during pregnancy compared with a group whose mean intake of marine products was 44 g per day (18).

Several other maternal factors are associated with an increasing risk of lower birth weight, such as insufficient caloric intake and weight gain during pregnancy, anemia, gestational diabetes, smoking, and adolescent pregnancy (28–33). In addition to these factors, environmental contaminants such as lead, mercury, and polychlorinated biphenyls (PCB) are also suspected to be related to adverse pregnancy outcomes and reduced growth (25,34–44).

The Nunavik region is located above the 55th parallel in the province of Québec (Canada) and is inhabited primarily by Inuit populations. Data from 1992 revealed that blood concentrations of organochlorines and mercury in these communities were at least 10 times higher among Inuit adults compared with a general population of adults living in southern regions of Québec (45,46). The traditional Inuit diet consists primarily of marine mammals [white whale (beluga) and seal], fish, and caribou, which are eaten fresh (raw or cooked) or dried, with use of the skin, blubber, liver, and fat in different meals (47,48). Consumption of fish and marine mammals, rich in n-3 HUFA, represents a significant part of the Inuit diet (47–50). In the Santé Québec Health Survey Among the Inuit of Nunavik

*To whom correspondence should be addressed at Public Health Research Unit, Laval University Medical Research Centre, Centre Hospitalier Universitaire de Québec (CHUQ), 945 Wolfe Ave., Sainte-Foy, Québec, Canada G1V 5B3.

Abbreviations: AA, arachidonic acid; ALA, α-linolenic acid; CI, confidence interval; DPA, docosapentaenoic acid; GA, gestational age; HUFA, highly unsaturated FA; LA, linoleic acid; LBW, low birth weight; PCB, polychlorinated biphenyl; PG, prostaglandin; PL, phospholipids.

(1992), mean consumption of marine products among women was 163 g per day (49). This consumption of marine products is far greater than that for other Québec women living in southern regions (established at 13 g per day) (50). Dewailly *et al.* (49,50) have shown that the mean concentration of EPA and DHA in plasma phospholipids (PL) of adults was significantly higher among Inuit [7.95 ± 0.21 (SE)] than non-Inuit populations [1.79 ± 0.51 (SE)]. Although the high consumption of marine products by Inuit women could be a benefit during pregnancy, it also represents a paradox: Marine foods provide n-3 HUFA that are beneficial for fetal growth, but they are also potentially harmful because of the high concentrations of contaminants.

From a public health standpoint, it is therefore important to examine the effects of the traditional Inuit diet on pregnancy outcomes. To our knowledge, only one epidemiological study conducted in the Faroe Islands has considered both FA and food chain contaminants (mercury and PCBs) in their analysis (25). The aim of the present study is primarily to determine the impact of marine n-3 HUFA on the GA of Nunavik mothers and the anthropometric characteristics of their newborns, while controlling for the effects of environmental contaminants.

SUBJECTS AND METHODS

Study population. Participants with placenta previa ($n = 1$), premature rupture of membranes ($n = 12$), preeclampsia ($n = 16$), intrauterine growth retardation ($n = 2$), GA ≤ 35 wk ($n = 2$), and LBW delivery (<2500 g) ($n = 5$) were excluded. Forty-four subjects failed to complete the questionnaire, but FA and environmental contaminant concentrations in cord blood were measured. Among the participating mothers, 51.5% ($n = 234$) came from Hudson Bay and 48.5% ($n = 220$) from Ungava Bay. The population under study is represented by Inuit women who lived in the 14 coastal villages of Nunavik as well as their infants born at the Tulattavik Health Centre (Ungava Bay) and Inuulitsivik Health Centre (Hudson Bay) between November 1993 and December 1996. During this period, 491 Inuit women agreed to participate. Women who delivered outside the Nunavik region or at their community nursing stations were not recruited.

Procedures and variables. The protocol was first approved by Laval University's Ethics Committee and also by the Physicians and Dentists Committee of each Health Centre involved in this project. Informed consent was obtained from each participant. The following information was obtained from medical records of the mothers: GA, pre-pregnancy weight, pre-delivery weight, weight gain during pregnancy, twin pregnancy, age, parity and previous deliveries, smoking status before and during pregnancy, anemia, gestational diabetes, other health problems occurring during pregnancy, and vitamin and drug use during pregnancy. The first day of the last menstrual period was used to estimate the GA. Birth date, gender, birth weight, length, head and thoracic circumferences, APGAR score at 5 min, intrauterine growth retardation, cardiac problems, and any other health problems were obtained from the medical records of newborns. Unfortunately, thoracic circumference measurements were available for newborns only from Ungava Bay, whereas GA values were unavailable.

Cord plasma samples from a southern Québec reference group were used only to compare FA and environmental contaminant concentrations with samples from Nunavik Inuit newborns. This group consisted of a subsample of full-term (>37 wk of gestation) newborns ($n = 29$) randomly selected for FA measurement among 1,109 newborns who had participated in a survey from June 1993 to July 1994 (52). The principal aim of this survey was to evaluate the cord blood concentrations of environmental contaminants in southern Québec Caucasian newborns. Owing to budgetary constraints, we analyzed FA concentrations only in a subsample of these newborns for the present project.

LABORATORY PROCEDURES

General procedure. After the cord was severed, blood was collected from the umbilical vein using a syringe. The blood was transferred into heparinized vacutainer tubes with EDTA. After centrifugation, plasma samples were stored in glass vials frozen at −20°C until the time of analyses.

Plasma PL FA. FA were determined from the PL fraction by the Lipid Analytical Labs, University of Guelph. To determine the PL fraction, 200-μL aliquots of plasma were extracted following the addition of chloroform/methanol (2:1, vol/vol) in the presence of a known amount of internal standard (diheptadecanoyl PL) (53). The total PL was isolated from the lipid extract by TLC using heptane/isopropyl ether/acetic acid (60:40:3, by vol) as the developing solvent. Following transmethylation using BF_3/methanol, the FA profile was determined by capillary GLC. The FA concentrations in plasma PL were expressed as percentages of the total area of all FA peaks from 14:0 to 24:1. In this study, plasma PL concentrations of FA correspond to relative percentages of total FA by weight. The detection limit for FA was 0.02% of the total FA in plasma PL. A total of 27 FA were identified in more than 75% of the subjects. For clarity, the concentrations of only 10 individual PUFA and 11 FA groups are reported.

Mercury and PCB analyses. Mercury and organochlorine compound analyses were performed at the Direction de la toxicologie humaine (Institut national de santé publique du Québec), a laboratory accredited by the Canadian Association for Environmental Analytical Laboratories. Lead (Pb) concentrations were determined in whole cord blood with a graphite furnace atomic absorption spectrometer (ZL-4100, PerkinElmer Corp., Norwalk, CT). The detection limit was 0.01 μmol/L. Cold-vapor atomic absorption spectrometry was used to measure total mercury (Hg) in cord blood. The blood was initially digested with nitric acid. Mercury was then reduced with anhydrous stannous chloride ($SnCl_2$). Metallic mercury was volatilized and detected by atomic absorption. The detection limit was 1 nmol/L. Quality control measures were described elsewhere (52).

To extract PCB congeners, a 1:1:3 mixture of ammonium sulfate/ethanol/hexane was first added to the plasma. The extracts were then concentrated and purified on two Florisil

columns (60–100 mesh; Fisher Scientific, Nepean, Ontario, Canada). The 14 most prevalent PCB congeners (IUPAC nos. 28, 52, 99, 101, 105, 118, 128, 138, 153, 156, 170, 180, 183, and 187) were measured in purified extracts with a Hewlett-Packard 5890 high-resolution gas chromatograph equipped with dual capillary columns (Hewlett-Packard Ultra I and Ultra II) and dual Ni-63 electron capture detectors (Hewlett-Packard, Palo Alto, CA). Quality control procedures were described elsewhere (52). The detection limit was 0.02 μg/L for PCB congeners. To adjust PCB concentrations on a lipid basis, standard enzymatic procedures were used to determine total cholesterol, free cholesterol, and TG in plasma samples; and plasma PL were determined according to the enzymatic method of Takayama *et al.* (54). Concentration of total plasma lipids was estimated according to the formula developed by Philips *et al.* (55). Lipid analyses were performed by the Centre de recherche sur les maladies lipidiques of the Centre hospitalier de l'Université Laval.

Statistical analysis. Frequency distribution of environmental contaminants displayed a lognormal distribution; therefore, we used the geometric mean and 95% confidence intervals (CI) to describe the results. Student's *t*-test was applied to compare cord blood FA and environmental contaminant concentrations between Nunavik and southern Québec newborns. The Pearson correlation coefficient was employed first to measure the intercorrelation between PUFA and then to evaluate associations between PUFA and the characteristics of mothers and newborns. In each tertile group of FA and contaminant concentrations, we analyzed the distribution of GA and birth weights. Arithmetic means of GA and birth weight distributions in each tertile were compared using ANOVA. Because an increased proportion of n-3 HUFA (in the total HUFA) of tissues is associated with a lower proportion of n-6 HUFA and a lower rate of formation of n-6 eicosanoids (56), the percentage of n-3 HUFA (of the total HUFA) was used as a surrogate indicator of n-6 eicosanoid production. Covariance analysis was used to calculate adjusted mean birth weight and GA according to tertiles of percentage of n-3 HUFA (of the total HUFA). Two-by-two comparisons of these means were performed using Scheffé's multiple-comparison test. The variables known to influence GA, birth weight, and PUFA were controlled for in the analysis. Covariates that were included in the models were: pre-pregnancy weight (kg), pre-delivery weight (kg), weight gain during pregnancy (kg), age (yr), parity (0, 1+), smoking status during pregnancy (yes, no), gestational diabetes (yes, no), anemia (yes, no), newborn gender (boy, girl), coastal region (Ungava Bay, Hudson Bay), and cord blood contaminants (Hg, Pb, PCB congener 153). Only those with a confounding effect were retained in covariance analyses, i.e., those that modified the n-3 HUFA and GA or the n-3 HUFA and birth weight relation by more than 10%. Congener 153 was used as a surrogate for PCB exposure in this population (57). Statistical analyses were performed using the SAS program for Windows v.8 (SAS Institute Inc., Cary, NC). Differences between groups and associations were considered significant at $P < 0.05$ (bilateral).

RESULTS

Characteristics of the Nunavik mothers are presented in Table 1. Sixteen percent (16.2%) of the mothers were under 18 yr of age, 45.5% between 18 and 24 yr, 35.6% between 25 and 34 yr, and only 3% over 35 yr. Despite the young age, more than 60% had more than three live births. Approximately 85% of the women smoked during pregnancy. The proportion of women who smoked 1–10 cigarettes/d and ≥11 cigarettes/d was, respectively, 60 and 40%. The results showed a higher average birth weight, height, and head circumference among boys than girls (Table 2).

Cord blood concentrations of mercury were 18 times higher in Nunavik than in southern Québec newborns (Table 3). Lead and PCB congener 153 concentrations in cord blood were, respectively, 2.4 and 3.6 times higher in Nunavik than in southern Québec neonates. Total saturated FA (ΣSAFA) concentrations in umbilical cord plasma were higher in the southern Québec group, whereas total monounsaturated FA (ΣMUFA) were lower (Table 4). The plasma concentrations of the n-6 precursor, linoleic acid (LA, 18:2n-6), were significantly higher in Nunavik newborns, whereas AA, total n-6 (Σn-6), and total n-6 HUFA (Σn-6 HUFA) concentrations were significantly higher in southern Québec newborns (Table 4). All n-3 HUFA concentrations were significantly higher in Nunavik than in southern Québec newborns, except for docosapentaenoic acid (DPA,

TABLE 1
Characteristics of Participants in a Study of Nunavik Mothers, Canada (1993–1996)

	n	Mean	%	95% CI[a]
Gestational age (d)	149	275.5	—	274.0–277.0
Mother's age (yr)	402	23.7	—	23.2–24.2
Pre-pregnancy weight (kg)	315	59.5	—	58.4–60.6
Pre-delivery weight (kg)	369	69.8	—	68.8–70.9
Weight gain during pregnancy (kg)	304	9.4	—	8.9–10.0
Smoked during pregnancy	341	—	85.6	81.9–89.3
Gestational diabetes	308	—	7.1	4.2–10.0
Parity	380			
0		—	17.9	14.0–21.8
1 or 2		—	20.5	16.4–24.6
>3		—	61.6	56.7–66.5

[a]95% confidence interval.

TABLE 2
Characteristics of Nunavik Newborns

	Mean (95% CI[a])			
	n	Male	*n*	Female
Birth weight (g)	197	3567 (3508–3626)	203	3438 (3377–3500)
Height (cm)	189	51.8 (51.5–52.1)	192	50.8 (50.4–51.2)
Head circumference (cm)	185	34.9 (34.7–35.1)	188	34.3 (34.1–34.6)
Thoracic circumference (cm)	90	34.8 (34.4–35.1)	99	34.5 (34.1–34.8)

[a]For abbreviation see Table 1.

TABLE 3
Means and 95% CI of Corn Blood Concentrations of Lead, Mercury, and Polychlorinated Biphenyls (PCB)

	GM[a] (95% CI)	
Contaminants	Nunavik (*n* = 439)	Southern Québec (*n* = 29)
Mercury (nmol/L)	70.5* (65.3–76.0)	3.8 (2.9–5.1)
Lead (μmol/L)	0.19* (0.18–0.21)	0.08 (0.07–0.10)
ΣPCB[b] (μg/kg lipid basis)	322.1* (303.5–341.9)	129.0 (109.3–152.1)
PCB congener 153 (μg/kg lipid basis)	94.2* (87.9–100.9)	26.1 (21.0–32.5)

[a]GM, geometric mean. (*) Difference between southern Québec and Nunavik significant at $P < 0.0001$ (P-value obtained by Student's t-test). For other abbreviation see Table 1.
[b]ΣPCB = sum of the 14 most prevalent PCB congeners (IUPAC nos. 28, 52, 99, 101, 105, 118, 128, 138, 153, 156, 170, 180, 183, and 187).

TABLE 4
Comparison of FA Concentrations in Umbilical Cord Plasma Phospholipids Between Nunavik and Southern Québec Newborns

FA[a]	Nunavik mean ± SE[b] *n* = 398	Southern Québec mean ± SE *n* = 29	Student's *t*-test *P*-value
ΣSAFA[c]	49.40 ± 0.11	52.51 ± 0.38	<0.0001
ΣMUFA[d]	17.85 ± 0.14	12.20 ± 0.29	<0.0001
18:2 (n-6) (LA)	9.58 ± 0.10	6.91 ± 0.16	<0.0001
20:2 (n-6)	0.74 ± 0.03	0.95 ± 0.06	0.0038
20:3 (n-6)	5.22 ± 0.04	5.12 ± 0.13	0.5496
20:4 (n-6) (AA)	10.12 ± 0.12	17.63 ± 0.26	<0.0001
22:4 (n-6)	0.52 ± 0.009	0.80 ± 0.04	<0.0001
22:5 (n-6) (DPAn-6)	0.28 ± 0.02	1.08 ± 0.06	<0.0001
Σn-6[e]	26.66 ± 0.15	32.61 ± 0.28	<0.0001
Σn-6HUFA[f]	16.14 ± 0.14	24.62 ± 0.26	<0.0001
18:3 (n-3) (ALA)	0.03 ± 0.003	0.02 ± 0.004	0.0002
20:5 (n-3) (EPA)	0.38 ± 0.02	0.20 ± 0.02	<0.0001
22:5 (n-3) (DPAn-3)	0.28 ± 0.009	0.53 ± 0.05	<0.0001
22:6 (n-3) (DHA)	3.66 ± 0.06	1.16 ± 0.04	<0.0001
EPA + DHA	4.04 ± 0.07	1.36 ± 0.04	<0.0001
Σn-3[g]	4.51 ± 0.08	2.02 ± 0.08	<0.0001
Σn-3HUFA[h]	4.44 ± 0.08	1.98 ± 0.08	<0.0001
ΣPUFA	31.18 ± 0.18	34.63 ± 0.24	<0.0001
ΣHUFA[i]	20.58 ± 0.19	26.60 ± 0.24	<0.0001
Σn-3/Σn-6	0.17 ± 0.003	0.06 ± 0.003	<0.0001
%n-3HUFA[j]	21.27 ± 0.28	7.48 ± 0.31	<0.0001

[a]LA, linoleic acid; AA, arachidonic acid; ALA, α-linolenic acid; DPA, docosapentaenoic acid.
[b]Arithmetic mean ± SE; relative concentrations are expressed as the percentage of total FA in umbilical cord plasma phospholipids.
[c]ΣSAFA = sum of saturated FA (14:0 + 15:0 + 16:0 + 18:0 + 20:0 + 22:0 + 24:0).
[d]ΣMUFA = sum of monounsaturated FA (14:1 + 18:1 + 20:1 + 22:1 + 24:1).
[e]Σn-6 = sum of n-6 PUFA (18:2 + 18:3 + 20:2 + 20:3 + 20:4 + 22:2 + 22:4 + 22:5).
[f]Σn-6 HUFA = sum of n-6 highly unsaturated FA (20:3 + 20:4 + 22:4 + 22:5).
[g]Σn-3 = sum of n-3 PUFA (18:3 + 18:4 + 20:3 + 20:4 + 20:5 + 22:5 + 22:6).
[h]Σn-3 HUFA = sum of n-3 highly unsaturated FA (20:3 + 20:4 + 20:5 + 22:5 + 22:6).
[i]ΣHUFA = Σn-6 HUFA+ Σn-3 HUFA.
[j]%n-3 HUFA = (Σn-3 HUFA/ΣHUFA) × 100.

TABLE 5
Unadjusted Mean Values of Birth Weight and Gestational Age by Tertile of Cord Blood FA[a], Mercury (nmol/L), and PCB Congener 153 (μg/kg lipid basis)

	Birth weight (g) (n = 351)		Gestational age (d) (n = 114)	
	Mean	P-value[c]	Mean	P-value
AA		0.07		0.52
<8.76	3542		274.7	
8.76–10.70	3570		276.3	
>10.70	3446		277.4	
EPA		0.42		0.25
<0.21	3474		273.6	
0.21–0.39	3541		276.0	
>0.39	3537		277.2	
DHA		0.06		0.18
<2.99	3486		273.7	
2.99–4.03	3469		276.2	
>4.03	3592		277.6	
Σn-3/Σn-6		0.006		0.15
<0.14	3446		273.6	
0.14–0.18	3486		275.6	
>0.18	3617		277.8	
%n-3 HUFA		0.003		0.02
<18.60	3415		272.7	
18.60–22.96	3526		274.8	
>22.96	3610		278.7	
Mercury		0.06		0.91
<48.0	3447		274.7	
48.0–102	3496		275.3	
>102	3575		275.6	
PCB congener 153		0.009		0.24
<71.83	3410		274.0	
71.83–126.33	3557		277.4	
>126.33	3549		275.1	

[a]Relative concentrations are expressed as the percentage of total FA in umbilical cord plasma phospholipids.
[b]P-values obtained by ANOVA. For abbreviations see Tables 3 and 4.

22:5n-3). Σn-3 and Σn-3 HUFA concentrations were 2.2 times higher in newborns of Nunavik. Moreover, DHA, the Σn-3/Σn-6 ratio, and the percentage of n-3 HUFA (of the total HUFA) were three times higher in Nunavik than in the comparison group.

Mean GA and mean birth weight according to the tertile group of FA, mercury (nmol/L), and PCB congener 153 (μg/kg lipid basis) are presented in Table 5. We observed a significant positive relationship between birth weight and the concentrations of Σn-3/Σn-6, percentage of n-3 HUFA (of the total HUFA), and congener 153. A positive trend in birth weight according to mercury concentrations was also found. Although

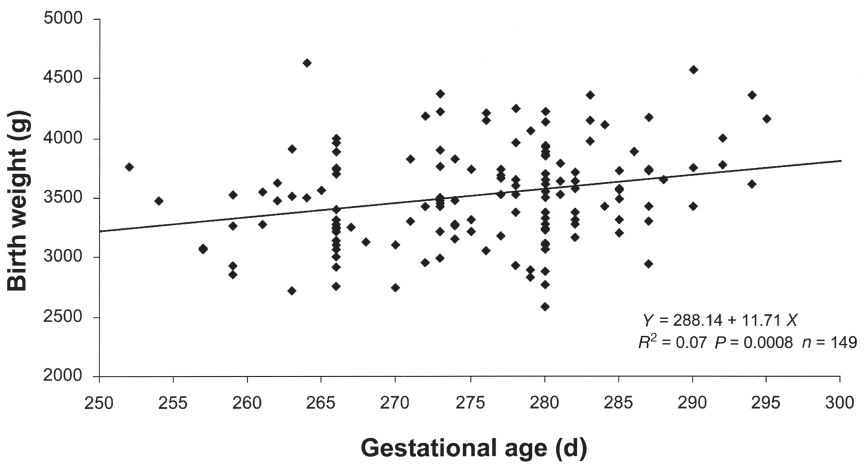

FIG. 1. Relationship between gestational age (d) and birth weight (g).

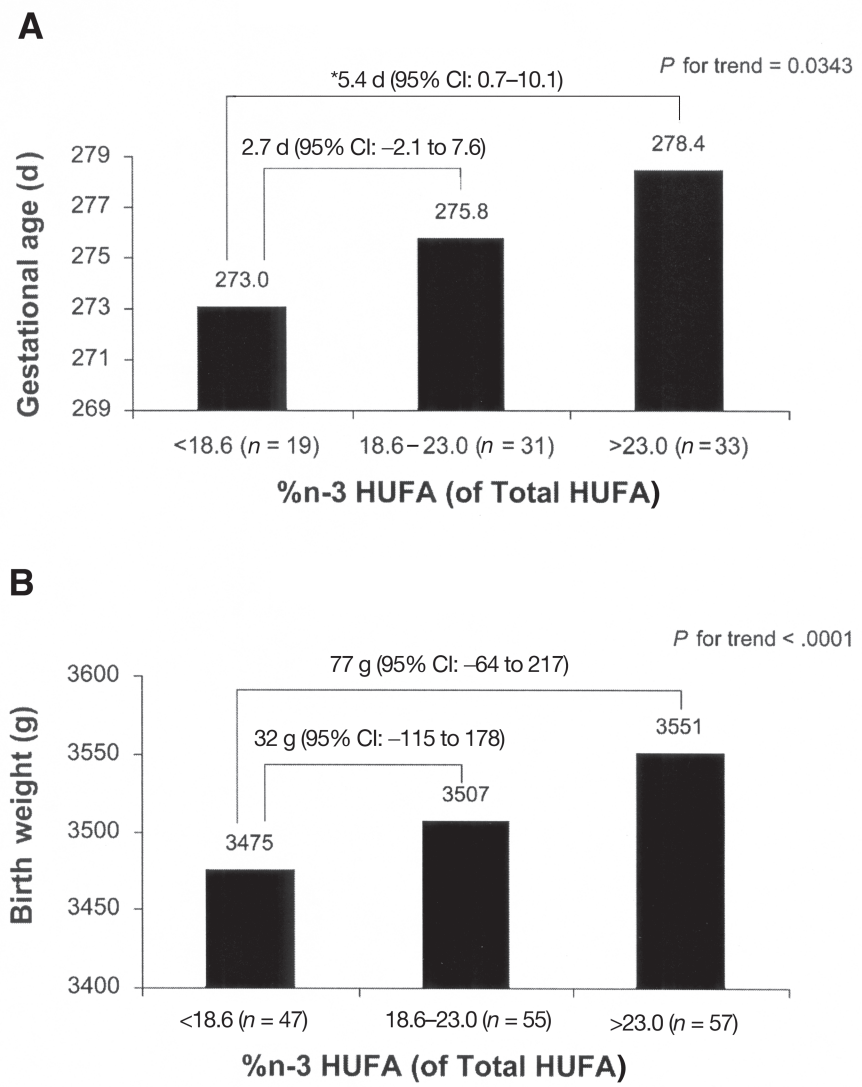

FIG. 2. Adjusted mean gestational age (A) and birth weight (B) according to tertiles of percentage n-3 HUFA (of the total HUFA) in umbilical cord blood. *P*-values for trends were obtained by analysis of covariance. *Difference significant, $P < 0.05$ (Scheffé's multiple-comparison test). (A) Adjusted for weight gain during pregnancy, gestational diabetes, cord blood mercury, lead, and PCB congener 153. (B) Adjusted for pre-pregnancy weight, weight gain during pregnancy, parity, smoking status during pregnancy, gestational diabetes, age, cord blood mercury, and PCB congener 153. CI, confidence interval; %n-3 HUFA, percentage of n-3 highly unsaturated FA; PCB, polychlorinated biphenyl.

the birth weight variance was explained by GA, these variables were weakly correlated ($R^2 = 0.07$) (Fig. 1). After controlling for confounders, the mean GA in the third tertile of percentage of n-3 HUFA (of the total HUFA) was significantly higher by 5.4 d (95% CI: 0.7–10.1) compared with the first tertile (Fig. 2A). A difference of 77 g (95% CI: –64 to 217) in the mean adjusted birth weight was observed in the third tertile of percentage of n-3 HUFA (of the total HUFA) compared with the first tertile, but this result was not statistically significant (Fig. 2B).

DISCUSSION

Our study suggests a positive relationship between the percentage of n-3 HUFA (over total HUFA) and the GA of newborns in Nunavik. After adjustment for various confounders, an increase in average GA of 5.4 d was reported among the newborns in the third tertile of percentage of n-3 HUFA (of the total HUFA) compared with the first tertile. After adjustment for confounding factors, Olsen *et al.* (20) observed in

Danes that a 20% increase in the [(EPA + DPAn-3 + DHA)/AA] ratio, measured in the erythrocyte membranes of mothers after delivery (<48 h), was associated with an increase of 5.7 d (95% CI: 1.4–10.1) of the pregnancy duration and 0.7 d (95% CI: −2.0 to 3.3) in women of the Faroe Islands. However, the results were not significant with GA in the combined groups. In Faroe Islands women, Grandjean *et al.* (25) reported a positive association between GA and DHA tertiles measured in cord plasma PL, but a negative relationship between birth weight and EPA tertiles. Helland *et al.* (58) observed a significantly longer GA (7.1 d) when comparing the last quartile of DHA concentrations measured in umbilical cord plasma PL with the first quartile. In the present study, no significant difference was noted between tertiles of DHA and the GA, and the birth weight (except for head circumference, data not shown).

The intensity of n-6 eicosanoid action depends in part on the rate of n-6 eicosanoid formation—which depends on the relative availability of the n-6 HUFA precursor to the oxygenase—which depends on the relative abundance of the n-6 HUFA in tissue PL (14). A high intake of n-3 HUFA during pregnancy may decrease the concentrations of AA, the most prevalent n-6 HUFA, in the tissues and therefore reduce the endogenous production of strong, biologically active PG (PGE_2 and $PGF_{2\alpha}$), which are involved in cervical ripening and myometrial contractions (8–10,13,14,59,60). Arntzen *et al.* (13) demonstrated that the production of PGE_2 and $PGF_{2\alpha}$ in decidual cells was significantly lower when EPA or DHA was added to the AA in the cell culture medium. It was suggested that n-3 HUFA may increase the fetal growth rate by decreasing thromboxane A_2 production and reducing blood viscosity and therefore facilitating placental blood flow (61,62). In a recent randomized clinical trial, almost the same results in GA and birth weight as our study were obtained with an increase in DHA intake of 100 mg/d from enriched eggs (63). Compared with the ordinary egg group, a significant increase in the gestation length of 6.0 ± 2.3 d ($P = 0.009$) and a nonsignificant difference of 83 ± 62 g ($P = 0.184$) were observed in the high-DHA egg group, after adjustment for confounders. Furthermore, two double-blind randomized experimental trials with fish oil conducted among pregnant women showed positive and significant relationships between supplementation with n-3 HUFA and GA as well as birth weight (26,27). However, Olsen *et al.* (27) did not observe, in comparison with a placebo group, significant effects of n-3 HUFA on GA and birth weight in women with any of the following gestational conditions: twin pregnancy, preeclampsia, or intrauterine growth retardation.

Because the human fetus cannot synthesize AA and DHA, it is therefore strongly dependent on the mothers' consumption and metabolism as well as on placental transport of these FA (5,64–67). In our study, FA were determined in cord blood as an indirect indicator of the FA in mothers. Van Houwelingen *et al.* (11) observed in newborns whose mothers had consumed fish oil supplement during pregnancy that EPA and DHA concentrations in umbilical plasma PL were significantly higher compared with a control group. Moreover, this association was related to a significant reduction of AA concentrations in umbilical cord plasma PL in newborns. The higher proportion of n-3 HUFA (of the total HUFA) reported in umbilical cord blood of Nunavik newborns, which was associated with a lower proportion of n-6 HUFA and a lower rate of formation of n-6 eicosanoids, could reflect a greater n-3 HUFA accumulation in the mothers' tissues through a high intake of marine foods.

Plasma concentrations of AA were lower in Nunavik newborns, whereas concentrations of LA (18:2n-6) were significantly higher in comparison with newborns of southern Québec. Surprisingly, lower concentrations of AA and adrenic acid (22:4n-6) were noted in Nunavik compared with southern Québec newborns in spite of comparable concentrations of their precursors, i.e., dihomo-γ-linolenic acid (20:3n-6), in both groups. These results may indicate a reduction in expression of Δ5-desaturase enzyme in Nunavik newborns. Other researchers have observed such results among Greenland Inuit (68–70). Decreased activity of this enzyme could reflect a different level of genetic expression or a different degree of regulation because of their high intake of n-3 HUFA (71). Grandjean and Weihe (72) recently found a negative association between PCB and AA plasma concentrations in maternal and umbilical cord serum (72). If Δ5-desaturase activity is genetically inhibited among the Inuit of Nunavik, this could have important implications.

In our sample, we noted that birth weight was significantly higher in the second and third tertiles of PCB congener 153 comparated with the first tertile (Table 5). Fein *et al.* (34) reported that newborns from Michigan state whose PCB concentration in cord blood was higher than or equal to 3.0 ng/mL had a smaller head circumference ($P < 0.001$) and a lower birth weight ($P < 0.05$) than those with concentrations under 3.0 ng/mL. The exposure level to PCB congener 153 in this Michigan cohort (120 ng/g serum lipid) was similar to what we have noted (100 ng/g serum lipid) in Nunavik Inuit and fourfold lower than in Faroe Islanders (74). In Faroe Islanders, no evidence of negative effects on birth weight or GA was seen in association with umbilical cord blood concentrations of either mercury or PCB (25). In another study carried out in the same area, Grandjean and Weihe (39) found a positive association between cord blood mercury concentrations and birth weight. In the present study, the higher birth weight seen in the third tertiles of PCB congener 153 and mercury compared with the first tertile could be due to the positive association between environmental contaminants and Σn-3 HUFA, which are found mainly in marine products. However, the Pearson correlation coefficients between contaminants and Σn-3 HUFA (0.125–0.239; $P < 0.0005$), and Σn-6 HUFA (−0.142 to −0.331; $P < 0.0005$), were not very high. Increasing birth weight also could be due to factors other than those measured in the present study. Finally, lead levels in our group were well below the negative association observed with gestational age (42,43).

The results of this study should be interpreted with caution. Estimating GA by using the last normal menstrual period of the mother may be subject to considerable error, especially because

of recall bias, bleeding after conception interpreted as normal menstruation, irregular menstrual cycles, or late ovulation (75,76). Contrary to GA, birth weight measurement is usually better reported in medical records (77). The power of the study could have been reduced because GA was not available among Ungava Bay women. Furthermore, no data were collected on the number of induced deliveries. Our sample is not necessarily representative of the Nunavik population. In fact, mean birth weight, proportion of premature births, and LBW in our sample were significantly lower than those reported for the Nunavik region in the Provincial birth registry for the 1993–1996 period. The exclusion from our sample of women suffering from complications during pregnancy, who were evacuated to southern Québec hospitals, could explain such results.

In this population having high intakes of seafood, an increase in the proportion of umbilical cord plasma PL of n-3 HUFA (of the total HUFA) was associated with a significantly longer GA. Furthermore, no evidence of negative effects of mercury or PCB concentrations on GA and birth weight was found. Marine sources of n-3 FA are important because they not only enhance the health of infants but also provide numerous advantages for adults (78–88). Before making recommendations to reduce the exposure of the fetus to contaminants contained in marine products, all the impacts they may have should be considered. As stated by the joint Food and Agriculture Organization/World Health Organization Expert Committee on Food Additives (89): "Fish makes an important contribution to nutrition, especially in certain regional and ethnic diets, and the Committee recommended that its nutritional benefits be weighed against the possibility of harm when limits on methylmercury concentrations in fish or on fish consumption are being considered." This statement particularly applies to populations such as the Inuit of Nunavik, where marine products play a major role in their cultural heritage. Further studies are needed to find out whether the lower AA concentrations observed among Nunavik newborns are related to the FA content of the diet or to a lower expression of Δ5-desaturase (by genetic expression or by PCB exposure) of their mothers.

ACKNOWLEDGMENTS

This work was supported by Indian and Northern Affairs Canada (1993–1994, 1996) and Health Canada (1995). We would like to express our appreciation to the Northern Contaminant Program (Indian and Northern Affairs Canada) and to Health Canada for their financial support. We would also like to express our gratitude to the Nunavik Health Centres' personnel and especially the mothers who participated in this study.

REFERENCES

1. Food and Agriculture Organization of the United Nations (FAO) and the World Health Organization (WHO) (1994). Fats and Oils in Human Nutrition, Report of a Joint Expert Consultation, Food and Nutrition Paper No. 57, Rome, 19–26 October 1993.
2. Kramer, M.S., Demissie, K., Yang, H., Platt, R.W., Sauve, R., and Liston, R. (2000) The Contribution of Mild and Moderate Preterm Birth to Infant Mortality. Fetal and Infant Health Study Group of the Canadian Perinatal Surveillance System, *JAMA 284*, 843–849.
3. Wilcox, A.J., and Skjaerven, R. (1992) Birth Weight and Perinatal Mortality: The Effect of Gestational Age, *Am. J. Public Health 82*, 378–382.
4. Mattison, D.R., Damus, K., Fiore, E., Petrini, J., and Alter, C. (2001) Preterm Delivery: A Public Health Perspective, *Paediatr. Perinat. Epidemiol. 15* (Suppl. 2), 7–16.
5. Crawford, M.A. (2000) Placental Delivery of Arachidonic and Docosahexaenoic Acids: Implications for the Lipid Nutrition of Preterm Infants, *Am. J. Clin. Nutr. 71*, 275s–284s.
6. Crawford, M., Costeloe, K., Ghebremeskel, K., Phylactos, A., Skirvin, L., and Stacey, F. (2000) Are Deficits of Arachidonic and Docosahexaenoic Acids Responsible for the Neural and Vascular Complications of Preterm Babies? *Am. J. Clin. Nutr. 66*, 1032S–1041S.
7. Godfrey, K.M., and Barker, D.J. (2000) Fetal Nutrition and Adult Disease, *Am. J. Clin. Nutr. 71*, 1344S–1352S.
8. Mitchell, M.D., Romero, R.J., Edwin, S.S., and Trautman, M.S. (1995) Prostaglandins and Parturition, *Reprod. Fertil. Dev. 7*, 623–632.
9. Calder, A.A. (1994) Prostaglandins and Biological Control of Cervical Function, *Aust. N.Z. J. Obstet. Gynaecol. 34*, 347–351.
10. Abayasekara, D., and Wathes D. (1999) Effects of Altering Dietary Fatty Acid Composition on Prostaglandin Synthesis and Fertility, *Prostaglandins Leukot. Essent. Fatty Acids 61*, 275–287.
11. Van Houwelingen, A.C., Sorensen, J.D., Hornstra, G., Simonis, M.M., Boris, J., Olsen, S.F., and Secher, N.J. (1995) Essential Fatty Acid Status in Neonates After Fish-Oil Supplementation During Late Pregnancy, *Br. J. Nutr. 74*, 723–731.
12. Boudreau, M.D., Chanmugam, P.S., Hart, S.B., Lee, S.H., and Hwang D.H. (1991) Lack of Dose Response by Dietary n-3 Fatty Acids at a Constant Ratio of n-3 to n-6 Fatty Acids in Suppressing Eicosanoid Biosynthesis from Arachidonic Acid, *Am. J. Clin. Nutr. 54*, 111–117.
13. Arntzen, K.J., Brekke, O.L., Vatten, L., and Austgulen, R. (1998) Reduced Production of PGE_2 and $PGF_{2\alpha}$ from Decidual Cell Cultures Supplemented with n-3 Polyunsaturated Fatty Acids, *Prostaglandins Other Lipid Mediat. 56*, 183–195.
14. Lands, W.E. (1992) Biochemistry and Physiology of n-3 Fatty Acids, *FASEB J. 6*, 2530–2536.
15. Ma, X.H., Wu, W.X., Brenna, J.T., and Nathanielsz, P.W. (2000) Maternal Intravenous Administration of Long Chain n-3 Polyunsaturates to the Pregnant Ewe in Late Gestation Results in Specific Inhibition of Prostaglandin h Synthase (PGHS) 2, but Not PGHS1 and Oxytocin Receptor mRNA in Myometrium During Betamethasone-Induced Labor, *J. Soc. Gynecol. Investig. 7*, 233–237.
16. Baguma-Nibasheka, M., Brenna, J.T., and Nathanielsz, P.W. (1999) Delay of Preterm Delivery in Sheep by Omega-3 Long-Chain Polyunsaturates, *Biol. Reprod. 60*, 698–701.
17. Olsen, S.F. (1993) Consumption of Marine n-3 Fatty Acids During Pregnancy as a Possible Determinant of Birth Weight, *Epidemiol. Rev. 15*, 399–413.
18. Olsen, S.F., and Secher, N.J. (2002) Low Consumption of Seafood in Early Pregnancy as a Risk Factor for Preterm Delivery: Prospective Cohort Study, *BMJ 324*, 447–450.
19. Olsen, S.F., Hansen, H.S., Sorensen, T.I.A., Jensen, B., Secher, N.J., Sommer, S., and Knudsen, L.B. (1986) Intake of Marine Fat, Rich in n-3 Polyunsaturated Fatty Acids, May Increase Birthweight by Prolonging Gestation, *Lancet 2*, 367–369.
20. Olsen, S.F., Hansen, H.S., Sommer, S., Jensen, B., Sorensen, T.I., Secher, N.J., and Zacchariassen, P. (1991) Gestational Age in Relation to Marine n-3 Fatty Acids in Maternal Erythrocytes: A Study of Women in the Faroe Islands and Denmark, *Am. J. Obstet. Gynecol. 164*, 1203–1209.

21. Olsen, S.F., Grandjean, P., Weihe, P., and Videro, T. (1993) Frequency of Seafood Intake in Pregnancy as a Determinant of Birth Weight: Evidence for a Dose Dependent Relationship, *J. Epidemiol. Community Health 47*, 436–440.
22. Harper, V., MacInnes, R., Campbell, D., and Hall, M. (1991) Increased Birth Weight in Northerly Islands: Is Fish Consumption a Red Herring? *BMJ 303*, 166.
23. Leaf, A.A., Leighfield, M.J., Costeloe, K.L., and Crawford, M.A. (1992) Long Chain Polyunsaturated Fatty Acids and Fetal Growth, *Early Hum. Dev. 30*, 183–191.
24. Reddy, S., Sanders, T.A.B., and Obeid, O. (1994) The Influence of Maternal Vegetarian Diet on Essential Fatty Acid Status of the Newborn, *Eur. J. Clin. Nutr. 48*, 358–368.
25. Grandjean, P., Bjerve, K.S., Weihe, P., and Steuerwald, U. (2001) Birthweight in a Fishing Community: Significance of Essential Fatty Acids and Marine Food Contaminants, *Int. J. Epidemiol. 30*, 1272–1278.
26. Olsen, S.F., Sorensen, J.D., Secher, N.J., Hedegaard, M., Henriksen, T.B., Hansen, H.S., and Grant, A. (1992) Randomised Controlled Trial of Effect of Fish-Oil Supplementation on Pregnancy Duration, *Lancet 339*, 1003–1007.
27. Olsen, S., Secher, N., Tabor, A, Weber, T., Walker, J., and Gluud, C. (2000) Randomised Clinical Trials of Fish Oil Supplementation in High Risk Pregnancies. Fish Oil Trials In Pregnancy (FOTIP) Team, *Br. J. Obstet. Gynaecol. 107*, 382–395.
28. Bjerregaard, P., and Hansen, J.C. (1996) Effects of Smoking and Marine Diet on Birthweight in Greenland, *Arctic Med. Res. 55*, 156–164.
29. Cnattingius, S., Bergstrom, R., Lipworth, L., and Kramer, M.S. (1998) Prepregnancy Weight and the Risk of Adverse Pregnancy Outcomes, *N. Engl. J. Med. 338*, 147–152.
30. Hellerstedt, W.L, Himes, J.H., Story, M., Alton, I.R., and Edwards, L.E. (1997) The Effects of Cigarette Smoking and Gestational Weight Change on Birth Outcomes in Obese and Normal-Weight Women, *Am. J. Public Health 87*, 591–596.
31. Scholl, T.O., Hediger, M.L., Khoo, C.S., Healey, M.F., and Rawson, N.L. (1991) Maternal Weight Gain, Diet and Infant Birth Weight: Correlations During Adolescent Pregnancy, *J. Clin. Epidemiol. 44*, 423-428.
32. Scholl, T.O., Hediger, M.L., Fischer, R.L., and Shearer, J.W. (1992) Anemia vs. Iron Deficiency: Increased Risk of Preterm Delivery in a Prospective Study, *Am. J. Clin. Nutr. 55*, 985–988.
33. American Diabetes Association (1998) Gestational Diabetes, *Diabetes Care 21*, 60S–61S.
34. Fein, G.G., Jacobson, J.L., Jacobson, S.W., Schwartz, P.M, and Dowler, J.K. (1984) Prenatal Exposure to Polychlorinated Biphenyls: Effects on Birth Size and Gestational Age, *J. Pediatr. 105*, 315–320.
35. Taylor, P.R., Stelma, J.M., and Lawrence, C.E. (1989) The Relation of Polychlorinated Biphenyls to Birth Weight and Gestational Age in the Offspring of Occupationally Exposed Mothers, *Am. J. Epidemiol. 129*, 395–406.
36. Dewailly, É., Bruneau, S., Ayotte, P., Laliberté, C., Gringras, S., Bélanger, D., and Ferron, L. (1993) Health Status at Birth of Inuit Newborns Prenatally Exposed to Organochlorines, *Chemosphere 27*, 359–366.
37. Dar, E., Kanarek, M.S., Anderson, H.A., and Sonzogni, W.C. (1992) Fish Consumption and Reproductive Outcomes in Green Bay, Wisconsin, *Environ. Res. 59*, 189–201.
38. Foldspang, A., and Hansen, J.C. (1990) Dietary Intake of Methylmercury as a Correlate of Gestational Length and Birth Weight Among Newborns in Greenland, *Am. J. Epidemiol. 132*, 310–317.
39. Grandjean, P., and Weihe, P. (1993) Neurobehavioral Effects of Intrauterine Mercury Exposure: Potential Sources of Bias, *Environ. Res. 61*, 176–183.
40. Rylander, L., Strömberg, U., Dyremark, E., Östman, C., Nilsson-Ehle, P., and Hagmar, L. (1998) Polychlorinated Biphenyls in Blood Plasma Among Swedish Female Fish Consumers in Relation to Low Birth Weight, *Am. J. Epidemiol. 147*, 493–502.
41. Vartiainen, T., Jaakkola, J.J.K., Saarikoski, S., and Tuomisto, J. (1998) Birth Weight and Sex of Children and the Correlation to the Body Burden of PCDDs/PCDFs and PCBs of the Mother, *Environ. Health Perspect. 106*, 61–66.
42. Moore, M.R., Goldberg, A., Pocock, S.J., Meredith, A., Stewart, I.M., MacAnespie, H., Lees, R., and Low, A. (1982) Some Studies of Maternal and Infant Lead Exposure in Glasgow, *Scott Med. J. 27*, 113–122.
43. McMichael, A.J., Vimpani, G.V., Robertson, E.F., Baghurst, P.A., and Clark, P.D. (1986) The Port Pirie Cohort Study: Maternal Blood Lead and Pregnancy Outcome, *J. Epidemiol. Community Health 40*, 18–25.
44. Satin, K.P., Neutra, R.R., Guirguis, G., and Flessel, P. (1991) Umbilical Cord Blood Lead Levels in California, *Arch. Environ. Health 46*, 167–173.
45. Ayotte, P., Dewailly, E., Ryan, J.J., Bruneau, S., and Lebel, G. (1997) PCBs and Dioxin-Like Compounds in Plasma of Adult Inuit Living in Nunavik (Arctic Quebec), *Chemosphere 34*, 1459–1468.
46. Dewailly, E., Ayotte, P., Bruneau, S., Lebel, G., Levallois, P., and Weber, J.P. (2001) Exposure of the Inuit Population of Nunavik (Arctic Quebec) to Lead and Mercury, *Arch. Environ. Health 56*, 350–357.
47. Santé Québec (1995) Report of the Santé Québec Health Survey Among the Inuit of Nunavik (1992) Diet, a Health Determining Factor, Ministère de la Santé et des Services Sociaux, Gouvernement du Québec, Montréal, pp. 47–124.
48. Blanchet, C., Dewailly, E., Ayotte, P., Bruneau, S., Receveur, O., and Holub, B. (2000) Contribution of Selected Traditional and Market Foods to the Diet of Nunavik Inuit Women, *Can. J. Diet. Pract. Res. 61*, 50–59.
49. Dewailly, E., Blanchet, C., Lemieux, S., Sauve, L., Gingras, S., Ayotte, P., and Holub, B.J. (2001) n-3 Fatty Acids and Cardiovascular Disease Risk Factors Among the Inuit of Nunavik, *Am. J. Clin. Nutr. 74*, 464–473.
50. Dewailly, E., Blanchet, C., Gingras, S., Lemjeux, S., Sauve, L., Bergeron, J., and Holub, B.J. (2001) Relations Between n-3 Fatty Acid Status and Cardiovascular Disease Risk Factors Among Quebecers, *Am. J. Clin. Nutr. 74*, 603–611.
51. Nettleton, J.A. (1991) n-3 Fatty Acids: Comparison of Plant and Seafood Sources in Human Nutrition, *J. Am. Diet. Assoc. 91*, 331–337.
52. Rhainds, M., Levallois, P., Dewailly, E., and Ayotte, P. (1999) Lead, Mercury, and Organochlorine Compound Levels in Cord Blood in Quebec, Canada, *Arch. Environ. Health 54*, 40–47.
53. Holub, B.J., Bakker, D.J., and Skeaff, C.M. (1987) Alterations in Molecular Species of Cholesterol Esters Formed *via* Plasma Lecithin–Cholesterol Acyltransferase in Human Subjects Consuming Fish Oil, *Atherosclerosis 66*, 11–18.
54. Takayama, M., Itoh, S., Nagasaki, T., and Tanimizu, I. (1977) A New Enzymatic Method for Determination of Serum Choline-Containing Phospholipids, *Clin. Chim. Acta 79*, 93–98.
55. Phillips, D.L., Pirkle, J.L., Burse, V.W., Bernert, J.T., Jr., Henderson, L.O., and Needham, L.L. (1989) Chlorinated Hydrocarbon Levels in Human Serum: Effects of Fasting and Feeding, *Arch. Environ. Contam. Toxicol. 18*, 495–500.
56. Lands, W.E. (1995) Long-Term Fat Intake and Biomarkers, *Am. J. Clin. Nutr. 61*, 721S–725S.
57. Muckle, G., Ayotte, P., Dewailly, E., Jacobson, S.W., and Jacobson, J.L. (2001) Determinants of Polychlorinated Biphenyls and Methylmercury Exposure in Inuit Women of Childbearing Age, *Environ. Health Perspect 109*, 957–963.
58. Helland, I.B., Saugstad, O.D., Smith, L., Saarem, K., Solvoll, K., Ganes, T., and Drevon, C.A. (2001) Similar Effects on Infants

of n-3 and n-6 Fatty Acids Supplementation to Pregnant and Lactating Women, *Pediatrics 108*, E82–E92.
59. Olsen, S., and Secher, N., (1990) A Possible Preventive Effect of Low-Dose Fish Oil on Early Delivery and Pre-eclampsia: Indications from a 50-Year-Old Controlled Trial, *Br. J. Nutr. 64*, 599–609.
60. Hansen, H.S., and Olsen, S.F. (1988) Dietary (n-3)-Fatty Acids, Prostaglandins, and Prolonged Gestation in Humans, *Prog. Clin. Biol. Res. 282*, 305–317.
61. Oates, J.A., Fitzgerald, G.A., Branch, R.A., Jackson, E.K., Knapp, H.R., and Roberts, L.J., II (1988) Clinical Implications of Prostaglandin and Thromboxane A_2 Formation (1), *N. Engl. J. Med. 319*, 689–698.
62. Secher, N.J., and Olsen, S.F. (1990) Fish-Oil and Pre-eclampsia, *Br. J. Obstet. Gynaecol. 97*, 1077–1079.
63. Smuts, C.M., Huang, M., Mundy, D., Plasse, T., Major, S., and Carlson, S.E. (2003) A Randomized Trial of Docosahexaenoic Acid Supplementation During the Third Trimester of Pregnancy, *Obstet. Gynecol. 101*, 469–479.
64. Al, M.D., Van Houwelingen, A.C., Kester, A.D., Hasaart, T.H., De Jong, A.E., and Hornstra, G. (1995) Maternal Essential Fatty Acid Patterns During Normal Pregnancy and Their Relationship to the Neonatal Essential Fatty Acid Status, *Br. J. Nutr. 74*, 55–68.
65. Al, M.D., Badart-Smook, A., Von Houwelingen, A.C., Hasaart, T.H., and Hornstra, G. (1996) Fat Intake of Women During Normal Pregnancy: Relationship with Maternal and Neonatal Essential Fatty Acid Status, *J. Am. Coll. Nutr. 15*, 49–55.
66. Dutta-Roy, A.K. (2000) Transport Mechanisms for Long-Chain Polyunsaturated Fatty Acids in the Human Placenta, *Am. J. Clin. Nutr. 71*, 315S–322S.
67. Ruyle, M., Connor, W.E., Anderson, G.J., and Lowensohn, R.I. (1990) Placental Transfer of Essential Fatty Acids in Humans: Venous-Arterial Difference for Docosahexaenoic Acid in Fetal Umbilical Erythrocytes, *Proc. Natl. Acad. Sci. USA 87*, 7902–7906.
68. Young, K.T., Gerrard, J.M., and O'Neil, J.D. (1999) Plasma Phospholipid Fatty Acids in the Central Canadian Artic: Biocultural Explanations for Ethnic Differences, *Am. J. Phys. Anthropol. 109*, 9–18.
69. Stark, K.D., Mulvad, G., Pedersen, H.S., Park, E.J., Dewailly, E., and Holub, B.J. (2002) Fatty Acid Compositions of Serum Phospholipids of Postmenopausal Women: A Comparison Between Greenland Inuit and Canadians Before and After Supplementation with Fish Oil, *Nutrition 18,* 627–630.
70. Hornstra, G., Al, M.D.M., Gerrard, J.M., and Simonis, M.M.G. (1992) Essential Fatty Acid Status of Neonates Born to Inuit Mothers: Comparison with Caucasian Neonates and Effect of Diet, *Prostaglandins Leukot. Essent. Fatty Acids 45*, 125–130.
71. Clandinin, M.T. (2002) Serum Long-Chain Polyenoic Fatty Acids in Postmenopausal Women, *Nutrition 18*, 680.
72. Grandjean, P., and Weihe, P. (2003) Arachidonic Acid Status During Pregnancy Is Associated with Polychlorinated Biphenyl Exposure, *Am. J. Clin. Nutr. 77*, 715–719.
73. Gibson, R.A., and Sinclair, A.J. (1981) Are Eskimos Obligate Carnivores? *The Lancet 1*, 1100.
74. Longnecker, M.P., Wolff, M.S., Gladen, B.C., Brock, J.W., Grandjean, P., Jacobson, J.L., Korrick, S.A., Rogan, W.J., Weisglas-Kuperus, N., Hertz-Picciotto, I., *et al.* (2003) Comparison of Polychlorinated Biphenyl Levels Across Studies of Human Neurodevelopment, *Environ. Health Perspect. 111*, 65–70.
75. David, R.J. (1980) The Quality and Completeness of Birthweight and Gestational Age Data in Computerized Birth Files, *Am. J. Public Health 70*, 964–973.
76. Treloar, A.E., Behn, B.G., and Cowan, D.W. (1967) Analysis of Gestational Interval, *Am. J. Obstet. Gynecol. 99*, 34–45.
77. Berkowitz, G.S., and Papiernik, E. (1993) Epidemiology of Preterm Birth, *Epidemiol. Rev. 15*, 414–443.
78. Hibbeln, J.R. (2002) Seafood Consumption, the DHA Content of Mothers' Milk and Prevalence Rates of Postpartum Depression: A Cross-National, Ecological Analysis, *J. Affect. Disord. 69*, 15–29.
79. Kris-Etherton, P.M., Harris, W.S., and Appel, L.J. (2002) Fish Consumption, Fish Oil, Omega-3 Fatty Acids, and Cardiovascular Disease, *Circulation 106*, 2747–2757.
80. Lee, R.M. (1994) Fish Oil, Essential Fatty Acids, and Hypertension, *Can. J. Physiol. Pharmacol. 72*, 945–953.
81. Kremer, J.M. (2000) n-3 Fatty Acid Supplements in Rheumatoid Arthritis, *Am. J. Clin. Nutr. 71*, 349S–351S.
82. Stoll, A.L., Severus, W.E., Freeman, M.P., Rueter, S., Zboyan, H.A., Diamond, E., Cress, K.K., and Marangell, L.B. (1999) Omega-3 Fatty Acids in Bipolar Disorder, *Arch. Gen. Psychiatry 56*, 407–412.
83. Hibbeln, J.R. (1998) Fish Consumption and Major Depression, *Lancet 351*, 1213.
84. Peet, M., and Horrobin, D.F. (2002) A Dose-Ranging Study of the Effects of Ethyl-Eicosapentaenoate in Patients with Ongoing Depression Despite Apparently Adequate Treatment with Standard Drugs, *Arch. Gen. Psychiatry 59*, 913–919.
85. Tanskanen, A., Hibbeln, J.R., Hintikka, J., Haatainen, K., Honkalampi, K., and Viinamaki, H. (2001) Fish Consumption, Depression, and Suicidality in a General Population, *Arch. Gen. Psychiatry 58*, 512–513.
86. Maillard, V., Bougnoux, P., Ferrari, P., Jourdan, M.L., Pinault, M., Lavillonniere, F., Body, G., Le Floch, O., and Chajes, V. (2002) n-3 and n-6 Fatty Acids in Breast Adipose Tissue and Relative Risk of Breast Cancer in a Case-Control Study in Tours, France, *Int. J. Cancer 98*, 78–83.
87. Terry, P., Lichtenstein, P., Feychting, M., Ahlbom, A., and Wolk, A. (2001) Fatty Fish Consumption and Risk of Prostate Cancer, *Lancet 357*, 1764–1766.
88. Belluzzi, A., Boschi, S., Brignola, C., Munarini, A., Cariani, G., and Miglio, F. (2000) Polyunsaturated Fatty Acids and Inflammatory Bowel Disease, *Am. J. Clin. Nutr. 71*, 339S–342S.
89. World Health Organization (2000) Evaluation of Certain Food Additives and Contaminants, Fifty-Third Report of the Joint FAO/WHO Expert Committee on Food Additives, Technical Report Series #896 (based on a meeting held in Rome, 1999), World Health Organization, Geneva.

[Received February 2, 2004; accepted August 26, 2004]

Supplementation and Delivery of n-3 Fatty Acids Through Spray-Dried Milk Reduce Serum and Liver Lipids in Rats

T.R. Ramaprasad[a], V. Baskaran[b], K. Sambaiah[b], and B.R. Lokesh[a,*]

Departments of [a]Lipid Science and Traditional Foods and [b]Biochemistry and Nutrition, Central Food Technological Research Institute (CFTRI), Mysore–570 020, India

ABSTRACT: Indian diets comprising staples such as cereals, millets, and pulses provide 4.8 energy % from linoleic acid (18:2n-6) but fail to deliver adequate amounts of n-3 FA. Consumption of long-chain n-3 PUFA such as EPA (20:5n-3) and DHA (22:6n-3) is restricted to those who consume fish. The majority of the Indian population, however, are vegetarians needing additional dietary sources of n-3 PUFA. The present work was designed to use n-3 FA-enriched spray-dried milk powder to provide n-3 FA. Whole milk was supplemented with linseed oil to provide α-linolenic acid (LNA, 18:3n-3), with fish oil to provide EPA and DHA, or with groundnut oil (GNO), which is devoid of n-3 PUFA, and then spray-dried. Male Wistar rats were fed the spray-dried milk formulations for 60 d. The rats given formulations containing n-3 FA showed significant increases ($P < 0.001$) in the levels of LNA or EPA/DHA in the serum and in tissue lipids as compared with those fed the GNO control formulation. Rats fed formulations containing n-3 FA had 30–35% lower levels of serum total cholesterol and 25–30% lower levels of serum TAG than control animals. Total cholesterol and TAG in the livers of rats fed the formulations containing n-3 FA were lower by 18–30% and 11–18%, respectively, compared with control animals. This study showed that spray-dried milk formulations supplemented with n-3 FA are an effective means of improving dietary n-3 FA intake, which may decrease the risk factors associated with cardiovascular disease.

Paper no. L9474 in *Lipids 39*, 627–632 (July 2004).

Over the past decades, the intake of n-6 FA has increased because of the increased use of vegetable oils in our diets (1). In addition to visible fats coming from vegetable oils, such as groundnut oil [GNO, i.e., peanut oil, with 32% linoleic acid (LA)], mustard oil (with 22% LA), and sunflower oil (with 70% LA), Indian diets comprising cereals, pulses, and millets also contain lipids termed "invisible fats." Based on surveys conducted on Indian dietary patterns, Ghafoorunissa (2,3) has estimated that Indians derive 12.6 g of LA per day, equivalent to 4.8 energy % (en%), from visible and invisible fats. The requirement for LA as an EFA is 3 en% (2). Hence, Indian diets provide adequate amounts of LA. However, the intake of n-3 FA by Indians is in the range of 0.3 g in the rural population and 0.6 g in the urban population, equivalent to 0.2–0.3 en% (3,4). A number of scientific and regulatory agencies, such as the Committee on Medical Aspects of Food Policy, Department of Health, in the United Kingdom; the British Nutrition Foundation; the European Commission's Scientific Committee on Food; and the Food and Agricultural Organization of the United Nations/World Health Organization have recommended that n-3 PUFA be increased to approximately 0.7–1.0 en%. These recommendations have been summarized in detail by Roche (5), Stanley (6), and Sanderson *et al*. (7). Recently, experts also have debated and agreed on the essentiality of n-3 PUFA in the diet (8,9). Even though India has no specific recommendations for the intake of n-3 PUFA, several studies conducted by the National Institute of Nutrition, an organization of the Indian Council of Medical Research, have suggested that an intake of 0.75 en% from α-linolenic acid (LNA) and 0.2 en% from EPA and DHA would have a positive impact on the prevention of coronary heart disease in India (3,10–12). Soybean, canola, perilla, and walnut oils, although good sources of LNA, are not used on a regular basis in India. Mustard oil, which contains about 10% LNA, is used in some parts of India. However, it also contains about 50% erucic acid (22:1*cis*-13), which is a concern for many individuals, as erucic acid levels higher than 7% in the oil of the diet are known to cause myocardial lipidosis and fibrosis in experimental animals (13). These observations of the dietary habits of normal Indian subjects, as well as biochemical indices such as the plasma and platelet phospholipid n-3 FA profiles, reinforce the need to improve the n-3 FA intake (3). Oily fish can provide sufficient amounts of n-3 FA such as EPA and DHA; however, many Indians refrain from eating fish, as it is a nonvegetarian food. Linseed (*Linum usitatissimum*), which is rich in LNA, is an economically important oilseed crop used for edible purposes in the central and northeastern regions of India. The beneficial properties of linseed oil (LSO) (14–16) and fish oil (FO) (17) have been discussed in detail in earlier research. LSO could be exploited as an alternate source of n-3 FA if it could be delivered in appropriate form. However, LSO has very limited utility because it polymerizes rapidly if not processed properly.

The direct use of these n-3 FA-rich oils, either as single oils or as blends, has certain limitations with respect to sensory qualities, acceptability, and accessibility. Hence, an alternate means of delivering dietary n-3 PUFA to the Indian population could be through enriching a food product such as milk, a beverage commonly consumed by all segments of the population. Milk also contains additional components that

*To whom correspondence should be addressed.
E-mail: brlokesh@yahoo.com

Abbreviations: FO, fish oil; GNO, groundnut oil; LA, linoleic acid; LNA, α-linolenic acid; LSO, linseed oil.

may have significant health benefits. Milk fat is a good source of CLA (18) with putative antiatherogenic properties (19). Milk also contains short- and medium-chain FA, which are more readily absorbed, digested, and oxidized through carnitine-independent pathways without hindering the formation of chylomicrons (20). Studies have emphasized the important traditional role of milk as a supplier of nutrients because of its versatility and high nutrient density (21). Bovine milk is widely used in India by people of different age groups. In spite of its high nutritional value, however, it is devoid of FA of the n-3 family such as LNA, EPA, and DHA. In this research, we developed a process for incorporating n-3 PUFA-rich oils into milk and then spray-drying it without affecting the overall quality (22). This spray-dried milk could then be reconstituted with water to provide n-3 FA.

The present experiment was designed to study the feasibility of using milk in spray-dried form to deliver n-3 FA from LSO or FO. The implications for several risk factors for cardiovascular disease were also studied.

MATERIALS AND METHODS

Materials. Cholesterol, dipalmitoyl PC, triolein, boron trifluoride in methanol, and alpha cellulose were purchased from Sigma Chemical Co. (St. Louis, MO). Heparin and $MnCl_2$ were obtained from Sisco Research Laboratory (Mumbai, India). Casein was purchased from Nimesh Corporation (Mumbai, India). Maltodextrin was purchased from Laxmi Starch Co. (Hyderabad, India). All solvents used were of analytical grade and were distilled prior to use. Milk was obtained from a state-owned dairy. GNO, LSO, and FO were purchased from a local market.

Experimental animals. The experimental protocol was approved by the institutional animal ethics committee. Male Wistar rats [OUTB-Wistar, IND-cft (2c)] weighing 49 ± 3 g were grouped by random distribution into individual cages and housed, under a 12-h light/dark cycle, in an approved animal facility at the Central Food Technological Research Institute in Mysore, India. Animals were given a fresh diet daily, and leftover diets were weighed and discarded. The gain in body weight of animals was monitored at regular intervals. The animals were given free access to food and water throughout the study.

Preparation of n-3 FA-enriched spray-dried milk powder. The FA profile of the milk used in the present study was as follows (in %): 12:0, 1.8; 14:0, 9.7; 16:0, 33.0; 16:1, 1.7; 18:0, 9.8; 18:1, 37.2; and 18:2, 6.1. Three batches (70 L of milk/batch) of spray-dried milk powder were prepared in a pilot plant after supplementation with GNO, LSO, or FO (23). The dried product, which was golden yellow in color and had a smooth texture, was collected in a humidity-controlled chamber and packed under nitrogen. The total fat content of the milk enriched with GNO, LSO, or FO was 16%. A GNO-enriched diet devoid of n-3 FA, which served as the control, and the LSO and FO n-3 FA-enriched diets were fed to rats *ad libitum* (24). After 60 d of feeding the formulations containing GNO, LSO, or FO, the rats were fasted overnight and sacrificed under ether anesthesia. Blood was drawn by cardiac puncture, and serum was separated by centrifugation at 1100 × *g* for 30 min. The liver and other organs were removed, rinsed with ice-cold saline, blotted, weighed, and stored at −20°C until analyzed.

Analysis of lipids. Lipids were extracted from serum and tissues by the method of Folch *et al.* (25). Serum and liver cholesterol levels were quantified by the method of Searcy and Bergquist (26). HDL cholesterol was estimated after precipitating LDL with a heparin–$MnCl_2$ reagent (27). Phospholipids were measured by the method of Stewart (28) using dipalmitoyl PC as a reference standard. TAG were estimated by the method of Fletcher (29). FAME were prepared by using boron trifluoride in methanol as described by Morrison and Smith (30) and then analyzed by GC (Shimadzu model 14B, fitted with an FID) using a 25 m × 0.25 mm fused-silica capillary column (Parma bond FFAP-DF-0.25; Macherey-Nagel GmBH; Düren, Germany). The operating conditions were as follows: initial column temperature, 160°C; injector temperature, 210°C; detector temperature, 250°C. The column temperature was programmed to ramp at 6°C per min to a final temperature of 240°C, and nitrogen was used as the carrier gas. Individual FA were identified by comparison with the retention times of standards (Nu-Chek-Prep. Inc., Elysian MN) and were quantified by an on-line Shimadzu Chromatopack CR6A integrator.

Statistical analysis. The results were analyzed statistically by ANOVA (31). P values of <0.001 were considered to be significantly different.

RESULTS

Proximate composition of spray-dried milk powder. Analysis of the proximate composition of spray-dried milk revealed that the amounts of carbohydrate (59 ± 0.7%), protein (17 ± 0.4%), and fat (16 ± 0.2%) in both the LSO and FO formulations were similar to that in the GNO control. There were no significant differences with respect to the caloric value (458 ± 1.6 cal), percent of total ash (4.4 ± 0.2%), and moisture content (3.28 ± 0.08%) (combined mean ± SD of all three formulations). Sensory qualities were evaluated by a panel of judges using a hedonic scale of 1 to 10, in which lower scores (<5) indicated poor acceptability and higher scores (>5) indicated good acceptability. Panelists assigned the milk formulations scores of 7.9 ± 0.9, 7.5 ± 1.3, and 7.5 ± 0.8, respectively, for flavor, mouthfeel, and overall acceptability of the products (combined mean ± SD of all three formulations). These values were comparable with those of bovine milk without any added n-3 FA.

FA composition of spray-dried milk formulations. Analysis of the FA composition of diets revealed that the spray-dried milk powder with LSO contained 20% LNA and that with FO contained 3 and 2% EPA and DHA, respectively. These FA were not detected in the spray-dried milk powder containing GNO (Table 1).

TABLE 1
FA Composition (%) of Diets[a]

FA	GNO	LSO	FO
12:0	1.2	1.9	1.6
14:0	6.9	7.9	11.0
16:0	27.7	25.8	35.0
16:1n-7	1.0	1.0	4.8
18:0	9.2	11.9	10.6
18:1n-9	41.3	24.2	25.0
18:2n-6	9.7	6.8	3.8
18:3n-3	ND	20.3	ND
20:0	1.9	ND	ND
20:4n-6	ND	ND	3.1
20:5n-3	ND	ND	2.9
22:0	0.8	ND	ND
22:6n-3	ND	ND	2.1
PUFA	9.7	27.1	11.9
SFA	47.7	47.5	58.2
PUFA/SFA	0.20	0.57	0.20

[a]Values are means of triplicate samples. ND, not detected; GNO, groundnut oil; LSO, linseed oil; FO, fish oil; SFA, saturated FA.

Effect of n-3 FA-enriched formulations on growth parameters. The fat level was kept constant at 16% in all three diet groups. The amounts of diet consumed in the different groups were comparable (Table 2). There were no significant changes in the food efficiency ratio and body weight gain of rats fed diets containing GNO, LSO, or FO. Weights of the heart, spleen, and brain of rats fed either the GNO-, LSO-, or FO-enriched diet were comparable. The liver weights of rats fed the FO diet were higher than those observed for rats fed the GNO or LSO diets (Table 3). The hematological parameters in different groups were comparable (hemoglobin 14.66 ± 1.37 g/dL; 9.82 ± 0.41 red blood cells × 10^6/μL; 6687 ± 442 total count; and 37.41 ± 1.25% packed-cell volume) (combined mean ± SD of all groups). These studies indicated that supplementation of milk with n-3 PUFA-rich oils (LSO or FO) had no adverse effect on the growth of animals.

TABLE 2
Effect of Feeding Spray-Dried Formulations Enriched with n-3 FA on the Growth of Rats[a]

Parameters	GNO	LSO	FO
Food intake (g/d/rat)	9.9 ± 0.8	10.2 ± 0.6	10.3 ± 1.0
Body weight gain (g)	191 ± 25	194 ± 30	188 ± 19
Food efficiency ratio	0.32 ± 0.04	0.31 ± 0.03	0.31 ± 0.04

[a]Values are means ± SD (n = 6 rats). None of the values within a row were statistically different. For abbreviations see Table 1.

TABLE 3
Effect of Feeding Spray-Dried Formulations Enriched with n-3 FA on Organ Weights in Rats (g/100 g body wt)[a]

Organs	GNO	LSO	FO
Liver	3.5 ± 0.2^b	3.5 ± 0.3^b	4.1 ± 0.2^c
Heart	0.32 ± 0.02^b	0.34 ± 0.03^b	0.33 ± 0.02^b
Spleen	0.26 ± 0.08^b	0.23 ± 0.03^c	0.24 ± 0.02^c
Brain	0.67 ± 0.11^b	0.66 ± 0.08^b	0.67 ± 0.07^b

[a]Values are means ± SD (n = 6 rats). Values not sharing a common superscript within a row are statistically significant ($P < 0.001$). For abbreviations see Table 1.

Effect of feeding milk formulations enriched with n-3 FA on serum lipid profiles. Rats fed spray-dried milk powder containing LSO or FO had 30 and 35% lower levels of serum total cholesterol compared with those given the formulation containing GNO. The serum TAG level was 26 and 29% lower in the LSO and FO diet groups, respectively, compared with rats fed the formulation containing GNO (Table 4). Significant changes were observed in the n-3 FA level in rats fed milk formulations with LSO or FO (Table 5). The LNA level in rats fed the LSO formulation was 6.8%. Significant increases in the EPA and DHA levels and a concomitant decrease in the arachidonic acid level were also observed in rats given the formulation containing LSO. LNA was not detected in the serum of rats fed the formulation containing GNO; n-3 FA-fed rats had 12–18% lower levels of oleic acid in the serum than those fed GNO. In those fed the FO formulation, the long-chain n-3 PUFA EPA and DHA were incorporated into serum at levels of 2.3 and 2.6%, respectively. These FA were not observed in rats given the formulation containing GNO.

Liver lipid profile of rats fed milk enriched with n-3 FA. The total cholesterol level in the liver decreased by 30 and 18%, respectively, in rats fed the LSO and FO formulations, and the TAG level decreased by 18 and 11%, respectively. No significant changes were observed in the phospholipid levels of the liver tissue when animals were fed different fat sources (Table 6). The oleic acid level decreased by 38–41% in the livers of rats fed the n-3 FA (Table 7). Significant amounts of

TABLE 4
Serum Lipid Profile (mg/dL) of Rats Fed Spray-Dried Formulations Enriched with n-3 FA[a]

Parameters	GNO	LSO	FO
Total cholesterol	90.2 ± 3.2^b	62.9 ± 5.7^c	58.2 ± 6.3^c
HDL cholesterol	37.6 ± 4.3^b	23.4 ± 3.2^c	23.4 ± 3.8^c
LDL + VLDL cholesterol	52.5 ± 4.0^b	39.5 ± 4.8^c	34.7 ± 4.8^c
Phospholipids	147.3 ± 10.7^b	119.1 ± 9.5^c	122.6 ± 10.8^c
TAG	136.4 ± 6.4^b	99.9 ± 12.9^c	96.4 ± 11.8^c

[a]Values are means ± SD (n = 6 rats). Values not sharing a common superscript within a row are statistically significant ($P < 0.001$). For diet abbreviations see Table 1.

TABLE 5
Serum FA Profile (%) of Rats Fed Spray-Dried Formulations Enriched with n-3 FA[a]

FA	GNO	LSO	FO
16:0	30.4 ± 3.0^{b,c}	29.1 ± 1.6^b	34.3 ± 2.0^c
16:1n-7	1.5 ± 0.3^b	2.1 ± 0.5^{b,c}	3.3 ± 0.7^c
18:0	11.9 ± 1.5^b	14.5 ± 2.3^{b,c}	15.5 ± 2.0^c
18:1n-9	41.0 ± 3.9^b	33.3 ± 2.1^c	35.8 ± 2.3^{b,c}
18:2n-6	8.7 ± 2.3^b	8.3 ± 1.9^b	3.1 ± 2.3^c
18:3n-3	ND	6.8 ± 0.8^b	ND
20:4n-6	6.3 ± 1.3^b	2.4 ± 1.0^c	2.6 ± 1.5^c
20:5n-3	ND	2.0 ± 0.6^b	2.3 ± 0.1^b
22:6n-3	ND	0.9 ± 0.1^b	2.6 ± 0.5^c

[a]Values are means ± SD (n = 4 rats). Values not sharing a common superscript within a row are statistically significant ($P < 0.001$). For abbreviations see Table 1.

TABLE 6
Liver Lipid Profile (mg/g tissue) of Rats Fed Spray-Dried Formulations Enriched with n-3 FA[a]

Parameters	GNO	LSO	FO
Total cholesterol	10.7 ± 0.5[b]	7.5 ± 1.2[c]	8.8 ± 0.6[c]
TAG	15.1 ± 0.8[b]	12.3 ± 1.0[c]	13.5 ± 0.7[c]
Phospholipids	28.2 ± 2.9[b]	30.7 ± 7.0[b]	29.7 ± 2.9[b]

[a]Values are means ± SD (n = 6 rats). Values not sharing a common superscript within a row are statistically significant ($P < 0.001$). For abbreviations see Table 1.

TABLE 7
Liver FA Profile (%) of Rats Fed Spray-Dried Formulations Enriched with n-3 FA[a]

FA	GNO	LSO	FO
16:0	22.7 ± 2.3[b]	21.1 ± 1.9[b]	28.2 ± 3.4[c]
16:1n-7	1.3 ± 0.2[b]	1.5 ± 0.3[b]	2.9 ± 0.2[c]
18:0	11.9 ± 2.1[b]	17.5 ± 3.4[c]	17.3 ± 1.6[c]
18:1n-9	41.2 ± 3.3[b]	25.3 ± 3.9[c]	24.0 ± 2.5[c]
18:2n-6	11.3 ± 1.8[b]	9.9 ± 2.0[b]	5.7 ± 1.8[c]
18:3n-3	ND	7.6 ± 0.8[b]	ND
20:4n-6	11.4 ± 1.1[b]	6.9 ± 0.4[c]	5.9 ± 0.6[c]
20:5n-3	ND	6.5 ± 1.0[b]	6.0 ± 1.1[b]
22:6n-3	ND	3.4 ± 0.6[b]	9.7 ± 0.9[c]

[a]Values are means ± SD (n = 4 rats). Values not sharing a common superscript within a row are statistically significant ($P < 0.001$). For abbreviations see Table 1.

LNA and long-chain n-3 FA accumulated in the livers of rats fed the LSO-enriched diets. The total n-3 PUFA level in LSO-fed rats was 17.5%. Similarly, FO-supplemented diets significantly enriched the EPA (6%) and DHA (9.7%) levels in liver lipids; however, n-3 FA enrichment decreased the levels of LA and arachidonic acid in the liver.

FA composition of adipose, brain, and heart tissues of rats fed n-3 FA. The dietary n-3 FA level influenced the FA composition of adipose (Table 8), brain (Table 9), and heart tissues (Table 10). Animals fed the LSO and FO formulations had 25 and 45% lower amounts of LA in the adipose tissue compared with those fed the GNO-containing formulation. The adipose tissue of rats fed the LSO formulation had 15% of total FA as LNA, whereas LNA was not detected in rats fed the GNO or FO formulation. EPA and DHA were found only in animals fed the FO formulation and were found to be 1.3 and 1.4%, respectively, of total FA. In the brain, rats fed the LSO formulation had 2.9% of total FA as LNA, whereas LNA was not detected in the other dietary groups. The basal level of DHA in rats fed the GNO formulation was 9.6% of total FA, whereas this amount increased to 12.7 and 14.4% of total FA, respectively, in rats fed the LSO and FO formulations. In the heart, the LNA levels of rats fed the LSO formulation were 4.9% of total FA, whereas LNA was not detected in the other dietary groups. The basal level of DHA was significantly enhanced in the heart tissue of rats given the FO diet. There was a 3.5-fold increase in the accumulation of DHA in the heart tissue of animals fed the FO formulation compared with those fed the GNO diet. The level of arachidonic acid in the heart tissue decreased when n-3 FA were fed.

TABLE 8
Adipose Tissue FA Profile (%) of Rats Fed Spray-Dried Formulations Enriched with n-3 FA[a]

FA	GNO	LSO	FO
14:0	6.7 ± 0.6[b]	7.5 ± 1.0[b]	10.6 ± 1.0[c]
16:0	26.6 ± 4.1[b]	28.2 ± 4.6[b]	33.1 ± 3.3[b]
16:1n-7	2.4 ± 0.6[b]	4.4 ± 1.1[c]	8.1 ± 1.2[d]
18:0	4.2 ± 0.3[b]	4.0 ± 0.6[b]	3.4 ± 0.3[b]
18:1n-9	48.9 ± 4.9[b]	39.1 ± 3.8[c]	35.3 ± 4.0[c]
18:2n-6	10.7 ± 2.1[b]	8.0 ± 0.9[c]	5.8 ± 1.1[d]
18:3n-3	ND	15.1 ± 1.2[b]	ND
20:4n-6	0.5 ± 0.04[b]	0.2 ± 0.04[c]	0.4 ± 0.06[b]
20:5n-3	ND	ND	1.3 ± 0.2[b]
22:6n-3	ND	ND	1.4 ± 0.3[b]

[a]Values are means ± SD (n = 4 rats). Values not sharing a common superscript within a row are statistically significant ($P < 0.001$). For abbreviations see Table 1.

TABLE 9
Brain Tissue FA Profile (%) of Rats Fed Spray-Dried Formulations Enriched with n-3 FA[a]

FA	GNO	LSO	FO
16:0	24.3 ± 2.9[b]	25.6 ± 3.6[b]	23.0 ± 3.0[b]
16:1n-6	0.4 ± 0.1[b]	0.5 ± 0.1[b]	0.4 ± 0.2[b]
18:0	20.9 ± 3.6[b]	20.1 ± 4.3[b]	19.0 ± 3.8[b]
18:1n-9	29.9 ± 3.6[b]	25.0 ± 4.2[b]	29.1 ± 2.8[b]
18:2n-6	1.8 ± 0.9[b]	1.6 ± 0.5[b]	1.4 ± 0.1[b]
18:3n-3	ND	2.9 ± 0.4[b]	ND
20:4n-6	11.6 ± 2.8[b]	9.2 ± 1.6[b]	8.1 ± 1.2[b]
20:5n-3	0.6 ± 0.2[b]	2.1 ± 1.2[c]	3.0 ± 0.9[c]
22:6n-3	9.6 ± 0.2[b]	12.7 ± 0.8[c]	14.4 ± 0.3[d]

[a]Values are means ± SD (n = 4 rats). Values not sharing a common superscript within a row are statistically significant ($P < 0.001$). For abbreviations see Table 1.

TABLE 10
Heart Tissue FA Profile (%) of Rats Fed Spray-Dried Formulations Enriched with n-3 FA[a]

FA	GNO	LSO	FO
16:0	14.3 ± 2.3[b]	13.5 ± 3.1[b]	14.8 ± 1.9[b]
16:1n-7	1.0 ± 0.2[b]	1.0 ± 0.3[b]	1.2 ± 0.1[b]
18:0	17.4 ± 2.5[b]	23.0 ± 3.1[c]	22.9 ± 3.5[c]
18:1n-9	29.7 ± 3.9[b]	22.2 ± 3.8[c]	19.4 ± 2.6[c]
18:2n-6	17.1 ± 2.1[b]	17.4 ± 3.1[b]	14.4 ± 3.2[b]
18:3n-3	ND	4.9 ± 0.4[b]	ND
20:4n-6	13.6 ± 3.1[b]	11.2 ± 1.9[b]	11.2 ± 1.6[b]
22:6n-3	ND	1.0 ± 0.1[b]	2.9 ± 0.5[c]
20:5n-3	4.6 ± 0.4[b]	5.7 ± 1.3[c]	15.8 ± 2.1[d]

[a]Values are means ± SD (n = 4 rats). Values not sharing a common superscript within a row are statistically significant ($P < 0.001$). For abbreviations see Table 1.

DISCUSSION

The present investigation was aimed at providing a formulation containing n-3 FA that could be consumed by those whose dietary intake of n-3 FA is inadequate. To cater to such populations, a milk-based instant beverage formulation was developed that can provide n-3 FA. Attempts have been made to enrich milk with n-3 FA by feeding dairy cows fish-based products (32). However, the metabolic state of animals, as

well as season and hormonal variations, may interfere with the level of n-3 FA in the milk. Because fresh milk cannot be stored for a long period of time, we developed two milk-based spray-dried formulations that are shelf stable and that contained n-3 FA, one from a vegetable source (LSO) and the other from a marine source (FO). The beverage provided 640 mg of LNA or 160 mg of EPA and DHA per serving when 20 g of formulation dissolved in 100 mL of water was consumed. The LSO and FO formulations provided 0.75 and 0.2 en%, respectively, of n-3 FA.

Rats were fed these milk-based formulations to study the delivery of n-3 FA to various tissues and its impact on several risk factors associated with cardiovascular diseases. The rats fed the spray-dried formulation containing LSO showed incorporation of LNA and its metabolites EPA and DHA into the serum, liver tissue, and heart tissue. Earlier studies have shown that feeding diets containing LNA can increase the level of this FA, as well as the level of long-chain metabolites, to varying degrees (33–35).

Zhong and Sinclair (36) observed that feeding a diet high in LNA to guinea pigs increased the EPA and DHA levels in liver, heart, and adipose tissues compared with a diet low in LNA. However, in our study EPA and DHA were not detected in adipose tissue when rats were fed the formulation containing LSO. Similarly, Lin and Connors (37) observed that an LNA-enriched diet resulted in the accumulation of LNA, but not EPA and DHA, in the adipose tissue. The investigation by Okuno *et al.* (38) on rats showed that feeding a diet containing perilla oil (60.3% LNA) resulted in an accumulation of only 0.9 and 0.4% EPA and DHA, respectively, whereas LNA made up 12.3% of the total FA in adipose tissue. These studies may indicate that at high intake levels, LNA can accumulate in adipose tissue but that its elongation to EPA and DHA is restricted. However, these FA can accumulate in adipose tissue when preformed long-chain n-3 PUFA are included in the diet.

The brain is a unique organ characterized by the presence of a high concentration of DHA, which influences its structural and functional properties (39). Feeding rats the formulations containing n-3 FA from LSO or FO further increased the DHA levels in the brain compared with feeding the control diet. We also observed that rats fed preformed DHA in the form of FO had a higher level of DHA in the brain compared with those fed the LSO formulation. This finding is in agreement with earlier reports showing that preformed DHA is incorporated efficiently into brain tissue (40,41). Feeding the LSO-enriched diet significantly increased the levels of LNA and of EPA and DHA in the brain. Earlier studies have also shown a small but significant increase in LNA and EPA levels in brain tissue when diets high in n-3 FA were administered (36,42,43). These studies may indicate different mechanisms for the accumulation of LNA and its conversion to long-chain n-3 PUFA in different tissues.

The n-3 FA obtained through spray-dried milk had significant effects on serum lipids. The serum total cholesterol, VLDL + LDL cholesterol, and TAG were significantly lower in rats fed formulations containing n-3 FA compared with the control. Similar to serum lipids, liver lipids decreased by feeding the n-3 FA-enriched formulation. The present investigation also showed that the FO formulation containing 5% n-3 PUFA as EPA and DHA was as effective as the LSO formulation containing 20% LNA in modulating serum lipids in a beneficial manner. The bioefficacy of long-chain n-3 PUFA is generally believed to be much greater than that of n-3 PUFA of shorter chain lengths. Our results are in agreement with this perception.

The present study indicates that spray-dried milk formulations enriched in LSO or FO can be used to provide n-3 FA. These formulations not only deliver n-3 FA but also modulate serum lipid levels. Such formulations may play an important role in providing n-3 PUFA to individuals whose regular diets provide inadequate amounts of these EFA. Whether these formulations have beneficial effects on cardiovascular risk factors, however, can only be determined by studies in human volunteers.

ACKNOWLEDGMENTS

The authors thank Dr. Vishweshwariah Prakash, director, CFTRI, and Dr. Santhoor G. Bhat, head, Department of Biochemistry and Nutrition, CFTRI, for their keen interest, encouragement, and support. We also thank Sankaran Jayaprakash, Department of Food Engineering, CFTRI, for help in the pilot plant. T.R. Ramaprasad acknowledges a Senior Research Fellowship grant from the Council of Scientific and Industrial Research, New Delhi, India.

REFERENCES

1. Simopoulos, A.P. (1999) Essential Fatty Acids in Health and Chronic Diseases, *Am. J. Clin. Nutr. 70*, S560–S569.
2. Ghafoorunissa (1990) Availability of Linoleic Acid from Cereal-Pulse Diets, *Lipids 25*, 763–766.
3. Ghafoorunissa (1996) Fats in Indian Diets and Their Nutritional Implications, *Lipids 31*, S287–S291.
4. Achaya, K.T. (1995) Fat Intake in India—An Update, *J. Sci. Ind. Res. 54*, 91–97.
5. Roche, H.M. (1999) Unsaturated Fatty Acids, *Proc. Nutr. Soc. 58*, 397–401.
6. Stanley, J. (2004) What is the Appropriate Balance Between Intakes of n-6 and n-3 PUFA in the Diet? *Lipid Technol. 16*, 61–63.
7. Sanderson, P., Finnegan, Y.E., Williams, C.M., Calder, P.C., Burdge, G.C., Wootton, S.A., Griffin, B.A., Millward, D.J., Pegge, N.C., and Bemelmans, W.J.E. (2002) UK Food Standards Agency α-Linolenic Acid Workshop Report, *Br. J. Nutr. 88*, 573–579.
8. Sinclair, A.J. (2003) Which of the n-3 PUFA Should Be Called Essential? *Lipids 38*, 1113–1114.
9. Lauritzen, L., and Hansen, H.S. (2003) Which of the n-3 FA Should Be Called Essential? *Lipids 38*, 889–891.
10. Ghafoorunissa, Vani, A., Laxmi, R., and Sesikeran, B. (2002) Effects of Dietary α-Linolenic Acid from Blended Oils on Biochemical Indices of Coronary Heart Disease in Indians, *Lipids 37*, 1077–1086.
11. Ghafoorunissa (1998) Requirement of Dietary Fats to Meet Nutritional Needs and Prevent the Risk of Atherosclerosis—An Indian Perspective, *Ind. J. Med. Res*. 108, 191–202.
12. Indu, M., and Ghafoorunissa (1992) n-3 Fatty Acids in Indian Diets—Comparison of the Effects of Precursor (α-linolenic

acid) vs. Product (long chain n-3 polyunsaturated fatty acids), *Nutr. Res. 12*, 569–582.
13. Beare-Rogers, J.A. (1977) Docosaenoic Acid in Dietary Fats, in *Progress in Chemistry of Fats and Other Lipids* (Holman, R.T. ed.), Vol. 15, pp. 29–56, Pergamon Press, Paris.
14. Caughey, G.E., Mantzioris, E., Gibson, R.A., Cleland, L.G., and James, M.J. (1996) The Effect on Human Tumor Necrosis Factor Alpha and Interleukin 1 Beta Production of Diets Enriched in n-3 Fatty Acids from Vegetable Oil or Fish Oil, *Am. J. Clin. Nutr. 63*, 116–122.
15. Cunnane, S.C., Ganguly, S., Menaard, C., Liede, A.C., Hamadeh, M.J., Chen, Z.Y., and Woolever, T. (1993) High α-Linolenic Acid Flaxseed (*Linum usitatissimum*). Some Nutritional Properties in Humans, *Br. J. Nutr. 69*, 443–453.
16. Jenkins, D.J.A., Kendall, C.W.C., Vidgen, E., Agarwal, S., Rao, A.V., Rosenberg, R.S., Diamandis, E.P., Novokmet, R., Mehling, C.C., Perera, T., *et al.* (1999) Health Aspects of Partially Defatted Flaxseed, Including Effects on Serum Lipids, Oxidative Measures and *ex vivo* Androgen and Progestin Activity: A Controlled Crossover Trial, *Am. J. Clin. Nutr. 69*, 395–402.
17. Schmidt, E.B. (1997) n-3 Fatty Acids and the Risk of Coronary Heart Disease, *Dan. Med. Bull. 44*, 1–22.
18. Aneja, R.P., and Murthy, T.N. (1991) Beneficial Effects of Ghee, *Nature 350*, 280.
19. Lee, K.N., Kritchevsky, D., and Pariza, M.W. (1994) Conjugated Linoleic Acid and Atherogenisis in Rabbits, *Atherosclerosis 108*, 19–25.
20. Bansal, P., and Kansal, V.K. (1996) Milk, Some Myths and Misconceptions, *Ind. Dairyman 48*, 25–31.
21. Gurr, M.I. (1999) *Lipids in Nutrition and Health: A Reappraisal*, Vol. 21, p. 240, The Oily Press, Dundee, Scotland.
22. Ramaprasad, T.R., Baskaran, V., Debnath, S., Sambaiah, K., Jayaprakasan, S.G., Shivakumara, M., and Lokesh, B.R. (2003) A Process for the Preparation of Cholesterol Lowering Health Beverage Mix, Indian Patent 526/Del/2003.
23. Nagendra, R., Mahadevamma, Baskaran, V., and Venkatrao, S. (1995) Shelf Life of Spray Dried Infant Formula Supplemented with Lactulose, *J. Food Proc. Preserv. 19*, 303–315.
24. American Institute of Nutrition (1997) Report on the American Institute of Nutrition *Ad Hoc* Committee on Standards for Nutritional Studies, *J. Nutr. 107*, 1340–1348.
25. Folch, J., Lees, M., and Sloane Stanley, G.H. (1957) A Simple Method for the Isolation and Purification of Total Lipids from Animal Tissues, *J. Biol. Chem. 226*, 497–509.
26. Searcy, R.L., and Bergquist, L.M. (1960) A New Color Reaction for the Quantification of Serum Cholesterol, *Clin. Chim. Acta 5*, 192–196.
27. Warnick, G.R., and Albers, J.J. (1978) A Comprehensive Evaluation of the Heparin–Manganese Chloride Precipitation Procedure for Estimating HDL-Cholesterol, *J. Lipid Res. 19*, 65–76.
28. Stewart, J.C.M. (1980) Colorimetric Estimation of Phospholipids with Ammonium Ferrothiocyanate, *Anal. Biochem. 104*, 10–14.
29. Fletcher, M.J. (1968) A Colorimetric Method for Estimating Serum Triacylglycerol, *Clin. Chim. Acta 22*, 303–307.
30. Morrison, M.R., and Smith, M. (1963) Preparation of Fatty Acid Methyl Esters and Dimethyl Acetyls from Lipids with Boron Fluoride Methanol, *J. Lipid Res. 5*, 600–608.
31. Fisher, R.A. (1970) *Statistical Methods for Research Workers*, 14th edn., Oliver and Boya, Edinburg.
32. Kitessa, S.M., Gulati, S.K., Simos, G.C., Ashes, J.R., Scott, T.W., Fleck, E., and Wynn, P.C. (2004) Supplementation of Grazing Dairy Cows with Rumen-Protected Tuna Oil Enriches Milk Fat with n-3 Fatty Acids Without Affecting Milk Production or Sensory Characteristics, *Br. J. Nutr.* 91, 271–277.
33. Gerster, H. (1998) Can Adults Adequately Convert α-Linolenic Acid (18:3n-3) to Eicosapentaenoic Acid (20:5n-3) and Docosahexaenoic Acid (22:6n-3), *Intl. J. Vit. Nutr. Res. 68*, 159–173.
34. Mantzioris, E., James, M.J., Gibson, R.A., and Cleland L.G. (1994) Dietary Substitution with α-Linolenic Acid-Rich Vegetable Oil Increases Eicosapentaenoic Acid Concentrations in Tissues, *Am. J. Clin. Nutr. 59*, 1304–1309.
35. Bazinet, R.P., McMillan, E.G., and Cunnane, S.C. (2003) Dietary α-Linolenic Acid Increases the n-3 PUFA Content of Sow's Milk and the Tissues of the Suckling Piglet, *Lipids 38*, 1045–1049.
36. Zhong, F., and Sinclair, A.J. (2000) Increased α-Linolenic Acid Intake Increases Tissue α-Linolenic Acid Content and Apparent Oxidation with Little Effect on Tissue Docosahexaenoic Acid in the Guinea Pig, *Lipids 35*, 395–400.
37. Lin, D.S., and Connors, W.E. (1990) Are the n-3 Fatty Acids from Dietary Fish Oil Deposited in the Triglyceride Stores of Adipose Tissue, *Am. J. Clin. Nutr. 51*, 535–539.
38. Okuno, M., Kajiwara, K., Imai, S., Kobayashi, T., Honma, N., Maki, T., Suruga, K., Goda, T., Takase, S., Muto, Y., and Moriwaki, H. (1997) Perilla Oil Prevents Excessive Growth of Visceral Adipose Tissue in Rats by Down-regulating Adipocyte Differentiation, *J. Nutr. 127*, 1752–1757.
39. Brenner, R.R. (1984) Effect of Unsaturated Acids on Membrane Structure and Kinetics, *Prog. Lipid Res. 23*, 69–96.
40. Abedin, L., Lien, E.L., Vingrys, A.J., and Sinclair, A.J. (1999) The Effect of Dietary α-Linolenic Acid Compared with Docosahexaenoic Acid on Brain, Retina, Liver, and Heart in the Guinea Pig, *Lipids 34*, 475–482.
41. Sheaff Greiner, R.C., Zhang, Q., Goodman, K.J., Giussani, D.A., Nathanielsz, P.W., and Brenna, J.T. (1996) Linoleate, α-Linolenate, and Docosahexaenoate Recycling into Saturated and Monounsaturated Fatty Acid Is a Major Pathway in Pregnant or Lactating Adults and Fetal or Infant Rhesus Monkeys, *J. Lipid Res. 37*, 2675–2686.
42. Anderson, G.J. (1994) Developmental Sensitivity of the Brain to Dietary n-3 Fatty Acids, *J. Lipid Res. 35*, 105–111.
43. Philbrick, D.J., Mahadevappa, V.G., Ackman, R.G., and Holub, B.J. (1987) Ingestion of Fish Oil or a Derived n-3 Fatty Acid Concentrate Containing Eicosapentaenoic Acid (EPA) Affects Fatty Acid Compositions of Individual Phospholipids of Rat Brain Sciatic Nerve and Retina, *J. Nutr. 117*, 1663–1670.

[Received March 26, 2004; accepted September 2, 2004]

Cigarette Smoke Negatively and Dose-Dependently Affects the Biosynthetic Pathway of the n-3 Polyunsaturated Fatty Acid Series in Human Mammary Epithelial Cells

Franca Marangoni[a,*], Claudio Colombo[a], Leonardo De Angelis[a], Veniero Gambaro[b], Carlo Agostoni[c], Marcello Giovannini[c], and Claudio Galli[a]

[a]Department of Pharmacological Sciences and [b]Institute of Pharmaceutical and Toxicological Chemistry, University of Milan, 20133 Milan, Italy, and [c]Department of Pediatrics, San Paolo Hospital, University of Milan, 20142 Milan Italy

ABSTRACT: Maternal smoking during pregnancy has been associated with a reduced content of n-3 long-chain PUFA (LC-PUFA) in breast milk, thereby reducing the intake of key nutrients by the infants. We postulated that the mammary gland is affected by maternal smoking in the process of n-3 LC-PUFA secretion into milk. This prompted us to investigate the effects of cigarette smoke on the synthesis of n-3 LC-PUFA *in vitro* by using a line of healthy epithelial cells from the human mammary gland, MCF-10A. Cells were exposed to cigarette smoke under controlled conditions by adding to the medium aliquots of horse serum containing smoke components, as analyzed by GC–MS. The major findings concern the inhibition of both the conversion of the precursor ^{14}C-ALA (α-linolenic acid) to n-3 LC-PUFA and of the Δ5 desaturation step (assessed by HPLC analysis with radiodetection of n-3 FAME) following exposure to minimal doses of smoke-enriched serum, and the dose-dependent relationship of these effects. The data indicate that exposure to cigarette smoke negatively affects the synthesis of n-3 LC-PUFA from the precursor in mammary gland cells.

Paper no. L9379 in *Lipids 39*, 633–637 (July 2004).

It is well established that maternal milk components are important determinants of infant development during the first period of extrauterine life, when milk represents the only source of nutrients (1). In particular, the early developmental stages of highly specialized organs, such as the brain and retina, are strongly dependent on adequate intakes of fatty acids (FA), especially the PUFA, which are exclusively derived from the diet and which are essential for several biological functions (2).

A previous study by our group (3) showed that FA in the maternal diet are only partly responsible for the FA composition of milk, especially the levels of long-chain PUFA (LC-PUFA). These results suggest a major role of the mammary gland in synthesizing and secreting LC-PUFA into milk (4,5). On the other hand, investigations into the role of the mammary gland in lactogenesis indicate that only 10% of milk FA, mainly medium-chain FA (6), are synthesized in the gland. The mechanisms that modulate the transfer through the mammary gland of the remainder of FA coming both from maternal tissues and directly from the diet, or the *in situ* formation of LC-PUFA and their secretion into milk, remain to be investigated.

Several studies have shown that maternal cigarette smoking during pregnancy negatively affects birth weight and the subsequent development of cognitive functions in the infant (7), but very limited information is available about the possible effects of maternal smoking during breastfeeding on metabolic processes relevant to the delivery of nutrients to the neonate.

There is evidence that women who smoke breastfeed their infants for a shorter duration than nonsmokers (8), indicating that maternal smoking is associated with an increased risk of early weaning. However, the possible relationships between cigarette smoke and quantitative and qualitative modifications of milk production have not been adequately investigated (9).

Cigarette smoke appears to affect this process independently of the mechanisms regulating the secretion of milk FA, since we have previously observed that in breastfeeding mothers who smoke, the increments of milk lipids during the first 3 mon of lactation are reduced, resulting in lower fat intakes by their infants (10), especially of DHA (22:6n-3), compared with nonsmoking mothers. Concomitantly, the typical reduction in plasma lipids associated with breastfeeding in the mother (3), especially triglycerides (TG), was also smaller.

These combined observations suggest that LC-PUFA in milk may be mainly produced directly from the 18-carbon precursors linoleic acid (LA, 18:2n-6) and α-linolenic acid (ALA, 18:3n-3) in the mammary gland and that maternal cigarette smoke may negatively affect the process. We therefore looked for a suitable *in vitro* model to evaluate the direct effects of cigarette smoke on the biosynthetic metabolic pathways of n-3 LC-PUFA in cells from the human mammary gland. The cellular composition of this tissue is highly complex; we therefore selected mammary epithelial cells, the major site of the synthesis and conversion of lipids deriving from mammary adipocytes and from other maternal tissues (11,12).

*To whom correspondence should be addressed at Department of Pharmacological Sciences, 9, Via Balzaretti, 20133 Milan, Italy.
E-mail: Franca.Marangoni@unimi.it

Abbreviations: ALA, α-linolenic acid; HS, horse serum; LA, linoleic acid; LC-PUFA, long-chain polyunsaturated fatty acids; PL, phospholipids; SE-HS, smoke-exposed horse serum; TG, triglycerides.

MATERIALS AND METHODS

A line of healthy epithelial cells from the human mammary gland, MCF-10A, purchased by ATCC (CRL-10317; American Type Culture Collection, Manassas, VA) was used. These cells, immortalized by changing Ca^{2+} levels in the culture medium, maintain the characteristics of nonmalignant cells, as demonstrated by several characteristics, namely, that anchorage-independent growth is absent, that they are unable to produce tumors in athymic mice, and that they require the same supplements as normal cells (13). Furthermore, it has been demonstrated that these cells are able to incorporate and metabolize both LA and ALA to LC-PUFA by desaturation and elongation processes at relatively high concentrations (24 μM) (14).

Cells were grown in T75 flasks with DMEM/Ham's Nutrient Mixture F-12 (1:1) with the addition of epidermal growth factor (20 ng/mL), cholera enterotoxin (100 ng/mL), insulin (10 μg/mL), and hydrocortisone (500 ng/mL) in the presence of 5% horse serum (HS). Before each experiment, cells were transferred into 100-mm dishes and maintained without HS for 24 h.

In the first experiment, different concentrations (1, 10, 50, 100 μM) of 9,12,15-1-^{14}C-ALA (NEC 779; NEN Life Science Products, Inc., Boston, MA) (5 μCi/plate) complexed with BSA were incubated for 24 h. To expose the cells to cigarette smoke in appropriate and reproducible conditions, a device was developed that allowed a controlled incorporation of cigarette smoke into the HS through aspiration by a pump under controlled vacuum. Specifically, smoke from each cigarette was bubbled through HS for 5 min at 3 puffs/min. The most popular brand of Italian cigarettes was used, MS with filter, and 5 mL of HS was exposed to smoke equivalent to 0.25–4 cigarettes. One hundred-microliter aliquots of smoke-exposed horse serum (SE-HS) were subsequently added to incubated cells, and the final exposure corresponded to the amounts of smoke generated from 0.005–0.08 cigarettes (0.5–8% of one cigarette).

To validate the procedure in terms of the correspondence of smoke components in aqueous systems and directly in gaseous smoke, the main components were analyzed by GC–MS in the electron-impact mode (Saturn 2100T™; Varian, Palo Alto, CA) with a DB5 capillary column (30 m; Hewlett-Packard, Palo Alto, CA) for the various types of samples. The temperature program was increased from 40 to 245°C at 6°C/min. To this end, smoke components were extracted directly without derivatization from cigarette smoke itself (to which the adsorbing fiber was exposed) from SE-HS, as well as from a buffer exposed to smoke, using a carbowax/divinyl benzene fiber (65 μm; Supelco, Bellefonte, PA). The fiber was desorbed for 5 min in the GC injector at 240°C. Qualitative reproducibility was assessed by three analyses of aliquots from the same sample.

In addition, we determined the FA percentage composition of total lipids in the control and in SE-HS by GC analysis of their methyl esters, which were prepared by transmethylation with methanolic HCl (Supelco) at 90°C for 1 h in a model 85.10 gas chromatograph (DANI SpA, Cologno Monzese, Italy) equipped with a capillary column (Omegawax™ 320; Supelco), programmable temperature vaporizer injector, and FID (temperature program from 120 to 220°C).

The amounts of lipid peroxides were measured by a thiobarbituric acid method, and conjugated dienes were measured by absorbance at 234 nm, as described previously (15).

The effects of SE-HS on the biosynthesis of n-3 LC-PUFA were evaluated by incubating MCF-10A with 0.5 μCi/plate of labeled C_{18} precursor, [1-^{14}C]ALA (0.96 μM), for 6 and 24 h. Each experiment was repeated at least three times. After extraction of cell total lipids (16), the FAME, prepared as described previously, were injected into a high-performance liquid chromatograph (model 880; Jasco, Easton, MD) equipped with a C18 RP column (LiChrosphere® 100 RP-18; Merck, Darmstadt, Germany) and connected to a radiodetector (Canberra Packard, Tampa, FL). A gradient mobile phase made up of acetonitrile and water (from 74:26% to 100:0%) (17) and Floscint-A (Canberra Packard) was used. FA were identified by the use of reference FA. The same amount of radioactivity was injected for control and smoke-exposed samples. The sum of the radioactivity associated with all the chromatographic peaks separated by HPLC corresponded to the radioactivity that was incubated with the sample, in both the control and the smoke-exposed samples, indicating that the reduced conversion of substrate to the long-chain derivatives in the treated samples was not related to enhanced degradation of these products.

We evaluated the total conversion of ^{14}C-ALA, expressed as the percentage of total radioactivity associated with its products, and indirectly measured the activity of the enzymes involved in LC-PUFA biosynthesis by evaluating the product/precursor ratios at each metabolic step.

To assess the effects on the incorporation of FA into lipid classes of exposing MCF-10 cells to SE-HS, total lipids were separated by TLC, on silica gel plates, using hexane/diethyl ether/acetic acid (70:30:1, by vol) as the mobile phase in the presence of reference compounds. After detection by exposure to iodine vapors, spots were scraped into plastic vials, and the radioactivity associated with each lipid class was determined using a beta counter with UltimaGold (Canberra Packard).

Student's *t*-test and ANOVA were used to compare data obtained from smoke-exposed cells with those from controls and to assess the relationships between conversion of total radioactivity and the 20:5/20:4 ratio, an index of Δ5 desaturation, with the number of cigarettes smoked.

RESULTS

By incubating MCF-10A with increasing concentrations of ALA (1, 10, 50, and 100 μM) in the presence of a constant amount of radioactivity, the conversion of precursors to products was progressively reduced, in relative terms, at the highest concentrations, i.e., as a percentage of the radioactivity

associated with longer-chain FA, but the total incorporation of DHA produced, and hence the absolute synthesis of this FA as nmol per plate, increased (Table 1). A correlation between the concentration of the substrate and the formation of the products was observed, indicating that the metabolic products responded to the availability of the FA precursor ($P \leq 0.005$). This may reflect what happens *in vivo* during lactogenesis, i.e., that the mammary gland responds to the large availability of FA from the maternal compartment for transfer into milk.

The cigarette smoke, serum, and buffer exposed to smoke were analyzed, and acetaldehyde (by GC, data not shown), nicotine, limonene, and phenol derivatives (by GC–MS) were detected in all samples as major and typical components. More specifically, the profiles of products in smoke and SE-HS were similar (Fig. 1), indicating that trapping smoke in serum was a reliable process with respect to exposure to smoke.

Parameters measured in 100 μL of SE-HS generated from 0, 4, and 8% of a cigarette are reported in Table 2 (means were obtained from duplicate analyses of three experiments with all the smoke concentrations). The levels of conjugated dienes and TBARS in SE-HS vs. the control HS rose significantly with exposure to smoke from an increasing number of cigarettes, and the increase in conjugated dienes rather than TBARS appeared to be more dose dependently associated with smoke concentration. Analysis of the FA composition of serum lipids revealed that 20- and 22-carbon PUFA, which were present in the control serum, were completely absent in SE-HS.

HPLC radiochromatograms of the FAME of MCF-10A total lipids after 6 h of incubation with ^{14}C-ALA without or with SE-HS (0.04 cigarettes/100 μL) are shown in Figure 2 (panels A and B). The conversion of ^{14}C-ALA to its products was lower in the SE-HS cells, as indicated by the lower radioactivity associated with the products and, conversely, by the higher radioactivity associated with the substrate. In addition, major changes involved a reduction in 20:5n-3 (EPA) and an increase in 20:3n-3, a product of ALA elongation that was not found in the control conditions. Calculations of the product/precursor ratios for each metabolic step indicated that the index of the Δ5 desaturation, i.e., the 20:5/20:4 ratio, was affected the most by smoke exposure. In addition, DHA was not detectable in these samples. The same parameter was evaluated at 6 and 24 h after incubation with ^{14}C-ALA and SE-HS generated from 0.04 cigarettes and, as shown in Figure 3, it was already markedly and significantly affected at the earlier time period.

TABLE 1
Total Conversion of ^{14}C-α-Linolenic Acid (^{14}C-ALA) and DHA Synthesized[a] at Different Precursor Concentrations (mean ± SEM)

	ALA concentrations (μM)			
Conversion rates	1	10	50	100
Total conversion of ^{14}C-ALA to products* (% of radioactivity)	92.8 ± 0.2	91.1 ± 0.4	79.7 ± 0.0	65.7 ± 0.1
DHA* (nmol/plate)	0.08 ± 0.01	2.9 ± 0.4	8.3 ± 0.2	12.9 ± 0.3

[a]An asterisk (*) indicates $P \leq 0.005$. ALA, α-linolenic acid.

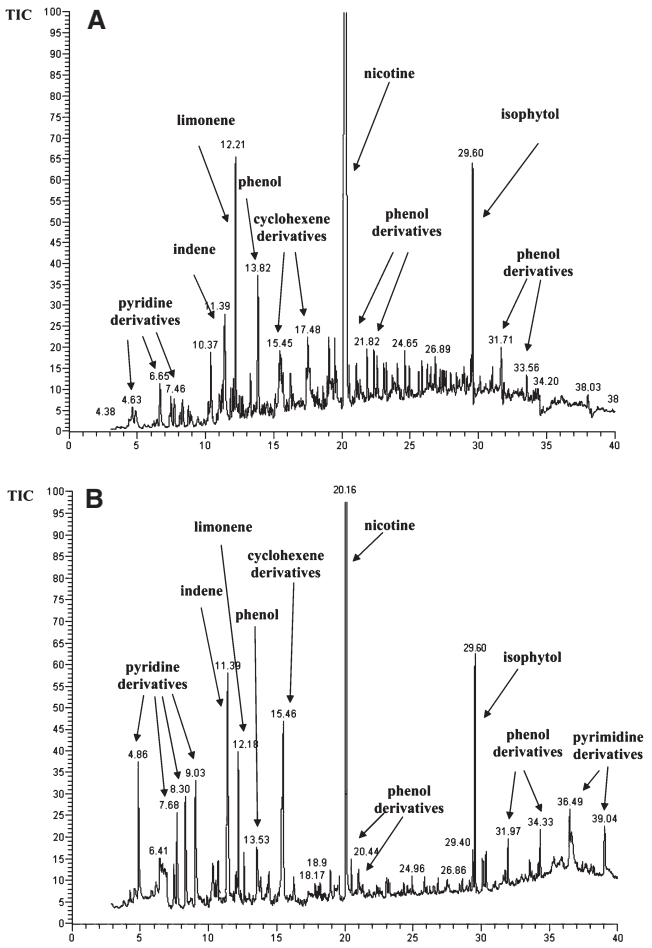

FIG. 1. GC–MS chromatograms of (A) cigarette smoke alone and (B) smoke-exposed horse serum (SE-HS) (EI = 70 eV). TIC, total ion current.

TABLE 2
Conjugated Diene, TBARS, and Long-Chain PUFA (LC-PUFA) Levels in Smoke-Exposed Horse Serum Generated from Different Numbers of Cigarettes[a] (mean ± SEM)

	Cigarette equivalents		
Parameters	0	0.04	0.08
Conjugated dienes** (μM)	163 ± 5	281 ± 1	556 ± 2
TBARS* (μM)	0.83 ± 0.01	4.73 ± 0.28	6.71 ± 0.57
LC-PUFA (%)	1.68 ± 0.04	ND	ND

[a]Duplicate analyses were performed in three experiments. *$P \leq 0.01$; **$P \leq 0.001$. ND, not detected.

Figure 4 shows the total conversion of ALA to products and the 20:5/20:4 ratios after 6 h of incubation with increasing cigarette concentrations per plate. Both parameters were significantly ($P \leq 0.001$) and dose-dependently reduced, and Δ5 desaturation was completely inhibited by serum exposed to smoke from less than one-tenth of a cigarette.

Also, the incorporation of radioactivity into lipid classes, assessed by TLC of the MCF-10A total lipid extracts,

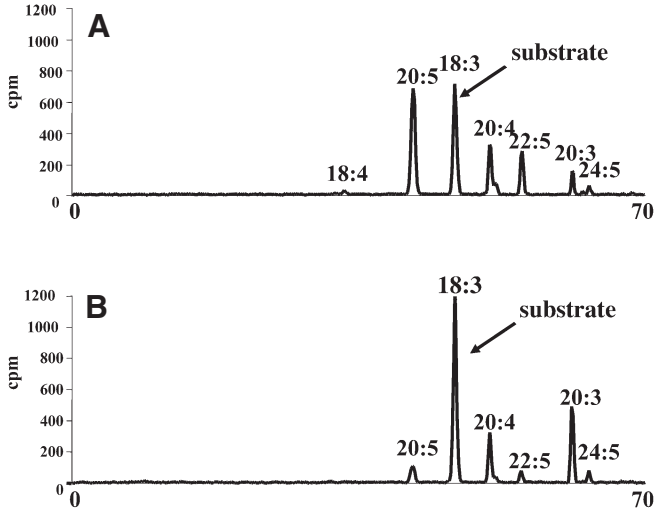

FIG. 2. HPLC chromatograms of methyl esters from MCF-10A total lipids after 6 h of incubation with ^{14}C-α-linolenic acid (^{14}C-ALA) and (A) the control or (B) SE-HS (0.04 cigarettes). For other abbreviation see Figure 1.

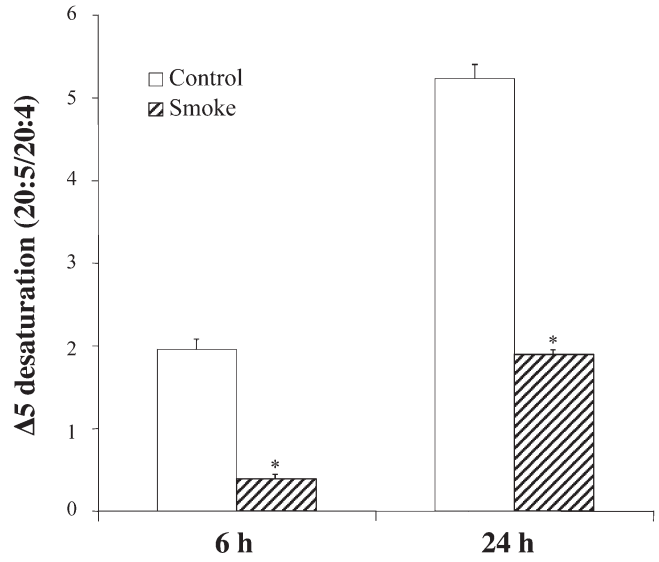

FIG. 3. Δ5 Desaturation activity (20:5/20:4) in MCF-10A cells exposed to the control and SE-HS (0.04 cigarettes) after 6 and 24 h of incubation with ^{14}C-ALA (mean ± SEM). An asterisk indicates $P \leq 0.01$. For abbreviations see Figure 2.

changed after exposure to an increasing number of cigarettes per plate (data not shown). A reduction in the incorporation into phospholipids (PL) (from 87 to 83% of total radioactivity) was associated with a concomitant incorporation into TG (from 4 to 14%).

DISCUSSION

A first consideration is that the experimental model used is suitable for studies on the effects of smoke on PUFA metabolism. MCF-10A cells incorporated the essential FA ALA into lipids and converted the substrate to its longer-chain and more

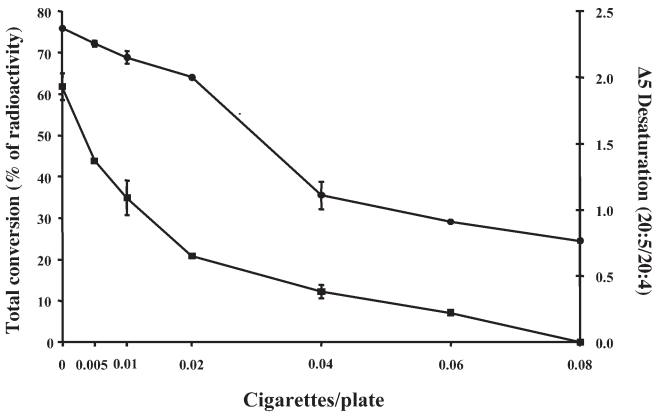

FIG. 4. Total ^{14}C-ALA conversion (●) and 20:5/20:4 ratio (■) in MCF-10A cells after 6 h of incubation with the horse serum control and SE-HS from an increasing number of cigarettes (mean ± SEM). For abbreviations see Figures 1 and 2.

highly unsaturated products. This biosynthetic pathway is regulated by the availability of the precursor, as demonstrated by the increasing amounts of DHA produced at increasing levels of ALA. We found similar results with linoleic acid as the substrate in relation to its n-6 derivatives (data not shown). This observation is in line with the situation occurring *in vivo*, since during lactation a marked reduction occurs in maternal plasma TG, which are rich in the 18-carbon PUFA, LA and ALA, suggesting enhanced delivery of these FA to the mammary gland. As for the conditions used when exposing biological samples to cigarette smoke, the similarities in the proportions of major cigarette smoke components (e.g., nicotine, acetaldehyde) in the smoke and in SE-HS indicate that incubation of cells with SE-HS is a valid *in vitro* model for studying the effects of cigarette smoke on cells. This approach is applicable to the study of effects on other types of cells and other metabolic pathways. Moreover, smoke exposure causes dose-dependent lipid peroxidation processes in HS, as demonstrated by the increase in conjugated dienes and TBARS and the disappearance of LC-PUFA. Since we observed the same inhibitory effects on PUFA metabolism by incubating cells with smoke-exposed buffer and serum (data not shown), we propose that exposure to smoke—and not to other degradation products generated in smoke-exposed serum—is in itself responsible for the observed changes in PUFA metabolism.

Major changes induced by cigarette smoke in cell lipids concern a reduction in the incorporation of radioactivity from ALA in 20:4 and 20:5, and finally, a reduction in the 20:4/20:5 ratio. This observation is in agreement with other studies, which have demonstrated that the Δ5-desaturation step is affected the most by toxic xenobiotics (18,19). Also, the increased incorporation of FA into TG associated with a reduction in their incorporation into PL, an index of PL synthesis, observed in smoke-exposed MCF-10A cells is characteristic of a wide range of toxic effects (20).

Hence, the present results appear to confirm that exposure to components of cigarette smoke, even in very low concen-

trations, affects the synthesis of LC-PUFA, in particular of DHA, in mammary cells, apparently mimicking the conditions that are operating *in vivo*. Characterization of the compounds in cigarette smoke that negatively affect LC-PUFA synthesis will be the next step in our research.

ACKNOWLEDGMENT

This study was supported by the Danone Institute.

REFERENCES

1. Innis, S.M., Gilley, J., and Werker, J. (2001) Are Human Milk Long-Chain Polyunsaturated Fatty Acids Related to Visual and Neural Development in Breast-Fed Term Infants? *J. Pediatr. 139*, 532–537.
2. Koletzko, B., and Rodriguez-Palmero, M. (1999) Polyunsaturated Fatty Acids in Human Milk and Their Role in Early Infant Development, *J. Mammary Gland Biol. Neoplasia 4*, 269–284.
3. Marangoni, F., Agostoni, C., Lammardo, A.M., Giovannini, M., Galli, C., and Riva, E. (2002) Polyunsaturated Fatty Acids in Maternal Plasma and in Breast Milk, *Prostaglandins Leukot. Essent. Fatty Acids 66*, 528–533.
4. Boersma, E.R., Offringa, P.J., Muskiet, F.A., Chase, W.M., and Simmons, I.J. (1991) Vitamin E, Lipid Fractions, and Fatty Acid Composition of Colostrum, Transitional Milk, and Mature Milk: An International Comparative Study, *Am. J. Clin. Nutr. 53*, 1197–204.
5. Neville, M.C., and Picciano, M.F. (1997) Regulation of Milk Lipid Secretion and Composition, *Annu. Rev. Nutr. 17*, 159–183.
6. Barber, M.A., Clegg, R.A., Travers, M.T., and Vernon, R.G. (1997) Lipid Metabolism in the Lactating Mammary Gland, *Biochim. Biophys. Acta 1347*, 101–126.
7. Wang, X., Zuckerman, B., Pearson, C., Kaufman, G., Chen, C., Wang, G., Niu, T., Wise, P.H., Bauchner, H., and Xu, X. (2002) Maternal Cigarette Smoking, Metabolic Gene Polymorphism, and Infant Birth Weight, *JAMA 287*, 195–202.
8. Hill, P.D., and Aldag, J.C. (1996) Smoking and Breastfeeding Status, *Res. Nursing Health 19*, 125–32.
9. Vio, F., Salazar, G., and Infante, C. (1991) Smoking During Pregnancy and Lactation and Its Effects on Breast-Milk Volume, *Am. J. Clin. Nutr. 54*, 1011–1016.
10. Agostoni, C., Marangoni, F., Giovannini, M., Lammardo, A.M., Grandi, F., Riva, E., and Galli C. (2003) Lipids and Polyunsaturated Fatty Acids Are Lower in Milk from Smoking Mothers, *Eur. J. Clin. Nutr. 57*, 1466–1472.
11. Neville, M.C., and Picciano, M.F. (1997) Regulation of Milk Lipid Secretion and Composition, *Ann. Rev. Nutr. 17*, 159–183.
12. Mather, I.H., and Keenan, T.W. (1998) Origin and Secretion of Milk Lipids, *J. Mammary Gland Biol. Neoplasia 3*, 259–273.
13. Soule, H.D., Maloney, T.M., Wolman, S.R., Peterson, W.D., Jr., Brenz, R., McGrath, C.M., Russo, J., Pauley, R.J., Jones, R.F., and Brooks, S.C. (1990) Isolation and Characterization of a Spontaneously Immortalized Human Breast Epithelial Cell Line, MCF 10, *Cancer Res. 50*, 6075–6086.
14. Grammatikos, S.I., Subbaiah, P.V., Victor, M., and Miller, W.M. (1994) n-3 and n-6 Fatty Acid Processing and Growth Effects in Neoplastic and Non-cancerous Human Mammary Epithelial Cell Lines, *Br. J. Can. 70*, 219–227.
15. Balla, G., Jacob, H.S., Eaton, J.W., Belcher, J.D., and Vercellotti, G.M. (1991) Hemin: A Possible Physiological Mediator of Low Density Lipoprotein Oxidation and Endothelial Injury, *Arterioscler. Thromb. 11*, 1700–1711.
16. Bligh, E.G., and Dyer, W.J. (1959) A Rapid Method of Total Lipid Extraction and Purification, *Can. J. Biochem. Physiol. 37*, 911–917.
17. Moore, S.A., Hurt, E., Yoder, E., Sprecher, H., and Spector, A.A. (1995) Docosahexaenoic Acid Synthesis in Human Skin Fibroblasts Involves Peroxisomal Retroconversion of Tetracosahexaenoic Acid, *J. Lipid Res. 36*, 2433–2443.
18. Brenner, R.R. (1990) Endocrine Control of Fatty Acid Desaturation, *Biochem. Soc. Trans. 18*, 773–775.
19. Grandjean, P., and Weihe, P. (2003) Arachidonic Acid Status During Pregnancy Is Associated with Polychlorinated Biphenyl Exposure, *Am. J. Clin. Nutr. 77*, 715–719.
20. Coleman, R.A., Lewin, T.M., and Muoio, D.M. (2000) Physiological and Nutritional Regulation of Enzymes of Triacylglycerol Synthesis, *Ann. Rev. Nutr. 20*, 77–103.

[Received September 10, 2003; in revised form and accepted September 15, 2004]

Diet and Lipoprotein Oxidation: Analysis of Oxidized Triacylglycerols in Pig Lipoproteins

Jukka-Pekka Suomela[a,*], Markku Ahotupa[b], Olli Sjövall[a,c], Juha-Pekka Kurvinen[a], and Heikki Kallio[a,d]

[a]Department of Biochemistry and Food Chemistry, University of Turku, FIN-20014 Turku, Finland, [b]MCA Research Laboratory, Department of Physiology, University of Turku, FIN-20014 Turku, Finland, [c]Department of Biochemistry and Pharmacy, Åbo Akademi University, FIN-20521 Turku, Finland, and [d]Functional Foods Forum, University of Turku, FIN-20520 Turku, Finland

ABSTRACT: Oxidized lipoproteins have a recognized role in atherogenesis, but molecular-level research on oxidized lipids in lipoproteins and the effect of diet on these molecules have been limited. In the present study, the effects of three sunflower seed oil diets differing in oxidation levels (PV in oils 1, 84, and 223 mequiv O_2/kg) on lipoprotein lipid oxidation in growing pigs were investigated. The emphasis was on the investigation of oxidized TAG molecules found in chylomicrons and VLDL. A method based on RP-HPLC and electrospray ionization-MS was used for the analysis of oxidized TAG molecules. The baseline diene conjugation method was used for the estimation of *in vivo* levels of lipoprotein lipid oxidation. Several oxidized TAG structures were found in the samples. These products consisted of TAG molecules with a hydroxy, an epoxy, or a keto group attached to a FA, and of TAG molecules containing an aldehyde structure derived from a FA. The lipoprotein lipids and TAG were more oxidized in the pigs fed on the most oxidized oil compared with those fed on nonoxidized oil. Oxidation of dietary fat was reflected in the lipoprotein oxidation. New, detailed information on oxidized TAG molecules of chylomicrons and VLDL was obtained.

Paper no. L9489 in *Lipids 39*, 639–647 (July 2004).

During the last 15 yr, the contribution of oxidized LDL to atherogenesis has become evident (1–5). Based on the results of various research groups, oxidized chylomicron remnants also seem to be potentially atherogenic (6–9). Some studies have shown that the oxidation of dietary lipids is reflected in the degree of oxidation of chylomicrons and VLDL (10,11). Like oxidation of LDL, oxidation of chylomicrons results in particles that may serve as a substrate for scavenger receptors (9). Oxidized chylomicrons seem to be taken up by phagocytic cells (9), and a study by Mamo and Wheeler (12) suggests that chylomicrons and their remnants may associate with arterial tissue with an even greater efficiency than LDL.

Lipids may be gradually oxidized during normal processing of food. Although diet may contribute to the burden of oxidized lipids in plasma lipoproteins, studies of the dietary effects on lipoprotein oxidation at the molecular level have been scarce. Only a few oxidized lipid species in lipoproteins have been studied. These are mainly cholesteryl esters and glycerophospholipids (13–15). Also, there are only a few methods for direct measurement of lipoprotein oxidation. Estimation of *in vivo* LDL oxidation has been largely based on determination of autoantibodies to oxidized LDL (16).

In our previous study (17) we used a novel approach based on HPLC-electrospray ionization (ESI)-MS and LDL baseline diene conjugation (LDL-BDC) method to investigate lipid oxidation in human LDL. HPLC-ESI-MS was applied to the analysis of the oxidized TAG molecular structures. The LDL-BDC method was used to evaluate the oxidation levels of the samples. The method has been developed for fast measurement of oxidized LDL in blood samples. All species of lipids containing oxidized FA residues with conjugated double bonds contribute to the diene conjugation value (16,18,19). The relationships between LDL-BDC and different health risk factors have been investigated in several studies (19–21).

Possible nonvolatile TAG autoxidation products are TAG with a hydroperoxy, hydroxy, epoxy, or oxo (aldehyde or ketone) group(s) or a combination of these groups. Structures of oxidized TAG molecules have been studied by different groups (22–29). Our approach was based on the work of Sjövall *et al.* (27), in which the elution factors of synthetic, oxidized TAG were obtained for RP-HPLC by plotting the retention times of the compounds against the theoretical carbon number.

In the present study, the methods validated in a previous study (17) were applied. The effects of oxidized dietary sunflower seed oils on the oxidation of pig lipoproteins were investigated. Owing to its wide applicability, the BDC method was used for the analysis of chylomicrons and VLDL in addition to the analysis of LDL. Detailed information on lipoprotein lipid oxidation and on the molecular structures of oxidized chylomicron and VLDL TAG was obtained.

MATERIALS AND METHODS

Chemicals and reagents. 3-Chloroperoxybenzoic acid, triphenyl phosphine (TPP), and activated manganese dioxide (MnO_2) were obtained from Aldrich Chemical Co. (Milwaukee, WI) and 2,4-dinitrophenylhydrazine (DNPH) was obtained from Sigma Chemical Co. (St. Louis, MO). Reagents were of reagent grade or better quality. All solvents were of chromatography or reagent grade and were purchased from local suppliers. HPLC standard (G-1) containing synthetic

*To whom correspondence should be addressed. E-mail: jusuom@utu.fi

Abbreviations: ACN:DB, acyl carbon number:number of double bonds; BDC, baseline diene conjugation; DNPH, 2,4-dinitrophenyl hydrazine; ESI, electrospray ionization; TPP, triphenyl phosphine.

monoacid TAG was obtained from Nu-Chek-Prep, Inc. (Elysian, MN). Synthetic 1,3-distearoyl-2-oleoyl-*sn*-glycerol was obtained from Sigma Chemical Co. 1,3-Didocosanoyl-2-oleoyl-*sn*-glycerol and 1-linoleoyl-2-oleoyl-3-palmitoyl-*sn*-glycerol were obtained from Larodan Fine Chemicals AB (Malmö, Sweden).

Preparation of reference compounds. The synthetic TAG and their oxidized derivatives prepared in this study are listed in Table 1. TAG standards containing aldehyde structures derived from FA (core aldehydes) (IIa, IIb, IVa, Vc, Vd, VIc, VId) were obtained by ozonization of TAG and reduction of the ozonides with TPP (30). TAG (5–40 mg) were dissolved in 4 mL hexane and ozonized for 40 min in an ice bath. The solvent was evaporated, and the ozonides were dissolved in 4 mL chloroform and reduced to aldehydes by treatment with 25–50 mg TPP for 1 h at room temperature. The aldehydes were purified by TLC as described below, and part of them were converted to DNPH derivatives (IIb, IVa, Vd, VId) by treatment with 1–4 mL DNPH reagent (1 mg DNPH in 2 mL of 1 M HCl) at 60°C for 30 min (31). The DNPH derivatives were extracted from the solution with chloroform/methanol (2:1, vol/vol).

Epoxides (Ia, IIIa, Va, VIa) were prepared by the method of Deffense (32). TAG (2–5 mg) were oxidized with 4–10 mg 3-chloroperoxybenzoic acid in 400 μL dichloromethane at room temperature for 1–2 h followed by purification using TLC as described below.

Hydroperoxides (Ib, IIIb, IIIc, Vb, VIb) were prepared by photosensitized oxidation (33). TAG (10–20 mg) were added to 3 mL methylene blue solution (0.1 mM methylene blue in dichloromethane) in a test tube that was placed in an ice bath under a 250-W photographer's lamp for 28 h. The distance between the sample solution and the lamp was approximately 20 cm. Hydroperoxides were purified by TLC as described below.

For the preparation of hydroxides (Ic, VIe), 1 mg hydroperoxide was dissolved in 2 mL chloroform and reduced to hydroxide by treatment with 15–20 mg TPP for 1 h at room temperature (34). The hydroxy compounds were purified by TLC as described below.

Ketone standards (Id, VIf) were prepared by oxidizing the corresponding hydroxides with activated manganese dioxide (35). The hydroxide (0.3 mg) was dissolved in 0.5 mL chloroform. The solution and 50 mg manganese dioxide were transferred to a test tube, which was placed in a shaker. The reaction was allowed to take place for 6 d at 37°C (Id) or for 3.25 h at 60°C (VIf).

Animals and diets. The study plan was approved by the Test Animal Committee of MTT Agrifood Research Finland, and the level of vitamin E in E supplementation was based on their guidelines. Nine growing pigs (castrated boars) from three different litters were used in the study. For 2 wk, three groups of three pigs (groups 1, 2, and 3) were fed a diet (Table 2) containing 14% sunflower seed oil varying in oxidation levels. In each group, there was one animal from each of the three litters. The average weight of the animals was 34.4 kg (SD 2.0 kg) at the beginning of the feeding period and 45.6 kg (SD 2.9 kg) at the end of the period. The oil of group 1 was not oxidized, whereas the oils of groups 2 and 3 were oxidized in convection ovens at 60°C until certain PV were reached. The PV of the oils were as follows: group 1, 1 mequiv O_2/kg; group 2, 84 mequiv O_2/kg; group 3, 223 mequiv O_2/kg. The PV determinations were made according to AOCS Official Method Cd 8-53 (36) and could be expressed as millimoles of FA hydroperoxy groups per kilogram of oil. This method does not assay oxo-FA other than hydroperoxides. The vitamin E contents of the oils were as follows: group 1, 566 mg/kg; group 2, 459 mg/kg; group 3, 1 mg/kg. The vitamin E determinations were made according to IUPAC 2.432/C112029 method (37). FA compositions of the oils (Table 3) were determined as described below.

TABLE 1
Reference Compounds Used in the Study[a]

Number	TAG[b]	Number	Derivatized TAG[b]
I	18:0-18:1-18:0	Ia	18:0-18:1 epoxy[c]-18:0
		Ib	18:0-18:1 OOH-18:0
		Ic	18:0-18:1 OH-18:0
		Id	18:0-18:1 keto-18:0
II	18:1-18:0-18:0	IIa	9:0 ALD-18:0-18:0
		IIb	9:0 ALD-18:0-18:0 DNPH
III	18:1-18:1-18:0	IIIa	18:1-18:1-18:0 diepoxy[c]
		IIIb	18:1 OOH-18:1-18:0
		IIIc	18:1 OOH-18:1 OOH-18:0
IV	18:2-18:1-16:0	IVa	9:0 ALD-9:0 ALD-16:0 di-DNPH
V	18:0-18:2-18:0	Va	18:0-18:2 diepoxy[c]-18:0
		Vb	18:0-18:2 OOH-18:0
		Vc	18:0-9:0 ALD-18:0
		Vd	18:0-9:0 ALD-18:0 DNPH
VI	22:0-18:1-22:0	VIa	22:0-18:1 epoxy[c]-22:0
		VIb	22:0-18:1 OOH-22:0
		VIc	22:0-9:0 ALD-22:0
		VId	22:0-9:0 ALD-22:0 DNPH
		VIe	22:0-18:1 OH-22:0
		VIf	22:0-18:1 keto-22:0
VII	Series of saturated TAG (24:0–54:0)		

[a]ALD, aldehyde; DNPH, 2,4-dinitrophenylhydrazine.
[b]Regioisomers (*sn*-1 and *sn*-3 positions not distinguished from each other).
[c]Position of an epoxy group is marked as an underlined double bond.

TABLE 2
Composition of the Feed of the Pigs[a]

Component	g/kg feed	Component	g/kg feed
Barley	437.9	Monocalcium phosphate	7.7
Granulated soy[b]	364.9	Xylitol-Selen-E Vita[c]	21.9
Sunflower seed oil	140.0	Mineral-vitamin mix[d]	16.5
Feeding lime	11.1		

[a]Total energy from fat: 1350–1460 kcal/kg feed.
[b]Contains 3.4–6.8% fat.
[c]In kg of feed: 0.2 mg Se; 77 mg vitamin E.
[d]In kg of feed: 2.8 g Ca; 1.0 g P; 0.7 g Mg; 4.1 g NaCl; 131 mg Fe; 28 mg Cu; 0.3 mg Se; 115 mg Zn; 30 mg Mn; 0.3 mg I; 6,567 IU vitamin A; 657 IU vitamin D; 63 mg vitamin E; 2.4 mg vitamin K; 2.4 mg vitamin B_1; 6.0 mg vitamin B_2; 3.5 mg vitamin B_6; 0.03 mg vitamin B_{12}; 0.3 mg biotin; 18 mg pantothenic acid; 25 mg niacin; 4.2 mg folic acid.

TABLE 3
FA Compositions of the Oils Fed to Pigs[a]

FA	Oil 1[b]	Oil 2[c]	Oil 3[d]
16:0	5.9	6.0	6.2
18:0	3.6	3.6	3.7
18:1n-9	24.7	25.1	25.7
18:1n-7	0.7	0.7	0.8
18:2n-6	64.1	63.6	62.6
18:3n-3	0.3	0.3	0.2
20:0	0.2	0.2	0.2
22:0	0.5	0.5	0.6

[a]Results expressed as percentage of total FA.
[b]PV 1 mequiv O_2/kg oil.
[c]PV 84 mequiv O_2/kg oil.
[d]PV 223 mequiv O_2/kg oil.

The pigs were fed twice a day. During the first week, the pigs were fed 170 g oil/d and during the second week 200 g oil/d, the only exception being pig 8 (see Table 7), which was fed 185 g oil/d during the second week due to its poor appetite. Because of the high fat load, the pigs were fed in total 155 mg vitamin E/kg feed, not including vitamin E from the oils (Table 2).

Sample preparation. Blood samples were obtained by venipuncture from the jugular vein at 3 and 4 h (time points 1 and 2, respectively) after the last meal (half of the daily dose). The blood was collected into tubes containing EDTA as an anticoagulant. Plasma was separated from cells by centrifugation at 3000 × *g* for 15 min. Chylomicrons and VLDL were separated from plasma by ultracentrifugation, and LDL was directly precipitated from EDTA plasma by buffered heparin as described (16,38). Lipids were extracted from plasma and lipoproteins using chloroform/methanol (2:1, vol/vol).

Purification of TAG and their oxidation products. For FA analysis, the TAG of chylomicrons and VLDL were purified using Sep-Pak® prepacked silica columns (Waters, Milford, MA) (39). Normal-phase TLC without added antioxidants was used to purify the reference compounds and the oxidation products of chylomicron and VLDL TAG (40). Heptane/di-isopropyl ether/acetic acid (60:40:4, by vol) solution was used as the mobile eluent. Samples were applied to silica G plates. Resolved components were scraped off the plates and were recovered from the silica gel by extraction with chloroform/methanol (2:1, vol/vol). When TLC was applied to the lipoprotein lipid samples, two fractions below the TAG band were scraped from the plate (TAG band, R_f = 0.59; fraction 1, R_f = 0.30–0.50; fraction 2, R_f = 0.10–0.30). The fractions contained the oxidized TAG molecules (27). The extracts were washed with distilled water. TAG and their hydroxy, hydroperoxy, ketone, and epoxy derivatives were detected in UV light after spraying with 2,7-dichlorofluorescein. Core aldehydes showed a purple color with a Schiff base reagent (40).

Derivatization of lipoprotein TAG core aldehydes. To derivatize TAG core aldehydes, part of the oxidized TAG of the lipoprotein samples was allowed to react with DNPH as described above for the reference compounds, the exception being that the reaction took place at 6°C overnight.

FA analysis. The FAME of TAG were prepared by sodium methoxide-catalyzed transesterification (41). Methyl esters were dissolved in hexane and analyzed by GC (PerkinElmer AutoSystem, Norwalk, CT) using a DB-23 column (30 m × 0.32 mm i.d., 0.25 μm film thickness; Agilent Technologies, Palo Alto, CA). The instrument was equipped with an FID. We did not attempt to detect or identify oxidized FA *via* GLC.

Analysis of samples by HPLC-UV/ELSD and HPLC-ESI-MS. TAG and their oxidation products were separated by RP-HPLC. The HPLC system consisted of a Hitachi (Tokyo, Japan) L-6200 Intelligent Pump with a Discovery® HS C18 column (250 mm × 4.6 mm i.d.; Supelco Inc., Bellefonte, PA). The column was eluted at 0.85 mL/min and a linear gradient was used: 20% 2-propanol in methanol was changed to 80% 2-propanol in 20 min. The final composition was held for 10 min. Eighty-five percent of the effluent (0.72 mL/min) was led to a Sedex 75 (S.E.D.E.R.E., Alfortville, France) ELSD through a Shimadzu (Kyoto, Japan) SPD-6AV UV/vis detector that was used for the analysis of DNPH derivatives of core aldehydes at 358 nm. An evaporation temperature of 70°C and nebulizer gas (air) pressure of 2.7 bar were used in the ELSD. Fifteen percent of the effluent (0.13 mL/min) was led to a Finnigan MAT TSQ 700 triple quadrupole mass spectrometer (Finnigan, San Jose, CA) equipped with a nebulizer-assisted electrospray interface. Full-scan MS spectra were collected in negative (*m/z* 600–1200) and positive (*m/z* 450–1100) ionization mode. The electrospray voltages used were −4.5 and +4.5 kV, respectively.

Determination of the oxidation level of plasma and lipoproteins. For the estimation of total lipid oxidation by the baseline level of diene conjugation in plasma and lipoproteins, extracted lipids of plasma, chylomicrons, VLDL, and LDL were dissolved in cyclohexane and analyzed spectrophotometrically at 234 nm. Absorbance units were converted to molar units using the molar extinction coefficient 2.95×10^4 M^{-1} cm^{-1}. The results were expressed as micromoles conjugated dienes in a liter of plasma to have an estimation of the actual level of oxidized lipoproteins in circulation (18). The proportions of oxidized TAG molecules were estimated by HPLC using the conditions described above. The estimations were based on the ELSD chromatograms of the HPLC runs in which an internal standard was used. The response of ELSD to the injected amount of a reference compound (Table 1, Ia) was tested before the estimations were made.

Statistical analysis. SPSS 10.0 and SPSS 12.0 (Chicago, IL) for Windows were used for data analysis. One-way ANOVA and the Kruskal–Wallis test were used to compare the BDC values and FA compositions of the different piglet groups.

RESULTS

FA compositions of the TAG of chylomicrons and VLDL are listed in Tables 4 and 5, respectively. Both lipoprotein classes reflected, to a large degree, the FA compositions of the test oils. Lipoprotein TAG contained more 16:0 (palmitic acid) and 18:3n-3 (α-linolenic acid), and less 18:2n-6 (linoleic

TABLE 4
FA Compositions of the TAG of Pig Chylomicrons[a]

FA	Group 1	Group 2	Group 3
Time point 3 h			
16:0	8.1 ± 0.3	8.8 ± 1.1	8.8 ± 1.5
16:1n-7	0.3 ± 0.2	0.2 ± 0.0	0.3 ± 0.0
18:0	3.3 ± 0.1	3.4 ± 0.5	3.5 ± 0.2
18:1[b]	26.0 ± 0.7	25.2 ± 0.1	26.0 ± 1.3
18:2n-6	59.7 ± 0.5	59.5 ± 1.8	58.4 ± 1.2
18:3n-3	0.8 ± 0.1	0.9 ± 0.2	0.6 ± 0.1
20:0	0.1 ± 0.0	0.2 ± 0.1	0.2 ± 0.0
20:1n-9	0.2 ± 0.0	0.3 ± 0.1	0.3 ± 0.1
20:2n-6	0.1 ± 0.0	0.2 ± 0.0	0.1 ± 0.1
20:4n-6	1.3 ± 0.1	1.1 ± 1.0	1.6 ± 0.3
Time point 4 h			
16:0	8.3 ± 0.2	9.7 ± 1.0	8.0 ± 1.2
16:1n-7	0.4 ± 0.2	0.3 ± 0.1	0.3 ± 0.0
18:0	3.4 ± 0.4	3.4 ± 0.5	3.4 ± 0.2
18:1[b]	25.6 ± 0.3	24.3 ± 1.3	26.3 ± 1.0
18:2n-6	59.4 ± 0.7	57.4 ± 2.2	58.6 ± 1.4
18:3n-3	1.0 ± 0.1	1.1 ± 0.4	0.6 ± 0.0
20:0	0.1 ± 0.0	0.1 ± 0.1	0.2 ± 0.0
20:1n-9	0.2 ± 0.0	0.3 ± 0.1	0.3 ± 0.1
20:2n-6	0.1 ± 0.0	0.2 ± 0.1	0.1 ± 0.1
20:4n-6	1.2 ± 0.0	3.1 ± 1.0	2.0 ± 1.0

[a]Results expressed as percentage of total FA (mean ± SD, $n = 3$).
[b]Includes FA of n-9 and n-7 series.
[c]$n = 2$.

TABLE 5
FA Compositions of the TAG of Pig VLDL[a]

FA	Group 1	Group 2	Group 3
Time point 3 h			
16:0	7.3 ± 0.1	7.7 ± 1.2	8.8 ± 2.7
16:1n-7	1.0 ± 0.1	0.7 ± 0.2	0.7 ± 0.2
18:0	2.6 ± 0.2	2.9 ± 0.6	2.7 ± 0.2
18:1[b]	23.8 ± 0.1[a]	24.2 ± 0.6	25.7 ± 1.0[b]
18:2n-6	58.7 ± 1.8	57.6 ± 2.6	55.3 ± 3.0
18:3n-6	1.3 ± 0.4	1.0 ± 0.5	1.4 ± 0.6
18:3n-3	0.7 ± 0.1	0.8 ± 0.2	0.6 ± 0.1
20:0	0.0 ± 0.1	0.1 ± 0.0	0.0 ± 0.0
20:1n-9	0.2 ± 0.0[a]	0.2 ± 0.0[a]	0.3 ± 0.0[b]
20:2n-6	0.4 ± 0.1	0.4 ± 0.1	0.5 ± 0.0
20:4n-6	3.4 ± 1.1	3.9 ± 2.0	3.3 ± 0.6
22:1n-9	0.0 ± 0.0	0.1 ± 0.1	0.2 ± 0.2
Time point 4 h			
16:0	8.0 ± 0.4	8.4 ± 1.8	9.2 ± 2.9
16:1n-7	0.9 ± 0.2	0.6 ± 0.3	0.9 ± 0.3
18:0	2.9 ± 0.4	3.4 ± 0.9	2.8 ± 0.4
18:1[b]	23.3 ± 0.6[a]	23.3 ± 0.8[a]	26.7 ± 1.8[b]
18:2n-6	58.7 ± 1.7	56.3 ± 3.8	54.5 ± 5.5
18:3n-6	0.7 ± 0.5	0.8 ± 0.4	0.4 ± 0.4
18:3n-3	0.9 ± 0.1	1.0 ± 0.3	0.5 ± 0.4
20:0	0.1 ± 0.1	0.1 ± 0.1	0.0 ± 0.0
20:1n-9	0.3 ± 0.0	0.3 ± 0.1	0.4 ± 0.2
20:2n-6	0.5 ± 0.0	0.6 ± 0.1	0.6 ± 0.1
20:4n-6	3.6 ± 0.8	4.8 ± 3.0	3.9 ± 0.7
22:1n-9	0.1 ± 0.1	0.2 ± 0.2	0.1 ± 0.1

[a]Results expressed as percentage of total FA (mean ± SD, $n = 3$). Different superscript roman letters indicate significant differences between diet groups ($P < 0.05$).
[b]Includes FA of n-9 and n-7 series.

acid) than the test oils. The differences between the lipoprotein TAG compositions of different diet groups were relatively small. Both 18:3n-6 (γ-linolenic acid) and 22:1n-9 were found in VLDL but not in chylomicrons. The presence of γ-linolenic acid in VLDL TAG indicates hepatic Δ6-desaturation of dietary linoleic acid and incorporation of the γ-linolenic acid formed into VLDL, or incorporation of endogenous γ-linolenic acid into VLDL.

The retention times obtained with the present HPLC column were longer than those obtained with the column used by Sjövall *et al.* (27). This is why the time of the linear gradient applied was shortened. Despite the change, the standard curve made with a series of saturated TAG (G-1) was linear between 10 and 30 min. The validity of the elution factors determined by Sjövall *et al.* for the present HPLC column and gradient program was tested with different TAG and with core aldehyde, hydroperoxide, hydroxide, and epoxide reference compounds (Table 1). It was concluded that the elution factors could be applied to the present column as such.

Several oxidation products of TAG were detected in the TLC fractions of chylomicron and VLDL lipids. The oxidized structures were found by extracting peaks of a specific *m/z* value from the MS chromatograms of HPLC runs (Fig. 1). Only $[M + Na]^+$ ions were formed from the molecules other than DNPH derivatives, which were seen as $[M - H]^-$ ions. This simplified identification. If the retention time for a peak of an *m/z* value suggested a certain type of oxidation product and a particular FA composition, and a homologous series of ions was found in the chromatogram, this was regarded as evidence of a certain molecular structure. Because of the small amount of oxidized TAG in the samples, individual oxidation products could not be quantified.

The postulated molecular structures of the oxidized TAG of chylomicrons and VLDL are listed in Table 6. No major differences were found between the oxidation products of the lipoprotein samples from different pigs. Most of the oxidized structures were found in all samples at both time points. In some cases (particularly chylomicron TAG ketones in time point 1), the peaks representing the oxidation products of TAG were slightly stronger in group 3 compared with the other groups. Typically, the oxidation products were formed from TAG with ACN:DB (acyl carbon number:number of double bonds) values of 52:2, 52:3, 52:4, 54:3, 54:4, 54:5, and 54:6.

In most oxidation products detected, oxidation had occurred in only one of the FA of a TAG molecule. These products consisted of TAG molecules with a hydroxy, an epoxy, or a keto group attached to a FA, and of TAG core aldehydes. Based on the intensities of the extracted peaks in the MS chromatograms (Fig. 1), hydroxides seemed to be the most abundant TAG oxidation product in the samples.

Autoxidation of TAG produces two distinct classes of epoxides (25): those in which the oxygen atom is added at the site where a double bond has been, and those in which the epoxide is added near a double bond so that no double bonds are lost (25). In our samples, oxygen seems to have been added mainly at the site of a double bond, again based on the

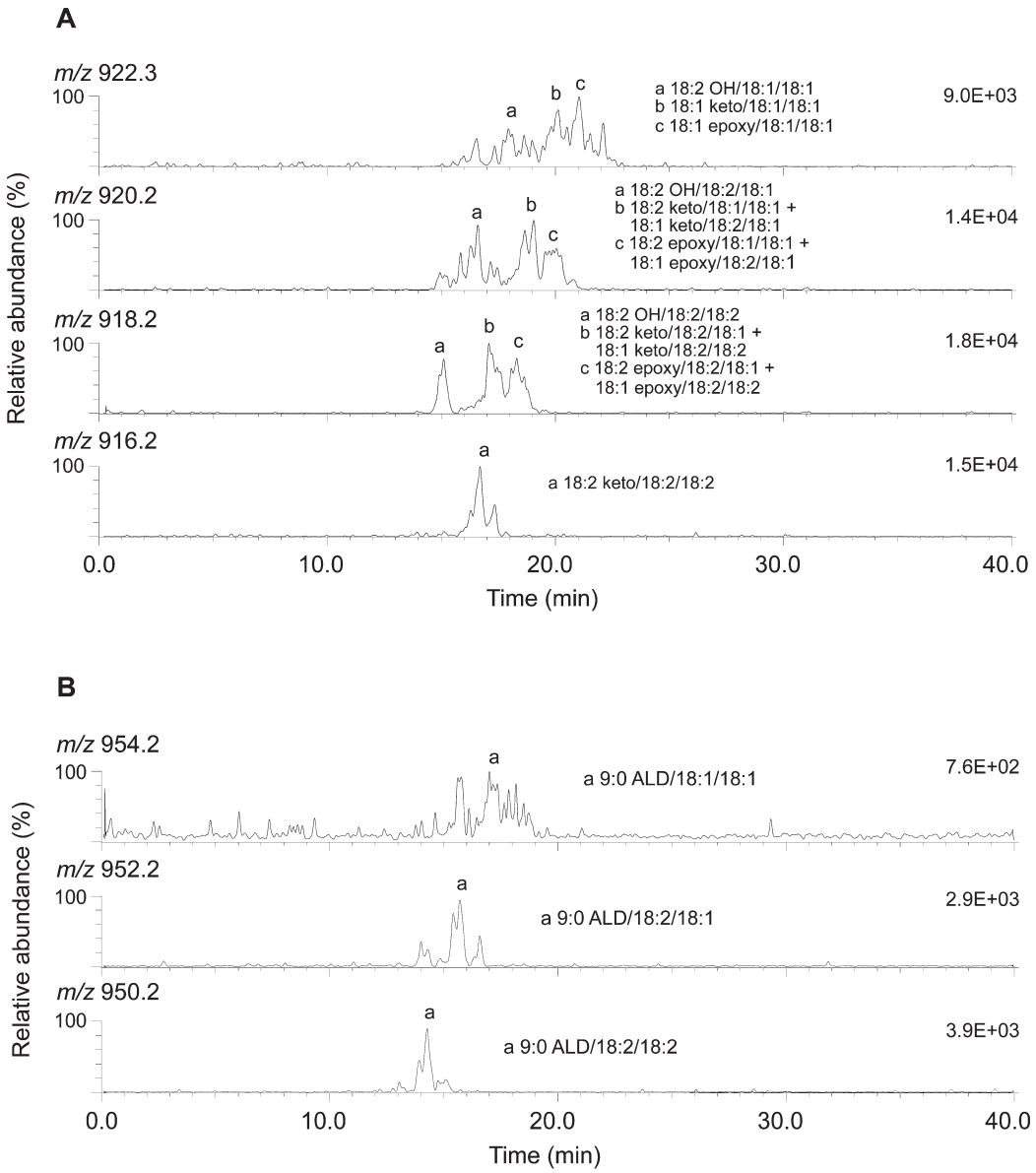

FIG. 1. Ion chromatograms showing the oxidized TAG molecules of pig chylomicrons. Postulated molecular structures (not regioisomers) are included in the chromatograms. (A) TAG of 54 acyl carbons with a hydroxy, a keto, or an epoxy group attached to a FA. The mass calibration was made using *m/z* values 0.5 units higher than the calculated isotopic masses; the ions have been detected accordingly. (B) TAG of 45 carbons (originally 54 carbons) with a FA core aldehyde (ALD) (as a 2,4-dintrophenyl hydrazine derivative).

intensities of the extracted peaks in the MS chromatograms (Fig. 1) and the FA composition of the TAG (Tables 4 and 5).

Since no elution factors were determined for ketone compounds in the work of Sjövall *et al.* (27), the postulated presence of ketones based on the extracted peaks in the MS chromatograms (Fig. 1) had to be confirmed. For this purpose, the retention times of the postulated ketone peaks were compared with the retention time of the ketone reference compounds (Table 1). The results showed that TAG molecules with a ketone group in one of the FA were present in our samples. The ketone structures may have formed in either of two ways: Either the number of double bonds between FA carbons had not changed (e.g., conversion of a hydroperoxide to a ketone by dehydration), or there was one less double bond (formation of a ketone at a site of unsaturation).

In accordance with our previous study on human LDL (17), virtually no hydroperoxides were found in the lipoprotein samples. This is in contrast to the oxidized test oils, where monohydroperoxides were the major class of oxidized TAG. In the test oils, monohydroperoxides were formed from TAG with ACN:DB 52:2, 52:3, 52:4, 54:3, 54:4, 54:5, and 54:6 (like most of the oxidized TAG molecules in the lipoprotein samples); also, some monoepoxides and mono-core aldehydes were formed from the same TAG molecules. Part of the test oil hydroperoxides as well as hydroperoxide reference compounds lost 18 mass units in the ion source, which

TABLE 6
Postulated Structures of the Oxidized TAG Molecules Found in the Chylomicron and VLDL Samples[a]

ACN[b]	Hydroxides	Epoxides	Ketones	Aldehydes
50			18:2 keto/16:0/16:0[c]	9:0 ALD/16:0/16:0[c]
			18:1 keto/16:0/16:0[c]	
52	18:3 OH/18:2/16:0[d]	18:2 epoxy/18:1/16:0	18:3 keto/18:2/16:0[d]	9:0 ALD/18:2/16:0[c]
	18:2 OH/18:2/16:0	18:1 epoxy/18:2/16:0	18:2 keto/18:2/16:0	9:0 ALD/18:1/16:0[c]
	18:2 OH/18:1/16:0	18:1 epoxy/18:1/16:0	18:2 keto/18:1/16:0	12:1 ALD/18:2/16:0[c]
	18:1 OH/18:1/16:0	18:1 epoxy/18:0/16:0	18:1 keto/18:2/16:0	13:2 ALD/18:2/16:0[c]
		18:0 epoxy/18:1/16:0	18:1 keto/18:1/16:0	
		18:0 diepoxy/18:2/16:0[c]		
		18:0 diepoxy/18:1/16:0[c]		
54	18:3 OH/18:2/18:2[d]	18:2 epoxy/18:2/18:1	18:2 keto/18:2/18:2	9:0 ALD/18:3/18:2[c]
	18:2 OH/18:2/18:2	18:1 epoxy/18:2/18:2	18:2 keto/18:2/18:1	9:0 ALD/18:2/18:2
	18:2 OH/18:2/18:1	18:2 epoxy/18:1/18:1	18:1 keto/18:2/18:2	9:0 ALD/18:2/18:1
	18:2 OH/18:1/18:1	18:1 epoxy/18:2/18:1	18:2 keto/18:1/18:1	9:0 ALD/18:1/18:1[c]
	18:1 OH/18:1/18:1	18:1 epoxy/18:1/18:1	18:1 keto/18:2/18:1	12:1 ALD/18:2/18:2
	18:1 OH/18:1/18:0[c]	18:1 epoxy/18:1/18:0	18:1 keto/18:1/18:1	12:1 ALD/18:2/18:1
		18:0 epoxy/18:1/18:1	18:1 keto/18:1/18:0[c]	12:1 ALD/18:1/18:1
		18:0 diepoxy/18:2/18:2[c]	18:0 keto/18:1/18:1[c]	12:1 ALD/18:1/18:0
		18:0 diepoxy/18:2/18:1[c]		13:2 ALD/18:2/18:1[c]
		18:0 diepoxy/18:1/18:1[c]		13:2 ALD/18:1/18:1[c]

[a]The most probable molecular structures based on *m/z* values, TAG FA compositions, and the assumption that the most unsaturated FA is oxidized; regioisomers are not distinguished. ALD, aldehyde.
[b]Acyl carbon number (ACN) of the original TAG molecule.
[c]Uncertain/very weak peak in chromatogram.
[d]More abundant in VLDL samples.

denotes cleavage of H_2O. The product formed could be a ketone or an epoxide without a loss of any double bonds. Neff and Byrdwell (25) discovered that in the atmospheric-pressure chemical ionization ion source, TAG hydroperoxides formed epoxides by loss of the outer –OH from the hydroperoxy group, followed by cyclization of the remaining oxygen. This reaction may also have taken place in our ESI source.

Figure 2 shows the BDC values of plasma and separate lipoproteins. The differences between groups 1 and 2 were relatively small in most cases, but the BDC values of group 3 were higher than those of groups 1 and 2 in all fractions and both time points. This indicates that feeding pigs on oxidized oil had an increasing effect on the oxidation of lipoprotein lipids. It is noteworthy, though, that the oxidized test oils contained less vitamin E than the nonoxidized oil, resulting in lower total vitamin E content in the feeds containing the oxidized oils.

The estimated proportions of oxidized TAG molecules in the total lipids of the test oils and chylomicrons are listed in Table 7. The oxidized molecules include all the oxidized TAG species that were detectable in HPLC-ELSD chromatograms. Proportions could not be determined for group 2 owing to the small amount of samples. The results show that the proportion of oxidized TAG was considerably lower in the chylomicron lipids of pigs fed on oxidized oil compared with the lipids of oxidized oils themselves. However, the proportion of oxidized TAG molecules was greater in group 3 compared with group 1. This is in agreement with the previously mentioned BDC determinations and the hypothesis that TAG contribute to the oxidation of lipoproteins.

In most cases, no peaks were found for oxidized TAG molecules of VLDL in ELSD chromatograms. Thus, estimations could not be made for VLDL.

DISCUSSION

As chylomicrons and VLDL contain approximately 90 and 55% TAG, respectively (42,43), it would be likely that the oxidation of lipoproteins was partly due to oxidized TAG molecules. This is supported by our earlier work, which demonstrated that TAG have a contribution of almost 30% to the diene conjugation of LDL, which contains considerably less TAG than chylomicrons and VLDL (Ahotupa, M., and Viikari, J., unpublished results). The present results on lipoprotein TAG oxidation also support this hypothesis.

The lack of TAG hydroperoxides in the lipoprotein samples is in accordance with the observation that only traces of unmodified hydroperoxy lipids are found in tissue and blood samples (44). According to Spiteller (44), lipid hydroperoxides are quickly converted to hydroxides in biological surroundings. In the studies of the group of Yamamoto (45), cholesteryl ester hydroperoxides were present in rat and human plasma whereas PC hydroperoxides were undetectable because of enzymatic and nonenzymatic reduction and conversion. Our results suggest that modification of hydroperoxy structures, particularly conversion to hydroxides, could also take place in the oxidized TAG molecules found in chylomicrons and VLDL. TAG hydroperoxides of dietary origin may, to a large degree, be reduced and decomposed to secondary oxidation products already in gastrointestinal tract (46,47).

The possibility that some decomposition of hydroperoxy structures had occurred during sample preparation cannot be excluded. However, our hydroperoxide reference compounds were observed to be relatively stable during storage and during TLC and HPLC-MS runs. Therefore, sample preparation probably does not explain the absence of hydroperoxides in the samples.

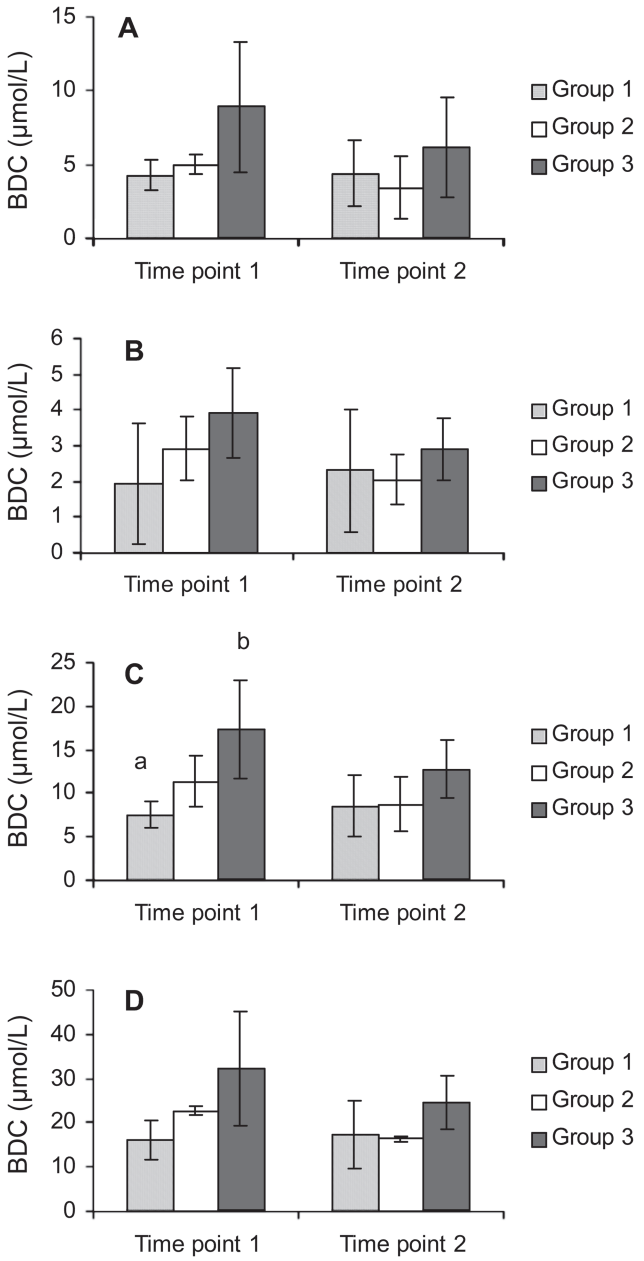

FIG. 2. Baseline diene conjugation (BDC) values (µmol/L plasma) of chylomicron (A), VLDL (B), LDL (C), and plasma (D) lipids. Time point 1, 3 h; time point 2, 4 h after the last test meal. Different letters indicate significant differences between the diet groups ($P < 0.05$). PV of the sunflower seed oil used in feed: group 1, 1 mequiv O_2/kg; group 2, 84 mequiv O_2/kg; group 3, 223 mequiv O_2/kg.

Oxidized TAG molecules could at least partly explain why lipoproteins rich in TAG seem to be important factors in the induction of atherogenesis (48). As already mentioned, TAG hydroxides seemed to be the most abundant group of oxidized TAG in our samples. An interesting detail is that linoleic acid hydroxides are found in atherosclerotic plaques (44). Also, linoleic acid hydroxides have been found to be endogenous activators and ligands of peroxisome proliferator activated receptor protein γ, which promotes monocyte/macrophage differentiation and uptake of oxidized LDL (49,50). Thus, linoleic acid hydroxides as well as those of other PUFA could have an influence on atherogenesis (44).

TABLE 7
Estimated Proportions of Oxidized TAG Molecules in the Total Lipids of the Test Oils and Chylomicrons Determined by ELSD[a]

Group 1[b]		Group 3[c]	
Oil	0.2	Oil	6.2
Time point 3 h			
Pig 1	0.0	Pig 7	0.4
Pig 2	0.1	Pig 8	0.4
Pig 3	0.2	Pig 9	1.9
Time point 4 h			
Pig 1	0.0	Pig 7	0.6
Pig 2	0.3	Pig 8	1.1
Pig 3	0.3	Pig 9	1.2

[a]Results expressed as g/100 g of total lipids.
[b]PV of the sunflower seed oil used in feed: 1 mequiv O_2/kg.
[c]PV of the sunflower seed oil used in feed: 223 mequiv O_2/kg.

In summary, new information on oxidized TAG molecules of chylomicrons and VLDL was obtained, which can aid future research of dietary effects on lipoprotein oxidation and atherogenesis. The results obtained by the BDC method show that the lipoprotein lipids of group 3 were more oxidized compared with group 2 and especially when compared with group 1. It was also shown that the chylomicron samples of group 3 contained more oxidized TAG molecules than the samples of group 1. Thus, our results suggest that the oxidation of dietary fat is reflected in lipoprotein oxidation. The present results will stimulate further research using larger groups of growing pigs to provide more detailed information on lipid oxidation and oxidized lipid molecules in disease processes.

ACKNOWLEDGMENTS

This work was supported by ABS Graduate School, Helsinki, Finland; Raisio Nutrition Ltd., Raisio, Finland; and Wäinö Edward Miettinen Foundation. Hilkka Siljander-Rasi and the staff of MTT Agrifood Research Finland, Swine Research Station (Hyvinkää, Finland) are thanked for pleasant co-operation. Tiina Ylinen, Anja Pirinen, Heidi Huotari, and Mika Kaimainen and the staff of MCA Research Laboratory Ltd. are thanked for technical assistance.

REFERENCES

1. Steinbrecher, U.P., Zhang, H., and Lougheed, M. (1990) Role of Oxidatively Modified LDL in Atherosclerosis, *Free Radic. Biol. Med. 9,* 155–168.
2. Esterbauer, H., Gebicki, J., Puhl, H., and Jurgens, G. (1992) The Role of Lipid Peroxidation and Antioxidants in Oxidative Modifications of LDL, *Free Radic. Biol. Med. 13,* 241–290.
3. Witztum, J.L. (1994) The Oxidation Hypothesis of Atherosclerosis, *Lancet 344,* 793–795.
4. Berliner, J.A., and Heinecke, J.W. (1996) The Role of Oxidized Lipoproteins in Atherogenesis, *Free Radic. Biol. Med. 20,* 707–727.
5. Jialal, I., and Devaraj, S. (1996) Low-Density Lipoprotein Oxidation, Antioxidants, and Atherosclerosis: A Clinical Biochemistry Perspective, *Clin. Chem. 42,* 498–506.
6. Grieve, D.J., Avella, M.A., Elliott, J., and Botham, K.M. (2000) The Interaction Between Oxidised Chylomicron Remnants and

the Aorta of Rats Fed a Normocholesterolaemic or Hypercholesterolaemic diet, *J. Vasc. Res. 37,* 265–275.
7. Napolitano, M., Rivabene, R., Avella, M., Amicone, L., Tripodi, M., Botham, K.M., and Bravo, E. (2001) Oxidation Affects the Regulation of Hepatic Lipid Synthesis by Chylomicron Remnants, *Free Radic. Biol. Med. 30,* 506–515.
8. Naruszewicz, M., Wozny, E., Mirkiewicz, E., Nowicka, G., and Szostak,W.B. (1987) The Effect of Thermally Oxidized Soya Bean Oil on Metabolism of Chylomicrons. Increased Uptake and Degradation of Oxidized Chylomicrons in Cultured Mouse Macrophages, *Atherosclerosis 66,* 45–53.
9. Umeda, Y., Redgrave, T.G., Mortimer, B.C., and Mamo, J.C.L. (1995) Kinetics and Uptake *in vivo* of Oxidatively Modified Chylomicrons, *Am. J. Physiol. 268,* G709–G716.
10. Staprans, I., Rapp, J.H., Pan, X.-M., Kim, K.Y., and Feingold, K.R. (1994) Oxidized Lipids in the Diet Are a Source of Oxidized Lipid in Chylomicrons of Human Serum, *Arterioscler. Thromb. 14,* 1900–1905.
11. Staprans, I., Rapp, J.H., Pan, X.-M., Kim, K.Y., and Feingold, K.R. (1996) Oxidized Lipids in the Diet Are Incorporated by the Liver into Very Low Density Lipoprotein in Rats, *J. Lipid Res. 37,* 420–430.
12. Mamo, J.C.L., and Wheeler, J.R. (1994) Chylomicrons or Their Remnants Penetrate Rabbit Thoracic Aorta as Efficiently as Smaller Macromolecules Including Low Density Lipoprotein, High Density Lipoprotein and Albumin, *Coron. Artery Dis. 5,* 695–705.
13. Kamido, H., Kuksis, A., Marai, L., and Myher, J.J. (1995) Lipid Ester-Bound Aldehydes Among Copper-Catalyzed Peroxidation Products of Human Plasma Lipoproteins, *J. Lipid Res. 36,* 1876–1886.
14. Karten, B., Boechzelt, H., Abuja, P.M., Mittelbach, M., and Sattler, W. (1999) Macrophage-Enhanced Formation of Cholesteryl Ester-Core Aldehydes During Oxidation of Low Density Lipoprotein, *J. Lipid Res. 40,* 1240–1253.
15. Niu, X., Zammit, V., Upston, J.M., Dean, R.T., and Stocker, R. (1999) Coexistence of Oxidized Lipids and α-Tocopherol in All Lipoprotein Density Fractions Isolated from Advanced Human Atherosclerotic Plaques, *Arterioscler. Thromb. Vasc. Biol. 19,* 1708–1718.
16. Ahotupa, M., Marniemi, J., Lehtimäki, T., Talvinen, K., Raitakari, O.T., Vasankari, T., Viikari, J., Luoma, J., and Yläherttuala, S. (1998) Baseline Diene Conjugation in LDL Lipids as a Direct Measure of *in vivo* LDL Oxidation, *Clin. Biochem. 31,* 257–261.
17. Suomela, J.-P., Ahotupa, M., Sjövall, O., Kurvinen, J.-P., and Kallio, H. (2004) New Approach to the Analysis of Oxidized Triacylglycerols in Lipoproteins, *Lipids 39,* 507–512.
18. Ahotupa, M., Ruutu, M., and Mäntylä, E. (1996) Simple Methods of Quantifying Oxidation Products and Antioxidant Potential of Low Density Lipoproteins, *Clin. Biochem. 29,* 139–144.
19. Ahotupa, M., and Vasankari, T.J. (1999) Baseline Diene Conjugation in LDL Lipids: An Indicator of Circulating Oxidized LDL, *Free Radic. Biol. Med. 27,* 1141–1150.
20. Gavella, M., Lipovac, V., Car, A., and Vucic, M. (2002) Baseline Diene Conjugation in LDL Lipids from Newly Diagnosed Type 2 Diabetic Patients, *Diabetes Metab. 28,* 391–396.
21. Vasankari, T., Fogelholm, M., Kukkonen-Harjula, K., Nenonen, A., Kujala, U., Oja, P., Vuori, I., Pasanen, P., Neuvonen, K., and Ahotupa, M. (2001) Reduced Oxidized Low-Density Lipoprotein After Weight Reduction in Obese Premenopausal Women, *Int. J. Obesity Related Metab. Disord. 25,* 205–211.
22. Byrdwell, W.C., and Neff, W.E. (1999) Non-volatile Products of Triolein Produced at Frying Temperatures Characterized Using Liquid Chromatography with Online Mass Spectrometric Detection, *J. Chromatogr. A 852,* 417–432.
23. Byrdwell, W.C., and Neff, W.E. (2001) Autoxidation Products of Normal and Genetically Modified Canola Oil Varieties Determined Using Liquid Chromatography with Mass Spectrometric Detection, *J. Chromatogr. A 905,* 85–102.
24. Frankel, E.N., Neff, W.E., and Miyashita, K. (1990) Autoxidation of Polyunsaturated Triacylglycerols. II. Trilinolenoylglycerol, *Lipids 25,* 40–47.
25. Neff, W.E., and Byrdwell, W.C. (1998) Characterization of Model Triacylglycerol (triolein, trilinolein and trilinolenin) Autoxidation Products *via* High-Performance Liquid Chromatography Coupled with Atmospheric Pressure Chemical Ionization Mass Spectrometry, *J. Chromatogr. A 818,* 169–186.
26. Steenhorst-Slikkerveer, L., Louter, A., Janssen, H.-G., and Bauer-Plank, C. (2000) Analysis of Nonvolatile Lipid Oxidation Products in Vegetable Oils by Normal-Phase High-Performance Liquid Chromatography with Mass Spectrometric Detection, *J. Am. Oil Chem. Soc. 77,* 837–845.
27. Sjövall, O., Kuksis, A., Marai, L., and Myher, J.J. (1997) Elution Factors of Synthetic Oxotriacylglycerols as an Aid in Identification of Peroxidized Natural Triacylglycerols by Reverse-Phase High-Performance Liquid Chromatography with Electrospray Mass Spectrometry, *Lipids 32,* 1211–1218.
28. Sjövall, O., Kuksis, A., and Kallio, H. (2001) Analysis of Molecular Species of Peroxide Adducts of Triacylglycerols Following Treatment of Corn Oil with *tert*-Butyl Hydroperoxide, *Lipids 36,* 1347–1356.
29. Sjövall, O., Kuksis, A., and Kallio, H. (2002) Formation of Triacylglycerol Core Aldehydes During Rapid Oxidation of Corn and Sunflower Oils with *tert*-Butyl Hydroperoxide/Fe^{2+}, *Lipids 37,* 81–94.
30. Ravandi, A., Kuksis, A., Myher, J.J., and Marai, L. (1995) Determination of Lipid Ester Ozonides and Core Aldehydes by High-Performance Liquid Chromatography with On-Line Mass Spectrometry, *J. Biochem. Biophys. Methods 30,* 271–285.
31. Esterbauer, H., and Cheeseman, K.H. (1990) Determination of Aldehydic Peroxidation Products: Malonaldehyde and 4-Hydroxynonenal, *Methods Enzymol. 186,* 407–421.
32. Deffense, E. (1993) Nouvelle Méthode d'Analyse pour Séparer, *via* HPLC, les Isomères de Position 1-2 et 1-3 des Triglycérides Mono-Insaturés des Graisses Végétales, *Rev. Fr. Corps Gras 40,* 33–39.
33. Neff, W.E., Frankel, E.N., and Weisleder, D. (1982) Photosensitized Oxidation of Methyl Linolenate. Secondary Products, *Lipids 17,* 780–790.
34. Chiba, T., Takazawa, M., and Fujimoto, K. (1989) A Simple Method for Estimating Carbonyl Content in Peroxide-Containing Oils, *J. Am. Oil Chem. Soc. 66,* 1588–1592.
35. Gritter, R.J., and Wallace, T.J. (1959) The Manganese Dioxide Oxidation of Allylic Alcohols, *J. Org. Chem. 24,* 1051–1056.
36. AOCS, *Standard Methods and Recommended Pratices of the AOCS,* 5th edn., AOCS Press, Champaign, 1997.
37. IUPAC (1987) *Standard Methods for the Analysis of Oils, Fats, and Derivatives,* 7th edn., Blackwell Science, Oxford.
38. Ågren, J.J, Vidgren, H.M., Valve, R.S., Laakso, M., and Uusitupa, M. (2001) Postprandial Responses of Individual Fatty Acids in Subjects Homozygous for the Threonine- or Alanine-Encoding Allele in Codon 54 of the Intestinal Fatty Acid Binding Protein 2 Gene, *Am. J. Clin. Nutr. 73,* 31–35.
39. Hamilton, J.G., and Comai, K. (1988) Rapid Separation of Neutral Lipids, Free Fatty Acids and Polar Lipids Using Prepacked Silica Sep-Pak Columns, *Lipids 23,* 1146–1149.
40. Skipski, V.P., and Barclay, M. (1969) Thin-Layer Chromatography, *Methods Enzymol. 14,* 542–548.
41. Christie, W.W. (1982) A Simple Procedure for Rapid Transmethylation of Glycerolipids and Cholesteryl Esters, *J. Lipid Res. 23,* 1072–1075.
42. Kuksis, A. (2000) Biochemistry of Glycerolipids and Formation of Chylomicrons, in *Fat Digestion and Absorption* (Christophe,

A.B., and De Vriese, S., eds.), pp. 119–181, AOCS Press, Champaign, IL.
43. Olson, R.E. (1998) Discovery of the Lipoproteins, Their Role in Fat Transport and Their Significance as Risk Factors, *J. Nutr. 128,* 439S–443S.
44. Spiteller, G. (1998) Linoleic Acid Peroxidation—The Dominant Lipid Peroxidation Process in Low Density Lipoprotein—And Its Relationship to Chronic Diseases, *Chem. Phys. Lipids 95,* 105–162.
45. Yamamoto, Y. (2000) Fate of Lipid Hydroperoxides in Blood Plasma, *Free Rad. Res. 33,* 795–800.
46. Aw, T.Y., Williams, M.W., and Gray, L. (1992) Absorption and Lymphatic Transport of Peroxidized Lipids by Rat Small Intestine *in vivo*: Role of Mucosal GSH, *Am. J. Physiol. 262,* G99–G106.
47. Kanazawa, K., and Ashida, H. (1998) Dietary Hydroperoxides of Linoleic Acid Decompose to Aldehydes in Stomach Before Being Absorbed into the Body, *Biochim. Biophys. Acta 1393,* 349–361.
48. Hamsten, A. (1993) Lipids as Coronary Risk Factor: Analysis of Hyperlipidaemias, *Postgrad. Med. J. 69,* S8–S11.
49. Nagy, L., Tontonoz, P., Alvarez, J.G.A., Chen, H., and Evans, R.M. (1998) Oxidized LDL Regulates Macrophage Gene Expression Through Ligand Activation of PPARγ, *Cell 93,* 229–240.
50. Tontonez, P., Nagy, L., Alvarez, J.G.A., Thomazy, V.A., and Evans, R.M. (1998) PPARγ Promotes Monocyte/Macrophage Differentiation and Uptake of Oxidized LDL, *Cell 93,* 241–252.

[Received April 19, 2004; accepted September 4, 2004]

β-Oxidation, Esterification, and Secretion of Radiolabeled Fatty Acids in Cultivated Atlantic Salmon Skeletal Muscle Cells

A. Vegusdal[a,*], T.K. Østbye[a], T.-N. Tran[b], T. Gjøen[c], and B. Ruyter[a]

[a]AKVAFORSK, Institute of Aquaculture Research, NO-1432 Ås, Norway,
[b]Institute of Clinical Biochemistry, Rikshospitalet University Hospital, Univerity of Oslo, NO-0027 Oslo, Norway,
and [c]Department of Microbiology, Institute of Pharmacy, University of Oslo, NO-0316 Oslo, Norway

ABSTRACT: The white muscle of Atlantic salmon metabolizes FA with different chain lengths and different saturations at different rates, but few details are available on the processes involved or the products formed. We have investigated how multinucleated muscle cells (myotubes) in culture metabolize [1-^{14}C]8:0, [1-^{14}C]18:1n-9, and [1-^{14}C]20:5n-3. The myotubes were formed by the differentiation of isolated myosatellite cells from the white skeletal muscle of salmon fry. Almost all (98%) of the [1-^{14}C]8:0 substrate was oxidized to acid-soluble products (ASP) and $^{14}CO_2$ after 48 h of incubation, whereas only approximately 50% of the [1-^{14}C]18:1n-9 and [1-^{14}C]20:5n-3 substrates were oxidized. However, only one cycle of β-oxidation was measured by the method used. For all three substrates, the main ASP were acetate and a combined fraction of oxaloacetate and malate. Nearly twice as much radioactivity from the [1-^{14}C]20:5n-3 substrate was found in the cellular lipids as radioactivity from [1-^{14}C]18:1n-9, indicating that [1-^{14}C]20:5n-3 was taken up into muscle cells more rapidly than [1-^{14}C]18:1n-9. Approximately 10% of the added [1-^{14}C]20:5n-3 substrate and 5% of the added [1-^{14}C]18:1n-9 substrate was secreted from the muscle cells into the culture media as esterified lipids. Immunocytochemical staining showed that the cells synthesized apolipoprotein A-I. Differentiated muscle cells also expressed peroxisome proliferator-activated receptor α (PPARα) and PPARβ, two transcription factors that are involved in regulating β-oxidation.

Paper no. L9462 in Lipids 39, 649–658 (July 2004).

Traditionally, lipids have not been considered an important fuel during exhaustive exercise and recovery in fish. Evidence is mounting, however, that many fish species have a relatively high capacity to utilize the FA in TAG as an important metabolic fuel for skeletal muscle (1,2), and that these species rely on lipid oxidation in muscle to produce the ATP needed for recovery after exhaustive exercise (3). Atlantic salmon can store a considerable proportion of the FA esterified in TAG in adipocytes of muscle myosepta (4) and also, to some extent, in white muscle cells. Both of these cell types can release nonesterified FA (NEFA) for β-oxidation in highly metabolically active tissues such as the liver and muscle. Several studies have shown that the β-oxidation activity per milligram of white muscle tissue is low in fish (1,5,6). However, white muscle constitutes approximately 60% of the total body weight (7); thus, the white muscle is probably more important for overall β-oxidation in fish than the liver or the red muscle (2,5). The NEFA in muscle cells probably enter different metabolic pathways, depending on their chain length and degree of saturation. This is the case for NEFA in salmon liver (8,9). Medium-chain FA (MCFA) such as 8:0 are believed to enter the mitochondria prior to β-oxidation independently of the carnitine transport system, whereas longer-chain FA (LCFA) such as 18:1n-9 use a carnitine–acylcarnitine exchange system to enter the mitochondria (reviewed in Ref. 10). LCFA thus cross the membrane at a lower rate than do MCFA. However, we do not know whether the rate of β-oxidation in salmon muscle cells is influenced by the rate of entry of FA into the mitochondria. Mitochondrial MCFA and LCFA both undergo β-oxidation to yield acetyl-CoA in mammals. The acetyl-CoA generated in this way by mitochondrial FA oxidation in the liver of mammals is channeled to the tricarboxylic acid (TCA) cycle and to ketogenesis (11,12). In contrast, we know very little about the major β-oxidation products from FA with different chain lengths in salmon muscle cells and what happens to them. Although it is true that most β-oxidation takes place in mitochondria, peroxisomes are also necessary for the β-oxidation of a wide range of FA. In Atlantic salmon, peroxisomal β-oxidation accounts for approximately 10% (5) of total β-oxidation, whereas it may account for as much as 50% of the total β-oxidation in some marine teleosts (13,14). Most acetyl-CoA units released during peroxisomal FA oxidation in mammalian liver cells are metabolized to acetate (15), but we do not know whether this is the case in fish.

Controlling the rate of FA oxidation is highly important, and it is important for us to understand which steps in the pathway

*To whom correspondence should be addressed at AKVAFORSK, Institute of Aquaculture Research, P.O. Box 5010, NO-1432 Ås, Norway.
E-mail: anne.vegusdal@akvaforsk.nlh.no

Abbreviations: AEC, 3-amino-9-ethylcarbazole; apoA-I, apolipoprotein A-I; ASP, acid-soluble product; BHB, β-hydroxybutyrate; HRP, horseradish peroxidase; LCFA, long-chain FA; MCFA, medium-chain FA; MDG, mono- and diacylglycerols; MLC2, myosin light-chain 2; NEFA, nonesterified fatty acid; ox-mal, oxaloacetate and malate; PBS-T, PBS with 0.05% Tween; PCNA, proliferating cell nuclear antigen; PL, phospholipid; PPAR, peroxisome proliferator-activated receptor; PVDF, polyvinylidene difluoride; RT-PCR; reverse-transcriptase polymerase chain reaction, TCA, tricarboxylic acid.

contribute significantly to controlling the FA flux so that we might better understand increases or decreases in the rate of fat breakdown. However, we do not know how FA metabolism is regulated in salmon muscle. This regulation is important since the selective FA oxidation capacity of the muscle may determine not only the fat content, but also the FA composition of the muscle, and in this way influence the nutritional quality of the fillet. Modern salmonid diets have high lipid contents, and in several fish species, such as rainbow trout (16,17) and Atlantic salmon (18–20), these diets have led to increased muscle lipid levels. Excess lipid levels in the muscle may undermine fish health and quality (reviewed in Ref. 21). It would therefore be beneficial if the fish used more of the lipid stored in the muscle for producing energy. This could be achieved by stimulating FA oxidation.

In mammals, different dietary FA regulate lipid metabolism by the activation of nuclear receptors such as the peroxisome proliferator-activated receptors (PPAR) (22). We have previously shown that PPARγ is expressed in salmon liver (23,24) and salmon adipocytes (25). PPAR genes have recently been identified in other fish species (26,27), but the function of PPAR in fish muscle is not known. PPARα in mammals stimulates the expression of genes involved in FA uptake, activation of FFA into acyl-CoA esters, peroxisomal and mitochondrial β-oxidation pathways, and ketone body synthesis (reviewed in Ref. 28). PPARβ is the most abundant receptor of the various PPAR in the skeletal muscle (29), and this receptor promotes FA oxidation and TAG utilization (30). It is not known whether PPARα and PPARβ have the same regulatory functions in fish.

Salmon myosatellite cells isolated from white striated muscle differentiate into functional muscle fibers in culture (31). These cells could provide an appropriate experimental system for investigating muscle-specific FA metabolism in Atlantic salmon. We have used this *in vitro* salmon muscle cell system to study how FA with different chain lengths and degrees of saturation are oxidized to different products or are esterified into different cellular and secreted lipids. We have also determined whether these cultivated muscle cells express PPAR known to be important for the regulation of β-oxidation in mammals.

MATERIALS AND METHODS

Materials. Atlantic salmon (*Salmo salar*) fry were obtained from Aqua Gen (Sunndalsøra, Norway) and raised in a local aquarium at the Agricultural University of Norway. A commercial feed containing 20% fat was used. The radiolabeled FA [1-^{14}C]8:0, [1-^{14}C]18:1n-9, and [1-^{14}C]20:5n-3 (50 mCi/mmol) were obtained from American Radiolabeled Chemicals, Inc. (St. Louis, MO). DMEM, FBS, antibiotics, HEPES, L-glutamine, collagenase, trypsin, EFA-free BSA, laminin, Thermanox cover slips, the rabbit anti-goat IgG horseradish peroxidase (HRP)-conjugated antibody used in Western blots, phenylethylamine, and phenylmethylsulfonyl fluoride (PMSF) were obtained from Sigma-Aldrich (St. Louis, MO). Acetic acid, chloroform, petroleum ether, diethyl ether, and methanol were obtained from Merck (Darmstadt, Germany). Benzene was obtained from Rathburn Chemicals Ltd. (Walkerburn, United Kingdom). Methanolic HCl and 2,2-dimethoxypropane were purchased from Supelco Inc. (Bellfonte, PA). Glass baked silica gel K6 plates were obtained from Whatman International Ltd. (Maidstone, United Kingdom). Tissue culture plasticware was obtained from Nalge-Nunc International (Naperville, IL). Paraformaldehyde was obtained from Electron Microscopy Sciences (Fort Washington, PA). The proliferating cell nuclear antigen (PCNA) immunodetection kit, Histomount, Clearmount, and Mayer's hematoxylin were supplied by Zymed Laboratories Inc. (South San Francisco, CA). Trizol was from Boehringer Mannheim (Indianapolis, IN), and the T-primed First Strand kit and polyvinylidene difluoride (PVDF) transfer membranes, ECL Plus Western blotting detection kit, and ECL high-performance chemiluminescence film were from Amersham Biosciences (Buckinghamshire, United Kingdom). The Gene Amp PCR system 2400 was from PerkinElmer (Boston, MA). All primers used in mRNA expression studies were from Invitrogen (Paisley, United Kingdom), and they were designed to exclude amplification of genomic DNA. The sequences were as follows: α-actin: sense: 5′-atgggtcagaaggactc-3′, antisense: 5′-gtctcatgaataccagcg-3′; myogenin: sense: 5′-ctaccctgggcctgcaa-3′, antisense: 5′-ccacgatggacgtcagaga-3′; myosin light-chain 2 (MLC2): sense: 5′-ggcccccatcaacttcac-3′, antisense: 5′-ctcctccttctcctctccgtg-3′; myostatin I: sense: 5′-cacgcaaatacatattcac-3′, antisense: 5′-gca cttcagccagctg-3′; apoA-I: sense: 5′-ccatcagccaggccataaa-3′, and antisense: 5′-tgagtgagaagggagggagaga-3′. The sequence of the β-actin primer used in the expression studies of structural proteins and myogenic regulatory factors was: sense: 5′-gaccttcaacacccccg-3′, antisense: 5′-agtacgacgagtctggc-3′, whereas the sequence of the β-actin primer used in the real-time expression study of apoA-I was: sense: 5′-gctgacagggatgcagaaggaaa-3′ and antisense: 5′- cctccgatccagacggagtatt-3′. The Mini Trans-blot apparatus was from Biorad (Hercules, CA). Normal goat IgG, normal rabbit IgG, and HRP–3-amino-9-ethylcarbazole (AEC) immunodetection kits were provided by R&D Systems, Ltd. (Abingdon, United Kingdom). Rabbit anti-human PPARα, rabbit anti-human PPARβ, and goat anti-human apoA-I were supplied by Santa Cruz Biotechnology (Santa Cruz, CA). The goat anti-rabbit IgG HRP-linked antibody used in Western blotting was from Southern Biotechnology Associates (Birmingham, AL). All antibodies were polyclonal. Cells in culture were observed using a Diaphot inverted light microscope (Nikon, Japan). A Leitz Laborlux S light microscope (Leica, Germany) was used to view all stained cells. Leica DC100 cameras integrated with the microscopes were used to capture digitized cell images. All image acquisitions were controlled by Image Pro Plus 4.0 software from Media Cybernetics (Silver Spring, MD).

Cell isolation and differentiation. We used Atlantic salmon fed a commercial diet and isolated myosatellite cells from the fish when they had reached an average length of 5 cm. Myosatellite cells were isolated essentially as described by Koumans *et al*. (32), with the modifications developed by Matchak and Stickland (31). The fish were stunned by a blow to the head and killed by decapitation. White epaxial muscle

was excised under sterile conditions and placed into 90% DMEM. The tissue was minced, centrifuged at 300 × *g* for 5 min, and washed twice in 90% DMEM. Collagenase (0.2%) digestion was allowed to proceed with gentle shaking for 90 min at 11°C. The resulting suspension was centrifuged at 300 × *g* for 5 min, and the pellet thus obtained was resuspended in 0.1% trypsin solution. The suspension was digested for 30 min with gentle agitation. It was then centrifuged for 1 min at 300 × *g*, and the supernatant was aspirated and collected in 2 vol of ice-cold DMEM containing FBS. The pellet was subjected to a second trypsin digestion, centrifuged at 300 × *g* for 1 min, and the supernatant was diluted in 2 vol of DMEM containing FBS. The resulting two supernatants were centrifuged at 300 × *g* for 15 min. The pellet was resuspended in growth medium (90% DMEM supplemented with 15% FBS, 10 mM HEPES, 2 mM L-glutamin, and antibiotics) and filtered through a 40-μm filter. The cells were washed once more, diluted in growth medium, and plated (day 0) on laminin-precoated plastic tissue-culture flasks or 24-well plates equipped with Thermanox coverslips. It was difficult to count the myosatellite cells before plating them because tissue debris and various other cell types were present in the final cell suspension. The muscle tissue was therefore weighed after excision, and cells were plated at a density of approximately 5 g of tissue/25 cm^2. After adhesion for 3 h, the cells were extensively washed with medium. Cells were incubated at 13°C without CO_2, and the medium was changed every 5 d. Cells were cultured for 4 wk in the growth medium, during which period they differentiated into a confluent layer of multinucleated muscle cells (myotubes). Cultures for proliferation assessment were fixed on days 1, 2, 4, and 28 after seeding. On day 14, cultures for immunocytochemical studies were fixed, and cells for mRNA analyses and Western blot analyses were harvested. Cultures that had reached confluent monolayers of differentiated muscle cells during the 4-wk cultivation period were used for the studies of FA metabolism.

Assessment of cell proliferation. Cell proliferation was assessed by the immunocytochemical detection of PCNA. Cells were washed in PBS and fixed in 70% ethanol for 30 min at 4°C. Endogenous peroxidase activity was blocked by adding 3% hydrogen peroxide in methanol for 10 min. The cells were washed three times in PBS and then incubated with a mouse anti-PCNA monoclonal antibody (clone PC10) using a PCNA immunodetection kit. The cells were counterstained with Mayer's hematoxylin for 2 min, washed in water, dehydrated in a graded series of alcohol solutions, cleared with xylene, and mounted with Histomount. PCNA-containing nuclei were stained dark brown. Two hundred cells were counted, and the percentage of proliferating cells was calculated.

Immunocytochemistry. Cells for immunocytochemical staining were washed in PBS and fixed in freshly prepared 4% paraformaldehyde in PBS (pH 7.4) for 30 min at 4°C. The cells were treated with 0.1% Triton X-100 in PBS for 15 min to improve immunoglobulin penetration. The cells were rinsed in PBS and incubated with blocking serum, and then with primary antibody. PPARα, PPARβ, and apoA-I antibodies were diluted 1:50 in a dilution buffer (PBS with 1.5% FBS and 0.01% Tween). All proteins were visualized using HRP–AEC (red color) detection kits. Rabbit primary antibodies were replaced by normal rabbit IgG, and the goat primary antibody was replaced by normal goat IgG in the negative controls. Another negative control was obtained by omitting the primary antibodies and using pure dilution buffer.

PAGE and Western blot analysis. Cells grown for 14 d were washed in PBS, incubated in ice-cold extraction buffer (0.1 M Tris-HCl, pH 8.3, 0.5 M NaCl, 5 mM DTT, 5 mM EDTA, and 2 mM PMSF) for 10 min at 4°C, and then harvested in the same buffer. Cells were subjected to ultrasound for 5 × 4 s on ice, and then centrifuged at 16,000 × *g* for 5 min at 4°C. Protein concentration was determined by the method of Lowry *et al*. (33). Approximately 40 μg of protein was loaded into each well on a 10% SDS polyacrylamide gel. Gel electrophoresis was performed at 100 V for about 1 h, and the polypeptides were transferred onto moist PVDF transfer membranes by electroblotting. The membranes were prewetted in 100% methanol and rinsed in distilled water before blotting for 1 h using a Mini Trans-Blot apparatus at 4°C. Protein blots were treated with a blocking solution (PBS containing 5% dry milk and 0.1% Tween) for 1 h at room temperature to block nonspecific binding. The blots were then incubated with anti-PPARα or anti-PPARβ (diluted 1:1500) in PBS-T (PBS with 0.1% Tween) overnight at 4°C. The blots were rinsed in PBS-T for 3 × 15 min and then incubated with HRP-conjugated anti-rabbit antibody (diluted 1:5000) in PBS-T for 1 h at room temperature. Binding was detected by luminescence using high-performance chemiluminescence film.

mRNA-expression of structural proteins and myogenic regulatory proteins. Total RNA (5 μg) was isolated from cells using Trizol and then reverse-transcribed into cDNA using a T-primed First Strand kit. Reverse-transcriptase polymerase chain reaction (RT-PCR) analyses were run on a Gene Amp PCR 2400 system by denaturation at 95°C for 10 min, followed by 35 cycles of amplification at 95°C for 30 s, at 60–62°C for 30 s, and at 72°C for 45 s. Amplified fragments were visualized by agarose gel electrophoresis.

mRNA-expression of apoA-I. Total RNA from cultured muscle cells or salmon head kidney cells (34) was isolated using the RNAeasy mini kit (Quiagen, Chatsworth, CA). RNA (2 μg) was used for cDNA synthesis with TaqMan reverse transcription reagents using oligo-dT primers. The real-time PCR reaction was set up on an ABI Prism 7000 with the SYBR Green PCR master mix reagents (ABI, Midland, Canada). The expression of apoA-I was calculated relative to actin expression using the $2^{-\Delta\Delta C}{}_T$ method (35).

Incubations with radiolabeled FA. Confluent layers of muscle cells were thoroughly washed with serum-free growth medium and incubated in serum-free growth medium containing one of three radiolabeled FA (1 μCi/mL, 20 μM). The radiolabeled FA were added to the media in the form of their potassium salts bound to BSA (the molar ratio of FA to BSA was 2.7:1). Each FA incubation was conducted in five independent parallel experiments (i.e., $n = 5$). Cells were incubated for 48 h at 13°C, and the medium from each culture flask was then removed

for the analysis of radiolabeled lipid classes, acid-soluble products (ASP), and amount of $^{14}CO_2$ produced. The cells were washed twice in PBS and harvested in PBS for the analysis of radiolabeled lipid classes.

Lipid extraction, and analysis of lipid classes and FA composition. Total lipids were extracted from culture media and cells using the method described by Folch *et al.* (36). The chloroform phase was dried under nitrogen gas, and the residual lipid extract was redissolved in hexane. FFA, phospholipids (PL), mono- and diacylglycerols (MDG), and TAG were separated by TLC using a mixture of petroleum ether, diethyl ether, and acetic acid (113:20:2, by vol) as the mobile phase. No sterol esters were found after the separation of lipid classes. The lipids were visualized by spraying the TLC plates with 0.2% (wt/vol) 2´,7´-dichlorofluorescein in methanol, and they were identified by comparison with known standards under UV light. The spots corresponding to FFA, PL, MDG, and TAG were scraped off into vials containing liquid scintillation fluid (InstaGel II Plus; Packard Instruments, Downers Grove, IL) for measurements of radioactivity using a liquid scintillation counter (TRI-CARB 1900 TR, Packard Instruments). The total FA compositions of muscle cells and serum were determined basically as described by Ruyter *et al.* (9). After Folch extraction and TLC, the lipids were transmethylated overnight with 2,2-dimethoxypropane, methanolic HCl, and benzene at room temperature, as described by Mason and Waller (37). The methyl esters of FA were separated in a gas chromatograph (Perkin-Elmer Autosystem GC equipped with an autoinjector and a programmable split/splitless injector) with a CP Wax 52 column (L = 25 m, i.d. = 0.25 mm, DF = 0.2 mm; PerkinElmer, Buckinghamshire, England), FID, and 1022 data system. Helium was used as the carrier gas, and the injector and detector temperatures were set at 280°C. The oven temperature was raised from 50 to 180°C at a rate of 10°C min^{-1}, and then raised to 240°C at a rate of 0.7°C min^{-1}. The relative quantity of each FA present was determined by measuring the area under the peak corresponding to a particular FA.

Measurement of $^{14}CO_2$ from [1-^{14}C]FA oxidation and analyses of ASP. FA oxidation was measured essentially as described by Christiansen *et al.* (38) with minor modifications. [1-^{14}C]-labeled FA, which enabled measurement of one cycle of β-oxidation, were used in the experiment. Gaseous $^{14}CO_2$ produced during the incubation was determined by transferring 1.5 mL of medium to a sealed glass vial with a center well containing Whatman filter paper moistened with 0.3 mL of phenylethylamine/methanol (1:1, vol/vol). The medium was acidified with 0.3 mL of 1 M $HClO_4$. After incubation for 1 h, the wells containing the filter paper were placed into vials for scintillation counting. The quantities of ASP present were determined by acidifying 1 mL of the medium with 0.5 mL of ice-cold 2 M $HClO_4$ and incubating it for 60 min at 4°C. The medium was then centrifuged, and an aliquot of the supernatant was collected for scintillation counting. The remaining supernatant was neutralized with NaOH and analyzed by HPLC on a ChromSep (250 mm × 4.6 mm stainless steel) Inertsil C8-3 column (Chrompack Varian, Inc., Palo Alto, CA). The sample was eluted at a flow rate of 1 mL/min with 0.1 M ammonium dihydrogenphosphate adjusted with phosphoric acid to pH 2.5. Eluted components were detected by a UV detector at 210 nm and an A-100 radioactive detector (Radiomatic Instrument & Chemicals, Tampa, FL) coupled in series to the UV detector. The components in the ASP were identified by co-chromatography with standards.

Statistical analysis. The data were subjected to a one-way ANOVA, and differences were ranked by Duncan's multiple range test. The significance level was set at 5%.

RESULTS

Proliferation and differentiation of myosatellite cells in vitro. Myosatellite cells and differentiated muscle cells (myotubes) in the microscope were easy to recognize by their characteristic morphology. One day after seeding, we observed myosatellite cells with a typical spindle shape, together with more triangularly shaped cells that we considered to be fibroblasts (Fig. 1A). On the second day in culture, most of the myosatellite cells had become more elongated, and some of them had fused with neighboring myosatellite cells. The myosatellite cells continually elongated and fused with other cells until they formed a continuous web of multinucleated muscle cells after 2 wk. However, the degree of differentiation reached by the cells at this stage was heterogenous: Differentiated muscle cells were present together with some cells that still showed a spindle-shaped morphology (Fig. 1B). Growth and differentiation continued during the subsequent days until the muscle cells formed a confluent layer that completely dominated the fibroblasts after 4 wk in culture (Fig. 1C). Cells first stained positive for PCNA on day 2 after seeding, showing that proliferation had started. Approximately 25% of the myosatellite cells stained positive for PCNA after 4 d in culture (Fig. 1D). Confluent cultures did not proliferate 4 wk after seeding. At this stage, the cultures consisted of terminally differentiated (postmitotic) muscle cells.

Expression of mRNA of muscle-specific proteins. The mRNA of α-actin, MLC2, myogenin, and myostatin I were all expressed after 14 d in culture (Fig. 2).

Expression of lipid regulatory proteins and apoA-I. Nuclei of both myosatellite cells and differentiated muscle cells stained intensely positive for PPARα, whereas the cytoplasm showed no staining (Fig. 3A). The staining pattern for PPARβ (Fig. 3B) was the same as that for PPARα. Immunolabeling of apoA-I resulted in an intense staining in the cytoplasm, which was especially prominent near the nuclei (Fig. 3C). Fibroblast-like cells were not stained in any experiment, irrespective of the primary antibody that was used. Controls for all antibodies were very weakly stained, if at all. The negative control for PPARα is shown in Figure 3D. PPARα and PPARβ primary antibodies both labeled one specific band at approximately 50 kDa on Western blots (Fig. 4). The M.W. of the bands corresponded approximately to the M.W. of the same proteins in mammals. The quantity of apoA-I transcripts (relative to actin) determined by real-time PCR showed that the level of apoA-I

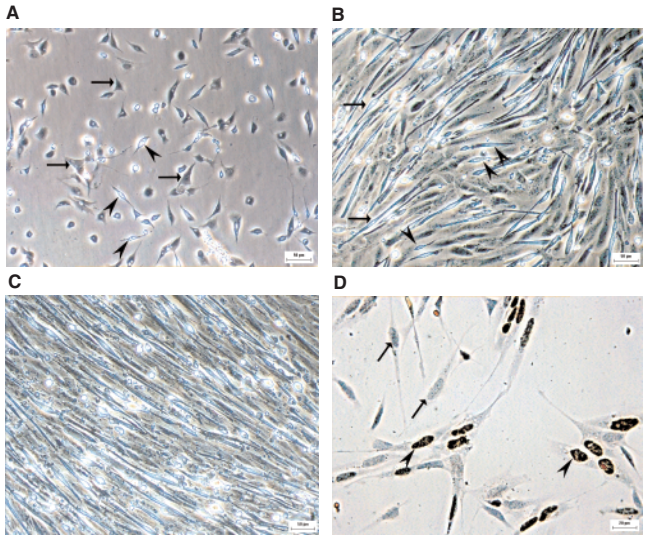

FIG. 1. Micrographs of salmon myosatellite cells and multinucleated muscle cells (myotubes) differentiated in primary culture. (A) Twenty-four hours after seeding, the myosatellite cells were small and showed a characteristic spindle shape (arrowheads), whereas fibroblast-like cells at this stage showed a more triangular shape (arrows). (B) During the following days, the myosatellite cells elongated, and after 14 d in culture, most of them had fused to a web of multinucleated muscle cells (arrows). Some cells still showed the characteristic spindle shape (arrowheads). (C) The muscle cells reached confluence after 4 wk in culture. At this stage, the cultures consisted of terminally differentiated (postmitotic) muscle cells with no fibroblast-like cells or myosatellite cells. (D) Cell proliferation was assessed by immunocytochemical detection of proliferating cell nuclear antigen (PCNA). PCNA-containing nuclei are stained dark brown (arrowheads). Counterstaining with Mayer's hematoxylin gave PCNA-negative nuclei a blue color (arrows). Approximately 25% of the myosatellite cells were labeled with PCNA after 4 d. Micrographs A, B, and C are unstained cells during cultivation; bars = 50 μm. Micrograph D: bar = 20 μm.

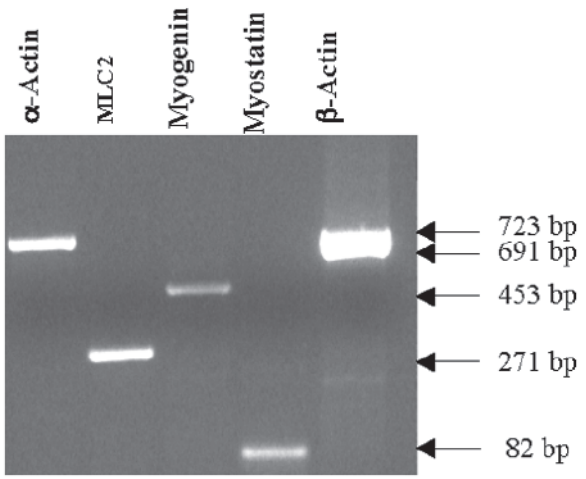

FIG. 2. Expression of structural and myogenic regulatory proteins in salmon muscle cells differentiated in primary culture. The cDNA sequences of α-actin, myosin light-chain 2 (MLC2), myogenin, and myostatin I were amplified by reverse-transcriptase PCR from total RNA. β-Actin cDNA was included as a positive control.

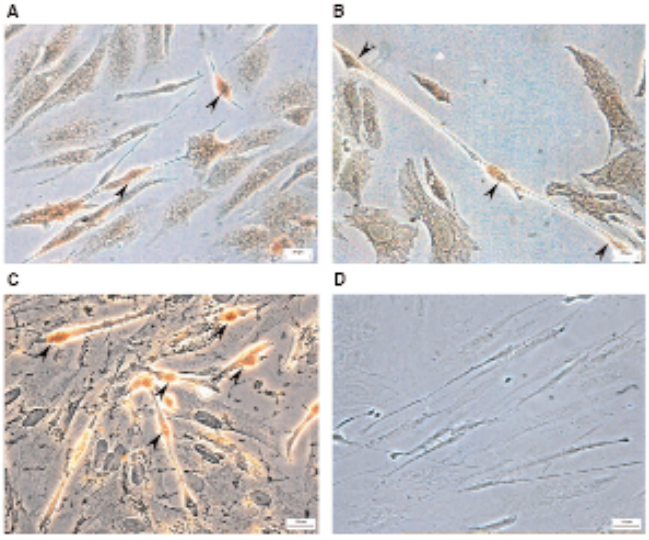

FIG. 3. Micrographs showing the immunocytochemistry of myosatellite cells and myotubes differentiated in primary culture. After 14 d in culture, the cells were immunostained (arrowheads) for (A) peroxisome proliferator-activated receptor α (PPARα), (B) PPARβ, and (C) apolipoprotein A-I (apoA-I). In all cases, the staining was positive in both myosatellite cells and differentiated muscle cells. Both PPAR were expressed in the nuclei, whereas intense apoA-I reactivity was detected in the cytoplasm, especially near the nucleus. Fibroblast-like cells were not stained. (D) Negative controls for all primary antibodies were without immunostaining; the control for PPARα is shown. Bars = 20 μm.

mRNA was about 10 times higher in cultured muscle cells than in a long-term cell line from the salmon head kidney.

FA composition of muscle cells and FBS. The endogenous FA composition of the muscle cells reflected the FA profile of the FBS in the growth medium (Table 1).

Distribution of [1-^{14}C]FA substrates into cellular and secreted lipids and oxidation products. Muscle cells were incubated for 48 h with [1-^{14}C]8:0, [1-^{14}C]18:1n-9, or [1-^{14}C]20:5n-3 to study FA uptake, oxidation, esterification, and secretion. Table 2 presents the incorporation of radioactivity from [1-^{14}C]8:0, [1-^{14}C]18:1n-9, and [1-^{14}C]20:5n-3 substrates into cellular and secreted lipids, oxidation products (ASP and CO_2), and FFA in the culture media. The amounts of radioactivity that were incorporated into each fraction during the 48-h incubation time are expressed as percentages of the recovered radioactivity. The [1-^{14}C]8:0 substrate was primarily oxidized (98%) to [1-^{14}C]ASP and $^{14}CO_2$, with less than 2% esterified into cellular and secreted lipids. Almost 50% of the [1-^{14}C]18:1n-9 and [1-^{14}C]20:5n-3 substrates were oxidized during the 48-h incubation time. However, in contrast to [1-^{14}C]20:5n-3, where 31% of the radioactivity was recovered in cellular lipids, only 18% of the radioactivity from the [1-^{14}C]18:1n-9 substrate was recovered in cellular lipids. Furthermore, nearly twice as much radioactivity was found in secreted lipids after cells had been incubated with [1-^{14}C]20:5n-3 (10%) than when they had been incubated with [1-^{14}C]18:1n-9 (5.3%). Twenty-nine percent of the radioactivity from 18:1n-9 was recovered as FFA in the culture medium, compared with 9% for [1-^{14}C]20:5n-3.

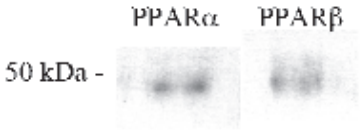

FIG. 4. Western blot showing a single protein band for both PPAR antibodies tested. For abbreviation see Figure 3.

Recovery of [1-^{14}C]FA in lipid classes of muscle cells and culture media. Figure 5A compares the proportional distribution of radioactivity from [1-^{14}C]8:0, [1-^{14}C]18:1n-9, and [1-^{14}C]20:5n-3 in PL, TAG, MDG, and FFA in muscle cells, whereas Figure 5B shows the corresponding results for culture media. Approximately 13% of the total radioactivity was esterified in the PL fraction of the cells with both the [1-^{14}C]20:5n-3 and the [1-^{14}C]18:1n-9 substrates, about 10% was esterified in the nonpolar lipids with the n-3 substrate, and about 3% was esterified with the n-9 substrate. Very small amounts of radioactivity from the 8:0 substrate were esterified in the PL (0.4%) and nonpolar lipids (0.6%) of muscle cells. Approximately 7% of the total radioactivity from the 20:5n-3 substrate was not esterified but was recovered as FFA in the cellular lipids, compared with 1.4% for the 18:1n-9 substrate and 0.1% for the 8:0 substrate. Approximately 5% of the total radioactivity was recovered in the PL fraction of the culture media with the n-3 substrate, and approximately 5% was recovered in nonpolar esterified lipids. Approximately 2% of the total radioactivity was recovered in the PL fraction of the culture media with the n-9 substrate, and approximately 3% was recovered in nonpolar esterified lipids. Almost no radioactivity was recovered in the culture media from the 8:0 substrate.

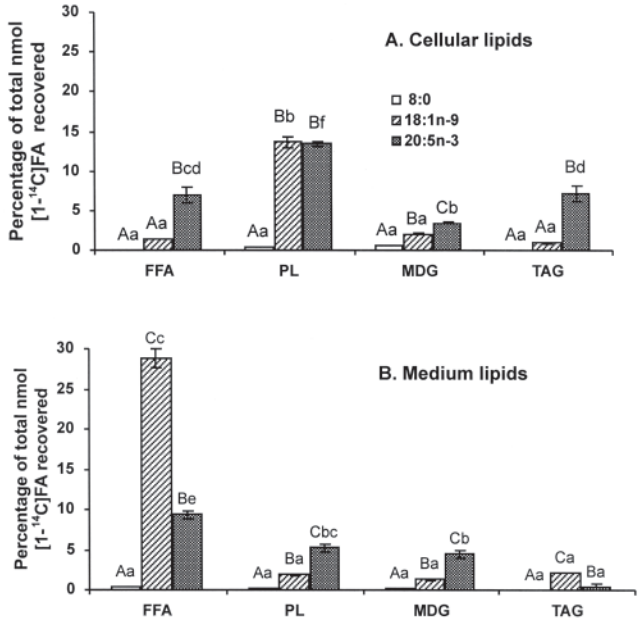

FIG. 5. Percentage distributions of radioactivity from [1-^{14}C]8:0, [1-^{14}C]18:1n-9, and [1-^{14}C]20:5n-3 in cellular and medium lipids. Muscle cells differentiated in primary culture were incubated with one of the radiolabeled FA for 48 h. Total radioactivity recovered in all analyzed fractions (sum of radioactivity incorporated into oxidation products and lipid fractions from cells and media) = 100%. Data are shown as mean ± SEM (n = 5). Different capital letters indicate significant differences between FA; different small letters indicate significant differences between lipid classes for each FA ($P < 0.05$).

TABLE 1
FA Composition of Total Lipid Fraction of Muscle Cells and FBS[a]

FA	Muscle cells	FBS
12:0	0.3 ± 0.31	0.3
14:0	1.1 ± 0.14	1.7
16:0	14.9 ± 0.38	22.3
18:0	8.9 ± 0.39	11.7
20:0	3.8 ± 1.92	0.2
22:0	0.2 ± 0.02	0.5
16:1n-7	2.3 ± 0.21	3.5
18:1n-7	2.1 ± 0.23	2.8
18:1n-9	20.8 ± 1.56	26.3
20:1n-9	1.5 ± 0.43	0.2
22:1n-7	0.3 ± 0.05	0.7
22:1n-11	1.4 ± 0.16	0.8
18:2n-6	12.1 ± 1.73	16.5
20:2n-6	0.4 ± 0.0	0.4
18:3n-3	2.1 ± 0.44	1.3
18:3n-6	0.4 ± 0.0	0.3
20:3n-3		0.3
20:3n-6	4.2 ± 0.19	1.4
18:4n-3	0.3 ± 0.04	0.2
20:4n-3	0.5 ± 0.0	2.2
20:4n-6	9.2 ± 2.50	3.8
22:4n-6	0.4 ± 0.14	0.2
20:5n-3	2.9 ± 0.10	0.7
22:5n-3	1.6 ± 0.39	0.8
22:5n-6	0.2 ± 0.06	0.3
22:6n-3	5.3 ± 0.48	0.8
Others	2.8 ± 1.93	1.3
ΣEPA + DHA	8.2 ± 0.60	1.5
Σ-n-3	12.7 ± 0.85	6.3
Σ-n-6	26.9 ± 0.82	22.9
Σ-n-9	22.3 ± 1.84	26.5

[a]The quantity of each FA is given as a percentage of the total FA. Data from muscle cell analysis are presented as means ± SEM (n = 3).

β-Oxidation products. The amounts of radioactive FA oxidized to $^{14}CO_2$ were similar for the three FA substrates, with approximately 20% of total radioactivity recovered as $^{14}CO_2$ after 48 h of incubation. Significantly more radioactivity from the 8:0 substrate was recovered in [1-^{14}C]-labeled ASP (78%) than was recovered from either of the other two substrates (26–30%) (Table 2). The [1-^{14}C]-labeled ASP fractions were separated by HPLC to determine the metabolic fates of oxidation products from β-oxidation of the FA. Acetate was the main oxidation product for all three FA substrates, accounting for 54 to 64% of the total radioactivity in ASP (Fig. 6). The TCA-cycle products oxaloacetate and malate (ox-mal) accounted for 28.5% of the total radioactivity in the ASP fraction with [1-^{14}C]20:5n-3 as the substrate, and a small amount of radioactivity was recovered in the β-hydroxybutyrate (BHB) fraction (7.5%). No radiolabeled BHB was recovered in the ASP fraction with the [1-^{14}C]8:0 and [1-^{14}C]18:1n-9 substrates. Ox-mal accounted for approximately 45% of the radioactivity in the ASP fraction for both these substrates.

TABLE 2
Percentage Distributions of [1-^{14}C]8:0, [1-^{14}C]18:1n-9, and [1-^{14}C]-20:5n-3 in Total Cellular Lipids (FFA, PL, MDG, TAG) and Secreted Esterified Lipids (PL, MDG, TAG), Medium FFA, Acid-Soluble Products (ASP), and CO_2[a]

	8:0	18:1n-9	20:5n-3
Recovery (nmol)	82.3 ± 5.38[a]	91.7 ± 3.67[a]	90.4 ± 4.18[a]
Cellular lipids	1.0 ± 0.02[a]	18.0 ± 0.23[b]	31.0 ± 0.57[c]
Secreted lipids	0.2 ± 0.01[a]	5.3 ± 0.09[b]	10.0 ± 0.33[c]
FFA in medium	0.4 ± 0.04[a]	28.9 ± 1.25[c]	9.3 ± 0.47[b]
ASP	78.1 ± 4.19[b]	26.5 ± 0.91[a]	30.4 ± 0.99[a]
CO_2	20.3 ± 4.24[a]	21.3 ± 0.31[a]	19.3 ± 0.73[a]

[a]Data are shown as means ± SEM (n = 5). Values with different letters indicate significant differences ($P \geq 0.05$) between FA. The number of nmol added in each incubation was 100. PL, phospholipids; MDG, mono- and diacylglycerols.

DISCUSSION

Morphology and biochemical identity of muscle cells during cultivation. The cells isolated from Atlantic salmon were recognized as myosatellite cells on the basis of their typical morphological spindle shape at an early stage in culture. The cells at a later stage became more elongated and fused with neighboring cells to form multinucleated muscle cells, as described by Matchak and Stickland (31). The myosatellite cell cultures were contaminated with other cell types, mainly fibroblast-like cells, early in the cultivation period. However, the muscle cells gradually became the dominating cell type during cultivation, and the cultures were nearly uncontaminated with other cell types after week 4. We verified the identity of the cells used in our study by verifying their myogenic identity. We did this by verifying their expression of mRNA for the muscle-specific factors α-actin, MLC2, myogenin, and myostatin I (39). The myosatellite cells tended to proliferate until they reached confluence, as do rainbow trout myosatellite cells in culture (40). This contrasts with previous studies of salmon and carp myosatellite cells in culture, in which a low proliferative activity has been reported (31,32).

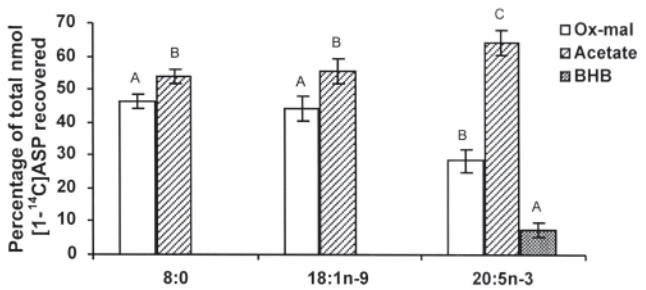

FIG. 6. Percentage distributions of radiolabeled oxaloacetate and malate (ox-mal), acetate, and β-hydroxybutyrate (BHB) from [1-^{14}C]8:0, [1-^{14}C]18:1n-9, and [1-^{14}C]20:5n-3 oxidation. Muscle cells differentiated in primary culture were incubated with one of the radiolabeled FA for 48 h. Total radioactivity recovered as acid-soluble products (ASP) for each FA = 100%. Data are shown as mean ± SEM (n = 5). Different letters indicate significant differences ($P < 0.05$) between the ASP for each FA.

FA oxidation. Nearly all (98.4%) of the 8:0 substrate was oxidized to ASP and CO_2 during the 48-h incubation period, compared with approximately 50% of the two other substrates, 18:1n-9 and 20:5n-3. The more rapid oxidation of the MCFA than of the two LCFA may be due to the effective uptake of [1-^{14}C]8:0 into the muscle cells and because the MCFA can freely pass the muscle cell mitochondrial membranes and does not require the presence of carnitine for transport into the mitochondria. Further, the MCFA does not need carnitine to become extensively oxidized. This agrees with several mammalian liver studies (reviewed in Ref. 10).

HPLC/radiochromatographic analysis of organic acids in ASP from Atlantic salmon muscle cells incubated with [1-^{14}C]8:0, [1-^{14}C]18:1n-9, or [1-^{14}C]20:5n-3 showed that 29–46% of the ASP fraction consisted of the TCA-cycle intermediates ox-mal. This shows that a significant proportion of the acetyl-CoA generated in the mitochondrial FA oxidation was channeled to the TCA-cycle for ATP production in the cultured salmon muscle cells, as is also the case in trout muscle *in vivo* (41). A small amount (7%) of the ASP fraction was found as the ketone body BHB after incubation with the [1-^{14}C]20:5n-3 substrate, whereas no ketone bodies were produced after incubation with the 8:0 or 18:1n-9 substrates. This shows that the fish muscle cells had a relatively low capacity to produce ketone bodies, which agrees with earlier studies (42). In contrast, MCFA usually result in increased ketogenesis in mammals, a result of the rapid and uncontrolled entry into the mitochondria (reviewed in Ref. 10). The major product found in ASP, however, was acetate, which accounted for 50–60% of the total radioactivity in the ASP for all three FA substrates. Several studies have shown that acetate is a major product of FA oxidation in neonatal piglets, which display a low ketogenic capacity (43,44). Acetogenesis can be considered an overflow mechanism for acetyl-CoA in species with a low ketogenic capacity, in the same way ketogenesis has been considered to be an overflow mechanism for acetyl-CoA in species with a high ketogenic capacity. Rat studies have demonstrated that most of the acetyl-CoA generated by FA oxidation in the peroxisomes of hepatocytes is transformed to acetate, whereas in mitochondria, conversion to acetate also occurs but at a minor rate relative to ketogenesis (11,12,15). Our results do not allow us to determine the subcellular origin (mitochondrial or peroxisomal) of the acetate produced in fish muscle cells.

Esterification of FA. Less than 2% of the radioactivity from the [1-^{14}C]8:0 substrate became esterified into cellular lipids during the 48-h incubation, showing that oxidation is the major metabolic fate of MCFA in fish muscle cells. This agrees with results from mammals (reviewed in Ref. 10). The radioactivity in esterified lipids was most probably from elongated forms of 8:0, since the 8:0 itself was unlikely to be incorporated unchanged into glycerolipids. Twice as much radioactivity (31%) from the [1-^{14}C]20:5n-3 substrate was esterified in cellular lipids than was esterified from the [1-^{14}C]18:1n-9 substrate. Nearly 30% of the 18:1n-9 substrate was recovered as FFA in the culture medium in our study, compared with 9% for 20:5n-3. This was probably unmetabolized FFA that had not been

internalized by the muscle cells. Both the higher percentage of [1-^{14}C]20:5n-3 than that of [1-^{14}C]18:1n-9 in the cellular and the secreted lipids, and the higher amount of unmetabolized [1-^{14}C]18:1n-9 showed that [1-^{14}C]20:5n-3 was taken up more rapidly than [1-^{14}C]18:1n-9. This agrees with previous work in our group showing that n-3 FA are more readily esterified than n-6 FA in cellular liver lipids in Atlantic salmon (9). Our results also agree with results from rainbow trout (45). The endogenous FA composition of the cells was strongly influenced by the FA composition of the lipid source of their growth medium, FBS, during the 4-wk growth period. The muscle cells became relatively rich in n-6 and n-9 FA, with relatively low levels of long-chain n-3 FA. The influence of FBS on the FA composition of cultured muscle cells resembles the influence of dietary vegetable oils on the muscle FA composition of Atlantic salmon *in vivo* (46,47). The lower uptake of [1-^{14}C]18:1n-9 into muscle cells, as compared with [1-^{14}C]20:5n-3, may have been affected by the higher endogenous level of 18:1n-9 (20.8%) than that of 20:5n-3 (2.9%).

Small amounts (4–10%) of both LCFA substrates were found esterified in PL and nonpolar lipids in the culture media. We believe that [1-^{14}C]18:1n-9 and [1-^{14}C]20:5n-3 had been assimilated into lipoproteins in the muscle cells and then further secreted into the culture media. Immunolabeling of the muscle cells with anti-apoA-I showed intense staining in an area close to the nucleus, which we believe was the Golgi region. mRNA for apoA-I was also expressed in the muscle cells. This shows that salmon muscle cells synthesize apoA-I, which is the most abundant protein in HDL, and that they probably also secrete lipids into the medium in the form of this lipoprotein. Our results agree with previous results from skeletal muscle in developing chicks, which synthesize and secrete apoA-I-containing HDL (48). In the course of spawning migration, which may be very long, salmon cease feeding. Lipids are mobilized during this period from reserve tissues such as liver, skeletal muscle, and visceral adipose tissue, not only to be used as an energy source, but also to ensure the formation of genital products. Carotenoids, particularly astaxanthin, are also transported from the muscle where they are stored in the skin and gonads during sexual maturation (reviewed in Ref. 49). Astaxanthin is transported by HDL and vitellogenin in the plasma of the chum salmon (reviewed in Ref. 49). It has been reported that the levels of VLDL and LDL decrease sharply in pink salmon during fasting, whereas that of HDL remains high even after a very long period without eating (50). It is therefore tempting to assume that HDL secreted from the muscle mediates a direct transport of excess lipid and astaxanthin to the gonads, comparable to the transport of lipids from the liver to the gonads that is mediated by vitellogenin and VLDL.

Lipid regulatory proteins. We used immunocytochemical staining with antibodies against PPARα and PPARβ to establish whether the muscle cells expressed proteins known to regulate lipid metabolism in mammals. Intense staining showed that both proteins were expressed in the cell nuclei. This is the first time these transcription factors have been shown to be present in salmon muscle cells. Future studies will focus on the function of these factors in fish muscle and the complex interrelationships of the factors that influence cellular uptake and intracellular metabolism of FA. In addition, it will be interesting to determine the mitochondrial and peroxisomal capacities for β-oxidation in salmon muscle cells, considering their relative contribution to total β-oxidation and their metabolic fuel preferences.

We have shown that salmon muscle cells differentiated in primary culture are well suited as a model system for studies of lipid metabolism in fish muscle. The muscle cells express lipid regulatory transcription factors and exhibit a high FA oxidative capacity. The major oxidation products are acetate and TCA-cycle intermediates (ox-mal), whereas only low levels of ketone bodies are produced.

ACKNOWLEDGMENTS

The authors are grateful to Inger Ø. Kristiansen for technical assistance during the project. We thank Harald Støkken for his skillful work in the aquarium division. The Norwegian Research Council and Nutreco ARC supported the work.

REFERENCES

1. Bilinski, E. (1963) Utilization of Lipids by Fish. I. Fatty Acid Oxidation by Tissue Slices from Dark and White Muscle of Rainbow Trout (*Salmo gairdnerii*), *Can. J. Biochem. Physiol. 41*, 107–112.
2. Frøyland, L., Madsen, L., Eckhoff, K.M., Lie, Ø., and Berge, R. (1998) Carnitine Palmitoyltransferase I, Carnitine Palmitoyltransferase II, and Acyl-CoA Oxidase Activities in Atlantic Salmon (*Salmo salar*), *Lipids 33*, 923–930.
3. Richards, J.G., Heigenhauser, G.J.F., and Wood, C.M. (2002) Lipid Oxidation Fuels Recovery from Exhaustive Exercise in White Muscle of Rainbow Trout, *Am. J. Physiol. 282*, R89–R99.
4. Zhou, S., Ackman, R., and Morrison, C. (1995) Storage of Lipids in the Myocepta of Atlantic Salmon (*Salmo salar*), *Fish Physiol. Biochem. 14*, 171–178.
5. Frøyland, L., Lie, Ø., and Berge, R. (2000) Mitocondrial and Peroxisomal β-Oxidation Capacities in Various Tissues from Atlantic Salmon (*Salmo salar*), *Aquacult. Nutr. 6*, 85–89.
6. Torstensen, B.E., Lie, Ø., and Frøyland, L. (2000) Lipid Metabolism and Tissue Composition in Atlantic Salmon (*Salmo salar* L.)—Effects of Capelin Oil, Palm Oil, and Oleic Acid-Enriched Sunflower Oil as Dietary Lipid Sources, *Lipids 35*, 653–664.
7. Hamre, K., and Lie, Ø. (1995) α-Tocopherol Levels in Different Organs of Atlantic Salmon (*Salmo salar*)—Effect of Smoltification, Dietary Levels of n-3 Polyunsaturated Fatty Acids and Vitamin E, *Comp. Biochem. Physiol. 111A*, 547–554.
8. Ruyter, B., and Thomassen, M.S. (1999) Metabolism of n-3 and n-6 Fatty Acids in Atlantic Salmon Liver: Stimulation by Essential Fatty Acid Deficiency, *Lipids 34*, 1167–1176.
9. Ruyter, B., Røsjø, C., Grisdal-Helland, B., Rosenlund, G., Obach, A., and Thomassen, M.S. (2003) Influence of Temperature and High Dietary Linoleic Acid Content on Esterification, Elongation, and Desaturation of PUFA in Atlantic Salmon Hepatocytes, *Lipids 38*, 833–840.
10. Papamandjaris, A.A., MacDougall, D.E., and Jones, P.J.H. (1998) Medium Chain Fatty Acid Metabolism and Energy Expenditure: Obesity Treatment Implications, *Life Sci. 14*, 1203–1215.
11. Tran, T.N., and Christophersen, B.O. (2001) Studies on the Transport of Acetyl Groups from Peroxisomes to Mitochondria in Isolated Liver Cells Oxidizing the Polyunsaturated Fatty Acid 22:4n-6, *Biochim. Biophys. Acta 1533*, 255–265.
12. Tran, T.N., and Christophersen, B.O. (2002) Partitioning of Polyunsaturated Fatty Acid Oxidation Between Mitochondria and Peroxisomes in Isolated Rat Hepatocytes Studied by HPLC

Separation of Oxidation Products, *Biochim. Biophys. Acta 1583*, 195–204.
13. Crockett, E.L., and Sidell, B.D. (1993a) Substrate Selectivities Differ for Hepatic Mitochondrial and Peroxisomal β-Oxidation in an Antarctic Fish, *Notothenia gibberifrons, Biochem. J. 289*, 427–433.
14. Crockett, E.L., and Sidell, B.D. (1993b) Peroxisomal β-Oxidation Is a Significant Pathway for Catabolism of Fatty Acids in a Marine Teleost, *Am. J. Physiol. 264*, R1004–R1009.
15. Leighton, F., Bergseth, S., Rørtveit, T., Christiansen, E.N., and Bremer, J. (1989) Free Acetate Production by Rat Hepatocytes During Peroxisomal Fatty Acid and Dicarboxylic Acid Oxidation, *J. Biol. Chem. 264*, 10347–10350.
16. Luzzana, U., Serrini, G., Moretti, V.M., Gianesini, C., and Valfre, F. (1994) Effect of Expanded Feed with High Fish Oil Content on Growth and Fatty Acid Composition of Rainbow Trout, *Aquacult. Int. 2*, 239–248.
17. Weatherup, R.N., McCracken, K.J., Foy, R., Rice, D., McKendry, J., Mairs, R.J., and Hoey, R. (1997) The Effects of Dietary Fat Content on Performance and Body Composition of Farmed Rainbow Trout (*Oncorhynchus mykiss*), *Aquaculture 151*, 173–184.
18. Bell, J.G., McEvoy, J., Webster, J.L., McGhee, F., Millar, R.M., and Sargent, J.R. (1998) Flesh Lipid and Carotenoid Composition of Scottish Farmed Atlantic Salmon (*Salmo salar*), *J. Agric. Food Chem. 46*, 119–127.
19. Hemre, G.-I., and Sandnes, K. (1999) Effect of Dietary Lipid Level on Muscle Composition in Atlantic Salmon (*Salmo salar*), *Aquacult. Nutr. 5*, 9–16.
20. Torstensen, B.E., Lie, Ø., and Hamre, K. (2001) A Factorial Experimental Design for Investigation of Effects of Dietary Lipid Content and Pro- and Antioxidants on Lipid Composition in Atlantic Salmon (*Salmo salar*) Tissues and Lipoproteins, *Aquacult. Nutr. 7*, 265–276.
21. Sargent, J.R., Tocher, D.R., and Bell, J.G. (2002) The Lipids, in *Fish Nutrition*, 3rd edn. (Halver, J.E., ed.), pp. 181–257, Academic Press, San Diego.
22. Göttlicher, M., Widmark, E., Li, Q., and Gustafsson, J.A. (1992) Fatty Acids Activate a Chimera of the Clofibric Acid Activated Receptor and the Rlucocorticoid Receptor, *Proc. Natl. Acad. Sci. USA 89*, 4653–4657.
23. Ruyter, B., Andersen, Ø., Dehli, A., Östlund Farrants, A.-K., Gjøen, T., and Thomassen, M.S. (1997) Peroxisome Proliferator Activated Receptors in Atlantic Salmon (*Salmo salar*): Effects on PPAR Transcription and Acyl-CoA Oxidase Activity in Hepatocytes by Peroxisome Proliferators and Fatty Acids, *Biochim. Biophys. Acta 1348*, 331–338.
24. Andersen, Ø., Eijsink, V.G., and Thomassen, M. (2000) Multiple Variants of the Peroxisome Proliferator-Activated Receptor (PPAR) γ Are Expressed in the Liver of Atlantic Salmon (*Salmo salar*), *Gene 255*, 411–418.
25. Vegusdal, A., Sundvold, H., Gjøen, T., and Ruyter, B. (2003) An *in vitro* Method for Studying the Proliferation and Differentiation of Atlantic Salmon Preadipocytes, *Lipids 38*, 289–296.
26. Leaver, M.J., Wright, J., and George, S.G. (1998) A Peroxisome Proliferator-Activated Receptor Gene from the Marine Flatfish, the Plaice (*Pleuronectes platessa*), *Mar. Environ. Res. 46*, 75–79.
27. Maglich, J.M., Caravella, J.A., Lambert, M.H., Willson, T.M., Moore, J.T., and Ramamurthy, L. (2003) The First Completed Genome Sequence from a Teleost Fish (*Fugu rubripes*) Adds Significant Diversity to the Nuclear Receptor Superfamily, *Nucleic Acids Res. 31*, 4051–4058.
28. Schoonjans, K., Staels, B., and Auwerx, J. (1996) The Peroxisome Proliferator-Activated Receptors (PPARs) and Their Effects on Lipid Metabolism and Adipocyte Differentiation, *Biochim. Biophys. Acta 1302*, 93–109.
29. Muoio, D.M., MacLean, P.S., Lang, D.B., Li, S., Houmard, J.A., Way, J.M., Winegar, D.A., Corton, J.C., Dohm, G.L., and Kraus, W.E. (2002) Fatty Acid Homeostasis and Induction of Lipid Regulatory Genes in Skeletal Muscles of Peroxisome Proliferator-Activated Receptor (PPAR) α Knock-Out Mice. Evidence for Compensatory Regulation by PPAR δ, *J. Biol. Chem. 277*, 26089–26097.
30. Wang, Y.-X., Lee, C.-H., Tiep, S., Yu, R.T., Ham, J., Kang, H., and Evans, R.M. (2003) Peroxisome Proliferator-Activated Receptor δ Activates Fat Metabolism to Prevent Obesity, *Cell 113*, 159–170.
31. Matchak, T.W., and Stickland, N.C. (1995) The Growth of Atlantic Salmon (*Salmo salar L.*) Myosatellite Cells in Culture at Two Different Temperatures, *Experientia 51*, 260–266.
32. Koumans, J.T.M., Akster, H.A., Dulos, G.J., and Osse, J.W.M. (1990) Myosatellite Cells of *Cyprinus carpio* (Teleostei) *in vitro*: Isolation, Recognition and Differentiation, *Cell Tissue Res. 261*, 173–181.
33. Lowry, O.H., Rosebrough, N.J., Farr, A.L., and Randall, R.J. (1951) Protein Measurement with the Folin Phenol Reagent, *J. Biol. Chem. 193*, 265–275.
34. Dannevig, B.H., Falk, K., and Press, C.M. (1995) Propagation of Infectious Salmon Anaemia (ISA) Virus in Cell Culture, *Vet. Res. 26*, 438–442.
35. Livak, K.J., and Schmittgen, T.D. (2001) Analysis of Relative Gene Expression Data Using Real-Time Quantitative PCR and the $2^{-\Delta\Delta C}_{T}$ Method, *Methods 25*, 402–408.
36. Folch, A.C., Lees, M., and Sloane Stanley, G.H. (1957) A Simple Method for the Isolation and Purification of Total Lipids from Animal Tissues, *J. Biol. Chem. 226*, 497–509.
37. Mason, M.E., and Waller, G.R. (1964) Dimethoxypropane Induces Transesterification of Fats and Oils in Preparation of Methylesters for Gas Chromatographic Analysis, *Anal. Chem. 36*, 583.
38. Christiansen, R., Borrebaeck, B., and Bremer, J. (1976) The Effect of (–)Carnitine on the Metabolism of Palmitate in Liver Cells Isolated from Fasted and Refed Rats, *FEBS Lett. 62*, 313–317.
39. Østbye, T.-K., Galloway, T.F., Nielsen, C., Gabestad, I., Bardal, T., and Andresen, Ø. (2001) The Two Myostatin Genes of Atlantic Salmon (*Salmo salar*) Are Expressed in a Variety of Tissues, *Eur. J. Biochem. 268*, 5249–5257.
40. Valente, L.M.P., Paboeuf, G., and Fauconneau, B. (2002) Effect of Genetic Origin of the Fish on *in vitro* Proliferation of Muscle Myosatellite Cells of Rainbow Trout, *J. Fish Biol. 61*, 594–605.
41. Moyes, C.D., Schulte, P.M., and Hochachka, P.W. (1992) Recovery Metabolism of Trout White Muscle: Role of Mitochondria, *Am. J. Physiol. 262*, R295–R304.
42. Soengas, J.L., Strong, E.F., Fuentes, J., Veira, J.A.R., and Andrés, M.D. (1996) Food Deprivation and Refeeding in Atlantic Salmon, *Salmo salar*: Effects on Brain and Liver Carbohydrate and Ketone Bodies Metabolism, *Fish Physiol. Biochem. 15*, 491–511.
43. Lin, X., Adams, S.H., and Odle, J. (1996) Acetate Represents a Major Product of Heptanoate and Octanoate β-Oxidation in Hepatocytes Isolated from Neonatal Piglets, *Biochem. J. 318*, 235–240.
44. Adams, S.H., Lin, X., Yu, X.X., Odla, J., and Drackley, J.K. (1997) Hepatic Fatty Acid Metabolism in Pigs and Rats: Major Differences in End Products, O_2 Uptake and β-Oxidation, *Am. J. Physiol. 272*, R1641–R1646.
45. Hagve, T.-A., Christophersen, B.O., and Dannevig, B.H. (1986) Desaturation and Chain Elongation of Essential Fatty Acids in Isolated Liver Cells from Rat and Rainbow Trout, *Lipids 21*, 202–205.
46. Grisdale-Helland, B., Ruyter, B., Rosenlund, G., Obach, A., Helland, S.J., Sandberg, M.G., Standal, H., and Røsjø, C. (2002) Influence of High Contents of Dietary Soybean Oil on Growth,

Feed Utilization, Tissue Fatty Acid Composition, Heart Histology and Standard Oxygen Consumption of Atlantic Salmon (*Salmo salar*) Raised at Two Temperatures, *Aquaculture 207*, 311–329.
47. Bell, J.G., Henderson, R.J., Tocher, D.R., McGhee, F., Dick, J.R., Porter, A., Smullen, R.P., and Sargent, J.R. (2002) Substituting Fish Oil with Crude Palm Oil in the Diet of Atlantic Salmon (*Salmo salar*) Affects Muscle Fatty Acid Composition and Hepatic Fatty Acid Metabolism, *J. Nutr. 132*, 222–230.
48. Tarugi, P., Reggiani, D., Ottaviani, E., Ferari, S., Tiozzo, R., and Calandra, S. (1989) Plasma Lipoproteins, Tissue Cholesterol Overload, and Skeletal Muscle Apolipoprotein A-I Synthesis in the Developing Chick, *J. Lipid Res. 30*, 9–22.
49. Babin, P.J., and Vernier, J.-M. (1989) Plasma Lipoproteins in Fish, *J. Lipid Res. 30*, 467–489.
50. Nelson, G.J., and Shore, V.G. (1974) Characterization of the Serum High Density Lipoproteins of Pink Salmon, *J. Biol. Chem. 249*, 536–542.

[Received March 5, 2004; accepted August 26, 2004]

Synthesis, Spectroscopic, and Biological Studies of Novel Estolides Derived from Anticancer Active 4-*O*-Podophyllotoxinyl 12-Hydroxyl-octadec-*Z*-9-enoate

Jamal Mustafa[a], Shabana I. Khan[a], Guoyi Ma[a], Larry A. Walker[a,b], and Ikhlas A. Khan[a,c,*]

[a]National Center for Natural Products Research, Research Institute of Pharmaceutical Sciences, [b]Department of Pharmacology, and [c]Department of Pharmacognosy, School of Pharmacy, University of Mississippi, University, Mississippi 38677

ABSTRACT: Podophyllotoxin is a well-known natural antitumor agent with severe side effects, which led us to synthesize its numerous analogs in search of product(s) of improved therapeutic potential. Here, we report an efficient method for the synthesis of a series of 4-*O*-podophyllotoxin estolides with spectral characteristics and their biological studies. The OH of a known molecule, 4-*O*-podophyllotoxinyl 12-hydroxyl-octadec-Z-9-enoate **2**, was coupled with the carboxylic groups of different FA with the help of dicyclohexylcarbodiimide and dimethyl aminopyridine (catalyst) to produce high yields of their respective $C_4\alpha$-estolides **3–11**. Spectroscopic techniques, particularly ^1H and ^{13}CNMR, proved to be suitable tools to characterize the new compounds. These molecules of greater lipophilic character were tested for their *in vitro* cytotoxicity against four human solid tumors, one human leukemia cell, and one noncancerous cell. Compounds **4–6** and **11** showed moderate antileukemic activity; unexpectedly, none were found to be active against solid tumors. Estolides were also investigated for their *in vitro* activity against tubulin and topoisomerase II proteins. All the compounds showed inhibition of the catalytic activity of topoisomerase II, whereas **6–8** also inhibited tubulin polymerization. These results suggest the need for further screening of these molecules against a larger panel of cancerous cells.

Paper no. L9503 in *Lipids 39*, 659–666 (July 2004).

Podophyllotoxin **1** is isolated from various plant species and is particularly abundant in those of the genus *Podophyllum* (1). It is one of the natural products widely known for its anticancer activity (1,2). However, clinical use of **1** and its analogs is restricted because of its severe side effects (3–5). Extensive chemical modifications of the structure of **1** have resulted in the development of glycosylated semisynthetic etoposide and teniposide for clinical use to treat several cancers (4,6–8). However, their aqueous solubility, bioavailability, metabolic inactivation, drug resistance, and myelosuppression have limited their clinical applications (9,10). The recent research in this area has focused mainly on the development of new podophyllotoxin analogs with the aim of overcoming these difficulties.

The progress of podophyllotoxins, from their early applications in folk medicine to the most recent chemical transformations, and their mechanism(s) of action, pharmacological potential, and structure–activity relationships are remarkable (1,10,11). However, the synthesis and possible therapeutic potential of FA-based podophyllotoxin formulations have been unexplored until recently, when Nagao *et al.* (12) first reported the synthesis of such congeners and their strong activity against P388 lymphocytic leukemia in mice. In a recent study, we demonstrated the synthesis of new $C_4\alpha$-FA analogs of podophyllotoxin and their *in vitro* cytotoxicity against a panel of human cancerous and normal cell lines (13). Some of them were as potent as the parent molecule against several tumor cell lines, and a noticeable feature was their selective inhibition toward cancerous cells.

The potential of FA to reduce or eliminate the multidrug resistance to cancers in humans or animals (14) and to prevent the side effects of chemotherapy (15) is known from the literature. There is also evidence that submicron-sized lipid emulsions with lipophilic drugs entrapped in the oil core can act as a novel drug carrier system with many potential applications (16). The quest for improved clinical activity may be an important stimulus for undertaking chemical and biological investigations of a variety of unusual FA derivatives of podophyllotoxin as we search for chemotherapeutic agents for human cancers. On the basis of these discoveries and considerations, we designed a new series of $C_4\alpha$-estolide derivatives of podophyllotoxin (Scheme 1). The hydroxyl group at the 12-carbon of the FA side chain in a previously reported (13) 4-*O*-podophyllotoxinyl 12-hydroxyl-octadec-*Z*-9-enoate[1] **2** molecule was exploited to incorporate further FA components to produce estolides (dimers and trimers). The FA used in this study had different degrees of Z-unsaturated (C_{18}, C_{20}), terminal unsaturated (C_{11}), saturated (C_{20}), and hydroxyl-*Z*-ene (C_{18}) functionalities. In the current study, we describe the method of synthesis and report the

*To whom correspondence should be addressed at National Center for Natural Products Research, Research Institute of Pharmaceutical Sciences, School of Pharmacy, University of Mississippi, University, MS 38677.
E-mail: ikhan@olemiss.edu

Abbreviations: BT549, ductal breast carcinoma cell line; DCC, dicyclohexylcarbodiimide; DMAP, dimethyl aminopyridine; HL-60, human leukemia cell line; IC_{50}, concentration of a test compound that prevented 50% of the substrate from being converted to the product; KB, human epidermal carcinoma cell line; kDNA, kinetoplast DNA; SK-MEL, human malignant melanoma cell line; SK-OV3, human ovary carcinoma cell line; VERO, monkey kidney fibroblast cell line.

[1]Selected by National Cancer Institute (Bethesda, MD) for *in vitro* anitumor screening; consists of 60 human tumor cell lines.

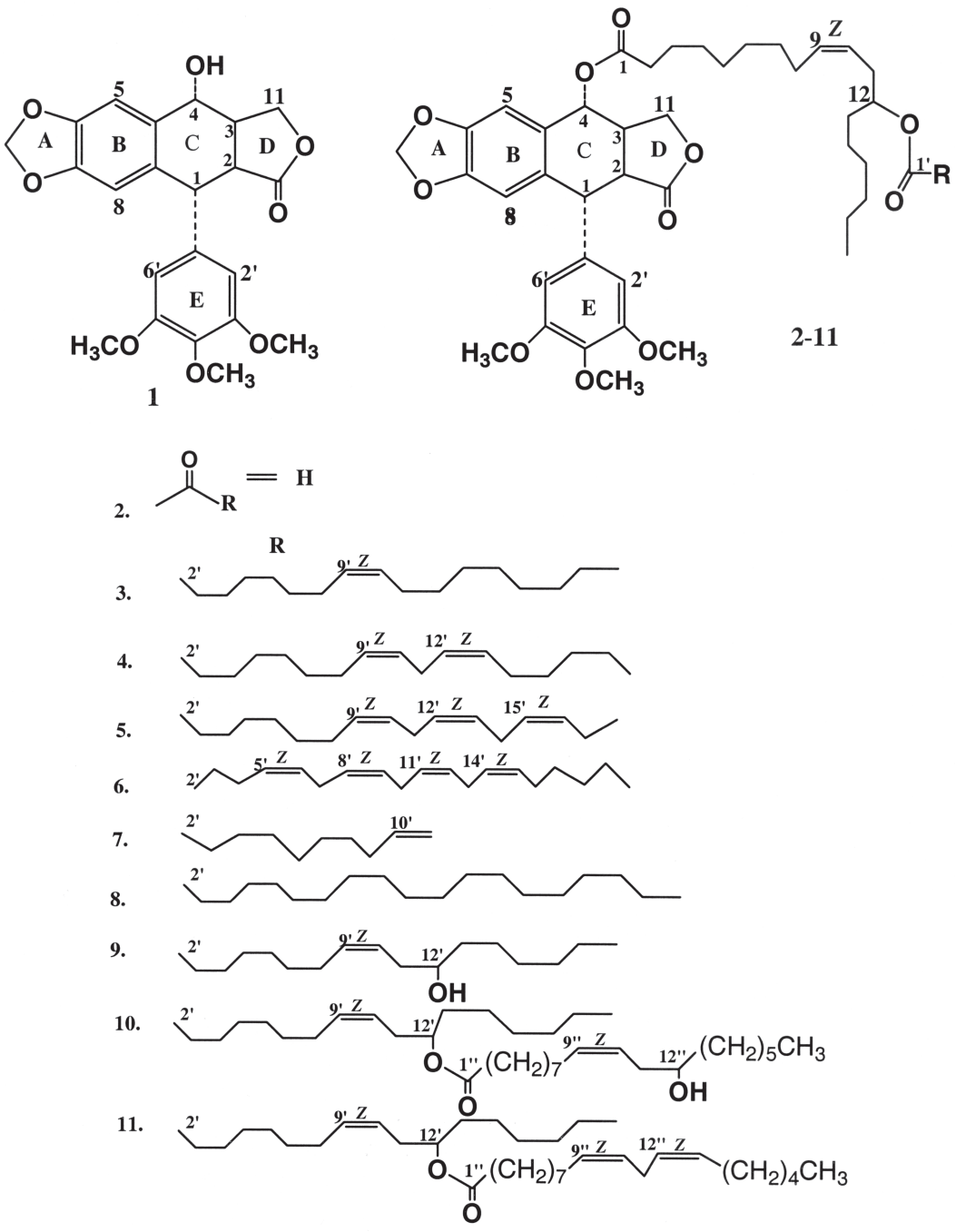

SCHEME 1

IR, ^{1}H NMR, ^{13}C NMR, and high-resolution MS data used to establish the structures of this new class of relatively complex $C_4\alpha$-estolides of podophyllotoxin. We also present the findings of our evaluation of this series of compounds for their *in vitro* effects against specific cancer cell lines, i.e., SK-MEL, KB, BT-549, SK-OV-3 (human solid tumors) and HL-60 (human leukemia), and their action on tubulin and topoisomerase II.

MATERIALS AND METHODS

The method of synthesizing 4-*O*-podophyllotoxinyl 12-hydroxyl-octadec-*Z*-9-enoate **2**, all the experimental procedures, the sources of reagents, dicyclohexylcarbodiimide (DCC), dimethyl aminopyridine (DMAP), FA, and podophyllotoxin were similar to those reported previously (13).

*Chemical procedures. (i) General method for the synthesis of podophyllotoxin $C_4\alpha$-estolides **3–11** (dimers and trimers).*

To a solution of 4-*O*-podophyllotoxinyl 12-hydroxyl-octadec-*Z*-9-enoate **2** (1 mmol) or 4-*O*-podophyllotoxinyl 12-(12′-hydroxyl-octadec-*Z*-9′-enacyloxy)octadec-*Z*-9-enoate **9** (1 mmol) in dry methylene chloride (5 mL) were added an appropriate FA (1 mmol) and a catalytic amount of DMAP under nitrogen atmosphere; the reaction mixture was then stirred for 10 min at room temperature. To this mixture was added DCC (1 mmol), and the reaction was stirred further. The progress of the reaction was monitored on a silica gel TLC plate, which showed the formation of a single product in all reactions. The reaction time for estolide-forming coupling reactions was recorded as 1 h. A white solid, dicyclohexylcarbonylurea, was removed by filtration. The organic layer was concentrated under vacuum at 20°C. The crude semisolid product was purified by silica gel flash column chromatography with *n*-hexane/ethyl acetate (1:1, vol/vol) as eluent.

(ii) 4-O-*Podophyllotoxinyl 12-(octadec-Z-9′-enacyloxy)-octadec-Z-9-enoate* ***3***. Viscous, colorless oil; R_f = 1.0 (*n*-hexane/ethyl acetate, 1:1 vol/vol, as developer), isolated yield, 99.5%. IR ($CHCl_3$, cm^{-1}): 1781, 1714, 1588, 1504, 1484, 1239, 1172, 1128, 1039, 990; ^1H NMR ($CDCl_3$, δ_H): 0.86 (*t*, *J* = 6.88 Hz, 6H), 1.31–1.26 (*br m*, 36H, $18CH_2$ of 2 × FA units), 1.53 (*m*, 2H), 1.60 (*m*, 2H), 1.60 (*m*, 2H), 1.99 (*m*, 6H), 2.28 (*m*, 4H), 2.42 (*m*, 2H), 2.81 (*m*, 1H), 2.90 (*dd*, $J_{1,2}$ = 4.41 Hz, $J_{2,3}$ = 14.50 Hz, 1H), 3.74 (*s*, 6H), 3.79 (*s*, 3H), 4.18 (*t*, *J* = 10.10 Hz, 1H), 4.34 (*dd*, *J* = 9.0 Hz, *J* = 7 Hz, 1H), 4.58 (*d*, $J_{1,2}$ = 4.26 Hz, 1H), 4.87 (*m*, 1H), 5.32 (*m*, 3H), 5.45 (*m*, 1H), 5.87 (*d*, $J_{3,4}$ = 9.1 Hz, 1H), 5.95 (*d*, *J* = 2.50 Hz, 1H), 5.96 (*d*, *J* = 2.50 Hz, 1H), 6.38 (*s*, 2H), 6.52 (*s*, 1H), 6.74 (*s*, 1H); ^{13}C NMR ($CDCl_3$, δ_C): 14.43, 14.64, 20.93, 22.94, 25.38, 25.49, 25.73, 25.92, 26.01, 27.59, 27.70, 29.51, 29.57, 29.91, 29.97, 32.12, 32.39, 34.02, 34.75, 35.05, 39.17, 44.15, 45.97, 56.54, 61.10, 71.76, 73.80, 74.05, 101.97, 107.36, 108.60, 110.11, 124.81, 127.51, 128.12, 128.63, 128.67, 128.86, 130.63, 132.32, 132.78, 135.22, 137.65, 147.99, 148.50, 153.04, 173.89, 174.02, 174.55; electrospray ionization (ESI)-MS found $[M + Na]^+$ 981.6062; $C_{58}H_{86}O_{11}Na$ $[M + Na]^+$ requires 981.60622.

(iii) 4-O-*Podophyllotoxinyl 12-(octadec-Z-9′,12′-dienacyloxy)octadec-Z-9-enoate* ***4***. Viscous colorless oil; R_f = 1.0 (*n*-hexane/ethyl acetate, 1:1 vol/vol, as developer), isolated yield, 99.5%. IR ($CHCl_3$, cm^{-1}): 1773, 1725, 1588, 1507, 1484, 1239, 1173, 1127, 1037, 998; ^1H NMR ($CDCl_3$, δ_H): 0.89 (*m*, 6H), 1.33–1.27 (*br m*, 30H, $15CH_2$ of 2 × FA units), 1.54 (*m*, 2H), 1.61 (*m*, 2H), 1.68 (*m*, 2H), 2.06 (*m*, 6H), 2.29 (*m*, 4H), 2.43 (*m*, 2H), 2.77 (*m*, 2H), 2.84 (*m*, 1H), 2.91 (*dd*, $J_{1,2}$ = 4.42 Hz, $J_{2,3}$ = 14.52 Hz, 1H), 3.75 (*s*, 6H), 3.80 (*s*, 3H), 4.19 (*t*, *J* = 10.03 Hz, 1H), 4.35 (*dd*, *J* = 9.01 Hz, *J* = 7.18 Hz, 1H), 4.59 (*d*, $J_{1,2}$ = 4.33 Hz, 1H), 4.88 (*m*, 1H), 5.40–5.32 (*br m*, 5H), 5.46 (*m*, 1H), 5.88 (*d*, $J_{3,4}$ = 9.13 Hz, 1H), 5.96 (*d*, *J* = 2.51 Hz, 1H), 5.97 (*d*, *J* = 2.5 Hz, 1H), 6.40 (*s*, 2H), 6.53 (*s*, 1H), 6.75 (*s*, 1H); ^{13}C NMR ($CDCl_3$, δ_C): 14.40, 22.91, 25.37, 25.48, 25.71, 26.01, 27.56, 27.68, 29.50, 29.55, 29.70, 29.89, 29.97, 31.88, 32.10, 32.39, 34.02, 34.74, 35.04, 39.17, 44.16, 45.96, 56.54, 61.06, 71.73, 73.81, 74.04, 101.94, 107.35, 108.64, 109.99, 110.09, 124.81, 128.30, 128.43, 128.89, 130.39, 130.56, 132.75, 135.21, 137.71, 147.99, 148.50, 153.05, 173.82, 173.97, 174.51; ESI-MS found $[M + Na]^+$ 979.5947; $C_{58}H_{84}O_{11}Na$ $[M + Na]^+$ requires 979.59052.

(iv) 4-O-*Podophyllotoxinyl 12-(octadec-Z-9′,12′,15′-trienacyloxy)octadec-Z-9-enoate* ***5***. Viscous colorless oil; R_f = 1.0 (*n*-hexane/ethyl acetate, 1:1 vol/vol, as developer), isolated yield, 99%. IR ($CHCl_3$, cm^{-1}): 1769, 1729, 1588, 1484, 1239, 1178, 1127, 1037, 998; ^1H NMR ($CDCl_3$, δ_H): 0.88 (*t*, *J* = 7.06 Hz, 3H), 0.98 (*t*, *J* = 7.54 Hz, 3H), 1.33–1.27 (*br m*, 26H, $13CH_2$ of 2 × FA units), 1.60 (*m*, 2H), 1.65 (*m*, 2H), 1.68 (*m*, 2H), 2.05 (*m*, 4H), 2.28 (*m*, 4H), 2.42 (*m*, 2H), 2.85–2.80 (*m*, 5H), 2.92 (*dd*, $J_{1,2}$ = 4.45 Hz, $J_{2,3}$ = 14.52 Hz, 1H), 3.76 (*s*, 6H), 3.81 (*s*, 3H), 4.20 (*t*, *J* = 9.64 Hz, 1H), 4.36 (*dd*, *J* = 9.14 Hz, *J* = 7.10, 1H), 4.61 (*d*, $J_{1,2}$ = 4.34 Hz, 1H), 4.88 (*m*, 1H), 5.40–5.30 (*m*, 7H), 5.45 (*m*, 1H), 5.89 (*d*, $J_{3,4}$ = 9.18 Hz, 1H), 5.98 (*d*, *J* = 2.51 Hz, 1H), 5.99 (*d*, *J* = 2.5 Hz, 1H), 6.40 (*s*, 2H), 6.54 (*s*, 1H), 6.75 (*s*, 1H); ^{13}C NMR ($CDCl_3$, δ_C): 14.47, 14.68, 20.93, 22.94, 25.38, 25.49, 25.73, 25.92, 26.01, 27.59, 27.70, 29.51, 29.57, 29.91, 29.97, 32.12, 32.39, 34.02, 34.75, 35.05, 39.17, 44.15, 45.97, 56.54, 61.10, 71.76, 73.80, 74.05, 101.97, 107.36, 108.60, 110.11, 124.81, 127.51, 128.12, 128.63, 128.67, 128.83, 130.65, 132.33, 132.72, 135.22, 137.65, 147.99, 148.50, 153.04, 173.89, 174.02, 174.55; EI-MS found $[M + Na]^+$ 977.5750; $C_{58}H_{82}O_{11}Na$ $[M + Na]^+$ requires 977.57492.

(v) 4-O-*Podophyllotoxinyl 12-(eicosa-Z-5′,8′,11′,14′-tetraenacyloxy)octadec-Z-9-enoate* ***6***. Viscous colorless oil; R_f = 1.0 (*n*-hexane/ethyl acetate, 1:1 vol/vol, as developer), isolated yield, 98.5%. IR ($CHCl_3$, cm^{-1}): 1779, 1729, 1588, 1504, 1463, 1239, 1173, 1127, 1038, 998; ^1H NMR ($CDCl_3$, δ_H): 0.88 (*m*, 6H), 1.38–1.27 (*br m*, 22H, $11CH_2$ of 2 × FA units), 1.54 (*m*, 2H), 1.70 (*m*, 4H), 2.06 (*m*, 4H), 2.11 (*m*, 2H), 2.30 (*m*, 4H), 2.44 (*m*, 2H), 2.86–2.81 (*m*, 7H), 2.92 (*dd*, $J_{1,2}$ = 4.47 Hz, $J_{2,3}$ = 14.53 Hz, 1H), 3.77 (*s*, 6H), 3.82 (*s*, 3H), 4.21 (*t*, *J* = 9.63 Hz, 1H), 4.37 (*dd*, *J* = 9.11 Hz, *J* = 7.05 Hz, 1H), 4.61 (*d*, $J_{1,2}$ = 4.39 Hz, 1H), 4.89 (*m*, 1H), 5.37–5.30 (*br m*, 9H), 5.47 (*m*, 1H), 5.90 (*d*, $J_{3,4}$ = 9.18 Hz, 1H), 5.98 (*d*, *J* = 2.52 Hz, 1H), 5.99 (*d*, *J* = 2.52 Hz, 1H), 6.40 (*s*, 2H), 6.55 (*s*, 1H), 6.76 (*s*, 1H); ^{13}C NMR ($CDCl_3$, δ_C): 14.43, 22.95, 25.38, 25.74, 26.02, 27.03, 27.61, 27.71, 29.53, 29.58, 29.70, 29.91, 31.90, 32.11, 32.37, 34.02, 34.47, 34.76, 39.18, 44.16, 45.99, 56.56, 61.11, 71.76, 73.81, 74.19, 101.97, 107.37, 108.63, 110.12, 124.77, 127.94, 128.26, 128.58, 128.60, 128.87, 128.97, 129.16, 129.43, 130.86, 132.75, 132.81, 135.22, 137.68, 148.00, 148.51, 153.06, 173.64, 174.01, 174.55; EI-MS found $[M + H]^+$ 981.6094; $C_{60}H_{85}O_{11}$ $[M + H]^+$ requires 981.6092.

(vi) 4-O-*Podophyllotoxinyl 12-(undec-10′-enacyloxy)-octadec-Z-9-enoate* ***7***. Viscous colorless oil; R_f = 1.0 (*n*-hexane/ethyl acetate, 1:1 vol/vol, as developer), isolated yield, 99.5%. IR ($CHCl_3$, cm^{-1}): 1781, 1732, 1588, 1504, 1484, 1462, 1239, 1172, 1127, 1067, 998; ^1H NMR ($CDCl_3$, δ_H): 0.84 (*t*, *J* = 6.82 Hz, 3H), 1.30–1.26 (*br m*, 26H, $13CH_2$ of 2 × FA units), 1.51 (*m*, 2H), 1.58 (*m*, 2H), 1.64 (*m*, 2H), 2.11 (*m*, 4H), 2.24 (*m*, 4H), 2.40 (*m*, 2H), 2.80 (*m*, 1H), 2.90 (*dd*, $J_{1,2}$ = 4.40 Hz, $J_{2,3}$ = 14.54 Hz, 1H), 3.73 (*s*, 6H), 3.78 (*s*, 3H), 4.17 (*t*, *J* = 9.60 Hz, 1H), 4.33 (*dd*, *J* = 9.12 Hz, *J* = 7.10 Hz, 1H), 4.57 (*d*, $J_{1,2}$ = 4.81 Hz, 1H), 4.98–4.85 (*m*, 3H), 5.34 (*m*, 1H), 5.44 (*m*, 1H),

5.78 (*m*, 1H), 5.86 (*d*, $J_{3,4}$ = 9.16 Hz, 1H), 5.95 (*d*, *J* = 2.51 Hz, 1H), 5.96 (*d*, *J* = 2.51 Hz, 1H), 6.36 (*s*, 2H), 6.51 (*s*, 1H), 6.72 (*s*, 1H); ^{13}C NMR ($CDCl_3$, δ_C): 14.45, 22.95, 25.38, 25.49, 25.73, 27.70, 29.27, 29.44, 29.52, 29.61, 29.69, 29.91, 32.13, 34.02, 34.16, 35.05, 39.16, 44.13, 45.94, 56.51, 61.11, 71.77, 73.78, 74.03, 101.98, 107.37, 108.50, 110.09, 114.53, 124.81, 128.83, 132.71, 132.79, 135.24, 137.54, 139.52, 147.97, 148.49, 153.01, 173.93, 174.04, 174.57; ESI-MS found $[M + Na]^+$ 883.4965; $C_{51}H_{72}O_{11}Na$ $[M + Na]^+$ requires 883.4972.

(vii) 4-O-*Podophyllotoxinyl 12-(eicosanacyloxy)octadec-Z-9-enoate* ***8***. Viscous colorless oil; R_f = 1.0 (*n*-hexane/ethyl acetate, 1:1 vol/vol, as developer), isolated yield, 99.5%. IR ($CHCl_3$, cm^{-1}): 1781, 1734, 1588, 1505, 1463, 1239, 1172, 1127, 1066, 998; ^{1}H NMR ($CDCl_3$, δ_H): 0.84 (*t*, *J* = 6.96 Hz, 6H), 1.30–1.23 (*br m*, 48H, $24CH_2$ in 2 × FA units), 1.51 (*m*, 2H), 1.56 (*m*, 2H), 1.65 (*m*, 2H), 2.01 (*m*, 2H), 2.25 (*m*, 4H), 2.38 (*m*, 2H), 2.79 (*m*, 1H), 2.87 (*dd*, $J_{1,2}$ = 4.39 Hz, $J_{2,3}$ = 14.53 Hz, 1H), 3.71 (*s*, 6H), 3.76 (*s*, 3H), 4.15 (*t*, *J* = 9.63 Hz, 1H), 4.32 (*dd*, *J* = 9.11 Hz, *J* = 7.03 Hz, 1H), 4.55 (*d*, $J_{1,2}$ = 4.29Hz, 1H), 4.85 (*m*, 1H), 5.30 (*m*, 1H), 5.43 (*m*, 1H), 5.84 (*d*, $J_{3,4}$ = 9.10 Hz, 1H), 5.92 (*d*, *J* = 2.50 Hz, 1H), 5.94 (*d*, *J* = 2.50 Hz, 1H), 6.36 (*s*, 2H), 6.48 (*s*, 1H), 6.72 (*s*, 1H); ^{13}C NMR ($CDCl_3$, δ_C): 14.39, 14.44, 22.91, 23.03, 25.34, 25.48, 25.70, 27.66, 29.49, 29.53, 29.65, 29.70, 29.85, 29.87, 29.97, 30.04, 32.10, 32.27, 32.37, 34.00, 34.69, 35.01, 39.13, 44.12, 45.85, 56.44, 60.98, 71.69, 73.77, 73.94, 101.93, 107.33, 108.55, 110.03, 124.80, 128.89, 132.71, 135.22, 137.59, 147.95, 148.45, 152.99, 173.77, 173.92, 174.41; ESI-MS found $[M + Na]^+$ 1011.6525; $C_{60}H_{92}O_{11}Na$ $[M + Na]^+$ requires 1011.65312.

(viii) 4-O-*Podophyllotoxinyl 12-(12′-hydroxyl-octadec-Z-9′-enacyloxy)octadec-Z-9-enoate* ***9***. Viscous colorless oil; R_f = 0.8 (*n*-hexane/ethyl acetate, 1:1 vol/vol, as developer), isolated yield, 98%. IR ($CHCl_3$, cm^{-1}): 3532, 1781, 1732, 1588, 1484, 1463, 1239, 1169, 1128, 1038, 1003; ^{1}H NMR ($CDCl_3$, δ_H): 0.88 (*m*, 6H), 1.33–1.27 (*br m*, 32H, $16CH_2$ of 2 × FA units), 1.46 (*m*, 2H), 1.54 (*m*, 2H), 1.60 (*m*, 2H), 1.66 (*m*, 2H), 2.04 (*m*, 4H), 2.21 (*m*, 2H), 2.27 (*m*, 4H), 2.43 (*m*, 2H), 2.82 (*m*, 1H), 2.93 (*dd*, $J_{1,2}$ = 4.38 Hz, $J_{2,3}$ = 14.52 Hz, 1H), 3.61 (*m*, 1H), 3.76 (*s*, 6H), 3.81 (*s*, 3H), 4.19 (*t*, *J* = 9.63 Hz, 1H), 4.35 (*dd*, *J* = 9.01 Hz, *J* = 7.01 Hz, 1H), 4.60 (*d*, $J_{1,2}$ = 4.22 Hz,1H), 4.88 (*m*, 1H), 5.57–5.31 (*br m*, 4H), 5.89 (*d*, $J_{3,4}$ = 9.15 Hz, 1H), 5.97 (*d*, *J* = 2.53 Hz, 1H), 5.98 (*d*, *J* = 2.53 Hz, 1H), 6.40 (*s*, 2H), 6.54 (*s*, 1H), 6.75 (*s*, 1H); ^{13}C NMR ($CDCl_3$, δ_C): 14.41, 22.92, 22.97, 25.37, 25.46, 25.71, 26.07, 27.69, 27.76, 29.49, 29.71, 29.90, 29.97, 32.10, 32.20, 32.39, 34.02, 34.75, 35.03, 35.77, 37.26, 39.18, 44.16, 45.98, 56.56, 61.08, 71.74, 71.87, 73.81, 74.06, 101.95, 107.36, 108.70, 110.11, 124.82, 125.67, 128.88, 132.76, 133.55, 135.20, 147.99, 148.51, 153.06, 173.86, 173.97, 174.53; ESI-MS found $[M + H]^+$ 976.6261; $C_{58}H_{88}O_{12}$ $[M + H]^+$ requires 976.6275.

(ix) 4-O-*Podophyllotoxinyl 12-[12′(12″-hydroxyl-octadec-Z-9″-enacyloxy)octadec-Z-9′-enacyloxy]octadec-Z-9-enoate* ***10***. Viscous colorless oil; R_f = 0.85 (*n*-hexane/ethyl acetate, 1:1 vol/vol, as developer), isolated yield, 98%. IR ($CHCl_3$, cm^{-1}): 3552, 1781, 1731, 1588, 1484, 1239, 1186, 1128, 1039, 1001; ^{1}H NMR ($CDCl_3$, δ_H): 0.88 (*m*, 9H), 1.33–1.27 (*br m*, 54H, $27CH_2$ of 3 × FA units), 1.46 (*m*, 2H), 1.54 (*m*, 2H), 1.61 (*m*, 2H), 1.67 (*m*, 2H), 2.04 (*m*, 4H), 2.21 (*m*, 2H), 2.30 (*m*, 8H), 2.41 (*m*, 2H), 2.83 (*m*, 1H), 2.93 (*i*, $J_{1,2}$ = 4.39 Hz, $J_{2,3}$ = 14.52 Hz, 1H), 3.61 (*m*, 1H), 3.76 (*s*, 6H), 3.83 (*s*, 3H), 4.19 (*t*, *J* = 10.13 Hz, 1H), 4.35 (*dd*, *J* = 9.10 Hz, *J* = 7.03 Hz, 1H), 4.60 (*d*, $J_{1,2}$ = 4.28 Hz, 1H), 4.88 (*m*, 2H), 5.72–5.30 (*br m*, 6H), 5.89 (*d*, $J_{3,4}$ = 9.15 Hz, 1H), 5.97 (*d*, *J* = 2.52 Hz, 1H), 5.98 (*d*, *J* = 2.52 Hz, 1H), 6.40 (*s*, 2H), 6.54 (*s*, 1H), 6.75 (*s*, 1H); ^{13}C NMR ($CDCl_3$, δ_C): 14.41, 22.92, 22.97, 25.37, 25.47, 25.71, 26.07, 27.71, 27.76, 29.52, 29.72, 29.91, 29.97, 32.10, 32.20, 32.39, 34.03, 34.74, 35.03, 35.77, 37.27, 39.18, 44.17, 45.98, 56.56, 61.07, 71.73, 71.86, 73.81, 74.05, 101.94, 107.35, 108.71, 110.10, 124.74, 124.81, 125.67, 128.89, 132.75, 132.85, 133.53, 135.20, 147.99, 148.50, 153.06, 173.82, 173.95, 174.50; ESI-MS found $[M + Na]^+$ 1277.8404; $C_{76}H_{118}O_{14}Na$ $[M + Na]^+$ requires 1277.8419.

(x) 4-O-*Podophyllotoxinyl 12-[12′(octadec-Z-9″,12″-dienacyloxy)octadec-Z-9′-enacyloxy]octadec-Z-9-enoate* ***11***. Viscous colorless oil; R_f = 1.0 (*n*-hexane/ethyl acetate, 1:1 vol/vol, as developer), isolated yield, 99.5%. IR ($CHCl_3$, cm^{-1}): 1781, 1738, 1588, 1505, 1463, 1339, 1173, 1128, 1039, 1005; ^{1}H NMR ($CDCl_3$, δ_H): 0.88 (*m*, 9H), 1.36–1.27 (*br m*, 50H, $25CH_2$ of 3 × FA units), 1.54 (*m*, 2H), 1.61 (*m*, 2H), 1.68 (*m*, 2H), 2.04 (*m*, 10H), 2.28 (*m*, 6H), 2.34 (*m*, 2H), 2.43 (*m*, 2H), 2.77 (*m*, 2H), 2.83 (*m*, 1H), 2.93 (*dd*, $J_{1,2}$ = 4.26 Hz, $J_{2,3}$ = 14.52 Hz, 1H), 4.20 (*t*, *J* = 9.98 Hz, 1H), 4.36 (*dd*, *J* = 9.13 Hz, *J* = 7.03 Hz, 1H), 4.60 (*d*, $J_{1,2}$ = 4.20 Hz, 1H), 4.88 (*m*, 2H), 5.39–5.30 (*br m*, 6H), 5.48–5.43 (*m*, 2H), 5.89 (*d*, $J_{3,4}$ = 9.10 Hz, 1H), 5.97 (*d*, *J* = 2.51 Hz, 1H), 5.99 (*d*, *J* = 2.51 Hz, 1H), 6.40 (*s*, 2H), 6.54 (*s*, 1H), 6.75 (*s*, 1H); ^{13}C NMR ($CDCl_3$, δ_C): 14.43, 22.94, 25.38, 25.49, 25.72, 26.02, 27.58, 27.72, 29.52, 29.57, 29.72, 29.93, 29.99, 31.90, 32.12, 32.39, 34.02, 34.20, 34.75, 35.05, 39.18, 44.15, 45.98, 56.54, 61.10, 71.76, 73.81, 74.07, 101.96, 107.36, 108.61, 110.11, 124.74, 124.80, 128.30, 128.43, 128.86, 130.41, 130.57, 132.77, 132.87, 135.22, 137.66, 147.99, 148.51, 153.05, 173.90, 174.03, 174.56; ESI-MS found $[M + Na]^+$ 1259.8275; $C_{76}H_{116}O_{13}Na$ $[M + Na]^+$ requires 1259.83072.

Biological. (i) Assay for anticancer activity. Compounds **3–11** (in the concentration range of 0.04 to 10 μM) were tested for their *in vitro* cytotoxicity against a panel of human cancer cell lines including SK-MEL (malignant, melanoma), KB (epidermal carcinoma, oral), BT-549 (ductal carcinoma, breast), SK-OV-3 (ovary carcinoma), and HL-60 (human leukemia) as well as noncancerous VERO cells (African green monkey kidney fibroblast) using procedures identical to those described previously (13). Cell viability was determined after exposing the cells to the test compounds for 48 h, either by the Trypan Blue exclusion method for HL-60 cells or by the Neutral Red assay for all other cells.

(ii) Assay for microtubule polymerization. The assay for microtubule polymerization was performed in Corning Costar 96-well plates using a CytoDYNAMIX Screen from Cytoskeleton Inc. (Denver, CO). The bovine brain tubulin used in the assay contained 90% tubulin and 10% microtubule-associated pro-

teins. The lyophilized tubulin was reconstituted to 2 mg/mL in G-PEM buffer consisting of 80 mM of PIPES sequisodium salt, 2 mM of $MgCl_2$, 0.5 mM of EGTA, and 1 mM of GTP, pH 6.9. When 100 µL of reconstituted tubulin was pipetted to a prewarmed well of the plate, it polymerized efficiently at 37°C. Tubulin polymerization was detected by measuring the increase in absorbance at 340 nm for 30 min on a Bio-Tek PowerwaveXS plate reader (Bio-Tek, Winooski, VT). Taxol (10 µM) and nocodazole (10 µM) were included as known ligands (stabilizer and inhibitor, respectively) for tubulin polymerization. Compounds **3–11** were tested at a concentration of 25 µM using a stock of 5 mM in DMSO. The final DMSO concentration was 0.5% in the assay and did not affect the rate of tubulin assembly.

(iii) Assay for topoisomerase II activity. Measurement of the catalytic activity of topoisomerase II was based on the conversion of kDNA to decatenated kDNA. kDNA and purified human topoisomerase II were purchased from TopoGEN, Inc. (Columbus, OH). The assay was performed in a total volume of 20 µL containing 250 ng of kDNA, the test sample (2–50 µM), and 2 units of topoisomerase II in the assay buffer (50 mM of TrisCl, pH 8.0, 120 mM of KCl, 10 mM of $MgCl_2$, 0.5 mM of ATP, 0.5 mM of dithiothreitol, and 30 µg of BSA/mL). The assay mixture was incubated at 37°C for 30 min, and the reaction was terminated by the addition of 1/5 vol of 5× stop buffer (5% sarkosyl, 0.025% bromophenol blue, 25% glycerol). DNA was analyzed by electrophoresis on agarose gel (1%) in TAE buffer (40 mM of Tris acetate, 2 mM of EDTA, pH 8.5). After staining with ethidium bromide, the gel was analyzed on a Gel Doc system (BioRad, Hercules, CA) for quantification of DNA. Enzyme activity was measured in terms of the percentage of substrate kDNA converted to product (decatenated kDNA). The concentration of the test compound that prevented 50% of the substrate from being converted to the product (IC_{50}) was calculated.

RESULTS AND DISCUSSION

To date, no reports have described the synthesis of podophyllotoxin derivatives bearing an estolide moiety. Estolides may be better drug carrier systems because of their higher lipophilic character (16,17). Encouraged by our recent findings (13) in which we described the selective anticancer activity of $C_4\alpha$-FA derivatives of podophyllotoxin, here we describe the synthesis of a series of $C_4\alpha$-estolides (Scheme 1). Estolides are a group of FA polyesters resulting from ester bond formation between the oxygen of a hydroxyl group of one FA and the carbonyl carbon of the terminal carboxylic group of another FA.

Synthetic methodology is based on the coupling of the hydroxyl function (12C-OH) present in the FA side chain of 4-*O*-podophyllotoxinyl 12-hydroxyl-octadec-*Z*-9-enoate **2** with the terminal carboxylic group of different FA to form various 4-*O*-podophyllotoxinyl estolides. Quantitative formation of estolides is achieved with the help of DCC as a coupling reagent and DMAP as a catalyst. The FA used in these reactions are octadec-*Z*-9-enoic, octadec-*Z*-9,11-dienoic, octadec-*Z*-9,12,15-trienoic, eicosa-*Z*-5,8,11,14-tetraenoic, 10-undecynoic, eicosanoic, and 12-hydroxyl-octadec-*Z*-9-enoic acids, to produce compounds **3**, **4**, **5**, **6**, **7**, **8**, and **9**, respectively (Scheme 1).

Further, 12′C-OH in the second FA unit of **9** was used to introduce a third FA unit as 12-hydroxy-octadec-*Z*-9-enoic and octadec-*Z*-9,12-dienoic acids under similar reaction conditions to furnish quantitative yields of compounds **10** and **11**, respectively (Scheme 1).

Compound **10** was detected as a minor product (–2%) in the coupling reaction of **2** with 12-hydroxyl-octadec-*Z*-9-enoic acid, the formation of which was completely suppressed when the reaction was conducted at –78°C for 90 min. During the preparation of **10**, a minor amount of a product was detected that contained four similar FA units bonded with three estolide bonds. This observation indicates the suitability of this method to form higher estolides.

The numbering system for **1** (Scheme 1) was used, which is widely in practice (1,10,11) and which we have already reported (13). The nature of bonds present between the podophyllotoxin nuclei and FA units are as follows: compounds **3–9**: an ester bond (podophyllotoxin $C_4\alpha \rightarrow$ 1C FA) and an estolide bond (12C FA $\rightarrow$ 1′C FA); compounds **10** and **11**: an ester bond (podophyllotoxin $C_4\alpha \rightarrow$ 1C FA) and two estolide bonds (12C FA $\rightarrow$ 1′C FA; 12′C FA $\rightarrow$ 1″C FA). The second FA unit in each of the estolide derivatives **3–9** differs in its chemical composition; they are as follows: the *Z*-monoene (18:1, $\Delta^{9'}$) in **3**; the *Z*-diene (18:2, $\Delta^{9',12'}$) in **4**; the *Z*-triene (18:3, $\Delta^{9',12',15'}$) in **5**; the *Z*-tetraene (20:4, $\Delta^{5',8',11',14'}$) in **6**; the terminal olefin (11:1) in **7**; the saturated (20:0) in **8**; and the hydroxyl-*Z*-ene (18:1, 12′C-OH, $\Delta^{9'}$) in **9**. Estolides **10** and **11** were structurally identical up to the first two FA units, but their third FA unit was formulated by hydroxyl-*Z*-ene (18:1, 12″C-OH, $\Delta^{9''}$) and *Z*-diene (18:2, $\Delta^{9'',12''}$), respectively.

The stereochemistry of all three stereogenic centers at which coupling reactions occurred—C-4 (podophyllotoxin), C-12 (first FA unit), and C-12′ (second FA unit)—were retained. The main factor for the retention of a configuration was the noncleavage of bonds at any of the three stereogenic centers, as revealed by the reaction mechanism. A similar observation was reported previously (13). The stereogenic carbon (C-12) of 12-hydroxyl-octadec-*Z*-9-enoate had an *R*-configuration (18).

The IR spectrum of **6** displayed two carbonyl bands at 1779 and 1729 cm^{-1}. The ^{13}C NMR spectrum illustrated three structure-revealing signals at δ_C 173.64, 174.01, and 174.55, which characterized the presence of three carbonyl groups. The signals at δ_C 174.01 and 174.55 were readily assigned to one ester carbonyl (1-C) of 12-hydroxyl-octadec-*Z*-9-enoate as the first FA unit and one estolide carbonyl (1′-C) of eicosa-*Z*-5,8,11,14-tetraenoate as the second FA unit. The remaining signal at δ_C 173.64 was for the lactone carbonyl in the D ring of the podophyllotoxin nuclei. The formation of an estolide bond at 12-C of the first FA unit to link it with the carboxylic (1′-C) group of the second FA unit exerted significant downfield chemical shifts to 12-H (δ_H 4.89, *m*) and 12-C (δ_C 73.81) signals. A broad multiplet for nine olefin protons (9-H, 5′/6′-H, 8′/9′-H, 11′/12′-H, 14′/15′-H) appeared in the olefinic region at

δ_H 5.37–5.30, which was correlated with eight carbons of the second FA unit at δ_C 127.94, 128.26, 128.58, 128.60, 128.97, 129.16, 129.43, 130.86 (5′/6′-C, 8′/9′-C, 11′/12′-C, 14′/15′-C) in addition to 9-C of the first unit at 124.77. The remaining first-unit olefinic proton (10-H) and carbon (10-C) resonated at δ_H 5.47 (*m*) and δ_C 132.81. A broad multiplet at δ_H 2.86–2.81 (7H) was assigned to three methylene-group protons (7′-C$\underline{H}_2$, 10′-C$\underline{H}_2$, 13′-C$\underline{H}_2$), which were flanked by four sets of Z-olefins in the second FA unit and 3-H (podophyllotoxin), and carbon correlations appeared at δ_C 25.38, 25.74, 26.02 (7′-C, 10′-C, 13′-C), and 45.99 (3-C, podophyllotoxin). The proton and carbon signals for two terminal methyl (18-CH_3, 20′-CH_3) groups of both FA units were merged to record at δ_H 0.88 (*m*, 6H) and δ_C 14.43 (2 × C, 18-C, 20′-C). Signals associated with 11-C$\underline{H}_2$ and 11-C of the first FA unit were distinguished at δ_H 2.44 (*m*) and δ_C 34.47. Carbon signals arising from 2-C and 2′-C from two FA units were recorded at δ_C 34.76 and 34.02 with a correlation at δ_H 2.30 (*m*, 4H, 2-C$\underline{H}_2$, 2′-C$\underline{H}_2$). The proton and carbon signals related to the A, B, C, D, and E rings in the podophyllotoxin structure were recorded as (i) a five-member A ring: O-C$\underline{H}_2$-O, with each of the two protons split into two separate doublets: δ_H 5.98 (J = 2.52 Hz) and 5.99 (J = 2.52 Hz), δ_C 101.97 (O–C–O); (ii) an aromatic B ring: δ_H 6.76 (*s*, 5-H), δ_C 107.37 (5-C); δ_H 6.55 (*s*, 8-H), δ_C 110.12 (8-C); (iii) a cyclohexyl C ring: δ_H 4.61 (*d*, $J_{1,2}$= 4.39 Hz, 1-H), δ_C 44.16 (1-C); δ_H 2.92 (*dd*, $J_{1,2}$ = 4.47 Hz, $J_{2,3}$ = 14.53 Hz, 2-H), δ_C 39.18 (2-C); δ_H 5.90 (*d*, $J_{3,4}$ = 9.18 Hz, 4-H), δ_C 74.19 (4-C); (iv) a lactone D ring: each of the two methylene protons (11-C$\underline{H}_2$) was split into two separate signals: δ_H 4.21 (*t*, J = 9.63 Hz) and 4.37 (*dd*, J = 9.11 Hz, J = 7.05 Hz), δ_C 71.76 (11-C); and (v) a pendant 3′,4′,5′-trimethoxy aromatic E ring: δ_H 6.40 (*s*, 2′-H, 6′-H), δ_C 108.63 (2′-C, 6′-C); δ_H 3.77 (*s*, 3′OC$\underline{H}_3$, 5′OC$\underline{H}_3$), δ_C 56.56 (3′-C, 5′-C); 4′OC$\underline{H}_3$, δ_H 3.82 (*s*, 4′OC$\underline{H}_3$), δ_C 61.11 (4′-C).

A characteristic feature of podophyllotoxin and its analogs was that the 2′,6′ protons and the 3′,5′ methoxy protons, even at 500 MHz, gave rise to single resonance peaks.

Carbon signals of three Z-olefinic groups (9′/10′-C, 12′/13′-C, 15′/16′-C) in the second FA unit of compound **5** were observed at δ_C 127.51, 128.12, 128.63, 128.67, 130.65, 132.33 and were correlated for protons (9′/10′-H, 12′/13′-H, 15′/16′-H) at δ_H 5.40–5.30 (*br m*). Two Z-olefinic protons and carbons of the first unit were assigned at δ_H 5.40–5.30 (*br m*, 9-H), δ_C 124.81 (9-C), and δ_H 5.45 (*m*, 10-H), 132.72 (10-C). Protons of two methylene groups (11′-C$\underline{H}_2$, 14′-C$\underline{H}_2$) interrupting the three olefin functionalities of the second FA unit and 3-H (podophyllotoxin) were distinguished at δ_H 2.85–2.80 (*m*) with correlations at δ_C 25.38, 25.73 (11′-C, 14′-C), and 45.97 (3-C). A striking feature of the NMR spectra was the splitting of both the proton and carbon signals of 18-CH_3 and 18′-CH_3, which appeared at δ_H 0.88 (*t*, J = 7.06 Hz, 18-C$\underline{H}_3$), δ_C 14.47 (18-C) and 0.98 (*t*, J = 7.54 Hz, 18′-C$\underline{H}_3$), 14.68 (18′-C). The deshielding effect on 18′CH_3 by a double bond at 15′/16′-C resulted in the downfield shift of its proton and carbon signals. The olefinic signals of **4** were absorbed at δ_H 5.40–5.32 (5H, *m*, 9-H, 9′/10′-H, 12′/13′-H), 5.46 (*m*, 10-H); δ_C 124.81 (9-C), 128.30, 128.43, 130.39, 130.56 (9′/10′-C, 12′/13′-C), 132.75 (10-C). Proton signals originating from 3-H (δ_H 2.84, *m*, δ_C 45.96, 3-C) in the C ring of the podophyllotoxin nuclei and 11′-C$\underline{H}_2$ (δ_H 2.77, *m*, δ_C 25.71,11′-C) were absorbed separately because there was less crowding of the methylene proton signals around δ_H 2.84–2.77. Interestingly, two triplets arising from 18-CH_3 and 18′-CH_3 in **3** overlapped so accurately that they produced a sharp triplet at δ_H 0.86 (6H, J = 6.88 Hz), but their carbon signals showed different chemical shifts at δ_C 14.43 and 14.64. A similar observation was noticed even for **8**, which contained FA units of different carbon chain lengths.

The FA units of compound **9** were identical. The structure establishing NMR signals were (i) one hydroxyl group: δ_H 3.61 (*m*, 12′-H), δ_C 71.87 (12′-C); (ii) two Z-double bond signals: δ_H 5.57–5.31 (4H, *br m*, 9/10-H, 9′/10′-H), δ_C 124.82, 125.67, 128.88, 132.76 (9/10-C, 9′/10′-C), (iii) IR: 3532 cm^{-1} (OH). The estolide part of **10** was constituted with three units of 12-hydroxy-octadec-9-*Z*-enoic acid. The structures contributing significant NMR signals were: δ_C 174.50, 173.95 (ester and estolide carbonyls), 173.82 (2 × C=O, estolide and lactone carbonyls); one hydroxyl group: δ_H 3.61 (*m*, 12″-H), δ_C 71.73 (12″-C); two estolide bond signals: δ_H 4.88 (*m*, 12-H, 12′-H), δ_C 74.05 (12-C, 12′-C); three Z-double bond signals: δ_H 5.72–5.30 (*br m*, 9/10-H, 9′/10′-H, 9″/10″-H), δ_C 124.74, 124.81, 125.67, 128.89, 132.75, 132.85 (9/10-C, 9′/10′-C, 9″/10″-C); IR: 3552 cm^{-1} (OH). Compound **11** differed from **10** in its third unit, which was a *Z*-9″,12″-diene C_{18} FA. Structural characteristic signals were exhibited as δ_C 174.56, 174.03 (ester and estolide carbonyls), 173.90 (2 × C=O, estolide and lactone carbonyls); two estolide bond signals: δ_H 4.88 (*m*, 12-H, 12′-H), δ_C 74.07 (12-C, 12′-C); four Z-double bond signals: 5.39–5.30 (*br m*, 9-H, 9′-H, 9″/10″-H, 12″/13″-H), δ_C 124.74, 124.80, 128.30, 128.43, 130.41, 130.57 (9-C, 9′-C, 9″/10″-C, 12″/13″-C), and δ_H 5.48–5.43 (*m*, 10-H, 10′-H), δ_C 132.77, 132.87 (10-C, 10′-C).

Present spectral studies have demonstrated that the presence of either estolide or mono-FA (13,19) moieties at αC_4 have no appreciable impact on the pattern of NMR signals of podophyllotoxin nuclei.

Biological activity. 4-*O*-Podophyllotoxin estolides **3–11** were assayed *in vitro* against four human solid tumor cell lines (SK-MEL, KB, BT-549, and SK-OV-3) and one human leukemia cell line (HL-60) as well as a noncancerous VERO cell culture (Table 1). Compound **2** possessed one FA chain and showed uniform *in vitro* antitumor activity against the above cell lines (13). The increase in the lipophilicity of **2** by incorporating a second FA unit (**3–9**) and a third FA unit (**10**, **11**) unexpectedly led to a loss of the growth inhibition activity of the new molecules against four solid tumor cells. Compounds **4**, **5**, **6,** and **11** were effective against leukemia cells (HL-60), although their growth suppression activity was lower than both podophyllotoxin, **1**, and their immediate precursor, **2** (13). Active molecules shared structural similarities by possessing PUFA with methylene-interrupted Z-unsaturated functionalities in their estolide part. Earlier studies on 4-*O*-podophyllotoxinyl analogs (monoesters of methylene-interrupted Z-unsaturation) revealed

TABLE 1
Cytotoxicity of Compounds 3–11 in a Panel of Cell Lines[a]

Compound[b]	Cell lines (IC_{50} μM)					
	SK-MEL	KB	BT549	SK-OV3	HL-60	VERO
1*	0.22	0.24	0.36	0.19	0.01	0.55
2*	0.21	0.31	0.22	0.26	0.07	NA
3	NA	NA	NA	NA	NA	NA
4	NA	NA	NA	NA	3.45	NA
5	NA	NA	NA	NA	4.08	NA
6	NA	NA	NA	NA	3.77	NA
7	NA	NA	NA	NA	NA	NA
8	NA	NA	NA	NA	NA	NA
9	NA	NA	NA	NA	NA	NA
10	NA	NA	NA	NA	NA	NA
11	NA	NA	NA	NA	1.21	NA

[a]The highest concentration tested was 10 μM. Values are means of two observations. NA, not active; SK-MEL, human malignant melanoma; KB, human epidermal carcinoma; BT549, ductal breast carcinoma; SK-OV3, human ovary carcinoma; HL-60, human leukemia; VERO, monkey kidney fibroblast.
[b]An asterisk (*) indicates values from Reference 13.

greater antileukemic activities both *in vivo* (12) and *in vitro* (13). Podophyllotoxin derivatives with one PUFA chain at αC_4 showed greater *in vitro* anticancer activity against a panel of cancer cell lines (13), whereas PUFA estolides against similar cell lines moderately inhibited leukemia (HL-60) cells and showed no inhibition against solid tumors. The estolides were nontoxic to the VERO cells.

Efforts were also directed at studying the *in vitro* interaction of 4-*O*-podophyllotoxin estolides **3–11** with tubulin (Fig. 1) and DNA topoisomerase II to understand their possible mechanisms of action. This is the first study of its type to investigate FA-derived podophyllotoxin derivatives.

The mechanism by which podophyllotoxin **1** blocks cell division was related to its inhibition of the microtubule assembly in the mitotic apparatus (1,20). Compounds **6–8** strongly inhibited tubulin polymerization to the same extent as **1** and resembled the reference compound nocodazole (Fig. 1). A significant, dose-dependent inhibition was observed in the concentration range of 12.5 to 50 μM. Representative data for a 25 μM concentration range is shown in Figure 1. Compound **2** did not affect tubulin polymerization and remained inactive.

Although **1** was not active toward topoisomerase II, compound **2** inhibited topoisomerase II with an IC_{50} of 17 μM. Interestingly, analogs **3–6** and **8–11** also inhibited the *in vitro* catalytic activity of topoisomerase II, with IC_{50} ranging from 3 to 32 μM. Analogs **4**, **5**, **6**, and **9** were found to be more active (with IC_{50} of 7.30, 3.10, 9.20, and 7.20 μM, respectively) than analogs **3**, **8**, **10**, and **11** (with IC_{50} of 18.80, 30.0, 32.0, and 20.20, respectively). Cleavage complex stabilization activity was not detected for any of the compounds with the topoisomerase II enzyme. Inhibition of the catalytic activity of topoisomerase II has been associated with the intercalating property of several molecules. Compounds of the epipodophyllotoxin (βC_4) series are potent inhibitors of topoisomerase II (21). Hence, the intercalation by $C_4\alpha$-estolides seems to be a significant biological observation. Antitumor aromatic agents carrying a side chain are found as topoisomerase II intercalators (21). Conformational investigations of PUFA possessing the estolide derivatives **3–11** may explain whether the presence of PUFA in the side chains of estolide moieties somehow participates in forming an intercalating chromophore to intercalate DNA. The antileukemic activity of compounds **4–6** and **11** can be correlated with their inhibition of topoisomerase II.

The observation that **6** and **8** (αC_4) are dual inhibitors of topoisomerase II (catalytic activity) and tubulin polymerization is noteworthy because only a few etoposide (βC_4) derivatives have been reported for such behavior (20).

Although the inhibition of tumor cell growth by podophyllotoxin and its analogs is correlated with their activity against either tubulin or topoisomerase II, in the present investigation

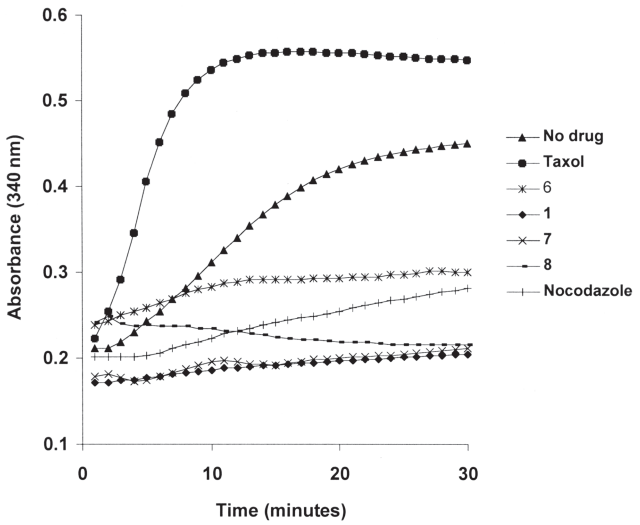

FIG. 1. Inhibition of *in vitro* microtubulin polymerization by compounds **1**, **6**, **7**, and **8** at a concentration of 25 μM. The assay was done in duplicate for concentration ranges of 12.5–50 μM, and the representative time curves for 25 μM of test compounds are shown here. Nocodazole at 10 μM was included in the assay as a positive control.

we discovered an apparent lack of such a correlation. This result might be because the biochemical assays were performed with the isolated enzyme topoisomerase II and tubulin. The effects may not be the same with living cells. Additional factors such as cellular uptake, metabolism, and the involvement of other target molecules may exert significant effects and cannot be excluded. Previously, the absence of such a correlation was reported for podophyllotoxin derivatives (21). The cell-based assay to determine the cytotoxicity of 4-*O*-podophyllotoxin estolides **3–11** examined in this report was also limited to only a few cancer cells. It will be worthwhile to test them in a variety of cancer cell lines to further investigate their anticancer potential.

In conclusion, we demonstrated for the first time an efficient and high-yielding stepwise synthetic method for the preparation of a series of 4-*O*-podophyllotoxin estolides. Their structures were determined by a combination of spectral data, particularly ^{1}H and ^{13}C NMR values. When these estolides were tested for their *in vitro* cytotoxicity, some exhibited moderate antileukemic potency against the HL-60 cell line but had no potency against the four solid tumors. Our preliminary investigations of *in vitro* anticancer bioassays and the inhibition of tubulin and topoisomerase II suggest that these molecules are attractive and that they require further biological profiling in a wide array of cancer cell cultures to explore their possible antitumor potential. Since this is the first study targeting different molecular components, such as tubulin and topoisomerase II, by FA derivatives of podophyllotoxin, further biochemical work is required to develop a better understanding of their mode of action and structure–activity relationships.

ACKNOWLEDGMENT

This work is supported in part by the United States Department of Agriculture Research Service, Specific Cooperation Agreement no. 58-6408-2-0009.

REFERENCES

1. Gordaliza, M., Castro, M.A., Miguel del Correl, J.M., and Feliciano, A.S. (2000) Antitumor Properties of Podophyllotoxin and Related Compounds, *Curr. Pharm. Design 6*, 1811–1839.
2. Brewer, C.F., Loike, J.D., Horwitz, S.B., Sternlicht, H., and Gensler, W.J. (1979) Conformational Analysis of Podophyllotoxin and Its Congeners. Structure–Activity Relationship in Microtuble Assembly, *J. Med. Chem. 22*, 215–221.
3. Jardine, I. (1980) Podophyllotoxin, in *Anticancer Agents Based on Natural Product Models* (Cassady, J.M., and Douras, J.D., eds.), Academic Press, New York, pp. 319–351.
4. Keller-Juslen, C., Kuhn, M., Stahelin, H., and von Wartburg, A. (1971) Synthesis and Antimitotic Activity of Glycosidic Lignan Derivatives Related to Podophyllotoxin, *J. Med. Chem. 14*, 936–940.
5. Weiss, S.G., Tin-wa, M., Perdue, R.E., Jr., and Farnsworth, N.R. (1975) Potential Anticancer Agents II: Antitumor and Cytotoxic Lignans from *Linum album* (Linaceae), *J. Pharm. Sci. 64*, 95–98.
6. O'Dwyer, P.J., Alonso, M.T., Leyland-Jones, B., and Marsoni, S. (1984) Teniposide: A Review of 12 Years of Experience, *Cancer Treat. Rep. 68*, 1455–1466.
7. Issell, B.F., Muggia, F.M., and Carter, S.K. (eds.) (1984) *Etoposide (VP-16) Current Status and New Developments*, Academic Press, New York.
8. VePesid® Product Information Overview, Bristol Lab, New York, 1983.
9. van Maanen, J.M.S., Retel, J., De Vries, J., and Pinedo, H.M. (1988) Mechanism of Action of Antitumor Drug Etoposide: A Review, *J. Natl. Cancer Inst. 80*, 1526–1533.
10. Damayanthi, Y., and Lown, J.W. (1998) Podophyllotoxins: Current Status and Recent Developments, *Curr. Med. Chem. 5*, 205–252.
11. Lee, K.H. (1999) Novel Anticancer Agents from Higher Plants, *Med. Res. Rev. 19*, 569–596.
12. Nagao, Y., Mustafa, J., Sano, S., Ochiai, M., Tazuko, T., and Shigeru, T. (1991) Different Mechanism of Action of Long Chain Fatty Acid Esters of Podophyllotoxin and Esters of Epipodophyllotoxin Against P388 Lymphocytic Leukemia in Mice, *Med. Chem. Res. 1*, 295–299.
13. Mustafa, J., Khan, S.I., Ma, G., Walker, L.A., and Khan, I.A. (2004), Synthesis and Anticancer Activities of Fatty Acid Analogs of Podophyllotoxin, *Lipids 39*, 167–172.
14. Coon, J.S. (1993) Methods and Compositions Using Fatty Acid Esters for Reducing Multi-drug Resistance in Cancer Treatment, *PCT Int. Appl. 38,* Application WO 92-US10563.
15. Scott, C.A., and Horrobin, D.F. (1998) Fatty Acids for the Prevention of Side Effects of Chemotherapy, *PCT Int. Appl. 17*, Application WO 97-GB2362 19970902.
16. Lundberg, B. (1994) The Solubilization of Lipophilic Derivatives of Podophyllotoxins in Sub-micron Sized Lipid Emulsions and Their Cytotoxic Activity Against Cancer Cells in Culture, *Int. J. Pharm. 109*, 73–81.
17. Levy, R.K., Hall, I.H., and Lee, K.L. (1983) Antitumor Agents LXII: Synthesis and Biological Evaluation of Podophyllotoxin Esters and Related Derivatives, *J. Pharm. Sci. 72*, 1158–1161.
18. Paddon-Jones, G.C., McErlean, C.S.P., Hayes, P., Moore, C.J., Konig, W.A., and Kitching, W. (2001) Synthesis and Stereochemistry of Some Bicyclic γ-Lactones from Parasitic Wasps (Hymenoptera: Braconidae). Utility of Hydrolytic Kinetic Resolution of Epoxides and Palladium(II)-Catalyzed Hydroxycyclization–Carbonylation–Lactonization of Ene-diols, *J. Org. Chem. 66*, 7487–7495.
19. Lie Ken Ji, M.S.F., Mustafa, J., and Pasha, M.K. (1999) Synthesis and Spectral Characteristics of Some Unusual Fatty Esters of Podophyllotoxin, *Chem. Phys. Lipids 100*, 165–170.
20. Shi, Q., Chen, K., Morris-Natschke, S.L., and Lee, K.H. (1998) Recent Progress in the Development of Tubulin Inhibitors as Antimitotic Antitumor Agents, *Curr. Pharm. Des. 4*, 219–248.
21. Wang, H.K., Morris-Natschke, S.L., and Lee, K.H. (1997) Recent Advances in the Discovery and Development of Topoisomerase Inhibitors as Antitumor Agents, *Med. Res. Rev. 4*, 367–425.

[Received May 5, 2004; accepted September 17, 2004]

Antibacterial and Xanthine Oxidase Inhibitory Cerebrosides from *Fusarium* sp. IFB-121, an Endophytic Fungus in *Quercus variabilis*

R.G. Shu, F.W. Wang, Y.M. Yang, Y.X. Liu, and R.X. Tan*

Institute of Functional Biomolecules, State Key Laboratory of Pharmaceutical Biotechnology, Nanjing University, Nanjing 210093, P.R. China

ABSTRACT: Two antibacterial and xanthine oxidase inhibitory cerebrosides, one of which is chemically new, were characterized from the chloroform–methanol (1:1) extract of *Fusarium* sp. IFB-121, an endophytic fungus in *Quercus variabilis*. By means of chemical and spectral methods [IR, electrospray ionization MS (ESI-MS), tandem ESI-MS, ^{1}H and ^{13}C NMR, distortionless enhancement by polarization transfer, COSY, heteronuclear multiple-quantum coherence, heteronuclear multiple-bond correlation, and 2-D nuclear Overhauser effect correlation spectroscopy], the structure of the new metabolite named fusaruside was established as (2*S*,2′*R*,3*R*,3′*E*,4*E*,8*E*,10*E*)-1-*O*-β-D-glucopyranosyl-2-*N*-(2′-hydroxy-3′-octadecenoyl)-3-hydroxy-9-methyl-4,8,10-sphingatrienine, and the structure of the other was identified as (2*S*,2′*R*,3*R*,3′*E*,4*E*,8*E*)-1-*O*-β-D-glucopyranosyl-2-*N*-(2′-hydroxy-3′-octadecenoyl)-3-hydroxy-9-methyl-4,8-sphingadienine. Both new and known cerebrosides, although inactive to *Trichophyton rubrum* and *Candida albicans*, showed strong antibacterial activities against *Bacillus subtilis*, *Escherichia coli*, and *Pseudomonas fluorescens*, with their minimum inhibitory concentrations being 3.9, 3.9, and 1.9 μg/mL, and 7.8, 3.9, and 7.8 μg/mL, respectively. Furthermore, both metabolites were inhibitory to xanthine oxidase, with the IC_{50} value of fusaruside being 43.8 ± 3.6 μM and the known cerebroside being 55.5 ± 1.8 μM.

Paper no. L9513 in *Lipids 39*, 667–673 (July 2004).

Cerebrosides, a group of glycosphingolipids, are essential components of a wide variety of tissues and organs in biological systems. Chemically, cerebrosides are composed of a hexose and a ceramide moiety usually consisting of a long-chain amino alcohol, trivially called a "sphingoid base" (i.e., a sphingosine or sphingol), and an amide-linked long-chain FA. Biologically, cerebrosides are ascertained to be structural support and textural determinants of cell membranes and to act, most likely through protein binding, as mediators of biological events such as activation, cell agglutination, intracellular communication, and cell development. Moreover, the cerebrosides play significant or even essential biological roles in cellular membranes as cell surface antigens and receptors. In particular, an increasing amount of evidence has indicated that cerebrosides perform a wide range of biological functions, all being potentially related to the common amphipathic and/or ionophoretic nature of this type of molecule (1).

As a continuation of our characterization of chemically new and/or bioactive constituents from various endophytic fungi (2–5), our attention was extended to cerebroside constituents that are usually abundant in fungal cells (6). Our co-bioassays with antibacterial and xanthine oxidase (XO) inhibitory tests demonstrated that the chloroform–methanol (1:1) extract from the culture of *Fusarium* sp., an endophytic fungus in *Quercus variabilis* Bl., was substantially bioactive. We therefore launched a project aimed at characterizing the active principle(s) it produces. This communication deals with our chemical and biological results regarding the two active cerebrosides afforded, cerebroside **1** and fusaruside **2** (Scheme 1), the latter being new.

EXPERIMENTAL PROCEDURES

Chromatographic and instrumental methods. IR spectra were obtained on a Nexus 870 FTIR spectrograph (Nicolet, Madison, WI) with a KBr wafer, and optical rotations were recorded on a Jasco DIP-181 polarimeter (JASCO, Tokyo, Japan). EI-MS spectra were taken on a VG-ZAB-HS mass spectrometer (Micromass, Manchester, United Kingdom) with the ionization energy at 70 eV and an accelerated pressure at 8000 V. Tandem ESI-MS (ESI-MS/MS) experiments were performed in the positive ion mode on an LCQ (Finnigan, San Jose, CA) spectrometer with a 4.5-kV source voltage and a 40-sheath gas flow rate, and high-resolution ESI-MS (HR-ESI-MS) was performed on a Mariner System 5304 instrument (Applied Biosystems, Foster City, CA). A *m/z* range of 200–1800 was scanned at a capillary temperature of 200°C for each quadrupole record. All NMR experiments were performed at 298 K on a Bruker DRX 500 spectrometer (Bruker, Karlsruhe, Germany) in DMSO-d_6 with ^{1}H and ^{13}C nuclei observed at 500 and 125 MHz, respectively. The chemical shifts were given in ppm (δ) relative to the internal standard, tetramethylsilane, with coupling constants (*J*) in Hz. Unequivocal assignment of all ^{1}H and ^{13}C signals

*To whom correspondence should be addressed at School of Life Sciences, Nanjing University, Nanjing 210093, P.R. China. E-mail: rxtan@nju.edu.cn

Abbreviations: ESI-MS, electrospray ionization MS; ESI-MS/MS, tandem electrospray ionization MS; HMBC, heteronuclear multiple-bond correlation; HMQC, heteronuclear multiple-quantum coherence; HR-ESI-MS, high-resolution electrospray ionization MS; MIC, minimum inhibitory concentration; NOESY, 2-D nuclear Overhauser effect correlation spectroscopy; PDA, potato–dextrose–agar; XO, xanthine oxidase.

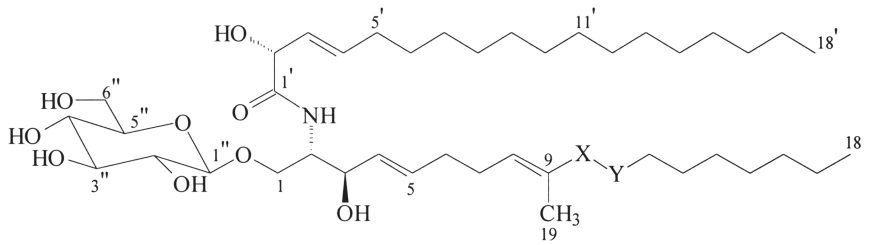

1 X–Y = CH_2CH_2

2 X–Y = CH=CH

SCHEME 1

was realized through a combination of 2-D NMR techniques including COSY, 2-D nuclear Overhauser effect correlation spectroscopy (NOESY), heteronuclear multiple-quantum coherence (HMQC), and heteronuclear multiple-bond correlation (HMBC) experiments.

Materials. Si-gel (200–300 mesh) was produced by Qingdao Marine Chemical Company (Qingdao, China), and Sephadex LH-20 by Pharmacia Biotec AB (Uppsala, Sweden). Precoated C_{18} reversed-phase TLC plates were purchased from Merck (Darmstadt, Germany), and normal-phase TLC was carried out on silica gel 60-precoated plates (Macherey-Nagel, Düren, Germany). Substances on all developed TLC plates were visualized under UV light, followed by heating after being stained with either 10% methanolic H_2SO_4 or 10% ethanolic phosphomolybdic acid as detailed earlier (7). XO from cow's milk, xanthine, and the standard inhibitor allopurinol were purchased from Sigma Chemical Co. (St. Louis, MO).

Microorganisms and cultures. Fusarium sp., identified according to the typical morphological characteristics of the culture, was an endophytic fungus isolated from the healthy bark of *Q. variabilis*, which grows well on the southern hillside of the Zijin Mountain in the eastern suburb of Nanjing, China. To prepare a "seed liquor," a lump (*ca.* 20 mL) of the fresh mycelia pregrown on potato–dextrose–agar (PDA) medium at 28°C for 5 d was uniformly distributed into 1000-mL flasks, each preloaded with 400 mL of a broth composed of potato, dextrose, and H_2O in a proportion of 10:1:50, followed by shaking at 140 rpm for 6 d at 28°C. The subsequent solid culture was completed by allowing it to stand at 28 ± 1°C for 30 d. Fifteen milliliters of the seed liquor was then distributed evenly into 420 bottles preloaded with a given amount of millet medium [composed of millet (7.5 g), bran (7.5 g), yeast extract (0.5 g), $FeSO_4 \cdot 7H_2O$ (0.01 g), sodium tartrate (0.1 g), sodium glutaminate (0.1 g), and pure corn oil (0.1 mL)] in 15 mL of water. The used blank medium was allowed to stand under the same conditions as a control.

Lipid extraction. The air-dried solid-state fungal culture was pulverized, followed by successive extractions with fourfold volumes of 1:1 $CHCl_3$/MeOH by standing overnight at room temperature. *In vacuo* evaporation of the solvents from the extract yielded 200 g of a dark-brown tarry mass, which was soaked in a 1.5-fold amount of MeOH with refluxing for 1 h. The afforded solution was gradually cooled to –20°C and allowed to stand for another 24 h to precipitate the lipids. Filtration of the refrigerated solution yielded the crude lipids as precipitate (*ca.* 60 g, not totally dry).

Isolation and purification of cerebrosides. The total crude lipids were first separated by chromatography on a silica gel column, which was eluted sequentially with $CHCl_3$/MeOH mixtures of increasing polarity (100:0, 99:1, 98:2, 96:4, 92:8, 84:16, 70:30, 50:50, and 0:100, vol/vol). A total of seven fractions (F-1, 15.6 g; F-2, 7.5 g; F-3, 6.2 g; F-4, 6.0 g; F-5, 6.9 g; F-6, 6.5 g; and F-7, 11.0 g) were combined according to a TLC comparison developed with A ($CHCl_3$/MeOH/H_2O, 80:20:1) or B ($CHCl_3$/Me_2CO/MeOH, 80:20:15). F-5, which showed pronounced antibacterial activity, was rechromatographed on a Si-gel column that was eluted with $CHCl_3$/Me_2CO/MeOH (80:20:10, 640 mL) to afford four subfractions (F-5-1, 2.5 g; F-5-2, 1.0 g; F-5-3, 1.2 g; and F-5-4, 1.7 g). F-5-3 was subjected to gel filtration on a Sephadex LH-20 column with MeOH to give the total cerebroside part (760 mg), which was further purified by preparative HPLC (Hitachi semipreparative column, 99:1 MeOH/H_2O; Hitachi, Tokyo, Japan) to yield cerebrosides **1** (73 mg) and **2** (24 mg). They accounted for about 0.12 and 0.04%, respectively, of the total crude lipids extracted.

Characterization of sugar, FA, and amino alcohols. A solution of **1** or **2** (15 mg) in MeOH (2 mL), water (0.2 mL), and 12 N HCl (0.2 mL) was refluxed for 7 h as described elsewhere (8,9). After cooling, the reaction mixture was dried with a stream of N_2 to yield a residue that was dissolved in 9:1 MeOH/H_2O (8 mL) and subsequently extracted three times with *n*-hexane (8 mL each). The combined hexane layer was concentrated to dryness and further purified by gel filtration on a Sephadex LH-20 column with 1:1 $CHCl_3$/MeOH to yield FAME, as identified by EI-MS. The aqueous methanol phase was adjusted to pH 11 with 2% NaOH and then extracted with ether. The ether layer was purified following the aforementioned procedure to yield an amino alcohol, as detected by EI-MS. The H_2O layer was evaporated *in vacuo* and then purified by gel filtration on a Sephadex LH-20 column with MeOH to afford methyl glucopyranoside ($[\alpha]^{27}_D$ +75.4°, *c* 0.01, MeOH), as identified by paper chromatographic and optical rotation comparisons with the authentic material ([α]

value of methyl D-glucopyranoside in the literature (10): +74.2°, *c* 0.01, MeOH). This observation established the D-glucose motif in the original cerebroside.

Antimicrobial test. Antimicrobial action was assessed by a liquid dilution method using three bacteria (*Bacillus subtilis*, *Escherichia coli*, and *Pseudomonas fluorescens*) and two human pathogenic fungi (*Trichophyton rubrum* and *Candida albicans*). A stock solution of each test compound at 500 μg/mL in 5% DMSO was serially diluted (twofold) up to 0.9 μg/mL. The diluted solution (50 μL each) was then mixed with an equal amount of precultured bacterial solution at 10^5 cells/mL, followed by incubation at 28°C for 24 h on 96-well plates. The lowest concentration at which no visible bacterial growth could be discerned was designated the minimum inhibitory concentration (MIC). The vehicle (5% DMSO in water) was the negative control, whereas amikacin sulfate and ketoconazole were co-assayed as positive references for antibacterial and antifungal actions, respectively.

XO inhibitory assay. XO inhibitory activity was measured according to our published method (11). Briefly, the reaction was initiated by adding 76 μL of 31 mU/mL XO to a mixture containing 724 μL of 50 mM K_2HPO_4 (pH 7.8), and 200 μL of 84.8 μg/mL xanthine in 50 mM K_2HPO_4. Because the reaction was found to have linear kinetics during the first 6 min, as reported previously (12), the reaction was monitored for 6 min at 295 nm, and the product was expressed as μmol uric acid per minute. Thus, quantified amounts of stock solutions of the test material in dimethylformamide were added separately to the reaction liquor, and the inhibition of cerebrosides on XO was described as the concentration at which the sample afforded a half-maximal enzyme catalytic velocity (IC_{50}).

RESULTS AND DISCUSSION

Fusarium sp. IFB-121 was isolated from the healthy bark of an abundantly growing strain of *Q. variabilis*. The endophytic nature of *Fusarium* sp. IFB-121 was reinforced by the vital test just outlined, and the specimen was deposited on a PDA slant in our laboratory at 4°C (5). This endophytic fungal strain became cultivatable *in vitro* independent of the host plant. The cerebroside fraction extracted with 1:1 $CHCl_3$/MeOH from the solid-state culture of the endophyte was first separated by a combination of Si-gel column chromatography and gel filtration on a Sephadex-LH 20 column, and the final purification was achieved by semipreparative HPLC to afford two antibacterial and XO inhibitory white amorphous solids (**1** and **2**). Subsequent TLC comparisons demonstrated that the polarity of both isolates was fairly close to, but different from, that of pinelloside, a new monohexosylceramide characterized recently from the tubers of *Perilla frutescens* (8). Furthermore, the ESI-MS/MS mass spectra of both compounds showed intense fragment peaks afforded through the elimination of a single hexose moiety from the protonated molecular ions. This observation led to the assumption that both cerebrosides could be monohexosylceramides.

In the ^{1}H NMR spectrum of **1**, a set of five olefinic proton signals was exhibited at δ 5.69, 5.59, 5.45, 5.40, and 5.10 accompanied by a three-proton singlet at δ 1.55 (Table 1), implying the existence of three double bonds, one of which carried a methyl group. The positive ESI-MS spectrum of compound **1** showed two quasimolecular ions at *m/z* 776 ($[M + Na]^+$) and 754 ($[M + H]^+$), coexistent with intense peaks at *m/z* 1529, 736, and 574 arising from $[2M + Na]^+$, $[M + H - H_2O]^+$, and $[M + H - \text{hexose}]^+$ ions, respectively. These ions, along with the protonated molecular ion at *m/z* 754.4953 in its HR-ESI-MS spectrum, demonstrated that the molecular formula of cerebroside **1** was $C_{43}H_{79}NO_9$. Further interpretation of its ^{1}H and ^{13}C NMR spectral data, exactly assigned with distortionless enhancement by polarization transfer, COSY, NOESY, HMQC, and HMBC techniques, led to the identification of compound **1** as (2*S*,2′*R*,3*R*,3′*E*,4*E*,8*E*)-1-*O*-β-D-glucopyranosyl-2-*N*-(2′-hydroxy-3′-octadecenoyl)-3-hydroxy-9-methyl-4,8-sphingadienine (13–15). Moreover, the structure of **1** was reinforced by methanolysis liberating the anticipated mixture of α- and β-anomers of methyl glucoside (**I**) and 2-hydroxyoctadeca-3-enoic acid methyl ester (**II**) in addition to amino alcohol (**1a)** (Scheme 2).

In the IR spectrum of compound **2**, a broadened absorption band due to N–H and O–H was seen at 3326 cm^{-1} in addition to those at 1628 and 1533 cm^{-1} (amide bands) and at 1059, 1016 (C–O), and 960 cm^{-1} (*trans*-1,2-disubstituted double bond). These IR spectral data, along with their resemblance by TLC to those of **1**, suggested that **2** was also a cerebroside. The HR-ESI-MS spectrum of compound **2** gave a protonated molecular ion at *m/z* 752.5117 together with $[M + Na]^+$ and $[2M + H]^+$ peaks at *m/z* 774.4263 and 1504.0464, respectively. These data demonstrated that the molecular formula of **2** was $C_{43}H_{77}NO_9$, two protons less than that of metabolite **1**.

In the ^{1}H NMR spectrum of **2**, a six-proton triplet (J = 7.0 Hz) at δ 0.85 and a methyl singlet at δ 1.65 as well as seven olefinic proton signals at δ 6.01, 5.68, 5.58, 5.51, 5.44, 5.39, and 5.35 could be readily recognized, together with a set of β-D-glucopyranosyl signals (Table 1), indicating that this cerebroside possessed a branched amino alcohol chain, as discerned with metabolite **1** and those previously reported for the fungi *Magnaporthe grisea*, *Tuber indicum*, and *Engleromyces goetzei* (16–18). This observation, along with eight olefinic carbon signals at δ 134.9, 133.6, 131.4, 131.3, 131.1, 129.8, 129.3, and 127.7, suggested the presence of three di- and one trisubstituted double bonds, the latter carrying a methyl group, as evidenced by a methyl singlet at δ 1.65. To assign the positions of these four vinyl groups unambiguously, compound **2** was subjected to methanolysis (with the products identified by optical rotation and EI-MS) to produce a mixture of α- and β-anomers of methyl glucoside (**I**) and 2-hydroxyoctadeca-3-enoic acid methyl ester (**II**) in addition to amino alcohol (**2a**) (Scheme 2). This co-detection of fragments **I** and **II** allowed the structure of the amide-linked acyl and saccharide moieties to be established, with both being identical to those of metabolite **1**. The aforementioned spectral and chemical evidence accommodated the planar structure of **2**, which was confirmed by its COSY, NOESY, HMQC, and HMBC spectra, allowing the unambiguous assignment of all proton and carbon-13 signals (Table 1). Thus, a clear HMBC correlation of C-1″ with H_2-1

TABLE 1
^{1}H and ^{13}C NMR Spectral Data of Cerebrosides 1 and 2 (in DMSO-d_6)[a]

	1			2		
Position	^{13}C	^{1}H	Multiplicity; *J* (Hz)	^{13}C	^{1}H	Multiplicity; *J* (Hz)
Hexose						
1″	103.9	4.13	*d*; 7.5	103.8	4.12	*d*; 7.5
2″	73.7	2.98	*t*; 8.0	73.7	2.97	*t*; 8.0
3″	76.8	3.15	*t*; 8.5	76.8	3.14	*t*; 8.5
4″	70.3	3.06	*t*; 9.5	70.3	3.05	*t*; 9.5
5″	77.3	3.12	*m*	77.2	3.11	*M*
6″a	61.4	3.46	*dd*; 5.5, 11.7	61.4	3.45	*dd*; 5.5, 11.7
6″b		3.68	*dd*; 5.5, 11.7		3.67	*dd*; 5.5, 11.7
Amino alcohol						
1a	69.0	3.55	*dd*; 6.0, 10.5	69.0	3.54	*dd*; 6.0, 10.5
1b		3.93	*dd*; 6.0, 10.5		3.93	*dd*; 6.0, 10.5
2	53.2	3.80	*m*	53.2	3.78	*m*
3	70.9	4.00	*t*; 6.5	70.8	3.98	*t*; 7.0
4	**131.2**	**5.40**	***br dd*; 15.5, 6.5**	**131.1**	**5.39**	***br dd*; 15.5, 7.0**
5	**131.4**	**5.59**	***br dt*; 15.5, 6.0**	**131.4**	**5.58**	***br dt*; 15.5, 6.0**
6	27.7	1.95	*m*	27.8	2.05	*m*
7	32.5	1.98	*m*	31.7	2.11	*m*
8	**123.9**	**5.10**	***br t*; 6.0**	**129.8**	**5.35**	***br t*; 6.5**
9	**135.3**			**133.6**		
10	39.3	1.93	*m*	**134.9**	**6.01**	*br d*; 15.5
11	27.7	1.35	*m*	**127.7**	**5.51**	***m***
12	29.3	1.24	*m*	32.6	2.03	*m*
13	29.3	1.24	*m*	28.0	1.33	*m*
14–16	29.3	1.24	*m*	29.2	1.23	*m*
17	22.4	1.28	*m*	22.4	1.26	*m*
18	14.3	0.85	*t*; 7.0	14.3	0.85	*t*; 7.0
19	16.1	1.55	*s*	12.7	1.65	*S*
NH		7.30	*d*; 9.5		7.23	*d*; 9.5
2-Hydroxy FA						
1′	172.5			172.5		
2′	72.3	4.30	*dd*; 1.0, 5.5	72.2	4.29	*dd*; 1.0, 5.5
3′	**129.4**	**5.45**	***br dd*; 5.5, 15.5**	**129.3**	**5.44**	***br dd*; 5.5, 15.5**
4′	**131.3**	**5.69**	***br ddd*; 1.5, 5.5, 15.5**	**131.3**	**5.68**	***br ddd*; 1.5, 5.5, 15.5**
5′	31.9	1.97	*m*	31.9	1.97	*M*
6′	29.4	1.30	*m*	29.4	1.30	*M*
7′–16′	29.4	1.24	*m*	29.4	1.23	*M*
17′	22.5	1.27	*m*	22.5	1.26	*M*
18′	14.3	0.85	*t*; 7.0	14.3	0.85	*t*; 7.0

[a]Vinylic resonance lines are in boldface for emphasis. Unequivocal assignments were allowed by COSY, 2-D nuclear Overhauser effect correlation spectroscopy, heteronuclear multiple-quantum coherence, and heteronuclear multiple-bond correlation experiments.

required the linkage of the β-glucopyranosyl residue at C-1, whereas that at C-1′ with H-2 indicated the presence of the 2-hydroxyoctadeca-3-enoyl chain at the 2-amino group (Scheme 3).

Starting from signals at $\delta_{C(H)}$ 69.0 (3.54 and 3.93, *dd* each, J = 10.5, 6.0 Hz) arising from the 1-oxygenated methylene of the amino alcohol chain, the chemical shifts of the methine signals from C-2 through C-5 were assigned at $\delta_{C(H)}$ 53.2 (3.78, *m*), 70.8 (3.98, *t*, J = 7.0 Hz), 131.1 (5.39, *br dd*, J = 15.5, 7.0 Hz), and 131.4 (5.58, *br dt*, J = 15.5, 6.0 Hz), respectively. The magnitude of $J_{4,5} = J_{3',4'}$ = 15.5 Hz demonstrated the *trans*-geometry of 3′,4′- and 4,5-double bonds. Furthermore, a 1,4-disubstituted-2-methyl-*trans*-diene system was connected to the 4,5-olefin through an ethylene "bridge," as required by the splitting pattern of the olefinic proton signals involved (Table 1), by clear HMBC correlations of C-6 with H-4, H-5, and H-8 (Scheme 3), and by the NOESY correlation of the 9-methyl group with H_2-7 and H-11 (Scheme 4). Furthermore, the presence of the 9-methyl group at the center of the conjugated diene system was reinforced by the H-19 and C-19 signals; the former shifted downfield by 0.1 ppm and the latter upfield by 3.4 ppm from those of **1**, owing to the paramagnetic and conjugative effects of the 10,11-double bond (Table 1). Finally, an *n*-heptyl group had to anchor on the C-11 to complete the full assignment of the formulated amino alcohol moiety of cerebroside **2** as (4*E*,8*E*,10*E*)-9-methyl-4,8,10-sphingatrienine. Regarding the absolute configuration, the chemical shifts from C-1 through C-7 and from C-1′ through C-18′ of compound **2**, which were

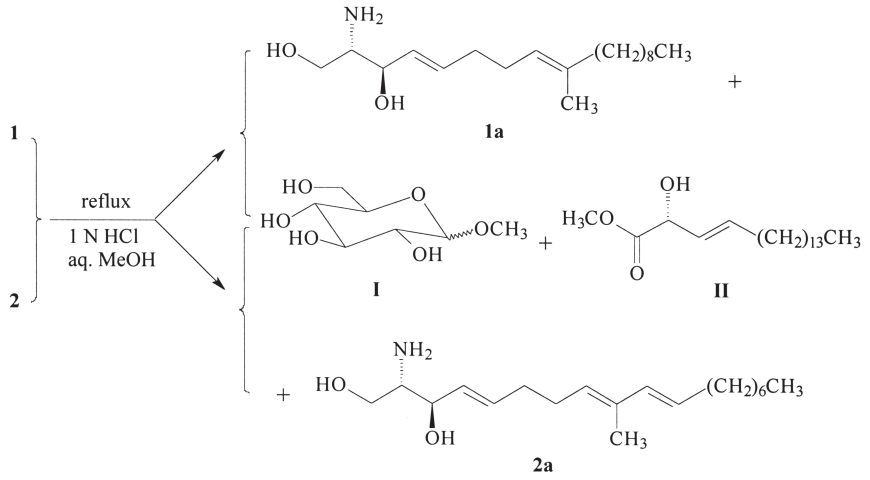

SCHEME 2

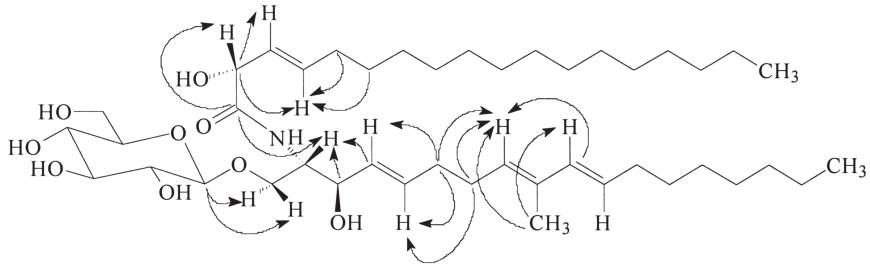

SCHEME 3

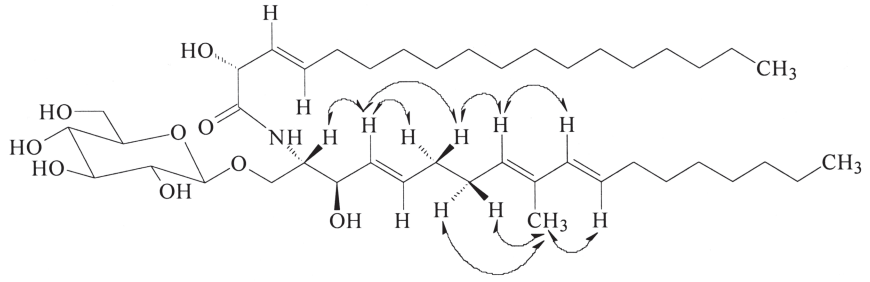

SCHEME 4

nearly identical to those of cerebroside **1** (Table 1) and which were shown to be the same as those of the natural cerebroside, **B** (13), indicated that it shared 2*S*,2′*R*,3*R*-configurations with cerebroside **1**. Morever, the specific rotations of **II** ($[\alpha]^{27}_{D}$ –5.1°) and **2** ($[\alpha]^{27}_{D}$ +6.2°) were nearly identical to those in the literature (see Ref. 10 and the related references cited therein), implying that the absolute configuration at C-2′ of **2** was *R* and that those at C-2 and C-3 were 2*S*,3*R*. In conclusion, the structure of cerebroside **2** was (2*S*,2′*R*,3*R*,3′*E*,4*E*,8*E*,10*E*)-1-*O*-β-D-glucopyranosyl-2-*N*-(2′-hydroxy-3′-octadecenoyl)-3-hydroxy-9-methyl-4,8,10-sphingatrienine. We have named compound **2** fusaruside.

In vitro antimicrobial/antibacterial tests showed that both cerebrosides were strongly active against *B. subtilis, E. coli*, and *P. fluorescens*, with the MIC of **1** being 7.8, 3.9, and 7.8 µg/mL, and that of **2** being 3.9, 3.9, and 1.9 µg/mL, respectively (Table 2). The MIC of the amikacin sulfate co-assayed as a positive reference against the three bacteria were 0.45, 3.9, and 3.9 µg/mL, respectively. However, no substantial inhibition against the two test fungi could be discerned with any of the cerebrosides at 125

TABLE 2
***In vitro* Antimicrobial Activities of 1 and 2**

Test microbes	MIC[a] (μg/mL)			
	1	**2**	Amikacin sulfate	Ketoconazole
Bacillus subtilis	7.8	3.9	0.45	—
Escherichia coli	3.9	3.9	3.9	—
Pseudomonas fluorescens	7.8	1.9	3.9	—
Trichophyton rubrum	>125	>125	—	3.9
Candida albicans	>125	>125	—	3.9

[a]MIC, minimum inhibitory concentration.

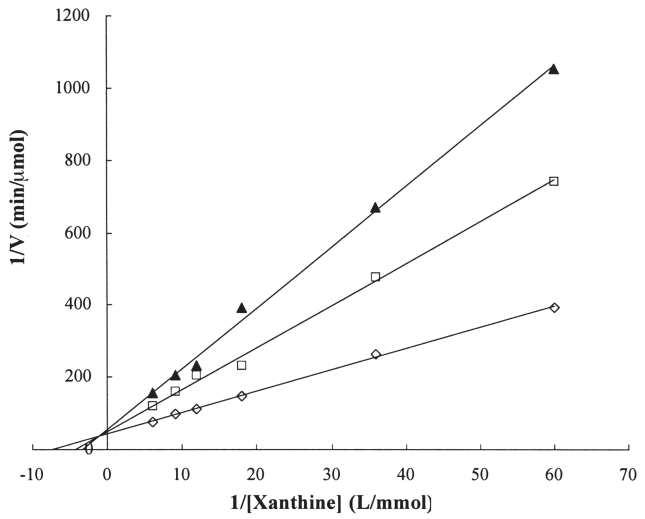

FIG. 1. Lineweaver–Burk plot of xanthine oxidase inhibition by cerebroside **1**. Xanthine oxidase assays were performed as described in the Experimental Procedures section, but with various concentrations of xanthine. Each experiment comprised three conditions: the control without any inhibitor (◇), in the presence of 47.2 μM cerebroside **1** (□), and in the presence of 74.1 μM of cerebroside **1** (▲). The Lineweaver–Burk-transformed data were plotted, followed by linear regression of the points. Data represent the average of two experiments.

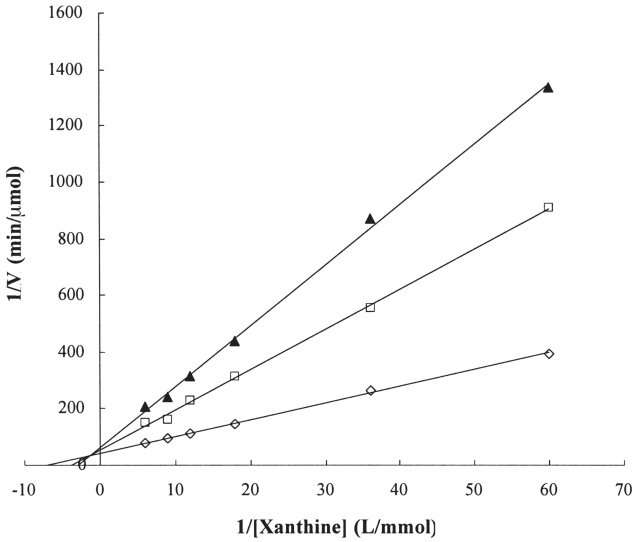

FIG. 2. Lineweaver–Burk plot of xanthine oxidase inhibition by fusaruside **2**. The experimental conditions and the subsequent data analyses were the same as in Figure 1, except that fusaruside **2** was used instead of cerebroside **1**: control without any inhibitor (◇), in the presence of 37.2 μM of fusaruside **2** (□), and in the presence of 58.4 μM of fusaruside **2** (▲). Data represent the average of two experiments.

μg/mL, whereas ketoconazole exhibited an MIC of 3.9 mg/mL with both fungi.

XO catalyzes the metabolism of hypoxanthine and xanthine to uric acid. The overproduction and/or underexcretion of this acid leads to complications of hyperuricemia, such as gout. Accordingly, one of the therapeutic approaches for treating gout is to use XO inhibitors that block the synthesis of uric acid. Allopurinol has been the sole XO inhibitor in clinical use during the past three decades, although other agents are being developed, as this drug gives rise to a number of adverse side effects (19). Therefore, there is an urgent need to search for new XO inhibitors. The XO inhibitory tests showed that cerebrosides **1** and **2** could inhibit the enzyme, as they had IC_{50} values of 55.5 ± 1.8 and 43.8 ± 3.6 μM, respectively. The IC_{50} datum for the allopurinol co-assayed in the study as a positive control was 9.8 ± 1.2 μM. Figure 1 shows a Lineweaver–Burk transformation of the data for XO assays performed as a function of different concentrations of xanthine in the absence or presence of cerebroside **1**. Parallel studies were carried out with fusaruside **2**, as shown in Figure 2. The data indicated that both of the cerebrosides shared with allopurinol (19) a mixed-type inhibition to XO.

Cerebrosides are central components of a wide variety of tissues and organs in biological systems that serve as structure and shape determinants of the cell membrane (20). The cerebrosides containing (4*E*,8*E*)-9-methylsphinga-4,8-dienine have been found in a number of fungi (10,21,22). Previously, some cerebrosides carrying a 9-methylated (4*E*,8*E*)-sphingadienine chain amidated by 2-hydroxylated FA of $C_{14–18}$ lengths have shown stronger fruit-inducing (23) and antibiotic activities (24–26). Recently, it was reported that monoclonal antibodies prepared against cerebroside **1** can be used as tools for evaluating the role of glucosylceramides in the morphological transition of *Colletotrichum gloeosporioides* (27). These results differ from those of Weiss *et al.* (28) and Duarte *et al.* (14). Weiss *et al.* (28) reported that the monohexosylceramides of *Fusarium lini* contain predominantly C_{18} and C_{20} phytosphingosines on the basis of hydrolysis, reduction, and periodate oxidation.

Duarte *et al.* (14) described two 9-methyl-4,8-sphingadiene glycosphingolipids from *F. solani* and *Fusarium* sp. using modern spectroscopic methods such as ^{1}H NMR, GC-MS, and FABMS. It is noteworthy that this is the first communication dealing with these two antibacterial and XO inhibitory glycosphingolipids including a new metabolite, fusaruside (**2**).

ACKNOWLEDGMENTS

This work was co-financed by a key project (No. 104195) from the Ministry of Education and as grants (Nos. 30171104 and 30270034) from the National Natural Science Foundation of China.

REFERENCES

1. Tan, R.X., and Chen, J.H. (2003) The Cerebrosides, *Nat. Prod. Rep. 20*, 509–534.
2. Liu, J.Y., Liu, C.H., Zou, W.X., Tian, X., and Tan, R.-X. (2002) Leptosphaerone, a Metabolite with a Novel Skeleton from *Leptosphaeria* sp. IV403, an Endophytic Fungus in *Artemisia annua, Helv. Chim. Acta 85*, 2664–2667.
3. Tan, R.X., and Zou, W.X. (2001) Endophytes: A Rich Source of Functional Metabolites, *Nat. Prod. Rep. 18*, 448–459.
4. Zou, W.X., Lu, H., Meng, J.C., Chen, G.X., Zhang, T.Y., and Tan, R.X. (2000) New and Bioactive Metabolites of *Colletotrichum gloeosporioides*, an Endophytic Fungus in *Artemisia mongolica*, *J. Nat. Prod. 63*, 1529–1530.
5. Lu, H., Zou, W.X., Meng, J.C., Hu, J., and Tan, R.X. (2000) New Bioactive Metabolites Produced by *Colletotrichum* sp., an Endophytic Fungi in *Artemisia annua, Plant Sci. 151*, 67–73.
6. Dickson, R.-C., and Lester, R.-L. (1999) Yeast Sphingolipids, *Biochim. Biophys. Acta 1426*, 347–357.
7. Batrakov, S.G., Konova, I.V., Sheichenko, V.I., Esipov, S.E., Galanina, L.A., and Istratova, L.N. (2002) Unusual Fatty Acid Composition of Cerebrosides from the Filamentous Soil Fungus *Mortierella alpina, Chem. Phys. Lipids 117*, 45–51.
8. Chen, J.H., Cui, G.Y., Liu, J.Y., and Tan, R.X. (2003) Pinelloside, an Antimicrobial Cerebroside from *Pinellia ternate, Phytochemistry 64*, 903–906.
9. Qi, J., Ojika, M., and Sakagami, Y. (2000) Termitomycesphins A–D, Novel Neuritogenic Cerebrosides from the Edible Chinese Mushroom *Termitomyces albuminosus, Tetrahedron 56*, 5835–5841.
10. Gao, J.M., Hu, L., Dong, Z.J., and Liu, J.K. (2001) New Glycosphingolipid Containing an Unusual Sphingoid Base from the Basidiomycete *Polyporus ellisii, Lipids 36*, 521–527.
11. Kong, L.D., Abliz, Z., Zou, C.X., Li, L.J., Cheng, C.H.K., and Tan, R.X. (2001) Glycosides and Xanthine Oxidase Inhibitors from *Conyzaa bonariensis, Phytochemistry 58*, 645–651.
12. Van Hoorn, D.E.C., Nijveldt, R.J., Van Leeuwen, P.A.M., Hofman, Z., M'Rabet, L., De Bont, D.B.A., and Van Norren, K. (2002) Accurate Prediction of Xanthine Oxidase Inhibition Based on the Structure of Flavonoids, *Eur. J. Pharmacol. 451*, 111–118.
13. Toledo, M.S., Levery, S.B., Straus, A.H., Suzuki, E., Momany, M., Glushka, J., Moulton, J.M., and Takahashi, H.K. (1999) Characterization of Sphingolipids from Mycopathogens: Factors Correlating with Expression of 2-Hydroxy Fatty Acyl (*E*)-Δ^3-Unsaturation in Cerebrosides of *Paracoccidioides brasiliensis* and *Aspergillus fumigatus, Biochemisry 38*, 7294–7306.
14. Duarte, R.S., Polycarpo, C.R., Wait, R. Hartmann, R., and Bergter, E.B. (1998) Structural Characterization of Neutral Glycosphingolipids from *Fusarium* Species, *Biochim. Biophys. Acta 1390*, 186–196.
15. Keusgen, M., Yu, C.-M., Curtis, J.M., Brewer, D., and Ayer, S.W. (1996) A Cerebroside from the Marine Fungus *Microsphaeropsis olivacea* (Bonord.) Höhn, *Biochem. Syst. Ecol. 24*, 465–468.
16. Umemura, K., Ogawa, N., Yamauchi, T., Iwata, M., Shimura, M., and Koga, J. (2000) Cerebroside Elicitors Found in Diverse Phytopathogens Activate Defense Responses in Rice Plants, *Plant Cell Physiol. 41*, 676–683.
17. Huang, Y., Dong, Z.J., and Liu, J.K. (2001) The Chemical Constituents from Basidiocarps of *Sarcodon aspratum, Acta Bot. Yunnanica 23*, 125–128.
18. Zhan, Z.J., Sun, H.D., Wu, H.M., and Yue, J.M. (2003) Chemical Components from the Fungus *Engleromyces goetzei, Acta Bot. Sin. 45*, 248–252.
19. Kong, L.D., Cai, Y., Huang, W.W., Cheng, C.H.K., and Tan, R.X. (2000) Inhibition of Xanthine Oxidase by Some Chinese Medicinal Plants Used to Treat Gout, *J. Ethnopharmacol. 73*, 199–207.
20. Barrett, A.G.M., Beall, J.C., Braddock, D.C., Flack, K., Gibson, V.C., and Salter, M.M. (2000) Asymmetric Allylboration and Ring Closing Alkene Metathesis: A Novel Strategy for the Synthesis of Glycosphingolipids, *J. Org. Chem. 65*, 6508–6514.
21. Tan, J.W., Dong, Z.J., and Liu, J.K. (2003) New Cerebrosides from the Basidiomycete *Cortinarius tenuipes, Lipids 38*, 81–84.
22. Boas, M.H.S.V., Egge, H., Pohlentz, G., Hartmann, R., and Bergter, E.B. (1994) Structural Determination of *N*-2′-Hydroxyoctadecenoyl-1-*O*-β-D-glucopyranosyl-9-methyl-4,8-sphingadienine from Species of *Aspergillus, Chem. Phys. Lipids 70*, 11–19.
23. Kawai, G. (1989) Molecular Species of Cerebrosides in Fruiting Bodies of *Lentimus edodes* and Their Biological Activity, *Biochim. Biophys. Acta 1001*, 185–190.
24. Sitrin, R.D., Chan, G., Dinger-dissen, J., DeBrosse, C., Mehta, R., Roberts, G., Rottschaefer, S., Staiger, D., Valenta, J., Snader, K.M., *et al.* (1988) Isolation and Structure Determination of *Pachybasium* Cerebrosides Which Potentiate the Antifungal Activity of Aculeacin, *J. Antibiot. 41*, 469–480.
25. Nishida, F., Mori, Y., Rokkaku, N., Isobe, S., Furuse, T., Suzuki, M., Meevootisom, V., Flegel, T.W., Thebtaranonth, Y., and Intararuangsorn, S., (1990) Structure Elucidation of Glycosidic Antibiotics Glykenins from *Basidiomycetes* sp. II. Absolute Structures of Unusual Polyhydroxylated C26-Fatty Acids, Aglycones of Glykenins, *Chem. Pharm. Bull. 38*, 2381–2389.
26. Nishida, F., Mori, Y., Sonobe, C., and Suzuki, M. (1991) Structure Elucidation of Glycosidic Glykenins from *Basidomycetes* sp. III, *J. Antibiot. 44*, 541–545.
27. da Silva, A.F.C., Rodrigues, M.L., Farias, S.E., Almeida, I.C., Pinto, M.R., and Barreto-Bergter, E. (2004) Glucosylceramides in *Colletotrichum gloeosporioides* Are Involved in the Differentiation of Conidia into Mycelial Cells, *FEBS Lett. 561*, 137–143.
28. Weiss, B., Stiller, R.L., and Jack, R.C. (1973) Sphingolipids of the Fungi *Phycomycetes blakesleeanus and Fusarium lini, Lipids 8*, 25–30.

[Received May 31, 2004, and in final form and accepted September 20, 2004]

2-Methoxylated Fatty Acids in Marine Sponges: Defense Mechanism Against Mycobacteria?

Néstor M. Carballeira[a,*], Heidyleen Cruz[a], Cecil D. Kwong[b], Baojie Wan[c], and Scott Franzblau[c]

[a]Department of Chemistry, University of Puerto Rico, San Juan, Puerto Rico 00931-3346, [b]Tuberculosis Antimicrobial Acquisition & Coordinating Facility, Birmingham, Alabama 35255-5305, and [c]Institute for Tuberculosis Research, College of Pharmacy, The University of Illinois at Chicago, Chicago, Illinois 60612-7231

ABSTRACT: A series of saturated 2-methoxylated FA having even-numbered chains with 8–14 carbons were synthesized, and their spectroscopic data are presented for the first time. The 2-methoxylated C_{10}–C_{14} acids were prepared from the corresponding 2-hydroxylated FA, whereas the 2-methoxyoctanoic acid was synthesized starting with heptaldehyde. All of the methoxylated FA displayed some degree of inhibition (between 2 and 99%) of *Mycobacterium tuberculosis* H_{37}Rv at 6.25 μg/mL. The most inhibitory FA was 2-methoxydecanoic acid, with a minimum inhibitory concentration of 200–239 μM against *M. tuberculosis* H_{37}Rv as determined by both the microplate Alamar Blue assay and the green fluorescent protein microplate assay. These results are discussed in terms of the possible role of the 2-methoxylated FA as antimicrobial lipids produced either by marine sponges, or the associated marine symbiotic bacteria, as a defense mechanism in a highly competitive environment.

Paper no. L9436 in *Lipids 39,* 675–680 (July 2004).

Marine organisms, in particular sponges, are a recognized source of antibacterial substances (1). In addition, bacteria present as symbionts in sponges also are sources of antibacterial compounds, which has led to the theory that microbial symbionts play a role in the defense of their host sponge (2). For example, a recent study revealed that 57% of bacteria isolated from a *Cliona* sp. produce antibacterial compounds against *Staphylococcus aureus* ATCC 6538, and predominating in these bacterial isolates were strains of *Aeromonas* spp. and *Vibrio* spp. (2).

Host specificity also has been recognized to operate in marine sponge-associated bacteria. For example, some sponges from Australia, such as *Callyspongia* sp. and *Stylinos* sp., contain unique specialized communities of microbes (3). Microbial communities vary little within each species of sponge, but changes among species are noteworthy. How do these different communities of microbes guarantee themselves a place in a competitive and beneficial habitat? It is evident that the antimicrobial defenses of such marine microbes, and their hosts, are mostly uncharacterized.

In looking for such antimicrobial substances, we have focused on the FA composition of several Caribbean marine sponges (4). One particular group of FA unique to marine sponges is the α-methoxylated FA, which have only been identified in small amounts in the PE and PS of these organisms (5). Recent examples of short-chain analogs (C_{14}–C_{18}) of these α-methoxylated FA, in particular those arising from a *Callyspongia* sp. sponge, have been postulated to originate from bacteria in symbiosis with the sponge (4). Could these FA be used by a yet unrecognized marine microbe, in symbiosis with the sponge, as an antibacterial lipid to gain preference in a competitive marine microbial community? To begin answering this question, we needed to determine the complete spectrum of the antibacterial potential of these lipids.

Little information is available regarding the antibacterial properties of α-methoxylated FA. In our first efforts in this direction, we synthesized two α-methoxylated FA, (*Z*)-2-methoxy-6-hexadecenoic acid and (*Z*)-2-methoxy-5-hexadecenoic acid, and showed that they displayed similar antimicrobial activity against the Gram-positive bacteria *S. aureus* [minimum inhibitory concentration (MIC) 0.35 μmol/mL] and *Streptococcus faecalis* (MIC 0.35 μmol/mL) but that they were inactive against Gram-negative bacteria (6). The saturated 2-methoxyhexadecanoic acid was not antimicrobial in these bioassays.

Although nothing is known about the antimycobacterial properties of these intriguing α-methoxylated FA, the mycobactericidal effect of FA has been known for some time (7–10). Earlier studies by Kondo and Kanai (7) established that among a series of straight-chain saturated FA (C_2–C_{20}), myristic acid displayed the strongest bactericidal activity at 0.04 mM against a highly virulent strain (Ravenel) of *Mycobacterium bovis* and an avirulent strain (H_{37}Ra) of *M. tuberculosis*. More recently, Saito and collaborators (9) studied the cytotoxicity of a selected number of FA against 71 strains of 15 species of rapidly growing mycobacteria using the agar dilution method at pH 7.0. Among a series of straight-chain saturated FA having between 2 and 20 carbons, lauric acid (12:0) was the most active (MIC values of 6.25–25 μg/mL), and capric acid (10:0) was the second-most active (MIC values of 50–100 μg/mL) (9). Other saturated FA between C_2 and C_{20} were essentially nontoxic to all the mycobacteria

*To whom correspondence should be addressed at Department of Chemistry, University of Puerto Rico, P.O. Box 23346, San Juan, Puerto Rico 00931-3346. E-mail: ncarball@upracd.upr.clu.edu

Abbreviations: FU, fluorescence units; GFPMA, green fluorescent protein microplate assay; MABA, microplate Alamar Blue assay; MIC, minimum inhibitory concentration; OADC, oleic acid, albumin, dextrose, catalase.

studied. Unsaturated FA with 16–20 carbons were also highly toxic to the Group IV mycobacteria: palmitoleic acid was highly toxic (MIC values of 3.2–6.25 μg/mL), and oleic acid showed a similar profile. The mechanisms of antibacterial activity were postulated to proceed *via* disruption of the bacterial cell membrane resulting in a change in membrane permeability (9).

To begin to understand the antimycobacterial properties of these interesting α-methoxylated FA, and guided initially by literature values defining suitable chain lengths, we present herein the susceptibility of *M. tuberculosis* $H_{37}Rv$ toward the 2-methoxylated acids **1–4** (Fig. 1). We also report spectral data for acids **1–3**, which have not previously been reported, although data for the saturated α-methoxylated FA having chain lengths between 14 and 24 carbons are available (5).

MATERIALS AND METHODS

Instrumentation. IR spectra were recorded on a Nicolet 600 FTIR spectrophotometer. ^1H and ^{13}C NMR spectra were recorded on either a Bruker DPX-300 or a Bruker DRX-500 spectrometer. ^1H NMR chemical shifts are reported with respect to internal $(CH_3)_4Si$, and ^{13}C NMR chemical shifts are reported in parts per million relative to $CDCl_3$ (77.0 ppm). Mass spectral data were acquired using a gas chromatograph–mass spectrometer (Hewlett-Packard 5972A MS ChemStation) at 70 eV equipped with a 30 m × 0.25 mm special performance capillary column (HP-5MS) of polymethylsiloxane cross-linked with 5% phenyl methylpolysiloxane. Elemental analyses were performed by Galbraith Laboratories, Inc. (Knoxville, TN).

(±)-2-Trimethylsilyloxyoctanonitrile. To heptaldehyde (5 g, 44 mmol) in 20 mL of anhydrous CH_2Cl_2 was added dropwise 4.3 g (44 mmol) of trimethylsilyl cyanide and catalytic amounts of Et_3N (10%) at 0°C. The reaction mixture was stirred for 2 h at 0°C. Then the solvent was removed *in vacuo*, affording 8.5 g (40 mmol) of (±)-2-trimethylsilyloxyoctanonitrile. ^1H NMR ($CDCl_3$, 300 MHz) δ 4.37 (1H, *t*, *J* = 6.6 Hz, H-2), 1.76 (2H, *m*, H-3), 1.43 (2H, *m*, H-4), 1.28 (6H, *brs*, CH_2), 0.87 (3H, *J* = 6.9 Hz, *t*, H-8), 0.19 (9H, *s*, $Si(CH_3)_3$); ^{13}C NMR ($CDCl_3$, 75 MHz) δ 120.0 (*s*, C-1), 61.4 (*d*, C-2), 36.1 (*t*), 31.5 (*t*), 28.5 (*t*), 24.4 (*t*), 22.4 (*t*), 13.9 (*q*), –0.4 (*q*). GC–MS *m/z* (relative intensity) M^+ 213 (0.1), 198 (40), 185 (4), 173 (4), 172 (15), 171 (100), 129 (14), 115 (20), 114 (24), 113 (7), 102 (21), 101 (35), 100 (11), 97 (28), 89 (7), 84 (27), 83 (2), 74 (81), 73 (64), 70 (19), 69 (14), 59 (17), 57 (12), 55 (94).

Methyl 2-hydroxyoctanoate. Into a 25-mL round-bottomed flask was placed the trimethylsilyloxy nitrile (6 g, 28 mmol) in 10 mL of dimethoxyethane. Concentrated HCl (10 mL) was added, and the reaction mixture was heated at 90°C for 24 h. The reaction mixture was then cooled (ice bath) and made alkaline by the slow addition of 50% NaOH (10 mL). The reaction mixture was heated again for 2 h at 90°C. The mixture was then acidified with 10 mL of 6 M HCl, and the product was extracted with ether (2 × 12 mL). The organic layer was dried over Na_2SO_4, filtered, and evaporated *in vacuo*, affording 3.7 g (21 mmol) of the 2-hydroxyoctanoic

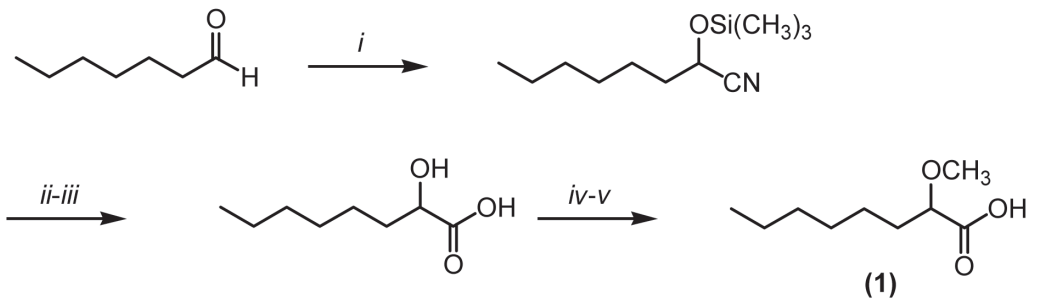

(*i*) TMS-CN, Et_3N, CH_2Cl_2, 0°C; (*ii*) HCl (conc.), DME 24 h; (*iii*) 50% NaOH, heat 3 h; (*iv*) NaH/DMSO, 2 = CH_3I; (*v*) KOH/EtOH

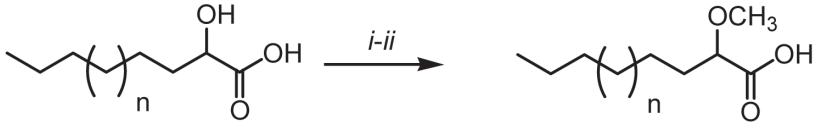

(*i*) NaH/DMSO, 2 equiv CH_3I; (*ii*)

(2), n = 3
(3), n = 5
(4), n = 7

FIG. 1. Synthesis of the 2-methoxylated FA 2-methoxyoctanoic acid (**1**), 2-methoxydecanoic acid (**2**), 2-methoxydodecanoic acid (**3**), and 2-methoxytetradecanoic acid (**4**). TMS-CN, trimethylsilyl cyanide; DME, dimethoxyethane.

acid, which was subsequently esterified (100% yield) with MeOH/HCl for final characterization. ^{1}H NMR ($CDCl_3$, 300 MHz) δ 4.18 (1H, *dd*, *J* = 7.4 and 7.35 Hz, H-2), 3.77 (3H, *s*, –OMe), 3.15 (1H, *s*, –OH), 1.76 (1H, *m*, H-3), 1.60 (1H, *m*, H-3), 1.27 (8H, *brs*, CH_2), 0.86 (3H, *t*, *J* = 6.9 Hz, H-8); ^{13}C NMR ($CDCl_3$, 75 MHz) δ 175.9 (*s*, C-1), 70.4 (*q*, –OCH_3), 52.4 (*d*, C-2), 34.3 (*t*), 31.6 (*t*), 28.9 (*t*), 24.6 (*t*), 22.5 (*t*), 14.0 (*q*, C-8); GC–MS *m/z* (relative intensity) M^+ 174 (0.1), 145 (1), 127 (2), 116 (3), 115 (39), 113 (4), 104 (1), 98 (5), 97 (68), 90 (25), 87 (3), 74 (1), 70 (4), 69 (18), 68 (2), 60 (1), 59 (8), 57 (14), 56 (6), 55 (100).

Methylation of the 2-hydroxy FAME. Into 15- or 50-mL round-bottomed flasks provided with magnetic stirrers and under a nitrogen atmosphere were placed 2 equiv of NaH in 3–25 mL of DMSO. Then the 2-hydroxy FAME (0.03–3.7 g, 0.11–21.3 mmol) dissolved in DMSO was added dropwise at room temperature for 10 min. An excess of CH_3I was then added dropwise, and the reaction mixture was further stirred for 20 min, after which it was diluted with 10 mL of hexane/ether (1:1) and washed with H_2O (2 × 10 mL) to remove the remaining DMSO. The organic phase was separated, dried over Na_2SO_4, filtered, and evaporated *in vacuo,* affording 0.02–3.2 g (0.08–17.0 mmol) of the 2-methoxylated methyl esters (74–80% isolated yields). The compounds were used as such for the next step without further purification.

Saponification of the 2-methoxy FAME. Into a 25-mL round-bottomed flask was added the 2-methoxymethyl ester (0.02–1.0 g, 0.08–5.5 mmol) in 15 mL of 1 M KOH/ethanol, and the mixture was refluxed for 1 h. The reaction mixture was cooled to room temperature, and the ethanol was then evaporated *in vacuo*. Hexane was added to the mixture, and the organic phase was washed twice with H_2O (2 × 10 mL). The aqueous phase was then acidified with 6 M HCl, and the acid was extracted with ether (2 × 10 mL). The organic phase was separated, dried over Na_2SO_4, and evaporated *in vacuo*, affording the 2-methoxylated FA (0.016–0.81 g, 0.065–4.65 mmol, 81–86% yield). Spectral data not previously reported in the literature are presented below.

*(i) 2-Methoxyoctanoic acid (**1**).* IR (neat) ν_{max} 2956, 2928, 2872, 2856, 2829, 1708, 1604, 1461, 1414, 1099, and 796 cm^{-1}; ^{1}H NMR ($CDCl_3$, 300 MHz) δ 9.13 (1H, *s*, –CO_2H), 3.77 (1H, *dd*, *J* = 6.4 and 5.4 Hz, H-2), 3.42 (3H, *s*, OCH_3), 1.75 (2H, *m*, H-3), 1.38 (2H, *m*, H-4), 1.26 (6H, *brs*, CH_2), 0.86 (3H, *t*, *J* = 6.9 Hz, CH_3); ^{13}C NMR ($CDCl_3$, 75 MHz) δ 178.0 (*s*, C-1), 80.1 (*d*, C-2), 58.2 (*q*, –OCH_3), 32.4 (*t*), 31.5 (*t*), 28.9 (*t*), 24.8 (*t*), 22.5 (*t*), 13.9 (*q*, C-8); GC–MS *m/z* (relative intensity) M^+ 174 (0.1), 130 (6), 129 (73), 113 (1), 101 (1), 98 (6), 97 (75), 95 (2), 90 (11), 84 (1), 72 (2), 71 (15), 69 (16), 68 (2), 67 (4), 61 (2), 59 (5), 58 (10), 56 (6), 55 (100). Anal. calcd. for $C_9H_{18}O_3$: C, 62.04; H, 10.41. Found: C, 58.86; H, 10.65.

*(ii) 2-Methoxydecanoic acid (**2**).* M.p. 40–42°C, IR (neat) ν_{max} 2992, 2923, 2908, 2848, 2838, 1706, 1467, 1423, 1354, 1285, 1263, 1227, 1210, 1144, 1119, 1053, 1015, 958, 835, 788, 755, 719 cm^{-1}; ^{1}H NMR ($CDCl_3$, 300 MHz) δ 8.55 (1H, *s*, –CO_2H), 3.78 (1H, *dd*, *J* = 6.9 and 6.8 Hz, H-2), 3.42 (3H, *s*, –OMe), 1.75 (2H, *m*, H-3), 1.40 (2H, *m*, H-4), 1.25 (10H, brs, CH_2), 0.85 (3H, *t*, *J* = 6.6 Hz, CH_3); ^{13}C NMR ($CDCl_3$, 75 MHz) δ 178.0 (*s*, C-1), 80.1 (*d*, C-2), 58.2 (*q*, –OCH_3), 32.4 (*t*), 31.8 (*t*), 29.3 (*t*), 29.2 (*t*), 29.1 (*t*), 24.9 (*t*), 22.6 (*t*), 14.0 (*q*, C-10); GC–MS *m/z* (relative intensity) M^+ 202 (0.1), 169 (1), 157 (73), 152 (1), 125 (2), 113 (2), 97 (3), 90 (12), 85 (3), 83 (55), 81 (5), 75 (2), 73 (5), 71 (20), 69 (100), 57 (22), 55 (41). Anal. calcd. for $C_{11}H_{22}O_3$: C, 65.31; H, 10.96. Found: C, 65.05; H, 11.09.

*(iii) 2-Methoxydodecanoic acid (**3**).* M.p. 49–51°C, IR (neat) ν_{max} 2948, 2895, 2848, 1705, 1474, 1422, 1270, 1244, 1221, 1145, 1119, 940, 916 cm^{-1}; ^{1}H NMR ($CDCl_3$, 300 MHz) δ 3.81 (1H, *dd*, *J* = 6.4 and 6.4 Hz, H-2), 3.45 (3H, *s*, OCH_3), 1.78 (2H, *m*, H-3), 1.40 (2H, *m*, H-4), 1.25 (14H, *brs*, CH_2), 0.87 (3H, *t*, *J* = 6.9 Hz, CH_3); ^{13}C NMR ($CDCl_3$, 75 MHz) δ 177.4 (*s*, C-1), 80.2 (*d*, C-2), 58.3 (*q*, –OCH_3), 32.0 (*t*), 31.9 (*t*), 29.55 (*t*), 29.51 (*t*), 29.4 (*t*), 29.3 (*t*), 29.2 (*t*), 24.7 (*t*), 22.7 (*t*), 14.1 (*q*, C-12); GC–MS *m/z* (relative intensity) M+ 230 (2), 186 (14), 185 (100), 152 (1), 138 (2), 127 (1), 113 (3), 111 (19), 109 (3), 103 (2), 97 (81), 90 (18), 85 (10), 83 (72), 71 (54), 69 (64), 57 (29), 55 (73). Anal. calcd. for $C_{13}H_{26}O_3$: C, 67.78; H, 11.38. Found: C, 67.72; H, 11.62.

Bacterial strains and growth conditions. Mycobacterium tuberculosis H_{37}Rv ATCC 27294 (H_{37}Rv) was obtained from the American Type Culture Collection (Rockville, MD). For the first three of four replicate experiments, H_{37}Rv was first passaged in radiometric 7H12 broth (BACTEC 12B; Becton Dickinson Diagnostic Instrument Systems, Sparks, MD) until the growth index (measurement of the radioactivity of the ^{14}C-CO_2 released by multiplying mycobacteria) reached 800 to 999. For the fourth replicate experiment, H_{37}Rv was grown in 100 mL of Middlebrook 7H9 broth (Difco, Detroit, MI) supplemented with 0.2% (vol/vol) glycerol (Sigma Chemical Co., St. Louis, MO), 10% (vol/vol) OADC (oleic acid, albumin, dextrose, catalase; Difco), and 0.05% (vol/vol) Tween 80 (Sigma). The complete medium was referred to as 7H9GC-Tween. Cultures were incubated in 500-mL nephelometer flasks on a rotary shaker (New Brunswick Scientific, Edison, NJ) at 150 rpm and 37°C until they reached an optical density of 0.4 to 0.5 at 550 nm. Bacteria were washed and suspended in 20 mL of PBS and passed through an 8-μm pore-size filter to eliminate clumps. The filtrates were aliquotted, stored at –80°C, and used within 30 d.

Media. The FA were solubilized, and stock solutions were filter sterilized (0.22 μm pore size) and stored at –70°C for not more than 30 d. MIC were determined four times on four different days. A common set of frozen drug stock solutions was used for all experiments, with a previously unthawed aliquot being used for each experiment. Maximal final drug concentrations in testing media were limited by compound solubility.

Microplate Alamar Blue susceptibility test (MABA). Antimicrobial susceptibility testing was performed in black, clear-bottomed, 96-well microplates (black view plates; Packard Instrument Company, Meriden, CT) to minimize background fluorescence. Outer perimeter wells were filled with sterile water to prevent dehydration in experimental wells. Initial drug dilutions were prepared in either DMSO or distilled deionized water, and subsequent dilutions were performed in 0.1 mL of

7H9GC (no Tween 80) in the microplates. BACTEC 12B-passaged inocula were initially diluted 1:2 in 7H9GC, and 0.1 mL was added to wells. Subsequent determination of bacterial titer yielded 1×10^6 CFU/mL in plate wells for $H_{37}Rv$. Frozen inocula were initially diluted 1:20 in BACTEC 12B medium followed by a 1:50 dilution in 7H9GC. Addition of 0.1 mL to wells resulted in a final bacterial titer of 2.0×10^5 CFU/mL for $H_{37}Rv$. Wells containing drug only were used to detect autofluorescence of compounds. Additional control wells consisted of bacteria only (B) and medium only (M). Plates were incubated at 37°C. Starting at day 4 of incubation, 20 μL of 10× Alamar Blue solutions (Alamar Biosciences/Accumed, Westlake, OH) and 12.5 μL of 20% Tween 80 were added to one B well and one M well, and plates were reincubated at 37°C. Wells were observed at 12 and 24 h for a color change from blue to pink and for a reading of >50,000 fluorescence units (FU). Fluorescence was measured in a Cytofluor II microplate fluorometer (PerSeptive Biosystems, Framingham, MA) in bottom-reading mode with excitation at 530 nm and emission at 590 nm. If the B wells became pink by 24 h, reagent was added to the entire plate. If the well remained blue or ≤50,000 FU was measured, additional M and B wells were tested daily until a color change occurred, at which time reagents were added to all remaining wells. Plates were then incubated at 37°C, and results were recorded at 24 h after addition of reagent. Visual MIC were defined as the lowest concentration of drug that had prevented a color change. For fluorometric MIC, a background subtraction was performed on all wells with a mean of triplicate M wells. Percent inhibition was defined as 1 – (test well FU/mean FU of triplicate B wells) × 100. The lowest drug concentration effecting an inhibition of ≥90% was considered the MIC.

Statistical analysis. All analyses were performed with the program SAS (SAS Institute Inc., Cary, NC). Correlation coefficients were defined according to Spearman for ranked data analysis and Pearson for raw data analysis to determine differences between the BACTEC system and the MABA either fluorometrically or visually for determination of MIC (11). A general linear model procedure using ANOVA of ranked data was performed for each of the three variables of MIC generation to determine significant differences between the replicate comparisons of the four experiments. Tukey's Studentized range test was also used for pairwise *post hoc* comparison of variable analysis of ranked measure for significant differences among techniques for individual antimicrobial agents for each bacterial strain. Significance was determined at $P \leq 0.05$.

*Determination of the MIC of 2-methoxydecanoic acid (**2**).* *Mycobacterium tuberculosis* $H_{37}Rv$ (ATCC 27294) was grown to late log phase (70–100 Klett units) in Middlebrook 7H9 broth supplemented with 0.2% vol/vol glycerol, 0.05% Tween 80, and 10% vol/vol OADC. Cultures were centrifuged 15 min at 4°C at $3150 \times g$, washed twice, and resuspended in PBS. Suspensions were then passed through an 8-μm filter to remove clumps, and aliquots were frozen at –80°C. The CFU was determined by plating on 7H11 agar plates.

Twofold dilutions of FA were prepared in Middlebrook 7H12 medium (7H9 broth containing 1 mg/mL% wt/vol casitone, 5.6 μg/mL palmitic acid, 5 mg/mL BSA, 4 mg/mL catalase, filter-sterilized) or in the same medium supplemented with 0.2% vol/vol glycerol but without palmitic acid. Medium was added to 96-well microplates in a volume of 100 μL. *Mycobacterium tuberculosis* $H_{37}Rv$ (100 μL continuing 2×10^4 CFU) was added, yielding a final testing volume of 200 μL. Cultures were incubated for 7 d at 37°C.

The MIC of FA for *M. tuberculosis* was assessed by the MABA (11) or by the green fluorescent protein microplate assay (GFPMA) (12). For determination of growth/inhibition by MABA, at the end of the incubation period 12.5 μL of 20% Tween 80 and 20 μL of Alamar Blue were added to cultures. After incubation at 37°C for 16–24 h, fluorescence was read (excitation, 530 nm; emission, 590 nm). For determination of MIC by the GFPMA, fluorescence of cultures was read at excitation, 485 nm; emission, 510 nm. The MIC for both assays was defined as the lowest concentration effecting a reduction in fluorescence of ≥90% relative to the mean of replicate bacteria-only controls. Rifampin was used as a reference antimycobacterial drug in the MIC determination.

Cytotoxicity. Evaluation of the cytotoxic activity of FA in Vero cells (African green monkey kidney cells) was performed as described earlier (13) using the CellTiter 96 aqueous nonradioactive cell proliferation assay (Promega Corp., Madison, WI). The IC_{50} was defined as the reciprocal dilution resulting in 50% inhibition of the Vero cells.

RESULTS AND DISCUSSION

To appraise the antimycobactericidal potential of straight-chain 2-methoxylated FA, a short series of four FA having even-numberd carbon chains of 8–14 carbons was synthesized. Of these four FA, only the 2-methoxytetradecanoic acid (4) is a naturally occurring FA, with antifungal activity against *Candida albicans*, and its synthesis has been described before (14). The synthesis of the other methoxylated FA was achieved as outlined in Figure 1. For example, the 2-methoxydodecanoic acid and the 2-methoxydecanoic acid were synthesized from commercially available (Matreya, Pleasant Gap, PA) 2-hydroxydodecanoic acid and 2-hydroxydecanoic acid, respectively, by simple double methylation with sodium hydride in DMSO followed by saponification with KOH in ethanol, which resulted in the desired 2-methoxylated FA in 60–69% isolated overall yields. The synthesis of 2-methoxyoctanoic acid required a more lengthy synthetic sequence (Fig. 1). For this synthesis heptaldehyde was chosen as the starting material, which was first reacted with trimethylsilyl cyanide and triethylamine affording 2-trimethylsilyloxyoctanonitrile in a 90% yield. The silyloxynitrile was then transformed into 2-hydroxyoctanoic acid by first reacting the nitrile with concentrated HCl in DME followed by saponification with 50% NaOH. The final acid was obtained, as described for the longer-chain analogs, by a simple

double methylation with sodium hydride and DMSO followed by saponification with KOH in ethanol, resulting in the desired 2-methoxyoctanoic acid (Fig. 1).

The preliminary survey of the mycobactericidal activity of the four even-numbered-chain 2-methoxylated FA **1–4** was performed against the *M. tuberculosis* strain $H_{37}Rv$ at the single concentration of 6.25 μg/mL using the Alamar Blue susceptibility test (11). At this concentration, the 2-methoxydec-anoic acid displayed the greatest potential as a mycobactericidal α-methoxylated FA, with an apparent 99% inhibition of *M. tuberculosis* $H_{37}Rv$. The second-most promising was the 2-methoxydodecanoic acid, which presented a 62% inhibition of the mycobacterium, and the third-most bactericidal was the 2-methoxytetradecanoic acid, with a 22% inhibition of *M. tuberculosis* $H_{37}Rv$. The 2-methoxyoctanoic acid displayed only a very weak 2% inhibition of *M. tuberculosis* $H_{37}Rv$ at 6.25 μg/mL. Therefore, the order of percent inhibition of the tested 2-methoxylated FA against *M. tuberculosis* $H_{37}Rv$ at 6.25 μg/mL was determined to be $C_{10} > C_{12} > C_{14} > C_8$.

Based on this preliminary survey, we then focused our attention on 2-methoxydecanoic acid and determined its exact MIC against *M. tuberculosis* $H_{37}Rv$. The activity was assessed using both the MABA and the GFPMA. In addition, decanoic acid was tested so as to compare its mycobactericidal activity with that of the methoxylated analog. The results of this more precise study are shown in Table 1. In both assays the 2-methoxydecanoic acid displayed a MIC of 200–239 μM against *M. tuberculosis* $H_{37}Rv$. On the other hand, decanoic acid presented a MIC of 149–200 μM against this same strain of *M. tuberculosis* $H_{37}Rv$. An interesting observation is that neither acid was toxic to mammalian Vero cells (African green monkey kidney cells) at $IC_{50} > 300$ μM.

From these results we can conclude that *M. tuberculosis* $H_{37}Rv$ is susceptible to the different α-methoxylated FA tested in this work, but that the 2-methoxydecanoic acid is the most bactericidal. However, the use by marine organisms of the α-methoxylated FA **2–4** as antimycobactericidal lipids is plausible despite the fact that acids **1–3** still need to be identified in marine sponges. However, acid **4** is known to occur in sponges (14). We should mention in this context that although most α-methoxylated FA are phospholipid bound, this presents no problem in their release since many sponges are known to have considerable phospholipase A_2 activity (15). Based on these results, the survey of these and other α-methoxylated FA against other strains of mycobacteria is certainly warranted.

TABLE 1
Minimum Inhibitory Concentrations (MIC) of 2-Methoxydecanoic Acid and Decanoic Acid Against *Mycobacterium tuberculosis* $H_{37}Rv$[a]

Compound	MIC (μM)		IC_{50} (μM)
	MABA	GFPMA	
2-Methoxydecanoic acid	239.51	200.12	>300
Decanoic acid	200.07	148.83	>300
Rifampin	0.05	0.04	

[a]GFPMA, green fluorescent protein microplate assay; MABA, microplate Alamar Blue assay.

In summary, we have presented the first synthesis and spectral data for the saturated 2-methoxylated FA **1–3**. This information should certainly facilitate their future identification in nature. All acids displayed some sort of bactericidal activity toward *M. tuberculosis* $H_{37}Rv$, but the 2-methoxydecanoic acid (**2**) displayed the best mycobactericidal activity at MIC of 200 μM. As to the mechanism of action of the 2-methoxydecanoic acid (**2**) we can only speculate at this point, but this methoxylated FA could also disturb the mycobacterial cytoplasmic membrane in a fashion similar to that postulated for the unmethoxylated FA (8). This preliminary work should lay the foundation for further studies on the antimycobacterial properties of this interesting group of marine FA.

ACKNOWLEDGMENTS

This work was supported by a grant from the SCORE program of the National Institutes of Health (grant no. S06GM08102). Heidyleen Cruz thanks the UPR-Río Piedras NIH-RISE program and Compañía de Fomento Industrial (PR) for financial assistance. The preliminary antimycobacterial data were provided by the Tuberculosis Antimicrobial Acquisition and Coordinating Facility (TAACF) through a research and development contract with the U.S. National Institute of Allergy and Infectious Diseases.

REFERENCES

1. Konig, G.M., Wright, A.D., and Franzblau, S.G. (2000) Assessment of Antimycobacterial Activity of a Series of Mainly Marine Derived Natural Products, *Planta Med. 66*, 337–342.
2. Castillo, I., Lodeiros, C., Nuñez, M., and Campos, I. (2001) *In vitro* Evaluation of Antibacterial Substances Produced by Bacteria Isolated from Different Marine Organisms, *Rev. Biol. Trop. 49*, 1213–1222.
3. Taylor, M.W., Schupp, P.J., Dahllof, I., Kjelleberg, S., and Steinberg, P.D. (2004) Host Specificity in Marine Sponge-Associated Bacteria, and Potential Implications for Marine Microbial Diversity, *Environ. Microbiol. 6*, 121–130.
4. Carballeira, N.M. (2001) New Methoxylated Fatty Acids from the Caribbean Sponge *Callyspongia fallax*, *J. Nat. Prod. 64*, 620–623.
5. Carballeira, N.M. (2002) New Advances in the Chemistry of Methoxylated Lipids, *Prog. Lipid Res. 41*, 437–456.
6. Carballeira, N.M., Emiliano, A., Hernández-Alonso, N., and González, F.A. (1998) Facile Total Synthesis and Antimicrobial Activity of the Marine Fatty Acids (*Z*)-2-Methoxy-5-hexadecenoic Acid and (*Z*)-2-Methoxy-6-hexadecenoic Acid, *J. Nat. Prod. 61*, 1543–1546.
7. Kondo, E., and Kanai, K. (1977) The Relationship Between the Chemical Structure of Fatty Acids and Their Mycobactericidal Activity, *Jpn. J. Med. Sci. Biol. 30*, 171–178.
8. Kanetsuna, F. (1985) Bactericidal Effect of Fatty Acids on Mycobacteria, with Particular Reference to the Suggested Mechanism of Intracellular Killing, *Microbiol. Immunol. 29*, 127–141.
9. Saito, H., Tomioka, H., and Yoneyama, T. (1984) Growth of Group IV Mycobacteria on Medium Containing Various Saturated and Unsaturated Fatty Acids, *Antimicrob. Agents Chemother. 26*, 164–169.
10. Kondo, E., and Kanai, K. (1985) Mechanism of Bactericidal Activity of Lysolecithin and Its Biological Implication, *Jpn. J. Med. Sci. Biol. 38*, 181–194.
11. Collins, L., and Franzblau, S.G. (1997) Microplate Alamar Blue Assay versus BACTEC 460 System for High-Throughput Screening of Compounds Against *Mycobacterium tuberculosis*

and *Mycobacterium avium, Antimicrob. Agents Chemother. 41*, 1004–1009.
12. Changsen, C., Franzblau, S.G., and Palittapongarnpim, P. (2003) Improved Green Fluorescent Protein Reporter Gene-Based Microplate Screening for Antituberculosis Compounds by Utilizing an Acetamidase Promoter, *Antimicrob. Agents Chemother. 47*, 3682–3687.
13. Cantrell, C.L., Lu, T., Fronczek, F.R., Fischer, N.H., Adams, L.B., and Franzblau, S.G. (1996) Antimycobacterial Cycloartanes from *Borrichia frutescens*, *J. Nat. Prod. 59*, 1131–1136.
14. Carballeira, N.M., Ortiz, D., Parang, K., and Sardari, S. (2004) Total Synthesis and *in vitro* Antifungal Activity of (±)-2-Methoxytetradecanoic Acid, *Arch. Pharm. Pharm. Med. Chem. 337*, 152–155.
15. Nevalainen, T.J., Quinn, R.J., and Hooper, J.N. (2004) Phospholipase A_2 in Porifera, *Comp. Biochem. Physiol. B Biochem. Mol. Biol. 137*, 413–420.

[Received January 15, 2004; accepted September 3, 2004]

Unusual C_{21} Linear Polyacetylenic Alcohols from an Atlantic Ascidian

Margherita Gavagnin[a,*], Francesco Castelluccio[a], Angelo Antonelli[a], Josè Templado[b], and Guido Cimino[a]

[a]Istituto di Chimica Biomolecolare (ICB), Consiglio Nazionale delle Ricerche-I 80078-Pozzuoli (Naples), Italy and [b]Museo Nacional de Ciencias Naturales (CSIC), 28006 Madrid, Spain

ABSTRACT: Four novel straight-chain polyacetylenic alcohols were isolated from a marine ascidian (Phylum Chordata, subphyllum Urochordata) collected off Vigo, along the Atlantic coast of northwestern Spain. The chemical structures, which exhibit an uncommon dienyne group, were characterized by spectroscopic methods, mainly mono- and bi-dimensional NMR. This is the first finding of acetylenic lipids from an organism belonging to phylum Chordata.

Paper no. L9518 in *Lipids 39,* 681–685 (July 2004).

Several examples of polyacetylenic compounds with different chain lengths, unsaturation degrees, and oxygenation patterns have been reported from marine organisms in the last few years (1). The main sources of these molecules have been selected genera of sponges (i.e., *Petrosia*, *Xestospongia*, *Callyspongia*) belonging to the order Haplosclerida, for which polyacetylenes are considered to be good chemotaxonomic markers (2). A few reports of polyacetylenes from marine organisms belonging to different plant and animal groups, such as red algae (3–8), nudibranch molluscs (9,10), and stony corals (11), also have appeared in the literature. Acetylenic compound biogenesis is a highly speculative field, with an almost total lack of experimentation. Still, there is enough evidence to hypothesize a likely biosynthesis *de novo* of most of the compounds even though a bacterial symbiont origin in the different organisms also could be possible. Notable biological activities including antifungal properties (12), HIV protease inhibition (13), and cytotoxicity (14,15) have been reported for several members of this class of compounds. In continuing our studies on secondary metabolites of marine benthic invertebrates, we analyzed an unclassified ascidian belonging to the family Polyclinidae, collected along the Atlantic coast of northwestern Spain. This chemical analysis led to the isolation of four novel C_{21} acetylene-containing lipids, the structures of which were determined by extensive spectral analysis.

*To whom correspondence should be addressed at Istituto di Chimica Biomolecolare (CNR), Via Campi Flegrei 34, 80078–Pozzuoli (Naples), Italy. E-mail: mgavagnin@icmib.na.cnr.it

Abbreviations: HMBC, heteronuclear multiple-bond correlation; HMQC, heteronuclear multiple-quantum correlation; HRESIMS, high-resolution electrospray ionization mass spectroscopy; ICB, Istituto di Chimica Biomolecolare.

EXPERIMENTAL PROCEDURES

Silica gel chromatography was performed using precoated Merck F_{254} plates and Merck Kieselgel 60 powder (Merck, Darmstadt, Germany). HPLC was carried out on a Shimadzu liquid chromatograph LC-10AD equipped with a UV SPD-10A wavelength detector. Optical rotations $[\alpha]_D$were measured on a JASCO DIP 370 digital polarimeter by using a 100×2 mm cell. The IR spectra were taken on a Bio-Rad FTS 7 spectrophotometer. ^1H and ^{13}C NMR spectra were recorded on Bruker WM 500 MHz and Bruker AM 300 MHz spectrometers in $CDCl_3$ solutions; chemical shifts are reported in ppm referenced to $CHCl_3$ as the internal standard (δ 7.26 for proton and δ 77.0 for carbon). CI-MS spectra were measured on a Shimadzu quadrupole LCMS-2010 instrument, equipped with both UV SPD-10A and LCMS-2010 mass detectors. Samples were analyzed on an LC solvent stream and ionized by an atmospheric pressure chemical ionization MS (APCIMS) source. High-resolution mass spectra were recorded on a Micromass Q-TOF MICRO spectrometer coupled with a Waters Alliance 2695 high-performance liquid chromatograph, equipped with a Waters 2996 photodiode and a Rheodyne 7725i injector. An electrospray ionization method was employed, and the instrument was calibrated by using a polyethylene glycol mixture of 200 to 1000 MW [resolution specification 5000 full width at half maximum (FWHM), deviation <5 ppm root mean square (RMS) in the presence of a known internal reference mass].

Collection, extraction, and isolation. The ascidian (belonging to the family Polyclinidae), which shows club-shaped colonies with a well-developed stalk, a globular head, and yellowish zooids, was collected by SCUBA (–15 m) off Vigo (northern Spain) during August 1999. The identification of the specimens to the species or genus level was not possible due their preservation conditions. After collection, the biological material was frozen, then transferred to ICB laboratories in Naples, where it was kept at –80°C until extraction. A voucher specimen is stored for inspection at ICB (sample VIG37). In a typical extraction procedure, a sample of frozen tunicate (dry weight 17.6 g) was cut into small pieces, immersed in acetone (100 mL), and extracted sequentially at room temperature by both ultrasonic vibration (5 min) and grinding by a pestle. The treatment was repeated three times. After concentration *in vacuo*, the aqueous residue was extracted with Et_2O (3×50 mL). The combined ether extracts were taken to dryness, yielding an

TABLE 1
NMR Data[a] for Compounds 1 and 2

	Compound **1**		Compound **2**		
	^{13}C	^{1}H	^{13}C	^{1}H	HMBC[b]
Position	(ppm)	δ, *m* (*J*, Hz)	(ppm)	δ, *m* (*J*, Hz)	^{13}C to ^{1}H
1	74.1	2.57 *d* (2.1)	72.9	2.46 *d* (2.1)	H-3
2	ND		87.6		H-1, H-3, H_2-4
3	62.7	4.83 *bd* (5.4)	62.3	4.37 *m*	H-3, H_2-4
4	128.5	5.62 *m*	37.6	1.73 *m*	H-3
5	134.2	5.90 *ddt* (1.0, 15.2, 6.7)	24.9	1.45 *m*	H-3, H_2-4, H_2-6
6	31.7	2.10 *m*	29.4	1.34 *m*	H_2-4
7	28.3	1.42 *m*	29.0	1.34 *m*	H_2-9
8	29.0	1.42 *m*	29.0	1.42 *m*	H_2-6, H_2-9
9	27.8	2.20 *m*	27.9	2.19 *m*	H-11
10	134.8	5.59 *m*	135.2	5.60 *m*	H-12, H_2-9
11	125.9	6.53 *dd* (11.2, 10.5)	125.7	6.53 *dd* (11.4, 12.0)	H-13, H_2-9
12	133.8	6.59 *dd* (10.1, 11.2)	133.9	6.58 *dd* (10.1, 11.4)	H-10
13	109.6	5.45 *bd* (10.1)	109.4	5.44 *d* (10.1)	H-12, H_2-16
14	ND		77.8		H-12, H_2-16
15	97.2		97.2		H_2-16, H_2-17
16	19.6	2.39 *m*	19.6	2.39 *m*	H_2-17
17	28.2	1.60 *m*	28.2	1.60 *m*	H_2-16, H_2-19
18	28.1	1.55 *m*	28.1	1.55 *m*	H_2-17, H_2-19, H-20
19	33.2	2.10 *m*	33.2	2.09 *m*	H_2-17, H_2-18, H-20, H_2-21
20	138.6	5.80 *ddt* (17.1, 10.2, 6.7)	138.6	5.82 *ddt* (17.1, 10.2, 6.8)	H_2-19
21	114.6	5.01 *dd* (17.1, 1.8) 4.96 *bd* (10.2)	114.7	5.02 *bd* (17.1) 4.96 *bd* (10.2)	H_2-19

[a]$CDCl_3$, 300 and 500 MHz. Assignments were supported by ^{1}H-detected heteronuclear multiple-quantum coherence (HMQC), distortionless enhancement by polarization transfer (DEPT) 135° and 90° experiments.
[b]^{1}H-Detected heteronuclear multiple-bond coherence (HMBC) (*J* = 10 Hz).

TABLE 2
NMR Data[a] for Compounds 3 and 4

	Compound **3**			Compound **4**	
	^{13}C	^{1}H	HMBC[b]	^{13}C	^{1}H
Position	(ppm)	δ, *m* (*J*, Hz)	^{13}C to ^{1}H	(ppm)	δ, *m* (*J*, Hz)
1	74.0	2.56 *d* (2.1)		72.8	2.46 *d* (2.1)
2	83.2		H-1, H-4	84.6	
3	62.8	4.83 *d* (5.1)	H-5	62.3	4.37 *dt* (1.9, 6.5)
4	128.6	5.63 *m*	H_2-6	37.6	1.71 *m*
5	134.1	5.90 *m*	H-4, H_2-6	24.9	1.45 *m*
6	31.7	2.08 *m*	H-4, H-5	29.3	1.34 *m*
7	28.3	1.42 *m*	H_2-6, H_2-8, H_2-9	29.3	1.34 *m*
8	29.0	1.42 *m*	H_2-6, H_2-7, H_2-9	29.0	1.42 *m*
9	27.8	2.20 *m*	H-11	27.9	2.19 *dt* (7.3, 6.8)
10	134.9	5.59 *m*	H_2-9	135.2	5.60 *m*
11	125.9	6.52 *dd* (10.6, 11.5)	H_2-9, H-13	125.8	6.51 *dd* (11.6, 10.7)
12	133.9	6.59 *dd* (10.9, 10.6)	H-10	134.0	6.60 *dd* (11.2, 10.7)
13	109.5	5.44 *d* (10.9)		109.3	5.44 *bd* (11.2)
14	78.0		H-11, H-12, H_2-16	77.8	
15	96.8		H_2-16	96.7	
16	19.6	2.43 *m*		19.6	2.43 *m*
17	24.6	1.69 *m*	H_2-16, H_2-18	24.6	1.69 *m*
18	36.1	1.68 *m*	H_2-16, H_2-17	36.1	1.69 *m*
19	72.8	4.15 *m*	H_2-21	72.8	4.16 *m*
20	141.0	5.88 *m*		141.0	5.88 *ddd* (6.2, 10.4, 17.2)
21	114.8	5.24 *d* (17.1) 5.12 *d* (10.2)		114.8	5.24 *d* (17.1) 5.12 *d* (10.4)

[a]$CDCl_3$, 300 and 500 MHz. Assignments were supported by ^{1}H-detected HMQC, DEPT 135° and 90° experiments.
[b]^{1}H-Detected HMBC (*J* = 10 Hz). For abbreviations see Table 1.

oily residue (1.4 g) that was chromatographed on a Si-gel column using a petroleum ether/Et_2O gradient as eluent. Nine different fractions (A–I) of increasing polarity were collected. Two selected fractions, D (20.1 mg) and G (26.6 mg), containing UV-vis spots at Rf 0.7 and 0.25 (light petroleum ether/diethyl ether, 1:1), respectively, were further purified by RP-HPLC (Phenomenex Kromasil 5µ C18, 4.6 × 250 mm column, MeOH/H_2O, 7:3, flow 1 mL/min). Four pure compounds were obtained: **1** (3.5 mg) and **2** (4.1 mg) from fraction D, **3** (2.0 mg) and **4** (2.5 mg) from fraction G.

*Physical data for **1–4***. Compound **1**: oil, $[\alpha]_D$ –21.4° (c 0.3, $CHCl_3$); IR (liquid film) ν_{max} 3320, 2930, 2860 cm^{-1}; UV (MeOH): λ_{max} 267 (ε = 7,500); ^1H and ^{13}C NMR, see Table 1; CI-MS (*m/z*) 279 (M + 1 – H_2O), 253 (M + 1 – H_2O – C_2H_2). Compound **2**: oil, $[\alpha]_D$ –6.6° (c 0.4, $CHCl_3$); IR (liquid film) ν_{max} 3306, 2930, 2860 cm^{-1}; UV (MeOH): λ_{max} 267 (ε = 7,320); ^1H and ^{13}C NMR, see Table 1; CI-MS (*m/z*) 299 (M + 1), 281 (M + 1 – H_2O), 273 (M +1 – C_2H_2); high-resolution electrospray ionization MS (HRESIMS) on sodiated molecule $[C_{21}H_{30}O + Na]^+$ found 321.2186, calculated 321.2194. Compound **3**: oil, $[\alpha]_D$ 1.2° (c 0.1, $CHCl_3$); IR (liquid film) ν_{max} 3390, 3301, 2930, 2865 cm^{-1}; UV (MeOH): λ_{max} 269 (ε = 8,650); ^1H and ^{13}C NMR, see Table 2; CI-MS (*m/z*) 313 (M + 1), 295 (M + 1 – H_2O), 287 (M + 1 – C_2H_2), 277 (M + 1 – $2H_2O$). Compound **4**: oil, $[\alpha]_D$ –2.5° (c 0.2, $CHCl_3$); IR (liquid film) ν_{max} 3405, 3313, 2932, 2860 cm^{-1}; UV (MeOH): λ_{max} 269 (ε = 3,600); ^1H and ^{13}C NMR, see Table 2; CI-MS (*m/z*) 315 (M + 1), 297 (M + 1 – H_2O), 289 (M + 1 – C_2H_2), 279 (M + 1 – $2H_2O$).

RESULTS AND DISCUSSION

A preliminary NMR analysis revealed that the four molecules (**1–4**, Fig. 1) were unsaturated lipids containing triple and double bonds and that they were structurally correlated with each other. In particular, ^1H NMR spectra were characterized by a series of signals attributable to olefinic protons (δ 5.0–6.5), oxygenated methines (δ 4.1–4.8), allylic methylene groups (δ 1.9–2.4), aliphatic methylenes (δ 1.2–1.4), and acetylenic protons (δ 2.5–3.1). All compounds were quite unstable in common organic solvents, and degradations occurred as the samples were held in solution to record NMR spectra. Reisolation from crude extract and repurification of these molecules were carried out repeatedly.

The main metabolite, compound **2** (Fig.1), was considered first. Its molecular formula, $C_{21}H_{30}O$, was established by analysis of the HRESIMS spectrum containing a sodiated molecule peak at *m/z* 321.2189 [calculated 321.2194 for ($C_{21}H_{30}O$ + Na)]. The CI-MS spectrum showed a base peak at *m/z* 299 (M + 1), along with diagnostic peaks at *m/z* 281 and 273, corresponding to the ions derived from the molecular ion by loss of H_2O and acetylene, respectively. The presence of six signals attributable to sp^2 carbons in the ^{13}C NMR spectrum [δ 109.4 (*d*, C-13), 125.7 (*d*, C-11), 133.9 (*d*, C-12), 135.2 (*d*, C-10), 138.6 (*d*, C-20), and 114.7 (*t*, C-21)] and of seven multiplets due to olefinic protons in the ^1H NMR spectrum was consistent with

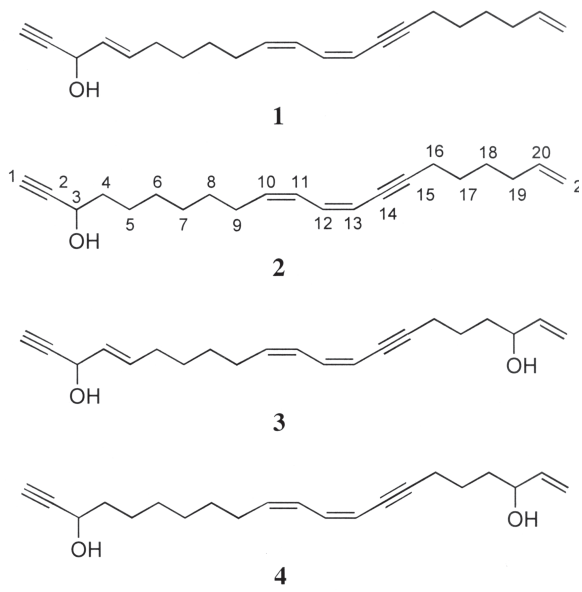

FIG. 1. Acetylene lipids isolated in this work.

three double bonds, one of which was trisubstituted and the other two of which were disubstituted. In particular, analysis of a COSY experiment allowed assignment of the two broad doublets at δ 5.02 (J = 17.1 Hz) and 4.96 (J = 10.2 Hz), both coupled with the multiplet at δ 5.82 (*ddt*, J = 17.1, 10.2, and 6.8 Hz), to the geminal protons of a terminal double bond (partial structure *a*, Fig. 2), whereas the signals at δ 6.53 (*dd*, J = 11.4 and 12.0 Hz, H-11) and δ 6.58 (*dd*, J = 10.1 and 11.4 Hz, H-12), which showed cross-peaks with a multiplet at δ 5.60 (H-10) and a doublet at δ 5.44 (J = 10.1 Hz, H-13), respectively, were attributed to the two internal protons of a conjugated diene system. The *cis*,*cis* stereochemistry of diene was indicated by both the coupling constants of olefinic protons ($J_{10.11}$ = 12.0 Hz, $J_{12.13}$ = 10.1 Hz) and the carbon chemical shift value of methylene linked to diene (δ 27.9, C-9). The presence of an internal triple bond in the molecule was indicated by typical *sp* carbon resonances in the ^{13}C NMR spectrum at δ 97.2 (*s*, C-15) and 77.8 (*s*, C-14). Furthermore, the up-shifted value of C-13 (δ 109.4) was consistent with linking of the internal triple bond to the diene system leading to a conjugated dienyne group (partial structure *b*, Fig. 2). This hypothesis was supported by the UV spectrum, which

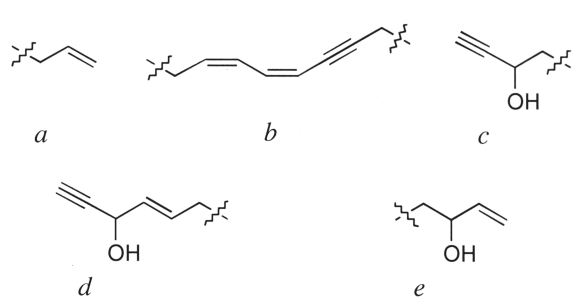

FIG. 2. Partial structures *a–e*.

showed an intense absorption at 267 nm (ε = 7,320) that was consistent with the conjugated dienyne system. An additional terminal triple bond was indicated by the presence in the ^{1}H NMR spectrum of a signal at δ 2.46 (*d*, *J* = 2.1 Hz, H-1) due to an acetylene proton and in the ^{13}C NMR spectrum of two resonance values at δ 72.9 (*d*, C-1) and 87.6 (*s*, C-2). This triple bond was suggested to be linked to a carbon bearing a hydroxyl group (δ_H 4.37, δ_C 62.3), as depicted in partial structure *c* (Fig. 2), by a diagnostic heteronuclear multiple-bond correlation (HMBC) between C-1 (δ 72.9) and H-3 (δ 4.37). A careful analysis of 2-D experiments [^{1}H-^{1}H COSY, heteronuclear multiple-quantum correlation (HMQC), and HMBC] allowed the assembly of partial structures *a*, *b*, and *c* through a series of methylene groups, to give structure **2** (Fig. 1).

All proton and carbon resonances were assigned as reported in Table 1.

Spectral data of compound **1** (Fig. 1) showed strong analogies with those of acetylene **2**. Analysis of both CI-MS and ^{13}C NMR spectra indicated the molecular formula $C_{21}H_{28}O$, which exhibited an additional unsaturation degree with respect to compound **2**. The mass spectrum showed a base peak at *m/z* 279 (M + 1 – H_2O), with two mass units less than the corresponding peak in compound **2**, whereas in the ^{13}C NMR spectrum eight signals attributable to sp^2 carbons were detected, indicating the presence in compound **1** of four double bonds instead of three. Analysis of both ^{1}H and ^{13}C NMR spectra revealed that the groups *a* and *b* were also present in the structure of **1**, and that the additional disubstituted double bond [δ_H 5.62 (*m*, H-4) and 5.90 (*ddt*, *J* = 1.0, 15.2, and 6.7 Hz, H-5); δ_C 128.5 (C-4) and 134.2 (C-5)] had to be located in the other part of the molecule. In particular, the chemical shifts of both H-1 and H-3, resonating at δ 2.57 and 4.83, respectively, were at a lower field compared with the corresponding values of compound **2**. In addition, ^{1}H-^{1}H COSY correlations that were observed between the signals at δ 4.83 (H-3) and δ 5.62 (H-4) were coherent with the location of the double bond near the carbon bearing the hydroxyl group, as depicted in partial structure *d* (Fig. 2). The *trans*-stereochemistry of this double bond was deduced by the coupling constant value of olefinic protons ($J_{4,5}$ = 15.3 Hz) and further supported by the carbon chemical shift value of allylic methylene (δ 31.7, C-6). Comparison of spectral data for compound **1** with those for **2** and analysis of ^{1}H-^{1}H COSY and HMQC experiments allowed the assembly of partial structures *a*, *b*, and *d*, as depicted in structure **1** (Fig. 1), and the assignment of all NMR resonances (Table 1).

The molecular formula of compound **3** (Fig. 1) was $C_{21}H_{28}O_2$, as deduced by LCMS and ^{13}C NMR spectra. In the mass spectrum, the base peak was observed at *m/z* 295 (M + 1 – H_2O), along with the molecular peak at *m/z* 313 (M + 1) and diagnostic fragmentation ions at *m/z* 287 (M + 1 – acetylene) and 277 (M + 1– $2H_2O$). These data clearly indicated the presence in the molecule of an additional hydroxyl function, with respect to compounds **1** and **2**. In particular, the ^{1}H NMR spectrum of **3** strongly resembled that of compound **1**, revealing the presence of the same partial structures *b* and *d* (Fig. 2), whereas the spin system due to protons of the terminal double bond resonated at a lower field [δ 5.88 (*m*, H-20), 5.24 (*d*, *J* = 17.1 Hz, H-21$_{trans}$), and 5.12 (*d*, *J* = 10.2 Hz, H-21$_{cis}$)]. Furthermore, a signal at δ 4.15 (*m*), which was attributed to the proton linked to the carbon bearing the additional hydroxyl, was observed to correlate with H-20 and H_2-21, clearly supporting the location of the additional hydroxyl group at C-19 (partial structure *e*, Fig. 2). All spectral data were consistent with structure **3** (Fig. 1). Analogously with compounds **1** and **2**, analysis of 2-D experiments (^{1}H-^{1}H COSY, HMQC, and HMBC) supported the assignment of all NMR resonances as reported in Table 2.

Compound **4** (Fig. 1) had the molecular formula $C_{21}H_{30}O_2$ and showed spectral data strongly similar to those of compound **2**. In the CI-MS spectrum, the molecular peak at *m/z* 315 (M + 1, base peak) was observed along with a series of peaks due to fragmentation ions at *m/z* 297 (M + 1 – H_2O), 289 (M + 1 – C_2H_2) and 279 (M + 1 – $2H_2O$). The ^{1}H NMR spectrum was characterized by multiplets that were coherent with the partial structures *b*, *c*, and *e* (Fig. 2), suggesting that **4** differs from **2** by the presence of an additional hydroxyl function at C-19. Proton and carbon values of **4** (Table 2) were attributed by direct homo- and heteronuclear experiments (^{1}H-^{1}H COSY and HMQC).

To establish the absolute configuration at C-3 for compounds **1** and **2**, and at both C-3 and C-19 for compounds **3** and **4**, we planned to apply the modified Mosher method, according to our previous stereochemical studies conducted on petroformynes, long-chain polyacetylenes from the sponge *Petrosia ficiformis* (16,17). Compounds **2** and **4** were considered. Unfortunately, every attempt to obtain a suitable Mosher derivative of either **2** or **4** failed due to its high instability in solution, so the absolute stereochemistry at chiral centers remained undetermined.

The reactivity of lipids **1**–**4** also prevented the evaluation of their biological activities. However, it is interesting to note that this is the first finding of polyacetylenes from a marine ascidian.

ACKNOWLEDGMENTS

The authors thank Drs. Ernesto Mollo and Guido Villani for collection of biological material, Raffaele Turco for drawing, and Carmine Iodice for spectroscopic measurements. The NMR spectra were recorded at the ICB NMR Service. This research was partially supported by Italian–Spanish bilateral cooperative project and PharmaMar (contract "Bioactive Marine Metabolites").

REFERENCES

1. Blunt, J.W., Copp, B.R., Munro, M.H.G., Northcote P.T., and Prinsep, M.R. (2004) Marine Natural Products, *Nat. Prod. Rep. 21*, 1–48.
2. Van Soest, R.W.M., Fusetani, N., and Andersen, R.J. (1998) Straight-Chain Acetylenes as Chemotaxonomic Markers of the Marine Haplosclerida, in *Sponge Sciences—Multidisciplinary Perspectives* (Watanabe, Y., and Fusetani, N., eds.), pp. 3–30, Springer-Verlag, Tokyo.
3. Kurosawa, E., Fukuzawa, A., and Irie, T. (1972) *Trans*- and *cis*-Laurediol: Unsaturated Glycols from *Laurencia nipponica* Yamada, *Tetrahedron Lett. 13*, 2121–2124.
4. Paul, V.J., and Fenical, W. (1980) Toxic Acetylene-Containing

Lipids from the Red Marine Alga *Liagora farinosa* Lamouroux, *Tetrahedron Lett. 21*, 3327–3330.
5. Kigoshi, H., Shizuri, Y., Niwa, H. and Yamada, K. (1981) Laurencenyne: Plausible Precursor of Various Nonterpenoid C_{15} Compounds and Neolaurencenyne from *Laurencia okamurai, Tetrahedron Lett. 22*, 4729–4732.
6. Gonzalez, A.G., Martin, J.D., Martin, V.S., Norte, M., Perez, R., Ruano, J.Z., Drexler, S.A., and Clardy, J. (1982) Non-terpenoid C-15 Metabolites from the Red Seaweed *Laurencia pinnatifida, Tetrahedron 38*, 1009–1014.
7. Kigoshi, H., Shizuri, Y., Niwa, H., and Yamada, K. (1986) Four New C15 Acetylenic Polyenes of Biogenetic Significance from the Red Alga *Laurencia okamurai*: Structure and Synthesis, *Tetrahedron 42*, 3781–3787.
8. Wright, A.D., Konig, G.M., de Nys, R., and Sticher, O. (1993) Seven New Metabolites from the Marine Red Alga *Laurencia majuscula, J. Nat. Prod. 56*, 394–401.
9. Castiello, D., Cimino, G., De Rosa, S., De Stefano, S., and Sodano, G. (1980) High Molecular Weight Polyacetylenes from the Nudibranch *Peltodoris atromaculata* and the Sponge *Petrosia ficiformis, Tetrahedron Lett. 21*, 5047–5050.
10. Walker, R.P., and Faulkner, D.J. (1981) Chlorinated Acetylenes from the Nudibranch *Diaulula sandiegensis*, *J. Org. Chem. 46*, 1475–1478.
11. Higa, T., Tanaka, J., Kohagura, T., and Wauke, T. (1990) Bioactive Polyacetylenes from Stony Corals, *Chem. Lett.*, 145–148.
12. Li, H.-Y., Matsunaga, S., and Fusetani, N. (1994) Bioactive Marine Metabolites. Corticatic Acids A–C, Antifungal Acetylenic Acids from the Marine Sponge *Petrosia corticata, J. Nat. Prod. 57*, 1464–1467.
13. Patil, A.D., Kokke, W.C., Cochran, S., Francis, T.A., Tomszek, T., and Westley, J.W. (1992) Brominated Polyacetylenic Acids from the Marine Sponge *Xestospongia muta*: Inhibitors of HIV Protease, *J. Nat. Prod. 55*, 1170–1177.
14. Kim, J.S., Lim, Y.J., Im, K.S., Jung, J.H., Shim, C.J., Lee, C.O., Hong, J., and Lee, H. (1999) Cytotoxic Polyacetylenes from the Marine Sponge *Petrosia* sp., *J. Nat. Prod. 62*, 554–559.
15. Lim, Y.J., Park, H.S., Im, K.S., Jung, J.H., Shim, C.J., Lee, C.O., Hong, J., Lee, M.Y., Kim, D. and Jung, J.H. (2001) Additional Cytotoxic Polyacetylenes from the Marine Sponge *Petrosia* Species, *J. Nat. Prod. 64*, 46–53.
16. Guo, Y.W., Gavagnin, M., Trivellone, E., and Cimino, G. (1994) Absolute Stereochemistry of Petroformynes, High Molecular Polyacetylenes from the Marine Sponge *Petrosia ficiformis, Tetrahedron 50*, 13261–13268.
17. Guo, Y.W., Gavagnin, M., Trivellone, E., and Cimino, G. (1995) Further Structural Studies on the Petroformynes, *J. Nat. Prod. 58*, 712–722.

[Received June 3, 2004; accepted September 26, 2004]

METHOD

Quantitative Determination of Low Density Lipoprotein Oxidation by FTIR and Chemometric Analysis

Henry S. Lam[a], Andrew Proctor[a,*], John Nyalala[b], Manford D. Morris[c], and W. Grady Smith[c]

[a]Department of Food Science, University of Arkansas, Fayetteville, Arkansas 72704, and Departments of [b]Internal Medicine, Division of Endocrinology and [c]Biochemistry and Molecular Biology, University of Arkansas for Medical Sciences, Little Rock, Arkansas 72205

ABSTRACT: This study was conducted to develop a quantitative FTIR spectroscopy method to measure LDL lipid oxidation products and determine the effect of oxidation on LDL lipid and protein. *In vitro* LDL oxidation at 37°C for 1 h produced a range of conjugated diene (CD) (0.14–0.26 mM/mg protein) and carbonyl contents (0.9–3.8 μg/g protein) that were used to produce calibration sets. Spectra were collected from the calibration set and partial least squares regression was used to develop calibration models from spectral regions 4000–650, 3750–3000, 1720–1500, and 1180–935 cm^{-1} to predict CD and carbonyl contents. The optimal models were selected based on their standard error of prediction (SEP), and the selected models were performance-tested with an additional set of LDL spectra. The best models for CD prediction were derived from spectral regions 4000–650 and 1180–935 cm^{-1} with the lowest SEP of 0.013 and 0.013 mM/mg protein, respectively. The peaks at 1745 (cholesterol and TAG ester C=O stretch), 1710 (carbonyl C–O stretch), and 1621 cm^{-1} (peptide C=O stretch) positively correlated with LDL oxidation. FTIR and chemometrics revealed protein conformational changes during LDL oxidation and provided a simple technique that has potential for rapidly observing structural changes in human LDL during oxidation and for measuring primary and secondary oxidation products.

Paper no. L9479 in *Lipids 39*, 687–692 (July 2004).

Human LDL is a major carrier of plasma cholesterol and plays an important role in the regulation of cholesterol metabolism. The LDL particle is spherical with a hydrophobic core of cholesterol esters, mainly cholesterol linoleate, and TAG. The core is surrounded by a monolayer of phospholipid, mainly PC, and unesterified cholesterol in which a single apolipoprotein B-100 (apoB-100) molecule is embedded (1).

Human LDL is more sensitive to oxidation than the other lipoproteins (2) because of the large proportion of unsaturated lipids (3). Oxidation of the polyunsaturated lipid in the core of the LDL particle produces hydroperoxides, which subsequently decompose to produce low-M.W. compounds, including aldehydes (4). These aldehydes modify the apoB-100 by binding to its lysine residues, resulting in the formation of Schiff bases. Oxidative modification of the LDL particle decreases its uptake by cells in the normal LDL receptor pathway, but it is degraded rapidly by blood macrophages through the acetyl-LDL receptor. These macrophages are the precursors of the lipid-laden foam cells whose presence indicates atherogenesis (5).

The oxidation of human LDL has been monitored by measuring a wide range of its oxidation products (6). The most commonly used method is measurement of TBARS. However, the method is nonspecific for the malondialdehyde it is intended to measure. Determination of conjugated diene (CD) is more specific because it measures one of the primary products of LDL dienoic acid autoxidation. Other methods include measuring apoB-100 fluorescence (7) and measuring the amount of oxysterols produced by cholesterol oxidation (6). These methods, however, have low sensitivity or require extensive sample preparation.

IR spectroscopy has been used for the investigation of changes in apoB-100 during LDL oxidation (8) and has provided insight into the changes in the α-helix, β-sheet, and β-turn structures. This technique is rapid, requires only a small sample size (9), and provides information on functional group composition. IR spectroscopy also can be used as a quantitative technique and has been used to determine the apoB-100 secondary structure of LDL (10,11). However, the application of IR spectroscopy to the investigation of LDL oxidation has been mostly qualitative. FTIR with chemometric analysis could provide a useful tool to quantify lipid oxidation products and protein changes simultaneously during LDL oxidation. Chemometric techniques are useful for obtaining information on chemical structures from complex spectral data (12). Lee *et al.* (10) used the methodology of factor analysis and multiple linear regression, and Dousseau and Pezolet (13) employed FTIR and a partial least squares (PLS) method to quantify the secondary structures of LDL proteins. The purpose of this study was to develop a new approach, based on FTIR and chemometrics, for measuring human LDL oxidation; this could be used as a noninvasive clinical diagnostic technique for coronary heart disease and related disorders and could evaluate efficacies of dietary interventions.

The objectives of the study were (i) to develop a rapid FTIR technique to measure primary (CD) and secondary (carbonyls)

*To whom correspondence should be addressed at Department of Food Science, 2650 N. Young Ave., Fayetteville, AR 72704.
E-mail: aproctor@uark.edu

Abbreviations: ApoB-100, apolipoprotein B-100; ATR, attenuated total reflection; CD, conjugated diene; 2,4-DNPH, 2,4-dinitrophenylhydrazine; PLS, partial least squares; PRESS, prediction error sum of squares; SEC, standard error of calibration; SEP, standard error of prediction.

LDL lipid oxidation products simultaneously by using chemometric techniques and (ii) to determine the changes in LDL lipid and apoB-100 structures with oxidation.

EXPERIMENTAL PROCEDURES

LDL preparation. Blood from four fasting male humans were obtained in vacutainers containing 1 mg/mL EDTA and centrifuged for 10 min at 2,000 × *g* to separate the plasma. Human LDL were isolated from the fresh human plasma by sequential floating ultracentrifugation according to the modified method of Jurgens *et al.* (14), as follows: EDTA plasma was raised to a density of 1.022 with solid KBr in SW40 tubes and overlayered with a 1.022 solution of KBr containing 0.05% thimerosal and 0.02% EDTA. The samples were centrifuged for 22 h at 200,000 × *g* in the SW 40 rotor of a Beckman ultracentrifuge (Beckman Coulter, Fullerton, CA). The top layer was removed by tube slicing, and the density of the lower layer was raised to 1.058 with KBr/thimerosal/EDTA solution and overlayered with the same density KBr solution. The samples were again centrifuged for 22 h at 200,000 × *g*. Following tube slicing, the isolated LDL were dialyzed against 1000 vol of 0.01% EDTA for 72 h at 4°C.

The protein content of LDL was determined according to the method of Lowry *et al.* (15) with BSA as a standard. LDL samples were desalted to remove EDTA using 3.5 mL PD-10 gel filtration columns (Supelco, Bellefonte, PA) pre-equilibrated with phosphate buffer (pH 7.4) immediately before the oxidation study.

LDL incubation. The *in vitro* oxidation of LDL was performed by a procedure modified from Esterbauer *et al*. (16). All LDL samples were diluted to a final concentration of 50 μg of protein/mL with EDTA-free phosphate buffer (pH 7.4). Oxidation was initiated by adding freshly prepared $CuCl_2 \cdot 2H_2O$ solution (final concentration 5 μmol/L). The IR spectra, CD, and carbonyls contents were recorded every 3 min for 1 h for the incubated LDL samples. Samples were incubated in duplicate.

CD determination. The primary products of LDL lipid oxidation were determined by measuring CD absorbance at 234 nm (17) by means of a UV-vis diode array spectrophotometer (Hewlett-Packard, Palo Alto, CA) using thermostated quartz cells with a 1.0 cm pathlength. Control LDL incubations were performed without $CuCl_2 \cdot 2H_2O$ but with EDTA and BHT added prior to incubation.

Total carbonyl determination. The total carbonyl contents of LDL samples were determined according to the methods of Yukawa *et al*. (18). An incubated LDL sample (1 mL) and 1 mL of 2,4-dinitrophenylhydrazine (2,4-DNPH) reagent were added to a test tube. The tube was stoppered, incubated for 30 min at 50°C, then cooled in an ice bath for 10 min; to this 5.0 mL of 10% KOH/80% ethanol was added. The samples were then centrifuged at 1300 × *g* for 20 min at 20°C, and absorbance was measured at 425 nm. The final data were expressed as micromoles of carbonyls per milligram of protein using a molar absorption coefficient of 1.81×10^{-4} M^{-1} cm^{-1} for the 2,4-DNPH derivatives.

IR spectroscopy. Duplicate 30 μL aliquots, drawn every 3 min for 1 h from LDL incubated at 37°C, were evenly spread on one side of multibounce attenuated total reflectance (ATR) windows. The aliquots were allowed to dry under a steady stream of nitrogen to produce films (19). The spectra of the phosphate buffer used to dilute the LDL samples were also collected under the same conditions as the LDL sample spectra. FTIR spectra of the films were recorded at 22°C using a Nexus 670 spectrometer (Thermo Electron Corp., Madison, WI) equipped with a deuterated triglycine sulfate detector scanning over the frequency range of 4000–400 cm^{-1} at a resolution of 4 cm^{-1}. Spectra were collected by using rapid scan software running under OMNIC (Nicolet, Madison, WI), and the spectrum for each sample was calculated from the average of 100 repetitive scans. The internal reflection element was a Spectra-Tech ZnSe ATR trough plate crystal with an aperture angle of 45° generating seven bounces. A reference background absorbance spectrum was taken by scanning the clean and dry ATR crystal. Difference spectra obtained by subtraction of the phosphate buffer spectrum from the spectrum of LDL samples were reported and used for PLS model development.

Spectral transformation. FTIR spectral data were converted into numerical data, transferred to a MS Excel file, and linked to the CD and carbonyl data. The MS Excel file was imported into the chemometrics software, The Unscrambler (Camo, Trondheim, Norway).

Variance spectrum. A total of 84 FTIR spectra were generated from the incubated LDL samples, which had a range of CD and carbonyl contents. A set of eight FTIR spectra representing different degrees of LDL oxidation were randomly selected and kept out of the calibration set to be used for external validation of the models. The remaining 76 FTIR spectra were used as the calibration set for LDL CD and carbonyls. Each spectrum represents the mean of duplicate spectra of a sample. FTIR spectral data were pretreated by mean centering and weighting by their SD. To determine the regions most appropriate for model development, spectra were examined to identify regions where the most changes occurred. Spectral regions with the highest degree of change were determined by obtaining the variance spectrum and plotted. PLS models were derived by taking second derivatives (nine-point Savitzky–Golay derivatives) of the original absorption spectra using the IR spectral region 4000–650 cm^{-1}, and regions 3750–3000, 1720–1500, and 1180–935 cm^{-1} identified by the variance spectrum.

PLS. The PLS regression analysis is based on optimizing a set of partial (separate) submodels by minimizing their lack-of-fit residuals through the principles of least squares (20). PLS is advantageous relative to the other IR analysis methods because it can model baseline variations and some types of nonlinearity associated with Beer's law. Detection of outliers from spectral residuals is also possible, and chemically interpretable spectral information can be obtained since PLS is a full-spectrum approach (21).

PLS is a bilinear regression model that projects a set of independent *x*-variables onto a few PLS components (22). The

PLS components, also known as "factors" or "latent variables," are extracted by means of noniterative partial least squares regressions on the *x*-variables and then used as regressors for the *y*-variable. PLS establishes a relationship between a single *y*-variable and set of *x*-variables, which can be represented by the polynomial

$$y = b_0 + b_1x_1 + b_2x_2 + b_nx_n + E \quad [1]$$

where *y* is the vector of the dependent variable (in this study, reference data for LDL CD or carbonyls), x_1–x_n are the absorbances at the selected wavenumbers, b_0–b_n are the regression coefficients vectors (b_0 is the intercept), and *E* is the residual matrix (error not accounted for by the model). The optimal number of PLS factors was determined by computing the prediction error sum of squares (PRESS) (22). The number of factors that gave the minimal PRESS for each model was used.

PLS regression analysis was performed for those spectral regions identified in the variance spectrum to obtain prediction models for CD and carbonyls and show how protein and lipid groups relate to LDL oxidation. The PLS calibration obtained was tested by "leave-one-out" full cross-validation and jackknifing as described by Lam *et al.* (23). Briefly, the data were restructured to stress the variation between the different spectra in such a way that this variation maximally correlated with variation in the CD and carbonyl contents. Models to correlate the restructured spectral data and the response variable were developed for leave-one-out calibration samples followed by the prediction of the sample left out by the model. The process was repeated for every sample in order to calculate an accurate prediction error. The results were reported as a weighted regression coefficient profile of the calibration model that shows regions of the LDL spectrum that correlated with the CD and carbonyl contents. Standardization was done by weighting the absorbances at a given wavelength with the reciprocal of their SD. The optimal model obtained to predict CD and the optimal model to predict carbonyl contents were selected and used to determine oxidation levels of additional LDL samples. These data were then correlated with those obtained by UV-vis spectrophotometry, as an external validation of the method.

RESULTS AND DISCUSSION

Human LDL carbonyls and CD analysis. The CD content of the LDL calibration set as determined by UV-vis analysis ranged from 0.14 mM/mg protein prior to incubation to 0.26 mM/mg protein after 1 h of incubation. The total carbonyl content ranged from 0.9 to 3.8 μg/g protein after 1 h of incubation.

IR spectroscopy. Figure 1A is a typical FTIR spectrum of an LDL film and shows high absorbance at wavenumbers characteristic of lipid and protein functional groups. The band centered at 3280 cm^{-1} corresponds to stretching of the N–H groups in the peptide linkage of the polypeptide chain and proteins of the apoB-100 (19). The dominant features between 3000 and 2800 cm^{-1} are attributable to the symmetric and asymmetric stretching vibrations of the lipid acyl CH_2 groups. The band at 1740 cm^{-1} arises predominantly from the ester C=O groups of LDL lipids. The absorptions present in the 1660–1500 cm^{-1} region arise from C=O stretching (1652 cm^{-1}, amide I band) and N–H bending (1550 cm^{-1}, amide II band) vibrations of the peptide group in apoB-100. The band in the 1300–1000 cm^{-1} region represents P=O symmetric and asymmetric and P–O–C vibrations of phospholipid groups and ester C–O–C stretching vibrations of phospholipids, cholesterol esters, and TAG (24).

Variance spectrum. To determine the variability of the LDL spectra relative to the mean LDL spectrum, a variance spectrum was obtained. The variance spectrum (Fig. 1B) identified the spectral regions with the most significant degree of variation that could be used to develop predictive models (25). The spectral regions identified as having the most variability were at 3750–3000 (due to N–H stretching), 1720–1500 (arising from C=O stretching and N–H bending of peptide groups), and

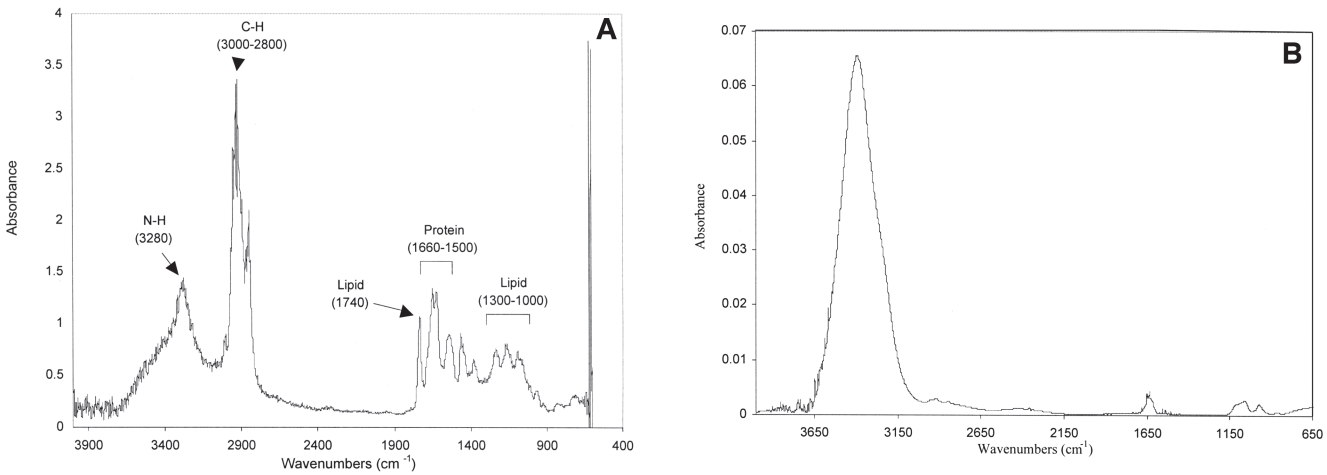

FIG. 1. (A) A Typical FTIR spectrum of LDL film identifying the relevant peaks associated with absorbance of groups in protein and lipids; (B) variance spectrum of 84 LDL samples showing the spectral regions with high degrees of variation from the overall mean spectrum.

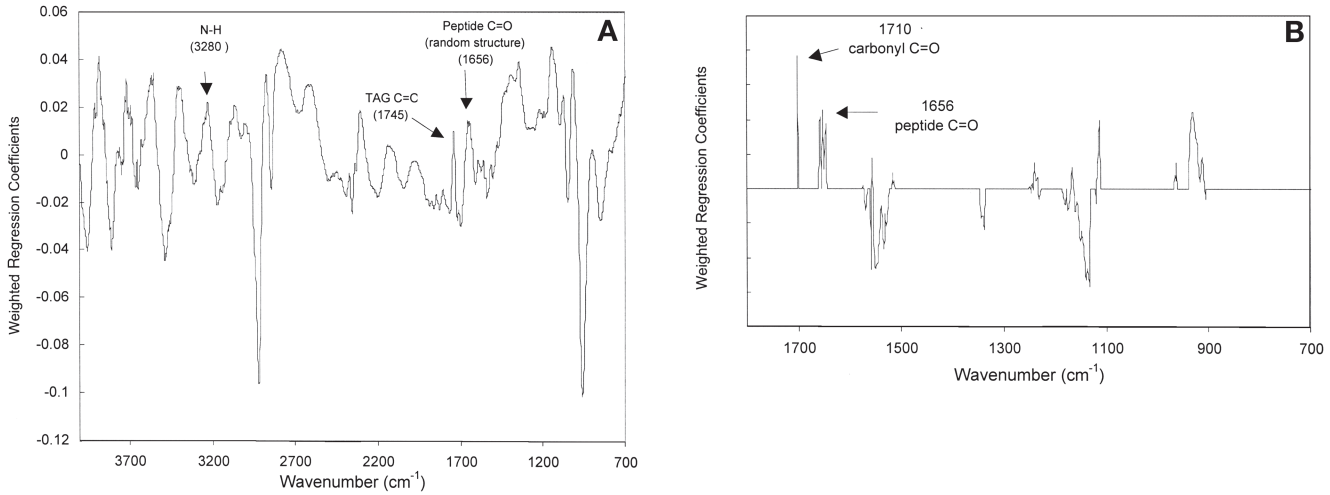

FIG. 2. Weighted regression coefficients of the calibration model showing LDL spectral regions that correlate with (A) conjugated diene content and (B) carbonyl content.

1180–935 cm^{-1} (due to asymmetric and symmetric stretching of ester C–O–C and PO_2^- of the phosphodiester group) (24). The changes identified by the variance spectrum could be due to exposure of the cholesterol and TAG esters that were previously in the interior of the LDL molecule and alteration in the phospholipid monolayer on the surface, suggesting disruption of the LDL complex.

PLS regression. The weighted regression coefficients assigned by PLS to the CD and carbonyls are presented in Figure 2. Figure 2A shows the most important wavenumbers related to the variability of CD and includes spectral regions associated with specific functional groups in LDL. The spectral peaks due to N–H at 3280 cm^{-1}, ester C=O stretching at 1745 cm^{-1}, unordered peptide C=O stretching at 1656 cm^{-1}, and PO_2^- double-bond stretching at 1120 cm^{-1} received positive regression coefficients (Fig. 2A), indicating that they correlated positively with LDL CD formation. The data confirm earlier findings that random or unordered structures are formed from the α-helix structure of the apoB-100 protein in oxidized LDL (26). The positive correlation for ester C=O absorbance with CD formation suggests that cholesterol ester and TAG interactions with IR radiation increased as LDL oxidation proceeded. This is further evidence that cholesterol ester and TAG, located at the LDL core, became exposed as oxidation proceeded.

The peak at 1710 cm^{-1}, associated with lipid carbonyl stretches (27), and 1656 cm^{-1}, assigned to an asymmetric amide I band (peptide C=O, random structure), was positively correlated with the formation of carbonyls in LDL (Fig. 2B). A positive correlation for the peak at 1710 cm^{-1} during LDL oxidation would imply that the carbonyl groups associated with this peak are probably those found in lipid oxidation products of LDL such as aldehydes and ketones (4). The positive correlation at 1656 cm^{-1} could have resulted from transition in the LDL peptide structures during LDL oxidation. Herzyk *et al.* (8) reported that a random secondary structure is formed from the LDL protein α-helix during LDL oxidation.

PLS models for CD and carbonyls. The PLS models for CD and carbonyls obtained using different spectral regions, including the optimal number of factors used, are summarized in Table 1. The PLS models for CD prediction generated from the spectral regions 4000–650 and 1180–935 cm^{-1} yielded analytical results with the lowest SEP, 0.013 and 0.012 mM/mg protein, respectively. This finding is in agreement with our previous work (23), where we found that analysis of the whole IR spectral region (4000–400 cm^{-1}) resulted in a better PLS model for predicting FFA on milled rice surfaces. The analysis of the 1720–1500 cm^{-1} spectral region gave the best PLS model for total carbonyl prediction with the lowest SEP of 0.73 μg/g protein.

External validation. The prediction capabilities of the optimal PLS models, 4000–650 cm^{-1} for CD and 1720–1500 cm^{-1}

TABLE 1
Prediction Errors Obtained from Different PLS Models and the Number of Factors Used[a]

	CD			Carbonyls		
Spectral region (cm^{-1})	SEC	SEP	PLS factors[b]	SEC	SEP	PLS factors
4000–650	0.009	0.013	10	0.55	0.77	10
3750–3000	0.012	0.015	12	0.56	0.79	15
1720–1500	0.013	0.015	10	0.44	0.73	9
1180–935	0.008	0.012	9	0.52	0.74	10

[a]SEC, standard error of calibration; SEP, standard error of prediction; PLS, partial least squares; CD, conjugated diene.
[b]Number of factors included in the PLS optimal calibration models.

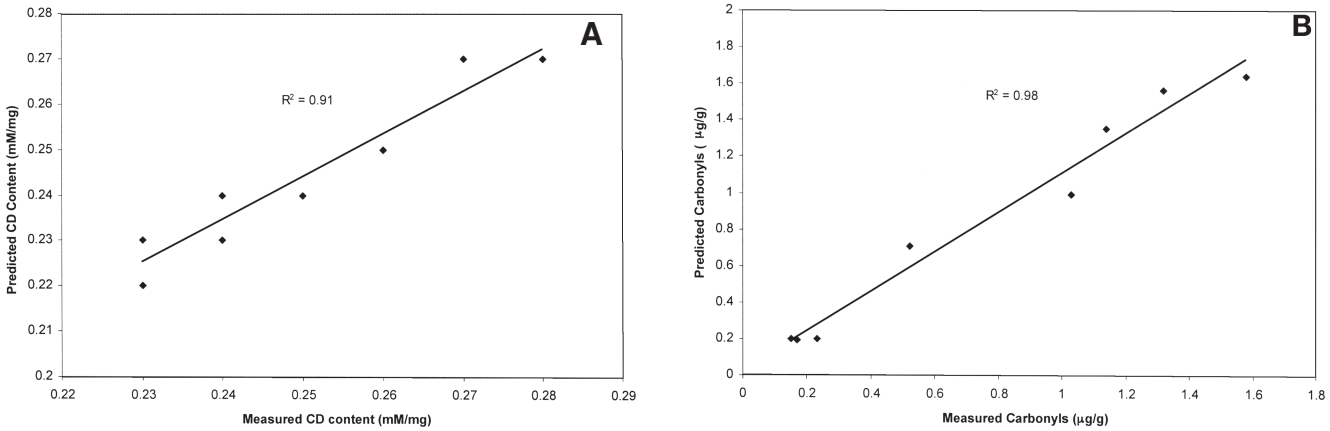

FIG. 3. (A) Correlation of LDL CD content predicted by optimal PLS model vs. measured LDL CD content; (B) correlation of LDL carbonyls content predicted by optimal PLS model vs. measured LDL carbonyls content. PLS, partial least squares; CD, conjugated diene.

for carbonyls, were tested by using the models to predict degrees of LDL oxidation for the eight FTIR spectra left out of the calibration set. Figure 3A shows the correlation curve between the LDL CD contents measured by absorbance at 234 nm and those predicted by the PLS model; a high correlation with an R^2 of 0.91 and prediction error of 0.01 was obtained. Figure 3B presents the correlation plot for PLS predicted and LDL total carbonyls as measured by UV-vis spectrophotometry. The data also yielded a high R^2 of 0.98 and prediction error of 0.10. The correlation coefficient for predicting carbonyl content was higher than that of CD content, partly due to the narrow range of CD content of LDL test set.

This study demonstrated that FTIR spectroscopy in combination with multivariate analysis can provide a simple and rapid method for measuring LDL primary and secondary lipid oxidation products. The technique also provided insight into how oxidation affects protein and lipids in the LDL complex. The technique requires a small LDL aliquot (30 µL) and analysis takes just 4 min, which makes it a potential alternative method for measuring LDL oxidation.

ACKNOWLEDGMENTS

The authors wish to thank the Arkansas Bioscience Institute for its financial support of this work and Dr. Fred Faas for the use of his laboratory for LDL preparation.

REFERENCES

1. Goormaghtigh, E., Cabiaux, V., and Ruysschaert, J.M. (1990) Secondary Structure and Dosage of Soluble and Membrane Proteins by Attenuated Total Reflection Fourier-Transform Infrared Spectroscopy on Hydrated Films, *Eur. J. Biochem. 193*, 409–420.
2. Schuh, J., Fairclough, G.F., and Haschenmeyer, R.H. (1978) Oxygen-Mediated Heterogeneity of Apo-Low-Density Lipoprotein, *Proc. Natl. Acad. Sci. USA 75*, 3173–3177.
3. Deckelbaum, R.J., Shipley, G.G., and Small, D.M. (1977) Structure and Interactions of Lipids in Human Plasma Low Density Lipoproteins, *J. Biol. Chem. 252*, 744–754.
4. Pinchuk, I., Schnitzer, E., and Lichtenberg, D. (1998) Kinetic Analysis of Copper-Induced Peroxidation of LDL, *Biochim. Biophys. Acta 1389*, 155–172.
5. Steinbrecher, U.P. (1987) Oxidation of Human Low Density Lipoprotein Results in Derivatization of Lysine Residues of Apolipoprotein B by Lipid Peroxide Decomposition Products, *J. Biol. Chem. 262*, 3603–3608.
6. Puhl, H., Waeg, G., and Esterbauer, H. (1994) Methods to Determine Oxidation of Low-Density Lipoproteins, *Methods Enzymol. 233*, 425–452.
7. Esterbauer, H., Jurgens, G., Quehenberger, O., and Koller, E. (1987) Autoxidation of Human Low Density Lipoprotein: Loss of Polyunsaturated Fatty Acids and Vitamin E and Generation of Aldehydes, *J. Lipid Res. 28*, 495–509.
8. Herzyk, E., Lee, D.C., Dunn, C., Bruckdorfer, K.R., and Chapman, D. (1987) Changes in the Secondary Structure of Apolipoprotein B-100 After Cu^{2+}-Catalyzed Oxidation of Human Low-Density Lipoproteins Monitored by Fourier Transform Infrared Spectroscopy, *Biochim. Biophys. Acta 922*, 145–154.
9. Goormaghtigh, E., and Ruysschaert, J.M. (1994) Subtraction of Atmospheric Water Contribution in Fourier Transform Infrared Spectroscopy of Biological Membranes and Proteins, *Spectrochim. Acta 50A*, 2137–2144.
10. Lee, D.C., Haris, P.I., Chapman, D., and Mitchell, R.C. (1990) Determination of Protein Secondary Structure Using Factor Analysis of Infrared Spectra, *Biochemistry 29*, 9185–9193.
11. Goormaghtigh, E., Cabiaux, V., De Meutter, J., Rosseneu, M., and Ruysschaert, J.-M. (1993) Secondary Structure of the Particle Associating Domain of Apolipoprotein B-100 in Low-Density Lipoprotein by Attenuated Total Reflection Infrared Spectroscopy, *Biochemistry 32*, 6104–6110.
12. Brown, S.D. (1995) Chemical Systems Under Indirect Observation: Latent Properties and Chemometrics, *Appl. Spectrosc. 49*, 14A–31A.
13. Dousseau, F., and Pezolet, M. (1990) Determination of the Secondary Structure Content of Proteins in Aqueous Solutions from Their Amide I and Amide II Infrared Bands. Comparison Between Classical and Partial Least-Squares Methods, *Biochemistry 29*, 8771–8779.
14. Jurgens, G., Hoff, H.F., Chisolm, G.M., and Esterbauer, H. (1987) Modification of Human Serum Low Density Lipoprotein by Oxidation. Characterization and Pathophysiological Implications, *Chem. Phys. Lipids 45*, 315–336.
15. Lowry, O.H., Rosebrough, N., Farr, A.L., and Randall, R.J. (1951) Protein Measurement with the Folin Phenol Reagent, *J. Biol. Chem. 193*, 265–275.

16. Esterbauer, H., Striegl, G., Puhl, H., and Rotheneder, M. (1989) Continuous Monitoring of *in vitro* Oxidation of Human Low Density Lipoprotein, *Free Radic. Res. Commun. 6*, 67–71.
17. Gieseg, S.P., and Esterbauer, H. (1994) Low Density Lipoprotein Is Saturable by Pro-oxidant Copper, *FEBS Lett. 343*, 188–194.
18. Yukawa, N., Takamura, H., and Matoba, T. (1993) Determination of Total Carbonyls Compounds in Aqueous Media, *J. Am. Oil Chem. Soc. 70*, 881–884.
19. Fringeli, U.P., and Gunthard, H.H. (1981) Infrared Membrane Spectroscopy, in *Membrane Spectroscopy* (Grell, E., ed.), pp. 270–332, Springer Verlag, New York.
20. Martens, M., and Marterns, H. (1986) Partial Least Squares Regression, in *Statistical Procedures in Food Research* (Piggott, J.R., ed.), pp. 293–360, Elsevier Applied Science, London.
21. Halaand, M.D., and Thomas, V.E. (1988) Partial Least-Squares Methods for Spectral Analyses. 2. Application to Simulated and Glass Spectral Data, *Anal. Chem. 60*, 1202–1208.
22. Geladi, P., and Kowalski, R.B. (1986) An Example of 2-Block Predictive Partial Least Squares Regression with Simulated Data, *Anal. Chim. Acta 185*, 19–32.
23. Lam, H.S., Proctor, A., and Meullenet, J.F. (2001) Free Fatty Acid Formation and Lipid Oxidation on Milled Rice, *J. Am. Oil Chem. Soc. 78*, 1271–1275.
24. Liu, K.-Z., Shaw, R.A., Man, A., Dembinski, T.C., and Mantsch, H.H. (2002) Reagent-Free, Simultaneous Determination of Serum Cholesterol in HDL and LDL by Infrared Spectroscopy, *Clin. Chem. 48*, 499–506.
25. Fuller, M.P., Ritter, G.I., and Draper, C.S. (1988) Partial Least Squares Quantitative Analysis of Infrared Spectroscopic Data. Part I. Algorithm Implementation, *Appl. Spectrosc. 42*, 217–227.
26. Surewicz, W.K., Mantsch, H.H., and Chapman, D. (1993) Determination of Protein Secondary Structure by Fourier Transform Infrared Spectroscopy: A Critical Assessment, *Biochemistry 32*, 389–394.
27. Chapman, D., Kamat, V.B., and Levene, R.J. (1968) Infrared Spectra and the Chain Organization of Erythrocyte Membranes, *Science 160*, 314–316.

[Received July 19, 2004; accepted September 21, 2004]

Re: Nomenclature of *trans*-Fatty Acids

Plea for Using the Term n-7 Fatty Acids in Place of C18:2*cis*-9,*trans*-11, and C18:1*trans*-11 or Their Trivial Names Rumenic Acid and Vaccenic Acid Rather than the Generic Term Conjugated Linoleic Acids

Sir:

Since the nineties of the former century an ever increasing number of papers about conjugated linoleic acid (CLA) is published yearly. From 1999 on it has become clear that different CLA-isomers have different physiological effects (1). This means that referring to CLA in general, and especially when CLA in milk fat is dealt with, it would be better to state clearly which isomer is meant. For milk, C18:2*cis*-9,*trans*-11 or rumenic acid is the main isomer and this name should be preferably used instead of the term CLA. It can be foreseen that in the future, the term CLA might be associated with negative health effects, as a result of the liver-fattening and liver-enlarging effects of CLA *trans*-10,*cis*-12 found in experimental animals (2,3). This could negatively influence the health image of dairy products.

Similarly, for C18:1*trans*-11 the name "vaccenic acid" could be used to avoid negative associations with *trans* fatty acids in general.

Rumenic acid and vaccenic acid have similar, positive health effects. Because rumenic acid and vaccenic acid are both omega-7, or n-7 fatty acids, which are naturally almost only present in milk and meat from ruminants, it could be advantageous to refer to them as n-7 fatty acids, or use their individual trivial names, in order to avoid confusion with other CLA-isomers or *trans* fatty acids.

Other n-7 fatty acids occur only sparsely in fats and oils (http://msdlocal.ebi.ac.uk/docs/chem_comp/fatty_acids.html) and their physiological effects are not well documented. Because these rare fatty acids are almost absent in the human diet, the term "n-7 fatty acids" would be appropriate to characterize rumenic and vaccenic acid as highly interesting components with positive health effects in milk fat.

REFERENCES

1. Martin, J.-C., and Valeille, K. (2002). Conjugated Linoleic Acid: All the Same or to Everyone Its Own Function? *Reprod. Nutr. Dev. 42*, 525–536.
2. De Deckere, E.A.M., Van Amelsvoort, J.M.M., McNeill, G.P., and Jones, P. (1999). Effects of Conjugated Linoleic Acid Isomers on Lipid Levels and Peroxisome Proliferation in the Hamster, *Br. J. Nutr. 82*, 309–317.
3. Warren, J.M., Simon, V.A., Bartolini, G., Erickson, K.L., Mackey, B.E., and Kelley, D.S. (2003) *Trans*-10,*cis*-12 CLA Increases Liver and Decreases Adipose Tissue Lipids in Mice: Possible Roles of Specific Lipid Metabolism Genes, *Lipids 38*, 497–504.

G. Ellen[a], and A. Elgersma[b]
[a]NIZO Food Research, P.O. Box 20, 6710 BA Ede, and [b]Department of Plant Sciences, Wageningen University, Haarweg 333, 6709 RZ Wageningen, The Netherlands

*This Letter to the Editor originally appeared in the *Journal of Dairy Science* [*87*, 1131 (2004)] and is reprinted with permission from the American Dairy Science Association.

The use of Total *trans*-11 Containing FA, Rather than Total "n-7" FA, Is Recommended to Assess the Content of FA with a Positive Health Image in Rumiant Fats

Sir:

Ellen and Elgersma (1) recently expressed concern that the term conjugated linoleic acids (CLA) is too vague. They encouraged the naming of individual isomers to avoid inclusion of isomers with a possible negative health image. They then proposed the term "n-7" FA, which they believed would encompass all beneficial CLA isomers and their precursors. A similar "n-x" designation is commonly used to identify naturally occurring unsaturated FA such as oleic (n-9), linoleic (n-6), and α-linolenic acid (n-3) and their family acids.

We previously questioned the accuracy of using the term CLA to describe conjugated FA and suggested that the term conjugated fatty acids (CFA) would be a more appropriate name, since CFA do not fit the strict definition of linoleic acid (*cis*-9,*trans*-12 octadecadienoic acid; *c*9,*t*12-18:2; or 18:2n-6) (2). We proposed the name "rumenic acid" (*cis*-9,*trans*-11 octadecadienoic acid; *c*9,*t*11-18:2) for the most abundant CFA isomer present in all ruminant fats (3).

We find use of the proposed "n-7" terminology (1) to encompass the beneficial CFA and their precursors unacceptable for the following reasons: (i) the "n-7" term is an incorrect usage of the "n-x" nomenclature; (ii) it is misleading; (iii) it includes potentially undesirable isomers (iv) while excluding others; and (v) the lack of caution to the reader regarding the use of appropriate analytical methods to determine rumenic and vaccenic acids may perpetuate the reporting of inaccurate data.

(i) The "n-x" (or ω-x) nomenclature was introduced as a convenient shorthand form to express metabolic conversions of the oleic (n-9), linoleic (n-6), and α-linolenic (n-3) acid families, where "n" is the chain length and "x" specifies the first double bond in the chain counting from the methyl end of the FA molecule. This terminology has two inherent assumptions: All double bonds are in the *cis* configuration, and if more than one double bond is involved, all double bonds are separated by methylene groups (methylene-interrupted). To use this "n-x" nomenclature to describe rumenic and vaccenic acids is incorrect because both of these FA are *trans* FA, and because the double bonds in rumenic acid are conjugated, not methylene-interrupted. One could modify the "n-x" term for unsaturated FA to "m-x" for CFA. However, such a new term would require additional specification of the conjugated double bond system, since each positional CFA isomer consists of four geometrical CFA isomers (*c,t*, *t,c*, *c,c*, *t,t*).

(ii) The authors indicate that the "n-7" FA are rare and occur only in dairy fats. Since the authors did not distinguish between all *cis*-containing "n-7" FA and *trans*-containing

"n-7" FA, this statement is misleading. *Cis* "n-7" FA, such as 16:1n-7 and 18:1n-7, are ubiquitous constituents of oilseed and animal lipids, whereas *trans*-containing "n-7" FA admittedly occur generally in dairy fats. Furthermore, by not distinguishing between "*cis*" and "*trans*" "n-7" FA, the authors leave the impression that "n-7" FA are similar, which is not the case. In natural products, *cis* "n-7" FA are generally produced by Δ9 desaturation of palmitic acid (16:0), giving rise to *c*9-16:1 (16:1n-7), followed by chain elongation to *c*11-18:1 (18:1n-7). On the other hand, the "n-7" FA containing a *trans* double bond are produced by isomerization and biohydrogenation of linoleic, α-linolenic, or γ-linolenic acids in rumen bacteria (4).

(iii) The authors thought that only the potentially beneficial CFA would be encompassed by using the "n-7" terminology (1). Unfortunately, "n-7" by definition includes all four naturally occurring geometric isomers of 9,11-18:2 (*c*9,*t*11-18:2; *t*9,*c*11-18:2; *c*9,*c*11-18:2; and *t*9,*t*11-18:2), all of which are present in dairy fats (5). However, except for *c*9,*t*11-18:2, little is known about the other "n-7" CFA. There is evidence to suggest that all the 9,11-CFA isomers have different effects based on the differences in platelet aggregation reported recently between *c*9,*c*11-, *c*9,*t*11-, and *t*9,*t*11-18:2 (6).

(iv) The production of the "*t*11" double bond in the rumen appears to be unique. In ruminants fed exclusively on pasture, virtually all the CFA (*c*9,*t*11-18:2; *t*11,*c*13-18:2; *t*11,*t*13-18:2; *t*9,*t*11-18:2) and *trans*-18:1 (*t*11-18:1) isomers contain the "*t*11" double bond. A very high content of these "*t*11" FA relative to the other isomers was reported in dairy cows raised at high altitudes in the Alps (7), and in grass fed to yak (8) and musk oxen (9). In fact, the "*t*11" double bond appears to reflect a "healthy rumen" and provides a more reasonable justification to assess the total beneficial CFA (plus precursors) in ruminant fats. On the other hand, the "n-7" designation does not include any of the 11,13 CFA isomers since they are all "n-5" (or "m-5") FA.

To include the "n-5" FA as those having a positive health image has no scientific basis and demonstrates why we object to the "n" nomenclature. Take, for instance, the two 11,13 CFA isomers *t*11,*c*13-18:2 and *c*11,*t*13-18:2, both of which are "n-5" FA. The former is found in ruminant fats (2,5) and may prove to be beneficial; see above. The latter is present in commercial CFA preparations (2,5) and has been associated with a negative image since it accumulates in tissue phospholipid classes, but particularly in diphosphatidylglycerol (cardiolipin) of pigs fed commercial CFA mixtures (10). This is of particular concern since diphosphatidylglycerol is a major component in inner mitochondrial membranes (10).

(v) This Letter to the Editor (1) is very unfortunate since it refers to rumenic and vaccenic acids without cautioning the reader to use proper methods for their analyses. The major CFA peak, as determined by GC, is usually designated as *c*9,*t*11-18:2, even though it is well known to include a substantial amount of another CFA isomer (*t*7,*c*9-18:2), which can only be resolved by silver-ion HPLC (2,5,8,11). To report the value of the GC peak "rumenic acid" without removing the contribution of *t*7,*c*9-18:2 leads to overestimation of rumenic acid. Furthermore, determining the *trans*-18:1 isomer composition is an estimate at best even when using a 100-m highly polar capillary column (see Fig. 1 below). The resolution of all *trans*-18:1 requires a prior separation of the *trans* fraction by silver-ion TLC followed by GC analysis at low-temperature isothermal conditions (8). Therefore, not to caution the reader to use proper analyses for both rumenic and vaccenic acids propagates the general use of inappropriate methods and reporting of inaccurate data.

Based on these arguments, we recommend that total "*t*11", rather than total "n-7", be used to assess the content of CFA and *trans*-18:1 isomers with a positive health image, as proposed by Ellen and Elgersma (1). The source of all "*t*11"-containing FA are rumen bacteria (i.e., *Butyrivibrio fibrisolvens*) that first isomerize the *c*12 double bond of unsaturated C_{18} FA, followed by successive biohydrogenation processes (4). In pasture-fed ruminants, the main *trans*-18:1 isomer is *t*11-18:1, whereas virtually all CFA are "*t*11"-containing FA. The exact biosynthetic pathway for the 11,13-CFA present in milk fat (*t*11,*c*13- and *t*11,*t*13-18:2) remains unknown, although it has been suggested that they are derived from α-linolenic acid (7). Furthermore, it is not clear whether *t*11,*t*13-18:2 is also a rumen metabolite or an artifact of the methylation procedure. The latter is highly unlikely since a base catalyst was used (12) for methylation. In addition, *t*11-18:1 is resynthesized to rumenic acid by Δ9 desaturase in most tissues of ruminants, mono-gastric animals, and humans.

The high content of "*t*11"-containing FA in tundra-grazed musk oxen is clearly demonstrated in the partial *trans*-18:1 (*t*4- to *t*12-18:1) and the complete CFA profiles obtained by GC. Figure 1 shows a comparison of backfat analyzed from pasture-fed musk ox and beef that were finished in feedlots on a high-concentrate diet. The FA composition of musk ox shows the high content of the "*t*11" containing CFA (95%) and *t*11-18:1 (56%) relative to total CFA and *trans*-18:1 (85% relative to the *t*4- to *t*12-18:1, i.e., the region shown in Fig. 1), respectively (9). Similar results were reported by Kraft *et al.*

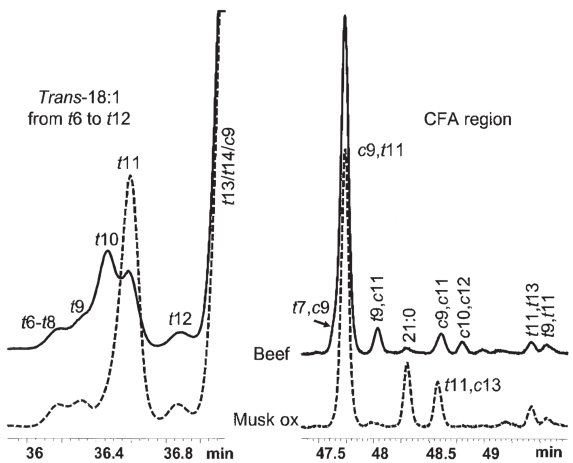

FIG. 1. A partial GC profile of the *trans*-18:1 (from *t*4- to *t*12-18:1) and conjugated fatty acid (CFA) region obtained from the FA analysis of backfat taken from tundra-grazed musk oxen and feedlot-finished beef fed a high-concentrate diet (9). See References 8, 10, and 12 for detailed GC conditions, column (100 m, CP Sil 88), and temperature program (45 to 215°C). The methyl ester of 21:0 elutes in the CFA region (2,8,10,12) and is prominent in tundra-grazed musk oxen.

(7). Even though the pathway of the formation of some "*t*11" CFA and their biochemical/pathological responses remains unknown, the "*t*11"-containing FA clearly reflect the biochemical processes in the healthy rumen and are associated with a "natural" and a positive image. We hypothesize that most, if not all, of the "*t*11"-containing FA in ruminant fats may prove to be equally beneficial to monogastric animals and humans.

REFERENCES

1. Ellen, G., and Elgersma, A. (2004) Plea for Using the Term n-7 Fatty Acids for C18:2*cis*-9,*trans*-11 and C18:1*trans*-11 or Their Trivial Names Rumenic Acid and Vaccenic Acid Rather Than the Generic Term Conjuaged Linoleic Acids, *J. Dairy Sci. 87*, 1131.
2. Kramer, J.K.G., Sehat, N., Fritsche, J., Mossoba, M.M., Eulitz, K., Yurawecz, M.P., and Ku, Y. (1999) Separation of Conjugated Linoleic Acid Isomers, in *Advances in Conjugated Linoleic Acid Research, Volume 1* (Yurawecz, M.P., Mossoba, M.M., Kramer, J.K.G., Pariza, M.P., and Nelson, G.J., eds.), pp. 83–109, AOCS Press, Champaign.
3. Kramer, J.K.G., Parodi, P.W., Jensen, R.G., Mossoba, M.M., Yurawecz, M.P., and Adlof, R.O. (1998) Rumenic Acid: A Proposed Common Name for the Major Conjugated Linoleic Acid Isomer Found in Natural Products, *Lipids 33*, 835.
4. Griinari, J.M., and Bauman, D.E. (1999) Biosynthesis of Conjugated Linoleic Acid and Its Conversion into Meat and Milk in Ruminants, in *Advances in Conjugated Linoleic Acid Research, Volume 1* (Yurawecz, M.P., Mossoba, M.M., Kramer, J.K.G., Pariza, M.P., and Nelson, G.J., eds.), pp. 180–200, AOCS Press, Champaign.
5. Sehat, N., Kramer, J.K.G., Mossoba, M.M., Yurawecz, M.P., Roach, J.A.G., Eulitz, K., Morehouse, K.M., and Ku, Y. (1998) Identification of Conjugated Linoleic Acid Isomers in Cheese by Gas Chromatography, Silver Ion High-Performance Liquid Chromatography and Mass Reconstructed Ion Profiles. Comparison of Chromatographic Elution Sequences, *Lipids 33*, 963–971.
6. Al-Madaney, M.M., Kramer, J.K.G., Deng, Z., and Vanderhoek, J.Y. (2003) Effects of Lipid-Esterified Conjugated Linoleic Acid Isomers on Platelet Function: Evidence for Stimulation of Platelet Phospholipase Activity, *Biochim. Biophys. Acta 1635*, 75–82.
7. Kraft, J., Collomb, M., Möckel, P., Sieber, R., and Jahreis, G. (2003) Differences in CLA Isomer Distribution of Cow's Milk Lipids, *Lipids 38*, 657–664.
8. Cruz-Hernandez, C., Deng, Z., Zhou, J., Hill, A.R., Yurawecz, M.P., Delmonte, P., Mossoba, M.M., Dugan, M.E.R., and Kramer, J.K.G. (2004) Methods for Analysis of Conjugated Linoleic Acids and *trans* 18:1 Isomers in Dairy Fats by Using a Combination of Gas Chromatography, Silver-Ion Thin-Layer Chromatography/Gas Chromatography, and Silver-Ion Liquid Chromatography, *J. AOAC Int. 87*, 545–562.
9. Dugan, M.E.R., Robertson, W.M., Rolland, D.C., and Kramer, J.K.G. (2004). The Fatty Acid Composition of Muskox Relative to Beef Backfat Including the Conjugated Linoleic and *trans*-Monoene Composition, *Can. J. Anim. Sci. 84*, in press.
10. Kramer, J.K.G., Sehat, N., Dugan, M.E.R., Mossoba, M.M., Yurawecz, M.P., Roach, J.A.G., Eulitz, K., Aalhus, J.L., Schaefer, A.L., and Ku, Y. (1998) Distribution of Conjugated Linoleic Acid (CLA) Isomers in Tissue Lipid Classes of Pigs Fed a Commercial CLA Mixture Determined by Gas Chromatography and Silver Ion High-Performance Liquid Chromatography, *Lipids 33*, 549–558.
11. Yurawecz, M.P., Roach, J.A.G., Sehat, N., Mossoba, M.M., Kramer, J.K.G., Fritsche, J., Steinhart, H., and Ku, Y. (1998) A New Conjugated Linoleic Acid Isomer, 7*trans*,9*cis*-Octadecadienoic Acid, in Cow Milk, Cheese, Beef and Human Milk and Adipose Tissue, *Lipids 33*, 803–809.
12. Kramer, J.K.G., Fellner, V., Dugan, M.E.R., Sauer, F.D., Mossoba, M.M., and Yurawecz, M.P. (1997) Evaluating Acid and Base Catalysts in the Methylation of Milk and Rumen Fatty Acids with Special Emphasis on Conjugated Dienes and Total *trans* Fatty Acids, *Lipids 32*, 1219–1228.

[Received March 11, 2004; accepted October 1, 2004]

John K.G. Kramer[a,*], Cristina Cruz-Hernandez[b], Mamun Or-Rashid[a], and Michael E.R. Dugan[c]
[a]Food Research Program, Agriculture and Agri-Food Canada, Guelph, Ontario, Canada, [b]Department of Food Science, University of Guelph, Guelph, Ontario, Canada, and [c]Lacombe Research Center, Agriculture and Agri-Food Canada, Lacombe, Alberta, Canada

*To whom correspondence should be addressed at Food Research Program, Agriculture and Agri-Food Canada, 93 Stone Road West, Guelph, Ontario, Canada. E-mail: kramerj@agr.gc.ca

---

Response from Authors

Sir:

First of all, we welcome the initiative of *Lipids* to provide a platform for discussion of the nomenclature of PUFA.

We appreciate the attention and welcome the support of Kramer *et al.* (1) regarding our idea (2) that most (if not all) of the *trans* n-7 (or *t*11) FA in ruminant fats are beneficial to monogastrics including humans. It appears there is a great similarity between their ideas and ours, including question marks pertaining to the use of the term CLA (albeit for different reasons) as well as the plea for naming of the individual isomers.

The authors state that we proposed the term "n-7" FA and that we believed this term would encompass all beneficial CLA isomers and their precursors. However, we indicated only that both the major CLA isomer in milk, rumenic acid (RA), and its precursor, *trans*-vaccenic acid (TVA), are indeed *trans* n-7 FA. These *trans* n-7 (or *t*11) FA are naturally present almost exclusively in milk and meat from ruminants. We also mentioned that other (*cis* and *trans*) n-7 FA do exist but occur only sparsely in fats and oils, and that they are almost absent in the human diet.

The detailed criticism by Kramer *et al.* (1) concerning our proposed n-7 terminology contains five aspects (i–v).

Point (i). We are aware that, strictly speaking, the "n-x" designation applies only to *cis*-unsaturated FA. The recommendation in 1967 of the International Union of Pure and Applied Chemistry (IUPAC)–International Union of Biochemistry and Molecular Biology (IUB) Joint Commission on Biochemical Nomenclature (JBN) to replace the "omega" symbol with "n-x" mentioned that this applies to FA with *cis* double bonds. Indeed, TVA and RA have the double bond between C11 and C12 in the *trans* configuration, which is nearly unique for ruminant fats. We agree that this should have been added to our proposal, which would then become "*trans* n-7 FA." The term "*trans* n-7 FA" would overcome the problem that, by convention, the "n-x" designation applies to *cis* FA. Just as the prefix

Re: Nomenclature of *trans*-Fatty Acids

Plea for Using the Term n-7 Fatty Acids in Place of C18:2*cis*-9,*trans*-11, and C18:1*trans*-11 or Their Trivial Names Rumenic Acid and Vaccenic Acid Rather than the Generic Term Conjugated Linoleic Acids

Sir:

Since the nineties of the former century an ever increasing number of papers about conjugated linoleic acid (CLA) is published yearly. From 1999 on it has become clear that different CLA-isomers have different physiological effects (1). This means that referring to CLA in general, and especially when CLA in milk fat is dealt with, it would be better to state clearly which isomer is meant. For milk, C18:2*cis*-9,*trans*-11 or rumenic acid is the main isomer and this name should be preferably used instead of the term CLA. It can be foreseen that in the future, the term CLA might be associated with negative health effects, as a result of the liver-fattening and liver-enlarging effects of CLA *trans*-10,*cis*-12 found in experimental animals (2,3). This could negatively influence the health image of dairy products.

Similarly, for C18:1*trans*-11 the name "vaccenic acid" could be used to avoid negative associations with *trans* fatty acids in general.

Rumenic acid and vaccenic acid have similar, positive health effects. Because rumenic acid and vaccenic acid are both omega-7, or n-7 fatty acids, which are naturally almost only present in milk and meat from ruminants, it could be advantageous to refer to them as n-7 fatty acids, or use their individual trivial names, in order to avoid confusion with other CLA-isomers or *trans* fatty acids.

Other n-7 fatty acids occur only sparsely in fats and oils (http://msdlocal.ebi.ac.uk/docs/chem_comp/fatty_acids.html) and their physiological effects are not well documented. Because these rare fatty acids are almost absent in the human diet, the term "n-7 fatty acids" would be appropriate to characterize rumenic and vaccenic acid as highly interesting components with positive health effects in milk fat.

REFERENCES

1. Martin, J.-C., and Valeille, K. (2002). Conjugated Linoleic Acid: All the Same or to Everyone Its Own Function? *Reprod. Nutr. Dev. 42*, 525–536.
2. De Deckere, E.A.M., Van Amelsvoort, J.M.M., McNeill, G.P., and Jones, P. (1999). Effects of Conjugated Linoleic Acid Isomers on Lipid Levels and Peroxisome Proliferation in the Hamster, *Br. J. Nutr. 82*, 309–317.
3. Warren, J.M., Simon, V.A., Bartolini, G., Erickson, K.L., Mackey, B.E., and Kelley, D.S. (2003) *Trans*-10,*cis*-12 CLA Increases Liver and Decreases Adipose Tissue Lipids in Mice: Possible Roles of Specific Lipid Metabolism Genes, *Lipids 38*, 497–504.

G. Ellen[a], and A. Elgersma[b]
[a]NIZO Food Research, P.O. Box 20, 6710 BA Ede, and [b]Department of Plant Sciences, Wageningen University, Haarweg 333, 6709 RZ Wageningen, The Netherlands

*This Letter to the Editor originally appeared in the *Journal of Dairy Science* [*87*, 1131 (2004)] and is reprinted with permission from the American Dairy Science Association.

The use of Total *trans*-11 Containing FA, Rather than Total "n-7" FA, Is Recommended to Assess the Content of FA with a Positive Health Image in Rumiant Fats

Sir:

Ellen and Elgersma (1) recently expressed concern that the term conjugated linoleic acids (CLA) is too vague. They encouraged the naming of individual isomers to avoid inclusion of isomers with a possible negative health image. They then proposed the term "n-7" FA, which they believed would encompass all beneficial CLA isomers and their precursors. A similar "n-x" designation is commonly used to identify naturally occurring unsaturated FA such as oleic (n-9), linoleic (n-6), and α-linolenic acid (n-3) and their family acids.

We previously questioned the accuracy of using the term CLA to describe conjugated FA and suggested that the term conjugated fatty acids (CFA) would be a more appropriate name, since CFA do not fit the strict definition of linoleic acid (*cis*-9,*trans*-12 octadecadienoic acid; *c*9,*t*12-18:2; or 18:2n-6) (2). We proposed the name "rumenic acid" (*cis*-9,*trans*-11 octadecadienoic acid; *c*9,*t*11-18:2) for the most abundant CFA isomer present in all ruminant fats (3).

We find use of the proposed "n-7" terminology (1) to encompass the beneficial CFA and their precursors unacceptable for the following reasons: (i) the "n-7" term is an incorrect usage of the "n-x" nomenclature; (ii) it is misleading; (iii) it includes potentially undesirable isomers (iv) while excluding others; and (v) the lack of caution to the reader regarding the use of appropriate analytical methods to determine rumenic and vaccenic acids may perpetuate the reporting of inaccurate data.

(i) The "n-x" (or ω-x) nomenclature was introduced as a convenient shorthand form to express metabolic conversions of the oleic (n-9), linoleic (n-6), and α-linolenic (n-3) acid families, where "n" is the chain length and "x" specifies the first double bond in the chain counting from the methyl end of the FA molecule. This terminology has two inherent assumptions: All double bonds are in the *cis* configuration, and if more than one double bond is involved, all double bonds are separated by methylene groups (methylene-interrupted). To use this "n-x" nomenclature to describe rumenic and vaccenic acids is incorrect because both of these FA are *trans* FA, and because the double bonds in rumenic acid are conjugated, not methylene-interrupted. One could modify the "n-x" term for unsaturated FA to "m-x" for CFA. However, such a new term would require additional specification of the conjugated double bond system, since each positional CFA isomer consists of four geometrical CFA isomers (*c,t*, *t,c*, *c,c*, *t,t*).

(ii) The authors indicate that the "n-7" FA are rare and occur only in dairy fats. Since the authors did not distinguish between all *cis*-containing "n-7" FA and *trans*-containing

(7). Even though the pathway of the formation of some "*t*11" CFA and their biochemical/pathological responses remains unknown, the "*t*11"-containing FA clearly reflect the biochemical processes in the healthy rumen and are associated with a "natural" and a positive image. We hypothesize that most, if not all, of the "*t*11"-containing FA in ruminant fats may prove to be equally beneficial to monogastric animals and humans.

REFERENCES

1. Ellen, G., and Elgersma, A. (2004) Plea for Using the Term n-7 Fatty Acids for C18:2*cis*-9,*trans*-11 and C18:1*trans*-11 or Their Trivial Names Rumenic Acid and Vaccenic Acid Rather Than the Generic Term Conjuaged Linoleic Acids, *J. Dairy Sci. 87*, 1131.
2. Kramer, J.K.G., Sehat, N., Fritsche, J., Mossoba, M.M., Eulitz, K., Yurawecz, M.P., and Ku, Y. (1999) Separation of Conjugated Linoleic Acid Isomers, in *Advances in Conjugated Linoleic Acid Research, Volume 1* (Yurawecz, M.P., Mossoba, M.M., Kramer, J.K.G., Pariza, M.P., and Nelson, G.J., eds.), pp. 83–109, AOCS Press, Champaign.
3. Kramer, J.K.G., Parodi, P.W., Jensen, R.G., Mossoba, M.M., Yurawecz, M.P., and Adlof, R.O. (1998) Rumenic Acid: A Proposed Common Name for the Major Conjugated Linoleic Acid Isomer Found in Natural Products, *Lipids 33*, 835.
4. Griinari, J.M., and Bauman, D.E. (1999) Biosynthesis of Conjugated Linoleic Acid and Its Conversion into Meat and Milk in Ruminants, in *Advances in Conjugated Linoleic Acid Research, Volume 1* (Yurawecz, M.P., Mossoba, M.M., Kramer, J.K.G., Pariza, M.P., and Nelson, G.J., eds.), pp. 180–200, AOCS Press, Champaign.
5. Sehat, N., Kramer, J.K.G., Mossoba, M.M., Yurawecz, M.P., Roach, J.A.G., Eulitz, K., Morehouse, K.M., and Ku, Y. (1998) Identification of Conjugated Linoleic Acid Isomers in Cheese by Gas Chromatography, Silver Ion High-Performance Liquid Chromatography and Mass Reconstructed Ion Profiles. Comparison of Chromatographic Elution Sequences, *Lipids 33*, 963–971.
6. Al-Madaney, M.M., Kramer, J.K.G., Deng, Z., and Vanderhoek, J.Y. (2003) Effects of Lipid-Esterified Conjugated Linoleic Acid Isomers on Platelet Function: Evidence for Stimulation of Platelet Phospholipase Activity, *Biochim. Biophys. Acta 1635*, 75–82.
7. Kraft, J., Collomb, M., Möckel, P., Sieber, R., and Jahreis, G. (2003) Differences in CLA Isomer Distribution of Cow's Milk Lipids, *Lipids 38*, 657–664.
8. Cruz-Hernandez, C., Deng, Z., Zhou, J., Hill, A.R., Yurawecz, M.P., Delmonte, P., Mossoba, M.M., Dugan, M.E.R., and Kramer, J.K.G. (2004) Methods for Analysis of Conjugated Linoleic Acids and *trans* 18:1 Isomers in Dairy Fats by Using a Combination of Gas Chromatography, Silver-Ion Thin-Layer Chromatography/Gas Chromatography, and Silver-Ion Liquid Chromatography, *J. AOAC Int. 87*, 545–562.
9. Dugan, M.E.R., Robertson, W.M., Rolland, D.C., and Kramer, J.K.G. (2004). The Fatty Acid Composition of Muskox Relative to Beef Backfat Including the Conjugated Linoleic and *trans*-Monoene Composition, *Can. J. Anim. Sci. 84*, in press.
10. Kramer, J.K.G., Sehat, N., Dugan, M.E.R., Mossoba, M.M., Yurawecz, M.P., Roach, J.A.G., Eulitz, K., Aalhus, J.L., Schaefer, A.L., and Ku, Y. (1998) Distribution of Conjugated Linoleic Acid (CLA) Isomers in Tissue Lipid Classes of Pigs Fed a Commercial CLA Mixture Determined by Gas Chromatography and Silver Ion High-Performance Liquid Chromatography, *Lipids 33*, 549–558.
11. Yurawecz, M.P., Roach, J.A.G., Sehat, N., Mossoba, M.M., Kramer, J.K.G., Fritsche, J., Steinhart, H., and Ku, Y. (1998) A New Conjugated Linoleic Acid Isomer, 7*trans*,9*cis*-Octadecadienoic Acid, in Cow Milk, Cheese, Beef and Human Milk and Adipose Tissue, *Lipids 33*, 803–809.
12. Kramer, J.K.G., Fellner, V., Dugan, M.E.R., Sauer, F.D., Mossoba, M.M., and Yurawecz, M.P. (1997) Evaluating Acid and Base Catalysts in the Methylation of Milk and Rumen Fatty Acids with Special Emphasis on Conjugated Dienes and Total *trans* Fatty Acids, *Lipids 32*, 1219–1228.

[Received March 11, 2004; accepted October 1, 2004]

John K.G. Kramer[a,*], Cristina Cruz-Hernandez[b], Mamun Or-Rashid[a], and Michael E.R. Dugan[c]
[a]Food Research Program, Agriculture and Agri-Food Canada, Guelph, Ontario, Canada, [b]Department of Food Science, University of Guelph, Guelph, Ontario, Canada, and [c]Lacombe Research Center, Agriculture and Agri-Food Canada, Lacombe, Alberta, Canada

*To whom correspondence should be addressed at Food Research Program, Agriculture and Agri-Food Canada, 93 Stone Road West, Guelph, Ontario, Canada. E-mail: kramerj@agr.gc.ca

---

Response from Authors

Sir:

First of all, we welcome the initiative of *Lipids* to provide a platform for discussion of the nomenclature of PUFA.

We appreciate the attention and welcome the support of Kramer *et al.* (1) regarding our idea (2) that most (if not all) of the *trans* n-7 (or *t*11) FA in ruminant fats are beneficial to monogastrics including humans. It appears there is a great similarity between their ideas and ours, including question marks pertaining to the use of the term CLA (albeit for different reasons) as well as the plea for naming of the individual isomers.

The authors state that we proposed the term "n-7" FA and that we believed this term would encompass all beneficial CLA isomers and their precursors. However, we indicated only that both the major CLA isomer in milk, rumenic acid (RA), and its precursor, *trans*-vaccenic acid (TVA), are indeed *trans* n-7 FA. These *trans* n-7 (or *t*11) FA are naturally present almost exclusively in milk and meat from ruminants. We also mentioned that other (*cis* and *trans*) n-7 FA do exist but occur only sparsely in fats and oils, and that they are almost absent in the human diet.

The detailed criticism by Kramer *et al.* (1) concerning our proposed n-7 terminology contains five aspects (i–v).

Point (i). We are aware that, strictly speaking, the "n-x" designation applies only to *cis*-unsaturated FA. The recommendation in 1967 of the International Union of Pure and Applied Chemistry (IUPAC)–International Union of Biochemistry and Molecular Biology (IUB) Joint Commission on Biochemical Nomenclature (JBN) to replace the "omega" symbol with "n-x" mentioned that this applies to FA with *cis* double bonds. Indeed, TVA and RA have the double bond between C11 and C12 in the *trans* configuration, which is nearly unique for ruminant fats. We agree that this should have been added to our proposal, which would then become "*trans* n-7 FA." The term "*trans* n-7 FA" would overcome the problem that, by convention, the "n-x" designation applies to *cis* FA. Just as the prefix

"conjugated" in CLA stipulates that we are not dealing with real linoleic acid but with a closely related compound, the prefex "*trans*" would indicate that these FA are not regular "n-x" FA, but something special.

In general, the Δ-designation is used by chemists, whereas nutritionists prefer the "n-x" designation, because it allows one to link diet with tissue FA composition. Both systems can unequivocally define any unsaturated FA. Because nutritionists have much more interaction with the general public, the generic term "omega fatty acids" is widely known.

In addition, if the "n-x" terminology has a biological meaning, in the case of *trans* n-7, its spatial structure—with a bend causing an apolar "tail" of seven-carbon atoms at the methyl end of the molecule—this could perhaps be essential for its functioning. After cleaving, the specific length and/or spatial structure of the fragments might also have functional relevance, but as we are no experts in this field, we would welcome other scientists to reflect on this hypothesis.

Point (ii). The improved name "*trans* n-7 FA" is more specific and excludes *cis* n-7 FA.

Point (iii). Indeed, all 9,11 isomers could have different effects, and knowledge is lacking on their precise biological functions. The improved name "*trans* n-7 FA" excludes the *t*9,*c*11 and *c*9,*c*11 18:2 isomers but does include the *t*9,*t*11 18:2 isomer (as would the term *t*11 FA).

Point (iv). We fully agree with the positive association the authors (1) make regarding the *t*11 (or *trans* n-7) double bond, both with a healthy rumen and with health effects for the consumer of ruminant products. As knowledge of the *t*11,13 isomers of 18:2 is still lacking, and as *t*11,*t*13 18:2 may even be an artifact of the methylation method, it would be prudent not to include these beforehand in the category of beneficial FA; therefore, *trans* n-7 would be preferred to *t*11 in our opinion.

Point (v). A terminology proposal for specific FA has no relation with the—justified—concern the authors (1) express regarding methodology and can in no way be associated with propagation of the use of inaccurate data.

In conclusion, we think the criticism regarding our terminology proposal is justified only with regard to a need for further specificity and that "*trans* n-7 FA" would be the preferred term.

We would again like to emphasize our other points, i.e., that the term CLA is confusing and should be avoided, and that names of FA should be mentioned individually. Our main concern is that health food stores sell food supplements designated as CLA that contain roughly equal amounts of the *c*9,*t*11 and *t*10,*c*12 isomer, together with some other compounds. There is evidence that at the doses applied, the *t*10,*c*12 isomer does not have the slimming effect in humans that is found in experimental animals. Moreover, adverse effects (e.g. liver fattening/enlarging) have been reported for the *t*10,*c*12 isomer. Milk fat should not be connected with these negative effects for the public by stating that it contains CLA. The advantage of using the term "*trans* n-7 FA" is that it includes the major CLA isomer (RA) and the major *trans* FA (TVA) in milk fat, the formation of which *in vivo* is closely related and which probably has positive health effects in humans; there are no documented negative effects in animals.

We (3–6) and others (e.g., 7,8) also consistently observed the highest levels of RA and TVA in milk of pasture-fed cows. This reflects the biochemical processes in the healthy rumen and is associated with a natural and positive image of the sector and the products. We therefore fully agree with the final statements in the letter of Kramer *et al.* (1).

The public is familiar with the terminology of saturated/unsaturated fat and, in recent years, also with *trans* fats. General terms such as CLA, omega FA, saturated fats (which includes butyric acid), and *trans* fats are simplifications and have the disadvantage that they might include compounds with positive as well as negative effects. Using specific trivial or scientific names for individual compounds precludes this confusion.

We hope this debate will initiate more discussion and lead to increased understanding and to a change in the widely misperceived general public—and scientific!—opinion that all *trans* FA are unhealthy! Unlike hardened *trans* FA from plant origin, *trans* n-7 FA in ruminant fats are beneficial, both to the animals themselves and to the consumers of their products.

REFERENCES

1. Kramer, J.K.G., Cruz-Hernandez, C., Or-Rashid, M. and Dugan, M.E.R. (2004) Letter to the Editor, *Lipids 39*, 601–603.
2. Ellen, G., and Elgersma, A. (2004) Plea for Using the Term n-7 Fatty Acids for C18:2 *cis*-9, *trans*-11 and C18:1 *trans*-11 or Their Trivial Names Rumenic Acid and Vaccenic Acid Rather Than the Generic Term CLA, *J. Dairy Sci 87*, 1131.
3. Elgersma, A., Ellen, G., Dekker, R.G., van der Horst, H., Boer, H., and Tamminga, S. (2003) Effects of Perennial Ryegrass (*Lolium perenne*) Cultivars with Different Linolenic Acid Contents on Milk Fatty Acid Composition, *Aspects Appl. Biol. 20*, 107–114.
4. Elgersma, A., Ellen, G., van der Horst, H., Boer, H., Dekker, P.R., and Tamminga, S. (2004) Quick Changes in Milk Fat Composition from Cows After Transition from Fresh Grass to a Silage Diet, *Animal Feed Sci. Technol. 117*, 13–27.
5. Elgersma, A., Ellen, G., and Tamminga, S. (2004) Rapid Decline of Contents of Beneficial Omega-7 Fatty Acids in Milk from Grazing Cows with Decreasing Herbage Allowance, *Grassland Sci. Eur. 9*, 1136–1138.
6. Elgersma, A., Tamminga, S., and Ellen, G. (2003) Effect of Grazing Versus Stall-Feeding of Cut Grass on Milk Fatty Acid Composition of Dairy Cows, *Grassland Sci. Eur. 8*, 271–274.
7. Kelly, M.L., Kolver, E.S., Bauman, D.E., van Amburgh, M.E., and Muller, L.D. (1998) Effect of Intake of Pasture on Concentrations of Conjugated Linoleic Acids in Milk of Lactating Cows, *J. Dairy Sci. 81*, 1630–1636.
8. Dhiman, T.R., Anand, G.R., Satter, D., and Pariza, M.W. (1999) Conjugated Linoleic Acid Content of Milk from Cows Fed Different Diets, *J. Dairy Sci. 82*, 2146–2156.

[Received and accepted October 5, 2004]

Anjo Elgersma[a,*] and Geert Ellen[b]
[a]Plant Sciences Group, Wageningen University, 6709 RZ Wageningen, The Netherlands, and
[b]NIZO Food Research, 6710 BA Ede, The Netherlands

*To whom correspondence should be addressed at Crop and Weed Ecology, Haarweg 333, 6709 RZ Wageningen, The Netherlands.
E-mail: anjo.elgersma@wur.nl
Personal web page: www.dpw.wageningen-ur.nl/cwe/organis/elgersma.htm

Recent Advances in Steroid Research

Presented at the 94th AOCS Annual Meeting & Expo
in Cincinnati, Ohio, May 2004

Edward J. Parish[a], Robert A. Moreau[b], Isao Ikeda[c], W. David Nes[d], and John R. Williams[e]

[a]Department of Chemistry, Auburn University, Auburn, Alabama 36849, [b]USDA, ARS, ERRC, Wyndmoor, Pennsylvania 19038, [c]Kyushu University, Fukuoka 812-8581, Japan, [d]Department of Chemistry and Biochemistry, Texas Tech University, Lubbock, Texas 79409, and [e]Department of Chemistry, Temple University, Philadelphia, Pennsylvania 19122

The AOCS has been a regular host to steroid symposia since 1970. The history of this symposium series has been published [Weete, J.D., Parish, E.J., and Nes, W.D. (2000) *Lipids 35*, 241]. These symposia have focused on current research in the areas of steroid structure, biosynthesis, chemistry, regulation, and function.

The 2004 Steroid Symposium, "Recent Advances in Steroid Research," was held at the AOCS Annual Meeting in Cincinnati, Ohio. This year the symposium held special significance, for it hosted the presentation of the second G.J. Schroepfer Jr. Award for steroid research. The Award was established to honor the memory of Dr. George J. Schroepfer Jr., a prominent steroid biochemist and chemist who made major and lasting contributions to the steroid field. Much of his research dealt with the biosynthesis of cholesterol and its regulation. In addition, he maintained a strong organic synthesis program to support his biochemical studies. A biography describing many of Dr. Schroepfer's contributions can be found in this journal [Wilson, W.K. (2000) *Lipids 35*, 242]. Dr. Schroepfer was scheduled to be the keynote speaker at the steroid symposium in Orlando, Florida, in 1999, but unfortunately, he passed away on December 11, 1998.

The second recipient of the G.J. Schroepfer Jr. Award for steroid research was Professor Jan Sjövall of the Department of Medical Biochemistry and Biophysics at the Karolinska Institutet in Stockholm, Sweden. Professor Sjövall has made major contributions to the steroid field, and we were pleased with his nomination. Professor Sjövall is well known for research on the metabolism of sterols and bile acids in human and animal tissues and the identification of steroids by MS.

As in past symposia, we are indebted to our corporate partners who helped make the symposium a success: Cargill Health & Food Technologies, and Steraloids, Inc. We appreciate their contribution and look forward to their continued support of our symposium series.

This symposium was sponsored by the Biotechnology Division of the AOCS. Speakers in the 2004 Sterol Symposium represented an international group of senior and junior scientists. This year the technical sessions were a joint effort with members of the Japan Oil Chemists' Society, and several of our symposium speakers were from Japan. We express here our appreciation to each of them for their cooperation during the planning process and for their participation in the symposium. By all accounts, the event was a success, and we are looking forward to the next steroid symposium.

Fifty Years with Bile Acids and Steroids in Health and Disease

Jan Sjövall*

Department of Medical Biochemistry and Biophysics, Karolinska Institutet, SE-171 77, Stockholm, Sweden

ABSTRACT: Cholesterol and its metabolites, e.g., steroid hormones and bile acids, constitute a class of compounds of great biological importance. Their chemistry, biochemistry, and regulation in the body have been intensely studied for more than two centuries. The author has studied aspects of the biochemistry and clinical chemistry of steroids and bile acids for more than 50 years, and this paper, which is an extended version of the Schroepfer Medal Award lecture, reviews and discusses part of this work. Development and application of analytical methods based on chromatography and mass spectrometry (MS) have been a central part of many projects, aiming at detailed characterization and quantification of metabolic profiles of steroids and bile acids under different conditions. In present terminology, much of the work may be termed steroidomics and cholanoidomics. Topics discussed are bile acids in human bile and feces, bile acid production, bacterial dehydroxylation of bile acids and steroids during the enterohepatic circulation, profiles of steroid sulfates in plasma of humans and other primates, development of neutral and ion-exchanging lipophilic derivatives of Sephadex for sample preparation and group separation of steroid and bile acid conjugates, profiles of steroids and bile acids in human urine under different conditions, hydroxylation of bile acids in liver disease, effects of alcohol-induced redox changes on steroid synthesis and metabolism, alcohol-induced changes of bile acid biosynthesis, compartmentation of bile acid synthesis studied with ^{3}H-labeled ethanol, formation and metabolism of sulfated metabolites of progesterone in human pregnancy, abnormal patterns of these in patients with intrahepatic cholestasis of pregnancy corrected by ursodeoxycholic acid, inherited and acquired defects of bile acid biosynthesis and their treatment, conjugation of bile acids and steroids with *N*-acetylglucosamine, sulfate-glucuronide double conjugates of hydroxycholesterols, extrahepatic 7α-hydroxylation and 3-dehydrogenation of hydroxycholesterols, and extrahepatic formation of C_{27} bile acids. The final part discusses analysis of free and sulfated steroids in brain tissue by capillary liquid chromatography-electrospray MS and suggests a need for reevaluation of the function of steroid sulfates in rat brain.

Paper no. L9527 in *Lipids 39,* 703–722 (August 2004).

It is a great honor for me to be selected as the second recipient of the Schroepfer Medal Award. I met George on several occasions at meetings and in Stockholm. He was a friend of my friend Henry Danielsson, who had also studied with Konrad Bloch at Harvard. His way of doing science appealed very much to me. His interest in analytical methodology was deep and critical, and he published beautiful, comprehensive papers on the separation and mass spectrometric analysis of unsaturated sterols, exemplified by References 1–3. Their application to studies of biosynthetic and metabolic pathways under normal and pathological conditions yielded reliable results and often corrected earlier misconceptions caused by unreliable methodology. George's analytical studies of sterol profiles were predecessors of what in the postgenomic era would be termed "sterolomics." They should be consulted by all those who are presently involved in studies of metabolism of sterols and their potential regulatory importance as ligands to nuclear receptors. The 194-page review of oxysterols with 1,231 references referred to as "critical, fairly comprehensive" (4) also illustrates George's mind and care in drawing conclusions from studies using methods that had not been well validated. He was probably convinced that certain oxysterols were important endogenous ligands to nuclear receptors and to the regulation of sterol and bile acid synthesis. However, all scientists are not fully convinced that this is the case (5). New methodology, probably based on mass spectrometry (MS), is required to actually prove that a certain oxysterol is bound to a nuclear receptor when this is bound to the regulatory sites on genes in the nucleus of the living cell.

Professor Geoffrey Gibbons, the first recipient of the Schroepfer Medal, gave an elegant description of the 200-yr history of cholesterol and then presented recent results on the regulation of cholesterol and lipid synthesis (6). I would like to be more egocentric and go back only in my own history and describe results from intertwined lines of research during the past 50 yr, particularly from the members and descendants of the Sune Bergström group. I will expand a little on studies that may be less well known and also permit myself to speculate freely.

REVERSED-PHASE AND QUANTITATIVE PAPER CHROMATOGRAPHY IN STUDIES OF METABOLISM AND TURNOVER OF BILE ACIDS

Two factors determined my introduction to bile acid research: golf and Sune Bergström (Nobel Laureate 1982 with B. Samuelsson and J. Vane). Bergström visited a biochemist

Dedicated to the memory of Sune Bergström, who died on August 15, 2004.

*E-mail: jan.sjovall@mbb.ki.se

Abbreviations: CID, collision-induced dissociation; CTX, cerebrotendinous xanthomatosis; CYP7A1, cholesterol 7α-hydroxylase; CYP7B1, oxysterol 7α-hydroxylase; CYP27A1, sterol 27-hydroxylase; DHEA, dehydroepiandrosterone (3β-hydroxyandrost-5-en-17-one); ES, electrospray; FAB, fast atom bombardment; FXR, farnesoid X receptor; GC/MS, gas chromatography–mass spectrometry; GlcNAc, *N*-acetylglucosamine; ICP, intrahepatic cholestasis of pregnancy; LXR, liver X receptor; MS, mass spectrometry.

friend who was the chairman of my golf club and a friend of my parents. At the age of 31 yr, he was a newly appointed professor of Physiological Chemistry at the University of Lund where I was a medical student. He had discovered the attraction of golf and in this way we came to play together. I was very impressed by his personality and decided to try to become his student. The next year, 1949, I was accepted as amanuens at the Department of Physiological Chemistry.

At about that time Bergström started a comprehensive project on the biosynthesis and metabolism of bile acids. In 1950 A.J.P. Martin and G.A. Howard published the first paper on reversed-phase chromatography of FA, and I was given the task to design reversed-phase systems for separation of bile acids. This was successful (7), and A. Norman extended the systems to cover more polar and conjugated bile acids. Reversed-phase chromatography was then used extensively during the following 10 yr in studies of the hepatic and bacterial metabolism of bile acids labeled with ^{14}C. As a parenthesis, the reversed-phase systems were essential in the isolation of prostaglandins, which turned out to have mobilities similar to that of cholic acid (8,9).

I also developed paper chromatographic systems for conjugated and free bile acids (10,11). These permitted direct analysis of bile acids in bile, and their application made it clear that chenodeoxycholic acid was a major bile acid in human bile (12). Ursodeoxycholic also was detected for the first time in human bile (13), and the method was made quantitative. When used for analysis of bile acid excretion in bile fistula rats and humans, the feedback regulation of bile acid biosynthesis was discovered. Thus, bile acid excretion increased markedly during the days following the insertion of a bile duct cannula (14,15). Bergström and Danielsson showed that infusion of taurochenodeoxycholic acid depressed cholic acid excretion in the bile fistula rat (16). It took another 10 yr to show that the site of feedback inhibition was the cholesterol 7α-hydroxylase (CYP7A1) reaction (17). It was shown that protein synthesis was required and that the half-life time for CYP7A1 was 2–3 h (18). The enzyme was cloned by several groups 20–25 yr later (19–21). When the presence of nuclear receptors for regulatory steroids became known about 35 yr ago, the search for potential bile acid receptors began. The last few years have seen unparalleled development in this area. About 5 yr ago several groups reported that bile acids were natural ligands for the farnesoid X receptor (FXR), the activation of which led to repression of bile acid synthesis. The understanding of mechanisms that control bile acid formation and excretion is increasing rapidly (22). A year ago the crystal structure of the FXR ligand-binding domain was reported with natural and synthetic ligands in the binding pocket (23,24). Thus, it took about 50 yr to elucidate the chemical nature of the feedback mechanism in bile acid synthesis. There is still much to be understood; one detail is how the large species differences in the regulation and pathways of bile acid synthesis and metabolism are explained. Ongoing work in several laboratories shows that the regulation of the CYP7A1 gene is very complex and involves a number of nuclear receptors and other proteins.

Quantitative paper chromatography also led to the discovery that the formation of deoxycholic acid required contact with intestinal bacteria. Thus, deoxycholic acid disappeared from bile during biliary drainage (15), and it was absent from bile of infants (25). Final proof of its formation by bacterial 7α-dehydroxylation of cholic acid was obtained by comparing the metabolism of cholic acid in intact and bile fistula rabbits (26). Detailed studies by A. Norman and others in collaboration with B.E. Gustafsson, later head of the Department of Germfree Research at Karolinska Institutet, showed that bacterial metabolism of bile acids during their enterohepatic circulation was extensive; besides 7α-dehydroxylation, oxidoreductions, epimerizations, and hydrolysis of conjugates took place (27,28). The detailed mechanism of 7α-dehydroxylation was elucidated by P. Hylemon and coworkers as one of the first examples of the application of molecular biology to the bile acid field, and was complete about 40 yr after the discovery of the reaction (29). The pathophysiological importance of bacterially modified, so-called secondary, bile acids is not yet clear. A possible role in colon cancer is still under debate. A recent finding is that lithocholic acid and 3-oxo-5β-cholanoic acid are ligands of the vitamin D receptor (and FXR and pregnane X receptors) (30).

Quantitative paper chromatography was also used to determine specific radioactivity in many studies of bile acid turnover in man and animals based on the Lindstedt method (31). For example, we studied the turnover of bile acids in rabbits first fed hydrogenated coconut oil, which greatly increased plasma cholesterol, and then corn oil, which drastically lowered the plasma cholesterol. In contrast to the large changes of plasma cholesterol levels, bile acid production and turnover remained the same (32). The results of these early studies can now be compared with measurements of levels and expression of regulatory molecules to get an understanding of underlying mechanisms. Recently Salen and coworkers studied the liver X receptor (LXR) and FXR regulation of bile acid synthesis in the rabbit and found that FXR-regulated depression of CYP7A1 overrides LXR-induced increase of this enzyme in the rabbit, making this animal more sensitive to cholesterol feeding than rat and man (33).

GC/MS, BILE ACIDS, AND STEROID SULFATES

In 1960 and 1962–1963, I spent postdoctoral periods in the laboratories of E.C. Horning at the U.S. National Institutes of Health and Baylor College of Medicine of Houston and of D. Turner at Sinai Hospital of Baltimore to learn how to analyze bile acids and steroids by GLC. We developed the first GLC methods for analysis of bile acids (34) and dehydroepiandrosterone sulfate in plasma (35). For the first time in steroid analysis, solid phase extraction was used instead of solvent extraction, employing a macroreticular anion exchanger to recover the compounds from plasma.

On returning to Stockholm, I started a series of studies on the profiles of bile acids in human feces (with P. Eneroth and K. Hellström), steroids in feces from germfree and conven-

tional rats (with B.E. Gustafsson and J.-Å. Gustafsson), and steroid sulfates in human plasma (with R. Vihko). I also became engaged in the project, led by R. Ryhage, to construct a combined GC/MS instrument, resulting in the first commercial GC/MS instrument manufactured by the LKB company (see Ref. 36). We used the prototypes of this instrument and later the commercial version to identify the compounds appearing in the effluents from the GLC columns.

The bile acid mixture in feces, after hydrolysis and deconjugation, was found to be very complex owing to the bacterial metabolism of the primary bile acids. Deoxycholic and lithocholic acids formed by 7α-dehydroxylation were predominant (37,38), but their 3β epimers were often present in considerable amounts. They were later shown to be partially esterified at C-3 with FA (39,40), a fact that may still be forgotten in present-day analyses of fecal bile acid excretion. Some samples also contain significant amounts of potentially toxic 3-oxo bile acids, which are usually lost in the analytical procedures (41). Since secondary bile acids have been suspected to be important in the development of colon cancer, there is an interest in quantification of fecal bile acid profiles. A reasonably comprehensive (using Schroepfer's definition) and critical review on fecal bile acids and their analysis was published by Setchell *et al.* in 1988 (42). Although collection of representative fecal samples is the major practical problem, the procedures for quantitative analysis still cannot be regarded as satisfactory with regard to specificity in analyses of individual bile acids and their conjugates, in spite of recent developments both in chromatographic and mass spectrometric methods (see below).

Analyses of steroid excretion in germfree and conventional rats were performed with B. Gustafsson and my student J.-Å. Gustafsson to evaluate the role of bacteria and enterohepatic circulation in the metabolism of steroid hormones. It appeared possible that bacterial formation of steroid metabolites, which were returned to the body, might be of pathophysiological importance. In addition to new information about the nature of the steroids present, we found a number of metabolic reactions catalyzed by the intestinal bacteria: hydrolysis of conjugates, oxidoreductions, and novel dehydroxylations. With our student H. Eriksson we discovered that bacterial elimination of the 16-hydroxy group in a 16α-hydroxy-20-oxo-C_{21} steroid lead to pregnane derivatives with either a 17α- or 17β-oriented side chain (43). This reaction was also observed in pregnant women (44). Bacterial elimination of the 21-hydroxy group in 21-hydroxy-20-oxo-C_{21} steroids was also an important reaction (45). In fact, whereas 3,11,15,21-tetrahydroxy-20-oxosteroids (in sulfated form) predominated in feces from female germfree rats, there were no free 21-hydroxysteroids in feces from the conventional rats (46). The pathophysiological importance of this bacterial metabolism is still unknown but remains an interesting question, considering the large number of nuclear receptors of the steroid family, some of which are promiscuous in their acceptance of ligand structures. The studies of steroid metabolism in germfree and conventional rats were continued by J.-Å. Gustafsson and his coworkers and led to the discovery of large sex differences in hepatic steroid metabolism in the rat, shown to be regulated by growth hormone secretory pattern and induction of a 15β-hydroxylase specific for sulfated steroids in the female rat. Gustafsson's later achievements in the field of nuclear receptors are well known and have been of great importance for this field.

With Gustafsson and postdoctoral student C.H.L. Shackleton, grandson of the explorer of the Antarctic, we also started a series of GC/MS studies of the metabolic profiles of steroids in infants (47,48). These studies were continued by Shackleton, who has made many important contributions both to analytical methodology and to the understanding and diagnosis of clinical conditions involving defects in the biosynthesis and metabolism of steroids (49). One of his present interests is steroid synthesis in infants with the Smith-Lemli-Opitz syndrome (7-dehydrocholesterol-7-reductase deficiency) (50). Part of this work is being carried out in collaboration with the department at Rice University, Houston, where Schroepfer did his beautiful methodological studies on unsaturated sterols (see introductory section) and applied the methods to studies of the unsaturated sterols in patients with the Smith-Lemli-Opitz syndrome (51).

My interest in steroid sulfates was stimulated by the studies of E.-E. Baulieu and coworkers (52), which showed that certain steroid sulfates, e.g., dehydroepiandrosterone (3β-hydroxyandrost-5-en-17-one; DHEA) sulfate, were primary products of steroid biosynthesis in endocrine organs and not secondary metabolites for excretion. With my student R. Vihko, a chromatographic method based on methylated Sephadex (later replaced by Sephadex LH-20, see next section) was developed for group isolation of mono- and disulfated steroids. These groups were solvolyzed and the steroids were analyzed as trimethylsilyl ethers by GLC and GC/MS (53–56). Vihko's thesis gave the first reliable values for DHEA sulfate in plasma and showed for the first time that the levels were lower in women than in men and decreased with age in both sexes (57). These findings have been confirmed many times up to the present day (see Ref. 58). Our studies in Horning's laboratory had already shown that the levels could be markedly increased by oral administration of DHEA (35). This has been confirmed repeatedly. A number of other C_{19} and C_{21} steroid sulfates in plasma were also identified and could be analyzed quantitatively to give profiles of mono- and disulfated steroids. The methods were used by several groups in studies of steroid sulfates in blood, urine, bile, and amniotic fluid under different conditions. Interest in DHEA has increased exponentially in recent years: A search for dehydroepiandrosterone in PubMed, when this lecture was being prepared, gave 9,528 hits. DHEA and/or its sulfate are neurosteroids and have a variety of effects on the nervous system. Effects of oral administration of DHEA on parameters in aging are under study in several laboratories (58).

Using these profiling methods, we found that pregnant women had a special pattern of steroid sulfates in plasma (59–61). This will be discussed in a separate section.

LIPOPHILIC GELS AND METABOLIC PROFILES ("STEROIDOMICS")

The work with complex matrices such as plasma and feces made it clear that appropriate sample preparation procedures were essential for successful analysis of complex mixtures of bile acids and steroids by GLC and GC/MS. Chromatography in conventional two-phase systems was not practical for this purpose because of the need for solvent equilibration. With a student, E. Nyström, we began to study how stationary phases could be prepared by chemical modification of cross-linked dextran gels. Methylated Sephadex was prepared that permitted molecular sieving in organic solvents as well as partition chromatography in miscible solvent systems where the solvent–gel constituted the stationary phase. High column efficiencies could be obtained by recycling chromatography or with capillary columns in Teflon tubing (62). We made the important observation that sodium and potassium salts of steroid sulfates were strongly retained by these columns when chloroform/methanol containing sodium or potassium chloride, respectively, was used as solvent. This became the basis for the analyses of profiles of steroid sulfates described above. When introduced by Pharmacia, Sephadex LH-20 replaced methylated Sephadex and also became widely used for purification of steroids prior to radioimmunoassays.

It was soon evident that a wider range of substituted Sephadex derivatives was desirable for sample preparation purposes. Less polar derivatives were required for establishment of better reversed-phase systems, and ion exchangers of variable polarity were desirable for group separation of biological extracts in which steroids and bile acids occurred in different forms of conjugation with charged moieties. The postdoctoral student J. Ellingboe reacted Sephadex LH-20 with long-chain olefin oxides to give lipophilic gels of desired hydrophobicity (63) and with epichloro- or epibromohydrin to yield intermediates for further substitution with functional groups suitable for ion exchange and ligand exchange purposes (64). In this way an array of stationary phases was obtained with which the biological sample could be subfractionated according to charge, polarity, and specific functional groups of the compounds to be analyzed by GC/MS (see 65,66).

Our sample preparation methods for analysis of metabolic profiles usually consist of passage of the sample solution through an appropriate sequence of lipophilic neutral and ion-exchanging gel beds. The strategy is to retain either the analytes or the interfering material (digital chromatography). Groups of unconjugated and conjugated metabolites differing in charge and acidity are sequentially eluted by stepwise displacements from the ion-exchanging beds that, unlike ion-exchange resins, do not show nonspecific adsorption. If the sample is a biological fluid, the initial step is a solid-phase extraction under conditions minimizing protein binding (66–69); if the sample is a tissue, a solvent extract is prepared that can then be transferred in different ways onto a suitable sorbent for subsequent elution (e.g., see Refs. 66,68,70) and subfractionation. It should be mentioned that lipophilic-hydrophobic derivatives of Sephadex (Lipidex 1000 and 5000) are very useful for extraction of less-polar steroids and bile acids since they do not extract polar conjugates and thus give cleaner extracts. Extraction with these derivatives is different from the common solid-phase extractions with substituted silica or polystyrenes and is comparable to solvent extractions without emulsion problems (68,71). Because of the cross-linked matrix, proteins do not enter the gel, and ligands to nuclear receptors can be extracted separately from weakly bound compounds by control of the temperature of the gel (72).

These principles of sample preparation were first applied to analyses of urinary bile acids and steroids by GC/MS (73–75). Detailed profiles of different groups of conjugates were obtained. Computerization of the mass spectrometric analyses was an important prerequisite. Ryhage's group constructed an interface for our LKB 9000 that permitted recording of spectra on a tape that could then be evaluated on an IBM 1800 computer (36). My engineer R. Reimendal wrote all the necessary programs for this evaluation (76,77), including programs for quantification of number and abundances of stable isotopes (78); now all of this is commercially available.

The bile acid profiles in urine revealed the presence of many previously unknown bile acids. Most of the mono- and dihydroxy bile acids were sulfated in addition to being glycine- or taurine-conjugated. Evidence was obtained for tetrahydroxycholanoic acids, predominantly taurine-conjugated, carrying hydroxyl groups in the 1,3,7,12- and 3,6,7,12-positions and excreted in increased amounts in liver disease (73,74,79). They were shown to be formed from cholic acid (80). Microbially synthesized 1β-hydroxydeoxycholic acid was identical with the 1-hydroxydeoxycholic acid found in urine, suggesting that the 1-hydroxylated bile acids in urine carried a 1β-hydroxy group (81). Extensive synthetic work by Japanese groups has provided the correct structures for these and other hydroxylated bile acids found by different groups in human urine. Thus, C_{24} bile acids in humans may occur hydroxylated at carbons 1, 2, 3, 4, 5, 6, 7, 12, 19, 22, and 23. Increased hydroxylation is seen in the neonatal period and in liver disease. The cytochromes P450 catalyzing hydroxylations of primary and secondary bile acids are only partly known, and the regulation of these hydroxylations are not known. The hydroxylations may serve to protect the hepatocytes from the hepatotoxic primary bile acids.

The analyses of metabolic profiles of bile acids also led to the detection of bile alcohol glucuronides in urine from healthy humans and patients with liver disease (82–84). The major bile alcohol had 26 instead of 27 carbon atoms but was formed from cholesterol (85). Ion exchange separation is of great value in this case, not only for isolation of glucuronidated bile alcohols as a group but also for the subsequent separation of neutral sterols from acidic steroids (bile acids). This is because the cholestane and methyl cholanoate skeletons differ by 2 Da and it can be very difficult to tell whether a peak in the GC/MS analysis is due to a substituted cholestane or a methyl cholanoate with a double bond. A prior ion exchange separation eliminates this problem.

E.C. Horning pioneered the analyses of metabolic profiles of steroids (86). However, since hydrolysis of conjugates was an initial step, these profiles represented a mixture of differently conjugated steroids, which may have different metabolic origins. In our strategy, different groups of conjugates were analyzed separately. The profiles of unconjugated, glucuronidated, and sulfated steroids were widely different, and pathological changes in the individual groups could now be detected. Examples are given in the sections below. Ion exchange fractionation also made it possible to analyze profiles of unconjugated and conjugated steroids in plasma (67,87).

ALCOHOL AND THE METABOLISM AND BIOSYNTHESIS OF STEROIDS AND BILE ACIDS

The metabolism of ethanol leads to a large production of NADH, particularly in the liver, and a change of the redox state in cells that metabolize ethanol. We thought that this could influence biosynthesis as well as metabolism of steroids and bile acids since a number of dehydrogenases and reductases using NAD(H) and NADP(H) are involved in these processes. In addition, alcohol dehydrogenase was found to be a 3β-hydroxy-5β-steroid dehydrogenase (88). My student T. Cronholm and I chose to analyze the profiles of steroid sulfates in human plasma to study whether ethanol affected the 17β-hydroxy-/17-oxosteroid or the 20α-hydroxy-/20-oxosteroid ratios. We found that the former but not the latter ratio was greatly increased by ethanol and ascribed this difference to the use of NAD(H) in the former reaction and NADP(H) in the latter (89). The effect of ethanol was dose dependent at low blood alcohol levels (<10 mM) but was maximal when alcohol dehydrogenase was saturated with substrate (i.e., at maximal production of NADH). When [1,1-$^2H_2$]ethanol was ingested, there was an extensive transfer of ^2H to androst-5-ene-3β,17β-diol 3-sulfate, which was parallel to the increase of the levels of this steroid. This result indicated a formation by reduction of DHEA sulfate with use of NAD^2H. The levels of the disulfate of the androstenediol were not affected by acute ethanol metabolism. However, chronic ingestion of moderate amounts of alcohol resulted in increased plasma levels and urinary excretion of the disulfate (90,91), reflecting the continuous ethanol-induced formation of the monosulfate.

The importance of the redox effect of ethanol on steroid hormone balance is not yet fully understood. Hormonal disturbances are known to occur in alcoholics. Since the hormones testosterone and estradiol both have a 17β-hydroxy group and since their inactive precursors with a 17-oxo group (androst-4-en-3,17-dione and estrone, respectively) are circulating in plasma, we analyzed the effect of ethanol on these potential redox couples. We found that the sulfated and glucuronidated forms of estradiol increased markedly after alcohol ingestion in men, whereas the levels of free testosterone and estradiol in plasma did not increase significantly (92). This does not exclude an increase of intracellular free estradiol by hydrolysis of its conjugates.

Interest in the redox effects of ethanol on steroid metabolism has recently been renewed. In studies of large groups of women ingesting moderate doses of alcohol, Sarkola and coworkers found significant increases of the plasma levels of estradiol and an increase of the estradiol/estrone ratio in women taking oral contraceptives (93). Välimäki *et al.* (94) and Mendelson *et al.* (95) previously described an acute elevation of plasma estradiol after alcohol administration in premenopausal women. Sarkola *et al.* also found that alcohol induced a fourfold increase of testosterone and a decrease of androstendione in women, which was abolished by pretreatment with the alcohol dehydrogenase inhibitor 4-methylpyrazole (96). The combined results of these and our studies show that alcohol, *via* its effect on the redox state of the liver, can influence the hormone balance and potentially induce estrogenic effects in men and androgenic effects in women. The effect on estrogen balance might influence the development of breast cancer.

The *de novo* biosynthesis of steroid hormones could conceivably also be affected by the redox effect of ethanol metabolism. The 3β-hydroxy-Δ^5-steroid dehydrogenase 4,5-isomerase required for conversion to the essential 3-oxo-Δ^4 structure utilizes NAD as coenzyme while 17β-hydroxysteroid dehydrogenase uses NADP. Together with student S. Andersson, we developed a method for analysis of profiles of unconjugated steroids in rat testis and applied it to a study of the effects of ethanol metabolism (97). The results showed that ethanol increased the ratios between 3β-hydroxy-Δ^5-/3-oxo-Δ^4-steroid couples, compatible with an inhibition of testosterone biosynthesis. Later studies with [1,1-$^2H_2$]ethanol indicated that this was a direct effect of testicular ethanol metabolism on the redox state, not mediated by lactic acid from the liver (98). Thus, it appears that ethanol-induced redox changes can be of endocrinological importance both *via* effects on the metabolism and the biosynthesis of steroid hormones.

Since bile acid metabolism also involves redox reactions and alcohol dehydrogenase is a 3β-hydroxy-5β-steroid dehydrogenase and is hepatotoxic, the postdoctoral student I. Makino studied effects of ethanol metabolism on oxidoreductions of bile acids in the bile fistula rat (99,100). However, ethanol had no effects on the reduction of 3-oxo bile acids or the oxidation of 3β-hydroxy bile acids and thus does not seem to affect bile acid metabolism directly. During metabolism of [1,1-$^2H_2$]ethanol, the bile acids became ^2H-labeled at C-3 to an extent indicating that at least 60% of the bile acid molecules underwent oxidoreduction during each passage through the liver. The extensive oxidoreduction at C-3 and the 3β-hydroxy-5β-steroid dehydrogenase activity of alcohol dehydrogenase may explain why all bile acids in bile have a 3α-hydroxy group in spite of the formation of 3β-hydroxy bile acids by intestinal bacteria during the enterohepatic circulation (see above).

Ethanol may stimulate bile acid biosynthesis in man. With M. Axelson we found a number of potential C_{27} neutral and acidic intermediates in bile acid biosynthesis in plasma, hav-

ing either a 3β-hydroxy-Δ^5 or a 3-oxo-Δ^4 structure (101,102). When these were analyzed after a moderate dose of ethanol, no immediate redox effect was noted. However, after about an hour the levels of 7α-hydroxycholest-4-en-3-one began to rise to reach a 5–15-fold increase after 3–4 h (103). The levels of 7α-hydroxycholesterol also increased in parallel to a similar extent. We had previously shown that the plasma level of 7α-hydroxycholest-4-en-3-one reflected rates of bile acid synthesis in man (104), a finding that has been confirmed and extended to show that it reflects the activity of CYP7A1 in man (105,106). If this is the case also after ingestion of alcohol, the data indicate that bile acid synthesis *via* the neutral (7α-hydroxycholesterol) pathway (102) is increased by alcohol in man. The mechanism of this increase is unknown but the time course indicates an indirect mechanism; it could involve changes of the enterohepatic circulation or indirect effects on the regulation of CYP7A1 by nuclear receptors, e.g., FXR, by alcohol, its metabolites, or the redox change. Studies with isolated hepatocytes may help to answer this question.

The alcohol-induced increase of 7α-hydroxycholest-4-en-3-one is interesting also from a clinical point of view. The etiology of alcoholic liver cirrhosis is not fully understood, and many theories have been put forward in the last 50 yr. About 15 yr ago, cholesta-4,6-dien-3-one was identified in fatty livers of alcoholic patients (107). This could reflect an increased formation of 7α-hydroxycholest-4-en-3-one, since the 7α-hydroxy group can be eliminated both in the liver and by intestinal bacteria (108). The hepatotoxicity of cholesta-4,6-dien-3-one is not known, but bile acids with a 3-oxo-Δ^4 structure induce liver disease (see section on defects in bile acid biosynthesis). Studies of this possible mechanism would be of interest, as would studies of ways to influence the alcohol-induced change of bile acid biosynthesis (or biosynthetic pathways).

The initial studies of ethanol effects on steroid and bile acid metabolism indicated that ethanol labeled with ^2H and ^{13}C might be used to investigate compartmentation of coenzyme and acetate pools, metabolism of steroids, and biosynthesis and biliary secretion of lipids. These studies were carried out in particular by T. Cronholm and T. Curstedt with participation of A. Burlingame and postdoctoral students S. and H. Matern. It is beyond the scope of this lecture to discuss the results, and the reader is referred to reviews (109–111). Only one example will be given. The ^2H-labeling pattern of bile acids and cholesterol in the above studies with $^2H_2$-ethanol indicated that bile acids and cholesterol in bile represented different pools of cholesterol (99). Earlier studies with other methods had indicated that bile acids might be formed from a special pool of cholesterol (see Ref. 112). By infusing [2,2,2-$^2H_3$]ethanol or [1-^{13}C,1-$^2H_2$]ethanol into bile fistula rats, we could show that this was indeed the case (113). The infusion resulted in formation and biliary excretion of polydeuterated bile acids, cholesterol, and allotetrahydrocorticosterone. The rate of disappearance of unlabeled molecules (i.e., molecules formed before the start of infusion) gave the half-life times of the cholesterol pools serving as precursors for the three types of compound. The turnover of the pool used for bile acid synthesis was about five times higher than that used for corticosterone synthesis and biliary cholesterol secretion. The labeling of the precursor acetate pool could be calculated from the composition of isotopomers of the compounds after correction for deuterium-protium exchange in the biosynthetic sequence (114). About 40% of the precursor acetate pool originated from ethanol. In these studies we had the pleasure to collaborate with A.L. Burlingame, who spent about a year in my laboratory as a Guggenheim fellow. The same method was used by visiting professor R. Vlahcevic to show that all 5β- and 5α-di- and trihydroxy bile acids and their sulfates in bile fistula rats were formed from kinetically the same pool of cholesterol (115). This is of interest in view of the presently accepted importance of at least two pathways of bile acid biosynthesis, one starting with 7α-hydroxylation of cholesterol in the endoplasmic reticulum and the other by 27-hydroxylation in the mitochondria. It is likely that the former, FXR-regulated, pathway predominates in the bile fistula rat and that mitochondrial cholesterol is an insignificant precursor in this case.

STEROID SULFATES IN PREGNANCY AND INTRAHEPATIC CHOLESTASIS OF PREGNANCY

As already mentioned, pregnant women were found to have a special pattern of steroid sulfates in plasma. In addition to the mono- and disulfated C_{19} and C_{21} steroids present in the nonpregnant state, there was a complex mixture of isomeric pregnanolone sulfates, pregnanediol mono- and disulfates, and pregnandiolone and pregnantriol mono- and disulfates (59,60,116). Their levels increased during the course of the pregnancy as determined by GLC and GC/MS by K. Sjövall (61). Their structures indicated that they were metabolites of progesterone. To evaluate the uniqueness of this pattern of steroid sulfates for the human species, we investigated the patterns in pregnant monkeys and great apes. Similar, although quantitatively different, profiles were found in plasma from the pregnant chimpanzee and orangutan whereas the pregnant rhesus monkey did not have any of these steroid sulfates in plasma (117). Thus, the metabolic profiles of steroid sulfates in plasma seem to reflect a late step in evolution specific for the higher primates. It remains to be determined whether any of these sulfated pregnane derivatives have a physiological role in pregnancy or parturition or only represent metabolites for elimination of progesterone.

The production, metabolism, and turnover rates of 3-sulfated pregnane derivatives with 3β-hydroxy-5α or 3α-hydroxy-5α structures were determined by injection of the corresponding pregnanolone sulfates labeled with deuterium at C-3 and C-11 and the pregnanediol mono- and disulfates labeled at C-3, C-11, and C-20. These studies were made possible by the synthetic efforts of visiting professor J.E. Herz and postdoctoral students T.A. Baillie and R.A. Andersson who prepared the labeled steroids in such a way that the turnover of the steroid skeleton (11,11-$^2H_2$-labeling), hydrolysis and oxidoreduction at C-3 (3-^2H-labeling), and oxidoreduction

(20-^{2}H-labeling) and sulfation at C-20 could be studied simultaneously (118–120). Detailed information was obtained about turnover rates (which varied greatly between the isomers), daily production, oxidoreduction, and sulfation at C-20, and metabolism of the individual steroid sulfates. It could be calculated that the excretion of sulfated 5α-pregnane derivatives corresponded to about 50% of the total progesterone production, contrary to the belief that 5β-pregnane derivatives were the predominant metabolites of progesterone in man. In contrast to 5β-pregnane derivatives, which are predominantly glucuronidated and excreted in urine, the sulfated 5α-pregnane derivatives are to a large extent excreted in bile and feces (121). The difficulty in analyzing feces explains why less attention has been paid to metabolites with a 5α than a 5β configuration. Among the interesting metabolic reactions of the sulfated 5α-pregnane derivatives were 16α-hydroxylation of the intact pregnanolone sulfates and 21-hydroxylation specific for the 3α-hydroxy-5α-pregnan-20-one/5α-pregnan-3α,20α-diol 3-sulfate couple to yield 5α-pregnan-3α,20α,21-triol 3-sulfate (120,122). The latter reaction was the exclusive pathway to this pregnanetriol sulfate, which together with its disulfate and the pregnanediol isomer disulfates constituted end products in the metabolism. Although the physiological function of the sulfated pregnane derivatives in pregnancy remains unknown, these studies underline the power of MS and use of appropriately labeled compounds in "steroidomics."

At this time the metabolism of ethinylestradiol was also of interest. Visiting professor David Collins performed elegant syntheses of 11ξ,12,12-trideutero- and 9α,11,11,12,12-pentadeuteroethinylestradiol (123,124), and methods for selective isolation of ethinyl steroids on a cation exchanger in silver form were developed (125–127). Unfortunately the project was not further supported, but labeled estradiols obtained as intermediates were used in studies of the turnover of estradiol in the rat uterus by H. Eriksson, M. Axelson, and postdoctoral student M. Tetsuo (128–130).

The patterns of steroid conjugates in plasma and urine of pregnant women have been studied in recent years using more refined group separation methods and capillary GLC and GC/MS (131,132). Also, fast atom bombardment (FAB) ionization made it possible to analyze the intact conjugates. In the course of these studies, double conjugates of pregnanediols and pregnanetriols with *N*-acetylglucosamine (GlcNAc) were found to be quantitatively important in urine (133). The GlcNAc moiety was attached to the 20α-hydroxy group, and the 3-hydroxy group was sulfated or glucuronidated. A GlcNAc conjugate of 5-pregnen-3α,20α-diol was first described by Arcos and Liebermann (134), but the physiological importance of this mode of conjugation of steroids and bile acids (see following discussion) remains unknown. However, it is of analytical interest since most methods will not include this type of conjugate in the analysis.

Some pregnancies are complicated by intrahepatic cholestasis (ICP), a condition clinically characterized by itching, which disappears shortly after delivery. Using the GLC method from 1965, we made the first studies of the profiles of bile acids in plasma from patients with ICP and showed that the bile acid levels were elevated except for that of deoxycholic acid, indicating a defective enterohepatic circulation (135). The results from that study have been confirmed and extended many times by many groups including our own, and, more recently, by L.J. Meng in collaboration with H. Reyes, professor of medicine in Santiago de Chile and an expert on the disease. My student P. Thomassen performed a detailed study of urinary bile acid excretion in patients with ICP (136) and found that the appearance of tetrahydroxylated bile acids was one of the first signs of the disease (137).

When the profiles of steroid sulfates were analyzed, marked differences from the normal patterns were detected (138). The levels of most steroid sulfates were elevated, particularly those of the disulfates (3α,5α, 3α,5β, and 3β,5α isomers). The ratio between the monosulfated 3α,5α and 3β,5α steroids was increased as were the levels of 5α-pregnan-3α,20α,21-triol sulfates. Recent studies using improved methods for group separation of conjugates and capillary column GLC and GC/MS have confirmed these findings and added more detailed information regarding the structures, plasma levels, and urinary excretion of steroid conjugates and bile acids in ICP (131,132). The changes are restricted to sulfated progesterone metabolites, including their double conjugates with GlcNAc, whereas levels of glucuronides are normal or decreased. Furthermore, the plasma levels and urinary excretion of the steroid metabolites are not correlated with those of the bile acids, indicating that the two classes of compounds do not share the same transport mechanisms for excretion. These results are compatible with a specific defect in the biliary excretion of certain steroid sulfates.

Methods of treatment of ICP were unsatisfactory until Reyes showed that administration of ursodeoxycholic acid in most cases gave relief of the itching and improved liver function tests (139). We analyzed the profiles of steroid conjugates in plasma and urine from his patients before and during treatment with ursodeoxycholic acid and found an improvement toward normal in almost all cases (140,141). These studies also provided information on the metabolism of ursodeoxycholic acid, which included hydroxylations in positions 1β, 4ξ,5β, 6α/β, and 22, as well as conjugation with GlcNAc (see next section). The importance of separate analysis of different groups of conjugates is emphasized by the finding that 4-hydroxylated bile acids were excreted as double conjugates with glycine/taurine and glucuronic acid. In fact, many steroid and bile acid metabolites are excreted in urine as double conjugates, which would not be detected by most methods used in clinical studies. An extensive study of ICP and its treatment in Sweden is presently being conducted by Glantz, Marschall, and Mattsson using electrospray MS (ES-MS) to monitor bile acids and steroids during treatment (142).

The etiology of ICP is still unknown and open for speculations (139,143,144). Our results indicate that it may be a disease of progesterone metabolism or a disease due to progesterone or its metabolites. Bacq *et al.* (145) made the interesting observation that 32 of 50 consecutive patients had been given progesterone orally shortly before the development of

ICP. There is a genetic (and geographical) component, and many patients with ICP develop the disease in a subsequent pregnancy. When we monitored a healthy pregnant woman, a change of steroid sulfate profiles in plasma was the first sign of a forthcoming ICP, which became clinically overt 6 wk later (137). An important question is whether the abnormal metabolic profiles of steroid sulfates are due to a change in progesterone metabolism or to an impaired biliary secretion of certain sulfated metabolites of progesterone. The production of large amounts of sulfated steroids in pregnancy may in some genetically predisposed individuals result in a saturation of the hepatic transport system(s) used for the biliary secretion of these (particularly disulfated) steroids. The contribution of unknown dietary factors could be related to a defective transport system shared by the dietary factor and the steroid sulfates. At present, research by several groups is focused on search for polymorphism/mutations in hepatic organic anion and bile acid transporters (144). A change in the regulation of such transporters by nuclear receptors is an alternative, since several isomers of the progesterone metabolites have a structure resembling those of ligands to nuclear receptors. The potential ligand activity of most of the steroids found in human pregnancy plasma has not been evaluated. Finally, it is possible that ICP is not a single entity (144). The majority of patients have normal values for γ-glutamyl transferase in plasma but some have elevated values, the severity of the disease varies greatly, some patients recover spontaneously before delivery, others do not respond to ursodeoxycholic acid, and in a few cases the liver is chronically damaged (139).

INHERITED AND ACQUIRED DISEASES OF BILE ACID BIOSYNTHESIS

The introduction of soft ionization methods greatly extended the application of MS to studies of steroid and bile acid metabolism. Shackleton (49) was the first to show that direct analysis of urine extracts by FAB-MS could be used to diagnose genetic defects in steroid biosynthesis. Depending on the type of enzyme deficiency, the negative ion mass spectrum showed different profiles of deprotonated steroid glucuronides (or sulfates). Postdoctoral student B. Egestad applied this method to patients of Professor S. Skredes, Oslo, having cerebrotendinous xanthomatosis (CTX) and found a very characteristic profile of bile alcohol glucuronides at *m/z* 611, 627, and 643 corresponding to deprotonated glucuronides of C_{27} bile alcohols carrying 4–6 hydroxyl groups (146). These were known from the work of G. Salen and coworkers to be metabolites of cholesterol in these patients, who were later shown by I. Björkhem and coworkers to lack mitochondrial sterol 27-hydroxylase (CYP27A1) (147). The first Swedish case of CTX was detected by ES-MS (which has now replaced FAB-MS) of a urine extract, and the diagnosis was confirmed by locating a mutation in the CYP27A1 gene (148). This case represented an unusual form of the disease, presenting as cholestatic liver disease in early infancy. Clayton and coworkers have reported a family with several similar cases (149) and Setchell has also found such a patient (personal communication).

FAB-MS was important in the diagnosis of the first deficiency of an enzyme involved in the transformation of the cholesterol ring system into a bile acid ring system (150). A patient with severe cholestasis, offspring of a first-cousin marriage, was investigated by P.T. Clayton, J.V. Leonard, K. Setchell, and A. Lawson in London. In spite of the cholestasis, bile acids were not found in plasma. Analysis of urinary bile acids by GC/MS gave results that could not be interpreted. Further studies with us indicated that labile bile acids with the allylic 3,7-dihydroxy-Δ^5 structure might be present that were converted into a mixture of artifact products by the analytical procedure. Analysis by FAB-MS showed peaks corresponding to anions of sulfated unsaturated di- and trihydroxy bile acids (*m/z* 469 and 485) and their glycine conjugates (*m/z* 526 and 542). Anion exchange separation and FAB-MS analyses of the fractions showed that the compounds had the mobility of bile acid sulfates. The method of solvolysis, suspected to produce the artifacts, was modified until the FAB spectrum showed the absence of artifacts and formation only of free and glycine-conjugated unsaturated bile acids. These could then be identified by GC/MS. This is an example of systematic unbiased bile acid analysis leading to the diagnosis of a deficiency of 3β-hydroxy-Δ^5-C_{27}-steroid dehydrogenase/4,5-isomerase. The genetic nature of the disease was indicated by other similar cases in the family (151). The absence of the enzyme was confirmed using fibroblasts from the patient (152); fibroblasts from the parents had half the normal activity of the enzyme. The gene was cloned and sequenced by M. Schwarz in D. Russell's laboratory in Dallas; the patient's gene was found to have a 2 bp deletion resulting in a truncated protein with no enzyme activity (153). As shown in many studies (see Ref. 151), the enzyme is different from those used in the synthesis of 3-oxo-Δ^4 steroid hormones, a fact that we noted in an early study of bile acid and steroid profiles in an infant who had a deficiency of 3β-hydroxysteroid dehydrogenase required for steroid hormone synthesis (154).

The patient (150) was treated with chenodeoxycholic acid on the assumption that this would inhibit the CYP7A1 reaction and formation of the pathological bile acids and would give the patient a normal bile acid needed for absorption of lipids and lipid-soluble vitamins. The treatment resulted in considerable clinical improvement and the sulfated bile acids and bile alcohols with a 3β-hydroxy-Δ^5 structure virtually disappeared (155). As far as I know the patient is still well, 17 yr after the beginning of the treatment. A number of new cases have been found by FAB- or ES-MS screening of patients with liver disease carried out in the laboratories of P. Clayton and my former postdoctoral student K. Setchell. It is of interest that some patients have presented at over 10 yr old while others have died in early infancy. This variability could be due to differences in the mutations and enzyme activity, but another possibility is that the bacterial flora has provided the necessary enzyme for formation of normal bile acids during an enterohepatic circulation of the sulfated precursors

excreted in bile. Whether this could form a basis for treatment of the disease remains to be studied.

Deficiency of 3-oxo-Δ^4-steroid 5β-reductase is another defect of bile acid synthesis, reflected by an excretion of 3-oxo-Δ^4 bile acids in urine (156,157). The two patients described by Setchell *et al.* (157) were suggested to have a genetic deficiency, but this has not yet been proven at the gene level. However, urinary excretion of 3-oxo-Δ^4 bile acids is a frequent finding in cases of severe liver disease of different etiologies accompanied by cholestasis (156). Studies of ATP-dependent bile acid transport in canalicular plasma membrane vesicles showed that the taurine conjugate of 7α-hydroxy-3-oxo-4-cholenoic acid strongly inhibited taurocholate transport and was not itself a substrate of the bile acid transporter (158). This provides an explanation for the intrahepatic cholestasis in patients with a deficiency of 5β-reductase and is consistent with the finding that the 3-oxo-Δ^4 bile acid is not excreted in bile, only in urine. The situation may be different for the 12α-hydroxy analog because glycine/taurine conjugated and free 7α,12α-dihydroxy-3-oxo-4-cholenoic acid is found in healthy subjects, and 12α-hydroxylation might serve as a detoxification in this case (see Refs. 132,159). Treatment of 5β-reductase deficiency with chenodeoxycholic acid seriously aggravates the disease, probably because of the hepatotoxicity of this bile acid and the inhibition of its biliary secretion by the 3-oxo-Δ^4 bile acids. In the same way a vicious circle also is created when chenodeoxycholic acid is not administered. Ursodeoxycholic acid is used in combination with cholic acid to improve the condition.

The taurine conjugate of 3β,7α-dihydroxy-5-cholenoic acid is also an inhibitor of ATP-dependent bile acid transport (and is not itself transported), which could explain the cholestasis in patients with deficiency of 3β-hydroxy-Δ^5-C_{27}-steroid dehydrogenase/4,5-isomerase. However, in this disease the abnormal bile acids are excreted in bile as sulfates, confirming that sulfated and nonsulfated bile acids are not transported by the same system.

The discovery of the two deficiencies described above led to programs for screening of urine from patients with cholestasis with FAB-MS (now usually replaced by ES-MS). Setchell screened thousands of samples and found a new inherited disease involving the nuclear modification of the cholesterol skeleton. In collaboration with the laboratories of Russell and Lathe, this disease was characterized as a deficiency of oxysterol 7α-hydroxylase (CYP7B1) (160). The FAB mass spectrum had peaks corresponding to sulfated monohydroxycholenoate and -cholestenoate, shown to have 3β-hydroxy-Δ^5 structures, and a lack of the common primary bile acids. Notably, the levels of 27-hydroxycholesterol were several thousand times higher than normal, indicating the importance of CYP7B1 for the metabolism of this oxysterol, which is formed in most tissues and also is the first compound in one of the pathways from cholesterol to bile acids. Analysis of the CYP7B1 gene revealed a mutation leading to a truncated inactive protein. This study is a beautiful example of the power of combining MS techniques with the methods of molecular biology. Setchell and coworkers have provided another example in the characterization of patients with neonatal liver disease lacking the ability to racemize (25*R*)tri- and -dihydroxy-5β-cholestanoic acids, intermediates in bile acid biosynthesis (161). In contrast to these enzyme deficiencies, human CYP7A1 deficiency was not discovered by analyses of bile acid profiles (162). However, patients with the latter deficiency were hypercholesterolemic and had a greatly reduced formation of bile acids with an expected predominance of chenodeoxycholic acid (162).

FAB- and ES-MS has been of great importance for detection and structure determination of previously unknown conjugated forms of steroids and bile acids. Two examples from our laboratory will be given.

One is the detection of bile acids conjugated with GlcNAc. Matern *et al.* (163) had found an enzyme catalyzing glucosidation of bile acids and sent their student H.-U. Marschall to us to find out whether bile acid glucosides were formed *in vivo* in humans. By using profiling methods and FAB-MS, we found them in urine at levels similar to those of bile acid glucuronides. The latter were first described by a former postdoctoral student P. Back (164), and we had found that 6α-hydroxylated bile acids were selectively glucuronidated at the 6-hydroxy group (165–167). Comprehensive studies of bile acid glucuronidation have been carried out, particularly by A. Radominska and coworkers (168).

When the glucoside fraction from urine was analyzed by GC/MS (following derivatization), peaks were also found that were identified as GlcNAc conjugates. The FAB-MS spectra supported the presence of GlcNAc conjugates of saturated and monounsaturated di- and trihydroxycholanoates (169). Six bile acids conjugated with GlcNAc could be identified by GC/MS following enzymatic hydrolysis. They were all found to carry a 7β-hydroxy group (170). When ursodeoxycholic acid with or without ^{13}C was administered to healthy or cholestatic subjects, at least 50% of its urinary metabolites, including the 3β isomer and hydroxylated and glycine/taurine-conjugated forms, were conjugated with GlcNAc (171).

The positions of conjugation of glucosides, glucuronides, and *N*-acetylglucosaminides were determined by MS by postdoctoral student W. Griffiths using collision-induced dissociation (CID) of the deprotonated molecules generated by FAB ionization (172). Product ion-linked scans were recorded on these ions using an AutoSpec double-focusing mass spectrometer. The sensitivity and the extent of charge-remote fragmentation of the steroid skeleton, important for the structure determinations, were increased by derivatization of the carboxyl group with taurine to yield a sulfonic acid side chain (173,174). These spectra clearly showed that conjugation with glucose was at the 3α-hydroxy group whereas GlcNAc was linked to the 7β-hydroxy group. The interesting question of whether the conjugation of ursodeoxycholic and isoursodeoxycholic acids with GlcNAc is of importance for the pharmacological effects of these acids remains to be answered. One may speculate about competitive effects on the pool of hepatic UDP-GlcNAc or on metabolic reactions utilizing this pool.

The other example is the identification of a double conjugate of 24-hydroxycholesterol in human plasma and urine. FAB and ES mass spectra of urine from cholestatic patients suggest the presence of a wide variety of conjugated bile acids and bile alcohols. As an example, a sample was fractionated on a lipophilic ion exchanger into groups of conjugates, which were then analyzed by capillary column LC–MS. In this way more than 150 different conjugated bile acids and bile alcohols could be detected as separate peaks in reconstructed ion chromatograms (175). One of the unknown compounds, observed as the deprotonated molecule at *m/z* 657, was selected for structural study because it was present in the most severe cases of cholestasis. The *m/z* value, the mobility on the ion exchanger, and the CID spectrum were compatible with a sulfated and glucuronidated conjugate of a hydroxycholesterol. Solvolysis of the sulfate gave the expected product at *m/z* 577, having the mobility of a glucuronide on the ion exchanger. CID of this ion showed that it was a 24-glucuronide. Enzymatic hydrolysis gave the free sterol(s), which were analyzed by GC/MS and found to consist predominantly of 24-hydroxycholesterol. Lesser amounts of other mono- and dihydroxycholesterols were also present that, by the method of isolation, must also have been sulfate glucuronide double conjugates.

The presence of the double conjugate of 24-hydroxycholesterol in plasma and urine of patients with severe cholestasis is interesting for several reasons. First, this conjugate requires special analytical methods to be included in studies of levels and metabolism of 24-hydroxycholesterol. As shown by Björkhem and Meaney, 24-hydroxycholesterol is the major metabolite of cholesterol in the brain (176). Under steady-state conditions its formation and efflux balance most of the *de novo* synthesis of cholesterol in the brain. The forms in which it exists in the peripheral circulation are important because all forms should be included in calculations of turnover and production rates. It has also been shown that neurological diseases can affect the levels of 24-hydroxycholesterol (176). The double conjugate was not included in these measurements. Consideration of the presence of a double conjugate is also of interest because 24-hydroxycholesterol is a potential endogenous ligand to the LXRs and may thus be of regulatory importance. We hypothesize that the high levels of the double conjugate in conditions of severe cholestasis reflect a hepatic encephalopathy with an increased output of 24-hydroxycholesterol from the brain followed by conversion to the sulfate and double conjugate in the liver. It may be added that 24-hydroxycholesterol sulfate was one of the first steroid sulfates found in our early studies of infant feces (177).

Analogous methods were used to show that DHA is an endogenous ligand of the retinoid X receptor, which is the heterodimerization partner of a number of nuclear receptors of the steroid family (178).

HEPATIC AND EXTRAHEPATIC 7α-HYDROXYLATION OF OXYSTEROLS

In the course of studies of alternative pathways in bile acid biosynthesis (102), M. Axelson, postdoctoral student J. Shoda, and I collaborated with K. Wikvall's group in Uppsala. We found that cholesterol could be converted to a 7α-hydroxy-3-oxocholest-4-enoic acid in pig liver mitochondria and that, besides the known cholesterol 27-hydroxylase, there was a sterol 7α-hydroxylase different from cholesterol 7α-hydroxylase (179). Pig liver microsomes were also found to contain a 7α-hydroxylase that catalyzed 7α-hydroxylation of 27-hydroxycholesterol, 3β-hydroxycholest-5-enoic, and 3β-hydroxychol-5-enoic acids (180). The same enzyme activity was also present in human liver microsomes and mitochondria (181). Owing to the presence of 3β-hydroxy-Δ^5-C_{27}-steroid dehydrogenase, end products with a 7α-hydroxy-3-oxo-Δ^4 structure were also formed. Interestingly, a metabolite with 3β,7β-dihydroxy-Δ^5 structure was formed by epimerization of the 7α-hydroxy precursor. In contrast, there was no product with a 7β-hydroxy-3-oxo-Δ^4 structure, showing that the 3β-hydroxy-Δ^5-C_{27}-steroid dehydrogenase does not oxidize substrates with a 7β- instead of a 7α-hydroxy group. This is of interest considering the species-specific formation of ursodeoxycholic acid in bears (*Ursus*) (182) and the nutria (182) and the finding of a considerable percentage of this bile acid in one child (13). The low percentage of ursodeoxycholic acid often present in human bile is usually ascribed to epimerization of chenodeoxycholic acid during the enterohepatic circulation, but this would be an unlikely mechanism for a species-specific formation. It would be interesting to sequence the gene and determine the specificity and structure of the active site of 3β-hydroxy-Δ^5-C_{27}-steroid dehydrogenase in bears and the nutria. This would also be interesting in view of the particular pharmacological effects of ursodeoxycholic acid.

Hydroxylation of 25- and 27-hydroxycholesterol by an oxysterol 7α-hydroxylase was independently confirmed by several groups (183,184). The gene has been cloned (185), and the enzyme (CYP7B1) is an essential component in the biosynthetic pathway (alternative or acidic pathway) starting with mitochondrial 27-hydroxylation of cholesterol, first proposed by Mitropoulos and Myant (186) and Javitt and coworkers (187).

The finding of an oxysterol 7α-hydroxylase changed the view that the classical pathway of bile acid biosynthesis, starting by cholesterol 7α-hydroxylation, was necessarily the predominant pathway. The relative importance of these two pathways and their regulation in different species and under different physiological and pathological conditions are presently being studied in many laboratories. Less attention is being paid to the question of compartmentation in bile acid biosynthesis. It is not clear whether the same enzyme pools are used in the two pathways, which start in the endoplasmic reticulum and mitochondria, respectively. Our finding that mitochondria can perform a sequence of reactions that, according to present views about enzyme distribution, should require shuttling from mitochondria to the endoplasmic reticulum needs to be explained. If the same enzyme pools are being used by the two pathways, which interactions between the pathways can be expected?

Intermediates in the pathways from cholesterol to bile acids were tested for their ability to inhibit the activity of HMG-CoA reductase in cultures of human diploid fibroblasts (188). The regulation of cholesterol biosynthesis by oxygenated sterol derivatives was one of George Schroepfer's major interests (4,6), and George gave us one of his favorite synthetic inhibitors, 3β-hydroxy-5α-cholest-8(14)-en-15-one to use for comparison. Together with M. Axelson, O. Larsson, J. Shoda, and J. Zhang, we studied the effect of 23 potential intermediates (188). Only a few specific intermediates were found to be of possible biological importance. 27-Hydroxycholesterol was previously well established as an inhibitor, and among the other intermediates only those having a 7α-hydroxy-3-oxo-Δ^4 nuclear structure and a 27-hydroxy group had a similar activity. So far none of these derivatives of 27-hydroxycholesterol has been tested for activity as LXR ligands. Cholestenoic acids and cholenoic acids with a 3-oxo-Δ^4-steroid structure (i.e., as present in patients with 3-oxo-Δ^4-steroid 5β-reductase deficiency) had a lower activity, as did precursors that could be converted into the active compounds by 27-hydroxylation or oxidation by 3β-hydroxy-Δ^5-C_{27}-steroid dehydrogenase in the fibroblasts. Although the activity of HMG-CoA reductase is not directly correlated to cholesterol biosynthesis, our results could perhaps indicate a connection between cholesterol and bile acid synthesis mediated *via* intermediates in the pathway(s) to chenodeoxycholic acid. This is of interest because chenodeoxycholic acid is regarded as the most important endogenous ligand of FXR. It is also the major bile acid synthesized in patients with liver cirrhosis (and diminished cholesterol synthesis), making a connection with my results of paper chromatographic analyses 45 yr ago (189).

The inhibitory activity of the intermediates in bile acid biosynthesis raised the question of whether 7α-hydroxylation of 27-hydroxycholesterol could occur in extrahepatic cells. We showed that this was indeed the case (190) (first reported at the 13th International Bile Acid Meeting, Falk Symposium 80, San Diego, 1994). Both 25- and 27-hydroxycholesterol were 7α-hydroxylated and then oxidized by the ubiquitous 3β-hydroxy-Δ^5-C_{27}-steroid dehydrogenase to the 25(27),7α-dihydroxy-3-oxo-Δ^4 sterols (see Ref. 152). Extrahepatic 7α-hydroxylation of the 3β-hydroxy-Δ^5 steroid dehydroepiandrosterone was first described by Sulcova and Starka in 1972 (191) and has since been shown by several groups to occur in many cell types. However, in our experiments pregnenolone and DHEA were hydroxylated to a much lower extent, if any, than the two oxycholesterols and they were only weak inhibitors of the hydroxylation of the latter. This result is difficult to understand considering the present view that these 7α-hydroxylations are being catalyzed by a single enzyme, CYP7B1 (192).

Our results showed that formation of intermediates in bile acid biosynthesis does not require a liver. Previous work by Björkhem and others had shown the widespread occurrence of cholesterol 27-hydroxylase (CYP27A1) (193). Previous and ongoing work by the Björkhems group has shown that hydroxylation of cholesterol in extrahepatic cells is of importance for cholesterol homeostasis in these cells. Thus, macrophages are dependent on formation and secretion of 27-hydroxycholesterol (5), the brain balances *de novo* synthesis of cholesterol by hydroxylation to and elimination of 24-hydroxycholesterol (176,194), and the lung is the major source of 3β-hydroxycholest-5-enoic acid in human plasma (195).

The bile acid precursors formed in extrahepatic cells are transported to the liver and converted into normal bile acids. Measurements of arterio-hepatic venous differences in humans showed an uptake of about 25 mg/24 h of bile acid precursors by the splanchnic area (liver) (193). About half of this uptake consisted of 7α-hydroxy-3-oxocholest-4-enoic acid, an end product of 27-hydroxycholesterol in the human fibroblasts (190). Thus the sequence of 27-hydroxylation, 7α-hydroxylation, and 3-dehydrogenation is a pathway for extrahepatic cholesterol metabolism in humans. However, data from Björkhem's laboratory suggest that circulating 7α-hydroxy-3-oxocholest-4-enoic acid also has a hepatic origin (195). Duane and Javitt have arrived at similar values for the flux of cholesterol metabolites to the liver by measuring the production rates of 27-hydroxycholesterol (196).

The importance of CYP7B1 for the metabolism of oxysterols is also obvious from the analyses of the patient with a genetic lack of the enzyme (160). The plasma levels of 27-hydroxycholesterol in this patient were more than a thousandfold elevated, and total oxysterols were over 4,500 times higher than normal. The extrahepatic contribution to these levels is not known.

The 7α-hydroxylation of 25- and 27-hydroxycholesterol was extensive in rat brain microsomes and in cultures of rat fetal astrocytes and neurons and newborn rat Schwann cells (197,198). As in the case of the human fibroblasts, the 7α-hydroxylated products from the cell cultures were 3-dehydrogenated into the 7α-hydroxy-3-oxo-Δ^4 steroids. A small fraction of 27-hydroxycholesterol and its 7α-hydroxylated metabolites was also oxidized to the corresponding cholestenoic acids. 3β-Hydroxycholest-5-enoic and 3β-hydroxychol-5-enoic acids were also 7-hydroxylated as were DHEA and pregnenolone. The products of the two latter compounds were not 3-dehydrogenated. Our findings regarding the metabolism of 27-hydroxycholesterol in glial cells may help to explain the high levels of 7α-hydroxy-3-oxocholest-4-enoic acid in chronic subdural hematoma (199) and suggest that this acid may be formed locally.

In the course of our studies, the presence in rodent hippocampus of high levels of a new cytochrome P450 was reported (200). This cytochrome, later shown to be CYP7B1, catalyzes the 7α-hydroxylation of DHEA, pregnenolone, and 25- and 27-hydroxycholesterol. It appears to be the major 7α-hydroxylase, perhaps the only one, for steroids with a 3β-hydroxy-Δ^5 structure in the brain (201). The potential function of this reaction in signaling has been discussed by Lathe (192).

In our experiments, 24-hydroxycholesterol was a notable exception in that it was not 7α-hydroxylated and 3-dehydrogenated, underlining the special role of this oxysterol in brain cholesterol metabolism (5). However, 24-hydroxycholesterol

as well as 27-hydroxycholesterol underwent 25-hydroxylation in the astrocytes. These cells also produced 7α,25-dihydroxy-4-cholesten-3-one *de novo* during the incubations. The importance of this finding is unknown; 25-hydroxycholesterol has been one of the most intensely studied oxysterols and is a ligand of LXR but it is not clear if it has a function *in vivo*. Our result could indicate that 25-hydroxylated metabolites of cholesterol have a function in the brain.

The question of whether 7α-hydroxylation and subsequent 3-dehydrogenation of oxysterols are of importance as an autocrine or paracrine mechanism in the cellular regulation of cholesterol homeostasis was independently addressed by Axelson and Larsson and ourselves (202,203). Several cancer cells and virus-transformed fibroblasts are resistant to the inhibitory effects of oxysterols on the activity of HMG-CoA reductase, and several of these cell types also lack the oxysterol 7α-hydroxylase. Whereas Axelson and Larsson found that 27-hydroxycholesterol was converted to 7α,27-dihydroxycholest-4-en-3-one before suppressing production of cholesterol in normal human fibroblasts (202), we did not find a correlation between the presence of an oxysterol 7α-hydroxylase and the ability of 25- or 27-hydroxycholesterol to suppress the activity of HMG-CoA reductase (203). It is possible that differences in the mode of addition of the sterols to the cell cultures affect the results and can explain the apparent contradiction. The 7α-hydroxylation in extrahepatic cells may be regulated since it was stimulated by glucocorticoids and interleukin-1β and inhibited by the glucocorticoid antagonist RU 486 (203,204). It was also inhibited by metyrapone, a known inhibitor of the 11β-hydroxylase.

The 7α-hydroxylation can be an inactivating reaction. It is known that 25-hydroxycholesterol can have immunosuppressing effects by inducing apoptosis of thymocytes. We found that thymic epithelial cells (but not thymocytes) converted 25- and 27-hydroxycholesterol by 7α-hydroxylation and 3-dehydrogenation into the corresponding sterols with a 7α-hydroxy-3-oxo-Δ^4 structure, which did not induce thymocyte apoptosis (204). As in the other cell types studied, cholestenoic acids were also formed from 27-hydroxycholesterol. Whether this is an important mechanism for protection of thymocytes against dietary or circulating oxysterols remains to be investigated. The mechanism by which 25-hydroxycholesterol induces thymocyte apoptosis is not known; our results with inhibitors indicate that it is different from the induction by glucocorticoids.

ANALYSIS OF NEUROSTEROIDS BY ES-MS

The term neurosteroids was coined by E.-E. Baulieu (205) and initially referred to steroids synthesized from cholesterol in the nervous system and their metabolites. The definition may now be somewhat broader. In contrast to classical steroid hormones, the neurosteroids exert their function by binding to neurotransmitter receptors. A PubMed search for "neurosteroids" during the preparation of this manuscript gave 974 hits, the majority of investigations being of a physiological or pharmacological nature. We collaborated with Baulieu's group in performing the mass spectrometric identification of the first steroids of this category in brain: DHEA and pregnenolone (206–208). The sulfates of these steroids were also identified indirectly by identifying the free steroids after solvolysis of fractions corresponding to steroid sulfates. However, recent work has shown that the steroids released by solvolysis in these studies were not sulfates (see below), and ongoing work with Baulieu's group has shown that pregnenolone and DHEA are present in rat brain in an unknown bound form, at concentrations much higher than those of the unconjugated steroids (209).

The extraordinary advances in ES-MS with nanospray and coupling to capillary LC columns prompted W. Griffiths and me to evaluate these methods for analysis of neurosteroids in brain, and we engaged a student, S. Liu, in the project. Detection limits and fragmentation of reference steroid sulfates during ES/CID MS were determined using a double-focusing instrument with a fourth orthogonal time-of-flight sector (AutoSpec-OATOF) (210). Monitoring of the deprotonated molecules gave a sensitivity in the low femtomole range, as did monitoring of precursor ions of *m/z* 97 (sulfate) in a triple quadrupole instrument. Since neutral steroids are poorly protonated in ES, resulting in low sensitivity of detection, they were derivatized prior to analysis. Conversion into oximes was chosen for four reasons: (i) oximes are easily prepared, (ii) most neurosteroids have an oxo group, (iii) oximes can be selectively isolated as a group from a biological extract on a lipophilic ion exchanger (41,211), and (iv) oximes gave a 20-fold increase in sensitivity. The oximes gave structurally informative spectra, also with low-energy collisions as obtained when using a triple quadrupole instrument (212). For example, oximes of 3-oxo-Δ^4 steroids gave typical fragment ions of the A/B rings at *m/z* 112, 124, and 138, and 20-oximes of pregnanolones and pregnenolone gave an intense fragment ion at *m/z* 86. Thus, it was possible to monitor either the protonated molecules, or specific product ions of selected precursors, or precursors of selected product ions. The sensitivity was in the low femtomole or mid-attomole range depending on the mode of detection (213).

A capillary precolumn-column (100 μm i.d. for flow rates around 200 nL/min) system was designed to fit the probe of the AutoSpec, or be connected to a UV-detector or a triple quadrupole instrument, and to permit use of gradients and injections of 1–20 μL of sample solution with simultaneous desalting (214). An important feature was the use of two splitters, one between the injector and precolumn (permitting low-flow gradients), the other between the precolumn and the analytical column (permitting injection of 20 μL at high flow rate). The system was evaluated by analyzing steroid sulfates in human plasma. It is remarkable that only 5 μL of plasma was used in the analysis as compared to 2 mL when our original analyses by GLC and GC/MS were developed 40 yr ago (53,56). Also, the LC–MS method is fast since the intact sulfates are analyzed directly preceded by a simple delipidation step, and the desalting occurs on the precolumn. On the other

hand, it is important to realize that the speed and resolution of capillary GLC are still much higher than that of packed column capillary LC, which is limited by the slow diffusion rates in the liquid phase. The CID spectra in ES-MS also give less information about the structure of the steroid skeleton than the electron impact spectra obtained in GC/MS analyses. Thus, combined analysis by LC–MS and GC/MS (after cleavage of conjugates) will give the most reliable identification of components in complex steroid mixtures.

In the course of these studies we found that electrochemical oxidations could occur on the precolumn or analytical column (215). Steroids with a 3β-sulfoxy-Δ^5 structure underwent reactions similar to those of autoxidation, so that DHEA and pregnenolone sulfates disappeared from the chromatograms. Appropriate grounding between the ES-needle and the columns eliminated the upstream current through the columns and prevented the reactions.

A sample preparation method was developed to permit amounts corresponding to 20 mg brain to be injected in the capillary LC–ES-MS system. It is based on our previous methods and consists of ethanol extraction of brain, passage of the extract through beds of C18 silica and a lipophilic cation exchanger to remove lipids, and application of that effluent to a lipophilic anion exchanger that separates the sample into neutral and sulfated compounds. The sulfated compounds are desalted and analyzed by capillary LC–ES-MS. The neutral fraction is reacted with hydroxyammonium chloride; the oximes formed are selectively isolated on a lipophilic cation exchanger and are then analyzed by capillary LC–ES-MS.

Analysis of rat brain by this method failed to show the expected presence of pregnenolone sulfate and DHEA sulfate. If present in rat brain, their levels must be less than 0.3 μg/g. Our results are supported by the results of Shimada *et al.* using immunossays specific for the sulfated steroids (216,217). Since this is 10–50 times less than previously assumed, our finding calls for a reevaluation of the functions of these steroids in the rat brain. Our ongoing work with Baulieu's group also stresses the need for further studies of neurosteroids in the rat brain as previously suggested by Prasad *et al.* (218).

The LC–ES-MS analyses of free steroids in rat brain show that the method is satisfactory. It confirms sex differences in levels of progesterone and testosterone, it is able to measure the low levels of DHEA (50–100 pg/g), and it shows the presence of several isomers of pregnanolone besides the most studied 3α-hydroxy-5α isomer (allopregnanolone) (219). The method should make it possible to perform more unbiased investigations of the occurrence of unknown steroids and to determine the distribution of steroids in different brain areas. There is a limitation, however, in that an oxo group is needed for derivatization and isolation of the steroids. Introduction of an enzymatic step, e.g., with cholesterol oxidase, might extend the applicability of the method. Quantification is also a problem with ES ionization, which is at best semiquantitative; steroids labeled with heavy isotopes are presently needed as internal standards for accurate quantification.

The successful use of oximes in ES-MS analyses of oxosteroids stimulated studies of alternative derivatives. Shackleton (220) had published on the use of the classical Girard T reagent in analyses of testosterone esters. With W. Griffiths we are evaluating the use of the Girard P reagent for analysis of oxysterols in brain. In using CID at low collision energies, the Girard P derivatives of 3-oxo-Δ^4 steroids give characteristic neutral losses of 79 and 107 Da, useful for high-sensitivity detection and monitoring of the protonated steroid derivatives in a triple quadrupole instrument (221). For analysis of brain, a fraction containing free oxysterols is isolated, oxidized with cholesterol oxidase, and derivatized. An intense peak at *m/z* 534 giving an identical CID spectrum to the product from 24-hydroxycholesterol is obtained, as expected. Products of dihydroxycholesterol are also seen (Griffiths, W.J., Alvelius, G., Tamasawa, N., and Sjövall, J., reported at the 18th International Bile Acid Meeting, Stockholm, June 18–19, 2004). The method should be useful in the search for compounds of the type described above to be formed in cultures of glial cells.

IMPORTANCE OF MS

I was fortunate to be introduced to organic MS by Bergström and Ryhage more than 40 yr ago. The development of biological MS has been truly amazing, particularly following the inventions of the soft ionization methods. These have made it possible to study not only small nonvolatile metabolites but also proteins. MS is now the major technique in the field of proteomics, and noncovalent interactions between proteins and between small molecules and proteins, e.g., steroid receptors, can now be investigated by MS. It is possible to distinguish between specific ligand binding and non-specific protein binding of bile acids (Lengqvist, J., Perlmann, T., Sjövall, J., and Griffiths, W.J., unpublished data). Clinical applications of MS are no longer limited to analyses of metabolic profiles of small molecules (metabonomics, lipidomics, steroidomics, sterolomics, etc.); the proteins can also be analyzed. A rate-limiting step in many or almost all cases of profile analysis is the preparation of the samples for ES-MS, as exemplified for small molecules in this paper. However, it should be possible to construct miniaturized and automated systems based on the principles used in our sample preparation procedures. Perhaps the future in clinical applications will be MS of tissue slices as demonstrated so elegantly by R. Caprioli and coworkers (222). Fourier transform ion cyclotron resonance MS with its remarkable resolution and sensitivity will permit previously inconceivable studies of proteins and metabolic studies with multiple isotope labeling. It has been exciting to have had the opportunity to follow this development during 50 yr of research on steroids and bile acids in health and disease.

ACKNOWLEDGMENTS

I thank all my coworkers and Ph.D. students for what they have done to make projects possible. Some names are given in the text, others are found in the list of references. I am particularly grateful to Sune

Bergström for his continuous support and friendship. Financial support was given from many sources: The Swedish Medical Research Council, the Council for Planning and Coordination of Research, the Knut and Alice Wallenberg Foundation, the Bank of Sweden Tercentenary Fund, Magnus Bergvalls Stiftelse, Stiftelsen Therese and Johan Anderssons Minne, Stiftelsen Lars Johan Hiertas Minne, Sune Bergström, and many funds at Karolinska Institutet. Without the early support from The National Institutes of Health to Sune Bergström the development of the bile acid project would not have been possible.

REFERENCES

1. Ruan, B., Shey, J., Gerst, N., Wilson, W.K., and Schroepfer, G.J. (1996) Silver Ion High Pressure Liquid Chromatography Provides Unprecedented Separation of Sterols: Application to the Enzymatic Formation of Cholesta-5,8-dien-3β-ol, *Proc. Natl. Acad. Sci. USA 93,* 11603–11608.
2. Gerst, N., Ruan, B., Pang, J., Wilson, W.K., and Schroepfer, G.J. (1997) An Updated Look at the Analysis of Unsaturated C_{27} Sterols by Gas Chromatography and Mass Spectrometry, *J. Lipid Res. 38,* 1685–1701.
3. Ruan, B., Gerst, N., Emmons, G.T., Shey, J., and Schroepfer, G.J. (1997) Sterol Synthesis. A Timely Look at the Capabilities of Conventional and Silver Ion High Performance Liquid Chromatography for the Separation of C_{27} Sterols Related to Cholesterol Biosynthesis, *J. Lipid Res. 38,* 2615–2626.
4. Schroepfer, G.J. (2000) Oxysterols: Modulators of Cholesterol Metabolism and Other Processes, *Physiol. Rev. 80,* 361–554.
5. Björkhem, I., and Diczfalusy, U. (2002) Oxysterols. Friends, Foes or Just Fellow Passengers, *Arterioscler. Thromb. Vasc. Biol. 22,* 734–742.
6. Gibbons, G.F. (2002) From Gallstones to Genes: Two Hundred Years of Sterol Research. A Tribute to George J. Schroepfer Jr., *Lipids 37,* 1153–1162.
7. Bergström, S., and Sjövall, J. (1951) Separation of Bile Acids with Reversed Phase Partition Chromatography, *Acta Chem. Scand. 5,* 1267–1270.
8. Bergström, S., and Sjövall, J. (1960) The Isolation of Prostaglandin F from Sheep Prostate Glands, *Acta Chem. Scand. 14,* 1693–1700.
9. Bergström, S., and Sjövall, J. (1960) The Isolation of Prostaglandin E from Sheep Prostate Glands, *Acta Chem. Scand. 14,* 1701–1705.
10. Sjövall, J. (1954) Separation of Conjugated and Free Bile Acids by Paper Chromatography. Bile Acids and Steroids 12, *Acta Chem. Scand. 8,* 339–345.
11. Sjövall, J. (1955) Quantitative Determination of Bile Acids on Paper Chromatograms. Bile Acids and Steroids 33, *Arkiv Kemi 8,* 317–324.
12. Sjövall, J. (1956) Quantitative Determination of Bile Acids in Human Bile, *Acta Chem. Scand. 10,* 1051.
13. Sjövall, J. (1959) The Occurrence of 7β-Hydroxylated Bile Acids in Human Bile. Bile Acids and Steroids 76, *Acta Chem. Scand. 13,* 711–716.
14. Eriksson, S. (1957) Biliary Excretion of Bile Acids and Cholesterol in Bile Fistula Rats, *Proc. Soc. Exp. Biol. Med. 94,* 578–582.
15. Ekdahl, P.-H., and Sjövall, J. (1957) On the Conjugation and Formation of Bile Acids in the Human Liver. I. On the Excretion of Bile Acids by Patients with Postoperative Choledochostomy Drainage. Bile Acids and Steroids 61, *Acta Chir. Scand. 114,* 439–452.
16. Bergström, S., and Danielsson, H. (1958) On the Regulation of Bile Acid Formation in the Rat Liver, *Acta Physíol. Scand. 43,* 1–7.
17. Danielsson, H., Einarsson, K., and Johansson, G. (1967) Effect of Biliary Drainage on Individual Reactions in the Conversion of Cholesterol to Taurocholic Acid. Bile Acids and Steroids 180, *Eur. J. Biochem. 2,* 44–49.
18. Einarsson, K., and Johansson, G. (1968) Effect of Actinomycin D and Puromycin on the Conversion of Cholesterol into Bile Acids in Bile Fistula Rats. Bile Acids and Steroids 206, *FEBS Lett. 1,* 219–222.
19. Noshiro, M., Nishimoto M., Morohashi, K., and Okuda, K. (1989) Molecular Cloning of cDNA for Cholesterol 7α-Hydroxylase from Rat Liver Microsomes. Nucleotide Sequence and Expression, *FEBS Lett.* 257, 97–100.
20. Jelinek, D.F., Andersson, S., Slaughter, S.A., and Russell D.W. (1990) Cloning and Regulation of Cholesterol 7α-Hydroxylase, the Rate-Limiting Enzyme in Bile Acid Biosynthesis, *J. Biol. Chem. 265,* 8190–8197.
21. Li, Y.C., Wang, D.P., and Chiang, J.Y. (1990) Regulation of Cholesterol 7α-Hydroxylase in the Liver. Cloning, Sequencing, and Regulation of Cholesterol 7α-Hydroxylase mRNA, *J. Biol. Chem. 265,* 12012–12019.
22. Edwards, P., Kast, H.R., and Anisfeld, A.M. (2002) BAREing It All: The Adoption of LXR and FXR and Their Roles in Lipid Homeostasis, *J. Lipid Res. 43,* 2–12.
23. Downes, M., Verdecia, M.A., Roecker, A.J., Hughes, R., Hogenesch, J.B., Kast-Woelbern, H.R., Bowman, M.E., Ferrer, J.-L., Anisfeld, A.M., Edwards, P., *et al.* (2003) A Chemical, Genetic, and Structural Analysis of the Nuclear Bile Acid Receptor FXR, *Mol. Cell 11,* 1079–1092.
24. Mi, L.-Z., Devarakonda, S., Harp, J.M., Han, Q., Pelliciari, R., Willson, T.M., Khorasanizadeh, S., and Rastinejad, F. (2003) Structural Basis for Bile Acid Binding and Activation of the Nuclear Receptor FXR, *Mol. Cell 11,* 1093–1100.
25. Encrantz, J.-C., and Sjövall, J. (1959) On the Bile Acids in Duodenal Contents of Infants and Children. Bile Acids and Steroids 72, *Clin. Chim. Acta 4,* 793–799.
26. Lindstedt, S., and Sjövall, J. (1957) On the Formation of Deoxycholic Acid from Cholic Acid in the Rabbit. Bile Acids and Steroids 48, *Acta Chem. Scand. 11,* 421–426.
27. Gustafsson, B.E., Midtvedt, T., and Norman A. (1966) Isolated Fecal Microorganisms Capable of 7α-Dehydroxylating Bile Acids, *J. Exp. Med. 123,* 413–432.
28. Gustafsson, B.-E., Midtvedt, T., and Norman A. (1968) Metabolism of Cholic Acid in Germfree Animals After the Establishments in the Intestinal Tract of Deconjugating and 7α-Dehydroxylating Bacteria, *Acta Pathol. Microbiol. Scand. 72,* 433–443.
29. Ye, H.-Q., Mallonee, D.H., Wells, J.E., Björkhem, I., and Hylemon, P.B. (1999) The Bile Acid Inducible *bai F* Gene from *Eubacterium* sp. Strain VPI 12708 Encodes a Bile Acid-Coenzyme A Hydrolase, *J. Lipid Res. 40,* 17–23.
30. Makishima, M., Lu, T.T., Xie, W., Whitfield, G.K., Domoito, H., Evans, R.M., Haussler, M.R., and Mangelsdorf, D.J. (2002) Vitamin D Receptor as an Intestinal Bile Acid Sensor, *Science 296,* 1313–1316.
31. Lindstedt, S. (1957) The Turnover of Bile Acids in Man. Bile Acids and Steroids 51, *Acta Physiol. Scand. 40,* 1–9.
32. Hellström, K., Sjövall, J., and Wigand, G. (1962) Influence of Semi-synthetic Diet and Type of Fat on the Turnover of Deoxycholic Acid in the Rabbit, *J. Lipid Res. 3,* 405–412.
33. Xu, G., Li, H., Pan, L., Shang, Q., Honda, A., Ananthanarayanan, M., Erickson, S.K., Shneider, B.L., Shefer, S., Bollineni, J., *et al.* (2003) FXR-Mediated Down-Regulation of CYP7A1 Dominates LXRα in Long-Term Cholesterol-Fed NZW Rabbits, *J. Lipid Res. 44,* 1956–1962.
34. Sandberg, D.H., Sjövall, J., Sjövall, K., and Turner, D.A. (1965) Measurement of Human Serum Bile Acids by Gas–Liquid Chromatography, *J. Lipid Res. 6,* 182–192.

35. Sjövall, K., Sjövall, J., Maddock, K., and Horning, E.C. (1966) Estimation of Dehydroepiandrosterone Sulfate in Human Serum by Gas–Liquid Chromatography, *Anal. Biochem. 14,* 337–346.
36. Ryhage, R. (1993) The Mass Spectrometry Laboratory at the Karolinska Institute 1944–1987, *Mass Spectrom. Rev. 12,* 1–49.
37. Eneroth, P., Gordon, B., Ryhage, R., and Sjövall, J. (1966) Identification of Mono- and Dihydroxy Bile Acids in Human Feces by Gas–Liquid Chromatography and Mass Spectrometry, *J. Lipid Res. 7,* 511–523.
38. Eneroth, P., Hellström, K., and Sjövall, J. (1968) A Method for Quantitative Determination of Bile Acids in Human Feces. Bile Acids and Steroids 195, *Acta Chem. Scand. 22,* 1729–1744.
39. Gustafsson, B.E., and Norman, A. (1968) Physical State of Bile Acids in Intestinal Contents of Germfree and Conventional Rats, *Scand. J. Gastroenterol. 3,* 625–631.
40. Korpela, J.T., Fotsis, T., and Adlercreutz, H. (1986) Multicomponent Analysis of Bile Acids in Faeces by Anion Exchange and Capillary Column Gas–Liquid Chromatography: Application in Oxytetracycline Treated Subjects, *J. Steroid Biochem. 25,* 277–284.
41. Axelson, M., and Sjövall, J. (1985) Studies on the Selective Analysis of Ketonic Bile Acids and Steroids in Faeces, in *Enterohepatic Circulation of Bile Acids and Sterol Metabolism* (Paumgartner, G., Stiehl, A., and Gerok, W., eds.), pp. 249–258, MTP Press, Lancaster.
42. Setchell, K.D.R., Street, J.M., and Sjövall, J. (1988) Fecal Bile Acids, in *The Bile Acids* (Setchell, K.D.R., Kritchevsky, D., and Nair, P., eds.), Vol. 4, pp. 441–570, Plenum Press, New York.
43. Eriksson, H., Gustafsson, J.-Å., and Sjövall, J. (1968) Steroids in Germfree and Conventional Rats. 4. Identification and Bacterial Formation of 17α-Pregnane Derivatives, *Eur. J. Biochem. 6,* 219–226.
44. Eriksson, H., Gustafsson, J.-Å., Sjövall, J., and Sjövall, K. (1972) Excretion of Neutral Steroids in Urine and Faeces of Women with Intrahepatic Cholestasis of Pregnancy, *Steroids Lipids Res. 3,* 30–48.
45. Eriksson, H., Gustafsson, J.-Å., and Sjövall, J. (1969) Steroids in Germfree and Conventional Rats. 21-Dehydroxylation by Intestinal Microorganisms, *Eur. J. Biochem. 9,* 550–554.
46. Eriksson, H., Gustafsson, J.-Å., and Sjövall, J. (1971) Studies on the Structure, Biosynthesis and Bacterial Metabolism of 15-Hydroxylated Steroids in the Female Rat, *Eur. J. Biochem. 19,* 433–441.
47. Gustafsson, J.-Å., Shackleton, C.H.L., and Sjövall, J. (1969) Steroids in Newborns and Infants. C_{19} and C_{21} Steroids in Faeces from Infants, *Eur. J. Biochem. 10,* 302–311.
48. Shackleton, C.H.L., Gustafsson, J.-Å., and Sjövall, J. (1971) Steroids in Newborns and Infants. Identification of Steroids in Urine from Newborn Infants, *Steroids 17,* 265–280.
49. Shackleton, C.H.L., Merdinck, J., and Lawson, A.M. (1990) Steroid and Bile Acid Analyses, in *Mass Spectrometry of Biological Materials* (McEwen, C.N., and Larsen, B.S., eds.), pp. 297–377, Marcel Dekker, New York.
50. Shackleton, C., Roitman, E., Guo, L.-W., Wilson, W.K., and Porter, F.D. (2002) Identification of 7(8) and 8(9) Unsaturated Adrenal Steroid Metabolites Produced by Patients with 7-Dehydrocholesterol-Δ^7-Reductase Deficiency (Smith-Lemli-Opitz syndrome), *J. Steroid Biochem. Mol. Biol. 82,* 225–232.
51. Ruan, B., Wilson, W.K., Pang, J., Gerst, N., Pinkerton, F.D., Tsai, J., Kelley, R.I., Whitby, F.G., Milewicz, D.M., Garbern, J., and Schroepfer, G.J. (2002) Sterols in Blood of Normal and Smith-Lemli-Opitz Subjects, *J. Lipid Res. 42,* 799–812.
52. Baulieu, E.-E., Corpéchot, C., Dray, F., Emiliozzi, R., Lebeau, M.C., Mauvais-Jarvis, P., and Robel, P. (1965) An Adrenal-Secreted "Androgen": Dehydroisoandrosterone Sulfate. Its Metabolism and a Tentative Generalization on the Metabolism of Other Steroid Conjugates in Man, *Recent Prog. Horm. Res. 21,* 411–500.
53. Sjövall, J., and Vihko, R. (1965) Determination of Androsterone and Dehydroepiandrosterone Sulfates in Human Serum by Gas–Liquid Chromatography, *Steroids 6,* 597–604.
54. Sjövall, J., and Vihko, R. (1966) Chromatography of Conjugated Steroids on Lipophilic Sephadex, *Acta Chem. Scand. 20,* 1419–1421.
55. Sjövall, J., and Vihko, R. (1968) Analysis of Solvolyzable Steroids in Human Plasma by Combined Gas Chromatography–Mass Spectrometry, *Acta Endocrinol. (Copenhagen) 57,* 247–260.
56. Jänne, O., Vihko, R., Sjövall, J., and Sjövall, K. (1969) Determination of Steroid Mono- and Disulfates in Human Plasma, *Clin. Chim. Acta 23,* 405–412.
57. Vihko, R. (1966) Gas Chromatographic–Mass Spectrometric Studies on Solvolyzable Steroids in Human Peripheral Plasma, *Acta Endocrinol. (Copenhagen) 52 (Suppl. 109),* 1–67.
58. Baulieu, E.-E. (2002) Androgens and Aging Men, *Mol. Cell. Endocrinol. 198,* 41–49.
59. Sjövall, J., Sjövall, K., and Vihko, R. (1968) Steroid Sulfates in Human Pregnancy Plasma, *Steroids 11,* 703–715.
60. Sjövall, J., and Sjövall, K. (1968) Identification of 5α-Pregnane-3α,20α,21-triol in Human Pregnancy Plasma, *Steroids 12,* 359–366.
61. Sjövall, K. (1970) Gas Chromatographic Determination of Steroid Sulphates in Plasma During Pregnancy, *Ann. Clin. Res. 2,* 393–408.
62. Sjövall, J., Nyström, E., and Haahti, E. (1968) Liquid Chromatography on Lipophilic Sephadex: Column and Detection Techniques, in *Advances in Chromatography* (Giddings, J., and Keller, R., eds.), Vol. 6, pp. 119–170, Marcel Dekker, New York.
63. Ellingboe, J., Nyström, E., and Sjövall, J. (1970) Liquid-Gel Chromatography on Lipophilic-Hydrophobic Sephadex Derivatives, *J. Lipid Res. 11,* 266–273.
64. Ellingboe, J., Almé, B., and Sjövall, J. (1970) Introduction of Specific Groups into Polysaccharide Supports for Liquid Chromatography, *Acta Chem. Scand. 24,* 463–467.
65. Sjövall, J., and Axelson, M. (1982) Newer Approaches to the Isolation, Identification and Quantitation of Steroids in Biological Materials, *Vitam. Horm. 39,* 31–144.
66. Sjövall, J., and Axelson, M. (1984) Sample Work-up by Column Techniques, *J. Pharm. Biomed. Anal. 2,* 265–280.
67. Axelson, M., and Sjövall, J. (1977) Analysis of Unconjugated Steroids in Plasma by Liquid-Gel Chromatography and Glass Capillary Gas Chromatography Mass Spectrometry, *J. Steroid Biochem. 8,* 683–692.
68. Sjövall, J. (1985) Column Techniques in the Preparation of Biological Samples for Gas Chromatography-Mass Spectrometry, in *Mass Spectrometry in the Health and Life Sciences* (Burlingame, A., and Castagnoli, N., Jr., eds.), pp. 303–317, Elsevier, Amsterdam.
69. Meng, L.J., and Sjövall, J. (1997) Method for Combined Analysis of Profiles of Conjugated Progesterone Metabolites and Bile Acids in Serum and Urine of Pregnant Women, *J. Chromatogr. Biomed. Sci. Appl. 688,* 11–26.
70. Andersson, S.H.G., and Sjövall, J. (1985) Analysis of Profiles of Unconjugated Steroids in Rat Testicular Tissue by Gas Chromatography–Mass Spectrometry, *J. Steroid Biochem. 23,* 469–475.
71. Dyfverman, A., and Sjövall, J. (1978) A Novel Liquid-Gel Chromatographic Method for Extraction of Unconjugated Steroids from Aqueous Solutions, *Anal. Lett. B11,* 485–499.
72. Banner, C.D., Goos-Nilsson, A., Sjövall, J., Gustafsson, J.-Å., and Rafter, J.J. (1992) A Method for Characterization of Endogenous Ligands to Orphan Receptors Belonging to the

Steroid Hormone Receptor Superfamily—Isolation of Progesterone from Pregnancy Plasma Using Progesterone Receptor Ligand-Binding Domain, *Anal. Biochem. 200,* 163–170.
73. Almé, B., Bremmelgaard, A., Sjövall, J., and Thomassen, P. (1975) Complexity of the Bile Acid Mixture in Human Urine, in *Advances in Bile Acid Research* (Matern, S., Hackenschmidt, J., Back, P., and Gerok, W., eds.), pp. 145–147, F.K. Schattauer Verlag, Stuttgart.
74. Almé, B., Bremmelgaard, A., Sjövall, J., and Thomassen, P. (1977) Analysis of Metabolic Profiles of Bile Acids in Urine Using a Lipophilic Anion Exchanger and Computerized Gas–Liquid Chromatography–Mass Spectrometry, *J. Lipid Res. 18,* 339–362.
75. Setchell, K.D.R., Almé, B., Axelson, M., and Sjövall, J. (1976) The Multicomponent Analysis of Conjugates of Neutral Steroids in Urine by Lipophilic Ion Exchange Chromatography and Computerised Gas Chromatography–Mass Spectrometry, *J. Steroid Biochem. 7,* 615–629.
76. Reimendal, R., and Sjövall, J. (1972) Analysis of Steroids by Off-Line Computerized Gas Chromatography–Mass Spectrometry, *Anal. Chem. 44,* 21–29.
77. Reimendal, R., and Sjövall, J. (1973) Computer Evaluation of Gas Chromatographic–Mass Spectrometric Analyses of Steroids from Biological Materials, *Anal. Chem. 45,* 1083–1089.
78. Axelson, M., Cronholm, T., Curstedt, T., Reimendal, R., and Sjövall, J. (1974) Quantitative Analysis of Unlabelled and Polydeuterated Compounds by Gas Chromatography–Mass Spectrometry, *Chromatographia 7,* 502-509.
79. Bremmelgaard, A., and Sjövall, J. (1979) Bile Acid Profiles in Urine of Patients with Liver Diseases, *Eur. J. Clin. Invest. 9,* 341–348.
80. Bremmelgaard, A., and Sjövall, J. (1980) Hydroxylation of Cholic, Chenodeoxycholic, and Deoxycholic Acids in Patients with Intrahepatic Cholestasis, *J. Lipid Res. 21,* 1072–1081.
81. Carlström, K., Kirk, D.N., and Sjövall, J. (1981) Microbial Synthesis of 1β- and 15β-Hydroxylated Bile Acids, *J. Lipid Res. 22,* 1225–1234.
82. Karlaganis, G., Almé, B., Karlaganis, V., and Sjövall, J. (1981) Bile Alcohol Glucuronides in Urine. Identification of 27-Nor-5β-cholestane-3α,7α,12α,24ξ,25ξ-pentol in Man, *J. Steroid Biochem. 14,* 341–345.
83. Karlaganis, G., Németh, A., Hammarskjöld, B., Strandvik, B., and Sjövall, J. (1982) Urinary Excretion of Bile Alcohols in Normal Children and Patients with α1-Antitrypsin Deficiency During Development of Liver Disease, *Eur. J. Clin. Invest. 12,* 399–405.
84. Karlaganis, G., and Sjövall, J. (1984) Formation and Metabolism of Bile Alcohols in Man, *Hepatology 4,* 966–973.
85. Karlaganis, G., Bremmelgaard, A., Karlaganis, V., and Sjövall, J. (1983) Precursor of 27-Nor-5β-cholestane-3α,7α,12α,24,25-pentol in Man, *J. Steroid Biochem. 18,* 725–729.
86. Horning, M.G., Chambaz, E.M., Brooks, C.J., Moss, A.M., Boucher, E.A., Horning, E.C., and Hill, R.M. (1969) Characterization and Estimation of Urinary Steroids of the Newborn Human by Gas-Phase Analytical Methods, *Anal. Biochem. 31,* 512–531.
87. Axelson, M., and Sahlberg, B.-L. (1983) Group Separation and Gas Chromatography–Mass Spectrometry of Conjugated Steroids in Plasma, *J. Steroid Biochem. 18,* 313–321.
88. Waller, G., Theorell, H., and Sjövall, J. (1965) Liver Alcohol Dehydrogenase as a 3β-Hydroxy-5β-cholanic Acid Dehydrogenase, *Arch. Biochem. Biophys. 111,* 671–684.
89. Cronholm, T., and Sjövall, J. (1970) Effect of Ethanol Metabolism on Redox State of Steroid Sulphates in Man, *Eur. J. Biochem. 13,* 124–131.
90. Belfrage, P., Berg, B., Cronholm, T., Elmqvist, D., Hägerstrand, I., Johansson, B., Nilsson-Ehle, P., Nordén, G., Sjövall, J., and Wiebe, T. (1973) Prolonged Administration of Ethanol to Young, Healthy Volunteers: Effects on Biochemical, Morphological and Neurophysiological Parameters. 6. Effects on Steroid Metabolites in Plasma, *Acta Med. Scand. Suppl. 552,* 32–37.
91. Axelson, M., Cronholm, T., Sahlberg, B.-L., and Sjövall, J. (1981) Changes in the Metabolic Profile of Steroids in Urine During Ethanol Metabolism in Man, *J. Steroid Biochem. 14,* 155–159.
92. Andersson, S.H.G., Cronholm, T., and Sjövall, J. (1986) Effects of Ethanol on the Levels of Unconjugated and Conjugated Androgens and Estrogens in Plasma of Men, *J. Steroid Biochem. 24,* 1193–1198.
93. Sarkola, T., Mäkisalo, H., Fukunaga, T., and Eriksson, C.J.P. (1999) Acute Effect of Alcohol on Estradiol, Estrone, Progesterone, Prolactin, Cortisol and Luteinizing Hormone in Premenopausal Women, *Alcohol Clin. Exp. Res. 23,* 976–982.
94. Välimäki, M., Härkönen, M., and Ylikahri, R. (1983) Acute Effects of Alcohol on Female Sex Hormones, *Alcohol Clin. Exp. Res. 7,* 289–293.
95. Mendelson, J.H., Lukas, S.E., Mello, N.K., Amass, L., Ellingboe, J., and Skupny, A. (1988) Acute Alcohol Effects on Plasma Estradiol Levels in Women, *Psychopharmacology 94,* 464–467.
96. Sarkola, T., Adlercreutz, H., von der Pahlen, B., and Eriksson, C.J.P. (2001) The Role of the Liver in the Acute Effect of Alcohol on Androgens in Women, *J. Clin. Endocrinol. Metab. 25,* 513–516.
97. Andersson, S.H.G., and Sjövall, J. (1986) Effects of Ethanol on Steroid Profiles in the Rat Testis, *Biochim. Biophys. Acta 876,* 352–357.
98. Norsten-Höög, C., Cronholm, T., Andersson, S.H.G., and Sjövall, J. (1992) Transfer of Deuterium from [1,1-$^2H_2$]Ethanol to Steroids and Organic Acids in the Rat Testis, *Biochem. J. 286,* 141–146.
99. Cronholm, T., Makino, I., and Sjövall, J. (1972) Steroid Metabolism in Rats Given [1-$^2H_2$]Ethanol. Biosynthesis of Bile Acids and Reduction of 3-Keto-5β-cholanoic Acid, *Eur. J. Biochem. 24,* 507–519.
100. Cronholm, T., Makino, I., and Sjövall, J. (1972) Steroid Metabolism in Rats Given [1-$^2H_2$]Ethanol. Oxidoreduction of Isomeric 3-Hydroxycholanoic Acids and Reduction of 3-Oxo-4-cholenoic Acid, *Eur. J. Biochem. 26,* 251–258.
101. Axelson, M., Mörk, B., and Sjövall, J. (1988) Occurrence of 3β-Hydroxy-5-cholestenoic Acid, 3β,7α-Dihydroxy-5-cholestenoic Acid, and 7α-Hydroxy-3-Oxo-4-Cholestenoic Acid as Normal Constituents in Human Blood, *J. Lipid Res. 29,* 629–641.
102. Axelson, M., and Sjövall, J. (1990) Potential Bile Acid Precursors in Plasma—Possible Indicators of Biosynthetic Pathways to Cholic and Chenodeoxycholic Acids in Man, *J. Steroid Biochem. 36,* 631–640.
103. Axelson, M., Mörk, B., and Sjövall, J. (1991) Ethanol Has an Acute Effect on Bile Acid Biosynthesis in Man, *FEBS Lett. 281,* 155–159.
104. Axelson, M., Aly, A., and Sjövall, J. (1988) Levels of 7α-Hydroxy-4-cholesten-3-one in Plasma Reflect Rates of Bile Acid Synthesis in Man, *FEBS Lett. 239,* 324–328.
105. Axelson, M., Björkhem, I., Reihner, E., and Einarsson., K. (1991) The Plasma Level of 7α-Hydroxy-4-cholesten-3-one Reflects the Activity of Hepatic Cholesterol 7α-Hydroxylase in Man, *FEBS Lett. 284,* 216–218.
106. Sauter, G., Berr, F., Beuers, U., Fischer, S., and Paumgartner, G. (1996) Serum Concentrations of 7α-Hydroxy-4-cholesten-3-one Reflect Bile Acid Synthesis in Humans, *Hepatology, 24,* 123–126.
107. Ryzlak, M.T., Fales, H.M., Russell, W.L., and Schaffner, C.P. (1990) Oxysterols and Alcoholic Liver Disease, *Alcohol Clin. Exp. Res. 14,* 490–495.

108. Skrede, S., Buchmann, M.S., and Björkhem, I. (1988) Hepatic 7α-Dehydroxylation of Bile Acid Intermediates, and Its Significance for the Pathogenesis of Cerebrotendinous Xanthomatosis, *J. Lipid Res. 29,* 157–164.
109. Cronholm, T., Curstedt, T., Eriksson, H., Matern, H., Matern, S., and Sjövall, J. (1974) Pathways of Hydrogen in the Metabolism of Ethanol, in *Alcohol and Aldehyde Metabolizing Systems* (Thurman, R., Yonetani, T., Williamson, J., and Chance, B., eds.), pp. 511–522, Academic Press, New York.
110. Cronholm, T., Curstedt, T., and Sjövall, J. (1982) Formation of Bile Acids and Glycerophosphatides in Liver, in *Metabolic Compartmentation* (Sies, H., ed.), pp. 331–359, Academic, London.
111. Andersson, S., Cronholm, T., and Sjövall, J. (1986) Redox Effects of Ethanol on Steroid Metabolism, *Alcohol Clin. Exp. Res. 10,* 55S–63S.
112. Danielsson, H., and Sjövall, J. (1975) Bile Acid Metabolism, *Ann. Rev. Biochem. 44,* 233–253.
113. Cronholm, T., Burlingame, A.L., and Sjövall, J. (1974) Utilization of the Carbon and Hydrogen Atoms of Ethanol in the Biosynthesis of Steroids and Bile Acids, *Eur. J. Biochem. 49,* 497–510.
114. Cronholm, T., Sjövall, J., Wilson, D.M., and Burlingame, A.L. (1979) Exchange of Methyl Hydrogens in Ethanol During Incorporation in Bile Acids *in vivo*, *Biochim. Biophys. Acta 575,* 193–203.
115. Vlahcevic, Z.R., Cronholm, T., Curstedt, T., and Sjövall, J. (1980) Biosynthesis of 5α- and 5β-Cholanoic Acid Derivatives During Metabolism of [1,1-^{2}H]- and [2,2,2-^{2}H]Ethanol in the Rat, *Biochim. Biophys. Acta 618,* 369–377.
116. Baillie, T.A., Anderson, R.A., Sjövall, K., and Sjövall, J. (1976) Identification and Quantitation of 16α-Hydroxy C_{21} Steroid Sulphates in Plasma from Pregnant Women, *J. Steroid Biochem. 7,* 203–209.
117. Axelson, M., Graham, C.E., and Sjövall, J. (1984) Identification and Quantitation of Steroids in Sulfate Fractions from Plasma of Pregnant Chimpanzee, Orangutan, and Rhesus Monkey, *Endocrinology 114,* 337–344.
118. Baillie, T.A., Sjövall, J., and Herz, J.E. (1975) Synthesis of Specifically Deuterium-Labelled Pregnanolone and Pregnanediol Sulphates for Metabolic Studies in Humans, *Steroids 26,* 438–457.
119. Baillie, T.A., Curstedt, T., Sjövall, K., and Sjövall, J. (1980) Production Rates and Metabolism of Sulphates of 3β-Hydroxy-5α-pregnane Derivatives in Pregnant Women, *J. Steroid Biochem. 13,* 1473–1486.
120. Anderson, R.A., Baillie, T.A., Axelson, M., Cronholm, T., Sjövall, K., and Sjövall, J. (1990) Stable Isotope Studies on Steroid Metabolism and Kinetics: Sulfates of 3α-Hydroxy-5α-pregnane Derivatives in Human Pregnancy, *Steroids 55,* 443–457.
121. Laatikainen, T., and Karjalainen, O. (1972) Excretion of Conjugates of Neutral Steroids in Human Bile During Late Pregnancy, *Acta Endocrinol. (Copenhagen) 69,* 775–788.
122. Baillie, T.A., Sjövall, J., and Sjövall, K. (1975) Origin of 5α-Pregnane-3α,20α,21-triol 3-Sulphate in Pregnant Women, *FEBS Lett. 60,* 145–148.
123. Collins, D.J., and Sjövall, J. (1979) Synthesis of 17α-Ethynyloestradiol Tri- and Pentadeuterated in Ring C, *Tetrahedron Lett. 7,* 629–632.
124. Collins, D.J., and Sjövall, J. (1983) The Structure and Function of Oestrogens. IV. Synthesis of 17α-Ethynyloestradiol Specifically Polydeuterated in Ring C, *Aust. J. Chem. 36,* 339–360.
125. Tetsuo, M., Axelson, M., and Sjövall, J. (1980) Selective Isolation Procedures for GC/MS Analysis of Ethynyl Steroids in Biological Material, *J. Steroid Biochem. 13,* 847–860.
126. Andersson, S.H.G., Axelson, M., Sahlberg, B.-L., and Sjövall, J. (1981) Simplified Method for the Isolation and Analysis of Ethynyl Steroids in Urine, *Anal. Lett. 14,* 783–790.
127. Sahlberg, B.-L., Axelson, M., Collins, D.J., and Sjövall, J. (1981) Analysis of Isomeric Ethynylestradiol Glucuronides in Urine, *J. Chromatogr. 217,* 453–461.
128. Axelson, M., Clark, J.H., Eriksson, H.A., and Sjövall, J. (1981) Estrogen Binding in Target Tissues; A GC/MS Method for Assessing Uptake, Retention and Processing of Estrogens in Target Cell Nuclei Under *in vivo* Conditions, *J. Steroid Biochem. 14,* 1253–1260.
129. Tetsuo, M., Eriksson, H., and Sjövall, J. (1982) Gas Chromatographic–Mass Spectrometric Analysis of Endogenous Levels of Estradiol in Plasma and in Cytosol from Rat Uterus, *J. Chromatogr. 239,* 287–300.
130. Tetsuo, M., Eriksson, H., Cronholm, T., Collins, D., and Sjövall, J. (1989) Concentration and Turnover of Estradiol in the Rat Uterus *in vivo*, *J. Steroid Biochem. 33,* 371–378.
131. Meng, L.J., and Sjövall, J. (1997) Method for Combined Analysis of Profiles of Conjugated Progesterone Metabolites and Bile Acids in Serum and Urine of Pregnant Women, *J. Chromatogr. Biomed. Sci. Appl. 688,* 11–26.
132. Meng, L.J., Reyes, H., Palma, J., Hernandez, I., Ribalta, J., and Sjövall, J. (1997) Profiles of Bile Acids and Progesterone Metabolites in the Urine and Serum of Women with Intrahepatic Cholestasis of Pregnancy, *J. Hepatol. 27,* 346–357.
133. Meng, L.J., Griffiths, W.J., and Sjövall, J. (1996) The Identification of Novel Steroid *N*-Acetylglucosaminides in the Urine of Pregnant Women, *J. Steroid Biochem. Molec. Biol. 58,* 585–598.
134. Arcos, M., and Liebermann, S. (1967) 5-Pregnene-3β,20α-diol-3-sulfate-20-(2′-acetamido-2′-deoxy-α-D-glucoside) and 5-Pregnene-3β,20α-diol-3,20-disulfate. Two Novel Urinary Conjugates, *Biochemistry 6,* 2032–2039.
135. Sjövall, K., and Sjövall, J. (1966) Serum Bile Acid Levels in Pregnancy with Pruritus. Bile Acids and Steroids 158, *Clin. Chim. Acta 13,* 207–211.
136. Thomassen, P. (1979) Urinary Bile Acids in Late Pregnancy and in Recurrent Cholestasis of Pregnancy, *Eur. J. Clin. Invest. 9,* 425–432.
137. Thomassen, P. (1979) Urinary Bile Acids During Development of Recurrent Cholestasis of Pregnancy, *Eur. J. Clin. Invest. 9,* 417–423.
138. Sjövall, J., and Sjövall, K. (1970) Steroid Sulphates in Plasma from Pregnant Women with Pruritus and Elevated Plasma Bile Acid Levels, *Ann. Clin. Res. 2,* 321–337.
139. Reyes, H., and Sjövall, J. (2000) Bile Acids and Progesterone Metabolites in Intrahepatic Cholestasis of Pregnancy, *Ann. Med. 32,* 94–106.
140. Meng, L.J., Reyes, H., Axelson, M., Palma, J., Hernandez, I., Ribalta, J., and Sjövall, J. (1997) Progesterone Metabolites and Bile Acids in Serum of Patients with Intrahepatic Cholestasis of Pregnancy—Effect of Ursodeoxycholic Acid Therapy, *Hepatology 26,* 1573–1579.
141. Meng, L.-J., Reyes, H., Palma, J., Hernandez, I., Ribalta, J., and Sjövall, J. (1997) Effects of Ursodeoxycholic Acid on Conjugated Bile Acids and Progesterone Metabolites in Serum and Urine of Patients with Intrahepatic Cholestasis of Pregnancy, *J. Hepatol. 27,* 1029–1040.
142. Glantz, A., Marschall, H.-U., and Mattsson, L.A. (2004) Intrahepatic Cholestasis of Pregnancy: Relationships Between Bile Acid Levels and Fetal Complication Rates, *Hepatology 40,* 467–474.
143. Lammert, F., Marschall, H.-U., Glantz, A., and Matern, S. (2000) Intrahepatic Cholestasis of Pregnancy: Molecular Pathogenesis, Diagnosis and Management, *J. Hepatol. 33,* 1012–1021.
144. Savander, M., Ropponen, A., Avela, K., Weerasekera, N., Cormand, B., Hirvioja, M.L., Riikonen, S., Ylikorkala, O., Lehesjoki, A.E., Williamson, C., and Aittomaki, K. (2003)

Genetic Evidence of Heterogeneity in Intrahepatic Cholestasis of Pregnancy, *Gut 52,* 1025–1029.
145. Bacq, Y., Sapey, T., Brechot, M.C., Pierre, F., Fignon, A., and Dubois, F. (1997) Intrahepatic Cholestasis of Pregnancy: A French Prospective Study, *Hepatology 26,* 358–364.
146. Egestad, B., Pettersson, P., Skrede, S., and Sjövall, J. (1985) Fast Atom Bombardment Mass Spectrometry in the Diagnosis of Cerebrotendinous Xanthomatosis, *Scand. J. Clin. Lab. Invest. 45,* 443–446.
147. Björkhem, I., Muri-Boberg, K., and Leitersdorf, E. (2001) Inborn Errors in Bile Acid Biosynthesis and Storage of Sterols Other Than Cholesterol, in *The Metabolic Basis of Inherited Disease* (Scriver, C.R., Beaudet, A.L., Sly, W.S., Valle, D., Childs, B., Kinzler, K.W., and Vogelstein, B., eds.), pp. 2961–2988, McGraw-Hill, New York.
148. von Bahr, S., Björkhem, I., van't Hooft, F., Alvelius, G., Nemeth, A., Sjövall, J., and Fischler, B. (in press) Mutation in the Sterol 27-Hydroxylase Gene Associated with Fatal Cholestasis in Infancy, *J. Pediatr. Gastroenterol. Nutr.*
149. Clayton, P.T., Verrips, A., Sistermans, E., Mann, A., Mieli-Vergani, G., and Wevers, R. (2001) Mutations in the Sterol 27-Hydroxylase Gene (CYP27A) Cause Hepatitis of Infancy as Well as Cerebrotendinous Xanthomatosis, *J. Inherit. Metab. Dis. 25,* 501–513.
150. Clayton, P.T., Leonard, J.V., Lawson, A.M., Setchell, K.D.R., Andersson, S., Egestad, B., and Sjövall, J. (1987) Familial Giant Cell Hepatitis Associated with Synthesis of 3β,7α-Dihydroxy- and 3β,7α,12α-Trihydroxy-5-cholenoic Acids, *J. Clin. Invest. 79,* 1031–1038.
151. Russell, A., Nazer, H., Shams, A., Sjövall, J., and Sutcliffe, R. (1995) No Linkage to the 3β-HSD Gene Cluster in a Kindred Affected with 3β-Hydroxy-Δ^5-C_{27}-steroid Dehydrogenase Deficiency and Early Onset Hepatic Failure, *Hum. Genet. 95,* 586–588.
152. Buchmann, M.S., Kvittingen, E.A., Nazer, H., Gunasekaran, T., Clayton, P.T., Sjövall, J., and Björkhem, I. (1990) Lack of 3β-Hydroxy-Δ^5-C_{27}-steroid Dehydrogenase/Isomerase in Fibroblasts from a Child with Urinary Excretion of 3β-Hydroxy-Δ^5-bile Acids. A New Inborn Error of Metabolism, *J. Clin. Invest. 86,* 2034–2037.
153. Schwarz, M., Wright, A.C., Davis, D.L., Nazer, H., Björkhem, I., and Russell, D.W. (2000) The Bile Acid Synthetic Gene 3β-Hydroxy-Δ^5-C_{27}-steroid Oxidoreductase Is Mutated in Progressive Intrahepatic Cholestasis, *J. Clin. Invest. 106,* 1175–1184.
154. Laatikainen, T., Perheentupa, J., Vihko, R., Makino, I., and Sjövall, J. (1972) Bile Acids and Hormonal Steroids in Bile of a Boy with 3β-Hydroxysteroid Dehydrogenase Deficiency, *J. Steroid Biochem. 3,* 715–719.
155. Ichimiya, H., Egestad, B., Nazer, H., Baginski, E.S., Clayton, P.T., and Sjövall, J. (1991) Bile Acids and Bile Alcohols in a Child with Hepatic 3β-Hydroxy-Δ^5-C_{27}-steroid Dehydrogenase Deficiency: Effects of Chenodeoxycholic Acid Treatment, *J. Lipid Res. 32,* 829–841.
156. Clayton, P.T., Patel, E., Lawson, A.M., Carruthers, R.A., Tanner, M.S., Strandvik, B., Egestad, B., and Sjövall, J. (1988) 3-Oxo-Δ^4 Bile Acids in Liver Disease, *Lancet ii,* 1283–1284.
157. Setchell, K.D., Suchy, F.J., Welsh, M.B., Zimmer-Nechemias, L., Heubi, J., and Balistreri, W.F. (1988) Δ^4-3-Oxosteroid 5β-Reductase Deficiency Described in Identical Twins with Neonatal Hepatitis. A New Inborn Error in Bile Acid Synthesis, *J. Clin. Invest. 82,* 2148–2157.
158. Stieger, B., Zhang, J., O'Neill, B., Sjövall, J., and Meier, P.J. (1997) Differential Interaction of Bile Acids from Patients with Inborn Errors of Bile Acid Synthesis with Hepatocellular Bile Acid Transporters, *Eur. J. Biochem. 244,* 39–44.
159. Wahlén, E., Egestad, B., Strandvik, B., and Sjövall, J. (1989) Ketonic Bile Acids in Urine of Infants During the Neonatal Period, *J. Lipid Res. 30,* 1847–1857.
160. Setchell, K.D., Schwarz, M., O'Connell, N.C., Lund, E.G., Davis, D.L., Lathe, R., Thompson, W.T.R., Sokol, R.J., and Russell, D.W. (1998) Identification of a New Inborn Error in Bile Acid Synthesis: Mutation of the Oxysterol 7α-Hydroxylase Gene Causes Severe Neonatal Liver Disease, *J. Clin. Invest. 102,* 1690–1703.
161. Setchell, K.D., Heubi, J.E., Bove, K.E., O'Connell, N.C., Brewsaugh, T., Steinberg, S.J., Moser, A., and Squires, R.H., Jr. (2003) Liver Disease Caused by Failure to Racemize Trihydroxycholestanoic Acid: Gene Mutation and Effect of Bile Acid Therapy, *Gastroenterology 124,* 217–232.
162. Pullinger, C.R., Eng, C., Salen, G., Shefer, S., Batta, A.K., Erickson, S.K., Verhagen, A., Rivera, C.R., Mulvihill, S.J., Malloy, M.J., and Kane, J.P. (2002) Human Cholesterol 7α-Hydroxylase (CYP7A1) Deficiency Has a Hypercholesterolemic Phenotype, *J. Clin. Invest. 110,* 109–117.
163. Marschall, H.-U., Egestad, B., Matern, H., Matern, S., and Sjövall, J. (1987) Evidence for Bile Acid Glucosides as Normal Constituents in Human Urine, *FEBS Lett. 213,* 411–414.
164. Back, P., Spaczynski, K., and Gerok, W. (1974) Bile Salt Glucuronides in Urine, *Hoppe-Seyler's Z. Physiol. Chem. 355,* 749–752.
165. Almé, B., Nordén, Å., and Sjövall, J. (1978) Glucuronides of Unconjugated 6-Hydroxylated Bile Acids in Urine of a Patient with Malabsorption, *Clin. Chim. Acta 86,* 251–259.
166. Almé, B., and Sjövall, J. (1980) Analysis of Bile Acid Glucuronides in Urine. Identification of 3α,6α,12α-Trihydroxy-5β-cholanoic Acid, *J. Steroid Biochem. 13,* 907–916.
167. Marschall, H.-U., Matern, H., Egestad, B., Matern, S. and Sjövall, J. (1987) 6α-Glucuronidation of Hyodeoxycholic Acid by Human Liver, Kidney and Small Bowel Microsomes, *Biochim. Biophys. Acta 921,* 392–397.
168. Radominska, A., Little, J.M., Lester, R., and Mackenzie, P.I. (1994) Bile Acid Glucuronidation by Rat Liver Microsomes and cDNA-Expressed UDP-Glucuronosyltransferases, *Biochim. Biophys. Acta 1205,* 75–82.
169. Marschall, H.-U., Egestad, B., Matern, H., Matern, S., and Sjövall, J. (1989) *N*-Acetylglucosaminides. A New Type of Bile Acid Conjugate in Man, *J. Biol. Chem. 264,* 12989–12993.
170. Marschall, H.-U., Matern, H., Wietholtz, B., Egestad, S., Matern, S., and Sjövall, J. (1992) Bile Acid N-Acetylglucosaminidation. *In vivo* and *in vitro* Evidence for a Selective Conjugation Reaction of 7β-Hydroxylated Bile Acids in Humans, *J. Clin. Invest. 89,* 1981–1987.
171. Marschall, H.-U., Griffiths, W.J., Götze, U., Zhang, J., Wietholtz, H., Busch, N., Sjövall, J., and Matern, S. (1994) The Major Metabolites of Ursodeoxycholic Acid in Human Urine Are Conjugated with *N*-Acetylglucosamine, *Hepatology 20,* 845–853.
172. Marschall, H.-U., Griffiths, W.J., Zhang, J., Wietholtz, H., Matern, H., Matern, S., and Sjövall, J. (1994) Positions of Conjugation of Bile Acids with Glucose and *N*-Acetylglucosamine *in vitro*, *J. Lipid Res. 35,* 1599–1610.
173. Zhang, J., Griffiths, W.J., Bergman, T., and Sjövall, J. (1993) Derivatization of Bile Acids with Taurine for Analysis by Fast Atom Bombardment Mass Spectrometry with Collision-Induced Fragmentation, *J. Lipid Res. 34,* 1895–1900.
174. Griffiths, W.J., Zhang, J., and Sjövall, J. (1994) Charge-Remote Fragmentation of Sulphated and Glucuronidated Bile Acids and Their 2-Aminoethanesulphonic Acid Derivatives, *Rapid Commun. Mass Spectrom. 8,* 227–236.
175. Yang, Y., Griffiths, W.J., Nazer, H., and Sjövall, J. (1997) Analysis of Bile Acids and Bile Alcohols in Urine by Capillary Column Liquid Chromatography–Mass Spectrometry Using Fast Atom Bombardment or Electrospray Ionization and Collision-Induced Dissociation, *Biomed. Chromatogr. 11,* 240–255.

176. Björkhem, I., and Meaney, S. (2004) Brain Cholesterol: Long Secret Life Behind a Barrier, *Arterioscler. Thromb. Vasc. Biol. 24,* 806–815.
177. Gustafsson, J.-Å., and Sjövall, J. (1969) Identification of 22-, 24- and 26-Hydroxycholesterol in the Steroid Sulphate Fraction of Faeces from Infants, *Eur. J. Biochem. 8,* 467–472.
178. Mata de Urquiza, A., Liu, S., Sjöberg, M., Zetterström, R.H., Griffiths, W.J., Sjövall, J., and Perlmann, T. (2000). Docosahexaenoic Acid, a Ligand for the Retinoid X Receptor in Mouse Brain, *Science 290,* 2140–2144.
179. Axelson, M., Shoda, J., Sjövall, J., Toll, A., and Wikvall, K. (1992) Cholesterol Is Converted to 7α-Hydroxy-3-oxo-4-cholestenoic Acid in Liver Mitochondria. Evidence for a Mitochondrial Sterol 7α-Hydroxylase, *J. Biol. Chem. 267,* 1701–1704.
180. Toll, A., Shoda, J., Axelson, M., Sjövall, J., and Wikvall, K. (1992) 7α-Hydroxylation of 26-Hydroxycholesterol, 3β-Hydroxy-5-cholestenoic Acid and 3β-Hydroxy-5-cholenoic Acid by Cytochrome P450 in Pig Liver Microsomes, *FEBS Lett. 296,* 73–76.
181. Shoda, J., Toll, A., Axelson, M., Pieper, F., Wikvall, K., and Sjövall, J. (1993) Formation of 7α- and 7β-Hydroxylated Bile Acid Precursors from 27-Hydroxycholesterol in Human Liver Microsomes and Mitochondria, *Hepatology 17,* 395–403.
182. Hagey, L.R., Crombie, D.L. Espinosa, E., Carey, M.C., Igimi, H., and Hofmann, A.F. (1993) Ursodeoxycholic Acid in the Ursidae: Biliary Bile Acids of Bears, Pandas, and Related Carnivores, *J. Lipid Res. 34,* 1911–1917.
183. Björkhem, I., Nyberg, B., and Einarsson, K. (1992) 7α-Hydroxylation of 27-Hydroxycholesterol in Human Liver Microsomes, *Biochim. Biophys. Acta 1128,* 73–76.
184. Martin, K.O., Budai, K., and Javitt, N.B. (1993) Cholesterol and 27-Hydroxycholesterol 7α-Hydroxylation: Evidence for Two Different Enzymes, *J. Lipid Res. 34,* 581–588.
185. Schwarz, M., Lund, E.G., and Russell, D.W. (1998) Two 7α-Hydroxylase Enzymes in Bile Acid Biosynthesis, *Curr. Opin. Lipidol. 9,* 113–118.
186. Mitropoulos, K.A., and Myant, N.B. (1967) The Formation of Lithocholic Acid, Chenodeoxycholic Acid, and α- and β-Muricholic Acids from Cholesterol Incubated with Rat-Liver Mitochondria, *Biochem. J. 103,* 472–479.
187. Wachtel, N., Emerman, S., and Javitt, N.B. (1968) Chemistry and Metabolism of Cholest-5-ene-3β,26-diol in the Rat and Hamster, *J. Biol. Chem. 243,* 5207–5212.
188. Axelson, M., Larsson, O., Zhang, J., Shoda, J., and Sjövall, J. (1994) Structural Specificity in the Suppression of HMG-CoA Reductase in Human Fibroblasts by Intermediates in Bile Acid Biosynthesis, *J. Lipid Res. 36,* 290–298.
189. Sjövall, J. (1960) Bile Acids in Man Under Normal and Pathological Conditions. Bile Acids and Steroids 73, *Clin. Chim. Acta 5,* 33–41.
190. Zhang, J., Larsson, O., and Sjövall, J. (1995) 7α-Hydroxylation of 25-Hydroxycholesterol and 27-Hydroxycholesterol in Human Fibroblasts, *Biochim. Biophys. Acta 1256,* 353–359.
191. Sulcova, J., and Starka, L. (1972) 7α-Hydroxylation of Dehydroepiandrosterone in Human Testis and Epididymis *in vitro*, *Experientia 28,* 1361–1362.
192. Lathe, R. (2002) Steroid and Sterol 7-Hydroxylation: Ancient Pathways, *Steroids 67,* 967–977.
193. Lund, E., Andersson, O., Zhang, J., Babiker, A., Ahlborg, G., Diczfalusy, U., Einarsson, K., Sjövall, J., and Björkhem, I. (1996) Importance of a Novel Oxidative Mechanism for Elimination of Intracellular Cholesterol in Humans, *Arterioscler. Thromb. Vasc. Biol. 16,* 208–212.
194. Björkhem, I., Lütjohann, D., Breuer, O., Sakinis, A., and Wennmalm, Å. (1997) Importance of a Novel Oxidative Mechanism for Elimination of Brain Cholesterol, *J. Biol. Chem. 272,* 30178–30184.
195. Meaney, S., Babiker, A., Lütjohann, D., Diczfalusy, U., Axelson, M., and Björkhem, I. (2003) On the Origin of the Cholestenoic Acids in Human Circulation, *Steroids 68,* 595–601.
196. Duane, W.C., and Javitt, N.B. (1999) 27-Hydroxycholesterol: Production Rates in Normal Human Subjects, *J. Lipid Res. 40,* 1194–1199.
197. Zhang, J., Akwa, Y., Baulieu, E.-E., and Sjövall, J. (1995). 7α-Hydroxylation of 27-Hydroxycholesterol in Rat Brain Microsomes, *C.R. Acad. Sci. Paris 318,* 345–349.
198. Zhang, J., Akwa, Y., El-Etr, M., Baulieu, E.-E., and Sjövall, J. (1997) Metabolism of 27-, 25- and 24-Hydroxycholesterol in Rat Glial Cells and Neurons, *Biochem. J. 322,* 175–184.
199. Nagata, K., Takakura, K., Asano, T., Seyama, Y., Hirota, H., Shigematsu, N., Shima, I., Kasama, T., and Shimizu, T. (1992) Identification of 7α-Hydroxy-3-oxo-4-cholestenoic Acid in Chronic Subdural Hematoma, *Biochim. Biophys. Acta 1126,* 229–236.
200. Stapleton, G., Steel, M., Richardson, M., Mason, J.O., Rose, K.A., Morris, R.G., and Lathe, R. (1995) A Novel Cytochrome P450 Expressed Primarily in Brain, *J. Biol. Chem. 270,* 29739–29745.
201. Rose, K., Allan, A., Gauldie, S., Stapleton, G., Dobbie, L., Dott, K., Martin, C., Wang, L., Hedlund, E., Seckl, J.R., Gustafsson, J.Å., and Lathe, R. (2001) Neurosteroid Hydroxylase CYP7B: Vivid Reporter Activity in Dentate Gyrus of Gene-Targeted Mice and Abolition of a Widespread Pathway of Steroid and Oxysterol Hydroxylation, *J. Biol. Chem. 276,* 23937–23944.
202. Axelson, M., and Larsson, O. (1996) 27-Hydroxylated Low Density Lipoprotein Cholesterol Can Be Converted to 7α,27-Dihydroxy-4-cholesten-3-one (cytosterone) Before Suppressing Cholesterol Production in Normal Human Fibroblasts. Evidence That an Altered Metabolism of LDL Cholesterol Can Underlie a Defective Feedback Control in Malignant Cells, *J. Biol. Chem. 271,* 12724–12736.
203. Zhang, J., Dricu, A., and Sjövall, J. (1997) Studies on the Relationships Between 7α-Hydroxylation and the Ability of 25- and 27-Hydroxycholesterol to Suppress the Activity of HMG-CoA Reductase, *Biochim. Biophys. Acta 1344,* 241–249.
204. Zhang, J., Xue, Y., Jondal, M., and Sjövall, J. (1997) 7α-Hydroxylation and 3-Dehydrogenation Abolish the Ability of 25-Hydroxycholesterol and 27-Hydroxycholesterol to Induce Apoptosis in Thymocytes, *Eur. J. Biochem. 247,* 129–135.
205. Baulieu, E.-E. (1997) Neurosteroids: Of the Nervous System, by the Nervous System, for the Nervous System, *Rec. Prog. Horm. Res. 52,* 1–32.
206. Corpéchot, C., Robel, P., Lachapelle, F., Baumann, N., Axelson, M., Sjövall, J., and Baulieu, E.E. (1981) Déhydroépiandrostérone Libre et Sulfo-Conjuguée dans le Cerveau de Souris Dysmyéliniques, *C.R. Acad. Sci. Paris 292 Série III,* 231–234.
207. Corpéchot, C., Robel, P., Axelson, M., Sjövall, J., and Baulieu, E.-E. (1981) Characterization and Measurement of Dehydroepiandrosterone Sulfate in Rat Brain, *Proc. Natl. Acad. Sci. USA 78,* 4704–4707.
208. Corpéchot, C., Synguelakis, M., Talha, S., Axelson, M., Sjövall, J., Vihko, R., Baulieu, E.-E., and Robel, P. (1983) Pregnenolone and Its Sulfate Ester in the Rat Brain, *Brain Res. 270,* 119–125.
209. Liere, P., Pianos, A., Eychenne, B., Cambourg, A., Liu, S., Griffiths, W., Schumacher, M., Sjövall, J., and Baulieu, E.E. (in press) Novel Lipoidal Derivatives of Pregnenolone and Dehydroepiandrosterone and Absence of Their Sulphated Counterparts, *J. Lipid Res.*
210. Griffiths, W.J., Liu, S., Yang, Y., Purdy, R.H., and Sjövall, J. (1999) Nano-electrospray Tandem Mass Spectrometry for the

Analysis of Neurosteroid Sulphates, *Rapid Commun. Mass Spectrom. 13,* 1595–1610.
211. Axelson, M., and Sjövall, J. (1979) Strong Non-polar Cation Exchangers for the Separation of Steroids in Mixed Chromatographic Systems, *J. Chromatogr. 186,* 725–732.
212. Liu, S., Sjövall, J., and Griffiths, W.J. (2000) Analysis of Oxosteroids by Nano-electrospray Mass Spectrometry of Their Oximes, *Rapid Commun. Mass Spectrom. 14,* 390–400.
213. Liu, S., Sjövall, J., and Griffiths, W.J. (2003) Neurosteroids in Rat Brain: Extraction, Isolation and Analysis by Nanoscale Liquid Chromatography–Electrospray Mass Spectrometry, *Anal. Chem. 75,* 5835–5846.
214. Liu, S., Griffiths, W.J., and Sjövall, J. (2003) Capillary Liquid Chromatography/Electrospray Mass Spectrometry for Analysis of Steroid Sulfates in Biological Samples, *Anal. Chem. 75,* 791–797.
215. Liu, S., Griffiths, W.J., and Sjövall, J. (2003) On-Column Electrochemical Reactions Accompanying the Electrospray Process, *Anal. Chem. 75,* 1022–1030.
216. Higashi, T., Daifu, Y., and Shimada, K. (2001) Studies on Neurosteroids XIV. Levels of Dehydroepiandrosterone Sulfate in Brain and Serum Determined with Newly Developed Enzyme-Linked Immunosorbent Assay, *Steroids 66,* 865–874.
217. Higashi, T., Sugitani, H., Yagi, T., and Shimada, K. (2003) Studies on Neurosteroids XVI. Levels of Pregnenolone Sulfate in Rat Brains Determined by Enzyme-Linked Immunosorbent Assay Not Requiring Solvolysis, *Biol. Pharm. Bull. 26,* 709–711.
218. Prasad, V.V.K., Vegesna, S.R., Welch, M., and Lieberman, S. (1994) Precursors of Neurosteroids, *Proc. Natl. Acad. Sci. USA 91,* 3220–3223.
219. Corpéchot, C., Young, J., Calvel, M., Wehrey, C., Veltz, J.N., Touyer, G., Mouren, M., Prasad, V.V.K., Banner, C., Sjövall, J., Baulieu, E.E., and Robel, P. (1993) Neurosteroids: 3α-Hydroxy-5α-pregnan-20-one and Its Precursors in the Brain, Plasma, and Steroidogenic Glands of Male and Female Rats, *Endocrinology 133,* 1003–1009.
220. Shackleton, C.H., Chuang, H., Kim, J., de la Torre, X., and Segura, J. (1997) Electrospray Mass Spectrometry of Testosterone Esters: Potential for Use in Doping Control, *Steroids 62,* 523–529.
221. Griffiths, W.J., Liu, S., Alvelius, G., and Sjövall, J. (2003) Derivatisation for the Characterisation of Neutral Oxosteroids by Electrospray and Matrix-Assisted Laser Desorption/Ionisation Tandem Mass Spectrometry: The Girard-P Derivative, *Rapid Commun. Mass Spectrom. 17,* 924–935.
222. Chaurand, P., Schwartz, S.A., and Caprioli, R.M. (2004) Assessing Protein Patterns in Disease Using Imaging Mass Spectrometry, *J. Proteome Res. 3,* 245–252.

[Received June 23, 2004; accepted July 27, 2004]

A Review of Tobacco BY-2 Cells as an Excellent System to Study the Synthesis and Function of Sterols and Other Isoprenoids

Andréa Hemmerlin[a], Esther Gerber[a], Jean-François Feldtrauer[a], Laurent Wentzinger[a], Marie-Andrée Hartmann[a], Denis Tritsch[b], Jean-François Hoeffler[b], Michel Rohmer[b], and Thomas J. Bach[a,*]

[a]Centre National de la Recherche Scientifique (CNRS), Institut de Biologie Moléculaire des Plantes (IBMP) (UPR 2357), Département "Fonctions et Biosynthèse des Isoprénoïdes," Université Louis Pasteur, F-67083 Strasbourg, France, and [b]Université Louis Pasteur/CNRS, Institut Le Bel, 67070 Strasbourg Cedex, France

ABSTRACT: In plants, two pathways are utilized for the synthesis of isopentenyl diphosphate (IPP), the universal precursor for isoprenoid biosynthesis. In this paper we review findings and observations made primarily with tobacco BY-2 cells (TBY-2), which have proven to be an excellent system in which to study the two biosynthetic pathways. A major advantage of these cells as an experimental system is their ability to readily take up specific inhibitors and stably- and/or radiolabeled precursors. This permits the functional elucidation of the role of isoprenoid end products and intermediates. Because TBY-2 cells undergo rapid cell division and can be synchronized within the cell cycle, they constitute a highly suitable test system for determination of those isoprenoids and intermediates that act as cell cycle inhibitors, thus giving an indication of which branches of the isoprenoid pathway are essential. Through chemical complementation, and use of precursors, intracellular compartmentation can be elucidated, as well as the extent to which the plastidial and cytosolic pathways contribute to the syntheses of specific groups of isoprenoids (e.g., sterols) *via* exchange of intermediates across membranes. These topics are discussed in the context of the pertinent literature.

Paper no. L9541 in *Lipids 39*, 723–735 (August 2004).

Isoprenoids represent the largest family of natural compounds with over 35,000 characterized molecules, most of them being described in plant systems (1). A prominent example is tobacco as a species, which contains nearly 500 isoprenoid molecules (2) out of 2500 identified compounds (3). The isoprenoid pathway in plants apparently is more intricate than that in other organisms and is consequently subjected to close regulation; it is presumably organized in metabolic channels (4). Moreover, the metabolic flux through different pathways and in different compartments of the plant cell can vary substantially, depending on particular requirements during development. Many isoprenoids are unique to plants. Among those are phytohormones (some cytokinins, absciscic acid, gibberellins, brassinosteroids), a number of molecules directly or indirectly implicated in photosynthesis (carotenoids, chlorophylls, plastoquinone), and others involved in secondary metabolism (an array of monoterpenes, sesquiterpenes, and diterpenes). Interestingly, plants are special in the biosynthesis of the universal precursor, isopentenyl diphosphate (IPP, C_5), and its chemically active isomer, dimethylallyl diphosphate (DMAPP), in that they utilize two distinct compartmentalized pathways. The first one, the well-known mevalonate (MVA) pathway (5), occurs in the cytosol/endoplasmic reticulum (ER), whereas the second one, the more recently discovered 2-*C*-methyl-D-erythritol 4-phosphate (MEP) pathway, is present in the plastidial compartment (6–10).

MVA-derived metabolites, such as phytosterols, prenylated proteins, ubiquinones, and cytochrome a 3, are mainly, but not strictly, implicated in vital cell functions. The key enzyme in the MVA pathway is 3-hydroxy-3-methylglutaryl-coenzyme A reductase (HMGR, E.C. 1.1.1.34). In plants, a family of genes encodes at least three isozymes, depending on the plant species (11,12). Based on sequence similarities, tobacco plants contain three families of genes, with more than seven closely related isogenes (13). In comparison with mammalian cells (14), this membrane-bound enzyme plays a key regulatory function in the biosynthesis not only of sterols (15–17), but also of some plant-specific isoprenoids (18). The enzyme is closely regulated at the transcriptional and post-transcriptional level (11,19). The importance of this enzymic reaction in nature is further emphasized by the existence of highly specific inhibitors of HMGR such as mevinolin, also referred to as lovastatin, found in ascomycetes (20).

Only recently has the MEP pathway been completely elucidated (21). Besides gibberellic acids and abscisic acid, which are vital phytohormones, and molecules having antioxidant

Part of this work was presented at the 95th Annual Meeting of the AOCS (Steroid session) in Cincinnati, Ohio, May 9–12, 2004.

*To whom correspondence should be addressed at CNRS-IBMP (UPR 2357) Département "Fonctions et Biosynthèse des Isoprénoïdes," Institut de Botanique, Université Louis Pasteur, 28 rue Goethe, F-67083 Strasbourg, France. E-mail: Thomas.Bach@bota-ulp.u-strasbg.fr

Abbreviations: CNRS, Centre National de la Recherche scientifique; DMAPP, dimethylallyl diphosphate; DX, 1-deoxy-D-xylulose; ER, endoplasmic reticulum; FPP, farnesyl diphosphate; GFP, green fluorescent protein; HMGR, HMG-CoA reductase; IBMP, Institut de Biologie Moléculaire des Plantes; IPA, isopentyladenine; IPP, isopentenyl diphosphate; ME, 2-*C*-methyl-D-erythritol; MEP, 2-*C*-methyl-D-erythritol 4-phosphate; MVA, mevalonate; PQ, plastoquinone; Q_{10}, ubiquinone; TBY-2, tobacco *Nicotiana tabacum* cv. Bright Yellow-2.

properties and/or functions in photosynthesis such as carotenoids, α-tocopherol, and plastoquinone, other MEP-derived compounds play a role mainly in secondary metabolism (22). Within the MVA-independent pathway it was expected that 1-deoxy-D-xylulose 5-phosphate reductoisomerase (DXR) would catalyze the limiting step, simply through the existence of the microbial antibiotic fosmidomycin, which specifically blocks this reaction (23). In the plant kingdom, studies with *Arabidopsis thaliana* supported this hypothesis (24). Other experiments, however, showed that the first enzyme, 1-deoxy-D-xylulose 5-phosphate synthase (DXS), also is rate-limiting (25,26).

The way these MVA and MEP pathways are regulated remains obscure. It seems clear that the accumulation of end products might exert a retro-inhibitory control on the activities of key enzymes (27), or that signal transduction pathways would be implicated (28,29). It is no surprise that environmental changes affect the biosynthetic pathways (30), but so far no regulatory elements or transcription factors have been clearly identified. Several recent independent studies found that the plastidial pathway can exchange isoprenoid precursors with the cytosolic pathway for the synthesis of normally MVA-derived compounds (6,31–36). The reverse exchange is observed under certain circumstances (e.g., in the presence of inhibitors), as will be discussed later, but is not as efficient. Other plant-specific cell components, with a mixed cytosolic and plastidial origin are synthesized starting from a prenyl group (6,32,37). However, it is still unknown whether the exchange of isoprenoid precursors between cell compartments can, for instance, play a rescue and/or regulatory function *in vivo*, and to what extent.

ADVANTAGES IN USING TOBACCO BRIGHT YELLOW-2 CELLS

Tobacco (*Nicotiana tabacum*) cv. Bright Yellow-2 (TBY-2) cells correspond to a pale-yellow cell suspension that has been used mainly for the elucidation of cellular functions. This is due to their rapid cell duplication, which is around 14 h (38). They do not agglomerate into calli as other plant cell suspensions often do, but can form a string of a few cells. Furthermore, they contain all organelles found in other cell types, with a considerable number of mitochondria (38). No chloroplast formation can be initiated, but they contain active proplastids or leucoplasts (38), which can also evolve into amyloplasts under some specific conditions (39). The plastids can easily be visualized by confocal microscopy after transient expression of specific plastid-targeted peptides fused to the N-terminal side of a green fluorescent protein (GFP) (Fig. 1). They frequently are uniformly distributed within the cytosol (Figs. 1A, 1B) but also sometimes accumulate around the nucleus (Figs. 1C, 1D), a situation we never observed for other tobacco or *Arabidopsis* cell lines. This effect is reproducible with different transit peptides from enzymes implicated in plastidial isoprenoid biosynthesis. In any case, because the cell suspension is unable to perform photosynthesis, it is conditioned to use exogenous nutrients. For this reason, the cells are

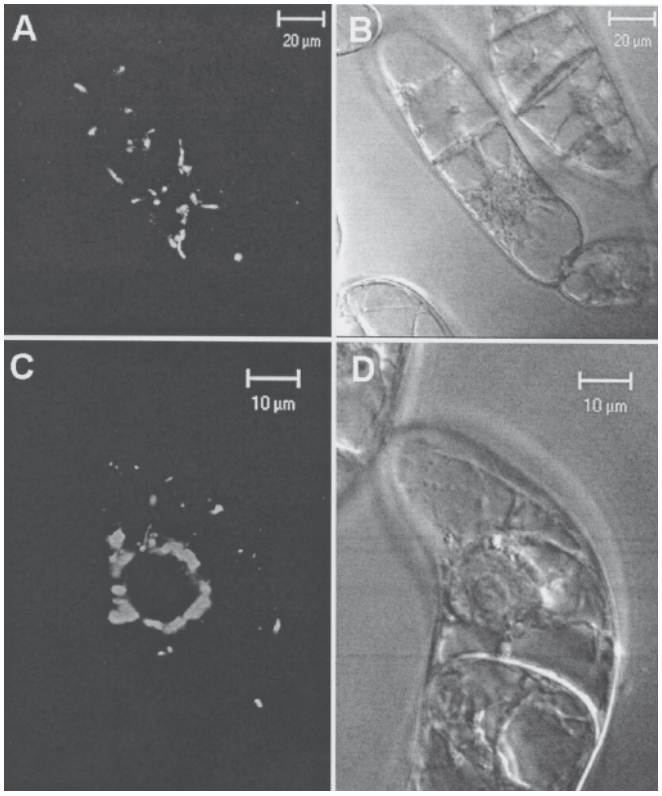

FIG. 1. Cellular localization of specific plastid-targeted peptides [of enzymes implicated in the 2-*C*-methyl-D-erythritol 4-phosphate (MEP) pathway of isoprenoid biosynthesis] fused to the N-terminal side of a green fluorescent protein (GFP) under the control of the constitutive cauliflower virus 35 S promoter. Tobacco *Nicotiana tabacum* cv. Bright-Yellow-2 (TBY-2) cells were transformed by tungsten particle shooting with an inflow gun. Transient expression was examined by confocal microscopy (LSM510 confocal laser-scanning microscope equipped with an inverted Zeiss Axiovert 10 M microscope) after 16 h of expression. GFP was excited at 488 nm using an argon laser, and emission spectra were recorded between 505 and 530 nm (panel A and C) compared with the corresponding bright field (panels B and D). Panels A and B represent plastids within the cytosol; panels C and D represent plastids accumulated around the nucleus.

adapted to absorb all kind of compounds readily from the medium, even those that are not needed for growth. In our experience, most inhibitors, biosynthetic intermediates, and precursors of the isoprenoid biosynthetic pathways penetrate TBY-2 cells very rapidly and efficiently (35,40–46), and thus do not present difficulties when time studies on induced effects are desired. By the same token, they provide an excellent system for incorporation studies (35,40,44–46) owing to their extremely high productivity. They also represent a highly suitable system for studying regulatory interactions between isoprenoid biosynthesis and fundamental processes such as cell division and growth (41,42,47,48), as guaranteed by high metabolic flux rates to end products of biosynthetic pathways (e.g., sterols). In addition, TBY-2 cells show high activities of putatively rate-limiting enzymes such as HMGR, which are otherwise difficult to measure in some other plant species. Indeed, the enzyme activity in TBY-2 cells is higher than that found in a sterol-overproducing

tobacco mutant (*sterov*) affected in HMGR activity, which is with stimulated several-fold as compared with the wild-type (15).

REPRESENTATIVE ISOPRENOIDS FOUND IN TBY-2 CELLS

TBY-2 cells, cultivated in suspension, contain several classes of isoprenoid compounds. Phytosterols, representing nearly 0.2% of the total dry weight, are the major one. The composition, described by Wentzinger *et al.* (46), showed a classical predominance of stigmasterol, 24-methylcholesterol (campesterol), and sitosterol, as described for other plant species (49). The cells also contain two major prenylquinones, plastoquinone PQ_9 and ubiquinone Q_{10} (40), which are implicated in electron transport in plastids and mitochondria, respectively. Consequently, each cell compartment is supposed to contain a complete metabolic pathway leading to the formation of highly represented end products (Fig. 2): Phytosterols are synthesized in the cytosolic/ER compartment, whereas the plastidial compartment contains mainly plastoquinone PQ_9, and mitochondria contain high amounts of ubiquinone Q_{10}. Starting from a reasonable cell-culture volume, enough of the three above-mentioned compounds can be purified for analysis by MS or even by NMR. Consequently, for analyzing the regulation of biosynthetic intermediates and final products, a cell line such as TBY-2, which contains only a limited array of products, appears to be quite advantageous.

In the cell suspension, as a heterotrophic system, some end products that are found in intact plants, are not produced. As an example, TBY-2 cells seem to be unable to synthesize phytol and/or phytyl diphosphate for the synthesis of the side chain of chlorophylls. Similarly, despite several attempts, we were not able to identify an accumulation of free solanesol, typical for tobacco plants. Solanesyl diphosphate is used for plastoquinone PQ_9 biosynthesis and is known to accumulate in large amounts in tobacco leaves. Its apparent absence in TBY-2 cells might be explained by the high turnover within the pathway. In contrast to what has been described by Goossens *et al.* (50), in the TBY-2 cell suspension we use,

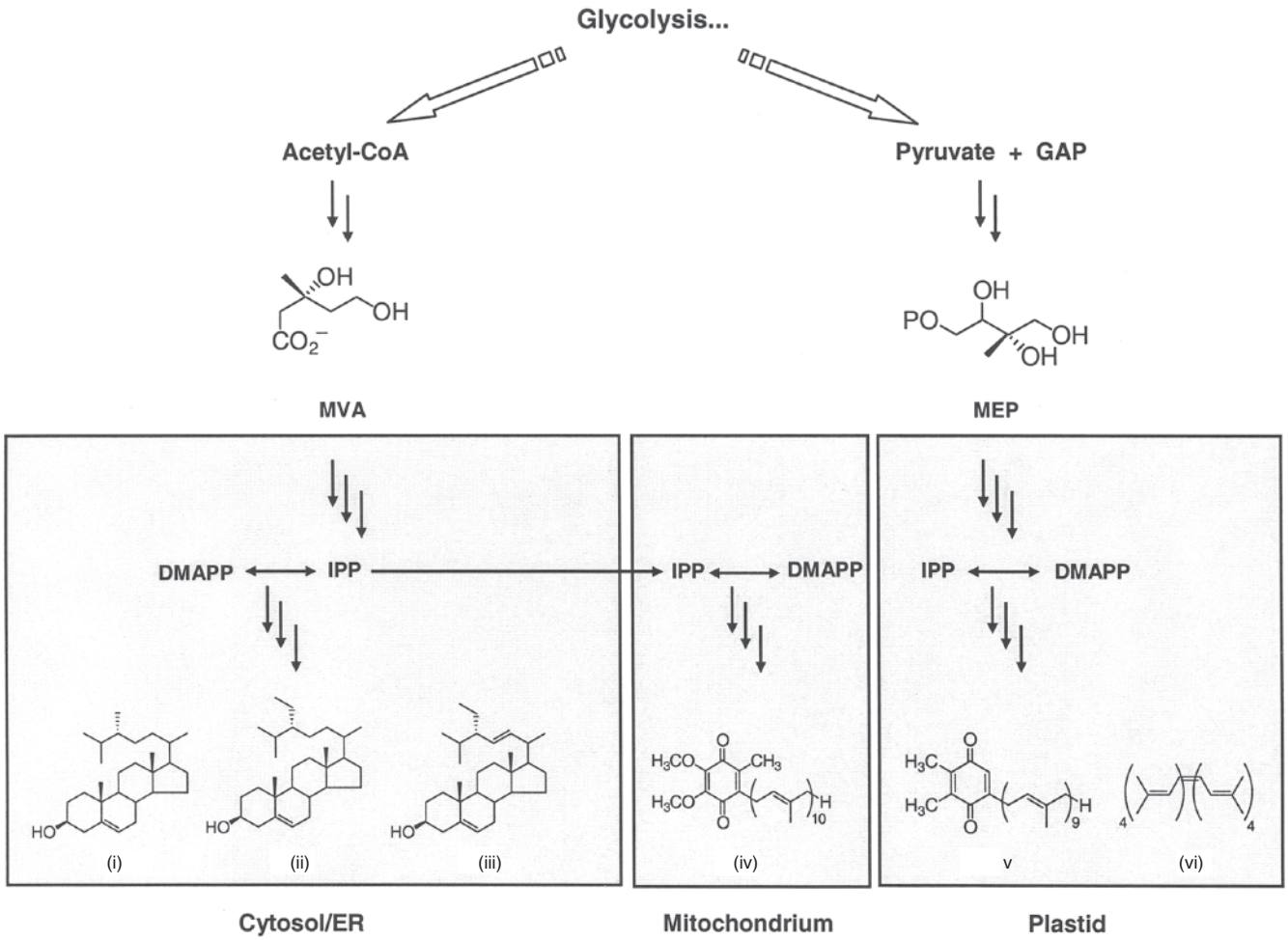

FIG. 2. Biosynthetic compartmentation of major isoprenoids found in TBY-2 cells. Cytosolic and mitochondrial isoprenoids derive from mevalonate (MVA), whereas plastidial compounds are synthesized starting from MEP. The most abundant isoprenoids in TBY-2 cells are (i) campesterol, (ii) sitosterol, (iii) stigmasterol, (iv) ubiquinone Q_{10}, (v) plastoquinone PQ_9, and (vi) phytoene. GAP, glyceraldehyde 3-phosphate; DMAPP, dimethylallyl diphosphate; IPP, isopentenyl diphosphate. For other abbreviations see Figure 1.

carotenoids are virtually nonexistent under standard culture conditions. Chemical analyses revealed that TBY-2 cells synthesize mainly phytoene, the first common carotenoid precursor (45), which suggests a near-absence of subsequent dehydrogenation steps. The concentration of phytoene increases after the culture medium is supplied with 1-deoxy-D-xylulose (DX). Phytoene, in combination with α-tocopherol and plastohydroquinone, may play an antioxidative function in the cell suspension.

Because TBY-2 cells grow under rather environmentally isolated conditions, isoprenoid secondary metabolites are almost nonexistent. TBY-2 cells are, for example, unable to produce capsidiol, a phytoalexin sesquiterpenoid (Fritig, B., IBMP, personal communication) that is commonly found in tobacco cell suspensions after elicitation with a necrotic lesion-inducing type of elicitor (51). For this reason, TBY-2 cells do not represent the most adapted model to study plant–pathogen interactions, although they display some of the early responses such as extracellular alkalinization, active oxygen species production, and so forth, but also cell death induction (50,52).

APPROACHES USED TO STUDY THE ISOPRENOID PATHWAYS

In previous experimental approaches aimed at elucidation of biosynthetic pathways, we demonstrated the usefulness of TBY-2 cells in combination with inhibitor treatments. Mevinolin especially (20) was revealed to be an excellent probe to evaluate the role of MVA in various physiological and biochemical processes in plants (53–56). In a quite early study, compactin, a homolog of mevinolin, was used in a celery cell suspension culture in an attempt to quantify a putative MVA pool (54). Fosmidomycin (57) is a mycotoxin and an inhibitor of the MEP pathway (23). It was subsequently used in several studies to block this pathway even in plants, where the inhibitor has to cross the plasma membrane and the plastid envelope before reaching its target enzyme. Treatments led to bleaching of plants and/or a decrease in the content of MEP-derived compounds (58,59). Similarly, other specific inhibitors can be used; some of them have been summarized previously (43,46,60). The aim is to achieve a block of metabolic flux rates *in vivo* in order to investigate physiological reactions, for instance to force the cells to use an alternative substrate for biosynthesis.

Metabolic pathways have been deciphered mainly by isotope labeling studies (61). To circumvent internal dilution and/or intracellular complementation by anaplerotic pathways during incorporation studies, application of inhibitors is the method of choice. When stable isotope-labeled precursors are used, the analysis by MS or NMR spectroscopy gives information on the pathway through which end products had been synthesized. A more sensitive technique is the use of radiolabeled precursors. However, especially in the case of isoprenoid biosynthesis, a frequent bias in the literature arises from the techniques used to isolate organelles and end products, whose radiochemical purity has not always been proven. Further, when cell suspension cultures are used, labeled biosynthetic precursors are incorporated *via* the culture medium; thus, they need to remain stable in the medium throughout the incubation period. Moreover, they need to cross first the cell wall (although this is quite rudimentary in TBY-2 cells), then at least the plasma membrane, in order to get into the cell before being integrated into a cytosolic pathway, or even more membranes, should integration occur in organelles. As with other plant species, both DX and MVA are easily absorbed by TBY-2 cells. In the latter case, in our experience they accept the free acid form of MVA much better than its uncharged lactone, which suggests the involvement of a membrane transporter. Whereas in *Escherichia coli* 2-*C*-methyl-D-erythritol (ME) can also be integrated into the MEP pathway (62), this compound is toxic for TBY-2 cells (Hemmerlin, A., unpublished observations). DX and ME need to be phosphorylated before their integration into the MEP pathway. The respective kinases capable of phosphorylating these sugar derivatives were identified in bacterial species and correspond to D-xylulose kinase, which accepts DX as an alternative substrate (63), and to sorbitol phosphotransferase, for ME (64). The inability of TBY-2 cells to use this latter precursor can be explained by the absence of such a type of transporter in plants.

An alternative method to study biosynthetic pathways is to characterize knockout mutant lines (65). With this approach, the use of TBY-2 cells has a certain disadvantage. However, TBY-2 cells were shown to be quite promising in attempts to perform RNA interference (66); thus, the targeted inactivation of genes and blockage of enzymes derived from them will be possible.

MODEL TO STUDY EARLY STEPS OF ISOPRENOID BIOSYNTHESIS

As discussed previously, HMGR catalyzes a key regulatory step in the MVA pathway. As in other organisms, as well as in TBY-2 cells, the enzyme activity is modulated in response to various treatments. For instance, exposure of TBY-2 cells to mevinolin led to induction of apparent HMGR activity, and an increase in the quantity of protein and mRNA, although it has to be noted that there is only a relative, but not a strict coupling, between those parameters (41,42). The increased protein level most likely represents two HMGR isozymes (35). Taking those and other observations together, it is not surprising that induction of apparent HMGR activity by mevinolin, to overcome the depletion of MVA-derived isoprenoid units, follows a biphasic behavior, with overlapping peak characteristics (35).

Enzyme activity is also stimulated by inhibitors acting downstream of HMGR, such as squalestatin, an inhibitor of squalene synthase, or terbinafin, an inhibitor of squalene epoxidase (46,67). Other compounds also were shown to stimulate HMGR activity, for instance farnesol (42), corresponding to the dephosphorylated form of farnesyl diphosphate (FPP), the

central C_{15} intermediate in the cytosolic biosynthetic pathway. *In vivo*, farnesol can be phosphorylated by two independent kinases (68), then be integrated into biosynthetic pathways. In animal systems, farnesol is considered to be the nonsterol compound that is responsible for the negative retro-control of HMGR (69,70). With the presence of HMGR isozymes in plants, the situation is different: Close inspection of the time course after treatment with farnesol revealed a rapid decrease of HMGR activity; however, after 24 h this was followed by an increase of activity (Fig. 3A). The estimation of mRNA by quantitative real-time polymerase chain reaction showed that transcription of mainly one isogene expressed in TBY-2 cells was stimulated quite significantly after 48 h of treatment (Fig. 3B). Therefore, we could assume that in TBY-2 cells, and maybe more generally in plants, the isoform responsible for the pathway regulation could be down-regulated as in animal cells,

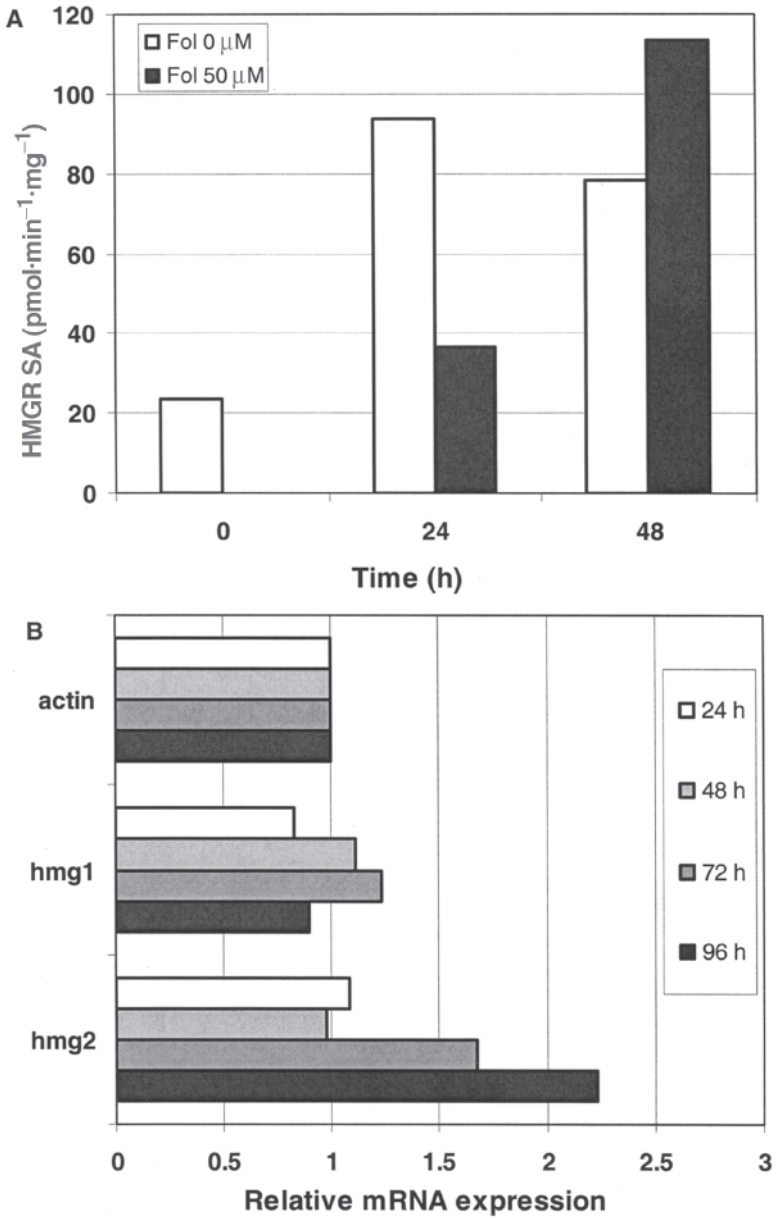

FIG. 3. Influence of farnesol (Fol) treatment on apparent activity of microsome-bound HMG-CoA reductase (HMGR). (A) TBY-2 cells were treated (Fol 50 µM) or not (Fol 0 µM) with Fol before isolation of membrane fractions. Activity was always measured in the presence of 30 µM *R,S*-[3-^{14}C]HMG-CoA (10-fold K_m) and 30 µg of microsomal protein. (B) Real-time polymerase chain reaction analysis of HMGR1 (-hmg1) and HMGR2 (-hmg2) gene expression. Actin was used as a standard for normalization. SA, specific activity. For other abbreviations see Figure 1.

whereas at the activity level this phenomenon is compensated for by activation of another isoform. This can be interpreted to mean that under our cultivation conditions we have two major forms of active enzyme, a housekeeping one that reacts slowly and a stress-induced one. We were able to discriminate two HMGR isoforms in TBY-2 cells that slightly differed in their molecular mass and could thus be resolved by high-resolution SDS-PAGE and Western blot analysis (35).

TBY-2 cells were also revealed to be helpful in studying the so-called branching of the MEP pathway. In *E. coli*, the last enzyme in the pathway, LytB forms IPP and DMAPP simultaneously (71,72). This phenomenon, called "branching," was discovered by demonstrating the nonessential function of IPP isomerase in bacteria (73,74). The situation was more obscure in plants, and some early studies suggested that the synthesized C_5 precursor was exclusively IPP, as it was for the MVA pathway (75,76). The enigma was solved when Rieder *et al.* (77) analyzed the monoterpene cineol in *Eucalyptus* plants and observed different labeling patterns in the isoprene units derived from IPP and DMAPP after [4-^{2}H]DX incorporation. The use of TBY-2 cells allowed us to confirm unambiguously that plants, like bacteria, synthesize IPP and DMAPP simultaneously in the MEP pathway; however, the situation seems to be more intricate than in bacteria, as IPP isomerase is apparently active in plastids (45). The differences found in several organisms were discussed in detail by Wolff *et al.* (78).

MODEL TO STUDY CELLULAR COMPARTMENTATION OF ISOPRENOID SYNTHESIS

The use of TBY-2 cells helped us to elucidate how and to what extent different plant compartments can exchange isoprenoid precursors. This was first examined with the cytosolic and mitochondrial compartments. As mitochondria contain neither the MVA nor the MEP pathway, we were interested in understanding what carbon source is used to build up ubiquinone Q_{10} as the major isoprenoid. It is noteworthy that, in the past, TBY-2 cells were optimized to obtain varieties producing high amounts of ubiquinone Q_{10} (79), an additive in cosmetics and nutrition. In an earlier study, it was suggested that in plants, plastoquinone PQ_9 and ubiquinone Q_{10} share a common origin (80), with both compounds being synthesized in the cytosol, followed by selective translocation to plastids and mitochondria, respectively. By using the TBY-2 cell line, we could prove that ubiquinone Q_{10} and plastoquinone PQ_9, the latter found in the plastids, are of different biosynthetic origin (40). Whereas the plastoquinone PQ_9 side chain is synthesized from MEP-derived IPP, the ubiquinone Q_{10} side chain is clearly a derivative of MVA. We also demonstrated that an exchange of isoprenoid precursors between the cytosol and mitochondria must exist (40). However, the compound crossing the membrane has not yet been identified. As a specific mitochondrial-targeted IPP isomerase occurs in *A. thaliana* (81), it is most likely IPP that is imported. In earlier work performed by Lütke-Brinkhaus *et al.* (82), IPP was taken up by mitochondria purified from different plant species. However, it was also shown that to some extent, farnesol, which is phosphorylated by cytosolic kinases (68), can be integrated into ubiquinone Q_{10} in TBY-2 cells (44). Therefore, it seems likely that at least FPP can also be translocated across the mitochondrial membrane.

We then focused our attention on the exchange of compounds between the cytosol and plastids. Whereas some biosynthetic spillover had already been shown in studies performed by the group of Duilio Arigoni at the ETH Zürich (6) using *Ginkgo biloba* embryos, we wanted to know whether this exchange could be activated and to what extent. Other groups performed comparable experiments (32,33,36,83). By using TBY-2 cells, we could, however, show that for the biosynthesis of sterols the cells can rely completely on a pool of MEP-derived precursors, so long as the MVA pathway is blocked (35). This was demonstrated by incorporation studies with [1,1,1,4-$^2H_4$]DX with TBY-2 cells treated by mevinolin. The unique aspect of our study was to show that this spillover could reach up to 100%, a much higher rate than that obtained in any other plant system studied so far. Addition of DX to the culture medium of mevinolin-treated cells complemented growth inhibition at the same low millimolar concentration range as did MVA, the product of the inhibited enzyme. Further, DX partially re-established feedback repression of mevinolin-induced HMGR activity. Inhibition by fosmidomycin (although much less active as a growth inhibitor), which blocks MEP synthase, could be partially overcome by addition of MVA, and chemical complementation was further substantiated by incorporation of [2-^{13}C]MVA into plastoquinone, representative of plastidial isoprenoids. The best rates of incorporation of exogenous stably-labeled precursors were observed in the presence of both inhibitors, thereby avoiding any internal isotope dilution. Thus, an exchange of isoprenoid precursors from the cytosol to the plastids seems possible, albeit at low efficiency.

REGULATION OF STEROL BIOSYNTHESIS IN TBY-2 CELLS

In plants, phytosterols play a role similar to that of cholesterol in animal cells. They are functional in the maintenance of membrane fluidity, thereby regulating permeability or controlling the activity of some membrane-associate proteins, and they are also implicated in the regulation of plant development (49). Under standard growth conditions TBY-2 cells synthesize these sterols from MVA (40), but sterol synthesis can also be achieved from MEP-derived precursors (35). TBY-2 cells are sensitive to inhibitors such as squalestatin or terbinafine, which decrease sterol content, and they display high activities of enzymes implicated in steroll biosynthesis (46). However, it is surprising to note that despite the high production of MVA, which is due to the elevated HMGR activity, the cells do not accumulate esterified intermediates into lipid droplets, as compared, for example, with the *sterov* mutant (84). This observation might be explained by the fact that in rapidly dividing and later expanding TBY-2 cells, the membranes always formed *de novo* constitute a metabolic sink for

sterols, which prevents a noticeable accumulation of esterified intermediates. The *sterov* mutant cells have a much slower growth rate, and the high HMGR activity, most likely due to a loss in feedback regulation, leads to accumulation of bulky sterol intermediates, which are detoxified through esterification with FA and storage in lipid droplets (84). For all these reasons, TBY-2 cells are highly suited as a plant model for the study of the regulation of the phytosterol biosynthetic pathway.

It has been hypothesized that in plants, HMGR, at least the isozyme possibly linked to sterol biosynthesis, is feedback-regulated (85). The overexpression of the soluble catalytic part of the hamster HMGR in a tobacco cell line led mainly to the accumulation of sterol intermediates such as cycloartenol (16), presumably as FA esters (17), whereas end-of-chain sterols were overaccumulated only to a very limited extent. We hypothesized that for this type of regulation, some intermediate, or close-to-end product, of the sterol pathway must always be synthesized *de novo*. When this "regulatory molecule" has been converted into an end-of-chain product and reached its putative final destination, for instance, the plasma membrane, it no longer exerts such a feedback control. More recent studies point exactly in this direction (46). HMGR was modulated in TBY-2 cells at a transcriptional level in response to a selective depletion of endogenous sterols at a different level of the biosynthetic pathway (86). Furthermore, these studies showed that in the presence of terbinafine (an inhibitor of squalene epoxidase), the cells accumulate squalene in cytosolic lipid droplets, which can later be remobilized for sterol biosynthesis (46). The signal that triggers, in parallel, the synthesis and accumulation of triglycerides (apparently needed as a matrix to dissolve squalene) remains to be identified.

Our studies with TBY-2 cells gave some indication that sterol biosynthesis might depend on different metabolic pools. In the studies partially described by Disch *et al.* (40), starting from various isotopomers of ^{13}C-labeled glucose, we observed two types of labeling: that arising from the conversion of glucose into acetyl-CoA, proceeding through glycolysis, and that from the oxidative pentose phosphate cycle. From the NMR spectra of sterols, it cannot be deduced whether the two types of putative labeling are found in one and the same or in two different sterol molecules, because of superposition of both phenomena. Nor could we distinguish between the two types of sterol isotopomers, which might correspond to a compartmentation of syntheses in space and time. However, incorporation of the much more specific precursor [2-^{13}C]MVA into the sterols of a TBY-2 cell culture shed light on the existence of clearly differentiated sterol pools, synthesized from carbon sources of different origins (35) and identified by MS (Fig. 4). A major sterol pool characterized by strong incorporation of [2-^{13}C]MVA, corresponding to the labeling of nearly all five isoprene units (i.e., to the maximal expected degree) was accompanied by a minor pool, which had only 0 to 3 labeled isoprene units and represented about 5% of the total sterols, as deduced from the spectra. This observation implies a significant contribution of nonlabeled MVA derived from *de novo* biosynthesis from the main carbon and energy source of the culture medium (sucrose in this case). In addition, both pools were differentiated by their composition according to the relative intensities of the pseudomolecular ions (M^+ – AcOH). The minor pool containing less label was, for instance, enriched in isofucosterol (35). Mass peaks arising from endogenous MVA nearly disappeared in mevinolin-treated cells, and especially in lipid extracts from cells that had been treated with mevinolin plus fosmidomycin. In this latter case, there was no longer any isotope dilution, and sterols became 100% labeled by [2-^{13}C]MVA (Fig. 4).

CELLULAR FUNCTION OF SOME ISOPRENOID MOLECULES

The TBY-2 cell line was mainly used for cell cycle and cytoskeleton studies (87). We had particularly been interested in the implication of MVA in plant cell cycle regulation (41,43). It previously was shown that mevinolin efficiently inhibits the growth of cultured TBY-2 cells (47). More precisely, we could prove that mevinolin acts as a G1-phase cell cycle inhibitor when MVA is not available at the end of the mitosis (41). We then investigated what MVA-derived molecules could be essential for plant cell cycle progression. Molecules of plastidial origin (e.g., the phytyl moiety of chlorophylls, and α-tocopherol; phylloquinone, carotenoids, and the nonaprenyl moiety of plastoquinone) are synthesized independently of MVA (7,8) and were therefore not considered as potential candidates. An approach to identify a molecule implicated in a cellular function is to chemically complement a deficiency with "candidate compounds." In this way, it was demonstrated that mevinolin-induced inhibition of cell division in TBY-2 cells can be reversed by addition of the inhibited enzyme's product MVA (41,47), by cytokinins (47), by partial alkalinization of the cytosolic pH (48), and also by DX (35). Further, MVA alone stimulates growth of TBY-2 cells over control values (48), which points to a limiting role of a putative MVA pool for cell growth and division. Nonphosphorylated intermediates such as farnesol could hardly overcome the inhibition and even became readily toxic (42).

Another strategy to identify the MVA-derived compound essential for cell cycle progression was to compare the inhibitory effect of mevinolin with those exerted by branch-specific inhibitors acting downstream in the pathway. Therefore, we focused on the effects of compounds interacting with (i) sterol biosynthesis, (ii) protein prenylation, and (iii) protein glycosylation (43). Interestingly, none of these compounds behaved or could exactly mimic the effect of mevinolin. The capacity of cytokinins, apparently with zeatin being the most efficient one, to release mevinolin-treated cells from cell cycle arrest was explained by the implication of these hormones in cell cycle regulation (88,89). However, the authors consider that cytokinins are strictly synthesized from MVA. But recently Kasahara *et al.* (37) demonstrated that in *A. thaliana,* some cytokinins are synthesized starting from MVA,

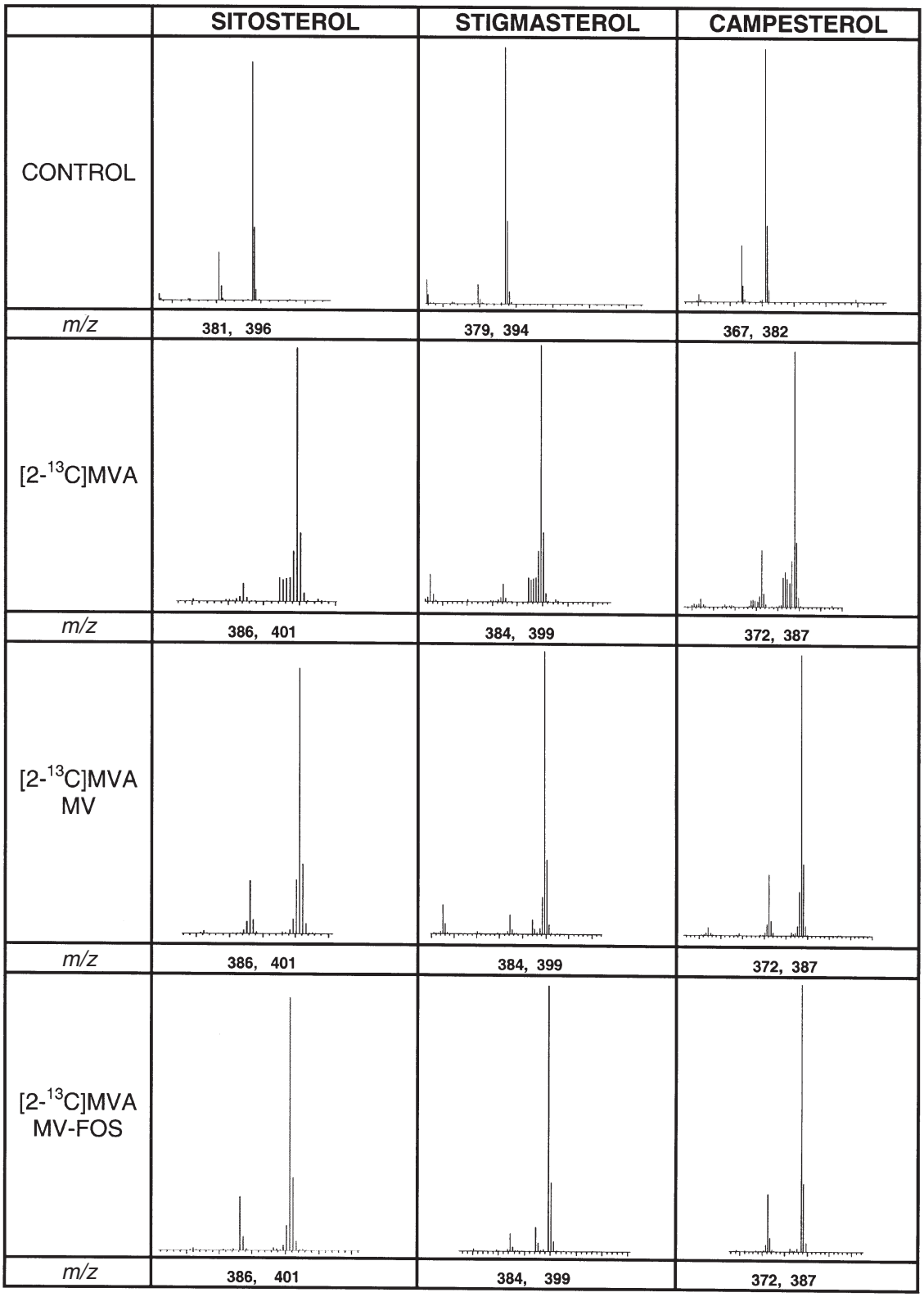

FIG. 4. MS analysis of phytosterols isolated from TBY-2 cells. Mass spectra of steryl acetates were recorded as described by Hemmerlin *et al.* (35). Isotopomer distribution was normalized in arbitrary units for each fragment. The treatments of TBY-2 cells were as follows: cells grown for 7 d in the presence of 2 mM [2-^{13}C]MVA ([2-^{13}C]MVA), cells grown for 7 d in the presence of 2 mM [2-^{13}C]MVA and 5 μM mevinolin ([2-^{13}C]MVA, MV), and cells grown for 7 d in the presence of 2 mM [2-^{13}C]MVA, 5 μM MV, and 20 μM fosmidomycin (FOS) ([E2-^{13}C]MVA, MV-FOS). The mass spectra were compared with those of nonlabeled compounds. Note the increasing loss of mass peaks from unlabeled sterols in the presence of MV, especially when both MV and FOS had been added. For other abbreviations see Figure 1.

others from MEP. Consequently, an application of mevinolin cannot be considered as sufficiently efficient to block cytokinin biosynthesis entirely. On the other hand, as we described earlier, mevinolin might exert pleiotropic effects, as it prevents the formation of a wide array of compounds implicated in cell division. Thus, the situation is complex. Furthermore, the reversion of cell cycle inhibition by cytokinins also seems to work in animal cell lines (90,91). Even the existence of a novel group of proteins, modified by isopentenyladenine (IPA), was proposed (91). To a certain extent, these proteins seem to be implicated in the modulation of DNA synthesis by an as yet unknown mechanism. Using monoclonal anti-IPA antibodies, kindly provided by Professor Roy O. Morris (University of Missouri, Columbia, MO), in membrane fractions isolated from TBY-2 cells, we could also detect proteins that were cross-reacting (92).

Several classes of phytohormones are of isoprenoid origin (93). A prominent example of MVA-derived phytohormones are brassinosteroids, which are synthesized *via* campesterol. Recently, Miyazawa *et al.* (94) characterized the positive effect of brassinolide on the proliferation of TBY-2 cells cultivated in the absence of auxin. These results are in contrast with those observed with LA6 cells, a cytokinin and auxin autotroph tobacco cell line (95), and even with TBY-2 cells (92), when the normal growth medium, containing auxin, was supplied with a synthetic brassinosteroid (epibrassinolide BR-1, kindly provided by Dr. Malcolm J. Thompson; USDA, ARS, Rockville, MD).

Taken together, our results suggested that protein prenylation, in details described for TBY-2 cells (96,97), in correlation with signaling, might be as important for cell proliferation as is the presence of membrane components such as sterols (43,98). One of the various possibilities of how an MVA-derived isoprenoid compound could be implicated in cell cycle regulation is the essential function of the prenylation of the Ras GTP-binding protein that is involved in signal transduction by activating mitogen-activated protein kinase cascades (99,100). In plants, however, ras proteins are absent, and only ras-related proteins have been described (101). Other hypotheses were developed to explain how mevinolin might interfere with the cell cycle. For a human breast cancer cell line, it was reported that mevinolin-induced cell cycle arrest could be independent of the inhibition of MVA production, but that the inhibitor might interfere with the proteasome (102). Because plant cells are able to synthesize isoprenoid precursors such as IPP/DMAPP by two different although compartmentalized pathways, the model described for this human cell line cannot explain why in TBY-2 cells the sugar DX can be used to rescue cells from inhibition by mevinolin. In our eyes, DX acts as a substitute for MVA by providing another source of isoprenoid precursors, as shown by stable isotope labeling of end products (35).

POSSIBLE TOXIC EFFECTS INDUCED BY PATHWAY DEREGULATION

The toxic effect of accumulation or deficiency of a metabolic intermediate must be considered in studying biosynthetic pathways. This is especially true when a strategy for overproduction of a commercially interesting compound (103) consists in overexpressing a key enzyme. That a product might somehow accumulate within the cell and might eventually interfere with cell integrity cannot be excluded. For instance, isoprenoid intermediates such as geranyl diphosphate, FPP, geranylgeranyl diphosphate, or longer chains are increasingly hydrophobic and might thus interfere with endomembranes, with deleterious consequences on their architecture. Thus, in addition to the deficiency in some end products, an excessive accumulation of isoprenoid intermediates could induce cell death in plant cells such as TBY-2 cells, as happens in animal cells. Because TBY-2 cells are very sensitive to treatments, they represent an excellent and very sensitive tool to study the potential toxicity of isoprenoid intermediates, for instance of farnesol. Further, their size and their frequent organization into tetrads considerably facilitate microscopical observations as compared with other plant cell cultures that often are organized as calli. Therefore, we have been able to compare cell death induction in mevinolin- and farnesol-treated TBY-2 cells (41,42), whereas sterol biosynthesis inhibitors were moderately or not at all toxic (43,46). Some toxic effect was also observed with some protein prenylation inhibitors (43) and with the 3-hydroxy-3-methylglutaryl coenzyme A synthase-specific inhibitor F-244 (92). All toxic effects described above were correlated with strong induction of HMGR activity as a result of treatment, which can be interpreted by the absence of the aforementioned regulatory cytoplasmic IPP-derived isoprenoid molecule, which cannot be formed under such conditions.

Mevinolin, besides affecting sterol synthesis and protein prenylation, also blocks biosynthesis of ubiquinone, a key component of cellular respiration. The resulting mitochondrial dysfunction can lead to programmed cell death (104). Hence, it is reasonable to assume that the ATP deficit that is a consequence of this dysfunction is somehow disadvantageous to cell cycle progression and favors cell death induction (105).

OUTLOOK AND CONCLUSION

The use of the TBY-2 cell suspension helped answer some questions concerning the organization and regulation of isoprenoid biosynthesis in higher plants.

More recently, we established a new system, using transformed TBY-2 cells that express carboxyterminal GFP fusions with a peptide containing an array of basic amino acyl residues and a terminal CaaX motif. If this fusion protein bears, for instance, a CaaL motif, it can be geranylgeranylated, and as a consequence will be integrated into the plasma membrane (Fig. 5A). If this is not possible, for instance through exchange of the cysteinyl residue by seryl, the GFP fusion protein will migrate into the nucleus (Fig. 5B). We are currently applying such transiently- or stably-transformed cells as a test system to visualize the metabolic origin of isoprenyl residues in the presence or absence of inhibitors and

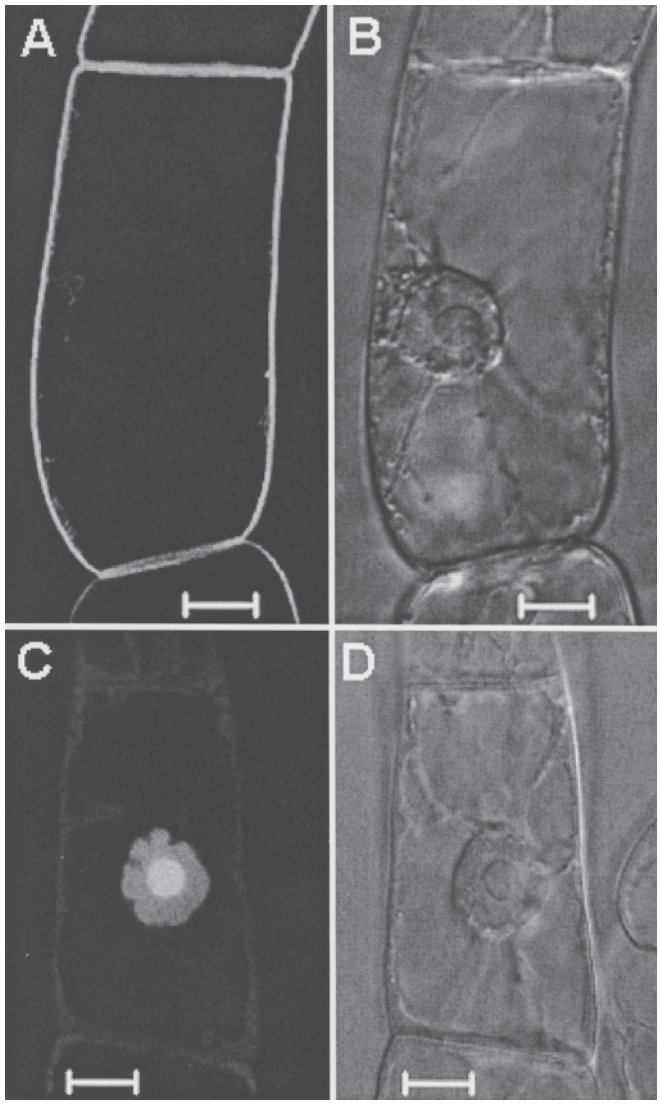

FIG. 5. Confocal microscopy of transformed TBY-2 cells expressing a GFP fusion protein with an extension containing the basic domain of rice CaM61 and either a carboxyterminal CaaL motif (A and B) or a SaaL motif (C and D). Expression was examined by confocal microscopy (LSM510 confocal laser-scanning microscope equipped with an inverted Zeiss Axiovert 10 M microscope). GFP was excited at 488 nm using an argon laser, and emission spectra were recorded between 505 and 530 nm (panels A and C) compared with the corresponding bright field (panels B and D). Note the localization of the isoprenylated GFP fusion protein to the plasma membrane (A), whereas prevention of this covalent modification (B) leads to migration into the nucleus. The white bar represents 10 μm. For other abbreviations see Figure 1.

exogenous intermediates. The preliminary results confirm this experimental approach. The system is also designed to allow for the determination of flux rates needed to satisfy the metabolic sink represented by increasingly expressed GFP fusion proteins.

However, there are still some drawbacks in using the TBY-2 cell suspension or tobacco plants in general, as compared with *A. thaliana* plants, mainly due to the absence of a systematic sequencing program. Some efforts are underway to solve this problem. Indeed, microarray analyses have been described recently for TBY-2 cells (50), as well as analysis of its protein expression by proteomics (106); this opens new avenues also to metabolic studies, particularly in the field of isoprenoid biosynthesis.

ACKNOWLEDGMENTS

Our work was supported by the CNRS, by the Université Louis Pasteur, and by the Institut Universitaire de France (MR). We are grateful to Prof. Toshiyuki Nagata (Tokyo University) for his authorization (more than 10 yr ago) to use the tobacco BY-2 cell suspension to perform our studies. We also thank the CNRS, the Université Louis Pasteur, the Région Alsace, and the Association pour la Recherche sur le Cancer for the support of the Inter-Institute confocal microscopy equipment at the Institut de Biologie Moléculaire des Plantes in Strasbourg. Finally, we are grateful to the anonymous referees for their suggestions to improve the manuscript.

REFERENCES

1. Connolly, J.D., and Hill, R.A. (1992) *Dictionary of Terpenoids*, Chapman & Hall, New York.
2. Wahlberg, I., and Enzell, C.R. (1987) Tobacco Isoprenoids, *Nat. Prod. Rep. 4,* 237–276.
3. Nugroho, L.H., and Verpoorte, R. (2002) Secondary Metabolism in Tobacco, *Plant Cell Tiss. Org. 68,* 105–125.
4. Newman, J.D., and Chappell, J. (1997) Isoprenoid Biosynthesis in Plants: Carbon Partitioning Within the Cytoplasmic Pathway, in *Biochemistry and Function of Sterols* (Parish, E.J., and Nes, D.W., eds.), pp. 123–134, CRC Press, Boca Raton, FL.
5. Bochar, D.A., Friesen, J.A., Stauffacher, C.V., and Rodwell, V.W. (1999) Biosynthesis of Mevalonic Acid from Acetyl-CoA, in *Comprehensive Natural Product Chemistry, Isoprenoids Including Steroids and Carotenoids* (Cane, D.E., ed.), Vol. 2, pp. 15–44, Pergamon Press, Tarrytown, NY.
6. Schwarz, M. (1994) Terpen-Biosynthese in *Ginkgo biloba:* Eine überraschende Geschichte, Dissertation 10951, Eidgenössische Technische Hochschule, Zürich, Switzerland.
7. Lichtenthaler, H.K., Rohmer, M., and Schwender, J. (1997) Two Independent Biochemical Pathways for Isopentenyl Diphosphate (IPP) and Isoprenoid Biosynthesis in Higher plants, *Physiol. Plant. 101,* 643–652.
8. Rohmer, M. (1999) The Discovery of a Mevalonate-Independent Pathway for Isoprenoid Biosynthesis in Bacteria, Algae and Higher Plants, *Nat. Prod. Rep. 16,* 565–574.
9. Schwarz, M., and Arigoni, D. (1999) Ginkgolide Biosynthesis, in *Comprehensive Natural Product Chemistry, Isoprenoids Including Steroids and Carotenoids* (Cane, D.E., ed.), Vol. 2, pp. 367–400, Pergamon Press, Tarrytown, NY.
10. Eisenreich, W., Rohdich, F., and Bacher, A. (2001) Deoxyxylulose Phosphate Pathway to Terpenoids, *Trends Plant Sci. 6,* 78–84.
11. Stermer, B.A., Bianchini, G.M., and Korth, K.L. (1994) Regulation of HMG-CoA Reductase Activity in Plants, *J. Lipid Res. 35,* 1133–1140.
12. Bach, T.J. (1995) Some New Aspects of Isoprenoid Biosynthesis in Plants—A Review, *Lipids 30,* 191–202.
13. Crévenat, P. (1997) Clonage de la mutation responsable de la surproduction de stérols chez un mutant de tabac (*Nicotiana tabacum*), Thèse Doctorale, Université Louis Pasteur, Strasbourg, France.
14. Goldstein, J.L., and Brown, M.S. (1990) Regulation of the Mevalonate Pathway, *Nature 343,* 425–430.
15. Gondet, L., Weber, T., Maillot-Vernier, P., Benveniste, P., and Bach, T.J. (1992) Regulatory Role of Microsomal 3-Hydroxy-3-methylglutaryl Coenzyme A Reductase in a Tobacco Mutant

That Overproduces Sterols, *Biochem. Biophys. Res. Commun. 186,* 888–893.
16. Chappell, J., Wolf, F., Proulx, J., Cuellar, R., and Saunders, C. (1995) Is the Reaction Catalyzed by 3-Hydroxy-3-methylglutaryl Coenzyme A Reductase a Rate-Limiting Step for Isoprenoid Biosynthesis in Plants? *Plant Physiol. 109,* 1337–1343.
17. Schaller, H., Graussem, B., Benveniste, P., Chye, M.-L., Tan, C.T., Song, Y.H., and Chua, N.H. (1995) Expression of the *Hevea brasiliensis* (H.B.K.) Müll. Arg. 3-Hydroxy-3-methylglutaryl Coenzyme A Reductase 1 in Tobacco Results in Sterol Overproduction, *Plant Physiol. 109,* 761–770.
18. Lange, B.M., Severin, K., Bechthold, A., and Heide, L. (1998) Regulatory Role of Microsomal 3-Hydroxy-3-methylglutaryl-coenzyme A Reductase for Shikonin Biosynthesis in *Lithospermum erythrorhizon* Cell Suspension Cultures, *Planta 204,* 234–241.
19. Dale, S., Arró, M., Becerra, B., Morrice, N.G., Boronat, A., Hardie, D.G., and Ferrer, A. (1995) Bacterial Expression of the Catalytic Domain of 3-Hydroxy-3-methylglutaryl-CoA Reductase (isoform HMGR1) from *Arabidopsis thaliana*, and Its Inactivation by Phosphorylation at Ser577 by *Brassica oleracea* 3-Hydroxy-3-methylglutaryl-CoA Reductase Kinase, *Eur. J. Biochem. 233,* 506–513.
20. Alberts, A.W., Chen, J., Kuron, G., Hunt, V., Huff, J., Hoffman, C., Rothrock, J., Lopez, M., Joshua, H., Harris, E., *et al.* (1980) Mevinolin, a Potent Competitive Inhibitor of Hydroxymethylglutaryl-Coenzyme A Reductase and a Cholesterol-Lowering agent, *Proc. Natl. Acad. Sci. USA 77,* 3957–3961.
21. Rodríguez-Concepción, M., and Boronat, A. (2002) Elucidation of the Methylerythritol Phosphate Pathway for Isoprenoid in Bacteria and Plastids. A Metabolic Milestone Achieved Through Genomics, *Plant Physiol. 130,* 1079–1089.
22. Lichtenthaler, H.K. (1999) The 1-Deoxy-D-xylulose 5-Phosphate Pathway of Isoprenoid Biosynthesis in Plants, *Annu. Rev. Plant Physiol. Plant Mol. Biol. 50,* 47–65.
23. Kuzuyama, T., Shimizu, T., Takahashi, S., and Seto, H. (1998) Fosmidomycin, a Specific Inhibitor of 1-Deoxy-D-xylulose 5-Phosphate Reductoisomerase in the Nonmevalonate Pathway for Terpenoid Biosynthesis, *Tetrahedron Lett. 39,* 7913–7916.
24. Carretero-Paulet, L., Ahumada, I., Cunillera, N., Rodríguez-Concepción, M., Ferrer, A., Boronat, A., and Campos, N. (2002) Expression and Molecular Analysis of the *Arabidopsis* DXR Gene Encoding 1-Deoxy-D-xylulose 5-Phosphate Reductoisomerase, the First Committed Enzyme of the 2*C*-Methyl-D-erythritol 4-Phosphate Pathway, *Plant Physiol. 129,* 1581–1591.
25. Lois, L.M., Rodríguez-Concepción, M., Gallego, F., Campos, N., and Boronat, A. (2000) Carotenoid Biosynthesis During Tomato Fruit Development: Regulatory Role of 1-Deoxy-D-xylulose 5-Phosphate Synthase, *Plant J. 22,* 503–513.
26. Estévez, J.M., Cantero, A., Reindl, A., Reichler, S., and León, P. (2001) 1-Deoxy-D-xylulose 5-Phosphate Synthase, a Limiting Enzyme for Plastidic Isoprenoid Biosynthesis in Plants, *J. Biol. Chem. 276,* 22901–22909.
27. Brooker, J.D., and Russell, D.W. (1979) Regulation of Microsomal 3-Hydroxy-3-methylglutaryl Coenzyme A Reductase from Pea Seedlings: Rapid Posttranslational Phytochrome-Mediated Decrease in Activity and *in vivo* Regulation by Isoprenoid Products, *Arch. Biochem. Biophys. 198,* 323–334.
28. Choi, D., and Bostock, R.M. (1994) Involvement of *de novo* Protein Synthesis, Protein Kinase, Extracellular Ca^{2+}, and Lipoxygenase in Arachidonic Acid Induction of 3-Hydroxy-3-methylglutaryl Coenzyme A Reductase Genes and Isoprenoid Accumulation in Potato (*Solanum tuberosum* L.), *Plant Physiol. 104,* 1237–1244.
29. Moore, K.B., and Oishi, K.K. (1994) 3-Hydroxy-3-methylglutaryl Coenzyme A Reductase Activity in the Endosperm of Maize *vivipary* Mutants, *Plant Physiol. 105,* 119–125.
30. Learned, R.M. (1996) Light Suppresses 3-Hydroxy-3-methylglutaryl Coenzyme A Reductase Gene Expression in *Arabidopis thaliana*, *Plant Physiol. 110,* 645–655.
31. Piel, J., Donath, J., Bandemer, K., and Boland, W. (1998) Induzierte und konstitutiv emitierte Pflanzendüfte: Mevalonat-unabhängige Biosynthese terpenoider Duftstoffe, *Angew. Chem. 110,* 2622–2625.
32. Adam, K.P., Thiel, R., and Zapp, J. (1999) Incorporation of 1-[1-^{13}C]Deoxy-D-xylulose in Chamomile Sesquiterpenes, *Arch. Biochem. Biophys. 369,* 127–132.
33. Kasahara, H., Hanada, A., Kuzuyama, T., Takagi, M., Kamiya, Y., and Yamagushi, S. (2002) Contribution of the Mevalonate and Methylerythritol Phosphate Pathways to the Biosynthesis of Gibberellins in *Arabidopsis*, *J. Biol. Chem. 277,* 45188–45194.
34. Bick, J.A., and Lange, B.M. (2003) Metabolic Cross-Talk Between Cytosolic and Plastidial Pathways of Isoprenoid Biosynthesis: Unidirectional Transport of Intermediates Across the Chloroplast Envelope Membrane, *Arch. Biochem. Biophys. 415,* 146–154.
35. Hemmerlin, A., Hoeffler, J.-F., Meyer, O., Tritsch, D., Kagan, I.A., Grosdemange-Billiard, C., Rohmer, M., and Bach, T.J. (2003) Cross-Talk Between the Cytosolic Mevalonate and the Plastidial Methylerythritol Phosphate Pathways in Tobacco Bright Yellow-2 Cells, *J. Biol. Chem. 278,* 26666–26676.
36. Laule, O., Fürholz, A., Chang, H.S., Zhu, T., Wang, X., Heifetz, P.B., Gruissem, W., and Lange, B.M. (2003) Crosstalk Between Cytosolic and Plastidial Pathways of Isoprenoid Biosynthesis in *Arabidopsis thaliana*, *Proc. Natl. Acad. Sci. USA 100,* 6866–6871.
37. Kasahara, H., Takei, K., Ueda, N., Hishiyama, S., Yamaya, T., Kamiya, Y., Yamaguchi, S., and Sakakibara, H. (2004) Distinct Isoprenoid Origins of *cis*- and *trans*-Zeatin Biosynthesis in *Arabidopsis*, *J. Biol. Chem. 279,* 14049–14054.
38. Nagata, T., Nemoto, Y., and Hasezawa, S. (1992) Tobacco BY-2 Cell Line as the "Hela" Cell Line in the Cell Biology of Higher Plants, *Int. Rev. Cytol. 132,* 1–30.
39. Miyazawa, Y., Kato, H., Muranaka, T., and Yoshida, S. (2002) Amyloplast Formation in Cultured Tobacco BY-2 Cells Requires a High Cytokinin Content, *Plant Cell Physiol. 43,* 1534–1541.
40. Disch, A., Hemmerlin, A., Bach, T.J., and Rohmer, M. (1998) Mevalonate-Derived Isopentenyl Diphosphate is the Biosynthetic Precursor of Ubiquinone Prenyl Side-chain in Tobacco BY-2 Cells, *Biochem. J. 331,* 615–621.
41. Hemmerlin, A., and Bach, T.J. (1998) Effects of Mevinolin on Cell Cycle Progression and Viability of Tobacco BY-2 Cells, *Plant J. 14,* 65–74.
42. Hemmerlin, A., and Bach, T.J. (2000) Farnesol Induced Cell Death and Stimulation of HMG-CoA Reductase Activity in Tobacco BY-2 Cells, *Plant Physiol. 123,* 1257–1268.
43. Hemmerlin, A., Fischt, I., and Bach, T.J. (2000) Differential Interaction of Branch-Specific Inhibitors of Isoprenoid Biosynthesis with Cell Cycle Progression in Tobacco BY-2 Cells, *Physiol. Plant. 110,* 343–350.
44. Hartmann, M.-A., and Bach, T.J. (2001) Incorporation of All-*trans*-Farnesol into Sterols and Ubiquinone in *Nicotiana tabacum* L. cv. Bright Yellow Cell Cultures, *Tetrahedron Lett. 42,* 655–657.
45. Hoeffler, J.F., Hemmerlin, A., Grosdemange-Billiard, C., Bach, T.J., and Rohmer, M. (2002) Isoprenoid Biosynthesis in Higher Plants and in *Escherichia coli*: On the Branching in the Methylerythritol Phosphate Pathway and the Independent Biosynthesis of Isopentenyl Diphosphate and Dimethylallyl Diphosphate, *Biochem. J. 366,* 573–583.
46. Wentzinger, L.F., Bach, T.J., and Hartmann, M.-A. (2002) *In vivo* Inhibition of Squalene Synthase and Squalene Epoxidase in Tobacco Cells Triggers an Up-regulation of 3-Hydroxy-3-methylglutaryl Coenzyme A Reductase, *Plant Physiol. 130,* 334–346.
47. Crowell, D.N., and Salaz, M.S. (1992) Inhibition of Growth of

Cultured Tobacco Cells at Low Concentrations of Lovastatin Is Reversed by Cytokinin, *Plant Physiol. 100,* 2090–2095.
48. Hemmerlin, A., Brown, S.C., and Bach, T.J. (1999) Function of Mevalonate and Derivatives in Tobacco BY-2 Cell Proliferation, *Acta Bot. Gall. 146,* 85–100.
49. Benveniste, P. (2002) Sterol Metabolism, in *The Arabidopsis Book,* pp. 1–31, American Society of Plant Biologists, Rockville, MD. Available at netlink: http://www.aspb.org/publications/.
50. Goossens, A., Häkkinen, S.T., Laakso, I., Seppänen-Laakso, T., Biondi, S., De Sutter, V., Lammertyn, F., Nuutila, A.M., Södeerlund, H., Zabeau, M., *et al.* (2003) A Functional Genomics Approach Toward the Understanding of Secondary Metabolism in Plant Cells, *Proc. Natl. Acad. Sci. USA 100,* 8595–8600.
51. Chappell, J., Nable, R., Fleming, P., Andersen, R.A., and Burton, H.R. (1987) Accumulation of Capsidiol in Tobacco Cell Cultures Treated with Fungal Elicitor, *Phytochemistry 26,* 2259–2260.
52. Houot, V., Etienne, P., Petitot, A.-S., Barbier, S., Blein, J.-P., and Suty, L. (2001) Hydrogen Peroxide Induces Programmed Cell Death Features in Cultured Tobacco BY-2 Cell, in a Dose-Dependent Manner, *J. Exp. Bot. 52,* 1721–1730.
53. Bach, T.J. (1987) Synthesis and Metabolism of Mevalonic Acid in Plants, *Plant Physiol. Biochem. 25,* 163–178.
54. Ryder, N.S., and Goad, L.J. (1980) The Effect of the 3-Hydroxy-3-methylglutaryl Coenzyme A Reductase Inhibitor ML-236 B on Phytosterol Synthesis in *Acer pseudoplatanus* Tissue Culture, *Biochim. Biophys. Acta 619,* 424–427.
55. Bach, T.J., and Lichtenthaler, H.K. (1983) Inhibition by Mevinolin of Plant Growth, Sterol Formation and Pigment Accumulation, *Physiol. Plant. 59,* 50–60.
56. Bach, T.J., Weber, T., and Motel, A. (1990) Some Properties of Enzymes Involved in the Biosynthesis and Metabolism of 3-Hydroxy-3-methylglutaryl-CoA in Plants, in *Recent Advances in Phytochemistry* (Towers, G.H.N., and Stafford, H.A., eds.), Vol. 24, pp. 1–82, Plenum Press, NY.
57. Okuhara, M., Kuroda, Y., Goto, T., Okamoto, M., Terano, H., Kohsaka, M., Aoki, H., and Imanaka, H. (1980) Studies on New Phosphonic Acid Antibiotics: III. Isolation and Characterization of FR-31564, FR-32863 and FR-33289, *J. Antibiot. 33,* 24–28.
58. Kamuro, Y., Kawai, T., and Kakiuchi, T. (1991) Herbicidal Methods and Compositions Comprising Fosmidomycin, U.S. Patent 5,002,602.
59. Zeidler, J., Schwender, J., Müller, C., Wiesner, J., Weidemeyer, C., Beck, E. Jomaa, H., and Lichtenthaler, H.K. (1998) Inhibition of the Non-mevalonate 1-Deoxy-D-xylulose 5-Phosphate Pathway of Plant Isoprenoid Biosynthesis by Fosmidomycin, *Z. Naturforsch. 53c,* 980–986.
60. Lange, B.M., Ketchum, R.E.B., and Croteau, R.B. (2001) Isoprenoid Biosynthesis. Metabolite Profiling of Peppermint Oil Gland Secretory Cells and Application to Herbicide Target Analysis, *Plant Physiol. 127,* 305–314.
61. Roscher, A., Kruger, N.J., and Ratcliffe, R.G. (2000) Strategies for Metabolic Flux Analysis in Plants Using Isotope Labelling, *J. Biotechnol. 77,* 81–102.
62. Duvold, T., Calí, P., Bravo, J.-M., and Rohmer, M. (1997) Incorporation of 2-*C*-Methyl-D-erythritol, a Putative Isoprenoid Precursor in the Mevalonate-Independent Pathway, into Ubiquinone and Menaquinone of *Escherichia coli*, *Tetrahedron Lett. 38,* 6181–6187.
63. Wungsintaweekul, J., Herz, S., Hecht, S., Eisenreich, W., Feicht, R., Rohdich, F., Bacher A., and Zenk, M.H. (2001) Phosphorylation of 1-Deoxy-D-xylulose by D-Xylulokinase of *Escherichia coli*, *Eur. J. Biochem. 268,* 310–316.
64. Testa, C.A., Cornish, R.M., and Poulter, C.D. (2004) The Sorbitol Phosphotransferase System Is Responsible for Transport of 2-*C*-Methyl-D-erythritol into *Salmonella enterica* Serovar *typhimurium*, *J. Bacteriol. 186,* 473–480.
65. Thoneycroft, D., Sherson, S.M., and Smith, S.M. (2001) Using Gene Knockouts to Investigate Plant Metabolism, *J. Exp. Bot. 52,* 1593–1601.
66. Akashi, H., Miyagishi, M., and Taira, K. (2004) RNAi Expression Vectors in Plant Cells, *Methods Mol. Biol. 252,* 533–543.
67. Hartmann, M.-A., Wentzinger, L., Hemmerlin, A., and Bach, T.J. (2000) Metabolism of Farnesyl Diphosphate in TBY-2 Cells Treated with Squalestatin, *Biochem. Soc. Trans. 28,* 794–796.
68. Thai, L., Rush, J.S., Maul, J.E., Devarenne, T., Rodgers, D.L., Chappell, J., and Waechter, C.J. (1999) Farnesol Is Utilized for Isoprenoid Biosynthesis in Plant Cells *via* Farnesyl Pyrophosphate Formed by Successive Monophosphorylation Reactions, *Proc. Natl. Acad. Sci. USA 96,* 13080–13085.
69. Bradfute, D.L., and Simoni, R.D. (1994) Non-sterol Compounds That Regulate Cholesterogenesis: Analogues of Farnesyl Pyrophosphate Reduce 3-Hydroxy-3-methylglutaryl Coenzyme A Reductase Levels, *J. Biol. Chem. 269,* 6645–6650.
70. Correll, C.C., Ng, L., and Edwards, P.A. (1994) Identification of Farnesol as the Non-sterol Derivative of Mevalonic Acid Required for the Accelerated Degradation of 3-Hydroxy-3-methylglutaryl Coenzyme A Reductase, *J. Biol. Chem. 269,* 17390–17393.
71. Adam, P., Hecht, S., Eisenreich, W., Kaiser, J., Grawert, T., Arigoni, D., Bacher, A., and Rohdich, F. (2002) Biosynthesis of Terpenes: Studies on 1-Hydroxy-2-methyl-2-(*E*)-butenyl 4-Diphosphate Reductase, *Proc. Natl. Acad. Sci. USA 99,* 12108– 12113.
72. Rohdich, F. Hecht, S. Gartner, K., Adam, P., Krieger, C., Amslinger, S., Arigoni, D., Bacher, A., and Eisenreich, W. (2002) Studies on the Nonmevalonate Terpene Biosynthetic Pathway: Metabolic Role of IspH (LytB) Protein, *Proc. Natl. Acad. Sci. USA 99,* 79–88.
73. Hahn, F.M., Hurlburt, A.P., and Poulter, C.D. (1999) *Escherichia coli* Open Reading Frame 696 Is *idi*, a Nonessential Gene Encoding Isopentenyl Diphosphate Isomerase, *J. Bacteriol. 181,* 4499–4504.
74. Rodríguez-Concepción, M., Campos, N., Lois, L.-M., Maldonado, C., Hoeffler, J.-F., Grosdemange-Billiard, C., Rohmer, M., and Boronat, A. (2000) Genetic Evidence of Branching in the Isoprenoid Pathway for the Production of Isopentenyl Diphosphate and Dimethylallyl Diphosphate in *Escherichia coli*, *FEBS Lett. 473,* 328–332.
75. Caskill, D., and Croteau, R. (1999) Isopentenyl Diphosphate Is the Terminal Product of the Deoxyxylulose-5-phosphate Pathway for Terpenoid Biosynthesis in Plants, *Tetrahedron Lett. 40,* 653–656.
76. Arigoni, D., Eisenreich, W., Latzel, C., Sagner, S., Rady kewicz, T., Zenk, M.H., and Bacher, A. (1999) Dimethylallyl Pyrophosphate Is Not the Committed Precursor of Isopentenyl Pyrophosphate During Terpenoid Biosynthesis from 1-Deoxyxylulose in Higher Plants, *Proc. Natl. Acad. Sci. USA 96,* 1309–1314.
77. Rieder, C., Jaun, B., and Arigoni, D. (2000) On the Early Steps of Cineol Biosynthesis in *Eucalyptus globulus*, *Helv. Chim. Acta 83,* 2504–2513.
78. Wolff, M., Seemann, M., Tse Sum Bui, B., Frapart, Y., Trisch, D., Garcia Estrabot, A., Rodríguez-Concepción, M., Boronat, A., Marquet, A., and Rohmer, M. (2003) Isoprenoid Biosynthesis *via* the Methylerythritol Phosphate Pathway: The (*E*)-4-Hydroxy-3-methylbut-2-enyl Diphosphate Reductase (LytB/IspH) from *Escherichia coli* Is a [4Fe-4S] Protein, *FEBS Lett. 541,* 115–120.
79. Ikeda, T., Matsumoto, T., Obi, Y., Kisaki, T., and Noguchi, M. (1981) Characteristics of Cultured Tobacco Cell strain's Producing High Levels of Ubiquinone-10 Selected by a Cell Cloning Technique, *Agric. Biol. Chem. 45,* 2259–2263.
80. Osowskarogers, S., Swiezewska, E., Andersson, B., and Dallner, G. (1994) The Endoplasmic Reticulum–Golgi System Is a

Major Site of Plastoquinone Synthesis in Spinach Leaves, *Biochem. Biophys. Res. Commun. 205,* 714–721.
81. Cunningham, F.X., Jr., and Gantt, E. (2000) Identification of Multi-Gene Families Encoding Isopentenyl Diphosphate Isomerase in Plants by Heterologous Complementation in *Escherichia coli*, *Plant Cell Physiol. 41,* 119–123.
82. Lütke-Brinkhaus, F., Liedvogel, B., and Kleinig, H. (1984) On the Biosynthesis of Ubiquinones in Plant Mitochondria, *Eur. J. Biochem. 141,* 537–541.
83. Jux, A., Gleixner, G., and Boland, W. (2001) Classification of Terpenoids According to the Methylerythritolphosphate or the Mevalonate Pathway with Natural $^{12}C/^{13}C$ Isotope Ratios: Dynamic Allocation of Resources in Induced Plants, *Angew. Chem. Int. Ed. 40,* 2091–2093.
84. Gondet, L., Bronner, R., and Benveniste, P. (1994) Regulation of Sterol Content in Membranes by Subcellular Compartmentation of Steryl-Esters Accumulation in a Sterol-Overproducing Tobacco Mutant, *Plant Physiol. 105,* 509–518.
85. Bach, T.J., Boronat, A., Caelles, C., Ferrer, A., Weber, T., and Wettstein, A. (1991) Aspects Related to Mevalonate Biosynthesis in Plants, *Lipids 26,* 637–648.
86. Wentzinger, L. (2002) Régulation de la voie de biosynthèse des isoprénoïdes cytoplasmiques chez le tabac, Thèse Doctorale, Université Louis Pasteur, Strasbourg, France.
87. Geelen, D.N.V., and Inzé, D.K. (2001) A Bright Future for the Bright Yellow-2 Cell Culture, *Plant Physiol. 127,* 1375–1379.
88. Laureys, F., Dewitte, W., Witters, E., Van Montagu, M., Inzé, D., and Van Onckelen, H. (1998) Zeatin is Indispensable for the G2-M Transition in Tobacco BY-2 Cells, *FEBS Lett. 426,* 29–32.
89. Laureys, F., Smets, R., Lenjou, M., Van Bockstaele, D., Inzé, D., and Van Onckelen, H. (1999) A Low Content in Zeatin Type Cytokinins Is Not Restrictive for the Occurrence of G1/S Transition in Tobacco BY-2 Cells, *FEBS Lett. 460,* 123–128.
90. Quesney-Huneeus, V., Wiley, M.H., and Siperstein, M.D. (1980) Isopentenyladenine as a Mediator of Mevalonate-Regulated DNA Replication, *Proc. Natl. Acad. Sci. USA 77,* 5842–5846.
91. Faust, J.R., and Dice, J.F. (1991) Evidence for Isopentenyladenine Modification on a Cell Cycle-Regulated Protein, *J. Biol. Chem. 266,* 9961–9970.
92. Hemmerlin, A. (1997) Etude du rôle de molécules d'origine isoprénique (dérivées du mévalonate) dans la régulation du cycle cellulaire d'une suspension de cellules Nicotiana tabacum Bright Yellow 2 (TBY-2), Thèse Doctorale, Université Louis Pasteur, Strasbourg, France.
93. Crozier, A., Kamiya, Y., Bishop, G., and Yokota, T. (2000) Biosynthesis of Hormones and Elicitor Molecules, in *Biochemistry and Molecular Biology of Plants* (Buchanan, B., Gruissem, W., and Jones, R.L., eds.), American Society of Plant Biologists, Rockville, MD.
94. Miyazawa, Y., Nakajima, N., Abe, T., Sakai, A., Fujioka, S., Kawano, S., Kuroiwa, T., and Yoshida, S. (2003) Activation of Cell Proliferation by Brassinolide Application in Tobacco BY-2 Cells: Effects of Brassinolide on Cell Multiplication, Cell-Cycle-Related Gene Expression, and Organellar DNA Contents, *J. Exp. Bot. 54,* 2669–2678.
95. Roth, P.S., Bach, T.J., and Thompson, M.J. (1989) Brassinosteroids: Potent Inhibitors of Growth of Transformed Tobacco Callus Cultures, *Plant Sci. 59,* 63–70.
96. Randall, S.K., Marshall, M.S., and Crowell, D.N. (1993) Protein Isoprenylation in Suspension-Cultured Tobacco Cells, *Plant Cell 5,* 433–442.
97. Morehead, T.A., Biermann, B.J., Crowell, D.N., and Randall, S.K. (1995) Changes in Protein Isoprenylation During the Growth of Suspension-Cultured Tobacco Cells, *Plant Physiol. 109,* 277–284.
98. Hemmerlin, A., Hartmann, M.-A., and Bach, T.J. (1998) Regulatory Interactions Between Cytoplasmic Isoprenoid Biosynthesis, Cell Cycle Progression and Viability of Tobacco BY-2 Cells, in *Advances in Plant Lipid Research* (Sánchez J., Cerdá-Olmedo E., and Martínez-Force, E., eds.), pp. 429–432, Secretario de Public, Universitad de Sevilla.
99. Itoh, T., Kaibuchi, K., Masuda, T., Yamamoto, T., Matsuura, Y., Maeda, A., Shimizu, K., and Takai, Y. (1993) The Post-translational Processing of Ras p21 Is Critical for Its Stimulation of Mitogen-Activated Protein Kinase, *J. Biol. Chem. 268,* 3025–3028.
100. Bassa, B.V., Roh, D.D., Vaziri, N.D., Kirschenbaum, M.A., and Kamanna, V.S. (1999) Effect of Inhibition of Cholesterol Synthetic Pathway on the Activation of Ras and MAP Kinase in Mesanglial Cells, *Biochim. Biophys. Acta 1449,* 137–149.
101. Randall, S.K., and Crowell, D.N. (1999) Protein Isoprenylation in Plants, *Crit. Rev. Biochem. Mol. Biol. 34,* 325–338.
102. Rao, S., Porter, D.C., Chen, X., Herliczek, T., Lowe, M., and Keyomarsi, K. (1999) Lovastatin-Mediated G1 Arrest Is Through Inhibition of the Proteasome, Independent of Hydroxy-methyl-glutaryl CoA Reductase, *Proc. Natl. Acad. Sci. USA 96,* 7797–7802.
103. Verpoorte, R., and Memelink, J. (2002) Engineering Secondary Metabolite Production in Plants, *Curr. Opin. Biotechnol. 13,* 181–187.
104. Richter, C., Schweizer, M., Cossarizza, A., and Franceschi, C. (1996) Control of Apoptosis by the Cellular ATP Level, *FEBS Lett. 378,* 107–110.
105. Nah, J., Song, S.J., and Back, K. (2001) Partial Characterization of Farnesyl and Geranylgeranyl Diphosphatases Induced in Rice Seedlings by UV-C Irradiation, *Plant Cell Physiol. 42,* 864–867.
106. Laukens, K., Deckers, P., Esmans, E., Van Onckelen, H., and Witters, E. (2004) Construction of a Two-Dimensional Gel Electrophoresis Protein Database for the *Nicotiana tabacum* cv. Bright Yellow-2 Cell Suspension Culture, *Proteomics 4,* 720–727.

[Received July 8, 2004, and in final form and accepted October 8, 2004]

Disruption of Ergosterol Biosynthesis, Growth, and the Morphological Transition in *Candida albicans* by Sterol Methyltransferase Inhibitors Containing Sulfur at C-25 in the Sterol Side Chain

Ragu Kanagasabai, Wenxu Zhou, Jialin Liu, Thi Thuy Minh Nguyen, Phani Veeramachaneni, and W. David Nes*

Department of Chemistry and Biochemistry, Texas Tech University, Lubbock Texas 79409

ABSTRACT: The sterol substrate analog 25-thialanosterol and its corresponding sulfonium salt were evaluated for their ability to serve as antifungal agents and to inhibit sterol methyltransferase (SMT) activity in *Candida albicans*. Both compounds inhibited cell proliferation, were fungistatic, interrupted the yeast-like-form to germ-tube-form transition, and resulted in the accumulation of zymosterol and related Δ^{24}-sterols concurrent with a decrease in ergosterol, as was expected for the specific inhibition of SMT activity. Feedback on sterol synthesis was evidenced by elevated levels of cellular sterols in treated vs. control cultures. However, neither farnesol nor squalene accumulated in significant amounts in treated cultures, suggesting that carbon flux is channeled from the isoprenoid pathway to the sterol pathway with minor interruption or redirection until blockage at the *C*-methylation step. Activity assays using solubilized *C. albicans* SMT confirmed the inhibitors impair SMT action. Kinetic analysis indicated that 25-thialanosterol inhibited SMT with the properties of a time-dependent mechanism-based inactivator K_i of 5 μM and apparent k_{inact} of 0.013 min^{-1}, whereas the corresponding sulfonium salt was a reversible-type transition state analog exhibiting a K_i of 20 nM. The results are interpreted to imply changes in ergosterol homeostasis as influenced by SMT activity can control growth and the morphological transition in *C. albicans*, possibly affecting disease development.

Paper no. L9576 in *Lipids 39*, 737–746 (August 2004).

Candida albicans is a dimorphic fungus responsible for superficial mucosal infections in immunocompromised patients and topical infections in healthy individuals (1). Drugs used to treat infections resulting from candidiasis are directed at the production and processing of ergosterol, a 24-alkyl sterol synthesized by the fungus (2). Current therapy is largely limited to two classes of antifungal agents, both of which are nonsteroidal compounds: the polyene antibiotics, which target membrane sterols, and the ergosterol biosynthesis inhibitors, which target membrane enzymes that act on sterol catalysis. The polyenes, such as amphotericin B, are fungicidal by binding to ergosterol, resulting in the formation of channels that disrupt normal membrane proton gradients (3). The azole antifungal agents, such as ketoconazole, are fungistatic by inhibiting lanosterol 14α-demethylase, thereby interrupting carbon flux from lanosterol to ergosterol (4) (Fig. 1; conversion of **1** to **2**). The azoles can bind to the 14α-demethylase of the host cholesterol pathway, but they are mostly more selective for the fungal enzyme. The mechanism of action of drug effectiveness has been primarily associated with the inhibition of fungal growth. However, *C. albicans* has the ability to switch from a yeast (blastospore) morphology to a hyphal (filamentous) morphology mainly in response to environmental conditions (5); the switch from a yeast form to a hyphal form often correlates with pathogenicity under physiological conditions (6). Regulatory substrates derived from the isoprenoid pathway, i.e., farnesol and farnesoic acid, that are capable of inhibiting the cell-to-hyphal transition have been identified (7–9). Recent work indicates that subinhibitory concentrations of azole drugs, including ketoconazole, inhibit hyphal development and maintain the cells in the yeast morphology (10,11). In the presence of the azole antifungals, farnesol efflux into the fungal medium increases dramatically (10), suggesting a redirection of carbon flux from sterol production to sesquiterpene production.

Because the polyenes have negative side effects and resistance to the azoles has been reported (12), fungal-specific enzymes of the ergosterol pathway have been considered in the design and testing of new antifungals (4,13–15). The sterol methyltransferase (SMT), a class of *S*-adenosyl-L-methionine (AdoMet)-dependent methyltransferases, represents a particularly good enzyme (gene = *ERG*6) to test because SMT is not found in the cholesterol pathway of the human host and because the *C*-methylation step, required in the construction of the ergosterol side chain, is essential to the "sparking" function of ergosterol (Fig. 1; conversion of **4** to **5**) (16–18). The corresponding *ERG*6 gene is necessary to ergosterol biosynthesis and for normal membrane function (19,20); in *C. albicans* the *ERG*6 and other sterol genes (21) can be transcriptionally regulated following drug treatment to prompt resistance or susceptibility (22–24).

*To whom correspondence should be addressed.
E-mail: wdavid.nes@ttu.edu

Abbreviations: AdoMet, *S*-adenosyl-L-methionine; HEI, high-energy intermediate; SMT, sterol methyltransferase; TMS, tetramethylsilane.

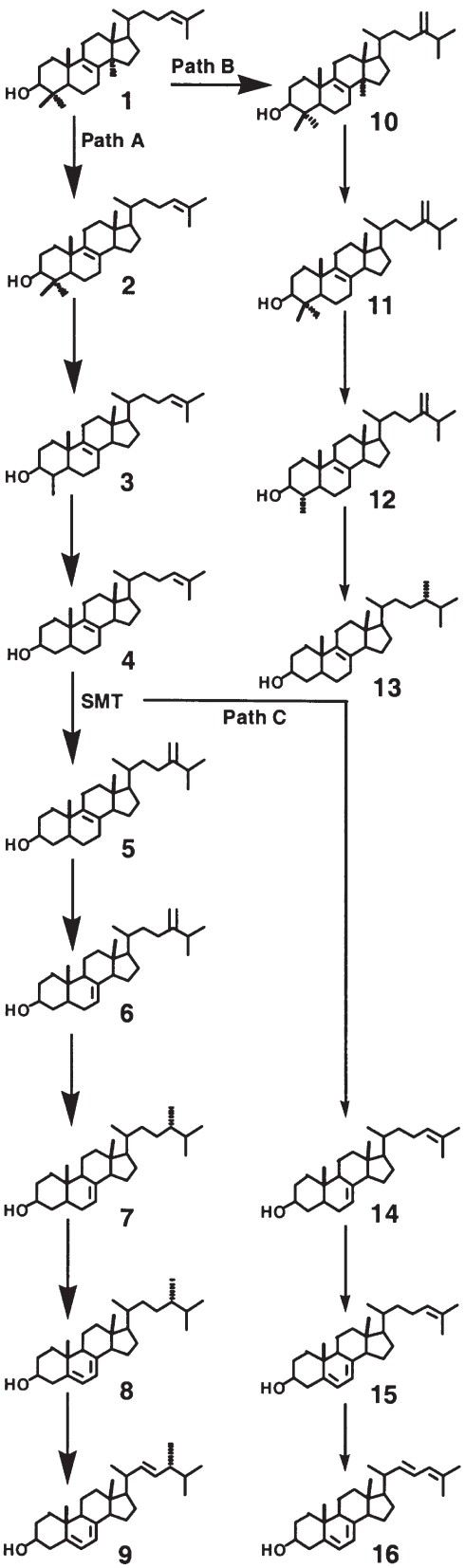

FIG. 1. Hypothetical pathway for ergosterol biosynthesis in *Candida albicans*. Alternate paths are illustrated that reveal redirection of carbon flux resulting from developmental regulation (path B) and blockade of the *C*-methylation step by 25-thialanosterol and its salt (path C).

Several groups, including ours, have shown that substrate analogs that are based on the *steric-electric plug* model of SMT action (25) and contain a nitrogen or sulfur substituent in the side chain inhibit SMT activity *in vitro*, decrease ergosterol production, and lead to the accumulation of ergosterol intermediates lacking a 24-methyl group in the side chain (13, 26–32). Because the ammonium structure is considered to be protonated under physiological conditions and the substrate mimics possess stereoelectronic properties very similar to the native ionic intermediate catalyzed by the SMT, they should behave as inhibitors. The efficacy of these compounds is, in part, related to the position of the SMT in the ergosterol pathway, i.e., whether the SMT enzyme is a first step or a late step in the post-lanosterol pathway, whether the compound is absorbed by the cells, and whether the heteroatom is located along the lateral side chain.

To assess further the value of rationally designed inhibitors of ergosterol biosynthesis as antifungal agents, we have begun to study the effects of sulfonium analogs assayed with *C. albicans*. Sulfur-based analogs have been studied as antifungals and antiprotozoan agents, but no clear rationale for the growth inhibition resulting from activity assay with these compounds has been reported. Thioether-bearing sterols can undergo *C*-methylation by SMT to give a charged sulfonium compound at the active site; therefore, these types of analogs were considered to mimic the nitrogen-containing compounds mechanistically (34). However, there are two possibilities for the mechanism of inhibition of sulfur-containing phytosterols on SMT action; they can act as either a mechanism-based inactivator or a high-energy-intermediate (HEI) analog (26,33). The nature of the fungal response to the different mechanisms of inhibition can possibly affect the physiological toxicity of the inhibitor. We report herein (i) a detailed analysis of the normal sterol composition of *C. albicans* at two stages of its life history (yeast cell and germ tube form), (ii) the synthesis of two new ergosterol biosynthesis inhibitors, (iii) the inhibition of growth and morphology transitions of *C. albicans* by 25-thialanosterol and 25-thialanosterol iodide, and (iv) the kinetic analysis of the test compounds *in vitro* with an SMT preparation. Thus, by employing a pair of sulfur analogs of the catalytic domain of the sterol substrate that differed in the electrostatic nature of the inhibitor function, we have uncovered new information about the enzymatic and physiological recognition of sulfur-containing ergosterol biosynthesis inhibitors.

MATERIALS AND METHODS

Organism and culture conditions. Candida albicans was obtained from American Type Culture Collection (ATCC 10231). A starter culture was prepared by inoculating 200 mL of medium with a loop of cells into a flask of YMPD medium containing 0.3% of yeast extract (Y), 0.3% of maltose (M), 0.5% of peptone (P), and 1% of dextrose (D) (wt/vol) at pH 7.0 and 30°C for 42 h. The inoculum culture of 20 mL (5×10^5 cells/mL) was added to 2.7-L Fernbach flasks containing

1 L each of YMPD medium and incubated with shaking (180 rpm) at 30°C for 48 h to reach a stationary phase of growth of 5×10^8 cells/mL. Growth arrested cells were harvested by centrifugation for 10 min at 10,000 × *g* and then stored at –20°C until used. Normally, 10 g fresh weight of cells was generated from 1 L of culture.

Separation of yeast and germ tube forms. Cells were transformed to the germ tube form by switching to an induction medium developed by Brayman and Wilks (35). Cell counting and germ tube measurements were determined using a hamocytometer set on an Olympus CH-2 microscope with magnification at 40×. Scanning electron micrographs were obtained on glutaraldehyde-fixed preparations at the Texas Tech University Medical School. The inoculum for germ tube production was established by culturing cells in a YPD medium containing 1% yeast extract, 2% peptone, and 2% glucose to growth arrest. About 10 mL of these cells were transferred to 7.5 mL Falcon tubes and cultured statically in YPD medium at 25°C for another 48 h. The Falcon tubes were centrifuged at room temperature for 15 min at 7,500 × *g*, and the resulting pellet was added to RPMI 1640 medium (Gibco BRL, Rockville, MD) and vortexed for 1 min to generate a stock solution of *ca.* 4.5×10^7 cells/mL. An aliquot of stock cells (0.9 mL) was resuspended in a conical flask containing 20 mL of prewarmed RPMI-1640 medium (or with inhibitor solution) to give 2×10^6 cells/mL. The cells were shaken at 100 rpm for 5 h at 37°C to generate hyphae. The percentage of germ tube formation, is derived from the ratio of germ tubes formed to the total number of cells times 100. In our control experiments, there was *ca.* 96% germ tube formation consistent with the report by Brayman and Wilks (35).

IC_{50} determination. Treated cultures containing the desired amount of test analog were grown in 50 mL medium in the same manner as the controls for 48 h. Inhibitors were dissolved in 100% ethanol (**17**) or 95% aqueous ethanol (**22**) and added to the culture medium (see Fig. 2); equal amounts of ethanol were added to all cultures in a given series of experiments. Curves of the concentration of inhibitor giving 50% inhibition relative to the growth of control provided the IC_{50}. To determine the relative potency of the inhibitor on ergosterol synthesis, cells treated at the IC_{50} value of inhibitor were harvested and the sterol composition analyzed by GC–MS.

Substrates and reagents. Sterols were isolated from nature or prepared synthetically and, in the case of the isoprenoids farnesol and squalene, purchased from Sigma (St. Louis, MO); farnesoic acid was from Echelon Biosciences (Salt Lake City, UT). [*methyl*-$^3H_3$]AdoMet was from PerkinElmer and diluted with nonradioactive AdoMet to 20 μCi/μmol for activity assay. Purity and identification of all the compounds studied were established by GC–MS and ^{1}H NMR (36–38). Other reagents were purchased from Fisher Scientific (Fairlawn, NJ) or Sigma unless indicated specifically.

Instrumentation. GLC was carried out on a Hewlett-Packard 5890 series II GC system with a 2 mm i.d. × 50 cm glass column (at 245°C) packed with Chromosorb W-HP coated with 3% SE-30 (Alltech Associates, Deefield, IL) and FID (300°C). Helium was used as the carrier gas. Spectra from GC–MS were recorded with a Hewlett-Packard 6890 GC interfaced to a 5973 mass selective detector at 70 eV. GC was achieved on a DB-5 capillary column (Agilent Technologies Inc., Palo Alto, CA) 0.25 mm i.d. × 30 m with film thickness of 0.25 μm. The chromatography was performed at a constant flow rate at 1.2 mL/min. The injection model was pulsed splitless at a pressure of 25.0 psi. For sterol analysis the oven temperature was programmed: initial temperature 170°C (1 min hold), then ramped from 170 to 280°C (20°C/min) and maintained at 280°C for the next 15 min. The operating conditions for the DB-5 were: initial temperature at 100°C for 3 min, then 20°/min to 280°C and hold for 13 min.

The temperatures for the GC to MS interface, MS ion source, and quadrapole were 280, 250, and 230°C, respectively. Helium at 8 psi was used as the carrier gas. In this system cholesterol elutes in 13 min, whereas farnesol, farnesoic acid, and squalene elute at 9.2, 10.2, and 15 min, respectively. TLC, to separate sterols based on the number of methyl group 5 substituted at C-4, was performed on Silica gel G plates and developed in benzene/ ether as described (39). Relevant reference specimens were available as part of the Nes steroid collection (36–39). HPLC chromatography was performed on an ISCO (Lincoln, Nebraska) HPLC system with a Selectosil C_{18} semipreparative column (Phenomenex, Palo Alto, CA) eluted with methanol at 4 mL/min at ambient temperature. Radioactivity measurements were obtained on a Beckman LS 6500 liquid scintillation counter with 5 mL of ScintiVerse BD cocktail (Fisher) and were automatically quench corrected. ^{1}H NMR spectroscopy was performed at 500 MHz at ambient temperature on a Varian Unity Inova 500, in $CDCl_3$, with tetramethylsilane (TMS) as internal standard.

Synthesis of inhibitors. The sulfonium compounds (25-thialanosterol, **17**, and 25-thionalanosterol-3-ol iodide **22**) were prepared by straightforward synthetic methods involving ozonolysis of the lanosterol side chain **1** and its reconstruction, introducing the sulfur atom at position 25 followed by methylation of the resulting sulfide, as shown in Figure 2. From 100 mg of starting material **1**, as the C3-acetate, was recovered 55 mg of **17**, as the free alcohol. The product was purified by HPLC eluted with 100% methanol. The characterization of **17** is as follows: GLC RRT_C (relative retention time of sterol compared with the retention time of cholesterol in GLC), 2.60; mass spectrum (*m/z*) (M^+ and other diagnostic ions in high mass region): 432, 417, 415; ^{1}H NMR (in ppm relative to TMS in $CDCl_3$): δ 0.811 (3H, *s*, H-19); 0.960 (3H, *s*, H-18); 3,13 (1H, *m*, H-3), 0.982 (3H, *s*, H-30), 0.874 (3H, *s*, H-32), 1.003 (3H, *s*, H-31), 2.102 (3H, *s*, H-26), 3.25 (2H, *m*, H-24). ^{13}C NMR (75 MHz, in $CDCl_3$): δ (terminal side chain signals) 34.82 (C-23); 25.49 (C-24); 24.25 (C-26).

Conversion of the sulfide **17** (5 mg) to the crystalline salt **22** generated crystals (*ca.* 40% yield) that were collected by filtration: ^{1}H NMR (in ppm relative to TMS at 500 MHz, in MeOH-d_4): δ 3.13 (*m*, 1H, H-3), 0.762 (3H, *s*, H-18), 0.802 (3H, *s*, H-19), 0.918 (3H, *s*, H-30), 0.981 (3H, *s*, H-32), 1.013 (3H, *s*, H-31), 2.908 (3H, *s*, H-26), 2.912 (3H, *s*, H-27), 3.25

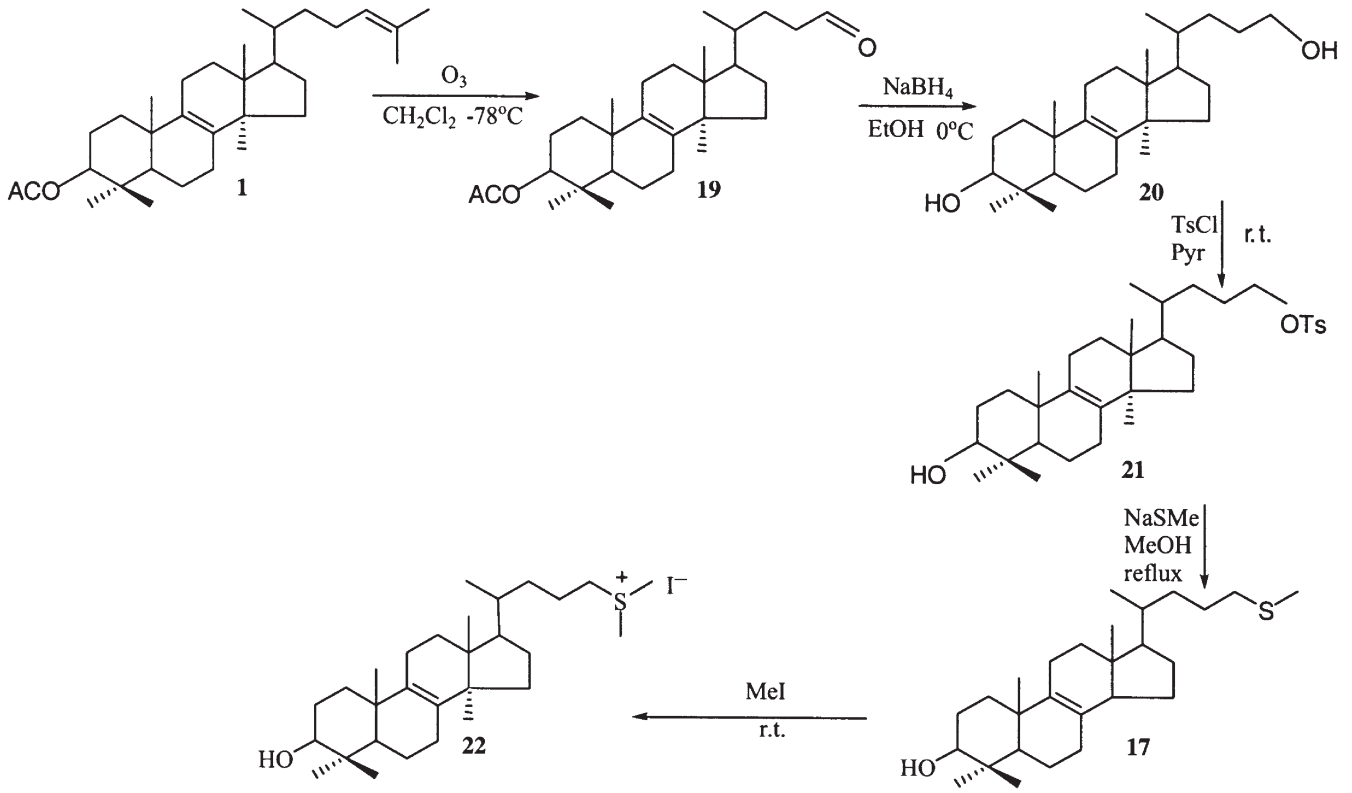

FIG. 2. Outline for the synthesis of sulfur-based drugs. Pyr, pyridine; TsCl, tosyl chloride; r.t., room temperature.

(2H, *m*, H-24). ^{13}C NMR: 135.583 (C-8); 136.104 (C-9); 79.638 (C-3): 22.0582 (C-26), 22.102 (C-27); 36.031 (C-24). m.p.: 128–129°C.

Sterol and isoprenoid analysis. Cells (10 g fr. wt) of normal and treated *C. albicans* cells were saponified with 10% methanolic KOH (300 mL) at reflux for 30 min. The reaction mixture was cooled to room temperature and diluted with 300 mL of water. Total sterols were extracted from the reaction mixture with *n*-hexane (3 × 600 mL). The hexane layers were pooled, and the solvent was removed under reduced pressure. The resulting nonsaponifiable lipid fraction was dissolved in 10 mL of acetone and an aliquot subjected to GC–MS analysis or, alternatively, purified further by TLC and HPLC to generate a set of 13 mg sterols. Total sterols were quantified with cholesterol as the external standard. Isoprenoids were extracted from the cells or spent medium with ethyl acetate. Sterols and isoprenoids were identified by comparing their chromatographic and spectral data with those of authentic standards.

Assays and inhibitor studies. The procedures for enzyme preparation and activity assay were adapted from that of Venkatramesh *et al.* (36) for *Saccharomyces cerevisiae* SMT. Briefly, frozen *C. albicans* cells (50 g) were thawed, suspended in 4 vol homogenate buffer A (50 mM TrisHCl, 2 mM β-mercaptoethanol, 2 mM $MgCl_2$, and 10% sucrose, pH 7.5). The cells were subsequently broken by five passes through a French press (SIM Aminco) at a pressure of 20,000 psi. Cell debris was removed by centrifugation (Beckman) at 10,000 × *g* for 30 min, and the supernatant was centrifuged at 100,000 × *g* for 1.30 h. The resulting microsomal pellets were suspended in ice-chilled buffer B (50 mM TrisHCl, 2 mM β-mercaptoethanol, 2 mM $MgCl_2$, and 20% glycerol pH 7.5; 3 mL/microsome) using a Wheaton glass homogenizer. Solubilization of SMT was achieved by adding detergent (emulphogen: polyoxyethylene 10 tridecylether) to the microsomal suspension to the final concentration of 0.4% and incubated on ice for 30 min with gentle stirring. Solubilized protein from the supernatant after the mixture was centrifuged at 100,000 × *g* for 1 h generated a concentration of 1 to 2 mg/mL. Total protein was determined by the Bradford dye-binding procedure (40) using the Bio-Rad laboratories (Richmond, CA) protein assay kit with BSA as the standard.

All assays were conducted under steady-state conditions in the relevant buffer system at pH 7.5 in the presence of saturating substrates. A general assay for the SMT preparation was performed in 600 µL of total volume, 1 to 2 mg total protein in buffer B (pH 7.5), 100 µM sterol, 100 µM [*methyl*-$^3H_3$] AdoMet (20 µCi/mmol) and Tween 80 (0.1% wt/vol). Samples were incubated at 30°C for 45 min at pH 7.5 with constant agitation. The reactions were terminated by adding 1 mL of 10% methanolic KOH, and total sterols were extracted three times with 2.5 mL each of *n*-hexane. The resulting organic layer was transferred to 10-mL scintillation vials and dried under a stream of nitrogen. The residue so prepared was counted by liquid scintillation spectrometry (in 5 mL of Scintiverse cocktail [Fisher]; ^3H efficiency 58%) on a Beckman

LS 6500 liquid scintillation counter. Buffer controls with labeled AdoMet were included with each set of assays, and nonenzymatic activity was negligible. For determination of kinetic constants (K_m, V_{max}, or K_i) for zymosterol and the two analogs, the zymosterol concentration was varied from 2.5 to 100 μM, and the inhibitor concentrations ranged from 1 to 10 μM for **17** and from 10 to 100 nM for **22**. Each set of experiments used the same fixed concentration of substrates, as relevant, and the same incubation conditions as described for the standard assay. All assays were conducted in triplicate, with appropriate boiled controls.

In studies to be reported elsewhere, we have partially purified the native SMT from *C. albicans* (Kanagasabai, R., and Nes, W.D., unpublished data) using protocols established for the purification of the wild-type SMT from *S. cerevisiae* (41). Product distribution and identity were verified by GC–MS and radio-HPLC; zymosterol **4** was converted to fecosterol **5** (36). The apparent kinetic constants for sterol and AdoMet were found to be *ca.* 30 μM each, and the substrate specificity of the *C. albicans* enzyme was very similar to the *S. cerevisiae* SMT, as would be expected based on similar primary sequences of their corresponding cDNA (21).

Data analysis. The initial velocity data were analyzed using a Sigmaplot 2001 Plus Sigma enzyme kinetics software package (SPSS Inc., Chicago, IL). Kinetic constants, determined by Lineweaver–Burk plotting, had SE of ±5% and R^2 values of 0.95 to 0.98. Steady-state inhibition patterns were determined with the software package in analogous fashion to the initial velocity data analysis as described elsewhere (42).

Mechanism-based inactivation experiments. Two experiments were performed. (i) Substrate protection; co-incubation of 50 μM of **17** and 100 mM of AdoMet with 100 or 300 μM zymosterol in the standard assay afforded protection against inactivation, conserving 46 and 73% of *C*-methylation activity after the incubation period, respectively. (ii) Time-dependent inactivation of SMT; a typical preincubation contained 1 mg/mL solubilized microsomal protein in buffer B. The inactivation reaction was initiated by the addition of AdoMet to give a final concentration of 100 μM, and the reaction was allowed to proceed at 30°C for up to 25 min. At the indicated times, 0 (control), 5, 25, and 50 μM of 25-thialanosterol-treated enzyme was put into a precooled (dry ice in ethanol) test tube to prevent catalysis. The samples were thawed on ice, diluted 20-fold in ice-cold buffer, and the amount of SMT activity remaining was determined as described above.

RESULTS

Yeast growth and sterol production. As a foundation for the antifungal susceptibility testing with sulfur-based drugs fed to *C. albicans*, a set of initial experiments was performed to examine the growth response, morphology, yeast-cell to germ-tube (adolescent forms that can mature into hyphae) transition, and sterol composition of the control. From an inoculum size of *ca.* 5×10^6 cells/mL, a stationary phase cell population of 5×10^8 cells/mL was observed at about 48 h of growth on YMPD medium (Fig. 3). By changing the culture medium to YPD and using inoculum from the growth-arrested cells, the hyphal form was induced (Fig. 3). In comparison with the morphology of *C. albicans* reported by others (8,22,43), our culture conditions generated cell forms and germ tube forms that appeared normal.

Although the sterol composition of *C. albicans* has been studied before (44–46), a more detailed analysis of the amounts and identities of minor sterols has not been carried out. The wild-type cells contained a sterol composition typical of ascomycetous fungi (47), with many of the same sterols reported by other investigators for *C. albicans*. The major sterol of the yeast cells and germ tubes (data not shown) was ergosterol, *ca.* 70 and 97% of the total sterols, respectively (Table 1). Cultures at growth arrest contained a set of 24-methyl(ene) sterols (**10–13**) at trace levels, and these sterols were in the germ tube form at trace levels as well (data not shown). Compounds **10–13** were not apparent in actively growing cells (within the limits of GC detection); they were found to accumulate at growth arrest (data not shown). The trace compounds can be arranged as a minor pathway (Fig. 1; path C). However, these compounds do not appear to contribute significantly to ergosterol production, and lanosterol will not bind productively to the SMT under the standard assay conditions (Nes, W.D., Kanagasabai, R., and Nguyen, T.T.M., unpublished data). We speculate that the onset of path C is developmentally delayed and the pathway interrupted at the stage of **13** formation. In addition, the *C*-methylated sterols produced hypothetically in path C can result from an increase in SMT at growth arrest or modulation of SMT activity by as yet unknown effectors that promote 4,4-dimethyl sterols to serve as substrates of the SMT.

Inhibition of growth and sterol analysis of C. albicans. In the second set of experiments, the cell response to sulfur-based drugs was tested. A dose-dependent inhibition of growth was observed between 5 and 50 μM of **17** (Fig. 4) and 0.1 and 2.0 μM of **22** (data not shown) with 100% growth

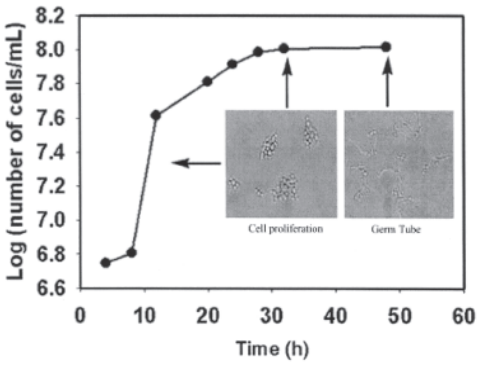

FIG. 3. Typical growth curve of wild-type *Candida albicans* cells. Insets are micrographs of yeast cells and germ tubes recorded on an Nikon-Labophot Fluorescent Microscope set at a magnification of 40×.

TABLE 1
Sterol Composition of Control and Treated *Candida albicans*[a]

Sterol (structure)		Sterol composition of cells (as % total sterol)		
		Control	**17**	**22**
Lanosterol	(**1**)	1	6	1
4,4-Dimethylcholesta-8,24-dienol	(**2**)	2	ND	ND
4-Methylcholesta-8,24-dienol	(**3**)	1	ND	2
Zymosterol	(**4**)	1	43	35
Fecosterol	(**5**)	2	4	2
Cholesta-7,24(28)-dienol	(**6**)	16	3	ND
Ergosta-7-enol	(**7**)	2	ND	1
Ergosta-5,7-dienol	(**8**)	3	3	ND
Ergosterol	(**9**)	69	25	Tr
Eburicol	(**10**)	Tr	Tr	ND
4,4-Dimethylergosta-8,24(28)-dienol	(**11**)	Tr	ND	ND
4-Methylergost-8,24(28)-dienol	(**12**)	1	1	ND
Ergost-8-enol	(**13**)	1	2	ND
Cholesta-7,24-dienol	(**14**)	1	9	14
Cholest-5,7,24-trienol	(**15**)	ND	2	42
Cholesta-5,7,22,24-trienol	(**16**)	ND	2	3

[a]Sterol composition of wild-type cells (yeast form) at stationary phase growth and treated cells at IC_{50}. ND, not detected; Tr, trace (<0.05%).

arrest at 100 μM of **17** and at 4 μM of **22**. The salt form of the drug **22** was more potent than the neutral form **17** at inhibiting growth and the cell to germ-tube transition, with IC_{50} values of 25 and 0.75 μM, respectively, for growth and 10 and 0.35 μM for the cell to germ-tube transition, respectively. Examination of the cell morphology of control and treated cells by scanning electron microscopy revealed that the control cells appeared elliptical with normal budding, whereas the cells treated with **17** and **22** possessed aberrant morphology. Treated cells appeared elongated with immature hyphae and some vacuolated cells with no distinct budding (Fig. 5).

To determine the basis for growth inhibition and explore which steps in the sterol biosynthesis pathway were blocked, we used sub-inhibitory concentrations of the drugs. At the IC_{50} of the drug, a decline in ergosterol production (Table 1) with a corresponding increase in total sterols was observed for both treatments (Table 2). Sterols lacking the 24-methyl group accumulated in treated cells (but not in the medium), including zymosterol after treatment with **17** and cholesta-5,7,24-trienol after treatment with **22** (Fig. 1; path C). In neither treatment did lanosterol or other 4-methyl sterols accumulate significantly.

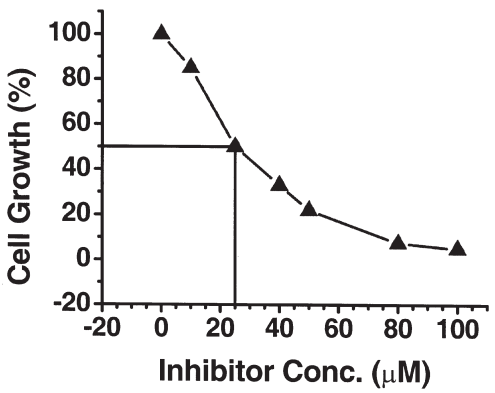

FIG. 4. Determination of the IC_{50} value for 25-thialanosterol.

The isoprenoid composition of the medium of cultures used to generate germ tubes contained insignificant amounts of autoregulatory substances, e.g., farnesol and farnesoic acid, which prevent the morphogenetic transition. In contrast to the accumulation of sterols after treatment of cells with the sulfur-based drugs, the isoprenoid compostion was not significantly affected by incubation with the drugs: (i) The control contained farnesol, 0.59 mg/g dry wt (0.5 mg/L of medium), farnesoic acid, 0.13 mg/g dry wt, and squalene, <0.001 mg/g dry wt; (ii) cells treated with **17** contained farnesol, 0.88 mg/g dry wt (0.3 mg/L of medium), farnesoic acid, 0.06 mg/g dry wt, squalene, <0.002 mg/g dry wt; (iii) the isoprenoid composition of the **22**-treated cells was similar to the **17**-treated cells (data not shown). These results showed that the two sulfur-based compounds inhibit the ergosterol pathway in *C. albicans* at the *C*-methylation step, resulting in impaired ergosterol synthesis, cell proliferation, and the cell-to-hyphae transition.

Enzyme inhibition studies. To examine the mode of action of the pair of sulfur-based compounds **17** and **22**, we studied *in vitro* inhibition kinetics using a cell-free preparation containing solubilized SMT. Plots of methyl product formation vs. sulfonium analog concentration in the 0.25 to 100 μM range afforded typical hyperbolic curves, and the double-reciprocal (Lineweaver–Burk) plots of each analog were linear from which the K_i values and patterns of inhibitions were determined. Analog **22**, in which the sulfur group at C-25 was ionized, generated a noncompetitive inhibition pattern and an apparent K_i value of 20 nM (B; Fig. 6), suggesting that the analog and sterol bind to different subsites in the active center. Alternatively, analog **17**, in which the carbon group at C-25 was substituted for sulfur, generated a competitive inhibition pattern and an apparent K_i value of 5 μM (A; Fig. 6), suggesting the inhibitor and sterol bind to the same subsite in the active center. Because competitive-type inhibition is consistent with a sulfur-based analog acting as a mechanism-based inactivator (26), additional work was performed with 25-thialanosterol.

Time-dependent inactivation of SMT by 25-thialanosterol. As anticipated for an active-site-directed process, incubation of increasing concentrations of **17** with solubilized SMT resulted in pseudo-first-order time-dependent inactivation of the SMT (Fig. 7). The rate of inactivation by zymosterol was saturable, with a maximum rate of inactivation of k_{inact} of 0.013 ± 0.005 min^{-1}, and a K_i of 5.5 ± 0.2 μM. These values compare very favorably with the steady-state kinetic parameters for the normal substrate zymosterol of $k_{cat} = 0.036$ min^{-1} and $K_m = 25$ μM (Kanagasabai, R., and Nes, W.D., unpublished data). Dialysis of the inactivated enzyme failed to restore SMT activity. However, similar treatment of the enzyme

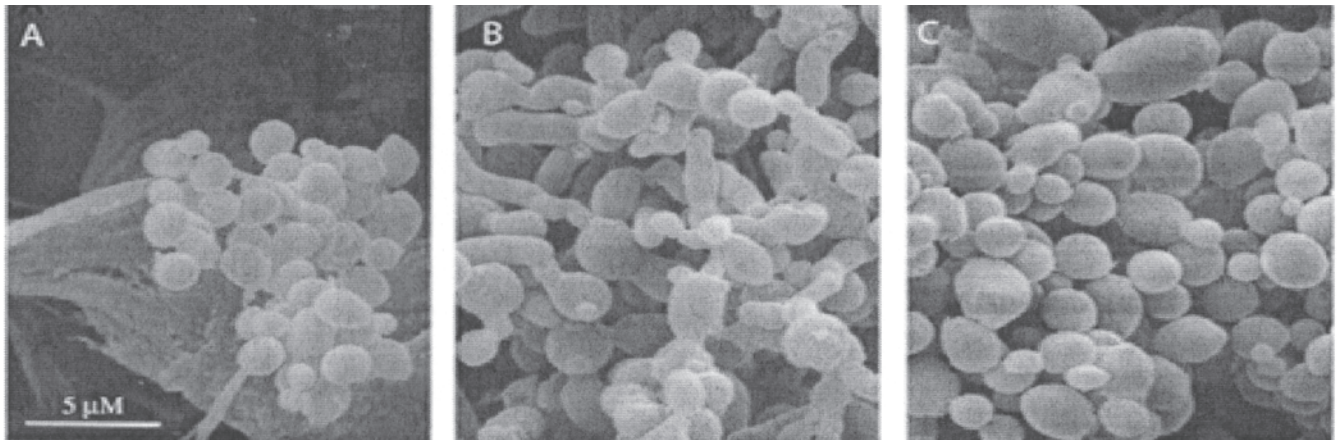

FIG. 5. Scanning electron micrographs (obtained on a Scanning Electron Microscopic , Power Tome XL-RMC Product Boeckeler) taken at 2500× of 48-h cultures of *Candida albicans*. (A) Control cells; (B) cells treated with the IC_{50} concentration of 25-thialanosterol; (C) cells treated with the IC_{50} concentration of 25-thialanosterol iodide.

with **22** resulted in a restoration of 80% of the SMT activity. These results and the observation reported in the Materials and Methods section that the SMT could be partially protected against inactivation by co-incubation with zymosterol is consistent with **17** acting as a mechanism-based inactivator of SMT activity. Efforts to trap the HEI formed by 25-thialanosterol catalysis were not successful, and low abundance of SMT in the enzyme preparation prevented further analysis of the putative SMT-$[^3H_3]CH_3$ complex resulting from assay with 25-thialanosterol.

DISCUSSION

The inhibition of ergosterol biosynthesis is a proven therapeutic target. Thus, we have considered the design and testing of novel antifungal drugs tailored for the unique aspects of fungal metabolism related to the SMT enzyme synthesized by opportunistic pathogens. As we discovered in this study, *C. albicans* can recognize sulfur-based drugs with varied effects on 24-methyl sterol biosynthesis/24-desalkyl sterol accumulation required before inhibition of cell proliferation or the cell to germ-tube (hyphae) transition. The target site in the ergosterol pathway blocked by the sulfur-based analogs was associated with the *C*-methylation step catalyzed by SMT. The mechanism of *C*-methylation in yeast (48) has been shown to involve an HEI; therefore, molecules that resemble the intermediate in the sequence can be inhibitors of the reaction, as shown in Figure 8. Conceivably, both inhibitors **17** and **22** can be charged in the active site and inhibit SMT action through a similar mechanism; therefore, we would expect a similar set of inhibition kinetic patterns. However, a dramatic difference in the kinetic patterns of the two compounds was observed, and only **17** exhibited a time-dependent inhibition against the SMT. The high specificity of the inhibition was related to the positive charge on the analog, which provided structural similarity to the predicted ionic intermediate and permitted the sterol side chain of **22** to bind the active center.

The fungus at two developmental stages was susceptible to the action of the sulfur-based drugs with **22**, compared with **17**, the more potent drug. The potencies of **17** and **22** are relatively similar to those of ketaconazole and amphotericin B tested for antifungal activity elsewhere (27). The fungus responded to the SMT inhibitors differently. For example, in the case of treatment with **22**, no ergosterol was detected in the cells, but there was an increase in total sterols. In the case of treatment with **17**, minor amounts of ergosterol that were present in a background of increased total sterol did not protect the fungus from the fungicidal behavior of the drug. Thus, a threshold level of ergosterol may be necessary to trigger the morphological transition in *C. albicans*. Interestingly, the up-regulation of sterol synthesis following treatment with **17** and **22** has been inferred by others studying gene expression patterns in the sterol pathway following treatment with

TABLE 2
Antifungal Activity, Sterol Analysis, and Inhibition of Sterol Methyl Transferase by Sulfur-Based Substrate Analogs[a]

Treatment	Cell count IC_{50}	Hyphal growth IC_{50}	Sterol cotent (fg/cell)	24-Methylsterol to 24-desmethyl sterol ratio	K_i	Pattern	k_{inact}
Control	ND	ND	32	4:1	ND	ND	ND
25-Thialanosterol **17**	25 µM	13 µM	100	1:1.5	5 µM	C	0.013 min^{-1}
25-Thialanosterol iodide **22**	0.75 µM	0.35 µM	118	1:97	0.02 µM	NC	ND

[a]ND, not determined; kinetic patterns are competitive (C) or noncompetitive (NC). For experimental details of growth and activity assays refer to the Materials and Methods section of the text.

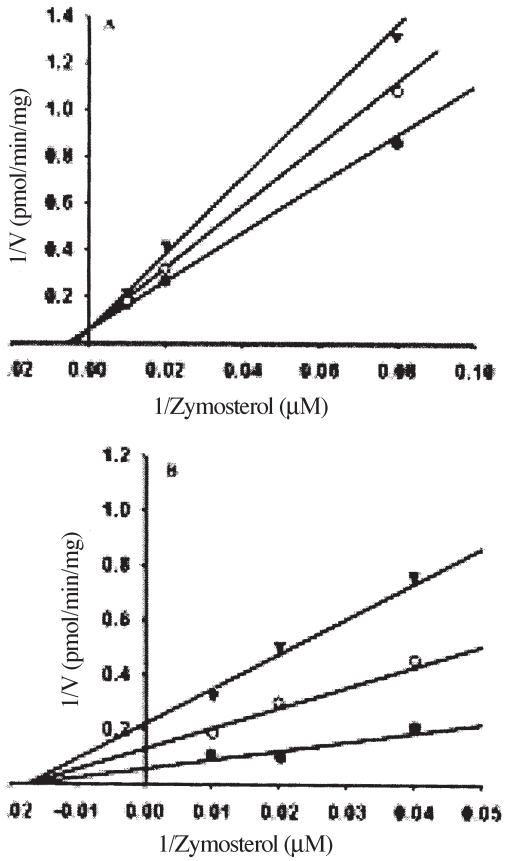

FIG. 6. Kinetic patterns for the *Candida albicans* sterol methyltransferase (SMT). Assays performed with 25-thialanosterol **17** (panel A) or 24(*R,S*)methyl-25-thionalanost-3β-ol iodide **22** (panel B) as inhibitors. *S*-Adenosyl-L-methionine (AdoMet) was added at a fixed concentration of 100 μM, and zymosterol was varied at several fixed concentrations at 12.5, 25, 50, and 100 μM. In the double reciprocal plots, inhibitor **17** concentrations were added at 25 (▼), 50 (○), and 75 μM (●), and inhibitor **22** concentrations were added at 25 (▼), 50 nM (○), and 75 nM (●). Results are the average of measurements from three separate experiments with variation among the trials at <10%.

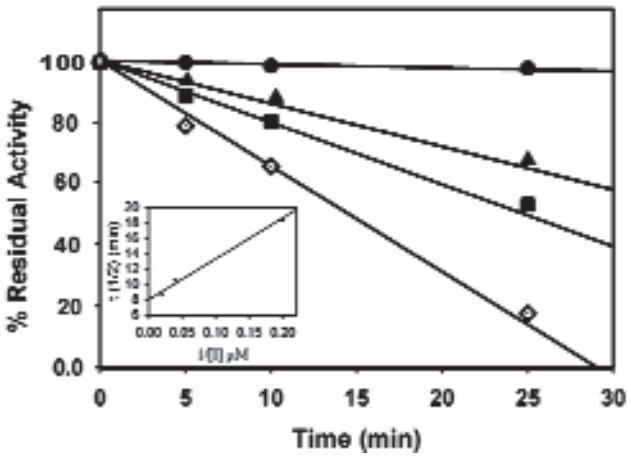

FIG. 7. Inactivation of *C. albicans* SMT with mechanism-based inactivator **17**. Semilog plots of residual activity vs. time at 0 (●), 5 (▲), 25 (■), and 50 μM (◆) concentrations of inhibitor (I). The times indicated are 0, 5, 10, and 25 min. (Inset) Plot of enzyme half life ($t_{1/2}$) for inactivation vs. 1/[I]. For abbreviations see Figure 6.

ergosterol biosynthesis inhibitors (23,24). The increase in carbon flux from the isoprenoid pathway to the ergosterol pathway was not accompanied by an efflux of signal molecules (farnesol or farnesoic acid), which might induce the morphological transition in *C. albicans* (10). Although a more precise formulation of sulfur-based analog inhibition of growth and sterol biosynthesis must await a means of assessing isoprenoid and ergosterol functions other than drugs targeted to pathway enzymes, the present studies, in conjunction with previous work (49), do give a preliminary indication of impaired ergosterol homeostasis disrupting growth and germ-tube formation, thereby affecting hyphal development.

The catalytic response of the *C. albicans* SMT to 25-thialanosterol is readily explained by the relative similarity of **17** to **5** and by the nature of the charge on the sulfur atom at binding. Thus, depending on whether the sulfur atom in the sterol side chain is in the neutral or charged state, the SMT can be rendered inactive through an irreversible or reversible mode of inhibitor binding, respectively. The irreversible binding mechanism is readily explained by a directional process in which *C*-methylation of 25-thialanosterol by SMT generates the intermediate **18** (Fig. 8), which is charged and activated to serve as the methyl donor. The latter compound can, when the enzyme assumes an appropriate conformation, react irreversibly with an active site base or a nearby nucleophilic amino acid side chain to inactivate catalysis covalently through enzyme methylation. Alternatively, when 25-thialanosterol is prepared as a salt and therefore "charged" as a consequence of methylation (**22**), the compound can bind to SMT in a manner that allows it to act as an HEI analog and block catalysis reversibly. The different molecular parameters of the inhibition ultimately generate the same end response to impair SMT action under physiological conditions. In addition to the mechanistic implications of this work for the development of antifungal agents that are fungal-specific, the SMT-catalyzed transformations of sulfur-based analogs are also relevant to providing a route to active site labeling complementary to the previously described use of 26,27-dehydrozymosterol to affinity-label the yeast SMT active site (50).

ACKNOWLEDGMENTS

This work was supported by grants from the National Institutes of Health (GM63477) and Welch Foundation (D-1276) to W.D.N.

REFERENCES

1. Calderone, R.A. (2002) Candida and *Candidiasis*, ASM Press, Washington, DC, pp. 10–15.
2. De Backer, M.D., Luyten, W.H.M.C., and Vanden Bossche, H.F. (2002) Antifungal Drug Discovery: Old Drugs, New Tools, in *Pathogen Genomics; Impact on Human Health* (Shaw, K.J., ed.), pp. 167–196, Humana Press, Totowa, NJ.

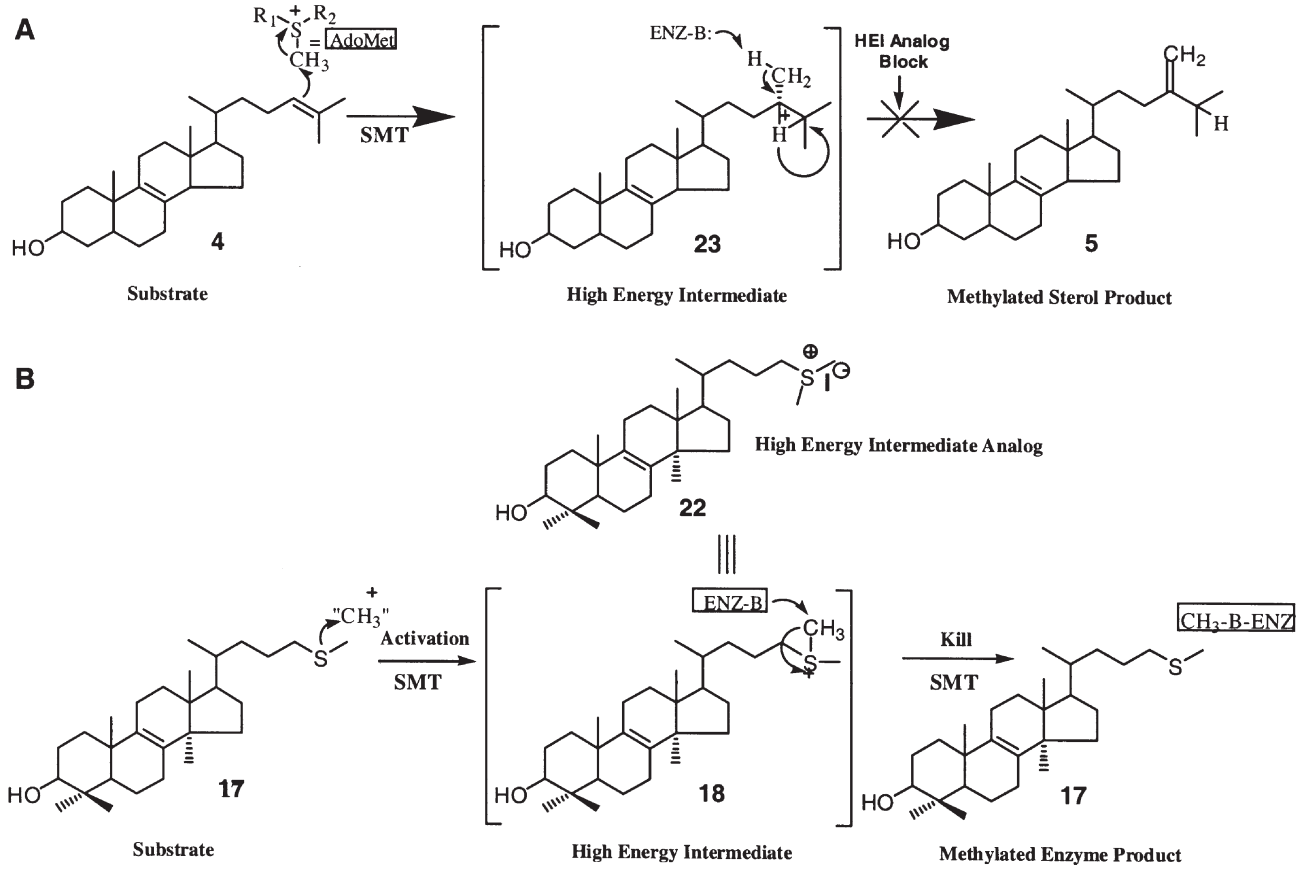

FIG. 8. Proposed mechanisms for the *C*-methylation of sterol substrate. Panel A illustrates catalysis of zymosterol by the SMT, and Panel B illustrates catalysis of 24-thialanosterol by the SMT. HEI, high-energy intermediate; ENZ:B, enzyme:base; for other abbreviations see Figure 6.

3. Ellis, D. (2002) Amphotericin B: Spectrum and Resistance, *J. Antimicrob. Chemother. 49*, 7–10.
4. Georgopapadakou, N.K., and Walsh, T.J. (1996) Antifungal Agents: Chemotherapeutic Targets and Immunologic Strategies, *Antimicrob. Agents Chemother. 40*, 279–291.
5. Brown, A.J., and Gow, N.A. (1999) Regulatory Networks Controlling *Candida albicans* morphogenesis,*Trends Microbiol. 7*, 333–338.
6. Lo, H.J., Kohler, J.R., DiDomenico, B., Loebenberg, D., Cacciapuoti, A., and Fink, G.R. (1997). Nonfilamentous *C. albicans* Mutants Are Avirulent, *Cell 90*, 939–949.
7. Hornby, J.M., Jensen, E.C., Lisec, A.D., Tasto, J.J., Jahnuke, B., Shoemaker, P., Dussault, P., and Nickerson, K.W. (2001) Quorum-Sensing in the Dimorphic Fungus *Candida albicans* Is Mediated by Farnesol, *Appl. Environ. Microbiol. 67*, 2982–2992.
8. Oh, K., Miyazawa, H., Naito, T., and Matsuoka, H. (2001) Purification and Characterization of an Autoregulatory Substance Capable of Regulating the Morphological Transition in *Candida albicans, Proc. Natl. Acad. Sci. USA 98*, 4664–4668.
9. Ramage, G., Saville, S.P., Wickes, B.L., and Lopez-Ribot, J.L. (2002) Inhibition of *Candida albicans* Biofilm Formation by Farnesol, a Quorum-Sensing Molecule, *Appl. Environ. Microbiol. 68*, 5459–5463.
10. Hornby, J.M., and Nickerson, K.W. (2004) Enhanced Production of Farnesol by *Candida albicans* treated with Four Azoles, *Antimicrob. Agents Chemother. 48*, 2305–2307.
11. Ha, K.C., and White, T.C. (1999) Effects of Azole Antifungal Drugs on the Transition from Yeast Cells to Hyphae in Susceptible and Resistant Isolates of the Pathogenic Yeast *Candida albicans, Antimicrob. Agents Chemother. 43*, 763–768.
12. Vanden Bossche, H. (1997) Mechanisms of Antifungal Resistance, *Rev. Iberoam. Micol. 14*, 44–49.
13. Boyle, F.T. (1990) Drug Discovery: A Chemist's Approach, in *Chemotherapy of Fungal Infections* (Ryley, J.F., ed.), pp. 3–30, Springer, Berlin.
14. Park, K., Kang, K., Kim, K., Jeong, P., Kim, J., Adams, D.J., Kim, J., and Paik, Y. (2001) HWY-289, A Novel Semi-synthetic Protoberberine Derivative with Multiple Target Sites in *Candida albicans, J. Antimicrob. Chemother. 47*, 513–519.
15. Guo, D., Mangla, A.T., Zhou, W., Lopez, M., Jia, Z., Nichols, S.D., and Nes, W.D. (1997) Antifungal Sterol Biosynthesis Inhibitors, *Subcell. Biochem. 28*, 89–116.
16. Rodriquez, R.J., Low, C., Bottema, C.D.K., and Parks, L.W. (1985) Multiple Functions for Sterols in *Saccharomyces cerevisiae*, *Biochim. Biophys. Acta 837*, 336–343.
17. Bloch, K.E. (1988) Sterol Structure and Function, *J. Am. Oil Chem. Soc. 65*, 1763–1766.
18. Pinto, W.J., and Nes, W.D. (1983) Stereochemical Specificity for Sterols in *Saccharomyces cerevisiae*, *J. Biol. Chem. 258*, 4472–4476.
19. Palermo, L.M., Leak, F.W., Tove, S., and Parks, L.W. (1997) Assessment of the Essentiality of *ERG*6 Genes Late in Ergosterol Biosynthesis in *Saccharomyces cerevisiae*, *Curr. Genetics 32*, 93–99.
20. Gaber, R.F., Copple, D.M., Kennedy, B.K., Vidal, M., and Bard, M. (1989) The Yeast Gene *ERG*6 Is Required for Normal Membrane Function but Is Not Essential for Biosynthesis of the Cell-Cycle-Sparking Sterol, *Mol. Cell. Biol. 9*, 3447–3456.
21. Jensen-Pergakes, K.L., Kennedy, M.A., Lees, N.D., Barbuch, R. ,

Koegel, C., and Bard, M. (1998) Sequencing, Disruption and Characterization of the *Candida albicans* Sterol Methyltransferase (*ERG*6) Gene: Drug Susceptibility, *Antimicrob. Agents Chemother. 42*, 1160–1167.
22. Young, J.Y., Hull, C.M., and Heitman, J. (2003) Disruption of Ergosterol Biosyntesis Confers Resistance to Amphotericin B in *Candida lusitaniae*, *Antimicrob. Agents Chemother. 47*, 2717–2724.
23. Henry, K.W., Nickels, J.T., and Edlind, T.D. (2000) Upregulation of *ERG*6 Genes in *Candida* Species by Azoles and Other Biosynthesis Inhibitors, *Antimicrob. Agents Chemother. 44*, 2693–2700.
24. Agarwal, A.K., Rogers, P.D., Baerson, S.R., Jacob, M.R., Barker, K.S., Cleary, J.D., Walker, L.A., Nagle, D.G., and Clark, A.M. (2003) Genome-wide Expression Profiling of the Response to Polyene, Pyrimidine, Azole and Echinocandin Antifungal Agents in *Saccharomyces cerevisiae*, *J. Biol. Chem. 278*, 34998–35015.
25. Nes, W.D. (2000) Sterol Methyltransferase: Enzymology and Inhibition, *Biochim. Biophys. Acta. 1529*, 63–88.
26. Ator, M.A., Schmidt, S.J., Adams, J.L., and Dolle, R.E. (1989) Mechanism and Inhibition of Δ^{24}-Sterol Methyltransferase from *Candida albicans* and *Candida tropicalis*, *Biochemistry 28*, 9633–9640.
27. Ator, M.A., Schmidt, S.J., Adams, J.L., Dolle, R.E., Kruse, L.I., Frey, C.L., and Barone, J.M. (1992) Synthesis, Specificity, and Antifungal Activity of Inhibitors of the *Candida albicans* Δ24-Sterol Methyltransferase, *J. Med. Chem. 35*, 100–106.
28. Oehlschlager, A.C., Angus, R.H., Pierce, A.M., Pierce, H.D., and Srinivasan, R. (1984) Azasterol Inhibition of Δ24-Sterol Methyltransferase in *Saccharomyces cerevisiae*, *Biochemistry 23*, 3582–3589.
29. Acuna-Johnson, A.P., Oehlschlager, A.C., Pierce, A.M., Pierce, H.D., Jr., and Czyzewska, E.K. (1997) Stereochemistry of Yeast Δ24-Sterol Methyltransferase, *Bioorg. Med. Chem. 5*, 821–832.
30. Nes, W.D., Guo, D., and Zhou, W. (1997) Substrate-Based Inhibitors of (*S*)-Adenosyl-L-methionine: $\Delta^{24(25)}$-to $\Delta^{24(28)}$-Sterol Methyltransferase from *Saccharomyces cerevisiae*, *Arch. Biochem. Biophys. 342*, 68–81.
31. Nes, W.D., Xu, S., and Parish, E.J. (1989) Metabolism of 24(*R,S*), 25-Epiminolanosterol to 25-Aminolanosterol and lanosterol by *Gibberella fujikuroi*, *Arch. Biochem. Biophys. 272*, 323–331.
32. Mangla, A.T., and Nes, W.D. (1999) Sterol C-Methyl Transferase from *Prototheca wickerhamii*. Mechanism, Sterol Specificity and Inhibition, *Bioorg. Med. Chem. 8*, 925–936.
33. Zhou, W., Song, Z., Liu, J., Miller, M.B., and Nes, W.D. (2004) 24-Thiacycloartanol, a Potent Mechanism-Based Inactivator of Plant Sterol Methyltransferase, *Tetrahedron Lett. 45*, 875–879.
34. Rahman, M.D., and Pascal, R.A., Jr. (1990) Inhibitors of Ergosterol Biosynthesis and Growth of the Trypanosomatid Protozoan *Crithidia fasciculata*, *J. Biol. Chem. 265*, 4989–4996.
35. Brayman, T.G., and Wilks, J.W. (2003) Sensitive Assay for Antifungal Activity of Glucan Synthase Inhibitors That Uses Germ Tube Formation in *Candida albicans* as an End Point, *Antimicrob. Agents Chemother. 47*, 3305–3310.
36. Venkatramesh, M., Guo, D., Jia, Z., and Nes, W.D. (1996) Mechanism and Structural Requirements for Transformation of Substrates by the (*S*)-Adenosyl-L Methionine: $\Delta^{24(25)}$-Sterol Methyl Transferase from *Saccharomyces cerevisiae*, *Biochim. Biophys. Acta. 1299*, 313–324.
37. Parish, E.J., and Nes, W.D. (1988) Synthesis of New Epiminoisopentenoids, *Synth. Commun. 18*, 221–226.
38. Nes, W.D., Koike, K., Jia, Z., Sakamoto, Y., Satou, T., Nikaido, T., and Griffin, J.F. (1998) 9β,19-Cyclosterol Analysis by ^{1}H- and ^{13}C-NMR, Crystallographic Observations and Molecular Mechanics Calculations, *J. Amer. Chem. Soc. 120*, 5970–5980.
39. Xu, S., Norton, R.A., Crumley, F.G., and Nes, W.D. (1988) Comparison of the Chromatographic Properties of Sterols, Select Additional Steroids and Triterpenoids: Gravity-Flow Liquid Chromatography, Thin-Layer Chromatography, Gas–Liquid Chromatography, and High-Performance Liquid Chromatography, *J. Chromatogr. 452*, 377–398.
40. Bradford, M.M. (1976) A Rapid and Sensitive Method for the Quantitation of Microgram Quantities of Protein Utilizing the Principle of Protein-Dye Binding, *Anal Biochem. 72*, 248–254.
41. Nes, W.D., McCourt, B.S., Zhou, W.-X., Ma., J., Marshall, J.A., Peek, L.A., and Brennan, M. (1998) Overexpression, Purification, and Stereochemical Studies of the Recombinant (*S*)-Adenosyl-L-Methionine: $\Delta^{24(25)}$- to $\Delta^{(24(28)}$-Sterol Methyl Transferase Enzyme from *Saccharomyces cerevisiae*, *Arch. Biochem. Biophys. 353*, 297–311.
42. Nes, W.D., Song, Z., Dennis, A.L., Zhou, W., Nam, J., and Miller, M. (2003) Biosynthesis of Phytosterols: Kinetic Mechanism for the Enzymatic *C*-Methylation of Sterols, *J. Biol. Chem. 278*, 34505–34516.
43. Ghannoum, M.A., Janini, G., Khamis, L., and Radwan, S.S. (1986) Dimorphism-Associated Variations in the Lipid Composition of *Candida albicans, J. Gen. Microbiol. 132*, 2367–2375.
44. Fryberg, M., Oehlschlager, A.C., and Unrau, A.M. (1975) Sterol Biosynthesis in Antibiotic Sensitive and Resistant *Candida, Arch. Biochem. Biophys. 173*, 171–177.
45. Subden, R.E., Safe, L., Morris, D.C., and Brown, R.G. (1977) Eburicol, Lichesterol, Ergosterol and Obtusifoliol from Polyene Antibiotic-Resistant Mutants of *Candida albicans, Can. J. Microbiol. 23*, 751–754.
46. Peyron, F., Favel, A., Calaf, R., Michel-Nguyen, A., Bonaly, R., and Coulon, J. (2002) Sterol and Fatty Acid Composition of *Candida lusitaniae* Clinical Isolates, *Antimicrob. Agents Chemother. 46*, 531–533.
47. Patterson, G.W. (1994) Phylogenetic Distribution of Sterols, *American Chemical Society Symposium Series 562*, 90– 611.
48. Nes, W.D. (2003) Enzyme Mechanisms for Sterol C-Methylations, *Phytochemistry 64*, 75–95.
49. Nes, W.D., Hanners, P.K., and Parish, E.J. (1986) Control of Fungal Sterol C-24 Transalkylation: Importance to Developmental Regulation, *Biochem. Biophys. Res. Commun. 139*, 410–415.
50. Nes, W.D., Marshall, J.A., Jia, Z., Jaradat, T.T., Song, Z., and Jayasimha, P. (2002). Active Site Mapping and Substrate Channelling in the Sterol Methyltransferase Pathway, *J. Biol. Chem. 277*, 42459–42556.

[Received August 9, 2004; accepted October 12, 2004]

A Mutation in Sphingolipid Synthesis Suppresses Defects in Yeast Ergosterol Metabolism

Martin Valachovic[a], Lisa J. Wilcox[b], Stephen L. Sturley[b,c], and Martin Bard[a,*]

[a]Biology Department, Indiana University–Purdue University Indianapolis, Indianapolis, Indiana 46202, and [b]Institute of Human Nutrition and [c]Department of Pediatrics, Columbia University Medical Center, New York, New York 10032

ABSTRACT: A mutation in an otherwise nonessential *ERG2* gene is synthetically lethal when combined with mutations in two transcription factors encoded by the *UPC2* and *ECM22* genes. Employing UV mutagenesis, we isolated a suppressor of the triple mutant *erg2*Δ *upc2*Δ *ecm22*Δ. The morpholine-resistant phenotype of the suppressor was used to identify the suppressor as a mutation in the *ELO3* gene. In an expression study on tridemorph-containing medium, using the inducible *GAL1* promoter fused to the *ELO3* open reading frame, we demonstrated that suppression occurred only when *ELO3* was not expressed. *ELO3* encodes an enzyme involved in sphingolipid synthesis required for long-chain FA synthesis. Surprisingly, a deletion of *ELO2*, also required for the synthesis of sphingolipid-containing long-chain FA, did not suppress the *erg2*Δ *upc2*Δ *ecm22*Δ triple mutant. The sterol composition of the *upc2*Δ *ecm22*Δ double mutant reflected regulation of the latter part of the ergosterol synthesis by the Upc2p and Ecm22p transcription factors. This study demonstrates a synergistic relationship between two lipid species, sterols and sphingolipids.

Paper no. L9507 in *Lipids 39,* 747–752 (August 2004).

The *ERG2* gene encodes a C-8 sterol isomerase enzyme functioning in the latter part of the ergosterol pathway. This gene is nonessential in most genetic backgrounds (1–4). FL100 is the only genetic background yet documented in which an *ERG2* deletion resulted in a lethal phenotype. Two suppressor mutations, *elo2/fen1* and *elo3/sur4*, were isolated that restored viability (5). Both Elo2p and Elo3p enzymes are involved in sphingolipid synthesis and are components of a FA elongation system that elongates a C_{16}/C_{18} to a C_{24}/C_{26} (6). Recently, Vik and Rine (7) showed that *erg2* is synthetically lethal when combined with a *upc2ecm22* double mutant. Upc2p and Ecm22p are two paralogous transcription factors involved in the regulation of sterol and cell wall metabolism. *UPC2* was originally identified as a semidominant allele, *upc2-1*, which allowed the uptake of sterol from the media under aerobic conditions (8). Besides regulating the import of exogenous sterols, Upc2p and Ecm22p also regulate the synthesis of endogenous ergosterol. Using lacZ fusion constructs of *ERG2* and *ERG3* genes, Vik and Rine (7) demonstrated transcriptional regulation of both genes by Upc2p and Ecm22p. In addition, they identified a sterol regulatory element (SRE)-binding site for Upc2p and Ecm22p in the promoter regions of both the *ERG2* and *ERG3* genes. An 11-bp SRE (5′-CTCGTATAAGC-3′) was noted as being present in promoters of several genes involved in ergosterol synthesis (e.g., *ERG1*, *ERG6*). In this study, the essentiality of the *ERG2* gene was simulated by introducing the double mutation *upc2*Δ *ecm22*Δ into the viable *erg2*Δ strain. The suppressor of the nonviable triple mutant u*pc2*Δ *ecm22*Δ *erg2*Δ was identified, and the sterol composition of the suppressed strain was analyzed.

MATERIALS AND METHODS

Strains, plasmids, media, and growth conditions. All mutants were constructed from the SCY325 strain (*MAT*α*, ade2-1, his3-11,15, leu2-3,112, trp1-1, ura-3-1*) with the exception of *elo2*Δ (*MAT*α*, elo2*Δ*::HIS3, ade2-1, his3-11,15, leu2-2,112, ura-3-1, can1-100*), *elo3*Δ (*MAT*α*, elo3*Δ*::HIS3, ade2-1, his3-11,15, leu2-2,112, ura-3-1, can1-100*), and DTY10A (*MAT*α*, ade2-1, his3-11,15, leu2-2,112, ura-3-1, can1-100*) strains. *elo2*Δ, *elo3*Δ, and the wild-type DTY10A were kindly provided by Dr. Charles Martin, as was the YCpGALELO3 plasmid (6). The pU6ΔSacI is a genomic complementing plasmid containing the wild-type *UPC2* allele in the YCp50 vector. Cells were grown on a rotary shaker at 30°C in rich media (YPAD: 1% yeast extract, 2% peptone, 2% glucose, 60 mg/mL adenine) or complete synthetic media [CSM: 0.67% yeast nitrogen base, 2% glucose, 0.5% ammonium sulfate, 0.8 g/L CSM (BIO101)], or in complete synthetic media lacking uracil [CSM-URA: 0.67% yeast nitrogen base, 2% glucose, 0.5% ammonium sulfate, 0.8 g/L CSM-URA (BIO101)]. For the expression of *GAL1-ELO3*, glucose in synthetic media was replaced with galactose at a final concentration of 2%. Cells were pregrown in synthetic media with rafinose (2%) instead of glucose before plating them onto galactose-containing medium. Tridemorph (Sigma, St. Louis, MO) was prepared in a 95% ethanol solution and added to the media after autoclaving. The 5-fluoroorotic acid (5-FOA) medium was prepared as a CSM-URA medium with the addition of 50 mg/L of uracil (Sigma) and 1 g/L of 5-FOA (Zymo Research, Orange, CA).

*To whom correspondence should be addressed at IUPUI, Biology Department, 723 W. Michigan St., Indianapolis, IN 46202. E-mail: mbard@iupui.edu

Abbreviations: CSM, complete synthetic media; CSM-URA, complete synthetic media lacking uracil; 5-FOA, 5-fluoroorotic acid; SRE, sterol regulatory element; YPAD, yeast extract, peptone, adenine, dextrose.

Lipid analysis. Cells grown in 50 mL of YPAD media to early stationary phase were resuspended in a solution of 3 mL of 50% ethanol and 25% KOH. After 1 h of incubation at 88°C, lipids were extracted into 3 mL of *n*-heptane and analyzed by GC.

Genetic methods and transformation procedures. Mating, sporulation, and tetrad analysis techniques were performed as in Burke *et al.* (9). *UPC2, ECM22, ERG2*, and *ELO2* genes were disrupted by one-step PCR deletion disruption (10) using the primers listed in Table 1. The disruptions were confirmed by PCR using the checking primers listed in Table 1.

RESULTS

The double mutation upc2ecm22 *inhibits ergosterol synthesis.* As previously shown, *erg2* mutants accumulate primarily ergosta-5,8,22-trien-3β-ol, zymosterol, fecosterol, and ergosta-8-en-3β-ol (1–4). In most backgrounds, these intermediates are sufficient to support the requirements of the cell for sterols. However, introduction of two additional mutations in the *UPC2* and *ECM22* genes resulted in synthetic lethality of the *erg2*Δ *upc2*Δ *ecm22*Δ triple mutant (7). Vik and Rine (7) showed that Upc2p and Ecm22p are transcriptional regulators of the *ERG2* and *ERG3* genes in the ergosterol pathway and suggested that several other ergosterol genes may be subject to Upc2p/Ecm22p regulation. Therefore, the sterol composition of *upc2*Δ and *ecm22*Δ single mutants and the *upc2*Δ *ecm22*Δ double mutant (Fig. 1) were analyzed. The sterol profiles of the *upc2*Δ and *ecm22*Δ single mutants were similar to the sterol profile of the wild-type strain. However, changes in the sterol composition were observed in the *upc2*Δ *ecm22*Δ double mutant. A decrease in the final product ergosterol resulted in significant increases of the sterol intermediates episterol and ergosta-5,7-dien-3β-ol. These sterol precursors are substrates of the Erg3p and Erg5p enzymes, respectively, suggesting their regulation by Upc2p and Ecm22p.

The sterol profile of the suppressed triple mutant upc2ecm 22erg2 *is unique.* To better understand the synthetic lethality of *erg2*Δ *upc2*Δ *ecm22*Δ, suppressors of the triple mutant were isolated. Since *erg2*Δ *upc2*Δ *ecm22*Δ is not viable, the

TABLE 1
List of Primers Used in This Study

Primer name	Primer sequence[a]	Purpose[b]
frwUPC2	CGGTAAACGTAAATTCCATAACAAATCAAAGAATGGGTGCGAT AACTGT AAAAGAAGAAGT**GGCGGGTGTCGGGGCTGGC**	Disruption of *UPC2*
revUPC2	CTATCAGGTTCAGATTGCCTTTGGTAGAAAGATCTAAAAGCTTA GCGATGTTACTGGTAC**TTGCCGATTTCGGCCTATTG**	
frwUPC2ck	GTTCAGCAGTATGAGCGAAG	Checking of the *upc2*ΔΔ
revUPC2ck	CTAACTCCGGTATGTAGTCC	
frwECM22	CCGATGATGGGAATGCTGGACAAGAAAGAGAGAAGGATGCTG AACTGATTGAGGTTGG**GGCGTACGCTGCAGGTCGAC**	Disruption of *ECM22*
revECM22	CGCGATGCAGTTTGTCCAAATATGCTAAAGTTATCAAGTACGGT GAATCAATTTCTACG**GATCGATGAATTCGAGCTCG**	
frwECM22ck	GGCACAAATAACATTTCGCC	Checking of the *ecm22*ΔΔ
revECM22ck	CATCGATGAGGTTCACATTC	
frwERG2	CCACTCCTTTTGTTGATTGGTGTTGTAGGCTACATTATGAACGTA TTGTTCACTACCTGGT**GGCGGGTGTCGGGGCTGGC**	Disruption of *ERG2*
revERG2	CAAGTTCTTACCCATGTCCCTGGCAGTCAGGTAGACAGTTCTATAT AGAGTGTATAAATC**TTGCCGATTTCGGCCTATTG**	
frwERG2ck	GCGGTAACGTTTGACACTGG	Checking of the *erg2*ΔΔ
revERG2ck	GCCGAATATATCCGTCGTCG	
frwELO2	ATGAATTCACTCGTTACTCAATATGCTGCTCCGTTGTTCGAGCG TTATCCCCAACTTCATT**GGCGGGTGTCGGGGCTGGC**	Disruption of *ELO2*
revELO2	TAGGAACGTTTTTCAAGTCAACGTTAACATACTCATTAACCTTT GCGGCAACACCGCCGT**TTGCCGATTTCGGCCTATTG**	
frwELO2ck	CGTATTCACATGTCCTGGCG	Checking of the *elo2*ΔΔ
revELO2ck	CAGTACGATCTCCATCCTCG	

[a]Bold letters correspond to conserved regions bordering the *TRP1, KAN*^{MX}*, HIS3*, and *LEU2* genes in the pRS304, pFA6, pRS303, and pRS315 vectors, respectively.
[b]The genes to replace *UPC2, ECM22, ERG2*, and *ELO3* were *TRP1, KAN*^{MX}*, HIS3*, and *LEU2*, respectively.

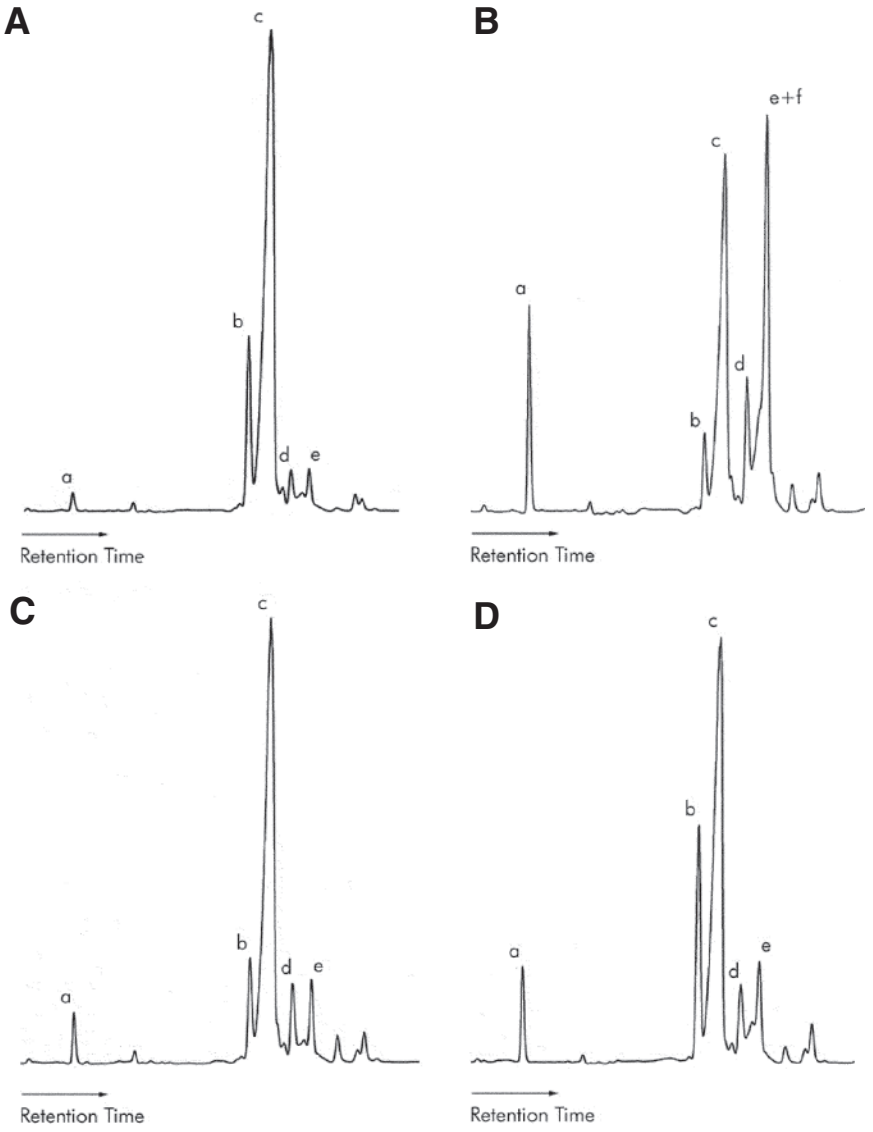

FIG. 1. Sterol profiles of the wild SCY325 cells (A), the *upc2*Δ *ecm22*Δ double mutant (B), the *upc2*Δ single mutant (C), and the *ecm22*Δ single mutant (D). Lowercase letters represent ergosterol or ergosterol precursors: (a) squalene, (b) zymosterol, (c) ergosterol, (d) fecosterol, (e) episterol, and (f) ergosta-5,7-dien-3β-ol.

triple mutant was prepared containing a plasmid (pU6ΔSacI) with the wild-type *UPC2* and *URA3* alleles. *erg2*Δ *upc2*Δ *ecm22*Δ (*UPC2*) was UV-mutagenized and plated on 5-FOA media (toxic to cells that retain the URA3 plasmid harboring the UPC2 allele) to isolate mutants that had lost this plasmid. Forty-six surviving colonies were isolated, and one (#21) was studied further. The suppressed strain, *erg2*Δ *upc2*Δ *ecm22*Δ *sup21*, was crossed to the wild-type strain to isolate the suppressor mutation in an otherwise wild-type background. Several of the spore colonies that were wild type for *UPC2, ECM22,* and *ERG2* were resistant to tridemorph, an inhibitor of sterol C-14 reductase and sterol C-8 isomerase encoded by *ERG24* and *ERG2*, respectively (11). One of these tridemorph-resistant colonies, *sup21*, was backcrossed to the parental *erg2*Δ *upc2*Δ *ecm22*Δ (*UPC2*) strain. Viability of the *erg2*Δ *upc2*Δ *ecm22*Δ *sup21* quadruple mutant indicated that *sup21* is a single gene suppressor of the triple mutant. Since both components of the triple mutant (*upc2*Δ *ecm22*Δ and *erg2*Δ) affected the sterol profile (Figs. 1B, 2A), the sterol composition of the quadruple mutant *upc2*Δ *ecm22*Δ *erg2*Δ *sup21* (Fig. 2B) was analyzed. In addition to increased levels of the sterol precursor squalene, the major sterols in the quadruple mutant were zymosterol, fecosterol, and ergosta-8-en-3β-ol. Loss of ergosta-5,8,22-trien-3β-ol, which is one of the predominant peaks in the *erg2*Δ sterol profile, is in agreement with our previous observation that the introduction of Δ5 and Δ22 double bonds catalyzed by Erg3p and Erg5p, respectively, involves regulation by Upc2 and Ecm22.

Identification of the upc2ecm22erg2 *suppressor.* Previously, Silve *et al.* (5) showed that in the FL100 genetic back-

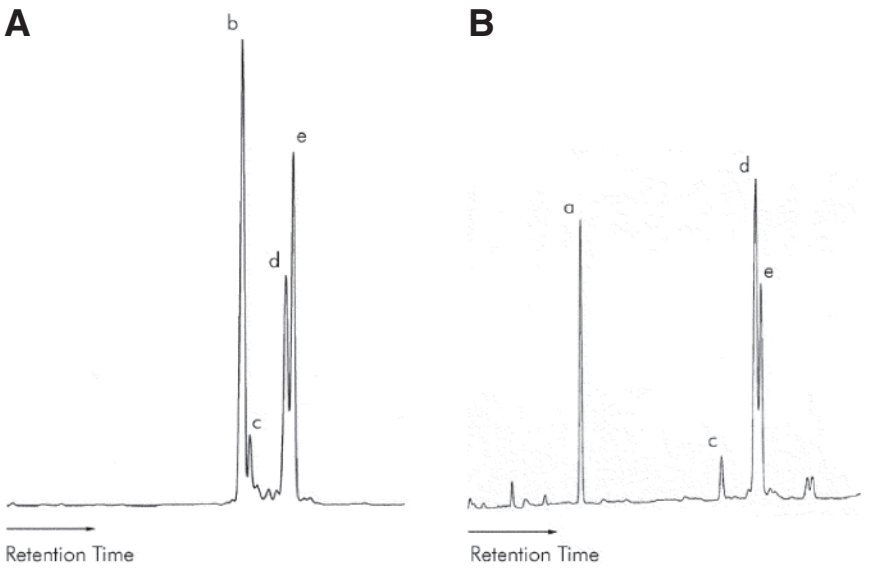

FIG. 2. Sterol profile of the *erg2*Δ (A) and the *upc2*Δ *ecm22*Δ *erg2*Δ *sup21* (B) strains. Lowercase letters represent ergosterol precursors: (a) squalene, (b) ergosta-5,8,22-trien-3β-ol, (c) zymosterol, (d) fecosterol, and (e) ergosta-8-en-3β-ol.

ground, an *erg2* mutant is nonviable. Mutants in sphingolipid synthesis *elo2/fen1* and *elo3/sur4* were shown to suppress their *erg2* strain. Since both mutants (*elo2* and *elo3*) were resistant to morpholines, as was the *sup21* suppressor, the possibility existed that *sup21* was *elo2* or *elo3* (Fig. 3). The *sup21* strain was crossed to both *elo2*Δ and *elo3*Δ mutants. Tridemorph sensitivity of the diploid, *sup21* × *elo2*Δ, and tridemorph resistance of the diploid, *sup21* × *elo3*Δ, suggested that *sup21* was an *elo3* mutant. Plasmid YCp-GALELO3 carrying *ELO3* fused to the GAL1- inducible promoter was transformed into the *sup21* strain (Fig. 4). When placed on a galactose medium, tridemorph sensitivity of the *sup21* strain was restored. A similar effect was observed with the *elo3*Δ control strain; however, overexpression of the *ELO3* gene had no effect on the tridemorph resistance of the wild-type strain, indicating that restored sensitivity was due to complementation by the wild-type *ELO3* allele. This confirmed that *sup21* was an *elo3* mutant. Further, a quadruple mutant strain, *erg2*Δ *upc2*Δ *ecm22*Δ *elo3*Δ carrying the wild-type *UPC2* allele on a plasmid, was constructed and placed on 5-FOA media to select for loss of the *UPC2*-containing plasmid. As shown in Figure 5, the triple mutant *erg2*Δ *upc2*Δ *ecm22*Δ (*UPC2*) plated on 5-FOA did not grow. In contrast, the quadruple mutant *erg2*Δ *upc2*Δ *ecm22*Δ *elo3*Δ plated on 5-FOA lost the plasmid and grew, demonstrating that *elo3*Δ suppresses the synthetic lethality of *erg2*Δ *upc2*Δ *ecm22*Δ. In addition, the sterol composition of *erg2*Δ *upc2*Δ *ecm22*Δ *elo3*Δ was the same as that in the suppressed triple mutant *upc2*Δ *ecm22*Δ *erg2*Δ *sup21* (not shown).

elo2 *does not suppress the* erg2upc2ecm22 *triple mutant.* Since *elo2* was also shown to suppress the nonviable *erg2* mutant (5), suppression of *erg2*Δ *upc2*Δ *ecm22*Δ by *elo2*Δ was also tested. The *elo2*Δ *upc2*Δ *ecm22*Δ (*UPC2*) triple mutant was constructed and crossed to *erg2*Δ *upc2*Δ *ecm22*Δ

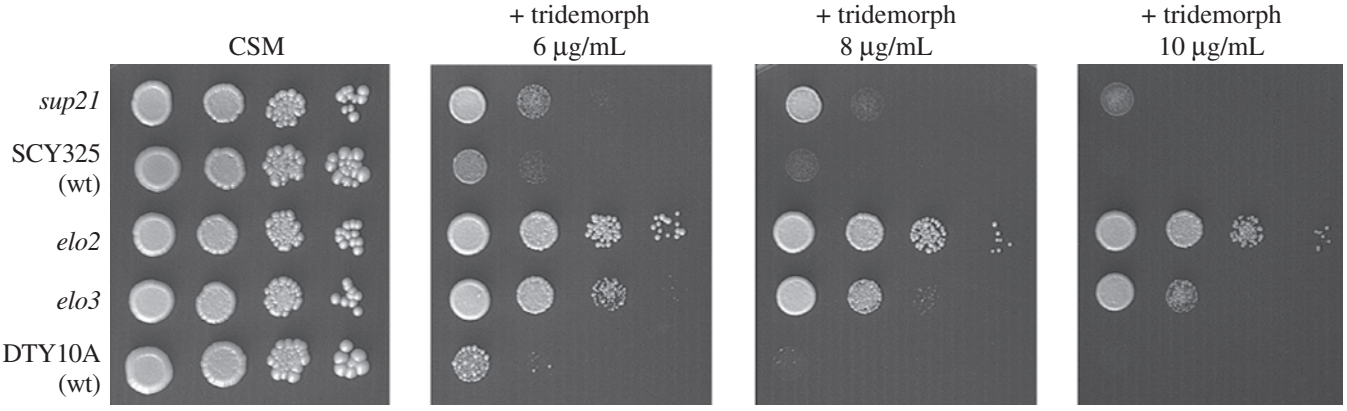

FIG. 3. Tridemorph resistance of the *sup21* suppressor and the corresponding wild-type SCY325 as well as the *elo2*Δ and *elo3*Δ mutants with the corresponding wild-type DTY10A. Colony growth assays represent 10-fold serial dilutions starting with 10^4 cells per spot. CSM, complete synthetic media.

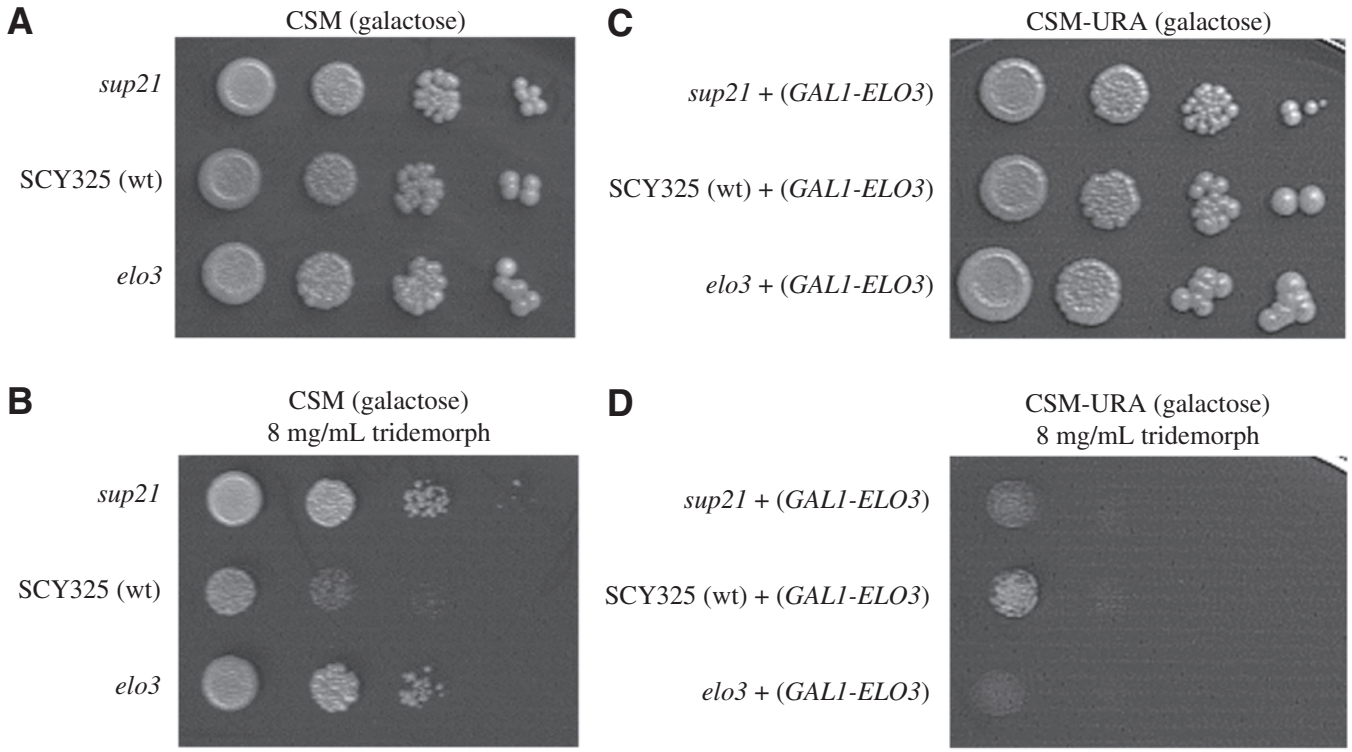

FIG. 4. Effect of tridemorph on *sup21* transformed with *GAL1-ELO3*. Strains *sup21*, SCY325, and *elo3*Δ grown on galactose medium without the *GAL1-ELO3* plasmid, and (A) without and (B) with tridemorph. Strains *sup21*, SCY325, and *elo3*Δ carrying the YCp*GAL1-ELO3* plasmid under inducible conditions (C) without and (D) with tridemorph. Colony growth assays represent 10-fold serial dilutions starting with 10^4 cells per spot. CSM-URA, complete synthetic media lacking uracil; for other abbreviation, see Figure 3.

(*UPC2*). The diploid was dissected and segregants from 16 tetrads were analyzed. Consistent with Vik and Rine's (7) results, none of the 10 segregating *erg2*Δ *upc2*Δ *ecm22*Δ (*UPC2*) triple mutants were viable when plated on 5-FOA medium. Surprisingly, all 12 of the *elo2*Δ *erg2*Δ *upc2*Δ *ecm22*Δ (*UPC2*) quadruple mutants from the cross failed to grow on 5-FOA media, suggesting an inability to lose the *UPC2*-containing plasmid. The nonviability of the *erg2*Δ *upc2*Δ *ecm22*Δ *elo2*Δ quadruple mutant indicated that a mutation in the *ELO2* gene could not suppress *erg2*Δ *upc2*Δ *ecm22*Δ.

DISCUSSION

Five enzymes from the late ergosterol pathway, encoded by *ERG6, ERG2, ERG3, ERG4,* and *ERG5*, are nonessential in the yeast *Saccharomyces cerevisiae* under normal conditions. There is, however, one genetic background (FL100) in which one of them, the *ERG2* gene, is essential (5). By crossing two different *erg2* strains, one viable and one nonviable, Silve *et al.* (5) showed that the *erg2* lethality phenotype is dependent on the genetic background. In this study, mutations in two transcription factors, Upc2p and Ecm22p, were introduced into a viable *erg2*Δ mutant. This resulted in a synthetic lethality of the triple mutant and thus simulated the genetic background, as described by Silve *et al.* (5), in which *erg2* alone is lethal. Sterol analysis of the *upc2*Δ *ecm22*Δ double mutant showed that deletion of these two transcription factors reduces the amount of ergosterol synthesized, although cells are still able to synthesize the final product ergosterol. This is in agreement with the results of Vik and Rine (7). To understand why the triple mutant *erg2*Δ *upc2*Δ *ecm22*Δ is lethal, the

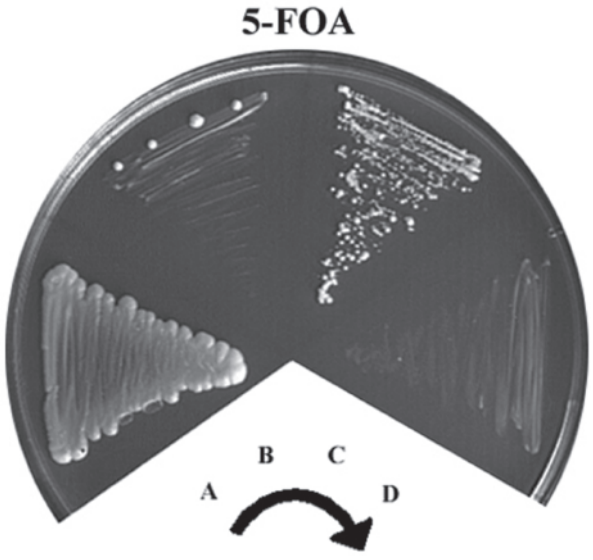

FIG. 5. Viability of the quadruple mutant *erg2*Δ *upc2*Δ *ecm22*Δ *elo3*Δ. The wild-type strain SCY325 (A) and the *erg2*Δ *upc2*Δ *ecm22*Δ (*UPC2*) triple mutant (B) served as positive and negative controls, respectively. *erg2*Δ *upc2*Δ *ecm22*Δ *elo3*Δ (*UPC2*) (C) and *erg2*Δ *upc2*Δ *ecm22*Δ (*UPC2*) (D) represent two segregants from the cross *erg2*Δ *upc2*Δ *ecm22*Δ (UPC2) × *elo3*Δ. 5-FOA, 5-fluoroorotic acid.

search for a suppressor was undertaken, and a mutation in the *ELO3* gene was revealed. The *ELO3* gene was previously shown to suppress *erg2* in the FL100 genetic background. Interestingly, *elo2* also suppressed *erg2* in this background but was not able to suppress the *erg2*Δ *upc2*Δ *ecm22*Δ mutant in this study. Both the *ELO2* and *ELO3* genes encode components of a complex involved in the production of very long chain FA, which are precursors for ceramide and sphingolipids. The Elo2p enzyme catalyzes the elongation of FA up to 24 carbons. Elo3p and Elo2p overlap in the production of 24-carbon FA. However, Elo3p is essential for the conversion of 24-carbon acids to 26-carbon species. Both sterols and sphingolipids are the main constituents of lipid rafts (12,13), which are lateral microdomains of cell membranes that have been implicated in numerous cellular processes such as signal transduction, lateral protein sorting, and cellular trafficking (14). It is proposed that sterols and sphingolipids are packed tightly together within these rafts, thus requiring a concerted physical interaction between them. Improper synthesis of both lipid molecules might result in nonfunctional rafts, as shown by Eisenkolb *et al.* (15). These authors demonstrated that simultaneous mutations in sterol and sphingolipid synthesis due to mutations in *erg6*Δ and *elo3*Δ, respectively, produced a synthetically lethal phenotype as a result of faulty raft biogenesis. This mutant incompatibility was highly specific, since *elo3*Δ was not lethal with any other mutant in the ergosterol pathway. Interestingly, results from this work show that the effects of alterations in sterol composition could be suppressed by specific changes in the structure of sphingolipids. Since only *elo3*Δ, which is essential for the production of 26-carbon FA, and not *elo2*Δ is the suppressor of *erg2*Δ *upc2*Δ *ecm22*Δ, it is apparent that the absence of sphingolipids with 26-carbon FA can suppress specific defects in the ergosterol pathway. Analysis of the sterol profile of the quadruple mutant *erg2*Δ *upc2*Δ *ecm22*Δ *elo3*Δ showed the accumulation of all sterol intermediates found in the *erg2* mutant alone, with the exception of ergosta-5,8,22-trien-3β-ol, which indicates that lethality of the triple mutant is not due to the accumulation of toxic sterols. Rather, it seems that a decrease in the flux through the ergosterol pathway caused by *upc2*Δ *ecm22*Δ and qualitative changes in the sterol species produced by the *erg2*Δ deletion resulted in abnormalities of cellular structures such as rafts. Again, our observations are consistent with those of Eisenkolb *et al.* (15), which demonstrate that mutations in *ELO2* and *ELO3* can behave very differently in combination with alterations in sterol synthesis.

ACKNOWLEDGMENTS

This work was supported by an NIH grant GM62104 to M.B. We thank Dr. Charles Martin for providing strains and plasmids.

REFERENCES

1. Bard, M., Woods, R.A., Barton, D.H., Corrie, J.E., and Widdowson, D.A. (1977) Sterol Mutants of *Saccharomyces cerevisiae*: Chromatographic Analyses, *Lipids 12,* 645–654.
2. Ashman, W.H., Barbuch, R.J., Ulbright, C.E., Jarrett, H.W., and Bard, M. (1991) Cloning and Disruption of the Yeast C-8 Sterol Isomerase Gene, *Lipids 26,* 628–632.
3. Palermo, L.M., Leak, F.W., Tove, S., and Parks, L.W. (1997) Assessment of the Essentiality of ERG Genes Late in Ergosterol Biosynthesis in *Saccharomyces cerevisiae, Curr. Genet. 32,* 93–99.
4. Munn, A.L., Heese-Peck, A., Stevenson, B.J., Pichler, H., and Riezman, H. (1999) Specific Sterols Required for the Internalization Step of Endocytosis in Yeast, *Mol. Biol. Cell 10,* 3943–3957.
5. Silve, S., Leplatois, P., Josse, A., Dupuy, P.H., Lanau, C., Kaghad, M., Dhers, C., Picard, C., Rahier, A., Taton, M., *et al.* (1996) The Immunosuppressant SR 31747 Blocks Cell Proliferation by Inhibiting a Steroid Isomerase in *Saccharomyces cerevisiae, Mol. Cell. Biol. 16,* 2719–2727.
6. Oh, C.S., Toke, D.A., Mandala, S., and Martin, C.E. (1997) *ELO2* and *ELO3*, Homologues of the *Saccharomyces cerevisiae ELO1* Gene, Function in Fatty Acid Elongation and Are Required for Sphingolipid Formation, *J. Biol. Chem. 272,* 17376–17384.
7. Vik, A., and Rine, J. (2001) Upc2p and Ecm22p, Dual Regulators of Sterol Biosynthesis in *Saccharomyces cerevisiae, Mol. Cell. Biol. 21,* 6395–6405.
8. Crowley, J.H., Leak, F.W., Jr., Shianna, K.V., Tove, S., and Parks, L.W. (1998) A Mutation in a Purported Regulatory Gene Affects Control of Sterol Uptake in *Saccharomyces cerevisiae, J. Bacteriol. 180,* 4177–4183.
9. Burke, D., Dawson, D., and Stearns, T. (2000) *Methods in Yeast Genetics, 2000 Edition: A Cold Spring Harbor Laboratory Course Manual,* 1st edn., pp. 161–167, Cold Spring Harbor Laboratory Press, Cold Spring Harbor, NY.
10. Baudin, A., Ozier-Kalogeropoulos, O., Denouel, A., Lacroute, F., and Cullin, C. (1993) A Simple and Efficient Method for Direct Gene Deletion in *Saccharomyces cerevisiae, Nucleic Acids Res. 21,* 3329–3330.
11. Baloch, R.I., and Mercer, E.I. (1987) Inhibition of Sterol $\Delta^8 \rightarrow \Delta^7$ Isomerase and Δ^{14} Reductase by Fenpropimorph, Tridemorph, and Fenpropidin in Cell Free Enzyme Systems from *Saccharomyces cerevisiae, Phytochemistry 26,* 663–668.
12. Brown, D.A., and London, E. (1998) Structure and Origin of Ordered Lipid Domains in Biological Membranes, *J. Membr. Biol. 164,* 103–114.
13. Bagnat, M., Keranen, S., Shevchenko, A., and Simons, K. (2000) Lipid Rafts Function in Biosynthetic Delivery of Proteins to the Cell Surface in Yeast, *Proc. Natl. Acad. Sci. USA 97,* 3254–3259.
14. Pike, L.J. (2003) Lipid Rafts: Bringing Order to Chaos, *J. Lipid Res. 44,* 655–667.
15. Eisenkolb, M., Zenzmaier, C., Leitner, E., and Schneiter, R. (2002) A Specific Structural Requirement for Ergosterol in Long-Chain Fatty Acid Synthesis Mutants Important for Maintaining Raft Domains in Yeast, *Mol. Biol. Cell. 13,* 4414–4428.

[Received May 21, 2004; accepted September 14, 2004]

Sterol Metabolism in the Opportunistic Pathogen *Pneumocystis*: Advances and New Insights

Edna S. Kaneshiro*

Department of Biological Sciences, University of Cincinnati, Cincinnati, Ohio 45221

ABSTRACT: *Pneumocystis* can transiently colonize healthy individuals without causing adverse symptoms, and most people test positive for exposure to this organism early in life. However, it can cause *Pneumocystis* pneumonia (PcP) in people with impaired immune systems and is a major cause of death in HIV/AIDS. Although it has close affinities to the Ascomycetes, *Pneumocystis* has features unlike those of any single group of fungi. For example, *Pneumocystis* does not synthesize ergosterol, which is consistent with the inefficacy of amphotericin B and some triazoles in clearing PcP. *Pneumocystis* sterols include distinct Δ^7 24-alkylsterols. Metabolic radiolabeling experiments demonstrated that *P. carinii* synthesizes sterols *de novo.* Cholesterol is the most abundant sterol in *Pneumocystis*; most, if not all, is scavenged from the mammalian host lung by the pathogen. The *P. carinii erg7, erg6,* and *erg11* genes have been cloned, sequenced, and expressed in heterologous systems. The recombinant *P. carinii S*-adenosyl-L-methionine:C-24 sterol methyl transferase (SAM:SMT) has a preference for lanosterol over zymosterol as substrate, and the enzyme can catalyze the transfer of either one or two methyl groups to the C-24 position of the sterol side chain. Two different sterol compositions were detected among human-derived *P. jirovecii*; one was dominated by C_{28} and C_{29} sterols, and the other had high proportions of higher molecular mass components, notably the C_{32} sterol pneumocysterol. The latter phenotype apparently represents organisms blocked at 14α-demethylation of the sterol nucleus. These studies suggest that SAM:SMT is an attractive drug target for developing new chemotherapy for PcP.

Paper no. L9538 in *Lipids 39,* 753–761 (August 2004)

Pneumocystis, the paradigm of opportunistic infections, causes life-threatening pneumonia (PcP) in individuals with defective immune systems, such as those with HIV/AIDS, and in solid organ transplant and cancer patients undergoing immunosuppressive therapy (1,2). Prior to the AIDS pandemic, PcP was rarely observed, but it is now a major killer among those with this disease. It is generally believed that the organism occurs worldwide, and there is evidence that it is ubiquitous in both indoor (3) and outdoor (4,5) environments and can survive for months outside the mammalian lung (6,7). Most people test seropositive for *Pneumocystis* early in life, indicating transient infections (colonization) are normally cleared in healthy individuals but reinfections occur and high anti-*Pneumocystis* antibody titers are maintained in adults (1,2).

*E-mail: Edna.Kaneshiro@uc.edu

Abbreviations: BALF, bronchoalveolar lavage fluid; 14DM, 14α-demethylase; PcP, *Pneumocystis* pneumonia; SAM:SMT, *S*-adenosyl-L-methionine:C-24 sterol methyltransferase.

We recently observed an extraordinarily high percentage of HIV-negative adult natives in the sub-Saharan country of Cameroon with antibodies against *Pneumocystis*. Analysis was performed by Western immunoblot techniques on sera from HIV-negative and -positive patients (Table 1) (Nkinin, S., Asonganyi, T., Medrano, F.J., Respaldiza, N., Calderón, E., and Kaneshiro, E.S., unpublished data). These data are in agreement with the suggestion that frequent, transient *Pneumocystis* infections normally occur in human populations. We believe that potential emerging pathogens can infect healthy individuals who normally tolerate invasions by various microbes. These can cause disease when changes occur in the microbe or host. Our data also showed that a lower percentage of the HIV-positive patients had anti-*Pneumocystis* antibodies compared with HIV-negative patients. These results verified that people infected with the virus have immune systems that are less able to produce antibodies.

The genus *Pneumocystis* is a genetically diverse group of organisms that infect several mammalian host species and are host species-specific (8,9). Different species can infect the same host species. *Pneumocystis* in humans is named *P. jirovecii* (10,11); *P. murina* is found in laboratory mice (12), and both *P. carinii* (13) and *P. wakefieldiae* (14) infect laboratory rats. Several different forms have been observed in lung infections; the most dominant stages are thick-walled cystic forms and vegetative pleiomorphic trophic forms (15). All life cycle stages are characterized by an evenly thick glycocalyx, and the trophic stages have unique extensions of their cell surfaces described as tubular extensions. The trophic forms form tight adhesions to alveolar type I epithelial cells probably held by disulfide links, as suggested by the separation of *Pneumocystis* from the pneumocytes using glutathione, DTT, and other sulfhydryl agents (16). Mature cysts (spore cases) contain eight ovoid intracystic bodies (spores); however, there are also thick-walled cysts with banana-shaped intracystic bodies that exhibit motility (17).

TABLE 1
Serology of HIV-Negative and HIV-Positive Patients in Cameroon[a,b]

Patient group	Number of samples	MSG-positive	MSG-negative	Not scored
HIV-negative	55	50 (91%)	5 (9%)	0 (0%)
HIV-positive	51	38 (75%)	12 (23%)	2 (4%)

[a]Nkinin, S., Asonganyi, T., Medrano, F.J., Respaldiza, N., Calderón, E., and Kaneshiro, E.S., unpublished data.
[b]Antibodies directed against the major surface glycoprotein (MSG) of *Pneumocystis* were detected by Western immunoblots.

Pneumocystis is classified as a lower ascomycete fungus, but most workers agree that it has several features that differ from those of most typical fungi. Among these atypical features are the nature and metabolism of its sterols. The structures of the *Pneumocystis* sterols resemble those described in basidiomycetous rust fungi (18), trypanosomatid flagellated protozoan parasites (19–23), and some plants (24–27).

PNEUMOCYSTIS STEROLS

The majority of antifungal drugs currently used clinically target ergosterol or its synthesis. In the initial period of the AIDS pandemic, it was found that some drugs used for protozoan parasite infections could clear PcP, but several antimycotics such as triazoles did not (28–32). Only higher concentrations of amphotericin B that would be toxic to humans were effective in reducing *P. carinii* viability and growth *in vitro* (31,32).

In the late 1980s, *Pneumocystis* was found not to contain ergosterol, and the major sterol in the organism was cholesterol (33). Later, the presence of distinct Δ^7 24-alkylsterols was reported (34–37); these constituted almost half of the noncholesterol sterols (34,36,38,39) (Fig. 1). Since there was no culture method available for *Pneumocystis*, those studies were performed on organisms isolated from infected lungs of animal models, primarily corticosteroid-immunosuppressed laboratory rats. There is still no culture method for indefinite passage of *Pneumocystis in vitro*, although improvements for the growth of small numbers of organisms have been reported (40). Thus, most direct biochemical experiments on sterols still rely primarily on organisms isolated from rat lungs. To ensure that the lipids analyzed do not include those from the host lung, a protocol was developed to isolate and purify *P. carinii* (16), and the purity of the preparations was shown to be >95 to 100% by light and electron microscopic, immunochemical, microbiological, biochemical, and enzyme analyses.

By using these purified preparations, at least 24 sterol components were detected in *P. carinii* 10 yr ago by GLC and MS (34). Analyses have since been refined, and 43 sterols recently were identified in *P. carinii* by using a combination of TLC and HPLC to separate individual sterols, which were then subjected to high-field (600 MHz) NMR spectroscopy (39) (Table 2). With structural identities that include their stereochemical features now available, we are in a better position to predict the origins of the compounds present. It appears that some are synthesized *de novo* by *P. carinii* whereas other sterols present in the mammalian lung are taken up (scavenged) by the pathogen and incorporated unchanged into its membranes. Also, it is hypothesized that some host-derived sterols are scavenged and then modified by enzymes in *Pneumocystis*.

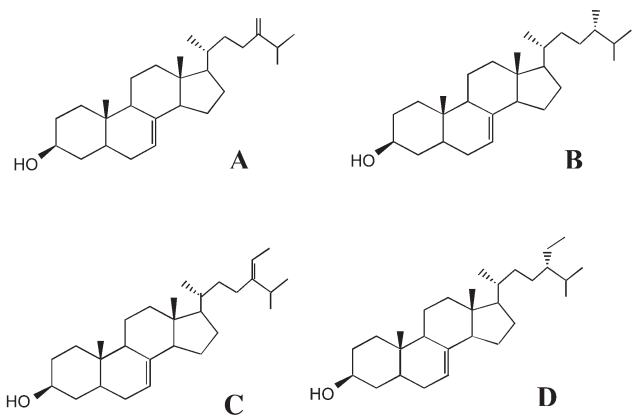

FIG. 1. The major *Pneumocystis carinii*-specific sterols. (A) Ergosta-7,24(28)-dien-3β-ol (24-methylenecholest-7-en-3β-ol); (B) (24*S*)-ergost-7-en-3β-ol (24β-methylcholest-7-en-3β-ol); (C) (*Z*)-stigmasta-7,24(28)-dien-3β-ol (24*Z*)-ethylidenecholest-7-en-3β-ol); and (D) (24*S*)-stigmast-7-en-3β-ol (24β-ethylcholest-7-en-3β-ol).

TABLE 2
Sterols Detected in *Pneumocystis carinii* Organisms Purified from Infected Rat Lungs[a]

Sterol	Total sterol mass (%)
Cholest-5-en-3β-ol (cholesterol)	81.16
(*Z*)-Stigmasta-7,24(28)-dien-3β-ol	2.60
(24*S*)-Ergost-7-en-3β-ol (fungisterol)	2.51
(24*S*)-Ergost-5-en-3β-ol	1.92
(24*R*)-Stigmast-5-en-3β-ol (β-sitosterol)	1.38
(24*S*)-Stigmast-7-en-3β-ol	1.30
Ergosta-7,24(28)-dien-3β-ol	1.16
(24*R*)-Ergost-5-en-3β-ol (campesterol)	0.96
(*Z*)-Stigmasta-5,24(28)-dien-3β-ol (isofucosterol)	0.68
Ergosta-5,24(28)-dien-3β-ol	0.65
(24*S*)-Ergost-8(14)-en-3β-ol	0.48
Lanosta-8,24-dien-3β-ol (lanosterol)	0.40
Cholesta-5,24-dien-3β-ol (desmosterol)	0.35
(24*S*)-Stigmast-5-en-3β-ol	0.35
Cholesta-7,24-dien-3β-ol	0.34
5β-Cholestan-3β-ol	0.33
(*Z*)-24-Ethylidenelanost-8-en-3β-ol (pneumocysterol)	0.31
24-Methylenelanost-8-en-3β-ol	0.29
Cholest-7-en-3β-ol (lathosterol)	0.29
(*Z*)-Stigmasta-8(14),24(28)-dien-3β-ol	0.29
4α-Methylergosta-8,24(28)-dien-3β-ol	0.27
(24*S*)-Stigmast-8(14)-en-3β-ol	0.24
4,4-Dimethylergosta-8,24(28)-dien-3β-ol	0.21
(24*S*)-Ergost-8-en-3β-ol	0.17
(*Z*)-Stigmasta-8,24(28)dien-3β-ol	0.15
4,4-Dimethylcholesta-8,24-dien-3β-ol	0.15
(24*S*)-5β-Ergostan-3β-ol	0.15
(24*R*)-5β-Stigmastan-3β-ol	0.13
Ergosta-8,24(28)-dien-3β-ol	0.11
(*Z*)-4,4-Dimethylstigmasta-8,24(28)-dien-3β-ol	0.10
4α-Methylcholesta-8,24-dien-3β-ol	0.10
4α-Methylcholest-7-en-3β-ol	0.09
(24*S*)-Stigmasta-7,25-dien-3β-ol	0.06
4α-Methylergosta-8(14),24(28)-dien-3β-ol	0.05
(24*S*)-Stigmasta-5,22-dien-3β-ol (stigmasterol)	0.05
24-Methylenecholest-8(14)-en-3β-ol	0.05
(Z)-4α-Methylstigmasta-8,24(28)-dien-3β-ol	0.04
(24*R*)-Ergosta-5,22-dien-3β-ol (brassicasterol)	0.04
(24*S*)-Stigmasta-5,25-dien-3β-ol	0.04
Cholesta-5,25-dien-3β-ol	0.03
Cholesta-8,24-dien-3β-ol (zymosterol)	0.03
25-Methylergosta-5,24(28)-dien-3β-ol	0.02
Cholest-8-en-3β-ol	0.01

[a]From Reference 39.

SCAVENGED STEROLS

Cholesterol constitutes approximately 75–85% of *P. carinii* total sterols (34,37,39). The pathogen proliferates in a milieu rich in lung surfactant. Lung surfactant is composed mainly of lipids, especially dipalmitoyl PC, but also includes substantial levels of cholesterol. Bronchoalveolar lavage fluid (BALF) from *P. carinii*-infected rats was shown to contain less phospholipids compared with uninfected controls (41–43). Also, total lipids and total phospholipids in BALF from HIV-positive, PcP-positive human patients were lower than normal, and this reduction was specifically correlated with PcP (44). These observations suggested that PcP enhanced phospholipase activity in the alveolus and/or that the lipids were removed by the proliferating organisms. Subsequently, BALF from PcP patients were found to contain 80% less sterols (3.06 μg/mL) than controls (16.25 μg/mL) (45). Although PcP might be accompanied by decreased alveolar phospholipids as a consequence of enhanced phospholipase activity, this alone cannot explain the reduction of sterols. Thus, these results strongly suggest that *Pneumocystis* takes up significant amounts of sterols from its environment in the lung.

Additional support for scavenging of host cholesterol by *Pneumocystis* comes from a metabolic radiolabeling experiment using [^{3}H]squalene. After incubation of *P. carinii* with the sterol precursor, sterols were isolated and crude fractions were collected by preparative GLC. The GLC fraction containing cholesterol plus some other minor components had only low levels of radioactivity (Table 3). In contrast, the other fractions representing a lower proportion of the total sterol mass had higher radioactivities; hence, the relative specific activity of the cholesterol-containing fraction was dramatically lower than that of the other fractions. We tentatively conclude that most, if not all, cholesterol in the organism is taken up from the environment in the host lung and is utilized unchanged by the organism to form new membranes.

The organism contains substantial amounts of Δ^5 sterols, including those with methyl and ethyl groups in the β configuration (39). However, there is no evidence that intrapulmonary *P. carinii* desaturates sterols at C-5 of the sterol nucleus. It has been suggested that *P. carinii* scavenges Δ^5 sterols, namely, desmosterol, that are available in the rat lung and modifies them (46). Data supporting this suggestion come from experiments showing that the recombinant *P. carinii S*-adenosyl-L-methionine:C-24 sterol methyltransferase (SAM:SMT) (see below) can transmethylate desmosterol and 24-methylenecholesterol (Worsham, D.N., and Kaneshiro, E.S., unpublished data). The Δ^5 24-alkylsterol products might be further modified by the *P. carinii* C-24 (28) reductase to produce methyl and ethyl groups in the β configuration.

Pneumocystis contains undetectable or only low amounts of Δ^{22} sterols. Thus, it is currently believed that intrapulmonary forms of the organism do not desaturate the sterol side chain at C-22.

TABLE 3
Incorporation of [^{3}H]Squalene into Major *P. carinii* Sterol GLC Fractions[a]

GLC fraction	% of total dpm	% of total mass[b]	Relative specific activity
Cholesterol-enriched[c]	13.4	75	0.17
All other sterol fractions	86.6	25	3.48

[a]Fractions were collected by preparative GLC using a 15% OV 101 packed glass column.
[b]Estimated from Reference 34.
[c]Cholesterol plus other minor components. For abbreviation see Table 1.

DE NOVO SYNTHESIS OF STEROLS

The distinct Δ^7 24-alkylsterols not found in mammalian lung controls (34) are not known to be formed by mammals; thus, it was inferred that *P. carinii* synthesized these *de novo* (34–36). The *P. carinii* Δ^7 24-alkylsterols with methyl and ethyl groups at C-24 are now known to occur in the β configuration. In contrast, most phytosterols found in uninfected lung controls are in the α configuration (39). Direct evidence for *de novo* sterol synthesis comes from several metabolic incorporation experiments. *Pneumocystis carinii* sterols were shown to become radioactive when intact organisms were incubated with a number of radiolabeled precursors of the acetate-mevalonate pathway. These included acetate, HMG-CoA, mevalonate, squalene, and isopentenyl diphosphate (47–50). It was also shown that the HMG-CoA reductase activity was highly sensitive to lovastatin inhibition; IC_{50} was 4 nM (48).

REACTIONS IN STEROL BIOSYNTHESIS AS DRUG TARGETS IN *PNEUMOCYSTIS*

Because *Pneumocystis* synthesizes its own distinct sterols despite the abundance of cholesterol and other sterols available for scavenging, it appears that the pathogen cannot rely entirely on them to grow and multiply. The 24-alkylsterols can be regarded as "metabolic sterols" (22). It was experimentally demonstrated that the kinetoplastid flagellate *Leishmania* can be depleted of its "metabolic sterols" (24-alkylsterols) by adapting it to an inhibitor (azasterol) over several subcultures (51). However, this has not been observed in pathogens causing natural infections. That *P. carinii* is sensitive to sterol biosynthesis inhibitors also has been demonstrated. A number of different compounds reduced *P. carinii* viability *in vitro* as indicated by decreased cellular ATP *in vitro* (Table 4) (32).

Terbinafine was among the compounds tested, and it showed high anti-*P. carinii* activity (32). Furthermore, consistent with the *in vitro* assay, terbinafine showed efficacy against PcP *in vivo* using laboratory rats (52). On other hand, an independent study on terbinafine did not show any effect on PcP in rats and mice (53). The disparity between the results obtained in the two studies using animal models is not known.

The effects of 14α-demethylase (14DM) inhibitors fell into two groups (32). Two of three imidazoles tested exhibited high anti-*P. carinii* activity, but fluconazole and two other triazoles tested had no effect on cellular ATP levels. Subse-

TABLE 4
Effects of Sterol Biosynthesis Inhibitors on *P. carinii* Viability by Measuring Cellular ATP[a]

Targeted sterol biosynthesis reaction step	IC_{50} (μM) Exposure times 24 h	48 h	72 h
HMG-CoA reductase			
Simvastatin (Merck)	—[b]	—	2,422
Lovastatin (Merck)	—	—	—
L-647,318 (prodrug similar to lovastatin and simvastatin; Merck)	—	—	—
L-654,164 (bromo- and chlorinated amine; Merck)	—	—	—
Squalene synthase			
CCI 14993 (naphthalene alkylamine derivative; Glaxo)	2,832	18	8
CCI 16543 (biphenyl alkylamine derivative; Glaxo)	434	68	33
Squalestatin (GR 105155X; Glaxo)	—	—	—
Squalene epoxidase			
Terbinafine	5,863	130	13
Tolnaftate (Sigma)	—	3,980	1,625
Squalene epoxide-lanosterol cyclase			
GR 90525A (phenylcyclohexylamine derivative; Glaxo)	7	4	3
GR 193018A (phenylcyclohexylamine derivative; Glaxo)	30	11	8
GR 54985A (bis-cyclohexyloxyalkylamine derivative; Glaxo)	121	16	9
GR 31149A (bis-cyclohexyloxyalkylamine derivative; Glaxo)	4,464	47	6
UI 8666A (3-β-[(diethylamino)ethoxy]androst-5-en-17-one	212	60	67
Lanosterol demethylase			
GR 40317A (imidazole derivative; Glaxo)	33	8	5
GR 42539X (imidazole derivative; Glaxo)	81	8	7
GR 40665X (imidazole derivative; Glaxo)	692	453	372
Fluconazole	—	—	—
GR 71539X (triazole derivative; Glaxo)	—	—	—
GR 77303X (triazole derivative; Glaxo)	—	—	—
Δ^8 to Δ^7 isomerase			
AY 9944 (Ayerst)	51	36	7
SAM:SMT			
24(25)-Epiminolanosterol (E.J. Parish)	—	4,737	—
24-Bromolanosterol (E.J. Parish)	—	—	—
24-Iodolanosterol (E.J. Parish)	—	—	—
Sinefungin (Sigma)	—	—	—

[a]From Reference 32.
[b]—, Inhibition was always less than 50%. SAM:SMT, *S*-adenosyl methionine:C-24 sterol methyl transferase; for other abbreviation see Table 1.

quently, it was reported that the triazole tebuconazole was effective in reducing *P. carinii* viability *in vitro* (54).

The azasterol 20-piperidin-2-yl-5α-pregnan-3β-20(*R*)-diol and 24-epiminolanosterol were tested on primary cultures of *P. carinii* isolated from infected rat lungs (36). Both of these compounds, which inhibit SAM:SMT, caused dramatic reductions in the total 24-alkysterol level, which was reduced by 40% after 2 d of exposure to 10 μM of azasterol. At the same inhibitor concentration and exposure time, cell proliferation declined by approximately 50% compared with untreated cultures. As 24-epiminolanosterol had no effect on ATP levels after exposure of organisms *in vitro* for 72 h (32), blocking production of 24-alkylsterols by SAM:SMT appears to have static rather than cidal effects on *P. carinii* growth.

Some steroidal allenic phosphonic acid derivatives also reduced *P. carinii* viability *in vitro* (55). Diethyl phosphono analogs of norethindrone and mestranol (Fig. 2) had potent activity against *P. carinii* ATP levels, but whether these compounds specifically inhibit SAM:SMT has not been demonstrated. The studies performed to date indicate that reactions in sterol biosynthesis are potential drug targets in *Pneumocystis*.

MOLECULAR BIOLOGY APPROACHES

Since methods are still not available for rapid growth of *Pneumocystis* in large numbers in continuous subcultures, molecular biology techniques are currently being applied to study sterol biosynthesis in this pathogen. Genes encoding

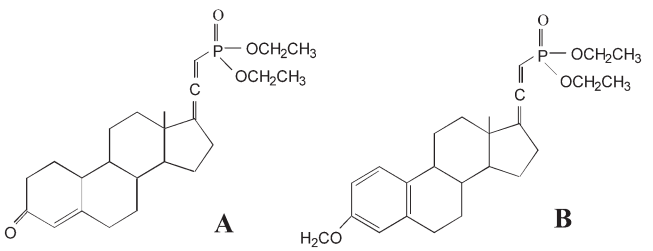

FIG. 2. Steroidal allenic phosphonic acid derivatives with anti-*Pneumocystis* activity *in vitro*. (A) 17[2-(Diethylphosphonato)ethylidienyl]-19-norpreg-4-en-3-one, a diethyl phosphono analog of norethindrone; (B) 17[2-(diethylphosphonato)ethylidienyl]-3-methoxy-19-norpregna-1,3,5-tirene, a diethyl phosphono steroid derived from mestranol.

TABLE 5
The *P. carinii* Recombinant SAM:SMT Expressed in *Escherichia coli*: Affinity of Sterol Substrates[a]

Sterol substrate	K_m (μM)	V_{max} (pmol mg^{-1} protein min^{-1})	Products
Lanosterol	11	155	24-Methylenelanost-8-en-3β-ol (eburicol); 24-ethylidenelanost-8-en-3β-ol (pneumocysterol)[b]
24-Methylenelanosterol	19	738	(*Z*)-24-Ethylidenelanost-8-en-3β-ol; (*E*)-24-ethylidenelanost-8-en-3β-ol[c]
Zymosterol	41	42	Structures not determined
Cycloartenol	ND		

[a]From Reference 59. Recombinant protein was expressed in *E. coli*, from a pET 30a vector, which contains an S- and 6 His-tags. Assays were performed on transformed bacterial homogenates; thus, V_{max} values do not represent rates of the pure enzyme protein. ND, not determined.
[b]The *Z* and *E* isomers were in a 2:1 ratio.

enzymes in sterol biosynthesis have been cloned, sequenced, and expressed in heterologous systems.

Matsuda and his colleagues (56) succeeded in expressing the recombinant *P. carinii* oxidosqualene cyclase (encoded by *erg7)* in the yeast *Saccharomyces cerevisiae*. The enzyme produced lanosterol (not cycloartenol); hence, the enzyme is a lanosterol synthase (56), which is consistent with our inability to detect cycloartenol in *P. carinii* by GLC–MS with sensitivity in the nanomolar range (38). Unlike the *S. cerevisiae* enzyme, the recombinant lanosterol synthase did not accumulate in lipid particles but remained in the endoplasmic reticulum of the yeast cell (56). The transformed yeast has been used to screen a number of potential inhibitors of this enzyme (57). Some compounds showed promise as potential anti-*Pneumocystis* drugs by exhibiting activity against *P. carinii* proliferation in short-term culture with little toxicity to mammalian tissue culture cells.

The *P. carinii* SAM:SMT (encoded *erg6*) was expressed in *S. cerevisiae* and in the bacterium *Escherichia coli* (58,59) by our group. Unlike most yeast SAM:SMT, the *P. carinii* recombinant enzyme expressed in *E. coli* can transfer one or two methyl groups to the C-24 position of the sterol side chain. Also, the enzyme can act on a number of sterol substrates and appears to prefer lanosterol over other sterols (Table 5). Experiments on the recombinant SAM:SMT showed that lanosterol is converted to 24-methylenelanost-8-en-3β-ol (eburicol) (Fig. 3). Eburicol is then converted to (*Z*)-24-ethylidenelanost-8-en-3β-ol (pneumocysterol) (58; Worsham, D.N., and Kaneshiro, E.S., unpublished data) as the major product; its stereoisomer (*E*)-24-ethylidenelanost-8-en-3β-ol is also produced (58). As described above, inhibition of SAM:SMT in *P. carinii* with an azasterol blocked the production of 24-alkylsterols and reduced organism proliferation (36). Thus, SAM:SMT is a particularly attractive target because it is absent in mammals and blocking this reaction in the pathogen may have little toxicity to the host.

The *P. carinii* 14DM (encoded by *erg11*) was also expressed in *S. cerevisiae* by Thomas and his colleagues (60). Compared with parental yeast cells, the transformed yeasts expressing the *P. carinii erg11* gene required higher concentrations of the azoles fluconazole and voriconazole to reduce culture proliferation; however, itraconazole was a potent inhibitor. Thus, the *P. carinii* 14DM appears to be relatively insensitive to some but not all azole drugs. These workers also identified two sites that were identical to those in a fluconazole-resistant strain of *Candida albicans,* and they altered the *P. carinii erg11* gene by site-directed mutagenesis at these two loci to those in the azole-sensitive *Candida*. The sites altered were E113 to D and T125 to K. However, D116E and D128T mutations are also found in azole-sensitive strains of *C. albicans* (61); thus, the importance of these amino acid substitutions in azole binding and susceptibility to fluconazole in *P. carinii* remains an open question. Studies on azole sensitivity of a native or recombinant *Pneumocystis* 14DM by direct enzyme analysis have yet to be reported.

Analysis of *erg* gene homolog expression under different environmental conditions has been initiated. The expression of several *erg* genes in response to anti-*Pneumocystis* drugs was evaluated using a macroarray protocol (54). After 24-h exposure to 0.1 μg/mL of chymostatin (inhibits HMG-CoA reductase), 25 μg/mL of tolnaftate (inhibits squalene epoxidase) (62), or 15 μg/mL of tebuconazole (inhibits 14DM) (63), putative *P. carinii erg11* and *erg8* expressions were down-regulated. These compounds increased expression of *erg1*, *erg4*, *erg6*, and *erg10*. On the other hand, *erg7*, *erg9*, and *erg13* were up-regulated by chymostatin and tebuconazole and down-regulated by tolnaftate. Pentamidine (inhibits mitochondrial DNA) (64) and atovaquone (inhibits electron transport) (65,66), used clinically against PcP, reduced expression of many *erg* genes, but a few exhibited increased expression. It should be noted that atovaquone not only inhibits the cytochrome bc_1 complex in the electron transport chain but also is a potent inhibitor of ubiquinone biosynthesis

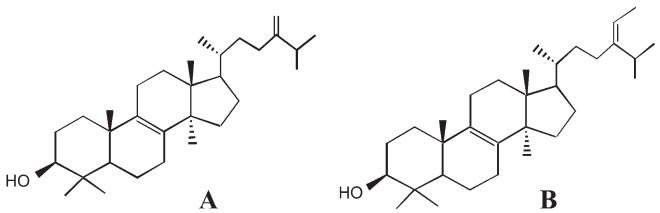

FIG. 3. Products of the recombinant *P. carinii* SAM:SMT on lanosterol. (A) 24-Methylenelanost-8-en-3β-ol (eburicol); (B) (*Z*)-24-ethylidenelanost-8-en-3β-ol. This was the dominant noncholesterol component in *P. jirovecii* 14DM$^-$. SAM:SMT, *S*-adenosyl methionine: C-24 sterol methyltransferase; 14DM, 14α-demethylase.

(67–70). Since the syntheses of sterols and ubiquinones share several steps of the isoprenoid pathway, the response of *erg* gene expression to atovaquone may be quite complex. Also, at this stage, the extent to which organism viability (ATP) influenced the expression of specific *erg* genes is not yet clear.

HUMAN-DERIVED *P. JIROVECII*: POSSIBLE *erg11* MUTANT POPULATION?

From the initial studies on *P. jirovecii* sterols, it was clear that the sterol composition of these organisms was more variable from sample to sample than those reported for *P. carinii* (71,72). It is expected that the biochemical nature of human-derived material would not be as uniform as that observed in laboratory animals kept under controlled conditions. However, the sterol compositions observed in different *P. jirovecii* samples spanned an unusually broad range. Two general types were noted (Fig. 4). One was characterized by C_{28} and C_{29} 24-alkylsterols with low proportions of $\geq C_{30}$ components, generally what was observed in *P. carinii* and *Pneumocystis* from SIV-positive monkeys, *scid/scid* mice, corticosteroid-immunosuppressed mice, and weanling rabbits (71). The other type had high proportions of $\geq C_{30}$ sterols, especially the C_{32} lanosterol derivative pneumocysterol (Fig. 3). It was a specimen of the latter type containing high concentrations of pneumocysterol that provided the material needed to describe this rare sterol (73). There was no obvious correlation between these two phenotypes and HIV/AIDS status, drug treatment, or other information available on patients' histories (71,72), but the effects of disease or therapy could not be ruled out at the time. It was proposed that the high $\geq C_{30}$ sterol phenotype resulted from low 14DM activity and that the sterols with compositions between the two extremes represented co-infections of the two genetically distinct organisms (72). However, one could not be absolutely sure that some patients might have taken drugs such as azoles that had not been prescribed for them, or that their diets might have included compounds that inhibit 14DM. Support for distinct *P. jirovecii* populations with different sterol compositions was provided by analysis of samples taken from different regions of the same pair of autopsied lungs obtained from a person who died of PcP. A broad range of sterol compositions was observed in different samples from the same individual; thus, it seems unlikely that the basis for these two phenotypes was caused by disease or drug treatment (74).

Most recently, definitive structural identities of 28 sterols were elucidated for *P. jirovecii* with blocked 14DM activity. Individual sterols were isolated by TLC and HPLC and analyzed by NMR (75). These analyses confirmed that the major noncholesterol components had a methyl group at C-14 of the sterol nucleus (Table 6). The observation of two different sterol composition phenotypes is most simply explained by mutation of the *erg11* gene. However, detailed genetic analysis of the *P. jirovecii erg11* gene from putative wild-type and mutant organisms has yet to be performed; thus, it cannot be ruled out that other factors regulating gene expression or enzyme activity are responsible. The putative $14DM^-$ phenotype has been observed in samples obtained from the United States and Europe (71,72). Thus, it appears that organisms of this phenotype have spread among different human populations, and it is possible that several putative *erg11* mutants developed independently. The rapid expression and high incidence of $14DM^-$ phenotype populations is consistent with the haploid nature of *Pneumocystis* organisms (76). The sterols of putative wild-type *P. jirovecii* with active 14DM have yet to be analyzed by NMR; however, it appears that the 14DM enzyme protein of *Pneumocystis* is unlike those of many other fungal pathogens.

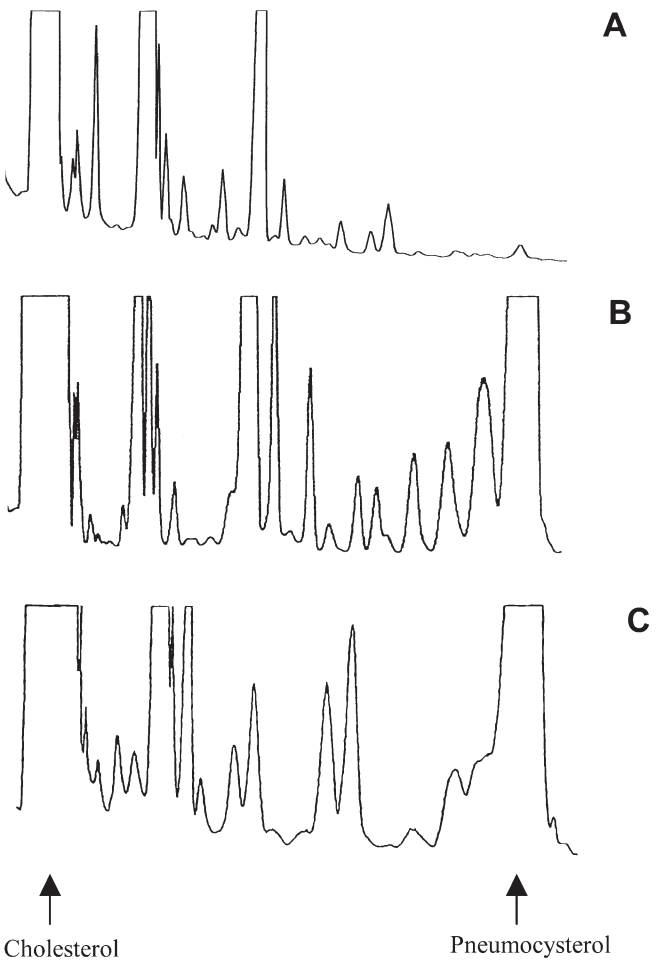

FIG. 4. GLC tracings of two sterol composition phenotypes in different *P. jirovecii* samples. (A) Purified cryopreserved *P. jirovecii* from an HIV-negative cancer patient from Denmark exhibiting low proportions of $\geq C_{30}$ sterols; (B) enriched preparation of cryopreserved *P. jirovecii* isolated from an AIDS patient in Italy with high ≥30 sterols (from Ref. 72); (C) formalin-fixed lung of an AIDS patient in the United States who died of *Pneumocystis* pneumonia.

SUMMARY

It is important to understand the natural history of *Pneumocystis* because it is an excellent example of an "emerging pathogen", that was not frequently encountered clinically 25

TABLE 6
Quantification of Sterol Categories Based on Nuclear Structures[a,b]

Sterol nucleus	Percentage of total mass[a]	
	P. jirovecii 14DM⁻	*P. carinii*[c]
4α,4α-Dimethyl-14α-methyl-Δ^8	88.82	5.30
4α-Methyl, 14α-methyl-Δ^8	2.42	0.00
4α-Methyl-Δ^8	0.00	2.17
Desmethyl-Δ^8	0.00	2.48
Desmethyl-Δ^7	0.12	43.75
Others	8.66	46.30

[a]Excluding cholesterol; data on *P. jirovecii* 14DM⁻ from Reference 74.
[b]*Pneumocystis jirovecii* with sterol compositional phenotype characterized by high proportions of $\geq C_{30}$ sterols is compared with those of *P. carinii*. Definitive structural analysis of sterols in *P. jirovecii* with high C_{27}–C_{29} sterols have yet to be reported.
[c]Data on *P. carinii* from Reference 39. 14DM, 14α-demethylase; for other abbreviations see Table 1.

yr ago, and was then regarded by most clinicians simply as a curiosity. Since the AIDS pandemic and the recognition that a variety of drug-resistant microbes are rapidly evolving, it is clear that more and diverse drugs need to be developed. Studying the sterols of *Pneumocystis* and their biosyntheses has broad relevance because some of these compounds are also found in some protozoan and fungal parasites that cause other devastating diseases. Furthermore, this organism has many unusual characteristics. A better understanding of how *Pneumocystis* functions would broaden our ability to study a larger range of organisms inhabiting our planet.

ACKNOWLEDGMENTS

Zunika Amit, Tazoacha Asonganyi, Mireille Basselin, Robert P. Baughman, David H. Beach, Enriquez Calderón, Carlo Contini, Melanie T. Cushion, José-Luis Giner, Koka Jayasimhulu, Scott Keely, Bettina Lundgren, F. Javier Medrano, Nieves Respaldiza, Stephenson W. Nkinin, Edward J. Parish, Jill A. Rosenfeld, Harry Rudney, A. George Smulian, James R. Stringer, D. Nicole Worsham, Michael A. Wyder, and Hui Zhao are among the collaborators who have participated in our sterol studies and are gratefully acknowledged. Supported by grants RO1 AI29316 and R21 AI49145 from the National Institute of Allergy and Infectious Diseases.

REFERENCES

1. Kaneshiro, E.S. (2002) Pneumocystis, in *Encyclopedia of Life Sciences*, Vol. 14, pp. 654–661, Nature Publishing Group, London (http://www.els.net).
2. Walzer, P.D. and Cushion, M.T. (eds.) (2004) Pneumocystis carinii *Pneumonia*, 3rd edn., Marcel Dekker, New York.
3. Bartlett, M.S., Vermund, S.H., Jacobs, R., Durant, P.J., Shaw, M.M., Smith, J.W., Tang, X., Lu, J.J., Li, B., Jin, S., and Lee, C.H. (1997) Detection of *Pneumocystis carinii* DNA in Air Samples: Likely Environmental Risk to Susceptible Persons, *J. Clin. Microbiol. 35*, 2511–2513.
4. Wakefield, A.E. (1996) DNA Sequences Identical to *Pneumocystis carinii* f. sp. *carinii* and *Pneumocystis carinii* f. sp. *hominis* in Samples of Air Spora, *J. Clin. Microbiol. 34*, 1754–1759.
5. Navin, T.R., Rimlan, D., Lennox, J.L., Jernigan, J., Cetron, M., Hightower, A., Roberts, J.M., and Kaplan, J.E. (2000) Risk Factors for Community-Acquired Pneumonia Among Persons Infected with Human Immunodeficiency Virus, *J. Infect. Dis. 181*, 158–164.
6. Kaneshiro, E.S., and Maiorano, J.N. (1996) Survival and Infectivity of *Pneumocystis carinii* Outside the Mammalian Host, *J. Eukaryot. Microbiol. 43*, 35S.
7. Chin, K., Luttrell, T.D., Roe, J.D., Shadzi, S., Wyder, M.A., and Kaneshiro, E.S. (1999) Putative *Pneumocystis* Dormant Forms Outside the Mammalian Host, and Long-Term Cultures Derived from Them: Initial Characterizations, *J. Eukaryot. Microbiol. 46*, 95S–99S.
8. Stringer, J.R. (1993) The Identity of *Pneumocystis carinii*: Not a Single Protozoan but a Diverse Group of Exotic Fungi, *Infect. Agents Dis. 2*, 109–117.
9. Stringer, J.R., Cushion, M.T., and Wakefield, A.E. (2001) New Nomenclature for the Genus *Pneumocystis, J. Eukaryot. Microbiol. 48*, 184S–189S.
10. Frenkel, J.K. (1976) *Pneumocystis jiroveci* n. sp. from Man: Morphology, Physiology, and Immunology in Relation to Pathology, *Natl. Cancer Inst. Monogr. 4*3, 13–30.
11. Frenkel, J.K. (1999) *Pneumocystis* Pneumonia, an Immunodeficiency-Dependent Disease (IDD): A Critical Historical Overview, *J. Eukaryot. Microbiol. 46*, 89S–92S.
12. Keely, S.P., Fischer, J.M., Cushion, M.T., and Stringer, J.R. (2004) Phylogenetic Identification of *Pneumocystis murina* sp. nov., a New Species in Laboratory Mice, *Microbiology 150*, 1153–1165.
13. Delanoë, P., and Delanoë, M. (1912) Sur les Rapports des Kystes de Carinii du Poumon des Rats avec le *Trypanosoma lewisii*, *C.R. Acad. Sci. (Paris) 155*, 658–660.
14. Cushion, M.T., Keely, S.P., and Stringer, J.R. (2004) Molecular and Phenotypic Description of *Pneumocystis wakefieldiae* sp. nov., a New Species in Rats, *Mycologia 96*, 429–438.
15. Yoshida, Y. (1989) Ultrastructural Studies of *Pneumocystis carinii, J. Protozool. 36*, 53–60.
16. Kaneshiro, E.S., Wyder, M.A., Zhou, L.H., Ellis, J.E., Voelker, D.R., and Langreth, S.G. (1993) Characterization of *Pneumocystis carinii* Preparations Developed for Lipid Analysis, *J. Eukaryot. Microbiol. 40*, 805–815.
17. Newsome, A.L., Durkin, M.M., Bartlett, M.S., and Smith, J.W. (1991) Videomicroscopic Recording of *Pneumocystis carinii* Motion, *J. Protozool. 38*, 207S–208S.
18. Weete, J.D. (1989) Structure and Function of Sterols in Fungi, *Adv. Lipid Res. 23*, 484–491.
19. Korn, E.D., von Brand, T., and Tobie, E.J. (1969) The Sterols of *Trypanosoma cruzi* and *Crithidia fasciculata, Comp. Biochem. Physiol. 30*, 601–610.
20. Goad, L.J., Keithly, J.S., Berman, J.D., Beach, D.H., and Holz, G.G., Jr. (1989) The Sterols of *Leishmania* Promastigotes and Amastigotes: Possible Implications for Chemotherapy, in *Leishmaniasis* (Hart, D.T., ed.), pp. 495–501, Plenum, New York.
21. Rahman, M.D., and Pascal, R.A. (1990) Inhibitors of Ergosterol Biosynthesis and Growth of the Trypanosomatid Protozoan *Crithidia fasciculata*, *J. Biol. Chem. 265*, 4986–4996.
22. Haughan, P.A., and Goad, L.J. (1991) Lipid Biochemistry of Trypanosomatids, in *Biochemical Protozoology* (Coombs, G.H., and North, M.D., eds.), pp. 312–328, Taylor & Frances, London.
23. Liendo, A., Visbal, G., Piras, M.M., and Urbina, J.A. (1999) Sterol Composition and Biosynthesis in *Trypanosoma cruzi* Amastigotes, *Mol. Biochem. Parasitol. 104*, 81–91.
24. Parish, E.J., Hanners, P.K., and Nes, W.D. (1987) Synthesis and Biological Evaluation of Fungal Bioregulators of Sterol Biosynthesis, in *The Metabolism, Structure and Function of Plant Lipids* (Stump, P.K., Mudd, J.B., and Nes, W.D., eds.), pp. 103–105, Plenum Press, New York.
25. Grebenok, R.J., Galbraith, D.W., and Penna, D.D. (1997) Characterization of *Zea mays* Endosperm C-24 Sterol Methyltrans-

ferase: One of Two Types of Sterol Methyltransferases in Higher Plants, *Plant Mol. Biol. 34*, 891–896.
26. Guo, D., Mangla, A.T., Zhou, W., Lopez, M., Jia, Z., Nichols, S.D., and Nes W.D. (1997) Antifungal Sterol Biosynthesis Inhibitors, in *Cholesterol: Its Functions and Metabolism in Biology and Medicine (Subcellular Biochemistry 28)* (Bittman, R., ed.), Kluwer Academic, pp. 91–116, Dordrecht, The Netherlands.
27. Nes, W.D. (2000) Sterol Methyl Transferase: Enzymology and Inhibition, *Biochim. Biophys. Acta 1529*, 63–88.
28. Hughes W.T. (1989) *Pneumocystis carinii*: Taxing Taxonomy, *Eur. J. Epidemiol. 5*, 265–269.
29. Bartlett, M.S., Queener, S.F., Shaw, M.M., Richardson, J.D., and Smith, J.W. (1994) *Pneumocystis carinii* Is Resistant to Imidazole Antifungal Agents, *Antimicrob. Agents Chemother. 38*, 1859–1861.
30. Cushion, M.T., Chen, F., and Kloepfer, N. (1997) A Cytotoxicity Assay for Evaluation of Candidate Anti-*Pneumocystis carinii* Agents, *Antimicrob. Agents Chemother. 41*, 379–384.
31. Bartlett, M.S., Eichholtz, R., and Smith, J.W. (1984) Antimicrobial Susceptibility of *Pneumocystis carinii* in Culture, *Diagn. Microbiol. Infect. Dis. 3*, 381–387.
32. Kaneshiro, E.S., Collins, M.S., and Cushion, M.T. (2000) Inhibitors of Sterol Biosynthesis and Amphotericin B Reduce the Viability of *Pneumocystis carinii* f. sp. *carinii*, *Antimicrob. Agents Chemother. 44*, 1603–1638.
33. Kaneshiro, E.S., Cushion, M.T., Walzer, P.D., and Jayasimhulu, K. (1989) Analyses of *Pneumocystis* Fatty Acids, *J. Protozool. 36*, 69S–72S.
34. Kaneshiro, E.S., Ellis, J.E., Jayasimhulu, K., and Beach, D.H. (1994) Evidence for the Presence of "Metabolic Sterols" in *Pneumocystis*: Identification and Initial Characterization of *Pneumocystis carinii* Sterols, *J. Eukaryot. Microbiol. 41*, 78–85.
35. Furlong, S.T., Samia, J.A., Rose, R.M., and Fishman, J.A. (1994*)* Phytosterols Are Present in *Pneumocystis carinii, Antimicrob. Agents Chemother. 38*, 2534–2540.
36. Urbina, J.A., Visbal, G., Contreras, L.M., McLaughlin, G., and Docampo, R. (1997) Inhibitors of $\Delta^{24(25)}$ Sterol Methyltransferase Block Sterol Synthesis and Cell Proliferation in *Pneumocystis carinii*, *Antimicrob. Agents Chemother. 41*, 1428–1432.
37. Zhou, W., Nguyen, T.T., Collins, M.S., Cushion, M.T., and Nes, W.D. (2002) Evidence for Multiple Sterol Methyl Transferase Pathways in *Pneumocystis carinii*, *Lipids 37*, 1177–1186.
38. Kaneshiro, E.S., and Wyder, M.A. (2000) The C_{27} to C_{32} Sterols in *Pneumocystis*, an Opportunistic Pathogen of Immunocompromised Mammals, *Lipids 35*, 317–324.
39. Giner, J.-L., Zhao, H., Beach, D.H., Parish, E.J., Jayasimhulu, K., and Kaneshiro, E.S. (2002) Comprehensive and Definitive Structural Identities of *Pneumocystis carinii* Sterols, *J. Lipid Res. 43*, 1114–1124.
40. Merali, S., Frevert, U., Williams, J.H., Chin, K., Bryan, R., and Clarkson, A.B., Jr. (1999) Continuous Axenic Cultivation of *Pneumocystis carinii, Proc. Natl. Acad. Sci. USA 96*, 2402–2407.
41. Kerbaum, S., Masliah, U., Alcindor, L.G., Bouton, C., and Cristol, D. (1983) Phospholipase Activities of Bronchoalveolar Lavage Fluid in Rat *Pneumocystis carinii* Pneumonia, *Br. J. Exp. Pathol. 64*, 75–80.
42. Sheehan, P.M., Stokes, D.C., Yeh, Y.-Y., and Hughes, W.T. (1986) Surfactant Phospholipids and Lavage Phospholipase A_2 in Experimental *Pneumocystis carinii* Pneumonia, *Am. Rev. Respir. Dis. 134*, 526–531.
43. Guo, Z., and Kaneshiro, E.S. (1995) Phospholipid Composition of *Pneumocystis carinii carinii* and the Effects of Methylprednisolone Immunosuppression on Rat Lung Lipids, *Infect. Immun. 63*, 1286–1290.
44. Hoffman, A.G., Lawrence, M.G., Ognibene, F., Suffredini, A.F., Lipschik, G.Y., Kovacs, J.A., Masur, H., and Shelhammer, J.H. (1992) Reduction of Pulmonary Surfactant in Patients with Human Immunodeficiency Virus Infection and *Pneumocystis carinii* Pneumonia, *Chest 102*, 1730–1738.
45. Chandra, J., Amit, Z., Baughman, R.P., Kleykamp, B., and Kaneshiro, E.S. (1999) *Pneumocystis* Infection Is Correlated with a Reduction in the Total Sterol Content of Human Bronchoalveolar Lavage Fluid, *J. Eukaryot. Microbiol. 46*, 146S–148S.
46. Worsham, D.N., Basselin, M., Smulian, A.G., Beach, D.H., and Kaneshiro, E.S. (2003) Evidence for Cholesterol Scavenging by *Pneumocystis* and Potential Modifications of Host-Synthesized Sterols by the *P. carinii* SAM:SMT, *J. Eukaryot. Microbiol. 50*, 678–679.
47. Florin-Christensen, M., Florin-Christensen, J., Wu, Y.-P., Zhou, L.H., Gupta, A., Rudney, H., and Kaneshiro, E.S. (1994) Occurrence of Specific Sterols in *Pneumocystis carinii*, *Biochem. Biophys. Res. Commun. 198*, 236–242.
48. Kaneshiro, E.S., Ellis, J.E., Zhou, L.H., Rudney, H., Gupta, A., Jayasimhulu, K., Setchell, K.D.R., and Beach, D.H. (1994) Isoprenoid Metabolism in *Pneumocystis carini, J. Eukaryot. Microbiol. 41*, 93S.
49. Ellis, J.E., Wyder, M.A., Zhou, L., Gupta, A., Rudney, H., and Kaneshiro, E.S. (1996) Composition of *Pneumocystis* Neutral Lipids and Identification of Coenzyme Q_{10} as the Major Ubiquinone Homolog in *P. carinii carinii*, *J. Eukaryot. Microbiol. 43*, 165–170.
50. Sul, D., and Kaneshiro, E.S. (2001) *Pneumocystis carinii* f. sp. *carinii* Biosynthesizes *de novo* Four Homologs of Ubiquinone, *J. Eukaryot. Microbiol. 48*, 184–189.
51. Haughan, P.A., Chance, M.L., and Goad, L.J. (1995) Effects of Azasterol Inhibitor of Sterol 24-Transmethylation on Sterol Biosynthesis and Growth of *Leishmania donovani* Promastigotes, *Biochem. J. 308*, 31–38.
52. Contini, C., Colombo, D., Cultrera, R., Prini, E., Sechi, T., Angelici, E., and Canipari, R. (1996) Employment of Terbinafine Against *Pneumocystis carinii* Infection in Rat Models, *Br. J. Dermatol. 134*, 30–32.
53. Walzer, P.D., and Ashbaugh, A. (2002) Use of Terbinafine in Mouse and Rat Models of *Pneumocystis carinii* Pneumonia, *Antimicrob. Agents Chemother. 46*, 514–516.
54. Collins, M.S., Bansil, S., and Cushion, M.T. (2003) Expression Profiling of the Responses of *Pneumocystis carinii* to Drug Treatment Using DNA Macroarrays, *J. Eukaryot. Microbiol. 50* (Suppl.), 605–606.
55. Beach, D.H., Chen, F., Cushion, M.T., Macomber, R.S., Krudy, G.A., Wyder, M.A., and Kaneshiro, E.S. (1997) Effects of Steroidal Allenic Phosphonic Acid Derivatives on the Parasitic Protists *Leishmania donovani, Leishmania mexicana mexicana* and *Pneumocystis carinii carinii*, *Antimicrob. Agents Chemother. 41*, 162–168.
56. Milla, P., Viola, F., Oliaro Bosso, S., Rocco, F., Cattel, L., Joubert, B.M., LeClair, R.J., Matsuda, S.P., and Balliano, G. (2002) Subcellular Localization of Oxidosqualene Cyclases from *Arabidopsis thaliana*, *Trypanosoma cruzi*, and *Pneumocystis carinii* Expressed in Yeast, *Lipids 37*, 1171–1176.
57. Hinshaw, J.C., Suh, D.-Y., Garnier, P., Buckner, F.S., Eastman, R.T., Matsuda, S.P.T., Joubert, B.M., Coppens, I., Joiner, K.A., Merali, S., *et al.* (2003) Oxidosqualene Cyclase Inhibitors as Antimicrobial Agents, *J. Med. Chem. 46*, 4240–4243.
58. Kaneshiro, E.S., Rosenfeld, J.A., Basselin, M., Bradshaw, S., Stringer, J.R., Smulian, A.G., and Giner, J.-L. (2001) *Pneumocystis carinii erg6* Gene: Sequencing and Expression of Recombinant SAM:Sterol Methyltransferase in Heterologous Systems, *J. Eukaryot. Microbiol. 48*, 144S–146S.
59. Kaneshiro, E.S., Rosenfeld, J.A., Basselin, M., Stringer, J.R., Keely, S., Smulian, A.G. and Giner, J.-L. (2002) The *Pneumocystis carinii* Drug Target *S*-Adenosyl-L-methionine:Sterol

Methyl Transferase Has a Unique Substrate Preference, *Mol. Microbiol*. *44*:989–999.
60. Morales, I.J., Vohra, P.K., Puri, V., Kottom, T.J., Limper, A.H., and Thomas, C.F. (2003) Characterization of a Lanosterol 14α-Demethylase from *Pneumocystis carinii*, *Am. J. Resp. Cell Mol. Biol*. *29*, 232–238.
61. Marichal, P., Koymans, L., Willemsens, S., Bellens, D., Verhasselt, P., Luyten, W., Borgers, M., Ramaekers, F.C.S., Odds, F.C., and Vanden Bossche, H. (1999) Contribution of Mutations in the Cytochrome P450 14α-Demethylase (Erg11p, Cyp51p) to Azole Resistance in *Candida albicans*, *Microbiology 145*, 2701–2713.
62. Vanden Bossche, H., Engelen, M., and Rochette F. (2003) Antifungal Agents of Use in Animal Health—Chemical, Biochemical and Pharmacological Aspects, *J. Vet. Pharmacol. Ther*. *26*, 5–29.
63. Isaacson, D.M., Tolman, E.L., Tobia, A.J., Rosenthale, M.E., McGuire, J.L., Vanden Bossche, H., and Janssen, P.A.J. (1988) Selective Inhibition of 14α-Desmethyl Sterol Synthesis in *Candida albicans* by Terconazole, a New Triazole Antimycotic, *J. Antimicrob. Chemother*. *21*, 333–343.
64. Ludewig, G., and Staben, C. (1994) Characterization of the PNT1 Pentamidine Resistance Gene of *Saccharomyces cerevisiae, Antimicrob. Agents Chemother*. *38*, 2850–2856.
65. Gutteridge, W. (1991) 566C80, An Antimalarial Hydroxynaphthoquinone with Broad Spectrum: Experimental Activity Against Opportunistic Parasitic Infections of AIDS Patients, *J. Eukaryot. Microbiol. 38*, 141S–143S.
66. Cushion, M.T., Collins, M., Hazra, B., and Kaneshiro, E.S. (2000) The Effects of Atovaquone and Diospyrin-Based Drugs on the ATP Content of *Pneumocystis carinii* f. sp. *carinii*, *Antimicrob. Agents Chemother*. 44, 713–719.
67. Kaneshiro, E.S., Sul, D., and Hazra, B. (2000) Effects of Atovaquone and Diospyrin-Based Drugs on Ubiquinone Biosynthesis in *Pneumocystis carinii*, *Antimicrob. Agents Chemother. 44*, 14–18.
68. Kaneshiro, E.S., Sul, D., Basselin, M., and Kayser, O. (2001) *Pneumocystis carinii* Synthesizes Four Ubiquinone Homologs: Inhibition by Atovaquone and Bupravaquone but Not by Stigmatellin*, J. Eukaryot. Microbiol*. *48*, 172S–173S.
69. Kaneshiro, E.S. (2001) Are Cytochrome b Gene Mutations the Only Cause of Atovaquone Resistance in *Pneumocystis*? *Drug Resist. Updat. 5*, 322–329.
70. Kaneshiro, E.S., Basselin, M., and Hunt, S.M. (2003) Evidence That Biosynthesis of Individual Ubiquinone Homologs in *Pneumocystis carinii* Is Under Homolog-Specific Negative Feedback (product) Control, *J. Eukaryot. Microbiol. 50*, 622–623.
71. Amit, Z. (1998) Analysis of *Pneumocystis carinii* Sterols from Various Mammalian Hosts, Including Humans, Ph.D. Thesis, 121 pp., University of Cincinnati, Cincinnati, Ohio. Available at the University of Cincinnati Chemistry/Biology Library.
72. Kaneshiro, E.S., Amit, Z., Chandra, J., Baughman, R.P., Contini, C., and Lundgren, B. (1999) The Sterol Composition of *Pneumocystis carinii hominis* Organisms Isolated from Human Lungs, *Clin. Diagn. Lab. Immunol*. *6*, 970–976.
73. Kaneshiro, E.S., Amit, Z., Swonger, M.M., Kreishman, G.P., Brooks, E.E., Kreishman, M., Jayasimhulu, K., Parish, E.J., Sun, H., Kizito, S.A., and Beach, D.H. (1999) Pneumocysterol [(24*Z*)-ethylidenelanost-8-en-3β-ol], a Rare Sterol Detected in the Opportunistic Pathogen *Pneumocystis carinii* f. sp. *hominis*: Structural Identity and Chemical Synthesis*, Proc. Natl. Acad. Sci. USA 96*, 97–102.
74. Amit, Z., and Kaneshiro, E.S. (2001) Heterogeneity of *Pneumocystis* Sterol Profiles in Samples from Different Sites of the Same Lung Suggests Co-infection by Distinct Organism Populations, *J. Clin. Microbiol*. *39*, 1137–1139.
75. Giner, J.-L., Zhao, H., Amit, Z., and Kaneshiro, E.S. (in press) Sterol Composition of *Pneumocystis jirovecii* with Blocked 14α-Demethylase Activity, *J. Eukaryot. Microbiol*.
76. Wyder, M.A., Rasch, E.M., and Kaneshiro, E.S. (1998) Quantitation of Absolute *Pneumocystis carinii* Nuclear DNA Content. Trophic and Cystic Forms Isolated from Infected Rat Lungs Are Haploid Organisms*, J. Eukaryot. Microbiol*. *45*, 233–239.

[Received July 6, 2004; accepted August 26, 2004]

Detailed Sterol Compositions of Two Pathogenic Rust Fungi

José-Luis Giner* and Hui Zhao

State University of New York, College of Environmental Science and Forestry, Syracuse, New York 13210

ABSTRACT: Teliospores of cedar-apple rust *Gymnosporangium juniperi-virginianae* were collected from the eastern red cedar *Juniperus virginiana,* and aeciospores of quince rust *G. clavipes* were collected from the fruit of English hawthorn *Crataegus laevigata.* The sterol fractions were separated by HPLC, and their identities were determined by 600 MHz ^{1}H NMR. Twenty-six sterols were isolated from *G. juniperi-virginianae* and 18 sterols were isolated from *G. clavipes.* The principal sterol of both fungi was (*Z*)-stigmasta-7,24(28)-dien-3β-ol. Other major sterols were (24*S*)-ergost-7-en-3β-ol, (24*S*)-stigmast-7-en-3β-ol, and (24*S*)-stigmasta-5,7-dien-3β-ol. The sterols of the hosts were found to be very different from those of the fungi. The 24-alkyl sterols of the fungi had the 24α-configuration, whereas those of the hosts had the 24β-configuration. Similarities to the sterol composition of the AIDS pneumonia fungus *Pneumocystis carinii* are discussed.

Paper no. L9550 in *Lipids 39,* 763–767 (August 2004).

The *Gymnosporangium* rusts are heterobasidiomycete fungi that have a complex life cycle alternating between evergreen hosts of the cypress family and members of the rose family. Cedar-apple rust *Gymnosporangium juniperi-virginianae* Schw. is widespread in the United States and southern Canada east of the Rocky Mountains, and the quince rust *G. clavipes* C. & P. is found throughout North America (1). These plant diseases have a significant economic impact on fruit orchards. Many of the fungicides used to control these plant diseases target fungal sterol metabolism (2,3), as do most clinical antifungal agents (4–6).

The sterol biosynthesis of the rust fungi differs significantly from that of other fungi (7–9). Although ergosterol is the predominant sterol in many fungi, the rusts contain mainly C_{29} sterols. The rust fungi also contain 24-ethyl or 24-ethylidene sterols and therefore carry out an extra *S*-adenosylmethionine (SAM)-dependent methylation. A similar pattern has been found in *Pneumocystis*, an opportunistic fungal pathogen that causes pneumonia in AIDS patients (10).

In publications over 30 yr old, the sterols of five species of rust fungi were reported based on mixed m.p., GC, MS, and low-field ^{1}H NMR (11–19). The structures of a total of four sterols were identified. In this study, by using RP-HPLC and 600 MHz NMR, a detailed analysis is presented of the sterols of *G. juniperi-virginianae* and *G. clavipe*. This is the first complete analysis of the sterols of rust fungi, and the first sterol analysis of these two disease organisms. The sterol content of the host plants, *Juniperus virginiana* and *Crataegus laevigata*, was also analyzed.

*To whom correspondence should be addressed at Department of Chemistry, SUNY-ESF, 1 Forestry Dr., Syracuse, NY 13210. E-mail: jlginer@syr.edu

Abbreviation: SAM, *S*-adenosylmethionine.

MATERIALS AND METHODS

Plant sample collection. The gall and telia of *G. juniperi-virginianae* were collected from five eastern red cedar trees, *J. virginiana,* on the campus of Syracuse University (Syracuse, NY). The telia (168 g) were cut off and stored at −20°C. Healthy twigs (2.1 g) were collected from the same trees and lyophilized using a Virtis 8XL freeze dryer (The Virtis Company, Gardiner, NY) to give 1.0 g of dry material. Fruits infected with *G. clavipes* were collected from English hawthorn trees *C. laevigata* on the campus of Syracuse University. The aecial peridia (12.2 g) containing the aeciospores of *G. clavipes* were removed from the surface of the fruit and stored at −20°C. Heathy fruits (62.9 g) were collected from the same trees and lyophilized to give 34.4 g of dry material.

Extraction and purification. All extraction and purification steps were carried out under low light conditions to minimize autoxidation. All solvent extractions were carried out with 100 mL of solvent at room temperature for 1 h, unless specified otherwise. Solvent extractions were repeated until TLC monitoring indicated complete extraction of sterols.

The sterols were extracted from *G. juniperi-virginianae* by stirring the telia with ethyl acetate overnight. After separation of the solvent, the fungal cells were further extracted several times with acetone. The organic extracts were combined and evaporated *in vacuo* to dryness.

The sterols of *G. clavipes* were similarly extracted from aecial peridia and aeciospores by stirring with ethyl acetate overnight, followed by extraction with several portions of acetone, several portions of dichloromethane, and sonication with methanol/dichloromethane (1:9, vol/vol). The organic solutions were combined, and the solvents were removed by evaporation *in vacuo* to dryness.

The sterols of lyophilized hawthorn fruits (*C. laevigata*) were extracted several times in a stainless steel blender (Waring Products Division, New Hartford, CT) with ethyl acetate. The solvent was evaporated *in vacuo*. The dry leaves of juniper (*J. virginiana*) were extracted by the same method as the hawthorn fruits.

The polar substances were removed from the four extracts by filtration through silica gel with ethyl acetate. The residues

were saponified with 5% ethanolic KOH at reflux for 1 h. The reaction mixtures were partitioned between water and ether, and the organic layers were evaporated *in vacuo*. Pigments were removed by Florisil chromatography using hexane/ethyl acetate (39:1 and 4:1, vol/vol). The sterol fractions from the hexane/ethyl acetate 4:1 eluate were evaporated to dryness with a stream of nitrogen.

Sterol analyses. The total sterols of each organism were fractionated by preparative TLC (0.25-mm Silica Gel 60 F254; EM Science, Gibbstown, NJ) using hexane/ethyl acetate (2:1, vol/vol) as the solvent. Four sterol fractions were obtained: *G. juniperi-virginianae* (17.2 mg); *G. clavipes* (16.1 mg); *J. virginiana* (1.4 mg); and *C. laevigata* (7.5 mg). Three 4,4-dimethyl sterol fractions were obtained: *G. juniperi-virginianae* (2.8 mg); *G. clavipes* (0.3 mg); and *C. laevigata* (2.4 mg). The different sterol fractions thus obtained were purified by RP-HPLC using a Waters 6000A pump, Waters 410 differential refractometer, and two Altex Ultrasphere ODS columns (5 μm, 10 × 250 mm) in series, at a flow rate of 3 mL/min of methanol. Some 4,4-dimethyl sterol fractions were still mixtures after HPLC. These were separated using acetonitrile/methanol/ethyl acetate (11:4:4, by vol) as the HPLC solvent. The isolated sterol fractions were evaporated with a stream of N_2 and characterized by ^{1}H NMR (600 MHz, $CDCl_3$). The structures of sterols were assigned by comparison with the NMR spectra of standards. The relative proportions of sterols within each fraction were determined from the HPLC integrals.

Spectral data. The structures of (24*S*)-stigmasta-5,7,25-trien-3β-ol (**Ej**) and (24*S*)-stigmast-5,7,9(11)-trien-3β-ol (**Fi**) have not been reported before (See Fig. 1 for structures—uppercase bold letters refer to the sterol nucleus, lowercase letters to the side chain). Their assignments were based on their ^{1}H NMR spectral data. Thus, the signals due to the sterol nucleus match those of other sterols with the same nucleus, and the signals due to the side chain match those of other sterols with the same side chain. The ^{1}H NMR data are also reported for 28-norurs-12-en-3β-ol, which previously has only been characterized as its acetate (20).

(24S)-Stigmasta-5,7,25-trien-3β-ol (**Ej**): ^{1}H NMR ($CDCl_3$, 600 MHz), δ5.58 (1H, *m*), 5.39 (1H, *m*), 4.73 (1H, *s*), 4.64 (1H, *s*), 3.64 (1H, *m*), 1.57 (3H, *s*), 0.95 (3H, *s*), 0.91 (3H, *d*, *J* = 6.6), 0.81 (3H, *t*, *J* = 7.2), 0.63 (3H, *s*).

(24S)-Stigmasta-5,7,9(11)-trien-3β-ol (**Fi**): ^{1}H NMR ($CDCl_3$, 600 MHz), δ5.68 (1H, *m*), 5.52 (1H, *m*), 5.41 (1H, *m*), 3.61 (1H, *m*), 1.25 (3H, *s*), 0.94 (3H, *d*, *J* = 6.4), 0.86 (3H, *t*, *J* = 7.4), 0.84 (3H, *d*, *J* = 6.8), 0.82 (3H, *d*, *J* = 6.8), 0.57 (3H, *s*).

28-Norurs-12-en-3β-ol: ^{1}H NMR ($CDCl_3$, 600 MHz), δ5.16 (1H, *t*, *J* = 3.6), 3.23 (1H, *m*), 1.06 (3H, *s*), 1.00 (3H, *s*), 0.95 (3H, *s*), 0.92 (3H, *d*, *J* = 6.5), 0.91 (3H, *s*), 0.80 (3H, *d*, *J* = 6.5), 0.80 (3H, *s*).

RESULTS

The sterols of cedar-apple rust *G. juniperi-virginianae* were 0.01% of the wet weight of the teliospores. The major sterol was (*Z*)-stigmasta-7,24(28)-dien-3β-ol (**Bg**) (58.7%). In total, 26 sterols were isolated, including three 4,4-dimethylsterols (12.4% of total sterols), two 4α-methyl sterols (1.2%), and 21 desmethyl sterols (86.4%) (Table 1). The desmethyl sterol fraction contained seven Δ^5 sterols (8.4% of the total sterols), five Δ^7 sterols (67.1%), two $\Delta^{8(14)}$ sterols (0.7%), two Δ^8 sterols (1.7%), four $\Delta^{5,7}$ sterols (7.9%), and one $\Delta^{5,7,9(11)}$ sterol (0.6%). The major sterol side chains were (*Z*)-$\Delta^{24(28)}$ stigmastane (**g**) (63.8%) and (24*S*)-stigmastane (**i**) (15.4%) (Fig. 1).

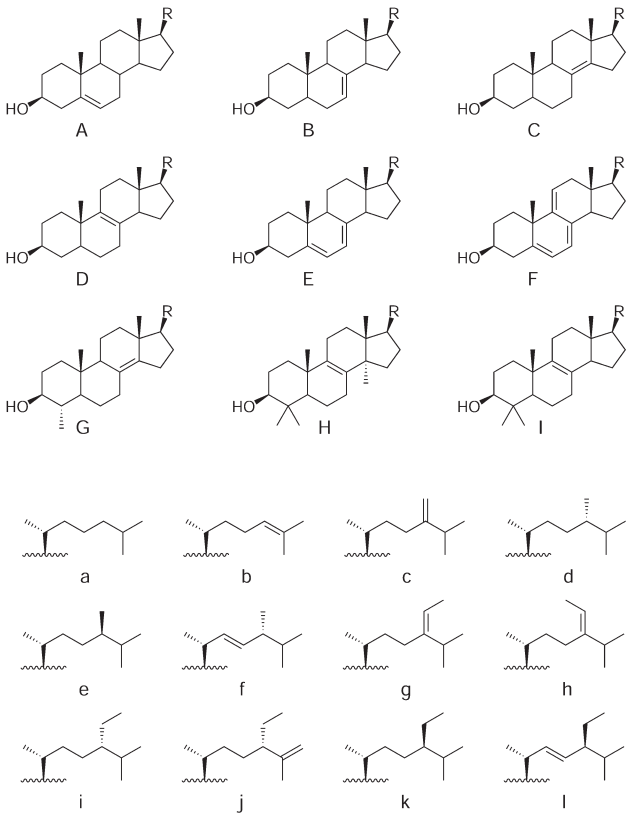

FIG. 1. Structures of sterol nuclei (uppercase letters) and sterol side chains (lowercase letters) isolated from *Gymnosporangium* rust fungi and their hosts. (R = sterol side chain).

The sterols of quince rust *G. clavipes* accounted for 0.13% of the wet weight of the aeciospores. The major sterols were (*Z*)-stigmasta-7,24(28)-dien-3β-ol (**Bg**) (40.9%), (24*S*)-ergost-7-en-3β-ol (**Bd**) (28.7%), and (24*S*)-stigmast-7-en-3β-ol (**Bi**) (12.2%). Eighteen sterols were found, including two 4,4-dimethylsterols (1.2% of total sterols), and 16 desmethyl sterols (98.8%) (Table 1). No 4α-methylsterols were found. The desmethyl sterols fraction contained four Δ^5 sterols (2.4% of the total sterols), five Δ^7 sterols (84.6%), three Δ^8 sterols (2.0%), three $\Delta^{5,7}$ sterols (8.8%), and one $\Delta^{5,7,9(11)}$ sterol (1.0%). The major sterol side chains were (*Z*)-$\Delta^{24(28)}$ stigmastane (**g**) (42.5%), (24*S*)-ergostane (**d**) (29.1%), and (24*S*)-stigmastane (**i**) (22.2%).

The leaves of *J. virginiana* contained desmethylsterols as 0.07% of the wet weight (Table 1). Four sterols were found; all are Δ^5 sterols. The principal sterol was (24*R*)-stigmast-5-en-3β-ol (sitosterol, **Ak**) (84.6%). No 4,4-dimethyl- or 4α-methylsterols were found.

TABLE 1
Sterol Contents of *Gymnosporangium* Rust Fungi and Their Hosts

		Percentage of total sterols[c]			
Sterols[a]	RT[b] (MeOH)	*Gymnosporangium juniperi-virginianae*	*Juniperus virginiana*	*G. clavipes*	*Crataegus laevigata*
Cholest-5-en-3β-ol (**Aa**)	45.0	—[d]	—	0.2	1.1
Cholesta-5,24-dien-3β-ol (**Ab**)	37.4	0.4	—	—	—
Ergosta-5,24(28)-dien-3β-ol (**Ac**)	39.0	0.04	—	0.2	—
(24*S*)Ergost-5-en-3β-ol (**Ad**)	49.9	0.9	—	—	—
(24*R*)Ergost-5-en-3β-ol (**Ae**)	49.3	—	9.5	—	—
(24*R*)Ergosta-5,22-dien-3β-ol (**Af**)	42.9	0.04	—	—	—
(*Z*)Stigmasta-5,24(28)-dien-3β-ol (**Ag**)	45.0	1.8	3.9	—	4.6
(*E*)Stigmasta-5,24(28)-dien-3β-ol (**Ah**)	45.0	—	—	—	0.3
(24*S*)Stigmast-5-en-3β-ol (**Ai**)	53.6	5.2	—	0.6	—
(24*S*)Stigmasta-5,25-dien-3β-ol (**Aj**)	42.3	0.02	—	—	0.8
(24*R*)Stigmast-5-en-3β-ol (**Ak**)	53.0	—	84.5	1.4	68.4
(24*S*)Stigmasta-5,22-dien-3β-ol (**Al**)	47.6	—	2.1	—	0.3
Ergosta-7,24(28)-dien-3β-ol (**Bc**)	38.0	2.6	—	2.5	—
(24*S*)Ergost-7-en-3β-ol (**Bd**)	49.9	1.6	—	28.7	—
(*Z*)Stigmasta-7,24(28)-dien-3β-ol (**Bg**)	45.0	58.7	—	40.9	—
(24*S*)Stigmast-7-en-3β-ol (**Bi**)	53.3	4.0	—	12.2	—
(24*S*)Stigmasta-7,25-dien-3β-ol (**Bj**)	42.9	0.2	—	0.3	—
Ergosta-8(14),24(28)-dien-3β-ol (**Cc**)	35.6	0.6	—	—	—
(*Z*)Stigmasta-8(14),24(28)-dien-3β-ol (**Cg**)	40.6	0.1	—	—	—
Cholesta-8,24-dien-3β-ol (**Db**)	37.5	0.2	—	—	—
Ergosta-8,24(28)-dien-3β-ol (**Dc**)	37.8	—	—	0.2	—
(24*S*)Ergost-8-en-3β-ol (**Dd**)	48.1	—	—	0.4	—
(*Z*)Stigmasta-8,24(28)-dien-3β-ol (**Dg**)	42.9	1.5	—	1.4	—
(24*R*)Ergosta-5,7,22-trien-3β-ol (**Ef**)	38.0	0.5	—	0.2	—
(*Z*)Stigmasta-5,7,24(28)-trien-3β-ol (**Eg**)	40.6	1.7	—	0.2	—
(24*S*)Stigmasta-5,7-dien-3β-ol (**Ei**)	48.1	5.6	—	8.4	—
(24*S*)Stigmasta-5,7,25-trien-3β-ol (**Ej**)	40.6	0.1	—	—	—
(24*S*)Stigmasta-5,7,9(11)-trien-3β-ol (**Fi**)	35.6	0.6	—	1.0	—
4α-Methylergosta-8(14),24(28)-dien-3β-ol (**Gc**)	39.8	0.9	—	—	—
(24*S*)4α-Methylergost-8(14)-en-3β-ol (**Gd**)	50.0	0.3	—	—	—
Lanosta-8,24-dien-3β-ol (**Hb**)	42.6	5.5	—	—	—
24-Methylenelanost-8-en-3β-ol (**Hc**)	44.9	6.5	—	0.3	—
4,4-Dimethylergosta-8,24(28)-dien-3β-ol (**Ic**)	50.0	0.4	—	—	—
α-Amyrin	49.4	—	—	0.9	1.3
β-Amyrin	45.2	—	—	—	0.9
δ-Amyrin	46.9	—	—	—	0.3
Butyrospermol	41.7	—	—	—	6.9
Cycloartenol	46.9	—	—	—	1.4
Lupeol	38.7	—	—	—	7.7
24-Methylenecycloartanol	49.4	—	—	—	1.3
28-Norurs-12-en-3β-ol	49.4	—	—	—	1.3
Δ^7 Tirucallol	43.5	—	—	—	3.4

[a]The structures of sterols are shown in Figure 1—uppercase bold letters refer to the sterol nucleus, lowercase letters to the side chain.
[b]HPLC retention times (min).
[c]Percentages determined by integration of the refractive index detection chromatogram.
[d]Em dash (—), not detected.

Fifteen sterols were isolated from hawthorn (*C. laevigata*) fruits (0.02% of the wet weight), including nine 4,4-dimethylsterols (24.5%) and six desmethyl sterols (75.5%) (Table 1). All of the desmethyl sterols had the Δ^5 sterol nucleus. All of the 4,4-dimethylsterols were nonsteroidal triterpene alcohols. No 4α-methylsterols were obtained from the fruits.

DISCUSSION

A 1958 analysis of wheat stem rust *Puccinia graminis* var. *tritici* indicated the presence of ergost-7-en-3β-ol (**Bd** or **Be**) in uredospores (11). The identification of this sterol was based on IR spectrometry, X-ray diffraction patterns, mixed m.p., and polarimetry. However, when the sample was later analyzed by GC, it was shown to be mainly stigmast-7-en-3β-ol (**Bi** or **Bk**) (13). In another study of this fungus, capillary GC and MS also showed stigmast-7-en-3β-ol (**Bi** or **Bk**) to be the predominant sterol, and minor amounts of ergost-7-en-3β-ol (**Bd** or **Be**) and a diunsaturated C_{28} sterol were detected (15). The same pattern was found in the closely related *P. striiformis* (15).

The investigation of the lipids of the flax rust *Melampsora lini* identified stigmast-7-en-3β-ol (**Bi** or **Bk**) and stigmasta-

7,24(28)-dien-3β-ol (**Bg** or **Bh**) in the uredospores using m.p., IR spectrometry, and 60 MHz NMR (12). Based on its GC retention time and UV spectrum, a third, minor sterol was suggested to be stigmasta-5,7-dien-3β-ol (**Ei** or **Ek**). It was proposed that the sterols are derived from the host by the parasite.

The major sterol of the uredospores of the bean rust *Uromyces phaseoli* was identified as (*Z*)-stigmasta-7,24(28)-dien-3β-ol (**Bg**) using m.p., GC, MS, and NMR (14). The stereochemical assignment of the side chain was made possible by Fourier transform 100 MHz NMR spectrometry. A second sterol was tentatively identified as stigmast-7-en-3β-ol (**Bi** or **Bk**) based on MS and IR spectrometry. Biosynthetic incorporation of ^{14}C-labeled methionine and acetate showed that the sterols were synthesized by the rust fungus (12,16). The isolation of a partially purified SAM-dependent sterol methyltransferase from the uredospores further strengthened the argument that the fungus synthesizes its own sterols (21).

In an analysis of the lipids of *Cronartium fusiforme*, the causative agent of fusiform pine rust, stigmasta-7,24(28)-dien-3β-ol (**Bg** or **Bh**) was identified as the major sterol in the aeciospores using GC–MS (17). Interestingly, basidiospores of the same species were shown by GC–MS to contain stigmast-7-en-3β-ol (**Bi** or **Bk**) as the major sterol, followed by stigmasta-5,7-dien-3β-ol (**Ei** or **Ek**) and ergost-7-en-3β-ol (**Bd** or **Be**) (18). These sterols were also detected in the mycelium of the germinating basidiospores in culture (19).

The detailed analysis presented here of cedar-apple and quince rusts confirms the earlier observations of stigmasta-7,24(28)-dien-3β-ol (**Bg** or **Bh**), stigmast-7-en-3β-ol (**Bi** or **Bk**), and ergost-7-en-3β-ol (**Bd** or **Be**) as the major sterols of rust fungi. Stigmasta-5,7-dien-3β-ol (**Ei** or **Ek**), which had been identified as a minor component in flax rust and pine rust, was detected in both cedar-apple and quince rusts at 5.6 and 8.4%, respectively. In contrast to the early studies, the stereochemical configuration of the sterol side chains, and thereby the absolute identity of each sterol, was determined. All of the 24-alkyl sterols in the *Gymnosporangium* rusts, with the exception of a small amount of sitosterol (**Bi**) (1.4%) found in *G. clavipes*, had the 24β-configuration. This is in marked contrast to the sterols of the host plants, which all bear the 24α-configuration, with the exception of a trace of clerosterol (**Aj**) found in the hawthorn fruit (0.8%).

The difference in stereochemical configuration of the 24-alkyl sterols of the host and the fungi indicates that the rust fungi have a $\Delta^{24(28)}$ sterol reductase that is opposite in its stereochemical outcome to that of the host plants. Evidence for *de novo* sterol biosynthesis in the rust fungi comes from the presence of lanosterol (**Hb**) and 24-methylenelanosterol (**Hc**), which are intermediates in fungal sterol biosynthesis but are rarely found in plants (22). This is consistent with the biosynthetic studies of Lin, Langenbach, and Knoche supporting sterol synthesis in rust fungi (14,16,21). Furthermore, fungicides that inhibit the enzyme 14-demethylase effectively control the rust fungi (2,3); therefore, the rust fungi depend on *de novo* sterol biosynthesis for the sterols required for propagation and growth.

However, some of the sterols detected may be scavenged from the host plants and subsequently modified. The small amount of sitosterol (1.4%, **Ak**) found in the quince rust probably comes from the host, where it is the major sterol (68.4%). Similarly, the trace of α-amyrin (0.9%) found in quince rust most likely originates from the host. Interestingly, none of the other triterpene alcohols found in the host was detected in the fungus, suggesting selective uptake. It is likely that the Δ^5 sterols found in the rust fungi are scavenged from the hosts. For example, (*Z*)-stigmasta-5,24(28)-dien-3β-ol (**Ag**) could be taken from the host and converted into (24*S*)-stigmast-5-en-3β-ol (**Ai**) using the fungal $\Delta^{24(28)}$ sterol reductase.

The rust fungi do not appear to be capable of producing Δ^{22}-desaturated sterols such as ergosterol (**Ef**) (7–9). Although ergosterol is the major sterol of many fungi (7–9), only traces were detected in the two *Gymnosporangium* rusts (0.5 and 0.2% of the total sterols). This may come from contamination with other types of fungi, such as yeast. Other $\Delta^{5,7}$ sterols (**Eg**, **Ei**, **Ej**) bearing side chains typical of rust fungi are found in substantial amounts, and it is therefore likely that the rust fungi are capable of synthesizing the $\Delta^{5,7}$ sterol nucleus.

The fungal pathogen that causes pneumonia in immunocompromised individuals, such as AIDS patients, has a very similar sterol composition to the rust fungi (10). The major sterol in *Pneumocystis* is cholesterol, which is thought to originate from the lungs of the host. However, as in the rust fungi, the major noncholesterol sterols are (*Z*)-stigmasta-7,24(28)-dien-3β-ol (**Bg**), ergost-7-en-3β-ol (**Bd**), and stigmast-7-en-3β-ol (**Bi**). Of the 30 sterols isolated from the two *Gymnosporangium* rusts, 25 of them were also found in *Pneumocystis carinii.* The same set of side chains (**b**, **c**, **d**, **g**, **i**, **j**) and nuclei (**A**–**D**, **G**–**I**) is found in both types of fungi, although the $\Delta^{5,7}$ sterol nucleus (**E**) was not detected in *P. carinii*. Neither the rusts nor *P. carinii* appears to be able to produce Δ^{22} sterols such as ergosterol (**Ef**). Finally, rust fungi contain the rare FA *cis*-9,10-epoxyoctadecanoic acid (8,23), which is also found in *Pneumocystis* (24). These similarities suggest that *Pneumocystis* is closely related to the rust fungi.

ACKNOWLEDGMENT

We thank Prof. C.J.K. Wang (Biology Department, SUNY-ESF) for identification of the rust fungi.

REFERENCES

1. Sinclair, W.A., Lyon, H.H., and Johnson, W.T. (1987) *Diseases of Trees and Shrubs*, pp. 240–249, Comstock Publishing Associates, Ithaca, New York.
2. Yoder, K.S., and Hickey, K.D. (1981) Sterol-Inhibiting Fungicides for Control of Certain Diseases of Apple in the Cumberland–Shenandoah Region, *Plant Dis. 65*, 998–1001.
3. Köller, W. (1991) Antifungal Agents with Target Sites in Sterol Functions and Biosynthesis, in *Target Sites of Fungicide Action* (Köller, W., ed.), pp. 119–206, CRC Press, Boca Raton.
4. Sisler, H.D., and Ragsdale, N.N. (1984) Biochemical and Cellular Aspects of the Antifungal Action of Ergosterol Biosynthesis Inhibitors, in *Mode of Action of Antifungal Agents* (Trinci,

A.P.J., and Ryley, J.F., eds.), pp. 257–282, Cambridge University Press, Cambridge, London.
5. St. Georgiev, V. (ed.) (1988) *Antifungal Drugs*, *Ann. N.Y. Acad. Sci. 544,* 1–613.
6. Chapman, S.W., Cleary, J.D., Rogers, P.D., Hamill, R.J., Como, J., Dismukes, W.E., Groll, A.H., Walsh, T.J., Pappas, P.G., Roilides, E., *et al.* (2003) Systemic Antifungal Drugs, in *Clinical Mycologe* (Dismukes, W.E., Pappas, P.G., and Sobel, J.D., eds.), pp. 31–140, Oxford University Press, New York.
7. Weete, J.D. (1973) Sterols of the Fungi: Distribution and Biosynthesis, *Phytochemistry 12*, 1843–1864.
8. Weete, J.D. (1980) *Lipid Biochemistry of Fungi and Other Organisms*, 2nd edn., pp. 237–243, Plenum Press, New York.
9. Patterson, G.W. (1994) Phylogenetic Distribution of Sterols, in *Isopentenoids and Other Natural Products: Evolution and Function* (Nes, W.D., ed.), pp. 90–108, American Chemical Society, Washington, DC.
10. Giner, J.-L., Zhao, H., Beach, D.H., Parish, E.J., Jayasimhulu, K., and Kaneshiro, K.S. (2002) Comprehensive and Definitive Structural Identification of *Pneumocystis carinii* Sterols, *J. Lipid Res. 43*, 1114–1124.
11. Hougen, F.W., Craig, B.M., and Ledingham G.A. (1958) The Oil of Wheat Stem Rust Uredospores I. The Sterol and Carotenes of the Unsaponifiable Matter, *Can. J. Microbiol. 4*, 521–529.
12. Jackson, L.L., and Frear, D.S. (1968) Lipid of Rust Fungi—II. Stigmast-7-enol and Stigmasta-7,24(28)-dienol in Flax Rust Uredospores, *Phytochemistry 7*, 651–654.
13. Nowak, R., Kim, W.K., and Rohringer, R. (1972) Sterols of Healthy and Rust-Infected Primary Leaves of Wheat and of Non-germinated and Germinated Uredospores of Wheat Stem Rust, *Can. J. Bot. 50*, 185–190.
14. Lin, H.-K., Langenbach, R.J., and Knoche, H.W. (1972) Sterols of *Uromyces phaseoli* Uredospores, *Phytochemistry 11*, 2319–2322.
15. Weete, J.D., and Laster, J.L. (1973) Distribution of Sterols in the Fungi I. Fungal Spores, *Lipids 9*, 575–581.
16. Lin, H.-K., and Knoche, H.W. (1974) Origins of Sterols in Uredospores of *Uromyces phaseoli*, *Phytochemistry 13*, 1795–1799.
17. Carmack, C.L., Weete, J.D., and Kelley, W.D. (1976) Hydrocarbons, Fatty Acids and Sterols of *Cronartium fusiforme* Aeciospores, *Physiol. Plant Pathol. 8*, 43–49.
18. Weete, J.D., and Kelley, W.D. (1977) Fatty Acids and Sterols of *Cronartium fusiforme* Basidiospores, *Lipids 12*, 398–401.
19. Weete, J.D., Kelley, W.D., and Hollis, C.A. (1979) Mycelial Lipids as an Aid in Identifying Rust Fungi in Culture—*Cronartium fusiforme*, *Can. J. Microbiol. 25*, 1481–1483.
20. Hota, R.K., and Bapuji, M. (1994) Triterpenoids from the Resin of *Shorea robusta*, *Phytochemistry 35*, 1073–1074.
21. Lin, H.-K., and Knoche, H.W. (1976) A Sterol Methyltransferase from Bean Rust Uredospores, *Uromyces phaseoli*, *Phytochemistry 15*, 683–687.
22. Nes, W.R., and Nes, W.D. (1980*) Lipids in Evolution*, 157 pp., Plenum Press, New York.
23. Tulloch, A.P., Craig, B.M., and Ledingham G.A. (1959) The Oil of Wheat Stem Rust Uredospores II. The Isolation of *cis*-9,10-epoxyoctadecanoic Acid and the Fatty Acid Composition of the Oil, *Can. J. Microbiol. 5*, 485–491.
24. Kaneshiro, E.S., Ellis, J.E., Guo, A., Jayasimhulu, K., Maiorano, J.N., and Kallam, K.A. (1996) Characterizations of Neutral Lipid Fatty Acids and *cis*-9,10-Epoxy Octadecanoic Acid in *Pneumocystis carinii carinii*, *Infect. Immunol. 64*, 4105–4114.

[Received July 20, 2004; accepted August 24, 2004]

The *in vitro* Hydrolysis of Phytosterol Conjugates in Food Matrices by Mammalian Digestive Enzymes

Robert A. Moreau* and Kevin B. Hicks

Crop Conversion Science and Engineering Research Unit, ERRC, ARS, USDA, Wyndmoor, Pennsylvania 19038

ABSTRACT: All fruits, vegetables, and grains contain phytosterols. Numerous clinical studies have documented that phytosterols lower LDL-cholesterol levels and thereby reduce the risk of cardiovascular disease. Most experts believe that the cholesterol-lowering mechanism of phytosterols requires that they be in their "free" form. In addition to their occurrence in the free form, phytosterols also occur as four common phytosterol conjugates: (i) fatty acyl esters, (ii) hydroxycinnamate esters, (iii) steryl glycosides, and (iv) fatty acylated steryl glycosides. This study was undertaken to investigate the extent of hydrolysis of four common phytosterol conjugates by mammalian digestive enzymes (cholesterol esterase and pancreatin, a mixture of pancreatic enzymes) and for comparison purposes, by KOH. Two types of purified hydroxycinnamate esters (sitostanyl ferulate and oryzanol, a mixture of hydroxycinnamate esters purified from rice bran oil) were hydrolyzed by cholesterol esterase and by pancreatin. Both cholesterol esterase and pancreatin hydrolyzed the phytosteryl esters in two functional food matrices, and they hydrolyzed the hydroxycinnamate esters in corn fiber oil. This is the first report to demonstrate that phytostanyl ferulate esters (which are present at levels of 3–6% in corn fiber oil) are hydrolyzed by pancreatic cholesterol esterase. It is also the first report that pancreatin contains enzymes that hydrolyze the fatty acyl moiety of fatty acylated steryl glycoside, converting it to steryl glycoside. Pancreatin had no effect on steryl glycosides. The ability of pancreatin to hydrolyze three other types of lipid conjugates was also evaluated. Phospholipids were completely hydrolyzed. About half of the galactolipids were hydrolyzed, and less than 10% of the polyamine conjugates were hydrolyzed. The extents of hydrolysis of phytosteryl esters by base (saponification) were also studied, and conditions commonly used for the saponification of acyl lipids (1.5 N methanolic KOH, 30 min at 70°C), were found to result in a nearly 100% hydrolysis of TAG but only about 35–45% hydrolysis of the phytosteryl fatty acyl esters or phytosteryl hydroxycinnamate esters.

Paper no. L9531 in *Lipids 39,* 769–776 (August 2004).

In recent years there has been much interest in phytosterols (plant sterols), mainly due to their ability to lower LDL-cholesterol by 10–15%, when consumed at dosages of 1–3 g/d and at still lower dosages in certain food matrices (1). In plants and in plant-derived foods, phytosterols can occur either in the "free" form (FS, with an OH group that is not bound), or as phytosterol conjugates: phytosterol fatty acyl esters (SE), hydroxycinnamate phytosterol esters (HSE), acylated steryl glycosides (ASG), and steryl glycosides (SG) (Fig. 1). FS, SE, ASG, and SG are ubiquitous in plants, but HSE are usually found only in cereals such as corn and rice. Very little is known about how phytosterol conjugates are hydrolyzed and metabolized during digestion. Two *in vivo* studies have demonstrated that SE are hydrolyzed in the upper portion of the small intestine (2,3). One *in vitro* study reported comparable rates of hydrolysis (23–34%)

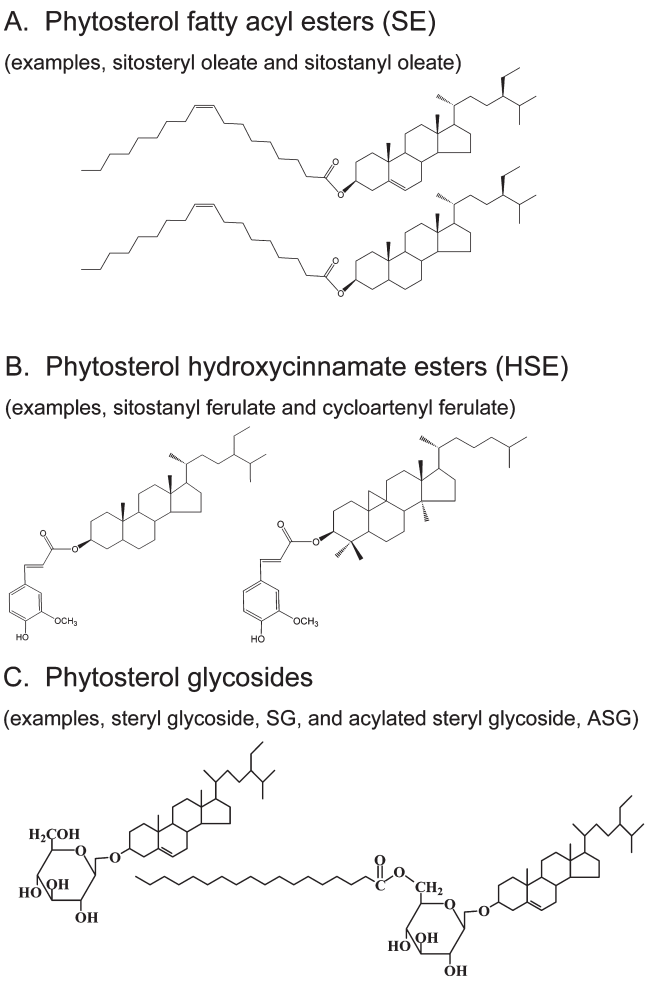

FIG. 1. Structures of some common phytosterol conjugates found in foods.

*To whom correspondence should be addressed at ERRC, ARS, USDA, 600 East Mermaid Lane, Wyndmoor, PA 19038.
E-mail : rmoreau@errc.ars.usda.gov

Abbreviations: ASG, acylated steryl glycosides; CFP, *p*-coumaroyl feruloylputrescine; DFP, diferuloylputrescine; FS, free phytosterol, i.e., with an unbound –OH group; HSE, hydroxycinnamate phytosterol esters; SE, phytosterol fatty acyl esters; SG, steryl glycosides.

of various oleate esters of sterols (cholesterol, sitosterol, and stigmasterol) using porcine pancreatic cholesterol esterase (4).

One *in vivo* study demonstrated that oryzanol (an HSE from rice bran oil) is hydrolyzed in the small intestine (5). Two recent *in vitro* studies demonstrated that some HSE (orzyanols comprising desmethyl phytosterols) were rapidly hydrolyzed by pancreatic enzymes whereas others (oryzanol, mainly comprising dimethyl phytosterols such as cycloartenol) were apparently hydrolyzed at much lower rates (6,7).

We are not aware of any previous *in vitro* reports of the ability of digestive enzymes to hydrolyze steryl glycosides or phytostanyl ferulate esters, which are found at levels of 3–6% in corn fiber oil (1). Some previous reports have provided evidence that certain plant β-glucosidases could hydrolyze phytosterol glycosides (8–12) whereas others (1,13), using more highly purified preparations of β-glucosidase, have reported that these enzyme preparations were not able to hydrolyze SG.

This study was undertaken to investigate the extents of *in vitro* hydrolysis of several phytosterol conjugates (especially the phytostanyl ferulate esters in corn fiber oil and steryl glycosides), and other lipid conjugates (Fig. 2), using two commercial mammalian digestive enzymes (bovine cholesterol esterase and pancreatin, of which the latter is a common commercial extract of the pancreas of hogs, containing cholesterol esterase, lipase, amylase, trypsin, and other enzymes) and to compare these enzymatic hydrolyses to those obtained *via* saponification (alkaline hydrolysis).

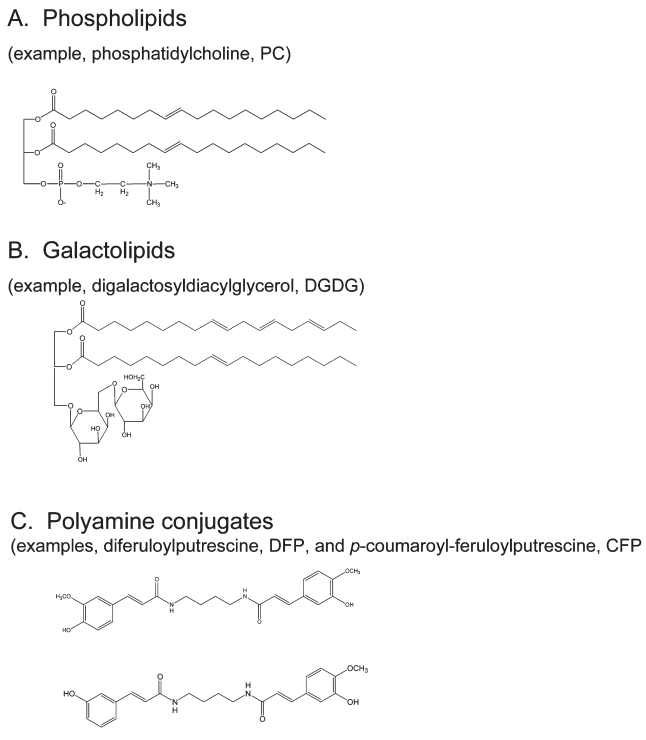

FIG. 2. The structures of some other common plant lipid conjugates found in foods.

MATERIALS AND METHODS

Oryzanol was purchased from CTS Organics (Atlanta, GA). Sitostanyl ferulate (~99%) was synthesized by the method of Condo *et al.* (14). Take Control® and Benecol® were purchased at a local supermarket. Lecithin Granules, 97% Soy Phosphatides (Vitamin Shoppe, North Bergen, NJ) were obtained from a local vitamin store. Oat oil was purchased from BioSeparations (Los Angeles, CA). Corn fiber oil was prepared as previously described (15). An extract rich in polyamine conjugates was prepared as previously described (16). All other reagents were purchased from Sigma (St. Louis, MO).

Lipids were added to the reaction mixture first by pipeting a stock solution containing lipids dissolved in isopropanol. Oryzanol and sitostanyl ferulate stock solutions were prepared by dissolving the pure compounds in isopropanol at a concentration of 0.005 M. Benecol, Take Control, and corn fiber oil stock solutions were prepared at a concentration of 40 mg/mL. Lecithin, oat oil, and corn bran ethanol extract stock solutions were prepared at a concentration of 10 mg/mL. Isopropanol was evaporated with a stream of nitrogen, and then the other reagents were added. All enzymatic reactions (5 mL) contained 0.05 M Trizma buffer and pH 7.0, 0.020 taurocholate. Both enzymes (see next) were dissolved in the above buffer at a concentration of 10 mg/mL. Pancreatin (2 mg, from porcine pancreas, Sigma P-7545) and cholesterol esterase (1 mg, from bovine pancreas, Sigma C-3766) were added to each 5-mL reaction mixture. Lipids were extracted by the method of Bligh and Dyer (17).

Nonpolar lipids (including SE, HSE, TAG, and FFA) were quantitatively analyzed by a normal-phase HPLC method with ELSD (15). These analyses were performed on a Model 1050 Hewlett-Packard HPLC, with autosampler, and detection was by both Model 1050 HP diode-array UV-vis detector (Agilent Technologies, Avondale, PA) and an MKII Alltech-Varex Evaporative Light Scattering Detector (Alltech Associates, Deerfield, IL), operated at 40°C and a nitrogen gas flow rate of 1.7 standard liters per minute. The column was a LiChrosorb 7 μ DIOL column (3 × 100 mm, packed by Chrompack, Raritan, NJ). The ternary gradient had a constant flow rate of 0.5 mL/min, with Solvent A = hexane/acetic acid, 1000:1, Solvent B = hexane/isopropanol, 100:1. The gradient timetable was as follows: at 0 min, 100:0 (%A/%B); at 8 min, 100:0; at 10 min, 75:25; at 40 min, 75:25; at 41 min, 100:0; and at 60 min, 100:0.

Polar lipids (including ASG, SG, glycolipids, phospholipids, and polyamine conjugates) were quantitatively analyzed by a similar HPLC-ELSD method (18), using a Model 1100 Hewlett-Packard HPLC, with autosampler, and detection by both a Model 1100 HP diode-array UV-vis detector (Agilent Technologies) and a Model 55 Sedex Evaporative Light Scattering Detector (Richard Scientific, Novato, CA), operated at 40°C and a nitrogen gas pressure of 2 bar. The diol column and flow rates were the same as above. The ternary gradient consisted of Solvent A = hexane/acetic acid, 1000:1; Solvent B = isopropanol; and Solvent C = water. Gradient timetable was as

TABLE 1
Hydrolysis of Nonpolar Phytosterol Conjugates (in purified samples) by Digestive Enzymes

		% Hydrolysis[a]	
Phytosterol conjugate	Enzyme	1 h	4 h
Sitostanyl ferulate	Cholesterol esterase	55.4 ± 3.9	84.7 ± 3.8
	Pancreatin	ND[b]	47.3 ± 8.3
Oryzanol	Cholesterol esterase	33.7 ± 4.3	56.3 ± 7.3
	Pancreatin	ND	0

[a]All reported in all tables are the mean ± SD (n = 3).
[b]Not determined.

follows: at 0 min, 90:10:0 (%A/%B/%C); at 30 min, 58:40:2; at 40 min, 45:50:5; at 50 min 45:50:5; at 51 min, 50:50:0; at 52 min, 90:10:0; and at 60 min 90:10:0. The minimum limit of quantitative detection with both HPLC methods was about 1 μg per injection. Mass vs. peak area calibration curves were constructed for the range of 1–20 μg per injection.

For enzymatic and saponification studies the extent of hydrolysis was calculated as the decrease in the levels of substrate (phytosteryl conjugates or other lipids). All enzymatic treatments were performed three times, twice with duplicate samples and once with triplicate samples. The enzymatic results presented are the means of the triplicate sample experiment ± SD. The saponification experiments were performed twice, each time with duplicate samples, and the data presented are the means from one experiment.

RESULTS AND DISCUSSION

The first set of experiments focused on evaluating the extent of enzymatic hydrolysis of phytosteryl and phytostanyl fatty acyl esters in two purified phytosteryl conjugates (Table 1). Our *in vitro* studies demonstrated that cholesterol esterase catalyzed a moderate extent of hydrolysis of both HSE, about 55–85% hydrolysis of sitostanyl ferulate (a desmethyl stanyl ester from corn) (Fig. 3), and about 35–55% hydrolysis of oryzanol (a steryl ferulate ester mixture comprising both dimethyl and desmethyl sterols from rice bran). Pancreatin catalyzed the hydrolysis of about half of the sitostanyl ferulate in 4 h, but none of the oryzanol (Table 1). We do not know why cholesterol esterase catalyzed the hydrolysis of both HSE (oryzanol and sitostanyl ferulate), whereas pancreatin (which contains cholesterol esterase) only hydrolyzed sitostanyl ferulate and not oryzanol. A possible explanation is that the cholesterol esterase was bovine and the pancreatin was porcine, and the amino acid sequences and substrate specificities of the two cholesterol esterases could have been different. Another possible explanation is that some of the other enzymes (lipases, proteases, etc.) or nonenzymatic components in pancreatin, or some of the products generated by some of the other enzymes, may alter the specificity of its cholesterol esterase.

This is the first study of any kind that demonstrates phytostanyl ferulate esters (which are present at levels of 3–6% in corn fiber oil) are hydrolyzed by mammalian digestive enzymes. These *in vitro* data predict that the phytostanyl ferulate esters in corn fiber oil potentially can be hydrolyzed and the free stanols can potentially lower LDL-cholesterol in the same manner as phytosteryl and phytostanyl fatty acyl esters. The efficacy of the phytostanyl and phytosteryl fatty acyl esters has been demonstrated in numerous clinical studies (1).

Huang (6) used reversed-phase HPLC to separate the individual molecular species in oryzanol, before and after incubation with cholesterol esterase, and presented qualitative data (chromatograms) suggesting that the esters with desmethyl phytosterols (sitosteryl and campesteryl ferulates) were hydrolyzed at a much faster rate than the esters of dimethyl phytosterols (cycloartenyl and 24-methylcycloartenyl ferulates). Miller *et al.* (7) performed similar incubations of individual molecular species of oryzanol HSE and demonstrated that desmethyl esters (sitosteryl and campesteryl ferulates) were hydrolyzed by cholesterol esterase and dimethyl esters (cycloartenyl and 24-methylcycloartenyl ferulates) were not. *In situ* experiments indicated that ^{14}C-γ-oryzanol was partially hydrolyzed in the intestine during absorption (5). The lower extents of *in vitro* hydrolysis of esters of dimethyl sterol-containing esters in the current study (oryzanol) and in previous *in vitro* studies may help to explain the lower *in vivo* cholesterol-lowering efficacy of dimethylsterols reported by Trautwein

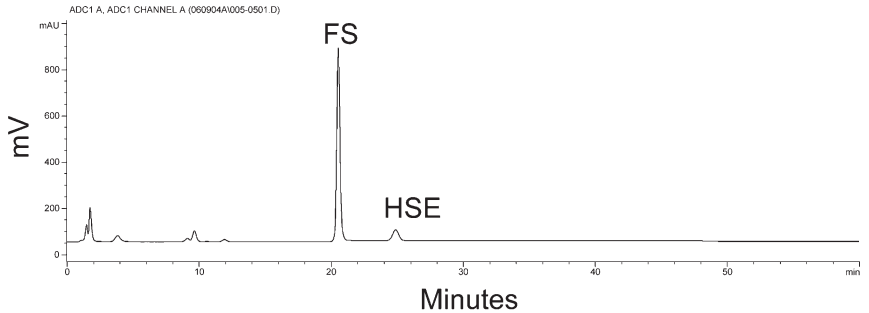

FIG. 3. HPLC chromatogram evaluating the hydrolysis of phytosterol hydroxycinnamate esters. The substrate was pure sitostanol ferulate (0.15 mg), the enzyme was cholesterol esterase (1 mg), in 5 mL reaction mixture or buffer and taurocholate, which was incubated for 1 h at 37°C. Abbreviations: FS, free phytosterols; HSE, sitostanyl ferulate.

TABLE 2
Hydrolysis of Nonpolar Phytosterol Conjugates (in food matrices) by Digestive Enzymes

Food matrix	Phytosterol conjugate	Concentration of conjugate in food matrix (wt% of total lipid)	Enzyme	% Hydrolysis 1 h	% Hydrolysis 4 h
Benecol®	Phytostanyl FA esters	~10%	Cholesterol esterase[a]	33.0 ± 2.8	44.6 ± 9.6
			Pancreatin	ND	8.0 ± 4.2
Take Control®	Phytosteryl FA esters	~10%	Cholesterol esterase	38.1 ± 2.4	46.0 ± 4.8
			Pancreatin	ND	35.6 ± 2.3
Corn fiber oil	Phytosteryl FA esters	~6%	Cholesterol esterase	9.6 ± 3.1	10.1 ± 5.4
			Pancreatin	ND	0
	Phytostanyl ferulate	~4%	Cholesterol esterase	26.7 ± 4.2	57.0 ± 1.1
			Pancreatin	ND	10.5 ± 4.4

[a]*Note:* With all three food matrices, the substrate also included TAG, and TAG were completely hydrolyzed in 4 h. ND, not determined.

et al. (19). It should be noted that the previous two *in vitro* reports did not include any phytostanyl esters, so our current report is the first *in vitro* report of the hydrolysis of a phytostanyl ferulate ester by mammalian digestive enzymes

Although these experiments demonstrated that *mammalian* cholesterol esterase is able to hydrolyze HSE, it should also be noted that in our previous report (20) the *microbial* cholesterol esterase (in a commercial spectrophotometric cholesterol test kit) was unable to hydrolyze sitostanyl ferulate.

The second experiment investigated the extent of hydrolysis of several phytosteryl ester-containing functional foods (Table 2). The phytosteryl and phytostanyl fatty acyl esters in the two margarines were hydrolyzed to a similar extent at both 1 h (33–38%) and 4 h (44–46%) (Table 2). An interesting observation was that in addition to hydrolyzing the steryl esters, the purified cholesterol esterase catalyzed the hydrolysis of almost all of the TAG in all three food matrices (Fig. 4). When the phytosteryl esters in both spreads were incubated with pancreatin, a slightly lower extent of hydrolysis was observed with the steryl esters in Take Control (about 36% hydrolysis), and a much lower extent of hydrolysis was observed with stanyl esters in Benecol (about 8% hydrolysis). When the cholesterol esterase was used to hydrolyze corn fiber oil, its phytosteryl fatty acyl esters (which constitute 4–6% of the oil) were hydrolyzed to a low extent (9–10%) and its hydroxycinnamate esters [predominantly sitostanyl ferulate according to Norton (21)] were hydrolyzed to a moderate extent (27–57%). When pancreatin was used to hydrolyze corn fiber oil, its phytostanyl ferulate was hydrolyzed to a low extent (about 11%); there was no apparent hydrolysis of its phytosteryl fatty acyl esters. This lower rate of hydrolysis of the corn fiber oil HSE than the rate of hydrolysis of pure sitostanyl ferulate (Table 1) may be attributed to the fact that the former is a mixture of esters that contains significant levels of campestanol and other esterified phytostanols and phytosterols (21). The phytosteryl fatty acyl esters in corn fiber oil were hydrolyzed to a lesser extent than those in both margarines. A possible explanation for the low extent of hydrolysis of phytosteryl fatty acyl esters in corn fiber oil is that the presence of other components (wax esters, squalene, and other hydrocarbons, which have retention times very close to that of phytosteryl fatty acyl esters), may interfere with the accurate quantification of these esters. Since the extent of hydrolysis was calculated as the disappearance of substrate, the presence of these compounds could contribute to the apparent lower extents of hydrolysis with corn fiber oil. In the future we will test this hypothesis using another HPLC system (reversed-phase or alumina) that better separates these very nonpolar components.

In a previous *in vitro* study, the rates of hydrolysis of several molecular species of phytosteryl fatty acyl esters by porcine pancreatic cholesterol esterase were shown to be similar to the rates of hydrolysis of cholesteryl esters (4). The

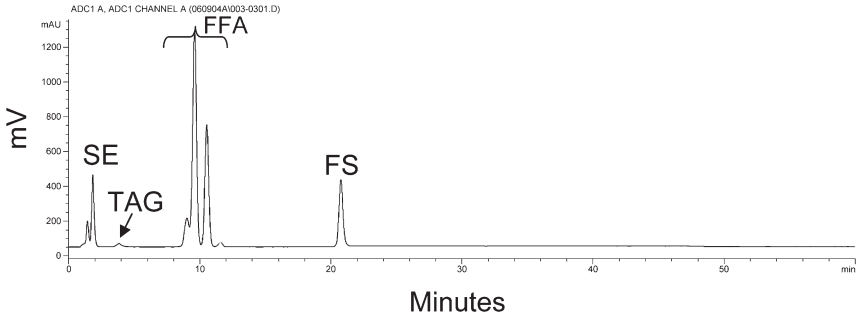

FIG. 4. HPLC chromatogram evaluating the hydrolysis of phytosterol fatty acyl esters (SE). The substrate was Take Control® (2 mg), the enzyme was cholesterol esterase (1 mg), in a 5-mL reaction mixture of buffer and taurocholate, incubated for 1 h at 37°C. Abbreviation: FS, free phytosterols.

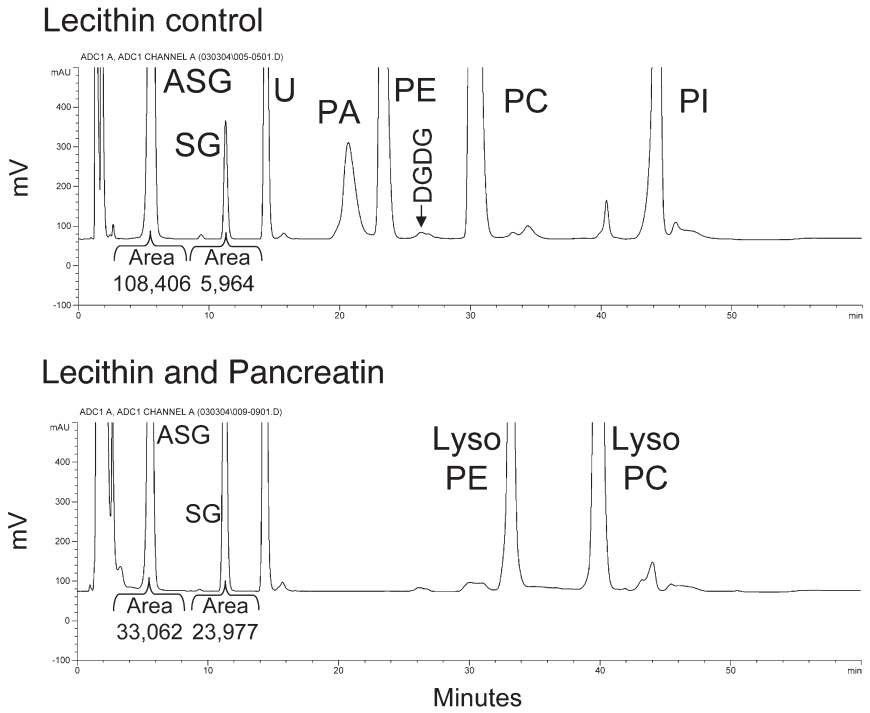

FIG. 5. HPLC chromatogram evaluating the hydrolysis of phytosterol glycosides (ASG and SG) and phospholipids. The substrate was soy lecithin (2 mg) and the enzyme was pancreatin (2 mg) in 5 mL of a reaction mixture of buffer and taurocholate that was incubated for 6 h at 37°C. U, unknown; DGDG, digalactosyldiacyglycerol; for other abbreviations see Figure 1.

current and previous *in vitro* results confirmed the *in vivo* reports (2,3) that phytostanyl and phytosteryl fatty acyl esters (SE) are hydrolyzed in the mammalian GI system.

The next several experiments were performed to evaluate the ability of pancreatin to hydrolyze phytosteryl glycosides and other polar lipid conjugates. An HPLC system designed to separate polar lipids was employed (Figs. 5,6) and the results are summarized in Table 3.

Among the steryl glycoside conjugates, pancreatin was found to hydrolyze the FA moiety from ASG, thus converting it to SG (Table 3). However, with three different food matrices (Table 3), the glycosidic bond in SG apparently was not hydrolyzed by pancreatin (Fig. 5). It is not widely known that "Soy Lecithin" or "Lecithin Granules" contain significant levels of sterol glycosides. Also, it is unfortunate that the word lecithin has two meanings: It is the common name for PC, and it is the name for a food supplement that is an enriched fraction of polar lipids, containing about 97% phosphatides. The manufacturer claims that the fraction contains 3% "other lipids;" our analytical data indicate that it contains about 3% phytosterols (~2.7% acylated steryl glycoside and ~0.2% steryl glycoside, Table 3). Oat oil and corn bran ethanol extract were evaluated as other food matrices that also contain SG and that contain other lipid conjugates. Because the levels of SG actually increased when all three food matrices were incubated with pancreatin (presumably owing to the hydrolysis of ASG), we feel that it will be important to confirm this observation (i.e., the inability of the enzyme to hydrolyze SG) in the future by evaluating the ability of pancreatin to hydrolyze a purified preparation of SG.

Weber (22) performed *in vivo* metabolic studies with rats. His results indicated that [4-^{14}C]sitosteryl β-D-glucosides were hydrolyzed at a low rate in the intestines, but they were not absorbed. In contrast, the current *in vitro* results indicate that SG is not hydrolyzed by mammalian digestive enzymes.

Although this is the first published *in vitro* report evaluating the potential hydrolysis of steryl glycosides by mammalian digestive enzymes, others have reported that some early preparations of β-glucosidase from almonds were useful for the hydrolysis of SG (8–12). However, it has been reported that more recent commercial preparations of almond β-glucosidase were unable to hydrolyze SG (1,13). A possible explanation is that there are multiple types of β-glucosidase in almond, and that the type(s) that hydrolyze SG are not the type(s) that are enriched in modern commercial preparations. Recent evidence suggests that one possible physiological role of steryl glycosides is to serve as primers for cellulose synthesis (23).

Among the other common plant lipid conjugates, pancreatin causes near-complete (>99%) hydrolysis of phospholipids in Lecithin Granules (Fig. 5) and a partial (about 40%) hydrolysis of digalactosydiacylglycerol (Fig. 6), a common plant galactolipid, which is present at a level of 1–5% in oat oil.

We recently reported (16) that the pericarp of corn kernels contains high levels of two unusual polyamine conjugates, diferuloylputrescine (DFP) and *p*-coumaroyl feruloylputrescine (CFP) (structures shown in Fig. 2). When corn bran

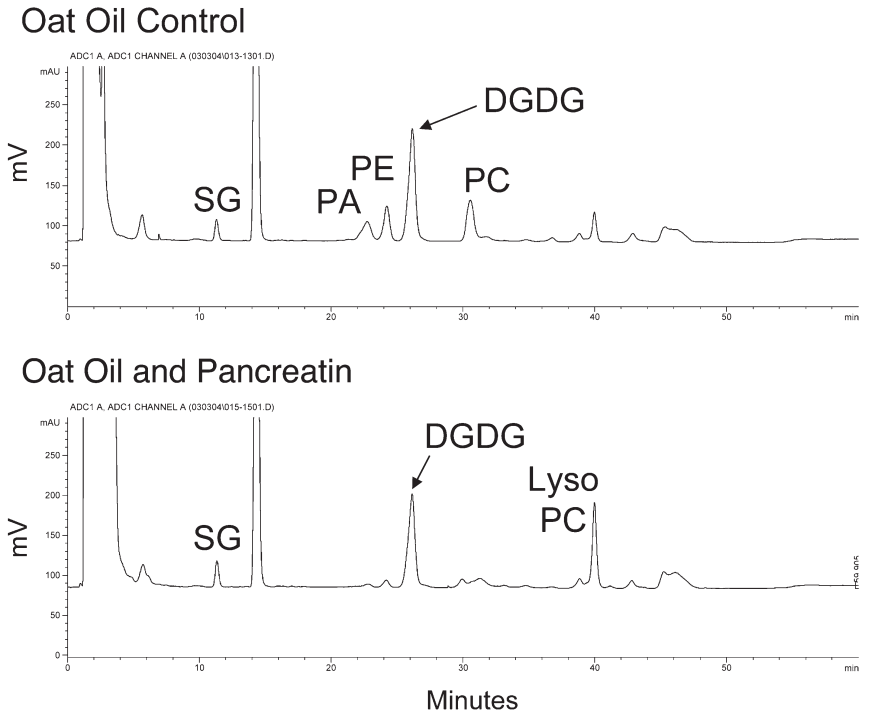

FIG. 6. HPLC chromatogram evaluating the hydrolysis of DGDG. The substrate was oat oil (2 mg) and the enzyme was pancreatin (2 mg) in 5 mL of a reaction mixture of buffer and taurocholate that was incubated for 6 h at 37°C. For abbreviations see Figures 1 and 5.

is extracted with hot ethanol, the extract contains about 10% DFP and 2% CFP (16). When the potential hydrolysis of this extract was evaluated, these two conjugates were hydrolyzed to a slight extent (about 2% hydrolysis of DFP and about 8% hydrolysis of CFP) (Table 3). In this HPLC system, the retention times for CFP and DFP were 24 and 25 min, respectively (data not shown).

Saponification (alkaline hydrolysis) of lipid extracts is a routine procedure to hydrolyze the ester bonds before analyzing the resulting FA or free phytosterols (Table 4). Christie (24) cautioned that saponification of steryl esters requires longer and more vigorous saponification than saponification of common acylglycerol esters. Thompson and Merola (25) reported that cholesteryl oleate was completely hydrolyzed in 8 min upon saponification with 0.5 N KOH in ethanol/pyrogallol (97:3) at 80°C. In the current study, 30 min was adequate for the complete (>99%) hydrolysis of the TAG in the two margarines, but it resulted in only about 35–65% hydrolysis of the four phytosterol ester conjugates (Table 4). Saponification for 2 h resulted in about 96 and 86% hydrolysis of the

TABLE 3
Hydrolysis of Phytosterol Conjugates (glycosides) and Other Polar Lipids (in food matrices) by Pancreatin

Food matrix	Phytosterol conjugate (or other lipid)	Concentration of conjugate in food matrix	% Hydrolysis at 6 h
Lecithin granules	Acylated steryl glycoside, ASG	~2.7%	54.3 ± 0.6
	Steryl glycoside, SG	~0.2%	0 (380% increase)
	Phospholipids, PC	~97%	>99
Oat oil	Acylated steryl glycoside, ASG	~0.1	NQ[a]
	Steryl glycoside, SG	~0.2%	0 (22% increase)
	Galactolipid, DGDG	~3%	39.7 ± 0.6
	Phospholipids, PC	~2%	>99
Corn bran ethanol extract	Acylated steryl glycoside, ASG	~0.1%	NQ
	Steryl glycoside, SG	~0.1%	0 (80 % increase)[a]
	Polyamines, DFP	~5%	1.8 ± 1.6
	CFP	~1%	7.8 ± 4.1
	Phospholipids, PC	~2%	>99

[a]NQ, not quantified. In oat oil and corn bran ethanol extract, the ASG peak was masked by other peaks and could not be accurately estimated. However, the increase in SG is evidence that ASG was present and it was hydrolyzed. DGDG, digalactosyldiacylglycerol; DFP, diferuloylputrescine; CFP, *p*-coumaroyl feruloylputrescine.

TABLE 4
Hydrolysis of Phytosterol Conjugates (esters) by Saponification with 1.5 N KOH in Methanol (10% water) at 70°C

Food matrix or pure compound	Phytosterol conjugate	% Hydrolysis at 30 min	% Hydrolysis at 120 min
Benecol®	Phytostanyl fatty acyl esters	52.2[a]	96.7
Take Control®	Phytosteryl fatty acyl esters	64.4[a]	97.4
Purified sample	Sitostanyl ferulate	34.7	87.0
Purified sample	Oryzanol	44.6	86.2

[a]*Note:* TAG in these samples were completely hydrolyzed within 30 min.

SE and HSE, respectively. Our results differ from those of Thomson and Merola (25) and indicate that any analyses that include alkaline hydrolysis of sterols should include methods to verify complete hydrolysis.

This report provides the first *in vitro* evidence that phytostanyl ferulate esters (a major component in corn fiber oil) are hydrolyzed by mammalian digestive enzymes. It is also the first report that provides evidence that ASG are hydrolyzed to steryl glycosides by mammalian digestive enzymes. However, the glycosidic linkage in steryl glycosides does not appear to be hydrolyzed by mammalian digestive enzymes. This study also reports the first *in vitro* data demonstrating the extent of hydrolysis of phytostanyl fatty acyl esters in food matrices by mammalian digestive enzymes. Because all plant-derived foods, including most functional foods, and some supplements (e.g., Lecithin Granules) contain steryl glycosides and most grains contain phytostanyl ferulate esters, these new findings have implications in the fields of food science, nutraceuticals, and pharmacology. It also confirms several previous reports of the *in vitro* hydrolysis of some phytosterol conjugates (phytosteryl fatty acyl esters, oryzanol, and other phytosteryl-ferulates). Our results indicate the bovine preparation of cholesterol esterase could be useful for those interested in using it as a tool to hydrolyze phytosteryl esters. On the other hand, the porcine pancreatin preparation used in these studies provided reasonable and repeatable hydrolysis of ASG to SG (and hydrolysis of phospholipids and galactolipids) but it appears to be less useful as a tool for the hydrolysis of the phytosteryl esters.

REFERENCES

1. Moreau, R.A., Whitaker, B.D., and Hicks, K.B. (2002) Phytosterols, Phytostanols, and Their Conjugates in Foods: Structural Diversity, Quantitative Analysis, and Health-Promoting Uses, *Prog. Lipid Res. 41,* 457–500.
2. Miettinen, T.A., Vuoristo, M., Nissinen, M., Jarvinen, H.J., and Gylling, J. (2000) Serum, Biliary and Fecal Cholesterol and Plant Sterols in Colectomized Patients Before and During Consumption of Stanol Ester Margarine, *Am. J. Clin. Nutr. 71,* 1095–1102.
3. de Jong, A., Plat, J., and Mensink, R.P. (2003) Metabolic Effects of Plant Sterols and Stanols, *J. Nutr. Biochem. 14,* 262–269.
4. Swell, L., Field, H., Jr., and Treadwell, C.R. (1954) Sterol Specificity of Pancreatic Cholesterol Esterase, *Proc. Soc. Exptl. Biol. Med. 87,* 216–218.
5. Fujiwara, S., Sakurai, S., Noumi, Sugimoto, I., and Awata, N. (1983) Absorption and Metabolism of γ-Oryzanol in Rats, *Chem. Pharm. Bull. 31*, 645–652.
6. Huang, C-C.J. (2003) Potential Functionality and Digestibility of Oryzanol as Determined Using *in vitro* Cell Culture Methods, Ph.D. Dissertation, Louisiana State University, pp. 119–139. Also available at netlink: http://etd02.lnx390.lsu.edu/docs/available/etd-0609103-135757/.
7. Miller, A., Majauskaite, L., and Engel, K-H. (2004) Enzyme-Catalyzed Hydrolysis of γ-Oryzanol, *Eur. Food Res. Technol. 218,* 349–354.
8. Kesselmeier, J., Eichenberger, W., and Urban, B. (1985) High-Performance Liquid Chromatography of Molecular Species of Free Sterols and Sterylglycosides Isolated from Oat Leaves and Seeds, *Plant Cell. Physiol. 26*, 463–471.
10. Moreau, R.A., Powell, M.J., Whitaker, B.D., Bailey, B.A., and Anderson, J.D. (1994) Xylanase Treatment of Plant Cells Induces Glycosylation and Fatty Acylation of Phytosterols, *Physiol. Plant. 91*, 575–580.
11. Palta, J., Whitaker, B.D., and Weiss, L. (1993) Plasma Membrane Lipids Associated with Genetic Variability in Freezing Tolerance and Cold Acclimation of *Solanum* Species, *Plant Physiol. 103,* 793–803.
12. Whitaker, B.D., Lee, E.H., and Rowland, R.A. (1990) EDU and Ozone Protection: Foliar Glycerolipids and Steryl Lipids in Snapbean Exposed to O_3, *Physiol. Plant. 80,* 286–293.
13. Holkeri, L.I. (2002) Enzymatic Hydrolysis of Steryl Conjugates II. Analysis of Sterols in Rye, M.Sc. Thesis, University of Helsinki, pp. 25–27.
14. Condo, A.M., Baker, D.C., Moreau, R.A., and Hicks, K.B. (2001) Improved Method for the Synthesis of *trans*-Feruloyl-β-sitostanol, *J. Agric. Food Chem. 49,* 4961–4964.
15. Moreau, R.A., Powell, M.J., and Hicks, K.B. (1996) Extraction and Quantitative Analysis of Oil from Commercial Corn Fiber, *Ibid. 44*, 2149–2154.
16. Moreau, R.A., Nuñez, A., and Singh, V. (2001) Diferuloylputrescine and *p*-Coumaroyl Feruloylputrescine, Abundant Polyamine Conjugates in Lipid Extracts of Maize Kernels, *Lipids 36,* 839–844.
17. Bligh, E.G., and Dyer, W.J. (1959) Rapid Method of Total Lipid Extraction and Purification, *Can. J. Biochem. Physiol. 37,* 911–917.
18. Moreau, R.A., Powell, M.J., and Singh, V. (2003) Pressurized Liquid Extraction of Polar and Nonpolar Lipids in Corn and Oats with Hexane, Methylene Chloride, Isopropanol, and Ethanol, *J. Am. Oil Chem. Soc. 80,* 1063–1067.
19. Trautwein, E.A., Schulz, C., Rieckhoff, D., Kunath-Rau, A., Erbersdobler, H.F., de Groot, W.A., and Meijer, G.W. (2002) Effect of Esterified 4-Desmethylsterols and -Stanols or 4,4′-Dimethylsterols on Cholesterol and Bile Acid Metabolism in Hamsters, *Br. J. Nutr. 87,* 227–237.
20. Moreau, R.A., Powell, M.J., and Hicks, K.B. (2003) Evaluation of a Commercial Enzyme-Based Serum Cholesterol Test Kit

for the Analysis of Phytosterol and Phytostanol Products, *J. Agric. Food Chem. 51,* 6663–6667.
21. Norton, R.A. (1995) Quantitation of Steryl Ferulate and *p*-Coumarate Esters from Corn and Rice, *Lipids 30,* 269–274.
22. Weber, N. (1988) Metabolism of Sitosteryl-β-D-glucoside and Its Nutritional Effects in Rats, *Lipids 23*, 42–47.
23. Peng, L., Kawagoe, Y., Hogan, P., and Delmer, D. (2002) Sitosterol-β-glucoside as Primer for Cellulose Synthase in Plants, *Science 295,* 147–150.
24. Christie, W.W. (2003) *Lipid Analysis: Isolation, Separation, Identification and Structural Analysis of Lipids,* 3rd edn., p. 206, The Oily Press, Bridgewater, United Kingdom.
25. Thompson, R.H., and Merola, G.V. (1993) A Simplified Alternative to the AOAC Official Method for Cholesterol in Multi-Component Foods, *JAOAC 76*, 1057–1068.

[Received June 28, 2004; accepted October 1, 2004]

Phospholipase D-Catalyzed Synthesis of Novel Phospholipid–Phytosterol Conjugates

Monjur Hossen and Ernesto Hernandez*

Food Protein R&D Center, Texas A&M University, College Station, Texas 77843-2476

ABSTRACT: In the present study, plant sterols were modified to form amphiphiles by synthesizing phospholipid derivatives from them so they could be formulated in different functional foods and possibly improve their effects as therapeutic agents. The new phosphatidyl derivatives, phosphatidyl-sitosterols, were synthesized by the transfer reaction of a phosphatidyl residue from PC to β-sitosterol by phospholipase D (PLD EC 3.1.4.4) from *Streptomyces* sp. in a biphasic medium.

Paper no. L9580 in *Lipids 39,* 777–782 (August 2004).

Cholesterol metabolism is important because it is related to two diseases that affect millions of people: atherosclerosis and gallstones. Cholesterol absorption and plasma cholesterol are directly related in some individuals. Although many steps in the absorption of cholesterol have been studied and drugs have been developed that inhibit cholesterol absorption, inhibition of cholesterol absorption by dietary plant sterols has also received much attention because of their claimed effectiveness in lowering plasma total and LDL cholesterol (1). The cholesterol-lowering effect of plant sterols (phytosterols) has been studied since the 1950s (2,3), but because of poor solubility and bioavailability, doses of sitosterol as high as 25 g/d are required for efficacy. The crystalline nature and poor solubility of free phytosterols also limit their application in foods. Recently, technological developments have allowed sterol and stanol esters to be incorporated successfully into spreads and margarines (4,5). The spreads supplemented with 8–10% plant sterols lower serum total cholesterol and LDL cholesterol by 8–13% (6,7). This is equivalent to the consumption of 1.6–2.0 g of plant sterols per day. Because the intakes of higher doses of plant sterol and stanol esters eventually increase the total fat intake, researchers are trying to incorporate plant sterols and stanols into fat-free or low-fat food systems (8). Low-fat yogurt enriched with plant sterol esters lowers LDL cholesterol within 1 wk to the same extent as do oil-based products (9). However, the intestinal bioavailability of plant sterols is still a major concern. The actual mechanism by which the plant sterols and stanols reduce cholesterol absorption is not completely understood. Several molecular mechanisms of phytosterol action on the level of serum cholesterol are believed to be of particular importance (10). Recently, an *in vitro* study on the effect of plant sterols on the solubilization of cholesterol by model dietary mixed micelles demonstrated that plant sterols and stanols reduce the concentration of cholesterol in dietary mixed micelles *via* a dynamic competition mechanism (11). Earlier, it was also reported that incorporation of phytosterols into the phospholipid (PL) vesicles improves their cholesterol lowering efficacy (12,13). Thus, it is desirable to develop biologically active phytosterol preparations that will require lower doses of phytosterols to have significant cholesterol-lowering effects and that are capable of being added to a variety of foods. Ramaswamy *et al.* (14) showed that a hydrophilic phytosterol composed of sitosterol- and campesterol-ascorbyl-phosphate had 15-fold greater inhibition of cholesterol uptake by Caco-2 cells than did free sterols. Recently, an aqueous dispersible sterol product was invented for beverage applications (15), and orange juice fortified with these plant sterols was effective in reducing LDL cholesterol (16). In the present study, an attempt has been made to produce amphiphilic sterols by synthesizing phospholipid derivatives of phytosterols *via* an enzymatic process catalyzed by phospholipase D.

EXPERIMENTAL PROCEDURES

Materials. Soybean PC (PC content not less than 94%) was donated by Lipoid GmbH (Ludwigshafen, Germany). β-Sitosterol (65% purity) was obtained from Fluka Chemie AG (Buchs, Switzerland). The enzyme phospholipase D (PLD) from *Streptomyces* sp. (PC phosphatidohydrolase, EC 3.1.4.4) was donated by Ashahi Kasei Corporation (Tokyo, Japan). Activity of the enzyme was determined by the manufacturer as 305 U/mg. Solvents (chloroform and methanol), the matrix (2,5-dihdroxybenzoic acid, DHB), and trifluoroacetic acid (TFA) were obtained from Sigma Chemical Company (St. Louis, MO).

Transphosphatidylation reaction. The transphosphatidylation reaction between PC and β-sitosterol was carried out according to reaction Scheme 1. In a typical reaction, 20 mg of PL and 104 mg of β-sitosterol (1:10 mol PL/mol sterol) were dissolved in 2 mL of chloroform (HPLC grade) and 100 μL of 0.2 M sodium acetate buffer (pH 5.6) containing 40 mM of $CaCl_2$ and 20 U of PLD (EC 3.1.4.4) and incubated at 40°C with stirring. Aliquots (50 μL) drawn from the reaction mixture

*To whom correspondence should be addressed at Food Protein R&D Center, Cater Mattil Hall, M.S. 2476 TAMU, College Station, TX 77843-2476. E-mail: erhernandez@tamu.edu

Abbreviations: DHB, 2,5-dihydroxybenzoic acid; DPPC, 1,2-dipalmitoyl-*sn*-glycero-3-phosphorylcholine; MALDI-TOF, matrix-assisted laser desorption and ionization time-of-flight; PC-sterol, PC–sitosterol; PG, phosphatidylglycerol; PL, phospholipid(s); PLD, phospholipase D; TFA, trifluoroacetic acid.

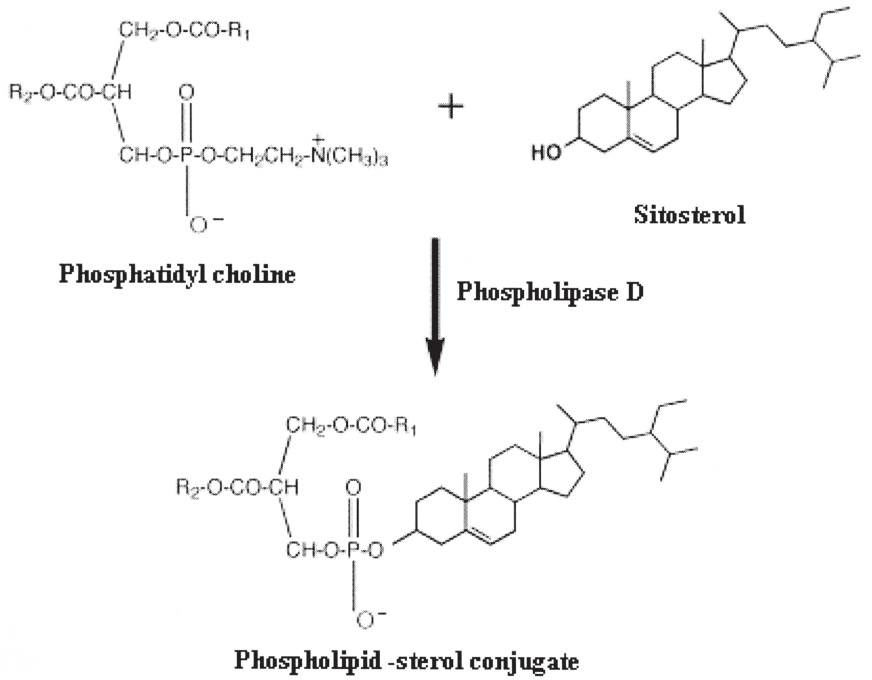

SCHEME 1

at different time intervals were extracted with 100 μL of chloroform/methanol (3:1, vol/vol) after adding 50 μL of 0.01 N HCl. The lower organic layer was separated and further extracted with chloroform and analyzed by TLC. To confirm the identity of the PC–sitosterol (PC-sterol) derivative, a similar reaction was carried out between 1,2-dipalmitoyl-*sn*-glycero-3-phosphorylcholine (DPPC, M.W. 734.1) obtained from Matreya, Inc. (Pleasant Gap, PA) and β-sitosterol (M.W. 414.7). Reaction aliquots collected in chloroform were analyzed by matrix-assisted laser desorption and ionization time-of-flight (MALDI-TOF) MS.

TLC analysis. Aliquots collected in chloroform were applied to TLC plates (silica gel 60 F254; E. Merck Co., Darmstadt, Germany). The plates were developed with chloroform/methanol/water (65:25:4, by vol). Eluted compounds were detected by spraying them with 5% phosphomolybdic acid in ethanol followed by heating.

Time-course analysis for the synthesis of PC-sterol. FA analysis of individual bands (PC, PC-sterol, and the PLD-hydrolysis product) on TLC plates was used to quantify the reaction products with time. About 80 μL of aliquots collected in chloroform was applied on 10 × 10 cm TLC plates and developed as just described. Individual bands were scraped from the plates and FAME were prepared by adding 1.0 mL of 0.25 M sodium methoxide in methanol/diethyl ether (1:1). After incubation for 5 min in a water bath shaker at 45°C, 200 μL of hexane was added, followed by 3 mL of saturated NaCl solution. After vortexing and centrifugation, the methyl esters extracted in hexane were collected from the upper layer and 1 μL of methyl esters with an internal standard (methyl behenate, 22:0; Nu-Chek-Prep, Inc., Elysian, MN) was injected into the gas chromatograph. A Varian Model 3400 GC system equipped with a split injector, an FID, and a fused-silica capillary column (Supelco SP 2560, 100 m, 0.25 mm i.d., 0.20 μm film; Supelco, Bellefonte, PA) was used for FAME analysis. The initial column oven temperature was 150°C for 3 min and then raised to 210°C at 6°C/min and held for 15 min. The injector and detector temperatures were 250 and 300°C, respectively. Hydrogen was used as a carrier gas. The amount of FA (mol) in each band was converted into reaction products (mol) after dividing it by two. The conversion of PC-sterol was calculated as mol% based on the relative amount in the total phosphatidyl compounds.

Spectral analysis. To confirm product identities, mass spectra were analyzed with a MALDI-TOF mass spectrometer (Voyager; PerSeptive Biosystems, Framingham, MA) in a linear mode. This system utilizes a pulsed nitrogen laser, emitting at 337 nm. The extraction voltage was set at 20 kV, and 100 single laser "shots" were averaged for each mass spectrum. For analysis, all samples were dissolved in a 0.5 M DHB matrix solution in methanol containing 1% TFA. Samples in chloroform (10 μL of aliquots) were premixed with the matrix (10 μL) and the sample/matrix mixtures (1.2 μL) were placed directly on the MALDI-TOF sample plate. Samples were crystallized in air without any flow before any spectra were acquired.

RESULTS AND DISCUSSION

As a model reaction for monitoring the catalytic activity of PLD, a transphosphatidylation reaction between glycerol and PC was carried out for 8 h according to the conditions mentioned in the Experimental Procedures section (Scheme 2). Synthe-

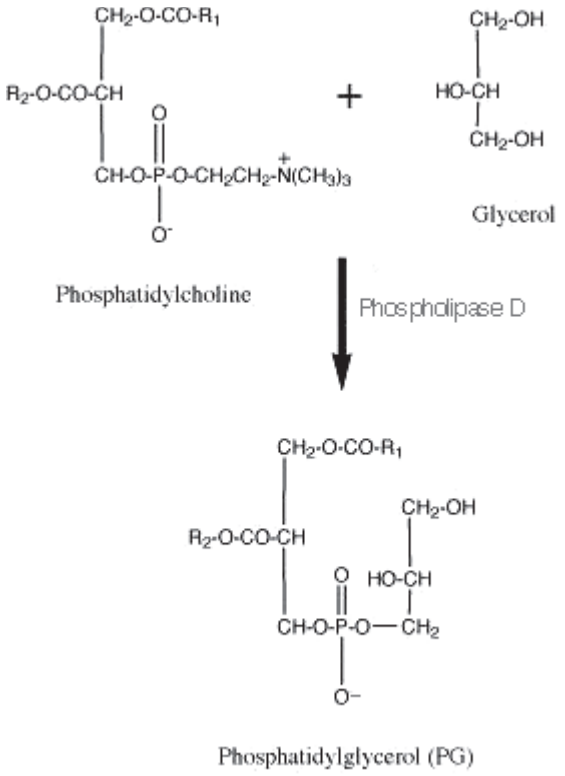

SCHEME 2

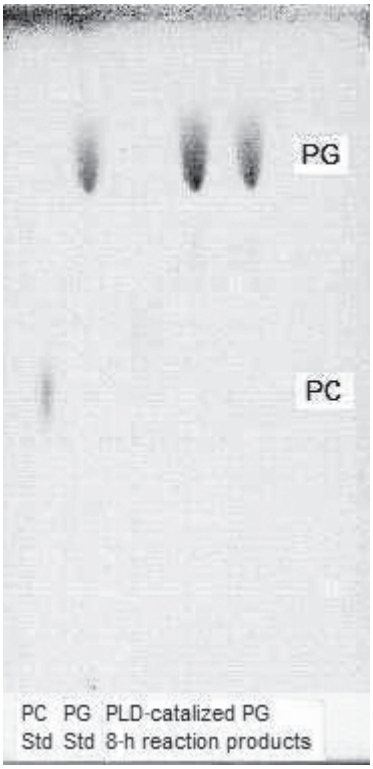

FIG. 1. TLC analysis of phospholipase D (PLD)-catalyzed transphosphatidylation of PC into phosphatidylglycerol (PG). Std, standard.

sis of phosphatidylglycerol (PG) was confirmed by TLC analysis of the reaction mixture, and the PG standard was PG obtained from Sigma (St. Louis, MO). Synthesized PG and the PG standard had similar R_f values (Fig. 1). The conversion of PC to PG was almost complete, as no spot was visible at an R_f value similar to the PC standard. The enzymatic synthesis of PG from PC by a transphosphatidylation reaction catalyzed by PLD from Savoy cabbage has been reported (17). Several preparative transphosphatidylation reactions between phospholipids and nucleophile alcohols of complex structure also have been reported (18,19). Because PLD catalyzes the transphosphatidylation reaction between PC and an alcohol group, we proposed that a similar reaction could be carried out between PC and sterol (having a hydroxyl group) to synthesize novel phospholipid–sterol conjugates. We first examined the reaction between natural PC and β-sitosterol catalyzed by PLD (from *Streptomyces* sp.) for 24 h. Samples in chloroform collected at different time intervals were placed on TLC plates. A new spot having a lower R_f value than that of sitosterol but higher than that of PC was observed by TLC (Fig. 2). For structural analysis, a similar reaction was carried out between DPPC and β-sitosterol for 72 h using reaction conditions similar to those mentioned in the Experimental Procedures section. The reaction products extracted in chloroform were isolated by silica gel (Wacogel C-200) column chromatography followed by TLC analysis (Fig. 3). Fractions collected with chloroform were identified as sitosterol, whereas fractions collected with chloroform/methanol (24:1, vol/vol) had the same R_f value as unknown spots observed by TLC analysis of the reaction mixture (Fig. 2). Fractions collected with chloroform/methanol (85:15, vol/vol) were identified as PC. Mass spectral analyses of all fractions collected were carried out to confirm the structure of DPPC and β-sitosterol and to identify the structure of the phospholipid–sterol conjugate synthesized from DPPC and β-sitosterol. Mass spectral analysis of the fractions collected with chloroform/methanol (24:1, vol/vol) confirmed the structure of the DPPC–sterol conjugate. The MALDI-TOF mass spectrum of this fraction showed a $[M - C_2H_6]$ ion at *m/z* 1013, a $[M - C_3H_8]$ ion at *m/z* 999, a $[M - C_4H_{12}]$ ion at *m/z* 984, and a $[M - C_7H_{17}]$ ion at *m/z* 942 because of the side-chain fragmentation of sitosterol in the DPPC–sterol conjugate (Fig. 4). The time-course analysis of the reaction mixture (Fig. 5) indicated that the synthesis of PC-sterol reached a maximum at 12 h and then gradually decreased with time. In parallel with the transphosphatidylation reaction, hydrolysis of PC and PC-sterol was observed and increased with time after 12 h. The amount of PC decreased with time, and the rate was much slower after 24 h.

The PC-sterol conjugates were synthesized by the reaction of PC with sterol catalyzed by PLD from *Streptomyces* sp. in a biphasic system of an organic solvent with an acetate buffer. We observed from the TLC analysis that the R_f value of the PC-sterol conjugate was lower than that of sitosterol; therefore, we can conclude that PC-sterol conjugates will have higher polarity than sterols. As far as we know, such types of

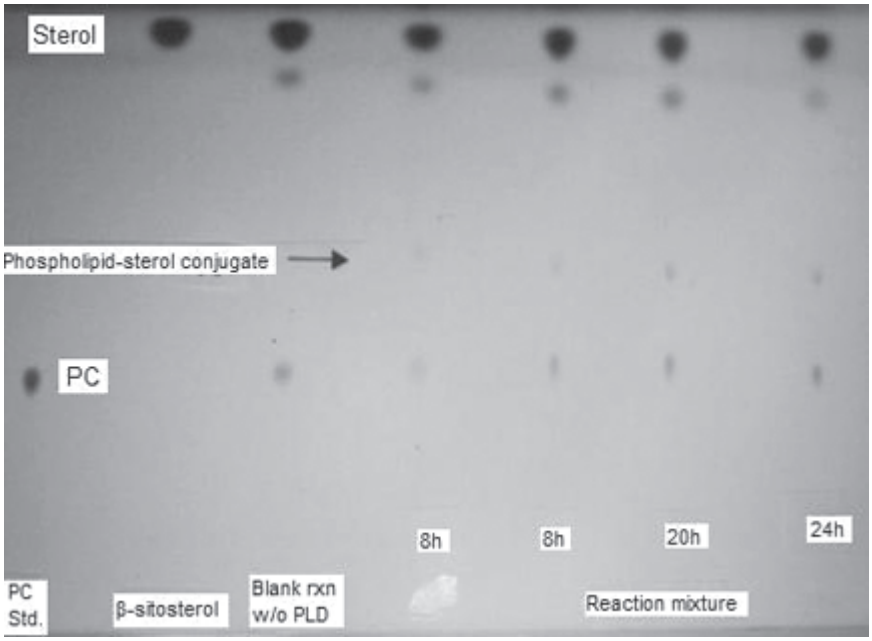

FIG. 2. TLC analysis of PLD-catalyzed transphosphatidylation of PC into the PC–sitosterol conjugate. Comparison with a standard and PC and β-sitosterol in all reaction products with time. The new unknown spots had R_f values higher than that of PC but lower than that of β-sitosterol. rxn, reaction; for other abbreviations see Figure 1.

PC-sterol conjugates have not yet been described in the literature. There is a demand to improve the efficacy of phytosterols and stanols to reduce total serum cholesterol levels by increasing their intestinal bioavailability, and more research is needed in this area. Ostlund *et al.* (13) reported that sitostanol administered in lecithin micelles reduced cholesterol absorption by 36.7 ± 4.2% (mean ± SD) compared with only 11.3 ± 7.4% when lecithin was not used. This result suggests that naturally occurring phytosterols may significantly affect cholesterol absorption, especially when added with PL. Unlike the prior study (13), in which sitostanol was physically mixed with phospholipids in solvent and lyophilized, in our present line of work we hypothesized that conjugating phytosterols or stanols directly with PL will increase their

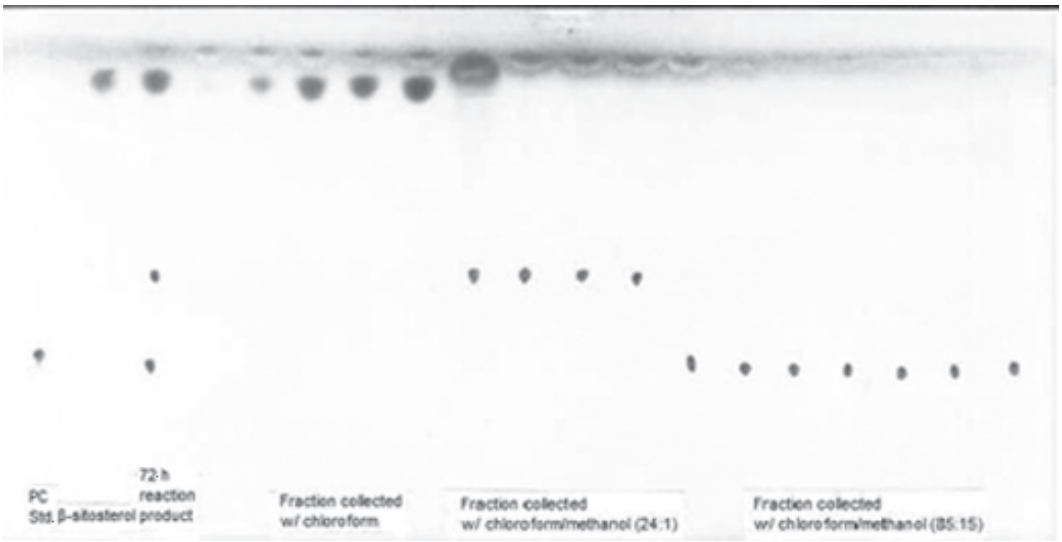

FIG. 3. TLC analysis of fractions collected from reaction products of PLD-catalyzed transphosphatidylation of 1,2-dipalmitoyl-*sn*-glycero-3-phosphorylcholine (DPPC) and β-sitosterol eluted from a silica gel column with gradient solvent. For other abbreviations see Figures 1 and 2.

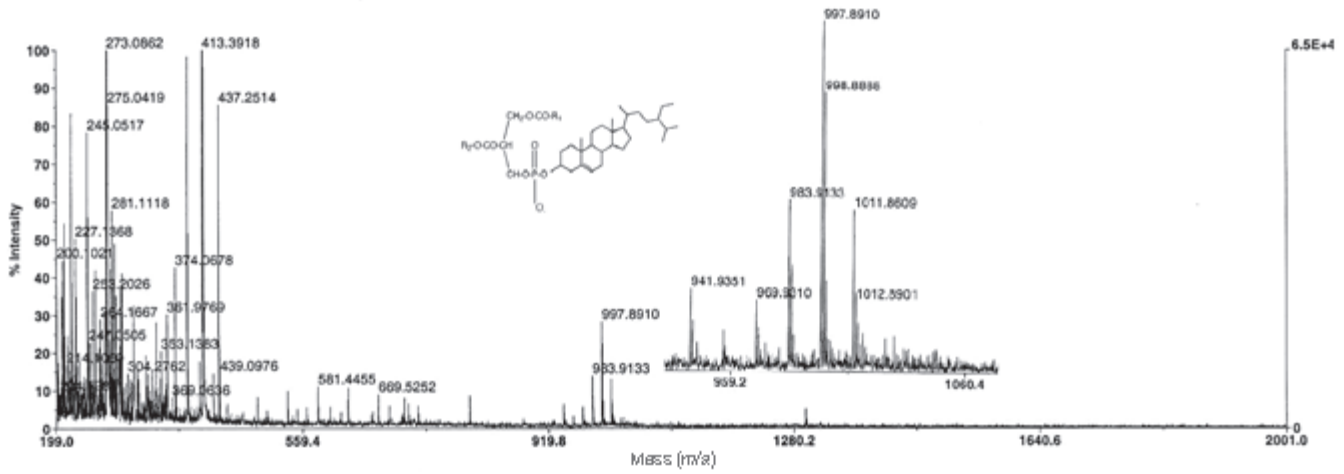

FIG. 4. Matrix-assisted laser desorption and ionization time-of-flight (MALDI-TOF) mass spectrum of dipalmitoyl PC–β-sitosterol.

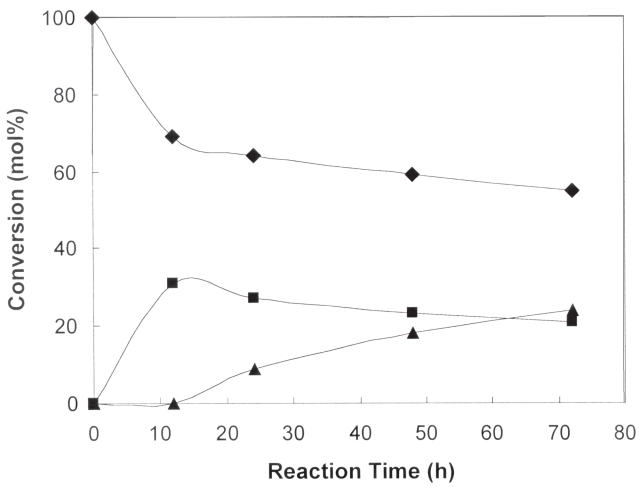

FIG. 5. Time-course analysis of the transphosphatidylation reaction of PC and sterol. (◆) PC; (■) PC-sterol; (▲) hydrolysis products of phosphatidyl compounds.

cholesterol-lowering efficacy even more. Studies to test this hypothesis are required. Recently, Ramaswamy *et al.* (14) synthesized a novel hydrophilic phytostanol phosphoryl ascorbate (chemical conjugation of stanol and ascorbic acid with a phosphodiester moiety) that has a 15-fold greater cholesterol inhibition activity than do the free sterols. Because commercially available phytosterols, phytostanols, and their FA ester form are hydrophobic and limited to oil-based foods such as margarine, more research in line with our present study is needed to produce amphiphilic phytosterols with improved food application and absorption characteristics.

ACKNOWLEDGMENTS

We thank Dr. Ronald Macfarlane and Dr. Zachlyn Farwig for the mass spectral analyses and Dr. Rosemary Walzem for valuable discussions with regard to the project. The study was supported in part by a Texas Food and Fiber Commission grant.

REFERENCES

1. Ostlund, R.E., Jr. (2002) Phytosterols in Human Nutrition, *Annu. Rev. Nutr. 22*, 533–549.
2. Pollak, O.J. (1953) Reduction of Blood Cholesterol in Man, *Circulation 7*, 702–706.
3. Peterson, D.W. (1951) Effect of Soybean Sterols in the Diet on Plasma and Liver Cholesterol in Chicks, *Proc. Soc. Exp. Biol. Med. 78*, 143–147.
4. Ntanios, F. (2001) Plant Sterol-Ester-Enriched Spreads as an Example of a New Functional Food, *Eur. J. Lipid Sci. Technol. 103*, 102–106.
5. Law, M. (2000) Plant Sterol and Stanol Margarines and Health, *Br. Med. J. 320*, 861–864.
6. Weststrate, J.A., and Meijer, G.W. (1998) Plant Sterol-Enriched Margarines and Reduction of Plasma Total- and LDL-Cholesterol Concentrations in Normocholesterolaemic and Mildly Hypercholesterolaemic Subjects, *Eur. J. Clin. Nutr. 52*, 334–343.
7. Hendrinks, H.F.J., Weststrate, J.A., Van, V.T., and Meijer, G.M. (1999) Spreads Enriched with Different Levels of Vegetable Oil Sterols and Degree of Cholesterol Lowering in Normocholesterolaemic and Mildly Hypercholesterolaemic Subjects, *Eur. J. Clin. Nutr. 53*, 319–327.
8. St-Onge, M.-P., and Jones, P.J.H. (2003) Phytosterols and Human Lipid Metabolism: Efficacy, Safety, and Novel Foods, *Lipids 38*, 367–375.
9. Ronald, P.M., Ebbing, S., Lindhout, M., Plat, J., Marjolien, M.A., and Heugten, V. (2002) Effects of Plant Stanol Esters Supplied in Low-Fat Yoghurt on Serum Lipids and Lipoproteins, Non-cholesterol Sterols and Fat Soluble Antioxidant Concentrations, *Atherosclerosis 160*, 205–213.
10. Trautwein, E.A., Duchateau, G.S.M.J.E., Lin, Y., Mel'nikov, S.M., Molhuizen, H.O.F., and Ntanios, F.Y. (2003) Proposed Mechanisms of Cholesterol-Lowering Action of Plant Sterols, *Eur. J. Lipid Sci. Technol. 105*, 171–185.
11. Mel'nikov, S.M., Seijen ten Hoorn, J.W.M., and Eijkelenboom, A.P.A.M. (2004) Effect of Phytosterols and Phytostanols on the Solubilization of Cholesterol by Dietary Mixed Micelles: An *in vitro* Study, *Chem. Phys. Lipids 127*, 121–141.
12. Datsenko, Z.M., Kholodova, Y.D., Kokunin, V.A., Klimashevsky, V.M., Peredery, O.F., and Timchenko, A.P. (1984) Effect of β-Sitosterol Incorporated into Liposomes on Some Patterns of Lipid-Metabolism in Experimental Hypercholesterolemia of Rats, *Vopr. Med. Khim. 30*, 33–38.
13. Ostlund, R.E., Jr., Spilburg, C.A., and Stenson, W.F. (1999)

Sitostanol Administered in Lecithin Micelles Potently Reduces Cholesterol Absorption in Humans, *Am. J. Clin. Nutr. 70*, 826–831.
14. Ramaswamy, M., Yau, E., and Wasan, K.M. (2002) Influence of Phytosterol Phosphoryl Ascorbate, FM-VP4, on Pancreatic Lipase Activity and Cholesterol Accumulation Within Caco-2 Cells, *J. Pharm. Pharmaceut. Sci. 5*, 29–38.
15. Stevens, L.A., and Schmelzer, W.N. (2003) Aqueous Dispersible Sterol Product, U.S. Patent 6,623,780.
16. Devaraj, S., Jialal, I., and Vega-Lópoez, S. (2004) Plant Sterol-Fortified Orange Juice Effectively Lowers Cholesterol Levels in Mildly Hypercholesterolemic Healthy Individuals, *Arterioscler. Thromb. Vasc. Biol. 24*, e25–e28.
17. Juneja, L.R., Hibi, N., Inagaki, N., and Yamane, T. (1987) Comparative Study on Conversion of Phosphatidylcholine to Phosphatidylglycerol by Cabbage Phospholipase D in Micelle and Emulsion Systems, *Enzyme Microb. Technol. 9*, 350–354.
18. Rich, J.O., and Khmelnitsky, Y.L. (2001) Phospholipase D-Catalyzed Transphosphatidylation in Anhydrous Organic Solvents, *Biotechnol. Bioeng. 72*, 374–377.
19. Takami, M., Hidaka, N., and Suzuki, Y. (1994) Phospholipase D-Catalyzed Synthesis of Phosphatidyl Aromatic Compounds, *Biosci. Biotechnol. Biochem. 58*, 2140–2144.

[Received September 13, 2004, and in revised form and accepted October 19, 2004]

Pearling Barley and Rye to Produce Phytosterol-Rich Fractions

Anna-Maija Lampi[a,*], Robert A. Moreau[b], Vieno Piironen[a], and Kevin B. Hicks[b]

[a]Department of Applied Chemistry and Microbiology, University of Helsinki, Finland, and
[b]USDA, ARS, Eastern Regional Research Center, Wyndmoor, Pennsylvania 19038,

ABSTRACT: Because of the positive health effects of phytosterols, phytosterol-enriched foods and foods containing elevated levels of natural phytosterols are being developed. Phytosterol contents in cereals are moderate, whereas their levels in the outer layers of the kernels are higher. The phytosterols in cereals are currently underutilized; thus, there is a need to create or identify processing fractions that are enriched in phytosterols. In this study, pearling of hulless barley and rye was investigated as a potential process to make fractions with higher levels of phytosterols. The grains were pearled with a laboratory-scale pearler to produce pearling fines and pearled grains. Lipids were extracted by accelerated solvent extraction, and nonpolar lipids were analyzed by normal-phase HPLC with ELSD and UV detection. Total sterol analyses were performed by GC. After a 90-s pearling, the amounts of pearling fines from hulless barley and rye were 14.6 and 20.1%, respectively, of the original kernel weights. During pearling, higher levels of phytosterols and other lipids were fractionated into the fines. The contents of free sterols and sterols esterified with FA in the fines were at least double those in the whole grains. Pearling fines of hulless barley and rye contained >2 mg/g phytosterol compounds, which makes them a good source of phytosterols and thus valuable raw materials for health-promoting foods.

Paper no. L9521 in *Lipids* 39, 783–787 (August 2004).

Phytosterols are being studied extensively because of their positive health effects. Research projects have focused on their biological functions, safety, and chemical and physical properties, as well as on attempts to develop new phytosterol-enriched foods (1,2). As the result of a recent workshop on sterols and stanols with 26 leading researchers as participants (i.e., the Stresa Workshop), an extensive review was published on the effects of using phytosterols and stanols to control serum cholesterol and the safety of phytosterol and stanol enrichments in foods (3). The authors concluded that daily consumption of 2 g of sterols or stanols decreases serum LDL cholesterol levels by approximately 10%.

Cereals are considered to be a good source of dietary phytosterols. Although their levels in whole grains are moderate (0.4–1.2 mg/g) (4,5), the total amount of phytosterols is significant because of the large amounts of cereals consumed. Phytosterols, like many other bioactive compounds (e.g., tocopherols, tocotrienols, and folates), are unevenly distributed in the kernels and are more concentrated in the outer layers than in the starch-rich endosperm (6,7). During the milling of some grains, pearling is a traditional way of gradually removing the hull, pericarp, and other outer layers of the kernels and germ as pearling fines to produce pearled grains. It is the most common technique used to fractionate barley (8). The abrasion of rye and barley to produce high-starch pearled grains also has been used to improve fuel ethanol production (9,10). There is a need to find new food uses for the pearling fines and other possible low-starch by-products remaining after separation of the high-starch pearled grain. The objective of this study was to evaluate pearling as a potential process to make fractions with higher levels of cereal phytosterols. The cereals studied were hulless barley and rye.

*To whom correspondence should be addressed at Dept. of Applied Chemistry and Microbiology, Latokartanonkaari 11, P.O. Box 27, FIN-00014 University of Helsinki, Finland. E-mail: anna-maija.lampi@helsinki.fi

MATERIALS AND METHODS

The grains used for pearling were a new winter hulless barley variety, Doyce, released in 2003 by the Virginia Polytechnic Institute and State University and grown in Virginia. The rye variety, Flesynt, was from the North Florida Research and Education Center, Institute of Food and Agricultural Services, University of Florida (Quincy, FL). Rye grains were also hulless. Both grains were harvested in the 2003 season, and the moisture content of the grains ranged between 11 and 14%.

Grains were pearled with a laboratory-scale barley pearler (30 grit carborundum stone, no. 7 mesh screen; Seedburo Equipment Co., Chicago, IL). For each pearling experiment, 50 g of grains were pearled, producing a fraction of pearling fines and a mixture of broken kernels and pearled grains.

The grains were first pearled sequentially to learn how phytosterols were localized in the kernels and to determine a relevant time for the production of pearling fractions. Sequential pearling consisted of five steps of 30 s each. After each pearling, fines were separated from the broken kernels by passing them through an 18-mesh sieve and collected as the product. Pearled grains and broken kernels were combined and pearled again. To obtain enough material, each pearling sequence was repeated five times, and the five fractions of pearling fines were extracted and analyzed separately. In the second experiment, the grains were pearled for 90 s. Pearling fines and pearled grains from three separate pearlings were combined and subjected to further analysis. Each pearling experiment was performed in duplicate.

The grains and pearled grains were ground to 20 mesh in a Wiley mill (Thomas Scientific, Swedesboro, NJ) before lipid

extraction. The pearling fines were extracted without additional grinding. Lipids were extracted using a Dionex ASE 200 accelerated solvent extractor (ASE) (Sunnyvale, CA) with 2.0-g sample sizes and 11-mL extraction vessels as reported earlier (11). In this study, the extraction mixture consisted of hexane and isopropanol (3:2, vol/vol) (12). The extracts were used for gravimetric measurements of lipid extracts and nonpolar lipid analyses by HPLC (13). The extracts were dried under nitrogen at ≤40°C and weighed for total extractable lipids. The extracts were redissolved in hexane for nonpolar lipid analysis and filtered through 0.2-μm polyvinylidene fluoride filters (Acrodisc LC 13; Pall Gelman Laboratory, Ann Arbor, MI) when needed. Each grain sample was extracted in triplicate. In each extraction batch, whole-grain rye flour (Hodgson Mill Inc., Effingham, IL) was included as an in-house reference sample to monitor the extraction procedure. Extraction efficacy was also verified by spiking the same flour with stigmasterol (95%; Sigma Chemical Co., St. Louis, MO) and calculating its recovery.

Nonpolar lipids were analyzed by normal-phase HPLC with LiChrosorb DIOL (5 μm, 3 × 100 mm) columns (Chrompack, Raritan, NJ) using instruments and running conditions as presented by Moreau *et al.* (13) except that the gradient was slightly modified. The linear gradient elution consisted of three steps followed by a 20-min stabilization period. In step 1 (0–8 min), the eluent consisted of 100% solvent A (hexane with 0.1% acetic acid); in step 2 (8–10 min), the proportion of solvent B (hexane with 1% isopropanol) was increased to 25%; and in step 3 (10–40 min), the eluent consisted of 75% solvent A and 25% solvent B. The flow rate was 0.5 mL/min. All lipids were detected using ELSD (Alltech-Varex Mark III; Alltech Assoc., Deerfield, IL) except for phytosterols esterified with ferulic acid, which were detected using UV at 280 nm. An external standard method was used for quantification (13). Performance of the nonpolar lipid HPLC was checked daily using corn fiber oil (13). The retention times of nonpolar lipid classes remained stable during the study and were 1.8 min for sterols esterified with FA (St-FA), 4.5 min for TAG, 9.2–10.6 min for FFA, 21.2 min for free stanols, 22.0 min for free sterols, and 26.6 min for sterols esterified with ferulic acid (St-Fer). All three lipid extracts for each sample were analyzed for nonpolar lipids.

Total phytosterols of the grains and pearling fines were analyzed by GC using FID after acid and alkaline hydrolysis (5). Pearling fractions were also analyzed for moisture and ash using AACC official methods AACC 44-15A and AACC 08-01 (14), respectively. Nonpolar lipid and total phytosterol results are presented as means and SD derived from three subsamples, and moisture and ash are given as means derived from two subsamples.

RESULTS AND DISCUSSION

Evaluation of the lipid analysis method. Reproducibility of the lipid extraction method was examined by analyzing nonpolar lipids of whole-grain rye flour at least once in each extraction batch during the study (N = 23). The contents of TAG, St-FA, stanols, sterols, and St-Fer were 3.65 ± 0.18, 0.74 ± 0.03, 0.06 ± 0.01, 0.20 ± 0.01, and 0.06 ± 0.01 mg/g, respectively. Recovery of spiked stigmasterol from the flour was 98% (N = 6). Detector responses of the nonpolar lipid analysis remained stable; the contents of TAG, St-FA, and St-Fer of corn fiber oil were 656 ± 22 mg/g (N = 29), 44.7 ± 2.9 mg/g (N = 59), and 44.9 ± 2.0 mg/g (N = 59), respectively.

Sequential pearling. When hulless barley and rye were pearled sequentially, the pearling fine yields were approximately 7 and 5%, respectively, from each 30-s pearling step. Barley grains contained free sterols and St-FA (Fig. 1). The total amount of sterol compounds in the whole barley grains was 0.70 mg/g. The highest level, 2.8 mg/g, was obtained in the fines from the first pearling step. The total sterol content of the fines decreased with each pearling step. Even the fifth fines had 2.2 times the amount of sterol compounds as the whole grains. The pearled barley grains still contained 65 and 80% of

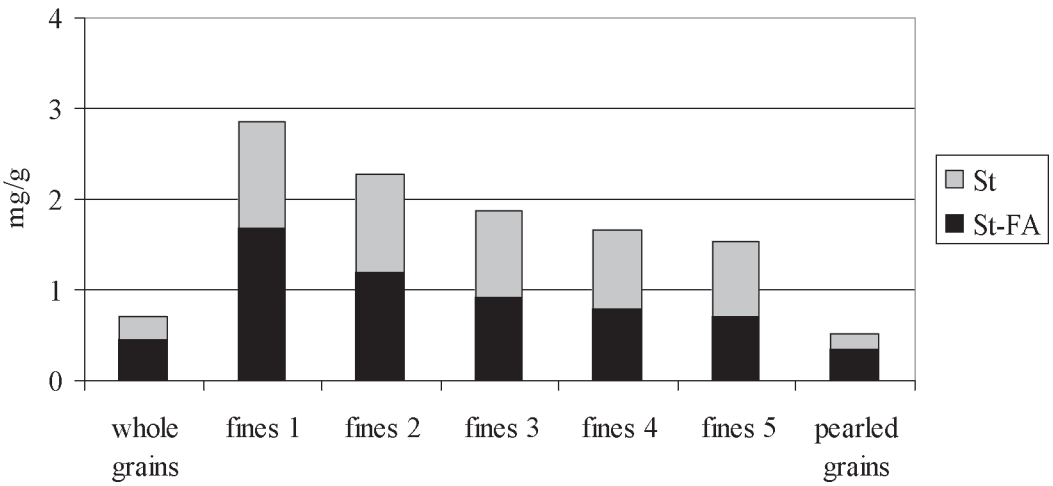

FIG. 1. Distribution of nonpolar sterol classes in hulless barley and its products from five 30-s sequential pearling steps. Values are given as means of two replicate experiments. St-FA, sterols esterified with FA; St, free sterols and stanols.

the free sterol and St-FA levels found in the whole grains. Nonpolar lipid profiles showed that free sterols were more concentrated in the outer layers of the kernels than were St-FA.

Rye grains contained free sterols, free stanols, St-FA, and St-Fer (Fig. 2). The total amount of sterol compounds in the whole grains was 1.1 mg/g. Phytosterols were concentrated in the pearling fines. All pearling fines contained ≥1.9 mg/g sterol compounds, with the highest level being found in the second pearling fines. After five steps, the pearled rye grains still contained 63 and 61% of the free sterol and St-FA levels found in the whole grains.

The levels of sterol compounds decreased more in hulless barley than in rye when comparing the inner layers of the kernels to the outer ones (Figs. 1, 2). In both cereals, the sterol levels were at least twice as concentrated in fines after the third pearling step than the whole grains. Thus, one 90-s pearling was chosen for further experiments to produce pearling fines with high phytosterol and lipid contents at a reasonable extraction rate.

Products from a 90-s pearling. The yields and composition of pearling fines and pearled grains from two replicate pearling experiments of each grain were similar (Table 1). The amounts of pearling fines of hulless barley and rye were 14.6 and 20.1% of the whole grains, and the percentages of extractable lipids in the products were 7.08 and 5.08%, respectively. Extractable lipid contents of the products were comparable with those in earlier studies (15,16). Since the yield of pearling fines from hulless barley was lower than that from rye, the pearling fines of barley contained proportionally more lipid-rich outer layers of the kernels than those of rye, and the lipid content of the pearling fines of barley was higher. Similarly, the ash contents showed that the pearling fines of barley were enriched in ash in the outer layers, because the ash content was 2.2 times higher than that of the whole grain, whereas in rye the ratio was 1.6.

Whole grains of hulless barley and rye contained 1.1% TAG and 0.1% FFA, two major lipid classes, and contributed >60% of the extractable lipids (Tables 1–3). After these lipids, the amounts of St-FA and free sterols were greatest. It should be remembered that, in addition to the nonpolar lipid classes, the lipid extracts also contained some polar lipids and nonlipid compounds that co-extracted under ASE conditions.

The pearling fines of hulless barley were rich in lipids. The sum of TAG and FFA accounted for 5.4% of the mass of fines. The contents of phytosterol compounds were also clearly greater in the fines than in the whole grains: 1.18 and 0.43 mg/g for St-FA, and 0.96 and 0.25 mg/g for free sterols, respectively. During the pearling of rye, the phytosterol compounds were fractionated into fines and pearled grains in a ratio similar to that of hulless barley. In the rye pearling fines, the level of St-FA, 1.34 mg/g, was double that of the whole grains, and the levels of free sterols increased almost threefold to 0.93 mg/g.

Although St-Fer were the least abundant sterol class in whole-grain rye, 0.07 mg/g, their presence is important, because they are considered to be potent antioxidants and are present in a number of cereals, e.g., corn, rice, wheat, and rye (17–20). St-Fer levels in the pearling fines were only slightly higher than those in the whole and pearled grains, which does not support earlier findings that the ferulates are concentrated in the outer and especially in the aleurone layer of the kernels (19,20). The small differences in St-Fer levels might be partly due to their overall low level in the extracts and the analytical uncertainty derived from that. In the sequential pearling experiments, however, St-Fer in the fines were clearly greater than in the pearled grains. St-Fer were not found in any barley products, which is in accordance with earlier studies (19).

After a 90-s pearling step, the pearled barley and rye grains still contained phytosterol compounds at levels of 0.5 and 0.8 mg/g, respectively, which means that even the pearled grains have an important impact on our natural dietary phytosterol intake. If phytosterols were isolated for the enrichment of their levels in regular foods, the pearling fines from hulless barley or rye would be a better source of phytosterols than the whole grains.

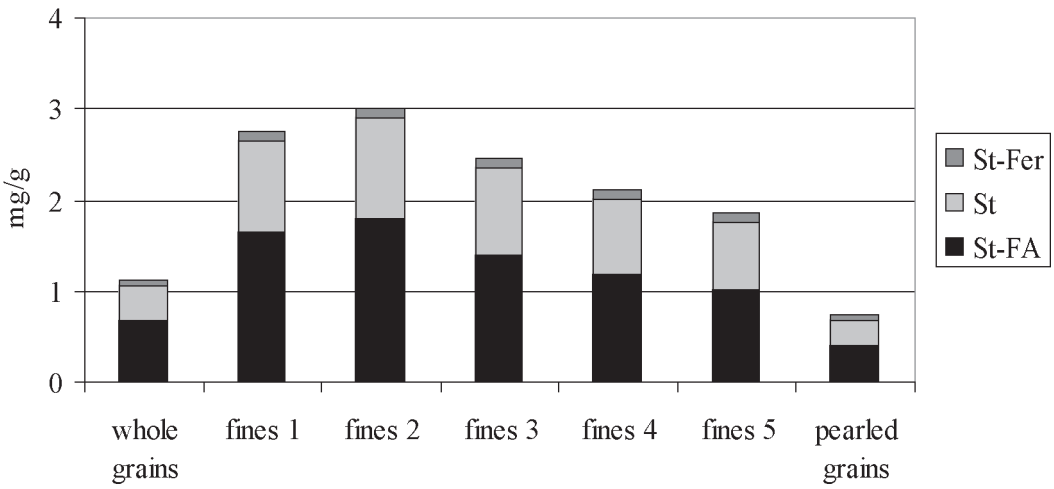

FIG. 2. Distribution of nonpolar sterol classes in rye and its products from five 30-s sequential pearling steps. Values are given as means of two replicate experiments. St-Fer, sterols esterified with ferulic acid; for other abbreviations, see Figure 1.

TABLE 1
Characterization of Two Replicate 90-s Pearlings (A and B) of Hulless Barley and Rye[a]

Sample	Yield (%)	Extractable lipids (%)	Ash (%)	Moisture (%)
Whole-grain barley	100	1.95 ± 0.07	1.8	12.4
Pearling fines, A	14.5	7.04 ± 0.10	4.0	10.7
Pearling fines, B	14.6	7.12 ± 0.06	3.9	10.7
Pearled grains, A	85.5	1.46 ± 0.06	1.4	12.2
Pearled grains, B	85.7	1.44 ± 0.02	1.4	12.3
Whole-grain rye	100	1.84 ± 0.04	2.1	10.6
Pearling fines, A	19.8	5.11 ± 0.05	3.4	9.4
Pearling fines, B	20.5	5.05 ± 0.01	3.4	9.4
Pearled grains, A	77.4	1.14 ± 0.02	1.7	10.7
Pearled grains, B	76.7	1.15 ± 0.02	1.7	10.3

[a]Data are mean ± SD (N = 3) or mean (N = 2).

The phytosterol contents obtained from the nonpolar lipid analyses were consistent with the total phytosterol analysis results obtained by GC. When sterol contents present in free sterols, St-FA, and St-Fer were calculated, most of the total phytosterols in barley and rye grains could be attributed to these classes. A small proportion of total phytosterols in the grains (35% in barley and 5% in rye) could thus occur as glycosides and acylated glycosides. Steryl glycosides may contribute to *ca.* 20% of total phytosterols in whole-grain wheat flour (21).

Three phytosterols, namely, sitosterol, campesterol, and stigmasterol, were the major sterols in barley and rye (Table 4), which is in accordance with earlier studies (4,5). Up to 18% of total sterols in rye consisted of saturated phytosterols, sitostanol, and campestanol. The amount of stanols in barley was lower than that in rye, which was also shown by the nonpolar lipid analysis. Phytosterol profiles of the pearling fines were comparable with those of the whole grains. In barley, the amounts of stanols in the fines were greater than those in the grains.

Potential food uses of pearling fines. Pearling fines are usually considered by-products of the milling and/or pearling industry, with the high-starch fractions as the main products. However, the by-products contain higher levels of many valuable bioactive compounds (e.g., vitamins and minerals, and dietary fiber) than the refined products. This study showed that the pearling fines of hulless barley and rye contained >2 mg/g phytosterol compounds, which makes them a reliable and inexpensive source of phytosterols. Recent studies have shown

TABLE 2
Nonpolar Lipids of Hulless Barley and Its Products After 90-s Pearling[a]

	Lipid contents (mg/g)					
Sample	TAG	FFA	St-FA	Stanols	Sterols	St-Fer
Whole grains	11.4 ± 0.2	1.00 ± 0.03	0.43 ± 0.01	+[b]	0.25 ± 0.00	ND[c]
Pearling fines, A	50.4 ± 1.2	3.08 ± 0.04	1.16 ± 0.02	+	0.94 ± 0.01	ND
Pearling fines, B	50.8 ± 1.0	3.17 ± 0.08	1.19 ± 0.01	+	0.99 ± 0.03	ND
Pearled grains, A	7.35 ± 0.5	0.81 ± 0.02	0.34 ± 0.01	+	0.20 ± 0.01	ND
Pearled grains, B	7.1 ± 0.2	0.80 ± 0.01	0.33 ± 0.00	+	0.20 ± 0.00	ND

[a]A and B refer to replicate pearling experiments. Data are mean ± SD (N = 3).
[b]+, present at <0.05 mg/g.
[c]ND, not detected.

TABLE 3
Nonpolar Lipids of Rye and Its Products After 90-s Pearling[a]

	Lipid contents, (mg/g)					
Sample	TAG	FFA	St-FA	Stanols	Sterols	St-Fer
Whole grains	11.1 ± 0.2	1.09 ± 0.02	0.62 ± 0.02	0.09 ± 0.00	0.33 ± 0.00	0.07 ± 0.01
Pearling fines, A	34.0 ± 0.7	1.87 ± 0.04	1.33 ± 0.06	+[b]	0.92 ± 0.01	0.07 ± 0.01
Pearling fines, B	34.4 ± 0.3	1.94 ± 0.05	1.34 ± 0.01	+	0.94 ± 0.01	0.08 ± 0.02
Pearled grains, A	4.75 ± 0.1	1.04 ± 0.02	0.45 ± 0.02	0.06 ± 0.00	0.20 ± 0.00	0.07 ± 0.00
Pearled grains, B	4.7 ± 0.2	1.06 ± 0.03	0.45 ± 0.00	0.06 ± 0.00	0.20 ± 0.00	0.06 ± 0.00

[a]A and B refer to replicate pearling experiments. Data are mean ± SD (N = 3).
[b]+, present at <0.05 mg/g.

TABLE 4
Total Phytosterol Compositions of Whole Grains and 90-s Pearling Fines of Hulless Barley and Rye[a]

	Total sterol contents, (μg/g)						
Sample	Campesterol	Campestanol	Sitosterol	Sitostanol	Stigmasterol	Minor sterols[b]	Total phytosterols
Whole-grain barley	181 ± 2	11 ± 0	476 ± 1	5 ± 0	39 ± 0	86 ± 1	797 ± 4
Pearling fines, A	391 ± 8	40 ± 0	925 ± 20	26 ± 0	120 ± 1	221 ± 9	1732 ± 38
Pearling fines, B	397 ± 5	40 ± 0	934 ± 10	25 ± 0	121 ± 1	227 ± 1	1744 ± 14
Whole-grain rye	133 ± 1	68 ± 1	452 ± 4	94 ± 1	29 ± 1	111 ± 1	886 ± 7
Pearled fines, A	297 ± 3	100 ± 2	795 ± 9	122 ± 2	74 ± 1	199 ± 3	1587 ± 19
Pearled fines, B	300 ± 6	105 ± 3	804 ± 12	126 ± 2	73 ± 1	212 ± 11	1620 ± 33

[a]A and B refer to replicate pearling experiments. Data are mean ± SD (N = 3).
[b]Minor sterols include, e.g., Δ5- and Δ7-avenasterols, Δ7-stigmastenol, and stigmastadienol.

that the phytosterol levels present in natural foods might also contribute to lowering cholesterol absorption (22,23). It also has been suggested that when phytosterols are combined with other bioactive compounds, they may have a greater impact on health. Moreover the LDL-lowering effect of phytosterols might be enhanced by other cholesterol-lowering compounds such as soluble fiber, guar gum, and soy protein (24), which may make the pearling fines valuable raw materials for health-promoting foods. More research is needed to understand the interactions between phytosterols and dietary fibers, and to develop processes to enable the efficient utilization of the milling industry by-products to yield improved food applications.

In addition to possible food uses of barley pearling fines, a new type of edible oil also could be obtained by the extraction of barley pearling fines. (Pearling fines contain about 4.5 times as much oil as whole grains.) From the data on pearling fines, we estimate that a "barley pearling fine oil" contains about 3% total phytosterols, which is several-fold higher than the levels of phytosterols in typical commercial vegetable oils. Since Ostlund *et al.* (25) demonstrated that the endogenous phytosterols in refined corn oil had a significant cholesterol-lowering effect, it is reasonable to assume that an oil from barley fines may have similar health-promoting properties.

ACKNOWLEDGMENTS

Collaboration between the Department of Applied Chemistry and Microbiology (University of Helsinki) and the USDA/ARS/ERRC was financially supported by the National Technology Agency of Finland. The authors would like to thank Drs. Mark Vaughn, Carl Griffey, and Wynse Brooks for providing us with the barley grains and Dr. Ronald Barnett for the rye grains.

REFERENCES

1. Piironen, V., Lindsay, D.G., Miettinen, T.A., Toivo, J., and Lampi, A.-M. (2000) Plant Sterols: Biosynthesis, Biological Function and Their Importance to Human Nutrition, *J. Sci. Food Agric. 80*, 939–966.
2. Moreau, R.A., Whitaker, B.D., and Hicks, K.B. (2002) Phytosterols, Phytostanols, and Their Conjugates in Foods: Structural Diversity, Quantitative Analysis, and Health-Promoting Uses, *Prog. Lipid Res. 41*, 457–500.
3. Katan, M.B., Grundy, S.M., Jones, P., Law, M., Miettinen, T., and Paoletti, R. (2003) Efficacy and Safety of Plant Stanols and Sterols in the Management of Blood Cholesterol Levels, *Mayo Clin. Proc. 78*, 965–978.
4. Normén, L., Bryngelsson, S., Johnsson, M., Evheden, P., Ellegård, L., Brants, H., Andersson, H., and Dutta, P. (2002) The Phytosterol Content of Some Cereal Foods Commonly Consumed in Sweden and in The Netherlands, *J. Food Comp. Anal. 15*, 693–704.
5. Piironen, V., Toivo, J., and Lampi, A.-M. (2002) Plant Sterols in Cereals and Cereal Products, *Cereal Chem. 79*, 148–154.
6. Liukkonen, K.-H., Katina, K., Wilhelmsson, A., Myllymäki, O., Lampi, A.-M., Kariluoto, S., Piironen, V., Heinonen, S.-M., Nurmi, T., Adlercreutz, H., *et al.* (2003) Process-Induced Changes on Bioactive Compounds in Whole Grain Rye, *Proc. Nutr. Soc. 62*, 117–122.
7. Piironen, V., Kariluoto, S., and Lampi, A.-M. (2004) Importance of Phytosterols, Folates and Other Bioactive Compounds in Cereals, in *Dietary Fiber Bioactive Carbohydrates for Food and Feed* (van der Kamp, J.W., Asp, N.-G., Miller Jones, J., and Schaafsma, G., eds.), pp. 135–140, Wageningen Academic Publishers, Wageningen.
8. Izydorczyk, M.S., Symons, S.J., and Dexter, J.E. (2002) Fractionation of Wheat and Barley, in *Whole-Grain Foods in Health and Disease* (Marquart, L., Slavin, L., and Fulcher, R.G., eds.), pp. 47–82, American Association of Cereal Chemists, St. Paul, MN.
9. Sosulski, K., Wang, S., Ingledew, W.M., Sosulski, F.W., and Tang, J. (1997) Preprocessed Barley, Rye, and Triticale as a Feedstock for an Integrated Fuel Ethanol-Feedlot Plant, *Appl. Biochem. Biotechnol. 63–65*, 59–70.
10. Wang, S., Sosulski, K., Sosulski, F., and Ingledew, M. (1997) Effect of Sequential Abrasion on Starch Composition of Five Cereals for Ethanol Fermentation, *Food Res. Intl. 30*, 603–609.
11. Moreau, R.A., Powell, M.J., and Singh, V. (2003) Pressurized Liquid Extraction of Polar and Nonpolar Lipids in Corn and Oats with Hexane, Methylene Chloride, Isopropanol, and Ethanol, *J. Am. Oil Chem. Soc. 80*, 1063–1067.
12. Hara, A., and Radin, N.S. (1978) Lipid Extraction of Tissues with a Low-Toxicity Solvent, *Anal. Biochem. 90*, 420–426.
13. Moreau, R.A., Powell, M.J., and Hicks, K.B. (1996) Extraction and Quantitative Analysis of Oil from Commercial Corn Fiber, *J. Agric. Food Chem. 44*:2149–2154.
14. American Association of Cereal Chemists (2000) *Approved Methods of the AACC*, 10th edn., AACC, St. Paul, MN.
15. Nilsson, M., Åman, P., Härkönen, H., Hallmans, G., Bach Knudsen, K.E., Mazur, W., and Adlercreutz, H. (1997) Content of Nutrients and Lignans in Roller Milled Fractions of Rye, *J. Sci. Food Agric. 73*, 143–148.
16. Yeung, J., and Vasanthan, T. (2001) Pearling of Hull-less Barley: Product Composition and Gel Color of Pearled Barley Flours as Affected by the Degree of Pearling, *J. Agric. Food Chem. 49*, 331–335.
17. Seitz, L.M. (1989) Stanol and Sterol Esters of Ferulic and *p*-Coumaric Acids in Wheat, Corn, Rye, and Triticale, *J. Agric. Food Chem. 37*, 662–667.
18. Moreau, R.A., Powell, M.J., Hicks, K.B., and Norton, R.A. (1998) A Comparison of the Levels of Ferulate-Phytosterol Esters in Corn and Other Seeds, in *Advances in Plant Lipid Research* (Sánchez, J., Cerdá-Olmedo, E., and Martínez-Force, E., eds.), pp. 472–474, Universidad de Sevilla, Sevilla.
19. Hakala, P., Lampi, A.-M., Ollilainen, V., Werner, U., Murkovic, M., Wähälä, K., Karkola, S., and Piironen, V. (2002) Steryl Phenolic Acid Esters in Cereals and Their Milling Fractions, *J. Agric. Food. Chem. 50*, 5300–5307.
20. Singh, V., Moreau, R.A., and Cooke, P.H. (2001) Effect of Corn Milling Practices on Aleurone Layer Cells and Their Unique Phytosterols, *Cereal Chem. 78*, 436–441.
21. Toivo, J., Phillips, K., Lampi, A.-M., and Piironen, V. (2001) Determination of Sterols in Foods: Recovery of Free, Esterified, and Glycosidic Sterols, *J. Food Comp. Anal. 14*, 631–643.
22. Ostlund, R.E., Jr., Racette, S.B., and Stenson, W.F. (2003) Inhibition of Cholesterol Absorption by Phytosterol-Replete Wheat Germ Compared with Phytosterol-Depleted Wheat Germ, *Am. J. Clin. Nutr. 77*, 1385–1389.
23. Ostlund, R.E., Jr. (2004) Phytosterols and Cholesterol Metabolism, *Curr. Opin. Lipidol. 15*, 37–41.
24. Jenkins, D.J.A., Kendall, C.W.C., Marchie, A., Faulkner, D.A., Wong, J.M.W., de Souza, R., Emam, A., Parker, T.L., Vidgen, E., Lapsley, K.G., Trautwein, E.A., Josse, R.G., Leiter, L.A., and Connelly, P.W. (2003) Effects of a Dietary Portfolio of Cholesterol-Lowering Foods vs. Lovastatin on Serum Lipids and C-Reactive Protein, *J. Am. Med. Assoc. 290*, 502–510.
25. Ostlund, R.E., Jr., Racette, S.B., Okeke, A., and Stenson, W.F. (2002) Phytosterols That Are Naturally Present in Commercial Corn Oil Significantly Reduce Cholesterol Absorption in Humans, *Am. J. Clin. Nutr. 75*, 1000–1004.

[Received June 14, 2004; accepted September 2, 2004]

Recovery of Sterols as Fatty Acid Steryl Esters from Waste Material After Purification of Tocopherols

Toshihiro Nagao[a,*], Yoshinori Hirota[b], Yomi Watanabe[a], Takashi Kobayashi[a], Noriaki Kishimoto[c], Tokio Fujita[c], Motohiro Kitano[b], and Yuji Shimada[a]

[a]Osaka Municipal Technical Research Institute, Osaka 536-8553, Japan, [b]Yashiro Co. Ltd., Osaka 547-0003, Japan, and [c]Department of Agricultural Chemistry, Faculty of Agriculture, Kinki University, Nara 631-8505, Japan

ABSTRACT: Tocopherols are purified industrially from soybean oil deodorizer distillate by a process comprising distillation and ethanol fractionation. The waste material after ethanol fractionation (TC waste) contains 75% sterols, but a purification process has not yet been developed. We thus attempted to purify sterols by a process including a lipase-catalyzed reaction. *Candida rugosa* lipase efficiently esterified sterols in TC waste with oleic acid (OA). After studying several factors affecting esterification, the reaction conditions were determined as follows: ratio of TC waste/OA, 1:2 (wt/wt); water content, 30%; amount of lipase, 120 U/g-reaction mixture; temperature, 40°C. Under these conditions, the degree of esterification reached 82.7% after 24 h. FA steryl esters (steryl esters) in the oil layer were purified successfully by short-path distillation (purity, 94.9%; recovery, 73.1%). When sterols in TC waste were esterified with FFA originating from olive, soybean, rapeseed, safflower, sunflower, and linseed oils, the FA compositions of the steryl esters differed somewhat from those of the original oils: The content of saturated FA was lower and that of unsaturated FA was higher. The m.p. of the steryl esters synthesized (21.7–36.5°C) were remarkably low compared with those of the steryl esters purified from high-b.p. soybean oil deodorizer distillate substances (56.5°C; *JAOCS 80*, 341–346, 2003). The low-m.p. steryl esters were soluble in rapeseed oil even at a final concentration of 10%.

Paper no. L9523 in *Lipids 39*, 789–794 (August 2004).

The cholesterol-lowering effect of phytosterols (referred to as sterols), which has been studied since the 1950s (1–5), is believed to be caused by an inhibition of cholesterol absorption resulting from the higher solubility of sterols than of cholesterol in bile salt micelles (4,5). FA steryl esters (referred to as steryl esters) show the same physiological effects as free sterols (6–8). This physiological activity has led to the development of several functional foods, such as salad oils with added sterols and margarines blended with steryl esters. The solubility of steryl esters in vegetable oil is extremely high compared with that of free sterols; thus, considerable attention is being focused on the addition of steryl esters to oil-based foods. Vegetable oil deodorizer distillate (VODD), which is produced in the final deodorization step of vegetable oil refining, contains mainly FFA, tocopherols, sterols, steryl esters, and unknown hydrocarbons. One industrial process for the purification of tocopherols in VODD consists of short-path distillation and ethanol fractionation (9). Short-path distillation results in tocopherol concentrate, which contains tocopherols, sterols, and unknown hydrocarbons, but not FFA and steryl esters. The sterols and hydrocarbons are precipitated by adding 5 vol parts of ethanol to the tocopherol concentrate and then cooling the mixture to 0°C with agitation (9). The filtrate is the tocopherol fraction, and the precipitate is an industrial waste (referred to as TC waste), although about 75% sterols are included. Recovery of sterols in the TC waste by distillation is difficult because TC waste contains contaminants (tocopherols and unknown hydrocarbons) whose M.W. are similar to those of sterols. However, relatively easy purification of sterols can be expected if only the sterols are converted to their FA esters by a selective reaction using a lipase.

That sterols can be converted to their FA esters by lipase-catalyzed esterification or transesterification is well known (10–13). Moreover, we recently reported that treatment of VODD using C*andida rugosa* lipase converts only the sterols to steryl esters (14,15), and that an enzymatic reaction is useful for the purification of tocopherols and for the recovery of sterols as steryl esters. This finding was also supported by Weber *et al*. (16). An enzymatic reaction was therefore introduced to recover the sterols in TC waste. This paper shows that a process comprising a lipase-catalyzed reaction and distillation is effective for the purification of sterols in TC waste as steryl esters. In addition, this process is applicable to low-m.p. steryl esters, which are desired for their applications in oil-based foods.

MATERIALS AND METHODS

Materials. TC waste was obtained from Yashiro Co. Ltd. (Osaka, Japan). Ethanol in the TC waste (*ca*. 50%) was evaporated under reduced pressure before beginning the enzymatic reactions. The ethanol-free waste (TC waste) was composed of 74.7 wt% sterols, 7.0 wt% tocopherols, 1.2 wt% steryl esters, and 17.1 wt% unknown hydrocarbons. The composition of sterols was 2.6 wt% brassicasterol, 27.4 wt%

*To whom correspondence should be addressed at Osaka Municipal Technical Research Institute, 1-6-50 Morinomiya, Joto-ku, Osaka 536-8553, Japan. E-mail: nagao@omtri.city.osaka.jp

Abbreviations: ALA, α-linolenic acid; LnA, linoleic acid; OA, oleic acid; PA, palmitic acid; SA, stearic acid; steryl ester, FA steryl ester; TC waste, waste material after purification of tocopherols; VODD, vegetable oil deodorizer distillate.

campesterol, 27.5 wt% stigmasterol, and 42.5 wt% β-sitosterol. The FA composition of a commercial product, oleic acid (OA; Tokyo Kasei Kogyo Co. Ltd., Tokyo, Japan), was 1.0 wt% palmitic acid (PA), 1.2 wt% stearic acid (SA), 92.7 wt% OA, 4.8 wt% linoleic acid (LnA), and 0.3 wt% α-linolenic acid (ALA). Olive oil was purchased from Wako Pure Chemical Industry Ltd. (Osaka, Japan), and soybean, rapeseed, and linseed oils were obtained from Yashiro. Safflower and high-oleic sunflower oils were purchased from Showa Sangyo Co. Ltd. (Tokyo, Japan). The FA compositions of these oils are shown in the Results section.

Lipases. *Geotrichum candidum* lipase was prepared according to Tsujisaka *et al*. (17). The cells were cultivated at 27°C for 24 h in a medium containing 5% corn steep liquor, 1% soybean oil, and 0.5% NH_4NO_3 (pH 6.0). The enzyme solution was prepared by ammonium sulfate fractionation, followed by dialysis against deionized water. The other lipases were obtained from the following companies: Lipases from *C. rugosa* (Lipase-OF), *Alcaligenes* sp. (Lipase-QLM), *Burkholderia cepacia* (Lipase-SL), and *Pseudomonas stutzeri* (Lipase-TL) were from Meito Sangyo Co. Ltd. (Aichi, Japan); lipases from *C. rugosa* (Lipase-AY) and *Pseudomonas* sp. (Lipases-PS and -AK) were from Amano Enzyme Inc. (Aichi, Japan); *Rhizopus oryzae* lipase was from Tanabe Seiyaku Co. Ltd. (Osaka, Japan); *Thermomyces lanuginosa* lipase was from Novozymes (Bagsvaerd, Denmark); *Burkholderia glumae* lipase was from Asahi Chemical Industry Co. Ltd. (Tokyo, Japan). Lipase activity was measured by titrating the FA liberated from olive oil with 50 mM of KOH as described previously (18). In brief, the hydrolysis of olive oil was conducted at 40°C with stirring at 500 rpm. One unit (U) of lipase activity was defined as the amount that liberated 1 μmol of FA per minute.

Preparation of FFA originating from vegetable oils. A mixture of 50 g of vegetable oil, 200 mL of ethanol, 20 mL of water, and 15 g of NaOH was heated at 60°C for 30 min with stirring in a 1-L round-bottomed flask overlain with nitrogen gas. After the reaction, 200 mL of water was added to the mixture, and its pH was adjusted to 2 with concentrated HCl. FFA were extracted three times with 200 mL of *n*-hexane, and the solvent was removed by evaporation.

Reactions. A small-scale reaction was performed in a 50-mL vessel. A standard reaction mixture containing 1.17 g of TC waste, 2.33 g of FFA (3.9 mol for sterols in the TC waste), 1.5 g of water, and 120 U/g-mixture of lipase was stirred at 30°C and 500 rpm for 20 h. A large-scale reaction was conducted at 40°C for 24 h in a 5-L reactor (MDL-500; Marubishi Bioengineering Co. Ltd., Tokyo, Japan) containing 333 g of TC waste, 667 g of OA, 430 g of water, and 171,600 U of *C. rugosa* lipase (120 U/g-mixture) with agitation at 250 rpm. The degree of esterification was expressed as the mol% of steryl esters based on the total content of sterols and steryl esters.

Purification of steryl esters. Small-scale purification of steryl esters was performed by a combination of *n*-hexane extraction and silica gel column chromatography as described previously (19). Large-scale purification was carried out by short-path distillation. In brief, the reaction mixture was allowed to stand at 90°C, and the resulting oil layer was dehydrated at 80°C and 5 mm Hg for 30 min with blowing nitrogen gas (water content, <100 ppm). The oil layer was applied to a distillation apparatus (Wiprene type 2-03; Kobelco Eco-Solutions Co. Ltd., Kobe, Japan) and was distilled stepwise as follows: step 1, at 180°C and 0.2 mm Hg; step 2, at 200°C and 0.2 mm Hg; step 3, at 240°C and 0.05 mm Hg.

Analyses. Contents of FFA, sterols, and steryl esters were analyzed with a Shimadzu GC-18A gas chromatograph (Kyoto, Japan) connected to a DB-1ht capillary column (0.25 mm × 5 m; J&W Scientific, Folsom, CA). The column temperature was raised from 120 to 280°C at 15°C/min and from 280 to 370°C at 10°C/min, and was then maintained for 1 min. The injector and detector temperatures were set at 370 and 390°C, respectively.

The FA composition was analyzed by GC after methylation. In brief, FFA (0.08 g) were methylated in 3 mL of methanol containing 0.45% boron trifluoride (Wako) by heating at 75°C for 5 min, and FA in the steryl esters (0.08 g) were converted to their methyl esters in 3 mL of methanol containing 5.8% Na-methylate (Wako) by heating at 75°C for 30 min. The FAME were analyzed by a gas chromatograph (model 5890; Hewlett-Packard, Avondale, PA) connected to a DB-23 capillary column (0.25 mm × 30 m; J&W Scientific). The column temperature was raised from 150 to 170°C at 4°C/min, from 170 to 190°C at 5°C/min, and from 190 to 215°C at 10°C/min, and was then maintained for 6 min. The injector and detector temperatures were set at 245 and 250°C, respectively.

The tocopherol contents were determined with a Hewlett-Packard 5890 gas chromatograph connected to a DB-5 capillary column (0.25 mm × 10 m; J&W Scientific) using tricaproin (Tokyo Kasei Kogyo, Tokyo, Japan) as an internal standard. The column temperature was raised from 190 to 290°C at 10°C/min and from 290 to 320°C at 5°C/min, and was then maintained for 1 min. The injector and detector temperatures were set at 250 and 330°C, respectively.

All analyses were conducted three to five times under the same experimental conditions. The relative SD were less than ±8.5% for the average value of <1%, less than ±2.9% for the value of 1–3%, less than ±2.3% for 3–10%, and less than ±1.5% for >10%.

The m.p. of steryl esters were determined according to the AOCS standard open tube melting point (slip melting point) method (20). The m.p. were measured three times, and the SD were less than ±0.5°C.

RESULTS AND DISCUSSION

Selection of lipase for the esterification of sterols in TC waste. To find a suitable lipase for selective esterification, a 5-g mixture of TC waste/OA (1:2, wt/wt), 30% water, and 250 U/g-mixture of lipase was stirred at 30°C for 20 h (Table 1). Among the lipases tested, *C. rugosa* lipases (Lipases-OF and -AY) were the most effective for the conversion of sterols to

TABLE 1
Esterification of Sterols from Waste Material After the Purification of Tocopherols Using Various Lipases[a]

Lipase	Content (wt%)			Esterification (%)
	FFA	Sterol	Steryl ester	
None[b]	65.7	25.3	0.4	—
Candida rugosa[c]	52.5	4.2	34.2	83.2
Candida rugosa[d]	52.7	4.4	33.8	82.3
Geotrichum candidum	60.3	17.0	13.9	32.4
Rhizopus oryzae	65.2	25.2	0.7	0.3
Thermomyces lanuginosa	65.1	24.7	1.2	2.4
Alcaligenes sp.	64.9	24.1	2.5	4.7
Burkholderia glumae	60.3	17.4	13.4	31.2
Burkholderia cepacia	59.0	15.5	16.4	38.3
Pseudomonas sp.[e]	64.9	24.2	2.2	4.3
Pseudomonas sp.[f]	65.3	24.8	1.0	2.0
Pseudomonas stutzeri	61.0	18.8	10.9	25.3

[a]A mixture of 1.17 g of waste material after purification of tocopherols (TC waste), 2.33 g of oleic acid (OA), and 1.50 g of water was stirred at 30°C for 20 h with a 250 U/g-mixture of lipase.
[b]Composition in a mixture of TC waste/OA (1:2, wt/wt).
[c]Lipase-OF (Meito Sangyo Co. Ltd., Aichi, Japan).
[d]Lipase-AY (Amano Enzyme Inc., Aichi, Japan).
[e]Lipase-PS (Amano Enzyme Inc.).
[f]Lipase-AK (Amano Enzyme Inc.).

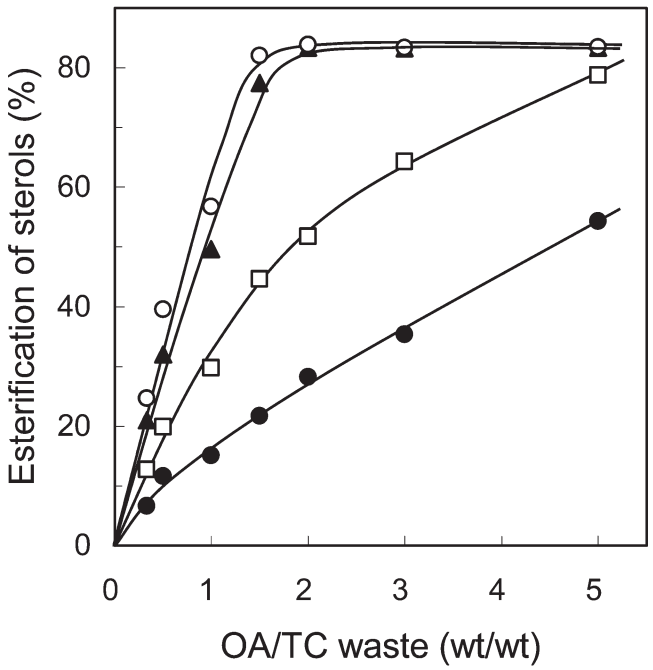

FIG. 1. Effect of oleic acid (OA) content on esterification of sterols in waste material after the purification of tocopherols (TC waste) using *Candida rugosa* lipase. A 5.0-g mixture composed of TC waste, various amounts of OA, 1.5 g of water, and a 120 U/g-mixture of lipase was stirred at 40°C for 3, 7, 20, and 40 h. After separating the reaction mixture into an oil and a water layer, the contents of sterols and steryl esters in the oil layer were analyzed. The degree of esterification was expressed as the mol% of steryl esters based on the total content of sterols and steryl esters. ●, 3 h; □, 7 h; ▲, 20 h; ○, 40 h.

steryl esters, and the degree of esterification reached 82.3–83.2%. In addition, reactions with these two lipases catalyzed only the esterification of sterols with OA. Based on this screening test, Lipase-OF was selected for subsequent studies.

Factors affecting the esterification of sterols. The effect of temperature on the esterification of sterols in TC waste was first studied. A 5-g mixture of TC waste/OA (1:2, wt/wt), 30% water, and 250 U/g-mixture of *C. rugosa* lipase was stirred at various temperatures (20–60°C) for 3, 7, and 20 h. The degree of esterification at 3 h increased with an increase in the reaction temperature and reached a maximum (57.2%) at 50°C, showing that the optimal temperature was around 50°C. The degree of esterification in the equilibrium state at 50°C was 79.6% and was slightly lower than that at 40°C (esterification, 82.7%); thus, the reaction temperature was fixed at 40°C in the following reactions.

The effect of the amount of lipase was next studied. A 5-g mixture of TC waste/OA (1:2, wt/wt), 30% water, and different amounts of *C. rugosa* lipase was stirred at 40°C. The degree of esterification after 20 h did not increase, even though more than 120 U/g-mixture of lipase was used (data not shown).

To study the effect of the amount of OA on esterification, sterols in the TC waste were esterified at 40°C with 0.33–5 weight parts of OA for TC waste using 120 U/g-mixture of *C. rugosa* lipase (Fig. 1). The degree of esterification after 3 h showed that the reaction was accelerated with an increasing amount of OA. The degree of esterification after 20 and 40 h depended on the ratio of TC waste/OA and reached an almost constant value (83.2–83.5%) at the ratio of 1:2 (wt/wt).

The effect of water content on esterification was finally studied. The reaction was conducted at 40°C for 3, 7, and 20 h in a 5.0-g mixture of TC waste/OA (1:2, wt/wt), various amounts of water, and 120 U/g-mixture of lipase (Fig. 2). The degree of esterification after 20 h was almost the same (81.0–83.3%) when the reactions were conducted in the presence of 5–65% water. The degree of esterification at 3 h was the highest in reactions including 20–40% water.

Time course of the esterification of sterols in TC waste. Based on the results described previously, the reaction conditions were determined as follows: temperature, 40°C; amount of lipase, 120 U/g-reaction mixture; ratio of TC waste/OA, 1:2 (wt/wt); water content, 30%. Figure 3 shows a typical time course under these conditions. The reaction proceeded rapidly during the first 10 h and gradually thereafter, and the decrease in sterols and FFA correlated with the increase in steryl esters. The degree of esterification reached 82.7% at 24 h, and the contents of sterols and steryl esters were 4.3 and 35.4 wt%, respectively.

Large-scale purification of steryl esters. The purification of steryl esters from TC waste is summarized in Table 2. A mixture of 1.0 kg of TC waste/OA (1:2, wt/wt) was agitated at 40°C for 24 h with 120 U/g-mixture of *C. rugosa* lipase in the presence of 30% water. The reaction mixture separated into oil and water layers, and the oil layer was dehydrated. The resulting oil layer (942 g) contained 52.2 wt% FFA, 4.5 wt% sterols, and 34.3 wt% steryl esters (esterification, 82.3%). FFA in the oil layer were removed by two-step distillation at 180°C/0.2 mm Hg and 200°C/0.2 mm Hg. The first

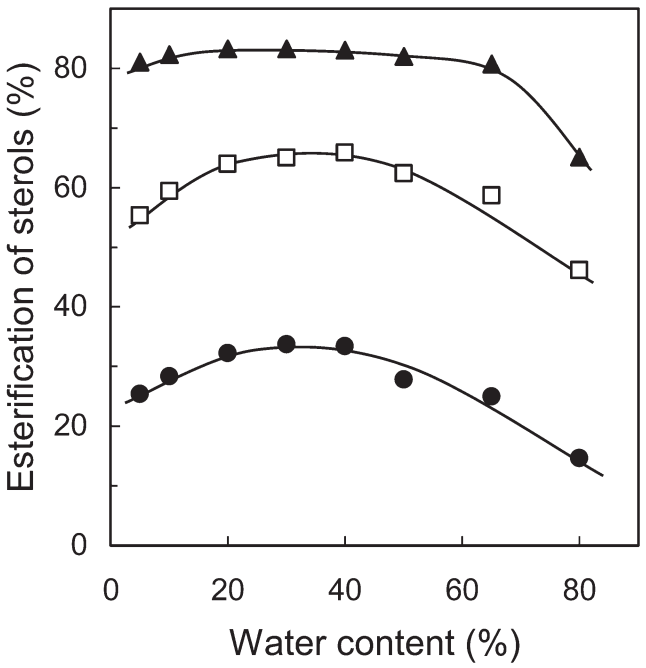

FIG. 2. Effect of water content on the esterification of sterols in TC waste using *C. rugosa* lipase. A 5.0-g mixture composed of TC waste/OA (1:2, wt/wt) and various amounts of water was stirred at 40°C for 3, 7, and 20 h with a 120 U/g-mixture of lipase. ●, 3 h; □, 7 h; ▲, 20 h. See Figure 1 for abbreviations.

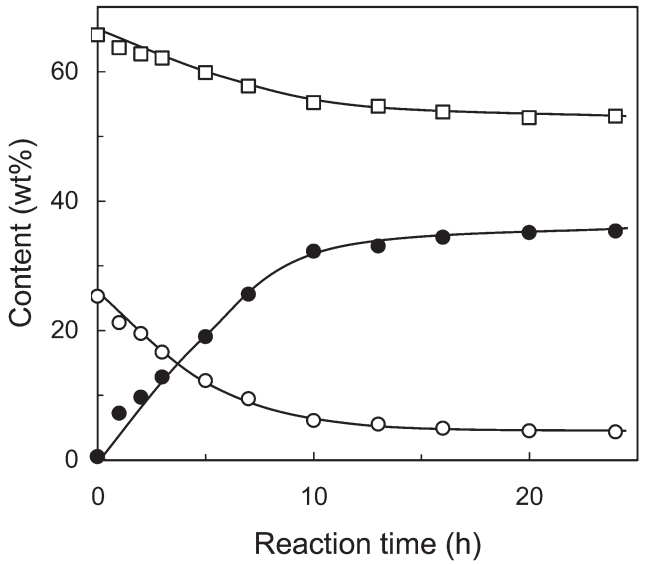

FIG. 3. Time course of the esterification of sterols in TC waste and OA using *C. rugosa* lipase. A mixture of 1.17 g of TC waste, 2.33 g of OA, and 1.50 g of water was stirred at 40°C with a 120 U/g-mixture of *C. rugosa* lipase. ●, Steryl esters; ○, sterols; □, FFA. See Figure 1 for abbreviations.

distillation step removed 47.4% FFA, and the second removed 44.3% FFA. Steryl esters were not detected in distillates 1 and 2. Residue 2 (448 g) contained 8.9 wt% FFA, 8.5 wt% sterols, 4.1 wt% tocopherols, and 71.0 wt% steryl esters. To remove the remaining FFA, sterols, and tocopherols, residue 2 was then distilled at 240°C and 0.05 mm Hg, and was fractionated into 128 g of distillate 3 and 314 g of residue 3. Residue 3 contained only small amounts of FFA (0.7 wt%) and sterols (1.3 wt%), and the purity of the steryl esters was 94.9%. Sterols in the TC waste were recovered as steryl esters in 73.1% yield for the initial contents. These results showed that a process comprising lipase treatment and short-path distillation is effective for the recovery of sterols in TC waste.

Esterification of sterols in TC waste with FFA originating from several vegetable oils. Sterols in TC waste were esterified at 40°C for 20 h with 2 weight parts of FFA originating from several vegetable oils in a 5-g mixture containing 30% water and 120 U/g-mixture of *C. rugosa* lipase (Table 3). The degree of esterification in all reactions was 81.5 to 83.2%. Steryl esters were purified from the reaction mixture by *n*-hexane extraction, followed by silica gel column chromatography. The composition of sterols in the purified steryl esters was almost the same as that of sterols in the TC waste, but the FA composition was slightly different (Table 3). The contents of PA and SA in the steryl esters were lower than those in the original FFA, and the contents of ALA and LnA were higher. These results can be explained by the FA specificity of *C. rugosa* lipase, which was in the order of ALA > LnA > OA > PA > SA (15,21).

The steryl esters purified previously from high-b.p. soybean oil deodorizer distillate substances (19) were solid at room temperature (slip melting point, 56.5°C), and they did not dissolve completely when mixed with 9 weight parts of rapeseed oil at 25°C. These results were attributed to the high content of saturated FA (PA, 16.5 wt%; SA, 3.8 wt%). In contrast, the contents of PA and SA in the steryl esters synthesized with FFA originating from vegetable oils (PA, 3.3–8.0 wt%; SA, 0.7–1.9 wt%) were lower than those of the steryl esters purified from soybean oil deodorizer distillate, and their m.p. were 21.7–36.5°C (Table 3). These results suggest that the m.p. of steryl esters are correlated with the saturated FA contents. The total contents of PA and SA in the steryl esters esterified with FFA from sunflower and linseed oils were similar (4.7–4.6 wt%), but the m.p. of steryl esters esterified with FFA from linseed oil (21.7°C) were lower than those esterified with FFA from sunflower oil (25.2°C). The low m.p. could be explained by the high content of ALA, which has a m.p. lower than that of OA.

The steryl esters synthesized with FFA originating from rapeseed, safflower, sunflower, and linseed oils (m.p., 21.7–27.4°C) dissolved completely in 9 weight parts of rapeseed oil at 25°C, and no precipitation occurred even after the mixture was kept at 15°C for 24 h. The low-m.p. steryl esters prepared in this study could be used as additives in oil-based foods.

Esterification of sterols in TC waste using TAG. Finally, we attempted the esterification of sterols using TAG. A mixture of 1.17 g of TC waste, 2.33 g of olive oil, and 1.50 g of water was stirred at 40°C with 120 U/g-mixture of *C. rugosa* lipase (Fig. 4). The TAG hydrolyzed rapidly, and the TAG content decreased to <0.4 wt% at 3 h. After FFA had accumu-

TABLE 2
Purification of Steryl Esters from TC Waste

Step	Weight (g)					
	Total	FFA	Sterol	Steryl ester	Tocopherol	Other
Enzymatic reaction[a]						
Before	1000	667	248	4	23	58
After	942	492	42	323	23	62
Distillation						
Distillate 1[b]	249	233	1	ND[e]	1	14
Distillate 2[c]	240	218	3	ND	3	16
Distillate 3[d]	128	37	33	18	17	23
Residue 3[d]	314	2	4	298	1	9

[a]A mixture of 333 g of TC waste, 667 g of OA, 430 g of water, and 171,600 U of *C. rugosa* lipase was agitated at 40°C for 24 h. After the reaction, the resulting oil layer was recovered.
[b]Distilled at 180°C and 0.2 mm Hg.
[c]Distilled at 200°C and 0.2 mm Hg.
[d]Distilled at 240°C and 0.05 mm Hg.
[e]ND, not detected (<0.5 g). See Table 1 for other abbreviations.

TABLE 3
Enzymatic Esterification of Sterols in TC Waste with FFA Originating from Various Vegetable Oils Using *C. rugosa* Lipase[a]

Origin of FFA	Esterification (%)	FA composition (wt%)					m.p.[b] (°C)
		16:0	18:0	18:1	18:2	18:3	
Olive							
Before	—	8.9	3.6	78.6	8.1	0.8	
After	82.6	7.9	1.5	80.6	9.0	1.0	36.5
Soybean							
Before	—	10.8	4.9	23.9	53.4	7.0	
After	83.2	8.0	1.9	21.6	60.2	8.3	34.4
Rapeseed							
Before	—	4.5	2.1	62.5	21.1	9.8	
After	82.0	3.4	0.7	64.0	21.6	10.3	24.5
Safflower							
Before	—	7.2	2.7	15.8	73.7	0.6	
After	82.5	5.1	0.9	14.9	78.4	0.7	27.4
Sunflower							
Before	—	3.8	4.1	81.8	9.2	1.1	
After	83.0	3.3	1.4	83.9	10.1	1.3	25.2
Linseed							
Before	—	6.0	3.6	21.2	16.8	52.4	
After	81.5	3.5	1.1	13.4	15.8	66.2	21.7

[a]A mixture of 1.17 g of TC waste, 2.33 g of FFA, 1.5 g of water, and 600 U of *C. rugosa* lipase was agitated at 40°C for 20 h.
[b]Slip melting point of steryl esters. See Table 1 for abbreviations.

lated by the hydrolysis of TAG, sterols were esterified using the FFA. The time course for the conversion of sterols to steryl esters in the reaction with TC waste and olive oil was quite similar to that in the reaction with TC waste and OA (Figs. 3, 4), and the degree of esterification reached 83.7% after 24 h. The reaction mixture in the equilibrium state contained only 0.4 wt% MAG, 0.4 wt% DAG, and 0.3 wt% TAG. These results suggest that sterols are converted to steryl esters mainly by their esterification with FFA generated by the hydrolysis of TAG and are slightly converted by their transesterification with TAG.

Features of a process comprising an enzymatic reaction and distillation. Tocopherols have been purified industrially from VODD by a combination of chemical methylation, distillation, methanol (ethanol) fractionation, and ion-exchange chromatography. Sterols have been highly purified from by-products after the recovery of tocopherols by fractionation with a solvent mixture whose main component is *n*-hexane, although the yield is low (*ca*. 50%). Steryl esters with unsaturated FA (whose solubility in TAG is high) can be synthesized by lipase-catalyzed esterification and transesterification (10–13), but the synthesis of high-purity steryl esters requires high-purity sterols as a starting material. In this study, sterols in a by-product generated from the purification of tocopherols were converted to the desired steryl esters by a selective reaction, and the resulting steryl esters were highly purified by short-path distillation in good yield because the M.W. of the steryl esters was the highest among those of components in the reaction mixture: The conversion served as one process in the purification of sterols (steryl esters). The new process es-

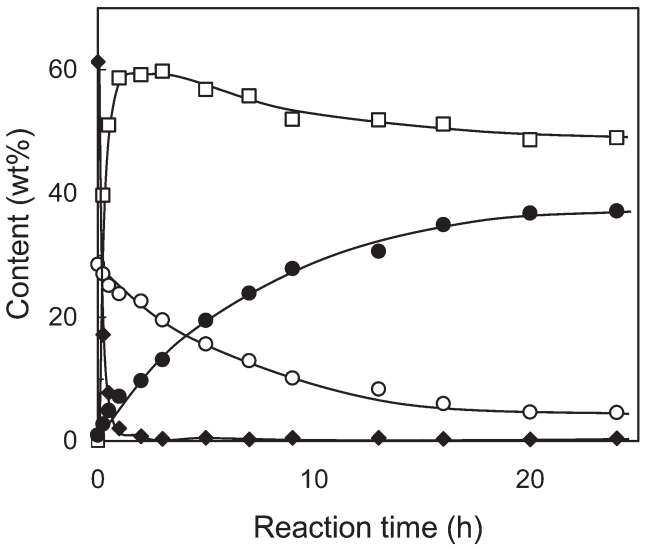

FIG. 4. Time course of the esterification of sterols in TC waste and olive oil using *C. rugosa* lipase. A mixture of 1.17 g of TC waste, 2.33 g of olive oil, and 1.50 g of water was stirred at 40°C with a 120 U/g-mixture of *C. rugosa* lipase. ●, Steryl esters; ○, sterols; □, FFA; ◆, TAG. See Figure 1 for abbreviations.

tablished in this study may contribute to the production of value-added steryl esters in response to requests from the oil and fat industry.

ACKNOWLEDGMENTS

We thank Seiich Nakai and Masaharu Suenaga of Yashiro Co. Ltd. for their valuable discussions, and Takayuki Utsumi of Kinki University for technical support.

REFERENCES

1. Peterson, D.W. (1951) Effect of Soybean Sterols in the Diet on Plasma and Liver Cholesterol in Chicks, *Proc. Soc. Exp. Biol. Med. 78*, 219–225.
2. Farquhar, J.W., Smith, R.E., and Dempasy, M.E. (1956) The Effect of β-Sitosterol on the Serum Lipids of Young Men with Arteriosclerotic Heart Disease, *Circulation 14*, 77–82.
3. Lees, A.M., Mok, H.Y., Lees, R.S., McCluskey, M.A., and Grundy, S.M. (1977) Plant Sterols as Cholesterol-Lowering Agents: Clinical Trials in Patients with Hypercholesterolemia and Studies of Sterol Balance, *Atherosclerosis 28*, 325–338.
4. Armstrong, M.J., and Carey, M.C. (1987) Thermodynamic and Molecular Determinants of Sterol Solubilities in Bile Salt Micelles, *J. Lipid Res. 28*, 1144–1155.
5. Ikeda, I., Tanabe, Y., and Sugano, M. (1989) Effects of Sitosterol and Sitostanol on Micellar Solubility of Cholesterol, *J. Nutr. Sci. Vitaminol. 35*, 361–369.
6. Sierksma, A., Weststrate, J.A., and Meijer, G.W. (1999) Spreads Enriched with Plant Sterols, Either Esterified 4,4-Dimethylsterols or Free 4-Desmethylsterols, and Plasma Total- and LDL-Cholesterol Concentrations, *Br. J. Nutr. 82*, 273–282.
7. Nomén, L., Dutta, P., Lia, A., and Andersson, H. (2000) Soy Sterol Esters and β-Sitosterol Ester as Inhibitors of Cholesterol Absorption in Human Small Bowel, *Am. J. Clin. Nutr. 71*, 908–913.
8. Jones, P.J., Raeini-Sarjaz, M., Ntanois, F.Y., Vanstone, C.A., Feng, J.Y., and Parsons, W.E. (2000) Modulation of Plasma Lipid Levels and Cholesterol Kinetics by Phytosterol Versus Phytostanol Esters, *J. Lipid Res. 41*, 697–705.
9. Hirota, Y., Shimada, Y., Nagao, T., Nakai, S., Urayama, A., Suenaga, M., Terai, T., and Kitano, M. (2003) Enzymatic Purification of Tocopherols and Sterols from Soybean Oil Deodorizer Distillate with Industrial Plants, *Kagaku to Kogyo 77*, 471–477.
10. Myojo, K., and Matsufune, Y. (1994) Process for Preparing Sterol Fatty Acid Esters with Enzymes, *Yukagaku*, *44*, 883–896.
11. Shimada, Y., Hirota, Y., Baba, T., Sugihara, A., Moriyama, S., Tominaga, Y., and Terai, T. (1999) Enzymatic Synthesis of Steryl Esters of Polyunsaturated Fatty Acids, *J. Am. Oil Chem. Soc. 76*, 713–716.
12. Weber, N., Weitkamp, P., and Mukherjee, K.D. (2001) Fatty Acid Steryl, Stanyl, and Steroid Esters by Esterification and Transesterification *in vacuo* Using *Candida rugosa* Lipase as Catalyst, *J. Agric. Food Chem. 49*, 67–71.
13. Negishi, S., Hidaka, I., Takahashi, I., and Kunita, S. (2003) Transesterification of Phytosterol and Edible Oil by Lipase Powder at High Temperature, *J. Am. Oil Chem. Soc. 80*, 905–907.
14. Shimada, Y., Nakai, S., Suenaga, M., Sugihara, A., Kitano, M., and Tominaga, Y. (2000) Facile Purification of Tocopherols from Soybean Oil Deodorizer Distillate in High Yield Using Lipase, *J. Am. Oil Chem. Soc. 77*, 1009–1013.
15. Watanabe, Y., Nagao, T., Hirota, Y., Kitano, M., and Shimada, Y. (2004) Purification of Tocopherols and Phytosterols by a Two-Step *in situ* Enzymatic Reaction, *J. Am. Oil Chem. Soc. 81*, 339–345.
16. Weber, N., Weitkamp, P., and Mukherjee, K.D. (2002) Cholesterol-Lowering Food Additives: Lipase-Catalysed Preparation of Phytosterol and Phytostanol Esters, *Food Res. Intl. 35*, 177–181.
17. Tsujisaka, Y., Iwai, M., and Tominaga, Y. (1973) Purification, Crystallization, and Some Properties of Lipase from *Geotrichum candidum* Link, *Agric. Biol. Chem. 37*, 1457–1464.
18. Sugihara, A., Shimada, Y., and Tominaga, Y. (1990) Separation and Characterization of Two Molecular Forms of *Geotrichum candidum* Lipase, *J. Biochem. 107*, 426–430.
19. Hirota, Y., Nagao, T., Watanabe, Y., Suenaga, M., Nakai, S., Kitano, M., Sugihara, A., and Shimada, Y. (2003) Purification of Steryl Esters from Soybean Oil Deodorizer Distillate, *J. Am. Oil Chem. Soc. 80*, 341–346.
20. American Oil Chemists' Society (AOCS) (1998) Slip Melting Point: AOCS Standard Open Tube Melting Point, *Official Methods and Recommended Practices of the AOCS*, 5th edn. (Firestone, D., ed.), AOCS Press, Champaign, Official Method Cc 3-25.
21. Shimada, Y., Sugihara, A., Maruyama, K., Nagao, T., Nakamura, S., Nakano, H., and Tominaga, Y. (1995) Enrichment of Arachidonic Acid: Selective Hydrolysis of a Single-Cell Oil from *Mortierella* with *Candida cylindracea* Lipase, *J. Am. Oil Chem. Soc. 72*, 1323–1327.

[Received June 15, 2004; accepted August 18, 2004]

Isolation and Synthesis of Shark-Repelling Saponins

John R. Williams* and Hua Gong

Department of Chemistry, Temple University, Philadelphia, Pennsylvania 19122

ABSTRACT: Saponins are complex compounds that are composed of a saccharide attached to a steroid or triterpene. They are natural surfactants, or detergents. Several important biological effects have been ascribed to saponins. They have been isolated from a great number of terrestrial plants. In the animal kingdom they are found in most sea cucumbers and starfish, whereas they are found only rarely in alcyonarians, gorgonians, sponges, and as shark-repelling compounds in fish. The present review deals with the isolation and some syntheses of the shark-repelling saponins mosesins-1 to -5 and pavoninins-1 to -6 obtained from the fish species *Pardachirus.*

Paper no. L9562 in Lipids 39, 795–799 (August 2004).

Saponins are complex compounds that are composed of a saccharide attached to a steroid or triterpene. They are natural surfactants, or detergents. Upon shaking with water, they form colloidal solutions, giving soapy lathers. A wide range of biological effects have been ascribed to saponins, such as membrane-permeabilizing, immunostimmulant, hypocholesterolemic, and anticancer properties (1,2). They can also kill protozoa and mollusks, be used as antioxidants, cause hypoglycemia, and act as antifungal and antiviral agents (1,2). They have been isolated from a great number of terrestrial plants and are most abundant in the desert plants yucca and quillaja. Saponins are uncommon constitutents among members of the animal kingdom. They are found in nearly all sea cucumbers and starfish, whereas they are rare in alcyonarians, in gorgonians sponges, and as shark-repelling compounds in fish (3). The present review deals with the isolation and some syntheses of shark-repelling saponins obtained from fish.

Ichthyocrinotoxic fish secrete biologically active compounds that repel their predators. In 1974 the Moses sole *Pardachirus marmoratus,* which lives in the Red Sea and the western Indian Ocean, was reported to emit a toxic secretion when it was about to be bitten (4). The structures of the shark-repelling compounds were shown to be the five steroidal saponins called mosesins-1 to -5 (**1–5**) (5). The mosesins have the β-bond of C-1 of the monosaccharide galactose attached at the 7α position of the (25)-3,7α,26-trihydroxycholestane 26-acetate skeleton with varying substitution and oxidation at C-3,4,5,6,12α and -15α on the steroid (**1–5**), as shown in Figure 1.

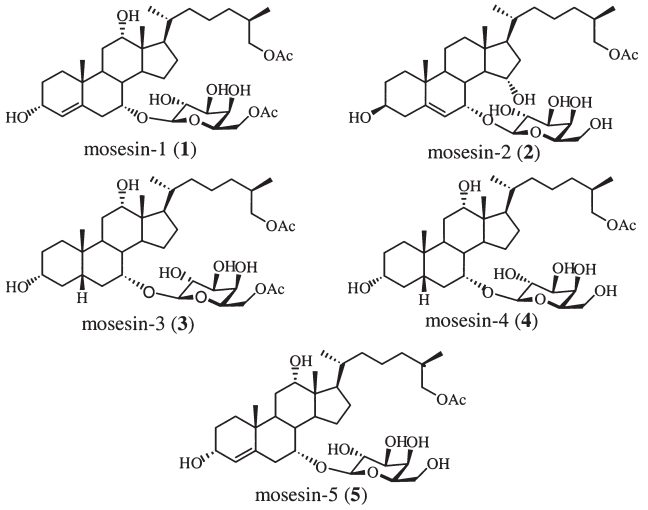

FIG. 1. Mosesins 1–5 (**1–5**).

The synthesis of mosesin-4 (**4**) is outlined in Scheme 1 (6). Cholic acid (**6a**) was used as the starting material since it has the hydroxy groups 3α, 7α, and 12α together with a *cis*-A,B ring junction. To synthesize **4**, the 26-hydroxy cholesterol side chain and the sugar need to be attached. The side chain was synthesized by photochemical decarboxylation/iodination of the cholic ester **6b** to yield the iodide **7a**. Conversion of the iodide **7a** to the alcohol **7b** followed by oxidation gave the aldehyde **8**. Wittig reaction of **8** with the appropriately substituted benzyl ether gave a mixture of 23*E* and *Z* isomers, **9**. The acetates were hydrolyzed, and the more reactive C-3α alcohol was protected as its ethyl carbonate **10**. The sugar was attached by reacting the steroidal diol **10** with β-galactose peracetate, using trimethylsilyl triflate as a promotor in 1,2-dichloroethane to yield the glycoside **11a** in 40% yield. To selectively introduce the C-26 acetate, the acetates in **11a** were hydrolyzed and replaced with silyl ethers, **12**. Catalytic reduction simultaneously reduced the double bond in the side chain and cleaved the benzyl ether. Acetylation at C-26 followed by cleaving the silyl ethers with hydrogen fluoride afforded mosesin-4 (**4**).

In 1984, six shark-repelling saponins, pavoninin-1 to -6 (**13–18**), were isolated from a related species of fish, *P. pavoninus,* living in the tropical regions of the western

*To whom correspondence should be addressed at Dept. of Chemistry, Temple University, 13 and Norris Sts., Philadelphia, PA 19122-2585. E-mail: john.r.williams@temple.edu

Abbreviations: LAH, lithium aluminum hydride; MEMCl, methoxyethoxymethyl chloride.

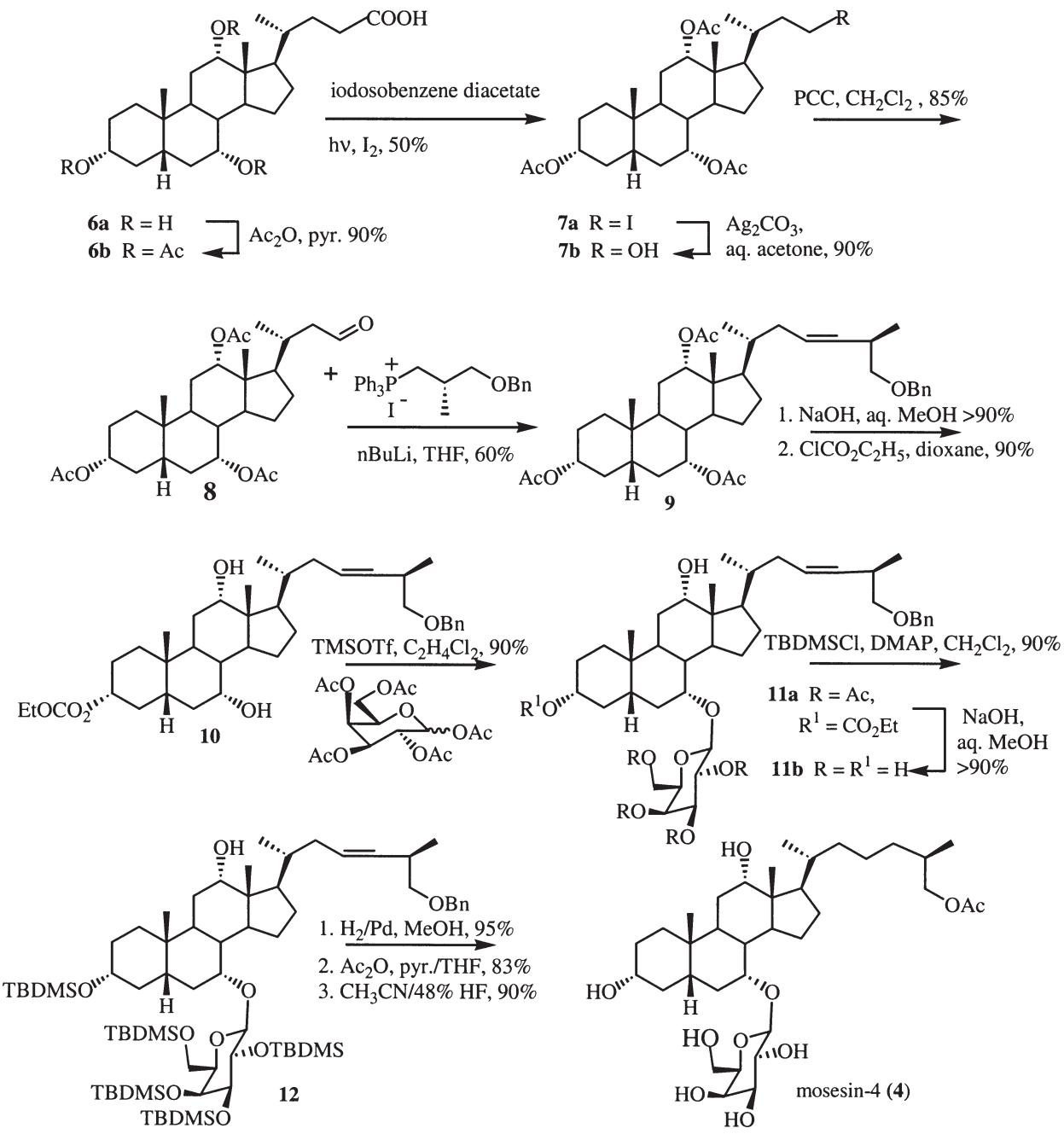

SCHEME 1. Synthesis of mosesin-4 (**4**) from cholic acid (**6a**).

Pacific and eastern Indian Oceans (7,8). The pavoninins have the β-bond of C-1 of *N*-acetylglucosamine attached at 7α or 15α to a (25*R*)-26-hydroxy- or -26-acetoxycholestane skeleton with varying oxidation at C-3,4,5,6, and -7 (**13–18**), as shown in Figure 2.

The first synthesis of the aglycones of pavoninin-1 and -2 (**28** and **27**, respectively), which contain 7α hydroxylation, was reported in 1997 and is outlined in Scheme 2 (9). 26-Hydroxycholesterol **21** was chosen as the starting material since it had been previously prepared by Clemmensen reduction of diosgenin **19** followed by C-16 deoxygenation of the resulting 3α,16β,26-triol **20** (10). Selective silylation of **21** at C-26 followed by Oppenauer oxidation of the C-3 alcohol in **22** and acetylation of the desilylated C-26 alcohol afforded the enone acetate **23**. The C-7α alcohol was prepared by lithium aluminum hydride (LAH) reduction of the C-6α epoxide **25**. The epoxide **25** was made by *meta*-chloroperoxybenzoic acid oxidation of the 4,6-dien-3-one **24**, itself obtained by 2,3-dichloro-5,6-dicycano-1,4-benzoquinone oxidation of the enone **23**. The aglycone of pavoninin-2, **27**, was prepared by treatment of the triol **26** with manganese dioxide. Selective acetylation of **27** afforded the aglycone of pavoninin-1, **28**.

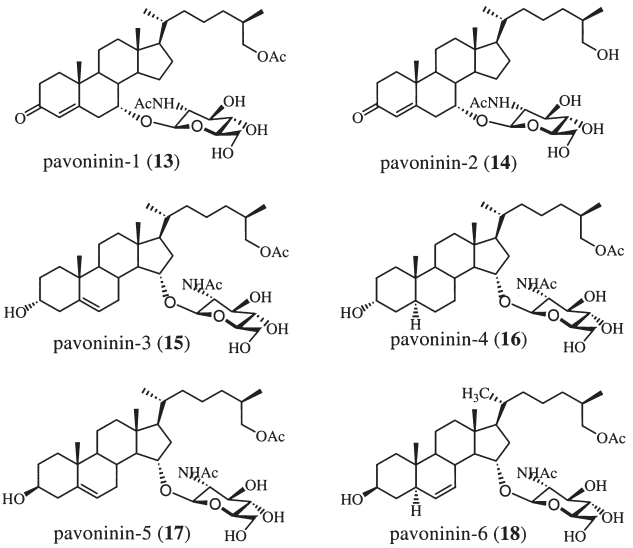

FIG. 2. Pavoninins 1–6 (**13–18**).

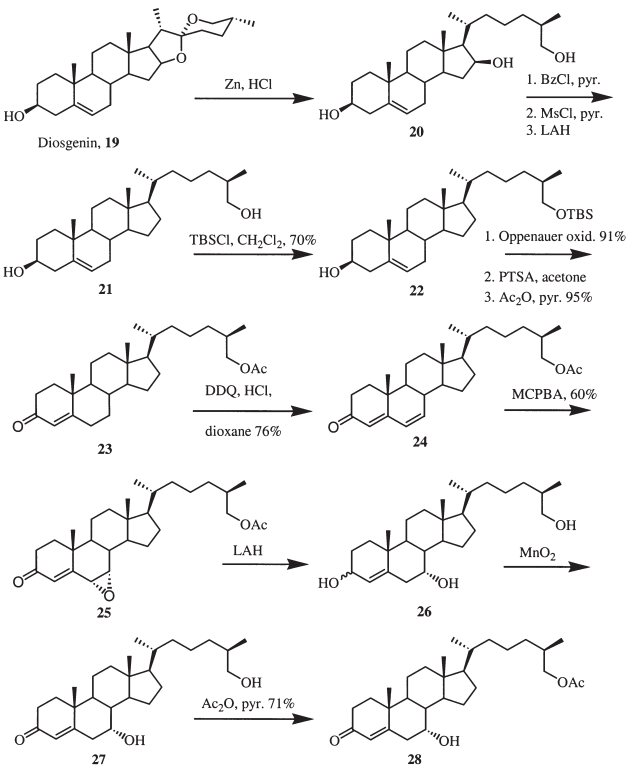

SCHEME 2. Synthesis of the aglycones of pavoninin-1 and -2 (**28** and **27**).

In the same year (1997), the first total synthesis of the saponin pavoninin-1 (**13**) was reported (11) and is outlined in Scheme 3. The synthesis of the aglycone started with commercially available chenodeoxycholic acid **29** being suitably oxidized at C-3 and C-7α. The side chain was elongated following the method used for mosesin-4, with some modifications. The aldehyde **30** was synthesized from the intermediate iodide by oxidation with DMSO and collidine. Wittig addition generated the *Z*-olefin **31**. Reductive cleavage of the acetates in **31** with LAH furnished a diol that was selectively protected at C-3. Catalytic hydrogenation simultaneously reduced the olefin and hydrogenolyzed the benzyl ether to yield the 7α,26-diol **32**. Reprotection of the C-26 alcohol as a methyl carbonate afforded the 7α alcohol **33**. Glycosylation of the hindered C-7α alcohol in **33** using a glycosyl sulfoxide gave the saponin **34**. Treatment with hydrogen fluoride liberated the C-3 alcohol, which was oxidized to the ketone with pyridinium dichromate and protected as its dimethoxy ether, **35**. Reduction of the azide group in **35** and removal of the methoxycarbonyl group with LAH followed by acetylation afforded the saponin **36**. The benzyl protecting groups on

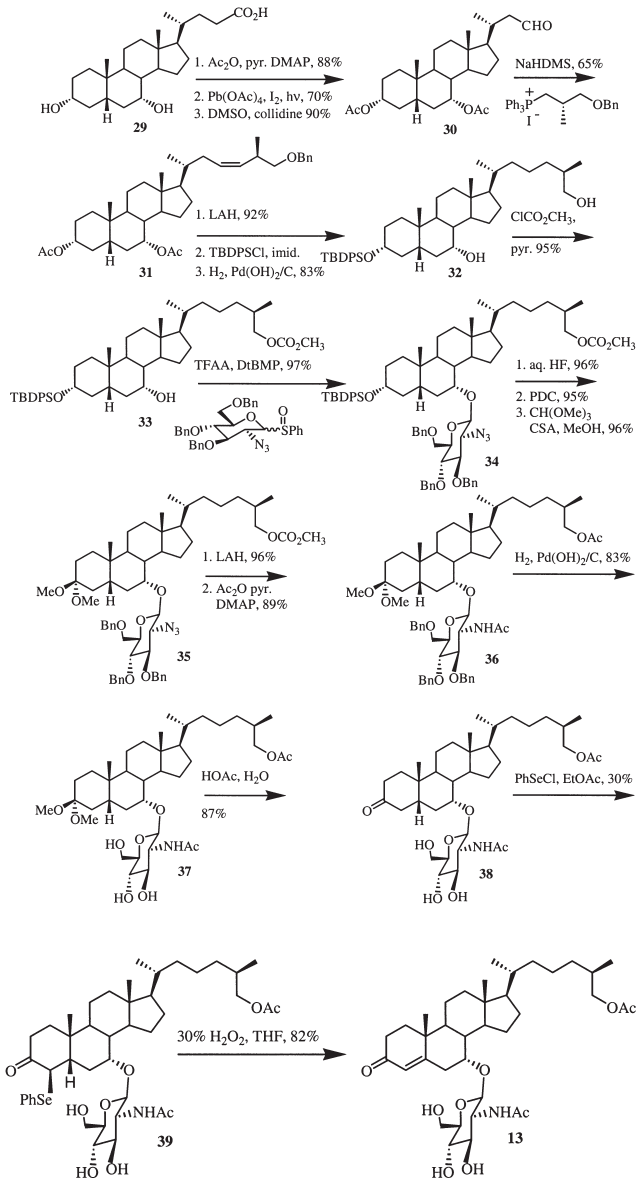

SCHEME 3. Synthesis of pavoninin-1 (**13**).

the sugar were removed by catalytic reduction to yield **37**. Hydrolysis of the ketal gave the dihydropavoninin-1 **38**. Treatment of **38** with phenyl selenyl chloride followed by hydrogen peroxide oxidation afforded pavoninin-1 (**13**) *via* the intermediate phenyl selenide **39**.

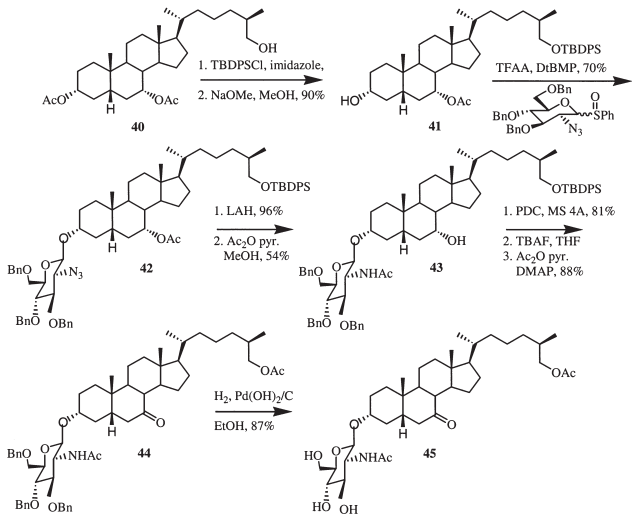

SCHEME 4. Synthesis of a structural analog of pavoninin-1 (**45**).

To test the structural requirements for biological activity, the analog **45** was synthesized as outlined in Scheme 4 (11). In this structure the C-3 and C-7 functionalities have been reversed. The synthesis of **45** started with catalytic reduction of the *Z*-olefin **31** prior to deacetylation and proceeded with simultaneous hydrogenolysis of the benzyl ether to yield the hydroxy diacetate **40**. Reprotection of the C-26 alcohol as its *tert*-butyldiphenylsilyl ether and selective hydrolysis of the C-3 acetate gave the 3α alcohol **41**. Glycosylation of **41** gave the glycoside **42**. LAH reduction and acetylation gave the saponin **43**. Oxidation of the C-7 alcohol and desilylation at C-26 followed by acetylation gave the acetate **44**. Hydrogenolysis of the benzyl ethers by catalytic reduction gave the structural analog **45**.

The ichthyotoxicity of pavoninin-1 **13**, the structural analog **45**, and the dihydropavoninin-1 intermediate **38** have been compared previously (11). The results showed that dihydropavoninin-1, **38**, was lethal to Japanese killifish at twice the concentration of pavoninin-1 **13**, showing it is less toxic. By contrast, twice the concentration of **45** was nontoxic to killifish. Thus, it appears that the saponins that are structurally unique, i.e., having the glycoside orthogonal to the steroid skeleton, have ichthyotoxicity activity. The structural analog **45**, which parallels the usual saponin structure, has significantly less or no ichthyotoxicity activity.

Pavoninins-3 to -6 (**15–18**) all have the sugar attached at C-15α on a cholesterol skeleton (7,8). A logical starting material for the synthesis of the C-15α pavoninins, as outlined in Scheme 5, is the commercially available diosgenin, **19**,which has functionality in positions suitable for conversion to the C-15α pavoninins. Recent modification of the Clemmensen reduction with the removal of mercury has resulted in a significant improvement in the yield of 3β,16β,26-triol, **20** (12). Dehydration of the 3,26-diprotected-16β-alcohol **46**, *via* a *syn* elimination of the 16β acetate **47**, afforded the C-15 olefin **48**. Chemo- and regioselective hydroxylation from the less hindered α face should yield the desired C-15α alcohol **49**. However, attempts to hydroxylate **48** regioselectively using substituted alkyl boranes were unsuccessful, as there was no reaction. When diborane followed by basic hydrogen peroxide oxidation was used, a mixture of C-15α and C-16α hydroxy steroids, **49** and **50**, was formed in the ratio of 1:2, with the undesired C-16α hydroxy steroid **50** as the major component.

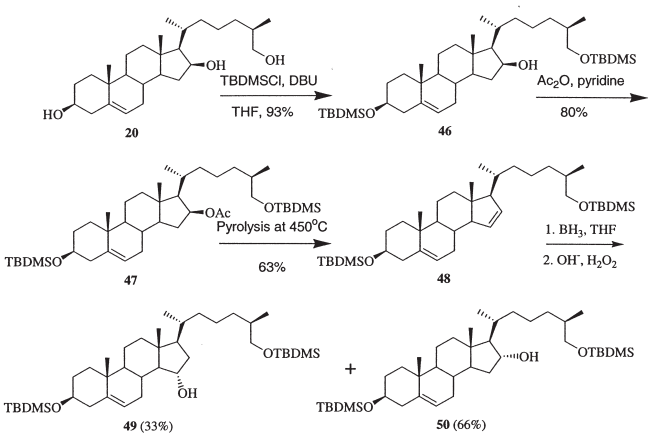

SCHEME 5. Hydroboration–oxidation of 3,26-disilyoxycholesta-5,15-diene (**48**).

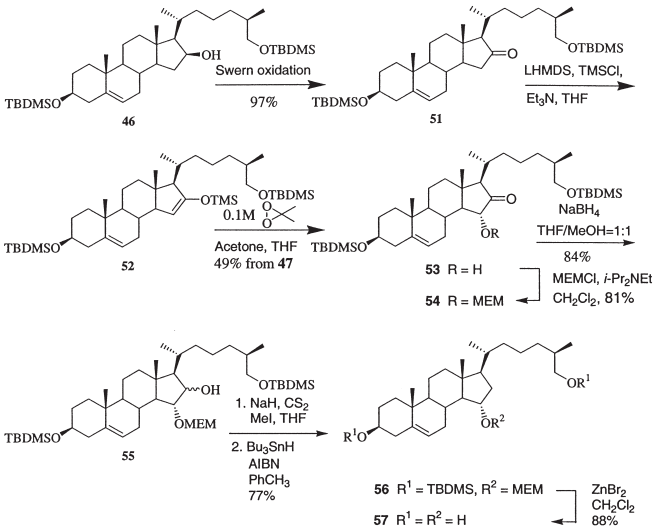

SCHEME 6. Synthesis of 26-*O*-deacetyl pavoninin-5 aglycone (**57**).

Another approach for the synthesis of the aglycone of 26-*O*-deacetyl pavonin-5, **57**, is outlined in Scheme 6 (13,14). The initial plan was to oxidize the C-16 alcohol in **46** to a ketone, introduce the C-15α hydroxyl, and then remove the ketone. Swern oxidation of 3,26-bissilyl ether **46** gave the C-15

ketone **51**. Because of the difficulty of direct hydroxylation of **51**, the ketone was hydroxylated through its silyl enol ether. The silyl enol ether, **52**, was synthesized by adding lithium hexamethyldisilazane to the solution of **51** and trimethylsilyl chloride, followed by triethylamine, then quenching the reaction with saturated $NaHCO_3$. The silyl enol ether, **52**, was not purified because it is sensitive to silica gel. Oxidation of **52** with dimethyldioxirane, followed by decomposition of the unstable intermediate C-15α,16α-epoxide under mildly acidic conditions, afforded the C-15α-hydroxy ketone **53**.

The next step was the deoxygenation of the 16-ketone. However, all methods used to deoxygenate the α-hydroxy ketone using Raney nickel on the dithioketal or Wolff–Kishner reduction failed. To remove the ketone, the carbonyl was reduced to a hydroxyl group, followed by deoxygenation using Barton's reaction. Since both C-15 and C-16 would be hydroxyl groups, a different protecting group for the hydroxyl group in the 15α-position was used. Protection of the C-15α alcohol in **53** with methoxyethoxymethyl chloride (MEMCl) gave the MEMCl ether **54**. Reduction of the C-16 ketone in **54** using sodium borohydride gave **55**, a mixture of epimeric alcohols at C-16. Deoxygenation of the alcohols, **55**, *via* the xanthate using the Barton reaction yielded the MEMCl ether, **56**. Treatment of the MEMCl ether, **56**, using dry zinc bromide in dry methylene chloride cleaved the MEMCl group as well as the *tert*-butyldimethylsilyl groups to yield the target 26-*O*-deacetyl pavoninin-5 aglycone, **57**.

There were 53 unprovoked shark attacks in the United States in 2000, with approximately a third being fatal. If one could develop a compound with shark-repelling properties, when applied appropriately, the risk of shark attacks could be greatly reduced. Fish belonging to the species *Pardachirus* are known to excrete saponins that have shark-repelling properties. These natural saponins, i.e., mosesins 1–5 (**1–5**) and pavoninins-1 to -6 (**13–18**), could act as lead compounds for the synthesis of more effective shark repellents. From the results thus far, two conclusions can be drawn: (i) Saponins with shark-repelling properties appear to have the saccharide toward the middle of the steroid and orthogonal to its axis. (ii) The monosaccharide can be varied, since both galactose and *N*-acetylglucosamine are both shark repellents when attached to the C-7α of (25*R*)-26-cholesterol. Because glucose is the most abundant, most widespread, and least expensive monosaccharide, the question is, does glucose work? That is to say, would a 7α glycoside of (25*R*)-26-hydroxycholesterol be a shark repellent? It is an obvious target for synthesis.

ACKNOWLEDGMENTS

This work was supported in part by grants from the Temple University Research Incentive Fund, Howard Hughes Medical Institute grant to the Undergraduate Biological Sciences Education Program at Temple University, GlaxoSmithKline, Wyeth, Merck, Incyte, and Bristol-Myers Squibb.

REFERENCES

1. Francis, G., Kerem, Z., Harinder, P.S., and Becker, K. (2002) The Biological Action of Saponins in Animal Systems: A Review, *Br. J. Nutr. 88,* 587–605.
2. Press, J.B., Reynolds, R.C., May, R.D., and Marciani, D.J. (2000) Structure/Function Relationships of Immunostimulating Saponins, *Stud. Nat. Prod. Chem. 24,* 131–174.
3. Minale, L., Ricco, R., and Zollo, F. (1993) Steroidal Oligoglycosides and Polyhydroxysteroids from Echinoderms, in *Progress in the Chemistry of Organic Natural Products* (Herz, W., Kirby, G.W., Moore, R.W., Steglich, W., and Tamm, Ch., eds.), Vol. 62, pp. 75–308, Springer-Verlag, New York.
4. Clark, E. (1974) The Red Sea's Sharkproof Fish, *Natl. Geographic 146,* 718–727.
5. Tachibana, K., and Gruber, S.H. (1988) Shark Repellent Lipophilic Constituentes in the Defense Secretion of the Moses Sole (*Pardachirus marmoratus*), *Toxicon 26,* 839–853.
6. Gariulo, D., Blizzard, T.A., and Nakanishi, K. (1989) Synthesis of Mosesin-4, a Naturally Occurring Steroid Saponin with Shark Repellent Activity, and Its Analog 7β-Galactosyl Ethyl Cholate, *Tetrahedron 45,* 5423–5432.
7. Tachibana, K., Sakaitani, M., and Nakanishi, K. (1984) Pavoninins: Shark-Repelling Ichthyotoxins from the Defense Secretion of the Pacific Sole, *Science 226*, 703–705.
8. Tachibana, K., Sakaitani, M., and Nakanishi, K. (1985) Pavoninins, Shark-Repelling and Ichthyotoxic Steroid *N*-Acetylglucosaminides from the Defense Secretion of the Sole *Pardachirus pavoninus* (Soleidae), *Tetrahedron 41,* 1027–1037.
9. Kim, H.S., Kim, I.C., and Lee, S.O. (1997) Synthesis of Two Marine Natural Products: The Aglycones of Pavoninin-1 and -2, *Tetrahedron 53,* 8129–8136.
10. Noam, M., Tamir, I., Breuer, E., and Mechoulam, R. (1981) Conversion of Ruscogenin into 1α- and 1β-Hydroxycholesterol Derivatives, *Tetrahedron 37,* 597–604.
11. Ohnishi, Y., and Tachibana, K. (1997) Synthesis of Pavoninin-1, a Shark Repellent Substance, and Its Structural Analogues Toward Mechanistic Studies on Their Membrane Perturbation, *Bioorg. Med. Chem. 5,* 2251–2265.
12. Williams, J.R., Chai, D., and Wright, D. (2002) Synthesis of (25*R*)-26-Hydroxycholesterol, *Steroids 67,* 1041–1044.
13. Williams, J.R., Chai, D., Gong, H., Zhao, W., and Wright, D. (2002) Studies Toward the Synthesis of the Shark Repellent Pavoninin-5, *Lipids 37,* 1193–1195.
14. Williams, J.R., Chai, D., Bloxton, J.D., II, Gong, H., and Solvibile, W.R. (2003) Synthesis of the Aglycone of 26-*O*-Deacetyl Pavoninin-5, *Tetrahedron 59,* 3183–3188.

[Received July 27, 2004; accepted August 12, 2004]

Review of Chemical Syntheses of 7-Keto-Δ^5-sterols

Edward J. Parish*, Stephen A. Kizito, and Zhihai Qiu

Department of Chemistry, Auburn University, Auburn, Alabama 36849

ABSTRACT: Steroids bearing ketone functionality at carbon-7 are found commonly in nature, and the most prevalent of these are the 7-keto-Δ^5-sterols. These substances have diverse biological properties and are present in biological samples and food products. For the purpose of studying this class of oxysterols, many chemical methods, involving the chemical oxidation of Δ^5-sterols to the corresponding 7-keto-Δ^5-sterol derivatives have been developed to produce these compounds. We have undertaken a review and evaluation of chemical methods for the synthesis of these compounds and have endeavored to enhance one of these procedures to yield products for chemical and biological investigations.

Paper no. L9537 in *Lipids 39,* 801–804 (August 2004).

Some of the most frequently encountered oxysterols are those with a ketone function at carbon-7. The major portion of these is the 7-keto-Δ^5-sterols, which originate from the oxidation of Δ^5-sterols. These compounds, which are found in animal tissues, food products (1,2), and certain folk medicines (3–6), are significant inhibitors of HMG-CoA reductase (7,8), sterol synthesis (7,9), and cell replication (10–12).

The chemical synthesis of 7-keto-Δ^5-sterols relies on the allylic oxidation of carbon-7 of Δ^5-sterols. We have studied a number of different synthetic methods and procedures and review our findings here.

In many chemical and biological studies, 7-keto-Δ^5-sterols containing the 3β-hydroxyl group are the desired compounds. During the chemical (allylic) oxidation of the corresponding Δ^5-sterols, the 3β-hydroxyl group must be protected, usually as the acetate or benzoate ester (13,14), to avoid oxidation of the C-3 hydroxyl group to a ketone. The benzoate derivative is usually preferred owing to its superior crystallinity (i.e., ease of crystal formation leading to higher yields) when purified by recrystallization. Figure 1A demonstrates the reaction paths of oxidation that occur when the 3β-hydroxyl is not protected (15–19).

The most common methods of allylic oxidation of Δ^5-sterols are those that rely on the use of chromium(VI) reagents. Early or "classical" methods of oxidation used chromium trioxide (CrO_3) (20–23) or sodium chromate (24–26) and *t*-butyl chromate (27,28) in acetic acid; these afforded only limited success and produced the 7-keto compounds in modest yields. For example, the allylic oxidation of cholesteryl benzoate with sodium chromate in acetic acid/acetic anhydride gave 7-ketocholesteryl benzoate in an optimal yield of 38% (29). Figure 1B demonstrates the reaction that occurs when the 3β-hydroxyl group is protected.

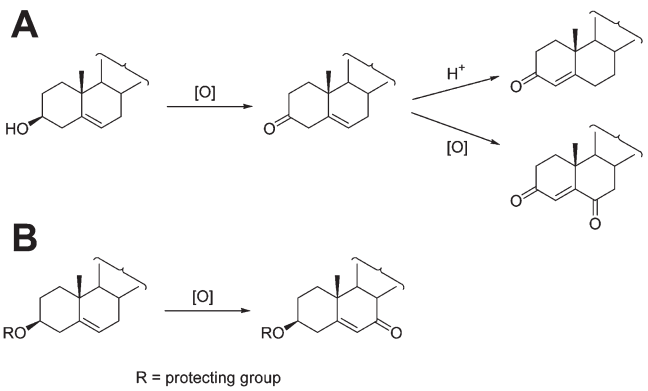

FIG. 1. Chemical oxidation of 3β-hydroxy-Δ^5-sterols (A) in the absence of a protection for the β-hydroxyl group and (B) in the presence of a protective group.

Synthetically useful changes in the properties and reactivity of chromium(VI) reagents have been brought about by the formation of amine complexes. The Collins reagent is formed by the complexation of chromium trioxide with pyridine (30,31). With this reagent, the allylic oxidation of cholesteryl benzoate gave a 68% yield of 7-ketocholesteryl benzoate (32), and in a related study, using anhydrous conditions, cholesteryl acetate was oxidized to 7-ketocholesteryl acetate in 72% yield (33). Similar complexes have been formed using chromium trioxide and pyrazole (34), 3,5-dimethylpyrazole (29), and benzotriazole (35) and have been shown to oxidize cholesteryl benzoate to 7-ketocholesteryl benzoate in 70–76% yields. These reactions require the preparation of the reagent complex before each reaction.

Commercially available pyridinium chlorochromate (PCC) has been widely used in organic synthesis for the oxidation of primary and secondary alcohols to carbonyl compounds (36). This reagent, in methylene chloride containing pyridine (37), other aromatic amines (38), pyrazole (39), 3,5-dimethylpyrazole (40), and benzotriazole (35), was reported to effect the selective oxidation of the allylic hydroxyl function of a number of steroidal alcohols. At room temperature, PCC in methylene chloride was an ineffective reagent for allylic oxidation (29). In contrast to these results, we have achieved moderate success by using PCC in refluxing methylene chloride for allylic and benzylic oxidations (41). PCC in DMSO also has been used for the oxidation of β-ionone to the corresponding diketone (42).

*To whom correspondence should be addressed. E-mail: parisej@auburn.edu

Abbreviations: PCC, pyridinium chlorochromate; PFC, pyridinium fluorochromate; TBHP, *t*-butyl hydroperoxide.

In a related study, we found that benzene was a superior solvent for allylic oxidations using PCC (43). PCC in refluxing benzene could effect a high-yield (87%) oxidation of cholesteryl benzoate to 7-ketocholesteryl benzoate. This conversion was accomplished with a 1:30 ratio of reagent (PCC) when 1–10 g of cholesteryl benzoate was oxidized. Oxidation of quantities of less than 1 g cholesteryl benzoate was successfully performed by using smaller quantities of reagent (1:25) with similar yields, thus demonstrating the usefulness of the described method for both large- and small-scale preparations. This efficient (i.e., high-yielding) procedure represents a significant improvement in both yield and convenience compared with other reported methods for the allylic oxidation of cholesteryl benzoate to 7-ketocholesteryl benzoate.

With the reaction conditions described (43), we conducted additional studies using other solvents with cholesteryl benzoate and PCC. Under these conditions, refluxing acetone, pyridine, *N,N*-dimethylformamide, and DMSO at 100°C yielded 7-ketocholesteryl benzoate in 2, 0, 18, and 77% yield, respectively. In an earlier study, we found that using refluxing methylene chloride as solvent yielded 54% of 7-ketocholesteryl benzoate from cholesteryl benzoate (41).

In another additional study, we showed that pyridinium fluorochromate (PFC), in refluxing benzene, was also an effective and convenient reagent for the efficient allylic oxidation of Δ^5-sterols to the corresponding C-7 unsaturated ketones in high yields (44). With this reagent, the allylic oxidation of cholesteryl benzoate resulted in an 88% yield of 7-ketocholesteryl benzoate. In the same study, cholesteryl acetate was oxidized to its 7-keto derivative in an 87% yield.

Other oxidation studies have used hydroperoxides [e.g., *t*-butyl hydroperoxide (TBHP)] with different types of catalysts. Chromium trioxide (45) and bis(tributyltin oxide)dioxochromium (46) have been used as catalysts to obtain 7-keto-Δ^5-sterols. However, epoxidation of the double bond was also observed. Good yields of these products were also reported when the reaction with the oxidizing agent TBHP was catalyzed by hexacarbonyl chromium (47,48) and ruthenium trichloride (49). However, the high toxicity of hexacarbonyl chromium, the high cost of the ruthenium catalyst, and potential safety risks have led researchers to explore other methods (50). The use of TBHP with catalysts such as Cu(I), Cu(II), or Cu metal (51) gave good yields in the allylic oxidation of Δ^5-sterols and required small amounts of reagents and solvents, and the copper catalysts were inexpensive and less toxic than the chromium reagents.

More environmentally friendly oxidations by molecular oxygen and *N*-hydroxyphthalimide as catalyst (52,53) give good yields of 7-keto-Δ^5-sterols. These methods are readily applicable and inexpensive, and the catalyst can be recovered. However, the required use of an oxygen atmosphere makes them inconvenient (50). In a related procedure, allylic oxidation at the C-7 position was accomplished using *N*-hydroxyphthalimide-catalyzed oxidation in air with benzoyl peroxide as a free radical initiator (54,55). The resulting C-7 hydroperoxide was dehydrated with copper(II) chloride in pyridine to produce the corresponding C-7 ketone of stigmasterol in 81–82% yield. In addition to being environmentally friendly, this procedure had an added advantage in that no protecting group was required for the 3β-hydroxyl group, since it was not oxidized under these reaction conditions.

Recently, TBHP has been used in the presence of copper(I) iodide, and tetra-*n*-butylammonium bromide was used as a phase-transfer catalyst in a two-phase system of water and methylene chloride (56,57). The allylic oxidation was found to proceed more efficiently when TBHP was added to the reaction mixture in portions. The high-yield conversion (>70%) of Δ^5-sterols into the corresponding C-7 unsaturated ketones in short reaction times was reported.

We have continued our studies on the allylic oxidation of Δ^5-sterols using PCC to produce the C-7 ketones. The use of both PCC and PFC in refluxing benzene represents one of the most convenient methods for the allylic oxidation of these substrates (43,44,58). However, long reaction times, large volumes of solvent, and high molar ratios of the oxidant are required.

To improve on these procedures, we tested the use of diphenyl diselenide as a catalyst to reduce reaction times and amounts of reagent required for oxidation and observed that lower quantities of the required reagent (PCC) were needed. That selenium reagents introduce a hydroxyl group at allylic positions in a substrate has long been known (59–61). In our case these substrates would be oxidized to a ketone. The involvement of the catalyst in this reaction would alter the mechanism and would be similar to that already described for the enhanced allylic chlorination of β-pinene using diphenyl diselenide as a catalyst (62).

When we modified our established procedure (43), PCC (1:5 molar ratio of steroid substrate/PCC) and catalytic amounts of diphenyl diselenide (1:0.1 molar ratio of steroid substrate/diphenyl diselenide) were heated together in refluxing benzene with cholesteryl benzoate; allylic oxidation at the

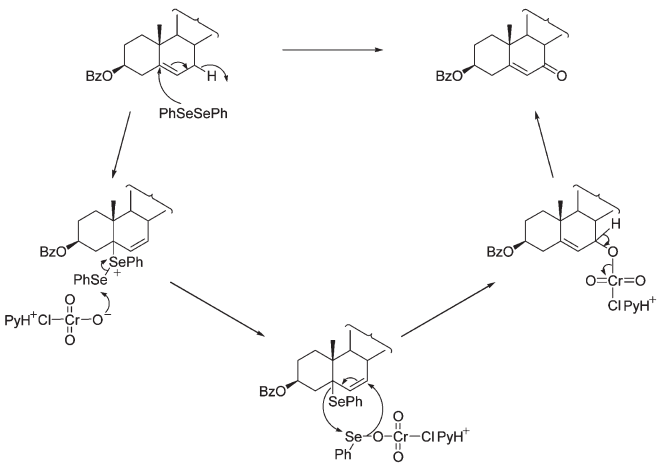

FIG. 2. Mechanism of allylic oxidation of cholesteryl benzoate by pyridinium chlorochromate and a diphenyl diselenide catalyst.

C-7 position occurred in 5 h, and 7-ketocholesteryl benzoate was obtained in 50% yield. Continued heating for a total of 24 h produced a 76% yield. When this reaction was conducted in the absence of a diphenyl diselenide catalyst, an 11% yield of the C-7 ketone was obtained after 24 h of reaction. Without the catalyst, a molar ratio of 1:30 of PCC was required for optimal product yield (87%). A proposed mechanism for the allylic oxidation of cholesteryl benzoate using PCC and diphenyl diselenide is shown in Figure 2. The ionic mechanism shown is supported by the addition of 2,2′-azobisisobutyronitrile, a radical initiator (63), which produced no observed enhancement of the reaction rate (monitored by TLC) or final yield of the reaction product.

In conclusion, we believe the results presented herein provide useful information concerning the chemical synthesis of 7-keto-Δ^5-sterols resulting from the allylic oxidation of Δ^5-sterols. The major methods of synthesis have been reviewed and the advantages of certain procedures have been indicated. In addition, we have attempted to develop novel and efficient approaches to the synthesis of these products.

REFERENCES

1. Smith, L.L. (1981) *Cholesterol Autoxidation*, Plenum Press, New York.
2. Guardiola, F., Dutta, P.C., Codony, R., and Savage, G.P. (eds.) (2002) *Cholesterol and Phytosterol Oxidation Products: Analysis, Occurrence, and Biological Effects*, AOCS Press, Champaign, 394 pp.
3. Hietter, H., Bischoff, P., Beck, J.P., Ourisson, G., and Luu, B. (1986) Comparative Effects of 7β-Hydroxycholesterol Towards Murine Lymphomas, Lymphoblasts and Lymphocytes: Selective Cytotoxicity and Blastogenesis Inhibition, *Cancer Biochem. Biophys. 9*, 75–83.
4. Cheng, K.P., Nagano, H., Luu, B., Ourisson, G., and Beck, J.P. (1977) Chemistry and Biochemistry of Chinese Drugs. Part I. Sterol Derivatives Cytotoxic to Hepatoma Cells, Isolated from the Drug Bombyx cum Botryte, *J. Chem. Res. (S)*, *217*; *(M)*, 2501–2521.
5. Nagano, H., Poyser, J.P., Cheng, K.-P., Luu, B., Ourisson, G., and Beck, J.P. (1977) Chemistry and Biochemistry of Chinese Drugs. Part II. Hydroxylated Sterols, Cytotoxic Towards Cancerous Cells: Synthesis and Testing, *J. Chem. Res. (S)*, 218; *(M)*, 2522–2571.
6. Zander, M., Koch, P., Luu, B., Ourisson, G., and Beck, J.P. (1977) Chemistry and Biochemistry of Chinese Drugs. Part III. Mechanism of Action of Hydroxylated Sterols on Cultured Hepatoma Cells, *J. Chem. Res. (S)*, 219; *(M)*, 2572–2584.
7. Kandutsch, A.A., Chen, H.W., and Heiniger, H.J. (1978) Biological Activity of Some Oxygenated Sterols, *Science 201*, 498–501.
8. Taylor, F.R., Saucier, S.E., Shown, E.P., Parish, E.J., and Kandutsch, A.A. (1984) Correlation Between Oxysterol Binding to a Cytosolic Binding Protein and Potency in the Repression of Hydroxymethylglutaryl Coenzyme A Reductase, *J. Biol. Chem. 259*, 12382–12387.
9. Schroepfer, G.J., Jr. (2000) Oxysterols: Modulators of Cholesterol Metabolism and Other Processes, *Physiol. Rev. 80*, 361–554.
10. Schroepfer, G.J., Jr. (1981) Sterol Biosynthesis, *Annu. Rev. Biochem. 50*, 585–621.
11. Parish, E.J., Chitrakorn, S., Luu, B., Schmidt, G., and Ourisson, G. (1989) Studies of the Oxysterol Inhibition of Tumor Cell Growth, *Steroids 53*, 579–596.
12. Guardiola, F., Codony, R., Addis, P.B., Rafecas, M., and Boatella, J. (1996) Biological Effects of Oxysterols: Current Status, *Food Chem. Toxicol. 34*, 193–211.
13. Kumar, V., Amann, A., Ourisson, G., and Luu, B. (1987) Stereospecific Syntheses of 7α- and 7β-Hydroxycholesterols, *Synth. Commun. 17*, 1279–1286.
14. Atwater, N.W. (1961) Oxasteroids. II. 6-Oxaandrostane Derivatives, *J. Am. Chem. Soc. 83*, 3071–3079.
15. Dhar, D.N., and Singh, A.K. (1977) Pyridinium Chlorochromate Oxidation of Some Steroidal Systems. Regioselective Opening of Ring 'F' in Spirostan, *Z. Naturforsch. B: Anorg Chem., Org. Chem. 32B*, 1476–1477.
16. Parish, E.J., Chitrakorn, S., Taylor, F.R., and Saucier, S.E. (1984) Chemical Synthesis of 4,4′-Dimethyl-7-oxygenated Sterols. Inhibitors of 3-Hydroxy-3-methylglutaryl Reductase, *Chem. Phys. Lipids 36*, 179–188.
17. Parish, E.J., and Honda, H. (1990) A Facile Synthesis of Steroidal Δ^4-3-Ketones Using Pyridinium Chlorochromate (PCC), *Synth. Commun. 20*, 1167–1174.
18. Parish, E.J., Honda, H., Chitrakorn, S., and Livant, P. (1991) A Facile Chemical Synthesis of Cholest-4-en-3-one. Carbon-13 Nuclear Magnetic Resonance Spectral Properties of Cholest-4-en-3-one and Cholest-5-en-3-one, *Lipids 26*, 675–677.
19. Parish, E.J., Kizito, S.A., and Heidepriem, R.W. (1993) A Novel Synthesis of Steroidal Δ^4-3,6-Diones Using Pyridinium Chlorochromate (PCC), *Synth. Commun. 23*, 223–230.
20. Marker, R.E., Kamm, O., Fleming, G.H., Popkin, A.H., and Wittle, E.L. (1937) Sterols. X. Cholesterol Derivatives, *J. Am. Chem. Soc. 59*, 619–621.
21. Stavely, H.E., and Bollenback, G.N. (1943) Steroids with Double Bonds Between Quaternary Carbon Atoms. I. The Oxidation of α-Ergostenyl Acetate, *J. Am. Chem. Soc. 65*, 1285–1289.
22. Klyne, W. (1951) Some 7-Substituted Derivatives of the 5α-Pregnane Series, *J. Chem. Soc.*, 3449–3451.
23. Kasal, A. (2000) Epalons: 6-Substituted Derivatives of 7-Norepiallopregnanolone, *Tetrahedron 56*, 3559–3565.
24. Marshall, C.W., Ray, R.E., Laos, I., and Riegel, B. (1957) 7-Oxo Steroids. II. Steroidal 3β-Hydroxy-Δ^5-7-ones and -$\Delta^{3,5}$-7-ones, *J. Am. Chem. Soc. 79*, 6308–6313.
25. Amann, A., Ourisson, G., and Luu, B. (1987) Stereospecific Syntheses of the Four Epimers of 7,22-Dihydroxycholesterol, *Synthesis*, 1002–1005.
26. Cook, R.P. (1958) *Cholesterol: Chemistry, Biochemistry, and Pathology*, pp. 56–57, Academic Press, New York.
27. Marshall, C.W., Ray, R.E., Laos, I., and Riegel, B. (1957) 7-Oxo Steroids. I. Steroidal 3-Hydroxy-3,5-dien-7-ones, *J. Am. Chem. Soc. 79*, 6303–6308.
28. Singh, H., Bhardwaj, T.R., and Paul, D. (1977) Steroids and Related Studies. Part 41. Schmidt Reaction with 3β-Acetoxypregn-5-ene-7,20-dione, *J. Chem. Soc., Perkin Trans. I*, 1987–1989.
29. Salmond, W.G., Barta, M.A., and Havens, J.L. (1978) Allylic Oxidation with 3,5-Dimethylpyrazole-Chromium Trioxide Complex. Steroidal Δ^5-7-Ketones, *J. Org. Chem. 43*, 2057–2059.
30. Collins, J.C., Hess, W.W., and Frank, F.J. (1968) Dipyridine-Chromium(VI) Oxide Oxidation of Alcohols in Dichloromethane, *Tetrahedron Lett.*, 3363–3366.
31. Dauben, W.G., Lorber, M.E., and Fullerton, D.S. (1969) Allylic Oxidation of Olefins with Chromium Trioxide Pyridine Complex, *J. Org. Chem. 34*, 3587–3592.
32. Cook, R.P. (1958) *Cholesterol: Chemistry, Biochemistry, and Pathology*, p. 100, Academic Press, New York.
33. Fullerton, D.S., and Chen, C.-M. (1976) *In situ* Allylic Oxidations with Collins Reagent, *Synth. Commun. 6*, 217–220.
34. Parish, E.J., Chitrakorn, S., and Todd, K.L., III (1985) Steroidal

Allylic Oxidation with Chromium Trioxide in the Presence of Pyrazole, *Org. Prep. Proced. Int. 17*, 192–194.
35. Parish, E.J., and Chitrakorn, S. (1985) Benzotriazole-Mediated Selective Chromium(VI) Oxidations, *Synth. Commun. 15*, 393–399.
36. Piancatelli, G., Scettri, A., and D'Auria, M. (1982) Pyridinium Chlorochromate: A Versatile Oxidant in Organic Synthesis, *Synthesis*, 245–258.
37. Parish, E.J., and Schroepfer, G.J., Jr. (1980) Selective Oxidation of Steroidal Allylic Alcohols, *Chem. Phys. Lipids 27*, 281–288.
38. Parish, E.J., Scott, A.D., Dickerson, J.R., and Dykes, W. (1984) Further Studies on the Selective Oxidation of Steroidal Allylic Alcohols, *Chem. Phys. Lipids 35*, 315–320.
39. Parish, E.J., Chitrakorn, S., and Lowery, S. (1984) Selective Oxidation of Steroidal Allylic Alcohols Using Pyrazole and Pyridinium Chlorochromate, *Lipids 19*, 550–552.
40. Parish, E.J., and Scott, A.D. (1983) Selective Oxidation of Steroidal Allylic Alcohols Using 3,5-Dimethylpyrazole and Pyridinium Chlorochromate, *J. Org. Chem. 48*, 4766–4768.
41. Parish, E.J., Chitrakorn, S., and Wei, T.Y. (1986) Pyridinium Chlorochromate-Mediated Allylic and Benzylic Oxidation, *Synth. Commun. 16*, 1371–1375.
42. Becher, E., Albrecht, R., Bernhard, K., Leuenberger, H.G.W., Mayer, H., Mueller, R.K., Schuep, W., and Wagner, H.P. (1981) Synthesis of Astaxanthin from β-Ionone. I. Enantiomeric C_{15}-Wittig Salts by Chemical and Microbial rResolution of (±)-3-Acetoxy-4-oxo-β-ionone, *Helv. Chim. Acta 64*, 2419–2435.
43. Parish, E.J., Wei, T.-Y., and Livant, P. (1987) A Facile Synthesis and Carbon-13 Nuclear Magnetic Resonance Spectral Properties of 7-Ketocholesteryl Benzoate, *Lipids 22*, 760–763.
44. Parish, E.J., Sun, H., and Kizito, S.A. (1996) Allylic Oxidation of Δ^5-Steroids with Pyridinium Fluorochromate, *J. Chem. Res. (S)*, 544–545.
45. Muzart, J. (1987) Synthesis of Unsaturated Carbonyl Compounds *via* a Chromium-Mediated Allylic Oxidation by 70% *tert*-Butyl Hydroperoxide, *Tetrahedron Lett. 28*, 4665-4668.
46. Muzart, J. (1989) Bimetallic Oxidation Catalysts: Oxidations with *tert*-Butyl Hydroperoxide Mediated by Bis(tributyltin oxide)dioxochromium(VI), *Synth. Commun. 19*, 2061–2067.
47. Pearson, A.J., Chen, Y.S., Hsu, S.Y., and Ray, T. (1984) Oxidation of Alkenes to Enones Using *tert*-Butyl Hydroperoxide in the Presence of Chromium Carbonyl Catalysts, *Tetrahedron Lett. 25*, 1235–1238.
48. Pearson, A.J., Chen, Y.S., Han, G.R., Hsu, S.Y., and Ray, T. (1985) A New Method for the Oxidation of Alkenes to Enones. An Efficient Synthesis of Δ^5-7-Oxo Steroids, *J. Chem. Soc., Perkin Trans. I*, 267–273.
49. Miller, R.A., Li, W., and Humphrey, G.R. (1996) A Ruthenium-Catalyzed Oxidation of Steroidal Alkenes to Enones, *Tetrahedron Lett. 37*, 3429–3432.
50. Harre, M., Haufe, R., Nickisch, K., Weinig, P., Weinmann, H., Kinney, W.A., and Zhang, X. (1998) Some Reaction Safety Aspects of Ruthenium-Catalyzed Allylic Oxidations of Δ^5-Steroids in the Pilot Plant, *Org. Proc. Res. Dev. 2*, 100–104.
51. Salvador, J.A.R., Sáe Melo, M.L., and Campos Neves, A.S. (1997) Copper-Catalyzed Allylic Oxidation of Δ^5-Steroids by *t*-Butyl Hydroperoxide, *Tetrahedron Lett. 38*, 119–122.
52. Ishii, Y., Nakayama, K., Takeno, M., Sakaguchi, S., Iwahama, T., and Nishiyama, Y. (1995) Novel Catalysis by N-Hydroxyphthalimide in the Oxidation of Organic Substrates by Molecular Oxygen, *J. Org. Chem. 60*, 3934–3935.
53. Foricher, J., Fuerbringer, C., and Pfoertner, K. (1991) Process for the Catalytic Oxidation of Isoprenoids Having Allylic Groups, U.S. Patent 5,030,739.
54. Jones, S.R., Selinsky, B.S., Rao, M.N., Zhang, X., Kinney, W.A., and Tham, F.S. (1998) Efficient Route to 7α-(Benzoyloxy)-3-dioxolane cholestan-24(*R*)-ol, a Key Intermediate in the Synthesis of Squalamine, *J. Org. Chem. 63*, 3786–3789.
55. Shu, Y., Jones, S.R., Kinney, W.A., and Selinsky, B.S. (2002) The Synthesis of Spermine Analogs of the Shark Aminosterol Squalamine, *Steroids 67*, 291–304.
56. Arsenou, E.S., Koutsourea, A.I., Fousteris, M.A., and Nikolaropoulos, S.S. (2003) Optimization of the Allylic Oxidation in the Synthesis of 7-Keto-Δ^5-steroidal Substrates, *Steroids 68*, 407–414.
57. Feldberg, L., and Sasson, Y. (1994) Copper-Catalyzed Oxidation of Hydroxy Compounds by *tert*-Butyl Hydroperoxide Under Phase-Transfer Conditions, *J. Chem. Soc., Chem. Commun.*, 1807.
58. Parish, E.J., and Wei, T.Y. (1987) Allylic Oxidation of Δ^5-Steroids with Pyridinium Chlorochromate (PCC) and Pyridinium Dichromate (PDC), *Synth. Commun. 17*, 1227–1233.
59. Fieser, L.F. (1953) Cholesterol and Companions. III. Cholestanol, Lathosterol, and Ketone 104, *J. Am. Chem. Soc. 75*, 4395–4403.
60. Petrow, V.A., Rosenheim, O., and Starling, W.W. (1943) Acyl Migration in Steroids, *J. Chem. Soc.*, 135–139.
61. Guillemonat, A. (1939) Oxidation of Ethylenic Hydrocarbons with Selenium Dioxide, *Ann. Chim. Appl. 11*, 143–211.
62. Hori, T., and Sharpless, K.B. (1979) Conversion of Allylic Phenylselenides to the Rearranged Allylic Chlorides by *N*-Chlorosuccinimide. Mechanism of Selenium-Catalyzed Allylic Chlorination of β-Pinene, *J. Org. Chem. 44*, 4208–4210.
63. Smith, M.B. (1994) *Organic Synthesis*, 1st edn., p. 156, McGraw-Hill, New York.

[Received September 14, 2004; accepted September 15, 2004]

Dioxirane Oxidation of 3β-Substituted Δ^5-Steroids

Edward J. Parish* and Zhihai Qiu

Department of Chemistry, Auburn University, Auburn, Alabama 36849

ABSTRACT: This article reviews the utility of dioxiranes in the oxidation of 3β-substituted Δ^5-sterols. Dioxiranes are the smallest cyclic peroxides that contain a carbon atom. They can be generated *in situ* from Oxone® ($2KHSO_5 \cdot KHSO_4 \cdot K_2SO_4$) and a ketone. Dioxiranes are versatile oxidizing agents. The most common reaction of dioxiranes is epoxidation, with nearly 1:1 ratios of α/β isomer products in all cases. Δ^5-Steroids with different side chains were epoxidized by dioxiranes generated *in situ* from several commercially available ketones. Although ketones function as catalyst, they were used in about an equivalent amount or large excess to accelerate the reaction.

Paper no. L9542 in *Lipids 39*, 805–809 (August 2004).

As a class of compounds, oxysterols can be defined as sterols bearing a second oxygen function in addition to that at carbon-3, and having an iso-octyl or modified iso-octyl side chain. These compounds have a variety of biological properties, including cytotoxicity, atherogenicity, carcinogenicity, mutagenicity, hypocholesterolemia, and effects on specific enzymes. Widely distributed in nature, they have been found in animal tissues and foodstuffs (1–4). Among these, the α- and β-epoxides of cholesterol (5,6α-epoxy-5α-cholestan-3β-ol and 5,6β-epoxy-5β-cholestan-3β-ol) are recognized to result from autoxidation rather than from enzymatic origin.

As a result of the interest in steroidal 5,6-epoxides, we have investigated new chemical methods to provide these compounds for biological and analytical studies of oxysterols. Dioxiranes, a class of environmentally friendly oxidants, had previously displayed a high efficiency for epoxidation of various alkenes, including polycyclic aromatic hydrocarbons, allenes, enol derivatives, and α,β-unsaturated carbonyl compounds (5,6). The very mild reaction conditions have allowed for the isolation of extremely labile epoxides.

Dioxiranes are molecules with three-membered peroxide rings. As powerful oxidants, dioxiranes, whether generated *in situ* or in isolated forms as solutions, have been used to carry out many synthetically useful transformations (7-11). In the *in situ* method, the reaction is run in a buffered aqueous system containing a ketone, caroate (Oxone®; DuPont Co., Wilmington, DE), and the substrate; otherwise, a buffered organic-aqueous cosolvent system together with a phase-transfer catalyst could be used for a water-insoluble substrate. Using isolated dioxiranes allows the reaction to be performed under extremely mild, strictly neutral nonhydrolytic conditions, whereas the *in situ* method is suitable for large-scale reactions.

Most of the known reactions involving dioxiranes are summarized in Scheme 1. These include quantitative oxidation of chloride ion to hypochlorite ion (transformation 1) (12), of sulfides to sulfoxides or of sulfoxides to sulfones (transformation 2) (oxidation of sulfides can be controlled at the sulfoxide stage by using stoichiometric amounts of the dioxirane) (5,6,13–19), and of phosphine or phosphine sulfides to phosphine oxides (transformation 3) (6,20). The latter two transformations have been used to determine concentrations of dioxirane solutions (6,13). Dioxiranes also display high efficiency for epoxidation of various alkenes as mentioned previously (transformation 4) (5,6). Tertiary amines, imines, pyridine, and diazo compounds are oxidized to the corresponding N-oxides (transformation 5) (6,21–24), secondary amines to hydroxylamines, which can be further oxidized, and primary amines to nitro compounds *via* hydroxylamine intermediates (transformation 6) (22,25–30). Nitro compounds are also produced in the oxidation of isocyanates (31). O-Insertions into C–H bonds of aldehydes (transformation 7) (6,32), of secondary or primary alcohols (transformation 8) (33–35), and of acyclic or cyclic ethers (transformation 9) (36) have been reported. Even oxyfunctionalizations of "unactivated" tertiary and secondary C–H bonds

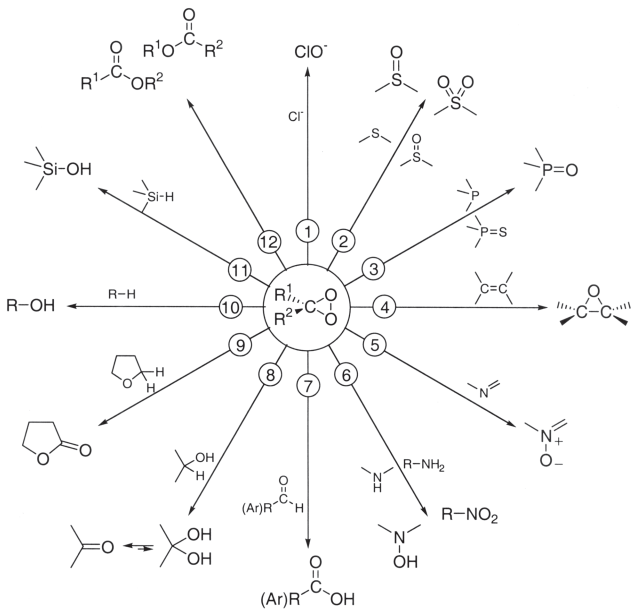

SCHEME 1

*To whom correspondence should be addressed. E-mail: parisej@auburn.edu

Abbreviations: Oxone®: $2KHSO_5 \cdot KHSO_4 \cdot K_2SO_4$ (caroate); R_f, relative forward mobility in TLC.

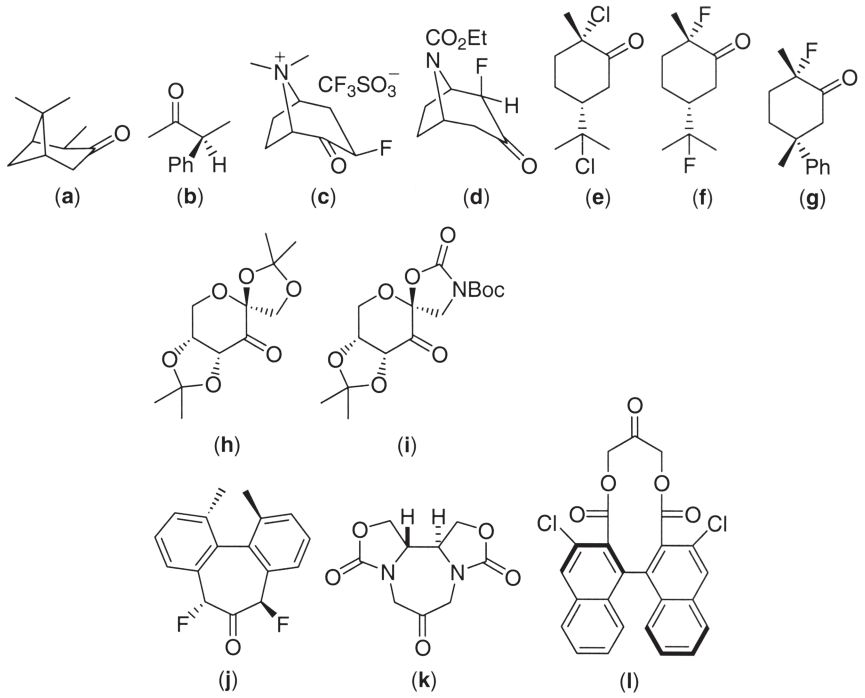

FIG. 1. Chiral ketones for asymmetric epoxidation by dioxiranes. Boc, *tert*-butoxycarbonyl protecting group.

of alkanes (transformation 10) (7,37–44) with high efficiency under extremely mild conditions have been described. O-Insertion into Si–H bonds of silanes (transformation 11) (45) has also been achieved with dioxiranes. As for self-decomposition of dioxiranes, esters are the main products from photochemical or thermal rearrangements (transformation 12) (6,7,13,46,47). It has been reported that BF_3 etherate catalyzes the thermal decomposition of dioxiranes (6).

The most extensively investigated chemical transformation with dioxiranes is their ability to convert a variety of alkenes into the corresponding epoxides, especially in asymmetric epoxidations (48). Using an optically active ketone (Fig. 1, compounds **A** and **B**) as precursors of dioxiranes, Curci *et al.* (49) presented the first example of enantioselective epoxidation with up to 12.5% enantiomeric excesses. Since then a variety of ketones (Fig. 1) (50–58) have been designed in a number of laboratories and tested for their selectivity with various unfunctionalized alkenes. Up to 96% enantiomeric excess has been achieved. Chiral dioxiranes generated *in situ* are very effective reagents for asymmetric epoxidation.

The goal of the present study was to apply dioxirane chemistry to the syntheses of oxysterols. Epoxidation of 3β-substituted Δ^5-steroids with various dioxiranes generated *in situ* is described herein. The three ketones used in this study to generate dioxiranes for the epoxidation of the 3β-substituted Δ^5-steroids were (i) acetone, (ii) 1,1,1-trifluoroacetone, and (iii) cyclohexanone. The six steroidal substrates shown in Figure 2 were used to explore the epoxidation potential of dioxiranes generated *in situ*.

The results are shown in Table 1. With a $KHCO_3/K_2CO_3$ buffer solution (pH 10–10.5) to control the pH, several Δ^5-steroids in acetone/water (3:4 vol/vol) were converted into the corresponding epoxides with Oxone. Under the same pH condition, epoxidations by 1,1,1-trifluoroacetone/Oxone or cyclohexanone/Oxone were carried out in CH_3CN/dimethoxymethane/water (1:2:4 by vol).

Epoxidation of steroids **4**–**9** by dioxiranes generated *in situ* from Oxone with acetone (Table 1, entries 1–6), 1,1,1-trifluoroacetone (Table 1, entries 7–10), or cyclohexanone (Table 1, entry 11) is very efficient (i.e., high-yielding). Among the three ketones, 1,1,1-trifluoroacetone displayed the highest catalytic activity. Although acetone is much less active than 1,1,1-trifluoroacetone, its ability to be used as solvent, i.e., used in large amount, completely suppressed its disadvantage. Cyclohexanone was also an effective ketone catalyst. Under the reaction conditions employed, secondary hydroxy groups were left intact (Table 1, entries 1–3, 7–9, 11). Another advantage of acetone and 1,1,1-trifluoroacetone is that their low b.p. (56 and 24°C, respectively) simplify the isolation and purification of final products.

5β,6β-Epoxide could not be separated from the corresponding 5α,6α-isomer on HPLC columns, but resolution on GC columns has been reported. Both isomers show almost the same R_f value on TLC plates for several common solvent pairs. The assignment of the stereochemistry to the epoxides and the calculation of α/β ratios depended on their ^{1}H NMR spectra. According to the research of Cross (59), the H-6β resonance of steroidal 5α,6α-epoxides appears in the range δ 2.82–2.94 as a doublet with a coupling constant *J* in the range 3.3–4.1 Hz, whereas the H-6α signal of the corresponding 5β,6β-epoxides

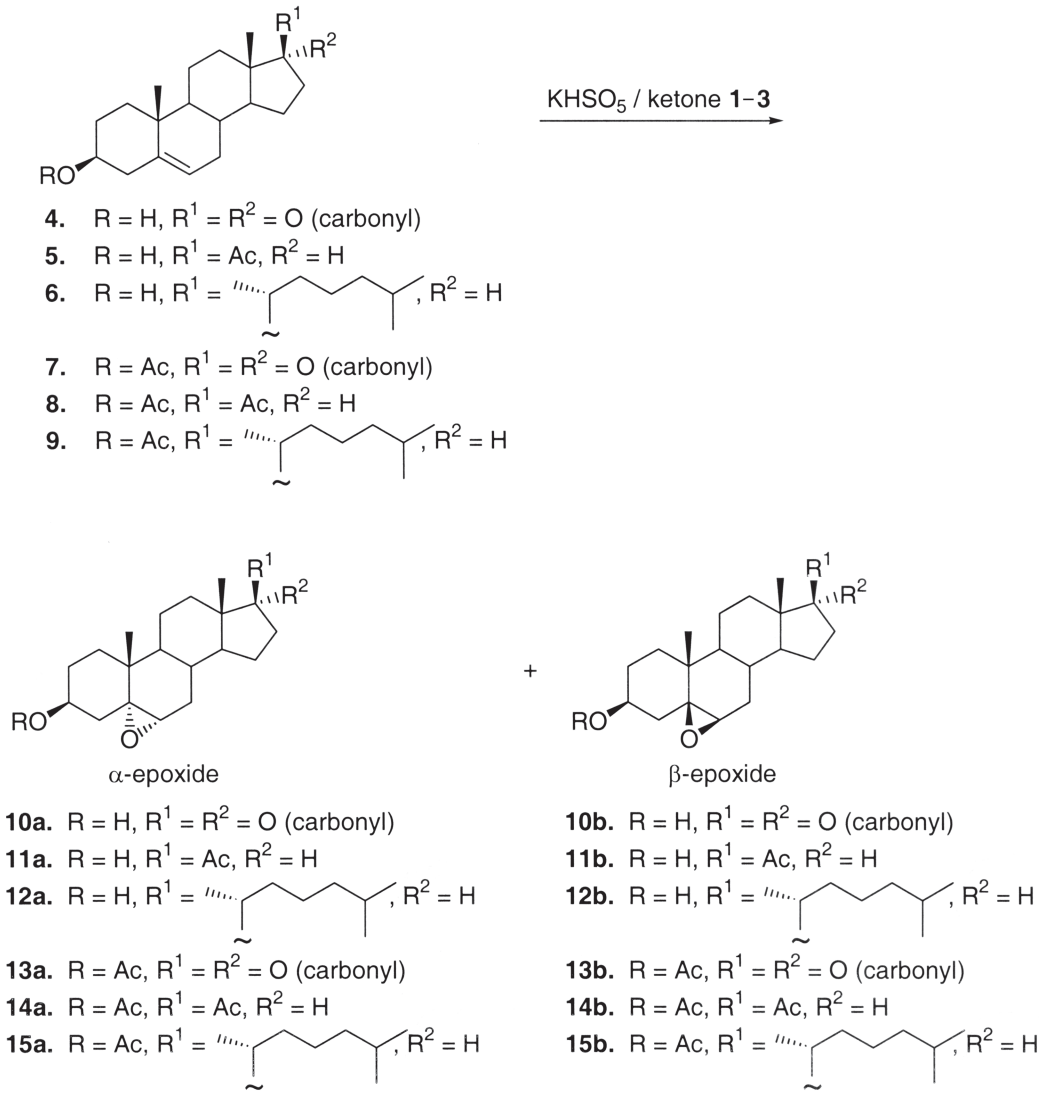

FIG. 2. Epoxidation of 3β-substituted Δ^5-steroids by dioxiranes generated *in situ* from caroate-ketone systems. Epoxidation products are presented in Table 1 as α/β epoxide ratios.

lies in the range δ 3.05–3.12, also as a doublet, with a smaller coupling constant *J* in the range 2.1–2.7 Hz; only one 6,7-proton coupling is observed in both cases. The integration values of H-6 peaks were used to calculate the α/β-ratio of the epoxidation products in Table 1. It was also found that the H-3α signal of 5α,6α-epoxides (δ 3.8–3.9 for 3β-hydroxy-substituted and δ 4.9–5.0 for 3β-acetoxy-substituted steroids) appeared downfield to the H-3α signal of the corresponding 5β,6β-epoxides (δ 3.6–3.7 and δ 4.7–4.8, respectively). The integration values of these peaks have been used to recheck the ratios calculated from integration of the H-6 peaks to within 5%.

Despite the relatively simple procedure for the reaction and purification when acetone, 1,1,1-trifluoroacetone, or cyclohexanone is employed as the precursor of the dioxirane, a major limitation associated with these ketones is the lack of stereoselectivity in the epoxidation of 3β-substituted Δ^5-steroids **4–9** (Table 1), just as reported by other authors (40,60). The α/β ratios of corresponding 5,6-epoxides were all very close to 1. This result differs from that observed for epoxidation by peracids (60), where the α/β ratio is about 4. Attempts to use 2,6-dimethylcyclohexanone or camphor as dioxirane precursors failed. The conversions were too low to give any reliable data.

Study of the epoxidation properties of dioxiranes has elucidated the formation of steroidal epoxides. Epoxidation of cyclohexene at 25°C by purified dimethyldioxirane in acetone solution is 74 times faster than by peroxybenzoic acid in methylene chloride (11). Because the procedure for the isolation of dioxiranes is rather cumbersome and because only some dioxiranes from simple ketones can be isolated (so far), epoxidation using dioxiranes generated *in situ* from caroate-ketone systems is generally preferred (Fig. 3). The *in situ* method allows the use of ketones with complex structures to achieve certain stereoselectivity. According to the mechanism depicted in Scheme 2,

TABLE 1
Epoxidation[a] of 3β-Substituted Δ^5-Steroids by Dioxiranes Generated *in situ* from Ketones 1, 2, and 3 with Oxone® at pH 10–10.5

Reaction no.	Steroidal substrate[b]	Ketone[c]	Ketone loading (equiv.)	$KHSO_5$ loading (equiv.)	Reaction temperature	Reaction time (h)	Isolated yield (%)	α/β-Epoxide ratio
1	**4**	**1**	204	3	RT	4	86	44:56
2	**5**	**1**	204	3	RT	4	84	52:48
3	**6**	**1**	204	5	RT	8	78	45:55
4	**7**	**1**	204	3	RT	4	88	45:55
5	**8**	**1**	204	4	RT	5	90	50:50
6	**9**	**1**	204	8	RT	12	81	43:57
7	**4**	**2**	1	2	0°C	4	80	45:55
8	**5**	**2**	1	2	0°C	4	81	50:50
9	**6**	**2**	1	4	0°C	6	77	44:56
10	**7**	**2**	1	2	0°C	4	90	44:56
11	**4**	**3**	19	3	RT	4	85	45:55

[a]Oxone®: 2 $KHSO_5 \cdot KHSO_4 \cdot K_2SO_4$ (caroate) (DuPont, Wilmington, DE). RT, room temperature.
[b]Compounds **4–7** are illustrated in Figure 2.
[c]Ketone **1**, acetone; **2**, 1,1,1-Trifluoroacetone; **3**, cyclohexanone.

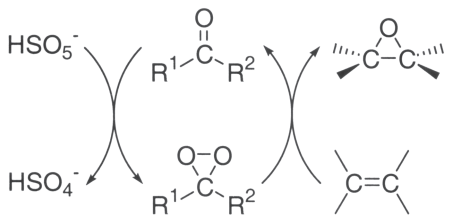

SCHEME 2

the ketone is regenerated upon epoxidation. Therefore, in principle, only a catalytic amount of ketone is required. Moreover, compared with most metal-based oxidants, Oxone is an environmentally friendly oxidant with no toxic by-products and is very inexpensive.

REFERENCES

1. Smith, L.L. (1981) *Cholesterol Autoxidation*, Plenum Press, New York.
2. Guardiola, F., Dutta, P.C., Codony, R., and Savage, G.P. (eds.) (2002) *Cholesterol and Phytosterol Oxidation Products: Analysis, Occurrence, and Biological Effects*, AOCS Press, Champaign.
3. Schroepfer, G.J., Jr. (2000) Oxysterols: Modulators of Cholesterol Metabolism and Other Processes, *Physiol. Rev. 80*, 361–554.
4. Guardiola, F., Codony, R., Addis, P.B., Rafecas, M., and Boatella, J. (1996) Biological Effects of Oxysterols: Current Status, *Food. Chem. Toxicol. 34*, 193–211.
5. Edwards, J.O., Pater, R.H., Curci, R., and Di Furia, F. (1979) On the Formation and Reactivity of Dioxirane Intermediates in the Reaction of Peroxoanions with Organic Substrates, *Photochem. Photobiol. 30*, 63–70.
6. Murray, R.W., and Jeyaraman, R. (1985) Dioxiranes: Synthesis and Reactions of Methyldioxiranes, *J. Org. Chem. 50*, 2847–2853.
7. Murray, R.W. (1988) Chemistry of Dioxiranes. Part 7. Organic Chemistry of Dioxiranes, in *Molecular Structure and Energetics. Modern Models of Bonding and Delocalization (Vol. 6)* (Liebman, J.F., and Greenberg, A., eds.), pp. 311–351, VCH Publishers, New York.
8. Adam, W., Curci, R., and Edwards, J.O. (1989) Dioxiranes: A New Class of Powerful Oxidants, *Acc. Chem. Res. 22*, 205–211.
9. Murray, R.W. (1989) Chemistry of Dioxiranes. 12. Dioxiranes, *Chem. Rev. 89*, 1187–1201.
10. Adam, W., Hadjiarapoglou, L.P., Curci, R., and Mello, R. (1992) Dioxiranes, Three-Membered Ring Cyclic Peroxides, in *Organic Peroxides* (Ando, W., ed.), pp. 195–219, John Wiley & Sons, Chichester.
11. Curci, R., Dinoi, A., and Rubino, M.F. (1995) Dioxirane Oxidations: Taming the Reactivity–Selectivity Principle, *Pure Appl. Chem. 67*, 811–822.
12. Montgomery, R.E. (1974) Catalysis of Peroxymonosulfate Reactions by Ketones, *J. Am. Chem. Soc. 96*, 7820–7821.
13. Adam, W., Chan, Y.Y., Cremer, D., Gauss, J., Scheutzow, D., and Schindler, M. (1987) Spectral and Chemical Properties of Dimethyldioxirane as Determined by Experiment and *ab initio* Calculations, *J. Org. Chem. 52*, 2800–2803.
14. Murray, R.W., Jeyaraman, R., and Pillay, M.K. (1987) Chemistry of Dioxiranes. 6. Electronic Effects in the Oxidation of Sulfides and Sulfoxides by Dimethyldioxirane, *J. Org. Chem. 52*, 746–748.
15. Adam, W., Haas, W., and Sieker, G. (1984) Thianthrene 5-Oxide as Mechanistic Probe in Oxygen-Transfer Reactions: The Case of Carbonyl Oxides vs. Dioxiranes, *J. Am. Chem. Soc. 106*, 5020–5022.
16. Colonna, S., and Gaggero, N. (1989) Enantioselective Oxidation of Sulfides by Dioxiranes in the Presence of Bovine Serum Albumin, *Tetrahedron Lett. 30*, 6233–6236.
17. Miyahara, Y., and Inazu, T. (1990) An Extremely Efficient Synthesis of Thiophene 1,1-Dioxides. Oxidation of Thiophene Derivatives with Dimethyldioxirane, *Tetrahedron Lett. 31*, 5955–5958.
18. Adam, W., and Hadjiarapoglou, L. (1992) α-Oxo Sulfones by Dimethyldioxirane Oxidation of Thiol Esters, *Tetrahedron Lett. 33*, 469–470.
19. Ballistreri, F.P., Tomaselli, G.A., Toscano, R.M., Bonchio, M., Conte, V., and Di Furia, F. (1994) The Relative Reactivity of Thioethers and Sulfoxides Toward Oxygen Transfer Reagents: The Case of Dioxiranes, *Tetrahedron Lett. 35*, 8041–8044.
20. Sánchez-Baeza, F., Durand, G., Barceló, D., and Messeguer, A. (1990) Dimethyldioxirane Conversion of Phosphine Sulfides and Phosphorothioates into Their Corresponding Oxygen Analogs, *Tetrahedron Lett. 31*, 3359–3362.
21. Gallopo, A.R., and Edwards, J.O. (1981) Kinetics and Mechanism of the Oxidation of Pyridine by Caro's Acid Catalyzed by Ketones, *J. Org. Chem. 46*, 1684–1688.
22. Murray, R.W., Jeyaraman, R., and Mohan, L. (1986) Chemistry of Dioxiranes. 5. A New Synthesis of Nitro Compounds Using Dimethyldioxirane, *Tetrahedron Lett. 27*, 2335–2336.

23. Boyd, D.R., Coulter, P.B., McGuckin, M.R., Sharma, N.D., Jennings, W.B., and Wilson, V.E. (1990) Imines and Derivatives. Part 24. Nitrone Synthesis by Imine Oxidation Using Either a Peroxyacid or Dimethyldioxirane, *J. Chem. Soc., Perkin Trans. 1*, 301–306.
24. Ferrer, M., Sánchez-Baeza, F., and Messeguer, A. (1997) On the Preparation of Amine *N*-Oxides by Using Dioxiranes, *Tetrahedron 53*, 15877–15888.
25. Zabrowski, D.L., Moormann, A.E., and Beck, K.R., Jr. (1988) The Oxidation of Aromatic Amines in the Presence of Electron-rich Aromatic Systems, *Tetrahedron Lett. 29*, 4501–4504.
26. Murray, R.W., and Singh, M. (1988) Chemistry of Dioxiranes. II. A Convenient High Yield Synthesis of Nitroxides, *Tetrahedron Lett. 29*, 4677–4680.
27. Murray, R.W., Rajadhyaksha, S.N., and Mohan, L. (1989) Chemistry of Dioxiranes. 13. Oxidation of Primary Amines by Dimethyldioxirane, *J. Org. Chem. 54*, 5783–5788.
28. Murray, R.W., and Singh, M. (1989) Chemistry of Dioxiranes. 14. A High Yield One Step Synthesis of Hydroxylamines, *Synth. Commun. 19*, 3509–3522.
29. Wittman, M.D., Halcomb, R.L., and Danishefsky, S.J. (1990) On the Conversion of Biologically Interesting Amines to Hydroxylamines, *J. Org. Chem. 55*, 1981–1983.
30. Murray, R.W., and Singh, M. (1990) Chemistry of Dioxiranes. 16. A Facile One Step Synthesis of C-Aryl Nitrones Using Dimethyldioxirane, *J. Org. Chem. 55*, 2954–2957.
31. Eaton, P.E., and Wicks, G.E. (1988) Conversion of Isocyanates to Nitro Compounds with Dimethyldioxirane in Wet Acetone, *J. Org. Chem. 53*, 5353–5355.
32. Baumstark, A.L., Beeson, M., and Vasquez, P.C. (1989) Dimethyldioxirane: Mechanism of Benzaldehyde Oxidation, *Tetrahedron Lett. 30*, 5567–5570.
33. Mello, R., Cassidei, L., Fiorentino, M., Fusco, C., Hümmer, W., Jäger, V., and Curci, R. (1991) Oxidations by Methyl(trifluoromethyl)dioxirane. 5. Conversion of Alcohols into Carbonyl Compounds, *J. Am. Chem. Soc. 113*, 2205–2208.
34. Bovicelli, P., Lupattelli, P., Sanetti, A., and Mincione, E. (1995) Efficient Desymmetrization of 1,2- and 1,3-Diols by Dimethyldioxirane, *Tetrahedron Lett. 36*, 3031–3034.
35. Bovicelli, P., Truppa, D., Sanetti, A., Bernini, R., and Lupattelli, P. (1998) Regioselective Oxidation of Azidodiols, Bromodiols and Triol Derivatives by Dimethyldioxirane, *Tetrahedron 54*, 14301–14314.
36. Curci, R., D'Accolti, L., Fiorentino, M., Fusco, C., Adam, W., González-Nuñez, M.E., and Mello, R. (1992) Oxidation of Acetals, an Orthoester, and Ethers by Dioxiranes Through α-Carbon-Hydrogen Insertion, *Tetrahedron Lett. 33*, 4225–4228.
37. Murray, R.W., Jeyaraman, R., and Mohan, L. (1986) Chemistry of Dioxiranes. 4. Oxygen Atom Insertion into Carbon–Hydrogen Bonds by Dimethyldioxirane, *J. Am. Chem. Soc. 108*, 2470–2472.
38. Mello, R., Fiorentino, M., Fusco, C., and Curci, R. (1989) Oxidations by Methyl(trifluoromethyl)dioxirane. 2. Oxyfunctionalization of Saturated Hydrocarbons, *J. Am. Chem. Soc. 111*, 6749–6757.
39. Mello, R., Cassidei, L., Fiorentino, M., Fusco, C., and Curci, R. (1990) Oxidations by Methyl(trifluoromethyl)dioxirane. 3. Selective Polyoxyfunctionalization of Adamantine, *Tetrahedron Lett. 31*, 3067–3070.
40. Bovicelli, P., Lupattelli, P., Mincione, E., Prencipe, T., and Curci, R. (1992) Oxidation of Natural Targets by Dioxiranes. Oxyfunctionalization of Steroids, *J. Org. Chem. 57*, 2182–2184.
41. Bovicelli, P., Lupattelli, P., Mincione, E., Prencipe, T., and Curci, R. (1992) Oxidation of Natural Targets by Dioxiranes. 2. Direct Hydroxylation at the Side Chain C-25 of Cholestane Derivatives and of Vitamin D3 Windaus-Grundmann Ketone, *J. Org. Chem. 57*, 5052–5054.
42. Asensio, G., González-Núñez, M.E., Bernardini, C.B., Mello, R., and Adam, W. (1993) Regioselective Oxyfunctionalization of Unactivated Tertiary and Secondary Carbon-Hydrogen Bonds of Alkylamines by Methyl(trifluoromethyl)dioxirane in Acid Medium, *J. Am. Chem. Soc. 115*, 7250–7253.
43. Curci, R., Detomaso, A., Prencipe, T., and Carpenter, G.B. (1994) Oxidation of Natural Targets by Dioxiranes. 3.1 Stereoselective Synthesis of (all-*R*)-Vitamin D3 Triepoxide and of Its 25-Hydroxy Derivative, *J. Am. Chem. Soc. 116*, 8112–8115.
44. Asensio, G., Castellano, G., Mello, R., and González Núñez, M.E. (1996) Oxyfunctionalization of Aliphatic Esters by Methyl(trifluoromethyl)dioxirane, *J. Org. Chem. 61*, 5564–5566.
45. Adam, W., Mello, R., and Curci, R. (1990) Oxygen Atom Insertion into Silicon–Hydrogen Bonds with Assistance by Dioxiranes. A Stereospecific and Direct Rearrangement of Silanes to Silanols, *Angew. Chem. 102*, 916–917.
46. Adam, W., Curci, R., González Nuñez, M.E., and Mello, R. (1991) Thermally and Photochemically Initiated Radical Chain Decomposition of Ketone-free Methyl(trifluoromethyl)dioxirane, *J. Am. Chem. Soc. 113*, 7654–7658.
47. Singh, M., and Murray, R.W. (1992) Chemistry of Dioxiranes. 21. Thermal Reactions of Dioxiranes, *J. Org. Chem. 57*, 4263–4270.
48. Frohn, M., and Shi, Y. (2000) Chiral Ketone-Catalyzed Asymmetric Epoxidation of Olefins, *Synthesis*, 1979–2000.
49. Curci, R., Fiorentino, M., and Serio, M.R. (1984) Asymmetric Epoxidation of Unfunctionalized Alkenes by Dioxirane Intermediates Generated from Potassium Peroxomonosulfate and Chiral Ketones, *J. Chem. Soc., Chem. Commun.*, 155–156.
50. Wang, Z.-X., Tu, Y., Frohn, M., Zhang, J.-R., and Shi, Y. (1997) An Efficient Catalytic Asymmetric Epoxidation Method, *J. Am. Chem. Soc. 119*, 11224–11235.
51. Denmark, S.E., Wu, Z., Crudden, C.M., and Matsuhashi, H. (1997) Catalytic Epoxidation of Alkenes with Oxone. 2. Fluoro Ketones, *J. Org. Chem. 62*, 8288–8289.
52. Yang, D., Wong, M.-K., Yip, Y.-C., Wang, X.-C., Tang, M.-W., Zheng, J.-H., and Cheung, K.-K. (1998) Design and Synthesis of Chiral Ketones for Catalytic Asymmetric Epoxidation of Unfunctionalized Olefins, *J. Am. Chem. Soc. 120*, 5943–5952.
53. Yang, D., Yip, Y.-C., Chen, J., and Cheung, K.-K. (1998) Significant Effects of Nonconjugated Remote Substituents in Catalytic Asymmetric Epoxidation, *J. Am. Chem. Soc. 120*, 7659–7660.
54. Tian, H., She, X., Shu, L., Yu, H., and Shi, Y. (2000) Highly Enantioselective Epoxidation of *cis*-Olefins by Chiral Dioxirane, *J. Am. Chem. Soc. 122*, 11551–11552.
55. Solladié-Cavallo, A., Bouérat, L., and Jierry, L. (2001) Asymmetric Epoxidation of *trans*-Olefins *via* Chiral Dioxiranes: A Possible Contribution of Axial Approaches in the Case of Tri- and Tetrasubstituted α-Fluoro Cyclohexanones, *Eur. J. Org. Chem.*, 4557–4560.
56. Denmark, S.E., and Matsuhashi, H. (2002) Chiral Fluoro Ketones for Catalytic Asymmetric Epoxidation of Alkenes with Oxone, *J. Org. Chem. 67*, 3479–3486.
57. Armstrong, A., Ahmed, G., Dominguez-Fernandez, B., Hayter, B.R., and Wailes, J.S. (2002) Enantioselective Epoxidation of Alkenes Catalyzed by 2-Fluoro-*N*-Carbethoxytropinone and Related Tropinone Derivatives, *J. Org. Chem. 67*, 8610–8617.
58. Matsumoto, K., and Tomioka, K. (2002) Chiral Ketone-Catalyzed Asymmetric Epoxidation of Olefins with Oxone, *Tetrahedron Lett. 43*, 631–633.
59. Cross, A.D. (1962) Steroids. CC. Spectra and Stereochemistry. Part 3. Steroidal 5,6-Epoxides, *J. Am. Chem. Soc. 84*, 3206–3207.
60. Marples, B.A., Muxworthy, J.P., and Baggaley, K.H. (1991) Dioxirane Mediated Steroidal Alkene Epoxidations and Oxygen Insertion into Carbon–Hydrogen Bonds, *Tetrahedron Lett. 32*, 533–536.

[Received July 8, 2004; accepted September 7, 2004]

Identification of a Neurosteroid Binding Site Contained Within the GluR2-S1S2 Domain

Vlad Spivak, Adam Lin, Patrick Beebe, Laura Stoll, and Lisa Gentile*

Department of Chemistry, Western Washington University, Bellingham, Washington 98225-9150

ABSTRACT: Glutamate receptors play a major role in neural cell plasticity, growth, and maturation. The degree to which ionotropic glutamate receptors (iGluR) conduct current is dependent on binding of extracellular ligands, of which glutamate is the native agonist. Although the glutamate binding site of the GluR2 class of amino-3-hydroxy-5-methyl-4-isoxazolepropionic acid (AMPA) iGluR has been structurally characterized, the allosteric sites attributed to neurosteroid binding have yet to be localized. Here, using intrinsic tryptophan fluorescence spectroscopy, we show that the extracellular glutamate binding core of the GluR2 class of AMPA receptors also binds to two neurosteroids, pregnenolone sulfate (PS) and 3α-hydroxy-5β-pregnan-20-one sulfate, both of which negatively modulate its activity. Interest in these sulfated neurosteroids stems from their differential modulation of other members of the iGluR family and their potential use as endogeneous agents for stroke therapy. In particular, whereas PS inhibits AMPA and other non-*N*-methyl-D-aspartate (NMDA) family members, it activates the NMDA receptor. In addition to providing evidence for binding of these neurosteroids to the glutamate binding core of the GluR2 class of AMPA receptors, our data suggests that both neurosteroids bind in a similar manner, consistent with their modulation of activity of this class of iGluR. Interestingly, the conformational change induced upon binding of these neurosteroids is distinct from that induced upon glutamate binding.

Paper no. L9515 in *Lipids 39*, 811–819 (August 2004).

Fast synaptic transmission between nerve cells is thought to be responsible for the formation of memory and learning and to result primarily from the depolarizing effect of ionotropic glutamate receptors (iGluR). Nature regulates a specific level of activity for the iGluR, and deviations from this lead to two major states of malfunction: hyper- and hypo-excitation. The physiology induced by hyperexcitation is similar, if not identical, to that resulting from states of ischemia, hypoglycemia, and physical trauma. Furthermore, it is believed that when these physical stresses are imposed upon the central nervous system, they may cause the chronic neuronal degeneration observed in diseases such as Huntington's, Alzheimer's, and Parkinson's (1). As the root of both these chronic and acute neurological diseases is believed to be overactivity of the iGluR, negative modulators of these receptors are attractive potential drug leads. In fact, the most potent anti-excitotoxic drugs identified thus far are noncompetitive *N*-methyl-D-aspartate (NMDA) receptor antagonists (1). 3-α-Hydroxy-5β-pregnan-20-one sulfate (PregaS; Fig. 1), an endogenous neurosteroid, has been shown to inhibit NMDA receptors in a noncompetitive manner (2). In addition, pregnenolone sulfate (PS), which differs from PregaS by only one double bond at the steroid A/B ring juncture (Fig. 1), is at least a partial inhibitor of all non-NMDA iGluR; however, PS potentiates the NMDA receptor response to glutamate by approximately 150% (2,3).

The iGluR are divided into three subcategories based on their agonist selectivity: amino-3-hydroxy-5-methyl-4-isoxazolepropionic acid (AMPA), kainate, and NMDA receptors—with AMPA and kainate receptors often grouped together as non-NMDA iGluR. Recent studies suggest that the functional glutamate-gated ion channels are composed of a dimer of dimers motif with the actual channel formed by the re-entrant loop of each subunit (4–8). Each of the subunits is composed of an extracellular amino terminus, a ligand-binding core (S1S2), three transmembrane-spanning domains, a re-entrant loop, and an intracellular carboxy-terminal tail (Fig. 2; 9–16). Upon binding of glutamate to the extracellular S1S2 ligand-binding core, a conformational change is transmitted that allows the channel to open. Molecular cloning of the iGluR has led to the development of a soluble extracellular GluR2-S1S2 domain that has been shown to possess near-native binding affinities for both agonists and antagonists (14–19). This AMPA receptor construct, which eliminates the first two transmembrane-spanning regions as well as the re-entrant loop, is composed of the S1 domain joined to the S2 domain by a two amino acid (GT, i.e., glycine + threonine) linker (the C-terminus of S2 ends prior to the start of the final transmembrane-spanning region). Since PregaS-binding to the NMDA receptor is known to occur extracellularly (3) and since modulation of activity of the receptor appears to be regulated by the S1S2 domain, this engineered GluR2-S1S2 construct was used to probe for PS and PregaS binding to the AMPA receptor. Based on intrinsic tryptophan fluorescence spectroscopy, we propose that the binding site for both of these neurosteroids is contained within the S1S2 domain of the GluR2 class of AMPA receptors.

*To whom correspondence should be addressed at Department of Chemistry, Western Washington University, 516 High St., Bellingham, WA 98225. E-mail: gentile@chem.wwu.edu

Abbreviations: AMPA, amino-3-hydroxy-5-methyl-4-isoxazolepropionic acid; CD, circular dichroism; HPLC-SEC, HPLC size-exclusion chromatography; iGluR, ionotropic glutamate receptors; LB, Luria broth; NMDA, *N*-methyl-D-aspartate; PregaS, 3α-hydroxy-5β-pregnan-20-one sulfate; PS, pregnenolone sulfate.

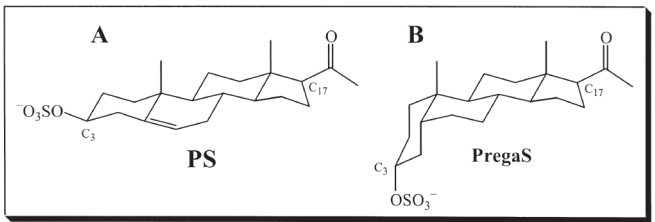

NMDA iGluR	positively regulates	negatively regulates
non-NMDA iGluR	negatively regulates	negatively regulates

FIG. 1. Neurosteroid structures and their physiological effect on members of the ionotropic glutamate receptor (iGluR) family. (A) Pregnenolone sulfate (PS); (B) 3α-hydroxy-5β-pregnan-20-one sulfate (PregaS).

EXPERIMENTAL PROCEDURES

Buffers. Buffer 8: 20 mM NaOAc, 4 M guanidine-HCl, 1 mM DTT, 1 mM EDTA, pH 4.5 (15,19). Buffer 9: 650 mM arginine-HCl, 400 μM KCl, 10 mM NaCl, 1 mM EDTA, pH 8.5 (15,19). Buffer 13: 150 mM NaH_2PO_4, 1 mM glutamate, pH 6.0. Buffer 14: 150 mM NaH_2PO_4, 1 mM glutamate, 1 M NaCl, pH 7.0. Buffer 15: 6 M urea, 150 mM NaH_2PO_4, pH 6.0. Buffer 16: 6 M urea, 150 mM NaH_2PO_4, 500 mM NaCl, pH 7.0. Buffer 17: 6 M urea, 50 mM NaH_2PO_4, 50 mM Tris, pH 8.5. Buffer 18: 6 M urea, 1 M imidazole, 50 mM NaH_2PO_4, 50 mM Tris, pH 8.5.

Protein expression, purification, and folding for circular dichroism (CD) studies (Fig. 3, Scheme A). GluR2 cDNA in

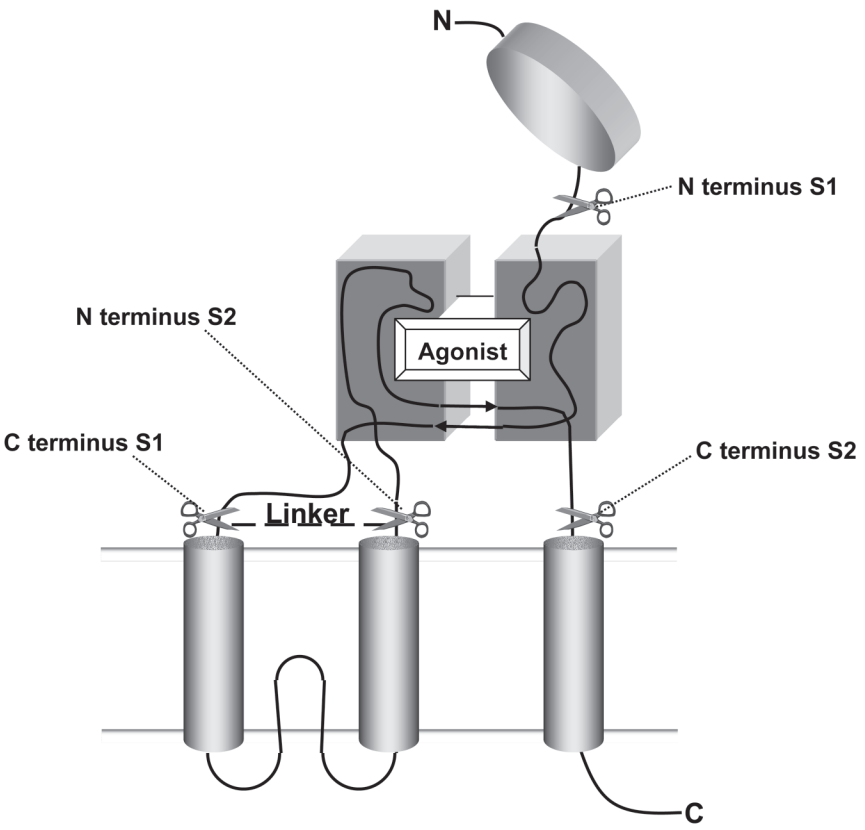

FIG. 2. Schematic representation of the GluR2-S1S2 domain. GluR2 subunits are composed of an extracellular amino terminus, a ligand-binding core (S1S2), three transmembrane-spanning domains, a re-entrant loop, and an intracellular carboxy-terminal tail (Ref. 16, modified Figure 1A used with permission).

the pETGQ vector was obtained from Eric Gouaux (Columbia University, New York, NY) and transformed into electrocompetent *Escherichia coli* BL21(DE3) cells. The amino acid sequence of this construct is as follows: M-H_8-SSG-LVPRGS(thrombin cut site)-AMG-S1(amino acids 383–524)-GT(linker)-S2(amino acids 627–791). Protein was expressed, harvested, solubilized, and folded as in Chen *et al.* (15,19). The folded GluR2-S1S2 protein was then dialyzed against 16 vol of buffer 13 (2 × 8 h) at 4°C, followed by centrifugation at 85,000 × *g*, 20°C for 1 h. The resultant supernatant was concentrated ~12-fold and loaded onto an SP-sepharose column (1.5 mL/min), which was then washed with 40 mL of buffer 13 and eluted with a gradient of 0–100% buffer 14 over a 100-mL range. Elution of the S1S2 protein began with approximately 200 mM NaCl, pH 6.2, and was more than 90% complete by 400 mM NaCl, pH 6.4. Aliquots (300 µL) of approximately 2 mg/mL were then loaded onto an HPLC size-exclusion chromatography (HPLC-SEC) column (Varian Prostar HPLC, Superdex 75 HR 10/30 SEC) at a flow rate of 0.5 mL/min in buffer 13, and the peak corresponding to monomer was collected (approximately 1:6 mol/mol ratio of GluR2-S1S2 dimer/monomer). The material was then concentrated to 16.1 µM, yielding approximately 0.5 mg of monomeric protein per liter of initial growth.

Protein expression, purification, and folding for fluorescence studies (Fig. 3, Scheme Bi). The GluR2-S1S2 protein was expressed, harvested, and solubilized as in Scheme A of Figure 3. The solubilized protein was then centrifuged at 110,000 × *g*, at 20°C for 1 h. The resultant supernatant was diluted with 350 mL of buffer 8, centrifuged again at 110,000 × *g*, 4°C for 1 h, and the supernatant was then dialyzed against 12.5 vol of buffer 15 (3 × 8 h). Aliquots (100 mL) of the unfolded protein solution were then loaded onto an SP-sepharose column (10 mL column volume, 2.0 mL/min), washed with 40 mL of buffer 15, and eluted with a gradient of 0–100% buffer 16 over a range of 100 mL. Elution of the S1S2 protein began with approximately 200 mM NaCl, pH 6.2, and was more than 90% complete by 400 mM NaCl, pH 6.4. The fractions containing GluR2-S1S2 were then loaded onto an HPLC-SEC column (Varian Prostar HPLC, Superdex

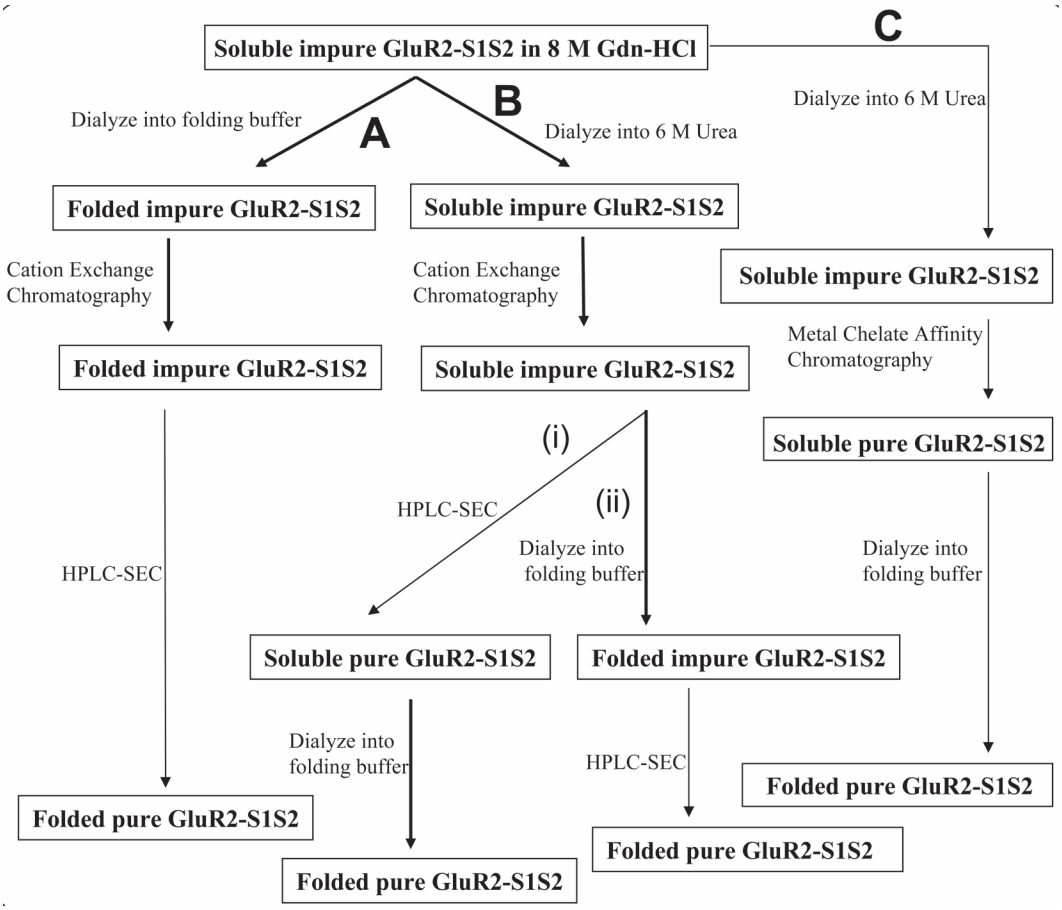

FIG. 3. Purification schemes for the GluR2-S1S2 domain. The pETGQ vector, transformed into *Escherichia coli* BL21(DE3) cells, is used to overexpress the GluR2-S1S2 domain in inclusion bodies. The protein can be solubilized, refolded, and then purified (Scheme A), or it can be solubilized, purified in the denatured state, and then refolded (Schemes B and C). Schemes B and C differ by the purification method employed in the denatured state [cation exchange chromatography followed by HPLC size-exclusion chromatography (HPLC-SEC) vs. chromatography on an immobilized metal affinity column].

75 HR 10/30 SEC) in 300-μL aliquots at a flow rate of 0.5 mL/min, and the peak corresponding to monomer was collected (no significant amounts of multimeric GluR2-S1S2 were detected). The pooled peaks were dialyzed against 12.5 vol of buffer 9 (4 × 8 h) followed by centrifugation at 85,000 × *g*, 20°C for 1 h. The supernatant was then treated with GSH/GSSG (1 mM/0.2 mM) at 4°C overnight, yielding approximately 15.5 mg of monomeric protein per liter of initial growth.

Protein expression, purification, and folding for fluorescence studies (Fig. 3, Scheme C). GluR2-S1S2 was expressed, harvested, and solubilized as in Schemes A and B (Fig. 3). Solubilized unfolded protein was centrifuged at 110,000 × *g*, 20°C for 1 h, and the supernatant was successively dialyzed against 35–50 vol of buffer 17 (3 × 4 h) at room temperature. The protein solution was again centrifuged at 110,000 × *g*, 20°C for 1 h. The supernatant [5 mL; 0.5 L Luria broth (LB) prep equivalent] was then loaded onto a His-Bind® Resin (Novagen, Madison, WI) column (30 mL column volume at 2.0 mL/min). Impurities were eluted with two gradients: a 50-mL gradient of 50 to 100 mM imidazole in buffer 17 followed by a 40-mL gradient of 100 to 250 mM imidazole in buffer 17. Buffer 18 (90 mL) was then used to elute the desired S1S2 protein, which was then diluted twofold with buffer 17 and, for folding, dialyzed against 35–50 vol of buffer 9 for 3 × 4 h at 4°C. The folded protein solution was then treated with GSH/GSSG (1 mM/0.2 mM) at 4°C overnight. The solution was centrifuged at 110,000 × *g*, 4°C for 1 h and the supernatant collected, yielding approximately 25 mg of pure S1S2 protein per liter of initial growth.

CD studies. The CD measurements plotted in Figure 4

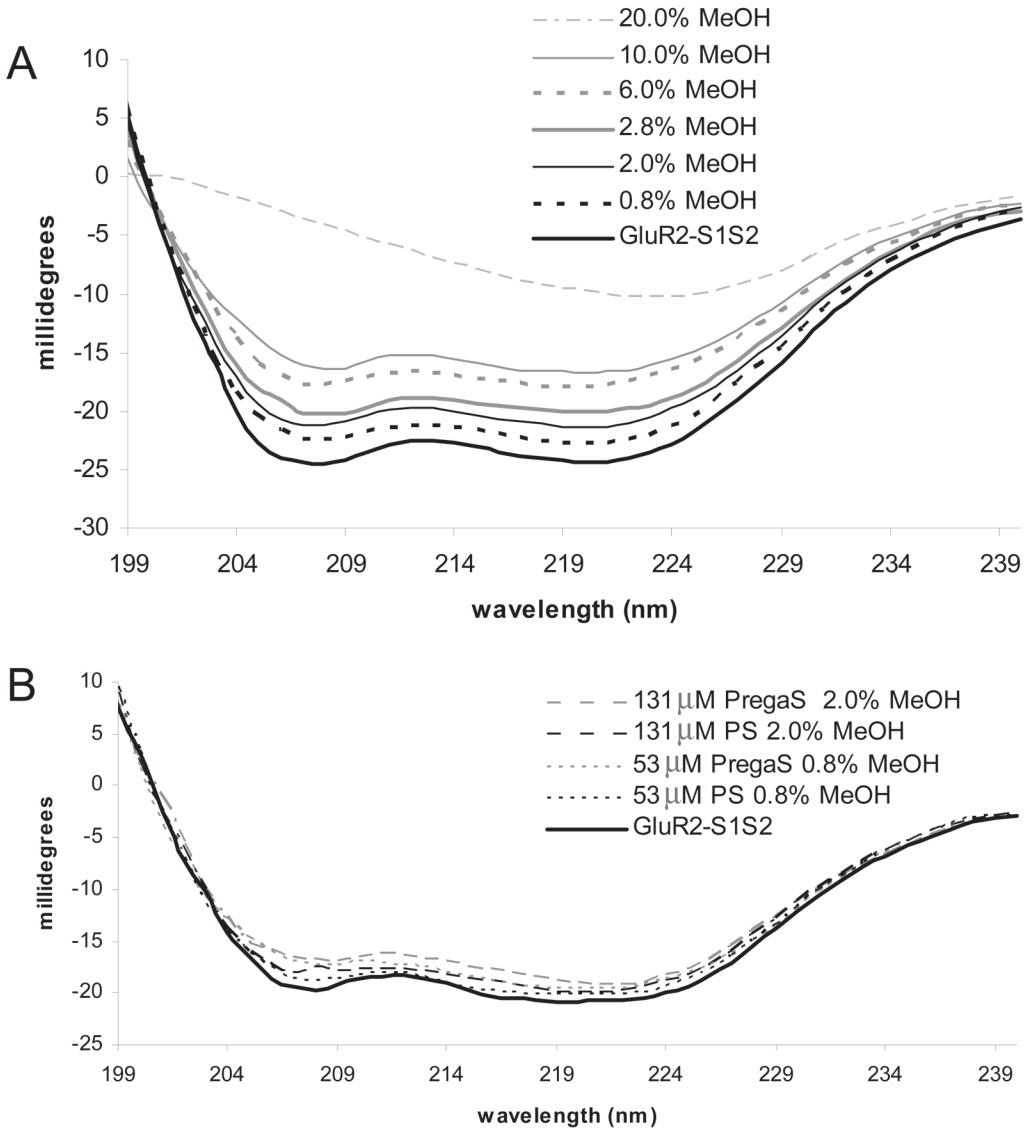

FIG. 4. Far-UV circular dichroism spectra of the GluR2-S1S2 domain. (A) Methanol titration of GluR2-S1S2 to verify that secondary structure remains intact under conditions necessary for addition of neurosteroid. (B) Addition of a 3.3-fold molar excess of either PS or PregaS in 0.8% methanol to GluR2-S1S2 (16 mM, buffer 13) leads to no global changes in secondary structure of the receptor domain. Addition of an 8.2-fold molar excess of either neurosteroid in 2.0% methanol shows similar results. For abbreviations see Figure 1.

were performed on an Olis DSM-10 CD spectrophotometer (Bogard, GA) at 25°C using a 0.5-mm slit width and a 1-mm pathlength quartz cell. All scans were performed from 190 to 240 nm with an integration time of 3 s. Five blank spectra of buffer 13 were recorded, which were then averaged and subtracted from subsequent experimental spectra. Protein samples, as prepared above, were at a concentration of 16 μM. PS (Sigma, St. Louis, MO) and PregaS (Steraloids, Newport, RI), solubilized in 100% methanol (10 mM stock solution), were added to protein samples to a final concentration of either 53 μM (3.3:1 molar ratio of neurosteroid/protein) or 131 μM (8.2:1 molar ratio of neurosteroid/protein) in 0.8 or 2.0% final methanol concentration, respectively.

Fluorescence studies. Fluorescence emission was measured on a Cary Eclipse fluorescence spectrophotometer (Varian) at 25°C using 2.5 nm excitation and emission slit widths. All scans were performed from 285 to 450 nm with a 280-nm excitation in a 1-cm pathlength cell. Each sample was equilibrated 90 s at 25°C in the sample holder before data acquisition. Upon addition of ligand, an additional 90-s equilibration at 25°C was performed before data were collected. Sample preparation times were also normalized to eliminate differences in the time frame over which each ligand was allowed to bind to the S1S2 domain.

Blanks were measured by adding the appropriate ligand to buffer 9. Since all blank signals were <1% of the total fluorescent signal at 339 nm, experimental data were reported without subtraction of a blank. Protein samples, as prepared above, were at a concentration of 7.1 μM. For the binding experiments (Fig. 5A), the neurosteroids were solubilized in methanol to a stock concentration of 50 mM. They were added to a final concentration of 25 to 1030 μM (3.5:1 to 145:1 molar ratio of neurosteroid/protein) in 2.1% methanol. To take into account any effects of 2.1% methanol on the protein, fluorescence emission in the absence of quencher was determined in the presence of 2.1% methanol, thus allowing a direct comparison between samples with and without neurosteroid. Percent binding is defined as [(fluorescence emission

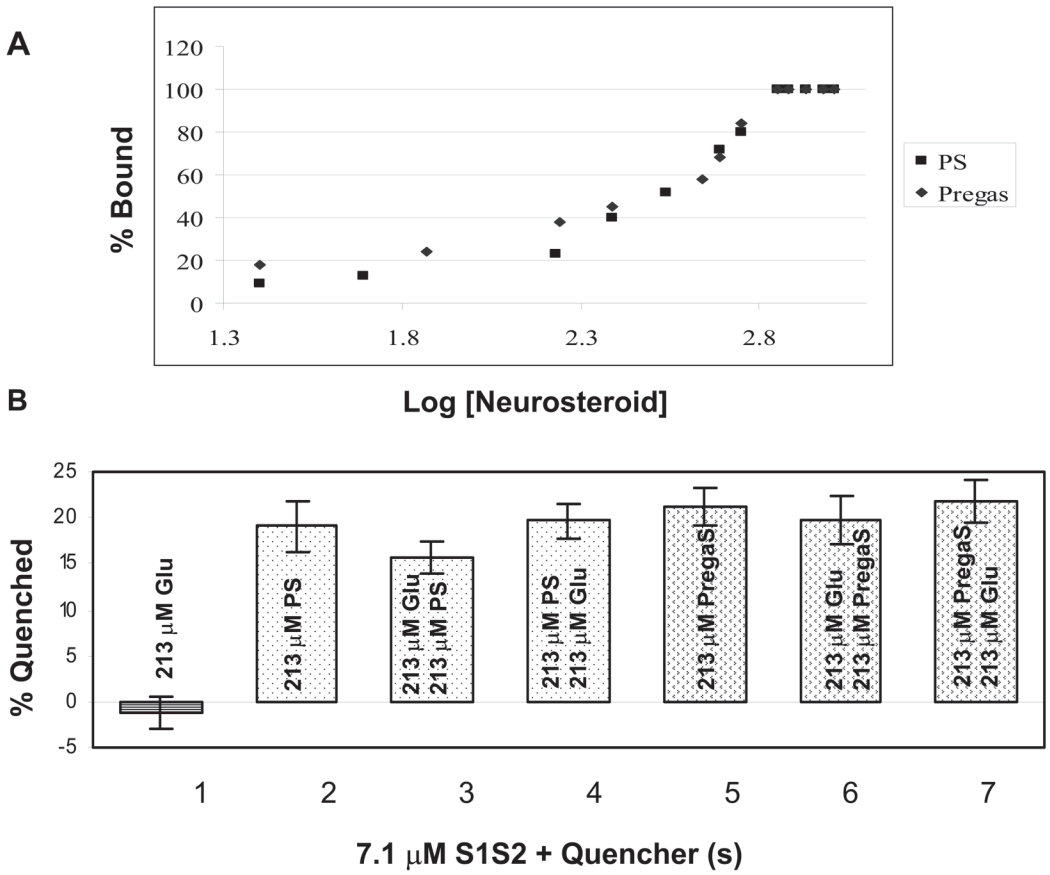

FIG. 5. Intrinsic fluorescence emission at 339 nm of the GluR2-S1S2 domain in the presence of ligand. (A) Percent binding of PregaS (◆) or PS (■) to the GluR2-S1S2 domain (7.1 μM in buffer 9). In each case, the neurosteroid was added (from a 50 mM stock solution) to a final concentration of 25–1030 μM (3.5:1 to 145:1 molar ratio of neurosteroid/protein) in 2.1% methanol. (B) Percent quenching of fluorescence emission of the GluR2-S1S2 domain (7.1 μM in buffer 9) plus: (1) 213 μM glutamate (Glu), (2) 213 μM PS, (3) 213 μM glutamate followed by 213 μM PS, (4) 213 μM PS followed by 213 μM glutamate, (5) 213 μM PregaS, (6) 213 μM glutamate followed by 213 μM PregaS, (7) 213 μM PregaS followed by 213 μM glutamate. In each case, the ligand was added from a 10 mM stock solution to 2.1% of the total volume of the solution. The mean value ± the error at a 95% confidence level is plotted.

in the absence of the quencher at 339 nm – fluorescence emission in the presence of a certain concentration of the quencher at 339 nm)/(fluorescence emission in the absence of the quencher at 339 nm – fluorescence emission in the presence of a saturating concentration of the quencher at 339 nm)] × 100. A saturating concentration is defined here as one for which there is no further quenching.

For the fluorescence quenching experiments (Fig. 5B), neurosteroids were solubilized in methanol to a stock concentration of 10 mM. They were added to a final concentration of 213 μM (30:1 molar ratio of neurosteroid/protein) in 2.1% methanol. To take into account any effects of 2.1% methanol on the protein, fluorescence emission in the absence of quencher was determined in the presence of 2.1% methanol, thus allowing a direct comparison between samples with and without neurosteroid. Glutamate was solubilized in buffer 9 to a stock concentration of 10 mM. It was added to a final concentration of 213 μM in buffer 9 (30:1 molar ratio of glutamate/protein). Percent fluorescence quenching is defined as [(fluorescence emission in the absence of the quencher at 339 nm − fluorescence emission in the presence of the quencher at 339 nm)/fluorescence emission in the absence of the quencher at 339 nm] × 100. Each data set in Figure 5B consists of emission spectra from independent scans of five identically prepared samples. The average spectrum of each data set was calculated by averaging the intensity at each individual wavelength between 285 and 450 nm. The wavelength at maximum intensity was determined to be at 339 nm for all data sets. The SD was calculated at 339 nm for each data set based on the five data points for each protein/ligand mixture, and the error at 95% confidence was determined. The 95% confidence interval (μ) was defined as average fluorescence intensity ± ($t \times$ SD)/(number of data points)$^{1/2}$, where t is the Student-t value for the appropriate degrees of freedom at the 95% confidence level.

RESULTS

Protein purification. Purification of the GluR2-S1S2 domain has been described by Gouaux and colleagues (15,19). In this protocol, protein is produced in inclusion bodies, solubilized, refolded, and then purified (Fig. 3, Scheme A). Owing to difficulties encountered after refolding, two purification protocols of the GluR2-S1S2 domain in the denatured state were devised. In our hands, purification in the denatured state followed by refolding increased protein yields up to 50-fold. The first of these denatured purification protocols (Fig. 3, Schemes Bi and Bii) involves cation exchange chromatography followed by HPLC-SEC. In this protocol, cation exchange chromatography is performed in buffers containing 6 M urea. The resultant material is either refolded and then subjected to HPLC-SEC for further purification (Scheme Bii) or subjected to HPLC-SEC for further purification while still in the denatured state (6 M urea) and then refolded (Scheme Bi). These protocols yielded approximately 15.5 mg of monomeric GluR2-S1S2 protein per liter (LB) of bacterial growth. Since HPLC-SEC is a low-throughput method, a denatured purification protocol has been developed (Fig. 3, Scheme C) that takes advantage of the octa-histidine tag on the N-terminus of the GluR2-S1S2 construct. By using a two-stage gradient elution of imidazole to remove undesired bacterial impurities, pure GluR2-S1S2 protein is then acquired from a 1 M imidazole elution. This protocol has the advantage of being amenable to efficient purification (one column) of larger quantities of the GluR2-S1S2 protein, yielding approximately 25 mg of monomeric GluR2-S1S2 protein per liter (LB) of bacterial growth.

Neurosteroid binding. An IC_{50} value for PS binding to the intact NMDA receptor of 37 μM has been reported (20). This weak binding necessitates the use of excess ligand in neurosteroid binding experiments to shift the equilibrium in favor of the protein–ligand complex. Before ligand binding experiments could commence, a solvent to solubilize the neurosteroids needed to be found that was compatible with the native folded state of the GluR2-S1S2 domain. DMSO and methanol were found to solubilize both PS and PregaS; however, because even low concentrations (0.1% vol/vol) of DMSO caused the GluR2-S1S2 domain to unfold, the neurosteroid binding studies described here were performed in methanol. Figure 4A shows far-UV CD spectra that confirm that the GluR2-S1S2 domain is folded, that it contains significant secondary structure that is consistent with an α/β protein, and that it remains stable upon addition of methanol up to concentrations of ~10%. From this titration, final methanol concentrations up to 2.8% were deemed acceptable. Upon addition of an excess of either PS or PregaS (3.3- or 8.2-fold molar excess) to the GluR2-S1S2 domain, no significant changes in global secondary structure were observed by CD spectroscopy (Fig. 4B). Similarly, addition of glutamate to the S1S2 domain (data not shown) resulted in no changes in overall secondary structure. The latter was not surprising as the findings of Gouaux and colleagues (16,21) document that the mechanism of glutamate binding entails a hinge motion closure of the S1 and S2 domains. Such a binding mechanism results in a dramatic change in tertiary structure but minimal changes in secondary structure. If PS and PregaS induce a conformational change upon binding to the S1S2 domain that involves a similar hinge-type motion of the S1 domain relative to the S2 domain, the data shown in Figure 4B would be expected.

Intrinsic fluorescence spectroscopy (upon excitation at 280 nm) was employed to monitor changes in the tertiary structure of the GluR2-S1S2 domain upon addition of each neurosteroid, because the near-UV CD spectrum of the S1S2 domain was dominated by the n–π* transition of the steroid C-17 carbonyl group. Before monitoring ligand binding by fluorescence, negative controls were performed to demonstrate that neither neurosteroid bound nonspecifically to proteins (ovalbumin or chymotrypsinogen) or to tryptophan (data not shown). The intrinsic tryptophan fluorescence intensity of ovalbumin and chymotrypsinogen was seen to change by less than 4% (within experimental error) in the presence of either

PS or PregaS, implying that these neurosteroids do not bind nonspecifically to protein. Although neither steroid binds to ovalbumin, we observed both to bind to BSA, as was originally reported by Romeu *et al.* (22). The minimal change in intrinsic fluorescence intensity of tryptophan on addition of either neurosteroid also implies that PS and PregaS do not nonspecifically bind to solvent-exposed tryptophan residues.

A study of each ligand binding to the GluR2-S1S2 domain was performed before quenching experiments were undertaken. Figure 5A shows this percent binding data at λ_{max} (339 nm) in the presence of 25 to 1020 μM neurosteroid (3.5- to 145-fold molar excess). There are three interesting features of this plot. First, the EC_{50} for quenching of the GluR2-S1S2 tryptophan fluorescence is similar upon binding of both neurosteroids (316 μM for PS and 327 μM for PregaS). In addition, the λ_{max} of emission at 339 nm indicates that the indole side chains of the tryptophan residue(s) contributing to this fluorescence intensity are at least partially solvent-exposed or in polar environments (see below). Finally, it is noteworthy that ligand binding to the S1S2 domain does not cause a shift in the wavelength of maximum emission; hence, the polarity of the environment around the responsible Trp residue(s) is not significantly altered.

The results of the intrinsic fluorescence quenching experiments are summarized in Figure 5B. In these experiments, a 30-fold molar excess (213 μM) of each neurosteroid was added to the GluR2-S1S2 domain. As seen in Figure 5A, this correlates to each neurosteroid being ~40% bound. A higher concentration of neurosteroid was not used in these experiments owing to the limited solubility of each neurosteroid (and the ability to make neurosteroid stock solutions of >10 mM reliably in methanol), as well as the need to limit the quantity of methanol to ensure that the GluR2-S1S2 domain remained structurally intact (Fig. 4A). Had a higher concentration of neurosteroid been used in these quenching experiments, one that corresponded to 100% binding, the percent quenching would have been ~55% rather than the ~20% shown in Figure 5B. In each plot of Figure 5B, five independent data sets were acquired and their mean values calculated. Note that in each data set, fluorescence emission in the absence of quencher was determined in the presence of 2.1% methanol, thus allowing a direct comparison between samples with and without neurosteroid. Error analysis was performed from the SD of each data set and used to calculate the 95% confidence level (error bars shown in Fig. 5B). These data show that the GluR2-S1S2 fluorescence intensity at a λ_{max} of 339 nm is partially quenched in the presence of either PS or PregaS, but no significant quenching was observed upon the addition of glutamate alone. From these data, it is clear that within the 95% confidence limit, there is no significant difference in fluorescence quenched (15.6–21.9%) if the S1S2 domain is incubated with only the neurosteroid, with the neurosteroid first and then glutamate, or with glutamate first and then the neurosteroid. Also, within the 95% confidence limit, there was no difference between the fluorescence quenched upon addition of PS or PregaS.

It is interesting to note that addition of either iodide, nitrate, or cesium ion, at concentrations up to 20 mM, had no effect on the fluorescence of the GluR2-S1S2 domain. Addition of these water-soluble quenchers after binding of each neurosteroid to the S1S2 domain also had no effect on its fluorescence.

DISCUSSION

Proteins contain three naturally occurring aromatic residues that may contribute to their fluorescence; however, it is well documented that, owing to the low quantum yield of phenylalanine and the ease of quenching of tyrosine (particularly by radiationless energy transfer to nearby tryptophan residues), tryptophan is the major contributor (23,24). In addition, phenylalanine and tyrosine have λ_{max} of emission (282 and 303 nm, respectively) that are distinct from that of tryptophan (348 nm). At higher pH values, including that used for these fluorescence studies, the possibility of tyrosinate formation exists. Although tyrosinate has a fluorescence emission maximum (330–350 nm) that could overlap with that of tryptophan, tyrosinate fluorescence is quenched (23). Thus, we believe that the observed fluorescent emission at 339 nm for the GluR2-S1S2 domain is predominantly due to one or more of its four tryptophan residues: Trp460, Trp671, Trp766, and Trp767 (Fig. 6). The observed decrease in fluorescence intensity with neurosteroid binding may occur through either one or two major modes of action: (i) the fluorescing residue is quenched as a direct result of neurosteroid binding; or (ii) a conformational change upon neurosteroid binding brings an appropriate functional group close enough to the fluorescing residue to result in quenching by either electron or proton transfer. A number of potential quenching species exist: (i)

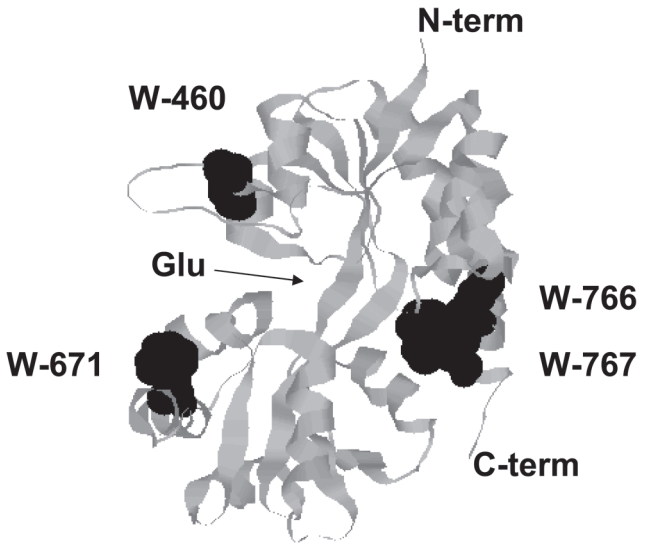

FIG. 6. Rasmol rendering of the apo GluR2-S1S2 domain (PDB: 1FTO; 16). The four tryptophan residues in the S1S2 domain (Trp 461, 671, 766, and 767) are space-filled and are shown in black. In addition, the location of the glutamate (Glu) binding pocket is illustrated.

water; (*ii)* peptide bond; (*iii)* lysine or tyrosine residues through excited-state proton transfer; or (*iv)* glutamate, aspartate, glutamine, asparagine, cysteine, or histidine residues through excited state electron transfer (23). The observed lack of quenching with iodide, nitrate, and cesium ion of the GluR2-S1S2 fluorescence intensity, either before or after binding of either neurosteroid, suggests that none of the four tryptophan residues in the apo S1S2 domain is on the surface (unless in small crevices not accessible to the quenchers), and likely not directly contacting neurosteroid upon binding, thus eliminating mode of action option (i). In addition, none are brought to the surface as a result of the conformational change induced upon neurosteroid binding. It is therefore likely that the tryptophans responsible for the observed quenching upon neurosteroid binding are moved to different partially buried regions (see below) of the protein as a consequence of to the conformational change associated with neurosteroid binding.

Analysis of the crystal structure of the GluR2-S1S2 domain in the apo state (PDB file 1FTO: 16) shows that three of its four tryptophan residues have an electron-donating group well within quenching distance; aspartate 668 is 6.4 Å from Trp671, aspartate 427 is 2.9 Å from Trp766, and glutamate 710 is 4.3 Å from Trp767. Theoretically therefore the only tryptophan residue retaining fluorescent capabilities within the apo state of the GluR2-S1S2 domain is Trp460. The hypothesis that only one tryptophan residue is responsible for the observed quenching, however, is inconsistent with the half-bandwidth of 66 nm for this fluorescence emission signal, which is larger than normally found for a single tryptophan residue and is more consistent with the superposition of more than one tryptophan emission band (25,26).

Although addition of neurosteroid to the GluR2-S1S2 domain causes quenching of fluorescence intensity, it does not cause a shift in the λ_{max} at 339 nm. This favors a quenching mechanism that does not change the polarity around the fluorophores. The observed λ_{max} at 339 nm suggests that the residues most responsible for the GluR2-S1S2 fluorescence signal are at least partially solvent-exposed or are in buried polar regions (25,27,28). As seen in Figure 8, all four tryptophan residues within the GluR2-S1S2 domain are somewhat exposed to solvent.

In summary, we have demonstrated that both PS and PregaS bind to the S1S2 domain of the GluR2 subunit of the AMPA receptor in a manner that is distinct from binding of the natural agonist glutamate. Results of intrinsic fluorescence emission experiments suggest that both neurosteroids bind to the S1S2 domain in a similar manner, which is consistent with both PS and PregaS similarly affecting the activity of the non-NMDA receptors (down-regulation). This binding causes a conformational change that affects the environment, although not the polarity, of more than one of the tryptophan residues in the S1S2 domain. The results described here are significant because knowing that these neurosteroids bind to the well-defined, structurally stable S1S2 domain of this receptor will allow for higher-resolution structural studies that could not have been performed on the intact receptor. These structural studies will address such questions as whether the observed fluorescence quenching is due to each neurosteroid binding at the same site within the GluR2-S1S2 domain, affecting the same tryptophan residues, and will also elucidate the fluorescence-observed conformational differences in the binding of glutamate and the neurosteroids to the S1S2 domain. The protocols elucidated for the efficient production of large quantities of the S1S2 domain will enable these higher resolution studies. In conjunction with similar studies of the S1S2 domain of the NMDA receptor, an understanding of inactivation of this receptor by PregaS will be facilitated. This inactivation, especially by compounds endogeneous to the mammalian central nervous system, is an exciting avenue to pursue to minimize or reverse the effects of the ischemic cascade in stroke patients.

ACKNOWLEDGMENTS

GluR2-S1S2 plasmid: Eric Gouaux, Columbia University; fluorescence facilities: Fred Federico, UBC, Molecular Biophysics Laboratory; financial support: Undergraduate Research and Creative Opportunity Award (VS, PB), Immunex on-campus summer stipend (VS, PB), Beckman Foundation (AL), Western Washington University startup funds and project development award (LG), and American Chkemical Society Petroleum Research Fund (33815-B4 to LG).

REFERENCES

1. Olney, J.W. (1990) Excitotoxic Amino Acids and Neuropsychiatric Disorders, *Annu. Rev. Pharmacol. Toxicol. 30*, 47–71.
2. Yaghoubi, N., Malayev, A.A., Russek, S.J., Gibbs, T.T., and Farb, D.H. (1998) Neurosteroid Modulation of Recombinant ionotropic Glutamate Receptors, *Brain Res.* 803, 153–160.
3. Park-Chung, M., Wu, F.S., Purdy, R.H., Malayev, A.A., Gibbs, T.T., and Farb, D.H. (1997) Distinct Site for the Inverse Modulation of the *N*-Methyl-D-aspartate Receptors by Sulfated Steroids, *Mol. Pharmacol. 52*, 1113–1123.
4. Seeburg, P.H. (1993) The TINS/TiPS Lecture. The Molecular Biology of the Mammalian Glutamate Receptor Channels, *Trends Neurosci. 16*, 359–365.
5. Nakanishi, S., and Masu, M. (1994) Molecular Diversity and Functions of Glutamate Receptors, *Annu. Rev. Biophys. Biomol. Struct.* 23, 319–348.
6. Laube, B., Kuhse, J., and Betz, H. (1998) Evidence for a Tetrameric Structure of Recombinant NMDA Receptors, *J. Neurosci. 18*, 2954–2961.
7. Mano, I., and Teichberg, V.I. (1998) A Tetrameric Subunit Stoichiometry for a Glutamate Receptor-Channel Complex, *NeuroReport* 9, 327–331.
8. Rosenmund, C., Stern-Bach, Y., and Stevens, C.F. (1998) The Tetrameric Structure of a Glutamate Receptor Channel, *Science* 280, 1596–1599.
9. O'Hara, P.J., Sheppard, P.O., Thogersen, H., Venezia, D., Haldeman, B.A., McGrane, V., Houamed, K.M., Thomsen, C., Gilbert, T.L., and Mulvihill, E.R. (1993) The Ligand-Binding Domain in Metabotropic Glutamate Receptors Is Related to Bacterial Periplasmic Binding Proteins, *Neuron 11*, 41–52.
10. Hollmann, M., Maron, C., and Heinemann, S. (1994) *N*-Glycosylation Site Tagging Suggests a Three Transmembrane Domain Topology for the Glutamate Receptor GluR1, *Neuron 13*, 1331–1343.
11. Stern-Bach, Y., Bettler, B., Hartley, M., Sheppard, P.O.,

O'Hara, P.J., and Heinemann, S.F. (1994) Agonist Selectivity of Glutamate Receptors Is Specified by Two Domains Structurally Related to Bacterial Amino Acid-Binding Proteins, *Neuron* 13, 1345–1357.
12. Wo, Z.G., and Oswald, R.E. (1994) Transmembrane Topology of Two Kainate Receptor Subunits Revealed by N-Glycosylation, *Proc. Natl. Acad. Sci. USA 91*, 7154–7158.
13. Bennett, J.A., and Dingledine, R. (1995) Topology Profile for a Glutamate Receptor: Three Transmembrane Domains and a Channel-Lining Reentrant Membrane Loop, *Neuron* 14, 373–384.
14. Kuusinen, A., Arvola, M., and Keinänen, K. (1995) Molecular Dissection of the Agonist Binding Site of an AMPA Receptor, *EMBO J.* 14, 6327–6332.
15. Chen, G-Q., Sun, Y., Jin, R., and Gouaux, E. (1998) Probing the Ligand Binding Domain of the GluR2 Receptor by Proteolysis and Deletion Mutagenesis Defines Domain Boundaries and Yields a Crystallizable Construct, *Protein Sci. 7*, 2623–2630.
16. Armstrong, N., and Gouaux, E. (2000) Mechanism for Activation and Antagonism of an AMPA-Sensitive Glutamate Receptor: Crystal Structure of the GluR2 Ligand Binding Core, *Neuron 28*, 165–181.
17. Ivanovic, A., Reilander, H., Laube, B., and Kuhse, J. (1998) Expression and Initial Characterization of a Soluble Glycine Binding Domain of the *N*-Methyl-D-aspartate Receptor NR1 Subunit, *J. Biol. Chem. 273*, 19933–19937.
18. Keinänen, K., Jouppila, A., and Kuusinen, A. (1998) Characterization of the Kainate-Binding Domain of the Glutamate Receptor GluR-6 Subunit, *Biochem. J. 330*, 1461–1467.
19. Chen, G-Q., and Gouaux, E. (1997) Overexpression of a Glutamate Receptor (GluR2) Ligand Binding Domain in *Escherichia coli*: Application of a Novel Protein Folding Screen, *Proc. Natl. Acad. Sci. USA* 94, 13431–13436.
20. Weaver, C.E., Wu, F.S., Gibbs, T.T., and Farb, D.H. (1998) Pregnenolone Sulfate Exacerbates NMDA-Induced Death of Hippocampal Neuron, *Brain Res. 803*, 129.
21. Armstrong, N., Mayer, M., and Gouaux, E. (2003) Tuning Activation of the AMPA-Sensitive GluR2 Ion Channel by Genetic Adjustment of Agonist-Induced Conformational Changes, *Proc. Nat. Acad. Sci. USA 100*, 5736–5741.
22. Romeu, A.M., Martino, E.E., and Stoppani, A.O.M. (1975) Structural Requirements for the Action of Steroids as Quenchers of Albumin Fluorescence, *Biochim. Biophysi. Acta 409*, 376–386.
23. Cowgill, R.W. (1976) *Biochemical Fluorescence, Concepts II* (Chen, R.F., and Edelhoch, H., eds.) pp. 441–486, Marcel Dekker, New York.
24. Chen, R.F. (1967) Fluorescence Quantum Yields of Tryptophan and Tyrosine, *Anal. Lett. 1*, 35–42.
25. Burstein, E.A., Vedenkina, N.S., and Ivkova, M.N. (1973) Fluorescence and the Location of Tryptophan Residues in Protein Molecules, *Photochem. Photobiol. 18*, 263–279.
26. Reutimann, H., Straub, B., Luisi, P.L., and Holmgren, A. (1981) A Conformational Study of Thioredoxin and Its Tryptic Fragments, *J. Biol. Chem. 256*, 6796–6803.
27. Yengo, C.M., Chrin, L., Rovner, A.S., and Berger, C.L. (1999) Intrinsic Tryptophan Fluorescence Identifies Specific Conformational Changes at the Actomyosin Interface upon Actin Binding and ADP Release, *Biochemistry 38*, 14515–14523.
28. Chen, Y., and Barkley, M.D. (1998) Toward Understanding Tryptophan Fluorescence in proteins, *Biochemistry 37*, 9976–9982.

[Received June 2, 2004; accepted October 11, 2004]

Identification of Genes Leading to Glucocorticoid-Induced Leukemic Cell Death

E.B. Thompson[a,*], M.S. Webb[a], A.L. Miller[a], Y. Fofanov[b] and B.H. Johnson[a]

[a]The University of Texas Medical Branch, Department of Human Biological Chemistry & Genetics, Galveston, Texas, and [b]Department of Computer Science, The University of Houston, Houston, Texas

ABSTRACT: Glucocorticoidal steroids (GC) are capable of causing apoptotic death of many varieties of lymphoid cells; consequently, GC are used in therapy for many lymphoid malignancies. Gene transcription in the GC-treated cells is required for subsequent apoptosis, but only a few of the actual genes involved have been identified. We employed gene microarray analysis to find the network of genes involved in GC-evoked cell death, using three clones derived from the CEM lymphoid leukemia cell line. Clone C1-15 was resistant to GC-evoked apoptosis, although not necessarily to GC-induced gene transcription; the other two underwent apoptosis in the presence of GC. Clone C7-14 was subcloned from the apoptosis-sensitive parental C7 clone to establish karyotypic uniformity. The second sensitive clone, C1-6, was a spontaneous revertant from parental resistant clone C1. A period of ≥24 h in the constant presence of receptor-occupying concentrations of synthetic GC dexamethasone (Dex) was necessary for apoptosis to begin. To identify the steps leading to this dramatic event, we identified the changes in gene expression in the 20-h period preceding the onset of overt apoptosis. Cells in the log phase of growth were treated with 10^{-6} M Dex, and 2–20 h later, mRNA was prepared and analyzed using the Affymetrix HG_U95Av2 chip, containing probes for about 12,600 genes. Of these, approximately 6,000 were expressed above background. Comparisons of the basal and expressed genes in the three clones led to several conclusions: The Dex-sensitive clones shared the regulation of a limited set of genes. The apoptosis-resistant clone C1-15 showed Dex effects on a largely different set of genes. Promoter analysis of the regulated genes suggested that primary gene targets for GC often lack a classic GC response element.

Paper no. L9533 in *Lipids 39,* 821–825 (August 2004).

Steroid hormones are powerful regulators of gene expression. This regulation is carried out by a complex and imperfectly understood series of interacting mechanisms. The general outline of the process is well known, however: After entering the cell, the steroid binds to a high-affinity protein receptor molecule, which functions as a ligand-activated transcription factor. The activated receptor can then bind to sequence-specific DNA sites termed response elements (REs) or can be tethered to DNA indirectly by interaction with other transcription factors bound to their own sequence-specific sites. Combinations of such interactions also may occur. The relative frequency of use of each of these options has not been determined, and until recently the tethering mechanism was thought to cause only gene repression. Consequent to localization at the proper DNA sites, the receptor associates with a number of additional proteins, and in combination with these proteins, assists the fundamental transcription machinery to induce or repress the transcription of specific genes. Ivarie and O'Farrell (1) showed long ago, in liver-derived cells, that steroid hormones affect a specific, limited array of proteins, but in no case have all of these been identified. Gene transcription that is altered directly by glucocorticoid (GC) receptor (GR) complexes consequent to steroid receptor activation is termed "primary." The changing levels of the protein and RNA products of the genes under primary regulation may in turn alter the transcription of "secondary" genes, those regulated as a consequence of the primary events. This implies a complex network of gene regulation stemming from the initial primary events. Only recently have the tools of genomics allowed a global investigation of such networks. With these tools, several groups have initiated studies of GC-regulated genes in lymphoid cell systems (2–10).

We investigated such a network (11–13) in a system of three cell clones, which we derived from the cultured cell line CEM. This line was grown from the cells of a pediatric patient with acute lymphoblastic leukemia. Without selective pressure, clones C7 (sensitive) and C1 (resistant) were derived from the CEM line (14). Subsequently, also without selective pressure, subclones C7-14, C1-6, and C1-15 were obtained from the parental clones. C7-14 and C1-15 retained the response phenotypes to Dex of their respective parental clones, whereas C1-6 was a spontaneous revertant to sensitivity. Sensitive clones of CEM cells are killed by GC such as dexamethasone (Dex) through an apoptotic process, whereas C1-derived clones are highly resistant. C1 and its subclones contain the apparatus necessary for apoptosis, however; activation of the cAMP/protein kinase A pathway restored sensitivity to Dex (15). The sensitive clones required Dex to be present constantly for many hours to initiate and then carry out apoptosis. We focused on the network of genes regulated by Dex during the interval preceding the onset of apoptosis.

*To whom correspondence should be addressed at Department of Human Biological Chemistry & Genetics, University of Texas Medical Branch, 301 University Boulevard, Galveston, TX 77555-1068.
E-mail: bthompso@utmb.edu

Abbreviations: Dex, dexamethasone; DSIPI/GILZ, delta sleep-inducing peptide; GC, glucocorticoid; GR, GC receptor; GRE, GC response element; GRU, GC response unit; nGRE, negative GRE; PEPCK, phosphoenol pyruvate carboxy kinase, pGRE, palindromic GC response element; RE, response element.

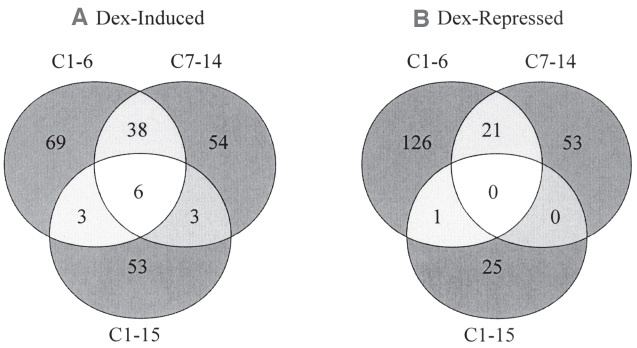

FIG. 1. Venn diagrams of CEM clones C1-6, C7-14, and C1-15 showing the number of genes induced (A) or repressed (B) after 20 h of dexamethasone treatment. For inclusion, genes had to of be "present" and induced ≥2.5-fold, or repressed ≥2-fold, in at least two of the three replicate experiments. (Modified from Ref. 11.)

In this paper, we briefly review our published results on the events in this interval. The results confirm the importance of c-*myc* repression for GC-evoked apoptosis and identify an additional limited set of genes regulated only in the two sensitive clones. Promoter analysis of the regulated genes in the sensitive clones suggests that primary induction of genes often occurs by mechanisms not employing classic GC response elements (GREs), a mechanism not yet widely recognized.

Basal gene expression. The pattern of gene expression in the absence of Dex was compared among the three clones. Clustering analysis showed that, overall, the expression of genes in this basal state differed between the C1-derived clones and clone C7-14. The basal gene expression patterns of the two C1-derived clones clustered more closely than did either clone with the C7-14 basal genes (12,13). There were, however, relative small sets of genes whose basal levels in both the sensitive clones differed from those of resistant clone, C1-15. One intriguing difference was found in caspase 4, a component of the caspase system that carries out apoptosis. Caspase 4 mRNA was expressed at somewhat higher levels in the two sensitive clones. Why such an increase would make cells selectively sensitive to GC is not clear. In general, inspection of the gene sets revealed no obvious explanations for the differing phenotypes. Thus, for example, activation of the NFκB pathway was shown in many cases to promote the viability of lymphoid cells (16). However, we found no obvious differences in the level of expression of known genes of the NFκB system that would explain the cells' sensitive/resistant phenotypes. A similar conclusion was reached for the genes of the Bcl2 family. Most of its pro- and anti-apoptotic members were expressed similarly in all three clones in the absence of Dex. DeRijk *et al.* (17) suggested that an excess of a dominant negative splice variant of the GR, GRβ, could account for some instances of GC resistance. We found no excess GRβ gene expression in the resistant clone, consistent with reports of coordinate regulation of GRα and GRβ in CEM-C7 cells (18) and a failure to find excess GRβ in childhood leukemias (19). However, many opportunities remain for tests of the relevance of other genes that did show basal differences.

Genes regulated after exposure to Dex. At a time chosen to be just at the onset of initiation of apoptosis, we identified 39 induced and 21 repressed genes regulated by Dex exclusively in the two closely related sensitive CEM clones, but not in the third closely related resistant clone (11). Based on statistical analyses, we chose cutoffs of ≥2.5-fold for induced genes and ≤2.0-fold for reduced genes to minimize the inclusion of random events. Other genes were found to be regulated exclusively in the resistant clone. The resistant clone was therefore not insensitive to GC altogether, but rather, differed in the genes it had available for regulation. A few genes were found to be regulated in both the sensitive and resistant clones (Fig. 1). From literature searches, we found that, unique to the sensitive clones, a number of the induced genes are known to promote apoptosis or inhibit cell growth in at least one cell type. Among the down-regulated genes we found c-*myc*, which we had shown previously to be important in the processes preceding apoptosis (15, 20–22). Detailed investigation of the importance of each of the newly identified genes is underway, and we have initiated a time-course analysis of the sequence of gene regulation.

Using somewhat less stringent criteria for induction, a clustering analysis was done on the induced gene sets. This analysis revealed that when Dex was added, gene expression in C1-6 shifted so that its gene expression profile more closely resembled that of the sensitive clone C7-14 (11). This result was consistent with our hypothesis that the genes found to be regulated in both sensitive clones would include those responsible for the initiation of apoptosis.

Each of the clones showed some uniquely regulated genes, allowing one to rule them out as relevant to the Dex-induced apoptosis. A few genes were induced robustly in all three clones, including that for the delta sleep-inducing peptide (DSIPI/GILZ). Kofler *et al.* (10) suggested that this gene is not induced as strongly in (most) resistant CEM cells. Our results showed that strong induction (20–30×) of DSIPI/GILZ can occur in resistant cells and therefore that such a loss of induction is not necessary for resistance.

Promoter analysis. We examined the nucleotide sequences of the promoters/regulatory regions up to approximately 2500 nt 5′ from the transcription initiation sites of the regulated genes of the sensitive clones (11). Only a minority of these genes contained a classic palindromic response element (pGRE) for the GC receptor. The pGRE consists of a specific hexanucleotide sequence followed by three nonspecific nucleotides, then the hexanucleotides in reverse order. For example, a *consensus* pGRE was TGTTCTnnnAGAACA. (In nature, few genes with a pGRE have a sequence that exactly matches the consensus.) Other genes were found to contain a half GRE (1/2 GRE), i.e., one hexamer of the classic pGRE. Many genes had neither form of the GRE. In the near vicinity of the partial or complete pGRE, we often found putative binding sites for other transcription factors with which the GC receptor could interact: AP-1, C/EBP, NFκB, OCT-1, and

CREB. This raised the question of whether the GRE-containing genes were primarily induced by Dex whereas the genes with 1/2 GRE or no GRE were secondarily induced. Our initial data from time-course studies of gene expression showed little correlation between the presence of a pGRE or 1/2 GRE and earlier induction or extent of induction (Webb, M.S., and Thompson, E.B., unpublished results). We therefore tentatively concluded that a large proportion of genes induced by Dex were activated to increase their transcription from GR tethered to heterologous sites or acting at GC response units (GRU) lacking a cognate GRE.

DISCUSSION

In this paper, we review our published data on the pre-apoptotic changes in gene expression from a single time point in three clones of CEM cells. Among these clones, after exposure to Dex for a sufficient time, two died by apoptosis whereas the third did not. All three were cloned, without selective pressure, from two initial CEM cell clones. Two of the subclones retained their parental phenotypes, one sensitive to Dex-induced apoptosis and the other resistant. These clones were pseudodiploid and karyotypically identical, with an extra chromosome 22 and a pericentric inversion of chromosome 9. The third clone was a revertant to sensitive and was pseudotetraploid. Overall, despite the closely related origins of the three clones, the pattern of gene expression in the resistant clone was quite different from the sensitive clone. The gene expression patterns of the revertant to sensitive clone resembled those of its resistant "sister" clone in the absence of Dex. When the steroid was added, the revertant showed a shift in expression of a significant number of genes, so that it then clustered with the sensitive clone. Thus, we hypothesized that a "molecular master switch" had been thrown in the revertant, allowing the response to Dex of an entire set of genes. Among these, we believe, were genes critical for the eventual apoptosis of the cells. We are now searching for the putative switch, as well as the genes critical for initiating apoptosis. Studies of the timing of regulation of the Dex-controlled genes also are underway.

To narrow the search for the critical genes, we adopted fairly stringent criteria for inclusion as induced or down-regulated. Although this could exclude some important genes truly regulated by Dex, our choice was to take criteria such that the genes identified were statistically unlikely to be random events. This led to the identification of 59 genes uniquely regulated in the sensitive cells. Some of these confirmed prior results, e.g., by showing c-*myc* down-regulation and GR up-regulation. This lent credence to the validity of the larger group of newly identified genes.

Promoter analysis of the regulated genes provided provocative information on the mechanisms through which steroids, particularly GC, and their receptors bring about gene induction. Historically, from the fact that GC induced the mouse mammary tumor virus from a regulatory region found to contain a specific GRE nucleotide sequence to which the GR bound with high affinity (23), it was concluded that such sequences would be found in all corticoid-induced genes. Careful analysis of the sequence led to the definition of the pGRE, consisting of inverted nucleotide hexamers separated by three nonspecific "spacer" nucleotides. Extensive work on other receptors in the protein family related to the GR led to the definition of other RE for each receptor class and "rules" for their structure (24–28).

Soon we found that GR–GRE interaction alone was insufficient for induction. Other proteins were found to be involved at the GR binding site and the nearby DNA in the phosphoenol pyruvate carboxy kinase (PEPCK) and tyrosine amino transferase genes, and the term GRU was proposed to indicate this more complex, multiprotein regulatory region (29,30). Elegant studies of the regulation of the PEPCK gene showed that a GRU need not contain GRE recognizable by its nucleotide sequence. In this case, the GR–DNA site binding, necessary for GC regulation of PEPCK transcription, requires simultaneous binding of adjacent heterologous, site-specific factors (31). Extensive work on several genes confirmed the general idea of a multiprotein complex, with the discovery of chromatin-modifying proteins that tether to the GR, on its GRE site (32).

Repression of transcription by the GR took a different course. Although one or two "negative GRE" (nGRE) in the regulatory DNA regions of specific genes were discovered (see the references in Ref. 11), they did not prove to be common. Repression also could be found in a case in which the GRE overlapped the TATA box of the osteocalcin gene, so that the GR and the essential TATA box-binding protein appeared to show steric competition (33). But a potentially more general mechanism of repression was revealed by the discovery that the GR could interact with several important and common transcription factors, such as the c-Jun component of AP-1, NFκB, CREB, and C/EBP. Some of these interactions could occur without DNA, but most often they were found to involve the GR tethered by the heterologous factor to the heterologous DNA site. In some cases, it was suggested that the GR simultaneously contacted a 1/2 GRE on the DNA (34,35).

It is not always recognized that a GRE need not be required for primary gene induction by the GR. In other words, is the type of regulation seen in PEPCK an exception or is it common? Our data suggest that primary GR-driven induction often occurs in genes lacking a full pGRE or even a 1/2 GRE in the –2.5 kb from the start of transcription. Several potential mechanisms could account for this. The GR could interact with site-specific repressors to block their repressive action. Or, as with PEPCK, the combination of GR with other proteins could bind to sites not discernable as GRE by inspection to act as positive inducers. A recent analysis of genes responding to estrogen receptors concluded that about 1/3 of the responsive genes bound estrogen receptors only indirectly (36). This is consistent with our findings for GR-responsive genes. Our data thus add to a growing body of evidence (35–37) that gene induction by GC occurs at a variety of DNA sites, many of which are not classical GRE.

We conclude: (i) Comparisons of genes expressed by closely related clones of human leukemic cells show that the clone resistant to GC-induced apoptosis has a pattern of gene expression broadly different from the sensitive clone. (ii) A clone that has spontaneously reverted from resistance to sensitivity has a pattern of gene expression close to that of its resistant sister clone in the basal state. Dex causes a switch in gene expression such that the gene expression pattern of the revertant moves closer to that of the sensitive clone. This suggests that a molecular master switch has changed the ability of many genes to respond to the steroid. (iii) By a set of stringent criteria, 38 Dex-induced and 21 Dex-repressed genes have been identified that are distinct from the sensitive clones. (iv) Promoter analysis of the regulated genes has revealed that many lack classic GREs.

ACKNOWLEDGMENT

Supported by grant NCI 2RO1 CA41407 to E.B.Thompson.

REFERENCES

1. Ivarie, R.D., and O'Farrell, P.H. (1978) The Glucocorticoid Domain: Steroid-Mediated Changes in the Rate of Synthesis of Rat Hepatoma Proteins, *Cell 13,* 41–55.
2. Tonko, M., Ausserlechner, M.J., Bernhard, D., Helmberg, A., and Kofler, R. (2001) Gene Expression Profiles of Proliferating vs. G1/G0 Arrested Human Leukemia Cells Suggest a Mechanism for Glucocorticoid-Induced Apoptosis, *FASEB J. 15*, 693–699.
3. Obexer, P., Certa, U., Kofler, R., and Helmberg, A. (2001) Expression Profiling of Glucocorticoid-Treated T-ALL Cell Lines: Rapid Repression of Multiple Genes Involved in RNA-, Protein- and Nucleotide Synthesis, *Oncogene 20*, 4324–4336.
4. Ferrando, A.A., Neuberg, D.S., Staunton, J., Loh, M.L., Huard, C., Raimondi, S.C., Behm, F.G., Pui, C.H., Downing, J.R., Gilliland, D.G. *et al.* (2002) Gene Expression Signatures Define Novel Oncogenic Pathways in T Cell Acute Lymphoblastic Leukemia, *Cancer Cell 1,* 75–87.
5. Wang, Z., Malone, M.H., He, H., McColl, K.S., and Distelhorst, C.W. (2003) Microarray Analysis Uncovers the Induction of the Proapoptotic BH3-Only Protein Bim in Multiple Models of Glucocorticoid-Induced Apoptosis, *J. Biol. Chem. 278,* 23861–23867.
6. Chauhan, D., Auclair, D., Robinson, E.K., Hideshima, T., Li, G., Podar, K., Gupta, D., Richardson, P., Schlossman, R.L., Krett, N., *et al.* (2002) Identification of Genes Regulated by Dexamethasone in Multiple Myeloma Cells Using Oligonucleotide Arrays, *Oncogene 21,* 1346–1358.
7. Maurer, M., Trajanoski, Z., Frey, G., Maurer, M., Trajanoski, Z., Frey, G., Hiroi, N., Galon, J., Willenberg, H.S., Gold, P.W., Chrousos, G.P., Scherbaum, W.A., and Bornstein, S.R. (2001) Differential Gene Expression Profile of Glucocorticoids, Testosterone, and Dehydroepiandrosterone in Human Cells, *Horm. Metab. Res. 33,* 691–695.
8. Galon, J., Franchimont, D., Hiroi, N., Frey, G., Boettner, A., Ehrhart-Bornstein, M., O'Shea, J.J., Chrousos, G.P., and Bornstein, S.R. (2002) Gene Profiling Reveals Unknown Enhancing and Suppressive Actions of Glucocorticoids on Immune Cells, *FASEB J. 16,* 61–71.
9. Yoshida, N.L., Miyashita, T., U, M., Yamada, M., Reed, J.C., Sugita, Y., and Oshida, T. (2002) Analysis of Gene Expression Patterns During Glucocorticoid-Induced Apoptosis Using Oligonucleotide Arrays, *Biochem. Biophys. Res. Commun. 293,* 1254–1261.
10. Kofler, R., Schmidt, S., Kofler, A., and Ausserlechner, M.J. (2003) Mechanisms of Steroid Action and Resistance in Inflammation. Resistance to Glucocorticoid-Induced Apoptosis in Lymphoblastic Leukemia, *J. Endocrinol. 178*, 19–27.
11. Medh, R.D., Webb, M.S., Miller, A.L., Johnson, B.H., Fofanov, Y., Li, Y., Wood, T., Luxon, B.A., and Thompson, E.B. (2003) Gene Expression Profile of Human Lymphoid CEM Cells Sensitive and Resistant to Glucocorticoid-Evoked Apoptosis, *Genomics 81,* 543–555.
12. Webb, M.S., Miller, A.L., Johnson, B.H., Fofanov, Y., Li, T., Wood, T., and Thompson, E.B. (2003) Gene Networks in Glucocorticoid-Evoked Apoptosis of Leukemic Cells, *J. Steroid Biochem. Mol. Biol. 85,* 183–193.
13. Thompson, E.B., and Johnson, B.H. (2003) Regulation of a Distinctive Set of Genes in Glucocorticoid-Evoked Apoptosis in CEM Human Lymphoid Cells, *Recent Prog. Horm. Res. 58*, 175–197.
14. Norman, M.R., and Thompson, E.B. (1977) Characterization of a Glucocorticoid-Sensitive Human Lymphoid Cell Line, *Cancer Res. 37*, 3785–3791.
15. Medh, R.D., Saeed, M.F., Johnson, B.H., and Thompson, E.B. (1998) Resistance of Human Leukemic CEM-C1 Cells Is Overcome by Synergism Between Glucocorticoid and Protein Kinase A Pathways: Correlation with c-*myc* Suppression, *Cancer Res.* 58, 3684–3693.
16. Li, X., and Stark, G.R. (2002) NFκB-Dependent Signaling Pathways, *Exper. Hematol. 30*, 285–296.
17. DeRijk, R.H., Schaaf, M., and de Kloet, E.R. (2002) Glucocorticoid Receptor Variants: Clinical Implications, *J. Steroid Biochem. Mol. Biol. 81*, 103–122.
18. Pedersen, K.B., and Vedeckis, W.V. (2003) Quantification and Glucocorticoid Regulation of Glucocorticoid Receptor Transcripts in Two Human Leukemic Cell Lines, *Biochemistry 42*, 10978–10990.
19. Haarman, E.G., Kaspers, G.J., Pieters, R., Rottier, M.M., and Veerman, A.J. (2004) Glucocorticoid Receptor α, β and γ Expression vs. *in vitro* Glucocorticoid Resistance in Childhood Leukemia, *Leukemia 18*, 530–537.
20. Yuh,Y.-S., and Thompson, E.B. (1989) Glucocorticoid Effect on Oncogene/Growth Gene Expression in Human T Lymphoblastic Leukemic Cell Line CCRF-CEM: Specific c-*myc* mRNA Suppression by Dexamethasone, *J. Biol. Chem. 264,* 10904–10910.
21. Thulasi, R., Harbour, D.V., and Thompson, E.B. (1993) Suppression of c-*myc* Is a Critical Step in Glucocorticoid-Induced Human Leukemic Cell Lysis, *J. Biol. Chem. 268,* 18306–18312.
22. Zhou, F., Medh, R.D., and Thompson, E.B. (2000) Glucocorticoid Mediated Transcriptional Repression of c-*myc* in Apoptotic Human Leukemic CEM Cells, *J. Steroid Biochem. Mol. Biol. 73,* 195–202.
23. Beato, M., Arnemann, J., Chalepakis, G., Slater, E., and Willmann, T. (1987) Gene Regulation by Steroid Hormones, *J. Steroid Biochem. 27(1–3)*, 9–14.
24. Dean, D.M., and Sanders, M.D. (1996) Ten Years After: Reclassification of Steroid-Responsive Genes, *Mol. Endocrinol. 10,* 1489–1495.
25. Payvar, F., Wrange, Ö., Carlstedt-Duke, J., Okret, S., Gustafsson, J.-Å., and Yamamoto, K.R. (1981) Purified Glucocorticoid Receptors Bind Selectively *in vitro* to a Cloned DNA Fragment Whose Transciption Is Regulated by Glucocorticoids *in vivo, Proc. Natl. Acad. Sci. USA 78*, 6628–6632.
26. Mangelsdorf, D.J., Thummel, C., and Beato, M. (1995) The Nuclear Receptor Superfamily: The Second Decade*, Cell 83,* 835–839.
27. Evans, R.M. (1988) The Steroid and Thyroid Hormone Receptor Superfamily, *Science 240,* 889–895.

28. Umesono, K., Murakami, K.K., Thompson, C.C., and Evans, R.M. (1991) Direct Repeats as Selective Response Elements for the Thyroid Hormone, Retinoic Acid, Vitamin D_3 Receptors, *Cell 65,* 1255–1266.
29. Imai, E., Stromstedt, P.E., Quinn, P.G., Carlstedt-Duke, J., Gustafsson, J.A., and Granner, D.K. (1990) Characterization of a Complex Glucocorticoid Response Unit in the Phosphoenolpyruvate Carboxykinase Gene, *Mol. Cell. Biol. 10,* 4712–4719.
30. Grange, T., Roux, J., Rigaud, G., and Pictet, R. (1991) Cell-Type Specific Activity of Two Glucocorticoid Responsive Units of Rat Tyrosine Aminotransferase Gene Is Associated with Multiple Binding Sites for C/EBP and a Novel Liver-Specific Nuclear Factor, *Nucleic Acids Res. 19,* 131–139.
31. Sutherland, C., O'Brien, R.M., and Granner, D.K. (1996) New Connections in the Regulation of PEPCK Gene Expression by Insulin, *Philos. Trans. R. Soc. Lond. B: Biol. Sci. 351,* 191–199.
32. Edwards, D.P. (1999) Coregulatory Proteins in Nuclear Hormone Receptor Action, *Vitam. Horm. 55,* 165–218.
33. Meyer, T., Gustafsson, J.A., and Carstedt-Duke, J. (1997) Glucocorticoid-Dependent Transcriptional Repression of the Osteocalcin Gene by Competitive Binding at the TATA Box, *DNA Cell Biol. 16,* 919–927.
34. Jonat, C., Stein, B., Ponta, H., Herrlich, P., and Rahmsdorf, H.J. (1992) Positive and Negative Regulation of Collagenase Gene Expression, *Matrix Suppl. 1,* 145–155.
35. Yamamoto, K.R., Darimont, B.D., Wagner, R.L., and Iniguez-Lluhi, J.A. (1998) Building Transcriptional Regulatory Complexes: Signals and Surfaces, *Cold Spring Harb. Symp. Quant. Biol. 63*, 587–598.
36. O'Lone, R., Frith, M.C., Karlsson, E.K., and Hansen, U. (2004) Genomic Targets of Nuclear Estrogen Receptors, *Mol. Endocrinol. 18*, 1859–1875.
37. Rogatsky, I., Leucke, H.F., Leitman, D.C., and Yamamoto, K.R. (2002) Alternate Surfaces of Transcriptional Coregulator GRIP1 Function in Different Glucocorticoid Receptor Activation and Repression Contexts, *Proc. Natl. Acad. Sci. USA 99*, 16701–16706.

[Received June 28, 2004; accepted October 10, 2004]

Comparison of the Lymphatic Transport of Radiolabeled 1,3-Dioleoylglycerol and Trioleoylglycerol in Rats

Teruyoshi Yanagita[a,*], Ikuo Ikeda[b], Yu-ming Wang[a], and Hideaki Nakagiri[b]

[a]Laboratory of Nutrition Biochemistry, Department of Applied Biological Sciences, Saga University, Saga 840-8502, Japan, and [b]Laboratory of Nutrition Chemistry, Division of Bioresource and Bioenviromental Science, Graduate School Kyushu University, Fukuoka 812-8581, Japan

ABSTRACT: It has been reported that, compared with TAG, DAG suppresses postprandial hypertriacylglycerolemia and reduces visceral fat levels in experimental animals and humans. To clarify the mechanism responsible for these beneficial effects, we compared the lymphatic transport of 1,3-DAG, a major isomer of DAG, and TAG in rats. Male SD rats, after insertion of a cannula into the thoracic duct, were given 1,3-di[1-^{14}C]oleoylglycerol or tri[1-^{14}C]oleoylglycerol *via* a stomach tube. The 24-h recovery of the radioactivity from 1,3-di[^{14}C]oleoylglycerol in the lymph was slightly but significantly lower than that from tri[^{14}C]oleoylglycerol (81.3 ± 1.0 vs. 86.5 ± 1.2%, respectively). However, in the first 1-h interval after administration, the recovery of radioactivity from 1,3-dioleoylglycerol was almost half of that from trioleoylglycerol (17.5 ± 2.0 vs. 31.1 ± 1.4%). The amount of TAG and phospholipids secreted into the lymph was significantly lower 1 h after the administration of 1,3-dioleoylglycerol compared with that after the administration of trioleoylglycerol. More than 90% of the radioactivity recovered in the lymph in the first 3 h was distributed in the TAG fraction for both 1,3-dioleoylglycerol and trioleoylglycerol. These results suggest that slower lymphatic transport of 1,3-DAG compared with TAG could be a factor in the suppression of postprandial hypertriacylglycerolemia. The possibility that the slower lymphatic transport of DAG contributes to the antiobesity action observed in the feeding of 1,3-DAG cannot be excluded.

Paper no. L9496 in *Lipids 39,* 827–832 (September 2004).

Because hyperlipidemia and obesity are risk factors of life style-related diseases such as diabetes, hypertension, and cardiovascular heart diseases, their prevention is an important issue in human health. Several human studies have shown that DAG, compared with the corresponding TAG, suppresses postprandial hypertriacylglycerolemia (1,2) and reduces body fat mass as a long-term effect (3,4). Antiobese effects of DAG oil have been demonstrated in obese model mice (5,6) and rats (7,8) although there are some arguments on its efficacy in Wistar rats (9,10). Murase *et al*. (5) proposed that the feeding of DAG caused an increase in β-oxidation in the liver of rats. However, since DAG is not known to reach the liver directly, the issue of how DAG stimulates β-oxidation in the liver is unclear. Murata *et al*. (11) showed that, when DAG was administered to the stomach of rats, the lymphatic transport of TAG was lower than when TAG was given. The low intestinal absorption of DAG may be one of the causes of the reduction of postprandial hypertriacylglycerolemia and body fat accumulation. However, Taguchi *et al*. (12) reported that the fecal excretion of lipids remained the same irrespective of whether DAG or TAG was fed to rats, suggesting that the intestinal absorption of DAG and TAG are the same. The causes of this inconsistency are not understood.

In the present study, the rate of lymphatic secretion of lipids after a stomach infusion of a DAG emulsion vs. a TAG emulsion was determined using [^{14}C]-labeled TAG and 1,3-DAG in rats that had been cannulated in the thoracic duct, as a means to compare the lymphatic transport of DAG and TAG.

MATERIALS AND METHODS

Materials. Tri[1-^{14}C]oleoylglycerol (98% purity, Amersham Pharmacia Biotech, Tokyo, Japan) and 1,3-di[1-^{14}C]oleoylglycerol (97% purity, Amersham Pharmacia Biotech) were kindly supplied by the Kao Co. Ltd. (Tokyo, Japan). The specific radioactivities were 492 MBq/mmol and 3.8 Gbq/mmol, respectively. Trioleoylglycerol and 1,3-dioleoylglycerol were purchased from Sigma (Tokyo, Japan). To prevent conversion to 1,2-DAG by acyl migration, 1,3-dioleoylglycerol was stored at −80°C upon receipt from the manufacturer. The other chemicals and reagents were purchased from Wako Pure Chemicals (Osaka, Japan).

Cannulation in the thoracic duct of rats. Male SD rats (8 wk old, body weight 280–330 g) were obtained from Seac Yoshitomi (Fukuoka, Japan). After a 1-wk adaptation period, a cannula was inserted into the left thoracic channel to collect lymphatic fluid and a catheter was also inserted into the stomach (13,14). After the surgery, a physiological solution containing 139 mM glucose and 85 mM NaCl was continuously infused overnight at a rate of 3.4 mL/h through the stomach cannula. The same solution was also provided as drinking water. On the next day, the rats were infused with 3 mL of an emulsion in the form of a single bolus through the stomach catheter. Emulsions containing 1 μCi 1,3-di[^{14}C]oleoylglycerol or tri[^{14}C]oleoylglycerol, 200 mg 1,3-dioleoylglycerol or trioleoylglycerol, 50 mg of FA-free albumin, and 200 mg of sodium taurocholate were prepared by ultrasonication. After infusing the DAG or TAG emulsions into the rats, the infusion of the glucose/NaCl solution was continued. Lymph was collected for analysis during the following intervals

*To whom correspondence should be addressed.
E-mail: yanagitt@cc.saga-u.ac.jp,

after the infusion: 0–1, 1–2, 2–3, 3–4, 4–5, 5–6, 6–8, and 8–24 h. All aspects of the experiment were conducted according to the guidelines provided by the ethical committees of experimental animal care at Kyushu University.

Measurement of lipid concentrations in lymph. Lymphatic TAG and total cholesterol concentrations were determined using commercial kits supplied by Wako Pure Chemicals following the procedure recommended by the manufacturer. Lipids were extracted and purified by the method of Bligh and Dyer (15). The concentration of phospholipids was quantified based on phosphorus content as reported previously (16).

Separation of radioactivity in lipid fractions. Neutral lipid subclasses were separated on silica gel type G TLC plates using petroleum ether/diethyl ether/acetic acid (80:20:1, by vol) (Wako Product, Osaka, Japan) as the eluent. The radioactivity was measured with an imaging plate and bio-imaging analyzer BAS 1000 system (Fuji Photograph Film Company Ltd., Kanagawa, Japan).

Statistical analyses. All values are presented as the mean ± SE. Significant differences in the means between the TAG and DAG groups at each interval were established using Student's *t*-test at the level of $P < 0.05$ (17).

RESULTS

Total recovery of radioactivity in lymph. Lymph flow rates were 141 ± 16 and 124 ± 10 mL/24 h in the TAG and DAG groups, respectively. There was no significant difference between the two groups. The cumulative recovery and secretion rate for each interval for the radioactivity in the lymph are shown in Figure 1. During the first 1 h after the administration of 1,3-di[^{14}C]acylglycerol, the recovery of radioactivity in the lymphatic fluid was almost half the amount obtained in the rats after the administration of tri[^{14}C]acylglycerol (17.5 ± 2.0 vs. 31.1 ± 1.4%). At 24 h after the infusion, the cumulative recovery of radioactivity for the infusion of DAG was slightly but significantly lower compared with that for TAG (81.3 ± 1.0 vs. 86.5 ± 1.2%).

Recovery of radioactivity in various lipid subfractions of lymph. The recovery of radioactivity in various lipid fractions of the lymph for the first three intervals is shown in Figure 2. The recoveries of radioactivity in the TAG, DAG, and phospholipid fractions were significantly lower in the case of the DAG group than in the TAG group 1 h after ingestion. The recovery for the free cholesterol fraction was significantly higher in the DAG group. The recovery for the esterified cholesterol and FFA fractions was comparable between the two groups. After these three intervals, no significant differences between treatment groups were observed for any of these lipid fractions.

Distribution of radioactivity in lipid subfractions of lymph. The distribution of radioactivity in TAG, phospholipids, free cholesterol, FFA, and cholesterol esters is shown in Table 1 for the first three intervals. More than 90% of the total radioactivity from both TAG and DAG was recovered in the TAG fraction at every time interval. During 0–1 h, the percentage incorporation into TAG for the DAG group was significantly lower and that for free cholesterol, FFA, and esterified cholesterol was significantly higher than that in the TAG group. The difference in these values was less in later intervals, except for free cholesterol.

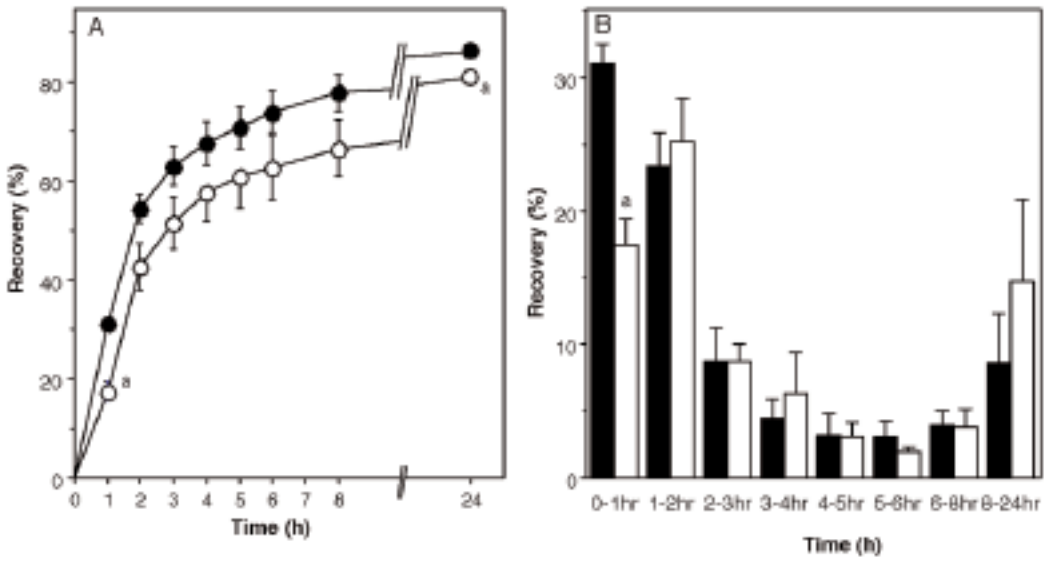

FIG. 1. Cumulative recovery (A) and secretion rate for each interval (B) for ^{14}C-radioactivity in the thoracic duct lymph of rats infused with an emulsion containing 1,3-di[^{14}C]oleoylglycerol or tri[^{14}C]oleoylglycerol. Values are expressed as the percent recovery of administered labeled dioleoylglycerol or trioleoylglycerol. Closed circles and closed bars denote the trioleoylglycerol group, and open circles and open bars denote the 1,3-dioleoylglycerol group. Each value represents the mean ± SE for seven rats. Values with a superscript "a" are significantly different from the corresponding values of the rats infused with ^{14}C-labeled trioleoylglycerol at $P < 0.05$.

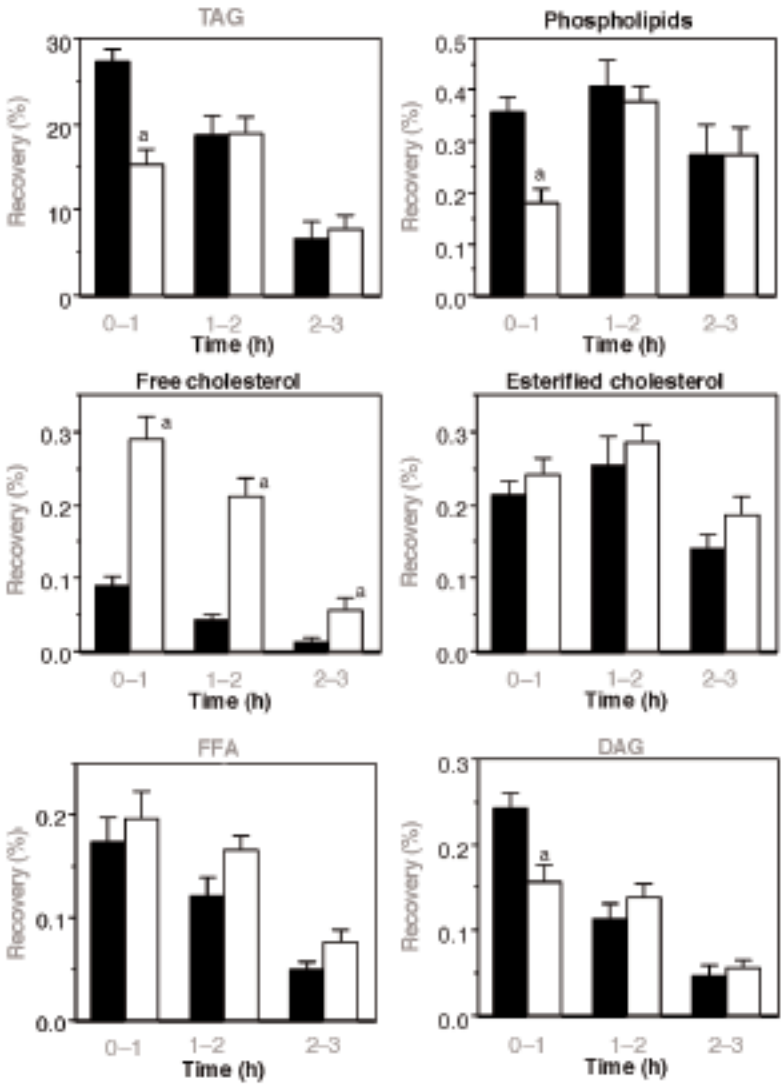

FIG. 2. Recovery of radioactivity in various lipid fractions for the first three time intervals in the thoracic duct lymph of rats infused with an emulsion containing 1,3-di[^{14}C]oleoylglycerol (open bars) or tri[^{14}C]oleoylglycerol (solid bars).Values are expressed as the percent recovery of administered labeled dioleoylglycerol or trioleoylglycerol. Each value represents the mean ± SE for seven rats. Values with a superscript "a" are significantly different from the corresponding values for the rats infused with ^{14}C-labeled trioleoylglycerol at $P < 0.05$.

Distribution of masses of various lipids in lymph. The amounts of TAG, cholesterol, and phospholipids secreted in the first three intervals after the infusion are shown in Figure 3. The amounts of TAG and phospholipids secreted into the lymph were significantly lower for the 0–1 h interval after the administration of dioleoylglycerol compared with that for trioleoylglycerol. There were no differences between the two groups in the rate of secretion of cholesterol into the lymphatic fluid.

DISCUSSION

These results clearly show that the lymphatic recovery of radioactivity in the first hour after the administration of ^{14}C-1,3-dioleoylglycerol was almost half that for ^{14}C-trioleoylglycerol, and that this accounts for 14% of the total radioactivity ingested (Fig. 1). The amount of TAG was also significantly lower in the DAG group 1 h after administration (Fig. 3), and this difference tended to continue for 8 h after the administration. However, the difference in total recovery at 24 h was only 5%, because the recovery of radioactivity at 8–24 h tended to be higher for the DAG group than in the TAG group (Fig. 1). More than 90% of the radioactivity was present in the TAG fraction for the administration of both dioleoylglycerol and trioleoylglycerol (Table 1). These results indicate that most of the FA that originate from dietary DAG are transported to the lymph as TAG and that their transport is delayed, compared with that for TAG. Taguchi *et al.* (1) and Tada *et al*. (2) showed that postprandial hypertriacylglycerolemia was suppressed when DAG

TABLE 1
Composition[a] of Radioactivity Incorporated into Lymphatic Lipids After Infusion (%)

Infused lipid	TAG	Phospholipids	Free cholesterol	FFA	Esterified cholesterol
0–1 h					
Trioleoylglycerol	96.2 ± 0.2	1.3 ± 0.1	0.3 ± 0.1	0.6 ± 0.1	0.8 ± 0.1
1,3-Dioleoylglycerol	93.4 ± 0.2*	1.1 ± 0.1	1.8 ± 0.1*	1.2 ± 0.1*	1.5 ± 0.1*
1–2 h					
Trioleoylglycerol	95.2 ± 0.3	2.1 ± 0.1	0.2 ± 0.1	0.6 ± 0.1	1.3 ± 0.2
1,3-Dioleoylglycerol	94.1 ± 0.4	1.9 ± 0.1	1.1 ± 0.1*	0.9 ± 0.1	1.5 ± 0.1
2–3 h					
Trioleoylglycerol	90.5 ± 1.5	4.7 ± 0.7	0.2 ± 0.1	1.0 ± 0.2	2.9 ± 0.7
1,3-Dioleoylglycerol	91.7 ± 0.8	3.4 ± 0.4	0.7 ± 0.2*	1.0 ± 0.1	2.6 ± 0.5

[a]Values are means ± SE for seven rats. Asterisk (*) indicates significant difference at $P < 0.05$ from the corresponding values for the rats infused with [^{14}C]-labeled trioleoylglycerol.

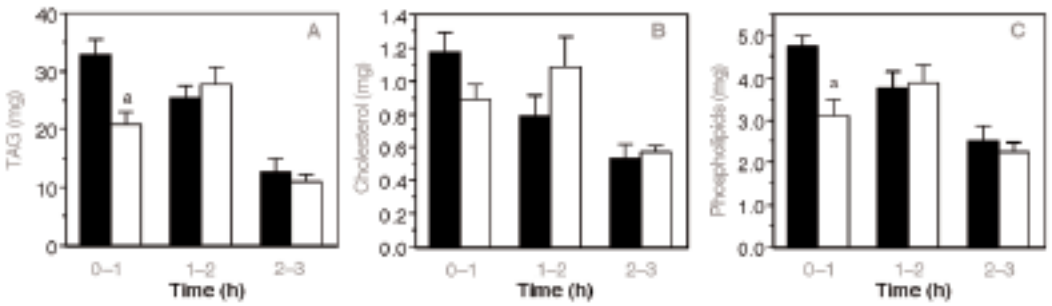

FIG. 3. Distribution of TAG mass (A), total cholesterol (B), and phospholipids (C) in the thoracic duct lymph in rats infused with an emulsion containing 1,3-di[^{14}C]oleoylglycerol (open bars) or tri[^{14}C]oleoylglycerol (solid bars). Each value represents the mean ± SEM for seven rats. Values with a superscript "a" are significantly different from the corresponding values for the rats infused with ^{14}C-labeled trioleoylglycerol at $P<0.05$.

was fed compared with TAG in humans. The present results strongly suggest that the suppression in postprandial hypertriacylglycerolemia by dietary DAG is mainly the result of the delayed transport of TAG from intestinal cells to the lymph.

In an earlier study, Murata *et al*. (11) followed the lymphatic recovery of TAG for 5 h after the infusion of TAG or DAG. They infused an emulsion containing DAG or TAG at a rate of 3 mL/h for 1 h and observed a lower recovery of TAG in the case of DAG infusion, compared with the TAG, at 2–3 h after the beginning of the infusion. Since they collected lymph for only 5 h, the cumulative recovery of TAG was significantly lower at 5 h in the DAG infusion. We conclude that the collection time for lymph was too short in that study to measure the total recovery of TAG and DAG absorbed in the intestine.

It is well established that ingested TAG is hydrolyzed to 2-MAG and FA in the small intestine (18). In contrast to TAG digestion, it has been shown, in an intragastric infusion experiment, that 1,3-DAG is hydrolyzed to 1- (or 3)-MAG and FA as the result of digestion by pancreatic lipase (7,19). Since 1(3)-monooleoylglycerol was detected in rat intestinal epithelial cells after the intraduodenal infusion of 1,3-di[1-^{14}C]oleoylglycerol, it is possible that it is directly incorporated into intestinal epithelial cells (19). Alternatively, it is possible that 1(3)-MAG is further hydrolyzed to a FA and glycerol in the intestinal lumen (19). 2-MAG is readily re-esterified to TAG in intestinal cells through the 2-MAG pathway (18). Although the direct pathway involved with the synthesis of TAG from 1(3)-MAG in intestinal cells is not known with certainty, it is thought that the 1(3)-MAG may be hydrolyzed to FA and glycerol in such cells. When ^{14}C-linoleic acid and 1(3)-MAG were incubated with intestinal epithelial cells, the radioactivity was detected as 1,3-DAG (19). Therefore, at least part of the 1(3)-MAG incorporated into intestinal epithelial cells may be enzymatically converted to 1,3-DAG. However, since the synthesis of TAG from 1,3-DAG is much lower than that from 1,2-DAG (15), 1,3-DAG must eventually be hydrolyzed to 1(3)-MAG, and then glycerol and FFA by yet unidentified lipases, which are known to be present in intestinal cells.

Most of the dietary 1,3-DAG are hydrolyzed to FFA and glycerol in intestinal cells. Although the TAG content of chylomicrons after the ingestion of DAG was slightly lower than that after the TAG ingestion, the majority of the chylomicron lipids were TAG (Table 1). These results indicate that most of the ingested DAG is resynthesized to TAG after its hydrolysis to FFA. Because 2-MAG cannot be supplied in sufficient quantity during the absorption of 1,3-DAG, TAG synthesis may proceed *via* the glycerol-3-phosphate pathway, which is less active than the 2-MAG pathway (18). Thus, the reduced rate of TAG synthesis could be a factor in the slow rate of TAG secretion to the lymph.

Our results show that the total 24-h recovery of di[1-^{14}C]oleoylglycerol was about 5% lower than that of tri[1-^{14}C]oleoylglycerol. Taguchi *et al.* (12) reported that the fecal excretion of FA after the feeding of DAG was almost the same as that for TAG, suggesting that the intestinal absorption of DAG is comparable to that of TAG. There are three possible causes for the slightly lower recovery of FA from 1,3-DAG in the lymph. First, a portion of the FA from DAG might have been transferred to the portal vein. Watanabe *et al.* (7) reported an increase in portal venous FA after the ingestion of DAG compared with TAG. They proposed that FA transported *via* the portal vein might undergo preferential β-oxidation in the liver (7). It is well-known that medium-chain FA are transported *via* the portal vein to the liver and are also preferentially β-oxidized. Although it is well established that most long-chain FA are nearly quantitatively absorbed as chylomicron TAG *via* the lymph (20), the portal venous transport of long-chain FA has been reported (21). It has been reported that the partitioning of long-chain FA between portal blood and lymph is dependent on the luminal milieu, the polarity of the FA and the rate of absorption (21). Therefore, the possibility that slower lymphatic secretion after DAG infusion might have increased the amount of FA partitioned to portal venous transport cannot be ruled out.

Second, the possibility that a portion of the FA from DAG are β-oxidized in intestinal cells cannot be excluded. Murase *et al.* (6) reported that, when DAG was fed to mice for 10 d, intestinal β-oxidation was stimulated. They also observed an increase in the expression of acyl-CoA oxidase mRNA, medium-chain acyl-CoA dehydrogenase mRNA, and uncoupling protein-2 mRNA in the intestine. We observed that when 1,3-di[1-^{14}C]oleoylglycerol or tri[1-^{14}C]oleoylglycerol was intragastrically administered to rats cannulated in the thoracic duct, a small but significantly higher radioactivity originating from 1,3-dioleoylglycerol was detected in the free cholesterol fraction of lymph lipids compared with that from TAG (Fig. 2). Therefore, the possibility that a small portion of [1-^{14}C]oleic acid released from di[1-^{14}C]oleoylglycerol was more effectively β-oxidized to acetyl CoA than that from TAG and then utilized as a substrate for cholesterol synthesis cannot be excluded.

Third, the intestinal absorption of DAG over a 24-h period might be less effective than that of TAG under the experimental conditions used here because the lymphatic transport of DAG was delayed. The lymphatic recovery of radioactivity at 8–24 h after the administration of DAG tended to be higher than that of TAG as shown in Figure 1. This suggests that a longer time might be required for the complete transport of radioactivity from DAG than from TAG. Therefore, if lymph were to be collected for more than 24 h, a greater fraction of the total radioactivity might be recovered in the DAG group than in the TAG group.

Dietary DAG reportedly has antiobesity activity and prevents postprandial hypertriacylglycerolemia in experimental animals and humans (1,3,5–7), and mechanisms have been proposed. Murata *et al.* (22) and Murase *et al.* (5) reported that hepatic β-oxidation may possibly be stimulated by the feeding of DAG compared with TAG in rats and mice. However, the issue of how dietary DAG stimulates hepatic β-oxidation has never been clearly explained. Both reports indicated that the feeding of DAG reduced hepatic TAG levels in rats and mice. Recently, Murase *et al.* (6) showed that intestinal β-oxidation was enhanced after the feeding of DAG in mice. Watanabe *et al.* (7) showed that postprandial oxygen consumption was increased in rats that were fed DAG for 7 d, compared with those fed TAG. These observations suggest that dietary DAG may activate hepatic and intestinal β-oxidation, thus increasing energy expenditure.

We propose here an alternative mechanism for the antiobese activity of DAG. Our findings indicate that the lymphatic transport of chylomicron TAG in rats that are fed DAG is delayed. This may be the reason why DAG suppresses postprandial hypertriacylglycerolemia in rats and humans (1,7). The delayed lymphatic transport of DAG, compared with TAG, may be an important determinant in preventing the accumulation of body fat. Han *et al.* (23,24) pointed out that slower absorption of dietary fat prevents body fat accumulation in mice. A nibbling meal pattern, in contrast to a gorging meal pattern, suppresses body fat accumulation in humans and experimental animals (25–27). Postprandial hypertriacylglycerolemia would be predicted to be higher in the case of a gorging meal pattern compared with a nibbling meal pattern. However, since these hypotheses cannot necessarily be experimentally proved, studies are now in progress to investigate the mechanism associated with the delayed lymphatic transport of FA from dietary DAG, which causes the suppression of body fat accumulation.

REFERENCES

1. Taguchi, H., Watanabe, H., Onizawa, K., Nagao, T., Gotoh, N., Yasukawa, T., Tsushima, R., Shimasaki, H., and Itakura, H. (2000) Double-Blind Controlled Study on the Effects of Dietary Diacylglycerol on Postprandial Serum and Chylomicron Triacylglycerol Responses in Healthy Humans, *J. Am. Coll. Nutr. 19*, 789–796.
2. Tada, N., Watanabe, H., Matsuo, N., Tokimitsu, I., and Okazaki, M. (2001) Dynamics of Postprandial Remnant-like Lipoprotein Particles in Serum After Loading of Diacylglycerol, *Clin. Chim. Acta 311*, 109–117.
3. Nagao, T., Watanabe, H., Goto, N., Onizawa, K., Taguchi, H., Matsuo, N., Yasukawa, T., Tsushima, R., Shimasaki, H., and Itakura, H. (2000) Dietary Diacylglycerol Suppresses Accumulation of Body Fat Compared to Triacylglycerol in Men in a Double-Blind Controlled Trial, *J. Nutr. 130*, 792–797.
4. Maki, K.C., Davidson, M.H., Tsushima, R., Matsuo, N., Tokimitsu, I., Umporowicz, D.M., Dicklin, M.R., Foster, G.S., Ingram, K.A., Anderson, B.D., *et al.* (2002) Consumption of Diacylglycerol Oil as Part of a Reduced-Energy Diet Enhances Loss of Body Weight and Fat in Comparison with Consumption of a Triacylglycerol Control Oil, *Am. J. Clin. Nutr. 76,* 1230–1236.
5. Murase, T., Mizuno, T., Omachi, T., Onizawa, K., Komine, Y., Kondo, H., Hase, T., and Tokimitsu, I. (2001) Dietary Diacylglycerol Suppresses High Fat and High Sucrose Diet-Induced Body Fat Accumulation in C57BL/6J Mice, *J. Lipid Res. 42*, 372–378.
6. Murase, T., Aoki, M., Wakisaka, T., Hase, T., and Tokimitsu, I. (2002) Anti-obesity Effect of Dietary Diacylglycerol in C57BL/6J Mice: Dietary Diacylglycerol Stimulates Intestinal Lipid Metabolism, *J. Lipid Res. 43*, 1312–1319.

7. Watanabe, H., Onizawa, K., Taguchi, H., Kobori, M., Chiba, H., Naito, S., Matsuo, N., Yasukawa, T., Hattori, M., and Shimasaki, H. (1997) Nutritional Characterization of Diacylglycerol in Rats, *J. Jpn. Oil Chem. Soc. 46*, 301–307 (in Japanese).
8. Meng, X. Zou, D., Shi, Z., Duan, Z.n., and Mao, Z. (2004) Dietary Diacylglycerol Prevents High-Fat Diet-Induced Lipid Accumulation in Rat Liver and Abdominal Adipose Tissue, *Lipids 39,* 37–41.
9. Sugimoto, T., Kimura, T., Fukuda, H., and Iritani, N. (2003) Comparison of Glucose and Lipid Metabolism in Rats Fed Diacylglycerol and Triacylglycerol Oils, *J. Nutr. Sci. Vitaminol. 49*, 47–55.
10. Sugimoto, T., Fukuda, H., Kimura, T., and Iritani, N. (2003) Dietary Diacylglycerol-rich Oil Stimulation of Glucose Intolerance in Genetically Obese Rats, *J. Nutr. Sci. Vitaminol. 49,* 139–144.
11. Murata, M., Hara, K., and Ide, T. (1994) Alteration by Diacylglycerol of the Transport and Fatty Acid Composition of Lymph Chylomicrons in Rats, *Biosci. Biotechnol. Biochem. 58*, 1416–1419.
12. Taguchi, H., Nagao, T., Watanabe, H., Onizawa, K., Matsuo, N., Tokimitsu, I., and Itakura, H. (2001) Energy Value and Digestibility of Dietary Oil Containing Mainly 1,3-Diacylglycerol Are Similar to Those of Triacylglycerol, *Lipids 36*, 379–382.
13. Ikeda, I., Kobayashi, M., Hamada, T., Tsuda, K., Goto, H., Imaizumi, K., Nozawa, A., Sugimoto, A., and Kakuda, T. (2003) Heat-Epimerized Tea Catechins Rich in Gallocatechin Gallate and Catechin Gallate Are More Effective to Inhibit Cholesterol Absorption Than Tea Catechins Rich in Epigallocatechin Gallate and Epicatechin Gallate, *J. Agric. Food Chem. 51*, 7303–7307.
14. Ikeda, I., Kumamaru, J., Nakatani, N., Sakono, M., Murota, I., and Imaizumi, K. (2001) Mechanism of Suppression of Postprandial Hypertriglyceridemia by Docosahexaenoic Acid-rich Fish Oil in Sprague-Dawley Rats, *J. Nutr. 131*, 1159–1164.
15. Bligh, E.G., and Dyer, W.J. (1959) A Rapid Method of Total Lipid Extraction and Purification, *Can. J. Biochem. Physiol. 37*, 911–917.
16. Ikeda, I., Cha, J.Y., Yanagita, T., Nakatani, N., Oogami, K., Imaizumi, K., and Yazawa, K. (1998) Effects of Dietary α-Linolenic, Eicosapentaenoic and Docosahexaenoic Acids on Hepatic Lipogenesis and β-Oxidation in Rats, *Biosci. Biotechnol. Biochem. 62*, 675–680.
17. Snedecor, G.W., and Cochran, W.G. (1967) *Statistical Methods*, 6th edn., pp. 258–338, Iowa State University Press, Ames.
18. Friedman, H.I., and Nylund, B. (1980) Intestinal Fat Digestion, Absorption, and Transport. A Review, *Am. J. Clin. Nutr. 33*, 1108–1139.
19. Kondo, H., Hase, T., Murase, T., and Tokimitsu, I. (2003) Digestion and Assimilation Features of Dietary DAG in the Rat Small Intestine, *Lipids 38*, 25–30.
20. Ikeda, I., Yoshida, H., and Imaizumi, K. (1997) Effect of Triolein or Oleic Acid on Lymphatic Recovery of Docosahexaenoic Acid Given as Ethyl Ester and Their Intramolecular Distribution in Lymph Triglyceride of Rats, *Lipids, 32*, 949–952.
21. McDonald, G.B., and Weidman, M. (1987) Partitioning of Polar Fatty Acid into Lymph and Portal Vein After Intestinal Absorption in the Rat, *Q.J. Exp. Physiol. 72,* 153–159.
22. Murata, M., Ide, T., and Hara, K. (1997) Reciprocal Responses of Dietary Diacylglycerol of Hepatic Enzymes of Fatty Acid Synthesis and Oxidation in the Rat, *Br. J. Nutr. 77*, 107–121.
23. Han, L.-K., Takaku, T., Li, J., Kimura, Y., and Okuda, H. (1999) Anti-obesity Action of Oolong Tea, *Int. J. Obesity 23*, 98–105.
24. Han, L.–K., Kimura, Y., and Okuda, H. (1999) Reduction in Fat Storage During Chitin,-Chitosan Treatment in Mice Fed a High-Fat Diet, *Int. J. Obesity 23*, 174–179.
25. Fabry, P., Hejl, Z., Fodor, J., Braun, T., and Zvolankova, K. (1964) The Frequency of Meals: Its Relation to Overweight, Hypercholesterolaemia, and Decreased Glucose Tolerance, *Lancet ii,* 614–615.
26. Bellisle, F., McDevitt, R., and Prentice, A.M. (1997) Meal Frequency and Energy Balance, *Br. J. Nutr. 77* (suppl. 1)*,* S57–S70.
27. Baker, N., and Huebotter, J. (1973) Lipogenic Activation After Nibbling and Gorging in Mice, *J. Lipid Res. 14*, 87–94.

[Received April 27, 2004; accepted October 4, 2004]

Lipids Rich in Phosphatidylethanolamine from Natural Gas-Utilizing Bacteria Reduce Plasma Cholesterol and Classes of Phospholipids: A Comparison with Soybean Oil

Hanne Müller[a,*], Lars I. Hellgren[b], Elisabeth Olsen[c], and Anders Skrede[a,d]

[a]Department of Animal and Aquacultural Sciences, Agricultural University of Norway, N-1432 Ås, Norway, [b]Technical University of Denmark, Biocentrum-DTU and Centre for Advanced Food Studies, Dk-2800 Lyngby, Denmark, [c]MATFORSK, Norwegian Food Research Institute, N-1430 Ås, Norway, and [d]Aquaculture Protein Centre, Centre of Excellence, N-1432 Ås, Norway

ABSTRACT: We compared the effects of three different high-lipid diets on plasma lipoproteins and phospholipids in mink (*Mustela vison*). The 18 mink studied were fed one of the three diets during a 25-d period in a parallel group design. The compared diets had 0, 17, and 67% extracted lipids from natural gas-utilizing bacteria (LNGB), which were rich in PE. The group with 0% LNGB was fed a diet for which the lipid content was 100% soybean oil. The total cholesterol, LDL cholesterol, and HDL cholesterol of animals consuming a diet with 67% LNGB (67LNGB-diet), were significantly lowered by 35, 49, and 29%, respectively, and unesterified cholesterol increased by 17% compared with the animals fed a diet of 100% lipids from soybean oil (SB-diet). In addition, the ratio of LDL cholesterol to HDL cholesterol was 27% lower in mink fed the 67LNGB-diet than those fed the SB-diet. When the mink were fed the 67LNGB-diet, plasma PC, total phospholipids, lysoPC, and PI were lowered significantly compared with the mink fed a SB-diet. Plasma total cholesterol was correlated with total phospholipids as well as with PC ($R = 0.8$, $P < 0.001$). A significantly higher fecal excretion of unesterified cholesterol, cholesteryl ester, PC, lysoPC, and PE was observed in the 67LNGB-fed mink compared with the SB-fed mink. We conclude that phospholipids from the 67LNGB-diet decreased plasma lipoprotein levels, the LDL/HDL cholesterol ratio, and plasma phospholipid levels, especially lysoPC and PC, compared with the highly unsaturated soybean oil. Our findings indicate that the decrease of plasma cholesterol is mainly caused by a specific mixture of phospholipids containing a high level of PE, and not by the dietary FA composition. The lack of significant differences in the level of plasma PE due to the diets indicates that most of the PE from LNGB has been converted to PC in the liver. Thus, plasma cholesterol may at least be partly regulated by phospholipid methylation from PE to PC in the liver.

Paper no. L9551 in *Lipids 39*, 833–841 (September 2004).

The main dietary lipids are TAG, but small amounts of phospholipids occur in most foods (1). Egg yolks, meat, fish, dairy products, and several grains are relatively rich in phospholipids (2).

Bacterial protein meal (BioProtein), produced by natural gas-utilizing bacteria (3), contains a high level of crude protein (70%) and also a high level of lipids (10%). Four different bacteria—*Methylococcus capsulatus* (Bath) (88%), *Alcaligenes acidovorans* (12%), *Bacillus brevis* (0.3%), and *B. firmus* (0.2%)—have been grown using natural gas (99% methane), ammonia, and mineral salts as fermentation substrates (3). Methanotrophs (methane-oxidizing bacteria) such as *M. capsulatus* are unique in their abilities to utilize methane as their sole source of carbon and energy, and they oxidize methane to carbon dioxide for energy generation and biomass production (4). Phospholipids are the main lipid components in *M. capsulatus*. PE constitutes 74% of the total phospholipids of *M. capsulatus*, with phosphatidylglycerol (PG) (13%), PC (8%), and cardiolipin (CL) (5%) making up the rest of the phospholipids, with a FA composition that is predominantly 16:0 and 16:1 (5).

Studies on the effects of dietary phospholipids on plasma lipoproteins have been few compared with the studies on the effects of TAG. Published studies show conflicting results on the effects of different exogenous phospholipids on plasma cholesterol in both rats and humans (6–11). It has been suggested that dietary PE and ethanolamine markedly lower plasma lipoprotein levels (6–8) and that free ethanolamine may slightly reduce serum TAG (6,12). Comparisons of a diet supplemented with egg yolk phospholipid containing PE and PC, a diet supplemented with soybean PC preparations, and a diet with no supplements showed that the egg yolk supplement decreased serum total cholesterol whereas soybean PC preparations showed no effect on serum lipoproteins (6). Additionally, ethanolamine reduced total plasma cholesterol in rats (8). A study with rats further showed that dietary PE decreased serum cholesterol, HDL cholesterol, and phospholipids but had no significant influence on the concentration of lipids in the LDL cholesterol fraction (7). The latter study also indicated that the capacity of PE to reduce plasma cholesterol is not mainly caused by the dietary FA composition.

The cholesterol-reducing capacity of PC (lecithin) intake is controversial. A meta-analysis showed no evidence for a

*To whom correspondence should be addressed at Department of Animal and Aquacultural Sciences, Agricultural University of Norway, P.O. Box 5003, N-1432 Ås, Norway. E-mail: hanne.muller@iha.nlh.no

Abbreviations: 17LNGB-diet, diet with 17% lipids from natural gas-utilizing bacteria (LNGB); 67LNGB-diet, diet with 67% LNGB and 33% soybean oil; CDP, cytidine diphosphate; CETP, cholesteryl ester transfer protein; CL, cardiolipin; HPTLC, high-performance TLC; PEMT, PE methyltransferase; PG, phosphatidylglycerol; PI, phosphatidylinositol; SB-diet, diet with 100% lipids from soybean oil; SM, sphingomyelin.

specific effect of PC on total plasma cholesterol, independent of its linoleic acid content (11). Knuiman *et al.* (11) concluded that any cholesterolemic response to PC could be due to its content of linoleic acid. The effects of PC on HDL cholesterol were not the focus of the meta-analysis (11), but other studies have shown that soybean PC may increase HDL cholesterol (13,14).

The mechanism involved in a possible plasma cholesterol-lowering effect of dietary PE or ethanolamine has not been established. In a recent study, Noga and Vance (15) suggested that PE methyltransferase (PEMT) activity plays a role in regulating the levels of plasma lipoproteins. However, the role of PEMT-derived PC in lipoprotein secretion and metabolism is not entirely understood. In the liver, PC is synthesized either through the cytidine diphosphate (CDP)-choline pathway or by PE methylation *via* PEMT (16). The CDP-choline pathway is the major pathway for the biosynthesis of PC in all mammalian nucleated cells (16). *S*-Adenosylmethionine is the major methyl-group donor in the stepwise methylation of PE to PC (16), although choline also has shown to be a methyl donor in the PEMT-catalyzed reaction (17). Sehayek *et al.* (18) have suggested that local canalicular membrane PC biosynthesis, in concert with the phospholipid transporter mdr2 and scavenger receptor class B type 1, promotes excretion of phospholipid and cholesterol into the bile.

Dietary intake of lipids extracted from natural gas-utilizing bacteria can possibly influence plasma cholesterol and the predicted risk of coronary heart disease. The relationships among different dietary phospholipids with regard to plasma cholesterol remain to be elucidated. No other studies have been published on the effects of plasma lipoproteins and phospholipids in lipids from LNGB rich in PE. The aim of the present study was to study the effects of dietary LNGB phospholipids on plasma lipoproteins and classes of phospholipids, compared with a control diet containing soybean oil as the major fat source. Mink (*Mustela vison*) were used as model animals for other mammals, because of considerations such as availability of animals and research facilities, and the mink's natural adaptation to a moist diet with a high lipid content (19).

MATERIALS AND METHODS

Lipids extracted from bacterial protein meal. Bacterial protein meal (BioProtein), used for the lipid extraction, was produced by continuous aerobic fermentation using natural gas as the carbon and energy source, and ammonia as the nitrogen source for protein biosynthesis (Norferm AS, Stavanger, Norway) (3). The bacterial culture consisted of prokaryotic bacteria containing 88% *M. capsulatus* (Bath), with smaller amounts of *A. acidovorans* (12%), *B. brevis* (0.3%), and *B. firmus* (0.2%) (3). This biomass was subjected to a short heat treatment at 140°C to produce a sterile product of dead bacteria, which was then spray-dried to form a reddish-brown meal with about 96% dry matter (3) and a particle size of 150–200 μm. The lipids from the biomass were extracted by 2:1 chloroform/methanol (vol/vol) (20). After mixing with the bacterial protein meal, the solvent was tapped from the mixing tank into several filter bags with 5 μm pore size. The extraction was performed twice, and the rest of the solvent was removed by mixing the lipids at reduced pressure and high temperature. The lipid extraction was performed at Natural ASA (Hovdebygda, Norway).

Animals and diets. Eighteen farm-bred male mink (*M. vison*) of genotype standard dark (21), with birth dates between the 1st and 15th of May 2002, were randomized and fed one of three diets for a 25-d period in a parallel group design at the Department of Animal and Aquacultural Sciences at the Agricultural University of Norway. The study ran from October 25 to November 25, 2002. The body weight of the animals was monitored before they entered the experiment and at the end of the study period. The average initial weight of the mink was 2221g (SD ± 316). There were no significant differences in the initial weights of the treatments groups. During a 7-d digestibility experiment (the first week of the study), the animals were housed individually in net cages (51 × 39 × 49 cm) designed for metabolic experiments with devices to minimize contamination of feces with urine and to catch spilled feed. The temperature was kept constant at 13°C, and the daily light–dark cycle was controlled by photocells and adapted to a natural photoperiod. After the digestibility experiment, the mink were kept under conventional farm housing conditions in net cages (75 × 30.5 × 38 cm), equipped with wooden nest boxes (35 × 26 × 22 cm) to provide a secluded rest area, for the remainder of the experimental period.

The three high-lipid diets were planned using a computer-based optimization program and were designed to have the same nutrient composition (Table 1), with each diet contain-

TABLE 1
Composition of Experimental Diets (g kg^{-1})

Ingredient	SB-diet[a]	17LNGB-diet[b]	67LNGB-diet[c]
Cornstarch	62.9	62.9	62.9
Coalfish fillet	611.5	651.4	651.4
Soybean oil	91.4	61.0	15.3
Lipids from natural gas-utilizing bacteria	—	30.5	76.2
Sunflower oil	2.29	2.29	2.29
Vitamin/mineral mix[d]	0.84	0.84	0.84
BHT (100 mg/kg)	0.08	0.08	0.08
Calcium phosphate	1.63	1.63	1.63
Calcium carbonate	1.85	1.85	1.85
Water	227.5	187.7	187.7
Gross energy[e] (kJ/g, dry weight)	24.53	25.43	22.69
Total feed intake (g/d)	241.9	249.0	235.1

[a]Diet with 100% soybean oil (SB) as lipid source.
[b]Diet with 17% of lipids from natural gas-utilizing bacteria (LNGB) and 83% from SB.
[c]Diet with 67% LNGB and 33% SB.
[d]AS Norsk Mineralnæring, Hønefoss, Norway, containing per kg diet: vitamin A, 504 μg; vitamin D_3, 4.2 μg; vitamin E, 42 mg; thiamine, 12.6 mg; riboflavin, 2.5 mg; vitamin B_6, 2.5 mg; vitamin B_{12}, 17 μg; pantothenic acid, 2.5 mg; niacin, 4.2 mg; biotin, 25 μg; folate, 0.25 mg; iron, 17 mg; zinc, 6 mg; manganese, 12.6 mg; copper, 1 mg.
[e]Determined on freeze-dried samples by bomb calorimetry.

ing adequate quantities of all nutrients known to be required by mink (22). Each diet had 29.7% energy (E%) derived from protein and 14.5% from carbohydrates. The three tested diets differed in their amounts of TAG, phospholipids, and individual FA. The lipids from the background diets were planned to provide a minimal amount of 1.14 E% lipids, whereas the test lipids were planned to provide 54.6 E% in the diets. Two different test lipids were used in the three diets: soybean oil (in the control diet) and lipids extracted from BioProtein. The three high-lipid diets contained the following added lipids: (i) 100% soybean oil (SB-diet), (ii) 83% soybean oil plus 17% extracted LNGB (17LNGB-diet), and (iii) 33% soybean oil and 67% extracted LNGB (67LNGB-diet). The lipids from BioProtein, which were solid at room temperature, were mixed with the soybean oil and heated before mixing with other ingredients.

Experimental design. All the mink consumed one of the three diets for 25 d. During the first week the mink were individually fed rations providing 1100 kJ of metabolizable energy per animal per day. Thereafter, the mink were fed *ad libitum* three times a day for the rest of the feeding period. Water was available *ad libitum*. The diets were stored at –20°C and thawed in a refrigerator for 24 h before feeding. Feces were stored at –20°C, and the diets and the feces were freeze-dried before analyses. Animal care followed the guidelines given by the Norwegian Animal Research Authority. National protocols of ethical standards concerning experiments involving animals were followed regarding animal care and method of sacrifice. The animals were killed by electrocution at the end of the experiment.

Bomb calorimetry. Duplicate portions of the three freeze-dried homogenates corresponding to an estimated intake of 1100 kJ were analyzed by a Parr 1281 bomb calorimeter (Parr Instrument Company, Moline, IL).

Chemical analysis of diets. Duplicate samples were taken from the three diets and frozen at –20°C, freeze-dried, and homogenized. The nitrogen content was determined by the Kjeldahl technique. The factor used for conversion of nitrogen content to crude protein was 6.25. Starch content (including free glucose) was determined as glucose after hydrolysis by α-amylase and amyloglucosidase as described by McCleary *et al.* (23).

The total fat content was determined gravimetrically after Bligh and Dyer extraction (24). The lipid phase was slowly evaporated under nitrogen (Hydro Gas, Oslo, Norway), and the lipids were redissolved in 1 mL of benzene (p.a.; Merck KGaA, Darmstadt, Germany).

FA analysis. The FA extracted from diets and plasma were converted to methyl esters using a modified version of a method described by Mason and Waller (25) and analyzed by GLC.

One milliliter of 3 N methanolic hydrochloric acid (Supelco, Bellefonte, PA) and 200 μL of 2,2-dimethoxy propane (Sigma-Aldrich Chemie GmbH, Steinheim, Germany) were added to the benzene solutions in 20-mL reagent tubes. The tubes were flushed with nitrogen, sealed, and left overnight at room temperature. FAME were subsequently extracted in 0.5 mL of isooctane (p.a.; Merck KGaA) and the reagent tubes were filled with a saturated solution of sodium chloride (p.a.; Merck KGaA). The isooctane layer was transferred to new vials, 1 mL of a 2% solution of sodium hydrogen carbonate (p.a.; Merck KGaA) in distilled water was added, and the phases were thoroughly mixed. The isooctane layer was again transferred to new tubes and dried with anhydrous sodium sulfate (p.a., Merck KGaA) prior to analysis.

One microliter of the FAME solutions was injected splitless into a gas chromatograph (HP model no. G1530A) equipped with an autosampler (HP 6890 Series Injector) and FID. The analytes were separated on a BPX70 column (0.25 mm i.d., 60 m, 0.25 μm film; SGE, Melbourne, Australia) with helium as the carrier gas, using a temperature program of 70°C for 1 min, increasing at 30°C min^{-1} to 170°C, then 1.5°C min^{-1} to 200°C, and at 3°C min^{-1} to 220°C, with a final hold of 5 min. Peaks were integrated with HP GC ChemStation software (rev. A.05.02) and identified by comparison of the retention times with those of pure standards.

Phospholipid, free cholesterol, and cholesteryl ester analysis. The extracted phospholipids from diets and plasma were analyzed by quantitative high-performance TLC (HPTLC) using a modified version of two methods described by Macala *et al.* (26) and Ruiz and Ochoa (27). Just prior to the analyses, the samples were dried under N_2 and redissolved in a defined volume of chloroform/methanol (2:1 vol/vol). Samples and a quantitative standard mixture (a six-point standard curve ranging from 160 to 2500 ng was applied on each plate) were applied on prewashed and activated silica HPTLC plates (Silica Gel-60; Merck GmbH) using a Desaga AS-30 HPTLC applicator (Desaga GmbH, Wiesloch, Germany). The standard mixture in the analysis of plasma phospholipids contained egg yolk sphingomyelin (SM), dioleoyl-PC, dioleoyl-PI, dioleoyl-PS, and dioleoyl-PE (Avanti Polar Lipids, Alabaster, AL). For the analysis of phospholipids in the diet, dioleoyl-PC, dioleoyl-PI, dioleoyl-PS, dioleoyl-PE, dioleoyl-PG, and CL from *Escherichia choli* (Avanti Polar Lipids) were used. In the analysis of phospholipids, the HPTLC plates were developed in chloroform/methanol/acetic acid/formic acid/dH_2O (70:30:12:4:2 by vol), and in the analysis of dietary phospholipids, development was carried out in three consecutive runs in methyl acetate/*n*-propanol/chloroform/methanol/aqueous 0.25% KCl (25:25:28:10:7), increasing the length of the development by 2 cm for each run. Analyses of cholesteryl esters and free cholesterol were performed using a solvent system consisting of heptane/diethyl ether/formic acid (85:15:1) with a standard curve consisting of cholesteryloleate and free cholesterol (Sigma, St. Louis). Development was performed in a Camag Horizontal TLC-chamber (Camag, Muttenz, Switzerland). Following development, the plates were soaked with charring reagent (633 mM $CuSO_4 \cdot 5 H_2O$ in 8% phosphoric acid (Sigma) and heated at 160°C for 6 min. Quantification was performed through densitometry at 420 nm, using a Desaga CD-60 HPTLC densitometer in reflectance mode (Fig. 1). R^2 values for the regression line were never below 0.991; interassay variability was 8% and intra-assay

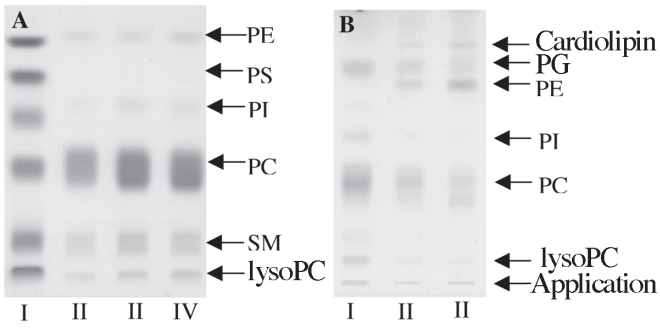

FIG. 1. Representative high-performance thin-layer chromatogram of classes of phospholipids. (A) Plasma phospholipids: Lane I is a reference mixture, lane II is the soybean oil-diet (SB-diet), lane III is the diet with 17% lipids from natural gas-utilizing bacteria (17LNGB), and lane IV is the diet with 67% lipids from natural gas-utilizing bacteria (67LNGB-diet). (B) Phospholipids in the diet: Lane I is the SB-diet, lane II is the 17LNGB-diet, and lane III is the 67LNGB-diet. SM, sphingomyelin; PG, phosphatidylglycerol; application, sample application point.

variability was 5%. All standards used were of 99% purity or higher.

Blood sampling and analyses. Blood samples were taken after an overnight fast in Na-heparin vacuum tubes immediately after electrocution and chilled on ice. Plasma was obtained by low-speed centrifugation for 15 min at 3000 × *g* within 15 min of heart puncture and the plasma was quickly separated and pipetted into plastic vials and stored at –80°C until analyzed.

Plasma cholesterol and serum TAG were measured by enzymatic methods (28,29) using Cobas® Integra enzyme kits and automated analyzer equipment (Cobas Mira, Hoffman-La Roche & Co., Basel, Switzerland). Plasma HDL cholesterol was measured by a similar enzymatic technique (28) after complexing the LDL, VLDL, and chylomicron fractions by polyanions (ABX Diagnostics HDL Cholesterol Direct) and using the same equipment as described above. LDL cholesterol was calculated using the Friedewald equation (30). The interassay coefficients of variation were the following: total cholesterol 2%, HDL- cholesterol 5%, TAG 3%.

Statistical methods. Data were analyzed by one-way ANOVA. *P* values <0.05 were considered significant. The Bonferroni method was used for a pairwise comparison between the three diet groups and for calculation of 95% confidence limits for the differences between the diets. The Bonferroni method encompasses a downward adjustment of significance limits for the differences between the diets. All *P*-values are two-tailed. Correlation coefficients (Pearson) between levels of plasma lipoproteins and classes of phospholipids are presented. The statistical package SPSS 11.0 (SPSS Inc., Chicago, IL) was used for the data analysis.

RESULTS

The gross energy level was slightly lower in the 67LNGB-diet than in the other two diets (Table 1). The feed intake (Table 1) and the final body mass did not differ significantly among the three groups.

When LNGB replaced soybean oil, dietary levels of oleic acid (18:1*c*,n-7) and linoleic acid (18:2*c*,n-6) were lower, and levels of palmitic acid (16:0) and palmitoleic acid (16:1, n-7), 16:1n-6, and 16:1n-5 were higher (Table 2). The LNGB-diets had a higher content of phospholipids than the SB-diet, and PE constituted a substantially higher percentage of the total phospholipids in the LNGB diets than in the SB-diet (Table 3). In the animals fed the 67LNGB-diet, total cholesterol,

TABLE 2
FA Composition of the Diets (mol% total FA)

FA	SB-diet[a]	17LNGB-diet[b]	67LNGB-diet[c]
14:0	0.2	0.4	1.2
14:1	—	—	0.2
16:0	11.6	14.0	24.7
16:1*t*,n-7		0.1	0.5
16:1*c*,n-7	0.3	2.6	12.6
16:1*c*,n-6	0.1	0.9	4.8
16:1*c*,n-5	0.1	0.5	2.3
18:0	3.5	3.3	2.3
18:1*c*,n-9	19.5	17.9	11.4
18:1*c*,n-7	1.5	1.4	1.1
18:2*c*,n-6	53.3	48.4	29.9
18:3*c*,n-3	5.7	5.1	3.0
20:0	0.4	0.3	0.2
20:1*c*,n-9	0.4	0.4	0.3
20:4*c*,n-6	0.1	0.1	0.1
20:5*c*,n-3	0.6	0.7	0.8
22:0	0.4	0.4	0.2
22:1*c*,n-11	0.2	0.1	0.1
22:5*c*,n-3		0.1	0.1
22:6*c*,n-3	1.6	2.4	2.9
24:0	0.2	0.1	0.1
P/S[d]	3.76	3.06	1.28

[a]Diet with 100% SB.
[b]Diet with 17% LNGB and 83% SB.
[c]Diet with 67% LNGB and 33% SB.
[d]Polyunsaturated/saturated ratio. For other abbreviations see Table 1.

TABLE 3
Phospholipid Content of the Diets (mg/g) (% of total phospholipids in parentheses)[a]

	SB-diet[b]	17LNGB-diet[c]	67LNGB-diet[d]
PC	3.3 ± 0.3 (74)	10.6 ± 0.8 (60)	25.7 ± 2.1 (44)
PI	0.4 ± 0.0 (9)	0.7 ± 0. 1 (4)	1.8 ± 0.2 (3)
PE	0.04 ± 0.0 (1)	2.6 ± 0.3 (15)	19.3± 2.3 (33)
Phosphatidylglycerol	0.7 ± 0.1 (17)	3.3 ± 0.3 (19)	8.8± 1.0 (15)
Cardiolipin	Traces	0.4 ± 0.0 (2)	2.9 ± 0.2 (5)
PE/PC ratio	0.01	0.25	0.75

[a]Values given as mean ± SD.
[b]Diet with 100% SB.
[c]Diet with 17% lipids from LNGB and 83% SB.
[d]Diet with 67% LNGB and 33% SB. For abbreviations see Table 1.

TABLE 4
Plasma Lipoprotein Levels (mmol/L) and Unesterified Cholesterol (% of total cholesterol) at the End of the Dietary Test Period[a,b]

	SB-diet[c]	17LNGB-diet[d]	67LNGB-diet[e]
Total cholesterol	6.76 ± 0.88[a]	6.51 ± 0.40[c]	4.43 ± 0.66[a,c]
Unesterified cholesterol	17.9 ± 1.22[d]	15.6 ± 1.69[a]	20.9 ± 1.53[a,d]
LDL cholesterol	1.87 ± 0.38[a]	1.67 ± 0.41[b]	0.95 ± 0.23[a,b]
HDL cholesterol	4.52 ± 0.41[a]	4.50 ± 0.26[c]	3.22 ± 0.50[a,c]
LDL/HDL cholesterol	0.41 ± 0.06[e]	0.37 ± 0.10	0.30 ± 0.05[e]
TAG	0.84 ± 0.36	0.76 ± 0.18	0.58 ± 0.10
VLDL cholesterol	0.37 ± 0.16	0.34 ± 0.82	0.26 ± 0.05

[a]Adjustment for multiple comparisons: Bonferroni.
[b]Values given as mean ± SD, $n = 6$. Means with common superscripts differ: [a,c], $P < 0.001$; [b], $P < 0.009$; [d], $P = 0.014$; [e], $P = 0.048$.
[c]Diet with 100 % SB.
[d]Diet with 17% lipids from LNGB and 83% SB.
[e]Diet with 67% LNGB and 33% SB. For abbreviations see Table 1.

LDL cholesterol, and HDL cholesterol were significantly lower, and unesterified cholesterol (as a percentage of total cholesterol) was significantly higher than in animals fed the 17LNGB-diet or the SB-diet (Table 4). No significant differences in the levels of total cholesterol, LDL cholesterol, HDL cholesterol, unesterified cholesterol (as a percentage of total cholesterol), or TAG were found between the 17LNGB-diet-fed animals and the SB-diet-fed animals. The ratio of LDL cholesterol to HDL cholesterol was significantly lower in mink fed the 67LNGB-diet than it was in mink fed the SB-diet.

No statistically significant differences among the three diets were found in plasma TAG and VLDL cholesterol in the present population ($n = 6$).

Plasma total phospholipids, PC, lysoPC, and PI were significantly lower in the 67LNGB-fed mink than in the mink fed solely with soybean oil (Table 5). Plasma SM was also lower in the mink on the 67LNGB-diet than the mink on the SB-diet, but the difference was below statistical significance ($P = 0.06$, Bonferoni adjusted). The highest percentage difference in the phospholipid classes in lysoPC and PC was observed between the 67LNGB-fed mink and the SB-fed mink. No significant differences in the concentration of plasma PE were found due to the diets (Table 5). However, PE constituted a significantly higher portion of the total phospholipids (Table 6) and PE/PC (Table 6), and plasma PE/total cholesterol ratios (Table 5) were also significantly higher for the 67LNGB-fed mink than for the SB-fed mink.

Plasma total cholesterol, LDL cholesterol, and HDL cholesterol were significantly correlated with total phospholipids, PC, lysoPC, SM, and PI (Table 7). There were no significant correlations between plasma total cholesterol and PE, LDL cholesterol and PE, or HDL cholesterol and PE. Fecal excretion of unesterified cholesterol, cholesteryl ester, PC, lysoPC, and PE (Table 8) was higher for the mink that were fed the 67LNGB-diet than those fed the SB-diet; it was also significantly higher in mink fed the 67LNGB-diet than those fed the 17LNGB-diet.

DISCUSSION

The most interesting findings of the present study were that dietary LNGB rich in PE, lowers total, LDL, and HDL choles-

TABLE 5
Plasma Phosolipid Composition and Ratios (μg/mL)[a–c]

	SB-diet[d]	17LNGB-diet[e]	67LNGB-diet[f]
Total phospholipids (PL)	4200 ± 1137[b]	3722 ± 558	2685 ± 251.0[b]
PC	3475 ± 1003[b]	3072 ± 506	2162 ± 256[b]
LysoPC	114 ± 22[a]	97 ± 15	61 ± 31[a]
Sphingomyelin (SM)	393 ± 110[e]	337 ± 49.6	280 ± 10[e]
PI	141 ± 31[c]	124 ± 21	99 ± 10[c]
PE	77 ± 24	94 ± 23	83 ± 21
PE/PC ratio	0.022 ± 0.005[d]	0.031 ± 0.010	0.039 ± 0.010[d]
PL/total cholesterol ratio	601 ± 92	570 ± 64	639 ± 99
PC/total cholesterol ratio	497 ± 86	470 ± 58	515 ± 88
PE/total cholesterol ratio	11.0 ± 2.79[a]	14.4 ± 3.6	19.4 ± 3.5[a]

[a]Adjustment for multiple comparisons: Bonferroni.
[b]Values given as mean ± SD, $n = 6$. Means with common superscripts differ: [a], $P < 0.001$; [b], $P < 0.02$; [c], $P = 0.03$; [d], $P = 0.039$.
[c]$P = 0.062$ ($P = 0.021$ without Bonferroni adjustment).
[d]Diet with 100% SB.
[e]Diet with 17% lipids from LNGB and 83% SB.
[f]Diet with 67% LNGB and 33% SB. For abbreviations see Table 1.

TABLE 6
Distribution of Phospholipids in Plasma (% of total phospholipids)[a]

	SB-diet[b]	17LNGB-diet[c]	67LNGB-diet[d]
PC	82.5 ± 2.3	82.4 ± 2.1	80.4 ± 1.9
LysoPC	2.8 ± 0.4	2.6 ± 0.2	2.3 ± 1.3
SM	9.5 ± 2.19	9.1 ± 1.3	10.49 ± 1.1
PI	3.40 ± 0.4	3.3 ± 0.5	3.7 ± 0.2
PE	1.8 ± 0.4[a]	2.6 ± 0.8	3.1 ± 0.8[a]
PE/PC	0.022 ± 0.005[a]	0.031 ± 0.100	0.039 ± 0.010[a]

[a]Values given as mean ± SD.
[b]Diet with 100% SB.
[c]Diet with 17% lipids from LNGB and 83% SB.
[d]Diet with 67% LNGB and 33% SB. For abbreviatioins see Table 1.

terol compared with soybean oil. These decreasing effects on plasma LDL and HDL cholesterol are unlikely to be due to FA composition. The 67LNGB-diet contained larger amounts of palmitic acid (16:0), known to raise cholesterol (31,32), than did the SB-diet, and also contained higher levels of palmitoleic acid (*cis* 16:1), suggested to raise plasma cholesterol (33,34). Palmitoleic acid has been shown to increase total and LDL cholesterol in humans similarly to palmitic acid and significantly more than oleic acid (18:1) (33). The results of a study with pigs support that palmitoleic acid increases cholesterol (34). The unsaturated FA in soybean oil, used as the main lipid source in the control diet of the present study, have been known to decrease total and LDL cholesterol in plasma (31). Further, it is established that, compared with saturated FA, n-6 PUFA have a lowering effect on HDL cholesterol (35). In this study the polyunsaturated/saturated (P/S) FA ratio was higher and the phospholipid concentrations were lower in the SB-diet than in the 67LNGB-diet. This means that the phospholipid content, rather than FA composition, is likely to have caused the greater reduction in plasma total cholesterol, LDL cholesterol, and HDL cholesterol in animals fed the 67LNGB-diet compared with those fed the SB-diet. Imaizumi *et al.* (7) showed that PE, but not PC, reduces serum cholesterol in rats. This was in contrast to our results, which showed effective reduction in plasma total, LDL, and HDL cholesterol with the 67LNGB-diet compared with the SB-diet). Imaizumi *et al.* (7) observed the most prominent effect of PE on the HDL fraction and no significant difference in the concentration of LDL cholesterol when comparing PE with soybean oil. However, our extracted bacterial lipids with high phospholipid content, especially PE, were not directly comparable with their purified PE prepared *via* transphosphatidylation of PC by cabbage phospholipase D (7). Thus, one cannot exclude that other components in the LNGB-diets, for instance, sterols, have hypocholesterolemic effects.

Our results showed a greater effect of LNGB on plasma LDL cholesterol than on HDL cholesterol, resulting in a lower LDL/HDL cholesterol ratio. This seems to be in line with another study that showed a reduction in plasma total and LDL cholesterol following a high intake of ethanolamine (8). Methylation of PE to PC by the liver-specific enzyme PEMT is an important reaction in PC homeostasis, and PEMT activity may play a role in regulating the levels of plasma

TABLE 7
Relationships Between Concentrations of Plasma Cholesterol and Classes of Phospholipid Concentrations[a]

	Total cholesterol	LDL cholesterol	HDL cholesterol
Total phospholipids R^b, P^c	0.841*, <0.001	0.850*, <0.001	0.726*, <0.001
PC R^b, P^c	0.830*, <0.001	0.839*, <0.001	0.716*, <0.002
LysoPC R^b, P^c	0.669*, <0.005	0.702*, <0.002	0.561*, 0.024
SM R^b, P^c	0.724*, <0.002	0.778*, <0.001	0.572*, 0.021
PI R^b, P^c	0.717*, <0.002	0.699*, <0.003	0.656*, <0.006
PE R^b, P^c	0.245 0.360	0.053, 0.847	0.352, 0.181

[a]Values given as mean ± SD, $P < 0.05$. *Correlation is significant. For other abbreviation see Table 5.
[b]R = Pearson correlation.
[c]P = P value.

TABLE 8
Fecal Excretion of Unesterified Cholesterol, Cholesteryl Ester, and Phospholipids[a,b]

	SB-diet[c]	17LNGB-diet[d]	67LNGB-diet[e]
Unesterified cholesterol (mg/d)	74.28 ± 11.43[a]	83.78 ± 10.90[b]	101.96 ± 9.02[a,b]
Cholesteryl ester (mg/d)	33.59 ± 20.86[a]	47.64 ± 10.03[c]	132.80 ± 27.46[a,c]
PC (µg/d)	0.94 ± 0.18[a]	2.06 ± 0.56[c]	12.57 ± 3.67[a,c]
LysoPC (µg/d)	0.28 ± 0.10[a]	1.78 ± 0.86[c]	16.64 ± 5.86[a,c]
PE (µg/d)	0.16 ± 0.05[a]	0.49 ± 0.13[c]	5.38 ± 2.04[a,c]

[a]Values given as mean ± SD, $n = 6$. Means with common superscripts differ: [a,c]$P < 0.001$, [b]$P = 0.027$.
[b]Adjustment for multiple comparisons: Bonferroni.
[c]Diet with 100 % SB.
[d]Diet with 17% lipids from LNGB and 83% SB.
[e]Diet with 67% LNGB and 33% SB. For abbreviations see Table 1.

lipoproteins (15). A study by Reo *et al.* (36), using NMR analysis of liver extracts from rats, showed that about 30% of liver PC was produced by PEMT. The significantly lower plasma PC in mink fed the PE-rich 67LNGB-diet compared with mink fed the SB-diet is in agreement with other studies (7,8). Imaizumi *et al.* (7) indicated that since the FA compositions of the PE and the purified PC were similar in their study, the different effects of these phospholipids on plasma cholesterol may be attributed to their constituent bases. However, a possible explanation of the effect on plasma cholesterol is a reduction of PC *via* the PE N-methylation pathway. Ethanolamine is used as substrate for the PE synthesis through the CDP-ethanolamine pathway (16). Since dietary PE is degraded to free ethanolamine, 2-MAG, and FFA in the intestine, it is possible that PE and ethanolamine may reduce plasma cholesterol in the same way.

The highly significant correlation between plasma total cholesterol and total phospholipids found in our study is in agreement with the results of Beynen and Terpstra (37). In their study, there was a positive correlation (more than 70%) between serum total cholesterol and phospholipid concentrations in humans, rabbits (*Oryctolagus cunicullus*), and calves (*Bos taurus*). Also, plasma phospholipid concentrations in the present study changed in a manner similar to that of plasma cholesterol, resulting in high correlation between these two variables. The findings in the present study that the plasma lipoproteins (total cholesterol, LDL cholesterol, HDL cholesterol) were correlated with total phospholipids, PC, lysoPC, SM, and PI indicate a close association between plasma cholesterol and classes of phospholipids and on the distribution of cholesterol over the various lipoprotein fractions. The lack of significant differences in the level of plasma PE due to the diets indicates that most of PE in LNGB has been converted to PC in the liver, although the PE/PC ratio of total plasma phospholipids was significantly higher in the 67LNGB-fed mink than the SB-fed mink.

The reduction in both plasma cholesterol and PC in the study by Noga and Vance (15) is in accordance with our results. The most abundant phospholipid in plasma lipoproteins is PC (38), but the relationships between PC, the other classes of phospholipids, and plasma cholesterol are not entirely understood and more studies are needed. It is likely that more than one mechanism regulates the cholesterol and PC content in lipoproteins.

Higher fecal excretion of unesterified cholesterol, cholesteryl ester, PC, lysoPC, and PE following feeding of the 67LNGB-diet compared with the SB-diet may be related to the high concentration of PE and possibly higher levels of PEMT-derived PC. Thus, PC biosynthesis *via* the PE methylation pathway may promote biliary excretion of phospholipids and cholesterol (18). It has been shown that relationships between biliary phospholipid and cholesterol excretion are complex (18). Increased biliary excretion of phospholipids and cholesterol from PC biosynthesis *via* the PE methylation pathway may at least partly explain the lower concentration of plasma cholesterol and PC in the 67LNGB-diet compared with the SB-diet. In another study, the secretion of PEMT-derived PC into bile was higher in mice fed a high-fat and -cholesterol diet (39). The liver has a major role in cholesterol homeostasis through excretion of cholesterol into the bile, by conversion to bile acids, and by secretion of lipoproteins (40). The lipoprotein systems in mink and humans are somewhat different: Most of the mink's plasma cholesterol is in the form of HDL, and they have very low levels of cholesteryl ester transfer protein (CETP) activity in plasma (41). Hence, the results obtained in this study should be validated in pigs, which have a more human-like lipoprotein metabolism.

The 67LNGB-diet contained more PC than the SB-diet did, and one cannot exclude the possibility that alternations of dietary phospholipids may decrease cholesterol absorption. However, Homan and Hamehle (42), working with Caco-2 cells (a human intestinal cell line with enterocyte-similar properties), have shown that cholesterol absorption from bile acid micelles is suppressed by PC in the micelles.

The fact that plasma unesterified cholesterol in our study was significantly higher for the mink on the 67LNGB-diet than for those on the SB-diet and for animals on the 67LNGB-diet compared with those on the 17LNGB-diet is not easy to explain. However, it has been suggested that phospholipid transfer protein activity on HDL can modulate the activities of lecithin:cholesterol acyltransferase and CETP *in vitro*, which could lead to a higher concentration of free cholesterol (43).

The synthesis of the VLDL components such as TAG and PC is strictly coordinated (16). The difference in plasma TAG concentrations among dietary treatments in our study was somewhat smaller than in total cholesterol, LDL cholesterol, and HDL cholesterol and was not statistically significant. However, soybean oil has a well-established reducing effect on plasma TAG levels (35). Furthermore, considering the interindividual variations in fasting values of TAG, the number of animals may have been too small to detect significant differences. Studies have shown that PEMT is essential for the incorporation of TAG into VLDL particles in liver cells (44), for secretion of TAG (15), and for normal concentration of plasma VLDL in mice (45). The study of Imaizumi *et al.* (7) showed no significant difference in plasma TAG between that in rats consuming PE and PC and consuming soybean oil (7). Furthermore, it has been shown that free ethanolamine may slightly reduce serum TAG (6,12).

From our comparison between the 67LNGB-diet and a diet of highly unsaturated soybean oil, we conclude that phospholipids from the 67LNGB-diet decrease plasma lipoproteins levels and the LDL/HDL cholesterol ratio. The diets containing bacterial lipids also cause lower levels of phospholipids, especially lysoPC and PC. Our findings show that the lowering effects on plasma cholesterol achieved with a specific dietary mixture of phospholipids are mainly caused by specific phospholipids, especially a high level of PE, and not the FA composition. The lack of significant differences in the level of plasma PE due to the diets indicates that most of the PE in the LNGB-diets has been converted to PC in the liver. Thus, plasma cholesterol is at least partly regulated by phospholipid methylation from PE to PC in the liver.

ACKNOWLEDGMENTS

We gratefully acknowledge the Research Council of Norway for financial support, Norferm AS for supplying the bacterial protein meal used for lipid extraction, and Helene Kingsley-Smith for technical assistance at the research farm. Also, we thank Øystein Ahlstrøm for drawing blood samples and Inger Johanne Jørgensen for help with performing the lipoprotein analyses.

REFERENCES

1. Åkesson, B. (1982) Content of Phospholipids in Human Diets Studied by the Duplicate-Portion Technique, *Br. J. Nutr. 47,* 223–229.
2. Lucas, C.C., and Ridout, J.H. (1967) Fats and Other Lipids, *Progr. Chem. 10,1*.
3. Skrede, A., Berge, G.M., Storebakken, T., Herstad, O., Aarstad, K.G., and Sundstøl, F. (1998) Digestibility of Bacterial Protein Grown on Natural Gas in Mink, Pigs, Chicken and Atlantic Salmon, *Anim. Feed. Sci. Technol. 76,* 103–116.
4. Hanson, R.S., and Hanson, T.E. (1996) Methanotrophic Bacteria, *Microbiol. Rev. 60,* 439–471.
5. Makula, R.A. (1978) Phospholipid Composition of Methane-Utilizing Bacteria, *J. Bacteriol. 134,* 771–777.
6. Murata, M., Imaizumi, K., and Sugano, M. (1982) Effect of Dietary Phospholipids and Their Constituent Bases on Serum Lipids and Apolipoproteins in Rats, *J. Nutr. 112,* 1805–1808.
7. Imaizumi, K., Mawatari, K., Murata, M., Ikeda, I., and Sugano, M. (1983) The Contrasting Effect of Dietary Phosphatidylethanolamine and Phosphatidylcholine on Serum Lipoproteins and Liver Lipids in Rats, *J. Nutr. 113,* 2403–2411.
8. Sugiyama, K., Ohishi, A., Siyu, H., and Takeuchi, H. (1989) Effects of Methyl-Group Acceptors on the Regulation of Plasma Cholesterol Level in Rats Fed High Cholesterol Diets, *J. Nutr. Sci. Vitaminol. 35,* 613–626.
9. Morrison, L.M. (1958) Serum Cholesterol Reduction with Lecithin, *Geriatrics 13,* 12–19.
10. Childs, M.T., Bowlin, J.A., Ogilvie, J.T., Hazzard, W.R., and Albers, J.J. (1981) The Contrasting Effects of a Dietary Soya Lecithin Product and Corn Oil on Lipoprotein Lipids in Normolipidemic and Familial Hypercholesterolemic Subjects, *Atherosclerosis 38,* 217–228.
11. Knuiman, J.T., Beynen, A.C., and Katan, M.B. (1989) Lecithin Intake and Serum Cholesterol, *Am. J. Clin. Nutr. 49,* 266–268.
12. Bondesson G., Hedbom, C., Magnusson, O., and Stjernstrom, N.E. (1974) Potential Hypolipidemic Agents. X. Plasma Lipid-Lowering Properties of Some Aliphatic Aminoalcohols, *Acta Pharm. Suec. 11,* 417–426.
13. O'Brien, B.C., and Andrews, V.G. (1993) Influence of Dietary Egg and Soybean Phospholipids and Triacylglycerols on Human Serum Lipoproteins, *Lipids 28,* 7–12.
14. Childs, M.T., Bowlin J.A., Ogilvie, J.T., Hazzard, W.R., and Albers, J.J. (1981) The Contrasting Effects of a Dietary Soya Lecithin Product and Corn Oil on Lipoprotein Lipids in Normolipidemic and Familial Hypercholesterolemic Subjects, *Atherosclerosis 38,* 217–228.
15. Noga, A.A., and Vance, D.E. (2003) A Gender-Specific Role for Phosphatidylethanolamine N-Methyltransferase-Derived Phosphatidylcholine in the Regulation of Plasma High Density and Very Low Density Lipoproteins in Mice, *J. Biol. Chem. 278,* 21851–21859.
16. Tijburg, L.B.M., Geelen, M.J.H., and van Golde, L.M.G. (1989) Regulation of the Biosynthesis of Triacylglycerol, Phosphatidylcholine and Phosphatidylethanolamine in the Liver, *Biochem. Biophys. Acta 1004,* 1–19.
17. DeLong, C.J., Hicks, A.M., and Cui, Z. (2002) Disruption of Choline Methyl Group Donation for Phosphatidylethanolamine Methylation in Hepatocarcinoma cells, *J. Biol. Chem. 277,* 17217–17225.
18. Sehayek, E., Wang, R., Ono, J.G., Zinchuk, V.S., Duncan, E.M., Shefer, S., Vance, D.E., Ananthanarayanan, M., Chait, B.T., and Breslow, J.L. (2003) Localization of the PE Methylation Pathway and SR-BI to the Canalicular Membrane: Evidence for Apical PC Biosynthesis That May Promote Biliary Excretion of Phospholipid and Cholesterol, *J. Lipid Res. 44,* 1605–1613.
19. Skrede, A., and Cheeke, P.R. (2004) Feeding and Nutrition of Fur-Bearing Animals, in *Applied Animal Nutrition*, 3rd edn., pp. 514–522. Pearson Prentice Hall, Upper Saddle River, NJ.
20. Folch, J., Lees, M., and Sloane Stanley, G.H. (1957) A Simple Method for the Isolation and Purification of Total Lipids from Animal tissues, *J. Biol. Chem. 226,* 497–509.
21. Nes, N., Einarsson, E.J., and Lohi, O. (1988) *Beautiful Fur Animals and Their Colour Genetics*, (Jørgensen, G., ed.), pp. 155–160, Scientifur, Hillerød, Denmark.
22. National Research Council (1982) *Nutrient Requirements of Mink and Foxes*, 2nd rev. edn., National Academy Press, Washington, DC.
23. McCleary, B.V., Solah, V., and Gibson, T.S. (1994) Quantitative Measurements of Total Starch in Cereal Flours and Products, *J. Cereal. Sci. 20,* 51–58.
24. Bligh, E.G., and Dyer, W.J. (1959) A Rapid Method of Total Lipid Extraction and Purification, *Can. J. Med. Sci. 37,* 911–917.
25. Mason, M.E., and Waller, G.R. (1964) Dimethoxypropane Induced Transesterification of Fats and Oils in Preparation of Methyl Esters for Gas Chromatographic Analysis, *Anal. Chem. 36,* 583–586.
26. Macala, L.J., Yu, R.K., and Ando, S. (1983) Analysis of Brain Lipids by High Performance Thin-Layer Chromatography and Densitometry, *J. Lipid Res. 24,* 1243–1249.
27. Ruiz, J.I., and Ochoa, B. (1997) Quantification in the Subnanomolar Range of Phospholipids and Neutral Lipids by Monodimensional Thin-Layer Chromatography and Image Analysis, *J. Lipid Res. 38,* 1482–1489.
28. Siedel, J., Rollinger, W., Rôschlau, P., and Ziegenhorn, J. (1985) Total Cholesterol, End-point and Kinetic Method, in *Methods of Enzymatic Analysis,* 3rd edn. (Bergmeyer, H.U., ed.), Vol. 8, pp. 139–148, Weinheim, Germany.
29. Nägele, U., Wahlefeld, A.W., and Ziegenhorn, J. (1985) Triglycerides: Colorimetric Method, in *Methods of Enzymatic Analysis,* 3rd edn. (Bergmeyer, H.U., ed.), Vol. 8, pp. 12–18, Weinheim, Germany.
30. Friedewald, W.T., Lewy, R.I., and Fredrickson. D.S. (1972) Estimation of the Concentration of Low-Density Lipoprotein Cholesterol in Plasma, Without Use of the Preparative Ultracentrifuge, *Clin. Chem. 18,* 499–502.
31. Yu, S., Derr, J., Etherton, T.D., and Kris-Etherton, P.M. (1995) Plasma Cholesterol-Predictive Equations Demonstrate That Stearic Acid Is Neutral and Monounsaturated Fatty Acids Are Hypocholesterolemic, *Am. J. Clin. Nutr. 61,* 1129–1139.
32. Müller, H., Kirkhus, B., and Pedersen, J.I. (2001) Serum Cholesterol Predictive Equations with Special Emphasis on *trans* and Saturated Fatty Acids. An Analysis from Designed Controlled Studies, *Lipids 36,* 783–791.
33. Nestel, P., Clifton, P., and Noakes, M. (1994) Effects of Increasing Dietary Palmitoleic Acid Compared with Palmitic and Oleic Acids on Plasma Lipids of Hypercholesterolemic Men, *J. Lipid Res. 35,* 656–662.
34. Smith, D.R., Knabe, D.A., Cross, H.R., and Smith, S.B. (1996) A Diet Containing Myristoleic Plus Palmitoleic Acids Elevates Plasma Cholesterol in Young Growing Swine, *Lipids 31,* 849–858.
35. Goodnight, S.H., Harris, W.S., Connor, W.E., and Illingworth, D.R. (1982) Polyunsaturated Fatty Acids, Hyperlipidemia, and Thrombosis, *Arteriosclerosis 2,* 87–113.
36. Reo, N.V., Adinehzadeh, M., and Foy, B.D. (2002) Kinetic Analyses of Liver Phosphatidylcholine and Phosphatidylethanolamine

Biosynthesis Using ^{13}C NMR Spectroscopy, *Biochim. Biophys. Acta. 1580,* 171–188.
37. Beynen, A.C., and Terpstra, A.H. (1983) Relationships Between Cholesterol and Phospholipid Concentrations in the Serum of Humans, Calves, Rabbits and Chickens, *Comp. Biochem. Physiol. B 76,* 737–740.
38. Kent, C. (1995) Eukaryotic Phospholipid Biosynthesis, *Ann. Rev. Biochem. 64,* 315–343.
39. Noga, A.A., and Vance, D.E. (2003) Insights into the Requirement of Phosphatidylcholine Synthesis for Liver Function in Mice, *J. Lipid Res. 44,* 1998–2005.
40. Dietschy, J.M., Turley, S.D., and Spady, D.K. (1993) Role of Liver in the Maintenance of Cholesterol and Low Density Lipoprotein Homeostasis in Different Animal Species, Including Humans. Review, *J. Lipid Res. 34,* 1637–1659.
41. Christophersen, B., Nordstoga, K., Shen, Y., Olivecrona, T., and Olivecrona, G. (1997) Lipoprotein Lipase Deficiency with Pancreatitis in Mink: Biochemical Characterization and Pathology, *J. Lipid Res. 38,* 837–846.
42. Homan, R., and Hamelehle, K.L. (1998) Phospholipase A_2 Relieves Phosphatidylcholine Inhibition of Micellar Cholesterol Absorption and Transport by Human Intestinal Cell Line Caco-2, *J. Lipid Res. 39,* 1197–1209.
43. Tu, A.Y., Nishida, H.I., and Nishida, T. (1993) High Density Lipoprotein Conversion Mediated by Human Plasma Phospholipid Transfer Protein, *J. Biol. Chem. 268,* 23098–23105.
44. Nishimaki-Mogami, T., Yao, Z., and Fujimori, K. (2002) Inhibition of Phosphatidylcholine Synthesis *via* the Phosphatidylethanolamine Methylation Pathway Impairs Incorporation of Bulk Lipids into VLDL in Cultured Rat Hepatocytes, *J. Lipid Res. 43,* 1035–10445.
45. Noga, A.A., Zhao, Y., and Vance, D.E. (2002) An Unexpected Requirement for Phosphatidylethanolamine N-Methyltransferase in the Secretion of Very Low Density Lipoproteins, *J. Biol. Chem. 277,* 42358–42365.

[Received October 20, 2004; accepted October 26, 2004]

Effect of Five Cysteine-Containing Compounds on Three Lipogenic Enzymes in Balb/cA Mice Consuming a High Saturated Fat Diet

Chun-che Lin[a], Mei-chin Yin[b,*], Cheng-chin Hsu[b], and Meng-pei Lin[b]

[a]Department of Internal Medicine, Chungshan Medical University Hospital, and [b]Department of Nutritional Science, Chungshan Medical University, Taichung City, Taiwan, Republic of China

ABSTRACT: The *in vivo* effects of N-acetyl cysteine (NAC), S-allyl cysteine, S-ethyl cysteine (SEC), S-methyl cysteine (SMC), and S-propyl cysteine (SPC) against hyperlipidemia development and oxidation stress in Balb/cA mice consuming a high saturated fat diet were examined. The influence of these agents on plasma levels of glucose, insulin, uric acid, TG, cholesterol, and the activity of three lipogenic enzymes—glucose-6-phosphate dehydrogenase, malic enzyme, and FA synthase—was determined. All mice consumed the coconut oil-basd, high saturated fat diet, water, and cysteine or one of the five cysteine-containing compounds for 4 wk. The diet with 18% saturated fat significantly elevated the activity of three lipogenic enzymes and significantly increased TG and cholesterol biosynthesis in plasma and liver ($P < 0.05$). When compared with the water and cysteine groups, the treatments from five cysteine-containing agents significantly reduced high saturated fat diet-increased malic enzyme and FA synthase activities, and significantly lowered TG levels in plasma and liver ($P < 0.05$); however, only NAC, SAC, and SMC treatments significantly reduced cholesterol levels in plasma and liver ($P < 0.05$). The five cysteine-containing agents significantly restored high saturated fat diet-decreased glutathione peroxidase (GPX) activity in liver ($P < 0.05$); however, only SMC and SPC significantly restored GPX activity in heart and kidney ($P < 0.05$). These agents also significantly improved high saturated fat diet-related hyperglycemia, hyperuricemia, and oxidation stress ($P < 0.05$). These data support the hypothesis that these compounds are potential multiply-protective agents for hyperlipidemia prevention or therapy.

Paper no. L9556 in *Lipids 39,* 843–848 (September 2004).

N-Acetyl cysteine (NAC), S-allyl cysteine (SAC), S-ethyl cysteine (SEC), S-methyl cysteine (SMC), and S-propyl cysteine (SPC) are five hydrophilic cysteine-containing compounds naturally formed in *Allium* plants such as garlic and onion (1,2). Several studies have indicated that SAC, SEC, and SPC could inhibit TG and cholesterol biosynthesis in cultured rat hepatocytes (3–6). The study of Liu and Yeh (4) further reported that SAC and SPC could decrease the activity of FA synthase, a lipogenic enzyme, in the cultured hepatocytes. Thus, these water-soluble organosulfur compounds are potent hypolipidemic agents. Our past animal study found that these compounds exhibit marked enzymatic antioxidant protection and reduce the TG level in normal diet-consuming mice (7). However, whether these agents are able to inhibit the biosynthesis of TG and cholesterol in animals consuming a high saturated fat diet remains unclear. Furthermore, the effect of these agents on the activity of other lipogenic enzymes such as glucose-6-phosphate dehydrogenase (G6PDH) and malic enzyme remains unknown.

Total plasma cysteine, based on its potential vascular toxicity, is a risk factor for cardiovascular diseases (8,9). The influence of a cysteine-enriched diet on lipid metabolism remains controversial (10–12). Although our previous animal study (7) found that a cysteine supplement elevated TG and cholesterol levels in normal diet-consuming mice, information regarding the impact of cysteine on the biosynthesis of TG and cholesterol in animals consuming a high saturated fat diet is lacking.

The major purpose of this study was to evaluate the *in vivo* effects of cysteine and five cysteine-containing compounds on hyperlipidemia development in mice consuming a high saturated fat diet. The impact of these agents on the plasma levels of glucose, insulin, TG, cholesterol, and the activity of three lipogenic enzymes was determined.

MATERIALS AND METHODS

Animals. Three- to 4-wk-old male Balb/cA mice were obtained from the National Laboratory Animal Center (National Science Council, Taipei City, Taiwan). Mice were housed on a 12-h light–12-h dark schedule and fed with water *ad libitum* and a rat and mouse standard diet containing by weight (g/100 g): 64 starch, 23 protein, 3.5 fat, 5 fiber, 1 vitamin mixture, and 3 salt mixture (PMI Nutrition International LLC, Brentwood, MO) (7) for 1 wk of acclimation. Use of the mice was reviewed and approved by the Chungshan Medical University animal care committee.

Organosulfur compound treatment. Cysteine (99.5%), NAC (99.5%), SMC (99%), and SEC (99.5%) were purchased from Sigma Chemical Co. (St. Louis, MO). SAC (99%) and SPC (99%) were supplied by Wakunaga Pharmaceutical Co.

*To whom correspondence should be addressed at Department of Nutritional Science, Chungshan Medical University, No. 110, Sec. 1, Chien-Kuo N. Rd., Taichung City, Taiwan, R.O.C. E-mail: mcyin@csmu.edu.tw

Abbreviations: ALT, alanine aminotransferase; AST, aspartate aminotransferase; FAS, fatty acid synthase; G6PDH, glucose-6-phosphate dehydrogenase; GPX, glutathione peroxidase; MDA, malondialdehyde; NAC, N-acetyl cysteine; RIA, radioimmunoassay; SAC, S-allyl cysteine; SEC, S-ethyl cysteine; SMC, S-methyl cysteine; SPC, S-propyl cysteine; TBA, thiobarbituric acid.

(Hiroshima, Japan). Each agent was added to the drinking water of mice at a rate of 1 g/L.

High saturated fat diet preparation and experimental design. Regular mouse chow (85 g) was mixed with 15 g coconut oil (Sigma-Aldrich Co., Ltd., Poole, United Kingdom). This prepared diet provided 18% fat, which contained 82.6% saturated FA such as lauric acid, myristic acid, palmitic acid, and stearic acid. All mice consumed the prepared high saturated fat diet, and these mice were divided into seven groups (n = 15) on the basis of their intake of water, cysteine, or one of five cysteine-containing compounds for 4 wk. All mice had free access at all times to food and water. Food and water intake was recorded daily. Body weight was measured every week. Plasma glucose level was measured every other week. After 4 wk, mice were killed with carbon dioxide. Heart, liver, and kidney from each mouse were collected and weighed. Blood was also collected, and plasma was separated from erythrocytes immediately. Two-tenths of a gram of each organ was homogenized in 2 mL PBS (pH 7.2), and the filtrate passing through number 1 filter paper was collected. The protein concentration of plasma, heart, liver, and kidney filtrate was determined by the method of Lowry *et al.* (13) using BSA as a standard. In all experiments, sample was diluted to a final concentration of 1 g protein/L using PBS, pH 7.2.

Analysis of alanine aminotrasferase (ALT) and aspartate aminotransferase (AST). Liver damage was assessed by measuring serum activities of ALT and AST, which were determined by using commercial assay kits (Randox Laboratories Ltd., Crumlin, United Kingdom).

Plasma level of glucose, insulin, and uric acid. Plasma glucose, insulin, and uric acid levels (mmol/L) were measured by a radioimmunoassay (RIA) using glucose HK kit (Sigma Chemical), rat insulin RIA kit (SRI-13K; Linco Research Inc., St. Charles, MO), and uric acid kit (Randox Laboratories Ltd.), respectively.

TG and cholesterol determination. TG and cholesterol levels (mmol/L) in plasma were determined by TG/GB kit and cholesterol/HP kit (Boehringer Mannheim, Indianapolis, IN), respectively. Total lipids were extracted from liver, and then liver TG and cholesterol concentrations (μmol/g wet tissue) were quantified by colorimetric assay (14).

Measurement of the activity of lipogenic enzymes in the liver. The activity of G6PDH was assayed by a commercial kit (Sigma-Aldrich Co., Ltd.), in which enzyme activity was determined by using a plate-reader spectrophotometer and measuring the rate of absorbance increase at 340 nm due to the conversion of $NADP^+$ to NADPH. The activities of malic enzyme and FA synthase (FAS) were measured by spectrophotometric assays based on the absorbance change at 340 nm, as described in Hsu and Lardy (15) and Nepokroeff *et al.* (16). The enzyme activity was calculated as nmol NADPH formed or oxidized/min/mg protein.

Glutathione peroxidase (GPX) assay. GPX activity (U/mg protein) in heart, liver, and kidney was determined by using a commercial GPX assay kit (Calbiochem, EMD Biosciences, Inc., San Diego, CA).

Lipid oxidation determination. Glucose at 50 mmol/L was added to the 1 mL filtrate from heart, liver, and kidney to initiate lipid oxidation (7). The lipid oxidation level in the filtrate was determined after 2 d of incubation at 37°C by measuring the level of malondialdehyde (MDA, μmol/L) *via* an HPLC method (17). Briefly, 0.5 mL trichloroacetic acid (30%) was added to the samples. After vortexing, samples were centrifuged at 1000 × g for 15 min. Supernatant (1 mL) was mixed with 0.25 mL thiobarbituric acid (TBA, 1%) and the mixture was kept in boiling water for 15 min. The concentration of MDA-TBA complex was assayed using a high-performance liquid chromatograph equipped with a reversed-phase Shodex KC-812 column (Showa Denko, Tokyo, Japan) with a UV-vis detector at 532 nm.

Statistical analysis. The effect on 15 mice (n = 15) of each treatment was analyzed. Data were subjected to one-way ANOVA and computed using the SAS General Linear Model (GLM) procedure (18). Differences having P-values <0.05 were considered to be significant.

RESULTS

The intake of water, cysteine, and various cysteine-containing compounds in conjunction with a high saturated fat diet did not significantly affect heart weight (0.16–0.19 g), liver weight (1.21–1.43 g), kidney weight (0.28–0.31 g), and the activity of ALT and AST in these mice ($P > 0.05$). The body weight, daily food intake, and daily water intake are presented in Table 1. All high saturated fat diet-consuming mice had significantly greater body weight, daily food intake, and water intake than normal diet-consuming mice ($P < 0.05$). When compared with the water and cysteine groups, the intake of five cysteine-containing compounds significantly reduced body weight ($P < 0.05$).

The plasma glucose, insulin, and uric acid levels from mice are presented in Table 2. High saturated fat diet consumption

TABLE 1
Final Body Weight, Daily Food Intake, and Daily Water Intake of Mice Treated with a Normal Diet and with a High Saturated Fat Diet Plus Water, Cysteine, or One of Five Cysteine-Containing Agents[a,b]

	Body weight[c] (g)	Food intake (g/d)	Water intake (mL/d)
Normal diet	23.7 ± 1.3[a]	3.6 ± 0.8[a]	4.3 ± 1.2[a]
High saturated fat diet			
Water	31.3 ± 2.6[c]	8.9 ± 1.8[b]	8.4 ± 1.0[b]
Cysteine	30.7 ± 1.7[c]	8.7 ± 1.4[b]	7.8 ± 1.7[b]
NAC	28.3 ± 1.2[b]	8.8 ± 1.0[b]	7.5 ± 1.3[b]
SAC	28.8 ± 1.3[b]	9.1 ± 1.6[b]	8.0 ± 0.8[b]
SEC	29.8 ± 0.8[b]	8.2 ± 2.0[b]	7.6 ± 1.2[b]
SMC	29.0 ± 1.4[b]	8.6 ± 1.2[b]	8.2 ± 0.5[b]
SPC	29.3 ± 1.1[b]	8.4 ± 1.1[b]	7.9 ± 1.5[b]

[a]Values are means ± SD, n = 15. Means in a column without a common superscript letter differ significantly, $P < 0.05$.
[b]Abbreviation: NAC, N-acetyl cysteine; SAC, S-allyl cysteine; SEC, S-ethyl cysteine; SMC, S-methyl cysteine; SPC, S-propyl cysteine.
[c]Initial body weight was 13.7 ± 1.1 g.

TABLE 2
Plasma Glucose, Insulin and Uric Acid Levels from Mice Treated with a Normal Diet and a High Saturated Fat Diet Plus Water, Cysteine, or One of Five Cysteine-Containing Agents[a]

	Glucose (mmol/L)	Insulin (nmol/L)	Uric acid (mmol/L)
Normal diet	6.9 ± 0.8[a]	11.7 ± 1.2[b]	46.6 ± 3.2[a]
High saturated fat diet			
Water	12.5 ± 1.1[c]	8.9 ± 1.0[a]	63.2 ± 5.3[c]
Cysteine	11.6 ± 1.0[c]	8.5 ± 0.6[a]	62.7 ± 4.8[c]
NAC	9.8 ± 0.7[b]	10.8 ± 1.2[b]	51.2 ± 2.5[b]
SAC	9.4 ± 1.2[b]	8.7 ± 0.9[a]	48.3 ± 3.2[a]
SEC	10.6 ± 1.4[b]	9.3 ± 0.4[a]	54.5 ± 3.0[b]
SMC	9.7 ± 0.7[b]	9.0 ± 0.7[a]	50.7 ± 2.7[b]
SPC	10.1 ± 1.1[b]	10.6 ± 1.0[b]	52.1 ± 3.1[b]

[a]Values are means ± SD, $n = 15$. Means in a column without a common letter differ, $P < 0.05$. See Table 1 for abbreviations.

significantly elevated plasma glucose and uric acid levels and decreased the plasma insulin level ($P < 0.05$). When compared with the water and cysteine groups, the treatments with five cysteine-containing agents significantly decreased plasma glucose and uric acid levels ($P < 0.05$); however, only NAC and SPC treatments significantly increased the insulin level ($P < 0.05$). As shown in Table 3, high saturated fat diet consumption significantly increased the TG and cholesterol levels in plasma and liver ($P < 0.05$); of these, the cysteine group had the greatest TG and cholesterol levels in plasma and liver ($P < 0.05$). When compared with the water and cysteine groups, the treatments from five cysteine-containing agents significantly decreased the TG level in plasma and liver ($P < 0.05$); however, only the NAC, SAC, and SMC treatments significantly reduced the cholesterol levels in plasma and liver ($P < 0.05$).

The influence of cysteine and five cysteine-containing agents on the activity of three lipogenic enzymes is presented in Table 4. A high saturated fat diet caused a significant increase in the activity of three test enzymes ($P < 0.05$). Cysteine intake further enhanced G6PDH activity significantly ($P < 0.05$). The administration of five cysteine-containing agents only slightly, but not significantly, reduced G6PDH when compared with the water group ($P > 0.05$). However, these five cysteine-containing agents significantly reduced high saturated fat diet-enhanced malic enzyme and FAS activities when compared with the water and cysteine groups ($P < 0.05$). The GPX activity from heart, liver, and kidney is presented in Table 5. High saturated fat intake significantly decreased GPX activity in these organs ($P < 0.05$). The intake of cysteine caused further reduction in GPX activity in heart only ($P < 0.05$). The administration of five cysteine-containing agents significantly restored GPX activity in liver ($P < 0.05$); however, only SMC and SPC significantly restored GPX activity in heart and kidney ($P < 0.05$). As shown in Table 6, the consumption of a high saturated fat diet containing cysteine significantly increased glucose-induced MDA formation in three organs ($P < 0.05$). The intake of cysteine-containing agents resulted in significantly lower MDA levels in three organs when compared with the cysteine group ($P < 0.05$).

DISCUSSION

Several studies of animals have reported that the consumption of coconut oil enhanced lipogenesis in liver, which was also reflected in increased TG and cholesterol levels in plasma (19,20). In our present study, mice were fed a coconut oil-supplemented diet (without extra cholesterol supplementation) for 4 wk, and these mice exhibited hypotriglyceridemia and hypercholesterolemia. Our results agreed with those previous studies and found that the enhanced lipogenesis by coconut oil was in part due to the elevated activity of three important lipogenic enzymes, G6PDH, malic enzyme, and FAS. Furthermore, we found the intake of five cysteine-containing agents could effectively down-regulate high coconut oil-induced lipogenesis by lowering the activity of malic enzyme and FAS, which consequently reduced the biosynthesis of TG and cholesterol as well as the body weight in these mice. Therefore, these results suggest that these cysteine-containing agents are able to alleviate hyperlipidemia development and might lower body fat accumulation.

TABLE 3
TG and Cholesterol Concentrations in Plasma and Liver from Mice Treated with Normal Diet and High Saturated Fat Diet Plus Water, Cysteine, or One of Five Cysteine-Containing Agents[a]

	TG		Cholesterol	
	Plasma (g/L)	Liver (mg/g wet liver)	Plasma (g/L)	Liver (mg/g wet liver)
Normal diet	2.15 ± 0.11[a]	28.3 ± 1.3[a]	1.51 ± 0.17[a]	3.26 ± 0.12[a]
High saturated fat diet				
Water	4.03 ± 0.21[c]	36.4 ± 2.1[d]	3.03 ± 0.20[c]	4.85 ± 0.28[c]
Cysteine	4.61 ± 0.23[c]	38.5 ± 2.6[d]	3.73 ± 0.29[d]	5.54 ± 0.30[d]
NAC	3.07 ± 0.17[b]	34.7 ± 1.7[c]	2.07 ± 0.12[b]	3.72 ± 0.21[b]
SAC	2.95 ± 0.16[b]	32.3 ± 1.0[b]	2.16 ± 0.07[b]	3.68 ± 0.18[b]
SEC	3.04 ± 0.19[b]	34.0 ± 2.0[c]	2.84 ± 0.14[c]	4.36 ± 0.17[c]
SMC	2.88 ± 0.14[b]	30.9 ± 1.0[b]	2.21 ± 0.23[b]	3.67 ± 0.20[b]
SPC	3.19 ± 0.10[b]	31.2 ± 1.1[b]	2.73 ± 0.21[c]	4.13 ± 0.19[c]

[a]Values are means ± SD, $n = 15$. Means in a column without a common letter differ, $P < 0.05$. See Table 1 for abbreviations.

TABLE 4
Enzyme Activity of Glucose-6-phosphate Dehydrogenase (G6PDH), Malic Enzyme, and Fatty Acid Synthase (FAS) in Liver from Mice Treated with a Normal Diet and a High Saturated Fat Diet Plus Water, Cysteine, or One of Five Cysteine-Containing Agents[a]

	G6PDH	Malic enzyme	FAS
	(nmol/min/mg protein)		
Normal diet	1.73 ± 0.38[a]	4.58 ± 0.23[a]	2.56 ± 0.11[a]
High saturated fat diet			
Water	3.63 ± 0.34[b]	6.35 ± 0.32[c]	5.48 ± 0.20[c]
Cysteine	4.43 ± 0.30[c]	6.77 ± 0.18[c]	5.24 ± 0.21[c]
NAC	3.16 ± 0.22[b]	5.17 ± 0.07[b]	4.17 ± 0.16[b]
SAC	3.32 ± 0.25[b]	5.63 ± 0.21[b]	3.89 ± 0.10[b]
SEC	3.42 ± 0.28[b]	5.58 ± 0.19[b]	4.25 ± 0.13[b]
SMC	2.84 ± 0.18[b]	5.22 ± 0.20[b]	4.04 ± 0.08[b]
SPC	3.08 ± 0.22[b]	5.53 ± 0.16[b]	3.68 ± 0.18[b]

[a]Values are means ± SD, $n = 15$. Means in a column without a common letter differ, $P < 0.05$. See Table 1 for abbreviations.

The inhibitory effect of SAC, SEC, and SPC on lipid and cholesterol biosynthesis in cultured rat hepatocytes has been examined (3–6). These authors indicated that these agents impaired TG biosynthesis by decreasing the activity of FAS in these cells. Our present *in vivo* study agreed that the three agents could effectively reduce FAS activity, and our results further found that these three agents as well as SMC and NAC effectively decreased the activity of malic enzyme, which consequently contributed to the reduction of TG biosynthesis. Our data partially explained the mode of action of these agents in inhibiting hypertriglyceridemia development. On the other hand, hypercholesterolemia was present in all high saturated fat-consuming mice, especially in the cysteine groups. Hypercholesterolemia induced by coconut oil was strongly correlated with an increase in acyl-CoA:cholesterol acyltransferase activity (21); thus, the observed hypercholesterolemia in our present study also might be due to the enhanced activity of this enzyme. However, previous cell-culture studies have reported that these cysteine-containing agents could inhibit cholesterol synthesis by changing the phosphorylation of HMG-CoA reductase in cultured cells (5,6). Thus, these agents might also affect HMG-CoA reductase in our present animal study and reduce cholesterol biosynthesis. Further study is necessary to elucidate the action mode of these agents in inhibiting hypercholesterolemia development.

TABLE 5
Glutathione Peroxidase Activity of Heart, Liver, and Kidney from Mice Treated with a Normal Diet and a High Saturated Fat Diet Plus Water, Cysteine, or One of Five Cysteine-Containing Agents[a]

	Heart	Liver	Kidney
	(U/mg protein)		
Normal diet	36.2 ± 3.2[d]	29.6 ± 1.1[c]	17.8 ± 1.3[b]
High saturated fat diet			
Water	28.3 ± 2.1[b]	24.0 ± 2.0[a]	13.5 ± 1.0[a]
Cysteine	22.6 ± 2.0[a]	23.2 ± 1.7[a]	14.0 ± 0.8[a]
NAC	29.3 ± 3.1[b]	26.7 ± 1.5[b]	14.3 ± 0.6[a]
SAC	28.4 ± 1.9[b]	27.4 ± 1.0[b]	13.8 ± 1.1[a]
SEC	29.8 ± 2.1[b]	26.7 ± 2.1[b]	14.6 ± 0.9[a]
SMC	32.7 ± 3.4[c]	27.0 ± 1.6[b]	17.8 ± 1.2[b]
SPC	33.0 ± 3.7[c]	27.2 ± 1.2[b]	18.2 ± 1.4[b]

[a]Values are means ± SD, $n = 15$. Means in a column without a common letter differ, $P < 0.05$. See Table 1 for abbreviations.

TABLE 6
Glucose-Induced MDA Concentration in Heart, Liver, and Kidney from Mice Treated with Normal Diet and High Saturated Fat Diet Plus Water, Cysteine, or One of Five Cysteine-Containing Agents[a]

	Heart	Liver	Kidney
	(μ/mg)		
Normal diet	0.96 ± 0.13[a]	1.08 ± 0.13[a]	1.23 ± 0.10[a]
High saturated fat diet,			
Water	1.43 ± 0.08[b]	1.56 ± 0.10[b]	1.73 ± 0.13[b]
Cysteine	2.06 ± 0.15[c]	2.43 ± 0.17[c]	2.31 ± 0.18[c]
NAC	1.03 ± 0.11[a]	1.33 ± 0.07[b]	1.34 ± 0.06[a]
SAC	1.14 ± 0.09[a]	1.25 ± 0.09[a]	1.48 ± 0.09[a]
SEC	1.28 ± 0.11[a]	1.16 ± 0.10[a]	1.34 ± 0.11[a]
SMC	1.23 ± 0.06[a]	1.40 ± 0.08[b]	1.59 ± 0.08[b]
SPC	1.21 ± 0.10[a]	1.37 ± 0.11[b]	1.42 ± 0.12[a]

[a]Values are means ± SD, $n = 15$. Means in a column without a common letter differ, $P < 0.05$. See Table 1 for abbreviations.

Dyslipidemia is implicated in a decline in renal function and causes hyperuricemia and hyperglycemia in humans and animals (22–24). The results of these studies indicated that a high saturated fat diet increased the risk of cardiovascular disease *via* impairing endothelial vasodilation function and caused endothelial damage. Our present study found these mice also developed hyperuricemia and hyperglycemia after they consumed a high saturated fat diet for 4 wk. Thus, our results agreed with earlier studies that high dietary saturated fat caused dyslipidemia and impaired glucose and uric acid metabolism. Furthermore, our present study observed that cysteine-containing agents improved hyperuricemia and hyperglycemia in these mice. This might be due to these agents alleviating dyslipidemia, which consequently improved glucose and uric acid metabolism. The other possibility was that these agents provided protection to renal function and affected glucose and uric acid metabolism.

The GPX activity-lowering effect from a coconut oil-rich diet has been reported (25). Our results agreed with that study, as GPX activity was lower in organs from coconut oil-consuming mice. Furthermore, we found that cysteine-containing agents could partially restore high saturated fat-reduced GPX activity, which consequently improved enzymatic antioxidant protection. Our previous animal study demonstrated that the administration of these cysteine-containing agents elevated the glutathione level and enhanced GPX activity in plasma and organs from mice consuming a normal diet (7). Thus, our results suggest these agents could improve hyperlipidemia-related oxidation damage *via* up-regulating GPX activity. In our present study, glucose was used to initiate oxidation. The purpose was to evaluate whether these agents could reduce high glucose-

induced oxidative stress as presented in diabetic conditions because hyperlipidemia is strongly associated with diabetic progression. The observed antioxidative protection from these cysteine-containing agents suggests these agents might prevent or delay the oxidation damage developed from the interaction of hyperlipidemia and hyperglycemia.

Cysteine administration markedly enhanced the activity of three lipogenic enzymes and reduced GPX activity, especially in heart. It is known the elevated G6PDH activity can cause abnormal carbohydrate and lipid metabolism, which then contributes to the development of metabolic diseases (26). Several studies have indicated that cysteine, based on its autooxidation property and vascular toxicity, should be considered as a risk factor for cardiovascular diseases (8,9). The results of our present study provide other evidence to elucidate the adverse role of cysteine in the progression of lipid metabolism disorder. Although the five cysteine-containing agents are hydrophilic amino acids and are naturally formed in *Allium* foods such as garlic, Benevenga *et al.* (27) indicated that excessive consumption of SMC leads to cytotoxicity. Therefore, the safety of these agents at effective dose levels needs further study. On the other hand, Krest *et al.* (28) reported that the content in *Allium* plants of these cysteine-containing compounds differed among species and varied over the vegetation period; for instance, the SMC content was 33–487 mg/100 g fresh garlic or 4–623 mg/100 g of stems or roots of *Allium* plants. Thus, it may not be appropriate to obtain these compounds by supplementing the diet with garlic or other *Allium* plants.

In conclusion, five cysteine-containing agents effectively reduced the activity of two lipogenic enzymes, malic enzyme and FAS, and suppressed TG and cholesterol biosynthesis in high saturated fat-consuming mice. These agents also improved hyperlipidemia-related hyperglycemia, hyperuricemia, and oxidation stress. These data support the contention that these compounds are potential multiply-protective agents for hyperlipidemia prevention or therapy.

ACKNOWLEDGMENTS

This study was supported by grants from National Science Council, Taiwan, ROC (NSC 93-2320-B-040-033). The authors would like to thank Wakunaga Pharmaceutical Co., Ltd. (Hiroshima, Japan) for kindly supplying SAC and SPC.

REFERENCES

1. Sheela, C.G., Kumud, K., and Augusti, K.T. (1995) Anti-Diabetic Effects of Onion and Garlic Sulfoxide Amino Acids in Rats, *Planta Med. 61,* 356–357.
2. Hatono, S., Jimenez, A., and Wargovich, M.J. (1996) Chemopreventive Effect of S-Allylcysteine and Its Relationship to the Detoxification Enzyme Glutathione S-Transferase, *Carcinogenesis 17,* 1041–1044.
3. Han, S.Y., Hu, Y., Anno, T., and Yanagita, T. (2002) S-Propyl Cysteine Reduces the Secretion of Apolipoprotein B100 and Triacylglycerol by HepG2 Cells, *Nutrition 18,* 505–509.
4. Liu, L., and Yeh, Y.Y. (2001) Water-Soluble Organosulfur Compounds of Garlic Inhibit Fatty Acid and Triglyceride Syntheses in Cultured Rat Hepatocytes, *Lipids 36,* 395–400.
5. Yeh, Y.Y., and Yeh, S.M. (1994) Garlic Reduces Plasma Lipids by Inhibiting Hepatic Cholesterol and Triacylglycerol Synthesis, *Lipids 29,* 189–193.
6. Gebhardt, R., and Beck, H. (1996) Differential Inhibitory Effects of Garlic-Derived Organosulfur Compounds on Cholesterol Biosynthesis in Primary Rat Hepatocyte Cultures, *Lipids 31,* 1269–1276.
7. Hsu, C.C., Huang, C.N., Hung, Y.C., and Yin, M.C. (2004) Five Cysteine-Containing Compounds Have Antioxidative Activity in Balb/CA Mice, *J. Nutr. 134,* 149–152.
8. Ozkan, Y., Ozkan, E., and Simsek, B. (2002) Plasma Total Homocysteine and Cysteine Levels as Cardiovascular Risk Factors in Coronary Heart Disease, *Int. J. Cardiol. 82,* 269–277.
9. Jacob, N., Bruckert, E., Giral, P., Foglietti, M.J., and Turpin, G. (1999) Cysteine Is a Cardiovascular Risk Factor in Hyperlipidemic Patients, *Atherosclerosis 146,* 53–59.
10. Kawasaki, M., Funabiki, R., and Yagasaki, K. (1998) Effects of Dietary Methionine and Cystine on Lipid Metabolism in Hepatoma-Bearing Rats with Hyperlipidemia, *Lipids 33,* 905–911.
11. Serougne, C., Felgines, C., Ferezou, J., Hajri, T., Bertin, C., and Mazur, A. (1995) Hypercholesterolemia Induced by Cholesterol- or Cystine-Enriched Diets Is Characterized by Different Plasma Lipoprotein and Apolipoprotein Concentrations in Rats, *J. Nutr. 125,* 35–41.
12. Serougne, C., Mathe, D., and Lutton, C. (1988) Induction of Long-lasting Hypercholesterolemia in the Rat Fed a Cystine-Enriched Diet, *Lipids 23,* 930–936.
13. Lowry, O.H., Rosebrough, N.J., and Farr, A.L. (1951) Protein Determination with the Folin Phenol Reagent, *J. Biol. Chem. 193,* 265–275.
14. Biggs, H.G., Erikson, J.M., and Moorehead, W.R. (1975) A Manual Colorimetric Assay of Triglycerides in Serum, *Clin. Chem. 21,* 437–441.
15. Hsu, R.Y., and Lardy, H.A. (1967) Pigeon Liver Malic Enzyme. II. Isolation, Crystallization, and Some Properties, *J. Biol. Chem. 242,* 520–526.
16. Nepokroeff, C.M., Lakshmanan, M.R., and Porter, J.W. (1975) Fatty-Acid Synthase from Rat Liver, *Methods Enzymol. 35,* 37–44.
17. Jain, S.K., and Palmer, M. (1997) The Effect of Oxygen Radical Metabolites and Vitamin E on Glycosylation of Proteins, *Free Radic. Biol. Med. 22,* 593–596.
18. SAS, *SAS/STAT User's Guide*, version 6, Statistical Analysis System Institute, Cary, NC, 1990.
19. Nishina, P.M., Lowe, S., Verstuyft, J., Naggert, J.K., Kuypers, F.A., and Paigen, B. (1993) Effects of Dietary Fats from Animal and Plant Sources on Diet-Induced Fatty Streak Lesions in C57BL/6J Mice, *J. Lipid Res. 34,* 1413–1422.
20. Oliveros, L.B., Videla, A.M., Ramirez, D.C., and Gimenez, M.S. (2003) Dietary Fat Saturation Produces Lipid Modifications in Peritoneal Macrophages of Mouse, *J. Nutr. Biochem. 14,* 370–377.
21. Jackson, B., Gee, A.N., Martinez-Cayuela, M., and Suckling, K.E. (1990) The Effects of Feeding a Saturated Fat-Rich Diet on Enzymes of Cholesterol Metabolism in the Liver, Intestine and Aorta of the Hamster, *Biochim. Biophys. Acta 1045,* 21–28.
22. Chu, N.F., Wang, D.J., Liou, S.H., and Shieh, S.M. (2000) Relationship Between Hyperuricemia and Other Cardiovascular Disease Risk Factors Among Adult Males in Taiwan, *Eur. J. Epidemiol. 16,* 13–17.
23. Wannamethee, S.G., Shaper, A.G., Durrington, P.N., and Perry, I.J. (1998) Hypertension, Serum Insulin, Obesity and the Metabolic Syndrome, *J. Human Hypertens. 12,* 735–741.
24. Amaral, M.E., Oliveira, H.C., Carneiro, E.M., Delghingaro-Augusto, V., Vieira, E.C., Berti, J.A., and Boschero, A.C. (2002) Plasma Glucose Regulation and Insulin Secretion in Hypertriglyceridemic Mice, *Horm. Metab. Res. 34,* 21–26.
25. D'Aquino, M., Benedetti, P.C., Di Felice, M., Gentili, V., Tomassi,

G., Maiorino, M., and Ursini, F. (1991) Effect of Fish Oil and Coconut Oil on Antioxidant Defence System and Lipid Peroxidation in Rat Liver, *Free Radic. Res. Commun. 13,* 147–152.
26. Takeuchi, H., Nakamoto, T., Mori, Y., Kawakami, M., Mabuchi, H., Ohishi, Y., Ichikawa, N., Koike, A., and Masuda, K. (2001) Comparative Effects of Dietary Fat Types on Hepatic Enzyme Activities Related to the Synthesis and Oxidation of Fatty Acid and to Lipogenesis in Rats, *Biosci. Biotechnol. Biochem. 65,* 1748–1754.
27. Benevenga, N.J., Yeh, M.H., and Lalich, J.J. (1976) Growth Depression and Tissue Reaction to the Consumption of Excess Dietary Methionine and S-Methyl-L-Cysteine, *J. Nutr. 106,* 1714–1729.
28. Krest, I., Glodek, J., and Keusgen, M. (2000) Cysteine Sulfoxides and Alliinase Activity of Some *Allium* Species, *J. Agric. Food Chem. 48,* 3753–3760.

[Received July, 2004; accepted September 30, 2004]

Alteration of 20:5n-3 and 22:6n-3 Fat Contents and Liver Peroxisomal Activities in Fenofibrate-Treated Rainbow Trout

Zhen-yu Du[a,b], Laurent Demizieux[a], Pascal Degrace[a], Joseph Gresti[a], Bastien Moindrot[a], Yong-jian Liu[b], Li-xia Tian[b], Jun-ming Cao[c], and Pierre Clouet[a,*]

[a]Unité Propre de Recherche de l'Enseignement Supérieur (UPRES) Lipides et Nutrition EA2422, Université de Bourgogne, 21000 Dijon, France, [b]Institute of Aquatic Economic Animals, School of Life Sciences, Sun Yat-sen University, 510275 Guangzhou, P.R. China, and [c]Guangdong Academy of Agriculture Science, 510640 Guangzhou, P.R. China

ABSTRACT: Fish easily accumulate n-3 PUFA of exogenous origin, but the underlying mechanisms are not well established in the whole animal. This study was undertaken to investigate whether this feature was physiologically associated with mitochondrial and peroxisomal capacities that differentially affect FA oxidation. For this purpose, peroxisomal FA oxidation was increased by treating rainbow trout with fenofibrate, which strongly stimulates the peroxisome proliferator-activated receptor-α in rodents. Diets containing EPA and DHA, with or without fenofibrate added, were administered to male trout for 12 d. After treatment, neither liver hypertrophy nor accumulation of fat was apparent within the liver and muscle cells. However, fenofibrate treatment decreased the contents of EPA and DHA in the liver, white muscle, and intraperitoneal fat tissue, which represented (per whole body) at least 280 mg less than in controls. Carnitine-dependent palmitate oxidation rates, expressed per gram of liver, were slightly increased by fenofibrate when measured from tissue homogenates and were unchanged when calculated from isolated mitochondria, relative to control fish. The treatment altered neither carnitine palmitoyltransferase I activity rates, expressed per gram of liver, nor the sensitivity of the enzyme to malonyl-CoA inhibition, but did increase the malonyl-CoA content (+45%). Meanwhile, fenofibrate increased (by about 30%) the peroxisome-related activities, i.e., catalase, carnitine-independent palmitate oxidation, acyl-CoA oxidase, and the peroxisomal FA-oxidizing system, relative to the control group. The data strongly suggest that the induction of peroxisomal activities, some of which being able to oxidize very long chain FA, was responsible for the lower contents of EPA and DHA in the body lipids of fenofibrate-treated trout.

Paper no. L9512 in *Lipids 39*, 849–855 (September 2004).

n-3 PUFA are essentially synthesized by the marine microorganisms that are massively ingested by many fish species. In the tissues of mammals, very long chain FA (VLCFA) of the n-3 and n-6 series are known to be ligands for peroxisome proliferator-activated receptors (PPAR) (1–5). Because peroxisomes contain enzymes that perform the partial chain-shortening of VLCFA (6,7), the cell contents of n-3 PUFA are expected to level off through β-oxidation, first in the peroxisomes and then in the mitochondria. However in fish, these n-3 PUFA, e.g., EPA and DHA, accumulate in body fats, suggesting that there is less control of their contents following the activation of PPAR than in mammals. Yet the tissue and cellular distribution of PPAR subtypes in *Danio rerio* has been shown to partially resemble that described in mammals (8). Differential activation of PPAR in the tissues of several animal species has been directly demonstrated from a number of chemical compounds, such as fibrates, that are widely used as hypolipidemic drugs (9,10). These compounds are known to increase dramatically the number and size of peroxisomes in liver cells, and to induce FA oxidation-related activities in peroxisomes and mitochondria, such as acyl-CoA oxidase (ACO) (11,12) and carnitine palmitoyltransferase I (CPT I) (13,14), respectively. Fenofibrate, clofibrate, ciprofibrate, and gemfibrozil all belong to the fibrate class and have been identified as strong peroxisome proliferators in rats and mice (9). However, their efficiency is much lower or null in hamsters, guinea pigs, and primates (15–17). The peroxisome proliferator effects of some of the fibrates mentioned are reportedly very weak in the rainbow trout (*Oncorhynchus mykiss*) and Japanese medaka (*Oryzias latipes*) (18–20), but no result regarding the actual efficiency of these weak increases in peroxisomal activities on the physiological status of n-3 VLCFA in tissues is available.

The above data prompted us to use as a model rainbow trout continuously fed a diet enriched in marine oil containing about 9% of total FA as EPA and DHA (on a molar basis), with or without fenofibrate treatment, under pair-feeding conditions. Our first objective was to investigate whether fenofibrate, as a strong peroxisome proliferator in rodents but not in fish, was capable of modifying the FA profile (with particular attention to EPA and DHA) in lipids of the liver, muscle, and intraperitoneal fat tissue of trout. The experimental design was also aimed at determining whether the change in tissue FA compositions might result from altered mitochondrial and/or peroxisomal enzyme activities involved in FA oxidation within the liver cells. Eventually, the data may provide information about the reactions induced in trout by chemical compounds biologically related to fibrates that are present in the environment and likely to alter the lipid composition of this fish species.

*To whom correspondence should be addressed at UPRES Lipides et Nutrition, Faculté des Sciences Gabriel, Université de Bourgogne, 21000 Dijon, France. E-mail: pclouet@u-bourgogne.fr

Abbreviations: ACO, acyl-CoA oxidase; ASP, acid-soluble products; bw, body weight; CPT I, carnitine palmitoyltransferase I; LCFA, long-chain FA; MUFA, monounsaturated FA; PFAOS, peroxisomal FA-oxidizing system; PPAR, peroxisome proliferator-activated receptor; SFA, saturated FA; VLCFA, very long chain FA.

EXPERIMENTAL PROCEDURES

Biochemicals. Fenofibrate and L-carnitine were gifts from Dr. François Bellamy (Laboratoires Fournier, Daix, France) and Dr. Gérard Lavianne (Sigma-Tau, Ivry-sur-Seine, France), respectively. [1-^{14}C]Palmitic acid and [^{3}H]acetyl-CoA were purchased from PerkinElmer Life Sciences (Courtaboeuf, France). L-[Methyl-^{3}H]carnitine was supplied by Amersham Biosciences (Saclay, France). Hyamine® and Ultima Gold XR™ were specific products provided by PerkinElmer. Biochemicals and chemicals were from Sigma-Aldrich (Saint-Quentin-Fallavier, France) and VWR International (Fontenay-sous-Bois, France), respectively.

Fish and diets. Male rainbow trout, weighing 230–250 g (about 11–12 mon old) and obtained from the Cordier-Gand fish farm (Corgoloin, France), were divided into two groups (6 per group). Fish were kept indoors on a 12-h/12-h light/dark cycle at 16–18°C in double-walled glass-fiber tanks, kindly lent by Michel Couturier (Drambon, France), containing 600 L of fresh water (3 trout per tank). Dissolved oxygen, pH, and ammonia were equilibrated to 7.1–8.1 mg/L, 7.10–7.26, and less than 0.2 mg/L, respectively, through pipes conveniently providing air and fresh water. Before the experiment, trout were fed a commercial diet, Aqualife 17 (BioMar, Nersac, France), containing 42% crude protein, 22% fat (see FA composition in the second column of Table 2), 17.6% nonnitrogenous extract, 8.6% ash, 2% cellulose, 1.23% total phosphate, 1.09% available phosphate, and 1.7% methionine + cysteine. Over the 12 d of the experiment, the same diet was administered to each trout by hand as small pasty balls of about 4–5 mm diameter, made from 0.9 g of dry pellets per 100 g of body weight (bw) per day, wetted before use and given as soon as they were swallowed (instant ingestion). For fenofibrate-treated trout, the drug was kneaded with the pasty balls (100 mg/kg bw per day). The dose of fenofibrate was the same as that usually administered to rats and known to trigger the maximum effect (21) in the minimum amount of time. Trout were food-deprived for 16 h, then stunned by a blow to the head; the spinal cord was then transected. Liver, intraperitoneal fat tissue, and white muscle (after removing the viscera, head, skin with fins, red muscle, and bones) were immediately weighed, and samples were frozen in liquid nitrogen and stored at –86°C for later analyses of total lipids for the three organs and of the crucial metabolites implied in FA oxidation (L-carnitine, malonyl-CoA) for the liver only.

Homogenate and mitochondrial fraction preparations. The rest of each liver was cut finely into ice-cold 0.25 mol/L sucrose medium containing 1 mmol/L of EGTA and 10 mmol/L of Tris/HCl, pH 7.4, rinsed five times in the same medium, blotted with absorbent paper, and weighed. The tissue was diluted (1:80, wt/vol) in the chilled sucrose medium and homogenized by only four strokes of a Teflon pestle rotating at 300 rpm in a Potter–Elvehjem homogenizer (Kontes, Vineland, NJ). Some samples of homogenate were kept apart for marker enzyme activity measurements and also for mitochondrial and peroxisomal palmitate oxidation analyses (see below). The rest of the homogenate was centrifuged at 2,000 × *g* for 4 min at 4°C, and the supernatant was immediately centrifuged at 13,000 × *g* for 6 min. The pellet was resuspended with the sucrose medium and centrifuged under the preceding conditions. The procedure was repeated once, and the pellet resuspended in buffered 0.3 mol/L sucrose was used as the mitochondrial fraction. The protein content of this fraction was roughly estimated by spectrophotometry (22) immediately before incubations for palmitate oxidation, and CPT I activity measurements were performed. Protein content was subsequently determined more accurately using the bicinchoninic acid method (23).

Carnitine, malonyl-CoA, and lipid contents. Carnitine esters were first hydrolyzed with KOH, and total carnitine was estimated by the radiochemical procedure of McGarry and Foster (24). Malonyl-CoA determination was carried out as previously described (25) on a Varian HPLC system (UV detection at 254 nm) equipped with a C18 column (Lichrocart, Superspher; 250 × 4 mm; Merck, Darmstadt, Germany). Total lipids were extracted with chloroform/methanol (2:1, vol/vol) according to the procedure of Folch *et al.* (26). Their constitutive FA were methylated through the action of boron trifluoride, separated by GLC (Chrompack CP9002) on a capillary column (CP Wax 52CB; 30 m × 0.32 mm; Varian, Les Ulis, France) and quantified using heptadecanoic acid as an internal standard (27).

Mitochondrial and peroxisomal enzyme assays. The presence of mitochondria was assessed by the activities of monoamine oxidase (EC 1.4.3.4) (28) and citrate synthase (EC 4.1.3.7) (29), whereas that of peroxisomes was revealed by the activities of urate oxidase (EC 1.7.3.3) (30), catalase (EC 1.11.1.6) (31), ACO (EC 1.3.3.6) (32), and CN^{-}-insensitive palmitoyl-CoA-dependent NAD^{+} reduction (32), a short sequence of the β-oxidation cycle, described as the peroxisomal FA-oxidizing system (PFAOS). CPT I (EC 2.3.1.21) activity and inhibition of CPT I by malonyl-CoA were carried out using tritiated L-carnitine with palmitoyl-CoA, as described previously (33), and by extraction of the palmitoyl-[^{3}H]carnitine produced with butan-1-ol. The associated radioactivity was counted after mixing with Ultima Gold XR.

Mitochondrial and peroxisomal palmitate oxidation. (i) From liver homogenates. Palmitate oxidation rates were measured from homogenates using two media as described in Reference 34, the first allowing mitochondrial and peroxisomal activities to occur, and the second allowing the peroxisomal activity only. After 30 min, the radioactivity initially held by [1-^{14}C]palmitate (bound to BSA in a 5:1 molar ratio) was recovered on labeled short molecules released from the β-oxidative cycle and soluble in perchloric acid (acid-soluble products, ASP) and on labeled CO_2 trapped in Hyamine. The radioactivity of ASP and of Hyamine containing CO_2 was measured after mixing each with Ultima Gold XR.

(ii) From liver mitochondria. The incubation medium described in Reference 22 contained [1-^{14}C]palmitate (bound to BSA in a 1.5:1 molar ratio), and the reaction was stopped with perchloric acid after 8 min. The radioactivity of CO_2 and ASP was measured as for the oxidation of palmitate by liver homogenates.

Statistics. Results are expressed as means ± SEM (n = 6 per group). Data were subjected to one-way ANOVA fol-

TABLE 1
Effects of Fenofibrate Treatment on Organ Weights and Lipid Contents of Rainbow Trout[a]

Parameters studied	Control	Fenofibrate-treated
Body and organ weights		
Total body (g)	247.1 ± 10.6	241.3 ± 6.9
Liver (% of bw)	1.29 ± 0.07	1.23 ± 0.03
White muscle (% of bw)	47.5 ± 2.2	46.7 ± 2.4
Intraperitoneal fat tissue (% of bw)	1.47 ± 0.15	1.41 ± 0.28
Total FA content (mg/g wet tissue)		
Liver	30.5 ± 5.7	28.9 ± 5.0
White muscle	12.7 ± 2.8	13.3 ± 7.4
Intraperitoneal fat tissue	709 ± 5	737 ± 8*

[a]Values are means ± SEM (n = 6 in each group). An asterisk (*) indicates that results between control and treated groups differ significantly at $P < 0.05$. bw, body weight.

lowed by a Student's t-test analysis. Differences were considered significant at $P < 0.05$.

RESULTS

Body parameters and lipid analysis. Fenofibrate treatment did not alter the weights of liver, white muscle, or intraperitoneal fat tissue (Table 1). The total FA content was increased in intraperitoneal fat tissue only, relative to controls. The FA composition of total lipids (Table 2) shows that the treatment did not modify the proportion of saturated FA (ΣSFA) and of monounsaturated FA (ΣMUFA) for each organ. Oleic and linoleic acids (18:1 and 18:2n-6), abundant in the dietary lipids, were low in the livers of both groups, but were always greater in the liver, white muscle, and intraperitoneal fat tissue of fenofibrate-treated fish than in the controls. Conversely, EPA and DHA, which were less than 9% of the dietary lipids, amounted to about 50% of the FA in liver, 40% of the FA in white muscle, and 30% of the FA in intraperitoneal fat tissue once they were ingested. However, the presence of EPA and DHA within the three tissues was always lower in fenofibrate-treated fish than in the controls. Taking into account the actual mass of organs and the corresponding content of total FA, the deficit of EPA and DHA attributable to fenofibrate was calculated at around 280 mg per whole fish from the three isolated organs only.

Parameters related to FA oxidation. From monoamine oxidase and citrate synthase activities, expressed per gram of liver and per milligram of mitochondrial protein, the content of mitochondrial protein calculated per gram of liver was 25% greater after treatment (Table 3). For the peroxisomal marker enzymes used, the activity of urate oxidase, expressed per gram of liver, was about 30% lower and that of catalase 30% greater in treated fish, relative to the controls (Table 3). In the mitochondrial fractions, the specific activities of contaminating catalase were low and quite similar in both groups (45 ± 12 and 68 ± 15 mIU/min·mg protein^{-1} in control and treated fish, respectively). As regards the parameters related to mitochondrial FA oxidation (Table 4), the L-carnitine content per gram of tissue was markedly decreased by fenofibrate. In treated fish, the carnitine-dependent palmitate oxidation rates per liver unit were only slightly greater when measured from crude tissue homogenates and not significantly different when calculated from isolated mitochondria and the

TABLE 2
FA Composition of Total Lipids in the Diet and in the Liver, White Muscle, and Intraperitoneal Fat Tissue of Control and Fenofibrate-Treated Rainbow Trout[a]

		Liver		White muscle		Intraperitoneal fat tissue	
FA (molar %)	Diet	Control	Treated	Control	Treated	Control	Treated
14:0	2.69	2.07 ± 0.20	1.40 ± 0.04*	4.48 ± 0.14	4.47 ± 0.13	6.83 ± 0.02	6.2 ± 0.11*
16:0	13.62	20.7 ± 0.3	20.1 ± 0.1	18.7 ± 0.5	16.4 ± 0.2*	14.7 ± 0.2	13.9 ± 0.2*
16:1	2.81	2.61 ± 0.13	1.32 ± 0.03*	6.34 ± 0.12	5.87 ± 0.17	8.5 ± 0.2	7.4 ± 0.3*
18:0	3.83	4.9 ± 0.3	6.7 ± 0.3*	4.1 ± 0.1	3.8 ± 0.1	3.1 ± 0.1	3.1 ± 0.2
18:1	21.06	8.7 ± 0.5	9.4 ± 0.2	13.1 ± 0.2	16.5 ± 0.3*	18.1 ± 0.5	20.0 ± 0.5*
18:2n-6	36.29	3.2 ± 0.3	7.5 ± 0.2*	3.8 ± 0.5	11.0 ± 0.3*	9.1 ± 0.5	14.4 ± 1.0*
18:3n-6	—	0.17 ± 0.03	0.21 ± 0.02	0.33 ± 0.01	0.38 ± 0.02	0.37 ± 0.03	0.46 ± 0.01
18:3n-3	5.39	0.56 ± 0.02	0.73 ± 0.07	0.89 ± 0.04	1.85 ± 0.02*	1.67 ± 0.2	2.29 ± 0.07*
20:1n-9	2.51	0.48 ± 0.05	0.82 ± 0.05*	3.02 ± 0.36	3.53 ± 0.15	3.34 ± 0.3	4.26 ± 0.60
20:2n-6	—	0.28 ± 0.07	0.91 ± 0.15*	0.35 ± 0.03	0.74 ± 0.01*	1.71 ± 0.15	00.87 ± 0.18*
20:3n-6	—	0.22 ± 0.04	1.09 ± 0.31	—	—	0.22 ± 0.01	0.30 ± 0.02*
20:4n-6	0.25	4.2 ± 0.2	4.1 ± 0.1	1.04 ± 0.02	0.85 ± 0.02*	0.76 ± 0.01	0.69 ± 0.01*
20:5n-3 (EPA)	3.58	9.6 ± 0.5	6.6 ± 0.6*	9.3 ± 0.2	7.8 ± 0.1*	8.6 ± 0.3	6.7 ± 0.2*
22:1n-9	1.89	—	—	—	—	—	—
22:5n-6	—	0.24 ± 0.03	0.26 ± 0.03	0.46 ± 0.03	0.34 ± 0.01*	0.39 ± 0.01	0.35 ± 0.01
22:5n-3	0.88	1.69 ± 0.05	1.51 ± 0.16	2.67 ± 0.12	2.63 ± 0.07	3.42 ± 0.03	3.22 ± 0.02*
22:6n-3 (DHA)	5.20	40.4 ± 0.9	37.2 ± 0.6*	31.5 ± 0.5	23.8 ± 0.8*	19.4 ± 0.6	16.0 ± 0.8*
ΣSFA	20.14	27.7 ± 0.5	28.2 ± 0.4	27.4 ± 0.6	24.7 ± 0.2*	24.6 ± 0.2	23.2 ± 0.4*
ΣMUFA	28.27	11.8 ± 0.5	11.6 ± 0.2	22.5 ± 0.4	25.9 ± 0.6*	29.9 ± 0.7	31.6 ± 0.7
Σn-6 PUFA	36.54	8.3 ± 0.4	14.1 ± 0.7*	6.0 ± 0.1	13.3 ± 0.3*	12.6 ± 0.4	17.1 ± 0.8*
Σn-3 PUFA	15.05	52.3 ± 1.3	46.2 ± 1.1*	44.3 ± 0.3	36.1 ± 0.7*	33.1 ± 1.0	28.2 ± 1.2*
EPA + DHA	8.78	50.0 ± 0.9	43.8 ± 0.6*	40.8 ± 0.6	31.6 ± 0.8*	28.0 ± 0.6	22.7 ± 0.8*
EPA + DHA (mg/organ)		52.9 ± 1.8	41.0 ± 1.3*	701 ± 12	586 ± 8*	796 ± 11	643 ± 9*

[a]Values are means ± SEM (n = 6 in each group). An asterisk (*) indicates that results between control and treated groups differ significantly at $P < 0.05$. SFA, saturated FA; MUFA, monounsaturated FA.

TABLE 3
Effects of Fenofibrate Treatment on Mitochondrial and Peroxisomal Marker Enzyme Activities in the Liver of Rainbow Trout[a]

Marker enzyme activities	Control	Fenofibrate-treated
Mitochondrial enzymes		
Monoamine oxidase activity		
In tissue homogenates (mIU/g wet tissue)	63 ± 6	89 ± 4*
In mitochondrial fractions (mIU/mg protein)	1.48 ± 0.07	1.53 ± 0.04
Citrate synthase activity		
In tissue homogenates (mIU/g wet tissue)	5471 ± 93	6982 ± 150*
In mitochondrial fractions (mIU/mg protein)	166 ± 5	191 ± 7*
Mitochondrial protein content[b] (mg protein/g wet tissue)	37.8 ± 1.4	47.3 ± 1.1*
Peroxisomal enzymes		
Catalase activity (IU·10^3/g wet tissue)	27.3 ± 0.5	35.5 ± 2.8*
Urate oxidase (IU/g wet tissue)	0.51 ± 0.05	0.37 ± 0.03*

[a]Values are means ± SEM (n = 6 in each group). An asterisk (*) indicates that results between control and treated groups differ significantly at $P < 0.05$.
[b]Calculated by dividing monoamine oxidase and citrate synthase activities, expressed per gram of wet tissue, by the corresponding specific activities in mitochondrial fractions.

mitochondrial protein content per gram of tissue, relative to the controls. The activity of CPT I, a key enzyme of the mitochondrial FA oxidation pathway, was comparable in both groups when expressed per gram of liver. Malonyl-CoA, as the physiological inhibitor of CPT I, was found to be 45% more concentrated within the liver cells of treated fish than those of the controls. The sensitivity of CPT I to malonyl-CoA inhibition was quite similar in both groups (Fig. 1), the enzyme activity being half reduced for the same malonyl-CoA concentration (IC_{50} = 0.2 μmol/L). In peroxisomes, palmitate oxidation rates measured using liver homogenates were 43% greater in fenofibrate-treated fish than in the controls. The activities of PFAOS, a sequence of the entire peroxisomal FA oxidation pathway, and of ACO, a key enzyme in this sequence, were increased by 32 and 65%, respectively.

DISCUSSION

DHA and EPA in body lipids. One of the main observations in this study was that, in trout fed a diet containing fish oil, EPA and DHA accumulated in body fats to a lesser extent when the fish were concomitantly treated with fenofibrate. In whole-body lipids, the EPA and DHA contents predominantly depended on their levels in the dietary oils ingested. For example, in a previous study, a mixture of fish oil and soybean oil given as the dietary lipid source to trout gave rise to a FA profile in the liver lipids close to that found in this study (35). Furthermore, replacing soybean oil in the diet with fish oil reportedly resulted in higher levels of EPA and DHA and in lower levels of n-6 FA in tissues of Atlantic salmon (*Salmo salar*) (36) and rainbow trout (37). However, DHA also originates within the liver cells from EPA or 18:3n-3 through microsomal desaturation/elongation steps, followed by a retroconversion process in peroxisomes, as demonstrated in mammals (38) and in rainbow trout (39). Nevertheless, when fish oil (or DHA) was added to the diet, as in the case of our model, the *de novo* synthesis of DHA from labeled 18:3n-3 was clearly reduced (39,40). Synthesis of EPA from α-linolenic acid occurs through the aforementioned microsomal reactions as well (39). EPA and DHA are also substrates for oxidation reactions, which are somehow likely to alter the levels of these VLCFA in tissue lipids. This last aspect constitutes the main concern of this study.

TABLE 4
Effects of Fenofibrate Treatment on Parameters Related to Mitochondrial and Peroxisomal FA Oxidation in the Liver of Rainbow Trout[a]

FA oxidation-related activities	Control	Fenofibrate-treated
Mitochondria-related parameters		
Total L-carnitine content (nmol/g wet tissue)	78.9 ± 4.2	56.9 ± 2.1*
Carnitine-dependent palmitate oxidation (nmol/min·g wet liver^{-1})		
Calculated from tissue homogenates	42.9 ± 2.6	49.9 ± 2.8*
Calculated from isolated mitochondria[b]	9.76 ± 0.60	9.00 ± 0.45
Carnitine palmitoyltransferase I[b] (nmol/min·g wet liver^{-1})	26.1 ± 1.5	26.0 ± 1.8*
Malonyl-CoA content (nmol/g wet liver)	56.2 ± 3.7	81.9 ± 6.4*
Peroxisomal-related activities in tissue homogenates (nmol/min·g wet liver^{-1})		
Carnitine-independent palmitate oxidation	4.1 ± 0.3	5.9 ± 0.5*
Acyl-CoA oxidase	350 ± 40	580 ± 50*
Peroxisomal FA oxidizing system	55.8 ± 3.9	73.7 ± 4.4*

[a]Values are means ± SEM (n = 6 in each group). An asterisk (*) indicates that results between control and treated groups differ significantly at $P < 0.05$.
[b]Calculated from activities of mitochondrial fractions (nmol/min·mg protein^{-1}) multiplied by the corresponding mitochondrial protein contents per gram of liver.

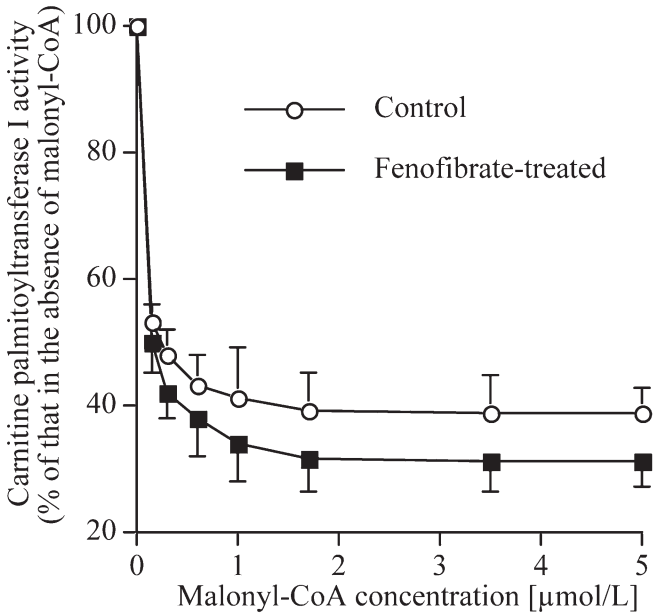

FIG. 1. Sensitivity of carnitine palmitoyltransferase I to malonyl-CoA inhibition in mitochondria isolated from the liver of rainbow trout with or without fenofibrate treatment. T-bars show SEM ($n = 6$ in each group). All malonyl-CoA concentrations checked gave rise to values between the control and fenofibrate-treated trout not significantly different at $P < 0.05$.

Alterations of liver growth. Fenofibrate-induced hepatic effects are well documented in mammals, but their levels appear to differ greatly in trout. In humans, the drug is used as a normolipidemic agent, as are other members of the fibrate family known to activate PPARα (9,10). In rodents, and rats in particular, the range of effects includes enlargement of the liver through anti-apoptotic mechanisms (41) and an increase in number and size of mitochondria and peroxisomes within the hepatic cells (42–44). In trout, however, we observed that the fenofibrate treatment did not enlarge the liver but did increase the content of mitochondrial protein per gram of tissue somehow. Interestingly, gemfibrozil administered to trout for 2 wk reportedly caused significant liver enlargement (20), which could be considered a secondary or belated effect of this fibrate. As regards peroxisome marker enzymes, catalase exhibited higher activity rates, which may correspond to an increase in hydrogen peroxide production, in accordance with observations made on rat perfused liver (45,46). On the contrary, urate oxidase activities were slightly depressed in treated fish, relative to controls. Urate oxidase is considered as a stable component of peroxisomes in hepatic cells irrespective of applied treatments (47), at least in rodents; thus, its activity rates were logically also affected little in trout, even when other peroxisomal activities were increased.

Effects on activities related to FA oxidation. In rodents, fenofibrate strongly induced peroxisomal and mitochondrial activities related to corresponding FA oxidation pathways within the liver (13,48), but in trout, these activities were affected at a much lower level after the same treatment. DHA, as a VLCFA, is a substrate for FA oxidation within peroxisomes (49,50), whereas long-chain FA (LCFA) containing 16 to 18 carbons are preferentially oxidized within mitochondria (47). EPA is reportedly degraded within both organelles (50). That the percentages of DHA and EPA were highest in hepatic lipids suggests that the liver is a crucial organ in the metabolism of these VLCFA and in their distribution to other organs through lipoprotein secretion. From Table 2, it is apparent that oleic, linoleic, and α-linolenic acids, which are abundant in the dietary lipids and are good substrates as CoA-derivatives for CPT I (22,51), were dramatically diminished within the liver lipids of both groups. This result suggests that oleic and linoleic acids are oxidized within the mitochondria for energy requirements, and that α-linolenic acid is a very good substrate for the β-oxidation pathway and also a precursor for EPA/DHA biosynthesis. Conversely, even though poorly represented in the dietary lipids, EPA and DHA accumulated markedly, but to a slightly lesser extent, in fenofibrate-treated fish. This fact was observed in the three organs studied, accounting for a notable deficit in EPA and DHA per whole trout.

Mitochondrial FA oxidation. Surprisingly, whereas fenofibrate treatment was reported to increase the total L-carnitine content of the rat liver more than fivefold (13), this content was markedly decreased when trout were treated under similar experimental conditions. Carnitine-dependent palmitate oxidation rates, as measured *in vitro* in the presence of exogenous L-carnitine, were slightly greater from crude liver homogenates but similar when calculated from isolated mitochondria of treated fish relative to the controls. This result is in accordance with the comparable activity found per gram of tissue of CPT I as the key enzyme of the mitochondrial FA oxidation pathway. In both groups, the controlling effect of malonyl-CoA on CPT I was very efficient, since the malonyl-CoA concentration that inhibited CPT I activity by 50% was around 0.2 μmol/L, as already reported in trout (52). Owing to the greater malonyl-CoA content per gram of liver in treated fish, a more marked decrease in CPT I activity would be expected *in vivo* and would reduce the activity of the mitochondrial FA oxidation pathway in this group. In this context, Osmundsen and Bjornstad (53) showed that DHA inhibits the mitochondrial β-oxidation of other FA, which could apply to both groups. As a result, the higher percentage of all the FA possessing 18 carbons in the hepatic lipids of fenofibrate-treated trout might indicate lower activities of the mitochondrial FA oxidation enzymes.

Peroxisomal FA oxidation. All the peroxisomal activities expressed per gram of liver and related to carnitine-independent FA oxidation were increased by about 30% by fenofibrate treatment. These increases could be considered modest relative to the greater effects of fenofibrate in rats on the same basis (13,54). In trout, the increase in peroxisomal FA oxidation capacities may be associated with an increase in the retroconversion of 24:6n-3 to DHA within the peroxisomes, as observed in mammals (38). Yet the abundance of DHA was slightly lower in treated trout, which suggests that the increase in peroxisomal FA oxidation by fenofibrate treatment was sufficient to significantly chain-shorten a greater part of the DHA (and also of the EPA), the shortened products then

being oxidized through the mitochondrial carnitine-dependent FA oxidation pathway (47).

Regulation of FA oxidation. It has been shown that, in cultured mammal cells, DHA is capable of enhancing the levels of mRNA expression of CPT I and ACO through PPARα activation, as did the fibrate-related drugs (55). Therefore, we were puzzled that, in trout, the continuous ingestion of EPA and DHA was not associated with high mitochondrial and peroxisomal enzyme activities. This suggests that, in trout, VLCFA are ligands with relatively poor affinity for PPARα. The use of fenofibrate, which is one of the more potent activators of PPAR in rodents, appeared to be inefficient in liver growth and mitochondrial activities and to be moderately effective on peroxisomal activities in trout. These data may indicate that the conformation of PPAR and/or their levels of mRNA expression in the liver of trout differ strongly from those in rats. The trout model also allowed us to demonstrate that the composition of VLCFA in lipids may be significantly altered, even through moderately increased peroxisomal FA oxidation activity. From a practical point of view, the impossibility of inducing a peroxisomal FA oxidation system in trout equal to that in rats suggests that fish are relatively insensitive to the fenofibrate-related xenobiotics accidentally present in the environment.

ACKNOWLEDGMENTS

We are grateful to Monique Baudoin for figure construction and for typing the manuscript. This work was supported by grants from the Ministère de la Recherche et de la Technologie and from the Région Bourgogne, Dijon.

REFERENCES

1. Gottlicher, M., Demoz, A., Svensson, D., Tollet, P., Berge, R.K., and Gustafsson, J.A. (1993) Structural and Metabolic Requirements for Activators of the Peroxisome Proliferator-Activated Receptor, *Biochem. Pharmacol. 46*, 2177–2184.
2. Forman, B.M., Chen, J., and Evans, R.M. (1997) Hypolipidemic Drugs, Polyunsaturated Fatty Acids, and Eicosanoids Are Ligands for Peroxisome Proliferator-Activated Receptors α and δ, *Proc. Natl. Acad. Sci. USA 94*, 4312–4317.
3. Krey, G., Braissant, O., L'Horset, F., Kalkhoven, E., Perroud, M., Parker, M.G., and Wahli, W. (1997) Fatty Acids, Eicosanoids, and Hypolipidemic Agents Identified as Ligands of Peroxisome Proliferator-Activated Receptors by Coactivator-Dependent Receptor Ligand Assay, *Mol. Endocrinol. 11*, 779–791.
4. Lin, Q., Ruuska, S.E., Shaw, N.S., Dong, D., and Noy, N. (1999) Ligand Selectivity of the Peroxisome Proliferator-Activated Receptor α, *Biochemistry 38*, 185–190.
5. Diep, Q.N., Touyz, R.M., and Schiffrin, E.L. (2000) Docosahexaenoic Acid, a Peroxisome Proliferator-Activated Receptor α Ligand, Induces Apoptosis in Vascular Smooth Muscle Cells by Stimulation of p38 Mitogen-Activated Protein Kinase, *Hypertension 36*, 851–855.
6. Osmundsen, H., Neat, C.E., and Norum, K.R. (1979) Peroxisomal Oxidation of Long Chain Fatty Acids, *FEBS Lett. 99*, 292–296.
7. Osmundsen, H., Bremer, J., and Pedersen, J.I. (1991) Metabolic Aspects of Peroxisomal β-Oxidation, *Biochim. Biophys. Acta 1085*, 141–158.
8. Ibabe, A., Grabenbauer, M., Baumgart, E., Fahimi, H.D., and Cajaraville, M.P. (2002) Expression of Peroxisome Proliferator-Activated Receptors in Zebrafish (*Danio rerio*), *Histochem. Cell Biol. 118*, 231–239.
9. Haubenwallner, S., Essenburg, A.D., Barnett, B.C., Pape, M.E., DeMattos, R.B., Krause, B.R., Minton, L.L., Auerbach, B.J., Newton, R.S., Leff, T., *et al.* (1995) Hypolipidemic Activity of Select Fibrates Correlates to Changes in Hepatic Apolipoprotein C-III Expression: A Potential Physiologic Basis for Their Mode of Action, *J. Lipid Res. 36*, 2541–2551.
10. Motojima, K. (2002) A Metabolic Switching Hypothesis for the First Step in the Hypolipidemic Effects of Fibrates, *Biol. Pharm. Bull. 25*, 1509–1511.
11. Bardot, O., Clemencet, M.C., Malki, M.C., and Latruffe, N. (1995) Delayed Effects of Ciprofibrate on Rat Liver Peroxisomal Properties and Proto-oncogene Expression, *Biochem. Pharmacol. 50*, 1001–1006.
12. Berthou, L., Duverger, N., Emmanuel, F., Langouet, S., Auwerx, J., Guillouzo, A., Fruchart, J.C., Rubin, E., Denefle, P., Staels, B., and Branellec, D. (1996) Opposite Regulation of Human Versus Mouse Apolipoprotein A-I by Fibrates in Human Apolipoprotein A-I Transgenic Mice, *J. Clin. Invest. 97*, 2408–2416.
13. Tsoko, M., Beauseigneur, F., Gresti, J., Demarquoy, J., and Clouet, P. (1998) Hypolipidaemic Effects of Fenofibrate Are Not Altered by Mildronate-Mediated Normalization of Carnitine Concentration in Rat Liver, *Biochimie 80*, 943–948.
14. Minnich, A., Tian, N., Byan, L., and Bilder, G. (2001) A Potent PPAR-α Agonist Stimulates Mitochondrial Fatty Acid β-Oxidation in Liver and Skeletal Muscle, *Am. J. Physiol. Endocrinol. Metab. 280*, E270–E279.
15. Pourbaix, S., Heller, F., and Harvengt, C. (1984) Effect of Fenofibrate and LF 2151 on Hepatic Peroxisomes in Hamsters, *Biochem. Pharmacol. 33*, 3661–3666.
16. Cornu-Chagnon, M.C., Dupont, H., and Edgar, A. (1995) Fenofibrate: Metabolism and Species Differences for Peroxisome Proliferation in Cultured Hepatocytes, *Fundam. Appl. Toxicol. 26*, 63–74.
17. Guo, Q., Wang, P.R., Milot, D.P., Ippolito, M.C., Hernandez, M., Burton, C.A., Wright, S.D., and Chao, Y. (2001) Regulation of Lipid Metabolism and Gene Expression by Fenofibrate in Hamsters, *Biochim. Biophys. Acta 1533*, 220–232.
18. Yang, J.H., Kostecki, P.T., Calabrese, E.J., and Baldwin, L.A. (1990) Induction of Peroxisome Proliferation in Rainbow Trout Exposed to Ciprofibrate, *Toxicol. Appl. Pharmacol. 104*, 476–482.
19. Donohue, M., Baldwin, L.A., Leonard, D.A., Kostecki, P.T., and Calabrese, E.J. (1993) Effect of Hypolipidemic Drugs Gemfibrozil, Ciprofibrate, and Clofibric Acid on Peroxisomal β-Oxidation in Primary Cultures of Rainbow Trout Hepatocytes, *Ecotoxicol. Environ. Saf. 26*, 127–132.
20. Scarano, L.J., Calabrese, E.J., Kostecki, P.T., Baldwin, L.A., and Leonard, D.A. (1994) Evaluation of a Rodent Peroxisome Proliferator in Two Species of Freshwater Fish: Rainbow Trout (*Onchorynchus mykiss*) and Japanese Medaka (*Oryzias latipes*), *Ecotoxicol. Environ. Saf. 29*, 13–19.
21. Legendre, C., Causse, E., Chaput, E., Salvayre, R., Pineau, T., and Edgar, A.D. (2002) Fenofibrate Induces a Selective Increase of Protein-Bound Homocysteine in Rodents: A PPARα-Mediated Effect, *Biochem. Biophys. Res. Commun. 295*, 1052–1056.
22. Clouet, P., Niot, I., and Bézard, J. (1989) Pathway of α-Linolenic Acid Through the Mitochondrial Outer Membrane in the Rat Liver and Influence on the Rate of Oxidation, *Biochem. J. 263*, 867–873.
23. Smith, P.K., Krohn, R.I., Hermanson, G.T., Mallia, A.K., Gartner, F.H., Provenzano, M.D., Fujimoto, E.K., Goeke, N.M., Olson, B.J., and Klenk, D.C. (1985) Measurement of Protein Using Bicinchoninic Acid, *Anal. Biochem. 150*, 76–85.

24. McGarry, J.D., and Foster, D.W. (1976) An Improved and Simplified Radioisotopic Assay for the Determination of Free and Esterified Carnitine, *J. Lipid Res. 17*, 277–281.
25. King, M.T., Reiss, P.D., and Cornell, N.W. (1988) Determination of Short-Chain Coenzyme A Compounds by Reversed-Phase High-Performance Liquid Chromatography, *Methods Enzymol. 166*, 70–79.
26. Folch, J., Lees, M., and Sloane Stanley, G.H. (1957) A Simple Method for the Isolation and Purification of Total Lipids from Animal Tissues, *J. Biol. Chem. 226*, 497–509.
27. Slover, H.T., and Lanza, E. (1979) Quantitative Analysis of Food Fatty Acids by Capillary Gas Chromatography, *J. Am. Oil Chem. Soc. 56*, 933–943.
28. Weissbach, H., Smith, T.E., Daly, J.W., Witkop, B., and Udenfriend, S. (1960) A Rapid Spectrophotometric Assay of Monoamine Oxidase Based on the Rate of Disappearance of Kynuramine, *J. Biol. Chem. 235*, 1160–1163.
29. Robinson, J.B., Jr., and Srere, P.A. (1985) Organization of Krebs Tricarboxylic Acid Cycle Enzymes in Mitochondria, *J. Biol. Chem. 260*, 10800–10805.
30. Leighton, F., Poole, B., Beaufay, H., Baudhuin, P., Coffey, J., Fowler, S., and De Duve, C. (1968) The Large-Scale Separation of Peroxisomes, Mitochondria, and Lysosomes from the Livers of Rats Injected with Triton WR-1339, *J. Cell. Biol. 37*, 482–513.
31. Aebi, H. (1974) Catalase, in *Methods of Enzymatic Analysis* (Bergmeyer, H.U., eds.), pp. 673–684, Academic Press, New York.
32. Bronfman, M., Inestrosa, N.C., and Leighton, F. (1979) Fatty Acid Oxidation by Human Liver Peroxisomes, *Biochem. Biophys. Res. Commun. 88*, 1030–1036.
33. Bremer, J. (1981) The Effect of Fasting on the Activity of Liver Carnitine Palmitoyltransferase and Its Inhibition by Malonyl-CoA, *Biochim. Biophys. Acta 665*, 628–631.
34. Veerkamp, J.H., Van Moerkerk, H.T., Glatz, J.F., and Van Hinsbergh, V.W. (1983) Incomplete Palmitate Oxidation in Cell-Free Systems of Rat and Human Muscles, *Biochim. Biophys. Acta 753*, 399–410.
35. Caballero, M.J., Obach, A., Rosenlund, J., Montero, D., Gisvold, M., and Izquierdo, M.S. (2002) Impact of Different Dietary Sources on Growth, Lipid Digestibility, Tissue Fatty Acid Composition and Histiology of Rainbow Trout (*Oncorhynchus mykiss*), *Aquaculture 214*, 253–271.
36. Hardy, R.W., Scott, T.M., and Harrell, L.W. (1987) Replacement of Herring Oil with Menhaden Oil, Soybean Oil, or Tallow in the Diets of Atlantic Salmon Raised in Marine Net-Pens, *Aquaculture 65*, 267–277.
37. Greene, D.H.S., and Selivonchick, D.P. (1990) Effects of Dietary Vegetable, Animal, and Marine Lipids on Muscle Lipid and Hematology of Rainbow Trout (*Oncorhynchus mykiss*), *Aquaculture 89*, 165–182.
38. Luthria, D.L., Mohammed, B.S., and Sprecher, H. (1996) Regulation of the Biosynthesis of 4,7,10,13,16,19-Docosahexaenoic Acid, *J. Biol. Chem. 271*, 16020–16025.
39. Buzzi, M., Henderson, R.J., and Sargent, J.R. (1996) The Desaturation and Elongation of Linolenic Acid and Eicosapentaenoic Acid by Hepatocytes and Liver Microsomes from Rainbow Trout (*Oncorhynchus mykiss*) Fed Diets Containing Fish Oil or Olive Oil, *Biochim. Biophys. Acta 1299*, 235–244.
40. Ruyter, B., Rosjo, C., Grisdale-Helland, B., Rosenlund, G., Obach, A., and Thomassen, M.S. (2003) Influence of Temperature and High Dietary Linoleic Acid Content on Esterification, Elongation, and Desaturation of PUFA in Atlantic Salmon Hepatocytes, *Lipids 38*, 833–840.
41. Roberts, R.A., James, N.H., Woodyatt, N.J., Macdonald, N., and Tugwood, J.D. (1998) Evidence for the Suppression of Apoptosis by the Peroxisome Proliferator Activated Receptor α (PPARα), *Carcinogenesis 19*, 43–48.
42. Hawkins, J.M., Jones, W.E., Bonner, F.W., and Gibson, G.G. (1987) The Effect of Peroxisome Proliferators on Microsomal, Peroxisomal, and Mitochondrial Enzyme Activities in the Liver and Kidney, *Drug Metab. Rev. 18*, 441–515.
43. Lock, E.A., Mitchell, A.M., and Elcombe, C.R. (1989) Biochemical Mechanisms of Induction of Hepatic Peroxisome Proliferation, *Annu. Rev. Pharmacol. Toxicol. 29*, 145–163.
44. Schoonjans, K., Staels, B., and Auwerx, J. (1996) Role of the Peroxisome Proliferator-Activated Receptor (PPAR) in Mediating the Effects of Fibrates and Fatty Acids on Gene Expression, *J. Lipid Res. 37*, 907–925.
45. Oshino, N., Chance, B., Sies, H., and Bucher, T. (1973) The Role of H_2O_2 Generation in Perfused Rat Liver and the Reaction of Catalase Compound I and Hydrogen Donors, *Arch. Biochem. Biophys. 154*, 117–131.
46. Handler, J.A., and Thurman, R.G. (1988) Catalase-Dependent Ethanol Oxidation in Perfused Rat Liver. Requirement for Fatty-Acid-Stimulated H_2O_2 Production by Peroxisomes, *Eur. J. Biochem. 176*, 477–484.
47. Mannaerts, G.P., Debeer, L.J., Thomas, J., and De Schepper, P.J. (1979) Mitochondrial and Peroxisomal Fatty Acid Oxidation in Liver Homogenates and Isolated Hepatocytes from Control and Clofibrate-Treated Rats, *J. Biol. Chem. 254*, 4585–4595.
48. Yamamoto, K., Fukuda, N., Zhang, L., and Sakai, T. (1996) Altered Hepatic Metabolism of Fatty Acids in Rats Fed a Hypolipidaemic Drug, Fenofibrate, *Pharmacol. Res. 33*, 337–342.
49. Hagve, T.A., and Christophersen, B.O. (1986) Evidence for Peroxisomal Retroconversion of Adrenic Acid (22:4(n-6)) and Docosahexaenoic Acids (22:6(n-3)) in Isolated Liver Cells, *Biochim. Biophys. Acta 875*, 165–173.
50. Madsen, L., Froyland, L., Dyroy, E., Helland, K., and Berge, R.K. (1998) Docosahexaenoic and Eicosapentaenoic Acids Are Differently Metabolized in Rat Liver During Mitochondria and Peroxisome Proliferation, *J. Lipid Res. 39*, 583–593.
51. Gavino, G.R., and Gavino, V.C. (1991) Rat Liver Outer Mitochondrial Carnitine Palmitoyltransferase Activity Toward Long-Chain Polyunsaturated Fatty Acids and Their CoA Esters, *Lipids 26*, 266–270.
52. Gutieres, S., Damon, M., Panserat, S., Kaushik, S., and Medale, F. (2003) Cloning and Tissue Distribution of a Carnitine Palmitoyltransferase I Gene in Rainbow Trout (*Oncorhynchus mykiss*), *Comp. Biochem. Physiol. 135B*, 139–151.
53. Osmundsen, H., and Bjornstad, K. (1985) Inhibitory Effects of Some Long-Chain Unsaturated Fatty Acids on Mitochondrial β-Oxidation. Effects of Streptozotocin-Induced Diabetes on Mitochondrial β-Oxidation of Polyunsaturated Fatty Acids, *Biochem. J. 230*, 329–337.
54. Van Veldhoven, P., Declercq, P.E., Debeer, L.J., and Mannaerts, G.P. (1984) Effects of Benfluorex and Fenofibrate Treatment on Mitochondrial and Peroxisomal Marker Enzymes in Rat Liver, *Biochem. Pharmacol. 33*, 1153–1155.
55. Totland, G.K., Madsen, L., Klementsen, B., Vaagenes, H., Kryvi, H., Froyland, L., Hexeberg, S., and Berge, R.K. (2000) Proliferation of Mitochondria and Gene Expression of Carnitine Palmitoyltransferase and Fatty Acyl-CoA Oxidase in Rat Skeletal Muscle, Heart and Liver by Hypolipidemic Fatty Acids, *Biol. Cell 92*, 317–329.

[Received June 1, 2004; accepted September 25, 2004]

Effects of EPA and DHA on Proliferation, Cytokine Production, and Gene Expression in Raji Cells

Rozangela Verlengia[a,b], Renata Gorjão[a], Carla Cristine Kanunfre[c], Silvana Bordin[a], Thais Martins de Lima[a], Edgair Fernandes Martins[a], Philip Newsholme[d], and Rui Curi[a,*]

[a]Department of Physiology and Biophysics, Institute of Biomedical Sciences, University of São Paulo, Brazil, [b]Methodist University of Piracicaba, Faculty of Sciences of Health, Physical Education, São Paulo, Brazil, [c]Department of Biology, University of Ponta Grossa, PR, Brazil, and [d]Department of Biochemistry, Conway Institute of Biomolecular and Biomedical Research, University College Dublin, Belfield, Dublin, Ireland.

ABSTRACT: The effects of EPA and DHA on the function and gene expression of a B-lymphocyte cell line (Raji) were investigated. Proliferation; production of interleukin-10 (IL-10), tumor necrosis factor (TNF)-α, and interferon (INF)-γ; and expression of pleiotropic genes were evaluated. Cell proliferation was increased in the presence of 12.5 μM EPA (approximately twofold) and 12.5 μM DHA (approximately 1.5-fold). EPA and DHA (25 μM) also decreased production of the key immunoregulatory cytokines IL-10, TNF-α, and INF-γ. EPA and DHA changed the expression of specific genes, but this effect was more marked for EPA (25.9% of genes investigated) compared with DHA (8.4% of genes investigated). EPA and DHA affected the expression of genes clustered as: cytokines, signal transduction, transcription, cell cycle, defense and repair, apoptosis, cell adhesion, cytoskeleton, and hormones. The most remarkable changes were observed in the genes of signal transduction and transcription. These results led us to conclude that the mechanism of DHA and EPA effects on B-lymphocyte functions includes regulation of gene expression. Thus, the ingestion of fish oil, a rich source of EPA and DHA, may have a strong effect on B-lymphocyte function *in vivo*. However, remarkable differences were observed between DHA and EPA, demonstrating that specific effects of these FA may be responsible for the marked differences in edible oil effects on immune function *in vivo* reported by others.

Paper no. L9475 in *Lipids 39,* 857–864 (September 2004).

Fish oil (FO) exerts beneficial effects with respect to the treatment of inflammatory diseases such as autoimmune disease and allergy (1,2). FO ingestion leads to enhanced production of the 3-series prostaglandins (PG) and thromboxanes and the 5-series of leukotrienes while reducing 2-series PG and 4-series leukotriene production (3). These changes in eicosanoid synthesis may regulate the isotype and production of antibodies *via* B-lymphocyte-dependent events (4,5). The beneficial effects of FO are related to the high content of n-3 fatty acids (FA) EPA (20:5) and DHA (22:6), which have potent regulatory effects on the function of many cell types (6,7). However, although EPA and DHA belong to the same family of FA (n-3), in general they provoke different effects on cell function (8–10).

In relation to B-lymphocyte function, antibody production, switching and secretion can be modulated by specific PG (11). n-3 and other long-chain PUFA administered orally modulate immune responses and hypersensitivity reactions (12–14). Mice fed γ-linoleate (n-6) have lower immunoglobulin E production than those fed α-linolenate (n-3) (15). Mice fed α-linolenate survive for longer periods of time than those fed γ-linoleate after antigen-induced anaphylactic shock (15) probably owing to suppression of eicosanoid production. An increase in the n-3 to n-6 FA ratio of the diet is effective in reducing the severity of immediate-type allergic hypersensitivity (16).

Several mechanisms by which FA influence lymphocyte function have been postulated (17–19). FA may modulate the amount and types of eicosanoids produced (such as those comprising specific classes of leukotrienes, thromboxanes, and PG). However, FA may also elicit some of their effects *via* eicosanoid-independent mechanisms, including actions upon intracellular signaling pathways (20,21), transcription factor activity (22), and cell metabolism (23). Long-chain FA can modulate calcium signaling (24), ceramide production (25), phospholipase C activation and subsequent production of inositol-1,4,5-triphosphate and DAG (19), and thus protein phosphorylation (26). In addition to the mechanisms described above, FA are also known to regulate gene expression and cause cell death (27–30).

To date, no study has determined the individual effects of EPA and DHA on B-lymphocytes, although the effect of these FA on T-lymphocyte function and viability has been investigated (31). The comparative effects of EPA and DHA on parameters of FA composition, cell survival, proliferation, cytokine production, and gene expression were determined in Raji cells, a well-known B-lymphocyte model established by Epstein *et al.* (32,33). Cell proliferation was determined by measuring [^{14}C]thymidine incorporation. Production of interleukin (IL)-10, interferon-gamma (INF-γ), and tumor necrosis factor-alpha (TNF-α) was determined by ELISA. Expression of some pleiotropic genes was analyzed by macroarray technique. The genes selected for analysis were related to several B-lymphocyte functions such as cytokines, signal transduction, transcription factors, defense against oxidative stress, and apoptosis.

*To whom correspondence should be addressed at Departamento de Fisiologia e Biofísica, Instituto de Ciências Biomédicas I, Universidade de São Paulo, Av. Prof. Lineu Prestes, 1524, 05508-900, Butantã, São Paulo, SP, Brasil. E-mail: ruicuri@icb.usp.br

Abbreviations: ConA, concanavalin A; FO, fish oil; IL, interleukin; INF-γ, interferon-gamma; PG, prostaglandins; RT, reverse transcriptase; TNF-α, tumor necrosis factor α.

MATERIAL AND METHODS

Culture conditions and FA treatment. Raji cells were obtained from the Dunn School of Pathology, Oxford University, England. The cells were cultured in RPMI 1640 medium supplemented with 10% fetal calf serum. EPA and DHA addition did not result in toxicity to Raji cells up to 50 μM as indicated by loss of membrane integrity and DNA fragmentation assessed by flow cytometric analysis (FACS-Calibur; Becton Dickinson, San Jose, CA) (34). The FA were first dissolved in ethanol before they were added to the serum protein-containing medium. The percentage of ethanol was always lower than 0.05% of the total volume of culture medium. This concentration of ethanol was not toxic to the cells as also observed by Siddiqui *et al.* (35).

Lipid extraction and determination of DHA and EPA content by HPLC. The lipids were extracted as previously described (36) from Raji cells cultured for 24 h in the presence of 25 μM DHA or EPA. The lipids were saponified using 2 mL of an alkaline methanol solution (1 mol NaOH/L in 90% methanol) at 37°C, for 2 h, in a shaking water bath. Afterward, the alkaline solution was acidified to pH 3 with HCl solution (1 mol/L). FA were then extracted three times with 2 mL hexane. After the extraction procedure and saponification (37–39), the FA were derivatized with 4-bromomethyl-7 methoxycoumarim (40), and the analysis performed on a Shimadzu model LC-10A liquid chromatograph. The samples were placed on a C8 column (25 cm × 4.6 mm i.d., 5 μm of particles) following a precolumn C8 (2.5 cm × 4.6 mm i.d., 5 μm of particles), with a flow rate of 1 mL/min of acetonitrile/water (77:23, vol/vol), and a fluorescence detector (325 nm excitation and 395 nm emission). The standard mixture of FA was obtained from Sigma Chemical Co. (St. Louis, MO). Margaric acid (17:0) was used to calculate recovery. The capacity factor (K'), elution sequence, linearity, recovery, precision, interference, and limit of detection were determined. The minimum limit of quantification of the FA ranged from 1 to 10 ng. One curve of calibration for each standard, determining coefficients of correlation and regression, was obtained.

Proliferation assay. Raji cells (3.3×10^5 cells/mL) were plated in 96 well microtiter plates and treated for 48 h with EPA and DHA (12.5, 25, 50, 75 μM). [^{14}C]Thymidine (1 μCi/mL) was added to the medium at the beginning of the experiment. Plates were incubated in a humidified atmosphere of 5% CO_2 and 95% air at 37°C. Cells were collected by using a Skatron Combi Multiple Cell Harvester (Suffolk, United Kingdom), and the radioactivity of the [^{14}C]thymidine incorporated into DNA was determined by using a β counter (Packard Tri-Carb 2100 TR counters; Downers Grove, IL). The incorporation of [^{14}C]thymidine was expressed as total counts per minute.

Measurement of cytokine secretion. The cells (2×10^5 cells per mL) were plated in 24-well plates and treated for 24 h with EPA and DHA at 25 μM. The cells were then cultured for another 24 h in the presence of 25 μg/mL concanavalin A (Con A). ConA receptors have been described in the surface membrane of B lymphocytes (41). Afterward, cell culture supernatant fluid was collected for determination of secreted cytokines.

The production of IL-10, INF-γ, and TNF-α was evaluated by ELISA using Kit OptEIA™ from Pharmingen (San Diego, CA). The detection limit of IL-10 and TNF-α was 7.8 pg/mL and of INF-γ was 4.7 pg/mL (according to the manufacturer).

Incubation of Raji cells with FA to evaluate pleiotropic gene expression. Cells were resuspended at a density of 2×10^6 cells/mL in 25-cm^3 flasks containing RPMI-1640 medium and 10% fetal calf serum. Cells were treated for 24 h with EPA and DHA at 25 μM concentration. A similar procedure was used in previous work (42).

Total RNA extraction. Total RNA was obtained from 0.5–1 $\times 10^7$ cells by lysis with 1 mL Trizol reagent (Life Technology, Rockville, MD). After 5 min of incubation at room temperature, 200 μL chloroform was added to the tubes, which were centrifuged at 12,000 × *g*. The aqueous phase was transferred to another tube, and the RNA was pelleted by centrifugation (12,000 × *g*) with cold ethanol and dried in air. Subsequently, RNA pellets were resuspended in RNase-free water and treated with DNase I. RNA samples were stored at −70°C until the time of the experiment. The RNA was quantified by measuring absorbance at 260 nm. The purity of the RNA was assessed by the ratio of the absorbances at 260 vs. 280 nm and on a 1% agarose gel stained with ethidium bromide at 5 μg/mL (43). These samples were used for macroarray and reverse transcription-polymerase chain reaction (RT-PCR) analysis.

Synthesis of cDNA probes. The cDNA probes were synthesized using the pure total RNA labeling system Atlas Kit™ according to manufacturer's recommendations (Clontech Laboratories, Palo Alto, CA). Briefly, 10 μg of total RNA and 2 μL primers mix "CDs" (a specific mix of primers relative to the genes present in the macroarray membrane) were heated at 70°C for 5 min in a Techne-Genius Thermal cycler (Oxford, United Kingdom). The temperature was decreased to 50°C and 13.5 μL of the mixture of the following reagents was added: 4 μL reaction buffer 5×, 0.5 μL 100 mM DTT, 2 μL 10× dNTP mix (dCTP, dGTP, dTTP), 5 μL of [α-^{33}P]ATP (at 10 μCi/μL), and 2 μL of reverse transcriptase enzyme (Invitrogen, Rockville, MD). The reaction was incubated for 25 min at 50°C and stopped by using 2 μL Termination Mix (Clontech Laboratories, Palo alto, CA). The ^{33}P-labeled probe was purified from unincorporated nucleotides by passing the reaction mixture through a push column (NucleoSpin Extraction Spin Column; Clontech Laboratories). Experiments using 20 μg total RNA were also performed, and the results indicated saturation of the hybridization process (data not shown).

Macroarray hybridization. All solutions for hybridization were obtained from Clontech Laboratories. The membrane was prehybridized for 30 min at 68°C in Express Hyb containing 50 μg freshly denatured salmon sperm DNA. Subsequently, the membrane was hybridized over 18 h at 68°C with 2×10^6 cpm/mL ^{33}P-labeled denatured probe. The membrane was washed twice at 68°C with 1 × SSC, 0.1% SDS; followed by two washes in 1 × SSC, 1% SDS; then exposed to phosphor screen for 48 h and scanned using a Storm 840 (Molecular Dynamics, Sunnyvale, CA).

Analysis of macroarray results. Changes in gene expression

induced by FA were analyzed by comparison with untreated cells using the software Array-Pro™ Analyzer, version 4 (Media Cybernetics®, Silver Spring, MD). Local ring background was subtracted from the density value of each spot to obtain a "net" value. Spots with a mean intensity greater than 1.2 times the mean local background intensity were further considered as "measurable spots." Normalization was done by calculating total intensity ratios and using the housekeeping gene β-actin (the same was used for RT-PCR analysis) present in the membrane. Duplicate hybridizations using separate sets of nylon membranes were performed for all conditions. Only signals that differed from the control by at least twofold in two independent experiments were considered as significant. A similar procedure was used by Yamazaki *et al.* (44).

RT-PCR. RT-PCR using specific primers was performed to confirm the differential expression of the mRNAs detected by macroarray analysis. The sequences of the primers were designed using information contained in the public database of the GeneBank of the National Center for Biotechnology Information (http://www.ncbi.nlm.nih.gov/BLAST).

The RT-PCR was performed using parameters described by Innis and Gelfand (45). The number of cycles used was selected to allow quantitative comparison of the samples in a linear way. For semiquantitative PCR analysis, the housekeeping β-actin gene was used as reference. The primer sequences and their respective PCR fragment lengths are shown in Table 1. Published guidelines were followed to guard against bacterial and nucleic acid contamination (46).

Analysis of the PCR products. The analysis of PCR amplification products was performed in 1.5% gels containing 0.5 μg/mL ethidium bromide and electrophoresed for 1 h at 100 V. The gels were photographed using a DC120 Zoom Digital Camera System from Kodak (Invitrogen). The images were processed and analyzed in the software Kodak Digital Science 1D Image Analysis (Invitrogen).

PCR band intensities were expressed as optical density normalized for β-actin expression. Data are presented as a ratio compared with the respective controls, which received an arbitrary value of 1 in each experiment.

Statistical analysis. The results of FA composition, proliferation assay and measurement of cytokine production were expressed as mean ± SEM of three experiments. Comparisons with control (ethanol) and between DHA and EPA treatments were performed by ANOVA. Significant differences were found by using the Tukey–Kramer method (INStat; Graph Pad Software, Inc., San Diego, CA).

RESULTS

Determination of FA composition by HPLC. FA analysis showed that cells cultured in the presence of EPA or DHA (25 μM) for 24 h were subsequently enriched with the corresponding n-3 FA. The proportion of EPA increased from 1.27 ± 0.41% in control cells to 21.35 ± 0.23% in EPA-treated cells. DHA content in these cells was not altered (3.77 ± 0.34% in control cells and 1.72 ± 0.07% in EPA-treated cells). The proportion of DHA increased from 3.77 ± 0.34 to 33.89 ± 1.94% in DHA-treated cells. EPA content in these cells was not altered (1.27 ± 0.41% in control cells, and 0.75 ± 0.04% in DHA-treated cells). The values are presented as mean ± SEM of determinations from three experiments. These findings confirm the incorporation of the FA into the cells and support the proposition that EPA is not converted into DHA in Raji cells.

Raji cell proliferation. [^{14}C]Thymidine incorporation by Raji cells was increased by both EPA and DHA. The increase was more marked with EPA (1.8-, 1.9-, 2.0-, and 2.0-fold at 12.5, 25, 50, and 75 μM, respectively; Fig. 1) compared with DHA (1.5-, and 1.3-fold at 12.5 and 25 μM, respectively; Fig. 1). DHA at 50 μM concentration had no effect on Raji cell proliferation and at 75 μM caused a decrease.

Production of cytokines. Cytokine production was assessed in the presence of 25 μM EPA and DHA. Both EPA and DHA significantly reduced the production of IL-10 (59 and 70%, respectively; Fig. 2), TNF-α (29 and 42%, respectively; Fig. 2), and INF-γ (23 and 28%, respectively; Fig. 2). Statistically significant differences between EPA and DHA were observed for the production of IL-10 only. Cytokine production without ConA stimuli was undetectable.

Pleiotropic gene expression. The comparative effects of

TABLE 1
The Standardized Conditions for Reverse Transcription-Polymerase Chain Reaction (RT-PCR) Analysis[a].

Genes	Primer sense	Primer antisense	Anneling temperature (°C)	PCR fragment lengths	Number of cycles
PLA_2	5′-AGCCCGTAGGTCATCTTGG-3′	5′-TGCTTCAGCTTCGTCTCCTTGG-3′	56	559 bp	30
CASP3[b]	5′-GTCGATGCAGCAAACCTCAGGG-3′	5′-TGTTTCAGCATGGCACAAAGCG-3′	56°C (15 cycles) plus 58°C (20 cycles)	470 bp	35
Bcl-xL[b]	5′-CATGGCAGCAGTAAAGCAAGC-3′	5′-GGTCAGTGTCTGGTCATTTCCG-3′	59	470 bp	45
Myc proto-oncogen	5′-TACCCTCTCAACGACAGCAGCT 3′	5′-TCTTGACATTCTCCTCGGTGTCC-3′	60	455 bp	35
Bcl-2	5′-GATGACTTCTCTCGTCGCTACC-3′	5′-TGAAGAGTTCCTCCACCACC-3′	60	111 bp	35
β-Actin	5′-GTGGGGCGCCCCAGGCACCA -3′	5′-CTCCTTAATGTCACGCACGATTTC-3′	56	545 bp	25

[a]The sequence of the primers, the PCR fragment lengths, and the number of cycles are shown for each gene under study. For all genes, 1.5 mM $MgCl_2$ was used.
[b]For CASP3 and Bcl-xL RT-PCR, formamide was used at 1.5 and 0.5% concentrations, respectively. PLA_2, phospholipase A_2; CASP3, caspase 3; Bcl 2, B-cell leukemia/lymphoma protein 2.

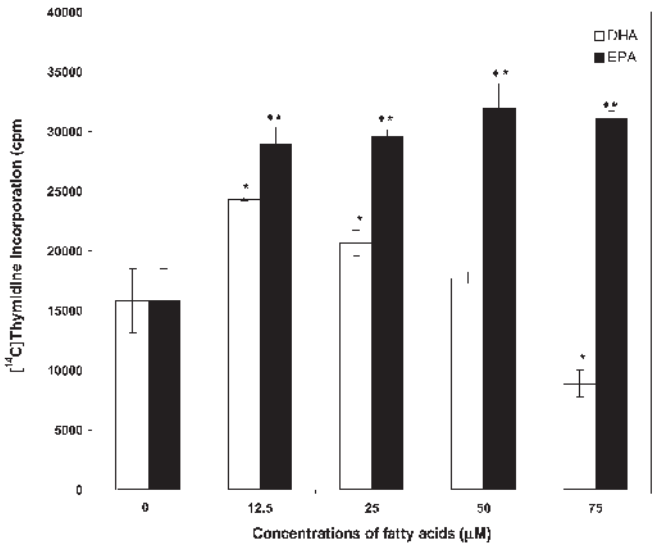

FIG. 1. Effect of EPA and DHA on Raji cell proliferation. Cells (3.3×10^5 cells/mL) were cultured in the presence of 12.5, 25, 50, and 75 mM EPA or DHA for 48 h. The cells harvested and radioactivity of the [14C] thymidine incorporated into DNA were determined by using a liquid scintillation counter. The incorporation of [^{14}C]thymidine is expressed as total cpm. The values are presented as mean ± SEM of three experiments. *$P < 0.05$ as compared with the corresponding controls. ◆$P < 0.05$ for comparison between DHA and EPA.

DHA and EPA on expression of B-lymphocyte genes related to several aspects of cell function including signaling pathways, cell defense and repair, apoptosis and cytokine production are described in Table 2. Of the surveyed genes (83 in total), 25 were modified by at least one of the FA tested. The proportion of genes changed by the FA was 8.4% for DHA and 25.9% for EPA. DHA raised the expression of seven genes, whereas EPA up-regulated 20 genes and down-regulated one gene (Table 2).

RT-PCR analysis. To validate the results of the macroarray analysis, five genes were selected for confirmation by RT-PCR (Fig. 3). Although the magnitude was not identical, the direction of change induced by the FA was the same for both macroarray and RT-PCR analysis. Therefore, macroarray analysis performed in duplicate using pooled cells from two experiments provides reliable observations (concerning FA-induced changes in gene expression). The genes selected for analysis by RT-PCR were those involved in important aspects of B-lymphocyte function including signal transduction and apoptosis. They were altered by the treatments with DHA and EPA as indicated by macroarray analysis. DHA increased the expression of Bcl2. EPA raised the expression of phospholipase A_2, caspase 3, apoptosis regulator bcl-x, and Myc-proto-oncogene.

DISCUSSION

Several studies have shown that FO rich in n-3 FA exerts immunomodulatory effects. However, it remains to be investigated whether the immunomodulation induced by FO is due to EPA or DHA, or a combined effect of these two n-3 PUFA. Peterson *et al.* (47) and Jolly *et al.* (25) have shown that both

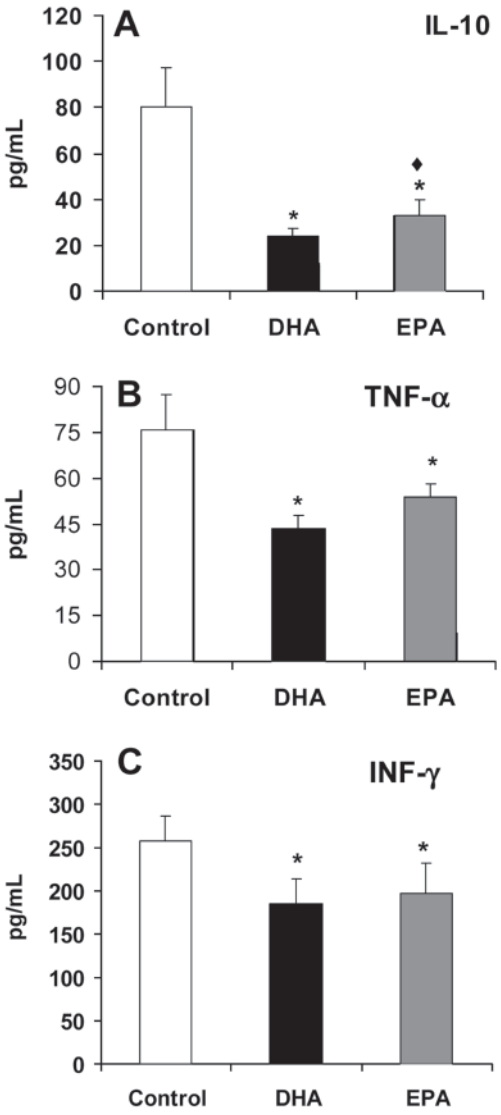

FIG. 2. Effect of FA on cytokine production by Raji cells. Cells were cultured in the presence of EPA and DHA (25 mM) for 24 h. Cells were then cultured for another period of 24 h in the presence of 25 μg/mL of concanavalin A and the FA. Afterward, the supernatant fluid was used for determination of the cytokines (by ELISA) as described in Materials and Methods section. Values are presented as mean ± SEM of three experiments. *$P < 0.05$ as compared with the corresponding controls (no FA added). ◆$P < 0.05$ for comparison between DHA and EPA. IL-10, interleukin-10; TNF-α, tumor necrosis factor α; INF-γ, interferon γ.

EPA and DHA have immunomodulatory effects in rats. However, some studies have shown that EPA and DHA may have different effects on inflammation. Tomobe *et al.* (48) observed that a DHA-rich diet, but not an EPA-rich one, reduces the infiltration of CD4-positive T lymphocytes after the induction of a hypersensitivity reaction in rats' ears. The mRNA levels of INF-γ, IL-6, IL-1 β, and IL-2 were also decreased. On the other hand, Volker *et al.* (49) observed that EPA-rich diets are more effective in ameliorating the destructive arthritic phase in hock joints than DHA-rich diets. In human subjects, a more pronounced immunomodulatory effect of EPA has been observed (50–52).

In the present study, several functions were altered by in-

TABLE 2
Modification in Raji Cell Gene Expression after Treatment with EPA and DHA at 25 μM[a–c]

Cluster/GAN*	Gene name	EPA	DHA
1. Cytokines and related receptors			
X02812	Transforming growth factor beta (TGF-beta)		+3.4
L08096; S69339	CD27 ligand (CD27LG); CD70 antigen	+4.7	
2. Signal transduction pathways			
L36719	Mitogen-activated protein kinase kinase 3 (MAPKK 3)	+2.7	
M31158	cAMP-dependent protein kinase type II beta regulatory subunit (PRKAR2B)		+2.6
Z29090	PI 3 kinase catalytic subunit alpha isoform (PI3 kinase)	+2.4	+2.0
U39657	Mitogen-activated protein kinase kinase 6 (MAPKK 6)	+4.0	+2.9
M86400	Phospholipase A_2 (PLA_2)	+2.2	
3. Transcription factors and related genes			
L26318	c-jun N-terminal Kinase 1 (JNK-1)		+2.0
M29366; M34309	ErbB3 proto-oncogene (HER3)	+2.5	
L19067	Nuclear factor of kappa light polypetide gene enhancer in B cells 3 (NFKB3)	+5.3	+2.5
V00568	Myc proto-oncogene	+2.1	
X13293	MYB-related protein B (B-MYB)	+2.8	
4. Cell cycle			
L33264	Cyclin-dependent kinase 10 (CDK10)	+2.3	
M73812	G1/S-specific cyclin E (CCNE)	+3.4	
5. Defense and repair			
K00065; X02317	Cytosolic superoxide dismutase 1 (SOD1)	+2.2	
X08058	Glutathione S-transferase pi (GSTP1)	+4.2	
M11717	Heat shock 70 kDa protein 1 (HSP70.1)	+2.5	
6. Apoptosis			
U13737	Caspase 3 (CASP3)	+2.1	
L22474	BCL-2-associated X protein membrane (BAX)	+2.8	
Z23115	Apoptosis regulator bcl-x (bcl-xL)	+2.3	
X89986; U34584	NBK apoptotic inducer protein; BCL-2 interacting killer protein (BIK)	+6.8	
M14745	B-cell leukemia/lymphoma protein 2 (Bcl2)		+3.9
8. Cell adhesion, cytoskeleton, and related genes			
M34064; X57548; X54315; S42303	Cadherin 2 (CDH2); neural cadherin (N-cadherin; NCAD)	+2.6	
Z15009	Laminin gamma 2 subunit (LAMC2)	+44	
9. Hormones			
M27544	Insulin-like growth factor (IGF1)	-5.3	

[a]Results are described as fold-changes in expression.
[b]Raji cells were treated for 24 h with EPA and DHA (25 μM). Total RNA was isolated, retrotranscribed, ^{33}P-labeled, and hybridized to the cDNA array presenting 83 transcripts of known genes. The signals were then analyzed by Pro-Analysis Software Array-Pro™ Analyzer, version 4 (Media Cybernetics®, Silver Spring, MD) and expressed as -fold increase (+) or decrease (–) in relation to untreated cells. Data are presented as means of two pools of cells from two different experiments. Only signals that differed from the untreated cells by at least wofold were considered as significant. For details of the calculations see the Material and Methods section.
[c]GAN, GeneBank accession number.

cubation of B-lymphocyte (Raji cells) in the presence of nontoxic concentrations of EPA or DHA. Cell proliferation was increased in the presence of EPA (by twofold over the concentration range of 12.5 to 75 μM; Fig. 1) and DHA (by 1.5-fold in the presence of 12.5 μM; Fig. 1). At a concentration of 75 μM, however, DHA reduced Raji cell proliferation, whereas the stimulatory effect of EPA remained. EPA and DHA (25 μM) significantly decreased the production of IL-10, TNF-α, and INF-γ (Fig. 2). This suppression of cytokine production was also observed in spleen lymphocytes from mice fed FO-rich diets and in mononuclear cells from septic patients who received a FO-rich infusion (53,54).

Expression of genes related to signal transduction, cell survival, apoptosis, and cytokine production was altered by the treatment of either EPA or DHA. The significant increase in expression of 20 selected genes and decrease in one gene by EPA and increase in seven selected genes by DHA argues for selective effects of these n-3 PUFA on gene transcription (Fig. 4). This may explain, at least in part, some of the distinct effects observed after treatment with these FA. For instance, the up-regulation of the cell cycle genes cyclin-dependent kinase 10 and G1/S-specific cyclin E by EPA may be related to the more pronounced increase in cell proliferation observed in cells treated with 25 μM of this FA. Cell cycle regulation by EPA and DHA has already been described by others. Yusufi *et al.* (55) noticed a more pronounced inhibition of mesangial cell proliferation by DHA when compared to EPA, probably due to down-regulation of extracellular signal-regulated kinase and cyclin E activity and induction of the cell cycle inhibitor p21 expression. A similar mechanism may be related to the inhibition of Raji cell proliferation by high doses of DHA observed in our study.

Gene expression of IL-10, TNF-α, and INF-γ was not altered by the treatment with both FA, although their production was decreased. These findings indicate that the modulatory effects of EPA and DHA on Raji cells are not due only to

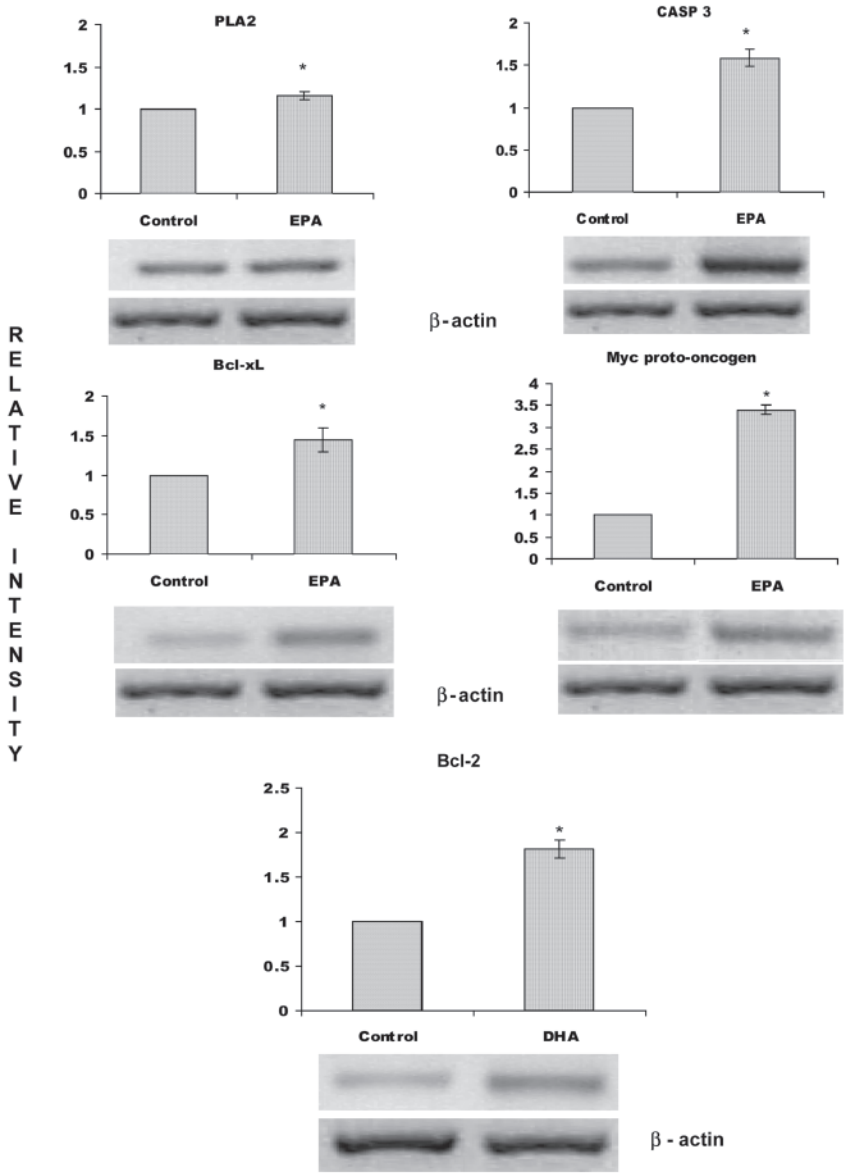

FIG. 3. Confirmation by reverse transcription-polymerase chain reaction (RT-PCR) of the genes modified by the FA as detected by macroarray analysis (Table 2). Raji cells (10^7 cell/condition) were exposed for 24 h to the following conditions: control (no FA added), DHA, and EPA (25 μM). After this time, the cells were harvested, mRNA was extracted, and RT-PCR was performed with the equivalent of 10^7 cells. PCR band intensities were expressed as optical density corrected for β-actin expression. Data are presented as the ratio with the respective controls, which received an arbitrary value of 1 in each experiment. The values are presented as mean ± SEM for four experiments. PLA_2, phospholipase A_2; CASP3, caspase 3; Bcl-xL, apoptosis regulator bcl-x; Bcl-2, B-cell leukemia/lymphoma protein 2. $^*P < 0.05$ as compared with the corresponding controls (no FA).

changes in gene expression. Indeed, as mentioned in the introductory section, FA can modulate calcium signaling (56), ceramide production (57), phospholipase C and D activation (19,58), and protein phosphorylation (10,59). We can then postulate that the modulatory effect of EPA and DHA on B-lymphocyte function involves several mechanisms that include regulation of gene expression.

In summary, this study provides evidence that EPA and DHA present different effects on B-lymphocyte proliferation and expression of genes related to its function (e.g., signal transduction). Thus, we postulate that FO with different proportions of DHA and EPA may have different therapeutic actions.

ACKNOWLEDGMENTS

The authors are indebted to the constant encouragement and support of Drs. Philip Calder and Parveen Yaqoob. The authors are also grateful for the technical assistance of José Roberto Mendonça,

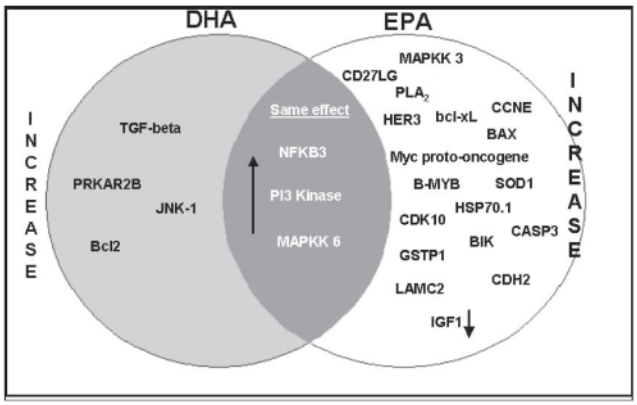

FIG. 4. Diagram with common and uncommon genes regulated by DHA and EPA treatment. Genes regulated by DHA only are shown on the left side. Genes regulated by EPA only are shown on the right side. Genes regulated by both FA are in the intersection. ↑ indicates increase and ↓ indicates decrease of gene expression. IGF1 expression was the only one reduced by the FA treatment. TGF-beta, transforming growth factor beta; CD27LG, CD27 ligand; MAPKK 3, 6, mitogen-activated protein kinase kinase 3, 6; PRKAR2B, cAMP-dependent protein kinase type II beta regulatory subunit; PI3 kinase, phosphatididylinositol 3 kinase catalytic subunit alpha isoform; PLA_2, phospholipase A_2; JNK-1, c-jun N-terminal kinase 1; HER3, ErbB3 proto-oncogene; NFKB3, nuclear factor of kappa light polypetide gene enhancer in B cells 3; B-MYB, MYB-related protein B; CDK10, cyclin-dependent protein kinase 10; CCNE, G1/S-specific cyclin E; SOD1, cytosolic superoxide dismutase 1; GSTP1, glutathione S-transferase pi; HSP70.1, heat shock 70 kDa protein 1; CASP3, caspase 3; BAX, BCL-2-associated X protein membrane; BIK, bcl-2 interacting killer; Bcl2, B-cell leukemia/lymphoma protein 2; CDH2, cadherin 2; LAMC2, laminin gamma 2 subunit; IGF1, insulin-like growth factor 1; bcl-xL, apoposis regulator bcl-x.

Geraldina de Souza, and Erica Portioli. FAPESP (Fudanção de Amparo à Pesquisa do Estado de Sào Paulo), Pronex, CNPq (Conselho Nacional de Desenvolvimento Cient¡ifico e Tecnol¡ogico), CAPES (Coordenação de Aperfeiçoamento de Pessoal de Nível Superior), Enterprise Ireland, The Health Research Board of Ireland, and the British Council supported this research.

REFERENCES

1. Harbige, L.S. (2003) Fatty Acids, the Immune Response, and Autoimmunity: A Question of n-6 Essentiality and the Balance Between n-6 and n-3, *Lipids 38*, 323–341.
2. Calder, P.C. (2001) Polyunsatured Fatty Acids, Inflammatory, and Immunity, *Lipids 36*, 1007–1024.
3. Calder, P.C. (2003) N-3 Polyunsatured Fatty Acids and Inflammatory: From Molecular Biology to the Clinic, *Lipids 38*, 343–352.
4. Kelley, D.S. (2001) Modulation of Human Immune and Inflammatory Responses by Dietary Fatty Acids, *Nutrition 17*, 669–673.
5. Simopoulos, A.P. (2002) Omega-3 Fatty Acids in Inflammation and Autoimmune Diseases, *J. Am. Coll. Nutr. 21*, 495–505.
6. Simopoulos, A.P. (2001) n-3 Fatty Acids and Human Health: Defining Strategies for Public Policy, *Lipids 36*, S83–S90.
7. Kew, S., Mesa, M.D., Tricon, S., Buckley, R., Minihane, A.M., and Yaqoob, P. (2004) Effects of Oils Rich in Eicosapentaenoic and Docosahexaenoic Acids on Immune Cell Composition and Function in Healthy Humans, *Am. J. Clin. Nutr. 79*, 674–681.
8. Kew, S., Gibbons, E.S., Thies, F., McNeill, G.P., Quinlan, P.T., and Calder, P.C. (2003) The Effect of Feeding Structured Triacylglycerols Enriched in Eicosapentaenoic or Docosahexaenoic Acids on Murine Splenocyte Fatty Acid Composition and Leucocyte Phagocytosis, *Br. J. Nutr. 90*, 1071–1080.
9. Hung, P., Kaku, S., Yunoki, S., Ohkura, K., Gu, J.Y., Ikeda, I., Sugano, M., Yazawa, K., and Yamada, K. (1999) Dietary Effect of EPA-rich and DHA-rich Fish Oils on the Immune Function of Sprague-Dawley Rats, *Biosci. Biotechnol. Biochem. 63*, 135–140.
10. Madani, S., Hichami, A., Cherkaoui-Malki, M., Khan, N.A., and Charkaoui-Malki, M. (2004) Diacylglycerols Containing Omega 3 and Omega 6 Fatty Acids Bind to RasGRP and Modulate MAP Kinase Activation, *J. Biol. Chem. 279*, 1176–1183.
11. Roper, R.L., Graf, B., and Phipps, R.P. (2002) Prostaglandin E2 and cAMP Promote B Lymphocyte Class Switching to IgG1, *Immunol. Lett. 84*, 191–198.
12. Yamasaki, M., Chujo, H., Hirao, A., Koyanagi, N., Okamoto, T., Tojo, N., Oishi, A, Iwata, T., Yamauchi-Sato, Y., Yamamoto, T., *et al.* (2003) Immunoglobulin and Cytokine Production from Spleen Lymphocytes is Modulated in C57BL/6J Mice by Dietary *cis*-9,*trans*-11 and *trans*-10,*cis*-12 Conjugated Linoleic Acid, *J. Nutr. 133*, 784–788.
13. Miyasaka, C.K., Mendonça, J.R., Nishiyama, A., de Souza, J. A., Pires de Melo, M., Pithon-Curi, T.C., and Curi, R. (2001) Comparative Effects of Fish Oil Given by Gavage and Fish Oil-Enriched Diet on Leukocytes, *Life Sci. 69*, 1739–1751.
14. Miyasaka, C.K., Mendonça, J.R., Silva, Z.L., de-Souza, J.A., Tavares-de Lima, W., and Curi, R. (1999) Modulation of Hypersensitivity Reaction by Lipids Given Orally, *Gen. Pharmacol. 32*, 597–602.
15. Oh-hashi, K., Watanabe, S., Kobayashi, T., and Okuyama, H. (1997) Reevaluation of the Effect of a High Alpha-Linolenate and a High Linoleate Diet on Antigen-Induced Antibody and Anaphylactic Responses in Mice, *Biol. Pharm. Bull. 20*, 217–223.
16. Watanabe, S., Sakai, N., Yasui, Y., Kimura, T., Kobayashi, T., Mizutani T., and Okuyama, H. (1994) A High Alpha-Linolenate Diet Suppresses Antigen-Induced Immunoglobulin E Response and Anaphylactic Shock in Mice, *J. Nutr. 124*, 1566–1573.
17. Arrington, J.L., McMurray, D.N., Switzer, K.C., Fan, Y.Y., and Chapkin, R.S. (2001) Docosahexaenoic Acid Suppresses Function of the CD28 Costimulatory Membrane Receptor in Primary Murine and Jurkat T Cells, *J. Nutr. 131*, 1147–1153.
18. McMurray, D.N., Jolly, C.A., and Chapkin, R.S. (2000) Effects of Dietary n-3 Fatty Acids on T Cell Activation and T Cell Receptor-Mediated Signaling in a Murine Model, *J. Infect. Dis. 182*, S103–S107.
19. Sanderson, P., and Calder, P.C. (1998) Dietary Fish Oil Appears to Prevent the Activation of Phospholipase C-γ in Lymphocytes, *Biochim. Biophys. Acta. 1392*, 300–308.
20. Graber, R., Sumida, C., and Nunez, E.A. (1994) Fatty Acids and Cell Signal Transduction, *J. Lipid Mediat. Cell Signal. 9*, 91–116.
21. Denys, A., Hichami, A., and Khan, N.A. (2001) Eicosapentaenoic Acid and Docosahexaenoic Acid Modulate MAP Kinase (ERK1/ERK2) Signaling in Human T Cells, *J. Lipid Res. 42*, 2015–2020.
22. Kliewer, S.A., and Willson, T.M. (1998) The Nuclear Receptor PPAR γ—Bigger Than Fat, *Curr. Opin. Genet. Dev. 8*, 576–581.
23. Butler, M., Huzel, N., and Barnabe, N. (1997) Unsaturated Fatty Acids Enhance Cell Yields and Perturb the Energy Metabolism of an Antibody-Secreting Hybridoma, *Biochem. J. 322*, 615–623.
24. Bonin, A. and Khan, N.A. (2000) Regulation of Calcium Signaling by Docosahexaenoic Acid in Human T-Cells: Implication of CRAC Channels, *J. Lipid Res. 41*, 277–284.
25. Jolly, C.A., Jiang, Y.H., Chapkin, R.S., and McMurray., D.N. (1997) Dietary (n-3) Polyunsaturated Fatty Acids Suppress Murine Lymphoproliferation, Interleukin-2 Secretion, and the Formation of Diacylglycerol and Ceramide, *J. Nutr. 127*, 37–43.

26. Terano, T., Tanaka, T., Tamura, Y., Kitagawa, M., Higashi, H., Saito, Y., and Hirai, A. (1999) Eicosapentaenoic Acid and Docosahexaenoic Acid Inhibit Vascular Smooth Muscle Cell Proliferation by Inhibiting Phosphorylation of Cdk2-cyclinE Complex, *Biochem. Biophys. Res. Commun. 254*, 502–506.
27. Jump, B.D., and Clarke, S.D. (1999) Regulation of Gene Expression by Dietary Fat, *Annu. Rev. Nutr. 19*, 63–90.
28. Khan, S., Minihane, A.M., Talmud, P.J., Wright, J.W., Murphy, M.C., Williams, C.M., and Griffin, B.A. (2002) Dietary Long-Chain n-3 PUFAs Increase LPL Gene Expression in Adipose Tissue of Subjects with an Atherogenic Lipoprotein Phenotype, *J. Lipid Res. 43*, 979–985.
29. Heimli, H., Giske, C., Naderi, S., Drevon, S., Drevon, C.A., and Hollung, K. (2002) Eicosapentaenoic Acid Promotes Apoptosis in Ramos Cells *via* Activation of Caspase-3 and -9, *Lipids 37*, 797–802.
30. Heimli, H., Hollung, K., and Drevon, C.A. (2003) Eicosapentaenoic Acid-Induced Apoptosis Depends on Acyl Coa-Synthetase, *Lipids 38*, 263–268.
31. Verlengia, R., Gorjão, R., Kanunfre, C.C., Bordin, S., Lima, T.M.D., and Curi, R. (2004) Comparative Effects of EPA and DHA on Proliferation Cytokines Production and Pleiotropic Genes Expression in Jurkat Cells, *J. Nutr. Biochem.,* in press.
32. Epstein, M.A., and Barr, V.M. (1965) Characteristics and Mode of Growth of Tissue Culture Strain (eb1) of Human Lymphoblasts from Burkitt's Lymphoma, *J Natl. Cancer Inst. 34*, 231–240.
33. Epstein, M.A., Achong, B.G., Barr, Y.M., Zajac, B., Henle, G., and Henle, W. (1966) Morphological and Virological Investigations on Cultured Burkitt Tumor Lymphoblasts (strain Raji), *J. Natl. Cancer Inst. 37*, 547–559.
34. Lima, T.M., Kanunfre, C.C., Pompeia, C., Verlengia, R., and Curi, R. (2002) Ranking the Toxicity of Fatty Acids on Jurkat and Raji Cells by Flow Cytometric Analysis, *Toxicol.* In Vitro *16*, 741–747.
35. Siddiqui, R.A., Jenski, L.J., Neff, K., Harvey, K., Kovacs, R.J., and Stillwell, W. (2001) Docosahexaenoic Acid Induces Apoptosis in Jurkat Cells by a Protein Phosphatase-Mediated Process, *Biochim. Biophys. Acta 1499*, 265–275.
36. Folch, J., Lee, M., and Sloane Stanley, G.H. (1957) A Simple Method for Isolation Purification of Total Lipid from Animal Tissue, *J. Biol. Chem. 226*, 497–503.
37. Beyer, R.S., and Jensen, L.S. (1989) Overestimation of the Cholesterol Content of Egg, *Agric Food Chem. 37*, 917.
38. Hamilton, S., Hamilton, R.J., and Sewell, P.A. (1992) Extraction of Lipids and Derivative Formation, in *Lipid Analysis—A Practical Approach*, 1st edn., (Hamilton, R.J., and Hamilton, S., eds.), pp. 13–64, IRL Press at Oxford University Press, Oxford.
39. Nishiyama-Naruke, A., de Sousa, J.A.A., Carnelós Filho, M., and Curi, R. (1998) HPLC Determination of Underivatized Fatty Acid Saponified at Low Temperature Analysis of Fatty Acids in Oils and Tissues, *Anal. Lett. 31*, 2565–2576.
40. Abushufa, R., Reed, P., and Weinkove, C. (1994) Fatty Acids in Erythrocytes Measured by Isocratic HPLC, *Clin. Chem. 40*, 1707–1712.
41. Ben-Bassat, H., Goldblum, N., Mitrani, S., Klein, G., and Johansson, B. (1976) Concanavalin A Receptors on the Surface Membrane of Lymphocytes from Patients with African Burkitt's Lymphoma and Lymphoma Cell Lines, *Int. J. Cancer 17*, 448–454.
42. Verlengia, R., Gorjão, R., Kanunfre, C.C., Bordin, S., Lima, T.M., Newsholme, P., and Curi, R. (2003) Genes Regulated by Arachidonic and Oleic Acids in Raji Cells, *Lipids 38*, 1157–1165.
43. Sambrook, J., and Russell, D.W. (2001) *Molecular Cloning: A Laboratory Manual,* 3rd edn., A8.21, Cold Spring Harbor Laboratory Press, Cold Spring Harbor, New York.
44. Yamazaki, K., Kuromitsu, J., and Tanaka, I. (2002) Microarray Analysis of Gene Expression Changes in Mouse Liver Induced by Peroxisome Proliferator-Activated Receptor Alpha Agonists, *Biochem. Biophys. Res. Commun. 290*, 1114–1122.
45. Innis, M.A., and Gelfand, D.H. (1990) Optimization of PCRs, in *PCR Protocols: A Guide to Methods and Applications* (Innis, M.A., Gelfand, D.H., Sninsky, J.J., and White, T.J., eds.), 1st edn., pp. 3–12, Academic Press, San Diego.
46. Kwok, S., and Higuch, R. (1989) Avoiding False Positives with PCR, *Nature 339*, 237–238.
47. Peterson, L.D., Thies, F., Sanderson, P., Newsholme, E.A., and Calder, P.C. (1998) Low Levels of Eicosapentaenoic and Docosahexaenoic Acids Mimic the Effects of Fish Oil upon Rat Lymphocytes, *Life Sci. 62*, 2209–2217.
48. Tomobe, Y.I., Morizawa, K., Tsuchida, M., Hibino, H., Nakano, Y., and Tanaka, Y. (2000) Dietary Docosahexaenoic Acid Suppresses Inflammation and Immunoresponses in Contact Hypersensitivity Reaction in Mice, *Lipids 35*, 61–69.
49. Volker, D.H., FitzGerald, P.E., and Garg, M.L. (2000) The Eicosapentaenoic to Docosahexaenoic Acid Ratio of Diets Affects the Pathogenesis of Arthritis in Lew/SSN Rats, *J. Nutr. 130*, 559–565.
50. Thies, F., Miles, E.A., Nebe-von-Caron, G., Powell, J.R., Hurst, T.L., Newsholme, E.A., and Calder, P.C. (2001) Influence of Dietary Supplementation with Long-Chain n-3 or n-6 Polyunsaturated Fatty Acids on Blood Inflammatory Cell Populations and Functions and on Plasma Soluble Adhesion Molecules in Healthy Adults, *Lipids 36*, 1183–1193.
51. Kelley, D.S., Taylor, P.C., Nelson, G.J. and Mackey, B.E. (1998) Dietary Docosahexaenoic Acid and Immunocompetence in Young Healthy Men, *Lipids 33*, 559–566.
52. Kelley, D.S., Taylor, P.C., Nelson, G.J., Schmidt, P.C., Ferretti, A., Erickson, K.L., Yu, R., Chandra, R.K., and Mackey, B.E. (1999) Docosahexaenoic Acid Ingestion Inhibits Natural Killer Cell Activity and Production of Inflammatory Mediators in Young Healthy Men, *Lipids 34*, 317–324.
53. Mayer, K., Gokorsch, S., Fegbeutel, C., Hattar, K., Rosseau, S., Walmrath, D., Seeger, W., and Grimminger, F. (2003) Parenteral Nutrition with Fish Oil Modulates Cytokine Response in Patients with Sepsis, *Am. J. Respir. Crit. Care Med. 167*, 1321–1328.
54. Wallace, F.A., Miles, E.A., Evans, C., Stock, T.E., Yaqoob, P., and Calder, P.C. (2001) Dietary Fatty Acids Influence the Production of Th1- but Not Th2-type Cytokines, *J. Leukoc. Biol. 69*, 449–457.
55. Yusufi, A.N., Cheng, J., Thompson, M.A., Walker, H.J., Gray, C.E., Warner, G.M. and Grande, J.P. (2003) Differential Effects of Low-Dose Docosahexaenoic Acid and Eicosapentaenoic Acid on the Regulation of Mitogenic Signaling Pathways in Mesangial Cells, *J. Lab. Clin. Med. 141*, 318–329.
56. Denys, A., Aires, V., Hichami, A., and Khan, N.A. (2004) Thapsigargin-Stimulated MAP Kinase Phosphorylation *via* CRAC Channels and PLD Activation: Inhibitory Action of Docosahexaenoic Acid, *FEBS Lett. 564*, 177–182.
57. Siddiqui, R.A., Jenski, L.J., Harvey, K.A., Wiesehan, J.D., Stillwell, W., and Zaloga, G.P. (2003) Cell-Cycle Arrest in Jurkat Leukaemic Cells: A Possible Role for Docosahexaenoic Acid, *Biochem. J. 37*1, 621–629.
58. Diaz, O., Berquand, A., Dubois, M., Di Agostino, S., Sette, C., Bourgoin, S., Lagarde, M., Nemoz, G., and Prigent, A.F. (2002) The Mechanism of Docosahexaenoic Acid-Induced Phospholipase D Activation in Human Lymphocytes Involves Exclusion of the Enzyme from Lipid Rafts, *J. Biol. Chem. 277*, 39368–39378.
59. Denys, A., Hichami, A., and Khan, N.A. (2002) Eicosapentaenoic Acid and Docosahexaenoic Acid Modulate MAP Kinase Enzyme Activity in Human T-Cells, *Mol. Cell Biochem. 232*, 143–148.

[Received March 26, 2004; accepted November 1, 2004]

Regulation of Diacylglycerol Acyltransferase in Developing Seeds of Castor

Xiaohua He, Grace Q. Chen, Jiann-Tsyh Lin, and Thomas A. McKeon*

Western Regional Research Center, USDA, Albany, California 94710, USA

ABSTRACT: We have previously reported the cloning of castor diacylglycerol acyltransferase (RcDGAT) based on its homology to other plant type 1 diacylglycerol acyltransferases (DGATs). To elucidate the physiological role of the RcDGAT, we have investigated the regulation of RcDGAT expression in developing seeds of castor. The RcDGAT transcript appeared at 12 d after pollination (DAP), reached the highest level at 26 DAP, and declined rapidly after that. However, the RcDGAT protein started to accumulate at 26 DAP, reached its peak at 47 DAP, then remained at this high level until 54 DAP. The significant difference between the expression of mRNA and protein indicates that gene expression of RcDGAT in maturing castor seeds is controlled at the posttranscriptional level. We found that DGAT activity measured in microsomal membranes isolated from seed at different stages of development was parallel to RcDGAT protein level, suggesting DGAT activity is mainly a function of the level of RcDGAT protein. We monitored the triacylglycerol (TG) composition and content during seed development. Compared with the overall rate of TG accumulation, DGAT activity appeared coincidently with the onset of lipid accumulation at 26 DAP; the highest DGAT activity occurred during the rapid phase of lipid accumulation at 40 DAP; and a decline in DGAT activity coincided with a decline in the accumulation rate of TG after 40 DAP. The ricinoleate-containing TG content was very low (only about 7%) in oil extracted from seeds before 19 DAP; however, it increased up to about 77% of the oil at 26 DAP. The relative amount of triricinolein in oil at 26 DAP was 53 times higher than that at 19 DAP, and it was about 76% of the amount present in oil from mature castor seeds. The close correlation between profiles of RcDGAT activity and oil accumulation confirms the role of RcDGAT in castor oil biosynthesis.

Paper no. L9612 in *Lipids 39,* 865–871 (September 2004).

The oil from castor seed (*Ricinus communis*) contains 90% ricinoleate, a hydroxy FA that is particularly useful because it is extremely viscous and is therefore an excellent source for biodegradable lubricants and greases (1). Worldwide, the annual production of castor oil is about 460,000 tons (1.1 million tons of seeds), produced mainly in India, Brazil, and China (http://www.hort.purdue.edu/newcrop/). The United States spends over $50 million annually to import castor for industrial applications including such diverse products as lubricants, greases, plasticizers, cosmetics, pharmaceuticals, paints, plastics, coatings, antifungal compounds, shampoo, and thermopolymers.

Conventional domestic production of castor oil, however, is seriously hindered owing to the presence of a toxic protein, ricin, as well as various allergenic albumins. Efforts to engineer other plants to produce oil with high levels of ricinoleate by expression of the oleoyl-hydroxylase gene have been unsuccessful as a result of the plants' inability to "move" ricinoleate through the lipid biosynthetic pathway into triacylglycerols (TG) (2). An understanding of how plants assemble TG, and specifically how a plant like castor can accumulate seed oil in which the FA composition exceeds 90% in a single FA, ricinoleate, is a prerequisite before such an effort can be undertaken successfully. Moreover, such basic biosynthetic information will be useful in engineering microbes that can convert surplus oils to higher-value industrial oils. It will also prove useful in reprogramming castor to produce other useful FA.

The regulatory factors that influence oil accumulation in castor seeds are largely unknown (3). Acyl-CoA-dependent diacylglycerol acyltransferase (DGAT) is thought to be a key enzyme in controlling the biosynthetic rate of TG in most oilseeds (4,5). It is the only enzyme in the Kennedy glycerol-3-P pathway that is exclusively committed to TG synthesis (6) although there are two types, DGAT1 and DGAT2. The DGAT is responsible for the acylation of 1,2-diacylglycerol (1,2-DG) at the *sn*-3 position using an acyl-CoA substrate. Genes encoding DGAT have been cloned and characterized from several plant species (7–9). Both DGAT1 and DGAT2 have been reported in plants. While the DGAT2 from fungi has been shown to have a stronger preference for acylating DG with medium-chain acyl groups, it does not apparently have a significant effect on the FA composition of the oil (10). We recently reported the identification of a cDNA encoding a castor DGAT (RcDGAT) and demonstrated that the RcDGAT preferentially incorporated diricinolein into TG (11). Determination of the content and composition of storage lipids in developing seeds has been reported in numerous oilseed crops (12–14); however, how the developmental profile of an enzyme participating in TG biosynthesis is regulated and correlated with oil accumulation remains poorly understood. In the present paper, we report our studies of the regulation of

*To whom correspondence should be addressed at USDA, 800 Buchanan St., Albany, CA 94710. E-mail: tmckeon@pw.usda.gov

Abbreviations: AG, acylglycerols; DAP, days after pollination; DG, diacylglycerol; DGAT, diacylglycerol acyltransferase; DIG, digoxigenin; PDAT, phospholipid:diacylglycerol transferase; RcDGAT, castor DGAT; TG, triacylglycerol.

RcDGAT protein expression and function during castor seed development. We also examine the correlation between RcDGAT activity and oil accumulation.

EXPERIMENTAL PROCEDURES

Northern blot analysis. RNA samples were extracted from castor seeds at different developmental stages using the method of Gu *et al.* (15). Five μg of total RNA was applied to each lane in a 1% agarose gel with 2% formaldehyde. The probe used for hybridization was generated by PCR labeling with digoxigenin (DIG-dUTP) using RcDGAT cDNA as template and the primers: 5′-AAGACCCCATGGCGATTCTC-GAAACGCCAGAA-3′ (HE-15F) and 5′-CTGAGAGCTT CAGAACCCTCTCAA-3′ (HE-6R). Northern analysis was performed based on the DIG Application Manual for Filter Hybridization (Roche Molecular Biochemicals, Mannhein, Germany).

Antibody production. Antibodies for RcDGAT were raised in two rabbits immunized with the peptide (CVLLYYHDLM-NRDGN), which corresponds to the C terminus of the native protein (Pacific Immunology Corp., Ramona, CA). The carrier protein, keyhole limpet hemocyanin, was conjugated to the N-terminal Cys of the peptide using *m*-maleimidobenzoyl-*N*-hydroxysuccinimide ester. Prior to immunization, serum samples were obtained and the rabbits were injected four times at 3-wk intervals with the linked peptide. Serum was collected 1 wk after the final injection and column-purified by affinity chromatography. The titer was determined using the remaining peptide.

Total protein and microsomal preparations. Castor seeds from different developmental stages were harvested and homogenized in a buffer (16) containing 400 mM sucrose, 100 mM Hepes-NaOH pH 7.5, 10 mM KCl, 1 mM $MgCl_2$, 5 mM EDTA, 2 mM DTT, and a protease inhibitor cocktail tablet per 10 mL from Boehringer Mannheim (Indianapolis, IN). The homogenate was centrifuged at 10,000 × *g* for 10 min to remove cell debris, and the supernatant (total protein fraction) was spun again at 100,000 × *g* for 90 min. The pellet was resuspended in the homogenizing buffer (microsomal fraction), and the protein concentration was determined using Bradford reagent (BioRad, Hercules, CA). These microsomal preparations were stored at –80°C and used for western blot and DGAT activity assay.

Western blot analysis. Thirty micrograms of total or microsomal proteins from different developmental stages were separated by SDS-PAGE, and electroblotted onto polyvinylidene difluoride membranes. The blot was incubated with the polyclonal rabbit antibodies described above (at 1:5,000 dilution). Horseradish peroxidase conjugated goat anti-rabbit (Amersham Pharmacia, Piscataway, NJ) secondary antibodies were diluted 1:3,000. Horseradish peroxidase activity was visualized using chemiluminescence (ECL kit; Amersham Pharmacia).

In vitro *DGAT assay.* The DGAT assay was performed as in Cases *et al.* (17) with minor modifications. Assay mixtures (100 μL) contained 0.1 M Tris-HCl pH 7.0, 20% glycerol, 400 μM 1,2-diricinolein, and 20 μM [^{14}C]oleoyl-CoA (200,000 cpm), and reactions were started by the addition of 100 μg microsomal protein. The reactions were incubated for 15 min at 30°C with shaking and stopped by the addition of 1 μL 10% SDS. The 1,2-diricinolein was prepared as a 10-mM stock in 0.5% Tween-20. Lipids were extracted from assay mixtures using chloroform/methanol as previously described (18). The molecular species of TG products were separated using C18 HPLC (25 × 0.46 cm, 5 μm, Ultrasphere C18; Beckman Instruments Inc., Fullerton, CA) (19). DGAT activity was determined based on the ^{14}C-label incorporated into the TG products from [^{14}C]oleoyl-CoA.

Quantification of RcDGAT protein and lipid contents. Total lipids were extracted from seeds by grinding in a 2:1 chloroform/methanol mixture (20). Following the addition of 0.9% NaCl, the chloroform phase was evaporated to dryness under a stream of N_2. Oil contents (%) were determined by dividing the extracted oil (g) by the sample's fresh weight. The abundance of RcDGAT proteins in seed samples was quantified by measuring the average intensity value of the protein bands on the western blot using Bio-Rad Quantity One Quantitation software. The relative amounts of oil content and RcDGAT protein were calculated by normalizing against the highest value as 100%.

HPLC. HPLC was carried out on a liquid chromatograph (Waters Associates, Milford, MA) using a flow scintillation analyzer (150TR; Packard Instrument Co., Downers Grove, IL) to detect [^{14}C]-labeled TG or an ELSD for mass quantification (MK III; Alltech Associates, Deerfield, IL) at a flow rate of 1 mL/min. The drift tube temperature of the ELSD was set at 80°C. The nitrogen gas flow of the nebulizer of the ELSD was set at 1.0 L/min. The nitrogen pressure on the regulator of the nitrogen tank was set at about 65 psi. Separation of lipid classes and molecular species of TG was performed as we reported previously (21,22). The quantification of different molecular species of TG in Table 1 was based on relative ELSD peak area (%) in the HPLC chromatogram. Our previous data indicated that ELSD responses of different amounts of the standards of molecular species of TG were nearly linear (22).

RESULTS AND DISCUSSION

Disparity of RcDGAT expression in mRNA and in protein. To investigate how the expression of RcDGAT is regulated in maturing castor seeds, Northern blot analysis was performed using RNA samples extracted from castor seeds at different developmental stages. Figure 1 shows that RcDGAT transcript was detectable at 12 d after pollination (DAP), reached a maximum at 26 DAP, and declined thereafter. Our previous results based on reverse transcription-polymerase chain reaction indicated that the highest transcript level appeared at 19 DAP; this discrepancy may be due to the variation in samples and detection methods used in the two experiments. To determine the expression pattern of RcDGAT protein, we raised

TABLE 1
Molecular Species of TG Identified and Their Contents (%) in Castor Oil at Different Stages of Seed Development[a]

TG species	19 DAP	26 DAP	61 DAP
RRR	1	53	70
RRLs	0	0.29	1.37
RRLn	0	2.92	1.14
RRL	5.71	9.22	9.26
RRO + RRP	0	10.2	6.51
RRS	0	0.99	0.69

[a]Abbreviations: TG, triacylglycerols; R, ricinoleic acid; Ls, lesquerolic acid; Ln, linolenic acid; L, linolenic acid; O, oleic acid; P, palmitic acid; S, stearic acid; DAP, days after pollination.

antibodies to a peptide of RcDGAT in rabbits. The synthetic peptide corresponded to a 15-amino acid peptide in the C-terminus of RcDGAT. Since the C-terminus of RcDGAT is not hydrophobic, this appears to be a suitable region from which to derive an epitope. Total proteins were extracted and analyzed with these antibodies by western blot. The protein started to appear at 26 DAP, kept increasing to 47 DAP, and remained at a high level to 54 DAP, then quickly decreased to a very low level at 61 DAP. The disparity of accumulation patterns between RcDGAT protein and mRNA was remarkable. Similar results were obtained from studies with cell cultures of oilseed rape (9). It could be that the mRNA for RcDGAT encodes a relatively stable protein because most of the protein is embedded in the membrane, and therefore resistant to endogenous proteases, or because some of the gene expression is regulated at the posttranscriptional level. The predicted size of the RcDGAT protein is 60 kDa; however, the polypeptide detected on the blot prepared from the total protein extracts is only about 50 kDa, which appears to be a product of posttranslational proteolytic processing of the native RcDGAT protein. The full-length RcDGAT protein was observed on the western blot prepared from microsomal samples isolated from 26 and 33 DAP (Fig. 2B), although it was

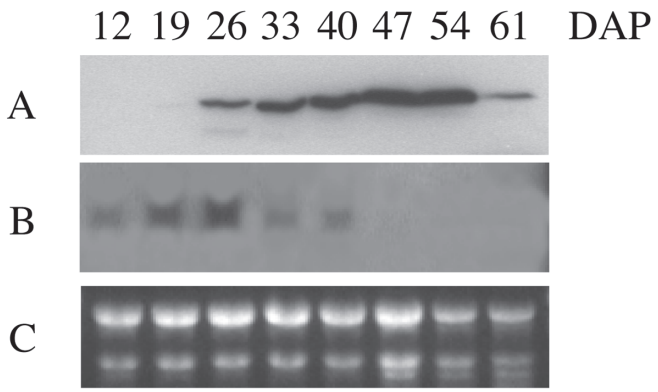

FIG. 1. Expression of castor diacylglycerol acyltransferase (RcDGAT) mRNA and protein. RNA samples were extracted from castor seeds at different stages of development from 12 to 61 d after pollination (DAP). Total RNA (5 μg) was used for northern analysis (B). Ethidium bromide staining is shown to demonstrate the equal loading of RNA in the blot (C). Another set of seeds was used to extract protein. Total protein (30 μg) was used for western blot analysis (A).

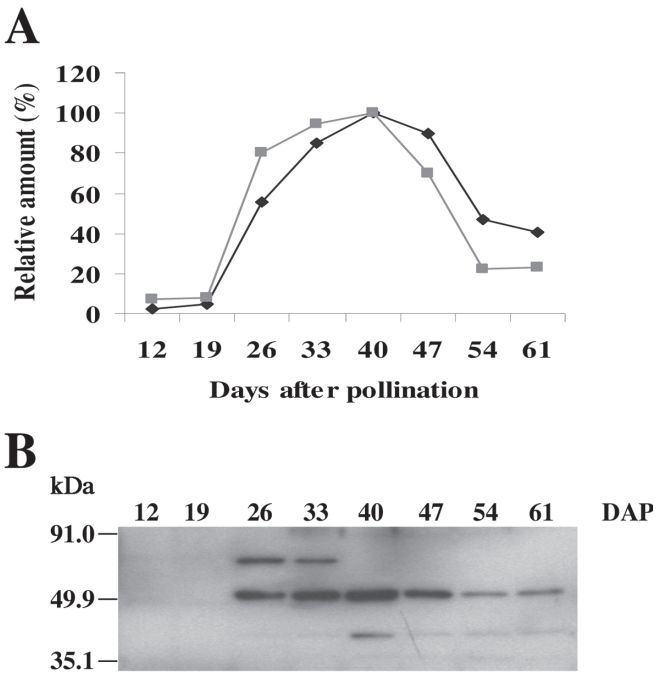

FIG. 2. Accumulation of RcDGAT proteins (■) and diacylglycerol acyltransferase (DGAT) activities (◆) during seed maturation (A). Microsomal fractions isolated from seeds at 12 to 61 DAP were used for DGAT assay and western blot analysis. The levels of RcDGAT protein and activity at 40 DAP were used for normalizing to 100% and calculating the relative amounts in other stages. The activity at 40 DAP was 412.72 pmol/min/ mg. The accumulation of RcDGAT protein in seed samples was quantified by measuring the average intensity value of the protein bands on the western blot (B) using Bio-Rad (Hercules, CA) Quantity One Quantitation software. Molecular masses of proteins are marked in the left margin, and 30 μg of microsomal protein was loaded in each lane on the blot. For other abbreviation see Figure 1.

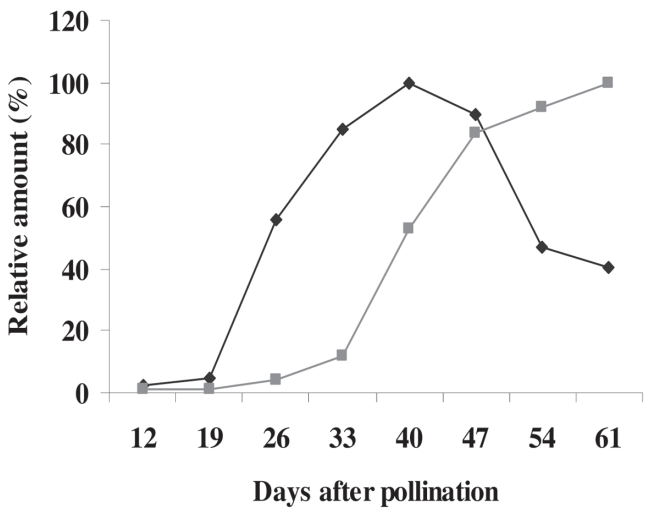

FIG. 3. Accumulation of oil (■) and DGAT activities (◆) during seed maturation. Extraction of lipids and determination of oil content in seed samples were performed as described in the Experimental Procedures section. The oil contents at 61 DAP (66% of the fresh weight) and the enzyme activity at 40 DAP (624 pmol/mg/min) were normalized to 100% to calculate the relative amounts in other stages. For abbreviations see Figures 1 and 2.

not the predominant form of the protein. Since RcDGAT is an integral membrane enzyme, most of the C-terminal region is embedded in the membrane (11), whereas the N-terminal region containing 119 amino acid residues is hydrophilic and thus accessible to proteases. Moreover, the antibody was raised against the C-terminal 15 amino acid residues of the RcDGAT protein, and it detects only protein containing the C-terminus of the protein. If the C-terminus is cleaved, there will be no signal on the western blot. The specificity of the antibody was confirmed by western blot of extracts from non-induced yeast and yeast induced to express RcDGAT protein (data not shown). Several groups have reported that DGAT activity was found in all particulate fractions prepared from developing seeds (23–25). We compared the RcDGAT levels in protein from total extracts and from microsomal fractions (Figs. 1A and 2B). The overall trends among multiple independent experiments showed that the accumulation patterns of RcDGAT protein from 12 to 40 DAP were identical in the two protein extracts but started to differentiate after 40 DAP. After 40 DAP, the protein level in the microsomal fraction declined, but it remained at a high level in the total protein fraction. This result suggests that the majority of the RcDGAT protein is present in microsomes from 12 to 40 DAP, but after 40 DAP a significant amount of the protein starts to accumulate in fractions other than microsomes. The specific particulate fractions with which RcDGAT may be associated and its biological function are under investigation.

DGAT activity was predominantly a function of the level of RcDGAT protein. Our previous studies showed that there were multiple phosphorylation sites based on functional motifs and critical amino acid residues in the deduced amino acid sequence of RcDGAT (11). It is possible that RcDGAT activity is controlled posttranslationally. It was known that most of the DGAT activity was recovered from the 100,000 × *g* pellet, so this microsomal pellet was chosen for further characterization. DGAT activity was measured in an *in vitro* assay with microsomal membranes isolated from maturing seeds. Enzyme activity was barely detectable before 19 DAP, increased to a significant amount at 26 DAP, reached a maximum at 40 DAP, then quickly decreased until 54 DAP (Fig. 2A). These changes in RcDGAT activity closely correlate with the expression pattern of RcDGAT proteins from microsomes (Figs. 2A and 2B). This result suggests that there is no posttranslational control in RcDGAT activity, which is consistent with the regulation of DGAT1 activity from mouse adipocytes (26). As indicated in Figure 2B, a majority of the RcDGAT proteins are present as partial products (50 kDa) of the entire DGAT protein (60 kDa) in microsomes of develop-

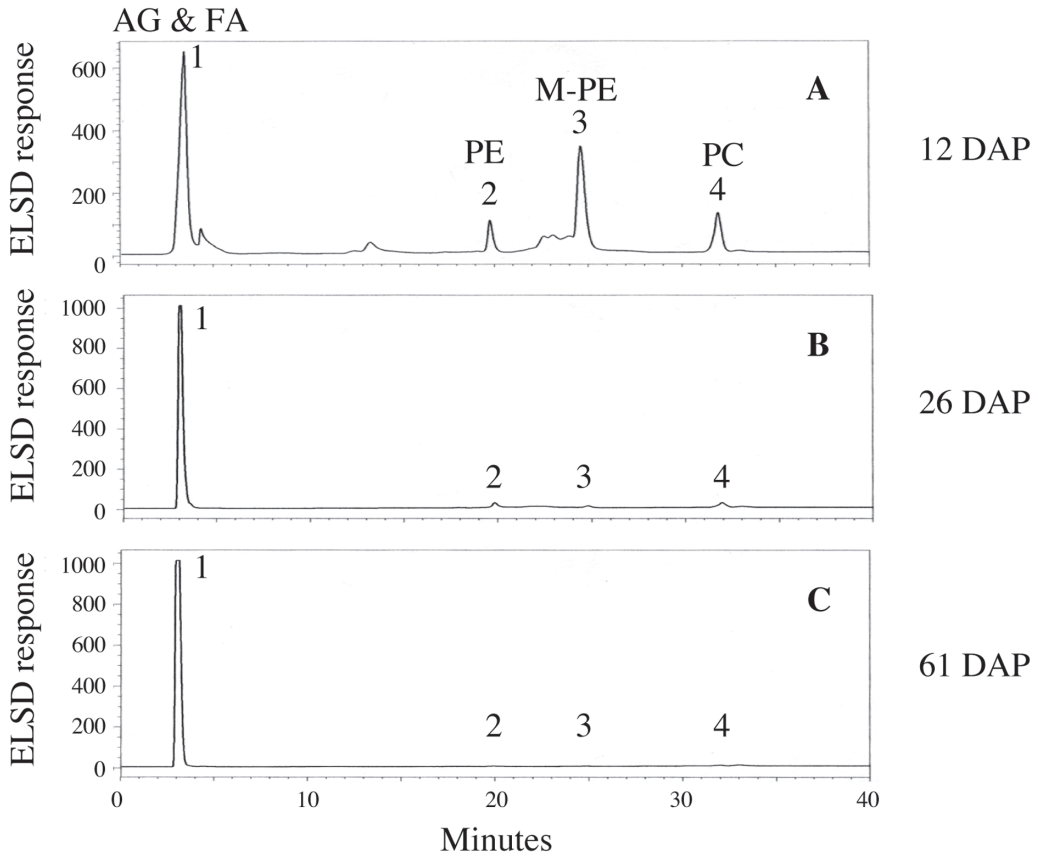

FIG. 4. Separation of lipid classes of total lipid (100 μg) extracted from castor seeds using a silica HPLC and ELSD detection system. (A) Lipid extracted from seeds at 12 DAP; (B) lipid extracted from seeds at 26 DAP; (C) lipid extracted from seeds at 61 DAP. (1) Acylglycerols (AG) and FFA; (2) PE; (3) *N*-methyl-PE (M-PE); (4) phosphatidylcholine (PC). Other peaks are unknown. For other abbreviation see Figure 1.

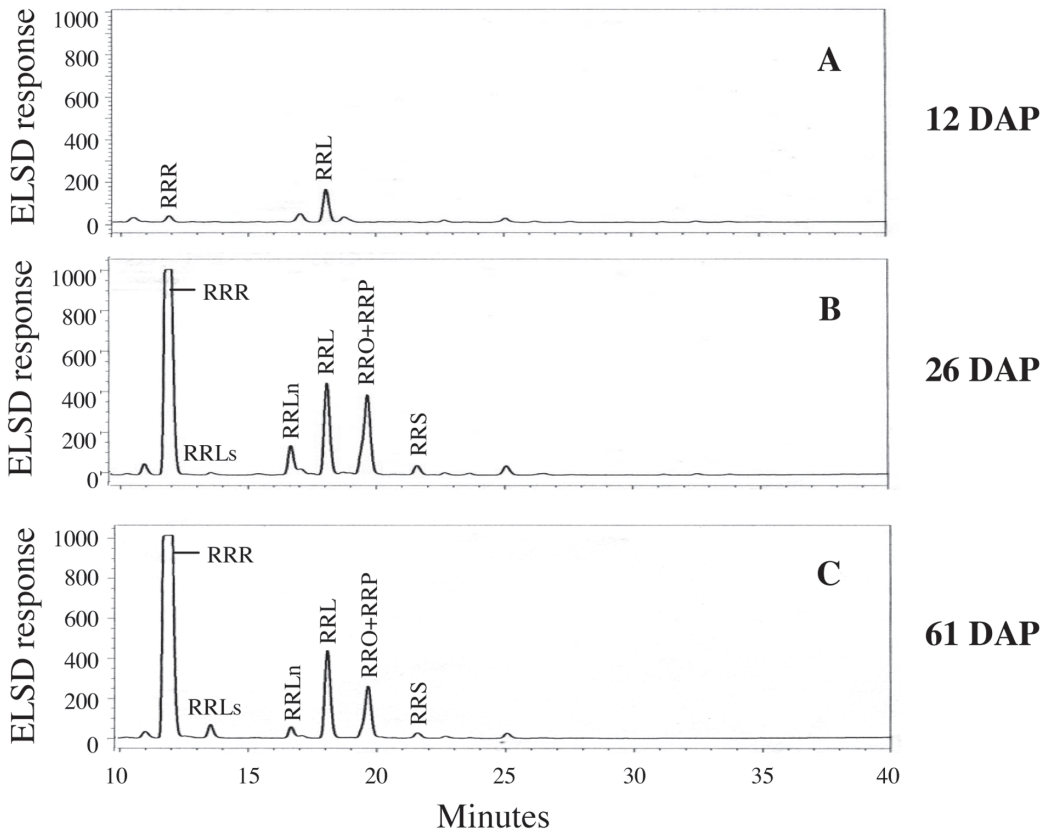

FIG. 5. Separation of molecular species of triacylglycerol (TG) (isolated from 100 μg of lipid) from castor seeds using C18 HPLC and ELSD detection system. (A) TG isolated from seeds at 12 DAP; (B) TG isolated from seeds at 26 DAP; (C) TG isolated from seeds at 61 DAP. For HPLC conditions, see the Experimental Procedures section. R, ricinoleic acid; L, linoleic acid; Ls, lesquerolic acid; Ln, linolenic acid; O, oleic acid; P, palmitic acid; S, stearic acid; for other abbreviation see Figure 1.

ing seeds. The same microsomal preparations were used when measuring the RcDGAT activities, suggesting that the cleavage of the 10-kDa peptide (possibly N-terminal hydrophilic region) from the intact protein does not seem to destroy the enzyme activity. It is possible that cleavage of the 10-kDa peptide represents a form of posttranslational regulation. Recently, DGAT2 was identified from animals, fungi, and plants (10,27). It is unclear whether a DGAT2 is present in castor seeds. We predict that the predominant activity in developing seeds of castor may come from DGAT1, based on the correlation between the total DGAT activity and the RcDGAT protein expression profile. However, we cannot exclude the possibility that DGAT2 is present, because the assay conditions have been optimized for DGAT1.

Developmental changes in oil accumulation of castor seeds. To determine the functionality of the changes in RcDGAT activity during seed development, oil content at each stage was determined. As shown in Figure 3, the onset of oil accumulation was coincident with the appearance of DGAT activity. The maximal rate of lipid accumulation occurred when the DGAT activity reached its peak at 40 DAP. The rate of oil accumulation slowed after 40 DAP, and that was the time at which the activity started to decrease. The tight correlation between DGAT activity and oil deposition also has been reported by other groups (28,29). For many years, acyl-CoA-dependent DGAT was thought to be the only enzyme directly involved in TG biosynthesis. Recently, an acyl-CoA-independent enzyme called phospholipid:diacylglycerol acyltransferase (PDAT) was identified in plants and yeast (30). This enzyme catalyzes the transfer of acyl groups from the *sn*-2 position of the major phospholipids to DG, thus forming TG and lysophospholipids. Based on the correlation of activity with oil accumulation, our results suggest that DGAT using acyl-CoA as a substrate for acyl transfer to DG is the main pathway for synthesis of TG, but we have not eliminated the possibility that PDAT may also display enzymatic activity levels similar to DGAT during seed development of castor.

Developmental changes in lipid classes and TG contents. Castor seed contains high levels of hydroxy FA in its TG. Much of the research concerning unusual plant FA has been focused on the identification of new structures. Little is known about how the synthesis and incorporation of these unusual FA is regulated. Because of the importance of maintaining membrane integrity, accumulation of unusual FA produced by plants is usually restricted to the TG. Plants that produce such

unusual FA must have mechanisms to ensure the removal of the modified FA from the membrane lipids. One of the possibilities is that these seeds may have selective acyltransferases to incorporate unusual FA into the neutral lipid fraction. Before testing this mechanism, we studied the FA distribution and TG accumulation and compared them with the expression profile of RcDGAT protein during seed development. The same amounts of lipids extracted from each stage were separated into lipid classes by silica HPLC as shown in Figure 4. Besides acylglycerols (AG), there were considerable amounts of PC and PE present in seeds at earlier developmental stages (before 19 DAP). At 26 DAP, the relative amounts of PC and PE in seeds dropped to very low levels. After 26 DAP, the FA were almost exclusively in AG. For analyses of TG composition and content during seed development, the AG fractions collected after silica HPLC were separated by C18 HPLC and quantified using ELSD. Figure 5 shows the separation of major molecular species of TG isolated from different developmental stages. The contents of these TG are shown in Table 1. The percentage of ricinoleate- containing TG in oil extracted from seeds at 19 DAP was only about 7, but it rapidly increased to 77 at 26 DAP. The relative amount of triricinolein in oil increased 53 times from 19 DAP to 26 DAP, but it increased only 1.32 times from 26 DAP to 61 DAP. The data shown here suggest that the time between 19 and 26 DAP is a critical stage for castor oil biosynthesis and that the significant switchover in lipid metabolism coincides with the obvious increase of RcDGAT protein and activity in this period.

We have examined the regulation of RcDGAT expression and function during seed development. We demonstrated that RcDGAT expression was regulated at a posttranscriptional level, since accumulation of transcript greatly precedes detectable translation. RcDGAT activity and its effect on the rate of TG accumulation depended primary on the levels of RcDGAT protein. We monitored changes of the relative amounts of different lipid classes in developing seeds of castor. A dramatic increase of TG and decrease of PC and PE were observed in seeds from 19 to 26 DAP. We also found that the major increase of the relative amount of triricinolein in oil happened at this period of time (increase from 1% at 19 DAP to 53% at 26 DAP). These noticeable changes closely correlated with the increase of RcDGAT protein and activity.

ACKNOWLEDGMENTS

This work was supported in part by ARS CRIS Project 5325-21000-006-00D, ARS Research Associate Program, and a cooperative agreement with Dow Chemical Company (Midland, MI).

REFERENCES

1. Caupin, H.J. (1997) Products from Castor Oil: Past, Present, and Future, in *Lipid Technologies and Applications* (Gunstone, F.D., and Padley, F.B., eds.), pp. 787–795, Marcel Dekker, New York.
2. McKeon, T.A. and Lin, J.T. (2002) Biosynthesis of Ricinoleic Acid for Castor Oil Production, in *Lipid Biotechnology* (Kuo, T.M., and Gardner, H.W., eds.), pp. 129–139, Marcel Dekker, New York.
3. Ohlrogge, J.B., and Jaworski, J.G. (1997) Regulation of Fatty Acid Synthesis, *Annu. Rev. Plant Physiol. Plant Mol. Biol. 48,* 109–136.
4. Ichihara, K., Takahashi, T., and Fujii, S. (1988) Diacylglycerol Acyltransferase in Maturing Safflower Seed: Its Influences on the Fatty Acid Composition and on the Rate of Triacylglycerol Synthesis, *Biochem. Biophys. Acta 958,* 125–129.
5. Perry, H.J., and Harwood, J.L. (1993) Changes in the Lipid Content of Developing Seeds of *Brassica napus, Phytochemistry 32,* 1411–1415.
6. Stymne, S., and Stobart, K. (1987) Triacylglycerol Biosynthesis, in *The Biochemistry of Plants* (Stumpf, P.K., and Conn, E.E., eds.), Vol. 9, 175–214, Academic Press, New York.
7. Hobbs, D.H., Lu, C.F., and Hill, M.J. (1999) Cloning of a cDNA Encoding Diacylglycerol Acyltransferase from *Arabidopsis thaliana* and Its Functional Expression, *FEBS Lett. 452,* 145–149.
8. Bouvier-Nave, P., Benveniste, P., Oelkers, P., Sturley, S.L., and Schaller, H. (2000) Expression in Yeast and Tobacco of Plant cDNAs Encoding Acyl CoA:Diacylglycerol Acyltransferase, *Eur. J. Biochem. 267,* 85–96.
9. Nykiforuk, C.L., Furukawa-Stoffer, T.L., Huff, P.W., Sarna, M., Laroche, A., Moloney, M.M., and Weselake, R.J. (2002) Characterization of cDNAs Encoding Diacylglycerol Acyltransferase from Cultures of *Brassica napus* and Sucrose-Mediated Induction of Enzyme Biosynthesis, *Biochim. et Biophys. Acta 1580,* 95–109.
10. Lardizabal, K.D., Mai, J.T., Wagner, N.W., Wyrick, A., Voelker, T., and Hawkins, D. (2001) DGAT2 Is a New Diacylglycerol Acyltransferase Gene Family, *J. Biol. Chem. 276,* 38862–38869.
11. He, X., Turner, C., Chen, G., Lin, J.-T., and McKeon, T.A. (2004) Cloning and Characterization of a cDNA Encoding Diacylglycerol Acyltransferase from Castor Bean, *Lipids,* 39, 311–318.
12. Wiberg, E., Banas, A., and Stymne, S. (1997) Fatty Acid Distribution and Lipid Metabolism in Developing Seeds of Laurate-Producing Rape (*Brassica napus* L.), *Planta 203,* 342–348.
13. Bao, X., and Ohlrogge, J.B. (1999) Supply of Fatty Acid Is One Limiting Factor in the Accumulation of Triacylglycerol in Developing Embryos, *Plant Physiol. 120,* 1057–1062.
14. O'Neill, C.M., Gill, S., Hobbs, D.H., Morgan, C., and Bancroft, I. (2003) Natural Variation for Seed Oil Composition in *Arabidopsis thaliana*, *Phytochemistry 64,* 1077–1090.
15. Gu, Y.Q., Yang, C., Thara, V.K., Zhou, J., and Martin, G.B. (2000) Pti4 Is Induced by Ethylene and Salicylic Acid, and Its Product Is Phosphorylated by the Pto Kinase, *Plant Cell 12,* 771–785.
16. Lu, C., Noyer, S.B., Hobbs, D.H., Kang, J., Wen, Y., Krachtus, D., and Hills, M. (2003) Expression Pattern of Diacylglycerol Acyltransferase-1, an Enzyme Involved in Triacylglycerol Biosynthesis, in *Arabidopsis thaliana, Plant Mol. Biol. 52,* 31–41.
17. Cases, S., Smith, S.J., Zheng, Y.W., Myers, H.M., Lear, S.R., Sande, E., Novak, S., Collins, C., Welch, C.B., Lusis, A.J., *et al.* (1998) Identification of a Gene Encoding an Acyl CoA:Diacylglycerol Acyltransferase, a Key Enzyme in Triacylglycerol Synthesis, *Proc. Natl. Acad. Sci. USA 95,* 13018–13023.
18. Lin, J.T., McKeon, T.A., Goodrich-Tanrikulu, M., and Stafford, A. E. (1996) Characterization of Oleoyl-12-hydroxylase in Castor Microsomes Using the Putative Substrate, 1-Acyl-2-oleoyl-*sn*-glycero-3-phosphocholine, *Lipids 31,* 571–577.
19. Lin, J.T., Woodruff, C.L., and McKeon, T.A. (1997) Non-aqueous Reversed-Phase High-Performance Liquid Chromatography of Synthetic Triacylglycerols and Diacylglycerols, *J. Chromatogr. A 782,* 41–48.

20. Smith, M.A., Moon, H., Chowrira, G., and Kunst, L. (2003) Heterologous Expression of a Fatty Acid Hydroxylase Gene in Developing Seeds of *Arabidopsis thaliana, Planta 217,* 507–516.
21. Lin, J.T., Lew, K.M., Chen, J.M., Iwasaki, Y., and McKeon, T.A. (2000) Metabolism of 1-Acyl-2-oleoyl-*sn*-glycero-3-phosphoethanolamine in Castor Oil Biosynthesis, *Lipids 35,* 481–486.
22. Lin, J.T., Turner, C., Liao, L.P., and McKeon, T.A. (2003) Identification and Quantification of the Molecular Species of Acylglycerols in Castor Oil by HPLC Using ELSD, *J. Liq. Chromatogr. Rel. Tech. 26,* 773–780.
23. Weselake, R.J., Taylor, D.C., Pomeroy, M.K., Lawson, S.L., and Underhill, E.W. (1991) Properties of Diacylglycerol Acyltransferase from Microspore-Derived Embryos of *Brassica napus, Phytochemistry 30,* 3533–3538.
24. Ichihara, K., Takahashi, T., and Fujii, S. (1988) Diacylglycerol Acyltransferase in Maturing Safflower Seeds: Its Influences on the Fatty Acid Composition of Triacylglycerol and on the Rate of Triacylglycerol Synthesis, *Biochim. Biophys. Acta. 958,* 125–129.
25. Bernerth, R., and Frentzen, M. (1990) Utilization of Erucoyl-CoA by Acyltransferases from Developing Seeds of *Brassica napus* (L.) Involved in Triacylglycerol Biosynthesis, *Plant Sci. 67,* 21–28.
26. Yu, Y., Zhang, Y., Oelkers, P., Sturley, S.L., Rader, D.J., and Ginsberg, H.N. (2002) Posttranscriptional Control of the Expression and Function of Diacylglycerol Acyltransferase-1 in Mouse Adipocytes, *J. Biol. Chem. 277,* 50876–50884.
27. Cases, S., Stone, S.J., Zhou, P., Yen, E., Tow, B., Lardizabal, K.D., Voelker, T., and Farese, R.V., Jr. (2001) Cloning of DGAT2, a Second Mammalian Diacylglycerol Acyltransferase, and Related Family Members, *J. Biol. Chem. 276,* 38870–38876.
28. Tzen, J.T.C., Cao, Y.Z., Laurent, P., Ratnayake, C., and Huang, A.H.C. (1993) Lipids, Proteins, and Structure of Seed Oil Bodies from Diverse Species, *Plant Physiol. 101,* 267–276.
29. Weselake, R.J., Pomeroy, M.K., Furukawa, T.L., Golden, J.L., Little, D.B., and Laroche, A. (1993) Developmental Profile of Diacylglycerol Acyltransferase in Maturing Seeds of Oilseed Rape and Safflower and Microspore-Derived Cultures of Oilseed Rape, *Plant Physiol. 102*, 565–571.
30. Dahlqvist, A., Stahl, U., Lenman, M., Banas, A., Lee, M., Sandager, L., Ronne, H., and Stymne, S. (2000) Phospholipid: Diacylglycerol Acyltransferase: An Enzyme That Catalyzes the Acyl-CoA-Independent Formation of Triacylglycerol in Yeast and Plants, *Proc. Natl. Acad. Sci. USA 97,* 6487–6492.

[Received September 16, 2004; accepted November 8, 2004]

Biomimetic Oxidation of Unactivated Carbons in Steroids by a Model of Cytochrome P-450, Oxorutheniumporphyrinate Complex

Takashi Iida[a,*], Shoujiro Ogawa[a], Shouhei Miyata[a], Takaaki Goto[b], Nariyasu Mano[b], Junichi Goto[b], and Toshio Nambara[b]

[a]Department of Chemistry, College of Humanities and Sciences, Nihon University, Sakurajousui, Setagaya, Tokyo 156-8550, Japan, and [b]Graduate School of Pharmaceutical Sciences, Tohoku University, Aobayama, Sendai 980-8578, Japan

ABSTRACT: Biomimetic oxidation of unactivated carbons for structurally different steroids was studied with a model of cytochrome P-450, oxorutheniumporphyrinate complex, which is generated *in situ* by 2,6-dichloropyridine *N*-oxide as an oxygen donor and (5,10,15,20-tetramesitylporphyrinate) ruthenium(II) carbonyl complex and HBr as catalysts. The O-insertion positions depended significantly on specific structural features of the substrates to give novel and remote-oxygenated steroids in one step. The electrophilic oxorutheniumporphyrinate attacked predominantly allylic and benzylic β-carbons adjacent to a π-bond and/or less hindered, electron-rich *tert*-methine carbons in the substrates to give regio- and stereoselectively the corresponding oxo and/or hydroxy derivatives.

Paper no. L9570 in *Lipids 39,* 873–880 (September 2004).

Oxyfunctionalization of unactivated carbon atoms of aliphatic saturated hydrocarbons and aromatic hydrocarbons is carried out efficiently by cytochrome P-450 enzymes *in vivo* (1). For instance, cytochrome P-450-dependent oxidations are the key steps for the biotransformations from cholesterol to various steroid hormones and bile acids. The active site of such enzymes carries a heme prosthetic group.

Many attempts have been made to mimic the action of the P-450 enzymes by synthetic metalloporphyrins as a catalyst and active oxygen species as an oxygen transfer agent (2–6). Grieco and colleagues (7–9) have prepared manganese(III) porphyrin covalently linked to steroid substrates. When the steroid–porphyrin complexes were oxidized with iodosylbenzene, they were capable of introducing oxygen-containing functions at specific, nonactivated sites in the steroid moieties *via* the corresponding oxomanganese(V) species.

In more recent work, a direct, true catalytic method for the oxyfunctionalization of unactivated carbons in steroids was attained by Breslow and co-workers (10–13). The method, termed a model of P-450, involved the hydroxylation of steroid derivatives carrying *tert*-butylphenyl groups with oxomanganeseporphyrinate, which is generated *in situ* from a catalytic amount of manganese porphyrin substituted with four β-cyclodextrins and excess amounts of iodosylbenzene. Extension of this work by these workers (14) to develop a more stable catalyst, chloro[5,10,15,20-tetrakis(pentafluorophenyl)porphyrinato] manganese(III), gave oxyfunctionalization products in one step without the need for prior sample derivatization.

An alternative model of the P-450 system was developed by Hirobe and colleagues (15–18). The system consisted of 2,6-dichloropyridine (DCP) *N*-oxide as an oxygen donor and (5,10,15,20-tetramesitylporphyrinate) ruthenium(II) carbonyl [Ru(TMP)CO] and HBr as catalysts. The oxidant system *via* the oxorutheniumporphyrinate(IV) complex, with a high stability as well as excellent catalytic turnover, permitted other selective oxidations of interest.

As part of our continuing efforts directed toward a convenient, efficient synthesis of biologically important and physiologically active steroids (19–21), we became interested in the oxorutheniumporphyrinate catalyst developed by Hirobe and colleagues (15–18). We report here the biomimetic oxyfunctionalization of structurally different steroids (**1–6**) by the complex to clarify factors governing the reactivity and O-insertion position on oxidative transformations of the substrates.

EXPERIMENTAL PROCEDURES

Melting points were determined on an electric micro hot stage and are uncorrected. IR spectra were obtained on a Bio-Rad FTS-7 FT-IR spectrometer (Philadelphia, PA) for samples in KBr pellets. ^{1}H and ^{13}C NMR spectra were obtained on a JEOL JNM-EX 270 FT instrument (Tokyo, Japan) at 270 and 67.8 MHz, respectively, with $CDCl_3$ containing 0.1% Me_4Si as the solvent; chemical shifts are expressed as δ-ppm relative to Me_4Si. ^{13}C NMR signals corresponding to methyl (CH_3), methylene (CH_2), methine (CH), and quaternary (C) carbons were differentiated by means of distortionless enhancement by polarization transfer experiments. Low-resolution MS (LR-MS) spectra were recorded on a JEOL JMS-303 liquid chromatograph-mass spectrometer at 70 eV with an electron ionization (EI) probe under the positive ion mode (PIM). High-resolution MS (HR-MS) spectra were performed using a JEOL JMS-LCmate and a JMS-700 double-focusing magnetic mass

*To whom correspondence should be addressed.
E-mail: takaiida@chs.nihon-u.ac.jp

Abbreviations: APCI, atmospheric pressure CI; DCP, 2,6-dichloropyridine; EI, electron ionization; ESI, electrospray ionization; Fr., fraction; HR-MS, high-resolution MS; LR-MS, low-resolution MS; MPLC, medium-pressure LC; NIM, negative ion mode; PIM, positive ion mode; SC, side chain; TMP, tetramesitylporphyrinate.

spectrometer equipped with an electrospray ionization (ESI) probe under the PIM and an atmospheric pressure CI (APCI) probe under the negative ion mode (NIM), respectively. A Shimadzu GC-2010 gas chromatograph equipped with an FID was used isothermally at 300°C; it was fitted with an SGE chemically bonded fused-silica capillary column (25QC$_3$/BPX5; 25 m × 0.32 mm i.d.; film thickness, 0.35 μm; SGE, Melbourne, Australia). The apparatus used for medium-pressure LC (MPLC) consisted of a Shimamura YRD-880 RI-detector (Tokyo, Japan) and a uf-3040s chromatographic pump using silica gel 60 (230–400 mesh; Nacalai Tesque, Kyoto, Japan) as adsorbent and benzene/EtOAc mixtures as eluent. TLC was performed on precoated silica gel plates (0.25 mm layer thickness; E. Merck, Darmstadt, Germany) using hexane/EtOAc/acetic acid mixtures (80:20:1–20:80:1, by vol) as the developing solvent.

The preparation of DCP *N*-oxide and Ru(TMP)CO has been described in a previous paper (21). Compounds **1–3** used in this study were purchased from Wako Pure Chemical Industries, Ltd. (Osaka, Japan). Compounds **4–6** were from our laboratory collection.

General procedure for the oxidation using DCP N*-oxide/Ru(TMP)CO/HBr*. To a magnetically stirred solution of steroid (1.3 mmol) in dry benzene (3 mL) and molecular sieves (850 mg, 4 Å), DCP *N*-oxide (630 mg, 3.8 mmol), Ru(TMP)CO (5 mg, 5.5 μmol), and HBr (50 μL) were successively added, and the mixture was stirred at 50°C for 48 h (the reaction was monitored by TLC). The reaction product was extracted with toluene, and the combined extracts were washed with water, dried with Drierite, and evaporated to dryness under reduced pressure. The residue was chromatographed on a column of silica gel (70–230 mesh, 50 g) eluting with benzene/EtOAc (8:2–6:4, vol/vol) mixtures and then by MPLC on silica gel (230–400 mesh, 20 g) eluting with benzene/EtOAc (9:1, vol/vol).

*Oxyfunctionalization products of estrone acetate (**1**). (i) 3-Acetoxyestra-1,3,5(10)-triene-6,17-dione (**7**).* Isolated from the reaction product of **1** as colorless thin plates [fraction (Fr.) 1] crystallized from EtOAc: m.p. 186–189°C; IR ν_{max}/cm 1767, 1738, 1680 (C=O). ^{1}H NMR δ 0.92 (3H, *s*, 18-H$_3$), 2.32 (3H, *s*, COCH$_3$), 7.27 (1H, *dd*, J_1 8.3, J_2 2.4 Hz, 2-H), 7.48 (1H, *d*, *J* 8.1 Hz, 1-H), 7.77 (1H, *d*, *J* 2.4 Hz, 4-H). LR-MS *m/z* 326 (18%, M), 284 (100%, M − part of ring D), 266 (5%, M − AcOH), 240 (12%), 227 (14%). HR-MS (EI-PIM) calc. for $C_{20}H_{22}O_4$ [M]$^+$: 326.1518. Found: *m/z* 326.1522.

*(ii) 3-Acetoxy-9α-hydroxyestra-1,3,5(10)-triene-6,17-dione (**8**).* Isolated from the reaction product of **1** as colorless needles (Fr. 2) crystallized from EtOAc: m.p. 216–219°C: IR ν_{max}/cm 3519 (OH), 1760, 1745 (C=O). ^{1}H NMR δ 0.91 (3H, *s*, 18-H$_3$), 2.32 (3H, *s*, COCH$_3$), 7.22 (1H, *dd*, J_1 8.8, J_2 2.4 Hz, 2-H), 7.41 (1H, *d*, *J* 8.3 Hz, 1-H), 7.77 (1H, *d*, *J* 2.4 Hz, 4-H). LR-MS *m/z* 342 (35%, M), 324 (1%, M − H$_2$O), 300 (100%, M − part of ring D), 282 (19%, M − H$_2$O − part of ring D), 243 (7%), 215 (23%). HR-MS (EI-PIM) calc. for $C_{20}H_{22}O_5$ [M]$^+$: 342.1467. Found: *m/z* 342.1469.

*Oxyfunctionalization products of estrone methyl ether (**2**). (i) 3-Methoxyestra-1,3,5(19)-triene-6,17-dione (**9**).* Isolated from the reaction product of **2** as colorless plates (Fr. 1) crystallized from EtOAc: m.p. 143–144°C. IR ν_{max}/cm 1745 (C=O). ^{1}H NMR δ 0.91 (3H, *s*, 18-H$_3$), 3.82 (3H, *s*, OCH$_3$), 7.03 (1H, *dd*, J_1 8.8 J_2 2.8 Hz, 2-H), 7.32 (1H, *d*, *J* 8.6 Hz, 4-H), 7.52 (1H, *d*, *J* 2.8 Hz, 1-H). LR-MS *m/z* 298 (100%, M), 280 (3%, M − H$_2$O), 256 (6%, M − part of ring D), 242 (14%, M − ring D), 213 (7%). HR-MS (EI-PIM) calc. for $C_{19}H_{22}O_3$ [M]$^+$: 298.1569. Found: *m/z* 298.1558.

*(ii) 9α-Hydroxy-3-methoxyestra-1,3,5(10)-triene-6,17-dione (**10**).* Isolated from the reaction product of **2** as colorless thin plates (Fr. 2) crystallized from methanol: m.p. 191–192°C [lit. (22), m.p. 195°C]. IR ν_{max}/cm 3490 (OH), 1738, 1680 (C=O). ^{1}H NMR δ 0.95 (3H, *s*, 18-H$_3$), 3.88 (3H, *s*, OCH$_3$), 7.12 (1H, *dd*, J_1 8.8 J_2 3.0 Hz, 2-H), 7.32 (1H, *d*, *J* 8.8 Hz, 4-H), 7.51 (1H, *d*, *J* 2.8 Hz, 1-H). LR-MS *m/z* 314 (100%, M), 296 (14%, M − H$_2$O), 281 (5%, M − H$_2$O − CH$_3$), 257 (11%), 229 (38%), 216 (13%).

*(iii) 6β-Hydroxy-3-methoxyestra-1,3,5(10)-triene-17-one (**11**).* Isolated from the reaction product of **2** as a noncrystalline substance (Fr. 3): IR ν_{max}/cm 3446 (OH), 1730 (C=O). ^{1}H NMR δ 0.93 (3H, *s*, 18-H$_3$), 3.81 (3H, *s*, OCH$_3$), 4.83 (1H, *m*, 6α-H), 6.87 (1H, *dd*, J_1 8.6 J_2 3.0 Hz, 2-H), 7.24 (1H, *d*, *J* 6.8 Hz, 4-H), 7.60 (1H, *d*, *J* 3.8 Hz, 1-H). LR-MS *m/z* 300 (100%, M), 282 (34%, M − H$_2$O), 256 (10%), 225 (10%). HR-MS (EI-PIM) calc. for $C_{19}H_{24}O_4$ [M]$^+$: 300.1725. Found: *m/z* 300.1707.

*Oxyfunctionalization products of progesterone (**3**). (i) 4β,5β-Epoxypregnane-3,20-dione (**12**).* Isolated from the reaction product of **3** as colorless needles (Fr. 1) crystallized from EtOAc: m.p. 132–134°C [lit. (23), m.p. 130–132°C]: IR ν_{max}/cm 1699 (C=O), 854 (C–O). ^{1}H NMR δ 0.62 (3H, *s*, 18-H$_3$), 1.12 (3H, *s*, 19-H$_3$), 2.09 (3H, *s*, 21-H$_3$), 2.96 (1H, *s*, 4α-H). LR-MS *m/z* 330 (67%, M), 312 (58%, M − H$_2$O), 302 (47%), 258 (100%), 215 (37%).

*(ii) 4-Pregnene-3,6,20-trione (**13**).* Isolated from the reaction product of **3** as a colorless amorphous solid (Fr. 2) crystallized from EtOAc-hexane: m.p. 180–182°C; IR ν_{max}/cm 1738 (C=O). ^{1}H NMR δ 0.69 (3H, *s*, 18-H$_3$), 1.18 (3H, *s*, 19-H$_3$), 2.15 (3H, *s*, 21-H$_3$), 6.19 (1H, *s*, 4-H). LR-MS *m/z* 328 (100%, M), 310 (54%, M − H$_2$O), 300 (66%), 243 (62%), 229 (16%). HR-MS (EI-PIM) calc. for $C_{21}H_{28}O_3$ [M]$^+$: 328.2038. Found: *m/z* 328.2032.

*Oxyfunctionalization products of dihydrolanosteryl acetate (**4**). (i) 7-Oxolanost-8-en-3β-yl acetate (**14**).* Isolated from the reaction product of **4** as an amorphous solid (Fr. 1) crystallized from aqueous methanol: m.p. 145–148°C [lit. (24), m.p. 150.5–152°C]: IR ν_{max}/cm 1738 (C=O). ^{1}H NMR δ 0.66 (3H, *s*, 18-H$_3$), 0.86 (3H, *d*, *J* .6.8 Hz, 26- and 27-H$_3$), 0.89 (3H, *s*, 28-H$_3$), 0.90 (3H, *d*, *J* 6.8 Hz, 21-H$_3$), 0.92 (3H, *s*, 30-H$_3$), 0.96 (3H, *s*, 29-H$_3$), 1.19 (3H, *s*, 19-H$_3$), 2.07 (3H, *s*, COCH$_3$), 4.51 (1H, *dd*, J_1 10.2 J_2 4.8 Hz, 3α-H). LR-MS *m/z* 484 (46%, M), 469 (100%, M − CH$_3$), 409 (3%, M − AcOH-CH$_3$), 371 [9%, M − side chain (SC)], 344 (6%), 302 (6%), 278 (7%), 243 (5%), 207 (5%).

*(ii) 11α-Hydroxy-7-oxolanost-8-en-3β-yl acetate (**15**).* Isolated from the reaction product of **4** as an amorphous solid (Fr. 2) crystallized from aqueous methanol: m.p. 167–169°C:

IR ν_{max}/cm 3329 (OH), 1699 (C=O). ^{1}H NMR δ 0.65 (3H, *s*, 18-H_3), 0.86 (3H, *d*, *J* 6.8 Hz, 26- and 27-H_3), 0.86 (3H, *s*, 28-H_3), 0.90 (3H, *d*, *J* 6.8 Hz, 21-H_3), 0.92 (3H, *s*, 30-H_3), 0.96 (3H, *s*, 29-H_3), 1.23 (3H, *s*, 19-H_3), 2.05 (3H, *s*, $COCH_3$), 4.48 (1H, *td*, J_1 4.9 J_2 4.9 Hz, 11β-H), 4.52 (1H, *dd*, J_1 10.2 J_2 4.9 Hz, 3α-H). LR-MS *m/z* 500 (100%, M), 440 (30%, M – AcOH), 425 (14%, M – AcOH – CH_3), 369 (5%, M – H_2O – SC), 318 (16%), 304 (18%), 294 (11%), 271 (4%, M – AcOH – CH_3 – SC). HR-MS (EI-PIM) calc. for $C_{32}H_{52}O_4$ $[M]^+$: 500.3866. Found: *m/z* 500.3885.

*(iii) 25-Hydroxy-7,11-dioxolanost-8-en-3β-yl acetate (**16**).* Isolated from the reaction product of **4** as colorless needles (Fr. 3), crystallized from EtOAc: m.p. 195–197°C: IR ν_{max}/cm 3490 (OH), 1709 (C=O). ^{1}H NMR δ 0.80 (3H, *s*, 18-H_3), 0.90 (3H, *d*, *J* 5.4 Hz, 21-H_3), 0.90 (3H, *s*, 30-H_3), 0.92 (3H, *s*, 28-H_3), 0.95 (3H, *s*, 29-H_3), 1.22 (3H, *s*, 19-H_3 and 26-H_3 and 27-H_3), 2.06 (3H, *s*, $OCOCH_3$), 4.67 (1H, *dd*, J_1 10.2 J_2 4.9 Hz, 3α-H). LR-MS *m/z* 514 (43%, M), 496 (100%, M – H_2O), 454 (20%, M – AcOH), 436 (8%, M – AcOH – H_2O), 385 (6%, M – SC), 332 (7%), 318 (19%), 292 (8%), 255 (5%). HR-MS (EI-PIM) calc. for $C_{32}H_{52}O_5$ $[M]^+$: 514.3658. Found: *m/z* 514.3646.

*Oxyfunctionalization products of ergostanyl acetate (**5**).*
*(i) (20S)-20-Hydroxy-5α-ergostan-3β-yl acetate (**17**).* Isolated from the reaction product of **5** as colorless needles (Fr. 1) crystallized from aqueous methanol: m.p. 87–88°C. IR ν_{max}/cm 3548 (OH), 1723 (C=O). ^{1}H NMR δ 0.78 (6H, *d*, *J* 6.5 Hz, 26- and 27-H_3), 0.82 (3H, *s*, 18-H_3), 0.84 (3H, *s*, 19-H_3), 0.85 (3H, *d*, *J* 6.5 Hz, 28-H_3), 1.25 (3H, *s*, 21-H_3), 2.02 (3H, *s*, $COCH_3$), 4.67 (1H, *br m*, 3α-H). LR-MS *m/z* 442 (19%, M – H_2O), 427 (4%, M – H_2O – CH_3), 361 (100%), 343 (57%), 301 (38%, M – SC), 258 (60%, M – AcOH – SC + H), 243 (32%), 216 (15%). HR-MS (EI-PIM) calc. for $C_{30}H_{50}O_2$ $[M – H_2O]^+$: 442.3817. Found: *m/z* 442.3811.

*(ii) (24R)-24-hydroxy-5α-ergostan-3β-yl acetate (**18**).* Isolated from the reaction product of **5** as colorless needles (Fr. 2), crystallized from aqueous methanol: m.p. 167–169°C [lit. (19), mp, 169–172°C]: IR ν_{max}/cm 3505 (OH), 1716 (C=O). ^{1}H NMR δ 0.65 (3H, *s*, 18-H_3), 0.82 (3H, *s*, 19-H_3), 0.87 (3H, *d*, *J* 6.5 Hz, 21-H_3), 0.90 (6H, *d*, *J* 5.4 Hz, 26- and 27-H_3), 1.07 (3H, *s*, 28-H_3), 2.02 (3H, *s*, $COCH_3$), 4.68 (1H, brm, 3α-H). LR-MS *m/z* 442 (19%, M – H_2O), 417 (26%, M – SC), 399 (21%), 358 (100%), 315 (38%, M – SC), 257 (60%, M – AcOH-SC), 216 (30%, M – AcOH – SC – ring D).

*(iii) 25-Hydroxy-5α-ergostan-3β-yl acetate (**19**).* Isolated from the reaction product of **5** as colorless needles (Fr. 3) crystallized from aqueous methanol: m.p. 157–160°C [lit. (19), mp, 160–163°C]: IR ν_{max}/cm 3505 (OH), 1716 (C=O); ^{1}H NMR δ 0.65 (3H, *s*, 18-H_3), 0.82 (3H, *s*, 19-H_3), 0.88 (3H, *d*, *J* 6.2 Hz, 21-H_3), 0.91 (3H, *d*, *J* 6.5 Hz, 28-H_3), 1.15 (3H, *s*, 27-H_3), 1.16 (3H, *s*, 26-H_3), 2.02 (3H, *s*, $COCH_3$), 4.68 (1H, *br m*, 3α-H); LR-MS *m/z* 442 (34%, M – H_2O), 402 (7%, M – SC), 358 (12%), 327 (24%), 315 (13%), 257 (100%, M – AcOH – SC), 215 (26%, M – AcOH – SC – ring D).

*(iv) (20S,24R)-20,24-Dihydroxy-5α-ergostan-3β-yl acetate (**20**).* Isolated from the reaction product of **5** as a noncrystalline substance (Fr. 4): IR ν_{max}/cm 3505 (OH), 1723 (C=O). ^{1}H NMR δ 0.82 (3H, *s*, 18-H_3), 0.84 (3H, *s*, 19-H_3), 0.87 (3H, *d*, *J* 6.8 Hz, 27-H_3), 0.91 (3H, *d*, *J* 7.0 Hz, 26-H_3), 1.25 (3H, *s*, 21-H_3), 2.02 (3H, *s*, $COCH_3$), 4.68 (1H, *br m*, 3α-H). LR-MS *m/z* 443 (4%, M – H_2O – CH_3), 415 (4%), 397 (12%, M – $2H_2O$ – $3CH_3$), 361 (26%), 343 (12%), 301 (24%), 283 (7%), 257 (10%, M – AcOH – SC), 243 (6%), 215 (6%, M – AcOH – SC – ring D). HR-MS (APCI-NIM) calc. for $C_{30}H_{51}O_4$ $[M – H]^–$: 475.3787. Found: *m/z* 475.3793.

*(v) (20S)-20,25-Dihydroxy-5α-ergostan-3β-yl acetate (**21**).* Isolated from the reaction product of **5** as a noncrystalline substance (Fr. 5): IR ν_{max}/cm 3565 (OH), 1723 (C=O). ^{1}H NMR δ 0.82 (3H, *s*, 18-H_3), 0.84 (3H, *s*, 19-H_3), 0.88 (3H, *d*, *J* 7.0 Hz, 28-H_3), 1.15 (3H, *s*, 27-H_3), 1.18 (3H, *s*, 26-H_3), 1.26 (3H, *s*, 21-H_3), 2.02 (3H, *s*, $COCH_3$), 4.68 (1H, *br m*, 3α-H). LR-MS *m/z* 440 (10%, M – H_2O), 383 (9%), 361 (79%), 343 (28%), 301 (49%), 283 (14%), 257 (17%, M – AcOH – SC), 243 (11%), 215 (9%, M – AcOH – SC – ring D). HR-MS (APCI-NIM) calc. for $C_{30}H_{51}O_4$ $[M – H]^–$: 475.3787. Found: *m/z* 475.3808.

*Oxyfunctionalization products of stigmastanyl acetate (**6**).*
*(i) (24S)-24-Hydroxy-5α-stigmastan-3β-yl acetate (**22**).* Isolated from the reaction product of **6** as a colorless amorphous solid (Fr. 1), crystallized from aqueous methanol: m.p. 150–152°C [lit. (19), m.p., 153–155°C]: IR ν_{max}/cm 3519 (OH), 1723, 1709 (C=O). ^{1}H NMR δ 0.65 (3H, *s*, 18-H_3), 0.82 (3H, *s*, 19-H_3), 0.88 (3H, *t*, *J* 7.0 Hz, 29-H_3), 0.88 (6H, *d*, *J* 6.8 Hz, 26- and 27-H_3), 0.91 (3H, *d*, *J* 6.8 Hz, 21-H_3), 2.02 (3H, *s*, $COCH_3$), 4.68 (1H, *br m*, 3α-H). EI-MS *m/z* 456 (10%, M – H_2O), 431 (29%), 413 (40%), 371 (31%). 358 (60%), 315 (44%, M – H_2O), 257 (67%, M – AcOH – SC), 215 (28%, M – AcOH – SC – ring D).

(ii) 25-Hydroxy-5α-stigmastan-3β-yl acetate (23). Isolated from the reaction product of **6** as a colorless amorphous solid (Fr. 2) crystallized from aqueous methanol: m.p. 195–197°C [lit. (19), m.p., 197–199°C]: IR ν_{max}/cm 3344 (OH), 1730 (C=O). ^{1}H NMR δ 0.65 (3H, *s*, 18-H_3), 0.82 (3H, *s*, 19-H_3), 0.92 (3H, *d*, *J* 5.4 Hz, 21-H_3), 0.95 (3H, *t*, *J* 4.6 Hz, 29-H_3), 1.17 (6H, *s*, 26- and 27-H_3), 2.02 (3H, *s*, $COCH_3$), 4.68 (1H, *br m*, 3α-H). EI-MS *m/z* 456 (28%, M – H_2O), 416 (11%), 381 (4%), 356 (26%), 341 (23%), 315 (12%), 257 (100%, M – AcOH – SC), 215 (22%, M – AcOH – SC – ring D).

*(iii) (24S)-24-Hydroxy-15-oxo-5α-stigmastan-3β-yl acetate (**24**).* Isolated from the reaction product of **6** as a colorless amorphous solid (Fr. 3) crystallized from aqueous methanol: m.p. 161–164°C: IR ν_{max}/cm 3534 (OH), 1730, 1716 (C=O). ^{1}H NMR δ 0.74 (3H, *s*, 18-H_3), 0.85 (3H, *t*, *J* 5.9 Hz, 29-H_3), 0.87 (3H, *s*, 19-H_3), 0.87 (6H, *d*, *J* 6.2 Hz, 26- and 27-H_3), 1.00 (3H, *d*, *J* 6.2 Hz, 21-H_3), 2.02 (3H, *s*, $COCH_3$), 4.68 (1H, *br m*, 3α-H). LR-MS *m/z* 488 (4%, M), 445 (80%), 428 (22%, M – AcOH), 385 (33%), 367 (60%), 331 (100%, M – SC), 271 (32%, M – AcOH – SC), 262 (10%), 216 (13%, M – AcOH – SC – ring D). HR-MS (APCI-NIM) calc. for $C_{31}H_{51}O_4$ $[M – H]^–$: 487.3787. Found: *m/z* 487.3758.

*(iv) (24*S*)-24,25-Dihydroxy-5α-stigmastan-3β-yl acetate (**25**).* Isolated from the reaction product of **6** as a colorless amorphous solid (Fr. 4), crystallized from aqueous methanol: m.p. 160–162°C: IR ν_{max}/cm 3505, 3446 (OH), 1730, 1709 (C=O). ^{1}H NMR δ 0.65 (3H, *s*, 18-H_3), 0.81 (3H, *s*, 19-H_3), 0.92 (3H, *t*, *J* 6.5 Hz, 29-H_3), 0.92 (3H, *d*, *J* 6.5 Hz, 21-H_3), 1.18 (6H, *s*, 26- and 27-H_3), 2.02 (3H, *s*, $COCH_3$), 4.68 (1H, *br m*, 3α-H). LR-MS *m/z* 430 (18%, M – AcOH,), 413 (74%), 371 (73%), 353 (100%), 315 (65%), 283 (10%), 257 (7%, M – AcOH – SC), 215 (12%, M – AcOH – SC – ring D). HR-MS (APCI-NIM) calc. for $C_{31}H_{53}O_4$ [M – H]$^-$: 489.3944. Found: *m/z* 489.3926.

*(v) 25-Hydroxy-15-oxo-5α-stigmastan-3β-yl acetate (**26**).* Isolated from the reaction product of **6** as a colorless amorphous solid (Fr. 5), crystallized from aqueous methanol: m.p. 149–151°C: IR ν_{max}/cm 3519 (OH), 1738, 1709 (C=O). ^{1}H NMR δ 0.74 (3H, *s*, 18-H_3), 0.82 (3H, *s*, 19-H_3), 0.94 (3H; *d*, *J* 6.9 Hz, 21-H_3), 1.18 (6H, *s*, 26- and 27-H_3), 2.02 (3H, *s*, $COCH_3$), 4.68 (1H, *br m*, 3α-H). LR-MS *m/z* 488 (1%, M), 470 (14%, M – H_2O), 430 (7%), 415 (5%), 370 (12%), 331 (100%), 303 (9%), 271 (23%), 262 (8%), 201 (9%, M – AcOH – CH_3 – SC – ring D). HR-MS (APCI-NIM) calc. for $C_{31}H_{51}O_4$ [M – H]$^-$: 487.3787. Found: *m/z* 487.3787.

*(vi) (20*S*)-20,25-Dihydroxy-5α-stigmastan-3β-yl acetate (**27**).* Isolated from the reaction product of **6** as a noncrystalline substance (Fr. 6): IR ν_{max}/cm 3490 (OH), 1723 (C=O). ^{1}H NMR δ 0.82 (3H, *s*, 18-H_3), 0.84 (3H, *s*, 19-H_3), 0.95 (3H, *t*, *J* 5.9 Hz, 29-H_3), 1.16 (6H, *s*, 26- and 27-H_3), 1.27 (3H, *s*, 21-H_3), 2.02 (3H, *s*, $COCH_3$), 4.68 (1H, *br m*, 3α-H). LR-MS *m/z* 445 (9%, M – $3CH_3$), 427 (7%, M – H_2O – $3CH_3$), 385 (10%, M – AcOH – $3CH_3$), 361 (75%), 343 (28%), 301 (50%, M – SC – CH_3), 257 (17%, M – AcOH – SC), 215 (14%, M – AcOH – SC – ring D). HR-MS (APCI-NIM) calc. for $C_{31}H_{53}O_4$ [M – H]$^-$: 489.3944. Found: *m/z* 489.3941.

*(vii) (20*S*)-20,25-Dihydroxy-15-oxo-5α-stigmastan-3β-yl acetate (**28**).* Isolated from the reaction product of **6** as colorless needles (Fr. 7), crystallized from aqueous methanol: m.p. 183–185°C: IR ν_{max}/cm 3505, 3446 (OH), 1723, 1716 (C=O). ^{1}H NMR δ 0.83 (3H, *s*, 18-H_3), 0.92 (3H, *s*, 19-H_3), 1.16 (6H, *s*, 26- and 27-H_3), 1.22 (3H, *s*, 21-H_3), 2.02 (3H, *s*, $COCH_3$), 4.68 (1H, *br m*, 3α-H). LR-MS *m/z* 486 (1%, M – H_2O), 468 (19%, M – $2H_2O$), 375 (9%, M – AcOH – $3H_2O$ – CH_3), 315 (6%), 272 (12%), 215 (10%, M – AcOH – SC – ring D). HR-MS (APCI-NIM) calc. for $C_{31}H_{53}O_4$ [M – H]$^-$: 503.3736. Found: *m/z* 503.3741.

RESULTS AND DISCUSSION

The series of steroid substrates **1–6** were found to react readily with the DCP *N*-oxide/Ru(TMP)CO/HBr system to form a variety of the novel oxygenated derivatives in one step (Scheme 1). Each of the reaction products was separated by chromatographic purification, and the structures of the individually isolated products (**7–28**) were determined on the basis of the ^{1}H and ^{13}C NMR and MS spectral data. The results are shown in Table 1. The reactivity and selectivity of the oxidation reactions depended significantly on the structures of the substrates.

In previous papers, the direct oxidation of estrone acetate (**1**) possessing an aromatic A-ring by using dimethyldioxirane as an oxygen atom source was effective for the 9α-hydroxylation (25,26). Treatment of estrone methyl ether (**2**) with *tert*-butyl hydroperoxide and cobalt acetate afforded the epimeric 6-oxo-11-hydroxylation products (22). On the other hand, the 6- and 11β-hydroxylations predominated for the catalytic oxidation of equilenin acetate with iodosylbenzene/manganese porphyrin (14). These intriguing results prompted us to examine **1** and **2** with DCP *N*-oxide/Ru(TMP)CO/HBr.

The oxidant system with **1** was found to be effective for the ketonization at C-6 and the hydroxylation at C-9 to give the corresponding benzylic 6-oxo (**7**, 55%) and 6-oxo-9α-hydroxy (**8**, 25%) derivatives under mild conditions as described in the Experimental Procedures section. An essentially identical result was also obtained for **2**, which was transformed into the 6-oxo (**9**, 82%) and 6-oxo-9α-hydroxy (**10**, 8%) derivatives, accompanied by a minute amount of the 6β-hydroxy compound (**11**, 2%). Since the C-3 functional groups in **1** and **2** are situated far apart from the methine and methylene carbons in the B–D rings, the variation of local electron density induced by the electron-withdrawing or -donating substituents is little affected on benzylic oxidation. In addition, that **11** was isolated may suggest that all of the 6-oxo compounds (**7**–**10**) are produced *via* the successive oxidation of possible 6β-hydroxy intermediates.

A preliminary experiment showed that saturated 5α-androstane-3,17-dione is completely inert with DCP *N*-oxide/Ru(TMP)CO/HBr, in analogy with a previous finding (18). However, when progesterone (**3**), having a conjugated enone moiety, was subjected to the oxidation reaction, it caused simultaneous β-epoxidation of the Δ^4-unsaturated bond and allylic ketonization of the β-methylene carbon at C-6 to give the corresponding 4β,5β-epoxide **12** (65%) and 6-oxo derivative **13** (10%), respectively. The high stereoselectivity of the epoxidation is very similar to that of cholesta-1,4-dien-3-one by dimethyldioxirane, in which the 4β,5β-epoxide was a major product, accompanied by the 4β,5β-epoxy-25-ol as a minor one (27). The DCP *N*-oxide/Ru(TMP)CO/HBr oxidant therefore catalyzes more predominantly the stereoselective epoxidation at a less hindered double bond than the ketonization at allylic and benzylic β-methylene carbon atoms (see also below).

As shown in Table 2, the position of the C-6 oxo group in **7–10** and **13** was determined by the appearance of a quaternary ^{13}C signal at *ca*. 196–201 ppm, which corresponds to the allylic or benzylic β-position with regard to a double bond (22,28). The olefinic 4-H signal appearing at 5.74 ppm in **3** was strongly deshielded by the 6-ketonization and resonated at 6.19 ppm in **13**. Similarly, the presence of the 9α-hydroxy group in **8** and **10** was confirmed by the occurrence of a quaternary ^{13}C signal at 69.3 ppm (C-9), tertiary signals at 40.8–41.1 (C-8) and 43.4 ppm (C-14), and a methyl signal at 12.7–12.8 ppm (C-18) (22,25,26). Meanwhile, the substituent effect of a 6β-hydroxy group on the ^{1}H and ^{13}C chemical shifts

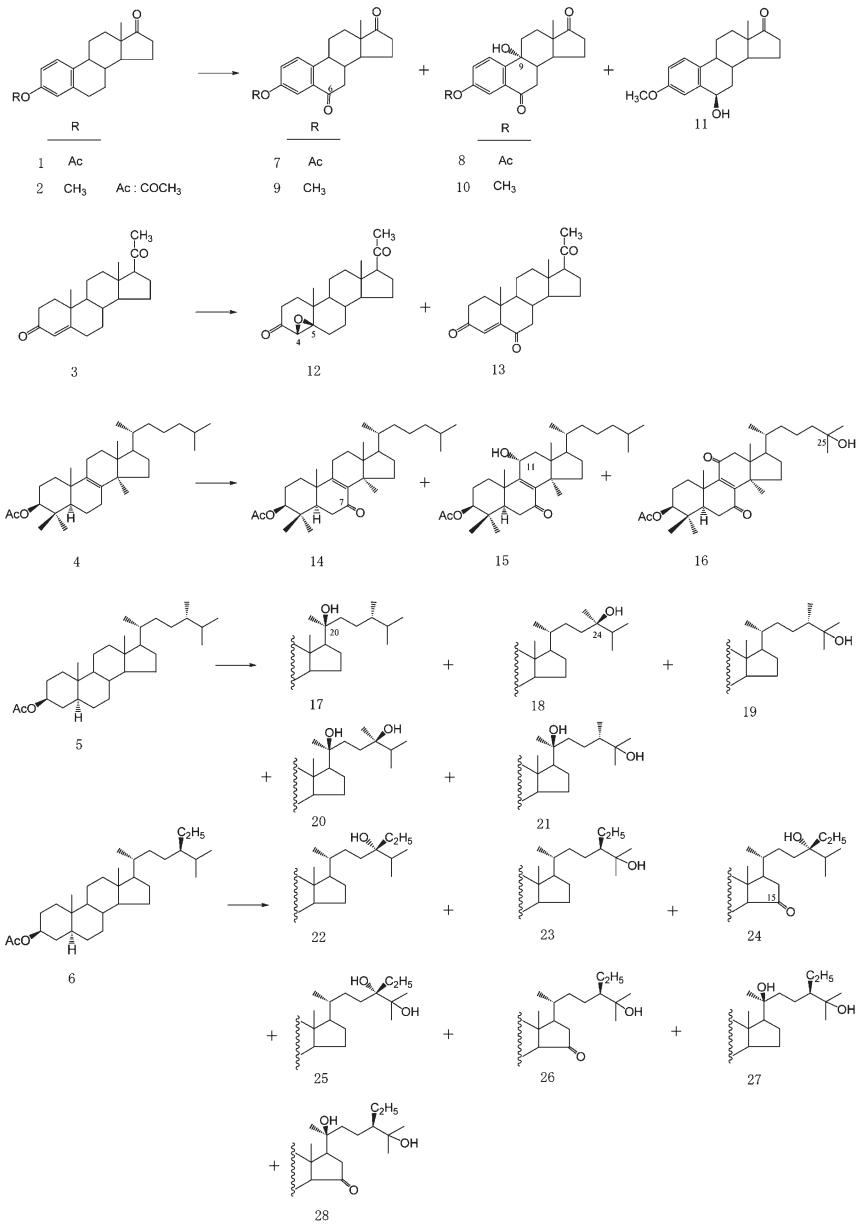

SCHEME 1

of **7** was used for the structural elucidation of **11** (28,29); the observed chemical shift values for the 18- and 19-methyl protons and the carbons at C-6, -7, -8, -9, and -10 were in good agreement with those for the calculated ones. The β-configuration of the epoxide ring in **12** was determined by the 19-methyl signal appearing at 1.12 ppm in the ^{1}H NMR (23).

TABLE 1
Oxidation Products of Steroids with DCP *N*-Oxide/Ru(TMP)CO/HBr

Substrate	Starting compound recovery[a] (%)	Product compounds[a] (yield, %)
1	20	**7** (55), **8** (25)
2	8	**9** (82), **10** (8), **11** (2)
3	25	**12** (65), **13** (10)
4	12	**14** (56), **15** (16), **16** (16)
5	22	**17** (7), **18** (30), **19** (32), **20** (5), **21** (4)
6	9	**22** (24), **23** (25), **24** (11), **25** (7), **26** (13), **27** (6), **28** (3)

[a]Determined by capillary GC; for conditions, see the Experimental Procedures section. DCP, 2,6-dichloropyridine; TMP, tetramesitylporphyrinate.

TABLE 2
^{13}C NMR Chemical Shifts for the Oxyfunctionalization Products (7–28) of Steroids 1–6[a]

Carbon	7	8	9	10	11	12	13	14	15	16	17	18	19	20	21	22	23	24	25	26	27	28
1	127.1	127.3	126.2	125.6	126.5	38.2	35.5	34.5	36.4	36.2	36.7	36.7	36.7	36.7	36.7	36.7	36.7	36.7	36.7	36.7	36.7	36.7
2	126.6	125.6	109.4	110.4	114.4	30.4	33.9	23.8	24.0	23.9	27.4	27.5	27.4	27.4	27.4	27.4	27.4	27.4	27.4	27.4	27.4	27.4
3	149.3	150.7	157.9	159.6	158.1	206.3	199.2[b]	79.6	79.6	79.3	73.7	73.7	73.7	73.7	73.7	73.7	73.8	73.5	73.8	73.5	73.7	73.5
4	120.1	120.8	121.1	121.4	114.1	63.2	125.7	37.7	37.9	37.7	33.9	34.0	34.0	34.0	34.0	34.0	34.0	33.9	34.0	33.8	33.9	33.8
5	143.3	144.4	138.6	139.7	138.9	69.9	160.4	49.8	49.9	50.1	44.6	44.6	44.6	44.6	44.6	44.6	44.6	44.6	44.6	44.6	44.6	44.7
6	196.3	196.6	196.7	197.5	67.6	25.8	201.6[b]	36.4	34.0	33.7	28.5[b]	28.6	28.5	28.5	28.5	28.6	28.6	28.1	28.3	28.1	28.0	28.1
7	43.0	36.6	42.8	36.8	35.8	29.5	46.5	198.7	200.0	202.4[b]	31.8	32.0	31.9	31.8	31.8	32.0	32.0	30.5	32.0	30.5	31.8	30.6
8	39.1	40.8	39.1	41.1	32.6	34.7	34.0	139.1	141.7	150.6[c]	34.8	35.4	35.4	34.8	34.8	35.4	35.7	33.9	35.4	35.5	34.7	31.4
9	43.0	69.3	42.5	69.3	44.0	46.0	50.7	164.7	160.1	151.7[c]	54.1	54.2	54.1	54.1	54.1	54.2	54.2	53.7	54.2	53.7	54.1	53.8
10	133.5	134.0	132.9	132.8	131.9	36.9	39.7	39.6	40.3	39.0	35.4	35.4	35.4	35.4	35.4	35.4	35.4	35.5	35.4	35.5	35.4	35.6
11	25.0	31.9[c]	24.8	32.0[c]	25.5	21.3	20.8	23.7	65.5	201.9[b]	21.0	21.2	21.1	21.0	21.0	21.2	21.2	20.7	21.2	20.7	21.0	20.6
12	31.1	27.3[c]	30.9	27.4[c]	31.5	38.2	38.1	30.1	44.4	51.6	40.3	39.9	39.9	40.3	40.3	39.9	39.9	39.8	39.9	39.9	40.3	40.2
13	47.5	47.4	47.3	47.5	48.1	43.8	43.8	44.8	47.5	49.0	42.8	42.6	42.5	42.9	42.9	42.6	42.6	42.3	42.6	42.3	42.9	43.1
14	50.2	43.4	49.8	43.4	50.0	55.7	56.5	47.8	48.1	47.5	56.5	56.4	56.3	56.5	56.5	56.4	56.4	65.8	56.4	65.8	56.5	66.0
15	21.3	20.9	21.0	21.1	21.4	24.1	24.1	32.0	32.8	32.1	23.6	24.2	24.1	23.7	23.7	24.2	24.2	215.8	24.2	216.0	24.5	215.5
16	35.6	35.6	35.3	35.7	35.4	22.5	22.8	28.7	0.0	27.3	22.3	28.2	28.1	22.4	22.4	28.3	28.3	41.9	28.6	41.9	26.8	43.8
17	219.5	219.4	219.2	219.6	220.8	62.3	63.1	49.0	50.2	49.0	57.4	55.9	55.9	58.1	57.6	56.0	56.0	51.3	55.9	51.2	57.9	53.6
18	13.6	12.7	13.3	12.8	13.9	13.1	13.2	15.8	16.9	16.8	12.2	12.0	12.0	13.8	13.9	12.0	12.0	12.9	12.0	13.0	13.7	13.7
19						18.7	17.5	18.4	18.6	17.5	13.8	12.2	12.1	12.2	12.2	12.2	12.2	12.1	12.2	12.1	12.2	12.1
20						208.9	208.8	36.4	36.2	36.2	75.2	36.1	36.3	75.0	75.3	36.4	36.3	36.0	36.7	35.8	75.4	74.8
21						31.2	31.4	18.8	19.9	18.5	26.4	18.7	18.9	26.2	26.4	18.7	18.6	19.0	18.7	19.0	26.1	28.5
22								36.4	36.8	36.4	41.8	29.1	34.8	36.8	42.6	29.0	35.7	29.0	30.7[b]	35.8	43.5	36.9
23								24.1	23.8	21.0	28.6[b]	36.2	27.8	29.7	25.9	31.8	26.9	31.7	30.3[b]	26.7	22.3	28.9
24								39.6	39.4	44.2	39.0	74.7	45.1	74.5	44.8	76.0	51.7	75.8	77.9	51.5	52.0	51.8
25								28.0	28.0	71.0	31.6	36.1	73.5	36.2	73.5	33.9	74.2	33.9	75.7	74.0	74.2	74.4
26								22.5	22.5	29.2	15.3	16.8	26.1	16.8	25.8	16.8	27.4	16.6	25.5	27.3	26.8	26.7
27								22.8	22.8	29.3	20.4	17.6	27.1	17.6	27.6	16.7	27.4	16.8	25.5	26.7	26.1	26.5
28								27.4	27.4	27.8	17.6	23.3	14.7	23.2	14.8	28.4	23.5	28.4	26.7	23.5	23.6	24.1
29								16.4	16.3	16.5						7.7	13.9	7.7	8.9	13.9	13.7	14.6
30								25.0	25.2	25.9												
$O\underline{C}H_3$			55.1	55.5	55.3																	
$O\underline{C}OCH_3$	169.3	169.3						170.8	170.7	170.8	170.6	170.7	170.7	170.7	170.7	170.7	170.7	170.7	170.7	170.7	170.7	170.7
$O\underline{C}OCH_3$	20.9	21.1						21.2	21.2	21.2	21.4	21.5	21.4	21.5	21.5	21.5	21.5	21.4	21.5	21.4	21.4	21.4

[a]In ppm downfield from tetramethylsilane.
[b,c]Assignments along a vertical column may be interchanged.

To clarify the difference in the reactivity between allylic (or benzylic) and methine carbons, we then examined for dihydrolanosteryl acetate (**4**), which has both a $\Delta^{8(9)}$-bond in the 5α-steroid nucleus and an C_8H_{17}-alkyl group in the side chain. The reaction of **4** with DCP *N*-oxide/Ru(TMP)CO/HBr resulted in the formation of the three variants of mono-, di-, and trioxygenated products, and those were identified as the 7-oxo (**14**, 56%), 7-oxo-11α-hydroxy (**15**, 16%), and 7,11-dioxo-25-hydroxy (**16**, 16%) derivatives. In the case of **4**, the tetrasubstituted $\Delta^{8(9)}$-bond was completely unreactive, probably owing to a large shielding of the axially β-oriented 18- and 19-methyl groups and the axial 14α-methyl. Again, the allylic ketonization at the C-7 and C-11 methylene carbons in **14–16** may be as a result of the subsequent oxidation of intermediary 7ζ- and/or 11α-hydroxy precursors. Of further note was that the reactivity was much larger for the allylic C-7 and -11 β-methylene carbons than for the C-21 and -25 *tert*-methine carbons (see below). The ^1H and ^{13}C NMR spectral data for **14** were in accord with those reported in a literature (24). The structures of **15** and **16** were determined on the basis of the substituent effects (29) of 11α-hydroxy and 11-oxo groups on the 18- and 19-methyl ^1H chemical shifts of the parent **14** and the typical ^{13}C chemical shifts (65.5 and 200.0 ppm for **15** and 201.9 and 202.4 ppm for **16**) of the allylic β-carbon signals (28).

Supporting evidence for the electrophilic nature of the oxoruthenium porphyrinate complex was achieved by the oxidation of saturated 5α-ergostanyl acetate (**5**) and 5α-stigmastanyl acetate (**6**), both of which possess an additional C-24 alkyl (methyl or ethyl) substituent at the C_8H_{17}-side chain in **4**. Thus, the methine carbons at C-20, -24, and -25 in **5** were oxyfunctionalized effectively to give the (24*R*)-24- (**18**, 30%) and 25-hydroxy (**19**, 32%) derivatives, along with small amounts of the (20*S*)-20-hydroxy (**17**, 7%), (20*S,*24*R*)-20,24- (**20**, 5%), and (20*S*)-20,25-dihydroxy (**21**, 4%) derivatives. The methine carbon at C-5 in the 5α-steroid nucleus and the methylene carbons in the side chain were not oxidized at all. Similarly, the 24- and 25-hydroxylations predominated for **6** to yield the (24*S*)-24-hydroxy (**22**, 24%) and 25-hydroxy (**23**, 25%) derivatives as the major products; the (24*S*)-24-hydroxy-15-oxo (**24**, 11%), 25-hydroxy-15-oxo (**25**, 7%), (20*S*)-20,25-dihydroxy (**26**, 13%), (24*S*)-24,25-dihydroxy (**27**, 6%), and (20*S*)-20,25-dihydroxy-15-oxo (**28**, 3%) derivatives were also isolated as the minor components. Both the methine protons (C-H) at the C-20 and -24 asymmetric center in **5** were completely replaced by hydroxy groups to give stereoselectively the corresponding (*20S*)-20- and (*24R*)-24-hydroxylated derivatives; on the other hand, **6** afforded only the (*20S*)-20- and (24*S*)-24-hydroxylation products. The position and stereochemical configuration of the oxyfunctionalizations in **17–28** were determined by comparison with the spectral data for analogous 15-, 20-, 24-, and 25-oxygenated steroids reported in the literature (19,30) and confirmed by the result of 5α-cholestan-3-one by using the same oxidizing system (18).

According to a previous study of 5α-cholestan-3-one without an alkyl substituent at C-24, hydroxylation took place only on the C-20 and -25 methine carbons by oxoruthenium porphyrinate (18). In **5** and **6**, however, the formation of appreciable amounts of the 24-hydroxy compounds (**18**, **20**, **22**, **24**, and **25**), together with the 20- and 25-hydroxy ones, implies that the O-insertion reaction depends somewhat on the degree of alkyl substitution of carbons under consideration. Thus, in general, the electrophilic attack of oxoruthenium porphyrinate is accelerated much more efficiently on an electron-rich *tert*-methine carbon rather than on a *sec*-methylene carbon. In addition, the relatively low reactivity at the C-20 methine carbon, rather the C-24 and -25 ones, is probably due to a steric hindrance of the axially oriented 18-methyl group, which prevents access of the oxidant to the C-20 and thereby decreases the formation of the stable substrate–catalyst complex. A similar steric hindrance also has been observed for the C-5 methine carbon in **4–6**, in contrast to the less hindered C-5 in 5β-steroids, which was readily hydroxylated (18,21).

In conclusion, the relatively bulky oxoruthenium porphyrinate complex attacks less sterically hindered methine and/or methylene carbons in steroid substrates. Geometrical and electronic interactions of unactivated carbons in the substrates with oxoruthenium porphyrinate also appear to be major factors controlling the reactivity and regioselectivity of the O-insertion reaction, which are interesting from a synthetic point of view.

ACKNOWLEDGMENTS

This work was supported by a Grant-in-Aid for Scientific Research from the Ministry of Education, Sciences, Sports and Culture of Japan and by Nihon University Multidisciplinary Research Grant for 2004.

REFERENCES

1. Omura, T., Ishimura, Y., and Fujii, Y. (eds.) (1993) *Cytochrome P-450*, Kodansha, Tokyo.
2. Meunier, B. (1992) Metalloporphyrins as Versatile Catalysts for Oxidation Reactions and Oxidative DNA Cleavage, *Chem. Rev. a2*, 1411–1456.
3. Reese, P.B. (2001) Remote Functionalization Reactions in Steroids, *Steroids 66*, 481–497.
4. Battioni, P., Renaud, J.P., Bartoli, J.F., Reina-Artiles, M., Fort, M., and Mansuy, D. (1988) Monooxygenase-like Oxidation of Hydrocarbons by H_2O_2 Catalyzed by Manganese Porphyrins and Imidazole: Selection of the Best Catalytic System and Nature of the Active Oxygen Species, *J. Am. Chem. Soc. 110*, 8462–8470.
5. Banfi, S., Maiocchi, A., Moggi, A., Montanari, F., and Quici, S. (1990) Hydrogen Peroxide Oxygenation of Alkanes Catalysed by Manganese(III)-Tetraarylporphyrins: The Remarkable Cocatalytic Effect of Lipophilic Carboxylic Acids and Heterocyclic Bases, *Chem. Commun*. 1794–1796.
6. Collman, J.P., Tanaka, H., Hembre, R.T., and Brauman, J.I. (1990) Metalloporphyrin-Catalyzed Oxidation of Saturated Hydrocarbons with Sodium Chlorite, *J. Am. Chem. Soc. 112*, 3689–3690.
7. Grieco, P.A., and Stuk, T.L. (1990) Remote Oxidation of Unactivated C–H Bonds in Steroids *via* Oxometalloporphinates, *J. Am. Chem. Soc. 112*, 7799–7801.

8. Stuk, T.L., Grieco, T.L., and Marsh, M.M. (1991) Site-Selective Hydroxylation of Steroids *via* Oxometalloporphinates Covalently Linked to Ring D: Introduction of Hydroxyl Groups into the C(9) and C(12) Position of 5α-Androstanes, *J. Org. Chem*. *56*, 2957–2959.
9. Kaufman, M.D., Grieco, P.A., and Bougie, D.W. (1993) Functionalization of Unactivated C–H bonds in Steroids *via* (Salen)Manganese(III) Complexes, *J. Am. Chem. Soc*. *115*, 11648–11649.
10. Breslow, R., Zhang, X., Xu, R., Maletic, M., and Merger, R. (1996) Selective Catalytic Oxidation of Substrates That Bind to Metalloporphyrin Enzyme Mimics Carrying Two or Four Cyclodextrin Groups and Related Metallosalens, *J. Am. Chem. Soc*. *118*, 11678–11679.
11. Breslow, R., Zhang, X., and Huang, Y. (1997) Selective Catalytic Hydroxylation of a Steroid by an Artificial Cytochrome P-450 Enzyme, *J. Am. Chem. Soc*. *119*, 4535–4536.
12. Breslow, R., Huang, Y., Zhang, X., and Yang, J. (1997) An Artificial Cytochrome P450 That Hydroxylates Unactivated Carbons with Regio- and Stereoselectivity and Useful Catalytic Turnovers, *Proc. Natl. Acad. Sci. USA, 94*, 11156–11158.
13. Breslow, R., Gabriele, B., and Yang, J. (1998) Geometrically Direct Selective Steroid Hydroxylation with High Turnover by a Fluorinated Artificial Cytochrome P-450, *Tetrahedron Lett*. *39*, 2887–2890.
14. Yang, J., Weinberg, R., and Breslow, R. (2000) The Hydroxylation and Amidation of Equilenin Acetate Catalyzed by Chloro [5,10,15,20-Tetrakis(pentafluorophenyl)porphyrinato]Manganese(III), *Chem. Commun*., 531–532.
15. Ohtake, H., Higuchi, T., and Hirobe, M. (1992) Highly Efficient Oxidation of Alkane and Alkyl Alcohols with Heteroaromatic *N*-Oxides Catalyzed by Ruthenium Porphyrins, *J. Am. Chem. Soc. 114*, 10660–10662.
16. Ohtake, H., Higuchi, T., and Hirobe, M. (1995) The Highly Efficient Oxidation Olefins, Alcohols, Sulfides, and Alkanes with Heteroaromatic *N*-Oxides Catalyzed by Ruthenium Porphyrins, *Heterocycles 40*, 867–903.
17. Higuchi, T., Satake, C., and Hirobe, M. (1995) Selective Quinone Formation by Aromatic Oxidation with Heteroaromatic *N*-Oxides Catalyzed by Ruthenium Porphyrin, *J. Am. Chem. Soc*. *117*, 8879–8880.
18. Shingaki, T., Miura, K., Higuchi, T., Hirobe, M., and Nagano, T. (1997) Regio- and Stereo-selective Oxidation of Steroids Using 2,6-Dichloropyridine *N*-Oxide Catalysed by Ruthenium Porphyrins, *Chem. Commun*., 861–862.
19. Iida, T., Yamaguchi, T., Nakamori, R., Hikosaka, M., Mano, N., Goto, J., and Nambara, T. (2001) A Highly Efficient, Stereoselective Oxyfunctionalization of Unactivated Carbons in Steroids with Dimethyldioxirane, *J. Chem. Soc. Perkin Trans. 1*, 2229–2236.
20. Iida, T., Ogawa, S., Shiraishi, K., Kakiyama, G., Goto, T., Mano, N., and Goto, J. (2003) A Comparative Study of Remote Oxy-functionalization of Unactivated Carbons in 5β-Steroids by Dimethyldioxirane and 2,6-Dichloropyridine *N*-Oxide/ Ruthenium Porphyrin/HBr, *ARKIVOC (Part viii)*, 170–179.
21. Ogawa, S., Iida, T., Goto, T., Mano, N., Goto, J., and Nambara, T. (2004) The Remote-Oxyfunctionalization of Unactivated Carbons in (5β)-3-Oxobile Acids by 2,6-Dichloropyridine *N*-Oxide Catalyzed by Ruthenium–Porphyrin and HBr: A Direct Lactonization at C-20, *Org. Biomol. Chem. 2*, 1013–1018.
22. Modica, E., Bombieri, G., Colombo, D., Marchini, N., Ronchetti, F., Scala, A., and Toma, L. (2003) Novel Estrones by Oxidation of the Benzylic Positions of the Estrane Skeleton with *tert*-Butyl Hydroperoxide and Cobalt Acetate, *Eur. J. Org. Chem*., 2964–2971.
23. Haase-Held, M., Hatzis, M., and Mann, J. (1993) New Routes to 4-Substituted Steroids: Synthesis of 4-Cyanoprogesterone, a Potent Inhibitor of the Enzyme 5α-Reductase, *J. Chem. Soc. Perkin Trans. 1*, 2907–2911.
24. Emmons, G.T., Wilson, W.K., and Schroepfer, G.J., Jr. (1989) ^{1}H and ^{13}C NMR Assignments for Lanostan-3β-ol Derivatives: Revised Assignments for Lanosterol, *Magn. Reson. Chem. 27*, 1012–1024.
25. Bovicelli, P., Lupattelli, P., and Mincione, E. (1992) Oxidation of Natural Targets by Dioxiranes: Oxyfunctionalization of Steroids, *J. Org. Chem. 57*, 2182–2184.
26. Brown, D.S., Marples, B.A., Muxworthy, J.P., and Baggaley, K.H. (1992) Preparation of 9α-Hydroxyestra-1,3,5(10)-trienes by Direct Benzylic Oxidation with Dimethyldioxirane, *J. Chem. Research (S)*, 28–29.
27. Bovicelli, P., and Lupattelli, P. (1994) Regio-and Stereoselective Epoxidation of Steroidal 1,4-Diene 3-Ones by Dimethyldioxirane: A New Access to A-Norsteroids and to a Class of Estrogen Synthetase Inhibitors, *J. Org. Chem. 59,* 4304–4307.
28. Blunt, J.W., and Stothers, J.B., (1977) ^{13}C NMR Spectra of Steroids: A Survey and Commentary, *Org. Magn. Reson. 9*, 439–464.
29. Kirk, D.N., Toms, H.C., Douglas, C., and White, K.A., (1990) A Survey of the High-Field ^{1}H NMR Spectra of the Steroid Hormones, Their Hydroxylated Derivatives, and Related Compounds, *J. Chem. Soc. Perkin Trans. 2*, 1567–1594.
30. Iida, T., Hikosaka, M., Kakiyama, G., Shiraishi, K., Schteingart, C.D., Hagey, L.R., Ton-Nu, H.-T., Hofmann, A.F., Mano, N., Goto, J., and Nambara, T. (2002) Potential Bile Acid Metabolites. 25. Synthesis and Chemical Properties of Stereoisomeric 3α,7α,16- and 3α,7α,15-Trihydroxy-5β-cholan-24-oic Acids, *Chem. Pharm. Bull. 50*, 1327–1334.

[Received August 4, 2004, and in revised form and accepted October 15, 2004]

Interaction Between Ferric Ions, Phospholipid Hydroperoxides, and the Lipid Phosphate Moiety at Physiological pH

Gene A. Morrill[a,*], Adele Kostellow[a], Lawrence M. Resnick[b], and Raj K. Gupta[a]

[a]Department of Physiology & Biophysics, Albert Einstein College of Medicine, Bronx, New York 10461, and
[b]Department of Medicine, Cornell University Medical Center, New York, New York 10021

ABSTRACT: Iron-catalyzed lipid peroxidation was examined using ^{1}H NMR in a biphasic aqueous-chloroform system. At physiological pH (7.4), mole ratios of phospholipids/Fe^{3+} as low as 1300:1 catalyzed the rapid disappearance of endogenous lipid hydroperoxides with a loss of two of the four double bonds in PC containing palmitic (16:0) and arachidonic (20:4) acids in the *sn*-1 and *sn*-2 positions, respectively. The predominant phospholipid products after 1 h at 20°C were a 9-carbon monounsaturated carbonyl and a phospholipid with an 11-carbon $\Delta^{5,8}$ FA in the *sn*-2 position. PC with linoleic acid (18:2) in the *sn*-2 position lost one double bond and formed a phospholipid with a 9-carbon FA. Cardiolipin (linoleic acid-rich) also lost about 40% of its double bonds. No detectable loss was seen for PC containing oleic acid (18:1) or neutral lipids with PUFA. At arachidonyl PC/Fe^{3+} ratios less than 20:1, significant broadening of the choline methyl proton peak was evident, indicating that Fe^{3+} may form a complex with the adjacent phosphate group and that the complex involves both the phosphate and the hydroperoxide adjacent to the Δ^{11} double bond. The results demonstrate that, at physiological pH, Fe^{3+}-catalyzed peroxidation in polyunsaturated phospholipids occurs selectively adjacent to specific double bonds (Δ^9 or Δ^{11}). These PC-derived products have been shown to activate components of the inflammatory system. This suggests that the episodic release of ferric ions may play a significant role in generating inflammatory mediators.

Paper no. L9539 in *Lipids 39*, 881–889 (September 2004).

Iron (Fe)-catalyzed phospholipid peroxidation is a recognized source of oxidative damage to cell membranes, lipoproteins, and other lipid-containing structures (reviewed in Refs. 1–3). Peroxidation can be initiated either by free radical species or by the iron-catalyzed breakdown of lipid hydroperoxides. H_2O_2 is formed continuously in cells and tissues, both spontaneously and by enzymatic action, and reacts with phospholipids to form hydroperoxides (4,5). Newly formed membrane lipid hydroperoxides are repaired by a membrane enzyme, phospholipid-hydroperoxide glutathione peroxidase (6), or, if metal ions such as Fe, Cu, or Ni are present, may undergo breakdown to form products such as malondialdehyde.

McIntyre and colleagues (7) proposed that oxidation of choline phospholipids results in chain-shortened fragments and oxygenated derivatives of polyunsaturated *sn*-2 fatty acyl residues, generating potent biological compounds that activate components of the immune and inflammatory systems. More recently, they have identified an abundant oxidatively fragmented alkyl phospholipid (hexadecyl azelaoyl PC, or azPC) derived from LDL and known to produce an inflammatory response (8). Similarly, Leitinger and colleagues (9) demonstrated that products of oxidized 1-palmitoyl-2-arachidonyl-*sn*-glycerol-3-phosphorylcholine, isolated from minimally modified LDL, activate endothelial cells to bind monocytes. More recent studies in our laboratory (10) have shown that micromolar levels of ferric ions catalyze lipid peroxidation in aortic cell membranes *in vitro*, and that extracellular ionized Mg^{2+} protects membrane lipids from peroxidation. Iron-catalyzed lipid peroxidation in the vascular system could thus both damage cell membranes and act on serum lipids to cause local inflammation.

We have developed a biphasic system for studying the iron-catalyzed modifications of phospholipids using ^{1}H NMR. This method allowed the analysis of sequential structural changes in phospholipids undergoing peroxidation as well as the nature of the structural modification of the FA in the *sn*-2 position. The studies were largely carried out with ferric ions, since at physiological pH, the ferrous ion undergoes rapid autoxidation to the ferric species (11,12). We have found that Fe^{3+} catalyzes the disappearance of endogenous lipid hydroperoxide and of the acyl double bonds in PC if either contains esterified FA having two or more double bonds in the *sn*-2 position. Fe^{3+} produced a significant broadening of the proton resonance associated with the choline methyl groups of PC, suggesting that Fe^{3+} is interacting with the phosphate moiety. No peroxidation was seen with PC-containing monounsaturated FA or with neutral lipids containing two or more double bonds. This indicates that Fe^{3+} interaction with specific FA double bonds as well as with the lipid phosphate group is essential for lipid peroxidation at physiological pH (7.4).

*To whom correspondence shoud be addressed at Department of Physiology & Biophysics, Albert Einstein College of Medicine, 1300 Morris Park Ave., Bronx, NY 10461. E-mail: morrill@aecom.yu.edu

Abbreviations: Arachidonyl PC, 1-palmitoyl-2-arachidonyl-*sn*-glycero-3-phosphocholine; azPC, hexadecyl azelaoyl phosphatidylcholine; BAPTA, 1,2,-bis (*o*-aminophenoxy)ethane-*N,N,N′,N′*-tetraacetic acid; NKRB, normal pH 7.4 Krebs–Ringer bicarbonate.

MATERIALS AND METHODS

Materials. Purified phospholipids [1-palmitoyl-2-arachidonyl-*sn*-glycero-3-phosphocholine (arachidonyl PC), 1-palmitoyl-2-linoleoyl-*sn*-glycero-3-phosphocholine, 1-palmitoyl-2-oleoyl-*sn*-glycero-3-phosphocholine, bovine heart cardiolipin] were obtained from Avanti Polar Lipids, Inc. (Alabaster, AL). Lipids were obtained dissolved in $CHCl_3$ in sealed ampules. After opening, lipids were transferred to brown bottles with Teflon-lined caps and stored at –35°C under N_2. Total lipids were extracted from rat aortic tissue (13), taken to dryness under nitrogen, and fractionated on 200 mg aminopropylsilyl minicolumns (Alltech, Deerfield, IL) as described below. The $CHCl_3$ fraction was used as a source of polyunsaturated TG. Deuterated solvents were obtained from Aldrich (Milwaukee, WI). Ferric and ferrous ammonium sulfate salts (dodecahydrate, cell culture grade) were obtained from Sigma Chemical Co. (St. Louis, MO). 5,5′-Difluoro-BAPTA [where BAPTA = 1,2,-bis (*o*-aminophenoxy)ethane-*N,N,N′,N′*-tetraacetic acid], tetrapotassium salt, was obtained from Molecular Probes, Inc. (Eugene, OR). Normal pH 7.4 Krebs–Ringer bicarbonate (NKRB) solution (prepared in D_2O or H_2O) contained (in mM): NaCl, 118; KCl, 4.7; $KHPO_4$, 1.2; $MgSO_4$, 1.2; $CaCl_2$, 2.5; and $NaHCO_3$, 25. Ferrous and ferric salts were dissolved in distilled water or D_2O (*ca.* pH 3) and diluted 1:1000 in the corresponding NKRB immediately before use. Tadolini and Hakim (11) and Welch *et al.* (12) have reported that Fe^{2+} undergoes autoxidation at pH 7.2–7.5 with a half-time of less than 5 min, indicating that the predominant species in NKRB is the ferric ion (traces of ferrous ion are invariably present). The solubilities of Fe^{2+} and Fe^{3+} at pH 7.0 are reported to be 10^{-2} and *ca.* 10^{-18} M, respectively (14). Precipitate formation of $Fe(OH)_3$ is slow, however, taking days to weeks unless a strong base is added to the solution (14). We have found that $Fe(OH)_3$ in NKRB at physiological pH forms a clear solution that is stable for hours.

^{1}H NMR measurements. ^{1}H NMR spectroscopy was used to quantify FA unsaturation and to estimate the average FA chain length in purified phospholipids (e.g., 10,15) following peroxidation by ferric and/or ferrous ions. One-pulse spectra were taken on a Varian VXR-500 spectrometer operating at a proton frequency of 500 MHZ (13). All spectra were taken at 25°C using a 60° pulse, a spectral width of 5000 Hz, and a repetition time of 10 s and 8K data points. Adequate signal/ noise ratios were generally attained by 256 acquisitions. Resonance intensities were measured as peak areas in fully relaxed spectra. The average number of double bonds per acyl chain and the average carbon chain length were determined as indicated in Figure 1. Successive NMR measurements on the same experimental sample indicated that minimal changes occurred following the termination of sample vortexing. The ^{1}H NMR spectra were analyzed using NUTS, v. 2002 (Acorn NMR, Inc., Livermore, CA).

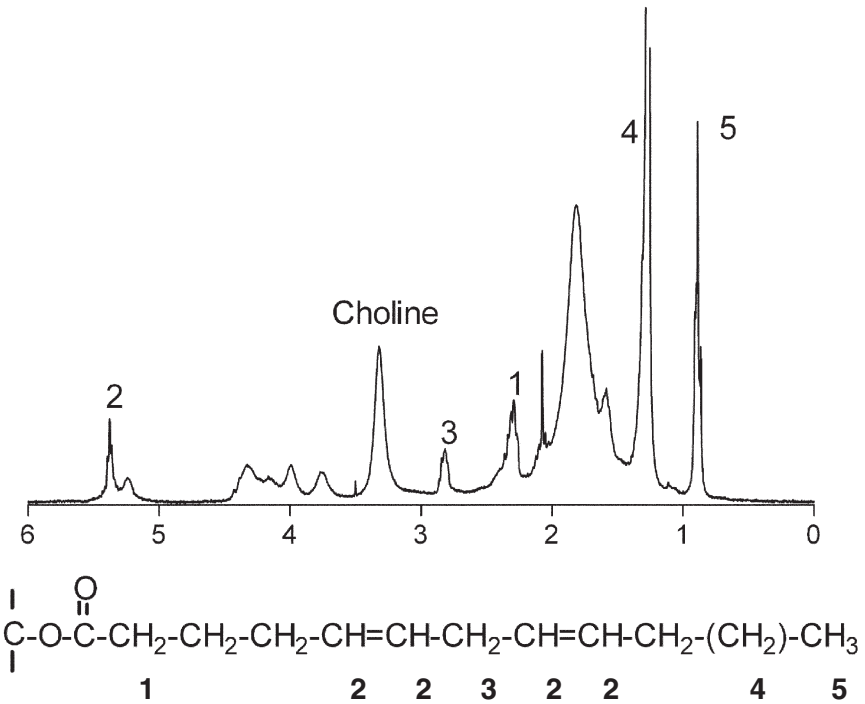

FIG. 1. (upper trace) Typical 500-MHz ^{1}H NMR spectrum of 1-palmitoyl-2-arachidonyl-*sn*-glycero-3-phosphocholine (arachidonyl PC) dissolved in $CDCl_3$. (lower formula) Numerically labeled peaks correspond to the protons indicated in the formula of a Δ^5 FA. Assignments important to this study include proton peaks associated with FA double bonds (peak 2, 5.3 ppm), the nine proton peaks associated with the choline methyl groups (3.33 ppm), the protons associated with the carbon alpha to the carboxyl group of the FA (peak 3, 2.3 ppm), the methylene groups (peak 4, 1.2 ppm), and the protons associated with the omega methyl groups of the FA (peak 5, 0.8 ppm).

Lipid peroxidation. Incubation of lipid and Fe salts was carried out at room temperature (20–22°C) in $CDCl_3/D_2O$ (50:1). Aliquots containing 1.0 mg of purified lipids were taken to dryness under N_2, redissolved in 1.0 mL of $CDCl_3$, and transferred to 5 × 70 mm Pyrex NMR tubes (New Era Enterprises, Inc., Vineland, NJ). Twenty microliters of NKRB in D_2O containing 0–200 μM of ferric ammonium sulfate and/or ferrous ammonium sulfate was added to the top of the $CDCl_3$ phase, and the tube was vortexed continuously at room temperature for the time periods indicated. Forty microliters of D_2O and 0.5 mL of CD_3OD were then added to the tube, and the tube was again vortexed for 30 s. The upper and lower phases were allowed to separate for 5 min. Under these conditions, the lower $CDCl_3$ phase contained the phospholipid and the upper phase contained D_2O, CD_3OD, and salts. Only the lower organic phase was situated in the NMR window. Alternatively, 20 μL of deuterated ethanol was added, the NMR tube was vortexed, and a single phase was formed. NMR measurements were taken within minutes after the treatment of each lipid sample. The above procedure has also been carried out in aqueous solution, with the final $CHCl_3$ phase taken to dryness under N_2. Residual water was removed using an Abderhalden pistol, and the lipid residue was redissolved in $CDCl_3$.

Fractionation of peroxidized lipids. Ferric ion-treated lipids were taken to dryness under nitrogen and fractionated on 200-mg aminopropylsilyl minicolumns. Columns were rinsed with 5 mL of hexane prior to addition of the lipid. The columns were eluted successively with 5 mL of $CHCl_3$ (neutral lipids, DG, methylated FA fraction), diethyl ether/acetic acid (98:2) (FFA, MG fraction), and methanol (N-containing phospholipids). Radiolabeled phospholipid and FA standards were used to monitor elution efficiency. Minicolumns were placed in conical 15-mL centrifuge tubes, and the mobile phase was collected by gentle centrifugation. (We found that using the vacuum filtration system developed by Alltech was unsuitable, as it caused a loss of lipid double bonds.) The fractions obtained by solid-state extraction were taken to dryness under N_2 and analyzed first by ^{1}H NMR in $CDCl_3$ and subsequently by TLC and/or HPLC. No detectable peroxidation of the purified lipids was seen after centrifugation. Column recovery was greater than 95%.

Analysis of lipid hydroperoxide. Aliquots of lipid were taken directly from the vial after opening or from the $CHCl_3$ phase prior to adding methanol (see the preceding section) and analyzed for hydroperoxides using the OxisResearch kit LPO-560 (OxisResearch, Portland, OR).

RESULTS

^{1}H NMR analysis of purified lipids. The ^{1}H NMR spectra of 1.0 mg of arachidonyl PC dissolved in 1.0 mL of $CDCl_3$ are shown in Figure 1. The peaks corresponding to the protons of the FA double bonds of the arachidonyl moiety appear around 5.3 ppm (peak 2 on Fig. 1). Protons associated with the FA backbone are shown in the 2.8–0.7 ppm region and include methylene protons (peak 4) and the omega methyl protons (peak 5). The protons associated with the methyl groups on the choline nitrogen are measurable at 3.33 ppm. Peaks in the 3.5 to 4.5 ppm region are associated with the protons of glycerol and the two carbons of the choline moiety. For assignment of the phospholipid protons, see Sze and Jardetzky (15) and Morrill *et al.* (13). Based on areas under the individual proton peaks, the purified lipid contained an average of 2.01 ± 0.03 double bonds per chain and an average chain length of 18.1 ± 0.24 per FA (mean ± SD for three batches of arachidonyl PC from Avanti Polar Lipids). This is consistent with the presence of palmitic acid (16:0) in the *sn*-1 position and arachidonic acid (20:4) in the *sn*-2 position.

Ferric ion-catalyzed peroxidation of arachidonyl-containing PC. The half-life of Fe^{2+} was estimated following addition of 4 mM of Fe^{2+} to the mixture containing 5 mM of 5,5′-difluoro-BAPTA at pH 7.4. Fe^{2+} forms a complex with 5,5′-difluoro-BAPTA (K_d = *ca.* 50 nM), exhibiting a characteristic peak downfield from those ascribed to other biological ions such as Ca^{2+} and Zn^{2+}. This Fe^{2+} peak disappears within 15 min, indicating conversion to Fe^{3+}, consistent with the findings by Tadolini and Hakim (11) and Welch *et al.* (12) that within the physiological pH range, and in the absence of chelators, ferrous iron autoxidation occurs with a half-time of less than 5 min. As noted in the Materials and Methods section, compared with ferrous ions, ferric ions are relatively insoluble at pH 7.4 (14). We found that the $Fe(OH)_3$ formed at physiological pH partitions into the hydrophobic phase ($CHCl_3$).

Figure 2 compares the loss of double bonds in arachidonyl-containing PC as a function of time after exposure to either 20 or 100 μM of Fe^{3+}. The reaction mixture contained a 50:1 $CDCl_3/D_2O$ ratio and an arachidonyl PC/ferric ion ratio of either 1300:1 or 260:1. The lower arachidonyl PC/ferric ion ratio approximates the episodic free ferric ion concentration under physiological conditions, whereas the higher ratio approximates that during hemolytic events (e.g., injury, surgery) or during kidney dialysis. Under the conditions used, loss of arachidonate double bonds was dose- and time-dependent, with a maximal loss of two of the four double bonds in ≥2 h at 20–22°C. Assuming no Fe^{3+}-induced changes in the palmitate in the *sn*-1 position, the number of residual carbons can be calculated from the areas in the 0.7 to 2.8 ppm region and from the number of remaining double bonds. The average chain length of the arachidonate moiety decreased by 9.6 ± 0.6 carbons over the 2-h time course in the presence of 100 μM Fe^{3+}, with an average of 3.5 carbons being lost over the first hour. When the aqueous phase was recovered at the end of the 2-h period and 5,5′-difluoro-BAPTA added, no peak characteristic of ferrous-BAPTA could be detected. This indicates that, as expected, no conversion of ferric to ferrous ions occurred under the conditions used.

Results were the same when either 100 μM of ferrous or ferric ions was used or when 50 μM of each were combined. However, the observed lipid peroxidation by Fe^{2+} may have been largely due to autoxidation of Fe^{2+} at physiological pH,

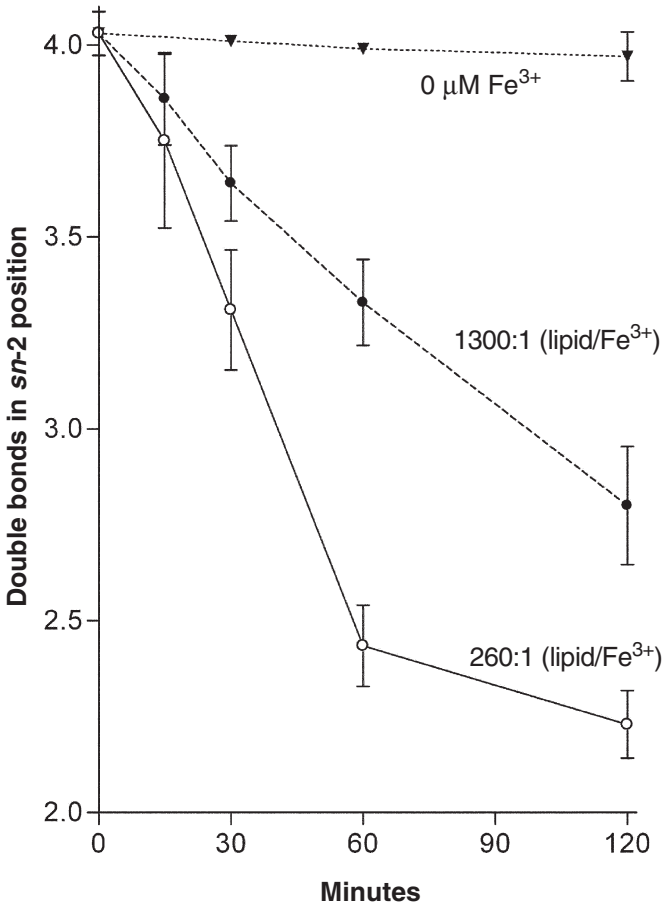

FIG. 2. Time-dependent changes in double bonds in the *sn*-2 position of arachidonyl PC as a function of ferric ion concentration. Aliquots of arachidonyl PC dissolved in $CDCl_3$ were incubated with an aqueous ferric ion solution (pH 7.4) by rapid mixing at 20–22°C as described in the Materials and Methods section. The reaction was stopped by addition of CD_3OD and immediately analyzed by ^1H NMR. The relative concentrations of ferric ions and arachidonyl PC in the biphasic mixture are expressed as mol/mol ratios. Values are means ± SD (n = 3). For abbreviation see Figure 1.

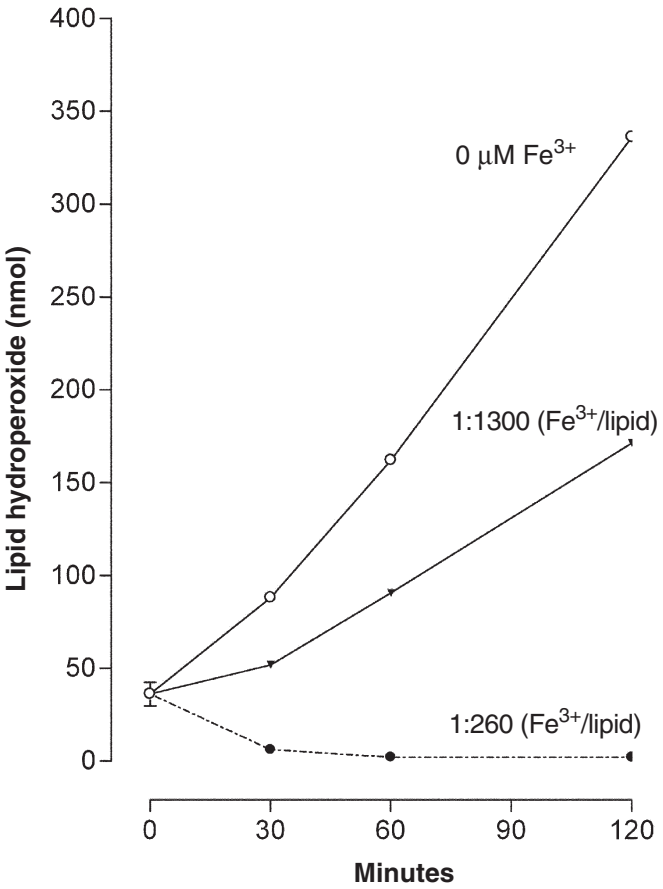

FIG. 3. Time-dependent changes in the hydroperoxide content of arachidonyl PC in the biphasic reaction system described in Figure 2. Total lipids were recovered at each time point and analyzed for hydroperoxide as described in the Materials and Methods section. Values are representative of two such experiments. For abbreviation see Figure 1.

followed by $Fe(OH)_3$ partitioning into the organic phase with the phospholipid. Since the solubility of $Fe(OH)_3$ in $CHCl_3$ is not known, the actual arachidonyl PC/ferric ion ratio may be lower than the calculated values (1300:1 or 260:1).

Lipid hydroperoxide formation: effect of Fe^{3+}. Figure 3 demonstrates that the arachidonyl PC in freshly opened vials contained detectable levels of lipid hydroperoxide and that the hydroperoxide content increased during the mixing action upon vortexing of the aqueous and organic phases. Assuming one hydroperoxide per PC molecule, about 0.3% of lipids in freshly opened vials had undergone peroxidation, increasing to about 3% at the end of 2 h. The zero-time values are for four preparations of arachidonyl PC from Avanti Polar Lipids sampled within minutes after opening the vial. A slow increase in peroxide content occurred during storage at –35°C in 1.0-mL brown bottles with minimal air space (data not shown). Addition of low levels of Fe^{3+} ions (1:1300, mol ratio Fe^{3+}/lipid) to the aqueous phase caused a disappearance of about 40% of the lipid hydroperoxide in the organic phase following mixing, whereas high Fe^{3+} levels (1:260 mol ratios of Fe^{3+}/lipid) largely eliminated hydroperoxide in the reaction mixture. The rate of disappearance of hydroperoxide at the lowest ferric ion concentration was about 80 nmol/h. The values shown are representative of two experiments using freshly opened vials of arachidonyl PC. Similar decomposition curves were seen with arachidonyl PC stored at –35°C.

Effect of the number of FA double bonds on sensitivity to iron-catalyzed peroxidation. Table 1 compares the Fe^{3+}-catalyzed loss of double bonds in PC containing palmitoyl (16:0) in the *sn*-1 (outer carbon) position of glycerol and either oleoyl (18:1), linoleoyl (18:2), or arachidonyl (20:4) in the *sn*-2 (middle carbon) position. No decrease in unsaturation was seen when oleic acid containing PC was used as a substrate, whereas both linoleic acid and arachidonic acid underwent peroxidation, as did linolenic acid (three double bonds, data not shown). Purified cardiolipin (beef heart) containing four FA (87% linoleic acid and 8% oleic acid) also underwent peroxidation comparable to that seen for arachidonic acid-containing PC. As also shown, a neutral lipid fraction con-

TABLE 1
Fe^{3+}-Catalyzed Lipid Peroxidation as a Function of FA Unsaturation

Lipid	Fe^{3+}/lipid (mol/mol)	*sn*-1	*sn*-2	Double bonds (%) compared with untreated phospholipid[a]
PC	1:1300	16:0	18:1	102 ± 1[b]
PC	1:1300	16:0	18:2	61.4 ± 3.1
PC	1:1300	16:0	20:4	55.0 ± 2.2
Cardiolipin (bovine heart)	1:650	16:0	18:2	57.9 ± 3.1
TG (rat aorta)	1:1100[c]	ND	ND	101.4 ± 1.5

[a]Percentage of residual double bonds in the *sn*-2 position as measured by ^{1}H NMR. Lipid (1.0 mg) was dissolved in 1.0 mL of $CDCl_3$, 20 µL of Fe^{3+} ammonium sulfate dissolved in normal pH 7.4 Krebs–Ringer bicarbonate prepared in D_2O (pH 7.4) was added, and the mixture was vortexed for 2 h as described in the Methods and Materials section. ND, not determined (neutral lipid fraction from rat aortic cells).
[b]Mean ± SD (n = 3).
[c]Estimated from the average M.W. of TG in preparation.

taining PUFA (isolated from rat aortic tissue; see the Materials and Methods section) failed to undergo significant ferric ion-catalyzed peroxidation under our conditions.

Ferric ions produce broadening of the ^{1}H peak associated with the choline moiety in arachidonyl-PC. Figure 4 compares ^{1}H NMR spectra of the choline moiety of arachidonyl PC exposed to low Fe^{3+} ion levels (1:1300, Fe^{3+}/lipid) with that after exposure to high Fe^{3+} ion concentrations (1:20, Fe^{3+}/lipid) in the biphasic reaction mixture. As shown, the choline peak became broader in the presence of elevated ferric ion and underwent a small downfield shift. Broadening of the choline peak became marked only when the molecular ratio of Fe^{3+}/PC in the reaction mixture was 1:100 or greater (data shown for 20:1). There was no significant difference between the choline proton peak in untreated arachidonyl PC and that exposed to low Fe^{3+} ion levels (data not shown). This broadening may reflect interaction between $Fe(OH)_3$ and the phospholipid dissolved in the $CHCl_3$ phase.

Analysis of the products of Fe^{3+}-catalyzed lipid peroxidation. The reaction products from the iron-catalyzed peroxidation of arachidonyl PC were taken to dryness under nitrogen, resuspended in hexane, and applied to aminopropylsilyl columns as described in the Materials and Methods section. Three fractions—(i) neutral lipids (including DG), (ii) FFA/MG, and (iii) N-containing phospholipids—were eluted

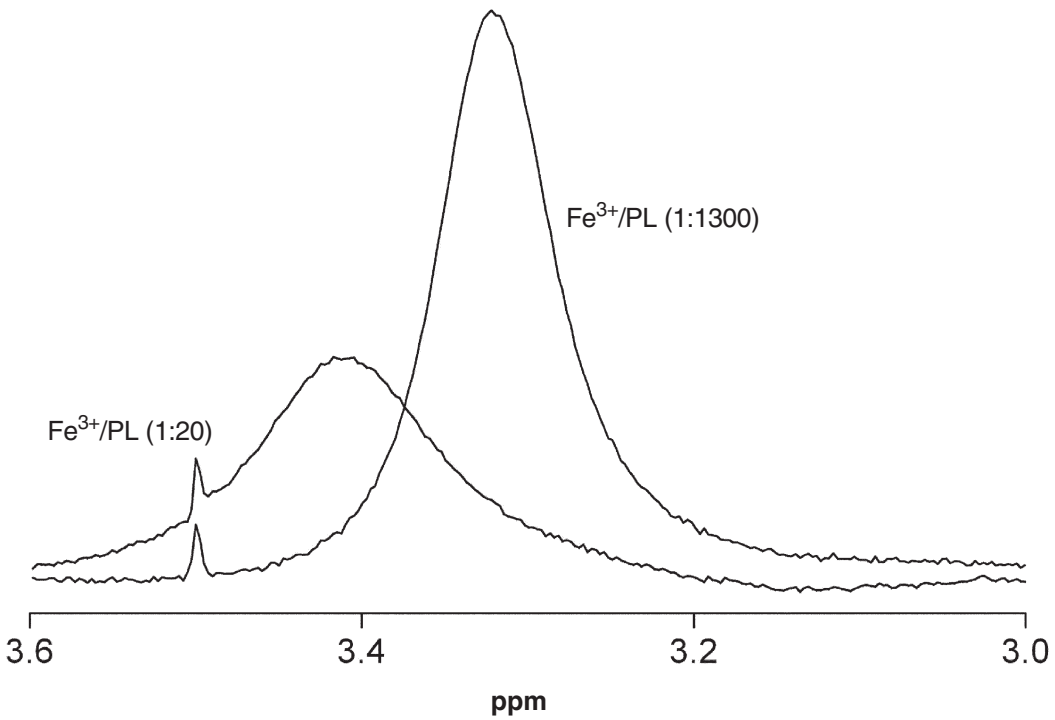

FIG. 4. Comparison of the effect of Fe^{3+} concentration on broadening of the proton peaks associated with the three methyl groups of the choline head group. The example shown was after a 1-h exposure to Fe^{3+} at 20–22°C. Ratios indicate phospholipids (PL)/Fe^{3+} (mol/mol).

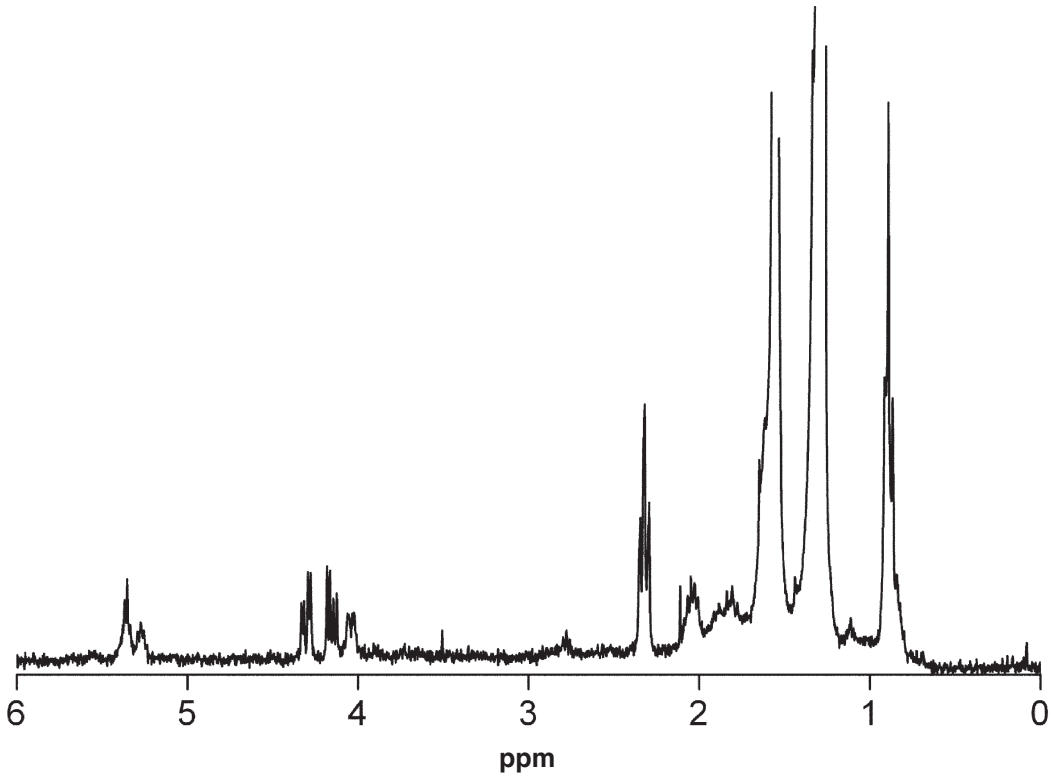

FIG. 5. ^{1}H NMR spectrum of the FA/MG fraction eluted from aminopropylsilyl minicolumns (Alltech, Deerfield, IL) as described in the Materials and Methods section. The spectrum shown represents the column fraction from the 1-h reaction mixture from the 1300:1 (PL/Fe^{3+}, mol/mol) sample in Figure 1. For abbreviation see Figure 4.

and analyzed by ^{1}H NMR. As is shown in Figure 5, material eluting with the FFA/MG fraction showed proton peaks corresponding to intact double bonds (5.4 ppm), carbons alpha to oxygen functions (4.0 to 4.3 ppm), methylene carbons (1.2 ppm), and omega terminal methyl protons (0.8 ppm). Material collected after a 1-h incubation in the presence of 20 μM of Fe^{3+} contained 0.96 ± 0.046 (SD, $N = 3$) double bonds per methyl group and an estimated chain length of 9 carbons. ^{1}H NMR analysis of the PC-rich fraction eluted by methanol from aminopropylsilyl minicolumns contained about two double bonds (5.4 ppm) and 3.2 ± 0.25 carboxyl groups (based on an α-methylene proton at about 2.8 ppm) per choline moiety. Correcting for the 16 carbons of the palmitic acid in the *sn*-1 position, it was estimated that the truncated moiety in the *sn*-2 position contained about 11 carbons (10.8 ± 0.35; SD, $N = 3$). This indicates that when arachidonic acid (20:4) was present in the *sn*-2 position of PC, Fe^{3+}-catalyzed peroxidation produced significant quantities of a modified phospholipid containing a truncated $\Delta^{5,8}$ alkyl chain. For comparison, material eluting in the FFA/MG fraction when PC containing linoleic acid (18:2) in the *sn*-2 position was exposed to Fe^{3+} for 1 h had essentially no remaining double bonds within an estimated chain length of about 9–10 carbons. The peroxidized phospholipids containing linoleic acid eluting with fraction 3 (N-containing phospholipids) were estimated to contain a truncated 8–9 carbon chain in the *sn*-2 position after a 2-h incubation.

DISCUSSION

The data presented here indicate that, at physiological pH, Fe^{3+}/phospholipid mole ratios as low as 1:1300 result in a decrease in the lipid hydroperoxides present in choline phospholipids containing linoleic or arachidonic acid, followed by the selective loss of one or two double bonds and chain-shortening of the FA in the *sn*-2 position (Fig. 2). Ferric ions had no measurable effect on the monounsaturated FA present in the *sn*-2 position of PC or on the PUFA present in TG. The failure of TG to undergo Fe^{3+}-catalyzed peroxidation and the observed broadening of the choline peak in arachidonyl PC (Fig. 4) suggest that interaction of ferric ions with the phosphate group may be critical to peroxidation.

An analysis of the exact role of iron in biological lipid peroxidation has often been complicated by a failure to use physiological conditions (pH and ion concentrations), failure to recognize the autoxidation of ferrous ions at or near neutral pH, and failure to consider the lipid solubility of ferric hydroxide complexes. Phospholipid hydroperoxides form continuously in cell membranes and in blood lipoproteins as well as during lipid isolation and/or during storage and handling. Catalysis of phospholipid peroxidation by some metals (Fe, Cu, Ni) occurs by oxidation or reduction of preformed lipid hydroperoxides (LOOH) to form a chain-carrying lipid oxyl radical (LO•) or lipid peroxyl radicals (LOO•) (reviewed in Refs. 1–3,16). For example, in the case of Fe^{3+},

$$LOOH + Fe^{3+} \rightarrow LOO\bullet + H^{+} + Fe^{2+} \quad [1]$$

As noted above, at physiological pH, the ferrous ions formed in the above reaction undergo rapid autoxidation and regeneration of ferric ions. Tadolini and Hakim (11) have shown that Fe^{3+} could not initiate lipid peroxidation in PC liposomes after the lipid hydroperoxides had been removed by treatment with triphenylphosphine, indicating that lipid hydroperoxides are essential for Fe-catalyzed peroxidation.

A peroxyl radical (LOO•) tends to abstract H from another lipid molecule, especially in the presence of a ferric ion, thus causing an autocatalytic chain reaction. The propagation stage of lipid peroxidation can be summarized as follows:

$$LOO\bullet + LH \rightarrow LOOH + L\bullet \quad [2]$$

Arachidonate has three active bis-allylic methylene groups and three 1,4-diene systems. Studies with methylarachidonate indicate that hydroperoxide substitution can occur on carbons 5, 8, 9, 11, 12, or 15 (reviewed in Ref. 16). ^{1}H NMR analysis of the fragment eluted from an aminopropylsilyl minicolumn following exposure of arachidonyl PC to ferric ions indicated that, following loss of one of the four double bonds, a 9-carbon fragment with one double bond was released. A similar analysis of the peroxidized PC-rich fraction indicated the presence of approximately three carbonyl groups (based on the α-methylene proton at about 2.8 ppm) per choline moiety. In other words, the predominant arachidonyl phospholipid peroxidation product contains a truncated chain in the *sn*-2 position with two ($\Delta^{5,8}$) double bonds and a chain length of 11 carbons. The omega carbon of the truncated chain in the *sn*-2 position is present as a carboxyl group. Thus, at low Fe^{3+} concentrations, a hydrogen on the alpha carbon between the double bonds at carbon 11 appears to participate in the hydroperoxide reaction, releasing a fragment containing the omega double bond. Examination of molecular models indicated that when arachidonic acid in the *sn*-2 position was in the all-*cis* configuration, the Δ^{11} double bond was in spatial proximity to the phosphate of the choline head group.

Metal ions are well known to interact with phosphate groups in biomolecules (e.g., Refs. 17–19). When metal ions are paramagnetic, this interaction would be expected to produce the observed large broadening of the adjacent choline methyl proton resonance due to electron–proton dipolar interaction (Fig. 5). Ferric ions could thus bind to the lipid phosphate of arachidonyl PC, and this bound metal ion would catalyze breakdown of the C-11 hydroperoxide that is in spatial proximity to the phosphate. A possible mechanism for the Fe^{3+}-catalyzed peroxidation of arachidonyl PC is illustrated in Figure 6, adapted from one proposed by Kaur *et al.* (20). The free-radical-induced oxidation of arachidonyl plasmalogen phospholipids has been reviewed by Murphy (21). As noted above, iron-catalyzed hydroperoxide decomposition of arachidonyl PC would yield a modified PC with an 11-carbon truncated chain in the *sn*-2 position. Linoleic acid forms a mixture of two conjugated diene 9- and 13-hydroperoxides (reviewed in Ref. 16). Iron-catalyzed hydroperoxide decomposition of linoleic acid-containing phospholipids would thus produce a modified phospholipid containing a chain-shortened 9- or 13-carbon alkyl moiety in the *sn*-2 position. In the chloroform–water system used here, Fe^{3+}-catalyzed breakdown of arachidonic or linoleic acid may be occurring both at the $CHCl_3/H_2O$ interphase and within the hydrophobic region, since the $Fe(OH)_3$ formed at physiological pH can distribute into the hydrophobic $CHCl_3$/lipid phase. For comparison, Wang *et al.* (22) studied the distribution of hydroperoxide positional isomers generated by free radical oxidation in arachidonyl PC in heterogeneous liposomes and in homogenous methanol solutions. They found that the distance between the hydrophilic region of PC and the water phase played an important role in influencing hydrogen abstraction. In biological systems, both aqueous–lipid (membranes) and hydrophobic regions (LDL, chylomicrons) exist, and both are exposed to ferric ions.

Davies *et al.* (8) have identified an abundant fragmented alkyl phospholipid in oxidized LDL as hexadecyl azelaoyl phosphatidylcholine (azPC, i.e., a 9-carbon saturated FA in the *sn*-2 position and an acyl ether in the *sn*-1 position) and have shown azPC to be a high-affinity ligand and agonist for peroxisome proliferator-activated receptor γ. Leitinger (23) demonstrated the presence of peroxidation products of arachidonyl PC in both "minimally modified LDL" and in atherosclerotic lesions and reported that they may modulate and/or trigger various signaling pathways involved in the inflammatory responses. As shown here, similar chain-shortened substances could result from Fe^{3+}-catalyzed peroxidation of choline phospholipids containing linoleic acid in the *sn*-2 position as well as from arachidonyl-containing PC. As reported by Barre (24), linoleic acid is the major unsaturated FA in choline phospholipids present in human LDL (*ca.* 22 mol%), with arachidonic acid constituting the next most prevalent FA (*ca.* 8 mol%).

There are a number of possible mechanisms for the transient release of ferric ions into circulation: (i) Free iron may be released from transferrin into circulation. Brieland and Fantone (25) showed that a decrease in plasma pH facilitated the release of Fe^{3+} from partially saturated transferrin by the polymorphonuclear leukocyte-derived superoxide anion ($O_2^{\bullet}$), reaching plasma Fe^{3+} concentrations greater than 1 μM. They suggest that since the plasma concentration of transferrin is approximately 25–35 μM, similar concentrations of Fe^{3+} may be released from transferrin at sites of acute inflammation. (ii) Nemoto *et al.* (26) showed that the hemolysis caused by cardiopulmonary bypass can lead to renal dysfunction, and other organ failure may be due at least in part to peroxidation caused by iron derived from hemoglobin. (iii) *In vitro* studies indicate that both transferrin (e.g., Refs. 27,28) and ferritin (e.g., Refs. 29–31) *per se* cause lipid peroxidation. For example, Saito *et al.* (27) reported that peroxidation of phospholipid liposomes could be catalyzed by iron from transferrin, since increasing the transferrin concentration increased rates of lipid peroxidation. Increasing xanthine oxidase activity in the presence of transferrin also caused

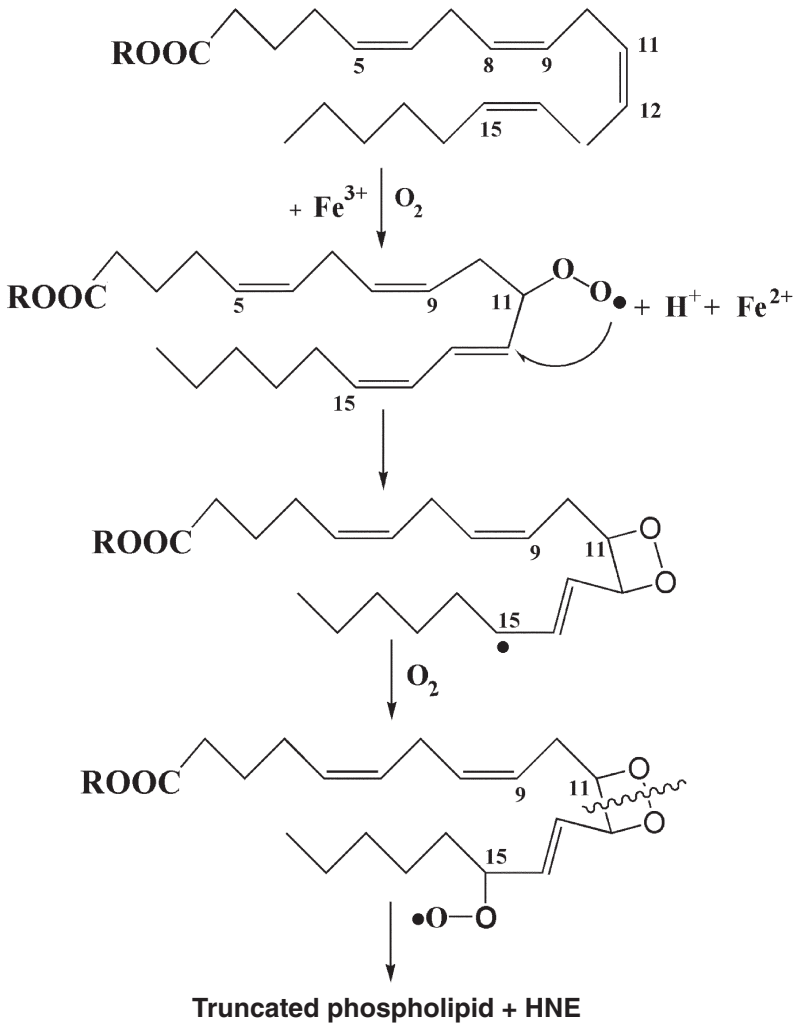

FIG. 6. Possible pathway for ferric ion-catalyzed peroxidation of arachidonic acid at physiological pH. The numbers indicate that hydroperoxide substitution can occur on carbons 5, 8, 9, 11, 12, or 15 (13). The example shown is for breakdown of the hydroperoxide isomer on the 11-carbon of arachidonic acid in the *sn*-2 position of PC and is adapted from a mechanism proposed by Kaur *et al.* (20). R, phosphorylglycerolcholine containing palmitic acid in the *sn*-1 position; HNE, 4-hydroxynonenal.

increased lipid peroxidation, suggesting that H_2O_2 formed by xanthine oxidase forms lipid hydroperoxides, with a resulting increase in iron-catalyzed peroxidation. Water proton relaxation NMR studies by Koenig and Schillinger (32) indicated that transferrin-bound ferric iron is accessible to water and may therefore participate in phospholipid peroxidation. An episodic rise in circulating ferric ion concentration may also occur during myocardial reperfusion injury (33) and during Fe supplementation in kidney dialysis patients (34,35).

In summary, at physiological pH (7.4), low concentrations of ferric ions are effective catalysts for peroxidation of PUFA in choline-containing phospholipids *in vitro*. As demonstrated here, Fe^{3+}-catalyzed peroxidation occurs selectively adjacent to specific double bonds (Δ^9 or Δ^{11}) in phospholipids, giving rise to linoleic and arachidonic acid-derived compounds known to be components of the inflammatory system. These results suggest that the transient release of ferric ions by hemolysis during surgery, dialysis, and/or injury may play a significant role in generating inflammatory mediators such as azPC.

ACKNOWLEDGMENTS

This work was supported by GM57421 and GM071324. The Albert Einstein NMR Research Facility is supported in part by NCI Core Grant CA-13330.

REFERENCES

1. Halliwell, B., and Gutteridge, J.M.C. (1990) Role of Free Radicals and Catalytic Metal Ions in Human Disease: An Overview, *Methods Enzymol. 186,* 1–85.
2. Schaich, K.M. (1992) Metals and Lipid Oxidation. Contemporary Issues, *Lipids 27,* 209–218.
3. Girotti, A.W. (1998) Lipid Hydroperoxide Generation, Turnover, and Effector Action in Biological Systems, *J. Lipid Res. 39,* 1529–1542.
4. Gamalei, I., and. Kliubin, I.V. (1996) Hydrogen Peroxide as a

Signal Molecule, *Tsitologiia 38,* 1233–1247.
5. Halliwell, B., Clement, M.V., Ramalingam, J., and Long, L.H. (2000) Hydrogen Peroxide. Ubiquitous in Cell Culture and *in vivo, IUBMB Life 5,* 251–257.
6. Thomas, J.P., Maiorino, M., Ursini, F., and Girotti, A.W. (1990) Protective Action of Phospholipid Hydroperoxide Glutathione Peroxidase Against Membrane-Damaging Lipid Peroxidation. *In situ* Reduction of Phospholipid and Cholesterol Hydroperoxides, *J. Biol. Chem. 265,* 454–461.
7. McIntyre, T.M., Zimmerman, G.A., and Prescott, S.M. (1999) Biologically Active Oxidized Phospholipids, *J. Biol. Chem. 274,* 25189–25192.
8. Davies, S.S., Pontsler, A.V., Marathe, G.K., Harrison, K.A., Murphy, R.C., Hinshaw, J.C., Prestwich, G.D., St. Hilaire, A., Prescott, S.M., Zimmerman, G.A., and McIntyre, T.M. (2001) Oxidized Alkyl Phospholipids Are Specific High Affinity Peroxisome Proliferator-Activated Receptor γ Ligands and Agonists, *J. Biol. Chem. 276,* 16015–16023.
9. Leitinger, N., Tyner, T.R., Oslund, L., Rizza, C., Subbanagounder, G., Lee, H., Shih, P.T., Mackman, N., Tigyi, G., Territo, M.C., Berliner, J.A., and Vora, D.K. (1999) Structurally Similar Oxidized Phospholipids Differentially Regulate Endothelial Binding of Monocytes and Neutrophils, *Proc. Natl. Acad. Sci. 96,* 12010–12015.
10. Kostellow, A.B., and Morrill, G.A. (2004) Iron-Catalyzed Lipid Peroxidation in Aortic Cells *in vitro*: Protective Effect of Extracellular Magnesium, *Atherosclerosis 175,* 15–22.
11. Tadolini, B., and Hakim, G. (1996) The Mechanism of Iron(III) Stimulation of Lipid Peroxidation, *Free Radic. Res. 25,* 221–227.
12. Welch, K.D., Davis, T.Z., and Aust, S.D. (2002) Iron Autoxidation and Free Radical Generation: Effects of Buffers, Ligands, and Chelators, *Arch. Biochem. Biophys. 397,* 360–369.
13. Morrill, G.A., Gupta, R.K., Kostellow, A.B., Ma, G.-Y., Zhang, A., Altura, B.T., and Altura, B.M. (1997) Mg^{2+} Modulates Membrane Lipids in Vascular Smooth Muscle: A Link to Atherogenesis, *FEBS Lett. 408,* 191–194.
14. Spiro, T.G., and Saltman, P. (1974) Inorganic Chemistry of Iron, in *Iron in Biochemistry and Medicine* (Jacobs, A., and Worwood, M., eds.), Academic Press, London, pp. 1–28.
15. Sze, D.Y., and Jardetzky, O. (1990) Characterization of Lipid Composition in Stimulated Human Lymphocytes by ^{1}H-NMR, *Biochim. Biophys. Acta 1054,* 198–206.
16. Frankel, E.N. (1998) Hydroperoxide Formation, in *Lipid Oxidation* (Frankel, E.N., ed.), The Oily Press, Dundee, Scotland, pp. 23–41.
17. Gupta, R.K., and Benovic, J.L. (1978) Magnetic Resonance Studies of the Interaction of Divalent Metal Cations with 2,3-Bisphosphoglycerate, *Biochem. Biophys. Res. Commun. 14,* 130–137.
18. Hettich, R.I. (1999) Formation and Characterization of Iron–Oligonucleotide Complexes with Matrix-Assisted Laser Desorption/Ionization Fourier Transform Ion Cyclotron Resonance Mass Spectrometry, *J. Am. Soc. Mass. Spectrom. 10,* 941–949.
19. Richter, Y., and Fischer, B. (2003) Characterization and Elucidation of Coordination Requirements of Adeninine Nucleotide Complexes with Fe(II) Ions, *Nucleosides Nucleotides Nucleic Acids 9,* 1757–1780.
20. Kaur, K., Solomon, R.G., O'Neil, J., and Hoff, H.F. (1997) (Carboxyalkly)pyrroles in Human Plasma and Oxidized Low Density Lipoproteins, *Chem. Res. Toxicol. 10,* 1387–1396.
21. Murphy, R.C. (2001) Free-Radical-Induced Oxidation of Arachidonyl Plasmalogen Phospholipids: Antioxidant Mechanism and Precursor Pathway for Bioactive Eicosanoids, *Chem. Res. Toxicol. 14,* 463–472.
22. Wang, X.H., Ushido, H., and Ohshima, T. (2003) Distributions of Hydroperoxide Positional Isomers Generated by Oxidation of 1-Palmitoyl-2-arachidonyl-*sn*-glycero-3-phosphocholine in Liposomes and in Methanol Solution, *Lipids 38,* 65–72.
23. Leitinger, N. (2003) Oxidized Phospholipids as Modulators of Inflammation in Atherosclerosis, *Curr. Opin. Lipidol. 14,* 421–430.
24. Barre, E. (2003) A More Detailed Fatty Acid Composition of Human Lipoprotein(a)—A Comparison with Low Density Lipoprotein, *Chem. Phys. Lipids. 123,* 99–105.
25. Brieland, J.K., and Fantone, J.C. (1991) Ferrous Iron Release from Transferrin by Human Neutrophil-Derived Superoxide Anion: Effect of pH and Iron Saturation, *Arch. Biochem. Biophys. 284,* 78–83.
26. Nemoto, S., Aoki, M., Dehua, C., and Imai, Y. (2000) Free Hemoglobin Impairs Cardiac Function in Neonatal Rabbit Hearts, *Ann. Thorac. Surg. 69,* 1484–1489.
27. Saito, M., Morehouse, L.A., and Aust, S.D. (1986) Transferrin-Dependent Lipid Peroxidation, *J. Free Radic. Biol. Med. 2,* 99–105.
28. Brieland, J.K., Clarke, S.J., Karmiol, S., Phan, S.H., and. Fantone, J.C. (1992) Transferrin: A Potential Source of Iron for Oxygen Free Radical-Mediated Endothelial Cell Injury, *Arch. Biochem. Biophys. 294,* 265–270.
29. Thomas, C.E., Morehouse, L.A., and Aust, S.D. (1985) Ferritin and Superoxide-Dependent Lipid Peroxidation, *J. Biol. Chem. 260,* 3275–3280.
30. Winterbourn, C.C., Monteiro, H.P., and Galilee, C.F. (1990) Ferritin-Dependent Lipid Peroxidation by Stimulated Neutrophils: Inhibition by Myeloperoxidase-Derived Hypochlorous Acid but Not by Endogenous Lactoferrin, *Biochim. Biophys. Acta 1055,* 179–185.
31. Miura, T., and Ogiso, T. (1991) Lipid Peroxidation of the Erythrocyte Membrane Caused by Stimulated Polymorphonuclear Leukocytes in the Presence of Ferritin, *Chem. Pharm. Bull. 39,* 1507–1509.
32. Koenig, S.H., and Schillinger, W.E. (1969) Nuclear Magnetic Relaxation Dispersion in Protein Solutions. II. Transferrin, *J. Biol. Chem. 244,* 6520–6526.
33. Shah, S.V., and Alam, M.G. (2003) Role of Iron in Atherosclerosis, *Am. J. Kidney Dis. 41,* S80-3.6.
34. Britton, R.S., Leicester, K.L., and Bacon, B.R. (2002) Iron Toxicity and Chelation Therapy, *Int. J. Hematol. 76,* 219–228.
35. Fishbane, S. (2003) Safety in Iron Management, *Am. J. Kidney Dis. 41,* S18–S26.

[Received July 6, 2004; accepted October 2, 2004]

Phosphatidylcholine Hydroperoxide Levels in Human Plasma Are Lower Than Previously Reported

Junko Adachi[a,*], Naoki Yoshioka[a], Rika Funae[a], Yasushi Nagasaki[a], Takeaki Naito[b], and Yasuhiro Ueno[a]

[a]Department of Legal Medicine, Kobe University Graduate School of Medicine, and [b]Kobe Pharmaceutical University, Kobe, Japan

ABSTRACT: The quantification of PC hydroperoxide (PCOOH) in human plasma was studied by HPLC with chemiluminescence detection (HPLC-CL). We identified for the first time the monohydroperoxide of 1-palmitoyl-2-linoleoyl-PC hydroperoxide (PC 16:0/18:2-OOH) in plasma by LC-MS and HPLC-CL. The standard compound, PC 16:0/18:2-OOH (synthetic PCOOH), as well as PCOOH from egg yolk, was used. Comparison of the PCOOH concentration in each participant's plasma as determined by use of a Finepak SIL NH_2 column with 2-propanol/methanol/water as the mobile phase (system A, the conventional method) gave a higher concentration than did an LC-18-DB column with methanol containing 0.01% triethylamine (system B). The mean PCOOH concentration for the 43 healthy volunteers was 55.1 ± 30.4 pmol/mL (mean ± SD) for system A and 16.3 ± 9.9 pmol/mL for system B. Moreover, the main peak of the plasma extract appeared at a different time from that of synthetic PCOOH or egg yolk PCOOH in system A, whereas in system B plasma sample retention time practically corresponded to that of standard PCOOH. These findings confirm that the PCOOH plasma concentration is not so high as previously reported.

Paper no. L9453 in *Lipids 39,* 891–896 (September 2004).

Free radicals are involved in the pathogenesis of atherosclerosis, liver disease, platelet aggregation, inflammation, cancer, diabetes, and aging. Lipid peroxidation in the cell membrane is a free radical-induced chain reaction that may result in cell membrane, protein, and DNA damage. Indeed, free radical-induced lipid peroxidation has been assessed in a number of studies including analyses of 4-hydroxynonenal (1), malondialdehyde (2), and isoprostanes (3), secondary products of phospholipid peroxidation.

Previously, we developed methods for quantifying cholesterol hydroperoxides by HPLC with chemiluminescence detection (HPLC-CL) (4) and oxysterols by HPLC with UV detection (5) and used these methods to investigate oxidative stress in various models. For example, administration of both paraquat and alcohol produces reactive oxygen species and induces membrane lipid peroxidation. We therefore investigated membrane cholesterol peroxidation by analyzing not only the 7-hydroperoxycholesterols present in rat liver and kidney after administration of a low dose of paraquat (6) but also the oxysterols present in human lung and kidney in paraquat intoxication (7). Concentrations of 7-hydroperoxycholesterols, as well as oxysterols, were significantly elevated in skeletal muscle (8), liver (9), and heart (5) of rats administered chronic alcohol and in the brains of CO-intoxicated rats (10). Results confirmed that 7-hydroperoxycholesterols and oxysterols are good markers of oxidative stress.

A method for quantifying PC hydroperoxide (PCOOH), reported in 1987, was developed and used to evaluate oxidative stress in various models (11). There is still contention, however, over whether the PCOOH concentration in the plasma is high enough to detect because of rapid enzymatic reduction of PCOOH to PC hydroxide (12,13). To address this issue, we investigated the method for analyzing PCOOH in two HPLC systems and compared PCOOH plasma concentration results for healthy volunteers.

MATERIALS AND METHODS

Materials. 3,5-Di-*tert*-butyl-4-hydroxytoluene (BHT), luminol (3-aminophthaloylhydrazine), and cytochrome C (from horse heart, type VI) were purchased from Wako Pure Chemical Co. (Osaka, Japan). PCOOH (from egg yolk), synthesized by reaction with methylene blue under tungsten lamp irradiation, was a gift from Prof. Junji Terao, Tokushima University. We named this *egg yolk PCOOH*. 1-Palmitoyl-2-linoleoyl-PC hydroperoxide (16:0/18:2-OOH) was synthesized as follows and named *synthetic PCOOH*. Methylene blue-4H_2O (2 mg) was dissolved in a 1:1 mixture (50 mL) of $CHCl_3$ and methanol. A solution of 1-palmitoyl-2-linoleoyl-L-PC (160 mg) in the methylene blue solution (20 mL) prepared above was irradiated with a tungsten lamp (30 W) at 15°C for 8 h with monitoring by HPLC and TLC. The whole reaction mixture was subjected to HPLC [Daiso-gel (Daiso, Osaka, Japan), SP-120-40/60-ODS-B; $CHCl_3$/methanol; UV 235 nm, 50 mL/min]. The product (67.3 mg) obtained was checked by MS, TLC, and HPLC. When we injected the synthetic PCOOH into the high-performance liquid chromatograph (a different system from either A or B) with UV detection at 235 nm, a small peak appeared whose area was 14%, while the area of the standard PCOOH was 86%. Thus, the purity of the standard compound may be 86%. When we determined the concentration of PCOOH in plasma, we used an HPLC-CL system. This system specifically detects the com-

*To whom correspondence should be addressed at Department of Legal Medicine, Kobe University Graduate School of Medicine, 7 Kusunoki-cho, Chuo-ku Kobe 650-0017, Japan. E-mail: adachi@med.kobe-u.ac.jp

Abbreviations: BMI, body mass index; CL, chemiluminescence detection; ESI, electrospray ionization; PCOOH, PC hydroperoxide.

pound with hydroperoxide. By this system the standard PCOOH appeared as a single peak. Moreover, there was a single spot on TLC. Additionally, the amount of phospholipid was analyzed quantitatively as 1.95 mg/mL. MS: 790.6 (MH^+, monoperoxide) and 812.6 ($[M + Na]^+$, monoperoxide). H NMR (δ): 6.8–5.2 [*m*, olefinic H and C<u>H</u>(OOH)], 5.20 (1H, *m*, 2‴-H), 4.4–4.0 [*m*, 1‴, 1″, and C<u>H</u>(OOH)], 3.95 (2H, *m*, 3‴-H_2), 3.75 (2H, *m*, 2″-H_2), 3.3 [10H, *m*, N(CH_3)$_3$ and OOH], 2.3 (2H, *m*, 2-H_2), 2.05 (2H, *m*, C<u>H</u>$_2$CH=CH–CH=CH–), 1.6 (4H, *m*, 3-H_2 and 3′-H_2), and 0.95 (6H, *m*, 16-CH_3 and 18′-CH_3) .

Subjects. Forty-three healthy volunteers, 33 men and 10 women, 20 to 79 yr old, body mass index (BMI) 22.2 ± 3.3 kg/m^2, were recruited after obtaining their informed consent. This study meets the ethical guidelines of the Helsinki Declaration.

Extraction. Three milliliters of blood was collected in a test tube containing 0.3 mg of EDTA·2Na, centrifuged at 4°C and 800 × *g* for 10 min, and the plasma fractionated. Total lipid was extracted by adding 0.5 mL of distilled water and 8 mL of ice-cold chloroform/methanol (3:1, vol/vol), containing 0.005% (vol/vol) BHT (as antioxidant) to 0.5 mL of plasma. The mixture was vortexed vigorously for 1 min then centrifuged at 800 × *g* for 20 min. The chloroform layer was aspirated off and concentrated in a rotary evaporator, then dried under a nitrogen stream. The phospholipid fraction then was isolated from the total lipid by solid-phase extraction. A silica column (Sep-Pak; Waters Co., Milford, MA) of 3-mL capacity packed with aminopropyl-derivatized silica (–NH_2) initially was conditioned by washing it with 5 mL of acetone and 10 mL of *n*-hexane. The total lipid sample, dissolved in a small amount of chloroform, was layered on the column, which then was flushed with a mixture of 2 mL chloroform and 1 mL isopropanol, giving an eluate consisting mainly of cholesterol. The column was next flushed with methanol containing 0.005% BHT, giving an eluate consisting mainly of phospholipid. This was concentrated in a rotary evaporator, dried under a nitrogen stream, then dissolved in 150 μL methanol; a 10-μL portion was injected onto the HPLC column.

LC-MS. The MS analysis was performed on a quadrupole orthogonal acceleration time-of-flight, Micromass Q-TOF Micro (Waters Corporation) equipped with an electrospray interface. The instrument was operated in positive ion mode with a capillary voltage of 3200 V and cone voltage of 40 V. The desolvation gas was set at 600 L/h with a desolvation temperature of 150°C and a source temperature of 80°C. The column effluent was 100 μL/min introduced into the mass spectrometer source. Full-scan spectra were recorded in profile mode. The range between *m/z* 100 and 1000 was recorded at a resolution of 5000 (full width at half maximum). The accumulation time was 1 s/spectrum.

Chromatography was performed using an Agilent 1100 HPLC (Agilent Technologies, Waldbronn, Germany). Injections of plasma samples (1 μL) were made onto a 150 × 1.0 mm Phenomenex (Torrance, CA) Luna C_8 5.0 μm column. The column was maintained at 40°C and eluted under gradient conditions at a flow rate of 100 μL/min; the mobile phase consisted of 5% methanol with 10 mM aqueous ammonium acetate (solvent A) and 95% methanol with 10 mM aqueous ammonium acetate (solvent B). Separation was carried out with a linear gradient starting with 90% solvent B followed by ramping up to 100% solvent B at 20 min and then maintaining for 17 min. The total run time was 37 min.

HPLC-CL analysis. PCOOH was analyzed by HPLC-CL. The apparatus consisted of two LC-10AD vp pumps (Shimadzu, Kyoto, Japan), a CLD-10A chemiluminescence detector (Shimadzu), and a Chromatopac C-R8A integrator (Shimadzu). Two columns and mobile phases were used: A Finepak SIL NH_2-5 column (250 × 4.6 mm i.d.; JASCO, Tokyo, Japan) with 2-propanol/methanol/water (115:65:20) as the mobile phase was designated system A. Both the mobile phase and chemiluminescent reagent were delivered at 0.7 mL/min.

An LC-18-DB column (250 × 4.6 mm i.d.; Supelco, Bellefonte, PA) with methanol containing 0.01% triethylamine as the mobile phase was designated system B. The mobile phase was delivered by one pump at 0.7 mL/min, and the chemiluminescent reagent by the other pump, also at 0.7 mL/min. The reagent consisted of cytochrome C and luminol (10 and 2 μL/mL, respectively) in alkaline borate buffer, pH 10. After the column eluant was passed through a UV detector (set at 210 nm in system A and at 234 nm in system B), it was mixed with the luminescent reagent in the postcolumn mixing joint of the chemiluminescence detector.

Individual peak areas were calculated with an integrator (Chromatopac C-R8A; Shimadzu). Synthetic PCOOH was injected at least three times a day to calculate the concentration, because the chemiluminescent intensity was sometime unstable, particularly during the early period of analysis.

Statistical analysis. All data are presented as means ± SD. Differences among age groups were assessed using two-way ANOVA followed by the *post hoc* tests of Fisher.

Recoveries from the plasma extracts were determined by comparison of the peak area obtained after injection of a plasma extract spiked with a known concentration (150 pmol). The recoveries were about 70%. The concentrations of plasma were calculated based on recovery.

RESULTS

Figure 1 shows the mass chromatograms from 5 to 17 min by LC-MS. Mass chromatograms of standard PCOOH (column 1) and plasma extract (columns 2 and 3) are shown. Coinciding peaks are seen originating from MH^+ of the standard PCOOH (16:0/18:2-OOH) at *m/z* 790.6 at a retention time of 10.6 min, from MH^+ of hydroperoxide of PC 16:0/18:2 at *m/z* 790.6 (column 2) at a retention time of 10.8 min, and from MH^+ of hydroperoxide of PC 18:0/18:2 at *m/z* 818.6 (column 3) at a retention time of 15.6 min. The electrospray ionization (ESI)-mass spectra of standard PCOOH and peak 2a show protonated and sodiated molecular ions as MH^+ of *m/z* 790.6 and $[M + Na]^+$ of *m/z* 812.6, respectively, as shown in Figure

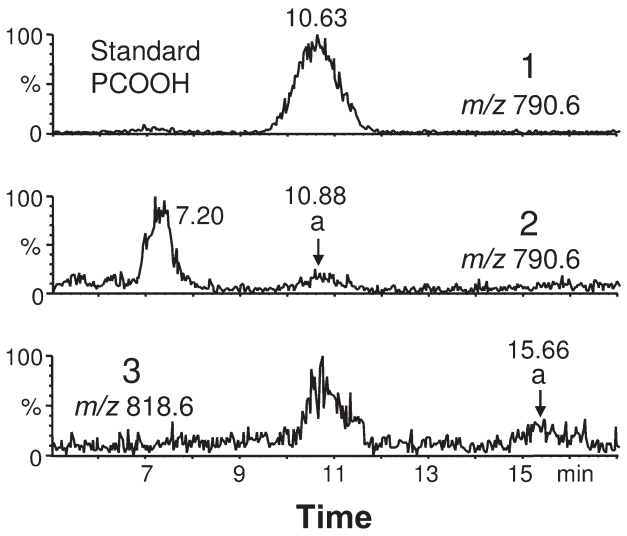

FIG. 1. Mass chromatograms of standard PCOOH (PC hydroperoxide) and lipid extract from human plasma in 8 to 16 min by LC-MS.

2. The ESI-mass spectrum of peak 3a contained ions as MH^+ of *m/z* 818.6 and $[M + Na]^+$ of *m/z* 840.6. Thus, peak 2a was identified as the monohydroperoxide of PC 16:0/18:2. Peak 3a seemed to be the monohydroperoxide of PC 18:0/18:2.

In Figure 3, typical HPLC-CL chromatograms for PCOOH are shown for standard solutions (1. synthetic PCOOH, 2. egg yolk PCOOH), plasma sample (3), and plasma + synthetic PCOOH (4) in the Finepak NH_2-5 column with 2-propanol/methanol/water as the mobile phase (system A). The respective peaks of synthetic and egg yolk PCOOH appeared at 10.83 and 10.78 min. The plasma extract peak at 10.07 min, however, was consistent with that of neither the synthetic nor egg yolk PCOOH. Moreover, when synthetic PCOOH was added to the plasma, the retention time was 10.18 min.

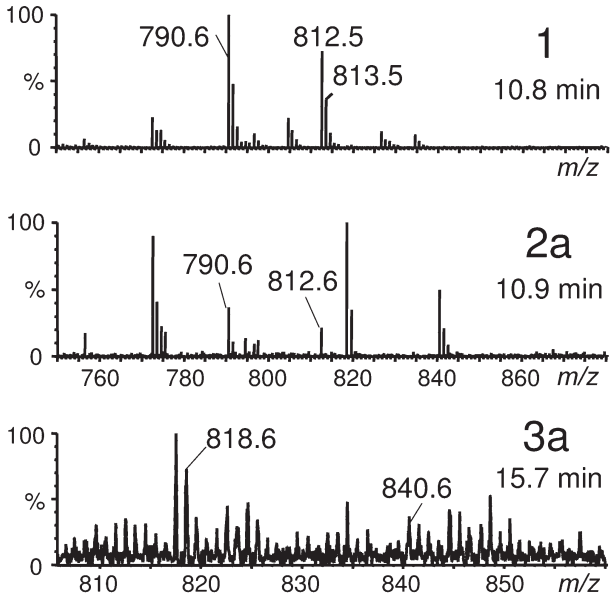

FIG. 2. Electrospray ionization mass spectra of standard PCOOH, peaks 2a and 3a, (from Fig. 1). For abbreviation see Figure 1.

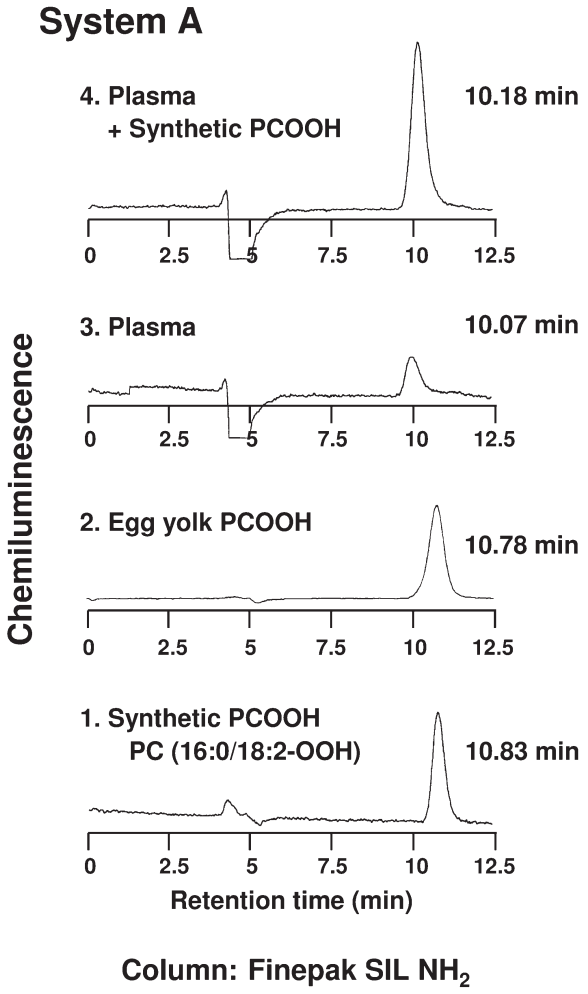

FIG. 3. HPLC analyses of standard PCOOH and a plasma sample by chemiluminescence detection in system A. For abbreviation see Figure 1.

The HPLC-CL chromatograms for PCOOH are shown in Figure 4 for PCOOH in standard solutions (1. synthetic PCOOH, 2. egg yolk PCOOH) and plasma sample (3) applied to the LC-18-DB column with methanol containing 0.01% triethylamine as the mobile phase (system B). Synthetic PCOOH gave a single peak at 7.82 min, whereas egg yolk PCOOH had two peaks at 7.83 and 9.42 min. The plasma extract had peak X at 7.81 and Y at 9.36 min, the retention time of peak X nearly coinciding with both the synthetic PCOOH peak and the earlier one of egg yolk PCOOH. Moreover, the retention time of peak Y nearly coincided with the later peak of egg yolk PCOOH. Accordingly, the retention time of the plasma extract peak corresponded to that of the standard PCOOH in system B but not in system A. When we used methanol without triethylamine as a mobile phase, PCOOH peak did not appear.

Comparison of the PCOOH concentration in systems A and B showed that the PCOOH concentration in the plasma is evidently higher in system A. The mean concentration in system A was 55.1 ± 30.4 pmol/mL, and in system B 16.3 ± 9.9 pmol/mL. The mean concentration ratio for systems A and B was 3.3 ± 0.9 (Table 1).

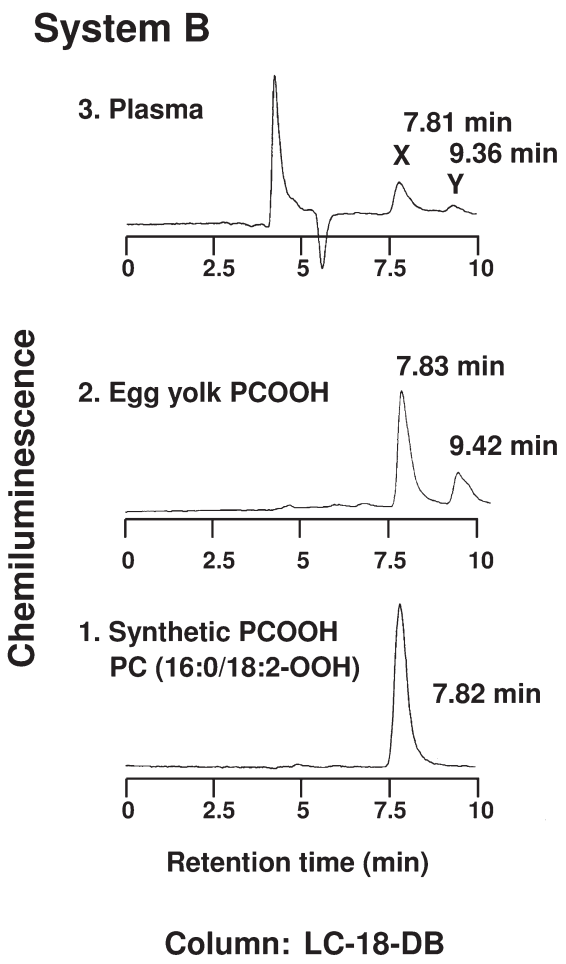

FIG. 4. HPLC analyses of standard PCOOH and a plasma sample in system B. For abbreviation see Figure 1.

PCOOH concentrations in the male and female subjects are shown in Table 1. There were no significant differences in the PCOOH concentrations between the two groups in either system, even though the number of subjects and mean ages differed. PCOOH concentrations for four age groups are shown in Table 2. The PCOOH concentration for age group 20–29 was the lowest in both systems. Although the BMI tended to increase with age, the PCOOH concentration for age group 50–79 was not the highest.

TABLE 1
PCOOH Concentrations[a] in Male and Female Subjects

Group	*n*	Age (yr)	BMI	PCOOH (pmol/mL) A. NH_2	PCOOH (pmol/mL) B. ODS	A/B ratio
Total	43	39.81 ± 14.17	22.26 ± 3.33	55.14 ± 30.43	16.38 ± 9.99	3.37 ± 0.97
Men	33	42.21 ± 14.62	22.96 ± 3.34	54.81 ± 30.69	16.57 ± 10.39	3.31 ± 1.04
Women	10	31.90 ± 9.27	19.56 ± 1.37	56.24 ± 31.17	15.81 ± 9.04	3.56 ± 0.74

[a]Values are means ± SD. PCOOH, PC hydroperoxide; BMI, body mass index calculated by body weight/(height)^2; A. NH_2: HPLC column, Finepak SIL NH_2-5 (JASCO, Tokyo, Japan); B. ODS: HPLC column, Supelco LC-18-DB (Bellefonte, PA).

TABLE 2
PCOOH Concentrations[a] in Four Age Groups

Age group	*n*	Age (yr)	BMI	PCOOH[b] (pmol/mL) A. NH_2	PCOOH[b] (pmol/mL) B. ODS	A/B ratio
20–29	12	23.83 ± 1.53	20.37 ± 2.67	32.31 ± 17.61	9.50 ± 6.36	3.66 ± 0.99
30–39	10	34.30 ± 2.82	21.41 ± 4.16	62.56* ± 28.67	18.95* ± 9.93	3.64 ± 1.16
40–49	10	44.10 ± 2.64	22.74 ± 3.45	66.87** ± 18.39	20.24** ± 8.72	3.57 ± 0.93
50–79	11	58.36 ± 9.57	24.00 ± 2.75	62.65* ± 40.30	18.08* ± 11.69	3.57 ± 0.94

[a]Values are mean ± SD.
[b]Different from group (20–29), $*P < 0.05$; $**P < 0.01$. For abbreviations see Table 1.

DISCUSSION

The major findings of this study were that (i) the hydroperoxide of PC 16:0/18:2 could be identified in plasma by LC-MS and HPLC-CL, (ii) the plasma PCOOH concentration obtained with system A (the conventional method) was 3.3 times that obtained with system B, and (iii) the main plasma peak in system A appeared at a different time from that of either synthetic or egg yolk PCOOH.

The mass spectrum of peak 2a showed that $[MH]^+$ and $[M + Na]^+$ ions at *m/z* 790.6 and 812.6, respectively, were not strong, because the concentration of hydroperoxide of PC 16:0/18:2 was very low (Fig. 2). When we analyzed the rat tissue sample with a higher concentration of PCOOH than in plasma, the mass chromatogram and MS spectra data were very similar to the plasma sample (14). The ESI-mass spectrum of peak 2a contained three pairs (A–C) of the MH^+ and $[M + Na]^+$ ions: (i) 772.6 and 794.5; (ii) 790.6 and 812.6; and (iii) 818.6 and 840.6 (Fig. 2). In addition, the retention time of peak 2a from plasma extract appearing on the mass chromatogram at *m/z* 790.6 was similar to the standard peak (Fig. 1). Moreover, we showed that the retention time of the standard PCOOH was consistent with that of plasma extract by HPLC-CL (System B) (Fig. 4). Thus, we identified peak 2a as the monohydroperoxide of PC 16:0/18:0. To our knowledge, this is the first report in which PCOOH is identified by LC-MS in human plasma. As for peak 3a, we assumed it was the monohydroperoxide of PC 18:0/18:2 based on the mass spectrum of 3a.

PC in plasma mainly consists of linoleic acid as unsaturated FA, whereas PE consists of linoleic acid as well as DHA.

Plasma PCOOH or egg yolk PCOOH also may contain molecular species of PC, of which PC 16:0/18:2-OOH is the most common and PC 18:0/18:2-OOH the second most common. A single main peak appeared in system A, whereas two peaks appeared in system B. The earlier peak (X) in system B, which appeared at a time similar to that of synthetic PCOOH, was PC 16:0/18:2-OOH. As we detected PC 16:0/18:2-OOH and PC 18:0/18:2-OOH in plasma extract by LC-MS, the later one (Y) must be PC 18:0/18:2-OOH. We estimated the concentration of peak Y by calculating the peak

TABLE 3
Human Plasma PCOOH Concentrations Reported in the Literature

System[a]	*n*	Age	PCOOH (pmol/mL)	HPLC columns[b]	Reference
A	47	49 ± 4	160 ± 65	Finepak SIL NH_2-5	15
	18	23–41	73.7 ± 32.4	Finepak SIL NH_2-5	16
	43	20–79	55.1 ± 30.4	Finepak SIL NH_2-5	Present study
	6	36 ± 6.1	36.0 ± 4.0	LiChrosphere 100 NH_2	17
			ND	Supelcosil LC-NH_2	12
B	43	20–79	16.3 ± 9.9	Supelcosil LC-18-DB	Present study
C	14	27.0 ± 6.8	227 ± 119	TSK-Gel SIL 60	18
	43		227 ± 68	TSK-Gel SIL 60	19
	11	42.3 ± 22.5	88.6 ± 14.3	Finepak SIL	20
			ND	Supelcosil LC-Si	13

[a]A, aminopropyl column; B, ODS column; C, silica gel column. ND, not detected.
[b]Finepak SIL and SIL NH_2-5 (JASCO Corp., Tokyo, Japan); L:Chrosphere 100 NH_2 (Kanto Chemical, Tokyo, Japan); Supelcosil LC-NH_2; LC-18-DB, and LC-Si (Supelco, Bellefonte, PA); TSK-Gel SIL 60 (Tosoh, Tokyo, Japan).

area based on PC 16:0/18:2-OOH. In the present study, the concentrations of PCOOH with system B were obtained by the sum of PC 16:0/18:2-OOH and PC 18:0/18:2-OOH. Measurement of the plasma PCOOH of healthy subjects showed a mean concentration of 55.1 pmol/mL with system A, which is more than 3.3 times the value obtained with system B (16.3 pmol/mL). The main peak in system A may therefore be contaminated.

Concentrations of phospholipid hydroperoxides in biological samples have been well studied, particularly PCOOH in plasma. Table 3 shows the reported plasma PCOOH concentrations in healthy volunteers, obtained with HPLC columns (12–20). Miyazawa *et al.* (15,16,18,19) developed an HPLC-CL method that uses a Finepak SIL-NH_2 column and a Finepak SIL column. They reported that the mean plasma PCOOH value was between 73 and 227 pmol/mL, whereas Yamamoto *et al.* (12,13) detected no PCOOH in human plasma. The reasons for its absence are that PCOOH is reduced to PCOH by plasma glutathione peroxidase (21) or apolipoprotein A-1 (22), and that PCOOH in HDL is converted to cholesteryl ester hydroperoxide by lecithin:cholesterol acyltransferase (23). When measuring the plasma PCOOH, Yamamoto *et al.* injected methanol extract corresponding to 10 μL of plasma onto the HPLC column. In examining their method, we recognized that 10 μL of plasma was too small to be detected. Comparison of the reported PCOOH concentrations with our results, 73 to 227 pmol/mL (15,16,18,19) as well as 88.6 pmol/mL (20), shows the reported values are far too high.

Reports of HPLC chromatograms showing the retention time of standard PCOOH are few (18). To our knowledge, there are no reports showing that the retention time of the plasma peak corresponds to that of standard PCOOH. Consequently, some contaminants in the main peak obtained with system A must be the cause of the inconsistency in the retention times.

Regarding age, the PCOOH concentration in red blood cell membranes was found to be significantly higher in older (56–92 yr) than younger (22–27 yr) subjects (24), and plasma PCOOH increased with age (15). Our findings indicate that the youngest group (22–29 yr) had the lowest PCOOH concentration. This is similar to the above results, but differs from a thiobarbituric acid study in which the total lipid peroxide of LDL was independent of age (25).

ACKNOWLEDGMENTS

We are grateful to Yasutaka Kosuge, KNC Laboratories Co., Ltd. for the PC 16:0/18:2-OOH preparation and Sanae Furusho, JASCO International Co., Ltd., Tokyo, Japan, for technical assistance. This work was supported in part by a Grant-in-Aid for Scientific Research from the Japanese Society for the Promotion of Science.

REFERENCES

1. Calabrese, V., Scapagnini, G., Latteri, S., Colombrita, C., Ravagna, A., Catalano, C., Pennisi, G., Calvani, M., and Butterfield, D.A. (2002) Long-Term Ethanol Administration Enhances Age-Dependent Modulation of Redox State in Different Brain Regions in the Rat: Protection by Acetyl Carnitine, *Int. J. Tissue React. 24*, 97–104.
2. Lasheras, C., Huerta, J.M., Gonzalez, S., Brana, A.F., Patterson, A.M., and Fernandes, S. (2002) Independent and Interactive Association of Blood Antioxidants and Oxidative Damage in Elderly People, *Free Radic. Res. 36*, 875–882.
3. Clejan, S., Japa, S., Clemetson, C., Hasabris, S.S., David, O., and Talano, J.V. (2002) Blood Histamine Is Associated with Coronary Artery Disease, Cardiac Events and Severity of Inflammation and Atherosclerosis, *J. Cell. Mol. Med. 6*, 583–592.
4. Adachi, J., Asano, M., Naito, T., Ueno, Y., and Tatsuno, Y. (1998) Chemiluminescent Determination of Cholesterol Hydroperoxides in Human Erythrocyte Membrane, *Lipids 33*, 1235–1240.
5. Adachi, J., Kudo, R., Ueno, Y., Hunter, R., Rajendram, R., Want, E., and Preedy, V.R. (2001) Heart 7-Hydroperoxycholesterol and Oxysterols Are Elevated in Chronically Ethanol-fed Rats, *J. Nutr. 131*, 2916–2920.
6. Adachi, J., Tomita, M., Yamakawa, S., Asano, M., Naito, T., and Ueno, Y. (2000) 7-Hydroperoxycholesterol as a Marker of Oxidative Stress in Rat Kidney Induced by Paraquat, *Free Radic. Res. 33*, 321–327.
7. Ishii, K., Adachi, J., Tomita, M., Kurosaka, M., and Ueno, Y. (2002) Oxysterols as Indices of Oxidative Stress in Man After Paraquat Ingestion, *Free Radic. Res. 36*, 163–168.
8. Fujita, T., Adachi, J., Ueno, Y., Peters, T.J., and Preedy, V.R. (2002) Chronic Ethanol Feeding Increases 7-Hydroperoxycho-

lesterol and Oxysterols in Rat Skeletal Muscle, *Metabolism 51*, 737–742.
9. Ariyoshi, K., Adachi, J., Asano, M., Ueno, Y., Rajendram, R., and Preedy, V.R. (2002) Effect of Chronic Ethanol Feeding on Oxysterols in Rat Liver, *Free Radic. Res. 36*, 661–666.
10. Kudo, R., Adachi, J., Uemura, K., Maekawa, T., Ueno, Y., and Yoshida, K. (2001) Lipid Peroxidation in the Rat Brain After CO Inhalation Is Temperature Dependent, *Free Radic. Biol. Med. 31*, 1417–1423.
11. Miyazawa, T., Yasuda, K., and Fujimoto, K., (1987) Chemiluminescence-High Performance Liquid Chromatography of Phosphatidylcholine Hydroperoxide, *Anal. Lett. 20*, 915–925.
12. Yamamoto, Y., Brodsky, M.H., Baker, J.C., and Ames, B.N. (1987) Detection and Characterization of Lipid Hydroperoxides at Picomole Levels by High-Performance Liquid Chromatography, *Anal. Biochem. 160*, 7–13.
13. Yamamoto, Y., Kambayashi, Y., and Ueda, T. (1998) Assay of Phosphatidylcholine Hydroperoxide by Chemiluminescence-Based High-Performance Liquid Chromatography, *Methods Mol. Biol. 108*, 63–70.
14. Adachi, J., Yoshioka, N., Funae, R., Nushida, H., Asano, M., and Ueno, Y. (2004) Determination of Phosphatidylcholine Monohydroperoxides Using Quadrupole Time-of-Flight Mass Spectrometry, *J. Chromatogr. B 806*, 41–46.
15. Kinoshita, M., Oikawa, S., Hayasaka, K., Sekikawa, A., Nagashima, T., Toyota, T., and Miyazawa, T. (2000) Age-related Increases in Plasma Phosphatidylcholine Hydroperoxide Concentrations in Control Subjects and Patients with Hyperlipidemia, *Clin. Chem. 46*, 822–828.
16. Nakagawa, K., Ninomiya, M., Okubo, T., Aoi, N., Juneja, L.R., Kim, M., Yamanaka, K., and Miyazawa, T. (1999) Tea Catechin Supplementation Increases Antioxidant Capacity and Prevents Phospholipid Hydroperoxidation in Plasma of Humans, *J. Agric. Food Chem. 47*, 3947–3973.
17. Yasuda, M., and Narita, S. (1997) Simultaneous Determination of Phospholipid Hydroperoxides and Cholesterol Ester Hydroperoxides in Human Plasma by High-Performance Liquid Chromatography with Chemiluminescence Detection, *J. Chromatogr. B 693*, 211–217.
18. Miyazawa, T., Yasuda, K., Fujimoto, K., and Kaneda, T. (1988) Presence of Phosphatidylcholine Hydroperoxide in Human Plasma, *J. Biochem. 103*, 744–746.
19. Sanaka, T., Takahashi, C., Sanaka, M., Higuchi, C., Shinobe, M., Hayasaka, Y., Miyazawa, T., Ishikawa, S., Nihei, H., and Omori, Y. (1995) Accumulation of Phosphatidylcholine-hydroperoxide in Dialysis Patients with Diabetic Nephropathy, *Clin. Nephrol. 44* (Suppl.), S33–S37.
20. Hirayama, A., Nagase, S., Gotoh, M., Takemura, K., Tomida, C., Ueda, A., Aoyagi, K., Terao, J., and Koyama, A. (2000) Hemodialysis Does Not Influence the Peroxidative State Already Present in Uremia, *Nephron 86*, 436–440.
21. Yamamoto, Y., Nagata, Y., Niki, E., Watanabe, K., and Yoshimura, Y. (1993) Plasma Glutathione Peroxidase Reduces Phosphatidylcholine Hydroperoxide, *Biochem. Biophys. Res. Commun. 193*, 133–138.
22. Mashima, R., Yamamoto, Y., and Yoshimura, S. (1998) Reduction of Phosphatidylcholine Hydroperoxide by Apolipoprotein A-1: Purification of the Hydroperoxide-Reducing Proteins from Human Blood Plasma, *J. Lipid Res. 39*, 1133–1140.
23. Nagata, Y., Yamamoto, Y., and Niki, E. (1996) Reaction of Phosphatidylcholine Hydroperoxide in Human Plasma: The Role of Peroxidase and Lecithin:Cholesterol Acyltransferase, *Arch. Biochem. Biophys. 329*, 24–30.
24. Miyazawa, T., Suzuki, T., Fujimoto, K., and Kinoshita, M. (1996) Age-Related Change of Phosphatidylcholine Hydroperoxide and Phosphatidylethanolamine Hydroperoxide Levels in Normal Human Red Blood Cells, *Mech. Ageing Devel. 86*, 145–150.
24. Sanderson, K.J., van-Rij, A.M., Wade, C.R., and Sutherland, W.H. (1995) Lipid Peroxidation of Circulating Low Density Lipoproteins with Age, Smoking and in Peripheral Vascular Disease, *Atherosclerosis 118*, 45–51.

[Received February 23, 2004; accepted November 2, 2004]

Multivariate Prediction of Clarified Butter Composition Using Raman Spectroscopy

J. Renwick Beattie[a], Steven E.J. Bell[a,*], C. Borgaard[b], A.M. Fearon[a], and Bruce W. Moss[c]

[a]School of Chemistry, Queen's University, Belfast BT9 5AG, Northern Ireland, [b]Danish Meat Research Institute, 4000 Roskilde, Denmark, and [c]School of Agriculture and Food Science, Queen's University, Belfast BT9 5AG, Northern Ireland

ABSTRACT: Raman spectroscopy has been used to predict the abundance of the FA in clarified butterfat that was obtained from dairy cows fed a range of levels of rapeseed oil in their diet. Partial least squares regression of the Raman spectra against FA compositions obtained by GC showed that good prediction of the five major (abundance >5%) FA gave R^2 = 0.74–0.92 with a SE of prediction (RMSEP) that was 5–7% of the mean. In general, the prediction accuracy fell with decreasing abundance in the sample, but the RMSEP was <10% for all but one of the 10 FA present at levels >1.25%. The Raman method has the best prediction ability for unsaturated FA (R^2 = 0.85–0.92), and in particular *trans* unsaturated FA (best-predicted FA was 18:1*t*Δ9). This enhancement was attributed to the isolation of the unsaturated modes from the saturated modes and the significantly higher spectral response of unsaturated bonds compared with saturated bonds. Raman spectra of the melted butter samples could also be used to predict bulk parameters calculated from standard analyzes, such as iodine value (R^2 = 0.80) and solid fat content at low temperature (R^2 = 0.87). For solid fat contents determined at higher temperatures, the prediction ability was significantly reduced (R^2 = 0.42), and this decrease in performance was attributed to the smaller range of values in solid fat content at the higher temperatures. Finally, although the prediction errors for the abundances of each of the FA in a given sample are much larger with Raman than with full GC analysis, the accuracy is acceptably high for quality control applications. This, combined with the fact that Raman spectra can be obtained with no sample preparation and with 60-s data collection times, means that high-throughput, on-line Raman analysis of butter samples should be possible.

Paper no. L9558 in *Lipids 39*, 897-906 (September 2004).

The composition, both physical and chemical, of fats is a major concern, from the health implications of saturated and n-3 and n-6 FA to the physical properties of shortening and of spreadable butter (1). In today's increasingly quality-conscious market, it is becoming more important to test products rigorously and extensively before they reach the processor or consumer. In this respect, the most favorable methods must be rapid with good repeatability and reliability and be capable of a high throughput. The best systems will allow on-line, nondestructive analysis of the product while analyzing for the maximal number of parameters possible.

*To whom correspondence should be addressed.
E-mail: S.Bell@QUB.ac.uk

Abbreviations: IV, iodine value; PLS, partial least squares; QC, quality control; RMSEP, standard error of prediction.

The potential of Raman spectroscopy for the analysis of fats and oils has been recognized for some decades. Raman spectroscopy already has been used successfully to determine important composition/physical structure parameters in a wide range of lipid sample types. These include: *cis/trans* geometrical isomer ratio (2), unsaturation (3), conjugated double bond content (4), chain length (5), FFA content (6), and crystal structure (7). The main advantages of Raman analysis are that no sample preparation is required (allowing *in situ* or on-line studies) and that it can be applied to any physical state including gases, liquids, gels, amorphous solids, and crystals. However, until recently, adoption of Raman methods for routine analysis of fats and oils has been hindered by the high cost and complexity of the instrumentation required. This situation is now changing rapidly. A number of technological advances such as holographic notch filters for rejection of elastically scattered light and the availability of long-wavelength (750–1064 nm) excitation lasers (which reduce background fluorescence problems) are making the technique more accessible than ever before, while the introduction of simple-to-use commercial instruments means that it is straightforward for nonspecialists to record good-quality Raman spectroscopic data. At present, the main problem Raman spectroscopy faces is that it is newer than competing techniques such as NIR, FTIR, and NMR spectroscopy, so there is not the same level of background information, such as widely agreed standard procedures and detailed best working practices for analysis of particular types of samples that are already available for the more established techniques. For example, NIR and FTIR spectroscopy have been shown to provide reasonably good predictions of FA composition in edible fats (8–11). However, although the proportion of the major unsaturated FA are well predicted (R^2 typically ≥0.95 for the most abundant unsaturated FA), the prediction ability is reduced considerably as the proportion of the FA decreases and as the saturation increases (e.g., R^2 for stearic acid is <0.8).

This paper is part of a series of investigations into the potential of Raman spectroscopy for routine analysis of lipid systems, which have also included experimental and theoretical studies (using density functional theory) on model systems (12–14) and the experimental analysis of adipose tissue from a range of animals (15). The aim of this work is to investigate the extent to which Raman spectroscopy can determine the composition of real-life edible fat samples, which are typically

composed of mixtures of TG. Two rather different types of compositional information might be extracted from Raman data. The first type is overall bulk properties, such as unsaturation, which *a priori* would be expected to be readily obtainable since they depend on measuring the spectroscopic signature of distinct entities in the samples, e.g., the C=C vibrations. The second type of information is the relative abundances of the FA in the sample, which would be expected to be much more difficult to obtain since the Raman spectra of homologous series of FA typically show smooth changes with increasing chain length, for example (12). Although subtle irregularities in these smooth trends have been found, the overall similarity in the spectra of 12:0, 14:0, 16:0, and 18:0 means that it must be more difficult to distinguish the relative proportions of each in a given sample than simply to extract the overall average chain length. In this paper the ability of Raman methods to determine both types of information for clarified butter will be examined.

Butter is a relatively simple food to analyze as it is generally *ca.* 82% fat (of which, *ca*. 98% are TG) with low concentrations of protein and water. This means that the Raman spectra are dominated by the fat bands, and interference from the other constituents is insignificant. The clarified butter samples used for this work were obtained from a large-scale investigation of the effect of dietary FA composition on the FA composition of cows' milk. These cows were offered feed that had been supplemented with varying amounts of seeds containing highly unsaturated oil. Results from the GC analysis of the clarified butter showed that the dietary feed affected the clarified butter composition, with a direct correlation between the FA composition of the feed and that of the clarified butter. This was found to have significant consequences on the physical properties, notably increased softness/spreadability in the clarified butter (see Ref. 16 for details). For the purposes of this work, the important point is that the dietary modification provided a set of butters with a range of different compositions and physical/chemical properties. Of course, if the method is shown to be successful, then, in addition to proving a point about the potential of the general approach, it would immediately provide an excellent method for routine quality control of modified butters of this type that could be adopted straightaway.

MATERIALS AND METHODS

Preparation of samples. The samples used in this investigation were anhydrous milk fat, prepared by clarifying butter (BSI 1961). Spectra were accumulated from samples held at 55°C using an insulated heating block controlled using a Eurotherm 91 temperature controller. This temperature was chosen because all the butter samples would be expected to be liquid, thus eliminating physical state effects and allowing the Raman spectra to be correlated with purely chemical changes. The butters used in this investigation were supplied from an experiment in which the FA composition of the milk fat (abundances of major FA 308, 195, and 139 g kg^{-1} on average for 16:0, 18:1*c*Δ9, and 14:0, respectively) was altered by inclusion of whole rapeseeds (containing 549, 294, and 103 g kg^{-1} 18:1*c*Δ9, 18: 2*c*Δ9,12, and 18:3*c*Δ9,12,15, respectively) in the pelleted concentrate offered to the dairy cows in the study. Full details of the experiment, along with all chemical and physical methods of analysis, are published elsewhere (16). Ninety-two clarified butter samples were analyzed by Raman spectroscopy.

Raman spectroscopy. Raman spectroscopic measurements were carried out using a point-focused 785 nm excitation wavelength (typically 100–120 mW at the sample) with a previously described home-built Raman spectrometer (12). Laser wavelength calibration was carried out using a neon emission lamp. The spectrograph was calibrated for Raman shift using a 50:50 (vol/vol) acetonitrile/toluene mixture [comparing to frequency standards from the American Standard Testing Method [ASTM E 1840 (1996)]. The Raman signal was recorded from 260 to 2000 cm^{-1}, the region containing the C–C, C=C, C–O and C=O, stretches and the C–H bends. Two spectra (30 s accumulation time) were obtained from each sample, and the individual spectra were averaged prior to regression analysis.

CSMA (17) spectral accumulation software was used to collect the raw data. The spectra were exported to SpectraCalc (Galactic Industries, Salem, NH), and the calibration was readjusted to allow for differences in the two file types. The spectra were then automatically baseline-subtracted using a modified visual basic program that allowed a standard 14-point subtraction to be carried out. The baseline points were at *ca.* 260, 340, 380, 500, 600, 690, 790, 1185, 1380, 1500, 1530, 1760, 1880, and 1990 cm^{-1}, but these values were adjusted as necessary to remove any effect due to slight daily variations in calibration. To eliminate cosmic rays, two sequential spectra were acquired and added together. Subtraction of the square root of the squared difference spectrum from this sum removed any cosmic rays. The spectra were exported as ASCII files to Microsoft Excel (Redmond, WA) and collated into spreadsheets, and regions known to contain no significant contribution from Raman scattering were removed.

Multivariate calibration. Standard partial least squares (PLS) analysis was carried out using The Unscrambler™ v. 7.5 (CAMO, Trondheim, Norway). Prior to regression analysis, the spectra were normalized around the intensity of the ν(C=O) band at 1745 cm^{-1}, and mean centering was applied to the spectra. During the PLS analysis of the data, the "jackknife" procedure included in the program was used to select the wavenumber shifts that correlated with the measured parameter and to reject data from wavenumber shifts not contributing to the prediction. Validation was carried out using leave-one-out cross-validation. The optimal number of PLS factors used for the regression was determined from the minimum residual validation variance. Outliers were detected using residual Y-validation variance.

GC Analysis. FAME were prepared from the anhydrous milk fat using BS684: 1980. Approximately 0.25–0.5 g of fat was dissolved in 10 mL of hexane, to which was added 0.5 mL of 2-N KOH in anhydrous methanol, and the sample con-

tainer was shaken vigorously for 20 s. Two milliliters of the hexane solution weas siphoned off and stored at –18°C until required.

For GC, an aliquot (0.1 μL) of the FAME was then injected onto a WCOT fused-silica coated capillary column (CP Sil 88, 0.32 mm i.d., 100 m length; Chrompack, London, United Kingdom) in a Varian Star 3400 gas chromatograph (Varian Associates Ltd., Walton-on-Thames, Surrey, United Kingdom) equipped with a Speta programmable injector and FID. The injection temperature was programmed from 50 to 250°C at a rate of 25.0°C/min, and the oven temperature was ramped from 50 to 125°C at 20°C/min, then from 120 to 225°C at 4°C/min to improve separation and resolution. Internal and external standards were used for identification and recovery efficiency purposes. Peaks with <0.5% of the total chromatogram area were rejected from the analysis.

Solid fat content and iodine value (IV). Solid fat content (%) of the clarified butter was measured using pulsed NMR in a Bruker Minispec PC 120 series NMR Analyzer (Bruker Spectrospin Ltd., Coventry). The clarified butter was melted at 60°C for 30 min followed by crystallization at 0°C for 90 min. Parallel measurements of solid fat content were made at 5, 10, 15, 20, and 25°C, after tempering of the milk fat for 30 min at the measuring temperature.

IV of the milk fat were determined using the AOCS Cd 1b-87 method (18), with results expressed as g of iodine per 100 g of fat.

RESULTS AND DISCUSSION

In this paper, our studies of model FA-based lipids are extended to the investigation of real fat systems (clarified butters) that are predominantly composed of TG. Figure 1 shows the average Raman spectrum at 55°C of clarified butter obtained from the milk of cows fed a standard diet and a high-oil diet. The spectra were normalized to the carbonyl stretching mode (*ca.* 1745 cm^{-1}), which is a molar standard since every FA contains only one carbonyl group. These spectra are very similar to those of the simple FAME we studied previously, which allowed the bands to be assigned easily, as shown in Table 1. In Figure 1 it is clear that all the major bands increase in intensity with respect to the carbonyl standard with higher oil content in the diet of the cows, but the modes arising from unsaturated bonds increase more than the others. This is expected, since comparison of the FA profiles of the standard diet butter and the rapeseed butter shows that the rapeseed contains >95% 18-carbon FA and unsaturated FA (many of which are polyunsaturated), whereas the butter contains large proportions of shorter–chain saturated FA (e.g., 16:0 and 14:0 account for 45% of the total FA). The central question is whether the obvious spectral changes associated with butter from cows fed the altered diet can be used to obtain quantitative information about the composition of the samples. Here we treat, in turn, prediction of the abundance of the various constituent FAME, the solid fat content, and the various bulk chemical composition parameters that can be used to characterize edible fats and oils.

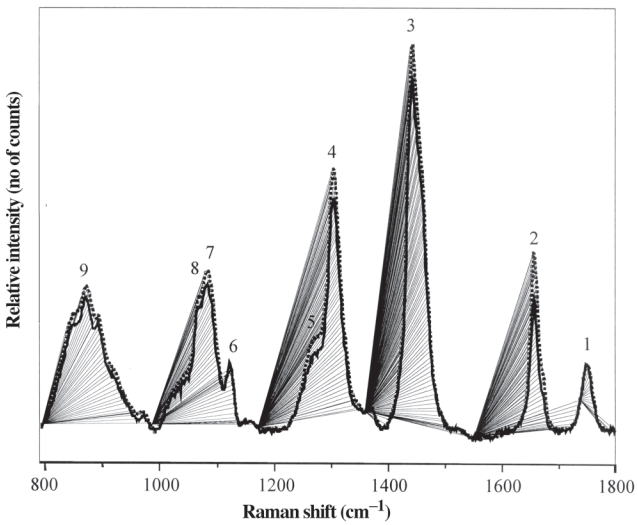

FIG. 1. Average Raman spectrum (acquired at 55°C) of the zero (solid line) and 600 g oil day^{-1} (dashed line) rapeseed diet clarified butter samples analyzed in this investigation. Numbering of peaks corresponds to the table of assignments (Table 1).

FA composition—PLS regression with GC data. In our previous studies of a model FAME system (12), we showed that Raman spectra carried information on the chemical composition of samples of the simple model compounds. In the current study, the Raman data were correlated with the results of GC analysis of all the clarified butter samples (all treatments

TABLE 1
Assignment of Bands in the Raman Spectra of Anhydrous Butter in the Liquid Phase

Band[a]	Band position	Assignment (ref. number)
1	1730–1750	ν(C=O) Carbonyl stretch (20)
2	1640–1680	ν(C=C) Olefinic stretch (4)
3	1400–1500	$\delta(CH_2)_{sc}$ Methylene scissor deformations (20)
4	1295–1305	$\delta(CH_2)_{tw}$ Methylene twisting deformations (21)
5	1250–1280	$\delta(=CH)_{ip}$ In-plane olefinic hydrogen bend (21)
6	1100–1135	$\nu(C–C)_{ip}$ In-phase aliphatic C–C stretch all-*trans* (22)
7	1080–1090	$\nu(C–C)_{g}$ Liquid: aliphatic C–C stretch in *gauche* (23)
8	1060–1065	$\nu(C–C)_{op}$ Out-of-phase aliphatic C–C stretch all-*trans* (24)
9	800–920	$\nu(C_1–C_2)$, $CH_{3,rk}$, ν(C–O) Complex broad table in liquid (25)

[a]The band number refers to the numbering in Figure 1.

TABLE 2
Prediction Correlation Coefficients and SE of Prediction (RMSEP) for PLS Regression of Raman Data with GC Data for Clarified Butterfat

	μ[a]	σ[b]	R^{2c}	RMSEP[d]	RMSEP % of μ	RMSEP % of 4σ	No. of factors[e]	No. of outliers
Raman vs. FA content								
4:0	1.12	0.34	0.609	0.214	19.10	15.73	4	1
6:0	1.15	0.34	0.724	0.181	15.72	13.29	3	1
8:0	0.93	0.27	0.814	0.117	12.60	10.85	3	1
10:0	2.25	0.75	0.86	0.278	12.36	9.27	5	0
12:0	2.87	0.9	0.903	0.278	9.68	7.72	4	1
14:0	10.19	1.91	0.869	0.690	6.77	9.03	5	0
14:1	0.96	0.19	0.621	0.117	12.18	15.38	5	0
15:0	1.26	0.17	0.769	0.084	6.63	12.28	5	0
16:0	25.32	3.38	0.86	1.261	4.98	9.33	3	0
16:1*c*	1.35	0.2	0.676	0.116	8.56	14.44	4	1
16:1*t*	0.49	0.03	0.116	0.036	7.39	30.17	1	0
17:0	0.61	0.13	0.235	0.493	80.89	94.88	5	2
18:0	13.26	1.93	0.736	0.946	7.13	12.25	3	0
18:1*c*	29.41	4.86	0.859	1.799	6.12	9.25	3	0
18:1*t*	5.26	1.3	0.924	0.298	5.66	5.73	5	1
18:2*c*	1.08	0.12	0.064	0.133	12.30	27.67	1	0
18:2*t*	0.3	0.07	0.819	0.031	10.37	11.11	2	2
18:3*c*	0.61	0.06	0.005	0.064	10.54	26.79	1	0
CLA	1.55	0.3	0.858	0.112	7.25	9.36	4	0

[a]Average % total mass of lipid.
[b]SD of the % total mass of lipid from the mean.
[c]Least squares regression correlation coefficient (validation).
[d]RMSEP is quoted as a percentage of the mean (RMSEP % of μ) and sample range (RMSEP % of 4σ). PLS, partial least squares.

and both lactation groups) to determine the ability of Raman spectra to predict the sample composition of more complex systems over a realistic range of compositions. The main difference between the work on the real and model systems is that in the clarified butter samples, there is a mixture of FA in each sample, so the relative proportions of each may be predicted as well as the overall average properties.

The prediction least squares regression correlation coefficients and SE of prediction for all the FA and bulk parameters analyzed in the course of the experiment are shown in Table 2. The FA are listed in order of chain length and unsaturation levels, with *cis* isomers before *trans*. The SE of prediction is quoted as a percentage of the mean, to give absolute error, and as a percentage of the SD, to give error relative to the range of the data. The major FA are 18:1*c*Δ9 (29.4% of total FA), 16:0 (25.3% of total FA), 18:0 (13.26% of total FA), and 14:0 (10.2% of total FA).

Not surprisingly, in general the best-predicted FA are those that are present in the higher amounts. Figure 2 shows, for example, the validation predictions plotted against the GC-measured values for the most abundant acid, 18:1*c*Δ9. Although the 18:1*c*Δ9 predictions are good ($R^2 = 0.859$ and an SE of prediction (RMSEP) of *ca*. 6% of the mean), the predictions for its *trans* near-analog 18:1*t*Δ11 were better ($R^2 = 0.924$ and an RMSEP of *ca*. 6% of both the mean and range) despite the *trans* only having the fifth-highest abundance. This good prediction for the *trans* can be explained by the isolation of the band corresponding to the olefinic modes of *trans* bonds at 1670 cm^{-1} and the relative scarcity of other *trans* FA (no others >0.5%). Notwithstanding these compound-specific effects, it is clear that the relative abundance of the fat is the major determining factor in the method's ability to predict it. Overall, the regression correlation coefficients for the prediction of FA content are comparable with the published NIR literature results quoted previously for the high-abundance acids (8–11), but here it is notable that the accuracy is not confined entirely to the major species. For the 10 most abundant FA, the root mean square error of prediction is <10% of the mean in all ex-

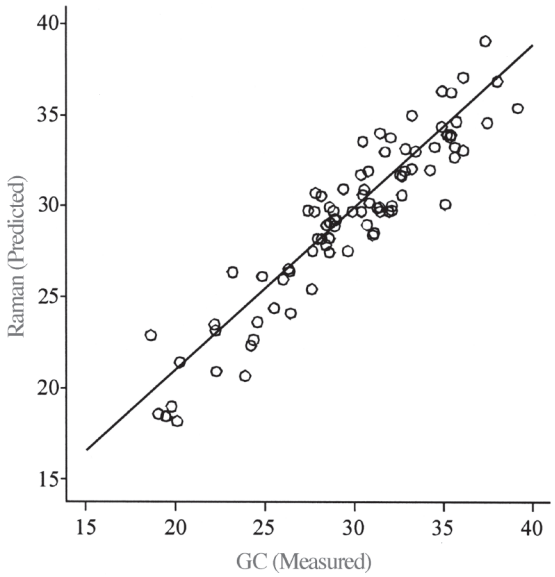

FIG. 2. Partial least squares (PLS) regression plot for the prediction of the relative abundance of 18:1*c*Δ9 FA in clarified butter using Raman spectroscopy.

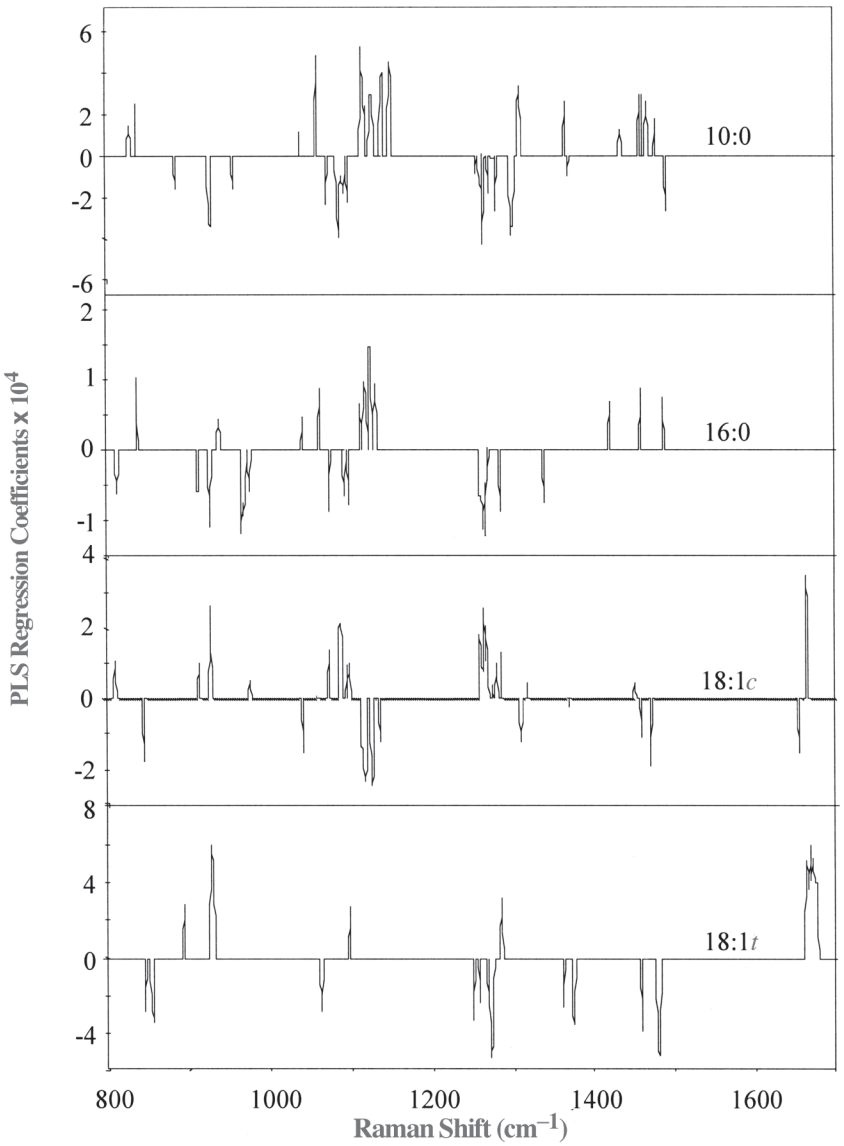

FIG. 3. PLS-1 regression coefficients used to predict the relative abundance of selected FA. For abbreviation see Figure 2.

cept one case; conversely, for the nine least abundant (all <1.25% of the sample), the error of prediction is >10% of the mean in all cases except one. For some of the least abundant FA (e.g., 16:1*t*Δ9), the optimal number of PLS factors was 1 since the residual validation variance increased with additional factors. CLA (18:2Δ*c*9,*t*11) is a FA of particular interest owing to its special role in health. In this investigation it was found that the amount of CLA in the clarified butter samples was well modeled, with RMSEP = 7.25% of the mean and an R^2 of 0.86.

The regression coefficients of the major FA show that the PLS regression uses the peaks that one might intuitively choose from knowledge of the Raman spectrum of FA-based lipids. Figure 3 shows the PLS regression coefficients for 16:0, 18:1*c*Δ9, and 18:1*t*Δ11, which are the major saturated, *cis*-unsaturated, and *trans*-unsaturated FA. Also included is 10:0 as a representative of the short-chain FA. From the regression coefficients it can readily be seen that the saturated FA (10:0 and 16:0) have positive correlations with saturated bands such as the $\nu(C–C)_{ip}$ (1120 cm^{-1}) and $\nu(C–C)_{op}$ (1060 cm^{-1}) bands (where op = out-of-plane and ip = in-plane), the twist (1300 cm^{-1}) bands, and scissor bands (1440 cm^{-1}). The saturated FA are negatively correlated with the unsaturated band at 1260 cm^{-1} and to the *gauche* C–C stretching band at 1080 cm^{-1}. The *cis* unsaturated FA show the opposite behaviour.

Figure 4 shows the loadings from principal components analyses of the GC data, which indicates that three groups of FA are present in the butter samples. One group contains the shorter-chain saturated FA from 4:0 to 16:0, along with 16:1*c*Δ8 and 14:1*c*Δ7, which are prevalent in native butter. A

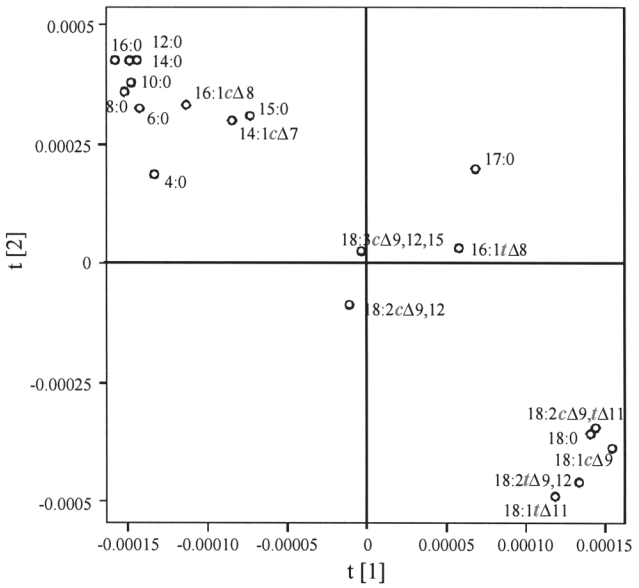

FIG. 4. Loadings for principal components analysis of the relative abundances of the FA in clarified butter samples as determined by GC.

second group contains FA (18:0, 18:1*c*Δ9, 18:1*t*Δ9, 18:2*t*Δ9,12, and 18:2*c*Δ9,*t*Δ11) that are more abundant either in rapeseed oils or as a result of biohydrogenation of rapeseed FA in the rumen. A third group, located near the origin, contains minor FA whose abundance does not vary significantly between rapeseed oil and butter. These three groups, of course, reflect the unusual origin of these samples, which means that the compositions of butters would be expected to change in the same way, but to a different degree, in the variously treated groups. The cross-correlation obvious from Figure 4 would be expected to enhance the apparent ability of analytical methods to predict minor FA that correlated with more abundant FA. For example, 8:0 was well-modeled (R^2 = 0.81, RMSEP 12.6% of the mean) despite constituting only 0.9% of the total FA. Of course, this apparent enhancement in the prediction accuracy will occur only for samples that show the same type of compositional variation as the calibration set, and lower accuracy would be expected for a sample set containing truly randomized FA. However, such a randomized data set rarely occurs naturally, and quality control (QC), for example, is generally concerned with samples where the abundances of the FA would be expected to be cross-correlated to some degree.

Finally, these observations should distract us from the principal conclusion, which is that for all but one of the most abundant FA (i.e., the 10 present at >1.5%), the RMSEP is <10%, even in these very complex mixed samples. This is an impressive result, considering the chemical similarity of the compounds analyzed and the fact that no separation step was used in the analytical procedure.

Bulk physical properties—PLS regression with solid fat content. Solid fat content is an important parameter in the food processing industry as this parameter will influence a range of properties in the final product. It is related to the spreadability of butters and margarines, the functional properties of pastries, and the physical properties of chocolate. Here we found that the Raman and GC data both predicted the solid fat content of lower-temperature samples better than higher-temperature samples (see Table 3). This is not surprising since the effect of the dietary modification was greater for the low-temperature solid fat contents than the high-temperature determinations, which has the consequence that the higher-temperature solid fat content data do not have as large a range over which to calibrate. In addition, the physical behavior of the clarified butter is extremely complex in the melting range, with low-m.p. TG softening the sample by dissolving higher-m.p. TG. This is a particular problem with clarified butter, which contains both

TABLE 3
Prediction Correlation Coefficients and RMSEP for PLS Regression of Raman Data with GC Data with Measured Solid Fat Content for Clarified Butterfat

	μ[a]	σ[b]	R^{2c}	RMSEP[d]	RMSEP % of μ	RMSEP % of 4σ	No. of factors	No. of outliers
Correlation of Raman spectroscopic data with solid fat content								
SF5[f]	47.05	5.79	0.865	2.35	4.54	9.22	3	2
SF10	37.60	4.71	0.764	2.12	6.05	12.08	4	1
SF15	27.27	2.85	0.721	1.63	5.46	13.06	4	1
SF20	15.44	1.41	0.671	0.81	5.24	14.34	5	1
SF25	9.25	1.50	0.463	1.18	12.02	18.53	3	2
Correlation of GC data with solid fat content								
SF5	47.05	5.79	0.884	1.97	4.19	8.50	5	5
SF10	37.60	4.71	0.901	1.83	4.87	7.96	5	5
SF15	27.27	2.85	0.750	1.42	5.22	12.47	5	5
SF20	15.44	1.41	0.692	0.79	5.12	13.97	5	5
SF25	9.25	1.50	0.613	0.94	10.19	15.68	5	5

[a]Average % total mass of lipid.
[b]SD of the % total mass of lipid from the mean.
[c]Least squares regression correlation coefficient (validation).
[d]RMSEP is quoted as a percentage of the mean (RMSEP % of μ) and sample range (RMSEP % of 4σ). For abbreviation see Table 2.
[e]SFX is the solid fat content at temperature X (°C).

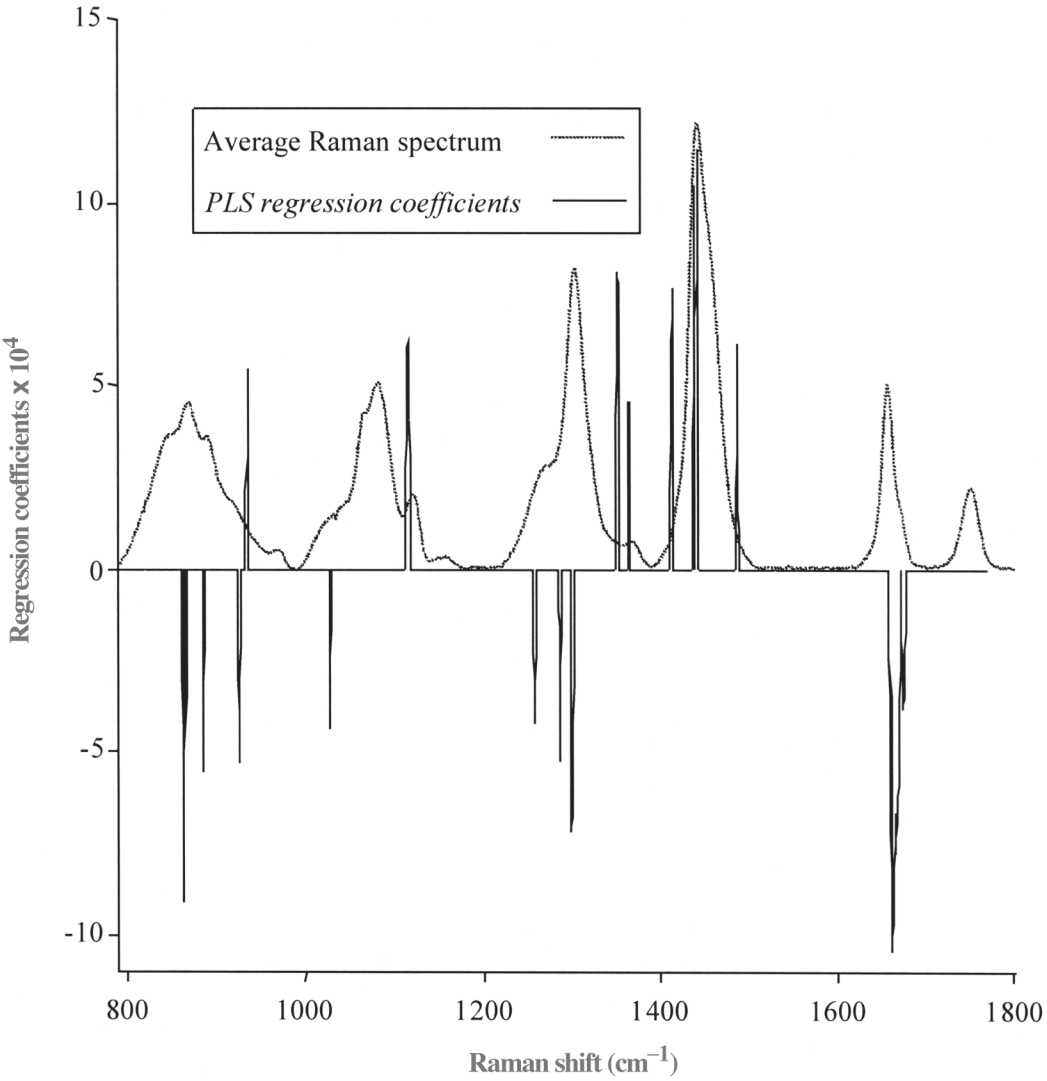

FIG. 5. PLS-1 regression coefficients used to predict the solid fat content of clarified butters from their Raman spectra. For abbreviation see Figure 2.

low-m.p. (short-chain and polyunsaturated) FA and long-chain saturated (high-m.p.) FA. The solid fat content prediction errors were found to be marginally lower for the GC data than the Raman data, but it should be noted that the Raman spectra used for the predictions of solid fat content at the various temperatures were all recorded at 55°C, where all the samples were liquid. It should be possible to improve the prediction by recording the spectra at lower temperatures since the spectra of solid and liquid fats are quite different and should thus provide additional information on physical state.

Figure 5 shows the regression coefficients used to determine the PLS regression of the Raman data (at 55°C) with solid fat content at 15°C. The positive contributors to the correlation are various peaks found in crystalline fats such as 1114, 1354, 1364, 1412, 1440, and 1486 cm^{-1}. Unsaturated peaks such as 1260 and 1660 have negative regression coefficients, as they reduce the m.p. of the lipids and thus raise the liquid fat content at any given temperature in the melting range. Peaks arising from disordered lipids such as the unresolved group of peaks at 800–950 cm^{-1}, the C–C *gauche* modes at 1028, 1071, and 1095 cm^{-1}, and the twist mode at 1300 cm^{-1} contribute the other negative regression coefficients.

Bulk chemical properties—PLS regression against composition parameters. One of the most important compositional parameters used to characterize fats and lipids is the IV, but other measures also give an indication of the composition of a mixed sample from a single numerical value. Table 4 lists measured (GC and IV) and predicted (Raman) values for a range of these parameters.

Since most of the bulk properties were calculated from the GC data, it is not surprising that these bulk properties have correlation coefficients similar to those for the individual FA that contribute most to that bulk property. The correlation for total carbon is similar to the average correlation (both 0.80) for all the FA present at >1%. For a number of reasons, unsaturation

TABLE 4
Prediction Correlation Coefficients and RMSEP for PLS Regression of Raman Data with Bulk Parameters Derived from GC and with Chemically Derived Iodine Value; Correlation of GC Profile with the Chemically Derived Iodine Value

	μ[a]	σ[b]	R^{2c}	RMSEP[d]	RMSEP % of μ	RMSEP % of 4σ	No. of factors[e]	No. of outliers
Correlation of Raman spectroscopic data with bulk parameters derived from GC								
Total carbon	16.21	0.36	0.797	0.160	0.99	11.11	4	3
Saturation	13.28	0.24	0.750	0.119	0.90	12.39	5	2
Unsaturation	0.84	0.11	0.850	0.043	5.12	9.77	5	2
Cis	0.35	0.05	0.831	0.018	5.23	9.15	4	2
Trans	0.063	0.014	0.847	0.0052	8.21	9.23	6	2
C=C/C–C	0.027	0.003	0.849	0.0012	4.43	9.97	5	2
Correlation of Raman spectroscopic data and GC with iodine value								
Raman	41.78	4.58	0.796	2.06	4.92	11.22	4	2
GC	41.78	4.78	0.511	3.21	7.68	17.52	3	0

[a]Average % total mass of lipid.
[b]SD of the % total mass of lipid from the mean.
[c]Least squares regression correlation coefficient (validation).
[d]RMSEP is quoted as a percentage of the mean (RMSEP % of μ) and sample range (RMSEP % of 4σ). For abbreviation see Table 2.
[e]Regression coefficients listed in Appendix F.
[f]SFX is the solid fat content at temperature X (°C).

(CH) is better modeled than saturation (CH_2) (0.85 compared to 0.75). First, the spectral response of one saturated bond (sum of the relative areas of the total scissor, twist, and C–C regions) is almost four times that of an unsaturated bond [sum of the relative areas of ν(C=C) and δ(=C–H), not including the effects on scissor, twist, or C–C regions]. Second, some of the Raman bands due to unsaturated bonds [ν(C=C) and δ(=C–H)] lie in regions where there is no interference from saturated peaks,

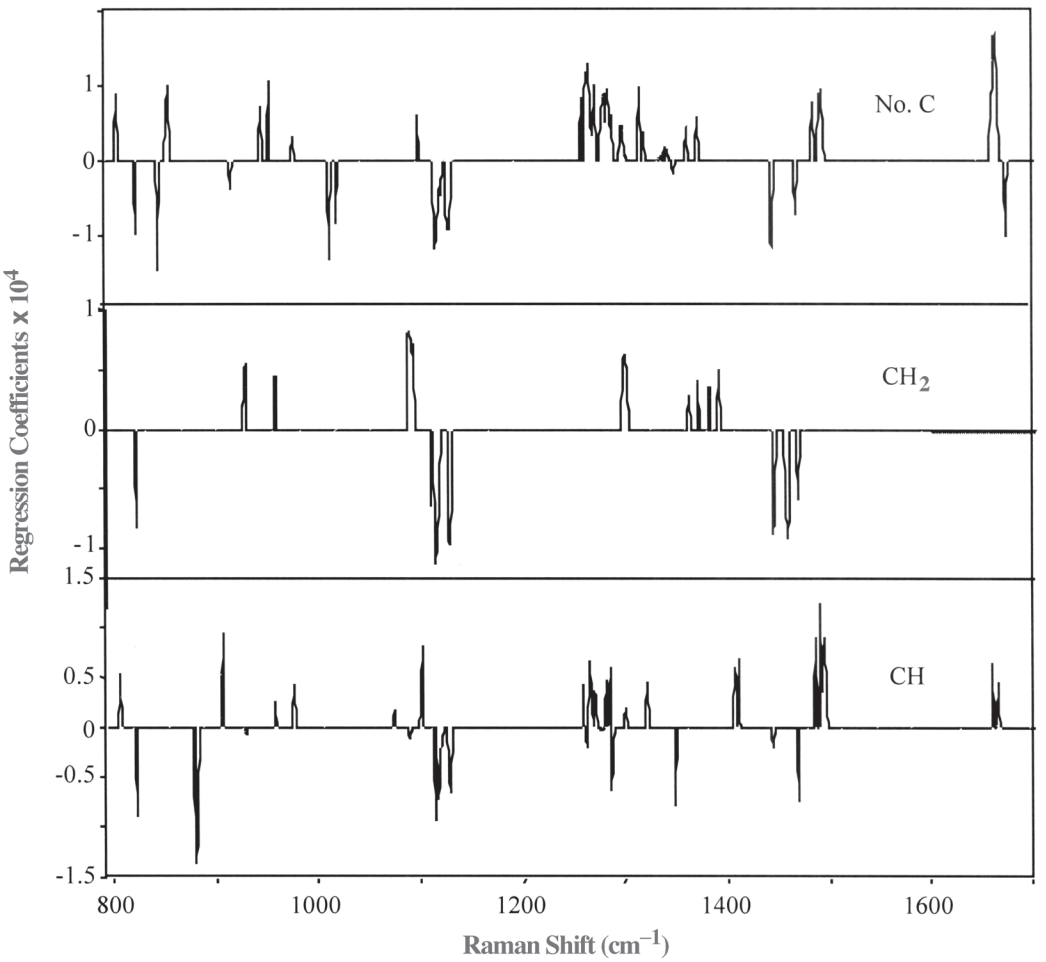

FIG. 6. PLS-1 regression coefficients used to predict selected bulk parameters of clarified butters from their Raman spectra.

whereas the $\delta(CH_x)$ and ν(C–C) regions contain contributions from unsaturated bonds in the sample. In addition, in a previous study of the relationship between chemical structure of FAME and their Raman spectra, we found that the saturated FAME did not show smooth spectral changes with chemical structure, whereas the unsaturated FAME did show a smooth relationship (12). Finally, although the absolute errors for the total carbon and the saturation are very low (<1%), the error relative to the SD is much higher (10–12%), as the range of values is small relative to the magnitude of the average.

The Raman data showed a significantly better correlation with the chemically determined IV than did the GC (R^2 = 0.80, compared to 0.51); the RMSEP from Raman (4.9% of the mean) was also better than the 7.7% value from GC. However, the unsaturation parameter calculated from the GC (i.e., C=C/C–C) is a more meaningful number than the chemically determined IV because they become nonlinear (19) with polyunsaturation and conjugation. In this study, the dietary modification increases the proportion of PUFA (particularly 18:2*c*Δ9,12 and 18:3*c*Δ9,12,15), and so would be expected to lead to nonlinearity problems. However, the Raman data correlate well with the GC unsaturation parameter (C=C/C–C, R^2 = 0.85) as well as the chemically determined IV and so can provide whichever unsaturation parameter is required.

As was the case for the determination of individual components, the Raman regression coefficients for the bulk properties (see Fig. 6) make physical sense. For example, prediction of total carbon includes contributions from both saturated and unsaturated bands, whereas prediction of molar unsaturation is positively correlated with unsaturated peaks and negatively correlated to saturated peaks. Prediction of saturation has no contribution from the unsaturated bands.

Thus, Raman spectroscopy is surprisingly effective for predicting the abundance of the major FA in clarified butter: The predictive power compares very favorably with alternative spectroscopic techniques such as NIR and FTIR spectroscopy. Of particular interest is the ability of Raman spectroscopy to predict the proportion of CLA, which is believed to be of relevance to health. Although the samples used in this study were butters whose FA composition had been altered by feeding the animals protected rapeseed oil, the method should be equally effective for more routine samples.

The accuracy in predicting the FA profile was also reflected in the ability to predict the bulk chemical parameters, which are derived from the FA profile, and physical parameters. For solid fat content, more work will be needed to improve the prediction of the Raman method to the same level as that of GC. This is not surprising as the physical state of clarified butter depends not only on the FA composition but also on a large range of other factors, including thermal history. Maintaining the samples above the m.p., as was done in this study, eliminates the effect of thermal history.

Finally, although Raman spectroscopy gives prediction errors for the abundances of each of the FA in a given sample that are good for a nondestructive spectroscopic method, the errors are still much larger than with full GC analysis. However, Raman spectra can be obtained with no sample preparation and with data collection times of 60 s. Moreover, the accuracy of the Raman method is acceptably high for QC applications because a complete, detailed FA composition profile often is not required. For example, the question of interest for QC is the extent to which a sample has the desirable properties conferred by dietary modification. Taken together, these properties make Raman methods much more suitable than GC for QC of samples of this type. Indeed more general, high-throughput, on-line analysis of clarified butter samples should be possible, particularly since extension to hydrated butter should be trivial because water gives a very low Raman signal compared with lipids.

REFERENCES

1. Fearon, A.M. (2001) Optimising Milkfat Composition and Processing Properties, *Austral. J. Dairy Technol. 56*, 104–108.
2. Johnson, G.L., Machado, R.M., Freidl, K.G., Achenbach, M.L., Clark, P.J., and Reidy, S.K. (2002) Evaluation of Raman Spectroscopy for Determining *cis* and *trans*-Isomers in Partially Hydrogenated Soybean Oil, *Org. Process Res. Dev. 6*, 637–644.
3. Barthus, R.C., and Poppi, R.J. (2001). Determination of the Total Unsaturation in Vegetable Oils by Fourier Transform Raman Spectroscopy and Multivariate Calibration, *Vib. Spectrosc. 26*, 99–105.
4. Chmielarz, B., Bajdor, K., Labudzinska, A., and Klukowskamajewska, Z. (1995) Studies on the Double-Bond Positional Isomerization Process in Linseed Oil by UV, IR and Raman Spectroscopy, *J. Mol. Struct. 348*, 313–316.
5. Beattie, J.R., Bell, S.E.J., and Moss, B.W. (2000) Raman Studies of Lipid Structure and Composition, in *XVII International Conference on Raman Spectroscopy* (Beattie, J.R., Bell, S.E.J., and Moss, B.W., eds.), pp. 708–709, John Wiley & Sons, Beijing.
6. Muik, B., Lendl, B., Molina-Diaz, A., and Ayora-Canada, M.J. (2003) Direct, Reagent-free Determination of Free Fatty Acid Content in Olive Oil and Olives by Fourier Transform Raman Spectrometry, *Anal. Chim. Acta 487*, 211–220.
7. Simpson, T.D., and Hagemann, J.W. (1982) Evidence of Two β′ Phases in Tristearin, *J. Am. Oil Chem. Soc. 59*, 169–171.
8. Sato, T., Takahashi, M., and Matsunaga, R. (2002) Use Of NIR Spectroscopy for Estimation of FA Composition of Soy Flour, *JAOCS J. Am. Oil Chem. Soc. 79*, 535–537.
9. Velasco, L., Mollers, C., and Becker, H.C. (1999) Estimation of Seed Weight, Oil Content and Fatty Acid Composition in Intact Single Seeds of Rapeseed (*Brassica napus* L) by Near-Infrared Reflectance Spectroscopy, *Euphytica 106*, 79–85.
10. Kohler, P., and Kallweit, E. (1999) Determination of Fatty Acid Composition of Intramuscular Fat in Sheep by Near-Infrared Transmission Spectroscopy (NIT) and Their Importance for the Meat Production, *Agribiol. Res.—Zeitschrift fur Agrarbiologie Agrikulturchemie Okologie 52*, 145–154.
11. Molette, C., Berzaghi, P., Zotte, A.D., Remignon, H., and Babile, R. (2001) The Use of Near-Infrared Reflectance Spectroscopy in the Prediction of the Chemical Composition of Goose Fatty Liver, *Poult. Sci. 80*, 1625–1629.
12. Beattie, J.R., Bell, S.J., and Moss, B.W. (2004). A Critical Evaluation of Raman Spectroscopy for the Analysis of Lipids: Fatty Acid Methyl Esters, *Lipids 39*, 407–419.
13. Oakes, R.E., Beattie, J.R., Moss, B., and Bell, S.E.J. (2002) Conformations, Vibrational Frequencies and Raman Intensities of Short Chain Fatty Acid Methyl Esters Using DFT with 6-31 G(d) and Sadlej pVTZ Basis Sets, *J. Mol. Struct. 586*, 91–110.
14. Oakes, R.E., Beattie, J.R., Moss, B.W., and Bell, S.E.J. (2003)

DFT Studies of Long-Chain FAMES: Theoretical Justification for Determining Chain Length and Unsaturation from Experimental Raman Spectra, *J. Mol. Struct.–Theochem. 626*, 27–45.
15. Beattie, J.R., Bell, S.E.J., and Moss, B.W. (1999). Preliminary Investigation on the Use of Raman Spectroscopy to Characterise Adipose Tissue, in *45th International Congress of Meat Science and Technology*, (Beattie, J.R., Bell, S.E.J., and Moss, B.W., eds.) Vol. 2, pp. 668–669, Yokohama, Japan.
16. Fearon, A.M., Mayne, C.S., Beattie, J.A.M., and Bruce, D.W. (2004) Effect of Level of Oil Inclusion in the Diet of Dairy Cows at Pasture on Animal Performance and Milk Composition and Properties, *J. Sci. Food Agric. 84*, 497–504.
17. Princeton (1993) *CSMA*, 2.3a ed., Princeton Instruments.
18. AOCS, Iodine Value of Fats and Oils Cyclohexane Method, in *Official Methods and Recommended Practices of the American Oil Chemists' Society*, 4th edn., American Oil Chemists' Society, Champaign, 1990, Method Cd 1b-87.
19. Pearson, D. (1970) *Chemical Analysis of Food*, J&A Churchill, London, p. 510.
20. Sadeghi-Jorabchi, H., Hendra, P.J., Wilson, R.H., and Belton, P.S. (1990) Determination of the Total Unsaturation in Oils and Fats by Fourier Transform Raman Spectroscopy, *J. Am. Oil Chem. Soc. 67*, 483–486.
21. Butler, M., Salem, N., Hoss, W., and Spoonhower, J. (1979) Raman Spectral Analysis of the 1300 cm^{-1} Region for Lipid and Membrane Studies, *Chem. Phys. Lipids 29*, 99–102.
22. Snyder, R.G., Cameron, D.G., Casal, H.L., Compton, D.A.C., and Mantsch, H.H. (1982) Studies on Determining Conformational Order in *N*-Alkanes and Phospholipids from the 1130 cm^{-1} Raman Band, *Biochim. Biophys. Acta. 684*, 111–116.
23. Lawson, E.E., Anigbogu, A.N.C., Williams, A.C., Barry, B.W., and Edwards, H.G.M. (1998) Thermally Induced Molecular Disorder in Human Stratum Corneum Lipids Compared with a Model Phospholipid System: FT-Raman Spectroscopy, *Spectrochim. Acta Part A: Mol. Biomol. Spectrosc. 54*, 543–558.
24. Susi, H., Sampugna, J., Hampson, J.W., and Ard, J.S. (1979) Laser-Raman Investigation of Phospholipid–Polypeptide Interactions in Model Membranes, *Biochemistry 18*, 297–301.
25. Kint, S., Wermer, P.H., and Scherer, J.R. (1992) Raman Spectra of Hydrated Phospholipid Bilayers. 2. Water and Headgroup Interactions, *J. Phys. Chem. 96*, 446–452.

[Received July 23, 2004; accepted October 18, 2004]

Novel Ceramides and a New Glucoceramide from the Roots of *Incarvillea arguta*

Yinggang Luo[a], Jinhai Yi[a,b], Bogang Li[a], and Guolin Zhang[a,*]

[a]Chengdu Institute of Biology, Chinese Academy of Sciences, Chengdu 610041, People's Republic of China, and [b]Sichuan Institute of Chinese Materia Medica, Chengdu 610041, People's Republic of China

ABSTRACT: Novel ceramides, *rel*-(3*S*,4*S*,5*S*)-3-[(2*R*)-2-hydroxycosanoyl~hexacosanoylamino]-4-hydroxy-5-[(4*Z*)-tetradecane-4-ene]-2,3,4,5-tetrahydrofuran (**1a–g**), and a new glucoceramide, 1-*O*-β-D-glucopyranosyl-(2*S*,3*S*,4*R*,8*E*)-2-[(2*R*)-2-hydroxytetracosanoylamino]-1,3,4-octodecanetriol-8-ene (**2**) were isolated from the aqueous ethanolic extract of the roots of *Incarvillea arguta*, together with eight known compounds: β-sitosterol (**3**), oleanolic acid (**4**), ursolic acid (**5**), piperin (**6**), maslinic acid (**7**), β-sitosterol 6′-*O*-acyl-β-D-glucopyranoside (**8**), 8-epideoxyloganic acid (**9**), and plantarenaloside (**10**). Their structures were elucidated on the basis of spectral data including IR, MS, NMR [^{1}H NMR, ^{13}C NMR (distortionless enhancement by polarization transfer), ^{1}H-^{1}H COSY, heteronuclear multiple-quantum coherence, and heteronuclear multiple-bond coherence correlations]. The relative configurations were established by nuclear Overhauser effect spectroscopy experiments and by comparison of the NMR spectral data and coupling constants with those already reported in the literature.

Paper no. L9529 in Lipids 39, 907–913 (September 2004).

The genus *Incarvillea* (Bignoniaceae) is widely distributed over southwest China. Plants of this genus are used in Chinese folk medicine to treat rheumatism and to relieve pain (1). Previous chemical investigation of this genus led to the isolation of alkaloids with antinociceptive activity from *I. sinensis* and *I. delavayi* (2–13), iridoids and their glycosides (14,15) from *I. olgae*, and a novel monoterpene glycoside (dissectol A) from *I. dissectifoliola* (16,17). A bacteriostatic compound, argutone, together with ursolic acid and hentriacontane, was isolated from *I. arguta*, which is used to treat hepatitis and infectious diseases (18,19).

Sphingolipids are ubiquitous constituents of eukaryotic cells and have been intensively investigated in mammals and yeast for decades. However, the biochemical aspects of sphingolipids in plants have been explored only recently (20). Sphingolipids are essential not only as structural components of cell membranes but also as key players in different physiological and pathophysiological cellular events such as regulating the proliferation, survival, and death of cells (21,22). Plant glucosylceramides are also important structural components of plasma and vacuole membranes. In the last few years, progress has been made in the cloning of plant genes coding for enzymes involved in sphingolipid metabolism. As found in yeast and mammals, the plant sphingolipid pathway is a potential generator of powerful cell signals (23). Ceramide, generated by the action of acid sphingomyelinase, has emerged as a biochemical mediator of stimuli as diverse as ionizing radiation, chemotherapy, heat, and reperfusion injury as well as infection with some pathogenic bacteria and viruses. The manipulation of ceramide metabolites and/or the function of ceramide-enriched membrane platforms may present novel therapeutic opportunities for the treatment of cancer, degenerative disorders, pathogenic infections, or cardiovascular diseases (24).

Herein we report the isolation and structure elucidation of novel 1,4-dehydrated ceramides, *rel*-(3*S*,4*S*,5*S*)-3-[(2*R*)-2-hydroxycosanoyl~hexacosanoylamino]-4-hydroxy-5-[(4*Z*)-tetradecane-4-ene]-2,3,4,5-tetrahydrofuran (**1a–g**), a new glucoceramide,1-*O*-β-D-glucopyranosyl-(2*S*,3*S*,4*R*,8*E*)-2-[(2*R*)-2-hydroxytetracosanoylamino]-1,3,4-octodecanetriol-8-ene (**2**), and eight known compounds: β-sitosterol (**3**), oleanolic acid (**4**), ursolic acid (**5**), piperin (**6**), maslinic acid (**7**), β-sitosterol 6′-*O*-acyl-β-D-glucopyranoside (**8**), 8-epideoxyloganic acid (**9**), and plantarenaloside (**10**) from the aqueous ethanolic extract of roots of *I. arguta*.

EXPERIMENTAL PROCEDURES

Instrumentation. Melting points were recorded on an XRC-1 apparatus (Sichuan University Scientific Instrument Factory, Sichuan University, People's Republic of China) and are uncorrected. Optical rotations were measured with a PerkinElmer 341 automatic polarimeter (Beaconsfield, United Kingdom). IR spectra were recorded on a PerkinElmer Spectrum One spectrometer. NMR spectra [^{1}H, ^{13}C distortionless enhancement by polarization transfer (DEPT), ^{1}H-^{1}H COSY, heteronuclear multiple-quantum coherence (HMQC), heteronuclear multiple-bond coherence (HMBC), and nuclear Overhauser effect spectroscopy (NOESY) experiments] were obtained on a Bruker Avance 500 (Bruker, Rheinstetten, Germany) at 500 MHz for ^{1}H NMR and at 125 MHz for ^{13}C NMR. Chemical shifts (δ) are given in parts per million (ppm) relative to tetramethylsilane as

*To whom correspondence should be addressed at Chengdu Institute of Biology, Chinese Academy of Sciences, P.O. Box 416, Chengdu 610041, P.R. China. E-mail address: ZHANGGL@cib.ac.cn

Abbreviations: CC, column chromatography, DEPT, distortionless enhancement by polarization transfer; Fr., fraction; Gly, glucosyl; HMBC, (^{1}H-detected) heteronuclear multiple-bond correlation; HMQC, (^{1}H-detected) heteronuclear multiple-quantum coherence; HRAPCIMS, high-resolution atmospheric pressure chemical ionization mass spectrum; NOESY, nuclear Overhauser effect spectroscopy.

internal standard and coupling constants in hertz (Hz). FABMS was carried out on a VG AutoSpec-3000 (glycerol as matrix; VG, Manchester, England). High-resolution atmospheric pressure chemical ionization mass spectra (HRAPCIMS) were obtained on a Bruker FTMS APEX3 mass spectrometer. Spots on TLC plates were visualized by spraying with Dragendorff's reagent and by spraying with 8% phosphomolybdic acid/ethanol solution followed by heating.

Materials. Silica gel for column chromatography (CC) (200–300 mesh) and for TLC plates (10–40 μm) was purchased from Qingdao Marine Chemical Ltd. (Qingdao, People's Republic of China).

The roots of *I. arguta* were collected from Mengwen County, Sichuan Province, People's Republic of China, in August 1998 and identified by Professor Shunchang Xiao (Chengdu Institute of Biology, the Chinese Academy of Sciences). A voucher specimen (Y-98-004) is deposited at the Herbarium of Chengdu Institute of Biology, the Chinese Academy of Sciences (Chengdu 610041, People's Republic of China).

Extraction and isolation. The dried and powdered roots (2.2 kg) were soaked with 95% EtOH (10 L × 3) at room temperature. After removing solvent under reduced pressure, the residue was successively partitioned between H_2O and EtOAc, and then partitioned between H_2O and *n*-BuOH, to provide an ethyl acetate-soluble fraction (22 g), and the *n*-BuOH extract, respectively. The EtOAc-soluble fraction was divided into eight fractions (Fr. 1–8) by CC using gradient elution with $CHCl_3$/MeOH (10:0–10:3, vol/vol). Fr. 3 was further separated by CC by elution with petroleum ether (b.p. 60–90°C)/EtOAc (10:2, vol/vol) to yield compounds **3** (57 mg), **4** (39 mg), and **5** (46 mg). Compound **6** (30 mg) was crystallized from the petroleum ether/EtOAc (1:1, vol/vol) solution of fraction (Fr. 4). Compounds **1a–g** (6 mg), **7** (23 mg), and **8** (25 mg) were obtained from Fr. 5 by CC by elution with $CHCl_3$/MeOH (10:0.5, vol/vol). The *n*-BuOH extract (35 g) was separated on a silica gel column eluted with the lower layer of $CHCl_3$/MeOH/H_2O (13:6:2, by vol) and further separated by reversed-phase chromatography (C-18) eluted with MeOH/H_2O (1:1, vol/vol) to yield compounds **2** (8 mg), **9** (41 mg), and **10** (28 mg).

rel-(*3*S,*4*S,*5*S)-*3*-[(*2*R)-*2-Hydroxycosanoyl~hexacosanoylamino]-4-hydroxy-5-[(4Z)-tetradecane-4-ene]-2,3,4,5-tetrahydrofuran (**1a–g**).* White powder; m.p. 202–204°C,$[\alpha]_D^{20}$ +9.2° [*c* 0.1, $CHCl_3$/MeOH (1:1, vol/vol)]. IR ν_{max}^{KBr} (cm^{-1}): 3392 (OH), 2924, 2854, 1643 and 1535 (C=O of amide), 1469, 1378, 1260, 1167, 1079, 1037, and 719. ^1H and ^{13}C NMR data, see Table 1. FABMS (positive ion mode) *m/z* (rel. int.): 692 ([M**g** + H]$^+$, 10), 678 ([M**f** + H]$^+$, 40), 664 ([M**e** + H]$^+$, 100), 650 ([M**d** + H]$^+$, 60), 636 ([M**c** + H]$^+$, 50), 622 ([M**b** + H]$^+$, 10) and 608 ([M**a** + H]$^+$, 5), 397 ([M**g** – sphingoid moiety + 2H]$^+$, 80), 383 ([M**f** – sphingoid moiety + 2H]$^+$, 20), 369 ([M**e** – sphingoid moiety + 2H]$^+$, 20), 355 ([M**d** – sphingoid moiety+ 2H]$^+$, 30), 341 ([M**c** – sphingoid moiety + 2H]$^+$, 30), 327 ([M**b** – sphingoid moiety + 2H]$^+$, 55), 313

TABLE 1
NMR Spectral Data of Compounds 1a–g in C_5D_5N

No.[a]	δ_H [b,c]	δ_C [b,c]	^1H-^1H COSY	HMBC	NOESY
2	4.51 (1H, *dd*, *J* = 15.0, 8.0 Hz) 3.92 (1H, *dd*, *J* = 15.0, 7.5 Hz)	71.6 (*t*)	H-3	C-3, C-4, C-5	H-3
3	4.77 (1H, *m*)	51.8 (*d*)	H-2, H-4	C-1′, C-5	H-2, H-4
4	4.30 (1H, *dd*, *J* = 6.5, 4.0 Hz)	74.6 (*d*)	H-3, H-5	C-2, C-3, C-5, C-1″	H-3, H-5
5	4.13 (1H, *dt*, *J* = 7.0, 5.0 Hz)	86.0 (*d*)	H-4, H-1″	C-4, C-2″	H-4
1″	1.98 (1H, *m*) 2.22 (1H, *m*)	33.8 (*t*)	H-5, H-2″	C-2″	
2″	1.97 (1H, *m*) 2.03 (1H, *m*)	26.4 (*t*)	H-1″, H-3″		
3″	1.99 (1H, *m*) 2.13 (1H, *m*)	32.8 (*t*)*	H-2″, H-4″		
4″	5.45 (1H, *dt*, *J* = 5.5, 2.5 Hz)	130.3 (*d*)**	H-3″, H-5″	C-2″, C-3″, C-5″	
5″	5.44 (1H, *dt*, *J* = 5.5, 2.5 Hz)	131.0 (*d*)**	H-4″, H-6″	C-3″, C-4″, C-6″	
6″	2.00 (1H, *m*) 2.19 (1H, *m*)	32.9 (*t*)*	H-5″	C-4″, C-5″	
7″-13″ and 5′-25′	1.21–1.32 (about 60 H, *m*)	22.9, 29.5–30.0, 32.1			
14″	0.84 (3H, *t*, *J* = 6.5 Hz)	14.3 (*q*)			
-NH	8.49 (1H, *d*, *J* = 7.5 Hz)		H-3	C-3, C-4, C-1′	H-3
1′		175.5 (*s*)			
2′	4.63 (1H, *dd*, *J* = 7.5, 3.5 Hz)	72.5 (*d*)	H-3′	C-1′, C-3′, C-4′	
3′	1.99 (1H, *m*) 2.15 (1H, *m*)	35.6 (*t*)	H-2′, H-4′		
4′	1.96 (2H, *m*)	25.8 (*t*)	H-3′		
26′	0.83 (3H, *t*, *J* = 6.5 Hz)	14.3 (*q*)			

[a]Numbers correspond to atoms in Figure 1.
[b]Signals were assigned by heteronuclear multiple-quantum coherence (HMQC), heteronuclear multiple-bond coherence (HMBC), and ^1H-^1H COSY experiments. *,** Signals having the same superscript could be interchangeable.
[c]Multiplicity was determined by distortionless enhancement by polarization transfer (DEPT); NOESY, nuclear Overhauser effect spectroscopy.

([M**a** — sphingoid moiety + 2H]$^+$, 26), 298 ([sphingoid moiety + 2H]$^+$, 10), 207, 177, and 147.

1-O-β-D-Glucopyranosyl-(2S,3S,4R,8E)-2-[(2R)-2-hydroxytetracosanoylamino]-1,3,4-octodecanetriol-8-ene (**2**). White powder; m.p. 203–205°C, $[\alpha]_D^{20}$ + 12.7° [*c* 0.1, $CHCl_3$/MeOH (1:1, vol/vol)]. IR ν_{max}^{KBr} (cm^{-1}): 3350 (–OH), 2920, 2851, 1624 and 1537 (C=O of amide), 1468, 1433, 1113, 1082, 1038, and 964. ^{1}H and ^{13}C NMR data, see Table 2. HRAPCIMS (positive ion mode) *m/z*: 867.6810 ($C_{48}H_{94}NO_{10}Na$, required for 867.6775, 3.4561 mDa error, 3.9831 ppm error). FABMS (positive ion mode) *m/z* (rel. int.): 844 ([M + H]$^+$, 35), 682 ([M – Glc + H]$^+$, 10), 478 ([M – Clc – FA moiety + 2H)$^+$, 5), 317 ([M – FA moiety + 2H)$^+$, 100), 299 ([sphingoid moiety + H]$^+$, 35), and 167 ([$CH_3(CH_2)_7CH_2CH{=}CHCH_2$]$^+$, 5).

RESULTS AND DISCUSSION

Compounds **1a–g** were obtained as a white powder. On TLC plates they appeared orange when reacted with Dragendorff's reagent. The FABMS (positive ion mode) of compounds **1a–g** showed seven quasi-molecular ion peaks that were 14 amu apart (*m/z* 692, 678, 664, 650, 636, 622, and 608, corresponding to $C_{38}H_{73}NO_4$ + n CH_2, n = 0–7), which suggested that **1a–g** was a mixture of homologs. The IR peak at 3392 cm^{-1} suggested the presence of hydroxyl groups. A secondary amide carbonyl group was deduced from the IR absorption at 1643 and 1535 cm^{-1} and the ^{13}C NMR signals (Table 1) at δ 175.5 (*s*, C-1′). The ^{1}H NMR signal (Table 1) at δ 8.49 (1 H, *d*, *J* = 7.5 Hz) suggested an amino group. A *Z*-disubstituted double bond was established by the ^{1}H NMR signals (Table 1) at δ 5.45 and 5.44 (each 1 H, *dt*, *J* = 5.5, 2.5 Hz, H-4″ and H-5″). The ^{13}C NMR signals (Table 1) at δ 86.0 (*d*, C-5), 74.6 (*d*, C-4), 72.5 (*d*, C-2′), and 71.6 (*t*, C-2) suggested the presence of four oxygenated carbons, which was confirmed by the HMQC correlations between δ 4.13 (1 H, *dt*, *J* = 7.0, 5.0 Hz) and 86.0 (*d*), between 4.30 (1 H, *dd*, *J* = 6.5, 4.0 Hz) and 74.6 (d), between 4.63 (1 H, *dd*, J = 7.5, 3.5 Hz) and 72.5 (*d*) and between 4.51 (1 H, *dd*, *J* = 15.0, 8.0 Hz), and 3.92 (1 H, *dd*, *J* = 15.0, 7.5 Hz) and 71.6 (*t*). The ^{13}C NMR signal (Table 1) at δ 51.8 should be assigned to the carbon atom substituted by a nitrogen atom considering the HMQC cross signal at δ 4.77 (1 H, *m*)/51.8 (*d*, C-3). The presence of methyl groups and long aliphatic chain was concluded from the ^{1}H NMR signals (Table 1) at δ 0.84 and 0.83 (each 3 H, *t*, *J* = 6.5 Hz) and 1.21–1.32 (about 60 H, *m*) and the ^{13}C NMR signals

TABLE 2
NMR Spectral Data of Compound 2 in C_5D_5N

No.[a]	δ_H[b,c]	δ_C[b,c]	^{1}H-^{1}H COSY	HMBC
1	4.69 (1H, *dd*, *J* = 10.2, 6.6 Hz) 4.52 (1H, *dd*, *J* = 10.2, 6.6 Hz)	70.5 (*t*)	H-2	C-2, C-3, C-1″
2	5.27 (1H, *m*)	51.9 (*d*)	H-1, H-3	C-1, C-3
3	4.28 (1H, *t*, *J* = 5.2 Hz)	76.0 (*d*)	H-2, H-4	C-1, C-2, C-4, C-5
4	4.18 (1H, *m*)	72.5 (*d*)	H-3, H-5	C-3, C-6
5	1.99 (1H, *m*) 2.18 (1H, *m*)	33.9 (*t*)	H-4, H-6	C-6
6	1.96 (1H, *m*) 2.05 (1H, *m*)	26.8 (*t*)	H-5, H-7	
7	1.99 (1H, *m*) 2.15 (1H, *m*)	33.0 (*t*)*	H-6, H-8	
8	5.52 (1H, *dt*, *J* =16.0, 6.0 Hz)	130.7 (*d*)**	H-7, H-9	C-6, C-7, C-9
9	5.47 (1H, *dt*, *J* =16.0, 6.0 Hz)	130.9 (*d*)**	H-8, H-10	C-7, C-8, C-10
10	2.06 (1H, *m*) 2.16 (1H, *m*)	33.3 (*t*)*	H-9	C-8, C-9
11-17 and 5′-23′	1.23–1.30 (about 52H, *m*)	22.9, 29.6–30.0, 32.1		
18	0.84 (3H, *t*, *J* = 6.6 Hz)	14.3 (*q*)		
–NH	8.54 (1H, *d*, *J* = 8.8 Hz)		H-2	C-2, C-1′
1′		175.6 (*s*)		
2′	4.55 (1H, *dd*, *J* = 7.2, 3.6 Hz)	72.5 (*d*)	H-3′	C-1′, C-3′, C-4′
3′	1.99 (1H, *m*) 2.15 (1H, *m*)	35.6 (*t*)	H-2′, H-4′	
4′	1.96 (2H, *m*)	25.9 (*t*)	H-3′	
24′	0.83 (3H, *t*, *J* = 7.3 Hz)	14.3 (*q*)		
1″	4.94 (1H, *d*, *J* = 7.2 Hz)	105.6 (*d*)	H-2″	C-1, C-3″
2″	3.98 (1H, *t*, *J* = 7.8 Hz)	75.2 (*d*)	H-1″, H-3″	C-1″, C-3″
3″	3.85 (1H, *brs*)	78.5 (*d*)	H-2″, H-4″	C-2″, C-4″
4″	4.16 (1H, *m*)	71.6 (*d*)	H-3″, H-5″	C-2″, C-3″
5″	4.16 (1H, *m*)	78.5 (*d*)	H-4″, H-6″	C-3″, C-6″
6″	4.31 (1H, *dd*, *J* = 12.8, 6.5 Hz) 4.46 (1H, *d*, *J* = 12.8 Hz)	62.8 (*t*)	H-5″	C-5″

[a]Numbers correspond to atoms in Figure 1.
[b]Signals were assigned by HMQC, HMBC, and ^{1}H-^{1}H COSY experiments. *,** Signals having the same superscript could be interchangeable.
[c]Multiplicity was determined by DEPT. For abbreviations see Table 1.

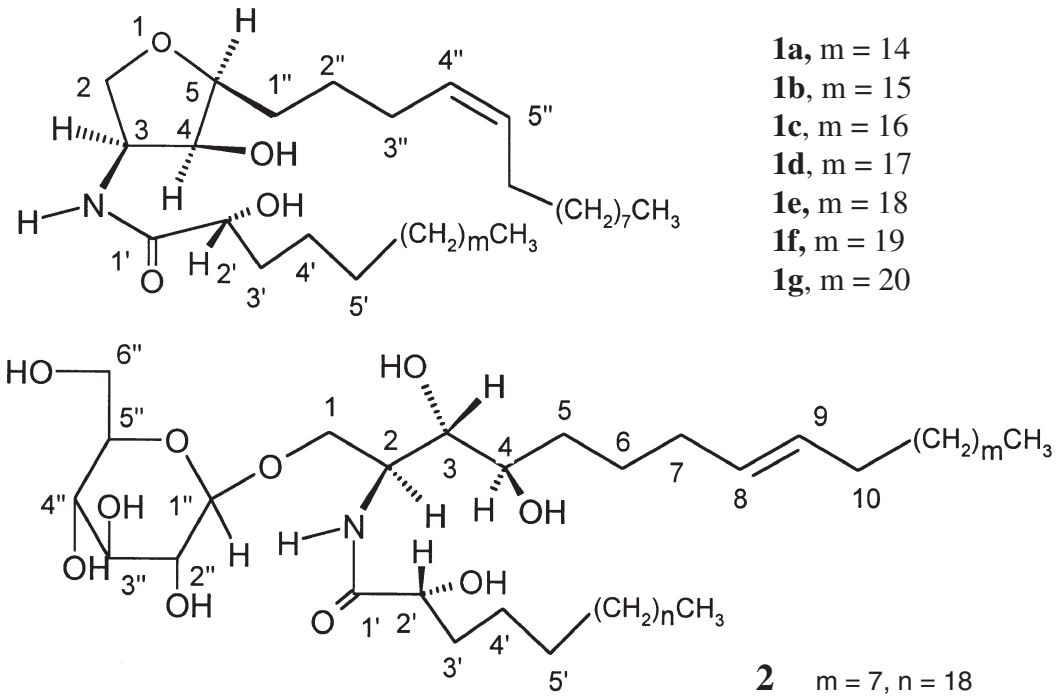

FIG. 1. The structures of compounds **1a–g** and **2**.

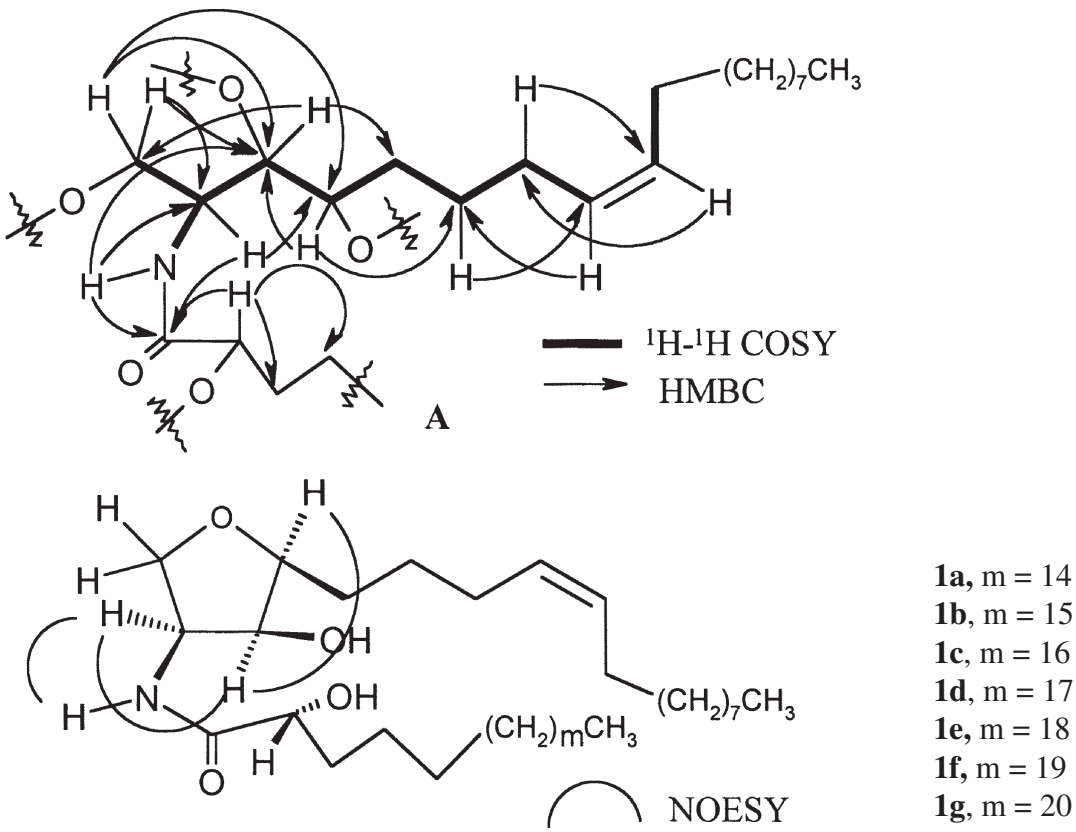

FIG. 2. The key heteronuclear multiple-bond coherence (HMBC) and nuclear Overhauser effect spectroscopy (NOESY) correlations of compounds **1a–g**.

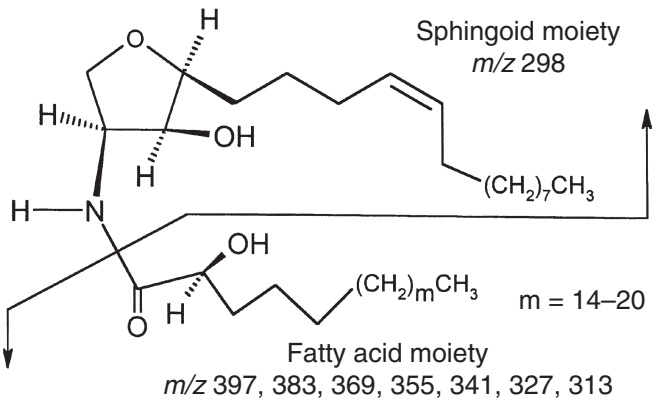

FIG. 3. The proposed fragmentation in the FABMS of compounds **1a–g**.

at δ 14.3 (*q*), and 29.5–30.0, respectively. The spectral data just discussed suggest that compounds **1a–g** should be ceramides possessing a 2-hydroxy fatty acyl moiety (Fig. 1).

Skeleton structure **A** was deduced from the ^{1}H-^{1}H COSY, HMQC, and HMBC correlations (Fig. 2, Table 1). C-2 and C-5 should be connected *via* an ether bond considering the key HMBC correlation between δ 4.51 (1 H, *dd*, *J* = 15.0, 8.0 Hz, Ha-2) and 86.0 (*d*, C-5) and the HMQC cross signal at δ 4.13 (1 H, *dt*, *J* = 7.0, 5.0 Hz)/86.0 (*d*, C-5) (Fig. 2), which suggested that compounds **1a–g** should be novel 1,4-dehydrated ceramides (Fig. 1). The *Z*-double bond was unambiguously assigned at C-4″ and C-5″ by ^{1}H-^{1}H COSY, HMQC, and HMBC correlations (Fig. 2).

The sphingoid base, 1,4-dehydrated 2-amino-1,3,4-trihydroxy-octadecane-8-ene (2-amino-4-hydroxy-5-[(4*Z*)-tetradecane-4-ene]-2,3,4,5-tetrahydrofuran) was postulated from the characteristic fragment ion peaks at *m/z* 298 (Fig. 3) (25). The ion peaks at *m/z* 397 ([M**g** – sphingoid moiety + 2H]$^{+}$), 383 ([M**f** – sphingoid moiety + 2H]$^{+}$), 369 ([M**e** – sphingoid moiety + 2H]$^{+}$), 355 ([M**d** – sphingoid moiety + 2H]$^{+}$), 341 ([M**c** – sphingoid moiety + 2H]$^{+}$), 327 ([M**b** – sphingoid moiety + 2H]$^{+}$), and 313 ([M**a** – sphingoid moiety + 2H]$^{+}$) suggested that m is 14–20 (Fig. 3).

The relative configurations of C-3, -4, and -5 were presumed as *S*, *S*, and *S*, respectively, which was confirmed from the NOESY cross signals (Table 1) between H-2 and H-3, between H-3 and H-4, between H-4 and H-5, and between –NH– and H-3 and by the coupling constants for those *cis*-protons (*J* < 7.2 Hz) at tetrahydrofuran (for *trans*-protons, *J* > 7.2 Hz) (26,27). The relative configuration of C-2′ was determined to be *R* by comparing the chemical shift and coupling constants of H-2′ with previously reported data (28–30). Thus, compounds **1a–g** could be elucidated as *rel*-(3*S*,4*S*,5*S*)-3-[(2*R*)-2-hydroxycosanoyl~hexacosanoylamino]-4-hydroxy-5-[(4*Z*)-tetradecane-4-ene]-2,3,4,5-tetrahydrofuran (Fig. 1). The complete assignments of proton and carbon signals (Table 1) were achieved by ^{1}H-^{1}H COSY, HMQC, and HMBC correlations.

Compound **2** was obtained as a white powder. The orange color on TLC with Dragendorff's reagent and the quasi-molecular ion peak at *m/z* 844 ([M + H]$^{+}$) in the FABMS (positive ion mode) suggested the presence of an odd nitrogen atom. The molecular formula $C_{48}H_{94}NO_{10}Na$ was calculated from the quasi-molecular ion peak at *m/z* 867.6810 in the HRAPCIMS of **2**. The ion peak at *m/z* 682 ([M + H – Glc]$^{+}$) and the six ^{13}C NMR signals (Table 2) at δ 105.6 (*d*, C-1″), 75.2 (*d*, C-2″), 78.5 (*d*, C-3″), 71.6 (*d*, C-4″), 78.5 (*d*, C-5″), and 62.8 (*t*, C-6″) indicated the presence of a glucosyl moiety, which was confirmed by hydrolyzing **2** in 10% HCl (aqueous) solution. The ^{1}H NMR signal (Table 2) at δ 4.94 (1 H, *d, J* = 7.2 Hz, H-1″) showed that it is the β-D-glucopyranosyl moiety. A secondary amide carbonyl group was deduced from the IR absorptions at 1624 and 1537 cm^{-1} and the ^{13}C NMR signal (Table 2) at δ 175.6 (*s*, C-1′). The ^{1}H NMR signal (Table 2) at δ 8.54 (1 H, *d*, *J* = 8.8 Hz) suggested an amino group. An *E*-disubstituted double bond was established by the ^{1}H NMR signals (Table 2) at δ 5.52 and 5.47 (each 1 H, *dt*, *J* = 16.0, 6.0 Hz, H-8 and H-9) and the IR absorption peak at 964 cm^{-1} (25). The ^{13}C NMR signals (Table 2) at δ 70.5 (*t*, C-1), 76.0 (*d*, C-3), and 72.5 (*d*, C-2′) suggested three oxygenated carbons. The ^{13}C NMR signal (Table 2) at δ 51.9 should be assigned to the carbon atom substituted by a nitrogen atom considering the HMQC cross-signal at δ 5.27 (1 H, *m*)/51.9 (*d*, C-2). The presence of methyl groups and a long-chain alkyl moiety was concluded from the ^{1}H NMR signals (Table 2) at δ 0.84 and 0.83 (each 3 H, *t, J* = 6.6 Hz) and 1.23–1.30 (about 52 H, *m*). Thus, compound **2** should be a glucoceramide.

The structure of compound **2** was concluded from the ^{1}H-^{1}H COSY, HMBC, and HMQC correlations (Table 2, Fig. 4). The ion peaks at *m/z* 478 ([M – FA moiety + 2H]$^{+}$) and 317 ([M – Glc – FA + H]$^{+}$) in the FABMS of compound **2** suggested that the FA chain is 2-hydroxytetracosanoyl. The sphingoid base, 2-amino-1,3,4-trihydroxy-octadecane-8-ene, was determined by the characteristic fragment ion peaks at *m/z* 299 ([sphingoid moiety + H]$^{+}$) and 167 ([$CH_3(CH_2)_7CH_2CH$=CH-CH_2]$^{+}$) (25).

The stereochemistry of C-2, -3, -4, and -2′ were determined to be *S, S, R*, and *R*, respectively, by comparing the ^{13}C NMR data and the optical rotation with those of compounds **11** and **12** (Table 3, Fig. 4) (30,31). The chemical shifts and the coupling constants of H-1, H-2, H-3, H-4, and H-2′ were in good agreement with those of the natural ceramide (31), supporting the above conclusion. Thus, the structure of **2** was determined as 1-*O*-β-D-glucopyranosyl-(2*S*,3*S*,4*R*,8*E*)-2-[(2*R*)-2-hydroxy-tetracosanoylamino]-1,3,4-octodecanetriol-8-ene (Fig. 1).

Recent studies show that various sphingolipids are being viewed as bioactive molecular and/or second messengers in different signal transduction pathways. In general, ceramides behave as pro-apoptotic mediators and mediate the death signal initiated by numerous stress agents, which either stimulate its *de novo* synthesis or activate sphingomyelinases that release ceramide from sphingomyelin (32–34). Ceramide itself produces apoptosis, but metabolic conversion of ceramide into either sphingosine 1-phosphate or glucosphingolipids leads to cell proliferation. The balance between these two aspects is missing in cancer cells, and yet intervention by stimulating or blocking only one or two of the pathways in a ceramide metabolite is very likely

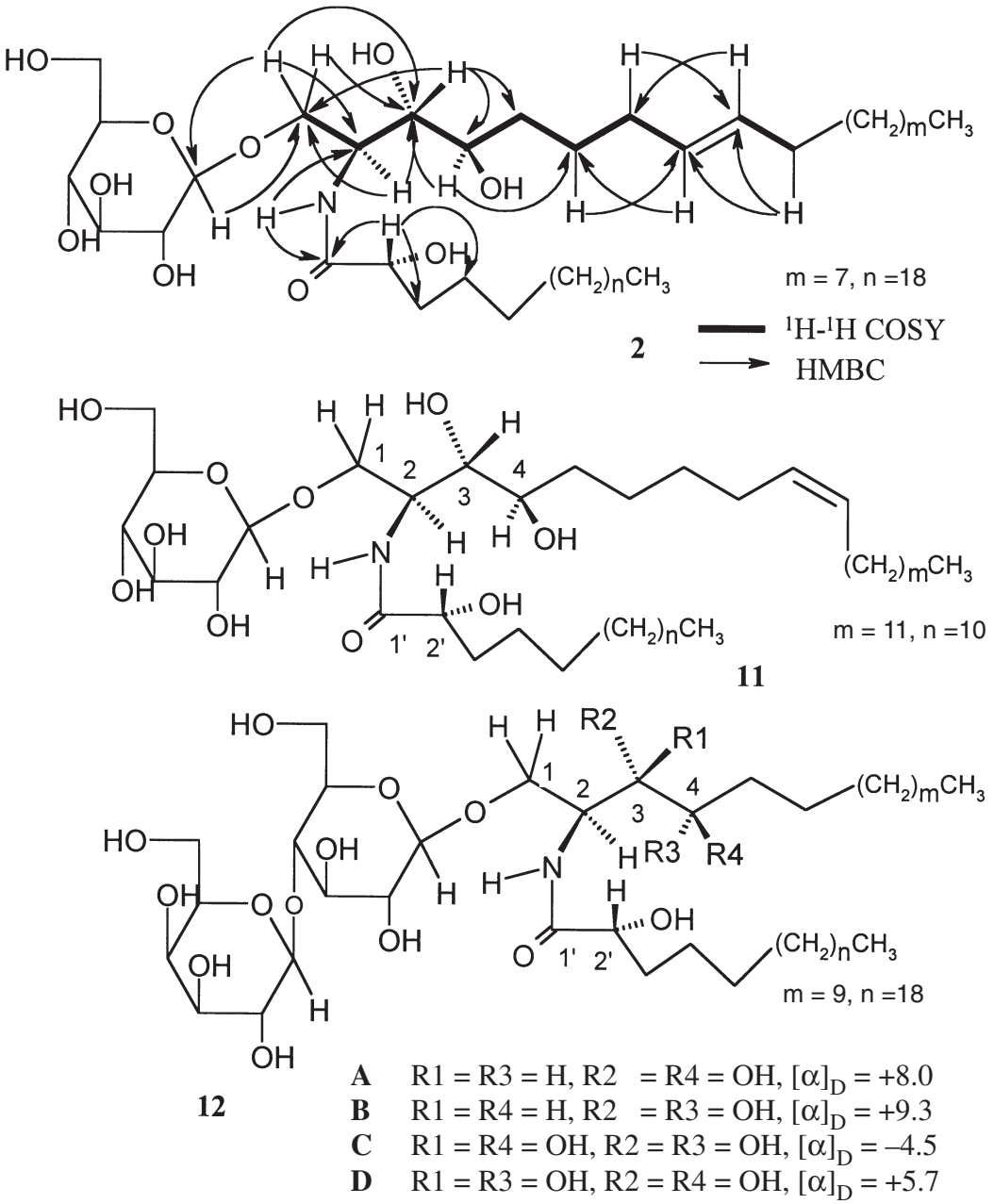

FIG. 4. The key HMBC and ^{1}H-^{1}H COSY correlations of compound **2**, and the structures and the optical rotations of compounds **11** and **12**.

TABLE 3
^{13}C NMR Chemical Shifts (δ values) of Compounds 2, 11, and 12 in C_5D_5N[a]

C	**2**	**11**[31]	**12A**[30]	**12B**[30]	**12C**[30]	**12D**[30]
1 (*t*)	70.5	70.5	70.3	70.3	70.9	70.7
2 (*d*)	51.9	51.7	51.6	52.2	50.4	50.5
3 (*d*)	76.0	75.8	75.8	75.2	75.2	75.2
4 (*d*)	72.5	72.4	72.6	73.0	73.3	72.5
=CH(*d*)	130.7	130.3	—	—	—	—
=CH(*d*)	130.9	130.1	—	—	—	—
1′ (*s*)	175.6	175.7	175.6	177.1	175.3	176.6
2′ (*d*)	72.5	72.4	72.6	72.3	72.5	71.6
CH_3 (*q*)	14.3	14.3	14.3	14.3	14.3	14.3

[a]Superscripts on column heads refer to reference numbers.

to fail. This may lead to the development of practical chemotherapy for cancer and other diseases of excess proliferation (35). Thus, those novel ceramides and glucoceramide may be the active components to treat hepatitis and infectious diseases.

The known compounds, piperin (**6**) (36), maslinic acid (**7**) (37), β-sitosterol 6′-*O*-acyl-β-D-glucopyranoside (**8**) (38), 8-epideoxyloganic acid (**9**) (39), and plantarenaloside (**10**) (40) were identified by their spectral data and by comparing their spectral data with those reported. β-Sitosterol (**3**), oleanolic acid (**4**), and ursolic acid (**5**) were identified by their spectral data and by co-TLC with authentic samples.

REFERENCES

1. Jiangsu New Medical College (1995) *Dictionary of Traditional Chinese Medicine*, pp. 2343, and 2437, Shanghai Science and Technology Press, Shanghai.
2. Chi, Y.M., Yan, W.M., and Li, J.S. (1990) An Alkaloid from *Incarvillea sinensis, Phytochemistry 29,* 2376–2378.
3. Chi, Y.M., Yan, W.M., Chen, D.C., Hiroshi, N., Yoichi, I., and Ushio, S. (1992) A Monoterpene Alkaloid from *Incarvillea sinensis, Phytochemistry 31,* 2930–2932.
4. Chi, Y.M., Hashimoto, F., Yan W.M., and Nohara, T. (1995) Incarvine A, a Monoterpene Alkaloid from *Incarvillea sinensis, Phytochemistry 40,* 353–354.
5. Chi, Y.M., Hashimoto, F., Yan, W.M., and Nohara, T. (1995) Two Alkaloids from *Incarvillea sinensis, Phytochemistry 39,* 1485–1487.
6. Chi, Y.M., Hashimoto, F., Yan, W.M., Nohara, T., Yamashita, M., and Marubayashi, N. (1997) Monoterpene Alkaloids from *Incarvillea sinensis*. VI. Absolute Stereochemistry of Incarvilline and Structure of a New Alkaloid, Hydroxyincarvilline, *Chem. Pharm. Bull. 45,* 495–498.
7. Chi, Y.M., Hashimoto, F., Yan, W.M., and Nohara, T. (1997) Five Novel Macrocyclic Spermine Alkaloids from *Incarvillea sinensis, Tetrahedron Lett. 38,* 2713–2716.
8. Chi, Y.M., Hashimoto, F., Yan, W.M., and Nohara, T. (1997) Four Monoterpene Alkaloid Derivatives from *Incarvillea sinensis, Phytochemistry 46,* 763-769.
9. Nakamura, M., Chi, Y.M., Yan, W.M., Nakasugi, Y., Yoshizawa, T., Irino, N., Hashimoto, F., Kinjo, J., Nohara, T., and Sakurada, S. (1999) Strong Antinociceptive Effect of Incarvillateine, a Novel Monoterpene Alkaloid from *Incarvillea sinensis, J. Nat. Prod. 62,* 1293–1294.
10. Nakamura, M., Chi, Y.M., Kinjo, J., Yan, W.M., and Nohara, T. (1999) Two Monoterpene Alkaloidal Derivatives from *Incarvillea sinensis, Phytochemistry 51,* 595–597.
11. Nakamura, M., Kido, K., Kinjo, J., and Nohara, T. (2000) Antinociceptive Substances from *Incarvillea delavayi, Phytochemistry 53,* 253–256.
12. Nakamura, M., Kido, K., Kinjo, J., and Nohara, T. (2000) Two Novel Actinidine-type Monoterpene Alkaloids from *Incarvillea delavayi, Chem. Pharm. Bull. 48,* 1826–1827.
13. Nakamura, M., Chi, Y.M., Yan, W.M., Yonezawa, A., Nakasugi, Y., Yoshizawa, T., Hashimoto, F., Kinjo, J., Nohara, T., and Sakurada, S. (2001) Structure–Antinociceptive Activity Studies of Incarvillateine, a Monoterpene Alkaloid from *Incarvillea sinensis, Planta Med. 67,* 114–117.
14. Maksudov, M.S., Umarova, R.U., Tashkhodzhaev, B., Saatov, Z., and Abdullaev, N.D. (1995) Iridoid Glycosides of the Genus *Incarvillea.* I. 7-*O*-Benzoyltecomoside, *Khim. Prir. Soedin*, 61– 69.
15. Maksudov, M.S., Faskhutdinov, M.F., Umarova, R.U., and Saatov, Z. (1995) Iridoids of *Incarvillea olgae* and *Dadartia orientalis, Khim. Prir. Soedin.* 751–752.
16. Chen, W., Shen, Y.M., and Xu, J.C. (2003) Dissectol A, a Novel Monoterpene Glycoside from *Incarvillea dissectifoliola, Chin. Chem. Lett. 14,* 385–388.
17. Chen, W., Shen, Y.M., and Xu, J.C. (2003) Dissectol A, an Unusual Monoterpene Glycoside from *Incarvillea dissectifoliola, Planta Med. 69,* 579–582.
18. Yang, M.K., Tang, Y.S., Cai, L.M., Xie, J.X., Shen, F.C., Lin, X.Y., and Zheng, Q.T. (1987) The Isolation and Structure of Argutone, a New Bacteriostatic Constituent of *Incarvillea arguta, Yaoxue Xuebao 22,* 711–715.
19. Yang, M.K., Tang, Y.S., Liao, R.H., Huang, Z.M., Ran, C.X., Yang, Q.L., and Cai, L.M. (1981) Studies on the Chemical Constituents of *Incarvillea arguta, Zhongcaoyao 12,* 489–490.
20. Lynch, D.V., and Dunn, T.M. (2004) An Introduction to Plant Sphingolipids and a Review of Recent Advances in Understanding Their Metabolism and Function, *New Phytol. 161,* 677–702.
21. Reynolds, C.P., Maurer, B.J., and Kolesnick, R.N. (2004) Ceramide Synthesis and Metabolism as a Target for Cancer Therapy, *Cancer Lett. 206,* 169–180.
22. Cinque, B., Di Marzio, L., Centi, C., Di Rocco, C., Riccardi, C., and Grazia Cifone, M. (2003) Sphingolipids and the Immune system, *Pharma. Res. 47,* 421–437.
23. Spassieva, S., and Hille, J. (2003) Plant Sphingolipids Today. Are They Still Enigmatic? *Plant Biol. 5,* 125–136.
24. Gulbins, E., and Kolesnick, R. (2003) Raft Ceramide in Molecular Medicine, *Oncogene 22,* 7070–7077.
25. Kraus, R., and Spiteller, G. (1991) Ceramides from *Urtica dioica* Roots, *Liebigs Ann. Chem.,* 125–128.
26. Martins, R.C.C., Lago, J.H.G., Albuquerque, S., and Kata, M.J. (2003) Trypanocidal Tetrahydrofuran Lignans from Inflorescences of *Piper solmsianum, Phytochemistry 64,* 667–670.
27. López, H., Valera, A., and Trujillo, J. (1995) Lignans from *Ocotea foetens, J. Nat. Prod. 58,* 782–785.
28. Gao, J.M., Dong, Z.J., and Liu, J.K. (2001) A New Ceramide from the Basidiomycete *Russula cyanoxantha, Lipids 36,* 175–180.
29. Zhan, Z.J., and Yue, J.M. (2003) New Glyceroglycolipid and Ceramide from *Premna microphylla, Lipids 38,* 1299–1303.
30. Sugiyama, S., Honda, M., Higuchi, R., and Komori, T. (1991) Stereochemistry of the Four Diastereomers of Ceramide and Ceramide Lactoside, *Liebigs Ann. Chem.,* 349–356.
31. Higuchi, R., Natori, T., and Komori, T. (1991) Isolation and Characterization of Acanthacerebroside B and Structure Elucidation of Related, Nearly Homogeneous Cerebrosides, *Liebigs Ann. Chem.,* 51–55.
32. Cuvillier, O., Andrieu-Abadie, N., Segui, B., Malagarie-Cazenave, S., Tardy, C., Bonhoure, E., and Levade, T. (2003) Sphingolipid-Mediated Apoptotic Signalling Pathways, *J. Soc. Biol. 197,* 217–221.
33. Angel, I., Bar, A., and Haring, R. (2002) Bioactive Lipids and Their Receptors, *Curr. Opin. Drug Discov. Devel. 5,* 728–740.
34. Kolesnick, R., and Fuks, Z. (2003) Radiation and Ceramide-Induced Apoptosis, *Oncogene 22,* 5897–5906.
35. Radin, N.S. (2003) Killing Tumours by Ceramide-Induced Apoptosis: A Critique of Available Drugs, *Biochem. J. 371,* 243–256.
36. Wenkert, E., Cochran, D.W., Hagaman, E.W., Lewis, R.B., and Schell, F.M. (1971) Carbon-13 Nuclear Magnetic Resonance Spectroscopy with the Aid of a Paramagnetic Shift Agent, *J. Am. Chem. Soc. 93,* 6271–6273.
37. Kuang, H.X., Kasai, R., Ohtani, K., Liu, Z.S., Yuan, C.S., and Tanaka, O. (1989) Chemical Constituents of Pericarps of *Rosa davurica* Pall., a Traditional Chinese Medicine, *Chem. Pharm. Bull. 37,* 2232–2233.
38. Sakakibara, J., Kaiya, T., Fukuda, H., and Ohki, T. (1983) 6β-Hydroxyursolic Acid and Other Triterpenoids of *Enkianthus cernuus, Phytochemistry 22,* 2553–2555.
39. Kobayashi, H., Karasawa, H., Miyase, T., and Fukushima, S. (1985) Studies on the Constituents of *Cistanchis herba*. VI. Isolation and Structure of a New Iridoid Glycoside, 6-Deoxycatalpol, *Chem. Pharm. Bull. 33,* 3645–3650.
40. Bianco, A., Massa, M., Oguakwa, J.U., and Passacantilli, P. (1982) 5-Deoxystansioside, an Iridoid Glucoside from *Tecoma stans, Phytochemistry 20,* 1871–1872.

[Received June 25; accepted October 8, 2004]

METHOD

Regiospecific Determination of Short-Chain Triacylglycerols in Butterfat by Normal-Phase HPLC with On-Line Electrospray–Tandem Mass Spectrometry

P. Kalo[a,*], A. Kemppinen[b], V. Ollilainen[a], and A. Kuksis[c]

[a]Department of Applied Chemistry and Microbiology and [b]Department of Food Technology, University of Helsinki, Helsinki, Finland, and [c]Banting and Best Department of Medical Research, University of Toronto, Toronto, Ontario, Canada

ABSTRACT: This study uses normal-phase HPLC with on-line positive ion electrospray mass spectrometry (ESI–MS) to obtain quantitative compositional data on both synthetic and butterfat short-chain TAG. The product ion tandem MS of standards averaged 11.1 times lower in abundance of the ion formed by cleavage of FA from the *sn*-2-position for the pairs of regioisomers in the TAG classes: L/L/S–L/S/L and L/S/S–S/L/S, where L denotes long and S short acyl chain (C_2–C_6). The molar correction factors, determined for 42 regioisomeric pairs of short-chain TAG of 20 randomized mixture of standards, differed by 1.4–80% as the ratios varied between 0.217 and 5.847. Butterfat TAG were resolved into four fractions on short flash chromatography grade silica gel columns. Pairs of regioisomers in the TAG classes L/S/S–S/L/S with predominance of L/S/S isomers and the sole regioisomers in the TAG classes L/L(M)/S were identified by tandem MS, where M denotes either 8:0 or 10:0 acyl chain. The total proportion of L/L(M)/S isomers was estimated at 34.7 and that of L/S/S–S/L/S at 1.0 mol%, including a small proportion of S/S/S. In contrast to previous work, the present data indicate the presence of a small proportion of butyric and caproic acids in the *sn*-1-position. The overall distribution of the FA in the short-chain TAG of butterfat, calculated from direct MS measurements, was consistent with the results of indirect determinations based on stereospecific analyses of total butterfat.

Paper no. L9549 in *Lipids* 39, 915–928 (September 2004).

The regioisomerism of short-chain TAG influences physicochemical, nutritional, and technological properties of butterfat and it has been the subject of numerous investigations. Specifically, regioisomerism of TAG affects the melting point, heat of fusion, solubility, crystal structure, and polymorphism (1). The lingual and gastric lipases preferentially release the short-chain FA from the *sn*-3-position of TAG to yield *sn*-1,2-DAG, which rapidly isomerize to *sn*-1,3-DAG, which are no longer subject to resynthesis *via* the 2-MAG pathway; as reviewed by Kuksis (2). Short- and medium-chain FA are absorbed mainly *via* portal vein unless they are esterified in the *sn*-2-position. Recent studies with structured TAG have provided further evidence for the critical role of regioisomerism in short- and medium-chain TAG metabolism (3).

Regiospecific analysis of TAG, especially short-chain TAG, however, still presents a challenge to the lipid analyst. Early stereospecific analyses of butterfat indicated that the C_4, C_6, and C_8 FA were preferentially, if not exclusively, associated with the *sn*-3-position (4–6), but did not provide a direct estimate of the regioisomers. Direct evidence for the presence of regioisomers in native, enzymatically, and chemically interesterified butterfats was not provided in numerous studies using GC–MS with positive EI and CI (7), LC–MS with positive and negative CI (8), capillary supercritical fluid chromatography–atmospheric pressure chemical ionization (APCI) MS (9), GC–MS with positive EI (10), direct inlet LC–MS with positive CI (11), LC–desorption tandem MS (12), and TLC and gel permeation chromatography in combination with reversed-phase–APCI–MS (13).

The potential applicability of MS, GC–MS, or LC–MS to differentiate regioisomers of long-chain TAG has been described in several publications (14–34). EI–MS allowed differentiation between FA esterified in the *sn*-1(3) and *sn*-2 positions, on the basis of the observation of the $[M - RCOOCH_2]^{+\cdot}$ formed by cleavage of the FA esterified in the *sn*-1(3)-position only (14). The abundance of the $[M - RCOO]^+$ ion cleaved from the *sn*-1(3)-position was four times that cleaved from *sn*-2 position in LC–CI–MS (15). In the collision-induced dissociation (CID) spectra produced by negative ion chemical ionization (NICI), the $[M–H–RCOO–100]^-$ ions were observed to be formed primarily by loss of FA from the *sn*-1(3)-positions (16–20).

Soft ionization methods applicable for interfacing with HPLC have been of great interest in the recent years. APCI has been found useful for differentiation of regioisomers of long-chain TAG owing to the lower abundance of $[M - RCOO]^+$ ions of FA esterified in the *sn*-2 position (21–24). Duffin *et al.* (25) reported the formation of abundant positive ion signals for ammonium adducts of MAG-, DAG-, and TAG, when a continuous flow of a sample dissolved in 10 mM ammonium acetate in chloroform/methanol was introduced through the electrospray (ESI) interface. In the low-energy CID of $[M + NH_4]^+$ ions of TAG generated by ESI, no

*To whom correspondence should be addressed at Department of Applied Chemistry and Microbiology, P.O. Box 27, Latokartanonkaari 11, FIN-00014 University of Helsinki, Finland.E-mail: Paavo.Kalo@Helsinki.Fi

Abbreviations: ACN, number of acyl group carbons, APCI, atmospheric pressure chemical ionization; CID, collision-induced dissociation; EIC, extracted ion chromatogram; ESI, electrospray ionization; ISTD, internal standard; L, long-chain acyl (C_{12}–C_{20}); M, medium-chain acyl (C_8, C_{10}); MCF, molar correction factor; MS/MS, tandem MS; NICI, negative ion chemical ionization; NP, normal-phase; R_S, resolution; S, short-chain acyl (C_2–C_6).

preferential loss of fatty acyl groups from either the *sn*-1(3)- or *sn*-2-position was observed. A similar result was obtained in the high-energy CID of $[M + NH_4]^+$ ions of TAG produced by ESI (26). A slightly greater loss of fatty acyl groups from the *sn*-1(3)-positions compared with the *sn*-2-position was found in low energy CID of $[M + NH_4]^+$ ions of long-chain TAG produced by ESI (28,29). An improved differentiation of long-chain TAG regioisomers using ESI–MSn of $[M + NH_4]^+$ ions and an ion trap instrument has been reported (30). In addition to CID fragmentation of ESI generated $[M + NH_4]^+$ ions, high-energy CID fragmentation of $[M + Na]^+$ and $[M + Li]^+$ ions of long-chain TAG produced by ESI has been shown to be applicable in the determination of regiospecific distribution of acyl groups in the molecular species of long-chain TAG (26,32). Sodiated precursor ions produced by FABMS and high-energy CID fragmentation have been used in the differentiation of regioisomers of short-chain TAG (33). According to a recent report (34), regioisomers of medium-chain TAG could not be differentiated by RP–HPLC/ESI–tandem MS.

Myher *et al.* (15) quantified separated TAG species of vegetable oils in direct inlet RP–LC–MS using response factors calculated from the ratio of the area percentage of total ion current and calculated TAG composition. Kallio and Currie (16) applied ammonia NICI–tandem MS (NICI–MS/MS) in the quantification of rapeseed oil TAG based on $[RCOO]^-$ ions in the daughter ion spectra of $[M - H]^-$ ions and correction factors calculated from respective spectra of standards in the analysis of proportions of the FA in each M.W. group. The ratio of $[M - H - RCOOH - 100]^-$ ions resulting from the release of FA from the *sn*-2- and *sn*-1(3)-positions was used for the determination of calibration curves obtained with mixtures of AAB- and ABA-type TAG standards. This method was applied in the regiospecific analyses of long-chain TAG in low erucic acid turnip rapeseed oil and human milk (16,17) and in several other fats and oils. Furthermore, the method has been used in the analysis of regioisomers of octanoic acid–containing structured TAG and chylomicron and VLDL TAG (18,20).

Byrdwell (35) and Byrdwell and Neff (36) used RP–LC/APCI–MS to evaluate four different approaches for quantifying of soybean oil and lard TAG. They proposed a method based on response factor ratios obtained from comparisons of FA values determined for TAG by GC with FID and summation of the areas of all DAG and protonated TAG peaks in the mass spectrometer. The method has been applied as well in the determination of TAG in animal fats (23). Recently, the ratio 1(3),2-dilinoleoyl-3(1)-oleoylglycerol and 1,3-dilinoleoyl-2-oleoylglycerol in vegetable oils has been determined by HPLC–APCI–MS from the mass abundances of $[LL]^+$ and $[LO]^+$ ions using a calibration curve (24). Han and Gross (27) quantified molecular species of long-chain TAG directly from lipid extracts of biological samples by positive ion ESI–MS/MS using product ion and neutral loss scanning, isotope corrections, and an odd carbon number TAG as internal standard (ISTD).

Recently, Kalo *et al.* (31) demonstrated the applicability of normal-phase HPLC with positive ESI–MS and –MS/MS for the quantification and identification of regioisomers of short-chain TAG in nine interesterified mixtures of monoacid TAG. For a successful application to natural mixtures, however, additional chromatographic resolution was clearly required. The present study describes the results of improved resolution of regioisomeric short-chain TAG of butterfat on normal-phase microbore HPLC columns followed by identification and quantification of regioisomers on the basis of positive ESI–MS/MS of ammonium adducts.

EXPERIMENTAL PROCEDURES

Materials. Anhydrous butterfat was purchased from Valio Ltd. (Helsinki, Finland) and dried under vacuum to a water content of 55–85 ppm. All solvents were purchased from Rathburn (Walkerburn, United Kingdom) and were HPLC grade. Monoacid TAG standards of 99% purity were purchased from Sigma (St. Louis, MO) and Fluka (Buchs, Switzerland). Silica gel 60 for column chromatography was purchased from Merck (Darmstadt, Germany). Characteristics of the gel given by the manufacturer were: particle size range 0.040–0.063 mm, pore volume 0.71–0.78 mL/g, specific area 490 m^2/g, drying loss <9.0%, pH 6.5–7.5.

Calibration standard mixtures. Mixtures of randomized TAG were prepared by chemical interesterification of equimolar amounts of three monoacid TAG at a time to yield the following 20 randomized mixtures labeled as follows: BCoE (mixture of tributyrin, tricaproin, and trienanthin), BLaS, BLaP, BLaM, BMS, BMP, BPS, CoLaP, CoMS, CoMP, CoPS, BLaO, BMO, BPO, BLaPo, BMPo, CoLaO, CoMO, CoPO, CoMPo (where B denotes tributyrin, Co tricaproin, E trienanthin, L trilaurin, M trimyristin, P tripalmitin, S tristearin, Po tripalmitolein, and O triolein). The interesterifications were performed using sodium methoxide as catalyst (1%) at 85–90°C (1 h). The TAG were isolated from the interesterification mixtures by TLC (37) or by flash chromatography grade silica gel column chromatography (31). All interesterified standard mixtures were analyzed for randomness by GC on polarizable phenyl(65%)methylsilicone capillary columns as described by Kemppinen and Kalo (37).

Flash column chromatography. The chromatographic column (5.4 × 1.5 cm) was prepared in a 15-mL isolute filtration column tube with micropore filters (International Sorbent Technology, Hengoed, United Kingdom) using a dry packing method. The column was solvated and equilibrated by introducing 50 mL of hexane through the sorbent. A flow of approximately 9 mL/min was achieved by applying vacuum to the lower end of column with Vac Elut Accessory (Analytichem International, Harbor City, CA). The fat sample (100 mg) was introduced in 0.5 mL of chloroform. A stepwise elution scheme was used in the fractionation (Table 1). Trinonanoin was added as internal standard to the TAG fractions. The total recovery of fractionation, determined gravimetrically, was 100%.

TABLE 1
Stepwise Elution Scheme for Fractionation of Triacylglycerols

Eluting solvent mixture (by vol)	Volume (mL)	Lipids eluted
A[a]/B[b] (22:78)	40	Cholesterol esters
A/B (60:40)	60	TAG fraction A
A/B (65:35)	40	TAG fraction B
A/B (85:15)	40	TAG fraction C
A/B (100:0)	40	TAG fraction D

[a]Dichloromethane.
[b]Hexane.

LC–ESI–MS. The TAG fractions and interesterified standard mixtures were analyzed by normal-phase HPLC (NP-HPLC) using two or three Phenomenex Luna 3-µm silica columns, 100 × 2.0 mm, and a 4 × 2.0-mm guard column, in series. For elution of TAG, multistage binary gradient of hexane (A) and hexane/methyl-*tert*-butyl ether/acetic acid (60:40:1, by vol) (B) in the analyses with three columns in series with the following parameters was applied (time in min/%B by vol/flow in mL/min): 0/0/0.1, 2/5/0.1, 18/18/0.1, 30/18/0.1, 31/90/0.1, 49/90/0.1, 50/99/0.5, 64/99/0.5, 65/0/0.5, and 75/0/0.5. In the analyses with two columns in series the respective parameters were: 0/0/0.1, 2/15/0.1, 16/15/0.1, 22/18/0.1, 30/18/0.1, 31/90/0.1, 49/90//0.1, 50/99/0.5, 64/99/0.5, and 65/0/0.5. An ion-trap Bruker Esquire LC-MS (Bruker Daltonic, Bremen, Germany) was operated in positive ESI mode. Capillary voltage was 3000 V, capillary exit offset 60 V, skimmer potential 20 V, and trap drive value of 55. Conventional ESI–MS were recorded using a scan range of 50–1000 *m/z* and summation of 15 spectra. Nebulizer (nitrogen) pressure was 40 psi, dry gas (nitrogen) flow 8 L/min, and dry temperature 300°C. Auto-MS/MS spectra for two most intense ions eluting concurrently were recorded using helium (99.996%) as the collision gas. The reagent solvent, chloroform/methanol/ammonia water (25%) 20:10:3 (by vol), was pumped with a flow rate of 6.0 mL/min *via* a 1:100 split device to effluent flow.

Linear calibration. Linear calibration was used in the determination of molar correction factors (MCF). Three solutions of each interesterified standard mixture with different analyte and internal standard (trinonanoin) ratios were prepared. The molar analyte/ISTD ratios of each regioisomer were calculated from GLC data (37) as follows. The molar amount of each molecular species was calculated from the areas of each analyte and ISTD and the amount of ISTD. Then the molar amount was divided in a random ratio (2:1) to get molar amounts of each regioisomer. The conventional ESI–MS were recorded for three analyte/ISTD ratios for each of the 22 interesterified standard mixtures using three silica gel columns in series. The ion chromatograms, recorded for the ammonium adducts of short-chain TAG in standard mixtures, butterfat fractions, and ISTD, were extracted from total ion current data and integrated. The plots $n(i)/n$(ISTD) vs. area (i)/area(ISTD) for each regioisomer of short-chain TAG in standard mixtures were produced for calculation of MCF by linear regression.

Normalization. The sum of $n(\text{mol})_i$, n_{tot}, was calculated for TAG containing two or three short acyl chain and for TAG containing one short acyl chain. In the previous GC study, the proportion of TAG containing one short acyl chain was shown to be 34.7 mol% of total TAG (37). The $\text{mol}\%_i$ was calculated using the equation: $\text{mol}\%_i/\text{mol}\%_{\text{tot}} = n_i/n_{\text{tot}}$. The $\text{mol}\%_{\text{tot}}$ for TAG containing two or three short acyl chain was calculated using the equation: $\text{mol}\%_{\text{tot(S/S/L + S/S/S)}}/\text{mol}\%_{\text{tot(S/L(M)/L)}} = n_{\text{tot(S/S/L + S/S/S)}}/n_{\text{tot(S/L(M)/L)}}$.

RESULTS

Ion chromatograms of ammonium adducts in interesterified standard mixtures. Each interesterified mixture of three monoacid TAG was composed of two diacid TAG with two short or medium-long acyl chain, two diacid TAG with one short- or medium-chain acyl, one three-acid TAG, and five long-chain TAG. The regioisomers of dibutyrate TAG were separated with baseline resolution, R_S values between 1.5 and 2.0 (Fig. 1A). The regioisomers of dicaproate TAG were resolved partially with R_S in the range 0.5–1.1 (Fig. 1C). Dicaprylate and dicapriate regioisomers were not separated. The regioisomers of monobutyrate TAG were separated to the baseline with R_S between 1.6 and 2.9 (Fig. 1B), those of saturated monocaproates close to the baseline with R_S in the range 1.0–1.5, and those of unsaturated monocaproates close to the baseline or partially with R_S in the range 0.5–1.3 (Fig. 1D). The ESI–MS showed only $[M + NH_4]^+$ ions. Sodium adducts and fragment ions were not observed except low intensity fragment ions in the spectra of ammonium adducts with molecular weight below 500.

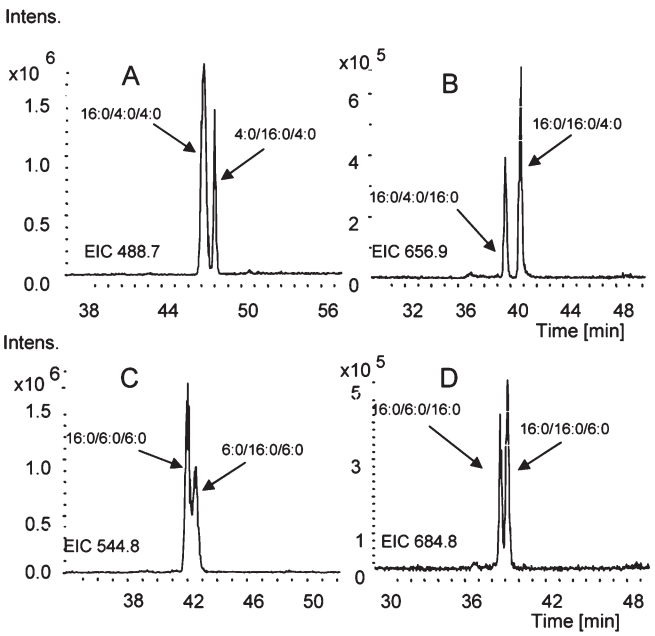

FIG. 1. Extracted ion chromatograms for ammonium adducts of short-chain TAG in standard mixtures. *m/z* 488, Regioisomers of dibutyroylpalmitoylglycerol (A), *m/z* 656, regioisomers of butyroyldipalmitoylglycerol (B), *m/z* 544, regioisomers of dicaproylpalmitoylglycerol (C), *m/z* 684, regioisomers of caproyldipalmitoylglycerol (D). EIC, extracted ion chromatograms.

Collision-induced dissociation spectra of short-chain TAG in standard mixtures. Figure 2 shows examples of the results obtained by the application of the LC–ESI–MS/MS method to the identification of regioisomers of a large number of short-chain TAG in standard mixtures. In the product ion tandem mass spectra $[(M + NH_4) - RCOONH_4]^+$ ions were formed. The abundance of the ion formed by cleavage of the FA from the *sn*-2 position was lower than that from the *sn*-1(3) positions. In the tandem MS of 1,2-dipalmitoyl-3-butyroyl-*rac*-glycerol and 1,3-dipalmitoyl-2-butyroyl-glycerol the relative abundance of $[(M + NH_4) - \text{butyroyloxy}–NH_4]^+$ ion (*m/z* 551) was 58.6 and 9.7%, respectively (Figs. 2A3 and A2). The relative abundance ratio $[(M + NH_4) - \text{butyroyloxy}–NH_4]^+/[(M + NH_4) - \text{long-chain acyloxy}–NH_4]^+$ varied between 1.022 and 1.416 for the former, and between 0.113 and 0.095 for the latter regioisomer. The ratios of these abundance ratios varied between 10.30 and 13.40 (data not shown). In the MS/MS of diacid TAG containing one butyroyl chain, the abundance of the ion formed by loss of butyric acid varied from 36.7 to 68.2 (n = 13) for L/L/4:0- and from 4.9 to 12.7% (n = 13) for L/4:0/L-isomers. The relative abundance ratio $[(M + NH_4) - \text{butyroyloxy}–NH_4]^+/[(M + NH_4) - \text{long-chain acyloxy}–NH_4]^+$ was in the range 0.580–2.140 for L/L/4:0- and in the range 0.051–0.146 for L/4:0/L-isomers. The ratio of the abundance ratios of the L/L/4:0- and L/4:0/L-isomers varied between 4.92 and 41.63 and was on the average 12.29 (SD 9.65, n = 13) (Table 2).

In the tandem MS of 1-oleoyl-2-lauroyl-3-butyroyl-*rac*-glycerol and 1-oleoyl-2-butyroyl-3-lauroyl-*rac*-glycerol the relative abundance of $[(M + NH_4) - \text{butyroyloxy}–NH_4]^+$ ion (*m/z* 521) was 50.6 and 8.0%, respectively (Figs. 2B3 and B2). The relative abundance ratio $[(M + NH_4) - \text{butyroyloxy}–NH_4]^+/[(M + NH_4) - \text{long-chain acyloxy}–NH_4]^+$ was 1.03 for the former and 0.087 for the latter regioisomer and the ratio of the abundance ratios of 18:1/12:0/4:0 and 18:1/4:0/12:0 was 11.81. In the MS/MS of triacid TAG containing one butyroyl chain the abundance of the ion formed by loss of butyric acid was in the range 39.9–79.7% for

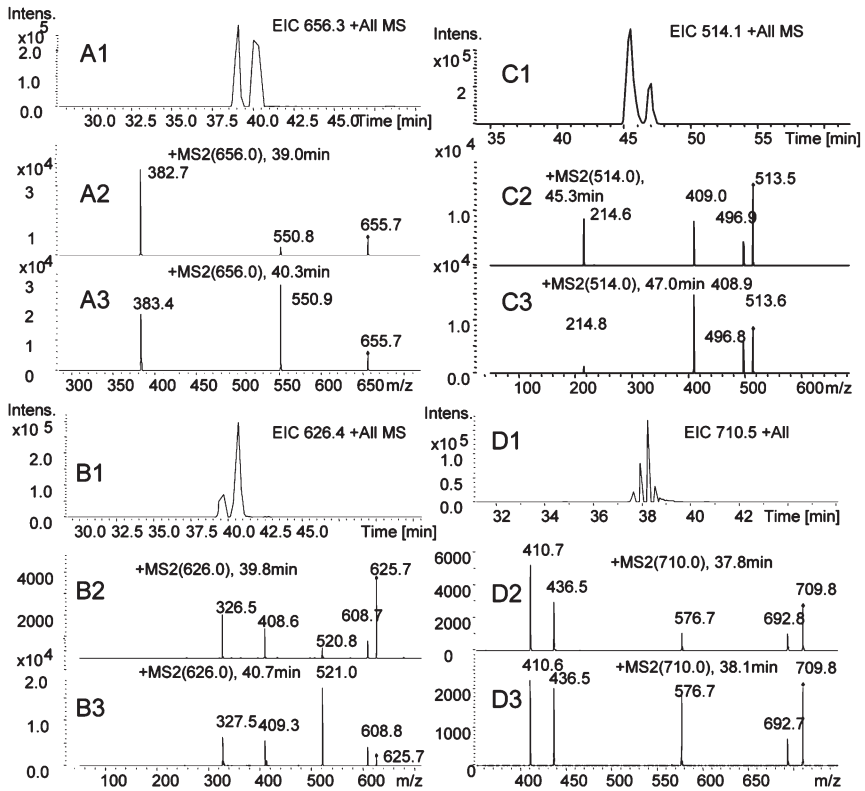

FIG. 2. EIC and collision-induced dissociation spectra for ammonium adducts of short-chain TAG in standard mixtures. (A1) EIC *m/z* 656: regioisomers of butyroyldipalmitoylglycerol. (A2) Tandem MS at 39.0 min: 1,3-dipalmitoyl-2-butyroyl-glycerol. (A3) Tandem MS at 40.3 min: 1,2-dipalmitoyl-3-butyroyl-*rac*-glycerol. (B1) EIC *m/z* 626: regioisomers of butyroyllauroyloleoylglycerol. (B2) Tandem MS at 39.8 min: 1-oleoyl-2-butyroyl-3-lauroyl-*rac*-glycerol. (B3) Tandem MS at 40.7 min: 1-oleoyl-2-lauroyl-3-butyroyl-*rac*-glycerol + 1-lauroyl-2-oleoyl-3-butyroyl-*rac*-glycerol. (C1) EIC *m/z* 514: regioisomers of dibutyroyloeloleoglycerol. (C2) Tandem MS at 45.3 min: 1-oleoyl-2,3-dibutyroyl-*rac*-glycerol. (C3) Tandem MS at 47 min: 1,3-dibutyroyl-2-oleoylglycerol. (D1) Auto-MS EIC *m/z* 710.5: regioisomers of caproylpalmitoyloleoylglycerol. (D2) Tandem MS at 37.8 min: 1-oleoyl-2-caproyl-3-palmitoyl-*rac*-glycerol. (D3) Tandem MS at 38.1 min: 1-oleoyl-2-palmitoyl-3-caproyl-*rac*-glycerol + 1-palmitoyl-2-oleoyl-3-caproyl-*rac*-glycerol. For abbreviation see Figure 1.

TABLE 2
The Ratios of Relative Abundance Ratios (RRAR) of the Ions Formed by Cleavage of FA from the Primary vs. Secondary Position[a]

Class of short-chain TAG	RRAR[a]			
	Range	Average	SD	*n*
A. L/L/4:0 vs. L/4:0/L	4.92–41.63	12.29	9.65	13
B. L/L′/4:0[b] vs. L/4:0/L′	5.35–24.53	12.27	6.08	7
C. L/L/6:0 vs. L/6:0/L	5.70–13.03	8.86	3.15	4
D. L/L′/6:0[c] vs. L/6:0/L′	6.79–12.75	9.33	3.08	3
E. L/4:0/4:0 vs. 4:0/L/4:0	7.02–35.89	16.68	8.21	8
F. L/6:0/6:0 vs. 6:0/L/6:0	4.15–12.70	7.32	2.93	6

[a]Ratio of [(M + NH_4) – short-chain acyloxy–NH_4]/[(M + NH_4) – long-chain acyloxy–NH_4] of the regioisomer pairs L/4:0/L vs. L/L/4:0, L/4:0/L′ vs. L/L′/4:0, L/6:0/L vs. L/L/6:0 , and L/6:0/L′ vs. L/L′/6:0. Ratio of [(M + NH_4) – long-chain acyloxy–NH_4]/[(M + NH_4) – short-chain acyloxy–NH_4] of the regioisomer pairs L/4:0/4:0 vs. 4:0/L/4:0 and L/6:0/6:0 vs. 6:0/L/6:0.
[b]Mixture of reverse isomers: L/L′/4:0 + L′/L/4:0.
[c]Mixture of reverse isomers: L/L′/6:0 + L′/L/6:0.

L/L′/4:0- and in the range 9.0–13.8% for L/4:0/L′-isomers. The relative abundance ratio [(M + NH_4) –butyroyloxy–NH_4]$^+$/[(M + NH_4) – long-chain acyloxy–NH_4]$^+$ varied between 0.794 and 3.931 for L/L′/4:0- and between 0.087 and 0.171 for L/4:0/L′-isomers. The ratio of the abundance ratios of L/L′/4:0- and L/4:0/L′-isomers was in the range 7.98–24.53 and on the average 12.27 (SD 6.08, n = 7) (Table 2).

In the MS/MS of 1-oleoyl-2,3-dibutyroyl-*rac*-glycerol and 1,3-dibutyroyl-2-oleoylglycerol the abundance of [(M + NH_4) – long-chain acyloxy–NH_4]$^+$ ion (*m/z* 215) varied between 51.0 and 67.0% for the former and between 2.8 and 10.7% for the latter regioisomer (Figs. 2C2 and C3). The relative abundance ratio [(M + NH_4) – long-chain acyloxy–NH_4]$^+$/[(M + NH_4) – butyroyloxy–NH_4]$^+$ was in the range 1.04–2.03 for 18:1/4:0/4:0 and in the range 0.029–0.120 for 4:0/18:1/4:0. The ratios of the abundance ratios of these pairs of regioisomers varied between 17.00 and 35.89 (data not shown). The relative abundance ratio [(M + NH_4) – long-chain acyloxy–NH_4]$^+$/[(M + NH_4) – butyroyloxy–NH_4]$^+$ of L/4:0/4:0-isomers was in the range 0.511–2.034 and that of 4:0/L/4:0-isomers in the range 0.021–0.120. The ratio of the abundance ratios of L/4:0/4:0- and 4:0/L/4:0-isomers was in the range 7.02–35.89 and on the average 18.68 (SD 8.21, n = 8) (Table 2).

In the MS/MS of diacid TAG containing one caproyl chain the abundance of the ion formed by loss of caproic acid varied from 43.6 to 60.5% for L/L/6:0- and from 9.5 to 14.5% for L/6:0/L-isomers. The relative abundance ratio [(M + NH_4) – caproyloxy–NH_4]$^+$/[(M + NH_4) – long-chain acyloxy–NH_4]$^+$ varied between 0.776 and 1.534 for the L/L/6:0- and between 0.105 and 0.169 for the L/6:0/L-isomers. The ratio of the abundance ratios of L/L/6:0- and L/6:0/L-isomers was in the range 5.70–13.03 and on the average 8.86 (SD 3.15, n = 4) (Table 2). In the tandem MS of 1-oleoyl-2-palmitoyl-3-caproyl-*rac*-glycerol and 1-oleoyl-2-caproyl-3-palmitoyl-*rac*-glycerol the abundance of [(M + NH_4) – caproyloxy–NH_4]$^+$ ion (*m/z* 577) was 46.8 and 11.5%, respectively (Figs. 2D3 and D2). The relative abundance ratio [(M + NH_4) – caproyloxy–NH_4]$^+$/[(M + NH_4) – long-chain acyloxy–NH_4]$^+$ was 0.880 for the former and 0.130 for the latter regioisomer. The ratio of the abundance ratios of 18:1/16:0/6:0 and 18:1/6:0/16:0 was 6.79 (data not shown). The ratio of the abundance ratios of L/L′/6:0- and L/6:0/L′-isomers varied between 6.79 and 12.75 and was on the average 9.33 (SD 3.08, n = 3) (Table 2).

In the tandem MS of diacid TAG containing two caproyl groups the abundance of [(M + NH_4) – caproyloxy–NH_4]$^+$ ion was in the range 22.0–62.1 and 4.2–22.2% for L/6:0/6:0- and 6:0/L/6:0-TAG, respectively. The relative abundance ratio [(M + NH_4) – long-chain acyloxy–NH_4]$^+$/[(M + NH_4) – caproyloxy–NH_4]$^+$ varied between 0.283 and 1.636 for L/6:0/6:0- and between 0.043 and 0.286 for 6:0/L/6:0-TAG. The ratio of the abundance ratios of L/6:0/6:0- and 6:0/L/6:0-isomers varied in the range 4.15–12.70 and was on the average 7.32 (SD 2.93, n = 6) (Table 2).

Determination of molar correction factors. GC of calibration standards on polarizable phenylmethylsilicone columns revealed random ratios of molecular species and regioisomers. Ratios of regioisomers L/L/4:0 and L/4:0/L of 17 molecular species in 11 standard mixtures were on the average 1.880 (SD 0.130, n = 108) and the deviation from the calculated random composition of the same molecular species was on the average 7.023% (SD 5.499). The data of regioisomer ratios included a few values around 1.5 for partially resolved (R_S < 1) regioisomers in three standard mixtures. However, the deviation from the random composition of these molecular species was below the average of all molecular species. Ratios of regioisomers L/L/6:0 and L/6:0/L of 12 molecular species in eight standard mixtures were on the average 1.992 (SD 0.271, n = 36) and the deviation from the calculated random composition of the same molecular species was on the average 5.849 (SD 6.179). Molar correction factors were determined for the 42 pairs of regioisomers of short-chain TAG. The ion chromatograms of ammonium adducts were extracted from total ion current data of three analyte/ISTD ratios and integrated. The area(i)/area(ISTD) for regioisomers of short-chain TAG was calculated from these ion chromatograms and n(i)/n(ISTD) ratio of each regioisomer was calculated from GLC data. The plots n(i)/n(ISTD) vs. area(i)/area(ISTD) in the ESI ion chromatograms for regioisomers of 4:0/16:0/16:0 (A and B), 4:0/16:0/18:1 (C and D), 4:0/4:0/16:0 (E and F), and 6:0/6:0/18:1 (G and H) demonstrate the linearity of response (Fig. 3). The regression analysis indicates linear relationship of n(i)/n(ISTD) and area(i)/area(ISTD), and different MCF for regioisomers. The coefficient of determination, R^2,varied between 0.692 and 0.999 and was on the average 0.933 (SD 0.058, n = 78). The experimentally determined MCF varied between 0.217 and 5.847. The MCF of regioisomers differed by 1.4–80.4%.

The plot of MCF vs. the number of acyl group carbons (ACN) for saturated butyrate regioisomers with long acyl chain present in the *sn*-2 position showed polynomial dependence with a minimum at ACN 22 (Fig. 4A). Regression analysis revealed polynomial dependence of MCF vs. ACN

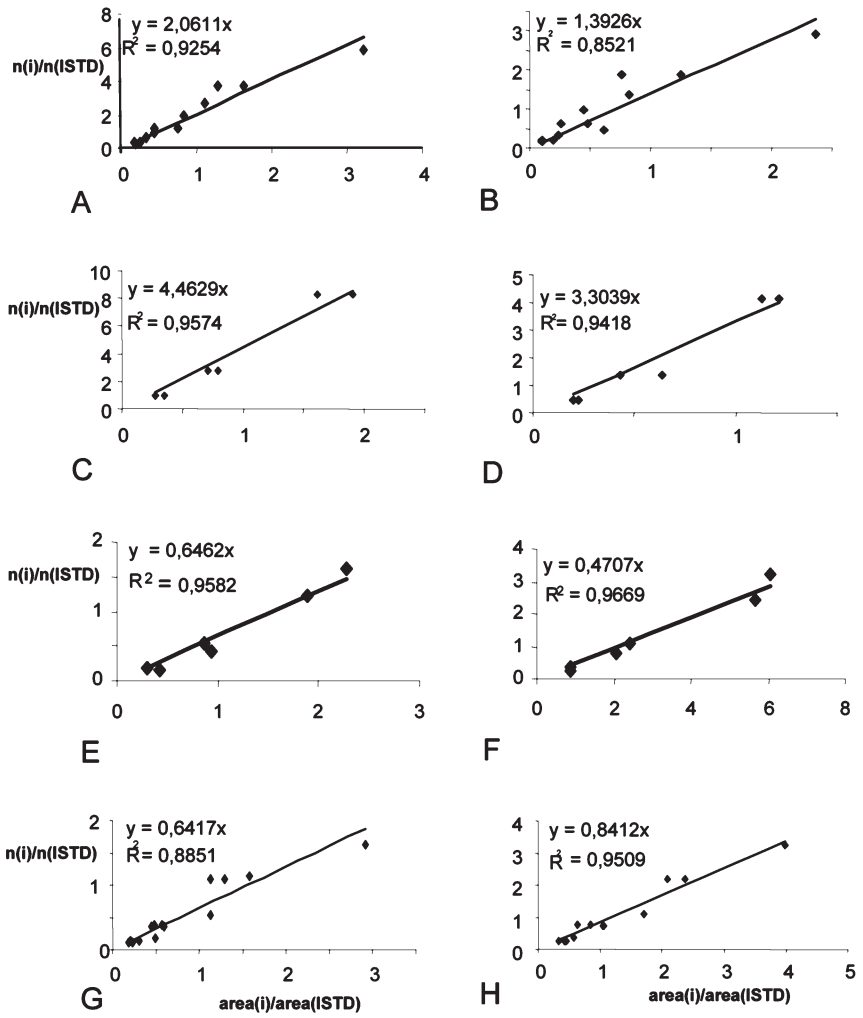

FIG. 3. Plots of *n*(*i*)/*n*(ISTD) vs. area(*i*)/area(ISTD). 1,2-Dipalmitoyl-3-butyroyl-*rac*-glycerol (A); 1,3-dipalmitoyl-2-butyroyl-*rac*-glycerol (B); 1-oleoyl-2-palmitoyl-3-butyroyl-*rac*-glycerol (C); 1-oleoyl-2-butyroyl-3-palmitoyl-*rac*-glycerol (D); 1,3-dibutyroyl-2-palmitoylglycerol (E); 1-palmitoyl-2,3-dibutyroyl-*rac*-glycerol (F); 1,3-dicaproyl-2-oleoylglycerol (G); 1-oleoyl-2,3-dicaproyl-*rac*-glycerol (H).

for saturated regioisomers with butyroyl in the *sn*-2-position (Fig. 4B). The minimum was at ACN 20. The regression curve shown in Figure 4B was calculated from MCF/ACN of diacid TAG with two butyroyl groups and symmetric diacid TAG with two identical long acyl chains. When, in addition, the asymmetric diacid TAG with two different long acyl chains were included in the calculation, the regression equation was $y = 0.005x2 - 0.1995x + 2.3936$ ($R^2 = 0.7098$). The MCF of asymmetric L/4:0/L′- isomers with ACN 32 and 36 were higher than those of corresponding symmetric acyl chain isomers (Fig. 4B). The regression curve for saturated caproate regioisomers with a long acyl chain in the *sn*-2-position showed polynomial dependence and minimum at ACN 18 (Fig. 4C). A similar trend with different parameters was observed for saturated regioisomers with caproyl in the *sn*-2 position, when the regression curve calculated from data points of diacid TAG with two caproyl groups and symmetric diacid TAG with two identical long acyl chains (Fig. 4D). The MCF of asymmetric L/6:0/L′-isomers with ACN 34 and 38 were distinctly higher compared to those of corresponding symmetric acyl chain isomers (Fig. 4D).

The plot of MCF vs. ACN for monoene butyrate regioisomers with a long acyl chain in the *sn*-2-position showed polynomial dependence with a minimum at ACN 28 (Fig. 4E). The corresponding plot of monoene regioisomers with butyrate in the *sn*-2-position showed also polynomial dependence and minimum at ACN 28 but different parameters and shape of the regression curve (Fig. 4F). The regression curves for monoene caproate TAG with a long acyl chain or caproyl present in the *sn*-2-position showed linear dependence with different parameters (Fig. 4G and H).

Identification of short-chain TAG in butterfat. For this purpose tandem mass spectra were recorded in automatic mode for four subfractions of butterfat. In all instances, the product ion tandem MS showed $[(M + NH_4) - \text{acyloxy}–NH_4]^+$ ions. Figure 5 demonstrates the structural analysis of a diacid TAG

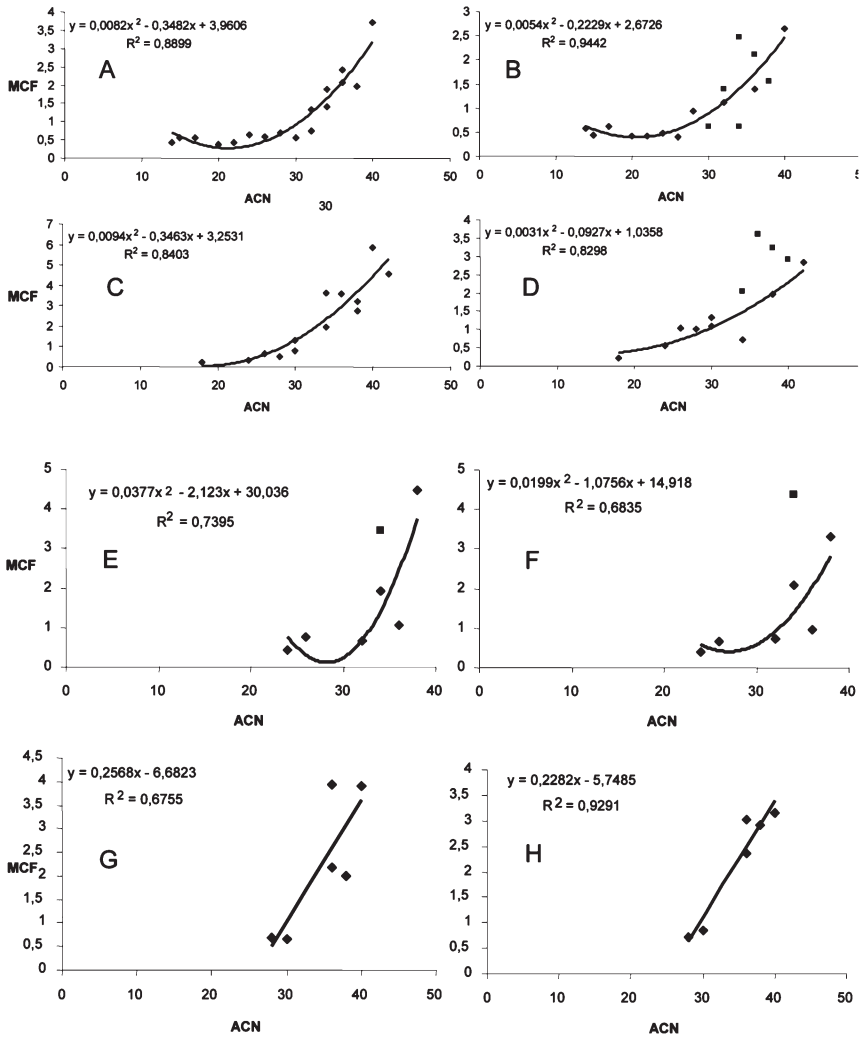

FIG. 4. The plots of molar correction factor vs. acyl carbon number. (A) Saturated: ◆ X/X/4:0-isomers. (B) Saturated: ◆ X/4:0/X-isomers, ■ X/4:0/X′-isomers. (C) Saturated ◆ X/X/6:0-isomers. (D) Saturated ◆ X/6:0/X-isomers, ■ X/6:0/X′-isomers. (E) Unsaturated ◆ X/X/4:0-isomers, ■ 18:1/12:0/4:0. (F) Unsaturated ◆ X/4:0/X-isomers, ■ 18:1/4:0/12:0. (G) Unsaturated ◆ X/X/6:0-isomers. (H) Unsaturated ◆ X/6:0/X-isomers.

containing two butyroyl groups. Extracted ion chromatogram *m/z* 514 corresponds to the ammonium adduct of TAG 26:1 (Fig. 5A). The MS/MS of the high intensity peak in the extracted ion chromatogram shows intense ions *m/z* 215 and *m/z* 409, which are formed in CID by loss of oleoyloxy–NH_4 and butyroyloxy–NH_4, respectively (Fig. 5B). The relative abundance of the former peak was 43.1%, and the relative abundance ratio $[(M + NH_4) - \text{oleoyloxy–}NH_4]^+/[(M + NH_4) - \text{butyroyloxy–}NH_4]^+$ was 0.757. The same fragment ions are shown in the MS/MS of the low-intensity peak eluting after the high-intensity peak in the extracted ion chromatogram *m/z* 514, but the relative abundance of ion *m/z* 215 was 5.5% and the relative abundance ratio $[(M + NH_4) - \text{oleoyloxy–}NH_4]^+/[(M + NH_4) - \text{butyroyloxy–}NH_4]^+$ was 0.0584 (Fig. 5C). The ratio of the relative abundance ratio of the former regioisomer to the latter regioisomer was 12.9. Comparison of this ratio to the MS/MS data for similar TAG in the standard mixtures indicated that the regioisomer eluting in the high-intensity peak was consistent with a pair of enantiomers: 1-oleoyl-2,3-dibutyroyl-*sn*-glycerol and 3-oleoyl-1,2-dibutyroyl-*sn*-glycerol. The regioisomer eluting in the low-intensity peak is 4:0/18:1/4:0. The same principles were applied in the identification of molecular species and pairs of regioisomers in the L/S/S–S/L/S- and L/S/S′–S/L/S′-classes shown in Table 3.

The three tandem mass spectra in Figure 6 are shown as an example of identification of acyl chain isomers of triacid TAG containing one short acyl chain. The MS/MS measured for the intense peak eluting at 38.1 min in the extracted ion chromatogram (EIC) 711, which corresponds to the ammonium adduct of TAG 40:1, shows fragment ions *m/z* 577, 437, and 411, which are formed by loss of caproyloxy–NH_4, palmitoyloxy–NH_4, and oleoyloxy–NH_4, respectively (Fig. 6B). The relative abundances for these ions, 61.1/17.7/21.2%, indicate a mixture of reverse isomers, 18:1/16:0/6:0 and 16:0/18:1/6:0. The relative abundance ratio $[(M + NH_4) - \text{caproyl-}$

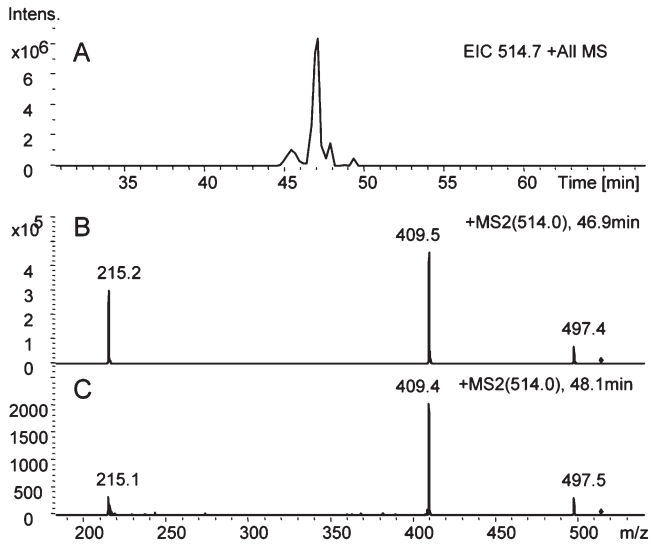

FIG. 5. Structural analysis of regioisomers of dibutyroyloleoylglycerol in butterfat. (A) EIC of ammonium adduct of 26:1, *m/z* 514. (B) Tandem MS at 46.9 min: 1-oleoyl-2,3-dibutyroyl-*sn*-glycerol + 1,2-dibutyroyl-3-oleoyl-*sn*-glycerol. (C) Tandem MS at 48.1 min: 1,3-dibutyroyl-2-oleoylglycerol. For abbreviation see Figure 1.

oxy–NH_4]$^+$/[(M + NH_4) – long-chain acyloxy–NH_4]$^+$ was 1.568, which slightly exceeds the range 0.776–1.534 measured for the L/L/6:0-isomers, in standard mixtures. The tandem MS recorded at the top of the less intense peak at 39.3 min shows fragment ions *m/z* 605, 411, and 409, which are formed by the cleavage of butyroyloxy–NH_4, oleoyloxy–NH_4, and stearoyloxy–NH_4, respectively (Fig. 6C). The relative abundances of these ions are 43.2/43.3/13.6%, which indicate that stearic acid is located in the *sn*-2-position. The relative abundance ratio [(M + NH_4) – butyroyloxy–NH_4]$^+$/[(M + NH_4) – long-chain acyloxy–NH_4]$^+$ was 0.758, which is slightly below the range 0.794– 3.931 for the L/L′/4:0-isomers in standard mixtures, but clearly higher than the range 0.087–0.171 for the L/4:0/L′-isomers. The data are consistent with a pair of enantiomers: 1-oleoyl-2-stearoyl-3-butyroyl-*sn*-glycerol and 1-butyroyl-2-stearoyl-3-oleoyl-*sn*-glycerol. Because the former enantiomer is more consistent with the results of stereospecific analyses, an abbreviation 18:1/18:0/4:0 is used (4–6). The tandem MS recorded at the tailing end of less intense peak at 39.5 shows the same fragment ions *m/z* 605, 411, and 409 with different relative abundance ratios, 39.0/5.0/56.0 (Fig. 6D). The relative abundance ratio [(M + NH_4) – butyroyloxy–NH_4]$^+$/[(M + NH_4) – long-chain acyloxy–NH_4]$^+$ was 0.640, which is slightly below the range for the L/L′/4:0-isomers in standard mixtures, but clearly higher than the range for the L/4:0/L′-isomers. The tandem MS is consistent with a pair of enantiomers: 1-stearoyl-2-oleoyl-3-butyroyl-*sn*-glycerol and 1-butyroyl-2-oleoyl-3-stearoyl-*sn*-glycerol and abbreviation 18:0/18:1/4:0.

A high number of molecular species of TAG containing two long acyl chains or one long and one medium-long acyl chain together with one short acyl chain, acetyl, butyroyl, or caproyl were identified (Table 4). Only L/L(M)/S- regioisomers were identified from tandem mass spectra. Saturated and unsaturated monocaproates and monobutyrates were identified in the ACN ranges 34–40 and 38–40, respectively.

When butterfat fractions C and D were analyzed using two silica gel columns in series, several TAG containing one acetyl with one short or medium, and one long acyl chain were identified. Figure 7 demonstrates the structural analysis

TABLE 3
Proportion of TAG Containing Two or Three Short Acyl Chains (acetyl, butyroyl, or caproyl) in Butterfat

ACN:DB[a]	RRT[b]	Major and (minor) molecular species of TAG[c,d]	Mol%[e,f]	RSD (%)[g]
12:0	1.219	4:0/4:0/4:0	0,0097^C	24.5
18:0	1.177	6:0/6:0/6:0	0,0188^C	37.0
20:0	1.184	6:0/10:0/4:0[d]	0.0012$^{C(D)}$	79.3
22:0	1.147	12:0/6:0/4:0, (8.0/8:0/6:0)[c]	0.0142$^{C(D)}$	29.7
	1.162	14:0/4:0/4:0[c]	0.0026^D	21.8
	1.214	4:0/16:0/2:0[d]	0.0007^D	13.2
24:0	1.118	14:0/6:0/4:0, (12:0/8:0/4:0 + 8:0/12:0/4:0)[c]	0.0453$^{C(D)}$	45.7
	1.135	6:0/14:0/4:0[d]	0.0341^D	21.6
	1.172	16:0/4:0/4:0[c]	0.0367^C	25.0
	1.187	4:0/16:0/4:0	0.0044^D	32.5
	1.216	16:0/6:0/2:0[c]	0.0033^D	3.5
26:1	1.140	16:1/6:0/4:0, 12:0/10:1/4:0[c]	0.0156$^{C(D)}$	28.4
	1.172	18:1/4:0/4:0[c]	0.0661$^{C(D)}$	37.8
	1.187	4:0/18:1/4:0	0.0049^D	95.4
26:0	1.088	16:0/6:0/4:0, (14:0/6:0/6:0)[c]	0.3206$^{C(D)}$	21.0
	1.125	6:0/16:0/4:0[d]	0.0396$^{C(D)}$	46.5
	1.152	18:0/4:0/4:0[c]	0.0223$^{C(D)}$	105.3
28:1	1.111	18:1/6:0/4:0[c], (16:1/6:0/6:0[c], 14:0/10:1/4:0[c], 6:0/18:1/4:0[d], 10:1/14:0/4:0[d])	0.1455$^{C(D)}$	27.3
28:0	1.088	18:0/6:0/4:0[c]	0.1249$^{C(D)}$	20.2
		NI,[h] 18:0, 20:0 22:1, 22:0, 23:0, 24:1 24:0, 26:2, 26:1, 26:0	0.0595	24.5
		Total	0.9699	

[a]The number of acyl group carbons:the number of double bonds.
[b]Relative retention time.
[c]Regiospecific analysis indicates a mixture of enantiomers: L/S/S′ + S′/S/L or L/S/S + S/S/L. The enantiomers L/S/S′ and L/S/S, which are more consistent with the results of stereospecific analyses (4–6), are presented.
[d]Regiospecific analysis revealed a mixture of enantiomers: S/L/S′ + S′/L/S. Only one enantiomer is presented.
[e]The mol percentage was calculated by normalizing the sum of the mean of *n*(mol) in fractions C (n = 5) and D (n = 3) to give the total proportion of 0.9699 mol%. This was calculated from the sums $n(\text{mol})_i$ of TAG containing two or three acetyl, butyroyl, or caproyl chains and TAG containing one butyroyl or caproyl chain.
[f]C or D after the value for mol% indicate the fraction of silica gel fractionation, where the molecular species was measured. Parentheses express that the minor part of molecular species was measured in the fraction in question.
[g]Relative standard deviation (RSD) (%) determined for the silica gel fraction, where the major part of the molecular species was measured (n = 5, fraction C; n = 3, fraction D).
[h]Not identified.

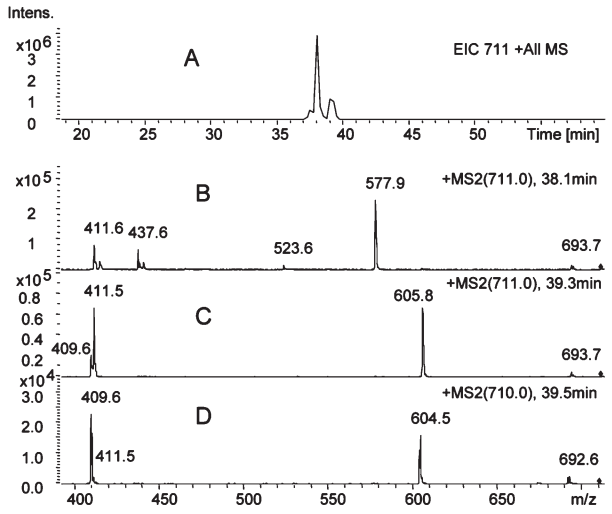

FIG. 6. Structural analysis of acyl chain isomers of TAG 40:1 in butterfat. (A) EIC of the ammonium adduct of 40:1, *m/z* 711. (B) Tandem MS at 38.1 min, mixture of two pairs of enantiomers (reverse isomers): (1-oleoyl-2-palmitoyl-3-caproyl-*sn*-glycerol + 1-caproyl-2-palmitoyl-3-oleoyl-*sn*-glycerol) + (1-palmitoyl-2-oleoyl-3-caproyl-*sn*-glycerol +1-caproyl-2-oleoyl-3-palmitoyl-*sn*-glycerol). (C) Tandem MS at 39.3 min: 1-oleoyl-2-stearoyl-3-butyroyl-*sn*-glycerol + 1-butyroyl-2-stearoyl-3-oleoyl-*sn*-glycerol. (D) Tandem MS at 39.5 min: 1-stearoyl-2-oleoyl-3-butyroyl-*sn*-glycerol + 1-butyroyl-2-oleoyl-3-stearoyl-*sn*-glycerol. For abbreviation see Figure 1.

of ammonium adduct of acetate TAG 24:0. The tandem MS recorded at 41.3 min shows fragment ions *m/z* 411, 383, and 187, which are formed by cleavage of acetyloxy–NH_4, butyroyloxy–NH_4, and stearoyloxy–NH_4, respectively. The relative abundances of these ions, 7.9/ 35.0/57.1%, indicate that acetic acid is in the *sn*-2-position and are consistent with 18:0/2:0/4:0 (Fig. 7B). The fragment ions of the tandem MS recorded at 42.5 min are *m/z* 411, 299, 271, formed by cleavage of acetyloxy–NH_4, caprioyloxy–NH_4, and lauroyloxy–NH_4, respectively. The relative abundances of these ions, 37.0/18.5/44.4%, are consistent with 12:0/10:0/2:0 (Fig. 7C). The relative abundances of the fragment ions *m/z* 411, 327, and 243, recorded at 43 min, 43.5/15.0/41.5%, and those of *m/z* 411, 355, and 215, recorded at 43.9 min, 39.0/ 17.2/43.7%, are consistent with 14:0/8:0/2:0 (Fig. 7D) and 16:0/6:0/2:0 (Fig. 7E), respectively.

Quantification of regioisomers of TAG in butterfat. The conventional mass spectra recorded at the maxima of total ion chromatogram of four fractions of butterfat revealed the ammonium adduct ions. These ions were extracted by computer from the total ion MS data and the ion chromatograms were integrated to obtain the area of different peaks of each ion chromatogram. For the calculation of *n*(mol) for each analyte peak by the method of internal standardization, the following principles were used in the choosing of MCF. Because the isomeric molecular species of the same regioisomer class showed different MCF (Fig. 4), the MCF of the isomer to be calculated was used, when available. If not, MCF was calculated using the appropriate regression equation. Among the triacid TAG containing two short acyl chains were identified several molecular species containing two different short acyl chains (two acyls of acetyl, butyroyl, or caproyl). For example, to calculate the MCF for L/6:0/4:0-regioisomers, ACN:DB 28:0, the MCF for ACN 28:0, was calculated first from equations for X/X/4:0 (Fig. 4A) and X/6:0/X-classes (Fig. 4D). The mean of these was used in the calculation of *n*(mol) of this molecular species in the fractions C and D.

Among the TAG containing two or three short acyl chains, small amounts of tributyrin and tricaproin were detected (Table 3). The molar ratio of the L/S/S′ + L/S/S- and S/L/S′ + S/L/S-isomers was 90.5:9.5. The short-chain TAG L/6:0/4:0- and L/4:0/4:0-classes, comprised approximately 69 and 13% of the TAG containing two or three short acyl chains. The proportion of dicaproates, acetobutyrates, and acetocaproates was small. The TAG containing one short acyl chain was composed of butyrate L/L(M)/4:0- (59.0%), caproate L/L(M)/6:0-isomers (40.9%), including caproates identified from retention data, and acetates (0.1%) (Table 4).

In the analyses using two silica gel columns in series, several molecular species of regioisomers of acetate TAG containing two short acyl chains (acetyl and butyroyl or caproyl) or one short and one medium acyl chain (acetyl and capryloyl or caprioyl) were identified in butterfat fractions C and D (Table 5). Regioisomer class X/X/2:0 predominated; only four molecular species of class X/2:0/X were detected. The area ratio of total regioisomer classes X/X/2:0 and X/2:0/X was 90.5:9.5.

To compare the regioisomer ratios determined using three silica gel columns in series to the results of regiospecific analyses, the distribution of short-chain FA among the three positions of glycerol backbone was calculated from $n(\text{mol})_i$ of all identified short-chain TAG on the basis of stereospecific analyses (4–6). The percentages of butyric acid esterified in the *sn*-1-, *sn*-2-, and *sn*-3-positions were 0.1, 0.7, and 99.2%, and those of caproic acid were 0.5, 6.1, and 93.4%, respectively. The percentages of short-chain FA (C_2–C_6) in the *sn*-1-, *sn*-2-, and *sn*-3-positions were 0.2, 2.7, and 97.0%, respectively. In the analysis using two silica gel columns in series, the area proportion of acetic acid in the *sn*-2-position in the acetate TAG was 9.5%.

DISCUSSION

Chromatographic resolution of regioisomers. The use of three normal-phase analytical columns in series instead of the two employed previously (31) in combination with a multistage binary gradient greatly improved the separation of TAG regioisomers containing one butyroyl or caproyl chain as well as those containing two caproyl chains per molecule. The present results on the separation of the regioisomers of short-chain TAG of butterfat are also superior to those obtained by a combined application of $AgNO_3$-TLC and polar capillary GLC on molecular distillates of butterfat, which had failed to recognize the presence of relatively high proportions of TAG containing caproic acid and minor proportions containing butyric acid in the *sn*-2-position (7).

TABLE 4
Composition of Short-Chain TAG Containing One Acetyl, Butyroyl, or Caproyl Chain in Butterfat

ACN:DB[a]	RRT[b]	Major and (minor) molecular species of triacylglycerols[c]	Mol%	RSD (%)[g]
28:0	1.010	NI[h]	0.054[B]	49.1
	1.048	16:0/8:0/4:0[c,d], 14:0/10:0/4:0[c,d], 18:0/6:0/4:0[c,d]	0.051[B]	21.3
30:1	1.018	NI	0.068[B]	8.3
30:1	1.048	18:1/8:0/4:0[c,d], 16:0/10:1/4:0[c,d], 12:1/14:0/4:0[c,d], 12:0/14:1/4:0[c,d], 14:0/12:1/4:0[c,d]	0.100[B,C,D]	29.2
30:0	1.000	NI	0.126[B]	9.2
	1.033	16:0/10:0/4:0[c,d], 14:0/12:0/4:0[c,d], 18:0/8:0/4:0[c,d]	0.455[B,C,D]	14.7
	1.223	18:0/10:0/2:0[c,d], 16:0/12:0/2:0[c,d],14:0/14:0/2:0[c]	0.035[C,D]	57.4
32:1	1.000	NI	0.061[B]	11.9
	1.028	18:1/10:0/4:0[c,d], 16:0/12:1/4:0[c,d], (16:1/12:0/4:0[c,d], 14:1/14:0/4:0[c,d])	0.359[B,C,D]	7.7
32:0	0.987	NI	0.315[B(A)]	12.3
	1.018	16:0/12:0/4:0[c,d], 14:0/14:0/4:0[c], 18:0/10:0/4:0[c,d]	1.093[B,C,D(A)]	6.7
34:1	1.000	NI	0.288[B(A)]	9.5
	1.015	16:0/14:1/4:0[c,d], 18:1/12:0/4:0[c,d], 16:1/14:0/4:0[c,d]	0.517[B(A)]	4.1
34:0	0.977	16:0/12:0/6:0[c,d], 14:0/14:0/6:0[c] (18:0/10:0/6:0[c,d])	0.894[B(A)]	5.4
	1.005	16:0/14:0/4:0[c,d], 18:0/12:0/4:0[c,d]	1.371[B(A)]	12.6
36:1	0.977	NI	0.575[B(A)]	8.1
	1.005	18:1/14:0/4:0[c,d], 16:1/16:0/4:0[c,d] (18:0/14:1/4:0[c,d])	0.716[B(A)]	4.5
36:0	0.970	16:0/14:0/6:0[c,d] (18:0/12:0/6:0[c,d])	2.227[B,A]	9.4
	0.995	16:0/16:0/4:0 (14:0/18:0/4:0[c,d])	2.130[B(A)]	14.1
38:2	0.977	NI	0.244[B]	19.6
	1.008	18:2/16:0/4:0[c,d]	0.807[B(A)]	9.0
38:1	0.967	18:1/14:0/6:0[c,d], 16:1/16:0/6:0[c,d]	0.908[B]	12.0
	0.992	18:1/16:0/4:0[c,d]	4.210[B]	19.7
38:0	0.949	18:0/14:0/6:0[c,d], 16:0/16:0/6:0[c]	2.062[B,A]	5.0
	0.962	18:0/16:0/4:0[c,d]	1.261[B,A]	15.3
40:2	0.970	NI	0.341[B]	12.3
40:2	0.990	18:1/18:1/4:0[c]	1.376[B,A]	23.4
40:1	0.960	18:1/16:0/6:0[c,d]	1.671[B,A]	7.7
	0.982	18:1/18:0/4:0[c] + 18:0/18:1/4:0[c]	3.416[B,A]	3.9
40:0	0.955	18:0/16:0/6:0[c,d]	0.447[B]	14.0
	0.980	18:0/18:0/4:0[c]	1.019[B]	8.2
42:2	0.955	18:1/18:1/6:0[c]	0.694[B,A]	2.8
42:1	0.952	18:1/18:0/6:0[c]	2.127[A(B)]	4.5
		NI, 31:0, 33:0, 35:1, 35:0, 37:1, 37:0, 39:1, 39:0	2.680	
			34.700	

[a]The number of acyl group carbons:the number of double bonds.
[b]Relative retention time.
[c]Regiospecific analysis indicates a mixture of enantiomers L/L′(M)/S + S/L′(M)/L. The enantiomers L/L′(M)/S, which are more consistent with the results of stereospecific analyses (4–6), are shown.
[d]Mixture of reverse isomers L/L′(M)/S and L′(M)/L/S.
[e]The mol percentage was calculated by normalizing the sum of the mean of *n*(mol) for each molecular species of triacylglycerols with one butyroyl or caproyl chain measured in fractions A ($n = 4$), B ($n = 4$), C ($n = 5$), and D ($n = 3$) to give the total proportion of 34.7 mol% determined by GC (37).
[f]A, B, C, or D after the value for mol% indicates the fraction of silica gel fractionation, where the molecular species was measured. Parentheses express that a minor part of the molecular species was measured in the fraction in question.
[g]Relative standard deviation (RSD) (%) determined for the silica gel fraction, where the major part of the molecular species was measured ($n = 4$, fractions A and B; $n = 5$, fraction C).
[h]Not identified.

The optimization of the analytical conditions to improve the separation of short-chain TAG containing one butyroyl or caproyl group per molecule in the analyses with three columns impaired the resolution and detection limit of acetate TAG, especially those of X/X/2:0-isomers. The results obtained with the two silica gel columns in series (Table 5) provided new data on the distribution of acetic acid in the short-chain TAG. As a result, it was possible to demonstrate significant amounts of acetate in the *sn*-2-position of TAG containing two short-chain FA or one short- and one medium-chain FA. Previously, Itabashi *et al.* (38) had shown by chiral phase HPLC that essentially all acetate was associated with the *sn*-3-position of acetic acid-enriched TAG in molecular distillates of butterfat. The TAG examined in their study, however, were made up exclusively of two long-chain FA and acetic acid. In the present work, acetic acid was found in the *sn*-3-position of the TAG containing two long-chain FA in the molecule.

Collision-induced dissociation spectra. The improved resolution of the regioisomers realized in the present study permitted much more accurate estimates of the relative ease of cleavage of the FA from the primary and secondary positions of the TAG. The relatively higher variation noted in the ion ratios of the regioisomers in the present study, compared to previous work (31), is probably due to the use of an automated MS/MS mode used in examining the large number of

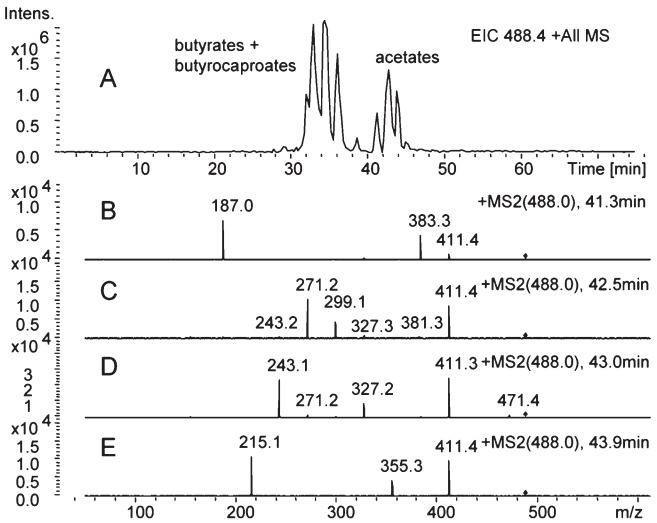

FIG. 7. Structural analysis of the acyl chain isomers of acetate TAG 24:0 in butterfat. (A) EIC of ammonium adduct of the TAG 24:0, *m/z* 488. (B) Tandem MS at 41.3 min: 1-stearoyl-2-acetyl-3-butyroyl-*sn*-glycerol + 1-butyroyl-2-acetyl-1-stearoyl-*sn*-glycerol. (C) Tandem MS at 42.5 min: 1-lauroyl-2-caprioyl-3-acetyl-*sn*-glycerol + 1-acetyl-2-caprioyl-3-lauroyl-*sn*-glycerol. (D) Tandem MS at 43.0 min: 1-myristoyl-2-capryloyl-3-acetyl-*sn*-glycerol + 1-acetyl-2-capryloyl-3-myristoyl-*sn*-glycerol. (E) Tandem MS at 43.9 min: 1-palmitoyl-2-caproyl-3-acetyl-*sn*-glycerol + 1-acetyl-2-caproyl-3-palmitoyl-*sn*-glycerol. For abbreviation see Figure 1.

TABLE 5
Area Proportions of Identified Regioisomer Species of Acetate TAG in Butterfat[a]

ACN:DB[b]	RRT[c]	Major and (minor) molecular species	X/X/2:0 area%[f]	X/2:0/X area%[f]
24:1	1.481	18:1/2:0/4:0		2.3[D]
	1.609	4:0/18:1/2:0	0.2[D]	
22:0	1.579	16:0/4:0/2:0.	0.6[D]	
24:0	1.451	18:0/2:0/4:0		1.2[D]
	1.510	12:0/10:0/2:0, 14:0/8:0/2:0	2.9[D]	
	1.549	16:0/6:0/2:0, 6:0/16:0/2:0	2.1[D]	
26:1	1.550	18:1/6:0/2:0, 14:0/10:1/2:0	2.5[D]	
26:0	1.332	16.0/2:0/8:0		3.2[C]
	1.472	14:0/10:0/2:0, (12:0/12:0/2:0)	7.0[D]	
	1.510	16:0/8:0/2:0, 18:0/6:0/2:0	8.0[D]	
28:1	1.332	18:1/2:0/8:0		2.8[C]
	1.538	18:1/8:0/2:0	3.2[C(D)]	
28:0	1.434	16:0/10:0/2:0, 18:0/8:0/2:0	23.5[C]	
30:1	1.488	18:1/10:0/2:0	10.4[C]	
30:0	1.455	16:0/12:0/2:0, (18:0/10:0/2:0)	30.1[C]	
	Sum		90.5	9.5

[a]Area proportions of identified regioisomer species of acetate TAG in butterfat determined by HPLC–ESI–MS/MS using two silica gel columns in series.
[b]The number of acyl group carbons:the number of double bonds.
[c]Relative retention time.
[f]C and D after the value for area% indicate the fraction of silica gel fractionation, where the regioisomer species was measured. Parentheses express that a minor part of the molecular species was measured in the fraction in question.

TAG species by tandem MS. The differences in the ion ratios, however, were so distinct that differentiation between regioisomers in butterfat fractions never became a problem. It should be noted that in LC–MS the observed reverse isomer ratio is dependent on the time point of MS/MS measurement. In automated MS/MS mode, the timing and identification of the reverse isomers of short-chain TAG is random, and resolution is not sufficient to allow quantitative estimation. On the average, our ion ratios are higher than those reported for long-chain TAG in ESI–MS by Marzilli *et al.* (30) and Han and Gross (27), in APCI–MS by Mottram and Evershed (21), and CI–MS by Myher *et al.* (15), as well as in NICI–MS by Kallio and Currie (16).

Quantitative estimation of TAG. Regioisomers of short-chain TAG of butterfat have not been quantified before by MS methods. Other methods have until now failed to provide quantitative data for short-chain TAG of butterfat.

Specifically, difficulties have been experienced in using by NICI–MS/MS methods for estimating regioisomers of TAG containing two C_8 FA per molecule (18). Fragmentation was less specific in the case of the TAG with a single 8:0 residue than in the case of TAG with two 8:0 residues. This finding made the exact quantification of this type of regioisomer in an unknown mixture impossible, although the predominant isomer could still be estimated, provided its proportion exceeded 50%. Similar difficulties are expected in the analysis of regioisomers of short-chain (C_4, C_6) TAG. In principle, the quantification of regioisomers of short-chain TAG should be possible by LC–APCI–MS, but relative to the present ESI method, more complicated calibration would be needed for a high number of regioisomer pairs, including response factors of $[M + H]^+$, up to three $[M - RCOO]^+$ and acyls for each regioisomer, and an algorithm for calculation of quantities. Probably owing to these complications, Mottram and Evershed (13) have recently reported only qualitative HPLC–APCI–MS data on milk fat TAG, while Mottram *et al.* (23) were able to obtain quantitative data on regioisomers of long-chain TAG of animal fat TAG. Application of the positive ESI–MS/MS method of Han and Gross (27) in the quantification of regioisomers of butterfat short-chain TAG would also need additional extensive calibration data.

The improved resolution of the regioisomers also permitted an improved determination of the different response factors, which varied with the chain length and degree of unsaturation of the FA chains and their association. In specific previous instances, this shortcoming has been overcome by employing various curve-fitting methods to correct for mass overlaps, chain length, degree of unsaturation, and the isotope effect (18,19,27). Although the present method also requires these corrections, they can be obtained from direct measurement, rather than from extrapolations. The improved resolution of regioisomers increased the reliability of the determination of MCF by allowing the examination of a much

larger number of regioisomers. A linear response was found for 42 pairs of regioisomers in 20 interesterified mixtures of standards. MCF varied widely among molecular species as well as between regioisomers. MCF and ACN showed a polynomial relationship in six classes of TAG containing short-chain FA in the *sn*-2- or *sn*-1(3)-position.

The present results differ from those obtained on the basis of silver ion solid-phase extraction and high-temperature GLC by Kemppinen and Kalo (37), who found the proportion of *sn*-2-butyrate isomers to vary between 0 and 10% and to be on the average 1.4% in the TAG containing one short acyl chain. That of *sn*-2-caproate isomers varied between 0 and 17% but was on the average only 0.3%. In the present study, *sn*-2-short-chain regioisomers L/4:0/L(M) and L/6:0/L(M) were not identified in butterfat. Comparison of relative retention times of standard mixtures showed that those of isobaric L/4:0/L- and L/L/6:0-species differed only slightly. It is therefore possible that small amounts of L/4:0/L-species had become eluted in the peak quantified as L/L/6:0-species. The CID spectra of 3 L/L/6:0-isomers showed very low abundance for ions, which could have been formed by cleavage of butyric acid from any coeluting L/4:0/L-isomers, while in other L/L/6:0-isomers, the respective ion was not detected at all. This suggests that the L/4:0/L-isomers are present, if at all, in trace amounts only.

Other unexpected complications arose from the observation that the MCF of isomeric saturated short-chain TAG varied depending on the overall symmetry of the TAG molecule. Thus, the MCF of asymmetric L/S/L′-isomers were consistently higher than those of the corresponding symmetric L/S/L-isomers. The greater the difference of the length of L and L′, the higher the MCF. This suggests easier ionization of symmetric than asymmetric TAG under soft ionization conditions. In monounsaturated TAG, the MCF of 18:1/4:0/12:0 was more than twice that of 16:1/4:0/14:0. Similar, but not as distinct differences were observed among L/L′/4:0-isomers: The greater the chain-length difference between the acyl chains in the primary positions, the higher the MCF.

The regioisomer ratio of butterfat TAG containing two short acyl chains per acylglycerol molecule has not been investigated previously. Myher *et al.* (39) identified and quantified the area percentages obtained by LC–MS and HPLC–ELSD for various short-chain TAG-species including L/S/S- and S/L/S-regioisomers, but not those originating from the same molecular species. Gresti *et al.* (40) used GLC of TAG and FAME analysis to characterize short-chain TAG subfractions obtained by RP-HPLC to identify several molecular species in the above category, but provided no information on regioisomers. Although the molar proportion of TAG containing two short acyl chains per molecule is approximately1% of total TAG and approximately 3% of short-chain TAG, the presence of 90.5% of L/S/S′ + L/S/S- and 69% of L/6:0/4:0-isomers along with S/L/S′ + S/L/S as regioisomers contributes significantly to the overall asymmetry of the FA distribution in the short-chain TAG of butterfat. The overall percentage of butyric acid esterified in the *sn*-1- (0.1), *sn*-2- (0.7), and *sn*-3- (99.2%) positions calculated from all identified short-chain TAG, is similar to the results of stereospecific analyses, except for the absence of butyric acid from the *sn*-1-position. Stereospecific analyses have indicated very low or zero percentage of butyric acid in the *sn*-2-position (4,5,41,42) and ^{1}H NMR data exclusion of butyric acid from the *sn*-2-position (43). Likewise, the percentages of caproic acid esterified at the *sn*-1- (0.5), *sn*-2- (6.1), and *sn*-3-positions (93.4%) resemble the results of stereospecific analyses (41), except for the absence of caproic acid from the *sn*-1-position. The detection of small amounts of tributyroylglycerol (0.0097%) and tricaproylglycerol (0.0188%) would also bolster the content of these short-chain acids in the *sn*-1- and *sn*-2-positions.

Significance of the results. The knowledge of the regioisomer distribution of FA in butterfat has a direct bearing on the understanding of milk fat biosynthesis and its digestion in the gastrointestinal tract and absorption by the intestine. The preferential attack of the lingual and gastric lipases upon the short-chain FA in the butterfat TAG followed by isomerization results in the formation of MAG- and DAG, which are subject to differential further hydrolysis by pancreatic lipase. The intestinal uptake and resynthesis of the regioisomeric lipolysis products determines the relative resynthesis of the milk fats *via* the monoacylglycerol and phosphatidic acid pathways, which determines their metabolic utilization. Likewise, the FA distribution and molecular association affects the dietary utilization of structured TAG synthesized to mimic milk fat TAG. The MS methodology developed in this study should be applicable also in studies on the interesterification and acidolysis reactions of milk fats and other fats used to improve their industrial and metabolic properties.

ACKNOWLEDGMENTS

Financial support from the Jenny and Antti Wihuri Foundation and Finnish Society of Dairy Science is gratefully acknowledged.

REFERENCES

1. Larsson, K. (1986) Physical properties—Structural and Physical Characteristics, in *The Lipid Handbook* (Gunstone, F.D., Harwood, J.L., and Padley, F.D., eds.), pp. 321–376, Chapman & Hall, London.
2. Kuksis, A. (2000) Biochemistry of Glycerolipids and Formation of Chylomicrons, in *Fat Digestion and Absorption* (Christophe, A., and Vriese, S.D., eds.), pp. 119–180, AOCS Press, Champaign.
3. Mu, H., and Høy, C.-E. (2000) Effects of Different Medium-Chain Fatty Acids on Intestinal Absorption of Structured Triacylglycerols, *Lipids 35,* 83–89.
4. Breckenridge, W.C., and Kuksis, A. (1968) Specific Distribution of Short-Chain Fatty Acids in Molecular Distillates of Bovine Milk Fat, *J. Lipid Res. 9,* 388–393.
5. Marai, L., Breckenridge, W.C., and Kuksis, A. (1969) Specific Distribution of Fatty Acids in the Milk Fat Triglycerides of Goat and Sheep, *Lipids 4,* 562–570.
6. Pitas, R.E., Sampugna, J., and Jensen, R.G. (1967) Triglyceride Structure of Cows' Milk Fat: I. Preliminary Observations on the

Fatty Acid Compositions of Positions 1, 2, and 3, *J. Dairy Sci. 50,* 1332–1336.
7. Myher, J.J., Kuksis, A., Marai, L., and Sandra, P. (1988) Identification of the More Complex Triacylglycerols in Bovine Milk Fat by Gas Chromatography–Mass Spectrometry Using Polar Capillary Columns, *J. Chromatogr. 452,* 93–118.
8. Kuksis, A., Marai, L., and Myher, J.J. (1991) Reversed-Phase Liquid Chromatography–Mass Spectrometry of Complex Mixtures of Natural Triacylglycerols with Chloride-Attachment Negative Chemical Ionization, *J. Chromatogr. 588,* 73–87.
9. Laakso, P., and Manninen, P. (1997) Identification of Milk Fat Triacylglycerols by Capillary Supercritical Fluid Chromatography–Atmospheric Pressure Chemical Ionization Mass Spectrometry, *Lipids 32,* 1285–1295.
10. Kalo, P., and Kemppinen, A. (1993) Mass Spectrometric Identification of Triacylglycerols of Enzymatically Modified Butterfat Separated on a Polarizable Phenylmethylsilicone Column, *J. Am. Oil Chem. Soc. 70,* 1209–1217.
11. Marai, L., Kuksis, A., and Myher, J.J. (1994) Reversed-Phase Liquid Chromatography–Mass Spectrometry of the Uncommon Triacylglycerol Structures Generated by Randomization of Butteroil, *J. Chromatogr. 672,* 87–99.
12. Spanos, G.A, Schwartz, R.B., van Breemen, R.B, and Huang, C.-H. (1995) High-Performance Liquid Chromatography with Light-Scattering Detection and Desorption Chemical–Ionization Tandem Mass Spectrometry of Milk Fat Triacylglycerols, *Lipids 30,* 85–90.
13. Mottram, H.R., and Evershed, R.P. (2001) Elucidation of the Composition of Bovine Milk Fat Triacylglycerols Using High-Performance Liquid Chromatography–Atmospheric Pressure Chemical Ionisation Mass Spectrometry, *J. Chromatogr. 926,* 239–253.
14. Ryhage, R., and Stenhagen, E. (1960) Mass Spectrometry in Lipid Research, *J. Lipid Res. 1,* 361–390.
15. Myher, J.J., Kuksis, A., Marai, L., and Manganaro, F. (1984) Quantitation of Natural Triacylglycerols by Reversed–Phase Liquid Chromatography with Direct Liquid Inlet Mass Spectrometry, *J. Chromatogr. 283,* 289–301.
16. Kallio, H., and Currie, G. (1993) Analysis of Low Erucic Acid Turnip Rapeseed Oil (*Brassica campestris*) by Negative Ion Chemical Ionization Tandem Mass Spectrometry: A Method Giving Information on the Fatty Acid Composition in Positions *sn*-2 and *sn*-1/3 of Triacylglycerols, *Lipids 28,* 207–215.
17. Kallio, H., and Rua, P. (1994) Distribution of the Major Fatty Acids of Human Milk Between *sn*-2, and *sn*-1,3 Positions of Triacylglycerols, *J. Am. Oil Chem. Soc. 71,* 985–992.
18. Kurvinen, J.-P., Mu, H., Kallio, H., Xu, X., and H_y, C.E. (2001) Regioisomers of Octanoic Acid–Containing Structured Triacylglycerols Analyzed by Tandem Mass Spectrometry Using Ammonia Negative Ion Chemical Ionization, *Lipids 36,* 1377–1382.
19. Kurvinen, J.-P., Rua, P., Sjovall, O., and Kallio, H. (2001) Software (MSPECTRA) for Automatic Interpretation of Triacylglycerol Molecular Mass Distribution Spectra and Collision Induced Dissociation Product Ion Spectra Obtained by Ammonia Negative Ion Chemical Ionuization Mass Spectrometry, *Rapid Commun. Mass Spectrom. 15,* 1084–1091.
20. Yli-Jokipii, K.M., Schwab, U.S., Tahvonen, R.L., Kurvinen, J.-P., Mykkänen, H., and Kallio, H.P.T. (2003) Chylomicron and VLDL TAG Structures and Postprandial Lipid Response Induced by Lard and Modified Lard, *Lipids 38,* 693–703.
21. Mottram, H.R., and Evershed, R.P. (1996) Structure Analysis of Triacylgycerol Positional Isomers Using Atmospheric Pressure Chemical Ionisation Mass Spectrometry, *Tetrahedron Lett. 37,* 8593–8596.
22. Mottram, H.R., Woodbury, S.E., and Evershed, R.P. (1997) Identification of Triacylglycerol Positional Isomers Present in Vegetable Oils by High Performance Liquid Chromatography/Atmospheric Pressure Chemical Ionization Mass Spectrometry, *Rapid Commun. Mass Spectrom. 11,* 1240–1252.
23. Mottram, H.R., Crossman, Z.M., and Evershed, R.P. (2001) Regiospecific Characterisation of the Triacylglycerols in Animal Fats Using High Performance Liquid Chromatography-Atmospheric Pressure Chemical Ionisation Mass Spectrometry, *Analyst 126,* 1018–1024.
24. Jakab, A., Jablonkai, I., and Forgács, E. (2003) Quantification of the Ratio of Positional Isomer of Dilinoleoyl-Oleoyl Glycerols in Vegetable Oils, *Rapid Commun. Mass Spectrom. 17,* 2295–2302.
25. Duffin, K.L., Henion, J.D., and Shieh, J.J. (1991) Electrospray and Tandem Mass Spectrometric Characterization of Acylglycerol Mixtures That Are Dissolved in Nonpolar Solvents, *Anal. Chem. 63,* 1781–1788.
26. Cheng, C., Gross, M.L., and Pittenauer, E. (1998) Complete Structural Elucidation of Triacylglycerols by Tandem Sector Mass Spectrometry, *Anal. Chem. 70,* 4417–4426.
27. Han, X., and Gross, R.W. (2001) Quantitative Analysis and Molecular Species Fingerprinting of Triacylglyceride Molecular Species Directly from Lipid Extracts of Biological Samples by Electrospray Ionization Tandem Mass Spectrometry, *Anal. Biochem. 295,* 88–100.
28. Hvattum, E. (2001) Analysis of Triacylglycerols with Non-Aqueous Reversed-Phase Liquid Chromatography and Positive Ion Electrospray Tandem Mass Spectrometry, *Rapid Commun. Mass Spectrom. 15,* 187–190.
29. Dorschel, C.A. (2002) Characterization of the TAG of Peanut Oil by Electrospray LC-MS-MS, *J. Am. Oil Chem. Soc. 79,* 749–753.
30. Marzilli, L.A., Fay, L.B., Dionisi, F., and Vouros, P. (2003) Structural Characterization of Triacylglycerols Using Electrospray Ionization-MSn Ion-Trap MS, *J. Am. Oil Chem. Soc. 80,* 195–202.
31. Kalo, P., Kemppinen, A., Ollilainen, V., and Kuksis, A. (2003) Analysis of Regioisomers of Short-Chain Triacylglycerols by Normal-Phase Liquid Chromatography–Electrospray Tandem Mass Spectrometry, *Int. J. Mass Spectrom. 229,* 167–180.
32. Hsu, F.-F., and Turk, J. (1999) Structural Characterization of Triacylglycerols as Lithiated Adducts by Electrospray Ionization Mass Spectrometry Using Low-Energy Collisionally Activated Dissociation on a Triple Stage Quadrupole Instrument, *J. Am. Soc. Mass Spectrom. 10,* 587–599.
33. Kim, Y.H., So, K.-Y., Limb, J.-K., Jhon, G.-J., and Han, S.-Y. (2000) Identification of Triacylglycerols Containing Two Short-Chain Fatty Acids at *sn*-2 and *sn*-3 Positions from Bovine Udder by Fast Atom Bombardment Tandem Mass Spectrometry, *Rapid Commun. Mass Spectrom. 14,* 2230–2237.
34. Segall, S.D., Artz, W.E., Raslan, D.S., Ferraz, V.P., and Takahashi, J.A. (2004) Ouricuri (*Syagrus coronata*) Triacylglycerol Analysis Using HPLC and Positive Ion Electrospray Tandem MS, *J. Am. Oil Chem. Soc. 81,* 143–149.
35. Byrdwell, W.C., Emken, E.A., Neff, W.E., and Adlof, R.O. (1996) Quantitative Analysis of Triglycerides Using Atmospheric Pressure Chemical Ionization–Mass Spectrometry, *Lipids 31,* 919–935.
36. Byrdwell, W.C., and Neff, W.E. (1996) Analysis of Genetically Modified Canola Varieties by Atmospheric Pressure Chemical Ionization Mass Spectrometric and Flame Ionization Detection, *J. Liq. Chrom. Rel. Technol. 19,* 2203–2225.
37. Kemppinen, A., and Kalo, P. (1998) Analysis of *sn*-1(3)- and *sn*-2-Short-Chain Acyl Isomers of Triacylglycerols in Butteroil by Gas–Liquid Chromatography, *J. Am. Oil Chem. Soc. 75,* 91–100.
38. Itabashi, Y., Myher, J.J., and Kuksis, A. (1993) Determination of Positional Distribution of Short-Chain Fatty Acids in Bovine

Milk Fat on Chiral Columns, *J. Am. Oil Chem. Soc. 70,* 1177–1181.
39. Myher, J.J., Kuksis, A., and Marai, L. (1993) Identification of the Less Common Isologous Short-Chain Triacylglycerols in the Most Volatile 2.5% Molecular Distillate of Butter Oil, *J. Am. Oil Chem. Soc. 70,* 1183–1191.
40. Gresti, J., Bugaut, M., Maniongui, C., and Bezard, J. (1993) Composition of Molecular Species of Triacylglycerols in Bovine Milk Fat, *J. Dairy Sci. 76,* 1850–1869.
41. Christie, W.W., and Clapperton, J.L. (1982) Structures of the Triglycerides of Cows' Milk, Fortified Milks (Including Infant Formulae), and Human Milk, *J. Soc. Dairy Technol. 35,* 22–24.
42. Parodi, P.W. (1982) Positional Distribution of Fatty Acids in Triglycerides from Milk of Several Species of Mammals, *Lipids 17,* 437–442.
43. Kalo, P., Kemppinen, A., and Kilpeläinen, I. (1996) Determination of Positional Distribution of Butyryl Groups in Milkfat Triacylglycerols, Triacylglycerol Mixtures, and Isolated Positional Isomers of Triacylglycerols by Gas Chromatography and ^{1}H Nuclear Magnetic Resonance Spectroscopy, *Lipids 31*, 331–336.

[Received July 20, 2004; accepted November 7, 2004]

α-Linolenic Acid and the Risk of Prostate Cancer

Sir:

Although the role of individual FA in cancer has been poorly investigated (1), a number of recent prospective epidemiological and case–control studies have shown a positive relationship between α-linolenic acid (ALA) in diet or blood and prostate cancer (2–8). In contrast, other epidemiological studies have found no significant relationship between ALA in diet, blood, or adipose tissue and prostate cancer (9–15). The association between ALA and prostate cancer has been reviewed recently by Attar-Bashi *et al.* (16), Brouwer *et al.* (17), and Astorg (18).

We have previously discussed the reliability of dietary assessment methods, such as food frequency questionnaires, in accurately capturing the intakes of certain nutrients, including ALA (16). One of the difficulties with dietary ALA is that food databases are unlikely to be up-to-date or to contain sufficient detail to reflect the ALA level in different foods, such as margarines. Indeed, of 13 margarines analyzed, reflecting all the major manufacturers in Australia, the ALA content varied from 0.2 to 5.9% of total margarine FA (19). Another issue is that the major food sources of ALA differ considerably among countries. In the United States, fats and oils provide 59% of dietary ALA (20), whereas fats and oils contribute only 16% of the total ALA intake in Australia (21).

Implicit in the epidemiological studies reported above is a causal relationship between dietary and/or plasma ALA and the incidence of prostate cancer. This raises several questions.

(i) Do dietary and/or plasma ALA levels reflect the ALA level in prostate tissue? To our knowledge, no studies have examined whether a relationship exists between the level of ALA in plasma and ALA in the prostate gland, apart from a pilot study by our group that *did not* find any significant relationship in 28 subjects undergoing exploratory surgery for prostate cancer (22).

(ii) Does the prostate accumulate ALA? We have found only three reports that discuss human prostate FA levels (13,23,24). Of these, only two have reported ALA levels in the prostate tissue, with values ranging from 0.5 to 2.7% of total FA (13,23). One of these studies showed that the ALA levels in prostate tissue were significantly lower in the patients with advanced cases of prostate cancer than in the control subjects (13). This finding would appear to be *opposite* that predicted by the epidemiological studies just mentioned. We have measured the FA content of prostate tissue in 20 subjects undergoing exploratory surgery (transurethral resection of the prostate) to aid in their diagnosis (25). All subjects were diagnosed with benign hyperplasia of the prostate on a subsequent histological examination. The main lipids in the tissue were TAG and phospholipids (PL), and in both fractions the levels of ALA were found to be very low in relation to the total n-3 PUFA. The proportion of ALA in the PL fraction was 0.03 ± 0.02% of total PL FA, whereas the proportion of total n-3 PUFA was 5.3 ± 0.9% of total FA. In the TAG fraction, the proportion of ALA was 0.5 ± 0.3% of the total TAG FA compared with a total proportion of n-3 PUFA of 2.5 ± 1.0%. The total ALA content of the prostate tissue was 0.3 mg/100 g tissue compared with a total n-3 PUFA content of 36 mg/100 g tissue. These data show that, as in many other human tissues, ALA is present in very low proportions compared with total n-3 PUFA. In our analyses, the main n-3 PUFA in the prostate tissue were 22:5n-3 and 22:6n-3 (25), which is consistent with what we reported in the dog (26), the only other mammal to develop prostate cancer spontaneously (27). The n-6 PUFA content of the human prostate tissue was five times that of the n-3, with the main n-6 PUFA being arachidonic acid (25).

(iii) What is the situation with breast and colon cancer? A recent study reported that a low ALA content in the breast adipose tissue was associated with an increased risk of breast cancer (28), whereas another study reported a significant reduction of risk for women in the highest tertile of both ALA and 22:6n-3 in breast adipose tissue (29). Another study, based on dietary data, found that both ALA and cholesterol intakes were significantly positively associated with an increased risk of breast cancer (30). A recent study reported that, in contrast, marine n-3 FA were inversely related to postmenopausal breast cancer in Chinese women from Singapore (31). The same group reported that women possessing high-activity genotypes of glutathione S-transferases showed no significant reduction in breast cancer risk (32). The authors suggested that the women in the high-activity genotype may have increased detoxification of hydroperoxides from the long-chain n-3 PUFA, leading to a reduction in possibly cytotoxic lipid oxidation products.

Clinical, case–control, and cohort studies have investigated the relationship between levels of ALA in the diet, plasma, and mucosal tissue and the risk of colorectal cancer in humans. Two studies found lower plasma or mucosal ALA levels in patients with cancer compared with controls (33,34), whereas six studies found no relationship between measures of ALA in the diet, blood, or mucosa and the risk of colon cancer (35–40). One study found a significant increase in ALA intake in subjects at high risk of colorectal cancer; however, no difference was found in the proportion of ALA in the plasma when compared with normal subjects (35).

Paper no. L9615 in *Lipids 39*, 929–932 (September 2004).

Abbreviations: ALA, α-linolenic acid; 13-HODE, 13-hydroxyoctadecadienoic acid; PL, phospholipid.

(iv) Is there a plausible biological mechanism by which ALA promotes prostate and other cancers? To our knowledge, there is no evidence that ALA metabolites, other than EPA and DHA, are formed in humans. Studies in animals and humans show that ALA is subject to extensive β-oxidation (41) and also that it is deposited in the adipose tissue and skin in animals (41). Hydroxy PUFA derivatives, such as 13-hydroxy-octadecadienoic acid (13-HODE), are known to be formed in mammals from linoleic acid *via* a lipoxygenase reaction (42). Perhaps ALA competes with linoleic acid, leading to a reduction in 13-HODE production. Pasqualini *et al.* (43) have suggested that 13-HODE and other hydroxy-PUFA might be related to the metastatic potential of cells. It is possible that ALA is also metabolized to hydroxy FA in mammals, since in plants, ALA is extensively metabolized by 15-lipoxygenase to a variety of active compounds (41). Most *in vitro* studies show no evidence of ALA promoting tumor cell growth; rather, they have shown that ALA and other n-3 PUFA *inhibit* the growth of prostate cancer cells *in vitro* (44,45). Studies in animals have shown that diets rich in ALA inhibit the growth of spontaneous or carcinogen-induced mammary tumors in animals (46–48) and inhibit the proliferation of human mammary tumor cells *in vitro* (49,50).

(v) Is it possible that ALA is a marker of another compound(s), found associated with ALA in foods, that is responsible for the associations seen in these epidemiological studies? In countries where there is widespread partial hydrogenation of ALA-containing oils, such as in the United States, it is possible that a strong association exists between ALA and *trans* isomers of ALA and other FA. Another possibility is that ALA may be a marker for lipids from the nonsaponifiable fraction of oils and fats, such as the sterols, hydrocarbons, and tocopherols. This aspect has received no attention in the published literature.

A recent pilot study in 15 men found that 6 mon of supplementation of their diet with 30 g of flaxseed daily (equivalent to approximately 5 g ALA/d) significantly reduced the circulating levels of prostate-specific antigen and the proliferation rates in the benign prostate epithelium (51). This pilot study is consistent with data from animal and cell-line studies showing a positive association between flaxseed or flaxseed lignans with the inhibition of growth and development of prostate cancer (52,53).

It is of interest that in a number of the studies cited above, the ALA longer-chain metabolites, 20:5n-3 and 22:6n-3, were associated with a reduced risk of prostate cancer (2) and breast cancer (31). It is difficult to rationalize how the parent n-3 FA (ALA) could be positively associated with certain cancers whereas the ALA metabolites (20:5n-3 and 22:6n-3) were protective against these same cancers, unless ALA is metabolized to an as yet undescribed novel metabolite.

We conclude that more basic research is needed before any conclusions can be drawn regarding the association between this essential nutrient and prostate and other cancers.

REFERENCES

1. Larsson, S.C., Kumlin, M., Ingelman-Sundberg, M., and Wolk, A. (2004) Dietary Long-Chain n-3 Fatty Acids for the Prevention of Cancer: A Review of Potential Mechanisms, *Am. J. Clin. Nutr. 79*, 935–945.
2. Leitzmann, M.F., Stampfer, M.J., Michaud, D.S., Augustsson, K., Colditz, G.C., Willett, W.C., and Giovannucci, E.L. (2004) Dietary Intake of n-3 and n-6 Fatty Acids and the Risk of Prostate Cancer, *Am. J. Clin. Nutr. 80*, 204–216.
3. Giovannucci, E., Rimm, E.B., Colditz, G.A., Stampfer, M.J., Ascherio, A., Chute, C.C., and Willett, W.C. (1993) A Prospective Study of Dietary Fat and Risk of Prostate Cancer, *J. Natl. Cancer Inst. 85*, 1571–1579.
4. De Stéfani, E., Deneo-Pellegrini, H., Boffetta, P., Ronco, A., and Mendilaharsu, M. (2000) α-Linolenic Acid and Risk of Prostate Cancer: A Case–Control Study in Uruguay, *Cancer Epidemiol. Biomarkers Prev. 9*, 335–338.
5. Ramon, J.M., Bou, R., Romea, S., Alkiza, M.E., Jacas, M., Ribes, J., and Oromi, J. (2000) Dietary Intake and Prostate Cancer Risk: A Case–Control Study in Spain, *Cancer Causes Control 11*, 679–685.
6. Gann, P.H., Hennekens, C.H., Sacks, F.M., Grodstein, F., Giovannucci, E.L., and Stampfer, M. (1994) Prospective Study of Plasma Fatty Acids and Risk of Prostate Cancer, *J. Natl. Cancer Inst. 86*, 281–286.
7. Harvei, S., Bjerve, K.S., Tretli, S., Jellum, E., Robsahm, T.E., and Vatten, L. (1997) Prediagnostic Level of Fatty Acids in Serum Phospholipids: ω-3 and ω-6 Fatty Acids and the Risk of Prostate Cancer, *Int. J. Cancer 71*, 545–551.
8. Newcomer, L.M., King, I.B., Wicklund, K.G., and Stanford, J.L. (2001) The Association of Fatty Acids with Prostate Cancer, *Prostate 47*, 262–268.
9. Andersson, S.O., Wolk, A., Bergstom, R., Giovannucci, E., Lindgren, C., and Baron, J. (1996) Energy, Nutrition Intake and Prostate Cancer Risk: A Population-Based Case–Control Study in Sweden, *Int. J. Cancer 68*, 716–722.
10. Schuurman, A.G., van den Brandt, P.A., Dorant, E., Brants, H.A., and Goldbohm, R.A. (1999) Association of Energy and Fat Intake with Prostate Carcinoma Risk: Results from The Netherlands Cohort Study, *Cancer 86*, 1019–1027.
11. Alberg, A.J., Kafonek, S., Huang, H.Y., Hoffman, S.C., Comstock, G.W., and Helzlsouer, K.J. (1996) Fatty Acid Levels and the Subsequent Development of Prostate Cancer, *Proc. Am. Assoc. Cancer Res. 37*, 281.
12. Godley, P.A., Campbell, M.K., Gallagher, P., Martinson, F., Mohler, J., and Sandler, R. (1996) Biomarkers of Essential Fatty Acid Consumption and Risk of Prostatic Carcinoma, *Cancer Epidemiol. Biomarkers Prev. 5*, 889–895.
13. Freeman, V.L., Meydani, M., Yong, S., Pyle, J., Flanigan, R.C., Waters, B., and Wojcik, E.M. (2000) Prostatic Levels of Fatty Acids and the Histopathology of Localized Prostate Cancer, *J. Urol. 164*, 2168–2172.
14. Mannisto, S., Pietinen, P., Virtanen, M.J., Salminen, I., Albanes, D., Giovannucci, E., and Virtamo, J. (2003) Fatty Acids and Risk of Prostate Cancer in a Nested Case–Control Study in Male Smokers, *Cancer Epidemiol. Biomarkers Prev. 12,* 1422–1428.
15. Ritch, C.R., Brendler, C.B., Wan, R.L., Pickett, K.E., and Sokoloff, M.H. (2004) Relationship of Erythrocyte Membrane Polyunsaturated Fatty Acids and Prostate-Specific Antigen Levels in Jamaican Men, *BJU Int. 93,* 1211–1215.
16. Attar-Bashi, N.M., Frauman, A.G., and Sinclair, A.J. (2004) α-Linolenic Acid and the Risk of Prostate Cancer. What Is the Evidence? *J. Urol. 171*, 1402–1407.
17. Brouwer, I.A., Katan, M.B., and Zock, P.L. (2004) Dietary α-Linolenic Acid Is Associated with Reduced Risk of Fatal Coronary

Heart Disease, but Increased Prostate Cancer Risk: A Meta-analysis, *J. Nutr. 134,* 919–922.
18. Astorg, P. (2004) Dietary n-6 and n-3 Polyunsaturated Fatty Acids and Prostate Cancer Risk: A Review of Epidemiological and Experimental Evidence, *Cancer Causes Control 15*, 367–386.
19. Mansour, M.P., and Sinclair, A.J. (1993) The *trans* Fatty Acid and Positional (*sn*-2) Fatty Acid Composition of Some Australian Margarines, Dairy Blends and Animal Fats, *Asia Pacific J. Clin. Nutr. 3*, 155–163.
20. Raper, N.R., Cronin, F.J., and Exler, J. (1992) n-3 Fatty Acid Content of the U.S. Food Supply, *J. Am. Coll. Nutr. 11*, 304–308.
21. Meyer, B.J., Mann, N.M., Jannie, L.L., Milligan, G.C., Sinclair, A.J., and Howe, P.R. (2003) Dietary Intake and Food Sources of Omega-6 and Omega-3 Polyunsaturated Fatty Acids, *Lipids 38*, 391–398.
22. Attar-Bashi, N.M., Frydenberg, M., Li, D., and Sinclair, A.J. (2004) Lack of Correlation Between Plasma and Prostate Tissue α-Linolenic Acid Levels, *Asia Pac. J. Clin. Nutr. 13* (Suppl.), S78.
23. Weisser, H., and Kreig, M. (1998) Fatty Acid Composition of Phospholipids in Epithelium and Stroma of Human Benign Prostatic Hyperplasia, *Prostate 36*, 235–243.
24. Chaudry, A., McClinton, S., Moffat, L.E.F., and Wahle, K.W.L. (1991) Essential Fatty Acid Distribution in the Plasma and Tissue Phospholipids of Patients with Benign and Malignant Prostatic Disease, *Br. J. Cancer 64*, 1157–1160.
25. Attar-Bashi, N.M. (2003) Metabolism and Biological Roles of α-Linolenic Acid in Humans and Animals, Ph.D. Thesis, RMIT University, Melbourne.
26. Attar-Bashi, N.M., Orzeszko, K., Slocombe, R.F., and Sinclair, A.J. (2003) Lipids and FA Analysis of Canine Prostate Tissue, *Lipids 38*, 665–668.
27. Cornell, K.K., Bostwick, D.G., Cooley, D.M., Hall, G., Harvey, H.J., Hendrick, M.J., Pauli, B.U., Render, J.A., Stoica, G., Sweet, D.C., and Waters, D.J. (2000) Clinical and Pathologic Aspects of Spontaneous Canine Prostate Carcinoma: A Retrospective Analysis of 76 Cases, *Prostate 45*, 173–183.
28. Klein, V., Chajes, V., Germain, E., Schulgen, G., Pinault, M., Malvy, D., Lefrancq, T., Fignon, A., Le Floch, O., Lhuillery, C., and Bougnoux, P. (2000) Low α-Linolenic Acid Content of Adipose Breast Tissue Is Associated with an Increased Risk of Breast Cancer, *Eur. J. Cancer 36*, 335–340.
29. Maillard, V., Bougnoux, P., Ferrari, P., Jourdan, M.L., Pinault, M., Lavillonniere, F., Body, G., Le Floch, O., and Chajes, V. (2002) N-3 and N-6 Fatty Acids in Breast Adipose Tissue and Relative Risk of Breast Cancer in a Case–Control Study in Tours, France, *Int. J. Cancer 98,* 78–83.
30. De Stefani, E., Deneo-Pellegrini, H., Mendilaharsu, M., and Ronco, A. (1998) Essential Fatty Acids and Breast Cancer: A Case–Control Study in Uruguay, *Int. J. Cancer 76*, 491–494.
31. Gago-Dominguez, M., Yuan, J.M., Sun, C.L., Lee, H.P., and Yu, M.C. (2003) Opposing Effects of Dietary n-3 and n-6 Fatty Acids on Mammary Carcinogenesis: The Singapore Chinese Health Study, *Br. J. Cancer 89*, 1686–1692.
32. Gago-Dominguez, M., Castelao, J.E., Sun, C.L., Van Den Berg, D., Koh, W.P., Lee, H.P., and Yu, M.C. (2004) Marine n-3 Fatty Acid Intake, Glutathione S-Transferase Polymorphisms and Breast Cancer Risk in Postmenopausal Chinese Women in Singapore, *Carcinogenesis* (July 15) [E-publication ahead of print].
33. Baro, L., Hermoso, J.C., Nunez, M.C., Jimenez-Rios, J.A., and Gil, A. (1998) Abnormalities in Plasma and Red Blood Cell Fatty Acid Profiles of Patients with Colorectal Cancer, *Br. J. Cancer 77*, 1978–1983.
34. Fernandez-Banares, F., Esteve, M., Navarro, E., Cabre, E., Boix, J., Abad-Lacruz, A., Klaassen, J., Planas, R., Humbert, P., Pastor, C., and Gassull, M.A. (1996) Changes of the Mucosal n-3 and n-6 Fatty Acid Status Occur Early in the Colorectal Adenoma–Carcinoma Sequence, *Gut 38*, 254–259.
35. Schloss, I., Kidd, M.S., Tichelaar, H.Y., Young, G.O., and O'Keefe, S.J. (1997) Dietary Factors Associated with a Low Risk of Colon Cancer in Coloured West Coast Fishermen, *Afr. Med. J. 87*, 152–158.
36. Tuyns, A.J., Haelterman, M., and Kaaks, R. (1987) Colorectal Cancer and the Intake of Nutrients: Oligosaccharides Are a Risk Factor, Fats Are Not. A Case–Control Study in Belgium, *Nutr. Cancer 10*, 181–196.
37. Neoptolemos, J.P., Clayton, H., Heagerty, A.M., Nicholson, M.J., Johnson, B., Mason, J., Manson, K., James, R.F., and Bell, P.R. (1988) Dietary Fat in Relation to Fatty Acid Composition of Red Cells and Adipose Tissue in Colorectal Cancer, *Br. J. Cancer 58*, 575–579.
38. Slattery, M.L., Potter, J.D., Duncan, D.M., and Berry, T.D. (1997) Dietary Fats and Colon Cancer: Assessment of Risk Associated with Specific Fatty Acids, *Int. J. Cancer 73*, 670–677.
39. Neoptolemos, J.P., Husband, D., Imray, C., Rowley, S., and Lawson, N. (1991) Arachidonic Acid and Docosahexaenoic Acid Are Increased in Human Colorectal Cancer, *Gut 32*, 278–281.
40. Terry, P., Bergkvist, L., Holmberg, L., and Wolk, A. (2001) No Association Between Fat and Fatty Acids Intake and Risk of Colorectal Cancer, *Cancer Epidemiol. Biomarkers Prev. 10*, 913–914.
41. Sinclair, A.J., Attar-Bashi, N.M., and Li, D. (2002) What Is the Role of α-Linolenic Acid for Mammals? *Lipids 37*, 1113–1123.
42. Ziboh, V.A., Miller, C.C., and Cho, Y. (2000) Significance of Lipoxygenase-Derived Monohydroxy Fatty Acids in Cutaneous Biology, *Prostaglandins Other Lipid Mediat. 63*, 3–13.
43. Pasqualini, M.E., Heyd, V.L., Manzo, P., and Eynard, A.R. (2003) Association Between E-Cadherin Expression by Human Colon, Bladder, and Breast Cancer Cells and the 13-HODE:15-HETE Ratio. A Possible Role of Their Metastatic Potential, *Prostaglandins Leukot. Essent. Fatty Acids 68*, 9–16.
44. du Toit, P.J., van Aswegen, C.H., and du Plessis, D.J. (1996) The Effect of Essential Fatty Acids on Growth and Urokinase-Type Plasminogen Activator Production in Human Prostate DU-145 Cells, *Prostaglandins Leukot. Essent. Fatty Acids 55*, 173–177.
45. Motaung, E., Prinsloo, S.E., van Aswegen, C.H., du Toit, P.J., Becker, P.J., and du Plessis, D. (1999) Cytotoxicity of Combined Essential Fatty Acids on a Human Prostate Cancer Cell Line, *Prostaglandins Leukot. Essent. Fatty Acids 61*, 331–337.
46. Kamano, K., Okuyama, H., Konishi, R., and Nagasawa, H. (1989) Effects of a High-Linoleate and High α-Linoleate Diet on Spontaneous Mammary Tumorigenesis in Mice, *Anticancer Res. 9*, 1903–1908.
47. Fritsche, K.L., and Johnston, P.V. (1990) Effect of Dietary α-Linolenic Acid on Growth, Metastasis, Fatty Acid Profile, and Prostaglandin Production of Two Murine Mammary Adenocarcinomas, *J. Nutr. 120*, 1601–1609.
48. Chen, J., Stavro, P.M., and Thompson, L.U. (2002) Dietary Flaxseed Inhibits Human Breast Cancer Growth and Metastasis and Downregulates Expression of Insulin-like Growth Factor and Epidermal Growth Factor Receptor, *Nutr. Cancer 43*, 187–192.
49. Begin, M.E., and Ells, G. (1987) Effects of C_{18} Fatty Acids on Breast Carcinoma Cells in Culture, *Anticancer Res. 7*, 215–217.
50. Chajes, V., Sattler, W., Stranzl, A., and Kostner, G.M. (1995) Influence of n-3 Fatty Acids on the Growth of Human Breast Cancer Cells *in vitro*: Relationship to Peroxides and Vitamin-E, *Breast Cancer Res. Treat. 34*, 199–212.
51. Demark-Wahnefried, W., Robertson, C.N., Walther, P.J., Polascik, T.J., Paulson, D.F., and Vollmer, R.T. (2004) Pilot Study to Explore Effects of Low-Fat, Flaxseed-Supplemented Diet on Proliferation of Benign Prostatic Epithelium and Prostate-Specific Antigen, *Urology 63*, 900–904.

52. Lin, X., Switzer, B.R., and Demark-Wahnefried, W. (2001) Effect of Mammalian Lignans on the Growth of Prostate Cancer Cell Lines, *Anticancer Res. 21*, 3995–3999.
53. Lin, X., Gingrich, J.R., Bao, W., Li, J., Haroon, Z.A., and Demark-Wahnefried, W. (2002) Effect of Flaxseed Supplementation on Prostatic Carcinoma in Transgenic Mice, *Urology 60*, 919–924.

[Received September 17, 2004, and in final form and accepted October 29, 2004]

Nadia M. Attar-Bashi[a], Duo Li[b], and Andrew J. Sinclair[a,*]
[a]School of Applied Sciences, RMIT University, Melbourne, Victoria, 3001, Australia, and [b]Zhejiang University, Hangzhou, China

*To whom correspondence should be addressed at Department of Food Science, RMIT University, Melbourne, Victoria, 3001, Australia.
E-mail: andrew.sinclair@rmit.edu.au

REVIEW

Astonishing Diversity of Natural Surfactants: 1. Glycosides of Fatty Acids and Alcohols

Valery M. Dembitsky*

Department of Organic Chemistry and School of Pharmacy, Hebrew University, Jerusalem, Israel

ABSTRACT: Alkyl and fatty acid glycosides have become of great commercial interest in general and specifically for the pharmaceutical, cosmetic, and food industries. Natural surfactants are good sources for future chemical preparation of these glycosides. This review article shows an astonishing diversity of natural surfactants that could be used in laboratories and industry. More than 250 natural surfactants, including their chemical structures and biological activities, are described in this review article.

Paper no. L9640 in *Lipids 39,* 933–953 (October 2004).

Many of the natural surfactant compounds are biological-chemical complexes that include molecules of fatty (carboxylic) and dicarboxylic (dioic) acids, fatty acid amides, alkylglycosides, lactones, and sugar molecules, which are connected by chemical bonds (1). Surfactants are molecules that have both a polar hydrophilic part and a nonpolar lipophilic part. They are adsorbed between phases of different natures and thus lower the interfacial tension between the phases. For this reason, surfactants are used as stabilization agents of emulsions or emulsifiers. The term *hydrophile–lipophile balance* (HLB) was first suggested by Clayton (2) in 1943 and refers to the balance in size and strength between the hydrophilic and lipophilic portions of a surfactant. Later, Griffin (3,4) developed the empirical concept of an HLB value for surfactants or emulsifiers on the basis of the solubility of these agents in water. These chemical complexes can also comprise other moieties such as flavonoids, iridoids, quinones, anthraquinones, carotenoids, steroids, and other molecular structures (1–15). Contemporary trends in the discovery of drugs from natural products emphasize investigation of the terrestrial and marine environments to yield numerous highly active compounds (5–7).

Low- and high-molecular-weight natural biosurfactants (fatty [or carboxylic] acid glycoside esters) are of great interest because of their physicochemical and biological properties, which can be exploited in the oil, food, cosmetic, and pharmaceutical industries (14,16). As for the general types of microbial amphiphiles, the data accumulated over recent years add to already well-known compounds another new interesting molecular structure. Fatty acid glycosides are active amphipathic molecules with hydrophobic and hydrophilic moieties. Surfactants constitute an important class of industrial chemicals widely used in modern industry (13,16). It is well established that many macrolactone glycosides are natural antibiotics that are used as antimicrobial agents in both clinical and veterinary medicine (15). Glyceroglycolipids and glycophospholipids have been reviewed recently (8) and are not included in this review except for some recent publications. Also we have not included methods for the synthesis and application of surfactants, as this field is well described in many books and review articles (see, for example, References 6, 11, 13, 14, and 16 and references cited in these papers).

The term *natural surfactant* is not unambiguous. In the strictest sense, this means that a natural surfactant is a surfactant taken directly from a natural source (14). The source may be a microorganism, plant, invertebrate, or an animal and the product should be obtained by some kind of separation procedure such as extraction, precipitation, or distillation. No organic synthesis should be involved, not even as an after-treatment. There are, in fact, not many surfactants in use today that fulfill these requirements. Different glycolipids, obtained from either plants or animals, are probably the best examples of truly natural surfactants.

In this review the term natural surfactant is used in its broadest sense. The article covers true, natural surfactants that were isolated from natural sources. Only glycosides of fatty (carboxylic) acids and alcohols with a well-defined structure are included.

GLYCOSIDES OF FATTY ACIDS

A great number of simple glycolipids are found in bacteria, yeasts, and lower marine invertebrates. These compounds are composed of a glycosyl moiety (one or several units) linked to a hydroxyl fatty acid or to one carboxyl group of a fatty acid (ester linkage). These compounds frequently possess interesting physical or biological properties (3,14,16).

The lipid composition of *Roseiflexus castenholzii,* a thermophilic filamentous phototrophic bacterium related to uncultivated filamentous phototrophic bacteria that predominate in hot-spring microbial mats, was reported (17). *Roseiflexus castenholzii* lipid extracts were dominated by components characterized by alkane-1-ol-2-alkanoate moieties **1–4** glycosidically bonded to a C6 sugar. Similar fatty glycosides, with

*Address correspondence at Department of Organic Chemistry, P.O. Box 39231, Hebrew University, Jerusalem 91391, Israel.
E-mail: dvalery@cc.huji.ac.il

Abbreviations: HG, heterocyst glycolipids; HLB, hydrophile-lipophile balance; MEL, mannosylerythritol lipids; SEFA, sucrose ester(s) of fatty acids; TAACF, Tuberculosis Antimicrobial and Acquisition Coordinating Facility.

an additional esterified fatty acid, were detected by HPLC-MS. In lipid extracts from the two nonsulfidic hot-spring microbial mats, similar alkane-1,2-diol-based lipids were detected in minor amounts. *Roseiflexus castenholzii* lipids are comparable to lipids of mats and other thermophilic mat isolates.

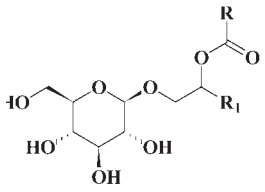

1 R = $C_{13}H_{27}$, R_1 = $C_{17}H_{35}$
2 R = $C_{15}H_{31}$, R_1 = $C_{18}H_{37}$

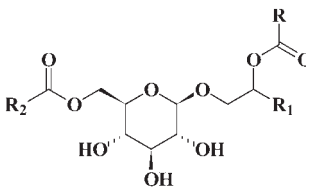

3 R = R_2 = $C_{13}H_{27}$, R_1 = $C_{18}H_{37}$
4 R = R_2 = $C_{15}H_{31}$, R_1 = $C_{18}H_{37}$

The determination of chemical structures of five novel compounds, that is, one multibranched polyunsaturated fatty acid (2*E*,4*E*,7*S*,8*E*,10*E*,12*E*,14*S*)-7,9,13,17-tetramethyl-7,14-dihydroxy-2,4,8,10,12,16-octadecahexaenoic acid) and its four glycosides, **5–8**, from seven different myxomycetes, was described (18). The glycosides contain glucose, mannose, and rhamnose only. Three of them were identified in *Arcyria cinerea*, two in *A. denudata*, and *A. nutans*, *Fuligo septica, Lycogala epidendrum*, *Physarum polycephalum,* and *Trichia varia* contained one of the identified glycosides each (18).

Fatty acid glucuronides **9–12** have been isolated from human liver as products of the action of UDP-glucuronosyltransferases and liver microsomes (19). Formation of fatty acid glucuronides **9–12** in human liver is shown in Scheme 1.

Řezanka and Dembitsky (20) found eight new brominated oxylipins, including two brominated glycosides, **13** and **14**.

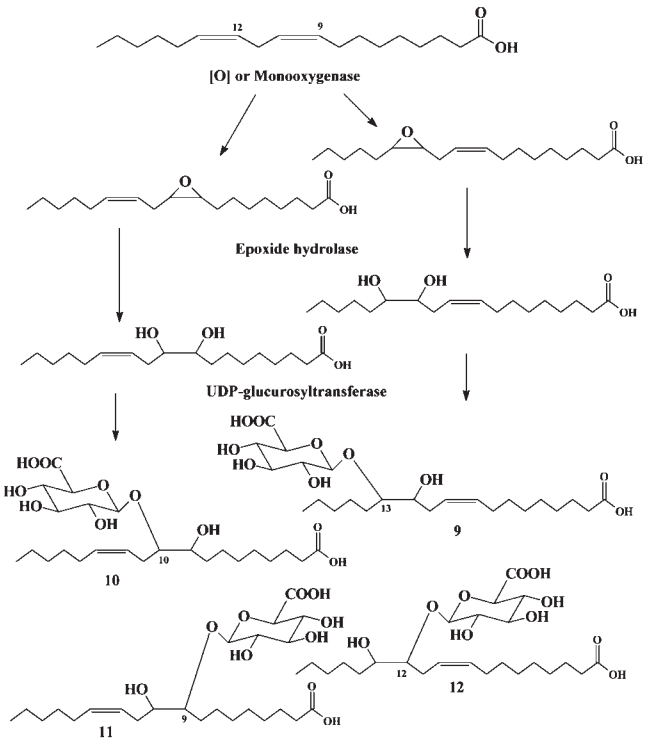

SCHEME 1

These compounds were isolated from the Red Sea invertebrates *Dendrophyllia* sp., *Dendronephthya* sp. (red variety), *Dendronephthya* sp. (yellow variety), and *Tubipora musica* and gave positive results in a brine shrimp toxicity assay, a sea urchin eggs test *(Paracentrotus lividu*s), and a crown gall tumor on potato disks test *(Agrobacterium tumefacien*s).

Tuberonic acid glucoside **15** and tuberonic acid glucoside methyl ester **16** were detected in the leaves of *Solanum tuberosum* (21). This was the first report of the isolation fatty acid glucosides from potatoes; **16** was also detected in Jerusalem artichoke (22,23) and **17** was isolated from *Salvia officinalis* (24).

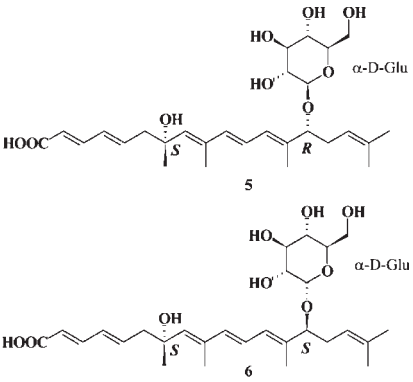

5 6

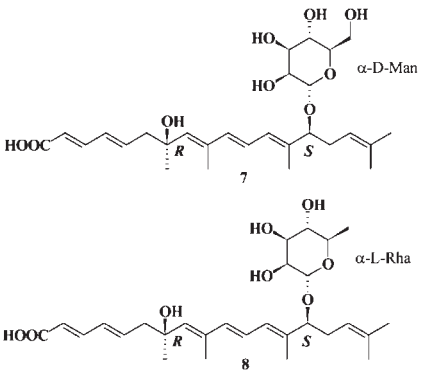

7 8

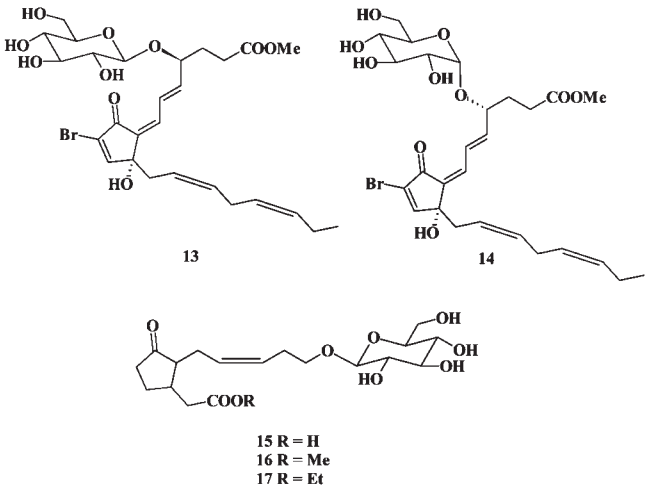

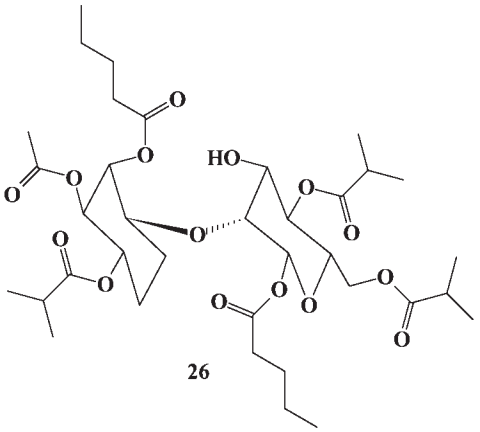

Four hydroxy fatty acid glucosides, **18–21**, were found at the time of ripening of the fruits of *Persoonia lenearis* × *pinifolia* (Proteacea) grown in Australia (25). The monoterpene glucoside ester **22** has been isolated from the leaves of the medicinal plant *Lantana lilacia*, used in the treatment of bronchitis (26). 2,6-Dimethyl-6-*O*-β-L-quinovo-pyranosyl-7-octadecanoic acid **23** has been isolated from the seeds of the *Albizia procera* (27). *Albizia procera,* belonging to the Leguminosae family and commonly known as "Safe Siris" in Hindi, is widely distributed in India. Ethyl 3-*O*-β-D-glucopyranosyl-butanoate **24** and butyl-*O*-3-β-D-glucopyranosyl-butanoate **25** were found in fruits of papaya, *Carica pubescens* (28).

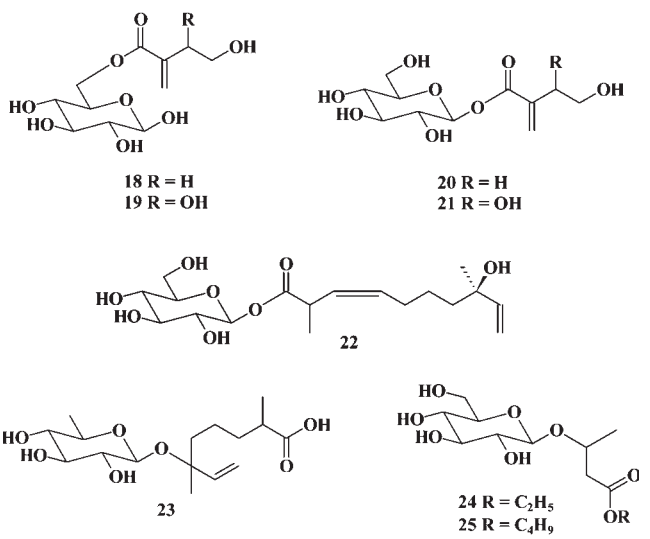

Bioassay-directed fractionation for *Staphylococcus aureus* multidrug resistance efflux pump inhibitors resulted in isolation of novel acylated neohesperidosides **26** from *Geranium caespitosum* (29). The more highly acylated compounds had no direct activity against *S. aureus,* but potentiated activity of the antibiotics berberine, rhein, ciprofloxacin, and norfloxacin. Cellular concentrations of berberine were greatly increased in the presence of active fatty acid esters.

Two novel glycolipids, emmyguyacin A **27** and emmyguyacin B **28**, were isolated from a potato dextrose agar fermentation of a sterile fungus species. The compounds inhibit replication of influenza A virus (A/X31) in MDCK cells by inhibiting the pH-dependent conformational change of hemagglutinin A (IC_{50} 9 μM) (30).

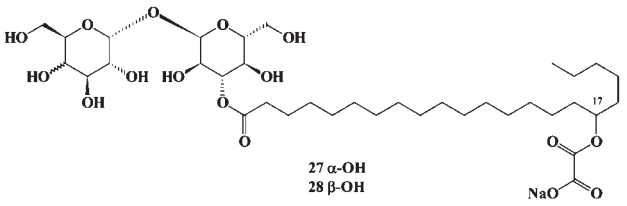

Many glucose and sucrose esters bearing a range of short- to medium-chain fatty acyl (usually C_2 to C_5) substitution patterns are known in the surface exudates from leaves of the Solanaceae genera: *Datura* (31), *Lycopersicon* (32), *Nicotiana* (33–36), and *Solanum* (37). It has been demonstrated that sucrose esters are formed in the glandular trichomes in tobacco leaves (38). These leaf surface lipids have biological activity against plants and microorganisms (39). It was reported that sucrose esters in leaf surface lipids of *Petunia hybrida* contain straight-chain fatty acids from C_4 to C_8 in addition to methylbutyryl groups (40). Investigations of leaf lipids of budworm-resistant tobacco revealed for the first time the presence of sucrose esters of fatty acids (33); saponification yielded sucrose and a series of C_2 to C_8 aliphatic acids, the major acids being acetic, 2-methylbutyric, and 3-methylvaleric acids. The major isomers are composed of an acetyl group (R_2) and three 3-methylvaleryl groups (R, R_1, and R_3)

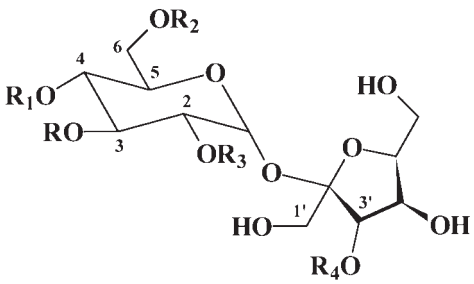

Sucrose esters of fatty acids

esterified to three hydroxyl groups of sucrose. Other short-chain acids are also present (propionic, butyric, valeric, caproic, methylcaproic, and heptanoic acids) (33).

The 2,3,4-triacyl sucrose esters of fatty acids (SEFA) have been isolated from *Datura hirsutum* f. (41) and *Nicotiana glutinosa* (42); 2,3,4-, 2,3,6-, and 2,3,1′-triacyl SEFA were found in *Lycopersicon peruvianum, Nicotiana tabacum, Salanum berthaultii,* and *Petunia multiflora nana* (33,34,43); 2,3,4,6-, 2,3,4,1′-, and 2,3,4,3′-, 2,3,6,3′-tetraacyl SEFA isolated from *Datura hirsutum* f., *Nicotiana glutinosa, N. tabacum, Petunia multiflora nana, Salanum berthaultii,* and *S. neocardenassi* (33,34,43–45). A rare type of 2,3,4,6,3′-pentaacyl SEFA has been isolated from *Nicotiana acuminata* [46].

The 2,3-diacyl glucose was found in *Datura metel* (31), and 1,2,3- and 2,3,4-triacyl glucose were isolated from *Solanum aethiopsicum* (47), *Lycopersicon pennellii* (48), and *Nicotiana acuminata* (46). 1,2,3,4- and 2,3,4,6-tetraacyl glucose have been isolated from *Nicotiana acuminata* (46) and *N. tabacum* (33); also a rare type of 1,2,3,4,6-pentaacyl glucose was found in *Nicotiana acuminata* (46).

SEFA are produced in large amounts in commercial manufacturing equipments as surfactants for the food industry (13,16). SEFA are nonionic surfactants consisting of a sugar (e.g., glucose or sucrose) as the hydrophilic group and a fatty acid as the lipophilic group. SEFA have broad applications in the food industry, cosmetics, detergents, oral-care products, and medical supplies (49), and they are also tasteless, odorless, nontoxic, nonirritating to the eyes and skin, and biodegradable (50).

Some interesting sucrose derivatives produced by colonies of sea pork, *Aplidium,* have been found recently. Shimofuridin A **29** is a cytototoxic metabolite of mixed biosynthesis from an Okinawan tunicate *A. multiplicatum* (51). Similar fatty acid sucrose derivatives, shimofuridin B–G **30–35**, are minor metabolites from the same organism (52).

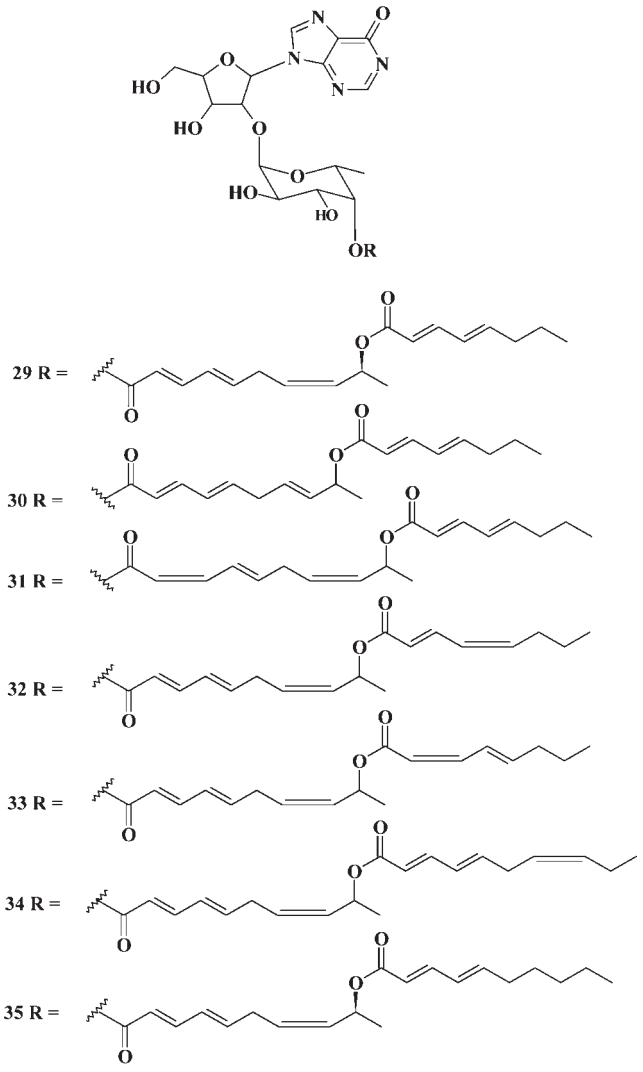

RHAMNOLIPIDS

Biosurfactants containing rhamnose and β-hydroxydecanoic acid and called rhamnolipids **36–41** with respect to microbial producers, their physiological role, biosynthesis and genetics, and especially their microbial overproduction, physicochemical properties, and potential applications, have been reviewed recently (53–58). Glycolipids containing rhamnose and β-hydroxydecanoic acid were found for the first time by Bergstrom *et al.* (59) in *Pseudomonas pyocyanea* after growth on glucose. This was achieved by Jarvis and Johnson (60), who demonstrated a glycosidic linkage of β-hydroxydecanoyl-β-hydroxydecanoate with two rhamnose molecules after cultivation of *Pseudomonas aeruginosa* on 3% glycerol and isolation of the product. However, the linkage between the two sugar units remained unclear. The structure was elucidated by Edwards and Hayashi (61), who were able to demonstrate a 1,2-linkage after periodate oxidation and methylation. The **39** was found to be the only rhamnose lipid produced when *P. aeruginosa* S7 B1 was cultivated on *n*-hexadecane and *n*-paraffins (C_{14}–C_{18}) (62). An additional new product, L-α-rhamnopyranosyl-β-hydroxydecanoyl-β-hydroxy-decanoate, rhamnolipid **36**, was isolated from a culture of *P. aeruginosa* KY 4025 with 10% *n*-alkane (63). Similar rhamnose lipids, rhamnolipids I **38** and II **41**, but with additional acylation by α-decenoic acid, have been described by Yamaguchi *et al.* (64). The methyl esters of the rhamnose

lipids **36** and **39** were the main products of *P. aeruginosa* (65). Two rhamnose lipids that are similar to **36** and **39** but contain only one β-hydroxydecanoyl unit, rhamnolipids III **37** and IV **40**, were detected after experiments with resting cells of *Pseudomonas* sp. DSM 2874 (66,67). Further structural variants of the rhamnose lipids containing hydroxy fatty acids with different chain lengths (C_8, C_{12}) have been enriched from cultures of a clinical isolate of *P. aeruginosa* (68). However, it can generally be stated that the latter variants represent minor components.

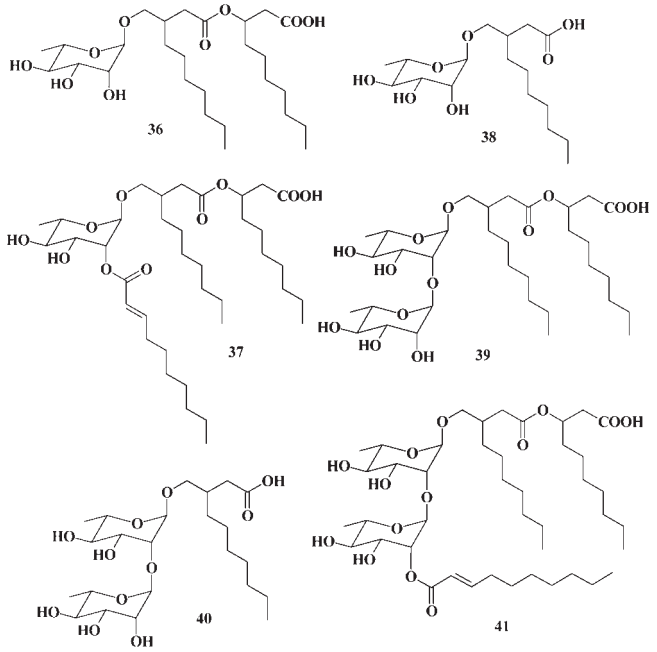

The rhamnolipids produced by *Pseudomonas aeruginosa* strains are often a mixture of several homologs. Up to seven species with different saturated and unsaturated fatty acids: $C_{10:0}$, $C_{12:0}$, $C_{12:1}$, $C_{12:2}$, and $C_{8:2}$ of **38** and **40** have been identified in cultures of *P. aeruginosa* AT10 (69). These compounds show excellent antifungal properties against *Aspergillus niger* and *Gliocadium virens* (16 μg/mL) and *C. globosum*, *P. crysogenum,* and *A. pullulans* (32 μg/mL), whereas the growth of the phytopathogenic fungi *Botrytis cinerea* and *Rhizotecnia solani* was inhibited at 18 μg/mL.

Mannosylerythritol lipids (MEL) **42–44**, yeast glycolipids, are one of the most promising biosurfactants already known and are abundantly produced from vegetable oils by *Pseudozyma* (previously *Candida*) *antarctica* T-34 to 47 g^{-1} (70). MEL exhibits excellent surface-active and vesicle-forming properties (71). They also induce cell differentiation in human leukemia cells (70), rat pheochromocytoma cells (72), and mouse melanoma cells (73). In addition, MEL was recently demonstrated to act as a potential antiagglomeration agent in an ice-water slurry system to be used for cold thermal storage (74). MEL, an extracellular glycolipid from yeast, induces the differentiation of HL-60 promyelocytic leukemia cells toward granulocytes. It was shown that MEL is also a potent inhibitor of the proliferation of mouse melanoma B16 cells (75). *n*-Alkanes ranging from C_{12} to C_{18} were converted into glycolipid biosurfactants, mannosylerythritol lipids **42–44**, by resting cells of *Pseudozyma (Candida) antarctica* T-34 (76a).

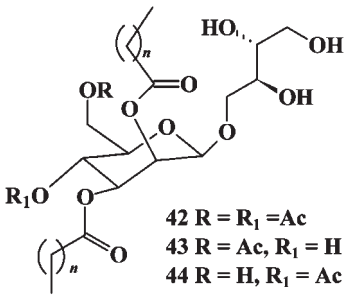

A novel resin glycoside, cuscutic resinoside A **45**, was isolated along with five known compounds from the extract from the seeds of *Cuscuta chinensis* (Convolvulaceae) (76b). The structure was deduced from its spectral data as (11*S*)-hydroxyhexadecanoic acid 11-*O*-α-L-(4-*O*-2*R*,3*R*-nilylrhamnopyranosyl)-(1→2)-*O*-α-L-rhamnopyranosyl-(1,2-lactone), forming a unique 15-membered macrocyclic lactone. The compound significantly stimulated not only MCF-7 cell proliferation but also T47D human breast cancer cells at a concentration of 10 μM.

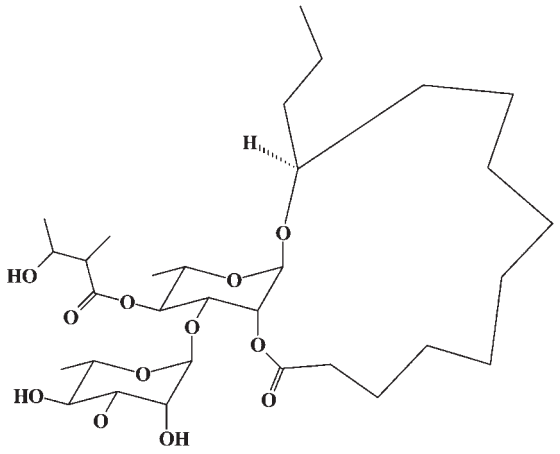

TREHALOSE LIPIDS

Fatty acid glycosides contain a nonreducing disaccharise α-D-trehalose occurring mainly in bacteria, fungi, algae, and insects, in which it seems to have a role as an energetic reserve compound (77). From lipids of *Mycobacterium fortuitum* (*M. minetti*) were isolated **46** with palmitic acid and also small amounts of saturated and saturated C_{19} and C_{20} acids (78). Similar but unsymmetrical compound **47** was also found in *M. fortuitum* (79). The occurrence of acylated trehalose **48** in the lipids of *Propionibacterium shermanii* with *myo*-inositol moiety was reported (80). Compounds **49** and **50**, in which α-D-trehalose acylated by micolic acids in the 6 and 6′ posi-

tions, were isolated from the cultures of virulent strains of the tubercle *Bacillus* sp. (81,82). Unusual lipids **51–53** and **54,55**, acylated by eight phleic acids, have been isolated from *Mycobacterium phlei* cells (83).

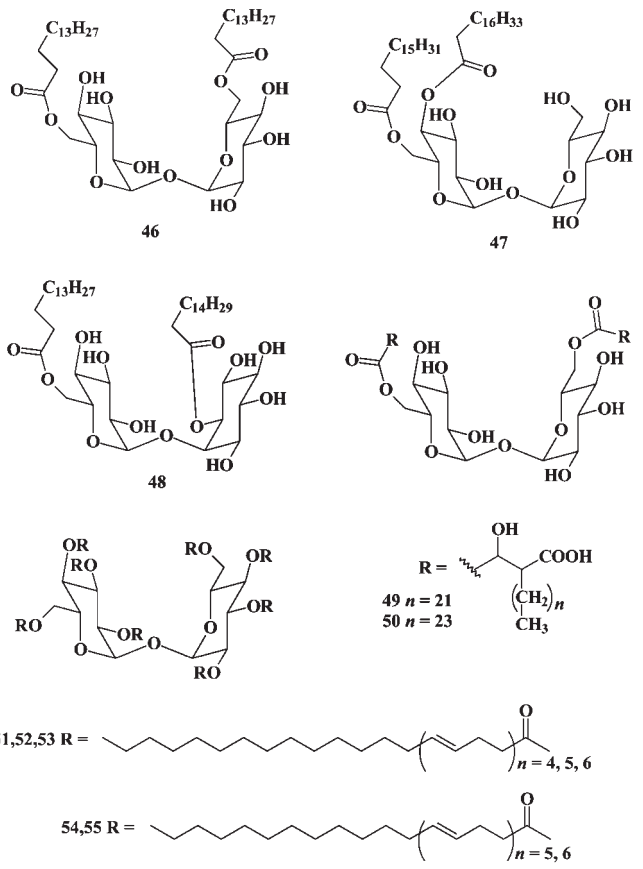

Structures of the two sulfolipids **56** and **57** from virulent tubercle bacilli were elucidated (84,85). A novel trisaccharide glycolipid biosurfactant containing trehalose bearing ester-linked hexanoate, succinate, and acyloxyacyl moieties, **58,** has been isolated from a gram-positive terrestrial actinomycete Q (86).

Fatty acid disaccharides **59–61**, the 3-*O*-β-D-glucopyranosyl-(1→6)-β-D-glucopyranoside of ethyl 3-hydroxyoctanoate and the diastereomeric 3-*O*-α-L-arabinopyranosyl-(1→6)-β-D-glucopyranosides of (3*R*) and (*3S*)-butyl 3-hydroxybutanoate, respectively, have been isolated from Colombian fruits of cape gooseberry (*Physalis peruviana*) (87). Glycosidically bound hydroxy acids: methyl 3-hydroxybutanoate, ethyl 3-hydroxy-butanoate, ethyl 3-hydroxyhexanoate, butyl 3-hydroxybutanoate, ethyl 3-hydroxyoctanoate, ethyl 5-hydroxyoctanoate; methyl-branched: 2-methyl

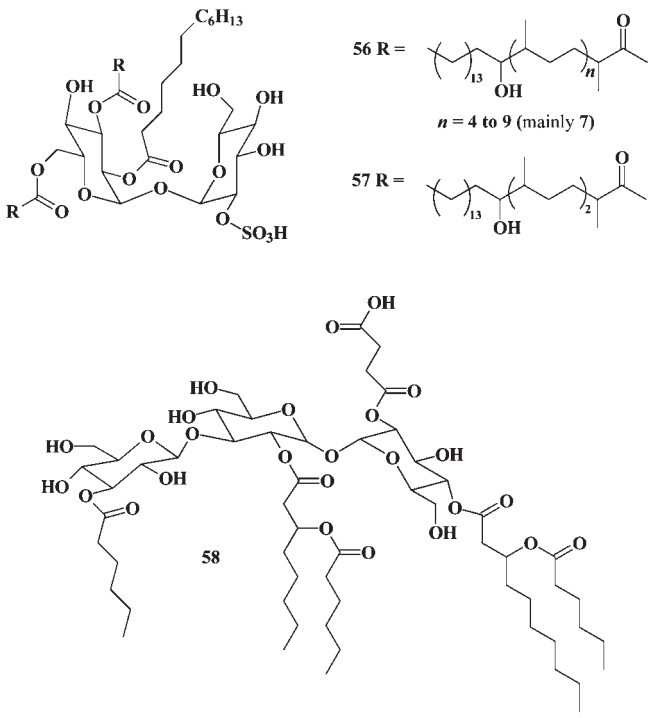

propanoic acid, 2-methylbutanoic acid, geranoic acid, saturated: butanoic acid, hexanoic acid, octanoic acid, decanoic acid, hexadecanoic acid, and unsaturated fatty acid: 9-(*Z*)-octadecenoic acid have also been detected after enzymatic hydrolysis using a nonselective pectinase (Rohapect D5L) in cape gooseberry *(P. peruviana*) (88).

The lower filamentous fungus *Absidia corymbifera* F-295 produced unusual glycolipids **62–67**: 2-*O*-(6′-*O*-β-D-galactopyranosyl)-β-D-galactopyranosides of 2-D-hydroxy and *erythro*-2,3-dihydroxy fatty acids C_9, C_{11}, and C_{13} (89).

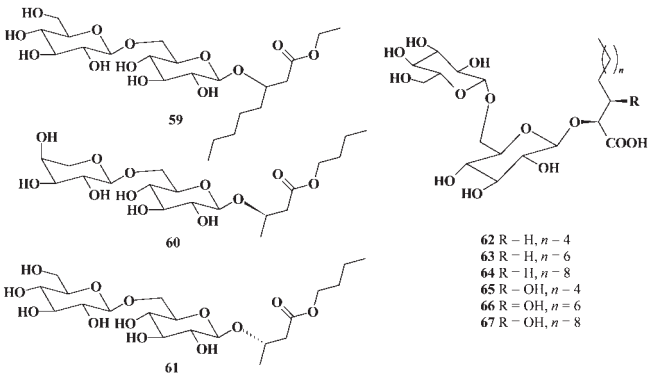

SOPHOROLIPIDS

Sophorolipids are microbial extracellular surface-active glycolipids. Cells of the yeast *Torulopsis bombicola* produce sophorolipids when they are grown on sugars, hydrocarbons, vegetable oils, or their mixtures. First described by Tulloch

(90) in 1961, sophorolipids occur as a mixture of macrolactone and free acid structures that are acetylated to various extents at the sophorose ring primarily in hydroxyl positions. Sophorolipids consist of a disaccharide glucosically linked to unsaturated ω- or (ω-1)-hydroxy C_{18} and C_{16} fatty acids. Careful examination has revealed that at least eight structurally different sophorolipids are produced **68–76** (91). The main component is 17-hydroxyoctadecanoic acid and its corresponding lactone (92,93). The yeast *Candida (Torulopsis) bombicola* ATCC 22214 secreted large amounts, up to 300 g/L^{-1}, of sophorolipids **68–76** (94). Some sophorolipids also were produced by *Torulopsis apicola* (95,96), *T. petrophilum* (97), and *Cryptococcus curvatus* ATCC 20509 (98). Microbial production of surfactants and their commercial potential have recently been reviewed (99).

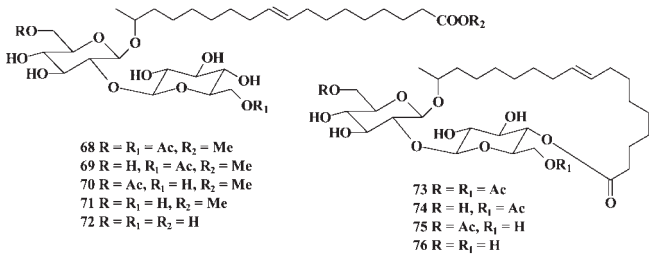

Tsukamurella sp. DSM 44370, isolated from an oil-containing soil sample, produced a high spectrum of di-**77** and **78**, tri-**79,80,** and tetrasaccharide **81,82** biosurfactant lipids from exogenous carbon sources: sugars and fatty acids (100); **77–82** showed antimicrobial activity against gram-positive and gram-negative bacteria *Bacillus megaterium*, *Escherichia coli, Ustilago viocea,* and *Chlorella fusca*.

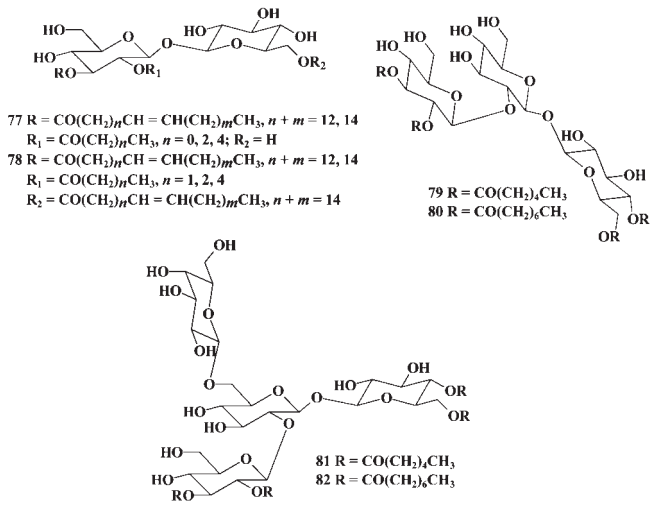

Noni, the common name for *Morinda citrifolia* L. (Rubiaceae), is a plant typically found in the Tahitian and Hawaiian islands (101). The bark, stem, root, leaf, and fruit have been used traditionally for many diseases, including diabetes, hypertension, and cancer (102,103), and all are mentioned as Hawaiian herbal remedies. Compounds **83** and **84** were isolated from fruits of this plant (104). β-1-*O*-Acyl-1,2-diglucosyl glycoside **85** has been isolated from the membrane of a gram-positive bacterium, *Sarcina ventriculi* (105).

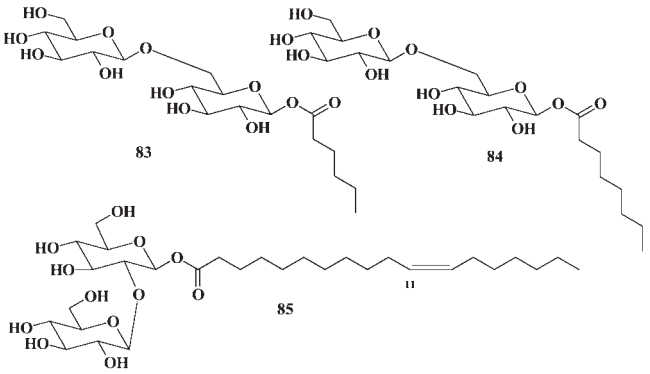

Unusual fatty acid glycosides **86–98** have been isolated from the Mexican scamimony roots (false jalap) of *Ipomoea orizabensis* (pelletan) (106). All isolated compounds inhibited cell cervix carcinoma and ovarian cancer cell lines (ED_{50} = 4–20 μg/mL), but the stronger effect was found against oral epidermoid carcinoma KB (ED_{50} = 1–5 μg/mL).

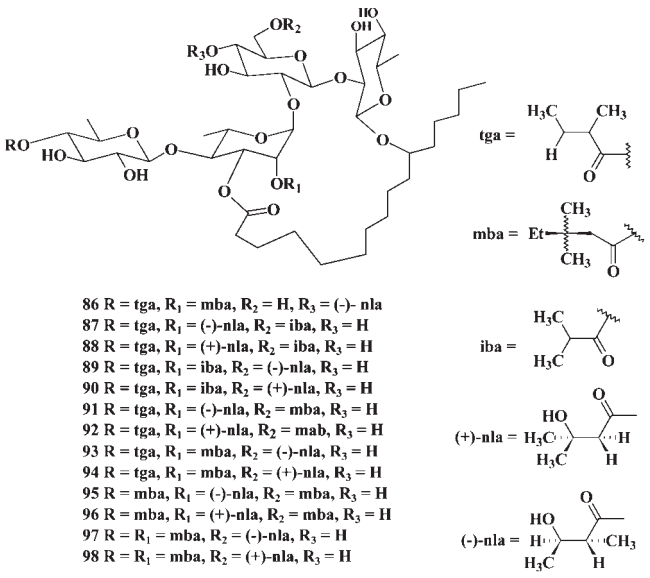

A nonlinear pentasaccharide resin glycoside soldanelline A **99**, which shows cytotoxic (UIDO, ED_{50} = 2 μg/mL) and antibacterial activity against *Bacillus subtilis* (MIC = 14.7 μg/mL), has been isolated from the plant *Calystegia soldanella* (Convolvulaceae) (107). This plant is used in Portuguese traditional medicine to cure hydropsy, paralysis, rheumatism, and scurvy (108).

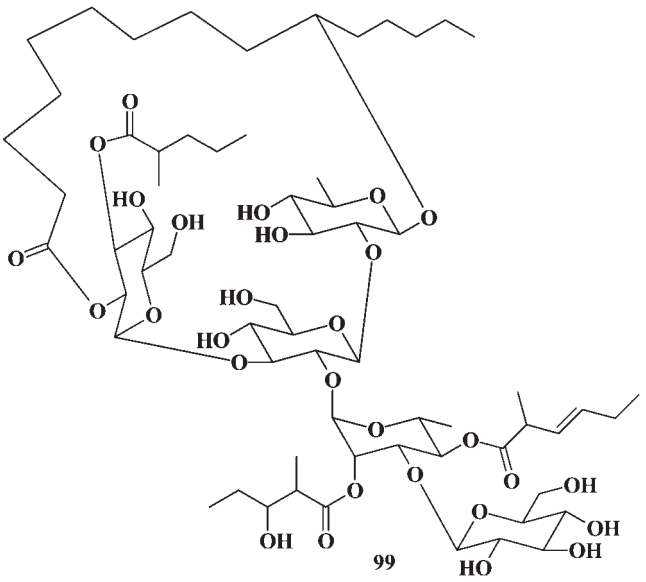

99

The unusual 3,11-dihydroxytetradecanoic acid 11-*O*-β-quinovopyranosyl-(1→2)-β-glucopyranosyl-(1→3)-[α-rhamnopyranosyl-(1→4)]-quinovopyranosyl-(1→2)-β-glucopyranosyl-(1→2)-β-fucopyranoside **100** has been isolated from the aerial parts of the Australian plant *Ipomoea lonchophylla* (109). Many species of *Ipomoea* were and often still are used in folk medicine in different parts of the world (110). Studies on ethanolic extracts of these plants have reported antimicrobial, analgesic, spasmogenic, spasmolytic, hypotensive, psychotomimetic, and anticancer effects (111). Fatty acid glycosides **101–103** have been isolated from the seeds of *Cuscuta chinesis* (Convolvulacea) or "Cuscula Semen," well known as a Chinese traditional medicine plant used as a tonic (112). Seven new ether-soluble resin glycosides, **105–111**, have been isolated from whole plants of *Ipomoea stolonifera* (113). These compounds were similar to the resin glycosides, **100–104** isolated previously from the plant *Ipomoea lonchophylla* (114).

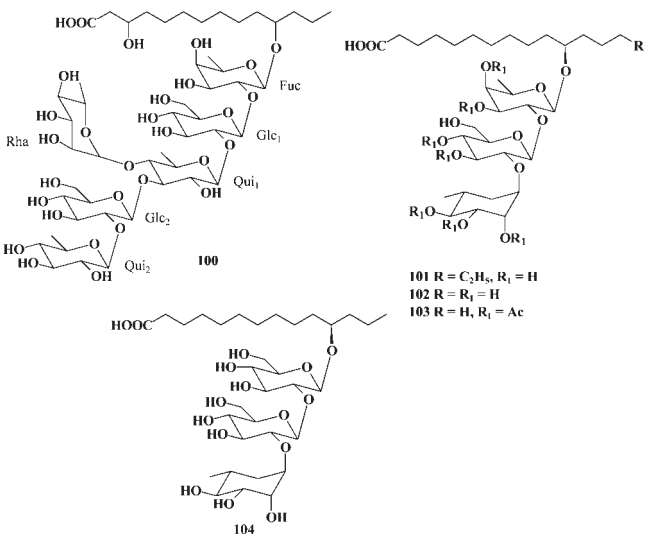

100

101 R = C_2H_5, R_1 = H
102 R = R_1 = H
103 R = H, R_1 = Ac

104

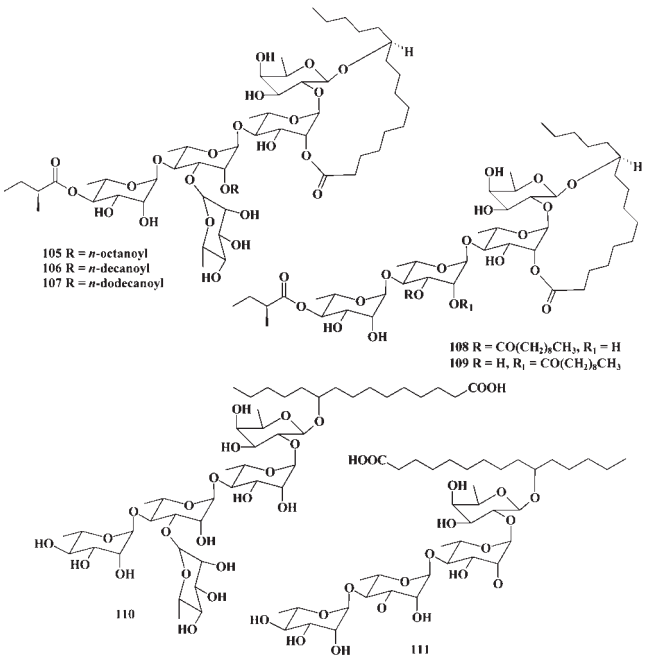

105 R = *n*-octanoyl
106 R = *n*-decanoyl
107 R = *n*-dodecanoyl

108 R = $CO(CH_2)_8CH_3$, R_1 = H
109 R = H, R_1 = $CO(CH_2)_8CH_3$

110 111

Antituberculosis resin glycosides **112–114**, isolated from the leaves of the native North American prairie plant *Ipomoea leptophylla* (big root morning glory), showed *in vitro* activity against *Mycobacterium tuberculosis* (115). The crude organic extract of *I. leptophylla* showed 92% inhibition (150 μg/mL) against *M. tuberculosis in vitro* in the antituberculosis assay performed by the Tuberculosis Antimicrobial and Acquisition Coordinating Facility (TAACF). Compound **112** showed 13% inhibition when tested at 6.25 μg/mL. The potency of **112** is insufficient to warrant further biological assessment by TAACF (100% protection at 6.25 μg/mL is required for a pure compound). The bioassay results indicate that the cinnamic acid residue is required for the observed antimicrobial activity.

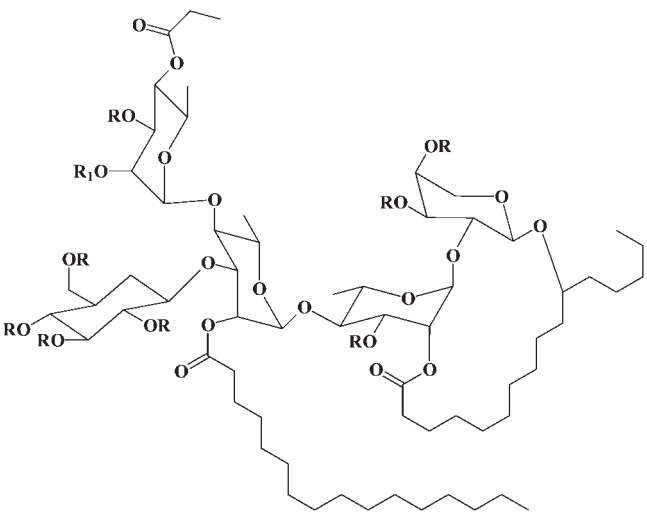

112 R = H, R_1 = *trans*-cinnamic acid
113 R = R_1 = H
114 R = Me, R_1 = *trans*-cinnamic acid

BUTANOLIDE GLYCOSIDES

Eight compounds **115–122** isolated from the extract of the central Asian lichens comprised new glycosides and glycoside esters having 18*R*-hydroxydihydroallo-protolichesterinic, 18*S*-hydroxydihydroprotolichesterinic, and 18*S*-hydroxyneodihydro-protolichesterinic acids, as the aglycones and a saccharide moiety linked at C-18 (**115–122**) and also at C-21 (**126–129**) made by glucose, xylose, or rhamnose (116). Eleven compounds isolated from the extract of the Central Asian lichens comprised seven new glycosides **123–129** having murolic, protoconstipatic, and allomurolic acids as the aglycones and a saccharide moiety linked at C-18 (in **123–125**) made up of one or two sugars (glucose and apiose or rhamnose, xylose, or arabinose) (117).

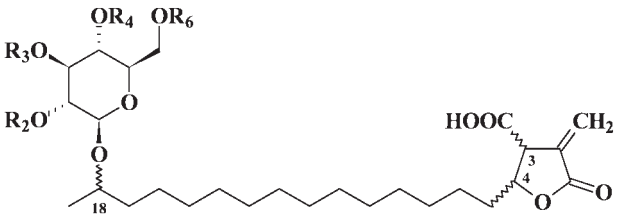

115 3S, 4S, 18R, R_2 = Glc, R_3 = R_4 = R_6 = H
116 3S, 4R, 18R, R_3 = Glc, R_2 = R_4 = R_6 = H
117 3R, 4S, 18S, R_6 = Glc, R_2 = R_3 = R_4 = H
118 3S, 4S, 18R, R_2 = R_3 = Glc, R_4 = R_6 = H
119 3S, 4S, 18R, R_2 = R_6 = Glc, R_3 = R_4 = H
120 3R, 4S, 18S, R_2 = Glc''2-1Glc''', R_3 = R_4 = R_6 = H
121 3S, 4R, 18R, R_3 = R_6 = Glc, R_2 = R_4 = H
122 3R, 4S, 18S, R_2 = Glc''6-1Glc''', R_3 = Glc, R_4 = R_6 = H

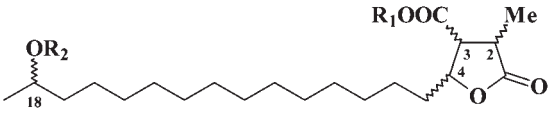

123 2R, 3S, 4S, 18R, R_1 = Rha, R_2 = H
124 2S, 3R, 4S, 18S, R_1 = Glc, R_2 = H
125 2R, 3R, 4S, 18S, R_1 = Glc, R_2 = H
126 2R, 3S, 4S, 18R, R_1 = Rha, R_2 = Glc
127 2S, 3R, 4S, 18S, R_1 = Glc, R_2 = Xyl
128 2R, 3R, 4S, 18S, R_1 = Glc, R_2 = Rha
129 2R, 3R, 4S, 18S, R_1 = Glc, R_2 = Glc

Three new glycoside butanolide derivatives having 18-hydroxy-dihydro-alloprotolichesternic, 18-hydroxy-neodihydroprotol chesternic, and 18-hydroxy-dihydroprotolichesternic acids as aglycones and a di- or trisaccharide moiety linked at C-18 and at the carboxylic group have been isolated from the lichen extract of *Acarospora gobiensis* grown in central Asia. These compounds, called gobienines A **130**, B **131**, and C **132**, were found to be di- or trisaccharides forming a macrolactone with the aglycone (116).

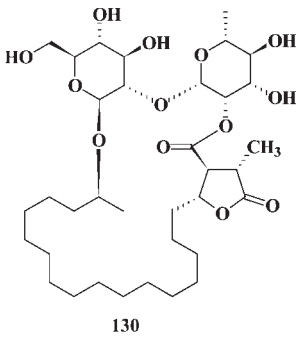

130

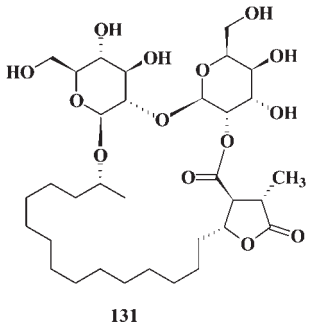

131

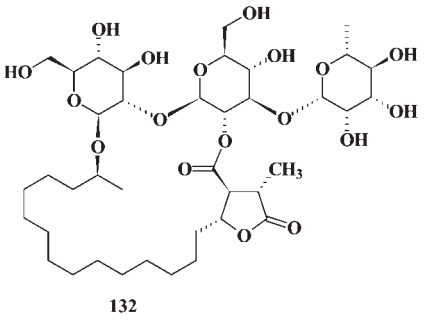

132

SORBITAN ESTERS OF FATTY ACIDS

Sorbitan fatty acid esters are called sorbitan ester, which originate from the esterification of sorbitol with fatty acids. They are a mixture of sorbitol ester and sorbide ester, which are produced simultaneously with sorbitan ester. There are many types of sorbitan esters with different kinds of fatty acids and varying degrees of esterification. Those are generally used as emulsifiers for creams and so on. Application is limited because special characteristics, other than its emulsifying capability, are few; however, it is widely used as a major emulsifier in combination with other emulsifiers with different functions (14b,16).

Vulfson (118) studied enzymatic synthesis of sorbitan esters and dehydration of sorbitol. According to resultant GC–MS data, more than 60 individual compounds were found, including various isomers of sorbitan, isosorbide (1,4:3,6-dianhydro-D-glucitol), and their mono-, di-, and triesters (for example, **133–138**). It has also been shown that sorbitan monolaurate dominated in reaction mixture. Structures of some identified dehydration products of sorbitol are shown in Figure 1.

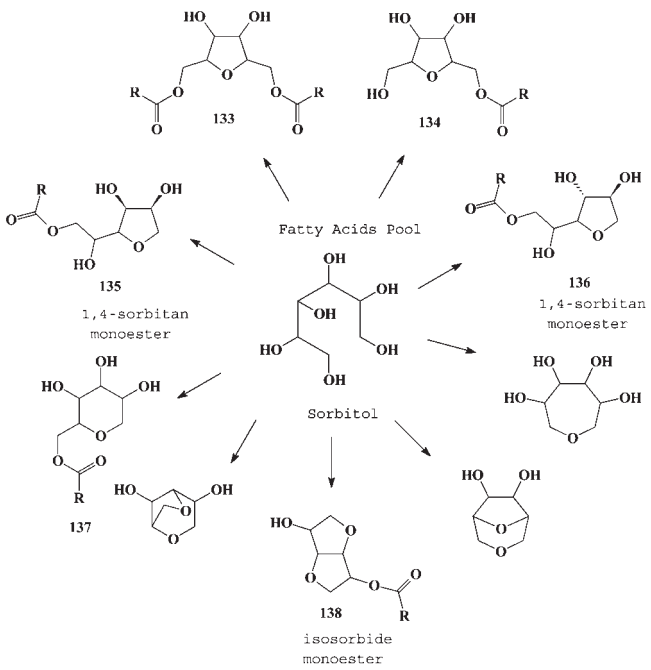

FIG. 1. Some sorbitol products identified by GC-MS.

Recently, Kikuchi *et al.* investigated secondary metabolites of the slime mold *Dictyostelium discoideum* and they found two novel amino sugar analogs, furanodictine A **139** and B **140** (119). These are the first 3,6-anhydrosugars (N-derivatives of isosorbide monoester **138**) isolated from natural sources. Their relative structures were elucidated by spectral means, and the absolute configurations were confirmed by asymmetric syntheses. The furanodictines **139** and **140** potently induce neuronal differentiation of rat pheochromocytoma (PC-12) cells (119).

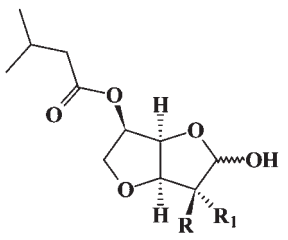

139 R = H, R_1 = NHAc
140 R = NHAc, R_1 = H

GLYCOSIDES OF FATTY ALCOHOLS

Alkylglycosides are surfactants that are arousing increased interest for several applications because, in addition to their excellent ecological and toxicological properties, they exhibit interesting interfacial properties (13,14,16,120). A comprehensive physicochemical characterization of surfactants must be based on our knowledge of not only their interfacial properties but also their phase behavior (121,122). Micellar aggregation, cloud-point, and phase formation have been studied (123).

A series of simple alkylglycosides has been isolated from different plant species. A small tree, *Crescentia cujete* L., is distributed in south Asian countries and has spherical or oval fruits. In Vietnam, the dried fruit is used in folk medicine (local name, Dao Tien) as an expectorant, antitussive, laxative, and a stomachic. The fruits of *C. cujete*, collected in Long Thanh, Ba Ria-Vung Tau province (Vietnam), afforded eight new compounds, *n*-alkylglycosides **141–148** (124).

Free and glycosidically bound flavor compounds of acerola (*Malphigia glabra*) fruit were isolated and identified by GC and GC–MS analysis. Among the 46 compounds identified in the volatile fraction, the alcohols 3-methyl-but-3-en-1-ol, 3-methyl-butan-1-ol, and 2-methyl-butan-1-ol were predominant among alkylglycosides **149–156** (125). Alkylglycosides **153** and **155** were also isolated from the essential oil of the dried leaves of *Origanum vulgare* L. ssp. *hirtum* (126). A new simple aliphatic glycoside, isopentyl-gentiobioside **157**, has been found in the cell cultures of *Lyco-persicon esculentum* (127). Methyl β-D-apiofuranosyl-(1→6)- β-D-glucopyranoside **158** and ethane-1,2-diol 1-*O*-β-D-apiofuranosyl-(1→6)-β-D-glucopyranoside **159** were isolated from the methanolic extract of cumin (fruit of *Cuminum cyminum* L.) (128), and isopentenol 1-*O*-β-D-apiofuranosyl-(1→6)-β-D-glucopyranoside **160** was found in the fruit of *Bupleurum falcatum* (129). An aliphatic alcohol glycoside, lunaroside 1-octen-3-yl *O*-β-apiofuranosyl-(1→6)-*O*-[β-glucopyranosyl-(1→2)]-β-glucopyranoside **161** was isolated from the aerial parts of *Phlomis lunariifolia* (130). Monoterpene glycoside **162**, in which a glucose unit was attached to a menthiafolic acid methyl ester, has been isolated during methanolysis of the leaves of *Jasminum hemsleyi* (131).

Two new fatty acid glucosides, (3*E*,8*Z*)-8-carboxy-1-(*O*-β-D-glucopyranosyl)-2,6-dihydroxytritriaconta-3,8-diene **163** and (8*Z*)-8-carboxy-1-(*O*-β-D-glucopyranosyl)-3,4-epoxy-2,6-dihydroxytritriacont-8-ene **164**, have been isolated from he root bark of *Ochna calodendron,* grown in southern Cameroon (132).

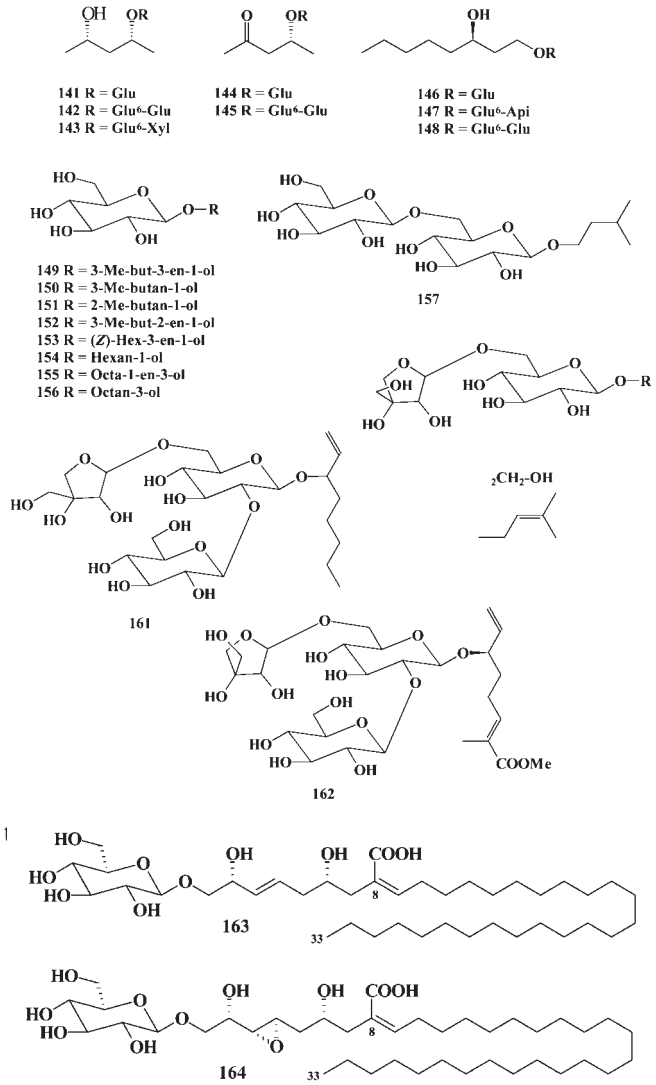

Heterocyst glycolipids have been reported to take part in the protection of the specialized cyanobacterial cells capable of N_2 fixation against the penetration of O_2. Such glycolipids have been isolated in a pure form from a cyanobacterium, *Nodularia harveyana*, and their structures have been established by spectroscopic and chemical means to be 1-(*O*-α-D-glucopyranosyl)-3*R*,25*R*-hexacosanediol **165**, 1-(*O*-α-D-glucopyranosyl)-3*S*,25*R*-hexacosanediol **166**, and 1-(*O*-α-D-glucopyranosyl)-3-keto-25*R*-hexacosanol **167** (133). The heterocyst glycolipids of the cyanobacterium *Cyanospira rippkae* have been isolated and their structures established to be 1-(*O*−α-D-glucopyranosyl)-3*R*,27*R*-octacosanediol **168** and 1-(*O*-α-D-glucopyranosyl)-27-keto-3*R*-octacosanol **169** (134). The akinetes of *C. rippkae* contain the same glycolipids.

The incorporation of [1-^{14}C] sodium acetate into the heterocyst glycolipids from 60- to 234-hour-old *Anabaena cylindrica* cultures was studied and radioactive lipids were isolated (135). In 60-hour and 88-hour cultures, about 90% of the radioactivity of the heterocyst glycolipids was found in the nonsaponifiable glycolipid fraction, whereas in older cultures this

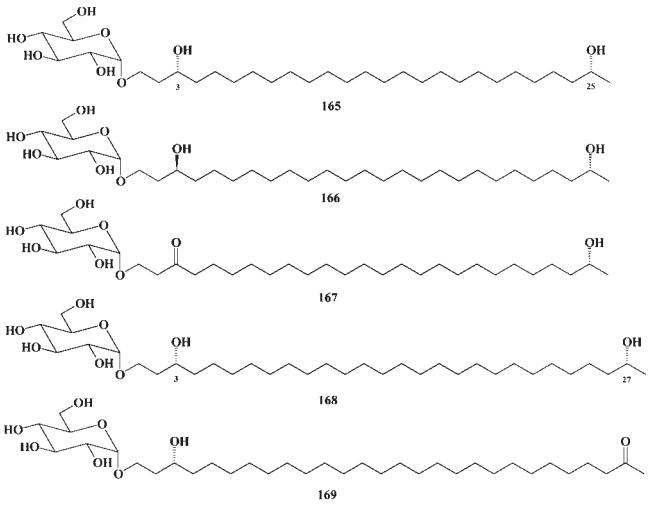

fraction contained only 75% of the radioactivity. Acid hydrolysis of nonsaponifiable heterocyst glycolipid fractions showed that in 60-hour cultures, 81% of the radioactivity occurred in the lipid moiety, whereas in older cultures a greater proportion (40–53%) of the radioactivity was found in the sugar residue. The lipid fraction obtained by acid hydrolysis contained a mixture of labeled long-chain mono-, di-, and trihydric alcohols. In young cultures the primary alcohol fraction was most heavily labeled (57.3% of the radioactivity in the nonsaponifiable glycosides) with much smaller amounts in the diol and triol (8.4 and 15.1%, respectively), whereas in older cultures the primary alcohol (23.6%), diol (22.5%), and triol (18.9%) fractions contained approximately equal amounts of radioactivity. The previously proposed structures for the heterocyst glycolipids of the nitrogen-fixing cyanobacterium *Anabaena cylindrica* (135) have been revised. ^{13}C-enriched acetonides have been utilized for the determination of the relative stereochemistry of the 1,3-diol moiety in the aglycone of two glycolipids. The same glycolipids, which are thought to protect the nitrogenase from O_2, have also been detected in *A. torulosa* (24); **165**,**167** and **170**,**171** have been isolated from cyanobacteria *A. cylindrica* and *A. torulosa* (24). Formation and functions of heterocyst glycolipids in cyanobacteria species have recently been reviewed (136).

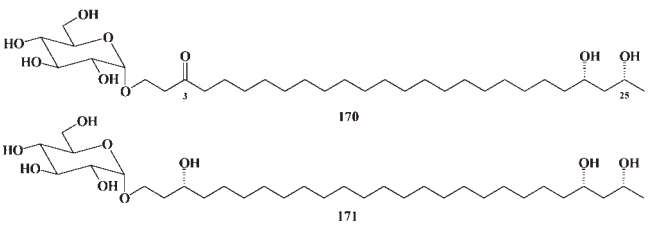

Six cyanobacteria representative of families able to form heterocysts, other than Nostocaceae, have been examined for their heterocyst glycolipids (HG) content (137). HG found in Nostocaceae were dominated by the presence of triols, and of the corresponding C-3 ketones as aglycones, those found in the other families were reported and characterized by tetrols

and by the corresponding ketones at the ω-3 position. A series of natural surfactants **172–194** was found in four of the six species examined: *Scytonema hofmanni, Calothrix desertica*, *Chlorogloeopsis fritschii*, and *Fischerella muscicola*. Triols and the corresponding ketone glycosides were found only in a *Microchaete* sp. and in *Tolypothrix tenuis*, the latter showing the most complex array of HG found so far. In *C. desertica* and *C. fritschii*, α-mannosides **179**, **181**, **191**, and **194** have been found for the first time (137).

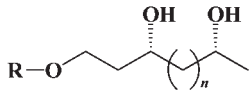

172 R = α-Glu, n = 23
173 R = α-Glu, n = 21
174 R = α-Gal, n = 23
175 R = β-Glu, n = 23

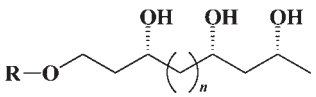

176 R = α-Glu, n = 23
177 R = α-Glu, n = 21
178 R = α-Gal, n = 23
179 R = α-Man, n = 21
180 R = α-Glu, n = 25
181 R = α-Man, n = 25

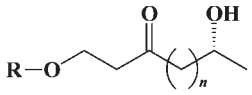

182 R = α-Glu, n = 23
183 R = α-Glu, n = 21
184 R = α-Gal, n = 23

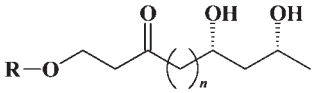

185 R = α-Glu, n = 23
186 R = α-Glu, n = 21
187 R = α-Gal, n = 23

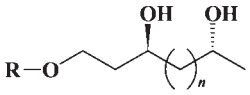

188 R = α-Glu, n = 21
189 R = α-Glu, n = 23

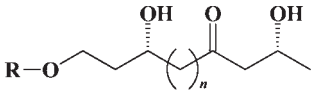

190 R = α-Glu, n = 21
191 R = α-Man, n = 21
192 R = α-Glu, n = 23
193 R = α-Glu, n = 25
194 R = α-Man, n = 25

The ethanolic extract of the stem bark of *Dimocarpus fumatus* showed cytotoxic activity *in vitro* against KB cancer cells. Fractionation of the extract gave compounds belonging to different classes, including two new glycosides with long-chain fatty alcohols, and structures were identified as 1-*O*-[α-L-rhamnopyranosyl-(1→2)-β-D-glucopyranosyl-(1→3)-α-L-rhamnopyranosyl-(1→6)-β-D-glucopyranosyl]hexadecanol **195** and 1-*O*-[[α-L-arabinopyranosyl-(1→3)]-α-L-rhamnopyranosyl-(1→2)-β-D-glucopyranosyl-(1→3)-α-L-rhamnopyranosyl-(1→6)-β-D-glucopyranosyl]hexadecanol **196**, and a mixture of three new diacylglycerylglucosides has been isolated (138). Extracts of the marine sponge *Caminus sphaeroconia* showed potent activity in a screen for bacterial type III secretion inhibitors. Bioassay-guided fractionation of the extract led to the isolation of the novel antimicrobial glycolipid caminoside A **197** (139).

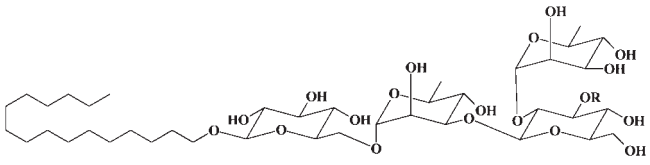

195 R = H

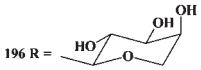

196 R =

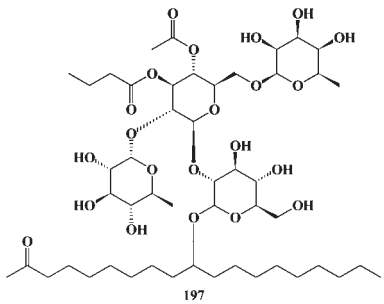

197

The series of aliphatic alcohol glycosides **198–204**, which have the aglycone (3*R*)-1-octen-3-ol or its derivatives, are rare in nature but have been isolated from some plant species. Ilicifolioside B **198**, ebracteatoside B **199**, and C **200** were isolated from the aerial parts of *Acanthus ilicifolius* (Acanthaceae) (140). This plant is widely distributed in southeastern Asia and is traditionally used in Chinese medicine as an anti-inflammatory and antihepatitis agent. Pharmaceutical studies on this plant revealed that the crude alcoholic extract of its leaves showed antioxidant, hepatoprotective, antitumor, and anticarcinogenic effects (141,142). A megastigmane glycoside (ebracteatoside A **201**), three aliphatic alcohol glycosides **[AUQ31]**(ebracteatoside B and C **199**, **200** and D **202**, respectively) were found in the aerial part of *Acanthus ebracteatus* (143). A new aliphatic alcohol glycoside, ilicifolioside C **203**, was also isolated from the aerial parts of *Acanthus ilicifolius* (144), and **204** from the *Asystasia intrusa* tree in Thailand (Thai name: Ya-Yaa) (145). Alkylglycosides **201**, **202**, and **204** have also been isolated from *Mentha spicata* (146), *Barleria lupulina*, and *B. strigosa* (147).

The new glycolipids, named simplexides **205–209**, have been isolated from the marine sponge *Plakortis simplex* (148). Simplexides are composed of long-chain secondary alcohols glycosylated by a disaccharide chain, and they represent a new structural kind of glycolipid. Simplexides **205–209** strongly inhibit proliferation of activated T cells by a noncytotoxic

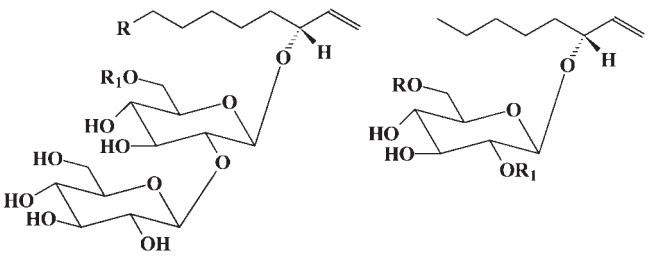

198 R = OH, R_1 = β-D-Xyl
199 R = H, R_1 = β-D-Xyl
200 R = OH, R_1 = H

201 R = β-D-Xyl, R_1 = β-D-Glu
202 R = β-D-Xyl, R_1 = H

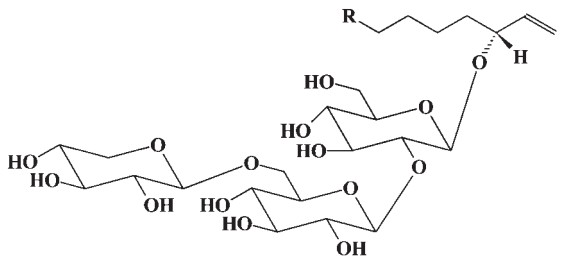

203 R = COOH
204 R = H

mechanism and can be regarded as simple molecular model for designing immunosuppressive drugs.

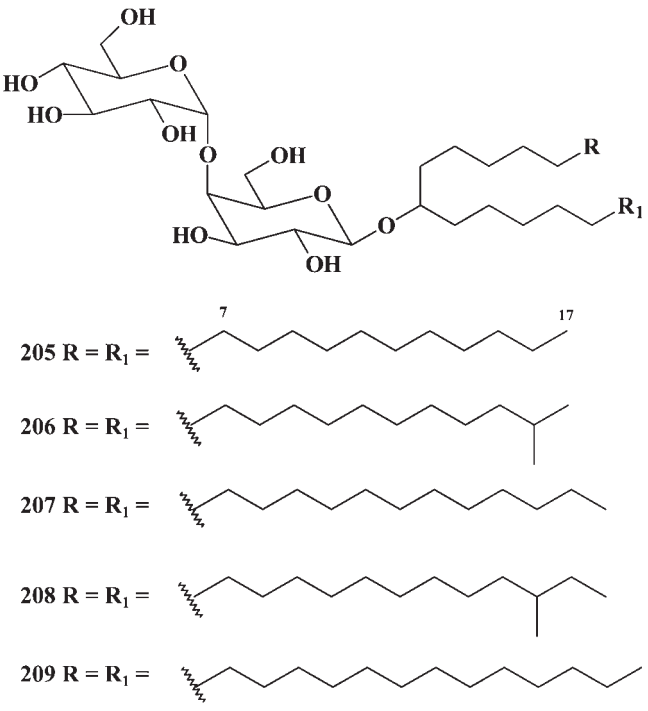

205 R = R_1 =
206 R = R_1 =
207 R = R_1 =
208 R = R_1 =
209 R = R_1 =

Glycosylated long-chain secondary alcohols can be considered the first members of a new, simple class of glycolipids. The most similar examples are the glycosylated hydroxy fatty acids isolated from some yeast (149). Another unusual feature of simplexides are the very long chains of alcohols, **205–209**, which are composed of 34–37 carbon atoms with the hydroxyl group nearly in the middle. Authors suggested that the lipid part of simplexides could be biosynthesized from the coupling of two molecules of fatty acid. A reasonable biogenetic hypothesis is sketched in Scheme 2.

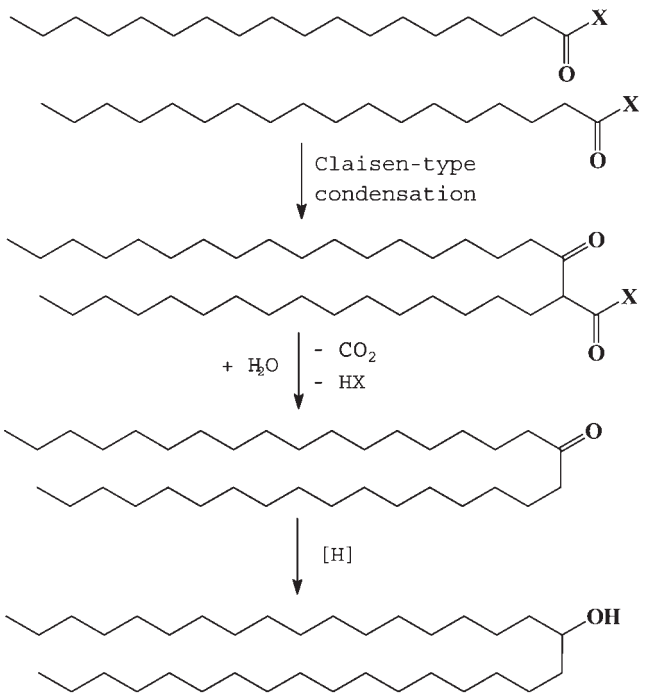

SCHEME 2. Proposed biosynthesis of the lipid part of simplexides (X = SCoA or any other acyl carrier).

Alkylglycoside, plakopolyprenoside **210**, with a unique cytotoxic glycolipid composed of a C_{35} linear polyisoprenoid alcohol and a dixylosyl carbohydrate chain, was isolated from the Caribbean sponge *Plakortis simplex* (150). Plakopolyprenoside **210** is cytotoxic against the J774 cell line. Plaxyloside **211**, a glycolipid also composed of a C_{35} linear polyisoprenoid alcohol aglycone and a linear carbohydrate chain made up of six α-xylopyranose units, has been isolated as its peracetate from the Caribbean sponge *P. simplex* (151).

Two novel polypropionate lactone glycosides, lycogalinosides A **212** and B **213**, were isolated from the slime mold *Lycogala epidendrum* (152). Compounds **212** and **213** are unique in structure, containing a 2-deoxy-α-L-fucopyranosyl-(1→4)-6-deoxy-β-D-gulopyranosyl unit and a β-D-olivopyranosyl-(1→4)-β-D-fucopyranosyl unit, respectively, and show growth-inhibitory activities against gram-positive bacteria.

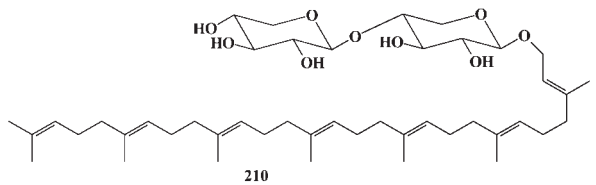

210

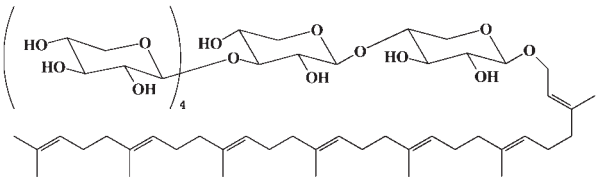

211

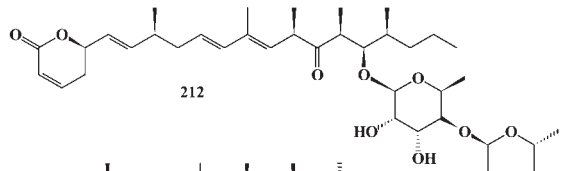

212

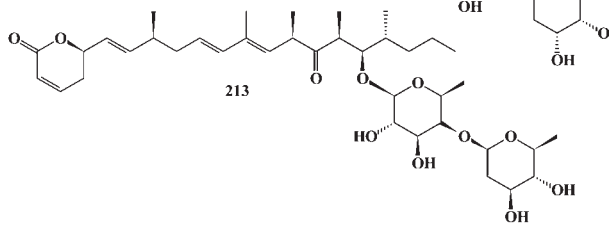

213

The marine fungus *Gliocladium roseum* KF-1040 produced unusual glycolipids roselipid 1A **214**, 1B **215**, 2A **216**, and 2B **217**. These compounds inhibit the enzyme diacylglycerol acyl transferase (153–155).

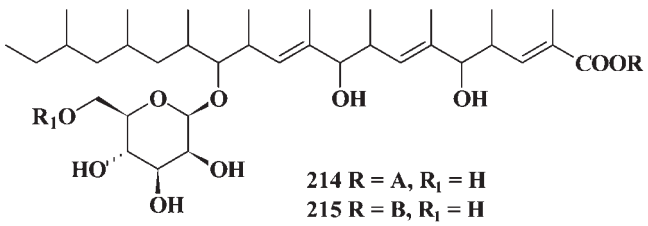

214 R = A, R_1 = H
215 R = B, R_1 = H
216 R = A, R_1 = Ac
217 R = B, R_1 = Ac

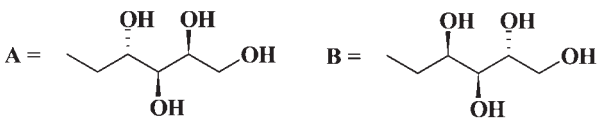

A novel glycoside, (4*S**,5*R**)-4-[(9*Z*)-2,13-di-(*O*-β-D-glucopyranosyl)-5,9,10-trimethyl-8-oxo-9-tetradecene-5-yl]-3,3,5-trimethylcyclohexanone, namely stenopaluside **218**, was isolated from the leaves of the medicinal plant *Stenochlaena palustris* (156).

Capsicum species are very important plants used as vegetable foods, spices, and external medicine, and capsaicinoids are the group of compounds responsible for the "heat" sensation of *Capsicum* fruits. Metabolites from *Capsicum* fruits are also used as pest repellants in agriculture, and there is interest in using them as synergists with organophosphate insecticides (157). Investigation of polar extracts from ripe fruits of *C. annuum* L. var. *acuminatum* yielded some new glycosides, capsianoside VII **219**, capsianoside II **220**, capsianoside III **221**, capsianoside A **222**, C **223**, E **224**, B **225**, D **226**, F **227**, and capsosides A **228** and B **229** (158–160, and references cited therein). Capsianosides showed many different biological activities and were described in a recent review article (161). Compounds **218** and **220–227** are a good sample of natural gemini surfactants.

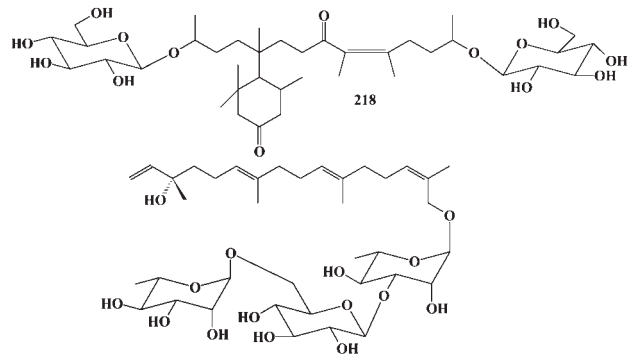

218

219

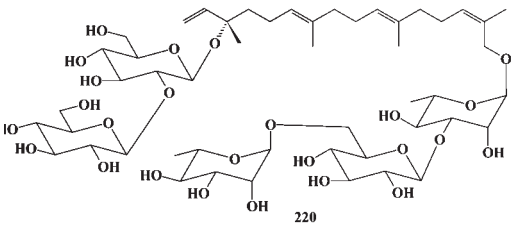

220

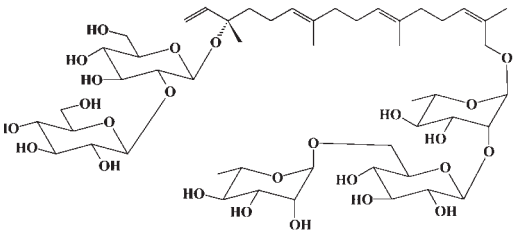

221

A new alcohol glycoside, 1-octyl *R*-D-arabinofuranosyl-(1→6)-α-D-glucopyranoside **230**, and some known compounds including three phenolics, isovitexin, astragalin, and the terpene glucosides have been isolated from the aerial parts of *Circaea lutetiana* ssp. *canadensis* (162). A new alkyl glycoside, oct-1-en-3-yl *R*-arabinofuranosyl-(1→6)-α-glucopyranoside **231**, has been isolated from methanolic extracts of the leaves, stems, and roots of *Phyllagathis rotundifolia* collected in Malaysia (163).

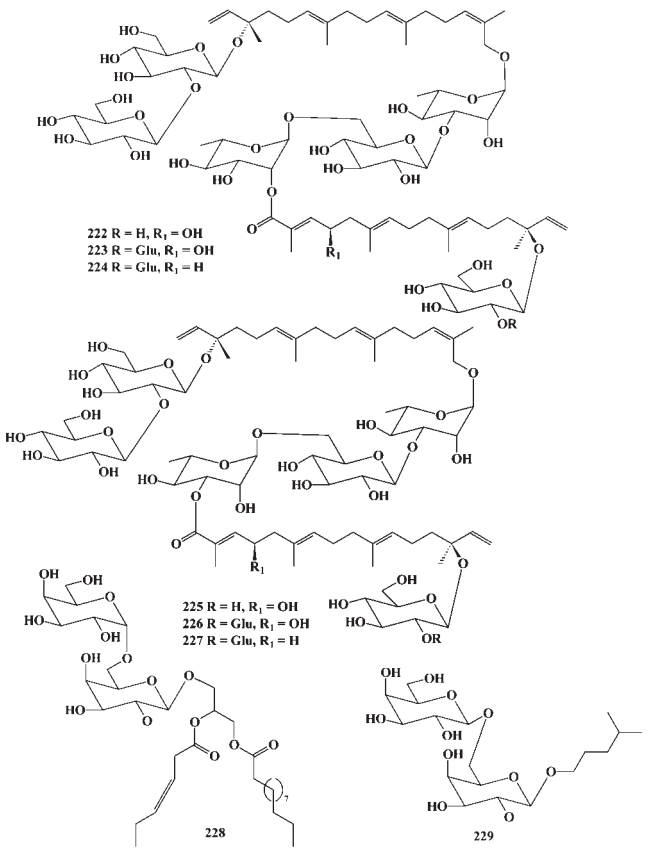

A unique ether glycolipid **232**, characterized by the glycosylation of two glycerol hydroxy groups, has been isolated from the Senegalese sponge *Trikentrion loeve* Carter (164). Cramerides **233–238**, six new glycolipid analogs in which the sugar moiety is replaced by an unprecedented five-membered cyclitol, were isolated as a mixture from the sponge *Pseudoceratina crassa* (165). Compounds **233–238** showed a high antifeedant activity on the fish *Carassius auratus,* which suggests their potential role as natural feeding deterrents.

An interesting group of polyacetylenic glycosides, **239–245**, has been discovered from plants belonging to the genus *Bidens*. Bidensyneosides A1 **239**, A2 **240**, B **241**, C **242**, and 3′-deoxy-C **243** are a group of five identified polyacetylenic glucosides from *B. parviflora* Willd (166). This plant is used in traditional Chinese medicine and contains many bioactive natural products (166). Authors showed that bidensyneosides **239–242** are effective inhibitors of both histamine release and nitric oxide production. Two polyacetylenic glucosides, **244** and **245**, were isolated from the aerial parts of *B. pilosa* Sch. Bip. var. *radiata* (Asteraceae) (167).

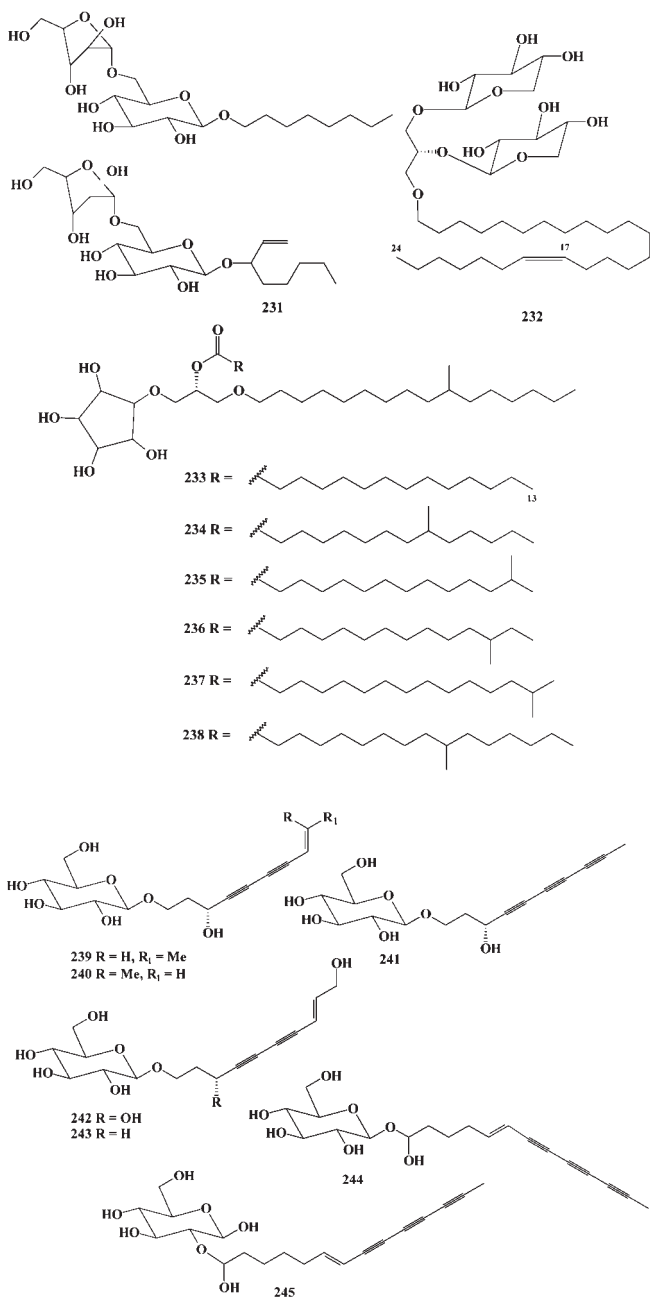

The importance of monoterpenes on the varietal flavor of grape and wines is known and has been partly studied and reviewed (168–173). These compounds were found linked mainly to sugar moieties (as alkylglycosides) in grape juice and wines, showing no olfactory characteristics. Figure 2 summarizes many publications that contain studies of alkylglycosides from grape species, apple, guava, raspberry, strawberry fruits, leaves and fruits of papaya, and some plants in which indicated compounds were found and isolated by

physicochemical methods (168–174). Major monoterpenoid alcohols that link with D-glucose and other sugars are shown in Figure 2.

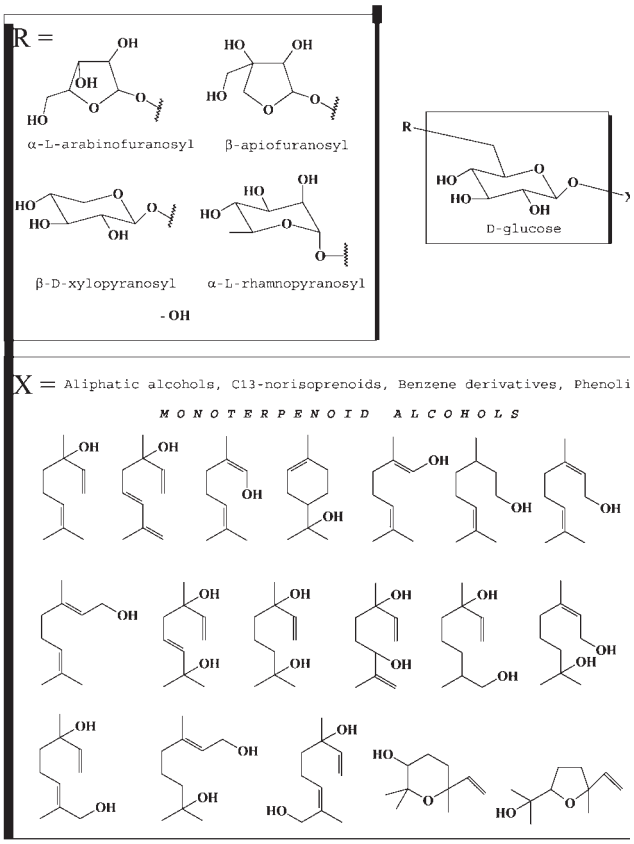

FIG. 2. Major monoterpene alcohols isolated as alkylglycerides from many fruits and some plant species.

SUMMARY

Glycosides of fatty acid and alcohols are of commercial interest for industry in general and specifically for the pharmaceutical and food industries (175,176). The past five years have seen significant progress in the understanding of the physical and chemical properties of alkyl glycosides. Remarkable results from studies concern the phase behavior, the oil/water interface, the microemulsions, and the adsorption of this new surfactant type on solid surfaces. Interesting differences between alkyl glycosides and other nonionic surfactants have been shown. An increasing importance of mixtures of alkyl glycosides and other surfactants led to more systematic studies of the influence of electrolytes and surfactants on the properties of alkyl glycosides. Gemini surfactants are a new generation of surfactants (177,178) and they belong to the family of surfactant molecules that possess more than one hydrophobic tail and hydrophilic head group. They have been used widely in industry because of their better properties. Geminis are used as promising surfactants in industrial detergency and have shown efficacy in skin care, as anti-HIV agents, in environmental protection, as antibacterial agents, in metal-encapped porphyrazine and vesicle formation, and in construction of high porosity materials which give new perspectives for medicine and pharmacology.

REFERENCES

1. Dembitsky, V.M. (2004) Chemistry and Biodiversity of Biologically Active Natural Glycosides, *Chem. Biodiver. 1*, 673–781.
2. Clayton, W. (1943) *Theory of Emulsions*, p. 127, McGraw-Hill, New York.
3. Griffin, W.C. (1949) Classification of Surface-Active Agents by "HLB," *J. Soc. Cosmet. Chem. 1*, 311–324.
4. Griffin, W.C. (1954) Calculation of HLB Values of Non-Ionic Surfactants, *J. Soc. Cosmet. Chem. 5*, 259–267.
5. Ikan, R. (ed.) (1999) *Naturally Occurring Glycosides,* John Wiley & Sons, Chichester, England.
6. Ernst, B., Hart, G.W., and Sinaÿ, P. (eds.) (2000) *Carbohydrates in Chemistry and Biology,* Wiley-VCH, Weinheim.
7. Levy, D.E., and Tang, C. (1995). *Chemistry of C-Glycosides,* Elsevier, Amsterdam.
8. Kates, M. (ed.) (1990) *Glycolipids, Phosphoglycolipids and Sulfoglycolipids. Handbook of Lipid Research,* Kluwer Academic/Plenum Publishers, New York.
9. Harborne, J.B., and Williams, C.A. (2001) Anthocyanins and Other Flavonoids, *Nat. Prod. Rep. 18*, 310–333.
10. Harborne, J.B. (1993) *Flavonoids: Advances in Research Since 1986*, CRC Press, Boca Raton, Florida.
11. Esko, J., Marth, J., Cummings, R., Freeze, H., Varki, A., and Hart, G. (eds.) (1999) *Essentials of Glycobiology*, Cold Spring Harbor Laboratory Press, Cold Spring Harbor, New York.
12. Frank, H.A., Young, A.J., Britton, G., and Cogdell, R.J. (eds.) (1999) *The Photochemistry of Carotenoids*. Kluwer Academic Publishers, Dordrecht.
13. Kosaric, N. (1993) *Biosurfactants: Production, Properties, Applications,* Marcel Dekker, New York.
14. (a) Holmberg, K. (2001) Natural Surfactants, *Curr. Opin. Colloid Interface Sci. 6*, 148–159; (b) Tyman, J.H.P. (ed.) (1992) *Surfactants in Lipid Chemistry: Recent Synthetic, Physical, and Biodegradative Studies,* Royal Society of Chemistry, London.
15. Satoshi, O. (ed.) (2002) *Macrolide Antibiotics: Chemistry, Biology, and Practice*, Academic Press, Amsterdam, Boston.
16. Rosen, M.J. (2004) *Surfactants and Interfacial Phenomena*, 3rd edn., p. 464, John Wiley & Sons, New York.
17. Van der Meer, M.T.J., Schouten, S., Hanada, S., Hopmans, E.C., Sinninghe Damsté, J.S., and Ward, D.M. (2002) Alkane-1,2-diol-Based Glycosides and Fatty Glycosides and Wax Esters in *Roseiflexus castenholzii* and Hot Spring Microbial Mats, *Arch. Microbiol. 178*, 229–237.
18. Rezanka, T. (2002) Glycosides of Polyenoic Branched Fatty Acids from Myxomycetes, *Phytochemistry 60,* 639–646.
19. Jude, A.R., Little, J.M., Freeman, J.P., Evans, J.E., Radominska-Pandya, A., and Grant, D.F. (2000) Linoleic Acid Diols Are Novel Substrates for Human UDP-Glucuronosyltransferases, *Arch. Biochem. Biophys. 380*, 294–302.
20. Řezanka, T., and Dembitsky, V.M. (2003) Brominated Oxylipins and Oxylipin Glycosides from Red Sea Corals, *Eur. J. Org. Chem. 14*, 309–316.
21. Simko, I., Omer, E.A., Ewing, E.E., McMurry, S., Koch, J.L., and Davies, P.J. (1996) Tuberonic (12-OH-jasmonic) Acid Glucoside and Its Methyl Ester in Potato, *Phytochemistry 43*, 727–730.
22. Matsuura, H., Yoshira, T., Ichihara, A., Kikuta, Y., and Koda, Y.

(1993) Tuber-forming Substances in Jerusalem Artichoke (*Helianthus tuberosus* L.), *Biosci. Biotech. Biochem. 57*, 1253–1256.
23. Matsuura, H., Yoshihara, T., and Ichihara, A. (1993) 4 New Polyacetylenic Glucosides, Methyl β-D-Glucopyranosyl Helianthenate C-F, from Jerusalem Artichoke (*Helianthus tuberosus* L.), *Biosci. Biotechnol. Biochem. 57,* 1492–1498.
24. Wang, M., Likuzaki, H., Zhu, N., Sang, N., Nakatani, N., and Ho, C.T. (2000) Isolation and Structural Elucidation of Two New Glycosides from Sage (*Salvia officinalis* L.), *J. Agric. Food Chem. 48,* 235–238.
25. MacLeod, J.K., Rasmussen, H.B., and Wills, A.C. (1997) A New Glycoside Antimicrobial Agent from *Persoonia linearis* × *pinifolia, J. Nat. Prod. 60,* 620–622.
26. Takeda, Y., Takechi, A., Masuda, T., and Otsuka, H. (1998) An Acyclic Monoterpene Glucosyl Ester from *Lantana lilacia, Planta Med. 64*, 78–79.
27. Yoshikawa, K., Satou, Y., Tokunaga, Y., Tanaka, M., Arihara, S., and Nigam, S.K. (1998) Four Acylated Triterpenoid Saponins from *Albizia procera, J. Nat. Prod. 61*, 440–445.
28. Krajewaski, D., Duque, C., and Schreier, P. (1997) Aliphatic β-D-Glucosides from Fruits of *Carica pubescens, Phytochemistry 45*, 1627–1631.
29. Stermitz, F.R., Cashman, K.K., Halligan, K.M., Morel, C., Tegos, G.P., and Lewis, K. (2003) Polyacylated Neohesperidosides from *Geranium caespitosum*: Bacterial Multidrug Resistance Pump Inhibitors, *Bioorg. Med. Chem. Lett. 13*, 1915–1918.
30. Boros, C., Katz, B., Mitchell, S., Pearce, C., Swinbank, K., and Taylor, D. (2002) Emmyguyacins A and B: Unusual Glycolipids from a Sterile Fungus Species That Inhibit the Low-pH Conformational Change of Hemagglutinin A During Replication of Influenza Virus, *J. Nat. Prod. 65,* 108–114.
31. King, R.R., and Calhoun, L.A. (1988) 2,3-Di-*O*- and 1,2,3-Tri-*O*-Acylated Glucose Esters from the Glandular Trichomes of *Datura metel, Phytochemistry 27*, 3761–3763.
32. King, R.R., Colhoun, L.A., Singh, P.R., and Boucher, A. (1993) Characterization of 2,3,4,3′-Tetra-*O*-acylated Sucrose Esters Associated with the Glandular Trichomes of *Lycopersicon typicum, J. Agric. Food Chem. 41*, 469–473.
33. Severson, R.F., Arrendale, R.F., Chortyk, O.T., Green, C.R., Thome, F.A., Stewart, J.L., and Johnson, A.W. (1985) Isolation and Characterization of the Sucrose Esters of the Cuticular Waxes of Green Tobacco Leaf, *J. Agric. Food Chem. 33*, 870–875.
34. Arrendale, R.F., Severson, R.F., Sisson, V.A., Costello, C.E., Leary, J.A., Himmelsbach, D.S., and Van Halbeek, H. (1990) Characterization of the Sucrose Esters from *Nicotiana glutinosa, J. Agric. Food Chem. 38*, 75–85.
35. Matsuzaki, T., Shinozaki, Y., Hagimori, M., Tobita, T., Shigematsu, H., and Koiwai, A. (1992) Novel Glycerolipids and Glycolipids from the Surface Lipids of *Nicotiana benthamiana*, *Biosci. Biotech. Biochem. 56*, 1565–1569.
36. Ohya, I., Shinozaki, Y., Tobita, T., Takahashi, H., Matsuzaki, T., and Koiwai, A. (1994) Sucrose Esters from the Surface Lipids of *Nicotiana cavicola, Phytochemistry 37*, 143–145.
37. King, R.R., Singh, R.P., and Calhoun, L.A. (1988) Elucidation of Structures for a Unique Class of 2,3,4,3′-Tetra-*O*-acylated Sucrose Esters from the Type B Glandular Trichomes of *Solanum neocardenusii* Hawkes and Hjerting (PI 498129), *Carbohydr. Res. 173*, 235–241.
38. Kandra, L., and Wagner, G.J. (1988) Studies of the Site and Mode of Biosynthesis of Tobacco Trichome Exudate Components, *Arch. Biochem. Biophys. 265*, 425–432.
39. Matsuzaki, T., Koseki, K., and Koiwai, A. (1988) Germination and Growth-Inhibition of Surface Lipids from *Nicotiana* Species and Identification of Sucrose Esters, *Agric. Biol. Chem. 52*, 1889–1897.
40. Ohya, I., Shinozaki, Y., Tobita, T., Takahashi, H., and Matsuzaki, T. (1996) Sucrose Esters from the Surface Lipids of *Petunia hybrida, Phytochemistry 41*, 787–789.
41. King, R.R., Calhoun, L.A., Singh, R.P., and Boucher, A. (1990) Sucrose Esters Associated with Glandular Trichomes of Wild *Lycopersicon* Species, *Phytochemistry 29,* 2115–2118.
42. King, R.R., Pelletier, Y., Singh, R.P., and Calhoun, L.A. (1986) 3,4-Di-*O*-isobutyryl-6-*O*-Caprylsucrose: The Major Component of a Novel Sucrose Ester Complex from the Type B Glandular Trichomes of *Solanum berthaultii* Hawkes (PI 473340), *J. Chem. Soc. Chem. Commun*., 1078–1079.
43. King, R.R., Singh, R.P., and Boucher, A. (1987) Variation in Sucrose Esters from the Type B Glandular Trichomes of Certain Wild Potato Species, *Am. Potato J. 64*, 529–534.
44. King, R.R., Singh, R.P., and Calhoun, L.A. (1987) Isolation and Characterization of 3,3′,4,6-Tetra-*O*-acylated Sucrose Esters from the Type B Glandular Trichomes of *Solanum berthaultii* Hawkes (PI 265857), *Carbohydr. Res. 166*, 113–121.
45. King, R.R., Singh, R.P., and Calhoun, L.A. (1988) Elucidation of Structures for a Unique Class of 2,3,4,3′-Tetra-*O*-acylated Sucrose Esters from the Type B Glandular Trichomes of *Solanum neocardenusii* Hawkes and Hjerting (PI 498129), *Carbohydr. Res. 173*, 235–241.
46. Matsuzaki, T., Shinozaki, Y., Suhara, S., Tobita, T., Shigematsu, H., and Koiwai, A. (1991) Leaf Surface Glycolipids from *Nicotiana acuminata* and *Nicotiana pauciflora, Agric. Biol. Chem. 55,* 1417–1419.
47. King, R.R., and Calhoun, L.A. (1988) 3,4-Di-*O*- and 2,3,4-Tri-*O*-acylated Glucose Esters from the Glandular Trichomes of Nontuberous *Solanum* species, *Phytochemistry 27*, 3765–3768.
48. Burke, B.A., Goldsby, G., and Mudd, J.B. (1987) Polar Epicuticular Lipids of *Lycopersicon pennellii, Phytochemistry 26,* 2567–2571.
49. Hill, K., and Rhode, O. (1999) Sugar-Based Surfactants for Consumer Products and Technical Applications, *FETT/Lipid 101*, 25–33.
50. Akoh, C.C., and Swanson, B.G. (1994) *Carbohydrate Polyesters as Fat Substitutes*, Marcel Dekker, New York.
51. Kobayashi, J., Doi, Y., and Ishibashi, M. (1994) Shimofuridin-A, a Nucleoside Derivative Embracing an Acylfucopyranoside Unit Isolated from the Okinawan Marine Tunicate *Aplidium multiplicatum*, *J. Org. Chem. 59*, 255–257.
52. Doi, Y., Ishibashi, M., and Kobayashi, J. (1994) Isolation and Structure of Shimofuridins B–G from the Okinawan Marine Tunicate *Aplidium multiplicatum, Tetrahedron 50*, 8651–8656.
53. Riva, S. (2002) Enzymatic Modification of the Sugar Moieties of Natural Glycosides, *J. Mol. Catal. B Enzymol. 19*, 43–54.
54. Lang, S., and Wullbrandt, D. (1999) Rhamnose Lipids—Biosynthesis, Microbial Production and Application Potential, *Appl. Microbiol. Biotechnol. 51*, 22–32.
55. Rosenberg, E., and Ron, E.Z. (1999) High- and Low-Molecular Mass Microbial Surfactants, *Appl. Microbiol. Biotechnol. 52*, 154–162.
56. Mailer, R.M., and Soberon-Chavez, G. (2000) *Pseudomonas aeruginosa* Rhamnolipids: Biosynthesis and Potential Applications, *Appl. Microbiol. Biotechnol. 54*, 625–633.
57. Lang, S. (2002) Biological Amphiphiles (Microbial Biosurfactants), *Curr. Opin. Colloid Interf. Sci. 7*, 12–20.
58. Ron, E.Z., and Rosenberg, E. (2002) Biosurfactants and Oil Bioremediation, *Curr. Opin. Biotechnol. 13*, 249–252.
59. Bergstrom, S., Theorell, H., and Davide, H. (1946) On a Metabolic Product of *Ps. pyocyanea*, Pyolipic Acid, Active Against *Myobacteria tuberculosis, Ark. Kem. Mineral Geol. 23A*, 1–12.
60. Jarvis, F.G., and Johnson, M.J. (1949) A Glyco-Lipide Produced by *Pseudomonas aeruginosa, J. Am. Chem. Soc. 71*, 4124–4126.
61. Edwards, J.R., and Hayashi, J.A. (1965) Structure of a Rhamnolipid from *Pseudomonas aeruginosa, Arch. Biochem. Biophys. 111,* 415–421.

62. Hisatsuka, K., Nakahara, T., Sano, N., and Yamada, K. (1971) Formation of Rhamnolipid by *Pseudomonas aeruginosa* and Its Function in Hydrocarbon Fermentation, *Agric. Biol. Chem. 35*, 686–692.
63. Itoh, S., Honda, H., Tomita, F., and Suzuki, T. (1971) Rhamnolipids Produced by *Pseudomonas aeruginosa* Grown on *n*-Paraffin, *J. Antibiot.* (*Tokyo) 24*, 855–859.
64. Yamaguchi, M., Sato, A., and Yukuyama, A. (1976) Microbial Production of Sugar-Lipids, *Chem. Ind. 4*, 741–742.
65. Hirayama, T., and Kato, I. (1982) Novel Methyl Rhamnolipids from *Pseudomonas aeruginosa, FEBS Lett. 139*, 81–85.
66. Syldatk, C., Lang, S., Wagner, F., Wray, V., and Witte, L. (1985) Chemical and Physical Characterization of Four Interfacial-Active Rhamnolipids from *Pseudomonas* Species DSM 2874 Grown on *n*-Alkanes, *Z. Naturforsch. 40*, 51–60.
67. Syldatk, C., Lang, S., Matulovic, U., and Wagner, F. (1985) Production of Four Interfacial Active Rhamnolipids from *n*-Alkanes or Glycerol by Resting Cells of *Pseudomonas* Species DSM 2874, *Z. Naturforsch. 40*, 61–67.
68. Rendell, N.B., Taylor, G.W., Somerville, M., Todd, H., Wilson, R., and Cole, J. (1990) Characterization of *Pseudomonas* Rhamnolipids, *Biochim. Biophys. Acta 1045*, 189–193.
69. Abalos, A., Pinazo, A., Infante, M.R., Casals, M., Garcýa, F., and Manresa, A. (2001) Physicochemical and Antimicrobial Properties of New Rhamnolipids Produced by *Pseudomonas aeruginosa* AT10 from Soybean Oil Refinery Wastes, *Langmuir 17*, 1367–1371.
70. Kitamoto, D., Yanagishita, H., Haraya, K., and Kitamoto, H.K. (1998) Contribution of a Chain-Shortening Pathway to the Biosynthesis of the Fatty Acids of Mannosylerythritol Lipid (Biosurfactant) in the Yeast *Candida antarctica*: Effect of β-Oxidation Inhibitors on Biosurfactant Synthesis, *Biotechnol. Lett. 20*, 813–818.
71. Kitamoto, D., Sangita, G., Ourisson, G., and Nakatani, Y. (2000) Formation of Giant Vesicles from Diacylmannosylerythritols, and Their Binding to Concanavalin A, *Chem. Commun.,* 861–862.
72. Wakamatsu, Y., Zhao, X., Jin, C., Day, N., Shibahara, M., Nomura, N., Nakahara, T., Murata, T., and Yokoyama, K.K. (2001) Mannosylerythritol Lipid Induces Characteristics of Neuronal Differentiation in PC12 Cells Through an ERK-Related Signal Cascade, *Eur. J. Biochem. 268*, 374–383.
73. Zhao, X., Wakamatsu, Y., Shibahara, M., Nomura, N., Geltinger, C., Nakahara, T., Murata, T., and Yokoyama, K.K. (1999) Mannosylerythritol Lipid Is a Potent Inducer of Apoptosis and Differentiation of Mouse Melanoma Cells in Culture, *Cancer Res. 59*, 482–486.
74. Kitamoto, D., Yanagishita, H., Endo, A., Nakaiwa, M., Nakane, T., and Akiya, T. (2001) Remarkable Antiagglomeration Effect of a Yeast Biosurfactant, Diacylmannosylerythritol, on Ice-Water Slurry for Cold Thermal Storage, *Biotechnol. Prog. 17*, 362–365.
75. Cameotra, S.S., and Makkar, R.S. (2004) Recent Applications of Biosurfactants as Biological and Immunological Molecules, *Curr. Opin. Microbiol. 7*, 262–266.
76. (a) Kitamoto, D., Ikegami, T., Suzuki, G.T., Sasaki, A., Takeyama, Y.I., Idemoto, Y., Koura, N., and Yanagishita, H. (2001) Microbial Conversion of *n*-Alkanes into Glycolipid Biosurfactants, Mannosylerythritol Lipids by *Pseudozyma* (*Candida antarctica*), *Biotechnol. Lett. 23*, 1709–1714; (b) Umehara, K., Nemoto, K., Ohkubo, T., Miyase, T., Degawa, M., and Noguchi, H. (2004) Isolation of a New 15-Membered Macrocyclic Glycolipid Lactone, Cuscutic Resinoside A from the Seeds of *Cuscuta chinensis***:** A Stimulator of Breast Cancer Cell Proliferation, *Planta Med. 70*, 299–304.
77. Asselineau, C., and Asselineau, J. (1978) Trehalose-Containing Glycolipids, *Prog. Chem. Fats Other Lipids 16*, 59–99.
78. Vilkas, E., and Rojas, A. (1964) On the Lipids of *Mycobacterium fortuitum*, *Bull. Soc. Chim. Biol. 46*, 689–701.
79. (a) Azuma, I., and Yamamura, Y.J. (1962) Studies on the Firmly Bound Lipids of Human *Tubercle bacillus*. I. Isolation of Arabinose Mycolate, *Biochemistry (Tokyo) 52*, 200–206; (b) Vilkas, E., Adam, A., and Senn, M. (1968) Isolation of a New Type of Trehalose Diester from *Mycobacterium fortuitum*, *Chem. Phys. Lipids 2*, 11–16.
80. (a) Prottey, C., and Ballou, C.E. (1968) Diacyl Myoinositol Monomannoside from *Propionibacterium shermanii, J. Biol. Chem. 243*, 6196–6201; (b) Shaw, N., and Dinglinger, F. (1969) The Structure of an Acylated Inositol Mannoside in the Lipids of Propionic Acid Bacteria, *Biochem. J. 112*, 769–775.
81. Noll, H., Bloch, H., Asselineau, J., and Lederer, E. (1956) The Chemical Structure of the Cord Factor of *Mycobacterium tuberculosis, Biochim. Biophys. Acta 20*, 299–309.
82. Asselieau, J., and Lederer, E. (1955) Constitution of the Cord Factor Isolated from a Human Strain of *Mycobacterium tuberculosis, Biochim. Biophys. Acta 17*, 161–168.
83. Asselineau, C., Montrozier, H., Prome, J.C., Savagnac, A., and Welby, M. (1972) Polyunsaturated Glycolipids Synthesized by *Mycobacterium phlei*, *Eur. J. Biochem. 28*, 102–109.
84. Goren, M.B. (1970) Sulfolipid I of *Mycobacterium tuberculosis*, Strain H37Rv: I. Purification and Properties, *Biochim. Biophys. Acta 210*, 116–126.
85. Goren, M.B. (1970) Sulfolipid I of *Mycobacterium tuberculosis*, Strain H37Rv: II. Structural Studies, *Biochim. Biophys. Acta 210*, 127–138.
86. Esch, S.W., Morton, M.D., Williams, T.D., and Buller, C.S. (1999) A Novel Trisaccharide Glycolipid Biosurfactant Containing Trehalose Bears Ester-Linked Hexanoate, Succinate, and Acyloxyacyl Moieties: NMR and MS Characterization of the Underivatized Structure, *Carbohydr. Res. 319*, 112–123.
87. Mayorga, H., Duqur, C., Knapp, H., and Winterhalter, P. (2002) Hydroxyester Disaccharides from Fruits of Cape Gooseberry (*Physalis peruviana*), *Phytochemistry 59*, 439–445.
88. Mayorga, H., Knapp, H., Winterhalter, P., and Duque, C. (2001) Glycosidically Bound Flavor Compounds of Cape Gooseberry *(Physalis peruviana* L.), *J. Agric. Food Chem. 49*, 1904–1908.
89. Batrakov, S.G., Konova, I.V., Sheichenko, V.I., and Galanina, L.A. (2003) Glycolipids of the Filamentous Fungus *Absidia corymbifera* F-295, *Chem. Phys. Lipids 123*, 157–164.
90. Tulloch, A.P. (1964) The Component Fatty Acids of Oils Found in Spores of Plant Rusts and Other Fungi. IV, *Can. J. Microbiol. 10*, 359–364.
91. Davila, A.M., Marchal, R., Monin, N., and Vandecasteele, J.P. (1993) Identification and Determination of Individual Sophorolipids in Fermentation Products by Gradient Elution High-Performance Liquid Chromatography with Evaporative Light-Scattering Detection, *J. Chromatogr. 648*, 139–149.
92. Tulloch, A.P., and Spencer, J.F. (1972) Formation of a Long-Chain Alcohol Ester of Hydroxy Fatty Acid Sophoroside by Fermentation of Fatty Alcohol by a *Torulopis* Species, *J. Org. Chem. 37*, 2868–2870.
93. Spencer, J.F., Gorin, P.A., and Tulloch, A.P. (1970) *Torulopsis bombicola* sp. N, *Antonie Van Leeuwenhoek. 36*, 129–133.
94. Rau, U., Hammen, S., Heckmann, R., Wray, V., and Lang, S. (2001) Sophorolipids: A Source for Novel Compounds, *Ind. Crops Prod. 13*, 85–92.
95. Hommel, R.K., Weber, L., Weiss, A., Himelreich, U., Rilke, O., and Kleber, H.P. (1994) Production of Sophorose Lipid by *Candida (Torulopsis) apicola* Grown on Glucose, *J. Biotechnol. 33*, 147–155.
96. Weber, L., Stach, J., Haufe, G., Hommel, R., and Kleber, H.-P. (1990) Structure Elucidation of an Unusual Glycolipid by Two-Dimensional N.M.R. Methods, *J. Mol. Struct. 219*, 353–358.
97. Cooper, D.G. (1986) Biosurfactants, *Microbiol. Sci. 3*, 145–149.

98. Otto, R.T., Daniel, H.J., Pekin, G., Muller-Decker, K., Furstenberger, G., Reuss, M., and Syldatk, C. (1999) Production of Sophorolipids from Whey. II. Product Composition, Surface Active Properties, Cytotoxicity and Stability Against Hydrolases by Enzymatic Treatment, *Appl. Microbiol. Biotechnol. 52*, 495–501.
99. Desai, J.D., and Banat, I.M. (1997) Microbial Production of Surfactants and Their Commercial Potential, *Microbiol. Mol. Biol. Rev. 61*, 47–64.
100. Vollbrecht, E., Rau, U., and Lang, S. (1999) Microbial Conversion of Vegetable Oils into Surface-Active Di-, Tri-, and Tetrasaccharide Lipids (Biosurfactants) by the Bacterial Strain *Tsukamurella* spec., *Fett/Lipid 101*, 389–394.
101. Levand, O., and Larson, H. (1979) Some Chemical Constituents of *Morinda citrifolia, Plant Med. 36*, 186–187.
102. Hirazumi, A., Furusawa, E., Chou, S.C., and Hokama, Y. (1994) Anticancer Activity of *Morinda citrifolia* (noni) on Intraperitoneally Implanted Lewis Lung Carcinoma in Syngeneic Mice, *Proc. West. Pharmacol. Soc. 37***,** 145–146.
103. Hirazumi, A., Furusawa, E., Chou, S.C., and Hokama, Y. (1996) Immunomodulation Contributes to the Anticancer Activity of *Morinda citrifolia* (noni) Fruit Juice, *Proc. West. Pharmacol. Soc. 39,* 7–9.
104. Wang, M., Kikuzaki, H., Jin, Y., Nakatani, N., Zhu, N., Csisar, K., Boyd, C., Rosen, R., Ghal, G., and Ho, C.T. (2000) Novel Glycosides from Noni (*Morinda citrifolia*), *J. Nat. Prod. 63*, 1182–1183.
105. Lee, J., and Hollingsworth, R.I. (1996) Isolation and Characterization of a β-1-O-Acyl-β-1,2-diglucosyl Glycoside from the Membranes of a Gram Positive Bacterium *Sarcina ventriculi, Tetrahedron 52*, 3873–3878.
106. Perda-Miranda, R., and Hernandez-Carlos, B. (2002) HPLC Isolation and Structural Elucidation of Diastereomeric Niloyl Ester Tetrasaccharides from Mexican Scammony Root, *Tetrahedron 58*, 3145–3154.
107. Gasper, E.M.M. (1999) New Pentasaccharide Macrolactone from the European Convolvulaceae *Calystegia soldanella, Tetrahedron Lett. 40*, 6861–6864.
108. Font Quer, P. (1962) *Plantas Medicinales*, Labor, S.A. (ed.), El Dioscorides Renovado, Madrid, p. 543.
109. MacLeod, J.K., Ward, A., and Oelrichs, P.B. (1997) Structural Investigation of Resin Glycosides from *Ipomoea lonchophylla, J. Nat. Prod. 60*, 467–471.
110. Heacock, R.A. (1975) Psychotomimetics of the Convolvulaceae, *Prog. Med. Chem. 11*, 91–118.
111. Bieber, L.W., Da Silva, F., Correa Lima, R.M.O., De Andrade Chiappeta, A., Do Naschimento, S.C., De Souza, I.A., De Mello, J.F., and Veith, H.J. (1986) Anticancer and Antimicrobial Glycosides from *Ipomoea bahiensis, Phytochemistry 25*, 1077–1081.
112. Du, X.M., Sun, N.S., Nishi, M., Lawasaki, T., Guo, Y.T., and Miyahara, K. (1999) Components of the Ether-Insoluble Resin Glycoside Fraction from the Seed of *Cuscuta australis, J. Nat. Prod. 62*, 722–723.
113. Noda, N., Takahashi, N., Miyahara, K., and Yang, C.R. (1998) Stoloniferins VIII–XII, Resin Glycosides, from *Ipomoea stolonifera, Phytochemistry 48*, 837–841.
114. MacLeod, J.K., and Ward, A. (1997) Structural Investigation of Resin Glycosides from *Ipomoea lonchophylla, J. Nat. Prod. 60*, 467–471.
115. Barnes, C.C., Smalley, M.K., Manfredi, K.P., Kindscher, K., Loring, H., and Sheeley, D.M. (2003) Characterization of an Anti-Tuberculosis Resin Glycoside from the Prairie Medicinal Plant *Ipomoea leptophylla, J. Nat. Prod. 66*, 1457–1462.
116. Rezanka, T., and Guschina, I.A. (2001) Glycoside Esters from Lichens of Central Asia, *Phytochemistry 58*, 509–516.
117. Rezanka, T., and Guschina, I.A. (2000) Glycosidic Compounds of Murolic, Protoconstipatic and Allo-murolic Acids from Lichens of Central Asia, *Phytochemistry 54*, 635–645.
118. Vulfson, E.N. (1992) Enzymatic Synthesis of Surfactans, in Tyman, J.H.P. (ed.), *Surfactants in Lipid Chemistry: Recent Synthetic, Physical, and Biodegradative Studies,* Royal Society of Chemistry, London, pp. 17–37.
119. Kikuchi, H., Saito, Y., Komiya, J., Takaya, Y., Honma, S., Nakahata, N., Ito, A., and Oshima, Y. (2001) Furanodictine A and B: Amino Sugar Analogues Produced by Cellular Slime Mold *Dictyostelium discoideum* Showing Neuronal Differentiation Activity, *J. Org. Chem. 66*, 6982–6987.
120. Milkereit, G., Morr, M., Thiem, J., and Vill, V. (2004) Thermotropic and Lyotropic Properties of Long Chain Alkyl Glycopyranosides: Part III: pH-Sensitive Headgroups, *Chem. Phys. Lipids 127*, 47–63.
121. Gradzielski, M. (2004) Vesicle Gels—Phase Behaviour and Process of Formation, *Curr. Opin. Colloid Interface Sci. 9*, 149–153.
122. Platz, G., Polike, J., and Thunig, C. (1995) Phase Behavior, Lyotropic Phases, and Flow Properties of Alkyl Glycosides in Aqueous Solution, *Langmuir 11,* 4250–4255.
123. Hoffmann, B., and Platz, G. (2001) Phase and Aggregation Behaviour of Alkylglycosides, *Curr. Opin. Colloid Interface Sci. 6*, 171–177.
124. Kaneko, T., Ohtani, K., Kasai, R., Yamasaki, K., and Duc, N.M. (1998) *n*-Alkyl Glycosides and *p*-Hydroxybenzoyloxy Glucose from Fruits of *Crescentia cujete, Phytochemistry 47*, 259–263.
125. Boulanger, R., and Crouzet, J. (2001) Identification of the Aroma Components of Acerola (*Malphigia glabra* L.): Free and Bound Flavour Compounds, *Food Chem. 74,* 209–216.
126. Milos, M., Mastelic, J., and Jerkovic, I. (2000) Chemical Composition and Antioxidant Effect of Glycosidically Bound Volatile Compounds from Oregano (*Origanum vulgare* L. ssp. *hirtum*), *Food Chem. 71*, 79–83.
127. De Rosa, S., De Giulio, A., and Tommonaro, G. (1996) Aliphatic and Aromatic Glycosides from the Cell Cultures of *Lycopersicon esculentum, Phytochemistry 42*, 1031–1034.
128. Takayanagi, T., Ishikawa, T., and Kitajima, J. (2003) Sesquiterpene Lactone Glucosides and Alkyl Glycosides from the Fruit of Cumin, *Phytochemistry 63*, 479–484.
129. Ono, M., Yoshida, A., Ito, Y., and Nohara, T. (1999) Phenethyl Alcohol Glycosides and Isopentenol Glycoside from Fruit of *Bupleurum falcatum, Phytochemistry 51*, 819–823.
130. Çalis, I., and Kirmizibekmez, H. (2004) Glycosides from *Phlomis lunariifolia, Phytochemistry 65,* 2619–2625.
131. Tanahashi, T., Shimada, A., Kai, M., Nagakura, N., Inoue, K., and Chen, C.C. (1996) An Iridoid Glucoside from *Jasminum hemsleyi, J. Nat. Prod. 59,* 798–800.
132. Messanga, B.B., fon Kimbu, S., Sondengam, B.L., and Bodo, B. (2001) Two New Fatty Acid Glucosides from the Root Bark of *Ochna calodendron, Fitoterapia 72*, 732–736.
133. Simko, I., Omer, E.A., Ewing, E.E., McMurry, S., Koch, J.L., and Davies, P.J. (1996) Tuberonic (12-OH-jasmonic) Acid Glucoside and Its Methyl Ester in Potato, *Phytochemistry 43*, 727–730.
134. Gambacorta, A., Soriente, A., Trincone, A., and Sodano, G. (1995) Biosynthesis of the Heterocyst Glycolipids in the Cyanobacterium *Anabaena cylindrica, Phytochemistry 39*, 771–774.
135. Lambein, F., and Wolk, C.P. (1973) Structural Studies on the Glycolipids from the Envelope of the Heterocyst of *Anabaena cylindrica, Biochemistry 12*, 791–798.
136. Adams, D.G., and Duggan, P.S. (1999) Tansley Review No. 107. Heterocyst and Akinete Differentiation in Cyanobacteria, *New Phytol. 144*, 3–33.
137. Soriente, A., Bisogno, T., Gambacorta, A., Romano, I., Sili, C., Trincone, A., and Sodano, G. (1995) Reinvestigation of Het-

erocyst Glycolipids from the Cyanobacterium, *Anabaena cylindrica, Phytochemistry 38*, 641–645.
138. Voutquenne, L., Lavaud, C., Massiot, G., Sevenet, T., and Hadi, H.A. (1999) Cytotoxic Polyisoprenes and Glycosides of Long-Chain Fatty Alcohols from *Dimocarpus fumatus, Phytochemistry 50*, 63–69.
139. Linington, R.G., Robertson, M., Gauthier, A., Finlay, B.B., van Soes, R., and Andersen, R.J. (2002) Caminoside A, an Antimicrobial Glycolipid Isolated from the Marine Sponge *Caminus sphaeroconia, Org. Lett. 4*, 4089–4092.
140. Wu, J., Zhang, S., Xiao, Q., Li, Q., Huang, J., Long, L., and Huang, L. (2003) Phenylethanoid and Aliphatic Alcohol Glycosides from *Acanthus ilicifolius, Phytochemistry 63*, 491–495.
141. Babu, B.H., Shylesh, B.S., and Padikkala, J. (2001) Antioxidant and Hepatoprotective Effect of *Acanthus ilicifolius, Fitoterapia 72*, 272–277.
142. Babu, B.H., Shylesh, B.S., and Padikkala, J. (2002) Tumour Reducing and Anticarcinogenic Activity of *Acanthus ilicifolius* in Mice, *J. Ethnopharmacol. 79*, 27–33.
143. Kanchanapoom, T., Kasai, R., Picheansoonthon, C., and Yamasaki, K. (2001) Megastigmane, Aliphatic Alcohol and Benzoxazinoid Glycosides from *Acanthus ebracteatus, Phytochemistry 58*, 811–817.
144. Wu, J., Zhang, S., Huang, J., Xiao, Q., Li, Q., Long, L., and Huang, L. (2003) New Aliphatic Alcohol and (*Z*)-4-Coumaric Acid Glycosides from *Acanthus ilicifolius, Chem. Pharm. Bull. 51*, 1201–1203.
145. Kanchanapoom, T., Ruchirawat, S., Kasai, R., and Otsuka, H. (2004) Aliphatic Alcohol and Iridoid Glycosides from *Asystasia intrusa, Chem. Pharm. Bull. 52*, 980–982.
146. Yamamura, S., Ozawa, K., Ohtani, K., Kasai, R., and Yamasaki, K. (1998) Antihistaminic Flavones and Aliphatic Glycosides from *Mentha spicata, Phytochemistry 48*, 131–136.
147. Kanchanapoom, T., Kasai, R., and Yamasaki, K. (2001) Iridoid Glucosides from *Barleria lupulina, Phytochemistry 58*, 337–341.
148. Costantino, V., Fattorusso, E., Mangoni, A., Di Rosa, M., and Ianaro, A. (1999) Glycolipids from Sponges: VII. Simplexides, Novel Immunosuppressive Glycolipids from the Caribbean Sponge *Plakortis simplex, Bioorg. Med. Chem. Lett. 9*, 271–276.
149. Gunstone, F.D., Harwood, J.L., and Padley, F.B. (1994) *The Lipid Handbook,* pp. 39–54, Chapman & Hall, London.
150. Costantino, V., Fattorusso, E., and Mangoni, A. (2000) Glycolipids from Sponges. Part 9: Plakoside C and D, Two Further Prenylated Glycosphingolipids from the Marine Sponge *Ectyoplasia ferox, Tetrahedron 56*, 5953–5957
151. Costantino, V., Fattorusso, E., Imperatore, C., and Mangoni, A. (2001) Plaxyloside from the Marine Sponge *Plakortis simplex*: An Improved Strategy for NMR Structural Studies of Carbohydrate Chains, *Eur. J. Org. Chem. 23*, 4457–4462.
152. Rezanka, T., and Dvoráková, R. (2003) Polypropionate Lactones of Deoxysugars Glycosides from Slime Mold, *Lycogala epidendrum, Phytochemistry 63*, 945–952.
153. Tabata, N., Ohyama, Y., Tomoda, H., Abe, T., Namikoshi, M., and Omura, S. (1999) Structure Elucidation of Roselipins, Inhibitors of Diacylglycerol Acyltransferase Produced by *Gliocladium roseum* KF-1040, *J. Antibiot. 52*, 815–822.
154. Tomoda, H., Ohyama, Y., Abe, T., Tabata, N., Namikoshi, M., Yamaguchi, Y., Masuma, R., and Omura, S. (1999) Roselipins, Inhibitors of Diacylglycerol Acyltransferase Produced by *Gliocladium roseum* KF-1040. Production, Isolation and Biological Properties, *J. Antibiot. 52*, 689–704.
155. Tabata, N., Ohyama, Y., Tomoda, H., Abe, T., Namikoshi, M., and Omura, S. (1999) Structure Elucidation of Roselipins, Inhibitors of Diacylglycerol Acyltransferase Produced by *Gliocladium roseum* KF-1040, *J. Antibiot. 52*, 815–826.
156. Liu, H., Orjala, J., Rali, T., and Sticher, O. (1998) Glycosides from *Stenochlaena palustris, Phytochemistry 49*, 2403–2408.
157. Thomas, B.V., Schreiber, A.A., and Weisskopf, C.P. (1988) Simple Method for Quantitation of Capsaicinoids in Pepper Using Capillary Gas Chromatography, *J. Agric. Food Chem. 46*, 2655–2663.
158. Iorizzi, M., Lanzotti, V., De Marino, S., Zollo, F., Blanco-Molina, M., Macho, A., and Munoz, E. (2001) New Glycosides from *Capsicum annuum* L. var. *acuminatum*. Isolation, Structure Determination, and Biological Activity, *J. Agric. Food Chem. 49*, 2022–2029.
159. Izumitani, Y., Yahara, S., and Nohara, T. (1990) Novel Acyclic Diterpene Glycosides, Capsianosides-A–F and Capsianosides-I–V from *Capsicum* Plants—Solanaceous Studies, *Chem. Pharm. Bull. 38*, 1299–1307.
160. Yahara, S., Kobayashi, N., Izumitani, Y., and Nohara, T. (1991) Studies on the Solanaceous Plants: 23. New Acyclic Diterpene Glycosides, Capsianoside-VI, Capsianoside-G and Capsianoside-H from the Leaves and Stems of *Capsicum annuum* L., *Chem. Pharm. Bull. 39*, 3258–3260.
161. Shimizu, M. (1999) Modulation of Intestinal Functions by Food Substances, *Nahrung/Food 43*, 154–158.
162. Kim, Y.C., and Kingston, D.G.I. (1996) A New Caprylic Alcohol Glycoside from *Circaea lutetiana* ssp. *canadensis, J. Nat. Prod. 59,* 1096–1098.
163. Ling, S.-K., Tanaka, T., and Kouno, I. (2002) New Cyanogenic and Alkyl Glycoside Constituents from *Phyllagathis rotundifolia, J. Nat. Prod. 65,*131–135.
164. Costantino, V., Fattorusso, E., Mangoni, A., Aknin, M., Fall, A., Samb, A., and Miralles, J. (1993) An Unusual Ether Glycolipid from the Senegalese Sponge *Trikentrion loeve* Carter, *Tetrahedron 49*, 2711–2716.
165. Costantino, V., Fattorusso, E., and Mangoni, A. (1993) Isolation of Five-Membered Cyclitol Glycolipids, Crasserides: Unique Glycerides from the Sponge *Pseudoceratina crassa, J. Org. Chem. 58,* 186–191.
166. Wang, N.L., Yao, X.S., Ishii, R., and Kitanaka, S. (2001) Antiallergic Agents from Natural Sources: 3. Structures and Inhibitory Effects on Nitric Oxide Production and Histamine Release of Five Novel Polyacetylene Glucosides from *Bidens parviflora* WILLD, *Chem. Pharm. Bull. 49*, 938–942.
167. Ubillas, R.P., Mendez, C.D., Jolad, S.D., Luo, J., King, S.R., Carlson, T.J., and Fort, D.M. (2000) Antihyperglycemic Acetylenic Glucosides from *Bidens pilosa, Planta Med. 66*, 82–83.
168. Mateo, J.J., and Jimenez, M. (2000) Monoterpenes in Grape Juice and Wines, *J. Chromatogr. A 881*, 557–567.
169. Mateo, J.J., Gentilini, N., Huerta, T., Jimnez, M., and Di Stefano, R. (1997) Fractionation of Glycoside Precursors of Aroma in Grapes and Wine, *J. Chromatogr. A 778*, 219–224.
170. Schneider, R., Charrier, F., Moutounet, M., and Baumes, R. (2004) Rapid Analysis of Grape Aroma Glycoconjugates Using Fourier-Transform Infrared Spectrometry and Chemometric Techniques, *Anal. Chim. Acta 513*, 91–96.
171. Ayestarán, B., Guadalupe, Z., and León, D. (2004) Quantification of Major Grape Polysaccharides (*Tempranillo* v.) Released by Maceration Enzymes During the Fermentation Process, *Anal. Chim. Acta 513*, 29–39.
172. Williams, P.J., Strauss, C.R., Wilson, B., and Massywestropp, R.A. (1982) Novel Monoterpene Disaccharide Glycosides of *Vitis vinifera* Grapes and Wines, *Phytochemistry 21*, 2013–2020.
173. Sarry, J.-E., and Günata, Z. (2004) Plant and Microbial Glycoside Hydrolases: Volatile Release from Glycosidic Aroma Precursors, *Food Chem. 87*, 509–521.

174. D'Incecco, N., Bartowsky, E., Kassara, S., Lante, A., Spettoli, P., and Henschke, P. (2004) Release of Glycosidically Bound Flavour Compounds of Chardonnay by *Oenococcus oeni* During Malolactic Fermentation, *Food Microbiol. 21*, 257–265.
175. Whitehurst, R.J. (ed.) (2004) *Emulsifiers in Food Technology*. Blackwell Publ., Ames, Iowa, p. 264.
176. De Roode, B.M., Franssen, A.C.R., Van Der Padt, A., Boom, R.M. (2003) Perspectives for the Industrial Enzymatic Production of Glycosides, *Biotechnol. Prog. 19*, 1391–1402.
177. Zhang, Q.S., Guo, B.N., and Zhang, H.M. (2004) Development and Application of Gemini Surfactants, *Prog. Chem. 16*, 343–348.
178. Hait, S.K., and Moulik, S.P. (2002) Gemini Surfactants: A Distinct Class of Self-Assembling Molecules, *Curr. Sci. 82*, 1101–1111.

[Received October 24, 2004; accepted November 13, 2004]

Dietary Fish Oil Dose- and Time-Response Effects on Cardiac Phospholipid Fatty Acid Composition

Alice J. Owen, Beata A. Peter-Przyborowska, Andrew J. Hoy, and Peter L. McLennan*

Smart Foods Center, Department of Biomedical Science, University of Wollongong, Wollongong, NSW 2522, Australia

ABSTRACT: Fish consumption is associated with reduced cardiovascular mortality, and elevated myocardial long-chain n-3 polyunsaturated FA (PUFA) content is implicated in this cardioprotection. This study examined the dose and time responses for incorporation of n-3 PUFA into cellular membranes in rats fed fish oil (FO)-containing diets. For the time course study, rats were fed a 10% FO diet for periods ranging from 0 to 42 d, after which myocardial and erythrocyte membrane fatty acid composition was determined. For the dose response study, rats ($n = 3$) were fed 0, 1.25, 2.5, 5, or 10% FO for 4 wk, with myocardial, erythrocyte, and skeletal muscle membrane FA determined. Myocardial DHA (22:6n-3) levels doubled in 2 d, stabilizing at levels ~200% higher than control after 28 d feeding with 10% FO. By comparison, DHA levels doubled after 4 wk of 1.25% FO feeding. In myocardium and skeletal muscle, EPA (20:5n-3) levels remained low, but in erythrocytes EPA levels reached 50% of DHA levels. The n-3 PUFA were incorporated at the expense of n-6 PUFA in myocardium and skeletal muscle, whereas erythrocytes maintained arachidonic acid levels, and total n-3 PUFA incorporation was lower. This study shows that low doses of FO produce marked changes in myocardial DHA levels; maximal incorporation takes up to 28 d to occur; and while erythrocytes are a good indicator of tissue n-3 incorporation in stable diets, they vary greatly in their time course and pattern of incorporation.

Paper no. L9631 in *Lipids 39*, 955–961 (October 2004).

Epidemiological evidence suggests that an inverse relationship exists between the consumption of very long chain n-3 polyunsaturated FA (PUFA) of marine origin and cardiovascular disease risk (1–3). This epidemiological evidence is supported by large-scale intervention trials such as the GISSI-Prevenzione Trial (4), which found fish oil (FO) intake was associated with a reduction in mortality among subjects with established cardiovascular disease. The link appears to be particularly strong in relation to sudden death from ischemic heart disease, which is often a result of cardiac arrhythmia.

Cardiac membrane FA composition can be altered by the fat composition of the diet (5). Previous studies examining the functional consequences of such changes have found significant anti-arrhythmic effects associated with an increase in the docosahexaenoic acid (DHA, 22:6n-3) content of myocardial membrane phospholipids from diets rich in marine oils (6-8). In addition, the economy of myocardial oxygen consumption and recovery from ischemia and reperfusion are improved in FO-fed compared to saturated fat-fed rats (9). Experimental animal studies have often used FO as the sole source of dietary fat, which could not be achieved in a free-living human diet. While one dose-response study of dietary DHA in rats has been reported (10), it was conducted over a relatively short period (2 wk) and it is not known whether this period of time is sufficient for the maximal incorporation of very long chain n-3 PUFA into membranes.

The current study had two major aims. The first was to examine the time course of FA incorporation into myocardial membrane phospholipids, and erythrocyte membrane FA, the latter being one of the most commonly used biomarkers of membrane FA composition in clinical and experimental studies. The second aim was to examine the dose-response effect of dietary n-3 PUFA on membrane lipid composition. Membrane phospholipid FA composition was determined in heart, erythrocyte and skeletal muscle in response to four doses of dietary FO fed for a period of 4 wk.

MATERIALS AND METHODS

All general chemicals and solvents were from Sigma (Sigma-Aldrich, Australia) and Merck (Crown Scientific, Australia). Chemicals were of ultra pure or analytical grade, and solvents were of at least high-performance chromatography grade. Pentobarbital sodium was from CenVet (NSW, Australia). Animals were sourced from the University of Technology Sydney, Gore Hill Laboratories (NSW, Australia). Nu-Mega high-DHA tuna FO, was kindly provided by Nu-Mega Ingredients (Australia) Ltd.

Animals and diets. Experiments were granted approval by the University of Wollongong Animal Ethics Committee, and all animals were treated in accordance with the Animal Welfare Guidelines set by the National Health and Medical Research Council, Australia. Animals were fed fully fabricated experimental diets containing (as a percentage of dry wt) 60% cornstarch, 10% sucrose, 9% casein, 5% cellulose, 10% oil, 5% gelatin and 1% vitamin/mineral mix. The 10% (% of dry wt) fat content is equivalent to approximately 22% of total energy. The lipid composition of the range of dietary oils used is given in Table 1. All animals were fed *ad libitum* and housed with a 12 h light/dark cycle at a constant temperature of 23–25°C.

*To whom correspondence should be addressed.

E-mail: petermcl@uow.edu.au

Abbreviations: EPA, eicosapentaenoic acid; DHA, docosahexaenoic acid, FO, fish oil; i.p., intraperitoneal; OO, olive oil; PUFA, polyunsaturated fatty acid(s).

Time response to dietary FO. For the time-response experiment all rats were fed fabricated diets for a total of 8 wk. Twenty-four male Sprague-Dawley rats aged 18–24 wk were fed an olive oil (OO) diet for at least 2 wk before being allocated to a 10% FO diet for the last 2 d ($n = 3$), 4 d ($n = 3$), 7 d ($n = 3$), 14 d ($n = 3$), 28 d ($n = 4$), or 42 d ($n = 4$) of the 8 wk prior to sacrifice or kept on the OO diet throughout (0 d FO, $n = 4$).

Dose response to dietary FO. For the dose-response experiment all rats were fed fabricated diets for a total of 6 wk. Fifteen male Wistar rats aged 8 wk and matched on the basis of body wt were fed an OO diet for 2 wk before being allocated to one of five dietary groups ($n = 3$); 10% OO as a 0% FO control, 1.25% FO (+8.75% OO), 2.5% FO (+7.5% OO), 5% FO (+5% OO), or 10% FO. All animals were fed the experimental diets for 4 wk prior to sacrifice.

Tissue collection. Animals were anesthetized (pentobarbital sodium (60 mg/kg i.p.) and euthanized by rapid removal of blood *via* cardiac puncture, then removal of the heart. Blood samples were collected into a syringe containing Na_2EDTA (final concentration 1 mg/mL) and subject to centrifugation at 800 × g for 10 min to separate the red cells, which were then frozen at –80°C. The heart was rinsed in ice-cold saline, cut into sections, snap-frozen in liquid nitrogen, and stored at –80°C. In the dose-response experiment, the vastus lateralis was also collected and rapidly frozen. A cross-section of the vastus lateralis, including both red and white muscle, was used for analysis.

Analytical procedure. Total lipids were extracted from duplicate 100–200 mg samples of cardiac and skeletal muscles using a modification of the method of Folch *et. al* (11). Phospholipids were isolated from the total muscle lipid by solid phase extraction, using silica Sep-Pak cartridges (Waters, Australia). Muscle phospholipid FA were methylated using 14% boron trifluoride in methanol and the FAME purified using Florisil Sep-Pak cartridges (Waters, Australia). Erythrocyte membranes (red cell ghosts) were collected by centrifugation (12), and derivatized using acetyl chloride. FAME were analyzed by GC using a Shimadzu GC-17A with FID. The column was a 30 m × 0.25 mm × 0.25 mm DB-225 (J&W Scientific, USA) with hydrogen used as the carrier gas and a temperature program rising from 150 to 23°C over a period of 28 min. FA were identified from authentic FAME standards (Sigma-Aldrich, Australia), and individual FA expressed as a percentage of total FA.

TABLE 1
Major FA Levels in the Experimental Diets[a]

	Dietary FA composition as a % of total fat				
Fat blend FA	10% OO	1.25% FO 8.75% OO	2.5% FO 7.5% OO	5% FO 5% OO	10% FO
14:0	ND	0.42	0.84	1.69	3.37
16:0	13.0	13.8	14.7	16.4	19.9
18:0	2.5	2.8	3.1	3.8	5.0
18:1n-9	69.1	62.4	55.7	42.3	15.6
18:2n-6	13.4	12.0	10.5	7.6	1.8
18:3n-3	ND	0.1	0.2	0.3	0.6
20:4n-6	ND	0.2	0.4	0.9	1.8
20:5n-3	ND	1.0	2.0	3.9	7.9
22:6n-3	ND	4.2	8.2	16.2	32.2

[a]Values are FA composition as a percentage of total dietary FA, determined by GC. The time response experiment used the 10% fish oil (FO) diet. The dose-response experiment used all incrementing doses of FO listed above with the 10% olive oil (OO) as a control. ND, not detected.

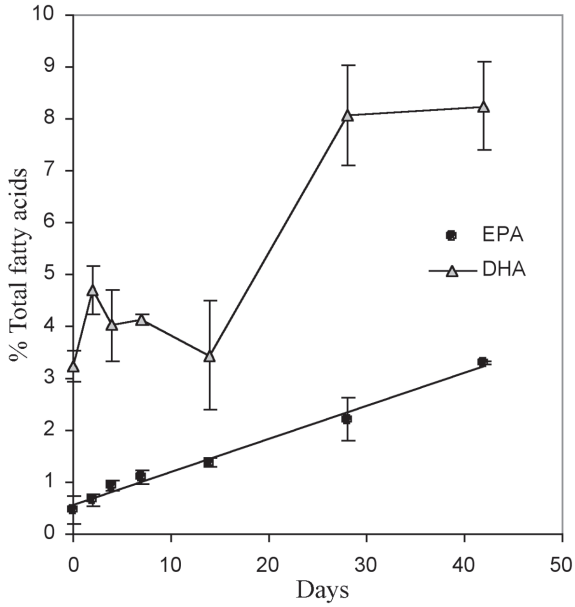

FIG. 1. Incorporation of eicosapentaenoic acid (EPA) and docosahexaenoic acid (DHA) into erythrocyte membranes with fish oil feeding over time. Values given are Mean ± SEM of DHA and EPA as a % of total erythrocyte FA.

Statistical analysis. Values are given as mean ± SE unless otherwise stated. Differences in FA composition between dietary groups within tissues in the dose response study were examined using ANOVA with Tukey HSD *post-hoc* tests. Pearson correlations were performed for individual FA between different tissue types. Statistical analyses were performed using SPSS v.10.0 and v.11.5 (SPSS Inc., Chicago, IL, USA) with significance accepted at $P < 0.05$.

RESULTS

Effect of dietary FO feeding duration on membrane lipid composition. (i) Myocardium. Significant changes in myocardial membrane FA composition were produced after only 2 d of FO feeding (Table 2): levels of the n-3 PUFA DHA (22:6n-3) and eicosapentaenoic acid (EPA, 20:5n-3) were increased, while levels of oleic acid (18:1n-9) and n-6 PUFA linoleic acid (18:2n-6) were reduced. Arachidonic acid (20:4n-6) levels were significantly reduced after 4 d of FO feeding. These changes were reflected in significant increases in total n-3 PUFA and decreases in total n-6 PUFA within 2 d. There were no significant changes in either individual or total saturated FA concentrations over the entire 42-d feeding period. No further significant differences in oleic acid occurred beyond 4 d, or in arachidonic acid and linoleic acid after 7 and 14 d respectively, although total n-6 PUFA concentration continued to decrease until 28 d of FO feeding. While the myocardial concentration of EPA increased up to 7 d, it did

TABLE 2
Time Response of Dietary Fish Oil on FA Composition of Myocardial Phospholipids[a]

FA	0 days (n = 4)	2 days (n = 3)	4 days (n = 3)	7 days (n = 3)	14 days (n = 3)	28 days (n = 4)	42 days (n = 4)
14:0	0.56 ± 0.04	0.73 ± 0.17	0.67 ± 0.09	0.70 ± 0.10	0.72 ± 0.09	0.68 ± 0.06	0.77 ± 0.02
16:0	8.49 ± 0.09	10.30 ± 0.74	10.56 ± 0.11	11.19 ± 0.26	10.88 ± 0.54	9.40 ± 0.54	7.53 ± 2.21
18:0	18.96 ± 0.11	20.86 ± 0.58	20.32 ± 0.99	21.80 ± 0.28	21.16 ± 1.15	18.97 ± 1.15	20.14 ± 1.12
18:1n-9	10.61 ± 0.18^{a}	6.33 ± 0.96^{b}	5.75 ± 0.93^{b,c}	3.40 ± 0.22^{c}	4.52 ± 0.35^{b,c}	3.45 ± 0.21^{c}	3.84 ± 0.41^{c}
18:2n-6	17.04 ± 0.81^{a}	13.30. ± 0.68^{b}	12.07 ± 0.91^{b,c}	9.82 ± 0.21^{c,d}	7.75 ± 0.03^{d,e}	5.17 ± 0.49^{e}	4.98 ± 0.30^{e}
20:4n-6	24.87 ± 0.32^{a}	21.91 ± 0.86^{a}	18.39 ± 0.59^{b}	15.83 ± 0.42^{b,c}	16.12 ± 0.48^{b,c}	13.36 ± 0.64^{c}	14.65 ± 0.90^{c}
20:5n-3	0.00 ± 0.00^{a}	0.44 ± 0.04^{b}	0.55 ± 0.06^{b}	0.71 ± 0.01^{b}	0.67 ± 0.01^{b}	0.70 ± 0.12^{b}	0.77 ± 0.11^{b}
22:6n-3	10.34 ± 0.36^{a}	19.17 ± 1.52^{b}	24.10 ± 1.23^{b}	30.78 ± 0.27^{c}	30.49 ± 0.77^{c}	39.13 ± 1.02^{d}	39.10 ± 1.34^{d}
SFA	27.86 ± 2.14	31.70 ± 0.67	31.56 ± 1.69	33.74 ± 0.24	32.41 ± 1.50	29.09 ± 1.48	28.38 ± 2.83
MUFA	15.98 ± 0.11^{a}	10.66 ± 1.25^{b}	10.03 ± 1.18^{b}	7.55 ± 0.07^{b}	8.95 ± 0.45^{b}	8.00 ± 0.52^{b}	8.31 ± 0.98^{b}
PUFA	54.23 ± 0.30^{a}	56.88 ± 1.08^{a,b}	57.31 ± 0.83^{a,b}	59.06 ± 0.24^{b}	56.76 ± 0.46^{a,b}	60.10 ± 1.10^{b}	60.89 ± 1.60^{b}
UI	220.73 ± 2.14^{a}	251.68 ± 5.87^{b}	264.08 ± 4.97^{b,c}	287.65 ± 0.73^{c}	282.93 ± 3.05^{c}	317.71 ± 6.02^{d}	321.37 ± 8.61^{d}
Total n-6	42.68 ± 0.52^{a}	35.84 ± 0.77^{b}	30.45 ± 1.32^{c}	26.33 ± 0.34^{c,d}	24.79 ± 0.74^{d,e}	18.53 ± 1.08^{f}	20.51 ± 1.35^{e,f}
Total n-3	11.55 ± 0.39^{a}	20.94 ± 1.75^{b}	25.82 ± 1.42^{b}	32.73 ± 0.27^{c}	31.97 ± 0.79^{c}	40.52 ± 1.20^{d}	40.37 ± 1.50^{d}
n-3/n-6	0.28 ± 0.01^{a}	0.59 ± 0.06^{a}	0.85 ± 0.08^{a,b}	1.24 ± 0.02^{c}	1.29 ± 0.07^{b}	2.22 ± 0.20^{d}	2.00 ± 0.19^{d}

[a]Values are given as mean ± SEM, where significant differences exist between duration of feeding. Within rows, numbers not sharing a common superscript differ significantly from one another, $P < 0.05$. MUFA, monounsaturated fatty acids; SFA, saturated fatty acids; UI, unsaturation index.

not get significantly greater beyond 2 d, whereas DHA levels continued to increase significantly until 28 d of FO feeding. The concentration of EPA rose from non-detectable levels to a maximum of 0.77% whereas DHA levels rose from 10% to a maximum of 39% after 28 d. In the n-6 PUFA, linoleic acid levels decreased from 17 to 5% and arachidonic acid decreased from 25 to 15% (Table 2).

(ii) Erythrocytes. Detectable levels of EPA (0.5%) were found in erythrocytes without FO feeding, and the incorporation of EPA into membranes appeared to be linear, reaching 3.3% of the FA content over the 42-d experimental period ($r^2 = 0.99$) (Fig. 1). In contrast, DHA showed only small changes in incorporation over 2–14 d, but exhibited a significant increase between 14 and 28 d of FO feeding (Table 3). Oleic acid levels tended to decline with increasing feeding period of FO diet but the changes did not reach significance until 28 d of feeding. Small, but significant, changes in linoleic acid levels were detected after only 2 d FO feeding, which were sustained until further significant decreases after 28 and 42 d. There were no significant changes in arachidonic acid levels in erythrocyte membranes during FO feeding. As a result of these changes in individual FA composition, n-3:n-6 PUFA ratio progressively increased with duration of feeding, while the unsaturation index remained unperturbed until after 28 d of FO feeding, when a large significant increase was noted (Table 3).

Effect of dietary FO concentration on membrane lipid composition. (i) Myocardium. Compared with the control diet (10% OO), increasing the levels of DHA-rich FO in the diet resulted in higher levels of DHA (22:6n-3) in myocardial membrane phospholipids, which achieved significance for all FO doses examined ($P < 0.01$) (Fig. 2). DHA comprised 9.29 ± 0.51% of total FA in myocardial membranes from control-fed

TABLE 3
Time Response of Dietary Fish Oil on FA Composition of Erythrocyte Membrane Lipids[a]

FA	0 days (n = 4)	2 days (n = 3)	4 days (n = 3)	7 days (n = 3)	14 days (n = 3)	28 days (n = 4)	42 days (n = 4)
14:0	0.56 ± 0.04	0.73 ± 0.17	0.66 ± 0.09	0.70 ± 0.10	0.72 ± 0.09	0.68 ± 0.06	0.77 ± 0.02
16:0	39.0 ± 0.49	43.38 ± 1.06	40.79 ± 1.20	42.07 ± 1.34	41.49 ± 0.28	40.18 ±1.01	39.89 ± 0.48
18:0	13.1 ± 0.99	14.16 ± 0.12	14.34 ± 0.44	15.45 ± 0.34	15.61 ± 0.83	15.47 ± 0.39	13.50 ± 0.26
18:1n-9	15.5 ± 0.99^{a}	13.14 ± 0.56^{a,b,c}	14.68 ± 1.88^{a,b}	11.59 ± 0.46^{a,b,c}	12.17 ± 0.04^{a,b,c}	11.11 ± 0.34^{b,c}	10.00 ± 0.37^{c}
18:2n-6	7.66 ± 0.38^{a}	5.55 ± 0.12^{b}	6.13 ± 0.18^{b}	5.11 ± 0.30^{b}	5.92 ± 0.18^{b}	4.03 ± 0.49^{c}	2.97 ± 0.28^{c}
20:4n-6	12.7 ± 0.84	10.02 ± 1.49	11.21 ± 0.52	12.06 ± 1.32	12.09 ± 0.53	12.93 ± 0.17	13.47 ± 0.14
20:5n-3	0.46 ± 0.27^{a}	0.66 ± 0.12^{a}	0.94 ± 0.09^{a}	1.09 ± 0.14^{a}	1.38 ± 0.08^{a,b}	2.21 ± 0.41^{b}	3.30 ± 0.02^{c}
22:6n-3	3.22 ± 0.30^{a}	4.69 ± 0.47^{a}	4.02 ± 0.68^{a}	4.12 ± 0.10^{a}	3.45 ± 1.06^{a}	8.06 ± 0.97^{b}	8.24 ± 0.85^{b}
SFA	39.72 ± 0.47	44.42 ± 1.24	41.84 ± 1.06	43.16 ± 1.37	42.60 ± 0.39	41.23 ± 1.00	41.09 ± 0.48
MUFA	20.06 ± 1.00^{a}	17.47 ± 0.56^{a,b,c}	19.31 ± 1.74^{a,b}	15.82 ± 0.95^{b,c,d}	15.80 ± 0.11^{b,c,d}	14.68 ± 0.45^{c,d}	13.27 ± 0.29^{c,d}
PUFA	25.92 ± 1.09^{a,b,c}	23.45 ± 1.71^{a}	24.23 ± 0.89^{a}	24.84 ± 1.26^{a,b}	25.26 ± 1.38^{a,b}	29.93 ± 1.30^{b,c}	31.00 ± 0.68^{c}
UI	116.1 ± 3.08	111.52 ± 6.87	114.14 ± 3.84	115.95 ± 3.93	115.08 ± 7.81	146.22 ± 8.00^{a}	152.93 ± 4.86^{a}
Total n-6	21.27 ± 1.06^{a}	16.50 ± 1.38^{b}	18.07 ± 0.67^{a,b}	17.99 ± 1.64^{a,b}	18.80 ± 0.39^{a,b}	18.13 ± 0.30^{a,b}	17.89 ± 0.39^{a,b}
Total n-3	4.65 ± 0.47^{a}	6.95 ± 0.34^{a}	6.16 ± 1.15^{a}	6.85 ± 0.91^{a}	6.50 ± 0.99^{a}	11.80 ± 1.39^{b}	13.11 ± 1.03^{b}
n-3/n-6	0.22 ± 0.02^{a}	0.42 ± 0.02^{b}	0.35 ± 0.07^{a,b}	0.39 ± 0.08^{a,b}	0.34 ± 0.04^{a,b}	0.65 ± 0.08^{c}	0.73 ± 0.07^{c}

[a]Values are given as mean ± SEM, where significant differences exist between duration of feeding. Within rows, numbers not sharing a common superscript differ significantly from one another, $P < 0.05$. MUFA, monounsaturated fatty acids; SFA, saturated fatty acids; UI, unsaturation index.

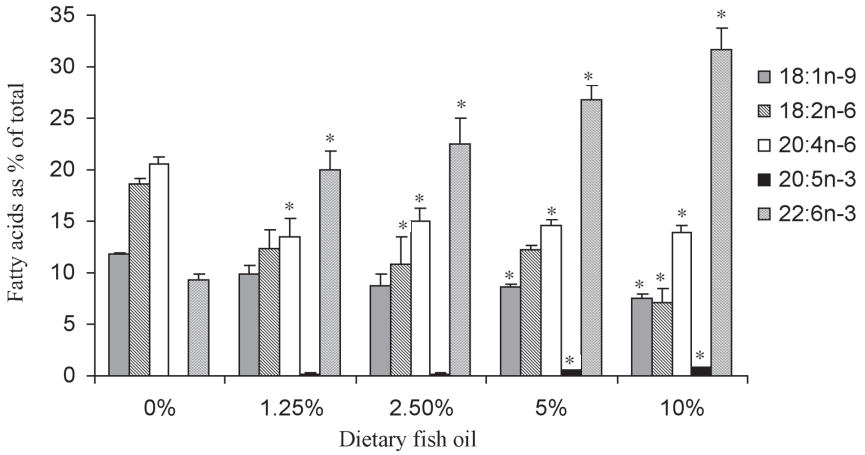

FIG. 2. Dose-response of dietary fish oil on FA composition of myocardial phospholipids from rats. Values are mean ± SEM. *Denotes significant difference from control (0%FO) diet, $P < 0.05$.

animals, whereas a diet containing 1.25% FO resulted in myocardial DHA levels of 20.06 ± 1.72% (Fig. 2). The lower OO content of the higher FO diets resulted in significantly lower oleic acid contents in myocardial phospholipids in the 5 and 10% FO groups ($P < 0.05$) (Fig. 2), but myocardial oleic acid levels from diets higher in olive oil (i.e., the control, 1.25 and 2.5% FO) did not differ significantly. Arachidonic acid (20:4n-6) levels in myocardial phospholipids were significantly lower at all FO doses compared to control ($P < 0.05$), but there was no further change with increasing FO beyond the 1.25% dose (Fig. 2). EPA was not detected in myocardial phospholipids in the control group, however it was increasingly incorporated with increasing FO dose at 0.14, 0.16, 0.50, and 0.81% on the 1.25, 2.5, 5 and 10% FO diets respectively, reaching significance at FO doses of 5 ($P = 0.011$) and 10% ($P < 0.001$).

(ii.) Skeletal muscle. Skeletal muscle FA composition with different doses of dietary FO is shown in Figure 3. There was considerable variability seen in the phospholipid FA composition of the skeletal muscle tissue samples (a mixed cross-section of vastus lateralis) (Fig. 3) and although linoleic acid and arachidonic acid tended to be reduced similarly across all doses, no statistically significant changes were observed. The dose-related effects of n-3 PUFA followed trends similar to those in myocardium, however, there was negligible incorporation of EPA into vastus lateralis membrane phospholipids. In controls, the levels of DHA in vastus lateralis were comparable to those of myocardium (12.7% of total FA), although levels plateaued at approximately 21% with FO diets of 2.5% and above, and did not reach the 30% DHA levels seen in the myocardium in these animals. DHA levels were significantly higher than control for the 2.5, 5, and 10% FO diets ($P = 0.032$, 0.018, and 0.009, respectively).

(iii) Erythrocytes. Erythrocyte membrane FA composition was significantly influenced by dietary fat composition (Fig. 4). With increasing dietary FO (and thus decreasing dietary OO content), the oleic acid content of total erythrocyte membrane FA was lowered, achieving significance at the level of 2.5% FO and above ($P < 0.003$). Erythrocytes showed significant incorporation of EPA, with EPA levels in the 10% FO dose being almost 30-fold greater than those seen in the control group (0.1 ± 0.1 for control and 2.89 ± 0.09 for 10% FO). The EPA content of erythrocyte membranes was at least three-fold higher than was seen in

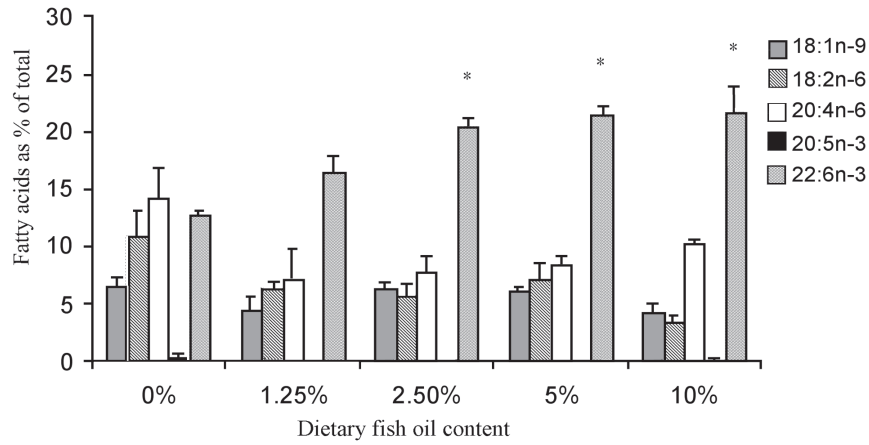

FIG. 3. Dose response of dietary fish oil on FA composition of skeletal muscle phospholipids from rats. Values are mean ± SEM. *Denotes significant difference from control diet (0%), $P < 0.05$.

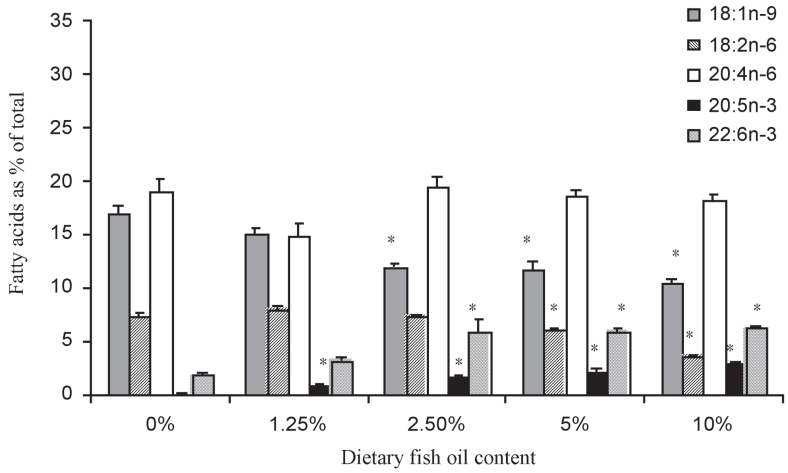

FIG. 4. Dose response of dietary fish oil on FA composition of rat erythrocyte membranes. Values are mean ± SEM. *Denotes significant difference from control diet (0%), $P < 0.05$.

either skeletal muscle or myocardium for all FO doses examined. Conversely, the level of DHA in erythrocyte membranes was only between a third and a quarter of those seen in myocardium for all dietary groups. DHA levels in erythrocyte membranes increased with increasing doses of FO, reaching significance ≥2.5% FO ($P < 0.001$) compared with control.

The level of oleic acid in myocardial membranes was highly correlated with the levels in erythrocyte membranes (r = 0.803, $P = 0.001$), but no significant correlations were seen between skeletal muscle and heart, nor skeletal muscle and erythrocyte for oleic acid. For the n-6 FA, arachidonic acid and linoleic acid, significant correlations existed between myocardium and skeletal muscle (r = 0.613, $P = 0.026$; and r = 0.586, $P = 0.036$, respectively), but not between erythrocytes and either myocardium or skeletal muscle. For the n-3 FA, EPA levels in erythrocytes and myocardium were well correlated (r = 0.871, $P < 0.001$), and significant correlations were observed for DHA between all three tissues (r = 0.806, 0.819 and 0.806, all $P < 0.005$ for skeletal muscle and myocardium, erythrocyte and myo-cardium, and erythrocyte and skeletal muscle respectively). The strongest correlations were seen between erythrocyte EPA + DHA and myocardial DHA (r = 0.883, $P < 0.001$) and skeletal muscle DHA (r = 0.943, $P < 0.001$) (Fig. 5), although with so little EPA in the myocardial and skeletal muscle membranes, the correlation was very similar for myocardial or skeletal muscle EPA + DHA.

DISCUSSION

This study has demonstrated a clear time course of incorporation of dietary long-chain n-3 PUFA into myocardial membranes in exchange for long-chain n-6 FA, with levels appearing to plateau within 28 d of feeding in mature adult rats. In adult Sprague-Dawley rats the n-3/n-6 PUFA ratio of myocardial membrane FA increased by 70% between 14 and 28 d of feeding. The myocardial phospholipid DHA levels reached in the time-response study were high (39% of total FA), but are comparable to those previously observed in Fisher rats fed a DHA-rich oil (at 25.6% of dietary energy) for 8 wk (13). In contrast to DHA, myocardial EPA levels were undetectable without FO feeding (i.e., on an OO diet) and after 42 d of FO supplementation still comstituted <1% of total FA, despite delivery of EPA and DHA in the ratio of 1:4 in the FO diet. The preferential incorporation of DHA over EPA is found even when EPA is the major n-3 PUFA in a rat diet (8). The EPA levels at all time points of FO feeding were significantly different from baseline (0 d FO) but there were no significant differences between the time points on the FO diet (2–42 d). The present study demonstrated the importance of the 4-wk feeding period in conducting dose response studies, with the only previous study examining the dose-response effect of FO FA on cardiac membranes being conducted over a 2-wk feeding period (10). While the pre-study acclimation to the fabricated OO diet from commercial chow was only conducted for a period of 2 wk, the baseline results from the time-response study differed only slightly to those seen after feeding the OO diet for a period of 4 wk in the dose-response study, despite strain differences. There is evidence to suggest that myocardial DHA levels change slightly with age (14), so the age differences between the rats used in the time course study and the dose response study may also have contributed to the differences seen in maximal DHA incorporation after 4 wk on the 10% FO diet in both arms of the study.

While the time course arm of the present study used a high-dose FO diet to maximize the ability to see changes in FA over the shortest period of time, the dose-response arm was able to demonstrate that lower doses of FO in the diet can result in marked changes to myocardial membrane composition. Inclusion of FO in the diet as 1.25% of diet wt (equivalent to approximately 2.8% of dietary energy) resulted in myocardial DHA levels that were more than double those seen with the control diet. While not examined in this study, the results suggest the possibility that even smaller amounts of FO in the diet might still result in significant changes to myocardial membrane n-3 PUFA content. Doses of EPA and DHA as low as 360 mg/kg body wt/d given by gavage have been found to increase the n-3 PUFA content of microsomal membranes

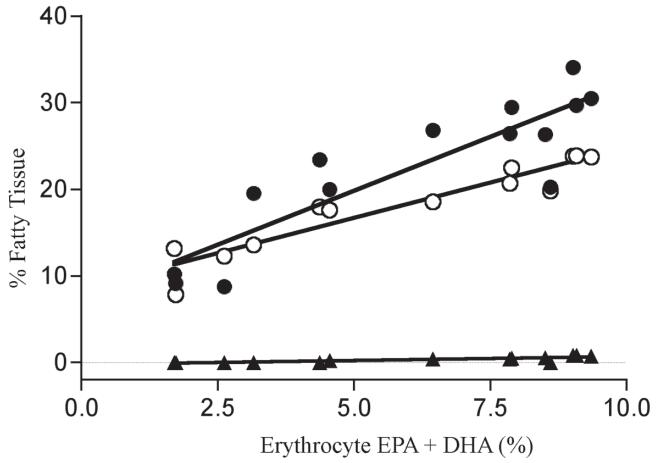

FIG. 5. Correlation between erythrocyte membrane EPA+DHA concentration, DHA concentration of myocardium (▲) and skeletal muscle (○) and EPA concentration of myocardium (●). For abbreviations see Figure 1.

compared to OO control in Wistar rats (15). However, gavage dosing of oil has previously been shown to place animals under significant stress (16), and catecholamine-induced stress has been shown to increase DHA in cardiac phospholipids at the expense of linoleic acid (14).

Erythrocytes are commonly used as a biomarker of tissue FA composition, and erythrocyte EPA + DHA has recently been proposed as a clinical marker of cardiovascular disease risk (the "Omega-3 index"), as it is thought to be reflective of cardiac membrane very long chain n-3 FA content (17). The time course of incorporation of high-FO diet into erythrocytes showed marked differences from that seen in myocardium. DHA levels in erythrocytes remained relatively steady over 0–14 d of feeding, but doubled between 14 and 28 d and appeared to plateau between 28 and 42 d, whereas EPA levels in erythrocyte membranes increased linearly over time, highlighting marked differences in incorporation of EPA and DHA. The lifespan of erythrocytes from Sprague-Dawley rats has been estimated to be approximately 60 d (18), so it is possible that the levels of EPA seen at the 42 d do not represent maximal EPA incorporation. Unlike myocardial membranes, the incorporation of EPA and DHA into erythrocyte membranes was at the expense of oleic and linoleic acids rather than the long-chain n-6 PUFA arachidonic acid, levels of which were largely preserved over time. The relative changes in phospholipid content of the n-6 PUFA linoleic acid and arachidonic acid in response to FO feeding also vary between the human blood components, plasma, platelets, and erythrocytes (19), with red blood cells showing the least change in arachidonic acid.

There was greater incorporation of DHA into myocardial membrane phospholipids compared with skeletal muscle and least incorporation into erythrocytes, with DHA levels increasing in a dose-dependent manner. The very low incorporation of EPA into myocardial phospholipids relative to the higher levels in the diet suggests a number of possibilities, including that DHA may be preferentially incorporated into myocardial lipids, that elongation and desaturation of EPA → DHA is more active in this tissue, and/or that little retroconversion of DHA → EPA occurs. The strong correlation between erythrocyte n-3 PUFA and myocardial n-3 PUFA, despite the difference in balance between EPA and DHA levels in the two tissues, highlights the importance of including both EPA and DHA in the "Omega-3 index" (17) and also confirms that the individual dietary or circulating FA are not reflected in equivalent changes in all tissue membranes (20).

The current study confirmed marked differences in lipid profile between different tissues in response to dietary fat intake. This has implications for the use of erythrocytes as a biomarker of cardiac FA composition. The relative concentrations of EPA, DHA, and other FA are known to vary between tissues within the same animal, with or without FO supplementation, as does the tissue total n-3 content (20). There are also clear differences between human and rat membrane composition, relating principally to lower PUFA content of human membranes. Nevertheless, limited human cardiac data from necropsy studies of subjects with all cause mortality show that myocardial DHA levels are 6–8 times higher than those of EPA, and n-3 PUFA content of myocardium exceeds that of serum (21), supporting the rat data. The relative differences between EPA and DHA levels in erythrocyte membranes of both humans and rats are less pronounced, with EPA more prominent and DHA less prominent in the FA profiles compared with heart (21). This contrasts with recent data from cardiac transplant patients, who despite comparable n-6 PUFA and n-3 PUFA in plasma to that of serum in the necropsy samples (21), display very low levels of both n-3 PUFA and n-6 PUFA in myocardium (22). In light of the potential importance of myocardial n-3 PUFA for healthy cardiac function (9, 23) it is possible that the low n-3 PUFA levels in the transplant biopsies compared to necropsy samples may be reflective of the failing heartor endothelial biopsy. While there were marked differences in the relative amounts and time course of incorporation of EPA and DHA into erythrocyte and myocardial membranes after 4 wk feeding, the overall correlations of n-3 PUFA content between these tissues were strong. This supports the use of erythrocyte highly unsaturated n-3 PUFA as a biomarker under conditions in which dietary fat intake is likely to be relatively stable. The use of erythrocytes as biomarkers for membrane levels of other FA (e.g., n-6 PUFA or monounsaturated FA) is not well supported by this study.

The FA composition of skeletal muscle is thought to affect insulin action, and the n-3 content of skeletal muscle phospholipids in rats is strongly related to insulin sensitivity (24). A study evaluating the use of erythrocyte FA composition as an index of abdominal rectus muscle membrane FA composition in humans concluded that skeletal muscle FA composition could not be extrapolated from erythrocytes (25). Our findings agree with those of Di Marino *et al*. (25) in terms of absolute percentages of individual FA, however, over the range of different diets we found strong correlations between either skeletal muscle or myocardial DHA and total n-3 PUFA content and erythrocyte EPA + DHA [the Omega-3 index (17)]. There was considerable variability in FA composition of the vastus lateralis cross-section taken in the present study. It has been sug-

gested that lipid composition differs significantly between white, red, and mixed muscle tissue and that these differences may be related to capacity for oxidative metabolism (26), which might account for the variability seen.

The results of the present study clearly illustrate both the time course and dose response of incorporation of FO-derived very long chain n-3 PUFA into rat cellular membranes, which is tissue specific and has implications for the use of erythrocytes as a membrane FA biomarker. Changes to cell membrane lipid composition are thought to significantly affect the function of cellular enzymes and ion channels (27), highlighting the importance of considering the effects of dietary fat on cellular membrane FA composition.

ACKNOWLEDGMENTS

This study was supported by a Strategic Partnership with Industry for Research and Training (SPIRT) grant from the Australian Research Council and Clover Corporation (Australia). The high DHA tuna FO was a gift from Nu-Mega Ingredients (Australia).

REFERENCES

1. Dyerberg J. and Bang H. O. (1982) A hypothesis on the development of acute myocardial infarction in Greenlanders. *Scand. J. Clin. Lab. Invest. Suppl. 161*, 7–13.
2. Oomen C. M., Feskens E. J., Rasanen L., Fidanza F., Nissinen A. M., Menotti A., Kok F. J. and Kromhout D. (2000) Fish consumption and coronary heart disease mortality in Finland, Italy, and The Netherlands. *Am. J. Epidemiol. 151*, 999–1006.
3. Albert C. M., Campos H., Stampfer M. J., Ridker P. M., Manson J. E., Willett W. C., and Ma J. (2002) Blood levels of long-chain n-3 FA and the risk of sudden death. *N. Eng. J. Med. 346*, 1113–1118.
4. GISSI-Prevenzione Investigators (1999) Dietary supplementation with n-3 polyunsaturated FA and vitamin E after myocardial infarction: results of the GISSI-Prevenzione trial. *Lancet. 354*, 447–455.
5. Charnock J. S., Abeywardena M. Y., and McLennan P. L. (1986) Comparative changes in the fatty-acid composition of rat cardiac phospholipids after long-term feeding of sunflower seed oil- or tuna fish oil-supplemented diets. *Ann. Nutr. Metab. 30*, 393–406.
6. McLennan P. L., Abeywardena M. Y., and Charnock J. S. (1988) Dietary fish oil prevents ventricular fibrillation following coronary artery occlusion and reperfusion. *Am. Heart. J. 116*, 709–717.
7. Nair S. S., Leitch J. W., Falconer J., and Garg M. L. (1997) Prevention of cardiac arrhythmia by dietary (n-3) polyunsaturated fatty acids and their mechanism of action. *J. Nutr. 127*, 383–393.
8. Pepe S. and McLennan P. L. (1996) Dietary fish oil confers direct antiarrhythmic properties on the myocardium of rats. *J. Nutr. 126*, 34–42.
9. Pepe S. and McLennan P. L. (2002) Cardiac membrane fatty acid composition modulates myocardial oxygen consumption and postischemic recovery of contractile function. *Circulation 105*, 2303-2308.
10. Saito M., Ueno M., Kubo K., and Yamaguchi M. (1998) Dose-Response Effect of Dietary Docosahexaenoic Acid on Fatty Acid Profiles of Serum and Tissue Lipids in Rats. *J. Agric. Food Chem. 46*, 184–193.
11. Folch J., Lees M., and Sloane Stanley G. H. (1957) A simple method for the isolation and purification of total lipids from animal tissues. *J. Biol. Chem. 226*, 497–509.
12. Steck T. L. and Kant J. A. (1974) Preparation of impermeable ghosts and inside-out vesicles from human erythrocyte membranes. *Methods. Enzymol. 31*, 172–180.
13. Atkinson T. G., Barker H. J., and Meckling-Gill K. A. (1997) Incorporation of long-chain n-3 fatty acids in tissues and enhanced bone marrow cellularity with docosahexaenoic acid feeding in post-weanling Fischer 344 rats. *Lipids 32*, 293–302.
14. Gudbjarnason S., Benediktsdottir V. E., and Skuladottir G. (1989) Effects of n-3 polyunsaturated fatty acids on coronary heart disease. *Bibl. Nutr. Dieta.,* 1–12.
15. Calviello G., Palozza P., Franceschelli P., and Bartoli G. M. (1997) Low-dose eicosapentaenoic or docosahexaenoic acid administration modifies fatty acid composition and does not affect susceptibility to oxidative stress in rat erythrocytes and tissues. *Lipids* 32, 1075–1083.
16. Brown A. P., Dinger N., and Levine B. S. (2000) Stress produced by gavage administration in the rat. *Contemp. Top. Lab. Anim. Sci. 39*, 17–21.
17. Harris W. S. and Von Schacky C. (2004) The Omega-3 Index: a new risk factor for death from coronary heart disease? *Prev. Med. 39*, 212–220.
18. Derelanko M. J. (1987) Determination of erythrocyte life span in F-344, Wistar, and Sprague-Dawley rats using a modification of the [^3H]diisopropylfluorophosphate ([^3H]DFP) method. *Fundam. Appl. Toxicol. 9*, 271–276.
19. von Schacky C. and Weber P. C. (1985) Metabolism and effects on platelet function of purified eicosapentaenoic and docosahexaenoic acids in humans. *J. Clin. Invest. 76*, 2446–2450.
20. Charnock J. S., Abeywardena M. Y., Poletti V. M., and McLennan P. L. (1992) Differences in fatty acid composition of various tissues of the marmoset monkey (*Callithrix jacchus*) after different lipid supplemented diets. *Comp. Biochem. Physiol. Comp. Physiol. 101*, 387–393.
21. Sexton P. T., Sinclair A. J., O'Dea K., Sanigorski A. J., and Walsh J. (1995) The relationship between linoleic acid level in serum, adipose tissue and myocardium in humans. *Asia Pacific J. Clin. Nutr. 4*, 314–318.
22. Harris W. S., Sands S. A., Windsor S. L., Ali H. A., Stevens T. L., Magalski A., Porter C. B., and Borkon A. M. (2004) Omega-3 fatty acids in cardiac biopsies from heart transplantation patients: correlation with erythrocytes and response to supplementation. *Circulation 110*, 1645–1649.
23. Tavazzi L., Tognoni G., Franzosi M. G., Latini R., Maggioni A. P., Marchioli R., Nicolosi G. L., and Porcu M. (2004) Rationale and design of the GISSI heart failure trial: a large trial to assess the effects of n-3 polyunsaturated fatty acids and rosuvastatin in symptomatic congestive heart failure. *Eur. J. Heart Fail. 6*, 635-641.
24. Storlien L. H., Pan D. A., Kriketos A. D., O'Connor J., Caterson I. D., Cooney G. J., Jenkins A. B., and Baur L. A. (1996) Skeletal muscle membrane lipids and insulin resistance. *Lipids 31 Suppl.*, S261–S265.
25. Di Marino L., Maffettone A., Cipriano P., Sacco M., Di Palma R., Amato B., Quarto G., Riccardi G., and Rivellese A. A. (2000) Is the erythrocyte membrane fatty acid composition a valid index of skeletal muscle membrane fatty acid composition? *Metabolism 49*, 1164–1166.
26. Okano G., Matsuzaka H., and Shimojo T. (1980) A comparative study of the lipid composition of white, intermediate, red and heart muscle in rats. *Biochim. Biophys. Acta 619*, 167–175.
27. Wu B. J., Hulbert A. J., Storlien L. H., and Else P. L. (2004) Membrane lipids and sodium pumps of cattle and crocodiles: an experimental test of the membrane pacemaker theory of metabolism. *Am. J. Physiol. 287*, R633–R641.

[Received October 14, 2004; accepted November 27, 2004]

Dietary Modulation of Fatty Acid Profiles and Oxidative Status of Rat Hepatocyte Nodules: Effect of Different n-6/n-3 Fatty Acid Ratios

S. Abel[a,*], M. De Kock[b], C.M. Smuts[c], C. de Villiers[d], S. Swanevelder[e], and W.C.A. Gelderblom[a]

[a]Programme on Mycotoxins and Experimental Carcinogenesis (PROMEC Unit), [c]Nutritional Intervention Research Unit, [d]Diabetes Research Group/Primate Unit, [e]Biostatistics Unit, Medical Research Council, Tygerberg, South Africa, and [b]Department of Physiology, University of the Western Cape, Bellville, South Africa

ABSTRACT: Male Fischer rats were fed the AIN 76A diet containing varying n-6/n-3 FA ratios using sunflower oil (SFO), soybean oil (SOY), and SFO supplemented with EPA-50 and GLA-80 (GLA) as fat sources. Hepatocyte nodules, induced using diethylnitrosamine followed by 2-acetylaminofluorene/partial hepatectomy promotion, were harvested, with surrounding and respective dietary control tissues, 3 mon after partial hepatectomy. The altered growth pattern of hepatocyte nodules in rats fed SFO is associated with a distinct lipid pattern entailing an increased concentration of PE, resulting in increased levels of 20:4n-6. In addition, there is an accumulation of 18:1n-9 and 18:2n-6 and a decrease in the end products of the n-3 metabolic pathway in PC, suggesting a dysfunctional Δ-6-desaturase enzyme. The hepatocyte nodules of the SFO-fed rats exhibited a significantly reduced lipid peroxidation level that was associated with an increase in the glutathione (GSH) concentration. The low n-6/n-3 FA ratio diets significantly decreased 20:4n-6 in PC and PE phospholipid fractions with a concomitant increase in 20:5n-3, 22:5n-3, and 22:6n-3. The resultant changes in the 20:4/20:5 FA ratio and the 20:3n-6 FA level in the case of the GLA diet suggest a reduction of prostaglandin synthesis of the 2-series. The GLA diet also counteracted the increased level of 20:4n-6 in PE by equalizing the nodule/surrounding ratio. The low n-6/n-3 ratio diets significantly increased lipid peroxidation levels in hepatocyte nodules, mimicking the level in the surrounding and control tissue while GSH was decreased. An increase in n-3 FA levels and oxidative status resulted in a reduction in the number of glutathione-S-transferase positive foci in the liver of the GLA-fed rats. Modulation of cancer development with low n-6/n-3 ratio diets containing specific dietary FA could be a promising tool in cancer intervention in the liver.

Paper no. L9492 in *Lipids 39,* 963–976 (October 2004).

Investigations into the lipid content of tumor tissue indicate that the process of carcinogenesis is associated with an altered lipid profile that appears to play an important role in cell survival and the subsequent development into neoplasia. FA, as integral components of cell membranes, may influence neoplastic development by altering cellular integrity, the activation state of pre-carcinogens, and the capacity of the cell to respond to growth regulatory signals (1). Studies by Dyerberg and Bang (2) indicated that dysfunctions in eicosanoid metabolism can lead to certain illnesses and disorders such as cardiovascular and gastrointestinal diseases as well as an increased incidence of cancer (3). These disorders have been linked to an imbalanced PUFA intake, related to diets with a high n-6 and/or low n-3 FA content (3). Diets high in n-6 FA content have been shown to promote colon and breast cancer which is associated with the up-regulation of cyclooxygenase-2 (COX-2) and p21*ras* expression (4,5). In the colon, phospholipase A_2 (PLA_2) and COX-2 (5) are overexpressed in neoplastic cells which may lead to the release of 20:4n-6 from membrane phospholipids with an increased production of prostaglandins such as PGE_2 (6–8). Overproduction of PGE_2 has been implicated in tumor initiation and promotion, cell proliferation, and differentiation and is shown to modulate cellular and humoral immune responses by inhibiting the production of lymphocytes, interleukin, and antibodies. It also has been shown to inhibit the macrophage mediated cytotoxicity to cancer cells (6). However, 20:4n-6 is an important FA in maintaining normal cellular homeostasis because of the multiple roles it plays: (i) structurally as part of membrane phospholipids, (ii) functionally as a precursor to the 2-series eicosanoids, and (iii) as an intermediate involved in signal transduction pathways regulating cell proliferation and apoptosis (9). As 20:4n-6 appears to be one of the major players in the progression of hepatocyte nodules into neoplasia, the modulation of the 20:4n-6 level is therefore of importance (10). The addition of n-3 PUFA in the diet is known to displace and therefore decrease the n-6 FA content of cellular membranes (3,6,11). This displacement and decrease are of particular importance with respect to 20:4n-6. To prevent excessive n-6 FA replacement, it is suggested that a dietary combination of 18:3n-6 and 20:5n-3 should be used to main-

*To whom correspondence should be addressed at PROMEC Unit, Medical Research Council, P.O. Box 19070, Tygerberg, 7505, South Africa.
E-mail: stefan.abel@mrc.ac.za

Abbreviations: 2-AAF, 2-acetylaminofluorene; CM, chloroform/methanol; CMS, chloroform/methanol/saline; COX-2, cyclo-oxygenase-2; DEN, diethylnitrosamine; GSH, glutathione (reduced form); GSSG, glutathione (oxidized form); $GSTP^+$, glutathione-S-transferase (placental) positive; LC-PUFA, long-chain PUFA; MDA, malondialdehyde; MUFA, monounsaturated fatty acid(s); SATS, saturated fatty acid(s); P/S, polyunsaturated to saturated fatty acid ratio; PGE_2, prostaglandin E_2; PLA_2, phospholipase A_2; SFO, sunflower oil; SOY, soybean oil; Δ6 SP, ratio of substrates to products of the Δ6-desaturase enzyme.

tain a critical level of 20:4n-6 in cell membranes (11,12). It has been shown, *in vitro* and *in vivo*, that supplementation with 18:3n-6 or evening primrose oil can maintain a steady state in the 20:4n-6 level (13,14). Dietary supplementation with 18:3n-6 and 20:5n-3 is also important with regard to supplying FA downstream of the Δ6-desaturase enzyme, which is known to be impaired in cancer tissue (15). In addition, 18:3n-6 is rapidly converted to 20:3n-6, a substrate for the 1-series prostaglandins that counteract the activities of the 2-series prostaglandins (11).

An important property of cancer cells is the low level of lipid peroxidation, partly due to unusually high levels of antioxidants such as vitamin E and 18:1n-9 (15,16). Another key molecule in determining the redox status in cells is the antioxidant glutathione which appears to be altered in cancer tissue (17,18). One of the main reasons, however, appears to be the low PUFA levels, especially n-3 PUFA, due to the impairment of the Δ6-desaturase enzyme (11,15). A previous study utilizing a liver cancer model in rats indicated that a distinct pattern with regard to FA metabolism exists in hepatocyte nodules (10). This entails low levels of the LCPUFA 22:5n-6 and 22:6n-3, and high levels of 18:1n-9 and 18:2n-6 typical of a Δ6-desaturase impairment. The decrease in the LCPUFA is also likely to be associated with a low oxidative status in hepatocyte nodules. Other important properties associated with hepatocyte nodule development include: (i) an increased concentration of the PE phospholipid fraction, resulting in a decrease in the PC/PE ratio and an increase in the level of 20:4n-6, (ii) elevated cholesterol, and (iii) an increase in membrane fluidity (10). Wood *et al.* (19) found similar elevations of PE in the plasma membrane and endoplasmic reticulum from hepatoma (7288CTC) cells grown in the hind legs of rats. With respect to FA levels, 18:1n-9 was increased in the PC and PE phospholipid fractions, while the level of 22:6n-3 was very low.

As tumors are dependent on host circulation for the type and amount of PUFA available, it should be possible to alter the FA composition by dietary means (20). Several studies have shown that the FA composition of cancer cells can be altered *in vitro* and *in vivo* by supplementation with dietary FA (21–23). The resultant changes in the FA content of the tumor may alter prostaglandin synthesis and relevant signaling pathways, thereby modulating the apoptotic/proliferative imbalance (24). The present study was conducted to monitor the effect of low n-6/n-3 FA ratio diets on the PUFA and oxidative status, and the modulating role on hepatocyte nodule development.

MATERIALS AND METHODS

Chemicals. Eicosapentaenoic acid (EPA-50) and GLA-80 were obtained from Callanish Ltd. (Breasclete, Scotland).

Animals and diets. The use of laboratory animals in this study was approved by the Ethics Committee of the Medical Research Council of South Africa. At weaning (body weight 50 g), male Fischer-344 rats were divided into three treatment groups (n = 20 rats per group) and their respective control groups (n = 5 rats per group) and fed the AIN 76A diet (25) containing fat (5% of diet) with varying n-6/n-3 FA ratios for the duration of the experiment. The different fat sources consisted of: (i) sunflower oil with a n-6/n-3 FA ratio of 250:1 (SFO, high n-6/n-3 ratio diet), (ii) SFO supplemented with EPA-50 and GLA-80, yielding a n-6/n-3 ratio of 12:1 (GLA, low n-6/n-3 ratio diet), and (iii) soybean oil yielding a n-6/n-3 ratio of 5:1 (SOY, low n-6/n-3 ratio diet).

To examine the influence of GLA on the nodule FA profile, a separate treatment group (n = 20) was fed the AIN 76A diet containing SFO and EPA-50 (without GLA) with an n-6/n-3 FA ratio of 12:1 (EPA diet). A schematic outline of the experimental design is illustrated in Figure 1.

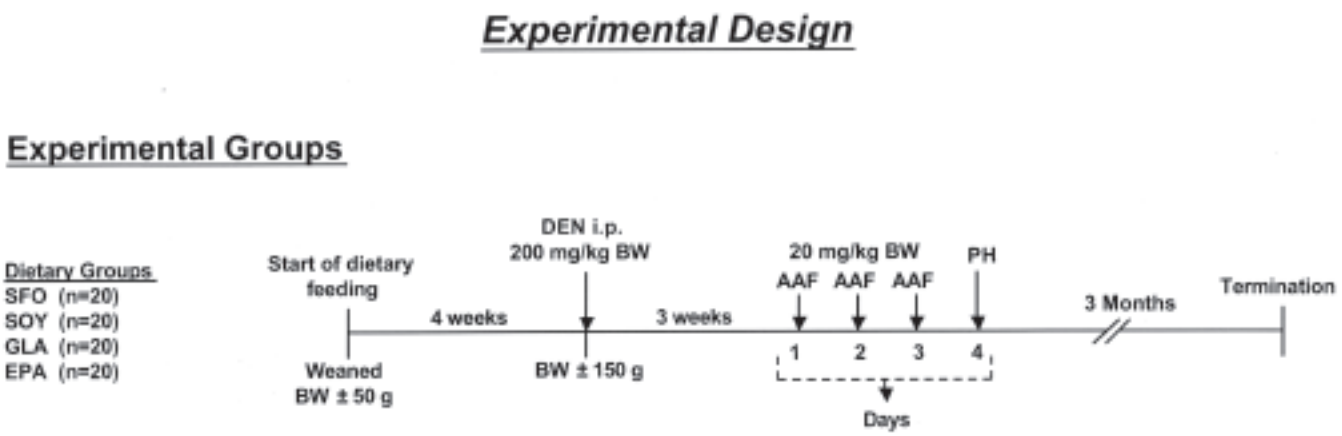

FIG. 1. The diagram depicts a timeline of the experimental procedure. Weaned male Fischer-344 rats (body weight, BW, 50 g) were divided into four experimental treatment groups (n = 20 rats per group) and were fed the AIN 76A diet containing fat (5% of diet) with varying n-6/n-3 FA ratios consisting of sunflower oil (SFO), soybean oil (SOY), sunflower/eicosapentaenoic acid-50/gamma-linolenic acid-80 (GLA) and sunflower/eicosapentaenoic acid-50 (EPA) for the duration of the experiment. Control groups included rats fed SFO, SOY, and GLA diets without the carcinogen treatment. Hepatocyte nodules were induced in the experimental treatment groups as described in the Materials and Methods section. Rats were terminated 3 mon after the cancer promotion treatment and hepatocyle nodules and surrounding tissue were collected.

TABLE 1
FA Content of the Oils (% of Total) Used in the Experimental Diets[a]

	Low n-6/n-3 FA ratio oils			
	Sunflower (SFO)	Soybean (SOY)	Sunflower EPA-50 GLA-80 (GLA)	Sunflower EPA-50 (EPA)
14:0	0.07	0.10	0.14	0.11
16:0	6.68	11.26	5.77	5.59
17:0	0.04	ND	0.24	0.22
18:0	4.45	4.20	4.23	4.15
20:0	0.29	0.36	0.29	0.32
22:0	0.75	0.43	0.79	0.77
24:0	0.25	ND	ND	ND
Total	12.53	16.35	11.46	11.16
16:1	0.06	0.06	1.17	1.02
18:1	25.17	25.60	24.35	22.08
20:1	0.21	0.24	0.28	0.24
22:1	0.01	0.01	0.04	0.02
24:1	0.05	ND	ND	ND
Total	25.50	25.91	25.84	23.36
n-6				
18:2	62.25	48.53	53.42	60.15
18:3	0.01	ND	6.2	0.12
20:2	0.02	ND	ND	ND
20:3	ND	ND	0.08	0.02
20:4	ND	ND	0.12	0.07
22:4	0.02	0.04	0.03	0.03
22:5	0.01	ND	0.01	0.02
Total	62.31	48.57	59.90	60.41
n-3				
18:3	0.25	9.20	0.31	0.40
18:4	ND	ND	0.35	0.30
20:3	ND	ND	0.05	0.13
20:5	ND	ND	3.40	3.58
22:5	ND	ND	0.27	0.23
22:6	ND	ND	0.56	0.44
Total	0.25	9.20	4.94	5.08
n-6/n-3	249.24	5.28	12.12	11.89
PUFA	62.56	57.77	64.84	65.49
P/S Ratio	4.99	3.53	5.66	5.87

[a]n-6/n-3 = n-6 FA to n-3 FA ratio, ND = not detected, P/S ratio = PUFA to saturated FA ratio.

The n-6/n-3 FA ratios of the different dietary oils used (Table 1) were determined by GC (Varian 3300, Palo, Alto, CA). The diets were prepared and stored at 4°C under nitrogen for the duration of the experiment. The rats were housed separately in wire-bottomed cages under controlled lighting (12-h cycles), humidity, and temperature (23–25°C) with free access to water. They were fed *ad libitum* and weighed three times weekly.

Induction and harvesting of hepatocyte nodules. Hepatocyte nodules were induced in the treatment groups according to the method described by Solt and Farber (26). Briefly, the rats (body weight approximately 150 g) were injected intraperitoneally (i.p.) with a single dose (200 mg/kg body weight) of diethylnitrosamine (DEN) to effect cancer initiation. Promotion was effected 3 wk later by a daily intragastric dose (20 mg/kg body weight) of 2-acetylaminofluorene (2-AAF) on three consecutive days followed by partial hepatectomy on the fourth day. The rats were terminated 3 mon following cancer promotion, and hepatocyte nodules and surrounding tissue were collected. Control tissue was collected from rats only fed the SFO, SOY, and GLA diets without the carcinogen treatment. Tissue sections were immediately frozen on dry ice and stored at –80°C prior to analyses.

Lipid extraction. Lipids were extracted with chloroform/methanol (CM; 2:1, vol/vol) containing 0.01% BHT as antioxidant (27,28). Approximately 100 to 150 mg of the liver tissue was ground to a fine powder in liquid nitrogen and weighed in glass-stoppered tubes. The tissue was suspended

in 0.5 mL saline (0.9% NaCl in distilled water), and the lipids were extracted with 24 mL CM. The CM mixture was filtered (sinterglass filters using Whatman glass microfiber filters, Cat. No. 1820 866; Whatman International, Ltd., Maidstone, England) and evaporated to dryness *in vacuo* at 40°C. The extract was transferred to glass-stoppered tubes, washed with saline saturated with CMS (chloroform/methanol/saline; 86:14:1, by vol) containing 0.01% BHT, and stored at 4°C until analyzed.

FA analyses. The lipid extracts were fractionated by TLC, and the major phospholipid fractions, PC and PE, were collected for phospholipid and FA analyses (29). For FA analyses, the phospholipid fractions were transmethylated with 2 mL methanol/18 M sulfuric acid (95:5, vol/vol) at 70°C for 2 h. The FAME were extracted in hexane and analyzed by GC on a Varian 3300 gas chromatograph equipped with 30-m fused silica Megabore DB-225 columns with a 0.53-mm internal diameter (cat. no. 125-2232; Agilent Technologies, Palo Alto, CA). The individual FAME were identified by comparison of the retention times to those of a standard mixture of free FA, 14:0 to 24:1 (Nu-Chek-Prep Inc., Elysian, MN) and quantified using an internal standard (17:0; Sigma-Aldrich, St. Louis) and expressed as μg FA/mg protein.

Phospholipid and cholesterol analyses. The phospholipid concentrations of PC and PE (μg/mg protein) were determined colorimetrically using malachite green after digestion with perchloric acid (16 N) at 170°C for approximately 1 h (30). Total cholesterol (μg/mg protein) from the lipid extracts was determined by an enzymatic iodide method (31) using cholesterin-oxidase and -esterase (Preciset Cholesterol kit, cat. no.125512; Indianapolis, IN). The cholesterol/phospholipid molar ratio (Chol/PL) was calculated by adding PC and PE together representing the major membrane phospholipids and using the M.W. of 386.7, 787, and 744 for cholesterol, PC, and PE, respectively.

Lipid peroxidation. Liver homogenates were prepared (1:19: m/vol) in a 1.15% KCl/0.01 M phosphate buffer (pH 7.4) on ice and a 0.5 mL aliquot (2 mg protein/mL) incubated with 2.5 mM ferrous sulfate for 1 h at 37°C (32). Malondialdehyde (MDA) was measured by determining the TBARS level according to the method of Hu *et al*. (33), and the results were expressed as TBARS representing the μmol MDA equivalents/mg protein, using a molar extinction coefficient of 1.56×10^5 M^{-1} cm^{-1} at 532 nm for MDA (34). Nonspecific lipid peroxidation was prevented by the incorporation of EDTA in the buffers and BHT in the reaction solutions for the TBARS assay.

Glutathione (GSH and GSSG) analysis. The glutathione, reduced (GSH) and oxidized forms (GSSG), was determined according to the method of Tietze (35). Tissue samples were homogenized (1:10 ratio) in a 15% TCA (wt/vol) and 1 mM EDTA solution for GSH and 6% perchloric acid (PCA, vol/vol), 3 mM M2VP (1-methyl-2-vinyl-pyridinium trifluoromethane sulfonate) and 1 mM EDTA solution for GSSG, on ice. The homogenates were centrifuged at $10{,}000 \times g$ for 10 min, and 50 μL of the supernatant was added to glutathione reductase (5 units) and 75 μM DTNB [5,5′ dithiobis-(2-nitrobenzoic acid)], in a microtiter plate. The reaction was initiated with the addition of 0.25 mM NADPH (50 μL) to a final reaction volume of 200 μL, the absorbance monitored at 410 nm for 5 min, and the levels of GSH and GSSG determined from standard GSH and GSSG curves, respectively. The results were expressed as mM GSH or GSSG/g wet liver weight.

Immunohistochemistry. Tissue sections of the major liver lobes were taken from all treatment and control groups at termination of the rats and preserved in buffered formalin for GSTP staining according to the method of Ogawa *et al.* (36). Dewaxed tissue sections (5 μm) were immunostained with a strepavidin-biotin-peroxidase complex and an affinity-purified biotin-labeled goat anti-rabbit IgG serum (Vector Laboratories, Burlingame, CA). Negative controls, without the antibody, were also included to test the specificity of the anti-GSTP antibody binding. The number and size (internal diameter using the largest transverse of longitudinal measurement) of the $GSTP^+$ foci were quantified microscopically (4× objective) and categorized according to the internal diameter of the foci (10 to 20, 21 to 50, 51 to 100, >100 μm, and total, i.e., >20 μm). The results were expressed as number per cm^2.

Protein determination. Powdered liver preparations (10–15 mg) from the liquid nitrogen homogenization step were first solubilized in 5% SDS at 37°C, and the protein content was determined using a modified method of Lowry (37). The protein content in the liver homogenate prepared for the lipid peroxidation determination was determined as described by Kaushal and Barnes (38).

Statistical analyses. Descriptive statistics performed on the data indicated that all groups were normally distributed (Kolmogorov–Smirnof Test) with homogeneity among the variances (Levene's Test). Initial statistical analyses included two-way ANOVA testing for interaction effects between diet and tissue type, which was followed by one-way ANOVA testing for diet effects across all tissue types and also testing for tissue effects across all dietary groups. One-way ANOVA were also used to test for dietary group differences within each tissue type separately, as well as for tissue type differences within each dietary group. When dietary group differences or tissue type differences were present, Tukey's Studentized Range Test was used, testing for multiple pairwise comparisons between the means of the different groups. As the data were unbalanced, the Tukey–Cramér adjustment was made automatically. When only two groups were present, group differences were tested using Student's *t*-test. Statistical significance was considered at $P < 0.05$.

RESULTS

FA content of dietary oils (Table 1). FA analyses of the dietary oils showed that with regard to PUFA, the SFO oil mainly contained 18:2n-6 (62.25%) with an n-6/n-3 FA ratio of approximately 250:1 consisting of total n-6 and n-3 FA levels of 62.31 and 0.25%, respectively. The SOY oil primarily con-

TABLE 2
Comparative Phospholipid and Cholesterol Content and Parameters in the Nodule, Surrounding and Control Liver of Rats Fed a Diet with Varying n-6/n-3 FA Ratios Phospholipid Concentration[a]

		Phospholipid concentration (μg/mg protein)			PC/PE phospholipid ratio		
Diet		Nodule	Surrounding	Control	Nodule	Surrounding	Control
SFO	PC	113.63 ± 31.56^{A}	102.32 ± 11.08^{A}	107.87 ± 14.55^{A}	1.99 ± 0.53^{a}	3.07 ± 0.46^{b}	2.83 ± 0.30^{b}
	PE	57.20 ± 5.08^{A}	35.58 ± 7.05^{B}	39.71 ± 5.68^{B}			
SOY	PC	104.76 ± 11.33^{A}	95.40 ± 13.13^{A}	91.94 ± 6.89^{A}	2.19 ± 0.30^{a}	3.09 ± 0.39^{b}	2.90 ± 0.32^{b}
	PE	51.77 ± 6.71^{A}	30.80 ± 5.46^{B}	32.05 ± 4.64^{B}			
GLA	PC	106.90 ± 20.70^{A}	87.82 ± 10.55^{A}	99.09 ± 9.30^{A}	2.17 ± 0.19^{a}	2.60 ± 0.17^{b}	2.91 ± 0.45^{b}
	PE	49.09 ± 8.45^{A}	35.29 ± 4.72^{B}	31.95 ± 8.60^{B}			
EPA	PC	101.95 ± 21.65^{A}	82.10 ± 12.70^{A}	—	2.19 ± 0.36^{a}	2.83 ± 0.49^{b}	—
	PE	48.73 ± 5.24^{A}	29.71 ± 8.23^{B}	—			
		Cholesterol Concentration (μg/mg protein)			Cholesterol/phospholipid Molar Ratio		
SFO		19.73 ± 3.30^{a}	15.88 ± 3.12a	14.82 ± 2.45	0.24 ± 0.05a	0.22 ± 0.05ab	0.20 ± 0.04
SOY		15.17 ± 2.02^{A}b	13.97 ± 2.14^{AB}ab	12.32 ± 1.98^{B}	0.19 ± 0.02ab	0.22 ± 0.04ab	0.20 ± 0.02
GLA		13.99 ± 2.22b	11.93 ± 1.66b	11.94 ± 2.98	0.18 ± 0.01b	0.19 ± 0.02a	0.19 ± 0.04
EPA		13.84 ± 1.67b	13.05 ± 1.06ab	—	0.18 ± 0.02^{A}b	0.25 ± 0.04^{B}b	—

[a]Values are means ± SD of 5 or 6 replications. Initial statistical analyses included two-way ANOVA testing for interaction effects between diet and tissue type, followed by one-way ANOVA testing for overall diet effects across all tissue types and testing for overall tissue effects across all dietary groups. Separate one-way ANOVA was performed to test for significance between different tissue types separately within the same dietary group, as indicated by superscript uppercase letters within a row ($P < 0.05$). One-way ANOVA was also used to test separately for differences within the same tissue type, but compared between the different dietary groups, as indicated by lowercase letters ($P < 0.05$) and identical color in a column. SFO = sunflower oil diet, SOY = soybean oil diet, GLA = sunflower/eicosapentaenoic acid-50/gamma-linolenic acid-80 oil diet, EPA = sunflower/eicosapentaenoic acid-50 oil diet. The cholesterol/phospholipid molar ratio was calculated using the sum of PC and PE, which constitute the two major phospholipid fractions in rat liver.

sisted of 18:2n-6 (48.53%) and 18:3n-3 (9.2%). The total n-6 and n-3 FA levels were 48.57 and 9.2%, respectively, with a n-6/n-3 ratio of approximately 5:1. The GLA dietary oil contained 18:2n-6 (53.42%) and 18:3n-6 (6.2%) compared to 60.15 and 0.12% in the EPA dietary oil. Both the GLA and EPA dietary oils contained total n-6 and n-3 FA levels of 60 and 5%, respectively, with an n-6/n-3 ratio of approximately 12:1. Both dietary oils also contained relatively high levels of 20:5n-3 (3.5%).

Due to the complexity and amount of data, all data for the lipid parameters and FA were first analyzed by two-way ANOVA for any diet and tissue interactions. Where a significant ($P < 0.05$) interaction occurred, the data were further analyzed by one-way ANOVA for diet effects across all tissue types and tissue effects across all dietary groups. Where no diet–tissue interactions were observed, the data were described as a diet and/or tissue effect, independent of each other. Because only overall interactions and effects were observed with this type of data analyses, the data were also separately analyzed by one-way ANOVA in which the different diet and tissue types were not grouped together as for the two-way ANOVA. The data in Tables 2, 3, and 4 and Figures 2 and 3 depict the results from these one-way ANOVA analyses.

Lipid parameters: phospholipid and cholesterol content (Table 2). (i) Phospholipids. No diet–tissue interaction was observed. Two-way ANOVA indicated significant ($P < 0.05$) effects due to the diet and tissue for PC and PE. Overall, the PC and PE levels were significantly ($P < 0.05$) higher in the nodule tissue. Overall the tissues, the EPA diet decreased ($P < 0.05$) the PC and PE levels in the nodules when compared to the SFO diet. The separate one-way ANOVA revealed a significantly ($P < 0.05$) higher PE level in the nodule tissue compared with the respective surrounding and control in all the diet groups (Table 2).

(ii) Cholesterol. No diet–tissue interaction was observed. Two-way ANOVA revealed significant ($P < 0.05$) effects due to the diet and tissue. The cholesterol level was significantly ($P < 0.05$) higher in the nodule tissue whereas the low n-6/n-3 ratio diets significantly ($P < 0.05$) decreased the cholesterol level when compared to the SFO dietary group. A similar effect was noticed when the data were analyzed by the separate one-way ANOVA. The GLA diet also significantly ($P < 0.05$) decreased the cholesterol level in the surrounding tissue compared with the SFO surrounding tissue.

(iii) Lipid parameter ratios (PC/PE and Chol/PL). No diet–tissue interaction was observed for the PC/PE ratio. Two-way ANOVA revealed a significant ($P < 0.05$) tissue effect with a lower PC/PE ratio in the nodule tissue. A significant ($P < 0.05$) diet and tissue interaction was observed for the Chol/PL ratio. Analyses by one-way ANOVA showed a significant ($P < 0.05$) diet effect reflected by a decrease in the Chol/PL ratio with the GLA diet when compared with the EPA diet. Separate one-way ANOVA revealed that the Chol/PL ratio was significantly ($P < 0.05$) decreased in the nodules by the GLA and EPA diets compared to the SFO diet (Table 2).

Comparative FA parameters: effect of SFO, SOY, GLA, and EPA diets on the FA content of the PC and PE phospholipid fraction of hepatocyte nodule, surrounding and control tissues (Tables 3 and 4). (i) Saturated FA (16:0, 18:0).

TABLE 3

Comparison of the Fatty Acid Profiles (μg fatty acid/mg protein) in the Phosphatidylcholine (PC) Phospholipid Fraction of the Nodule, Surrounding and Control Liver of Rats Fed a Diet with Varying n-6/n-3 Fatty Acid Ratios[a]

Diet		SFO			SOY			GLA			EPA	
	∀	Nodule	Surrounding	Control	Nodule	Surrounding	Control	Nodule	Surrounding	Control	Nodule	Surrounding
SATS												
16:0	N	13.96 ± 1.41	10.30 ± 0.91	9.13 ± 2.87	14.78 ± 1.49	11.68 ± 1.36	10.38 ± 0.72	14.59 ± 2.54	9.45 ± 1.51	9.10 ± 2.94	13.62 ± 2.09	9.04 ± 3.02
18:0	N	10.35 ± 2.31a	10.41 ± 1.47	13.25 ± 1.41	7.10 ± 0.81b	9.66 ± 1.02	12.10 ± 0.87	8.68 ± 1.51ab	9.65 ± 1.71	11.91 ± 3.04	8.24 ± 1.01ab	7.71 ± 2.49
Total	N	24.31 ± 3.23	20.71 ± 1.66	22.37 ± 3.88	21.88 ± 2.28	21.34 ± 2.21	22.47 ± 1.48	23.28 ± 3.76	19.10 ± 3.05	21.02 ± 5.45	21.87 ± 3.06	16.75 ± 5.50
MUFA												
16:1	Y	0.80 ± 0.13^{A}	0.49 ± 0.17^{B}	0.40 ± 0.11^{B}a	0.73 ± 0.09^{A}	0.43 ± 0.11^{B}	0.27 ± 0.07^{C}b	0.98 ± 0.20^{A}	0.45 ± 0.10^{B}	0.17 ± 0.05^{C}b	0.95 ± 0.18^{A}	0.44 ± 0.15^{B}
18:1	Y	7.53 ± 0.99^{A}	4.69 ± 0.88^{B}	4.78 ± 0.60^{B}a	6.04 ± 0.56^{A}	4.81 ± 0.50^{B}	3.73 ± 0.37^{C}b	7.14 ± 1.24^{A}	4.76 ± 0.70^{B}	3.37 ± 0.61^{C}b	7.08 ± 0.90^{A}	3.72 ± 1.34^{B}
Total	Y	8.33 ± 1.03^{A}	5.18 ± 0.91^{B}	5.18 ± 0.72^{B}a	6.78 ± 0.64^{A}	5.25 ± 0.60^{B}	4.01 ± 0.39^{C}b	8.12 ± 1.35^{A}	5.21 ± 0.73^{B}	3.54 ± 0.60^{C}b	8.03 ± 1.05^{A}	4.16 ± 1.49^{B}
n-6												
18:2	N	8.89 ± 1.38	5.50 ± 1.07	5.30 ± 1.36	8.99 ± 1.22	6.30 ± 0.45	5.02 ± 0.58	8.24 ± 1.46	5.91± 0.87	5.03 ± 1.11	10.28 ± 1.32	5.77 ± 2.62
18:3	Y	0.23 ± 0.05a	0.24 ± 0.05ab	0.32 ± 0.05a	0.14 ± 0.02^{A}b	0.22 ± 0.02^{B}ab	0.17 ± 0.04^{A}b	0.26 ± 0.05a	0.28 ± 0.05a	0.20 ± 0.03b	0.19 ± 0.02a	0.18 ± 0.07b
20:3	Y	0.23 ± 0.05^{A}	0.33 ± 0.10A^{B}a	0.41 ± 0.10^{B}	0.24 ± 0.04^{A}	0.32 ± 0.02^{B}a	0.36 ± 0.08^{B}	0.32 ± 0.06^{A}	0.57 ± 0.09^{B}b	0.36 ± 0.09^{A}	0.30 ± 0.06	0.41 ± 0.16ab
20:4	N	18:32 ± 2.85a	15.57 ± 2.38	19.10 ± 1.75a	11.47 ± 1.21b	14.56 ± 1.37ab	16.10 ± 1.15b	14.12 ± 2.48ab	15.84 ± 2.65a	15.83 ± 1.80b	13.36 ± 1.68b	11.97 ± 2.38b
22:4	N	0.41 ± 0.1a	0.56 ± 0.14a	0.44 ± 0.11	0.08 ± 0.01b	0.19 ± 0.11b	0.11 ± 0.03b	0.12 ± 0.02b	0.13 ± 0..03b	0.12 ± 0.04b	0.09 ± 0.01b	0.07 ± 0.03b
22:5	Y	1.24 ± 0.32^{A}a	2.43 ± 0.32^{B}a	2.33 ± 0.18^{B}a	0.05 ± 0.02^{A}b	0.16 ± 0.05^{B}b	0.19 ± 0.02^{B}b	0.08 ± 0.02b	0.12 ± 0.03b	0.16 ± 0.07b	0.05 ± 0.02^{A}b	0.09 ± 0.02^{B}b
Total	N	28.42 ± 5.39a	25.21 ± 4.47a	27.90 ± 3.07a	20.97 ± 2.30b	22.08 ± 2.16ab	21.94 ± 1.79b	23.14 ± 4.04ab	22.85 ± 3.67ab	21.69 ± 4.88b	24.26 ± 2.94ab	17.54 ± 6.12b
n-3												
18:3	Y	004 ± 0.01a	0.05 ± 0.01a	0.05 ± 0.02a	0.13 ± 0.02b	0.10 ± 0..02b	0.08 ± 0.01b	0.08 ± 0.01c	0.08 ± 0.02bc	0.05 ± 0.01a	0.08 ± 0.04bc	0.06 ± 0.02ac
20:5	Y	ND	ND	ND	0.16 ± 0.03a	0.11 ± 0.02a	0.15 ± 0.05	0.25 ± 0.05^{A}b	0.27 ± 0.11^{A}b	0.09 ± 0.05^{B}	0.30 ± 0.04b	0.27 ± 0.12b
22:5	Y	0.02 ± 0.01a	0.03 ± 0.01a	0.03 ± 0.01a	0.34 ± 0.05b	0.45 ± 0.12b	0.47 ± 0.10b	0.60 ± 0.15c	0.65 ± 0.15b	0.44 ± 0.12b	0.52 ± 0.06c	0.46 ± 0.24b
22:6	Y	0.17 ± 0.04^{A}a	0.24 ± 0.06^{AB}a	0.30 ± 0.06^{B}a	1.03 ± 0.20^{A}b	2.61 ± 1.02^{B}b	3.45 ± 0.47^{B}b	1.96 ± 0.44^{A}c	3.04 ± 0.54^{B}b	3.28 ± 1.10^{B}b	1.78 ± 0.37^{A}c	2.49 ± 0.65^{B}b
Total	Y	0.23 ± 0.06^{A}a	0.31 ± 0.08^{AB}a	0.37 ± 0.07^{B}a	1.66 ± 0.25^{A}b	3.27 ± 1.16^{B}b	4.15 ± 0.55^{B}b	2.90 ± 0.58^{A}c	4.04 ± 0.78^{B}b	3.86 ± 1.23^{B}b	2.69 ± 0.46c	3.28 ± 0.97b
PUFA	N	28.66 ± 5.45	25.53 ± 4.54	28.27 ± 3.13	22.63 ± 2.47	25.36 ± 1.72	26.10 ± 2.24	26.04 ± 4.51	26.89 ± 4.43	25.55 ± 6.01	26.95 ± 3.31	20.82 ± 7.07
LCPUFA	N	19.49 ± 0.43a	19.74 ± 3.30	22.61 ± 1.21	13.36 ± 1.33b	18.74 ± 1.25	20.83 ± 1.50	17.47 ± 2.80ab	20.62 ± 3.22	20.27 ± 4.46	16.40 ± 1.96ab	14.81 ± 4.09
FA ratios												
20:4 N/S		1.18 ± 0.09a		——	0.79 ± 0.12b		—	0.87 ± 0.14b		—	1.12 ± 0.15a	
20:4/20:5	Y	3.23 ± 0.08a	3.20 ± 0.08a	3.28 ± 0.04a	1.87 ± 0.06^{A}b	2.12 ± 0.11^{B}b	2.04 ± 0.11^{AB}b	1.75 ± 0.04^{A}bc	1.80 ± 0.15^{A}c	2.27 ± 0.24^{B}b	1.65 ± 0.02c	1.63 ± 0.06c
Δ6 S/P	Y	5.86 ± 0.73^{A}a	2.11 ± 0.31^{B}	1.96 ± 0.34^{B}	8.11 ± 1.77^{A}b	2.18 ± 0.36^{B}	1.50 ± 0.15^{B}	4.01 ± 0.73^{A}c	1.97 ± 0.04^{B}	1.60 ± 0.18^{B}	5.52 ± 0.79^{A}ac	2.24 ± 0.56^{B}
n-6/n-3	Y	123.21 ± 10.67^{A}a	81.42 ± 6.70^{B}a	76.85 ± 11.30^{B}a	12.79 ± 1.64^{A}b	7.94 ± 2.13^{B}b	5.32 ± 0.50^{B}b	8.07 ± 1.02^{A}c	5.69 ± 0.36^{B}b	5.80 ± 1.08^{B}b	9.12 ± 0.92^{A}c	5.28 ± 0.41^{B}b
P/S	Y	1.17 ± 0.10a	1.23 ± 0.17ab	1.29 ± 0.21	1.03 ± 0.06^{A}b	1.19 ± 0.06^{B}a	1.16 ± 0.03^{B}	1.12 ± 0.09^{A}ab	1.42 ± 0.15^{B}b	1.23 ± 0.15^{AB}	1.24 ± 0.05a	1.24 ± 0.03ab

[a]Values are means ± SD of 5 or 6 replications. ∀, A dietary group–tissue type interaction, analyzed by two-way ANOVA, Y = a significant ($P < 0.05$) diet–tissue interaction and N = no interaction. Initial statistical analyses included two-way ANOVA testing for interaction effects between diet and tissue type, followed by one-way ANOVA testing for overall diet effects across all tissue types and testing for overall tissue effects across all dietary groups. Separate one-way ANOVA was performed to test for significance between different tissue types separately within the same dietary group, as indicated by superscript uppercase letters within a row ($P < 0.05$). One-way ANOVA was also used to test separately for differences within the same tissue type across the different dietary groups, as indicated by lowercase letters ($P < 0.05$) in a row. SFO = sunflower dietary oil, SOY = soybean dietary oil, GLA = sunflower/eicosapentaenoic acid-50/gamma-linolenic acid-80 dietary oil, EPA = sunflower/eicosapentaenoic acid-50 dietary oil, SATS = saturated fatty acids, MUFA = monounsaturated fatty acids, LC PUFA, long-chain PUFA, ND = not detected, 20:4/20:5 = log ratio of 20:4n-6 to 20:5n-3, n-6/n-3 = n-6 to n-3 fatty acid ratio, P/S = polyunsaturated to saturated FA ratio, Δ6 S/P=ratio of the substrates to products of the Δ-6-desaturase enzyme, 20:4 N/S = 20:4n-6 nodule to surrounding tissue ratio.

TABLE 4

Comparison of the Fatty Acid Profiles (μg fatty acid/mg protein) in the Phosphatidylethanolamine (PE) Phospholipid Fraction of the Nodule, Surrounding and Control Liver of Rats Fed a Diet with Varying n-6/n-3 Fatty Acid Ratios[a]

Diet		SFO			SOY			GLA			EPA	
	∀	Nodule	Surrounding	Control	Nodule	Surrounding	Control	Nodule	Surrounding	Control	Nodule	Surrounding
SATS												
16:0	N	2.98 ± 0.63a	3.06 ± 0.60	2.43 ± 0.72	3.77 ± 0.44ab	3.14 ± 0.55	2.72 ± 0.45	3.92 ± 0.63b	3.01 ± 0.50	2.46 ± 0.72	3.73 ± 0.48ab	2.65 ± 1.27
18:0	N	8.18 ± 1.20	4.17 ± 0.85	5.67 ± 1.69	6.40 ± 0.85	3.84 ± 0.30	4.73 ± 0.44	6.84 ± 1.92	4.97 ± 1.04	4.89 ± 1.96	7.13 ± 0.98	3.43 ± 1.43
Total	N	11.16 ± 1.44	7.24 ± 1.05	8.10 ± 1.31	10.17 ± 1.24	6.98 ± 0.66	7.45 ± 0.88	10.77 ± 2.08	7.98 ± 1.36	7.34 ± 2.48	10.86 ± 1.31	6.08 ± 2.66
MUFA												
16:1	N	0.13 ± 0.03	0.09 ± 0.04	0.07 ± 0.04	0.14 ± 0.03	0.08 ± 0.04	0.05 ± 0.02	0.15 ± 0.03	0.07 ± 0.01	0.03 ± 0.01	0.16 ± 0.03	0.05 ± 0.02
18:1	Y	3.97 ± 0.50^{A}a	1.56 ± 0.36^{B}	1.76 ± 0.36^{B}a	2.93 ± 0.24^{A}b	1.62 ± 0.30^{B}	1.05 ± 0.15^{C}b	3.00 ± 0.58^{A}b	1.79 ± 0.25^{B}	1.02 ± 0.27^{C}b	3.36 ± 0.46^{A}ab	1.22 ± 0.55^{B}
Total	Y	4.10 ± 0.50^{A}a	1.66 ± 0.34^{B}	1.83 ± 0.33^{B}a	3.07 ± 0.25^{A}b	1.70 ± 0.33^{B}	1.09 ± 0.16^{C}b	3.15 ± 0.58^{A}b	1.86 ± 0.26^{B}	1.05 ± 0.27^{C}b	3.52 ± 0.46^{A}ab	1.27 ± 0.57^{B}
n-6												
18:2	N	2.61 ± 0.34	1.27 ± 0.35	1.36 ± 0.43	2.35 ± 0.17	1.46 ± 0.67	0.98 ± 0.16	2.06 ± 0.26	1.51 ± 0.18	0.99 ± 0.21	2.55 ± 0.34	1.25 ± 0.68
18:3	Y	0.02 ± 0.01^{A}	0.02 ± 0.01^{A}	0.04 ± 0.01^{B}	0.01 ± 0.01	0.01 ± 0.01	0.02 ± 0.01	0.01 ± 0.01^{A}	0.03 ± 0.01^{B}	0.02 ± 0.01^{AB}	0.01 ± 0.01	0.01 ± 0.01
20:3	Y	0.10 ± 0.02^{AB}	0.09 ± 0.04^{A}a	0.17 ± 0.07^{B}a	0.08 ± 0.04	0.05 ± 0.03a	0.08 ± 0.02b	0.09 ± 002^{A}	0.15 ± 0.03^{B}b	0.08 ± 0.03^{A}b	0.08 ± 0.01	0.09 ± 0.05ab
20:4	Y	10.25 ± 1.54^{A}a	5.66 ± 1.49^{B}ab	7.78 ± 2.92^{AB}	6.56 ± 0.72^{A}b	4.60 ± 0.75^{B}ab	5.20 ± 0.59^{B}	7.93 ± 1.41^{A}b	6.87 ± 1.34^{AB}a	5.36 ± 2.05^{B}	7.93 ± 1.07^{A}b	4.23 ± 1.83^{B}b
22:4	Y	1.04 ± 0.20^{A}a	0.63 ± 0.20^{B}a	0.69 ± 0.35^{AB}a	0.22 ± 0.02b	0.21 ± 0.08b	0.15 ± 0.02b	0.21 ± 0.08^{A}b	0.24 ± 0.06^{AB}b	0.15 ± 0.05^{B}b	0.21 ± 0.04^{A}b	0.12 ± 0.05^{B}b
22:5	N	2.38 ± 0.45a	2.13 ± 0.45a	2.74 ± 1.09a	0.10 ± 0.02b	0.16 ± 0.04b	0.14 ± 0.01b	0.14 ± 0.02b	0.14 ± 0.04b	0.12 ± 0.06b	0.09 ± 0.02b	0.07 ± 0.02b
Total	N	16.40 ± 2.49^{A}a	9.80 ± 2.40^{B}a	12.78 ± 4.83^{AB}a	9.32 ± 0.82b	6.68 ± 1.44ab	6.55 ± 0.79b	10.43 ± 1.85b	8.92 ± 1.62ab	6.73 ± 2.39b	10.87 ± 1.46b	5.78 ± 2.63b
n-3												
18:3	N	0.03 ± 0.01a	0.02 ± 0.01a	0.02 ± 0.01a	0.08 ± 0.01b	0.06 ± 0.01b	0.04 ± 0.01b	0.05 ± 0.02c	0.04 ± 0.01ab	0.02 ± 0.01a	0.05 ± 0.01c	0.03 ± 0.02ab
20:5	Y	ND	ND	ND	0.09 ± 0.01^{A}a	0.05 ± 0.02^{B}a	0.08 ± 0.04^{AB}	0.14 ± 0.03^{A}b	0.15 ± 0.03^{A}b	0.05 ± 0.02^{B}	0.19 ± 0.03b	0.13 ± 0.07b
22:5	Y	0.05 ± 0.01^{A}a	0.03 ± 0.01^{B}a	0.04 ± 0.02^{AB}a	0.65 ± 0.09^{A}b	0.34 ± 0.12^{B}b	0.39 ± 0.08^{B}b	0.99 ± 0.30^{A}c	0.83 ± 0.19^{A}c	0.40 ± 0.17^{B}b	0.94 ± 0.14^{A}c	0.47 ± 0.29^{B}b
22:6	Y	0.35 ± 0.06^{A}a	0.23 ± 0.08^{B}a	0.37 ± 0.16^{AB}a	2.32 ± 0.23^{A}b	2.10 ± 0.76^{A}b	3.07 ± 0.39^{B}b	3.63 ± 0.56c	3.91 ± 0.75c	3.26 ± 1.49b	3.45 ± 0.52^{A}c	2.31 ± 0.76^{B}b
Total	Y	0.42 ± 0.07^{A}a	0.28 ± 0.09^{B}a	0.43 ± 0.19^{AB}a	3.14 ± 0.31^{AB}b	2.55 ± 0.93^{A}b	3.58 ± 0.48^{B}b	4.80 ± 0.88c	4.94 ± 0.98c	3.74 ± 1.66b	4.62 ± 0.69^{A}c	2.94 ± 1.11^{B}b
PUFA	N	16.83 ± 2.56a	10.08 ± 2.49ab	13.21 ± 5.00	12.46 ± 1.05b	9.23 ± 1.87a	10.13 ± 1.25	15.23 ± 2.71ab	13.86 ± 2.57b	10.47 ± 4.04	15.49 ± 2.06ab	8.72 ± 3.73a
LCPUFA	Y	14.17 ± 1.06^{A}a	8.77 ± 1.99^{B}ab	11.80 ± 1.10^{B}	10.01 ± 0.90^{A}b	7.70 ± 1.15^{B}a	9.10 ± 0.98^{AB}	13.23 ± 2.17a	12.28 ± 2.19b	9.44 ± 3.41	12.88 ± 1.59^{A}a	7.42 ± 2.77^{B}a
FA ratios												
20:4 N/S		1.81 ± 0.31a		——	1.43 ± 0.27ab		—	1.15 ± 0.25b		—	1.87 ± 0.24a	
20:4/20:5	Y	3.01 ± 0.06^{A}a	2.74 ± 0.10^{B}a	2.87 ± 0.13^{AB}a	1.89 ± 0.02b	1.99 ± 0.08^{A}b	1.83 ± 0.12^{B}b	1.76 ± 0.02^{A}c	1.65 ± 0.05^{B}c	2.00 ± 0.10^{C}b	1.63 ± 0.02^{A}d	1.53 ± 0.03^{B}d
Δ6 S/P	Y	1.37 ± 0.11^{A}a	0.82 ± 0.13^{B}	0.68 ± 0.10^{B}a	1.37 ± 0.13^{A}a	0.83 ± 0.18^{B}	0.48 ± 0.03^{C}b	0.86 ± 0.08^{A}b	0.65 ± 0.03^{B}	0.49 ± 0.08^{C}ab	1.06 ± 0.09^{A}b	0.75 ± 0.21^{B}
n-6/n-3	N	39.03 ± 2.49a	36.11 ± 5.01a	31.67 ± 7.64a	2.98 ± 0.24b	2.61 ± 1.47b	1.84 ± 0.09b	2.17 ± 0.09b	1.82 ± 0.11b	1.86 ± 0.17b	2.36 ± 0.20b	1.92 ± 0.21b
P/S	Y	1.51 ± 0.12a	1.39 ± 0.26	1.61 ± 0.38	1.23 ± 0.10b	1.32 ± 0.20	1.36 ± 0.04	1.43 ± 0.17^{A}a	1.74 ± 0.20^{B}	1.43 ± 0.26^{AB}	1.43 ± 0.05a	1.45 ± 0.12

[a]Values are means ± SD of 5 or 6 replications. ∀, A dietary group–tissue type interaction, analyzed by two-way ANOVA, Y = a significant ($P < 0.05$) diet–tissue interaction and N = no interaction. Initial statistical analyses included two-way ANOVA testing for interaction effects between diet and tissue type, followed by one-way ANOVA testing for overall diet effects across all tissue types and testing for overall tissue effects across all dietary groups. Separate 1-way ANOVA was performed to test for significance between different tissue types separately within the same dietary group, as indicated by superscript uppercase letters within a row ($P < 0.05$). One-way ANOVA was also used to test separately for differences within the same tissue type across the different dietary groups, as indicated by lowercase letters ($P < 0.05$) in a row. SFO = sunflower dietary oil, SOY = soybean dietary oil, GLA = sunflower/eicosapentaenoic acid-50/gamma-linolenic acid-80 dietary oil, EPA=sunflower/eicosapentaenoic acid-50 dietary oil, SATS=saturated fatty acids, MUFA=monounsaturated fatty acids, ND=not detected, 20:4/20:5=log ratio of 20:4n-6 to 20:5n-3, n-6/n-3 = n-6 to n-3 fatty acid ratio, LCPUFA = long-chain PUFA, P/S = polyunsaturated to saturated fatty acid ratio, Δ6 S/P = ratio of the substrates to products of the Δ6-desaturase enzyme, 20:4 N/S = 20:4n-6 nodule to surrounding tissue ratio.

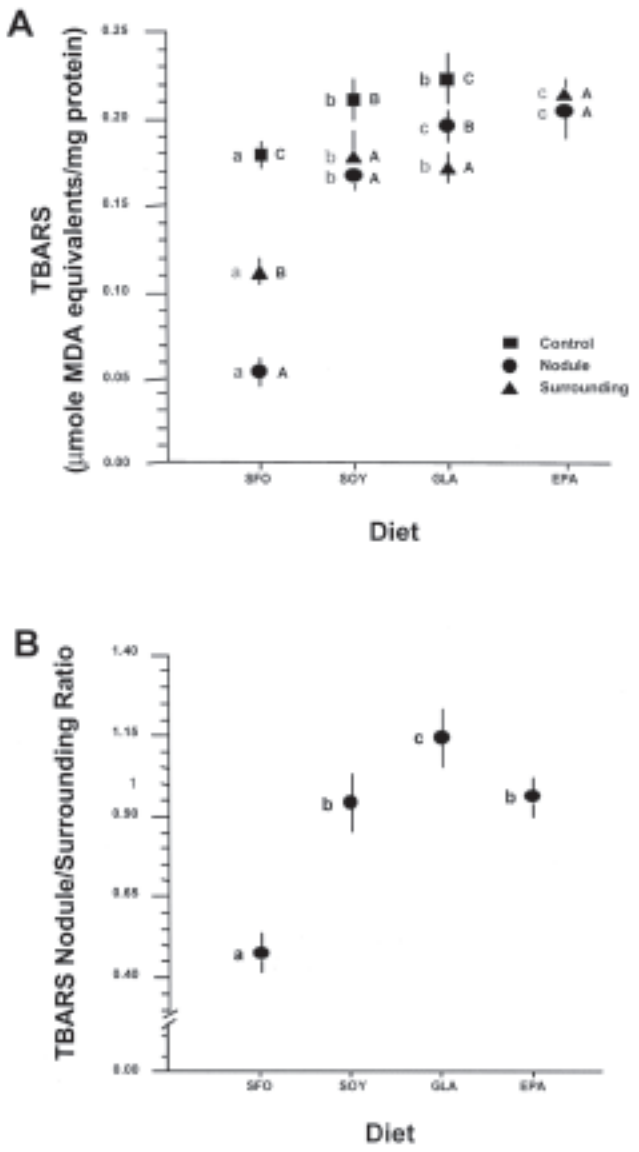

FIG. 2. The TBARS level (µmole MDA equivalents/mg protein) was determined in hepatocyte nodules, surrounding and control tissue samples from rat livers modulated with diets containing sunflower oil (SFO), soybean oil (SOY), sunflower/eicosapentaenoic acid-50/gamma-linolenic acid-80 (GLA) and sunflower/eicosapentaenoic acid-50 (EPA) as fat sources (Fig. 2A). Two-way ANOVA indicated a significant diet-tissue interaction. One-way ANOVA showed that the overall TBARS level was significantly ($P < 0.05$) increased by the low n-6/n-3 ratio diets compared with the SFO-fed group. Over all the diets, the lowest TBARS level ($P < 0.05$) was observed in the nodules compared with the control tissue. Statistical analyses by one-way ANOVA of the separate tissue types and dietary groups were also done. This was performed to test for significance between different tissue types within the same dietary group, as indicated by uppercase letters, and for differences within the same tissue type, but compared between the different dietary groups, as indicated by lowercase letters ($P < 0.05$). Control (a,b); surrounding (c–e); nodules (f–h). Figure 2B represents the change in ratio between nodule and surrounding tissue (nodule/surrounding ratio) compared with a theoretically value of 1 (i.e., no difference between nodule and surrounding tissue). Statistical analysis by one-way ANOVA was performed to test for significance ($P < 0.05$) between different dietary groups, as indicated by lowercase letters.

PC fraction. No significant diet–tissue interactions were observed. Two-way ANOVA showed a significant ($P < 0.05$) tissue effect for 16:0, 18:0, and the total saturated FA (SATS), as well as a diet effect ($P < 0.05$) for 18:0. Overall, the levels of 16:0 and the total SATS were higher in the nodule tissue than in the surrounding and control, except for 18:0 which was higher in the control tissue. Separate one-way ANOVA showed that the level of 18:0 was also significantly ($P < 0.05$) decreased in the nodules by the SOY diet when compared with the SFO diet (Table 3).

PE fraction. There were no diet–tissue interactions. Two-way ANOVA revealed a significant ($P < 0.05$) tissue effect for 16:0, 18:0, and total SATS. Overall, the levels of 16:0, 18:0, and total SATS were higher in the nodules than in surrounding and control tissues. Separate one-way ANOVA revealed that 16:0 was significantly ($P < 0.05$) increased in the nodules by the GLA diet when compared with the SFO diet (Table 4).

(ii) Monounsaturated FA (16:1, 18:1). PC fraction. A significant ($P < 0.05$) diet-tissue interaction was observed for 16:1, 18:1, and the total monounsaturated FA (MUFA). Analyses by one-way ANOVA showed a significant ($P < 0.05$) tissue effect for these FA and the total MUFA. Overall, these FA levels were highest in the nodules compared with surrounding and control tissue. Separate one-way ANOVA indicated that the SOY and GLA diets significantly ($P < 0.05$) decreased the levels of these FA in the control tissue when compared with the SFO diet (Table 3).

PE fraction. A significant ($P < 0.05$) diet–tissue interaction was observed for 18:1 and the total MUFA only. One-way analyses revealed a significant ($P < 0.05$) tissue effect with the highest levels observed in the nodule tissue compared with the surrounding and control. Two-way ANOVA for 16:1 indicated a significant ($P < 0.05$) tissue effect with the highest level observed in the nodules. Separate one-way ANOVA revealed that 18:1 and total MUFA were significantly ($P < 0.05$) decreased in the nodule and control tissues by the SOY and GLA diets when compared with the SFO diet (Table 4).

(iii) n-6 PUFA (18:2, 18:3, 20:3, 20:4, 22:4, 22:5). PC fraction. Significant ($P < 0.05$) diet–tissue interactions were observed for 18:3, 20:3, and 22:5. One-way ANOVA showed a significant ($P < 0.05$) diet effect for 18:3 and 22:5, whereas a diet and tissue effect ($P < 0.05$) was observed for 20:3. Overall, the SOY and EPA diets decreased 18:3 when compared with the SFO and GLA fed groups. The GLA diet also increased 20:3 when compared with the other diets, and 22:5 was decreased by the low n-6/n-3 ratio diets. The tissue effect of 20:3 was reflected by a lower level in the nodule tissue. Separate one-way ANOVA indicated that the SOY diet significantly ($P < 0.05$) decreased 18:3 in the nodule tissue while 22:5 was decreased by the low n-6/n-3 ratio diets (Table 3).

Two-way ANOVA revealed significant ($P < 0.05$) tissue effects for 18:2, a diet effect for the total n-6 PUFA level, and both diet and tissue effects for 20:4 and 22:4. Overall, the 18:2 level was the highest in the nodule tissue, whereas 20:4

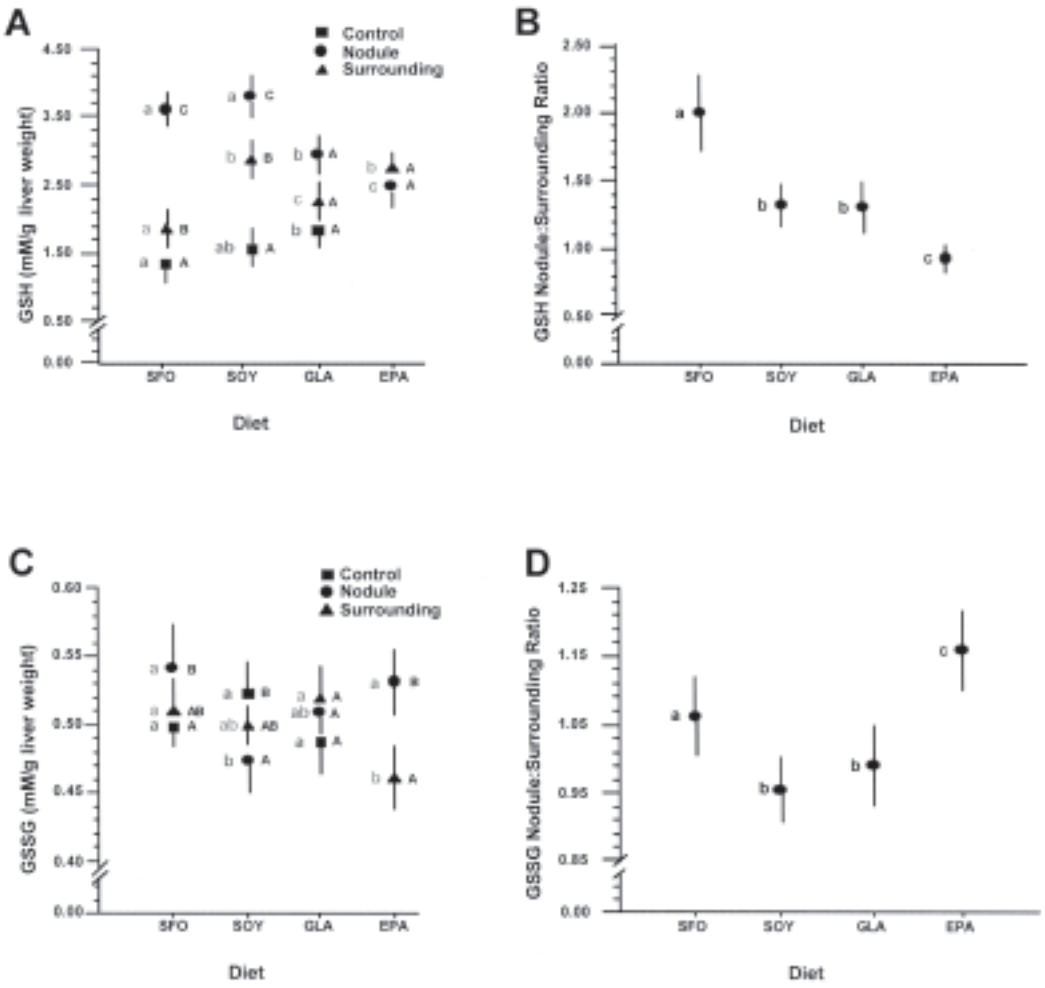

FIG. 3. The GSH (Fig. 3A) and GSSG (Fig. 3B) levels were determined in hepatocyte nodules, surrounding and control tissue from rats fed diets containing sunflower oil (SFO), soybean oil (SOY), sunflower/eicosapentaenoic acid-50/gamma-linolenic acid-80 (GLA), and sunflower/eicosapentaenoic acid-50 (EPA) as fat sources. Two-way ANOVA indicated a significant ($P < 0.05$) diet–tissue interaction for GSH and GSSG, although only a significant ($P < 0.05$) effect due to tissue was observed for GSH. Over all the diets, the GSH level was significantly ($P < 0.05$) higher in the nodule tissue. Statistical analyses by one-way ANOVA of the separate tissue types and dietary groups were also done. These were performed to test for significance between different tissue types within the same dietary group, as indicated by uppercase letters, and for differences within the same tissue type, but compared between the different dietary groups, as indicated by lowercase letters ($P < 0.05$). Control (a,b); surrounding (b–e); nodules (d–h).Figures 3C and 3D indicate the change in ratio in GSH and GSSG between nodule and surrounding tissue, respectively. Statistical analysis by one-way ANOVA was performed to test for significance ($P < 0.05$) between different dietary groups, indicated by lowercase letters.

and 22:4 were decreased. With regard to the diet, 20:4 was decreased by the SOY and EPA diets compared to the SFO and GLA dietary groups, whereas 22:4 and the total n-6 PUFA levels were decreased by the low n-6/n-3 ratio diets. A similar effect was noticed when conducting the separate one-way ANOVA on the levels of 20:4 and 22:4 in the nodules, surrounding and control tissues (Table 3).

PE fraction. Significant ($P < 0.05$) diet–tissue interactions were observed for 18:3, 20:3, 20:4, and 22:4. One-way ANOVA showed a significant ($P < 0.05$) diet effect for 20:3 and 22:4, whereas a diet and tissue effect was observed for 18:3 and 20:4. 20:3 was decreased by the SOY diet while 22:4 was decreased by the low n-6/n-3 ratio diets when compared to the SFO diet. Overall, 18:3 was decreased by the SOY and EPA diets, while the level was lower in the nodule tissue when compared to the control. The SOY diet decreased the 20:4 level when compared to the SFO diet but, overall, this FA remained higher in the nodule tissue compared with surrounding and control. 22:4 was decreased by the low n-6/n-3 ratio diets when compared to the SFO fed group.

Two-way ANOVA revealed a significant ($P < 0.05$) tissue effect for 18:2, a diet effect for 22:5 and a diet–tissue effect for the total n-6 PUFA. Overall, 18:2 was the highest in the nodule tissue. With regard to diet, 22:5 was decreased by the low n-6/n-3 ratio diets compared with the SFO-fed group. Although the total n-6 PUFA level was decreased by the low n-6/

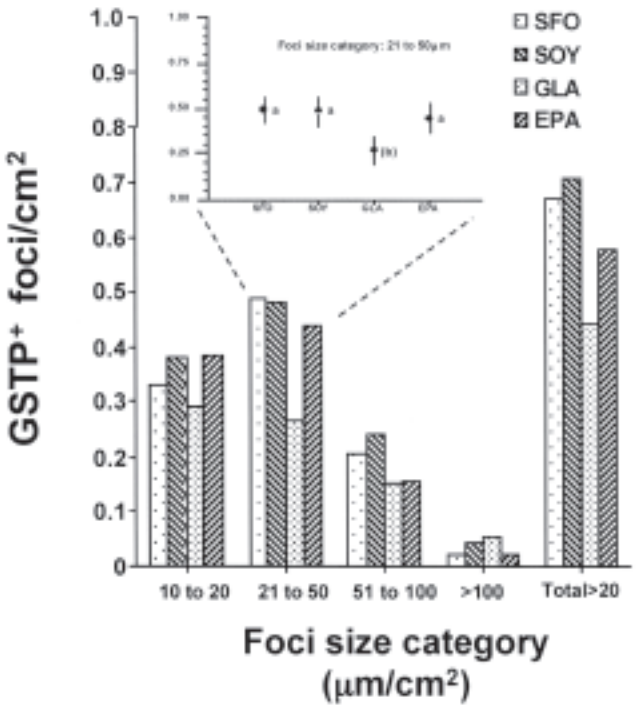

FIG. 4. Effect of diets containing sunflower oil (SFO), soybean oil (SOY), sunflower/eicosapentaenoic acid-50/gamma-linolenic acid-80 (GLA), and sunflower/eicosapentaenoic acid-50 (EPA) as fat sources on number of $GSTP^+$ foci in liver sections. The number and size of the $GSTP^+$ foci were quantified by microscope (4x objective) and categorized according to the internal diameter of the foci as follows: 10 to 20, 21 to 50, 51 to 100, >100 μm/cm^2 and total >20. Statistical analysis by one-way ANOVA was performed to test for significance between different dietary groups within a foci size category. The graph insert shows the number of $GSTP^+$ foci in the 21 to 50 μm/cm^2 foci size category of the different dietary groups. The letter in parentheses (b) indicates a marginally significant ($P < 0.1$) effect.

n-3 ratio diets, overall the level remained the highest in the nodules. When considering the separate one-way ANOVA, 20:4 was decreased in the nodules while 22:4 and 22:5 were decreased in all the tissues by the low n-6/n-3 ratio diets. This resulted in a significant decrease in the total n-6 FA in the nodules (Table 4).

(iv) n-3 PUFA (18:3, 20:5, 22:5, 22:6). PC fraction. Significant ($P < 0.05$) diet–tissue interactions were observed for 18:3, 20:5, 22:5, and 22:6 as well as for the total n-3 PUFA. One-way ANOVA showed a significant ($P < 0.05$) diet and tissue effect for 18:3, 20:5 and 22:6, but only a diet effect ($P < 0.05$) for 22:5 and the total n-3 PUFA. The 18:3, 20:5, and 22:6 levels were increased by the low n-6/n-3 ratio diets compared with the SFO-fed group. Overall, 18:3 and 20:5 were higher in the nodule tissue, whereas 22:6 was lower when compared with surrounding and control tissue. The overall levels of 22:5 and total n-3 PUFA were increased by the low n-6/n-3 ratio diets.

Separate one-way ANOVA indicated that 18:3 was increased by the low n-6/n-3 ratio diets in the nodule, with the highest level obtained with the SOY diet. 20:5 was increased significantly ($P < 0.05$) by the GLA and EPA diets when compared with the SOY diet. 22:5, 22:6, and total n-3 PUFA were significantly increased by the low n-6/n-3 ratio diets in the nodules, with the highest levels obtained with the GLA and EPA diets (Table 3).

PE fraction. Two-way ANOVA showed a significant ($P < 0.05$) diet and tissue effect for 18:3. The low n-6/n-3 ratio diets increased the 18:3 level when compared with the SFO-fed group, with the highest level achieved by the SOY diet. Overall, 18:3 was highest in the nodule tissue. Significant ($P < 0.05$) diet–tissue interactions were observed for 20:5, 22:5, 22:6, and the total n-3 PUFA. One-way ANOVA showed significant ($P < 0.05$) effects due to the diet and tissue for 20:5 and 22:5, but only a diet effect for 22:6 and the total n-3 PUFA. The low n-6/n-3 ratio diets increased the levels of 20:5, 22:5, 22:6, and the total n-3 PUFA. However, of the three diets, the level of 22:5 was lowest in the SOY-fed group, whereas 22:6 and the total n-3 PUFA were the highest in the GLA-fed group. Over all the tissue, 20:5 and 22:5 were the highest in the nodules when compared to the control tissue. Separate one-way ANOVA showed a significant ($P < 0.05$) increase of the n-3 FA in all the tissues when compared to the SFO diet. The highest incorporation was obtained with the GLA and EPA diets (Table 4).

(v) PUFA and long-chain PUFA (LCPUFA). PC fraction. No significant diet–tissue interactions were observed. Two-way ANOVA only revealed significant ($P < 0.05$) effects due to the diet and tissue for LCPUFA. Over all the tissue, the LCPUFA level was decreased by the SOY and EPA diets when compared with the SFO diet in contrast to the GLA diet, where the tissue level of LCPUFA was not affected. The level of the LCPUFA was significantly ($P < 0.05$) lower in the nodule and surrounding tissue when compared with the control. Separate one-way ANOVA indicated that the LCPUFA was decreased in the nodules only by the SOY diet when compared to the SFO diet (Table 3).

PE fraction. Two-way ANOVA for PUFA revealed a significant ($P < 0.05$) diet and tissue effect. The PUFA level was lowered by the SOY diet when compared with the SFO and GLA diets. Overall, PUFA were the highest in the nodule tissue compared with surrounding and control. A significant ($P < 0.05$) diet–tissue interaction was observed for the LCPUFA while the one-way ANOVA indicated a significant diet and tissue effect. Over all the tissue, the GLA diet effected a higher level of LCPUFA when compared with the SOY diet, while the level was higher in the nodule tissue compared to the surrounding and control. Separate one-way ANOVA indicated that the SOY diet significantly ($P < 0.05$) decreased the levels of LCPUFA and PUFA in the nodules (Table 4).

(vi) Membrane FA ratios (Tables 3 and 4). 20:4/20:5, Δ6 S/P, n-6/n-3, P/S ratios. PC fraction. A significant ($P < 0.05$) diet–tissue interaction was observed for the 20:4n-6 to 20:5n-3 FA ratio (20:4/20:5), Δ6-desaturase FA substrate to product ratio (n-6 S/P), total n-6 to total n-3 PUFA ratio (n-6/n-3), and the polyunsaturated to saturated FA ratio (P/S). One-way ANOVA indicated a significant ($P < 0.05$) diet effect for the

20:4/20:5 and n-6/n-3 ratios, a tissue effect for the Δ6 S/P ratio and a diet and tissue effect for the P/S ratio. Over all the tissues, the 20:4/20:5 and n-6/n-3 ratios were decreased by the low n-6/n-3 ratio diets, with the lowest 20:4/20:5 ratio observed in the EPA dietary group. The Δ6 S/P ratio was overall the highest in the nodule tissue. The SOY diet significantly decreased the P/S ratio when compared with the GLA diet. Overall, the ratio was lower in the nodule tissue.

Separate one-way ANOVA indicated that the 20:4/20:5 and n-6/n-3 ratios were decreased in the nodules by the low n-6/n-3 ratio diets, with the highest decrease obtained with the GLA and EPA diets. The Δ6 S/P ratio was increased by the SOY diet but decreased by the GLA diet when compared with the SFO diet. The P/S ratio was decreased only by the SOY diet (Table 3).

PE fraction. A significant ($P < 0.05$) diet–tissue interaction was observed for the 20:4/20:5, Δ6 S/P, and the P/S ratios. One-way ANOVA indicated a significant ($P < 0.05$) diet effect for the 20:4/20:5 and P/S ratios and a diet and tissue effect for the Δ6 S/P ratio. Over all the tissues, the 20:4/20:5 ratio was decreased by the low n-6/n-3 ratio diets, with the EPA diet exhibiting the lowest ratio. The P/S ratio was decreased by the SOY diet when compared with the SFO and GLA diets. The Δ6 S/P ratio was decreased by the GLA diet compared with the SFO diet, while overall the ratio was the higher in the nodule tissue. Separate one-way ANOVA indicated that the 20:4/20:5 ratio was decreased in the nodules with the low n-6/n-3 ratio diets, with the lowest ratio obtained with the EPA diet. The Δ6 S/P ratio was decreased in the nodules by the GLA and EPA diets. The P/S ratio was reduced in the nodules by the SOY diet (Table 4).

The 20:4n-6 nodule to surrounding ratio (20:4n-6 N/S) was significantly ($P < 0.05$) decreased by both the SOY and GLA diets in PC and the GLA diet ($P < 0.05$) in PE.

Lipid peroxidation (Fig. 2). Significant ($P < 0.05$) diet and tissue interactions were revealed for the TBARS level. For the diet, one-way ANOVA showed that the overall TBARS level was significantly ($P < 0.05$) increased by the low n-6/n-3 ratio diets compared with the SFO diet (Fig. 2A). Over all the diets, the lowest TBARS level ($P < 0.05$) was observed in the nodules compared with the control tissue.

Separate one-way ANOVA showed that the TBARS level in the nodules of the low n-6/n-3 ratio diets was significantly ($P < 0.05$) increased to a similar level as the respective surrounding tissue (Fig. 2A). This resulted in a significant ($P < 0.05$) increase in the TBARS nodule/surrounding ratio in the low n-6/n-3 ratio diets with the highest ($P < 0.05$) ratio observed in the GLA diet (Fig. 2B). The low n-6/n-3 ratio diets exhibited a shift in the ratio toward an equilibrium of 1 between the nodule and surrounding tissue (Fig. 2B). The TBARS level in the nodules of the EPA and GLA diets was significantly higher than the SOY diet (Fig. 2A).

Glutathione (GSH and GSSG; Fig. 3). Both the GSH and GSSG levels showed a significant ($P < 0.05$) diet–tissue interaction, although this was related to a significant ($P < 0.05$) tissue effect in the case of GSH only. Over all the diets, the GSH level was significantly ($P < 0.05$) higher in the nodule tissue.

Separate one-way ANOVA showed that the GSH level was significantly higher ($P < 0.05$) in the nodules of the SFO dietary group compared with the respective surrounding and control tissue (Fig. 3A). A similar pattern was also observed with the SOY diet, although the level was significantly increased ($P < 0.05$) in the surrounding tissue. The EPA and GLA diets significantly reduced ($P < 0.05$) the GSH levels in the nodules (Fig. 3A), while the GLA diet significantly ($P < 0.05$) increased the level in control tissue. These changes resulted in a significant ($P < 0.05$) reduction in the GSH nodule to surrounding ratio (Fig. 3B) with the low n-6/n-3 ratio diets. The lowest GSH nodule to surrounding ratio was observed with the EPA diet, while the SOY and GLA diets exhibited similar ratios. With respect to GSSG, only the SOY diet significantly ($P < 0.05$) reduced the level in the nodules (Fig. 3C). The GSSG nodule to surrounding ratio (Fig. 3D) was significantly ($P < 0.05$) lowered by the SOY and GLA diets and significantly ($P < 0.05$) increased with the EPA diet compared to the SFO diet.

Induction of GSTP$^+$ foci (Fig. 4). No significant effect on the induction of GSTP$^+$ foci was observed with the SOY and EPA diets as compared to the SFO diet (Fig. 4). The GLA diet markedly lowered foci in all the size categories when compared to the SFO and SOY diets, except for the size category >100 μm/cm^2. The GLA diet marginally ($P = 0.052$) reduced the 21 to 50 μm/cm^2 focal size category when compared to the SFO, SOY, and EPA diets (Fig. 4 insert). This size category constituted 70 to 76% of the total focal count in these diets compared with the 64% obtained with the GLA diet.

DISCUSSION

Alterations in lipid metabolism are associated with cancer development affecting the function and growth of neoplastic cells (6,10). It appears that the regulatory mechanisms related to normal lipid metabolism are disrupted, thereby altering the growth and survival of preneoplastic cells (10,39). The interaction between cholesterol, phospholipids, and FA is of importance in maintaining the integrity and functioning of cell membranes (40,41). A study by Blom *et al.* (42) reported that, in response to cholesterol loading, there was an increase in the phospholipid species containing PUFA, resulting in an increased membrane unsaturation. In the present study, increased levels of cholesterol and PE in hepatocyte nodules were associated with changes in the SATS, MUFA, and PUFA. The low n-6/n-3 FA ratio diets mainly altered the LCPUFA content of the major phospholipid fractions as well as the cholesterol level and Chol/PL ratio in the nodule tissue, while the PC and PE phospholipid concentrations were decreased. These changes were shown to affect the membrane fluidity of hepatocyte nodules in a previous study (10). Alterations in these parameters could be of importance when considering the potential role of lipid rafts in controlling certain cell signaling events by modulating the activity of raft proteins (43,44).

PUFA are known to affect various cellular processes including proliferation and/or apoptosis through the formation of oxidation products and prostaglandins (11,45). In the pres-

ent study, the low n-6/n-3 ratio diets significantly increased the n-3 FA content, especially 20:5n-3 and 22:6n-3, with a concomitant decrease in the n-6 PUFA levels. The regulation of 20:4n-6 in cancer cells by dietary FA intervention utilizing 20:5n-3, a precursor of the 3-series prostaglandins, has been suggested as it competes for the cyclooxygenase enzyme. The 20:4n-6 to 20:5n-3 FA ratio is therefore of importance, indicating a shift in the type of prostaglandin synthesized (46). The low n-6/n-3 ratio diets significantly decreased 20:4n-6 and increased 20:5n-3 in PC and PE resulting in a decreased 20:4/20:5 ratio. The kinetics of changes in these parameters differed between the diets with the EPA diet inducing the largest effect. However, as 20:4n-6 has been implicated in the induction of apoptosis *via* the stimulation of ceramide release (47,48), excessive reduction of 20:4n-6 could impact negatively on the apoptotic rate in the nodules in counteracting the enhanced cell proliferation in this tissue type. Therefore, control over the level of 20:4n-6 by dietary intake of 20:5n-3 and 22:6n-3 can be exercised, due to their feedback inhibition on the activity of the Δ5- and Δ6-desaturases (8,12). Dietary GLA also modulates the levels of 20:3n-6 and 20:4n-6, thereby influencing prostaglandin synthesis (49,50). In the present study, the GLA diet modulated the 20:4/20:5 ratio by stabilizing the replacement/decrease of 18:3n-6, 20:3n-6, and 20:4n-6 by the SOY diet and 18:3n-6 and 20:4n-6 by the EPA diet. The characteristic difference in the 20:4n-6, PUFA, and LCPUFA pattern between the nodule and surrounding tissue was equalized by the GLA diet in PE. GLA decreased the 20:4n-6 nodule/surrounding ratio to approximately 1 by bypassing the impaired Δ-6-desaturase. This could compensate for the increased level of 20:4n-6 due to the persistent high concentration of PE in the nodule tissue. In contrast, the EPA diet had a comparable nodule to surrounding ratio to the SFO diet, as the replacement of 20:4n-6 by the n-3 PUFA was similar in the nodule and surrounding tissue. Therefore, changes in the levels of both 18:3n-6 and 20:3n-6, together with a shift in the 20:4 nodule/surrounding and 20:4/20:5 ratios in hepatocyte nodules, are likely to direct prostaglandin synthesis away from 20:4n-6. In addition, the n-3 PUFA inhibit the phospholipase-induced release of 20:4n-6 (51,52), while 20:5n-3 has a potentiating effect on the growth regulatory effects of 20:3n-6 presumably *via* the production of the 1-series prostaglandins and 15-OH-dihomo-GLA, which inhibits cell proliferation (11). This potentiating effect is manifested by the lack of interference of n-3 PUFA in the elongation of 18:3n-6 to 20:3n-6, which will favor the formation of PGE_1, thereby further modulating PGE_2 formation (11).

High LCPUFA and lipid peroxidation levels have been shown to be important mechanisms in the inhibition of cancer cell proliferation (15,53). Impairment of the Δ6-desaturase enzyme could therefore play an important role in maintaining low LCPUFA levels, contributing to a low oxidative status in cancer tissue, with respect to hepatocyte nodules (10,12). Changes in cholesterol, phospholipids, and FA unsaturation level of PC have been shown to be important for the optimal functioning of the Δ6-desaturase enzyme (54,55). In the present study the dysfunctional desaturase enzyme was not affected by the low n-6/n-3 ratio diets, indicated by the persistent elevated levels of 18:1n-9 and 18:2n-6 in the nodule PC and PE fractions and persistent lower level of 22:6n-3 in the nodule tissue. The increase in lipid peroxidation can therefore be attributed to the increase in the n-3 LCPUFA, specifically 22:6n-3, which is known to be a good substrate for lipid peroxidation (56). Although 22:6n-3 was increased by the low n-6/n-3 ratio diets, it remained lower in the nodules in comparison to the surrounding and control tissue. This is probably due to the impaired Δ-6-desaturase enzyme, which also catalyzes the conversion of 22:5n-3 to 22:6n-3. Of interest is that the level of 18:1n-9, reported to be an effective antioxidant (16), was decreased in PE by the SOY and GLA diets which could contribute to the increased lipid peroxidation level in the nodules. 18:1n-9 also promotes cell proliferation and is a negative regulator of apoptosis (57).

The regulation of the oxidative status by GSH is of importance with regard to tumor growth (58). A higher GSH level in breast cancer tumors is associated with an increased level of cell proliferation (59). GSH is also elevated in a number of drug-resistant tumor cell lines and tumor cells isolated from patients resistant to drug therapy (60). In the present study, the GSH level was significantly increased in the nodules of the SFO- and SOY-fed dietary rats, but was decreased in the nodules of the GLA and EPA dietary groups, which coincided with the increased TBARS formation. A study by Kokura *et al.* (61) showed a similar effect with respect to an increased lipid peroxidation and decreased GSH levels in tumor cells of rats dosed with 20:5n-3. The decreased GSH, associated with the EPA and GLA diets, can be attributed to the high level of dietary 20:5n-3, which lies downstream of the Δ6-desaturase. In contrast, the SOY diet did not decrease the GSH level in the nodules, presumably, as stated above, due to the source of dietary n-3 FA, i.e., 18:3n-3, which lies upstream of the Δ6-desaturase. As mentioned earlier, the nodules of the SOY dietary group had lower n-3 FA levels in contrast to the GLA and EPA groups (Tables 3 and 4). The increased lipid peroxidation mainly targeted the hepatocyte nodules with a far less significant impact on the oxidative status in the surrounding and control tissue. In the case of the GLA diet, the increased oxidative status in the nodule tissue contributed to the reduced number of $GSTP^+$ foci and/or nodules in the foci category comprising the largest number of foci. This decrease can be ascribed to the so-called "GLA effect", which seems to stabilize the level of 20:4n-6, when considering the 20:4n-6 nodule/surrounding ratio. In addition to the potential modulating effect of 18:3n-6, *via* 20:3n-6, and 20:5n-3 on prostaglandin synthesis in tumor cells, these PUFA, including 20:4n-6, also elicit responses by directly influencing intracellular signaling pathways and transcription factor activity (6,8,12,23). Other FA such as 18:1n-9 have also been shown to exhibit antiapoptotic effects and stimulate cell proliferation in MDA-MB-231 breast cancer cells. This effect was found to be linked to 18:1n-9 stimulation of PI 3-kinase (PI3-K) activity, a key signal transduction enzyme involved in the control of cell

growth (57). Of interest is that both the SOY and GLA diets significantly reduced the level of 18:1n-9 in the PE phospholipid fraction of the nodules.

The decrease in LCPUFA levels, due to impairment of the Δ6-desaturase in hepatocyte nodules, is likely to play an important role in the subsequent modulatory effect on nodule development. In this regard, the role of dietary FA in controlling cellular homeostasis seems to be important in balancing events related to apoptosis and cell proliferation to sustain normal growth. Certain dietary n-6 and n-3 FA, therefore, could create a multiple control mechanism for regulating cancerous growth depending on the dietary n-6/n-3 FA ratio as well as the type of FA constituting this ratio.

ACKNOWLEDGMENTS

The authors wish to thank the Nutritional Intervention Research Unit for the use of their GC equipment, J. van Wyk for her expertise in the laboratory, Sonja Swanevelder of the Biostatistics Department of the Medical Research Council and Dirk van Schalkwyk from the UK Renal Registry, Southmead Hospital, Bristol, United Kingdom, for the statistical analyses. With thanks also to Amelia Damons and John Mokotary for washing and cleaning all the glassware. This study was partly funded by the Cancer Association of South Africa (CANSA).

REFERENCES

1. Kolonel, L.N., Nomura, A.M.Y., and Cooney, R.V. (1999) Dietary Fat and Prostate Cancer: Current Status, *J. Nat. Cancer Institute 91*, 414–428.
2. Dyerberg, J., and Bang, H.O. (1979) Haemostatic Function and Platelet Polyunsaturated Fatty Acids in Eskimos, *Lancet 2*, 433–435.
3. Gill, I., and Valivety, R. (1997) Polyunsaturated Fatty Acids, Part 1: Occurrence, Biological Activities and Applications, *TIBTECH 15*, 401–409.
4. Singh, J., Hamid, R., and Reddy, B.S. (1997) Dietary Fat and Colon Cancer: Modulation of Cyclooxygenase-2 by Types and Amount of Dietary Fat During the Postinitiation Stage of Colon Carcinogenesis, *Cancer Res. 57,* 3465–3470.
5. Badawi, A.F., El-Sohemy, A., Stephen, L.L., Ghoshal, A.K., and Arcger, M.C. (1998) The Effect of Dietary n-3 and n-6 Polyunsaturated Fatty Acids on the Expression of Cyclooxygenase 1 and 2 and Levels of $P21^{ras}$ in Rat Mammary Glands, *Carcinogenesis 19*, 903–910.
6. Bartsch, H., Nair, J., and Owen, R.W. (1999) Dietary Polyunsaturated Fatty Acids and Cancers of the Breast and Colorectum: Emerging Evidence for Their Role as Risk Modifiers, *Carcinogenesis 20*, 2209–2218.
7. Marks, F., Müller-Decker, K., and Fürstenberger, G. (2000) A Causal Relationship Between Unscheduled Eicosanoid Signaling and Tumor Development: Cancer Chemoprevention by Inhibitors of Arachidonic Acid Metabolism, *Toxicology 153*, 11–26.
8. Rose, D.P., and Connolly, J.M. (1999) Omega-3 Fatty Acids as Cancer Chemopreventive Agents, *Pharm. Therap. 83*, 217–244.
9. Khan, W.A., Blobe, G.C., and Hannun, Y.A. (1995) Arachidonic Acid and Free Fatty Acids as Second Messengers and the Role of Protein Kinase C, *Cell Signaling 7*, 171–184.
10. Abel, S., Smuts, C.M., de Villiers, C., and Gelderblom, W.C.A. (2001) Changes in Essential Fatty Acid Patterns Associated with Normal Liver Regeneration and the Progression of Hepatocyte Nodules in Rat Hepatocarcinogenesis, *Carcinogenesis 22*, 795–804.
11. Horrobin, D.F. (1992) Nutritional and Medical Importance of Gamma-Linolenic Acid, *Prog. Lipid Res. 31*, 163–194.
12. Tapiero, H., Ba, G.N., Couvreur, P., and Tew, K.D. (2002) Polyunsaturated Fatty Acids (PUFA) and Eicosanoids in Human Health and Pathologies, *Biomed. Pharmacother. 56*, 215–222).
13. Fujiyama-Fujiwara, Y., Ohmori, C., and Igarashi, O. (1989) Metabolism of γ-Linolenic Acid in Primary Cultures of Rat Hepatocytes and in Hep G2 Cells, *J. Nutr. Sci. Vitaminol. 35*, 597–611.
14. Ishikawa, T., Fujiyama, Y., Igarashi, O., Morino, M., Tada, N., Kagami, A., Sakamoto, T., Nagano, M., and Nakamura, H. (1989) Effect of Gammalinolenic Acid on Plasma Lipoproteins and Apolipoproteins, *Atherosclerosis 75*, 95–104.
15. Horrobin, D.F. (1994) Unsaturated lipids and cancer, in *New Approaches to Cancer Treatment: Unsaturated Lipids and Photodynamic Therapy* (Horrobin, D.F., ed.), pp. 3–64, Churchill Communications, Nordic House, London.
16. Diplock, A.T., Balasubramanian, K.A., Manohar, M., Mathan, V.I., and Ashton, D. (1988) Purification and Chemical Characterization of the Inhibitor of Lipid Peroxidation from Intestinal Mucosa, *Biochim. Biophys. Acta 962*, 42–50.
17. Klein, C.B., Snow, E.T., and Frenkel, K. (1998) Molecular Mechanisms in Metal Carcinogenesis: Role of Oxidative Stress, in *Molecular Biology of Free Radicals in Human Diseases* (Aruoma, O.I., and Halliwell, B., eds.), pp. 79–138, OICA International, London.
18. Pastore, A., Federici, G., Bertini, E., and Piemonte, F. (2003) Analysis of Glutathione: Implication in Redox and Detoxification, *Clin. Chim. Acta 333*, 19–39.
19. Wood, R., Upreti, G.C., and de Antueno, R.J. (1986) A Comparison of Lipids from Liver and Hepatoma Subcellular Membranes, *Lipids 21*, 292–300.
20. Burns, C.P., and Spector, A.A. (1994) Biochemical Effects of Lipids on Cancer Therapy, *J. Nutr. Biochem. 5*, 114–123.
21. Conklin, K.A. (2002) Dietary Polyunsaturated Fatty Acids: Impact on Cancer Chemotherapy and Radiation, *Altern. Med. Rev. 7*, 4–21.
22. Kokura, S., Nakagawa, S., Hara, T., Boku, Y., Naito, Y., Yoshida, N., and Yoshikawa, T. (2002) Enhancement of Lipid Peroxidation and of the Antitumor Effect of Hyperthermia upon Combination with Oral Eicosapentaenoic Acid, *Cancer Lett. 185*, 139–144.
23. Diggle, C.P. (2002) *In vitro* Studies on the Relationship Between Polyunsaturated Fatty Acids and Cancer: Tumour or Tissue Specific Effects? *Prog. Lipid Res. 41*, 240–253.
24. Baronzio, G.F., Solbiati, L., Ierace, T., Barzaghi, F., Suter, F., Airold, M., Belloni, G., Ravagnani, F., Notti, P., Gramalia, A., *et al.* (1995) Adjuvant Therapy with Essential Fatty Acids (EFA) for Primary Liver Tumours: Some Hypotheses, *Medical Hypotheses 44*, 149–154.
25. American Institute of Nutrition (AIN) (1980) Second Report of the *Ad Hoc* Committee on Standards for Nutritional Studies, *J. Nutr. 110*, 1726.
26. Solt, D., and Farber, E. (1976) New Principles for the Analysis of Chemical Carcinogenesis, *Nature 263*, 701–703.
27. Folch, J., Lees, M., and Sloane Stanley, G.H. (1957) A Simple Method for the Isolation and Purification of Total Lipids from Animal Tissues, *J. Biol. Chem. 226*, 497–509.
28. Smuts, C.M., Weich, H.F.H., Weight, M.J., Faber, M., Kruger, M., Lombard, C.J., and Benadé, A.J.S. (1994) Free Cholesterol Concentrations in the High-Density Lipoprotein Subfraction-3 as a Risk Indicator in Patients with Angiographically Documented Coronary Artery Disease, *Cor. Art. Dis. 5*, 331–338.
29. Gilfillan, A.M., Chu, A.J., Smart, D.A., and Rooney, S.A. (1983) Single Plate Separation of Lung Phospholipids Including

Disaturated Phosphatidylcholine, *J. Lipid Res. 24*, 1651–1656.
30. Itaya, K., and Ui, M. (1966) A New Micromethod for the Colorimetric Determination of Inorganic Phosphate, *Clin. Chim. Acta 14*, 361–366.
31. Richmond, W. (1973) Preparation and Properties of a Cholesterol Oxidase from *Nocardia* sp. and Its Application to the Enzymatic Assay of Total Cholesterol in Serum, *Clin. Chem. 19*, 1350–1356.
32. Yen, G.C., and Hsieh, C.L. (1998) Antioxidant Activity of Extracts from Du-Zhong (*Eucommia ulmoides*) Toward Various Lipid Peroxidation Models In Vitro, *J. Agric. Food Chem. 46*, 3952—3957.
33. Hu, M.L, Frankel, E.N., Leibovitz, B.E., and Tappel, A.L. (1989) Effect of Dietary Lipids and Vitamin E on *in vitro* Lipid Peroxidation in Rat Liver and Kidney Homogenates, *J. Nutr. 119*, 1574–1582.
34. Esterbauer, H., and Cheeseman, K.H. (1990) Determination of Aldehydic Lipid Peroxidation Products: Malonaldehyde and 4-Hydroxynonenal, *Methods Enzymol. 186*, 407–421.
35. Tietze, F. (1969) Enzymatic Method for Quantitative Determination of Nanogram Amounts of Total and Oxidized Glutathione: Applications to Mammalian Blood and Other Tissues, *Anal. Biochem. 27*, 502—522.
36. Ogawa, K. Solt, D., and Farber, E. (1980) Phenotypic Diversity as an Early Property of Putative Preneoplastic Cells in Liver Carcinogenesis, *Cancer Res. 40*, 725–733.
37. Markwell, M.A.K., Haas, S.M., Bieber, L.L., and Tolbert, N.E. (1978) A Modification of the Lowry Procedure To Simplify Protein Determination in Membrane and Lipoprotein Samples, *Anal. Biochem. 87*, 206–210.
38. Kaushal, V., and Barnes, L.D. (1986) Effect of Zwitterionic Buffers on Measurement of Small Masses of Protein with Bicinchoninic Acid, *Anal. Biochem. 157*, 291–294.
39. Mahler, S.M., Wilce, P.A., and Shanley, B.C. (1988) Studies on Regenerating Liver and Hepatoma Plasma Membranes—II. Membrane Fluidity and Enzyme Activity, *Int. J. Biochem. 20*, 613–619.
40. Tabas, I. (2001) Consequences of Cellular Cholesterol Accumulation: Basic Concepts and Physiological Implications, *J. Clin. Invest. 110*, 905–911.
41. Darnell, J., Lodisch, H., and Baltimore, D. (1986) The Plasma Membrane, in *Molecular Cell Biology* (Darnell, J., Lodisch, H., and Baltimore, D., eds.), pp. 576–577, Scientific American Books, New York.
42. Blom, T.S., Koivusalo, M., Kuismanen, E., Kostiainen, R., Somerharju, P., and Ikonen, E. (2001) Mass Spectrometric Analysis Reveals an Increase in Plasma Membrane Polyunsaturated Phospholipid Species upon Cellular Cholesterol Loading, *Biochemistry 40*, 14635–14644.
43. Stulnig, T.M., Huber, J., Leitinger, N., Imre, E-M., Angelisová, P., Nowotny, P., and Waldhäusl, W. (2001) Polyunsaturated Eicosapentaenoic Acid Displaces Proteins from Membrane Rafts by Altering Raft Lipid Composition, *J. Biol. Chem. 276*, 37335–37340.
44. Zajchowski, L.D., and Robbins, S.M. (2002) Lipid Rafts and Little Caves: Compartmentalized Signaling in Microdomains, *Eur. J. Biochem. 269*, 737–752.
45. Kohlmeier, L. (1997) Biomarkers of Fatty Acid Exposure and Breast Cancer Risk, *Am. J.. Clin. Nutr. 66*, 1548S–1556S.
46. Sears, B. (2002) *The Omega Rx Zone*, 1st edn., pp. 149, 184, HarperCollins, New York.
47. Jayadev, S., Linardic, C.M., and Hannun, Y.A. (1994) Identification of Arachidonic Acid as a Mediator of Sphingomyelin Hydrolysis in Response to Tumor Necrosis Factor-α, *J. Biol. Chem. 269*, 5757–5763.
48. Surette, M.E., Fonteh, A.N., Bernatchez, C., and Chilton, F.H. (1999) Perturbations in the Control of Cellular Arachidonic Acid Levels Block Cell Growth and Induce Apoptosis in HL-60 Cells, *Carcinogenesis 20*, 757–763.
49. Tocher, D.R., Bell, J.G., Farndale, B.M., and Sargent, J.R. (1997) Effects of Dietary γ-Linolenic Acid-Rich Borage Oil Combined with Marine Fish Oils on Tissue Phospholipid Fatty Acid Composition and Production of Prostaglandins E and F of the 1-, 2- and 3-Series in a Marine Fish Deficient in Δ5 Fatty Acyl Desaturase, *Prostaglandins Leukotrienes Essent. Fatty Acids 57*, 125–134.
50. Barham, J.B., Edens, M.B., Fonteh, A.N., Johnson, M.M., Easter, L., and Chilton, F.H. (2000) Addition of Eicosapentaenoic Acid to γ-Linolenic Acid-Supplemented Diets Prevents Serum Arachidonic Acid Accumulation in Humans, *J. Nutr. 130*, 1925–1931.
51. Calder, P.C. (2001) Polyunsaturated Fatty Acids, Inflammation and Immunity, *Lipids 36*, 1007–1024.
52. Lands, W.E.M., Le Tillier, P.R., Rome, L.H., and Vanderhoek, J.Y. (1973) Inhibition of Prostaglandin Biosynthesis, *Adv. Biosci. 9*, 15–17.
53. Bougnoux, P. (1999) n-3 Polyunsaturated Fatty Acids and Cancer, *Curr. Opin. Clin. Nutr. Metab. Care 2*, 121–126.
54. Leikin, A., and Shinitzky, M. (1995) Characterization of the Lipid Surrounding the Δ6-Desaturase of Rat Liver Microsomes, *Biochim. Biophys. Acta 1256*, 13–17.
55. Shimada, Y., Morita, T., and Sugiyama, K. (2003) Dietary Eritadenine and Ethanolamine Depress Fatty Acid Desaturase Activities by Increasing Liver Microsomal Phophatidylethanolamine in Rats, *J. Nutr. 133*, 758–765.
56. Song, J.H., Fujimoto, K., and Miyazawa, T. (2000) Polyunsaturated (n-3) Fatty Acids Susceptible to Peroxidation Are Increased in Plasma and Tissue Lipids of Rats Fed Docosahexaenoic Acid-Containing Oils, *J. Nutr. 130*, 3028–3033.
57. Hardy, S., Langelier, Y., and Prentki, M. (2000) Oleate Activates Phosphatidylinositol 3-Kinase and Promotes Proliferation and Reduces Apoptosis of MDA-MB-231 Breast Cancer Cells, Whereas Palmitate Has Opposite Effects, *Cancer Res. 60*, 6353–6358.
58. Navarro, J., Obrador, E., Carretero, J., Petschen, I., Perez, P., and Estrela, J.M. (1999) Changes in Glutathione Status and the Antioxidant System in Blood and in Cancer Cells Associated with Tumour Growth *in vivo*, *Free Rad. Biol. Med. 26*, 410–418.
59. Perquin, M., Oster, T., Maul, A., Froment, N., Untereiner, M., and Bagrel, D. (2001) The Glutathione-Related Detoxification System Is Increased in Human Breast Cancer in Correlation with Clinical and Histopathological Features, *J. Cancer Res. Clin. Oncol. 127*, 368–374.
60. Huang, Z.Z., Chen, C., Zeng, Z., Yang, H., Oh, J., Chen, L., and Lu, S.C. (2001) Mechanism and Significance of Increased Glutathione Level in Human Hepatocellular Carcinoma and Liver Level in Human Hepatocellular Carcinoma and Liver Regeneration, *FASEB 15*, 19–21.
61. Kokura, S., Nakagawa, S., Hara, T., Boku, Y., Naito, Y., Yoshida, N., and Yoshikawa, T. (2002) Enhancement of Lipid Peroxidation and of the Antitumor Effect of Hyperthermia upon Combination with Oral Eicosapentaenoic Acid, *Cancer Lett. 185*, 139–144.

[Received April 22, 2004; Accepted November 24, 2004]

Inhibitory Action of Conjugated C_{18}-Fatty Acids on DNA Polymerases and DNA Topoisomerases

Yoshiyuki Mizushina[a,b,*], Tsuyoshi Tsuzuki[c], Takahiro Eitsuka[c], Teruo Miyazawa[c], Kanako Kobayashi[a], Hiroshi Ikawa[a], Isoko Kuriyama[a], Yuko Yonezawa[a], Masaharu Takemura[d], Hiromi Yoshida[a,b], and Kengo Sakaguchi[e]

[a]Laboratory of Food & Nutritional Sciences, Department of Nutritional Science and [b]High Technology Research Center, Kobe-Gakuin University, Nishi-ku, Kobe, Hyogo 651-2180, Japan, [c]Food and Biodynamic Chemistry Laboratory, Graduate School of Life Science and Agriculture, Tohoku University, Sendai 981-8555, Japan, [d]Life Science Research Center, Mie University, Tsu, Mie 514-8507, Japan, and [e]Department of Applied Biological Science, Frontier Research Center for Genomic Drug Discovery, Tokyo University of Science, Noda-shi, Chiba 278-8510, Japan

ABSTRACT: We reported previously that unsaturated linear-chain FA of the *cis*-configuration with a C_{18}-hydrocarbon chain such as linoleic acid (18:2Δ9c,12c) could potently inhibit the activities of mammalian DNA polymerases and DNA topoisomerases, but their saturated forms could not. There are chemically two classes of unsaturated FA, normal and conjugated, but only the conjugated forms show potent antitumor activity. In this report, we study the inhibitory effects of chemically synthesized conjugated C_{18}-FA on mammalian DNA polymerases and DNA topoisomerases as compared with normal unsaturated FA. The conjugated α-eleostearic acid (18:3Δ9*c*,11*t*,13*t*) was the strongest of all the FA tested. For the inhibition, the conjugated form is crucially important. The energy-minimized 3-D structures of the FA were calculated, and both a length of less than 20 Å and a width of 8.13–9.24 Å in the C_{18}–FA structure were found to be important for enzyme inhibition. The 3-D structure of the active site of both DNA polymerases and topoisomerases must have had a pocket to join α-eleostearic acid, and this pocket was 12.03 Å long and 9.24 Å wide.

Paper no. L9577 in *Lipids 39,* 977–983 (October 2004)

We have screened inhibitors of mammalian DNA polymerases (1,2), and found that mammalian DNA polymerase α and β (pol α and β) are inhibited by linear-chain FA with the following characteristics: a hydrocarbon chain containing 18 or more carbons, a free carboxyl end, and the double bonds with the *cis*-configuration (1–3). The mode of binding of linear-chain FA to pol β has been studied extensively using NMR spectroscopy; FA were shown to specifically bind to the proteolytic N-terminal 8-kDa domain fragment of pol β at the DNA-binding groove (4). FA could also strongly inhibit the activities of human DNA topoisomerase I and II (topo I and II), with a degree of inhibition almost the same as that of the polymerases (5). In these studies, we realized the importance of the 3-D structure of FA and the presence of two classes of unsaturated linear FA, normal and conjugated. In this report, we describe the relationship between FA and the mode of inhibition, concentrating on the actions of conjugated FA.

Conjugated FA are positional and geometrical isomers in which conjugated double bonds are present. Among such FA, CLA, a mixture of 9*c*-, 11*t*-, 10*t*-, and 12*c*-octadecadienoic acids (18:2Δ9*c*,11*t* and 18:2Δ10*t*,12*c*, respectively) as major constituents, is known to have various physiological properties (6–10). It has been reported that dietary supplementation of conjugated linoleic acid reduces the incidence of mammary tumors in mice (11). CLA has also been shown to inhibit the proliferation of human breast cancer cells (12), colon cancer cells (13), and lung cancer cells (14) in culture. Additionally, n-3 highly unsaturated FA such as α-linolenic acid have been shown to have anticarcinogenic activity *in vitro* and *in vivo* (15–18). We previously reported the effect of *in vivo* tumor growth suppression by conjugated FA (19,20). Therefore, we prepared conjugated C_{18}-FA converted from linoleic acid (18:2Δ9*c*,12*c*), α-linolenic acid (18:3Δ9*c*,12*c*,15*c*), and stearidonic acid (18:4Δ6*c*,9*c*,12*c*,15*c*). The conjugated FA could also act as inhibitors of DNA polymerases and topoisomerases, and could be even stronger inhibitors than linoleic acid. As expected, some conjugated FA were strong inhibitors. Using computer modeling and 3-D structural analysis, we suggest the 3-D site where the enzyme binds to the conjugated FA. The molecular design method may be useful in creating agents for cancer chemotherapy.

MATERIALS AND METHODS

Materials. The linear-chain FA were named using the nomenclature described by Weete (21). In the following symbols, (A:B_2 ΔC_1*c*,C_2*t*), "A" refers to the number of carbon atoms, "B_2" refers to the number of double bonds, "C_1,C_2" represents the position of each double bond from the carboxyl end of the molecule, and "*c*" and "*t*" refer to the *cis*- and *trans*-configurations of the double bond, respectively. Saturated C_{18}-FA; *n*-octadecanoic acid (stearic acid, 18:0), and the *cis*-configuration of unsaturated C_{18}-FA such as *cis*-9-octadecenoic acid (oleic acid, 18:1Δ9*c*), *cis*-9,12-octadecadienoic acid (linoleic acid, 18:2Δ9*c*,12*c*), *cis*-9,12,15-octadeca-

*To whom correspondence should be addressed at the Department of Nutritional Sciences, Kobe-Gakuin University, Nishi-ku, Kobe, Hyogo 651-2180, Japan. E-mail: mizushin@nutr.kobegakuin.ac.jp

Abbreviations: dsDNA, double-stranded DNA; dTTP, [^{3}h]2′-deoxythymidine 5′-triphosphate; NP-40, Nonidet P-40; oligo(dT)$_{12–18}$, oligo(12–18) deoxyribothymidylic acid; pol, DNA-directed DNA polymerase (EC 2.7.7.7); poly(dA), polydeoxyriboadenylic acid; poly(rC), polycytidylic acid; topo, DNA topoisomerase.

trienoic acid (α-linolenic acid, 18:3Δ9*c*,12*c*,15*c*), and *cis*-6,9,12,15-octadecatetraenoic acid (stearidonic acid, 18:4Δ6*c*,9*c*,12*c*,15*c*) were purchased from Nu-Chek-Prep Inc. (Elysian, MN). Nucleotides such as [^{3}H]2′-deoxythymidine 5′-triphosphate (dTTP, 43 Ci/mmol) and chemically synthesized template-primers such as polydeoxyriboadenylic acid [poly(dA)] and oligo(12–18) deoxyribothymidylic acid [oligo(dT)$_{12–18}$] were purchased from Amersham Biosciences (Buckinghamshire, United Kingdom). All other reagents were of analytical grade and were purchased from Wako Ltd. (Osaka, Japan).

Preparation of conjugated C_{18}-FA by alkaline treatment. Conjugated C_{18}-FA were prepared by using alkaline treatment following an AOAC method with slight modifications (22). Potassium hydroxide at a concentration of the 6.6 or 21% (w/w) in ethylene glycol was prepared, and the potassium hydroxide solution was bubbled for 5 min with nitrogen gas. Ten milligrams of linoleic acid, linolenic acid, or stearidonic acid was added to 1 mL of 6.6 or 21% potassium hydroxide solution in a test tube (10 mL volume). The mixture was bubbled with nitrogen gas and then screw-capped and allowed to stand for 5 or 10 min at 180°C. The reaction mixture was cooled and 1 mL of methanol was added. The mixture was acidified to below pH 2 with 2 mL of 6 N HCl. After dilution with 2 mL of distilled water, the conjugated FA was extracted with 5 mL of hexane. The hexane extract was then washed with 3 mL of 30% methanol and with 3 mL of distilled water before being evaporated under a stream of nitrogen gas. Each isomer of converted C_{18}-FA was separated using a Shimadzu HPLC system. The conjugated FA were stored at −20°C after being purged with nitrogen gas. UV/Vis spectrophotometric analysis of the conjugated FA was performed with a Shimadzu UV-2400PC. Spectrophotometric readings confirmed the conjugated FA of diene (at 235 nm), triene (268 nm), and tetraene (315 nm) (22,23).

Enzymes. DNA polymerase α (pol α) was purified from calf thymus by immuno-affinity column chromatography, as described previously (24). Recombinant rat pol β was purified from *Escherichia coli* JMpβ5 as described by Date *et al.* (25). The human pol γ catalytic gene was cloned into pFastBac. Histidine-tagged enzymes were expressed using the BAC-TO-BAC HT Baculovirus Expression System according to the supplier's manual (Life Technologies, Rockville, MD) and purified using ProBoundresin (Invitrogen Japan, Tokyo, Japan) (Mizushina, Y., Yoshida, H., and Sakaguchi, K., unpublished data). Human pol δ and ε were purified from the nuclear fraction of human peripheral blood cancer cells (Molt-4) using the second subunit of pol δ- and ε-conjugated-affinity column chromatography, respectively (26). Human recombinant DNA topoisomerase I (topo I) and DNA topoisomerase IIα (topo II) (2 units/μL each) were purchased from TopoGen, Inc. (Columbus, OH).

DNA polymerase assays. Activities of DNA polymerases were measured by methods described previously (2,3). For DNA polymerases, poly(dA)/oligo(dT)$_{12–18}$ and [^{3}H]-2′-deoxythymidine 5′-triphosphate were used as the template-primer DNA and nucleotide substrate, respectively. Prepared conjugated C_{18}-FA were dissolved in DMSO at various concentrations and sonicated for 30 s. Aliquots of 4 μL of sonicated samples were mixed with 16 μL of each enzyme (final, 0.05 units) in 50 mM Tris-HCl (pH 7.5) containing 1 mM DTT, 50% glycerol, and 0.1 mM EDTA, and held at 0°C for 10 min. These inhibitor-enzyme mixtures (8 μL) were added to 16 μL of each of the enzyme standard reaction mixtures, and incubation was carried out at 37°C for 60 min, except for Taq DNA polymerase, which was incubated at 74°C for 60 min. The activity without the inhibitor was considered 100%, and the remaining activities at each concentration of inhibitor were determined relative to this value. One unit of DNA polymerase activity was defined as the amount of enzyme that catalyzed the incorporation of 1 nmol of dTTP into synthetic template-primers [i.e., poly(dA)/oligo(dT)$_{12–18}$, A/T = 2:1] in 60 min at 37°C under normal reaction conditions for each enzyme (2,3).

DNA topoisomerase (topo) assays. Relaxation activities of DNA topoisomerases were determined by detecting the conversion of supercoiled plasmid DNA to its relaxed form. The topo II reaction was performed in 20-μL reaction mixtures containing 50 mM Tris-HCl buffer (pH 8.0), 120 mM KCl, 10 mM $MgCl_2$, 0.5 mM ATP, 0.5 mM DTT, pBR322 plasmid DNA (200 ng), 2 μL of inhibitor solution (10% DMSO), and one unit of topo II. The reaction mixtures were incubated at 37°C for 30 min and terminated by adding 2 μL of loading buffer consisting of 5% sarkosyl, 0.0025% bromophenol blue, and 25% glycerol. The mixtures were subjected to 1% agarose gel electrophoresis in Tris-acetate-EDTA running buffer. The agarose gels were stained with ethidium bromide, and DNA was visualized on a UV transilluminator. Zero-D scan (version 1.0; M&S Instruments Trading Inc., Tokyo, Japan) was used for densitometric quantitation of the plasmid DNA products. Relaxation activity of topo I was analyzed in the same manner as described above, except that the reaction mixtures contained 10 mM Tris-HCl (pH 7.9), pUC19 plasmid DNA (200 ng), 1 mM EDTA, 150 mM NaCl, 0.1% BSA, 0.1 mM spermidine, 5% glycerol, and one unit of topo I. One unit was defined as the amount of enzyme capable of relaxing 0.25 μg of DNA in 15 min at 37°C.

Computational analysis of C_{18}-FA. A compound model was constructed and simple-minimized. Compound models were simulated with force field parameters based on the Consistent Valence Force Field. Group-based cutoffs, 0.95 nm for van der Waals and 0.95 nm for Coulomb interactions, were introduced. The temperature was set at 298 K. Calculations based on simulation images were carried out using INSIGHT II (Accelrys Inc., San Diego, CA).

RESULTS AND DISCUSSION

Conjugated C_{18}-FA-mediated inhibition of mammalian DNA polymerases and human topo. First of all, we tested whether several classes of linear-chain conjugated C_{18}-FA have the ability to inhibit calf DNA pol α, rat pol β, and human DNA topo I and II. Twenty micromoles of saturated FA with an 18-hydrocarbon chain

(i.e., stearic acid, 18:0) inhibited pol α activity (Fig. 1A), with an IC_{50} value of 15.0 μM, but had no inhibitory effect on pol β, topo I, or topo II (Figs. 1B–D). On the other hand, monounsaturated linear-chain C_{18}-FA of the *cis*-configuration (i.e., oleic acid, 18:1Δ9*c*) significantly inhibited the activities of all enzymes tested. Only the conjugated FA inhibited the activities of pol β, topo I, and topo II, which could be molecular targets for anticancer chemotherapy. We therefore systematically tested the inhibitory effect of the three purified $C_{18:2}$-conjugated FA (18:2Δ9*c*,11*c*, 18:2Δ9*t*,11*t*, and 18:2Δ10*t*,12*c*) converted from linoleic acid (18:2Δ9*c*,12*c*), the six purified $C_{18:3}$-conjugated FA [jacaric acid (18:3Δ8*c*,10*t*,12*c*), calendic acid (18:3Δ8*t*,10*t*,12*c*), punicic acid (18:3Δ9*c*,11*t*,13*c*), α-eleostearic acid (18:3Δ9*c*,11t,13t), β-eleostearic acid (18:3Δ9*t*,11*t*,13*t*)] converted from linolenic acid (18:3Δ9*c*,12*c*,15*c*), and a purified $C_{18:4}$-conjugated FA (18:4Δ9*c*,11*t*,13*t*,15*c*) converted from stearidonic acid (18:4Δ6*c*,9*c*,12*c*,15*c*), toward the DNA polymerases and topoisomerases.

As shown in Figure 1, at 20 μM, conjugated C_{18}-FA of the *cis*-configuration were more potent inhibitors than unsaturated C_{18}-FA of the *cis*-configuration. Notably, the inhibitory effect of 18:2Δ10*t*,12*c* was stronger than that of linoleic acid, and similarly, the $C_{18:4}$-conjugated FA was a stronger inhibitor than the $C_{18:4}$ FA. Among $C_{18:3}$-FA, α-eleostearic acid was the strongest inhibitor of the DNA polymerases and topoisomerases. On the other hand, no *trans*-conjugated FA

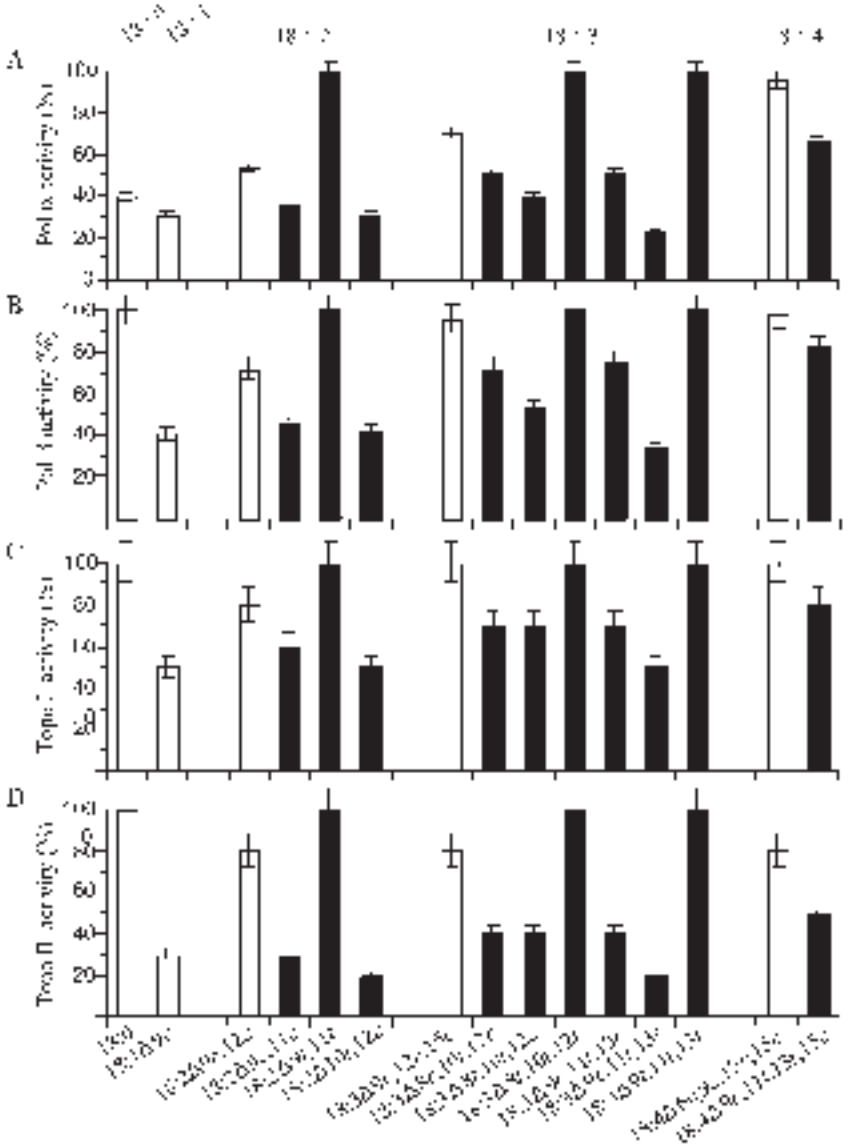

FIG. 1. Inhibitory effect of conjugated linear-chain C_{18}-FA (20 μM each) on DNA polymerases and DNA topoisomerases. (A) calf pol (DNA-directed DNA polymerase) α; (B) rat pol β; (C) human topo (DNA topoisomerase) I; (D) human topo II. The white bars are normal FA and the black bars are conjugated FA. Enzyme activity in the absence of FA was taken as 100%. Data are shown as means ± SEM of three independent experiments.

completely inhibited the activities of DNA polymerases and topoisomerases. These results suggest that conjugated unsaturating carbohydrate bonds of the *cis*-configuration in these FA play a critical role in the pol α, pol β, topo I, and topo II inhibitions, but the number of conjugated unsaturating carbohydrate bonds seems to have no relation to the inhibitory effect.

Figure 2 shows the dose–response curves for each of the normal or conjugated unsaturated linear-chain C_{18}-FA against calf pol α and rat pol β. The inhibition by these C_{18}-FA was dose dependent. Among $C_{18:2}$- and $C_{18:3}$-FA, conjugated FA were stronger pol α and β inhibitors than nonconjugated FA. The inhibitory effect of α-eleostearic acid was the strongest, with 50% inhibition for pol α and β observed at doses of 10.7 and 13.4 μM, respectively. Table 1 shows IC_{50} values for mammalian pol α to ε and human topos I and II. The inhibitory effect of five mammalian DNA polymerases by normal and conjugated C_{18}-FA was the same as that of human DNA topoisomerases, suggesting that pol α to ε and topo I and II have the same inhibitory mechanism.

Double reciprocal plots of the results indicated that the inhibition of both calf pol α and rat pol β by α-eleostearic acid was through competition with the DNA template primer [i.e., poly(dA)/oligo$(dT)_{12–18}$] (data not shown), suggesting that α-eleostearic acid might compete with the template primer to bind to the catalytic site of the DNA polymerases.

To determine the effects of a nonionic detergent on the binding of α-eleostearic acid to the DNA polymerases and topoisomerases, a neutral detergent, Nonidet P-40 (NP-40), was added to the reaction mixture at a concentration of 0.1%. In the absence of α-eleostearic acid, the enzyme activity was taken as 100%. As shown in Table 2, the inhibitory effect on pol α, pol β, topo I, and topo II by α-eleostearic acid at 25 μM was largely reversed by the addition of NP-40 to the reaction mixture, suggesting that the binding to the enzyme by α-eleostearic acid is hydrophobic. To determine whether the effects of the compound were due to nonspecific adhesion to the enzymes or to selective binding at specific sites, we also tested whether an excess amount of a substrate analogue, polycytidylic acid [poly(rC)] (100 μg/mL), or a protein, BSA (100 μg/mL), could prevent the inhibitory effects of α-eleostearic acid (Table 2). Poly(rC) and BSA showed little or no influence on the effects of α-eleostearic acid, suggesting that the binding to the DNA polymerases and topoisomerases occurs selectively.

3-D modeling of conjugated C_{18}-FA. The conjugated C_{18}-FA, α-eleostearic acid, was the strongest inhibitor of DNA polymerases and topoisomerases and was considered to bind directly to the template-primer binding site in the DNA polymerases. Therefore, the inhibition of DNA topoisomerase by α-eleostearic acid occurs in a similar manner between chemical structures of the enzyme protein and the FA, as previously described for the DNA polymerases and normal FA (2,3). Based on the previous computer modeling data, we carried out a 3-D structural analysis of the linear-chain conjugated C_{18}-FA, and speculated on the model of the DNA polymerases and topoisomerases with the FA. The energy-minimized 3-D C_{18}-FA obtained by computer modeling are shown in Figure 3. Oleic acid and α-eleostearic acid formed a V-shaped curve, with molecular widths of 8.50 and 9.24 Å, respectively (Table 3). The hydrocarbon chain in the saturated and *trans*-unsaturated FA molecule was linear because of the zero or low width, and did not inhibit the enzyme activities

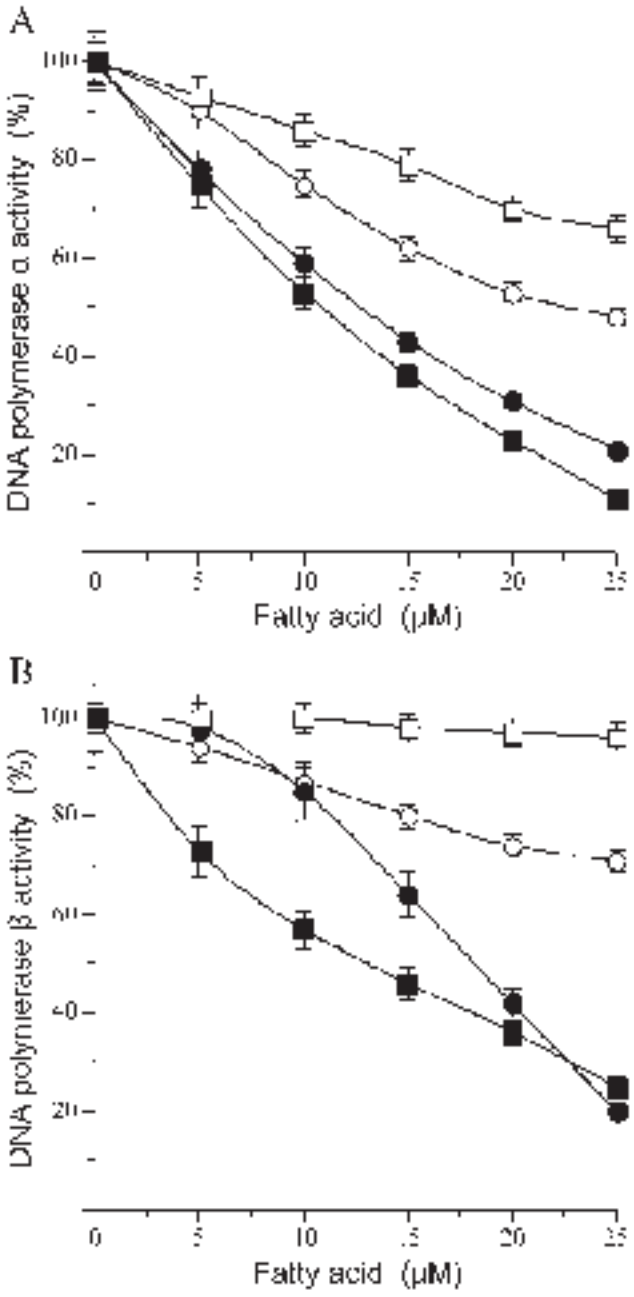

FIG. 2. Dose–response curves of conjugated linear-chain C_{18}-FA for DNA polymerases. (A) Calf pol α; (B) rat pol β. $C_{18:2}$-FA are linoleic acid (18:2Δ9*c*,12*c*, open circle) and 18:2Δ10*t*,12*c* (closed circle). $C_{18:3}$-FA are linolenic acid (18:3Δ9*c*,12*c*,15*c*, open square) and α-eleostearic acid (18:2Δ9*c*,11*t*,13*t*, closed square). The DNA polymerase activity in the absence of FA was taken as 100%. Data are shown as means ± SEM of three independent experiments. For abbreviations see Figure 1.

TABLE 1
IC_{50} Values (μM) of Enzymatic Inhibition Against Mammalian DNA Polymerases and Human DNA Topoisomerases

	Mammalian DNA polymerases				
FA	Pol α	Pol β	Pol γ	Pol Δ	Pol ε
18:0	15.0 ± 0.6	>100	52.5 ± 1.8	50.2 ± 2.2	62.8 ± 2.2
18:1Δ9*c*	11.7 ± 0.5	33.5 ± 1.7	10.4 ± 0.4	33.8 ± 1.8	36.3 ± 1.4
18:2Δ9*c*,12*c*[a]	22.5 ± 0.7	56.0 ± 2.7	22.2 ± 0.9	33.8 ± 1.5	39.7 ± 1.6
18:2Δ10*t*,12*c*	12.8 ± 0.5	18.0 ± 1.2	10.6 ± 0.4	22.0 ± 1.3	29.3 ± 1.0
18:3Δ9*c*,12*c*,15*c*	40.4 ± 1.2	>100	31.7 ± 1.4	68.3 ± 2.8	66.7 ± 2.0
18:3Δ9*c*,11*t*,13*t*[a]	10.7 ± 0.4	13.4 ± 0.8	10.6 ± 0.3	14.0 ± 0.8	22.0 ± 0.7
18:4Δ6*c*,9*c*,12*c*,15*c*	>100	>100	>100	>100	>100
18:4Δ9*c*,11*t*,13*t*,15*c*[a]	46.5 ± 1.9	83.1 ± 3.0	>100	71.0 ± 3.3	>100

	Human topisomerases	
FA	Topo I	Topo II
18:0	>100	>100
18:1Δ9*c*	22.5 ± 2.0	7.5 ± 0.5
18:2Δ9*c*,12*c*	35.0 ± 3.0	45.0 ± 3.5
18:2Δ10*t*,12*c*[a]	20.0 ± 2.0	5.0 ± 0.5
18:3Δ9*c*,12*c*,15*c*	>100	50.0 ± 4.0
18:3Δ9*c*,11*t*,13*t*[a]	20.0 ± 2.0	5.0 ± 0.5
18:4Δ6*c*,9*c*,12*c*,15*c*	>100	60.0 ± 0.4
18:4Δ9*c*,11*t*,13*t*,15*c*[a]	37.5 ± 3.5	40.0 ± 2.5

[a]Conjugated FA. Data are shown as means ± SEM of three independent experiments. Pol, DNA-directed DNA polymerase; topo, DNA topoisomerase.

(Table 3, Fig. 1). Because the hydrocarbon chains in their FA fold up at the position of the double bonds in the *cis*-configuration, di- and more unsaturated FA of the *cis*-configuration lost molecular length and did not form a V-shaped curve as seen in α-eleostearic acid. Therefore, both the molecular width and length of the FA appeared to be important for enzyme inhibition. The molecular lengths and widths of normal and conjugated linear-chain C_{18}-FA are compared in Table 3. A molecular length of more than 12 Å and molecular width of 8.5 to 9.5 Å influenced the activities of DNA polymerases and topoisomerases. The conjugated position of double bonds in the FA must affect these enzymes directly.

Several anticancer agents in clinical use have been shown to be potent inhibitors of DNA topoisomerases. For example, adriamycin (Doxorubicin), amsacrine (m-AMSA), and ellipticine have shown significant activity as inhibitors of topo II. The plant alkaloid camptothecin and its synthetic derivatives such as CPT-11 are extensively studied topo I inhibitors. All of these agents inhibit the rejoining reaction of topoisomerases by stabilizing a covalent topoisomerase–DNA complex termed the "cleavable complex." To determine whether conjugated FA bind to DNA, the melting temperature (T_m) of double-stranded DNA (dsDNA) in the presence of more than 100 μM of α-eleostearic acid was measured. The thermal transition of T_m was not observed, whereas 15 μM of ethidium bromide, a typical intercalating agent, caused the thermal transition (data not shown). Thus, none of the conjugated FA bound to the dsDNA, suggesting that it must inhibit the enzyme activities by interacting with the enzymes directly.

TABLE 2
Effects of Polyoxyriboadenylic Acid [poly(rC)], Bovine Serum Albumin (BSA), or Nonidet P-40 (NP-40) on the Inhibition of DNA Polymerase and Topoisomerase Activities by α-Eleostearic Acid (18:2Δ9*c*,11*t*,13*t*)[a]

	Relative activity (%)			
Compounds added to the reaction mixture	Pol α	Pol β	Topo I	Topo II
Without the compounds				
None (control)	100 ± 1.0	100 ± 2.0	100 ± 5.0	100 ± 5.0
+100 μg/mL poly(rC)	100 ± 0.5	100 ± 1.0	100 ± 2.5	100 ± 2.5
+100 μg/mL BSA	100 ± 2.0	100 ± 2.5	100 ± 5.0	100 ± 5.0
+0.1% NP-40	100 ± 2.5	100 ± 3.0	100 ± 5.0	100 ± 5.0
With 25 μM α-eleostearic acid				
25 μM α-eleostearic acid	11.0 ± 0.4	12.3 ± 0.5	50.0 ± 3.0	10.0 ± 1.0
25 μM α-eleostearic acid + 100 μg/mL poly(rC)	9.8 ± 0.3	12.5 ± 0.5	50.0 ± 2.5	10.0 ± 1.0
25 μM α-eleostearic acid + 100 μg/mL BSA	10.5 ± 0.8	13.3 ± 0.7	50.0 ± 4.0	10.0 ± 1.5
25 μM α-eleostearic acid + 0.1% NP-40	95.6 ± 3.5	98.0 ± 4.2	100 ± 6.5	100 ± 5.5

[a]100 μM poly(rC) and 100 μg/mL BSA or 0.1% NP-40 were added to the reaction mixture. In the absence of α-eleostearic acid, DNA polymerase activity was taken to be 100%. Data are shown as means ± SEM of three independent experiments. For abbreviations see Table 1.

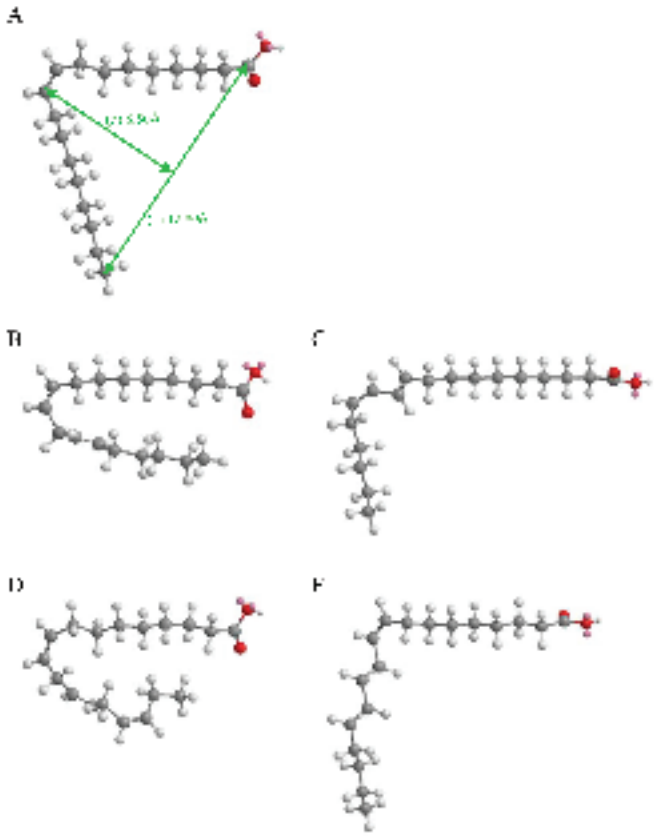

FIG. 3. Computer graphics of linear-chain C_{18}-FA. (A) Oleic acid (18:1Δ9c); (B) linoleic acid (18:2Δ9*c*,12*c*); (C) 18:2Δ10*t*,12*c*; (D) linolenic acid (18:3Δ9*c*,12*c*,15*c*); (E) α-eleostearic acid (18:2Δ9*c*,11*t*,13*t*). The length (a) and width (b) of the FA molecular structure are shown. The carbons, oxygens, and hydrogens of the compounds are indicated in gray, red, and white, respectively. These figures were prepared using Insight II (Accelrys, San Diego, CA). For abbreviations see Figure 1.

Suzuki *et al.* (27) reported that *cis*-unsaturated C_{18}-FA were to be of the noncleavable complex type of topo II inhibitors. The conjugated C_{18}-FA may be the same mode of topo II inhibition as the *cis*-unsaturated FA.

Inhibitors of DNA polymerases could also be anticancer agents, as reported previously (28,29), and polymerases and topoisomerases have recently emerged as important cellular targets for chemical intervention in the development of anticancer agents. The chemical frames of FA containing conjugated double bonds could, moreover, be used for screening new anticancer chemotherapy agents. They can be pursued by three-dimentionally using data on the structural heterogeneity of the FA binding pockets of the target enzymes, since the conjugated FA can be chemically synthesized in great variety. Therefore, the computer-simulated drug design of compounds, especially of inhibitors of the polymerases and topoisomerases, could be of great interest and may in theory be a promising approach to developing new agents for anticancer chemotherapy.

TABLE 3
Molecular Length and Width of the FA Calculated by 3-D Computer Simulation

FA	Length (Å)	Width (Å)
18:0 (stearic acid)	21.40	0
18:1Δ9*c* (oleic acid)	12.80	8.50
18:2Δ9*c*,12*c* (linoleic acid)	4.45	10.58
18:2Δ9*c*,11*c*[a]	4.68	10.28
18:2Δ9*t*,11*t*[a]	20.29	4.75
18:2Δ10*t*,12*c*[a]	14.64	8.68
18:3Δ9*c*,12*c*,15*c* (α-linolenic acid)	5.54	10.30
18:3Δ8*c*,10*t*,12*c*[a]	6.16	11.00
18:3Δ8*t*,10*t*,12*c*[a]	12.66	8.13
18:3Δ8*t*,10*t*,12*t*[a]	20.61	5.34
18:3Δ9*c*,11*t*,13*c*[a]	5.79	11.24
18:3Δ9*c*,11*t*,13*t*[a]	12.03	9.24
18:3Δ9*t*,11*t*,13*t*[a]	20.54	5.12
18:4Δ6*c*,9*c*,12*c*,15*c* (stearidonic acid)	Uncalculated	
18:4Δ9*c*,11*t*,13*t*,15*c*[a]	14.49	8.66

[a]Conjugated FA. These data were obtained using INSIGHT III (Accelrys, San Diego, CA). A restrained molecular dynamics method was used to calculate the energetically minimum structures of compounds.

ACKNOWLEDGMENTS

This work was partly supported by a Grant-in-Aid for Kobe Gakuin University Joint Research (B) (Y.M. and H.Y.). Y.M. acknowledges Grants-in-Aid from the Hyogo Science and Technology Association, The Japan Food Chemical Research Foundation, and Grant-in-Aid 14780466 for Scientific Research from the Ministry of Education, Culture, Sports, Science and Technology, Japan.

REFERENCES

1. Mizushina, Y., Yagi, H., Tanaka, N., Kurosawa, T., Seto, H., Katumi, K., Onoue, M., Ishida, H., Iseki, A., Nara, T., *et al.* (1996) Screening of Inhibitor of Eukaryotic DNA Polymerases Produced by Microorganisms, *J. Antibiot. (Tokyo) 49*, 491–492.
2. Mizushina, Y., Tanaka, N., Yagi, H., Kurosawa, T., Onoue, M., Seto, H., Horie, T., Aoyagi, N., Yamaoka, M., Matsukage, A., *et al*. (1996) Fatty Acids Selectively Inhibit Eukaryotic DNA Polymerase Activities *in vitro, Biochim. Biophys. Acta 1308*, 256–262.
3. Mizushina, Y., Yoshida, S., Matsukage, A., and Sakaguchi, K. (1997) The Inhibitory Action of Fatty Acids on DNA Polymerase β, *Biochim. Biophys. Acta 1336*, 509–521.
4. Mizushina, Y., Ohkubo, T., Date, T. Yamaguchi, M., Saneyoshi, F., Sugawara, K., and Sakaguchi, K. (1999) Mode Analysis of a Fatty Acid Molecule Binding to the N-Terminal 8-kDa Domain of DNA Polymerase β, *J. Biol. Chem. 274*, 25599–25607.
5. Mizushina, Y., Sugawara, F., Iida, A., and Sakaguchi, K. (2000) Structural Homology Between DNA Binding Sites of DNA Polymerase β and DNA Topoisomerase II, *J. Mol. Biol. 304*, 385–395.
6. Ha, Y.L., Grimm, N.K., and Pariza, M.W. (1987) Anticarcinogens from Fried Ground Beef: Heat-Altered Derivatives of Linoleic Acid, *Carcinogenesis 8*, 1881–1887.
7. Lee, K.N., Kritchevsky, D., and Pariza, M.W. (1994) Conjugated Linoleic Acid and Atherosclerosis in Rabbits, *Atherosclerosis 108*, 19–25.
8. Fritsche, J., and Steinhart, H. (1998) Analysis, Occurrence, and Physiological Properties of *trans* Fatty Acids (TFA) with Particular Emphasis on Conjugated Linoleic Acid Isomers (CLA)—A Review, *Fett/Lipid 100*, 190–210.

9. Park, Y., Albright, K.J., Storkson, J.M., Liu, W., Cook, M.E., and Pariza, M.W. (1999) Changes in Body Composition in Mice During Feeding and Withdrawal of Conjugated Linoleic Acid, *Lipids 34*, 243–248.
10. Chin, S.F., Liu, W., Storkson, J.M., Ha, Y.L., and Pariza, M.W. (1992) Dietary Sources of Conjugated Dienoic Isomers of Linoleic Acid, a Newly Recognized Class of Anticarcinogens, *J. Food Comp. Anal. 5,* 185–197.
11. Ip, C., Chin, S.F., Scimeca, J.A., and Pariza, M.W. (1991) Mammary Cancer Prevention by Conjugated Dienoic Derivative of Linoleic Acid, *Cancer Res. 51*, 6118–6124.
12. Durgam, V.R., and Fernandes, G. (1997) The Growth Inhibitory Effect of Conjugated Linoleic Acid on MCF-7 Cells Is Related to Estrogen Response System, *Cancer Lett. 116*, 121–130.
13. Shultz, T.D., Chew, B.P., Seaman, W.R., and Luedecke, L.O. (1992) Inhibitory Effect of Conjugated Dienoic Derivatives of Linoleic Acid and β-Carotene on the *in vitro* Growth of Human Cancer Cells, *Cancer Lett. 63*, 125–133.
14. Schonberg, S., and Krokan, H.E. (1995) The Inhibitory Effect of Conjugated Dienoic Derivatives (CLA) of Linoleic Acid on the Growth of Human Tumor Cell Lines Is in Part Due to Increased Lipid Peroxidation, *Anticancer Res. 15*, 1241–1246.
15. Cave, W.T., Jr. (1991) Dietary n-3 (omega-3) Polyunsaturated Fatty Acid Effects on Animal Tumorigenesis, *FASEB J. 5*, 2160–2166.
16. Begin, M.E., Ells, G., and Horrobin, D.F. (1988) Polyunsaturated Fatty Acid-Induced Cytotoxicity Against Tumor Cells and Its Relationship to Lipid Peroxidation, *J. Natl. Cancer Inst. 80*, 188–194.
17. Das, U.N. (1990) γ-Linolenic Acid, Arachidonic Acid, and Eicosapentaenoic Acid as Potential Anticancer Drugs, *Nutrition 6*, 429–434.
18. Begin, M.E., Ells, G., Das, U.N., and Horrobin, D.F. (1986) Differential Killing of Human Carcinoma Cells Supplemented with n-3 and n-6 Polyunsaturated Fatty Acids, *J. Natl. Cancer Inst. 77*, 1053–1062.
19. Tsuzuki, T., Igarashi, M., and Miyazawa, T. (2004) Conjugated Eicosapentanoic Acid Inhibits Transplanted Tumor Growth *via* Membrane Lipid Peroxidation in Nude Mice, *J. Nutr. 134*, 1162–1166.
20. Tsuzuki, T., Tokuyama, Y., Igarashi, M., and Miyazawa, T. (2004) Tumor Growth Suppression by α-Eleostearic Acid, a Linolenic Acid Isomer with a Conjugated Triene System, *via* Lipid Peroxidation, *Carcinogenesis 25*, 1417–1425.
21. Weete, J.D. (1974) *Fungal Lipid Biochemistry*, Plenum Press, New York.
22. Association of Official Analytical Chemists (1990) Acids (polyunsaturated) in Oil and Fats, in *Official Methods of Analysis of the Association of Official Analytical Chemists (*Helrich, K., ed.), pp. 960–963, AOAC, Arlington, VA.
23. Pitt, G.A.J., and Morton, R.A. (1957) Ultra-violet Spectrophotometry of Fatty Acids, *Prog. Chem. Fats Other Lipids 4*, 227–278.
24. Tamai, K., Kojima, K., Hanaichi, T., Masaki, S., Suzuki, M., Umekawa, H., and Yoshida, S. (1988) Structural Study of Immunoaffinity-Purified DNA Polymerase α-DNA Primase Complex from Calf Thymus, *Biochim. Biophys. Acta 950*, 263–273.
25. Date, T., Yamaguchi, M., Hirose, F., Nishimoto, Y., Tanihara, K., and Matsukage, A. (1988) Expression of Active Rat DNA Polymerase β in *Escherichia coli, Biochemistry 27*, 2983–2990.
26. Oshige, M., Takeuchi, R., Ruike, R., Kuroda, K., and Sakaguchi, K. (2004) Subunit Protein-Affinity Isolation of *Drosophila* DNA Polymerase Catalytic Subunit, *Protein Expr. Purif. 35*, 248–256.
27. Suzuki, K., Shono, F., Kai, H., Uno, T., and Uyeda, M. (2000) Inhibition of Topoisomerases by Fatty Acids, *J. Enzyme Inhib. 15*, 357–366.
28. Sahara, H., Hanashima, S., Yamazaki, T., Takahashi, S., Sugawara, F., Ohtani, S., Ishikawa, M., Mizushina, Y., Ohta, K., Shimozawa, K., *et al*. (2002) Anti-tumor Effect of Chemically Synthesized Sulfolipids Based on Sea Urchin's Natural Sulfonoquinovosylmonoacylglycerols, *Jpn. J. Cancer Res. 93*, 85–92.
29. Sakaguchi, K., Sugawara, F., and Mizushina, Y. (2002) Inhibitors of Eukaryotic DNA Polymerases, *Seikagaku 74*, 244–251.

[Received August 10, 2004; accepted November 13, 2004]

Fasting and Postprandial Lipid Response to the Consumption of Modified Milk Fats by Guinea Pigs

Geneviève Asselin[a], Charles Lavigne[a,b], Nathalie Bergeron[a], Paul Angers[a], Khaled Belkacemi[a], Joseph Arul[a], and Hélène Jacques[a,b,*]

[a]Department of Food Science and Nutrition and Nutraceuticals and Functional Foods Institute, Laval University, Ste-Foy, Québec, G1K 7P4, Canada, and [b]Lipid Research Unit, University Medical Center of Québec City, Ste-Foy, Québec, G1V 4G2, Canada

ABSTRACT: The objective of the present study was to investigate the effect of three modified milk fats with different melting profiles on fasting and postprandial lipid responses and on fecal fat content in guinea pigs. We hypothesized that the consumption of modified milk fat with a high m.p. results in reduced fasting and postprandial lipid responses compared with that of modified milk fat fractions with lower m.p. To test this hypothesis, male Hartley guinea pigs were fed isoenergetic diets containing 110 g of fat/kg, either from one of the three modified milk fats with high (HMF), medium (MMF), or low melting profiles (LMF), or from one of the two reference fats as whole milk fat (MF) or a fat blend similar to that of nonhydrogenated soft margarine (MA) for 28 d. Food intake ($P < 0.05$) and body weight gain ($P < 0.05$) were reduced in the animals fed the HMF diet compared with the other groups. In the fasting state, plasma LDL cholesterol was highest in animals fed the LMF diet, intermediary in those fed the MMF and MF diets, and lowest in those fed the HMF and MA diets ($P < 0.05$). Postprandially, the areas under the 0- to 3-h curves for the changes in plasma TG were lower in the HMF group than in the MA- and LMF-fed guinea pigs ($P < 0.05$). The fecal fat content was higher ($P < 0.05$) in the HMF group compared to the other milk fat groups. The present results suggest that modified milk fats can impact food intake, body weight gain, fasting cholesterolemia, and postprandial triglyceridemia, and these changes may be attributed to an altered fat absorption.

Paper no. L9536 in *Lipids* 39, 985–992 (October 2004).

Numerous studies have demonstrated that the consumption of milk fat compared with soft margarine causes an elevation of plasma LDL cholesterol and apolipoprotein B (apoB) (1–4) and can increase the risk of cardiovascular diseases in humans. Evidence indicates that the high levels of two saturated FA (SFA), myristic and palmitic acids (5), and of cholesterol (6) would be the major dietary factors in milk fat raising cholesterolemia.

Over the past decade, new technologies have enabled food scientists to design new foods to reduce the cholesterol-raising properties of milk fat. These technologies involve the transformation of milk fat composition either by interesterification, cow-feeding, or fractionation technology. Chemical or enzymatic interesterification is a random process exchanging FA positions on the glycerol molecule. Although this procedure is largely used in the fat and oil industry to modify physical and chemical properties, there is scepticism about the impact of interesterified fats on the lipid profile because of their negligible effect on fasting plasma lipids in adults (7). Nevertheless, Mutanen *et al.* (8) showed that enzymatic interesterified milk fat compared with natural milk fat can lower postprandial TG concentrations in women, and they attributed this reduction to reduced fat absorption.

Feeding cows on rations supplemented with unsaturated oils encapsulated with formaldehyde-casein yields a milk fat with reduced SFA and increased monounsaturated FA (MUFA) and PUFA levels. Noakes *et al.* (9) observed that the consumption of products containing this unsaturated FA-enriched milk fat lowered plasma total and LDL cholesterol by 4–5% after a 4-week dietary intervention in 33 men and women.

Fractionation technology is widely used to modify physicochemical and nutritional properties of fats and oils. Vacuum steam distillation, a process generally used for oil refining, has been used to reduce cholesterol concentration in animal fats (including milk fat and lard). A cholesterol-reduced animal fat lowered plasma TG and cholesterol concentrations by 14 and 3%, respectively, compared with a regular animal fat in normolipidemic postmenopausal women (10). Various methods have been developed to reduce cholesterol and to fractionate milk fat into fractions with different melting profiles. They involve melt crystallization, short-path distillation, and dense gas extraction (11). These processes yield milk fat fractions with low-melting TG enriched in short- and medium-chain FA, medium-melting TG, or high-melting TG enriched in long-chain FA. A study conducted in our laboratory (12) showed that a modified milk fat, reduced in cholesterol and with a high-m.p., induced beneficial reductions in plasma total TG (–20%), VLDL TG (–27%), and VLDL cholesterol (–39%) compared with both whole milk fat and nonhydrogenated margarine in 21 normolipidemic men. We hypothesized that the high solid fat and high viscosity of the melting

*To whom correspondence should be addressed at Department of Food Science and Nutrition, Laval University at Ste-Foy, Québec, Canada G1K 7P4. E-mail: helene.jacques@aln.ulaval.ca

Abbreviations: apoB, apolipoprotein B; AUC, area under the curve; DP, dropping point; HMF, modified milk fat fraction with high melting profile; LMF, modified milk fat with low melting profile; MA, fat blend similar to that of nonhydrogenated soft margarine; MF, whole milk fat; MMF, modified milk fat fraction with medium melting profile; MUFA, monounsaturated FA; mRNA, messenger ribonucleic acid; *P/S*, polyunsaturated to saturated FA ratio; SFA, saturated FA; TRL, triglyceride-rich lipoprotein.

TG of this modified milk fat at body temperature might reduce fat digestion and absorption.

Thus, the objective of this study was to investigate the fasting and postprandial lipid as well as the fecal fat responses to the consumption of whole milk fat (MF), three milk fat fractions produced by fractionation with high (HMF), medium (MMF), or low (LMF) m.p., and a fat blend similar to that of nonhydrogenated margarine (MA) in guinea pigs. Our hypothesis was that consumption of modified milk fat with a high m.p. results in a reduced lipid response compared with that of the two other modified milk fat fractions with low and medium m.p. Whole milk fat and fat blend similar to that of nonhydrogenated margarine were considered as reference fats. With these two reference fats, it was possible to characterize more accurately the specific effects of the modified milk fats on plasma lipids, as we did in our previous human study (12).

MATERIALS AND METHODS

Animals. Male Hartley guinea pigs (Charles River, St. Constant, QC, Canada), weighing 299 ± 2 g, were individually housed in plastic cages in a temperature (21–22°C) and humidity- (40–50%) controlled room and with a daily dephased 12:12-h light/dark cycle (lights on at 20:00 to 08:00). Upon arrival, all animals were fed a ground nonpurified commercial diet (Purina Guinea Pig chow; St. Louis, MO) for at least 4 d. At the end of this baseline period, the guinea pigs were randomly assigned to one of the five diet groups. Free access to the purified diets and tap water was provided for 28 d. Food intake was recorded daily and body weight was measured three times a week. The animal facilities met the guidelines of the Canadian Council on Animal Care and the protocol was approved by the Laval University Animal Care Committee.

Experimental fats: FA and cholesterol composition. The FA and cholesterol compositions of the five experimental fats are shown in Table 1. The modified milk fats were prepared from the same lot of whole milk fat. The fat blend similar to that of nonhydrogenated margarine was a blend of 460 g/kg canola oil (Briska Inc., Montreal, QC, Canada), 460 g/kg sunflower oil (Briska Inc.), and 80 g/kg modified palm oil (CanAmera Foods, Toronto, ON, Canada). This fat blend similar to nonhydrogenated margarine contained no cholesterol whereas the LMF fraction had the highest content, and the HMF fraction the lowest content in cholesterol among the milk fat fractions. The dropping points (DP) of each experimental fats were: MA, 29–30°C; MF, 33–34°C; LMF, 13–14°C; MMF, 22–23°C; HMF, 42–44°C. DP represents the temperature at which a solid fat turns into a liquid, measured by warming the solid fat until it forms a drop of liquid. It corresponds to the temperature at which about 90% of the solid fat is melted, and provides a good indication of the melting behavior of solid fats.

Diets. Animals were assigned to one of the five purified powdered diets varying only in fat source, which consisted of fat blend similar to that of nonhydrogenated margarine, whole milk fat, or modified milk fat with a high, medium, or a low melting profile. The diets were formulated according to the National Research Council (13) recommendations for guinea pigs and stored in the dark at 4ºC. Soybean oil (30 g/kg) was added to the diets to provide essential FA. The protein level of the diets was adjusted to 30% on the basis of the nitrogen content of casein determined by a 1612 Kjell-Foss autoanalyzer (Foss, Hillerod, Denmark). The composition of each purified diet is detailed in Table 2. The energy content of the diets was measured with an automatic adiabatic calorimeter (Model 1241; Parr Instruments, Moline, IL). The diets were found isoenergetic: MA, 20.7 kJ/g; MF, 21.1 kJ/g; LMF, 20.4 kJ/g; MMF, 20.4 kJ/g; HMF, 20.9 kJ/g. The lipid content of the diets was also determined by using a 35001 Goldfish Lipid Extractor (Labconco, Kansas City, MO): MA, 135 g/kg; MF, 130 g/kg; LMF, 132 g/kg; MMF, 132 g/kg; HMF, 135 g/kg. The cholesterol content of the diets was: MA, 0.0 g/kg; MF, 0.2 g/kg; LMF, 0.3 g/kg; MMF, 0.2 g/kg; HMF, 0.1 g/kg. Differences in cholesterol content of the three modified milk fat diets are due to fractionation processes to produce each modified milk fat fraction.

Feces collection. On day 21, guinea pigs were transferred to metabolic cages for feces collection on a 24-h basis. The cages were suspended over absorbent paper to facilitate feces collection. Feces were freeze-dried, weighed, and stored at –20°C until further analysis. The FA content in feces was de-

TABLE 1
FA and Cholesterol Composition of the Experimental Fats[a]

			Modified milk fats		
FA	MA	MF	LMF	MMF	HMF
			(g/kg)		
4:0	0.0	42.0	60.0	57.0	30.0
6:0	0.0	24.0	31.0	30.0	17.0
8:0	1.0	14.0	17.0	15.0	10.0
10:0	1.0	31.0	36.0	32.0	25.0
12:0	16.0	35.0	39.0	35.0	34.0
13:0	0.0	13.0	2.0	10.0	2.0
14:0	9.0	111.0	112.0	112.0	128.0
14:1	0.0	11.0	14.0	12.0	7.0
15:0	0.0	12.0	17.0	19.0	22.0
16:0	90.0	304.0	252.0	299.0	382.0
16:1	2.0	15.0	21.0	18.0	11.0
17:0	1.0	6.0	7.0	8.0	12.0
18:0	27.0	125.0	74.0	96.0	149.0
18:1	391.0	226.0	274.0	232.0	151.0
18:2	365.0	24.0	30.0	18.0	11.0
18:3	94.0	7.0	13.0	15.0	9.0
20:0	4.0	2.0	1.0	1.0	3.0
ΣSFA	149.0	719.0	647.0	705.0	812.0
ΣMUFA	393.0	252.0	309.0	262.0	169.0
ΣPUFA	459.0	31.0	43.0	33.0	20.0
P/S ratio	3.1	0.04	0.07	0.05	0.02
Cholesterol	0	2.0	3.0	2.0	1.0

[a]MA, fat blend similar to that of nonhydrogenated soft margarine; MF, whole milk fat; LMF, modified milk fat with a low melting profile; MMF, modified milk fat with a medium melting profile; HMF, modified milk fat with a high melting profile; ΣSFA, ΣMUFA, ΣPUFA, sum of saturated, monounsaturated, and polyunsaturated FA, respectively; P/S ratio, polyunsaturated to saturated FA ratio.

TABLE 2
Composition of the Experimental Diets[a]

Ingredients	MA	MF	Modified milk fats		
			LMF	MMF	HMF
			(g/kg)		
Casein[b,c]	336	336	336	336	336
DL-Methionine[b]	3	3	3	3	3
L-Arginine[b]	3	3	3	3	3
Sucrose[b]	200	200	200	200	200
Cornstarch[b]	108	108	108	108	108
Experimental fat[d]					
MA	110				
MF		110			
LMF			110		
MMF				110	
HMF					110
Soya oil[e]	30	30	30	30	30
Cellulose[b]	130	130	130	130	130
Minerals[b,f]	68	68	68	68	68
Vitamins[b,g]	10	10	10	10	10
Folic acid[b]	0.1	0.1	0.1	0.1	0.1
Choline bitartrate[b]	2	2	2	2	2

[a]MA, fat blend similar to that of nonhydrogenated soft margarine; MF, whole milk fat; LMF, modified milk fat with a low melting profile; MMF, modified milk fat with a medium melting profile; HMF, modified milk fat with a high melting profile.
[b]Purchased from ICN Nutritional Biochemicals, Cleveland, Ohio.
[c]Casein, 89.2% protein.
[d]MA was a blend of 460 g/kg canola oil (Briska Inc., Montreal, Canada), 460 g/kg sunflower oil (Briska Inc.), and 80 g/kg modified palm oil (CanAmera Foods, Toronto, ON). The modified milk fats were prepared from the same lot of whole milk fat. The composition of the experimental fats is in Table 1.
[e]Purchased from Briska Inc.
[f]ICN Guinea Pig Mineral Mix provides the following (g/kg mix): calcium carbonate, 221.32; calcium phosphate dibasic, 301.00; magnesium sulfate•7 H_2O, 224.27; potassium chloride, 169.68; sodium chloride, 73.77; ferric citrate, 5.16; manganese sulfate•H_2O, 2.36; zinc carbonate, 1.48; cupric sulfate•5 H_2O, 0.59; chromium potassium sulfate•12 H_2O, 0.32; potassium iodide, 0.03; sodium selenite, 0.02.
[g]ICN Vitamin Mix Fortification provides the following (g/kg mix): vitamin A acetate (500,000 IU/g), 1.80; vitamin D_2 (850,000 IU/g), 0.125; DL-α-tocopherol acetate, 22.00; ascorbic acid, 45.00; inositol, 5.00; choline chloride, 75.00; menadione, 2.25; *p*-aminobenzoic acid, 5.00; niacin, 4.25; riboflavin, 1.00; pyridoxine hydrochloride, 1.00; thiamine hydrochloride, 1.00; calcium pantothenate, 3.00; biotin, 0.02; folic acid, 0.09; vitamin B_{12}, 0.00135; dextrose, 833.46.

termined by one-step methylation using chloroform, according to an adapted method of Sukhija and Palmquist (14), followed by an analysis by GC. Briefly, the one-step methylation procedure uses 5 mL of a solvent mixture consisting of methanol/chloroform/acetyl chloride (20:27:3, by vol) for 500 mg of feces sample. The capped tubes were vortex mixed for 1 minute at low speed and heated for 2 h in a water bath at 70°C. After the content of the tubes was cooled to room temperature, 5 mL of K_2CO_3 (6%) and 4 mL of chloroform were added. Tubes were then centrifuged at 1000 × *g* for 10 min and the lower chloroform layer was removed. Another washing of the aqueous layer with 4 mL of chloroform completely removed the methyl esters. The chloroform layer was pooled and filtered through silica gel and dried under nitrogen. The dry residue was then resuspended in 1 mL chloroform and analyzed with a gas chromatograph (Model 5890 Series II; Hewlett-Packard) connected to a computer with a Hewlett-Packard ChemStation. Sample volumes (1.0 μL) were injected on a DB-225 capillary column (30 m × 0.25 mm i.d., 0.2 μm film thickness; J&W, Folsom, CA). The total FA content was calculated as the sum of individual FA.

Cannulation and blood sampling. At day 25, guinea pigs were cannulated *via* the jugular vein under isoflurane anesthesia (Aerrane; Janssen, North York, ON, Canada). Catheters were externalized from the nape of the neck, and the guinea pigs were allowed to recover. The experimental procedures were conducted in unrestrained conscious animals 3 d after surgery, when their food intake and body weight were nearly normal postoperatively. On day 28, after a 12-h fast and at the beginning of the dark period, a test meal, corresponding to 30% of the energy intake of their previously assigned diet, was given for 15 min. Blood samples for total cholesterol and TG measurements were obtained before the beginning of the test meal (–15 min) and at 0.5, 1, 1.5, 2, and 3 h after the meal, a postprandial time period known to reflect gastric emptying and intestinal absorption (15). Blood samples were collected in tubes containing EDTA (0.05%) and benzamidine (0.03%) to prevent scission of apoB-100 (16). The plasma was isolated by low speed centrifugation (700 × *g*, 10 minutes). Erythrocytes were suspended in saline and reinjected into the animals to prevent a fall in the hematocrit and to minimize stress. At the completion of the test meal, guinea pigs returned to their cages for 2 days. After a second 12-h fast, the guinea pigs were sacrificed by using CO_2. The liver, the epididymal white adipose tissues, and the perirenal adipose tissues were rapidly excised, weighed, and frozen in liquid nitrogen, and stored at –80°C.

Lipoprotein separation and hepatic lipid extraction. Fresh plasma (1.2 mL) from two or three animals was pooled and ultracentrifuged (TL-100 Tabletop Ultracentrifuge; Beckman, Palo Alto, CA) at 543,000 × *g* at 15°C for 120 min using the TLA-100.4 rotor, according to the method described by Sattler *et al.* (17) to separate lipoproteins. Plasma samples in the fasting state and at different times in the postprandial state were pooled to get enough plasma for the fasting and postprandial plasma lipoprotein measurements. Plasma samples were adjusted to a density of 1.24 g/mL by the addition of 381.6 mg of solid KBr per milliliter of plasma. A density gradient was formed by layering the density-adjusted plasma underneath phosphate-buffered saline (d = 1.006 g/mL). Plasma lipoproteins were fractionated into TG-rich lipoproteins (TRL) (chylomicrons and VLDL) (d < 1.006 g/mL) and LDL (1.006 < d < 1.063 g/mL). To facilitate the visualization of the single lipoprotein bands after ultracentrifugation, Coomassie Brilliant Blue R-250 (5% w/w; Bio-Rad Laboratories, Hercules, CA) was added to plasma samples before ultracentrifugation. The TRL supernatants from fasting and postprandial samples were removed and brought to a final volume of 1 mL with saline. LDL were also collected, but only in the fasting state. HDL were obtained after precipitation of apoB-containing lipoproteins with phosphotungstic acid and magnesium ion (HDL Cholesterol precipitant; Boehringer Mannheim, Laval, QC, Canada) from the fasting plasma of all animals. Finally, hepatic lipids were ex-

tracted according to the method of Folch *et al.* (18). Fasting and postprandial total plasma, lipoprotein, and hepatic TG and cholesterol were measured by using the enzymatic TG and the CHOD-PAP kits supplied by Roche Diagnostics (Laval, QC, Canada), respectively.

Statistical analyses. Results were analyzed by the general linear model program of the SAS statistical package for personal computers. Data on body weight gain, food intake, epididymal and perirenal fat pads, and fasting plasma and hepatic lipids were analyzed by using ANOVA. Data obtained from serial sampling (fasting and postprandial plasma total and TRL-TG) were analyzed by using ANOVA with repeated measures, with time as the repeated variable. Postprandial responses, in mmol/L, were also expressed as area under the curve (AUC) measurements calculated by the trapezoidal method (19). ANOVA was then followed by the Tukey test to identify significant differences between dietary fat groups at each time point. We also employed analysis of covariance (ANCOVA) on fasting and postprandial lipid responses as the dependent variables and body weight gain as the covariate. There were no changes in statistical significance after adjustment for body weight gain. Pearson correlation coefficients were calculated to assess the relationship between variables. Differences between diet groups were considered significant at $P < 0.05$. Data were expressed as means ± SEM.

RESULTS

Body weight gain, food intake, and fasting plasma cholesterol and TG. At the end of the experimental period, body weight gain ($P < 0.05$) and food intake ($P < 0.0001$) were significantly lower in the HMF group than in the other groups (Table 3). In the HMF-fed animals, epididymal and perirenal fat pads, which are variables responding to food intake, were lower compared with the MA and MMF groups ($P < 0.0008$). The food intake of the test meal was similar between the dietary groups.

Fasting plasma total, LDL and HDL cholesterol, as well as total plasma and hepatic TG are also presented in Table 3. Total plasma cholesterol was higher in the LMF group compared with the other groups ($P < 0.0001$). The LMF group had the highest LDL cholesterol values followed by the animals fed the MF and MMF diets, whereas the MA and HMF groups showed the lowest values ($P < 0.05$). No differences were observed in fasting plasma total TG and HDL cholesterol concentrations nor in hepatic TG concentrations among the dietary groups.

Postprandial responses. Expressed as change from fasting values (Δ), time course of plasma total TG responses is shown in Figure 1A. Visual comparison of the postprandial responses to various test meals showed that the TG concentrations peaked 1.5–2 h in all dietary groups. In the early postprandial period (0–0.5 h after the test meals), plasma TG changes were not different among the dietary groups. One hour after the test meal, the increments of plasma TG were significantly ($P < 0.05$) lower in animals fed various milk fat fractions than in the MA-fed animals. Guinea pigs fed the HMF, MMF, and MF diets showed significantly ($P < 0.05$) lower plasma total TG increases than guinea pigs fed the MA diet 1–2 h after the meal. Moreover, guinea pigs fed the HMF

TABLE 3
Body Weight Gain, Food Intake, Epididymal and Perirenal Fat Pads, and Fasting Plasma and Hepatic Lipids[a]

			Modified milk fats		
	MA	MF	LMF	MMF	HMF
Body weight gain (g)	83 ± 7^{A} (19)	82 ± 6^{A} (20)	76 ± 6^{A} (19)	74 ± 5^{A} (20)	42 ± 7^{B} (21)
Food intake (g/d)	17.1 ± 0.4^{A} (19)	17.6 ± 0.3^{A} (20)	17.7 ± 0.4^{A} (19)	17.3 ± 0.5^{A} (20)	14.4 ± 0.5^{B} (21)
Food intake (test meal) (g)	2.3 ± 0.1 (19)	2.7 ± 0.2 (20)	2.4 ± 0.2 (19)	2.2 ± 0.1 (20)	2.4 ± 0.2 (21)
Epididymal and perirenal fat pads (g)	2.0 ± 0.3^{A} (19)	1.6 ± 0.2^{AB} (20)	1.6 ± 0.2^{AB} (19)	1.8 ± 0.3^{A} (20)	1.0 ± 0.2^{B} (21)
Fasting plasma lipids (mmol/L)					
Total cholesterol	3.0 ± 0.2^{B} (19)	3.2 ± 0.2^{B} (20)	4.7 ± 0.3^{A} (19)	3.6 ± 0.2^{B} (20)	2.7 ± 0.3^{B} (21)
LDL-cholesterol[b]	2.2 ± 0.1^{C} (7)	2.9 ± 0.2^{B} (8)	4.2 ± 0.5^{A} (9)	3.1 ± 0.2^{B} (9)	2.1 ± 0.2^{C} (11)
HDL-cholesterol[c]	0.13 ± 0.02 (13)	0.13 ± 0.02 (12)	0.21 ± 0.03 (13)	0.17 ± 0.02 (12)	0.13 ± 0.02 (17)
Total TG	0.82 ± 0.1 (19)	0.75 ± 0.1 (20)	0.88 ± 0.2 (19)	0.89 ± 0.1 (20)	0.83 ± 0.1 (21)
Hepatic TG (μmol/g)	24 ± 5 (13)	20 ± 3 (12)	27 ± 3 (13)	21 ± 3 (12)	19 ± 4 (17)

[a]Values are means ± SEM of the number of observations given in parentheses. Values in the same row with a different superscript are significantly different; MA, fat blend similar to that of nonhydrogenated soft margarine; MF, whole milk fat; LMF, modified milk fat with a low melting profile; MMF, modified milk fat with a medium melting profile; HMF, modified milk fat with a high melting profile.
[b]LDL-cholesterol was measured from pools of two or three guinea pigs.
[c]HDL-cholesterol was measured from remaining plasma of individual guinea pigs.

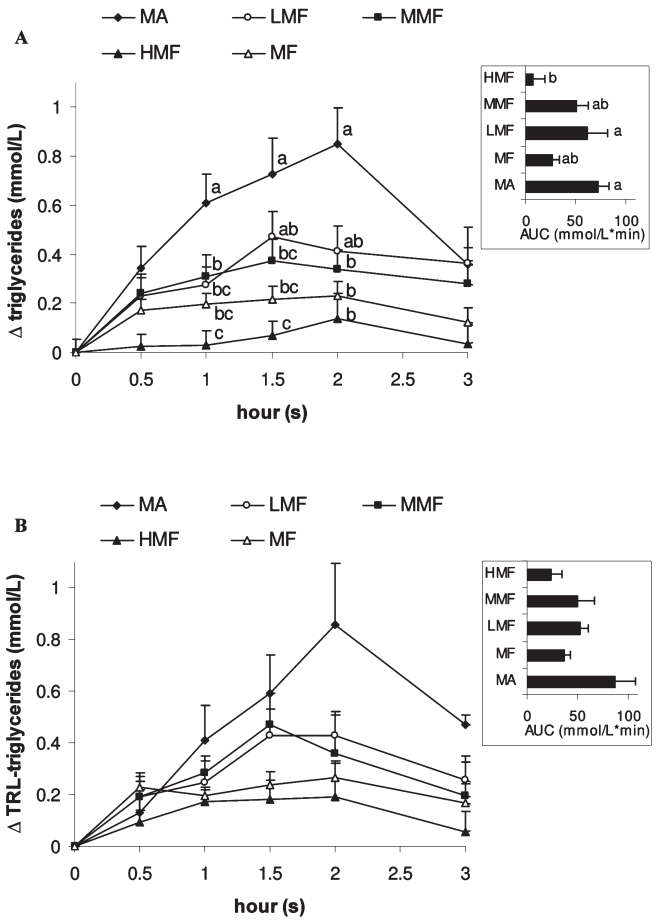

FIG. 1. TG changes in plasma of guinea pigs (n = 19–21 animals per group) (A) and TG-rich lipoprotein (TRL) (n = 7–11 animals per group) (B) concentrations after the ingestion of a meal containing 110 g/kg fat blend similar to that of nonhydrogenated soft margarine (MA), whole milk fat (MF), or one of the three modified milk fats with a low (LMF), medium (MMF), or high (HMF) melting profile during the 3-h postprandial period. Values are means ± SEM. At a given time, significant differences among the groups are represented by different superscripts, $P < 0.05$. Areas under the curves for the changes in the plasma triglycerides and TRL-TG (AUC) were calculated from 0 to 3 h after the ingestion of the meal; significant differences among the groups are represented by different superscripts, $P < 0.05$.

diet induced lower plasma total TG increase than those fed the LMF diet 1.5 h after the meal ($P < 0.05$). The areas under the 0- to 3-h curves for the changes in plasma TG were lower in the HMF-fed animals than in the MA- and LMF-fed animals ($P < 0.05$).

After guinea pigs had consumed the experimental diets for 28 days, fasting plasma TRL-TG were not significantly different among groups (data not shown). Postprandially, the change in TG of TRL is illustrated in Figure 1B. No difference was observed among the five dietary groups; a high variability in pooled TG responses as well as the low number of available guinea pig pools (n = 7–11) could have reduced the possibility to detect significant differences between the five diets. The areas under the 0- to 3-h curves for the changes in plasma TRL-TG were not significantly different between diets. However, there were significant positive correlations between the areas under the 0- to 3-h curves for the changes in plasma TG and plasma TRL-TG (r = 0.94; n = 24; P = 0.0001) suggesting that the postprandial response of TRL-TG was coupled to that of plasma total TG.

FA content of feces. The effects of experimental fat sources on total fecal FA content of guinea pigs are shown in Figure 2A. There were significant differences ($P < 0.0001$) in total fecal FA content: the HMF-fed guinea pigs showed the highest total fecal FA content; the MMF- and MF-fed guinea pigs, intermediary values; and the LMF- and MA-fed guinea pigs, the lowest values.

The saturated (14:0, 16:0, and 18:0) and unsaturated (18:1 and 18:2, n-6) FA content of fecal fat is presented in Figure 2B and Figure 2C, respectively. Significant ($P < 0.01$) differences were observed in the FA content of fecal fat. The HMF-fed animals showed the highest levels of myristic, palmitic, and stearic acids; the MA- and LMF-fed animals, the lowest levels; and the MF- and MMF-fed animals exhibited intermediate levels of these SFA (Fig. 2B). The fecal oleic acid con-

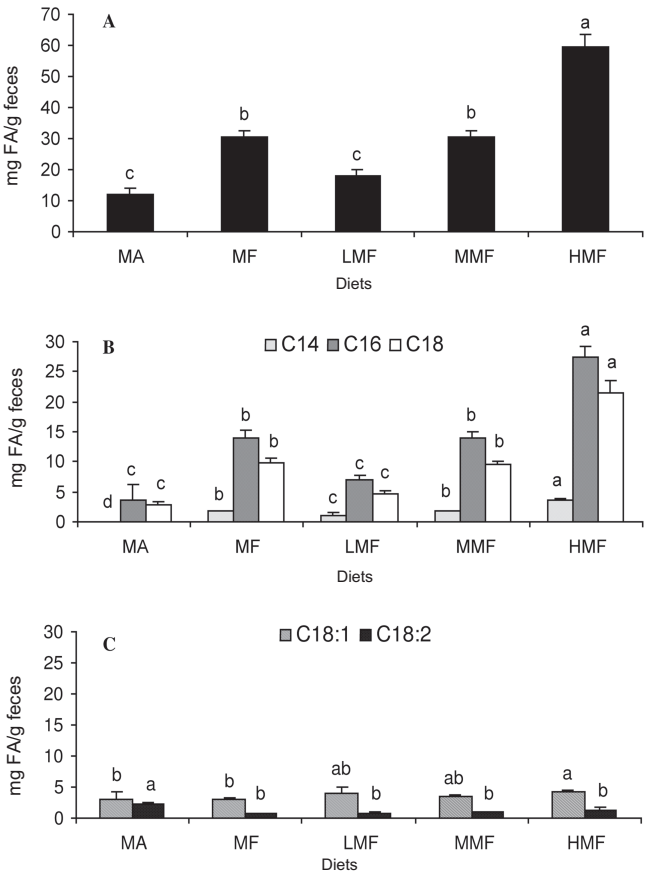

FIG. 2. Total (A), saturated (B), and unsaturated (C) FA distribution in feces collected from guinea pigs fed one of the five experimental diets: fat blend similar to that of nonhydrogenated soft margarine (MA), whole milk fat (MF), or one of the three modified milk fats with a low (LMF), medium (MMF), or high (HMF) melting profile. Values are means ± SEM, n = 15–19 animals per group. Bars with different superscripts within the same FA are significantly different; $P < 0.0001$ for total fecal FA and $P < 0.01$ for fecal saturated and unsaturated FA.

tent was higher in the HMF-animals than in the MA- and MF-fed animals, whereas the linoleic acid content of feces was higher in the MA-fed guinea pigs than in the other dietary groups (Fig. 2C). No differences were noted in the α-linolenic acid (18:3, n-3) content of feces among the five experimental groups (data not shown).

DISCUSSION

We have shown previously that a modified milk fat with a high m.p. reduced plasma TG in normolipidemic men (12). In this study, we observed that the melting profile of milk fat fractions can affect plasma fasting cholesterol and postprandial TG in guinea pigs. In particular, the modified milk fat with a high melting profile lowered fasting LDL cholesterol and the postprandial increase in plasma TG, suggesting an altered absorption of this modified milk fat fraction. The guinea pig was chosen for this study because this animal shows similar characteristics with humans with respect to cholesterol and lipoprotein metabolism. Like humans, guinea pigs have a negligible (<1%) apoB-48 mRNA editing in the liver (20), carry the majority of their cholesterol in LDL, and respond to dietary interventions by modifying their plasma LDL cholesterol response (21).

The consumption of the five experimental fats modified the fasting plasma cholesterol response differently. In agreement with previous observations in humans (1,3), the consumption of MF with a low PUFA to SFA ratio (*P/S* = 0.04) in the present study induced higher plasma LDL cholesterol levels compared with the consumption of MA with a high P/S ratio (*P/S* = 3.1). These results are in good agreement with numerous reports that dietary SFA increase plasma cholesterol levels compared with PUFA in guinea pigs (22,23). LMF (*P/S* = 0.07) and MMF (*P/S* = 0.05) also brought on higher plasma LDL cholesterol concentrations than MA for the same reason. Interestingly, in our study where diets provided 140 g fat/kg, LMF induced the highest plasma total and LDL cholesterol levels. There is a possibility that the higher cholesterol content of the LMF diet (0.3 g/kg), compared with the HMF diet (0.1 g/kg), may be partly responsible for the observed higher plasma cholesterol concentration with LMF. This explanation, however, is not supported by the results of Lin *et al.* (24,25) who, for diets providing 150 g of fat/kg, observed no effect of 0.8 g of cholesterol/kg on plasma total and LDL cholesterol levels compared to basal intakes (0 g of cholesterol/kg) in guinea pigs. As reported by the same authors (24,25), guinea pigs maintain stable plasma cholesterol levels until cholesterol intake (1.7 g of cholesterol/kg) equals or exceeds the mass of endogenous cholesterol synthesis. Nevertheless, it will be helpful in further studies to normalize the dietary cholesterol content of each diet to verify whether the variation in LDL cholesterol concentrations induced by the consumption of the various modified milk fat fractions would be attributed, at least in part, to the difference in cholesterol content of these fats. A factor other than the cholesterol content of modified milk fats should also be considered in their effect on plasma cholesterol. Among the three modified milk fat fractions, plasma LDL cholesterol concentrations were lowest in the HMF group, despite that this fraction had the lowest *P/S* ratio (*P/S* = 0.02). The cholesterol-reducing effect of HMF could be due, at least in part, to the lower body weight gain observed in the HMF-fed animals. It is indeed well established that a reduction in body weight gain generally induces a reduction in plasma cholesterol concentrations (26). In this respect, we used weight gain as covariate and we observed no changes in statistical significance after adjustment for body weight gain. Thus, the present results suggest that the consumption of the five experimental fats altered the fasting plasma cholesterol response not only by variation in body weight gain but also by factors inherent to each testing fat. Interestingly, the 17% lower food intake observed in the HMF group was in part responsible for their 45% lower weight gain, suggesting that other factors, such as intestinal fat absorption, may also be involved.

The early increase in plasma TG after the consumption of a fat-rich meal is thought to primarily reflect gastric emptying and intestinal fat absorption (15). In the present study, HMF, MF, and MMF diets induced significantly lower plasma TG changes 1–2 h after a test meal, suggesting a decreased absorption of these fats compared with the MA diet. In addition, the 0- to 3-h area under the curves for the changes in plasma TG was 90, 64, and 34% lower after HMF, MF, and MMF test meals, respectively, compared with that after the MA test meal. These results are in good agreement with those of Mekki *et al.* (27) who observed that butter significantly lowered the postprandial increase in serum TG (–38% AUC for the 0–7 h) compared with olive and sunflower oils in healthy young men consuming a meal containing 40 g of fat. These findings are also consistent with those of Bergeron and Havel (28) who reported in normolipidemic young men a smaller increase in TRL-TG and TRL-apoB-48 3 h after a SFA-rich test diet and meal (*P/S* = 0.2) than after an n-6 PUFA test diet and meal (*P/S* = 1.3). Furthermore, Tholstrup *et al.* (29) observed a relatively lower lipemia after test meals high in stearic and palmitic acids and the lipemic response took longer to return to fasting values than did intake of unsaturated FA in 16 healthy young men. These results suggested that PUFA, which have a lower melting profile and a greater affinity for the FA-binding protein in the intestine (30), are absorbed more rapidly than SFA. Conversely, highly saturated TG have been shown to decrease fat absorption rates (31). Another issue is that, compared to MA, whole milk fat and modified milk fat fractions also contained greater amount of short- and medium-chain FA. It is well recognized that these FA are efficiently hydrolyzed by the preduodenal lipases, absorbed by the gastric mucosa through the portal vein and therefore are not incorporated into lymph TG (31). Thus, it is not surprising that the postprandial TG responses are lower with the whole and modified milk fat diets compared with the MA diet. Consequently, factors inherent to MF, MMF, and HMF such as their high levels of SFA, including short- and medium-chain FA, and their low levels of unsatu-

rated FA, may have contributed to the decreased postprandial TG levels following consumption of these milk fat fractions.

Melting behavior is a physical characteristic that may influence the digestion and absorption of dietary fats. As reported by Small (32), fats containing a higher solid fat content at body temperature, such as HMF (DP = 42–44°C), could reduce the rate of enzymatic TG hydrolysis and cause higher viscosity of the fat emulsion compared with fats containing TG liquid at body temperature, such as LMF (DP = 13–14°C). To evaluate whether the postprandial lipid responses to the consumption of modified milk fats with variable melting profiles may result from changes in intestinal fat absorption, we estimated intestinal fat absorption by measuring FA content in feces (Fig. 2). Total FA content was the highest with the animals fed the HMF diet, intermediary with those fed MMF and MF diets, and the lowest in the LMF and MA diets. These data, together with the blunted postprandial plasma TG response 0- to 3-h after the HMF rich meal, support the hypothesis that a decreased intestinal fat absorption is associated with the HMF diet. This hypothesis was also supported by the negative correlation between the area under the 0- to 3-h curves for the changes in plasma TG and the total FA content in feces ($r = –0.57$; $n = 26$; $P = 0.002$) as well as between the area under the 0–3-h curves for the changes in plasma TRL-TG and the total FA content in feces ($r = –0.49$; $n = 25$; $P = 0.01$). Moreover these results suggest strongly that the MA diet can increase fat absorption compared with the whole milk fat diet. It is also relevant to point out that these potential differences in intestinal fat absorption may account for the variations in cholesterolemia. Interestingly, we also observed negative correlations between plasma total ($r = –0.54$; $n = 66$; $P = 0.0001$) and LDL cholesterol ($r = –0.59$; $n = 35$; $P = 0.0002$) concentrations and the saturated fecal FA content in guinea pigs fed whole milk fat and the various modified milk fat fractions. Two key points should be highlighted regarding the relationship between fecal fat content and cholesterolemia. First, the HMF diet induced higher fecal FA content, indicating lower fat and energy absorption and leading to lower body weight gain, LDL cholesterol concentrations, and postprandial TG response 1.5 h following the consumption of the test meal. The reduction of body weight in guinea pigs can be explained by an intestinal discomfort following the HMF diet consumption, and thus, leading to a lower food intake. Second, although the LMF and MA diets resulted in approximately the same low total fecal FA content, LMF ($P/S = 0.07$) induced higher plasma total and LDL cholesterol levels than MA ($P/S = 3.1$); and this is presumably due to its low *P/S* ratio.

In conclusion, the present results indicate that the melting profile of modified milk fat fractions can impact food intake, body weight, and fasting and postprandial lipid response in guinea pigs. The lowering effects of high-melting modified milk fat on food intake, body weight gain, cholesterolemia in the fasting state, and TG response in the early postprandial period may be attributed to a lower intestinal FA absorption, as shown by an increased fat content in feces. The beneficial effects of HMF on lipid profile can be worthwhile in reducing the incidence of lipid abnormalities and cardiovascular diseases.

ACKNOWLEDGMENTS

The authors are grateful to Dr. Benoit Lamarche for his helpful suggestions in statistical analysis. We are indebted to Dr. Dave Forster from CanAmera Foods Inc. for the supply of modified palm oil. This research was supported by Dairy Farmers of Canada and Natural Sciences and Engineering Research Council of Canada Collaborative Research and Development.

REFERENCES

1. Wood, R., Kubena, K., O'Brien, B., Tseng, S., and Martin, G. (1993) Effect of Butter, Mono- and Polyunsaturated Fatty Acid-Enriched Butter, Trans Fatty Acid Margarine, and Zero Trans Fatty Acid Margarine on Serum Lipids and Lipoproteins in Healthy Men, *J. Lipid Res. 34,* 1–11.
2. Chisholm, A., Mann, J., Sutherland, W., Duncan, A., Skeaff, M., and Frampton, C. (1996) Effect on Lipoprotein Profile of Replacing Butter with Margarine in a Low Fat Diet: Randomised Crossover Study with Hypercholesterolaemic Subjects, *Br. Med. J. 312,* 931–934.
3. Judd, J.T., Baer, D.J., Clevidence, B.A., Muesing, R.A., Chen, S.C., Weststrate, J.A., Meijer, G.W., Wittes, J., Lichtenstein, A.H., Vilella-Bach, M., and Schaefer, E.J. (1998) Effects of Margarine Compared with Those of Butter on Blood Lipid Profiles Related to Cardiovascular Disease Risk Factors in Normolipemic Adults Fed Controlled Diets, *Am. J. Clin. Nutr. 68,* 768–777.
4. Tonstad, S., Strom, E.C., Bergei, C.S., Ose, L., and Christophersen, B. (2001) Serum Cholesterol Response to Replacing Butter with a New Trans-Free Margarine in Hypercholesterolemic Subjects, *Nutr. Metab. Cardiovasc. Dis. 11*, 320–326.
5. Kris-Etherton, P.M., and Yu, S. (1997) Individual Fatty Acid Effects on Plasma Lipids and Lipoproteins: Human Studies, *Am. J. Clin. Nutr. 65,* 1628S–1644S.
6. Huff, M.W. (2003) Dietary Cholesterol, Cholesterol Absorption, Postprandial Lipemia and Atherosclerosis, *Can. J. Clin. Pharmacol. 10,* 26–32.
7. Hunter, J.E. (2001) Studies on Effects of Dietary FA as Related to Their Position on Triglycerides, *Lipids. 36,* 655–668.
8. Mutanen, M., Jauhiainen, M., Freese, R., and Valsta, L.M. (1996) Comparison of the Effects of Interesterified Butter Oil, Natural Butter Oil, Rapeseed Oil and Sunflower Oil on Postprandial Lipoprotein Levels in Healthy Females, *Nutr. Metab. Cardiovasc. Dis. 6,* 6–12.
9. Noakes, M., Nestel, P.J., and Clifton, P.M. (1996) Modifying the Fatty Acid Profile of Dairy Products Through Feedlot Technology Lowers Plasma Cholesterol of Humans Consuming the Products, *Am. J. Clin. Nutr. 63,* 42–46.
10. Labat, J.B., Martini, M.C., Carr, T.P., Elhard, B.M., Olson, B.A., Bergmann, S.D., Slavin, J.L., Hayes, K.C., and Hassel, C.A. (1997) Cholesterol-Lowering Effects of Modified Animal Fats in Postmenopausal Women, *J. Am. Coll. Nutr. 16,* 570–577.
11. Boudreau, A., and Arul, J. (1993) Cholesterol Reduction and Fractionation Technologies for Milk Fat: An Overview, *J. Dairy Sci. 76,* 1772–1781.
12. Jacques, H., Gascon, A., Arul, J., Boudreau, A., Lavigne, C., and Bergeron, J. (1999) Modified Milk Fat Reduces Plasma Triacylglycerol Concentrations in Normolipidemic Men Compared with Regular Milk Fat and Nonhydrogenated Margarine, *Am. J. Clin. Nutr. 70,* 983–991.
13. National Research Council (1995) *Nutrient Requirements of Laboratory Animals*, pp. 103–124, National Academy Press, Washington, D.C. [AOQ]

14. Sukhija, P.S., and Palmquist, D.L. (1988) Rapid Method for Determination of Total Fatty Acid Content and Composition of Feedstuffs and Feces, *J. Agric. Food Chem. 36,* 1202–1206.
15. Bergeron, N., and Havel, R.J. (1997) Assessment of Postprandial Lipemia: Nutritional Influences, *Curr. Opin. Lipidol. 8,* 43–52.
16. Cardin, A.D., Witt, K.R., Chao, J., Margolius, H.S., Donaldson, V.H., and Jackson, R.L. (1984) Degradation of Apolipoprotein B-100 of Human Plasma Low Density Lipoproteins by Tissue and Plasma Kallikreins, *J. Biol. Chem. 259,* 8522–8528.
17. Sattler, W., Bone, P., and Stocker, R. (1992) *Isolation of Human VLDL, LDL, HDL and Two Subclasses in the TL-100 Tabletop Centrifuge Using the TLA-100.4 Rotor. Application Note DS-850,* pp. 1–4, Beckman Instruments Inc., Spinco Division, Palo Alto, California.
18. Folch, J., Lees, M., and Sloane-Stanley, G.H. (1957) A Simple Method for Isolation and Purification of Total Lipids from Animals Tissues, *J. Biol. Chem. 226,* 497–509.
19. Matthews, J.N.S., Altman, D.G., Campbell, M.J., and Royston, P. (1990) Analysis of Serial Measurements in Medical Research, *Br. Med. J. 300,* 230–235.
20. Greeve, J., Altkemper, I., Dieterich, J.H., Greten, H., and Windler, E. (1993) Apolipoprotein B mRNA Editing in 12 Different Mammalian Species: Hepatic Expression Is Reflected in Low Concentrations of ApoB-Containing Plasma Lipoproteins, *J. Lipid Res. 34,* 1367–1383.
21. Fernandez, M.L. (2001) Guinea Pigs as Models for Cholesterol and Lipoprotein Metabolism, *J. Nutr. 131,* 10–20.
22. Abdel-Fattah, G., Fernandez, M.L., and McNamara, D.J. (1998) Regulation of Very Low Density Lipoprotein Apo B Metabolism by Dietary Fat Saturation and Chain Length in the Guinea Pig, *Lipids 33,* 23–31.
23. Fernandez, M.L., and McNamara, D.J. (1994) Dietary Fat Saturation and Chain Length Modulate Guinea Pig Hepatic Cholesterol Metabolism, *J. Nutr. 124,* 331–339.
24. Lin, E.C.K., Fernandez, M.L., and McNamara, D.J. (1992) Dietary Fat Type and Cholesterol Quantity Interact to Affect Cholesterol Metabolism in Guinea Pigs, *J. Nutr. 122,* 2019–2029.
25. Lin, E.C.K., Fernandez, M.L., Tosca, M.A., and McNamara, D.J. (1994) Regulation of Hepatic LDL Metabolism in the Guinea Pig by Dietary Fat and Cholesterol, *J. Lipid Res. 35,* 446–457.
26. Hecker, K.D., Kris-Etherton, P.M., Zhao, G., Coval, S., and St. Jeor, S. (1999) Impact of Body Weight and Weight Loss on Cardiovascular Risk Factors, *Curr. Atheroscler. Rep. 1,* 236–242.
27. Mekki, N., Charbonnier, M., Borel, P., Leonardi, J., Juhel, C., Portugal, H., and Lairon, D. (2002) Butter Differs from Olive Oil and Sunflower Oil in Its Effects on Postprandial Lipemia and Triacylglycerol-Rich Lipoproteins After Single Mixed Meals in Healthy Young Men, *J. Nutr. 132,* 3642–3649.
28. Bergeron, N., and Havel, R.J. (1995) Influence of Diets Rich in Saturated and Omega-6 Polyunsaturated Fatty Acids on the Postprandial Responses of Apolipoproteins B-48, B-100, E, and Lipids in Triglyceride-Rich Lipoproteins, *Arterioscler. Thromb. Vasc. Biol. 15,* 2111–2121.
29. Tholstrup, T., Sandström, B., Bysted, A., and Holmer, G. (2001) Effect of 6 Dietary Fatty Acids on the Postprandial Lipid Profile, Plasma Fatty Acids, Lipoprotein Lipase, and Cholesterol Ester Transfer Activities in Healthy Young Men, *Am. J. Clin. Nutr. 73,* 198–208.
30. Ockner, R.K., Pittman, J.P., and Yager, J.L. (1972) Differences in the Intestinal Absorption of Saturated and Unsaturated Long Chain Fatty Acids, *Gastroenterology 62*, 981–992.
31. Bracco, U. (1994) Effect of Triglyceride Structure on Fat Absorption, *Am. J. Clin. Nutr. 60,* 1002S–1009S.
32. Small, D.M. (1991) The Effects of Glyceride Structure on Absorption and Metabolism, *Annu. Rev. Nutr. 11,* 413–434.

[Received July 1, 2004, and in revised form accepted November 9, 2004]

Rapid Clearance of Hexachlorobenzene from Chylomicrons

Ronald J. Jandacek*, Shuqin Zheng, Qing Yang, and Patrick Tso

The University of Cincinnati, Department of Pathology, Cincinnati, Ohio

ABSTRACT: Toxic organochlorines that are present in food are lipophilic and carried by chylomicrons. We have studied the clearance of an organochlorine, hexachlorobenzene, from chylomicrons. Chylomicrons were obtained from mesenteric lymph of rats that were intraduodenally given ^{14}C-hexachlorobenzene and ^{3}H-triolein. The labeled chylomicrons were injected intravenously into recipient rats, and the clearance of isotopes was followed. Surprisingly, the hexachlorobenzene disappeared from the plasma more rapidly than the triolein. This unexpected result raises questions about the manner in which hexachlorobenzene is delivered to tissues. The tissue distribution of the hexachlorobenzene is consistent with its rapid uptake.

Paper no. L9614 in *Lipids 39,* 993–995 (October 2004).

Organochlorines are ubiquitous in nature and are found in human tissues throughout the world. For several decades they have been recognized as significant issues in ecology and health. The principal route of entry for these lipophilic compounds into humans is in foods. They are associated with fat and its digestion products during absorption from the intestine and subsequently in chylomicrons in lymph. Much attention has focused on the toxicity and metabolism of these compounds, but their initial absorption and distribution to tissues remain poorly understood.

Hexachlorobenzene (HCB) is sparingly metabolized, with 98% of the body burden in rodents remaining as the parent compound (1). We have investigated the clearance and tissue deposition of HCB introduced intravenously in chylomicrons (prior to their metabolism by the liver).

MATERIALS AND METHODS

Materials. ^{14}C-HCB (uniformly labeled; 2.8 μg/μCi) was purchased from Sigma-Aldrich (St. Louis, MO). [9,10 ^{3}H]Triolein (0.017 μg/μCi) was purchased from PerkinElmer Life Sciences (Boston, MA).

Animals. (i). Collection of labeled chylomicrons. The protocol was approved by the University of Cincinnati Animal Care and Use Committee. Male Sprague-Dawley rats fitted with mesenteric lymph cannula were gastrically intubated with 10 μCi of ^{14}C-HCB and 50 μCi of ^{3}H-triolein in 1 mL olive oil, and lymph was collected. Glutathione and gentamicin were added to the lymph at final concentrations of 0.5 and 0.1 mg/mL, to prevent oxidation and bacterial degradation, respectively. KBr was added to the lymph to bring it to a density of 1.1, and chylomicrons were floated to the top of the 1.006 layer of a NaCl density gradient after centrifugation (150,000 × *g*, SW41 rotor) for 45 min at room temperature. The chylomicrons were used for injection as described below after standing overnight.

(ii) Chylomicron metabolism studies. Chylomicrons suspended in saline were injected *via* the jugular vein into six nonfasted recipient animals (male Sprague-Dawley rats, 384–426 g). Each animal received 0.1 μCi of ^{14}C-HCB and 2.0 μCi of ^{3}H-triolein (40 mg of TAG). Blood (300 μL) was sampled from the carotid vein at 3, 5, 8, 12, 20, and 30 min and the plasma was analyzed for ^{14}C and ^{3}H. Animals were sacrificed after the final blood sample, and tissue samples were analyzed for ^{14}C and ^{3}H after oxidation with the Harvey Instruments OX-700 oxidizer (R.J. Harvey Instrument Corp., Hillsdale, NJ.)

Analyses. Blood clearance data were analyzed with the numerical analysis program of the SAAMII^{TM} software (SAAM Institute, Inc., University of Washington, Seattle, WA). Biexponential curves were calculated for each rat that received chylomicrons, and statistical comparisons were made based on the six curves. Fractional clearance was calculated from the 3- to 12-min monoexponential fit of the data (3). Initial clearance was calculated from the 3-min measurements. Means were compared by two-tailed *t*-test and/or Mann–Whitney Rank Sum test (SigmaStat 2.03; SPSS, Inc., Chicago, IL) with significance attained at $P < 0.05$.

RESULTS

HCB clearance from chylomicrons and tissue concentrations. The clearance of the ^{3}H and ^{14}C in the recipient animals is shown in Figure 1. There was rapid clearance of each isotope from the plasma. The clearance of HCB during the first 3 min (23.5 ± 0.7%/min; mean ± SEM) was faster than triolein (10.1 ± 1.8%/min) ($P < 0.001$). During the 3–12 min time period, the mean fractional clearance rates of the two compounds were not different. The fractional clearance rate for triolein was 0.149 ± 0.023 min^{-1} (mean ± SEM), and that for HCB was 0.145 ± 0.022 min^{-1} during the 3–12-min period. The ^{3}H and ^{14}C in tissues (percentage of dose in total organ, or percentage of dose/g concentration, when noted) is given in Table 1.

*To whom correspondence should be addressed at Department of Pathology, University of Cincinnati, Genome Research Institute, 2120 East Galbraith Rd., Bldg. A, Cincinnati, OH, 45237.
E-mail: ronald.jandacek@uc.edu

Abbreviations: DDT, dichlorodiphenyl-trichloroethane; HCB, hexachlorobenzene.

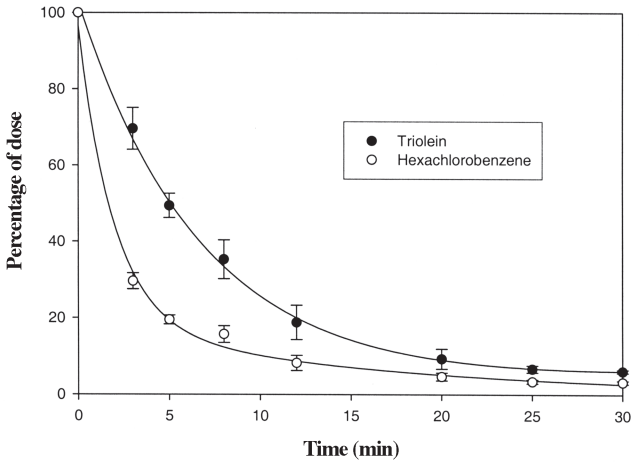

FIG. 1. Clearance from plasma of ^{3}H-triolein and ^{14}C-hexachlorobenzene in chylomicrons injected intravenously into rats. The curves are from the means from six animals. The values at individual time points are significantly different with the exception of that at 20 min.

TABLE 1
^{14}C and ^{3}H in Tissues[a] of Recipient Animals 30 min After Intravenous Injection of Chylomicrons Containing ^{14}C-Hexachlorobenzene (HCB) and ^{3}H-Triolein

	^{14}C (HCB)	^{3}H (Triolein)	HCB/Triolein (%)
Tissue (% of dose/tissue)			
Liver	7.5 ± 0.55[b]	15.7 ± 1.6	49 ± 3
Epididymal fat pad	1.08 ± 0.21	0.58 ± 0.19	263 ± 55
Heart	0.43 ± 0.03[b]	1.0 ± 0.12	43 ± 3
Spleen	0.22 ± 0.04[b]	1.1 ± 0.22	20 ± 2
Brain	0.54 ± 0.04[b]	0.31 ± 1.07	191 ± 19
Tissue (% of dose/g)			
Abdominal fat	0.60 ± 0.09	0.36 ± 0.03	187 ± 46
Muscle	0.16 ± 0.02	0.21 ± 0.02	79 ± 10

[a]*n*-6; mean ± SEM.
[b]HCB and triolein are different ($P < 0.05$).

DISCUSSION

HCB is highly lipophilic, with a $\log_{10}$ of its octanol/water partition coefficient equal to 5.7 (4) and of its aqueous solubility (mol/L) equal to −6.78 (5). Given this affinity for an oil phase, it is unlikely that HCB partitioned from the chylomicrons into the saline solution prior to injection. As would be expected from its lipophilicity, HCB is stored predominantly in adipose tissue (1). There is no evidence of its metabolism in the enterocyte or during the absorption process (1).

We found that the HCB that is absorbed in chylomicrons is distributed rapidly to tissues. The initial clearance was more rapid than that of triolein, and after 3 min, the fractional clearance was similar for the two compounds. The transport into adipose tissue of HCB was more rapid than that of triolein, consistent with rapid distribution to peripheral tissues implied by the rate of disappearance from blood.

This behavior differs from that of the large hydrophobic molecules, retinyl palmitate and squalene. These compounds have been used as markers for the chylomicron lipid core and are cleared from the blood at a markedly slower rate than TAG (3). They provide a means for following the disappearance of chylomicron remnants by hepatic uptake.

It is of interest that dichlorodiphenyl-trichloroethane (DDT), a relatively large and lipophilic molecule, was also observed to disappear from chylomicrons in blood more rapidly than TAG (2). HCB and DDT are both very lipophilic molecules that would be expected to be carried in the core of the chylomicrons. Nevertheless, they are rapidly removed from chylomicrons.

It is possible that rapid exchange between chylomicrons and other carriers such as albumin occurs in the circulation. Rapid exchange of other halogenated hydrocarbons among human lipoproteins was found by Maliwal and Guthrie (6). It is also possible that rapid diffusion of HCB allows it to be delivered to peripheral tissues during hydrolysis of TAG. This latter explanation may not completely account for the rapid clearance of DDT. Vost and Maclean (2) found that HDL has a strong affinity for DDT and that transfer from chylomicrons was correlated with TAG hydrolysis.

Our study utilized a trace mass of hexachlorobenzene HCB in the gavage preparation. This level was used to label the chylomicrons to mimic the absorption of trace levels of lipophilic toxins typical of that in foods. Human consumption of HCB has been estimated to be 0.2 μg/d (7). The amount of TAG (40 mg) injected as chylomicrons in this study approximates the mass that can be attained after a fatty meal. Although higher than average human consumption, the injected mass of HCB (0.3 μg) is readily soluble in the TAG phase. Nevertheless, it is possible that the rate of clearance could depend on the ratio of HCB to TAG.

We have observed that HCB absorbed *via* chylomicrons is rapidly cleared from chylomicrons and distributed into tissues. This observation and the tissue measurements are consistent with the uptake of newly absorbed HCB by peripheral tissues prior to uptake by the liver. Recently absorbed organochlorines may therefore be deposited in tissues without alteration by metabolism in the liver.

There is evidence for detrimental effects of organochlorine compounds in many systems including reproduction, development, and testicular cancer (8). They are also implicated in effects on energy metabolism that may contribute to obesity (9). The entry of organochlorines into tissues can be important in these processes, and our data contribute to understanding the initial absorption steps.

ACKNOWLEDGMENTS

This work was supported by the National Research Initiative of the USDA Cooperative State Research Education and Extension Service, Grant number 02-00824 and National Institute of Health grants DK 56863 and DK 56910.

REFERENCES

1. Koss, G., and Koransky, W. (1975) Studies on the Toxicology of Hexachlorobenzene I. Pharmacokinetics, *Arch. Toxicol. 34*, 203–212.
2. Vost, A., and Maclean, N. (1984) Hydrocarbon Transport in Chylomicrons and High-Density Lipoproteins in Rat, *Lipids 19*, 423–435.
3. Phan, C.T., Mortimer, B., Martins, I.J., and Redgrave, T.G. (1999) Plasma Clearance of Chylomicrons from Butterfat Is Not Dependent on Saturation: Studies with Butterfat Fractions and Other Fats Containing Triacylglycerols with Low or High Melting Points, *Am. J. Clin. Nutr. 69*, 1151–1161.
4. Fisk, A.T., Rosenberg, G., Cymbalisty, C.D., Stern, G.A., and Muir, D.C.G. (1999) Octanol/Water Partition Coefficients of Toxaphene Congeners Determined by the "Slow-Stirring" Method, *Chemosphere 39*, 2549–2562.
5. Huibers, P.D.T., and Katritzky, A.R. (1998) Correlation of the Aqueous Solubility of Hydrocarbons with Molecular Structure, *J. Chem. Inf. Comput. Sci. 38*, 283–292.
6. Maliwal, B.P., and Guthrie, F.E. (1982) *In vitro* Uptake and Transfer of Chlorinated Hydrocarbons Among Human Lipoproteins, *J. Lipid Res. 23*, 474–479.
7. Burton, M.A., and Bennett, B.G. (1987) Exposure of Man to Environmental Hexachlorobenzene (HCB)—An Exposure Commitment Assessment, *Sci. Total Environ. 66*, 137–146.
8. Toft, G., Hagmar, L., Giwercman, A., and Bonde, J.P. (2004) Epidemiological Evidence on Reproductive Effects of Persistent Organochlorines in Humans, *Reprod. Toxicol. 19*, 5–26.
9. Pelletier, C., Imbeault, P., and Tremblay, A. (2003) Energy Balance and Pollution by Organochlorines and Polychlorinated Biphenyls, *Obes. Rev. 4*, 17–24.

[Received September 17, 2004; accepted November 19, 2004]

Lipid and FA Composition of the Pearl Oyster *Pinctada fucata martensii*: Influence of Season and Maturation

Hiroaki Saito

National Research Institute of Fisheries Science Fisheries Research Agency, Yokohama-shi 236-8648, Japan

ABSTRACT: The lipid and FA composition of the total lipids of the pearl oyster *Pinctada fucata martensii*, in different seasons and in different areas, were analyzed to clarify its lipid physiology and to estimate the possible influence of its prey phytoplankton. TAG and sterols were the major components in the neutral lipids in all conditions, whereas high levels of phospholipids (PE and PC) were found in the polar lipids. The major FA in the TAG in all samples were 14:0, 16:0, and 18:0 as saturated FA (saturates); 16:1n-7, 18:1n-9, and 18:1n-7 as monoenoic FA (monoenes); and 20:4n-6 (arachidonic acid: AA), 20:5n-3 (EPA), and 22:6n-3 (DHA) as PUFA. The major components found in the polar lipids were 16:0 and 18:0 as saturates; 22:2n-9,15 and 22:2n-7,15 as non-methylene-interrupted dienes (NMID), and AA, 22:3n-6,9,15, EPA, and DHA as PUFA. Although it is a marine animal, characteristically high levels of AA were found in both the TAG and phospholipids. This result suggests that lipids of *P. fucata* may be influenced by those of its phytoplanktonic prey. The increase in levels of NMID from TAG to PE with a decrease in those of monoenes suggests that the tissues of this species are able to biosynthesize only the less unsaturated PUFA, such as NMID. In particular, NMID derivatives are considered to be biosynthesized in the PE; thus, they might play a particular role in the membrane, because NMID were characteristically localized only in the PE.

Paper no. L9451 in *Lipids 39*, 997–1005 (October 2004).

The chemical components of pelagic seawater fishes, the FA of fish in particular, have been reported on in detail, with growing recognition of the beneficial uses of dietary fish oils. As for FA determinations of bivalve species, only oyster (Ostreidae), scallop (Pectinidae), and mussel (Mytilidae) lipids have been investigated in detail (for oysters: Refs. 1–3; for scallops: Refs. 4 and 5; for mussels: Refs. 6 and 7). Although the biological and ecological influences on their chemical components are gradually being determined, little information is available as yet on the biochemical constituents of other bivalve species, especially the lipid and FA compositions of bivalves. The pearl oyster, *Pinctada fucata martensii,* is aquacultured in the sea off the coast of Japan and is an important marine resource for pearls in Japan. Although the production of pearls is a key industry in Japan, the other portions of the animals, the soft parts in particular, are mostly thrown away as offal after taking pearls from the shell of the bivalve. Only a few people in a very limited locale in Japan eat the adductor muscle of this bivalve.

On the other hand, recent animal studies have indicated that dietary supplements of n-3 PUFA, such as DHA (22:6n-3), may have beneficial effects on cardiovascular diseases, certain forms of cancer, and aging. Studies of lipids in marine organisms suggest that fish and shellfish can be unique sources of n-3 PUFA such as EPA (20:5n-3) and DHA, which are otherwise not provided in terrestrial oils (8,9).

To clarify the physiology of *P. fucata* and to examine its soft parts as a potential source of n-3 PUFA, the lipid and FA compositions of the total lipids collected in different seasons and in different areas were analyzed. In addition, the relationship between the lipids of this species and those of its prey are discussed (9,10).

MATERIALS AND METHODS

Materials. The samples of *P. fucata* are described in Table 1. Samples 1 and 4 were taken from specimens collected during the spawning season (June and July; seawater temperature, 20 and 23°C), and samples 2 and 3 were from specimens collected during the growing season (November and March; seawater temperature, 11 and 16°C). A total of 41 live specimens of *P. fucata* were obtained from the three different localities and at four different times: Uwajima Bay in the Pacific Ocean (sample 1: latitude 33°19′ N and longitude 132°30′ E in July 1998), the Ago Bay in the Pacific Ocean (samples 2 and 3: latitude 34°22′ N and longitude 136°40′ E in November 1998 and March 1999), and the seashore of Tsushima Island in the Japan Sea (replicate sample 4: latitude 34°22′N and longitude 129°12′E in June 2000). Samples 1 and 4 were from cultivated specimens collected about 1 yr after hatching, and samples 2 and 3 were from cultivated specimens about 1.5 yr after hatching. All the samples were cultivated in the wild and were not provided with artificial food.

Lipid extraction and the analysis of lipid classes. The total soft parts of live samples were immediately immersed in a mixture of chloroform and methanol (2:1, vol/vol) after rinsing them briefly in distilled water and were kept frozen at −40°C under an argon atmosphere for 2 d prior to lipid extraction. Each sample was homogenized in a mixture of chloroform

*Address correspondence at National Research Institute of Fisheries Science, Fisheries Research Agency, 2-12-4, Fuku-ura, Kanazawa-ku,, Yokohama-shi 236-8648, Japan. E-mail: hiroakis@nrifs.affrc.go.jp

Abbreviations: AA, arachidonic acid; CAEP, ceramide aminoethyl phosphonate; DMA, dimethylacetals; DMOX, 4,4-dimethyloxazoline; GE, diacylglyceryl ether(s); NMID; non-methylene-interrupted dienes, PL, phospholipids; SE, steryl ester(s); SFA, saturated fatty acids (saturates); ST, sterols; TFA, total fatty acids; TL, total lipids; WE, wax ester(s).

TABLE 1
Cultivation Locality and Biological Data of the Akoya Pearl Oyster *Pinctada fucata martensii*[a]

Sample no.	Date	Locality				Temperature (°C)	Replicate animals (*n*)	Length (cm)	Width (cm)	Weight (g)
1	July 8, 1998	Uwajima Bay	Pacific Ocean	33°19' N	132°30' E	23	10	5.7 ± 0.2	5.8 ± 0.1	18.6 ± 0.7
2	November 21, 1998	Ago Bay	Pacific Ocean	34°22' N	136°40' E	16	10	7.3 ± 0.2	7.3 ± 0.2	40.0 ± 1.5
3	March 11, 1999	Ago Bay	Pacific Ocean	34°22' N	136°40' E	11	11	7.7 ± 0.2	7.6 ± 0.1	47.1 ± 1.4
4	June 2, 2000	Tsushima Island	Japan Sea	34°22' N	129°20' E	20	10	5.8 ± 0.1	5.5 ± 0.1	28.7 ± 1.3

[a]Results are expressed as mean ± SE (n =10–11). The sex of samples of 2 and 3 was not confirmed, and the sex of samples of 1 and 4 could not be determined because of immaturity.

and methanol (2:1, vol/vol), and a portion of each homogenized sample was extracted according to the procedure of Folch *et al.* (11). The crude total lipids (TL) were separated into classes on silicic acid columns (Kieselgel 60, 70–230 mesh; Merck and Co. Ltd., Darmstadt, Germany), and a quantitative analysis of the lipid constituents was performed using gravimetric analysis of fractions collected by column chromatography. The first eluate (dichloromethane/*n*-hexane, 2:3, vol/vol) was collected as the steryl ester (SE), wax ester (WE), and diacylglyceryl ether (GE) fraction. This was followed by dichloromethane eluting the TAG; dichloromethane/ether (35:1, vol/vol) eluting the sterols (ST); dichloromethane/ether (9:1, vol/vol) eluting the DAG; dichloromethane/methanol (9:1, vol/vol) eluting the FFA; dichloromethane/methanol (1:5, vol/vol) eluting the PE; dichloromethane/methanol (1:20, vol/vol) eluting the ceramide aminoethyl phosphonate (CAEP) with other minor phospholipids (PL); and dichloromethane/methanol (1:50, vol/vol) eluting the PC (12).

Individual lipids from each lipid class, such as PL classes, were identified qualitatively by comparison of the R_f values with standards using TLC (Kieselgel 60, thickness of 0.25 mm for analysis; Merck & Co. Ltd.) and by identifying characteristic peaks using NMR. All sample lipids were dried under argon at room temperature and stored at –40°C.

NMR spectrometry and the determination of lipid classes. Spectra were recorded on a GSX-270 NMR spectrometer (JEOL Co. Ltd., Tokyo, Japan) in the pulsed Fourier transform mode at 270 MHz in a deuterochloroform solution using tetramethylsilane as an internal standard (13).

Some fractions often contained several classes; for instance, the first fraction contained WE, SE, and GE. The molar ratios of WE, GE, and SE were determined by quantitative analysis of NMR results. In NMR, the amount of WE was obtained by the total amount of the combined integrations of the triplet peaks (from 3.90 to 4.20 ppm) as the two protons at the ester alcohol, the amount of GE was obtained by that of the singlet peak (3.50–3.80 ppm) as the two ether protons linked with glycerol carbons, and the amount of SE was obtained by that of the multiplet peak (4.30–4.80 ppm) as one proton at the carbon-linked esterized C-3 alcohol of the sterol. The actual ratio of the WE, SE, and GE in the first fraction was determined as the respective integration divided by the sum of total integrations of the three combined peaks from 3.50 to 4.80 ppm. The actual weight of each class was obtained by calculating the ratio and multiplying by the total weight of the first fraction. Similarly, the third fraction sometimes contained TAG and ST, and had two characteristic peaks: for TAG (3.90–4.40 ppm) an octet-like peak for four protons, and for ST (3.40–3.60 ppm) a multiplet peak for one proton. The actual weights of TAG and ST in the third fraction were obtained by calculating the integration of each divided peak and multiplying by the total weight of the third fraction.

Preparation of methyl esters and GLC of the esters. Individual components of the TAG, PE, and PC fractions were converted to FAME by direct transesterification with boiling methanol containing 1% of concentrated hydrochloric acid under reflux for 1.5 h as previously reported. These methyl esters were purified by using silica gel column chromatography and eluting with dichloromethane/*n*-hexane (2:1, vol/vol).

The composition of the FAME was determined by GLC. Analysis was performed on a Shimadzu GC-8A (Shimadzu Seisakusho Co. Ltd., Kyoto, Japan) and an HP-5890 (Hewlett-Packard Co., Yokogawa Electric Corporation, Tokyo, Japan) gas chromatograph equipped with an Omegawax-250 fused-silica capillary column (30 m × 0.25 mm i.d.; 0.25 μm film; Supelco Japan Co. Ltd., Tokyo, Japan). The injector and column temperatures were held at 230 and 215°C, respectively, and the split ratio was 1:76. Helium was used as the carrier gas at a constant inlet rate of 0.7 mL/min.

Quantification of individual components was performed by means of a Shimadzu Model C-R3A (Shimadzu Seisakusho Co. Ltd.) and an HP ChemStation System (A, 06 revision, Yokogawa HP Co. Ltd., Tokyo, Japan) electronic integrator.

Preparation of 4,4-dimethyloxazoline derivatives (DMOX) and analysis of DMOX by GC–MS. The DMOX derivatives were prepared by adding an excess amount of 2-amino-2-methyl propanol to a small amount of the FAME in a test tube under an argon atmosphere. The mixture was heated at 180°C for 48 h. The reaction mixture was cooled and poured onto saturated brine and extracted three times with *n*-hexane. The extract was then washed with saturated brine and dried over anhydrous sodium sulfate. The solvent was removed under reduced pressure, and the samples were again dissolved in *n*-hexane for analysis by GC–MS (13).

Analysis of the DMOX derivatives was performed on an HP G1800C GCD Series II (Hewlett-Packard Co.) gas chromatograph–mass spectrometer equipped with the same capillary column for determining the respective FA with HP WS software (HP Kayak XA, G1701BA version, PC workstations; Hewlett-Packard Co.). The temperatures of the injector and the column

were held at 230 and 215°C, respectively. The split ratio was 1:75, and the ionization voltage was 70 eV, respectively. Helium was used as the carrier gas at a constant inlet rate of 0.7 mL/min.

FAME were identified (i) using marine lipid methyl esters as standards (Omegawax test mixture No. 4-8476; Supelco Japan Ltd.) and (ii) by comparison of mass spectral data obtained by GC–MS.

RESULTS AND DISCUSSION

Lipid content of P. fucata. Biological data on the *P. fucata* samples are listed in Table 1. The sizes and weights of samples 2 and 3 were markedly greater than those of samples 1 and 4, showing that the *P. fucata* grew during the growing season. The TL content and lipid classes are shown in Table 2. The TL content was 0.4–2.0% in all culture conditions; all the mean lipid contents were very low, similar to those of other oysters (*Crassostrea* spp.; Ref. 2). In addition, the lipid contents were slightly higher (1.0–2.0%) during the spawning season (June and July) than in the growing season (0.4–0.7%, November and March); the comparatively high lipid levels in the spawning season suggest that the lipids may play some role in maturation (14), similar to that in finfishes (15); this phenomenon differed from the tendency toward seasonal variation of glycogen, whose levels are higher in the growing season (16). Otherwise, the higher lipid contents in June and July suggest that the warm seawater might have promoted accumulation of lipids related to a high metabolic activity in this season. The lowest lipid content, seen in sample 3, suggests that the most unfavorable condition, i.e., the low temperature in this season, disturbed the normal lipid metabolism; the most suitable temperature for this bivalve is from 18 to 25°C, and its lowest survival temperature is generally known to be about 13°C.

Lipid classes in the total lipids of P. fucata. The lipid classes of *P. fucata* are shown in Table 2. TAG [7.4–27.3% of the total FA (TFA)] and ST (13.6–39.6% of TFA) were the major components in the neutral lipids in all specimens, with low levels of WE (0.1–0.4% of TFA), SE (0.5–7.4% of TFA), GE (0.9–3.1% of TFA), and DAG (0.3–0.9% of TFA). In contrast, the species had high levels of PL (PE, 20.9–29.9% of TFA; PC, 8.7–13.8% of TFA). In addition, significant levels of CAEP (7.1–11.9% of TFA) were found in the polar lipids with low levels of sphingolipids. The low level of neutral lipids reflected the low lipid content in the species (0.4–2.0%), because it is a lean organism (17,18). In general, the proportions of PL in tissue TL are constant in all animals because they are important as cell membrane lipids, except for the *Euphausia* sp. (*Euphausia pacifica*; Ref. 19), whereas the levels of depot lipids vary (9). The mean PL contents in tissues of all marine organisms can be less than 1% of their tissue weight (17,18). In fact, all of its actual PL levels (0.12–0.76% of total tissue weight) were less than 1% of the tissue weight, similar to those of other marine animals.

The lipid classes in sample 3 differed from those in other samples; in particular, the levels of ST in the sample were highest (7.4 ± 0.9% for SE and 39.6 ± 1.9% for ST). This result may also have been caused by a less favorable condition such as the lower seawater temperature; the high levels of SE and ST might be viewed as the result of low levels of depot TAG.

Similar to data on the Pacific oyster reported by Soudant *et al*. (3), significant levels of FFA (6.9–10.8% of TFA) were found in TL; this may be a result of digested products of glycerol derivatives in its viscera that were degraded by enzymatic metabolism, because the sampling of the whole soft part contained digestive glands that may have contained active enzymes for digestion.

The lipids of *P. fucata* contained mainly glycerol derivatives (TAG, FFA, PE, and PC), and the total proportion of these derivatives reached about 48–73%, with low levels of other depot lipids such as WE and GE. Comparatively high levels of ST (13.2–39.6%) were found, and the ST fractions were considered to contain several kinds of sterols; NMR analysis displayed at least two singlet peaks of C-18-positional methyl moieties of ST.

These lipid classes may be a characteristic of this bivalve species except for the differences in the SE and ST levels in sample 3, which grew under less favorable conditions, all other

TABLE 2
Lipid Contents and Lipid Classes of *Pinctada fucata martensii*[a]

Sample no.	No. of replicates	Lipid contents[b]	WE[c]	SE[c]	GE[c]	TAG[c]	ST[c]
1	9	2.0 ± 0.2	0.1 ± 0.0	0.5 ± 0.2	1.5 ± 0.3	27.3 ± 3.7	13.6 ± 2.2
2	10	0.7 ± 0.0	0.3 ± 0.1	0.9 ± 0.3	1.6 ± 0.4	13.9 ± 1.5	24.7 ± 1.5
3	11	0.4 ± 0.0	0.4 ± 0.2	7.4 ± 0.9	0.9 ± 0.1	7.4 ± 1.0	39.6 ± 1.9
4	10	1.0 ± 0.1	0.2 ± 0.1	0.7 ± 0.2	3.6 ± 0.4	14.0 ± 1.8	22.9 ± 1.5
		DAG[c]	FFA[c]	PE[c]	CAEP[c,d]	PC[c,e]	
1	9	0.9 ± 0.2	6.9 ± 1.4	24.2 ± 4.1	11.9 ± 2.0	13.8 ± 2.9	
2	10	0.7 ± 0.1	10.8 ± 2.5	24.4 ± 1.2	10.9 ± 2.2	12.8 ± 2.1	
3	11	0.8 ± 0.5	10.1 ± 1.5	20.9 ± 2.4	11.2 ± 2.4	8.7 ± 1.9	
4	10	0.3 ± 0.1	9.3 ± 0.6	30.8 ± 1.1	6.3 ± 1.8	12.5 ± 0.9	

[a]Data are mean ± SE (n = 9–11). WE, wax esters; SE, steryl esters; GE, glyceryl ethers; ST, sterols; CAEP, ceramide aminoethyl phosphate.
[b]Results are expressed as weight percent of wet tissue.
[c]Results are expressed as weight percent of total lipids.
[d]CAEP fractions contain small amounts of other minor phospholipids.
[e]PC fractions contain small amounts of sphingomyerlin.

TABLE 3
FA Composition of TAG of *Pinctada fucata martensii* Examined[a]

	1	2	3	4
Entry	Mean SE	Mean SE	Mean SE	Mean SE
Total saturated	30.2 ± 1.9	31.2 ± 1.0	29.8 ± 1.0	28.6 ± 0.6
14:0	5.7 ± 0.6	6.0 ± 0.3	1.5 ± 0.1	2.9 ± 0.1
16:0	15.3 ± 2.0	15.3 ± 0.5	12.4 ± 0.6	15.1 ± 0.5
17:0	1.0 ± 0.2	1.3 ± 0.1	2.2 ± 0.1	1.7 ± 0.1
18:0	5.9 ± 0.3	6.4 ± 0.4	10.1 ± 0.6	7.0 ± 0.2
Total monoenoic	17.5 ± 0.4	23.0 ± 0.5	20.9 ± 0.9	16.6 ± 0.3
16:1n-7	6.3 ± 0.6	8.6 ± 0.3	2.1 ± 0.2	4.1 ± 0.2
18:1n-9	2.1 ± 0.3	3.5 ± 0.1	7.5 ± 1.1	3.7 ± 0.1
18:1n-7	3.9 ± 0.1	5.0 ± 0.2	3.4 ± 0.4	4.1 ± 0.1
18:1n-5	0.2 ± 0.0	0.2 ± 0.0	0.3 ± 0.0	0.2 ± 0.0
19:1n-9	0.4 ± 0.0	0.8 ± 0.0	0.3 ± 0.1	0.2 ± 0.0
20:1n-11	1.5 ± 0.3	1.8 ± 0.1	4.3 ± 0.5	1.1 ± 0.0
20:1n-9	0.9 ± 0.0	1.0 ± 0.0	1.2 ± 0.1	1.1 ± 0.0
20:1n-7	1.3 ± 0.1	1.4 ± 0.1	1.1 ± 0.2	0.8 ± 0.0
Total NMID	3.3 ± 0.5	3.5 ± 0.2	6.7 ± 0.4	3.0 ± 0.1
20:2n-7,15	0.2 ± 0.0	0.2 ± 0.1	0.8 ± 0.3	0.1 ± 0.0
22:2n-9,15	0.9 ± 0.2	0.9 ± 0.1	1.7 ± 0.2	1.2 ± 0.0
22:2n-7,15	1.9 ± 0.3	2.0 ± 0.1	4.0 ± 0.2	1.5 ± 0.1
Total polyenoic	47.2 ± 2.0	40.3 ± 1.3	39.4 ± 1.2	48.9 ± 0.7
Total n-4 polyenoic	2.5 ± 0.2	4.7 ± 0.2	2.5 ± 0.2	1.5 ± 0.1
16:2n-4	0.6 ± 0.1	1.3 ± 0.1	0.2 ± 0.0	0.3 ± 0.0
16:3n-4	0.5 ± 0.1	1.2 ± 0.1	0.4 ± 0.0	0.5 ± 0.0
16:4n-1	0.7 ± 0.3	1.0 ± 0.1	1.1 ± 0.2	0.3 ± 0.0
Total n-6 polyenoic	13.0 ± 0.3	6.4 ± 0.2	11.6 ± 0.4	8.7 ± 0.3
18:2n-6	1.2 ± 0.1	1.6 ± 0.1	1.3 ± 0.1	2.2 ± 0.1
20:2n-6	0.6 ± 0.0	0.7 ± 0.1	1.0 ± 0.1	1.3 ± 0.1
20:4n-6	8.6 ± 0.4	2.1 ± 0.1	5.3 ± 0.4	2.4 ± 0.1
22:3n-6,9,15	1.0 ± 0.1	1.2 ± 0.1	2.3 ± 0.1	1.5 ± 0.1
22:4n-6	0.9 ± 0.1	0.2 ± 0.0	0.6 ± 0.0	0.3 ± 0.0
22:5n-6	0.4 ± 0.0	0.4 ± 0.0	0.7 ± 0.0	0.6 ± 0.1
Total n-3 polyenoic	31.6 ± 2.0	29.2 ± 1.1	25.3 ± 1.2	38.6 ± 0.6
18:3n-3	1.0 ± 0.1	2.4 ± 0.1	0.8 ± 0.1	2.3 ± 0.1
18:4n-3	1.6 ± 0.2	3.7 ± 0.2	0.7 ± 0.1	3.0 ± 0.1
20:4n-3	0.6 ± 0.1	0.7 ± 0.0	0.5 ± 0.1	1.1 ± 0.0
20:5n-3	18.0 ± 1.9	12.3 ± 0.5	8.5 ± 0.7	12.2 ± 0.2
22:5n-3	1.1 ± 0.1	0.8 ± 0.0	1.4 ± 0.1	1.2 ± 0.1
22:6n-3	9.1 ± 0.4	9.0 ± 0.5	13.0 ± 0.5	18.2 ± 0.4
Total FA	94.8 ± 0.4	94.6 ± 0.2	90.0 ± 0.7	94.6 ± 0.1

[a]Data are mean ± SE for several samples (n = 9–29).
[b]In Tables 3–5, the major FA were selected if at least one mean datum was detected at a level of 0.8% or more of total FA.
NMID, non-methylene interrupted diene(s).

samples analyzed which were collected from different areas and in different seasons (samples 1, 2, and 4) were similar to each other (Table 2).

FA composition of TAG depot lipids in P. fucata. FA in the TAG (more than 0.8% of TFA) are shown in Table 3. More than 60 kinds of FA were found in the TAG and PL of *P. fucata*. The wide range of FA detected in the lipids might have been caused by its omnivorous behavior (16), similar to that of higher trophic marine animals (9). Although the FA composition of TAG varied among specimens because of the seasonal and spatial variations of the prey lipids, the major FA were almost the same under the four different conditions. Nine dominant FA (more than about 2% of TFA) in TAG were found among the four different conditions—14:0 (1.5–6.0%), 16:0 (12.4–15.3%), and 18:0 (5.9–10.1%) as saturates; 16:1n-7 (2.1–8.6%), 18:1n-9 (2.1–7.5%), and 18:1n-7 (3.4–5.0%) as monoenes; arachidonic acid (AA) (2.1–8.6%) as n-6 PUFA; and EPA (8.5–18.0%) and DHA (9.0–18.8%) as n-3 PUFA—with significant levels of 11 FA—17:0 as saturates; 20:1n-11, 20:1n-9, and 20:1n-7 as monoenes; 18:2n-6 as dienes; 22:2n-9,15 and 22:2n-7,15 as non-methylene-interrupted dienoic (NMID) FA; 22:3n-6,9,15 as n-6 PUFA; and 18:3n-3, 18:4n-3, and 22:5n-3 (DPA: docosapentaenoic acid) as n-3 PUFA.

In general, both the short-chain saturates (14:0, 16:0, 17:0, and 18:0) and unsaturates (16:1n-7, 18:1n-7, 18:1n-9, 18:2n-6, 18:3n-3, 18:4n-3, and EPA) are also contained in the lipids of

phytoplankton (Bacillariophyceae, Haptophyceae, Cryptophyceae, Eustigmatophytes, and Euglenophyceae: Ref. 20). For example, several species of diatoms (Bacillariophyceae: Refs. 21 and 22) and Eustigmatophytes (23) have markedly high EPA contents (more than 20% of TFA). Furthermore, some phytoplankton lipids often contain significant levels of AA, with high levels of FA, such as 14:0 and 16:0, 16:1n-7, and EPA (Bacillariophyceae, Ref. 24; Rhodophyceae, Refs. 25 and 26; Haptophyceae, Refs. 27 and 28). Taking into account the microalgal biomass and species variety of phytoplankton in the sea, these results suggest that diatoms might be the major prey of *P. fucata* as an EPA and AA source.

On the other hand, it is well known that some phytoplankton, such as dinoflagellates, contain noticeable levels of DHA (more than 3% of TFA), with significant levels of EPA (more than 5% of TFA) (Bacillariophyceae: Refs. 20,22,28; dinoflagellates: Refs. 24,28–30; Haptophyceae: Ref. 27,28,31; Chrysophyceae and Xanthophyceae: Ref. 24). The DHA in the TAG of *P. fucata* might have originated specifically from these phytoplankton classes, mainly supplied by dinoflagellates.

Even though the TAG are only depot lipids, the three PUFA—AA (2.1–8.6%), EPA (8.5–18.0%), and DHA (9.0–18.8%)—in the TAG of *P. fucata* were significantly high. The high EPA levels might be similar to the TAG of other marine bivalves (5,32). Furthermore, the high level of AA in the TAG is an unusual characteristic, because this FA is a minor component in the depot lipids of other marine animals; only trace amounts are usually found in the depot TAG of other marine animals, such as copepods, which are at the same trophic level. Compared with the FA composition of phytoplankton, the high levels of both AA and EPA in TAG of *P. fucata* correspond well with those in some diatom lipids, except for NMID.

FA composition in tissue PL in P. fucata. In contrast to the FA composition of the TAG, the major FA (more than 3% of TFA) of the PL were more limited, as shown in Tables 4 and 5. In the FA composition of PE, low levels of dimethylacetals (DMA), such as DMA 18:0, were included (Table 4). The theoretical values of the FA composition were obtained by deleting the DMA from the TFA of PE. After this treatment, seven major FA were consistently found in the PE of all specimens under the four different conditions (2% or more of the TFA)—18:0 (5.4–7.7%) as saturates; 22:2n-9,15 (7.8–12.9%) and 22:2n-7,15 (2.4–8.2%) as NMID; AA (8.8–11.4%) and 22:3n-6,9,15 (4.3–7.2%) as n-6 PUFA; EPA (7.7–12.8%) and DHA (20.1–33.2%) as n-3 PUFA—with significant amounts of seven other FA—16:0 as saturates; 20:1n-11 and 20:1n-9 as monoenes; 22:4n-6 as n-6 PUFA; and DPA as n-3 PUFA.

The five FA were also the major components in the PC: 16:0 (14.9–20.0%) and 18:0 (3.6–6.9%) as saturates, 22:2n-7,15 (1.1–3.5%) as NMID; AA (3.7–9.5%) as n-6 PUFA; and EPA (7.6–8.8%) and DHA (23.2–40.9%) as n-3 PUFA. Significant amounts of 10 FA—17:0 as saturates; 18:1n-9, 18:1n-7, and 20:1n-11 as monoenes; 22:2n-9,15 as NMID; 22:3n-6,9,15 and 22:5n-6 as n-6 PUFA; and DPA as n-3 PUFA—were found in the PC. Although the detailed FA levels of the PE differed slightly from those of the PC, the profile of these major components of the PE were close to those of the PC. In particular, the total amounts of PUFA in both PE and PC (40.3–60.6% for PE and 51.4–59.0% for PC) were high under all four conditions; therefore, the PE and PC of the *P. fucata* were rich sources of PUFA, similar to those in other marine animals (17,18).

The high levels of total PUFA in the PL suggest the accumulation of PUFA in the tissue, because bivalves may not be able to biosynthesize PUFA such as AA and DHA (10,33). In particular, the high levels of AA, EPA, and DHA might be the result of a concentration of these PUFA in the tissue, because high levels of PUFA were consistently found in the PL, compared with those in the depot lipids. Moreover, significant levels of n-6 PUFA, such as 22:4n-6, which is a the elongation product of AA, were found in the PL, compared with the trace levels found in the TAG. Similarly, the level of AA in the PL increased slightly, compared with that in the TAG. As for n-3 PUFA, the level of DHA increased markedly in both the PE and PC, and DPA increased slightly in the PL, whereas the shorter-chain unsaturates 18:4n-3 and EPA decreased in the PL compared with those in the TAG. The species may selectively concentrate longer and more highly unsaturated FA in its tissues as membrane lipids.

During the spawning season, the DHA content in PC fluctuated between 23.2 and 40.8% of TFA (samples 1 and 4). This amount may be influenced by environmental and seasonal differences in the prey phytoplankton lipids, because the total PUFA levels (NMID, n-4, n-6, and n-3 PUFA: 58.9% of TFA for specimens of sample 1, and 59.0% for those of sample 4) in the spawning season did not differ much from each other. Otherwise, in the spawning season, the fluctuation of its FA composition might be influenced by maturation, because differences in the concentrations of specific chemical components in the tissues were often found between before and after spawning.

Biosynthesis of the NMID in the P. fucata *tissues.* The notable levels of C_{22} NMID in TAG, PC, and in particular PE, suggest that this species may have enzymes in its tissues, for the biosynthetic elongation to 22-carbon chains and for the desaturation to NMID by Δ5 desaturase, similar to the synthetic pathway in other bivalves (10,33–37), because these dienes increased with a decrease in the saturates and monoenes (from TAG to PL). For instance, the levels of long-chain NMID 22:2n-9,15 and 22:2n-7,15 increased markedly, while there were decreases of 14:0, 16:1n-7, 18:1n-9, and 18:1n-7 in the PE, compared with high levels of the shorter-chain and less unsaturated FA in the TAG. This result suggests that these NMID might originate from 18:1n-9 and 18:1n-7. The significantly high level of 22:3n-6,9,15, which is considered to be derived by Δ5 desaturation after the elongation of linoleic acid (18:2n-6,9), also suggests the presence of the desaturase, similar to other NMID derivatives.

All changes in FA from depot to tissue lipids under the four different conditions had the same tendency, in which shorter-chain and less unsaturated FA decreased in the polar lipids. These facts suggest that elongation and desaturation mechanisms exist in *P. fucata*.

TABLE 4
FA Composition of PE of *Pinctada fucata martensii* examined[a]

	1 Mean ± SE	Calcd. 1 Mean ± SE	2 Mean ± SE	Calcd. 2 Mean ± SE	3 Mean ± SE	Calcd. 3 Mean ± SE	4 Mean ± SE	Calcd. 4 Mean ± SE
Total saturated	12.9 ± 1.6	12.8 ± 1.1	7.9 ± 0.4	10.1 ± 0.4	7.7 ± 0.5	9.3 ± 0.3	7.9 ± 0.2	10.7 ± 0.3
14:0	1.4 ± 0.2	1.3 ± 0.1	1.1 ± 0.1	1.4 ± 0.1	0.6 ± 0.1	0.7 ± 0.1	0.7 ± 0.1	0.9 ± 0.1
16:0	2.2 ± 0.5	2.0 ± 0.3	0.9 ± 0.1	1.1 ± 0.1	1.1 ± 0.2	1.3 ± 0.2	0.6 ± 0.0	0.8 ± 0.1
17:0	0.8 ± 0.1	0.9 ± 0.1	0.5 ± 0.1	0.7 ± 0.1	0.5 ± 0.0	0.6 ± 0.0	0.4 ± 0.0	0.6 ± 0.0
18:0	7.2 ± 0.8	7.3 ± 0.6	4.4 ± 0.2	5.6 ± 0.2	4.5 ± 0.3	5.4 ± 0.2	5.7 ± 0.2	7.7 ± 0.2
Total monoenoic	10.1 ± 0.8	10.4 ± 0.5	6.1 ± 0.2	7.8 ± 0.4	4.6 ± 0.3	5.7 ± 0.4	7.6 ± 0.2	10.2 ± 0.2
16:1n-7	0.5 ± 0.2	0.4 ± 0.1	0.5 ± 0.0	0.6 ± 0.1	0.4 ± 0.1	0.5 ± 0.1	0.4 ± 0.0	0.5 ± 0.1
18:1n-9	0.7 ± 0.1	0.7 ± 0.1	0.5 ± 0.1	0.6 ± 0.1	0.2 ± 0.0	0.3 ± 0.0	1.3 ± 0.0	1.8 ± 0.1
18:1n-7	0.8 ± 0.1	0.9 ± 0.1	0.6 ± 0.1	0.8 ± 0.1	0.7 ± 0.2	0.9 ± 0.2	0.5 ± 0.1	0.7 ± 0.1
18:1n-5	0.2 ± 0.0	0.2 ± 0.0	0.3 ± 0.1	0.5 ± 0.2	0.1 ± 0.0	0.1 ± 0.0	0.1 ± 0.0	0.2 ± 0.0
19:1n-9	0.2 ± 0.0	0.2 ± 0.1	0.3 ± 0.1	0.3 ± 0.1	0.4 ± 0.1	0.5 ± 0.1	0.1 ± 0.0	0.1 ± 0.0
20:1n-11	2.5 ± 0.2	2.7 ± 0.1	1.2 ± 0.1	1.6 ± 0.1	0.6 ± 0.1	0.7 ± 0.1	1.7 ± 0.1	2.2 ± 0.1
20:1n-9	2.8 ± 0.3	3.0 ± 0.2	1.6 ± 0.1	2.0 ± 0.1	0.9 ± 0.1	1.1 ± 0.1	2.3 ± 0.1	3.0 ± 0.1
20:1n-7	1.5 ± 0.2	1.5 ± 0.2	0.7 ± 0.0	0.9 ± 0.0	0.4 ± 0.0	0.4 ± 0.0	0.7 ± 0.0	1.0 ± 0.0
Total NMID	19.1 ± 0.9	20.7 ± 0.7	17.6 ± 0.8	22.5 ± 0.8	9.2 ± 0.9	11.0 ± 0.6	14.4 ± 0.3	19.3 ± 0.3
20:2n-7,15	0.4 ± 0.1	0.5 ± 0.1	0.5 ± 0.1	0.6 ± 0.1	0.3 ± 0.0	0.3 ± 0.0	0.5 ± 0.0	0.7 ± 0.0
22:2n-9,15	11.7 ± 0.6	12.6 ± 0.5	10.1 ± 0.6	12.8 ± 0.6	6.5 ± 0.6	7.8 ± 0.5	9.6 ± 0.3	12.9 ± 0.3
22:2n-7,15	6.4 ± 0.3	6.8 ± 0.2	6.4 ± 0.2	8.2 ± 0.2	2.1 ± 0.3	2.4 ± 0.3	3.7 ± 0.1	4.9 ± 0.2
Total polyenoic	46.7 ± 1.2	51.8 ± 1.1	44.6 ± 1.8	56.9 ± 0.6	59.0 ± 2.4	71.8 ± 0.7	42.5 ± 0.7	56.9 ± 0.4
Total n-4 polyenoic	0.3 ± 0.0	0.3 ± 0.0	0.2 ± 0.0	0.3 ± 0.1	0.1 ± 0.0	0.1 ± 0.0	0.2 ± 0.0	0.3 ± 0.0
16:2n-4	0.0 ± 0.0	0.0 ± 0.0	0.1 ± 0.0	0.1 ± 0.1	0.0 ± 0.0	0.0 ± 0.0	0.1 ± 0.0	0.1 ± 0.0
16:3n-4	0.0 ± 0.0	0.0 ± 0.0	0.0 ± 0.0	0.0 ± 0.0	0.0 ± 0.0	0.0 ± 0.0	0.0 ± 0.0	0.0 ± 0.0
16:4n-1	0.0 ± 0.0	0.0 ± 0.0	0.0 ± 0.0	0.0 ± 0.0	0.0 ± 0.0	0.0 ± 0.0	0.0 ± 0.0	0.0 ± 0.0
Total n-6 polyenoic	18.1 ± 0.7	20.2 ± 0.5	14.9 ± 0.7	19.0 ± 0.4	17.5 ± 1.0	21.3 ± 0.7	14.6 ± 0.3	19.6 ± 0.3
18:2n-6	0.3 ± 0.0	0.3 ± 0.1	0.3 ± 0.0	0.4 ± 0.1	0.3 ± 0.0	0.4 ± 0.1	0.3 ± 0.0	0.3 ± 0.0
20:2n-6	1.0 ± 0.2	1.1 ± 0.2	0.5 ± 0.1	0.6 ± 0.1	0.2 ± 0.0	0.3 ± 0.0	0.3 ± 0.0	0.4 ± 0.0
20:4n-6	8.6 ± 0.6	9.6 ± 0.7	6.9 ± 0.4	8.8 ± 0.3	9.4 ± 0.5	11.4 ± 0.5	6.9 ± 0.2	9.3 ± 0.2
22:3n-6,9,15	4.3 ± 0.2	4.7 ± 0.2	4.2 ± 0.2	5.3 ± 0.2	3.6 ± 0.2	4.3 ± 0.2	5.4 ± 0.1	7.2 ± 0.1
22:4n-6	3.0 ± 0.2	3.4 ± 0.1	1.8 ± 0.1	2.3 ± 0.1	2.5 ± 0.2	3.1 ± 0.2	1.1 ± 0.1	1.5 ± 0.1
22:5n-6	0.8 ± 0.1	1.0 ± 0.1	1.1 ± 0.1	1.4 ± 0.1	1.5 ± 0.1	1.8 ± 0.1	0.5 ± 0.0	0.7 ± 0.0
Total n-3 polyenoic	26.4 ± 2.1	31.3 ± 1.5	29.5 ± 1.2	37.6 ± 0.7	41.3 ± 1.8	50.3 ± 1.2	27.7 ± 0.6	37.0 ± 0.4
18:3n-3	0.0 ± 0.0	0.0 ± 0.0	0.1 ± 0.0	0.1 ± 0.0	0.0 ± 0.0	0.1 ± 0.0	0.2 ± 0.0	0.3 ± 0.0
18:4n-3	0.0 ± 0.0	0.0 ± 0.0	0.0 ± 0.0	0.0 ± 0.0	0.0 ± 0.0	0.0 ± 0.0	0.1 ± 0.0	0.1 ± 0.0
20:4n-3	0.3 ± 0.0	0.4 ± 0.0	0.1 ± 0.0	0.2 ± 0.0	0.2 ± 0.0	0.2 ± 0.0	0.1 ± 0.0	0.1 ± 0.0
20:5n-3	6.6 ± 0.5	7.7 ± 0.6	7.0 ± 0.2	9.0 ± 0.4	10.4 ± 0.6	12.8 ± 0.7	7.5 ± 0.2	10.1 ± 0.3
22:5n-3	2.2 ± 0.2	2.6 ± 0.2	2.4 ± 0.1	3.0 ± 0.0	3.1 ± 0.2	3.8 ± 0.1	1.8 ± 0.1	2.5 ± 0.0
22:6n-3	16.7 ± 1.7	20.1 ± 1.1	19.6 ± 1.1	24.8 ± 0.9	27.3 ± 1.4	33.2 ± 1.0	17.7 ± 0.5	23.6 ± 0.4
Total FA	86.8 ± 2.1	95.7 ± 0.3	76.3 ± 2.6	97.3 ± 0.4	80.5 ± 3.6	97.8 ± 0.3	72.5 ± 1.0	97.0 ± 0.2
DMA 15:0	0.0 ± 0.0		0.0 ± 0.0		0.0 ± 0.0		0.1 ± 0.0	
DMA 16:0	0.2 ± 0.1		0.6 ± 0.1		0.5 ± 0.1		0.9 ± 0.1	
DMA 17:0	0.4 ± 0.1		0.9 ± 0.1		0.7 ± 0.1		1.2 ± 0.1	
DMA 17:0i	0.1 ± 0.0		0.0 ± 0.0		0.0 ± 0.0		0.1 ± 0.1	
DMA 18:0	6.6 ± 1.7		17.0 ± 2.1		13.8 ± 3.0		20.1 ± 0.8	
DMA 18:0i	0.3 ± 0.1		0.7 ± 0.1		0.9 ± 0.2		1.1 ± 0.1	
DMA 19:0	0.2 ± 0.0		0.2 ± 0.1		0.0 ± 0.0		0.2 ± 0.0	
DMA 19:0i	0.6 ± 0.1		0.9 ± 0.1		1.1 ± 0.2		1.0 ± 0.1	
DMA 20:0	0.1 ± 0.0		0.1 ± 0.0		0.1 ± 0.0		0.2 ± 0.0	
DMA 18:1	0.8 ± 0.2		0.8 ± 0.1		0.3 ± 0.1		0.2 ± 0.0	
DMA 20:1	0.1 ± 0.0		0.4 ± 0.1		0.2 ± 0.1		0.3 ± 0.0	
Total DMA	9.4 ± 2.2		21.6 ± 2.7		17.7 ± 3.6		25.3 ± 1.0	

[a]Data are mean ± SE for several samples (n = 9–29).
[b]In Tables 3–5, the major FA were selected if at least one mean datum was detected at a level of 0.8% or more of total FA. DMA, dimethyl acetals; i, abbreviation of the "iso"-compound. For other abbreviations see Table 3.

Accumulation of n-3 PUFA in the lipids of P. fucata. In the marine food chain, many pelagic fishes accumulate n-3 PUFA, such as DHA, which may originate from the phytoplankton (8). In general, DHA is the dominant PUFA in both the PE and PC of almost all higher trophic-level marine animals after accumulation in the food chain (17,18,38). Moreover, DHA is required by all marine fish because they are unable to biosynthesize this EFA (8,39,40). Although the high levels of n-3 PUFA in *P. fucata* PL were also similar to the results reported for other marine animals (17), fluctuations of the respective PUFA were

TABLE 5
FA Composition of PC of *Pinctada fucata martensii* Examined[a]

	1	2	3	4
Entry	Mean ± SE	Mean ± SE	Mean ± SE	Mean ± SE
Total saturated	26.9 ± 0.7	28.1 ± 1.1	23.8 ± 1.1	24.9 ± 0.7
14:0	0.8 ± 0.1	0.5 ± 0.0	0.3 ± 0.0	0.3 ± 0.0
16:0	16.7 ± 2.1	20.0 ± 0.8	14.9 ± 1.2	17.8 ± 0.5
17:0	1.5 ± 0.1	2.1 ± 0.1	2.9 ± 0.2	1.9 ± 0.1
18:0	6.9 ± 1.8	4.2 ± 0.4	4.3 ± 0.4	3.6 ± 0.2
Total monoenoic	12.5 ± 0.5	12.6 ± 1.0	9.9 ± 0.7	8.1 ± 0.2
16:1n-7	1.2 ± 0.1	1.3 ± 0.1	0.6 ± 0.1	0.5 ± 0.0
18:1n-9	2.0 ± 0.3	2.4 ± 0.1	2.8 ± 0.2	1.2 ± 0.2
18:1n-7	2.7 ± 0.2	3.1 ± 0.1	1.4 ± 0.1	2.2 ± 0.1
18:1n-5	0.1 ± 0.0	0.1 ± 0.0	0.1 ± 0.0	0.9 ± 0.2
19:1n-9	0.2 ± 0.1	0.1 ± 0.0	0.1 ± 0.0	0.1 ± 0.0
20:1n-11	3.2 ± 0.5	3.3 ± 0.6	2.3 ± 0.4	0.8 ± 0.1
20:1n-9	0.9 ± 0.1	0.8 ± 0.1	0.8 ± 0.1	0.6 ± 0.0
20:1n-7	1.1 ± 0.1	0.8 ± 0.1	0.6 ± 0.1	0.4 ± 0.0
Total NMIDs	5.3 ± 1.4	5.0 ± 0.4	5.9 ± 0.7	2.5 ± 0.1
20:2n-7, 15	0.2 ± 0.1	0.2 ± 0.0	0.3 ± 0.0	0.1 ± 0.0
22:2n-9, 15	2.1 ± 0.9	1.3 ± 0.2	1.8 ± 0.3	1.1 ± 0.1
22:2n-7, 15	2.7 ± 0.4	3.4 ± 0.3	3.5 ± 0.5	1.1 ± 0.1
Total polyenoic	53.6 ± 1.5	53.2 ± 2.0	58.0 ± 1.3	62.4 ± 0.7
Total n-4 polyenoic	1.6 ± 0.3	1.4 ± 0.2	1.0 ± 0.1	1.4 ± 0.1
16:2n-4	0.1 ± 0.0	0.1 ± 0.0	0.1 ± 0.0	0.2 ± 0.0
16:3n-4	0.2 ± 0.0	0.2 ± 0.0	0.2 ± 0.0	0.3 ± 0.0
16:4n-1	1.1 ± 0.3	0.9 ± 0.2	0.6 ± 0.1	0.9 ± 0.1
Total n-6 polyenoic	16.4 ± 0.5	10.9 ± 0.3	12.8 ± 0.4	8.6 ± 0.1
18:2n-6	0.9 ± 0.1	1.0 ± 0.0	0.6 ± 0.0	1.0 ± 0.0
20:2n-6	0.6 ± 0.0	0.5 ± 0.0	0.4 ± 0.1	0.4 ± 0.0
20:4n-6	9.5 ± 0.4	4.5 ± 0.1	6.1 ± 0.3	3.7 ± 0.1
22:3n-6,9,15	1.5 ± 0.3	1.9 ± 0.0	2.6 ± 0.1	1.3 ± 0.1
22:4n-6	2.2 ± 0.2	0.9 ± 0.1	1.1 ± 0.1	0.8 ± 0.0
22:5n-6	1.4 ± 0.1	1.8 ± 0.1	1.9 ± 0.1	1.4 ± 0.0
Total n-3 polyenoic	35.6 ± 1.1	41.0 ± 1.7	44.1 ± 1.2	52.3 ± 0.7
18:3n-3	0.6 ± 0.1	1.0 ± 0.0	0.5 ± 0.0	0.6 ± 0.0
18:4n-3	0.4 ± 0.1	0.6 ± 0.0	0.2 ± 0.0	0.5 ± 0.0
20:4n-3	0.2 ± 0.0	0.2 ± 0.0	0.2 ± 0.0	0.3 ± 0.0
20:5n-3	8.6 ± 0.6	7.6 ± 0.4	8.4 ± 0.6	7.9 ± 0.2
22:5n-3	2.6 ± 0.1	2.0 ± 0.1	2.5 ± 0.1	2.1 ± 0.1
22:6n-3	23.2 ± 1.1	29.6 ± 1.2	32.3 ± 1.1	40.9 ± 0.8
Total FA	93.0 ± 1.5	93.9 ± 0.5	91.7 ± 0.9	95.4 ± 0.2

[a]Data are mean ± SE for several samples (n = 9–29).
[b]In the Tables 3–5, the major FA are selected, if at least one mean datum was detected at a level of 0.8% or more of total FA.

found in the polar lipids. For example, the DHA in PE fluctuated from 18.4 to 33.2%, and that in PC fluctuated from 23.2 to 40.9%; the AA (9.5% of TFA) seemingly compensated for the lack of DHA (23.2% of TFA) in the FA composition of PC in sample 1. This result suggests that mollusks might not have an absolute requirement for DHA as an EFA, and that *P. fucata* might maintain the higher PUFA only for the fluidity of the cell membranes. This speculation is supported by some reports of extremely low levels of DHA in tissue lipids of some gastropod mollusks (10,34,35,41).

Relationship between prey lipids and the concentration of AA in the lipids of P. fucata. With respect to the level of PUFA, freshwater fish generally take in terrestrial prey rich in n-6 PUFA; consequently, they have comparatively high levels of n-6 PUFA, such as linoleic acid and AA, in their lipids (42). In contrast, marine organisms have mainly n-3 FA as PUFA; therefore, AA is usually undetectable or negligible in marine animal lipids. However, we found that *Siganus canaliculatus*, which is a typical subtropical coral fish, has significant levels of AA with consistently high DHA levels in its lipids (43). It is an herbivorous animal that prefers some seaweeds (macroalgae), such as *Cladosiphon* spp., and accumulates AA that originates from the lipids of brown algae. This species has a vegetarian feeding habit, and its lipids therefore differ from those of carnivorous marine fish species. The high levels of both n-3 and n-6 PUFA in *S. canaliculatus* tissues tended to be similar

to the high PUFA levels in *P. fucata* tissues. As for the difference between *S. canaliculatus* and *P. fucata* in the n-3 and n-6 PUFA levels we found that the levels of DHA in *P. fucata* fluctuated among the different conditions, even though consistently high levels of DHA were observed in *S. canaliculatus* tissues.

Although the role of n-6 PUFA in marine organisms is not clearly determined, *P. fucata* may accumulate AA similarly to n-3 PUFA. Differing from the essentiality of n-3 PUFA for marine subtropical fish, this bivalve may accumulate n-6 PUFA as a substitute for n-3 PUFA to maintain the fluidity of its cell membranes. All marine animals may have a tendency to accumulate PUFA in their tissues, and the difference in n-6 and n-3 PUFA levels among bivalve species may be caused only by their feeding habits.

Although *P. fucata* is omnivorous, similar to many other plankton feeders such as zooplankton, its lipid profile suggests that its prey may differ from those of zooplankton, which are primary consumers on the same trophic level as *P. fucata*. This suggests that *P. fucata* mainly filters specific or limited small phytoplankton, whereas many other animals ingest various prey, such as small animals (copepods, ciliates, and flagellates), phytoplankton, and detritus. In particular, high levels of AA and EPA in its lipids also suggest the effect of the lipids of specific phytoplankton.

Consequently, we determined that the lipids in *P. fucata* tissues contained comparatively high levels of both n-3 and n-6 PUFA, and more specifically, that AA and EPA and their derivatives were characteristic FA in both the depot TAG and the tissue PE and PC. Furthermore, the *P. fucata* may transform biosynthetically from shorter, monoenoic FA to longer NMID localized in the PE; AA may thus be useful as a lipid biomarker of herbivorous animals, because most marine animals do not have high levels of AA.

ACKNOWLEDGMENTS

The author thanks the Ehime Prefectural Fisheries Experimental Station, Dr. Akio Machii, Yamakatsu Shinju Co. Ltd., and Mr. Mituhiko Yoshida, Japan Aquatic Science Co. Ltd., for donating the specimens that made this work possible. The author also thanks Prof. Mutsumi Sugita, Shiga University, for kindly donating the authentic CAEP originating from the freshwater clam *Corbicula sandai* and for his valuable discussion of bivalve lipids. The author is grateful to Dr. Yanic Marty, West Bretagne University in Brest, Dr. Gerhard Kattner, Alfred Wegener Institute in Bremerhaven, and Dr. Masahiko Awaji, National Research Institute of Fisheries Science, for their valuable discussions of the lipid biosynthesis of marine organisms. The author also thanks Mikiko Tanaka, Akihito Takashima, and Junko Watanabe for their skilled technical assistance. This work was supported in part by the research project "Development of New Technology for Treatment and Local Recycling of Biomass" from the Ministry of Agriculture, Forestry, and Fisheries of Japan.

REFERENCES

1. Watanabe, T., and Ackman, R.G. (1974) Lipids and Fatty Acids of the American Virginica (*Crassostrea virginica*) and European Flat (*Ostrea edulis*) Oysters from a Common Habitat, and After One Feeding with *Dictateria iornata* or *Isochrysis galbana*, *J. Fish. Res. Board Canada. 31*, 403-409.
2. Dunstan, G.A., Volkman, J.K., and Barrett, S.M. (1993) The Effect of Lyophilization on the Solvent Extraction of Lipid Classes, Fatty Acids, and Sterols from the Oyster *Crassostrea gigas*, *Lipids. 28*, 937–944.
3. Soudant, P., Ryckeghem, K.V., Marty, Y., Moal, J., Samain, J.F., and Sorgeloos, P. (1999) Comparison of the Lipid Class and Fatty Acid Composition Between a Reproductive Cycle in Nature and a Standard Hatchery Conditioning of the Pacific Oyster *Crassostrea gigas, Comp. Biochem. Physiol. 123B*, 209–222.
4. Soudant, P., Marty, Y., Moal, J., Masski, H., and Samain, J.F. (1998) Fatty Acid Composition of Polar Lipid Classes During Larval Development of Scallop *Pecten maximus* (L.), *Comp. Biochem. Physiol. 121A*, 279–288.
5. Pazos, A.J., Sánchez, J.L., Román, G., Pérez-Parallé, M.L., and Abad, M. (2003) Lipid Classes Fatty Acid Composition in the Female Gonad of *Pecten maxima* in Relation to Reproductive Cycle and Environmental Variables, *Comp. Biochem. Physiol. 134B*, 367–380.
6. Kluytmans, J.H., Boot, J.H., Oudejand, R.C.H.M., and Zandee, D.I. (1985) Fatty Acid Synthesis in Relation to Gametogenesis in the Mussel *Mytilus edulis* L., *Comp. Biochem. Physiol. 81B*, 959–963.
7. Freites, L., Fernandez-Reiriz, M.J., and Labarta, U. (2002) Fatty Acid Profiles of *Mytilus galloprovincialis* (Lmk) Mussel of Subtidal and Rocky Shore Origin, *Comp. Biochem. Physiol. 132B*, 453–461.
8. Bell, M.V., Henderson, R.J., and Sargent, J.R. (1986) The Role of Polyunsaturated Fatty Acids in Fish, *Comp. Biochem. Physiol. 83B*, 711–719.
9. Morris, R.J., and Culkin, F. (1989) Fish, in *Marine Biogenic Lipids, Fats, and Oils* (Ackman, R.G., ed.), Vol. 2, pp. 145–178, CRC Press, Boca Raton, FL.
10. Joseph, J.D. (1989) Distribution and Composition of Lipids in Marine Invertebrates, in *Marine Biogenic Lipids, Fats, and Oils* (Ackman, R.G., ed.), Vol. 2, pp. 49–143, CRC Press, Boca Raton, FL.
11. Folch, J., Lees, M., and Sloane Stanley, G.H. (1957) A Simple Method for the Isolation and Purification of Total Lipids from Animal Tissues, *J. Biol. Chem. 226*, 497–509.
12. Saito, H., and Murata, M. (1998) The Origin of the Monoene Fats in the Lipid of Midwater Fishes: Relationship Between the Lipids of Myctophids and Those of Their Prey, *Mar. Ecol. Prog. Ser. 168*, 21–33.
13. Saito, H., and Kotani, Y. (2000) Lipids of Five Boreal Species of the Calanoid Copepod: Origin of the Monoene Fats of Marine Animals at the Higher Trophic Levels in the Grazing Food Chain of Subarctic Ocean Ecosystem, *Mar. Chem. 71*, 69–82.
14. Awaji, M., and Suzuki, T. (199) The Pattern of Cell Proliferation During Pearl Sac Formation in the Pearl Oyster, *Fish. Sci. 61*, 745–751.
15. Henderson R.J., Sargent, J.R., and Hopkins, C.C.E. (1984) Changes in the Content and Fatty Acid Composition of Lipid in an Isolated Population of the Capelin *Mallotus villosus* During Sexual Maturation and Spawning, *Mar. Biol. 78*, 255–263.
16. Numaguchi, K. (1994) Growth and Physiological Condition of the Japanese Pearl Oyster, *Pinctada fucata martensii* (Dunker, 1850) in Ohmura Bay, Japan, *J. Shellfish Res. 13*, 93–99.
17. Takama, K., Suzuki, T., Yoshida, K., Arai, H., and Anma, H. (1994) Lipid Content and Fatty Acid Composition of Phospholipids in White-Flesh Fish Species, *Fish. Sci. 60*, 177–184.
18. Medina, I., Santiago, P., Aubourg, P., and Martin, R.P. (1995) Composition of Phospholipids of White Muscle of Six Tuna Species, *Lipids 30*, 1127–1135.
19. Saito, H., Kotani, Y., Keriko, J.M., Xue, C., Taki, K., Ishihara,

K., Ueda, T., and Miyata, S. (2002) High Levels of n-3 Polyunsaturated Fatty Acids in *Euphausia pacifica* and Its Role as a Source of Docosahexaenoic and Icosapentaenoic Acids for Higher Trophic Levels, *Mar. Chem. 78*, 9–28.
20. Kayama, M., Araki, S., and Sato, S. (1989) Lipids of Marine Plants, in *Marine Biogenic Lipids, Fats, and Oils* (Ackman, R.G., ed.), Vol. 2, pp. 3–48, CRC Press, Boca Raton, FL.
21. Nichols, D.S., Nichols, P.D., and Sullivan, C.W. (1993) Fatty Acid, Sterol and Hydrocarbon Composition of Antarctic Sea Ice Diatom Communities During the Spring Bloom in McMurdo Sound, *Antarctic Sci. 5*, 271–278.
22. Henderson, R.J., Hegseth, E.N., and Park, M.T. (1998) Seasonal Variation in Lipid and Fatty Acid Composition of Ice Algae from the Barents Sea, *Polar Biol. 20*, 48–55.
23. Volkman, J.K., Jeffrey, S.W., Nichols, P.D., Rogers, G.I., and Garland, C.D. (1989) Fatty Acid and Lipid Composition of 10 Species of Microalgae Used in Mariculture, *J. Exp. Mar. Biol. Ecol. 128*, 219–240.
24. Ackman, R.G., Tocher, C.S., and McLachlan, J. (1968) Marine Phytoplankter Fatty Acids, *J. Fish. Res. Board Canada 25*, 1603–1620.
25. Cohen, Z., Shiran, D., Khozin, I., and Heimer, Y.M. (1997) Fatty Acid Unsaturation in the Red Alga *Porphyridium cruentum.* Is the Methylene Interrupted Nature of Polyunsaturated Fatty Acids an Intrinsic Property of the Desaturase? *Biochim. Biophys. Acta 1344*, 59–64.
26. Alonso, D.L., Belarbi, E.-H., Rodriguez-Ruiz, J., Segura, C.I., and Giménez, A. (1998) Acyl Lipid of Three Microalgae, *Phytochemistry 47*, 1473–1481.
27. Eichenberger, W., and Gribi, C. (1997) Lipids of *Pavlova luteri*: Cellular Site and Metabolic Role of DGCC, *Phytochemistry 45*, 1561–1567.
28. Reuss, N., and and Poulsen, L.K. (2002) Evaluation of Fatty Acids as Biomarkers for a Natural Plankton Community. A Field Study of a Spring Bloom and a Post-bloom Period off West Greenland, *Mar. Biol. 141*, 423–434.
29. Mansour, M.P., Volkman, J.K., Jackson, A.E., and Blackburn, S.I. (1999) The Fatty Acid and Sterol Composition of Five Marine Dinoflagellates, *J. Phycol. 35*, 710–720.
30. Zhukova, N.V., and Titlyanov, E.A. (2003) Fatty Acid Variation in Symbiotic Dinoflagellates from Okinawan Corals, *Phytochemistry 62*, 191-195.
31. Bell, M.V., and Pond, D. (1996) Lipid Composition During Growth of Motile and Coccolith Forms of *Emiliania huxleyi*, *Phytochemistry 41*, 465–471.
32. Napolitano, G.E., MacDonald, B.A., Thompson, R.J., and Ackmann, R.G. (1992) Lipid Composition of Eggs and Adductor Muscle in Giant Scallops (*Placopecten magellanicus*) from Different Habitats, *Mar. Biol. 113*, 71–76.
33. Cook, H.W. (1991) Fatty Acid Desaturation and Chain Elongation in Eucaryotes, in *Biochemistry of Lipids, Lipoproteins, and Membranes* (Vance, D.E., and Vance, J.E., eds.), pp. 181–212, Elsevier Science, Amsterdam.
34. Ackman, R.G., and Hooper, S.N. (1973) Non-methylene-interrupted Fatty Acids in Lipids of Shallow-Water Marine Inverterbrates: A Comparison of Two Molluscs (*Littorina littorea* and *Lunatia triseriata*) with the Sand Shrimp (*Crangon septemspinosus*), *Comp. Biochem. Physiol. 46B*, 153–165.
35. Joseph, J.D. (1982) Lipid Composition of Marine and Estuarine Invertebrates. Part II: Mollusca, *Prog. Lipid Res. 21*, 109–153.
36. Ackman, R.G. (1989) Fatty Acids, in *Marine Biogenic Lipids, Fats, and Oils* (Ackman, R.G., ed.), Vol. 1., pp. 103–137, CRC Press, Boca Raton, FL.
37. Zhukova, N.V. (1991) The Pathway of the Biosynthesis of Non-methylene-interrupted Dienoic Fatty Acids in Mollusks, *Comp. Biochem. Physiol. 100B*, 801–804.
38. Saito, H., Yamashiro, R., Ishihara, K., and Xue, C. (1999) The Lipids of Three Highly Migratory Fishes: *Euthynnus affinis*, *Sarda orientalis*, and *Elagatis bipinnulata*, *Biosci. Biotechnol. Biochem. 63*, 2028–2030.
39. Owen, J.M., Adron, J.W., Middleton, C., and Cowey, C.B. (1975) Elongation and Desaturation of Dietary Fatty Acids in Turbot *Scophthalmus maximus* L., and Rainbow Trout *Salmo gairdnerii* Rich, *Lipids 10*, 528–531.
40. Yamada, K., Kobayashi, K., and Yone, Y. (1980) Conversion of Linolenic Acid to 3-Highly Unsaturated Fatty Acids in Marine Fishes and Rainbow Trout, *Bull. Jap. Soc. Sci. Fish. 46*, 1231–1233.
41. Johns, R.B., Nichols, P.D., and Perry, G.J. (1980) Fatty Acid Components of Nine Species of Molluscs of the Littoral Zone from Australian Waters, *Comp. Biochem. Physiol. 65B*, 207–214.
42. Lawan, S., Dalan, W., Punyachewin, S., and Lawan, T. (2000) Amount of n-3 Fatty Acid in Freshwater Fish Found in Northeast Thailand, *J. Jpn. Oil Chem. Soc. 49*, 263–266.
43. Saito, H., Yamashiro, R., Alasalvar, C., and Konno, T. (1999) Influence of Diets on Fatty Acids of Three Subtropical Fish, Subfamily Caesioninae (*Caesio diagramma* and *C. tile*) and Family Siganidae (*Siganus canaliculatus*), *Lipids 34*, 1073–1082 (1999).

[Received February 19, 2004; accepted November 28, 2004]

Umbelliferone Aminoalkyl Derivatives as Inhibitors of Oxidosqualene Cyclases from *Saccharomyces cerevisiae, Trypanosoma cruzi,* and *Pneumocystis carinii*

Simonetta Oliaro-Bosso[a], Franca Viola[a], Seiichi Matsuda[b], Giancarlo Cravotto[a], Silvia Tagliapietra[a], and Gianni Balliano[a,*]

[a]Dipartimento di Scienza e Tecnologia del Farmaco, Università di Torino, 10125 Turin, Italy, and [b]Departments of Chemistry and of Biochemistry and Cell Biology, Rice University, Houston, Texas 77005

ABSTRACT: A series of umbelliferone aminoalkyl derivatives, previously studied as inhibitors of squalene-hopene cyclase, were tested as inhibitors of yeast (*Saccharomyces cerevisiae*) oxidosqualene cyclase (OSC) and OSC from *Trypanosoma cruzi* and *Pneumocystis carinii* expressed in yeast. Enzymes from these pathogens were included in this study to provide a preliminary screening for antiparasitic activity. Tests were carried out both on cell homogenates incubated with radiolabeled oxidosqualene and on spheroplasts incubated with radiolabeled acetate. Derivatives bearing a methylallylamino group were the most effective on all of the three enzymes. The *P. carinii* enzyme was the most susceptible to the action of the inhibitors, with IC_{50} values for almost all of them ranging from 0.1 to 1 μM. The *T. cruzi* enzyme was appreciably inhibited (IC_{50} 4–5 μM) only by derivatives bearing a methylallylaminoalkyl flexible chain. Results identify a particularly promising new family of OSC inhibitors, for the development of novel antiparasitic agents.

Paper no. L9600 in *Lipids 39,* 1007–1012 (October 2004).

In both photosynthetic and nonphotosynthetic organisms, oxidosqualene cyclases (OSC) catalyze the key reaction of sterol biosynthesis, namely, the formation of a cyclic intermediate from an acyclic precursor, oxidosqualene (1,2). This cyclization is one of the most complex, efficient, and highly stereoselective reactions catalyzed by a single enzyme (3).

For decades it has attracted the interest of researchers not only for its fascinating mechanism, but also as a potential target in drug-development projects. Selective inhibition of OSC would offer a promising approach to the control of blood cholesterol levels in humans (4–8).

A series of OSC inhibitors has recently been tested on *Trypanosoma cruzi*, *T. brucei*, *Pneumocystis carinii*, and *Leishmania mexicana* (9,10) with the aim of developing new drugs to treat the severe diseases that are caused by these microorganisms. Along the same line, we turned to a series of coumarin derivatives we had previously studied as inhibitors of squalene-hopene cyclase (SHC) of *Alicyclobacillus acidocaldarius* (11–13), the bacterial counterpart of eukaryotic OSC. SHC, whose structure was elucidated a few years ago (14,15), is thought to possess an active center cavity very similar to that of OSC (16). Having proved the most effective on SHC within the coumarin family (13), aminoalkyl derivatives were tested in the present work on OSC from yeast (*Saccharomyces cerevisiae)* as well as on OSC from *T. cruzi* and *P. carinii* expressed in yeast (17,18). Their inhibitory potency has been assayed both on cell homogenates and, for the first time, on spheroplasts. Recombinant enzymes from pathogens are a convenient and safe model for screening new molecules as antiparasitic agents.

MATERIALS AND METHODS

Materials. Chemicals and culture media were obtained from Sigma-Aldrich (Milan, Italy) unless otherwise specified. Coumarin derivatives (Fig. 1) and the OSC substrate, 2,3-oxidosqualene (OS), were synthesized as reported previously (13,19). Labeled [^{14}C](3*S*)OS was prepared according to the method of Popják (20) by incubating pig liver S_{10} supernatant with *R*,S[2-^{14}C]mevalonic acid (55 mCi/mmol, 2.04 GBq/mmol) (Amersham Pharmacia Biotech, Little Chalfont, Buckinghamshire, United Kingdom) in the presence of the OSC inhibitor 3β-(β-dimethylaminoethoxy)-androst-5en-17one (DMAE-DHA) (21). [2-^{14}C]Acetate (50 mCi/mmol) and *R,S*[2-^{14}C] mevalonic acid (55 mCi/mmol, 2.04 GBq/mmol) were obtained from Amersham Pharmacia Biotech.

Strains of S. cerevisiae *and cultural conditions*. The aploid mating type alpha (*MAT*α) strain of *S. cerevisiae* FL100 (*MAT*α *ura3-1 trp1-1*) having no mutation in the enzymes of the sterol biosynthesis pathway (wild type) was kindly provided by Francis Karst (Colmar, France) (22). Cells were grown aerobically at 30°C to early stationary phase in YPD medium, containing 1% yeast extract (Oxoid, Basingstoke, Hampshire, England), 2% peptone (Oxoid), and 2% glucose (Merck, Darmstadt, Germany), to which 20 μg/mL ergosterol was added from a stock solution of 2 mg/mL ergosterol in ethanol/Tween 80 (1:1 vol/vol). Inocula (0.5 mL per 100 mL culture medium) were taken from precultures grown aerobically for 18 h. The following recombinant strains of *S. cerevisiae*

*To whom correspondence should be addressed at Dipartimento di Scienza e Tecnologia del Farmaco, via P. Giuria, 9–10125 Torino, Italy.
E-mail: gianni.balliano@unito.it

Abbreviations: OS, 2,3-oxidosqualene; OSC, oxidosqualene cyclase; SHC, squalene-hopene cyclase; YPD medium, 1% yeast extract, 2% peptone, 2% glucose; YPG medium, 1% yeast extract, 2% peptone, 2% galactose.

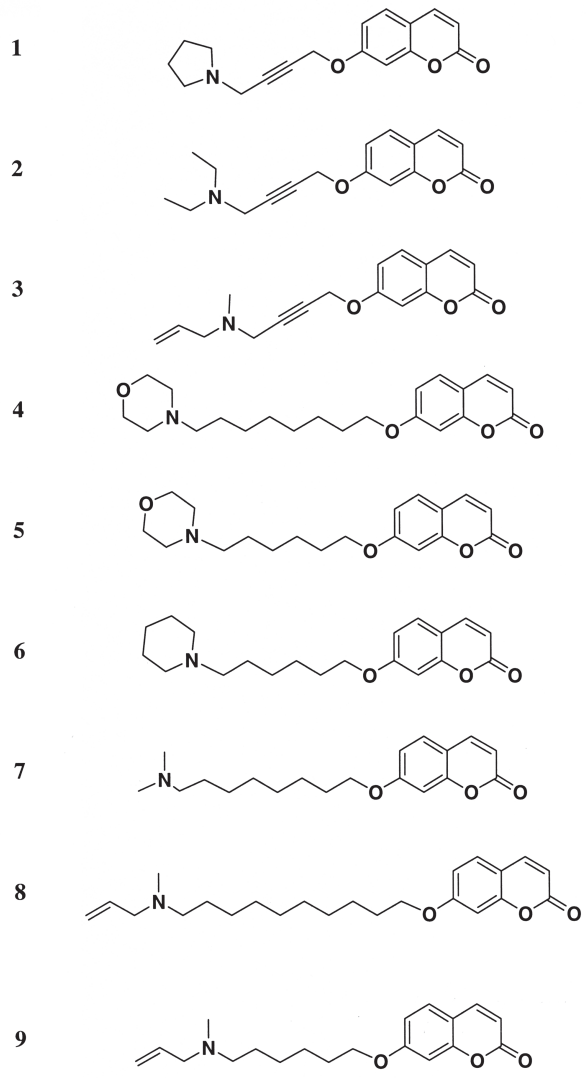

FIG. 1. Structure of umbelliferone derivatives investigated as oxidosqualene cyclase inhibitors. 7-[4′-(*N*-pyrrolidyn)-but-2-ynyloxy]chromen-2-one (**1**); 7-[4′-(*N*-diethylamino)-but-2-ynyloxy]chromen-2-one (**2**); 7-(4′-allylmethylamino-but-2-ynyloxy)chromen-2-one (**3**); 7-(morpholinyl-*N*-octanyloxy)-chromen-2-one (**4**); 7-(morpholinyl-*N*-hexyloxy)chromen-2-one (**5**); 7-(piperidinyl-*N*-hexyloxy)chromen-2-one (**6**); 7-[8′-(dimethylamino-*N*-octyloxy)]chromen-2-one (**7**); 7-[10-(allylmethylamino)-decyloxy]chromen-2-one (**8**); 7-[6-(allylmethylamino)-hexyloxy]-chromen-2-one (**9**).

were used: SMY8[pSM61.21] (*MATa erg7::HIS3 hem1::TRP1 ura3-52 trp1-Δ63 LEU2::OSC S. cerevisiae his3-Δ200 ade2 Gal+*) expressing wild-type yeast OSC; SMY8[pBJ1.21] (*MATa erg7::HIS3 hem1::TRP1 ura3-52 trp1-Δ63 LEU2::OSC T. cruzi his3-Δ200 ade2 Gal+*) expressing the *T. cruzi* OSC; and SMY8[pBJ4.21] (*MATa erg7::HIS3 hem1::TRP1 ura3-52 trp1-Δ63 LEU2::OSC P. carinii his3-Δ200 ade2 Gal+*) expressing the *P. carinii* OSC. Recombinant strains were obtained as described previously (17) by transformation with a galactose-inducible integrative yeast expression vector of the SMY8 *S. cerevisiae* strain, an aploid (*MATa*) lanosterol synthase mutant (erg7) strain. All strains, preserved in 40% glycerol at –80°C, were cultured as previously reported (18). Briefly, cells were grown aerobically as we have described with the addition to the culture medium of heme (13 μg/mL, added from a stock solution of 1.3 mg/mL heme in 1:1 ethanol/10 mM NaOH) and of ergosterol (20 μg/mL, added from a stock solution of 2 mg/mL ergosterol in 1:1 ethanol/Tween 80). Precultures were grown aerobically for 48 h. For OSC expression, 1 mL of inocula was grown for 48–72 h in 100 mL of YPG expression medium (1% yeast extract, 2% peptone, 2% galactose) and 13 μg/mL heme.

Enzyme assays. OSC activity was assayed in cell-free homogenates obtained from cultures grown to late exponential phase in YPG at 30°C. Cells were centrifuged at 3000 × *g* for 10 min, and their walls were lysed with lyticase (2 mg/g wet cells were suspended for 60 min at 30°C in 0.02 M KH_2PO_4 buffer, pH 7.4, containing 1.2 M sorbitol at a final concentration of 0.15 g of cell wet weight/mL). Spheroplasts were collected by centrifugation at 3000 × *g* for 10 min, washed twice with the same buffer, and homogenized with a Potter device in 10 mM MES/Tris buffer, pH 6.9, containing 0.2 mM EDTA and 1 mM PMSF at a final concentration of 0.5 g of cell wet weight/mL. Proteins were quantified in the homogenate with the Sigma Protein Assay Kit (Sigma, St. Louis, MO), based on the method of Lowry *et al.* (23) using BSA as standard. Homogenates could be used either fresh or after storage at –80°C for several months. For the assay, 0.5-mL aliquots of homogenate were incubated in the presence of labeled [^{14}C](3*S*)OS (1000 cpm) diluted with unlabeled (*R,S*)OS to a final concentration of 25 μM. Substrate and inhibitors, when added, were first dissolved in $CHCl_3$, aliquots were pipetted into test tubes containing Tween-80 (final conc. 0.2 mg/mL) and Triton X-100 (final conc. 1 mg/mL), and the solvent was evaporated under a stream of nitrogen. Residues were redissolved in 50 μL of 10 mM MES/Tris buffer, pH 6.9, containing 0.2 mM EDTA, then the amount of homogenate necessary to obtain a 20% substrate transformation was added and volumes were made up with buffer to 250 μL. After a 30-min incubation at 35°C, the enzymatic reaction was stopped by adding 1 mL of KOH in methanol (10% wt/vol) and heating at 80°C for 30 min in a water bath. The resulting mixtures were extracted with 2 mL petroleum ether, and extracts were evaporated under a stream of nitrogen. Residues, dissolved in a small amount of CH_2Cl_2, were spotted on TLC plates (Alufolien Kieselgel 60F254; Merck), which were developed with CH_2Cl_2. The percent conversion of the labeled substrate to lanosterol was estimated by integration from radioactivity scans with a System 2000 Imaging Scanner (Hewlett-Packard, Palo Alto, CA).

IC_{50} values (inhibitor concentrations that reduced the enzymatic conversion by 50%) were calculated by nonlinear regression analysis of the residual activity vs. the log of inhibitor concentration (duplicate determinations in two different experiments) using statistical software from Genstat (NAG, Oxford, United Kingdom).

Incorporation of [2-^{14}C]acetate into the nonsaponifiable lipids of spheroplasts. Tween-80 (final conc. 0.2 mg/mL) and inhibitors (when required) were dissolved in $CHCl_3$ and

TABLE 1
Effect of Umbelliferone Derivatives on the Activities of Squalene-Hopene Cyclase (SHC) and Oxidosqualene Cyclase (OSC)

	IC_{50} (μM)[a]			
Compound	SHC[b] *Alicyclobacillus acidocaldarius*	OSC *Saccharomyces cerevisiae*	OSC *Trypanosoma cruzi*	OSC *Pneumocystis carinii*
1	5.23	10.28	106.28	0.52
2	4.92	20.35	72.66	1.85
3	0.75	3.42	>100	1.12
4	7.35	30.67	102.38	5.35
5	6.28	102.82	95.83	78.76
6	8.17	31.54	>100	2.48
7	7.15	6.03	25.43	1.04
8	2.10	3.21	4.14	0.18
9	4.48	1.04	4.06	0.15

[a]Values are the means of two separate experiments, each with duplicate incubations. The maximal deviations from the mean were less than 10%.
[b]Data from Ref. 13.

added to 10-mL conical flasks. After the solvent was removed under a stream of nitrogen, spheroplasts from 3×10^8 cells, prepared and collected as we have described, were resuspended in 2.5 mL of 25 mM KH_2PO_4/NaOH buffer, pH 7.4, containing 1.2 M sorbitol, 1% glucose, and 0.5 μCi of [2-^{14}C]acetate (50 mCi/mol) and then added to each flask. After a 2-h incubation at 30°C under gentle shaking, spheroplasts were collected by centrifugation and saponified in 50% MeOH containing 15% KOH for 30 min at 80°C. Nonsaponifiable lipids were extracted twice with 1 mL of light petroleum and separated on silica gel plates (Merck) using *n*-hexane/ethyl acetate (85:15; vol/vol) as a developing solvent and authentic standards of ergosterol, lanosterol, dioxidosqualene, oxidosqualene, and squalene. Radioactivity in separated bands was measured using a System 2000 Imaging Scanner (Hewlett-Packard).

RESULTS

Effects of umbelliferone aminoalkyl derivatives on OSC from S. cerevisiae. In the presence of these compounds, we determined the OSC activity of the homogenate prepared from the wild-type yeast strain. Results (Table 1) are compared with those we obtained previously (13) with recombinant SHC of *A. acidocaldarius*, a bacterial counterpart of eukaryotic OSC. The majority of these derivatives proved less effective than they were on SHC. On yeast OSC, the most active inhibitors (IC_{50} 1–3 μM) were compounds **3**, **8**, and **9**, all of them bearing an allylmethylamino group.

Effects of umbelliferone aminoalkyl derivatives on recombinant OSC from T. cruzi and P. carinii. Homogenates, prepared (see *Enzyme assays* section) from yeast strains expressing OSC from *T. cruzi* and *P. carinii*, were about as active as those prepared from the wild-type strain FL100 (18). As shown in Table 1, only compounds **8** and **9**, both bearing a flexible chain with a terminal allylmethylamino group, had good inhibitory activity (IC_{50} 4 μM) on *T. cruzi* OSC. On the other hand, the majority of the listed compounds were active on the *P. carinii* enzyme, some of them with IC_{50} values ranging from 0.1 to 1 μM. On the whole, these compounds proved to be from 20- to 200-fold more active on the *P. carinii* than on the *T. cruzi* enzyme. Kinetic analysis was carried out on the *T. cruzi* enzyme only for compound **7**, which we consider as representative of the whole series. The double-reciprocal Lineweaver–Burk plot gave evidence of competitive inhibition (Fig. 2).

Effects of umbelliferone aminoalkyl derivatives on sterol biosynthesis in spheroplasts. Recognizing that inhibitors would enter yeast spheroplasts (cells deprived of cell wall) more easily than intact cells, and that spheroplasts would represent a better model than intact yeast cells for a eukaryote such as *T. cruzi* that is devoid of cell walls, we incubated spheroplasts from the above-mentioned yeast strains with radiolabeled acetate in the presence of inhibitors. A recombinant strain expressing the OSC of *S. cerevisiae* was also used to control the effect of genetic manipulation on the integrity of the sterol biochemical pathway. Comparison of wild-type FL100 and SMY8[pSM61.21] strains (Table 2), both expressing the *S. cerevisiae* OSC, showed that spheroplasts from both strains can make sterols, although in spheroplasts from the recombinant strain, the biosynthetic pathway seemed to run more slowly, as indicated by a higher squalene/sterols ratio in the nonsaponifiable extract. Because spheroplasts from SMY8[pBJ1.21] and SMY8[pBJ4.21], expressing *T. cruzi* and *P. carinii* OSC, respectively, behaved like those from SMY8[pSM61.21], expressing yeast OSC (Table 2), we could confirm that OSC genes from *T. cruzi* and *P. carinii* perfectly complemented the yeast OSC (12), in the spheroplast background as well. Results obtained with inhibitors **8** and **9** (Table 2) confirmed that *P. carinii* OSC was more susceptible to umbelliferone aminoalkyl derivatives. In fact, spheroplasts from the yeast strain expressing *P. carinii* OSC, when treated

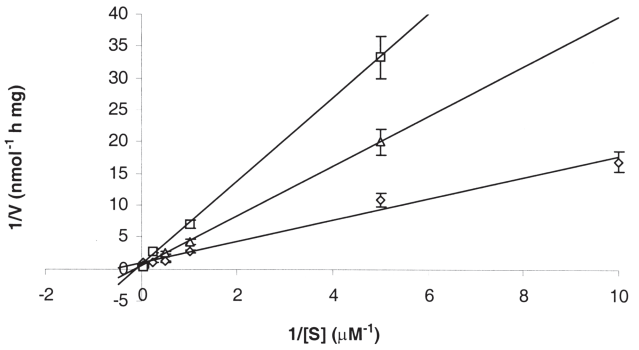

FIG. 2. Lineweaver–Burk analysis of the inhibition of *Trypanosoma cruzi* OSC by compound **7**. Oxidosqualene cyclase activity of the homogenate was determined over a range of oxidosqualene concentrations, in the absence (◇) or in the presence of compound **7** at 10 μM (△) or 50 μM (□). Error bars indicate the standard errors.

with compound **8** (1 μM), incorporated more label into the oxidosqualene fraction than those from the *T. cruzi* yeast strain treated with 10 times more inhibitor (21.04 and 17.72% of radioactivity found in the nonsaponifiable lipids, respectively).

DISCUSSION

Nine 7-aminoalkylumbelliferone derivatives, previously found to be active on recombinant SHC from *A. acidocaldarius* (13), were tested as inhibitors of OSC from *S. cerevisiae*, *T. cruzi*, and *P. carinii*. They all shared a basic structure consisting of a coumarin nucleus bearing a side chain with a terminal tertiary amino function. The kind of amino group, the flexibility of the chain, and the unsaturation of the chain all influenced the inhibitory activity very strongly, a result we had not found with SHC (13). Among these inhibitors, OSC from *T. cruzi* was the most sensitive to structural differences. Fairly good activity was shown only by compounds **8** and **9**, in which a flexible carbon chain bore a terminal allylmethylamino group. Interestingly, the same group is present in the well-known cholesterol-lowering agent RO048871 (4), as well as in other orally active nonterpenoid OSC inhibitors (8). Compound **7**, having a simple dimethylamino group at the end of a flexible chain, was less effective (Table 1). A quick kinetic study with the *T. cruzi* enzyme showed that compound **7** behaved as a competitive inhibitor (Fig. 2). The higher susceptibility of the *T. cruzi* enzyme to structural differences between inhibitors may depend on an architectural feature of the active site of the enzyme. Joubert *et al.* (17), in a comparative study on OSC, recently provided indirect evidence of this special feature by identifying a critical residue in a conserved motif of oxidosqualene-lanosterol synthases. This residue (position 384, *S. cerevisiae* numbering), which is tyrosine in *T. cruzi* and *T. brucei* OSC and threonine in animal and fungal OSC, has been recognized as catalytically important in a mutagenesis study (17). We can speculate that a bulky tyrosine residue sitting close to the active site could hinder the access of coumarin derivatives, and as a consequence, derivatives bearing a flexible linear chain would enter more easily. Of course, it is not possible to predict structural interactions between inhibitors and enzyme reliably until the tridimensional structure of the enzyme is elucidated.

Although OSC from *S. cerevisiae* and, especially, from *P. carinii* were less sensitive to structural differences among the inhibitors, compounds **8** and **9** proved to be the most active for all three enzymes. With the exception of **5**, which showed a uniformly poor activity, all our compounds were more effective on yeast and *P. carinii* enzymes than on the *T. cruzi* enzyme. The difference was particularly marked between *P. carinii* and *T. cruzi*: Compound **1**, one of the most active on the former enzyme (IC_{50} 0.52 μM), was almost inactive on the latter (IC_{50} 106 μM). Interestingly, the greatest difference between *P. carinii* and *T. cruzi* enzymes was observed with **1**, **2**, and **3**, compounds that bear a rigid triple-bond-containing chain. This may confirm the suggested crucial difference in the architecture of the active site. An interesting, structurally dependent difference was observed between two of the weakest inhibitors of the series, the morpholino derivatives **4** and **5**. Compound **4**, bearing a longer chain, was more active on *S. cerevisiae* and, especially, on *P. carinii* OSC. The different susceptibilities of *P. carinii* and *T. cruzi* OSC toward this family of inhibitors were also confirmed by our experiments with spheroplasts incubated with radiolabeled acetate.

Molecular recognition between the inhibitor and enzyme might not fully account for the different responses to inhibitors observed in the present work. In a recent study (18) on the subcellular distribution of *Arabidosis thaliana*, *T. cruzi*, and *P. carinii* OSC expressed in yeast, we reported that whereas the first two enzymes were bound to lipid particles, as was the yeast enzyme (24), none of the third enzyme was found in this fraction (18). One might argue that a different subcellular distribution of the enzymes could actually affect delivery of the inhibitors to target enzymes, enough to account for the different results we obtained with the aforementioned yeast strains. A clarification of this point can only come from experiments with purified enzymes, which are not available at this time.

A similar consideration arises from comparison of the present tests with previous ones carried out with the same umbelliferone derivatives on SHC from *A. acidocaldarius* (13). Although the interaction between these inhibitors and eukaryotic cyclases appears to be strongly dependent on the size and shape of their aminoalkyl moieties, inhibitory potencies toward SHC were not. This discrepancy probably results from a different architecture of the active site cavity, which in OSC seems to be more spatially restricted than in SHC (26). The study of interactions between inhibitors and OSC should derive great advantage from modeling studies based on comparisons between SHC and OSC (25,26), especially after SHC has been cocrystallized, for the first time, with a substrate-like inhibitor (27). However, the great leap forward in this field will occur only when the crystal structure of the first eukaryotic OSC is solved.

In conclusion, the present results prove that 7-aminoalky-

TABLE 2
Inhibitory Effects of Compounds 8 and 9 on Sterol Biosynthesis in Spheroplasts Incubated with Radiolabeled Acetate

	Radioactivity incorporated into nonsaponifiable lipids (%)					
Strain	Squalene	Oxidosqualene	Dioxidosqualene	Lanosterol and other 4,4-dimethylsterols	4-Monomethylsterolsa	Ergosterol and other 4-desmethylsterols
FL100 (wt)	24.2	3.4	0.9	27.2	10.2	34.1
+ **8** (10 μM)	19.9	14.0	–	29.0	4.3	32.8
+ **8** (100 μM)	32.0	40.3	5.2	9.6	4.8	8.1
SMY8 [pSM61.21] (*S. cerevisiae* OSC)	63.1	ND	ND	16.8	2.2	18.9
SMY8 [pBJ1.21] (*T. cruzi* OSC)	64.4	ND	ND	12.5	5.4	17.7
+ **8** (1 μM)	68.6	5.7	ND	12.6	1.9	11.2
+ **8** (10 μM)	54.2	17.7	–	17.1	3.1	7.8
+ 9 (10 μM)	45.2	12.1	4.22	32.0	1.2	5.3
SMY8 [pBJ4.21] (*P. carinii* OSC)	79.1	1.2	ND	10.8	1.8	6.9
+ 8 (1 μM)	70.8	21.0	ND	6.2	ND	1.0

[a]4-Monomethylsterol fraction includes the biosynthetic intermediates between lanosterol and ergosterol, having R_f values on TLC ranging from R_f ergosterol and R_f lanosterol. All results are the means of two separate experiments, each with duplicate incubations. The maximum deviations from the mean were less than 10%. ND, not detectable.

lumbelliferone derivatives are a promising family from which effective OSC inhibitors can be selected, particularly for the development of novel antiparasitic agents. As an added note, while the present work was under review, the structure of human OSC was published (28). This outstanding achievement, which represents a milestone in the field of oxidosqualene cyclase research, will give great impetus not only to the design of inhibitors that may act as cholesterol-lowering drugs but also in the development of novel antiparasitic agents. From now on, architectural differences in the active sites of target enzymes will be easier to predict from molecular modeling studies, as these can now take their bearings from the established structure of a eukaryotic OSC.

ACKNOWLEDGMENT

The authors are very grateful to MIUR (COFIN-project) the University of Turin for financial support.

REFERENCES

1. Nes, W.D. (1990) Control of Sterol Biosynthesis and Its Importance to Developmental Regulation and Evolution, *Recent. Adv. Phytochem. 24*, 283–327.
2. Abe, I., Rohmer, M., and Prestwich, G.D. (1993) Enzymatic Cyclization of Squalene and Oxidosqualene to Sterols and Triterpenes, *Chem. Rev. 90*, 2189–2206.
3. Wendt, K.U., Schulz, G.E., Corey, E.J., and Liu, D.R. (2000) Enzyme Mechanism for Polycyclic Triterpene Formation, *Angew. Chem. Int. Ed. 2000 39*, 2812–2833.
4. Mark, M., Müller, P., Maier, R., and Eisele, B. (1996) Effect of a Novel 2,3-Oxidosqualene Cyclase Inhibitor on the Regulation of Cholesterol Biosynthesis in HepG2 Cells, *J. Lipid Res. 37*, 148–158.
5. Morand, O.H., Aebi, J.D., Dehmlow, H., Ji, Y.H., Gains, N., Langsfeld, H., and Himber, J. (1997) Ro48-8071, a New 2,3-Oxidosqualene:Lanosterol Cyclase Inhibitor Lowering Plasma Cholesterol in Hamsters, Squirrel Monkeys, and Minipigs: Comparison to Simvastatin, *J. Lipid Res. 38*, 373–390.
6. Eisele, B., Budzinski, R., Müller, P., Maier, R., and Mark, M. (1997) Effects of a Novel 2,3-OSC Inhibitor on Cholesterol Biosynthesis and Lipid Metabolism in vivo, *J. Lipid Res. 38*, 564–575.
7. Brown, G.R., Hollinshead, D.M., Stokes, E.S.E., Clarke, D.S., Eakin, M.A., Foubister, A.J., Glossop, S.C., Griffiths, D., Johnson, M.C., McTaggart, F., Mirrlees, D.J., Smith, G.J., and Wood, R. (1999) Quinuclidine Inhibitors of 2,3-Oxidosqualene Cyclase-Lanosterol Synthase: Optimization from Lipid Profiles, *J. Med. Chem. 42*, 1306–1311.
8. Dehlmlow, H., Aebi, J.D., Jolidon, S., Ji, Y.-H., von der Mark, E.M., Himber, J., and Morand, O.H. (2003) Synthesis and Structural Activity Studies of Novel Orally Active non-Terpenoic 2,3-Oxidosqualene Cyclase Inhibitors, *J. Med. Chem. 46*, 3354–3370.
9. Buckner, F.S., Griffin, J.H, Wilson, A.J., and van Voorhis, W.C. (2001) Potent anti-*Trypanosoma cruzi* Activities of OSC Inhibitors, *Antimicrob. Agents Chemother. 45*, 1210–1215.
10. Hinshaw, J.C., Suh, D.-Y., Garnier, P., Buckner, F.S., Eastman, R.T., Matsuda, S.P.T., Joubert, B.M., Coppens, I., Joiner, K.A., Merali, S., Nash, T.E., and Prestwich, G.D. (2003) OSC Inhibitors as Antimicrobial Agents. *J. Med. Chem. 46*, 4240–4243.
11. Cravotto, G., Balliano, G., Chimichi, S., Robaldo, B., Oliaro-Bosso, S., and Boccalini, M. (2004)Farnesyloxycoumarins, a New Class of Squalene-Hopene Cyclase Inhibitors, *Bioorg. Med. Chem. Lett. 14*, 1931–1934.
12. Cravotto, G., Balliano, G., Tagliapietra, S., Oliaro-Bosso, S., and Nano, G.M. (2004) Novel Squalene-Hopene Cyclase Inhibitors Derived from Hydroxycoumarins and Hydroxyacetophenones, *Chem. Pharm. Bull. 52*, 1171–1174.
13. Cravotto, G., Balliano, G., Tagliapietra, S., Palmisano, G., and Penoni, A. (2004) Umbelliferone Aminoalkyl Derivatives, a New Class of Squalene-Hopene Cyclase Inhibitors, *Eur. J. Med. Chem. 39*, 917–924.

14. Wendt, K.U., Poralla, K., and Schulz, G.E. (1997) Structure and Function of Squalene Cyclase, *Science 277*, 1811–1815.
15. Wendt, K.U., Lenhart, A., and Schulz, G.E. (1999) The Structure of the Membrane Protein Squalene-Hopene Cyclase at 2 Å Resolution, *J. Mol. Biol. 286*, 175–187.
16. Lenhart, A., Reinert, D.J., Aebi, J.D., Dehmlow, H., Morand, O.H., and Schulz, G.E. (2003) Binding Structures and Potencies of OSC Inhibitors with the Homologous Squalene-Hopene Cyclase, *J. Med. Chem. 46*, 2083–2092.
17. Joubert, B.M., Buckner, F.S., and Matsuda, S.P.T. (2001) Trypanosome and Animal Lanosterol Synthases Use Different Catalytic Motif, *Org. Lett. 3*, 1957–1960.
18. Milla, P., Viola, F., Oliaro-Bosso, S., Rocco, F., Cattel, L., Joubert, B.M., LeClair, R.J., Matsuda, S.P.T., and Balliano, G. (2002) Subcellular Localization of OxidoSqualene Cyclases from *Arabidopsis thaliana, Trypanosoma cruzi,* and *Pneumocystis carinii* Expressed in Yeast, *Lipids 37*, 1171–1176.
19. Ceruti, M., Balliano, G., Viola, F., Cattel, L., Gerst, N., and Schuber, F. (1987) Synthesis and Biological Activity of Azasqualenes, Bis-azasqualenes and Derivatives, *Eur. J. Med. Chem. 22*,199–208.
20. Popják, G. (1969) *Methods in Enzymology, Steroids and Terpenoids* (Clayton, R.B., ed.), Vol. 15, pp. 438–443, Academic Press, New York.
21. Field, R.B., Holmlund, C.E., and Whittaker, N.F. (1979) The Effect of the Hypocholesteremic Compound 3β-(β-dimethylaminoethoxy)-Androst-en17-one on the Sterol and Steryl Ester Composizion of *Saccharomyces cerevisiae*, *Lipids 14*, 741–747.
22. Servouse, M., and Karst, F. (1986) Regulation of Early Enzyme of Ergosterol Biosynthesis in *Saccharomyces cerevisiae*, *Biochem. J. 240*, 541–547.
23. Lowry, O.H., Rosenbrough, N.J., Farr, A.L., and Randall, R.J. (1951) Protein Measurement with the Folin Phenol Reagent, *J. Biol. Chem. 193*, 265–275.
24. Milla, P., Athenstaedt, K., Viola, F., Oliaro-Bosso, S., Kohlwein, S.E., Daum, G., and Balliano. G. (2002) Yeast Oxidosqualene Cyclase (Erg7p) Is a Major Component of Lipid Particles, *J. Biol. Chem. 277*, 2406–2412.
25. Binet, J., Thomas, D., Benmbarek, A., de Fornel, D., and Renaut, P. (2002) Structure–Activity Relationships of New Inhibitors of Mammalian 2,3-Oxidosqualene Cyclase Designed from Isoquinoline Derivatives, *Chem. Pharm. Bull. 50*, 316–329.
26. Schulz-Gasch, T., and Sthal, M. (2003) Mechanistic Insights into Oxidosqualene Cyclizations Through Homology Modeling, *J. Comput. Chem. 24*, 741–753.
27. Reinert, D.J., Balliano, G., and Schulz, G.E. (2004) Conversion of Squalene to the Pentacarbocyclic Hopene, *Chem. Biol. 11*, 121–126.
28. Thoma, R., Schulz-Gasch, T., D'Arcy, B., Benz, J., Aebi, J., Dehmlow, H., Hennig, M., Stihle, M., and Ruf, A. (2004) Insight into Steroid Scaffold Formation from the Structure of Human Oxidosqualene Cyclase, *Nature 432*, 118–122.

[Received September 1, 2004; accepted November 19, 2004]

Asymmetric *in vitro* Synthesis of Diastereomeric Phosphatidylglycerols from Phosphatidylcholine and Glycerol by Bacterial Phospholipase D

Rina Sato[a], Yutaka Itabashi[a,*], Tadashi Hatanaka[b], and Arnis Kuksis[c]

[a]Graduate School of Fisheries Sciences, Hokkaido University, Hakodate 041-8611, Japan,
[b]Research Institute for Biological Sciences, Okayama, 716-1241, Japan, and
[c]Banting and Best Department of Medical Research, University of Toronto, Toronto, Ontario M5G 1L6, Canada

ABSTRACT: Using chiral-phase HPLC, we determined the stereochemical configuration of the phosphatidylglycerols (PtdGro) synthesized *in vitro* from 1,2-diacyl-*sn*-glycero-3-phosphocholine (PtdCho, *R* configuration) or 1,2-diacyl-*sn*-glycero-3-phosphoethanolamine (PtdEtn, *R* configuration) and glycerol by transphosphatidylation with bacterial phospholipase D (PLD). The results obtained with PLD preparations from three *Streptomyces* strains (*S. septatus* TH-2, *S. halstedii* K5, and *S. halstedii* subsp. *scabies* K6) and one *Actinomadura* species were compared with those obtained using cabbage and peanut PLD. The reaction was carried out at 30°C in a biphasic system consisting of diethyl ether and acetate buffer. The resulting PtdGro were then converted into bis(3,5-dinitrophenylurethane) derivatives, which were separated on an (*R*)-1-(1-naphthyl)ethylamine polymer. In contrast to the cabbage and peanut PLD, which gave equimolar mixtures of the *R,S* and *R,R* diastereomers, as previously established, the bacterial PLD yielded diastereomixtures of 30–40% 1,2-diacyl-*sn*-glycero-3-phospho-1′-*sn*-glycerol (*R,S* configuration) and 60–70% 1,2-diacyl-*sn*-glycero-3-phospho-3′-*sn*-glycerol (*R,R* configuration). The highest disproportionation was found for the *Streptomyces* K6 species. The present study demonstrates that bacterial PLD-catalyzed transphosphatidylation proceeds to a considerable extent stereoselectively to produce PtdGro from PtdCho or PtdEtn and prochiral glycerol, indicating a preference for the sn-3′ position of the glycerol molecule.

Paper no. L9480 in *Lipids 39*, 1013–1018 (October 2004).

Phospholipase D (PLD, EC 3.1.4.4) catalyzes hydrolysis of the terminal phosphodiester bond of phospholipids to produce phosphatidic acid (PtdOH) and alcohols. PLD also catalyzes transphosphatidylation, which can produce new phospholipids with polar head groups modified in the presence of alcohols (1–4). Thus, by using PLD, less-abundant natural phospholipids such as phosphatidylethanolamine (PtdEtn), phosphatidylglycerol (PtdGro), and phosphatidylserine can be easily amplified, and unnatural phospholipids can be prepared from a naturally abundant phosphatidylcholine (PtdCho) (5–7).

PLD-catalyzed transphosphatidylation is usually carried out in water–organic solvent emulsion systems, and the yield of products depends on the enzyme sources, the nature of the alcohols, and the reaction conditions. Most primary alcohols serve as good acceptors in the reaction; secondary alcohols react less effectively than primary alcohols (2,3,6,7). Thus, the two primary hydroxy groups of glycerol react readily with PtdCho to produce two PtdGro diastereomers (Fig. 1). Using chemical and enzymatic methods, Yang *et al.* (1) first reported that PtdGro generated from natural PtdCho (1,2-diacyl-*sn*-glycero-3-phosphocholine, *R* configuration) with cabbage PLD was an equimolar mixture of 1,2-diacyl-*sn*-glycero-3-phospho-1′-*sn*-glycerol (*sn*-3,*sn*-1; *R,S* configuration) and 1,2-diacyl-*sn*-glycero-3-phospho-3′-*sn*-glycerol (*sn*-3,*sn*-3′; *R,R* configuration). Using circular dichroism, on the other hand, Batrakov *et al.* (8) reported that the PtdGro generated from egg yolk PtdCho with cabbage PLD was a 100% naturally occurring *R,S* isomer. To resolve these conflicting experimental results, Joutti and Renkonen (9) reexamined them and concluded that the configuration of PtdGro prepared from egg yolk PtdCho with cabbage PLD was a 1:1 mixture of the *R,S* and *R,R* isomers. They demonstrated that only 50% of the PtdGro was hydrolyzed with phospholipase C, and that the released glycerophosphate had the *sn*-1 configuration, as determined using *sn*-glycero-3-phosphate dehydrogenase. Thus, the PLD-catalyzed transphosphatidylation reaction was shown to produce the *R,S* and *R,R* isomers nonstereoselectively. Using chiral-phase HPLC, however, Itabashi and Kuksis (10) reported that some commercially available PtdGro did not contain the anticipated equimolar mixture of *R,S* and *R,R* isomers (10), suggesting some stereoselectivity of PLD used in their preparation as well as a possible influence of substrate acyl groups. These observations prompted us to examine the configuration of the Ptd-Gro synthesized by transphosphatidylation with PLD from different origins. For this purpose, we examined several PLD preparations from *Actinomycetes* (*Streptomyces septatus* TH-2, *St. halstedii* K5, *S. halstedii* subsp. *scabies* K6, and *Actinomadura* sp.), and cabbage and peanuts. The *Streptomyces* strains had been isolated from soil and yielded PLD preparations

*To whom correspondence should be addressed at Laboratory of Bioresources Chemistry, Graduate School of Fisheries Sciences, Hokkaido University, 3-1-1 Minato-cho, Hakodate, Hokkaido 041-8611, Japan.
E-mail: yutaka@pop.fish.hokudai.ac.jp

Abbreviations: DNPU, 3,5-dinitrophenylurethane; GroPCho, glycerophosphocholine; GroPEtn, glycerophosphoethanolamine; *sn*-3,*sn*-3′ (*R,R*), 1,2-diacyl-*sn*-glycero-3-phospho-3′-*sn*-glycerol; *sn*-3,*sn*-1′ (*R,S*), 1,2-diacyl-*sn*-glycero-3-phospho-1′-*sn*-glycerol; GroPGro, glycerophosphoglycerol; PLD, phospholipase D; PtdCho, phosphatidylcholine; PtdEtn, phosphatidylethanolamine; PtdGro, phosphatidylglycerol; PtdOH, phosphatidic acid.

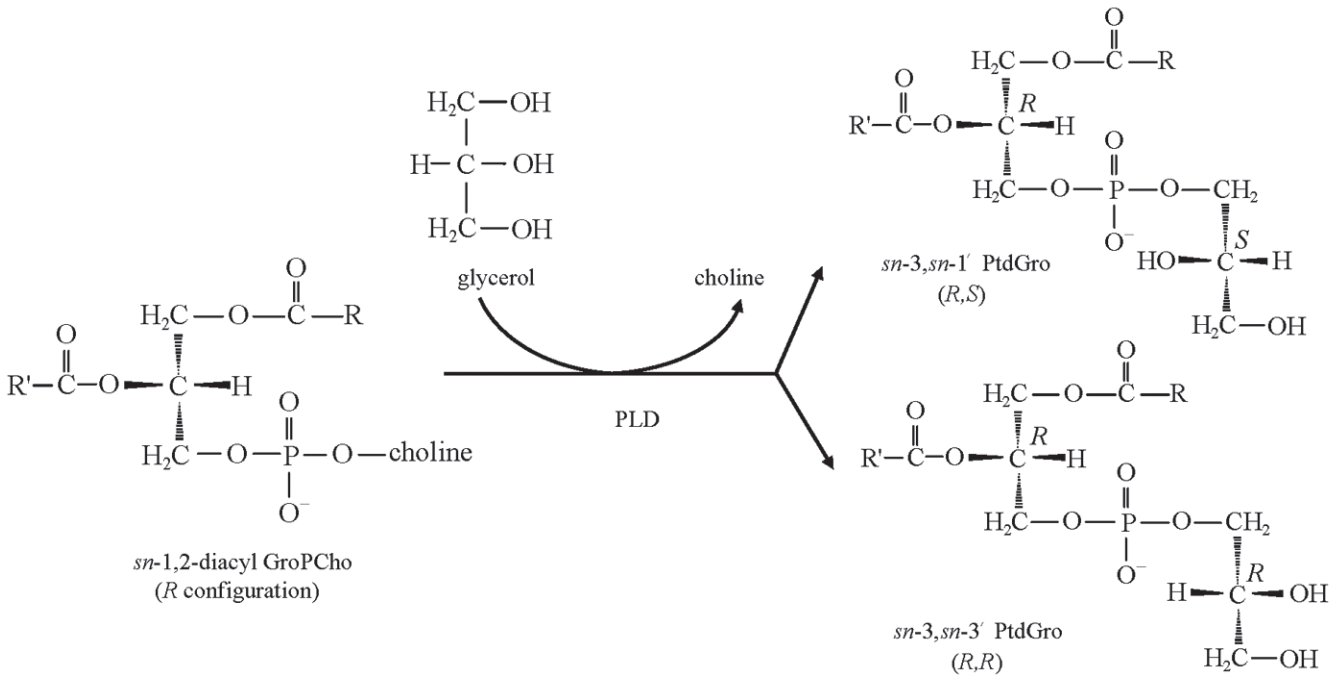

FIG. 1. Phospholipase D-catalyzed transphosphatidylation of 1,2-diacyl-*sn*-glycero-3-phosphocholine (*R* configuration) to phosphatidylglycerol. PLD, phospholipase D; GroPCho, glycerophosphocholine; PtdGro, phosphatidylglycerol; *sn*-3,*sn*-1′, 1,2-diacyl-*sn*-glycero-3-phospho-1′-*sn*-glycerol (*R,S* configuration); *sn*-3,*sn*-3′, 1,2-diacyl-*sn*-glycero-3-phospho-3′-*sn*-glycerol (*R,R* configuration).

with high transphosphatidylation activity (11–13). These PLD enzymes belong to the superfamily of the HKD-PLD, and their primary structures show approximately 70% identity to each other (13).

MATERIALS AND METHODS

PLD. Commercially available PLD from *Actinomadura* sp. (50 U/mg solid), cabbage leaves (0.29 U/mg solid), and peanut seeds (44 U/mg solid) were obtained from Seikagaku Kogyo (Tokyo, Japan), Fluka (Buchs, Switzerland), and Sigma (St. Louis, MO), respectively. One unit of the enzyme activities has been described in their catalogs as the amount that hydrolyzes 1 μmol PtdCho per min at pH 5.5 (50°C), 5.6 (37°C), and 5.5 (30°C), respectively. PLD from *S. septatus* TH-2 (3.3 U/mL), *S. halstedii* K5 (5.3 U/mL), and *S. halstedii* subsp. *scabies* K6 (3.2 U/mL), which were isolated from soils, were purified to homogeneity from culture supernatants for transphosphatidylation, as described in a previous paper (13). One unit of the activities of these bacterial PLD was defined as the amount that released 1 μmol of *p*-nitrophenol from phosphatidyl-*p*-nitrophenol per minute at pH 7.5 (37°C) (14).

Chemicals. Synthetic 1,2-dimyristoyl-*sn*-glycero-3-phosphocholine (14:0–14:0 GroPCho), 1,2-dipalmitoyl-*sn*-glycero-3-phosphocholine (16:0–16:0 GroPCho), and 1,2-distearoyl-*sn*-glycero-3-phosphocholine (18:0–18:0 GroPCho) were obtained from Sigma. Synthetic 1,2-dioleoyl-*sn*-glycero-3-phosphocholine (18:1–18:1 GroPCho) and 1,2-dilinoleoyl-*sn*-glycero-3-phosphocholine (18:2–18:2 GroPCho), and 1,2-dioleoyl-*sn*-glycero-3-phosphoethanolamine (18:1–18:1 GroPEtn) were obtained from Avanti Polar Lipids (Alabaster, AL). Egg yolk PtdCho was a product of Q.P. (Tokyo, Japan). Salmon (*Oncorhynchus keta*) roe PtdCho was isolated from the total lipids by silicic acid TLC as described previously (15). Glycerol was obtained from Nacalai Tesque (Kyoto, Japan). HPLC-grade solvents (hexane, dichloro-methane, and methanol) were obtained from Wako Pure Chemicals (Osaka, Japan). 3,5-Dinitrophenyl isocyanate was a product of Sumika Analysis Service (Osaka, Japan). All other chemicals and solvents were of reagent grade or better and were also obtained from Wako Pure Chemicals.

Transphosphatidylation. PtdGro was prepared according to the method described by Yang *et al.* (1). In brief, a mixture containing 5 mg of PtdCho or PtdEtn, 1 mL of 0.4 M acetate buffer (pH 5.6), 1 mL of 0.2 M $CaCl_2$, 1 mL of glycerol/0.4 M acetate buffer (1:4, vol/vol), and 2 mL of water was pre-incubated in the absence of PLD at 30°C for 10 min. The reaction was initiated by the addition of a suitable amount of buffered enzyme (S*treptomyces* TH-2, 0.033 U; *Streptomyces* K5, 0.053 U; *Streptomyces* K6, 0.032 U) and 2.5 mL of diethyl ether, and the mixture was stirred vigorously at 30°C for 1 to 9 h. After the reaction was terminated by the addition of 0.5 mL of 1 N HCl, the products were extracted with 10 mL of chloroform/methanol (2:1, vol/vol) and recovered from the chloroform layer formed by centrifuging at 1,500 × *g* for 5 min. To identify the lipid components, an aliquot of the reaction products was spotted on a TLC plate (Silica gel 60 F_{254}; Merck, Darmstadt, Germany) and developed with chloroform/methanol/

acetic acid (70:30:8, by vol). Spots were detected by spraying with the Dittmer–Lester reagent (16). Quantitative analysis was carried out with a TLC-FID analyzer (Iatroscan TH10; Iatron, Tokyo, Japan) according to the method described by Juneja *et al.* (17), with a slight modification of the mobile phase. The samples (5 μL each) dissolved in chloroform (1 mg/0.1 mL) were spotted on Chromarod S-III quartz rods coated with silica gel (Iatron) and developed with chloroform/acetone/ methanol/formic acid/water (65:25:10:1:2, by vol).

Preparation of derivatives. The PtdGro produced was converted into bis(3,5-dinitrophenylurethane) (bis-DNPU) derivatives without prior isolation from the reaction products as described by Itabashi and Kuksis (10) with a slight modification. To the transphosphatidylation products (less than 1 mg) dissolved in 1 mL of dry toluene were added 5 mg of 3,5-dinitrophenyl isocyanate and 20 μL of dry pyridine, and the solution was stirred gently at 30°C. After 3 h, the solvent was evaporated to dryness, and the resulting bis-DNPU derivatives were purified by TLC (Silica gel 60 F_{254}, 20 × 20 cm), using chloroform/methanol/water (40:10:1, by vol) as the developing solvent. Bands were visualized under UV irradiation, and the bis-DNPU derivatives were extracted three times with chloroform/methanol/acetic acid (20:10:0.1, by vol). The solution was washed once with water/30% ammonium hydroxide (3:1, vol/vol), then dried over sodium sulfate, and the solvent was evaporated to dryness.

Chiral-phase HPLC. The diastereomer composition of PtdGro obtained by transphosphatidylation was determined by chiral-phase HPLC (10). The separation was performed on a Shimadzu LC-6A liquid chromatograph (Shimadzu, Kyoto, Japan) equipped with an (*R*)-1-(1-naphthyl)ethylamine column (YMC-Pack A-K03, 25 cm × 4.6 mm i.d.; YMC, Kyoto, Japan). The analysis was done isocratically at 10°C using hexane/dichloromethane/methanol/trifluoroacetic acid (60:20:20:0.2, by vol) as the mobile phase at a flow rate of 1 mL/min. Several microliters of the purified bis-DNPU derivatives dissolved in dichloromethane (1 mg/mL) was injected on the column through a Rheodyne Model 7125 loop (20 μL) injector. Peaks were monitored at 254 nm UV with a Shimadzu SPD-6A variable-wavelength detector having an 8-μL flow cell, and chromatograms were recorded on a Shimadzu Chromatopac C-R3A.

RESULTS AND DISCUSSION

Transphosphatidylation. The progress of the PLD-catalyzed transphosphatidylation reaction was monitored on a thin-layer chromatograph with FID. The composition of the reaction products obtained with PLD from *Streptomyces* and *Actinomadura* is given in Table 1. Most of the PtdCho were transformed into PtdGro and PtdOH after 1–1.5 h of reaction. Of the four bacterial PLD examined, *Actinomadura* PLD gave the highest yield of PtdGro (95%), whereas the lowest one (64%) was observed for *Streptomyces* TH-2 PLD, which produced 36% PtdOH. With PLD from *Streptomyces* TH-2 and K5, the PtdOH contents increased greatly as the reaction time elapsed, i.e., accounting for 86 and 46% of the total phospholipids, respectively, after 9 h of reaction (Table 1). This phenomenon suggests that the resulting PtdGro was hydrolyzed to PtdOH during the transphosphatidylation reaction. As described next, the diastereomer composition of PtdGro produced with some bacterial PLD changes somewhat with the progress of transphosphatidylation. In this study, therefore, the configuration of PtdGro was determined in the early stage of the reaction, as soon as the parent PtdCho had disappeared.

Configuration of PtdGro. Figure 2 shows the typical HPLC chromatograms of the bis-DNPU derivatives of PtdGro generated from PtdCho (*R* configuration) and glycerol by transphosphatidylation with *Streptomyces* TH-2 PLD. The derivatives were clearly separated into the two diastereomers showing different proportions on the A-K03 column. The broad peaks of PtdGro obtained from salmon roe PtdCho, which was mainly composed of 18:1–20:5 GroPCho (5%), 16:0–20:5 GroPCho (19%), 16:0–22:6 GroPCho (23%), 16:0–22:5 GroPCho (6%), 18:0–20:5 GroPCho (7%), and 18:0–22:6 GroPCho (11%) (15), were due to differences in retention times of the different molecular species of PtdGro on the chiral column (10). Similar chromatograms were obtained for all the PtdGro analyzed.

Figure 3 shows the time course of diastereomer formation during preparation from PtdCho and glycerol by transphosphatidylation with PLD from *Streptomyces* and *Actinomadura.* The proportions of the *R,R* isomers generated with PLD from *Streptomyces* TH-2, *Streptomyces* K5, and *Actinomadura* sp. decreased gradually with time, showing a drop from 62, 66, and

TABLE 1
Composition (peak area%) of Phosphatidylglycerol (PtdGro) and Phosphatidic Acid (PtdOH) Prepared from Egg Yolk Phosphatidylcholine (PtdCho) and Glycerol by a Bacterial Phospholipase D (PLD)-Catalyzed Reaction[a]

PLD	Reaction time (h)	PtdGro	PtdOH	PtdCho
Streptomyces septatus TH-2	1.5	63.7	34.1	2.2
	9.0	14.1	85.9	Trace[b]
S. halstedii K5	1.5	78.9	17.3	3.8
	9.0	54.2	45.8	Trace
S. halstedii subsp. *scabies* K6	1.5	90.4	7.2	2.5
	9.0	80.6	19.4	Trace
Actinomadura sp.	1.0	94.8	0	5.2
	9.0	98.5	1.5	Trace

[a]Unreacted substrate.
[b]Trace (less than 0.1%).

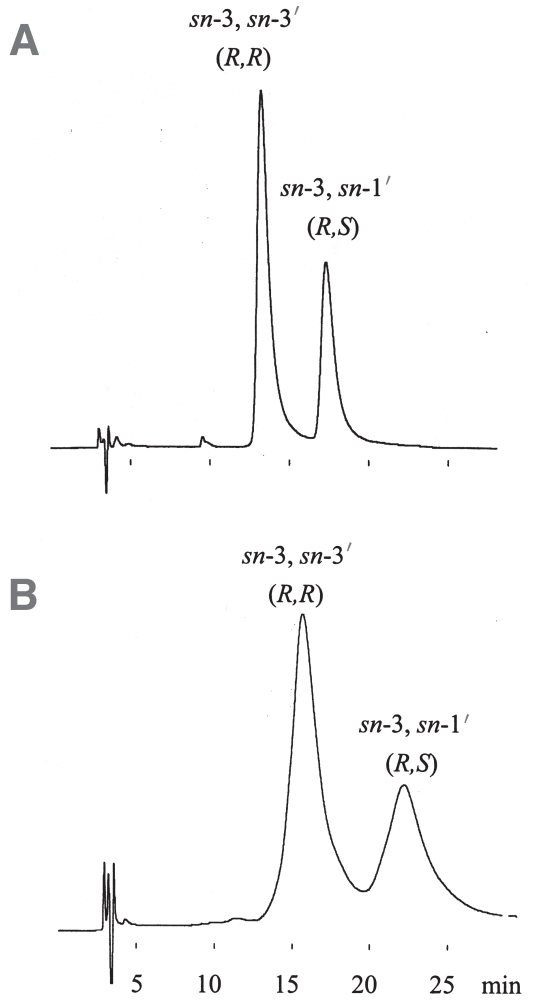

FIG. 2. Chiral-phase HPLC profiles of the bis(3,5-dinitrophenyl-urethane) derivatives of the PtdGro generated from 1,2-diacyl-*sn*-glycero-3-phosphocholine (*R* configuration) and glycerol by transphosphatidylation with PLD from *Streptomyces septatus* TH-2. (A) PtdGro generated from synthetic 1,2-dioleoyl-*sn*-glycero-3-phosphocholine (*R* configuration); (B) PtdGro generated from salmon roe phosphatidylcholine (PtdCho). HPLC conditions as given in text. For other abbreviations see Figure 1.

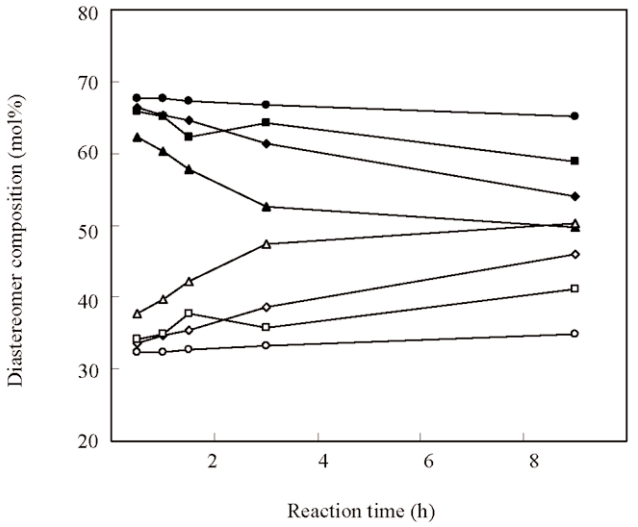

FIG. 3. Time course of alteration in the configuration of PtdGro generated from egg yolk PtdCho and glycerol by transphosphatidylation with bacterial PLD. ▲, ◆, ●, and ■ represent *sn*-3,*sn*-3′ (*R,R* configuration) generated with PLD from *S. septatus* TH-2, *S. halstedii* K5, *S. halstedii* subsp. *scabies* K6, and *Actinomadura* sp., respectively; △, ◇, ○, and □ represent the corresponding *sn*-3,*sn*-1′ (*R,S* configuration). For abbreviations see Figures 1 and 2.

66% after 0.5 h of reaction to 50, 54, and 59% after 9 h of reaction, respectively. These time-dependent changes of the diastereomer compositions demonstrate that the *R,R* isomer produced by transphosphatidylation was hydrolyzed to PtdOH faster than the *R,S* isomer; that is, the bacterial PLD would also have greater stereoselectivity toward the *sn*-3′ position than toward the *sn*-1′ position of the glycerol moiety of PtdGro in the hydrolysis reaction. The proportion of the two isomers changed most significantly for *Streptomyces* TH-2 PLD, with the highest hydrolytic activity, whereas *Streptomyces* K6 PLD, with a lower hydrolytic activity, showed almost constant values within the reaction times employed (0–9 h), giving a mixture of 65% *R,R* and 35% *R,S*.

Table 2 summarizes the diastereomer compositions of PtdGro prepared by bacterial PLD-catalyzed transphosphatidylation from PtdCho having different acyl groups. The data clearly show an excess amount of the *R,R* isomer, which occupied 60 to 70% of the total PtdGro. The maximum proportion of the *R,R* isomer (74.0%) was observed for PtdGro generated from 14:0–14:0 GroPCho with *Streptomyces* K6 PLD, whereas the minimum proportion (59.4%) was obtained for PtdGro synthesized from 18:2–18:2 GroPCho with *Streptomyces* K5 PLD. These observations suggest that the number of double bonds and the carbon numbers of the alkyl chains may slightly affect the introduction of a second chiral center in the free glycerol moiety, in addition to the 1,2-diacyl-*sn*-glycero-3-phosphate group having a chiral center (*R* configuration) (10). However, the proportions of the *R,R* isomer (30–40% *R,S* and 60–70% *R,R*) generated from salmon roe PtdCho and egg yolk PtdCho with *Streptomyces* and *Actinomadura* PLD were low compared with those prepared from synthetic PtdCho using the same PLD enzymes (Table 2). These results suggest that the molecular species containing polyunsaturated acyl groups (e.g., 20:5 and 22:6) of the PtdCho used as the substrates had little effect on the proportions of the *R,R* and *R,S* isomers of newly synthesized PtdGro. The diastereomer compositions of PtdGro prepared from PtdEtn were also almost the same as those from PtdCho (Table 2), showing no effect of the head group of phospholipids on the stereoselectivity of bacterial PLD.

Table 3 gives the diastereomer compositions of PtdGro prepared from PtdCho and glycerol by transphosphatidylation with PLD from cabbage and peanuts. In contrast to the bacterial PLD, cabbage and peanut PLD produced a 1:1 mixture of the *R,R* and *R,S* diastereomers from PtdCho having different acyl groups, although a slight excess of the *R,R* isomer was observed for 18:0–18:0 glycerophosphoglycerol (GroPGro) (cabbage PLD) and 18:2–18:2 GroPGro (peanut PLD). A slight excess of the

TABLE 2
Diastereomer Composition of the PtdGro Prepared from PtdCho or Phospatidylethanolamine (PtdEtn) and Glycerol by Transphosphatidylation with Bacterial PLD (mol%)[a]

	S. septatus TH-2		*S. halstedii* K5		*S. halstedii* subsp. *scabies* K6		*Actinomadura* sp.	
Substrate *sn*-1,2-diacyl	*sn*-3,*sn*-3′ (*R,R*)[b]	*sn*-3,*sn*-1′ (*R,S*)[c]	*sn*-3,*sn*-3′ (*R,R*)	*sn*-3,*sn*-1′ (*R,S*)	*sn*-3,*sn*-3′ (*R,R*)	*sn*-3,*sn*-1′ (*R,S*)	*sn*-3,*sn*-3′ (*R,R*)	*sn*-3,*sn*-1′ (*R,S*)
14:0–14:0 GroPCho	65.3 ± 1.4	34.7 ± 1.4	72.6 ± 0.2	27.4 ± 0.2	74.0 ± 0.6	26.0 ± 0.6	65.3 ± 0.9	34.7 ± 0.9
16:0–16:0 GroPCho	65.4 ± 1.0	34.6 ± 1.0	68.7 ± 1.0	31.3 ± 1.0	70.9 ± 0.9	29.1 ± 0.9	63.9 ± 0.4	36.0 ± 0.4
18:0–18:0 GroPCho	64.6 ± 1.0	35.4 ± 1.0	67.6 ± 1.4	32.4 ± 1.4	67.8 ± 0.9	32.2 ± 0.9	64.5 ± 0.5	35.5 ± 0.5
18:1–18:1 GroPCho	63.7 ± 1.1	36.3 ± 1.1	63.5 ± 0.8	36.5 ± 0.8	68.4 ± 0.7	31.6 ± 0.7	61.7 ± 0.5	38.3 ± 0.5
18:1–18:1 GroPEtn	61.7 ± 0.9	38.3 ± 0.9	65.4 ± 0.4	34.6 ± 0.4	70.0 ± 0.4	30.0 ± 0.4	63.5 ± 1.4	36.5 ± 1.4
18:2–18:2 GroPCho	64.5 ± 0.4	35.5 ± 0.4	59.4 ± 0.9	40.6 ± 0.9	65.3 ± 0.5	34.8 ± 0.5	67.4 ± 0.1	32.6 ± 0.1
Egg yolk PtdCho	59.6 ± 1.0	40.4 ± 1.0	61.0 ± 0.3	39.0 ± 0.3	69.6 ± 0.7	30.4 ± 0.7	63.5 ± 0.6	36.5 ± 0.6
Salmon roe PtdCho	62.5 ± 0.4	37.6 ± 0.4	65.7 ± 0.6	34.3 ± 0.6	66.5 ± 0.9	33.5 ± 0.9	60.5 ± 0.3	39.5 ± 0.3

[a]Reactions with PLD from *Streptomyces* and *Actinomadura* were carried out at 30°C for 1.5 and 1 h, respectively. Results are expressed as means (mol%) ± SD of triplicate HPLC analyses. GroPCho, glycerophosphocholine; GroPEtn, glycerophosphoethanolamine; for other abbreviations see Table 1.
[b]1,2-diacyl-*sn*-glycero-3-phospho-3′-*sn*-glycerol (*R,R* configuration).
[c]1,2-diacyl-*sn*-glycero-3-phospho-1′-*sn*-glycerol (*R,S* configuration).

TABLE 3
Diastereomer Composition of PtdGro Prepared from PtdCho and Glycerol by Transphosphatidylation with PLD from Cabbage and Peanuts

	Substrate	Diastereomer (mol%)[a]	
PLD	*sn*-1,2-diacyl	*sn*-3,*sn*-3′ (*R,R*)[b]	*sn*-3,*sn*-1′ (*R,S*)[c]
Cabbage	14:0–14:0 GroPCho	50.7 ± 1.4	49.3 ± 1.4
	16:0–16:0 GroPCho	47.6 ± 0.1	52.4 ± 0.1
	18:0–18:0 GroPCho	54.4 ± 0.4	45.6 ± 0.4
	18:1–18:1 GroPCho	48.5 ± 0.8	51.5 ± 0.8
	18:2–18:2 GroPCho	50.7 ± 0.6	49.3 ± 0.6
	Egg yolk PtdCho	51.5 ± 0.6	48.5 ± 0.6
Peanut	16:0–16:0 GroPCho	51.5 ± 0.9	48.5 ± 0.9
	18:1–18:1 GroPCho	52.1 ± 0.7	47.9 ± 0.7
	18:2–18:2 GroPCho	53.6 ± 0.8	46.4 ± 0.8

[a]Reactions with PLD from cabbage and peanuts were conducted at 30°C within 3–6 h and 15–82 h, respectively. Results are expressed as means (mol%) ± SD of triplicate HPLC analyses. For abbreviations see Tables 1 and 2.
[b]1,2-diacyl-*sn*-glycero-3-phospho-3′-*sn*-glycerol (*R,R* configuration).
[c]1,2-diacyl-*sn*-glycero-3-phospho-1′-*sn*-glycerol (*R,S* configuration).

R,R isomer also has been observed for a commercially available PtdGro, which was produced from egg yolk PtdCho and glycerol with cabbage PLD, showing 55% *R,R* and 45% *R,S* (10). The length of the reaction time had almost no effect on the diastereomer composition produced by the cabbage and peanut PLD, as shown by comparison of the product ratios at 3–6 h and 15–82 h. The results demonstrate that, unlike the bacterial PLD, the plant PLD do not discriminate clearly between the two primary hydroxyl groups of prochiral glycerol, as previously reported by Yang *et al.* (1), Joutti and Renkonen (9), and Itabashi and Kuksis (10). The slight excess of the *R,R* isomer, which was also observed for a commercially available PtdGro generated from egg yolk PtdCho and glycerol with cabbage PLD (10), suggests that the stereoselectivity is slightly influenced by the acyl groups of PtdCho. Further investigation on the effect of the acyl groups on the stereoselectivity of PLD is now in progress.

The reasons for the difference in the stereospecificity of the plant and bacterial PLD are not immediately obvious. Both are believed to belong to the PLD superfamily, which is characterized by the highly conserved HKD motif. Several bacterial PLD from *Streptomyces* have been sequenced. PLD from *S. halstedii, S. septatus*, and the *Streptomyces* sp. PMF strain have shown significant sequence similarity and similar enzymatic properties including high transphosphatidylation activity, high optimal reaction temperatures, and Ca^{2+}-independent activity (12,18). In contrast, the PLD from *S. chromofuscus* is Ca^{2+}-dependent and has very little sequence homology (19) with other *Streptomyces* PLD enzymes. The primary amino acid sequence of *S. chromofuscus* PLD (20,21) exhibits no HKD motif. Although the plant PLD also require micromolar Ca^{2+} for activation, they posses the HKD motifs (22) and that the conserved histidine, lysine, and aspartate residues are believed to form a catalytic triad responsible for the formation of phosphodiester bonds. The cabbage PLD exists as two isozymes, PLD1 and PLD2, which belong to the alpha-type of plant PLD and have an overall homology of 96% (23). The PLD2 is labile, but its

activity can be stabilized by immobilization of appropriate supports (24). The stereospecificity of the PLD1 and PLD2 from cabbage has not been separately assessed.

We conclude that bacterial PLD-catalyzed transphosphatidylation proceeds stereoselectively to produce the diastereomer mixtures of 30–40% *R,S* and 60–70% *R,R* from PtdCho and glycerol. These asymmetric proportions are distinct from those obtained by cabbage and peanut PLD, which give approximately equimolar amounts of the *R,S* and *R,R* isomers, as previously established.

ACKNOWLEDGMENTS

The authors thank Ayami Nakane for her technical assistance, and Q.P. Co-op for providing the egg yolk PtdCho. This study was supported in part by a Grant-in-Aid for Scientific Research from the Ministry of Education, Sciences, Sports and Culture of Japan (Scientific Research B 13460088).

RERERENCES

1. Yang, S.F., Freer, S., and Benson, A.A. (1967) Transphosphatidylation by Phospholipase D, *J. Biol. Chem. 242*, 477–484.
2. Heller, M. (1978) Phospholipase D, *Adv. Lipid Res. 16*, 267–326.
3. Waite, M. (1987) Plant Phospholipases, in *The Phospholipases* (Hanahan, D.J., ed.), Handbook of Lipid Research 5, pp. 61–77, Plenum Press, New York.
4. Ulbrich-Hofmann, R. (2003) Enzyme-Catalysed Transphosphatidylation, *Eur. J. Lipid Sci. Technol. 105*, 305–307.
5. Juneja, L.R., Kazuoka, T., Goto, N., Yamane, T., and Shimizu, S. (1989) Conversion of Phosphatidylcholine to Phosphatidylserine by Various Phospholipase D in the Presence of L- or D-Serine, *Biochim. Biophys. Acta 1003*, 277–283.
6. D'Arrigo, P., and Servi, S. (1997) Using Phospholipases for Phospholipid Modification, *Trends Biotechnol. 15*, 90–96.
7. Ulbrich-Hofmann, R. (2000) Phospholipases, in *Enzymes in Lipid Modification* (Bornscheuer, U., ed.), pp. 219–262, Wiley-VCH, Weinheim.
8. Batrakov, S.G., Panosyan, A.G., Kogan, G.A., and Bergelson, L.D. (1975) Steric Analysis of Glycerophospholipids by Circular Dichroism, Stereospecificity of Phospholipase D Catalyzed Transesterification, *Biochem. Biophys. Res. Commun. 66*, 755–762.
9. Joutti, A., and Renkonen, O. (1976) The Structure of Phosphatidyl Glycerol Prepared by Phospholipase D-Catalyzed Transphosphatidylation from Egg Lecithin and Glycerol, *Chem. Phys. Lipids 17*, 264–266.
10. Itabashi, Y., and Kuksis, A. (1997) Reassessment of Stereochemical Configuration of Natural Phosphatidylglycerols by Chiral-Phase High-Performance Liquid Chromatography and Electrospray Mass Spectrometry, *Anal. Biochem. 254*, 49–56.
11. Hagishita, T., Nishikawa, M., and Hatanaka, T. (2000) Isolation of Phospholipase D Producing Microorganisms with High Transphosphatidylation Activity, *Biotech. Lett. 22*, 1587–1590.
12. Hatanaka, T., Negishi, T., Kubota-Akizawa, M., and Hagishita, T. (2002) Purification, Characterization, Cloning and Sequencing of Phospholipase D from *Streptomyces septatus* TH-2, *Enzyme Microb. Technol. 31*, 233–241.
13. Hatanaka, T., Negishi, T., Kubota-Akizawa, M., and Hagishita, T. (2002) Study on Thermostability of Phospholipase D from *Streptomyces* sp., *Biochim. Biophys. Acta 1598*, 156–164.
14. Hagishita, T., Nishikawa, M., and Hatanaka, T. (1999) A Spectrophotometric Assay for the Transphosphatidylation Activity of Phospholipase D Enzyme, *Anal. Biochem. 276*, 161–165.
15. Okabe, H., Itabashi, Y., and Ota, T. (1999) Determination of Molecular Species of Phosphatidylcholines as 2-Anthrylurethanes by Reversed-Phase HPLC with Fluorescence Detection and Online Electrospray Ionization Mass Spectrometry, *J. Jpn. Oil Chem. Soc. 48*, 559–567.
16. Dittmer, J.C., and Lester, R.L. (1964) A Simple, Specific Spray for the Detection of Phospholipids on Thin-Layer Chromatograms, *J. Lipid Res. 5*, 126–127.
17. Juneja, L.R., Hibi, N., Inagaki, N., and Yamane, T. (1987) Comparative Study on Conversion of Phosphatidylcholine to Phosphatidylglycerol by Cabbage Phospholipase D in Micelle and Emulsion Systems, *Enzyme Microb. Technol. 9*, 350–354.
18. Shimbo, K., Iwasaki, Y., Yamane, T., and Ina, K. (1993) Purification and Properties of Phospholipase D from *Streptomyces antibioticus*, *Agric. Biol. Chem. 57*, 1946–1948.
19. Iwasaki, Y., Nakano, H., and Yamane, T. (1994) Phospholipase D from *Streptomyces antibioticus*: Cloning, Sequencing, Expression, and Relationship to Other Phospholipases, *Appl. Microbiol. Biotechnol. 42*, 290–299.
20. Yoshioka, K., Mizoguchi, M., Takahara, M., Imamura, S., Beppu, T., and Horinuchi, S. (1991) DNA Having the Genetic Information of Phospholipase D and Its Uses, European Patent 0435725B1.
21. Yang, H., and Roberts, M.F. (2002) Cloning, Overexpression, and Characterization of a Bacterial Ca^{2+}-Dependent Phospholipase D, *Protein Sci. 11*, 2958–2968.
22. Pappan, K., and Wang, X. (1999) Molecular and Biochemical Properties and Physiological Roles of Plant Phospholipase D, *Biochim. Biophys. Acta 1439*, 151–166.
23. Schäffner, I., Rücknagel, K.-P., Mansfeld, J., and Ulbrich-Hofmann, R. (2002) Genomic Structure, Cloning and Expression of Two Phospholipase D Isoenzymes from White Cabbage, *Eur. J. Lipid Sci. Technol. 104*, 79–87.
24. Younus, H., Rajcani, J., Ulbrich-Hofmann, R., and Saleemuddin, M. (2004) Behaviour of a Recombinant Cabbage (*Brassica oleracea*) Phospholipase D Immobilized on CNBr-Activated and Antibody Supports, *Biotechnol. Appl. Biochem. 40*, 95–99.

[Received April 2, 2004; accepted November 7, 2004]

Effect of Temperature on the Stereoselectivity of Phospholipase D Toward Glycerol in the Transphosphatidylation of Phosphatidylcholine to Phosphatidylglycerol

Rina Sato[a], Yutaka Itabashi[a,*], Akira Suzuki[a], Tadashi Hatanaka[b], and Arnis Kuksis[c]

[a]Graduate School of Fisheries Sciences, Hokkaido University, Hakodate 041-8611, Japan, [b]Research Institute for Biological Sciences, Okayama 716-1241, Japan, and [c]Banting and Best Department of Medical Research, University of Toronto, Toronto, Ontario M5G 1L6, Canada

ABSTRACT: In this study, the effect of temperature on the stereoselectivity of phospholipase D (PLD) toward the two primary hydroxyl groups of glycerol in the transphosphatidylation reaction of phosphatidylcholine to phosphatidylglycerol (PtdGro) was investigated. For this purpose, PLD from bacteria (*Streptomyces septatus* TH-2, *S. halstedii* subsp. *scabies* K6, and *Actinomadura* sp.) and cabbage were tested. At the reaction temperatures employed (0–60°C), the proportions of the two PtdGro diastereomers, namely, 1,2-dioleoyl-*sn*-glycero-3-phospho-3′-*sn*-glycerol (*R,R* configuration) and 1,2-dioleoyl-*sn*-glycero-3-phospho-1′-*sn*-glycerol (*R,S* configuration), which were produced with PLD from *Streptomyces* TH-2 and *Actinomadura* sp., changed gradually from 50% *R,R* and 50% *R,S* at 50–60°C to 70% *R,R* and 30% *R,S* at 0°C. These alterations suggested that the stereoselectivity of the bacterial PLD toward the two primary hydroxyl groups of prochiral glycerol was significantly influenced by reaction temperature. PLD from *Streptomyces* K6 showed relatively little effect of temperature on stereoselectivity, giving 65–69% *R,R* in the temperature range of 60–10°C examined. The plots of ln ([*R,R*]/[*R,S*]) vs. 1/*T* gave good linear fits for these three bacterial PLD. No temperature effect was observed for cabbage PLD, which gave an almost equimolar mixture of the *R,R* and *R,S* diastereomers in the range from 0 to 40°C. The temperature-dependent change in enantiomeric selectivity of the bacterial PLD promises potentially profitable commercial exploitation.

Paper no. L9481 in *Lipids 39,* 1019–1023 (October 2004).

Phospholipase D (PLD) is an enzyme that hydrolyzes the phosphodiester bond of various phospholipids including phosphatidylcholine (PtdCho) to form phosphatidic acid and a nonphosphorylated base. PLD also catalyzes a transphosphatidylation reaction in which the phosphatidyl moiety from phospholipids is transferred to alcohols (1–3). By the latter reaction, natural 1,2-diacyl-*sn*-glycero-3-phosphocholine (*R* configuration) in the presence of glycerol is readily converted to a mixture of diastereomeric phosphatidylglycerols (PtdGro), that is, 1,2-diacyl-*sn*-glycero-3-phospho-1′-*sn*-glycerol (*R,S* configuration) and 1,2-diacyl-*sn*-glycero-3-phospho-3′-*sn*-glycerol (*R,R* configuration) (4–6).

It is well known that the PtdGro prepared from PtdCho (*R* configuration) and glycerol by transphosphatidylation with cabbage PLD is an almost equimolar mixture of the *R,S* and *R,R* diastereomers (4–6). This means that the cabbage PLD shows no stereoselectivity toward the two primary hydroxyl groups of prochiral glycerol in the reaction. Hagishita *et al.* (7) have recently reported that the extracellular PLD isolated from microorganisms belonging to *Actinomycetes* possessed high transphosphatidylation activity. We have recently found that the bacterial PLD-catalyzed transphosphatidylation proceeds stereoselectively to produce a mixture of 30–40% *R,S* and 60–70% *R,R* diastereomers, discriminating to some extent between the two primary hydroxyl groups of prochiral glycerol (8). Interestingly, Hatanaka *et al.* (9) have observed that PLD enzymes from *Streptomyces* strains differed significantly in their thermostability, with *S. halstedii* K1 losing its activity at 45°C. Hatanaka *et al.* (10) later showed that substitution of Asp for Glu346 by site-directed mutagenesis tended to restore the thermostability of the K1 PLD. On the other hand, Sakai *et al.* (11,12) have reported a low-temperature method (–40°C at best) for enhancing enantioselectivity in lipase-catalyzed kinetic resolutions of some chiral alcohols. Other studies have shown that temperature can affect the enantioslectivity of dehydrogenases and esterases (13–15). To examine this observation further and to test its applicability to transphosphatidylation, we determined the effect of temperature on the course of the stereochemical reaction of several PLD enzymes from *Actinomyces* and from cabbage in the range of 0 to 60°C.

MATERIALS AND METHODS

Materials. PLD (*S. septatus* TH-2, *S. halstedii* subsp. *scabies* K6, *Actinomadura* sp., and cabbage), 1,2-dioleoyl-*sn*-glycero-3-phosphocholine, glycerol, 3,5-dinitrophenyl isocyanate, and HPLC-grade solvents (hexane, dichloromethane, and methanol) were those described previously (8).

*To whom correspondence should be addressed at Laboratory of Bioresources Chemistry, Graduate School of Fisheries Sciences, Hokkaido University, 3-1-1 Minato-cho, Hakodate, Hokkaido 041-8611, Japan.
E-mail: yutaka@pop.fish.hokudai.ac.jp

Abbreviations: DNPU, 3,5-dinitrophenylurethane; PLD, phospholipase D; PtdCho, phosphatidylcholine; PtdGro, phosphatidylglycerol.

Preparation, derivatization, and analysis of PtdGro. PtdGro was generated from PtdCho and glycerol by transphosphatidylation with PLD in a biphasic system consisting of diethyl ether and 0.4 M acetate buffer (pH 5.6) using a slight modification of a previously described procedure (8). Briefly, the reaction was performed at various temperatures (0–60°C) with vigorous stirring for 1, 1.5, and 3 h with PLD from *Actinomadura*, *Streptomyces*, and cabbage, respectively. At the selected reaction times, most of the PtdCho was transformed into PtdGro. The PtdGro was converted into bis(3,5-dinitrophenylurethane) (bis-DNPU) derivatives, followed by chiral-phase HPLC on an (*R*)-1-(1-naphthyl)ethylamine column (YMC-Pack A-K03, 25 cm × 4.6 mm i.d.; YMC, Kyoto, Japan) using hexane/dichloromethane/methanol/trifluoroacetic acid (60:20:20:0.2, by vol) as the mobile phase at a flow rate of 1 mL/min (6,8).

RESULTS AND DISCUSSION

Temperature effect. Figure 1 shows the chiral-phase HPLC profiles of the bis-DNPU derivatives of PtdGro generated from PtdCho and glycerol by transphosphatidylation at 0 and 60°C with PLD from *Streptomyces* TH-2. Clear resolution was observed for the *R,R* and *R,S* diastereomers with peak area ratios of 3:1 (0°C) and 1:1 (60°C), demonstrating a clear temperature effect on the stereoselectivity toward the two primary hydroxy groups of prochiral glycerol by the bacterial PLD. Similar chromatograms were also obtained for PLD from *Streptomyces* K6 and *Actinomadura* sp. Table 1 summarizes the proportions of diastereomers measured in the temperature range from 0 to 60°C using bacterial and cabbage PLD preparations. The reproducibility of the method was examined for *Streptomyces* TH-2 PLD, and the data were obtained within ±1.9 SD on repeated runs. The PtdGro formed at 60 and 50°C with PLD from *Streptomyces* TH-2 and *Actinomadura* sp., respectively, were comprised of equimolar amounts of the *R,R* and *R,S* isomers, whereas at 30 and 0°C the PtdGro proportions changed to 6:4 and 7:3 of the *R,R* and *R,S* isomers, respectively. Thus, in the range of 0–60°C, the proportion of the *R,R* isomer produced with PLD from *Streptomyces* TH-2 and *Actinomadura* sp. increased gradually as the temperature was lowered. On the other hand, PLD from *Streptomyces* K6 showed relatively little effect of temperature on stereoselectivity, giving 65–69% *R,R* in the temperature range of 60–10°C. The highest diastereomer excess (43.2%) was obtained at 0°C with PLD from *Actinomadura* sp., and an inversion of the configurational preference occurred at 50°C (Table 1). Pure stereoisomers also were not obtained when the *Actinomadura* enzyme was tested in the temperature range of 0 to –30°C using anhydrous organic solvents (16). A 3:7 mixture of the *R,S* and *R,R* isomers was recovered at –30°C. These results clearly show that the reaction temperature significantly affected the stereoselectivity of the three bacterial PLD used in this study. This finding is in agreement with the thermodynamics of the reaction (see following discussion), which suggests that lowering the temperature increases the enantioselectivity so long as the reaction is carried out below the racemic temperature (13). In contrast, cabbage PLD gave an almost equimolar mixture of the *R,S* and *R,R* isomers in the range of 0 to 40°C (Table 2), indicating no significant effect on the stereoselectivity of this enzyme.

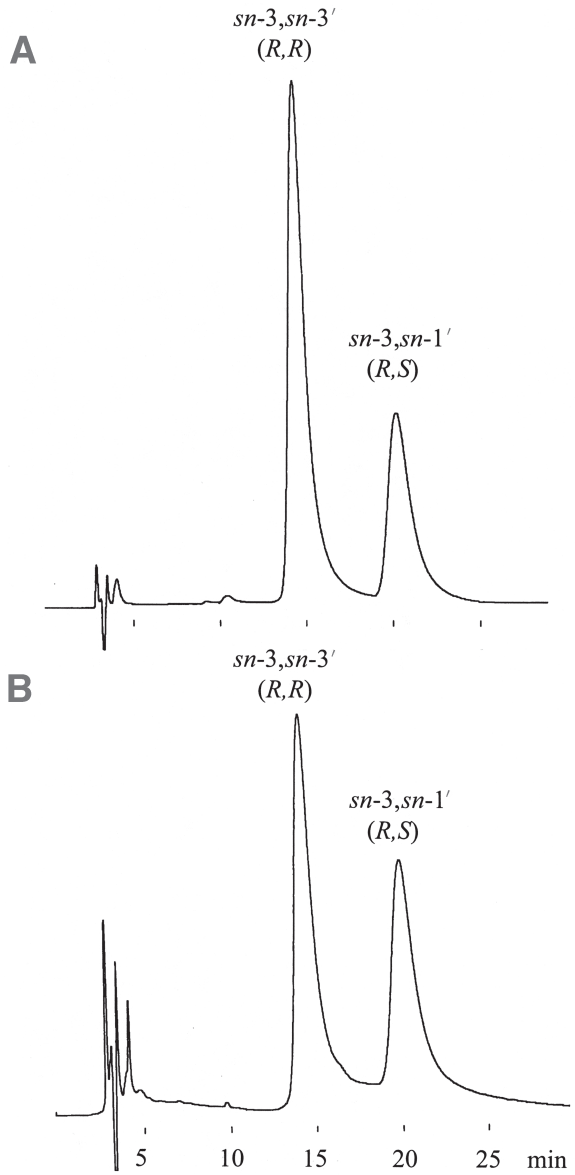

FIG. 1. Chiral-phase HPLC profiles of the bis(3,5-dinitrophenylurethane) derivatives of the phosphatidylglycerols generated from 1,2-dioleoyl-*sn*-glycero-3-phosphocholine and glycerol by transphosphatidylation with phospholipase D (PLD) from *Streptomyces septatus* TH-2, (A) 0°C; (B) 60°C. *sn*-3,*sn*-1′,1,2-dioleoyl-*sn*-glycero-3-phospho-1′-*sn*-glycerol (*R,S* configuration); *sn*-3,*sn*-3′, 1,2-dioleoyl-*sn*-glycero-3-phospho-3′-*sn*-glycerol (*R,R* configuration). Column temperature, 10°C; detection, 254 nm UV. Other HPLC conditions are as given in the text.

Thermodynamic parameters. To confirm that the temperature effects were real, we examined the thermodynamic parameters of the reaction using the Eyring equation. This equation

TABLE 1
Effect of Temperature on the Stereoselectivity of Bacterial Phospholipase D Toward Glycerol in the Transphosphatidylation of Phosphatidylcholine to Phosphatidylglycerol

Phospholipase D	Temperature (°C)	Diastereomer (mol%)		Diastereomer excess[c] (%)
		sn-3,*sn*-3′ (*R,R*)[a]	*sn*-3,*sn*-1′ (*R,S*)[b]	
Streptomyces septatus TH-2	0	66.4	33.6	32.8 (*R,R*)
	10	62.8	37.2	25.6 (*R,R*)
	30	57.9	42.1	15.8 (*R,R*)
	50	54.3	45.7	8.6 (*R,R*)
	60	52.0	48.0	4.0 (*R,R*)
S. halstedii subsp. *scabies* K6	10	69.0	31.0	38.1 (*R,R*)
	20	68.6	31.4	37.1 (*R,R*)
	30	67.7	32.3	35.4 (*R,R*)
	60	64.8	35.2	29.6 (*R,R*)
Actinomadura sp.	0	71.6	28.4	43.2 (*R,R*)
	10	64.3	35.7	28.7 (*R,R*)
	30	58.6	41.4	17.1 (*R,R*)
	50	48.4	51.6	2.6 (*R,S*)
Cabbage	0	48.3	51.7	3.4 (*R,S*)
	20	52.4	47.6	4.8 (*R,R*)
	40	50.6	49.4	1.2 (*R,R*)

[a]1,2-dioleoyl-*sn*-glycero-3-phospho-3′-*sn*-glycerol (*R,R* configuration).
[b]1,2-dioleoyl-*sn*-glycero-3-phospho-1′-*sn*-glycerol (*R,S* configuration).
[c]Diastereomer excess (%) = {([*R,S*] − [*R,R*])/([*R,S*] + [*R,R*])} × 100, where [*R,S*] and [*R,R*] denote the composition of the *R,S* and *R,R* diastereomers, respectively.

is derived from the transition-state theory (13) as shown in Equation 1:

$$k = [(k_B T)/h]\exp[-\Delta G^{\ddagger}/(RT)] = [(k_B T)/h]\exp[(\Delta S^{\ddagger}/R) - (\Delta H^{\ddagger}/R)(1/T)] \quad [1]$$

where k, k_B, h, $\Delta G^{\ddagger}$, $\Delta S^{\ddagger}$, and $\Delta H^{\ddagger}$ are the reaction rate constant, the Boltzmann constant, the Plank constant, the free energy of activation, the entropy of activation, and the enthalpy of activation, respectively. PLD-catalyzed transphosphatidylation toward the two primary hydroxyl groups at the *sn*-1′ and *sn*-3′ positions of glycerol on the basis of the Eyring equation (Eq. 1) can be defined as shown in Equations 2 and 3:

$$k_{R,S} = [(k_B T)/h]\exp[(\Delta S^{\ddagger}_{R,S}/R) - (\Delta H^{\ddagger}_{R,S}/R)(1/T)] \quad [2]$$

$$k_{R,R} = [(k_B T)/h]\exp[(\Delta S^{\ddagger}_{R,R}/R) - (\Delta H^{\ddagger}_{R,R}/R)(1/T)] \quad [3]$$

Combining Equations 2 and 3 leads to Equation 4:

$$\ln(k_{R,R}/k_{R,S}) = (\Delta\Delta S^{\ddagger}_{R,R\text{-}R,S}/R) - [\Delta\Delta H^{\ddagger}_{R,R\text{-}R,S}/(RT)] \quad [4]$$

On the other hand, the stereochemical purity of a chiral substance is often evaluated by the *E* value (11,12,14,15,17), meaning the enantiospecificity ratio. Defining *E* as the diastereospecificity ratio for the *R,R* and *R,S* diastereomers, it is expressed as Equation 5:

$$k_{R,R}/k_{R,S} = [R,R]/[R,S] \quad [5]$$

If the reverse reactions of diastereomer formation are negligible, the *E* value is approximately equal to the ratio of the rate constant as

$$E = k_{R,R}/k_{R,S} \quad [6]$$

Equations 4–6 lead to

$$\ln E = \ln([R,R]/[R,S]) = (\Delta\Delta S^{\ddagger}_{R,R\text{-}R,S}/R) - [\Delta\Delta H^{\ddagger}_{R,R\text{-}R,S}/(RT)] \quad [7]$$

Equation 7 describes a plot of ln *E* vs. $1/T$ that yields a straight line.

TABLE 2
Effect of Temperature on the Stereoselectivity of Cabbage Phospholipase D Toward Glycerol in the Transphosphatidylation of Phosphatidylcholine to Phosphatidylglycerol

Temperature (°C)	Diastereomer (mol%)		Diastereomer excess[c] (%)
	sn-3,*sn*-3′ (*R,R*)[a]	*sn*-3,*sn*-1′ (*R,S*)[b]	
0	48.3	51.7	3.4 (*R,S*)
20	52.4	47.6	4.8 (*R,R*)
40	50.6	49.4	1.2 (*R,R*)

[a]1,2-dioleoyl-*sn*-glycero-3-phospho-3′-*sn*-glycerol (*R,R* configuration).
[b]1,2-dioleoyl-*sn*-glycero-3-phospho-1′-*sn*-glycerol (*R,S* configuration).
[c]Diastereomer excess (%) = {([*R,S*] − [*R,R*])/([*R,S*] + [*R,R*])} × 100, where [*R,S*] and [*R,R*] denote the composition of the *R,S* and *R,R* diastereomers, respectively.

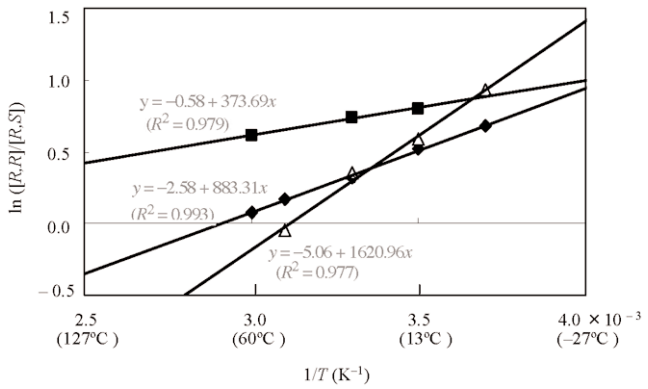

FIG. 2. Plots of ln ([*R,R*]/[*R,S*]) vs. 1/*T* for bacterial PLD-catalyzed transphosphatidylation of phosphatidylcholine to phosphatidylglycerol. The lines shown were obtained by linear regression fitting of the data from Table 1. The 1/*T* (K^{-1}) values of the two intersection points of the straight lines were 3.4×10^{-3} (25°C) and 3.6×10^{-3} (3°C). (u) PLD from *S. septatus* TH-2; (n) PLD from *S. halstedii* subsp. *scabies* K6; (s) PLD from *Actinomadura* sp. For abbreviation see Figure 1.

The plots of ln *E* vs. 1/*T* for the PtdGro diastereomers produced by bacterial PLD-catalyzed transphosphatidylation are shown in Figure 2. Good linear relationships were obtained for all the PLD examined. The differential free energy of activation ($\Delta\Delta G^{\ddagger}$) (13) can be given by Equation 8, where $\Delta\Delta H^{\ddagger}$ and $\Delta\Delta S^{\ddagger}$ denote the differences in activation enthalpy and entropy, respectively:

$$\Delta\Delta G^{\ddagger} = -RT \ln E = \Delta\Delta H^{\ddagger} - T\Delta\Delta S^{\ddagger} \quad [8]$$

When no diastereomeric discrimination in the formation of the *R,S* and *R,R* isomers occurs, $E = 1$; hence, $\Delta\Delta G^{\ddagger} = 0$. Equation 8 then results in Equation 9, and the reaction temperature refers to the racemic temperature, T_r (13):

$$T_r = \Delta\Delta H^{\ddagger}/\Delta\Delta S^{\ddagger} \quad [9]$$

Table 3 gives $\Delta\Delta H^{\ddagger}_{R,R\text{-}R,S}$, $\Delta\Delta S^{\ddagger}_{R,R\text{-}R,S}$, and T_r for the formation of the *R,R* and *R,S* isomers by PLD-catalyzed transphosphatidylation, as determined from the corresponding ln *E* vs. 1/*T* plots shown in Figure 2.

Mechanism of reaction. Sakai *et al*. (11) remarked that $\Delta\Delta H^{\ddagger}$ originated from the difference in the steric interactions operating between the enantiomers in the transition state. The high selectivity of PLD from *Actinomadura* sp. toward glycerol caused the large negative difference in $\Delta\Delta H^{\ddagger}_{R,R\text{-}R,S}$, whereas the low selectivity of PLD from *Streptomyces* K6 arose from the smaller negative values in $\Delta\Delta H^{\ddagger}_{R,R\text{-}R,S}$. The negative $\Delta\Delta S^{\ddagger}$ values indicate that the *R,R* isomer is more tightly bound to the enzyme in the transition state than is the *R,S* isomer. This is presumably due to favorable van der Waals interactions and hydrogen bonding between the *R,R* isomer and the amino acid side chains lining the binding sites in the complex (13,15).

Leiros *et al*. (18) have determined the tertiary structure of PLD from *Streptomyces* sp. strain PMF. The enzyme was found to consist of 18 α helices and 17 β sheets, with the overall structure being an α-β-α-β-α-sandwich configuration. The active site is made up of two identical sequence repeats of an HKD motif, positioned around an approximately two-fold axis. The reaction proceeds *via* a phosphohistidine intermediate and identifies a catalytic water molecule positioned for an apical attack on the phosphorus, consistent with an associative in-line phosphoryl transfer reaction. Hatanaka *et al.* (10) have discussed the nature of the amino acid residues critical for the thermostability of PLD, but the selectivity of interaction of specific amino acid residues with the chiral or prochiral glycerolipid derivatives has not been established.

Since the *E* value decreases with increasing temperatures at temperatures above T_r (13), the *R,S* isomer should be produced in excess over the *R,R* isomer at temperatures above the T_r values. On the other hand, at temperatures below T_r, the *E* value increases with a decrease in temperature (13). In this study, the *E* value was maximal at 0°C, the lowest temperature employed, and the *R,R* isomer was produced predominantly over the *R,S* isomer. These results suggest that the stereoselectivity of the bacterial PLD toward the two primary hydroxyl groups of glycerol is temperature-predictive in the range of 0–60°C examined. PLD from *Streptomyces* K6 exhibited a much higher T_r value than that of PLD from *Streptomyces* TH-2 and *Actinomadura* sp. The $\Delta\Delta H^{\ddagger}$ and $\Delta\Delta S^{\ddagger}$ values of *Streptomyces* K6 PLD were also higher than those observed for PLD from *Streptomyces* TH-2 and *Actinomadura* sp. These results show that *Streptomyces* K6 PLD has a high stereoselectivity over a wide range of reaction temperatures. The stereoselectivity of *Actinomadura* PLD was markedly influenced by temperature, as indicated by the lowest values of

TABLE 3
Thermodynamic Parameters and Racemic Temperature of Bacterial Phospholipase D Toward Glycerol in the Transphosphatidylation of Phosphatidylcholine to Phosphatidylglycerol[a]

	Phospholipase D		
	S. septatus TH-2	*S. halstedii* subsp. *scabies* K6	*Actinomadura* sp.
$\Delta\Delta H^{\ddagger}_{R,R\text{-}R,S}$ (kcal/mol)	–1.8	–0.7	–3.2
$\Delta\Delta S^{\ddagger}_{R,R\text{-}R,S}$ (cal/deg·mol)	–5.1	–1.0	–10.1
T_r (°C)	70.6	466.9	46.9

[a]$\Delta\Delta H^{\ddagger}_{R,R\text{-}R,S}$, difference of activation enthalpy; $\Delta\Delta S^{\ddagger}_{R,R\text{-}R,S}$, difference of activation entropy; T_r, racemic temperature.

$\Delta\Delta H^{\ddagger}$ and $\Delta\Delta S^{\ddagger}$ in the three bacterial PLD employed, although the highest stereoselectivity (72% *R,R*) was observed at temperatures below 3°C. On the other hand, the selectivity of *Streptomyces* TH-2 PLD was intermediate between that of PLD from *Streptomyces* K6 and *Actinomadura* sp.

Significance of the study. PtdGro is widely distributed in plants, animals, and bacteria, and is known to have a single *R,S* configuration (19). Using chiral-phase HPLC, however, Itabashi and Kuksis (6) and Fujishima *et al.* (20) have recently found that PtdGro from some bacteria, including *Escherichia coli,* contain a nonnegligible amount of the *R,R* isomer. The differences between the *R,S* and *R,R* isomers in the physical and biochemical properties and physiological functions are unknown. Thus, pure *R,S* and *R,R* isomers are necessary to determine the biological significance of the PtdGro diastereomers. Although chemical methods for preparing these diastereomers have been established (21,22), the products are not commercially available. The present study shows that the proportion of *R,R* isomers is significantly increased by conducting the reaction below the racemic temperature, but that a pure *R,R* isomer was not obtained with the enzymes tested. Since the bacterial PLD enzymes exhibit significant differences in reactivity, it is possible that a species or mutant may be found that exhibits higher temperature-dependent enantioselectivity. The present work suggests that it might be difficult to obtain pure *R,R* isomers even if much lower temperatures were applied. Likewise, pure *R,S* isomers are unlikely to be obtained even if mutant PLD of increased thermostability became available. Nevertheless, the study indicates that preparing glycerophospholipids of high enantiomeric excess by transphosphatidylation and by manipulating the reaction temperature is feasible.

ACKNOWLEDGMENT

This study was supported in part by a Grant-in-Aid for Scientific Research from the Ministry of Education, Sciences, Sports and Culture of Japan (Scientific Research B 13460088).

REFERENCES

1. Heller, M. (1978) Phospholipase D, *Adv. Lipid Res. 16*, 267–326.
2. Waite, M. (1987) Plant Phospholipases, in *The Phospholipases*, (Hanahan, D.J., ed.), *Handbook of Lipid Research 5*, pp. 61–77, Plenum Press, New York.
3. Ulbrich-Hofmann, R. (2003) Enzyme-Catalysed Transphosphatidylation, *Eur. J. Lipid Sci. Technol. 105*, 305–307.
4. Yang, S.F., Freer, S., and Benson, A.A. (1967) Transphosphatidylation by Phospholipase D, *J. Biol. Chem. 242*, 477–484.
5. Joutti, A., and Renkonen, O. (1976) The Structure of Phosphatidyl Glycerol Prepared by Phospholipase D-Catalyzed Transphosphatidylation from Egg Lecithin and Glycerol, *Chem. Phys. Lipids 17*, 264–266.
6. Itabashi, Y., and Kuksis, A. (1997) Reassessment of Stereochemical Configuration of Natural Phosphatidylglycerols by Chiral-Phase High-Performance Liquid Chromatography and Electrospray Mass Spectrometry, *Anal. Biochem. 254*, 49–56.
7. Hagishita, T., Nishikawa, M., and Hatanaka, T. (2000) Isolation of Phospholipase D Producing Microorganisms with High Transphosphatidylation Activity, *Biotech. Lett. 22*, 1587–1590.
8. Sato, R., Itabashi, Y., Hatanaka, T., and Kuksis, A. (2004) Asymmetric *in vitro* Synthesis of Diastereomeric Phosphatidylglycerols from Phosphatidylcholine and Glycerol by Bacterial Phospholipase D, *Lipids 39*, 1013–1018.
9. Hatanaka, T., Negishi, T., Kubota-Akizawa, M., and Hagishita, T. (2002) Study on the Thermostability of Phospholipase D from *Streptomyces* sp., *Biochim. Biophys. Acta 1598*, 156–164.
10. Hatanaka, T., Negishi, T., and Mori, K. (2004) A Mutant Phospholipase D with Enhanced Thermostability from *Streptomyces* sp., *Biochim. Biophys. Acta 1696*, 75–82.
11. Sakai, T., Kishimoto, T., Tanaka, Y., Ema, T., and Utaka, M. (1998) Low-Temperature Method for Enhancement of Enantioselectivity in the Lipase-Catalyzed Kinetic Resolutions of Solketal and Some Chiral Alcohols, *Tetrahedron Lett. 39*, 7881–7884.
12. Sakai, T., Kawabata, I., Kishimoto, T., Ema, T., and Utaka, M. (1997) Enhancement of the Enantioselectivity in Lipase-Catalyzed Kinetic Resolutions of 3-Phenyl-2*H*-azirine-2-methanol by Lowering the Temperature to −40°C, *J. Org. Chem. 62*, 4906–4907.
13. Phillips, R.S. (1996) Temperature Modulation of the Stereochemistry of Enzymatic Analysis: Prospects for Exploitation, *Trends Biotechnol. 14*, 13–16.
14. Pham, V.T., and Phillips, R.S. (1990) Effects of Substrate Structure and Temperature on the Stereospecificity of Secondary Alcohol Dehydrogenase from *Thermoanaerobacter ethanolicus*, *J. Am. Chem. Soc. 112*, 3629–3632.
15. Sehgal, A.C., and Kelly, R.M. (2002) Enantiomeric Resolution of 2-Aryl Propionic Esters with Hyperthermophilic and Mesophilic Esterases: Contrasting Thermodynamic Mechanisms, *J. Am. Chem. Soc. 124*, 8190–8191.
16. Rich, J.O., and Khmelnitsky, Y.L. (2001) Phospholipase D-Catalyzed Transphosphatidylation in Anhydrous Organic Solvents, *Biotechnol. Bioeng. 32*, 374–377.
17. Chen, C.-S., Fujimoto, Y., Girdaukas, G., and Sih, C.J. (1982) Quantitative Analysis of Biochemical Kinetic Resolutions of Enantiomers, *J. Am. Chem. Soc. 104*, 7294–7299.
18. Leiros, I., McSweeney, S., and Hough, E. (2004) The Reaction Mechanism of Phospholipase D from *Streptomyces* sp. Strain PMF. Snapshots Along the Reaction Pathway Reveal a Pentacoordinate Reaction Intermediate and an Unexpected Final Product, *J. Mol. Biol. 339*, 805–820.
19. Hostetler, K.Y. (1982) Polyglycerophospholipids: Phosphatidylglycerol, Diphosphatidylglycerol and Bis(monoacylglycero)phosphate, in *Phospholipids* (Hawthorne, J.N., and Ansell, G.B., eds.), pp. 215–261, Elsevier Biochemical Press, Amsterdam.
20. Fujishima, H., Gamano, T., Taoka, Y., Sawabe, T., and Itabashi, Y. (2004) Stereoisomers of Marine Bacterial Phosphatidylglycerols, *Nippon Suisan Gakkaishi* (in Japanese) *70*, 200–202.
21. Baer, E., and Buchnea, D. (1958) Synthesis of Saturated and Unsaturated Phosphatidyl Glycerols. III. Cardiolipin Substitutes, *J. Biol. Chem. 232*, 895–901.
22. Woolley, P., and Eibl, H. (1988) Synthesis of Enantiomerically Pure Phospholipids Including Phosphatidylserine and Phosphatidylglycerol, *Chem. Phys. Lipids 47*, 55–62.

[Received April 2, 2004; accepted November 7, 2004]

Simple Synthesis of Diastereomerically Pure Phosphatidylglycerols by Phospholipase D-Catalyzed Transphosphatidylation

Rina Sato[a], Yutaka Itabashi[a,*], Hironori Fujishima[a], Hidetoshi Okuyama[b], and Arnis Kuksis[c]

[a]Graduate School of Fisheries Sciences, Hokkaido University, Hakodate 041-8611, Japan, [b]Graduate School of Environmental Earth Science, Hokkaido University, Sapporo 060-0810, Japan, and [c]Banting and Best Department of Medical Research, University of Toronto, Toronto, Ontario M5G 1L6, Canada

ABSTRACT: A simple method for synthesizing diastereomerically pure phosphatidylglycerols (PtdGro), namely, 1,2-diacyl-*sn*-glycero-3-phospho-3′-*sn*-glycerol (*R,R* configuration) and 1,2-diacyl-*sn*-glycero-3-phospho-1′-*sn*-glycerol (*R,S* configuration), was established. For this purpose, diastereomeric 1,2-*O*-isopropylidene PtdGro were prepared from 1,2-diacyl-*sn*-glycero-3-phosphocholine (PtdCho) and enantiomeric 1,2-*O*-isopropylideneglycerols by transphosphatidylation with phospholipase D (PLD) from *Actinomadura* sp. This species was selected because of its higher transphosphatidylation activity and lower phosphatidic acid (PtdOH) formation than PLD from some *Streptomyces* species tested. The reaction proceeded well, giving almost no hydrolysis of PtdCho to PtdOH in a biphasic system consisting of diethyl ether and acetate buffer at 30°C. The isopropylidene protective group was removed by heating the diastereomeric isopropylidene PtdGro at 100°C in trimethyl borate in the presence of boric acid to obtain the desired PtdGro diastereomers. The purities of the products, which were determined by chiral-phase HPLC, were exclusively dependent on the optical purities of the original isopropylideneglycerols used. The present method is simple and can be utilized for the synthesis of pure PtdGro diastereomers having saturated and unsaturated acyl chains.

Paper no. L9482 in *Lipids 39,* 1025–1030 (October 2004).

Phosphatidylglycerol (PtdGro) is known to be widely distributed in animals, plants, and microorganisms (1), where it plays important roles as one of the acidic polyglycerophospholipids (2–4). The structure of naturally occurring PtdGro may be 1,2-diacyl-*sn*-glycero-3-phospho-1′-*sn*-glycerol (*sn*-3,*sn*-1′, *R,S* configuration) (1,5–7). However, Itabashi and Kuksis (8) and Fujishima *et al.* (9) have recently found that PtdGro from some bacteria, including *Escherichia coli*, contain a nonnegligible amount of 1,2-diacyl-*sn*-glycero-3-phospho-3′-*sn*-glycerol (*sn*-3,*sn*-3′, *R,R* configuration). Y. Itabashi, H. Fujishima, and A. Kuksis (unpublished results) also have found that the content of the *R,R* isomer in *E. coli* PtdGro increases with increasing growth temperature. This observation suggests that the bacterium adapts to temperature by alternating not only the degree of unsaturation but also the stereoisomer composition of PtdGro. To clarify the differences in biochemical properties and physiological functions between the *R,S* and *R,R* diastereomers in bacteria, we concerned ourselves with the synthesis of the pure PtdGro diastereomers, which are not commercially available.

Although the enantiomeric and diastereomeric PtdGro can be synthesized chemically *via* several steps involving phosphorylation of enantiomeric DAG (10,11), in this study we investigated a simpler enzymatic method using phospholipase D (PLD). PLD catalyzes transphosphatidylation in which the phosphatidyl moiety of substrate phospholipids is transferred to acceptor alcohols to produce phosphatidyl alcohols (12,13). Thus, 1,2-diacyl-*sn*-glycero-3-phosphocholine (*R* configuration) in the presence of glycerol is readily converted into PtdGro, which is a mixture of the *R,R* and *R,S* diastereomers (8,14–16). In this study, to obtain diastereomerically pure *R,R* and *R,S* PtdGro, we used enantiomerically pure 1,2- and 2,3-*O*-isopropylidene-*sn*-glycerols instead of glycerol, which are the general intermediates for the synthesis of chiral glycerolipids (17,18). The sequence of reactions used is shown in Figure 1. D'Arrigo *et al.* (16) reported a similar enzymatic method for obtaining the diastereomeric PtdGro from phosphatidylcholine (PtdCho) and isopropylideneglycerols by transphosphatidylation using PLD from *Streptomyces* species; the diastereomeric nature of the products was implied from the starting materials (1,2- and 2,3-*O*-isopropylidene-*sn*-glycerols), which were not enantiomerically characterized or their source indicated. The previous paper (16) claims that the two PtdGro diastereomers could be easily differentiated from their ^{1}H NMR spectra. However, there is no indication of which particular feature of the ^{1}H NMR spectra of the PtdGro diastereomers permits the degree of purity of either diastereomer to be established, chiral-shift reagents were not used. In the present study, we established the enantiomeric purities of the starting materials (1,2- and 2,3-*O*-isopropylidene-*sn*-glycerols) and the diastereomeric purities of the products (*R,R* and *R,S* PtdGro) using chiral-phase HPLC (8,19). In addition, we selected PLD from *Actinomadura* sp. because of its higher transphophatidylation activity and lower phosphatidic acid formation when compared with the *Streptomyces* species tested (20).

*To whom correspondence should be addressed at Graduate School of Fisheries Sciences, Hokkaido University, 3-1-1 Minato-cho, Hakodate, Hokkaido 041-8611, Japan. E-mail: yutaka@pop.fish.hokudai.ac.jp

Abbreviations: DNPU, 3,5-dinitrophenylurethane; ESI-MS, electrospray ionization mass spectrometry; PLD, phospholipase D; PtdCho, phosphatidylcholine; PtdGro, phosphatidylglycerol.

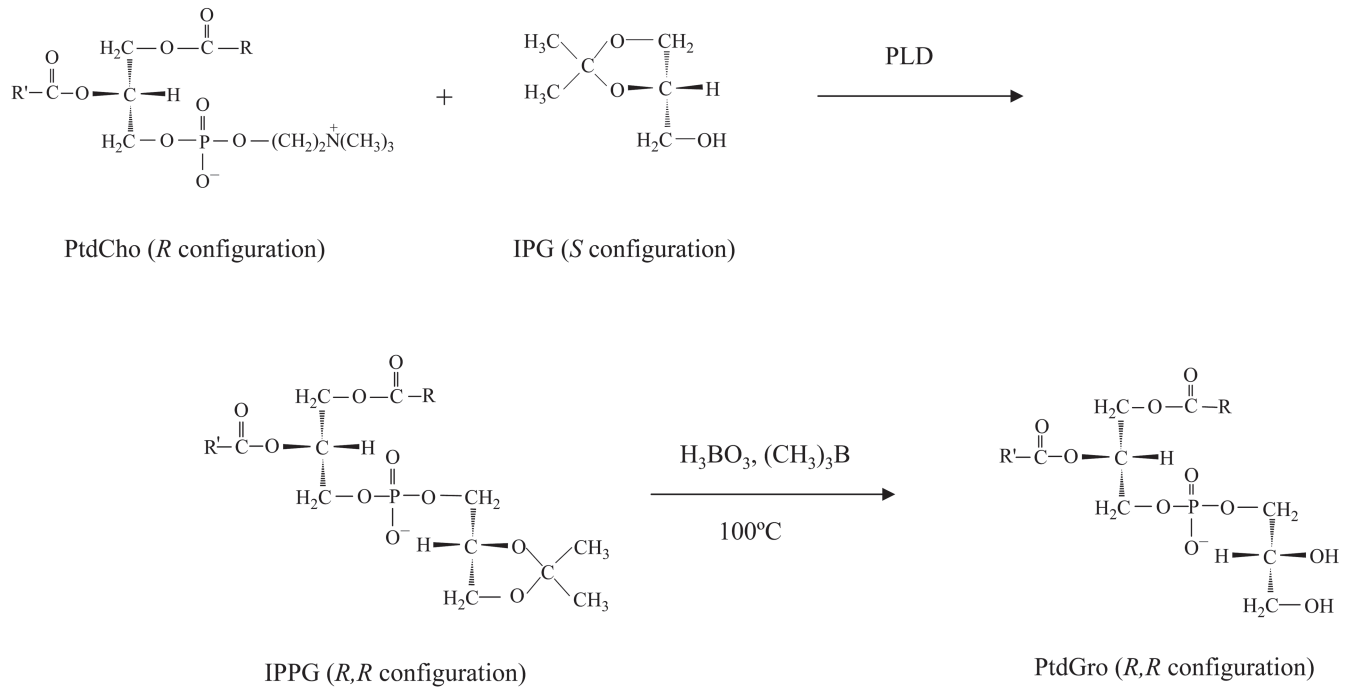

FIG. 1. Synthesis of a diastereomerically pure phosphatidylglycerol using phospholipase D (PLD)-catalyzed transphosphatidylation. PtdCho, phosphatidylcholine (1,2-diacyl-*sn*-glycero-3-phosphocholine, *R* configuration); IPG, isopropylideneglycerol (1,2-*O*-isopropylidene-*sn*-glycerol, *S* configuration); IPPG, isopropylidene phosphatidylglycerol (1,2-diacyl-*sn*-glycero-3-phospho-1′,2′-*O*-isopropylidene-*sn*-glycerol, *R,R,* configuration); PtdGro, phosphatidylglycerol (1,2-diacyl-*sn*-glycero-3-phospho-3′-*sn*-glycerol, *R,R,* configuration).

MATERIALS AND METHODS

Materials. PLD from *Actinomadura* sp. (Seikagaku Kogyo, Tokyo, Japan) was used for transphosphatidylation. (+)-1,2-*O*-Isopropylidene-*sn*-glycerol (*S* configuration) and (−)-2,3-*O*-isopropylidene-*sn*-glycerol (*R* configuration) were obtained from Sigma (St. Louis, MO) and Tokyo Kasei Kogyo (Tokyo, Japan), respectively. The optical purities of these enantiomers were determined as 98.6% (enantiomeric excess, e.e.) and 86.2% (e.e.), respectively, by chiral-phase HPLC (19). 1,2-*O*-Isopropylidene-*rac*-glycerol was a product of Tokyo Kasei Kogyo. Pure 1,2-dipalmitoyl-*sn*-glycero-3-phosphocholine (16:0–16:0) and 1,2-dioleoyl-*sn*-glycero-3-phosphocholine (18:1–18:1) were obtained from Sigma and Avanti Polar Lipids (Alabaster, AL), respectively. Fresh salmon (*Oncorhynchus keta*) roe was purchased at a fish market in Hakodate, and the PtdCho fraction was isolated from the total lipids by TLC as described previously (21). The major molecular species of the roe PtdCho were as follows: 16:0–22:6 (23%), 16:0–20:5 (19%), 16:0–22:5 (6%), 18:0–22:6 (11%), 18:0–20:5 (7%), and 18:1–20:5 (5%). Trimethyl borate and boric acid were obtained from Aldrich (Milwaukee, WI) and Kanto Kagaku (Tokyo, Japan), respectively. HPLC-grade solvents (hexane, dichloromethane, methanol, and trifluoroacetic acid) were obtained from Wako Pure Chemicals (Osaka, Japan). All other chemicals and solvents were of analytical grade or better from commercial sources.

Preparation of diastereomeric isopropylidene PtdGro. 1,2-Diacyl-*sn*-glycero-3-phospho-1′,2′-*O*-isopropylidene-*sn*-glycerol (*R,R* configuration) was prepared from PtdCho and 1,2-*O*-isopropylidene-*sn*-glycerol by PLD-catalyzed transphosphatidylation (Fig. 1), whereas 1,2-diacyl-*sn*-glycero-3-phospho-2′,3′-*O*-isopropylidene-*sn*-glycerol (*R,S* configuration) was prepared by using enantiomeric 2,3-*O*-isopropylidene-*sn*-glycerol instead of 1,2-*O*-isopropylidene-*sn*-glycerol. The transphosphatidylation reaction was carried out according to the procedures described previously (20). Briefly, a mixture containing 10 mg of PtdCho, 1.9 mL of 0.4 M acetate buffer (pH 5.6), 1 mL of 0.2 M $CaCl_2$, 0.1 mL of 1,2- or 2,3-*O*-isopropylidene-*sn*-glycerol/0.4 M acetate buffer (1:4, vol/vol), and 2 mL of water was preincubated at 30°C for 10 min, and the buffered PLD preparation (0.4 M acetate buffer, pH 5.6) from *Actinomadura* sp. (1.25 U) was then added. The reaction was initiated by the addition of 2.5 mL of diethyl ether and performed at 30°C for 1.5 h with stirring. The progress of the reaction was monitored by TLC on Silica gel $60F_{254}$ (Merck, Darmstadt, Germany) using chloroform/methanol/water (65:25:4, by vol) as the developing solvent. The reaction was stopped by the addition of 10 mL of chloroform/methanol (2:1, vol/vol). After centrifugation for 5 min, the lower phase was collected and dehydrated under anhydrous sodium sulfate. The lipids were obtained by evaporating the solvent under a stream of nitrogen.

Preparation of diastereomeric PtdGro. To the isopropylidene PtdGro diastereomers (*ca.* 10 mg each) dissolved in 1.5 mL of trimethyl borate was added 80 mg of boric acid, and the mixture was heated at 100°C for 2.5 h. After the solvent was evaporated under a stream of nitrogen, the reaction mixture was dissolved in 6 mL of chloroform/methanol (2:1,

vol/vol), then washed with 1 mL of distilled water. The suspension formed was centrifuged at 1500 × *g* for 5 min, and the resulting chloroform layer was recovered and dried over anhydrous sodium sulfate. After the solvent was evaporated, the crude PtdGro were purified by preparative TLC on a Silica gel $60F_{254}$ plate (Merck) using chloroform/methanol/water (65:25:4, by vol) as the developing solvent. The PtdGro band was detected by spraying with 0.2% 2′,7′-dichlorofluorescein ethanol and extracted from the adsorbent with three portions of chloroform/methanol/acetic acid (20:10:1, by vol). The purified PtdGro showed single spots on analytical TLC using the same solvent system as described above and the Dittmer–Lester reagent for detection (22).

MS. Aliquots of the transphosphatidylation products were analyzed by electrospray ionization MS (ESI-MS) in the negative ion mode on a LCQ mass spectrometer to confirm product identities. Samples dissolved in chloroform/methanol (2:1, vol/vol, *ca.* 10 μg/mL) were introduced directly into the ESI probe by flow injection (3 μL/min). The heated capillary temperature was 200°C, and the spray voltage was 4.2 kV. The nitrogen sheath gas was set at 30 arb (arbitrary units) by the software. Mass spectra were taken in the mass range of 150–2000 *m/z*.

Chiral-phase HPLC. To determine the purities of the *R,R* and *R,S* diastereomers, the resulting PtdGro were converted to bis(3,5-dinitrophenylurethane) (bis-DNPU) derivatives and analyzed by chiral-phase HPLC on an (*R*)-1-(1-naphthyl)ethylamine column (YMC A-K03, 25 cm × 4.6 mm i.d.; YMC, Kyoto, Japan) using hexane/dichloromethane/methanol/trifluoroacetic acid (60:20:20:0.2, by vol) as the mobile phase at a flow rate of 1 mL/min (8,20).

RESULTS AND DISCUSSION

Synthesis of diastereomeric isopropylidene PtdGro. PLD-catalyzed transphosphatidylation has usually been carried out in a biphasic system containing water and an organic solvent such as diethyl ether or ethyl acetate (12–16,23), although the reaction also has been tried in anhydrous organic solvents (24,25). Organic solvents play an important role by dissolving the PtdCho and preserving the modified phospholipid. A serious drawback of the biphasic reaction system containing water is the possibility of undesirable PLD-catalyzed hydrolysis of PtdCho, which would lower the yield of PtdGro. However, in this study, almost no PtdOH was detected in the reaction products by TLC and MS. Figure 2 shows the negative ESI-MS spectra of the 1,2-dipalmitoyl-*sn*-glycero-3-phospho-1′,2′-*O*-isopropylidene-*sn*-glycerol generated from 1,2-dipalmitoyl-*sn*-glycero-3-phosphocholine (*R* configuration) and 1,2-*O*-isopropylidene-*sn*-glycerol by PLD-catalyzed transphosphatidylation. In the negative ion mode, isopropylidene PtdGro (*R,R* configuration) gave a prominent singly charged $[M - H]^-$ ion (*m/z* 763), but no fragment ions showing PtdOH were seen in the spectrum. A similar simple spectrum was also observed for 1,2-dipalmitoyl-*sn*-glycero-3-phospho-2′,3′-*O*-isopropylidene-*sn*-glycerol, which was generated using 2,3-*O*-isopropylidene-*sn*-glycerol instead of 1,2-*O*-isopropylidene-*sn*-glycerol (spectrum not shown). No PtdOH was observed in the reaction products on TLC. These results demonstrate that the transphosphatidylation reaction with PLD from *Actinomadura* sp. proceeds without the hydrolysis of PtdCho to produce isopropylidene PtdGro. This is probably due to the high transphosphatidylation activity of *Actinomadura* PLD and the physicochemical properties of isopropylideneglycerol as an accepter in the reaction. The high transphosphatidylation activity of *Actinomadura* PLD also has been observed for the synthesis of PtdGro from PtdCho and glycerol (20).

Preparation of diastereomeric PtdGro. The isopropylidene group was easily removed by heating at 100°C in the presence of boric acid and trimethyl borate as established previously (17,18). Like the *R,R* isomer of isopropylidene PtdGro, the *R,R* isomer of PtdGro also gave a simple ESI-MS spectrum, showing a prominent singly charged $[M - H]^-$ ion (*m/z* 722) and a weak $[M + K]^-$ ion (*m/z* 763) for 16:0–16:0 (Fig. 2B). A similar spectrum also was observed for the *R,S* isomer (spectrum not shown). Figures 3 and 4 show the chiral-phase HPLC profiles of the bis-DNPU derivatives of PtdGro synthesized from PtdCho and enantiomeric and racemic 1,2-*O*-isopropylideneglycerols. Under the conditions employed (8), PtdGro produced from PtdCho and racemic 1,2-*O*-isopropylideneglycerol were clearly resolved into the *R,R* and *R,S* diastereomers and had almost the same peak areas (Figs. 3C, 4C). These chromatograms showed that no racemization occurred during the removal of the protective isopropylidene group and that the purity of each *R,R* and *R,S* isomer could be measured accurately.

The partially resolved and broad peaks seen in the chromatograms of salmon roe PtdGro (Fig. 4) are due to the shifts of retention times of different molecular species including polyunsaturated ones. Itabashi and Kuksis (8) previously showed that the bis-DNPU derivatives of synthetic PtdGro were eluted in the order of increasing double bonds and decreasing carbon numbers on chiral-phase HPLC under the same conditions as those used in this study. The small peaks appearing ahead of or behind the major ones (Figs. 3A, 3B; Figs. 4A, 4B) arise from small amounts of enantiomers contained in the original 1,2- and 2,3-*O*-isopropylideneglycerols, the optical purities of which were 99% (e.e.) and 86% (e.e.), respectively (19). Accordingly, the purities (diastereomer excess) of the *R,S* and *R,R* diastereomers of saturated and unsaturated PtdGro obtained in this study were 85–91% and 96–98%, respectively (Table 1). The overall yield of the reaction was about 65%. Losses were mainly due to incomplete recoveries of the isopropylidene PtdGro and PtdGro from the adsorbent on silicic acid TLC.

Comparison of the methods. This study emphasizes the diastereomeric purity of the products produced by PLD-catalyzed transphosphatidylation. Only recently has it become possible to establish the diastereomeric nature of the transphosphatidylation products of various PLD enzymes and to characterize their relaxed substrate specificity (20,26). In an earlier study (16), the diastereomeric nature of the products was implied from the starting

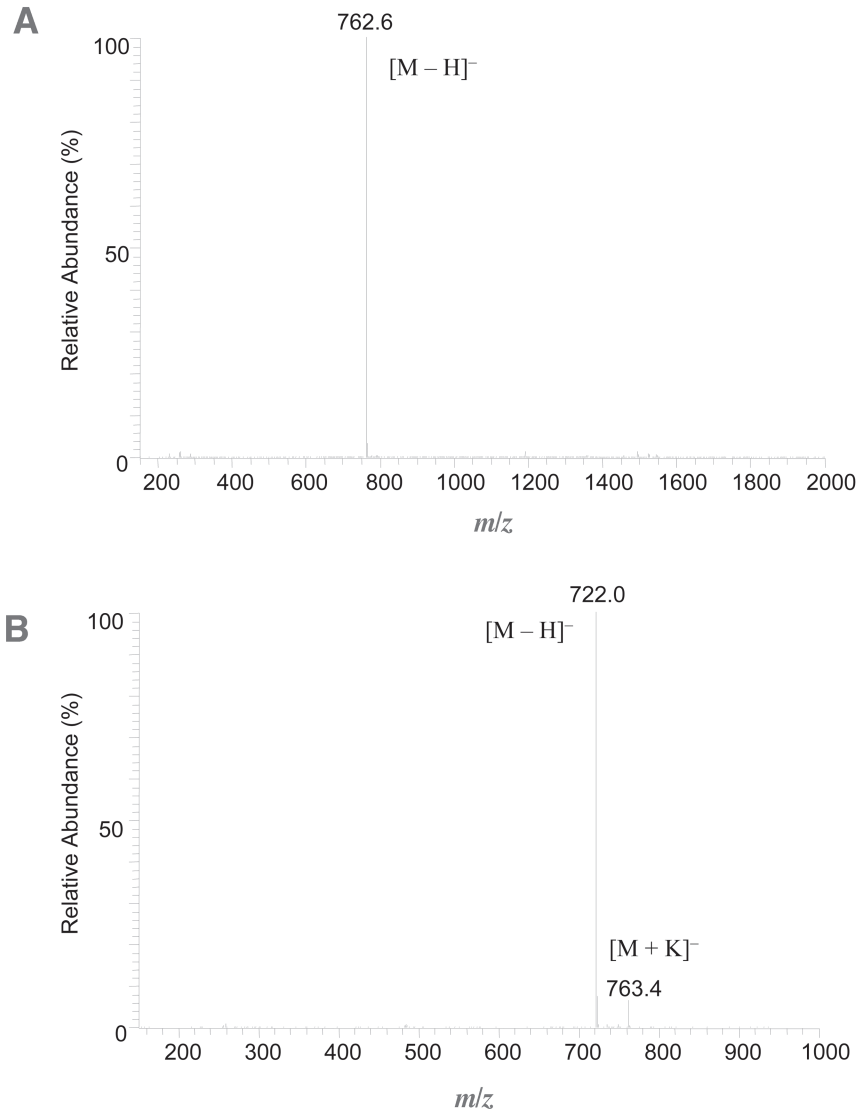

FIG. 2. Negative electrospray ionization (ESI)-MS spectra of (A) 1,2-dipalmitoyl-*sn*-glycero-3-phospho-1′,2′-*O*-isopropylidene-*sn*-glycerol (*R,R* configuration) and (B) 1,2-dipalmitoyl-*sn*-glycero-3-phospho-3′-*sn*-glycerol (*R,R,* configuration) generated from 1,2-dipalmitoyl-*sn*-glycero-3-phosphocholine (*R* configuration) and 1,2-*O*-isopropylidene-*sn*-glycerol (*S* configuration) by PLD-catalyzed transphosphatidylation. ESI-MS conditions are as given in the text.

materials (isopropylideneglycerols), which were not enantiomerically characterized or their source indicated. In the present study, the enantiomeric purities of the commercially available 1,2- and 2,3-*O*-isopropylidene-*sn*-glycerols were established as 99 and 86%, respectively, by chiral-phase HPLC (19). Until now, adequate methods did not exist for establishing the purity of enantiomeric isopropylideneglycerols or for their resolution. In the earlier study (16), the PtdGro were hydrolyzed in aqueous methanol in the presence of toluene-*p*-sulfonic acid. It has been well established that removal of the protective isopropylidene groups by acid hydrolysis involves some acyl migration, which is difficult to control. A much more effective method of removing the isopropylidene groups involves refluxing with trimethylborate in the presence of boric acid, which results in replacing the isopropylidine groups with trimethylborate groups. The latter are readily removed by hydrolysis in water at room temperature without altering the structure (17,18,27,28), as shown in this study.

In conclusion, this study establishes a method for preparing diastereomerically pure PtdGro by PLD-catalyzed transphosphatidylation. The reaction of PtdCho with enantiomeric 1,2-*O*-isopropylideneglycerols using *Actinomadura* PLD was shown to proceed efficiently, giving isopropylidene PtdGro under mild conditions and high yield. The isopropylidene protective group was decomposed chemically using boric acid and trimethylborate to produce the desired PtdGro diastereomers without racemiza-

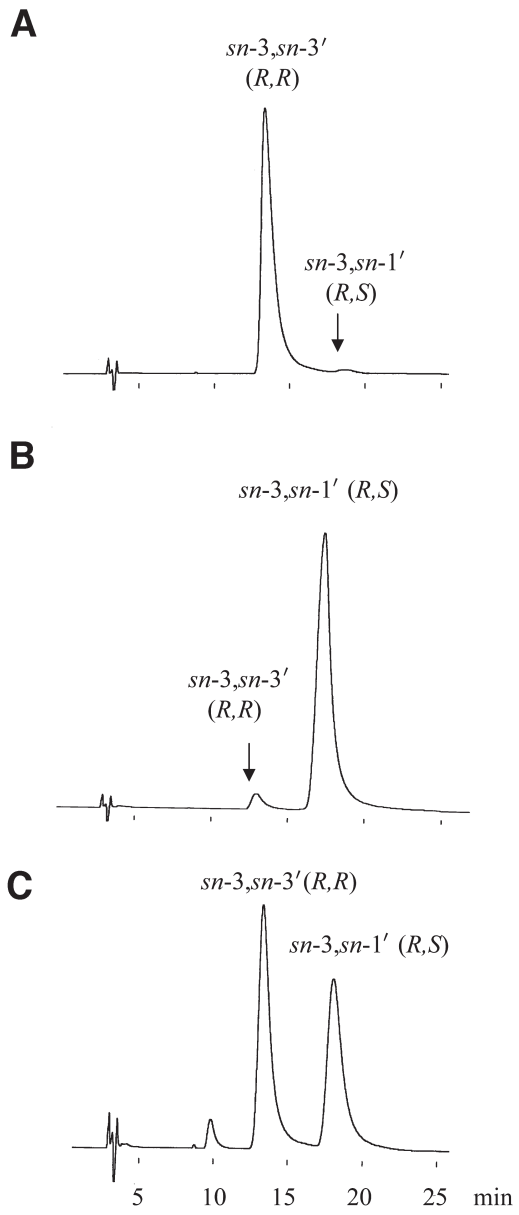

FIG. 3. Chiral-phase HPLC profiles of the bis(3,5-dinitrophenylurethane) derivatives of the PtdGro generated from 1,2-dioleoyl-*sn*-glycero-3-phosphocholine (*R* configuration) and 1,2-*O*-isopropylideneglycerols by PLD-catalyzed transphosphatidylation. (A) PtdGro from 1,2-*O*-isopropylidene-*sn*-glycerol; (B) PtdGro from 2,3-*O*-isopropylidene-*sn*-glycerol; (C) 1,2-*O*-isopropylidene-*rac*-glycerol. Column temperature, 10°C; detection, 254 nm UV. Other HPLC conditions are as given in the text. For abbreviations see Figure 1.

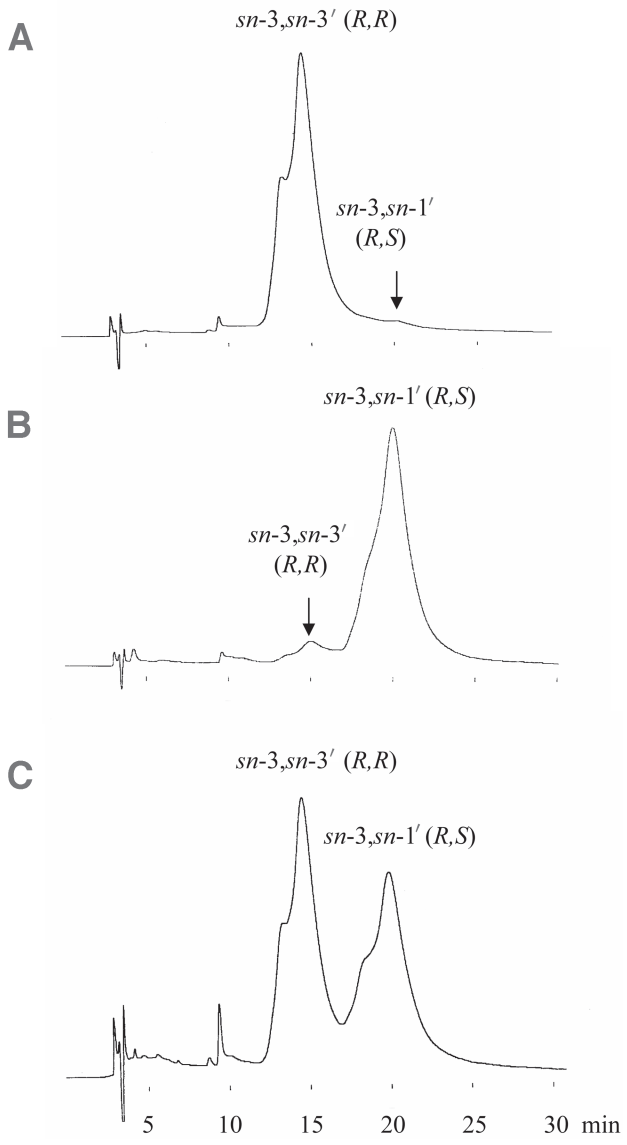

FIG. 4. Chiral-phase HPLC profiles of the bis(3,5-dinitrophenylurethane) derivatives of the PtdGro generated from salmon roe PtdCho and 1,2-*O*-isopropylideneglycerols by PLD-catalyzed transphosphatidylation. (A) PtdGro from 1,2-isopropylidene-*sn*-glycerol; (B) PtdGro from 2,3-*O*-isopropylidene-*sn*-glycerol; (C) 1,2-*O*-isopropylidene-*rac*-glycerol. HPLC conditions and abbreviations are as given in the text. For abbreviations see Figure 1.

tion. The present method is simple and can be utilized for the synthesis of diastereomerically pure saturated and unsaturated PtdGro.

ACKNOWLEDGMENT

This study was supported in part by a Grant-in-Aid for Scientific Research from the Ministry of Education, Sciences, Sports and Culture of Japan (Scientific Research B 13460088).

REFERENCES

1. Hostetler, K.Y. (1982) Polyglycerophospholipids: Phosphatidylglycerol, Diphosphatidylglycerol and Bis(monoacylglycero)-phosphate, in *Phospholipids* (Hawthorne, J.N., and Ansell, G.B., eds.), pp. 215–261, Elsevier Biochemical Press, Amsterdam.
2. Shibuya, I. (1992) Metabolic Regulation and Biological Functions of Phospholipids in *Escherichia coli, Prog. Lipid Res. 31*, 245–299.
3. Gombos, Z., Várkonyi, Z., Hagio, M., Iwaki, M., Kovács, L.,

TABLE 1
Diastereomer Composition of Phosphatidylglycerols Synthesized from Phosphatidylcholine and 1,2-*O*-Isopropylideneglycerols by Transphosphatidylation with Phospholipase D from *Actinomadura* sp.

Phosphatidylcholine[a]	1,2-*O*-Isopropylideneglycerol	Diastereomer (mol%)		Diastereomer excess (%)[d]
		sn-3,*sn*-3′ (*R,R*)[b]	*sn*-3,*sn*-1′ (*R,S*)[c]	
16:0–16:0	*rac*-1,2-	48.3	51.7	3.4 (*R,S*)
16:0–16:0	*sn*-1,2- (*S*)	98.1	1.9	96.2 (*R,R*)
16:0–16:0	*sn*-2,3- (*R*)	7.6	92.4	84.8 (*R,S*)
18:1–18:1	*rac*-1,2-	51.8	48.2	3.6 (*R,R*)
18:1–18:1	*sn*-1,2- (*S*)	98.3	1.7	96.6 (*R,R*)
18:1–18:1	*sn*-2,3- (*R*)	5.3	94.7	89.4 (*R,S*)
Salmon roe	*rac*-1,2-	49.5	50.5	1.0 (*R,S*)
Salmon roe	*sn*-1,2- (*S*)	98.8	1.2	97.6 (*R,R*)
Salmon roe	*sn*-2,3- (R)	4.5	95.5	91.0 (R,S)

[a]1,2-Diacyl-*sn*-glycero-3-phosphocholine (*R* configuration).
[b]1,2-Diacyl-*sn*-glycero-3-phospho-3′-*sn*-glycerol (*R,R* configuration).
[c]1,2-Diacyl-*sn*-glycero-3-phospho-1′-*sn*-glycerol (*R,S* configuration).
[d]Diastereomer excess (%) = $\{([R,S] - [R,R])/([R,S] + [R,R])\} \times 100$, where [*R,S*] and [*R,R*] denote the composition of the *R,S* and *R,R* diastereomers, respectively.

Masamoto, K., Itoh, S., and Wada, H. (2002) Phosphatidylglycerol Requirement for the Function of Electron Acceptor Plastoquinone Q_B in the Photosystem II Reaction Center, *Biochemistry 41*, 3796–3802.
4. Veldhuizen, R., Nag, K., Orgeig, S., and Possmayer, F. (1998) The Role of Lipids in Pulmonary Surfactant, *Biochim. Biophys. Acta 1408*, 90–108.
5. Hanahan, D.J. (1997) *A Guide to Phospholipid Chemistry*, pp. 165–194, Oxford University Press, New York.
6. Haverkate, F., and Van Deenen, L.L.M. (1963) The Stereochemical Configuration of Phosphatidyl Glycerol, *Biochem. Biophys. Acta 84*, 106–108.
7. Ruettinger, R.T., and Brewer, G.J. (1978) Strereoconfiguration of Phosphatidylglycerol in the Membrane of Bacteriophage PM2 and in Its Host, *Pseudomonas* BAL-31, *Biochim. Biophys. Acta 529*, 181–185.
8. Itabashi, Y., and Kuksis, A. (1997) Reassessment of Stereochemical Configuration of Natural Phosphatidylglycerols by Chiral-Phase High-Performance Liquid Chromatography and Electrospray Mass Spectrometry, *Anal. Biochem. 254*, 49–56.
9. Fujishima, H., Gamano, T., Taoka, Y., Sawabe, T., and Itabashi, Y. (2004) Stereoisomers of Marine Bacterial Phosphatidylglycerols, *Nippon Suisan Gakkaishi* (in Japanese) *70*, 200–202.
10. Baer, E., and Buchnea, D. (1958) Synthesis of Saturated and Unsaturated Phosphatidyl Glycerols. III. Cardiolipin Substitutes, *J. Biol. Chem. 232*, 895–901.
11. Woolley, P., and Eibl, H. (1988) Synthesis of Enantiomerically Pure Phospholipids Including Phosphatidylserine and Phosphatidylglycerol, *Chem. Phys. Lipids 47*, 55–62.
12. D'Arrigo, P., and Servi, S. (1997). Using Phospholipases for Phospholipid Modification, *Trends Biotechnol. 15*, 90–96.
13. D'Arrigo, P., de Ferra, L., Piergianni, V., Selva, A., Servi, S., and Strini, A. (1996) Preparative Transformation of Natural Phospholipids Catalysed by Phospholipase D from *Streptomyces, J. Chem. Soc. Perkin Trans. 1*, 2651–2656.
14. Yang, S.F., Freer, S., and Benson, A.A. (1967) Transphosphatidylation by Phospholipase D, *J. Biol. Chem. 242*, 477–484.
15. Joutti, A., and Renkonen, O. (1976) The Structure of Phosphatidyl Glycerol Prepared by Phospholipase D-Catalyzed Transphosphatidylation from Egg Lecithin and Glycerol, *Chem. Phys. Lipids 17*, 264–266.
16. D'Arrigo, P., de Ferra, L., Giuseppe, P.-F., Scarcelli, D., Servi, S., and Strini, A. (1996) Enzyme-Mediated Synthesis of Two Diastereoisomeric Forms of Phosphatidylglycerol and of Diphosphatidylglycerol (cardiolipin), *J. Chem. Soc. Perkin Trans. 1*, 2657–2660.
17. Buchnea, D. (1978) Stereospecific Synthesis of Enantiomeric Acylglycerols, in *Fatty Acids and Glycerides* (Kuksis, A., ed.), Handbook of Lipid Research 1, pp. 233–287, Plenum Press, New York.
18. Eibl, H. (1980) Synthesis of Glycerophospholipids, *Chem. Phys. Lipids 26*, 405–429.
19. Itabashi, Y., Fujishima, H., and Sato, R. (2004) Chiral Phase High-Performance Liquid Chromatographic Separation of Enantiomeric 1,2- and 2,3-*O*-Isopropylidene-*sn*-glycerols as 3,5-Dinitrophenylurethanes, *J. Oleo Sci. 53*, 405–412.
20. Sato, R., Itabashi, Y., Hatanaka, T., and Kuksis, A. (2004) Asymmetric *in vitro* Synthesis of Diastereomeric Phosphatidylglycerols from Phosphatidylcholine and Glycerol by Bacterial Phospholipase D, *Lipids 39,* 1013–1018.
21. Okabe, H., Itabashi, Y., and Ota, T. (1999) Determination of Molecular Species of Phosphatidylcholines as 2-Anthrylurethanes by Reversed-Phase HPLC with Fluorescence Detection and On-line Electrospray Ionization Mass Spectrometry, *J. Jpn. Oil Chem. Soc. 48*, 559–567.
22. Dittmer, J.C., and Lester, R.L. (1964) A Simple, Specific Spray for the Detection of Phospholipids on Thin-Layer Chromatograms. *J. Lipid Res. 5*, 126–127.
23. Juneja, L.R., Kazuoka, T., Goto, N., Yamane, T., and Shimizu, S. (1989) Conversion of Phosphatidylcholine to Phosphatidylserine by Various Phospholipase D in the Presence of L- or D-Serine, *Biochim. Biophys. Acta 1003*, 277–283.
24. Simpson, T.D. (1991) Phospholipase D Activity in Hexane, *J. Am. Oil Chem. Soc. 68*, 176–178.
25. Rich, J.O., and Khmelnitzky, Y.L. (2001) Phospholipase D-Catalyzed Transphosphatidylation in Anhydrous Organic Solvents, *Biotechnol. Bioeng. 32*, 374–377.
26. Sato, R., Itabashi, Y., Suzuki, A., Hatanaka, T., and Kuksis, A. (2004) Effect of Temperature on the Stereoselectivity of Phospholipase D Toward Glycerol in the Transphosphatidylation of Phosphatidylcholine to Phosphatidylglycerol, *Lipids 39*, 1019–1023.
27. Hartman, L. (1959) Hydrolysis of Isopropylidene Esters of Fatty Acids, *J. Chem. Soc.*, 4134–4135.
28. Mattson, F.H., and Volpenhein, R.A. (1962) Synthesis and Properties of Glycerides, *J. Lipid Res. 3*, 281–296.

[Received April 2, 2004; accepted November 11, 2004]

Separation of Vitamin E (tocopherol, tocotrienol, and tocomonoenol) in Palm Oil

Mei Han Ng[b], Yuen May Choo[a,*], Ah Ngan Ma[a], Cheng Hock Chuah[b], and Mohd. Ali Hashim[c]

[a]Malaysian Palm Oil Board (MPOB), 43000 Kajang, Selangor, Malaysia, and Departments of [b]Chemistry and [c]Chemical Engineering, University Malaya, Kuala Lumpur, Malaysia

ABSTRACT: Previous reports showed that vitamin E in palm oil consists of various isomers of tocopherols and tocotrienols [α-tocopherol (α-T), α-tocotrienol, γ-tocopherol, γ-tocotrienol, and δ-tocotrienol), and this is normally analyzed using silica column HPLC with fluorescence detection. In this study, an HPLC-fluorescence method using a C_{30} silica stationary phase was developed to separate and analyze the vitamin E isomers present in palm oil. In addition, an α-tocomonoenol (α-T_1) isomer was quantified and characterized by MS and NMR. α-T_1 constitutes about 3–4% (40 ± 5 ppm) of vitamin E in crude palm oil (CPO) and is found in the phytonutrient concentrate (350 ± 10 ppm) from palm oil, whereas its concentration in palm fiber oil (PFO) is about 11% (430 ± 6 ppm). The relative content of each individual vitamin E isomer before and after interesterification/transesterification of CPO to CPO methyl esters, followed by vacuum distillation of CPO methyl esters to yield the residue, remained the same except for α-T and γ-T_3. Whereas α-T constitutes about 36% of the total vitamin E in CPO, it is present at a level of 10% in the phytonutrient concentrate. On the other hand, the composition of γ-T_3 increases from 31% in CPO to 60% in the phytonutrient concentrate. Vitamin is present at 1160 ± 43 ppm, and its concentrations in PFO and the phytonutrient concentrate are 4,040 ± 41 and 13,780 ± 65 ppm, respectively. The separation and quantification of α-T_1 in palm oil will lead to more in-depth knowledge of the occurrence of vitamin E in palm oil.

Paper no. L9502 in *Lipids 39*, 1031–1035 (October 2004).

The presence of vitamin E in palm oil has been known since the early 1980s (1,2), when palm oil was found to contain not only tocopherols but also tocotrienols. In fact, palm oil is the richest source of tocotrienols among all vegetable oils, with the only other tocotrienol-containing vegetable oil being rice bran oil (3). Vitamin E is present in crude palm oil (CPO) and residual oil from palm pressed fiber (PFO) at concentrations of about 600–1000 and 2000–4000 ppm, respectively (1,2). The vitamin E isomers that are present in palm oil include α-tocopherol (α-T), α-tocotrienol (α-T_3), γ-tocotrienol (γ-T_3), and δ-tocotrienol (δ-T_3).

*To whom correspondence should be addressed at [a]MPOB, No. 6 Persiaran Institusi, Bandar Baru Bangi, 43000 Kajang, Selangor, Malaysia.
E-mail: Choo@mpob.gov.my

Abbreviations: CPO, crude palm oil; MDT, marine-derived tocopherol; MPOB, Malaysian Palm Oil Board; PFO, palm fiber oil; α-T, α-tocopherol; α-T_1, α-tocomonoenol; α-T_3, α-tocotrienol, γ-T_3, γ-tocotrienol; δ-T_3, δ-tocotrienol.

Vitamin E is a family of potent antioxidative compounds (4), and has also been suggested to be an anticancer agent (5–8). Some *in vitro and in vivo* studies have found that tocotrienol is a more potent antioxidant, and *in vivo* that it is a more effective anticancer agent than the tocopherols (9–11). This property of tocotrienols is believed to be related to the presence of an unsaturated side chain, which can more easily be incorporated into cells. The tocopherols nevertheless still possess potent antioxidant and anticancer properties in animal models of chemical-induced carcinogenesis.

Tocopherols differ from tocotrienols in that there are three double bonds in the side chain of the tocotrienols. There is a possibility that vitamin E isomers with only one or two double bonds in the side chain are present in palm oil.

A vitamin E isomer with a monounsaturated side chain has been detected in marine organisms. This compound was extracted from the lipophilic fraction of chum salmon eggs (12) and from the tissues of a variety of fish (13). Japanese workers reported the presence of another α-tocomonoenol (α-T_1) in palm oil (14), and Drotleff and Ternes (15) reported its occurrence in hardened palm oil. This plant-derived isomer of α-T_1 has only a slight structural difference from the marine-derived one, as shown in Scheme 1. This study is the first to report on the quantification of tocomonoenol in palm oil.

An investigation of the presence of the tocomonoenol isomers in CPO, PFO, and a phytonutrient concentrate is presented in this study. (The phytonutrient concentrate is the residue from the vacuum distillation of CPO methyl esters.) As the bulk of the esters has been removed from the residue, the amount of vitamin E in the phytonutrient concentrate is much higher than in CPO. Since the phytonutrient concentrate is derived from CPO, it is anticipated that the patterns of occurrence of individual vitamin E components in CPO and the phytonutrient concentrate would be identical.

In contrast, PFO (i.e., the residual oil extracted from the fiber that remains after the processing or pressing of the oil palm fruits) contains vitamin E with a different profile from that of CPO. In CPO, γ-T_3 is the main vitamin E constituent, whereas α-T is the major vitamin E in PFO (16).

EXPERIMENTAL PROCEDURES

Materials. Crude palm oil and palm pressed fiber were obtained from the MPOB Experimental Mill in Labu, Negri

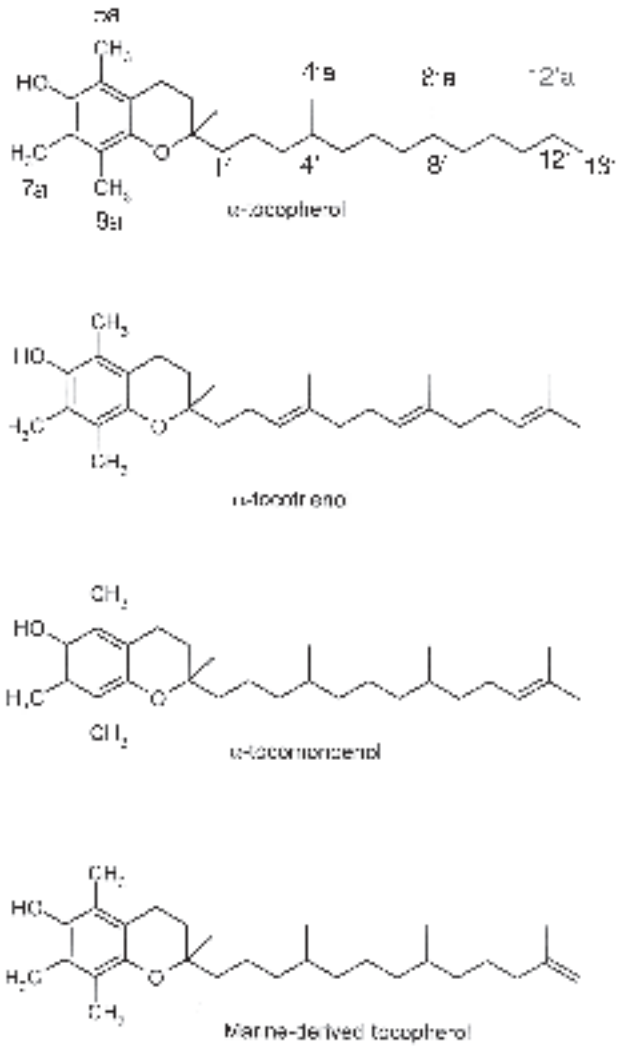

SCHEME 1

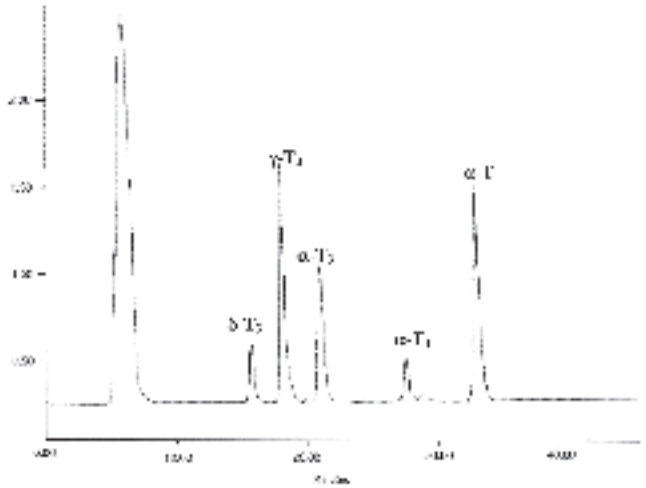

FIG. 1. HPLC profile of vitamin E in crude palm oil. Separation by Develosil RP (Phenomenex, Torrance, CA) aqueous column with 100% methanol. δ-T_3, δ-tocotrienol; γ-T_3, γ-tocotrienol; α-T_3, α-tocotrienol; α-T_1, α-tocomonoenol; α-T, α-tocopherol.

Sembilan, Malaysia. The Phytonutrient concentrate was obtained as the residue from vacuum distillation of CPO methyl esters. All solvents used were of analytical or chromatographic grade and were purchased from Merck (Darmstadt, Germany) and J.T.Baker (Phillipsburg, NJ). Solvents for chromatography were degassed before use. Tocopherol and tocotrienol standards were purchased from Calbiochem (San Diego, CA).

Extraction of residual oil from palm pressed fiber. Palm pressed fiber obtained fresh from the palm oil mill was soaked overnight in absolute ethanol. The extract was then filtered to separate the fiber from the solvents. The ethanol in the extract was distilled off, and the palm pressed fiber oil was dried *in vacuo*.

HPLC. A Waters 600 Controller equipped with a Waters 996 PDA high-performance liquid chromatograph system (Milford, MA) was used. The column was a Develosil RP Aqueous 4.6 mm i.d. × 250 mm length purchased from Phenomenex (Torrance, CA). The mobile phase was 100% methanol at a flow rate of 1.0 mL/min. Samples were dissolved in ethanol prior to injection. NMR spectra of samples dissolved in $CDCl_3$ (Sigma, St. Louis, MO) were recorded using a JEOL GSX270 spectrometer.

Sample pretreatment. CPO (5 g) was dissolved in 20 mL of ethanol and centrifuged for 15 min at 3000 rpm. The supernatant was separated from the sediment, the ethanol in the supernatant was distilled off, and the sample was redissolved in 5 mL of ethanol prior to injection into the high-performance liquid chromatograph. The same procedures were followed using 3 g of palm pressed fiber oil and 1 g of phytonutrient concentrate.

RESULTS AND DISCUSSION

Vitamin E isomers were separated from palm oil samples, and comparison with authentic standards showed that these compounds corresponded to δ-T_3, γ-T_3, α-T_3, and α-T. Figures 1–3 show the HPLC profiles of vitamin E in CPO, PFO, and the phytonutrient concentrate. An unknown compound was found to elute between α-T_3 and α-T. Mass and NMR spectra confirmed this compound to be α-T_1.

As shown in Scheme 1, α-T_1 has the same chroman structure as α-T and α-T_3. Thus, its major mass spectral data are typical of these tocols with the common tropylium ion of *m/z* 165. From the mass spectra (Fig. 4), the *m/z* of the molecular ion of α-T_1 is 428: 2 mass units less than α-T (M^+ = 430) and 4 mass units more than α-T_3 (M^+ = 424). An ion with *m/z* 69 distinguished α-T_3 and α-T_1 from α-T. This ion arises from the fragmentation of the α-T_3 isoprenoid side chain or terminal allenic side chain of α-T_1. The mass spectral data of α-T α-T_1, and α-T_3 are depicted in Table 1.

α-T_1 was distinguishable by means of MS, whereby its molecular mass and fragmentations showed it to be an α isomer of the tocols with a monounsaturated side chain. NMR spectra provided further confirmation of the identity of this compound.

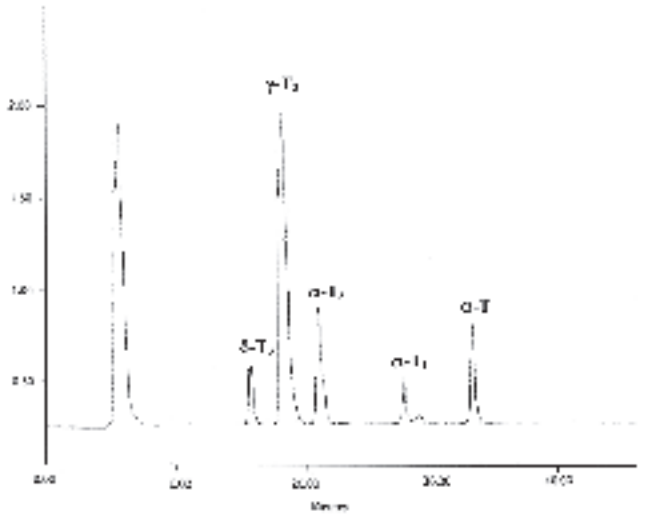

FIG. 2. HPLC profile of Vitamin E in the phytonutrient concentrate. For conditions and abbreviations see Figure 1.

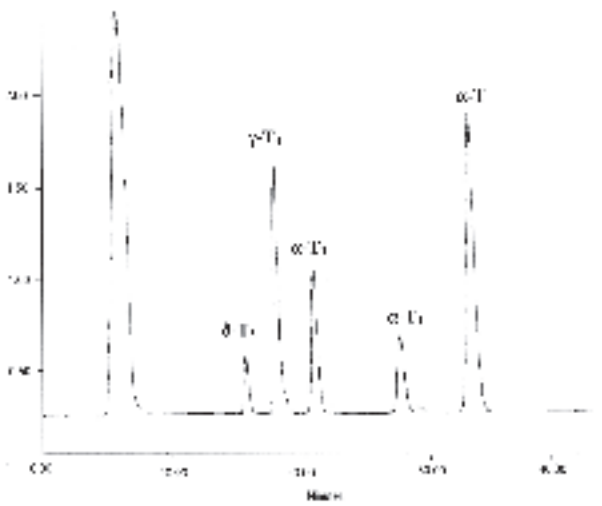

FIG. 3. HPLC profile of vitamin E in palm fiber oil. For conditions and abbreviations see Figure 1.

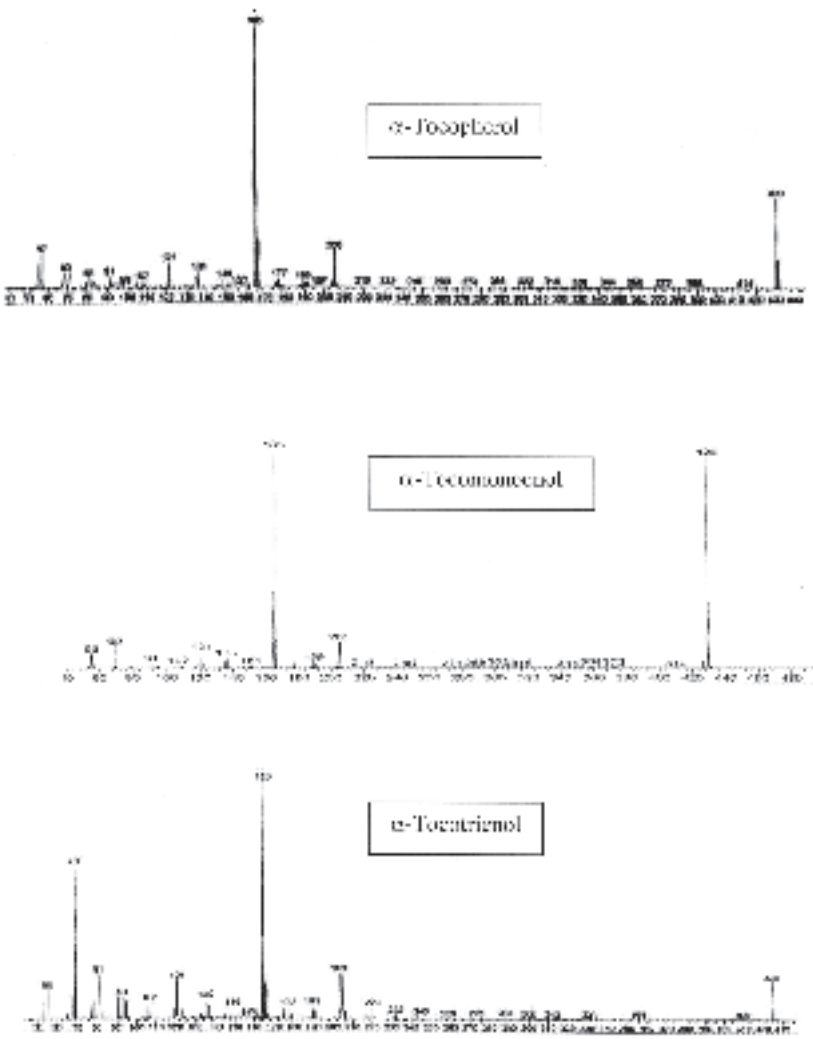

FIG. 4. Mass spectra of α-tocopherol, α-tocotrienol, and α-tocomonoenol. Major mass spectral data are shown in Table 1.

TABLE 1
Mass Spectral Data[a] of α-T, α-T_1, and α-T_3

Tocols	Formula	Major MS peaks (*m/z*)
α-T	$C_{29}H_{50}O_2$	430 (M^+), 205, 165, 164
α-T_1	$C_{29}H_{48}O_2$	428 (M^+), 205, 165, 164, 69
α-T_3	$C_{29}H_{44}O_2$	424 (M^+), 205, 165, 164, 69

[a]α-T, α-tocopherol; α-T_1, α-tocomonoenol; α-T_3, α-tocotrienol.

TABLE 2
^{1}H NMR Spectral Data of α-T, α-T_1, and α-T_3[a]

Proton	α-T	α-T_1	α-T_3
3′,7′,11′-CH (olefinic)	—	—	5.06
11′-CH (olefinic)	—	5.12	—
6-OH (phenolic)	4.21	4.22	4.09
4-CH_2	2.53	2.60	2.55
5a-CH_3	2.08	1.99	2.04
7a-CH_3	2.00	1.99	2.04
8a-CH_3	2.00	1.99	2.04
1′,2′,5′,6′,9′,10′-CH_2	—	1.95	1.99
3-CH_2	1.75	1.75	1.75
13′-CH_3	—	1.68	1.69
4′a,8′a,12′a-CH_3	1.15	—	1.60
2a-CH_3	1.17	1.22	1.17

[a]Measured in $CDCl_3$. For abbreviations see Table 1.

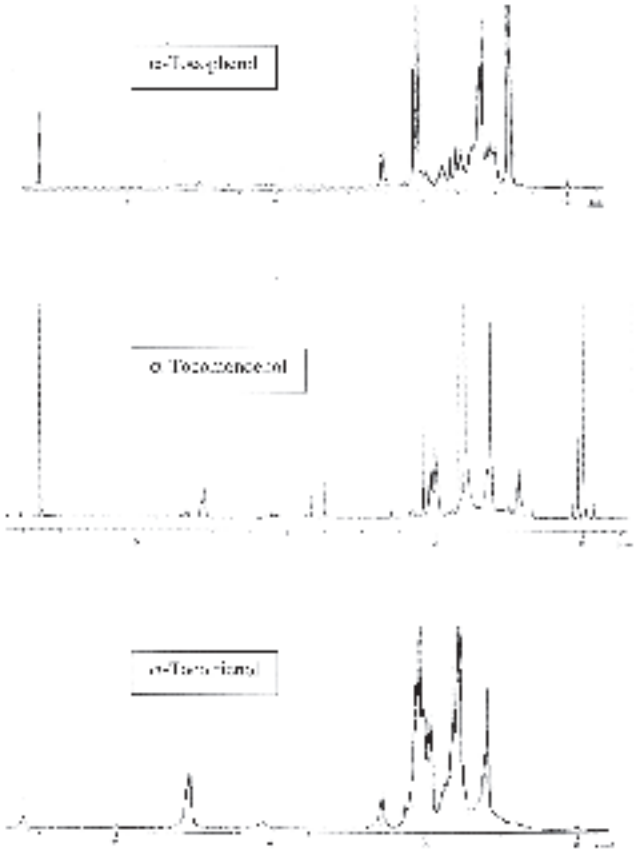

FIG. 5. ^{1}H NMR of α-tocopherol, α-tocotrienol, and α-tocomonoenol. Chemical shifts are shown in Table 2.

The ^{1}H NMR spectrum of α-T_1 is also typical of those of α-T and α-T_3, as shown in Figure 5. However, α-T_1 is distinguishable from α-T by the presence of proton signals in the aliphatic region of δ 1.68 ppm, which denotes the presence of two methyl groups attached to a double bond. The proton assignments of these three types of α-isomers of the tocols are shown in Table 2.

Concentrations of vitamin E in CPO, PFO, and the phytonutrient concentrate were calibrated using authentic standards and are depicted in Tables 3 and 4. The major constituent of vitamin E isomer in CPO and the phytonutrient concentrate is γ-T_3. This is not surprising as the phytonutrient concentrate was derived from esterification/transesterification of CPO. On the other hand, the major vitamin E isomer in PFO is α-T. The newly identified α-T_1 constitutes about 3–4% of the total vitamin E in CPO and the phytonutrient concentrate, whereas its content in PFO is about 11% of the

TABLE 3
Concentrations (ppm) of Vitamin E in CPO, PFO, and the Phytonutrient Concentrate[a]

Sample	α-T	α-T_1	α-T_3	γ-T_3	δ-T_3	Total
CPO	420 ± 15	40 ± 5	260 ± 10	360 ± 10	80 ± 3	1160 ± 43
PFO	1810 ± 10	430 ± 6	760 ± 5	930 ± 5	110 ± 5	4040 ± 31
Phytonutrient concentrate	1400 ± 20	350 ± 10	2430 ± 10	8320 ± 15	1280 ± 10	13780 ± 65

[a]CPO, crude palm oil; PFO, palm fiber oil; γ-T_3, γ-tocotrienol; δ-T_3, δ-tocotrienol; for other abbreviations see Table 1.

TABLE 4
Compositions (%) of Vitamin E in CPO, PFO, and the Phytonutrient Concentrate[a]

Sample	α-T	α-T_1	α-T_3	γ-T_3	δ-T_3
CPO	36	4	22	31	7
PFO	44	11	19	23	3
Phytonutrient concentrate	10	3	18	60	9

[a]For abbreviations see Tables 1 and 3.

total vitamin E present, which is even higher than the δ-T_3 content in PFO. α-T_1 has been shown to be present in hardened palm oil, although no data on its concentration are reported (15).

Both the esterification/transesterification process of CPO and the vacuum distillation of CPO methyl esters permit the retention of most of the vitamin E except for α-T and γ-T_3. The relative content of α-T in the total vitamin E present dropped from 36% in CPO to 10% in the phytonutrient concentrate. On the other hand, the content of γ-T_3 doubled from 31% in CPO to 60% in the phytonutrient concentrate.

REFERENCES

1. Goh, S.H., Choo, Y.M., and Ong, A.S.H. (1985) Minor Constituents of Palm Oil, *J. Am. Oil Chem. Soc. 62*, 237–240.
2. Choo, Y.M., Yap, S.C., Ooi, C.K., Ma, A.N., Goh, S.H., and Ong, A.S.H. (1996) Recovered Oil from Palm-Pressed Fiber: A Good Source of Natural Carotenoids, Vitamin E and Sterols, *J. Am. Oil Chem. Soc. 73*, 599–602.
3. Qureshi, A.A., Mo, H.B., Packer, L.A., and Peterson, D.M. (2000) Isolation and Identification of Novel Tocotrienols from Rice Bran with Hypocholesterolemic, Antioxidant and Antitumor Properties, *J. Agric. Food Chem. 48*, 3130–3140.
4. Sundram, K., Khor, H.T., Ong, A.S.H., and Pathmanathan, R. (1989) Effect of Dietary Palm Oil on Mammary Carcinogenesis in Female Rats Induced by 7,12-Dimethylbenz(a)anthracene, *Cancer Res. 49*, 1447–1451.
5. Yurttas, H.C., and Addis, P.B. (2001) Antioxidant Activity of Palm Tocotrienols in Meat Systems, in *2001 PORIM International Conference*, Kuala Lumpur, Malaysia.
6. Goh, S.H., Hew, N.F., Norhanom, A.E., and. Yadar, M.C. (1994) Inhibition of Tumour Growth Promotion by Various Palm Oil Tocotrienols, *Int. J. Cancer 57*, 529–531.
7. Guthrie, N., Nesaretnam, K., Chambers, A.F., and Carroll, K.K. (1993) Inhibition of Breast Cancer Cell Growth by Tocotrienols, *FASEB J*. 7, A70.
8. Nesaretnam, K., Kor, H.T., Ganesan, J., Chong, Y.H., Sundram, K., and Gapor. A. (1992) The Effect of Vitamin E Tocotrienols from Palm Oil on Chemically-Induced Mammary Carcinogenesis in Female Rats, *Nutr. Res. 12,* 63–75.
9. Kato, A., Yamaoka, M., Tanaka, A., Komiyama, K., and Umezawqa, L. (1985) Physiological Effects of Tocotrienols, *Abura Kagaku 34*, 375–376.
10. Komiyama, K., Izuka, K., and Yamaoka, M. (1989) Studies on Biological Activity of Tocotrienols, *Chem. Pharm. Bull. 37*, 1369–1371.
11. Kamar, J.P., Sarma, H.D., Devasageyam, T.P.A., Nesaretnam, K., and Basiron, Y. (1997) Tocotrienols from Palm Olein as Effective Inhibitors of Protein Oxidation and Lipid Peroxidation in Rat Liver Microsomes, *Mol. Cell. Biochem. 170*, 131–138.
12. Yamamoto, Y., Maita, N., Fujisawa, A., Takashira, J., Ishiii, Y., and Dunlap, W.C. (1999) A New Vitamin E (α-tocomonoenol) from Eggs of the Pacific Salmon *Oncorhynchus keta*, *J. Nat. Prod. 62*, 1685–1687.
13. Yamamoto, Y., Fujisawa, A., Hara, A., and Dunlap, W.C. (2001) An Unusual Vitamin E Constituent (α-tocomonoenol) Provides Enhanced Antioxidant Protection in Marine Organisms Adapted to Cold-Water Environments, *Proc. Natl. Acad. Sci. USA 98*, 13144–13148.
14. Matsumoto, A., Takahashi, S., Nakano, K., and Kijima, S. (1995) Identification of a New Vitamin E in a Plant Oil, *J. Jpn. Oil Chem. Soc. 44*, 593–597.
15. Drotleff, A.M., and Ternes, W. (1999) *Cis/trans* Isomers of Tocotrienols—Occurrence and Bioavailability, *Eur. Food Res. Technol. 210*, 1–8.
16. Tay, B.Y.P., and Choo, Y.M. (2000) Valuable Minor Constituents of Commercial Red Palm Olein: Carotenoids, Vitamin E, Ubiquinones and Sterols, *J. Oil Palm Res. 12*, 14–24.

[Received May 12, 2004, and in revised form September 28, 2004; revision accepted October 3, 2004]

COMMUNICATION

A New Glucoceramide from the Watermelon Begonia, *Pellionia repens*

Yinggang Luo, Yan Liu, Huayi Qi, and Guolin Zhang*

Chengdu Institute of Biology, Chinese Academy of Sciences, Chengdu 610041, People's Republic of China

ABSTRACT: A new glucoceramide named pellioniareside (**1**) was isolated from the aqueous ethanolic extract of whole plants of *Pellionia repens*, together with lupeol (**2**), uracil (**3**), (22*E*,20*S*,24*R*)-5α,8α-epidioxyergosta-6,22-dien-3-β-ol (**4**), and daucosterol (**5**). The structure and relative configurations of pellioniareside were identified as (2*S*,3*S*,4*R*,6*E*,8*E*)-1-*O*-β-D-glucopyranosyl-2-[(2*R*)-2-hydroxytetracosanoylamino]-1,3,4-octadecanetriol-6,8-diene by analysis of spectral data and by chemical evidence.

Paper no. L9594 in *Lipids 39*, 1037–1042 (October 2004).

The genus *Pellionia* Gaud. (Urticaceae) is distributed over the tropical regions in Asia (1). Whole plants of *P. repens* (Lour) Merr., grown at an altitude of 800–1100 m (2,3), was used to treat icterus, acute and chronic hepatitis, and allergic dermatitis in traditional Chinese medicine (4,5). Previous chemical studies only lead to the isolation of cholesterol and daucosterol from *P. scabra* (6).

Sphingolipids, a diverse group of lipids, are ubiquitous constituents of eukaryotic cells and have been intensively investigated in mammals and yeast for decades (7). Plant glucosylceramides are important structural components of plasma and vacuole membranes (8). However, the biochemistry of sphingolipid in plants has been explored only recently (7). Significant attention has been paid to the simple sphingolipids, particularly ceramide, and glucosylceramide, each of which appears to be involved in the regulation of specific aspects of neuronal proliferation, differentiation, survival, and apoptosis (9,10). Eukaryotic life is characterized by internal membranes of various components, and sphingolipids are a small but important part of these membranes. Cell biologists have recently focused on inherited sphingolipid-storage diseases (11). Glycosphingolipids are implicated in the pathogenesis of various diseases, including glycosphingolipidoses, peripheral neuropathies caused by antiganglioside antibodies, and secretory diarrhea (12).

*To whom correspondence should be addressed at Chengdu Institute of Biology, the Chinese Academy of Sciences, P.O. Box 416, Chengdu 610041, P.R. China. E-mail: ZHANGGL@cib.ac.cn

Abbreviations: CC, column chromatography; DEPT, distortionless enhancement by polarization transfer; DMDS, dimethyl disulfide; EI-MS, electron impact mass spectrum; ESI-MS, electrospray ionization mass spectrum; Fr., fraction; Glc, glucopyranosyl; HMBC, (^{1}H-detected) heteronuclear multiple-bond correlation; HR-APCI-MS, high-resolution atmospheric pressure chemical ionization mass spectrum; HR-EI-MS, high-resolution electron impact mass spectrum; HSQC, (^{1}H-detected) heteronuclear single-quantum coherence.

Here we report the isolation and structure elucidation of sphingolipid, a new glucoceramide named pellioniareside (**1**), together with lupeol (**2**), uracil (**3**), (22*E*,20*S*,24*R*)-5α,8α-epidioxyergosta-6,22-dien-3-β-ol (**4**), and daucosterol (**5**). Their structures and relative configurations were established by analysis of spectral data and by chemical evidence.

EXPERIMENTAL PROCEDURES

Instrumentation. Melting points were recorded on an X-6 apparatus (Beijing Fukai Science and Technology Co. Ltd., Beijing, People's Republic of China) and are uncorrected. Optical rotations were measured with a PerkinElmer 341 automatic polarimeter (Beaconsfield, United Kingdom). IR spectra were recorded on a PerkinElmer Spectrum One spectrometer. NMR spectra [^{1}H, ^{13}C distortionless enhancement by polarization transfer (DEPT); ^{1}H-^{1}H COSY, (^{1}H-detected) heteronuclear single-quantum coherence (HSQC); and (^{1}H-detected) heteronuclear multiple-bond correlation (HMBC) experiments] were obtained on a Bruker Avance 600 (Bruker, Rheinstetten, Germany) spectrometer at 600 MHz for ^{1}H NMR and at 150 MHz for ^{13}C NMR. Chemical shifts (δ) are given in ppm relative to tetramethylsilane as internal standard and coupling constants in Hertz (Hz). Electrospray ionization mass spectra (ESI-MS) were carried on a Finnigan LCQ^{DECA} mass spectrometer. High-resolution atmospheric pressure chemical ionization mass spectra (HR-APCI-MS) were obtained on a Bruker FTMS APEX3 mass spectrometer. Electron impact mass spectra (EI-MS) and high-resolution electron impact mass spectra (HR-EI-MS) were obtained on a VG 7070E (70 eV) mass spectrometer. Spots on TLC plates were visualized by spraying with Dragendorff's reagent and by spraying with 8% phosphomolybdic acid/ethanol solution followed by heating.

Materials. Silica gel for column chromatography (CC) (200–300 mesh) and for TLC plates (10–40 μm) was purchased from Qingdao Marine Chemical Ltd. (Qingdao, People's Republic of China).

Whole plants of *P. repens* were collected from Xishuangbanna, Yunnan Province, People's Republic of China, in August 2002 and identified by Professor Jingyun Cui (Xishuangbanna Tropical Botanical Garden, the Chinese Academy of Sciences). A voucher specimen (GF-110) is deposited at the Herbarium of Chengdu Institute of Biology (the Chinese Academy of Sciences Chengdu 610041, People's Republic of China).

Extraction and isolation. Aliquots of dried and powdered whole plants (3 kg) were soaked with 95% EtOH (20 L × 3) at room temperature. After removing solvent under reduced pressure, the residue (100 g) was partitioned between H_2O and EtOAc to provide an ethyl acetate-soluble fraction (32 g), which was divided into eight fractions (Fr. 1–8) by gradient elution CC using $CHCl_3$/MeOH (10:0–10:5, vol/vol). Fr. 3 was subjected to CC with elution by $CHCl_3$/MeOH (20:1, vol/vol) to yield three subfractions (Fr. 3A–3C). Compound **4** (4 mg) was obtained from Fr. 3B by CC using cyclohexane/acetone (6:1, vol/vol). Fr. 3C was separated on CC by elution with petroleum ether (60–90C)/acetone (10:1, vol/vol) to yield lupeol (**2**, 30 mg). Daucosterol (**5**, 408 mg) was precipitated from Fr. 5. The mother liquid of Fr. 5 was further separated on CC with elution by $CHCl_3$/MeOH (5:1, vol/vol) to yield compound **3** (6 mg). Compound **1** (30 mg) was obtained from Fr. 7 eluted by $CHCl_3$/MeOH (5:1, vol/vol).

*Pellioniareside ((2*S*,3*S*,4*R*,6*E*,8*E*)-1*-O-*β*-D-glucopyranosyl-2-[(2*R*)-2-hydroxytetracosanoyl amino]-1,3,4-octadecanetriol-6,8-diene, **1**)*. White powder ($CHCl_3$/MeOH, 5:1, vol/vol). m.p. 212–214°C, $[\alpha]_D^{20}$ +10.0° [*c* 0.2, $CHCl_3$/MeOH (1:1, vol/vol)]. IR ν_{max}^{KBr} cm^{-1}: 3429 (–OH), 2921, 2852, 1636 and 1541 (C=O of amide), 1467, 1433, 1113, 1079, 1038, 964, and 720. ^1H and ^{13}C NMR data are given in Table 1. HR-APCI-MS (positive-ion mode) *m/z*: 864.6572 ($C_{48}H_{91}NO_{10}Na$, required for 864.6541, 3.1068 mDa error, 3.5931 ppm error). ESI-MS (positive-ion mode) *m/z* (relative intensities, %): 842 ($[M + H]^+$, 30), 680 ($[M + H - Glc]^+$, 100, where Glc = glucopyranosyl 384), ($[M + H - Glc - sphingoid\ moiety]^+$, 100), 296 ($[sphingoid\ moiety + H]^+$, 35), 278 ($[sphingoid\ moiety + H - H_2O]^+$, 10), and 260 ($[sphingoid\ moiety + H - 2\times H_2O]^+$, 5).

*Acetylation of **1***. Compound **1** (6 mg) was dissolved in 0.3 mL of triethylamine and 0.3 mL of acetic anhydride. The reaction mixture was stirred at room temperature for 24 h. To the reaction solution was added 2 mL of water. Ethyl acetate was introduced to extract the acetylation product (1 mL × 3). The organic layers were combined and washed with brine and dried over anhydrous sodium sulfate. The ethyl acetate extract was subjected to elution on CC by *n*-hexane/ethyl acetate (5:1, vol/vol) to give 7 mg of its peracetate derivative **1a**.

*(2*S*,3*S*,4*R*,6*E*,8*E*)-1*-O-*(2,3,4,6-tetra*-O-*acetyl-*β*-D-glucopyranosyl)-3,4*-O-*diacetyl-2-[(*R*)-2-acetoxytetracosanoyl-amino]-6,8-octadecanediene (**1a**)*. White powder. $[\alpha]_D^{20}$ +5.5° (*c* 0.2, $CHCl_3$). IR ν_{max}^{KBr} cm^{-1}: 2926, 2856, 1749 (C=O of ester), 1633 and 1523 (C=O of amide), 1456, 1373, 1235, 1044, and 797. ^1H NMR ($CDCl_3$, 600 MHz): δ 6.77 (1H, *d*, *J* = 8.7 Hz, H–NHCO), 5.70 (1H, *m*), 5.68 (1H, *m*), 5.40 (1H, *m*), 5.39 (1H, *m*), 5.19 (1H, *t*, *J* = 9.6 Hz), 5.13 (3H, *m*), 5.07 (1H, *t*, *J* = 9.6 Hz), 4.90 (1H, *dt*, *J* = 9.5, 3.8 Hz), 4.86 (1H, *m*), 4.48 (1H, *d*, *J* = 8.0 Hz), 4.26 (1H, *m*), 4.24 (1H, *d*, *J* = 4.2

TABLE 1
NMR Spectral Data of Compound 1 in C_5D_5N

Position	δ_H[a]	δ_C[a,b]	^1H-^1H COSY	HMBC (selected)
1	4.69 (1H, *dd*, *J* = 10.0, 5.6 Hz)	70.5 (*t*)	H-2	C-2, C-1″
	4.51 (1H, *dd*, *J* = 10.0, 6.4 Hz)			
2	5.29 (1H, *m*)	51.9 (*d*)	H-1, H-3	
3	4.29 (1H, *m*)	76.0 (*d*)	H-2, H-4	
4	4.22 (1H, *m*)	72.7 (*d*)	H-3, H-5	C-3, C-6
5	2.04 (1H, *m*), 1.98 (1H, *m*)	33.8 (*t*)	H-4, H-6	C-6, C-7
6	6.00 (1H, *dt*, *J* = 15.6, 6.4 Hz)	136.3 (*d*)	H-5, H-7	C-4
7	5.79 (1H, *dd*, *J* = 15.6, 10.0 Hz)	131.6 (*d*)	H-6, H-8	C-5, C-6
8	5.85 (1H, *dd*, *J* = 16.0, 10.0 Hz)	131.1 (*d*)	H-7, H-9	C-7
9	5.80 (1H, *dt*, *J* = 16.0, 6.0 Hz)	131.1 (*d*)	H-8, H-10	C-10
10	2.06 (1H, *m*)	30.3 (*t*)	H-9	C-8, C-9
	2.16 (1H, *m*)			
11–17 and 5′–23′	1.20–1.33 (about 52 H, *m*)	22.9, 29.6–30.0, 32.1		
18	0.86 (3H, *t*, *J* = 6.6 Hz)	14.4 (*q*)		
–NH	8.56 (1H, *d*, *J* = 8.8 Hz)		H-2	C-2, C-1′
1′		175.8 (*s*)		
2′	4.56 (1H, *dd*, *J* = 7.2, 3.6 Hz)	72.5 (*d*)	H-3′	C-1′, C-4′
3′	2.18 (1H, *m*), 1.98 (1H, *m*)	35.6 (*t*)	H-2′, H-4′	
4′	1.74 (2H, *m*)	26.0 (*t*)	H-3′	
24′	0.85 (3H, *t*, *J* = 6.6 Hz)	14.4 (*q*)		
1″	4.93 (1H, *d*, *J* = 7.6 Hz)	105.7 (*d*)	H-2″	C-1, C-3″
2″	3.99 (1H, *t*, *J* = 7.2 Hz)	75.2 (*d*)	H-1″, H-3″	
3″	3.85 (1H, *brs*)	78.6 (*d*)	H-2″, H-4″	
4″	4.22 (1H, *m*)	71.6 (*d*)	H-3″, H-5″	
5″	4.18 (1H, *m*)	78.5 (*d*)	H-4″, H-6″	
6″	4.47 (1H, *dd*, *J* = 12.0, 4.5 Hz)	62.7 (*t*)	H-5″	C-5″
	4.32 (1H, *dd*, *J* = 12.0, 5.3 Hz)			

[a]Signals were assigned by (^1H-detected) heteronuclear single-quantum coherence (HSQC), (^1H-detected) heteronuclear multiple-bond correlation (HMBC), and ^1H-^1H COSY experiments.
[b]Multiplicities were determined by distortionless enhancement by polarization transfer (DEPT).

Hz), 4.14 (1H, *d*, *J* = 10.4 Hz), 3.86 (1H, *brd*, *J* = 11.0 Hz), 3.70 (1H, *m*), 3.67 (1H, *m*), 2.09 (3H, *s*), 2.07 (3H, *s*), 2.05 (3H, *s*), 2.04 (3H, *s*), 2.03 (3H, *s*), 2.02 (3H, *s*), 2.00 (3H, *s*), 1.84 (3H, *m*), 1.68 (9H, *m*), 1.26–1.35 (56H, *m*), and 0.88 (6H, *t*, *J* = 7.0 Hz). ^{13}C NMR ($CDCl_3$, 150 MHz): δ 171.0, 170.6, 170.3, 170.2, 170.0, 169.8, 169.4, 169.3, 134.8, 134.7, 128.0, 127.9, 100.4, 74.6, 73.9, 72.7, 71.9, 71.2, 68.1, 66.7, 61.8, 48.1, 34.5, 34.2, 34.1, 32.2, 31.9, 31.8, 31.7, 30.9, 29.2–29.7, 29.0, 25.0, 22.7, 20.96, 20.91, 20.71, 20.68, 20.66, 20.57, 20.54, and 14.1. ESI-MS (positive-ion mode) *m/z* (relative intensities, %): 1136 ($[M + H]^+$, 100), 806 ($[M + H - Glc(OAc)_4]^+$, 10), 747 ($[M + H - Glc(OAc)_4 - OAc]^+$, 10).

*Methanolysis of **1***. To 3 mL of 0.9 mol/L HCl in 82% aqueous methanol solution was added 8 mg of compound **1**. The mixture was refluxed with stirring for 20 h. The resultant reaction mixture was extracted with *n*-hexane (1 mL × 3). The combined organic layers were washed with brine and dried over sodium sulfate. Concentration of the *n*-hexane extract gave a fatty acid methyl ester (**1b**), which was purified by elution with *n*-hexane/acetone on silica gel CC (5:1, vol/vol).

*Methyl (2*R*)-2-hydroxytetracosanate (**1b**)*. White powder. $[\alpha]_D^{20}$ –4.0° (*c* 0.1, $CHCl_3$). IR ν_{max}^{KBr} cm^{-1}: 3428 (OH), 2920, 2851, 1741 (C=O of ester), 1467, 1384, 1261, 1098, 802, 751, and 722. ^{1}H NMR ($CDCl_3$, 600 MHz): δ 4.22 (1H, *dd*, *J* = 7.6, 4.2 Hz, H-2), 3.82 (3H, *s*, H–$COOCH_3$), 2.73 (1H, *brs*, OH), 1.81 (2H, *m*, H-3), 1.28 (*brs*, H-methylenes), and 0.90 (3H, *t*, *J* = 7.1 Hz, terminal methyl). EI-MS *m/z* (relative intensities, %): 398 ($[M]^+$, 31), 370 ($[M - H_2O]^+$, 4), 339 ($[M - COOCH_3]^+$, 13), 111 (22), 97 (54), 83 (50), 69 (43), 57 (80), and 43 (100).

*2-Acetoamino-1,3,4-triacetoxy-6,8-octadecanediene (**1e**)*. The aqueous methanolic layer of the methanolysis of **1** was neutralized with saturated sodium bicarbonate, concentrated to remove methanol, and extracted with ethyl ether. The organic layer was washed with brine, dried over sodium sulfate, and concentrated to give a long-chain base (**1d**), which was dissolved in 0.5 mL of acetic anhydride and 0.5 mL of triethylamine. The resultant solution was refluxed for 2 h. To the reaction mixture was added 2 mL of water and then the mixture was extracted with ethyl acetate (1 mL × 5). The organic layer was combined and washed with brine, dried over sodium sulfate, and then concentrated to give a residue that was subjected to CC on silica gel by elution with *n*-hexane/acetone (4:1, vol/vol) to yield a peracetate of the long-chain base (**1e**, 3 mg) as a white solid. $[\alpha]_D^{20}$ +9.0° (*c* 0.1, $CHCl_3$). IR ν_{max}^{KBr} cm^{-1}: 2947, 2920, 2854, 1740 (C=O of ester), 1630 (C=O of amide), 1445, 1377, 1347, 1309, 1264, 1200, 1176, 1143, 1098, 1065, 907, 850, and 670. ^{1}H NMR ($CDCl_3$, 600 MHz): δ 7.20 (1H, *d*, *J* = 8.8 Hz, H–NHCO), 5.77 (1H, *m*), 5.70 (1H, *m*), 5.55 (1H, *m*), 5.52 (1H, *m*), 5.20 (1H, *t*, *J* = 9.6 Hz), 4.28 (1H, *m*), 4.15 (2H, *dd*, *J* = 12.6, 5.4 Hz), 3.96 (1H, *m*), 2.19 (9H, *s*, 3×OAc), 2.13 (3H, *s*), 1.60 (2H, *m*), 1.23–1.31 (18H, *m*), and 0.88 (3H, *t*, *J* = 7.0 Hz). ESI-MS (negative-ion mode) *m/z* (relative intensities, %): 437 ($[M - H - Ac]^-$, 10), 396 ($[M - 2\times Ac]^-$, 100), 315 ($[M - H - Ac - 2\times HOAc]^-$, 30).

*1-*O*-Methyl-*β*-*D*-glucopyranoside (**1c**)*. The remaining water layer was evaporated *in vacuo*. The residue was then subjected to silica gel CC by elution with $CHCl_3/CH_3OH/H_2O$ (7:3:0.5, by vol) to yield 1-*O*-methyl-β-D-glucopyranoside (**1c**). $[\alpha]_D^{20}$ +78.1° (*c* 0.016, CH_3OH) literature (13) $[\alpha]_D^{20}$ +77.3° (*c* 0.1, CH_3OH). ESIMS (positive-ion mode) *m/z* (relative intensities, %): 399 ($[2M + H]^+$, 100).

*Dimethyl disulfide (DMDS) derivative of compound **1***. Compound **1** (2 mg) was dissolved in 0.2 mL of carbon disulfide and 0.2 mL of dimethyl disulfide (DMDS). Iodine (1 mg) was added to this solution. The reaction mixture was kept at 60°C for 40 h in a small sealed vial. The reaction was quenched with aqueous sodium thiosulfate, and the reaction mixture was extracted with *n*-hexane (0.3 mL). The extract was concentrated to give a residue that was purified by silica gel CC with elution by $CHCl_3$/acetone (8.5:1.5, vol/vol) to give the DMDS derivative (**1f**) as an amorphous powder. HR-EI-MS *m/z*: 187.1528 ($C_{11}H_{23}S$, required for 187.1520, 0.7863 mDa error, 4.2014 ppm error).

RESULTS AND DISCUSSION

Compound 1 was obtained as a white powder. The orange color visualization on TLC with Dragendorff's reagent and the quasi-molecular ion peak at *m/z* 842 ($[M + H]^+$) in the ESI-MS (positive-ion mode) suggested the presence of an odd nitrogen atom. The molecular formula $C_{48}H_{91}NO_{10}Na$ was calculated from the quasi-molecular ion peak at *m/z* 864.6572 in the HR-APCI-MS (positive-ion mode) of **1**. The ion peak at *m/z* 680 ($[M + H - Glc]^+$) and the six ^{13}C NMR signals (Table 1) at δ 105.7 (*d*), 75.2 (*d*), 78.5 (*d*), 71.6 (*d*), 78.6 (*d*), and 62.7 (*t*) indicated the presence of a glucosyl moiety, which was confirmed by the product 1-*O*-methyl-β-D-glucopyranoside (**1c**) from the methanolysis of **1** in 0.9 mol/L HCl in 82% aqueous methanol solution. The ^{1}H NMR signal (Table 1) at δ 4.93 (1H, *d*, *J* = 7.6 Hz, H-1″) also suggested it is β-D-Glc moiety. A secondary amide carbonyl group was deduced from the IR peaks at 1636 and 1541 cm^{-1}, the ^{13}C NMR signal (Table 1) at δ 175.8 (*s*, C-1′), and the ^{1}H NMR signal (Table 1) at δ 8.56 (1H, *d*, *J* = 8.8 Hz, H–NHCO). Two conjugated *E*-disubstituted double bonds were established by the ^{1}H NMR signals (Table 1) at δ 6.00 (1H, *dt*, *J* = 15.6, 6.4 Hz, H-6), 5.79 (1H, *dd*, *J* = 15.6, 10.0 Hz, H-7), 5.85 (1H, *dd*, *J* = 16.0, 10.0 Hz, H-8), and 5.80 (1H, *dt*, *J* = 16.0, 6.0 Hz, H-9), the IR absorption peak at 964 cm^{-1} (14), and the ^{1}H-^{1}H COSY correlations between H-6 and H-7, between H-7 and H-8, and between H-8 and H-9. The ^{13}C NMR signals (Table 1) at δ 70.5 (*t*), 76.0 (*d*), 72.7 (*d*), and 72.5 (*d*) suggested four oxygenated carbons. The ^{13}C NMR signal (Table 1) at δ 51.9 should be assigned to the carbon atom substituted by a nitrogen atom considering the HSQC cross signal at δ 5.29 (1 H, *m*)/51.9 (*d*). Two methyl groups and a long-chain alkyl moiety were concluded from the ^{1}H NMR signals (Table 1) at δ 0.86 and 0.85 (each 3 H, *t*, *J* = 6.6 Hz) and 1.20–1.33 (about 52 H, *m*). Thus, compound **1** could be a glucoceramide (Fig. 1).

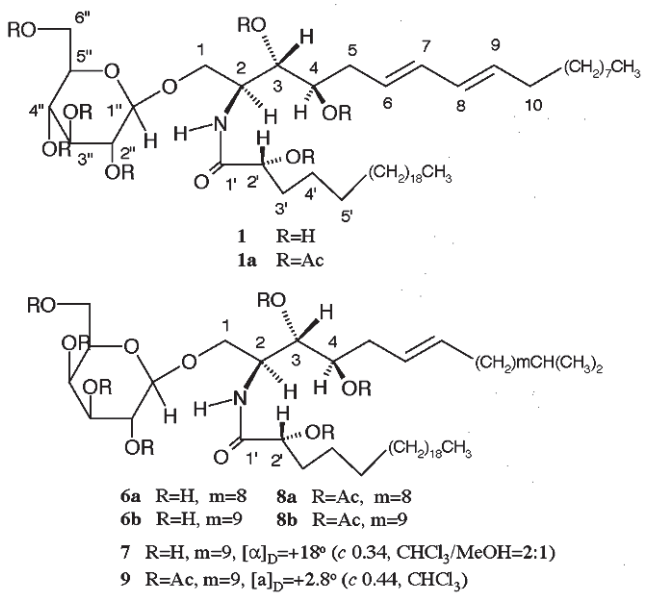

FIG. 1. The structures of compound **1**, its acetylated product **1a**, and structurally related compounds **6a**, **6b**, **7**, **8a**, **8b**, and **9**.

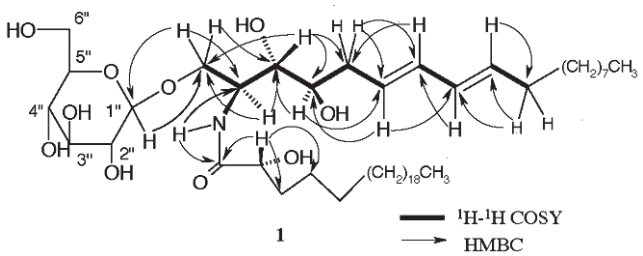

FIG. 2. The key ^{1}H-^{1}H COSY and HMBC correlations of compound **1**.

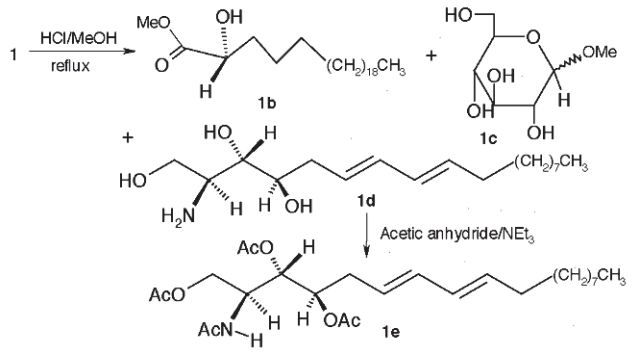

SCHEME 1

To determine the number of hydroxyl groups, compound **1** was acetylated with acetic anhydride/triethylamine at room temperature to yield its peracetate derivative **1a**, which displayed a quasi-molecular ion peak at *m/z* 1136 ([M + H]$^{+}$, 100) in its ESI-MS (positive-ion mode). A Glc moiety was also confirmed by the fragment ion peak at *m/z* 806 ([M + H − Glc(OAc)$_4$]$^{+}$, 10). Seven methyl signals of acetyl were observed at δ 2.09, 2.07, 2.05, 2.04, 2.03, 2.02, and 2.00 (each 3H, *s*) in the ^{1}H NMR spectrum and at δ 20.96, 20.91, 20.71, 20.68, 20.66, 20.57, and 20.54 in the ^{13}C NMR spectrum, and carbonyl signals at δ 171.0, 170.6, 170.3, 170.2, 170.0, 169.8, 169.4, and 169.3 in the ^{13}C NMR spectrum of compound **1a**, respectively. Thus, seven hydroxyl groups were present in compound **1**.

The structure of compound **1** was concluded from the ^{1}H-^{1}H COSY, HMBC, and HSQC correlations (Table 1, Fig. 2), which was confirmed by the chemical degradation (Scheme 1). A fatty acid methyl ester (**1b**), a methyl glucopyranoside (**1c**), and a long- chain base (**1d**), which was acetylated later by acetic anhydride/triethylamine to give compound **1e**, were obtained from the methanolysis solution of compound **1** (Scheme 1) (15). Compound **1b**, methyl 2-hydroxytetracosanate, was identified by its EI-MS and by comparing its ^{1}H NMR data and optical rotations with those reported (16). Thus, the relative configuration of C-2′ was proposed as *R* (16). The β-D-Glc moiety in **1** was concluded by the optical rotations and ESI-MS (positive-ion mode) of the methyl glucopyranoside **1c** (13).

The ion peaks at *m/z* 384 ([M + H − Glc − sphingoid moiety]$^{+}$, 100) in the ESI-MS (positive-ion mode) of compound **1** also suggested that the Fatty Acid chain is 2-hydroxytetracosanoyl. The sphingolipid base, 2-amino-1,3,4-trihydroxyoctadecane-6,8-diene, was also determined by the characteristic fragment ion peaks at *m/z* 296 ([sphingoid moiety + H]$^{+}$, 35) (Fig. 3).

The locations of the two *E*-double bonds were assigned by the ^{1}H-^{1}H COSY and HMBC correlations and by the characteristic fragment ion peaks at *m/z* 187.1528 for $C_{11}H_{23}S$ in the HR-EI-MS of the DMDS derivative **1f** (17,18).

The stereochemistry of C-2, -3, and -4 were determined to be *S*, *S*, and *R*, respectively, by comparing the NMR data, the coupling constants of H-1, H-2, H-3, and H-4, and the optical rotations of compound **1** with those of **6** and its synthetic glycoceramide **7** and by comparing the data of the acetylated product **1a** with those of the acetylated product of **8** and its synthetic glycoceramide **9** (19,20) (Tables 2, 3; Fig. 1). Thus, the structure of **1** was determined as (2*S*,3*S*,4*R*,6*E*,8*E*)-1-*O*-β-D-glucopyranosyl-2-[(2*R*)-2-hydroxytetracosanoylamino]-1,3,4-octadecanetriol-6,8-diene (Fig. 1).

Sphingolipids play an important role in the cells of the vasculature, and cell regulation, specifically in colon cancer cells, and proposes signaling pathways that dietary sphingolipids utilize in

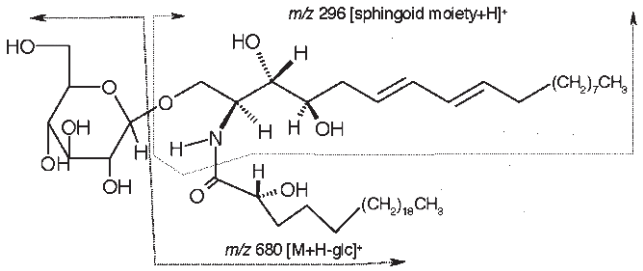

FIG. 3. The proposed fragmentation in the ESI-MS of compound **1**.

TABLE 2
Relevant NMR Data of Compounds 1, 6, and 7

	δ_H		δ_C		
Position	**1**	**7**[20]	**1**	**6**[19]	**7**[20]
1	4.69 (1H, *dd*, 10.0, 5.6)		70.5		70.6
	4.51 (1H, *dd*, 10.0, 6.4)				
2	5.29 (1H, *m*)	5.29 (1H, *m*)	51.9	51.39	51.6
3	4.29 (1H, *m*)		76.0	75.82	75.3
4	4.22 (1H, *m*)		72.7		72.8
5	2.04 (1H, *m*), 1.98 (1H, *m*)		33.8		33.3
6	6.00 (1H, *dt*, 15.6, 6.4)	5.99 (1H, *dt*, 14.6, 7.2)	136.3	133.67	132.7
7	5.79 (1H, *dd*, 15.6, 10.0)	5.74 (1H, *dt*, 14.5, 7.1)	131.6	126.60	128.3
8	5.85 (1H, *dd*, 16.0, 10.0)		131.1		
9	5.80 (1H, *dt*, 16.0, 6.0)		131.1		
10	2.06 (1H, *m*)		30.3		30.3
	2.16 (1H, *m*)				
–NH	8.56 (1H, *d*, 8.8)	8.57 (1H, *d*, 9.6)			
1′			175.8	175.61	175.7
2′	4.56 (1H, *dd*, 7.2, 3.6)		72.5		72.6
3′	2.18 (1H, *m*), 1.98 (1H, *m*)		35.6		35.6

the suppression of colon cancer, are being viewed as bioactive molecules and/or second messengers (29–31) in the suppression of colon cancer because of signaling pathways that have been proposed messengers (21–23). Significant strides have been made in this field over the past 10 yr, from identifying metabolites of the sphingomyelin pathway as second messengers to discerning the molecular biology and biophysics of these lipid-derived second messengers. Scientists from multiple disciplines began to translate manipulations of endogenous sphingolipid metabolites and targets into therapeutic initiatives (32). Chemotherapy has been the primary treatment for disseminated neuroblastoma, but it has often failed because of drug resistance. It has become apparent that sphingolipid metabolites and the generation of sphingolipid species, such as ceramide, play a role in this drug resistance, which involves a variety of cellular mechanisms, including increased drug efflux through expression of ATP-binding cassette transporters and the inability of tumor cells to activate or propagate the apoptotic response. This may be an autonomous mechanism, related to direct effects of sphingolipids on the apoptotic response, while there is also a subtle interplay between sphingolipids and ATP-binding cassette transporters (33). Pellioniareside, a new sphingolipid, may be the active components of this medicinal plant to treat icterus, acute and chronic hepatitis, and allergic dermatitis.

TABLE 3
Relevant ^{1}H NMR Data (δ_H) of Compounds 1a and 9

Position	**1a**	**9**[20]
1	3.86 (1H, *brd*, 11.0)	3.86 (1H, *dd*, 10.9, 3.6)
	3.67 (1H, *m*)	3.68 (1H, *dd*, 10.9, 3.6)
2	4.26 (1H, *m*)	4.33 (1H, *m*)
3	5.19 (1H, *t*, 9.6)	5.19 (1H, *m*)
4	4.90 (1H, *dt*, 9.5, 3.8)	4.92 (1H, *dt*, 9.1, 3.7)
–NH	6.77 (1H, *d*, 8.7)	6.78 (1H, *d*, 8.9)
2′	5.07 (1H, *t*, 9.6)	5.08 (1H, *m*)

The known compounds, uracil (**3**) (21) and (22*E*,20*S*,24*R*)-5α,8α-epidioxyergosta-6,22-dien-3-β-ol (**4**) (22–26) were identified by comparing their spectral data with those reported. Lupeol (**2**) (27) and daucosterol (**5**) (28) were identified by their spectral data and by co-TLC and co-m.p. with authentic samples.

REFERENCES

1. How, F.C. (1998) *A Dictionary of the Families and Genera of Chinese Seed Plants*, 2nd edn., 363 pp., Science Press, Beijing.
2. Delectis Florae Reipublicae Popularis Sinincae Agendae Academiae Sinicae Edita (1984) *Flora Reipublicae Popularis Sinincae, Tomus 53 (1)*, pp. 165–167, Science Press, Beijing.
3. Yunnan Institute of Tropical Botany, Academia Sinica (1984) *List of Plants in Xishuang Banna*, 208 pp., Yunnan Nationality Press, Kunming.
4. Ran, X.D. (1996) *Zhonghua Yaohai*, pp. 677–678, Harbin Press, Harbin.
5. Institutum Botanicum Kunmingense Academiae Sinicae Edita (1984) *Index Florae Yunnanensis (Tomus 1)*, 730 pp., The People's Publishing House, Kunmin.
6. Zhu, G.D., and Qiu, C.B. (1994) Chemical Components of *Pellionia scabra*, *Zhongyaocai 17*, 33.
7. Lynch, D.V., and Dunn, T.M. (2004) An Introduction to Plant Sphingolipids and Review of Recent Advances in Understanding Their Metabolism and Function, *New Phytol. 161*, 677–702.
8. Spassieva, S., and Hille, J. (2003) Plant Sphingolipids Today. Are They Still Enigmatic? *Plant Biol. 5*, 125–136.
9. Buccoliero, R., and Futerman, A.H. (2003) The Roles of Ceramide and Complex Sphingolipids in Neuronal Cell Function, *Pharm. Res. 47*, 409–419.
10. Buccoliero, R., Bodennec, J., and Futerman, A.H. (2002) The Role of Sphingolipids in Neuronal Development: Lessons from Models of Sphingolipid Storage Diseases, *Neurochem. Res.* 27, 565–574.
11. Sillence, D.J., and Platt, F.M. (2003) Storage Diseases: New Insights into Sphingolipid Functions, *Trends Cell Biol. 13*, 195–203.
12. Zhang, X., and Kiechle, F.L. (2004) Glycosphingolipids in Health and Disease, *Ann. Clin. Lab. Sci. 34*, 3–13.

13. Jin, W., Rinehart, K.L., and Jares-Erijman, E.A. (1994) Ophidiacerebrosides: Cytotoxic Glycosphingolipids Containing a Novel Sphingosine from a Sea Star, *J. Org. Chem. 59*, 144–147.
14. Kraus, R., and Spiteller, G. (1991) Ceramides from *Urtica dioica* Roots, *Liebigs Ann. Chem*., 125–128.
15. Natori, T., Morita, M., Akimoto, K., and Koezuka, Y. (1994) Agelasphins, Novel Antitumor and Immunostimulatory Cerebrosides from the Marine Sponge *Agelas mauritianus*, *Tetrahedron 50*, 2771–2784.
16. Tan, J.W., Dong, Z.J., and Liu, J.K. (2003) New Cerebrosides from the Basidiomycete *Cortinarius tenuipes*, *Lipids 38*, 81–84.
17. Inagaki, M., Isobe, R., Kawano, Y., Miyamoto, T., Komori, T., and Higuchi, R. (1998), Isolation and Structure of Three New Ceramides from the Starfish *Acanthaster planci*, *Eur. J. Org. Chem.,* 129–131.
18. Hua, H.M., Cheng, M.S., and Li, X. (2000) Studies on the Ceramides of *Linaria vulgaris* Mill., *Chin. J. Med. Chem. 10*, 57–59.
19. Endo, M., Nakagawa, M., Hamamoto, Y., and Ishihama, M. (1986) Pharmacologically Active Substances from Southern Pacific Marine Invertebrates, *Pure Appl. Chem. 58*, 387–394.
20. Honda, M., Ueda, Y., Sugiyama, S., and Komori, T. (1991) Synthesis of a New Cerebroside from a *Chondropsis* sp. Sponge, *Chem. Pharm. Bull. 39*, 1385–1391.
21. Blicharska, B., and Kupka, T. (2002) Theoretical DFT and Experimental NMR Studies on Uracil and 5-Fluorouracil, *J. Mol. Struct. 613*, 153–166.
22. Takaishi, Y., Uda, M., Ohashi, T., Nakano, K., Murakami, K., and Tomimatsu, T. (1991) Glycosides of Ergosterol from *Hericum erinacens*, *Phytochemistry 30*, 4117–4120.
23. Fisch, M.H., and Ernst, R. (1973) Identity of Ergosterol 5β,8β-Peroxide, *J. Chem. Soc., Chem. Comm.,* 530.
24. Ma, W.G., Li, X.C., Wang, D.Z., and Yang, C.R. (1994) Ergosterol Peroxide from *Cryptoporus volvatus*, *Yunnan Zhiwu Yanjiu 16*, 196–200.
25. He, L.W., and Mong, Z.M. (1995) Studies on Constituents of *Alternanthera philoxeroides* (Mart) Gresib., *Zhongguo Yaoke Daxue Xuebao 25*, 263–267.
26. Sheikh, Y.M., and Djerassi, C. (1974) Steroids from Sponges, *Tetrahedron 30*, 4095–4103.
27. Sholichin, M., Yamasaki, K., Kasai, R., and Tanaka, O. (1980) ^{13}C Nuclear Magnetic Resonance of Lupane-Type Triterpenes, Lupeol, Betulin and Betulinic Acid, *Chem. Pharm. Bull. 28*, 1006–1008.
28. Kojima, H., Sato, N., Hatano, A., and Ogura, H. (1990) Sterol Glucosides from *Prunella vulgaris, Phytochemistry 29*, 2351–2355.
29. Cuvillier, O., Andrieu-Abadie, N., Segui, B., Malagarie-Cazenave, S., Tardy, C., Bonhoure, E., and Levade, T. (2003) Sphingolipid-Mediated Apoptotic Signalling Pathways, *J. Soc. Biol. 197*, 217–221.
30. Schmelz, E.M. (2003) Sphingolipids: A New Strategy for Cancer Treatment and Prevention, *Mol. Nutr.,* 187–199.
31. Argraves, K.M., Obeid, L.M., Hannun, Y.A. (2002) Sphingolipids in Vascular Biology, *Adv. Exp. Med. Biol. 507*, 439–444.
32. Kester, M., and Kolesnick, R. (2003) Sphingolipids as Therapeutics, *Pharm. Res. 47*, 365–371.
33. Sietsma, H., Dijkhuis, A.J., Kamps, W., and Kok, J.W. (2002) Sphingolipids in Neuroblastoma: Their Role in Drug Resistance Mechanisms, *Neurochem. Res. 27*, 665–674.

[Received August 30, 2004; accepted October 29, 2004]

Structure and Function of Animal Fatty Acid Synthase

Subrahmanyam S. Chirala and Salih J. Wakil*

Verna and Marrs McLean Department of Biochemistry and Molecular Biology, Baylor College of Medicine, Houston, Texas 77030

ABSTRACT: Fatty acid synthase (FAS; EC 2.3.1.85) of animal tissues is a complex multifunctional enzyme consisting of two identical monomers. The FAS monomer (~270 kDa) contains six catalytic activities and from the N-terminus the order is β-ketoacyl synthase (KS), acetyl/malonyl transacylase (AT/MT), β-hydroxyacyl dehydratase (DH), enoyl reductase (ER), β-ketoacyl reductase (KR), acyl carrier protein (ACP), and thioesterase (TE). Although the FAS monomer contains all the activities needed for palmitate synthesis, only the dimer form of the synthase is functional. Both the biochemical analyses and the small-angle neutron-scattering analysis determined that in the dimer form of the enzyme the monomers are arranged in a head-to-tail manner generating two centers for palmitate synthesis. Further, these analyses also suggested that the component activities of the monomer are organized in three domains. Domain I contains KS, AT/MT, and DH, domain II contains ER, KR, and ACP, and domain III contains TE. Approximately one fourth of the monomer protein located between domains I and II contains no catalytic activities and is called the interdomain/core region. This region plays an important role in the dimer formation. Electron cryomicrographic analyses of FAS revealed a quaternary structure at approximately 19 Å resolution, containing two monomers (180 × 130 × 75 Å) that are separated by about 19 Å, and arranged in an antiparallel fashion, which is consistent with biochemical and neutron-scattering data. The monomers are connected at the middle by a hinge generating two clefts that may be the two active centers of fatty acid synthesis. Normal mode analysis predicted that the intersubunit hinge region and the intrasubunit hinge located between domains II and III are highly flexible. Analysis of FAS particle images by using a simultaneous multiple model single particle refinement method confirmed that FAS structure exists in various conformational states. Attempts to get higher resolution of the structure are under way.

Paper no. L9623 in *Lipids 39,* 1045–1053 (November 2004).

Fatty acid synthase (FAS) of animal tissues is a homodimer, and the monomer is a multifunctional protein containing seven catalytic domains and a site for the prosthetic group, 4′-phosphopantetheine. The FAS dimer complex catalyzes the synthesis of saturated fatty acids, myristate, palmitate, and stearate by using the substrates acetyl-CoA, malonyl-CoA, and NADPH (1–4). It is noteworthy that nearly every tissue in the human body has some level of FAS expression, but FAS is highly expressed in tissues like liver, adipose, and lactating mammary glands (5).

FAS plays an important role in energy homeostasis by converting the excess food consumed into lipids for storage and providing energy when needed via β-oxidation. FAS is also required for the generation of milk lipids during lactation. Besides being the apolar constituent of various membrane lipids required for membrane functions and its biogenesis, the products of FAS myristate (C14:0) and palmitate (C16:0) are involved in the myristoylation and palmitoylation of cellular and viral proteins for membrane targeting. Also, the products palmitate and stearate serve as substrates for chain elongation to produce very long chain fatty acids, which are important constituents of sphingolipids, ceramides, and glycolipids needed for cell division progression, brain structures, and neurological functions (6). Furthermore, increased FAS levels in cancer tissues indicate a poor prognosis and inhibition of FAS and leads to apoptosis of cancer cells (7,8). Inhibition of FAS also suppresses HER2/neu (erbB-2) oncogene overexpression in cancer cells (9). When mice were treated with FAS inhibitor c75, their food intake and body weight were reduced (10). However, saturated fatty acids synthesized by FAS are readily available from food sources.

To understand the importance and contribution of the *de novo* fatty acid synthesis catalyzed by FAS in animals, transgenic knockout mice were generated (11). Studies of these mice showed that not only did the $Fasn^{-/-}$ null mutant embryos die before their implantation in the uterus, but that due to haploid insufficiency most of the $Fasn^{+/-}$ heterozygotes also died at various stages of their embryonic development (11). Whole-mount *in situ* hybridization performed to detect FAS mRNA expression in E7.5–E10.5-day-old embryos, using digoxigenin-labeled anti-sense FAS mRNA probes, showed that the FAS gene was expressed broadly in the mouse embryos, but the regions of strong FAS mRNA expression varied in the developmental stages examined. These observations suggest that the sites of most intense FAS expression coincide with regions known to be undergoing tissue-tissue interactions, tissue outgrowth, and progressive modeling/remodeling (11); hence, FAS is essential during embryonic development.

In animal and human tissues palmitate (16:0 fatty acid), the major saturated constituent of lipids, is synthesized *de novo* by FAS. FAS was the first to make an entry into the most sophisticated class of multifunctional proteins in which a single polypeptide contained all the required constituent activities and performs all of the reactions involved in the synthesis of a metabolite. In addition to FAS, the polyketide syn-

*To whom correspondence should be addressed at Department of Biochemistry and Molecular Biology, Baylor College of Medicine, One Baylor Plaza, Houston, TX 77030. E-mail: swakil@bcm.tmc.edu

Abbreviations: ACP, acyl carrier protein; AT/MT, acetyl/malonyl transacylase; DH, dehydratase; DI to DIII, domains I to III; ER, enoyl reductase; FAS, fatty acid synthase; KR, ketoacyl reductase; KS, ketoacyl synthase; and TE, thioesterase.

thases, the nonribosomal peptide synthases, and the eukaryotic carboxylases such as acetyl-CoA, propionyl-CoA, and pyruvate carboxylases, fall into this category of multifunctional proteins; however, much of our knowledge and appreciation of these multifunctional proteins came from the studies of fatty acid synthesis in animal tissues. There are several extensive reviews describing the structure and function of FAS (1–4), but this review will focus mainly on the recent findings related to the structure and function of FAS and will give a brief introductory description of the pertinent earlier findings.

FATTY ACID SYNTHESIS BY ANIMAL FAS

FAS synthesizes palmitate from acetyl-CoA and malonyl-CoA, which is produced according to the following equation:

$$CH_3COS\text{-}CoA + 7HOOCCH_2COS\text{-}CoA + 14NADPH + 14H^+ \rightarrow CH_3(CH_2CH_2)_7COOH + 14NADP^+ + 8CoA\text{-}SH + 7CO_2 + 6H_2O$$

The synthesis of palmitate is carried out by a very complex overall reaction that involves sequential condensation of seven C_2 units derived from malonyl-CoA to the primer acetyl moiety derived from acetyl-CoA. The individual reactions involved in the synthesis became known from studies of the multienzyme complex of *Escherichia coli* FAS (type 2) in which each reaction is catalyzed by a separate specific enzyme of the FAS complex (1,2,12). These studies identified three important characteristics of fatty acid biosynthesis. First, ATP and CO_2 are required for the synthesis of the key substrate, malonyl-CoA, catalyzed by a biotin enzyme, acetyl-CoA carboxylase (13). Second, the essentiality of the acyl carrier protein (ACP) containing 4′-phosphopantetheine prosthetic group in fatty acid synthesis (14), and third, that all of the acyl intermediates in fatty acid synthesis are bound to ACP as thioester derivatives. The observation that ACP-bound acyl-intermediates are involved in fatty acid synthesis distinguished the pathway of synthesis from that of fatty acid oxidation, which utilizes the acyl-CoA intermediates (12,13). The fatty acid synthesis reactions, however, are catalyzed by several component enzymes of the multifunctional animal FAS (type 1) as illustrated in Figure 1. The transfer of substrates, acetate to β-ketoacyl synthase (KS), and malonate to acyl carrier protein (ACP), from the respective CoA derivatives is catalyzed by acetyl and malonyl transacylases respectively. KS catalyzes the condensation of these substrates to form acetoacetyl-ACP with the release of carbon dioxide. The reduction of acetoacetyl to β-hydroxyacyl chain is catalyzed by β-ketoacyl reductase (KR). The product then undergoes dehydration by β-hydroxyacyl dehydratase (DH) and is followed by a second reduction by enoyl reductase (ER) leading to the formation of a saturated four-carbon fatty acid attached to ACP. KS mediates the transfer of the saturated fatty acyl chain to its own Cys-SH, thus freeing ACP to accept malonate from malonyl-CoA for the next round of elongation. Thus sequential addition of two carbon moieties derived from malonyl-CoA to the growing acyl chain leads to the synthesis of palmitate attached to ACP, which is then hydrolyzed by thioesterase (TE) and released as palmitic acid (1–4).

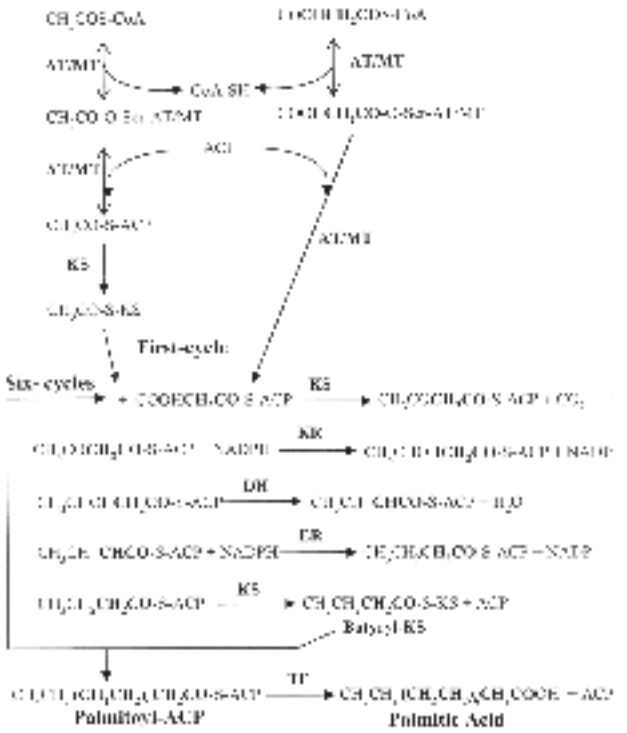

FIG. 1. Catalytic reactions involved in the synthesis of palmitate by animal fatty acid synthase (FAS). Acetyl and malonyl groups from their respective coenzyme A derivatives are transferred to the enzyme by acetyl/malonyl transacylase (AT/MT). In the first cycle the condensation of the acetyl group bound to β-ketoacyl synthase (KS) with the malonyl moiety bound to the acyl carrier protein (ACP) and subsequent β-carbon processing reactions involving β-ketoacyl reductase (KR), β-hydroxy-acyl dehydratase (DH), and enoyl reductase (ER) leads to the formation of butyryl-ACP. The butyryl group is then transferred to KS, thus freeing ACP-SH to accept malonyl moiety from its CoA derivative for the next round of elongation. After an additional six cycles of elongation reactions, the palmitate bound to ACP and is released by thioesterase (TE) to initiate next round of palmitate synthesis. Excluding the reversible steps, there are more than 50 reactions involved in the synthesis of one palmitate molecule, although most of them are repeti-

ORGANIZATION OF COMPONENT ACTIVITIES IN THE MULTIFUNCTIONAL FAS

Initially, the animal FAS was thought to be a multienzyme enzyme complex like *E. coli* FAS due to the presence of several protein bands on SDS-PAGE. By controlling proteolysis during isolation and denaturing immediately before electrophoresis, it was determined that FAS contains a single polypeptide of approximately 250 kDa (15). Active enzyme centrifugation analysis revealed that it is a homodimer (15,16). FAS dimer dissociates in low ionic-strength buffers and at cold temperatures, and the FAS monomer was found to be inactive in fatty acid synthesis (1,2). Even before cDNA derived, amino acid sequences were available, the order of the component activities in the monomer was established by partial proteolysis using various proteases, isolation of various compo-

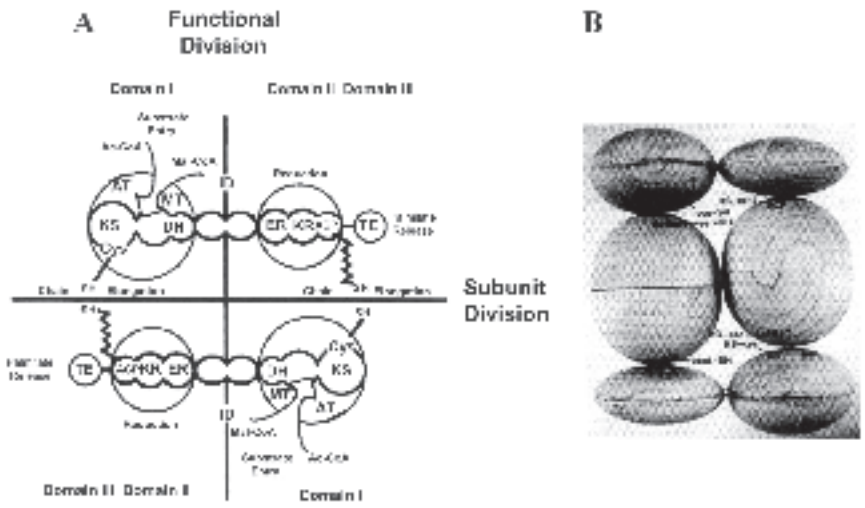

FIG. 2. The structural and functional organization of animal and human FAS dimer. In A, the model is based on the biochemical data in which FAS monomer has three domains. The two subunits with their domains I, II, and III are drawn in an antiparallel arrangement (subunit division) so that two sites of palmitate synthesis are constructed (functional division). Domain I contains KS, AT/MT, and DH. Domain II contains ER, KR and ACP. Domain III contains TE. The wavy line represents the 4′-phosphopantetheine prosthetic group of ACP. The domains I and II are separated by the interdomain peptide, consisting of about 640 amino acids, with no known catalytic function. In the head-to-tail arrangement of the monomers, two sites for the synthesis of palmitate are generated (functional division). Each of these sites is composed of domain I of one monomer and the domains II and III of the other monomer. In B, a model proposed based on the small-angle neutron-scattering analyses (26). Abbreviations used are indicated for Figure 1.

nent fractions, and by determining the FAS-related activities contained in them (1,2,17). These analyses revealed that the FAS monomer contains all the component activities in the following order: NH2-KS, acetyl/malonyl transacylase (AT/MT), DH, ER, KR, ACP, and TE (1,2,17).

The multifunctional FAS cDNA sequences of chicken (18–20), rat (21,22), human (5), and mouse (23) have been determined. Comparison of the amino acid sequences of animal and human FAS showed them to be highly homologous. In the deduced amino acid sequences, the already known active site peptide sequences of KS, AT/MT, the putative nucleotide binding motifs, Gly-X-Gly-X-X-Gly of ER and KR, the phosphopantetheine binding site of ACP, and the active site Ser of TE could be readily located (5,18–24). Comparisons of the amino acid sequences derived from cDNA sequences of animal and human FAS, with those of the subunits of prokaryotic FAS complex and polyketide synthases helped in defining the boundaries of the FAS component enzyme sequences (3,4,24). Interestingly, the highly conserved sequences of component enzymes are separated by short peptide stretches (linker regions) of least conserved sequences. Furthermore, there is a long, less conserved sequence of approximately 640 amino acids, termed the interdomain/core region, located between DH and ER, which does not code for any known functional activity of FAS (Fig. 2). The determination of the N-terminal sequences of chicken FAS peptides, which retained component activities (24) generated by limited proteolysis using kallikrein (2,17), revealed that most of the protease cleavage sites are located in the linker regions. Thus, in FAS monomer, the protein sequences of component activities are folded independently and are organized like beads on a string, an arrangement that suggests that fusion of genes coding for individual type 2 FAS activities resulted in complex multifunctional type 1 FAS.

Proteolytic analyses of animal FAS, described above, also suggested that these activities are organized in three domains (1,2,17). The domain organization was further refined by using the available amino acid sequences of animal and human synthases and heterologous expression of various segments of the cDNA. As shown in Figure 2, Domain I contains KS, AT/MT, and DH. Domain II contains ER, KR, and ACP, and domain III contains TE (1,2). Domains I and II are separated by the interdomain/core region. In addition, thiol cross-linking reagent experiments using 1,3-dibromo-2-propanone showed that the active site Cys-SH of KS and phosphopantetheine thiol of ACP were cross-linked, and the cross-linked enzyme fractionated as a dimer (~500 kDa) in SDS-PAGE (25). Hence, in the FAS homodimer, the two monomers are arranged in a head-to-tail fashion, bringing the amino terminal KS-Cys-SH of one monomer within 2 Å distance to the carboxy terminally located ACP-phosphopantetheine-SH of the other monomer (25). This arrangement generates two active centers for fatty acid synthesis as shown in Figure 2A. The domain organization and the dimeric nature of FAS were further supported by physical studies of the chicken FAS by using electron microscopy of the dibromopropanone cross-linked enzyme and the small-angle neutron-scattering analysis of native enzyme (26). These studies suggested a struc-

tural model with dimensions of $160 \times 146 \times 73$ Å and an overall appearance of two side-by-side cylinders arranged in an antiparallel fashion. Each cylinder has a length of 160 Å and a diameter of 36.5 Å, and is divided into three domains with lengths of 32, 82, and 46 Å. In the antiparallel arrangement of these cylinders, two crevices are generated on the major axis of the model at the opposite ends of the molecular diad. These two crevices probably represent the two active centers of the FAS dimer (Fig. 2B). This model was further substantiated by the observation that the two sites of palmitate synthesis function simultaneously (27).

COMPONENT ENZYMATIC ACTIVITIES OF ANIMAL FAS

Biochemical studies, heterologous expression of various constituent activities and full length enzyme, and mutational analysis of amino acid residues of active sites have helped in refining the organization of component activities and their mechanism of action. The substrates acetyl-CoA and malonyl-CoA enter the reaction cycle through a common component enzyme acetyl/malonyl transacylase. This component activity of chicken FAS (amino acids 455 to 726), when expressed with a His6 fusion in *E. coli,* was found to be in the insoluble inclusion bodies (24). However, the enzyme protein can be extracted from the insoluble pellet with denaturing agents such as guanidinium-HCL and urea, purified using Talon column, and can be renatured by removing the denaturing agents to obtain a protein that had approximately 60% of the native AT/MT activity (24,28). AT/MT has a serine at its active center in a highly conserved motif Gly-His-Ser (28) and binds either acetyl or malonyl moieties from their CoA derivatives. The serine-bound acetyl moiety is transferred to the active site Cys-SH of KS via ACP, and the malonyl group is transferred to the pantetheine-SH of ACP (Fig. 1). Mutation of the active site Ser581, of the AT/MT to Ala in rat FAS, resulted in the loss of both acetyl and malonyl transacylase activities (28). Mutation of another conserved His683 to Ala also resulted in the loss of both transacylase activities (28). Hence, His683 is considered as a proton acceptor from the hydroxyl of Ser581 to increase its nucleophilicity. Interestingly, when the conserved Arg606 mutated to Ala, the enzyme has reduced activity with the substrate malonyl-CoA. In addition, the Arg606A mutant enzyme showed a dramatically increased acetyl transacylase activity (29). Thus, Arg606 is essential for the malonyl transacylase activity due to its role in positioning the free carboxyl anion of malonate at the active center (29). Since the active site serine of AT/MT can accept both acetyl-CoA and malonyl-CoA as substrates, and the primer acetyl-CoA is needed only once in the synthesis of a palmitate molecule, the AT/MT has to scan for the required substrate at any given time and transfers the substrate that is not required to CoA. Hence, free CoA is required for fatty acid synthesis (1–4).

The condensing enzyme, KS, has a highly reactive cysteine at its active center (1–4,25). KS performs condensation reaction between acetyl/acyl chains bound to its Cys-SH and malonyl moiety bound to the phosphopantetheine thiol of ACP, generating a β-ketoacyl chain attached to ACP. KS also functions as an acyl transferase, since it transfers the growing saturated acyl chains from ACP to its own active site Cys-SH (1–4). In doing so, KS frees the ACP-SH so that it can accept the malonyl group from malonyl-CoA, to continue the next round of elongation (Fig. 1). The amino acid sequence of KS is highly conserved across all species. Mutation of the active site Cys161 of rat FAS to Ala, Ser, or Thr, resulted in a practically inactive enzyme (30); however, mutation of Cys161 to Gln led to the loss of condensation activity but this mutant enzyme was able to decarboxylate malonate (31). The decarboxylation of malonyl-CoA may be facilitated by His293 and His331 (31,32).

The β-ketoacyl fatty acid, generated by KS, is reduced by KR to the β-hydroxy fatty acid, which is dehydrated by the dehydratase to the enoyl derivative, which is then reduced by ER to the saturated fatty acyl derivative. Both ER and KR contain a typical nucleotide binding motif, GX(X)GXXG, identified in a Rossmann fold. In ER, the sequence GSGGVG, and in KR, the sequence GGLGGFG, are highly conserved, and as was expected, mutation of some of these glycine residues (underlined) in ER and KR of rat FAS resulted in loss of the reductase functions (33). Similarly, in DH, mutation of a conserved histidine, His873, in rat FAS led to the loss of its activity, which suggests that this histidine may be involved in the DH active site (34).

Thioesterase performs the ultimate step in fatty acid synthesis by releasing the long chain fatty acid palmitate from ACP. The cloning and expression of chicken FAS ACP-TE in *E. coli* showed that the animal ACP can be phosphopantetheinylated by *E. coli* holo-ACP synthase (35). Mutagenesis of TE active site residues of chicken FAS, Ser2302 or His2475 to Ala, resulted in an inactive enzyme, suggesting that these two residues are part of Ser-His-Asp catalytic triad of serine esterases (36). Conversion of Ser2302 to Cys made the TE function like a thiol-active thioesterase and was inhibited by iodoacetamide (36). In addition, the double mutant containing Ser2302Cys and His2475Ala showed diminished reactivity to iodoacetamide, and bound palmitate as palmitoyl-*S*-intermediate without hydrolyzing the thioester. These results suggested that Ser2302 is a strong nucleophile and that His2475 is the general base required to withdraw the proton from Ser2302/Cys2302 (36). Likewise, in the rat mammary gland-specific thioesterase (TEII), which binds to FAS and releases medium chain fatty acids during lactation, Ser101 and His237 are required for the esterase function (37). By collaborating with Quiocho and his associates, we have recently determined the 3-D structure of the human FAS TE domain. The structure revealed that the active site pocket of TE contains the conserved residues, Ser2308, His2481, and Asp2338, that constitute the active site catalytic triad (38). Mutagenesis of these conserved amino acids in human FAS TE to Ala, individually, confirmed their importance in the catalysis (38), suggesting that FAS-TE and TEII evolved from serene proteases.

DIMERIC STRUCTURE OF FAS AND THE ROLE OF THE INTERDOMAIN/CORE

As shown in Figure 2A, each palmitate synthesis center is constituted by the N-terminal KS, AT/MT, and DH compo-

nents of one monomer and the C-terminal ER, KR, ACP, and TE components of the other monomer. Synthesis of palmitate involves seven cycles of 2-carbon additions to the primer acetyl group and involves more than 50 reactions (Fig. 1). Based on the average specific activity of purified human FAS (~70 nmol of palmitate/min/mg), one molecule of FAS dimer generates approximately 40 molecules of palmitate per minute by catalyzing more than 2000 individual reactions/min/dimer. Hence, the two centers of palmitate synthesis in the dimer are highly dynamic and flexible, and it is difficult to imagine that the component activities can hold the dimer together while performing palmitate synthesis. However, the interdomain/core region, which constitutes approximately 25% of the FAS monomer (Fig. 2A) and has no catalytic function, is thought to play an essential role in dimer formation and holding it together during palmitate synthesis. Based on the head-to-tail arrangement of the monomers in the FAS dimer, the interdomain dimer regions of the two monomers also interact with each other in a head-to-tail manner (Fig. 2). Hence, the FAS model (Fig. 2A) predicts that the two halves of a FAS monomer could associate to form a functional FAS dimer containing one catalytic center. To demonstrate such an association, recombinant proteins containing domain I and the N-terminal half of interdomain and domains II–III containing the C-terminal half of the interdomain at its N-terminus (Fig. 3) were expressed in *E. coli* and purified (39). Recombinant proteins containing no interdomain regions were also produced. All of these recombinant proteins contained N-terminal thioredoxin and His6 tag fusions. As shown in Figure 3, fatty acid synthesis could be reconstituted only when the reaction mixture contained both the domain I with the N-terminal half of interdomain and the C-terminal

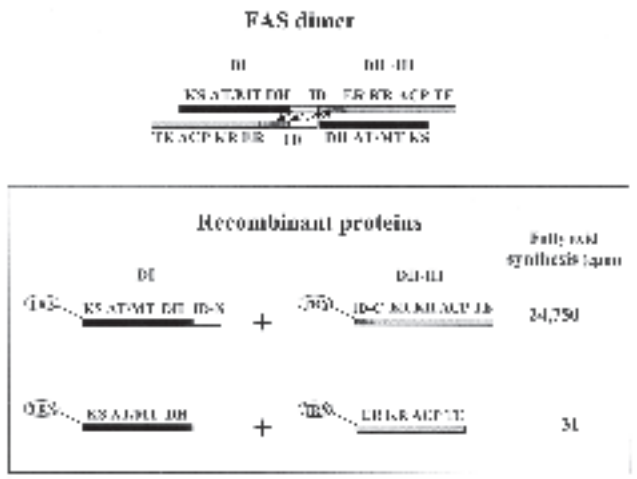

FIG. 3. Requirement of interdomain region in the FAS dimer formation. FAS dimer is shown in a schematic representation (not drawn to scale). Arrows indicate the interaction between the interdomain regions (ID) of the monomers. The interaction of the two halves of the FAS monomer to generate a palmitate synthesis site is shown in the boxed region. The recombinant proteins of domain I (DI), and domains II–III (DII–III) either containing or lacking interdomain regions were expressed in *E. coli* as thioredoxin (TRX) fusion proteins, purified, and used in the reconstitution of FAS activity. Abbreviations used are indicated for Figure 1.

half of the interdomain containing domain II–III proteins (39). The addition to the reconstitution mixture containing a constant amount of either domain I or domain II–III protein and increasing amounts of domain II–III or domain I protein, respectively, showed that the rate of fatty acid synthesis was determined by the limiting amount of the recombinant domain protein present in the reaction mixture (39). Hence, to generate an active center for fatty acid synthesis, stoichiometric amounts of interdomain containing domain I and domain II–III proteins were needed. As expected, the bifunctional reagent dibromopropanone cross-linked these two proteins and inhibited the fatty acid synthesis (39). That the two halves of a FAS monomer can generate palmitate synthesis further confirmed the antiparallel arrangement of FAS monomers in the dimer. In addition, these studies also showed that the interdomain region has an important structural role in the FAS dimer formation and function. That the interdomain regions interact with each other *in vivo* was further confirmed by using the yeast two-hybrid system (40).

As described above, the two sites of palmitate synthesis of the FAS dimer function simultaneously and independently (20); however, some variations to this theme were reported (4,30,33,41–44). Smith and his associates analyzed fatty acid synthesis by several combinations of mutant FAS dimers in which one monomer had a mutation in one component activity and the other monomer had a mutation in a different component activity (4,30,33,41–44). These analyses mostly supported the FAS dimer model with two active centers shown in Figure 2; however, it was observed that KS and AT/MT can work partially with the ACPs located in both of the palmitate synthesis centers (41). Although this observation can be explained by the flexible nature of the monomers in the FAS dimer as described below, however, the observation that DH functions only with the ACP of the same monomer (4,33) appears to be inconsistent with the functional division of the FAS dimer (Fig. 2) and our finding that the two halves of FAS monomer can form a fatty acid synthesis center as shown in Figure 3 (39). To explain the inter- and intrasubunit catalytic domain interactions observed, Smith and his colleagues have proposed an alternative model in which KS, AT/MT, and ACP domains of the opposite subunits are in structural and functional contact with each other and with the rest of the functional units that spread in the opposite directions (4,33). Although this model might explain the observations of Smith and his associates, it ignores the importance of interdomain region in the formation of FAS dimer shown in Figures 2 and 3 (39,40). Furthermore, the mutation complementation analyses performed by Smith and his colleagues showed fatty acid synthesis levels in the range of 16–20% (except for a few that showed 30–40%), a less than expected level of FAS activity (4,33). Even when one of the active centers was supposed to be active (for example, KS mutant monomer when combined with ACP mutant monomer), the FAS activity was only 19% (33). This variation in complemented FAS activity and the less than expected activity might be due to alteration in the structures of the individual monomers because of mutations

or to structural constraints and catalytic inefficiencies related to sharing of activities between the two fatty acid synthesis centers. Nonetheless, the apparent redundancy of KS and AT/MT functions might provide small but measurable (~20%) catalytic advantage to the FAS dimer function (4,33). In the head-to-tail dimer model depicted in Figure 2, dibromopropanone cross-links Cys-SH of KS of one monomer with the pantetheine-SH of ACP present in the other monomer, and hence, there will be two cross-links/dimers (25). Analysis of the dibromopropanone cross-linking showed that 45% of FAS dimers contained two cross-linkers, 15% contained one cross-link/dimer, and 35% of the molecules were monomers containing intramolecular KS and ACP thiol cross-linking (43). The presence of cross-linked monomers shows another degree of FAS flexibility. This flexibility could also explain how a FAS dimer formed by using a nonfunctional monomer, in which all of the component activities and ACP were mutated, and a fully functional monomer can synthesize fatty acids, albeit at 16% of the normal FAS dimer activity (44). Taken together, these observations suggest that monomers of the FAS dimer also have the ability to fold in such a way that the KS and ACP of the monomer may be close enough to generate some FAS activity. However, based on the dibromopropanone cross-linking analysis (25,26,43), which showed that head-to-tail dimer is the predominant form of FAS, the dimer with two distinct active centers proposed in Figure 2 is the most favorable and catalytically preferred structure. When some of the component enzymes are nonfunctional, the built-in flexibility of the monomers in the dimer described below might help in *de novo* fatty acid synthesis.

QUATERNARY STRUCTURE OF FAS

Attempts to crystallize FAS have not been successful thus far. Hence, we resorted to determining the structure of the highly pure human FAS using electron cryomicroscopy, by collaborating with Chiu and his associates (45). Electron cryomicroscopy showed FAS particles as dimers in all possible orientations (Fig. 4). A variety of shapes are observed in the micrograph, all consistent with the model of two roughly cylindrical particles in an antiparallel orientation with a linker region, forming an H-shaped molecule. X-ray solution-scattering analysis (45) confirmed FAS is a dimer consistent with dimensions described previously by small angle neutron-scattering analysis (26). Standard single particle reconstruction methodologies were then followed (46). Briefly, a dimer of two featureless the ellipsoids with dimensions $160 \times 146 \times 73$ Å (26) was used as an initial model. Projections of this model in all possible orientations were generated, and individual FAS particles selected from micrograph were compared to each projection. This classification process determines the orientation of each particle image. Particles in nearly identical orientations were then aligned relative to each other (in the image plane) and averaged together to generate class averages (Fig. 5). Finally, the class averages were combined to produce a new 3-D model (45). The procedure was repeated by using the new model as an initial model. This process was iterated until convergence was achieved. The analysis was performed both with and without imposing 2-fold symmetry (Fig. 6A and B). Both models showed dimensions of $180 \times 130 \times 75$ Å with monomers separated by about 19 Å and arranged in an antiparallel orientation, which is consistent with biochemical data (1,2,17–20). Each monomer subunit appears to be subdivided into three structural domains. The two clefts between the monomers, while asymmetric, may be the two active centers of fatty acid synthesis (Fig. 6). Recent studies on the structure of TE domain of human FAS (38), and the preliminary electron cryomicroscopy of the structure of FAS lacking TE indicated that the C-terminal TE domain is located at the end of the structural domain I (functional do-

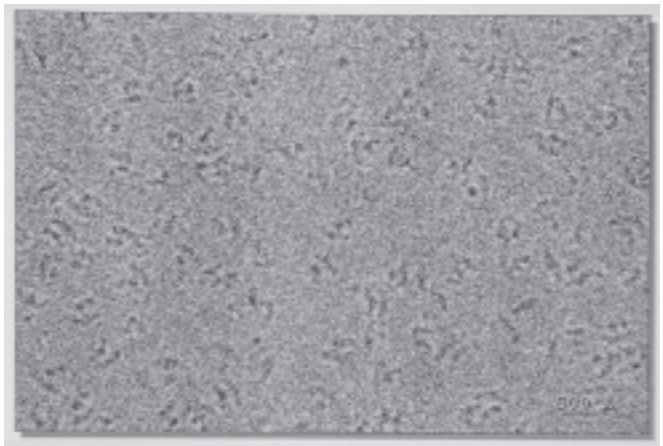

FIG. 4. Typical micrograph of fatty acid synthase (FAS) embedded in vitreous ice at 2.7-μm defocus. Particles can be observed in numerous different views ranging from dumbbell shape to double arches. Images are collected as focal pairs; image shown here is a far-from-focus image. The close-to-focus image is used for actual image processing.

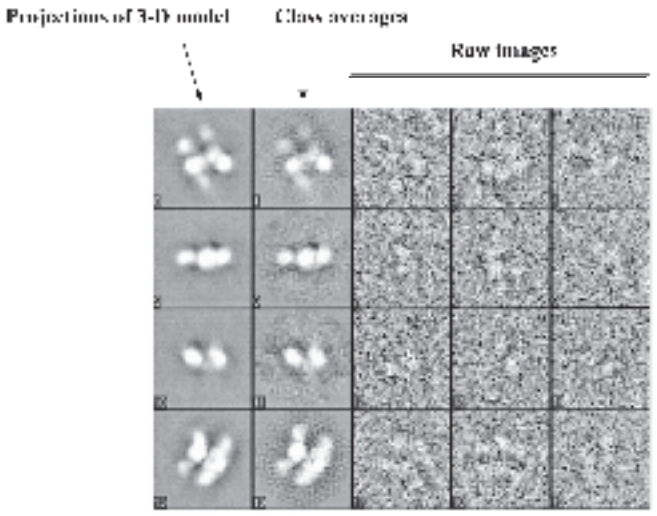

FIG. 5. Several projections of the final refined 3-D model in four orientations are shown with the corresponding class average and some individual particle images corresponding to each. In a properly refined structure, the projections and class averages will be identical except for noise. In cases of particle heterogeneity often small discrepancies will appear between the two.

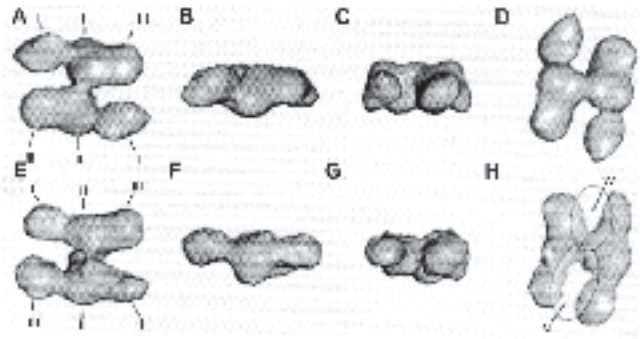

FIG. 6. Three-dimensional structure of fatty acid synthase (FAS). In A–D, the structure was obtained by applying C2 symmetry and in E–H, without symmetry. From left to right, different views of the molecule are shown, i.e., top view (A and E), side view (B and F), end-on view (C and G), and the view corresponding to the double-arch view visible in Figure 5 (D and H). Individual domains of the subunits have been indicated as I–III (A and E). In H, the asymmetric structure, the two clefts formed by the monomers are labeled as narrow (N) and wide (W). The proposed locations of the active sites of FAS are indicated by the two gray oval regions.

main III) of each monomer (Fig. 6), further confirming the antiparallel arrangement of FAS dimer. A strong bridge connects the two monomers, which may be the combination of the interdomain regions of both monomers (Fig. 6).

Although the FAS particle images (Fig. 6) are similar to what we have proposed based on partial proteolysis and biochemical analysis (Figs. 2), the resolution of the structure even after analyzing approximately 25,000 particles is only approximately 20 Å, suggesting that failure to get a much higher resolution may be due to inter- and intramolecular flexibility of the FAS dimer. To understand the inherent conformational flexibility of the FAS supermolecular complex, the domain movements of FAS were analyzed by using a computational method called quantized elastic deformational model (normal mode analysis) based on the electron density maps of the synthase at 19 Å, shown in Figure 6A, with the assumption that the monomers of FAS have enormous flexibility (47). This method has the ability to predict large-scale conformational changes such as domain movements by treating the protein as an elastic object without the knowledge of protein primary sequence and atomic coordinates (48). As shown in Figure 7, this analysis suggested that FAS is a very flexible molecule. FAS structure has two types of flexible hinges (Fig. 7). One is the intersubunit connection (interdomain) and the other is an intrasubunit hinge located between the structural domains I and II (Fig. 7), which are equivalent to functional domains III and II (Fig. 2). Despite that the dimeric FAS has a symmetric structure, large domain movements around the hinge region occur in various directions and allow the molecule to adopt a wide range of conformations (47). These domain movements are likely to be important in facilitating and regulating the entire palmitate synthesis by coordinating the communication between components of the molecule, for instance, adjusting the distance between various active sites inside the catalytic reaction centers.

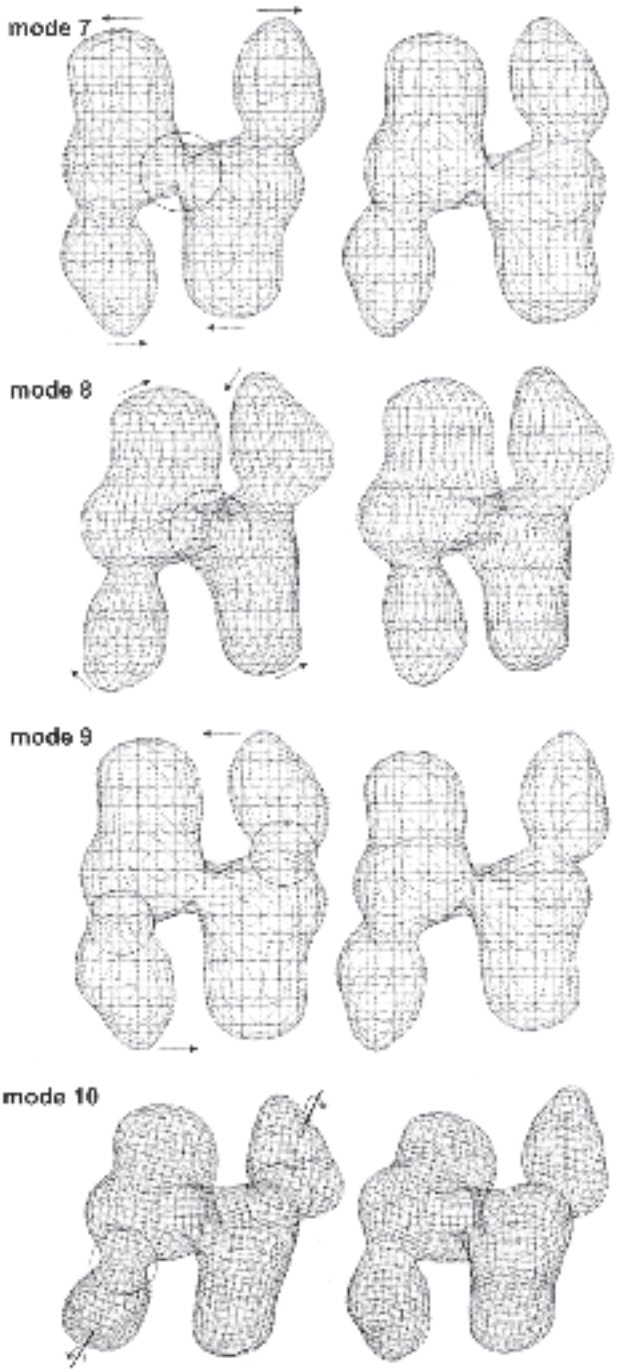

FIG. 7. The motional patterns of the fatty acid synthase (FAS) dimer. Four lowest-frequency deformational modes are shown. Mode 7 describes an in-plane bending motion around the hinge between two monomers (intersubunit hinge). This is the most flexible hinge in the system. Mode 8 describes an out-of-plane bending motion around the same hinge. Modes 9 and 10 describe the motions around two smaller intrasubunit hinges. They are smaller in magnitude. For each mode, two opposite conformations (left and right) during harmonic vibration are shown to illustrate the direction of the motion. The amplitude of the motion was arbitrarily chosen for visual clarity. The arrows are used to indicate the directions of the motions. The larger circles in modes 7 and 8 indicate the intersubunit hinge, and the smaller circles in mode 9 and mode10 indicate the intrasubunit hinges. The dotted lines in mode 10 indicate the longest axes of the subunits.

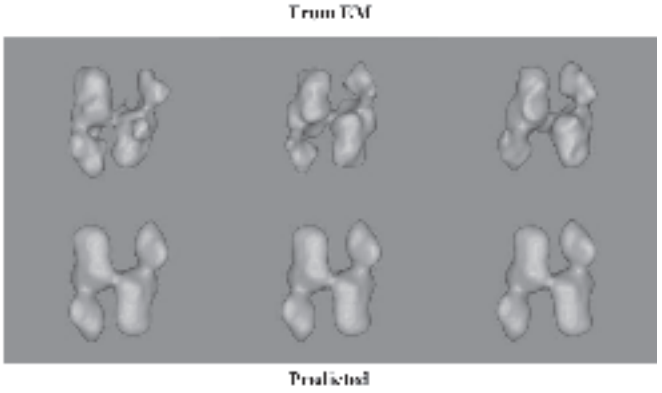

FIG. 8. Experimental verification of conformational variation in fatty acid synthase (FAS) predicted by normal mode analysis. FAS particle images (~20,000) were processed by using simultaneous multiple model single particle analysis (48). This single data set was used to simultaneously produce all three structures shown in the top row. The bottom row shows predicted structures from normal mode analysis (mode 7) as applied to the symmetric structure from Figure 7.

Based on this theoretically predicted flexibility described above, FAS dimer might exist in several different conformational states. To demonstrate the existence of this flexibility in FAS dimer, approximately 20,000 FAS particle images were processed by using a simultaneous multiple model single particle refinement method to search for their presence (49). For this analysis only the extreme conformational states shown in Figure 7 (mode 7) were used. This analysis confirmed the presence of these conformational states of FAS dimers in the electron cryomicrographic images (Fig. 8). This implies that the resolution limiting factor in our current structures is structural heterogeneity among the data. That is, our final structure consists of the average of many different states. To improve the resolution will require splitting the data up into many more groups, each of which will then be more structurally homogeneous. While this type of analysis would require approximately 10^6 FAS particles to be analyzed, it will provide multiple FAS dimer structures at much higher resolution instead of a single FAS structure at low resolution.

ACKNOWLEDGMENTS

The authors would like to express their thanks to the National Institutes of Health for their support of this research (GM19091, GM63115 and GM068826). We thank Drs. Steven J. Ludtke and Jianpeng Ma for their critical review of the manuscript and providing some of the figures.

REFERENCES

1. Wakil, S.J., Stoops, J.K., and Joshi, A.C. (1983) Fatty Acid Synthesis and Its Regulation, *Annu. Rev. Biochem. 52*, 537–579.
2. Wakil, S.J. (1989) The Fatty Acid Synthase: A Proficient Multifunctional Enzyme, *Biochemistry 28*, 4523–4530.
3. Smith, S. (1994) The Animal Fatty Acid Synthase: One Gene, One Polypeptide, Seven Enzymes, *FASEB J. 8*, 1248–1259.
4. Smith, S., Witkowski, A., and Joshi, A.K. (2003) Structural and Functional Organization of Animal Fatty Acid Synthase, *Prog. Lipid Res. 42*, 289–317.
5. Jayakumar, A., Tai, M.-H., Huang, W.-Y., Al-Feel, W., Hsu, M., Abu-Elheiga, L., Chirala, S.S., and Wakil, S.J. (1995) Human Fatty Acid Synthase: Properties and Molecular Cloning, *Proc. Natl. Acad. Sci. USA 92*, 8695–8699.
6. Hannun, Y.A., and Obeid, L.M. (2002) The Ceramide-Centric Universe of Lipid-Mediated Cell Regulation: Stress Encounters of the Lipid Kind, *J. Biol. Chem. 277*, 25847–25850.
7. Kuhajda, F.P., Jenner, K., Wood, F.D., Hennigar, R.A., Jacobs, L.B., Dick, J.D., and Pasternack, G.R. (1994) Fatty Acid Synthesis: A Potential Selective Target for Antineoplastic Therapy, *Proc. Natl. Acad. Sci. USA 91*, 6379–6383.
8. Pizer, E.S., Thupari, J., Han, W.F., Pinn, M.L., Cherst, F.J., Frehywot, G.L., Townsend, C.A., and Kuhajda, F.P. (2000) Malonyl-CoA Is a Potential Mediator of Cytotoxicity Induced by Fatty Acid Synthase Inhibition in Human Breast Cancer Cells and Xenografts, *Cancer Res. 60*, 213–238.
9. Menendez J.A., Vellon, L., Mehmi, I., Oza, B.P., Ropero, S., Colomer, R., and Lupu, R. (2004) Inhibition of Fatty Acid Synthase (FAS) Suppresses HER2/neu (erbB-2) Oncogene Overexpression in Cancer Cells, *Proc. Natl. Acad. Sci. USA 101*, 10715–10720.
10. Loftus, T.M., Jaworsky, D.E., Frehywot, G.L., Towsand, C.A., Ronnett, G.V., Lane, M.D., and Kuhajda, F.P. (2000) Reduced Food Intake and Body Weight in Mice Treated with Fatty Acid Synthase Inhibitors, *Science 288*, 2379–2381.
11. Chirala, S.S., Chang, H., Matzuk, M., Abu-Elheiga, L., Mao, J., Mahon, K., Finegold, M., and Wakil, S.J. (2003) Fatty Acid Synthesis Is Essential in Embryonic Development: Fatty Acid Synthase Null Mutants and Most of the Heterozygotes Die *In Utero, Proc. Natl. Acad. Sci. USA 100*, 6358–6363.
12. Wakil, S.J. (1970) Fatty Acid Metabolism, in *Lipid Metabolism* (Wakil, S.J., ed.), pp. 1–48, Academic Press, New York.
13. Wakil, S.J. (1958) Requirement of Bicarbonate in Fatty Acid Synthesis, *J. Am. Chem. Soc. 80*, 2908.
14. Wakil, S.J., Pugh, E.L., and Sauer, F. (1964) The Mechanism of Fatty Acid Synthesis, *Proc. Natl. Acad. Sci. USA 52*, 106–114.
15. Stoops, J.K., Arslanian, A.W., Oh, Y.H., Aune, K.C., Vanaman, T.C., and Wakil, S.J. (1975) Presence of Two Polypeptide Chains Comprising Fatty Acid Synthetase, *Proc. Natl. Acad. Sci. USA 75*, 1940–1944.
16. Stoops, J.K., Arslanian, A.W., Chalmers, J.H., Joshi, V.C., and Wakil, S.J. (1977) Fatty Acid Synthase Complexes, in *Bioorganic Chemistry* (Van Tamelien, E.E., ed.), Vol. 1, pp. 339–370, Academic Press, New York.
17. Tsukamoto, Y., and Wakil, S.J. (1988) Isolation and Mapping of the Beta-Hydroxyacyl Dehydratase Activity of Chicken Liver Fatty Acid Synthase, *J. Biol. Chem. 263,* 16225–16229.
18. Chirala, S.S., Kasturi, R., Pazirandeh, M., Stolow, D.T., Huang, W.-Y., and Wakil, S.J. (1989) A Novel cDNA Extension Procedure: Isolation of Chicken Fatty Acid Synthase cDNA Clones, *J. Biol. Chem. 264***,** 3750–3757.
19. Holzer, K.R., Liu, W., and Hammes, G.G. (1989) Molecular Cloning and Sequencing of Chicken Liver Fatty Acid Synthase cDNA, *Proc. Natl. Acad. Sci. USA 86***,** 4387–4391.
20. Haung, W.-Y., Chirala, S.S., and Wakil, S.J. (1994) Amino-Terminal Blocking Group and Sequence of the Animal Fatty Acid Synthase, *Arch. Biochem. Biophys. 314*, 45–49.
21. Amy, C.M., Witkowski, A., Naggert, J., Williams, B., Randhawa, Z., and Smith, S. (1989) Molecular Cloning and Sequencing of cDNAs Encoding the Entire Rat Fatty Acid Synthase, *Proc. Natl. Acad. Sci. USA 86***,** 3114–3118.
22. Beck, K.-I., Schreglmann, R., Stathopulos, I., Klein, H., Hoch, J., and Schweizer, M. (1992) The Fatty Acid Synthase (FAS) Gene and Its Promoter in Rattus Norvegicus, *DNA Seq. 2,* 359–386.
23. Paulauskis, J.D., and Sul, H.S. (1989) Structure of Mouse Fatty

Acid Synthase mRNA: Identification of the Two NADPH Binding Sites, *Biochem. Biophys. Res. Commun. 158,* 690–695.
24. Chirala, S.S., Huang, W.-Y., Jayakumar, A., Sakai, K., and Wakil, S.J. (1997) Animal Fatty Acid Synthase: Functional Mapping and Cloning and Expression of the Domain I Constituent Activities, *Proc. Natl. Acad. Sci. USA 94*, 5588–5593.
25. Stoops, J.K., and Wakil, S.J. (1981) Animal Fatty Acid Synthase: A Novel Arrangement of the β-Ketoacyl Synthase Site Comprising Domains of the Subunits, *J. Biol. Chem. 256*, 5128–5133.
26. Stoops, J.K., Wakil, S.J., Uberbacher, E.C., and Bunick, G.J. (1987) Small-Angle Neutron-Scattering and Electron Microscopic Studies of the Chicken Liver Fatty Acid Synthase, *J. Biol. Chem. 262*, 10246–10251.
27. Singh, N., Wakil, S.J., and Stoops, J.K. (1984) On the Question of Half or Full-Site Reactivity of Animal Fatty Acid Synthetase, *J. Biol. Chem. 259*, 3605–3611.
28. Rangan, V.S., and Smith, S. (1996) Expression in Escherichia Coli and Refolding of the Malonyl-Acetyltransferase Domain of the Multifunctional Animal Fatty Acid Synthase, *J. Biol. Chem. 271*, 31749–31755.
29. Rangan, V.S., and Smith, S. (1997) Alteration of the Substrate Specificity of the Malonyl-CoA/Acetyl-CoA:Acyl Carrier Protein S-Acyltransferase Domain of the Multi Functional Fatty Acid Synthase by Mutation of a Single Arginine Residue, *J. Biol. Chem. 272*, 11975–11978.
30. Joshi, A.K., Witkowski, A., and Smith, S. (1997) Mapping of Functional Interactions Between Domains of the Animal Fatty Acid Synthase by Mutant Complementation *In Vitro, Biochemistry 36*, 2316–2322.
31. Witkowski, A., Joshi, A.K., Lindqvist, Y., and Smith, S. (1999) Conversion of β-Ketoacyl Synthase to a Malonyl Decarboxylase by Replacement of the Active-Site Cysteine with Glutamine, *Biochemistry 38*, 11643–11650.
32. Witkowski, A., Joshi, A.K., and Smith, S. (1996) Mechanism of the _-Ketoacyl Synthase Reaction Catalyzed by the Animal Fatty Acid Synthase, *Biochemistry 41*, 10887–10887.
33. Rangan, V.S., Joshi, A.K., and Smith, S. (2001). Mapping the Functional Topology of the Animal Fatty Acid Synthase by Mutant Complementation In Vitro*, Biochemistry 40*, 10792–10799.
34. Joshi, A.K., and Smith, S. (1993). Construction, Expression, and Characterization of a Mutated Animal Fatty Acid Synthase Deficient in the Dehydrase Function, *J. Biol. Chem. 268*, 22508–22513.
35. Pazirandeh, M., Chirala, S.S., Huang, W.-Y., and Wakil, S.J (1989) Characterization of Recombinant Thioesterase and Acyl Carrier Protein Domains of Chicken Fatty Acid Synthase Expressed in Escherichia Coli, *J. Biol. Chem. 264*, 18195–18201.
36. Pazirandeh, M., Chirala, S.S**.,** and Wakil, S.J. (1991) Site-Directed Mutagenesis Studies on the Recombinant Thioesterase Domain of Chicken Fatty Acid Synthase Expressed in Escherichia Coli, *J. Biol. Chem. 266***,** 20946–20952.
37. Tai, M.H., Chirala, S.S., and Wakil, S.J. (1993) Roles of Ser101, Asp236, and His237 in Catalysis of Thioesterase II and of the C-terminal Region of the Enzyme in Its Interaction with Fatty Acid Synthase, *Proc. Natl. Acad. Sci. USA 90*, 1852–1856.
38. Chakravarty, B., Gu, Z., Chirala, S., S., Wakil, S.J., and Quiocho, F.A. (2004) Human Fatty Acid Synthase: Structure and Substrate Selectivity of the Thioesterase Domain, *Proc. Natl. Acad. Sci. USA 101*, 15567–15572.
39. Jayakumar, A., Chirala, S.S., and Wakil, S.J. (1997) Human Fatty Acid Synthase: Assembling Recombinant Halves of the Fatty Acid Synthase Subunit Protein Reconstitutes Enzyme Activity*, Proc. Natl. Acad. Sci. USA 94*, 12326–12330.
40. Chirala, S.S., Jayakumar, A., Gu, Z.-W., and Wakil, S.J. (2001) Human Fatty Acid Synthase: Role of Interdomain in the Formation of Catalytically Active Synthase Dimer, *Proc. Natl. Acad. Sci. USA 98*, 3104–3108.
41. Joshi, A.K., Witkowski, A., and Smith, S. (1998) The Malonyl/Acetyltransferase and β-Ketoacyl Synthase Domains of the Animal Fatty Acid Synthase Can Cooperate with the Acyl Carrier Protein Domain of Either Subunit, *Biochemistry 37*, 2515–2523.
42. Rangan, V.S., Joshi, A.K., and Smith, S. (1998) Differential Affinity Labeling of the Two Subunits of the Homodimeric Animal Fatty Acid Synthase Allows Isolation of Heterodimers Consisting of Subunits that Have Been Independently Modified, *J. Biol. Chem. 273*, 4937–4943.
43. Witkowski, A., Joshi, A.K., Rangan, V.S., Falick, A.M., Witkowska, H.E., and Smith, S. (1999). Dibromopropanone Cross-Linking of the Phosphopantetheine and Active-Site Cysteine Thiols of the Animal Fatty Acid Synthase Can Occur Both Inter- and Intrasubunit. Reevaluation of the Side-by-Side, Antiparallel Subunit Model, *J. Biol. Chem. 274*, 11557–11563.
44. Joshi, A.K., Rangan, V.S., Witkowski, A., and Smith, S. (2003). Engineering of an Active Animal Fatty Acid Synthase Dimer with Only One Competent Subunit, *Chem. Biol. 10*, 169–173.
45. Brink, J., Ludtke, S.J., Yang, C.-Y., Gu, Z.-W., Wakil, S.J., and Chiu, W. (2002) Quaternary Structure of Human Fatty Acid Synthase by Electron Cryomicroscopy*, Proc. Natl. Acad. Sci. USA 99*, 13–143.
46. Ludtke, S.J., Baldwin, P.R., and Chiu, W. (1999). EMAN: Semiautomated Software for High-Resolution Single-Particle Reconstructions, *J. Struct. Biol. 128,* 82–97.
47. Ming, D., Kong, Y., Wakil, S.J., Brink, J., and Ma, J. (2002) Domain Movements in Human Fatty Acid Synthase by Quantized Elastic Deformational Model*, Proc. Natl. Acad. Sci. USA 99*, 7895–7899.
48. Ming, D., Kong, Y., Lambert, M.A, Huang, Z., and Ma, J. (2002). How To Describe Protein Motion Without Amino Acid Sequence and Atomic Coordinates, *Proc. Natl. Acad. Sci. USA 99*, 8620–8625.
49 Brink, J., Ludtke, S.J., Kong, Y., Wakil, S.J., Ma, J., and Chiu, W. (2004) Experimental Verification of Conformational Variation of Human Fatty Acid Synthase as Predicted by Normal Mode Analysis, *Structure (Cambr.) 12,* 185–191.

[Received October 4, 2004; accepted November 4, 2004]

The Reductase Steps of the Type II Fatty Acid Synthase as Antimicrobial Targets

Yong-Mei Zhang[a], Ying-Jie Lu[a], and Charles O. Rock[a,b,*]

[a]Department of Infectious Diseases, St. Jude Children's Research Hospital, Memphis, Tennessee 38105, and [b]Department of Molecular Sciences, University of Tennessee Health Science Center, Memphis, Tennessee 38163

ABSTRACT: The increasing of multidrug resistance of clinically important pathogens calls for the development of novel antibiotics with unexploited cellular targets. FA biosynthesis in bacteria is catalyzed by a group of highly conserved proteins known as the type II FA synthase (FAS II) system. Bacterial FAS II organization is distinct from its mammalian counterpart; thus the FAS II pathway offers several unique steps for selective inhibition by antibacterial agents. Some known antibiotics that target the FAS II system include triclosan, isoniazid, and thiolactomycin. Recent years have seen remarkable progress in the understanding of the genetics, biochemistry, and regulation of the FAS II system with the availability of the complete genome sequence for many bacteria. Crystal structures of the FAS II pathway enzymes have been determined for not only the *Escherichia coli* model system but also other gram-negative and gram-positive pathogens. The protein structures have greatly facilitated structure-based design of novel inhibitors and the improvement of existing antibacterial agents. This review discusses new developments in the discovery of inhibitors that specifically target the two reductase steps of the FAS II system, β-ketoacyl-acyl carrier potein (ACP) reductase and enoyl-ACP reductase.

Paper no. L9543 in *Lipids 39,* 1055–1060 (November 2004).

TYPE II FA SYNTHASE

FA biosynthesis is a fundamental component of the cellular metabolic network, providing the essential building blocks for membrane phospholipid formation. Bacteria synthesize FA using a series of discrete monofunctional proteins, each catalyzing one reaction in the pathway [for reviews see (1–3)]. The bacterial system, also known as the dissociated, type II FA synthase (FAS II), contrasts with the yeast and animal type I FA synthase (FAS I), which contains polypeptides with multiple active sites that perform all the catalytic reactions in the pathway. Although the structural organizations of FAS I and FAS II are different, the chemical reactions and the catalytic mechanisms for FA synthesis are essentially the same.

*To whom correspondence should be addressed at Department of Infectious Diseases, Protein Science Division, St. Jude Children's Research Hospital, 332 N. Lauderdale, Memphis, TN 38105-2794.
E-mail: charles.rock@stjude.org

Abbreviations: ACP, acyl carrier protein; EGCG, epigallocatechin gallate; FabG, β-ketoacyl-ACP reductase; FabI, enoyl-ACP reductase I; FabK, enoyl-ACP reductase II; FabL, enoyl-ACP reductase III; FAS I, type I fatty acid synthase; FAS II, type II fatty acid synthase; INH, isoniazid acid hydrazide; SAR, structure-activity relationship; Ts, temperature sensitive.

Escherichia coli FAS II has been extensively studied and the biochemical properties of the individual enzymes are the paradigm for type II FA synthase (1). Acetyl-CoA carboxylase catalyzes the first committed reaction of FA biosynthesis. The product of the reaction is malonyl-CoA, and the malonate group is then transferred to acyl carrier protein (ACP) by malonyl-CoA:ACP transacylase (FabD) to form malonyl-ACP. The FA elongation cycle is initiated by the Claisen condensation of malonyl-ACP with acetyl-CoA catalyzed by β-ketoacyl-ACP synthase III (FabH) to form β-ketobutyryl-ACP. Four enzymes catalyze each cycle of elongation. The β-keto group is reduced by the NADPH-dependent β-ketoacyl-ACP reductase (FabG), and the resulting β-hydroxy intermediate is dehydrated by the β-hydroxyacyl-ACP dehydratase (FabA or FabZ) to an enoyl-ACP. Next, the reduction of the enoyl chain by the NAD(P)H-dependent enoyl-ACP reductase (FabI, FabK, or FabL) produces an acyl-ACP. Additional cycles of elongation are initiated by the β-ketoacyl-ACP synthase (FabB or FabF), which elongates the acyl-ACP by two carbons to form a β-ketoacyl-ACP. Elongation ends when the fatty acyl chain reaches 14–18 carbons in length, at which point it is used for membrane phospholipid or lipopolysaccharide synthesis.

Because the organization of the bacterial FAS II is distinct from its mammalian counterpart FAS I, the FAS II enzymes have become attractive targets for new antimicrobial drug discovery [for reviews see (4–6)]. Established inhibitors of FAS II enzymes include triclosan (7,8), isoniazid (9), and thiolactomycin (10). The discovery of a type II FA synthase in the malaria-causing agent *Plasmodium falciparum* stimulated the search for antimalarials that operate by inhibiting the FAS II enzymes (11–13).

This review focuses on the recent development of inhibitors that target the two reductase steps of FAS II, namely, β-ketoacyl-ACP reductase and enoyl-ACP reductase. The reactions catalyzed by these two reductases are outlined in Scheme 1. Only one isoform of FabG has been identified. Although FabG is essential and a valid antimicrobial target, there are not many known inhibitors of this enzyme. On the other hand, there are three isoforms of the enoyl-ACP reductase: the NAD(P)H-dependent FabI, the NADH-dependent FabK, and the NADPH-dependent FabL. The enoyl-ACP reductases are the primary targets of triclosan (7,14) and isoniazid (isonicotinic acid hydrazide, INH) (9). Due to the emergence of resistance to triclosan and isoniazid, there has been

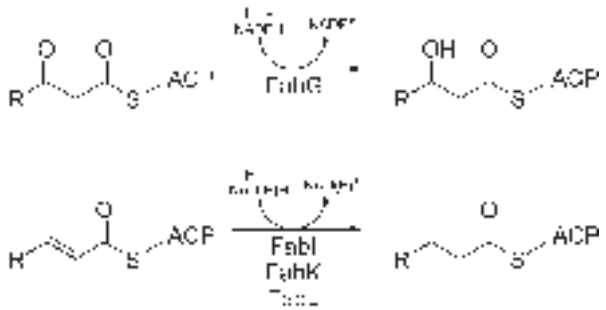

SCHEME 1. FabG catalyzes the NADPH-dependent reduction of β-ketoacyl-acyl carrier protein (ACP) intermediates to β-hydroxyacyl-ACP in the fatty acid elongation cycles. Three isoforms of enoyl-ACP reductase, FabI, FabK, and FabL, catalyze the reduction of the *trans*-2 enoyl-ACP to acyl-ACP using either NADH or NADPH, depending on the isoform.

tremendous effort aimed toward the development of analogs of the existing drugs and also novel inhibitors of the enoyl reductase.

Enoyl-ACP reductases (FabI, FabK, and FabL). The *trans*-2-enoyl-ACP reductase catalyzes the last step of the FA elongation cycle and plays a key regulatory role controlling the rate of elongation in the pathway (15). The NADH-dependent FabI is the single isoform in *E. coli* and FabI is essential for completion of the FA elongation cycles. The *fabI*(Ts) mutant accumulates β-hydroxybutyryl-ACP at the nonpermissive temperature (15). Antimicrobial agents such as diazaborine (16) and 2-hydroxydiphenyl ethers including triclosan (7,8,14) and hexachlorophene (17) primarily inhibit FabI. *Staphylococcus aureus* FabI is highly homologous to the *E. coli* enzyme, but, unlike the *E. coli* FabI, *S. aureus* FabI is specific for NADPH (17).

Streptococcus pneumoniae, *Bacillus subtilis,* and *Pseudomonas aeruginosa* are resistant to triclosan. Investigation of the molecular basis of the triclosan resistance in these organisms led to the discovery of two new enoyl-ACP reductases, FabK and FabL. FabK is present in streptococci, enterococci, and clostridia species (18,19). FabK requires NADH for activity, does not exhibit any sequence similarity with FabI, and is resistant to triclosan inhibiton (18,19). FabK is an FMN-containing enzyme although it is not known if the flavin is required for the enoyl reductase activity. Because FabK is the only isoform of enoyl-ACP reductase in *S. pneumoniae*, it can serve as a specific antibiotic target for this pathogen. *Bacillus subtilis* possesses two enoyl-ACP reductases, FabI and a distant FabI homolog FabL, the latter of which requires NADPH for catalysis and is reversibly inhibited by triclosan (20). The FabI deletion strain of *B. subtilis* is as sensitive to triclosan as is the wild-type strain, whereas the FabL deletion strain becomes much more sensitive to triclosan, demonstrating that FabL is responsible for the triclosan resistance in this organism (20). InhA is the enoyl-ACP reductase in *Mycobacterium tuberculosis* and the primary target of the antituberculosis drug isoniazid (INH) (9,21). Triclosan also inhibits *M. tuberculosis* by targeting InhA in both INH-susceptible and -resistant strains (22).

Triclosan is a slow, tight-binding, and irreversible inhibitor of FabI (7,8). The tight binding of triclosan to FabI is dependent on the presence of the cofactor. The crystal structure of the ternary complex of *E. coli* FabI-NAD^+-triclosan shows that triclosan binds to the enoyl-ACP substrate site on FabI, and hydrophobic interactions and hydrogen bonds between the inhibitor and both the protein and cofactor stabilize the complex (14,23). Mutations in the FabI active site that disrupt the cofactor binding site confer resistance to triclosan (7,8,14,24,25). A mutation of Gly93 to Val in *E. coli* FabI causes triclosan resistance by reducing the binding of the inhibitor to the enzyme. The MIC value of triclosan against the *E. coli* mutant with the Gly93 to Val mutation increases 100-fold in comparison to that of the wild-type strain. Two other mutations, Met159 to Thr and Phe203 to Leu, also significantly increase the triclosan resistance of *E. coli* (7,14). A mutation of Phe204 (equivalent to Phe203 in *E. coli* FabI) to Cys in *S. aureus* FabI prevents the formation of stable FabI-triclosan-NAD^+ and in turn causes triclosan resistance in the mutant *S. aureus* (24).

Similar to the mechanism of triclosan inhibition, INH inhibits mycobacterial InhA activity by forming a covalent complex with the bound NAD^+ at the enzyme active site (21,26). Mutations of InhA active site residues, such as Ile16 to Thr and Ser94 to Ala (equivalent to Gly93 of *E. coli* FabI) decrease the enzyme affinity for NADH and INH and strains with such mutations are resistant to INH (21). Structural studies of the InhA mutants show that INH resistance is directly related to a perturbed hydrogen bonding network that stabilizes NADH binding in the wildtype enzyme (21). An INH-resistant strain exhibits cross-resistance to triclosan, indicating that both inhibitors bind to the InhA active site at the cofactor binding region in a similar manner (27).

The human malaria parasite *P. falciparum* synthesizes FA using a type II pathway that is similar to the bacterial FAS II. Plasmodium enoyl-ACP reductase resembles bacterial FabI in both the primary sequence and overall folding of the protein (28). The parasite FabI is sensitive to triclosan and can form a ternary complex with the inhibitor and NAD^+ cofactor like its bacterial counterparts (28,29). Triclosan efficiently inhibits *P. falcifarum* growth both *in vitro* and in mice infected with the parasite (13). Inhibition of acetate and malonyl-CoA incorporation into FA by triclosan both *in vivo* and *in vitro* validates the theory that the FA synthesis pathway is the target.

With the potential for emerging resistance of bacteria to triclosan coupled with its poor bioavailability, researchers have begun the search for triclosan analogs and novel FabI inhibitors. Structure-activity relationship (SAR) analyses of triclosan analogs show that the hydroxyl group at position 2 in ring A (1, Scheme 2) is essential for triclosan activity and cannot be replaced with methoxy group or sulfur derivatives (28,30). Although the two ring-B chlorine atoms are not essential, the chlorine atom in ring A is required for tight binding of triclosan to FabI (30). The π-π stacking interaction between ring A and the nicotinamide ring of the cofactor is also important for stabilizing the ternary complex (28).

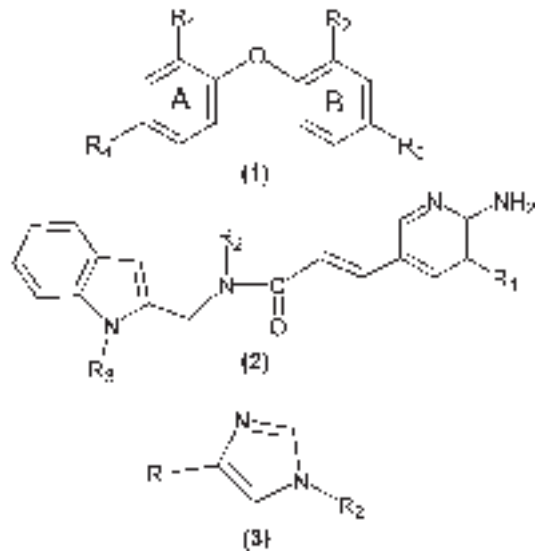

SCHEME 2. Structures of FabI inhibitors. (**1**) Diphenyl ethers including triclosan, in which R_1 is a hydroxyl group and R_2, R_3, and R_4 are each chlorine atoms; (**2**) aminopyridines, in which the amide and E-double bond is required for activity, substitution on the aminopyridine ring is restricted to R1, and the activity is optimal when R_2 and R_3 are methyl groups; (**3**) 1,4-disubstituted imidazoles at R_1 and R_2 positions.

New FabI inhibitors have also been identified by high-throughput screening of compound libraries. Examples of such leads are 1,4-disubsituted imidazoles (**3**, Scheme 2) and benzodiazepines, which inhibit FabI from both *E. coli* and *S. aureus* with submicromolar IC_{50} values (31,32). Their antibacterial activities are attributed to FabI inhibition, and this is confirmed by an increase in MIC in strains overexpressing FabI (31,32). The initial screening leads are further optimized with iterative medicinal chemistry and structure-based design to improve the inhibitory potency. This optimization process led to the discovery of the aminopyridine derivatives (**2**, Scheme 2) as inhibitors of FabI and the triclosan-resistant FabK (33–35). These compounds bind to the FabI active site in a slightly different manner from that of triclosan, suggesting that they will be active against triclosan-resistant strains (35). The subtle differences in the binding characteristics may also explain the inhibitory effect of aminopyridines against the triclosan-resistant FabK. The indole naphthyridinones achieve a similar spectrum of antimicrobial activity against gram-negative pathogens in comparison to triclosan and, significantly, have exquisite antistaphylococcal activity against multidrug-resistant *S. aureus* with MIC values considerably lower than those of the commercial antibiotics tested (33,35). Two indole naphthyridinone derivatives have exhibited excellent *in vivo* efficacy in a *S. aureus* infection model in rats (33,35). Because of their inhibitory activities on the triclosan-resistant FabK, the indole naphthyridinones are also active inhibitors of *S. pneumoniae,* which depends on FabK for its enoyl-ACP redutase activity (33). Compounds with both FabI and FabK inhibitory activity can inhibit the growth of *Enterococcus faecalis,* which has both enoyl-ACP reductases. A high-throughput screen against the mycobacterial InhA have identified two compounds, Genz-8575 and Genz-10850, that demonstrate activity against drug-resistant strains of both *M. tuberculosis* and the parasite *P. falciparum* (22).

Bacteria can be categorized into four groups based on which isoform(s) of enoyl-ACP reductase they have: only FabI, such as *E. coli* and *S. aureus*; only FabK, such as *S. pneumoniae*; both FabI and FabK, such as *E. faecalis* and *P. aeruginosa*; and both FabI and FabL, such as *B. subtilis*. Considering the diversity of these isoforms, it is difficult to find broad spectrum antimicrobial compounds by targeting this enzyme. However, inhibitors of one or two isoforms can become excellent antibacterials for specific pathogens. The structure-activity relationship analyses of triclosan analogs and the identification of additional novel inhibitors have provided valuable information about the molecular basis of inactivation of enoyl-ACP reductases and serve as a guide for future efforts to develop new inhibitors of this enzyme.

β-Ketoacyl-ACP reductase (FabG). FabG catalyzes the NADPH-dependent reduction of the β-ketoacyl-ACP intermediate to β-hydroxyacyl-ACP in the elongation cycles of FAS II. FabG has a monomeric M.W. of 25.5 kDa and exists as a tetramer in solution (36). FabG catalyzes the keto reduction by a compulsory ordered mechanism with the NADPH cofactor as the leading substrate and $NADP^+$ the last product to leave (37,38). FabG exhibits negative cooperativity in the binding of NADPH, and this effect is enhanced by the presence of ACP (38). The crystal structure of *E. coli* FabG has been solved in both the native form and in binary complex with $NADP^+$ (38,39). The side chains of the active site residues, Ser138, Tyr151, and Lys155, are in a nonproductive conformation in the FabG native conformation without bound cofactor (38). The structure of the binary complex of FabG with $NADP^+$ reveals that binding of the cofactor leads to the reorganization of the active site residues into a catalytically competent conformation (39). A proton relay conduit is also established upon cofactor binding to replenish the Tyr151 proton donated to the substrate during catalysis. The MabA protein catalyzes the NADPH-dependent reduction of the long-chain β-ketoacyl-AcpM intermediates of FAS II in *M. tuberculosis*. Like *E. coli* FabG, the crystal structure of MabA shows that it shares the conserved folds of the short-chain dehydrogenase/reductase superfamily (40) with additional features that allow MabA to accommodate substrates with longer acyl chains.

FabG exhibits all the characteristics required to be a broad spectrum antimicrobial target. First, only one isoform of FabG has been identified so far. Second, FabG is ubiquitously expressed and highly conserved in bacteria. Furthermore, it has been shown by indirect transcriptional analysis that FabG is essential for the growth of *E. coli* (41). Recently, direct evidence for the essentiality of FabG has been obtained by the isolation of temperature-sensitive (Ts) *fabG* mutants of *E. coli* and *Salmonella enterica* (42). All of the point mutations in the *fabG*(Ts) mutants localize to or near the interface of the homotetrameric FabG protein, disrupting salt bridges and hydrogen bonds and in turn the protein's quaternary structure at nonpermissive temperature.

Despite the growing collection of antibacterial agents that inhibit the FAS II enzymes, there are a very limited number of FabG inhibitors. We have recently evaluated plant polyphenols such as the major green tea extract component epigallocatechin gallate (EGCG) as FabG inhibitors (43). EGCG and related catechins strongly inhibit FabG activity with IC_{50} values between 5 and 15 μM. When tested against FabI, EGCG shows a similar inhibitory effect on the enoyl reductase (43). However, EGCG exhibits only weak antibacterial activity against gram-negative bacteria with a MIC value of 500 μM against *E. coli*. Overexpression of FabG and FabI fails to rescue cells from EGCG inhibition, demonstrating that FabG/FabI inhibition is not the sole antibacterial target of EGCG *in vivo* (43). EGCG is a competitive inhibitor of FabI and a mixed-type inhibitor of FabG, indicating that EGCG interferes with cofactor binding in both enzymes. The ability of EGCG and related plant secondary metabolites to interfere with the activity of multiple NAD(P)H-dependent cellular process may account for their numerous biological activities.

Mycobacterial β-ketoacyl-ACP reductase (MabA) is inhibited by the first-line antituberculosis antibiotic INH, whose primary target *in vivo* is the enoyl-ACP reductase, InhA (44). The *in vitro* action of INH on MabA protein is similar to the mechanism previously described for InhA (45,46). Oxidized INH covalently binds to $NADP^+$, forming an isonicotinoyl-NADP adduct that binds to the MabA active site (44). However, overexpression of *mabA* fails to confer INH resistance *in vivo* (47), suggesting that the most relevant INH target in mycobacteria is InhA.

The above two groups of β-ketoacyl-ACP reductase inhibitors both interfere with cofactor binding and also possess cross-inhibitory activity against the enoyl reductase. The conservation of the cofactor binding sites between the two reductases explains the cross reactivity of the inhibitors (Fig. 1). A structural comparison was made with *E. coli* FabG-$NADP^+$ (Protein DataBank ID 1Q7B) and FabI-NAD^+ (Protein DataBank ID 1C14) complexes, which exhibit a high degree of conformational similarity at the cofactor binding site. The structural conservation of cofactor binding between the *E. coli* enzymes is also reflected in the sequence homology of the two reductases from different species, including gram-positive *S. aureus*, *M. tuberculosis,* and the malaria-causing agent *P. falciparum* (Fig. 1C). The similarity of the cofactor

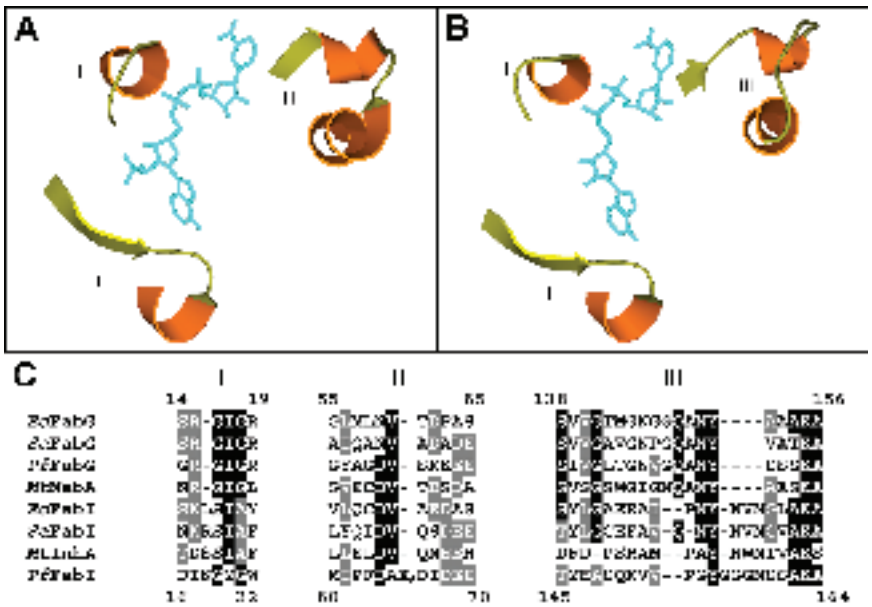

FIG. 1. Comparison of the cofactor binding site of the two reductases of type II FA synthase (FAS II). The crystal structures of *Escherichia coli* FabG (panel A, Protein DataBank ID 1Q7B) and FabI (panel B, Protein DataBank ID 1C14) with bound cofactor were used to compare the binding sites of NAD(P)H. Three regions involved in the cofactor binding (labeled I, II, and III) are conformationally conserved between the *E. coli* FabG and FabI. The bound cofactor $NAD(P)^+$ was shown in cyan, helices of the protein were colored orange, and β-sheets and coils were colored lime. The amino acid sequences of the three regions for cofactor binding are homologous between FabG and FabI from different species, including gram-negative *E. coli,* gram-positive *Staphylococcus aureus, Mycobacterium tuberculosis,* and *Plasmodium falciparum* (panel C). The three segments of sequence shown correspond to the three domains in the structure diagram. In block II, X_6 indicates a six-residue insertion (SFDTAN) in *Pf*FabI. The completely conserved residues were highlighted in black and the conservatively substituted residues were highlighted in gray. The numbers at the beginning and end of each segments are the *E. coli* proteins' numbering. Note that in *M. tuberculosis,* β-ketoacyl-ACP reductase is MabA and the enoyl reductase is ImhA.

binding site between the two reductases allows structure-based drug design of new inhibitors that could potentially target both enzymes by interfering with cofactor binding. The existence of multiple targets can increase the efficacy of the inhibitors and decrease the likelihood of development of drug resistance in bacteria.

DISCUSSION AND FUTURE PROSPECTS

Bacterial enoyl-ACP reductase has been extensively exploited as an antimicrobial target and there are some good antimicrobials that inhibit this enzyme, such as triclosan and INH. However, it is hard to find inhibitors with broad antibacterial spectrum by targeting the enoyl-ACP reductase because of the existence of multiple isoforms and their distribution among different organisms. On the other hand, the relatively untouched β-ketoacyl-ACP reductase may prove to be an excellent target for broad spectrum antimicrobials because there is only one highly conserved isoform of this enzyme. Structure-based design of FabG inhibitors and high-throughput screening of chemical libraries should help researchers discover novel antibiotics to combat the emerging drug-resistant infections.

ACKNOWLEDGMENTS

The work in this laboratory was supported by National Institutes of Health Grant GM 34496, Cancer Center (CORE) Support Grant CA 21765, and the American Lebanese Syrian Associated Charities.

REFERENCES

1. Cronan, J.E., Jr., and Rock, C.O. (1996) Biosynthesis of Membrane Lipids, in Escherichia coli *and* Salmonella typhimurium: *Cellular and Molecular Biology* (Neidhardt, F.C., Curtis, R., Gross, C.A., Ingraham, J.L., Lin, E.C.C., Low, K.B., Magasanik, B., Reznikoff, W., Riley, M., Schaechter, M., and Umbarger, H.E., eds.), pp. 612–636, American Society for Microbiology, Washington, D.C.
2. Rock, C.O.. and Cronan, J.E., Jr. (1996) *Escherichia coli* as a Model for the Regulation of Dissociable (Type II) FA Biosynthesis, *Biochim. Biophys. Acta 1302*, 1–16.
3. Rock, C.O., and Jackowski, S. (2002) Forty Years of FA Biosynthesis, *Biochem. Biophys. Res. Commun. 292*, 1155–1166.
4. Heath, R.J., and Rock, C.O. (2004) FA Biosynthesis as a Target for Novel Antibacterials, *Curr. Opin. Investig. Drugs 5*, 146–153.
5. Heath, R.J., White, S.W., and Rock, C.O. (2001) Lipid Biosynthesis as a Target for Antibacterial Agents, *Prog. Lipid Res. 40*, 467–497.
6. Campbell, J.W., and Cronan, J.E., Jr. (2001) Bacterial FA Biosynthesis: Targets for Antibacterial Drug Discovery, *Annu. Rev. Microbiol. 55*, 305–332.
7. McMurray, L.M., Oethinger, M., and Levy, S. (1998) Triclosan Targets Lipid Synthesis, *Nature (London) 394*, 531–532.
8. Heath, R.J., Yu, Y.-T., Shapiro, M.A., Olson, E., and Rock, C.O. (1998) Broad Spectrum Antimicrobial Biocides Target the FabI Component of FA Synthesis, *J. Biol. Chem. 273*, 30316–30321.
9. Banerjee, A., Dubnau, E., Quémard, A., Balasubramanian, V., Um, K.S., Wilson, T., Collins, D., de Lisle, G., and Jacobs, W.R., Jr. (1994) *inhA*, a Gene Encoding a Target for Isoniazid and Ethionamide in *Mycobacterium tuberculosis*, *Science 263*, 227–230.
10. Hayashi, T., Yamamoto, O., Sasaki, H., and Okazaki, H. (1984) Inhibition of FA Synthesis by the Antibiotic Thiolactomycin, *J. Antibiot. (Tokyo) 37*, 1456–1461.
11. Foth, B.J., Ralph, S.A., Tonkin, C.J., Struck, N.S., Fraunholz, M., Roos, D.S., Cowman, A.F., and McFadden, G.I. (2003) Dissecting Apicoplast Targeting in the Malaria Parasite *Plasmodium falciparum*, *Science 299*, 705–708.
12. Waller, R.F., Ralph, S.A., Reed, M.B., Su, V., Douglas, J.D., Minnikin, D.E., Cowman, A.F., Besra, G.S., and McFadden, G.I. (2003) A Type II Pathway for FA Biosynthesis Presents Drug Targets in *Plasmodium falciparum*, *Antimicrob. Agents Chemother. 47*, 297–301.
13. Surolia, N., and Surolia, A. (2001) Triclosan Offers Protection Against Blood Stages of Malaria by Inhibiting Enoyl-ACP Reductase of *Plasmodium falciparum*, *Nat. Med. 7*, 167–173.
14. Heath, R.J., Rubin, J.R., Holland, D.R., Zhang, E., Snow, M.E., and Rock, C.O. (1999) Mechanism of Triclosan Inhibition of Bacterial FA Synthesis, *J. Biol. Chem. 274*, 11110–11114.
15. Heath, R.J., and Rock, C.O. (1995) Enoyl-acyl Carrier Protein Reductase (*fabI*) Plays a Determinant Role in Completing Cycles of FA Elongation in *Escherichia coli*, *J. Biol. Chem. 270*, 26538–26542.
16. Turnowsky, F., Fuchs, K., Jeschek, C., and Högenauer, G. (1989) *envM* Genes of *Salmonella typhimurium* and *Escherichia coli*, *J. Bacteriol. 171*, 6555–6565.
17. Heath, R.J., Li, J., Roland, G.E., and Rock, C.O. (2000) Inhibition of the *Staphylococcus aureus* NADPH-Dependent Enoyl-acyl Carrier Protein Reductase by Triclosan and Hexachlorophene, *J. Biol. Chem. 275*, 4654–4659.
18. Heath, R.J., and Rock, C.O. (2000) A Triclosan-Resistant Bacterial Enzyme, *Nature (London) 406*, 145–146.
19. Marrakchi, H., DeWolf, W.E., Jr., Quinn, C., West, J., Polizzi, B.J., So, C.Y., Holmes, D.J., Reed, S.L., Heath, R.J., Payne, D.J., *et al*. (2003) Characterization of *Streptococcus pneumoniae* Enoyl-[Acyl Carrier Protein] Reductase (FabK), *Biochem. J. 370*, 1055–1062.
20. Heath, R.J., Su, N., Murphy, C.K., and Rock, C.O. (2000) The Enoyl-[Acyl-Carrier-Protein] Reductases FabI and FabL from *Bacillus subtilis*, *J. Biol. Chem. 275*, 40128–40133.
21. Dessen, A., Quémard, A., Blanchard, J.S., Jacobs, W.R., Jr., and Sacchettini, J.C. (1995) Crystal Structure and Function of the Isoniazid Target of *Mycobacterium tuberculosis*, *Science 267*, 1638–1641.
22. Kuo, M.R., Morbidoni, H.R., Alland, D., Sneddon, S.F., Gourlie, B.B., Staveski, M.M., Leonard, M., Gregory, J.S., Janjigian, A.D., Yee, C., *et al*. (2003) Targeting Tuberculosis and Malaria Through Inhibition of Enoyl Reductase: Compound Activity and Structural Data, *J. Biol. Chem. 278*, 20851–20859.
23. Stewart, M.J., Parikh, S., Xiao, G., Tonge, P.J., and Kisker, C. (1999) Structural Basis and Mechanism of Enoyl Reductase Inhibition by Triclosan, *J. Mol. Biol. 290*, 859–865.
24. Fan, F., Yan, K., Wallis, N.G., Reed, S., Moore, T.D., Rittenhouse, S.F., DeWolf, J.W., Jr., Huang, J., McDevitt, D., Miller, W.H., *et al*. (2002) Defining and Combating the Mechanisms of Triclosan Resistance in Clinical Isolates of *Staphylococcus aureus*, *Antimicrob. Agents Chemother. 46*, 3343–3347.
25. Sivaraman, S., Zwahlen, J., Bell, A.F., Hedstrom, L., and Tonge, P.J. (2003) Structure-Activity Studies of the Inhibition of FabI, the Enoyl Reductase from *Escherichia coli*, by Triclosan: Kinetic Analysis of Mutant FabIs, *Biochemistry 42*, 4406–4413.
26. Rawat, R., Whitty, A., and Tonge, P.J. (2003) The Isoniazid-NAD Adduct Is a Slow, Tight-Binding Inhibitor of InhA, the *Mycobacterium tuberculosis* Enoyl Reductase: Adduct Affinity and Drug Resistance, *Proc. Natl. Acad. Sci. USA 100*, 13881–13886.
27. McMurry, L.M., McDermott, P.F., and Levy, S.B. (1999) Genetic Evidence that InhA of *Mycobacterium smegmatis* Is a Target for Triclosan, *Antimicrob. Agents Chemother. 43*, 711–713.

28. Perozzo, R., Kuo, M., Sidhu, A.S., Valiyaveettil, J.T., Bittman, R., Jacobs, W.R., Jr., Fidock, D.A., and Sacchettini, J.C. (2002) Structural Elucidation of the Specificity of the Antibacterial Agent Triclosan for Malarial Enoyl Acyl Carrier Protein Reductase, *J. Biol. Chem. 277*, 13106–13114.
29. Kapoor, M., Dar, M.J., Surolia, A., and Surolia, N. (2001) Kinetic Determinants of the Interaction of Enoyl-ACP Reductase from *Plasmodium falciparum* with Its Substrates and Inhibitors, *Biochem. Biophys. Res. Commun. 289*, 832–837.
30. Sivaraman, S., Sullivan, T.J., Johnson, F., Novichenok, P., Cui, G., Simmerling, C., and Tonge, P.J. (2004) Inhibition of the Bacterial Enoyl Reductase FabI by Triclosan: A Structure-Reactivity Analysis of FabI Inhibition by Triclosan Analogues, *J. Med. Chem. 47*, 509–518.
31. Heerding, D.A., Chan, G., DeWolf, W.E., Fosberry, A.P., Janson, C.A., Jaworski, D.D., McManus, E., Miller, W.H., Moore, T.D., Payne, D.J., *et al*. (2001) 1,4-Disubstituted Imidazoles Are Potential Antibacterial Agents Functioning as Inhibitors of Enoyl Acyl Carrier Protein Reductase (FabI), *Bioorg. Med. Chem. Lett. 11*, 2061–2065.
32. Seefeld, M.A., Miller, W.H., Newlander, K.A., Burgess, W.J., Payne, D.J., Rittenhouse, S.F., Moore, T.D., DeWolf, W.E., Jr., Keller, P.M., Qiu, X., *et al*. (2001) Inhibitors of Bacterial Enoyl Acyl Carrier Protein Reductase (FabI): 2,9-Disubstituted 1,2,3,4-Tetrahydropyrido[3,4-b]indoles as Potential Antibacterial Agents, *Bioorg. Med. Chem. Lett. 11*, 2241–2244.
33. Payne, D.J., Miller, W.H., Berry, V., Brosky, J., Burgess, W.J., Chen, E., DeWolf, J.W., Jr., Fosberry, A.P., Greenwood, R., Head, M.S., *et al*. (2002) Discovery of a Novel and Potent Class of FabI-Directed Antibacterial Agents, *Antimicrob. Agents Chemother. 46*, 3118–3124.
34. Miller, W.H., Seefeld, M.A., Newlander, K.A., Uzinskas, I.N., Burgess, W.J., Heerding, D.A., Yuan, C.C., Head, M.S., Payne, D.J., Rittenhouse, S.F., *et al*. (2002) Discovery of Aminopyridine-Based Inhibitors of Bacterial Enoyl-ACP Reductase (FabI), *J. Med. Chem. 45*, 3246–3256.
35. Seefeld, M.A., Miller, W.H., Newlander, K.A., Burgess, W.J., DeWolf, W.E., Jr., Elkins, P.A., Head, M.S., Jakas, D.R., Janson, C.A., Keller, P.M., *et al*. (2003) Indole Naphthyridinones as Inhibitors of Bacterial Enoyl-ACP Reductases FabI and FabK, *J. Med. Chem. 46*, 1627–1635.
36. Sheldon, P.S., Kekwick, R.G., Smith, C.G., Sidebottom, C., and Slabas, A.R. (1992) 3-Oxoacyl-[ACP] Reductase from Oilseed Rape (*Brassica napus*), *Biochim. Biophys. Acta 1120*, 151–159.
37. Fawcett, T., Copse, C.L., Simon, J.W., and Slabas, A.R. (2000) Kinetic Mechanism of NADH-Enoyl-ACP Reductase from *Brassica napus*, *FEBS Lett. 484*, 65–68.
38. Price, A.C., Zhang, Y.-M., Rock, C.O., and White, S.W. (2001) The Structure of β-Ketoacyl-[Acyl Carrier Protein] Reductase from *Escherichia coli*: Negative Cooperativity and Its Structural Basis, *Biochemistry 40*, 12772–12781.
39. Price, A.C., Zhang, Y.-M., Rock, C.O., and White, S.W. (2004) Cofactor-Induced Conformational Rearrangements Establish a Catalytically Competent Active Site and a Proton Relay Conduit in β-Ketoacyl-Acyl Carrier Protein Reductase (FabG), *Structure 12*, 417–428.
40. Cohen-Gonsaud, M., Ducasse, S., Hoh, F., Zerbib, D., Labesse, G., and Quemard, A. (2002) Crystal Structure of MabA from *Mycobacterium tuberculosis*, a Reductase Involved in Long-Chain FA Biosynthesis, *J. Mol. Biol. 320*, 249–261.
41. Zhang, Y., and Cronan, J.E., Jr. (1996) Polar Allele Duplication for Transcriptional Analysis of Consecutive Essential Genes: Application to a Cluster of *Escherichia coli* FA Biosynthetic Genes, *J. Bacteriol. 178*, 3614–3620.
42. Lai, C.Y., and Cronan, J.E., Jr. (2004) Isolation and Characterization of β-Ketoacyl-Acyl Carrier Protein Reductase (*fabG*) Mutants of *Escherichia coli* and *Salmonella enterica* Serovar Typhimurium, *J. Bacteriol. 186*, 1869–1878.
43. Zhang, Y.-M., and Rock, C.O. (2004) Evaluation of Epigallocatechin Gallate and Related Plant Polyphenols as Inhibitors of the FabG and FabI Reductases of Bacterial Type II FA Synthase, *J. Biol. Chem. 279*, 30994–31001.
44. Ducasse-Cabanot, S., Cohen-Gonsaud, M., Marrakchi, H., Nguyen, M., Zerbib, D., Bernadou, J., Daffe, M., Labesse, G., and Quemard, A. (2004) *In vitro* Inhibition of the *Mycobacterium tuberculosis* β-Ketoacyl-Acyl Carrier Protein Reductase MabA by Isoniazid, *Antimicrobiol. Agents Chem. 48*, 242–249.
45. Lei, B., Wei, C.J., and Tu, S.C. (2000) Action Mechanism of Antitubercular Isoniazid. Activation by *Mycobacterium tuberculosis* KatG, Isolation, and Characterization of InhA Inhibitor, *J. Biol. Chem. 275*, 2520–2526.
46. Rozwarski, D., Grant, G., Barton, D., Jacobs, W., and Sacchettini, J.C. (1998) Modification of NADH of the Isoniazid Target (InhA) from *Mycobacterium tuberculosis*, *Science 279*, 98–102.
47. Banerjee, A., Sugantino, M., Sacchettini, J.C., and Jacobs, W.R., Jr. (1998) The *mabA* Gene from the *inhA* Operon of *Mycobacterium tuberculosis* Encodes a 3-Ketoacyl Reductase That Fails to Confer Isoniazid Resistance, *Microbiology 144*, 2697–2704.

[Received July 19, 2004; accepted September 30, 2004]

Regulation of Stearoyl-CoA Desaturase Expression

James M. Ntambi[a,b,*], Makoto Miyazaki[a], and Agnieszka Dobrzyn[a]

[a]Department of Biochemistry and [b]Department of Nutritional Sciences, University of Wisconsin, Madison, Wisconsin 53706

ABSTRACT: Stearoyl-CoA desaturase (SCD) is a regulatory enzyme in lipogenesis, catalyzing the rate-limiting step in the overall *de novo* synthesis of monounsaturated FA, mainly oleate and palmitoleate from stearoyl- and palmitoyl-CoA, respectively. Oleate and palmitoleate are the major monounsaturated FA of membrane phospholipids, TG, wax esters, cholesterol esters, and alkyldiacylglycerol. Several SCD gene isoforms (SCD1, SCD2, SCD3, and SCD4) exist in mice, and two have been characterized in humans. SCD1 gene expression in liver cells is regulated by numerous stimuli including diet and hormones. We are interested in why SCD is such a highly regulated enzyme even though oleate, the major product of this enzyme, is one of the most abundant FA in the diet and is therefore readily available. Dietary oleate is also well known for its TG-lowering effects and, as a major component of olive oil, is expected to have beneficial effects. However, high SCD activity has been implicated in diabetes, obesity, atherosclerosis, and cancer in several animal models; therefore, the role that *de novo* oleate plays in these disease states has to be carefully evaluated. By using SCD1–/– mice, which are deficient in tissue oleate, we begin to learn more about the physiological role of SCD gene expression and oleate in normal and disease states.

Paper L9589 in *Lipids 39,* 1061–1065 (November 2004)

EXPRESSION AND REGULATION OF STEAROYL-CoA DESATURASE 1 GENES

Stearoyl-CoA desaturase (SCD) is an endoplasmic reticulum enzyme that catalyzes the biosynthesis of monounsaturated FA from saturated FA that are either synthesized *de novo* or derived from the diet. SCD in conjunction with NADH, the flavoprotein cytochrome b_5 reductase, and the electron acceptor cytochrome b_5, as well as molecular oxygen, introduces a single double bond in a spectrum of methylene-interrupted fatty acyl-CoA substrates. The preferred substrates are palmitoyl- and stearoyl-CoA, which are converted into palmitoleoyl- and oleoyl-CoA, respectively (1–6). These products are the most abundant monounsaturated FA in various kinds of lipids, including phospholipids, TG, cholesteryl esters, wax esters, and alkyldiacylglycerols (7–10). Apart from being components of lipids, monounsaturated FA also serve as mediators of signal transduction and cellular differentiation, including neuronal differentiation (11–13). Oleate has been shown to regulate food intake in the brain (14). Monounsaturated FA also influence apoptosis (15) and may have some role in mutagenesis in some tumors (16). Therefore, given the multiple roles of monounsaturated FA, variation in stearoyl-CoA desaturase activity in mammals would be expected to affect physiological variables including differentiation, insulin sensitivity, metabolic rate, adiposity, atherosclerosis, cancer, and obesity.

The genes for SCD have been cloned from different species including yeast, drosophila, *Caenorhabditis elegans*, sheep, fish, hamster, rat, mice, and humans (5–6). In mice, four isoforms (SCD1, SCD2, SCD3, and SCD4) have been identified (17–19), whereas in rats, two isoforms have been characterized (20). Two SCD isoforms have been characterized in humans (21,22). In many different mouse strains, all of the SCD genes are localized in close proximity on chromosome 19 (23). Although the mouse isoforms share 85 to 88% identity in their amino acid sequence (5–6), their 5′-flanking regions differ somewhat, resulting in divergent tissue-specific gene expression.

Under normal dietary conditions, SCD1 mRNA is highly expressed in white adipose tissue, brown adipose tissue (BAT), meibomium gland, Harderian gland, and preputial gland (5,9,24) and is dramatically induced in liver and heart in response to a high-carbohydrate diet (18,25,26). The SCD1 isoform is also induced by cholesterol (27–29), LXR agonists (19), vitamin A (30,31), and peroxisomal proliferators (32). On the other hand, PUFA, thyroid hormone, glucagon, thiazolidinediones, and leptin repress the expression of SCD1 (18,33–37). PUFA, especially the n-3 series, are such potent repressors of SCD1 in liver that when added to diets they override the stimulatory effects of high carbohydrates on SCD1 gene expression (25). The SCD2 isoform is predominantly expressed in brain (18) and is developmentally induced during neonatal peripheral myelination (38). Similar to SCD1, SCD2 mRNA is expressed to a lesser extent in kidney, spleen, lung, and heart, where it is induced in response to a high-carbohydrate diet (18). In addition, SCD2 mRNA is expressed in B-cells and is down-regulated during lymphocyte development (39,40). In some tissues, such as adipose and eyelid, both SCD1 and SCD2 genes are expressed, whereas in skin, Harderian glands, and preputial gland SCD1, SCD2, and SCD3 gene isoforms are expressed (5,9). SCD4 is mainly expressed in the heart, where it is induced by high-carbohydrate feeding and LXRα agonists but not repressed by PUFA (19). In the heart, leptin represses SCD4 but not SCD1 or

*To whom correspondence should be addressed at Department of Biochemistry, University of Wisconsin, 433 Babcock Drive, Madison, WI 53706. E-mail: ntambi@biochem.wisc.edu

Abbreviations: ACC, acetyl-CoA carboxylase; AMPK, AMP-activated protein kinase; BAT, brown adipose tissue; CPT-1, carnitine palmitoyltransferase-1; PPARα, peroxisome proliferator-activated receptor-α; SCD, stearoyl-CoA desaturase; SRE, sterol response element; SREBP-1c, sterol regulatory element-binding protein-1c.

SCD2 expression (19). In skin, SCD1 expression is restricted to the undifferentiated sebocytes, whereas SCD3 is expressed mainly in the differentiated sebocytes (41). SCD2 is expressed in hair follicles (41). The reason for expression of two or more SCD isoforms in the same tissue is not known but seems to be related to the substrate specificity of the isoforms and their regulation by hormonal and dietary factors through tissue-specific expression (4–6).

ROLE OF SCD1 ISOFORM IN METABOLISM

Dietary oleate is well known for its TG-lowering effects and, being a major component of olive oil, it is expected to have beneficial effects. However, high SCD activity has been implicated in diabetes, obesity, atherosclerosis, and cancer in several animal models; therefore, the role that *de novo* synthesized oleate plays in these disease states has to be carefully evaluated. To investigate the physiological function of SCD and oleate in normal and disease states, we created mice with a targeted disruption of the SCD1 gene (SCD1–/–) (8). We established that SCD1–/– mice have reduced body adiposity, increased insulin sensitivity, and are resistant to diet-induced weight gain relative to wild-type mice (42). The resistance to diet-induced obesity is due to increased energy expenditure and thermogenesis (42,43). The thermogenesis is through activation of the β3-adrenergic receptor-mediated pathway (Fig. 1). In SCD1–/– mice, the expression of several genes encoding enzymes of FA oxidation are up-regulated, whereas genes encoding enzymes of lipid synthesis are down-regulated (42). The mechanisms by which SCD deficiency leads to these metabolic changes are presently unknown.

Role in lipid biosynthesis. Feeding high-carbohydrate diets induces FA and TG synthesis in both humans and rodents (44). The induction of hepatic FA and TG synthesis is mediated by sterol regulatory element binding protein-1c (SREBP-1c). SREBP belong to the basic helix-loop-helix family of transactivators and act on genes containing novel sequences called sterol response elements (SRE) in their promoter regions and activate their transcription (45). There are three SREBP isoforms. SREBP-1a and 1c are encoded by the same gene and differ at their N-terminus, whereas SREBP-2 is encoded by a separate gene. SREBP-1c is the predominant isoform in rodent and human liver and is now recognized as a key regulator of FA and TG synthesis in response to insulin.

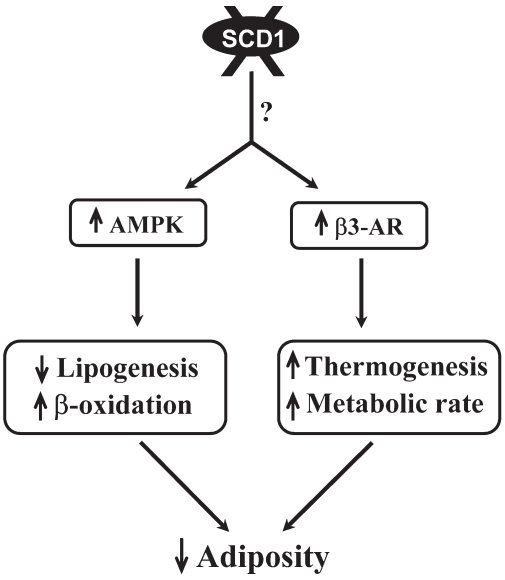

FIG. 1. Mechanism of reduced adiposity in the SCD1–/– mouse. The mechanisms of AMP-activated kinase (AMPK) activation and β3-adrenergic receptor (β3-AR) activation by SCD1 deficiency are not known at present. SCD, stearoyl-CoA desaturase.

We showed recently that when fed to SCD1–/– mice, a high-carbohydrate diet does not induce SREBP-1c or lipogenic gene expression, and liver TG levels are not increased (46). The failure to induce lipogenic gene expression could not be rescued by supplementing the diet with 5% by weight of oleate normally present in the diet. However, very high levels of oleate (20% by weight) supplemented to a high-fructose diet followed by long-term feeding increased the mRNA levels for SREBP-1c and lipogenic genes and increased plasma TG, but not to levels found in the wild-type mice fed the fructose diet. These results suggest that the endogenously synthesized oleate is a more readily accessible FA pool than the dietary pool for the synthesis of TG and regulation of lipogenic gene expression.

The fructose diet supplemented with 20% tripalmitin (16:0), tristearin (18:0), or trilinolein (18:2n-6) did not increase the mRNA levels for SREBP-1c and lipogenic genes in SCD1–/– mice and the liver TG levels were not increased. The inability of triolinolein to increase SREBP1 gene expression was not unexpected since PUFA in general repress SREBP1 gene expression and protein maturation *in vitro* and *in vivo* (47,48). Supplementation of the diet with tristearin or tripalmitin did not increase TG. Surprisingly, the content of the 16:0 or 18:0 FA did not increase in the SCD1–/– mice upon tripalmitin or tristearin supplementation, respectively, although the food intake was similar between the wild-type and SCD1–/– mice. The fate of these saturated FA is not clear at the moment, but we speculate that in oleate deficiency, they are channeled into FA β-oxidation so that a constant ratio of monounsaturated to saturated FA is maintained.

Role in lipid oxidation. Loss of SCD1 function activates genes of FA oxidation (42). Most of these genes, which include acyl-CoA oxidase, very long chain acyl-CoA dehydrogenase, carnitine palmitoyltransferase-1 (CPT-1), and fasting-induced adipocyte factor, are known targets of peroxisome proliferator-activated receptor-α (PPARα) (49,50) and contain PPARα response regions in their promoters (51–53). Because PPARα is a key transcription factor that induces the transcription of β-FA oxidation and thermogenic genes, we hypothesized that SCD1 deficiency may generate a PPARα ligand and that upon activation of the receptor, the transcription of PPARα-target genes would be activated, leading to increased FA β-oxidation. However, when we crossed the SCD1–/– mice with the PPARα-null mice, we found that the double knockout (SCD1–/–/PPARα–/–) mice were still protected

against adiposity, had increased energy expenditure, and had maintained high expression of PPARα-target genes in liver and BAT (46). The findings indicated that the increased expression of PPARα target genes associated with SCD1 deficiency is independent of activation of the PPARα pathway. The signals induced by SCD1 deficiency leading to increased expression of FA oxidation genes are therefore not known.

Leptin is an adipocyte-derived hormone that plays a pivotal role in regulating food intake and energy expenditure. Leptin stimulates the oxidation of FA and uptake of glucose and reduces the accumulation of lipids in non-adipose tissues. Recently, leptin was found to repress RNA levels and enzymatic activity of SCD1 in liver (37). Ob/ob mice with SCD1 mutations were significantly less obese than ob/ob controls and had markedly increased energy expenditure with reduced TG storage in liver (37). However, the signaling pathways that mediate the metabolic effects of leptin remain largely unknown. We hypothesized that leptin acts in part by suppressing SCD1 activity, which in turn activates a metabolic pathway that promotes FA oxidation. Leptin has been found to selectively stimulate phosphorylation and activation of the α2 catalytic subunit of AMP-activated protein kinase (AMPK), an enzyme that has been found to be a principal mediator of the effects of leptin on FA oxidation in muscle (54). However, the effects of leptin on AMPK in liver are not fully known. We recently found that SCD1 deficiency also activates AMPK, leading to increased acetyl-CoA carboxylase (ACC) phosphorylation, a well-known mechanism for ACC inactivation, thereby resulting in reduced malonyl-CoA levels (55). The reduction in malonyl-CoA levels derepresses CPT-1 leading to an increase in the transport of FA into mitochondria and their subsequent oxidation. Since SCD1 gene expression is repressed by leptin in liver and SCD1 deficiency has been shown to mimic the metabolic effects of leptin in ob/ob mice (37), we hypothesized that activation of AMPK by SCD1 deficiency in liver was leptin-dependent. Instead, we found that the activation of AMPK in the liver of SCD1–/– mice is leptin-independent because increased AMPK phosphorylation and enzymatic activity, and increased ACC phosphorylation were still observed in the livers of ab^J/ab^J;ob/ob double mutant mice (55). AMPK activation also suppresses the expression of SREBP-1c, a key transcription factor regulating genes of FA and TG biosynthesis (56), suggesting that the reduction in lipid synthesis observed in SCD1 deficiency could be mediated by AMPK activation. The observations indicate that SCD1 expression is involved in regulating AMPK function in mouse liver. The mechanism of AMPK activation in SCD1 deficiency is currently unknown.

The recent studies using the knockout mouse models have revealed the phenotypes generated as a result of SCD1 gene deficiency. SCD1 expression is critical in the biosynthesis of TG. When SCD1 expression is high, such as in response to high-carbohydrate diets and insulin, the switch is flipped in the direction of storing fat. When SCD1 expression is low, such as in response to diets rich in PUFA, the switch is flipped in the direction of burning fat (57). The mechanisms are not yet fully worked out, but we propose that through the activation of AMPK, SCD1 deficiency induces a signal that partitions FA toward oxidation rather than synthesis and that through activation of the β3-adrenergic receptor, SCD1 deficiency increases energy expenditure and thermogenesis (Fig. 1). The combined effect of these processes results in a decrease in adiposity. SCD1 therefore appears to be an important metabolic control point and is emerging as a promising therapeutic target that could be used in the treatment of obesity, diabetes, and other metabolic diseases.

ACKNOWLEDGMENTS

Our work has been supported by NIH grant NIDDK-RO162388 (J.M.N.) and AHA Postdoctoral Fellowship 0420051Z (A.D.).

REFERENCES

1. Enoch, H.G., Catala, A., and Strittmatter, P. (1976) Mechanism of Rat Liver Microsomal Stearyl-CoA Desaturase. Studies of the Substrate Specificity, Enzyme–Substrate Interactions, and the Function of Lipid, *J. Biol. Chem. 251*, 5095–5103.
2. Enoch, H.G., and Strittmatter, P. (1978) Role of Tyrosyl and Arginyl Residues in Rat Liver Microsomal Stearyl Coenzyme A Desaturase, *Biochemistry 17*, 4927–4932.
3. Ntambi, J.M. (1999) Regulation of Stearoyl-CoA Desaturase by Polyunsaturated Fatty Acids and Cholesterol, *J. Lipid Res. 40*, 1549–1558.
4. Ntambi, J.M. (1995) The Regulation of Stearoyl-CoA Desaturase (SCD), *Prog. Lipid Res. 34*, 139–150.
5. Miyazaki, M., and Ntambi, J.M. (2003) Role of Stearoyl-CoA Desaturase in Lipid Metabolism, *Prostaglandins Leukot. Essent. Fatty Acids 68*, 113–121.
6. Ntambi, J.M., and Miyazaki, M. (2003) Recent Insights into Stearoyl-CoA Desaturase-1, *Curr. Opin. Lipidol. 14*, 255–261.
7. Miyazaki, M., Kim, Y.C., Gray-Keller, M.P., Attie, A.D., and Ntambi, J.M. (2000) The Biosynthesis of Hepatic Cholesterol Esters and Triglycerides Is Impaired in Mice with a Disruption of the Gene for Stearoyl-CoA Desaturase 1, *J. Biol. Chem. 275*, 30132–30138.
8. Miyazaki, M., Man, W.C., and Ntambi, J.M. (2001) Targeted Disruption of Stearoyl-CoA Desaturase 1 Gene in Mice Causes Atrophy of Sebaceous and Meibomian Glands and Depletion of Wax Esters in the Eyelid, *J. Nutr. 131*, 2260–2268.
9. Miyazaki, M., Kim, H.J., Man, W.C., and Ntambi, J.M. (2001) Oleoyl-CoA Is the Major *de novo* Product of Stearoyl-CoA Desaturase 1 Gene Isoform and Substrate for the Biosynthesis of the Harderian Gland 1-Alkyl-2,3-diacylglycerol, *J. Biol. Chem. 276*, 39455–39461.
10. Miyazaki, M., Kim, Y.C., and Ntambi, J.M. (2001) A Lipogenic Diet in Mice with a Disruption of the Stearoyl-CoA Desaturase 1 Gene Reveals a Stringent Requirement of Endogenous Monounsaturated Fatty Acids for Triglyceride Synthesis, *J. Lipid Res. 42*, 1018–1024.
11. Velasco, A., Tabernero, A., and Medina, J.M. (2003) Role of Oleic Acid as a Neurotrophic Factor Is Supported *in vivo* by the Expression of GAP-43 Subsequent to the Activation of SREBP-1 and the Up-regulation of Stearoyl-CoA Desaturase During Postnatal Development of the Brain, *Brain Res. 977*, 103–111.
12. Medina, J.M., and Tabernero, A. (2002) Astrocyte-Synthesized Oleic Acid Behaves as a Neurotrophic Factor for Neurons, *J. Physiol. Paris 96*, 265–271.
13. Tabernero, A., Lavado, E.M., Granda, B., Velasco, A., and Medina, J.M. (2001) Neuronal Differentiation Is Triggered by Oleic

Acid Synthesized and Released by Astrocytes, *J. Neurochem. 79*, 606–616.
14. Obici, S., Feng, Z., Morgan, K., Stein, D., Karkanias, G., and Rossetti, L. (2002) Central Administration of Oleic Acid Inhibits Glucose Production and Food Intake, *Diabetes 51*, 271–275.
15. Listenberger, L.L., Han, X., Lewis, S.E., Cases, S., Farese, R.V., Ory, D.S., Jr., and Schaffer, J.E. (2003) Triglyceride Accumulation Protects Against Fatty Acid-Induced Lipotoxicity, *Proc. Natl. Acad. Sci. USA 100*, 3077–3082.
16. Hardy, S., Langelier, Y., and Prentki, M. (2000) Oleate Activates Phosphatidylinositol 3-Kinase and Promotes Proliferation and Reduces Apoptosis of MDA-MB-231 Breast Cancer Cells, Whereas Palmitate Has Opposite Effects, *Cancer Res. 60*, 6353–6358.
17. Ntambi, J.M., Buhrow, S.A., Kaestner, K.H., Christy, R.J., Sibley, E., Kelly, T.J., Jr., and Lane, M.D. (1988) Differentiation-Induced Gene Expression in 3T3-L1 Preadipocytes. Characterization of a Differentially Expressed Gene Encoding Stearoyl-CoA Desaturase, *J. Biol. Chem. 263*, 17291–17300.
18. Kaestner, K.H., Ntambi, J.M., Kelly, T.J., Jr., and Lane, M.D. (1989) Differentiation-Induced Gene Expression in 3T3-L1 Preadipocytes. A Second Differentially Expressed Gene Encoding Stearoyl-CoA Desaturase, *J. Biol. Chem. 264*, 14755–14761.
19. Miyazaki, M., Jacobson, M.J., Man, W.C., Cohen, P., Asilmaz, E., Friedman, J.M., and Ntambi, J.M. (2003) Identification and Characterization of Murine SCD4: A Novel Heart-Specific Stearoyl-CoA Desaturase Isoform Regulated by Leptin and Dietary Factors, *J. Biol. Chem. 278*, 33904–33911.
20. Mihara, K. (1990) Structure and Regulation of Rat Liver Microsomal Stearoyl-CoA Desaturase Gene, *J. Biochem. (Tokyo) 108*, 1022–1029.
21. Zhang, L., Ge, L., Parimoo, S., Stenn, K., and Prouty, S.M. (1999) Human Stearoyl-CoA Desaturase: Alternative Transcripts Generated from a Single Gene by Usage of Tandem Polyadenylation Sites, *Biochem. J. 340,* 255–264.
22. Beiraghi, S., Zhou, M., Talmadge, C.B., Went-Sumegi, N., Davis, J.R., Huang, D., Saal, H., Seemayer, T.A., and Sumegi, J. (2003) Identification and Characterization of a Novel Gene Disrupted by a Pericentric Inversion inv(4)(p13.1q21.1) in a Family with Cleft Lip, *Gene 309*, 11–21.
23. Tabor, D.E., Xia, Y.R., Mehrabian, M., Edwards, P.A., and Lusis, A.J. (1998) A Cluster of Stearoyl CoA Desaturase Genes, Scd1 and Scd2, on Mouse Chromosome 19, *Mamm. Genome 9*, 341–342.
24. Miyazaki, M., Gomez, F.E., and Ntambi, J.M. (2002) Lack of Stearoyl-CoA Desaturase-1 Function Induces a Palmitoyl-CoA Δ^6 Desaturase and Represses the Stearoyl-CoA Desaturase-3 Gene in the Preputial Glands of the Mouse, *J. Lipid Res. 43*, 2146–2154.
25. Ntambi, J.M. (1992) Dietary Regulation of Stearoyl-CoA Desaturase 1 Gene Expression in Mouse Liver, *J. Biol. Chem. 267*, 10925–10930.
26. Waters, K., and Ntambi, J.M. (1994) Insulin and Dietary Fructose Induce Stearoyl-CoA Desaturase 1 Gene Expression in Liver of Diabetic Mice, *J. Biol. Chem. 269*, 27773–27777.
27. Repa, J.J., Liang, G., Ou, J., Bashmakov, Y., Lobaccaro, J.M., Shimomura, I., Shan, B., Brown, M.S., Goldstein, J.L., and Mangelsdorf, D.J. (2000) Regulation of Mouse Sterol Regulatory Element-Binding Protein-1c Gene (SREBP-1c) by Oxysterol Receptors, LXR-α and LXR-β, *Genes. Dev. 14*, 2819–2830.
28. Landau, J.M., Sekowski, A., and Hamm, M.W. (1997) Dietary Cholesterol and the Activity of Stearoyl CoA Desaturase in Rats: Evidence for an Indirect Regulatory Effect, *Biochim. Biophys. Acta 1345*, 349–357.
29. Kim, H.J., Miyazaki, M., and Ntambi, J.M. (2002) Dietary Cholesterol Opposes PUFA-Mediated Repression of the Stearoyl-CoA Desaturase-1 Gene by SREBP-1 Independent Mechanism, *J. Lipid Res. 43*, 1750–1757.
30. Miller, C.W., Waters, K.M., and Ntambi, J.M. (1997) Regulation of Hepatic Stearoyl-CoA Desaturase Gene 1 by Vitamin A, *Biochem. Biophys. Res. Commun. 231*, 206–210.
31. Samuel, W., Kutty, R.K., Nagineni, S., Gordon, J.S., Prouty, S.M., Chandraratna, R.A., and Wiggert, B. (2001) Regulation of Stearoyl Coenzyme A Desaturase Expression in Human Retinal Pigment Epithelial Cells by Retinoic Acid, *J. Biol. Chem. 276*, 28744–28750.
32. Miller, C.W., and Ntambi, J.M. (1996) Peroxisome Proliferators Induce Mouse Liver Stearoyl-CoA Desaturase 1 Gene Expression, *Proc. Natl. Acad. Sci. USA 93*, 9443–9448.
33. Waters, K.M., Miller, C.W., and Ntambi, J.M. (1997) Localization of a Negative Thyroid Hormone-Response Region in Hepatic Stearoyl-CoA Desaturase Gene 1, *Biochem. Biophys. Res. Commun. 233*, 838–843.
34. Waters, K.M., and Ntambi, J.M. (1996) Polyunsaturated Fatty Acids Inhibit Hepatic Stearoyl-CoA Desaturase-1 Gene in Diabetic Mice, *Lipids 31*, S33–S36.
35. Kurebayashi, S., Hirose, T., Miyashita, Y., Kasayama, S., and Kishimoto, T. (1997) Thiazolidinediones Downregulate Stearoyl-CoA Desaturase 1 Gene Expression in 3T3-L1 Adipocytes, *Diabetes 46*, 2115–2118.
36. Kim, Y.-C., Gomez, E., Fox, B.G., and Ntambi, J.M. (2000). Differential Regulation of the Stearoyl-CoA Desaturase Genes by Thiazolidinediones in 3T3-L1 Adipocytes, *J. Lipid Res. 41*, 1310–1316.
37. Cohen, P., Miyazaki, M., Socci, N.D., Hagge-Greenberg, A., Liedtke, W., Soukas, A.A., Sharma, R., Hudgins, L.C., Ntambi, J.M., and Friedman, J.M. (2002) Role for Stearoyl-CoA Desaturase-1 in Leptin-Mediated Weight Loss, *Science 297*, 240–243.
38. Garbay, B., Boiron-Sargueil, F., Shy, M., Chbihi, T., Jiang, H., Kamholz, J., and Cassagne, C. (1998) Regulation of Oleoyl-CoA Synthesis in the Peripheral Nervous System: Demonstration of a Link with Myelin Synthesis, *J. Neurochem. 71*, 1719–1726.
39. Tebbey, P.W., and Buttke, T.M. (1992) Stearoyl-CoA Desaturase Gene Expression in Lymphocytes, *Biochem. Biophys. Res. Commun. 186*, 531–536.
40. Buttke, T.M., Van Cleave, S., Steelman, L., and McCubrey, J.A. (1989) Absence of Unsaturated Fatty Acid Synthesis in Murine T Lymphocytes, *Proc. Natl. Acad. Sci. USA 86*, 6133–6137.
41. Zheng, Y., Prouty, S.M., Harmon, A., Sundberg, J.P., Stenn, K.S., and Parimoo, S. (2001) SCD3—A Novel Gene of the Stearoyl-CoA Desaturase Family with Restricted Expression in Skin, *Genomics 71*, 182–191.
42. Ntambi, J.M., Miyazaki, M., Stoehr, J.P., Lan, H., Kendziorski, C.M., Yandell, B.S., Song, Y., Cohen, P., Friedman, J.M., and Attie, A.D. (2002) Loss of Stearoyl-CoA Desaturase-1 Function Protects Mice Against Adiposity, *Proc. Natl. Acad. Sci. USA 99*, 11482–11486.
43. Lee, S.H., Dobrzyn, A., Dobrzyn, P., Rahman, S.M., Miyazaki, M., Ntambi, J.M. (2004) Lack of Stearoyl-CoA Desaturase 1 Upregulates Basal Thermogenesis but Causes Hypothermia in a Cold Environment, *J. Lipid Res. 45,* 1674–1682.
44. Attie, A.D., Krauss, R.M., Gray-Keller, M.P., Brownlie, A., Miyazaki, M., Kastelein, J.J., Lusis, J.J., Stalenhoef, A.F.H., Stoehr, J.P., Hayden, M.R., and Ntambi, J.M. (2002) Plasma Triglycerides in Human and Mouse Hypertriglyceridemia, *J. Lipid Res. 43*, 1899–1907.
45. Osborne, T.F. (2000) Sterol Regulatory Element-Binding Proteins (SREBPs): Key Regulators of Nutritional Homeostasis and Insulin Action, *J. Biol. Chem. 275*, 32379–32382.
46. Miyazaki, M., Dobrzyn, A., Sampath, H., Lee, S.H., Man, W.C., Chu, K., Peters, J.M., Gonzalez, F.J., and Ntambi, J.M. (2004) Reduced Adiposity and Liver Steatosis by Stearoyl-CoA Desat-

urase Deficiency Are Independent of Peroxisome Proliferator-Activated Receptor-α, *J. Biol. Chem. 279,* 35017–35024.
47. Hannah, V.C., Ou, J., Luong, A., Goldstein, J.L., and Brown, M.S. (2001) Unsaturated Fatty Acids Down-regulate SREBP Isoforms 1a and 1c by Two Mechanisms in HEK-293 Cells, *J. Biol. Chem. 276*, 4365–4372.
48. Xu, J., Teran-Garcia, M., Park, J.H., Nakamura, M.T., and Clarke, S.D. (2001) Sterol Regulatory Element Binding Protein-1 Expression Is Suppressed by Polyunsaturated Fatty Acids. A Mechanism for the Coordinate Suppression of Lipogenic Genes by Polyunsaturated Fats, *J. Biol. Chem. 276*, 9800–9807.
49. Kersten, S., Seydoux, J., Peters, J.M., Gonzalez, F.J., Desvergne, B., and Wahli, W. (1999) Peroxisome Proliferator-Activated Receptor α Mediates the Adaptive Response to Fasting, *J. Clin. Invest. 103*, 1489–1498.
50. Kersten, S., Mandard, S., Tan, N.S., Escher, P., Metzger, D., Chambon, P., Gonzalez, F.J., Desvergne, B., and Wahli, W. (2000) Characterization of the Fasting-Induced Adipose Factor FIAF, a Novel Peroxisome Proliferator-Activated Receptor Target Gene, *J. Biol. Chem. 275*, 28488–28493.
51. Varanasi, U., Chu, R., Huang, Q., Castellon, R., Yeldandi, A.V., and Reddy, J.K. (1996) Identification of a Peroxisome Proliferator-Responsive Element Upstream of the Human Peroxisomal Fatty Acyl Coenzyme A Oxidase Gene, *J. Biol. Chem. 271*, 2147–2155.
52. Tugwood, J.D., Issemann, I., Anderson, R.G., Bundell, K.R., McPheat, W.L., and Green, S. (1992) The Mouse Peroxisome Proliferator Activated Receptor Recognizes a Response Element in the 5′ Flanking Sequence of the Rat Acyl-CoA Oxidase Gene, *Embo. J. 11*, 433–439.
53. Mascaro, C., Acosta, E., Ortiz, J.A., Rodriguez, J.C., Marrero, P.F., Hegardt, F.G., and Haro, D. (1999) Characterization of a Response Element for Peroxisomal Proliferator Activated Receptor (PPRE) in Human Muscle-Type Carnitine Palmitoyltransferase I, *Adv. Exp. Med. Biol. 466*, 79–85.
54. Minokoshi, Y., Kim, Y.B., Peroni, O.D., Fryer, L.G.D., Müller, C., Carling, D., and Kahn, B.B. (2002) Leptin Stimulates Fatty-Acid Oxidation by Activating AMP-Activated Protein Kinase, *Nature 415*, 339–343.
55. Dobrzyn, P., Dobrzyn, A., Miyazaki, M., Cohen, P., Asilmaz, E., Hardie, G.D., Friedman, J.M., and Ntambi, J.M. (2004) Stearoyl-CoA Desaturase-1 (SCD1) Deficiency Increases Fatty Acid Oxidation by Activating AMP-Activated Protein Kinase in Liver, *Proc. Natl. Acad. Sci. USA 101*, 6409–6414.
56. Yamauchi, T., Kamon, J., Minokoshi, Y., Ito, Y., Waki, H., Uchida, S., Yamashita, S., Noda, M., Kita, S., Ueki, K., *et al.* (2002) Adiponectin Stimulates Glucose Utilization and Fatty-Acid Oxidation by Activating AMP-Activated Protein Kinase, *Nat. Med. 8*, 1–8.
57. Dobrzyn, A., and Ntambi, J.M. (2004) The Role of Stearoyl-CoA Desaturase in Body Weight Regulation, *Trends Cardiovasc. Med. 14*, 77–81.

[Received August 26, 2004; accepted October 11, 2004]

Progress Toward the Production of Long-Chain Polyunsaturated Fatty Acids in Transgenic Plants

Johnathan A. Napier[a,*], Olga Sayanova[a], Baoxiu Qi[b,c], and Colin M. Lazarus[b]

[a]Rothamsted Research, Harpenden, Herts AL5 2JQ, United Kingdom, [b]School of Biological Sciences, University of Bristol, Bristol BS8 1UG, United Kingdom, and [c]Department of Biology and Biochemistry, University of Bath, Bath BA2 7AY, United Kingdom

ABSTRACT: Long-chain PUFA such as eicosapentaenoic and docosahexaenoic acids are prevalent in fish oils, and these compounds have been demonstrated to play important roles in human health and nutrition. In particular, these n-3/omega-3 long-chain PUFA provide protection from cardiovascular disease and a collection of symptoms (termed metabolic syndrome) associated with progression toward type 2 diabetes and obesity. Within Western populations, a large increase in the occurrence of these conditions represents a major public health concern. Unfortunately, both marine fish stocks and (consequentially) consumption of fish oils are in steep decline, limiting the protective role of long-chain PUFA in human health. One alternative approach to the provision of these health-beneficial FA is *via* their synthesis in transgenic plants. This review will describe recent advances in the production of transgenic plant oils nutritionally enhanced to produce long-chain PUFA.

Paper no. L9606 in *Lipids 39,* 1067–1075 (November 2004).

It is now clear from a plethora of scientific publications that human diet plays a central role in our acquisition of (or progression to) diseased states; for recent reviews see (1,2). Although this observation may have already been perceived as an intuitive truth, controlled clinical studies have now identified multiple important components of the human diet (3,4). More recently, the significance of genetic makeup in the responsiveness of an individual or population to any particular dietary regime has also revealed so-called "diet–gene" interactions (5). The completion of the human genome sequence and the parallel genotyping of large numbers of individuals have revealed considerable genetic variation among humankind globally; it is estimated that there are in excess of 5 million polymorphisms in the human population, with these variations mainly taking the form of single nucleotide polymorphisms (6). It is therefore also important (if slightly daunting) to consider these genetic components in our attempts to understand and modulate human health through optimizing our diet (7).

Among the first clear examples identified as being important components of the human diet were the so-called EFA linoleic acid (18:2n-6; LA) and α-linolenic acid (18:3n-3; ALA). Initial work by Burr and Burr (8,9) demonstrated the importance of these FA in the mammalian diet. Forty years later, Bang, Dyerberg, and colleagues (10,11) studied the role of diet–gene interactions in their pioneering study on the prevalence of cardiovascular disease (CVD) in Inuit (Eskimo) communities whose diet was rich in oily fish. These data led the authors to campaign for large-scale dietary intervention studies to determine the efficacy of diets rich in fish oils containing n-3 long-chain PUFA (LC-PUFA). As a result of these studies, it is now widely accepted that n-3 LC-PUFA are not only a pivotal component of the human diet, but they are also actively health-beneficial, providing a protective role against a range of diseases (and progressions to diseased states) (4,12). Such human pathologies include not only CVD but also "metabolic syndrome," which is a collective description for a number of indicators of risk of type 2 diabetes and obesity (13). These indicators (such as high blood pressure, high plasma TAG, and abnormal fasting blood glucose) are more and more prevalent in Western populations, and although the precise (presumably multifactorial) causes of these symptoms are unclear, they are of considerable concern. In particular, the apparent increases in both obesity and type 2 diabetes represent a major public health problem (13). However, the observation that n-3 LC-PUFA can provide some degree of pangenotypic protection from these diseases has focused research on the biosynthesis and production of these important FA (14).

Currently, LC-PUFA for human nutrition are primarily from fish oil sources, although there is also a considerable minority market for microorganism-derived LC-PUFA (14). In particular, two LC-PUFA found in fish oils, eicosapentaenoic acid (20:5n-3; EPA) and docosahexaenoic acid (22:6n-3; DHA), are known to play an active role in the prevention of both CVD and metabolic syndrome (13,14). It has been shown that a modest intake of fatty fish may reduce mortality in men who have recovered from myocardial infarction (15). The GISSI (Gruppo Italiano per lo Studio della Sopravvivenza nell'Infanto Miocardico)-Prevenzione trial confirmed these findings in a large intervention study in patients surviving myocardial infarction (4). Treatment with n-3 LC-PUFA significantly lowered the risk of CVD and death. Dietary EPA and DHA reduce blood coagulation, blood lipids, and blood pressure and have antiarrhythmic effects in adults. They may increase HDL cholesterol, suppress inflammatory and allergic processes, and benefit mental disorders (3,16,17). Unfortunately, just as the importance of n-3 LC-PUFA is finally being recognized by health protection agencies and the general public at large, the natural resources that provide these oils have been grossly overexploited. For example, stocks of common marine fish in north-

*To whom correspondence should be addressed at Crop Performance and Improvement Division, Rothamsted Research, Harpenden, Herts AL5 2JQ, UK. E-mail: johnathan.napier@bbsrc.ac.uk

ern Europe have been overfished for decades, resulting in continual reduction in catch size (in terms of both numbers and maturity of fish) (14,18). Thus, there is considerable pressure to identify a sustainable source of important fish oil FA such as DHA and EPA for use in the protection and improvement of human health.

LC-PUFA IN HUMAN DIETS

The synthesis of LC-PUFA is usually carried out by an aerobic process involving the sequential introduction of double bonds and two-carbon elongation into a FA substrate, although an anaerobic process similar to polyketide synthesis has been described in several marine microorganisms (19,20) In the case of mammals, this process is dependent on the dietary intake of LA and ALA (hence their already-mentioned designation EFA), since higher animals have lost the capacity to synthesize these FA (21). Moreover, the efficiency of LC-PUFA biosynthesis in mammals, in terms of the conversion of dietary EFA to EPA or DHA, appears to be relatively poor, emphasizing the desirability of supplementing this endogenous biosynthetic route with dietary LC-PUFA. This appears to be particularly critical at certain stages of human life; for example, LC-PUFA are important in the development of ocular vision in infants and may also play a role in aspects of neurological and brain development (22), and at the other end of the human life span, these same LC-PUFA may help alleviate a number of symptoms in geriatric patients (23). These data are in addition to those of intervention studies such as the GISSI-Prevenzione trial (4), which demonstrated the role of relatively modest (<1 g/d) consumption of n-3 LC-PUFA in protection against CVD. Current recommendations for regular dietary consumption of n-3 LC-PUFA vary, but are usually in the range 0.2–0.5 g/d (12–14).

As mentioned above, the primary dietary source of LC-PUFA is *via* fish-derived oils. Fish have a similar inefficient LC-PUFA biosynthetic pathway, depending on the dietary acquisition of FA to supplement their endogenous synthesis (24). However, the aquatic environment is rich in microorganisms that synthesize (with high efficiency) n-3 LC-PUFA such as EPA and DHA. Thus, it is *via* the consumption of these n-3 LC-PUFA-rich microbes that fish accumulate (either directly or *via* carnivorous consumption of other fish) EPA and DHA, rather than *via* any innate capacity for their synthesis. This progression of n-3 LC-PUFA up the aquatic food web has implications for attempts to supplement fish stocks by aquaculture (i.e., fish farming), not least of all because farmed fish still require dietary n-3 LC-PUFA (18). Aquaculture is currently the largest consumer of fish-derived oils, and so is clearly not capable of operating in a sustainable manner. Conversely, the greater part of human dietary FA intake is in the form of plant-derived "vegetable" oils rich in LA and ALA. However, higher plants lack the capacity to synthesize LC-PUFA, and so oils derived from them are devoid of FA such as EPA and DHA. It is for this reason that vegetable oils are unable to substitute for fish oils in aquaculture (25). Moreover, most plant oils are rich in n-6 FA such as LA, rather than the n-3 ALA. The preponderance of vegetable oils in the modern diet has resulted in a dietary "flood" of n-6 FA, with a ratio of n-6/n-3 of greater than 10:1. This contrasts considerably with the human diet of ~150 years ago, which probably reflected a ratio of 2:1, and was more likely to contain fish oils rich in n-3 LC-PUFA (22).

Considering all of the factors just described, it seems that there is ample evidence for the health-beneficial properties of dietary consumption of n-3 LC-PUFA such as EPA and DHA. Simultaneously, the overexploitation of natural reserves has precipitously affected marine fish stocks to a point where they are predicted to be unviable. This imminent reduction or absence of fish oils should therefore be considered a major driver for seeking and developing alternative sources of LC-PUFA. One approach that we believe is now emerging as a viable and sustainable source of LC-PUFA is the genetic engineering of plants to synthesize these FA (26–28). The remainder of this article will review the latest progress on the process of "reverse engineering" plants to synthesize and accumulate these non-native FA.

TOWARD THE REVERSE ENGINEERING OF LC-PUFA BIOSYNTHESIS

As outlined in the previous section, higher plants do not usually synthesize LC-PUFA, although over 400 different types of FA have been identified across the collective taxa of the plant kingdom. The vast majority of this chemical diversity in FA is found in the TAG of seed oils, presumably to compartmentalize these unusual FA away from the phospholipid membranes (27). Paradoxically, most of the plant enzymes identified as mediating the synthesis of these unusual FA utilize glycerolipid-linked acyl chains as their substrates, indicating the presence of (multiple) enzymes responsible for the channeling of FA from one form of lipid to another. The presence of compartmentalized storage lipids in the form of TAG is also of potential benefit in attempts to introduce non-native FA into a transgenic oilseed, as it may represent a "sink" into which the desired product (e.g., n-3 LC-PUFA) could be channeled, thus avoiding interference with endogenous biological processes such as membrane bilayer composition and oxylipin synthesis (29).

The process of generating transgenic plants producing n-3 LC-PUFA requires the heterologous reconstitution of the biosynthetic pathway in the new host. This in turn depends on the identification and functional characterization of the genes encoding this biosynthetic pathway from an appropriate LC-PUFA-synthesizing organism (such as a marine microorganism), followed by the transfer of these genes to the new host (a transgenic plant). In that respect, the process could be considered analogous to reverse engineering, a term used to describe the dismantling of a system to facilitate understanding, improvement, and replication of the system's processes and output. Whereas reverse engineering is generally associated with the computing and electronics industries, it also

serves as a useful descriptor for attempting to produce n-3 LC-PUFA in transgenic plants. In particular, dictionary exemplification of the term states, "Reverse engineering is usually undertaken in order to redesign the system for better maintainability or to produce a copy of a system without access to the design from which it was originally produced." This latter sentence encapsulates the challenges of attempting to reconstitute n-3 LC-PUFA biosynthesis in transgenic plants.

The last decade has witnessed considerable progress in the identification of the genes involved in LC-PUFA biosynthesis (see Ref. 27 for a recent review). Prior to the first identification of the microsomal FA Δ^6-desaturase in 1997 (30), no molecular identification of any LC-PUFA biosynthetic enzyme had been successfully achieved, despite considerable efforts. Since then, all the activities involved in this biochemical pathway have been functionally characterized at the molecular level. To some extent, these advances have been facilitated by the plethora of genomic and transcript sequences now available, but they also reflect the considerable interest in n-3 LC-PUFA biosynthesis *per se*. These genes (and the polypeptides they encode) can be classified into the two distinct enzymatic reactions that catalyze the primary biosynthetic process. The first of these is the microsomal FA desaturases, which underpin LC-PUFA biosynthesis (31). These LC-PUFA desaturases belong to the N-terminal cytochrome b_5 fusion superfamily, and the presence of this diagnostic N-terminal electron transport domain may be associated with the "front-end" desaturation process catalyzed by these enzymes (32). Many LC-PUFA desaturases have been identified from animals, fungi, and algae, and also from the few plant species that carry out limited PUFA desaturation (primarily Δ^6-desaturation of LA and ALA). One crucial observation regarding these microsomal desaturases is that very many of these enzymes utilize glycerolipid-linked substrates, in particular FA at the *sn-2* position of PC. For recent reviews of progress in the characterization of LC-PUFA desaturases, see Napier *et al.* (31) and Sperling *et al.* (32).

The second key enzymatic reaction in the synthesis of LC-PUFA is elongation, which also occurs in the microsomes. Elongation, in which a C_{18} substrate FA (usually containing a "front-end" Δ^6-desaturation) is C_2-elongated to yield the C_{20} PUFA, comprises the activities of four distinct and sequential enzymes, namely, condensation (of malonyl-CoA and the PUFA acyl-CoA), β-ketoreduction, dehydration, and enoyl-reduction (21). Additional rounds of elongation then occur to synthesize C_{22} and C_{24} LC-PUFA. In contrast to microsomal desaturation, microsomal elongation requires acyl-CoA substrates. A number of open reading frames (ORF) from LC-PUFA-synthesizing organisms such as *Caenorhrabditis elegans* and *Mortierella alpina* were identified as elongating activities by "gain-of-function" (i.e., acquisition of the ability to elongate C_{18} PUFA) in yeast (33,34). These nematode and fungal ORF showed homology to the yeast ELO genes, which are required for the synthesis of saturated very long chain (VLC) FA found in sphingolipids. Although the ELO-like genes are assumed to be condensing enzymes, this remains to be demonstrated unequivocally (23). Perhaps one of the more surprising observations in the identification of the ELO-like PUFA-elongating activities was that the expression of these single ORF was still able to reconstitute a PUFA-specific elongase; there was no requirement for the co-expression of any other (heterologous) components of the elongase. The identification of PUFA-specific elongating activities as members of the ELO-like gene family capable of reconstituting LC-PUFA elongation in yeast has facilitated the rapid cloning and functional characterization of LC-PUFA elongating activities from a number of species including mammals, fungi, and aquatic algae (27). For recent reviews on the identification and phylogenetics of the ELO gene family see Leonard *et al.* (23).

All the primary biosynthetic enzymes required for LC-PUFA synthesis have been identified and functionally characterized from a wide range of organisms (27). These include the cytochrome b_5 fusion desaturases of the so-called conventional pathway (see Fig. 1), in which the first committed step is the Δ^6-desaturation of LA or ALA to yield γ-linolenic acid (18:3n-6; GLA) and stearidonic acid (18:4n-3; STA), respectively. These Δ^6-desaturated FA are then elongated by a specific elongating activity to yield di-homo-γ-linolenic acid (20:3n-6; DHGLA) and eicosatetraenoic acid (20:4n-3; ETetA), respectively, with these products then undergoing Δ^5-desaturation to generate arachidonic acid (20:4n-6; ARA) and EPA. Importantly (especially from a human nutrition perspective), mammals have no capacity to convert n-6 FA to n-3 forms, whereas many lower organisms contain ω3-desaturases capable of performing this reaction (21). Recently, we and others have focused on the so-called alternative pathway for the synthesis of ARA and EPA, which has been described in a number of microorganisms. This biosynthetic pathway utilizes the same substrates (LA and/or ALA) but instead commences with the C_2-elongation of these FA, mediated by a specific C_{18} Δ^9-elongating activity (27). This reaction yields eicosadienoic acid (20:2n-6; EDA) and eicosatrienoic acid (20:3n-3; ETriA), which then undergo Δ^8-desaturation to yield DHGLA and ETetA. These two products are then Δ^5-desaturated as for the conventional pathway. Although the alternative Δ^9-elongase/Δ^8-desaturase pathway differs in the order of reactions, the enzymes mediating this process are closely related (in terms of sequence similarity) to those of the conventional pathway.

Recently, the genes encoding the biosynthetic enzymes required for the synthesis of DHA from EPA have additionally been identified. Previously, it was considered that the synthesis of DHA occurred *via* two C_2-elongation reactions, Δ^6-desaturation and peroxisomal β-oxidation (the so-called Sprecher shunt) (23). This somewhat complicated biosynthetic route appears to be prevalent in mammals, but a simpler system has been identified in a number of DHA-synthesizing algal species. In these aquatic microbes, DHA is synthesized by the specific Δ^5-elongation of EPA (to yield docosapentaenoic acid, 22:5n-3), which is then Δ^4-desaturated to yield DHA. Several Δ^4-desaturases have recently been isolated and functionally characterized (14,27), and very recently, the Δ^5-elongating activity has been identified (35,36). Again, the desaturase and elongating activity required

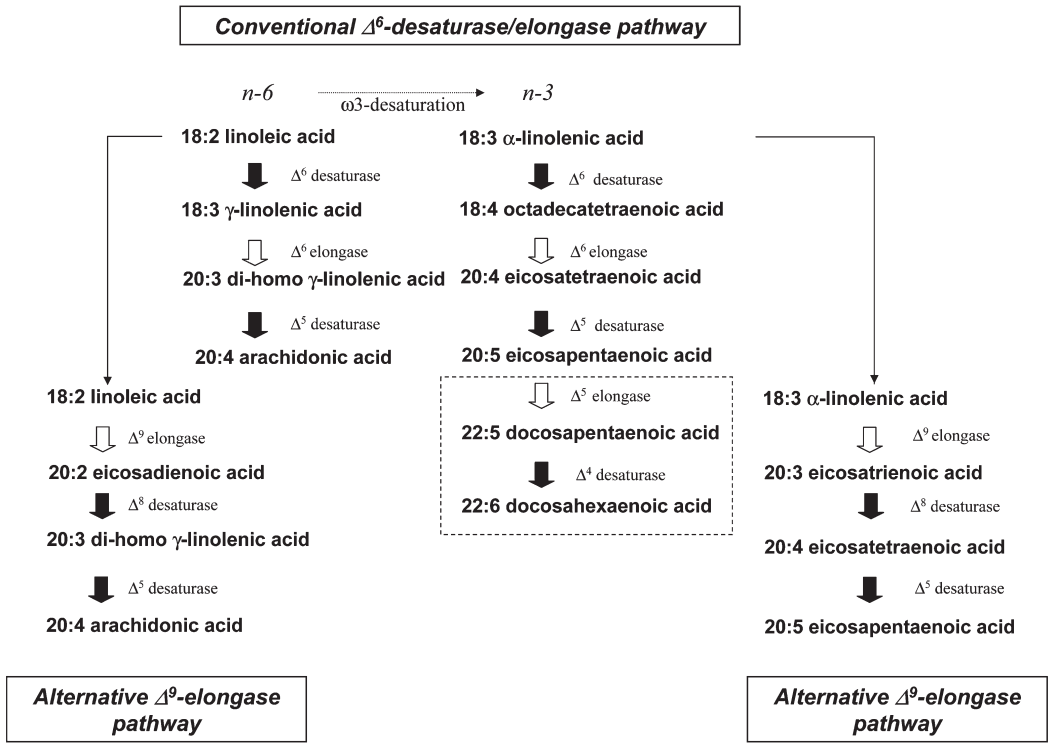

FIG. 1. Generalized representation of long-chain PUFA (LC-PUFA) biosynthesis. The conventional Δ^6-desaturase/elongase pathway for the synthesis of arachidonic acid and eicosapentaenoic acid from the EFA linoleic and α-linolenic acids is shown, as is the alternative Δ^9-elongase route. The Δ^5-elongase/Δ^4-desaturase route for docosahexaenoic acid synthesis is also indicated (boxed), as is the potential role of ω3-desaturation in the conversion of n-6 substrates to n-3 forms. The "substrate dichotomy" of PUFA biosynthesis is represented *via* solid arrows for glycerolipid-linked reactions and open arrows for acyl-CoA reactions.

for DHA synthesis are closely related to the ORF required for the synthesis of ARA and EPA, and as such likely to indicate a common ancestry.

In conclusion, all the primary biosynthetic components required for the synthesis of the C_{20} PUFA ARA and EPA, as well as the C_{22} PUFA DHA have now been identified. All these components can be categorized as either cytochrome b_5-fusion "front-end" desaturases or ELO-like elongating activities.

THE SUCCESSFUL SYNTHESIS OF LC-PUFA IN TRANSGENIC PLANTS

As described in the previous section, there is considerable need to identify an alternative source of LC-PUFA to replace the decreasing marine fish stocks and serve human nutritional requirements. Over the last 20 years, the advent of plant genetic engineering has opened new opportunities for genetic approaches to crop improvement. One major target for such projects has been the nutritional enhancement of plants, in particular the lipids and FA found in oilseeds (29,37). Although there are many examples of genetically engineered plants with so-called input traits (i.e., herbicide tolerance, insecticidal properties, etc.), there are far fewer for output traits such as nutritional enhancement (38). This is perhaps unfortunate, since the consumer benefits of herbicide tolerance are less obvious than (for example) the production of health-promoting FA, especially when the general public remains skeptical of the use of genetic modification (GM). Several reports have now been published regarding improving the vitamin E content of plants (38,39), and the feasibility of manipulating endogenous plant FA composition has previously been demonstrated (37). Importantly, two studies on the production of LC-PUFA have recently confirmed the possibility of making these products in transgenic plants, although each utilized distinct strategies toward the efficient reconstitution of the process.

The first study utilized the alternative pathway, after the serendipitous isolation of a C_{18} Δ^9-elongase from the marine alga *Isochrysis galbana*, an organism not previously described as utilizing the alternative LC-PUFA biosynthetic route (40). The second reaction in the alternative pathway, the C_{20} Δ^8-desaturase, had been isolated from the freshwater alga *Euglena gracilis* (41). The identification of the *Isochrysis* C_{18} Δ^9-elongating activity provided an opportunity to assess the function of a heterologous PUFA elongase in transgenic plants, since appropriate substrates for the elongase would be present (i.e., LA and ALA CoA esters). Expression of the *Isochrysis* C_{18} Δ^9-elongase in transgenic *Arabidopsis* under the control of the constitutive CaMV 35S promoter resulted in the synthesis of EDA and ETriA, with their accumulation

to significant levels (~15% of total FA) in all vegetative tissues (42). These data demonstrated the efficient reconstitution of an LC-PUFA elongase in transgenic plants, and confirmed the feasibility of engineering transgenic plants to accumulate C_{20} FA. In particular, it was clear that although C_{20} di- and trienoic FA accumulated to relatively high levels, this did not result in any disruption to normal plant form or function (42). This was in contrast to previous studies on the constitutive expression of the *Arabidopsis* FAE1 gene, a condensing enzyme responsible for the synthesis of $C_{20–22}$ monounsaturated FA in seed lipids, which resulted in profound disruptions to plant morphology when levels of >10% C_{20} + monounsaturates were present in vegetative tissue (43). A more detailed analysis of the distribution of EDA and ETriA in transgenic *Arabidopsis* expressing the *Isochrysis* Δ^9-elongase has revealed a number of insights into the channeling of FA into different lipid classes (44). For example, the levels of EDA vs. ETriA vary among different tissues, and do not necessarily reflect the ratios of the elongase substrates (LA and ALA). Moreover, the accumulation (and ratio) of the two novel FA differs dramatically for different lipid species. For example, n-3 ETriA was particularly abundant in the plastidial galactolipid DGDG, accumulating to almost 30% of the total FA at the *sn*-1 position. Conversely, n-6 EDA was the predominant C_{20} FA in phospholipids, and accumulated to ~20% of total FA present at the *sn*-2 position of either PC or PA (44). It might be possible to explain some of the galactolipid ETriA levels *via* the activity of the plastidial ω3-desaturases FAD7 and FAD8 (assuming they can utilize C_{20} substrates). However, it is also likely that lipids containing novel C_{20} FA are incorporated into DAG *via* the microsomal Kennedy pathway, and then incorporated in galactolipids *via* the action of plastidial MGDG and DGDG synthases. It is of interest that high levels of EDA were detected at the *sn*-2 position of PC, consistent with the reacylation of elongated LA. Such a process would be central to efficient reconstitution of C_{20} LC-PUFA biosynthesis, since front-end desaturation usually occurs on glycerolipid-linked substrates, in contrast to the cytosolic acyl-CoA-dependent elongation reaction (45).

The observation that the *Isochrysis* Δ^9-elongase was capable of directing the synthesis of significant levels of EDA and EtriA prompted us to attempt to fully reconstitute the alternative LC-PUFA biosynthetic pathway for ARA and EPA (see Fig. 1). We therefore coexpressed the *Isochrysis* Δ^9-elongase with the *Euglena* Δ^8 desaturase and the *M. alpina* Δ^5-desaturase; each transgene was under the control of the same constitutive 35S promoter, and the different constructs were introduced into *Arabidopsis* by sequential transformation using different selectable markers (42). The resulting transgenic plants were morphologically indistinguishable from wild type *Arabidopsis*, although analysis of their FA compositions revealed the presence of several C_{20} LC-PUFA including ARA and EPA. These two LC-PUFA accumulated in leaf tissues of transgenic *Arabidopsis* plants to a combined level of ~10% total FA, the majority being ARA (n-6); again, this does not reflect the levels of n-6/n-3 substrates, which are predominantly ALA (n-3). As well as the accumulation of ARA and EPA, additional C_{20} PUFA identified in the transgenic *Arabidopsis* were sciadonic acid ($20{:}3\Delta^{5,11,14}$) and juniperonic acid ($20{:}4\Delta^{5,11,14,17}$) (42). These two nonmethylene-interrupted PUFA are likely to have resulted from the "promiscuous" activity of the Δ^5-desaturase, acting on substrates that might usually be expected to undergo Δ^8-desaturation. Whether this represents some form of perturbation to substrate channeling for the reconstituted alternative LC-PUFA biosynthetic pathway remains unclear, although both desaturases are assumed to utilize similar substrates (C_{20} acyl chains at the *sn*-2 position of PC). Although sciadonic and juniperonic acids were not primary targets for the synthesis and accumulation in transgenic plants, recent evidence suggests that these VLC-PUFA may also be health-beneficial and play a role in modulating some aspects of human metabolism (46). Importantly, both sciadonic and juniperonic acids are found in a number of species of pine seeds, and as such have been previously consumed by humans without demonstrating any antinutritional effects (46). It is also worth noting that the *M. alpina* Δ^5-desaturase used in the reconstitution of the alternative LC-PUFA biosynthetic pathway was previously observed to utilize unexpected substrates when individually expressed in transgenic canola, resulting in the accumulation of the unusual Δ^5-desaturated C_{18} FA, taxoleic and pinolenic acids (47). This may indicate that the determinants affecting the substrate specificity of this desaturase are not fully understood at present.

The use of the alternative Δ^9-elongase/Δ^8-desaturase to successfully reconstitute LC-PUFA biosynthesis in transgenic plants has been recognized as an important breakthrough in the production of these nutritional compounds in a sustainable manner (48). However, whereas these current data represent an elegant proof-of-concept demonstration in vegetative tissues, it remains to be demonstrated that a similar efficient reconstitution of the alternative LC-PUFA biosynthetic pathway is possible in seeds, with the concomitant accumulation of AA and (more preferably) EPA in TAG.

In that respect, the complementary studies of Abbadi *et al.* (49) on the expression of the conventional Δ^6-desaturase/elongase pathway have provided greater insights into LC-PUFA synthesis when specifically heterologously expressed in the developing seeds of transgenic oilseeds. Using genes encoding enzyme activities from a number of different LC-PUFA-accumulating species, transgenic linseed and tobacco lines were engineered to express the three primary components of the conventional pathway, the Δ^6-desaturase, the Δ^6-elongase, and the Δ^5-desaturase (49). In contrast to the study previously described (42), in which components of the alternative pathway were constitutively expressed, these three activities were placed under the transcriptional regulation of a seed-specific promoter. Additionally, these three heterologous genes were introduced into the transgenic plant as a single integration event, rather than *via* sequential transformation. Analysis of homozygous T3 seeds of transgenic tobacco and linseed revealed very high levels of Δ^6-desaturated FA yet only relatively low amounts of ARA and EPA (49). These

data clearly demonstrated the seed-specific reconstitution of the conventional LC-PUFA biosynthetic pathway in transgenic oilseeds; they also paralleled earlier observations in yeast on the efficient synthesis of C_{20} PUFA (33,45). These previous studies had revealed a potential "bottleneck" at the elongation step in the pathway that had been ascribed to the inefficient acyl-exchange between the glycerolipid and acyl-CoA pools (45). Further detailed analysis of transgenic linseed expressing these activities revealed a number of subtle observations (49). First, although the Δ^6-desaturase and the Δ^6-elongase appeared to function at very different efficiencies (as measured by the accumulation of their products), the two transgenes were transcribed at similar levels (as determined by Q-PCR). Second, *in vitro* elongation assays carried out on microsomal fractions isolated from these transgenic developing linseed seeds clearly demonstrated the activity of the heterologous Δ^6-elongase when supplied with exogenous acyl-CoA substrates. Third, although high levels of Δ^6-desaturated FA accumulated in the microsomal membranes, particularly at the *sn*-2 position of PC, this was not reflected in a concomitant increase in the Δ^6-desaturated acyl-CoAs (49). Although it is obvious that a lack of Δ^6-desaturated FA in the acyl-CoA pool will prevent the Δ^6-elongase from functioning efficiently, it is less clear why these substrates remain in the microsomal membrane lipids; this may reflect an inefficient exchange from PC into the acyl-CoA pool (a process essential for the heterologous reconstitution of LC-PUFA biosynthesis) (50). A further subtlety was identified on analysis of the FA composition of TAG from these transgenic seeds, which revealed the presence of high levels of the n-3 Δ^6-desaturated FA STA, compared with the distribution of this FA in other lipid classes such as PC, PE, and DAG. In contrast, although the n-6 Δ^6-desaturated FA GLA was abundant in PC, STA was present at a very much lower level, even though the relevant substrates (LA, ALA) were present at similar levels (49). The authors then carried out very sophisticated positional analysis of TAG to determine the precise distribution of these novel FA, and found STA predominantly at the *sn*-3 position, whereas GLA was found at both the *sn*-2 and *sn*-3 positions. These data allowed the authors to consider a number of possibilities regarding the channeling of FA into different lipid classes. The absence of Δ^6-desaturated FA in the acyl-CoA pool could reflect a number of scenarios including (i) inefficient exchange between the CoA and PC pools; (ii) rapid channeling into lipids of any Δ^6-desaturated acyl-CoA such that their presence is not detected; and (iii) channeling into lipids *via* an acyl-CoA-independent process, such as the enzyme phospholipid:DAG acyltransferase (PDAT) (49,50). In that respect, it seems most likely that the n-3 Δ^6-desaturated FA STA is channeled from PC into TAG by the PDAT enzyme, precluding it from further elongation and desaturation. In addition, it may be that exchange of any Δ^6-desaturated FA (n-3 or n-6) from PC into the acyl-CoA pool is inefficiently catalyzed by the endogenous *lyso*-PC:acyltransferase (LPCAT) enzyme (which would not previously have been adapted to these non-native FA) and so substrate limits the activity of the heterologous LC-PUFA elongase. The combination of (at least) these two channeling activities contributes to the observed low levels of C_{20} LC-PUFA in the transgenic oilseeds (i.e., <10% of the novel C_{18} Δ^6-PUFA, and a skew toward the accumulation of n-6). Taking these observations together, it seems likely that a major constraint on the efficient reconstitution of C_{20} LC-PUFA *via* the conventional Δ^6-desaturase/elongase route is the dichotomy of substrate requirements for glycerolipid desaturation and acyl-CoA elongation (45,49,50). However, the levels of ARA and EPA obtained in the seed lipids of transgenic linseed are still significant, even allowing for the clearly suboptimal exchange and channeling of acyl substrates. Thus, these results should be taken as a highly encouraging pointer toward the future successful seed-specific synthesis of LC-PUFA *via* this pathway.

In addition, the study discussed earlier (49) not only identified potential bottlenecks in the conventional LC-PUFA biosynthetic route, but also highlighted a number of possible solutions. These include the additional coexpression of a LPCAT transgene, ideally from an organism carrying out endogenous LC-PUFA synthesis (49). This would be predicted to mediate the accumulation of Δ^6-desaturated FA in the acyl-CoA pool, facilitating their elongation to C_{20} FA (50). An alternative strategy might be to avoid the use of glycerolipid-

TABLE 1
Comparison of the Two Recent Demonstrations of Long-Chain-PUFA Synthesis in Transgenic Plants

Study	Plant	Pathway	Transgenes	Expression	Insertions	C_{20} PUFA	Comments
Abbadi *et al.*	Linseed (and tobacco)	Conventional Δ^6-desaturase	*Phaeodactylum tricornutum* Δ^6 *P. patens* ELO *P. tricornutum* Δ^5	Seed-specific	Single T-DNA	3.6% Total 0.9% ARA 0.8% EPA	Bottleneck in acyl exchange between PC and CoA pools, with high levels of C_{18} Δ^6-desaturated FA. First demonstration of seed-specific accumulation of C_{20} PUFA in TAG.
Qi *et al.*	*Arabidopsis*	Alternative Δ^9-elongase	*I. galbana* ELO *E. gracilis* Δ^8 *Mortierella alpina* Δ^5	Constitutive (vegetative)	Three unlinked T-DNA	22% Total 6.6% ARA 3.0% EPA	Efficient reconstitution of PUFA biosynthesis, although unexpected products such as sciadonic and juniperonic acids formed. Accumulation in TAG not determined.

dependent desaturases, but instead use microsomal acyl-CoA desaturases such as those found in animals. Thus, the entire LC-PUFA biosynthetic pathway could proceed *via* acyl-CoA intermediates, negating any requirement for acyl exchange during primary biosynthesis. A third approach suggested is the use of the alternative Δ^9-elongase pathway, which (as already discussed) may currently represent the most efficacious route for aerobically synthesizing C_{20} PUFA in transgenic plants (42,44,49).

FUTURE DIRECTIONS AND PROSPECTS

It is clear from the two studies described in this article (and summarized in Table 1) that heterologous reconstitution of C_{20} LC-PUFA synthesis in transgenic plants has now been demonstrated. This has been achieved by the reverse engineering of the primary biosynthetic enzymes, and has yielded significant levels of nutritionally important C_{20} LC-PUFA such as ARA and EPA. Perhaps of equal relevance, these data have indicated that our understanding of the biochemical processes that underpin the synthesis of these FA is still incomplete. In particular, the role of acyl channeling, either in terms of substrate presentation or compartmentalization of lipids, is still an emerging topic. Another consideration arises from the initial rationale for our attempts to synthesize LC-PUFA in transgenic plants, the wish to replace diminishing stocks of fish oils. Although transgenic plants can clearly synthesize and accumulate LC-PUFA, these are a mixture of n-6 and n-3 FA. This is in contrast to the aquatic food web (i.e., algae and the fish that consume these primary producers of LC-PUFA), which is predominantly rich in n-3 FA such as EPA and DHA. From the perspective of human health and nutrition, the n-3 LC-PUFA are beneficial because they have a protective effect in relation to metabolic syndrome and CVD (13,14), whereas n-6 LC-PUFA such as ARA may give rise to pro-inflammatory responses through their metabolism *via* the eicosanoid pathway. In that respect, the channeling of n-3 FA into storage lipids (i.e., TAG) observed in linseed may represent another potential bottleneck in the efficient synthesis of n-3 LC-PUFA (49). However, it may also be that current linseed cultivars were generated by plant breeders who inadvertently selected germplasm containing a highly active n-3-specific PDAT, since a desired trait in linseed was very high ALA in seed TAG. Thus, it remains to be seen if other oilseeds display the same strong channeling of n-3 FA into TAG. Even in the absence of such an activity, it may be desirable to convert any C_{20} LC-PUFA from n-6 to n-3. This reaction could be mediated by the coexpression of ω3-desaturases that recognize C_{20} substrates. Such an enzyme was recently identified from the fungus *Saprolegnia diclina* (51), and may represent a useful tool in the synthesis of n-3 LC-PUFA in transgenic plants. Similarly, the use of primary LC-PUFA biosynthetic enzymes with strong preferences for n-3 substrates, such as the Δ^6-desaturase identified from *Primula* (52), may provide additional skews toward EPA.

The demonstration that EPA can be synthesized in transgenic plants and specifically accumulated in seed TAG is a major step toward providing a sustainable source of LC-PUFA, but an additional goal must also be the production of DHA. In that respect, the very recent identification of the C_{20} Δ^5-elongase (which elongates EPA to 22:5), together with the earlier functional characterization of the C_{22} Δ^4-desaturase, will facilitate the heterologous reconstitution of DHA synthesis (35,36). Initial proof-of-concept experiments have been carried out in yeast and reveal low but significant levels of DHA in strains that have been engineered to contain activities of the conventional LC-PUFA biosynthetic pathway (i.e., the C_{18} Δ^6-elongase, C_{20} Δ^5-desaturase, C_{20} Δ^5-elongase, and the C_{22} Δ^4-desaturase). A very high proportion of the n-3 C_{18} STA supplied to the transgenic yeast was elongated to ETetA, probably due to the high availability of the substrate as an acyl-CoA. Although EPA is efficiently elongated to DPA by the newly identified Δ^5-elongase, and DPA is correctly Δ^4-desaturated to DHA, the resultant levels of DHA are low (~1% of total FA) (35). However, this appears to be due to the very poor conversion of ETetA to EPA by the Δ^5-desaturase. As discussed earlier, the microsomal front-end desaturation reaction that underpins LC-PUFA biosynthesis utilizes substrates at the *sn*-2 position of PC, and the inefficiency of the Δ^5-desaturase may simply reflect the lack of glycerolipid-linked substrate (even though total levels of ETetA are high) (35,45). In that respect, the data on the heterologous reconstitution of the C_{22} LC-PUFA biosynthetic pathway in yeast confirm the observations on the C_{20} pathway in both yeast and transgenic plants, in that the dichotomy of substrates required for elongation and desaturation indicates the need for additional factors (such as acyltransferases) to improve the efficiency of this process (45,49,50). Currently, enzymes such as LPCAT can be invoked as potential mediators of enhanced reconstitution of C_{22} LC-PUFA biosynthesis, although it remains to be determined whether one individual enzyme is responsible for exchange of all LC-PUFA substrates (C_{18}, C_{20}, and C_{22}). Recently, the functional identification of cDNA clones encoding LPCAT activities has been orally reported (Abbadi, A., and Heinz, E., University of Hamburg), so it is anticipated that the answers to these questions will soon be clear. It will also be important to try to generate transgenic plants with the activities required for DHA synthesis, in addition to those for C_{20} LC-PUFA biosynthesis. Since this will require the introduction of two additional genes into the transgenic plant, the approach used by Abbadi *et al.* (49) (in which the three genes for C_{20} LC-PUFA synthesis were all contained within one single T-DNA) is much more amenable to the introduction of further transgenes.

The efficient biosynthesis of C_{20} LC-PUFA in transgenic plants has now been conclusively demonstrated, using two different approaches. Not only do these data clearly indicate the potential to use transgenic plants as an alternative sustainable source of these important FA, but they also provide new insights into our understanding of lipid biochemistry, in particular the channeling of FA into various different lipids. In that respect, the realization that much deeper reverse engi-

neering is required to fully deconstruct, understand, and replicate LC-PUFA biosynthesis is both daunting and, at the same time, fascinating. Moreover, the provision of transgenic plants synthesizing non-native FA provides a unique tool with which to study the intricacies of plant lipid metabolism, not least of all the interchange between the so-called prokaryotic and eukaryotic pools.

ACKNOWLEDGMENTS

Rothamsted Research receives grant-aided support from the Biological Sciences and Biotechnology Research Council (BBSRC) United Kingdom. The authors thank BASF Plant Sciences for financial support.

REFERENCES

1. Go, V.L., Butrum, R.R., and Wong, D.A. (2003) Diet, Nutrition, and Cancer Prevention: The Postgenomic Era, *J. Nutr. 133*, 3830S–3836S.
2. Paoloni-Giacobino, A., Grimble, R., and Pichard, C. (2003) Genetics and Nutrition, *Clin. Nutr. 22*, 429–435.
3. von Schacky, C. (2003) The Role of Omega-3 Fatty Acids in Cardiovascular Disease, *Curr. Atheroscler. Rep. 5*,139–145.
4. GISSI-Prevenzione Investigators (1999) Dietary Supplementation with *n-3* Polyunsaturated Fatty Acids and Vitamin E after Myocardial Infarction: Results of the GISSI-Prevenzione Trial. Gruppo Italiano per lo Studio della Sopravvivenza nell'Infarto Miocardico, *Lancet 354,* 447–455.
5. German, J.B., Roberts, M.A., and Watkins, S.M. (2003) Genomics and Metabolomics as Markers for the Interaction of Diet and Health: Lessons from Lipids, *J. Nutr. 133*, 2078S–2083S.
6. Zhao, Z., Fu, Y.X., Hewett-Emmett, D., and Boerwinkle, E. (2003) Investigating Single Nucleotide Polymorphism (SNP) Density in the Human Genome and Its Implications for Molecular Evolution, *Gene 312*, 207–213.
7. Shastry, B.S. (2002) SNP Alleles in Human Disease and Evolution, *J. Hum. Genet. 47*, 561–566.
8. Burr, G.O., and Burr, M.M. (1929) A New Deficiency Disease Produced by the Rigid Exclusion of Fat from the Diet, *J. Biol. Chem. 82*, 345–367.
9. Burr, G.O. (1981) The Essential Fatty Acids Fifty Years Ago, *Prog. Lipid Res. 20*, xxvii–xxix.
10. Dyerberg, J., Bang, H.O. (1982) A Hypothesis on the Development of Acute Myocardial Infarction in Greenlanders, *Scand. J. Clin. Lab. Invest. Suppl. 161*, 7–13.
11. Bang, H.O., Dyerberg, J., and Hjoorne, N. (1976) The Composition of Food Consumed by Greenland Eskimos, *Acta Med. Scand. 200*, 69–73.
12. Simopoulos, A.P. (2000) Human Requirement for n-3 Polyunsaturated Fatty Acids, *Poult. Sci. 79*, 961–970.
13. Nugent, A.P. (2004) The Metabolic Syndrome, *Nutr. Bull. 29*, 36–43.
14. Graham, I.A., Cirpus, P., Rein, D., and Napier, J.A. (2004) The Use of Very Long Chain Polyunsaturated Fatty Acids to Ameliorate Metabolic Syndrome: Transgenic Plants as an Alternative Sustainable Source to Fish Oils, *Nutr. Bull. 29*, 228–233.
15. Burr, M.L., Fehily, A.M., Gilbert, J.F., Rogers, S., Holliday, R.M., Sweetnam, P.M., Elwood, P.C., and Deadman, N.M. (1989) Effects of Changes in Fat, Fish, and Fibre Intakes on Death and Myocardial Reinfarction: Diet and Reinfarction Trial (DART), *Lancet 2(8666)*, 757–761.
16. Hu, F.B., Manson, J.E., and Willett, W.C. (2001) Types of Dietary Fat and Risk of Coronary Heart Disease: A Critical Review, *J. Am. Coll. Nutr. 20*, 5–19.
17. Simopoulos, A.P. (2002) Omega-3 Fatty Acids in Inflammation and Autoimmune Diseases, *J. Am. Coll. Nutr. 21*, 495–505.
18. Opsahl-Ferstad, H.-G., Rudi, H., Ruyter, B., and Refstie, S. (2003) Biotechnological Approaches to Modify Rapeseed Oil Composition for Applications in Aquaculture, *Plant Sci. 165*, 349–357.
19. Metz, J.G., Roessler, P., Facciotti, D., Levering, C., Dittrich, F., Lassner, M., Valentine, R., Lardizabal, K., Domergue, F., Yamada, A., Yazawa, K., Knauf, V., and Browse, J. (2001) Production of Polyunsaturated Fatty Acids by Polyketide Synthases in Both Prokaryotes and Eukaryotes, *Science 293*, 290–293.
20. Napier, J.A. (2002) Plumbing the Depths of PUFA Biosynthesis: A Novel Polyketide Synthase-like Pathway from Marine Organisms, *Trends Plant Sci. 7*, 51–54.
21. Wallis, J.G., Watts, J.L., and Browse, J. (2002) Polyunsaturated Fatty Acid Synthesis: What Will They Think of Next? *Trends Biochem. Sci. 27*, 467–470.
22. Simopoulos, A.P. (1999) Essential Fatty Acids in Health and Chronic Disease, *Am. J. Clin. Nutr. 70*, 560S–569S.
23. Leonard, A.E., Pereira, S.L., Sprecher, H., and Huang, Y.S. (2004) Elongation of Long-Chain Fatty Acids, *Prog. Lipid Res. 43*, 36–54.
24. Tocher, D.R., and Ghioni, C. (1999) Fatty Acid Metabolism in Marine Fish: Low Activity of Fatty Acyl Δ^5 Desaturation in Gilthead Sea Bream (*Sparus aurata*) Cells, *Lipids 34*, 433–440.
25. Sargent, J.R., and Tacon, A.G. (1999) Development of Farmed Fish: A Nutritionally Necessary Alternative to Meat, *Proc. Nutr. Soc. 58*, 377–383.
26. Abbadi, A., Domergue, F., Meyer, A., Riedel, K., Sperling, P., Zank, T., and Heinz, E. (2001) Transgenic Oilseeds as Sustainable Source of Nutritionally Relevant C_{20} and C_{22} Polyunsaturated Fatty Acids? *Eur. J. Lipid Sci. Technol. 103*, 106–113.
27. Sayanova, O., and Napier, J.A. (2004) Eicosapentaenoic Acid: Biosynthetic Routes and the Potential for Synthesis in Transgenic Plants, *Phytochemistry 65*, 147–158.
28. Napier, J.A. (2004) The Production of Long Chain Polyunsaturated Fatty Acids in Transgenic Plants: A Sustainable Source for Human Health and Nutrition, *Lipid Technol. 16*, 103–107.
29. Thelen, J.J., and Ohlrogge, J.B. (2002) Metabolic Engineering of Fatty Acid Biosynthesis in Plants, *Metab. Eng. 4*, 12–21.
30. Sayanova, O., Smith, M.A., Lapinskas, P., Stobart, A.K., Dobson, G., Christie, W.W., Shewry, P.R., and Napier, J.A. (1997) Expression of a Borage Desaturase cDNA Containing an N-Terminal Cytochrome b_5 Domain Results in the Accumulation of High Levels of Δ^6-Desaturated Fatty Acids in Transgenic Tobacco, *Proc. Natl. Acad. Sci. USA 94*, 4211–4216.
31. Napier, J.A., Michaelson, L.V., and Sayanova, O. (2003) The Role of Cytochrome b_5 Fusion Desaturases in the Synthesis of Polyunsaturated Fatty Acids, *Prostaglandins Leukot. Essent. Fatty Acids 68*, 135–143.
32. Sperling, P., Ternes, P., Zank, T.K., and Heinz, E. (2003) The Evolution of Desaturases, *Prostaglandins Leukot. Essent. Fatty Acids 68*, 73–95.
33. Beaudoin, F., Michaelson, L.V., Hey, S.J., Lewis, M.J., Shewry, P.R., Sayanova, O., and Napier, J.A. (2000) Heterologous Reconstitution in Yeast of the Polyunsaturated Fatty Acid Biosynthetic Pathway, *Proc. Natl. Acad. Sci. USA 97*, 6421–6426.
34. Parker-Barnes, J.M., Das, T., Bobik, E., Leonard, A.E., Thurmond, J.M., Chaung, L.T., Huang, Y.S., and Mukerji, P. (2000) Identification and Characterization of an Enzyme Involved in the Elongation of n-6 and n-3 Polyunsaturated Fatty Acids, *Proc. Natl. Acad. Sci. USA 97*, 8284–8289.
35. Meyer, A., Kirsch, H., Domergue, F., Abbadi, A., Sperling, P., Bauer, J., Cirpus, P., Zank, T.K., Moreau, H., Roscoe, T.J., *et al*. (2004) Novel Fatty Acid Elongases and Their Use for the Reconstitution of Docosahexaenoic Acid Biosynthesis, *J. Lipid Res. 45*, 1899–1909.

36. Pereira, S.L., Leonard, A.E., Huang, Y.S., Chuang, L.T., and Mukerji, P. (2004) Identification of Two Novel Microalgal Enzymes Involved in the Conversion of the Omega 3-Fatty Acid, Eicosapentaenoic Acid (EPA), to Docosahexaenoic Acid (DHA), *Biochem. J. 384*, 357–366.
37. Drexler, H., Spiekermann, P., Meyer, A., Domergue, F., Zank, T., Sperling, P., Abbadi, A., and Heinz, E. (2001) Metabolic Engineering of Fatty Acids for Breeding of New Oilseed Crops: Strategies, Problems and First Results, *J. Plant Physiol. 160*, 779–802.
38. Tucker, G. (2003) Nutritional Enhancement of Plants, *Curr. Opin. Biotechnol. 14*, 221–225.
39. Cahoon, E.B., Hall, S.E., Ripp, K.G., Ganzke, T.S., Hitz, W.D., and Coughlan, S.J. (2003) Metabolic Redesign of Vitamin E Biosynthesis in Plants for Tocotrienol Production and Increased Antioxidant Content, *Nat. Biotechnol. 21*, 1082–1087.
40. Qi, B., Beaudoin, F., Fraser, T., Stobart, A.K., Napier, J.A., and Lazarus, C.M. (2002) Identification of a cDNA Encoding a Novel C_{18}-Δ^9 Polyunsaturated Fatty Acid-Specific Elongating Activity from the Docosahexaenoic Acid (DHA)-Producing Microalga, *Isochrysis galbana*, *FEBS Lett. 510*, 159–165.
41. Wallis, J.G., and Browse, J. (1999) The Δ^8-Desaturase of *Euglena gracilis*: An Alternate Pathway for Synthesis of 20-Carbon Polyunsaturated Fatty Acids, *Arch. Biochem. Biophys. 365*, 307–316.
42. Qi, B., Fraser, T., Mugford, S., Dobson, G., Sayanova, O., Butler, J., Napier, J.A., Stobart, A.K., and Lazarus, C.M. (2004) The Production of Very Long Chain Polyunsaturated Omega-3 and Omega-6 Fatty Acids in Transgenic Plants, *Nat. Biotechnol. 22*, 739–745.
43. Millar, A.A., Wrischer, M., and Kunst, L. (1998) Accumulation of Very-Long-Chain Fatty Acids in Membrane Glycerolipids Is Associated with Dramatic Alterations in Plant Morphology, *Plant Cell 10*, 1889–1902.
44. Fraser, T.C.M., Qi, B., Elhussein, S., Chatrattanakunchai, S., Stobart, A.K., and Lazarus, C.M. (2004) Expression of the Isochrysis C_{18}-Δ^9 Polyunsaturated Fatty Acid Specific Elongase Component Alters *Arabidopsis* Glycerolipid Profiles, *Plant Physiol. 135*, 859–866.
45. Domergue, F., Abbadi, A., Ott, C., Zank, T.K., Zahringer, U., and Heinz, E. (2003) Acyl Carriers Used as Substrates by the Desaturases and Elongases Involved in Very Long-Chain Polyunsaturated Fatty Acids Biosynthesis Reconstituted in Yeast, *J. Biol. Chem. 278*, 35115–35126.
46. Nakane, S., Tanaka, T., Satouchi, K., Kobayashi, Y., Waku, K., and Sugiura, T. (2000) Occurrence of a Novel Cannabimimetic Molecule 2-Sciadonoylglycerol (2-eicosa-5′,11′,14′-trienoylglycerol) in the Umbrella Pine *Sciadopitys verticillata* Seeds, *Biol. Pharm. Bull. 23*, 758–761.
47. Knutzon, D.S., Thurmond, J.M., Huang, Y.S., Chaudhary, S., Bobik, E.G., Jr., Chan, G.M., Kirchner, S.M., and Mukerji, P. (1998) Identification of Δ^5-Desaturase from *Mortierella alpina* by Heterologous Expression in Bakers' Yeast and Canola, *J. Biol. Chem. 273*, 29360–29366.
48. Green, A.G. (2004) From Alpha to Omega-Producing Essential Fatty Acids in Plants, *Nat. Biotechnol. 22*, 680–682.
49. Abbadi, A., Domergue, F., Fahl, A., Ott, C., Bauer, J., Napier, J.A., Welti, R., Cirpus, P., and Heinz, E. (2004) Biosynthesis of Very Long Chain Polyunsaturated Fatty Acids in Transgenic Oilseeds: Constraints on Their Accumulation, *Plant Cell 16,* 2734–2748.
50. Beaudoin, F., and Napier, J.A. (2004) Biosynthesis and Compartmentalisation of Triacyglycerol in Higher Plants, *Topics Curr. Genetics 6*, 267–287.
51. Pereira, S.L., Huang, Y.S., Bobik, E.G., Kinney, A.J., Stecca, K.L., Packer, J.C., and Mukerji, P. (2004) A Novel Omega-3-Fatty Acid Desaturase Involved in the Biosynthesis of Eicosapentaenoic Acid, *Biochem. J. 378*, 665–671.
52. Sayanova, O.V., Beaudoin, F., Michaelson, L.V., Shewry, P.R., and Napier, J.A. (2003) Identification of *Primula* Fatty Acid Δ^6-Desaturases with n-3 Substrate Preferences, *FEBS Lett. 542*, 100–104.

[Received September 8, 2004; accepted October 12, 2004]

Mechanisms of Regulation of Gene Expression by Fatty Acids

Manabu T. Nakamura*, Yewon Cheon, Yue Li, and Takayuki Y. Nara

Department of Food Science and Human Nutrition and Division of Nutritional Sciences, University of Illinois at Urbana-Champaign, Urbana, Illinois 61801

ABSTRACT: Fatty acids (FA) regulate the expression of genes involved in lipid and energy metabolism. In particular, two transcription factors, sterol regulatory element binding protein-1c (SREBP-1c) and peroxisome proliferator activated receptor α (PPARα), have emerged as key mediators of gene regulation by FA. SREBP-1c induces a set of lipogenic enzymes in liver. Polyunsaturated fatty acids (PUFA), but not saturated or monounsaturated FA, suppress the induction of lipogenic genes by inhibiting the expression and processing of SREBP-1c. This unique effect of PUFA suggests that SREBP-1c may regulate the synthesis of unsaturated FA for incorporation into glycerolipids and cholesteryl esters. PPARα plays an essential role in metabolic adaptation to fasting by inducing the genes for mitochondrial and peroxisomal FA oxidation as well as those for ketogenesis in mitochondria. FA released from adipose tissue during fasting are considered as ligands of PPARα. Dietary PUFA, except for 18:2 n-6, are likely to induce FA oxidation enzymes *via* PPARα as a "feed-forward " mechanism. PPARα is also required for regulating the synthesis of highly unsaturated FA, indicating pleiotropic functions of PPARα in the regulation of lipid metabolic pathways. It is yet to be determined whether FA regulate other transcription factors such as liver-X receptor, hepatocyte nuclear factor 4, and carbohydrate response element binding protein.

Paper no. L9544 in *Lipids 39,* 1077–1083 (November 2004).

The mammalian body is capable of adjusting its metabolism in response to a wide variety of nutritional conditions such as starvation and large changes in diet. The regulation of gene expression plays a critical role in this adaptive response, in addition to altering the activity of enzymes in relevant metabolic pathways. Key transcription factors that regulate this adaptive response have been identified in the last decade. These include peroxisome proliferator activated receptors (PPAR) (1,2), sterol regulatory element binding protein (SREBP) (3), and carbohydrate response element binding protein (ChREBP) (4). Importantly, activities of these transcription factors are regulated not only by hormones but also by nutrients and metabolites (5,6). The objective of this article is to provide a brief review of recent developments in research on the transcriptional regulation of lipid metabolism by FA. Broader topics on the transcriptional regulation of energy metabolism, including hormonal regulation and carbohydrate metabolism, have been reviewed previously (7). An in-depth review on the regulation of unsaturated FA metabolism is also available (8).

*To whom correspondence should be addressed at Department of Food Science and Human Nutrition, University of Illinois at Urbana-Champaign, 905 South Goodwin Avenue, Urbana, IL 61801. E-mail: mtnakamu@uiuc.edu

Abbreviations: ChREBP, carbohydrate response element binding protein; coA, coenzyme A; D6D, delta-6 desaturase; HNF4, hepatocyte nuclear factor 4; LXR, liver-X receptor; HUFA, highly unsaturated fatty acid; PPAR, peroxisome proliferator activated receptor; SCD, stearoyl-CoA desaturase; SREBP, sterol regulatory element binding protein.

SREBP-1c REGULATES FA SYNTHESIS

SREBP are transcription factors of the basic helix-loop-helix leucine zipper family. A negatively charged basic helix acts as a DNA binding domain, and another helix with a leucine zipper is required for dimerization. SREBP were first identified as factors that bind sterol regulatory element in the low density lipoprotein receptor promoter (9,10), and independently as a nucleotide E-box binding factor in adipocytes (11). There are three isoforms of SREBP: SREBP-1a, SREBP-1c, and SREBP-2. SREBP-1 and SREBP-2 are transcribed from different genes (10,12). SREBP-1c and SREBP-1a are encoded from the same gene through the use of alternative promoters (13). SREBP-1 is also called adipocyte differentiation and determination factor-1 (11).

SREBP-2 mainly activates the transcription of genes involved in cholesterol synthesis and metabolism, whereas SREBP-1a can activate genes of both FA and cholesterol synthesis (3,14). As shown in Figure 1, SREBP-1c activates many genes involved in FA and glycerolipid synthesis in liver, but it is unable to activate genes for cholesterol metabolism (3). Sterol regulatory element is identified in most of the SREBP-1c responsive genes listed in Figure 1. SREBP-1c is expressed in many tissues, with high expression in liver, adrenal gland, adipose, and brain tissues (13). Though SREBP-1a expression is unaffected, SREBP-1c expression in liver is diminished in fasting and is rapidly increased in refeeding in an insulin-dependent manner (3,15–17). When the SREBP-1c gene is knocked out, the induction of lipogenic genes by refeeding after fasting is largely abolished in liver, demonstrating a critical role of SREBP-1c in the induction of FA and glycerolipid synthesis by refeeding (18).

PUFA SUPPRESS SREBP-1c ACTIVITY

SREBP are synthesized as larger precursor proteins that remain in the endoplasmic reticulum membrane. After proteolytic cleavage, the amino terminal domain migrates to the nucleus and activates target genes (Fig. 2) (14). Refeeding stimulates this proteolytic processing of both SREBP-1c and SREBP-2 but not of SREBP-1a (15,19). In addition, refeed-

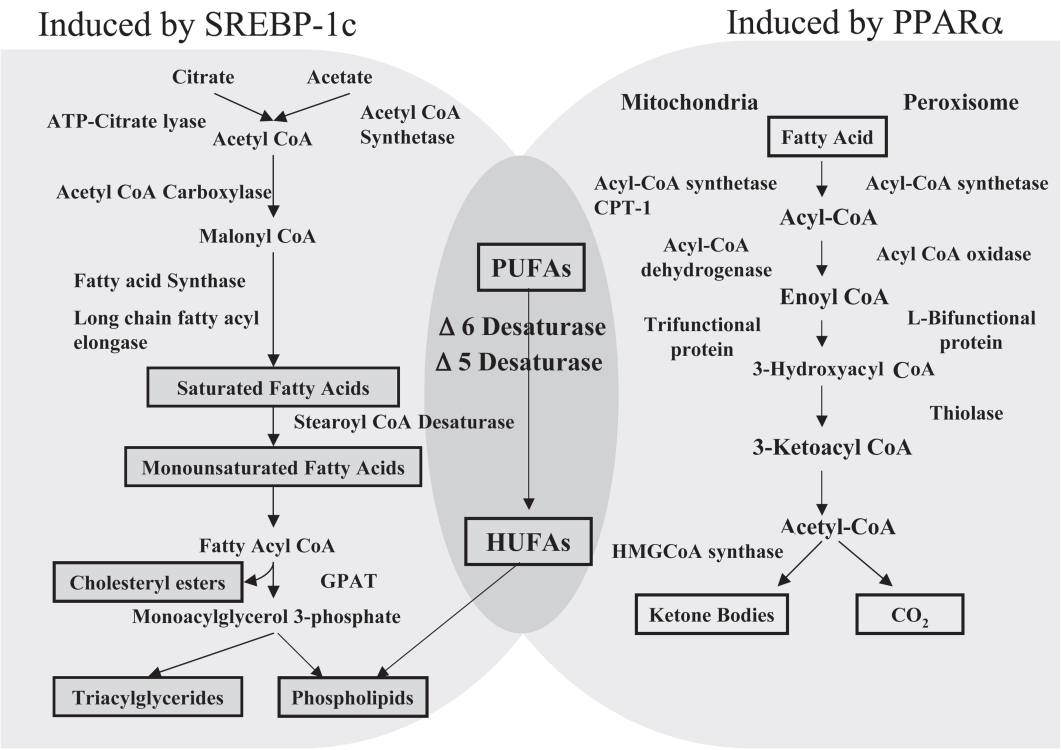

FIG. 1. Genes activated by SREBP-1c and PPARα. Sterol regulatory element binding protein-1c (SREBP-1c) and peroxisome proliferator activated receptor α (PPARα) induce mutually exclusive sets of genes except for all three acyl coenzyme A (CoA) desaturases in mammals. CPT-1, carnitine palmitoyltransferase-1; GPAT, glycerol-3-phosphate acyltransferase; HUFA, highly unsaturated fatty acid; PUFA, polyunsaturated fatty acid.

ing markedly increases expression of SREBP-1c mRNA. The proteolytic activation of SREBP-2 is regulated by cholesterol. SREBP cleavage-activating protein, which is associated with SREBP in the endoplasmic reticulum, has a cholesterol-sensing sequence and initiates SREBP-2 activation when membrane cholesterol is low (20). However, the mechanisms of proteolytic activation and gene expression of SREBP-1c are not well understood.

PUFA at 2% to 3% diet weight suppress the induction of hepatic lipogenic genes caused by refeeding (21). This suppression is exerted at the transcriptional step and is unique to PUFA. Other FA such as saturated and monounsaturated FA do not have such an effect (22,23). Although PUFA responsive regions had been mapped in several gene promoters, the transcription factor that mediates the PUFA suppression proved elusive for some time (22,24–26). Subsequently, SREBP-1c was identified as the factor that binds the PUFA response sequence and mediates the PUFA effect in FA synthase (27), S14 (28) , stearoyl CoA desaturase (SCD) (29,30), and delta-6 desaturase (D6D) (31) genes.

PUFA counteract the activation of SREBP-1c at two regulatory steps: (i) proteolytic processing and (ii) mRNA abundance (Fig. 2) (19,27,28,32,33). Consistent with early observations (21–23), this effect on SREBP-1c is unique to PUFA, as saturated and monounsaturated FA have no effect. The mechanism by which PUFA suppress proteolytic activation of SREBP-1c is not known. In Drosophila, phosphatidylethanolamine, but not cholesterol, inhibits the SREBP processing (34). In rat liver, increased membrane phosphatidylethanolamine resulted in down regulation of three desaturases: D6D, delta-5 desaturase, and SCD (35). Although these desaturases are targets of SREBP-1c, it is yet to be determined whether phosphatidylethanolamine regulates

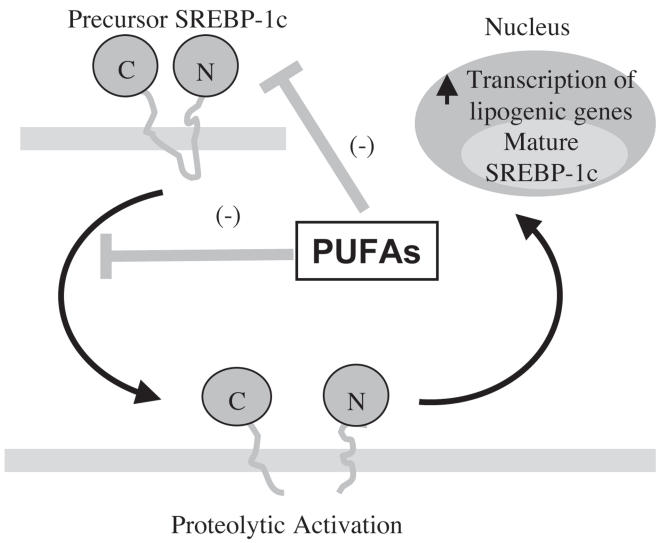

FIG. 2. Regulation of SREBP-1c by PUFA. PUFA suppress proteolytic activation of SREBP-1c. PUFA also reduce precursor SREBP-1c by suppressing expression of SREBP-1c mRNA. For abbreviations, see Figure 1.

SREBP-1c activation in mammalian liver. Additionally, PUFA also suppress SREBP-1c mRNA (Fig. 2) (19,27,28,32, 33). A nuclear run-on assay indicates that PUFA do not suppress transcription of the SREBP-1c gene in rat liver (27). Instead, PUFA accelerate the degradation of SREBP-1c mRNA although the mechanism is not known (36).

Targets of SREBP-1c include all three mammalian desaturases: SCD, D6D, and delta-5 desaturase. The products of SCD, 18:1 n-9 and 16:1 n-7, are incorporated into a wide range of lipids such as phospholipids, triglycerides, and cholesteryl esters. However, the products of D6D and delta-5 desaturase, 20:4 n-6 and 22:6 n-3, are mostly incorporated into phospholipids and not triglycerides (37,38). In addition, one of the target genes of SREBP-1c is cytosine triphosphate: phosphocholine cytidylyltransferase, which is an enzyme specific for phospholipid synthesis (39). Moreover, only PUFA, not long-chain FA in general, can suppress the SREBP-1c activity. Taken together, the profile of SREBP-1c target genes and FA species that exert suppression suggests that the physiological role of SREBP-1c in liver may be the regulation of unsaturated FA synthesis for glycerolipids and cholesteryl esters. If this is the case, induction of lipogenesis by SREBP-1c and its suppression by PUFA may not have a significant role in fat storage from excess dietary glucose.

PPARα REGULATES FA OXIDATION

PPAR are transcription factors of the nuclear receptor family. Transcription factors of this group have a ligand-binding domain and are activated by binding an agonistic ligand. Activated PPAR form a heterodimer with retinoid-X receptor and bind a peroxisome proliferator response element in the promoters of target genes (Fig. 3). There are three isotypes of PPAR: α, β (also called δ), and γ. Long-chain FA and eicosanoids can bind and activate these PPAR isotypes. High expression of PPARα mRNA is observed in organs that utilize FA for energy, such as brown fat, liver, heart, and gastrointestinal mucosa. PPARγ is expressed primarily in adipose tissues and lymphoid tissues, and PPARβ is expressed ubiquitously (1,2).

As shown in Figure 1, PPARα is required for the induction of genes involved in mitochondrial and peroxisomal β-oxidation (40–42). Liver plays a critical role in energy metabolism during fasting, by providing glucose and ketone bodies to other organs. This metabolic adaptation to fasting is largely achieved by the induction of enzymes for gluconeogenesis, FA oxidation, and ketogenesis. PPARα plays a central role in the latter two processes. The essential role of PPARα in adaptation to fasting was demonstrated by a targeted disruption of the gene. PPARα-null mice grew phenotypically normal as long as animals were fed *ad libitum.* However, when the animals were fasted, they showed hypoglycemia, hypoketonemia, hypothermia, and impairment in the induction of FA oxidation and ketogenic enzymes in liver (40,42,43). Some of the PPARα-null mice died after fasting for less than 48 hours (40). These studies demonstrated that PPARα plays a critical role in the transcriptional adaptation of energy metabolism to fasting.

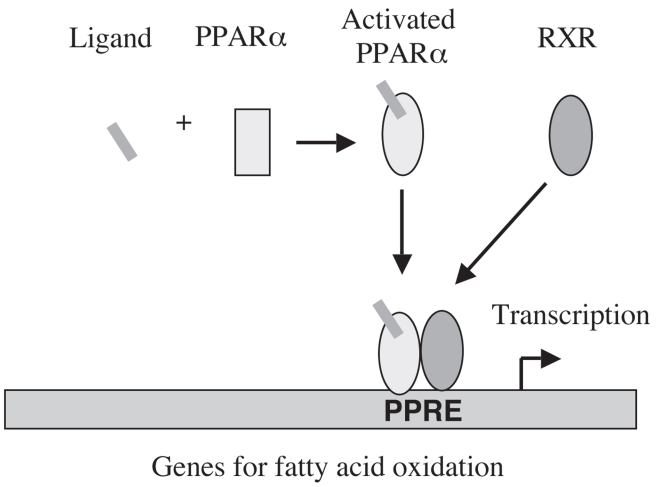

FIG. 3. Activation of PPARα by FA. Long-chain FA are likely endogenous ligands during fasting. Hypolipidemic agents and dietary n-3 HUFA induce peroxisomal β-oxidation genes in a PPARα-dependent manner. PPRE, peroxisome proliferator response element; RXR, retinoid-X receptor; for other abbreviations, see Figure 1.

Various long-chain FA act as ligands of PPARα (44,45). In liver, nonesterified FA are increased during fasting (46). Thus, FA released from adipose tissue are considered to act as endogenous ligands of PPARα during fasting. FA have strong binding affinity to PPARα with reported K_d values in the low nanomolar range (47,48). However, nonesterified FA are present at micromolar levels in liver (46), suggesting that a small pool of free FA at lower concentration works as a regulator of PPARα. A group of hypolipidemic drugs (peroxisome proliferators) such as fibrates also act as potent ligands of PPARα (44,45). PPARα mediates the hypolipidemic effect of such peroxisome proliferators (49).

Although the role of PPARα in the adaptation to fasting is well established in rodents, a physiological role of PPARα in other species including humans is somewhat controversial. This is partly because there is a marked difference between rodents and other species in the response to peroxisome proliferators such as fibrates. These PPARα ligands cause rapid peroxisome proliferation and liver enlargement in rats and mice, and chronic administration leads to liver carcinogenesis. However, other species show neither peroxisome proliferation nor tumor development (2). Furthermore, expression of PPARα in livers from humans, and from other species that do not undergo peroxisome proliferation, is reportedly lower than in livers from rats and mice (50,51). In contrast, other studies show that the pattern of PPARα expression in human tissues is similar to that of rodents; tissues with high FA utilization expressed higher PPARα mRNA (52,53). A recent study has shown that pigs express higher PPARα mRNA in liver than do rats and mice, and that β-oxidation enzymes were induced by both fasting and peroxisome proliferator administration without peroxisome proliferation (54). Consider-

ing all the evidence, it seems likely that PPARα acts as a key inducer of the genes for FA oxidation in nonrodents.

INDUCTION OF β-OXIDATION ENZYMES BY DIETARY PUFA

Dietary fish oil rich in docosahexaenoic acid (22:6 n-3) and eicosapentaenoic acid (20:5 n-3) increases activities and mRNA of FA oxidation enzymes in both mitochondria and peroxisomes (55–57). This induction is mediated by PPARα (58). Because FA with a chain length of 20 carbons or higher are primarily oxidized in peroxisomes, it is likely that excess amounts of 20:5 n-3 and 22:6 n-3 act as PPARα ligands and induce their own degradation pathway as a "feed-forward" mechanism. Other PUFA such as α-linolenic acid (18:3 n-3) (57,59) and γ-linolenic acid (18:3 n-6) (60) have similar effects, whereas linoleic acid (18:2 n-6) does not have a significant effect over saturated fats (55,57). An underlying mechanism for the differential effects among 18 carbon PUFA is yet to be elucidated. A possible mechanism is that 18:3 FA may be readily available for highly unsaturated FA (HUFA) synthesis and may generate more excess HUFA than 18:2 n-6 because 18:3 n-3 and 18:3 n-6 are poor substrates for phospholipid synthesis, whereas 18:2 n-6 is readily incorporated into phospholipids (38,59). Although the induction of FA oxidation by these dietary PUFA could affect energy utilization and fat deposition, the quantitative significance of this is unknown in humans.

Dietary fish oil also decreases plasma triglyceride concentration. The hypotriglyceridemic effect of fish oil does not appear to be due to the PPARα-mediated induction of FA oxidation enzymes (58). Studies with cell models suggest that fish oil may reduce very low density lipoprotein secretion by stimulating the insulin-signaling pathways (61,62).

PPAR-α REGULATION OF HUFA SYNTHESIS

As shown in Figure 1, SREBP-1c and PPARα induce nearly mutually exclusive sets of genes. Paradoxically, synthetic PPARα ligands also strongly induce acyl CoA desaturases (46,63). In addition to sterol regulatory element, a functional peroxisome proliferator response element was identified in promoters of SCD-1 (63) and D6D (64). A recent study has shown that PPARα-null mice were unable to induce D6D mRNA under an essential FA deficient condition (65). Moreover, PPARα target genes such as acyl-CoA oxidase, L-bifunctional protein, and cytochrome P450 4A10 are induced in wild type animals by essential FA deficiency, suggesting that an endogenous PPARα ligand is generated in this condition (65). These findings suggest that PPARα, together with SREBP-1c, acts as a sensor of HUFA status and exerts feedback induction of D6D when HUFA are low.

OTHER TRANSCRIPTION FACTORS

Hepatocyte nuclear factor 4α (HNF4α) is another transcription factor of the nuclear receptor family and is highly expressed in liver. The target DNA sequence of HNF4α is similar to peroxisome proliferator response element, consisting of a direct repeat-1 nucleotide motif. Liver-specific knockout of HNF4α demonstrated the essential nature of this factor for differentiated hepatocyte functions (66). Fatty acyl CoAs have been proposed as ligands that regulate HNF4α activity (67). However, a crystal structure study revealed that a FA molecule was bound tightly to the ligand pocket of HNF4α, and was very difficult to remove (68), suggesting that HNF4α may be constitutively active and that its activity may not be regulated by ligand binding. A recent study has shown that HNF4α binds more than 1000, or about 12%, of genes expressed in the liver and the pancreatic islets (69). These studies suggest that the primary physiological role of HNF4α is to direct tissue-specific gene expression rather than the regulation of metabolic pathways.

Liver-X receptors (LXR) are transcription factors that also belong to the nuclear receptor family. Two isoforms are identified: LXRα is the most abundant in liver, while LXRβ is expressed ubiquitously (70). Cholesterol metabolites known as oxysterols activate LXRs as natural ligands. LXRs activate a group of genes involved in reverse cholesterol transport, including cholesterol/bile acid transporters, and genes involved with bile acid synthesis (70,71). In addition, synthetic LXR agonists induce SREBP-1c, and the LXR response element is identified in the mouse SREBP-1c, promoter (72). A physiological role for this SREBP-1c induction by LXRα in liver may be to provide FA for the synthesis of cholesteryl esters to sequester excess cholesterol, and for phospholipids that are an essential component of bile. In cell studies, PUFA suppress SREBP-1c transcription by antagonizing a synthetic LXR agonist (73,74). However, an *in vivo* study showed that PUFA reduced SREBP-1c mRNA without affecting its transcription rate in rat liver (27). A recent cell study reported that, whereas 20:5 n-3 counteracted the SREBP-1c induction by an LXR agonist, 20:5 n-3 had no effect on the induction of other LXR responsive genes involved with bile acid metabolism (75). Thus, it is unclear whether PUFA suppress LXR activity *in vivo*.

ChREBP is a transcription factor of the basic helix-loop-helix leucine zipper family and is expressed in liver (76) and adipose tissue (77). Protein phosphatase 2A, which is activated by xylulose-5-phosphate (an intermediate of the pentose phosphate cycle), dephosphorylates and activates ChREBP (78). A ChREBP binding sequence, carbohydrate response element, has been identified in the promoters of liver-type pyruvate kinase (79), fatty acid synthase (80), acetyl CoA carboxylase (81), and S14 (79). Adenosine monophosphate-activated kinase is capable of phosphorylating and inactivating ChREBP. Addition of FA to hepatocyte culture medium induces a rapid increase in adenosine monophosphate concentration, leading to the activation of adenosine monophosphate-activated kinase (82). However, it is yet to be determined whether FA suppress ChREBP activity *in vivo*.

ACKNOWLEDGMENTS

This work was supported in part by research grant no. 0330394Z from the American Heart Association.

REFERENCES

1. Lee, C.-H., Olson, P., and Evans, R.M. (2003) Minireview: Lipid Metabolism, Metabolic Diseases, and Peroxisome Proliferator-Activated Receptors, *Endocrinology 144,* 2201–2207.
2. Desvergne, B., and Wahli, W. (1999) Peroxisome Proliferator-Activated Receptors: Nuclear Control of Metabolism, *Endocr. Rev. 20,* 649–688.
3. Horton, J.D., Goldstein, J.L., and Brown, M.S. (2002) SREBPs: Activators of the Complete Program of Cholesterol and Fatty Acid Synthesis in the Liver, *J. Clin. Invest. 109,* 1125–1131.
4. Uyeda, K., Yamashita, H., and Kawaguchi, T. (2002) Carbohydrate Responsive Element-Binding Protein (ChREBP): A Key Regulator of Glucose Metabolism and Fat Storage, *Biochem. Pharmacol. 63,* 2075–2080.
5. Clarke, S.D., and Jump, D.B. (1993) Regulation of Gene Transcription by Polyunsaturated Fatty Acids, *Prog. Lipid Res. 32,* 139–149.
6. Jump, D.B., and Clarke, S.D. (1999) Regulation of Gene Expression by Dietary Fat, *Annu. Rev. Nutr. 19,* 63–90.
7. Nakamura, M.T. (2004) Transcriptional Regulation of Energy Metabolism in Liver, In *Genomics and Proteomics in Nutrition*, Moustaid-Moussa, N., and Berdanier, C.D., editors,, Marcel Dekker, New York, pp. 119–143.
8. Nakamura, M.T., and Nara, T.Y. (2004) Structure, Function, and Dietary Regulation of Delta6, Delta5, and Delta9 Desaturases, *Annu. Rev. Nutr. 24,* 345–376.
9. Briggs, M.R., Yokoyama, C., Wang, X., Brown, M.S., and Goldstein, J.L. (1993) Nuclear Protein that Binds Sterol Regulatory Element of Low Density Lipoprotein Receptor Promoter. I. Identification of the Protein and Delineation of its Target Nucleotide Sequence, *J. Biol. Chem. 268,* 14490–14496.
10. Hua, X., Yokoyama, C., Wu, J., Briggs, M.R., Brown, M.S., Goldstein, J.L., and Wang, X. (1993) SREBP-2, a Second Basic-Helix-Loop-Helix-Leucine Zipper Protein that Stimulates Transcription by Binding to a Sterol Regulatory Element, *Proc. Natl. Acad. Sci. USA 90,* 11603–11607.
11. Tontonoz, P., Kim, J.B., Graves, R.A., and Spiegelman, B.M. (1993) ADD-1: A Novel Helix-Loop-Helix Transcription Factor Associated with Adipocyte Determination and Differentiation, *Mol. Cell Biol. 13,* 4753–4759.
12. Yokoyama, C., Wang, X., Briggs, M.R., Admon, A., Wu, J., Hua, X., Goldstein, J.L., and Brown, M.S. (1993) SREBP-1, a Basic-Helix-Loop-Helix-Leucine Zipper Protein that Controls Transcription of the Low Density Lipoprotein Receptor Gene, *Cell 75,* 187–197.
13. Shimomura, I., Shimano, H., Horton, J.D., Goldstein, J.L., and Brown, M.S. (1997) Differential Expression of Exons 1a and 1c in mRNAs for Sterol Regulatory Element Binding Protein-1 in Human and Mouse Organs and Cultured Cells, *J. Clin. Invest. 99,* 838–845.
14. Brown, M.S., and Goldstein, J.L. (1997) The SREBP Pathway: Regulation of Cholesterol Metabolism by Proteolysis of a Membrane-Bound Transcription Factor, *Cell 89,* 331–340.
15. Horton, J.D., Bashmakov, Y., Shimomura, I., and Shimano, H. (1998) Regulation of Sterol Regulatory Element Binding Proteins in Livers of Fasted and Refed Mice, *Proc. Natl. Acad. Sci. USA 95,* 5987–5992.
16. Shimomura, I., Bashmakov, Y., Ikemoto, S., Horton, J.D., Brown, M.S., and Goldstein, J.L. (1999) Insulin Selectively Increases SREBP-1c mRNA in the Livers of Rats with Streptozotocin-Induced Diabetes, *Proc. Natl. Acad. Sci. USA 96,* 13656–13661.
17. Foretz, M., Pacot, C., Dugail, I., Lemarchand, P., Guichard, C., Le Liepvre, X., Berthelier-Lubrano, C., Spiegelman, B., Kim, J.B., Ferre, P., and Foufelle, F. (1999) ADD1/SREBP-1c is Required in the Activation of Hepatic Lipogenic Gene Expression by Glucose, *Mol. Cell Biol. 19,* 3760–3768.
18. Liang, G., Yang, J., Horton, J.D., Hammer, R.E., Goldstein, J.L., and Brown, M.S. (2002) Diminished Hepatic Response to Fasting/Refeeding and Liver X Receptor Agonists in Mice with Selective Deficiency of Sterol Regulatory Element-Binding Protein-1c, *J. Biol. Chem. 277,* 9520–9528.
19. Xu, J., Cho, H., O'Malley, S., Park, J.H., and Clarke, S.D. (2002) Dietary Polyunsaturated Fats Regulate Rat Liver Sterol Regulatory Element Binding Proteins-1 and -2 in Three Distinct Stages and by Different Mechanisms, *J. Nutr. 132,* 3333–3339.
20. Yang, T., Espenshade, P.J., Wright, M.E., Yabe, D., Gong, Y., Aebersold, R., Goldstein, J.L., and Brown, M.S. (2002) Crucial Step in Cholesterol Homeostasis: Sterols Promote Binding of SCAP to INSIG-1, a Membrane Protein that Facilitates Retention of SREBPs in ER, *Cell 110,* 489–500.
21. Clarke, S.D., Romsos, D.R., and Leveille, G.A. (1976) Specific Inhibition of Hepatic Fatty Acid Synthesis Exerted by Dietary Linoleate and Linolenate in Essential Fatty Acid Adequate Rats, *Lipids 11,* 485–490.
22. Jump, D.B., Clarke, S.D., MacDougald, O., and Thelen, A. (1993) Polyunsaturated Fatty Acids Inhibit S14 Gene Transcription in Rat Liver and Cultured Hepatocytes, *Proc. Natl. Acad. Sci. USA 90,* 8454–8458.
23. Clarke, S.D., and Jump, D.B. (1994) Dietary Polyunsaturated Fatty Acid Regulation of Gene Transcription, *Annu. Rev. Nutr. 14,* 83–98.
24. Soncini, M., Yet, S.-F., Moon, Y., Chun, J.-Y., and Sul, H.S. (1995) Hormonal and Nutritional Control of the Fatty Acid Synthase Promoter in Transgenic Mice, *J. Biol. Chem. 270,* 30339–30343.
25. Fukuda, H., Iritani, N., Katsurada, A., and Noguchi, T. (1996) Insulin/Glucose-, Pyruvate- and Polyunsaturated Fatty Acid-Responsive Region(s) of Rat Fatty Acid Synthase Gene Promoter, *Biochem Mol Biol Int 38,* 987–996.
26. Waters, K.M., Miller, C.W., and Ntambi, J.M. (1997) Localization of a Polyunsaturated Fatty Acid Response Region in Stearoyl-CoA Desaturase Gene 1, *Biochim. Biophys. Acta 1349,* 33–42.
27. Xu, J., Nakamura, M.T., Cho, H.P., and Clarke, S.D. (1999) Sterol Regulatory Element Binding Protein-1 Expression is Suppressed by Dietary Polyunsaturated Fatty Acids: A Mechanism for the Coordinate Suppression of Lipogenic Genes by Polyunsaturated Fats, *J. Biol. Chem. 274,* 23577–23583.
28. Mater, M.K., Thelen, A.P., Pan, D.A., and Jump, D.B. (1999) Sterol Response Element-Binding Protein 1c (SREBP1c) Is Involved in the Polyunsaturated Fatty Acid Suppression of Hepatic S14 Gene Transcription, *J. Biol. Chem. 274,* 32725–32732.
29. Tabor, D.E., Kim, J.B., Spiegelman, B.M., and Edwards, P.A. (1999) Identification of Conserved *cis*-Elements and Transcription Factors Required for Sterol-Regulated Transcription of Stearoyl-CoA Desaturase 1 and 2, *J. Biol. Chem. 274,* 20603–20610.
30. Ntambi, J.M. (1999) Regulation of Stearoyl-CoA Desaturase by Polyunsaturated Fatty Acids and Cholesterol, *J. Lipid Res. 40,* 1549–1558.
31. Nara, T.Y., He, W.S., Tang, C., Clarke, S.D., and Nakamura, M.T. (2002) The E-box like Sterol Regulatory Element Mediates the Suppression of Human Delta-6 Desaturase Gene by Highly Unsaturated Fatty Acids, *Biochem. Biophys. Res. Commun. 296,* 111–117.
32. Kim, H.J., Takahashi, M., and Ezaki, O. (1999) Fish Oil Feeding Decreases Mature Sterol Regulatory Element-Binding Protein 1 (SREBP-1) by Down-Regulation of SREBP-1c mRNA in Mouse Liver. A possible Mechanism for Down-Regulation of Lipogenic Enzyme mRNAs, *J. Biol. Chem. 274,* 25892–25898.
33. Yahagi, N., Shimano, H., Hasty, A.H., Amemiya-Kudo, M., Okazaki, H., Tamura, Y., Iizuka, Y., Shionoiri, F., Ohashi, K., Osuga, J., Harada, K., Gotoda, T., Nagai, R., Ishibashi, S., and

Yamada, N. (1999) A Crucial Role of Sterol Regulatory Element-Binding Protein-1 in the Regulation of Lipogenic Gene Expression by Polyunsaturated Fatty Acids, *J. Biol. Chem. 274,* 35840–35844.
34. Dobrosotskaya, I.Y., Seegmiller, A.C., Brown, M.S., Goldstein, J.L., and Rawson, R.B. (2002) Regulation of SREBP Processing and Membrane Lipid Production by Phospholipids in *Drosophila, Science 296,* 879–883.
35. Shimada, Y., Morita, T., and Sugiyama, K. (2003) Dietary Eritadenine and Ethanolamine Depress Fatty Acid Desaturase Activities by Increasing Liver Microsomal Phosphatidylethanolamine in Rats, *J. Nutr. 133,* 758–765.
36. Xu, J., Teran-Garcia, M., Park, J.H., Nakamura, M.T., and Clarke, S.D. (2001) Polyunsaturated Fatty Acids Suppress Hepatic Sterol Regulatory Element-Binding Protein-1 Expression by Accelerating Transcript Decay, *J. Biol. Chem. 276,* 9800–9807.
37. Nakamura, M.T., Tang, A.B., Villanueva, J., Halsted, C.H., and Phinney, S.D. (1992) Reduced Tissue Arachidonic Acid Concentration with Chronic Ethanol Feeding in Miniature Pigs, *Am. J. Clin. Nutr. 56,* 467–474.
38. Phinney, S.D., Tang, A.B., Thurmond, D.C., Nakamura, M.T., and Stern, J.S. (1993) Abnormal Polyunsaturated Lipid Metabolism in the Obese Zucker Rat, with Partial Metabolic Correction by Gamma-Linolenic Acid Administration, *Metabolism 42,* 1127–1140.
39. Kast, H.R., Nguyen, C.M., Anisfeld, A.M., Ericsson, J., and Edwards, P.A. (2001) CTP:Phosphocholine Cytidylyl Transferase, a New Sterol- and SREBP-Responsive Gene, *J. Lipid Res. 42,* 1266–1272.
40. Leone, T.C., Weinheimer, C.J., and Kelly, D.P. (1999) A Critical Role for the Peroxisome Proliferator-Activated Receptor Alpha (Pparalpha) in the Cellular Fasting Response: The PPARalpha-Null Mouse as a Model of Fatty Acid Oxidation Disorders, *Proc. Natl. Acad. Sci. USA 96,* 7473–7478.
41. Le May, C., Pineau, T., Bigot, K., Kohl, C., Girard, J., and Pegorier, J.P. (2000) Reduced Hepatic Fatty Acid Oxidation in Fasting PPARalpha-Null Mice is due to Impaired Mitochondrial Hydroxymethylglutaryl-CoA Synthase Gene Expression, *FEBS Lett. 475,* 163–166.
42. Hashimoto, T., Cook, W.S., Qi, C., Yeldandi, A.V., Reddy, J.K., and Rao, M.S. (2000) Defect in Peroxisome Proliferator-Activated Receptor Alpha-Inducible Fatty Acid Oxidation Determines the Severity of Hepatic Steatosis in Response to Fasting, *J. Biol. Chem. 275,* 28918–28928.
43. Kersten, S., Seydoux, J., Peters, J.M., Gonzalez, F.J., Desvergne, B., and Wahli, W. (1999) Peroxisome Proliferator-Activated Receptor Alpha Mediates the Adaptive Response to Fasting, *J. Clin. Invest. 103,* 1489–1498.
44. Forman, B.M., Chen, J., and Evans, R.M. (1997) Hypolipidemic Drugs, Polyunsaturated Fatty Acids, and Eicosanoids are Ligands for Peroxisome Proliferator-Activated Receptors Alpha and Delta, *Proc. Natl. Acad. Sci. USA 94,* 4312–4317.
45. Kliewer, S.A., Sundseth, S.S., Jones, S.A., Brown, P.J., Wisely, G.B., Koble, C.S., Devchand, P., Wahli, W., Wilson, T.M., Lenhard, J.M., and Lehmann, J.M. (1997) Fatty Acids and Eicosanoids Regulate Gene Expression Through Direct Interaction with Peroxisome Proliferator-Activated Receptors Alpha and Gamma, *Proc. Natl. Acad. Sci. USA 94,* 4318–4323.
46. He, W.S., Nara, T.Y., and Nakamura, M.T. (2002) Delayed Induction of Delta-6 and Delta-5 Desaturases by a Peroxisome Proliferator, *Biochem. Biophys. Res. Commun. 299,* 832–838.
47. Lin, Q., Ruuska, S.E., Shaw, N.S., Dong, D., and Noy, N. (1999) Ligand Selectivity of the Peroxisome Proliferator-Activated Receptor Alpha, *Biochemistry 38,* 185–190.
48. Cowart, L.A., Wei, S., Hsu, M.-H., Johnson, E.F., Krishna, M.U., Falck, J.R., and Capdevila, J.H. (2002) The CYP4A Isoforms Hydroxylate Epoxyeicosatrienoic Acids to Form High Affinity Peroxisome Proliferator-Activated Receptor Ligands, *J. Biol. Chem. 277,* 35105–35112.
49. Peters, J.M., Hennuyer, N., Staels, B., Fruchart, J.C., Fievet, C., Gonzalez, F.J., and Auwerx, J. (1997) Alterations in Lipoprotein Metabolism in Peroxisome Proliferator-Activated Receptor Alpha-Deficient Mice, *J. Biol. Chem. 272,* 27307–27312.
50. Tugwood, J.D., Holden, P.R., James, N.H., Prince, R.A., and Roberts, R.A. (1998) A Peroxisome Proliferator-Activated Receptor-Alpha (PPARalpha) cDNA Cloned from Guinea-Pig Liver Encodes a Protein with Similar Properties to the Mouse PPARalpha: Implications for Species Differences in Responses to Peroxisome Proliferators, *Arch. Toxicol. 72,* 169–177.
51. Palmer, C.N., Hsu, M.H., Griffin, K.J., Raucy, J.L., and Johnson, E.F. (1998) Peroxisome Proliferator Activated Receptor-Alpha Expression in Human Liver, *Mol. Pharmacol. 53,* 14–22.
52. Mukherjee, R., Jow, L., Noonan, D., and McDonnell, D.P. (1994) Human and Rat Peroxisome Proliferator Activated Receptors (PPARs) Demonstrate Similar Tissue Distribution but Different Responsiveness to PPAR Activators, *J. Steroid Biochem. Mol. Biol. 51,* 157–166.
53. Auboeuf, D., Rieusset, J., Fajas, L., Vallier, P., Frering, V., Riou, J.P., Staels, B., Auwerx, J., Laville, M., and Vidal, H. (1997) Tissue Distribution and Quantification of the Expression of mRNAs of Peroxisome Proliferator-Activated Receptors and Liver X Receptor-Alpha in Humans: No Alteration in Adipose Tissue of Obese and NIDDM Patients, *Diabetes 46,* 1319–1327.
54. Cheon, Y.W., Wallig, M.A., Band, M.R., Beever, J.E., and Nakamura, M.T. (2004) Role of Peroxisome Proliferator Activated Receptor-Alpha in Adaptation to Fasting in a Pig Model (abstract), *FASEB J. 18,* A863.
55. Halminski, M.A., Marsh, J.B., and Harrison, E.H. (1991) Differential Effects of Fish Oil, Safflower Oil and Palm Oil on Fatty Acid Oxidation and Glycerolipid Synthesis in Rat Liver, *J. Nutr. 121,* 1554–1561.
56. Baillie, R.A., Takada, R., Nakamura, M., and Clarke, S.D. (1999) Coordinate Induction of Peroxisomal Acyl-CoA Oxidase and UCP-3 by Dietary Fish Oil: A Mechanism for Decreased Body Fat Deposition, *Prostaglandins Leukot. Essent. Fatty Acids 60,* 351–356.
57. Ide, T., Kobayashi, H., Ashakumary, L., Rouyer, I.A., Takahashi, Y., Aoyama, T., Hashimoto, T., and Mizugaki, M. (2000) Comparative Effects of Perilla and Fish Oils on the Activity and Gene Expression of Fatty Acid Oxidation Enzymes in Rat Liver, *Biochim. Biophys. Acta 1485,* 23–35.
58. Dallongeville, J., Bauge, E., Tailleux, A., Peters, J.M., Gonzalez, F.J., Fruchart, J.C., and Staels, B. (2001) Peroxisome Proliferator-Activated Receptor Alpha is Not Rate-Limiting for the Lipoprotein-Lowering Action of Fish Oil, *J. Biol. Chem. 276,* 4634–4639.
59. Kabir, Y., and Ide, T. (1996) Activity of Hepatic Fatty Acid Oxidation Enzymes in Rats Fed Alpha- Linolenic Acid, *Biochim. Biophys. Acta 1304,* 105–119.
60. Takada, R., Saitoh, M., and Mori, T. (1994) Dietary γ-Linolenic Acid-Enriched Oil Reduces Body Fat Content and Induces Liver Enzyme Activities Relating to Fatty Acid β-Oxidation in Rats, *J. Nutr. 124,* 469–474.
61. Fisher, E.A., Pan, M., Chen, X., Wu, X., Wang, H., Jamil, H., Sparks, J.D., and Williams, K.J. (2001) The Triple Threat to Nascent Apolipoprotein B. Evidence for Multiple, Distinct Degradative Pathways, *J. Biol. Chem. 276,* 27855–27863.
62. Murata, M., Kaji, H., Iida, K., Okimura, Y., and Chihara, K. (2001) Dual Action of Eicosapentaenoic Acid in Hepatoma Cells: Up-Regulation of Metabolic Action of Insulin and Inhibition of Cell Proliferation, *J. Biol. Chem. 276,* 31422–31428.
63. Miller, C.W., and Ntambi, J.M. (1996) Peroxisome Proliferators Induce Mouse Liver Stearoyl-Coa Desaturase 1 Gene Expression, *Proc. Natl. Acad. Sci. USA* 93, 9443–9448.
64. Tang, C., Cho, H.P., Nakamura, M.T., and Clarke, S.D. (2003)

Regulation of Human Delta-6 Desaturase Gene Transcription: Identification of a Functional Direct Repeat-1 Element, *J. Lipid Res. 44,* 686–695.
65. Li, Y., Nara, T.Y., and Nakamura, M.T. (2004) Regulation of Highly Unsaturated Fatty Acid Synthesis: A New Physiological Role of Peroxisome Proliferator-Activated Receptor Alpha (abstract), *FASEB J. 18,* A863.
66. Hayhurst, G.P., Lee, Y.H., Lambert, G., Ward, J.M., and Gonzalez, F.J. (2001) Hepatocyte Nuclear Factor-4alpha (Nuclear Receptor 2A1) is Essential for Maintenance of Hepatic Gene Expression and Lipid Homeostasis, *Mol. Cell Biol. 21,* 1393–1403.
67. Hertz, R., Magenheim, J., Berman, I., and Bar-Tana, J. (1998) Fatty Acyl-CoA Thioesters are Ligands of Hepatic Nuclear Factor-4alpha, *Nature 392,* 512–516.
68. Dhe-Paganon, S., Duda, K., Iwamoto, M., Chi, Y.I., and Shoelson, S.E. (2002) Crystal Structure of the HNF4alpha Ligand Binding Domain in Complex with Endogenous Fatty Acid Ligand, *J. Biol. Chem. 277,* 37973–37976.
69. Odom, D.T., Zizlsperger, N., Gordon, D.B., Bell, G.W., Rinaldi, N. J., Murray, H.L., Volkert, T.L., Schreiber, J., Rolfe, P.A., Gifford, D.K., Fraenkel, E., Bell, G.I., and Young, R.A. (2004) Control of Pancreas and Liver Gene Expression by HNF Transcription Factors, *Science 303,* 1378–1381.
70. Repa, J.J., and Mangelsdorf, D.J. (2002) The Liver X Receptor Gene Team: Potential New Players in Atherosclerosis, *Nat. Med. 8,* 1243–1248.
71. Edwards, P.A., Kast, H.R., and Anisfeld, A.M. (2002) BAREing it All: The Adoption of LXR and FXR and Their Roles in Lipid Homeostasis, *J Lipid Res. 43,* 2–12.
72. Repa, J.J., Liang, G., Ou, J., Bashmakov, Y., Lobaccaro, J.M., Shimomura, I., Shan, B., Brown, M. S., Goldstein, J. L., and Mangelsdorf, D. J. (2000) Regulation of Mouse Sterol Regulatory Element-Binding Protein-1c Gene (SREBP-1c) by Oxysterol Receptors, LXRalpha and LXRbeta, *Genes Dev. 14,* 2819–2830.
73. Ou, J., Tu, H., Shan, B., Luk, A., DeBose-Boyd, R.A., Bashmakov, Y., Goldstein, J.L., and Brown, M.S. (2001) Unsaturated Fatty Acids Inhibit Transcription of the Sterol Regulatory Element-Binding Protein-1c (SREBP-1c) Gene by Antagonizing Ligand- Dependent Activation of the LXR, *Proc. Natl. Acad. Sci. USA 98,* 6027–6032.
74. Yoshikawa, T., Shimano, H., Yahagi, N., Ide, T., Amemiya-Kudo, M., Matsuzaka, T., Nakakuki, M., Tomita, S., Okazaki, H., Tamura, Y., Iizuka, Y., Ohashi, K., Takahashi, A., Sone, H., Osuga Ji, J., Gotoda, T., Ishibashi, S., and Yamada, N. (2002) Polyunsaturated Fatty Acids Suppress Sterol Regulatory Element-Binding Protein 1c Promoter Activity by Inhibition of Liver X Receptor (LXR) Binding to LXR Response Elements, *J. Biol. Chem. 277,* 1705–1711.
75. Pawar, A., Botolin, D., Mangelsdorf, D.J., and Jump, D.B. (2003) The Role of Liver X Receptor-{alpha} in the Fatty Acid Regulation of Hepatic Gene Expression, *J. Biol. Chem. 278,* 40736–40743.
76. Yamashita, H., Takenoshita, M., Sakurai, M., Bruick, R.K., Henzel, W.J., Shillinglaw, W., Arnot, D., and Uyeda, K. (2001) A Glucose-Responsive Transcription Factor that Regulates Carbohydrate Metabolism in the Liver, *Proc. Natl. Acad. Sci. USA 98,* 9116–9121.
77. Letexier, D., Pinteur, C., Large, V., Frering, V., and Beylot, M. (2003) Comparison of the Expression and Activity of the Lipogenic Pathway in Human and Rat Adipose Tissue, *J. Lipid Res. 44,* 2127–2134.
78. Kabashima, T., Kawaguchi, T., Wadzinski, B.E., and Uyeda, K. (2003) Xylulose 5-Phosphate Mediates Glucose-Induced Lipogenesis by Xylulose 5-Phosphate-Activated Protein Phosphatase in Rat Liver, *Proc. Natl. Acad. Sci. USA 100,* 5107–5112.
79. Shih, H.M., and Towle, H.C. (1992) Definition of the Carbohydrate Response Element of the Rat S14 Gene. Evidence for a Common Factor Required for Carbohydrate Regulation of Hepatic Genes, *J. Biol. Chem. 267,* 13222–13228.
80. Rufo, C., Teran-Garcia, M., Nakamura, M.T., Koo, S.H., Towle, H.C., and Clarke, S.D. (2001) Involvement of a Unique Carbohydrate-Responsive Factor in the Glucose Regulation of Rat Liver Fatty-Acid Synthase Gene Transcription, *J. Biol. Chem. 276,* 21969–21975.
81. O'Callaghan, B.L., Koo, S.H., Wu, Y., Freake, H.C., and Towle, H.C. (2001) Glucose Regulation of the Acetyl-CoA Carboxylase Promoter PI in Rat Hepatocytes, *J. Biol. Chem. 276,* 16033–16039.
82. Kawaguchi, T., Osatomi, K., Yamashita, H., Kabashima, T., and Uyeda, K. (2002) Mechanism for Fatty Acid "Sparing" Effect on Glucose-Induced Transcription: Regulation of Carbohydrate-Responsive Element-Binding Protein by AMP-Activated Protein Kinase, *J. Biol. Chem. 277,* 3829–3835.

[Received July 19, 2004; accepted November 15, 2004]

Molecular Characterization of Three Peroxisome Proliferator-Activated Receptors from the Sea Bass (*Dicentrarchus labrax*)

Evridiki Boukouvala[a], Efthimia Antonopoulou[a], Laurence Favre-Krey[a], Amalia Diez[b], José M. Bautista[b], Michael J. Leaver[c], Douglas R. Tocher[c], and Grigorios Krey[a,*]

[a]National Agricultural Research Foundation—Fisheries Research Institute, Nea Peramos, 64007 Kavala, Greece, [b]Departamento de Bioquimica y Biologia Molecular IV, Facultad de Veterinaria, Universidad Complutenses de Madrid, Madrid 28040, Spain, and [c]Institute of Aquaculture, University of Stirling, Stirling FK9 4LA, Scotland

ABSTRACT: Peroxisome proliferator-activated receptors (PPAR) are nuclear hormone receptors that control the expression of genes involved in lipid homeostasis in mammals. We searched for PPAR in sea bass, a marine fish of particular interest to aquaculture, after hypothesizing that the physiological and molecular processes that regulate lipid metabolism in fish are similar to those in mammals. Here, we report the identification of complementary DNA and corresponding genomic sequences that encode three distinct PPAR from sea bass. The sea bass PPAR are the structural homologs of the mammalian PPARα, β/δ, and γ isotypes. As revealed by RNase protection, the tissue expression profile of the fish PPAR appears to be very similar to that of the mammalian PPAR homologs. Thus, PPARα is mainly expressed in the liver, PPARγ in adipose tissue, and PPARβ in all tissues tested, with its highest levels in the liver, where it is also the dominant isotype expressed. Like mammalian PPAR, the sea bass isotypes recognize and bind to PPAR response elements of both mammalian and piscine origin, as heterodimers with the 9-*cis* retinoic acid receptor. Through the coactivator-dependent receptor ligand assay, we also demonstrated that natural FA and synthetic hypolipidemic compounds can act as ligands of the sea bass PPARα and β isotypes. This suggests that the sea bass PPAR act through similar mechanisms and perform the same critical lipid metabolism functions as mammalian PPAR.

Paper no. L9546 in *Lipids 39*, 1085–1092 (November 2004).

In all species, energy homeostasis is achieved through the efficiencies of caloric intake, storage of excess calories, and fuel mobilization. In higher vertebrates under normal conditions, two classes of biological molecules, lipids and carbohydrates, provide essentially all of the necessary fuel. In fish and especially in the carnivorous species, which includes most marine fish, dietary lipids are the major provider of energy while carbohydrates play only a minor role due to their low abundance in natural diets.

Interest in fish FA and lipid metabolism has grown in the last decade as a result of the rapid expansion of intensive aquaculture. As a result, issues relating to physiology [e.g. excess deposition of fat in the carcass and liver of farmed fish (2)] or nutrition [e.g. the substitution of fish oils in fish diets by vegetable oils (3)], have become areas of considerable interest (see review in Ref. 1).

It is generally accepted that the biosynthesis and catabolism of FA involve equivalent pathways in mammals and fish (4). However, it remains to be determined whether the same molecular mechanisms control these pathways. In mammals, peroxisome proliferator-activated receptors (PPAR) have emerged as central factors in sensing FA levels and in regulating FA metabolism. PPAR are ligand-induced transcription factors belonging to the nuclear hormone receptor superfamily. Three PPAR isotypes, termed α, β/δ, and γ, have been identified from different organisms, including mammals, birds, and amphibians. PPAR activate the transcription of target genes by binding as heterodimers with the 9-*cis* retinoic acid receptor (RXR) to specific enhancer elements of the DR-1 (direct repeat of the hexanucleotide sequence 5′-AGCTCA, spaced by one nucleotide) type, known as peroxisome proliferator or PPAR response elements (PPRE). Ligand binding induces conformational changes to the receptor, resulting in both the recruitment of transcriptional coactivators in the promoter region of the target gene and in increased transcription. Specific ligands for each PPAR isotype have been identified and include a number of unsaturated FA, eicosanoids, and hypolipidemic and antidiabetic agents (5,6).

In contrast to the large amount of information available on mammalian PPAR, reports for PPAR in fish are scarce and, thus far, limited to the identification of the PPARγ isotype in two species (7,8). The presence of even a single PPAR isotype in lower vertebrates raises intriguing questions for the evolution of the structure and function of these receptors. In addition, the possibility that PPAR in fish fulfill the same functions as in mammals presents possibilities for manipulating FA metabolism in fish by interventions targeted specifically at these key regulatory factors. To begin to address these

*To whom correspondence should be addressed at National Agricultural Research Foundation—Fisheries Research Institute, Nea Peramos, GR-64007 Kavala, GR. E-mail: krey@otenet.gr

Present address of second author: Department of Biology, Laboratory of Physiology, Aristotelio University of Thessaloniki, GR-54124 Thessaloniki, GR

Abbreviations: bp, base pair; CARLA, coactivator-dependent receptor ligand assay; DR-1, direct repeat of the hexanucleotide sequence 5′-AGCTCA, spaced by one nucleotide; EMSA, electrophoretic mobility assay; GST, glutathione-*S* tranferase; nt., nucleotide(s); LBD, ligand binding domain; PPAR, peroxisome proliferator-activated receptors; PPRE, PPAR response elements; RACE, rapid amplification of cDNA ends; RT, reverse transcription; RXR, retinoic acid receptor; SRC-1, steroid receptor coactivator-1.

possibilities, we searched for PPAR in the sea bass (*Dicentrarchus labrax*), a species of particular interest to aquaculture. We report here the isolation of cDNA (the Genbank accession numbers of cDNA sequences reported here are AY590300 for sea bass PPARα, AY590302 for sea bass PPARβ, and AY590303 for sea bass PPARγ) and genes encoding three PPAR isotypes from this species. We also provide a preliminary account of the functions of these receptors.

EXPERIMENTAL PROCEDURES

PPAR gene isolation. Sea bass genomic DNA was prepared from muscle tissue with the DNeasy tissue kit (Quiagen, GmbH, Hilden, Germany) according to the manufacturer's instructions. PPAR genomic clones were isolated by direct PCR amplification of the DNA using isotype-specific primers. A partial genomic PPARα clone was obtained with primers 5′-CCA AAA GAA GAA CCG CAA CAA G and 5′-TTG CAG GAG CGG GTG CAA CGA CG. A PPARβ partial clone was obtained with primers 5′-ATG GAA GGG TTT CAA CAA ACT G and 5′-CTA ATA CAT GTC TTT GTA GAT CTC CTG. For PPARγ, primer pairs 5′-GTC GAC ATG GTG GAC AC and 5′-TGT AAT CCA TGT TCG TCA GG were used to amplify the genomic sequences encoding for the A/B domain; primers 5′-TTC AAT CAA GAT GGA GCC and 5′-TCA CAG GCA TGG ACG CC were used to amplify the exon encoding the first Zn finger of the C domain; and primers 5′-GCT GCA AGG GTT TCT TCA G-3′ and 5′-CGT TGT GTG ACA TGC CG-3′ were used to amplify the genomic sequences encoding the second Zn finger of the receptor's C domain. In all of the PCR reactions, high fidelity polymerase (Expand High Fidelity PCR system; Roche Applied Science, Mannheim, Germany) was used to minimize errors in the amplified products.

PPAR cDNA isolation. Total sea bass liver RNA was reverse transcribed with Expand Reverse Transcriptase (Roche). The resulting cDNA was used as a template for RACE PCR for the amplification of the 5′-ends of the receptors, with primers derived from partial genomic sequences. Either the SMART RACE kit (Clonetech) or the 5′/3′ RACE kit (Roche) was used in these experiments. The gene-specific primers 5′-GCC ACC TCT TTC TCC ACC A and 5′-CGG CCC TCT TCT TGG TCA T for PPARα and β, respectively, were used. Isolation of the entire coding sequences of the PPAR isotypes was done with RT-PCR (Expand Reverse Transcriptase; Roche) on total liver RNA with primers 5′-ACG CGG GTG GTA TTT ATC TTC T and 5′-TCA GTA CAT GTC CCT GTA GAT TTC TTG C for PPARa; 5′-ATG GAA GGG TTT CAA CAA ACT G and 5′-CTA ATA CAT GTC TTT GTA GAT CTC CTG for PPARβ; and 5′-GTC GAC ATG GTG GAC AC and 5′-CTA ATA CAA GTC TTT CAT GAT CTC for PPARγ (initiation and termination codons underlined). All cDNA were cloned into the pCR Script vector (Stratagene, La Jolla, CA) for further analyses.

Riboprobes and RNase protection assay. For the synthesis of sea bass PPAR isotype-specific riboprobes, the fragment encoding the D domain of each isotype was amplified by PCR. For PPARα, primers 5′-TTG GAT CCG CCA TTC GGT TTG GTC and 5′-AGA ATT CCT TGC TTG TCT TTC C were used to amplify a 197 base pair (bp) fragment [nucleotides (nt.) 554–751 of cDNA)]. For PPARβ, primers 5′-TTG GAT CCG CGA TCC GAT ACG GAC and 5′-AGA ATT CGA TGC TGC GGG CCC T were used to amplify a 175 bp fragment (nt. 631–806 of cDNA). For PPARγ, primers 5′ TTG GAT CCG CTA TTC GTT TTG and 5′-AGA ATT CCG CGT TAT CTC CGG T were used to amplify a 201 bp fragment (nt. 598–799 of cDNA). For directional cloning into the pBluescript KS vector (Stratagene), all upstream primers contained a *Bam*HI restriction enzyme site and all downstream primers an *Eco*RI site (underlined in the preceding primer sequences). A 203 bp β-actin fragment (nt. 228–431 of Genbank accession number AY148350) was amplified by reverse transcription (RT)-PCR from sea bream liver total RNA, with primers 5′-GAC CAA CTG GGA TGA CAT GG and 5′-GCA TAC AGG GAC AGC ACA GC and was cloned into the pCR Script vector (Stratagene).

Antisense PPAR riboprobes were synthesized by T3 RNA polymerase (Promega, Madison, WI) transcription on the *Bam*HI-digested plasmids. The β-actin plasmid construct was digested with *Not*I and the antisense riboprobe was synthesized by T7 RNA polymerase (Promega) transcription.

Total RNA from sea bass tissues, eggs, and larvae was extracted with the RNeasy tissue kit (Qiagen) according to the manufacturer's instructions. Intestine refers to the gut region adjacent to the cecum. Adipose is mesenteral adipose.

Sea bass PPAR mRNA expression was assessed by the RNase protection assay using a commercial kit (RNase protection kit; Roche), according to the manufacturer's instructions. All riboprobes were labeled with [α-^{32}P]CTP (800 Ci/mmol; Amersham Biosciences Europe GmbH, Freiburg, Germany) and their specific activity was quantified as described in the manual of the RNase protection kit. For PPAR expression, 8 μg of total RNA from each tissue sample were hybridized with the isotype-specific probes (approximately 3 fmol of each) before being subjected to digestion by RNases. For β-actin expression, 5 μg of total RNA were used with approximately 80,000 cpm of the riboprobe. The protected fragments were separated on a 6% polyacrylamide gel containing 7 M urea. Signals were visualized by autoradiography.

Electrophoretic mobility shift assay. Sea bass and mouse retinoic acid receptor (RXR)β (mRXRβ, 9) PPAR proteins were obtained by *in vitro* transcription and translation using the TNT coupled reticulocyte lysate system (Promega). Electrophoretic mobility assay (EMSA) was performed as previously described (9). The acyl-CoA oxidase and Cyp4A6-Z PPRE have been previously described (10). The GSTA1.1-3 probes correspond to the presumed PPRE elements of the plaice GSTA1 promoter (11). Specifically, these are between nucleotide positions 3713 and 3734 (GSTA1.1), 3718 and 3740 (GSTA1.2), and 3771 and 3793 (GSTA1.3) of Genbank accession number X95199. For antibody-induced supershifts, 2 μL of PPARγ antibody or pre-immune serum were intro-

duced to the reaction mix simultaneously with the proteins and probe.

Coactivator-dependent receptor ligand assay (CARLA) screen. The sequences encoding the D and E domains of the sea bass PPAR (nt. positions 504–1510 and 631–1533 of the cDNA for α and β isotypes, respectively) were amplified by PCR and cloned into the pGEX-2TK vector (Amersham Biosciences Europe GmbH) for high expression as glutathione-*S* transferase (GST) fusion proteins in *Escherichia coli* (BL21-pLysS; Stratagene). The correct sequence of all recombinant constructs was confirmed by sequencing. Recombinant proteins were purified and the CARLA screen was performed as previously described (12). The concentration of all compounds tested was 10^{-4} M. All compounds were obtained from Cayman Chemical (SPI-BIO; Massy, France), except for Wy14,643 (pirinixic acid) and CLA, mixed isomers (Sigma Aldrich, St. Louis, MO). Signals were quantified either by phosphor analysis (Molecular Imager FX system; Bio-Rad Laboratories, Richmond, CA) or image analysis (Gel-Pro, Media Cybernetics, Silver Springs, MD). Statistical analysis of data (ANOVA) was done using the STATGRAPHICS*Plus*, version 5, package (Manugistics, Inc., North Reading, MA).

RESULTS

Genomic sequences and cDNA encoding three distinct PPAR from sea bass. Using primers designed from sequences conserved in PPAR from other phyla, as well as from other fish species (7), PCR was performed on sea bass DNA. With this approach, distinct genomic fragments were isolated and, upon sequence analysis, revealed regions with significant homology to known PPAR. Specifically, the genomic regions amplified included all of the coding exons of the presumed PPARβ gene and the exons encoding the carboxy terminus, that is, part of the C domain and the D and E domains of the presumed PPARα receptor were amplified (Fig. 1). For the PPARγ gene, we were successful in amplifying only two individual exons, namely, those encoding the A/B domain and the second Zn finger of the C domain of the receptor. Notable is the small size of the introns in both the PPARβ gene and in the characterized portion of the PPARα gene. Therefore, these two sea bass genes are several times smaller than their mammalian counterparts. Interestingly, the proposed gene structures suggest that the E domain of the fish receptors is encoded by three exons. This is in contrast to mammalian or amphibian PPAR, where this domain is encoded by only two exons (13,14). Also of interest is that, with the exception of the additional exon in the E domain, all exon/intron boundaries in the characterized regions of the sea bass PPAR genes are in essentially identical positions in the mammalian genes (Fig. 2).

To confirm that the isolated genomic fragments constitute parts of functional genes, we performed 5′ RACE and RT-PCR

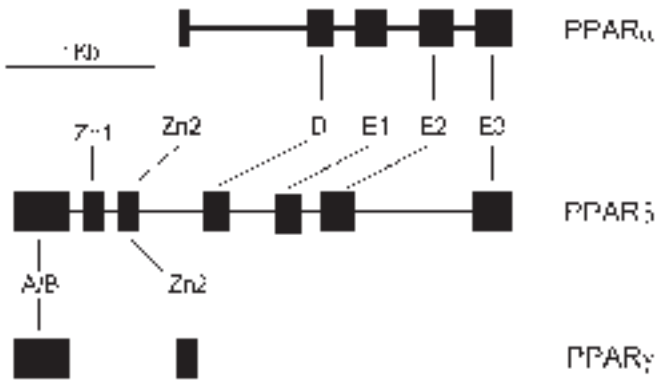

FIG. 1. Schematic representation of the sequenced portions of the peroxisome proliferator-activated receptor (PPAR) genes. Equivalent exons between isotypes are indicated by lines. Zn1 and Zn2 are the exons of the DNA-binding domain and E1–E3 are the exons of the ligand-binding domain.

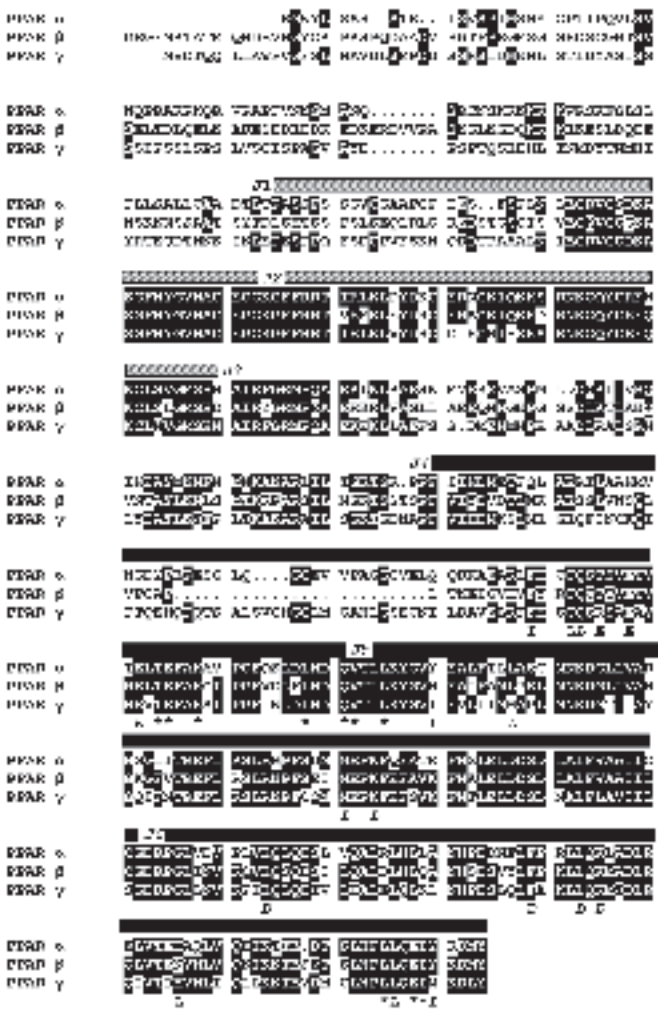

FIG. 2. Amino acid sequence alignment of the three sea bass PPAR isotypes. Identical residues between the three sequences are shaded. The DNA- and ligand-binding domains are indicated by gray and black bars, respectively. *J1–J6* indicate positions of corresponding introns (see Fig. 1). Italicized letters below a sequence indicate corresponding residues involved in ligand binding (*L*), ligand entry (*E*), and dimerization (*D*) in mammalian PPAR (20). Similarly, asterisks indicate residues involved in PPAR–SRC-1 (steroid receptor coactivator-1) interactions. See Figure 1 for abbreviation.

on sea bass liver-derived cDNA, using PPAR isotype-specific primers that were designed according to the distinct genomic sequences. These experiments resulted in the isolation of three cDNA, each encoding a distinct PPAR isotype. The cDNA corresponding to the PPARβ and γ isotypes apparently contained the entire coding sequence and, in the case of PPARβ, the 5′ untranslated region. For PPARα, none of the 5′ RACE products that we analyzed contained the complete 5′-end sequence, as no translation initiation codon conforming to the Kozak consensus could be located within the sequences obtained. Therefore, the cDNA for the sea bass PPARα must be considered partial.

The deduced amino acid sequences of the sea bass PPAR are shown in Figure 2. The encoded proteins have a length of 510 and 522 amino acids for the β and γ isotypes, respectively, while the obtained open reading frame for PPARα encodes a protein of 502 residues. The alignment in Figure 2 also demonstrates that the highest identity between isotypes is observed within the C and E domains.

When the sea bass PPAR proteins are compared to their human counterparts (Fig. 3), the region of highest identity is the C domain, where ≥90% of the residues are common among the corresponding homologs. Identity is lower at the E domain, where 67, 78, and 66% of the residues are common in the α, β, and γ isotypes, respectively. It should be noted that this reduced identity results in part from the insertion of 20 and 25 amino acid residues at the amino terminus of the domain in the sea bass α and γ isotypes, respectively. This insertion may be related to the fact that the E domain of the sea bass receptors is encoded by three exons, as opposed to two exons for the corresponding region in the human receptors. However, it is notable that the sea bass PPARβ E domain, which is also encoded by three exons, contains exactly the same number of residues as its human counterpart.

The region with the lowest identity between the sea bass and human receptors is the A/B domain, which is considerably longer in the isotypes of the fish species than in mammals.

Sea bass PPAR are differentially expressed in tissues and during development. The expression of PPAR in different tissues of sea bass was determined by the RNase protection assay. As the results in Figure 4A demonstrate, relatively abundant transcripts of PPARα are detected in liver, gills, heart, red muscle, and brain. The highest expression, relative to the other two subtypes, was observed in red muscle. PPARα is weakly expressed in intestine and spleen, while no expression is detected in either kidney or adipose tissue. In general, the tissue expression profile of this isotype is very similar to its mammalian counterpart in tissues with high β-oxidation capacity (15). Also, like its mammalian homolog, PPARβ is expressed in all the tissues of sea bass that were tested, with the liver being the site where mRNA for this receptor is most abundant. Like the α isotype, PPARγ exhibits a restricted tissue distribution and, like its mammalian homolog, is most abundantly expressed in adipose tissue. Relatively high amounts of PPARγ transcripts are also detected in the gills and lower amounts in red muscle and the intestine. Only trace amounts of PPARγ are detected in the liver. Notable is the absence of expression of this isotype in spleen and kidney, two tissues known to express PPARγ in mammals and amphibians (16,17).

PPAR expression is differentially regulated during development in both mammals and amphibians (18,19). Therefore, we also examined the expression of these receptors at stages considered critical during the development of sea bass. These included the fertilized egg (mostly, the neurula stage in our sample), the day following the first feeding (day 6, post-hatch), and different stages leading to metamorphosis (day 50 post-hatch).

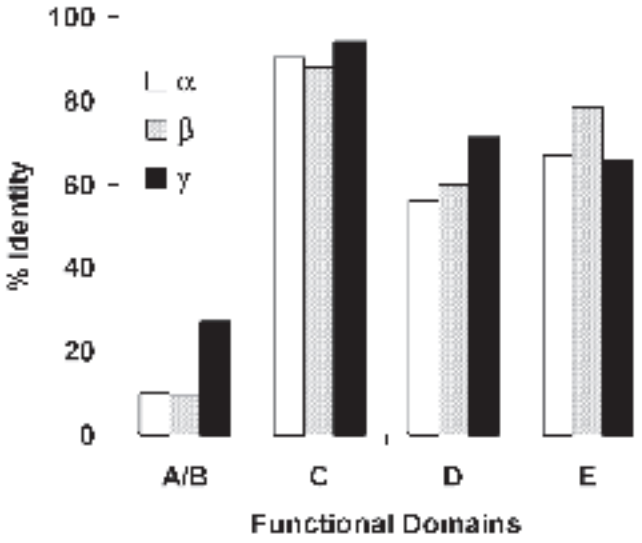

FIG. 3. Amino acid sequence identity between the functional domains of the sea bass and human PPAR isotypes. Open, gray, and black bars correspond to the α, β, and γ isotypes, respectively. For the C domain, only the residues in the two Zn fingers and the carboxy-terminal extension are compared. See Figure 1 for abbreviation.

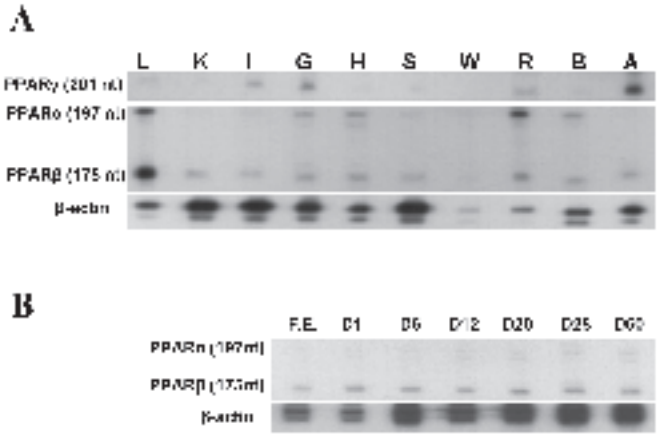

FIG. 4. Tissue and developmental stage expression of the sea bass PPAR. (A) Expression of PPAR and β-actin in the liver (L), kidney (K), intestine (I), gills (G), heart (H), spleen (S), white muscle (W), red muscle (M), brain (B), and adipose tissue (A) of sea bass, as determined by RNase protection. The length in nucleotides (nt) of the corresponding riboprobe for each PPAR isotype is indicated. (B) Expression of the sea bass PPARα and β isotypes during development. F.E. is fertilized egg and D indicates the number of days post-hatch of the larvae tested. See Figure 1 for abbreviation.

As demonstrated in Figure 4B, PPARβ transcripts were detectable in fertilized eggs and persisted at an approximately constant level in all the larval stages that we examined. The early expression of this receptor is in agreement with observations made in *Xenopus* sp. (16,18) and also in mammals (19).

Also like the expression in other species, sea bass PPARα zygotic transcripts appeared to accumulate at later embryonic stages as compared to PPARβ. Thus, PPARα mRNA was detected in one day post-hatch larvae, albeit at low levels, and in all subsequent larval stages (Fig. 4B).

With the approach used, we were not able to detect PPARγ transcripts in any of the larval stages examined. However, it should be noted that these experiments were performed in whole larvae and it is possible that PPARγ transcripts, which in the adult fish exhibit the most restricted tissue distribution (Fig. 4), have been discriminated against.

The sea bass PPAR bind to DR-1 elements. As previously mentioned (Fig. 3), the DNA binding domains of the three sea bass PPAR exhibit high levels of identity with their homologs from other species. Furthermore, residues shown to contribute to the PPAR:RXR dimerization interface in the human PPARγ (20) are apparently conserved in the sea bass receptors. Thus, it is expected that the sea bass PPAR also form heterodimers with RXR and that the sea bass PPRE are also of the DR-1 type. To test this, we performed EMSA with *in vitro* translated sea bass PPAR and mRXRβ. As probes, we used the well-characterized mammalian PPRE of the acyl-CoA oxidase and Cyp4A6 promoter (Cyp4A6-Z) (13), as well as potential PPRE derived from the promoter of the plaice GSTA1 gene, a piscine gene previously shown to be positively regulated by peroxisome proliferators (11). The sequences of these PPRE are shown in Figure 5A. In contrast to the sea bass PPARα, which lacks a proper initiation codon, both the β and γ isotypes were efficiently translated *in vitro* (not shown) and were used in EMSA. As shown in Figure 5B, both receptors bound efficiently to all the PPRE that were

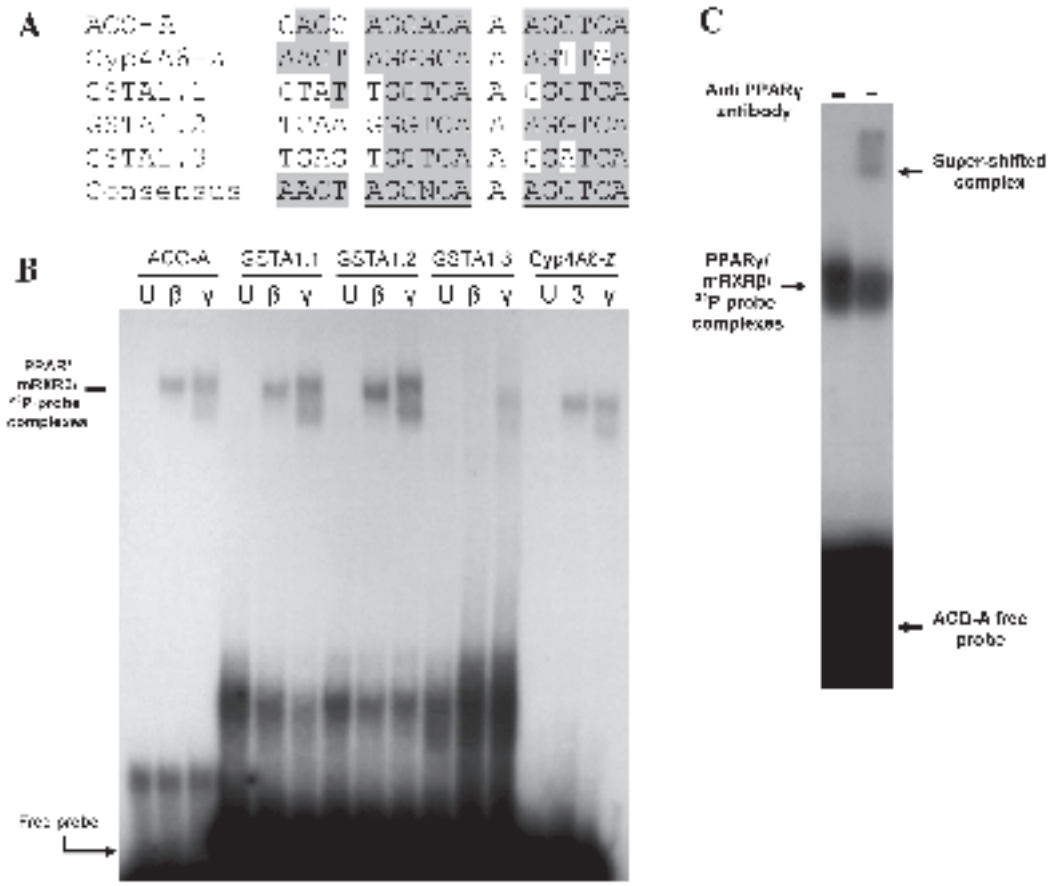

FIG. 5. The sea bass PPAR bind to PPAR response elements (PPRE) as heterodimers with retinoic acid receptors (RXR). (A) The sequences, including the 5′ flanking sequences, of the different PPRE tested. Residues identical to the consensus element, which is a direct repeat of the hexanucleotide sequence 5′-AGCTCA, spaced by one nucleotide (DR-1) (10), are shaded and the hexanucleotide repeats are underlined. (B) Specific complex formation with *in vitro* translated sea bass PPARβ and γ and mRXRβ on the ^{32}P-labeled PPRE indicated. Arrows indicate the position of the specific complexes and of the free probe. U is unprogrammed reticulocyte lysate. (C) The PPARγ/mRXRβ heterodimer on the acyl-CoA oxidase (ACO-A) probe is supershifted with the PPARγ -specific antibody (+) but not with the preimmune serum (–). Cyp46-z, z element in the promoter of the cyp4A6 gene; GST, glutathione-*S* transferase. See Figure 1 for other abbreviation.

tested, with the exception of the GSTA1.3 element. Indeed, the GSTA1.3 element exhibited the least identity with the consensus PPRE sequence (Fig. 5A) and, according to this assay's criteria, it does not constitute a functional DR-1 element. However, a detailed analysis of the plaice GSTA1 promoter is required in order to conclude whether this element is functional or not. The presence of PPAR in the above EMSA complexes was confirmed, in the case of PPARγ, by the use of a marine fish PPARγ-specific antibody (Diez, A., and Bautista, J.M., unpublished data) (Fig. 5C). For the β isotype, competition experiments with specific and nonspecific probes were performed and confirmed that the observed complexes require both the presence of the PPAR protein and the DR-1 element (results not shown).

FA and hypolipidemic drugs are ligands of sea bass PPARα and β. Residues that have been implicated both in ligand binding and in interactions with coactivator proteins in well-characterized PPAR (20,21) appear to also be conserved in the sea bass PPAR (Fig. 2). Therefore, we applied the CARLA screen, an assay based on the ligand-induced interactions of the receptor's ligand-binding domain (LBD) with coactivators (12), to determine whether the sea bass PPAR share common ligands with their mammalian and amphibian counterparts.

Sea bass PPARα and β LBD were expressed in *E. coli*, as GST fusions and the CARLA screen were performed with these two proteins, immobilized on glutathione-sepharose beads, ^{35}S-radiolabeled human steroid receptor coactivator-1 (SRC-1), and a variety of natural and synthetic compounds (22). As shown in Figure 6, statistically significant SRC-1 interactions with either the PPARα or β LBD were observed with the FA linoleic, linolenic, and CLA. Regarding CLA, all three isomers tested, in addition to a mixture of isomers, acted as ligands of PPARβ, while only the 10E, 12Z and 9E, and 11E isomers in addition to the mixed isomers, promoted interactions of the PPARα LBD with SRC-1. Similarly, the arachidonic acid analog eicosatetraynoic acid (ETA), a known ligand of both PPARα and β from other species (12,23,24), also interacted with the two sea bass isotypes. As is the case in other species (12,23,24), the hypolipidemic drug pirinixic acid (Wy-14,643) was able to interact only with the sea bass PPARα.

Neither of the FA phytanic, EPA, or DHA, nor the prostaglandin J_2 metabolite 15d-$\Delta^{12,14}$-PGJ_2, a well characterized mammalian PPARγ-specific ligand (25), were efficient in promoting LBD–SRC-1 interactions. Thus, from these results and at least for the compounds tested, the sea bass α and β PPAR isotypes appear to share the ligand binding properties of their mammalian and amphibian homologs.

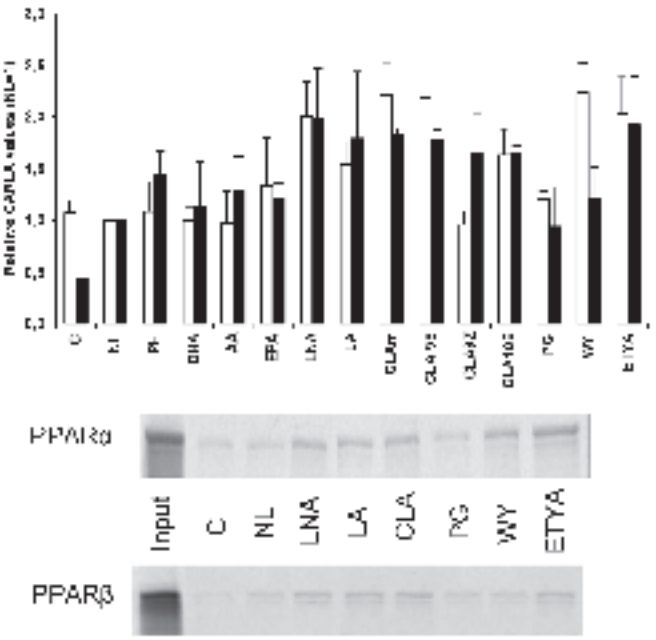

FIG. 6. Coactivator-dependent receptor ligand assay (CARLA) screen for the identification of ligands for the PPARα and β isotypes of sea bass. Upper panel: quantification of interactions (averages, with SD, of at least three independent experiments) of the PPARα (empty bars) and PPARβ (black bars) ligand binding domains (LBD) with SRC-1. A relative CARLA value of 1 is the amount of SRC-1 retained by the glutathione-*S* tranferase (GST)-PPAR LBD in the absence of ligand (NL). The compounds tested were: phytanic acid (PH); DHA; arachidonic acid (AA); eicosapentaenoic acid (EPA); linolenic acid (LNA); linoleic acid (LA); mixed isomers of CLA (CLAm); the 9*E*,11*E* (CLA9*E*), 9*Z*,11*E* (CLA9*Z*), and 10*E*,12*Z* (CLA10*E*) isomers of CLA; 15d-$\Delta^{12,14}$-PGJ_2 (PG); pirinixic acid-Wy-14,643 (WY); and eicosatetraynoic acid (ETYA). C is the control (immobilized GST in the presence of 10^{-4} M CLAm. Statistically significant interactions ($P < 0.05$) of the PPARα LBD with SRC-1 were observed with LNA, LA, CLAm, CLA9*E*, CLA10*E*, WY, and ETYA. The same compounds resulted in significant interactions of the PPARβ LBD with SRC-1 with the addition of CLA9*Z* and the exception of WY. Lower panel: Autoradiogram of ^{35}S-labeled SRC-1 retained by the PPAR LBD in the presence of selected compounds. See Figures 1 and 2 for abbreviations.

The genes of the sea bass PPAR are organized in a manner similar to that of their mammalian homologs in terms of different exons encoding distinct functional regions of the receptors, implying a modular organization of the proteins' domains. Thus, as with other species, the A/B and D domains of the receptors are encoded by individual exons, while two exons—one for each of the Zn fingers—encode the C domain. The main difference in the gene structure between the fish and mammalian receptors lies within the exons coding for the E domain. In the sea bass PPARα and β genes, this domain is encoded by three exons, while in all other known PPAR genes, it is encoded by only two exons (5).

The deduced protein products of the sea bass genes and cDNA show extended amino acid sequence identity with their mammalian homologs, especially at the C and E domains. Regarding the E domain, it is important to note that residues involved in ligand binding, heterodimerization with RXR, and

DISCUSSION

We have isolated genes and cDNA encoding three distinct PPAR from sea bass, and we have provided evidence that these receptors are the structural and functional homologs of the mammalian PPARα, β, and γ.

association with coactivators in the mammalian receptors (20,21) are also present in the sea bass PPAR. However, as a result of sequence insertion in the region corresponding to the additional exon present in the fish genes, both the sea bass PPARα and γ E domains are longer than their mammalian counterparts. Whether this insertion affects the overall structure of the domain, and therefore its function, remains to be determined.

The structure–function relationships between sea bass PPAR and PPAR from other species were assessed by comparing two fundamental properties of these receptors: DNA binding and ligand recognition. The sea bass PPAR recognize and bind to DR-1 elements as heterodimers with RXR. This implies that the sea bass receptors are expected to regulate transcription of piscine genes, which contain this type of elements in their promoter regions (6). Furthermore, sea bass PPAR-mediated transcription must involve similar mechanisms to those operating in mammals since, in terms of transcription complex assembly, we have shown that these receptors are capable of ligand-induced interactions with SRC-1, a mammalian PPAR coactivator (22).

This latter property, as is applied in the CARLA screen, allowed us to demonstrate that the sea bass receptors share common ligands with their mammalian or amphibian counterparts. Thus, both the α and β isotypes selectively associate with FA and hypolipidemic compounds that have been shown to be *bona fide* ligands of PPAR in other species (12,23,24). In addition, we have confirmed that the specificity of the hypolipidemic compound pirinixic acid for PPARα extends to this fish species.

Finally, the results presented herein demonstrate that the sea bass PPAR genes exhibit a tissue expression pattern resembling that observed in other species (17,18). Thus, the sea bass PPARα isotype is mainly expressed in tissues with increased β-oxidation activity, implicating this receptor in the regulation of FA catabolism. Similarly, PPARγ, which as a key factor in adipogenesis in mammals mainly expressed in adipose tissue (26), is also expressed principally in this tissue in sea bass. PPARβ, which has been recently proposed to function as a widespread regulator of fat burning in mammals (27), also exhibits a ubiquitous expression pattern in sea bass tissues. Furthermore, the expression of the β isotype during early development in sea bass suggests its involvement in the mobilization of energy stored in the yolk sac and other critical functions (e.g., differentiation, membrane lipids synthesis and turnover), as these have been proposed for mammals (19).

Although a more detailed analysis is required to fully elucidate the function of the sea bass PPAR, our results provide sufficient evidence that PPAR structure and function evolved before the divergence of the fish, amphibian, and mammalian lines. Thus, the ancestral PPAR gene and the duplication events that led to the appearance of distinct PPAR isotypes are likely to precede the osteicthyan lineage and must be located in the early vertebrates or the provertebrates. Interestingly, partial PPAR gene sequences have been reported from both lamprey (an early vertebrate) and amphioxus (a cephalocord), although no information is available concerning the presence of distinct PPAR isotypes in these organisms (28).

It should also be noted that we have recently isolated and functionally characterized the three PPAR isotypes from additional marine fish species (Boukouvala, E., Leaver, M.J., Antonopoulou, E., Diez, A., Favre-Krey, L., Bautista, J.M., Tocher, D.R., and Krey, G., manuscript in preparation). This will allow us to confirm the observations made with the sea bass PPAR, as far as the gene structure, expression, DNA binding, and transcriptional activation properties are concerned. The availability of these genes and cDNA will provide useful tools for the study of lipid metabolism in fish species.

ACKNOWLEDGMENTS

We thank W. Wahli and M.G. Parker for gifts of plasmids. This work was supported by the European Union (5FP, Project Q5RS-2000-30360).

Competing interests statement

The authors declare that they have no competing financial interests.

REFERENCES

1. Sargent, J.R., Tocher, D.R., and Bell, J.G. (2002) The Lipids, in *Fish Nutrition*, 3rd edn. (Halver, J. E. and Hardy, R.W, eds.), pp. 181–257, Academic Press, San Diego.
2. Hillestad, M., Jonsen, F., Austreng, E., and Asgard, T. (1998) Long Term Effects of Dietary Fat Level and Feeding Rate on Growth, Feed Utilization and Carcass Quality of Atlantic Salmon, *Aquacult. Nutr. 4*, 89–97.
3. Caballero, M.J., Lopez-Calero, G., Socorro, J., Roo, F.J., Izquierdo, M.S., and Fernandez, A.J. (1999) Combined Effect of Lipid Level and Fish Meal Quality on Liver Histology of Gilthead Sea Bream (*Sparus aurata*), *Aquaculture 179*, 277–290.
4. Buzzi, M., Henderson, R.J., and Sargent, J.R. (1996) The Desaturation and Elongation of Linolenic Acid and Eicosapentaenoic Acid by Hepatocytes and Liver Microsomes from Rainbow Trout (*Oncorhynchus mykiss*) Fed Diets Containing Fish Oil or Olive Oil, *Biochim. Biophys. Acta 1299*, 235–244.
5. Desvergne, B., and Wahli, W. (1999) Peroxisome Proliferator-Activated Receptors: Nuclear Control of Metabolism, *Endocr. Rev. 20*, 649–688.
6. Berger, J., and Moller, D.E. (2002) The Mechanisms of Action of PPAR, *Annu. Rev. Med. 53*, 409–435.
7. Leaver, M.J, Wright, J., and George, S.G. (1998) A Peroxisomal Proliferator-Activated Receptor Gene from the Marine Flatfish, the Plaice (*Pleuronectes platessa*), *Mar. Env. Res. 46*, 75–79.
8. Andersen, O., Eijsink, V.G., and Thomassen, M. (2000) Multiple Variants of the Peroxisome Proliferator-Activated Receptor (PPAR) γ are Expressed in the Liver of Atlantic Salmon (*Salmo salar*), *Gene 255*, 411–418.
9. Keller, H., Dreyer, C., Medin, J., Mahfoudi, A., Ozato, K., and Wahli, W. (1993) Fatty Acids and Retinoids Control Lipid Metabolism Through Activation of Peroxisome Proliferator-Activated Receptor-Retinoid X Receptor Heterodimers, *Proc. Natl. Acad. Sci. USA 90*, 2160–2164.
10. Ijpenberg, A., Jeannin, E., Wahli, W., and Desvergne, B. (1997) Polarity and Specific Sequence Requirements of Peroxisome

Proliferator-Activated Receptor (PPAR)/Retinoid X Receptor (RXR) Heterodimer Binding to DNA, *J. Biol. Chem. 274*, 20108–20117.
11. Leaver, M.J., Wright, J., and George, S.G. (1997) Structure and Expression of a Cluster of Glutathione S-Transferase Genes from a Marine Fish, the Plaice (*Pleuronectes platessa*), *Biochem. J. 321*, 405–412.
12. Krey, G., Braissant, O., L'Horset, F., Kalkhoven, E., Perroud, M., Parker, M.G., and Wahli, W. (1997) Fatty Acids, Eicosanoids, and Hypolipidemic Agents Identified as Ligands of Peroxisome Proliferator-Activated Receptors by Coactivator-Dependent Receptor Ligand Assay, *Mol. Endo. 11*, 779–791.
13. Krey, G., Keller, H., Mahfoudi, A., Medin, J., Ozato, K., Dreyer, C., and Wahli, W. (1993) *Xenopus* Peroxisome Proliferator-Activated Receptors: Genomic Organisation, Response Element Recognition, Heterodimer Formation with Retinoid X Receptor and Activation by Fatty Acids, *J. Steroid Biochem. Mol. Biol. 47*, 65–73.
14. Zhu, Y., Qi, C., Korenberg, J.R., Chen, X.N., Noya, D., Rao, M.S., and Reddy, J.K. (1995) Structural Organisation of Mouse Peroxisome Proliferator-Activated Receptor γ, mPPARγ Gene: Alternative Promoter Use and Different Splicing Yield Two mPPAR Isoforms, *Proc. Natl. Acad. Sci. USA 92*, 7921–7925.
15. Braissant, O., Foufelle, F., Scotto, C., Dauça, M., and Wahli, W. (1996) Differential Expression of Peroxisome Proliferator-Activated Receptors, PPAR: Tissue Distribution of PPARα, β, and γ in the Adult Rat, *Endocrinology 137*, 354–366.
16. Dreyer, C., Krey, G., Keller, H., Givel, F., Helftenbein, G., and Wahli, W. (1992) Control of the Peroxisomal β-Oxidation Pathway by a Novel Family of Nuclear Hormone Receptors, *Cell 68*, 879–887.
17. Escher, P., Braissant, O., Basu-Modak, S., Michalik, L., Wahli, W., and Desvergne, B. (2001) Rat PPAR; Quantitative Analysis in Adult Rat Tissues and Regulation in Fasting and Refeeding, *Endocrinology 142*, 4195–4202.
18. Dreyer, C., Keller, H., Mahfoudi, A., Laudet, V., Krey, G., and Wahli, W. (1993) Positive Regulation of the Peroxisomal β-Oxidation Pathway by Fatty Acids Through Activation of Peroxisome Proliferators-Activated Receptors (PPAR), *Biol. Cell 77*, 67–76.
19. Braissant, O., and Wahli, W. (1998) Differential Expression of Peroxisome Proliferator-Activated Receptor-α, -β, and –γ During Rat Embryonic Development, *Endocrinology 139*, 2748–2754.
20. Nolte, R.T., Wisely, G.B., Westin, S., Cobb, J.E., Lambert, M.H., Kurokawa, R., Rosenfeld, M.G., Willson, T.M., Glass, C.K., and Milburn, MV. (1998) Ligand Binding and Coactivator Assembly of the Peroxisome Proliferator-Activated Receptor-γ, *Nature 395*, 137–143.
21. Xu, H.E., Lambert, M.H., Montana, V.G., Plunket, K.D., Moore, L.B., Collins, J.L., Oplinger, J.A., Kliewer, S.A., Gampe Jr, R.T., McKee, D.D., Moore, J.T., and Willson, T.M. (2001) Structural Determinants of Ligand Binding Selectivity Between the Peroxisome Proliferator-activated Receptors, *Proc. Natl. Acad. Sci. USA 98*, 13919–13929.
22. Kalkhoven, E., Valentine, J.E., Heery, D., and Parker, M.G. (1998) Isoforms of Steroid Receptor Coactivator 1 Differ in their Ability to Potentiate Transcription by the Oestrogen Receptor, *EMBO J. 17*, 232–243.
23. Forman, B.M., Chen, J., and Evans, R.M. (1997) Hypolipidemic Drugs, Polyunsaturated Fatty Acids, and Eicosanoids are Ligands for Peroxisome Proliferator-Activated Receptors α and δ, *Proc. Natl. Acad. Sci. USA 94*, 4312–4317.
24. Kliewer, S.A., Sundseth, S.S., Jones, S.A., Brown, P.J., Wisely, G.B., Koble, C.S., Devchand, P., Wahli, W., Willson, T.M., Lenhard, J.M., and Lehmann, J.M. (1997) Fatty Acids and Eicosanoids Regulate Gene Expression Through Direct Interactions with Peroxisome Proliferator-Activated Receptors α and γ, *Proc. Natl. Acad. Sci. USA 94*, 4318–4323.
25. Kliewer, S.A., Lenhard, J.M., Willson, T.M., Patel, I., Morris, D.C., and Lehmann, J.M. (1995) A Prostaglandin J2 Metabolite Binds Peroxisome Proliferator-Activated Receptor γ and Promotes Adipocyte Differentiation, *Cell 83*, 813–819.
26. Tontonoz, P., Hu, E., Graves, R.A., Budavari, A.I., and Spiegelman, B.M. (1994) mPPARγ2: Tissue Specific Regulator of an Adipocyte Enhancer, *Genes Dev. 8*, 1224–1234.
27. Wang Y.X., Lee, C.H., Tiep, S., Yu, R.T., Ham, J., Kang, H., and Evans, R.M. (2003) Peroxisome Proliferator-Activated Receptor δ Activates Fat Metabolism to Prevent Obesity, *Cell 113*, 159–170.
28. Robinson-Rechavi, M., Marchand, O., Escriva, H., Bardet, P.L., Zelus, D., Hughes, S., and Laudet, V. (2001). Euteleost Fish Genomes are Characterised by Expansion of Gene Families, *Genome Res. 11*, 781–788.

[Received July 19, 2004; accepted November 20, 2004]

Functions of Peroxisome Proliferator-Activated Receptors (PPAR) in Skin Homeostasis

Nicolas Di-Poï, Liliane Michalik, Béatrice Desvergne, and Walter Wahli*

Center for Integrative Genomics, NCCR Frontiers in Genetics, University of Lausanne, CH-1015 Lausanne, Switzerland

ABSTRACT: The peroxisome proliferator-activated receptors (PPAR) are ligand-activated transcription factors that belong to the nuclear hormone receptor family. Three isotypes (PPARα, PPARβ or δ, and PPARγ) with distinct tissue distributions and cellular functions have been found in vertebrates. All three PPAR isotypes are expressed in rodent and human skin. They were initially investigated for a possible function in the establishment of the permeability barrier in skin because of their known function in lipid metabolism in other cell types. *In vitro* studies using specific PPAR agonists and *in vivo* gene disruption approaches in mice indeed suggest an important contribution of PPARα in the formation of the epidermal barrier and in sebocyte differentiation. The PPARγ isotype plays a role in stimulating sebocyte development and lipogenesis, but does not appear to contribute to epidermal tissue differentiation. The third isotype, PPARβ, regulates the late stages of sebaceous cell differentiation, and is the most effective isotype in stimulating lipid production in these cells, both in rodents and in humans. In addition, PPARβ activation has pro-differentiating effects in kera-tinocytes under normal and inflammatory conditions. Finally, preliminary studies also point to a potential role of PPAR in hair follicle growth and in melanocyte differentiation. By their diverse biological effects on cell proliferation and differentiation in the skin, PPAR agonists or antagonists may offer interesting oppotunities for the treatment of various skin disorders characterized by inflammation, cell hyperproliferation, and aberrant differentiation.

Paper no. L9545 in *Lipids 39,* 1093–1099 (November 2004).

Peroxisome proliferator-activated receptors (PPAR) belong, together with the receptors for thyroid hormones, retinoids, steroid hormones, and vitamin D, to the nuclear hormone receptor family. They require heterodimerization with the retinoid X receptors (RXR, NR2B) for binding to DNA as ligand-activated transcription factors that regulate the expression of target genes containing peroxisome proliferator response elements (PPRE) in their promoters. The PPAR subfamily consists of three isotypes, which are named PPARα (NR1C1), PPARβ or δ (NR1C2), and PPARγ (NR1C3). Each isoform is characterized by a distinct tissue distribution and specific functions (1). PPARα has a main function in FA catabolism in the liver, and regulates amino acid metabolism, urea synthesis, and inflammatory responses (1,2). PPARγ plays a pivotal role in adipocyte differentiation and then in maintenance of the differentiated state, as well as in lipid storage. Furthermore, like PPARα, it has been implicated in the downregulation of multiple inflammatory processes (1,2). PPARβ is the most ubiquitously expressed isotype, but little is known about its functions, mainly because of the lack, until recently, of selective PPARβ agonists. Nevertheless, recent studies have suggested a role for PPARβ in embryonic development, colon tumorigenesis, skin wound healing, fat catabolism, and oligodendrocyte differentiation (3,4).

Specific roles for PPAR in vertebrate development have emerged from both *in vitro* and *in vivo* models, in particular during the differentiation of adipose tissue, brain, and placenta in mice (5). The importance of PPAR in lipid metabolism in various cell types has led to the investigation of PPAR expression and function during the differentiation of skin, which is a tissue with high rates of FA and cholesterol metabolism largely devoted to the formation of the epidermal permeability barrier. During skin development, several nuclear hormone receptors, including the estrogen, thyroid, androgen, and retinoid receptors, and their respective ligands have been implicated in the ontogeny of the epidermal barrier, hair follicle growth, and skin homeostasis (6,7).

In this review, we will summarize the PPAR functions recently identified in skin homeostasis, including epidermal barrier formation, hair follicle growth, sebocyte differentiation, and melanogenesis.

MAIN FUNCTIONS OF PPARα AND PPARβ IN THE HEALTHY AND INJURED EPIDERMIS

The epidermis is renewed continuously and its integrity is dependent on a tightly regulated balance between cell proliferation, differentiation, and apoptosis. During its maturation, which happens mainly in the latest stages of fetal development, the epidermis evolves from a single layer of epithelial cells (periderm) to a fully stratified and differentiated epithelium (Fig. 1). This process involves the sequential expression of structural proteins (keratins, involucrin, loricrin, and filaggrin) and synthesis of specific lipids (sphingolipids, FFA, and cholesterol). The outermost layer of the epidermis, the stratum corneum, is the end product of keratinocyte differentiation and consists of a layer of cross-linked proteins and lipids,

*To whom correspondence should be addressed at Center for Integrative Genomics (CIG), University of Lausanne, Biology Building, CH-1015 Lausanne, Switzerland. E-mail: walter.wahli@unil.ch

Abbreviations: ADRP, adipose differentiation-related protein; E, embryonic day; FIAF, fasting-induced adipose factor; PPAR, peroxisome proliferator-activated receptor; PPRE, peroxisome proliferator response element; RXR, retinoid X receptor; TNF, tumor necrosis factor; TPA, tetradecanoylphorbol acetate.

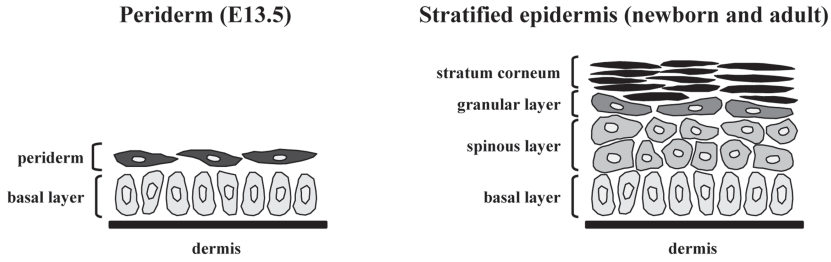

Mouse:	**α, β and γ**	**α, β and γ in newborn, undetectable in adult**
Rat:	**α and β (γ below detection)**	**α and β in newborn, undetectable in adult**
Human:	**nd**	**α, β and γ detected in adult**

FIG. 1. Schematic representation of interfollicular epidermis development. During late fetal development (between embryonic day E13.5 and the end of gestation) in mouse skin, the epidermis changes from a single basal undifferentiated layer (basal layer) covered by a transient superficial layer of cells (periderm), to a fully stratified and differentiated epithelium, with sequential formation of suprabasal layers (spinous and granular layers). The end product of differentiation resides on the surface of the epidermis (stratum corneum) and provides the main permeability barrier of the skin. Expression patterns of PPARα (α), PPARβ (β), and PPARγ (γ) determined or not (nd) during mouse (3) and rat (8,9) epidermal development, and in human adult interfollicular epidermis (10,11), are summarized in the bottom panel.

which functions as a barrier to transepidermal water loss and as a defense against physical damage, microbes, and xenobiotics.

During mouse and rat embryonic development, all three PPAR isotypes, and predominantly PPARβ, have been detected in the interfollicular epidermis from embryonic day 13.5 (E13.5) onward (3,8). Interestingly, PPAR expression is associated with all major events of the fetal maturation of the epidermal barrier. After birth, PPAR gradually disappear from the interfollicular epidermis to become undetectable in the adult animals (Fig. 1) (3,9). In contrast, the three PPAR isotypes are highly expressed in the basal and suprabasal layers of human adult interfollicular epidermis (Fig. 1), with PPARβ being again the predominant subtype (10,11). Consistent with the expression pattern of PPAR in the developing rodent skin, several reports have concentrated on the involvement of PPAR in processes such as cell proliferation, differentiation, and permeability barrier development (see Table 1). A variety of PPARα activators, including clofibrate, were shown to accelerate the morphologic and functional maturation of the epidermal permeability barrier in fetal rat skin both *in vitro* and *in vivo* (12–14). This is evidenced by decreased transepidermal water loss, increased epidermal stratification, and increased expression of the two specific late keratinocyte differentiation markers, loricrin and filaggrin. PPARα ligands also inhibit epidermal proliferation and induce keratinocyte differentiation in adult mouse epidermis *in vivo* (15,16). Furthermore, these activators restore epidermal homeostasis in murine models of hyperproliferative epidermis (17). In contrast, the two PPARγ ligands, troglitazone and prostaglandin J2, did not affect the development of barrier function or epidermal morphology in fetal rat skin (12), and no specific function in skin maturation has been attributed so far to this isotype (Table 1). In favor of a potential role of PPARβ in epidermal differentiation in rodents, the pan PPAR(α/β) activator linoleic acid (18) was shown to accelerate epidermal barrier development in fetal rat skin explants (12). In addition, an important role of PPARβ in mediating keratinocyte differentiation induced by inflammation was demonstrated in mouse primary keratinocytes (19). Importantly, the PPARβ-selective agonist GW1514 stimulated mouse epidermal differentiation without affecting cell proliferation *in vivo*, by inducing the expression of the late differentiation markers filaggrin and loricrin (20). Also, topical treatment of mice with GW1514 accelerates the restoration of permeability barrier functions after disruption by tape stripping, solvent, or detergent treatment (20), in support of the importance of the pro-differentiating effect of PPARβ activation.

Novel information on the role of PPAR in epidermis homeostasis also came from PPAR mutant mouse models. Although normal skin architecture was initially reported in PPARα-knockout mice (5,21), these animals show delayed fetal skin development between E18.5 and birth, with defects in the formation of the stratum corneum (22). Morphologic analysis of adult PPARα-null epidermis revealed a thinned stratum granulosum, with focal parakeratosis, indicative of impaired keratinocyte differentiation (15). Thus, consistent with its expression pattern, PPARα might be important for the maturation of the epidermis during late embryogenesis, but dispensable for normal renewal of the epidermis in the adult animals. Interestingly, PPARα also regulates the early inflammation phase during skin wound healing, as the recruitment of immune cells to the wound site is impaired in PPARα-null mice (3). PPARγ heterozygous mice, or PPARγ-null mice born after placental rescue, show no defect in

TABLE 1
Effects of Peroxisome Proliferator-Activated Receptor Agonists in Various Cell Types of the Skin[a]

Cell types		Rodents	Human
Keratinocytes	α	↗ differentiation *in vitro* (WY; CLO; OA) (12;14;17) and *in vivo* (WY; CLO) (13;15) ↘ proliferation *in vivo* (WY; CLO) (15;17)	↗ differentiation (WY; CLO; OA) (15;30;31) ↗ lipid accumulation (WY) (20;30) ↘ proliferation (WY; CLO) (10;31)
	β	↗ differentiation *in vitro* (LD; LA) (12;19) and *in vivo* (GW) (20) No effect on proliferation *in vivo* (GW) (20)	↗ differentiation (LD; GW; TTA) (10;20) ↗ lipid accumulation (GW) (20) No effect on proliferation (LD) (10)
	γ	No significant effect on differentiation *in vitro* (TRO; PGJ2) (12)	No effect on differentiation (BRL; PGJ2) (10;31) ↘ proliferation (TRO; BRL) (10;33)
Hair follicles and melanocytes	α	nd	↗ survival of cultured hair follicles (CLO) (34) ↘ proliferation and ↗ melanogenesis in melanocytes (WY) (42)
	β	nd	No effect on proliferation and melanogenesis in melanocytes (BEZ) (42)
	γ	nd	↘ proliferation and ↗ melanogenesis in melanocytes (CIG) (42)
Sebocytes	α	↗ differentiation (WY) (36;37;39) No effect on proliferation (WY) (39)	No effect on differentiation (WY) (38)
	β	↗ differentiation (LA; PGI2) (36;37;39) ↗ proliferation (PGI2) (39)	↗ differentiation (LA) (38)
	γ	↗ differentiation (TRO; BRL) (36;37;39) No effect on proliferation (TRO) (39)	No effect on differentiation (CIG) (38)

[a]This table summarizes the stimulatory (↗) or inhibitory (↘) effects of treatment with PPARα (α), PPARβ (β), and PPARγ (γ) agonists on the differentiation and proliferation in various cell types derived from rat and mouse (Rodents) as well as human (Human) skin. These results were obtained in *in vitro* studies, except in rodent keratinocytes where both *in vitro* and *in vivo* experiments were performed. Effects of PPAR ligands on the differentiation of hair follicles and melanocytes in rodents have not been determined (nd). PPAR agonists used in each study are indicated as follows: BEZ, bezafibrate; BRL, BRL-49653; CIG, ciglitazone; CLO, clofibrate; GW, GW1514; LA, linoleic acid; LD, L-165041; OA, oleic acid; PGI2, carbaprostacyclin; PGJ2, 15-deoxy-prostaglandin J2; TRO, troglitazone; TTA, tetradecylthoacetic acid; WY, Wy-14,643.

epidermal maturation (3,23). In addition, PPARγ-null cells are able to participate in the formation of the epidermal tissue in PPARγ-null and wild-type chimeric mice, suggesting very little or no contribution of PPARγ in this process (24). Analysis of PPARβ-mutant skin reveals no defect in fetal and adult epidermal architecture, or in the expression of keratinocyte differentiation markers (3). However, epidermal hyperplasia in response to tetradecanoylphorbol acetate (TPA) treatment was enhanced in PPARβ-mutant animals, emphasizing the role for PPARβ in the control of keratinocyte proliferation and differentiation (3,25). Similarly, the slightly increased keratinocyte proliferation index in PPARβ heterozygous animals is also in favor of the existence of such a control (3). Consistent with these observations, PPARβ expression is rapidly upregulated following challenges that stimulate keratinocyte proliferation, such as hair plucking or cutaneous injury, and skin wound healing is altered in PPARβ-mutant mice (3), largely due to a disrupted balance between proliferation and apoptosis (19,26), as well as to defects in kera-tinocyte adhesion and migration (3,27).

Important roles of PPARα and PPARβ in human keratinocyte differentiation were also reported (see Table 1). As already mentioned, PPARβ is the predominant isotype in these keratinocytes (10,11,28,29). Its expression remains high and unchanged during the differentiation of cultured keratinocytes, or during the stratification and keratinization of the epidermis in *in vitro* reconstructed skin (10,28), whereas it increases upon squamous differentiation in human tracheobronchial epithelial cells (29). PPARα and PPARγ are expressed at lower levels, but their expression increases upon keratinocyte differentiation in similar models (10,28). In human keratinocytes, PPARβ- (L-165041 and GW1514) and PPARα (clofibrate and Wy-14,643)-selective agonists induce the expression of a number of epidermal differentiation markers, including involucrin (10,20,30), whereas PPARγ ligands (BRL-49653 and prostaglandin J2) have no effect (10,31). The hypothesis that PPAR may also affect the metabolism of lipids in keratinocytes is supported by the observation that PPARα ligand Wy-14,643 increased both the synthesis of cer-amides and cholesterol derivatives in a human skin equivalent model (30). Also, the PPARβ selective agonist GW1514 increases TG accumulation and induces the adipose differentiation-related protein (ADRP) and fasting-induced adipose factor (FIAF) expression in human keratinocytes, two proteins that have potential important roles in lipid metabolism (20).

IMPLICATION OF PPAR IN HYPERPROLIFERATIVE SKIN DISEASES

Based on their diverse biological effects on keratinocyte proliferation and differentiation, PPAR ligands may become interesting compounds for the treatment of various epidermal disorders characterized by inflammation, keratinocyte hyperproliferation, and aberrant differentiation, such as psoriasis. In support of an involvement of PPAR in psoriatic epidermis, PPARβ expression was reported to be dramatically increased in the hyperproliferative lesional skin from psoriatic patients (11,28), probably as a response to pro-inflammatory signals in the lesions. It is indeed well established that PPARβ gene

expression is upregulated in mouse skin in response to inflammatory cytokines, such as tumor necrosis factor alpha (TNF-α) (19). In addition, putative PPARβ ligands, such as lipoxygenase products, are generated at high levels in psoriatic skin lesions, and may therefore activate the increased amount of PPARβ (11). The fact that PPARβ is probably naturally highly active in the psoriatic lesions may explain why the PPARβ agonist tetradecylthioacetic acid has no strong antipsoriatic effect when applied topically (32). By contrast to PPARβ expression, no or little change in the cutaneous levels of PPARα and PPARγ was observed in lesional psoriatic skin (11,28), and the PPARα (clofibrate) and PPARγ (rosiglitazone) agonists had no effect when applied on psoriasis plaques (32). Nevertheless, it is encouraging to note that treatment with the synthetic PPARγ agonist troglitazone was reported to normalize the histological characteristics of psoriatic skin in organ culture, and to reduce the epidermal hyperplasia of psoriasis in the severe combined immunodeficient mouse and human skin transplant model of psoriasis (33). Finally, two PPARα ligands (Wy-14,643 and clofibrate) were able to restore epidermal homeostasis in subacute and chronic models of hyperproliferative epidermis in hairless mice (17), even though these models do not perfectly mimic psoriatic or other human disorders. Obviously, further *in vivo* and clinical studies are needed to better define the potentially beneficial roles of PPAR in this pathology.

ROLE OF PPARS IN HAIR FOLLICLE AND SEBOCYTE DIFFERENTIATION

Skin epithelial progenitor cells give rise to the epidermis, as well as to the epithelial component of skin appendages, including hair follicles and their associated sebaceous glands. Hair follicle morphogenesis is governed by complex bidirectional interactions between epithelial keratinocytes and the underlying dermal cells of the mesenchymal condensations (Fig. 2). These interactions control a tight balance between keratinocyte proliferation and apoptosis. In rodents, all three PPAR isotypes are expressed in the differentiating hair follicles from the early embryonic developmental stages (Fig. 2). PPAR remain highly expressed in postnatal and adult hair follicles, whereas they disappear from the interfollicular epider-

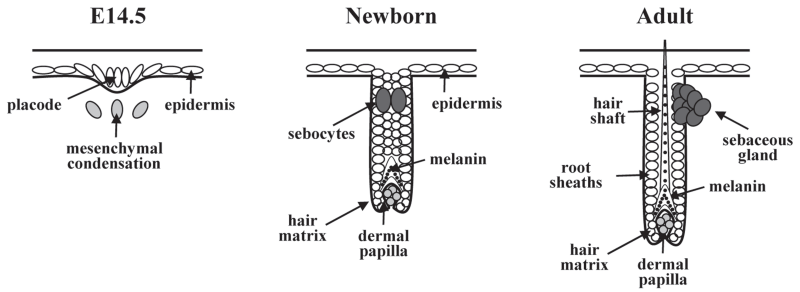

Hair follicles:	E14.5	Newborn	Adult
Mouse:	α, β and γ	α, β and γ	α, β and γ
Rat:	nd	nd	α and β (γ below detection)
Human:	nd	nd	α, β and γ

Sebaceous glands:	E14.5	Newborn	Adult
Mouse:	nd	nd	γ (α and β not tested)
Rat:	nd	nd	α and β (γ below detection)
Human:	nd	nd	γ (α and β not tested)

FIG. 2. Schematic representation of murine hair follicle morphogenesis. Hair follicle development occurs between embryonic day 14.5 (E14.5) and postnatal day 7 (P7) in mouse, and is governed by bidirectional epithelial–mesenchymal interactions between epithelial keratinocytes and dermal fibroblasts of underlying mesenchymal condensations. Following dermal induction, hair follicle precursors appear first as thickening of the uniform epithelial surface (placode, E14.5). Follicular epithelial cells will next proliferate, followed by downgrowth into the dermis, leading to the elongation of hair follicles (Newborn), and will finally differentiate into the typical structures of mature hair follicles, including root sheaths, hair matrix, and hair shaft (Adult) (46). In parallel, melanin starts to be produced in the precortex region, and the first sebocytes form the sebaceous gland (Newborn). Expression patterns of PPARα (α), PPARβ (β), and PPARγ (γ) determined or not (nd) in mouse (8), rat (10), and human (35) hair follicles at indicated stages, as well as in mature sebaceous glands (8,28,39), are given in the bottom panels.

mis after birth (3,8), as already mentioned (see Figs. 1, 2). A detailed analysis of the expression of PPAR in human hair follicles shows that they are specifically located in both epithelial and dermal hair follicle cells (34). In addition, the PPARα ligand clofibrate was reported to increase the survival of human hair follicles *in vitro*, within a narrow range of concentrations (Table 1) (34). Although a possible function of the two other PPAR isotypes in hair follicle growth has not yet been examined, it is interesting to note that conditional ablation in the murine epidermis of RXRα, the most abundant heterodimeric partner of PPARs in keratinocytes, results in delayed hair follicle maturation and alopecia (35).

Chronologically, the latest differentiated cell type to appear in the developing follicle is the oil-rich sebocytes. They arise from cells within the superficial hair follicle and will eventually form a gland located outside the hair follicle. Sebaceous lipogenesis, leading to the accumulation of lipid droplets and finally to sebum excretion, represents a major step in the differentiation process and differentiated state of sebaceous gland cells. Rodent and human sebocytes were shown to express the three PPAR, either in cell culture or *in vivo* (Fig. 2), the predominant isotype being PPARβ (9,24,36–38). Consistently, and in addition to androgens that are well known to regulate the growth and maturation of sebocytes, PPAR agonists and retinoids were recently found to affect sebaceous gland differentiation (see Table 1). Activation of PPARγ and PPARα by respective selective agonists has no effect on sebocyte growth (39), but stimulates lipid droplet accumulation in cultured rat preputial sebocytes, as assessed histochemically using Oil Red O staining (36,37). This effect was not observed in epidermal cells (37) or in cultured human sebocytes (38), possibly due to the different selective PPAR agonists or to various ligand concentrations used in each study. In parallel, RXR selective ligands have prominent differentiative and weak proliferative effects on sebocytes (40). The RXRα selective rexinoid CD2809 also amplified the prodifferentiative effect of PPAR in preputial sebocytes, suggesting a cooperation between PPAR and RXR agonists in promoting differentiation of these cells (39). In both rat and human cultured sebocytes, the pan PPAR(α/β) activators carbaprostacyclin and linoleic acid were more effective than PPARα or PPARγ agonists in stimulating sebocyte lipid droplet formation, suggesting an important contribution of PPARβ in this process (37–39). Interestingly, PPARβ seems more important in the late stages of sebocyte differentiation (37,38), whereas it was involved in the early adipocyte differentiation (41), suggesting that it plays different roles in the differentiation program of each cell type.

It is noteworthy that, in spite of the relative importance of PPAR in lipid metabolism and their high expression in sebocytes, in neither PPARα nor PPARβ mutant mouse models has sebaceous gland function been closely examined so far. In contrast, inactivation of the PPARγ gene has underscored a crucial contribution of PPARγ in sebocyte differentiation, although it appears dispensable for epidermal differentiation. Indeed, and as already discussed, chimeric mice for PPARγ-null and wild-type cells showed little or no contribution of mutant cells to the development of sebaceous glands, suggesting that PPARγ-null cells cannot develop into sebocytes (24).

NEW PUTATIVE FUNCTION OF PPARS IN MELANOCYTE DIFFERENTIATION

The pigment-producing cells of the skin are called melanocytes and their activity is the major determinant of the color of the hair and skin. Melanocytes originate from the neural crest and migrate to the basal layer of the epidermis and the hair matrix during embryogenesis. Interestingly, all three PPAR were detected in cultured human melanocytes (42) and in melanoma cells (43). Consistent with the role of PPAR agonists in cellular proliferation and differentiation in keratinocytes, PPARα (Wy-14,643) and PPARγ (ciglitazone) ligands were shown to inhibit the proliferation and to stimulate the melanin synthesis of cultured melanocytes (Table 1), whereas bezafibrate, a preferential activator for PPARβ in *Xenopus* (44), had no effect on melanin content (42). In agreement with this study, several PPARγ agonists, including troglitazone and rosiglitazone, were previously demonstrated to inhibit cell growth in human malignant melanoma (43), and topical application of retinoic acid was shown to improve hyperpigmented skin lesions such as melasma (45). Because of their antiproliferative and prodifferentiative effect on melanocytes, it is tempting to suggest that PPAR and RXR ligands may be beneficial in the treatment of melanomas. However, too little is known in this context for the moment, and further investigation is needed.

DISCUSSION AND HYPOTHESIS

These studies suggest that PPARα may contribute to sebaceous gland differentiation and epidermal permeability barrier formation by increasing both lipid metabolism and expression of structural differentiation markers, whereas PPARγ plays a unique role in stimulating sebocyte function. Furthermore, PPARβ was identified as the predominant isotype in the skin, and as a modulator of cell differentiation in both keratinocytes and sebocytes.

Because of their diverse biological activities in epidermal processes such as keratinocyte proliferation and differentiation, PPAR may represent a major research target for the understanding and treatment of many skin diseases resulting in disturbance of normal tissue homeostasis and epidermal hyperproliferation, such as benign epidermal tumors, papillomas, melanomas, and psoriasis. In addition, due to the increasing number of studies implicating PPAR in the control of sebocyte differentiation, the development of PPAR antagonists that can interfere selectively with sebum production may constitute an important element in the prevention of acne vulgaris, characterized by excess sebum production.

ACKNOWLEDGMENTS

This work was supported by the Swiss National Science Foundation (grants to Walter Wahli and to Béatrice Desvergne) and by the Etat de Vaud.

REFERENCES

1. Desvergne, B., and Wahli, W. (1999) Peroxisome Proliferator-Activated Receptors: Nuclear Control of Metabolism, *Endocr. Rev. 20*, 649–688.
2. Kersten, S., Desvergne, B., and Wahli, W. (2000) Roles of PPARs in Health and Disease, *Nature 405*, 421–424.
3. Michalik, L., Desvergne, B., Tan, N.S., Basu-Modak, S., Escher, P., Rieusset, J., Peters, J.M., Kaya, G., Gonzalez, F.J., Zakany, J., Metzger, D., Chambon, P., Duboule, D., and Wahli, W. (2001) Impaired Skin Wound Healing in Peroxisome Proliferator-Activated Receptor (PPAR)α and PPARβ Mutant Mice, *J. Cell Biol. 154*, 799–814.
4. Michalik, L., Desvergne, B., and Wahli, W. (2003) Peroxisome Proliferator-Activated Receptors β/δ: Emerging Roles for a Previously Neglected Third Family Member, *Curr. Opin. Lipidol. 14*, 129–135.
5. Michalik, L., Desvergne, B., Dreyer, C., Gavillet, M., Laurini, R.N., and Wahli, W. (2002) PPAR Expression and Function During Vertebrate Development, *Int. J. Dev. Biol. 46*, 105–114.
6. Alonso, L.C., and Rosenfield, R.L. (2003) Molecular Genetic and Endocrine Mechanisms of Hair Growth, *Horm. Res. 60*, 1–13.
7. Williams, M.L., Hanley, K., Elias, P.M., and Feingold, K.R. (1998) Ontogeny of the Epidermal Permeability Barrier, *J. Investig. Dermatol. Symp. Proc. 3*, 75–79.
8. Braissant, O., and Wahli, W. (1998) Differential Expression of Peroxisome Proliferator-Activated Receptor-α, -β, and -γ During Rat Embryonic Development, *Endocrinology 139*, 2748–2754.
9. Braissant, O., Foufelle, F., Scotto, C., Dauca, M., and Wahli, W. (1996) Differential Expression of Peroxisome Proliferator-Activated Receptors (PPARs): Tissue Distribution of PPAR-α, -β, and -γ in the Adult Rat, *Endocrinology 137*, 354–366.
10. Westergaard, M., Henningsen, J., Svendsen, M.L., Johansen, C., Jensen, U.B., Schroder, H.D., Kratchmarova, I., Berge, R.K., Iversen, L., Bolund, L., Kragballe, K., and Kristiansen, K. (2001) Modulation of Keratinocyte Gene Expression and Differentiation by PPAR-Selective Ligands and Tetradecylthioacetic Acid, *J. Invest. Dermatol. 116*, 702–712.
11. Westergaard, M., Henningsen, J., Johansen, C., Rasmussen, S., Svendsen, M.L., Jensen, U.B., Schroder, H.D., Staels, B., Iversen, L., Bolund, L., Kragballe, K., and Kristiansen, K. (2003) Expression and Localization of Peroxisome Proliferator-Activated Receptors and Nuclear Factor κB in Normal and Lesional Psoriatic Skin, *J. Invest. Dermatol. 121*, 1104–1117.
12. Hanley, K., Jiang, Y., Crumrine, D., Bass, N.M., Appel, R., Elias, P.M., Williams, M.L., and Feingold, K.R. (1997) Activators of the Nuclear Hormone Receptors PPARα and FXR Accelerate the Development of the Fetal Epidermal Permeability Barrier, *J. Clin. Invest. 100*, 705–712.
13. Hanley, K., Komuves, L.G., Bass, N.M., He, S.S., Jiang, Y., Crumrine, D., Appel, R., Friedman, M., Bettencourt, J., Min, K., Elias, P.M., Williams, M.L., and Feingold, K.R. (1999) Fetal Epidermal Differentiation and Barrier Development *in vivo* Is Accelerated by Nuclear Hormone Receptor Activators, *J. Invest. Dermatol. 113*, 788–795.
14. Komuves, L.G., Hanley, K., Jiang, Y., Elias, P.M., Williams, M.L., and Feingold, K.R. (1998) Ligands and Activators of Nuclear Hormone Receptors Regulate Epidermal Differentiation During Fetal Rat Skin Development, *J. Invest. Dermatol. 111*, 429–433.
15. Komuves, L.G., Hanley, K., Lefebvre, A.M., Man, M.Q., Ng, D.C., Bikle, D.D., Williams, M.L., Elias, P.M., Auwerx, J., and Feingold, K.R. (2000) Stimulation of PPARα Promotes Epidermal Keratinocyte Differentiation *in vivo*, *J. Invest. Dermatol. 115*, 353–360.
16. Hanley, K., Komuves, L.G., Ng, D.C., Schoonjans, K., He, S.S., Lau, P., Bikle, D.D., Williams, M.L., Elias, P.M., Auwerx, J., and Feingold, K.R. (2000) Farnesol Stimulates Differentiation in Epidermal Keratinocytes *via* PPARα, *J. Biol. Chem. 275*, 11484–11491.
17. Komuves, L.G., Hanley, K., Man, M.Q., Elias, P.M., Williams, M.L., and Feingold, K.R. (2000) Keratinocyte Differentiation in Hyperproliferative Epidermis: Topical Application of PPARα Activators Restores Tissue Homeostasis, *J. Invest. Dermatol. 115*, 361–367.
18. Yu, K., Bayona, W., Kallen, C.B., Harding, H.P., Ravera, C.P., McMahon, G., Brown, M., and Lazar, M.A. (1995) Differential Activation of Peroxisome Proliferator-Activated Receptors by Eicosanoids, *J. Biol. Chem. 270*, 23975–23983.
19. Tan, N.S., Michalik, L., Noy, N., Yasmin, R., Pacot, C., Heim, M., Fluhmann, B., Desvergne, B., and Wahli, W. (2001) Critical Roles of PPAR β/δ in Keratinocyte Response to Inflammation, *Genes Dev. 15*, 3263–3277.
20. Schmuth, M., Haqq, C.M., Cairns, W.J., Holder, J.C., Dorsam, S., Chang, S., Lau, P., Fowler, A.J., Chuang, G., Moser, A.H., *et al.* (2004) Peroxisome Proliferator-Activated Receptor (PPAR)-β/δ Stimulates Differentiation and Lipid Accumulation in Keratinocytes, *J. Invest. Dermatol. 122*, 971–983.
21. Lee, S.S., Pineau, T., Drago, J., Lee, E.J., Owens, J.W., Kroetz, D.L., Fernandez-Salguero, P.M., Westphal, H., and Gonzalez, F.J. (1995) Targeted Disruption of the α Isoform of the Peroxisome Proliferator-Activated Receptor Gene in Mice Results in Abolishment of the Pleiotropic Effects of Peroxisome Proliferators, *Mol. Cell Biol. 15*, 3012–3022.
22. Schmuth, M., Schoonjans, K., Yu, Q.C., Fluhr, J.W., Crumrine, D., Hachem, J.P., Lau, P., Auwerx, J., Elias, P.M., and Feingold, K.R. (2002) Role of Peroxisome Proliferator-Activated Receptor α in Epidermal Development in Utero, *J. Invest. Dermatol. 119*, 1298–1303.
23. Barak, Y., Nelson, M.C., Ong, E.S., Jones, Y.Z., Ruiz-Lozano, P., Chien, K.R., Koder, A., and Evans, R.M. (1999) PPAR γ Is Required for Placental, Cardiac, and Adipose Tissue Development, *Mol. Cell 4*, 585–595.
24. Rosen, E.D., Sarraf, P., Troy, A.E., Bradwin, G., Moore, K., Milstone, D.S., Spiegelman, B.M., and Mortensen, R.M. (1999) PPAR γ Is Required for the Differentiation of Adipose Tissue *in vivo* and *in vitro*, *Mol. Cell 4*, 611–617.
25. Peters, J.M., Lee, S.S., Li, W., Ward, J.M., Gavrilova, O., Everett, C., Reitman, M.L., Hudson, L.D., and Gonzalez, F.J. (2000) Growth, Adipose, Brain, and Skin Alterations Resulting from Targeted Disruption of the Mouse Peroxisome Proliferator-Activated Receptor β(δ), *Mol. Cell Biol. 20*, 5119–5128.
26. Di Poï, N., Tan, N.S., Michalik, L., Wahli, W., and Desvergne, B. (2002) Antiapoptotic Role of PPARβ in Keratinocytes *via* Transcriptional Control of the Akt1 Signaling Pathway, *Mol. Cell 10*, 721–733.
27. Di Poï, N., Michalik, L., Tan, N.S., Desvergne, B., and Wahli, W. (2003) The Anti-apoptotic Role of PPARβ Contributes to Efficient Skin Wound Healing, *J. Steroid Biochem. Mol. Biol. 85*, 257–265.
28. Rivier, M., Safonova, I., Lebrun, P., Griffiths, C.E., Ailhaud, G., and Michel, S. (1998) Differential Expression of Peroxisome Proliferator-Activated Receptor Subtypes During the Differentiation of Human Keratinocytes, *J. Invest. Dermatol. 111*, 1116–1121.

29. Matsuura, H., Adachi, H., Smart, R.C., Xu, X., Arata, J., and Jetten, A.M. (1999) Correlation Between Expression of Peroxisome Proliferator-Activated Receptor β and Squamous Differentiation in Epidermal and Tracheobronchial Epithelial Cells, *Mol. Cell Endocrinol. 147*, 85–92.
30. Rivier, M., Castiel, I., Safonova, I., Ailhaud, G., and Michel, S. (2000) Peroxisome Proliferator-Activated Receptor-α Enhances Lipid Metabolism in a Skin Equivalent Model, *J. Invest. Dermatol. 114*, 681–687.
31. Hanley, K., Jiang, Y., He, S.S., Friedman, M., Elias, P.M., Bikle, D.D., Williams, M.L., and Feingold, K.R. (1998) Keratinocyte Differentiation Is Stimulated by Activators of the Nuclear Hormone Receptor PPARα, *J. Invest. Dermatol. 110*, 368–375.
32. Kuenzli, S., and Saurat, J.H. (2003) Effect of Topical PPARβ/δ and PPARγ Agonists on Plaque Psoriasis. A Pilot Study, *Dermatology 206*, 252–256.
33. Ellis, C.N., Varani, J., Fisher, G.J., Zeigler, M.E., Pershadsingh, H.A., Benson, S.C., Chi, Y., and Kurtz, T.W. (2000) Troglitazone Improves Psoriasis and Normalizes Models of Proliferative Skin Disease: Ligands for Peroxisome Proliferator-Activated Receptor-γ Inhibit Keratinocyte Proliferation, *Arch. Dermatol. 136*, 609–616.
34. Billoni, N., Buan, B., Gautier, B., Collin, C., Gaillard, O., Mahe, Y.F., and Bernard, B.A. (2000) Expression of Peroxisome Proliferator Activated Receptors (PPARs) in Human Hair Follicles and PPARα Involvement in Hair Growth, *Acta Derm. Venereol. 80*, 329–334.
35. Li, M., Chiba, H., Warot, X., Messaddeq, N., Gerard, C., Chambon, P., and Metzger, D. (2001) RXR-α Ablation in Skin Keratinocytes Results in Alopecia and Epidermal Alterations, *Development 128*, 675–688.
36. Rosenfield, R.L., Deplewski, D., Kentsis, A., and Ciletti, N. (1998) Mechanisms of Androgen Induction of Sebocyte Differentiation, *Dermatology 196*, 43–46.
37. Rosenfield, R.L., Kentsis, A., Deplewski, D., and Ciletti, N. (1999) Rat Preputial Sebocyte Differentiation Involves Peroxisome Proliferator-Activated Receptors, *J. Invest. Dermatol. 112*, 226–232.
38. Chen, W., Yang, C.C., Sheu, H.M., Seltmann, H., and Zouboulis, C.C. (2003) Expression of Peroxisome Proliferator-Activated Receptor and CCAAT/Enhancer Binding Protein Transcription Factors in Cultured Human Sebocytes, *J. Invest. Dermatol. 121*, 441–447.
39. Kim, M.J., Deplewski, D., Ciletti, N., Michel, S., Reichert, U., and Rosenfield, R.L. (2001) Limited Cooperation Between Peroxisome Proliferator-Activated Receptors and Retinoid X Receptor Agonists in Sebocyte Growth and Development, *Mol. Genet. Metab. 74*, 362–369.
40. Kim, M.J., Ciletti, N., Michel, S., Reichert, U., and Rosenfield, R.L. (2000) The Role of Specific Retinoid Receptors in Sebocyte Growth and Differentiation in Culture, *J. Invest. Dermatol. 114*, 349–353.
41. Grimaldi, P.A. (2001) The Roles of PPARs in Adipocyte Differentiation, *Prog. Lipid Res. 40*, 269–281.
42. Kang, H.Y., Chung, E., Lee, M., Cho, Y., and Kang, W.H. (2004) Expression and Function of Peroxisome Proliferator-Activated Receptors in Human Melanocytes, *Br. J. Dermatol. 150*, 462–468.
43. Mossner, R., Schulz, U., Kruger, U., Middel, P., Schinner, S., Fuzesi, L., Neumann, C., and Reich, K. (2002) Agonists of Peroxisome Proliferator-Activated Receptor γ Inhibit Cell Growth in Malignant Melanoma, *J. Invest. Dermatol. 119*, 576–582.
44. Krey, G., Braissant, O., L'Horset, F., Kalkhoven, E., Perroud, M., Parker, M.G., and Wahli, W. (1997) Fatty Acids, Eicosanoids, and Hypolipidemic Agents Identified as Ligands of Peroxisome Proliferator-Activated Receptors by Coactivator-Dependent Receptor Ligand Assay, *Mol. Endocrinol. 11*, 779–791.
45. Kang, W.H., Chun, S.C., and Lee, S. (1998) Intermittent Therapy for Melasma in Asian Patients with Combined Topical Agents (Retinoic Acid, Hydroquinone and Hydrocortisone): Clinical and Histological Studies, *J. Dermatol. 25*, 587–596.
46. Paus, R., Muller-Rover, S., Van Der Veen, C., Maurer, M., Eichmuller, S., Ling, G., Hofmann, U., Foitzik, K., Mecklenburg, L., and Handjiski, B. (1999) A Comprehensive Guide for the Recognition and Classification of Distinct Stages of Hair Follicle Morphogenesis, *J. Invest. Dermatol. 113*, 523–532.

[Received July 19, 2004; accepted October 17, 2004]

What's So Special About Cholesterol?

Ole G. Mouritsen[a,*] and Martin J. Zuckermann[b]

[a]MEMPHYS—Center for Biomembrane Physics, Department of Physics, University of Southern Denmark, DK-5230 Odense M, Denmark, and [b]Department of Physics, Simon Fraser University, Burnaby, British Columbia, Canada

ABSTRACT: Cholesterol (or other higher sterols such as ergosterol and phytosterols) is universally present in large amounts (20–40 mol%) in eukaryotic plasma membranes, whereas it is universally absent in the membranes of prokaryotes. Cholesterol has a unique ability to increase lipid order in fluid membranes while maintaining fluidity and diffusion rates. Cholesterol imparts low permeability barriers to lipid membranes and provides for large mechanical coherence. A short topical review is given of these special properties of cholesterol in relation to the structure of membranes, with results drawn from a variety of theoretical and experimental studies. Particular focus is put on cholesterol's ability to promote a special membrane phase, the liquid-ordered phase, which is unique for cholesterol (and other higher sterols like ergosterol) and absent in membranes containing the cholesterol precursor lanosterol. Cholesterol's role in the formation of special membrane domains and so-called rafts is discussed.

Paper no. L9572 in *Lipids 39*, 1101–1113 (November 2004).

LIPIDS IN THE POST-GENOMIC ERA

Among the molecules of life, proteins and nucleic acids (DNA, RNA, and genes) have by far received the major attention among scientists as well as the public during the second half of the 20th century. Owing to the tremendous focus on genomics and protein-based biological functioning, lipids and FA have remained outside the mainstream of most areas of the life sciences. In many respects, lipids were becoming an overlooked class of molecules (1). The status of lipids is, however, in the process of changing. It is becoming clear that not all the answers to biological function can be derived from the genome. For example, it is not written in the genome how the molecular building blocks are assembled into macromolecular assemblies, organelles, and whole cells. Nor can one read in the genome how biological activity is regulated or how cells are molecularly organized.

Biological membranes are outstanding examples of molecular assemblies of extreme complexity whose structure and function cannot be determined from the genome alone and which present some grand challenges to science (2,3). However, progress in the fundamental understanding of membranes has not been impressive compared with that related to proteins and DNA. There are no genes coding for lipids as such, only for the enzymes that build and modify the lipids and FA. It is somewhat paradoxical that the preoccupation with well-defined molecular structure, which led to so many successes in structural biology during the 20th century, may be the reason why an advance in the understanding of lipid membrane structure, and structure–function relationships for membranes, has been rather slow. The problem is that if one searches for well-defined structures in membranes in the same way as investigations are made of the structure of genes and proteins, one is likely to be unsuccessful. The reason is that membranes are self-assembled molecular aggregates in which subtle elements of structure arise out of a state of considerable disorder. Disordered and partly ordered systems are notoriously difficult to characterize quantitatively. The role of certain sterols such as cholesterol for ordering of membranes is of particular importance in this context.

Lipids are now known not to be only structural builders of the cell and an energy source for cell functioning. In the form of membranes, lipids are crucial for controlling indirectly a great variety of biological functions that take place at or are mediated by membranes. Recent research has shown that the functional role of membrane lipids may be as important as that of the proteins. Not only do lipids act as a passive solvent for the proteins and as a means of compartmentalization, they are also an integral part of cellular function (4). Many lipid species are now known to play a very active role, serving as second messengers that pass on signals and information in the cell. Lipids also play the roles of enzymes, receptors, and drugs, as well as regulators of, e.g., neurotransmitter activity. Disorder in the lipid spectrum of cells has recently been related not only to atherosclerosis but also to major psychiatric illnesses (5). It has been proposed that polyunsaturated lipids provide an evolutionary driving force supplementing Darwinian natural selection (6). All these factors emphasize a necessary shift from a one-eyed genocentric approach to lipids and membranes toward a more balanced organocentric view. This puts the study of the physical properties of membranes at a very central position. It is for good reasons that a recent review paper in a physiology journal could carry the title "Getting Ready for the Decade of the Lipids" (7).

Lipids and membranes are coming back on the scene as a key research area in the postgenomic era, and there is a tremendous need for knowledge about the ways in which lipids are in-

*To whom correspondence should be addressed.
E-mail: ogm@memphys.sdu.dk

Abbreviations: 7DHC, 7-dihydrocholesterol; DMPC, 1,2-dimyristoyl phosphocholine; DOPC, 1,2-dioleoyl phosphocholine; DPPC, 1,2-palmitoyl-3-phosphocholine; GPL, glycerophospholipid; PI, phosphoinositol; POPC, phosphocholine; PPet-PC, 1-palmitoyl-2-petroselinoyl-3-phosphocholine; SC, Saccharomyces cerevisiae; SLOS, Smith–Lemli–Opitz syndrome..

volved in the various stages of cell function. In particular, it is necessary to achieve deeper knowledge about the lateral structure and molecular organization of lipid membranes, e.g., in terms of lipid domains or "rafts", on length scales that are relevant to the particular membrane phenomena in question. This puts emphasis on the nanometer scale and makes membrane science a true nanoscience. In fact, biological membranes as a microencapsulation technology can be seen as Nature's preferred nanotechnology. Membranes are ultra-thin layers only about 5 nm thick, and they have delicate structural features over scales from 1 to 1000 nm. Biological membranes are optimized by evolutionary processes to function on the nanometer scale. Also in this respect, cholesterol is an important player.

In the present topical review we shall describe our current understanding of the way in which cholesterol and related sterols affect the physical properties of lipid membranes with focus on simple lipid bilayers and liposomes as model membranes. Hence, we shall focus attention on cholesterol as a structural element of membranes, and refer to the literature for information on cholesterol's signaling functions (8). After a short note on the role of cholesterol in the evolution of membranes, we describe the particular phase equilibria that cholesterol induces in lipid membranes. We characterize the special *liquid-ordered phase* that is unique for membranes containing cholesterol. We shall compare cholesterol with other sterols, such as ergosterol, and point out that the precursor for the formation of the higher sterols, lanosterol, does not support the liquid-ordered phase and hence is not able to form rafts. The particular properties that cholesterol imparts to lipid bilayers will be described based on the phase diagram, in particular, permeability, binding capacity for solutes such as alcohols, mechanical stiffness, lipid-chain ordering, lateral diffusion, membrane thickness, lateral membrane organization, and aspects of protein function.

A NOTE ON MEMBRANE EVOLUTION

Lipids or other interface-forming molecules were required for forming the capsules that could separate useful enzymes and genes from the environment. Obviously, life as it evolved since its first appearance on Earth about 3.8 billion years ago used the molecules available, either those already existing or the new ones that were produced by various living organisms. The life forms that were fit would survive according to the Darwinian selection principles. Cholesterol or related higher sterols such as ergosterol and sitosterol (see Fig. 1) were not available for a very long time for the very reason that the chemical conditions for the biochemical synthesis of these sterols were not there. Molecular oxygen was lacking. For convenience, we shall in the present section refer mostly to cholesterol in our discussion; consequently, the discussion is pertinent to animal life. In the case of plants and fungi, cholesterol is replaced by phytosterols (e.g., sitosterol) and ergosterol, respectively. The differences in molecular structure of these three higher sterols, as shown in Figure 1, are of minor importance for the general arguments presented below.

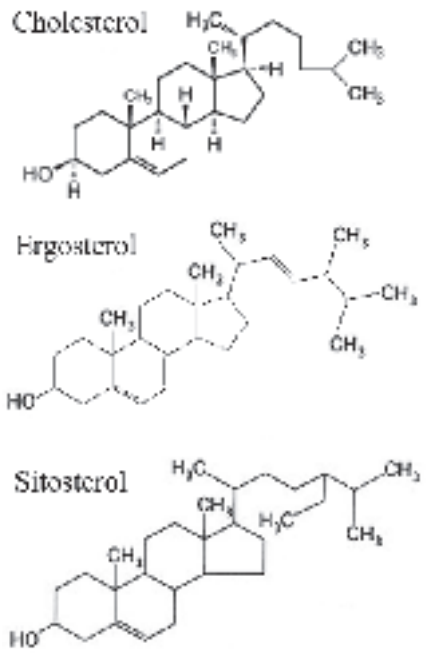

FIG. 1. Structural formulas for higher sterols: cholesterol, ergosterol, and sitosterol.

For an appreciation of how the advent of cholesterol released new driving forces for the evolution of higher organisms, it is instructive to study the variation in the concentration of molecular oxygen in the atmosphere of Earth since its creation almost five billion years ago. One then finds that the oxygen partial pressure in the atmosphere correlates with major events in the evolution of life (9). Before the evolution of the blue-green cyanobacteria that could produce O_2 by photosynthesis, the partial pressure of O_2 was as low as one part of in 10 million of an atmosphere. It increased gradually to concentrations that were large enough to support life forms that exploit oxygen by respiration, possibly around 2.8 to 2.4 billion years ago. Up until then, eubacteria and archaebacteria were the only forms of life. Along with the availability of O_2, eukaryotic life came on the scene. From then on, as the oxygen pressure was rising, there was a proliferation of eukaryotic diversity. This suggests that there is a conspicuous coincidence between the rise of the eukaryotes and the availability of molecular oxygen.

It has been proposed (9) that the availability of molecular oxygen removed a bottleneck in the evolution of species and that the crucial molecular entity in this process is cholesterol (and related sterols). This proposal is supported by the fact that eukaryotes universally contain high concentrations of cholesterol in their plasma membranes, whereas cholesterol is universally absent in prokaryotes (10). It should be added that the internal membranes of eukaryotes contain very low concentrations of cholesterol. There is a striking gradient in the cholesterol concentration from the mitochondria (3 wt%), over endoplasmic reticulum (6 wt%), to the Golgi (8 wt%). The fact that mitochondria have almost no cholesterol is in line with Lynn Margulis' symbiosis theory, according to which the mitochon-

dria in eukaryotes are ancient prokaryotes that were engulfed by the eukaryotes to take care of the respiratory process.

The background for assigning to cholesterol a unique role in evolution is to be found in the fundamental work by Konrad Bloch (11,12) who worked out the biochemical pathway for the synthesis of cholesterol. According to Figure 2, this pathway ranges from squalene, over lanosterol, to cholesterol. The path starts with the linear molecule squalene that becomes cyclized into the characteristic steroid ring structure. Bloch showed that there is no plausible way of cyclizing squalene in the absence of oxygen, and it is even more unlikely, if not impossible, to perform the next steps that lead from lanosterol to cholesterol. These steps can be seen as a successive streamlining of the hydrophobic surface of the sterol by removing from one to three of the methyl ($-CH_3$) groups that protrude from the flat face of the molecule. Chemical evolution in the absence of molecular oxygen along the sterol pathway would therefore have to stop with squalene. Bloch has termed the oxidative process leading to cholesterol "the evolutionary perfection of a small molecule" and thereby pointed out that not only genes changed during evolution; so did lipids and, in particular, sterols.

The significant difference in molecular smoothness between lanosterol and cholesterol can be seen in Figure 3. The three additional methyl groups on lanosterol make this molecule rougher and more bulky than cholesterol. It is surmised that Darwinian evolution has selected cholesterol for its ability, *via* its smoothness, to optimize certain physical properties of the membranes. It is unclear, however, which physical properties are the relevant ones in this context; moreover, the degree of optimization that can be provided by cholesterol is uncertain.

A clue to these questions may come from considering the actual biosynthetic pathway to cholesterol as the living "fossil" of the evolutionary pathway to cholesterol. Along this pathway, lanosterol is a precursor to cholesterol. In other words, the temporal sequence of the biosynthetic pathway could be taken to represent the evolutionary sequence. The evidence for this viewpoint comes from Konrad Bloch's studies of sterol biochemistry and organism evolution. This evidence appears highly convincing. The concept of living molecular fossils offers a framework for a research program geared toward identifying the physical properties that are relevant to evolutionary optimization, without having to face the impossible problem of performing experiments on evolutionary time scales. Such a

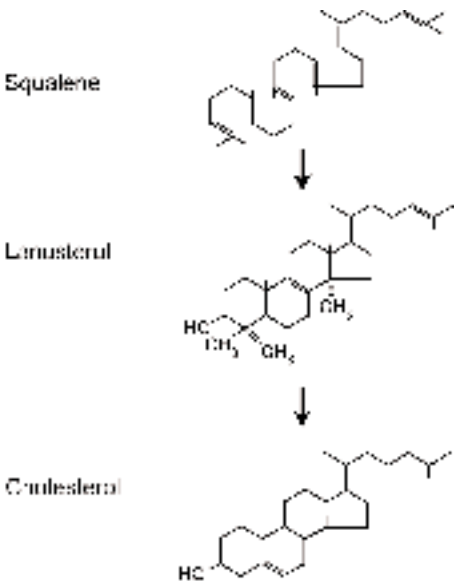

FIG. 2. Biosynthetic pathway for synthesis of sterols from squalene, to lanosterol, to cholesterol.

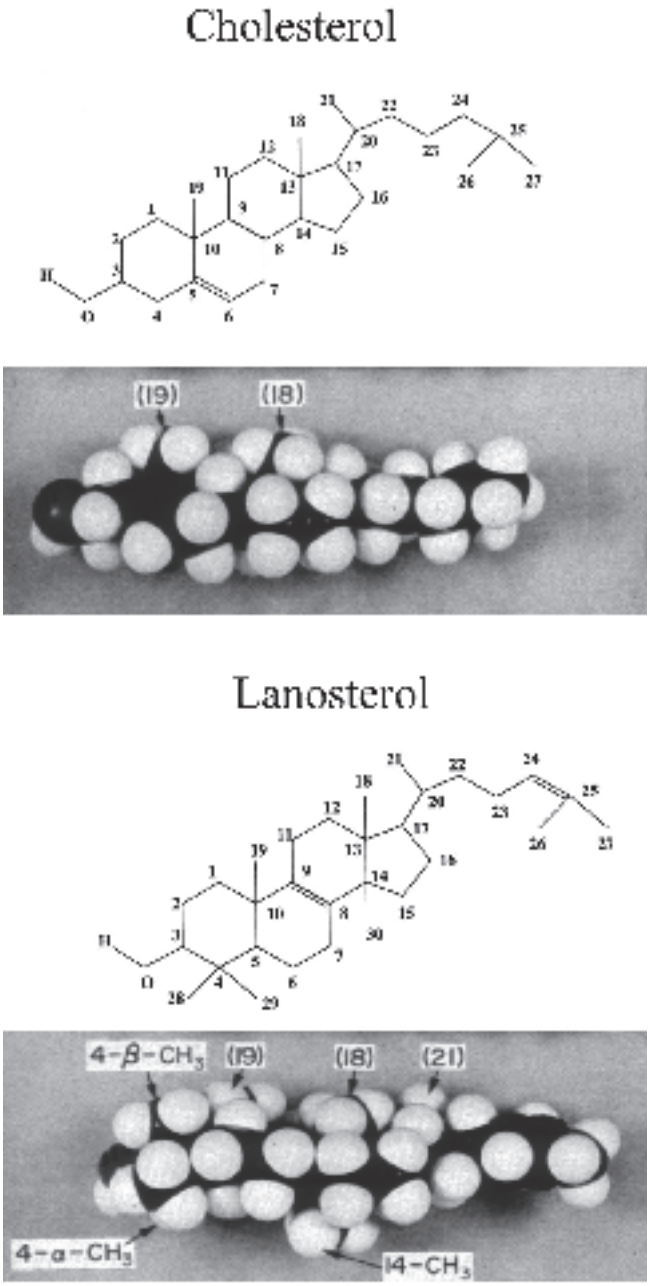

FIG. 3. Chemical structures and space-filling models of cholesterol and lanosterol, highlighting lanosterol's extra three methyl groups that lead to a hydrophobically less smooth surface of the molecule.

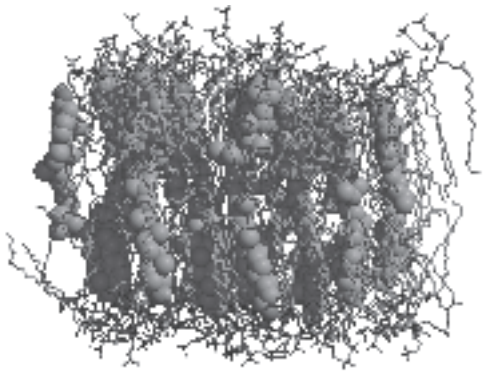

FIG. 4. Patch of a fluid 1,2-palmitoyl-3-phosphocholine (DPPC) lipid bilayer incorporated with 20% cholesterol. The picture is obtained from Molecular Dynamics simulations. The DPPC molecules are shown in thin lines, and the cholesterol molecules are highlighted in a space-filling representation. Water molecules are not shown. Courtesy of Mr. Michael Petra and Dr. Ilpo Vattulainen.

research program has been initiated in the laboratories of the present authors and their colleagues, and some of the results derived from this program are reported below.

CHOLESTEROL-INDUCED ORDER AND PHASE EQUILIBRIA

Membrane sterols are amphiphilic molecules that, with their small hydrophilic –OH head group, intercalate in lipid bilayers as illustrated in Figure 4 in the case of cholesterol. A cholesterol molecule can span about half a bilayer. It is well known that cholesterol regulates lipid chain order. Indeed, the lipid molecules depicted in Figure 4 are subject to a substantial ordering induced by the presence of the cholesterol molecules. The membrane patch shown in Figure 4 is in a liquid (fluid) state that, in the absence of cholesterol, is characterized by translational disorder and rapid lateral diffusion and by a substantial degree of lipid chain disorder. The bilayer phase is hence termed a *liquid-disordered* phase. On lowering the temperature, the lipid bilayer undergoes a phase transition (at a temperature T_m) that takes the bilayer to a state with in-plane translational order (as in a 2-D crystal) and slow lateral diffusion, and a substantial degree of lipid-chain order. This phase is therefore termed the *solid-ordered* phase. The presence of cholesterol complicates this picture.

In Figure 5 is shown experimental data for the lipid-chain order as measured by deuterium NMR (13) on lipid bilayers formed of 1-palmitoyl-2-petroselinoyl-3-phosphocholine (PPEt-PC) mixed with various amounts of either cholesterol or lanosterol. Pure PPEt-PC bilayers have a phase transition from the solid-ordered phase to the liquid-disordered phase at 16.8°C. For both sterols, there is a progressive ordering of the lipid chains above the transition and a suppression of order below the transition. However, lanosterol's ability to induce order in the fluid phase is considerably less than that of cholesterol, as shown in Figure 6. Moreover, whereas cholesterol only

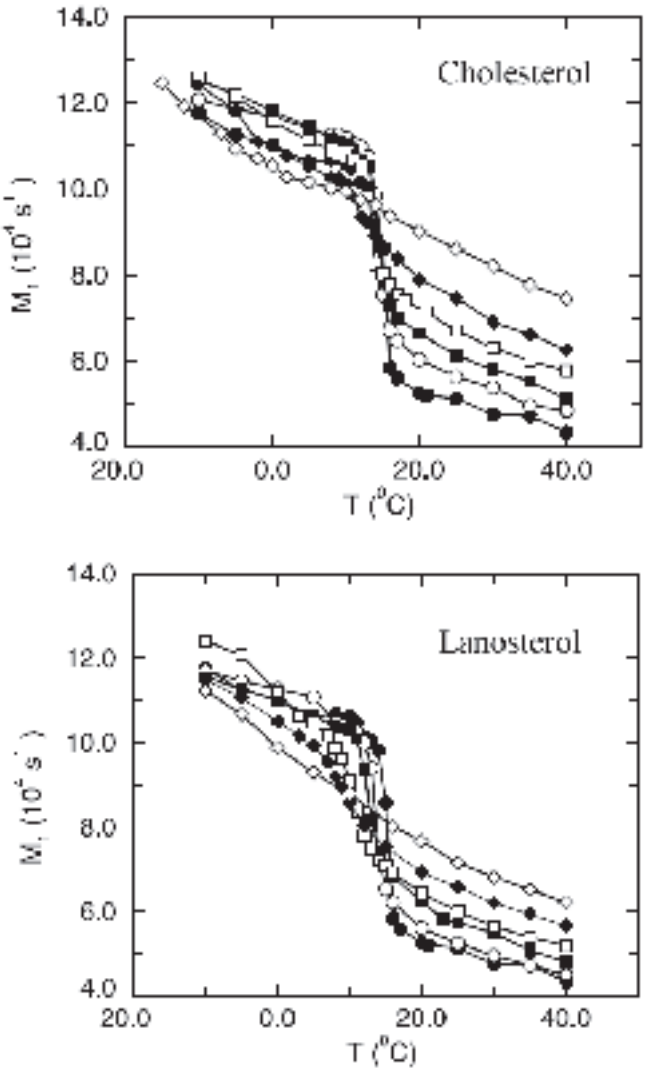

FIG. 5. Lipid-chain order as monitored by the first moment, M_1, of the quadrupolar NMR spectrum of 1-palmitoyl-2-petroselinoyl-3-phosphocholine (PPEt-PC)-cholesterol and PPEt-PC-lanosterol lipid bilayers. The sterol concentration is counted from the bottom of the curves seen from the right-hand side as: 0, 5, 10, 15, 20, and 30%. Adapted from Reference 13.

slightly changes the position of the transition region, lanosterol leads to a substantial broadening and downward shift of the transition region.

Data of the type presented in the top part of Figure 5, together with data from thermodynamic measurements as well as results from theoretical calculations, have laid the foundations for proposing a generic phase diagram for lipid–cholesterol mixtures as presented in Figure 7. This phase diagram has a peculiar feature: There is a remarkably small effect of freezing-point depression, which leads into an invariant three-phase line, signaling the appearance of a new phase, the liquid-ordered phase, first proposed by Ipsen *et al.* (14) on basis of some seminal experimental data obtained by Vist and Davis (15). The liquid-ordered phase is a liquid in the sense that there is translational disorder and rapid diffusion in the plane of the bilayer,

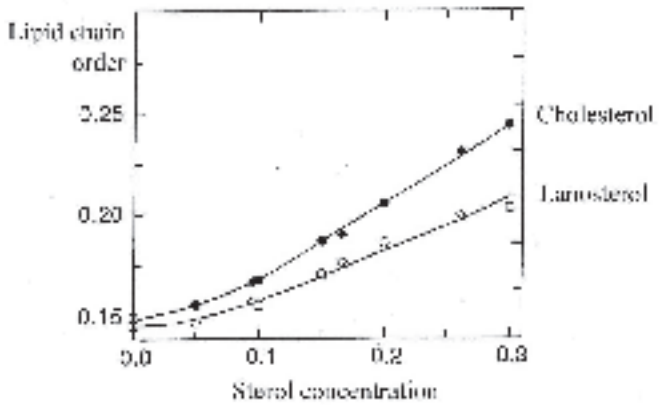

FIG. 6. Ordering, *S*, of lipid chains in PPEt-PC bilayers induced by lanosterol and cholesterol as a function of sterol concentration (mol%). Adapted from Reference 13. The ordering, *S*, is related to the first moment, M_1, of the quadrupolar NMR spectrum, as $M_1 = \pi e^2 qQS/(3^{1/2}h)$, where e^2qQS/h is the static quadrupolar coupling constant. For abbreviation see Figure 5. Symbols refer to experimental data and solid lines to theoretical predictions.

but at the same time this phase has a high lipid-chain conformational order. Owing to the high order in the liquid-ordered phase, the bilayer is almost as thick here as in the solid-ordered phase and hence has, as we shall see later, many of the desirable mechanical properties of a solid membrane without actually being crystalline. The liquid-ordered phase is unique for cholesterol and other higher sterols!

Lanosterol is unable to stabilize a liquid-ordered phase as shown in Figure 8, where the phase diagrams for the PPEt-PC bilayer with, respectively, lanosterol and cholesterol are displayed. Hence, it may be surmised that an evolutionary advantage of cholesterol may be its ability to promote and stabilize a liquid-ordered phase over a substantial range of temperatures

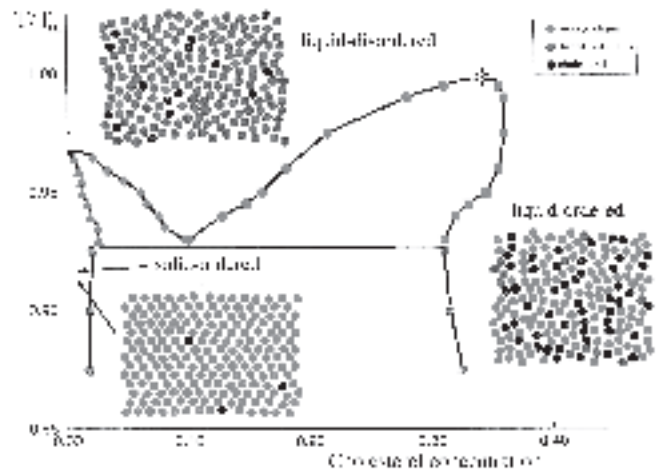

FIG. 7. Generic phase diagram for phosphocholine lipid bilayers mixed with cholesterol. A simple representation is given of the lateral structure and organization of the bilayers as composed of ordered and disordered lipid chains and cholesterol. The critical point is marked by an asterisk. The cholesterol concentration is given in mol%. *T* = temperature; T_m, temperature of phase transition.

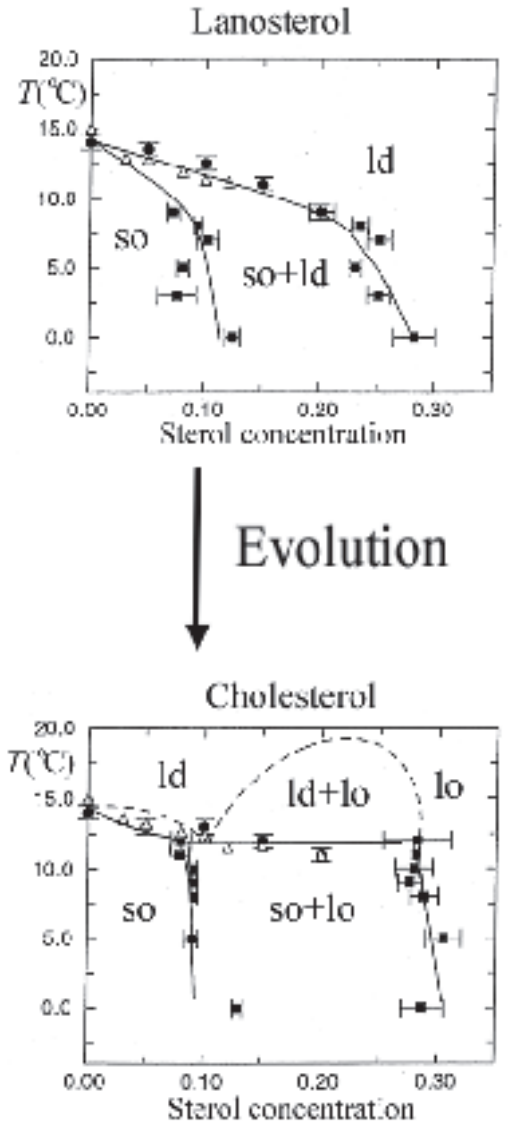

FIG. 8. Evolution from lanosterol to cholesterol, seen as an evolution in the phase equilibria toward a situation with a stable liquid-ordered membrane phase. The labels on the different phases correspond to the liquid-disordered (**ld**) phase, the solid-ordered (**so**) phase, and the liquid-ordered (**lo**) phase. The sterol concentration is given in mol%. Adapted from Reference 13. The error bars indicate experimental confidence limits.

and sterol concentrations. In particular, the evolution from lanosterol to cholesterol may be pictured as an evolution in the phase equilibria toward a situation with a stable liquid-ordered membrane phase (*cf.* Figure 8).

Owing to the difficulty in reliably extracting phase equilibria from experimental studies of lipid bilayers with sterols, only very few systems have been investigated in detail. The general trend is, however, that cholesterol in lipid bilayers made of different kinds of lipids leads to a phase diagram of the type shown in Figure 7. Recently, the phase equilibria in 1,2-palmitoyl-3-phosphocholine (DPPC) lipid bilayers with ergosterol have been investigated (16), and the resulting phase diagram has been deduced as

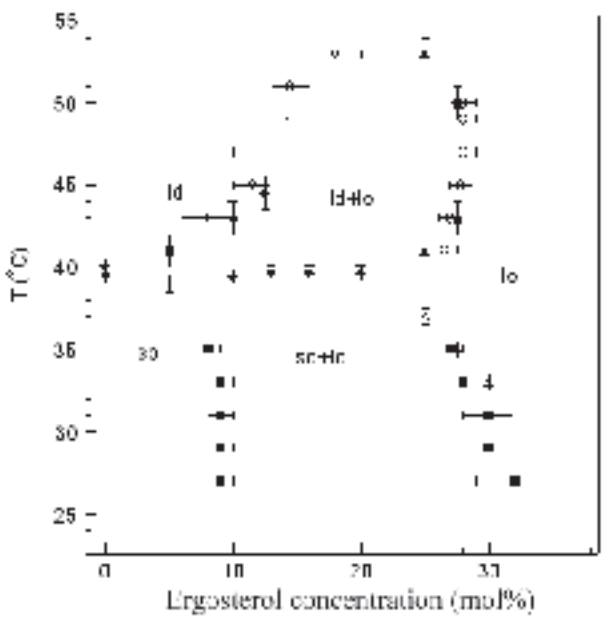

FIG. 9. Phase diagram for DPPC lipid bilayers mixed with ergosterol. The labels on the different phases correspond to the liquid-disordered (**ld**) phase, the solid-ordered (**so**) phase, and the liquid-ordered (**lo**) phase. Adapted from Reference 16.

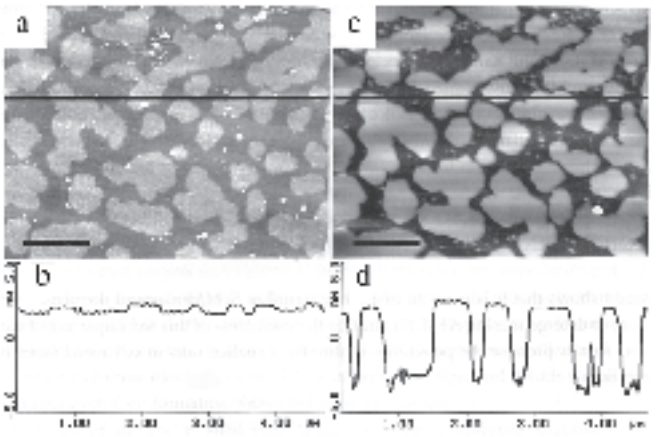

FIG. 10. Atomic force microscopy image of lipid bilayers made of raft mixtures of 1:1 dioleoyl phosphocholine (DOPC)/sphingomyelin containing 25% cholesterol. Before (a) and after (c) treatment with the detergent Triton X-100 at 4°C. Underneath the images are shown in (b) and (d) the corresponding cross sections of the height profile along the horizontal lines shown at the images above. The images are 5 × 5 μm and the scale bars are 1 μm. Adapted from Reference 29.

shown in Figure 9. This phase diagram shows that ergosterol also promotes a liquid-ordered phase leading to the proposal that a unique feature of all higher sterols is that they can stabilize a liquid-ordered phase in lipid membranes.

LATERAL ORGANIZATION

In addition to its ability to increase lipid-chain order in fluid membranes, cholesterol is believed to play a crucial role in the lateral organization of lipid membranes on a small scale, in the form of specialized lipid domains (17–19) or rafts (20–23). The presence of small-scale lateral structure in biological membranes and its importance for biological activity has received increasing attention in recent years. There are several reasons for this situation. First, single-particle tracking techniques revealed that labeled lipid or protein molecules performed a peculiar lateral diffusive motion that suggested they were temporarily confined to a small region of the membrane surface (24). Second, in the biochemical treatment of cold membrane samples with often rather harsh detergents, such as Triton X-100, a certain fraction of the membranes was discovered to be resistant to the detergent, and it was suggested that this fraction corresponds to supramolecular entities floating around in fluid membranes as a kind of *raft*. Rafts were surmised to behave as functional units supporting various functions (20). However, there is yet to be found an unambiguous structural correlate of the biochemically defined raft.

A common characteristic of the rafts is that they contain high levels of cholesterol and sphingolipids as well as saturated phospholipids (25–28). The presence of sphingolipids, such as sphingomyelin or glycosphingolipids, which often have high phase transition temperatures, and cholesterol, which promotes ordering of the lipid chain, led to the suggestion that the rafts had a structure similar to the liquid-ordered phase in the lipid–cholesterol phase diagram in Figure 7. However, at present there is only very limited evidence for the phospholipids in the rafts actually having a liquid-ordered structure. Moreover, the general understanding of the term liquid-ordered and where it comes from seems to be fairly limited (22).

Rafts are believed to be associated with peripheral and *trans* membrane proteins that stabilize the rafts and function in connection with the rafts. Raft-like entities are, however, also found in simple lipid mixtures containing sphingomyelin, cholesterol, and phospholipids. This is demonstrated in Figure 10, which shows images obtained from atomic force microscopy of the mixture dioleoyl phosphocholine (DOPC)/sphingomyelin/cholesterol in the form of lipid bilayers on solid supports (29). Domains of micrometer and submicrometer size are seen in the image to the left, and the frame to the right demonstrates that these domains or rafts resist treatment with detergent.

Further evidence for the presence of domain structures in native membrane extracts can be found in Figure 11 (left image), which shows fluorescence microscopy images of giant unilamellar vesicles formed of native pulmonary surfactant containing both lipids and the native proteins (30). The image displays large micrometer-sized domains of coexisting liquid-disordered and liquid-ordered phases. Further analysis has demonstrated that the integral pulmonary surfactant proteins reside in the fluid-disordered domains (30). On extraction of the proteins, the general structure of the domain pattern remains, suggesting that the proteins are not crucial for the domain formation.

Native pulmonary surfactant contains about 8–15% cholesterol, which is believed to be important for the mechanical

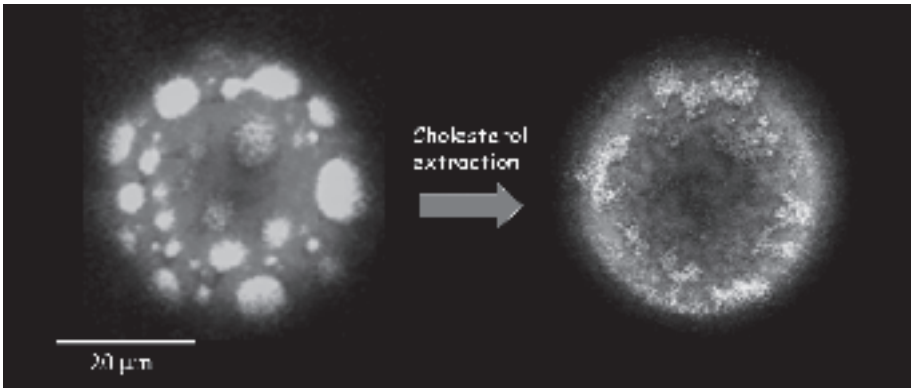

FIG. 11. Lipid domains in native pulmonary surfactant membranes consisting of lipids and proteins. Confocal fluorescence microscopy images of giant unilamellar vesicles composed of native pulmonary surfactant membranes before and after cholesterol extraction by methyl-β-cyclodextrin at 37°C. Adapted from Reference 30. Courtesy of Dr. Luis Bagatolli.

functioning of the lung film. It is shown in Figure 11 (right image) that, whereas the proteins are not important for domain formation, cholesterol certainly is. Following extraction of cholesterol from the vesicles by cyclodextrin, the domain pattern changes into a more ramified and fractal structure characteristic of liquid–solid phase equilibria (30). Hence, it appears that cholesterol is an important regulator of small-scale membrane organization in native membranes.

Little quantitative knowledge is available about the lateral structure of lipid–sterol mixtures in the liquid-ordered phase as well in the region of coexistence of the liquid-disordered and liquid-ordered phases (*cf.* the generic phase diagram in Fig. 7). Recent analysis of NMR data for the DPPC-ergosterol system has, however, revealed interesting results pointing to the possibility that the coexistence region does not consist of macroscopically separated phases but rather very small, nanometer-scale domains (16). Concerning the lateral structure of the liquid-ordered phase, some insight has been obtained from computer-simulation calculations (13), which indicate, as illustrated in Figure 12a, that very small dynamic domains indeed prevail in the liquid-ordered phase. These domains can be described as a stringy pattern of alternating rows of cholesterol molecules and rows of conformationally ordered lipid molecules. This dynamic small-scale structure is best picked up by the structure factor shown in Figure 12b, which shows a small peak corresponding to a 5-Å coherence length. It is a remarkable observation that when cholesterol is replaced by lanosterol, this peak disappears and there is no sign of a small-scale structure in the simulations. A related structure of lipid–cholesterol systems has been observed by McConnell and Radhakrishnan in terms of so-called complexes (31).

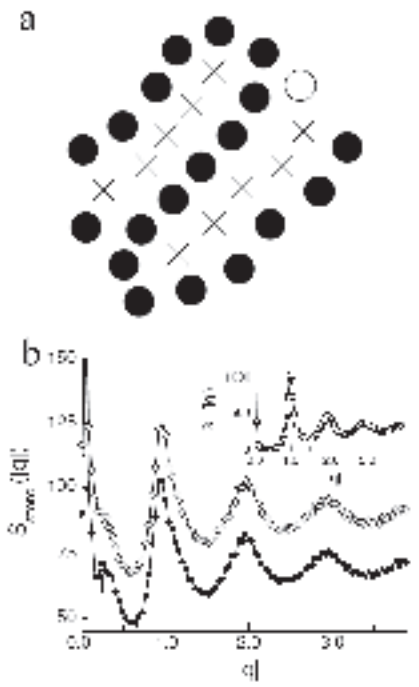

FIG. 12. (a) A local configuration of lipid and cholesterol molecules as obtained from a computer-simulation calculation on a simple model of lipid–cholesterol bilayers. The configuration shows a threadlike distribution of lipid and cholesterol molecules. Lipid chains in the ordered state are shown by filled circles, lipid chains in the disordered state are shown by open circles, and cholesterol molecules are shown by crosses. (b) The partial structure factor describing the distribution of the sterol molecules in the membranes, $S_{sterol}(|q|)$, calculated by computer simulation at $T = 0.9806\,T_m$ and $x_{sterol} = 0.367$. $S_{chol}(|q|)$ is shown by the filled circles and $S_{lan}(|q|)$ by the open diamonds. For clarity, the curve for $S_{lan}(|q|)$ has been shifted along the *y* axis. The values of the wave vector $|q|$ are given in units of $2\pi/d$, where *d* is a hard-core diameter assigned to the lipid and sterol particles in the simulational model. The arrows indicate an unusual structural signal in addition to the usual peaks characteristic of liquid structure. The inset shows the total structure factor, $S_T(|q|)$, for the two lipid–sterol systems. Adapted from Reference 13.

MEMBRANE PROPERTIES REGULATED BY CHOLESTEROL

We now briefly describe how physical, physicochemical, and certain functional properties of membranes are modulated and

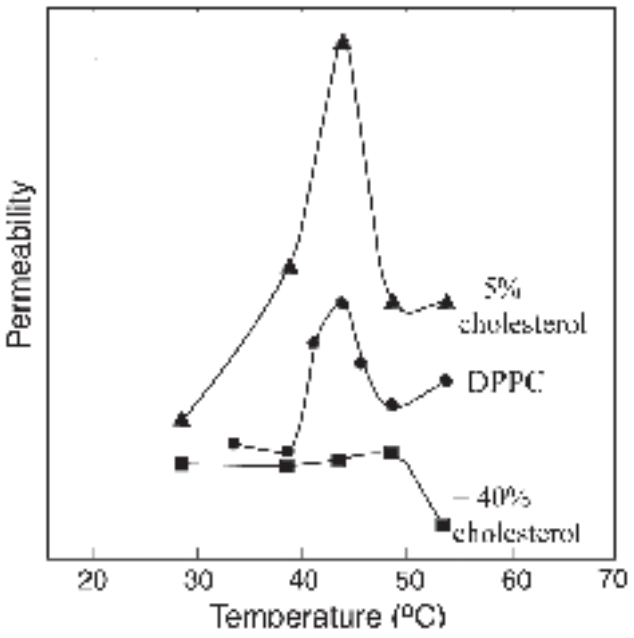

FIG. 13. The effect of cholesterol on the passive permeability (in arbitrary units) of sodium ions through DPPC lipid bilayers. Adapted from Reference 35. For abbreviation see Figure 4.

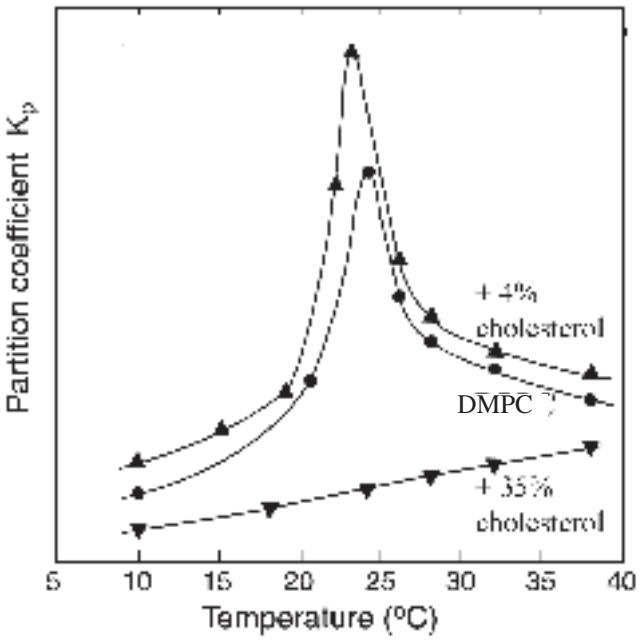

FIG. 14. The effect of cholesterol on the binding of ethanol to dimyristoyl phosphocholine (DMPC) lipid bilayers. Adapted from Reference 37. The partitioning coefficient is given in arbitrary units.

regulated by cholesterol. The account is in no way exhaustive, and the reader is referred to full review papers that provide more information (32–34).

Permeability. One of the primary reasons for the presence of cholesterol in eukaryotic membranes is probably its ability to regulate passive membrane permeability. In Figure 13 is shown a set of data for the passive permeation of Na^+ ions through lipid bilayers of DPPC (35). In the absence of cholesterol, a dramatic peak at the phase transition demonstrates that the bilayer becomes very leaky in this region. The reason for this anomalous behavior is the lateral structural heterogeneity of the bilayer, which is caused by the strong density fluctuations at the transition. In the presence of large amounts of cholesterol (here 40 mol%), the peak disappeared, implying that cholesterol increased the permeability barrier. The reason for this suppression is twofold. First, the lateral density fluctuations at the transition are suppressed. Second, by ordering the lipid chains (*cf.* Figs. 5 and 6) the bilayer is thickened, leading to an increase in the permeability barrier. Conversely, low levels of cholesterol have the opposite effect. This is explained *via* the phase diagram in Figure 7, which at low cholesterol concentrations exhibits only a very small freezing-point depression and a very narrow solid-ordered–liquid-disordered phase-separation region.

Cholesterol's ability to suppress passive permeability also has been found for a large variety of other compounds, suggesting that the mechanisms described above are fairly generic (36).

Binding of solutes. As a consequence of fluctuations prevailing at the pure lipid-bilayer phase transition as just described, the bilayer becomes not only prone to permeation but also susceptible to peripheral penetration and binding of various compounds, such as simple alcohols. An example is shown in Figure 14, where the bilayer/water partition coefficient of ethanol is shown for dimyristoyl phosphocholine (DMPC) lipid bilayers as a function of temperature (37). A dramatic peak at the phase transition is observed, implying that the bilayer strongly adsorbs ethanol as a result of the density fluctuations. These fluctuations and the concomitant lateral bilayer heterogeneity presumably provide for more binding sites at the bilayer–water interface where the ethanol molecules are know to associate preferentially. Large amounts of cholesterol (here 35 mol%) are found to lead to a substantial reduction in the partition coefficient. Hence, cholesterol acts as an antagonist to alcohol binding to membranes. In line with the foregoing observation regarding passive permeability, small levels of cholesterol lead to the opposite effect, i.e., stronger binding of ethanol, again presumably because the particular properties of the lipid–cholesterol phase diagram at low cholesterol concentrations imply an enhancement of the lateral density fluctuations of the bilayer.

Thermomechanics. The density fluctuations at the lipid-bilayer phase transition also have consequences for the thermomechanical properties of the bilayer. A lipid bilayer can be described in terms of a number of mechanical modules, specifically the area–compressibility modulus, $K(T)$, and the bending elastic modulus, $\kappa(T)$. At the transition, both of these modules are known to display a dramatic minimum, implying that the bilayer becomes softened at the phase transition both in terms of bending and compression. As a consequence, properties that are functions of these modules also become dramatically renor-

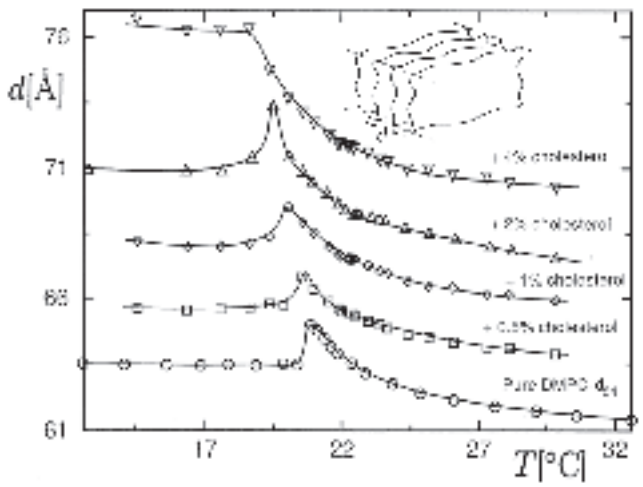

FIG. 15. Repeat distance, *d,* between perdeuterated DMPC lipid bilayers in a multi-lamellar stack shown as a function of cholesterol concentration. Adapted from Reference 38. For abbreviation see Figure 14.

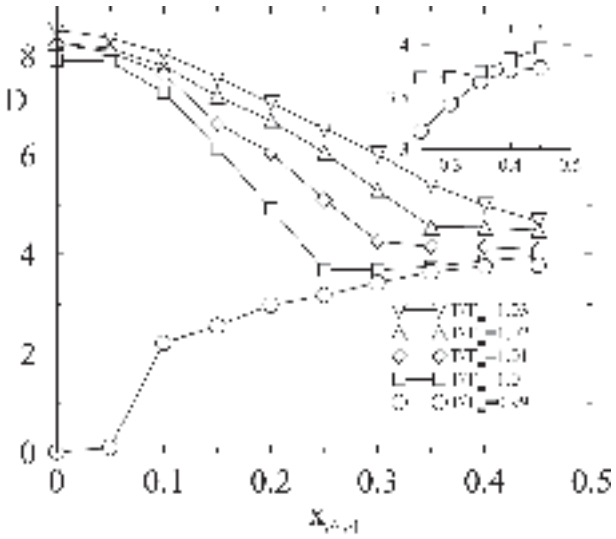

FIG. 16. Diffusion coefficient D (in arbitrary units) vs. cholesterol mole fraction x_{chol}. The inset shows the data for $T = 0.99T_m$ and $1.0T_m$ in an expanded scale in order to illustrate the increase in D with x_{chol} in the liquid-ordered phase. Adapted from Reference 41. For abbreviations see Figure 7.

malized in the transition region (38). One such property is the interlamellar, entropic undulation force that operates between a stack of lipid bilayers organized in a multilamellar stack as illustrated in the inset to Figure 15. The smaller the bending modulus, the larger the interlamellar force and hence the larger the equilibrium (repeat) distance, *d*, between adjacent layers. This effect is illustrated in Figure 15 for the case of perdeuterated DMPC bilayers in the phase-transition region, where *d* vs. *I* exhibits a peak at the transition temperature, suggesting that anomalous swelling has set in. On incorporation of more than about 4 mol% cholesterol, the anomalous swelling disappears. This may be explained by the ability of cholesterol to increase the bending modulus κ and hence diminish the repulsive undulation force. This in turn leads to a decrease in the equilibrium separation between adjacent lamellae. In contrast, small levels of cholesterol have the opposite effect. Again we rationalize this in terms of the lipid–cholesterol phase equilibria and the enhanced density fluctuations for small cholesterol concentrations.

Recently, *K* and κ have been measured quantitatively for giant unilamellar vesicles using vesicle fluctuation analysis and micropipette aspiration techniques [39; Henriksen, J.R., Rowat, A.C., Thewalt, J., Brief, E., Zuckermann, M.J., and Ipsen, J.H., (unpublished data)], and results have been obtained for palmitoyl-oleoyl phosphocholine (POPC) vesicles containing cholesterol, ergosterol, and lanosterol. The general finding from these experiments, which all have been carried out at room temperature (i.e., in the fluid phase of the POPC bilayers), is that all sterols in the concentration range from 0 to 30 mol% lead to an increase in the modules, i.e., the sterols lead to a mechanical stiffening of the bilayer in terms of both bending and area compression. In addition, it was found [39; Henriksen, J.R., Rowat, A.C., Thewalt, J., Brief, E., Zuckermann, M.J., and Ipsen, J.H., (unpublished data)] that the ability to stiffen the membranes decreased in the order cholesterol > lanosterol > ergosterol. So far, no explanation of this sequence has been found. In the same work, a universal relationship was found between, respectively, *K* and κ on the one side and the lipid-chain order (i.e., membrane thickness) on the other side.

Lateral diffusion. Cholesterol's unique ability on the one hand to increase lipid-chain order, and hence optimize mechanical and permeation properties of the membrane, and on the other hand to maintain the liquid character, and hence provide for lateral diffusion (40), is most clearly demonstrated by the variation of the lateral diffusion coefficient across the lipid-cholesterol phase diagram as shown in Figure 16 (41). This figure shows data obtained from a computer-simulation study of a simple model of lipid–cholesterol interactions in bilayers. The figure demonstrates that the tracer diffusion coefficient *D* increases monotonically with increasing temperature and this qualitative trend is independent of cholesterol concentration. The cholesterol concentration dependence of *D*, however, shows more interesting behavior. At higher temperatures, *D* decreases with increasing x_{chol}, whereas at temperatures below T_m, *D* increases monotonically with x_{chol}. At temperatures slightly greater than T_m, *D* first decreases, then increases slightly with increasing x_{chol}, as can be seen more clearly in the inset to Figure 16. A qualitative interpretation of the physical origin of this behavior is provided by the free volume theory of diffusion. An increase in *D* with x_{chol} is due to an increase in the free area per molecule with increasing x_{chol}. Decreases in *D* arise from the fact that cholesterol also promotes conformational ordering of the lipid chains, which in turn causes the chains to interact more effectively and thus increases the effective activation energy for particle movement. These two effects compete with one another and give rise to the nonmonotonic variation of *D* with x_{chol} at intermediate temperatures. The dif-

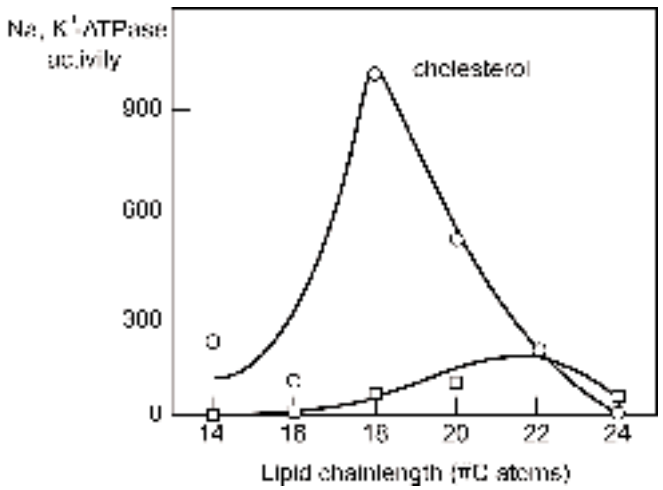

FIG. 17. Activity of the membrane-bound enzyme Na^+,K+-ATPase as a function of the hydrophobic thickness of the lipid bilayers into which it is incorporated. The hydrophobic thickness is given by the number of carbon atoms of monounsaturated phosphocholine lipids. The activity exhibits a clear maximum. When cholesterol is incorporated in the amount of 40%, the maximum is moved toward membranes made of shorter lipids. Adapted from Reference 46.

fusion results of Figure 16 are qualitatively consistent with those of fluorescence recovery after photo-bleaching studies of lateral DMPC–cholesterol binary mixture model membranes (42).

Protein function. Many examples exist that document the influence of cholesterol on the biochemical functioning of various cellular functions. We shall here focus attention on cases where cholesterol exerts an effect on protein function *via* modulation of certain physical properties of lipid bilayers. Possible candidates for such physical properties include hydrophobic bilayer thickness (4) and the lateral pressure profile of bilayers (43). Both of these properties are strongly influenced by the presence of cholesterol. Specifically, cholesterol tends to increase the thickness of lipid bilayers in the fluid phase and to shift the balance of the lateral pressures toward the interior of the bilayer.

A vast amount of experimental evidence strongly suggests that the hydrophobic matching principle, or some other physical principle related to it, is relevant for membrane organization as well as for membrane function (44,45). For example, a number of membrane channels, ion pumps, and sugar transporters, when incorporated into lipid bilayers of different thicknesses, function optimally for a certain narrow range of thicknesses, where they presumably are hydrophobically well matched. Thickness alterations induced internally or by external stimuli may therefore be seen as a way of triggering these proteins to enhance or suppress their function. To illustrate this principle, we shall describe the example of the transmembrane pump Na^+,K^+-ATPase that takes care of the delicate balance of sodium and potassium ions across biological membranes (46). Figure 17 shows that the activity of the pump is maximal for a certain lipid type and hence for a specific membrane thickness. If cholesterol is added to the membrane, the data demonstrate that the maximum moves toward lipid membranes composed of shorter lipids. This can be rationalized *via* the hydrophobic matching principle, recalling that cholesterol tends to thicken fluid membranes, which in turn will compensate for the shorter lipids.

The latter observation suggests a more general principle to be operative by which cholesterol may be used as a regulator of membrane function and the sorting and targeting of proteins, possibly *via* hydrophobic matching. The following serves as an illustration. Proteins are synthesized at the ribosomes placed in the endoplasmatic reticulum. From there they are transported *via* the Golgi to the various parts of the cell where they belong, e.g., in the plasma membrane. This transport, which is referred to as the secretory pathway, requires a sorting of the proteins, which is performed in the Golgi. Some proteins carry specific tags that will actively target them to their destination; others will flow passively through the cell. The question arises as to how these flowing proteins end up in the right membranes. It has been proposed (47) that the sorting along the secretory pathway may be performed by means of a gradient in the hydrophobic thickness of the membrane systems that the proteins have to pass on their way to their target. Indeed, the membrane contents of cholesterol and sphingomyelin, which both tend to enlarge membrane thickness, are found to increase going from the endoplasmatic reticulum, *via* the Golgi, to the plasma membrane. Furthermore, there is evidence that the proteins that are supposed to stay in the Golgi have hydrophobic domains that are shorter by about five amino acids compared with those of the plasma membrane. The set of different membranes along the secretory pathway may hence act as a molecular sieve, exploiting the hydrophobic matching condition. It is possible that this sieving mechanism is controlled by membrane rafts. Since cholesterol has a significant effect on membrane thickness and since integral membrane proteins are hydrophobically matched to their membranes, it is likely that the transmembrane proteins have closely co-evolved along with the sterols. The proposed sorting mechanism has recently been challenged by data that show that the bilayer thickness of exocytic pathway membranes is modulated by membrane proteins rather that cholesterol (48).

Certain proteins seem to prefer association with rafts and hence with cholesterol-rich membrane domains. An illustration of such a putative raft is provided in Figure 18. Many of these proteins carry a hydrocarbon chain anchor that fits snugly into the tight packing of the raft. Recruitment of proteins to the rafts or detachment of proteins from the rafts can conveniently be facilitated by enzymatic cleavage or attachment of appropriate hydrocarbon chains. For example, long saturated acyl chain anchors have affinity for the ordered raft structure, whereas the more bulky isoprenyl chain anchors prefer to be in the liquid-disordered phase outside the rafts.

Rafts have been shown to facilitate the communication between the two monolayer leaflets of the bilayer and to be involved in cell surface adhesion and motility. Furthermore, there are indications that rafts are involved in cell surface signaling and the intracellular trafficking and sorting of lipids and pro-

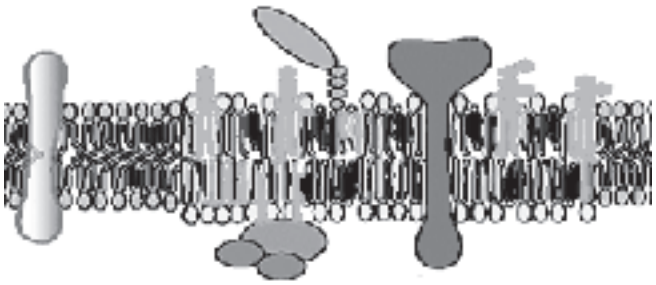

FIG. 18. Schematic illustration of a membrane raft, consisting of a lipid patch enriched in sphingolipids, glycolipids, and cholesterol (highlighted in black) to which certain proteins are attached. The raft is pictured thicker than the bilayer in which it is embedded. Adapted from www.glycoforum.gr.jp/science/word/glycolipid/GLD01E.html.

teins (21). It is interesting to note that some of these functions become impaired when cholesterol, which appears to be a necessary molecular requirement for raft formation, is extracted from the membranes.

A particularly important type of membrane domain is the so-called caveolae that appear as invaginations of the membrane (49). Caveolae are specialized lipid domains enriched in cholesterol and glycosphingolipids that are formed by the small transmembrane protein caveolin. Caveolae are found in a number of cell types, e.g., endothelial cells, and are involved in cholesterol transport, cytosis, and signal transduction.

CHOLESTEROL—EFFECTS OF ITS ABSENCE: COMPARISON WITH OTHER STEROLS.

So far, we have described the effects of cholesterol and lanosterol on the physical properties of lipid bilayer membranes with a view to understanding the related physical and biological implications. In this context, it must be noted that any significant decrease in the concentration of cholesterol in the body can result in severe health problems. A case in point is the autonomal recessive syndrome, known as the Smith-Lemli-Opitz syndrome (SLOS), which is found when infants are born with a decreased body concentration of the enzyme 7-dihydrocholesterol (7DHC) reductase. This enzyme converts 7DHC to cholesterol at the final stage of cholesterol synthesis by the removal of one double bond. SLOS is manifested by a variety of conditions including microcephalus, mental retardation, and second and third toe syndactaly; the severity of these depends on the magnitude of the decrease in cholesterol concentration (50).

As pointed out above, cholesterol is predicted to be important for several plasma membrane-based properties, which include raft formation, protein sorting, and cell signaling; e.g., cholesterol acts as precursor to mammalian steroid hormones and insect ecdysones. There must, therefore, be important changes in plasma membrane properties resulting from the deficiency in cholesterol. These are as yet unknown and should be investigated. The greater abundance of 7DHC does not appear to compensate for the concomitant absence of cholesterol.

The presence of sterols is ubiquitous in the plasma membranes of eukaryotic cells. For example, ergosterol is the dominant sterol in the plasma membranes of fungal cells, whereas phytosterols (such as campesterol, sitosterol, and stigmasterol) are found in plant plasma membranes. It has been shown that these sterols, when ingested, are recognized by the body and decomposed in the liver. There is a disease, however, known as sitosterolemia (51) for which these three phytosterols are not decomposed. Under these circumstances they remain in the body and are shown to be detrimental to human health. If not treated, sitosterolemia can lead to severe coronary problems leading to premature death. Furthermore, mammalian cells cannot use phytosterols and their presence may lead to a reduction in cholesterol concentration (51).

These considerations show that cholesterol is vital for human and, by extension, vertebrate health and that other sterols would not be able to substitute fully for it in the body. But this alone does not totally address the unique properties of cholesterol. Since relatively little is known about the detailed interaction of phytosterols with lipids, we begin by examining the plasma membrane environment of ergosterol in baker's yeast (*Saccharomyces cerevisiae,* or SC). In this context, Low *et al.* (52) prepared sterol auxotrophs of SC (from which the sterols had been removed) and then grew them in a medium containing exogenous sterols (cholesterol, ergosterol, sitosterol, or stigmasterol). Analysis of the resultant growth products revealed that the exogenous sterols regulated the phospholipid content and sterol concentration in the yeast auxotrophs, thus creating their optimal membrane environment.

As to the specific lipid content of SC, Schneiter *et al.* (53) identified specific lipid molecules of both the plasma membrane and the membranes of organelles of the X2180-IF wild-type strain of SC by using ionization tandem MS, which requires only small samples. The results for the plasma membrane are as follows. The phosphoinositol (PI)-based sphingolipids form 30% of the total phospholipid content of the plasma membrane, the other 70% being composed of glycerophospholipids (GPL); this observation is in agreement with the results of Patton and Lester (54). Interestingly, the acyl chain of the sphingolipids was highly saturated (26:0), and free ceramide with the same chain length was also present in abundance. It is not known, however, whether the ceramide is present as a precursor of the sphingolipids or whether it has a specific function in the plasma membrane. The GPL were mostly composed of a saturated acyl chain (e.g., 14:0 and 16:0) and a monounsaturated acyl chain (e.g., 16:1). In contrast to the case of higher eukaryotic cells, however, neither glycolipids nor lipids with polyunsaturated acyl chains were found. Schneiter *et al.* (53) also found that the concentration of disaturated lipids in all SC membranes was very small.

The range of polar heads of the GPL had already been found by Zinser *et al.* (55,56) for the same strain of SC in the same growth medium (YPD). The major GPL polar heads were found to be phosphatidylcholine at 16.8%, PI at 17.1%, phosphatidylserine at 33.6%, and phosphatidylethanolamine at 20.3%.

The specific lipid content of plant plasma membranes (57) is again different in that the lipid acyl chain content includes a high concentration of doubly and triply unsaturated acyl chains

(18:2) and (18:3) in, for example, barley roots and cauliflower. Also, unlike the case of both vertebrate and fungal plasma membranes, there appears to be no unique sterol species in plant plasma membranes. For example, barley root plasma membrane contains 16% campesterol, 24% stigmasterol, and 60% sitosterol, again indicating that plasma membrane stability requires specific lipid and sterol content depending on the species.

With respect to lipid-sterol interactions (excepting cholesterol) the only related phase diagram investigated in detail is that of DPPC-ergosterol using deuterium-NMR (16). This phase diagram is qualitatively identical to that of DPPC-cholesterol. This shows that ergosterol stabilizes the liquid-ordered phase in the same manner as cholesterol, whereas lanosterol does not. This correlates well with the result that raftlike behavior has been observed in SC (58) since DPPC is a reasonable model for saturated sphingolipids. The case of POPC-ergosterol bilayers is completely different from the case of POPC-cholesterol. POPC has one monounsaturated oleoyl chain and one saturated palmitoyl chain and is therefore a good model for fungal plasma membrane lipids. Urbina *et al.* (59) observed that POPC-cholesterol bilayers have properties similar to DPPC-cholesterol bilayers, but at lower temperatures, whereas POPC-ergosterol bilayers behave in a strange manner. Recent work by Hsueh *et al.* (16) shows that the concentration maximum of ergosterol in POPC bilayers at room temperature is 20 mol%, above which excess ergosterol probably forms a monohydride with water. The biological significance of this result is as yet unknown, but we are investigating the phase behavior of other fungal-lipid bilayer systems containing ergosterol to determine whether this effect is ubiquitous.

In the context of raft formation, Xu *et al.* (60) used ternary mixtures containing a high-T_m lipid, a low-T_m lipid, and various sterols together with fluorescence spectroscopy to find the effect of natural sterols and sphingolipids on the formation of ordered raft domains. They showed that the extent of domain (raft) formation is greatest for ergosterol followed by stigmasterol, sitosterol, and cholesterol. Clearly, further work is required to study the phase diagrams of other lipid-sterol bilayers systems, particularly those related to plant plasma membranes. Finally, a precise understanding of the nature of rafts in eukaryotic plasma membranes is still unavailable.

ACKNOWLEDGMENTS

MEMPHYS—Center for Biomembrane Physics is supported by the Danish National Research Foundation. M.J.Z. is supported by the National Science and Engineering Research Council of Canada (NSERC).

REFERENCES

1. Mouritsen, O.G. (2005) *Life—As a Matter of Fat. The Emerging Science of Lipidomics*, Springer-Verlag, Heidelberg.
2. Mouritsen, O.G., and Andersen, O.S. (eds.) (1998) In Search of a New Biomembrane Model, *Biol. Skr. Dan. Vid. Selsk. 49,* pp. 1–214.
3. Kinnunen, P.K.J. (1991) On the Principles of Functional Ordering in Biological Membranes, *Chem. Phys. Lipids 57*, 375–399.
4. Jensen, M.Ø., and Mouritsen, O.G. (2004) Lipids do influence protein function—The hydrophobic matching hypothesis revisited, *Biochim. Biophys.* Acta 1666, 205–226.
5. Peet, M., Glen, I. and Horrobin, D.F. (eds.) (1999) *Phospholipid Spectrum Disorder in Psychiatry*, Marius Press, Carnforth, United Kingdom.
6. Crawford, M., and Marsh, D. (1989) *The Driving Force*, Harper & Row, New York.
7. Hilgeman, D.W. (2003) Getting ready for the decade of the lipids, *Annu. Rev. Physiol. 65*, 697–700.
8. Kurzchalia, T.V., and Ward, S. (2003) Why do worms need cholesterol? *Nature Cell. Biol. 5*, 684–688.
9. Bloom, M., and Mouritsen, O.G. (1995) The evolution of membranes, in *Handbook of Biological Physics Vol. I: Structure and Dynamics of Membranes* (Lipowsky, R., and Sackmann, E., eds.), pp. 65–95 Elsevier Science B.V., Amsterdam.
10. Cavalier-Smith, T. (1987) The origin of eukaryote and archaebacterial cells, *Ann. NY Acad. Sci. 503*, 17–54.
11. Bloch, K. (1983) Sterol structure and membrane function, *CRC Crit. Rev. 14*, 47–92.
12. Bloch, K. (1994) *Blondes in Venetian Paintings, the Nine-Banded Armadillo, and Other Essays in Biochemistry*, Yale University Press, New Haven, MA.
13. Miao, L., Nielsen, M., Thewalt, J., Ipsen, J.H., Bloom, M., Zuckermann, M.J., and Mouritsen, O.G. (2002) From lanosterol to cholesterol: Structural evolution and differential effects on lipid bilayers, *Biophys. J. 82*, 1429–1444.
14. Ipsen, J.H., Mouritsen, O.G., Karlström, G., Wennerström, H., and Zuckermann, M.J. (1987) Phase equilibria in the lecithin–cholesterol system, *Biochim. Biophys. Acta 905*, 162–172.
15. Vist, M., and Davis, J.H. (1990) Phase equilibria of cholesterol/dipalmitoylphosphatidylcholine. ^{2}H nuclear magnetic resonance and differential scanning calorimetry, *Biochemistry 29,* 451–464.
16. Hsueh, Y.-W., Gilbert, K., Trandum, C., Zuckermann, M.J., and Thewalt, J. (2004) The effect of ergosterol on DPPC bilayers: A deuterium NMR and calorimetric study, *Biophys. J.,* in press.
17. Mouritsen, O.G., and Jørgensen, K. (1994) Dynamical order and disorder in lipid bilayers, *Chem. Phys. Lipids 73*, 3–26.
18. Bergelson, L.O., Gawrisch, K., Feretti, J.A., and Blumenthal, R. (eds.) (1995) Domain organization in biological membranes, *Mol. Membr. Biol. 12*, 1–162.
19. Mouritsen, O.G., and Jørgensen, K. (1997) Small-scale lipid-membrane structure: Simulation vs. experiment, *Curr. Opin. Struct. Biol. 7*, 518–527.
20. Simons, K., and Ikonen, E. (1997) Functional rafts in cell membranes, *Nature 387*, 569–572.
21. Edidin, M. (2003) The state of lipid rafts: From model membranes to cells, *Annu. Rev. Biophys. Biomol. Struct. 32*, 257–283.
22. McMullen, T.P.W., Lewis, R.N.A.H., and McElhaney, R.N. (2004) Cholesterol-phospholipid interactions, the liquid-ordered phase in model and biological membranes, *Curr. Opin. Colloid Interface. Sci. 8*, 459–468.
23. Maxfield, F.R. (2002) Plasma membrane microdomains, *Curr. Opin. Cell Biol.14,* 483–487.
24. Dietrich, C., Yang, B., Fujiwara, T., Kusumi, A., and Jacobson, K. (2002) The relationship of lipid rafts to transient confinement zones detected by single particle tracking, *Biophys. J. 82*, 274–284.
25. Xu, X., and London, E. (2000) The effect of sterol structure on membrane lipid domains reveals how cholesterol can induce lipid domain formation, *Biochemistry 39*, 843–849.
26. Dietrich, C., Bagatolli, L.A., Volovyk, Z., Thompson, N.L., Levi, M., Jacobson, K., and Gratton, E. (2001) Lipid rafts reconstituted in model membranes, *Biophys. J. 80*, 1417–1428.

27. Milhiet, P.E., Giocondi, M.-C., and Le Grimmelec, C. (2002) Cholesterol is not crucial for the existence of microdomains in kidney brush-border membrane models, *J. Biol. Chem. 277*, 875–878.
28. Silvius, J.R. (2003) Role of cholesterol in lipid raft formation: Lessons from lipid model systems, *Biochim. Biophys. Acta 1610*, 174–83.
29. Rinia, H.A., Snel, M.M.E., van der Eerden, J.P.J.M., and de Kruijff, B. (2001) Visualizing detergent resistant domains in model membranes with Atomic Force Microscopy, *FEBS Lett. 501*, 92–96.
30. Bernardino de la Serna, J., Perez-Gil, J., Simonsen, A.C., and Bagatolli, L.A. (2004) Cholesterol rules: Direct observation of the coexistence of two fluid phases in native pulmonary surfactant membranes at physiological temperatures, *J. Biol. Chem.* 279, 40715–40722.
31. McConnell, H.M. and Radhakrishnan, A. (2003) Condensed complexes of cholesterol and phospholipids, *Biochim. Biophys. Acta 1610*, 159–173.
32. Yeagle, P.L. (ed.) (1988) *Biology of Cholesterol*, CRC Press, Boca Raton, Florida.
33. Finegold, L.X. (ed.) (1993) *Cholesterol and Membrane Models,* CRC Press, Boca Raton, Florida.
34. Vance, D.E. and Van den Bosch, H. (eds.) (2000) Cholesterol in the year 2000, *Biochim. Biophys. Acta 152*, 1–373 (2000).
35. Corvera, E., Mouritsen, O.G., Singer, M.A., and Zuckermann, M.J. (1992) The permeability and the effect of acyl-chain length for phospholipid bilayers containing cholesterol: Theory and experiments, *Biochim. Biophys. Acta 1107*, 261–270.
36. Disalvo, A. and Simon, S.A. (eds.) (1995) *Permeability and Stability of Lipid Bilayers*, CRC Press, Boca Raton, FL.
37. Trandum, C., Westh, P., Jørgensen, K., and Mouritsen, O.G. (2000) A thermodynamic study of the effects of cholesterol on the interaction between liposomes and ethanol, *Biophys. J. 78*, 2486–2492.
38. Lemmich, J., Hønger, T., Mortensen, K., Ipsen, J.H., Bauer, R., and Mouritsen, O.G. (1996) Solutes in small amounts provide for lipid-bilayer softness: Cholesterol, short-chain lipids, and bola lipids, *Eur. Biophys. J. 25*, 61–65.
39. Henriksen, J.R., Rowat, A.C., and Ipsen, J.H. (2004) Vesicle fluctuation analysis of the effects of sterols on membrane bending rigidity, *Eur. Biophys. J. 33*, 732–741.
40. Vattulainen, I., and Mouritsen, O.G. (2004) Diffusion in membranes, in *Diffusion in Condensed Matter* (Kärger, J., Heitjans, P., and Haberlandt, R., eds.), Springer-Verlag, Berlin.
41. Polson, J.M., Vattulainen, I., Zhu, H., and Zuckermann, M.J. (2001) Simulation study of lateral diffusion in lipid-sterol bilayer mixtures, *Eur. Phys. J. E Soft Matter 5*, 485–497.
42. Almeida P.F., Vaz, W.L., and Thompson, T.E. (1992) Lateral diffusion in the liquid phases of dimyristoylphosphatidylcholine/cholesterol lipid bilayers: A free volume analysis, *Biochemistry 31*, 6739–6747.
43. Cantor, R.S. (1999) The influence of membrane lateral pressures on simple geometric models of protein conformational equilibria, *Chem. Phys. Lipids 101*, 45–56.
44. Dumas, F., Lebrun, M.C., and Tocanne, J.F. (1999) Is the protein/lipid hydrophobic matching principle relevant to membrane organization and functions? *FEBS Lett. 458*, 271–277.
45. Lee, A.G. (2003) Lipid-protein interactions in biological membranes: A structural perspective, *Biochim. Biophys. Acta 1612*, 1–40.
46. Cornelius, F. (2001) Modulation of Na,K-ATPase and Na-ATPase activity by phospholipids and cholesterol. I. Steady-state kinetics, *Biochemistry 40*, 8842–8851.
47. Munro, S. (1998) Localization of proteins to the Golgi apparatus, *Trends Cell. Biol. 8*, 11–15.
48. Mitra, K., Ubarretxena-Belandia, I., Taguchi, T., Warren, G., and Engelman, D.M. (2004) Modulation of the bilayer thickness of exocytic pathway membranes by membrane proteins rather that cholesterol, *Proc. Natl. Acad. Sci. USA 101*, 4083–4088.
49. Anderson, R.G.W., and Jacobson, K. (2002) A role for lipid shells in targeting proteins to caveolae, rafts, and other lipid domains, *Science 296*, 1821–1825.
50. Porter, F.D. (2000) RSH/Smith-Lemli-Opitz syndrome: a multiple anomaly/mental retardation syndrome due to an inborn error of cholesterol biosynthesis, *Mol. Genet. Metab. 71*, 163–174 (2000).
51. Steiner, R.D. (2004) Sterolemia, http://www.emedicine.com/ped/topic2110.htm.
52. Low, C., Rodriguez, R.J., and Parks. L.W. (1985) Modulation of Yeast Plasma Membrane Composition of a Yeast Auxotroph as a Function of Exogenous Sterol, *Arch. Biochem. Biophys. 260*, 530–538.
53. Schneiter, R., Brügger, B., Sandhoff, R., Zellnig, G., Leber, A., Lampl, M., Athenstaedt, K., Hrastnik, C., Eder, S., Daum, G., *et al.* (1999) Electrospray ionization tandem mass spectrometry (ESI-MS/MS) analysis of the lipid molecular species composition of yeast subcellular membranes reveals acyl chain-based sorting/remodeling of distinct molecular species en route to the plasma membrane, *J. Cell Biol. 146*, 741–754.
54. Patton, J.L., and Lester, R.L. (1991) The phosphoinositol sphingolipids of *Saccharomyces cerevisiae* are highly localized in the plasma membrane, *J. Bacteriol. 173*, 3101–3108.
55. Zinser, E., Sperka-Gottlieb, C.D., Fasch, E.V., Kohlwein, S.D., Paltauf, F., and Daum, G. (1991) Phospholipid synthesis and lipid composition of subcellular membranes in the unicellular eukaryote *Saccharomyces cerevisiae*, *J. Bacteriol. 173*, 2026–2034.
56. Zinser, E., Paltauf, F., and Daum, G. (1993) Sterol composition of yeast organelle membranes and subcellular distribution of enzymes involved in sterol metabolism, *J. Bacteriol. 175*, 2853–2858.
57. Larsson, C., and Møller, I.M. (eds.) (1990) *The Plant Plasma Membrane; Structure Function and Molecular Biology*, pp. 6–9, Springer Verlag, Heidelberg. .
58. Bagnat, M.S., Shevchenko, A., and Simons, K. (2000) Lipid rafts function in biosynthetic delivery of proteins to the cell surface in yeast, *Proc. Natl. Acad. Sci. USA 97*, 3254–3259.
59. Urbina, J.A., Pekerar, S., Le, H.B., Patterson, J., Montez, B., and Oldfield, E. (1995) Molecular order and dynamics of phosphatidylcholine bilayer membranes in the presence of cholesterol, ergosterol and lanosterol: A comparative study using ^{2}H-, ^{13}C- and ^{31}P-NMR spectroscopy, *Biochim. Biophys. Acta. 1238*, 163–176.
60. Xu, X., Bittman, R., Duportail, G., Heissler, D., Vilcheze, C., and London, E. (2001) Effect of the structure of natural sterols and sphingolipids on the formation of ordered sphingolipid/sterol domains (rafts). Comparison of cholesterol to plant, fungal, and disease-associated sterols and comparison of sphingomyelin, cerebrosides, and ceramide, *J. Biol. Chem. 276*, 33540–33546.

[Received August 5, 2004; accepted November 22, 2004]

Transient Confinement Zones: A Type of Lipid Raft?

Yun Chen[a], Bing Yang[a], and Ken Jacobson[a,b,*]

[a]Department of Cell and Developmental Biology and [b]Lineberger Comprehensive Cancer Center, University of North Carolina at Chapel Hill, Chapel Hill, North Carolina 27599-7090

ABSTRACT: Many important signaling events are initiated at the cell membrane. To facilitate efficient signal transduction upon stimulation, membrane microdomains, also known as lipid rafts, are postulated to serve as platforms to recruit components involved in the signaling complex, but few methods exist to study rafts *in vivo*. Single particle tracking provides an approach to study the plasma membrane of living cells on the nano-scale. The trajectories of single gold particles bound to membrane proteins and lipids are characterized in terms of both random and confined diffusion; the latter occurs in "transient confinement zones". Here we review transient confinement zones and some of their implications for membrane structure and function.

Paper no. L9571 in *Lipids 39*, 1115–1119 (November 2004).

In the Singer-Nicolson fluid mosaic model, the cell membrane is considered as a 2-D oriented solution of integral proteins in a viscous phospholipid bilayer (1). However, more recent single particle tracking (SPT) experiments suggest the need to modify the original model (2). In addition, over the past decade, numerous biochemical studies have demonstrated that a significant fraction of plasma membrane lipids including cholesterol, saturated phospholipids, and sphingolipids exhibit some degree of detergent resistance. This fraction also includes glycosylphosphatidylinositol (GPI)-anchored proteins and certain transmembrane proteins (3–5). Although detergent-resistant membranes (DRM) are postulated to represent putative submicron-sized lipid rafts on the cell surface (for reviews, see Refs. 6–10), the *in vivo* correlate of DRM has not been established. In detergent extraction experiments, the lipid and protein compositions of DRM depend strongly on the nature and concentration of the nonionic detergent used, as well as the time and the temperature of the extraction (11,12). Moreover, it has been observed that the nonionic detergent Triton-X can promote formation of microdomains in model membranes (13). Therefore, assuming DRM are lipid rafts could provide a grossly misleading view of membrane microstructure. Different approaches other than detergent extraction are required to test the lipid raft hypothesis.

*To whom correspondence should be addressed at Department of Cell and Developmental Biology, 220 Taylor Hall, University of North Carolina, Chapel Hill, NC 27599-7090. E-mail: frap@med.unc.edu

Abbreviations: DOPE, 1,2-dioleoyl-*sn*-glycero-3-phosphoethanolamine; DRM, detergent-resistant membrane(s); Fabs, single-valence fragments; GFP, green fluorescent protein; GPI, glycosylphosphatidylinositol; GSL, glycosphingolipids; RCT, relative confinement time; SFK, Src family kinase; SPT, single particle tracking; TCZ, transient confinement zone(s).

Usually, light microscopy resolution is limited to ~250 nm, meaning that microdomains smaller than this cannot be measured, although they can be detected if they are bright enough. By fluorescence microscopy, many raft components, as defined by detergent extraction, appear uniformly distributed although there are notable exceptions (14); but clustering can be seen by fluorescence resonance energy transfer in some cases (15,16).

SPT provides an alternative way to investigate the heterogeneity of cell membranes. By attaching antibody-coated submicron-sized colloidal gold particles to molecules on the cell membrane, the dynamics of a small number of molecules or even a single molecule can be recorded and studied by tracing trajectories of the particles. SPT has two advantages: (i) The particles used give a signal that does not photobleach, thereby extending the observation time; and (ii), 40-nm gold particles are small enough to reduce the chance for perturbation. Available detection methods are based on the intense Rayleigh scattering, which can be applied to submicron particles down to 30 nm in diameter. Although SPT presents insights about membrane structures, it does have limitations. The path of single particles is not controllable, and SPT only covers a small area of the cell membrane. Also, when coating specific antibodies on the gold particles, it is very difficult to achieve precise valence control, meaning that more than one surface molecule may anchor the particle to the cell membrane.

Rather than being exclusively 2-D random walks, the trajectories of single particles that are attached to surface molecules on the cell membrane often exhibit a variety of trajectories in addition to random walks. These include directed movement, confined movement, and anchored behavior (Fig. 1) (17,18), a result not explicitly anticipated by the Singer-Nicolson fluid mosaic model. Temporary confinements (Fig. 1B) are detected in the trajectories of membrane proteins that cannot be accounted for by the large family of random walks (17). These temporary confinements are termed transient confinement zones (TCZ). The existence of TCZ supplies another piece of evidence supporting membrane lateral heterogeneity, although the mechanism of transient confinement remains to be elucidated.

DETECTION OF TCZ AND THEIR SIGNIFICANCE

When the lateral mobility of surface molecules on the cell membrane is examined by SPT, careful analysis is required to characterize the molecular trajectories. To be able to distin-

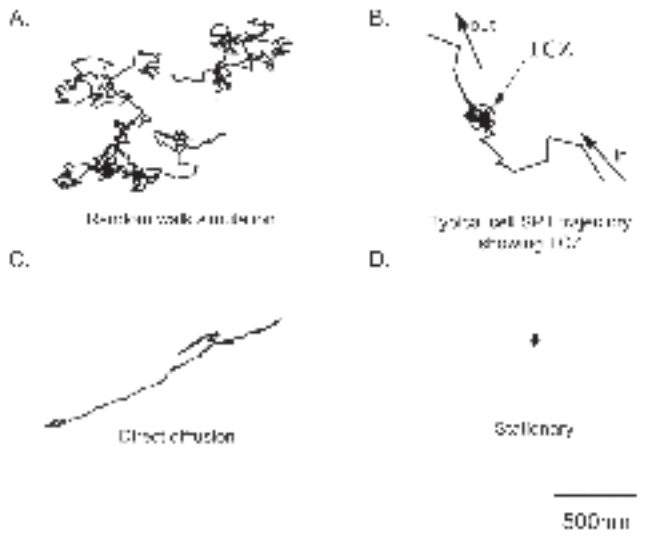

FIG. 1. Various trajectories from single-particle tracking (SPT) experiment on murine fibroblasts or simulation: (A) a typical 2-D random walk by computer simulation; (B) a transient confinement zone (TCZ) is encountered when the particle diffuses on the cell membrane; (C) directed movement; (D) an anchored particle.

guish confined diffusion or directed transport, both of which reveal interesting biological features, from simple Brownian motion, it is necessary to establish algorithms that can justifiably reject those random walks that might look confined or directed. Saxton (19) has studied the 2-D diffusion in a series of Monte Carlo simulations. For 2-D random walkers, the probability φ that a molecule, having diffusion coefficient D, will stay in a region of radius R, for a period of time t is given as:

$$\log \varphi = 0.2048 - \frac{2.5117\, Dt}{R^2} \qquad [1]$$

This allowed Simson *et al.* (17) to develop an algorithm that detects confinements due to nonrandom means. Simson *et al.* introduced the probability level index L to characterize the probabilities of nonrandom confinements. The relationship between L and ϕ is:

$$L = \begin{cases} -\log(\varphi) - 1 & \varphi \le 0.1 \\ 0 & \varphi > 0.1 \end{cases} \qquad [2]$$

The higher the value of L is, the more likely a particle is confined due to a nonrandom mechanism. Because a random walk can temporarily mimic confinement, the goal of this algorithm is to reject those random walks that look like transient confinement. To achieve this goal, the algorithm takes advantage of the fact that the peaks of probability profiles arising from mimicked confinement in random walks are usually lower and narrower than genuine ones. By experimenting with both actual and simulated data, an optimized threshold (L_c) value is obtained so that the algorithm is able to detect real confinement with a minimal error rate less than 0.07% and to reject mimicked ones with an accuracy of about 98.5%. Simson's algorithm also implements a low pass filter to smooth the probability profile (17), thereby suppressing short-lived mimicked confinement from Brownian motion. After applying the algorithm to SPT trajectories, TCZ are detected, and the sizes and dwell time of particles in the TCZ are computed. The computed sizes of confinements and dwell time of particles in TCZ are dependent on the time resolution of SPT. That is because with greater time resolution, two different confinements that are very close are more likely to be distinguished. At lower time resolution, such a structure will appear as a single bigger confinement with a longer dwell time. For this reason, before comparing transient confinement analysis results in terms of size and dwell time, it is important ensure the data were acquired at similar time resolution.

EXAMPLES OF TCZ

Previous papers from our group have reported TCZ being detected by SPT for GPI-anchored proteins, glycosphingolipids (GSL), and phospholipids (17,18,20,21). These TCZ are of a size ranging from 100 to 300 nm in diameter, and the diffusing particles are trapped for several seconds. Moreover, upon the suppression of GSL synthesis (20) or depletion of cholesterol (21), the abundance and the size of the zones were markedly diminished. Dietrich *et al.* (21) also found that TCZ could be revisited after particles escaped, suggesting that zones could be stable for tens of seconds and that diffusion within the zones was reduced by a factor of ~2, which was consistent with the particle diffusing within in a cholesterol-rich, liquid-ordered state. These experiments indicate that TCZ exhibit some of the physical and chemical characteristics postulated for hypothetical lipid rafts.

A few other examples of confinement have appeared in the literature. Daumas *et al.* (22,23) have studied the diffusion of a G-protein-coupled receptor, the μ-opioid receptor, by gold particle SPT. In their experiments, they observed transient confinement as well. However, they fitted the data to a different mathematical model, in which the diffusing surface proteins are confined to a domain which itself diffuses, the confinement being due to "long-range attraction between membrane proteins." In other words, the surface proteins belong to a "walking confined diffusion mode" composed of long-term random diffusion of a domain characterized by $D = 1.3 \times 10^{-3}$ μm^2/s and short-term confined diffusion within the domain characterized by $D \sim 10^{-1}$ μm^2/s.

SPT has been applied to the study of the kinetics of membrane-bound receptors as well. Instead of gold particles, Meier and colleagues (24) used 0.5 μm latex beads to track the movement of gephyrin, a ligand for glycine receptor, by SPT. They observed that particles attached to glycine receptor subunits expressed without gephyrin moved rapidly in the plane of the membrane for most of the time, with an estimated diffusion coefficient of ~2.7×10^{-2} μm^2/s, whereas co-expression of glycine receptors that contain the gephyrin binding domain and gephyrin-green fluorescent protein (GFP) resulted in long periods of confinement characterized by very limited slow movement interspersed with periods of rapid particle movement. The

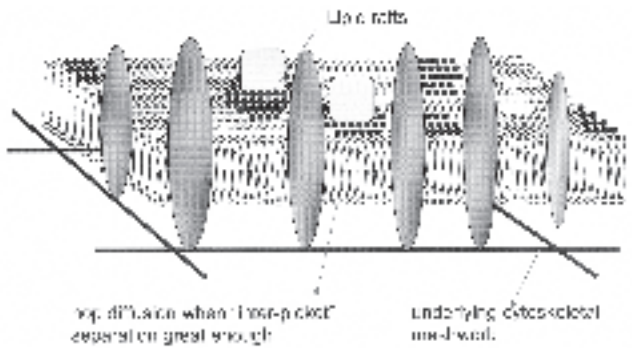

FIG. 2. Fence and picket structure of the plasma membrane model proposed by Ritchie *et al.* (28): a schematic representation of the fundamental microstructure on cell membranes. The plasma membrane consists of a lipid bilayer with embedded proteins. These "picket" proteins are immobilized by being bound to the underlying actin-based cytoskeleton network and serve to separate the cell membrane into numerous small compartments. Mobile lipids and protein tissue within one compartment translocate to an adjacent one when fluctuations in the separation between pickets permit "hop diffusion." Putative elementary lipid rafts (filled circles with tails) must disassemble on a time scale of milliseconds in order to allow raft proteins to "hop" to the adjacent compartment.

transient confinements were spatially associated with gephyrin-GFP clusters visualized by fluorescence microscopy. And diffusion coefficients of particles during confined periods were 1–1.5 orders of magnitude lower than those measured during rapidly moving periods. Based on these observations, Meier and colleagues (24) speculated that limited diffusion of receptors during the confined state may be due to slow diffusion of the entire gephyrin cluster with bound receptors.

TRANSIENT CONFINEMENT IS INDUCED BY CROSS-LINKING

Fine details of membrane lateral diffusion. A continuing puzzle is why diffusion coefficients of membrane lipids are reduced by a factor of 5–20 from those on artificial bilayers (25–29). To address the problem, Fujiwara *et al.* (30,31) measured the movement of 1,2-dioleoyl-*sn*-glycero-3-phosphoethanolamine (DOPE), which by virtue of its two unsaturated acyl chains, is considered to be a typical nonraft lipid. By using SPT with an ultra-high temporal resolution of 25 μs per frame, as opposed to the conventional video sampling rate of 33 ms per frame, they found that the cell membrane is compartmentalized with regard to translational diffusion of DOPE. That is, a single DOPE molecule is temporarily confined within a 30 to 230-nm compartment, the size depending on cell type (31), for several milliseconds on average before it hops to a neighboring compartment. This compartmentalization is dependent on the actin-based cytoskeleton underneath the cell membrane but is not sensitive to the removal of extracellular matrix or cholesterol. To explain their results, they proposed a membrane picket fence model (Fig. 2) (28,30). In the model, both lipids and proteins, regardless of their raft association, exhibit free diffusion—at rates comparable to those on artificial membranes—within plasma membrane compartments that are delimited by immobilized transmembrane proteins as anchored-pickets linked to the subjacent membrane cytoskeleton. The occasional hop to an adjacent compartment, which occurs roughly once every 11 ms, rate-limits the long-range diffusion. However, even if the effect from hop diffusion is taken into account, it does not completely explain the smaller long-range diffusion coefficients of GPI-anchored proteins such as Thy1 measured by SPT at 33 ms time resolution (21). The implication is that aggregation of proteins and/or lipids is the major reason for the reduced motion of surface molecules, primarily because the gold particles are pauci-valent. Indeed, it is plausible to regard the TCZ as a membrane domain that attracts certain cross-linked entities and thereby transiently confines these surface complexes.

Cleavage of antibodies that recognize the specific surface proteins into single-valence fragments (Fabs), followed by careful titration, permits coating gold particles in an apparent one-to-one ratio with these Fabs or ligands to surface proteins, making the particle effectively monovalent. Gold particles that recognize CD59, another GPI-anchored protein, exhibit similar diffusion rates and hop intervals when compared to DOPE at 25-μs resolution. Moreover, under these apparently monovalent conditions, no TCZ were observed at 33-ms resolution (7,29). By contrast, when the gold particles were deliberately made multivalent by coating the particles with intact antibodies at high concentration, short-range CD59 diffusion was considerably slower and TCZ were detected at 33-ms time resolution (7,29). This suggests that some form of cross-linking is required to observe TCZ. Interestingly, cross-linking-induced TCZ required cholesterol, intact actin filaments, and Src family kinase (SFK) activity. Intracellular calcium signals were closely associated in time with the formation of the TCZ. Taking all their data together, the Kusumi group (28) now suggests that lipid rafts are so small and short-lived in resting cells (Fig. 2) that a non-cross-linked single raft protein has almost the same short-range diffusion coefficient as a nonraft lipid molecule. However, upon cross-linking, the molecular cluster caused by multivalent gold particles not only diffuses more slowly but also triggers processes that stabilize lipid rafts. These cross-linked complexes are termed "cluster rafts." Cluster rafts are formed by various cross-linking agents including antibodies, and they are more stable and may be bigger than lipid rafts in resting cells. The cluster raft-stabilizing process is speculated to be caused by transient tethering onto the actin-based membrane skeleton. The likely involvement of signaling molecules in stabilizing cluster rafts suggests that lipid rafts serve as platforms that could locally initiate signal transduction (10).

To examine and verify the model proposed by Kusumi group (28), our laboratory now is investigating the behavior of other GPI-anchored proteins by SPT. To achieve maximal cross-linking, we incubated C3H fibroblast cells first with biotinylated anti-Thy1 antibodies, then anti-biotin antibody-coated colloidal gold particles, after which anti-mouse IgG an-

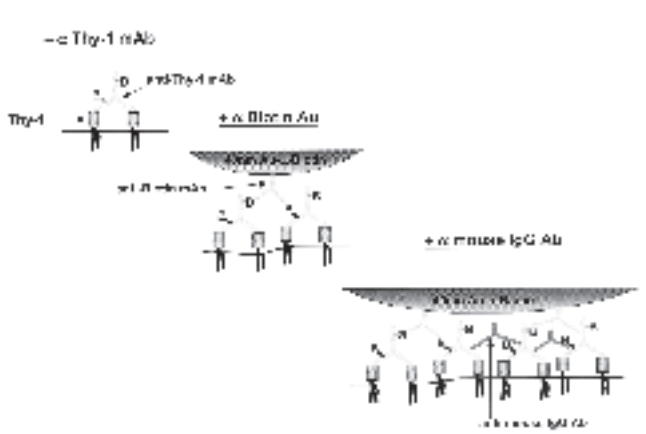

FIG. 3. Cross-linking scheme to cluster Thy-1 molecules on the cell surface: Biotinylated anti-Thy1 mouse antibodies are first incubated with cells to bind to Thy1 molecules on the cell membrane. The gold particle is coated with anti-biotin antibodies, which can bind to biotinylated anti-Thy1 monoclonal antibodies, and then added on the cell membrane to form gold-antibody-antigen complex. The complex under the gold particle is further cross-linked by an anti-mouse IgG secondary antibody, presumably forming clusters of Thy1 molecules on the cell surface.

tibodies were added (Fig. 3). We observed that maximal cross-linking increased the percentage of time (the relative confinement time, RCT) that a single particle spends in TCZ by more than twofold compared with control treatments without anti-mouse IgG applied. Under these conditions, we observed repeated transient anchorage, which means, in our experiments, that the displacement range of the particles is within ~20 nm for several seconds before the gold particles resume their trajectories on the cell membrane. The transient anchorage observed in maximal cross-linking experiments is distinct from conventional transient confinement. Whereas in normal transient confinement gold particles are localized in an area ranging from 100 to 300 nm in diameter, in which the particles move with a reduced diffusion coefficient, transient anchorage apparently stops the gold particles (to <20 nm). Addition of SFK inhibitor 4-amino-5-(4-chlorophenyl)-7-(*t*-butyl) pyrazolo(3,4-d) pyrimidine (PP2) reversed the RCT increase owing to transient anchorage, indicating SFK play a role in cross-linking-dependent TCZ formation/stabilization. Cholesterol depletion further reduced the RCT to 2%, indicating that cholesterol is essential for both TCZ existence and transient anchorage. Another GPI-anchored protein, CD73, a 5′-ectonucleotidase, exhibited qualitatively similar behavior in IMR-90 human fibroblasts, suggesting that these cross-linking-induced effects are quite general. In summary, confined behavior can be broken into two classes: true in-plane transient confinement and transient anchorage (SFK-mediated) of cluster rafts, as depicted in Figure 4. It appears that SPT can be used to reveal details of the early steps in cross-linking-induced signal transduction.

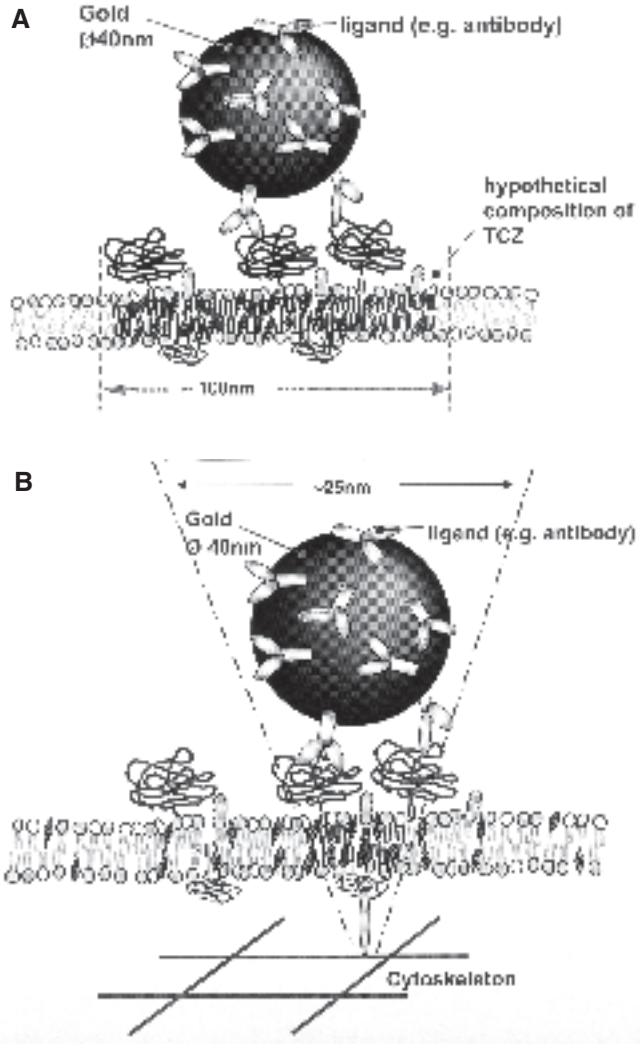

FIG. 4. Two different types of confinement induced by cross-linking. (A) At lower levels of cross-linking, the gold particle diffuses within the transient confinement zone, which has a diameter of ~100 nm; (B) at a higher level of cross-linking, the gold particle anchors to one spot for several seconds with a movement range of <25 nm due to temporary tethering to the cytoskeleton, mediated by Src family kinases.

ACKNOWLEDGEMENT

This work was supported by NIH grant GM41402.

REFERENCES

1. Singer, S.J., and Nicolson, G.L. (1972) The fluid mosaic model of the structure of cell membranes, *Science 175*(23):720–31.
2. Jacobson, K., Sheets, E.D. and Simson, R. (1995) Revisiting the fluid mosaic model of membranes, *Science 268*:1441–1442.
3. Brown, D.A. and J.K. Rose (1992) Sorting of GPI-anchored proteins to glycolipid-enriched membrane subdomains during transport to the apical cell surface, *Cell 68*:533–44.
4. Brown, D.A. and London, E. (1997) Structure of detergent-resistant membrane domains: does phase separation occur in bio-

logical membranes? *Biochem. Biophys. Res. Commun. 240*:1–7.
5. Brown, D.A. and London, E. Functions of lipid rafts in biological membranes, *Annu. Rev. Cell Dev. Biol. 14*:111–36.
6. Simons, K. and Ikonen, E. (2000) How cells handle cholesterol, *Science 290*:1721–1726.
7. Kusumi, A., Koyama-Honda, I. and Suzuki, K. (2004) Molecular dynamics and interactions for creation of stimulation-induced stabilized rafts from small unstable steady-state rafts, *Traffic 5*:213–230.
8. Jacobson, K., and Dietrich, C., Looking at lipid rafts? *Trends Cell Biol. 9*:87–91.
9. Simons, K., and Ikonen, E. (1997) Functional rafts in cell membranes, *Nature 387*:569–572.
10. Simons, K., and Toomre, D. (2000) Lipid rafts and signal transduction, *Nat. Rev. Mol. Cell Biol. 1*:31–9.
11. Shogomori, H., and Brown, D.A. (2003) Use of detergents to study membrane rafts: the good, the bad, and the ugly, *Biol. Chem. 384*:1259–1263.
12. Schuck, S., Honsho, M., Ekroos, K., ShevchenKo, A., and Simons, K. (2003) Resistance of cell membranes to different detergents, *Proc. Natl. Acad. Sci. USA 100*:5795–5800.
13. Heerklotz, H. (2002) Triton promotes domain formation in lipid raft mixtures, *Biophys. J. 83*:2693–2701.
14. Malinska, K., Malinsky, J., Opekarova, M., and Tanner, W. (2003) Visualization of protein compartmentation within the plasma membrane of living yeast cells. *Mol. Biol. Cell 14*:4427–4436.
15. Zacharias, D.A., Violin, J.D., Newton, A.C., and Tsien, R.Y. (2002) Partitioning of lipid-modified monomeric GFPs into membrane microdomains of live cells, *Science 296*:913–916.
16. Sharma, P., Varma, R., Sarasij, R.C., Ira, Groussel, K., Krishnamoorthy, G., Rao, M., and Mayor, S. (2004) Nanoscale organization of multiple GPI-anchored proteins in living cell membranes, *Cell 116*:577–89.
17. Simson, R., Sheets, E.D. and Jacobson, K. (1995) Detection of temporary lateral confinement of membrane proteins using single-particle tracking analysis. *Biophys. J. 69*:989–993.
18. Simson, R., Yang, B., Moore, S.E., Doherty, P., Walsh, F.S., and Jacobson, K.A. (1998) Structural mosaicism on the submicron scale in the plasma membrane. *Biophys J. 74*:297–308.
19. Saxton, M.J. (1993) Lateral diffusion in an archipelago. Single-particle diffusion, *Biophys. J. 64*:1766–1780.
20. Sheets, E.D., Lee, G.M., Simson, R., and Jacobson, K. (1997) Transient confinement of a glycosylphosphatidylinositol-anchored protein in the plasma membrane, *Biochemistry 36*: 12449–12458.
21. Dietrich, C., Yang, B., Fujiwara, T., Kusumi, A., and Jacobson, K. (2002) Relationship of lipid rafts to transient confinement zones detected by single particle tracking, *Biophys. J. 82*:274–284.
22. Daumas, F., Destainville, N., Millot, C., Lopez, A., Dean, D., and Salome, L. (2003) Confined diffusion without fences of a g-protein-coupled receptor as revealed by single particle tracking, *Biophys. J. 84*:356–366.
23. Daumas, F., Vannier, C., Serge, A., Triller, A., and Choquet, D. (2001) Interprotein interactions are responsible for the confined diffusion of a G-protein-coupled receptor at the cell surface, *Biochem. Soc. Trans. 31*:1001–1005.
24. Meier, J., Vannier, C., Serge, A., Triller, A., and Choquet, D. (2001) Fast and reversible trapping of surface glycine receptors by gephyrin, *Nat. Neurosci. 4*:253–260.
25. Jacobson, K., Ishihara, A., and Inman, R.(1987) Lateral diffusion of proteins in membranes, *Annu. Rev. Physiol. 49*:163–75.
26. Sonnleitner, A., Schutz, G.J., and Schmidt, T. (1999) Free brownian motion of individual lipid molecules in biomembranes, *Biophys. J. 77*:2638–2642.
27. Lee, G.M., Zhang, F., Ishihara, A., McNeil, C.L., and Jacobson, K.A. (1993) Unconfined lateral diffusion and an estimate of pericellular matrix viscosity revealed by measuring the mobility of gold-tagged lipids, *J. Cell Biol. 120*:25–35.
28. Ritchie, K., Iino, R., Fujiwara, T., Murase, K., and Kusumi, A. (2003) The fence and picket structure of the plasma membrane of live cells as revealed by single molecule techniques (Review), *Mol. Membr. Biol. 20*:13–18.
29. Subczynski, W.K. and Kusumi, A. (2003) Dynamics of raft molecules in the cell and artificial membranes: approaches by pulse EPR spin labeling and single molecule optical microscopy, *Biochim. Biophys. Acta. 1610*:231–243.
30. Fujiwara, T., Ritchie, K., Murakoshi, H., Jacobson, K., and Kusumi, A. (2002) Phospholipids undergo hop diffusion in compartmentalized cell membrane, *J. Cell Biol. 157*:1071–1081.
31. Murase, K., Fujiwara, T., Umemura, Y., Suzuki, K., Iino, R., Yamashita, H., Saito, M., Murakoshi, H., Ritchie, K., and Kusumi, A. (2004) Ultrafine Membrane Compartments for Molecular Diffusion as Revealed by Single Molecule Techniques, *Biophys. J. 86*:4075–4093.

[Received August 5, 2004; accepted December 9, 2004]

Environmental Light and Heredity Are Associated with Adaptive Changes in Retinal DHA Levels that Affect Retinal Function

Robert E. Anderson[a,*] and John S. Penn[b]

[a]Departments of Cell Biology and Ophthalmology, University of Oklahoma Health Sciences Center, and Dean A. McGee Eye Institute, Oklahoma City, OK; [b]Department of Ophthalmology and Visual Sciences, Vanderbilt University School of Medicine, Nashville, TN

ABSTRACT: Retinas of rats and mice react to environmental and genetic stimuli by altering the level of DHA in their rod outer segment membranes. We propose that this adaptation is a neuroprotective response to control the number of photons captured by rhodopsin and the efficiency of visual transduction, under conditions where excessive activation of the transduction cascade could lead to cell death.

Paper no. L9575 in *Lipids 39,* 1121–1124 (November 2004).

DHA (22:6n-3) is the most abundant FA in the retina, reaching levels of 50% in the rod outer segment (ROS) membranes (1), which also contain the photopigment rhodopsin. The largest amounts are found in the serine and ethanolamine phospholipids (PS and PE, respectively), but significant levels are found also in PC. DHA is esterified primarily in the 2-position of these phospholipids (2), although di-DHA molecular species occur in all three (3,4).

The retina tenaciously retains DHA and other n-3 PUFA during n-3 deprivation. Attempts to reduce the n-3 PUFA level by feeding weanling rats n-3-deficient diets produced only modest changes in retinal DHA levels (5). More significant changes could be produced by feeding pregnant rats an n-3-deficient diet in the last trimester of pregnancy and throughout the nursing period and by continuing to feed the weaning rats the same diet for 10–12 wk (6,7). Under these conditions, the levels of DHA in the ROS were reduced by half and were replaced by nearly equal amounts of 22:5n-6. Even further reductions could be achieved by raising several generations on an n-3-deficient diet (8,9). Moriguchi *et al.* (10) developed an artificial rearing system and recently reported rapid, profound changes in retinal and brain DHA in rats fed an n-3-deficient diet from birth.

DIET-INDUCED CHANGES IN DHA AFFECT RETINAL FUNCTION

Reduction in DHA in ROS membranes leads to significant changes in the electroretinographic (ERG) response of the retina. The ERG is a noninvasive measure of retinal function and is accomplished by placing electrodes on the cornea and tongue and then providing millisecond (MS) flashes of light starting at subthreshold levels and increasing in intensity until a saturating response is obtained. Two waveforms are generated: The cornea negative a-wave arises in photoreceptor cells and the cornea positive b-wave is generated at more proximal locations within the neural retina. Benolken *et al.* (8) raised two generations of rats on fat-free diets and found significant reductions in the a- and b-waves of the ERG, the a-wave being affected more than the b-wave. In a subsequent experiment (11), 14 wk-old female albino rats were fed diets containing no fat, 2% 18:1n-9, 2% 18:2n-6, 1% 18:2n-6 plus 1% 18:3n-3, or 2% 18:3n-3 for 40 d. Comparison of the relative ERG responses showed that the greatest amplitudes were present in animals fed n-3 FA. These studies were the first to indicate an effect of ROS n-3 FA on retinal membrane function and were confirmed by other laboratories in rats (12,13) and guinea pigs (14–17). Neuringer and colleagues (18–22) subsequently demonstrated a functional role of n-3 FA in nonhuman primates fed semipurified diets containing safflower (trace n-3) or soybean (adequate n-3) oils as the only source of fat. In the last decade, clinical trials in term and pre-term human infants also revealed an essential role for n-3 FA in the development of retinal function (23–30). Thus, it is clear from these and a large number of other studies that optimal retinal function depends on a lipid bilayer that contains high levels of DHA.

ENVIRONMENTAL LIGHT INTENSITY AFFECTS DHA LEVELS IN ROS

Penn and Anderson (31,32) explored the lipid makeup of ROS in rats from bright and dim environments. The authors raised groups of albino rats in cyclic light environments that differed in illuminance level during the light-on part of the cycle and found dramatic differences in the FA content of ROS membranes under the two light conditions (31). The molar ratio of DHA to palmitic acid, for example, was 6.5 in ROS of rats raised in the dim (<10 lux) light environment and only 0.6 in bright (400 lux) light. Interestingly, the reduction in DHA was not accompanied by an increase in 22:5n-6. No-

*To whom correspondence should be addressed at 608 S.L. Young Blvd., Oklahoma City, OK 73104. E-mail: robert-anderson@ouhsc.edu

Abbreviations: ERG, electroretinogram; G_t, transducin; *prcd*, progressive rod-cone degeneration; PUFA, polyunsaturated fatty acid; ROS, rod outer segments.

tably, this light environment-induced effect on ROS FA composition was reversible (32). Three weeks after rats were moved from high illuminance to low, the ratio changed to 4.7. The turnover rates of phospholipid molecular species containing two DHA molecules was similar in the two light groups for PC and PS, but di-22:6-PE turned over faster in ROS from bright light-raised rats (Penn, J.S., and Anderson, R.E., unpublished results). Finally, after injection of tracer, radio-labeled DHA-containing species (particularly di-22:6-PE, PS and PC) were significantly lower in ROS of rats from the bright environment (Penn, J.S., and Anderson, R.E., unpublished results). Thus, decreased synthesis of DHA-containing ROS phospholipid species was a clear component of the membrane modifications dictated by light environment. This could result from a lower level of DHA in the acyl CoA pool or a selective reduction in incorporation of DHA into newly synthesized glycerolipids.

HEREDITY AFFECTS DHA LEVELS IN ROS

Animals with inherited retinal degeneration have reduced DHA in ROS membranes. The FA composition of these animal models of human degeneration resemble chemically the membranes from the animals raised in bright cyclic light. To date, dogs with progressive rod-cone degeneration (*prcd*) (33); mice containing mutations in rds/peripherin (34), Rom1 (Anderson, R.E., and McInnis, R., unpublished results), and rhodopsin (35); rats with two different mutations in rhodopsin (36); and transgenic pigs expressing mutant rhodopsin (Anderson, R.E., and Wong, F., unpublished results) all have reduced DHA compared with controls. In each of these studies, there was no accumulation of 22:5n-6, which occurs during diet-induced reduction of DHA (37,38). Also, in each of the transgenic rat lines expressing mutant opsins, the animals with the highest levels of transgene expression had the fastest rate of retinal degeneration and lowest levels of DHA (36). The reason for the low levels of DHA in these animal models of human retinitis pigmentosa is not known. They clearly are not a result of n-3 deficiency, since there was no increase in 22:5n-6. Trials in animals testing the efficacy of fish oil or flaxseed oil on the rate of retinal degeneration showed no protection or rescue of photoreceptor cells in *prcd*-affected dogs (33) or in rats expressing P23H or S334ter mutant opsins (39), respectively. Interestingly, in both studies, supplementation with n-3 FA did not bring the DHA level in the ROS membranes of the mutant animals to that in the wild-type animals. Since wild-type n-3-deficient animals had less DHA in their ROS membranes than affected supplemented animals, yet showed no evidence of retinal degeneration, the degeneration observed in the mutant animals is not caused by the low levels of DHA in these membranes.

MECHANISM OF DHA EFFECTS IN ROS MEMBRANES

The mechanism by which DHA participates in maintenance of retinal function has remained elusive. Recent work by Litman and coworkers has shed enormous light in this area. Niu *et al.* (9) raised several generations of rats on diets that were deficient or adequate in n-3 FA and produced substantial changes in the ROS FA composition and in the distribution of DHA in molecular species of PE, PC, and PS. For example, the levels of DHA in PC, PS, and PE were changed from 29, 45, and 50 mole percentage, respectively, to 6, 9, and 14 in n-3-deficient animals. As a consequence and in contrast to the studies outlined above, the levels of 22:5n-6 were increased substantially in the deficient group to compensate for the reduction in DHA (37,38). ROS membranes from these two groups of animals were prepared from dark-adapted retinas and used in a series of experiments. In the n-3-deficient ROS, there was reduced rhodopsin activation, reduced rhodopsin-transducin (G_t) coupling, reduced cGMP phosphodiesterase activity, and slower formation of metarhodopsin II-G_t complex, relative to the animals fed the n-3-adequate diet. Thus, the reduction in DHA provoked dramatic changes in the efficiency of visual transduction, which should lead to a reduced visual response to a known quantity of photons.

IS THERE A PHYSIOLOGICAL BASIS FOR REDUCING DHA LEVELS IN ROS MEMBRANES?

Almost two decades ago, Penn and Williams (40) discovered that albino rats have the remarkable ability to adapt to ambient light in order to catch a constant number of photons per day. They named this phenomenon "photostasis." Their studies were the first to compare rats raised in light environments of varying illuminance. After 15 wk in dim or bright light, rats were subjected to measurements of several retinal parameters, including: (i) dark-adapted and steady-state (daytime) retinal rhodopsin levels, (ii) ROS length and photoreceptor cell density, and (iii) rhodopsin regeneration rate *in vivo*. Photon catch was calculated using these parameters and the following equation: $(k_f \cdot I) \cdot R_{ss} = k_r \cdot B_{ss}$, where R_{ss} equals unbleached rhodopsin at steady state and B_{ss} equals rhodopsin bleached at steady state. k_f and k_r are the rate constants for bleaching and regeneration, respectively, and I is the illuminance or light level. The number of photons absorbed during a light cycle is the product of k_r (the rhodopsin regeneration rate) and B_{ss}, converted to appropriate time units.

When this equation was applied to albino rats exposed to cyclic light environments with daytime light levels varying from 3 to 400 lux, the result was an equal photon catch per day in all groups. The rats raised in bright light environments had fewer photoreceptors, shorter ROS with poorly organized disc membranes, lower ROS rhodopsin concentration, and altered rhodopsin regeneration rates. Photons were plentiful in the bright environment, but the capacity of photoreceptors to absorb them was limited by these features. Notably, as was the case for ROS FA composition, all parameters were reversible when rats were removed from bright to dim light environments except photoreceptor number. However, even this parameter was compensated in these "transferred" rats by extremely high rhodopsin concentrations and abnormally long

photoreceptors with tightly stacked and well-organized disc membranes.

PHYSIOLOGICAL CONSEQUENCES OF PHOTOSTASIS

The concept of photostasis implies that the retina can adapt both morphologically and biochemically to capture a constant number of photons in a normal daily light cycle. The reason this may be desirable, especially in a rod-dominant animal, is that bright light can readily damage photoreceptor cells (41). In fact, albino rats born and raised in dim cyclic light (5 lux) can lose most of their rod photoreceptor cells after a 24-h exposure to light of 2,700 lux intensity (about the intensity of a bright, sunny day). In several animal models of inherited retinal degeneration, light has been shown to exacerbate the loss of photoreceptor cells (42,43). Thus, control of photon capture and the efficiency of visual transduction may be survival mechanisms that have been evolutionarily derived. The former is accomplished by reducing the level of rhodopsin in the ROS, shortening the length of the ROS, and disorganizing the membranes (44,45), whereas the latter is accomplished by reducing the levels of DHA in the membranes (9).

The rats raised by Penn and Anderson and those raised by the Litman group represent experimental homologs. In the former case, ROS FA composition was affected by environmental light level; in the latter, it was affected by n-3 FA-deficient diets. In the photostasis and lipid composition studies, Penn and his colleagues focused exclusively on events upstream from rhodopsin activation, whereas in the diet studies, Littman and coworkers emphasized downstream events. Both treatments, however, resulted in decreased transduction of photons into a neural signal. It remains to be determined whether changes in DHA are directly responsible for modulating photon catch, for example, by altering the lateral diffusion or membrane dichroism of rhodopsin. Clearly, DHA is directly responsible for the loss of efficiency of visual transduction, since retinas of animals raised on n-3-deficient diets have morphologically intact ROS (46).

CONCLUDING REMARKS

The n-3 family of essential PUFA has been found to have a number of physiological properties that are important in both normal and diseased tissues. Our studies have shown that the retina has the remarkable ability to adapt to genetic and environmental stimuli, in part by altering the levels of DHA in the photoreceptor outer segment membranes. We propose that one reason for this is to reduce photon capture and visual transduction efficiency under conditions where excessive activation of rhodopsin may exacerbate underlying pathologies that lead to cell death. It remains to be determined whether this phenomenon extends to other tissues.

ACKNOWLEDGMENTS

These studies were supported by grants from National Institutes of Health/National Eye Institute (EY04149, EY00871, and EY12190 to REA and EY07533 and EY08126 to J.S.P.); National Institutes of Health/National Center for Research Resources (RR17703); Research to Prevent Blindness, Inc.; and the Foundation Fighting Blindness, Inc.

REFERENCES

1. Fliesler, S.J., and Anderson, R.E. (1983) Chemistry and metabolism of lipids in the vertebrate retina, in *Progress in Lipid Research* (Holman, R.T., ed.), Vol. 22, pp. 79–131, Pergamon Press, Elmsford, New York.
2. Anderson, R.E., and Sperling, L. (1971) Lipids of ocular tissues: VII. Positional distribution of the fatty acids in the phospholipids of bovine retina rod outer segments, *Arch. Biochem. Biophys. 144*, 673–677.
3. Wiegand, R.D., and Anderson, R.E. (1983) Phospholipid molecular species of frog rod outer segment membranes, *Exp. Eye Res. 37*, 159–173.
4. Stinson, A.M., Wiegand, R.D., and Anderson, R.E. (1991) Fatty acid and molecular species compositions of phospholipids and diacylglycerols from rat retinal membranes, *Exp. Eye. Res. 52*, 213–218.
5. Anderson, R.E., and Maude, M.B. (1972) Lipids of ocular tissues: VII. The effects of essential fatty acid deficiency on the phospholipids of the photoreceptor membranes of rat retina, *Arch. Biochem. Biophys. 151*, 270–276.
6. Wiegand, R.D., Koutz, C.A., Chen, H., and Anderson, R.E. (1995) Effect of dietary fat and environmental lighting on the phospholipid molecular species of rat photoreceptor membranes, *Exp. Eye Res. 60*, 291–306.
7. Koutz, C.A., Anderson, R.E., Rapp, L.M., and Wiegand, R.D. (1995) Effect of dietary fat and environmental lighting on the response of the rat retina to chronic and acute light stress, *Exp. Eye Res. 60*, 307–316.
8. Benolken, R.M., Anderson, R.E., and Wheeler, T.G. (1973) Membrane fatty acids associated with the electrical response in visual excitation, *Science 182*, 1253–1254.
9. Niu, S.L., Mitchell, D.C., Lim, S.Y., Wen, Z.M., Kim, H.Y., Salem, N., Jr., and Litman, B.J. (2004) Reduced G protein-coupled signaling efficiency in retinal rod outer segments in response to n-3 fatty acid deficiency, *J. Biol. Chem. 279*, 31098–31104.
10. Moriguchi, T., Lim, S.Y., Greiner, R., Lefkowitz, W., Loewke, J., Hoshiba, J., and Salem, N., Jr. (2004) Effects of an n-3-deficient diet on brain, retina, and liver fatty acyl composition in artificially reared rats, *J. Lipid Res. 45*, 1437–1445.
11. Wheeler, T.G., Benolken, R.M., and Anderson, R.E. (1975) Visual membranes: Specificity of fatty acid precursors for the electrical response to illumination, *Science 188*, 1312–1314.
12. Watanabe, I., Kato, M., Aonuma, H., Hishimoto, A., Naito, Y., Moriuchi, A., and Okuyama, H. (1987) Effect of dietary alpha-linolenate/linoleate balance on the lipid composition and electroretinographic responses in rats, in *Advances in the Biosciences, Vol. 62: Research in Retinitis Pigmentosa* (Zrenner, E., Krastel, H., and Goebel, H.H., eds.), pp. 563–570, Pergamon Journals Ltd., Oxford, United Kingdom.
13. Bourre, J., Francois, M., Youyou, A., Doumont, O., Piciotti, M., Pascal, G., and Durand, G. (1989) The effects of dietary α-linolenic acid on the composition of nerve membranes, enzymatic activity, amplitude of electrophysiological parameters, resistance poisons and performance of learning tasks in rats, *J. Nutr. 119*, 1880–1892.
14. Weisinger, H., Vingrys, A., and Sinclair, A. (1996) Effect of dietary n-3 deficiency on the electroretinogram in the guinea pig. *Ann. Nutr. Metab. 40*, 91–98.
15. Weisinger, H., Vingrys, A., and Sinclair, A. (1996) The effect of docosahexaenoic acid on the electroretinogram of the guinea pig. *Lipids 31*, 65–70.

16. Weisinger, H.S., Vingrys, A.J., Abedin, L., and Sinclair, A.J. (1998) Effect of diet on the rate of depletion of n-3 fatty acids in the retina of the guinea pig, *J. Lipid Res. 39*, 1274–1279.
17. Weisinger, H.S., Vingrys, A.J., Bui, B.V., and Sinclair, A.J. (1999) Effects of dietary n-3 fatty acid deficiency and repletion in the guinea pig retina, *Invest. Ophthalmol. Vis. Sci. 40*, 327–338.
18. Neuringer, M., Connor, W.E., Van Patten, C., and Barstad, L. (1984) Dietary omega-3 fatty acid deficiency and visual loss in infant rhesus monkeys, *J. Clin. Invest. 73*, 272–276.
19. Neuringer, M., Connor, W.E., Lin, D.S., Barstad, L., and Luck, S. (1986) Biochemical and functional effects of prenatal and postnatal ω-3 fatty acid deficiency on retina and brain in rhesus monkeys*, Proc. Natl. Acad. Sci. USA 83*, 4021–4025.
20. Neuringer, M., and Connor, W.E. (1986) n-3 fatty acids in the brain and retina: Evidence for their essentiality, *Nutr. Rev. 44*, 285–294.
21. Neuringer, M. and Connor, W.E. (1987) The importance of dietary n-3 fatty acids in the development of the retina and nervous system, in *Proceedings of the AOCS Short Course on Polyunsaturated Fatty Acids and Eicosanoids* (Lands, W.E.M. ed.), pp. 301–311, American Oil Chemists' Society, Champaign, Illinois.
22. Neuringer, M., Connor, W.E., Lin, D.S., Anderson, G.J., and Barstad, L. (1991) Dietary omega-3 fatty acids: effects on retinal lipid composition and function in primates, in *Retinal Degenerations*, (Anderson, R.E., Hollyfield, J.G., and LaVail, M.M., eds.), pp. 1–13, CRC Press, New York.
23. Uauy, R.D., Birch, D.G., Birch, E.E., Tyson, J.E., and Hoffman, D.R. (1990) Effect of dietary omega-3 fatty acids on retinal function of very-low-birth-weight neonates, *Pediatr. Res. 28*, 485–492.
24. Carlson, S.E., Werkman, S.H., Rhodes, P.G., and Tolley, E.A. (1993) Visual-acuity development in healthy preterm infants: Effect of marine oil supplementation, *Am. J. Clin. Nutr. 58*, 35–42.
25. Carlson, S.E., Cooke, R.J., Werkman, S.H., and Tolley, E.A. (1992) First year growth of preterm infants fed standard compared to marine oil n-3 supplemented formula, *Lipids 27*, 901–907.
26. Carlson, S.E., Werkman, S.H., Peeples, J.M., Cooke, R.J., and Tolley, E.A. (1993). Arachidonic acid status correlates with first year growth in preterm infants, *Proc. Natl. Acad. Sci. USA 90*, 1073–1077.
27. Gibson, R.A. and Makrides, M. (1998) The role of long chain polyunsaturated fatty acids (LCPUFA) in neonatal nutrition, *Acta Paediatr. 87*, 1017–1022.
28. Birch, E.E., Birch, D.G., Hoffman, D.R., and Uauy, R. (1992) Dietary essential fatty acid supply and visual acuity development, *Invest. Ophthalmol. Vis. Sci. 33*, 3242–3253.
29. Birch, E.E., Hoffman, D.R., Uauy, R., Birch, D.G., and Prestidge, C. (1998) Visual acuity and the essentiality of docosahexaenoic acid and arachidonic acid in the diet of term infants, *Pediatr. Res. 44,* 201–209.
30. Uauy, R.D., Birch, E.E., Birch, D.G., and Peiran, P. (1992) Visual and brain function measurements in studies of n-3 fatty acid requirements of infants, *J. Pediatr. 120*, S168–S178.
31. Penn, J.S., and Anderson, R.E. (1987) Effect of light history on rod outer-segment membrane composition in the rat, *Exp. Eye Res. 44*, 767–778.
32. Penn, J.S., Thum, L.A., and Naash, M.I. (1989) Photoreceptor physiology in the rat is governed by the light environment, *Exp. Eye Res. 49,* 205–215.
33. Aguirre, G.D., Acland, G.M., Maude, M.B., and Anderson, R.E. (1997) Diets enriched in docosahexaenoic acid fail to correct progressive rod-cone degeneration (*prcd*) phenotype, *Invest. Ophthalmol. Vis. Sci. 38*, 2387–2407.
34. Anderson, R.E., Maude, M.B., and Bok, D. (2001) Low docosahexaenoic acid levels in rod outer segment membranes of mice with *rds*/peripherin and P216L peripherin mutations, *Invest. Ophthalmol. Vis. Sci. 42*, 1715–1720.
35. Anderson, R.E., Sieving, P.A., Maude, M.B., and Naash, M.I. (2001) Mice with G90D rhodopsin mutations have lower DHA in rod outer segment membranes than control mice, in *New Insights into Retinal Degenerative Diseases* (Anderson, R.E., Hollyfield, J.G., and LaVail, M.M. eds.), pp. 235–245, Plenum Press, New York.
36. Anderson, R.E., Maude, M.B., McClellan, M., Matthes, M.T., Yasumura, D., and LaVail, M.M. (2002) Low docosahexaenoic acid levels in rod outer segments of rats with P23H and S334ter rhodopsin mutations, *Mol. Vis. 8*, 351–358.
37. Galli, C., Trzeciak, H.I., and Paoletti, R. (1971) Effects of dietary fatty acids on the fatty acid composition of the brain ethanolamine phosphoglyceride: reciprocal replacement of n-6 and n-3 polyunsaturated fatty acids, *Biochim. Biophys. Acta 248*, 449–454.
38. Anderson, R.E., and Maude, M.B. (1972) Lipids of ocular tissues: VII. The effects of essential fatty acid deficiency on the phospholipids of the photoreceptor membranes of rat retina, *Arch. Biochem. Biophys. 151*, 270–276.
39. Martin, R.E., Ranchon-Cole, I., Brush, R.S., Williamson, C.R., Hopkins, S.A., Li, F., and Anderson, R.E. (2004) P23H and S334ter opsin mutations: Increasing photoreceptor outer segment n-3 fatty acid content does not affect the course of retinal degeneration, *Molec. Vis. 10*, 199–207.
40. Penn, J.S., and Williams, T.P. (1986) Photostasis: Regulation of daily photon-catch by rat retinas in response to various cyclic illuminances, *Exp. Eye Res. 43*, 915–928.
41. Noell, W.K., Walker, V.S., Kang B.S., and Berman, S. (1966) Retinal damage by light in rats, *Invest. Ophthalmol. 5*, 450–473.
42. Sanyal, S., and Hawkins, R.K. (1986) Development and degeneration of retina in rds mutant mice: effects of light on the rate of degeneration in albino and pigmented homozygous and heterozygous mutant and normal mice, *Vision Res. 26*, 1177–1785.
43. LaVail, M.M., Gorrin, G.M., Yasumura, D., and Matthes, M.T. (1999) Increased susceptibility to constant light in nr and pcd mice with inherited retinal degeneration, *Invest. Ophthalmol Vis. Sci. 40*, 1020–1024.
44. Penn, J.S., Naash, M.I., and Anderson, R.E. (1987) Effect of light history on retinal antioxidants and light damage susceptibility in the rat, *Exp. Eye Res. 44*, 779–788.
45. Penn, J.S., and Anderson, R.E. (1992) Effects of light history on the rat retina, in *Progress in Retinal Research* (Osborne, N., and Chader, G., eds.), Vol. 11, pp. 75–98, Pergamon Press, New York.
46. Dudley, P.A., Landis, D.J., and Anderson, R.E. (1975) Further studies on the chemistry of photoreceptor membranes of rats fed an essential fatty acid deficient diet, *Exp. Eye Res. 21*, 523–530.

[Received Agust 6, 2004; accepted December 10, 2004]

Resolvins, Docosatrienes, and Neuroprotectins, Novel Omega-3-Derived Mediators, and Their Endogenous Aspirin-Triggered Epimers

Charles N. Serhan*, Makoto Arita, Song Hong, and Katherine Gotlinger

Center for Experimental Therapeutics and Reperfusion Injury, Department of Anesthesiology, Perioperative and Pain Medicine, Brigham and Women's Hospital and Harvard Medical School, Boston, Massachusetts 02115

ABSTRACT: The molecular basis for the beneficial impact of essential omega-3 (n-3) FA remains of interest. Recently, we identified novel mediators generated from eicosapentaenoic acid (EPA) and docosahexaenoic acid (DHA) that displayed potent bioactions identified first in resolving inflammatory exudates and in tissues enriched with DHA. The trivial names *resolvin* (resolution phase interaction products) and *docosatrienes* were introduced for the bioactive compounds from these novel series since they possess potent anti-inflammatory and immunoregulatory actions. Compounds derived from EPA carrying potent biological actions (i.e., 1–10 nM range) are designated E series and denoted resolvins of the E series (resolvin E1 or RvE1), and those biosynthesized from the precursor DHA are denoted resolvins of the D series (resolvin D1 or RvD1). The number 1 designates the bioactive compounds in this family (e.g., 1–4). Bioactive members from DHA-containing conjugated triene structures or docosatrienes (DT) that possess immunoregulatory and neuroprotective actions were termed neuroprotectins. Aspirin treatment initiates a related epimeric series by triggering endogenous formation of the 17*R*-D series resolvins and docosatrienes. These epimers are denoted as aspirin-triggered (AT)-RvD and DT, and possess potent anti-inflammatory actions *in vivo* essentially equivalent to their 17*S* series pathway products. These include five distinct series: (i) 18*R* resolvins from EPA (i.e., RvE1); (ii) 17*R* series (AT) resolvins from DHA (RvD1 through RvD4); (iii) 17*S* series resolvins from DHA (RvD1 through RvD4), (iv) DT from DHA; and (v) their AT form 17*R* series DT. In this article, we provide an overview of the formation and actions of these newly uncovered pathways and products.

Paper no. L9568 in *Lipids 39,* 1125–1132 (November 2004).

The beneficial impact of essential omega-3 fatty acids was uncovered as early as 1929 (1). These observations were consistently observed for the next several decades (2–5). More recently, inflammation has emerged as playing a central role in many prevalent diseases not previously known to involve inflammation including Alzheimer's disease, cardiovascular disease (6), and cancer (7,8), in addition to those well known to be associated with inflammation such as arthritis and periodontal disease (9,10). Recently, we identified novel oxygenated products generated from precursors eicosapentaenoic acid (EPA) and docosahexaenoic acid (DHA) that possess potent actions within resolving inflammatory exudates (11–13). Hence, the terms *resolvin* (resolution phase interaction products) and *docosatrienes* (DT) were first introduced from initial studies since the new compounds displayed both potent anti-inflammatory and immunoregulatory properties.

In this article, we give a brief overview of the novel compounds and biosynthetic pathways from EPA that carry potent biological actions, resolvins of the E series (resolvin E1 or RvE1) and those from DHA, resolvins of the D series (resolvin D1 or RvD1), as well as bioactive members from these biosynthetic pathways carrying conjugated triene structures denoted as DT that are both anti-inflammatory (12,13) and neuroprotective (14,15), recently termed neuroprotectins (NPD1) (Ref. 15). Unlike other products identified earlier from omega-3 fatty acids that are similar in structure to eicosanoids but less potent or devoid of bioactions, the resolvins, DT, and neuroprotectins evoke potent biological actions *in vitro* and *in vivo* (11–15).

NOVEL LIPID MEDIATORS IDENTIFIED DURING RESOLUTION OF ACUTE INFLAMMATION: ARACHIDONIC ACID VS. EPA AND DHA

It is often questioned whether essential fatty acids, such as the omega-3 EPA or DHA, are converted to potent lipid mediators as is the case with arachidonic acid. In short, yes, both DHA and EPA are important precursors; we now appreciate that intimate cell–cell interactions within vessel walls, that is, adherent platelets that are studded with polymorphonuclear neutrophils (PMN), converge on the endothelium and can be visualized by intravital microscopy (16,17) and promote transcellular lipid mediator biosynthesis (18–20). During platelet-leukocyte interactions, arachidonic acid is converted to lipoxins (LX), which are generated to act as "stop" signals on PMN in the nanomolar range *via* specific receptors we identified (21,22) and as confirmed by others (23,24), and stimulated monocytes (25) and macrophages to promote resolution (26).

These forms of cell–cell interactions in the vasculature are impinged upon by aspirin (ASA) (27,28). ASA inhibits throm-

*To whom correspondence should be addressed at Center for Experimental Therapeutics and Reperfusion Injury, Brigham and Women's Hospital, 75 Francis St., Thorn Building for Medical Research, Room 724, Boston, MA 02115. E-mail: cnserhan@zeus.bwh.harvard.edu

Abbreviations: 17*R*-HDHA, 17*R*-hydroxy-docosahexaenoic acid; 18*R*-HEPE, 18*R*-hydroxy-5*Z*,8*Z*,11*Z*,14*Z*,16*E*-eicosapentaenoic acid; ASA, aspirin; AT, aspirin-triggered; ATL, aspirin-triggered lipoxin; COX, cyclooxygenase; DHA, docosahexaenoic acid; DT, docosatrienes; EPA, eicosapentaenoic acid; IL, interleukin; LOX, lipoxygenase; LX, lipoxins; PMN, polymorphonuclear neutrophils; RvD1, resolvin D1; RvE1, resolvin E1; TNF, tumor necrosis factor α.

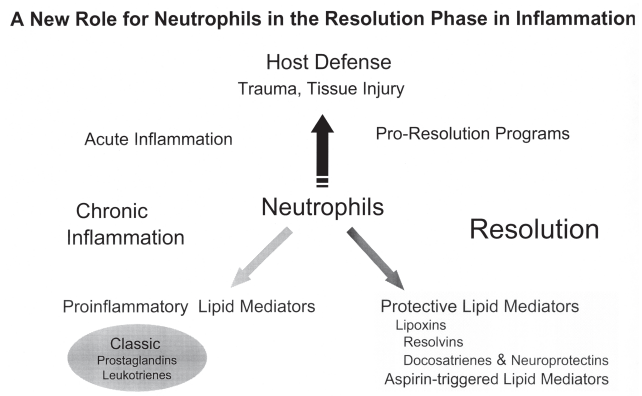

FIG. 1. Resolution phase role for neutrophils in the formation of protective lipid mediators.

boxane production by platelets and prostacyclin biosynthesis in vascular endothelial cells (29,30). During PMN-endothelial and/or PMN–epithelial interactions, aspirin triggers the biosynthesis of 15-epi-LX (aspirin-triggered LX, ATL) (Fig. 1) (27); both LX and ATL and their respective stable analogs are potent regulators of transendothelial/transepithelial migration of PMN across these cells and endothelial cell proliferation, *in vitro* and *in vivo* (31–33). Also, transgenic mice overexpressing the human LXA_4 receptor with myeloid-specific promoter display reduced PMN infiltration in peritonitis and heightened sensitivity to LXA_4 and ATL (34). Transgenic rabbits overexpressing 15-lipoxygenase (LOX) type I generate enhanced levels of LX, have an enhanced anti-inflammatory status, and are protected from the inflammatory bone loss of periodontal disease (35). Hence, the results of these studies have heightened our awareness that PMN, in addition to their host defense position and the possibility that they can spill proinflammatory agents (36) and mediators such as the classic eicosanoids, prostanoids, and leukotrienes (37,38), which amplify inflammatory responses, can also produce novel protective lipid mediators that actively counterregulate the inflammation (Fig. 1).

In view of the compelling results from the GISSI study, which showed improvements in more than 11,000 cardiovascular patients (39,40), namely, reduction in sudden death by approximately 45% by taking almost a gram of omega-3 per day, we addressed a potential role of omega-3 PUFA recently. Inspection of their methods indicated that all the patients also took daily ASA that was unaccounted for in their analysis. Despite very large doses (milligrams to grams daily), an abundant literature with omega (n-3) PUFA suggests beneficial actions in many human diseases including periodontal (41), anti-inflammatory, and antitumor actions (2,42). The three major mammalian LOX (5-LOX, 12-LOX, and 15-LOX) can each convert DHA to various monohydroxy-containing products; however, at the time their *in vivo* functions were either not apparent or they did not display bioactivity (43–45). Also, DHA can be nonenzymatically oxygenated to isoprostane-like compounds termed neuroprostanes that reflect oxidative stress in the brain (46) or autooxidized to products that are monohydroxy racemates (47) of the compounds that are now known to be enzymatically produced during biosynthesis of the resolvins and DT (12–15). Overall, it is noteworthy that the molecular basis and mechanisms underlying omega-3's immunoprotective actions remained to be established and appreciated, and their direct connection to human disease and treatment are still important biomedical challenges (48).

ASPIRIN UNVEILS NEW DIRECTIONS: ASPIRIN-TRIGGERED LIPID MEDIATORS

ASA is an active ingredient in more than 60 over-the-counter remedies, making it a difficult substance to control for in some human studies. What is the molecular basis for omega-3's protective action, and are there overlap(s) in their actions? To address this in an experimental setting, we used murine dorsal skin pouches (11,12). This model of inflammation is known to spontaneously resolve in rats (48). We adapted this for mice in order to include both genetics and to set up lipidomics employing LC-UV-MS-MS-based analyses geared to evaluating whether potential novel lipid mediators are indeed generated during the resolution phase of inflammation (11,12). In this pouch (experimental contained inflammation) after 4 h, PMN numbers begin to drop within exudates (11,12). Exudates were taken at timed intervals, focusing on the period of "spontaneous resolution," and lipid mediator profiles were determined by using tandem LC-UV-MS-MS. We constructed lipid mediator libraries with physical properties (i.e., MS and MS/MS spectra, elution times, UV spectra, etc.) for matching and to assess whether known and/or potential novel lipid mediators were present within the exudates and are presently expanding these libraries and the software for their matching (49). If novel lipid mediators were encountered, their structures were elucidated by carrying out retrograde analysis for both biogenic enzymatic synthesis and total organic synthesis. This approach permitted assessment of structure–activity relationships as well as the scale-up required to confirm the bioactions of novel compounds identified (11,12).

18*R* E SERIES RESOLVINS AND 17*R* D SERIES RESOLVINS

Resolving exudates in mice contain 18R-hydroxy-5*Z*,8*Z*,11*Z*,14*Z*,16*E*-eicosapentaenoic acid (18*R*-HEPE) as well as several related bioactive compounds (11). These novel compounds are produced from EPA by at least one biosynthetic pathway operative in human cells. This pathway is shown in Figure 2; blood vessel-derived vascular endothelial cells treated with aspirin convert EPA to 18*R*-hydro(peroxy)-EPE that is reduced to 18*R*-HEPE and released from endothelium and rapidly converted by activated human PMN to a 5(6) epoxide-containing intermediate that is further transformed to the bioactive 5,12,18*R*-trihydroxy-EPE, which we initially termed "resolvin," specifically resolvin E1 (RvE1), because it was identified in the resolution phase in mice, appeared as cell-cell interaction/transcellular biosynthetic products with isolated human cells, and importantly, proved to be a potent regulator of PMN and inflammation. In the absence of aspirin, 18*R*-

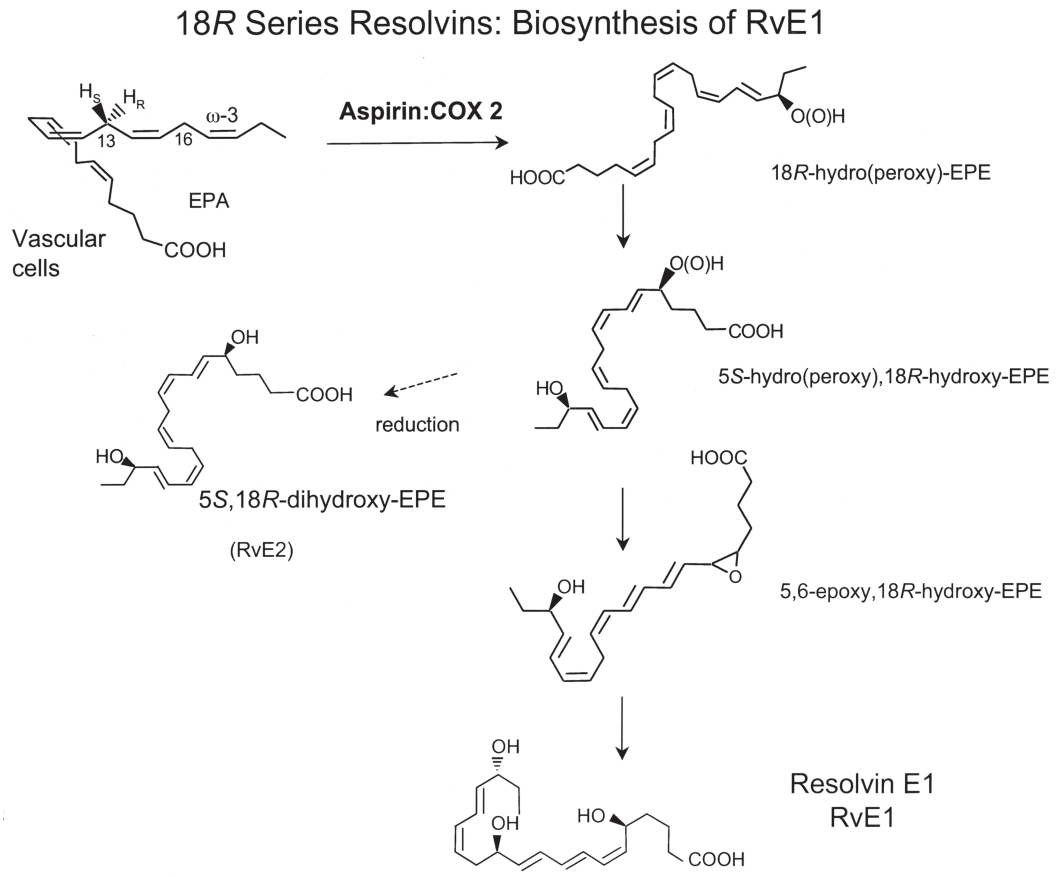

FIG. 2. Resolvin E1 (RVE1) biosynthesis from EPA. Human endothelial cells expressing cyclooxygenase (COX)-2 treated with ASA transform EPA by abstracting hydrogen at C16 to give *R* insertion of molecular oxygen to yield 18*R*-hydro(peroxy)-eicosapentaenoic acid (EPE), which is reduced to 18*R*-hydroxy-HEPE (not shown). They are next converted *via* sequential actions of a leukocyte 5-lipoxygenase (LOX)-like reaction that lead to the formation of 5,12,18*R*-triHEPE (RvE1) (12,51).

HEPE can be produced *via* a P450-like mechanism (50). Organic synthesis was achieved and its complete stereochemical assignment was recently established as 5*S*,12*R*,18*R*-trihydroxy-6*Z*,8*E*,10*E*,14*Z*,16*E*-eicosapentaenoic acid (51).

In resolving exudates from mice given aspirin and DHA, we found novel 17*R*-hydroxy-docosahexaenoic acid (17*R*-HDHA) and several related bioactive compounds (Fig. 3). Human microvascular endothelial cells, also aspirin-treated in hypoxia, generate 17*R*-HDHA. DHA is converted by human recombinant cyclooxygenase (COX)-2, which was surprising, since earlier literature indicated that DHA is not a substrate of COX (52,53). However, these investigations were before knowledge of the COX-2 isoform and used organs rich in COX-1. Human recombinant COX-2 converts DHA to 13-hydroxy-DHA. With aspirin, this switches to 17*R*-oxygenation to give epimeric aspirin-triggered (AT) forms, also in brain (12,13), of both resolvins (RvD1 through RvD6) and DT (i.e., 10,17*R*-DT) (see Fig. 3).

17*S* D SERIES RESOLVINS

Using our new mediator-lipidomic analyses, we learned that without aspirin or added DHA, the endogenous DHA was converted *in vivo* to a 17*S* series of resolvins (RvD1 through RvD6) as well as DT (10,17*S*-DT) (13,14). As in most structural elucidation experiments, added substrates were used to confirm biosynthesis, and to isolate quantities of the novel active principle for bioassay. In this case, given the large doses in humans, experimental animals, and *in vitro* cell culture studies needed to observe effects in omega-3 supplement studies reported in the literature (see Ref. 2–5 and references therein), we expected that these precursors needed to be added in the present studies. This proved not to be the case. Tissues such as normal mouse tissue and isolated human neural cells contain DHA that is available upon activation to produce 17*S*-containing DT and RvD *in vivo* (11–15) (Table 1).

ANTI-INFLAMMATORY PROPERTIES

With microglial cells that liberate cytokines in the brain, the D class resolvins block tumor necrosis factor α (TNFα)-induced interleukin (IL)-1β transcripts and are potent regulators of PMN infiltration in brain, skin, and peritonitis *in vivo* (13,14). Of the DT-derived family, 10,17*S*-DT, the neuroprotectin D1 pathway shown in Figure 4, proved a potent regulator of PMN influx in exudates at sites where it is formed from

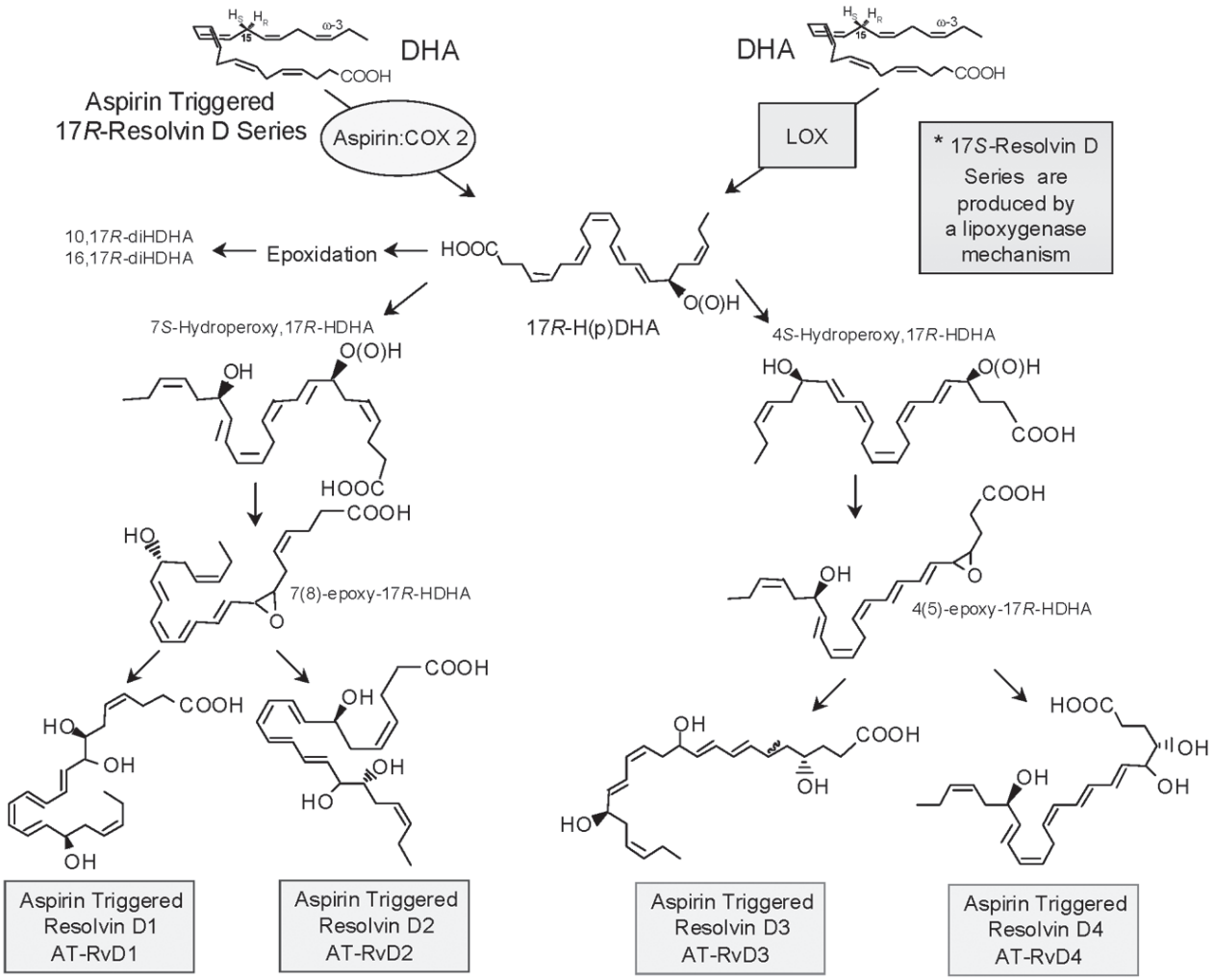

FIG. 3. Aspirin-triggered (AT) D series resolvins. The 17*R* series resolvins are produced from DHA in the presence of ASA (aspirin). Human endothelial cells expressing COX-2 treated with ASA transform DHA to 17*R*-hydroxy-DHA (17*R*-HDHA). Human polymorphonuclear neutrophils (PMN) convert 17*R*-HDHA to two compounds *via* 5-lipoxygenation (modeled with the potato 5-LOX) (11,12) that are each rapidly transformed into two epoxide intermediates: a 7(8)-epoxide (left side) and the other a 4(5)-epoxide. These two novel epoxide intermediates open to bioactive products denoted 17*R* series ATRvD1 through ATRvD6. Note: Stereochemistry depicted in likely configuration based on results with recombinant enzymes [see Refs. 12 and 13 for further details]. For other abbreviations see Figure 2.

TABLE 1
Biosynthesis of Resolvins and Protectins in Cells, Tissues, and Organs[a]

Compound	Cells, tissues, or organs	Compound	Cells, tissues, or organs
RvE1	Murine exudates (11); human blood (51); coincubations of human endothelial cells and human PMN (11)	RvD6	Human whole blood, human PMN, human glial cells (13)
		AT-RvD1	Murine inflammatory exudates (12); murine brain stroke (14)
Neuroprotectin D1 (10,17*S*-docosatriene)	Human whole blood, human PMN and its omega carbon-22 oxidation product, human glial cells (13); murine brain stroke (14); human retinal pigment epithelium (15)	AT-RvD2	Murine inflammatory exudates (12)
		AT-RvD3	Murine inflammatory exudates (12)
		AT-RvD4	Murine inflammatory exudates (12)
RvD2	Human whole blood (13)	AT-RvD5	Murine inflammatory exudates (12)
RvD4	Human whole blood (13)	AT-RvD6	Murine inflammatory exudates (12)
RvD5	Human whole blood glial cells (13)		

[a]AT denotes the aspirin-triggered *R* epimer; RvE1, resolvin E1; RvD1–RvD6, resolvin D1–D6.

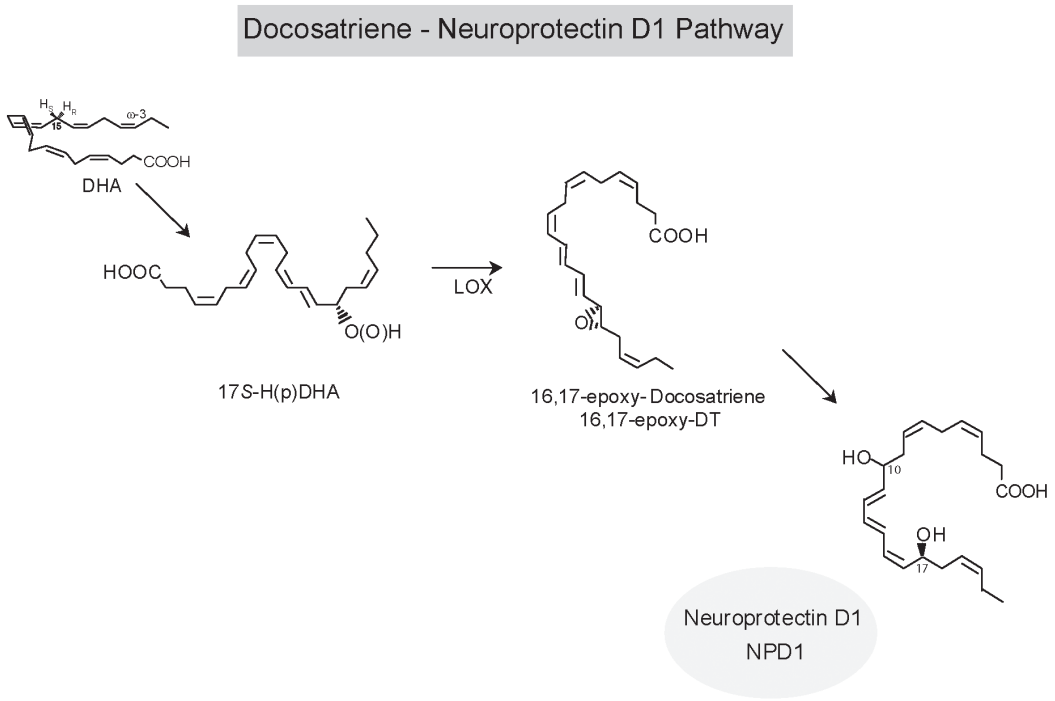

FIG. 4. Docosatriene (DT) formation and neuroprotectin (NP) D1 pathway. The LOX product 17*S*-H(p)DHA is converted to a 16(17)-epoxide and enzymatically converted to the 10,17-dihydroxy product (13) denoted as 10,17*S*-DT (14) and recently coined NPD1 based on its potent actions *in vivo* (14,56). The complete stereochemistries are currently being established in work in progress and are depicted in their tentative configurations based on enzymatic biosynthesis and biogenic synthesis. For other abbreviations see Figures 2 and 3.

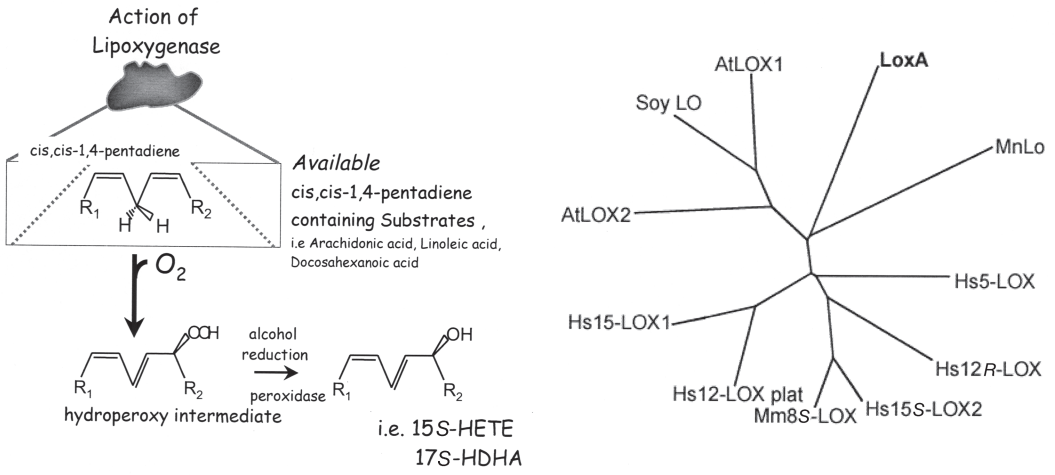

FIG. 5. Enzymatic action of LOX (left panel). Dendogram illustrating the diversity in different animal and plant LOX (right panel). The following LOX sequences were aligned using clustal x (GenBank accession ID indicated): LoxA (*Pseudomonas aeruguinosa* LOX, PA1169/A83499), MnLo (*Gaeumannomyces graminis* manganese LOX, AY040824), Hs5-LOX (*Homo sapiens* 5-LOX, P09917), Hs12*R*-LOX (*Homo sapiens* 12*R*-LOX, AF038461), Hs 15*S*-LOX2 (*Homo sapiens* 15*S*-lipoxygenase type 2, NM_001141), Mm8*S*-LOX (*Mus musculus* 8*S*-lipoxygenase, U93277), Hs 12-LOX plat (*Homo sapiens* platelet 12-LOX, P18054), Hs 15-LOX1 (*Homo sapiens* 15-LOX type I, M23892), AtLOX2 (*Arabidopsis thaliana* LOX 2, JQ2391), Soy LO (soybean LOX 5, U50075), and AtLOX1 (*Arabidopsis thaliana* LOX 1, JQ2267). The alignment was used to construct this unrooted tree dendrogram (see Vance *et al.*, Ref. 60, for further details). For other abbreviations see Figures 2 and 3.

endogenous precursors (12,13), limiting stroke brain injury (14) and retinal pigmented cellular damage (15). Other dihydroxydocosanoids were less active in these bioassay settings (13,15).

Direct comparisons of resolvin E class versus the D classes (17*R* and 17*S* epimer series) for their ability to regulate PMN *in vivo* were carried out (12,13,35). Both the D and E classes of resolvins are potent regulators of PMN infiltration. Resolvins D class 17*R* series, triggered by aspirin, and 17*S* series give essentially similar results (DHA-derived trihydroxy resolvins), indicating that the *S* to *R* switch does not diminish their bioactions. When injected intravenously at 100 ng/mouse, they both gave approximately 50% inhibition, and the RvE1 gave approximately 75–80% inhibition. In comparison, indomethacin at 100 ng/mouse (or ~3 μg/kg) gave roughly 25% inhibition (see Refs. 12, 13).

The main bioactive resolvins and DT as representative members are shown in Figures 2–4. The formation of these compounds may involve enzymes that are also known to convert arachidonic acid as substrate. It is possible that, in view of the many LOX identified to date with unknown function(s) and/or specific PUFA as substrates (54,55), strategically positioned enzymes may be specifically involved in pathways that produce these novel compounds. In general, LOX are defined by their ability to convert PUFA that contain *cis,cis*-1,4-pentadiene subunits to hydroperoxy-containing products that can serve as intermediates. The best-appreciated substrate in human tissues is arachidonic acid; the main LOX convert arachidonic acid to the corresponding 5*S*-, 12*S*-, or 15*S*-hydroperoxyeicosatetraenoic acids. Hence these enzymes came to be known as the arachidonate:oxygen 5-oxidoreductase (5-LOX), arachidonate:oxygen 12-oxidoreductase (12-LOX), and arachidonate:oxygen 15-oxidoreductase (15-LOX). The release and availability of substrate is critical to indicating the preferred substrate of a given LOX, which appears to be best appreciated only in the case of 5-LOX in leukotriene biosynthesis (56). With the identification of LOX *via* molecular cloning, many additional LOX have been discovered, but their preferred substrates are not established. These include 12*R*-LOX, 15-LOX-type 2, soluble 15-LOX (LoxA), and 8*S*-LOX (see Fig. 5 and legend for details). Each was cataloged according to its position of molecular insertion into arachidonate (see Refs. 57–60 and see supplemental materials therein). It follows that specific hydrolase(s), synthase(s), and related enzymes specialized to act on DHA- and EPA-derived intermediates are likely to be involved in these novel compounds and pathways. Hence, it remains to be established whether EPA and DHA are each converted by either specific pathways to biosynthesize these novel bioactive products or whether they simply commandeer the eicosanoid pathways as competitive substrates in these routes to generate the new bioactive products (Figs. 2–4).

Also note that 5*S*,18*R*-diHEPE (RvE2) carries a conjugated diene structure that is separate and distinct from the novel triene plus diene structure and chromophore present in RvE1. These compounds display potent actions *in vivo* and with isolated cells Recent results indicate that the ligand-specific receptor for RvE1 proved to be ChemR23 (51).

In summation, resolvin and DT are novel families comprised of five separate chemical series of lipid-derived mediators, each with unique structures and apparent complementary anti-inflammatory properties and actions. Both families of compounds, Rv and DT (protectins; see Fig. 1), are also generated in their respective epimeric forms when aspirin is given in mammalian systems (11,12). The resolvins and DT each dampen inflammation and PMN-mediated injury from within, key culprits in many human diseases. The results of these initial studies underscore a role in resolution as well as in catabasis. Catabasis is defined as a decline of disease (see www.merckmedicus.com). Here the term catabasis is used to denote the active biosynthesis of resolvins and protectins as local mediators of and during the resolution phase of inflammatory diseases. They also give a possible therapeutic potential for this new arena of immunomodulation and host protection. Hence, it is likely that the resolvins, DT, and their AT-related forms may play roles in other tissues and organs involved in physiological and pathological processes. It is of note that fish, for example, trout, generate LOX products such as LXA_5 from endogenous EPA (54), and also biosynthesize 17*S*-series RvD and DT from endogenous DHA (Hong S., Tjonahen E., Morgan E.L., Serhan C.N., and Rowley A.F., unpublished data). Together our findings suggest that these novel lipid mediators (e.g., resolvins, DT, and neuroprotectins) are conserved in evolution as self-protective and host-protective mediators. These pathways and their actions are the subject of our current investigations. In view of the important roles of DHA and EPA in human biology and medicine uncovered to date (2–5,11), the physiologic relevance of the resolvins and protectins is likely to extend well beyond our current appreciation (11–15).

ACKNOWLEDGMENTS

We thank Mary Halm Small for assistance in preparing the manuscript. This work was supported in part by National Institutes of Health grants GM38675, P01-DE13499, and P50-DE016191.

REFERENCES

1. Burr, G.O., and Burr, M.M. (1929) A New Deficiency Disease Produced by the Rigid Exclusion of Fat from the Diet, *J. Biol. Chem. 82*, 345.
2. Lands, W.E.M. (ed.) (1987) *Proceedings of the AOCS Short Course on Polyunsaturated Fatty Acids and Eicosanoids*, American Oil Chemists' Society, Champaign, IL.
3. Bazan, N.G. (1990) Supply of n-3 Polyunsaturated Fatty Acids and Their Significance in the Central Nervous System, in *Nutrition and the Brain* (Wurtman, R.J., and Wurtman, J.J., eds.), pp. 1–22, Raven Press, New York.
4. Simopoulos, A.P., Leaf, A., and Salem, N., Jr. (1999) Workshop on the Essentiality of and Recommended Dietary Intakes for Omega-6 and Omega-3 Fatty Acids, *J. Am. Coll. Nutr. 18*, 487–489.
5. Salem, N., Jr., Litman, B., Kim, H.-Y., and Gawrisch, K. (2001) Mechanisms of Action of Docosahexaenoic Acid in the Nervous System, *Lipids 36*, 945–959.
6. Helgadottir, A., Manolescu, A., Thorleifsson, G., Gretarsdottir, S., Jonsdottir, H., Thorsteinsdottir, U., Samani, N.J., Godmunds-

son, G., Grant, S.F.A., Thorgeirsson, G., Sveinbjornsdottir, S., Valdimarsson, E.M., Matthiasson, S.E., Johannsson, H., Gudmundsdottir, O., Gurney, M.E., Sainz, J., Thorhallsdottir, M., Andresdottir, A., Frigge, M.L., Topol, E.J., Kong, A., Gudnason, V., Hakonarson, H., Gulcher, J.R., and Stefansson, K. (2004) The Gene Encoding 5-Lipoxygenase Activating Protein Confers Risk of Myocardial Infarction and Stroke, *Nat. Genet. 36*, 233–239.

7. Erlinger, T.P., Platz, E.A., Rifai, N., and Helzlsouer, K.J. (2004) C-Reactive Protein and the Risk of Incident Colorectal Cancer, *JAMA 291*, 585–590.
8. Pasche, B., and Serhan, C.N. (2004) Is C-Reactive Protein an Inflammation Opsonin that Signals Colon Cancer Risk? *JAMA 291*, 623–624.
9. Gallin, J.I., Snyderman, R., Fearon, D.T., Haynes, B.F., and Nathan, C. (eds.) (1999) *Inflammation: Basic Principles and Clinical Correlates*, Lippincott Williams & Wilkins, Philadelphia, 1360 pp.
10. Van Dyke, T.E., and Serhan, C.N. (2003) Resolution of Inflammation: A New Paradigm for the Pathogenesis of Periodontal Diseases, *J. Dent. Res. 82*, 82–90.
11. Serhan, C.N., Clish, C.B., Brannon, J., Colgan, S.P., Chiang, N., and Gronert, K. (2000) Novel Functional Sets of Lipid-Derived Mediators with Antiinflammatory Actions Generated from Omega-3 Fatty Acids *via* Cyclooxygenase 2-Nonsteroidal Antiinflammatory Drugs and Transcellular Processing, *J. Exp. Med. 192*, 1197–1204.
12. Serhan, C.N., Hong, S., Gronert, K., Colgan, S.P., Devchand, P.R., Mirick, G., and Moussignac, R.-L. (2002) Resolvins: A Family of Bioactive Products of Omega-3 Fatty Acid Transformation Circuits Initiated by Aspirin Treatment that Counter Proinflammation Signals, *J. Exp. Med. 196*, 1025–1037.
13. Hong, S., Gronert, K., Devchand, P., Moussignac, R.-L., and Serhan, C.N. (2003) Novel Docosatrienes and 17*S*-Resolvins Generated from Docosahexaenoic Acid in Murine Brain, Human Blood and Glial Cells: Autacoids in Anti-inflammation, *J. Biol. Chem. 278*, 14677–14687.
14. Marcheselli, V.L., Hong, S., Lukiw, W.J., Hua Tian, X., Gronert, K., Musto, A., Hardy, M., Gimenez, J.M., Chiang, N., Serhan, C.N., and Bazan, N.G. (2003) Novel Docosanoids Inhibit Brain Ischemia-Reperfusion-Mediated Leukocyte Infiltration and Pro-inflammatory Gene Expression, *J. Biol. Chem. 278*, 43807–43817.
15. Mukherjee, P.K., Marcheselli, V.L., Serhan, C.N., and Bazan, N.G. (2004) Neuroprotectin D1: A Docosahexaenoic Acid-Derived Docosatriene Protects Human Retinal Pigment Epithelial Cells from Oxidative Stress, *Proc. Natl. Acad. Sci. USA 101*, 8491–8496.
16. Lehr, H.-A., Olofsson, A.M., Carew, T.E., Vajkoczy, P., von Andrian, U.H., Hübner, C., Berndt, M.C., Steinberg, D., Messmer, K., and Arfors, K.E. (1994) P-Selectin Mediates the Interaction of Circulating Leukocytes with Platelets and Microvascular Endothelium in Response to Oxidized Lipoprotein *in vivo*, *Lab. Invest. 71*, 380–386.
17. Mora, J.R., Bono, M.R., Manjunath, N., Weninger, W., Cavanagh, L.L., Rosemblatt, M., and von Andrian, U.H. (2003) Selective Imprinting of Gut-Homing T Cells by Peyer's Patch Dendritic Cells, *Nature 424*, 88–93.
18. Serhan, C.N., Hamberg, M., and Samuelsson, B. (1984) Lipoxins: Novel Series of Biologically Active Compounds Formed from Arachidonic Acid in Human Leukocytes, *Proc. Natl. Acad. Sci. USA 81*, 5335–5339.
19. Serhan, C.N., and Sheppard, K.A. (1990) Lipoxin Formation During Human Neutrophil–Platelet Interactions. Evidence for the Transformation of Leukotriene A_4 by Platelet 12-Lipoxygenase *in vitro*, *J. Clin. Invest. 85*, 772–780.
20. Marcus, A.J. (1999) Platelets: Their Role in Hemostasis, Thrombosis, and Inflammation, in *Inflammation: Basic Principles and Clinical Correlates* (Gallin, J.I., and Snyderman, R., eds.), pp. 77–95, Lippincott Williams & Wilkins, Philadelphia.
21. Fiore, S., Ryeom, S.W., Weller, P.F., and Serhan, C.N. (1992) Lipoxin Recognition Sites. Specific Binding of Labeled Lipoxin A_4 with Human Neutrophils, *J. Biol. Chem. 267*, 16168–16176.
22. Fiore, S., Maddox, J.F., Perez, H.D., and Serhan, C.N. (1994) Identification of a Human cDNA Encoding a Functional High Affinity Lipoxin A_4 Receptor, *J. Exp. Med. 180*, 253–260.
23. Bae, Y.-S., Park, J.C., He, R., Ye, R.D., Kwak, J.-Y., Suh, P.-G., and Ryu, S.H. (2003) Differential Signaling of Formyl Peptide Receptor-Like 1 by Trp-Lys-Tyr-Met-Val-Met-$CONH_2$ or Lipoxin A_4 in Human Neutrophils, *Mol. Pharmacol. 63*, 721–730.
24. Gewirtz, A.T., Collier-Hyams, L.S., Young, A.N., Kucharzik, T., Guilford, W.J., Parkinson, J.F., Williams, I.R., Neish, A.S., and Madara, J.L. (2002) Lipoxin A_4 Analogs Attenuate Induction of Intestinal Epithelial Proinflammatory Gene Expression and Reduce the Severity of Dextran Sodium Sulfate-Induced Colitis, *J. Immunol. 168*, 5260–5267.
25. Maddox, J.F., and Serhan, C.N. (1996) Lipoxin A_4 and B_4 Are Potent Stimuli for Human Monocyte Migration and Adhesion: Selective Inactivation by Dehydrogenation and Reduction, *J. Exp. Med. 183*, 137–146.
26. Godson, C., Mitchell, S., Harvey, K., Petasis, N.A., Hogg, N., and Brady, H.R. (2000) Cutting Edge: Lipoxins Rapidly Stimulate Nonphlogistic Phagocytosis of Apoptotic Neutrophils by Monocyte-Derived Macrophages, *J. Immunol. 164*, 1663–1667.
27. Clària, J., and Serhan, C.N. (1995) Aspirin Triggers Previously Undescribed Bioactive Eicosanoids by Human Endothelial Cell–Leukocyte Interactions, *Proc. Natl. Acad. Sci USA 92*, 9475–9479.
28. Perretti, M., Chiang, N., La, M., Fierro, I.M., Marullo, S., Getting, S.J., Solito, E., and Serhan, C.N. (2002) Endogenous Lipid- and Peptide-Derived Anti-inflammatory Pathways Generated with Glucocorticoid and Aspirin Treatment Activate the Lipoxin A(4) Receptor, *Nat. Med. 8*, 1296–1302.
29. Vane, J.R. (2002) Back to an Aspirin a Day? *Science 296*, 474–475.
30. Cheng, Y., Austin, S.C., Rocca, B., Koller, B.H., Coffman, T.M., Grosser, T., Lawson, J.A., and FitzGerald, G.A. (2002) Role of Prostacyclin in the Cardiovascular Response to Thromboxane A_2, *Science 296*, 539–541.
31. Fierro, I.M., Colgan, S.P., Bernasconi, G., Petasis, N.A., Clish, C.B., Arita, M., and Serhan, C.N. (2003) Lipoxin A_4 and Aspirin-Triggered 15-Epi-Lipoxin A_4 Inhibit Human Neutrophil Migration: Comparisons Between Synthetic 15 Epimers in Chemotaxis and Transmigration with Microvessel Endothelial Cells and Epithelial Cells, *J. Immunol. 170*, 2688–2694.
32. Fierro, I.M., Kutok, J.L., and Serhan, C.N. (2002) Novel Lipid Mediator Regulators of Endothelial Cell Proliferation and Migration: Aspirin-Triggered-15*R*-Lipoxin A_4 and Lipoxin A_4, *J. Pharmacol. Exp. Ther. 300*, 385–392.
33. Kieran, N.E., Doran, P.P., Connolly, S.B., Greenan, M.-C., Higgins, D.F., Leonard, M., Godson, C., Taylor, C.T., Henger, A., Kretzler, M., et al. (2003) Modification of the Transcriptomic Response to Renal Ischemia/Reperfusion Injury by Lipoxin Analog, *Kidney Int. 64*, 480–492.
34. Devchand, P.R., Arita, M., Hong, S., Bannenberg, G., Moussignac, R.-L., Gronert, K., and Serhan, C.N. (2003) Human ALX Receptor Regulates Neutrophil Recruitment in Transgenic Mice: Roles in Inflammation and Host-Defense, *FASEB J. 17*, 652–659.
35. Serhan, C.N., Jain, A., Marleau, S., Clish, C., Kantarci, A., Behbehani, B., Colgan, S.P., Stahl, G.L., Merched, A., Petasis,

N.A., Chan, L., and Van Dyke, T.E. (2003) Reduced Inflammation and Tissue Damage in Transgenic Rabbits Overexpressing 15-Lipoxygenase and Endogenous Anti-inflammatory Lipid Mediators, *J. Immunol. 171*, 6856–6865.
36. Weissmann, G., Smolen, J.E., and Korchak, H.M. (1980) Release of Inflammatory Mediators from Stimulated Neutrophils, *N. Engl. J. Med. 303*, 27–34.
37. Samuelsson, B. (1982) From Studies of Biochemical Mechanisms to Novel Biological Mediators: Prostaglandin Endoperoxides, Thromboxanes and Leukotrienes, in *Les Prix Nobel: Nobel Prizes, Presentations, Biographies and Lectures*, pp. 153–174, Almqvist & Wiksell, Stockholm.
38. Vane, J.R. (1982) Adventures and Excursions in Bioassay: The Stepping Stones to Prostacyclin, in *Les Prix Nobel: Nobel Prizes, Presentations, Biographies and Lectures*, pp. 181–206, Almqvist & Wiksell, Stockholm.
39. GISSI-Prevenzione Investigators. (1999) Dietary Supplementation with n-3 Polyunsaturated Fatty Acids and Vitamin E After Myocardial Infarction: Results of the GISSI-Prevenzione Trial. Gruppo Italiano per lo Studio della Sopravvivenza nell'Infarto miocardico, *Lancet 354*, 447–455.
40. Marchioli, R., Barzi, F., Bomba, E., Chieffo, C., Di Gregorio, D., Di Mascio, R., Franzosi, M.G., Geraci, E., Levantesi, G., Maggioni, A.P., et al. (2002) Early Protection Against Sudden Death by n-3 Polyunsaturated Fatty Acids After Myocardial Infarction: Time-Course Analysis of the Results of the Gruppo Italiano per lo Studio della Sopravvivenza nell'Infarto Miocardico (GISSI)-Prevenzione, *Circulation 105*, 1897–1903.
41. Rosenstein, E.D., Kushner, L.J., Kramer, N., and Kazandjian, G. (2003) Pilot Study of Dietary Fatty Acid Supplementation in the Treatment of Adult Periodontitis, *Prostaglandins Leukot. Essent. Fatty Acids 68*, 213–218.
42. Bazan, N.G. (1992) Supply, Uptake, and Utilization of Docosahexaenoic Acid During Photoreceptor Cell Differentiation, *Nestle Nutrition Workshop Series 28*, 121–133.
43. Lee, T.H., Mencia-Huerta, J.-M., Shih, C., Corey, E.J., Lewis, R.A., and Austen, K.F. (1984) Effects of Exogenous Arachidonic, Eicosapentaenoic, and Docosahexaenoic Acids on the Generation Of 5-Lipoxygenase Pathway Products by Ionophore-Activated Human Neutrophils, *J. Clin. Invest. 74*, 1922–1933.
44. Sawazaki, S., Salem, N., Jr., and Kim, H.-Y. (1994) Lipoxygenation of Docosahexaenoic Acid by the Rat Pineal Body, *J. Neurochem. 62*, 2437–2447.
45. Reich, E.E., Zackert, W.E., Brame, C.J., Chen, Y., Roberts, L.J., II, Hachey, D.L., Montine, T.J., and Morrow, J.D. (2000) Formation of Novel D-Ring and E-Ring Isoprostane-Like Compounds (D_4/E_4-Neuroprostanes) In Vivo from Docosahexaenoic Acid, *Biochemistry 39*, 2376–2383.
46. VanRollins, M., Baker, R.C., Sprecher, H.W., and Murphy, R.C. (1984) Oxidation of Docosahexaenoic Acid by Rat Liver Microsomes, *J. Biol. Chem. 259*, 5776–5783.
47. Lands, W.E.M. (2003) Diets Could Prevent Many Diseases, *Lipids 38*, 317-321.
48. Winyard, P.G., and Willoughby, D.A. (eds.) (2003) *Inflammation Protocols*, Humana Press, Totowa, NJ.
49. Lu, Y., Hong, S., Tjonahen, E., and Serhan, C.N. (2003) Lipid Mediator Lipidomics: Databases and Search Algorithms of Electric Spray Ionization/Tandem Mass and Ultraviolet Spectra for Structural Elucidation, Paper presented at the 5th Winter Eicosanoid Conference, Baltimore, March 9–12.
50. Capdevila, J.H., Wei, S., Helvig, C., Falck, J.R., Belosludtsev, Y., Truan, G., Graham-Lorence, S.E., and Peterson, J.A. (1996) The Highly Stereoselective Oxidation of Polyunsaturated Fatty Acids by Cytochrome P450BM-3, *J. Biol. Chem. 271*, 22663–22671.
51. Arita, M., Bianchini, F., Aliberti, J., Sher, A., Chiang, N., Hong, S., Yang, R., Tetasis, N.A., and Serhan, C.N. (2005) Stereochemical Assignment, Anti-inflammatory Properties, and Receptor for the Omega-3 Lipid Mediator Resolvin E1, *J. Exp. Med.*, in press.
52. Corey, E.J., Shih, C., and Cashman, J.R. (1983) Docosahexaenoic Acid Is a Strong Inhibitor of Prostaglandin but Not Leukotriene Biosynthesis, *Proc. Natl. Acad. Sci. USA 80*, 3581–3584.
53. Serhan, C.N., and Oliw, E. (2001) Unorthodox routes to Prostanoid Formation: New Twists in Cyclooxygenase-Initiated Pathways, *J. Clin. Invest. 107*, 1481–1489.
54. Coffa, G., and Brash, A.R. (2004) A Single Active Site Residue Directs Oxygenation Stereospecificity in Lipoxygenases: Stereocontrol Is Linked to the Position of Oxygenation, *Proc. Natl. Acad. Sci. USA 101*, 15579–15584.
55. Hessler, T.G., Thomson, M.J., Benscher, D., Nachit, M.M., and Sorrells, M.E. (2002) Association of a Lipoxygenase Locus, *Lpx-B1*, with Variation in Loxygenase Activity in Durum Wheat Seeds, *Crop Sci. 42*, 1695–1700.
56. Rådmark, O. (2002) Arachidonate 5-Lipoxygenase, *Prostaglandins Other lipid Mediat. 68–69*, 211–234.
57. Funk, C.D., Chen, X.S., Johnson, E.N., and Zhao, L. (2002) Lipoxygenase Genes and Their Targeted Disruption, *Prostaglandins Other Lipid Mediat. 68–69*, 303–312.
58. Kuhn, H., and Thiele, B.J. (1999) The Diversity of the Lipoxygenase Family. Many Sequence Data but Little Information on Biological Significance, *FEBS Lett. 449*, 7–11.
59. Furstenberger, G., Marks, F., and Krieg, P. (2002) Arachidonate 8(*S*)-Lipoxygenase, *Prostaglandins Other Lipid Mediat. 68–69*, 235–243.
60. Vance, R.E., Hong, S., Gronert, K., Serhan, C.N., and Mekalanos, J.J. (2004) The Opportunistic Pathogen *Pseudomonas aeruginosa* Carries a Novel Secretable Arachidonate 15-Lipoxygenase, *Proc. Natl. Acad. Sci. USA 101*, 2135–2139.
61. Rowley, A.F., Lloyd-Evans, P., Barrow, S.E., and Serhan, C.N. (1994) Lipoxin Biosynthesis by Trout Macrophages Involves the Formation of Epoxide Intermediates, *Biochemistry 33*, 856–863.

[Received August 8, 2004, and in revised form November 19, 2004]

Cytochrome c Release Is Required for Phosphatidylserine Peroxidation During Fas-Triggered Apoptosis in Lung Epithelial A549 Cells

Jianfei Jiang, Vidisha Kini, Natalia Belikova, Behice F. Serinkan, Grigory G. Borisenko, Yulia Y. Tyurina, Vladimir A. Tyurin, and Valerian E. Kagan*

Department of Environmental and Occupational Health, Center for Free Radical and Antioxidant Health, University of Pittsburgh, Pittsburgh, Pennsylvania 15260

ABSTRACT: Oxidation of phosphatidylserine (PtdSer) has been shown to play a pivotal role in signaling during cell apoptosis and subsequent recognition of apoptotic cells by phagocytes. However, the redox catalytic mechanisms involved in selective PtdSer oxidation during apoptosis remain poorly understood. Here we employed anti-Fas antibody CH-11-treated A549 cells as a physiologically relevant model to investigate the involvement of PtdSer oxidation and its potential mechanism during apoptosis. We demonstrated that ligation of CH-11 with its cognate receptor initiated execution of apoptotic program in interferon gamma-pretreated A549 cells as evidenced by activation of caspase and DNA fragmentation. A significant increase of cytochrome c (cyt c) content in the cytosol as early as 2 h after CH-11 exposure was detected indicating that Fas-induced apoptosis in A549 cells proceeds *via* extrinsic type II pathway and includes mitochondrial signaling. PtdSer was selectively oxidized 3 h after anti-Fas triggering while two more abundant phospholipids—phosphatidylcholine (PtdCho) and phosphatidylethanolamine (PtdEtn) —and the major intracellular antioxidant, glutathione, remained nonoxidized. A pan-caspase inhibitor, z-VAD, fully blocked cyt c release and oxidation of PtdSer in Fas-treated A549 cells. On the other hand, z-DQMD, a caspase-3 inhibitor, completely inhibited caspase-3 activity but did not fully block caspase-8 activation and release of cyt c. Importantly, z-DQMD failed to protect PtdSer from oxidation. In addition, in a model system, we demonstrated that peroxidase activity of cyt c was greatly enhanced in the presence of dioleoylphosphatidylserine containing liposomes by monitoring oxidation of 2′,7′-dichlorodihydrofluorescein to 2′,7′-dichlorofluorescein. We further showed that peroxidase activity of cyt c catalyzed oxidation of 1-palmitoyl-2-arachidonoyl-3-glycero-phosphoserine using a newly developed HPLC assay. MS analysis of 1-palmitoyl-2-arachidonoyl-3-glycero-phosphoserine revealed that in addition to its mono- and dihydroperoxides, several different PtdSer oxidation products can be formed. Overall, we concluded that cyt c acts as a catalyst of PtdSer oxidation during Fas-triggered A549 cell apoptosis.

Paper no. L9557 in Lipids 39, 1133–1142 (November 2004).

Oxidative stress and free radicals generated by either pro-oxidant chemicals or redox-cycling agents [e.g., H_2O_2 (1), diamide (2), and semiquinones (3)] or physical agents [e.g., UV irradiation (4)] are commonly associated with triggering of apoptosis. Generation of reactive oxygen species (ROS) and subsequent oxidative stress has also been demonstrated to occur in cells upon initiation of both intrinsic and extrinsic apoptosis by different nonoxidant stimuli such as staurosporine, melphalan, and Fas (5–7). In the latter case, a specific role for ROS in apoptosis has not been well established although their production is likely essential for the execution of the programmed death (6). We have recently documented the preferential oxidation of phosphatidylserine (PtdSer) during cell apoptosis on various stimuli and identified oxidized PtdSer (oxPtdSer) as a meaningful signaling molecule acting as a fine-tuning enhancer of PtdSer externalization and subsequent recognition of apoptotic cells by macrophages (8,9).

The preferential oxidation of PtdSer was only observed in intact living cells undergoing apoptosis but not in liposomes incubated with oxidants (10). Oxidation of PtdSer preceded its externalization during apoptosis and was blocked by the anti-apoptotic protein Bcl-2 (11,12). While these observations imply that PtdSer oxidation may be an indispensable part of PtdSer signaling pathways in apoptosis, the specific mechanisms involved in its selective oxidation remain to be elucidated. Since oxidative stress during apoptosis is largely due to disrupted electron transport in mitochondria and departure of cytochrome c (cyt c) from mitochondria into cytosol, we hypothesized that this specific oxidative pathway involves cyt c. We have speculated that positively charged cyt c [pI = 10.3 (13)] released from mitochondria into cytosol may interact with negatively charged PtdSer in the inner leaflet of plasma membrane and utilize H_2O_2 formed by disrupted mitochon-

*To whom correspondence should be addressed at Department of Environmental and Occupational Health, University of Pittsburgh, 3343 Forbes Ave., Pittsburgh, PA 15260. E-mail: kagan@pitt.edu

Abbreviations: Cyt c, cytochrome c; DCF, 2′,7′-dichlorofluorescein; DCFH, 2′,7′-dichlorodihydrofluorescein; dioleoyl-GroPCho, 1,2-dioleoyl-3-glycero-phosphocholine; dioleoyl-GroPSer, 1,2-dioleoyl-3-glycero-phosphoserine; dipalmitoyl-GroPSer, 1, 2-dipalmitoyl-3-glycero-phosphoserine; GSH, glutathione; IFN-γ, interferon gamma; NAO, 10-*N*-nonyl acridine orange; ox-PtdSer, oxidized phosphatidylserine; 1-palmitoyl-2-arachidonyl-GroPSer, 1-palmitoyl-2-arachidonyl-3-glycero-phosphoserine; 1-palmitoyl-2-arachidonyl-GroPCho, 1-palmitoyl-2-arachidonyl-3-glycero-phosphocholine; PnA, *cis*-parinaric acid; PtdCho, phosphatidylcholine; PtdEtn, phosphatidylethanolamine; PtdIns, phosphatidylinositol; PtdOH, phosphatidic acid; PtdSer, phosphatidylserine; ROS, reactive oxygen species; SOD, superoxide dismutase.

dria electron transport to catalyze preferential PtdSer oxidation (14).

In normal lung, elimination of apoptotic cells by macrophages is a highly regulated physiological process that is carried out without injury to neighboring cells and with minimum inflammation. The apoptotic cells that are not cleared by macrophages may undergo secondary necrosis with discharge of injurious cell contents. A wide array of pathological conditions like emphysema, pulmonary fibrosis, cystic fibrosis, and obliterative bronchiolitis in lung transplantation have been associated with excessive apoptosis and/or reduced clearance of apoptotic cells (15–19). Thus it is essential to investigate the factors, including oxPtdSer, that control the signaling pathways leading to effective cell removal.

Fas/FasL has been recently implicated in apoptosis in lung both under physiologic conditions as well as in disease. Fas, a member of the TNF receptor superfamily, is a 36-kDa transmembrane receptor (20). Upon binding of Fas to its cognate ligands, a Fas expressing cell commits to the extrinsic apoptotic pathway via recruitment of accessory proteins and formation of a death-inducing signaling complex (DISC) that contains the adaptor protein Fas-associated death domain protein (FADD) and caspase-8 that initiates apoptosis (21,22). In certain cell types (type II cells), the receptor-mediated pathway of apoptosis recruits the mitochondrial mechanisms to enhance apoptosis through caspase-8-mediated cleavage of Bid and the two pathways converge at the level of caspase-3 activation (21,22).

Herein, we report that anti-Fas antibody CH-11-induced apoptosis in interferon gamma (IFN-γ)-pretreated A549 cells resulted in selective PtdSer oxidation, preceded by release and accumulation of cyt c in the cytosol. Moreover, PtdSer oxidation was sensitive to a pan-caspase inhibitor, z-VAD, which blocked cyt c release from mitochondria but was insensitive to a caspase-3 inhibitor, z-DQMD, which did not prevent mitochondrial disruption and cyt c release. Furthermore, using cell-free systems, we showed that interaction with PtdSer (but not with PtdCho) converts cyt c in a peroxidase-catalyzing oxidation of PtdSer.

EXPERIMENTAL PROCEDURES

Materials. IFN-γ was purchased from Biosource International (Camarillo, CA). Anti-Fas monoclonal antibody (CH-11) was obtained from MBL (Nagoya, Japan). Anti-cyt c antibody was from BD Biosciences (Pharmingen, San Diego, CA). Z-VAD and z-DQMD were from Calbiochem (San Diego, CA). Enzchek Caspase-3 Assay Kit, *cis*-parinaric acid (PnA), Amplex Red Reagent (10-acetyl-3,7-dihydroxyphenoxazine), and 10-*N*-nonyl acridine orange (NAO) were purchased from Molecular Probes (Eugene, OR). Horse heart cyt c, superoxide dismutase (SOD), and catalase were from Sigma (St. Louis, MO). Mitochondria/Cytosol Fractionation Kit and Caspase-8/FLICE Fluorometric Protease Assay Kit were from Biovision (Mountain View, CA). Cyt c ELISA kit was from Oncogene (Boston, MA). 1-Palmitoyl-2-arachidonoyl-3-glycero-phosphocholine (1-palmitoyl-2-arachidonoyl GroP-Cho), 1-palmitoyl-2-arachidonoyl-3-glycero-phosphoserine (1-palmitoyl-2-arachidonoyl-GroPSer), 1,2-dioleoyl-3-glycero-phosphocholine (dioleoyl-GroPCho), 1,2-dipalmitoyl-3-glycerol-phosphoserine (dipalmitoyl-GroPSer), and 1,2-dioleoyl-3-glycero-phosphoserine (dioleoyl-GroPSer) were from Avanti Polar Lipids (Alabaster, AL).

Cell culture and treatments. A549 cells were cultured in F-12K medium with 10% heat-inactivated FBS. For apoptosis induction, cells were exposed to IFN-γ and CH-11 as described previously (23,24) with modifications. In brief, cells were plated in six-well plates at 0.1×10^6/well and allowed to adhere overnight, and then incubated with 1000 U/mL of IFN-γ for 24 h and subsequently loaded with 1 μg/mL of CH-11 for indicated time periods. The protease inhibitors, z-VAD or z-DQMD, were added 30 min before CH-11 treatment at the concentration of 40 μM in 0.4% DMSO. Parallel dishes received an equivalent volume of the solvent (0.4% DMSO) and were cultured under identical conditions. At the end of incubation, attached cells were harvested by trypsinization and pooled with detached cells.

Analysis of caspase activity. Caspase-3 and caspase-8 protease activities were assessed using Enzchek Caspase-3 Assay Kit and Caspase-8/FLICE Fluorometric Protease Assay Kit as described by the respective manufacturer's protocols. The fluorescence of cleaved substrates was determined using a Fusion a plate reader (PerkinElmer, Downers Grove, IL), and enzyme activity was expressed as arbitrary fluorescence units per microgram of protein.

Measurements of DNA fragmentation. Cells were collected at the end of incubation, after being washed once with PBS, fixed with 70% ethanol at 4°C overnight. Cells were then resuspended in PBS [containing 10 mg/mL propidium iodide (PI) and 0.2 mg/mL DNase-free RNase] for 30 min at room temperature in the dark. DNA fragmentation was analyzed on a FACscan flow cytometer using Cell Quest software (Becton-Dickinson, San Jose, CA).

Assay for cytochrome c release. Cytosolic fraction was separated using a Mitochondria/Cytosol Fractionate Kit. Content of cyt c was determined using a Cyt c ELISA Kit according to the manufacturer's protocol.

Assessment of membrane phospholipid oxidation. IFN-γ-pretreated A549 cells were metabolically labeled with PnA as described previously (25,26) before addition of CH-11. Total lipids were extracted at the end of incubation using the procedure of Folch *et al.* (27) in the presence of butylated hydroxytoluene to inhibit subsequent oxidations; lipids were then separated by normal phase HPLC using a 5-μm Microsorb-MV Si column (4.6 mm × 250 mm) employed with the following mobile phase at 1 mL/min: solvent A (isopropanol/hexane/water, 57:43:1, by vol) and solvent B (isopropanol/hexane/40 mM aqueous ammonium acetate, 57:43:10, by vol, pH 6.7), 0–3 min linear gradient from 10 to 37% B, 3–15 min with an isocratic at 37% B, 15–23 min with a linear gradient to 100% B, and 23–45 min with an isocratic

gradient at 100% B. The separations were performed using a Shimadzu HPLC system (LC-600) (Kyoto, Japan) equipped with a fluorescence detector (RF-10A) (Kyoto, Japan). Data were processed and stored in digital form using Shimadzu Ezchrom software. The amount of lipid phosphorus was determined using a micro method (28). To identify the HPLC peaks, two approaches were used: (i) The fractions of phospholipids were collected and analyzed by two-dimensional HPTLC on silica-gel plates. The phospholipids were visualized by exposure to iodine vapors and identified by comparing them with the R_f values measured for the authentic phospholipid standards. (ii) Authentic phospholipids standards were subjected to HPLC with UV detection and their R_f values compared with those of biological samples.

Assay for cyt c peroxidase activity and lipid binding constant. Liposomes were prepared from either dioleoyl-GroPCho or from a mixture of dioleoyl-GroPCho and dioleoyl- (or dipalmitoyl-)GroPSer at a ratio of 1:1 (4 mM total lipid) by tip sonicator (Ultrasonic Homogenizer 4710 Series, Cole-Palmer-Instrument Co., Chicago, IL). To determined peroxidase activity, 2′,7′-dichlorodihydrofluorescein (DCFH) was prepared from its diacetate by alkaline hydrolysis as previously reported (29). Cyt c (2 μM) was preincubated with (or without) small unilamellar phospholipid liposomes (100 μM) for 1 h in HEPES buffer (50 mM, pH 7.0), and then H_2O_2 (10 μM) and DCFH (10 μM) were added for 5-min incubation. Peroxidase activity of cyt c was assessed by monitoring the oxidation of DCFH to 2′,7′-dichlorofluorescein (DCF) by fluorescence spectroscopy (excitation, 502 nm; emission, 522 nm). To estimate the binding constant, liposomes (4 mM) were incubated with cyt c (40 μM) in the presence of different concentrations (2–12 mM) of NAO (1 h at room temperature in dark), which is known to strongly bind cardiolipin. The samples were electrophoresed in native-PAGE with 7.5% polyacrylamide in HEPES-Imidazol buffer (pH 7.4), and free cyt c was determined using Coomassie Blue staining. The lipid-cyt c binding constant was calculated based on known binding constant of lipid-NAO ($[NAO]/[Cyt\ c]_{free} = K_{lipid\text{-}cytc}/K_{lipid\text{-}NAO}$) (30).

Determination of cyt c-catalyzed oxidation of 1-palmitoyl-2-arachidonyl-GroPSer. 1-palmitoyl-2-arachidonyl-GroPSer or 1-palmitoyl-2-arachidonyl-GroPCho was incubated with cyt c (50 μM) in reaction buffer [50 mM phosphate buffer containing 100 μM diethylenetriaminepentaacetic acid (DTPA), pH 7.4) in the presence of H_2O_2 (100 μM of H_2O_2 was added every 15 min during incubation) for 1 h at 37°C. At the end of incubation, 100 U of catalase was added for additional 5-min incubation to remove excess of H_2O_2. Lipids were then extracted using the procedure by Folch *et al.* (27).

Determination of lipid hydroperoxides using HPLC. Lipid hydroperoxides were determined by fluorescence HPLC of products formed in microperoxidase-catalyzed reaction of specific lipid hydroperoxides with a fluorogenic substrate, Amplex Red, according to our newly developed protocol (31). The assay was started by addition of 10 μL of reaction mixture containing 50 μM Amplex Red to 40 μL of basic reaction mixture containing 25 mM NaH_2PO_4, (pH 7.0 at 21°C) and an aliquot (2 μL) of PtdSer treated with cyt c and H_2O_2. After addition of 1 μL of microperoxidase (1.0 μg/μL) samples were incubated at 37°C for 15 min. The reaction was stopped by addition of 100 μL of solution of 10 mM HCl in acetonitrile. After centrifugation at 15,000 × *g* for 5 min, aliquots of supernatant (5 μL) were injected into Eclipse XDB-C18 column (5 μm, 150 × 4.6 mm). Mobile phase was composed of 25 mM NaH_2PO_4 (pH 7.0)/methanol (50:50, v/v). The flow rate was 1 mL/min. The resorufin (an Amplex Red oxidation product) fluorescence was measured at 590 nm after excitation at 560 nm. Shimadzu LC-100AT vp HPLC system equipped with fluorescence detector (RF-10Axl) and autosampler (SIL-10AD vp) was used. Data were processed and stored in digital form with Class-VP software.

Elecrospray ionization mass spectrometry of 1-palmitoyl-2-arachidonoyl-GroPSer. Lipids were analyzed by electrospray ionization spectrometry by direct infusion into a triple quadrupole mass spectrometer (Finnigan MAT TSQ 700, San Jose, CA). Samples were evaporated under N_2, resuspended in chloroform/methanol (1:2, v/v; 10 pmol/μL) and directly utilized for acquisition of negative-ion ESI mass spectra using a syringe pump (KDS100; KDS Scientific, Holliston, MA) at a flow rate of 2 μL/min. The electrospray probe was operated at a voltage differential of –4.5 kV. Mass spectra for the $(M–H)^-$ PtdSer species were obtained by scanning in the range of 750–850 every 0.75 s and summing individual spectra. Source temperature was maintained at 70°C.

Statistics. All data were expressed as mean ± SD values. Paired *t*-tests were used for single comparisons. Differences were considered significant when $P < 0.05$.

RESULTS

Anti-Fas antibody-triggered apoptosis in IFN-γ-pretreated A549 cells. In agreement with previous reports (23,24), addition of CH-11 antibody to IFN-γ-pretreated A549 cells resulted in apoptosis as evidenced by an increase in caspase-3 activity. Figure 1A demonstrates that a 12-fold increase in caspase-3 activity was achieved after stimulation with CH-11 antibody for 3 h compared to control (nontreated) cells. No activation of caspase-3 was detected in IFN-γ-pretreated cells devoid of CH-11 exposure or in cells treated with CH-11 antibody without IFN-γ pretreatment (data not shown). Figure 1B shows the results of flow cytometric analysis revealing typical for apoptotic cells substantial DNA fragmentation after exposure to IFN-γ/CH-11. The characteristic DNA fragmentation was observed in 27.6% of CH-11-triggered IFN-γ-pretreated A549 cells *vs.* 3.9% of IFN-γ-pretreated cells without CH-11 exposure.

Although receptor-mediated extrinsic pathway can function independently of intrinsic mitochondrial mechanisms, in most cases both pathways are activated simultaneously and are reciprocally augmented. To delineate the role of mitochondria in regulating IFN-γ-/CH-11-induced apoptosis, we determined the release of cyt c from mitochondria into the cy-

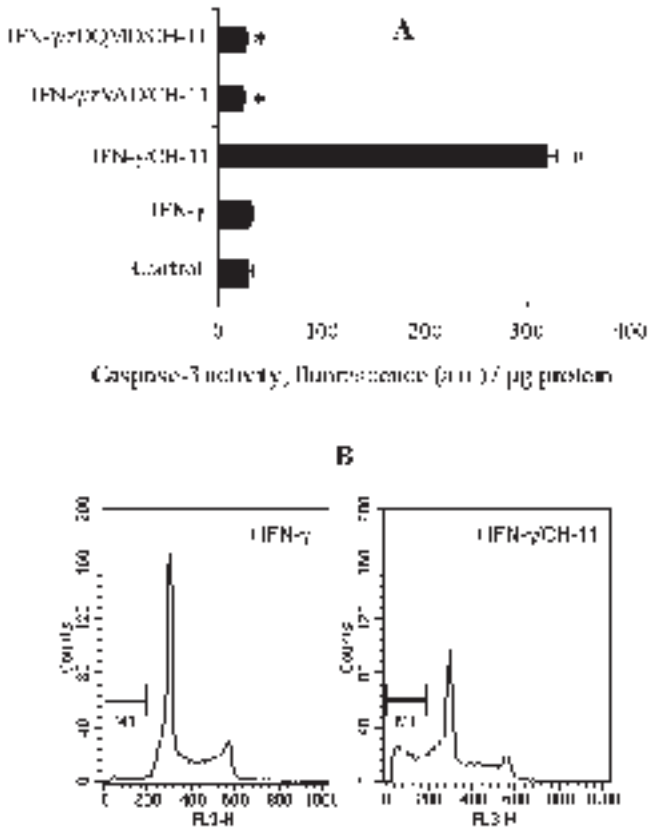

FIG. 1. Anti-Fas agonistic antibody CH-11 induces apoptosis in A549 cells. A549 cells were pretreated with 1000 U/mL of interferon-γ (IFN-γ) for 24 h, cells were then incubated with 1 μg/mL of CH-11 for 3 h. (A) Caspase-3 activity assayed by cleavage of the peptide substrate DEVD-AMC. Values are means ± SD ($n = 3$). #$P < 0.01$, compared with cells without any treatment, *$P < 0.01$, compared with IFN-γ/CH-11 triggered cells. (B) FACscan analysis demonstrating DNA fragmentation in A549 cells after IFN-γ/CH-11 treatment. The relative number of cells found in the region marked as M1 was defined as the percentage of apoptotic cells.

tosol by ELISA assay. Compared with control (nontreated) cells (72.2 ng/mg of protein), there were no changes in the cytosolic cyt c content in cells pretreated with IFN-γ without CH-11 exposure (Table 1) or cells incubated with CH-11 alone (data not shown). Significantly increased levels of cyt c were detected in the cytosol of IFN-γ-pretreated cells as early as 2 h after activation of Fas receptor by CH-11 (152.9 ng/mg of protein, $P < 0.05$) and the cyt c content mounted up to 397.2 ng/mg of protein after 3 h of incubation ($P < 0.05$) (Table 1).

TABLE 1
Accumulation of Cytochrome c (Cyt c) in Cytosol of A549 Cells Treated with CH-11[a]

	Cyt c, ng/mg of protein	
Time, h	IFN-γ	CH-11/IFN-γ
0	72.2 ± 19.2	/
1	80.3 ± 17.6	67.2 ± 14.3
2	86.4 ± 7.9	152.9 ± 17.2*
3	73.6 ± 10.3	397.2 ± 32.4*

[a]Apoptosis was induced by exposure of cells to CH-11 antibody after interferon-γ (IFN-γ) pretreatment for 1, 2, or 3 h. Cells were then harvested at various time points, cytosolic fractions were separated, and cyt c content was determined using Elisa assay. Cells without any treatment were used as a control at 0 point. Data represent means ± SD ($n = 3$). *$P < 0.05$, compared with control.

Fas-triggered phospholipid oxidation in A549 cells. To determine whether Fas-ligation induced phospholipid peroxidation in A549 cells, IFN-γ-pretreated cells were metabolically labeled with a natural fluorescent fatty acid, PnA, before the addition of CH-11. Figure 2A shows a typical fluorescence HPLC profile of major PnA-labeled membrane phospholipids extracted from A549 cells. Oxidation of phospholipids was determined by the decrease in fluorescence intensity of PnA esterified in four major classes of phospholipids, namely, phosphatidylcholine (PtdCho), phosphatidylethanolamine (PtdEtn), PtdSer, and phosphatidylinositol (PtdIns). Figure 2B illustrates that PtdSer was the only phospholipid that experienced significant Fas-induced oxidation. PtdSer was

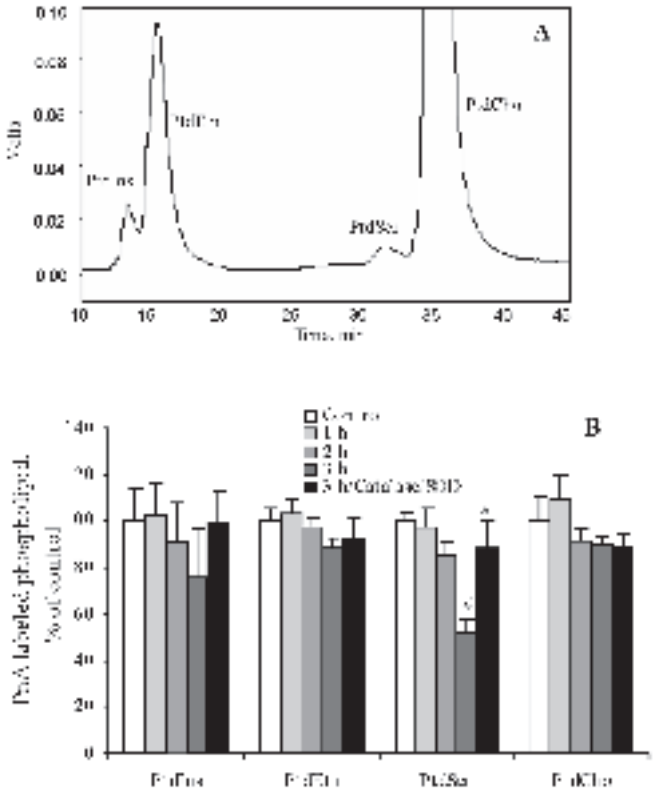

FIG. 2. CH-11-induced phospholipid oxidation in A549 cells. IFN-γ-pretreated A549 cells were metabolically labeled with *cis*-PnA for 2 h at 37°C, then incubated with 1 μg/mL of CH-11 for 1, 2, or 3 h. (A) Typical fluorescence HPLC tracing of PnA-labeled membrane phospholipids extracted from A549 cells. (B) Fas-triggered oxidation of membrane phospholipids. Note that PtdSer was preferentially oxidized among major classes of phospholipids in A549 cells after 3-h incubation, which was significantly protected by SOD (50 U/mL) and catalase (50 U/mL). Antioxidant enzymes were added simultaneously with CH-11 to IFN-γ-pretreated/PnA-labeled A549 cells and incubated for 3 h. Data are means ± SD ($n = 3$). #$P < 0.05$, compared with control cells without CH-11 treatment. *$P < 0.05$, compared with IFN-γ/CH-11-treated cells. PtdCho, phosphatidylcholine; PtdEtn, phosphatidylethanolamine; PtdIns, phosphatidylinositol; PtdSer, phosphatidylserine; SOD, superoxide dismutase; PnA, parinaric acid; for other abbreviation see Figure 1.

slightly (by ~15.0%) but not significantly oxidized as early as 2 h after addition of CH-11. A twofold decrease of fluorescently labeled PnA-PtdSer (down to 52.0% of its initial level, $P < 0.05$), demonstrating a pronounced PtdSer oxidation, was observed after 3-h exposure of cells to CH-11. In contrast, no significant peroxidation was detected in two more abundant phospholipid classes, PtdCho and PtdEtn. PtdIns, another major acidic phospholipid in the cytosolic leaflet of plasma membrane, demonstrated a slightly enhanced oxidation during Fas-induced apoptosis; the effect, however, did not reach the level of statistical significance. Fas-induced PtdSer oxidation was blocked ($P < 0.05$) by a combination of exogenously added antioxidant enzymes, SOD (50 U/mL) and catalase (50 U/mL) (Fig. 2B). Importantly, intracellular concentrations of glutathione (GSH), the most abundant thiol and major scavenger of radicals in the cytosol were also found to be unchanged during Fas-triggered apoptosis in A549 cells (data not shown).

Oxidation of PtdSer is dependent on accumulation of cyt c in the cytosol. We hypothesized that cyt c released from mitochondria into the cytosol—through its interactions with PtdSer in the presence of endogenously formed H_2O_2—may act as a specific catalyst responsible for predominant oxidation of PtdSer (rather than random oxidation of other more abundant phospholipids or GSH). This notion was supported by the fact that PtdSer oxidation was preceded by accumulation cyt c in CH-11-triggered A549 cells.

To further explore the potential role of cyt c in PtdSer oxidation, two caspase inhibitors—a pan-caspase inhibitor, z-VAD, and a specific caspase-3 inhibitor, z-DQMD, were used to manipulate cyt c release in Fas-triggered A549 cells. Preincubation of cells with the z-VAD completely prevented both caspase-8 (Fig. 3A) and capase-3 activation (Fig. 1A) in Fas-triggered A549 cells. Caspase-3 activity was also completely blocked in cells pretreated with z-DQMD (Fig. 1A), whereas caspase-8 activity was only partially inhibited ($P < 0.05$, compared with IFN-γ-/CH-11-treated cells, or IFN-γ-pretreated cells without CH-11 exposure) (Fig. 3A).

Since mitochondrial events are believed to occur downstream of caspase-8 activation but upstream of caspase-3 activation, release of cyt c is anticipated to have different sensitivity to z-VAD or z-DQMD treatment. As shown in Figure 3B, Fas-induced cyt c accumulation in the cytosol was completely blocked in the presence of z-VAD (77.9 ng/mg of protein; $P < 0.05$, compared with Fas-triggered apoptotic cells). In contrast, z-DQMD failed to prevent cyt c accumulation in CH-11-triggered cells (232.2 ng/mg of protein), although the concentration of cytosolic cyt c was lower than that in Fas-triggered A549 cells in the absence of z-DQMD.

If the presence of cyt c in the cytosol is critical for its catalytic role in PtdSer oxidation, then z-VAD and z-DQMD should affect PtdSer oxidation according to their ability to regulate cyt c release from mitochondria. Indeed, z-VAD, which blocked the release of cyt c from mitochondria, completely inhibited PtdSer oxidation in Fas-triggered A549 cells as evidenced by the lack of loss of PnA-labeled PtdSer (Fig. 4). In contrast, z-DQMD, which did not prevent release of cyt c, exerted no significant effect on Fas-triggered PtdSer oxidation (Fig. 4). These results allude to a close association between cyt c accumulations in the cytosol with PtdSer oxidation during Fas-triggered apoptosis in A549 cells.

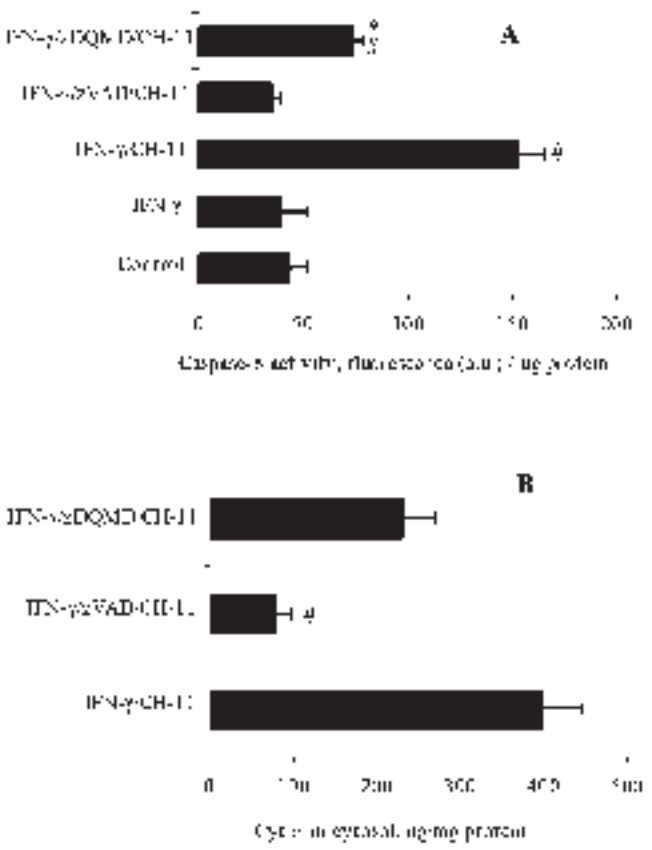

FIG. 3. Effect of caspase inhibitors on Fas-induced caspase-8 activation and cytochrome c (cyt c) release in A549 cell. IFN-γ-pretreated A549 cells were preincubated with z-VAD (40 μM) or z-DQMD (40 μM) for 30 min before addition of CH-11 antibody (1 μg/mL) after which the cells were additionally incubated with the inhibitors for 3 h. (A) Measurements of caspase-8 activity. (B) Assay of cyt c content in the cytosolic fraction. Data represent means ± SD ($n = 3$). #$P < 0.05$, compared with IFN-γ-pretreated cells without CH-11 exposure. *$P < 0.05$, compared with IFN-γ-/CH-11-treated cells. For other abbreviation see Figure 1.

Cyt c-catalyzed oxidation of DCFH or lipids. Once in the cytosol, positively charged cyt c may interact with negatively charged PtdSer in the inner leaflet of plasma membrane. Initial electrostatic binding of cyt c to acidic phospholipids is followed by strong hydrophobic interactions (at cyt c C-site) leading to profound conformational changes and rupture of the Fe-Met80 coordination bond with heme iron (32–34). As a result, peroxidase activity of cyt c may be enhanced resulting in selective oxidation of PtdSer. Here we assessed the effect of PtdSer binding on the peroxidase activity of cyt c using as substrate of DCFH, a probe that undergoes oxidation to fluorescent DCF (35). As shown in Figure 5, a low level of DCFH oxidation was detected in the presence of 10 μM H_2O_2 and the presence of cyt c slightly increased the rate of DCF formation. Dioleoyl-GroPCho containing liposome did not

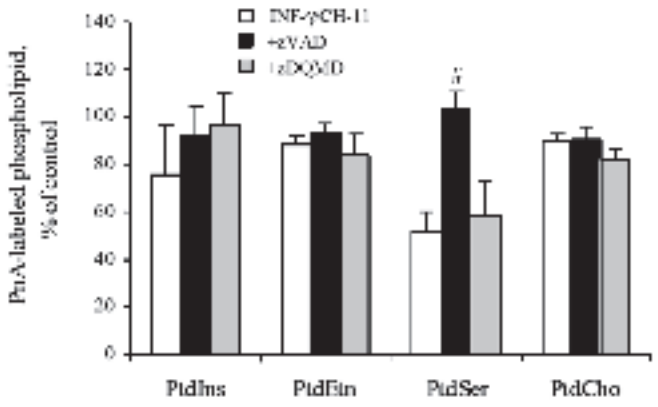

FIG. 4. Effect of caspase inhibitors on Fas-induced phospholipid oxidation in A549 cells. Note that z-VAD (but not z-DQMD) protected PtdSer against Fas-induced peroxidation. PnA-labeled/IFN-γ-pretreated A549 cells were preincubated with z-VAD (40 μM) or z-DQMD (40 μM) for 30 min before addition of CH-11 antibody (1 μg/mL), after which the cells were additionally incubated with the inhibitors for 3 h. Total lipids were extracted from harvested cells and resolved by fluorescence-HPLC. Data are means ± SD ($n = 3$), #$P < 0.05$, compared with IFN-γ-/CH-11-treated cells. PnA, *cis*-parinaric acid; for other abbreviations see Figures 1 and 2.

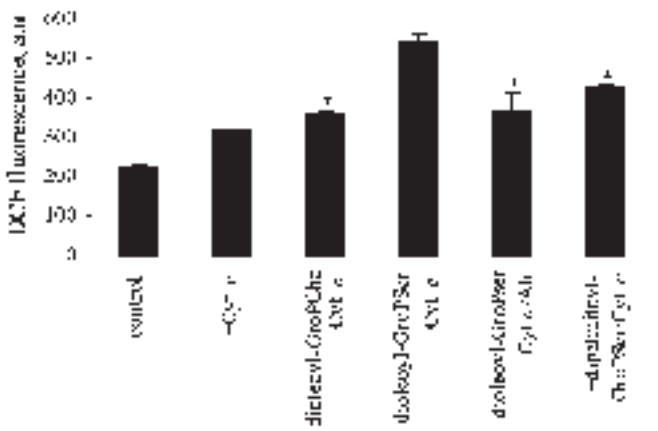

FIG. 5. Effect of PtdSer on peroxidase activity of cyt c. Cyt c (2 μM) was preincubated with (or without) small unilamellar phospholipid liposomes (100 μM) for 1 h in HEPES buffer (50 mM, pH 7.0), and then H_2O_2 (10 μM) and DCFH (10 μM) was added for 5-min incubation. Peroxidase activity of cyt c was evaluated by monitoring the formation of DCF with fluorescence spectroscopy (excitation, 502 nm; emission, 522 nm). In the experiment of peroxidase activity inhibition, anti-cyt c antibody (2 μM) was added 30 min before addition of H_2O_2 and DCFH. Sample without cyt c was considered as control. Data shown are representative of three independent experiments. *$P < 0.01$, compared with dioleoyl-GroPSer/cyt c. DCFH, 2′,7′-dichlorodihydrofluorescein; dioleoyl-GroPCho, 1,2-dioleoyl-3-glycero-phosphocholine; dioleoyl-GroPSer, 1,2-dioleoyl-3-glycerophosphoserine; dipalmitoyl-GroPSer, 1,2-dipalmitoyl-3-glycero-phosphoserine; for other abbreviation see Figure 3.

significantly change H_2O_2/cyt c-catalyzed DCFH oxidation. In contrast, dioleoyl-GroPCho/dioleoyl-GroPSer containing liposome markedly enhanced oxidation of DCFH to DCF. The peroxidase activity was fully abolished in the presence of anti-cyt c antibody. Though fully saturated dipalmitoyl-GroPSer also slightly increased oxidation of DCFH to DCF, its effect was significantly less pronounced than that of dioleoyl-GroPSer ($P < 0.01$).

Binding of acidic phospholipids to cyt c is essential for its activation to a peroxidase and subsequent phospholipid oxidation. Therefore, we compared binding of different phospholipids with cyt c and established that it decreased in the following order: tetraoleoyl-cardiolipin (data not shown) >> dioleoyl-GroPSer ($3.84 \pm 1.76 \times 10^6$ M^{-1}) >> dioleoyl-GroPCho (essentially no binding). We further established that even for cardiolipin, which demonstrates a remarkably high affinity for cyt c when unsaturated molecular species of cardiolipin are used for its activation to a peroxidase, both binding and peroxidase activity are essentially undetectable in the presence of cardiolipin-saturated molecular species (e.g., tetramyristoyl-cardiolipin; data not shown). These results are consistent with the hypothesis that both the negatively charged headgroup and unsaturated fatty acid residue were critical for the tight binding of cyt c and activation of cyt c peroxidase activity

Most important, when 1-palmitoyl-2-arachinodyl-GroPSer was incubated with cyt c in the presence of H_2O_2, marked oxidation of 1-palmitoyl-2-arachidonoyl-GroPSer was detected by Amplex Red-based assay of lipid hydroperoxides (Fig. 6) as well as by ESI-MS-analysis (Fig. 7). As can be seen from the spectrum, 1-palmitoyl-2-arachidonoyl-GroPSer molecular ion is represented by a peak with *m/z* 782.83. After incubation with cyt c/H_2O_2, mono-(814.85 *m/z*) and di-(847.37 *m/z*) hydroperoxides were detected as the major peaks along with other hydroperoxide oxidation products. In sharp contrast, cyt c/H_2O_2 did not cause any oxidation of 1-palmitoyl-

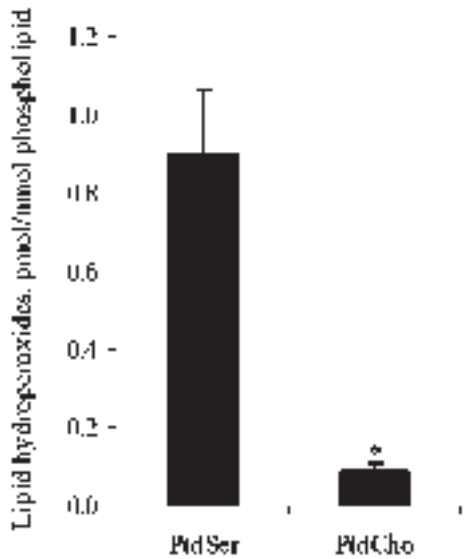

FIG. 6. Cyt c catalyzed oxidation of lipids. 1-Palmitoyl-2-arachidonyl-GroPSer or 1-palmitoyl-2-arachidonyl-GroPCho (1 mM) were incubated with cyt c (50 μM) in the presence of H_2O_2 (100 μM of H_2O_2 was added every 15 min during 1-h incubation at 37°C). Lipid hydroperoxides were assessed by determining the formation of resorufin in microperoxidase catalyzed reaction of specific lipid hydroperoxides with a fluorogenic substrate, Amplex Red, using HPLC. Data are mean ± SD ($n = 3$) (*$P < 0.01$, compared with 1-palmitoyl-2-arachidonyl-GroPSer). 1-Palmitoyl-2-arachidonyl-GroPSer, 1 palmitoyl-2-arachidonyl-3-glycero-phosphoserine; 1-palmitoyl-2-arachidonyl-GroPCo, 1-palmitoyl-2-arachidonyl-3-glycero-phosphocholine; for other abbreviation see Figure 3.

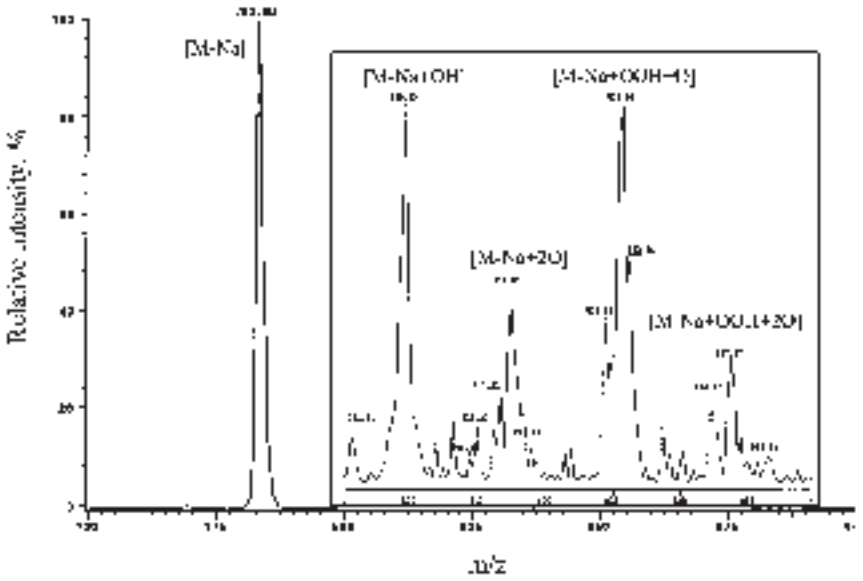

FIG. 7. Typical negative-ion ESI-MS profiles of 1-palmitoyl-2-arachidonyl-GroPSer before and after (inset) oxidation catalyzed by cyt c/H_2O_2. 1-Palmitoyl-2-arachidonyl-GroPSer or 1-palmitoyl-2-arachidonyl-GroPCho (1 mM) were incubated with cyt c (50 μM) in the presence of H_2O_2 (100 μM of H_2O_2 was added every 15 min during 1-h incubation at 37°C). Lipids were extracted and directly utilized for acquisition of negative-ion ESI mass spectra. The electrospray probe was operated at a voltage differential of –4.5 kV. 1-Palmitoyl-2-arachidonyl-GroPSer, 1-palmitoyl-2-arachidonyl-3-glycero-phosphoserine; 1-palmitoyl-2-arachidonyl-GroPCho, 1-palmitoyl-2-arachidonyl-3-glycero-phosphocholine; for other abbreviation see Figure 3.

2-arachidonoyl-GroPCho in spite of the presence of highly oxidizable substrate, 1-palmitoyl-2-arachidonoyl-GroPCho. Thus, once attracted by PtdSer in the cytosol, cyt c is likely activated to a peroxidase, which further catalyzes PtdSer oxidation using H_2O_2 formed by disrupted respiratory chain as a source of oxidizing equivalents.

DISCUSSION

In addition to its major commission as an electron transporter between complexes III and IV in mitochondria, cyt c may play an important role as an antioxidant by redox regulating electron transport and scavenging erroneously generated superoxide radicals (36,37). Moreover, as a heme-containing protein, cyt c can fulfill another antioxidant function by acting as a peroxidase to control the content of H_2O_2 generated as a by-product of mitochondrial electron transport. The latter, however, requires sources of oxidizing equivalents (H_2O_2) and activation of cyt c by anionic phospholipids, such as PtdSer or cardiolipin in mitochondria (38–40).

We hypothesized that disruption of electron transport during apoptosis and release of both cyt c and H_2O_2 in the cytosol create conditions for interactions of cyt c with PtdSer in the inner leaflet of plasma membrane, thus activating it as a peroxidase (40). PtdSer is distributed nonrandomly in the inner leaflet of plasma membrane but rather colocalizes with sphingomyelin and cholesterol in lipid rafts where its concentration is four times higher than in the surrounding membrane phospholipids (41). High affinity (K_d = 0.017 μM) binding of cyt c to negatively charged phospholipids including PtdSer *via* electrostatic (A-site) and hydrophobic interactions (C-site) has been demonstrated (42–45). Moreover, C-site-mediated binding of cyt c to negatively charged membrane phospholipids induces disruption of Fe-Met80 heme iron coordination bond, unfolding of native structure of cyt c, and concomitant opening of heme crevice, which allows close interaction of the heme with the lipid phosphate headgroup (32). The conformational changes of cyt c dramatically enhanced its peroxidase activity, which was confirmed in the present study. Remarkable increase of DCF formation was only observed in the presence of dioleoyl-GroPSer containing liposomes, while dioleoyl-GroPCho or dipalmitoyl-GroPSer exerted limited effects on peroxidase activity of cyt c. The peroxidase activity was fully abolished in the presence of anti-cyt c antibody, reconfirming that interaction of PtdSer with cyt c was responsible for the peroxidase activity observed. Most important, using a cell-free model system, we found that catalytic activity of cyt c may be directed toward the oxidation of PtdSer, a phospholipid that induced its peroxidase activity. This indicates that interaction of cyt c with PtdSer during apoptosis can, indeed, be involved in selective oxidation of the latter.

Here we demonstrated that ligation of anti-Fas antibody with its cognate receptor initiates execution of apoptotic program in A549 cells as evidenced by activation of caspase-3 and DNA fragmentation. Accumulation of cyt c in the cytosol was detected as early as 2 h after treatment with CH-11, indicating that Fas-induced apoptosis in A549 cells proceeds *via*

extrinsic type II pathway and includes mitochondrial signaling. PtdSer was found to be preferentially oxidized after 3-h incubation with CH-11. Strikingly, two more abundant membrane phospholipids (PtdCho and PtdEtn), and the most abundant cytosolic antioxidant, GSH, did not undergo any significant Fas-induced oxidation. Z-VAD, a peptidyl fluoromethylketone that acts as a pan-caspase inhibitor, fully blocked caspase-8 activation and all downstream events, including cyt c release and PtdSer oxidation. Application of z-DQMD, a specific caspase-3 inhibitor, completely suppressed caspase-3 activity. Partial inhibition of caspase-8 by z-DQMD implies that the activation of caspase-8 is partly due to a positive feedback loop involving caspase-3 activation, thus further supporting the type II mechanism of FAS-triggered apoptosis in A549 cells. Interestingly, z-DQMD exerted no significant effect on Fas-induced cytosolic cyt c accumulation, implying that remaining caspase-8 activity was sufficient to induce release of cyt c. Most important, z-DQMD provided no protection against PtdSer oxidation. Since the PnA-labeled phospholipids account for less than 1% of membrane phospholipid unsaturated fatty-acid residues (25), it is unlikely that membrane structure and characteristics are changed by the presence of such a small amount of incorporated PnA. Collectively, these data strongly suggest that PtdSer oxidation is specifically associated with apoptosis, and PtdSer oxidation relies on accumulation of cyt c in the cytosol (but does not depend on caspase-3 activation).

At neutral pH, cyt c bears a net positive charge of +8 and binds avidly acid phospholipids including PtdSer, PtdIns, phosphatidic acid (PtdOH), and cardiolipin. Thus, it is possible that other acid phospholipids, particularly cardiolipin, PtdOH, and PtdIns, may also undergo oxidative modification during cell apoptosis. It is likely that oxidation will be dependent on their abundance at the sites of cyt c location during apoptosis as well as on their affinity for cyt c. In the cytosolic leaflet of plasma membrane, another major acidic phospholipid, PtdIns, is also a potentially good oxidizable substrate for peroxidase activity of cyt c released from mitochondria during apoptosis. In line with this, we found that PtdIns demonstrated a slightly enhanced oxidation during Fas-induced apoptosis; the effect, however, did not reach the level of statistical significance.

Cardiolipin, a polyunsaturated acidic phospholipid in the inner mitochondrial membrane and intermembrane contact sites, is known to bind several basic mitochondrial proteins including cyt c. It has been suggested that oxidation of cardiolipin plays a role in permeabilization of mitochondria and release of pro-apoptotic factors during apoptosis. However, direct assessments of cardiolipin oxidation during apoptosis are scarce and its redox catalytic mechanisms have not been identified. Thus, it is important to establish potential involvement of cyt c in cardiolipin oxidation in apoptotic cells. Unfortunately, the integration of PnA into cardiolipin was insufficient for accurate analysis of its oxidation. However, using a newly developed HPTLC/fluorescence HPLC-based Amplex Red assay (31), we demonstrated that cardiolipin indeed was oxidized during actinomycin D-induced apoptosis in wild-type (cyt $c^{+/+}$) mouse embryonic cells, but remained unoxidized in cyt c-deficient cells (cyt $c^{-/-}$) (Kagan, V.E., Tyurin, V.A., Jiang, J., Tyurina, Y.Y., Ritov, V.B., Amoscato, A.A., Osipov, A.N. Belikova, N., Kapralov, O.O., Borisenko, G.G., Kini, V., and Lysytsya, A., unpublished data). This suggests that a fraction of cardiolipin tightly bound to cyt c may undergo peroxidation during early mitochondrial stages of apoptosis (39).

There are several additional experimental findings that are compatible with the hypothesis of cyt c-catalyzed PtdSer oxidation. Our previous work has established that when HL-60 cells were gently sonicated in the presence of excess of cyt c resulting in its integration into cells, preferential oxidation of PtdSer (compared to other phospholipids) occurred upon addition of H_2O_2 (46). Furthermore, in a separate series of experiments (38), we used a different approach to disrupt mitochondria and release cyt c into cytosol. It is based on utilization of DP-1 peptide, a conjugate of protein transduction domain PTD-5 and antibiotic peptide KLA [$(KLAKLAK)_2$]. DP-1-induced cyt c release was accompanied by ROS production and selective PtdSer oxidation in Jurkat cells.

Interestingly, another apoptosis-related protein, AIF, has been shown to act as an important H_2O_2-regulating antioxidant in mitochondria (47). Collapse of mitochondria reveals the pro-apoptotic nature of cyt c released into the cytosol where it interacts with Apaf-1 to cause caspase activation, the function seemingly dissociated from its redox properties (48,49). Our results demonstrate that redox activity of cyt c may be essential for PtdSer oxidation and its subsequent externalization during apoptosis. In our previous study, preferential oxidation of PtdSer during apoptosis has been shown to play an essential role in PtdSer externalization and its subsequent recognition by macrophages (8,9). Our MS analysis of PtdSer oxidation by peroxidase activity of cyt c showed that, in addition to its mono- and dihydroperoxides, several different PtdSer oxidation products can be formed. Further studies are necessary to characterize their specific roles as recognition signals interacting with macrophage receptors directly or *via* bridging proteins [review Lauber *et al.* (50)].

In summary, the results obtained suggest that generation of ROS in Fas-triggered apoptosis in A549 cells may play an important role in apoptotic signaling *via* a PtdSer-dependent pathway rather than represent a trivial and meaningless side effect. It is likely that cyt c released from mitochondria catalyzed selective PtdSer oxidation together with H_2O_2 from disrupted mitochondrial electron transport.

ACKNOWLEDGMENTS

This work was supported by Grant HL70755 from the National Institutes of Health.

REFERENCES

1. Choi, D.W. (1988) Glutamate Neurotoxicity and Diseases of the Nervous System, *Neuron 8*, 623–634.

2. Coyle, J.T., and Puttfarcken, P. (1993) Oxidative Stress, Glutamate, and Neurodegenerative Disorders, *Science 262*, 689–695.
3. Duprat, F., Guillemare, E., Romey, G., Fink, M., Lesage, F., Lazdunski, M., and Honore, E. (1995) Susceptibility of Cloned K+ Channels to Reactive Oxygen Species, *Proc. Natl. Acad. Sci. USA 92*, 11796–11800.
4. Nishi, J., Ogura, R., Sugiyama, M., Hidaka, T., and Kohno, M. (1991) Involvement of Active Oxygen in Lipid Peroxide Radical Reaction of Epidermal Homogenate Following Ultraviolet Light Exposure, *J. Invest. Dermatol. 97*, 115–119.
5. Suzuki, Y., Ono, Y., and Hirabayashi, Y. (1998) Rapid and Specific Reactive Oxygen Species Generation via NADPH Oxidase Activation during Fas-Mediated Apoptosis, *FEBS Lett. 425*, 209–212.
6. Matsura, T., Kai, M., Jiang, J., Babu, H., Kini, V., Kusumoto, C., Yamada, K., and Kagan, V.E. (2004) Endogenously Generated Hydrogen Peroxide is Required for Execution of Melphalan-Induced Apoptosis as well as Oxidation and Externalization of Phosphatidylserine, *Chem. Res. Toxicol. 17*, 685–696.
7. Kruman, I., Guo, Q., and Mattson, M.P. (1998) Calcium and Reactive Oxygen Species Mediate Staurosporine-Induced Mitochondrial Dysfunction and Apoptosis in PC12 Cells, *J. Neurosci. Res. 51*, 293–308.
8. Kagan, V.E., Gleiss, B., Tyurina, Y.Y., Tyurin, V.A., Elenstrom-Magnusson, C., Liu, S.X., Serinkan, F.B., Arroyo, A., Chandra, J., Orrenius, S., and Fadeel, B. (2002) A Role for Oxidative Stress in Apoptosis: Oxidation and Externalization of Phosphatidylserine is Required for Macrophage Clearance of Cells Undergoing Fas-Mediated Apoptosis, *J. Immunol. 169*, 487–499.
9. Shvedova, A.A., Tyurina, Y.Y., Kawai, K., Tyurin, V.A., Kommineni, C., Castranova, V., Fabisiak, J.P., and Kagan, V.E. (2002) Selective Peroxidation and Externalization of Phosphatidylserine in Normal Human Epidermal Keratinocytes during Oxidative Stress Induced by Cumene Hydroperoxide, *J. Invest. Dermatol. 118*, 1008–1018.
10. Fabisiak, J.P., Tyurina, Y.Y., Tyurin, V.A., Lazo, J.S., and Kagan, V.E. (1998) Random versus Selective Membrane Phospholipid Oxidation in Apoptosis: Role of Phosphatidylserine, *Biochemistry 37*, 13781–13790.
11. Koty, P. P., Tyurina, Y.Y., Tyurin, V.A., Liu, S.X., and Kagan, V.E. (2002) Depletion of Bcl-2 by an Antisense Oligonucleotide Induces Apoptosis Accompanied by Oxidation and Externalization of Phosphatidylserine in NCI-H226 Lung Carcinoma Cells, *Mol. Cell. Biochem. 234–235*, 125–133.
12. Fabisiak, J. P., Kagan, V.E., Ritov, V.B., Johnson, D.E., and Lazo, J.S. (1997) Bcl-2 Inhibits Selective Oxidation and Externalization of Phosphatidylserine during Paraquat-Induced Apoptosis, *Am. J. Physiol. 272*, C675–C684.
13. Lilja, H., Laurell, C.B., and Jeppsson, J.O. (1984) Characterization of the Predominant Basic Protein in Human Seminal Plasma, One Cleavage Product of the Major Seminal Vesicle Protein, *Scand. J. Clin. Lab. Invest. 44*, 439–446.
14. Kagan, V. E., Fabisiak, J. P., Shvedova, A.A., Tyurina, Y.Y., Tyurin, V.A., Schor, N. F., and Kawai. K. (2000) Oxidative Signaling Pathway for Externalization of Plasma Membrane Phosphatidylserine During Apoptosis, *FEBS Lett. 477*, 1–7.
15. Uhal, B.D., Joshi, I., Hughes, W.F., Ramos, C., Pardo, A., and Selman, M. (1998) Alveolar Epithelial Cell Death Adjacent to Underlying Myofibroblasts in Advanced Fibrotic Human Lung, *Am. J. Physiol. 275*, L1192–L1199.
16. Kasahara, Y., Tuder, R.M., Cool, C.D., Lynch, D.A., Flores, S.C., and Voelkel, N.F. (2001) Endothelial Cell Death and Decreased Expression of Vascular Endothelial Growth Factor and Vascular Endothelial Growth Factor Receptor 2 in Emphysema, *Am. J. Respir. Crit. Care Med. 163*, 737–744.
17. Barbas-Filho, J.V., Ferreira, M.A., Sesso, A., Kairalla, R.A., Carvalho, C.R., and Capelozzi, V.L. (2001) Evidence of Type II Pneumocyte Apoptosis in the Pathogenesis of Idiopathic Pulmonary Fibrosis (IFP)/Usual Interstitial Pneumonia (UIP), *J. Clin. Pathol. 54*, 132–138.
18. Lethem, M.I., James, S.L., Marriott, C., and Burke, J.F. (1990) The Origin of DNA Associated with Mucus Glycoproteins in Cystic Fibrosis Sputum, *Eur. Respir. J. 3*, 19–23.
19. Yagyu, K., and van Breda Vriesman, P.J. (1997) Apoptosis in Bronchiolitis Obliterans, Chronic Rejection and Infection after Lung Transplantation in Rats, Transplant Proc. 29, 1532–1535.
20. Itoh, N., Yonehara, S., Ishii, A., Yonehara, M., Mizushima, S., Sameshima, M., Hase, A., Seto, Y., and Nagata, S. (1991) The Polypeptide Encoded by the cDNA for Human Cell Surface Antigen Fas can Mediate Apoptosis, *Cell 166*, 233–243.
21. Scaffidi, C., Fulda, S., Srinivasan, A., Friesen, C., Li, F., Tomaselli, K.J., Debatin, K.M., Krammer, P. H., and Peter, M.E. (1998) Two CD95 (APO-1/Fas) Signaling Pathways, *EMBO J. 17*, 1675–1687.
22. Herr, I., and Debatin, K.M. (2001) Cellular Stress Response and Apoptosis in Cancer Therapy, *Blood 98*, 2603–2614.
23. Maeyama, T., Kuwano, K., Kawasaki, M., Kunitake, R., Hagimoto, N., Matsuba, T., Yoshimi, M., Inoshima, I., Yoshida, K., and Hara, N. (2001) Upregulation of Fas-Signalling Molecules in Lung Epithelial Cells from Patients with Idiopathic Pulmonary Fibrosis, *Eur. Respir. J. 17*, 180–189.
24. Wen, L.P., Madani, K., Fahrni, J.A., Duncan, S.R., and Rosen, G.D. (1997) Dexamethasone Inhibits Lung Epithelial Cell Apoptosis Induced by IFN- and Fas, *Am. J. Physiol. 273*, L921–L929.
25. Kagan, V.E., Ritov, V.B., Tyurina, Y.Y., and Tyurin, V.A. (1998) Sensitive and Specific Fluorescent Probing of Oxidative Stress in Different Classes of Membrane Phospholipids in Live Cells Using Metabolically Integrated *cis*-Parinaric Acid, *Methods Mol. Biol. 108*, 71–87.
26. Ritov V.B., Banni S., Yalowich, J.C., Day, B.W., Claycamp, H.G., Corongiu, F.P., Kagan, V.E. (1996) Non-Random Peroxidation of Different Classes of Membrane Phospholipids in Live Cells Detected by Metabolically Integrated cis-Parinaric Acid, *Biochim. Biophys. Acta 1283*, 127–140.
27. Folch, J., Lees, M., and Sloane Stanley, G.H. (1957) A Simple Method for the Isolation and Purification of Total Lipids from Animal Tissues, *J. Biol. Chem. 226*, 497–509.
28. Chalvardjian, A., and Rudnicki, E. (1970) Determination of Lipid Phosphorous in Nanomolar Range, *Anal. Biochem. 36*, 225–226.
29. LeBel, C.P., Ischiropoulos, H., and Bondy S.C. (1992) Evaluation of the Probe 2′,7′-dichlorofluorescin as an Indicator of Reactive Oxygen Species Formation and Oxidative Stress, *Chem. Res. Toxicol. 5*, 227–231.
30. Petit, J.M., Maftah, A., Ratinaud, M.H., and Julien, R. 10N-Nonyl Acridine Orange Interacts with cardiolipin and allows the quantification of this phospholipid in isolated mitochondria, *Eur. J. Biochem. 209*, 267–273.
31. Ritov, V.B., Tyurin, V.A., Tyurina, Y.Y., and Kagan, V.E. (2004) Ouantitative Analysis of Phospholipids Peroxidation: Appearanceof Oxidized Phosphatidylserine on the Surface of HL-60 Cells During Intrinsic Apoptosis, Abstract of 43rd Annual Meeting for Society of Toxicology, Baltimore.
32. Pinheiro, T.J., Elove, G.A., Watts, A., and Roder, H. (1997) Structural and Kinetic Description of Cytochrome c Unfolding Induced by the Interaction with Lipid Vesicles, *Biochemistry 36*, 13122–13132.
33. Cortese, J.D., Voglino, L.A., and Hackenbrock, C.R. (1998) Multiple Conformations of Physiological Membrane-Bound Cytochrome c, *Biochemistry 37*, 6402–6409.
34. Sanghera, N., and Pinheiro, T,J. (2000) Unfolding and Refolding of Cytochrome c Driven by the Interaction with Lipid Micelle, *Protein Sci. 9*, 1194–1202.

35. Burkitt, M.J., and Wardman, P. (2001) Cytochrome c is a Potent Catalyst of Dichlorofluorescin Oxidation: Implications for the Role of Reactive Oxygen Species in Apoptosis, *Biochem. Biophys. Res. Commun. 282*, 329–333.
36. Skulachev, V.P. (1998) Cytochrome c in the Apoptotic and Antioxidant Cascades, *FEBS Lett. 423*, 275–280.
37. Korshunov, S.S., Krasnikov, B.F., Pereverzev, M.O., and Skulachev, V.P. (1999) The Antioxidant Functions of Cytochrome c, *FEBS Lett. 462*, 192–198.
38. Jiang, J., Serinkan, B.F., Tyurina, Y.Y., Borisenko, G.G., Mi, Z., Robbins, P.D., Schroit, A.J., and Kagan, V.E. (2003) Peroxidation and Externalization of Phosphatidylserine Associated with Release of Cytochrome c from Mitochondria, *Free Rad. Biol. Med. 35*, 814–825.
39. Kagan V.E., Borisenko, G.G., Tyurina,Y.Y., Tyurin, V.A., Jiang, J., Potapovich, A.I., Kini, V., Amoscato, A.A., and Fujii, Y. (2004) Oxidative Lipidomics of Apoptosis: Redox Catalytic Interactions of Cytochrome c with Cardiolipin and Phosphatidylserine, *Free Rad. Biol. Med. 37*, 1963–1985.
40. Kagan, V.E., Borisenko, G.G., Serinkan, B.F., Tyurina, Y.Y., Tyurin, V.A., Jiang, J., Liu, S.X., Shvedova, A.A., Fabisiak, J.P., Uthaisang, W., and Fadeel, B. (2002) Appetizing Rancidity of Apoptotic Cells for Macrophages: Oxidation, Externalization, and Recognition of Phosphatidylserine, *Am. J. Physiol. Lung Cell. Mol. Physiol. 285*, L1–17.
41. Pike, L.J., Han, X., Chung, K.N., and. Gross, R.W. (2002) Lipid rafts are Enriched in Arachidonic Acid and Plasmenylethanolamine and their Composition is Independent of Caveolin-1 Expression: a Quantitative Electrospray Ionization/mass Spectrometric Analysis, *Biochemistry 41*, 2075–2088.
42. Sijens, P., Verkleij, A.J., and De Kruijff, B. (1983) Clonal Isolation of Hybridomas by Manual Single-Cell Isolation, *EMBO J. 2*, 907–913.
43. Rietveld, A., Jordi, W., and de Kruijff, B. (1986) Studies on the Lipid Dependency and Mechanism of the Translocation of the Mitochondrial Precursor protein Apocytochrome c Across Model Membranes, *J. Biol. Chem. 261*, 3846–3856.
44. Demel, R.A., Jordi, W., Lambrechts, H., van Damme, H., Hovius, R., and de Kruijff, B. (1989) Differential Interactions of Apo- and Holocytochrome c with Acidic Membrane Lipids in Model Systems and the Implications for their Import into Mitochondria, *J. Biol. Chem. 264*, 3988–3997.
45. Silvius, J.R. (1990) Fluorescence Studies Using Carbazole-Labeled and Brominated Phospholipids, *Biochemistry 29*, 2930–2938.
46. Kawai, K., Tyurina, Y., Tyurin, V.,. Kagan, V.E., and Fabisiak, J.P. (2000) Peroxidation and Externalization of Phosphatidylserine in Plasma Membrane of HL-60 Cells During *tert*-butyl Hydroperoxide-Induced Apoptosis: Role of Cytochrome c, *Toxicologist 54*, 165 (abstract).
47. Klein, J.A., Longo-Guess, C.M., Rossmann, M.P., Seburn, K.L., Hurd, R.E., Frankel, W.N., Bronson, R.T., and Ackerman, S.L. (2002) The Harlequin Mouse Mutation Downregulates Apoptosis-Inducing Factor, *Nature 419*, 367–374.
48. Kluck, R.M., Martin, S.J., Hoffman, B.M., Zhou, J.S., Green, D.R., and Newmeyer, D.D. (1997) Cytochrome c Activation of CPP32-Like Proteolysis Plays a Critical Role in a Xenopus Cell-Free Apoptosis System, *EMBO J. 16*, 4639–4649.
49. Hampton, M.B., Zhivotovsky, B., Slater, A.F., Burgess, D.H., and Orrenius, S. (1998) Importance of the Redox State of Cytochrome c During Caspase Activation in Cytosolic Extracts, *Biochem. J. 329*, 95–99.
50. Lauber, K., Blumenthal, S.G., Waibel, M., and Wesselborg, S. (2004) Clearance of Apoptotic Cells: Getting Rid of the Corpses, *Mol. Cell. 14*, 277–287.

[Received July 23, 2004; accepted November 24, 2004]

Conjugated Linoleic Acids (CLA) as Precursors of a Distinct Family of PUFA

Sebastiano Banni[a,*], Anna Petroni[b], Milena Blasevich[b], Gianfranca Carta[a], Lina Cordeddu[a], Elisabetta Murru[a], Maria Paola Melis[a], Anne Mahon[c], and Martha A. Belury[c]

[a]Università degli Studi di Cagliari, Dipartimento di Biologia Sperimentale, Cittadella Universitaria, Cagliari, Italy, [b]Università degli Studi di Milano, Dipartimento di Scienze Farmacologiche, Milan, Italy, and [c]Department of Human Nutrition, The Ohio State University, Columbus, Ohio 43221

ABSTRACT: One of the possibilities for distinct actions of *c*9,*t*11- and the *t*10,*c*12-conjugated linoleic acid (CLA) isomers may be at the level of metabolism since the conjugated diene structure gives to CLA isomers and their metabolites a distinct pattern of incorporation into the lipid fraction and metabolism. In fact, CLA appears to undergo similar transformations as linoleic acid but with subtle isomer differences, which may account for their activity in lowering linoleic acid metabolites in those tissues rich in neutral lipids where CLA is preferentially incorporated. Furthermore, *c*9,*t*11 and *t*10,*c*12 isomers are metabolized at a different rate in the peroxisomes, where the shortened metabolite from *t*10,*c*12 is formed at a much higher proportion than the metabolite from *c*9,*t*11. This may account for the lower accumulation of *t*10,*c*12 isomer into cell lipids. CLA isomers may therefore be viewed as a "new" family of polyunsaturated fatty acids (PUFA) producing a distinct range of metabolites using the same enzymatic system as the other (i.e., n-3, n-6 and n-9) PUFA families. It is likely that perturbation of PUFA metabolism by CLA will have an impact on eicosanoid formation and metabolism, closely linked to the biological activities attributed to CLA.

Paper no. L9618 in *Lipids 39*, 1143–1146 (November 2004).

Conjugated linoleic acid (CLA) has received considerable attention for the several biological activities shown in different experimental conditions (1). Recently, studies have focused on the activity of distinct CLA isomers (2). In particular, studies have addressed the isomer *c*9,*t*11-CLA, which is the main isomer found in milk and dairy products and the *t*10,*c*12-CLA isomer, formed mainly through synthesis by alkalization of linoleic acid. When CLA is synthetically formed through alkalization, these two isomers are the most concentrated and are found in approximately equal proportions. A mixture of these two isomers is found in most CLA supplements available in the market and consequently the most readily available for research.

Several mechanisms of action have been proposed for the biological activities of both isomers, but still there is not agreement on these. The two isomers, *t*10,*c*12-CLA and *c*9,*t*11-CLA, have different biological activities depending on the experimental system. While both have been shown to exert anticarcinogenic (3) and antiatherogenic activities (4), it seems that reduction of body fat and reduced milk fat synthesis is specific to *t*10,*c*12-CLA (2). One crucial question is whether mechanisms exist by which both isomers exert some similar activities but also have some distinct properties. One of the possibilities for distinct actions of CLA isomers may be at the level of metabolism whereby CLA appears to undergo similar transformations as linoleic acid (LA) (5) (Fig. 1) but with subtle isomer differences. In this regard, CLA isomers may be viewed as a "new" family of PUFA producing a distinct range of metabolites using the same enzymatic system as the other (i.e., n-3, n-6, and n-9) PUFA families (Fig. 1).

CLA METABOLISM

Since the first reports in 1996 of detection of CLA metabolites on rats fed a partial hydrogenated oil (6) and in lamb liver (7), further reports have added improved characterization of CLA metabolites (8,9). In fact, a detailed cascade of metabolism of the *c*9,*t*11 and *t*10,*c*12 isomers has been thoroughly described (8) and it seems that the two isomers show some differences in their metabolism. While *c*9,*t*11 seems

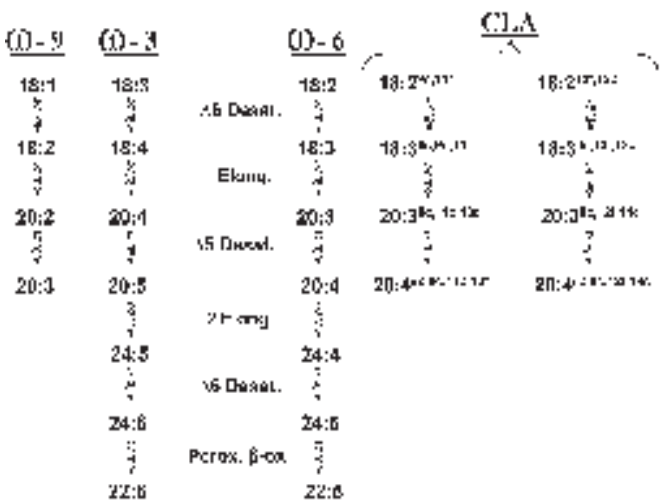

FIG. 1. Metabolism of ω-9, ω-3, ω-6, and CLA isomers.

*To whom correspondence should be addressed at Universita degli Studi di Cagliari, Dipartimento di Biologia Sperimentale, Cittadella Universitaria, S.S. 554, km. 4,500, 09042 Monserrato, Cagliari, Italy. E-mail: banni@unica.it

Abbreviations: CD, conjugated diene; CLA, conjugated linoleic acid; LA, linoleic acid; NL, neutral lipid; PL, phospholipids; PPAR, peroxisome proliferator-activated receptor.

well metabolized up to CD 20:4, the *t*10,*c*12 isomer appears to be resistant to CD 20:3 and CD 20:4 formation (10). There is no ready explanation for this, but it may be due to CD 18:3 formed from *t*10,*c*12 being resistant to elongation.

CLA and CLA metabolites differ from LA by distinct patterns of incorporation into tissues (11). In fact, while CLA isomers are mainly incorporated into neutral lipids (NL), with the exception of CD 20:4, LA and its metabolites are mainly distributed in phospholipids (PL) (11). It is well known that an increasing number of *cis* double bonds favor the incorporation into PL rather than into NL. It is likely that the presence of a CD structure drives the preferential incorporation into NL. Perhaps one extra double bond in CD 18:3 and CD 20:3 is not sufficient for their incorporation into PL. On the other hand, CD 20:4 with two extra double bonds besides the CD structure might allow the molecule to be incorporated into PL. Therefore, the CD structure seems fundamental for targeting to a particular lipid fraction in cells.

Metabolism of CLA has been characterized in rats and may be similar in different species including humans. In a recent trial on diabetic patients described in a study by Belury *et al.* (12) we measured CLA isomers and metabolites in plasma total lipids (Belury et al., unpublished data). We detected CD 18:3 and CD 20:3. Again, as described in rats (10) and humans (unpublished data), *t*10,*c*12 yielded CD 18:3 derived from Δ6 desaturation, but no CD 20:3 derived from this isomer was detected. In contrast, CD 18:3 from Δ6 desaturation of *c*9,*t*11 CLA accumulated to a lesser extent, but CD 20:3 was formed at higher concentrations. Only a few studies have reported the detection of CD 20:4 in animal or human tissues or serum, and in all cases this was when LA was low in the diet.

CLA COMPETITION WITH LINOLEIC ACID

In experimental diets used for rats, the level of LA is usually derived from corn oil and is relatively high (2.5–3% as a proportion of the diet by weight). Usually, the amount of CLA used in different experimental models ranges from 0.5 to 2% because it has been shown that this is also the range where CLA exerts its biological activities (1). Consequently, the ratio of LA to CLA ranges from 5:1 to 1.5:1. In humans it has been estimated that LA intake is about 10–20 g/d (13). The amount of CLA used in different experimental trials ranges from 1.5 to 6 g/d with a ratio of LA to CLA ranging from 7–14:1 to 1.5–3:1 and an average amount used in most trials of 3 g/d. This average level provides a ratio of approximately 3–6:1, therefore, translating to a similar range found in experimental animal studies.

Based on the similarity of the ratio of LA to CLA used in human and animal studies, it is not surprising that CLA metabolism in rats and humans appears to to be similar. When LA was low or absent from the diet, as in the case of rats reared on a free fat diet before the CLA treatment by gavage, high levels of CD 20:4 were detected (8). CD 20:4 was also detected in liver of rats fed butterfat, which is low in LA, irrespective of CLA concentration (11). It is clear that the ratio between LA and CLA is important for the detection of CD 20:4. With regard to other metabolites of CLA, there seems to be little, if any, dependence on the LA content of the diet. Currently, no data are available as to whether α-linolenic acid is also able to compete with CLA. An important point concerning the metabolism of CLA is to understand whether competition of CLA isomers with other PUFA is at the level of formation or incorporation. It is likely that competition may occur by both ways. Probably, in the liver it is more likely at the level of the formation of metabolites. In contrast, competition of CLA with other PUFA in extrahepatic tissues may occur more at the level of incorporation. It has been shown, for example, that in those tissues rich in neutral lipids, such as adipose and mammary tissues, CLA was able, in a dose-dependent manner, to decrease the concentration of LA metabolites; this was not true in the liver (14), where CD 20:4 was not detected. It is therefore possible that regulation of the formation of CD 20:4 is more likely to be due to competition in formation, whereas a decrease of LA metabolites is due to competition at the level of lipid incorporation.

CATABOLISM OF CLA BY PARTIAL β-OXIDATION IN PEROXISOMES

It is well known that several FA may undergo partial β-oxidation in peroxisomes. Most of them are unusual FA such as eicosanoids (15–17), isoprostanes (18), and branched FA (19). However, it has been shown that arachidonic acid is also β-oxidized in peroxisomes (20), and the biosynthesis of DHA requires a step in peroxisomal oxidation (21).

Therefore, it seems that peroxisomes are quite active in FA metabolism. Furthermore, it is believed that FA that are able to upregulate the enzymes involved in peroxisomal β-oxidation are also good ligands of peroxisome proliferators-activated receptor (PPAR)-α (17). In addition, peroxisomal β-oxidation activity was also increased in livers of partially hydrogenated fish oil-fed rats (22). In this case, both *cis* and

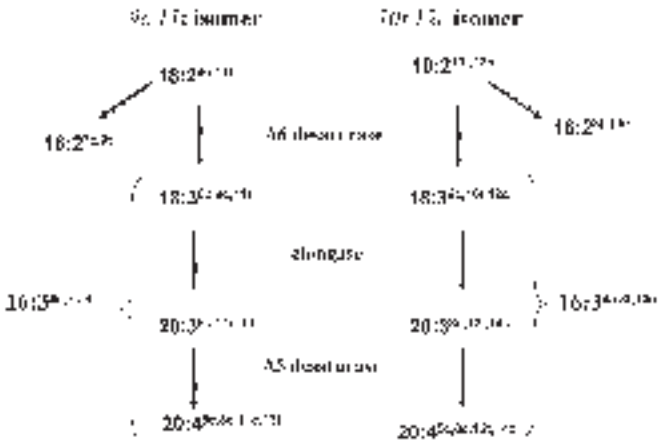

FIG. 2. Scheme of formation of partial β-oxidation products of CLA isomers and their metabolites.

trans isomers of 22:1 have been imputed to upregulate peroxisomal β-oxidation even though other components in dietary oils, different from 22:1 *cis* and *trans* FA, may be responsible for this effect (23). It is highly likely that partially hydrogenated fish oil may contain CLA (24). We have shown recently that naturally occurring CLA yields CD 16:2 probably from partial β-oxidation in peroxisomes (25) (Fig. 2). Furthermore, it has also been shown that *t*10,*c*12 gives rise to CD 16:2 (10). When we incubated human skin fibroblast, as described previously (25), with a mixture of the two isomers we found that both isomers yield CD 16:2, identified as *c*7,*t*9 CD 16:2 and *t*8,*c*10 CD 16:2, respectively, by HPLC (9). Interestingly, most of the CD 16:2 formed (about 70%) was found in the medium.

Further studies are in progress to find out why only 30% is incorporated into cells. As indirect evidence of an involvement of peroxisomes in the partial β-oxidation of CLA, we incubated human skin fibroblasts from adrenoleukodistrophy (ALD) patients with CLA. As can be seen in Figure 3, the CD 16:2 level was much lower than that found in control human skin fibroblasts.

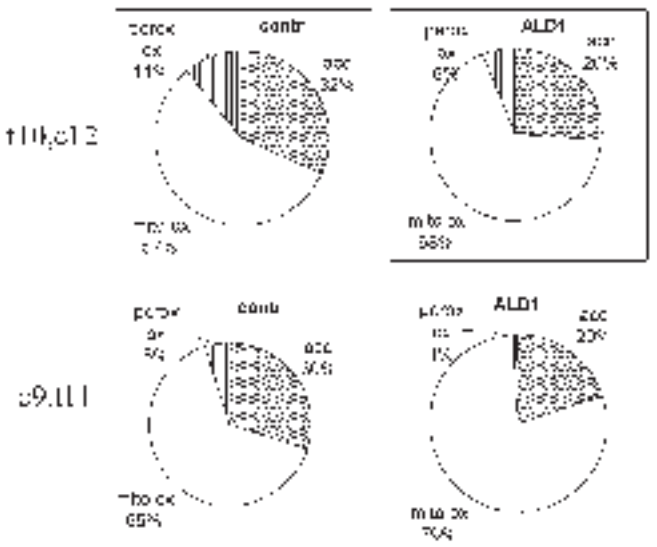

FIG. 3. Metabolism of CLA isomers *t*10,*c*12 and *c*9,*t*11 in human skin fibroblasts from control subjects (contr) and adrenoleukodistrophy patients (ALD1). Cell cultures were grown in minimum essential medium (MEM) containing 10% fetal calf serum (FCS), nonessential amino acids, tricine, penicillin/streptomycin, and maintained at 37°C, in 95% air and 5% CO_2. In the experiments ALD and control fibroblasts were used at the same passages, at confluence; 100 μM of CLA mixture of *t*10,*c*12 and *c*9,*t*11CLA (90% purity; Natural ASA, Hovdebygda, Norway) was dissolved in FCS according to Spector *et al.* (27), added to MEM, and supplemented to the cells for 18 h at 37°C, in 95% air and 5% CO_2. At the end of the incubation time the cells were washed with PBS and scraped off (25). Perox ox = total CD 16:2 (CD 16:2 found incorporated into cells + CD 16:2 found in the medium after incubation); acc = accumulation of CLA (CLA found incorporated into cells); mito ox = CLA oxidized in mitochondria [CLA present in the medium before incubation – (CLA found incorporated into cells + CLA found in the medium after incubation + total CD 16:2).

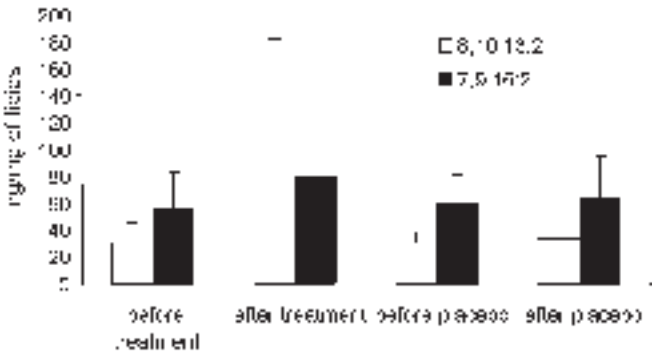

FIG. 4. CD 16:2 isomers in plasma of type 2 diabetes mellitus patients with a CLA daily intake of 6 g for 8 wk as described in the study by Belury *et al.* (12).

We also checked whether CD 16:2 was formed in humans *in vivo*. In a pilot trial (12) where subjects with type 2 diabetes mellitus were supplemented with 6 g/d of a CLA mixture, we detected CD 16:2 from both isomers; however, CD 16:2 from *t*10,*c*12 was more abundant Fig. 4), reflecting the data obtained i*n vitro* with skin fibroblasts. Therefore, it seems that in experimental animals or humans, both isomers are efficiently partially β-oxidized probably in peroxisomes *in vivo* and *in vitro*. More studies are needed to find out whether the metabolism of CLA is directly linked to its activity as a ligand of PPAR-α. It has been actually found that CLA is able to upregulate acyl CoA oxidase, the key enzyme of peroxisomal β-oxidation (26). If this link is definitely proven, CD 16:2 could be used as a marker of PPAR-α activation.

In summary, in the last 10 years research on CLA has grown exponentially. While studies on experimental animals have been shown to be very promising in terms of health benefits, the following studies on humans have been somewhat disappointing because they did not give the results expected. Among the many confounding factors that should be considered is the overall diet and, in particular, consumption of other PUFA. We and others have reported clear evidence that incorporation and metabolism of isomers of CLA is responsive to dietary composition and dietary habits. It is likely that changes in dietary PUFA will result in perturbation of overall PUFA metabolism, which will have an impact on incorporation, metabolism, the formation of eicosanoids, and ultimately the cellular events involved in signal transduction and gene expression, all of which are known to be attributed to CLA. The partial β-oxidation of CLA may also imply that CLA acts in peroxisomal metabolism that is modulated by PPAR-α.

Differences in yields of peroxisomal β-oxidation between *t*10,*c*12 and *c*9,*t*11 might be responsible, at least in part, for the differences observed in some biological systems between the effects of these two isomers. Further studies are needed to fill the gaps between CLA metabolism and eicosanoid formation and to verify whether different dietary fats are able to modulate CLA activity. These pieces of information could

then serve as a foundation for designing human trials in order to find whether CLA exerts its biological activity in humans to improve human health.

ACKNOWLEDGMENTS

This work was supported by a grant from EU Project No. QLK1-2002-02362. The authors thank Mr. Giacomo Satta for technical assistance.

REFERENCES

1. Belury, M.A. (2002) Dietary Conjugated Linoleic Acid in Health: Physiological Effects and Mechanisms of Action [Review], *Annu. Rev. Nutr. 22*, 505–531.
2. Pariza, M.W., Park, Y., and Cook, M.E. (2001) The Biologically Active Isomers of Conjugated Linoleic Acid [Review], *Prog. Lipid Res. 40*, 283–298.
3. Ip, C., Dong, Y., Ip, M.M., Banni, S., Carta, G., Angioni, E., Murru, E., Spada, S., Melis, M.P., and Saebo, A. (2002) Conjugated Linoleic Acid Isomers and Mammary Cancer Prevention, *Nutr. Cancer 43*, 52–58.
4. Kritchevsky, D. (2003) Conjugated Linoleic Acid in Experimental Atherosclerosis, in *Advances in Conjugated Linoleic Acid Research (Sébédio, J.-L., Christie, W.W., and Adlof, R., eds.)*, Vol. 2, pp. 292–301, AOCS Press, Champaign, IL.
5. Banni, S. (2002) Conjugated Linoleic Acid Metabolism [Review], *Curr. Opin. Lipidol. 13*, 261–266.
6. Banni, S., Day, B.W., Evans, R.W., Corongiu, F.P., and Lombardi, B. (1995) Detection of Conjugated Diene Isomers of Linoleic Acid in Liver Lipids of Rats Fed a Choline-Devoid Diet Indicates that the Diet Does Not Cause Lipoperoxidation, *J. Nutr. Biochem. 6*, 281–289.
7. Banni, S., Carta, G., Contini, M.S., Angioni, E., Deiana, M., Dessi, M.A., Melis, M.P., and Corongiu, F.P. (1996) Characterization of Conjugated Diene Fatty Acids in Milk, Dairy Products, and Lamb Tissues, *J. Nutr. Biochem. 7*, 150–155.
8. Sebedio, J.L., Juaneda, P., Dobson, G., Ramilison, I., Martin, J.C., Chardigny, J.M., and Christie, W.W. (1997) Metabolites of Conjugated Isomers of Linoleic Acid (CLA) in the Rat, *Biochim. Biophys. Acta 1345*, 5–10.
9. Melis, M.P., Angioni, E., Carta, G., Murru, E., Scanu, P., Spada, S., and Banni, S. (2001) Characterization of Conjugated Linoleic Acid and Its Metabolites by RP-HPLC with Diode Array Detector, *Eur. J. Lipid Sci. Technol. 103*, 617–621.
10. Sébédio, J.L., Angioni, E., Chardigny, J.M., Gregoire, S., Juaneda, P., and Berdeaux, O. (2001) The Effect of Conjugated Linoleic Acid Isomers on Fatty Acid Profiles of Liver and Adipose Tissues and Their Conversion to Isomers of 16:2 and 18:3 Conjugated Fatty Acids in Rats, *Lipids 36*, 575–582.
11. Banni, S., Carta, G., Angioni, E., Murru, E., Scanu, P., Melis, M.P., Bauman, D.E., Fischer, S.M., and Ip, C. (2001) Distribution of Conjugated Linoleic Acid and Metabolites in Different Lipid Fractions in the Rat Liver, *J. Lipid Res. 42*, 1056–1061.
12. Belury, M.A., Mahon, A., and Banni, S. (2003) The Conjugated Linoleic Acid (CLA) Isomer, *t*10*c*12-CLA, Is Inversely Associated with Changes in Body Weight and Serum Leptin in Subjects with Type 2 Diabetes Mellitus, *J. Nutr. 133*, 257S–260S.
13. Zhou, L., and Nilsson, A. (2001) Sources of Eicosanoid Precursor Fatty Acid Pools in Tissue, *J. Lipid Res. 42*, 1521–1542.
14. Banni, S., Angioni, E., Casu, V., Melis, M.P., Carta, G., Corongiu, F.P., Thompson, H., and Ip, C. (1999) Decrease in Linoleic Acid Metabolites as a Potential Mechanism in Cancer Risk Reduction by Conjugated Linoleic Acid, *Carcinogenesis 20*, 1019–1024.
15. Gordon, J.A., Figard, P.H., and Spector, A.A. (1990) Hydroxyeicosatetraenoic Acid Metabolism in Cultured Human Skin Fibroblasts: Evidence for Peroxisomal β-Oxidation, *J. Clin. Invest. 85*, 1173–1181.
16. Hadjiagapiou, C., Travers, J.B., Fertel, R.H., and Sprecher, H. (1990) Metabolism of 15-Hydroxy-5,8,11,13-Eicosatetraenoic Acid by MOLT-4 Cells and Blood T-Lymphocytes, *J. Biol. Chem. 265*, 4369–4373.
17. Reddy, J.K., and Hashimoto, T. (2001) Peroxisomal Beta-Oxidation and Peroxisome Proliferator-Activated Receptor α: An Adaptive Metabolic System [Review], *Annu. Rev. Nutr. 21*, 193–230.
18. Chiabrando, C., Valagussa, A., Rivalta, C., Durand, T., Guy, A., Zuccato, E., Villa, P., Rossi, J.C., and Fanelli, R. (1999) Identification and Measurement of Endogenous β-Oxidation Metabolites of 8-Epi-Prostaglandin F_2 α, *J. Biol. Chem. 274*, 1313–1319.
19. Singh, H., Beckman, K., and Poulos, A. (1994) Peroxisomal β-Oxidation of Branched Chain Fatty Acids in Rat Liver—Evidence that Carnitine Palmitoyltransferase-I Prevents Transport of Branched Chain Fatty Acids into Mitochondria, *J. Biol. Chem. 269*, 9514–9520.
20. Gordon, J.A., Heller, S.K., Kaduce, T.L., and Spector, A.A. (1994) Formation and Release of a Peroxisome-Dependent Arachidonic Acid Metabolite by Human Skin Fibroblasts, *J. Biol. Chem. 269*, 4103–4109.
21. Moore, S.A., Hurt, E., Yoder, E., Sprecher, H., and Spector, A.A. (1995) Docosahexaenoic Acid Synthesis in Human Skin Fibroblasts Involves Peroxisomal Retroconversion of Tetracosahexaenoic Acid, *J. Lipid Res. 36*, 2433–2443.
22. Berge, R.K., Flatmark, T., and Christiansen, E.N. (1987) Effect of a High-Fat Diet with Partially Hydrogenated Fish Oil on Long-Chain Fatty Acid Metabolizing Enzymes in Subcellular Fractions of Rat Liver, *Arch. Biochem. Biophys. 252*, 269–276.
23. Flatmark, T., Nilsson, A., Kvannes, J., Eikhom, T.S., Fukami, M.H., Kryvi, H., and Christiansen, E.N. (1988) On the Mechanism of Induction of the Enzyme Systems for Peroxisomal β-Oxidation of Fatty Acids in Rat Liver by Diets Rich in Partially Hydrogenated Fish Oil, *Biochim. Biophys. Acta 962*, 122–130.
24. Banni, S., Day, B.W., Evans, R.W., Corongiu, F.P., and Lombardi, B. (1994) Liquid Chromatographic Mass Spectrometric Analysis of Conjugated Diene Fatty Acids in a Partially Hydrogenated Fat, *J. Am. Oil Chem. Soc. 71*, 1321–1325.
25. Banni, S., Petroni, A., Blasevich, M., Carta, G., Angioni, E., Murru, E., Day, B.W., Melis, M.P., Spada, S., and Ip, C. (2004) Detection of Conjugated C_{16} PUFAs in Rat Tissues as Possible Partial β-Oxidation Products of Naturally Occurring Conjugated Linoleic Acid and Its Metabolites, *Biochim. Biophys. Acta 1682*, 120–127.
26. Belury, M.A., Moya-Camarena, S.Y., Liu, K.L., and Vanden Heuvel, J.P. (1997) Dietary Conjugated Linoleic Acid Induces Peroxisome-Specific Enzyme Accumulation and Ornithine Decarboxylase Activity in Mouse Liver, *J. Nutr. Biochem. 8*, 579–584.
27. Spector, A.A., Hoak, J.C., Fry, G.L., Denning, G.M., Stoll, L.L., and Smith, J.B. (1980) Effect of Fatty Acid Modification on Prostacyclin Production by Cultured Human Endothelial Cells, *J. Clin. Invest. 65*, 1003–1012.

[Received September 21, 2004, accepted November 20, 2004]

n-3 Fatty Acids, Inflammation, and Immunity—Relevance to Postsurgical and Critically Ill Patients

Philip C. Calder

Institute of Human Nutrition, School of Medicine, University of Southampton, Bassett Crescent East, Southampton SO16 7PX, United Kingdom

ABSTRACT: Excessive or inappropriate inflammation and immunosuppression are components of the response to surgery, trauma, injury, and infection in some individuals and these can lead, progressively, to sepsis and septic shock. The hyperinflammation is characterized by the production of inflammatory cytokines, arachidonic acid-derived eicosanoids, and other inflammatory mediators, while the immunosuppression is characterized by impairment of antigen presentation and of T helper cell type-1 responses. Long-chain n-3 FA from fish oil decrease the production of inflammatory cytokines and eicosanoids. They act both directly (by replacing arachidonic acid as an eicosanoid substrate and by inhibiting arachidonic acid metabolism) and indirectly (by altering the expression of inflammatory genes through effects on transcription factor activation). Thus, long-chain n-3 FA are potentially useful anti-inflammatory agents and may be of benefit in patients at risk of developing sepsis. As such, an emerging application of n-3 FA is in surgical or critically ill patients where they may be added to parenteral or enteral formulas. Parenteral or enteral nutrition including n-3 FA appears to preserve immune function better than standard formulas and appears to partly prevent some aspects of the inflammatory response. Studies to date are suggestive of clinical benefits from these approaches, especially in postsurgical patients.

Paper no. L9565 in *Lipids 39*, 1147–1161 (December 2004).

SEPTIC SYNDROMES

The systemic inflammatory response syndrome is the name given to the uncontrolled inflammatory response to insult or injury involving excessive production of inflammatory cytokines such as tumor necrosis factor (TNF)-α, interleukin (IL)-1β, IL-6, and IL-8 (1,2). Sepsis has been defined as "the systemic inflammatory response syndrome that occurs during infection" (1). Sepsis is the leading cause of death in critically ill patients in Western countries. Using records from 1995 for state hospitals in the United States it was estimated that there were more than 750,000 cases of sepsis with a 28.6% mortality rate (215,000 deaths) and a total cost of almost US$17 billion (3). Death from septic shock is the result of multiple organ failures and represents the extreme end of a continuum of events of increasing severity and decreasing likelihood of survival (4,5; Fig. 1). The systemic inflammatory response syndrome, sepsis, and septic shock may together be termed as "septic syndromes."

The involvement of inflammatory cytokines in septic syndromes has been long recognized and Vervloet *et al.* (6) wrote "these mediators [i.e., inflammatory cytokines] are largely, if not completely, responsible for the clinical signs and symptoms of the septic response to bacterial infection." In support of this idea, patients with sepsis were found to have markedly elevated circulating concentrations of TNF-α, TNF receptor 1, IL-1β, IL-1 receptor antagonist (IL-1ra), and IL-6, and those patients with the highest concentrations were more likely to die (6–9). In addition, circulating white cells from septic patients exhibited high levels of activated nuclear factor kappa B (NFκB), a transcription factor that promotes the expression of numerous genes associated with inflammation, and again levels of activated NFκB were higher in those patients who went on to die (9). Animal studies also support a role for inflammatory cytokines in the septic response. These studies have often used bacterial endotoxin (also called lipopolysaccharide) as a surrogate for infection, although endotoxin is a fragment of the gram-negative bacterial cell wall

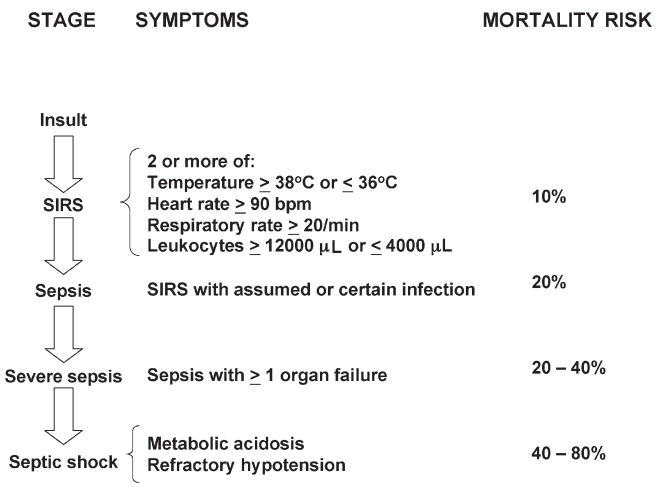

FIG. 1. The progression to septic shock and the risk of mortality at the different stages. bpm, beats per minute; SIRS, systemic inflammatory response syndrome.

*Address correspondence at Institute of Human Nutrition, School of Medicine, University of Southampton, Bassett Crescent East, Southampton SO16 7PX, United Kingdom. E-mail: pcc@soton.ac.uk

Abbreviations: COX, cyclooxygenase; DHA, docosahexaenoic acid; EPA, eicosapentaenoic acid; HEPE, hydroxyeicosapentaenoic acid; HETE, hydroxyeicosatetraenoic acid; HLA, human leukocyte antigen; IFN, interferon; IκB, inhibitory subunit of nuclear factor kappa B; IL, interleukin; IL-1ra, interleukin-1 receptor antagonist; LOX, lipoxygenase; LT, leukotriene; NFκB, nuclear factor kappa B; PG, prostaglandin; SNPs, single nucleotide polymorphisms; Th, T helper; TNF, tumor necrosis factor; TX, thromboxane.

and not a viable organism. Mice injected with endotoxin exhibit high circulating concentrations of TNF-α, IL-1β, IL-6, and IL-8, and survival of these animals can be improved by administering anti-cytokine antibodies (10,11), cytokine receptor antagonists (12), or anti-inflammatory cytokines such as IL-10 (13), or by knocking out the TNF-α receptor (14). Despite this evidence, it is important to note that some studies report that many septic patients do not show detectable or elevated circulating concentrations of TNF-α or IL-1β (15–18). Furthermore, it appears that inflammatory cytokines do play a beneficial role in sepsis. For example, in some animal models, blocking TNF-α increases mortality (19–21), while a TNF-α antagonist increased mortality in a clinical trial (22). Thus, the situation regarding the pathological role of inflammatory cytokines in sepsis is unclear; it may be that a little is beneficial but that excess is harmful and that complete blocking negates the beneficial effects. Another consideration is that there may be large between-individual differences in the generation of inflammatory cytokines, in the sensitivity to the harmful effects of these cytokines, and in the effects of blocking these cytokines. Thus, there may be significant variation in the susceptibility of individuals to exhibit the systemic inflammatory response syndrome and to progress toward septic shock. This may partly relate to the extent and site of the initial injury, partly to the nature and site of the infection, if any, and partly to aspects of the patient's well-being prior to receiving the injury (e.g., nutritional state). It is now recognized that genetics may also play a role. In fact there are likely to be genetic variations in many aspects of the septic response to infection and injury. These most likely relate to adaptations of various population groups to withstand infection and injury in different ecological settings. In the context of this article, genetic variations in the propensity to produce inflammatory cytokines are of relevance. It is now recognized that there are single base variations in genes or in their promoter regions called single nucleotide polymorphisms or SNPs (pronounced "snips").

SNPs have been described for TNF-α, TNF-β, IL-1β, IL-6, IL-10, TNF receptors, IL-1 receptors, IL-1ra, and for many other genes involved in the septic response (23). These SNPs are of functional significance since they partly determine the extent of expression of the gene once it is activated (23). Thus TNF-α production by monocytes in response to endotoxin is higher in individuals who have a G rather than an A at –308 in the TNF-α gene promoter region (24). Intriguingly, TNF-α production is also affected by a polymorphism in the TNF-β gene: TNF-α production by monocytes in response to endotoxin was higher if there was an A at +252 in the TNF-β gene than if there was a G (25). Genotypes affecting TNF-α production appear to be of relevance with respect to sepsis mortality. For example, possession of a G at –308 in the TNF-α gene was found in 39% of patients with septic shock compared with 18% of controls, and among patients with septic shock this polymorphism was significantly more common among patients who died (52% vs. 24% among survivors) (26). In controlling for age, it was identified that, for the same clinical score, patients with a G at –308 of the TNF-α gene had a 3.7-fold higher risk of death than those without a G (26). In another study, patients with sepsis who were homozygous for A at +252 in the TNF-β gene displayed significantly higher plasma TNF-α concentrations than heterozygotes or homozygotes for G, and they showed 88% mortality compared with 37% for heterozygotes and 25% for G homozygotes (27). In a more recent study, postoperative patients who were homozygous for A at +252 in the TNF-β gene had a 1.5-fold higher risk of developing severe complications than heterozygotes (28). Furthermore, among the patients who developed sepsis, those who were homozygous for A at +252 in the TNF-β gene were more likely to die (71 vs. 20% for heterozygotes and 0% for homozygotes for G) (28). These findings raise the possibility of being able to identify patients at high risk of complications and mortality on the basis of genetic polymorphisms.

Although there has been much focus on the potential detrimental role of inflammatory cytokines in sepsis, other mediators including arachidonic acid-derived eicosanoids, reactive oxygen species, nitric oxide, and adhesion molecules are involved in the pathological processes that accompany critical illness. Prostaglandin (PG) E_2 is implicated in sepsis, burns, and critical illness (29,30), while leukotriene (LT) B_4 and oxidants released by neutrophils are involved in acute respiratory distress syndrome [see Kollef and Schuster (31)].

In addition to hyperinflammation, patients with sepsis also display immunosuppression (32–34). There are reports that septic patients have high circulating concentrations of the anti-inflammatory cytokine IL-10 and that these are strongly correlated with mortality (35,36). Note that this is contrary to the predicted effect of IL-10 since this cytokine down-regulates TNF-α production and its early administration is protective in murine endotoxemia (37–39). However, the apparently harmful effect of IL-10 may relate to the timing of its production. Lymphocytes from patients with burns or trauma produce low levels of the T helper (Th) 1-type cytokines [e.g., interferon (IFN)-γ] associated with host defense against bacteria and viruses but high levels of the Th2- and Treg-type cytokines (IL-4, IL-10) associated with inhibition of host defense against bacteria and viruses (33,35). There also appears to be decreased monocyte expression of human leukocyte antigens (HLA) (40–43), the proteins involved in antigen presentation to T cells, and this is associated with impaired ability of monocytes to stimulate T cells (43). Interestingly, IL-10 downregulates both Th1-type cytokine production and HLA expression (44,45), and this might be the origin of the harmful effect of this cytokine in septic patients. Recent studies have revealed impaired proliferative or secretory functions of T cells from patients with sepsis, trauma, or burns (46,47).

The traditional view is that the immunosuppressed phase of septic syndromes lags behind the hyperinflammatory phase (Fig. 2); that is, initially sepsis is characterized by increased generation of inflammatory mediators (the systemic inflammatory response syndrome), but as it persists there is a shift toward an anti-inflammatory, immunosuppressed state sometimes called the compensatory anti-inflammatory response syndrome. However, some recent studies challenge this and

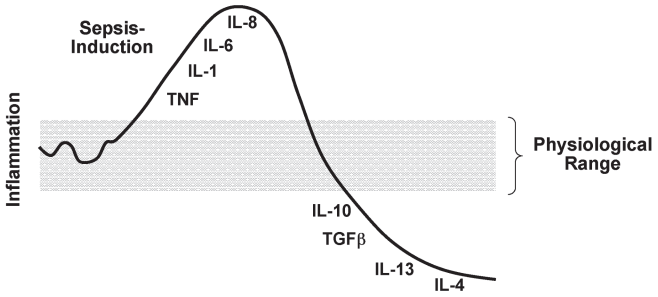

FIG. 2. Hypothetical biphasic immunoinflammatory response to a traumatic insult. IL, interleukin; TGF, transforming growth factor; TNF, tumor necrosis factor.

suggest that the hyperinflammatory and immunosuppressed states coexist. Some authors report that immunosuppression is present at the onset of sepsis (46,48,49), rather than being a later compensatory response. For example, Tschaikowsky *et al.* (49) identified that significantly decreased monocyte expression of HLA-DR was evident at the onset of severe sepsis in postsurgical patients; in survivors there was some recovery of expression but in nonsurvivors there was a further decrease or even a permanent suppression of HLA-DR expression. These authors identified that the timing of the peak of the systemic inflammatory reaction (identified as the time of maximum C-reactive protein concentration) coincided with the timing of the lowest monocyte expression of HLA-DR. From this they concluded that decreases in monocyte HLA-DR expression occur simultaneously with "signs of hyperinflammation" and as early as the onset of severe sepsis (49).

Thus, it appears that immune cells and cytokines have both detrimental and protective roles in patients as they move through the stages of sepsis. However, the traditional view that hyperinflammation precedes immunosuppression, as shown in Figure 2, may be a simplification of the real situation, and this increases the challenge to finding interventions that might benefit high-risk patients.

POTENTIAL RELEVANCE OF n-6 AND n-3 FA TO IMMUNOINFLAMMATORY RESPONSES

Human immune and inflammatory cells are rich in polyunsaturated FA (PUFA), especially arachidonic acid (20:4n-6) [see Calder (50)]. Classically the influence of PUFA on immunity and inflammation has been viewed as relating to their influence on eicosanoid generation (51–54). Arachidonic acid is the principal substrate for cyclooxygenase (COX) and lipoxygenase (LOX) enzymes giving rise to 2-series PG and thromboxanes (TX) or 5-hydroxyeicosatetraenoic acids (HETE) and 4-series LT, respectively. These mediators have cell- and stimulus-specific sources and frequently have opposing effects (Table 1). For example, PGE_2 is produced mainly by monocytes, macrophages, and, to a lesser extent, neutrophils and inhibits the production of TNF-α and IL-1β [see Miles *et al.* (55) and references therein; 56,57] and IL-12 (57,58), while LTB_4 is produced mainly by neutrophils, other granulocytes, and, to a lesser extent, monocytes and macrophages and increases the production of TNF-α and IL-1β [see Rola-Pleszczynski *et al.* (59) and references therein]. Thus, the overall physiological (or pathophysiological) outcome will depend upon the cells present, the nature of the stimulus, the timing of eicosanoid generation, the concentrations of different eicosanoids generated, and the sensitivity of target cells and tissues to the eicosanoids generated. Recent studies have demonstrated that PGE_2 induces COX-2 in fibroblasts cells and so upregulates its own production (60), induces production of IL-6 by macrophages (60), inhibits 5-LOX and so decreases production of 4-series LT (61), and induces 15-LOX so promoting the formation of lipoxins (61,62) that have been found to have anti-inflammatory effects (63,64). Thus, PGE_2 possesses both pro- and anti-inflammatory actions. PGE_2 also inhibits T-cell proliferation [see Calder *et al.* (65) and references therein] and the production of Th1-type cytokines especially IFN-γ [see Miles *et al.* (66) and references therein; 56].

It is frequently considered that the effects of arachidonic acid are solely related to its role as an eicosanoid precursor. Cell culture studies have shown that arachidonic acid acti-

TABLE 1
Some Immunoinflammatory Effects of PGE_2 and LTB_4[a]

PGE_2	LTB_4
Proinflammation	Proinflammation
Induces fever	Increases vascular permeability
Increases vascular permeability	Enhances local blood flow
Increases vasodilatation	Chemotactic agent for leukocytes
Causes pain	Induces release of lysosomal enzymes
Enhances pain caused by other agents	Induces release of reactive oxygen species by granulocytes
	Increases production of TNF, IL-1, and IL-6
Anti-inflammation	
Inhibits production of TNF and IL-1	
Inhibits 5-LOX	
Induces lipoxin production	
Immunosuppression	
Inhibits production of IL-2 and IFN-γ	
Inhibits lymphocyte proliferation	

[a]PG, prostaglandin; LT, leukotriene; TNF, tumor necrosis factor; IL, interleukin; LOX, lipoxygenase.

vates NFκB in a monocytic cell line (67), and induces TNF-α, IL-1α and IL-1β in osteoblasts (68), IL-6 in macrophages (60) and osteoblasts (69), and COX-2 in fibroblasts (60), and it appears that these effects are exerted directly by arachidonic acid rather than by an eicosanoid metabolite. What is evident from these studies is that arachidonic acid may be able to regulate inflammatory mediator production in its own right and, if so, that it has effects that are sometimes the opposite of those of PGE_2, for example, with respect to TNF-α production.

A series of cell culture-based studies with human endothelial cells has suggested that another n-6 FA, linoleic acid (18:2n-6), may also play a role in inflammation through activation of NFκB and increased production of TNF-α, IL-6, and other inflammatory mediators (70–76).

Increased consumption of long-chain n-3 PUFA, usually as components of fish oil, by humans results in increased amounts of EPA (20:5n-3) and DHA (22:6n-3) in cells involved in immunity and inflammation [see Calder (50)]. The incorporation of these FA from the diet into immune/inflammatory cells of humans is near-maximal within a few weeks (77,78) and occurs in a dose-dependent manner (79). Incorporation of EPA and DHA into human cells is partly at the expense of arachidonic acid [see Calder (50)], and the functional significance of this is that it decreases the amount of arachidonic acid available as a substrate for eicosanoid synthesis. Thus, fish oil supplementation of the human diet has been shown to result in decreased production of PGE_2 (80–83), TXB_2 (82), LTB_4 and 5-HETE (84,85), and LTE_4 (86) by inflammatory cells. However, the mechanism of the effect of long-chain n-3 FA on eicosanoid generation extends beyond simply decreasing the amount of arachidonic acid substrate. For example, EPA competitively inhibits metabolism of arachidonic acid by COX (87–89) and 5-LOX (87,90). *In vitro* studies also report that DHA can inhibit COX activity (91,92) but not that of 5-LOX (90,92). Interestingly, however, both EPA and DHA suppressed cytokine-induction of COX-2 and 5-LOX gene expression in cultured bovine chondrocytes and in human osteoarthritic cartilage explants (93,94). By inhibiting COX and LOX activities and by suppressing the up-regulation of the genes for these enzymes in response to inflammatory stimuli, long-chain n-3 FA act to oppose generation of eicosanoids from arachidonic acid. The final element of the effects of long-chain n-3 FA on eicosanoid production is the ability of EPA to act as a substrate for COX and LOX enzymes, so giving rise to a different family of eicosanoids: the 3-series PG and TX, the 5-series LT, and the hydroxyeicosapentaenoic acids (HEPE). EPA, which appears to be a good substrate for 5-LOX (86,90), is also a substrate for COX enzymes (95,96). Thus, fish oil supplementation of the human diet has been shown to result in increased production of LTB_5, LTE_5, and 5-HEPE by inflammatory cells (84–86), although generation of PGE_3 has been more difficult to demonstrate (97). The functional significance of this is that the mediators formed from EPA are believed to be less potent than those formed from arachidonic acid. For example, LTB_5 is 10- to 100-fold less potent as a neutrophil chemotactic agent than LTB_4 (98,99). Recent studies have compared the effects of PGE_2 and PGE_3 on production of cytokines by cell lines and by human cells. Bagga *et al.* (60) reported that PGE3 was a less potent inducer of COX-2 gene expression in fibroblasts and of IL-6 production by macrophages. PGE_2 and PGE_3 had equivalent inhibitory effects upon production of TNF-α (55,56) and IL-1β (55) by human mononuclear cells stimulated with endotoxin and upon production of IFN-γ production by mononuclear cells stimulated with mitogen (56,66). However, IL-2 production appeared to be less sensitive to PGE_3 than PGE_2 (66).

Studies using the isolated, perfused rabbit lung have identified contrasting effects of arachidonic acid- and EPA-derived eicosanoids. Infusion of *Escherichia coli* hemolysin caused hypertension mediated by TXB_2 and increased vascular leakage mediated by 4-series LT (100). Inclusion of arachidonic acid in the perfusate increased TXB_2 and 4-series LT generation, arterial pressure, and vascular leakage (100,101). In contrast, inclusion of EPA in the perfusate decreased TXB_2 and 4-series LT generation, decreased arterial pressure and vascular leakage, and increased generation of TXB_3 and 5-series LT (100). Perfusion with fish oil attenuated the hypertension induced by calcium ionophore (102). Compared with soybean oil infusion, fish oil decreased the concentration of LTC_4 by 50% and increased the concentration of LTC_5 from barely detectable to very similar to that of LTC_4 (102).

In addition to long-chain n-3 FA modulating the generation of eicosanoids from arachidonic acid and to EPA acting as substrate for the generation of alternative eicosanoids, recent studies have identified a novel group of mediators, termed E-series resolvins, formed from EPA by COX-2 that appear to exert anti-inflammatory actions (103–105). In addition, DHA-derived mediators termed D-series resolvins, docosatrienes, and neuroprotectins also produced by COX-2 have been identified, and these too appear to be anti-inflammatory (106–108). This is an exciting new area of n-3 FA and inflammatory mediators, and the implications for a variety of conditions may be of great importance.

Cell culture studies investigating the direct effects of arachidonic acid on inflammatory mediator production have also investigated effects of long-chain n-3 FA. EPA did not activate NFκB in a monocytic cell line (67), while EPA and DHA inhibited endotoxin-stimulated production of IL-6 and IL-8 by cultured human endothelial cells (109,110). More recent studies showed that EPA did not induce TNF-α, IL-1β, or IL-1α (68) or IL-6 (69) in osteoblasts, and even countered the upregulating effect of arachidonic acid (68); that EPA and DHA could totally abolish cytokine-induced up-regulation of TNF-α, IL-1α, and IL-1β in cultured bovine chondrocytes and in human osteoarthritic cartilage explants (93,94); and that EPA or fish oil inhibited endotoxin-induced TNF-α production by monocytes (111–114). EPA was also less potent than arachidonic acid in inducing COX-2 expression by fibroblasts and IL-6 expression by macrophages (60). EPA prevented NFκB activation by TNF-α in cultured pancreatic cells, an effect that involved decreased degradation of the in-

hibitory subunit of NFκB (IκB), perhaps through decreased phosphorylation (115). Similarly, EPA or fish oil decreased endotoxin-induced activation of NFκB in human monocytes (111,113,114), and this was associated with decreased IκB phosphorylation (113,114), perhaps due to decreased activation of mitogen-activated protein kinases (116). These observations suggest direct effects of long-chain n-3 FA on inflammatory gene expression *via* inhibition of activation of the transcription factor NFκB.

Animal feeding studies with fish oil support the observations made in cell culture with respect to the effects of long-chain n-3 FA on NFκB activation and inflammatory cytokine production. Compared with feeding corn oil, fish oil lowered NFκB activation in endotoxin-activated murine spleen lymphocytes (117). Feeding fish oil to mice decreased *ex vivo* production of TNF-α, IL-1β, and IL-6 by endotoxin-stimulated macrophages and decreased circulating TNF-α, IL-1β, and IL-6 concentrations in mice injected with endotoxin [Sadeghi *et al.* (118) and references therein].

Several studies in humans involving supplementation of the diet with fish oil have demonstrated decreased production of TNF-α, IL-1β, and IL-6 by endotoxin-stimulated monocytes or mononuclear cells (a mixture of lymphocytes and monocytes) (80–82,119). The study of Caughey *et al.* (82) reported a significant inverse correlation between the EPA content of mononuclear cells and the ability of those cells to produce TNF-α and IL-1β in response to endotoxin. Recent studies have confirmed the ability of dietary fish oil to decrease production of TNF-α (120) and IL-6 (120,121) by human mononuclear cells. Furthermore, these studies provide for the first time information on the dose-response relationship between dietary intake of long-chain n-3 FA and production of these cytokines. It should be noted that there are also several studies that fail to show effects of dietary long-chain n-3 FA on production of inflammatory cytokines in humans [see Calder (50) for references]. It is not clear what the reason for this is, but the dose of n-3 FA used and other technical factors are likely to be contributing factors. One other factor that has recently been identified is polymorphisms in genes affecting cytokine production (122). It was found that the effect of dietary fish oil on cytokine production by human mononuclear cells was dependent on the nature of the –308 TNF-α and the +252 TNF-β polymorphisms. This study raises the possibility of being able to identify those who are more likely and those who are less likely to experience specific anti-inflammatory effects of fish oil.

Thus, examination of FA composition and of eicosanoid profiles, cell and tissue culture work, and animal and human feeding studies have revealed a range of anti-inflammatory actions of long-chain n-3 FA (Table 2). These may be of benefit in sepsis, particularly during the "early" hyperinflammatory phase. The benefits of fish oil in animal models of experimental endotoxemia have been clearly demonstrated. For example, dietary fish oil or fish oil infused intravenously significantly enhanced survival of guinea pigs to intraperitoneal endotoxin compared with safflower oil (123,124). Dietary fish oil resulted in a decreased concentration of circulating postendotoxin eicosanoids (PGE_2, TXB_2, 6-keto-$PGF_{1\alpha}$) in rats and in decreased eicosanoid generation by alveolar macrophages (125,126). Furthermore, compared with dietary safflower oil, fish oil resulted in lower circulating TNF-α, IL-1β, and IL-6 concentrations following endotoxin administration to mice (118). Dietary fish oil also appears to decrease sensitivity to inflammatory cytokines (127,128). Fish oil decreased endotoxin-induced metabolic perturbations in guinea pigs and rats (129,130) and improved heart and lung function and decreased lung edema in endotoxic rats (126,131–133) and pigs (134–136).

In addition to effects on production of inflammatory eicosanoids and inflammatory cytokines, long-chain n-3 FA

TABLE 2
Summary of the Anti-inflammatory Effects of Long-Chain n-3 FA

Anti-inflammatory effect	Mechanism(s)[b]
Decreased generation of arachidonic acid-derived eicosanoids (many with inflammatory actions)	Partial replacement of arachidonic acid in cell membrane phospholipids Inhibition of arachidonic acid metabolism by phospholipase A_2, COX, and 5-LOX Decreased induction of COX-2, 5-LOX, and 5-LOX-activating protein
Increased generation of EPA-derived eicosanoids (many with less inflammatory and some with anti-inflammatory actions)	Increased cell membrane phospholipid content of EPA
Increased generation of DHA-derived docosanoids (some with anti-inflammatory actions)	Increased cell membrane phospholipid content of DHA
Decreased generation of inflammatory cytokines (TNF-α, IL-1β, IL-6, IL-8)	Decreased activation of NFκB (via decreased phosphorylation of IκB) ? Activation of peroxisome proliferation-activated receptor γ* ? Differential effects arachidonic acid vs. EPA ? Differential effects of arachidonic acid- vs. EPA-derived eicosanoids
Decreased expression of adhesion molecules[a]	Decreased activation of NFκB (*via* decreased phosphorylation of IκB) ? Other transcription factors

[a]Not discussed here [see Calder (54)].
[b]COX, cyclooxygenase; NFκB, nuclear factor kappa B; IκB, inhibitory subunit of NFκB.

also exert effects on cell-mediated immunity [see Kinsella *et al.* (51), Calder (52), and Calder *et al.* (137) for reviews]. Large amounts of fish oil in the diet of laboratory animals have been reported to exert immunosuppressive effects [see Kinsella *et al.* (51), Calder (52), and Calder *et al.* (137)]. However, it is the effects of lower amounts of long-chain n-3 FA that are of relevance to the patient setting. Several studies in humans, typically providing long-chain n-3 FA as fish oil, and investigating aspects of cell-mediated immunity have been performed. Phagocytic uptake of *Escherichia coli* appears unaffected by dietary long-chain n-3 FA in humans (138–141). One study reported that fish oil decreased expression of HLA-DP, -DQ, and -DR on human monocytes (142), suggesting impaired ability to present antigen, but there have been no studies attempting to confirm this finding. Meydani *et al.* (81) reported that fish oil providing 2.4 g EPA plus DHA per day decreased T-lymphocyte proliferation in older but not younger women. However, that study also reported increased oxidative stress in the older subjects (143), and it may be that the effect of n-3 FA was due to excessive lipid peroxidation. Several other studies report no effect of various doses of long-chain n-3 FA on lymphocyte proliferation (78,121,140), although there are studies reporting a decrease (144,145). One recent study reported that long-chain n-3 FA caused a dose-dependent increase in proliferation of T cells (83). It is noteworthy that the fish oil used was given in combination with an antioxidant mix. This might be important in terms of preventing excessive lipid peroxidation and so in determining the overall effect of n-3 FA. The study by Meydani *et al.* (81) also reported decreased production of IL-2 in the older women, but this effect has not been confirmed by others in either older (145), young (121,141), or mixed-age (78,140) subjects. A recent study reported a dose-dependent increase in IFN-γ production following n-3 FA supplementation as fish oil (83). That antioxidants were given in combination with fish oil may have been important in generating this finding.

Thus, the effects of long-chain n-3 FA on aspects of cell-mediated immunity are rather unclear, although recent human studies suggest that adverse immune effects are not exerted at modest doses (see previous discussion for references) and that enhanced T-cell responses (proliferation and IFN-γ production) may occur at modest doses so long as antioxidants are also given (83). In terms of sepsis, the true test of immunocompetence occurs when live pathogens are administered. This is a different situation from using endotoxin that is not living and that therefore does not require a robust cell-mediated immune response to eliminate it. As indicated previously, it is clear that long-chain n-3 FA protect against the deleterious effects of endotoxin. However, the situation regarding live pathogens is much less clear. This is because animal studies, frequently using high intakes of n-3 FA, report opposing findings. Infusion of fish oil into rats also receiving low-dose endotoxin decreased the number of viable bacteria in mesenteric lymph nodes and liver (146). Fish oil did not decrease bacterial translocation across the gut, and so the authors concluded that fish oil must have improved bacterial killing. Compared with linoleic acid-rich vegetable oils, fish oil fed to rats before exposure to live bacteria (147,148) resulted in increased survival, which was associated with decreased production of PGE_2. More recently, infusion of fish oil after induction of sepsis by cecal ligation and puncture decreased mortality (and PGE_2 production) compared with vegetable oil (149). Intragastric administration of fish oil into chow-fed rats before cecal ligation and puncture improved survival compared with saline or vegetable oil infusion (150). Compared with vegetable oil feeding to mice, fish oil feeding increased survival to an intramuscular injection of *Klebsiella pneumoniae* (151). The findings from these studies (146–151) contrast with those reporting that fish oil feeding decreases the survival of mice to oral *Salmonella typhimurium* (152) and to intraperitoneal *Listeria monocytogenes* (153), of guinea pigs to *Mycobacterium tuberculosis* (154), and of neonatal rabbits to *Staphylococcus aureus* (155). Thus, animal studies do not provide a clear picture of the effect of high-dose fish oil on ability to survive an infectious challenge. There are few human studies that address exposure to long-chain n-3 FA and infection; most intervention studies performed to date have been too small and of too short duration to monitor infection as an outcome. However, it is worth noting that an epidemic of measles in Greenland triggered by its introduction to a naive population by an infected Danish sailor showed the same characteristics as previous epidemics in other naive populations (156). This suggests that the very n-3 FA-rich diet of the Greenland Inuits did not worsen their response to the virus and this could indicate that these FA do not increase infectious susceptibility in humans.

STUDIES OF LONG-CHAIN n-3 FA IN SURGICAL PATIENTS

Surgery is typically accompanied by an inflammatory response that may be exaggerated in some patients, especially if the surgery is major. If the patient is exposed to pathogenic organisms and is unable to cope with these, then sepsis may develop. Artificial nutrition is frequently used post-surgery and this may involve parenteral (i.e., intravenous) infusions, especially where the gastrointestinal tract is not fully functional (e.g., post-abdominal surgery). Lipids are included in parenteral nutrition to provide an alternative source of calories to glucose and the lipid source used most frequently has been soybean oil, which is rich in the n-6 FA linoleic acid, although it also contains a proportion of α-linolenic acid (18:3n-3). A meta-analysis of total parenteral nutrition suggested that inclusion of lipids might be detrimental ($P = 0.09$ for lipids vs. no lipids) (157), at least in very ill patients. It is not clear why this is, although a number of *in vitro* experiments have shown that soybean oil-based lipid emulsions can exert immunosuppressive effects [see Calder *et al.* (158) for references], which would clearly be detrimental in patients at risk of infection and sepsis. Clinical trials provide conflicting evidence, some showing some immunosuppressive effects (159,160) and others not (161–163), at least in some patient

groups. The concern about potential harm, the view of sepsis as a hyperinflammatory state followed by an immunosuppressed state (Fig. 2), and the idea that n-6 FA might be "proinflammatory and immunosuppressive" has led to the development of alternative lipid emulsions for parenteral applications. Emulsions using a mix of medium-chain triglycerides and soybean oil or based upon olive oil instead of soybean oil have been developed, but these will not be discussed here. However, of relevance to the present discussion is the development of emulsions that include fish oil as a partial replacement for soybean oil. Several such emulsions have been tested in surgical patients.

Intravenous infusion of a lipid emulsion containing fish oil for 5 d into patients who had undergone major abdominal surgery resulted in much higher LTC_5 production by blood leukocytes stimulated *ex vivo* at 6 d postoperation (164). In another study, patients who had undergone abdominal surgery received soybean oil or a mix of medium-chain triglycerides, soybean oil, and fish oil (50:40:10, by vol) for 5 d post surgery (165). Leukocytes from these patients produced more LTB_5 and LTB_5 isomers at postoperative days 6 and 8. Patients who had undergone major gastrointestinal surgery received a medium-chain triglyceride/soybean oil mix (50:50, vol/vol) or a mix of medium-chain triglycerides, soybean oil, and fish oil (50:30:20, by vol) for 5 d postsurgery (166). Patients receiving fish oil got 3 (days 1 and 2) and 6 g (days 3, 4, and 5) of long-chain n-3 FA per day. Neutrophils from these patients produced less LTB_4 and more LTB_5 at postoperative days 6 and 10. Plasma TNF-α concentrations were lower in the fish oil group at day 6, while plasma IL-6 concentrations were lower at day 10. The study did not report clinical outcomes. A more recent study infused a fish oil-rich formula on the day before abdominal surgery and on days 1 to 5 following abdominal surgery (167). On days 4 and 5 the patients also received standard total parenteral nutrition that included 50 g of fat/d (n = 12; n = 11 in the control group). TNF-α production by endotoxin-stimulated whole blood tended to be lower at postoperative day 5 in the fish oil group, but this was not significant. Serum IL-6 concentrations were significantly lower at days 0, 1, and 3 in the fish oil group. Monocyte expression of HLA-DR was preserved in the fish oil group but declined at postsurgery days 3 and 5 in the control group. No differences in infection rates or mortality were observed. However, postoperative stay in intensive care tended to be shorter in the fish oil group (4.1 vs. 9.1 d) as did total hospital stay (17.8 vs. 23.5 days), although neither of these was a significant effect. Postoperative stay on medical wards was significantly shorter in the fish oil group. Another recent study compared the effects of lipid-free total parenteral nutrition or parenteral nutrition including 10% soybean oil or 8.3% soybean oil plus 1.7% fish oil for 5 d after large bowel surgery (168). There were no differences between the groups with respect to the numbers of circulating lymphocytes, B cells, $CD4^+$ cells, $CD8^+$ cells, or natural killer cells before surgery or at days 3 and 6 postsurgery, although these were affected by surgery itself. There were no differences between groups with respect to T-lymphocyte proliferation, but IL-2 production was increased in the fish oil group and the postsurgery decline in IFN-γ production was prevented by fish oil. These studies indicate that inclusion of fish oil in parenteral nutrition regimens for gastrointestinal surgical patients modulates generation of inflammatory eicosanoids (164–166) and cytokines (166,167) and may help to counter the surgery-induced declines in antigen-presenting cell activity (167) and T cell cytokine production (168). Importantly, these studies do not reveal deleterious immunologic effects of fish oil infusion in these patients. Furthermore, the only one of these fairly small studies to have examined hard end points like length of hospital stay suggests some clinical benefit from fish oil infusion in these patients (167). However, larger studies are required to evaluate the effects of this approach on complication rates, hospital stay, and mortality rate. A very recent report from a larger cohort of patients receiving parenteral nutrition postsurgery does indicate benefit of inclusion of fish oil in the regimen (169). Patients received fish oil postoperatively (n = 86) or controls received a 50:50 medium-chain triglyceride-soybean oil mix (n = 110). There were no differences between the two groups with respect to the proportions of patients who died or developed wound infections or with respect to length of hospital stay. However, the proportion of patients who were readmitted to intensive care (5%) was significantly lower in the fish oil than in the control group (17%). A group of patients also received the fish oil-containing emulsion for 2 d preoperatively (n = 53). Here there were a number of very significant benefits. This group showed a significantly decreased need for mechanical ventilation (17 vs. 31% in the control group), a significantly shorter length of hospital stay (22 vs. 29 d), significantly less need for readmission to intensive care (5 vs. 17%), and a significantly lower mortality rate (3 vs. 15%) (169). This study demonstrates a benefit from the inclusion of long-chain-3 FA in parenteral nutrition regimens used in abdominal surgery patients. However, it also demonstrates a much greater benefit if the FA are additionally provided before surgery, which, of course, is only possible in elective surgery. The greater benefit of preoperative infusion of long-chain n-3 FA may relate to better incorporation of the FA into leukocytes and other tissues.

Enteral nutrition is an alternative form of artificial nutrition. It describes provision of nutrients directly into the gastrointestinal tract *via* a tube and is sometimes referred to as "tube feeding." Enteral nutrition is used in patients with a functional gastrointestinal tract and is considered preferable to parenteral nutrition. The influence of enteral feeds including long-chain n-3 FA in their composition has been examined in surgical patients, generally in those who have undergone surgery to remove cancerous regions of the intestine. These studies have frequently used an enteral formula named Impact® (Novartis, Basel, Switzerland), which contains arginine, long-chain n-3 FA, and nucleotides, each of which is lacking from control formulas. Thus, any effects observed cannot be ascribed to a particular component of Impact. The effect of Impact on immunoinflammatory outcomes in surgical

patients has been widely examined. Daly *et al.* (170) reported that Impact results in time-dependent incorporation of EPA into mononuclear cells and that this is associated with a time-dependent decrease in PGE_2 production. Studies have reported that Impact increases phagocytosis by monocytes but not by neutrophils (171,172), increases T-cell proliferation (173) and cell-mediated immunity (172,174), and decreases circulating concentrations of IL-6 (172,175). Several of these studies report significantly improved clinical outcomes related to lower infection rate (170,172,173,175) and decreased length of hospital stay (170,172,175). Studies of Impact and similar enteral formulas investigating clinical outcomes in postsurgical patients have been subject to meta-analyses (176–178), which conclude that this approach to enteral nutrition significantly decreases infectious complications and length of hospital stay in elective surgery patients. It is possible that the modulation of inflammation and the improvements in immune function reported in these patients receiving Impact contribute to the improved clinical outcomes. However, it is not possible to ascribe these benefits to long-chain n-3 FA.

STUDIES OF LONG-CHAIN n-3 FA IN CRITICALLY ILL PATIENTS

Critically ill patients frequently require artificial support, depending upon the extent of organ damage or failure, and this will include nutritional support. The influence of enteral feeds including long-chain n-3 FA has been examined in critically ill patients; again, many of these studies have involved Impact. A study in intensive care unit patients (a mix of trauma, sepsis, and major surgery patients) reported that Impact resulted in higher T-cell proliferation at days 3 and 7 (179), while a study of severe trauma patients reported greater HLA-DR expression at day 7 (180). These studies did not report improvements in clinical outcomes. Studies of Impact and similar enteral formulas investigating clinical outcomes in trauma and critically ill patients have been subject to meta-analysis (176–178). The most recent of these concluded that this approach to enteral nutrition decreases length of hospital stay but has no effect on infectious complications or mortality in critically ill patients (178).

Another trial performed in patients with moderate and severe acute respiratory distress syndrome used an enteral preparation that differed mainly in lipid source from the control (181). The control group of patients (n = 72) received a formula in which the lipid source was 97% corn oil plus 3% soy lecithin. The experimental group (n = 70) received a lipid source that was 32% canola oil, 25% medium-chain triglycerides, 20% borage oil, 20% fish oil, and 3% soy lecithin. The experimental formula also contained more vitamin C and vitamin E than the control and it contained β-carotene, taurine, and carnitine, which the control formula did not. Patients receiving the experimental formula got about 7 g of EPA, 3 g of DHA, 6 g of γ-linolenic acid, 1.1 g of vitamin C, 400 IU of vitamin E, and 6.6 mg of β-carotene per day for 6 d. By 4 d the numbers of total leukocytes and of neutrophils in the alveolar fluid declined significantly in the experimental group and were lower than in the control group. Arterial oxygenation and gas exchange were improved in the experimental group. These patients had a significantly decreased requirement for supplemental oxygen, decreased time on ventilation support (11.0 vs. 16.3 d), and a shorter length of stay in intensive care (12.8 vs. 17.5 d). Total length of hospital stay tended to be shorter in the experimental group (29.6 vs. 34.6 d). Significantly fewer patients in the experimental group developed new organ failure (8 vs. 28%). The mortality rate was 12% in the experimental group and 19% in the control group, but this difference was not statistically significant. More recently, new data from this study have become available (182). Patients receiving the experimental formula had significantly lower concentrations of IL-8 in their alveolar fluid and tended to have lower concentrations of LTB_4 and TNF-α. It is possible that the lower concentrations of LTB_4 and IL-8, both of which are potent leukocyte chemoattractants, may have been responsible for the lower neutrophil infiltration reported in the experimental group, and indeed neutrophil counts were significantly associated with these concentrations (182). This study establishes that the experimental treatment decreases production of inflammatory mediators and infiltration of inflammatory leukocytes and that this can result in significant clinical improvement in extremely ill patients. Because of the many differences in composition between the experimental and control formulas used it is not possible to ascribe the effects and benefits to any particular nutrient. However, the effects on LTB_4, IL-8 and TNF-α concentrations are consistent with effects of long-chain n-3 FA reported elsewhere.

Recently, data from studies using parenteral nutrition with fish oil in sepsis patients have become available (183,184). Patients received a standard soybean oil-based emulsion or an emulsion containing fish oil for 5 (178) or 10 (177) d. Blood leukocyte counts and serum C-reactive protein concentration tended to be lower, and production of LTB_5 by stimulated neutrophils was significantly higher in patients receiving long-chain n-3 FA (177). Production of TNF-α, IL-1β, IL-6, IL-8, and IL-10 by endotoxin-stimulated mononuclear cells did not increase during infusion of the fish oil-containing emulsion whereas production of the four proinflammatory cytokines was markedly elevated during the first 2 d of soybean oil infusion (178). These studies establish that infusion of long-chain n-3 FA into patients with sepsis can modulate inflammatory mediator production and related inflammatory processes. However, the impact of this on hard clinical outcomes in these patients is not yet clear.

In summary, long-chain n-3 PUFA from fish oil decrease the production of inflammatory cytokines and eicosanoids. They act both directly, by replacing arachidonic acid as an eicosanoid substrate and by inhibiting arachidonic acid metabolism, and indirectly, by altering the expression of inflammatory genes through effects on transcription factor activation. Thus, long-chain n-3 PUFA are potentially useful anti-inflammatory agents and may be of benefit in patients at risk of developing sepsis. An emerging application of n-3 PUFA is in surgical or

critically ill patients where they may be added to parenteral or enteral formulas. Parenteral or enteral nutrition including n-3 PUFA appears to preserve immune function better than standard formulas and appears to partly prevent some aspects of the inflammatory response. Studies to date are suggestive of clinical benefits from these approaches, especially in post-surgical patients.

REFERENCES

1. Bone, R.C., Balk, R.A., Cerra, F.B., Dellinger, R.P., Fein, A.M., Knaus, W.A., Schein, R.M., and Sibbald, W.J. (1997) Definitions for Sepsis and Organ Failure and Guidelines for the Use of Innovative Therapies in Sepsis, *Chest 101*, 1644–1655.
2. Warren, H.S. (1997) Strategies for the Treatment of Sepsis, *N. Engl. J. Med. 336*, 952–953.
3. Angus, D.C., Linde-Zwirble, W.T., Lidicker, J., Clermont, G., Carcillo, J., and Pinsky, M.R. (2001) Epidemiology of Severe Sepsis in the United States: Analysis of Incidence, Outcome, and Associated Costs of Care, *Crit. Care Med. 29*, 1303–1310.
4. Friedman, G., Silva, E., and Vincent, J.-L. (1998) Has the Mortality of Septic Shock Changed with Time? *Crit. Care Med. 26*, 2078–2086.
5. Brun-Buisson, C. (2000) The Epidemiology of the Systemic Inflammatory Response Syndrome, *Intensive Care Med. 26*, S64–S74.
6. Vervloet, M.G., Thijs, L.G., and Hack, C.E. (1998) Derangements of Coagulation and Fibrinoloysis in Critically Ill Patients with Sepsis and Septic Shock, *Semin. Thromb. Hemostas. 24*, 33–44.
7. Girardin, E., Grau, G.E., Dayer, J.-M., Roux-Lombard, P., J5 Study Group, and Lambert, P.H. (1988) Tumor Necrosis Factor and Interleukin-1 in the Serum of Children with Severe Infectious Purpura, *N. Engl. J. Med. 319*, 397–400.
8. Hatherill, M., Tibby, S.M., Turner, C., Ratnavel, N., and Murdoch, I.A. (2000) Procalcitonin and Cytokine Levels: Relationship to Organ Failure and Mortality in Pediatric Septic Shock, *Crit. Care Med. 28*, 2591–2594.
9. Arnalich, F., Garcia-Palomero, E., Lopez, J., Jimenez, M., Madero, R., Renart, J., Vazquez, J.J., and Montiel, C. (2000) Predictive Value of Nuclear Factor κB Activity and Plasma Cytokine Levels in Patients with Sepsis, *Infect. Immun. 68*, 1942–1945.
10. Beutler, B., Milsark, I.W., and Cerami, A.C. (1985) Passive Immunization Against Cachectin/Tumor Necrosis Factor Protects Mice from Lethal Effect of Endotoxin, *Science 229*, 869–871.
11. Tracey, K.J., Fong, Y., Hesse, D.G., Manogue, K.R., Lee, A.T., Kuo, G.C., Lowry, S.F., and Cerami, A.C. (1987) Anti-Cachectin/TNF Monoclonal Antibodies Prevent Septic Shock During Lethal Bacteraemia, *Nature 330*, 662–664.
12. Alexander, H.R., Doherty, G.M., Buresh, C.M., Venzon, D.J., and Norton, J.A. (1991) A Recombinant Human Receptor Antagonist to Interkeukin 1 Improves Survival After Lethal Endotoxemia in Mice, *J. Exp. Med. 173*, 1029–1032.
13. Marchant, A., Bruyns, C., Vandenabeele, P., Ducarme, M., Gerard, C., Delvaux, A., De Groote, D., Abramowicz, D., Velu, T., and Goldman, M. (1994) Interleukin-10 Controls Interferon-Gamma and Tumor Necrosis Factor Production During Experimental Endotoxemia, *Eur. J. Immunol. 24*, 1167–1171.
14. Pfeffer, K., Matsuyama, T., Kundig, T.M., Wakeham, A., Kishihara, K., Shahinlan, A., Wiegmann, K., Ohashi, P.S., Kronke, M., and Mak, T.W. (1993) Mice Deficient for the 55 Kd Tumor Necrosis Factor Receptor are Resistant to Endotoxic Shock, Yet Succumb to *L. monocytogenes* Infection, *Cell 73*, 457–467.
15. Debets, J.M.H., Kampmeijer, R., van der Linden, M.P.M.H., Buurman, W.A., and van der Linden, C.J. (1989) Plasma Tumor Necrosis Factor and Mortality in Critically Ill Septic Patients, *Crit. Care Med. 17*, 489–494.
16. Rogy, M.A., Coyle, S.M., Oldenburg, H.S., Rock, C.S., Barie, P.S., Van Zee, K.J., Smith, C.G., Moldawer, L.L., and Lowry, S.F. (1994) Persistently Elevated Soluble Tumor Necrosis Factor Receptor and Interleukin-1 Receptor Antagonist Levels in Critically Ill Patients, *J. Am. Coll. Surg. 178*, 132–138.
17. Pruitt, J.H., Welborn, M.B., Edwards, P.D., Harward, T.R., Seeger, J.W., Martin, T.D., Smith, C., Kenney, J.A., Wesdorp, R.I., Meijer, S., Cuesta, M.A., Abouhanze, A., Copeland, E.M. 3rd, Giri, J., Sims, J.E., Moldawer, L.L., and Oldenburg, H.S. (1996) Increased Soluble Interleukin-1 Type II Receptor Concentrations in Postoperative Patients and in Patients with Sepsis Syndrome, *Blood 87*, 3282–3288.
18. Oberholzer, A., Oberholzer, C., and Moldawer, L.L. (2000) Cytokine Signalling—Regulation of the Immune Response in Normal and Critically Ill States, *Crit. Care Med. 28* (Suppl.), N3–N12.
19. Eskandari, M.K., Bolgos, G., Miller, C., Nguyen, D.T., DeForge, L.E., and Remick, D.G. (1992) Anti-Tumor Necrosis Factor Antibody Therapy Fails to Prevent Lethality After Cecal Ligation and Puncture or Endotoxemia, *J. Immunol. 148*, 2724–2730.
20. Opal, S.M., Cross, A.S., Jhung, J.W., Young, L.D., Palardy, J.E., Parejo, N.A., and Donsky, C. (1996) Potential Hazards of Combination Immunotherapy in the Treatment of Experimental Septic Shock, *J. Infect. Dis. 173*, 1415–1421.
21. Echtenacher, B., Weigl, K., Lehn, N., and Mannel, D.N. (2001) Tumor Necrosis Factor-Dependent Adhesions as a Major Protective Mechanism Early in Septic Peritonitis in Mice, *Infect. Immun. 69*, 3550–3555.
22. Fisher, C.J., Jr., Agosti, J.M., Opal, S.M., Lowry, S.F., Balk, R.A., Sadoff, J.C., Abraham, E., Schein, R.M., and Benjamin, E. (1996) Treatment of Septic Shock with the Tumor Necrosis Factor Receptor:Fc Fusion Protein, *N. Engl. J. Med. 334*, 1697–1702.
23. Howell, W.M., Calder, P.C., and Grimble, R.F. (2002) Gene Polymorphisms, Inflammatory Diseases and Cancer, *Proc. Nutr. Soc. 61*, 447–456.
24. Louis, E., Franchimont, D., Piron, A., Gevaert, Y., Schaaf-Lafontaine, N., Roland, S., Mahieu, P., Malaise, M., De Groote, D., Louis, R., and Belaiche, J. (1998) Tumour Necrosis Factor (TNF) Gene Polymorphism Influences TNF-Alpha Production in Lipopolysaccharide (LPS)-Stimulated Whole Blood Cell Culture in Healthy Humans, *Clin. Exp. Immunol. 113*, 401–406.
25. Pociot, F., Briant, L., Jongeneel, C.V., Molvig, J., Worsaae, H., Abbal, M., Thomsen, M., Nerup, J., and Cambon-Thomsen, A. (1993) Association of Tumor Necrosis Factor (TNF) and Class II Major Histocompatibility Complex Alleles with the Secretion of TNF-Alpha and TNF-Beta by Human Mononuclear Cells: A Possible Link to Insulin-Dependent Diabetes Mellitus, *Eur. J. Immunol. 23*, 224–231.
26. Mira, J.P., Cariou, A., Grall, F., Delclaux, C., Losser, M.-R., Heshmati, F., Cheval, C., Monchi, M., Teboul, J.-L., Riche, F., Leleu, G., Arbibe, L., Mignon, A., Delpech, M., and Dhainaut, J.-F. (1999) Association of TNF_2, a TNF-α Promoter Polymorphism, with Septic Shock Susceptibility and Mortality, *J. Am. Med. Assoc. 282*, 561–568.
27. Stuber, F., Peterson, M., Bokelmann, F., and Schade, U. (1996) A Genetic Polymorphism Within the Tumor Necrosis Factor Locus Influences Plasma Tumor Necrosis Factor-α Concentrations and Outcome of Patients with Severe Sepsis, *Crit. Care Med. 24*, 381–384.
28. Kahlke, V., Schafmayer, C., Schniewind, B., Seegert, D., Schreiber, S., and Schroder, J. (2004) Are Postoperative Com-

plications Genetically Determined by TNF-β NcoI Gene Polymprophism? *Surgery 135*, 365–373.
29. Grbic, J.T, Mannick, J.A., Gough, D.B., and Rodrick, M.L. (1991) The Role of Prostaglandin E2 in Immune Suppression Following Injury, *Ann. Surg. 214*, 253–263.
30. Ertel, W., Morrison, M.H., Meldrum, D.R., Ayala, A., and Chaudry, I.H. (1992) Ibuprofen Restores Cellular Immunity and Decreases Susceptibility to Sepsis Following Hemorrhage, *J. Surg. Res. 53*, 55–61.
31. Kollef, M.H., and Schuster, D.P. (1995) The Acute Respiratory Distress Syndrome, *N. Engl. J. Med. 332*, 27–37.
32. Meakins, J.L., Pietsch, J.B., Bubenick, O., Kelly, R., Rode, H., Gordon, J., and MacLean, L.D. (1977) Delayed Hypersensitivity: Indicator of Acquired Failure of Host Defenses in Sepsis and Trauma, *Ann. Surg. 186*, 241–250.
33. Lederer, J.A., Rodrick, M.L., and Mannick, J.A. (1999) The Effects of Injury on the Adaptive Immune Response, *Shock 11*, 153–159.
34. Oberholzer, A., Oberholzer, C., and Moldawer, L.L. (2001) Sepsis Syndromes: Understanding the Role of Innate and Acquired Immunity, *Shock 16*, 83–96.
35. O'Sullivan, S.T., Lederer, J.A., Horgan, A.F., Chin, D.H.L., Mannick, J.A., and Rodrick, M.L. (1995) Major Injury Leads to Predominance of the T Helper-2 Lymphocyte Phenotype and Diminished Interleukin-12 Production Associated with Decreased Resistance to Infection, *Ann. Surg. 222*, 482–492.
36. Opal, S.M., and DePalo, V.A. (2000) Anti-Inflammatory Cytokines, *Chest 117*, 1162–1172.
37. Gerard, C., Bruyns, C., Marchant, A., Abramowicz, D., Vandenabeele, P., Delvaux, A., Fiers, W., Goldman, M., and Velu, T. (1993) Interleukin 10 Reduces the Release of Tumor Necrosis Factor and Prevents Lethality in Experimental Endotoxemia, *J. Exp. Med. 177*, 547–550.
38. Howard, M., Muchamuel, T., Andrade, S., and Menon, S. (1993) Interleukin 10 Protects Mice from Lethal Endotoxemia, *J. Exp. Med. 177*, 1205–1208.
39. Smith, S.R., Terminelli, C., Kenworthy-Bott, L., Calzetta, A., and Donkin, J. (1994) The Cooperative Effects of TNF-α and IFN-γ are Determining Factors in the Ability of IL-10 to Protect Mice from Lethal Endotoxemia, *J. Leuk. Biol. 55*, 711–718.
40. Hershman, M., Cheadle, W., Wellhausen, S., Davidson, P., and Polk, H. (1990) Monocyte HLA-DR Antigen Expression Characterises Clinical Outcome in the Trauma Patients, *Br. J. Surg. 77*, 204–207.
41. Wakefield, C., Carey, P., Fould, S., Monson, J., and Guillou, P. (1993) Changes in Major Histocompatibility Complex Class II Expression in Monocytes and T Cells of Patients Developing Infection After Surgery, *Br. J. Surg. 80*, 205–209.
42. Astiz, M., Saha, D., Lustbader, D., Lin, R., and Rackow, E. (1996) Monocyte Response to Bacterial Toxins, Expression of Cell Surface Receptors, and Release of Anti-Inflammatory Cytokines During Sepsis, *J. Lab. Clin. Med. 128*, 594–600.
43. Manjuck, J., Saha, D.C., Astiz, M., Eales, L.-J., and Rackow, E.C. (2000) Decreased Response to Recall Antigens is Associated with Depressed Costimulatory Receptor Expression in Septic Critically Ill Patients, *J. Lab. Clin. Med. 135*, 153–1260.
44. Munoz, C., Carlet, J., Fitting, C., Missett, B., Bieriot, J., and Cavaillon, J. (1991) Dysregulation of *in vitro* Cytokine Production by Monocytes During Sepsis, *J. Clin. Invest. 88*, 1747–1754.
45. Brandtzaeg, P., Osnes, L., Ovstebo, R., Joo, G., Westvik, A., and Kierulf, P. (1996) Net Inflammatory Capacity of Human Septic Shock Plasma Evaluated by a Monocyte-Based Target Cell Assay: Identification of Interleukin-10 as a Major Functional Deactivator of Human Monocytes, *J. Exp. Med. 184*, 51–60.
46. Heidecke, C.D., Hensler, T., Weighardt, H., Zantl, N., Wagner, H., Siewert, J.R., and Holzmann, B. (1999) Selective Defects of T Lymphocyte Function in Patients with Lethal Intraabdominal Infection, *Am. J. Surg. 178*, 288–292.
47. Pellegrini, J.D., De, A.K.K., Puyana, J.C., Furse, R.K., and Miller-Graziano, C. (2000) Relationships Between T Lymphocyte Apoptosis and Anergy Following Trauma, *J. Surg. Res. 88*, 200–206.
48. Weighardt, H., Heidecke, C.D., Emmanuilidis, K., Maier, S., Bartels, H., Siewert, J.R., and Holzmann, B. (2000) Sepsis After Major Visceral Surgery is Associated with Sustained and Interferon-γ-Resistant Defects of Monocyte Cytokine Production, *Surgery 127*, 309–315.
49. Tschaikowsky, K., Hedwig-Geissing, M., Schiele, A., Bremer, F., Schywalsky, M., and Schutter, J. (2002) Coincidence of Pro- and Anti-Inflammatory Responses in the Early Phase of Severe Sepsis: Longitudinal Study of Mononuclear Histocompatibility Leukocyte Antigen-DR Expression, Procalcitonin, C-Reactive Protein, and Changes in T-Cell Subsets in Septic and Postoperative Patients, *Crit. Care Med. 30*, 1015–1023.
50. Calder, P.C. (2001) n-3 Polyunsaturated FA, Inflammation and Immunity: Pouring Oil on Troubled Waters or Another Fishy Tale? *Nutr. Res. 21*, 309–341.
51. Kinsella, J.E., Lokesh, B., Broughton, S., and Whelan, J. (1990) Dietary Polyunsaturated Fatty Acids and Eicosanoids: Potential Effects on the Modulation of Inflammatory and Immune Cells: An Overview, *Nutrition 6*, 24–44
52. Calder, P.C. (2001) Polyunsaturated Fatty Acids, Inflammation and Immunity, *Lipids 36*, 1007–1024.
53. Calder, P.C. (2002) Dietary Modification of Inflammation with Lipids, *Proc. Nutr. Soc. 61*, 345–358.
54. Calder, P.C. (2003) n-3 Polyunsaturated Fatty Acids and Inflammation: From Molecular Biology to the Clinic, *Lipids 38*, 342–352.
55. Miles, E.A., Allen, E., and Calder, P.C. (2002) *In vitro* Effects of Eicosanoids Derived from Different 20-Carbon Fatty Acids on Production of Monocyte-Derived Cytokines in Human Whole Blood Cultures, *Cytokine 20*, 215–223.
56. Dooper, M.M.B.W., Wassink, L., M'Rabet, L., and Graus, Y.M.F. (2002) The Modulatory Effects of Prostaglandin-E on Cytokine Production by Human Peripheral Blood Mononuclear Cells are Independent of the Prostaglandin Subtype, *Immunology 107*, 152–159.
57. Vassiliou, E., Jing, H., and Ganea, D. (2003) Prostaglandin E2 Inhibits TNF Production in Murine Bone Marrow-Derived Dendritic Cells, *Cell. Immunol. 223*, 120–132.
58. van der Pouw Kraan, T.C., Boeije, L.C., Smeenk, R.J., Wijdenes, J., and Aarden, L.A. (1995) Prostaglandin E2 is a Potent Inhibitor of Human Interleukin 12 Production in Murine Bone Marrow-Derived Dendritic Cells, *J. Exp. Med. 181*, 775–779.
59. Rola-Pleszczynski, M., Thivierge, M., Gagnon, N., Lacasse, C., and Stankova, J. (1993) Differential Regulation of Cytokine and Cytokine Receptor Genes by PAF, LTB_4 and PGE_2, *J. Lipid Mediat. 6*, 175–181.
60. Bagga, D., Wang, L., Farias-Eisner, R., Glaspy, J.A., and Reddy, S.T. (2003) Differential Effects of Prostaglandin Derived From ω-6 and ω-3 Polyunsaturated Fatty Acids on COX-2 Expression and IL-6 Secretion, *Proc. Natl. Acad. Sci. USA 100*, 1751–1756.
61. Levy, B.D., Clish, C.B., Schmidt, B., Gronert, K., and Serhan, C.N. (2001) Lipid Mediator Class Switching During Acute Inflammation: Signals in Resolution, *Nature Immunol. 2*, 612–619.
62. Vachier, I., Chanez, P., Bonnans, C., Godard, P., Bousquet, J., and Chavis, C. (2002) Endogenous Anti-Inflammatory Mediators from Arachidonate in Human Neutrophils, *Biochem. Biophys. Res. Commun. 290*, 219–224.
63. Gewirtz, A.T., Collier-Hyams, L.S., Young, A.N., Kucharzik,

T., Guilford, W.J., Parkinson, J.F., Williams, I.R., Neish, A.S., and Madara, J.L. (2002) Lipoxin A4 Analogs Attenuate Induction of Intestinal Epithelial Proinflammatory Gene Expression and Reduce the Severity of Dextran Sodium Sulfate-Induced Colitis, *J. Immunol. 168*, 5260–5267.
64. Serhan, C.N., Jain, A., Marleau, S., Clish, C., Kantarci, A., Beh-behani, B., Colgan, S.P., Stahl, G.L., Merched, A., Petasis, N.A., Chan, L., and Van Dyke, T.E. (2003) Reduced Inflammation and Tissue Damage in Transgenic Rabbits Overexpressing 15-Lipoxygenase and Endogenous Anti-Inflammatory Lipid Mediators, *J. Immunol. 171*, 6856–6865.
65. Calder, P.C., Bevan, S.J., and Newsholme, E.A. (1992) The Inhibition of T-Lymphocyte Proliferation by Fatty Acids is Via an Eicosanoid-Independent Mechanism, *Immunology 75*, 108–115.
66. Miles, E.A., Aston, L., and Calder, P.C. (2003) In Vitro Effects of Eicosanoids Derived from Different 20-Carbon Fatty Acids on T Helper Type 1 and T Helper Type 2 Cytokine Production in Human Whole-Blood Cultures, *Clin. Exp. Allergy 33*, 624–632.
67. Camandola, S., Leonarduzzi, G., Musso, T., Varesio, L., Carini, R., Scavazza, A., Chiarpotto, E., Baeuerle, P.A., and Poli, G. (1996) Nuclear Factor κB is Activated by Arachidonic Acid but Not by Eicosapentaenoic Acid, *Biochem. Biophys. Res. Commun. 229*, 643–647.
68. Priante, G., Bordin, L., Musacchio, E., Clari, G., and Baggio, B. (2002) Fatty Acids and Cytokine mRNA Expression in Human Osteoblastic Cells: A Specific Effect of Arachidonic Acid, *Clin. Sci. 102*, 403–409.
69. Bordin, L., Prianti, G., Musacchio, E., Giunco, S., Tibaldi, E., Clari, G., and Baggio, B. (2003) Arachidonic Acid-Induced IL-6 Expression is Mediated by PKC-α Activation in Osteoblastic Cells, *Biochemistry 42*, 4485–4491.
70. Hennig, B., Toborek, M., Joshi-Barve, S., Barger, S.W., Barve, S., Mattson, M.P., and McClain, C.J. (1996) Linoleic Acid Activates Nuclear Transcription Factor-Kappa B (NF-kappa B) and Induces NF-kappa B-Dependent Transcription in Cultured Endothelial Cells, *Am. J. Clin. Nutr. 63*, 322–328.
71. Hennig, B., Meerarani, P., Ramadass, P., Watkins, B.A., and Toborek, M. (2000) Fatty Acid-Induced Activation of Vascular Endothelial Cells, *Metabolism 49*, 1006–1013.
72. Toborek, M., Blanc, E.M., Kaiser, S., Mattson, M.P., and Hennig, B. (1997) Linoleic Acid Potentiates TNF-Mediated Oxidative Stress, Disruption of Calcium Homeostasis, and Apoptosis of Cultured Vascular Endothelial Cells, *J. Lipid Res. 38*, 2155–2167.
73. Toborek, M., Lee, Y.W., Garrido, R.S., and Hennig, B. (2002) Unsaturated Fatty Acids Selectively Induce an Inflammatory Environment in Human Endothelial Cells, *Am. J. Clin. Nutr. 75*, 119–125.
74. Young, V.M., Toborek, M., Yang, F.J., McClain, C.J., and Hennig, B. (1998) Effect of Linoleic Acid on Endothelial Cell Inflammatory Mediators, *Metabolism 47*, 566–572.
75. Park, H.J., Lee, Y.W., Hennig, B., and Toborek, M. (2001) Linoleic Acid-Induced VCAM-1 Expression in Human Microvascular Endothelial Cells is Mediated by the NF-kappa B-Dependent Pathway, *Nutr. Cancer 41*, 126–134.
76. Dichtl, W., Ares, M.P.S., Niemann Jonson, A., Jovinge, S., Pachinger, O., Giachelli, C.M., Hamsten, A., Eriksson, P., and Nilsson, J. (2002) Linoleic Acid-Stimulated Vascular Adhesion Molecule-1 Expression in Endothelial Cells Depends on Nuclear Factor-κB Activation, *Metabolism 51*, 327–333.
77. Gibney, M.J., and Hunter, B. (1993) The Effects of Short- and Long-Term Supplementation with Fish Oil on the Incorporation of n-3 Polyunsaturated Fatty Acids into Cells of the Immune System in Healthy Volunteers, *Eur. J. Clin. Nutr. 47*, 255–259.
78. Yaqoob, P., Pala, H.S., Cortina-Borja, M., Newsholme, E.A., and Calder, P.C. (2000) Encapsulated Fish Oil Enriched in α-Tocopherol Alters Plasma Phospholipid and Mononuclear Cell Fatty Acid Compositions but not Mononuclear Cell Functions, *Eur. J. Clin. Invest. 30*, 260–274.
79. Healy, D.A., Wallace, F.A., Miles, E.A., Calder, P.C., and Newsholme, P. (2000) The Effect of Low to Moderate Amounts of Dietary Fish Oil on Neutrophil Lipid Composition and Function, *Lipids 35*, 763–768.
80. Endres, S., Ghorbani, R., Kelley, V.E., Georgilis, K., Lonnemann, G., van der Meer, J.M.W., Cannon, J.G., Rogers, T.S., Klempner, M.S., Weber, P.C., Schaeffer, E.J., Wolff, S.M., and Dinarello, C.A. (1989) The Effect of Dietary Supplementation with n-3 Polyunsaturated Fatty Acids on the Synthesis of Interleukin-1 and Tumor Necrosis Factor by Mononuclear Cells, *N. Eng. J. Med. 320*, 265–271.
81. Meydani, S.N., Endres, S., Woods, M.M., Goldin, B.R., Soo, C., Morrill-Labrode, A., Dinarello, C., and Gorbach, S.L. (1991) Oral (n-3) Fatty Acid Supplementation Suppresses Cytokine Production and Lymphocyte Proliferation: Comparison Between Young and Older Women, *J. Nutr. 121*, 547–555.
82. Caughey, G.E., Mantzioris, E., Gibson, R.A., Cleland, L.G., and James, M.J. (1996) The Effect on Human Tumor Necrosis Factor a and Interleukin 1β Production of Diets Enriched in n-3 Fatty Acids from Vegetable Oil or Fish Oil, *Am. J. Clin. Nutr. 63*, 116–122.
83. Trebble, T.M., Wootton, S.A., Miles, E.A., Mullee, M., Arden, N.K., Ballinger, A.B., Stroud, M.A., and Calder, P.C. (2003) Prostaglandin E2 Production and T-Cell Function After Fish-Oil Supplementation: Response to Antioxidant Co-supplementation, *Am. J. Clin. Nutr. 78*, 376–382.
84. Lee, T.H., Hoover, R.L., Williams, J.D., Sperling, R.I., Ravalese, J., Spur, B.W., Robinson, D.R., Corey, E.J., Lewis, R.A., and Austen, K.F. (1985) Effects of Dietary Enrichment with Eicosapentaenoic Acid and Docosahexaenoic Acid on In Vitro Neutrophil and Monocyte Leukotriene Generation and Neutrophil Function, *N. Eng. J. Med. 312*, 1217–1224.
85. Sperling, R.I., Benincaso, A.I., Knoell, C.T., Larkin, J.K., Austen, K.F., and Robinson, D.R. (1993) Dietary ω-3 Polyunsaturated Fatty Acids Inhibit Phosphoinositide Formation and Chemotaxis in Neutrophils, *J. Clin. Invest. 91*, 651–660.
86. Von Schacky, C., Kiefl, R., Jendraschak, E., and Kaminski, W.E. (1993) n-3 Fatty Acids and Cysteinyl-Leukotriene Formation in Humans *in vitro*, *ex vivo and in vivo*, *J. Lab. Clin. Med. 121*, 302–309.
87. Needleman, P., Whitaker, M.O., Wyche, A., Watters, K., Sprecher, H., and Raz, A. (1980) Manipulation of Platelet Aggregation by Prostaglandins and Their Fatty Acid Precursors: Pharmacological Basis for a Therapeutic Approach, *Prostaglandins 19*, 165–181.
88. Kulmacz, R.J., Pendleton, R.B., and Lands, W.E.M. (1994) Interaction Between Peroxidase and Cyclooxygenase Activities in Prostaglandin-Endoperoxide Synthase, *J. Biol. Chem. 269*, 5527–5536.
89. Obata, T., Nagakura, T., Masaki, T., Maekawa, K., and Yamashita, K. (1999) Eicosapentaenoic Acid Inhibits Prostaglandin D2 Generation by Inhibiting Cyclo-oxygenase-2 in Cultured Human Mast Cells, *Clin. Exp. Allergy 29*, 1129–1135.
90. Lee, T.H., Mencia-Huerta, J.M., Shih, C., Corey, E.J., Lewis, R.A., and Austen, F.A. (1984) Effects of Exogenous Arachidonic, Eicosapentaenoic, and Docosahexaenoic Acids on the Generation of 5-Lipoxygenase Pathway Products by Ionophore-Activated Human Neutrophils, *J. Clin. Invest. 74*, 1922–1933.
91. Rao, G.H., Radha, E., and White, J.G. (1983) Effect of Docosahexaenoic Acid (DHA) on Arachidonic Acid Metabolism and Platelet Function, *Biochem. Biophys. Res. Commun. 16*, 549–55.

92. Corey, E.J., Shih, C., and Cashman, J.R. (1983) Docosahexaenoic Acid is a Strong Inhibitor of Prostaglandin but Not Leukotriene Biosynthesis, *Proc. Natl. Acad. Sci. USA 80*, 3581–3584.
93. Curtis, C.L., Hughes, C.E., Flannery, C.R., Little, C.B., Harwood, J.L., and Caterson, B. (2000) n-3 Fatty Acids Specifically Modulate Catabolic Factors Involved in Articular Cartilage Degradation, *J. Biol. Chem. 275*, 721–724.
94. Curtis, C.L., Rees, S.G., Little, C.B., Flannery, C.R., Hughes, C.E., Wilson, C., Dent, C.M., Otterness, I.G., Harwood, J.L., and Caterson, B. (2002) Pathologic Indicators of Degradation and Inflammation in Human Osteoarthritic Cartilage are Abrogated by Exposure to n-3 Fatty Acids, *Arthritis Rheum. 46*, 1544–1553.
95. Laneuville, O., Breuer, D.K., Xu, N., Huang, Z.H., Gage, D.A., Watson, J.T., Lagarde, M., DeWitt, D.L., and Smith, W.L. (1995) Fatty Acid Substrate Specificities of Human Prostaglandin-Endoperoxide H Synthase-1 and -2, *J. Biol. Chem. 270*, 19330–19336.
96. Malkowski, M.G., Thuresson, E.D., Lakkides, K.M., Rieke, C.J., Micielli, R., Smith, W.L., and Garavito, R.M. (2001) Structure of Eicosapentaenoic and Linoleic Acids in the Cyclooxygenase Site of Prostaglandin Endoperoxidase H Synthase-1, *J. Biol. Chem 276*, 37547–37555.
97. Hawkes, J.S., James, M.J., and Cleland, L.G. (1991) Separation and Quantification of PGE3 Following Derivatization with Panacyl Bromide by High Pressure Liquid Chromatography with Fluorometric Detection, *Prostaglandins 42*, 355–368.
98. Goldman, D.W., Pickett, W.C., and Goetzl, E.J. (1983) Human Neutrophil Chemotactic and Degranulating Activities of Leukotriene B5 (LTB5) Derived from Eicosapentaenoic Acid, *Biochem. Biophys. Res. Commun. 117*, 282–288.
99. Lee, T.H., Mencia-Huerta, J.M., Shih, C., Corey, E.J., Lewis, R.A., and Austen, K.F. (1984) Characterization and Biologic Properties of 5,12-Dihydroxy Derivatives of Eicosapentaenoic Acid, Including Leukotriene-B5 and the Double Lipoxygenase Product, *J. Biol. Chem. 259*, 2383–2389.
100. Grimminger, F., Mayer, K., Kiss, L., Wahn, H., Walmrath, D., Bahkdi, S., and Seeger, W. (1997) Synthesis of 4-Series and 5-Series Leukotrienes in the Lung Microvasculature Challenged with *Escherichia coli* Hemolysin: Critical Dependence on Exogenous Free Fatty Acid Supply, *Am. J. Resp. Cell Mol. Biol. 16*, 317–324.
101. Grimminger, F., Wahn, H., Mayer, K., Kiss, L., Walmrath, D., and Seeger, W. (1997) Impact of Arachidonic Acid Versus Eicosapentaenoic Acid on Exotoxin-Induced Lung Vascular Leakage—Relation to 4-Series Versus 5-Series Leukotriene Generation, *Am. J. Resp. Crit. Care Med. 155*, 513–519.
102. Breil, I., Koch, T., Heller, A., Schlotzer, E., Grunert, A., van Ackern, K., and Neuhof, H. (1996) Alteration of n-3 Fatty Acid Composition in Lung Tissue After Short-Term Infusion of Fish Oil Emulsion Attenuates Inflammatory Vascular Reaction, *Crit. Care Med. 24*, 1893–1902.
103. Serhan, C.N., Clish, C.B., Brannon, J., Colgan, S.P., Gronert, K., and Chiang, N. (2000) Anti-Inflammatory Lipid Signals Generated From Dietary n-3 Fatty Acids via Cyclooxygenase-2 and Transcellular Processing: A Novel Mechanism for NSAID and n-3 PUFA Therapeutic Actions, *J. Physiol. Pharmacol. 4*, 643–654.
104. Serhan, C.N., Clish, C.B., Brannon, J., Colgan, S.P., Chiang, N., and Gronert, K. (2000) Novel Functional Sets of Lipid-derived Mediators with Anti-inflammatory Actions Generated From Omega-3 Fatty Acids *Via* Cyclooxygenase 2-Nonsteroidal Antiinflammatory Drugs and Transcellular Processing, *J. Exp. Med. 192*, 1197–1204.
105. Serhan, C.N., Hong, S., Gronert, K., Colgan, S.P., Devchand, P.R., Mirick, G., and Moussignac, R-L. (2002) Resolvins: A Family of Bioactive Products of Omega-3 Fatty Acid Transformation Circuits Initiated by Aspirin Treatment That Counter Pro-Inflammation Signals, *J. Exp. Med. 196*, 1025–1037.
106. Hong, S., Gronert, K., Devchand, P., Moussignac, R.-L., and Serhan, C.N. (2003) Novel Docosatrienes and 17S-Resolvins Generated from Docosahexaenoic Acid in Urine Brain, Human Blood and Glial Cells: Autocoids in Anti-inflammation, *J. Biol. Chem. 278*, 14677–14687.
107. Marcheselli, V.L., Hong, S., Lukiw, W.J., Hua Tian, X., Gronert, K., Musto, A., Hardy, M., Gimenez, J.M., Chiang, N., Serhan, C.N., and Bazan, N.G. (2003) Novel Docosanoids Inhibit Brain Ischemia-Reperfusion-Mediated Leukocyte Infiltration and Pro-Inflammatory Gene Expression, *J. Biol. Chem. 278*, 43807–43817.
108. Mukherjee, P.K., Marcheselli, V.L., Serhan, C.N., and Bazan, N.G. (2004) Neuroprotectin D1: A Docosahexaenoic Acid-Derived Docosatriene Protects Human Retinal Pigment Epithelial Cells from Oxidative Stress, *Proc. Natl. Acad. Sci. USA 101*, 8491–8496.
109. De Caterina, R., Cybulsky, M.I., Clinton, S.K., Gimbrone, M.A., and Libby, P. (1994) The Omega-3 Fatty Acid Docosahexaenoate Reduces Cytokine-Induced Expression of Proatherogenic and Proinflammatory Proteins in Human Endothelial Cells, *Arterioscler. Thromb. 14*, 1829–1836.
110. Khalfoun, B., Thibault, F., Watier, H., Bardos, P., and Lebranchu, Y. (1997) Docosahexaenoic and Eicosapentaenoic Acids Inhibit *in vitro* Human Endothelial Cell Production of Interleukin-6, *Adv. Exp. Biol. Med. 400*, 589–597.
111. Lo, C.J., Chiu, K.C., Fu, M., Lo, R., and Helton S. (1999) Fish Oil Decreases Macrophage Tumor Necrosis Factor Gene Transcription by Altering the NFκB Activity, *J. Surg. Res. 82*, 216–222.
112. Babcock, T.A., Novak, T., Ong, E., Jho, D.H., Helton, W.S., and Espat, N.J. (2002) Modulation of Lipopolysaccharide-Stimulated Macrophage Tumor Necrosis Factor-α Production by ω-3 Fatty Acid Is Associated with Differential Cyclooxygenase-2 Protein Expression and is Independent of Interleukin-10, *J. Surg. Res. 107*, 135–139.
113. Novak, T.E., Babcock, T.A., Jho, D.H., Helton, W.S., and Espat, N.J. (2003) NF-κB Inhibition by ω-3 Fatty Acids Modulates LPS-Stimulated Macrophage TNF-α Transcription, *Am. J. Physiol. 284*, L84–L89.
114. Zhao, Y., Joshi-Barve, S., Barve, S., and Chen, L.H. (2004) Eicosapentaenoic Acid Prevents LPS-Induced TNF-α Expression by Preventing NF-κB Activation, *J. Am. Coll. Nutr. 23*, 71-78.
115. Ross, J.A., Moses, A.G.W., and Fearon, K.C.H. (1999) The Anti-catabolic Effects of n-3 Fatty Acids, *Curr. Opin. Clin. Nutr. Metab. Care 2*, 219–226.
116. Lo, C.J., Chiu, K.C., Fu, M.J., Chu, A., and Helton, S. (2000) Fish Oil Modulates Macrophage P44/42 Mitogen-Activated Protein Kinase Activity Induced by Lipopolysaccharide, *J. Parent. Ent. Nutr. 24*, 159–163.
117. Xi, S., Cohen, D., Barve, S., and Chen, L.H. (2001) Fish Oil Suppressed Cytokines and Nuclear Factor kappaB Induced by Murine AIDS Virus Infection, *Nutr. Res. 21*, 865–878.
118. Sadeghi, S., Wallace, F.A., and Calder, P.C. (1999) Dietary Lipids Modify the Cytokine Response to Bacterial Lipopolysaccharide in Mice, *Immunology 96*, 404–410.
119. Abbate, R., Gori, A.M., Martini, F., Brunelli, T., Filippini, M., Francalanci, I., Paniccia, R., Prisco, D., Gensini, G.F., and Serneri, G.G.N. (1996) n-3 PUFA Supplementation, Monocyte PCA Expression and Interleukin-6 Production, *Prostaglandins Leukot. Essent. Fatty Acids 54*, 439–444.
120. Trebble, T., Arden, N.K., Stroud, M.A., Wootton, S.A., Burdge, G.C., Miles, E.A., Ballinger, A.B., Thompson R.L., and Calder, P.C. (2003) Inhibition of Tumour Necrosis Factor-α and Inter-

leukin-6 Production by Mononuclear Cells Following Dietary Fish-Oil Supplementation in Healthy Men and Response to Antioxidant Co-Supplementation, *Br. J. Nutr. 90*, 405–412.
121. Wallace, F.A., Miles, E.A., and Calder, P.C. (2003) Comparison of the Effects of Linseed Oil and Different Doses of Fish Oil on Mononuclear Cell Function in Healthy Human Subjects, *Br. J. Nutr. 89*, 679–689.
122. Grimble, R.F., Howell, W.M., O'Reilly, G., Turner, S.J., Markovic, O., Hirrell, S., East, J.M., and Calder, P.C. (2002) The Ability of Fish Oil to Suppress Tumor Necrosis Factor-α Production by Peripheral Blood Mononuclear Cells in Healthy Men is Associated with Polymorphisms in Genes that Influence Tumor Necrosis Factor α Production, *Am. J. Clin. Nutr. 76*, 454–459.
123. Mascioli, E.A., Leader, L., Flores, E., Trimbo, S., Bistrian, B., and Blackburn, G. (1988) Enhanced Survival to Endotoxin in Guinea Pigs Fed IV Fish Oil Emulsion, *Lipids 23*, 623–625.
124. Mascioli, E.A., Iwasa, Y., Trimbo, S., Leader, L., Bistrian, B.R., and Blackburn, G.L. (1989) Endotoxin Challenge After Menhaden Oil Diet: Effects on Survival of Guinea Pigs, *Am. J. Clin. Nutr. 49*, 277–282.
125. Utsunomiya, T., Chavali, S.R., Zhong, W.W., and Forse, R.A. (1994) Effects of Continuous Tube Feeding of Dietary Fat Emulsions on Eicosanoid Production and on Fatty Acid Composition During an Acute Septic Shock in Rats, *Biochim. Biophys. Acta 1214*, 333–339.
126. Sane, S., Baba, M., Kusano, C., Shirao, K., Andoh, T., Kamada, T., and Aikou, T. (2000) Eicosapentaenoic Acid Reduces Pulmonary Edema in Endotoxemic Rats, *J. Surg. Res. 93*, 21–27.
127. Mulrooney, H.M., and Grimble, R.F. (1994) Influence of Butter and of Corn, Coconut and Fish Oils on the Effects of Recombinant Human Tumour Necrosis Factor-α in Rats, *Clin. Sci. 84*, 105–112.
128. Pomposelli, J., Mascioli, E.A., Bistrian, B.R., and Flores, S.M. (1990) Attenuation of the Febrile Response in Guinea Pigs by Fish Oil Enriched Diets, *J. Parent. Ent. Nutr. 13*, 136–140.
129. Pomposelli, J.J., Flores, E.A., Blackburn, G., Zeisel, S.H., and Bistrian, B.R. (1991) Diets Enriched with n-3 Fatty Acids Ameliorate Lactic Acidosis by Improving Endotoxin-Induced Tissue Hypoperfusion in Guinea Pigs, *Ann. Surg. 213*, 166–176.
130. Teo, T.C., Selleck, K.M,. Wan, J.M.F., Pomposelli, J.J., Babayan, V.K., Blackburn, G.L., and Bistrian, B.R. (1991) Long-Term Feeding with Structured Lipid Composed of Medium-Chain and N-3 Fatty Acids Ameliorates Endotoxic Shock in Guinea-Pigs, *Metabolism 40*, 1152–1159.
131. Murray, M.J., Kanazi, G., Moukabary, K., Tazelaar, H.D., and DeMichele, S.J. (2000) Effects of Eicosapentaenoic and γ-Linolenic Acids (Dietary Lipids) on Pulmonary Surfactant Composition and Function During Porcine Endotoxemia, *Chest 117*, 1720–1727.
132. Mancuso, P., Whelan, J., DeMichele, S.J., Snider, C.C., Guszcza, J.A., and Karlstad, M.D. (1997) Dietary Fish Oil and Fish and Borage Oil Suppress Intrapulmonary Proinflammatory Eicosanoids Biosynthesis and Attenuate Pulmonary Neutrophil Accumulation in Endotoxic Rats, *Crit. Care Med. 25*, 1198–1206.
133. Mancuso, P., Whelan, J., DeMichele, S.J., Snider, C.C., Guszcza, J.A., Claycombe, K.J., Smith, G.T., Gregory, T.J., and Karlstad, M.D. (1997) Effects of Eicosapentaenoic and Gamma-Linolenic Acid on Lung Permeability and Alveolar Macrophage Eicosanoid Synthesis in Endotoxic Rats, *Crit. Care Med. 25*, 523–532.
134. Murray, M.J., Svinger, B.A., Holman, R.T., and Yaksh, T.L. (1991) Effects of a Fish Oil Diet on Pig's Cardiopulmonary Response to Bacteremia, *J. Parent. Ent. Nutr. 15*, 152–158.
135. Murray, M.J., Svinger, B.A., Yaksh, T.L., and Holman, R.T. (1993) Effects of Endotoxin on Pigs Prefed Omega-3 Vs. Omega-6 Fatty Acids-Enriched Diets, *Am. J. Physiol. 265*, E920–E927.
136. Murray, M.J., Kumar, M., Gregory, T.J., Banks, P.L., Tazelaar, H.D., and DeMichele, S.J. (1995) Select Dietary Fatty Acids Attenuate Cardiopulmonary Dysfunction During Acute Lung Injury in Pigs, *Am. J. Physiol. 269*, H2090–H2097.
137. Calder, P.C., Yaqoob, P., Thies, F., Wallace, F.A., and Miles, E.A. (2002) Fatty Acids and Lymphocyte Functions, *Br. J. Nutr. 87*, S31–S48.
138. Halvorsen, D.A., Hansen, J-B., Grimsgaard, S., Bonna, K.H., Kierulf, P., and Nordoy, A. (1997) The Effect of Highly Purified Eicosapentaenoic and Docosahexaenoic Acids on Monocyte Phagocytosis in Man, *Lipids 32*, 935–942.
139. Thies, F., Miles, E.A., Nebe-von-Caron, G., Powell, J.R., Hurst, T.L., Newsholme, E.A., and Calder, P.C. (2001) Influence of Dietary Supplementation with Long-Chain N-3 or N-6 Polyunsaturated Fatty Acids on Blood Inflammatory Cell Populations and Functions and on Plasma Soluble Adhesion Molecules in Healthy Adults, *Lipids 36*, 1183–1193.
140. Kew, S., Banerjee, T., Minihane, A.M., Finnegan, Y.E., Muggli, R., Albers, R., Williams, C.M., and Calder, P.C. (2003) Lack of Effect of Foods Enriched with Plant- or Marine-Derived N-3 Fatty Acids on Human Immune Function, *Am. J. Clin. Nutr. 77*, 1287–1295.
141. Miles, E.A., Banerjee, T., Dooper, M.W.B.W., M'Rabet, L., Graus, Y.M.F., and Calder, P.C. (2004) The Influence of Different Combinations of γ-Linolenic Acid, Stearidonic Acid and EPA on Immune Function in Healthy Young Male Subjects, *Brit. J. Nutr. 91*, 893–903.
142. Hughes, D.A., Pinder, A.C., Piper, Z., Johnson, I.T., and Lund, E.K. (1996) Fish Oil Supplementation Inhibits the Expression of Major Histocompatibility Complex Class II Molecules and Adhesion Molecules on Human Monocytes, *Am. J. Clin. Nutr. 63*, 267–272.
143. Meydani, M., Natiello, F., Goldin, B., Free, N., Woods, M., Schaefer, E., Blumberg, J.B., and Gorbach, S.L. (1991) Effect of Long-Term Fish Oil Supplementation on Vitamin E Status and Lipid Peroxidation in Women, *J. Nutr. 121*, 484–491.
144. Molvig, J., Pociot, F., Worsaae, H., Wogensen, L.D., Baek, L., Christensen, P., Mandruppoulsen, T., Andersen, K., Madsen, P., Dyerberg, J., and Nerup, J. (1991) Dietary Supplementation with Omega 3 Polyunsaturated Fatty Acids Decreases Mononuclear Cell Proliferation and Interleukin 1 Beta Content but Not Monokine Secretion in Healthy and Insulin Dependent Diabetic Individuals, *Scand. J. Immunol. 34*, 399–410.
145. Thies, F., Nebe-von-Caron, G., Powell, J.R., Yaqoob, P., Newsholme, E.A., and Calder, P.C. (2001) Dietary Supplementation with γ-Linolenic Acid or Fish Oil Decreases T Lymphocyte Proliferation in Healthy Older Humans, *J. Nutr. 131*, 1918–1927.
146. Pscheidl, E., Schywalsky, M., Tschaikowsky, K., and Boke-Prols, T. (2000) Fish Oil-Supplemented Parenteral Diets Normalize Splanchnic Blood Flow and Improve Killing of Translocated Bacteria in a Low-Dose Endotoxin Rat Model, *Crit. Care Med. 28*, 1489–1496.
147. Barton, R.G., Wells, C.L., Carlson, A., Singh, R., Sullivan, J.J., and Cerra, F.B. (1991) Dietary Omega-3 Fatty Acids Decrease Mortality and Kupffer Cell Prostaglandin E2 Production in a Rat Model of Chronic Sepsis, *J. Trauma 31*, 768–774.
148. Rayon, J.I., Carver, J.D., Wyble, L.E., Wiener, D., Dickey, S.S., Benford, V.J., Chen, L.T., and Lim, D.V. (1997) The Fatty Acid Composition of Maternal Diet Affects Lung Prostaglandin E2 Levels and Survival from Group B Streptococcal Sepsis in Neonatal Rat Pups, *J. Nutr. 127*, 1989–1992.
149. Lanza-Jacoby, S., Flynn, J.T., and Miller, S. (2001) Parenteral Supplementation with a Fish Oil Emulsion Prolongs Survival and Improves Lymphocyte Function During Sepsis, *Nutrition 17*, 112–116.

150. Johnson, J.A., Griswold, J.A., Muakkassa, F.F., Meyer, A.A., Maier, R.V., Chaudry, I.H., and Cerra, F. (1993) Essential Fatty Acids Influence Survival in Stress, *J. Trauma 35*, 128–131.
151. Blok, W.L., Vogels, M.T.E., Curfs, J.H.A.J., Eling, W.M.C., Buurmann, W.A., and van der Meer, J.M.W. (1992) Dietary Fish Oil Supplementation in Experimental Gram Negative Infection and in cerebral malaria in Mice, *J. Infect. Dis. 165*, 898–903.
152. Chang, H.R., Dulloo, A.G., Vladoianu, I.R., Piguet, P.F., Arsenijevic, D., Girardier, L., and Pechere, J.C. (1992) Fish Oil Decreases Natural Rresistance of Mice to Infection with *Salmonella typhimurium*, *Metabolism 41*, 1–2.
153. Fritsche, K.L., Shahbazian, L.M., Feng, C., and Berg, J.N. (1997) Dietaey Fish Oil Reduces Survival and Impairs Bacterial Clearance in C3H/Hen Mice Challenged with *Listeria monocytogenes*, *Clin. Sci. 92*, 95–101.
154. Mayatepek, E., Paul, K., Leichsenring, M., Pfisterer, M., Wagener, D., Domann, M., Sonntag, H.G., and Brener, H.J. (1994) Influence of Dietary (n-3) Polyunsaturated Fatty Acids on Leukotriene B4 and Prostaglandin E2 Synthesis and the Time Course of Experimental Tuberculosis in Guinea Pigs, *Infection 22*, 106–112.
155. D'Ambola, J.B., Aeberhard, E.E., Trang, N., Gaffar, S., Barrett, C.T., and Sherman, M.P. (1991) Effect of Dietary (n-3) and (n-6) Fatty Acids on *in vivo* Pulmonary Bacterial clearance by Neonatal Rabbits, *J. Nutr. 121*, 1262–1269.
156. Kronberg, D., Hansen, B., and Aaby, P. (1992) Analysis of the Incubation Period for Measles in the Epidemic in Greenland in 1951 Using a Variance Components Model, *Stat. Med. 11*, 579–590.
157. Heyland, D.K., MacDonald, S., Keefe, L., and Drover, J.W. (1998) Total Parenteral Nutrition in the Critically Ill Patient: A Meta-Analysis, *JAMA 280*, 2013–2019.
158. Calder, P.C., Sherrington, E.J., Askanazi, J., and Newsholme, E.A. (1994) Inhibition of Lymphocyte Proliferation *in vitro* by Two Lipid Emulsions with Different Fatty Acid Compositions, *Clin. Nutr. 13*, 69–74.
159. Battistella, F.D., Widergren, J.T., Anderson, J.T., Siepler, J.K., Weber, J.C., and MacColl, K. (1997) A Prospective, Randomized Trial of Intravenous Fat Emulsion Administration in Trauma Victims Requiring Total Parenteral Nutrition, *J. Trauma 43*, 52–58.
160. Furukawa, K., Yamamori, H., Takagi, K., Hayashi, N., Suzuki, R., Nakajima, N., and Tashiro, T. (2002) Influences of Soybean Oil Emulsion on Stress Response and Cell-Mediated Immune Function in Moderately or Severely Stressed Patients, *Nutrition 18*, 235–240.
161. Gogos, C.A., Kalfarentzos, F.E., and Zoumbos, N.C. (1990) Effect of Different Types of Total Parenteral Nutrition on T-Lymphocyte Subpopulations and NK Cells, *Am. J. Clin. Nutr. 51*, 119–122.
162. Sedman, P.C., Somers, S.S., Ramsden, C.W., Brennan, T.G., and Guillou, P.J. (1991) Effects of Different Lipid Emulsions on Lymphocyte Function During Total Parenteral Nutrition, *Br. J. Surg. 78*, 1396–1399.
163. Lenssen, P., Bruemmer, B.A., Bowden, R.A., Gooley, T., Aker, S.N., and Mattson, D. (1998) Intravenous Lipid Dose and Incidence of Bacteremia and Fungemia in Patients Undergoing Bone Marrow Transplantation, *Am. J. Clin. Nutr. 67*, 927–933.
164. Morlion, B.J., Torwesten, E., Lessire, A., Sturm, G., Peskar, B.M., Furst, P., and Puchstein, C. (1996) The Effect of Parenteral Fish Oil on Leukocyte Membrane Fatty Acid Composition and Leukotriene-Synthesizing Capacity in Postoperative Trauma, *Metabolism 45*, 1208–1213.
165. Koller, M., Senkal, M., Kemen, M., Konig, W., Zumtobel, V., and Muhr, G. (2003) Impact of Omega-3 Fatty Acid Enriched TPN on Leukotriene Synthesis by Leukocytes After Major Surgery, *Clin. Nutr. 22*, 59–64.
166. Wachtler, P., Konig, W., Senkal, M., Kemen, M., and Koller, M. (1997) Influence of a Total Parenteral Nutrition Enriched with ω-3 Fatty Acids on Leukotriene Synthesis of Peripheral Leukocytes and Systemic Cytokine Levels in Patients with Major Surgery, *J. Trauma 42*, 191–198.
167. Weiss, G., Meyer, F., Matthies, B., Pross, M., Koenig, W., and Lippert, H. (2002) Immunomodulation by Perioperative Administration of n-3 Fatty Acids, *Br. J. Nutr. 87*, S89–S94.
168. Schauder, P., Rohn, U., Schafer, G., Korff, G., and Schenk, H.-D. (2002) Impact of Fish Oil Enriched Total Parenteral Nutrition on DNA Synthesis, Cytokine Release and Receptor Expression by Lymphocytes in the Postoperative Period, *Br. J. Nutr. 87*, S103–S110.
169. Tsekos, E., Reuter, C., Stehle, P., and Boeden, G. (2004) Perioperative Administration of Parenteral Fish Oil Supplements in a Routine Clinical Setting Improves Patient Outcome After Major Abdominal Surgery, *Clin. Nutr. 23*, 325–330.
170. Daly, J.M., Weintraub, F.N., Shou, J., Rosato, E.F., and Lucia, M. (1995) Enteral Nutrition During Multimodality Therapy in Upper Gastrointestinal Cancer Patients, *Ann. Surg. 221*, 327–338.
171. Schilling, J., Vranjes, N., Fierz, W., Joller, H., Gyurech, D., Ludwig, E., Marathias, K., and Geroulanos, S. (1996) Clinical Outcome and Immunology of Postoperative Arginine, ω-3 Fatty Acids, and Nucleotide-Enriched Enteral Feeding: A Randomized Prospective Comparison with Standard Enteral and Low Calories/Low Fat IV Solutions, *Nutrition 12*, 423–429.
172. Braga, M., Vignali, A., Gianotti, L., Cestari, A., Profili, M., and Di Carlo, V. (1996) Immune and Nutritional Effects of Early Enteral Nutrition After Major Abdominal Operations, *Eur. J. Surg. 162*, 105–112.
173. Daly, J.M., Lieberman, M.D., Goldfine, J., Shou, J., Weintraub, F., Rosato, E.F., and Lavin, P. (1992) Enteral Nutrition with Supplemental Arginine, RNA, and Omega-3 Fatty Acids in Patients after Operation: Immunologic, Metabolic, and Clinical Outcome, *Surgery 112*, 56–67.
174. Gianotti, L., Braga, M., Fortis, C., Soldini, L., Vignali, A., Colombo, S., Radaelli, G., and Di Carlo, V. (1999) A Prospective, Randomised Clinical Trial on Perioperative Feeding with an Arginine-, Omega-3 Fatty Acid-, and RNA-Enriched Enteral Diet: Effect on Host Response and Nutritional Status, *J. Parent. Ent. Nutr. 23*, 314–320.
175. Braga, M., Gianotti, L., Radaelli, G., Vignali, A., Mari, G., Gentilini, O., and Di Carlo, V. (1999) Perioperative Immunonutrition in Patients Undergoing Cancer Surgery, *Arch. Surg. 134*, 428–433.
176. Heys, S.D., Walker, L.G., Smith, I., and Eremin, O. (1999) Enteral Nutritional Supplementation with Key Nutrients in Patients with Critical Illness and Cancer—A Meta-Analysis of Randomized Controlled Clinical Trials, *Ann. Surg. 229*, 467–477.
177. Beale, R.J., Bryg, D.J., and Bihari, D.J. (1999) Immunonutrition in the Critically Ill: A Systematic Review of Clinical Outcome, *Crit. Care Med. 27*, 2799–2805.
178. Heyland, D.K., Novak, F., Drover, J.W., Jain, A., Su, X.Y., and Suchner, U. (2001) Should Immunonutrition Become Routine in Critically Ill Patients? A Systematic Review of the Evidence, *JAMA 286*, 944–953.
179. Cerra, F.B., Lehman, S., Konstantinides, N., Konstantinides, F., Shronts, E.P., and Holman, R. (1990) Effect of Enteral Nutrition on *in vitro* Tests of Immune Function in ICU Patients: A Preliminary Report, *Nutrition 6*, 84–87.
180. Weimann, A., Bastian, L., Bischoff, W.E., Grotz, M., Hansel, M., Lotz, J., Trautwein, C., Tusch, G., Schlitt, H.J., and Regel, G. (1998) Influence of Arginine, Omega-3 Fatty Acids and Nucleotide-Supplemented Enteral Support on Systemic Inflammatory Response Syndrome and Multiple Organ Failure in Patients After Severe Trauma, *Nutrition 14*, 165–172.

181. Gadek, J.E., DeMichele, S.J., Karlstad, M.D., Pacht, E.R., Donahoe, M., Albertson, T.E., Van Hoozen, C., Wennberg, A.K., Nelson, J., Noursalehi, M., and the Enteral Nutrition in ARDS Study Group (1999) Effect of Enteral Feeding with Eicosapentaenoic Acid, γ-Linolenic Acid, and Antioxidants in Patients with Acute Respiratory Distress Syndrome, *Crit. Care Med. 27*, 1409–1420.
182. Pacht, E.R., DeMichele, S.J., Nelson, J.L., Hart, J., Wennberg, A.K., and Gadek, J.E. (2003) Enteral Nutrition with Eicosapentaenoic Acid, Gamma-Linolenic Acid, and Antioxidants Reduces Alveolar Inflammatory Mediators and Protein Influx in Patients with Acute Respiratory Distress Syndrome, *Crit. Care Med. 31*, 491–500.
183. Mayer, K., Fegbeutel, C., Hattar, K., Sibelius, U., Kramer, H.J., Heuer, K.U., Temmesfeld-Wollbruck, B., Gokorsch, S., Grimminger, F., and Seeger, W. (2003) ω-3 vs, ω-6 Lipid Emulsions Exert Differential Influence on Neutrophils in Septic Shock Patients: Impact on Plasma Fatty Acids and Lipid Mediator Generation, *Intensive Care Med. 29*, 1472–1481.
184. Mayer, K., Gokorsch, S., Fegbeutel, C., Hattar, K., Rosseau, S., Walmrath, D., Seeger, W., and Grimminger, F. (2003) Parenteral Nutrition with Fish Oil Modulates Cytokine Response in Patients with Sepsis, *Am. J. Respir. Crit. Care Med. 167*, 1321–1328.

[Received July 30, 2004, accepted November 26, 2004]

Effects of Dietary n-3 Polyunsaturated Fatty Acids on T-Cell Membrane Composition and Function

Kirsten C. Switzer[a], David N. McMurray[a,b,c], and Robert S. Chapkin[a,b,*]

[a]Molecular and Cell Biology Section, Faculty of Nutrition, [b]Center for Environmental and Rural Health, Texas A&M University, and [c]Department of Microbiology and Immunology, Texas A&M University Health Science Center, College Station, Texas

ABSTRACT: Dietary n-3 PUFA have been shown to attenuate T-cell-mediated inflammation, in part, by suppressing T-cell activation and proliferation. n-3 PUFA have also been shown to promote apoptosis, another important mechanism for the prevention of chronic inflammation by maintaining T-cell homeostasis through the contraction of populations of activated T cells. Recent studies have specifically examined Fas death receptor-mediated activation-induced cell death (AICD), since it is the form of apoptosis associated with peripheral T-cell deletion involved in immunological tolerance and T-cell homeostasis. Data from our laboratory indicate that n-3 PUFA promote AICD in T helper 1 polarized cells, which are the mediators of chronic inflammation. Since Fas and components of the death-inducing signaling complex are recruited to plasma membrane microdomains (rafts), the effect of dietary n-3 PUFA on raft composition and resident protein localization has been the focus of recent investigations. Indeed, there is now compelling evidence that dietary n-3 PUFA are capable of modifying the composition of T-cell membrane microdomains (rafts). Because the lipids found in membrane microdomains actively participate in signal transduction pathways, these results support the hypothesis that dietary n-3 PUFA influence signaling complexes and modulate T-cell cytokinetics *in vivo* by altering T-cell raft composition.

Paper no. L9553 in *Lipids 39,* 1163–1170 (December 2004).

Among dietary factors, there is strong evidence for a protective effect of n-3 PUFA found in fish oil (FO) on autoimmune and inflammatory diseases (1,2). In contrast, n-6 PUFA can be deleterious with respect to the incidence and severity of such diseases (1–3). This is significant because the typical Western diet contains 10–20 times more n-6 than n-3 PUFA (4).

Inflammatory and autoimmune diseases are characterized by an overactive immune response, resulting from excessive immune cell accumulation. The suppressive effects of n-3 PUFA on the accumulation of inflammatory T-cells may result from either reduced proliferation or enhanced apoptosis of activated T cells, or both. T cells, particularly $CD4^+$ T cells, are involved in the induction of inflammation, orchestrating a cell-mediated immune response by stimulating monocytes and macrophages to secrete inflammatory cytokines such as interleukin (IL)-1, IL-6, and tumor necrosis factor (TNF)α (5). $CD4^+$ T cells also stimulate B cells to produce immunoglobulins. Activated $CD4^+$ T cells are functionally heterogeneous, differentiating into T helper (Th) 1 or Th2 cells, as defined by their different cytokine profiles. Th1 cells, characterized by the production of IL-2, interferon γ, and TNFβ, are required to mount a cell-mediated immunity against intracellular pathogens. Th2 cells are characterized by the production of IL-4, IL-5, and IL-10 and are important in humoral immunity and as a defense against extracellular pathogens (6). In addition to their protective roles in host defense, both subsets have been implicated in pathological responses. Th1 cells are proinflammatory and can mediate autoimmune and inflammatory diseases, whereas Th2 cells have been implicated in the pathogenesis of asthma and allergy (7). The two helper subsets cross-regulate each other to maintain a balanced heterogeneous response using cytokines; Th1 cells inhibit Th2 responses with interferon γ, and Th2 cells inhibit Th1 responses with IL-10 (8).

EFFECT OF n-3 PUFA ON T-CELL PROLIFERATION

Activation of naive T cells leads to proliferation and differentiation into effector cells, a process known as clonal expansion. Several studies in humans, rodents, and cell-culture systems have examined the effect of n-3 PUFA on lymphoproliferation. Three clinical studies in which subjects were fed diets containing 2.4–18 g/d of EPA and DHA reported significant reductions in mitogen-induced proliferation and IL-2 production in peripheral blood mononuclear cells (PBMC) (9–11). Another human study found similar reductions in proliferation and IL-2 secretion when 180 g/d of fish was fed rather than FO (12). Additionally, Grimble *et al.* (13) found that a diet containing 6 g/d of FO was able to decrease TNFα production. Similar immunosuppressive effects were reported in other studies (14–16).

Complementary studies have been conducted in rodents. Jolly *et al.* (17,18) fed mice diets containing 10 g/kg EPA or DHA for 10 d and reported a significant decrease in concanavalin A-stimulated splenocyte proliferation in both diet groups. This was accompanied by a decrease in IL-2 and IL-2

*To whom correspondence should be addressed at 442 Kleberg Center, 2471 TAMU, Texas A&M University, College Station, TX 77843-2471.
E-mail: r-chapkin@tamu.edu

Abbreviations: AA, arachidonic acid; AICD, activation-induced cell death; DD, death domain; DED, death-effector domain; DISC, death-inducing signaling complex; FADD, Fas-associated DD protein; FO, fish oil; IL, interleukin; IL-2Rα, IL-2 receptor α; MS, homologous mouse serum; NK, natural killer; PBMC, peripheral blood mononuclear cells; PKC, protein kinase c; PL, phospholipid; PMA, phorbol-12-myristate-13-acetate; PPAR, peroxisome proliferator-activated receptor; TCR, T-cell receptor; Th, T helper cell; TNF, tumor necrosis factor; TNFR, TNF receptor.

receptor α (IL-2Rα) expression, and reductions in DAG and ceramide, lipid second messengers. Feeding rats a diet containing 20% (wt/wt) FO for 10 wk, a much higher level of fat and longer feeding duration, also suppressed splenocyte proliferation (19). More recently, Arrington *et al.* (20) reported decreased splenocyte IL-2 secretion from the T-cells of mice fed diets containing 1% DHA by weight only when cultures were stimulated with antibodies against CD3 and CD28 (αCD3/αCD28). Thus, in certain experimental systems, dietary n-3 PUFA appear to alter T-cell receptor (TCR)-dependent or costimulatory (CD28) signal transduction. Using the same set of stimuli, Sasaki *et al.* (21) showed a decrease in $CD4^+$ and $CD8^+$ and an increase in CD28 surface expression (0.73 ± 0.11 vs. 0.33 ± 0.12 for a palm oil control diet [values given as fluorescence intensity]) in DHA-fed mouse splenocytes. In a further attempt to elucidate a mechanism of action, Arrington *et al.* (22) isolated $CD4^+$ and $CD8^+$ T-cell populations from mice following a 14-d diet of 2% (wt/wt) FO. They found that an effect on proliferation was dependent on the stimulus used in culture. FO suppressed $CD8^+$ T-cell proliferation in cells stimulated with αCD3/αCD28. In contrast, FO increased $CD4^+$ T-cell proliferation when cells were stimulated with αCD3 plus phorbol-12-myristate-13-acetate (PMA), an agonist that stimulates protein kinase C (PKC). Interestingly, this stimulation combination directs cells toward a Th2-like phenotype (22,23). Another study reported a decrease in reduction in phospholipase Cγ tyrosine phosphorylation in mitogen-stimulated rat splenocytes fed 20% (wt/wt) FO (24).

In cell-culture experiments, mouse splenocytes and human PBMC cultured in DHA or EPA exhibited reduced levels of proliferation, IL-2, and IL-2Rα expression following mitogen stimulation (25–27). In more mechanistic studies, Denys *et al.* (28) noted a decrease in PMA-stimulated PKC activation and ERK1/ERK2 signaling in Jurkat T-cells that were cultured in the presence of up to 60 μM EPA and DHA. Diaz *et al.* (29) showed that mitogen-stimulated human PBMC had increased phospholipase D activity, a regulator of T-cell proliferation and apoptosis, following culture in 5–15 μM DHA. Taken together, there is substantial evidence from several different experiments for the antiproliferative properties of n-3 PUFA.

EFFECT OF n-3 PUFA ON T-CELL APOPTOSIS

Apoptosis is an important mechanism for regulating immune responses by means of shaping the lymphocyte repertoire through selection of maturing thymocytes and maintaining homeostasis in the mature lymphocyte pool after antigenic expansion. There are at least two major pathways of apoptosis: (i) passive cell death, resulting from the absence of growth factors and other survival stimuli, and (ii) activation-induced cell death (AICD), induced by chronic antigen stimulation (30). Passive cell death is important in the elimination of cells that fail to undergo positive selection in the thymus (31). AICD plays an essential role in peripheral deletion involved in tolerance and homeostasis and is important in negative selection in the thymus (31–33). The biochemical mechanisms of passive cell death and AICD are distinct. However, both are mediated by the action of caspases, cysteine proteases with specificity for aspartate residues. Caspases exist as inactive zymogens (proenzymes) in the cytoplasm until activated by proteolytic cleavage. They are organized in cascades that amplify the initial death signal (34).

Passive cell death results from activation of the intrinsic mitochondrial death-mediated pathway. When cells are deprived of survival stimuli, there is an increase in mitochondrial permeability and breakdown of mitochondrial membrane potential. As a consequence, cytochrome c is released into the cytoplasm and binds to Apaf-1. Pro-caspase 9 associates with this complex, leading to its proteolytic activation. Active caspase 9 subsequently activates downstream caspases including caspase 3, leading to cell death (30,35). Mitochondrial membrane permeability is highly regulated by members of the Bcl-2 family. Anti-apoptotic members of the Bcl-2 family, including Bcl-2 and Bcl-x_L, prevent membrane permeability and the release of cytochrome c. Pro-apoptotic members, including Bax, Bak, Bid, and Bad, enhance membrane permeability, in part resulting in cytochrome c release (36).

In the immune system, AICD acts as a feedback mechanism for terminating an ongoing immune response and serves to maintain peripheral tolerance. T-cells responding to an antigenic stimulus first expand in number and then decrease as a result of AICD. Repeated antigen stimulation leads to the expression of death receptors that link extracellular signals to apoptosis. Death receptors belong to the TNF receptor (TNFR) superfamily and include Fas, TNFR1, and TRAIL-R (37). They are characterized by multiple cysteine-rich repeats in their extracellular domain and a protein–protein interaction death domain (DD) in their cytoplasmic tail (38). Fas (CD95, apo-1) is the best-studied receptor and is the principal mediator of $CD4^+$ T-cell AICD (30). Fas-mediated apoptosis is initiated by its interaction with FasL (CD95L), which is a TNF-related type II transmembrane molecule (38). Unlike Fas, which is expressed in a wide variety of tissues including thymus, spleen, lymph node, kidney, liver, and heart (39), FasL is expressed primarily in activated T cells and natural killer (NK) cells (38,40). Interestingly, although IL-2 plays a critical role in cell growth, it also sensitizes the same cells to apoptosis. When high levels of IL-2 are present, this cytokine promotes FasL expression (41). Fas trimerization, necessary for apoptosis transduction, is triggered by FasL binding and immediately recruits a complex of associated proteins known as the death-inducing signaling complex (DISC). The adaptor molecule, Fas-associated DD protein (FADD), binds to Fas *via* its DD. In addition, FADD also has a death-effector domain (DED) with which it recruits the DED-containing procaspase 8 into the DISC (38). Pro-caspase 8 is then cleaved, and active caspase 8 dissociates from the DISC to cleave procaspase 3, initiating the caspase cascade that results in cell death. The importance of Fas/FasL in AICD is illustrated by the development of lymphoproliferative disorders in *lpr/lpr* and *gld/gld* mice due to mutations in the genes encoding Fas and FasL, respectively (30).

T cells are not equally sensitive to AICD (42). In addition to their differential cytokine production and functions, Th1 and Th2 cells have different susceptibilities to AICD, with Th1 cells reported to be AICD sensitive and Th2 cells reported to be AICD resistant (42,43). The selective death of Th1 cells has been attributed to a preferential requirement for phorbol ester-sensitive PKC isoforms (44) and the upregulation of Fas (44) and FasL (44,45). In contrast, the resistance of Th2 cells to AICD has been linked to expression of c-FLIP, an enzymatically inert homolog of caspase 8 (46), and phosphatidylinositol-3′-kinase (PI-3K) activity (47).

With respect to the effect of dietary n-3 PUFA on apoptosis, there are relatively few data on lymphocyte apoptosis. The few studies that have addressed this issue have examined mixed cell populations, that is, whole splenocytes (48,49). Avula and Fernandes (50) showed that feeding young (4 mon) and old (9 mon) mice 5% (wt/wt) FO resulted in increased splenocyte apoptosis in both age groups. Fernandes *et al.* (48) reported an increase in mouse splenocyte apoptosis following a 10% (wt/wt) FO diet, and this was associated with an increase in the surface expression of Fas, a death receptor and mediator of apoptosis. In a similar study, FasL was upregulated and Bcl-2 was decreased in mouse splenocytes after consumption of a 4% (wt/wt) FO diet (49). Additionally, Jurkat T cells cultured in 0–90 μM DHA for up to 48 h produced higher levels of activated caspase 3 (51). Avula *et al.* (49) examined $CD4^+$ and $CD8^+$ T-cell subset apoptosis; however, this effect was quantified in the subset populations after stimulation of the mixture using flow cytometry, rather than in cultures of purified T-cell subsets.

These observations provided the rationale to investigate the effect of n-3 PUFA on the $CD4^+$ Th1 cell subset, since this class of polarized cells actively mediates chronic inflammation. Consistent with this rationale, we specifically examined the AICD apoptotic pathway, as it is the form of apoptosis associated with the deletion of cells involved in chronic inflammation and autoimmune disease. Our initial investigation of the effect of dietary n-3 PUFA on T-cell apoptosis showed that n-3 PUFA enhanced T-cell apoptosis following *in vitro* incubation with selective stimuli (52). Purified splenic T cells from diet-fed mice were stimulated with either αCD3/αCD28, αCD3/PMA, or PMA/Ionomycin for 24 h. T cells from 2% FO (wt/wt)-fed mice had a significantly increased percentage of apoptotic cells relative to both safflower oil (n-6 PUFA) and olive oil (n-9 monounsaturated FA) control diets only in PMA/Ionomycin-stimulated T cells. Cytokine analyses of cell culture supernatants revealed that αCD3/PMA-stimulated T cells secreted significantly more IL-4 and IL-10, Th2 cytokines. In comparison, PMA/Ionomycin-stimulated T cells secreted significantly more IL-2, and much less IL-4, indicative of a Th1 phenotype. Thus, in agreement with previous studies (22), αCD3/PMA drove T cells toward a Th2-biased cytokine profile, whereas PMA/Ionomycin drove T cells toward a Th1-biased cytokine profile. Experiments designed to examine T-cell AICD generated similar results. n-3 PUFA significantly increased AICD only following PMA/Ionomycin stimulation, that is, in Th1-biased cells (52). Furthermore, a comparison of dietary n-3 PUFA dose (4% FO vs. 9% FO) demonstrated that there was no difference in AICD. Thus, T-cell AICD can occur just as efficiently at low n-3 PUFA intake. In an attempt to determine whether the pro-apoptotic effects of dietary FO were specifically mediated by DHA, we fed mice diets composed of 1% DHA (wt/wt) ethyl esters. To our surprise, DHA did not enhance apoptosis (Fig. 1), suggesting that DHA, by itself, may not be the active molecule in FO with respect to AICD. Similarly, Thies *et al.* (53) observed that human NK cell activity was decreased only after 12 wk of consumption of 4 g/d FO, but not DHA. Additionally, 75 μM EPA was shown to suppress human PBMC proliferation by inhibiting IL-2Rα expression and IL-2 production and to promote the cell death of activated T cells (26).

Based on our results that n-3 PUFA enhanced AICD in T cells induced to secrete a Th1-biased cytokine profile, we hypothesized that n-3 PUFA would also promote AICD in $CD4^+$ T cells driven to differentiate more completely *in vitro* toward a Th1 cytokine pole using standard polarization methodology. Due to the extended time in culture necessary to achieve polarization, a set of cells from each diet group was cultured in diet-matched homologous mouse serum (MS), rather than FBS. This approach prevented culture-induced loss of n-3 PUFA from membrane phospholipids (PL) (19,54). Following flow cytometric verification that the cells were appropriately polarized toward a Th1 phenotype, it was demonstrated that dietary corn oil suppressed Th1 polarization relative to FO and that this effect occurred only in cells cultured in the presence of homologous MS (54). AICD was enhanced significantly in $CD4^+$ T cells from FO-fed mice cultured in the presence of homologous MS. Therefore, the diet and culture conditions that promoted the greatest number of Th1 cells also enhanced AICD to the greatest extent. Since Th1 cells are susceptible to AICD (42,43), our data suggest that dietary

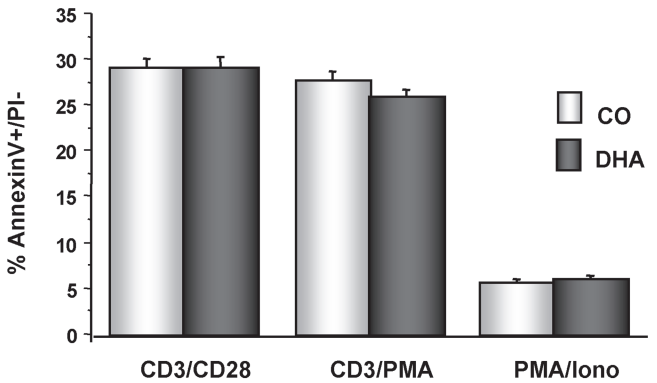

FIG. 1. DHA does not affect T-cell AICD. Splenic T cells from corn oil (5%, wt/wt) and DHA ethyl ester (1%, wt/wt)-fed mice were initially activated as follows: αCD3/αCD28, PMA/αCD3, or PMA/Ionomycin for 48 h. Following an overnight rest period in RPMI-complete medium, T cells were reactivated with the initial stimuli for 5 h. Apoptosis was analyzed with Annexin V/PI. Data represent the mean ± SEM, $n = 6$ per diet group. AICD, activation-induced cell death; PMA, phorbol-12-myristate-13-acetate; RPMI, media only control.

n-3 PUFA may indirectly enhance AICD *via* promotion of a Th1 phenotype.

ROLE OF LIPID RAFTS IN REGULATING T-CELL FUNCTION: MODULATION BY DIET

The plasma membrane is an asymmetrical lipid bilayer composed of PL, cholesterol, sphingolipids, and integral proteins. In 1972, Singer and Nicolson (55) proposed the fluid-mosaic model, which described the fluid nature of the membrane bilayer. The fluidity of the membrane affects the organization and dynamics of both lipids and proteins within the membrane, and thus its biological function. Fluidity of the membrane depends, in part, on its composition. The length and saturation of the fatty acyl chain of PL influences the ability of the PL molecules to pack against one another (56). A shorter chain length reduces the tendency of the acyl chains to interact with one another, and *cis*-double bonds create kinks in the chains that prevent them from packing together. The presence of cholesterol and sphingolipids promotes rigidity (57). Saturation is more prevalent in sphingolipid acyl chains, and the sterol structure of cholesterol causes the fatty acyl chains to become closely packed. It is also known that cholesterol preferentially interacts with sphingolipids (58) and, together with glycosylphosphatidylinositol-anchored proteins, they form liquid-ordered microdomains that float in the liquid-disordered bulk membranes (59). These "rafts" are resistant to solubilization by nonionic detergents, facilitating isolation for study (60).

Lipid rafts have been implicated in an ever-increasing number of biologically important phenomena such as signaling. Rafts play an important role in cell signaling, particularly through the organization and distribution of surface receptors, including Fas, at specific sites in the plasma membrane (61,62). Recent studies have shown that the formation of macromolecular complexes containing the T-cell receptor, CD4, and CD45 is believed to contribute to sustained TCR interaction with its ligand (63). Lipid rafts are important for the formation and stabilization of these TCR signaling complexes, acting as platforms that facilitate intramolecular associations and propagation of signal transduction cascades (63). Interestingly, conditions that modify raft structure can disrupt early steps in T-cell activation (64). Rafts appear to differ, depending on the developmental state of the T cell, and these differences probably contribute to markedly different outcomes of signaling (65). Effector and memory T cells have more surface rafts than naive T cells, and activated Th1 cells differ from activated Th2 cells in raft organization. Stimulation of Th1 cells results in a stable association of TCR components with raft domains, whereas Th2 stimulation fails to form these signaling complexes (65).

With respect to AICD, raft structures are required for efficient propagation of apoptotic signals. The death receptor and primary initiator of AICD, Fas, has been shown to require clustering and capping at the membrane to effectively signal to downstream apoptotic molecules (66). This clustering and capping occurs in rafts, a location that best facilitates the trapping of Fas, recruitment of additional intracellular molecules of the DISC, and exclusion of inhibitory pathways. Th1 and Th2 cells have different susceptibilities to AICD, possibly explained in part by their distinct lipid raft compositions (65).

Not surprisingly, changes in raft lipid and/or protein composition can alter cell function and phenotype. Fan *et al.* (67) have recently shown that dietary n-3 PUFA remodel the PL composition of murine T-cell rafts. They found that the sphingomyelin content of lipid rafts was significantly decreased in T cells from n-3 PUFA-fed mice. This novel observation is noteworthy because sphingolipids are required to facilitate raft formation and T-cell activation (57). In addition, it has been reported that Jurkat T cells cultured *in vitro* with n-3 PUFA undergo modification of lipid raft composition and suppression of signal transduction (68,69). Fan *et al.* (70) have recently shown that $CD3^+$ T cells from 4% FO (wt/wt)-fed mice had decreased PKCθ colocalization with lipid rafts after αCD3/αCD28 stimulation. PKCθ is an important molecule in the regulation of T-cell proliferation and apoptosis and requires translocation to lipid rafts to be active (71). Therefore, our data are noteworthy, because this is one of the first studies to examine the effect of diet on raft modification and its relationship to T-cell activation (Fig. 2).

The loss of phenotype observed in Th1 AICD responses when cells are cultured in FBS, rather than homologous MS, led us to hypothesize that homologous MS would maintain diet-induced changes in membrane microdomain FA composition during culture *in vitro*. In addition, previous research has shown that the lipid content of serum added to tissue culture medium has a significant effect on cell FA composition (72,73). Therefore, we examined the effect of culture conditions on $CD4^+$ T-cell rafts. Analysis of the FA composition of raft PL showed that the inclusion of MS prevented the culture-induced rearrangement of T-cell lipids. Detailed examination of membrane microdomains revealed that the significant enhancement of EPA and DHA observed in the $CD4^+$ T cells from FO-fed mice, compared with corn oil-fed mice, immediately *ex vivo* was lost in cells cultured in FBS. Further analysis revealed that only in rafts isolated from $CD4^+$ T cells from FO-fed mice did the addition of homologous MS prevent the culture-induced loss of cholesterol (54). Since cholesterol is critical for raft integrity (57), these results indicate that culture conditions have a profound effect on lipid raft composition and structure. Additionally, these observations suggest that caution should be taken when culturing cells *ex vivo*.

ALTERNATIVE MECHANISMS BY WHICH N-3 PUFA MAY MODULATE T-CELL PROLIFERATION AND APOPTOSIS

n-3 PUFA may exert their anti-inflammatory effects through a variety of alternative mechanisms. One mechanism may be by alterating eicosanoid synthesis. Eicosanoids are signaling molecules that include prostaglandins, thromboxanes, leukotrienes, and hydroxy and hydroperoxy derivatives (HETE,

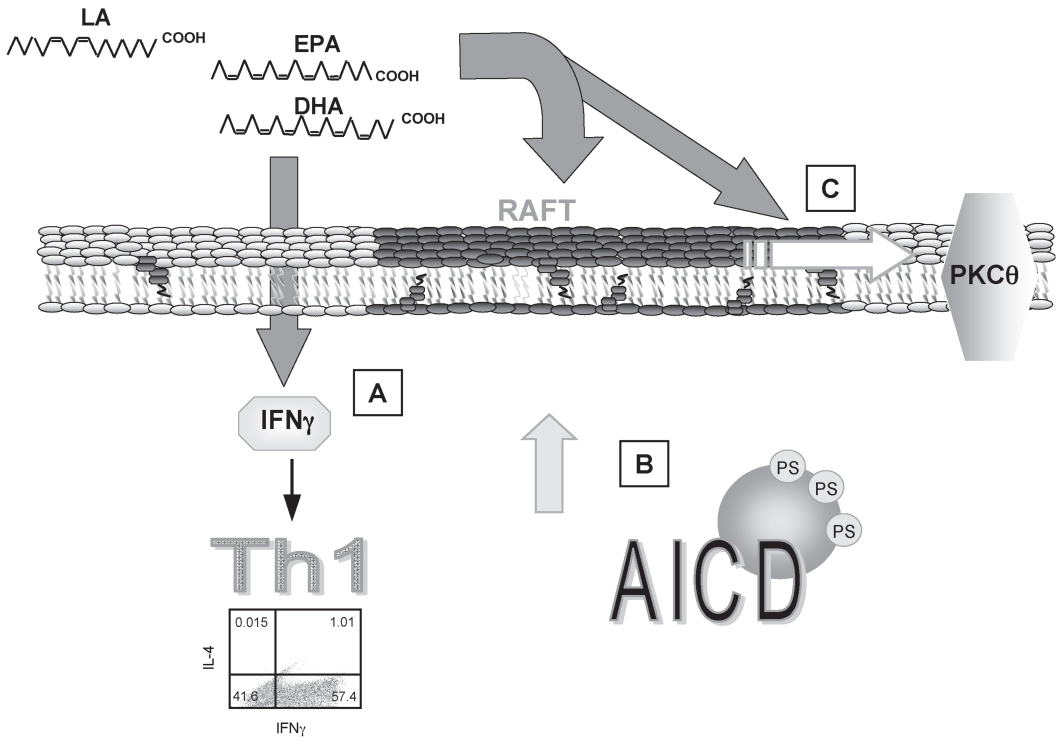

FIG. 2. Model depicting the effects of n-3 PUFA on T-cell lipid rafts and downstream signaling. Dietary n-3 PUFA alter lipid raft composition that may affect the following: the n-3 PUFA enhancement of Th1 cell polarization (A); the n-3 PUFA enhancement of Th1 cell AICD (B); the n-3 PUFA decrease in PKCθ colocalization with lipid rafts (C). Th1, T helper 1; PKC, protein kinase C. For other abbreviation see Figure 1.

HPETE). Nonesterified arachidonic acid (AA; 20:4n-6) released from membrane PL by phospholipases acts as a substrate for cyclooxygenases (COX-1, a constitutive enzyme, or COX-2, an inducible enzyme) and lipoxygenases. Cyclooxygenase products of AA give rise to prostaglandins and thromboxanes, which are mostly proinflammatory due to vascular permeability and vasodilation enhancement. Lipoxygenases give rise to leukotrienes, HETE, and HPETE, which are involved in vascular permeability and vasoconstriction (74). Compared to AA, EPA and DHA are substrates for cyclooxygenase and lipoxygenase, respectively; thus, the cell's ability to produce eicosanoids and resulting inflammatory responses is strongly influenced by the FA composition of membrane PL (74,75). Increasing dietary n-3 PUFA will decrease AA substrate availability for eicosanoid synthesis as shown by Endres *et al.* (76), who observed a decrease in prostaglandin E_2 production following n-3 PUFA feeding.

Another mechanism by which n-3 PUFA could alter T-cell proliferation and apoptosis might involve peroxisome proliferator-activated receptors (PPAR), specifically PPARγ. PPARγ has been shown to inhibit IL-4 production in $CD4^+$ T cells (77). However, PPARγ also reduces interferon γ and IL-2 in human T cells (78), indicating that PPARγ is not selective in T-cell subset repression. Additionally, PPARγ binds both n-3 and n-6 PUFA with equal affinity and lacks FA class specificity (79,80). Finally, we have already shown that our short-term feeding of n-3 PUFA does not induce PPARγ mRNA (52). Therefore, the effects of n-3 PUFA are likely not mediated by PPAR, at least not PPARγ. With regard to the propensity of PUFA to mediate metabolic oxidative stress, from an *in vivo* perspective, antioxidant cosupplementation in human subjects has been shown not to alter the suppressive effect of FO feeding on T-cell proliferation (81). Consistent with this observation, we have shown that there is no change in systemic oxidative stress following the ingestion of experimental diets containing n-3 PUFA in a murine model system (52). This is not surprising because the experimental diets utilized by our laboratory typically contain 120 IU vitamin E/kg to help protect against *in vivo* peroxidation. This exceeds the estimated minimal requirement of a 75 IU vitamin E/kg diet (82). With respect to *in vitro* cell culture conditions that can affect murine $CD4^+$ cell responses, Pompos and Fritsche (73) recently demonstrated that alterations in lipid peroxidation are not important with respect to n-3 PUFA-mediated suppression of T-cell proliferation. Collectively, these data suggest that the immunosuppressive effects of n-3 PUFA are not mediated by oxidative stress.

In conclusion, we have summarized several recent studies describing the anti-inflammatory properties of n-3 PUFA, especially EPA (20:5n-3) and DHA (22:6n-3). In general, consumption of diets rich in n-3 PUFA are associated with a reduced T-cell proliferative response and increased apoptotic response. Importantly, we found that dietary n-3 PUFA selectively modulate T-cell subset function. Additionally, we

showed that n-3 PUFA alterations of membrane microdomain (lipid raft) composition may be a key mechanism influencing these effects. Finally, we have shown that cell culture conditions (e.g., serum source) are critical to observe the biological impact of diet on cell function *in vitro*. Studies such as these will aid in the establishment of dietary guidelines designed to promote a balanced immune system, so that protective host responses (e.g., to infectious agents) can be maintained, while potentially detrimental host responses (e.g., chronic inflammation and hypersensitivity) can be controlled.

Future studies are needed to determine the precise cellular and molecular mechanisms by which dietary n-3 PUFA affect the proliferative and apoptotic functions of Th1 cells.

ACKNOWLEDGMENTS

This work was supported by NIH grants DK53055 and P30-ES09106, and USDA grant 2003-35200-13338.

REFERENCES

1. Calder, P.C. (1998) Dietary Fatty Acids and the Immune System, *Nutr. Rev. 56,* S70–S83.
2. Kremer, J.M. (2000) n-3 Fatty Acid Supplements in Rheumatoid Arthritis, *Am. J. Clin. Nutr. 71*, 349S–351S.
3. Wander, R.C., Hall, J.A., Gradin, J.L., Du, S.H., and Jewell, D.E. (1997) The Ratio of Dietary (n-6) to (n-3) Fatty Acids Influences Immune System Function, Eicosanoid Metabolism, Lipid Peroxidation and Vitamin E Status in Aged Dogs, *J. Nutr. 127*, 1198–1205.
4. Spector, A.A. (1999) Essentiality of Fatty Acids, *Lipids 34* (Suppl.), S1–S3.
5. Choy, E.H., and Panayi, G.S. (2001) Cytokine Pathways and Joint Inflammation in Rheumatoid Arthritis, *N. Engl. J. Med. 344*, 907–916.
6. Abbas, A.K., Murphy, K.M., and Sher, A. (1996) Functional Diversity of Helper T Lymphocytes, *Nature 383*, 787–793.
7. Murphy, K.M., and Reiner, S.L. (2002) The Lineage Decisions of Helper T Cells, *Nat. Rev. Immunol. 2*, 933–944.
8. Rengarajan, J., Szabo, S.J., and Glimcher, L.H. (2000) Transcriptional Regulation of Th1/Th2 Polarization, *Immunol. Today 21,* 479–483.
9. Endres, S., Meydani, S.N., Ghorbani, R., Schindler, R., and Dinarello, C.A. (1993) Dietary Supplementation with n-3 Fatty Acids Suppresses Interleukin-2 Production and Mononuclear Cell Proliferation, *J. Leukoc. Biol. 54,* 599–603.
10. Meydani, S.N., Endres, S., Woods, M.M., Goldin, B.R., Soo, C., Morrill-Labrode, A., Dinarello, C.A., and Gorbach, S.L. (1991) Oral (n-3) Fatty Acid Supplementation Suppresses Cytokine Production and Lymphocyte Proliferation: Comparison Between Young and Older Women, *J. Nutr. 121,* 547–555.
11. Thies, F., Nebe-von-Caron, G., Powell, J.R., Yaqoob, P., Newsholme, E.A., and Calder, P.C. (2001) Dietary Supplementation with γ-Linolenic Acid or Fish Oil Decreases T Lymphocyte Proliferation in Healthy Older Humans, *J. Nutr. 131,* 1918–1927.
12. Meydani, S.N., Lichtenstein, A.H., Cornwall, S., Meydani, M., Goldin, B.R., Rasmussen, H., Dinarello, C.A., and Schaefer, E.J. (1993) Immunologic Effects of National Cholesterol Education Panel Step-2 Diets With and Without Fish-Derived n-3 Fatty Acid Enrichment, *J. Clin. Invest. 92*, 105–113.
13. Grimble, R.F., Howell, W.M., O'Reilly, G., Turner, S.J., Markovic, O., Hirrell, S., East, J.M., and Calder, P.C. (2002) The Ability of Fish Oil to Suppress Tumor Necrosis Factor Alpha Production by Peripheral Blood Mononuclear Cells in Healthy Men Is Associated with Polymorphisms in Genes That Influence Tumor Necrosis Factor Alpha Production, *Am. J. Clin. Nutr. 76,* 454–459.
14. Kelley, D.S., Branch, L.B., Love, J.E., Taylor, P.C., Rivera, Y.M., and Iacono, J.M. (1991) Dietary α-Linolenic Acid and Immunocompetence in Humans, *Am. J. Clin. Nutr. 53,* 40–46.
15. Kramer, T.R., Schoene, N., Douglass, L.W., Judd, J.T., Ballard-Barbash, R., Taylor, P.R., Bhagavan, H.N., and Nair, P.P. (1991) Increased Vitamin E Intake Restores Fish-Oil-Induced Suppressed Blastogenesis of Mitogen-Stimulated T Lymphocytes, *Am. J. Clin. Nutr. 54,* 896–902.
16. Kelley, D.S., Taylor, P.C., Nelson, G.J., Schmidt, P.C., Ferretti, A., Erickson, K.L., Yu, R., Chandra, R.K., and Mackey, B.E. (1999) Docosahexaenoic Acid Ingestion Inhibits Natural Killer Cell Activity and Production of Inflammatory Mediators in Young Healthy Men, *Lipids 34,* 317–324.
17. Jolly, C.A., Jiang, Y.H., Chapkin, R.S., and McMurray, D.N. (1997) Dietary (n-3) Polyunsaturated Fatty Acids Suppress Murine Lymphoproliferation, Interleukin-2 Secretion, and the Formation of Diacylglycerol and Ceramide, *J. Nutr. 127,* 37–43.
18. Jolly, C.A., McMurray, D.N., and Chapkin, R.S. (1998) Effect of Dietary n-3 Fatty Acids on Interleukin-2 and Interleukin-2 Receptor Alpha Expression in Activated Murine Lymphocytes, *Prostaglandins Leukot. Essent. Fatty Acids 58,* 289–293.
19. Yaqoob, P., Newsholme, E.A., and Calder, P.C. (1994) The Effect of Dietary Lipid Manipulation on Rat Lymphocyte Subsets and Proliferation, *Immunology 82*, 603–610.
20. Arrington, J.L., McMurray, D.N., Switzer, K.C., Fan, Y.Y., and Chapkin, R.S. (2001) Docosahexaenoic Acid Suppresses Function of the CD28 Costimulatory Membrane Receptor in Primary Murine and Jurkat T Cells, *J. Nutr. 131*, 1147–1153.
21. Sasaki, T., Kanke, Y., Kudoh, K., Misawa, Y., Shimizu, J., and Takita, T. (1999) Effects of Dietary Docosahexaenoic Acid on Surface Molecules Involved in T Cell Proliferation, *Biochim. Biophys. Acta 1436*, 519–530.
22. Arrington, J.L., Chapkin, R.S., Switzer, K.C., Morris, J.S., and McMurray, D.N. (2001) Dietary n-3 Polyunsaturated Fatty Acids Modulate Purified Murine T-Cell Subset Activation, *Clin. Exp. Immunol. 125*, 499–507.
23. Noble, A., Truman, J.P., Vyas, B., Vukmanovic-Stejic, M., Hirst, W.J., and Kemeny, D.M. (2000) The Balance of Protein Kinase C and Calcium Signaling Directs T Cell Subset Development, *J. Immunol. 164,* 1807–1813.
24. Sanderson, P., and Calder, P.C. (1998) Dietary Fish Oil Appears to Prevent the Activation of Phospholipase C-γ in Lymphocytes, *Biochim. Biophys. Acta 1392*, 300–308.
25. Scherer, J.M., Stillwell, W., and Jenski, L.J. (1997) Spleen Cell Survival and Proliferation Are Differentially Altered by Docosahexaenoic Acid, *Cell. Immunol. 180*, 153–161.
26. Terada, S., Takizawa, M., Yamamoto, S., Ezaki, O., Itakura, H., and Akagawa, K.S. (2001) Suppressive Mechanisms of EPA on Human T Cell Proliferation, *Microbiol. Immunol. 45*, 473–481.
27. Wallace, F.A., Miles, E.A., Evans, C., Stock, T.E., Yaqoob, P., and Calder, P.C. (2001) Dietary Fatty Acids Influence the Production of Th1- but Not Th2-Type Cytokines, *J. Leukocyte Biol. 69,* 449–457.
28. Denys, A., Hichami, A., and Khan, N.A. (2001) Eicosapentaenoic Acid and Docosahexaenoic Acid Modulate MAP Kinase (ERK1/ERK2) Signaling in Human T Cells, *J. Lipid Res. 42*, 2015–2020.
29. Diaz, O., Berquand, A., Dubois, M., Di Agostino, S., Sette, C., Bourgoin, S., Lagarde, M., Nemoz, G., and Prigent, A.F. (2002) The Mechanism of Docosahexaenoic Acid-Induced Phospholipase D Activation in Human Lymphocytes Involves Exclusion of the Enzyme from Lipid Rafts, *J. Biol. Chem. 277*, 39368–39378.

30. Refaeli, Y., Van Parijs, L., and Abbas, A.K. (1999) Genetic Models of Abnormal Apoptosis in Lymphocytes, *Immunol. Rev. 169*, 273–282.
31. Palmer, E. (2003) Negative Selection—Clearing Out the Bad Apples from the T-Cell Repertoire, *Nat. Rev. Immunol. 3*, 383–391.
32. Green, D.R., Droin, N., and Pinkoski, M. (2003) Activation-Induced Cell Death in T Cells, *Immunol. Rev. 193*, 70–81.
33. Refaeli, Y., Van Parijs, L., London, C.A., Tschopp, J., and Abbas, A.K. (1998) Biochemical Mechanisms of IL-2-Regulated Fas-Mediated T Cell Apoptosis, *Immunity 8*, 615–623.
34. Holtzman, M.J., Green, J.M., Jayaraman, S., and Arch, R.H. (2000) Regulation of T Cell Apoptosis, *Apoptosis 5,* 459–471.
35. Scaffidi, C., Kirchhoff, S., Krammer, P.H., and Peter, M.E. (1999) Apoptosis Signaling in Lymphocytes, *Curr. Opin. Immunol. 11*, 277–285.
36. Green, D.R. (2003) Overview: Apoptotic Signaling Pathways in the Immune System, *Immunol. Rev. 193*, 5–9.
37. Aggarwal, B.B. (2003) Signalling Pathways of the TNF Superfamily: A Double-Edged Sword, *Nat. Rev. Immunol. 3,* 745–756.
38. Krammer, P.H. (2000) CD95's Deadly Mission in the Immune System, *Nature 407*, 789–795.
39. Watanabe-Fukunaga, R., Brannan, C.I., Itoh, N., Yonehara, S., Copeland, N.G., Jenkins, N.A., and Nagata, S. (1992) The cDNA Structure, Expression, and Chromosomal Assignment of the Mouse Fas Antigen, *J. Immunol. 148*, 1274–1279.
40. Suda, T., Takahashi, T., Golstein, P., and Nagata, S. (1993) Molecular Cloning and Expression of the Fas Ligand, a Novel Member of the Tumor Necrosis Factor Family, *Cell 75*, 1169–1178.
41. Van Parijs, L., Refaeli, Y., Lord, J.D., Nelson, B.H., Abbas, A.K., and Baltimore, D. (1999) Uncoupling IL-2 Signals That Regulate T Cell Proliferation, Survival, and Fas-Mediated Activation-Induced Cell Death, *Immunity 11*, 281–288.
42. Zhang, X., Brunner, T., Carter, L., Dutton, R.W., Rogers, P., Bradley, L., Sato, T., Reed, J.C., Green, D., and Swain, S.L. (1997) Unequal Death in T Helper Cell (Th)1 and Th2 Effectors: Th1, but Not Th2, Effectors Undergo Rapid Fas/FasL-Mediated Apoptosis, *J. Exp. Med. 185*, 1837–1849.
43. Varadhachary, A.S., Perdow, S.N., Hu, C., Ramanarayanan, M., and Salgame, P. (1997) Differential Ability of T Cell Subsets To Undergo Activation-Induced Cell Death, *Proc. Natl. Acad. Sci. USA 94*, 5778–5783.
44. Yahata, T., Abe, N., Yahata, C., Ohmi, Y., Ohta, A., Iwakabe, K., Habu, S., Yagita, H., Kitamura, H., Matsuki, N., Nakui, M., Sato, M., and Nishimura, T. (1999) The Essential Role of Phorbol Ester-Sensitive Protein Kinase C Isoforms in Activation-Induced Cell Death of Th1 Cells, *Eur. J. Immunol. 29*, 727–732.
45. Ramsdell, F., Seaman, M.S., Miller, R.E., Picha, K.S., Kennedy, M.K., and Lynch, D.H. (1994) Differential Ability of Th1 and Th2 T Cells to Express Fas Ligand and to Undergo Activation-Induced Cell Death, *Int. Immunol. 6*, 1545–1553.
46. Kirchhoff, S., Muller, W.W., Li-Weber, M., and Krammer, P.H. (2000) Up-Regulation of c-FLIPshort and Reduction of Activation-Induced Cell Death in CD28-Costimulated Human T Cells, *Eur. J. Immunol. 30*, 2765–2774.
47. Varadhachary, A.S., Edidin, M., Hanlon, A.M., Peter, M.E., Krammer, P.H., and Salgame, P. (2001) Phosphatidylinositol 3′-Kinase Blocks CD95 Aggregation and Caspase-8 Cleavage at the Death-Inducing Signaling Complex by Modulating Lateral Diffusion of CD95, *J. Immunol. 166*, 6564–6569.
48. Fernandes, G., Chandrasekar, B., Luan, X., and Troyer, D.A. (1996) Modulation of Antioxidant Enzymes and Programmed Cell Death by n-3 Fatty Acids, *Lipids 31* (Suppl.), S91–S96.
49. Avula, C.P., Zaman, A.K., Lawrence, R., and Fernandes, G. (1999) Induction of Apoptosis and Apoptotic Mediators in Balb/C Splenic Lymphocytes by Dietary n-3 and n-6 Fatty Acids, *Lipids 34*, 921–927.
50. Avula, C.P., and Fernandes, G. (2002) Inhibition of H_2O_2-Induced Apoptosis of Lymphocytes by Calorie Restriction During Aging, *Microsc. Res. Tech. 59*, 282–292.
51. Siddiqui, R.A., Jenski, L.J., Neff, K., Harvey, K., Kovacs, R.J., and Stillwell, W. (2001) Docosahexaenoic Acid Induces Apoptosis in Jurkat Cells by a Protein Phosphatase-Mediated Process, *Biochim. Biophys. Acta 1499*, 265–275.
52. Switzer, K.C., McMurray, D.N., Morris, J.S., and Chapkin, R.S. (2003) (n-3) Polyunsaturated Fatty Acids Promote Activation-Induced Cell Death in Murine T Lymphocytes, *J. Nutr. 133,* 496–503.
53. Thies, F., Nebe-von-Caron, G., Powell, J.R., Yaqoob, P., Newsholme, E.A., and Calder, P.C. (2001) Dietary Supplementation with Eicosapentaenoic Acid, but Not with Other Long-Chain N-3 or N-6 Polyunsaturated Fatty Acids, Decreases Natural Killer Cell Activity in Healthy Subjects Aged >55 Y, *Am. J. Clin. Nutr. 73*, 539–548.
54. Switzer, K.C., Fan, Y.Y., Wang, N., McMurray, D.N., and Chapkin, R.S. (2004) Dietary n-3 Polyunsaturated Fatty Acids Promote Activation-Induced Cell Death in Th1-Polarized Murine $CD4^+$ T-Cells, *J. Lipid Res. 45,* 1482–1492.
55. Singer, S.J., and Nicolson, G.L. (1972) The Fluid Mosaic Model of the Structure of Cell Membranes, *Science 175*, 720–731.
56. Raza Shaikh, S., Dumaual, A.C., LoCassio, D., Siddiqui, R.A., and Stillwell, W. (2003) Acyl Chain Unsaturation in PEs Modulates Phase Separation from Lipid Raft Molecules, *Biochem. Biophys. Res. Commun. 311*, 793–796.
57. Brown, D.A., and London, E. (2000) Structure and Function of Sphingolipid- and Cholesterol-Rich Membrane Rafts, *J. Biol. Chem. 275,* 17221–17224.
58. Ramstedt, B., and Slotte, J.P. (2002) Membrane Properties of Sphingomyelins, *FEBS Lett. 531,* 33–37.
59. Simons, K., and Ikonen, E. (1997) Functional Rafts in Cell Membranes, *Nature 387,* 569–572.
60. Brown, D.A., and Rose, J.K. (1992) Sorting of GPI-Anchored Proteins to Glycolipid-Enriched Membrane Subdomains During Transport to the Apical Cell Surface, *Cell 68,* 533–544.
61. Hueber, A.O., Bernard, A.M., Herincs, Z., Couzinet, A., and He, H.T. (2002) An Essential Role for Membrane Rafts in the Initiation of Fas/CD95-Triggered Cell Death in Mouse Thymocytes, *EMBO Rep. 3*, 190–196.
62. Muppidi, J.R., and Siegel, R.M. (2004) Ligand-Independent Redistribution of Fas (CD95) into Lipid Rafts Mediates Clonotypic T Cell Death, *Nat. Immunol. 5*, 182–189.
63. Balamuth, F., Leitenberg, D., Unternaehrer, J., Mellman, I., and Bottomly, K. (2001) Distinct Patterns of Membrane Microdomain Partitioning in Th1 and Th2 Cells, *Immunity 15*, 729–738.
64. Xavier, R., Brennan, T., Li, Q., McCormack, C., and Seed, B. (1998) Membrane Compartmentation Is Required for Efficient T Cell Activation, *Immunity 8*, 723–732.
65. Leitenberg, D., Balamuth, F., and Bottomly, K. (2001) Changes in the T Cell Receptor Macromolecular Signaling Complex and Membrane Microdomains During T Cell Development and Activation, *Semin. Immunol. 13*, 129–138.
66. Grassme, H., Jekle, A., Riehle, A., Schwarz, H., Berger, J., Sandhoff, K., Kolesnick, R., and Gulbins, E. (2001) CD95 Signaling *via* Ceramide-Rich Membrane Rafts, *J. Biol. Chem. 276*, 20589–20596.
67. Fan, Y.Y., McMurray, D.N., Ly, L.H., and Chapkin, R.S. (2003) Dietary (n-3) Polyunsaturated Fatty Acids Remodel Mouse T-Cell Lipid Rafts, *J. Nutr. 133*, 1913–1920.
68. Stulnig, T.M., Berger, M., Sigmund, T., Raederstorff, D., Stockinger, H., and Waldhausl, W. (1998) Polyunsaturated Fatty Acids Inhibit T Cell Signal Transduction by Modification of Detergent-Insoluble Membrane Domains, *J. Cell Biol. 143*, 637–644.

69. Stulnig, T.M., Huber, J., Leitinger, N., Imre, E.M., Angelisova, P., Nowotny, P., and Waldhausl, W. (2001) Polyunsaturated Eicosapentaenoic Acid Displaces Proteins from Membrane Rafts by Altering Raft Lipid Composition, *J. Biol. Chem. 276*, 37335–37340.
70. Fan, Y.Y., Ly, L.H., Barhoumi, R., McMurray, D.N., and Chapkin, R.S. (2004) Dietary Docosahexaenoic Acid Suppresses T Cell Protein Kinase Cθ Lipid Raft Recruitment and IL-2 Production, *J. Immunol. 173*, 6151–6160.
71. Bi, K., and Altman, A. (2001) Membrane Lipid Microdomains and the Role of PKCθ in T Cell Activation, *Semin. Immunol. 13*, 139–146.
72. Yaqoob, P., Newsholme, E.A., and Calder, P.C. (1995) Influence of Cell Culture Conditions on Diet-Induced Changes in Lymphocyte Fatty Acid Composition, *Biochim. Biophys. Acta 1255*, 333–340.
73. Pompos, L.J., and Fritsche, K.L. (2002) Antigen-Driven Murine $CD4^+$ T Lymphocyte Proliferation and Interleukin-2 Production Are Diminished by Dietary (n-3) Polyunsaturated Fatty Acids, *J. Nutr. 132*, 3293–3300.
74. Funk, C.D. (2001) Prostaglandins and Leukotrienes: Advances in Eicosanoid Biology, *Science 294*, 1871–1875.
75. Mukherjee, P.K., Marcheselli, V.L., Serhan, C.N., and Bazan, N.G. (2004) Neuroprotectin D1: A Docosahexaenoic Acid-Derived Docosatriene Protects Human Retinal Pigment Epithelial Cells from Oxidative Stress, *Proc. Natl. Acad. Sci. USA 101*, 8491–8496.
76. Endres, S., Ghorbani, R., Kelley, V.E., Georgilis, K., Lonnemann, G., van der Meer, J.W., Cannon, J.G., Rogers, T.S., Klempner, M.S., Weber, P.C., *et al.* (1989) The Effect of Dietary Supplementation with n-3 Polyunsaturated Fatty Acids on the Synthesis of Interleukin-1 and Tumor Necrosis Factor by Mononuclear Cells, *N. Engl. J. Med. 320*, 265–271.
77. Chung, S.W., Kang, B.Y., and Kim, T.S. (2003) Inhibition of Interleukin-4 Production in $CD4^+$ T Cells by Peroxisome Proliferator-Activated Receptor-γ (PPAR-γ) Ligands: Involvement of Physical Association Between PPAR-γ and the Nuclear Factor of Activated T Cells Transcription Factor, *Mol. Pharmacol. 64*, 1169–1179.
78. Marx, N., Kehrle, B., Kohlhammer, K., Grub, M., Koenig, W., Hombach, V., Libby, P., and Plutzky, J. (2002) PPAR Activators as Antiinflammatory Mediators in Human T Lymphocytes: Implications for Atherosclerosis and Transplantation-Associated Arteriosclerosis, *Circ. Res. 90*, 703–710.
79. Fan, Y.Y., Spencer, T.E., Wang, N., Moyer, M.P., and Chapkin, R.S. (2003) Chemopreventive n-3 Fatty Acids Activate RXRα in Colonocytes, *Carcinogenesis 24*, 1541–1548.
80. Xu, H.E., Lambert, M.H., Montana, V.G., Parks, D.J., Blanchard, S.G., Brown, P.J., Sternbach, D.D., Lehmann, J.M., Wisely, G.B., Willson, T.M., Kliewer, S.A., and Milburn, M.V. (1999) Molecular Recognition of Fatty Acids by Peroxisome Proliferator-Activated Receptors, *Mol. Cell 3*, 397–403.
81. Trebble, T.M., Wootton, S.A., Miles, E.A., Mullee, M., Arden, N.K., Ballinger, A.B., Stroud, M.A., Burdge, G.C., and Calder, P.C. (2003) Prostaglandin E_2 Production and T Cell Function After Fish-Oil Supplementation: Response to Antioxidant Cosupplementation, *Am. J. Clin. Nutr. 78*, 376–382.
82. National Research Council (1995) Nutrient *Requirements of Laboratory Animals*, pp. 80–102. National Research Council, Washington, DC.

[Received July 22, 2004; accepted November 20, 2004]

Immunomodulation by Polyunsaturated Fatty Acids: Impact on T-Cell Signaling

Thomas M. Stulnig* and Maximilian Zeyda

Division of Endocrinology and Metabolism, Department of Internal Medicine III, University of Vienna, Vienna, Austria, and CeMM-Center of Molecular Medicine, Austrian Academy of Sciences, Vienna, Austria

ABSTRACT: In recent years the potential application of the immunomodulatory effects of polyunsaturated FA (PUFA), particularly those of the n-3 series, in a variety of inflammatory disorders has been of considerable interest. However, the mechanisms underlying inhibition of T-cell activation have so far been unclear. In this short review we summarize possible mechanisms for the modulation of immune responses by PUFA. Effects of PUFA on T-cell signal transduction pathways and underlying molecular mechanisms are described in detail. These recent results add considerably to the understanding of mechanisms of PUFA actions, but their relevance in the *in vivo* situation must still be elucidated.

Paper no. L9554 in *Lipids 39*, 1171–1175 (December 2004).

PUFA exert a variety of immunomodulatory effects. Long-chain PUFA of the n-3 series such as EPA (20:5n-3) and DHA (22:6n-3) that are abundant in marine fish oils appear most effective in this respect. Also PUFA of the n-6 series, for example, GLA (18:3n-6), provide some beneficial effects on distinct inflammatory disorders, but their amounts in health food supplements are rather small. The efficacy of GLA could be taken as an indication that mechanisms common to PUFA but not specific for n-3 PUFA, such as some alterations in membrane function, could underlie modulation of the immune system by this FA (1). Notably, PUFA do not appear to adversely affect the immune system of healthy individuals, emphasizing that PUFA exert moderate effects in states of selected misdirected immune responses. Previous studies have shown that T lymphocytes are a primary target for PUFA-mediated immunomodulation (1). This short review summarizes effects of PUFA on T-cell activation with particular emphasis on the elucidation of underlying molecular mechanisms.

*To whom correspondence should be addressed at Division of Endocrinology and Metabolism, Department of Internal Medicine III, University of Vienna, Währinger Gürtel 18-20, A-1090 Vienna, Austria.
E-mail: Thomas.Stulnig@meduniwien.ac.at

Abbreviations: AA, arachidonic acid; ADC, antigen-presenting cells; COX, cyclooxygenase; GPI, glycosyl phosphatidylinositol; IFN, interferon; IL, interleukin; LAT, linker for activation of T cells; LT, leukotrienes; MAPK, mitogen-activated protein kinase; NF, nuclear factor; PAG, phosphoprotein associated with glycolipid-enriched membrane domains; PG, prostaglandins; PLCγ1, phospholipase C γ1; PPAR, peroxisome proliferator-activated receptor; TCR, T-cell receptor; TX, thromboxanes; ZAP, zeta-associated protein.

PRINCIPAL MECHANISMS OF IMMUNOMODULATION BY PUFA

Three modes of PUFA action have been primarily discussed with respect to their immunomodulatory action. First, PUFA of the n-3 series interfere with the biosynthesis of lipid mediator molecules. Eicosanoid messenger molecules such as prostaglandins (PG), leukotrienes (LT), and thromboxanes (TX) are usually derived from arachidonic acid (AA) that is liberated from membrane phospholipids. Metabolism of AA by cyclooxygenases (COX) leads to generation of PG and TX of the 2-series, whereas metabolism *via* 5-lipoxygenases gives rise to, for example, LT of the 4-series. PUFA of the n-3 series inhibit eicosanoid synthesis from AA and/or give rise to chemically altered molecules. When EPA is metabolized instead of AA by the COX, PG and TX of the 3-series are produced that in some cases have different biological effects, as reviewed in detail elsewhere (2,3). In addition to directly interfering with enzymes of eicosanoid synthesis, PUFA can also affect protein levels of involved enzymes by altering gene expression as shown for COX-2 in monocytes (4). Although n-6 and n-3 PUFA exert clearly different effects on eicosanoid synthesis, the functional outcome of these changes with respect to immunomodulation are often not predictable due to parallel pro- and anti-inflammatory effects and often unknown *in vivo* interactions of the generated messenger molecules. Moreover, due to great species differences (5) and differences between *in vitro* and *in vivo* eicosanoid production (6,7) *in vivo* extrapolations of experimental data have turned out to be extremely difficult.

A second principal mechanism for modulation of immune responses by PUFA is by direct alteration of gene expression by modification of transcription factor activity. This can be achieved either by direct interaction with ligand-binding transcription factors, so-called nuclear receptors, or by interference with membrane or cytoplasmic signaling pathways that finally lead to altered transcription factor activation. Peroxisome proliferator-activated receptor (PPAR) γ preferentially binds a variety of PUFA and their derivatives and has been shown to be involved in lymphocyte activation and macrophage differentiation (8–10). Since PUFA activate PPARγ, this could be a mechanism of PUFA-mediated immunomodulation. However, PPARγ is also activated by the abundant monounsaturated FA. In addition to PPARγ, PPARα, and PPARδ can bind FA, but with even less specificity for PUFA. PPARγ

is highly abundant in myeloid cells but T lymphocytes, which constitutively express PPARα, express PPARγ only upon stimulation. Liver X receptors α and β are inhibited by mono- and polyunsaturated FA (11). Retinoid X receptors, the heterodimer partner for a variety of nuclear receptors including those mentioned above, are activated by DHA with some selectivity compared to AA (12). However, nuclear receptors generally lack adequate specificity for PUFA to explain PUFA's immunomodulatory effects. Moreover, suppressive effects *in vitro* have mostly been found with rather unselective nuclear receptor ligands so that the impact of nuclear receptors in general, and PPARγ in particular, on PUFA-mediated immunomodulation is doubtful.

PUFA EFFECTS ON LIPID RAFT COMPOSITION

PUFA are incorporated into membrane phospholipids and hence modulate membrane structure and function. Based on the original fluid mosaic model of cellular membranes (13), incorporation of highly unsaturated FA alter their general biophysical properties such as microviscosity. However, PUFA affect the composition of particular microdomains of the plasma membrane called lipid rafts. Lipid rafts are built up by a particular lipid composition rich in sphingolipids and cholesterol (14). Phospholipid side chains are highly enriched in saturated FA compared to the plasma membrane proper. This special lipid composition leads to a particular biophysical property called the liquid-ordered state. Due to this special lipid composition, proteins that are modified by saturated FA (palmitoyl or myristoyl moieties) on their cytoplasmic side and cell surface proteins that are attached *via* a glycosyl phosphatidylinositol (GPI) anchor are highly concentrated within lipid rafts. Many proteins involved in signal transduction, for example, Src family kinases, are acylated and are hence predominantly found in lipid rafts. Therefore, lipid rafts have turned out to be implicated in signaling processes elicited by a variety of cell surface receptors including the T-cell receptor (TCR)/CD3 complex, and insulin receptors (15). Although the exact nature of lipid rafts is still a matter of discussion (16), a plethora of publications suggest lipid rafts and the location of particular proteins within rafts to be functionally important dynamic substructures of the plasma membrane that are crucial, for example, for lymphocyte activation (17).

PUFA treatment alters lipid rafts in a particular manner. Using GPI-anchored proteins and sphingolipids such as the ganglioside GM1 as marker molecules of the outer (exoplasmic) membrane lipid leaflet of the membrane bilayer, PUFA did not interfere with the concentration of these molecules in rafts. However, acylated proteins that are anchored to the inner (cytoplasmic) lipid leaflet are displaced from rafts when peripheral blood or Jurkat T lymphocytes are treated with n-3 PUFA and to a somewhat lower extent also with n-6 PUFA (18). Thus, PUFA selectively alter the protein composition of the inner membrane lipid leaflet while leaving the outer leaflet virtually unaffected. Notably, the extent of displacement of acylated proteins from lipid rafts strictly correlates with impairment of calcium signaling, indicating a functional impact of these alterations (18).

PUFA may principally alter lipid rafts by two different mechanisms: PUFA could replace saturated palmitoyl moieties of acylated proteins by PUFA residues. Polyunsaturated fatty acyl residues might then no longer be able to incorporate into the predominantly saturated lipid environment of lipid rafts. On the other hand, PUFA could be incorporated in membrane phospholipids, thereby altering the lipid environment, which would then no longer prefer fatty acyl moieties of proteins to be concentrated in rafts. Incorporation of polyunsaturated fatty acyl moieties has been shown to occur due to a partial nonselectivity of palmitoyl transferases (19). However, PUFA acylation of proteins is a rather inefficient process. On the other hand, PUFA readily attach to the *sn*-2 position of membrane phospholipids of both lipid rafts and the plasma membrane proper. Notably, PUFA are incorporated not only in lipids that predominantly reside in the outer membrane lipid leaflet (PC, sphingomyelin), but are also found in the PE that predominantly occurs in the inner membrane leaflet, whose protein composition is altered by PUFA treatment. Recent data with diets enriched with fish oils revealed that n-3 PUFA are readily incorporated into membrane lipids from rafts as well as soluble membrane fractions (20). Interestingly, these analyses revealed that dietary PUFA dramatically reduced raft content of sphingomyelin that is also involved in stabilizing lipid rafts (21). Moreover, when using tritiated palmitate for metabolic labeling, we could show that labeled acylated proteins such as the Src family kinase Lck are found displaced from rafts to a similar extent as the protein itself (22). Since palmitate cannot be transformed to PUFA, these data reveal that PUFA treatment leads to displacement from rafts of proteins that are not acylated with PUFA. Hence, incorporation of PUFA into membrane lipids is likely to be a mechanism for proteins to be displaced from rafts by PUFA treatment (Fig. 1). That only proteins from the inner leaflet are displaced from rafts by PUFA treatment, although PUFA are incorporated in lipids of both leaflets, may be due to additional raft-stabilizing effects of lipid head groups, for example, of sphingolipids, that are only present at the outer membrane surface.

FUNCTIONAL EFFECTS OF RAFT DISRUPTION BY PUFA

A number of acylated proteins are involved in T-cell signaling, including Src family kinases and the adaptor protein linker for activation of T cells (LAT). Virtually all acylated proteins tested are displaced from rafts by PUFA treatment. To elucidate which of the displaced proteins is critical for the inhibitory effect of PUFA on calcium signaling, we performed a step-by-step analysis of T-cell signaling cascades stimulated *via* the TCR/CD3 complex that mediates antigen-specific stimuli to T lymphocytes *in vivo*. Tyrosine phosphorylation of CD3ζ chains, which is presumably catalyzed by the Src-family kinase Lck, binding of the zeta-associated protein (ZAP)-70

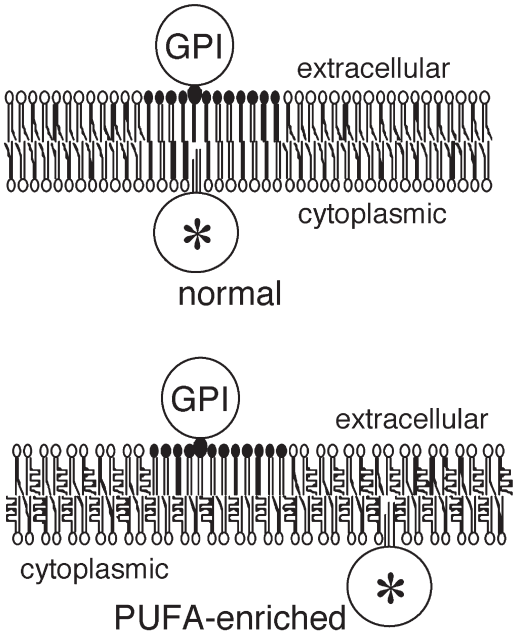

FIG. 1. A model for PUFA-mediated alteration of lipid rafts. GPI, GPI-anchored protein; *, acylated signaling proteins, for example, Src family kinases, LAT (linker for activation of of T cells).

to phospho-CD3ζ, and phosphorylation of ZAP-70 by Lck are not diminished in PUFA-treated T cells (23) (Fig. 2). However, subsequent phosphorylation of the central adaptor protein LAT turned out to be the most upstream signaling event inhibited by PUFA treatment. This inhibition is followed by diminished phosphorylation of phospholipase C (PLC) γ1, which liberates the inositol-1,4,5-trisphosphate needed for elevation of cytoplasmic calcium concentration, an early key event in T-cell activation.

Based on these data, we hypothesized that LAT displacement from lipid rafts is the critical event leading to diminished calcium signaling in PUFA-treated T cells. LAT is a double-acylated transmembrane protein with a short exoplasmic domain.

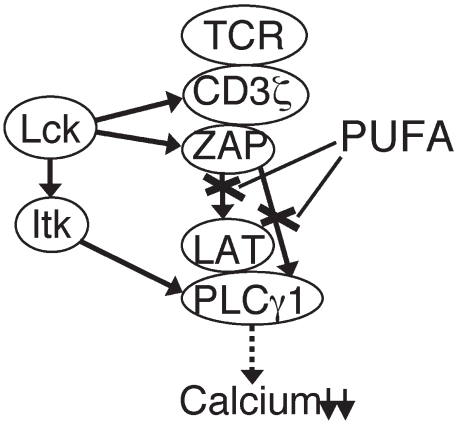

FIG. 2. PUFA-induced alterations in membrane-proximal T-cell signaling events. Arrows, tyrosine phosphorylation events. TCR, T cell receptor; ZAP, zeta-associated protein; PLCγ1, phospholipase Cγ1; for other abbreviations see Figure 1.

If LAT displacement from rafts is the critical alteration leading to diminished calcium signaling in PUFA-treated T cells, then reconstitution with a LAT molecule that cannot be displaced from rafts by PUFA treatment should render T cells insensitive to the inhibitory effects of PUFA. The recently cloned adaptor protein phosphoprotein associated with glycolipid-enriched membrane domains (PAG) is a transmembrane protein that turned out to not be displaced from rafts when T cells were treated with PUFA. We used the exoplasmic and transmembrane domains (including palmitoylation sites) of PAG to generate a chimeric molecule including the functional cytoplasmic domain of LAT (PAG-LAT). A LAT-deficient Jurkat line (ANJ3) was reconstituted with either wild-type LAT or the chimeric PAG-LAT protein. As we anticipated, the chimeric PAG-LAT remained localized to rafts irrespective of whether cells had been treated with PUFA or saturated FA. Notably, PUFA treatment did not inhibit PLCγ1 phosphorylation and calcium response in cells reconstituted with PAG-LAT in contrast to cells reconstituted with wild-type LAT (23). Thus, a PUFA-insensitive LAT protein is able to rescue T cells from PUFA-mediated inhibition of PLCγ1 and calcium signaling. Thus LAT displacement from lipid rafts is a molecular mechanism by which PUFA inhibit membrane-proximal signaling of T cells *in vitro*. Of note, a recent study for the first time links *in vivo* alterations of lipid rafts by PUFA with functional consequences (24).

IMPACT OF PUFA ON DOWNSTREAM SIGNALING

Signaling pathways in T lymphocytes comprise a rather complex network. Therefore, we elucidated whether the high specificity of PUFA-mediated signaling defects at the very early signaling events is maintained during downstream signaling (Fig. 3). At the level of mitogen-activated protein kinases (MAPK) we found a highly selective inhibition of c-jun N-terminal

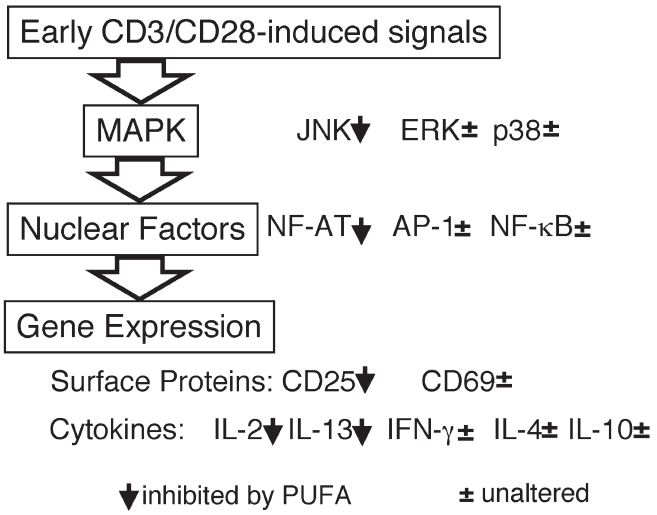

FIG. 3. PUFA inhibit T-cell downstream signaling on different levels in a highly selective manner. MAPK, mitogen-activated protein kinases; JNK, C-jun N-terminal kinase; NF-AT, nuclear factor of activated T cells; NF-κB, nuclear factor κB; IL, interleukin; IFN, interferon.

kinase (JNK) phosphorylation and activation, whereas phosphorylation of p38 MAPK and ERK-1,2 remained essentially unaltered by PUFA treatment of Jurkat and peripheral blood T cells (25). When analyzing transcription factor activation we found inhibition by PUFA of nuclear factor (NF) of activated T cells (NF-AT). In contrast, activation of AP-1 and NF-κB were not affected by PUFA treatment. These experiments showed that selectivity of PUFA is apparent also at the MAPK and transcription factor level.

When analyzing PUFA effects on cytokine signaling, we found inhibition only for interleukin (IL)-2 and IL-13, but not for interferon (IFN)-γ, IL-4, IL-9, or IL-10, further indicating selectivity of PUFA effects rather than general T-cell inhibition (25). Half-maximal effects for inhibition of IL-2 occurred at about 5 μM, suggesting significance also for *in vivo* PUFA treatment. In addition, expression of the cell surface activation marker CD25, but not of CD69, was strikingly inhibited by PUFA treatment. Thus, PUFA inhibit T-cell downstream signaling in a highly selective manner.

In contrast to these *in vitro* data, *in vivo* data on PUFA effects on T-cell-driven immune responses have not shown such high selectivity in inhibition but more general effects, for example, including reduction of serum concentrations of IFN-γ (26). These differences could be due to different ways of T-cell activation *in vivo* compared to *in vitro*. *In vivo*, T helper cells that drive immune responses are stimulated *via* antigen-presenting cells (APC). For efficient T-cell stimulation, the contact site between T cell and APC requires a complex organization known as "immunological synapse." Recent data from our laboratory indicate that formation of the immunological synapse is altered when T cells have been treated with PUFA (Geyeregger, R., Zeyda, M., and Stulnig, T.M., unpublished data). Such alterations could underlie deficient T-cell activation *in vivo*, leading to diminished activation of pathways that are not intrinsically altered in PUFA-treated T cells stimulated *via* antibodies to cell surface receptors. However, more *in vivo* studies are needed to elucidate how PUFA affect the initiation of immune responses at a molecular level.

In summary, recent advances in the elucidation of mechanisms leading to inhibition of T-cell activation by PUFA point to a critical involvement of lipid rafts. Although data are mostly confined to *in vitro* PUFA treatment, recent publications suggest that T-cell lipid rafts are also altered after dietary PUFA treatment. Hence, lipid rafts could be a key for the understanding of the immunomodulatory action of PUFA beyond alterations in eicosanoid production and nuclear receptor interactions.

ACKNOWLEDGMENTS

The work was supported by the Austrian Science Foundation (P16778-B13) and the CeMM–Center for Molecular Medicine, a basic research institute within the companies of the Austrian Academy of Sciences, Vienna, Austria.

REFERENCES

1. Stulnig, T.M. (2003) Immunomodulation by Polyunsaturated Fatty Acids: Mechanisms and Effects, *Int. Arch. Allergy Immunol. 132*, 310–321.
2. Calder, P.C., Yaqoob, P., Thies, F., Wallace, F.A., and Miles, E.A. (2002) Fatty Acids and Lymphocyte Functions, *Br. J. Nutr. 87* (Suppl. 1), S31–S48.
3. Calder, P.C. (1997) n-3 Polyunsaturated Fatty Acids and Cytokine Production in Health and Disease, *Ann. Nutr. Metab. 41*, 203–234.
4. Lee, J.Y., Ye, J., Gao, Z., Youn, H.S., Lee, W.H., Zhao, L., Sizemore, N., and Hwang, D.H. (2003) Reciprocal Modulation of Toll-like Receptor-4 Signaling Pathways Involving Myd88 and Phosphatidylinositol 3-Kinase/AKT by Saturated and Polyunsaturated Fatty Acids, *J. Biol. Chem. 278*, 37041–37051.
5. Morita, I., Takahashi, R., Saito, Y., and Murota, S. (1983) Effects of Eicosapentaenoic Acid on Arachidonic Acid Metabolism in Cultured Vascular Cells and Platelets: Species Difference, *Thromb. Res. 31*, 211–217.
6. Knapp, H.R., Reilly, I.A., Alessandrini, P., and FitzGerald, G.A. (1986) *In vivo* Indexes of Platelet and Vascular Function During Fish-Oil Administration in Patients with Atherosclerosis, *N. Engl. J. Med. 314*, 937–942.
7. Saito, J., Terano, T., Hirai, A., Shiina, T., Tamura, Y., and Saito, Y. (1997) Mechanisms of Enhanced Production of PGI_2 in Cultured Rat Vascular Smooth Muscle Cells Enriched with Eicosapentaenoic Acid, *Atherosclerosis 131*, 219–228.
8. Yang, X.Y., Wang, L.H., Chen, T., Hodge, D.R., Resau, J.H., DaSilva, L., and Farrar, W.L. (2000) Activation of Human T Lymphocytes Is Inhibited by Peroxisome Proliferator-Activated Receptor γ (PPARγ) Agonists: PPARγ Co-association with Transcription Factor NFAT, *J. Biol. Chem. 275*, 4541–4544.
9. Clark, R.B., Bishop-Bailey, D., Estrada-Hernandez, T., Hla, T., Puddington, L., and Padula, S.J. (2000) The Nuclear Receptor PPAR γ and Immunoregulation: PPAR γ Mediates Inhibition of Helper T Cell Responses, *J. Immunol. 164*, 1364–1371.
10. Marx, N., Sukhova, G., Murphy, C., Libby, P., and Plutzky, J. (1998) Macrophages in Human Atheroma Contain PPARγ: Differentiation-Dependent Peroxisomal Proliferator-Activated Receptor γ (PPARγ) Expression and Reduction of MMP-9 Activity Through PPARγ Activation in Mononuclear Phagocytes *in vitro*, *Am. J. Pathol. 153*, 17–23.
11. Desvergne, B., and Wahli, W. (1999) Peroxisome Proliferator-Activated Receptors: Nuclear Control of Metabolism, *Endocr. Rev. 20*, 649–688.
12. Mata de Urquiza, A., Liu, S., Sjoberg, M., Zetterstrom, R.H., Griffiths, W., Sjovall, J., and Perlmann, T. (2000) Docosahexaenoic Acid, a Ligand for the Retinoid X Receptor in Mouse Brain, *Science 290*, 2140–2144.
13. Singer, S.J., and Nicolson, G.L. (1972) The Fluid Mosaic Model of the Structure of Cell Membranes, *Science 175*, 720–731.
14. Simons, K., and Ikonen, E. (1997) Functional Rafts in Cell Membranes, *Nature 387*, 569–572.
15. Saltiel, A.R., and Pessin, J.E. (2002) Insulin Signaling Pathways in Time and Space, *Trends Cell Biol. 12*, 65–71.
16. Munro, S. (2003) Lipid Rafts: Elusive or Illusive? *Cell 115*, 377–388.
17. Pizzo, P., and Viola, A. (2003) Lymphocyte Lipid Rafts: Structure and Function, *Curr. Opin. Immunol. 15*, 255–260.
18. Stulnig, T.M., Berger, M., Sigmund, T., Raederstorff, D., Stockinger, H., and Waldhäusl, W. (1998) Polyunsaturated Fatty Acids Inhibit T Cell Signal Transduction by Modification of Detergent-Insoluble Membrane Domains, *J. Cell Biol. 143*, 637–644.
19. Liang, X., Nazarian, A., Erdjument-Bromage, H., Bornmann, W., Tempst, P., and Resh, M.D. (2001) Heterogeneous Fatty

Acylation of Src Family Kinases with Polyunsaturated Fatty Acids Regulates Raft Localization and Signal Transduction, *J. Biol. Chem. 276*, 30987–30994.
20. Fan, Y.Y., McMurray, D.N., Ly, L.H., and Chapkin, R.S. (2003) Dietary (n-3) Polyunsaturated FA Remodel Mouse T-Cell Lipid Rafts, *J. Nutr. 133*, 1913–1920.
21. Brown, D.A., and London, E. (2000) Structure and Function of Sphingolipid- and Cholesterol-Rich Membrane Rafts, *J. Biol. Chem. 275*, 17221–17224.
22. Stulnig, T.M., Huber, J., Leitinger, N., Imre, E.-M., Angelisová, P., Nowotny, P., and Waldhäusl, W. (2001) Polyunsaturated Eicosapentaenoic Acid Displaces Proteins from Membrane Rafts by Altering Raft Lipid Composition, *J. Biol. Chem. 276*, 37335–37340.
23. Zeyda, M., Staffler, G., Horejsi, V., Waldhausl, W., and Stulnig, T.M. (2002) LAT Displacement from Lipid Rafts as a Molecular Mechanism for the Inhibition of T Cell Signaling by Polyunsaturated Fatty Acids, *J. Biol. Chem. 277*, 28418–28423.
24. Fan, Y.Y., Ly, L.H., Barhoumi, R., McMurray, D.N., and Chapkin, R.S. (2004) Dietary Docosahexaenoic Acid Suppresses T Cell Protein Kinase Cθ Lipid Raft Recruitment and IL-2 Production, *J. Immunol. 173*, 6151–6160.
25. Zeyda, M., Szekeres, A.B., Saemann, M.D., Geyeregger, R., Stockinger, H., Zlabinger, G.J., Waldhausl, W., and Stulnig, T.M. (2003) Suppression of T Cell Signaling by Polyunsaturated Fatty Acids: Selectivity in Inhibition of Mitogen-Activated Protein Kinase and Nuclear Factor Activation, *J. Immunol. 170*, 6033–6039.
26. Fritsche, K.L., Anderson, M., and Feng, C. (2000) Consumption of Eicosapentaenoic Acid and Docosahexaenoic Acid Impair Murine Interleukin-12 and Interferon-γ Production *in vivo*, *J. Infect. Dis. 182* (Suppl. 1), S54–S61.

[Received July 22, 2004; accepted November 29, 2004]

Omega-3 PUFA of Marine Origin Limit Diet-Induced Obesity in Mice by Reducing Cellularity of Adipose Tissue

Jana Ruzickova[a], Martin Rossmeisl[a], Tomas Prazak[a], Pavel Flachs[a], Jana Sponarova[a], Marek Vecka[b], Eva Tvrzicka[b], Morten Bryhn[c], and Jan Kopecky[a,*]

[a]Department of Adipose Tissue Biology and Centre for Integrated Genomics, Institute of Physiology, Academy of Sciences of the Czech Republic, 142 20 Prague, Czech Republic, [b]4th Department of Medicine,1st Medical Faculty, Charles University, 128 08 Prague, Czech Republic, and [c]Pronova Biocare a.s., N-1327 Lysaker, Norway

ABSTRACT: Omega-3 PUFA of marine origin reduce adiposity in animals fed a high-fat diet. Our aim was to learn whether EPA and DHA could limit development of obesity and reduce cellularity of adipose tissue and whether other dietary FA could influence the effect of EPA/DHA. Weight gain induced by composite high-fat diet in C57BL/6J mice was limited when the content of EPA/DHA was increased from 1 to 12% (wt/wt) of dietary lipids. Accumulation of adipose tissue was reduced, especially of the epididymal fat. Low ratio of EPA to DHA promoted the effect. A higher dose of EPA/DHA was required to reduce adiposity when admixed to diets that did not promote obesity, the semisynthetic high-fat diets rich in EFA, either α-linolenic acid (ALA, 18:3 n-3, the precursor of EPA and DHA) or linoleic (18:2 n-6) acid. Quantification of adipose tissue DNA revealed that except for the diet rich in ALA the reduction of epididymal fat was associated with 34–50% depression of tissue cellularity, similar to the 30% caloric restriction in the case of the high-fat composite diet. Changes in plasma markers and adipose gene expression indicated improvement of lipid and glucose metabolism due to EPA/DHA even in the context of the diet rich in ALA. Our results document augmentation of the antiadipogenic effect of EPA/DHA during development of obesity and suggest that EPA/DHA could reduce accumulation of body fat by limiting both hypertrophy and hyperplasia of fat cells. Increased dietary intake of EPA/DHA may be beneficial regardless of the ALA intake.

Paper no. L9552 in *Lipids 39*, 1177–1185 (December 2004).

Many studies in rodents have demonstrated that PUFA, especially n-3 PUFA EPA (20:5n-3) and DHA, 22:6n-3, which are abundant in marine fish oils, are less effective in promoting accumulation of adipose tissue than saturated fats (1–5). Dietary n-3 PUFA admixed to high-fat (HF) diets do not affect food consumption (2,6–8), but they do modulate fuel partitioning by downregulating lipogenesis and stimulating lipid oxidation. Such modulation of metabolism is associated with changes of gene expression in many tissues including liver, muscle, and adipose tissue (4,9,10). A preferential reduction of epididymal compared with subcutaneous white adipose tissue due to enrichment of diet with fish oil or EPA/DHA concentrates was observed (2,7,10,11). However, the mechanism for the reduction of body fat stores is still unclear [see the following discussion and Azain (4), Lapillonne *et al.* (9), and Raclot and Oudart (10)]. Both in animals (6,10) and humans (12,13), EPA/DHA lower blood TG and may improve insulin sensitivity. They also exert prophylactic effects on cardiovascular disease (12,14). Data on the effects of n-3 PUFA on adiposity in humans are scarce (13,15).

The effect of EPA/DHA on adiposity was mostly studied in rats using semisynthetic HF (sHF) diets and compared with saturated FA or n-6 PUFA (1,2,5,10,11,16,17). Especially DHA-rich diets were potent in reducing body fat storage, and the reduction was explained by limited accumulation of lipids in adipocytes rather than by a decreased number of fat cells (2,11). A drawback of the above studies was that they were not conducted under conditions promoting obesity, since the body weight gain of control animals was very small. Also studies in mice fed sHF diets have documented the reduction of adiposity by n-3 PUFA (6,7,18,19) and indicated that EPA and DHA could be more effective than n-3 PUFA of plant origin, that is, α-linolenic acid [ALA, 18:3 n-3; Ikemoto *et al.* (6)]. This compound is a precursor of EPA and DHA in mammals, but it is oxidized very rapidly in the organism and its conversion to EPA and DHA is quite inefficient (4,12,14).

Inbred and genetically modified strains of mice are being increasingly used to study the pathophysiology of obesity and its related disorders. For instance, the C57BL/6J inbred strain of mice represents a common model of obesity and diabetes induced by composite HF diets [cHF diets (20–23)]. The previous mouse strain has been already used to study the effects of different dietary oils admixed to sHF diets on body fat accumulation and glucose metabolism (6). The goal of this study was to learn whether EPA and DHA could limit the obesity and proliferation of adipose tissue cells induced in the C57BL/6J mice by the cHF diet. To understand the influence of other dietary lipids, namely EFA of plant origin (i.e., 18:3n-3 and 18:2n-6), on the potency of EPA and DHA to reduce the mass and cellularity of adipose tissue, experiments were also

*To whom correspondence should be addressed at Institute of Physiology, Academy of Sciences of the Czech Republic, Videnska 1083, 142 20 Prague, Czech Republic. E-mail: kopecky@biomed.cas.cz

Abbreviations: ALA, α-linolenic acid; CR, caloric restriction by 30% compared with *ad libitum* fed mice; HF, high-fat; cHF diet, composite high-fat diet; cHF-F1 and cHF-F2, composite high-fat diets enriched with fish oil concentrate; sHFc, semisynthetic high-fat diet based on corn oil; HFc-F1, sHFc-F2, semisynthetic high-fat diets based on corn oil enriched with fish oil concentrate; sHFf, semisynthetic high-fat diet based on flaxseed oil; sHFf-F1, sHFf-F2, semisynthetic high-fat diets based on flaxseed oil enriched with fish oil concentrate; NEFA, nonesterified FA; and sHF diet, semisynthetic high-fat diet.

performed using sHF diets based on flaxseed or corn oils. The effects on gene expression in adipose tissue, as well as the plasma levels of lipids, leptin, and insulin in the mice fed sHF diets were also analyzed.

EXPERIMENTAL PROCEDURES

Animals and diets. Male mice were housed in a controlled environment (20°C; 12-h light/dark cycle; light from 6:00 a.m.) with free access to water and a standard chow diet [Velaz, Prague, Czech Republic; Kopecky *et al.* (22)]. At the age of 2.5 mon mice were single-caged. At 3 to 4 mon of age, the animals were randomly assigned to experimental HF diets: (i) obesity-promoting cHF diet derived from the standard chow (20,22); or (ii) sHF diet of a similar composition like the one previously used for rats (2,11), containing (in g/kg) 479 sucrose, 266 casein, 200 plant oil [either flaxseed oil rich in ALA, 18:3 n-3; or corn oil rich in linoleic acid, 18:2 n-6; Table 2], 45 agar-agar, 10 vitamin and mineral mix (Biofaktory, Prague, Czech Republic), and α-tocopherol (300 mg/kg). Macronutrient composition and energy density of the chow, cHF, and sHF diets are described in Table 1. When indicated, 15 or 44% (wt/wt) of a fat component in the HF diets was replaced by the concentrate of n-3 PUFA of marine origin rich in DHA (EPAX 1050 TG or EPAX 2050 TG) or EPA (EPAX 4510 TG; Pronova Biocare a.s., Lysaker, Norway). EPA and DHA collectively form 45–64% (wt/wt) of the concentrates and they are present as TG. The lipid composition and abbreviations of diets are given in Table 2. FA composition of all diets used in this study was determined by GC (Table 3). Mice were weighed weekly, while individual food intake was determined daily, when a new ration was given. In some experiments, the ration was reduced by 30% compared with *ad libitum* fed mice on the same type of diet (caloric restriction; CR). At the end of the feeding study, at 5 to 6.5 mon of age, mice were killed by cervical dislocation between 9:00 and 10:00 a.m., subcutaneous (dorsolumbar) and epididymal white fat [for the anatomical description of fat depots, see Cinti (24)], as well as the liver, were dissected. Plasma was obtained from truncal blood using EDTA and stored at –70·C for the analysis of metabolites and hormones (see the following discussion).

TABLE 1
Macronutrient Composition and Energy Density of Experimental Diets

	Diet		
	Chow	cHF	sHF
Lipids (% diet, wt/wt)	3.4	35.2	20.0
Carbohydrates (% diet, wt/wt)	56.2	35.4	47.9
Proteins (% diet, wt/wt)	20.9	20.5	26.6
Energy density (kJ/g)	14.2	22.8	10.1

Tissue content of TG and DNA and TG in feces. Content of TG in liver and feces was estimated in alcoholic KOH solubilizates prepared according to Salmon and Flatt (25), using a kit (Catalog No. 320-A) from Sigma Diagnostic (Procedure No.320-UV, Sigma, St. Louis, MO), as described previously (22). DNA was estimated fluorometrically in tissue samples digested with proteinase K as before (26).

Plasma concentrations of metabolites and hormones. Insulin, leptin, and TG were estimated in plasma of fed animals (22). Concentrations of nonesterified FA (NEFA) in plasma were evaluated enzymatically using a NEFA C kit (Wako Chemicals, Richmond, CA). Plasma leptin and insulin were assessed by using a Mouse Leptin RIA Kit and Sensitive Rat Insulin RIA Kit, respectively, from LINCO Research (St. Charles, MO). Blood glucose was measured by the use of a SmartScan glucometer (Life Scan, Milpitas, CA).

Gene expression. Total RNA was isolated by using TRIzol Reagent (Invitrogen, Carlsbad, CA). RNA was treated with RNase-free DNase. Gene expression was analyzed by reverse transcription followed by the real-time quantitative PCR (LightCycler Instrument, F. Hoffman-La Roche Ltd., Basel,

TABLE 2
Lipid Composition and Abbreviations of Experimental Diets[a]

	Oil (% lipid, wt/wt)						
Diet	Rapeseed	Sunflower	Flaxseed	Corn	EPAX 1050TG	EPAX 2050TG	EPAX 4510TG
Control diets							
cHF[b]	95	5	—	—	—	—	—
sHFf	—	—	100	—	—	—	—
sHFc	—	—	—	100	—	—	—
EPA/DHA-enriched diets							
EPA < DHA[c]							
cHF-F1[b]	81	4	—	—	15	—	—
cHF-F2[b]	53	3	—	—	44	—	—
sHFf-F1	—	—	85	—	—	15	—
sHFf-F2	—	—	56	—	—	44	—
sHFc-F1	—	—	—	56	44	—	—
EPA > DHA[c]							
sHFc-F2	—	—	—	56	—	—	44

[a]Lipid composition of all experimental diets prepared at the laboratory.
[b]The composition of plant oils used to prepare the cHF diets [see Kopecky *et al.* (22) for further details].
[c]EPA-to-DHA ratio in diet.

TABLE 3
FA Composition of Dietary Lipids[a]

	Control diets			EPA/DHA-enriched diets						
FA (g/100 g)	Chow	cHF	sHFf	sHFc	cHF-F1	cHF-F2	sHFf-F1	sHFf-F2	sHFc-F1	sHFc-F2
12:0	0.1	1.5	—	—	1.5	1.5	NE	NE	—	NE
14:0	1.3	2.4	—	—	2.4	2.4	—	0.1	—	0.2
14:1n-5	—	0.2	—	—	0.2	0.2	NE	NE	—	NE
16:0	20.9	11.3	4.2	10.3	10.8	9.8	3.7	2.6	6.3	6.4
16:1n-9	0.2	0.1	—	—	0.1	0.1	0.1	0.2	—	0.3
16:1n-7	1.9	0.5	—	0.1	0.6	0.6	NE	NE	0.2	NE
18:0	6.7	3.7	3.1	1.8	3.9	4.2	3.0	2.7	2.3	3.8
18:1n-9	23.3	50.8	18.1	28.5	42.3	25.9	15.9	11.5	18.9	21.3
18:1n-7	1.8	2.5	0.6	0.5	2.2	1.7	0.6	0.7	0.7	2.3
18:2n-6	32.0	19.4	14.9	52.7	16.6	11.1	12.7	8.6	31.5	30.1
18:3n-6	0.1	—	—	0.1	—	0.1	NE	NE	0.1	0.4
18:3n-3	3.3	4.1	57.9	1.6	3.3	1.9	49.3	32.7	1.1	2.6
18:4n-3	0.4	0.1	—	—	0.2	0.3	0.2	0.6	0.1	NE
20:0	0.2	0.4	0.1	0.4	0.5	0.5	NE	NE	0.5	NE
20:1n-9	0.7	0.9	0.1	3.6	0.9	0.9	0.4	1.0	2.5	4.1
20:2n-6	0.1	0.2	—	0.1	0.2	0.3	0.1	0.2	0.2	NE
20:3n-6	—	—	—	0.1	—	0.1	NE	NE	0.1	NE
20:4n-6	0.2	0.1	—	—	0.4	1.0	0.2	0.5	0.9	1.4
20:3n-3	0.1	—	—	—	—	0.1	NE	NE	0.1	NE
20:4n-3	0.1	—	—	—	0.1	0.2	0.3	0.8	0.2	1.1
20:5n-3	2.4	0.2	—	—	1.3	3.3	3.6	10.6	3.0	21.3
22:0	0.2	0.3	0.1	0.1	0.3	0.3	NE	NE	0.2	NE
22:1n-9	0.1	0.2	—	—	0.2	0.2	0.1	0.2	0.1	0.4
22:4n-6	—	—	—	—	0.2	0.4	NE	NE	0.3	NE
22:5n-6	0.1	0.1	—	—	0.8	2.2	0.2	0.5	2.0	NE
22:5n-3	0.4	0.1	0.2	—	0.4	1.1	0.9	2.4	1.0	0.7
22:6n-3	2.8	0.9	—	—	10.5	29.2	8.0	23.6	27.0	3.7
24:0	0.2	—	0.1	—	0.1	0.1	NE	NE	—	NE
24:1n-9	0.2	0.2	0.3	0.1	0.3	0.6	NE	NE	0.6	NE
Sum SFA	29.7	19.6	7.7	12.6	19.3	18.7	7.0	5.7	9.3	10.6
Sum MUFA	28.3	55.2	19.2	32.8	46.7	30.1	17.3	13.8	23.0	28.4
Sum n-6 PUFA	32.5	19.8	14.9	52.9	18.2	15.2	13.2	9.8	35.2	31.0
Sum n-3 PUFA	9.6	5.4	58.1	1.7	15.8	36.1	62.4	70.7	32.5	29.7

[a]SFA, saturated FA; MUFA, monounsaturated FA; —, <0.1%; NE, not estimated.

Switzerland) with primers specific for mouse leptin (F: CCGCCAAGCAGAGGGTCAC; R: GCATTCAGGGCTAACATCCAACT) and GLUT4 (F: ACCGGCTGGGCTGATGTGTCT; R: GCCGACTCGAAGATGCTGGTTGAATAG). Expression levels of eukaryotic translational elongation factor-1α (F: TGACAGCAAAAACGACCCACCAAT; R: GGGCCATCTTCCAGCTTCTTACCA) and cyclophilin-β (F: ACTACGGGCCTGGCTGGGTGAG; R: TGCCGGAGTCGACAATGATGA) mRNA were used to correct for inter-sample variations with similar results. Expression of these two genes was not affected by the dietary treatments (not shown). The detailed protocol has been described before (27).

Statistics. The data were analyzed by a one-way (diet) or a two-way (depot × diet) ANOVA, using SigmaStat statistical software. Logarithmic transformation was used to stabilize variance in cells when necessary. The Student–Newman–Keuls, or Dunnett's method, applied to separate variance t-test between pairs of groups, was used for multiple comparisons. All comparisons were judged to be significant at $P = 0.05$.

RESULTS

Reduction of cHF diet-induced obesity by EPA/DHA. Adult mice offered a control cHF diet started to gain body weight at a much higher rate than their littermates maintained on the chow diet. Weight gain was apparent after about 2 wk of habituation on the cHF diet and reached about 6.5 g within the next 5 wk of the experiment (Fig. 1). Body weight gain was about 2.7 g lower in mice fed a cHF-F1 diet enriched with EPA/DHA compared with cHF diet (for diets, see Tables 2 and 3) and even higher enrichment resulted in a net loss of body weight of about 3 g over the 5-wk feeding period (Fig. 1, the cHF-F2 mice). Weight loss of about 6 g was observed in food restricted (CR) animals fed the control cHF diet. However, a combination of CR and the cHF-F1 diet had no further effect on body weight compared with CR alone (Fig. 1). The intake of EPA/DHA did not affect food consumption of the animals (Table 4, cHF *vs.* cHF-F2).

A dose-dependent effect of dietary EPA/DHA on body weight could be attributed to a reduced adiposity of both epi-

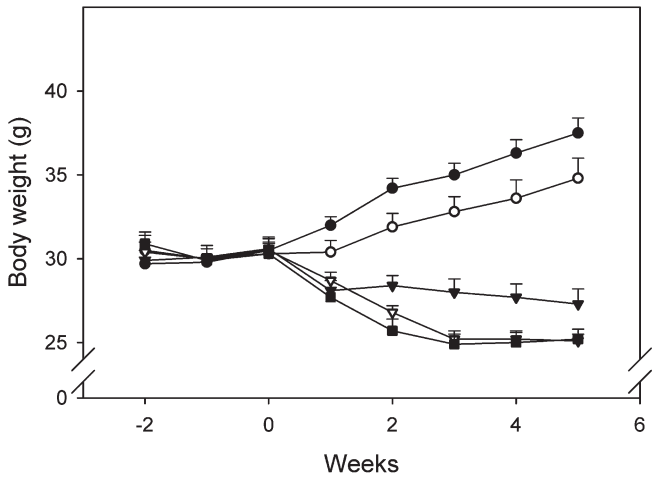

FIG 1. Effects of EPA/DHA and caloric restriction (CR) on body weight and fat accumulation in mice fed a composite high-fat (cHF) diet. At 4 mon of age (wk –2), the chow diet was replaced by the control cHF diet. Two weeks later (week 0), animals were divided into 5 subgroups and fed *ad libitum* the control cHF diet (●), cHF-F1 diet (○), or cHF-F2 diet (▼). Mice on the CR regime were fed either the control cHF diet (▽) or the cHF-F1 diet (■). After 5 wk, the animals were sacrificed. Data are means ± SE (n = 10). See also Table 4.

didymal and subcutaneous (dorsolumbar) fat depots. However, the former depot appeared to be more affected, and even the lower dose of EPA/DHA was effective (Table 4, cHF *vs.* cHF-F1). In fact, both higher dose of EPA/DHA (cHF-F2 diet) and CR reduced adiposity of the depots to a similar extent. No further decrease of fat content was observed when cHF-F1 diet was combined with CR (Table 4). Only CR but not EPA/DHA decreased liver mass (Table 4).

DNA concentration was higher in the dorsolumbar than epididymal fat and increased about 2-fold in both fat depots due to the higher dose of EPA/DHA (Table 4, cHF *vs.* cHF-F2) while the lower dose had no effect (Table 4, cHF *vs.* cHF-F1). In epididymal but not dorsolumbar fat the total DNA amount decreased about 2-fold due to both cHF-F1 and cHF-F2 diets. CR, either alone or in combination with the cHF-F1 diet, increased DNA concentration in both fat depots similarly as the cHF-F2 diet (Table 4). CR alone resulted in about 2-fold depression of total DNA in epididymal fat, while it did not affect DNA content of dorsolumbar fat. The combination of CR and cHF-F1 diet tended to decrease total DNA content in both depots, compared with the effect of CR alone (Table 4).

Depression of adiposity by EPA/DHA admixed to sHF diets. To understand whether the potency of n-3 PUFA of marine origin to reduce adiposity depends on the composition of the bulk of dietary lipids, experiments were performed using the sHF diets based on either flaxseed (sHFf diets) or corn oil (sHFc diets; see Tables 2 and 3). Control sHFf diet did not promote obesity during 2 mon of the experiment and the animals gained similar body weight as those maintained on a chow diet (Table 5, sHFf). The moderate enrichment of the diet with EPA/DHA had no significant effect on body weight; however, the weight of both epididymal and dorsolumbar fat depots tended to increase whereas DNA concentration decreased (Table 5, sHFf *vs.* sHFf-F1). The higher enrichment of the diet with EPA/DHA elicited significant reduction in body weight and adipose tissue mass as well as increase of DNA concentration in epididymal but not dorsolumbar adipose tissue (Table 5, sHFf *vs.* sHFf-F2). However, total content of DNA in neither fat depot was changed.

The next experiment was performed using the sHFc diets, that is, the control sHFc diet and the diets enriched with EPA/DHA, containing either more DHA (as in all the experiments described above) or more EPA (Table 6, sHFc-F1 and sHFc-F2, respectively). Compared to chow diet (not shown), 2.5 mon of feeding the sHFc diet did not affect body weight or mass of fat depots. However, treatment by both sHFc-F1 and sHFc-F2 diets resulted in a depression of body weight and the mass of epididymal fat. The DHA-rich sHFc-F1 diet exhibited a stronger effect compared to the EPA-rich sHFc-F2 diet (Table 6). Weight of dorsolumbar fat depot also tended to decrease, but the differences were not statistically

TABLE 4
Effects of EPA/DHA and CR on Fat Depots, Liver, and Food Consumption of Mice Fed cHF Diets

	Diet[a]				
	cHF	cHF-F1	cHF-F2	CR	cHF-F1 and CR
Epididymal fat					
Weight (mg of tissue)	1701 ± 124	1180 ± 190[b]	437 ± 60[b,c]	293 ± 60[b,c]	296 ± 50[b,c]
DNA (μg/mg of tissue)	0.39 ± 0.03	0.34 ± 0.04	0.74 ± 0.07[b,c]	0.76 ± 0.10[b,c]	0.65 ± 0.09[b,c]
(μg/depot)	652 ± 58	345 ± 47[b]	329 ± 63[b]	271 ± 50[b]	220 ± 20[b,c,d]
Dorsolumbar fat					
Weight (mg of tissue)	620 ± 40	552 ± 79	209 ± 16[b,c]	229 ± 24[b,c]	252 ± 14[b,c]
DNA (μg/mg of tissue)	0.56 ± 0.04	0.56 ± 0.05	1.20 ± 0.14[b,c]	1.41 ± 0.16[b,c]	1.05 ± 0.10[b,c]
(μg/depot)	323 ± 26	323 ± 40	244 ± 28[b]	348 ± 56	255 ± 15
Liver weight (mg)	1687 ± 85	1639 ± 74	1550 ± 120	915 ± 38[b,c,d]	935 ± 98[b,c,d]
Food consumption (kJ/d per animal)[e]	65 ± 3	NE	60 ± 3	NA	NA

[a]Animals described in Figure 1 were analyzed.
[b,c,d]Statistically significant differences compared to cHF, cHF-F1, and cHF-F2, respectively.
[e]Food consumption was estimated during the second week of feeding (week 2 in Fig. 1). There are different effects of diet on tissue weight and DNA content in various depots (ANOVA). CR, caloric restriction by 30% compared with *ad libitum*-fed mice; NA, not applicable; NE, not estimated.

TABLE 5
Effects of EPA/DHA on Body Weight and Fat Depots of Mice Fed sHFf Diet

	Diet[a]			
	Chow	sHFf	sHFf-F1	sHFf-F2
Body weight (g)				
Initial	25.5 ± 1.2	24.4 ± 0.9	25 ± 0.6	25.1 ± 0.8
Final	26.4 ± 0.8	24.3 ± 0.8	24.8 ± 0.6	22.2 ± 0.4[b,c]
Change	1.0 ± 0.4	0.6 ± 0.6	−0.15 ± 0.4	−2.9 ± 0.6[b,c]
Epididymal fat				
Weight (mg of tissue)	312 ± 45	357 ± 57	425 ± 52	182 ± 13[b,c]
DNA (μg/mg of tissue)	0.77 ± 0.07	0.77 ± 0.08	0.58 ± 0.04[b]	1.19 ± 0.14[b,c]
(μg/depot)	228 ± 24	213 ± 7	233 ± 11	211 ± 17
Dorsolumbar fat				
Weight (mg of tissue)	223 ± 18	236 ± 28	280 ± 18	207 ± 12[c]
DNA (μg/mg of tissue)	1.67 ± 0.26	1.22 ± 0.09	1.00 ± 0.04	1.57 ± 0.14[b,c]
(μg/depot)	352 ± 35	293 ± 21	279 ± 13	320 ± 23

[a]At 3 mon of age, chow diet-fed mice were divided into 4 groups (n = 8) and fed a chow, control sHFf, sHFf-F1 or sHFf-F2 diet. Animals were sacrificed at 5 months of age.
[b,c]Statistically significant differences compared to sHFf and sHFf-F1 diet, respectively. There are different effects of diet on tissue weight in various depots (ANOVA). See also Figures 2 and 3 for additional data from this experiment.

TABLE 6
Effects of EPA and DHA on Body Weight, Fat Depots, Lipid Content in Feces and Liver, and Plasma TG in Mice Fed sHFc Diets

	Diet[a]		
	sHFc	sHFc-F1	sHFc-F2
Body weight (g)			
Initial	26.9 ± 0.4	27.2 ± 0.5	27.1 ± 0.6
Final	28.1 ± 1.1	25.4 ± 0.7	26.2 ± 0.7
Change	1.7 ± 0.7	−1.4 ± 0.4[b]	−0.7 ± 0.6[b]
Epididymal fat weight (mg)	722 ± 132	355 ± 39[b]	450 ± 79
DNA (μg/mg of tissue)	0.51 ± 0.07	0.66 ± 0.08	0.74 ± 0.09
(μg/depot)	325 ± 26	216 ± 7.1[b]	339 ± 36
Dorsolumbar fat weight (mg)	268 ± 44	189 ± 12	205 ± 22
DNA (μg/mg of tissue)	0.76 ± 0.09	1.12 ± 0.11	1.29 ± 0.17[b]
(μg/depot)	190 ± 24	209 ± 19	253 ± 27
Food consumption (kJ/d per animal)[c]	73 ± 1	75 ± 2	73 ± 1
TG in feces (mg TG/g)	58 ± 9	76 ± 6	60 ± 7
TG in liver (mg TG/g)	159 ± 25	112 ± 6	91 ± 6[b]
Plasma TG (mg/dL)[d]	123 ± 9	49 ± 7[b]	36 ± 13[b]

[a]At 4 mon of age, chow diet-fed mice were divided into groups (n = 7) and fed by control sHFc, sHFc-F1, or sHFc-F2 diets. Animals were sacrificed at 6 and 1/2 mon of age.
[b]Statistically significant differences compared to sHFc diet.
[c]Mean food consumption during last 2 months of the experiment.
[d]At the time of sacrifice. In animals fed the control sHFf diet (see Table 5), food consumption was 78 ± 1 kJ/d per animal. There are different effects of diet on tissue DNA content in various depots (ANOVA).

significant (Table 6). Marked reduction of the epididymal fat due to sHFc-F1 diet was associated with a significant loss of tissue DNA (Table 6), indicating a reduction of tissue cellularity. On the other hand, the weak effect of sHFc-F2 diet on adiposity was accompanied by an increase in DNA concentration in both fat depots, but total DNA content in fat depots did not change. Food consumption was similar in all dietary groups (Table 6) including those fed the chow diet (not shown). Concentration of TG in feces was similar in all animals fed the sHF diets, whereas it was reduced in the liver of the sHFc-F2 compared with the sHFc mice (Table 6). Liver weight was similar in all groups of mice [data not shown; see also Hun *et al.* (7)].

Systemic consequences of dietary EPA/DHA. In the experiment, where the effects of EPA/DHA were tested using the sHFf diets, based on flaxseed oil (see Table 5), plasma levels of TG, NEFA, leptin, and insulin were also measured (Fig. 2). In parallel, the expression of leptin and GLUT4 genes in fat depots was also characterized (Fig. 3). Plasma TG levels were similar in mice fed the standard chow or sHFf diets, whereas they were decreased in proportion to the content of EPA/DHA in the diet. The levels of NEFA were similar in all groups of mice (Fig. 2). Leptin levels in plasma were greatly suppressed by the higher dose of EPA/DHA in the diet, whereas in all other dietary groups plasma leptin levels were similar (Fig. 2). The suppression of leptin concentrations by EPA/DHA

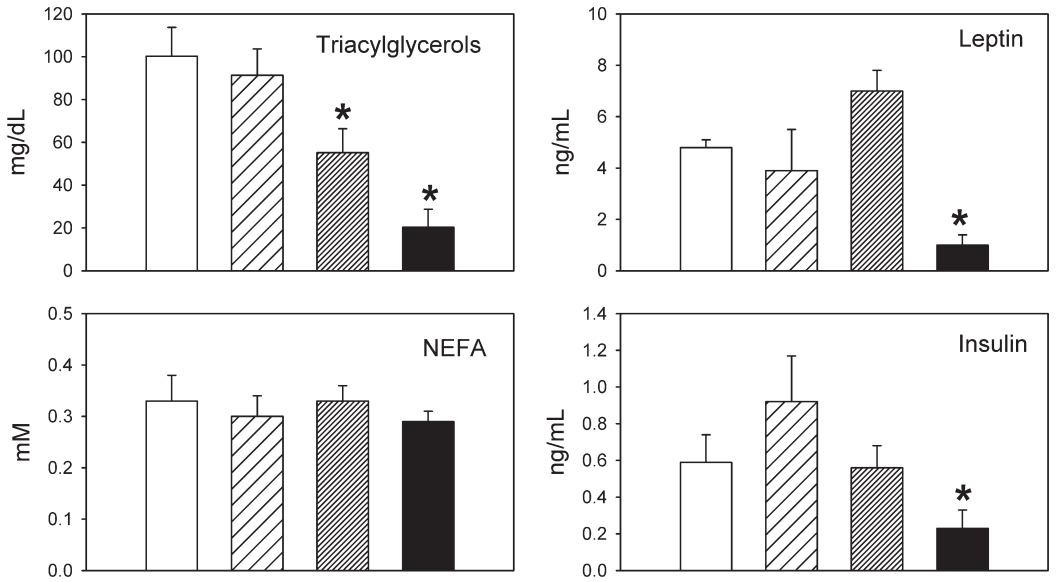

FIG 2. The effect of diet composition on plasma levels of TG, NEFA, leptin, and insulin. Metabolites and hormones were estimated in plasma of 5-mon-old mice fed either chow diet (open bars), control sHFf diet (coarse hatched bars), sHFf-F1 diet (fine hatched bars), or sHFf-F2 diet (filled bars). See Table 5 for further details. Data are means ± SE (n = 8). Asterisks indicate statistically significant differences compared with control sHFf diet.

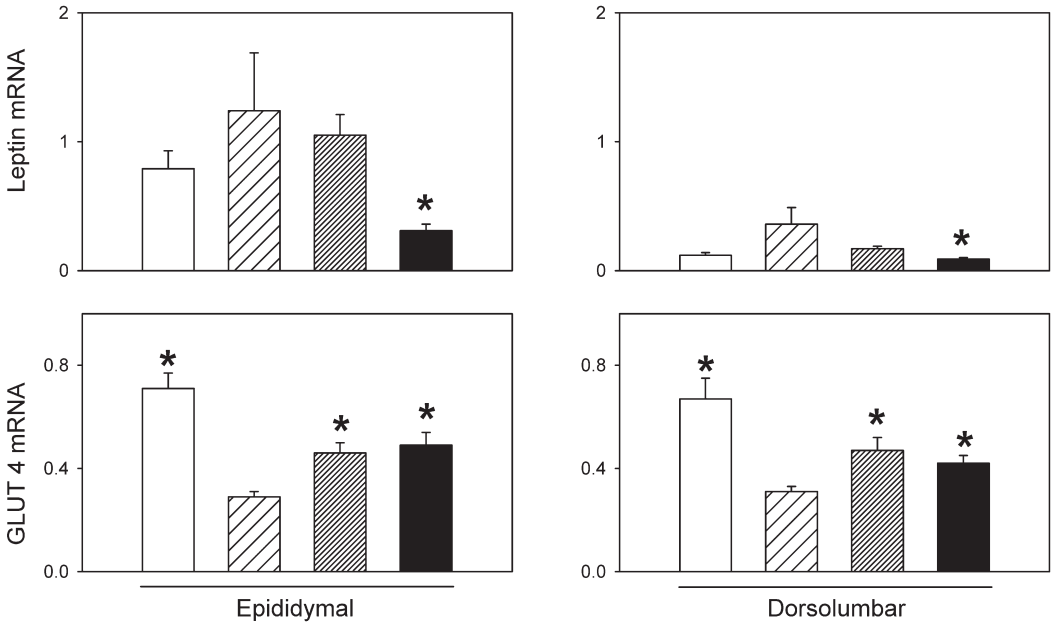

FIG 3. The effect of diet composition on transcript levels of leptin and GLUT4 in epididymal and dorsolumbar fat. Gene expression (arbitrary units) was estimated in total RNA isolated from different fat depots of 5-mon-old mice by using real-time quantitative PCR and standardized by using cyclophilin-β. For descriptions of the bars and other details, see Figure 2 and Table 5.

corresponded well with the changes in leptin gene expression in adipose tissue, namely, in epididymal fat, where the expression was in general much higher than in dorsolumbar fat (Fig. 3). The levels of insulin were similar in mice fed the control chow or sHFf diets, but were lowered proportionally to the content of the n-3 PUFA product in the diet (Fig. 2). On the contrary, blood glucose levels were not affected by dietary EPA/DHA (not shown). Expression of the GLUT4 gene, the insulin-regulated form of glucose transporters in adipocytes, was similar in both fat depots; however, it was about 2-fold higher in mice fed a standard chow compared to mice fed the sHFf diet. The expression was partially rescued by both sHFf-F1 and sHFf-F2 diets (Fig. 3).

In contrast to the differential effect of the sHFc diet rich in

DHA (sHFc-F1 diet) or EPA (sHFc-F2 diet) on weight and DNA content of the epididymal fat, plasma TG levels were lowered by both diets to a similar extent (Table 6).

DISCUSSION

In accordance with the previous studies (see introductory section) our results showed limited accumulation of epididymal fat by n-3 PUFA of marine origin admixed to various types of HF diets. Subcutaneous fat was less affected. During the development of obesity induced by cHF diet, accumulation of epididymal fat was significantly reduced when only 15% of dietary fat was replaced by lipids of marine origin and the content of EPA/DHA increased from about 1 to 12% (wt/wt) of dietary lipids. On the other hand, a larger part of dietary lipids had to be replaced by EPA/DHA for a significant reduction of adiposity in mice fed sHF diets, which did not promote obesity. A similar concentration of EPA/DHA in the sHF diet reduced adiposity also in rats (2,11). Extrapolation of our findings in mice fed cHF diets to an obese human, with a typical daily intake of about 100 g of dietary fat, suggests that additional daily intake of about 11 g of EPA/DHA would be required to limit obesity. In a clinical study conducted over 4 mon (13), daily fish meal (3.65 g of n-3 PUFA) in combination with a fat-restricted diet improved glucose metabolism and plasma lipid profile more effectively than the weight loss alone, whereas the combined treatment also tended to depress body weight more than the restriction of the dietary fat alone. In another clinical study, substitution of 6g/d of dietary fat by fish oil (1.8 g of n-3 EPA/DHA) resulted in a significant decrease of body fat over 3 weeks of treatment (15).

In accordance with the previous experiments (11), our study demonstrated that reduced accumulation of body fat in the EPA/DHA-treated animals did not result from a lower food consumption. The effect may be secondary to the stimulation of mitochondrial and peroxisomal FA oxidation in liver and muscle (2,9,11,13,28) and inhibition of hepatic lipogenesis and VLDL formation (1,2,4,9,13). These metabolic changes underlie the hypolipidemic effect of n-3 EPA/DHA, thus limiting the supply of FA to adipocytes. This idea is in accordance with our observation that an already low concentration of EPA/DHA contained in the sHFf-F1 diet, that did not affect adiposity, was sufficient to induce depression of plasma TG.

Development of obesity and accumulation of body fat may be also reduced by the modulation of gene expression in adipocytes. For example, EPA/DHA downregulate lipogenic genes (1,2,4,9,13) and stimulate expression of mitochondrial uncoupling proteins 2 and 3 (7,29) in adipose tissue. In our experiments, both DHA- and EPA-rich sHF diets (sHFc-F1 and sHFc-F2 diets, respectively) lowered plasma TG levels to a similar extent, whereas adiposity was preferentially decreased by the former diet (Table 4). These observations support the idea that the antiadipogenic effect does not result from the liver- and muscle-mediated hypolipidemia but depends, at least in part, on another mechanism. Changes in adipose tissue metabolism induced specifically by DHA could be involved. It has been observed before that natural fish oil (containing more EPA than DHA) was less potent in reducing the content of abdominal fat than an EPA/DHA mixture containing more of the latter PUFA (2).

The use of sHF diets in our experiments allowed us to characterize the significance of EFA, that is, ALA (18:3 n-3) and linoleic (18:2 n-6) acid for the antiadipogenic effect of EPA/DHA. ALA, abundant in the sHFf diets, is a precursor of EPA and DHA, but the efficiency of the conversion is low (see introductory section). Hence, dietary fish oil supplement is a more effective source of tissue DHA than is dietary ALA (4,14,30). In agreement with the above data, accumulation of epididymal fat was reduced by the sHFf-F2 diet, documenting that increased dietary intake of EPA/DHA reduces adiposity even in the presence of a high content of ALA. FA of the n-3 series are further metabolized to the group 3 series of eicosanoids, which could be involved in the antiadipogenic effect of EPA/DHA in adipocytes [for references, see Lapillonne *et al.* (9) and Raclot and Oudart (10)]. Linoleic acid (abundant in sHFc diets) serves as a precursor of arachidonic acid (20:4n-6) and groups 1 and 2 series of eicosanoids that promote adipogenesis [for references, see Azain (4), Massiera *et al.* (31), and Sessler and Ntambi (32)]. Competition between EFA occurs at the level of their desaturation and elongation since this metabolic pathway is shared by both FA. Therefore, abundance of ALA in the sHFf diets limits formation of arachidonic acid from linoleic acid and, in turn, inhibits the synthesis of the adipogenic eicosanoids of the n-6 series (30,31). Moreover, DHA inhibits cyclooxygenase, the key enzyme involved in the synthesis of these compounds (33). All these mechanisms could contribute to the reduction of fat storage due to EPA/DHA admixed to diets rich in ALA.

Enrichment of cHF diet with EPA/DHA at the low dose resulted in a depression of total amount of DNA in epididymal fat. Since each cell contains a constant amount of DNA, tissue DNA concentration and its amount could be used as markers of mean cell size and tissue cellularity, respectively. Apparently, the decrease of adipose tissue weight under these conditions was due to the reduction in number of cells in the tissue and not in the mean cell size. Only the higher dose of EPA/DHA increased DNA concentration in adipose tissue, indicating a decrease of mean cell size. DNA content of the epididymal fat was not affected by EPA/DHA-enriched sHFf diets. The different effect of EPA/DHA on DNA content and cellularity in animals fed the cHF (and also sHFc), compared with sHFf diets, could involve the inhibition of the conversion of arachidonic acid into proadipogenic eicosanoids by DHA, which probably occurs in sHFc and cHF diets. Such an effect of DHA may not take place in the sHFf diet since formation of arachidonic acid from linoleic acid in this diet is already inhibited by substrate competition with ALA (see previous discussion).

That the effect on cellularity was not noticed in the previous study (11) may be related to the fact that the number of mature fat cells rather than the content of DNA was evalu-

ated. However, DNA content of adipose tissue also decreases under other circumstances leading to depression of adiposity, such as the induction of energy dissipation by ectopic uncoupling protein 1 in adipocytes (34,35) or due to CR (3,36). Recent studies have shown a selective reduction of fat cell numbers by CR in male but not female rats (36) as well as stronger effect of CR on fat mass and gene expression in visceral than subcutaneous fat in humans (37).

Plasma leptin concentrations as well as leptin gene expression in epididymal fat positively correlated with adiposity under different dietary regimens, suggesting that leptin secretion from adipose cells followed the changes in adiposity [see also Hun *et al.* (7)]. Interestingly, EPA/DHA significantly reduced circulating insulin levels in a dose-dependent manner, suggesting improved whole-body insulin sensitivity and/or direct effect on pancreatic β-cells [see also Ikemoto *et al.* (6)]. The expression of glucose transporter GLUT4 partially restored in adipose tissue of mice treated with EPA/DHA suggests that improved insulin sensitivity of adipose tissue could be responsible, at least partly, for the enhancement in whole-body insulin sensitivity.

In summary, our results document augmentation of the anti-adipogenic effect of EPA/DHA during development of obesity and suggest that EPA/DHA could reduce accumulation of body fat by limiting both hypertrophy and hyperplasia of fat cells. Low EPA-to-DHA ratio potentiates the antiadipogenic effect. Increased dietary intake of EPA/DHA may be beneficial for prevention and treatment of obesity and related diseases regardless of ALA intake.

ACKNOWLEDGMENTS

We thank J. Bemova, S. Hornova, and D. Salkova for their technical assistance. This work was supported by the Grant Agency of the Czech Republic (grants 303/02/1220 and 303/03/P127), the research project AVOZ 5011922, and by Pronova Biocare a.s. (Norway).

REFERENCES

1. Takahashi, Y., and Ide, T. (1999) Effect of Dietary Fats Differing in Degree of Unsaturation on Gene Expression in Rat Adipose Tissue, *Ann. Nutr. Metab. 43*, 86–97.
2. Raclot, T., Groscolas, R., Langin, D., and Ferre, P. (1997) Site-Specific Regulation of Gene Expression by n-3 Polyunsaturated Fatty Acids in Rat White Adipose Tissues, *J. Lipid Res. 38*, 1963–1972.
3. Shillabeer, G., and Lau, D.C. (1994) Regulation of New Fat Cell Formation in Rats: The Role of Dietary Fats, *J. Lipid Res. 35*, 592–600.
4. Azain, M.J. (2004) Role of Fatty Acids in Adipocyte Growth and Development, *J. Anim. Sci. 82*, 916–924.
5. Hill, J.O., Peters, J.C., Lin, D., Yakubu, F., Greene, H., and Swift, L. (1993) Lipid Accumulation and Body Fat Distribution Is Influenced by Type of Dietary Fat Fed to Rats, *Int. J. Obes. Relat. Metab. Disord. 17*, 223–236.
6. Ikemoto, S., Takahashi, M., Tsunoda, N., Maruyama, K., Itakura, H., and Ezaki, O. (1996) High-Fat Diet-Induced Hyperglycemia and Obesity in Mice: Differential Effects of Dietary Oils, *Metabolism 45*, 1539–1546.
7. Hun, C.S., Hasegawa, K., Kawabata, T., Kato, M., Shimokawa, T., and Kagawa, Y. (1999) Increased Uncoupling Protein2 mRNA in White Adipose Tissue, and Decrease in Leptin, Visceral Fat, Blood Glucose, and Cholesterol in KK-Ay Mice Fed with Eicosapentaenoic and Docosahexaenoic Acids in Addition to Linolenic Acid, *Biochem. Biophys. Res. Commun. 259*, 85–90.
8. Oudart, H., Groscolas, R., Calgari, C., Nibbelink, M., Leray, C., Le Maho, Y., and Malan, A. (1997) Brown Fat Thermogenesis in Rats Fed High-Fat Diets Enriched with n-3 Polyunsaturated Fatty Acids, *Int. J. Obes. Relat. Metab. Disord. 21*, 955–962.
9. Lapillonne, A., Clarke, S.D., and Heird, W.C. (2004) Polyunsaturated Fatty Acids and Gene Expression, *Curr. Opin. Clin. Nutr. Metab. Care 7*, 151–156.
10. Raclot, T., and Oudart, H. (1999) Selectivity of Fatty Acids on Lipid Metabolism and Gene Expression, *Proc. Nutr. Soc. 58*, 633–646.
11. Belzung, F., Raclot, T., and Groscolas, R. (1993) Fish Oil n-3 Fatty Acids Selectively Limit the Hypertrophy of Abdominal Fat Depots in Growing Rats Fed High-Fat Diets, *Am. J. Physiol. 264*, R1111–R1118.
12. Ruxton, C.H., Reed, S.C., Simpson, M.J., and Millington, K.J. (2004) The Health Benefits of Omega-3 Polyunsaturated Fatty Acids: A Review of the Evidence, *J. Hum. Nutr. Diet. 17*, 449–459.
13. Mori, T.A., Bao, D.Q., Burke, V., Puddey, I.B., Watts, G.F., and Beilin, L.J. (1999) Dietary Fish as a Major Component of a Weight-Loss Diet: Effect on Serum Lipids, Glucose, and Insulin Metabolism in Overweight Hypertensive Subjects, *Am. J. Clin. Nutr. 70*, 817–825.
14. Sinclair, A.J., Attar-Bashi, N.M., and Li, D. (2002) What Is the Role of α-Linolenic Acid for Mammals? *Lipids 37*, 1113–1123.
15. Couet, C., Delarue, J., Ritz, P., Antoine, J.-M., and Lamisse, F. (1997) Effect of Dietary Fish Oil on Body Fat Mass and Basal Fat Oxidation in Healthy Adults, *Int. J. Obes. 21*, 637–643.
16. Benhizia, F., Hainault, I., Serougne, C., Lagrande, D., Hajduch, E., Guichard, C., Malewiak, M.-I., Quignard-Boulange, A., Lavau, M., and Griglio, S. (1994) Effects of Fish Oil–Lard Diet on Rat Plasma Lipoproteins, Liver FAS, and Lipolytic Enzymes, *Am. J. Physiol. 267*, E975–E982.
17. Parrish, C.C., Pathy, D.A., and Angel, A. (1990) Dietary Fish Oils Limit Adipose Tissue Hypertrophy in Rats, *Metabolism 39*, 217–219.
18. Cha, S.H., Fukushima, A., Sakuma, K., and Kagawa, Y. (2001) Chronic Docosahexaenoic Acid Intake Enhances Expression of the Gene for Uncoupling Protein 3 and Affects Pleiotropic mRNA Levels in Skeletal Muscle of Aged C57BL/6njcl Mice, *J. Nutr. 131*, 2636–2642.
19. Tsuboyama-Kasaoka, N., Takahashi, M., Kim, H., and Ezaki, O. (1999) Up-Regulation of Liver Uncoupling Protein-2 mRNA by Either Fish Oil Feeding or Fibrate Administration in Mice, *Biochem. Biophys. Res. Commun. 257*, 879–885.
20. Surwit, R.S., Kuhn, C.M., Cochrane, C., McCubbin, J.A., and Feinglos, M.N. (1988) Diet-Induced Type II Diabetes in C57BL/6J Mice, *Diabetes 37*, 1163–1167.
21. West, D.B., Boozer, C.N., Moody, D.L., and Atkinson, R.L. (1992) Dietary Obesity in Nine Inbred Mouse Strains, *Am. J. Physiol. 262*, R1025–R1032.
22. Kopecky, J., Hodny, Z., Rossmeisl, M., Syrovy, I., and Kozak, L.P. (1996) Reduction of Dietary Obesity in the aP2-*Ucp* Transgenic Mice: Physiology and Adipose Tissue Distribution, *Am. J. Physiol. 270*, E768–E775.
23. Parekh, P.I., Petro, A.E., Tiller, J.M., Feinglos, M.N., and Surwit, R.S. (1998) Reversal of Diet-Induced Obesity and Diabetes in C57BL/6J Mice, *Metabolism 47,* 1089–1096.
24. Cinti, S. (1999) *The Adipose Organ*, Editrice Kurtis, Milano, Italy.
25. Salmon, D.M., and Flatt, J.P. (1985) Effect of Dietary Fat Content on the Incidence of Obesity Among *ad libitum* Fed Mice, *Int. J. Obes. 9*, 443–449.

26. Stefl, B., Janovska, A., Hodny, Z., Rossmeisl, M., Horakova, M., Syrovy, I., Bemova, J., Bendlova, B., and Kopecky, J. (1998) Brown Fat Is Essential for Cold-Induced Thermogenesis but Not for Obesity Resistance in aP2-*Ucp* Mice, *Am. J. Physiol. 274*, E527–E533.
27. Flachs, P., Novotny, J., Baumruk, F., Bardova, K., Bourova, L., Miksik, I., Sponarova, J., Svoboda, P., and Kopecky, J. (2002) Impaired Noradrenaline-Induced Lipolysis in White Fat of aP2-*Ucp*1 Transgenic Mice Is Associated with Changes in G-Protein Levels, *Biochem. J. 364*, 369–376.
28. Christiansen, E.N., Flatmark, T., and Kryvi, H. (1981) Effects of Marine Oil Diet on Peroxisomes and Mitochondria of Rat Liver: A Combined Biochemical and Morphometric Study, *Eur. J. Cell Biol. 26*, 11–20.
29. Oudart, H., Trayhurn, P., and Rayner, D.V. (2000) Effect of n-3 Polyunsaturated Fatty Acids on Uncoupling Protein 1-3 Gene Expression, *Int. J. Obes. Metab. Disord. 24 (Suppl. 1)*, S130 (Abstract No. 424).
30. Amusquivar, E., and Herrera, E. (2003) Influence of Changes in Dietary Fatty Acids During Pregnancy in Placental and Fetal Fatty Acid Profile in the Rat, *Biol. Neonate 83*, 136–145.
31. Massiera, F., Saint-Marc, P., Seydoux, J., Murata, T., Kobayashi, T., Narumiya, S., Guesnet, P., Amri, E.Z., Negrel, R., and Ailhaud, G. (2003) Arachidonic Acid and Prostacyclin Signaling Promote Adipose Tissue Development: A Human Health Concern? *J. Lipid Res. 44*, 271–279.
32. Sessler, A.M., and Ntambi, J.M. (1998) Polyunsaturated Fatty Acid Regulation of Gene Expression, *J. Nutr. 128*, 923–926.
33. Ringbom, T., Huss, U., Stenholm, A., Flock, S., Skattebol, L., Perera, P., and Bohlin, L. (2001) COX-2 Inhibitory Effects of Naturally Occurring and Modified Fatty Acids, *J. Nat. Prod. 64*, 745–749.
34. Kopecky, J., Clarke, G., Enerback, S., Spiegelman, B., and Kozak, L.P. (1995) Expression of the Mitochondrial Uncoupling Protein Gene from the aP2 Gene Promoter Prevents Genetic Obesity, *J. Clin. Invest. 96*, 2914–2923.
35. Kopecky, J., Rossmeisl, M., Hodny, Z., Syrovy, I., Horakova, M., and Kolarova, P. (1996) Reduction of Dietary Obesity in the aP2-*Ucp* Transgenic Mice: Mechanism and Adipose Tissue Morphology, *Am. J. Physiol. 270*, E776–E786.
36. Porter, M.H., Fine, J.B., Cutchins, A.G., Bai, Y., and DiGirolamo, M. (2004) Sexual Dimorphism in the Response of Adipose Mass and Cellularity to Graded Caloric Restriction, *Obes. Res. 12*, 131–140.
37. Li, Y., Bujo, H., Takahashi, K., Shibasaki, M., Zhu, Y., Yoshida, Y., Otsuka, Y., Hashimoto, N., and Saito, Y. (2003) Visceral Fat: Higher Responsiveness of Fat Mass and Gene Expression to Calorie Restriction than Subcutaneous Fat, *Exp. Biol. Med. (Maywood) 228*, 1118–1123.

[Received and accepted November 29, 2004]

Effect of Cancer Cachexia on Triacylglycerol/Fatty Acid Substrate Cycling in White Adipose Tissue

S.A. Beck and M.J. Tisdale*

Pharmaceutical Sciences Research Institute, Aston University, Aston Triangle, Birmingham, B4 7ET, UK

ABSTRACT: The effect of cancer cachexia on the TAG/FA substrate cycle in white adipose tissue was determined *in vivo* using the MAC16 murine model of cachexia. When compared with non-tumor-bearing animals, the rate of TAG-glycerol production was found to be increased almost threefold in animals bearing the MAC13 tumor, which does not induce cachexia, but was not further elevated in animals bearing the MAC16 tumor. In both cases TAG-glycerol production and *de novo* synthesis of TAG-FA were also increased above non-tumor-bearing animals. In animals bearing the MAC16 tumor, the TAG-FA rates were significantly higher than in animals bearing the MAC13 tumor. This suggests that the presence of the tumor alone is sufficient to cause an increase in cycling rate, and in the absence of an elevated energy intake (MAC16) this may contribute to the depletion of adipose tissue.

Paper no. L9569 in *Lipids 39,* 1187–1189 (December 2004).

Cancer cachexia is associated with a marked loss of host body weight with depletion of both skeletal muscle and adipose tissue mass. In cancer patients, depletion of lipid stores may reach 85% of the values found in controls matched for pre-illness stable weight of the cancer patient (1). In animals bearing an experimental model of cachexia (MAC16 adenocarcinoma), depletion of adipose tissue occurs in the absence of anorexia (2) and early in the development of the tumor. Lipid mobilization in this model appears to arise from the production by the tumor and adipose tissue of a lipid-mobilizing factor (LMF) identical with the plasma protein zinc α_2-glycoprotein (3), the expression of which increases as weight loss increases (4).

The adipose tissue mass is a balance between the rate of lipolysis and the rate of esterification of nonesterified FA (NEFA) into TAG. Both processes can occur simultaneously, i.e., a high proportion of the NEFA released is immediately re-esterified, and these reactions are referred to as the TAG/FA substrate cycle. Using direct injection of tracer into the interstitial fluid of fat pads, Ookhtens *et al.* (5) showed a large decrease in the fractional rate of NEFA esterification in the epididymal fat pads of mice bearing the Ehrlich ascites carcinoma with accumulation of NEFA within fat pads. Such a decreased cycle was suggested as an energy conservation mechanism to prevent rapid depletion of adipose tissue in the tumor-bearing state.

To whom correspondence should be addressed at Pharmaceutical Research Institute, Aston University, Aston Triangle, Birmingham, B4 7ET, United Kingdom. E-mail: m.j.tisdale@aston.ac.uk

Abbreviations: LMF, liquid-mobilizing factor; NEFA, non-esterified FA.

In view of the rapid depletion of adipose tissue in the cachectic state, the rate of the TAG/FA substrate cycle was measured *in vivo* in non-tumor-bearing animals and compared with that in animals bearing two types of transplantable colonic adenocarcinomas, the MAC16, which induces mobilization of fat stores, and the MAC13, which is of the same histological type, but which grows without a significant loss of body fat (6).

EXPERIMENTAL PROCEDURES

Pure-strain male NMRI mice (average weight 26 g) were bred in our own colony and were transplanted with fragments (1 × 2 mm) of either the MAC13 or MAC16 tumors into the flank by means of a trochar as described previously (2). Animals were given free access to both food (Special Diet Services, Essex, United Kingdom) and water. For animals bearing the MAC16 tumor, experiments were performed when the animals had an average weight loss of 5.58 ± 0.53 g (21%), and for animals bearing the MAC13 tumor, experiments were performed when the tumor volume was comparable with that in animals bearing the MAC16 tumor.

Each animal was injected with ^3H_2O (10 mCi/kg) i.p. and after 3 h adipose tissue was removed and immediately frozen. The frozen tissue was weighed, homogenized in 15 mL of chloroform/methanol (2:1 vol/vol), and washed with 3 mL of water and twice with 3 mL of methanol/water (1:1 vol/vol) as described previously (7). The aqueous layer was removed and the lipid phase was evaporated under a stream of nitrogen. To each sample 3 mL of ethanol and 3 mL of 30% (wt/vol) KOH were added together with tracer [^{14}C]glycerol (1000 dpm), and saponification was achieved by heating at 70°C for 2 h. The cooled samples were acidified with 1.8 mL of 60% (wt/vol) $HClO_4$, and the NEFA was extracted twice with 10 mL of petroleum ether (b.p. 40–60°C). After evaporation of the petroleum ether under a stream of N_2, the radioactivity in the residue was determined in Optiphase Hisafe II scintillation fluid. The aqueous phase was neutralized with 20% KOH, and the insoluble $KClO_4$, was removed by centrifugation (1000 × *g*). A portion (0.5 mL) of the supernatant was dried under N_2 at 60–70°C, and the radioactivity was determined as described above with a Packard Tri-carb 2000CA liquid-scintillation analyzer programmed to yield dpm for ^{3}H and ^{14}C. The rate of cycling was calculated as described in Hansson *et al.* (7). *De novo* synthesis of TAG-FA was calculated by dividing the ^{3}H radioactivity of the NEFA in the pe-

troleum ether extract by the specific activity of ^3H_2O times 13.3. Synthesis of TAG-glycerol was calculated from the ^3H radioactivity of the aqueous sample (corrected for recovery of [^{14}C] glycerol) divided by three times the specific radioactivity. The cycling rate is the total esterification rate minus the esterification rate of FA synthesized *de novo*, i.e., three times the TAG synthesis rate minus the TAG-FA synthesis rate. ^3H_2O (sp act 5 mCi/mL) was purchased from Amersham Life Science Products (Buckinghamshire, United Kingdom, and [^{14}C]glycerol (sp act 157 mCi/mmol) from New England Nuclear (Stevenage, Herts, United Kingdom). Another group of animals received Tyloxapol [Triton WR 1339; 0.1 mL of a 10% (wt/vol) aqueous solution per 26 g mouse] by tail-vein injection 1 h prior to the ^3H_2O. Control animals received 0.1 mL of 0.9% NaCl. The plasma TAG concentrations were determined with a TAG diagnostic kit (Sigma Diagnostic, Dorset, United Kingdom). Results are presented as mean ± SEM Differences between means was determined by one-way ANOVA, followed by Tukey's post-test.

RESULTS

The effect of exogenous NEFA on the synthesis rate of TAG and the cycling rate were determined by the use of Tyloxapol, an inhibitor of lipoprotein lipase (8). Administration of Tyloxapol to both non-tumor-bearing animals and to animals bearing either the MAC13 or MAC16 tumors caused an increase in the plasma TAG concentration (Table 1). However, there was no effect of this agent on either the synthesis rate of TAG-glycerol or the cycling rate, as shown in Table 2, suggesting that the rate of esterification of exogenous FA is low and does not affect the rate of cycling.

The rates of TAG-glycerol production, *de novo* synthesis of TAG-FA and the TAG/FA substrate cycling rate in epididymal adipose tissue of non-tumor-bearing mice or in animals bearing either the MAC13 or MAC16 tumors are shown in Table 2. In non-tumor-bearing animals, the *in vivo* rate of TAG/FA cycling is similar to that reported by Hansson *et al.* (7) in white adipose tissue in fed virgin rats. In animals bearing both the MAC13 and MAC16 tumors, both the TAG-glycerol and TAG-FA synthesis rates were significantly elevated over those found in the epididymal adipose tissue of non-tumor-bearing mice. In addition, in animals bearing the MAC13 tumor, the rate of TAG/FA cycling was increased almost threefold over that found in non-tumor-bearing animals, but was not further elevated in animals bearing the MAC16 tumor. Only the synthesis of TAG-FA was significantly elevated in animals bearing the MAC16 tumor when compared with animals bearing the MAC13 tumor.

TABLE 1
The Effect of Tyloxapol on Plasma TAG Concentration[a]

Group	Plasma TAG (mg/100 mL)	
	NaCl	Tyloxapol
Non-tumor-bearing	249 ± 50	569 ± 107
MAC13	141 ± 60	276 ± 21
MAC16	137 ± 35	437 ± 142

[a]Results are expressed as mean ± SEM for six animals per group.

TABLE 2
Effect of the Tumor-Bearing State and Cachexia on Rates of TAG-Glycerol and TAG-FA Synthesis and Rate of TAG/FA Substrate Cycling in Epididymal Adipose Tissue[a]

Group	Rate (μmol/h/g wet wt.)		
	TAG-glycerol	TAG-FA	TAG/FA cycling
Non-tumor-bearing	0.77 ± 0.14	0.060 ± 0.005	2.25 ± 0.40
+ Tyloxapol	0.92 ± 0.21	0.070 ± 0.02	2.62 ± 0.47
MAC13	2.18 ± 0.21[c]	0.20 ± 0.01[c]	6.34 ± 0.62[c]
+ Tyloxapol	2.41 ± 0.19	0.22 ± 0.01	7.39 ± 0.70
MAC16	2.53 ± 0.28[c]	0.34 ± 0.02[b,c]	7.25 ± 0.81[c]
+ Tyloxapol	3.02 ± 0.31	0.36 ± 0.02	8.44 ± 1.31

[a]Results are expressed as mean ± SEM for six animals per group.
[b]$P < 0.01$ compared with animals bearing the MAC13 tumor.
[c]$P < 0.001$ compared with non-tumor-bearing controls.

DISCUSSION

The method employed in the present study for the measurement of the TAG/FA cycling rates assumes a negligible esterification of exogenous NEFA. This assumption was shown to be correct by the use of Tyloxapol, which decreases the rate of removal of TAG from the plasma by inhibiting lipoprotein lipase activity (8). However, despite the increase in plasma TAG concentration, neither the synthesis rate of TAG-glycerol nor the cycling rate was decreased. This suggests that the rate of esterification of exogenous FA is low under the conditions of the present experiment and consequently does not affect the rate of cycling.

This study shows that the futile cycle of NEFA esterification and hydrolysis is significantly enhanced in tumor-bearing animals, although surprisingly, is not further elevated in the cachectic state. This may arise from the fact that both glycerol and NEFA released from adipose tissue and utilized are not taken into account using the present methodology. The increase in cycling rate in animals bearing the MAC13 tumor (4.09 μmol/h per g wet wt) would result in an ATP consumption of 13.6 μmol/h per g wet wt, assuming 3.33 molecules of ATP are hydrolyzed per molecule of re-esterified FA (7). Such an effect would result in depletion of adipose tissue if energy intake remained normal. However, animals bearing the MAC13 tumor show an increased food intake (16.4 ± 0.3 kcal/d) compared with non-tumor-bearing controls (15.3 ± 0.3 kcal/d), reflecting an increased energy requirement in the tumor-bearing state (6). In contrast, animals bearing the MAC16 tumor showed no change in energy consumption (15.1 ± 0.3 kcal/d) compared with non-tumor-bearing animals. Such an inability to compensate for an increased energy demand would contribute to the loss of adipose tissue in animals bearing the MAC16 tumor.

ACKNOWLEDGMENT

We thank Mr. M. Wynter for the tumor transplantations.

REFERENCES

1. Fearon, K.C.H. (1992) The Mechanism and Treatment of Weight Loss in Cancer, *Proc. Nutr. Soc. 51*, 251–265.
2. Beck, S.A., and Tisdale, M.J. (1987) Production of Lipolytic and Proteolytic Factors by a Murine Tumor-Producing Cachexia in the Host, *Cancer Res. 47*, 5919–5923.
3. Todorov, P.T., McDevitt, T.M., Meyer, D.J., Ueyama, H., Ohkubo, I., and Tisdale, M.J. (1998) Purification and Characterization of a Tumor Lipid-Mobilizing Factor, *Cancer Res. 58*, 2353–2358.
4. Bing, C., Bao, Y., Jenkins, J., Sanders, P., Manieri, M., Cinti, S., Tisdale, M.J., and Trayhum, P. (2004) Zinc-α_2-glycoprotein, a Lipid Mobilizing Factor, Is Expressed in Adipocytes and Is Up-regulated in Mice with Cancer Cachexia, *Proc. Natl. Acad. Sci. USA 101*, 2500–2505.
5. Ookhtens, M., Montisano, D., Lyon, I., and Baker, N. (1986) Inhibition of Fatty Acid Incorporation into Adipose Tissue Triglycerides in Ehrlich Ascites Tumor-Bearing Mice, *Cancer Res. 46*, 633–638.
6. Mulligan, H.D., and Tisdale, M.J. (1991) Lipogenesis in Tumour and Host Tissues in Mice Bearing Colonic Adenocarcinomas, *Br. J. Cancer 63*, 719–722.
7. Hansson, P., Newsholme, E.A., and Williamson, D.H. (1987) Effects of Lactation and Removal of Pups on the Rate of Triacylglycerol/Fatty Acid Substrate Cycling in White Adipose Tissue of the Rat, *Biochem. J. 243*, 267–271.
8. Scanu, A.M. (1965) Factors Affecting Lipoprotein Metabolism, *Adv. Lipid Res. 3*, 63–138.

[Received August 4, 2004; accepted October 27, 2004]

A Randomized Controlled Trial of the Effect of Fish Oil Supplementation in Late Pregnancy and Early Lactation on the n-3 Fatty Acid Content in Human Breast Milk

Jane Boris[a], Benny Jensen[b], Jannie Dalby Salvig[a], Niels J. Secher[c], and Sjúrdur F. Olsen[d,*]

[a]Perinatal Epidemiologic Research Unit, Department of Obstetrics & Gynecology, Aarhus University Hospital, DK-8000 Aarhus C, Denmark, [b]Ministry of Agriculture and Fisheries, Danish Institute for Fisheries Research, Department of Seafood Research, Technical University of Denmark, DK-2800 Lyngby, Denmark, [c]Department of Obstetrics and Gynaecology, Hvidovre University Hospital, Copenhagen, Denmark, and [d]Maternal Nutrition Group, Danish Epidemiology Science Centre, Statens Serum Institut, Copenhagen, Denmark.

ABSTRACT: The aim of this research was to investigate the effect of fish oil supplementation, in the third trimester of pregnancy and early lactation period of healthy pregnant Danish women. Forty-four pregnant women were randomly allocated to fish oil supplementation (1.3 g EPA and 0.9 g DHA per day) from week 30 of gestation (FO-group) or to a control regimen (olive oil or no oil; controls). The FO-group was randomly subdivided into women stopping fish oil supplementation at delivery [FO(pregn)], and women continuing supplementation for an additional 30 d [FO(pregn/lact)]. Thirty-six women agreed to collect milk samples at days 4, 16, and 30 postpartum. The FA composition of the milk samples was determined by GLC. At days 4, 16, and 30 in lactation, FO(pregn/lact) women (n = 12) had, respectively 2.3 (P = 0.001), 4.1 (P = 0.001), and 3.3 (P = 0.001) times higher mean contents of LCPUFA(n-3) in their breast milk compared with controls (n = 13), and 1.7 (P = 0.005), 2.8 (P = 0.001), and 2.8 (P = 0.001) times higher LCPUFA(n-3) contents, respectively, at these days compared with FO(pregn) women (n = 11). The latter group did not differ significantly from controls with regard to LCPUFA(n-3) content in the breast milk. Similar results were obtained when analyzing separately for effects on the milk content of DHA. Dietary supplementation with 2.7 g LCPUFA(n-3) per day from week 30 of gestation and onward more than tripled the LCPUFA(n-3) content in early breast milk; supplementation limited to pregnancy only was much less effective.

Paper no. L9607 in *Lipids 39*, 1191–1196 (December 2004).

Docosapentaenoic acid (DPA, 22:5n-3) is a main component of structural lipids in the human brain and retina, as is docosahexaenoic acid (DHA), 22:6n-3) (1,2). In the early months postnatally, DHA increases substantially and constitutes between 25 and 60% of the phospholipid FA in these tissues (3,4). Earlier studies demonstrated that growing rats and monkeys fed a diet deficient in n-3 FA had behavioral changes, abnormal retinal responses to light, and poorer visual acuity development as compared with controls (3,5). These disturbances seem to be irreversible, since visual acuity did not reverse when the animals were fed long-chain n-3 PUFA [LCPUFA(n-3)] as adults, indicating an early critical period for the accumulation of DHA in neural tissues (6). Data suggest that these findings can be applied to humans, since preterm as well as term infants fed breast milk or diets supplemented with LCPUFA(n-3) had a better visual acuity (7–11) and mental capacity (12) than infants fed diets low in DHA.

The issue of essentiality of DHA and other LCPUFA(n-3) for newborn infants has primarily been discussed in relation to infant milk formulas, which as commercial products have been supplemented relatively recently with LCPUFA(n-3). However, the exact quantities of n-3 FA needed by newborn infants remain to be established, and it is possible that the content of these FA in breast milk is also critical. It is therefore important to identify factors determining the LCPUFA (n-3) level of early human breast milk.

Several observational studies (13–18), two nonrandomized intervention studies (19,20), and one randomized controlled trial (21) strongly suggest that the dietary supply of LCPUFA(n-3) to lactating women is the major determinant of the LCPUFA(n-3) content in breast milk. However, little seems to be known about the relationship of fish oil intake in pregnancy to the pattern of LCPUFA(n-3) concentration in breast milk in the early lactation period. Since recent evidence suggests an effect of LCPUFA(n-3) ingested in pregnancy on the duration of pregnancy and on preterm delivery (22,23), pregnant women may be recommended to increase their n-3 FA intake for this reason alone. We set out to test the hypotheses that (i) dietary supplementation of n-3 FA solely during pregnancy increases the n-3 FA content in the early breast milk, and also that (ii) continued supplementation after delivery is needed for a sustained increase over a longer period of time.

We have undertaken a randomized, controlled trial to compare the effects on the n-3 FA content of human breast milk during the first 30 d after delivery of the following three treatment regimens: (i) fish oil supplementation from week 30 of gestation until delivery, (ii) fish oil supplementation from week

*To whom correspondence should be addressed at Maternal Nutrition Group, Danish Epidemiology Science Centre, Statens Serum Institut, 5 Artillerivej, DK-2300 Copenhagen S, Denmark. E-mail: SFO@SSI.DK.

Abbreviations: control-1, olive oil supplemented during pregnancy; control-2, women receiving no oil capsules; controls, control-1 and control-2 combined; DHA, docosahexaenoic acid (22:6n-3); DPA, docosapentaenoic acid (22:5n-3); EPA, eicosapentaenoic acid (20:5n-3); FO(pregn), fish oil supplemented during pregnancy only; FO(pregn/lact), fish oil supplemented during both pregnancy and lactation; FO-group, fish oil supplemented from week 30 of gestation; LCPUFA(n-3), long-chain n-3 PUFA.

30 of gestation and continued after delivery during the period of milk collection; and (iii) no fish oil supplementation.

SUBJECTS AND METHODS

Trial design. The present study is part of a larger community-based randomized controlled trial of fish oil supplementation in pregnancy (22). The aim of the larger trial was to test whether fish oil supplementation among pregnant Danish women could prolong the duration of pregnancy and thereby explain the increased birth weight and longer gestation periods in the Faroe Islands compared with Denmark (22). Since, at the time the trial was planned, which types of controls would be most appropriate was not clear, we decided to use two different control groups, one receiving olive oil and the other receiving no oil; thus, women were randomized in the ratio 2:1:1 to receive fish oil capsules (FO-group), olive oil capsules (control-1), or no oil capsules (control-2). For the purpose of the present study, we combined the two control groups into one since we expected olive oil to be inert in relation to the outcome studied (DHA content of maternal milk). A consecutive sample of 44 of the women enrolled in the trial were asked to participate in the present study involving the collection of milk samples; 36 women accepted. The women allocated to treatment with fish oil in pregnancy were further divided randomly into two groups, one of which followed the usual regimen of stopping supplementation at delivery [FO(pregn), $n = 11$)], and the other of which was asked to continue fish oil supplementation for an additional 30 d [FO(pregn/lact), $n = 12$]. Women who had been allocated to the control group (controls, $n = 13$) received in pregnancy one of two control treatments: One was given olive oil until delivery (control-1), and the other was given no supplementation at all (control-2); no treatment was given postpartum. A sketch of the design is given in Figure 1.

The study protocol was approved by the Regional Scientific-Ethical Committee of the County of Aarhus, Denmark.

The oil supplements. The fish oil supplement consisted of four 1-g gelatine capsules with Pikasol® (Lube A/S, Hadsund, Denmark) fish oil TAG [32% eicosapentaenoic acid (EPA, 20:5n-3), 23% DHA, and 2 mg tocopherol/mL)], corresponding to 1.3 g EPA and 0.9 g DHA acid per day (the dose used was determined in such a way that it exceeded the difference between intake of marine n-3 FA in the Faroe Islands and Denmark, see the *Trial design* section). The olive oil supplement consisted of four 1-g capsules of olive oil per day [72% oleic acid (18:1n-9) and 12% linoleic acid (18:2n-6)].

Milk collection, handling, and storage. The day after delivery, the women received written information about the procedure for collecting the milk samples. Milk samples were hand-expressed by the mothers at days 4, 16 and 30 after delivery at the hospital or at home. For each milk sample, 1–3 mL of breast milk was collected into two plastic containers, one from the very beginning and one from the end of a milk-giving (24). All samples were taken from a morning milk-giving and from one breast only.

The milk samples were stored in a refrigerator (5°C) until collected by one of the research workers (i.e., .5–8 h after expression) and then stored for 3 to 6 mon at −52°C until transfer to the lipid laboratory. Before freezing, four drops of BHT (0.01%, 100 mg/L ethanol) was added to each container to prevent oxidation (24).

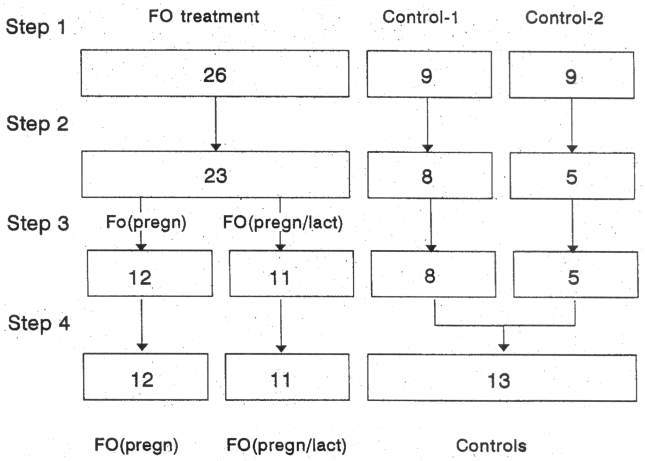

FIG. 1. Step 1: A consecutive sample of 44 women was drawn from the larger trial (see Ref. 22). Step 2: Women were asked to participate in the milk study. Step 3: The fish oil group was randomly divided (1:1) into two groups. Step 4: The control groups were combined for statistical analysis. FO treatment, fish oil supplemented from week 30 of gestation; FO(pregn), fish oil supplemented during pregnancy only; FO(pregn/lact), fish oil supplemented during both pregnancy and lactation; control-1, olive oil supplemented during pregnancy; control-2, women receiving no oil capsules; controls, control-1 and control-2 combined.

All samples were stored and analyzed, with the only identification being the original cryptographed numbers.

Milk analyses. All solvents were of analytical grade. The extraction procedure was based on the method of Bitman *et al.* (25), as recommended by Jensen *et al.* (24). However, lipase inactivation by heating was omitted. At the lipid laboratory, samples were stored at −30°C for up to 2 wk before analysis. The samples were slowly thawed at room temperature and placed in a water bath at 38°C for 15 min. The tubes were gently inverted 10 times to mix the cream layer. For each milk sample, aliquots with equal volumes of milk (usually 600 L) from the beginning and end of a milk-giving were transferred to a mixing tube. The tube was held at 38°C for a few minutes and inverted several times before 1 mL was taken for extraction, according to Bitman *et al.* (25), using 18 mL of dichloromethane + methanol (2 + 1, vol/vol), with 0.01% BHT. The headspace above the sample was flushed with nitrogen, covered, and mechanically homogenized (UltraTurrax) for 30 s. Saline (0.7% sodium chloride, 6 mL) was then added, the headspace was flushed with nitrogen, and the tubewas shaken 10 times and then centrifuged at 10°C for 10 min at $260 \times g_{aver}$.

The extracts were used for gravimetric determination of the extracted lipid (in duplicate) and for preparation of methyl esters for GC (in duplicate, with and without internal standards). For gravimetry, the solvent was removed under a nitrogen flow

at 30–35°C, and the weighing glass was held at 105°C for 2 h. Methyl ester preparation was carried out essentially as described in AOCS method Ce 1b-89 (26), using saponification and transmethylation by methanolic sodium hydroxide, followed by boron trifluoride-catalyzed methylation. After addition of a saturated sodium chloride solution, methyl esters were extracted into heptane. Heptadecanoic and tricosanoic acids were added as internal standards.

GC. An HP-5890 gas chromatograph (Hewlett-Packard, Avondale, PA) with a capillary injection port, an HP-7673A autosampler, and an FID was used. Samples (2.0 L) were injected in split mode (split ratio 1:50) onto an SP-2330 (Supelco, Bellefonte, PA) fused-silica capillary column (30 m × 0.32 mm; 0.2 m of 68% cyanopropyl phenylpolysilooxane as the stationary phase). The injection and detection temperatures were 250 and 240°C, respectively. The initial oven temperature of 140°C was immediately raised at a rate of 3°C/min to 200°C, held for 1 min, increased further at the same rate to 220°C, and finally held at this temperature for 9 min. Helium was used as carrier gas at a flow of 21 cm/s. Integration was carried out by an HP-3396A integrator with data transfer to a computer using HP-3393A/3396A file- server software (Hewlett-Packard).

Calculations. Relative FA composition (% distribution) was calculated as area percent (area%) distribution without the use of a response. FA shorter than 10 carbons were not determined by the method used. BHT-derived peaks did not coelute with FAME, and their areas were excluded from calculations.

The total lipid contents are shown as results from the basic gravimetric determinations.

Statistics. Differences between group means were tested by Student's *t*-test or ANOVA.

RESULTS

The three study groups were similar in baseline characteristics with regard to maternal age at delivery, prepregnant weight, parity, and percentage of smokers (data not shown).

General pattern. In the course of lactation we observed a decline in total milk LCPUFA(n-3) content among all three study groups (Table 1). A drastic decline in DHA and total LCPUFA(n-3) content of the very first breast milk (colostrum) was seen in the FO(pregn) group, which stopped fish oil supplementation at delivery; at the end of the study period these women had nearly reached the levels of the respective controls. Total lipid concentration was independent of the treatment regimen throughout the study period.

FO(pregn/lact) vs. controls. Compared with the controls, women who received fish oil during pregnancy and lactation had 2.3 ($P = 0.001$), 4.1 ($P = 0.001$), and 3.3 ($P = 0.001$) times higher levels of LCPUFA(n-3) at days 4, 16, and 30, respectively. The DHA levels in milk from mothers who continued fish oil supplementation were 2.1 ($P = 0.001$), 3.6 ($P = 0.001$), and 2.8 ($P = 0.001$) times higher than the levels found in milk from controls.

FO(pregn/lact) vs. FO(pregn). Women who received fish oil during both pregnancy and lactation had 1.7 ($P = 0.005$), 2.8 ($P = 0.001$), and 2.8 ($P = 0.001$) times higher levels of LCPUFA(n-3) at days 4, 16, and 30, respectively, than did women who received fish oil only during pregnancy. Estimations of DHA at days 4, 16, and 30, respectively, showed 1.5 ($P = 0.05$), 2.6 ($P = 0.001$), and 2.4 ($P = 0.001$) times higher DHA levels in milk from women who received fish oil supplements during both pregnancy and lactation compared with women who received supplements only during pregnancy.

FO(pregn) vs. controls. Women who received fish oil only during pregnancy tended to have somewhat higher levels (although not significant) of LCPUFA(n-3) and DHA in their breast milk, compared with the controls.

DISCUSSION

Our results demonstrate that supplementing the maternal diet of Danish women, who have an estimated mean intake of 0.25 g LCPUFA(n-3) (27) per day, with 2.7 g LCPUFA(n-3) per day, from week 30 of gestation through the first month of lactation, more than tripled the n-3 FA content and doubled the concentration of DHA in early human milk.

The steady decline in total milk LCPUFA(n-3) observed during the first month of lactation is in agreement with findings from observational studies of human milk (28,29). We observed a very rapid decrease in the LCPUFA(n-3) content in milk from women who stopped fish oil supplementation at delivery; thus, already at day 4 after delivery the LCPUFA(n-3) level in milk from women who stopped supplementation differed significantly from the LCPUFA(n-3) level measured in milk from women who continued supplementation. This prompt decline in LCPUFA(n-3) content is in agreement with established knowledge of the mechanisms of regulation and incorporation of dietary FA into milk TAG (30,31). In milk TAG most of the long-chain FA—which usually constitute about 95% of milk FA—are derived from dietary fat and mobilized adipose stores, in contrast to the relatively small proportion of medium-chain FA, which are synthesized by the mammary gland itself (32,33). During lactation, the activity of lipoprotein lipase, the enzyme that regulates extrahepatic uptake of dietary FA from plasma, is markedly increased in the mammary gland and is decreased in adipose tissue (31), thereby leading the milk TAG more exclusively to reflect the dietary FA intake.

Mean levels of EPA and DHA in this study are comparable to the findings of Innis and Kuhnlein (14), who studied the n-3 FA in breast milk of Inuit women consuming traditional foods. Compared with a control group of women living in Vancouver, Canada, they report levels of EPA and DHA, as the percentage of total FA (±SEM), of 1.1% (±0.3) and 1.4% (±0.4), respectively, for Inuit women and 0.2% (±0.2) and 0.4% (±0.1), respectively, for Vancouver women. In our study the respective findings at the end of the study period were 0.7% (±0.11) EPA and 1.4% (±0.17) DHA for women who received supplements of fish oil during pregnancy and lactation, and 0.1% (±0.02) EPA and 0.5% (±0.04) DHA for the control group. The levels of DHA and EPA in the control group are in agreement with another Danish study reporting DHA levels in breast milk of

TABLE 1
FA Pattern of Human Breast Milk at Days 4, 16, and 30 After Delivery[a]

Group	FO(pregn/lact)[b]			FO(pregn)[c]			Controls		
Day	4	16	30	4	16	30	4	16	30
Number	12	11	10	10	11	11	13	12	11
10:0	0.3	0.7	0.8	0.3	0.6	0.7	0.3	0.6	0.6
	(0.04)	(0.09)	(0.10)	(0.04)	(0.10)	(0.08)	(0.04)	(0.07)	(0.05)
12:0	2.2	4.1	4.0	2.0	3.4	3.7	1.9	2.8	2.7
	(0.32)	(0.63)	(0.57)	(0.23)	(0.52)	(0.37)	(0.19)	(0.38)	(0.27)
14:0	4.9	5.8	6.1[a]	5.1	5.2	7.6[a,b]	4.5	4.8	4.4[b]
	(0.43)	(0.60)	(0.65)	(0.42)	(0.61)	(1.80)	(0.30)	(0.38)	(0.28)
16:0	24.5	22.9	23.6	25.7	24.2	21.8	25.0	23.2	23.3
	(0.60)	(0.62)	(0.54)	(0.57)	(0.66)	(2.05)	(0.64)	(0.51)	(0.61)
16:1n-7	2.7	2.5	2.5	2.5	3.2	3.1	2.7	2.4	2.7
	(0.20)	(0.22)	(0.21)	(0.25)	(0.39)	(0.39)	(0.23)	(0.16)	(0.19)
17:0	0.7	0.6	0.6	0.6	0.5	0.7	0.6	0.6	0.5
	(0.08)	(0.11)	(0.04)	(0.09)	(0.06)	(0.25)	(0.06)	(0.07)	(0.06)
18:0	7.7	9.0	9.2	8.0	8.4	8.1	8.0	8.8	8.0
	(0.32)	(0.38)	(0.29)	(0.39)	(0.54)	(0.55)	(0.30)	(0.32)	(0.77)
18:1n-9	35.1	32.7	31.2	34.3	36.0	35.5	36.2	37.6	36.9
	(1.03)	(2.93)	(3.20)	(0.81)	(1.37)	(0.93)	(0.84)	(0.92)	(0.97)
18:2n-6	10.7	11.2	11.1	10.7	11.2	11.9	10.7	12.3	12.9
	(0.29)	(0.60)	(0.64)	(0.38)	(0.64)	(0.80)	(0.45)	(0.66)	(0.97)
18:3n-3	0.9	1.1	1.0	1.0	1.1	1.1	0.9	1.2	1.2
	(0.05)	(0.09)	(0.11)	(0.06)	(0.16)	(0.16)	(0.08)	(0.10)	(0.14)
20:0	0.3	0.3	0.3	0.3	0.3	0.3	0.3	0.3	0.3
	(0.02)	(0.02)	(0.03)	(0.02)	(0.02)	(0.02)	(0.03)	(0.03)	(0.03)
20:2n-6	0.7	0.4	0.4	0.7	0.5	0.4	0.8	0.5	0.4
	(0.03)	(0.01)	(0.02)	(0.05)	(0.02)	(0.01)	(0.06)	(0.04)	(0.02)
20:3n-6	0.6	0.4	0.3[a]	0.6	0.4	0.4[b]	0.6	0.4	0.4[b]
	(0.03)	(0.03)	(0.02)	(0.06)	(0.04)	(0.02)	(0.06)	(0.03)	(0.04)
20:4n-6+20:3n-3	0.9	0.7	0.5[a]	0.9	0.7	0.6[a]	0.9	0.7	0.7[b]
	(0.03)	(0.04)	(0.04)	(0.05)	(0.05)	(0.03)	(0.05)	(0.04)	(0.03)
20:4n-3	0.3	0.3	0.2[a]	0.2	0.1	0.1[b]	0.2	0.1	0.1[b]
	(0.02)	(0.03)	(0.02)	(0.01)	(0.01)	(0.02)	(0.03)	(0.01)	(0.01)
20:5n-3	0.6	0.9	0.7[a]	0.2	0.2	0.2[b]	0.2	0.1	0.1[c]
	(0.11)	(0.14)	(0.11)	(0.05)	(0.02)	(0.03)	(0.03)	(0.02)	(0.02)
22:5n-3	0.9	0.7	0.6[a]	0.6	0.3	0.3[b]	0.4	0.2	0.2[c]
	(0.07)	(0.12)	(0.09)	(0.06)	(0.02)	(0.01)	(0.06)	(0.03)	(0.02)
22:6n-3	1.8	1.8	1.4[a]	1.2	0.7	0.6[b]	0.9	0.5	0.5[b]
	(0.18)	(0.24)	(0.17)	(0.14)	(0.04)	(0.05)	(0.06)	(0.04)	(0.04)
Others[d]	4.2	3.9	5.5	5.1	3.0	2.9	4.9	2.9	4.1
LCPUFA(n3)[e]	3.3	3.4	2.8[a]	2.0	1.2	1.0[b]	1.5	0.8	0.8[b]
	(0.32)	(0.46)	(0.34)	(0.22)	(0.08)	(0.09)	(0.12)	(0.05)	(0.08)
n-3[f]	4.5	4.8	4.0[a]	3.2	2.5	2.3[b]	2.5	2.1	2.1[b]
	(0.36)	(0.49)	(0.41)	(0.25)	(0.13)	(0.25)	(0.10)	(0.13)	(0.18)
n-6[g]	12.0	12.0	11.8	12.0	12.1	12.8	12.1	13.3	13.8
	(0.30)	(0.59)	(0.65)	(0.38)	(0.64)	(0.80)	(0.48)	(0.71)	(0.98)
TLC[h]	38.2	41.6	44.9	29.5	42.5	48.2	36.9	49.8	42.0
	(3.2)	(3.4)	(4.1)	(3.4)	(3.1)	(3.3)	(3.5)	(5.4)	(2.5)

[a]Results are given as % of total FA. Numbers in parentheses indicate SEM. Pairwise significance tests for differences between means were performed only for samples taken at day 30. Different superscript roman letters (a, b, or c) indicate statistically significant different means ($P < 0.05$) in pairwise comparisons.
[b]Study group receiving fish oil supplementation in both pregnancy and the first month of lactation.
[c]Study group receiving fish oil supplementation only in pregnancy.
[d]Other FA include 6:0, 8:0, 18:1n-7, 18:3n-6, 20:1n-11/n-9, 22:1n-11/n-9, 24:0, and 24:1.
[e]LCPUFA(n-3), 20:5n-3 + 22:5n-3 + 22:6n-3.
[f]n-3, 18:3n-3 + 20:4n-3 + 20:5n-3 + 22:5n-3 + 22:6n-3.
[g]n-6, 18:2n-6 + 20:2n-6 + 20:3n-6.
[h]TLC, total lipid content, g/L (SEM).

women who received no fish or supplements of 0.49% (0.20) [mean (SD)] and EPA levels of 0.13% (0.07) (34).

The dietary requirements of DHA and other LCPUFA(n-3) for the newborn infant are still unknown, but recommendation of a daily intake of essential PUFA (n-3 and n-6) of 600–800 mg/kg, with a total proportion of n-3 FA 70-150 mg/kg/d, has been proposed (10). Recent evidence suggests that the desaturation and elongation systems are not fully active during the early postnatal period and that the newborn child may therefore be dependent on preformed dietary sources of the long-chain derivatives of EFA (35). It has been proposed that at least half the n-3 FA supply should be provided as LCPUFA(n-3) (i.e., 40–75 mg/kg/d), and preformed dietary DHA is known to be incorporated into developing brain at 10 times the rate of its precursor, α-linolenic acid (36). When dealing with an approximate daily intake of 500–600 mL breast milk by newborn term infants, the infants in our study would have an average supply of 700–850 mg LCPUFA(n-3)/d (i.e., 200–240 mg/kg/d) when nursed by mothers receiving fish oil supplements, and a supply of 200–240 mg LCPUFA(n-3) (i.e., 55–70 mg/kg/d) if no supplements had been given. Most Danish lactating women on a normal unsupplemented diet thus meet the recommendations of Uauy *et al.* (10) and supply sufficient levels of LCPUFA (n-3) to their infants. However, adequate data for estimating the optimal intake of n-3 FA during pregnancy and infancy are still lacking, and the question may be particularly critical when discussing aspects of the nutrition of preterm neonate who have not benefited from a placental supply of LCPUFA(n-3) in the last trimester.

With a total lipid concentration of 3 to 5% (15,37,38) in human breast milk, lipids account for about half of the energy supply to the newborn. Whether dietary fish oil intake in the lactation period reduces the total lipid concentration in breast milk has been discussed (39), as it may interfere critically with normal growth and development. In our study, we did not find significant effects on the total milk lipid content after fish oil supplementation. There is also evidence to suggest that dietary arachidonic acid (20:4n-6) is needed to obtain normal growth in infancy (40,41). With the GC column used for our analyses, 20:3n-3 and 20:4n-6 were not quantified separately. Usually, however, 20:3n-3 occurs primarily as an intermediate from the anabolism of α-linolenic acid and is of minor quantitative importance in the dietary supply of FA. Ferris and Jensen (42) have reviewed the literature on breast milk and have found that in two (out of six) papers both figures, 20:3n-3 represented between 5 and 15% of 20:4n-6 (43,44). In our study, later analyses of six milk samples allowed calculation of the area% of 20:3n-3. In all cases, the area% of this FA was below 0.1%, and in five out of six samples, it was less than 10% of the arachidonate area. On the basis of these findings, we consider the mixed peak area% to be usable as an n-6 FA area and conclude that no significant effect seems to be present on the arachidonic acid content in the breast milk of mothers receiving fish oil supplements.

This randomized study confirms the findings from earlier observational (14,15,19), (45) and intervention studies (21,46) that the DHA content in particular, and the n-3 FA content in general, of breast milk is strongly influenced by the amount of LCPUFA(n-3) ingested by the woman. Furthermore, the results demonstrate the need for a continued intake of dietary LCPUFA(n-3) into the lactation period if one wishes to maintain an increase in the LCPUFA(n-3) content in breast milk.

ACKNOWLEDGMENTS

The skilled laboratory work of Majbrit T. Andersen and the competent work of Jakob Hjort in making the data ready for analyses are greatly appreciated. We thank Kim Fleischer Michaelsen for comments on the article. The University of Aarhus (Aarhus, Denmark) supported the research financially with 2 mon salary. Lube A/S (Hadsund, Denmark), supplied us with Pikasol® fish oil and olive oil capsules. We are grateful for technical assistance from Ghita Holten-Lund and M.A. Inger Kristine Meder.

REFERENCES

1. Clandinin, M.T., Chappell, J.E., Leong, S., Heim, T., Swyer, P.R., and Chance, G.W. (1980) Intrauterine Fatty Acid Accretion Rates in Human Brain: Implications for Fatty Acid Requirements, *Early Hum. Dev. 4*, 121–129.
2. Clandinin, M.T., Chappell, J.E., and van Aerde, J.E. (1989) Requirements of newborn infants for long chain polyunsaturated fatty acids, *Acta Paediatr. Scand. Suppl. 351*, 63–71.
3. Neuringer,M., Anderson,G.J., and Connor,W.E. (1988) The essentiality of n-3 fatty acids for the development and function of the retina and brain, *Annu. Rev. Nutr. 8*, 517–541.
4. Anderson, R.E., Benolken, R.M., Dudley, P.A., Landis, D.J., and Wheeler, T.G. (1974) Proceedings: Polyunsaturated fatty acids of photoreceptor membranes, *Exp. Eye Res. 18*, 205–213.
5. Neuringer,M. and Connor,W.E. (1986) n-3 fatty acids in the brain and retina: Evidence for their essentiality, *Nutr. Rev. 44*, 285–294.
6. Connor, W., Neuringer, M., and Lin, D. (1985) The incorporation of docosahexaenoic acid into the brain of monkeys deficient in ω-3 essential fatty acids, *Clin Res 33*, 598 (abstr.).
7. Birch, E., Birch, D., Hoffman, D., Hale, L., Everett, M., and Uauy, R. (1993) Breast-feeding and optimal visual development, *J. Pediatr. Ophthalmol. Strabismus. 30*, 33–38.
8. Birch, E.E., Birch, D.G., Hoffman, D.R., and Uauy, R. (1992) Dietary essential fatty acid supply and visual acuity development, *Invest. Ophthalmol. Vis. Sci. 33*, 3242–3253.
9. Uauy, R., Birch, E., Birch, D., and Peirano, P. (1992) Visual and brain function measurements in studies of n-3 fatty acid requirements of infants [published erratum appears in *J. Pediatr. 121*(2), 329], *J. Pediatr. 120*, S168–S180.
10. Uauy, R. (1990) Are omega-3 fatty acids required for normal eye and brain development in the human? *J. Pediatr. Gastroenterol. Nutr. 11*, 296–302.
11. Carlson, S., Cooke, R., Peeples, J., Werkman, S., and Tolley, E. (1996) Docosahexaenoate (DHA) and eicosapentaenoate (EPA) status of preterm infants: Relationship to visual acuity in n-3 supplemented infants, *Pediatr Res 25*, 285A (abstr.).
12. Lucas, A., Morley, R., Cole, T.J., Lister, G., and Leeson Payne, C. (1992) Breast milk and subsequent intelligence quotient in children born preterm [see comments], *Lancet 339*, 261–264.
13. Read, W.W., Lutz, P.G., and Tashjian, A. (1965) Human milk lipids. II. The influence of dietary carbohydrates and fat on the fatty acids of mature milk. A study in four ethnic groups, *Am, J, Clin, Nutr, 17*, 180–183.
14. Innis, S.M. and Kuhnlein, H.V. (1988) Long-chain n-3 fatty acids in breast milk of Inuit women consuming traditional foods, *Early Hum. Dev. 18*, 185–189.

15. Finley, D.A., Lönnerdal, B., Dewey, K.G., and Grivetti, L.E. (1985) Breast milk composition: Fat content and fatty acid composition in vegetarians and non-vegetarians, *Am. J. Clin. Nutr. 4*, 787–800.
16. Silber, G.H., Hachey, D.L., Schanler, R.J., and Garza, C. (1988) Manipulation of maternal diet to alter fatty acid composition of human milk intended for premature infants, *Am. J. Clin. Nutr. 47*, 810–814.
17. Jensen, R.G., Ferris,A.M., Lammi-Keefe, C.J., Stewart, C.A., and DelSavio, G.C. (1990) Hypocholesterolemic human milk, *J. Pediatr. Gastroenterol. Nutr 10*, 148–150.
18. Hall, B. (1979) Uniformity of human milk, *Am. J. Clin. Nutr. 32*, 304–312.
19. Harris, W.S., Connor, W.E., and Lindsey, S. (1984) Will dietary omega-3 fatty acids change the composition of human milk? *Am. J. Clin. Nutr. 40*, 780-785.
20. Henderson, R.A., Jensen, R.G., Lammi-Keefe, C.J., Ferris, A.M., and Dardick, K.R. (1992) Effect of fish oil on the fatty acid composition of human milk and maternal and infant erythrocytes, *Lipids 27*, 863–869.
21. Dunstan, J.A., Roper, J., Mitoulas, L., Hartmann, P.E., Simmer, K., and Prescott, S.L. (2004) The effect of supplementation with fish oil during pregnancy on breast milk immunoglobulin A, soluble CD14, cytokine levels and fatty acid composition, *Clin. Exp. Allergy 34*, 1237–1242.
22. Olsen, S.F., Sorensen, J.D., Secher, N.J., Hedegaard, M., Henriksen, T.B., Hansen, H.S., and Grant, A. (1992) Randomised controlled trial of effect of fish-oil supplementation on pregnancy duration, *Lancet 339*, 1003–1007.
23. Olsen, S.F., Secher, N.J., Tabor, A., Weber, T., Walker, J.J., and Gluud, C. (2000) Randomised clinical trials of fish oil supplementation in high risk pregnancies. Fish Oil Trials In Pregnancy (FOTIP) Team, *BJOG. 107*, 382–395.
24. Jensen, R.G., Sicher, R.C., Jr., and Bahr, J.T. (1978) Regulation of Ribulose 1,5-Bisphosphate carboxylase in the chloroplast, *Basic Life Sci. 11*, 95–112.
25. Bitman, J., Wood, D.L., Mehta, N.R., Hamosh, P., and Hamosh, M. (1983) Lipolysis of triglycerides of human milk during storage at low temperatures: a note of caution, *J. Pediatr. Gastroenterol. Nutr 2*, 521–524.
26. AOCS, *Official Methods and Recommended Practices of the American Oil Chemists' Society*, 4th edn. (Firestone, D., ed.), American Oil Chemists' Society, Champaign, 1989.
27. Olsen, S.F., Hansen, H.S., Sandström, M., and Jensen, B. (1995) Erythocyte levels compared with reported dietary intake of marine n-3 fatty acids in pregnant women, *British Journal of Nutrition 73*, 387–395.
28. Gibson, R.A., and Kneebone, G.M. (1981) Fatty acid composition of human colostrum and mature breast milk, *Am. J. Clin. Nutr. 34*, 252–257.
29. Harzer, G., Haug, M., Dieterich, I., and Gentner, P.R. (1983) Changing patterns of human milk lipids in the course of the lactation and during the day, *Am. J. Clin. Nutr. 37*, 612–621.
30. Hachey, D.L., Thomas, M.R., Emken, E.A., Garza, C., Brown-Booth, L., Adlof, R.O., and Klein, P.D. (1987) Human lactation: Maternal transfer of dietary triglycerides labeled with stable isotopes, *J. Lipid Res. 28*, 1185–1192.
31. Scow, R., Blanchette-Mackie, E.J., Mendelson, C., Hamosh, M., and Zinder, O. (1975) Incorporation of Dietary Fatty Acids into Milk Triglyceride: Mechanism and Regulation, in *Milk and Lactation* (Kretchmer, N., Ross; E., and Sereni, F., eds), Karger, Basel.
32. Insull, W., Jr., Hirsch, J., James, T., and Ahrens, E.H., Jr. (1959) The fatty acids of human milk. II. Alterations produced by manipulation of caloric balance and exchange of dietary fats, *J. Clin. Invest. 38*, 443–450.
33. Jensen, R.G., Ferris, A.M., and Lammi-Keefe, C.J. (1992) Lipids in human milk and infant formulas, *Annu. Rev. Nutr 12*, 417–441.
34. Jorgensen, M.H., Hernell, O., Lund, P., Holmer, G., and Michaelsen, K.F. (1996) Visual acuity and erythrocyte docosahexaenoic acid status in breast-fed and formula-fed term infants during the first four months of life, *Lipids 31*, 99–105.
35. Kohn, G., Sawatzki, G., and van Biervliet, J.P. (1994) Long-chain polyunsaturated fatty acids in infant nutrition, *Eur. J. Clin. Nutr. 48* (Suppl 2), S1–7.
36. Sinclair, A.J. (1975) Incorporation of radioactive polyunsaturated fatty acids into liver and brain of developing rat, *Lipids 10*, 175–184.
37. Hall, B. (1979) Uniformity of human milk, *Am. J. Clin. Nutr. 32*, 304–312.
38. Jensen, R.G., Ferris, A.M., Lammi-Keefe, C.J., and Henderson, R.A. (1990) Lipids of bovine and human milks: A comparison, *J. Dairy Sci. 73*, 223–240.
39. Jensen, R.G., Lammi-Keefe, C.J., Henderson, R.A., Bush, V.J., and Ferris, A.M. (1992) Effect of dietary intake of n-6 and n-3 fatty acids on the fatty acid composition of human milk in North America, *J. Pediatr. 120*, S87–S92.
40. Carlson, S.E., Werkman, S.H., Peeples, J.M., Cooke, R.J., and Tolley, E.A. (1993) Arachidonic acid status correlates with first year growth in preterm infants, *Proc. Natl. Acad. Sci. U.S.A 90*, 1073–1077.
41. Carlson, S.E., Cooke, R.J., Werkman, S.H., and Tolley, E.A. (1992) First year growth of preterm infants fed standard compared to marine oil n-3 supplemented formula, *Lipids 27*, 901–907.
42. Ferris, A.M. and Jensen, R.G. (1984) Lipids in human milk: A review. 1: Sampling, determination, and content, *J. Pediatr. Gastroenterol. Nutr. 3*, 108–122.
43. Koletzko, B., Mrotzek, M., and Bremer, H.J. (1988) Fatty acid composition of mature human milk in Germany, *Am. J. Clin. Nutr. 47*, 954–959.
44. Dotson, K.D., Jerrell, J.P., Picciano, M.F., and Perkins, E.G. (1992) High-performance liquid chromatography of human milk triacylglycerols and gas chromatography of component fatty acids, *Lipids 27*, 933–939.
45. Cant, A., Shay, J., and Horrobin, D.F. (1991) The effect of maternal supplementation with linoleic and γ-linolenic acids on the fat composition and content of human milk: A placebo-controlled trial, *J. Nutr. Sci. Vitaminol.* (Tokyo) *37*, 573–579.
46. Henderson, R.A., Jensen, R.G., Lammi-Keefe, C.J., Ferris, A.M., and Dardick, K.R. (1992) Effect of fish oil on the fatty acid composition of human milk and maternal and infant erythrocytes, *Lipids 27*, 863–869.

[Received September 6, 2004; accepted December 10, 2004]

Modifying Milk Fat Composition of Dairy Cows to Enhance Fatty Acids Beneficial to Human Health

Adam L. Lock and Dale E. Bauman*

Department of Animal Science, Cornell University, Ithaca, New York 14853

ABSTRACT: There is increased consumer awareness that foods contain microcomponents that may have beneficial effects on health maintenance and disease prevention. In milk fat these functional food components include EPA, DHA, and CLA. The opportunity to enhance the content of these FA in milk has improved as a result of recent advances that have better defined the interrelationships between rumen fermentation, lipid metabolism, and milk fat synthesis. Dietary lipids undergo extensive hydrolysis and biohydrogenation in the rumen. Milk fat is predominantly TG, and *de novo* FA synthesis and the uptake of circulating FA contribute nearly equal amounts (molar basis) to the FA in milk fat. Transfer of dietary EPA and DHA to milk fat is very low (<4%); this is, to a large extent, related to their extensive biohydrogenation in the rumen, and also partly due to the fact that they are not transported in the plasma lipid fractions that serve as major mammary sources of FA uptake (TG and nonesterified FA). Milk contains over 20 isomers of CLA but the predominant one is *cis*-9,*trans*-11 (75–90% of total CLA). Biomedical studies with animal models have shown that this isomer has anticarcinogenic and anti-atherogenic activities. *cis*-9,*trans*-11-CLA is produced as an intermediate in the rumen biohydrogenation of linoleic acid but not of linolenic acid. However, it is only a transient intermediate, and the major source of milk fat CLA is from endogenous synthesis. Vaccenic acid, produced as a rumen biohydrogenation intermediate from both linoleic acid and linolenic acid, is the substrate, and Δ9-desaturase in the mammary gland and other tissues catalyzes the reaction. Diet can markedly affect milk fat CLA content, and there are also substantial differences among individual cows. Thus, strategies to enhance milk fat CLA involve increasing rumen outflow of vaccenic acid and increasing Δ9-desaturase activity, and through these, several-fold increases in the content of CLA in milk fat can be routinely achieved. Overall, concentrations of CLA, and to a lesser extent EPA and DHA, can be significantly enhanced through the use of diet formulation and nutritional management of dairy cows.

Paper no. L9574 in *Lipids 39,* 1197–1206 (December 2004).

Historically, the goal of agricultural research has been to increase yield and productive efficiency, with little focus given to improving the nutrient profile of food products. Mounting research evidence and consumer awareness of the potential health benefits of various microcomponents in foods has given rise to the concept of functional foods and helped create a demand for foods with improved nutrient profiles (1). Thus, producers and scientists are interested in research and agricultural practices that may improve the nutrient profile of food products (2). One such example is the dairy industry and recent efforts to modify the composition of milk fat.

Milk and dairy products are recognized as important sources of nutrients in human diets, providing energy, high quality protein, and essential minerals and vitamins (3,4). Milk fat is responsible for many of the sensory, physical, and manufacturing properties of dairy products (5). However, milk fat is relatively more saturated than most plant oils, and this has led to a negative consumer perception and a public health concern related to excessive intake of saturated fats.

Milk fat content and FA composition can be significantly altered through nutrition of the dairy cows, offering the opportunity to respond to market forces and human health recommendations (6). The impact of dairy cow nutrition on fat content and FA composition of milk has been extensively reviewed (6–12). Due to increased consumer awareness of the link between diet and health, research has focused on altering the FA composition of cows' milk to achieve a FA profile consistent with consumer perceptions and health recommendations. In the past, much of this work has involved studies in which whole-scale changes have been the goal, whereby large shifts in the saturated to PUFA ratio have been sought. Modest changes have been achievable, but this can lead to problems relating to product quality and stability.

Recent research has demonstrated that generalizations about fat and FA are of little value and often lead to misleading and erroneous public understanding. Instead, one must consider the biological effects and nutritional value on the basis of individual FA. The focus of this review is on the nutritional manipulation of omega-3 FA and CLA, and possible constraints to their enhancement in milk and dairy products. These FA are of particular interest because of their potential benefits to human health. However, modification of the FA content of milk fat in dairy cows is impacted significantly by the extensive metabolism of lipids that occurs in the rumen. Hence, we will also provide a brief background on lipid metabolism in the rumen and milk fat synthesis.

RUMINANT LIPID METABOLISM

Lipid metabolism in the rumen. Our understanding of lipid metabolism in the rumen and the effect of specific FA on ruminant metabolism has increased significantly in recent years.

*To whom correspondence should be addressed at 262 Morrison Hall, Department of Animal Science, Cornell University, Ithaca, NY 14853-4801. E-mail: deb6@cornell.edu

Abbreviations: NEFA, nonesterified fatty acid.

Analytical developments that improved our ability to quantify the intermediates of FA metabolism have played a major role in these advances. Diets consumed by lactating dairy cows are low in fat content, generally containing only about 4–5% lipid. The predominant PUFA in ruminant diets are linolenic acid and linoleic acid, the former derived principally from forage crops and the latter being a major component of the oilseeds and concentrates that are fed to dairy cows.

The rumen of a dairy cow has a 40- to 50-L fluid volume with 10^{10} to 10^{11} bacteria and 10^5 to 10^6 protozoa per milliliter of rumen contents. When dietary lipids enter the rumen, the initial step in lipid metabolism is the hydrolysis of the ester linkages found in TG, phospholipids, and glycolipids, and this is primarily carried out by hydrolases produced by rumen bacteria. The extent of hydrolysis is generally high (>85%), and a number of factors that affect the rate and extent of hydrolysis have been identified [see reviews by Doreau and Ferlay (13), Doreau and Chilliard (14), and Harfoot and Hazlewood (15)].

Biohydrogenation of unsaturated FA is the second major transformation that dietary lipids undergo in the rumen, and it requires an FFA to proceed. As a consequence, rates are always lower than those for hydrolysis, and factors that affect hydrolysis also affect biohydrogenation. In addition, the rate of rumen biohydrogenation of FA typically increases as the extent of unsaturation in the FA increases (16). Biohydrogenation involves only a few of the species of rumen bacteria, and they carry out these reactions as a protection mechanism against the toxic effects of PUFA. Biohydrogenation is extensive, and for most diets linoleic and linolenic acid are hydrogenated 70–95% and 85–100%, respectively (13–15,17). Classical pathways of biohydrogenation were established using pure cultures of rumen organisms (Fig. 1). Based on their metabolic pathways, the bacteria involved in biohydrogenation have been classified into two groups: Group A bacteria hydrogenate PUFA to *trans* 18:1 FA, and Group B bacteria hydrogenate the *trans* 18:1 FA to stearic acid (15). Thus, in general no single species catalyzes the full sequence of reactions to convert linoleic and linolenic acid to stearic acid (18). For a more in-depth review of rumen bacteria and their role in rumen biohydrogenation and lipid metabolism, the reader is directed to the recent review by Palmquist *et al.* (19).

As a consequence of the extensive hydrolysis and biohydrogenation occurring in the rumen, the FA that reach the small intestine are mainly saturated FFA. Some biohydrogenation intermediates can also escape from the rumen, and two of the major ones are *trans*-11 18:1 (vaccenic acid) formed from both linoleic and linolenic acid and *cis*-9,*trans*-11 CLA formed during the biohydrogenation of linoleic acid (Fig. 1); these are discussed in more detail in a following section. However, as analytical techniques have improved, it has become clear that biohydrogenation processes are considerably more complex than first thought because a remarkable range of *trans* 18:1 and CLA isomers have been identified in rumen outflow [see review by Bauman *et al.* (16)]. Thus, in addition to the major pathway involving the formation of *cis*-9,*trans*-11 CLA and vaccenic acid as intermediates, there must be many more pathways of biohydrogenation. Furthermore, modifications in diet and rumen environment influence biohydrogenation pathways, thereby causing substantial changes in FA intermediates produced in the rumen.

Milk fat synthesis. Milk fat consists of droplets of TG that are coated with cell membrane. Thus, 96–98% of milk fat is TG with the remainder mainly representing small amounts of phopholipids, cholesterol, and cholesterol esters found in the milk fat globule membrane (20). The TG comprise over 400 FA, with a large portion of these produced as intermediates during lipid metabolism in the rumen (9). However, most of these FA are present in trace amounts, and it is generally recognized that the major FA in milk fat include saturated FA from 4:0 to 18:0 plus palmitoleic, oleic, linoleic, and *trans*-18:1 FA.

The FA that compose milk TG are derived from two sources, *de novo* synthesis and the uptake of preformed FA (20). Substrates for *de novo* synthesis are acetate and β-hydroxybutyrate derived from rumen fiber digestion. They are used by the mammary epithelial cell to synthesize short- and medium-chain FA (4:0 to 14:0) plus a portion of the 16-carbon FA. Mammary uptake of circulating long-chain FA is the other source of the FA in milk. This source provides a portion of the 16-carbon and all of the longer-chain FA, and represents FA absorbed from digestion and mobilized from body fat reserves. Those from the diet are transported as TG in VLDL, and mammary uptake depends on the action of lipoprotein lipase residing in the capillary wall. The long-chain FA from body fat reserves are transported as nonesterified FA (NEFA), and mammary uptake is proportional to plasma concentration. Under typical conditions, on a molar basis, about one-half of the FA in milk are synthesized *de novo* within the mammary gland. Although plasma TG and NEFA represent less than 3% of total plasma lipids, they contribute the remaining one-half (molar basis) of milk FA. However, this can vary according to physiological state. In particular, the contribution of FA from body reserves can vary from about 5% in a well-fed animal to

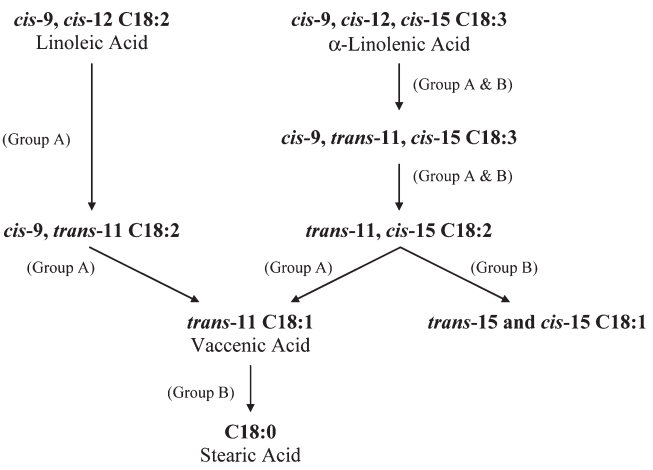

FIG. 1. Classical biochemical pathways for the biohydrogenation of linoleic and linolenic acid in the rumen. Adapted from Harfoot and Hazlewood (15).

over 20% of milk FA in early lactation when cows are in a negative energy balance (21).

OMEGA-3 FA

Background. Milk fat contents of EPA (20:5n-3) and DHA (22:6n-3) are of interest because of their potential benefits to human health. The effects of these omega-3 FA on reducing the risk of cardiovascular disease, type 2 diabetes, hypertension, cancer, and certain disruptive neurological functions and their potential mechanisms of action have been extensively reviewed (22–25). In human nutrition, there is an effort to increase consumption of these functional food components due to the low intake of omega-3 and the relationship of the intake of omega-3/omega-6 FA; Western diets typically have an omega-6 to omega-3 ratio of 20–30:1, whereas the ideal ratio is thought to be 4:1 or less (26). As a consequence, opportunities to enhance omega-3 FA in many foods, including dairy products, are being explored.

EPA and DHA are absent or at a minimal level in traditional dairy cow diets; consequently, they are typically present in very low amounts in ruminant products (<0.1% of total FA). However, fish oils, fish by-products, and marine algae are often available as dairy feedstuffs, and these are rich sources of EPA and DHA. Hence, there is an increasing use of fish oils and fish meal in dairy cattle diets. Despite this, only modest increases in the enrichment of EPA and DHA contents in milk fat have been achieved. For example, EPA and DHA in milk fat before fish oil supplementation averaged less than 0.1% of total FA and after supplementation were only marginally increased to 0.2 to 0.3% of total FA [see review by Chilliard *et al.* (27)]. The extent to which dietary supplements of FA enhance their secretion in milk fat is referred to as "transfer efficiency." In general, the literature indicates that the transfer efficiency of EPA and DHA to milk fat is low. A review of several studies showed that transfer efficiencies averaged 2 and 4% for EPA and DHA, respectively (27), and similar values were observed in more recent studies (Table 1). Interestingly, the transfer efficiency for docosapentaenoic acid (22:5n-3) appears to be higher than for EPA and DHA (27); transfer efficiencies of 20–30% were observed following the supplementation of 250 g/d fish oil (28,29).

Transfer efficiencies to milk fat are greater when fish oil is directly administered postruminally or fed in a "rumen-protected" form. McConnell (33) reported average transfer efficiencies of 30 and 25% for EPA and DHA, respectively, when 150 g/d of a fractionated fish oil (~40 g/d each of EPA and DHA) was infused into the abomasum. Similar values were reported during duodenal infusions of fish oil (Table 1). Rumen-protected formulations of fish oil have produced similar results; transfer efficiencies were 32% for EPA and 18% for DHA during supplementation of a formaldehyde-protected tuna orbital oil supplement in lactating dairy cows (34). Likewise, rumen-protected marine algae resulted in a transfer efficiency of 17% for EPA (35). Transfer efficiencies also tend to be greater when the FA are supplied by feeding fish meal (36), compared with dietary treatments in which fish oil has been used; thus, the matrix within which the oil is encased provides a degree of protection from rumen biohydrogenation, similar to that seen when oilseeds are fed.

Limitations in the transfer to milk fat. The basis for the low transfer efficiencies for EPA and DHA into milk fat is an active area of research, and two possibilities have been proposed. One hypothesis suggests the low transfer efficiency is because EPA and DHA are biohydrogenated by rumen bacteria. Support for this comes from comparisons showing that the transfer efficiency is about 10-fold greater when the EPA and DHA are provided in a manner to bypass metabolism in the rumen (Table 1). Studies utilizing duodenal or omasal sampling in sheep, steers, and lactating dairy cows during fish oil supplementation have quantified the extent of biohydrogenation as 78–100% for EPA and 74–98% for DHA (28,37–39).

Results from *in vitro* studies have been less consistent. Gulati *et al.* (40) and Ashes *et al.* (41) have suggested that there is little biohydrogenation of EPA and DHA; however, more recent *in vitro* studies have reported substantial biohydrogenation of these FA (42,43). Such discrepancies are likely due to the concentration of fish oil used in different studies. It is known that when the proportion of fish oil increases, the percentage of biohydrogenation declines (40,42,43), which is most likely due to the toxic effects of PUFA to certain rumen bacteria. For example, Gulati *et al.* (40) reported very little biohydrogenation when greater than 5 mg/mL (fish oil/mL rumen fluid) was incubated *in vitro*, but biohydrogenation

TABLE 1
EPA and DHA Transfer Efficiencies in Ruminal and Postruminal Fish Oil Supplementation Studies

	Source	EPA (% transfer)	DHA (% transfer)
Rumen			
Offer *et al.* (29)	Fish oil	2.0	2.0
Chilliard *et al.* (27)	Fish oil	2.0	4.0
Shingfield *et al.* (28)	Fish oil	1.4	1.9
McConnell *et al.* (30)	Menhaden fish oil	2.0	4.0
Postrumen			
Chilliard and Doreau (31)	Menhaden fish oil; duodenal infusion	20.0	18.0
Hagemeister *et al.* (32)	Menhaden fish oil; duodenal infusion	35.0–40.0	35.0–40.0
McConnell (33)	Menhaden fish oil; abomasal infusion	26.0–35.0	22.0–30.0

was extensive when less than 1 mg/mL was used. Overall, it would appear that, within the normal range of omega-3 FA supplied in dairy cow diets, EPA and DHA will be extensively biohydrogenated unless suitable technologies can be developed to provide protection from rumen bacteria.

The second possibility to explain the low transfer efficiency of EPA and DHA to milk fat may be a result of their partitioning into plasma lipid fractions that are less available to the mammary gland (29,44,45). As discussed earlier, the TG fraction of chylomicrons and VLDL is the form of esterified lipid used most extensively by the mammary gland. Brumby *et al.* (45) first suggested that EPA and DHA were packaged into lipid classes not readily used by the mammary gland. Recent studies have shown that supplements of EPA and DHA give only marginal enhancements in the TG and FFA lipid classes of plasma compared with the cholesterol ester and phospholipid fractions (29,44).

Transfer efficiencies of abomasally infused EPA and DHA (27,33,46) are similar to transfer efficiencies for abomasally infused isomers of CLA, which have been reported to have transfer efficiencies ranging from 20 to 32% (47–51). Such values are still low compared with transfer efficiencies reported for linoleic and linolenic acid. Although linoleic acid transfer efficiencies have been shown to be variable (10–90%), the majority of low values reported in the literature are when large amounts of linoleic acid were infused in cows in early to peak lactation. The majority of studies in established lactation observed transfer efficiencies in the 40–70% range; similar values have been reported for linolenic acid [see review by Chilliard *et al.* (46)]. Overall, these results suggest that preferential packaging of EPA and DHA into plasma cholesterol ester and phospholipid fractions may limit mammary uptake and their use for milk fat synthesis.

Finally, potential limitations on the use of fish oils in ruminant diets to increase the EPA and DHA content of milk must be considered. In some instances, fish oil can cause a shift in rumen biohydrogenation, which leads to a reduction in milk fat synthesis in the mammary gland and the production of milk with a low fat content. Although this may be beneficial in some circumstances [see Griinari and Bauman (52)], milk production with a low fat content is often detrimental, both financially and for many manufacturing processes (21). The second possible drawback to enhancing the omega-3 content of milk fat relates to the organoleptic properties of milk. Off-flavors due to FA oxidation are of prime concern because of the shift toward greater unsaturation of the milk fat when fish oils are fed. Although some studies have reported flavor problems in milk when fish oil supplements were fed to dairy cows (53), other investigations have observed no adverse effects on flavor score or peroxide index (54–56).

CONJUGATED LINOLEIC ACIDS

Background. The intake of CLA in humans is of interest because of the potential health benefits these FA may confer. The anticarcinogenic activity of CLA has been clearly established with *in vitro* cell culture systems and *in vivo* animal models for a wide range of cancer types [see reviews by Banni *et al.* (57), Belury (58), and Ip *et al.* (59)] . As biomedical studies with animal models expanded in scope, an impressive range of additional health effects were discovered for CLA, including antidiabetogenic, anti-atherogenic, immunomodulation, anti-obesity, and modulation of bone growth (58). The predominant source of CLA in human diets is ruminant-derived food products, with dairy products contributing about 75% of the total (60–62). CLA is a component of the fat in milk; hence, research has concentrated on increasing the CLA content per unit of fat. Processing has little effect on CLA, so the content in food products is related to the CLA concentration in the starting fat (61).

The presence of CLA in milk fat was first noted in the 1930s by scientists at the University of Reading, United Kingdom (63,64), with Parodi (65) later identifying *cis*-9,*trans*-11 CLA as a milk FA that contained a conjugated double bond pair. Subsequent research established that *cis*-9,*trans*-11 CLA was the major CLA isomer in ruminant fat representing about 75 to 90% of the total CLA (61,66), and the common name of "rumenic acid" has been proposed for this isomer because of its unique relationship to ruminants (67). As analytical techniques improved, numerous other isomers of CLA were identified in ruminant fat; these are present at much lower concentrations, and they differ by position (e.g., 7–9, 8–10, 9–11, 10–12, or 11–13) or geometric orientation (*cis-trans*, *trans-cis*, *cis-cis,* and *trans-trans*) of the double bond pair (Table 2). Thus far, the biological effects have been extensively examined for only two of the CLA isomers, *cis*-9,*trans*-11 and *trans*-10,*cis*-12, and there are clear differences. In the context of dairy products, biomedical studies with animal models have documented the anticarcinogenic and antiatherogenic effects of *cis*-9,*trans*-11 CLA (58,59,68). Since *cis*-9,*trans*-11 CLA is, by a considerable margin, the most predominant CLA isomer in milk fat, enhancing the CLA content of milk is realistically related only to increases in this isomer. The anti-obesity effects of CLA are due to the *trans*-10,*cis*-12 isomer; while this isomer can vary in milk fat, it never represents more than 1 or 2% of total CLA, and food products derived from ruminants are thus unlikely to provide sufficient amounts of this isomer to have biological effects on body fat.

Origin of CLA. The major pathways for rumen biohydrogenation of linoleic and linolenic acid are shown in Figure 2. Note that *cis*-9,*trans*-11 CLA is the first intermediate in the pathway, and it is formed only during the biohydrogenation of linoleic acid. In contrast, vaccenic acid is an intermediate formed from both linoleic and linolenic acid. Vaccenic acid and CLA are both present in ruminant fat, and it was generally assumed they were of rumen origin and represented intermediates that had escaped complete biohydrogenation. However, *cis*-9,*trans*-11 CLA is only a transitory intermediate in rumen biohydrogenation, whereas vaccenic acid tends to accumulate. Based on this and other considerations, Griinari and Bauman (69) proposed that endogenous synthesis

could be an important source of *cis*-9,*trans*-11 CLA in milk fat, with synthesis involving the enzyme Δ9-desaturase and vaccenic acid as the substrate.

The importance of endogenous synthesis of *cis*-9,*trans*-11 CLA has been examined in a series of *in vivo* investigations encompassing a range of diets characteristic of lactating dairy cows [see reviews by Palmquist *et al.* (19) and Bauman *et al.* (66)]. One of the strategies to investigate the importance of endogenous synthesis was a direct inhibition of Δ9-desaturase. For these *in vivo* studies, sterculic oil isolated from the nuts of *Sterculia foetida* was used. Sterculic oil contains about 60% sterculic acid [8-(2-octyl-1-cyclopropenyl) octanoic acid], a cyclopropenoic FA that is a potent inhibitor of Δ9-desaturase. Another approach was to compare values of estimated rumen outflow of CLA with the quantity of CLA secreted in milk fat. This indirect method provided an estimate of the maximum proportion of milk fat CLA that could originate from rumen production. Overall, results from these different approaches and investigations were consistent; endogenous synthesis accounted for the majority of the *cis*-9,*trans*-11 CLA present in milk fat with over 70 to over 90% originating from the conversion of vaccenic acid catalyzed by Δ9-desaturase (19,66).

In 1998, Yurawecz *et al.* (70) discovered that ruminant fat contained *trans*-7,*cis*-9 CLA. This CLA isomer had not been reported previously because it co-elutes with *cis*-9,*trans*-11 CLA under typical conditions with GC analysis. The milk fat content of *trans*-7,*cis*-9 CLA is generally about 10% of *cis*-9,*trans*-11 CLA, making it the second most prevalent CLA isomer. Endogenous synthesis is also the source of this CLA isomer; it is derived by the action of Δ9-desaturase on *trans*-7 18:1 that is produced in the rumen (71,72). In contrast to *cis*-9,*trans*-11 and *trans*-7,*cis*-9 CLA, other CLA isomers in milk fat appear to be exclusively of rumen origin. There are no specific mammalian desaturases analogous to Δ9-desaturase that could account for their presence. Rather, they are detected in rumen and duodenal contents, and estimates of rumen outflow are sufficient to account for the trace amounts of these CLA isomers secreted in milk fat (28,72).

Two of the minor CLA isomers merit further mention, *trans*-11,*cis*-13 CLA and *trans*-10,*cis*-12 CLA. Kraft *et al.* (74) recently reported that *trans*-11,*cis*-13 CLA was found at concentrations of approximately 8% of the total CLA present in milk fat produced by dairy cattle grazing Alpine regions of Switzerland. The rumen biohydrogenation pathways that produce this CLA isomer and the physiological basis for the relatively greater concentrations in milk fat from cattle grazing Alpine pastures are unknown. The *trans*-10,*cis*-12 CLA isomer is of interest because it is often produced in relatively greater quantities in the rumen of cows fed diets associated with milk fat depression. Indeed, this isomer has been shown to be a potent inhibitor of milk fat synthesis [see reviews by Bauman and Griinari (21) and Bauman *et al.* (66)].

Altering milk fat content. Diet is the major determinant of milk CLA content, and over the last decade, numerous experiments have been carried out with the objective of enhancing the milk fat content of CLA [see reviews by Chilliard *et al.* (27,46), Bauman *et al.* (79), and Stanton *et al.* (80)]. The key to increasing milk CLA is to increase rumen vaccenic acid output, allowing for increased endogenous synthesis in the mammary gland. Maximizing rumen output of vaccenic acid can be achieved in two ways: by increasing the supply of 18-carbon PUFA precursors and by inhibiting vaccenic acid reduction to stearic acid. Increasing the dietary supply of 18-carbon PUFA substrates is most easily achieved by the addition of plant oils high in linoleic and/or linolenic acids. The effects of different types and amounts of plant oils have been investigated, and a range of plant oils have been shown to be effective in increasing milk CLA content. The coat of oilseeds offers some protection from rumen biohydrogenation; thus, the use of different oilseeds and processing techniques has also been investigated (81–83). Oilseeds high in linoleic and/or linolenic acid, processed so that oil was accessible to biohydrogenating bacteria, resulted in greater increases in milk CLA compared with whole oil seeds, but were not as efficient as using the pure oil. Plant oils are often added to dairy cattle diets as calcium salts of FFA, and

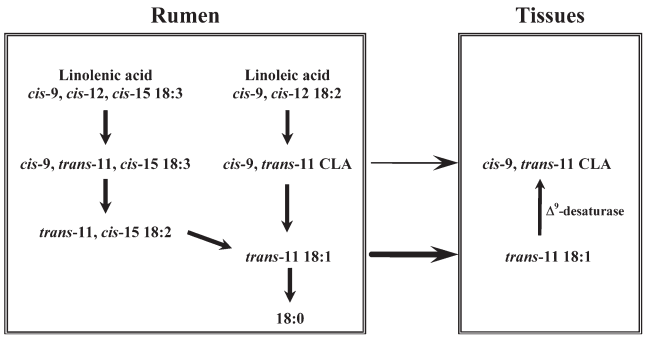

FIG. 2. Pathways for ruminal and endogenous synthesis of *cis*-9,*trans*-11 CLA in the dairy cow. Adapted from Bauman *et al.* (66)

TABLE 2
Range of Positional and Geometric Isomers (% of Total Isomers) of *trans* 18:1 and Conjugated 18:2 FA in Milk and Dairy Products[a]

Trans 18:1		Conjugated 18:2	
Isomer	% of total *trans* 18:1 isomers	Isomer	% of total CLA isomers
trans-4	0.30–2.30	*trans*-7,*cis*-9	1.20–8.89
trans-5	<0.01–1.40	*trans*-7,*trans*-9	0.02–2.39
trans-6–8	0.50–11.30	*trans*-8,*cis*-10	0.06–1.47
trans-9	3.00–18.20	*trans*-8,*trans*-10	0.19–0.37
trans-10	3.40–29.80	*cis*-9,*trans*-11	72.56–91.16
trans-11	24.50–74.90	*trans*-9,*trans*-11	0.77–2.87
trans-12	1.90–17.60	*trans*-10,*cis*-12	0.03–1.51
trans-13 + 14	<0.01–23.10	*trans*-10,*trans*-12	0.28–1.31
trans-15	3.30–11.10	*cis*-11,*trans*-13	0.18–4.70
trans-16	1.70–12.50	*trans*-11,*cis*-13	0.07–8.00
		trans-11,*trans*-13	0.28–4.24
		cis-12,*trans*-14	0.04–0.80
		trans-12,*trans*-14	0.33–2.76
		cis,*cis* isomers	0.06–4.80

[a]Data are derived from eight studies in which FA analyses were carried out on milk samples (28,72–76), butter (77), and cheese (78).

Chouinard *et al.* (82) fed calcium salts of canola (rape), soybean, and linseed oil. All three increased the CLA content of milk fat; however, those containing the greatest amounts of linoleic and linolenic (soybean and linseed, respectively) caused the greatest increases.

The lipid content of ruminant diets is generally restricted to less than 7% because higher amounts adversely affect the metabolism of rumen bacteria, thereby impairing rumen fermentation and animal performance (84,85). Thus, there is a limit to the extent that one can provide dietary lipid supplements to increase rumen output of vaccenic acid and CLA. Even at a modest level of plant oil supplementation, the rumen environment can be modified so that a portion of the biohydrogenation pathways are shifted to produce *trans*-10 18:1 and *trans*-10,*cis*-12 CLA as intermediates. These dietary situations are associated with milk fat depression, and increasing the CLA content of fat while reducing total milk fat secretion is often unacceptable to producers [see reviews by Bauman and Griinari (21,86)].

Dietary factors that affect rumen bacteria involved in biohydrogenation, either directly or indirectly *via* changes in the rumen environment, can also affect the CLA content of milk fat. These changes typically involve an inhibition of the final biohydrogenation step, which converts vaccenic acid to stearic acid. Several examples have been well characterized including alterations in the forage/concentrate ratio, dietary supplements of fish oil, and restricted feeding (79). The most effective of these is the use of fish oil, and the general trend is that equivalent amounts of dietary fish oil compared with plant oils result in a greater increase in milk CLA content (28–30,87–89). Fish oils supply only minimal amounts of 18-carbon PUFA; therefore, the increases are most likely the result of a reduction in the final biohydrogenation step where vaccenic acid is converted to stearic acid (69). In support, DHA has been shown to promote vaccenic acid accumulation in mixed ruminal cultures when incubated with linoleic acid (90).

Last, a combination of dietary supply of PUFA and modification of the rumen environment can be especially effective in increasing the CLA content of milk fat. Seasonal effects on milk CLA have been known for some time (91–94), and these appear related to this. Fresh pasture results in a two- to threefold increase in the CLA content of milk fat, but the effect diminishes as the pasture matures (81,92,93,95,96). These results cannot be totally explained in terms of the FA composition and supply of PUFA that grass provides; therefore, additional factors or components of grass must promote the production of vaccenic acid in the rumen, and these lessen in effect as the pasture matures.

Physiological factors that affect milk fat content of CLA have also been examined, and differences among individuals are particularly striking. Even when diet and other physiological variables are similar, there is still a two- to threefold range among individuals in the milk fat concentration of CLA (93,97–99). A similar level of variation also occurs in the milk fat desaturase index (a proxy for Δ9-desaturase activity), with a several-fold range among cows (93,97–99). These animal differences appear to have a genetic basis, although this has not been examined rigorously. Cows maintain a consistent hierarchy in milk CLA content and desaturase index over time when fed the same diet and when switched between diets (99). The effect of breed (Holstein vs. Brown Swiss) was examined in a large study (>200 cows) by Kelsey *et al.* (97), and no differences were observed. Although some have proposed breed differences in the CLA content of milk fat (89,100–102), these studies have often involved very few animals, were confounded by diet, or both. Thus, if breed differences do exist in the CLA content of milk fat and desaturase index, they must be minor compared with the effect of diet and individual animal variations (19,66). Differences in milk CLA among cows are presumably related to individual variations in expression of the Δ9-desaturase gene and rumen outflow of vaccenic acid and CLA. Examination of other physiological factors has established that the milk fat content of CLA and desaturase index have little relation to milk or milk fat yield, parity, or stage of lactation (97,103).

We have used such feeding regimes and taken advantage of individual animal variation to produce CLA-enriched butter for use in biomedical studies with animal models. Ip *et al.* (104) first showed that *cis*-9,*trans*-11 CLA was a potent anticarcinogen when supplied as a natural food component; dietary consumption of CLA-enriched butter was effective in reducing the incidence of tumors in a rat model of mammary carcinogenesis. We have subsequently shown that vaccenic acid derived from CLA-enriched butter increased tissue content of CLA and reduced mammary tumorogenesis (105) and that the anticarcinogenic effect of vaccenic acid is mediated predominantly, perhaps exclusively, by its conversion to *cis*-9,*trans*-11 CLA (106). These findings highlight the fact that vaccenic acid should also be considered as a FA with particular benefits to human health. Given that humans convert approximately 20% of dietary vaccenic acid to *cis*-9,*trans*-11 CLA *via* Δ9-desaturase (107), Parodi (61) has suggested that CLA intake multiplied by 1.4 would provide an estimate of the effective physiological dose of CLA derived from ruminant products.

CLA-enriched dairy products have been evaluated for taste, organoleptic properties, and storage characteristics in comparisons with standard dairy products. Off-flavors due to FA oxidation are of prime concern because of the shift toward greater unsaturation of the milk fat. We recently produced 2% fat milk with high CLA and vaccenic acid (47 and 121 mg/g FA, respectively) and compared this with a standard 2% milk (5 and 14 mg/g FA, respectively). Evaluations of the milk for up to 14 d postpasteurization indicated no differences in sensory and triangle taste tests, or in susceptibility to develop oxidized flavors under both light and dark storage conditions (56). Similar results have been observed by others, with milk that had a less marked enrichment of CLA (54,55,108–110).

In summary, there are four areas to consider when designing diets to increase the CLA content of milk fat: (i) increase 18-carbon PUFA precursors in the diet (linoleic and linolenic acids); (ii) maintain normal biohydrogenation pathways

(vaccenic acid pathway); (iii) inhibit the final biohydrogenation step (vaccenic acid to 18:0); (iv) increase desaturation of vaccenic acid to *cis*-9,*trans*-11 CLA in the mammary gland. Future strategies will thus involve establishing dietary and nutritional conditions that maximize rumen outflow of vaccenic acid and *cis*-9,*trans*-11 CLA, optimizing the amount and activity of Δ9-desaturase in mammary tissue, and identifying the genetic basis for the large differences among individuals in CLA-related variables. Obviously, before CLA-enriched foods are widely marketed, studies would need to examine commercial applications and be extended to a wide range of food products.

FUTURE CONSIDERATIONS

Consumers are increasingly aware of "functional food" components that can have positive effects on health maintenance and disease prevention. A number of specific FA are now recognized as having beneficial effects on human health, and these include the omega-3 FA and *cis*-9,*trans*-11 CLA that are present in milk fat. Enhancing their content in milk fat requires an understanding of the interrelationship between dietary supply of lipid, rumen fermentation, and mammary synthesis of milk fat. Milk and dairy products normally contain very low amounts of EPA and DHA, and increasing their content is limited primarily because their biohydrogenation in the rumen is extensive and secondarily because they circulate in specific plasma lipid fractions that contribute minimally to the mammary supply of FA. These challenges must be addressed to achieve substantial increases in EPA and DHA levels in milk fat, and the formulation of supplements of EPA and DHA that are protected from metabolism by rumen bacteria has potential to address the biohydrogenation problem.

The predominant source of *cis*-9,*trans*-11 CLA in milk fat is endogenous synthesis from vaccenic acid, and thus strategies that center on enhancing rumen output of vaccenic acid and increasing tissue activity of Δ9-desaturase. Diet has a major effect on milk fat content of CLA, and there is also a wide variation among individuals. Through modification of dairy cow diets and selection of cows with the highest milk CLA content, it is possible to produce milk that is significantly enriched with CLA. Vaccenic acid is also present in milk fat, and its contribution to CLA must be considered because it supplies precursor for the endogenous synthesis of CLA in humans. On this basis, vaccenic acid would also be considered as a functional food component in dairy products with potential benefits to human health. Finally, the education of the public that not all FA are equal is required. This is of special importance with the introduction of *trans* FA labeling of foods as undesirable and the fact that both vaccenic acid and *cis*-9,*trans*-11 CLA are *trans* FA.

ACKNOWLEDGMENTS

The authors gratefully acknowledge the helpful discussions of C. McConnell and D. Palmquist during the preparation of the manuscript.

REFERENCES

1. Milner, J.A. (1999) Functional Foods and Health Promotion, *J. Nutr. 129*, 1395S–1397S.
2. National Research Council (2003) *Frontiers in Agricultural Research: Food, Health, Environment and Communities*, National Academy Press, Washington, DC.
3. National Research Council (1998) *Designing Foods: Animal Product Options in the Marketplace*, National Academy Press, Washington, DC.
4. Demment, M.W., and Allen, L.H. (2004) Animal Source Foods to Improve Micronutrient Nutrition and Human Function in Developing Countries, *J. Nutr. 133* (Suppl. 11-S II).
5. Kaylegain, K.E., and Lindsay, R.C. (1995) *Handbook of Milk Fat Fractionation Technology and Applications*, AOCS Press, Champaign, IL.
6. Lock, A.L., and Shingfield, K.J. (2004) Optimising Milk Composition, in *UK Dairying: Using Science to Meet Consumers' Needs* (Kebreab, E., Mills, J., and Beever, D.E, eds.), pp. 107–188, Nottingham University Press, Nottingham, United Kingdom.
7. Ashes, J.R., Gulati, S.K., and Scott, T.W. (1997) Potential to Alter the Content and Composition of Milk Fat Through Nutrition, *J. Dairy Sci. 80*, 2204–2212.
8. Grummer, R.R. (1991) Effect of Feed on the Composition of Milk-Fat, *J. Dairy Sci. 74*, 3244–3257.
9. Jensen, R.G. (2002) The Composition of Bovine Milk Lipids: January 1995 to December 2000, *J. Dairy Sci. 85*, 295–350.
10. Kennelly, J.J. (1996) The Fatty Acid Composition of Milk Fat as Influenced by Feeding Oilseeds, *Anim. Feed Sci. Technol. 60*, 137–152.
11. Palmquist, D.L., Beaulieu, A.D., and Barbano, D.M. (1993) Feed and Animal Factors Influencing Milk Fat Composition, *J. Dairy Sci. 76*, 1753–1771.
12. Sutton, J.D. (1989) Altering Milk-Composition by Feeding, *J. Dairy Sci. 72*, 2801–2814.
13. Doreau, M., and Ferlay, A. (1994) Digestion and Utilization of Fatty Acids by Ruminants, *Anim. Feed Sci. Technol. 45*, 379–396.
14. Doreau, M., and Chilliard, Y. (1997) Digestion and Metabolism of Dietary Fat in Farm Animals, *Br. J. Nutr. 78*, S15–S35.
15. Harfoot, C.G., and Hazlewood, G.P. (1997) Lipid Metabolism in the Rumen, in *The Rumen Microbial Ecosystem*, 2nd edn. (Hobson, P.N., and Stewart, D.S., eds.), pp. 382–426, Chapman & Hall, London.
16. Bauman, D.E., Perfield, J.W., de Veth, M.J., and Lock, A.L. (2003) New Perspectives on Lipid Digestion and Metabolism in Ruminants, in *Proceedings of the Cornell Nutritional Conference,* pp. 175–189, Cornell University, Ithaca, NY.
17. Beam, T.M., Jenkins, T.C., Moate, P.J., Kohn, R.A., and Palmquist, D.L. (2000) Effects of Amount and Source of Fat on the Rates of Lipolysis and Biohydrogenation of Fatty Acids in Ruminal Contents, *J. Dairy Sci. 83*, 2564–2573.
18. Kemp, P., and Lander, D.J. (1984) Hydrogenation *in vitro* of α-Linolenic Acid to Stearic-Acid by Mixed Cultures of Pure Strains of Rumen Bacteria, *J. Gen. Microbiol. 130*, 527–533.
19. Palmquist, D.L., Lock, A.L., Shingfield, K.J., and Bauman, D.E. (2004) Biosynthesis of Conjugated Linoleic Acid in Ruminants and Humans, in *Advances in Food and Nutrition Research* (Taylor, S.L., ed.), Elsevier, San Diego, CA.
20. McGuire, M.A., and Bauman, D.E. (2002) Milk Biosynthesis and Secretion, in *Encyclopedia of Dairy Sciences* (Roginski, H., Furquay, J.W., and Fox, P.F., eds.), pp. 1828–1834, Elsevier Sciences, London.
21. Bauman, D.E., and Griinari, J.M. (2003) Nutritional Regulation of Milk Fat Synthesis, *Annu. Rev. Nutr. 23*, 203–227.
22. Connor, W.E. (2000) Importance of n-3 Fatty Acids in Health and Disease, *Am. J. Clin. Nutr. 71* (Suppl.), 171S–175S.

23. Williams, C.M. (2000) Dietary Fatty Acids and Human Health, *Ann. Zootech. 49*, 165–180.
24. Wijendran, V., and Hayes, K.C. (2004) Dietary n-6 and n-3 Fatty Acid Balance and Cardiovascular Health, *Annu. Rev. Nutr. 24*, 597–615.
25. Larsson, S.C., Kumlin, M., Ingelman-Sundberg, M., and Wolk, A. (2004) Dietary Long-Chain n-3 Fatty Acids for the Prevention of Cancer: A Review of Potential Mechanisms, *Am. J. Clin. Nutr. 79*, 935–945.
26. Simopoulos, A.P. (1999) Essential Fatty Acids in Health and Chronic Disease, *Am. J. Clin. Nutr. 70* (Suppl.), 560S–569S.
27. Chilliard, Y., Ferlay, A., and Doreau, M. (2001) Effect of Different Types of Forages, Animal Fat or Marine Oils in Cow's Diet on Milk Fat Secretion and Composition, Especially Conjugated Linoleic Acid (CLA) and Polyunsaturated Fatty Acids, *Livest. Prod. Sci. 70*, 31–48.
28. Shingfield, K.J., Ahvenjarvi, S., Toivonen, V., Arola, A., Nurmela, K.V.V., Huhtanen, P., and Griinari, J.M. (2003) Effect of Dietary Fish Oil on Biohydrogenation of Fatty Acids and Milk Fatty Acid Content in Cows, *Anim. Sci. 77*, 165–179.
29. Offer, N.W., Marsden, M., Dixon, J., Speake, B.K., and Thacker, F.E. (1999) Effect of Dietary Fat Supplements on Levels of n-3 Polyunsaturated Fatty Acids, *trans* Acids and Conjugated Linoleic Acid in Bovine Milk, *Anim. Sci. 69*, 613–625.
30. McConnell, C., Lock, A.L., McGadden, J.W., and Bauman, D.E. (2004) Fish Oil Supplementation in Dairy Cows Causes a Reduction in Milk Fat Secretion and Enhances Milk Fatty Acids of Interest in Human Health, *FASEB J. 18,* A129 (Abstr.).
31. Chilliard, Y., and Doreau, M. (1997) Effects of Ruminal or Postruminal Fish Oil Supply on Cow Milk Yield and Composition, *Reprod. Nutr. Dev. 37*, 338–339 (Abstr.).
32. Hagemeister, H., Precht, D., and Barth, C.A. (1988) Zum Transfer von Omega-3-Fettsäuren in das Milchfett bei Kühen, *Milchwissenschaft 43*, 153–158.
33. McConnell, C. (2004) The Effects of Omega-3 Fatty Acids on Milk Fat Synthesis and Composition in Dairy Cows, M.S. Thesis, Cornell University, Ithaca, NY.
34. Kitessa, S.M., Gulati, S.K., Simos, G.C., Ashes, J.R., Scott, T.W., Fleck, E., and Wynn, P.C. (2004) Supplementation of Grazing Dairy Cows with Rumen-Protected Tuna Oil Enriches Milk Fat with n-3 Fatty Acids Without Affecting Milk Production or Sensory Characteristics, *Br. J. Nutr. 91*, 271–277.
35. Franklin, S.T., Martin, K.R., Baer, R.J., Schingoethe, D.J., and Hippen, A.R. (1999) Dietary Marine Algae (*Schizochytrium* sp.) Increases Concentrations of Conjugated Linoleic, Docosahexaenoic and *trans* Vaccenic Acid in Milk of Dairy Cows, *J. Nutr. 129*, 2048–2054.
36. Wright, T.C., Holub, B.J., and McBride, B.W. (1999) Apparent Transfer Efficiency of Docosahexaenoic Acid from Diet to Milk in Dairy Cows, *Can. J. Anim. Sci. 79*, 565–568.
37. Scollan, N.D., Dhanoa, M.S., Choi, N.J., Maeng, W.J., Enser, M., and Wood, J.D. (2001) Biohydrogenation and Digestion of Long Chain Fatty Acids in Steers Fed on Different Sources of Lipid, *J. Agric. Sci. 136*, 345–355.
38. Wachira, A.M., Sinclair, L.A., Wilkinson, R.G., Hallett, K., Enser, M., and Wood, J.D. (2000) Rumen Biohydrogenation of n-3 Polyunsaturated Fatty Acids and Their Effects on Microbial Efficiency and Nutrient Digestibility in Sheep, *J. Agric. Sci. 135*, 419–428.
39. Chikunya, S., Demirel, G., Enser, M., Wood, J.D., Wilkinson, R.G., and Sinclair, L.A. (2004) Biohydrogenation of Dietary n-3 PUFA and Stability of Ingested Vitamin E in the Rumen, and Their Effects on Microbial Activity in Sheep, *Br. J. Nutr. 91*, 539–550.
40. Gulati, S.K., Ashes, J.R., and Scott, T.W. (1999) Hydrogenation of Eicosapentaenoic and Docosahexaenoic Acids and Their Incorporation into Milk Fat, *Anim. Feed Sci. Technol. 79*, 57–64.
41. Ashes, J.R., Siebert, B.D., Gulati, S.K., Cuthbertson, A.Z., and Scott, T.W. (1992) Incorporation of n-3 Fatty Acids of Fish Oil into Tissue and Serum Lipids of Ruminants, *Lipids 27*, 629–631.
42. AbuGhazaleh, A.A., and Jenkins, T.C. (2004) Disappearance of Docosahexaenoic and Eicosapentaenoic Acids from Cultures of Mixed Ruminal Microorganisms, *J. Dairy Sci. 87*, 645–651.
43. Dohme, F., Fievez, V., Raes, K., and Demeyer, D.I. (2003) Increasing Levels of Two Different Fish Oils Lower Ruminal Biohydrogenation of Eicosapentaenoic and Docosahexaenoic Acid *in vitro*, *Anim. Res. 52*, 309–320.
44. Offer, N.W., Speake, B.K., Dixon, J., and Marsden, M. (2001) Effect of Fish Oil Supplementation on Levels of (n-3) Polyunsaturated Fatty Acids in the Lipoprotein Fractions of Bovine Plasma, *Anim. Sci. 73*, 523–531.
45. Brumby, P.E., Storry, J.E., and Sutton, J.D. (1972) Metabolism of Cod-Liver Oil in Relation to Milk Fat Secretion, *J. Dairy Res. 39*, 167–182.
46. Chilliard, Y., Ferlay, A., Mansbridge, R.M., and Doreau, M. (2000) Ruminant Milk Fat Plasticity: Nutritional Control of Saturated, Polyunsaturated, *trans* and Conjugated Fatty Acids, *Ann. Zootech. 49*, 181–205.
47. Baumgard, L.H., Sangster, J.K., and Bauman, D.E. (2001) Milk Fat Synthesis in Dairy Cows Is Progressively Reduced by Increasing Supplemental Amounts of *trans*-10, *cis*-12 Conjugated Linoleic Acid (CLA), *J. Nutr. 131*, 1764–1769.
48. Chouinard, P.Y., Corneau, L., Barbano, D.M., Metzger, L.E., and Bauman, D.E. (1999) Conjugated Linoleic Acids Alter Milk Fatty Acid Composition and Inhibit Milk Fat Secretion in Dairy Cows, *J. Nutr. 129*, 1579–1584.
49. Chouinard, P.Y., Corneau, L., Saebo, A., and Bauman, D.E. (1999) Milk Yield and Composition During Abomasal Infusion of Conjugated Linoleic Acids in Dairy Cows, *J. Dairy Sci. 82*, 2737–2745.
50. Perfield, J.W., Saebo, A., and Bauman, D.E. (2004) Use of Conjugated Linoleic Acid (CLA) Enrichments to Examine the Effects of *trans*-8,*cis*-10 CLA, and *cis*-11,*trans*-13 CLA on Milk-Fat Synthesis, *J. Dairy Sci. 87*, 1196–1202.
51. Peterson, D.G., Baumgard, L.H., and Bauman, D.E. (2002) Short Communication: Milk Fat Response to Low Doses of *trans*-10,*cis*-12 Conjugated Linoleic Acid (CLA), *J. Dairy Sci. 85*, 1764–1766.
52. Griinari, J.M., and Bauman, D.E. (2003) Update on Theories of Diet-Induced Milk Fat Depression and Potential Applications, in *Recent Advances in Animal Nutrition 2003* (Garnsworthy, P.C., and Wiseman, J., eds.), pp. 115–156, Nottingham University Press, Nottingham, United Kingdom.
53. Lacasse, P., Kennelly, J.J., Delbecchi, L., and Ahnadi, C.E. (2002) Addition of Protected and Unprotected Fish Oil to Diets for Dairy Cows. I. Effects on the Yield, Composition and Taste of Milk, *J. Dairy Res. 69*, 511–520.
54. Baer, R.J., Ryali, J., Schingoethe, D.J., Kasperson, K.M., Donovan, D.C., Hippen, A.R., and Franklin, S.T. (2001) Composition and Properties of Milk and Butter from Cows Fed Fish Oil, *J. Dairy Sci. 84*, 345–353.
55. Ramaswamy, N., Baer, R.J., Schingoethe, D.J., Hippen, A.R., Kasperson, K.M., and Whitlock, L.A. (2001) Composition and Flavor of Milk and Butter from Cows Fed Fish Oil, Extruded Soybeans, or Their Combination, *J. Dairy Sci. 84*, 2144–2151.
56. Lynch, J.M., Lock, A.L., Dwyer, D.A., Noorbakhsh, R., Barbano, D.M., and Bauman, D.E. (2004) Flavor and Stability of Pasteurized Milk with Elevated Levels of Conjugated Linoleic Acid and Vaccenic Acid, *J. Dairy Sci.,* in press.
57. Banni, S., Heys, S.D., and Wahle, K.W.J. (2003) Conjugated Linoleic Acids as Anticancer Nutrients: Studies *in vivo* and

Cellular Mechanisms, in *Advances in Conjugated Linoleic Acid Research, Volume 2* (Sébédio, J.-L., Christie, W.W., and Adlof, R.O., eds.), AOCS Press, pp. 267–282, Champaign, IL.
58. Belury, M.A. (2002) Dietary Conjugated Linoleic Acid in Health: Physiological Effects and Mechanisms of Action, *Annu. Rev. Nutr. 22*, 505–531.
59. Ip, M.M., Masso-Welch, P.A., and Ip, C. (2003) Prevention of Mammary Cancer with Conjugated Linoleic Acid: Role of the Stroma and Epithelium, *J. Mammary Gland Biol. Neoplasia 8*, 103–118.
60. Ritzenthaler, K.L., McGuire, M.K., Falen, R., Shultz, T.D., Dasgupta, N., and McGuire, M.A. (2001) Estimation of Conjugated Linoleic Acid Intake by Written Dietary Assessment Methodologies Underestimates Actual Intake Evaluated by Food Duplicate Methodology, *J. Nutr. 131*, 1548–1554.
61. Parodi, P.W. (2003) Conjugated Linoleic Acid in Food, in *Advances in Conjugated Linoleic Acid Research, Volume 2* (Sébédio, J.-L., Christie, W.W., and Adlof, R.O., eds.), pp. 101–122, AOCS Press, Champaign, IL.
62. Fritsche, J., and Steinhart, H. (1998) Amounts of Conjugated Linoleic Acid (CLA) in German Foods and Evaluation of Daily Intake, *Z. Lebensm. Unters. Forsch. 206*, 77–82.
63. Booth, R.G., Dann, W.J., Kon, S.K., and Moore, T. (1933) A New Variable Factor in Butter Fat, *Chem. Ind. 52*, 270.
64. Moore, T. (1939) Spectroscopic Changes in Fatty Acids VI: General, *Biochem. J. 33*, 1635–1638.
65. Parodi, P.W. (1977) Conjugated Octadecienoic Acids of Milk Fat, *J. Dairy Sci. 60*, 1550–1553.
66. Bauman, D.E., Corl, B.A., and Peterson, D.G. (2003) The Biology of Conjugated Linoleic Acids in Ruminants, in *Advances in Conjugated Linoleic Acid Research, Volume 2* (Sébédio, J.-L., Christie, W.W., and Adlof, R.O., eds.), pp. 146–173, AOCS Press, Champaign, IL.
67. Kramer, J.K.G., Parodi, P.W., Jensen, R.G., Mossoba, M.M., Yurawecz, M.P., and Adlof, R.O. (1998) Rumenic Acid: A Proposed Common Name for the Major Conjugated Linoleic Acid Isomer Found in Natural Products, *Lipids 33*, 835.
68. Kritchevsky, D. (2003) Conjugated Linoleic Acids in Experimental Atherosclerosis, in *Advances in Conjugated Linoleic Acid Research, Volume 2* (Sébédio, J.-L., Christie, W.W., and Adlof, R.O., eds.), pp. 293–301, AOCS Press, Champaign, IL.
69. Griinari, J.M., and Bauman, D.E. (1999) Biosynthesis of Conjugated Linoleic Acid and Its Incorporation into Meat and Milk in Ruminants, in *Advances in Conjugated Linoleic Acid Research, Volume 1* (Yurawecz, M.P., Mossoba, M.M., Kramer, J.K.G., Pariza, M.W., and Nelson, G., eds.), pp. 180–200, AOCS Press, Champaign, IL.
70. Yurawecz, M.P., Roach, J.A.G., Sehat, N., Mossoba, M.M., Kramer, J.K.G., Fritsche, J., Steinhart, H., and Ku, Y. (1998) A New Conjugated Linoleic Acid Isomer, 7 *trans*,9 *cis*-Octadecadienoic Acid, in Cow Milk, Cheese, Beef, and Human Milk and Adipose Tissue, *Lipids 33*, 803–809.
71. Corl, B.A., Baumgard, L.H., Griinari, J.M., Delmonte, P., Morehouse, K.M., Yuraweczc, M.P., and Bauman, D.E. (2002) *trans*-7,*cis*-9 CLA Is Synthesized Endogenously by Δ9-Desaturase in Dairy Cows, *Lipids 37*, 681–688.
72. Piperova, L.S., Sampugna, J., Teter, B.B., Kalscheur, K.F., Yurawecz, M.P., Ku, Y., Morehouse, K.M., and Erdman, R.A. (2002) Duodenal and Milk *trans* Octadecenoic Acid and Conjugated Linoleic Acid (CLA) Isomers Indicate That Post-absorptive Synthesis Is the Predominant Source of *cis*-9-Containing CLA in Lactating Dairy Cows, *J. Nutr. 132*, 1235–1241.
73. Kay, J.K., Mackle, T.R., Auldist, M.J., Thomson, N.A., and Bauman, D.E. (2004) Endogenous Synthesis of *cis*-9,*trans*-11 Conjugated Linoleic Acid in Dairy Cows Fed Fresh Pasture, *J. Dairy Sci. 87*, 369–378.
74. Kraft, J., Collomb, M., Mockel, P., Sieber, R., and Jahreis, G. (2003) Differences in CLA Isomer Distribution of Cow's Milk Lipids, *Lipids 38*, 657–664.
75. Precht, D., and Molkentin, J. (1997) *Trans*-Geometrical and Positional Isomers of Linoleic Acid Including Conjugated Linoleic Acid (CLA) in German Milk and Vegetable Fats, *Fett-Lipid 99*, 319–326.
76. Lock, A.L., Perfield, J.W., Putnam, D., and Bauman, D.E. (2004) Evaluation of the Degree of Rumen Inertness and Bioavailability of *trans*-10,*cis*-12 CLA in a Lipid Encapsulated Supplement, *J. Dairy Sci. 87* (Suppl. 1), 335 (Abstr.).
77. Bauman, D.E., Barbano, D.M., Dwyer, D.A., and Griinari, J.M. (2000) Technical Note: Production of Butter with Enhanced Conjugated Linoleic Acid for Use in Biomedical Studies with Animal Models, *J. Dairy Sci. 83*, 2422–2425.
78. Rickert, R., Steinhart, H., Fritsche, J., Sehat, N., Yurawecz, M.P., Mossoba, M.M., Roach, J.A.G., Eulitz, K., Ku, Y., and Kramer, J.K.G. (1999) Enhanced Resolution of Conjugated Linoleic Acid Isomers by Tandem-Column Silver-Ion High Performance Liquid Chromatography, *J. High Resol. Chromatogr. 22*, 144–148.
79. Bauman, D.E., Baumgard, L.H., Corl, B.A., and Griinari, J.M. (2001) Conjugated Linoleic Acid (CLA) and the Dairy Cow, in *Recent Advances in Animal Nutrition 2001* (Garnsworthy, P.C., and Wiseman, J., eds.), pp. 221–250, Nottingham University Press, Nottingham, United Kingdom.
80. Stanton, C., Murphy, J., McGrath, E., and Devery, R. (2003) Animal Feeding Strategies for Conjugated Linoleic Acid Enrichment of Milk, in *Advances in Conjugated Linoleic Acid Research, Volume 2* (Sébédio, J.-L., Christie, W.W., and Adlof, R.O., eds.), pp. 123–145, AOCS Press, Champaign, IL.
81. Stanton, C., Lawless, F., Kjellmer, G., Harrington, D., Devery, R., Connolly, J.F., and Murphy, J. (1997) Dietary Influences on Bovine Milk *cis*-9,*trans*-11 Conjugated Linoleic Acid Content, *J. Food Sci. 62*, 1083–1086.
82. Chouinard, P.Y., Corneau, L., Butler, W.R., Chilliard, Y., Drackley, J.K., and Bauman, D.E. (2001) Effect of Dietary Lipid Source on Conjugated Linoleic Acid Concentrations in Milk Fat, *J. Dairy Sci. 84*, 680–690.
83. Dhiman, T.R., Satter, L.D., Pariza, M.W., Galli, M.P., Albright, K., and Tolosa, M.X. (2000) Conjugated Linoleic Acid (CLA) Content of Milk from Cows Offered Diets Rich in Linoleic and Linolenic Acid, *J. Dairy Sci. 83*, 1016–1027.
84. Jenkins, T.C. (1993) Lipid Metabolism in the Rumen, *J. Dairy Sci. 76*, 3851–3863.
85. Palmquist, D.L., and Jenkins, T.C. (1980) Fat in Lactation Rations: Review, *J. Dairy Sci. 63*, 1–14.
86. Bauman, D.E., and Griinari, J.M. (2001) Regulation and Nutritional Manipulation of Milk Fat: Low-Fat Milk Syndrome, *Livest. Prod. Sci. 70*, 15–29.
87. AbuGhazaleh, A.A., Schingoethe, D.J., Hippen, A.R., and Kalscheur, K.F. (2003) Milk Conjugated Linoleic Acid Response to Fish Oil Supplementation of Diets Differing in Fatty Acid Profiles, *J. Dairy Sci. 86*, 944–953.
88. AbuGhazaleh, A.A., Schingoethe, D.J., Hippen, A.R., and Kalscheur, K.F. (2003) Conjugated Linoleic Acid and Vaccenic Acid in Rumen, Plasma, and Milk of Cows Fed Fish Oil and Fats Differing in Saturation of 18 Carbon Fatty Acids, *J. Dairy Sci. 86*, 3648–3660.
89. Whitlock, L.A., Schingoethe, D.J., Hippen, A.R., Kalscheur, K.F., Baer, R.J., Ramaswamy, N., and Kasperson, K.M. (2002) Fish Oil and Extruded Soybeans Fed in Combination Increase Conjugated Linoleic Acids in Milk of Dairy Cows More Than When Fed Separately, *J. Dairy Sci. 85*, 234–243.
90. AbuGhazaleh, A.A., and Jenkins, T.C. (2004) Short Communication: Docosahexaenoic Acid Promotes Vaccenic Acid Accumulation in Mixed Ruminal Cultures When Incubated with Linoleic Acid, *J. Dairy Sci. 87*, 1047–1050.

91. Banni, S., Carta, G., Contini, M.S., Angioni, E., Deiana, M., Dessi, M.A., Melis, M.P., and Corongiu, F.P. (1996) Characterization of Conjugated Diene Fatty Acids in Milk, Dairy Products and Lamb Tissues, *Nutritional Biochemistry 7*, 150–155.
92. Auldist, M.J., Kay, J.K., Thomson, N.A., Napper, A.R., and Kolver, E.S. (2002) Brief Communication: Concentrations of Conjugated Linoleic Acid in Milk from Cows Grazing Pasture or Fed a Total Mixed Ration for an Entire Lactation, *Proc. New Zealand Soc. Anim. Prod. 62*, 240–247.
93. Lock, A.L., and Garnsworthy, P.C. (2003) Seasonal Variation in Milk Conjugated Linoleic Acid and Δ9-Desaturase Activity in Dairy Cows, *Livest. Prod. Sci. 79*, 47–59.
94. Riel, R.R. (1963) Physico-chemical Characteristics of Canadian Milk Fat: Unsaturated Fatty Acids, *J. Dairy Sci. 46*, 102–106.
95. Dhiman, T.R., Anand, G.R., Satter, L.D., and Pariza, M.W. (1999) Conjugated Linoleic Acid Content of Milk from Cows Fed Different Diets, *J. Dairy Sci. 82*, 2146–2156.
96. Kelly, M.L., Kolver, E.S., Bauman, D.E., Van Amburgh, M.E., and Muller, L.D. (1998) Effect of Intake of Pasture on Concentrations of Conjugated Linoleic Acid in Milk of Lactating Cows, *J. Dairy Sci. 81*, 1630–1636.
97. Kelsey, J.A., Corl, B.A., Collier, R.J., and Bauman, D.E. (2003) The Effect of Breed, Parity, and Stage of Lactation on Conjugated Linoleic Acid (CLA) in Milk Fat from Dairy Cows, *J. Dairy Sci. 86*, 2588–2597.
98. Lock, A.L., and Garnsworthy, P.C. (2002) Independent Effects of Dietary Linoleic and Linolenic Fatty Acids on the Conjugated Linoleic Acid Content of Cows' Milk, *Anim. Sci. 74*, 163–176.
99. Peterson, D.G., Kelsey, J.A., and Bauman, D.E. (2002) Analysis of Variation in *cis*-9,*trans*-11 Conjugated Linoleic Acid (CLA) in Milk Fat of Dairy Cows, *J. Dairy Sci. 85*, 2164–2172.
100. Lawless, F., Stanton, C., L'Escop, P., Devery, R., Dillon, P., and Murphy, J.J. (1999) Influence of Breed on Bovine Milk *cis*-9,*trans*-11 Conjugated Linoleic Acid Content, *Livest. Prod. Sci. 62*, 43–49.
101. White, S.L., Bertrand, J.A., Wade, M.R., Washburn, S.P., Green, J.T., and Jenkins, T.C. (2001) Comparison of Fatty Acid Content of Milk from Jersey and Holstein Cows Consuming Pasture or a Total Mixed Ration, *J. Dairy Sci. 84*, 2295–2301.
102. Dhiman, T.R., Zaman, M.S., Kilmer, L., and Gilbert, D. (2002) Breed of Dairy Cows Has Influence on Conjugated Linoleic Acid (CLA) Content of Milk, *J. Dairy Sci. 85* (Suppl. 1), 315 (Abstr.).
103. Lock, A.L., Bauman, D.E., and Garnsworthy, P.C. (2003) Effects of Milk Yield and Milk Fat Production on Milk *cis*-9, *trans*-11 CLA and D9-Desaturase Activity, *J. Dairy Sci. 86* (Suppl. 1), 245 (Abstr.).
104. Ip, C., Banni, S., Angioni, E., Carta, G., McGinley, J., Thompson, H.J., Barbano, D.M., and Bauman, D.E. (1999) Conjugated Linoleic Acid-Enriched Butter Fat Alters Mammary Gland Morphogenesis and Reduces Cancer Risk in Rats, *J. Nutr. 129*, 2135–2142.
105. Corl, B.A., Barbano, D.M., Bauman, D.E., and Ip, C. (2003) *cis*-9, *trans*-11 CLA Derived Endogenously from *trans*-11 18:1 Reduces Cancer Risk in Rats, *J. Nutr. 133*, 2893–2900.
106. Lock, A.L., Corl, B.A., Barbano, D.M., Bauman, D.E., and Ip, C. (2004) The Anticarcinogenic Effect of trans-11 18:1 is Dependent on Its Conversion to *cis*-9, *trans*-11 CLA by Δ9-Desaturase in Rats, *J. Nutr. 134*, 2698–2704.
107. Turpeinen, A.M., Mutanen, M., Aro, A., Salminen, I., Basu, S., Palmquist, D.L., and Griinari, J.M. (2002) Bioconversion of Vaccenic Acid to Conjugated Linoleic Acid in Humans, *Am. J. Clin. Nutr. 76*, 504–510.
108. Avramis, C.A., Wang, H., McBride, B.W., Wright, T.C., and Hill, A.R. (2003) Physical and Processing Properties of Milk, Butter, and Cheddar Cheeses from Cows Fed Supplemental Fish Meal, *J. Dairy Sci. 86*, 2568–2576.
109. Gonzalez, S., Duncan, S.E., O'Keefe, S.F., Sumner, S.S., and Herbein, J.H. (2003) Oxidation and Textural Characteristics of Butter and Ice Cream with Modified Fatty Acid Profiles, *J. Dairy Sci. 86*, 70–77.
110. Ramaswamy, N., Baer, R.J., Schingoethe, D.J., Hippen, A.R., Kasperson, K.M., and Whitlock, L.A. (2001) Short Communication: Consumer Evaluation of Milk High in Conjugated Linoleic Acid, *J. Dairy Sci. 84*, 1607–1609.

[Received August 6, 2004; accepted October 18, 2004]

Increasing Homicide Rates and Linoleic Acid Consumption Among Five Western Countries, 1961–2000

Joseph R. Hibbeln*, Levi R.G. Nieminen, and William E.M. Lands
Laboratory of Membrane Biochemistry and Biophysics, National Institute on Alcohol Abuse and Alcoholism, National Institutes of Health, Bethesda, Maryland

ABSTRACT: Clinical intervention trials and animal studies indicate that increasing dietary intakes of long chain n-3 FA or reducing linoleic acid intake may reduce aggressive and violent behaviors. Here we examine if economic measures of greater n-6 consumption across time and countries correlate with greater risk of homicide. Linoleic acid available for human consumption was calculated from World Health Organization disappearance data for 12 major seed oils in the food supply for the years 1961 to 2000 in Argentina, Australia, Canada, the United Kingdom, and the United States (US). Homicide mortality rates, adjusted for age, were obtained from the central judicial authority of each country. Apparent linoleic acid intake from seed oil sources ranged from 0.29 en% (percentage of daily food energy) (Australia 1962) to 8.3 en% (US 1990s). Greater apparent consumption of linoleic acid correlated with higher rates of homicide mortality over a 20-fold range (0.51–10.2/100,000) across countries and time in an exponential growth regression model ($r = 0.94$, $F = 567$, $P < 0.00001$). Within each country, correlations between greater linoleic acid disappearance and homicide mortality over time were significant in linear regression models. Randomized controlled trials are needed to determine if reducing high intakes of linoleic acid by seed oils with alternative compositions can reduce the risk of violent behaviors. These dietary interventions merit exploration as relatively cost-effective measures for reducing the pandemic of violence in Western societies, just as dietary interventions are reducing cardiovascular mortality. Low linoleate diets may prevent behavioral maladies that correctional institutions, social service programs, and mental health providers intend to treat.

Paper no. L9643 in *Lipids 39*, 1207–1213 (December 2004).

For 2–3 million years of human evolution, diets rich in seafood and range-fed animals likely provided appreciable amounts of the n-3 essential FA eicosapentaenoic acid (EPA) and docosahexaenoic acid (DHA) (1,2). As both n-3 and n-6 FA are essential, diets are dominant determinants of the proportions of essential FA in brain and body tissues. DHA is selectively concentrated in synaptic neuronal membranes and is necessary for optimal neuronal function (3,4). Seed oils, including soy, corn, and canola, are rich in the n-6 FA linoleic acid, and these oils have displaced other dietary fats and calories in the food supply in developed countries during the 20th century. In the United States in 1909, soy oil accounted for approximately 0.02 en% (percentage of daily food energy) of all calories available for food consumption compared to 20 en% in 2000 (5). High dietary linoleate can depress tissue and membrane levels of the n-3 FA EPA and DHA by competing with α-linolenic for conversion to 20- and 22-carbon highly unsaturated FA (HUFA) (6). We previously proposed that the increase in linoleic acid in Western diets, especially relative to EPA and DHA intake, has been a risk factor contributing to the increasing rates of major depression and violence in the 20th century (7). The observation that greater intakes of seafood rich in EPA and DHA correlated with lower rates of homicide mortality across 36 countries ($r = –0.63$, $P < 0.00001$) (8) is consistent with observational studies reporting that lower tissue levels of EPA and/or DHA predict greater hostility measures among 4,000 subjects in the CARDIA epidemiological study (9), among aggressive cocaine addicts (10), and violent prisoners (11). Homicide mortality data are robust indicators of violence, have clear diagnostic criteria with unequivocal importance, and have been prospectively collected. We postulated that greater consumption of seed oils, the major dietary source of linoleic acid, would correlate with greater rates of homicide mortality across time and among Western countries with similar socioeconomic and background seafood intake levels. The positive association reported here is striking.

METHODS

Data on age-adjusted homicide mortality were obtained from the U.S. Department of Justice (12), the United Kingdom Office of National Statistics on Criminal Justice (13), Statistics Canada (14), the Argentina Ministry of Justice (15), and the Australian Bureau of Statistics (16). Seed oils, in particular soybean oil, are the dominant sources of the linoleic acid in the United States. Economic data on the disappearance of 12 primary seed oils as a percentage of available food energy for all commodities from 1961 to 2000 were obtained from the World Health Organization (WHO) Statistical Information Services (17). Disappearance (apparently used for human consumption) was defined as production plus imports plus existing stocks minus exports and remaining stocks (5). The nutrient content of each seed oil was calculated using version 13 of the National Nutrient Database of the United States Department of Agriculture (5). For each year, linoleate availability from each food oil

*To whom correspondence should be addressed at Section on Nutritional Neurochemistry, LMBB, NIAAA, 31 Center Drive, Building 31/ 1B 58, Bethesda, MD 20892. E-mail: jhibbeln@mail.nih.gov

Abbreviations: DHA, docosahexaenoic acid; en%, percentage of daily food energy; EPA, eicosapentaenoic acid; WHO, World Health Organization.

was summed and expressed as a percentage of total calories (en%) from all food available for human consumption. No seed oil disappearance or mortality data available for these countries were excluded and no adjustments were made for possible food wastage. Both the food commodity and the homicide mortality data were prospectively collected, and they reflect changes for the whole population of each country. Statistical analyses included both simple linear Pearson's regressions using Statview 5.0 (SAS Institute, Cary, NC) and iterative curve fitting for linear and nonlinear regressions using Sigma Plot 8.0 (SPSS Inc., Chicago, IL).

RESULTS

Linoleic acid from seed oil sources, in apparent consumption as food, ranged from 0.29 en% (Australia 1962) to 8.3 en% (US 1990s). Rates of homicide mortality nearly tripled in the United States and in the United Kingdom from 1961 to 2000. Time trends were first considered separately by country. Greater linoleate disappearance was correlated with greater homicide mortality over time in linear regression models for the United States ($r = 0.61$, $P < 1.0 \times 10^{-6}$), the United Kingdom ($r = 0.89$, $P < 1.0 \times 10^{-14}$), Australia ($r = 0.74$, $P < 1.0 \times 10^{-10}$), Canada ($r = 0.53$, $P < 0.0004$), and Argentina ($r = 0.75$, $P < 0.0001$). When data from all countries and time points were combined, greater apparent consumption of linoleic acid correlated with higher rates of homicide mortality over a 20-fold range (0.51–10.2/100,000) in an exponential growth regression model ($r = 0.94$, $F = 567$, $P < 0.00001$) (see Fig. 1). A significant correlational relationship remains ($r = 0.51$, $F = 20.5$, $P < 0.00001$) in a similar three-factor exponential growth model after exclusion of the United States.

DISCUSSION

This comparison indicates a striking correlation between greater apparent consumption of linoleic acid from seed oils and greater risk of homicide mortality across time, from 1961 to 2000, among five Western countries (see Figs. 2–6). These findings suggest, but do not demonstrate, that increased availability of linoleic acid might be a causal factor contributing to the increased rates of homicide during the last half of the 20th century among these five countries. To our knowledge, this is the first examination of a risk factor for homicide across both countries and time. Greater linoleic acid consumption is not proposed here as a sole determinant factor for greater homicide mortality, but as a readily modifiable potential risk factor.

These findings may be due to secondary hidden covariates, which are fairly well established factors that increase the risk of homicide. For example, the availability of firearms is a rea-

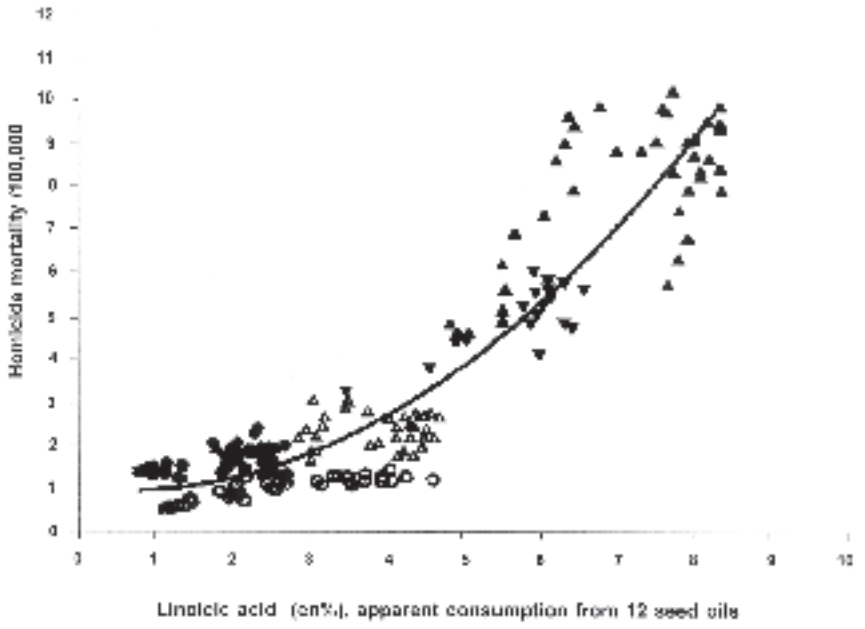

FIG. 1. Homicide rates and linoleic acid disappearance for human consumption among five countries, 1961–2000. The following symbols indicate dates within each country for the years 1961–2000: ↧ Australia; ↧ United Kingdom; ▪, Canada; ▾, Argentina; ▫, United States. The disappearance for human consumption of linoleic acid from 12 seed oils [18:2n-6 (en%)/cap/d] was derived as a percentage of energy available from all commodities available for use as human food, from the Food and Agriculture Organization/WHO database as indicated for each year. Other dietary sources of linoleic acid are not included. Corresponding homicide rates were adjusted for age, expressed per 100,000 population, and obtained from criminal justice statistics for each country. Iterative curve fitting for three-factor exponential growth equations resulted in the following fit: $f = 1.02788 - 0.162742x + 0.145575x^2$, $r = 0.94$, $r^2 = 0.87$, $F = 567$, $P < 0.00001$.

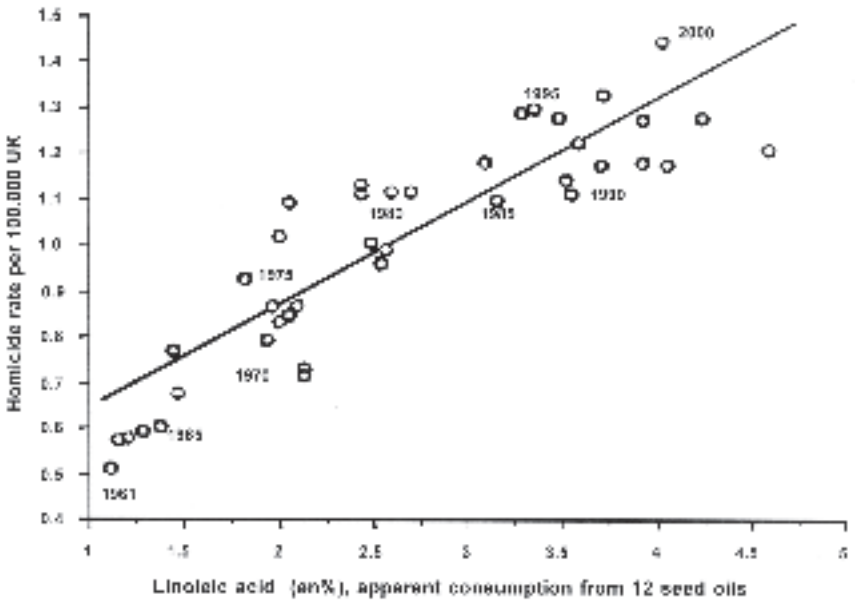

FIG. 2. Homicide mortality and consumption of linoleic acid from seed oils, 1961–2000, in the United Kingdom. The **o** symbol indicates dates 1961–2000 within the United Kingdom. A linear regression model resulted in the following fit: $r = 0.89$, $r^2 = 0.80$, $F = 150.6$, $P < 1 \times 10^{-14}$.

sonable confounding variable that could account for the findings reported here. Unfortunately, data on availability measured by per capita ownership or the percentage of households with firearms is not readily obtainable or reliable across countries in the time periods examined. Alternatively, data are more uniformly available expressing homicides attributable to firearms as a percentage of total homicides. This parameter also has the advantage of being a more direct assessment of the use of the firearms in the commission of homicides than surveys of availability or percent household ownership (18). In Canada, both firearm availability and the percentage of homicides related to firearms decreased during this time as the result of progressively restrictive gun legislation in 1977, 1991, and 1995 (19). In Australia, the percentage of homicides related to

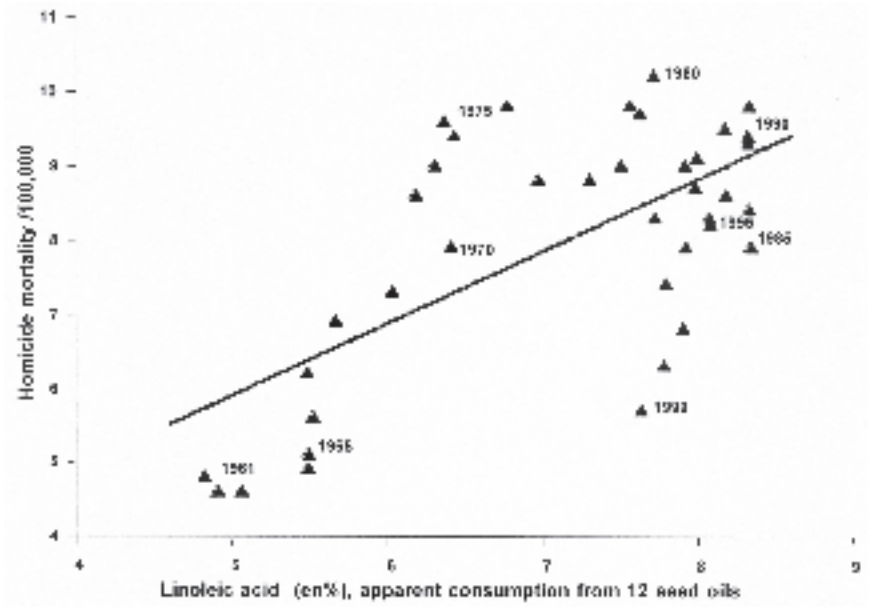

FIG. 3. Homicide mortality and consumption of linoleic acid from seed oils, 1961–1999, in the United States. The s symbol indicates dates 1961–1999 within the United States. A linear regression model resulted in the following fit: $r = 0.65$, $r^2 = 0.43$, $F = 27.7$, $P < 0.000001$.

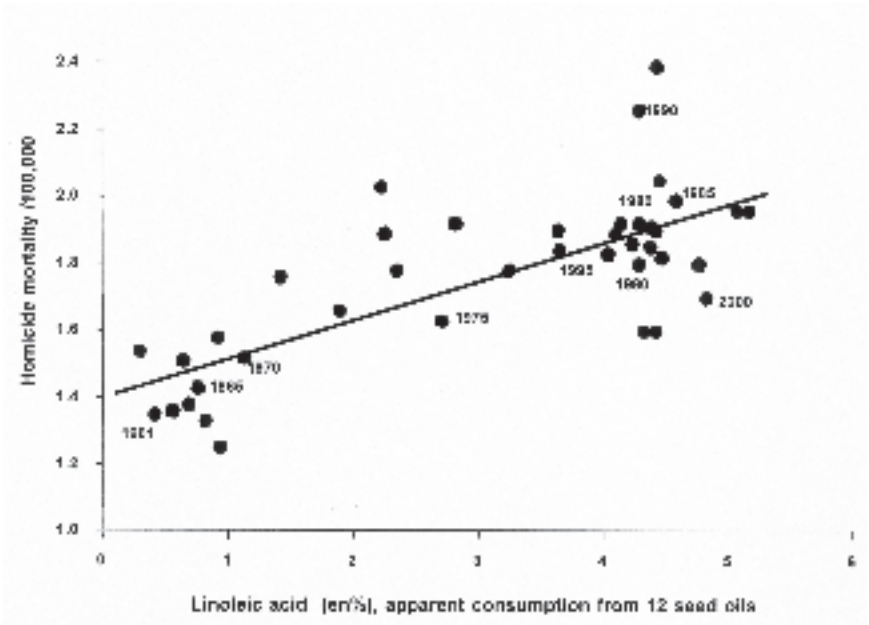

FIG. 4. Homicide mortality and consumption of linoleic acid from seed oils, 1961–2000, in Australia. The ı symbol indicates dates 1961–1999 within Australia. A linear regression model resulted in the following fit: $r = 0.74$, $r^2 = 0.54$, $F = 44$, $P < 1 \times 10^{-10}$.

firearms significantly decreased from 1960 to 2000 (20). Homicide rates by all methods rose in these countries, but, in general, for the period between 1960 and 2000 the percentage of homicides attributable to firearms decreased over time in Canada or Australia and changed little in the United Kingdom (21) or the United States (22). Since the availability of firearms as measured by their use in homicides has a negative or neutral trend in this analysis, availability is unlikely to be a hidden causal factor underlying the positive relationships between greater linoleate intake and greater homicide mortality in these countries over time. Since the United States has a higher rate of firearm availability and a higher percentage of firearm-related homicides, it may be a driving force confounding the cross-national relationship. However, a significant correlational

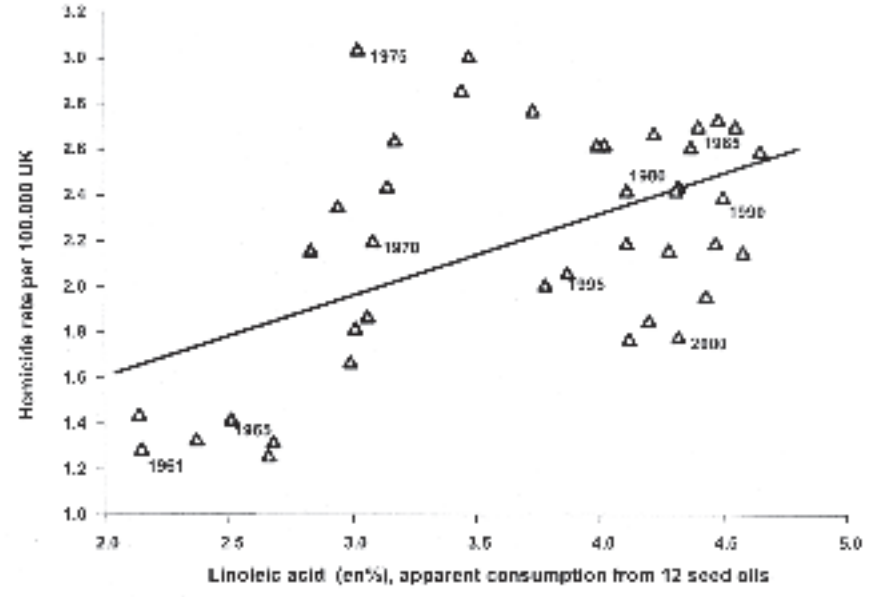

FIG. 5. Homicide mortality and consumption of linoleic acid from seed oils, 1961–2000, in Canada. The Δ symbol indicates dates 1961–2000 within Canada. A linear regression model resulted in the following fit: $r = 0.53$, $r^2 = 0.28$, $F = 15.1$, $P < 0.0004$.

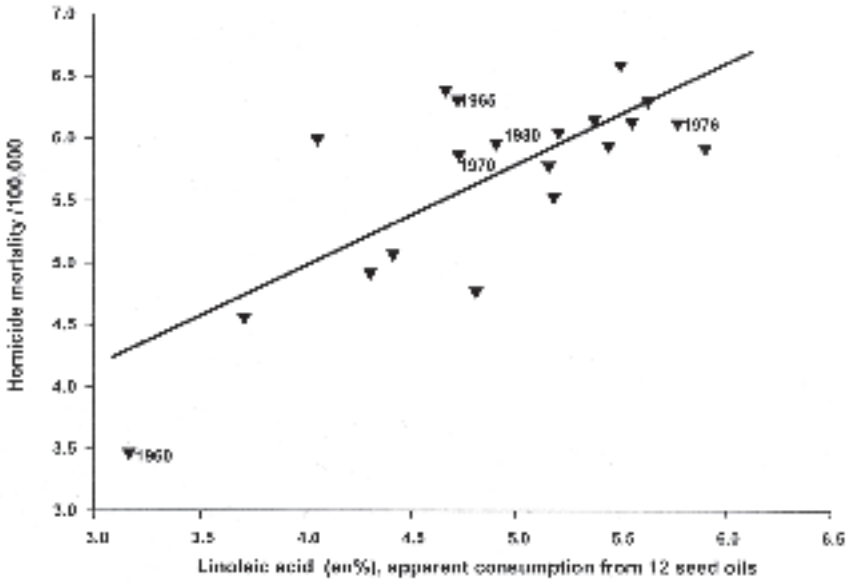

FIG. 6. Homicide mortality and consumption of linoleic acid from seed oils, 1960–1981, in Argentina. The t symbol indicates dates 1961–1985 within Argentina. A linear regression model resulted in the following fit: $r = 0.75$, $r^2 = 0.56$, $F = 23.2$, $P < 0.0001$.

relationship remained after excluding the United States. The magnitude of the relationships between homicide rates and linoleate disappearance ($r = 0.93$ including and $r = 0.51$ excluding the United States) reported here is similar to, or greater than, the magnitude of the relationship between firearm availability and homicide mortality in a cross-national analysis of 26 countries ($r = 0.69$ including and $r = 0.25$ excluding the United States) (23). In summary, it is unlikely that the correlational relationships between linoleate availability and homicide mortality are caused by differences in the availability or use of firearms when examined across countries and across time.

We do not propose that increased linoleate consumption during 1961 to 2000 can be isolated from many other societal, cultural, economic, or nutritional factors that might contribute to increased risk of homicide. However, the epidemiological associations in this report can help support a rationale for designing future controlled clinical intervention studies that directly alter linoleate intake and test for changes in aggressive behavior. The large differences in homicide mortality rates among the five countries suggest that many societal and economic factors contribute to greater risk of homicide (24). The American Academy of Pediatrics and five other prominent medical societies (25) cited exposure of youth to violent media *via* videogames, cable television, and the Internet as a contributing factor to societal violence. In the 40 years spanning the data examined here this media exposure has increased. These years have included the perception that the integrity of social systems declined in the United States and other countries, accompanying progressively higher divorce rates, a possible marker of disintegration of the family unit. In addition, drug and alcohol use have become widespread, along with gang behaviors, teenage pregnancy, sexually transmitted diseases, and an increasing population of generally dysphoric, discontented youth, each of which is a potential risk to greater social disintegration. Many of these social and cultural factors are difficult to quantify, and comparable data sets are not available across time and countries. As direct data are not available on a yearly basis for all potential risk factors, we do not attempt here to create a statistical model comparing the relative contributions of each potential risk factor, and thus we do not conclude that these epidemiological associations constitute causal proof that increasing linoleate availability increases homicide risk.

There was wide diversity in the apparent consumption of linoleic acid from seed oils as a percentage of energy, ranging from 0.29 en% in Australia, in 1962, to 8.3 en% in the United States, 1985–1992. The disappearance data for comparable seed oil and other commodities were used to examine the relative differences in apparent linoleate intakes across time and countries. Clearly, seed oils are the major but not the sole source of linoleic acid in the diet, and no attempt was made here to determine the absolute per capita ingestion of total linoleic acid and total calories. Estimates of linoleic acid that included other food sources during comparable time periods were higher in the United Kingdom (26) and lower in the Australian diet (27) than those reported here. Differential degrees of hydrogenation, waste, spoilage, reports of total calorie disappearance, and oil composition not reflected by the nutritional composition tables were likely to have increased variability in estimates of linoleic acid intake as a percentage of energy and reduced the strength of the robust correlations reported here.

The ecological associations between greater risks of homicide mortality and both greater linoleate intake and lower seafood intake (28) are consistent with animal studies and controlled intervention trials in humans that reported decreased

measures of aggression or violence by increasing intakes of long chain n-3 FA relative to n-6 intake. This proposition that dietary differences in essential FA status can alter aggressive behavior has been supported by six placebo-controlled, randomized clinical trials where supplementation with EPA, DHA, or both reduced violent behaviors or measures of aggression (29–33). A trial using essential FA, multivitamins, and minerals also reported a substantial reduction in aggression among prisoners (34). Aggressive behavior was also markedly higher among the adult pups of mothers who were fed diets containing 43 en% from soy oil throughout gestation (35). Muricidal behavior was induced in adult rats by diets rich in linoleic acid (36), and DHA was lower in the brains of rats with isolation-induced muricidal behavior (37).

One mechanism that may link excessive linoleic acid intake or deficient EPA and DHA status is a deficit in serotonergic neurotransmission in the frontal cortex, which has been repeatedly implicated in the pathophysiology of lifelong impulsive and violent behaviors (38,39). Higley (39) reported that at 2 weeks of age, low concentrations of a marker of frontal serotonergic function, cerebrospinal fluid 5-hydroxyindolacetic acid, predicted a lifetime predisposition toward aggressive behavior among rhesus monkeys. Dietary deficiencies of n-3 intake during fetal life and early in development resulted in residual deficits in serotonergic neurotransmission (40). This four fold lower serotonin release stimulated by fenfluramine, measured at 60 days old, could be prevented by restoring dietary α-linolenic acid, but only if done before 14 days of life (40). When piglets' infant formulas were supplemented with arachidonic acid and DHA, frontal cortex concentrations of serotonin, dopamine, and their respective metabolites increased by nearly 50% (41). Reduction in serotonergic neurotransmission in the medial prefrontal cortex is one plausible mechanism of action that can be tested in randomized placebo controlled trials designed to specifically decrease intakes of linoleic acid and/or increase the intakes of EPA and DHA. Dietary interventions that reduce linoleate intake and improve the tissue status of n-3 FA and other basic nutrients (34) can potentially become relatively cost-effective measures for reducing the pandemic of violence in Western societies, just as dietary interventions are reducing cardiovascular mortality. Low linoleate diets may prevent behavioral maladies that correctional institutions, social service programs, and mental health providers intend to treat.

REFERENCES

1. Broadhurst, C., Cunnane, S., and Crawford, M. (1998) Rift Valley Lake Fish and Shellfish Provided Brain-Specific Nutrition for Early Homo, *Br. J. Nutr. 79,* 3–21.
2. Walter, R.C., Buffler, R.T., Bruggemann, J.H., Guillaume, M.M., Berhe, S.M., Negassi, B., Libsekal, Y., Cheng, H., Edwards, R.L., von Cosel, R., Neraudeau, D., and Gagnon, M. (2000) Early Human Occupation of the Red Sea Coast of Eritrea During the Last Interglacial, *Nature 405,* 65–69.
3. Niu, S.L., Mitchell, D.C., Lim, S.Y., Wen, Z.M., Kim, H.Y., Salem, N., Jr., and Litman, B.J. (2004) Reduced G Protein-Coupled Signaling Efficiency in Retinal Rod Outer Segments in Response to n-3 Fatty Acid Deficiency, *J. Biol. Chem. 279,* 31098–31104.
4. Salem, N., Jr., and Niebylski, C.D. (1995) The Nervous System Has an Absolute Molecular Species Requirement for Proper Function, *Mol. Membr. Biol. 12,* 131–134.
5. Gerrior, S., and Bente, L. (2002) Nutrient Content of the U.S. Food Supply, 1909–1999: A Summary Report, Home Economics Research Report. No 55, U.S. Department of Agriculture, Center for Nutrition Policy and Promotion, Washington, DC., Netlink: http://www.usda.gov/cnpp/nutrient_content.html (accessed December 2004).
6. Rahm, J.J., and Holman, R.T. (1964) Effect of Linoleic Acid upon the Metabolism of Linolenic Acid, *J. Nutr. 84,* 15–19.
7. Hibbeln, J.R., and Salem, N., Jr. (1995) Dietary Polyunsaturated Fatty Acids and Depression: When Cholesterol Does Not Satisfy, *Am. J. Clin. Nutr. 62,* 1–9.
8. Hibbeln, J.R. (2001) Seafood Consumption and Homicide Mortality, *World Rev. Nutr. Diet 85,* 41–46.
9. Iribarren, C., Markovitz, J.H., Jacobs, D.R., Schreiner, P.J., Daviglus, M., and Hibbeln, J.R. (2004) Dietary Intake of n-3, n-6 Fatty Acids and Fish: Relationship with Hostility in Young Adults—The CARDIA Study, *Eur. J. Clin. Nutr. 58,* 24–31.
10. Buydens-Branchey, L., Branchey, M., McMakin, D.L., and Hibbeln, J.R. (2003) Polyunsaturated Fatty Acid Status and Aggression in Cocaine Addicts, *Drug Alcohol Depend. 71,* 319–323.
11. Virkkunen, M.E., Horrobin, D.F., Jenkins, D.K., and Manku, M.S. (1987) Plasma Phospholipids, Essential Fatty Acids and Prostaglandins in Alcoholic, Habitually Violent and Impulsive Offenders, *Biol. Psychiatry 22,* 1087–1096.
12. Federal Bureau of Investigation. (2000) Homicide Trends in the United States. Uniform Crime Reports, 1950–99, Department of Justice, US Federal Government, Netlink: www.ojp.usdoj.gov/bjs/homicide (accessed December 2004).
13. Home Office. (2002) Criminal Statistics, National Statistics of the United Kingdom. http://www.homeoffice.gov.uk/rds/crimstats02.html (accessed September 2004)
14. Statistics Canada. (2001) Homicide in Canada, 85-002-XPE Government of Canada, Netlink: www.statcan.ca (accessed December 2004).
15. Ministerio de Justicia de la Nación. (2003) *Registro Nacional de Reincidencia y Estadística Criminal,* Government of Argentina, Buenos Aires.
16. Australian Institute of Criminology. (2002) Adapted from *Causes of Death Australia,* Catalogue No. 3303.0, Australian Bureau of Statistics, Netlink: http://www.abs.gov.au/ausstats/abs@nsf/Lookup/C86E6B498E247877CA256889000CCDE0 (accessed December 2004).
17. FAO/WHO. (2004) FAOSTAT Database, Food and Agricultural Organization of the United Nations, Sept 9, 2004, Netlink: http://faostat.fao.org/faostat/collections (accessed September 2004).
18. Krug, E.G., Powell, K.E., and Dahlberg, L.L. (1998) Firearm-Related Deaths in the United States and 35 Other High- and Upper-Middle-Income Countries, *Int. J. Epidemiol. 27,* 214–221.
19. Dandurand, Y. (1998) Firearms, Accidental Deaths, Suicide and Violent Crime: An Updated Review of the Literature with Special Reference to the Canadian Situation, WD1998-4e International Centre for Criminal Law Reform and Criminal Justice Policy, Netlink:http://canada.justice.gc.ca/en/ps/rs/rep/wd98-4a-e.html (accessed December 2004).
20. Australian Institute on Criminality. (2000) Australian Crime: Facts and Figures 2000. Homicide Involving Firearms as a Percentage of Total Homicide, 1915 to 1998, Australian Government, Netlink: http://www.aic.gov.au/publications/facts/2000/sec3.html (accessed December 2004).
21. Smith, C., and Allen, J. (2004) Violent Crime in England and Wales, Home Office Online Report 18/04, Home Office Re-

search, Development and Statistics Directorate Communication Development Unit, Netlink: http://www.homeoffice.gov.uk/rds/pdfs04/rdsolr1804.pdf (accessed December 2004).
22. Department of Justice. (2004) FBI Uniform Crime Reports Online, U.S. Federal Government, Netlink: http://bjsdata.ojp.usdoj.gov/dataonline/ (accessed December 2004).
23. Hemenway, D., and Miller, M. (2000) Firearm Availability and Homicide Rates Across 26 High-Income Countries, *J. Trauma 49,* 985–988.
24. Krug, E.G., Dahlberg, L., Mercy, J.C., Zwi, A.B., and Lozano, R. (2002) *World Report on Violence and Health,* World Health Organization, Netlink: http://www.who.int/violence_injury_prevention/violence/world_report/en (accessed December 2004).
25. American Academy of Pediatrics. (2000) Joint Statement on the Impact of Entertainment Violence on Children: Congressional Public Health Summit, Dec. 6, Netlink: http://www.aap.org/advocacy/releases/jstmtevc.htm (accessed December 2004).
26. Sanders, T.A. (2000) Polyunsaturated Fatty Acids in the Food Chain in Europe, *Am. J. Clin. Nutr. 71,* 176S–178S.
27. Meyer, B.J., Mann, N.J., Lewis, J.L., Milligan, G.C., Sinclair, A.J., and Howe, P.R. (2003) Dietary Intakes and Food Sources of Omega-6 and Omega-3 Polyunsaturated Fatty Acids, *Lipids 38,* 391–398.
28. Hibbeln, J.R. (2001) Seafood Consumption and Homicide Mortality: A Cross-National Ecological Analysis, *World Rev. Nutr. Diet. 88,* 41–46.
29. Zanarini, M.C., and Frankenburg, F.R. (2003) Omega-3 Fatty Acid Treatment of Women with Borderline Personality Disorder: A Double-Blind, Placebo-Controlled Pilot Study, *Am. J. Psychiatry 160,* 167–169.
30. Stevens, L., Zhang, W., Peck, L., Kuczek, T., Grevstad, N., Mahon, A., Zentall, S.S., Arnold, L.E., and Burgess, J.R. (2003) EFA Supplementation in Children with Inattention, Hyperactivity, and Other Disruptive Behaviors, *Lipids 38,* 1007–1021.
31. Hirayama, S., Hamazaki, T., and Terasawa, K. (2004) Effect of Docosahexaenoic Acid-Containing Food Administration on Symptoms of Attention-Deficit/Hyperactivity Disorder—A Placebo-Controlled Double-Blind Study, *Eur. J. Clin. Nutr. 58,* 467–473.
32. Hamazaki, T., Thienprasert, A., Kheovichai, K., Samuhaseneetoo, S., Nagasawa, T., and Watanabe, S. (2002) The Effect of Docosahexaenoic Acid on Aggression in Elderly Thai Subjects—A Placebo-Controlled Double-Blind Study, *Nutr. Neurosci. 5,* 37–41.
33. Hamazaki, T., Sawazaki, S., and Kobayashi, M. (1996) The Effect of Docosahexaenoic Acid on Aggression in Young Adults. A Double-Blind Study, *J. Clin. Invest. 97,* 1129–1134.
34. Gesch, C.B., Hammond, S.M., Hampson, S.E., Eves, A., and Crowder, M.J. (2002) Influence of Supplementary Vitamins, Minerals and Essential Fatty Acids on the Antisocial Behaviour of Young Adult Prisoners: Randomised, Placebo-Controlled Trial, *Br. J. Psychiatry 181,* 22–28.
35. Raygada, M., Cho, E., and Hilakivi-Clarke, L. (1998) High Maternal Intake of Polyunsaturated Fatty Acids During Pregnancy in Mice Alters Offsprings' Aggressive Behavior, Immobility in the Swim Test, Locomotor Activity and Brain Protein Kinase C Activity, *J. Nutr. 128,* 2505–2511.
36. Miachon, S., Augier, S., Jouvenet, M., Boucher, P., and Vallon, J.J. (2001) Nutritional Parameters Modify Muricidal Behavior of Male Wistar Rats: Preventive Effects Of Amino Acids and 4′ Cl Diazepam, *Life Sci. 69,* 2745–2757.
37. Augier, S., Penes, M.C., Debilly, G., and Miachon, A.S. (2003) Polyunsaturated Fatty Acids in the Blood of Spontaneously or Induced Muricidal Male Wistar Rats, *Brain Res. Bull. 60,* 161–165.
38. Stanley, B., Molcho, A., Stanley, M., Winchel, R., Gameroff, M.J., Parsons, B., and Mann, J.J. (2000) Association of Aggressive Behavior with Altered Serotonergic Function in Patients Who Are Not Suicidal, *Am. J. Psychiatry 157,* 609–614.
39. Highley, J.D. (2001) Individual Differences in Alcohol-Induced Aggression: A Nonhuman-Primate Model, *Alcohol Res. Health 25,* 12–19.
40. Kodas, E., Galineau, L., Bodard, S., Vancassel, S., Guilloteau, D., Besnard, J.C., and Chalon, S. (2004) Serotoninergic Neurotransmission Is Affected by n-3 Polyunsaturated Fatty Acids in the Rat, *J. Neurochem. 89,* 695–702.
41. de la Presa Owens, S., and Innis, S.M. (1999) Docosahexaenoic and Arachidonic Acid Prevent a Decrease in Dopaminergic and Serotoninergic Neurotransmitters in Frontal Cortex Caused by a Linoleic and α-Linolenic Acid Deficient Diet in Formula-Fed Piglets, *J. Nutr. 129,* 2088–2093.

[Received November 4, 2004, and in final form and accepted December 7, 2004]

Long-Chain Polyunsaturated Fatty Acids in Childhood Developmental and Psychiatric Disorders

Alexandra J. Richardson*

University Lab of Physiology and Mansfield College, Oxford, United Kindgdom

ABSTRACT: Both omega-3 and omega-6 long-chain PUFA (LC-PUFA) are crucial to brain development and function, but omega-3 LC-PUFA in particular are often lacking in modern diets in developed countries. Increasing evidence, reviewed here, indicates that LC-PUFA deficiencies or imbalances are associated with childhood developmental and psychiatric disorders including ADHD, dyslexia, dyspraxia, and autistic spectrum disorders. These conditions show a high clinical overlap and run in the same families, as well as showing associations with various adult psychiatric disorders in which FA abnormalities are already implicated, such as depression, other mood disorders, and schizophrenia. Preliminary evidence from controlled trials also suggests that dietary supplementation with LC-PUFA might help in the management of these kinds of childhood behavioral and learning difficulties. Treatment with omega-3 FA appears most promising, but the few small studies published to date have involved different populations, study designs, treatments, and outcome measures. Large-scale studies are now needed to confirm the benefits reported. Further research is also required to assess the durability of such treatment effects, to determine optimal treatment compositions and dosages, and to develop reliable ways of identifying those individuals most likely to benefit from this kind of treatment. Childhood developmental and psychiatric disorders clearly reflect multifactorial influences, but the study of LC-PUFA and their metabolism could offer important new approaches to their early identification and management. Heterogeneity and comorbidity are such, however, that a focus on specific traits or symptoms may prove more fruitful than an exclusive reliance on current diagnostic categories.

Paper no. L9638 in *Lipids 39,* 1215–1222 (December 2004).

Increasing evidence indicates that disturbances of FA and phospholipid metabolism can play a part in a wide range of psychiatric, neurological, and developmental disorders in adults (1). In recent years it has also become clear that the same factors have a role to play in many childhood neurodevelopmental and psychiatric disorders (2). The latest evidence for this proposal, reviewed here, indicates that a better understanding of the role of long-chain PUFA (LC-PUFA) in these conditions could offer important new approaches to their identification and management.

ADHD, DYSLEXIA, DYSPRAXIA, AND AUTISTIC SPECTRUM DISORDERS

The most common developmental and psychiatric disorders of childhood include attention-deficit/hyperactivity disorder (ADHD), dyslexia, dyspraxia, and autistic spectrum disorders, which between them affect 10–20% of the school-age population. Each is defined by a different and relatively specific pattern of difficulties in behavior and/or learning. Thus in ADHD, the core features involve attentional problems and/or hyperactive-impulsive behaviors; in dyslexia, specific difficulties with reading and writing; in dyspraxia or developmental coordination disorder (DCD), specific weaknesses in the planning and coordination of actions; and in the autistic spectrum, impaired social and communication skills. In practice, however, the overlaps between these conditions are high, and their boundaries with normal variation in behavioral and cognitive function are not at all clear-cut (3–5). "Pure" cases are the exception, not the rule, and within each category there is substantial heterogeneity.

Many features associated with ADHD, dyslexia, dyspraxia, and autistic spectrum disorders are consistent with deficiencies or imbalances in omega-3 and/or omega-6 FA, as discussed in more detail elsewhere (6,7). These include the excess of males affected, slightly increased tendencies for pregnancy and birth complications and minor physical anomalies, and an increased frequency of atopic or autoimmune disorders in affected individuals and their relatives. FA abnormalities could also help to account for some of the key cognitive and behavioral features of these conditions, such as anomalous visual, motor, attentional, or language processing, as well as associated difficulties with mood, digestion, temperature regulation, and sleep.

These developmental conditions all tend to cluster within families, and they also show familial and other associations with certain psychiatric disorders including depression and bipolar disorder as well as schizophrenia spectrum and personality disorders (8–11). This and other evidence points to some common genetic factors in the predisposition to all of these conditions, which may include constitutional anomalies of FA and phospholipid metabolism (12).

THE IMPORTANCE OF LC-PUFA IN BRAIN DEVELOPMENT AND FUNCTION

Omega-3 and omega-6 FA are crucial for normal brain structure

*To whom correspondence should be addressed at University Lab of Physiology, Parks Road, Oxford OX1 3PT, United Kingdom.
E-mail: alex.richardson@physiol.ox.ac.uk

Abbreviations: AA, arachidonic acid; ADHD, attention deficit/hyperactivity disorder; ALA, α-linolenic acid; DCD, developmental coordination disorder; DGLA, di-homo-γ-linolenic acid; DSM-IV, Diagnostic and Statistical Manual of the American Psychiatric Association, Version IV; GLA, γ-linolenic acid; LA, linoleic acid; LC-PUFA, long-chain polyunsaturated fatty acids; PLA_2, phospholipase A_2; PPAR, peroxisome proliferator-activated receptor; RBC, red blood cell; RCT, randomized controlled trial.

and function, but must be derived from dietary sources. Four LC-PUFA are particularly important to the brain: the omega-6 FA arachidonic acid (AA) and dihomo-γ-linolenic acid (DGLA) and the omega-3 FA EPA and DHA. If not provided directly by the diet, these LC-PUFA must be manufactured *via* desaturation and elongation processes from linoleic acid (LA) in the case of omega-6, or α-linolenic acid (ALA) in the case of omega-3.

Structurally, AA and DHA are key components of neuronal membranes, making up 15–20% of the brain's dry mass and more than 30% of the retina. In early life, both omega-3 and omega-6 LC-PUFA are critical for supporting brain growth and maturation. During prenatal development, adequate supplies are so essential that the placenta doubles the levels circulating in maternal plasma (13), and severe deficits may have permanent effects if they occur during critical periods of early development. AA is crucial to brain growth, and mild deficiencies are associated with low birth weight and reduced head circumference. It also plays a key role in the cellular processes underlying learning and memory. DHA is particularly concentrated in highly active membranes such as synapses and photoreceptors, and adequate supplies are essential for normal visual and cognitive development (14,15). Pre-formed LC-PUFA are found naturally in breast milk, and although some controlled studies have shown advantages to both visual and cognitive development from their addition to infant formula (16), it is not yet clear whether the established benefits of such supplementation for preterm infants may also extend to well-nourished term infants (17).

Throughout life, adequate supplies of LC-PUFA remain crucial for optimal brain function. They increase the fluidity of neuronal membranes, essential for efficient signal transduction, and some act as second messengers in chemical neurotransmitter systems as well as contributing to many other aspects of cell signalling (18) Functionally, three LC-PUFA (DGLA, AA, and EPA) are particularly important as substrates for the eicosanoids—highly bioactive hormone-like substances including prostaglandins, leukotrienes, and thromboxanes. These derivatives play key roles in regulating blood flow and endocrine and immune functions and can modulate ion channels, neurotransmitter uptake, synaptic transmission, apoptosis, and many other biological processes.

An adequate and appropriately balanced supply of LC-PUFA is thus required for normal brain function, both during early development and throughout life. Unfortunately, there are many possible reasons why their availability may be less than optimal, particularly in the case of omega-3 FA.

POSSIBLE REASONS FOR FUNCTIONAL DEFICIENCIES OR IMBALANCES IN LC-PUFA

First, these FA are scarce in many modern diets, especially those in which highly processed foods predominate. This particularly applies to the omega-3 LC-PUFA most important for the brain (EPA and DHA), which are found in appreciable quantities only in fish and seafood. Their precursor, ALA, is found in green vegetables and some nuts and seeds, but its conversion to EPA and DHA is limited, as discussed further below. Omega-6 fats are much more plentiful, because most vegetable oils are rich in LA, and AA is provided directly by meat and dairy products. Overall, the last century has seen dramatic increases in the ratios of omega-6 to omega-3 in average Western-type diets, from approximately 3:1 to more than 20:1 in some cases (19). Gene transfer studies have recently provided powerful evidence that the earlier ratios were much closer to the optimum for healthy human cells (20), and this relative disappearance of omega-3 FA from the diet has already been explicitly linked with increased rates of many disorders of both physical and mental health, including cardiovascular disease, immune disorders, depression, and schizophrenia (19,21–23). Similar effects seem likely with respect to childhood developmental and psychiatric disorders.

Second, there may be difficulties in the synthesis of LC-PUFA from LA or ALA. *In vivo* studies indicate that this conversion process is not very efficient in humans (24,25), but it can also be affected by diet and lifestyle as well as constitutional factors. Males appear particularly vulnerable to LC-PUFA deficiency, as testosterone can impair LC-PUFA synthesis, whereas estrogen helps to protect these FA from breakdown (26,27). Some *in vivo* synthesis of DHA from ALA was observed in adult females (28), but none was detectable in adult males studied using the same methodology (29). These sex differences are interesting in view of the excess of males affected by most of the developmental and psychiatric disorders considered here. LC-PUFA synthesis may also be impaired in atopic conditions such as eczema (30), which are commonly associated with ADHD, dyslexia, autism, and related conditions. From these and other observations, constitutional inefficiencies in LC-PUFA synthesis were explicitly proposed in the first study implicating FA abnormalities in ADHD (31).

Constitutional factors affecting other aspects of FA metabolism may also reduce the availability of LC-PUFA. FA are constantly replaced and recycled during the normal turnover and remodeling of cell membranes and in the chemical cascades triggered by normal cell signalling processes. Phospholipase A_2 (PLA_2) enzymes cleave highly unsaturated FA from the *sn*-2 position of membrane phospholipids, creating FFA and lyso-phospholipids that are highly vulnerable to oxidation and require rapid recycling via at least two further enzyme steps. A huge number of other enzymes are involved in the transport and utilization of FA in the brain and body. Individual differences in their efficiency will have implications for optimal dietary requirements for LC-PUFA, and genetic influences on them may contribute to the risks for various developmental and psychiatric disorders (12).

A ROLE FOR LC-PUFA IN CURRENT THEORIES OF CHILDHOOD NEURODEVELOPMENTAL AND PSYCHIATRIC DISORDERS

The etiologies of ADHD, dyslexia, autism, and related disorders are obviously highly complex and multifactorial. Furthermore, LC-PUFA have such profound and widespread influences on brain development and function that their potential roles in

these conditions are innumerable. In current theories of these neurodevelopmental disorders, however, a few themes seem particularly relevant to possible mechanisms by which FA deficiencies or imbalances could play a contributory role.

Immune function. Many aspects of normal brain development and plasticity are influenced by the immune system (32), and abnormal immune reactivity is increasingly implicated in a wide range of neurodevelopmental and psychiatric disorders (33–37) Imbalances in LC-PUFA will give rise to imbalances in eicosanoid production, and although the relative effects of omega-3 and omega-6 FA on immune function are complex (38), derivatives of AA and EPA generally have opposing actions such that a relative lack of omega-3 increases tendencies toward inflammation and autoimmune reactivity via these and other mechanisms (39).

The minor neuroanatomical abnormalities reported in dyslexic brains postmortem are consistent with inflammatory processes that could plausibly reflect low dietary omega-3 during early development (40). Similarly, some of the visual processing deficits associated with dyslexia are thought to reflect autoimmune influences *in utero* (41). However, functionally inadequate levels of DHA at any developmental stage could play a part, given the crucial importance of this omega-3 FA for visual function, and whether visual deficits in dyslexia may respond to treatment with omega-3 LC-PUFA is the subject of ongoing studies. In addition to its unique role in visual signal transduction (42), DHA also gives rise to derivatives that have anti-inflammatory properties (43,44). These recent findings invite further exploration of the relative contributions of EPA and DHA to immune system changes following LC-PUFA administration, although preliminary evidence suggests that EPA may be more effective in the treatment of neurodevelopmental and psychiatric disorders, as discussed later.

Gut–brain interactions. The gut is a key interface in psychoneuroimmunological reactions—the highly complex interactions between the immune system and the brain, and digestive disorders are highly prevalent in children with neurodevelopmental disorders, especially within the autistic spectrum. In early life, dietary LC-PUFA are important to the establishment and maintenance of healthy gut flora and can influence Th1 and Th2 programming by gut-associated lymphoid tissues, with consequences for autoimmune or allergic responses (45). Relative omega-3 deficiencies may predispose a person to gut inflammation and associated increases in membrane permeability in a variety of ways (46), with negative effects on nutrient absorption and detoxification processes. The potential implications of immune–gut disturbances of this kind are widespread, and include deleterious effects on brain function.

Neurotransmitter function. The limitations of simplistic neurotransmitter-imbalance models of psychiatric illness have long been apparent, but the many ways in which FA and their metabolism can affect the functioning of conventional neurotransmitter systems—and the implications of this for many disorders of mental health and development—are only just starting to be fully appreciated (1,21). These also relate to the issues already mentioned, because many substances regarded primarily as neurotransmitters also play crucial signaling roles in the gut. Furthermore, pro-inflammatory cytokines have been shown to alter the function of monoamine neurotransmitters implicated in stress, sleep disorders, and depression (47,48).

Omega-3 supplementation can modulate the adrenal activation induced by mental stress (49), and dietary omega-3 FA are known to affect serotonergic function, which may help to explain their beneficial effects as reported in controlled trials of depression (50–52) and in preventing or reducing hostility and aggression (53,54). These clinical features are commonly associated with the childhood disorders considered here, raising the possibility that LC-PUFA could also help in the management of these conditions.

ADHD is routinely treated using stimulant medications that increase the availability of dopamine, a fact reflected in all pharmacological theories of this condition. It is thus of interest that chronic omega-3 deficiency reduces dopamine (and its binding to D_2 receptors) in the frontal cortex and is associated with comparable attentional and behavioral dysfunction in animal studies (55,56). Recent evidence from such studies indicates that some effects of early omega-3 deficiency on dopaminergic systems may be more amenable to subsequent dietary interventions than others (57), but whether ADHD symptoms in children can be reduced by LC-PUFA treatment still requires further exploration in clinical trials, as discussed later.

EVIDENCE FOR FA ABNORMALITIES IN CHILDHOOD DEVELOPMENTAL AND PSYCHIATRIC DISORDERS

Physical signs consistent with FA deficiency—such as excessive thirst; frequent urination; rough, dull, or dry hair and skin; and soft or brittle nails—have been repeatedly linked with ADHD, dyslexia, and autistic spectrum disorders (31,58–63). These kinds of physical symptoms can obviously have other causes, but their association with these neurodevelopmental disorders merits further investigation.

Reduced blood concentrations of LC-PUFA in ADHD children compared with controls have been found in several studies (62–66). The precise pattern of results has varied, but reductions of AA as well as DHA have usually been apparent, and plasma concentrations appear to show the most consistent findings. One recent study still found reduced plasma LC-PUFA in ADHD children despite significantly elevated concentrations of the same FA in red cell membranes (67). Relationships between blood biochemical and behavioral or health measures have also been explored in some studies. In 16 boys with ADHD, behavior problems were inversely correlated with γ-linolenic acid (GLA), but not its precursor LA, in serum TG (68), which was interpreted as reflecting a possible bottleneck in this conversion pathway. In a larger study of 96 ADHD and control boys, behavioral and learning problems were greater in those with low vs. high plasma phospholipid concentrations of omega-3 FA, irrespective of clinical diagnosis; but no such association was found for low and high omega-6 FA groups (65).

In autistic spectrum subjects LC-PUFA abnormalities have been reported in both plasma (69) and red blood cell (RBC) membranes (59,60). Findings include particular reductions in omega-3 LC-PUFA, an elevated AA/EPA ratio and an apparent increased susceptibility to the breakdown of membrane FA, possibly reflecting increased oxidative stress (70).

In dyslexia, blood biochemical studies to date are few, but include one early case report of FA deficiency in a dyslexic child (71) and the finding of elevated levels of a Type IV PLA_2 enzyme in RBC membranes of dyslexic adults relative to controls (72). New studies have also yielded interesting preliminary results. Omega-3 concentrations in RBC polar lipids were directly correlated with reading ability in both dyslexic and nondyslexic adults, although they did not differ significantly between the two groups (73). Poor working memory performance—a hallmark of dyslexia—was associated with low omega-3 status only in dyslexic adults, not in controls; and the same was true of schizotypal personality traits involving attentional dysfunction (74).

Although these kinds of studies broadly support the proposal that LC-PUFA may play a part in these childhood developmental and psychiatric disorders, the interpretation of blood biochemical measures remains difficult. They reflect complex interactions between influences of diet and other environmental factors with constitutional aspects of FA metabolism, and not enough is yet known about normal variability in LC-PUFA in compartments such as RBC vs. plasma, or TG vs. phospholipid fractions. Further investigations of the clinical significance of these kinds of measures are needed, ideally using samples drawn from the general community.

RANDOMIZED CONTROLLED TRIALS OF FA TREATMENT IN ADHD, DYSLEXIA, AND RELATED CONDITIONS

Intervention studies provide the most direct evidence that FA can play a role in developmental and psychiatric disorders of childhood. Anecdotal evidence, case reports, and open studies all suggest possible benefits from FA treatment in these conditions (71,75,76), but randomized controlled trials (RCT) are essential to demonstrate causality. Published studies of this kind remain few, although others are in progress. Only an overview summary can be provided here, but a recent review provides further details (77).

Two of the earliest RCT assessed the effects of evening primrose oil (providing the omega-6 FA GLA) in hyperactive or ADHD children (78,79). Unfortunately, the study designs were not optimal in either case, involving treatment periods of only one month as well as potential confounds from the use of full-treatment crossover. Few benefits from such supplementation were apparent from these trials, although some positive trends were noted.

Since then, emphasis has shifted toward omega-3 FA, but two studies have shown no benefits from supplementation with DHA alone. In the first of these (80), 63 U.S. children aged 6–12 yr with a formal DSM-IV diagnosis of ADHD were randomized to treatment with either 345 mg/d of pure algal-source DHA or placebo for 4 mon in addition to maintenance stimulant medication. Outcome measures included scores on computer-presented tests of inattention and impulsivity as well as clinical and parent ratings of ADHD symptoms. Compared with the placebo, active treatment significantly increased DHA in plasma phospholipids, but no group differences were found for any behavioral outcomes. The second such RCT involved 40 Japanese children aged 6–12 yr attending a summer camp for their ADHD-type difficulties (81). They received either foods fortified with DHA (at a dosage of approximately 0.5 g/d) or indistinguishable control foods for 2 mon. A wide range of measures was used pre-and post-treatment, but the only significant difference between treatment groups involved greater improvements over time on visual and auditory memory tests for those on placebo.

In contrast to these negative results for DHA, two other studies have shown some reduction in ADHD symptoms in children treated with combined omega-3/omega-6 supplements. One involved 50 ADHD-type children, preselected for physical signs consistent with FA deficiency and treated for 4 months with a supplement containing fish oil and evening primrose oil in a 4:1 ratio (providing 480 mg DHA, 80 mg EPA, 96 mg GLA, 40 mg AA, and 24 mg alpha-tocopheryl acetate daily) or an olive oil placebo (82). Both groups showed improvements, but significant benefits for active treatment over placebo were found for 2 of 16 outcomes—parent-rated conduct problems and teacher-rated attentional difficulties. In addition, oppositional defiant behavior dropped from clinical to subclinical levels in significantly more children receiving active treatment.

The other positive study used very similar treatments but involved children with a primary diagnosis of dyslexia who were selected for above-average ADHD-related symptoms (83). After 12 wk of supplementation (providing 480 mg DHA, 186 mg EPA, 96 mg GLA, 42 mg AA, and 60 IU vitamin E as DL-α tocopherol per day), scores for anxiety, attentional difficulties, and general behavior problems were significantly lower for the 15 children on active treatment than the 14 on the olive oil placebo. In a 12-wk follow-up stage involving one-way treatment crossover, similar improvements in ADHD-related symptoms were then seen in the placebo group when they switched to active treatment (84).

These contrasting results still require elucidation *via* further research. Two particular issues worth considering here, however, include the populations studied and the nature of the treatments used.

Populations studied. Research into the underlying biology of ADHD, dyslexia, and related conditions is complicated by the descriptive and categorical nature of these diagnoses, as there is always substantial heterogeneity within such clinically defined populations. In both of the negative studies using DHA, participants were selected using purely behavioral criteria rather than from a biochemical perspective. The U.S. study (80) involved full psychiatric evaluation and included only children formally diagnosed with "pure" DSM-

IV ADHD. Given the high comorbidity within ADHD, this would rule out a large proportion of children otherwise eligible for this diagnosis and might even equate to "throwing out the baby with the bathwater." In adults, omega-3 FA have already shown promise in the treatment of unipolar depression (50–52), bipolar disorder (85), and borderline personality disorder, (54) so excluding those ADHD children with comorbid difficulties of this kind might well eliminate those most likely to benefit from this type of treatment. Many children receiving the ADHD diagnosis have comorbid anxiety or mood disorders. Furthermore, stimulant medications appear to be ineffective in up to 70% of ADHD children with this profile (86–88), and their negative side effects more likely (89). Given the evidence from studies of adults with mood-related disorders, omega-3 treatment trials seem well warranted in these subsets of ADHD children, as well as in children with a primary diagnosis of depression.

In the Japanese study showing negative results for DHA-fortified foods (81), children were again selected for ADHD, although formal diagnostic information was limited. Biochemical measures were not available to assess FA status, but background diet might have been a factor given that Japanese diets are traditionally fairly rich in omega-3.

By contrast, the U.S. study showing some benefits from LC-PUFA (82) took a biochemical perspective, in that subjects were preselected for physical signs consistent with FA deficiency that had previously been found to relate to blood FA concentrations (63). Formal psychiatric diagnoses of ADHD were not used, although all children were under clinical care for this condition. Instead, recruitment was by advertisement, so that comorbidity probably reflected the usual high levels found in community samples. The other positive study (83) involved dyslexic children who were selected for above-average scores on dimensional measures of ADHD-related symptoms. Similar findings have now emerged from a larger, but as yet unpublished, trial of children with a primary diagnosis of dyspraxia/DCD (see Ref. 77), although biochemical measures were not included in either of these studies.

Preliminary evidence therefore suggests that treatment with LC-PUFA can ameliorate ADHD-related symptoms in at least some groups of children who show these kinds of behavioral and learning difficulties. Careful consideration of comorbidity issues seems worthwhile in further studies, although the inclusion of biochemical measures of FA status would also be an obvious advantage.

Composition of FA treatments. The optimal composition of LC-PUFA treatments also requires further investigation. There is no convincing evidence that omega-6 FA alone are of benefit in these conditions, although this has only been explored in the first small studies using evening primrose oil. With respect to omega-3, two studies found DHA ineffective in reducing ADHD symptoms (80,81), and two others found some advantages over placebo for supplements containing both EPA and DHA (as well as some omega-6) (82,83). Evidence from several RCT involving adult psychiatric patients suggests that EPA may be more effective than DHA in the treatment of functional disturbances of attention, cognition, or mood. Thus, DHA has been found ineffective in treating both depression (90) and schizophrenia (91), whereas pure EPA has shown significant benefits in these conditions (50,51,92).

Findings to date therefore suggest that EPA may be more effective than DHA in the conditions discussed here, which may seem counterintuitive given that DHA is undeniably more important than EPA in the structure of neuronal membranes. EPA nonetheless appears to play many key functional roles in the brain. Its eicosanoid derivatives are key regulators of immune, endocrine, and cardiovascular functions, and direct actions of EPA on cyclo-oxygenases, lipoxygenases, phospholipases, acylating systems, ion channels, mitochondria, and peroxisome proliferator-activated receptors (PPAR) are the focus of current investigations across many different fields of study. No studies have yet shown any benefits from pure DHA in developmental or psychiatric disorders, but direct comparisons of EPA and DHA—and of treatments containing these in different proportions—are needed to establish with any certainty their relative merits in the treatment of these conditions.

SUMMARY AND CONCLUSIONS

The childhood developmental and psychiatric disorders considered here are complex, multidimensional syndromes with considerable overlap at the individual and familial levels. The evidence reviewed here suggests that they share some common biological risk factors, and that these may include abnormalities of FA metabolism that increase dietary requirements for these essential nutrients.

Findings from controlled trials suggest that LC-PUFA supplements may be of some value in the management of these conditions. Modest benefits in reducing ADHD-related symptoms have been observed in two studies using combined omega-3/omega-6 FA from fish oil and evening primrose oil, but other studies using GLA or DHA alone have been negative. Together with similar evidence from studies of adult psychiatric disorders, these findings raise the possibility that the omega-3 FA EPA may be the most effective component of FA treatments aimed at improving behavior, learning, and mood. Larger studies involving direct comparisons of different treatments are needed to resolve these issues

In conclusion, a biochemical/nutritional approach focusing on FA and their metabolism offers considerable promise in identifying at least some factors contributing to childhood developmental and psychiatric disorders, and could lead to better methods for early identification and treatment of these conditions. It is argued here, however, that an exclusive focus on current diagnostic categories may be unhelpful given the substantial heterogeneity and comorbidity involved. Dimensional measures of specific traits and symptoms may prove more useful in identifying those individuals most likely to benefit from this approach.

REFERENCES

1. Peet, M., Glen, I. and Horrobin, D.F. (eds.) (2003) *Phospholipid spectrum disorders in psychiatry and neurology*. Marius Press, Carnforth.
2. Richardson, A.J., and Ross, M.A. (2000) Fatty Acid Metabolism in Neurodevelopmental Disorder: A New Perspective on Associations between Attention-Deficit/Hyperactivity Disorder, Dyslexia, Dyspraxia and the Autistic Spectrum, *Prostaglandins Leukot. Essent. Fatty Acids 63*, 1–9.
3. Jones, G.S. (2000) Autistic Spectrum Disorder: Diagnostic Difficulties, *Prostaglandins Leukot. Essent. Fatty Acids 63(1–2)*, 33–36.
4. Kadesjo, B., and Gillberg, C. (1999) Developmental Coordination Disorder in Swedish 7-Year-Old Children, *J. Am. Acad. Child Adolesc. Psychiatry 38*, 820–828.
5. Willcutt, E.G., and Pennington, B.F. (2000) Psychiatric Comorbidity in Children and Adolescents with Reading Disability, *J. Child Psychol. Psychiatry 41(8)*, 1039–1048.
6. Richardson, A.J., Cyhlarova, E., and Puri, B.K. (2003) Clinical and Biochemical Fatty Acid Abnormalities in Dyslexia, Dyspraxia, and Schizotypy: An Overview. *Phospholipid Spectrum Disorders in Psychiatry and Neurology* (Peet, M., Glen, I., Horrobin, D.F., eds.), Marius Press, Carnforth, pp. 477–490.
7. Richardson, A.J., and Puri, B.K. (2000) The Potential Role of Fatty Acids in Attention-Deficit/Hyperactivity Disorder, *Prostaglandins Leukot. Essent. Fatty Acids 63*, 79–87.
8. Biederman, J., Munir, K., Knee, D., Armentano, M., Autor, S., Waternaux, C., and Tsuang, M. (1987) High Rate of Affective Disorders in Probands with Attention Deficit Disorder and in Their Relatives: A Controlled Family Study, *Am. J. Psychiatry 144*, 330–333.
9. Hellgren, L., Gillberg, I.C., Bagenholm, A., and Gillberg, C. (1994) Children with Deficits in Attention, Motor Control and Perception (DAMP) almost Grown up: Psychiatric and Personality Disorders at Age 16 Years, *J. Child Psychol. Psychiatry 35(7)*, 1255–1271.
10. Horrobin, D.F., Glen, A.I., and Hudson, C.J. (1995) Possible Relevance of Phospholipid Abnormalities and Genetic Interactions in Psychiatric Disorders: The Relationship Between Dyslexia and Schizophrenia, *Med. Hypotheses 45*, 605–613.
11. Rasmussen, P., and Gillberg, C. (2000) Natural Outcome of ADHD with Developmental Coordination Disorder at Age 22 Years: A Controlled, Longitudinal, Community-Based Study, *J. Am. Acad. Child Adolesc. Psychiatry 39(11)*, 1424–1431.
12. Bennett, C.N., and Horrobin, D.F. (2000) Gene Targets Related to Phospholipid and Fatty Acid Metabolism in Schizophrenia and Other Psychiatric Disorders: An Update, *Prostaglandins Leukot. Essent. Fatty Acids 63*, 47–59.
13. Crawford, M.A. (2000) Placental Delivery of Arachidonic and Docosahexaenoic Acids: Implications for the Lipid Nutrition of Preterm Infants, *Am. J. Clin. Nutr. 71(1 Suppl)*, 275S–284S.
14. Neuringer, M., Reisbick, S., and Janowsky, J. (1994) The Role of n-3 Fatty Acids in Visual and Cognitive Development: Current Evidence and Methods of Assessment, *J. Pediatr. 125(5 Pt 2)*, S39–S47.
15. Uauy, R., Hoffman, D.R., Peirano, P., Birch, D.G., and Birch, E.E. (2001) Essential Fatty Acids in Visual and Brain Development, *Lipids 36*, 885–895.
16. Willatts, P., and Forsyth, J.S. (2000) The Role of Long-Chain Polyunsaturated Fatty Acids in Infant Cognitive Development, *Prostaglandins Leukot. Essent. Fatty Acids 63(1–2)*, 95–100.
17. Simmer, K. (2001) Long-chain Polyunsaturated Fatty Acid Supplementation in Infants Born at Term, *Cochrane Database Syst. Rev. 4*.
18. Yehuda, S., Rabinovitz, S., and Mostofsky, D.I. (1999) Essential Fatty Acids Are Mediators of Brain Biochemistry and Cognitive Functions, *J. Neurosci. Res. 56*, 565–570.
19. Simopoulos, A.P. (2002) The Importance of the Ratio of Omega-6/Omega-3 Essential Fatty Acids, *Biomed. Pharmacotherapy 56*, 365–379.
20. Kang, J.X. (2003) The Importance of Omega-6/Omega-3 Fatty Acid Ratio in Cell Function: The Gene transfer of Omega-3 Fatty Acid Desaturase, *World Rev. Nutr. Diet 92*, 23–36.
21. Haag, M. (2003) Essential Fatty Acids and the Brain, *Can. J. Psychiatry 48*, 195–203.
22. Holman, R.T. (1998) The Slow Discovery of the Importance of Omega 3 Essential Fatty Acids in Human Health, *J. Nutr. 128* (2 Suppl.), 427S–433S.
23. Rudin, D.O. (1981) The Major Psychoses and Neuroses as Omega-3 Essential Fatty Acid Deficiency Syndrome: Substrate Pellagra, *Biol. Psychiatry 16*, 837–850.
24. Pawlosky, R.J., Hibbeln, J.R., Novotny, J.A., and Salem, N., Jr. (2001) Physiological Compartmental Analysis of α-Linolenic Acid Metabolism in Adult Humans, *J. Lipid Res. 42(8)*, 1257–1265.
25. Salem, N., Jr., Pawlosky, R., Wegher, B., and Hibbeln, J. (1999) *In Vivo* Conversion of Linoleic Acid to Arachidonic Acid in Human Adults, *Prostaglandins Leukot. Essent. Fatty Acids 60 (5–6)*, 407–410.
26. Huang, Y.S., and Horrobin, D.F. (1987) Sex Differences in n-3 and n-6 Fatty Acid Metabolism in EFA-Depleted Rats, *Proc. Soc. Exp. Biol. Med. 185(3)*, 291–296.
27. Marra, C.A., and de Alaniz, M.J. (1989) Influence of Testosterone Administration on the Biosynthesis of Unsaturated Fatty Acids in Male and Female Rats, *Lipids 24*, 1014–1019.
28. Burdge, G.C., and Wootton, S.A. (2002) Conversion of α-Linolenic Acid to Eicosapentaenoic, Docosapentaenoic and Docosahexaenoic Acids in Young Women, *Br. J. Nutr. 88*, 411–420.
29. Burdge, G.C., Jones, A.E., and Wootton, S.A. (2002) Eicosapentaenoic and Docosapentaenoic Acids Are the Principal Products of α-Linolenic Acid Metabolism in Young Men, *Br. J. Nutr. 88*, 355–363.
30. Horrobin, D.F. (2000) Essential Fatty Acid Metabolism and Its Modification in Atopic Eczema, *Am. J. Clin. Nutr. 71*, 367S–372S.
31. Colquhoun, I., and Bunday, S. (1981) A Lack of Essential Fatty Acids as a Possible Cause of Hyperactivity in Children, *Med. Hypotheses 7*, 673–679.
32. Huh, G.S., Boulanger, L.M., Du, H., Riquelme, P.A., Brotz, T.M., and Shatz, C.J. (2000) Functional Requirement for Class I MHC in CNS Development and Plasticity, *Science 290*, 2155–2159.
33. Anderson, J.L. (1996) The Immune System and Major Depression, *Adv. Neuroimmunol. 6*, 119–129.
34. Jyonouchi, H., Sun, S.N., and Itokazu, N. (2002) Innate Immunity Associated with Inflammatory Responses and Cytokine Production against Common Dietary Proteins in Patients with Autism Spectrum Disorder, *Neuropsychobiology 46*, 76–84.
35. Krause, I., He, X.S., Gershwin, M.E., and Shoenfeld, Y. (2002) Immune Factors in Autism: A Critical Review, *J. Autism Dev. Disord. 32*, 337–345.
36. Muller, N., Riedel, M., Gruber, R., Ackenheil, M., and Schwarz, M.J. (2000) The Immune System and Schizophrenia. An Integrative View, *Ann. NY Acad. Sci. 917*, 456–467.
37. O'Brien, S.M., Scott, L.V., and Dinan, T.G. (2004) Cytokines: Abnormalities in Major Depression and Implications for Pharmacological Treatment, *Hum. Psychopharmacol. 19*, 397–403.
38. Harbige, L.S. (2003) Fatty Acids, the Immune Response, and Autoimmunity: A Question of n-6 Essentiality and the Balance Between n-6 and n-3, *Lipids 38*, 323–341.
39. Calder, P.C. (2003) n-3 Polyunsaturated Fatty Acids and Inflammation: From Molecular Biology to the Clinic, *Lipids 38*, 343–352.

40. Taylor, K.E., Richardson, A.J., and Stein, J.F. (2001). Could Platelet Activating Factor Play a Role in Developmental Dyslexia? *Prostaglandins Leukot. Essent. Fatty Acids 64*, 173–180.
41. Stein, J., and Walsh, V. (1997) To See But Not to Read: The Magnocellular Theory of Dyslexia, *Trends Neurosci. 20(4)*, 147–152.
42. Litman, B.J., Niu, S.L., Polozova, A., and Mitchell, D.C. (2001) The Role of Docosahexaenoic Acid Containing Phospholipids in Modulating G Protein-Coupled Signaling Pathways: Visual Transduction, *J. Mol. Neurosci. 16(2–3)*, 237–242; discussion, 279–284.
43. Hong, S., Gronert, K., Devchand, P.R., Moussignac, R.L., and Serhan, C.N. (2003) Novel Docosatrienes and 17S-Resolvins Generated from Docosahexaenoic Acid in Murine Brain, Human Blood, and Glial Cells. Autacoids in Anti-inflammation, *J. Biol. Chem. 278*, 14677–14687.
44. Serhan, C.N., Gotlinger, K., Hong, S., and Arita, M. (2004) Resolvins, Docosatrienes, and Neuroprotectins, Novel Omega-3-Derived Mediators, and Their Aspirin-Triggered Endogenous Epimers: An Overview of Their Protective Roles in Catabasis, *Prostaglandins Other Lipid Mediat. 73*, 155–172.
45. Das, U.N. (2002) Essential Fatty Acids as Possible Enhancers of the Beneficial Actions of Probiotics, *Nutrition 18*, 786.
46. Teitelbaum, J.E., and Allan Walker, W. (2001) Review: The Role of Omega 3 Fatty Acids in Intestinal Inflammation, *J. Nutr. Biochem. 12*, 21–32.
47. Leonard, B.E., and Song, C. (2002) Changes in the Immune System in Rodent Models of Depression, *Int. J. Neuropsychopharmacol. 5*, 345–356.
48. Song, C., Lin, A., Bonaccorso, S., Heide, C., Verkerk, R., Kenis, G., Bosmans, E., Scharpe, S., Whelan, A., Cosyns, P., de Jongh, R., and Maes, M. (1998) The Inflammatory Response System and the Availability of Plasma Tryptophan in Patients with Primary Sleep Disorders and Major Depression, *J. Affect. Disord. 49*, 211–219.
49. Delarue, J., Matzinger, O., Binnert, C., Schneiter, P., Chiolero, R., and Tappy, L. (2003) Fish Oil Prevents the Adrenal Activation Elicited by Mental Stress in Healthy Men, *Diabetes Metab. 29*, 289–295.
50. Nemets, B., Stahl, Z., and Belmaker, R.H. (2002) Addition of Omega-3 Fatty Acid to Maintenance Medication Treatment for Recurrent Unipolar Depressive Disorder, *Am. J. Psychiatry 159*, 477–479.
51. Peet, M., and Horrobin, D.F. (2002) A Dose-Ranging Study of the Effects of Ethyl-Eicosapentaenoate in Patients with Ongoing Depression Despite Apparently Adequate Treatment with Standard Drugs, *Arch. Gen. Psychiatry 59*, 913–919.
52. Su, K.P., Huang, S.Y., Chiu, C.C., and Shen, W.W. (2003) Omega-3 Fatty Acids in Major Depressive Disorder. A Preliminary Double-Blind, Placebo-Controlled Trial, *Eur. Neuropsychopharmacol. 13(4)*, 267–271.
53. Hamazaki, T., Sawazaki, S., Itomura, M., Asaoka, E., Nagao, Y., Nishimura, N., Yazawa, K., Kuwamori, T., and Kobayashi, M. (1996) The Effect of Docosahexaenoic Acid on Aggression in Young Adults. A Placebo-Controlled Double-Blind Study, *J. Clin. Invest. 97*, 1129–1133.
54. Zanarini, M.C., and Frankenburg, F.R. (2003) Omega-3 Fatty Acid Treatment of Women with Borderline Personality Disorder: A Double-Blind, Placebo-Controlled Pilot Study, *Am. J. Psychiatry 160*, 167–169.
55. Delion, S., Chalon, S., Guilloteau, D., Besnard, J.C., and Durand, G. (1996) α-Linolenic Acid Dietary Deficiency Alters Age-Related Changes of Dopaminergic and Serotoninergic Neurotransmission in the Rat Frontal Cortex, *J. Neurochem. 66(4)*, 1582–1591.
56. Zimmer, L., Hembert, S., Durand, G., Breton, P., Guilloteau, D., Besnard, J.C., and Chalon, S. (1998) Chronic n-3 Polyunsaturated Fatty Acid Diet-Deficiency Acts on Dopamine Metabolism in the Rat Frontal Cortex: A Microdialysis Study, *Neurosci. Lett. 240*, 177–181.
57. Levant, B., Radel, J.D., and Carlson, S.E. (2004) Decreased Brain Docosahexaenoic Acid During Development Alters Dopamine-Related Behaviors in Adult Rats That Are Differentially Affected by Dietary Remediation, *Behav. Brain Res. 152*, 49–57.
58. Taylor, K.E., Higgins, C.J., Calvin, C.M., Hall, J.A., Easton, T., McDaid, A.M., and Richardson, A.J. (2000) Dyslexia in Adults Is Associated with Clinical Signs of Fatty Acid Deficiency, *Prostaglandins Leukot. Essent. Fatty Acids 63*, 75–78.
59. Bell, J.G., Dick, J.R., MacKinlay, E.E., Glen, A.C.A., MacDonald, D.J., Ross, M.A., Riordan, V., and Sargent, J.R. (2004a) Apparent Fatty Acid Deficiency in Autistic Spectrum Disorders, *Prostaglandins Leukot. Essent. Fatty Acids*, in press.
60. Bell, J.G., Sargent, J.R., Tocher, D.R., and Dick, J.R. (2000) Red Blood Cell Fatty Acid Compositions in a Patient with Autistic Spectrum Disorder: A Characteristic Abnormality in Neurodevelopmental Disorders? *Prostaglandins Leukot. Essent. Fatty Acids 63*, 21–25.
61. Richardson, A.J., Calvin, C.M., Clisby, C., Schoenheimer, D.R., Montgomery, P., Hall, J.A., Hebb, G., Westwood, E., Talcott, J.B., and Stein, J.F. (2000) Fatty Acid Deficiency Signs Predict the Severity of Reading and Related Difficulties in Dyslexic Children, *Prostaglandins Leukot. Essent. Fatty Acids 63*, 69–74.
62. Stevens, L.J., Zentall, S.S., Abate, M.L., Kuczek, T., and Burgess, J.R. (1996) Omega-3 Fatty Acids in Boys with Behavior, Learning, and Health Problems, *Physiol.-Behav. 59*, 915–920.
63. Stevens, L.J., Zentall, S.S., Deck, J.L., Abate, M.L., Watkins, B.A., Lipp, S.R., and Burgess, J.R. (1995) Essential Fatty Acid Metabolism in Boys with Attention-Deficit Hyperactivity Disorder, *Am. J. Clin. Nutr. 62*, 761–768.
64. Bekaroglu, M., Aslan, Y., Gedik, Y., Deger, O., Mocan, H., Erduran, E., and Karahan, C. (1996) Relationships Between Serum Free Fatty Acids and Zinc, and Attention Deficit Hyperactivity Disorder: A Research Note, *J. Child Psychol. Psychiatry 37*, 225–227.
65. Burgess, J.R., Stevens, L., Zhang, W., and Peck, L. (2000) Long-Chain Polyunsaturated Fatty Acids in Children with Attention-Deficit Hyperactivity Disorder, *Am. J. Clin. Nutr. 71*, 327S–330S.
66. Mitchell, E.A., Aman, M.G., Turbott, S.H., and Manku, M. (1987) Clinical Characteristics and Serum Essential Fatty Acid Levels in Hyperactive Children, *Clin. Pediatr. Phila. 26*, 406–411.
67. Burgess, J.R., and Stevens, L.J. (2003) Essential Fatty Acids in Relation to Attention Deficit Hyperactivity Disorder. *Phospholipid Spectrum Disorders in Psychiatry and Neurology* (Peet, M., Glen, I., and Horrobin, D.F., eds.). Marius Press, Carnforth, pp. 511–519.
68. Arnold, L.E., Kleykamp, D., Votolato, N., Gibson, R.-A., and Horrocks, L. (1994) Potential Link Between Dietary Intake of Fatty Acids and Behavior: Pilot Exploration of Serum Lipids in Attention-Deficit Hyperactivity Disorder, *J. Child Adolesc. Psychopharmacol. 4*, 171–182.
69. Vancassel, S., Durand, G., Barthelemy, C., Lejeune, B., Martineau, J., Guilloteau, D., Andres, C., and Chalon, S. (2001) Plasma Fatty Acid Levels in Autistic Children, *Prostaglandins Leukot. Essent. Fatty Acids 65(1)*, 1–7.
70. Ross, M.A. (2000) Could Oxidative Stress Be a Factor in Neurodevelopmental Disorders? *Prostaglandins Leukot. Essent. Fatty Acids 63*, 61–63.
71. Baker, S.M. (1985) A Biochemical Approach to the Problem of Dyslexia, *J. Learn. Disabil. 18(10)*, 581–584.
72. MacDonell, L.E., Skinner, F.K., Ward, P.E., Glen, A.I., Glen,

A.C., Macdonald, D.J., Boyle, R.M., and Horrobin, D.F. (2000) Increased Levels of Cytosolic Phospholipase A_2 in Dyslexics, *Prostaglandins Leukot. Essent. Fatty Acids 63(1–2)*, 37–39.
73. Bell, J.G., Ross, M.A., Cyhlarova, E., Shrier, A., Dick, J.R., Henderson, R.J., and Richardson, A.J. (2004) Membrane Fatty Acids, Reading and Spelling in Dyslexic and Non-dyslexic Adults, *ISSFAL 6th International Congress*, Brighton, United Kingdom.
74. Ross, M.A., Cyhlarova, E., Shrier, A., Henderson, R.J., MacKinlay, E.E., Dick, J.R., Bell, J.G., and Richardson, A.J. (2004) Working Memory and Schizotypal Traits in Relation to Fatty Acid Status in Dyslexia, *ISSFAL 6th International Conference*, Brighton, United Kingdom.
75. Stordy, B.J. (1995) Benefit of Docosahexaenoic Acid Supplements to Dark Adaptation in Dyslexics, *Lancet 346*, 385.
76. Stordy, B.J. (2000) Dark Adaptation, Motor Skills, Docosahexaenoic Acid, and Dyslexia, *Am. J. Clin. Nutr. 71*, 323S–326S.
77. Richardson, A.J. (2004) Clinical Trials of Fatty Acid Treatment in ADHD, Dyslexia, Dyspraxia and the Autistic Spectrum, *Prostaglandins Leukot. Essent. Fatty Acids 70*, 383–390.
78. Aman, M.G., Mitchell, E.A., and Turbott, S.H. (1987) The Effects of Essential Fatty Acid Supplementation by Efamol in Hyperactive Children, *J. Abnorm. Child Psychol. 15*, 75–90.
79. Arnold, L.E., Kleykamp, D., Votolato, N.A., Taylor, W.A., Kontras, S.B., and Tobin, K. (1989) γ-Linolenic Acid for Attention-Deficit Hyperactivity Disorder: Placebo-Controlled Comparison to D-Amphetamine, *Biol. Psychiatry 25*, 222–228.
80. Voigt, R.G., Llorente, A.M., Jensen, C.L., Fraley, J.K., Berretta, M.C., and Heird, W.C. (2001) A Randomized, Double-Blind, Placebo-Controlled Trial of Docosahexaenoic Acid Supplementation in Children with Attention-Deficit/Hyperactivity Disorder, *J. Pediatr. 139*, 189–196.
81. Hirayama, S., Hamazaki, T., and Terasawa, K. (2004) Effect of Docosahexaenoic Acid-Containing Food Administration on Symptoms of Attention-Deficit/Hyperactivity Disorder—A Placebo-Controlled Double-Blind Study, *Eur. J. Clin. Nutr. 58*, 467–473.
82. Stevens, L., Zhang, W., Peck, L., Kuczek, T., Grevstat, N., Mahon, A., Zentall, S.S., Arnold, L.E., and Burgess, J.R. (2003) EFA Supplementation in Children with Inattention, Hyperactivity and Other Disruptive Behaviours, *Lipids 38*, 1007–1021.
83. Richardson, A.J., and Puri, B.K. (2002) A Randomized Double-Blind, Placebo-Controlled Study of the Effects of Supplementation with Highly Unsaturated Fatty Acids on ADHD-Related Symptoms in Children with Specific Learning Difficulties, *Prog. Neuropsychopharmacol. Biol. Psychiatry 26*, 233–239.
84. Richardson, A.J. (2003) Clinical Trials of Fatty Acid Supplementation in Dyslexia and Dyspraxia. *Phospholipid Spectrum Disorders in Psychiatry and Neurology* (Peet, M., Glen I., and Horrobin, D.F., eds.). Marius Press, Carnforth, pp. 491–500.
85. Stoll, A.L., Freeman, M.P., Severus, W.E., Rueter, S., Zboyan, H.A., Diamond, E., Cress, K.K., and Marangell, L.B. (1999) Omega 3 Fatty Acids in Bipolar Disorder: A Preliminary Double-Blind, Placebo-Controlled Trial, *Arch. Gen. Psychiatry 56*, 407–412.
86. Buitelaar, J.K., Van-der-Gaag, R.J., Swaab-Barneveld, H., and Kuiper, M. (1995) Prediction of Clinical Response to Methylphenidate in Children with Attention-Deficit Hyperactivity Disorder, *J. Am. Acad. Child Adolesc. Psychiatry 34(8)*, 1025–1032.
87. Pliszka, S.R. (1989) Effect of Anxiety on Cognition, Behavior, and Stimulant Response in ADHD, *J. Am. Acad. Child Adolesc. Psychiatry 28*, 882–887.
88. Taylor, E., Schachar, R., Thorley, G., Wieselberg, H.M., Everitt, B., and Rutter, M. (1987) Which Boys Respond to Stimulant Medication? A Controlled Trial of Methylphenidate in Boys with Disruptive Behaviour, *Psychol. Med. 17*, 121–143.
89. DuPaul, G.J., Barkley, R.A., and McMurray, M.B. (1994) Response of Children with ADHD to Methylphenidate: Interaction with Internalizing Symptoms, *J. Am. Acad. Child Adolesc. Psychiatry 33*, 894–903.
90. Marangell, L.B., Martinez, J.M., Zboyan, H.A., Kertz, B., Kim, H.F., and Puryear, L.J. (2003) A Double-Blind, Placebo-Controlled Study of the Omega-3 Fatty Acid Docosahexaenoic Acid in the Treatment of Major Depression, *Am. J. Psychiatry 160*, 996–998.
91. Peet, M., Brind, J., Ramchand, C.N., Shah, S., and Vankar, G.K. (2001) Two Double-Blind Placebo-Controlled Pilot Studies of Eicosapentaenoic Acid in the Treatment of Schizophrenia, *Schizophr. Res. 49*, 243–251.
92. Peet, M., Horrobin, D.F., and E-E-Multicentre-Study-Group. (2002) A Dose-Ranging Exploratory Study of the Effects of Ethyl-Eicosapentaenoate in Patients with Persistent Schizophrenic Symptoms, *J. Psychiatr. Res. 36(1)*, 7–18.

[Received October 21, 2004; accepted November 16, 2004]

Olive Oil and Modulation of Cell Signaling in Disease Prevention

Klaus W.J. Wahle[a,*], Donatella Caruso[b], Julio J. Ochoa[c], and Jose L. Quiles[c]

[a]School of Life Sciences, The Robert Gordon University, Aberdeen, AB25 1HG, Scotland, United Kingdom, [b]Department of Pharmacological Sciences, University of Milan, Italy, and [c]Institute of Nutrition and Food Technology, Department of Physiology, University of Granada, Spain

ABSTRACT: Epidemiological studies show that populations consuming a predominantly plant-based Mediterranean-style diet exhibit lower incidences of chronic diseases than those eating a northern European or North American diet. This observation has been attributed to the greater consumption of fruits and vegetables and the lower consumption of animal products, particularly fat. Although total fat intake in Mediterranean populations can be higher than in other regions (ca. 40% of calories), the greater proportion is derived from olive oil and not animals. Increased olive oil consumption is implicated in a reduction in cardiovascular disease, rheumatoid arthritis, and, to a lesser extent, a variety of cancers. Olive oil intake also has been shown to modulate immune function, particularly the inflammatory processes associated with the immune system. Olive oil is a nonoxidative dietary component, and the attenuation of the inflammatory process it elicits could explain its beneficial effects on disease risk since oxidative and inflammatory stresses appear to be underlying factors in the etiology of these diseases in man. The antioxidant effects of olive oil are probably due to a combination of its high oleic acid content (low oxidation potential compared with linoleic acid) and its content of a variety of plant antioxidants, particularly oleuropein, hydroxytyrosol, and tyrosol. It is also possible that the high oleic acid content and a proportionate reduction in linoleic acid intake would allow a greater conversion of α-linolenic acid (18:3n-3) to longer-chain n-3 PUFA, which have characteristic health benefits. Adoption of a Mediterranean diet could confer health benefits in high-risk populations.

Paper no. L9617 in *Lipids 39,* 1223–1231 (December 2004).

THE MEDITERRANEAN DIET AND HEALTH

The main reason for the interest shown by nutritionists and health professionals in the "Mediterranean diet" relates to epidemiological observations that certain populations living in and around the Mediterranean area have very low incidences of chronic diseases, particularly those with an inflammatory etiology such as heart disease, cancer and rheumatoid arthritis (RA), and that they display greater longevity when compared with northern European and American populations (1–3). Although a great deal has been published that suggests a specific, clearly defined Mediterranean diet exists, this is patently not the case since diets in this region vary significantly between countries. There are, however, strong similarities in the traditional diets from the Mediterranean region that distinguish them from those consumed in northern Europe and North America in that they are largely plant based. The characteristics are not uniform throughout the region but generally include a high consumption of vegetables, fruit, legumes, and grain (in the form of whole-grain bread), a relatively low consumption of meat, particularly red meat, a moderate consumption of dairy products other than cheese, a moderate intake of alcohol (mainly wine at meals), and a relatively high intake of olive oil as the major fat source when compared to Northern European and North American traditional diets (3,4).

This review will focus on the possible health benefits of olive oil, which is the major culinary fat in the classical Mediterranean diet. The total fat intake in this diet can be relatively high, as in Greece with *ca.* 40% of total calories as fat which is higher than in many North American populations, or moderate, as in Italy with *ca.* 30% of calories as fat, but the greater proportion of this fat is derived from olive oil and consequently the diet is rich in monounsaturated FA (MUFA). Fish consumption and the intake of omega-3 PUFA (n-3 PUFA) also vary considerably between different Mediterranean populations, depending mainly on their proximity to the sea. However, the ratio of MUFA to saturated FA is always much greater than in northern Europe and America due to the relatively high olive oil intake in these areas (3,4). The Seven Countries Study (1–5) in the 1950s and 1960s clearly showed that, despite having higher total fat intake (*ca.* 40% of energy), populations in Greece, particularly on Crete where adherence to the traditional diet was most pronounced, have lower disease incidence, particularly cardiovascular disease (CVD), and lower death rates from all causes in middle age than those in northern Europe and North America. This implicated the type, rather than the amount, of dietary fat as a prime causal factor in the etiology of disease, particularly CVD. This is important since positive associations between high fat consumption (*ca.* 40% of energy) and diseases such

*To whom correspondence should be addressed.
E-mail k.wahle-l@rgu.ac.uk

ARA, arachidonic acid; cGPx1, cytosolic glutathione peroxidase; COX, cyclooxygenase: CVD, cardiovascular disease; GPX1, glutathione peroxidase; GPX4, phospholipid glutathione peroxidase; HUVEC, human umbilical vein endothelial cells; ICAM-1, intercellular adhesion molecule 1; IL, interleukin; LOX, lipoxygenase; LT, leukotriene; MUFA, monounsaturated FA; NK, natural killer; PGE_2, prostaglandin E_2; RA, rheumatoid arthritis; ROS, reactive oxygen species; VCAM-1, vascular cell adhesion molecule 1.

as cancer of the colon (6), breast (7,8), prostate (8,9), and ovary (10) as well as atherosclerosis (11) and coronary heart disease (12) are reported. However, the link between total fat intake and cancer of the breast and colon has been refuted (13,14) and, as with CVD, it appears that the type rather than the amount of fat is important in the etiology of some cancers (15). This was supported by evidence from Greece and Israel where the average daily fat intakes are 140 and 100 g, respectively, with higher animal fat (60 vs. 40 g) and vegetable fat (80 vs. 60 g) in the former. However, the lower mortality from breast cancer in Greece than in Israel (16) may be explained by the fact that the vegetable fat in Greece was mainly olive oil whereas that in Israel was mainly sunflower oil (17). Increasing intakes of MUFA as olive oil would be expected to reduce the relative intake of saturated fat as seen in the high MUFA/saturated FA ratios in Mediterranean diets. Replacement of saturated fat with either MUFA or PUFA has been shown to confer health benefits, particularly in relation to CVD (18,19). The relative importance of the MUFA content of the Mediterranean diet to its recognized health benefits will be discussed in this review.

Although the MUFA content of olive oil (*ca.* 85% oleic acid, on average) is important in conferring certain health benefits attributable to this dietary constituent, recent studies have shown that the minor components of this oil may be equally, if not more, important. Although the content of the anti-oxidant vitamin E (α-tocopherol) is low in olive oil compared with corn or safflower oil, the content of other antioxidants such as squalene, simple phenols (e.g., oleuropein, ligstroside-aglycones, tyrosol, hydroxytyrosol, elenolic acid, caffeic acid, apigenin, terpenes, plus numerous others), secoiridoids, and the lignans (e.g., acetoxypinoresinol and pinoresinol) is relatively much higher, particularly in cold-pressed extra virgin olive oil (20). Other dietary sources of phenolic antioxidants are tea, fruit (including grapes, particularly red grapes), and vegetables. Phenols from tea and fruit are water-soluble, whereas those from olive oil are partly lipid-soluble (21). A Mediterranean-type diet rich in olive oil will supply about 10–20 mg of a mixture of these phenols per day (22). These phenolic compounds are absorbed from the diet in humans (*ca.* 55–66% of intake; 23,24) in a dose-dependent manner, appear in plasma, and are excreted in the urine as glucuronide conjugates of mainly tyrosol and hydroxytyrosol. The level of excretion depends on the amount ingested, but only a small fraction of that amount is recovered in urine (23–26). It appears to be impossible to completely eliminate hydroxytyrosol from biological fluids despite strict dietary control preventing its ingestion. This is attributable to the fact that this phenolic compound is also a metabolite (dihydroxyphenylethanol) of dopamine in the body (26). The lipid-soluble phenolic compounds are transported in the lipoprotein fraction of plasma and have been shown to attenuate the oxidation of LDL fractions *in vitro*, and this attenuation has been promulgated as a major factor in the antiatherogenic effects of olive oil (22,27,28).

MECHANISMS OF DISEASE PREVENTION

(i) Cardiovascular disease. As mentioned above, olive oil is the main source of dietary lipids in the Mediterranean regions where mortality and incidence rates for coronary heart disease are the lowest in Europe (1,29,30). This protective effect against heart disease has been attributed, at least in part, to the high content of MUFA in olive oil (*ca.* 85% oleic acid and only 4–5% linoleic acid), which generally results in a concomitant reduction in intake of saturated FA and PUFA. This results in LDL particles that are more resistant to oxidation *in vitro* because of the lower susceptibility to oxidation of MUFA compared with PUFA. In several dietarey studies in humans and experimental animals, virgin olive oil and oleic acid-rich diets that do not contain the phenolic anti-oxidants of olive oil, have been shown to decrease LDL susceptibility to oxidation and to lower LDL-cholesterol levels without affecting HDL-cholesterol; both effects are regarded as antiatherogenic (31–34). Western diets contain an excess of linoleic acid (18:2n-6) (ratio of n-6/n-3 is 15–20:1 instead of the recommended 4–5:1), which has a recognized cholesterol-lowering effect. It is now also recognized that dietary linoleic acid favors such deleterious effects as oxidative modification of LDL-cholesterol, increased platelet aggregation, and suppressed immune function (35). The Cretan diet also contains significant levels of α-linolenic acid (18:3n-3), and the low n-6 PUFA content should allow a greater metabolism of α-linolenic acid to its longer-chain metabolites EPA (20:5n-3) and DHA (22:2n-3), which are the precursors of different, possibly less inflammatory series of prostanoids [III series prostaglandins (PG) and V series leukotrienes (LT) mainly from EPA] than the n-6 PUFA with potential benefits to cardiovascular parameters. This was evident from the greater levels of the latter FA in plasma from Cretan as compared with plasma from Dutch volunteers. Similarly, in the Lyon intervention study, where European volunteers consumed an adapted Mediterranean diet, high plasma concentrations of oleic acid, enhanced 18:3n-3 to 18:2n-6 ratios, and longer-chain n-3 PUFA as well asand higher plasma concentrations of vitamin E and C were observed (35). The intervention group had no sudden deaths (35), suggesting anti-arrhythmic effects similar to those observed for long-chain n-3 PUFA from fish oil (36–38). A previous study showed that high intakes of 18:3n-3 (*ca.* threefold greater than that of control intake at 0.25% of calories vs. 0.755% of calories, respectively) were associated with increased plasma and platelet 20:5n-3 when 18:2n-6 intake was 4.8% of energy but not when it was 8.9% of energy (39). Similar observations were reported by Emken *et al.* (40) in human volunteer studies using isotope tracers. The conversion of deuterated 18:3n-3 to its longer-chain metabolites (EPA and DHA) was reduced by about 50% when dietary intake of 18:2n-6 was increased from 4.7 to 9.3% of energy. This can be explained by the competition between the n-6 and n-3 PUFA families for the desaturation pathway, where an excess of 18:2n-6 will inhibit desaturation of 18:3n-3. In Mediterranean countries, 18:2n-6 in-

take is generally at the moderate level of about 3–4% of dietary energy, thereby allowing adequate 18:3n-3 desaturation. Such effects of high oleic acid intakes have not been given sufficient recognition. Wahle *et al.* (8) observed a marked increase in 22:6n-3 and 20:4n-6, and an even greater decrease in 18:2n-6 of cardiac phospholipids (both PC and PE), when synthetic high-triolein diets were fed to obese Zucker rats. This again suggested an increased desaturation of dietary 18:3n-3 to 22:6n-3 because no fish oil was present in the diets. The beneficial effects of long-chain n-3 PUFA on cardiac arrhythmias in animals are well documented (see above), and it is conceivable that MUFA can elicit similar effects through modulation of desaturation mechanisms by decreasing the competitive inhibition of the high levels of 18:2n-6. This is a mechanism that offers a further explanation for the putative benefits of olive oil consumption, in tandem with 18:3n-3 intake, on CVD. The antiatherogenic effects of olive oil and oleic acid on classical plasma lipid risk factors have been well documented and have already been mentioned in this article.

MUFA-rich, Mediterranean-type diets also elicit significant beneficial, antithrombogenic effects on endothelial products such as von Willebrand factor (vWF), thrombomodulin, Tissue Factor Pathway Inhibitor, and E-selectin, which were all decreased in healthy male volunteers receiving a MUFA-rich diet (41). These decreases correlated with an increase in lag-time for LDL oxidation (41). Precisely how MUFA elicit these effects on endothelial products is not clear, but the mechanism could involve decreased oxidative stimuli and/or changes in FA composition.

In recent years there has been increasing interest in the presence of antiatherogenic and antithrombogenic effects of the minor phenolic components of olive oil as a way to explain the health benefits of the "Mediterranean diet." There is increasing evidence that certain of these compounds, but not all of them, display significant antioxidant activity, can increase the resistance of LDL particles to oxidation *in vivo* and *in vitro* (20–22,27), and inhibit platelet aggregation *in vitro* (42). Since atherogenesis and CVD are increasingly being regarded as an oxidative-inflammatory stress disorder (43), these dietary phenolic compounds offer another explanation for the observed cardiovascular health benefits, as well as other oxidative or inflammatory stress-induced diseases (see following discussion), of dietary olive oil. Phenolic compounds from virgin olive oil and red wine elicit protection in animal models against inflammation, inhibit vascular smooth muscle cell migration, and, at the cellular level, enhance the expression and activity of endothelial nitric oxide synthase (44–46).

Leukocyte/monocyte adhesion to the endothelium and their extravasation into the vessel wall is a very early stage of the atherogenic process leading to vascular disease and the first indication of endothelial dysfunction. The mechanism to explain this process appears to be predominantly the oxidative stress and/or inflammatory cytokine-induced increase in expression at the endothelial cell surface of specific endothelial-leukocyte adhesion molecules that tether the circulating cells prior to their invasion of the intima of the vessel wall (47,48). Circulating cancer cells utilize the same process prior to the development of metastatic secondary loci in various tissues (49).

The expression of these adhesion molecules in cells at the transcriptional and translational level (mRNA and protein) as well as the activity level appears to be largely regulated by redox-sensitive mechanisms in the cells, with enhanced redox state leading to decreased expression (50–53). n-3 Long-chain PUFA from fish, despite their reported enhancement of LDL oxidation *in vitro*, decrease the expression of cytokine-induced adhesion molecules such as intercellular adhesion molecule 1 (ICAM-1), vascular cell adhesion molecule 1 (VCAM-1), E-selectin, and P-selectin that are present on activated endothelial cells, and leukocytes/monocytes at the mRNA, protein, and activity level (54–59). A possible explanation for the effect of n-3 PUFA on adhesion molecule expression is the observation that these FA can up-regulate the expression and activity of the redox enzymes glutathione peroxidase (GPX1) and phospholipid glutathione peroxidase (GPX4) when compared with the n-6 arachidonic acid (ARA; 20:4n-6), a process that would be expected to decrease expression of the adhesion molecules (51). Inhibition of adhesion molecule expression in human umbilical vein endothelial cells (HUVEC) by CLA could also be due to the observed up-regulation of these redox enzymes when these FA are present (60,61).

Phenolic compounds from both olive oil and red wine such as oleuropein, tyrosol, hydroxytyrosol, apigenin and resveratrol at concentrations of *ca.* 30 μM can significantly attenuate the inflammatory cytokine-induced activation of endothelial cells and the transcriptional/translational up-regulation of adhesion molecules like ICAM-1, VCAM-1, and E-selectin by *ca.* 40–70% (61–63) and decrease monocyte cell adhesion to activated endothelial cells by *ca.* 20–30% (63). Surprisingly, a total phenolic extract of olive oil at concentrations from 10 to 250 μM actually increased the expression of ICAM-1 and E-selectin mRNA in HUVEC by about 25 to 550% in the presence of 10 U/mL interleukin-1β but elicited no effect on expression without the cytokine (61). The explanation for this is not clear, since hydroxytyrosol, apigenin and, to a lesser extent, tyrosol at similar concentrations inhibited the mRNA expression of these adhesion molecules (61). The lesser effect of tyrosol was to be expected since this phenolic compound is less of an antioxidant than hydroxytyrosol (20).

The effects of olive oil and red wine phenolics on gene expression of adhesion molecules are mostly determined individually, and little is known of any interactions or synergisms between these compounds and other components of the diet. We have investigated the interaction of the polyphenolics from green tea, quercetin, and kaempferol, and have observed a significant synergism between these compounds and n-3 PUFA in inhibiting the cytokine-induced expression of adhesion molecules on HUVEC. The presence of either n-3 PUFA or phenolics alone resulted in a *ca.* 50% inhibition of expression compared with control, but this was not as great an inhi-

bition as when the compounds were present in combination, where a further *ca.* 50% inhibition of the individual effects was observed (64). This is a reminder that the effects of dietary components should not be investigated or interpreted in isolation and that diets are a complex mixture of compounds that can have surprising interactions. Another case in point is the observation that, when phenolics are extracted together as a mixture from olive oil, they appear to have the opposite effect to the individual phenolic compounds. Whether similar interactions between n-3 PUFA and the phenolics from olive oil also occur is presently being investigated in our laboratory.

(ii) Cancer. The overall incidence of cancer is significantly lower in countries adhering to or partly adhering to the traditional Mediterranean diet when compared with northern Europe and North America, but differences are not as dramatic as seen with CVD (65,66). The differences are largely due to the lower incidence of colorectal cancer and cancer of the breast, prostate, and endometrium in these regions. The etiology of these specific cancers appears to have a strong dietary element and includes low intakes of fruit, vegetables, and whole-grain products and relatively high intakes of animal products (meat and fat) (3,4,67). It has been estimated that about 25% of colorectal cancer, 15% of breast cancer, and 10% of prostate, endometrial, and pancreatic cancers could be prevented if the populations of the more developed northern European countries and North America adopted a traditional Mediterranean type diet (3,4).

(iii) Cell mechanisms affected by diet. Although the traditional Mediterranean diet, particularly the intake of fruit, vegetables, and olive oil, is capable of reducing the incidence of various cancers, the cellular mechanisms by which this is achieved are not clearly understood. It is conceivable that the lower intake of linoleic acid and higher intakes of oleic and α-linolenic acids could play an important role in prevention/amelioration of certain cancers. In animal models of various cancers, the feeding of high levels of linoleic acid enhanced tumor growth, development, and metastasis whereas feeding long-chain n-3 PUFA from fish (EPA and DHA) elicited the opposite effect (68). As already mentioned, the high oleic acid intake and lower linoleic acid intake in olive oil-based Mediterranean diets would allow greater metabolism of 18:3n-3 to the longer-chain n-3 derivatives found in fish oils (EPA and possibly DHA) and could possibly elicit a similar effect to that of fish oil in reducing tumor growth and metastasis (68–70).

The beneficial effects of these n-3 PUFA in both vascular disease and animal models of cancer (and possibly in other immune/inflammatory-based diseases) appear to reside in their ability to attenuate the effects of oxidative and inflammatory processes, partly by inhibiting the expression of inflammatory cytokines at the level of gene transcription and partly by ameliorating the actions of these cytokines on cells through down-regulation of the cellular signal mechanisms (kinases, transcription factors: see following paragraphs) and inhibition of inflammatory eicosanoid formation (mainly reduction of PGE_2). The excessive production of PGE_2 is a characteristic of many tumors and is apparently a mechanism to enhance tumor growth and development (69). Inhibition of PGE_2 formation by inhibition of the cyclooxygenase-2 (COX-2) enzyme with aspirin has been shown to reduce colon cancer significantly (71). Reduced incidence of certain cancers in populations consuming Mediterranean-type diets with high 18:3n-3 and oleic acid but low 18:2n-6 contents compared with the average European and North American diets could be associated with lower PGE_2 production in tissues in response to an oxidative stress or/and an inflammatory insult and a lower capacity to produce the cytokines responsible for such an insult.

Our group has shown that the important constituents of olive oil, namely, oleic acid and phenolics like hydroxytyrosol, tyrosol, caffeic acid, and apigenin (the latter is present only as a minor component in olive oil but is a constituent of other edible plant species in the diet) can significantly attenuate the gene expression of eicosanoid-synthesizing enzymes such as 5-lipoxygenase (5-LOX) and its co-enzyme 5-LOX-activating protein by 20–25%. The most marked inhibition was observed with apigenin followed by hydroxytyrosol and oleic acid, with tyrosol and caffeic acid having little or no effect. The LOX enzyme system, which is responsible for the production of pro-inflammatory LT formation from n-6 PUFA, was affected to a greater extent than the COX system (COX-1 and -2), which produces the pro-inflammatory prostaglandins from n-6 PUFA (72). However, the formation of PGE2 was significantly decreased by hydroxytyrosol (and to a lesser extent by tyrosol and caffeic acid) in prostate cancer cells. This suggests that the olive oil components may have an effect on the gene expression of the LOX pathway and that the observed phenolic effects on PGE_2 reduction are most likely posttranscriptional effects. It also indicates the possibility that this LOX pathway is more important for enhancing the development and progression of tumors than hitherto thought. Increasing EPA (20:5n-3) availability in cells may alter the pro-inflammatory eicosanoid profile derived from ARA (20:4n-6) by decreasing PGE_2 synthesis and increasing the formation of three series PG and five series LT by substituting for ARA in the enzyme reactions (73). Since the high oleic acid, relatively high α-linolenic acid, and relatively lower linoleic acid contents in Mediterranean diets favor an increased conversion of 18:3n-3 to 20:5n-3 (and to a lesser extent 22:6n-3) and since this diet also incorporates significant amounts of fish, it is possible, but not proven, that the lower cancer incidence in these countries is related in part to reduced inflammation and eicosanoid production in response to specific stimuli. This is supported by epidemiological evidence of reduced incidence of certain types of cancer (large bowel, breast, prostate) in some populations with relatively high fish consumption (74).

Oxidative stress and an inability to counteract its consequences were suggested to be a component in the etiology of a number of cancers. Hydrogen peroxide and reactive oxygen species (ROS) formed during metabolic processes in the cell can result in damage to cellular components including lipids,

proteins, and, most importantly, DNA (75). These actions of ROS can result in lipid peroxide formation, cell dysfunction, DNA damage, and cell death. DNA damage can result in mutations and impairment of cell-cycle regulation, leading to the uncontrolled cell proliferation that is a characteristic of tumor growth (75). The relatively high intake of antioxidants in the traditional Mediterranean diet would tend to attenuate oxidative stress and reduce its deleterious cancer-promoting effects (3,4).

Our group showed that DNA damage, induced by H_2O_2 treatment of prostate cells, was decreased by olive oil phenolics and by increasing the amount of oleic acid presented to cells. The most effective compound was hydroxytyrosol, followed by caffeic acid, with tyrosol, as expected from its lower antioxidant capabilities (20), being the least effective but still affording protection at higher concentrations. The amelioration of DNA damage by these phenolics increased with their increasing concentration, with beneficial effects observed in physiological concentration ranges (10–50 μM) . However, the greatest effect of each compound was observed at relatively high and possibly nonphysiological concentrations (>200 μM) (76). The only phenolic eliciting significant inhibition of hydroperoxide formation in these cells, a biomarker of ROS-induced lipid peroxidation, was hydroxytyrosol, and the effect was not influenced by increasing its concentration. Tyrosol, in contrast, elicited a slight but significant increase in hydroperoxide production, whereas caffeic acid produced a nonsignificant, small decrease in this marker of ROS damage (76). The effects on hydroperoxide formation by the olive oil phenolics were mirrored by their effects on the gene expression of the important intrinsic redox enzyme, cytosolic glutathione peroxidase (cGPX1). The abundance of stable mRNA of cGPX1 was significantly and markedly decreased by hydroxytyrosol at all concentrations from 10 μM to nonphysiological 250 μM. Caffeic acid was less effective than hydroxytyrosol but still decreased expression significantly, whereas tyrosol elicited an increase in expression. Similar but less marked effects of these phenolics were observed on GPX4 mRNA expression. This enzyme is responsible for reducing hydroperoxides formed by ROS action in cell membranes, particularly mitochondrial membranes (76). The attenuation of the hydroperoxide formation and redox enzyme expression by phenolics, particularly hydroxytyrosol, is a strong indication that these extrinsic dietary compounds are functioning as antioxidants and decreasing the requirement for the induction of the intrinsic antioxidant enzymes. However, an induction of the expression of these cell antioxidant enzymes by dietary components such as n-3 PUFA also has been suggested to play a beneficial role in the prevention of cell dysfunction and disease states so long as the inducing stimuli do not overwhelm the cells' capacity for up-regulating these enzymes. (77). It has also been suggested that an individual's inability to up-regulate these intrinsic antioxidants, possibly due to polymorphisms (SNPs) in gene expression, may explain individual susceptibilities to cancer within populations, particularly if the intake of dietary antioxidants is low (77).

Although the efficacy of the Mediterranean diet in reducing incidence of cancer is not so marked as the reduction in CVD, it is nevertheless significant and is strongly correlated with the intake of olive oil on an epidemiological basis (2–4). Whether these effects are entirely due to the overall lower oxidative potential of classical Mediterranean diets or to specific components such as the phenolics present in the oil or antioxidants derived from other components of the diet is not clear and warrants further research. Similarly, it is not clear whether the hydroxytyrosol or tyrosol from olive oil is capable of augmenting the effects of specific FA in the diet as observed for DHA and the polyphenolic flavonoid quercetin (61). These aspects of olive oil are currently being investigated in our laboratory.

IMMUNE FUNCTION AND RA

Animal studies have shown that dietary olive oil has a significant suppressive effect on lymph node lymphocyte proliferation *ex vivo* in response to the T-cell mitogen Concanavalin A in comparison with diets rich in coconut oil or safflower oil or diets low in total fat. The effect of the olive oil diets was found to be similar to diets containing either fish oil or evening primrose oil (78). To determine whether the effects of olive oil feeding were due to components other than the high oleic acid content of these oils, these authors investigated the effects of diets containing high-oleic acid sunflower oil and compared the findings with the diets just described. Feeding either olive oil or high oleic acid sunflower oil significantly decreased lymphocyte proliferation by *ca.* 20% compared with the other diets (79). This suggested that these specific effects of the olive oil diets on lymphocyte proliferation were due largely to their content of oleic acid and not to the content of antioxidant phenolic compounds. This suppression of lymphocyte proliferation does not occur in middle-aged male volunteers consuming highly refined olive oil (lacking the phenolic antioxidants) (80). These contrasting effects may be explained by the fact that the rat diets were extreme (30% energy) compared with human diets (18% energy) or by species differences (81). Similar inhibitory effects on natural killer (NK) cell activity were observed in rats fed a high olive oil diet (20% by weight) or a diet high in oleic acid (30% of total energy), again suggesting effects are due to the oleic acid content of the diet (79). This was supported by the findings of a significant linear relationship between oleic acid content of a diet and NK cell activity (79). Again, the effects of oleic acid on immune function in healthy middle-aged male volunteers contrasted with findings in rats, and no significant effects on NK cell activity were evident after 1 mon on the diet although slight suppression was observed after 2 mon on the diet (80).

Expression of various adhesion molecules in the blood vascular system is up-regulated by immune-inflammatory stimuli and is a significant component of the thromboatherogenic process in animals and humans (82). In a dietary study in animals, the expression of adhesion molecules [ICAM-1, LFA-1 (lymphocytle function antigen-1) and CD2 (cluster of

differentiation 2)] on rat spleen lymphocytes was decreased by both olive oil and fish oil feeding (83). Similarly, after 2 mon on a high oleic acid diet, a significant reduction in ICAM-1 was observed in middle-aged male volunteers (80). No changes were found with the control diet, again suggesting that oleic acid content of the diet has specific effects on inflammatory responses. It is not clear whether the effects observed with high oleic acid diets are due to changes in other FA on a proportional basis. Increasing oleic acid will decrease the relative proportion of other FA consumed. A decrease in linoleic acid, as previously mentioned, could allow greater conversion of α-linolenic acid to long-chain n-3 PUFA. This might explain the similarities between olive oil or high-MUFA diets and fish oil diets (already discussed). The other possibility is that high-MUFA diets like the Mediterranean diet are less likely to induce oxidative stress, which is the stimulus for adhesion molecule up-regulation in the vascular system. The n-3 PUFA are known to enhance the expression and activity of intrinsic redox enzymes (GPX1 and GPX4) significantly, and this enhancement could be pivotal in their ability to reduce adhesion molecule expression since these enzymes are involved in the regulation of the nuclear factor κB (NF-κB) oxidative stress-activation pathway (51,56).

High olive oil diets (*ca.* 20% by weight) also attenuated the response of the immune system to endotoxins and the anorexia induced by increased production of the inflammatory cytokine tumor necrosis factor-α and the graft vs. host responses in animals (83,84). Again, the results indicate a similar effect of olive oil to that of fish oil in the diet. The expression of adhesion molecules in popliteal lymph nodes of animals following graft vs. host responses was significantly lower in animals fed olive oil or fish oil compared with low-fat or coconut fat diets (83). It appeared that olive oil was able to modulate *in vivo* responses involving B cells but not cytotoxic T lymphocytes whereas fish oil could modulate both responses (83).

Anti-inflammatory effects of olive oil consumption have also been reported for RA. In a Greek population, consumers of high amounts of olive oil (almost every day throughout life) were four times less likely to develop RA than those subjects who consumed the oil less than six times per month (85). Interestingly, in the light of similar effects of fish oil and olive oil in other studies, fish oil was without significant effect in this study (85). This contrasts with some other studies that showed a beneficial effect of dietary fish oil in reducing the symptoms of RA. Kremer *et al.* (86) showed significant attenuating effects of both fish oil and olive oil on RA and the production of the inflammatory cytokine IL-1, with the former eliciting the greater benefit in reducing both IL-1β production and the symptoms of RA. In conclusion, olive oil apparently is able to attenuate the activity of certain immune cells in animals, albeit to a lesser extent than dietary fish oil. Some evidence suggests that the effect of olive oil is primarily due to its monounsaturated oleic acid content, but this requires verification. Studies with human volunteers do not show the same attenuating effects of MUFA/olive oil on immune function and could reflect the high content of these components in the animal diets (*ca.* 20% by weight). The effect of high MUFA/olive oil on adhesion molecule expression in the blood vascular cells in both animals and humans could be an important effect of these dietary components, as increased expression of these molecules appears in a number of inflammatory diseases including CVD, cancer, and RA. Clearly, a Mediterranean diet with high oleic acid and relatively high content of a-linolenic as well as the various antioxidant components in both olive oil and other plant foods (mono- and polyphenolics) presents a low potential for oxidation in the body. This could be an additional factor in the benefits elicited by such a diet since the oxidative-inflammatory processes are associated with the most common diseases in industrialized societies. Adoption of a diet similar to the traditional Mediterranean diet with its high intakes of fruit, vegetables, whole-grain products and olive oil and low intakes of refined carbohydrates and red meat would also reduce the disease risk and enhance the life expectancy of northern European populations.

ACKNOWLEDGMENTS

The authors are grateful for financial support from The International Olive Oil Council (IOOC), Madrid, Spain; the Scottish Executive Environmental and Rural Affairs Department (SEERAD) and the Research Development Initiative (RDI) at Robert Gordon University, Aberdeen.

REFERENCES

1. Keys, A. (1980) Seven Countries: A Multivariate Analysis of Diet and Coronary Heart Disease, (Cambridge, and Landar), Harvard University Press, Boston.
2. Trichopoulou, A., Kouris-Blazos, A., Wahlqvist, M.L., Gnardellis, C., Lagiou, P., Polychronopoulos, E., Vassilakou, T., Lipworth, L., and Trichopoulos, D. (1995) Diet and Overall Survival in Elderly People, *Br. Med. J. 34*, 1457–1460.
3. Trichopoulou, A., Katsouyanni, K., Stuvers, S., Tzala, L., Gnardellis, C., Rimm, E., and Trichopoulos, D. (1995). Consumption of Olive Oil and Specific Food Groups in Relation to Breast Cancer Risk in Greece, *J. Natl. Cancer Instit. 87*, 110–116.
4. Trichopoulou, A., Lagiou, P., Kuper, H., and Trichopoulos, D. (2000) Cancer and Mediterranean Diet Traditions, *Cancer Epidemiol. Biomark. Prev. 9*, 869–873.
5. Keys, A., Mennotti, A., Karvonen, M.J., Aravanis, S.C., Blackburn, H., Buzina, R., Djordjevic, B.S., Dontas, A.S., Fidanza, F., Keys, A., *et al.* (1986) The Diet and 15 Year Death Rate in Seven Countries, *Am. J. Epidemiol. 124*, 903–915.
6. Armstrong, B., and Doll, R. (1975) Environmental Factors and Cancer Incidence and Mortality in Different Countries, with Special Reference to Dietary Practice, *Int. J. Cancer 15*, 617–631.
7. La Vecchia, C., Favero, A., and Franceschi, S. (1998) Monounsaturated and Other Types of Fat and Risk of Breast Cancer, *Eur. J. Cancer Prev. 7*, 461–464.
8. Wahle, K.W.J., Milne, L., and McIntosh, G. (1991) Regulation of Polyunsaturated Fatty Acid Metabolism in Tissue Phospholipids of Obese (fa/fa) and Lean (Fa/–) Zucker Rats. 1. Effect of Dietary Lipids on Cardiac Tissues, *Lipids 26*, 16–22.
9. Chan, J.M., Stampfer, M.J., and Giovannucci, E.L. (1998) What Causes Prostate Cancer? A Brief Summary of the Epidemiology, *Semin. Cancer Biol. 8*, 263–273.

10. Risch, H.A., Jain, M., Marrett, L.D., and Howe, G.R. (1994) Dietary Fat Intake and Risk of Epithelial Ovarian Cancer, *J. Natl Cancer Instit. 86*, 1409–1415.
11. Kuller, L.N. (1997) Dietary Fat and Chronic Diseases: Epidemiological Overview, *J. Am. Diet. Assoc. 97*, S9–S15.
12. Gerber, M. (1994) Olive Oil and Cancer, in *Epidemiology of Diet and Cancer,* (Ed Hill, M.J., Giacosa, A., and Caygill, C.P.G., eds), pp. 263–275, Ellis Horwood, Chichester, United Kingdom.
13. Giovannucci, E., Rimm, E.B., Stampfer, M.J., Colditz, G.A., Ascherio, A., and Willett, W.C. (1994) Intake of Fat, Meat and Fibre in Relation to Risk of Colon Cancer in Men, *Cancer Res. 54*, 2390–2397.
14. Holmes, M.D., Hunter, D.J., Colditz, G.A., Stampfer, M.J., Hankinson, S.E., Speizer, F.E., Rosner, B. and Willett, W.C. (1999) Association of Dietary Intake of Fat and Fatty Acids with Risk of Breast Cancer, *J. Am. Med. Assoc. 281*, 914–920.
15. Bartsch, H., Nair, J., and Owen, R.W. (1999). Dietary Polyunsaturated Fatty Acids and Cancer of the Breast and Colorectum: Compelling Evidence for Their Role as Risk Modifiers, *Carcinogenesis 20*, 2209–2218.
16. Berry, E.M., Eisenberg, S., Haratz, D., Friedlander, Y., Norman, Y., Kaufmann, N.A., and Stein, Y. (1991). Effect of Diets Rich in MUFA on Plasma Lipoproteins—The Jerusalem Nutrition Study: High MUFA Versus High PUFA, *Am. J. Clin. Nutr. 53*, 899–902.
17. Rose, D.P., Boyar, A.P., and Wynder, E.L. (1986) International Comparisons of Mortality Rates for Cancer of the Breast, Ovary, Prostate and Colon, and Per Capita Food Consumption, *Cancer 58*, 2363–2371.
18. Mensink, R.P., and Katan, M.B. (1987) Effect of Monounsaturated Fatty Acids Versus Complex Carbohydrates on High-Density Lipoprotein in Healthy Men and Women, *Lancet 1*, 122–124.
19. Mata, P., Alvarez-Silva, L.A., Rubio, M.J., Nuno, J., and De Oya, M.(1996) Effects of Long-Term Polyunsaturated Versus Monounsaturated-Enriched Diets on Lipoproteins in Healthy Men and Women, *Am. J. Clin. Nutr. 55*, 846–850.
20. Owen, R.W., Mier, W., Giacosa, A., Hull, W.E., Spiegelhalder, B., and Bartsch, H. (2000) Phenolic Compounds and Squalene in Olive Oils: The Concentration and Antioxidant Potential of Total Phenols, Simple Phenols, Secoridoids, Lignans and Squalene, *Food Chem. Toxicol. 38*, 647–659.
21. Moschandreas, J., Vissers, M.N., Wiseman, S., van Pute, K.P., and Kafetos, A. (2002) Extra Virgin Olive Oil Phenols and Markers of Oxidation in Greek Smokers: A Randomised Crossover Study, *Eur. J. Clin. Nutr. 56*, 1024–1029.
22. Visioli, F., Bellomo, G., Montedoro, G., and Galli, C. (1995) Low Density Lipoprotein Oxidation is Inhibited by *in vitro* Olive Oil Constituents, *Atherosclerosis 117*, 25–32.
23. Visioli, F., Galli, C., Bornet, F., Matteu, A., Pattelli, R., Galli, G., and Caruso, D. (2000) Olive Oil Phenolics Are Dose-Dependently Absorbed in Humans, *FEBS Lett. 468*, 159–160.
24. Caruso, D., Visioli, F., Pattelli, R., Galli, C., and Galli, G. (2001). Urinary Excretion of Olive Oil Phenols and Their Metabolites in Humans, *Metabolism 50*, 1426–1428.
25. Vissers, M.N., Zock, P.L., Roodenburg, A.J.C., Leenen, R., and Katan, M.B. (2002) Olive Oil Phenols Are Absorbed in Humans, *J. Nutr. 132*, 409–417.
26. Miro-Casas, E., Covas, M-I., Fito, M., Farre-Albadalejo, M., Marrugat, J., and de la Torre, R. (2003) Tyrosol and Hydroxytyrosol Are Absorbed from Moderate and Sustained Doses of Virgin Olive Oil in Humans, *Eur. J. Clin. Nutr. 57*, 186–190.
27. Caruso, D., Berra, B., Giavarini, F., Cortesi, N., Fedeli, E., and Galli, C. (1999) Effect of Virgin Olive Oil Phenolic Compounds on *in vitro* Oxidation of Human Low Density Lipoprotein, *Nutr. Metab. Cardiovasc. Dis. 9*, 102–107.
28. Fito, M., Covas, M.I., Lamuella-Raventos, R.M., Vila, J., Torrents, L., de la Torre, C., and Marrugat, J. (2000) Protective Effect of Olive Oil and Its Phenolic Compounds Against Low Density Lipoprotein Oxidation, *Lipids 35*, 633–638.
29. Tunstall-Pedo, H., Kuulasmaa, K., Mahonen, M., Tolonen, H., Ruokokoski, E., and Amouyel, P. (1999) Contribution of Trends in Survival and Coronary-Event Rates to Changes in Coronary Heart Disease Mortality. Ten Year Results from 37 WHO MONICA Project Populations. Monitoring Trends and Determinants in Cardiovascular Disease, *Lancet 353*, 1547–1557.
30. Fernandez-Jarne, E., Martinez-Losa, E., Prado-Santamaria, M., Brugarolas-Brufau, C., Serrano-Martinez, M., and Martinez-Gonzalez, M.A. (2002) Risk of First Non-fatal Myocardial Infarction is Negatively Associated with Olive Oil Consumption: Case Control Study in Spain, *Int. J. Epidemiol. 31*, 474–486.
31. Katan, M.B. (1999) Nutrition and Blood Lipids, *Nutr. Metab. Cardiovasc. Dis. 9*, 2–5.
32. Ramirez-Tortosa, M.C., Urbano, G., Lopez-Jurado, M., Nestares, T., Gomez, M.C., Mir, A., Ros, E., Mataix, J., and Gil, A. (1999) Extra Virgin Olive Oil Increases the Resistance of LDL to Oxidation More Than Refined Olive Oil in Free-Living Men with Peripheral Vascular Disease, *J. Nutr. 129*, 2177–2183.
33. Parthasaraty, S., Koo, J.C., Miller, E., Barnett, J., Witztum, J.C., and Steinberg, D. (1990) Low Density Lipoprotein Rich in Oleic Acid is Protected Against Oxidative Modification: Implications for Dietary Prevention of Atherosclerosis, *Proc. Natl. Acad. Sci. USA 87*, 3894–3898.
34. Fito, M., Gimeno, E., Covas, M.I., Miro, E., Lopez-Sabater, M.C., Farré, M., de la Torre, R., and Marrugat, J. (2002) Postprandial Short-Term Effects of Dietary Virgin Olive Oil on Oxidant/Antioxidant States, *Lipids 37*, 245–251.
35. Renaud, S., de Lorgeril, M., Delaye, J., Guidollet, J., Jacquard, F., Mamelle, N., Martin, J.L., Monjaud, I., Salen, P., and Toubol, P. (1995) Cretan Mediterranean Diet for Prevention of Coronary Heart Disease, *Am. J. Clin. Nutr. 61*, 1360S–1367S.
36. Riemersma, R.A., and Sargent, S.A. (1989) Dietary Fish Oil and Ischaemic Arrhythmias, *J. Int. Med. 225*, 111–116.
37. McLennan, P.L. (1993) Relative Effect of Dietary Saturated, Monounsaturated and Polyunsaturated Fatty Acids on Cardiac Arrhythmias in Rats, *Am. J. Clin. Nutr. 57*, 207–212.
38. Kris-Etherton, P.M., Harris, W.S., and Appel, L.J. (2003) Nutrition Committee of the American Heart Association. Fish Consumption, Fish Oil, Omega-3 Fatty Acids and Cardiovascular Disease, *Arterioscler. Thromb. Vasc. Biol. 23*, 151–152.
39. Renaud, S., Morazain, R., Godsey, F., Dumont, E., Thevenon, C., Martin, J.L., and Mendy, F. (1986) Nutrients, Platelet Function and Composition in Nine Groups of French and British Farmers, *Atherosclerosis 60*, 37–48.
40. Emken, E.A., Adlof, R.O., and Gulley, R.M. (1994) Dietary Linoleic Acid Influences Desaturationand Acylation of Deuterium-Labelled Linoleic Acid and Linolenic Acid in Young Adult Males, *Biochim. Biophys. Acta 1213*, 277–288.
41. Perez-Jimenez, F., Castro, P., Lopez-Mirando, J., Paz-Rojas, E., Blanco, A., Lopez-Segura, F., Velasco, F., Marin, C., Fuentes, F., and Ordovas, J.M. (1999) Circulating Levels of Endothelial-Function Regulators are Modulated by Dietary Monounsaturated Fat, *Atherosclerosis 145*, 351–358.
42. Petroni, A., Blasevic, M., Salami, M., Papini, N., Montedoro, G.F., and Galli, C. (1995) Inhibition of Platelet Aggregation and Eicosanoid Production by Phenolic Components of Olive Oil, *Thromb. Res. 78*, 151–160.
43. Ross, R. (1993) The Pathogenesis of Atherosclerosis: A Perspective for the 1990s, *Nature 362*, 801–809.
44. Martinez-Dominguez, E., de la Puerta, R., and Ruiz-Gutierrez, V. (2001) Protective Effects upon Experimental Inflammation of a Phenol-Supplemented Virgin Olive Oil Diet, *Inflamm. Res. 50*, 102–106.

45. Iijima, K., Yoshizumi, M., and Ouchi, Y. (2002) Effect of Red Wine Polyphenols on Vascular Smooth Muscle Cell Function: Molecular Mechanisms of the "French paradox," *Mech. Ageing Dev. 123*, 1033–1039.
46. Wallerath, T., Deckert, G., Ternes, T., Anderson, H., Li, H., Witte, K., and Forstermann, U. (2002) Reveratrol, a Polyphenolic Phytoalexin Present in Red Wine Enhances Expression and Activity of Endothelial Nitric Oxide Synthase, *Circulation 106*, 1652–1658.
47. Steinberg, D. (2000) Is There a Potential Therapeutic Role for Vitamin E or Other Antioxidants in Atherosclerosis? *Curr. Opin. Lipidol. 11*, 603–607.
48. Lusis, A.J. (2000) Atherosclerosis, *Nature 407*, 233–241.
49. Wahle, K.W.J., and Heys, S.D. (2002) Cell Signal Mechanisms, Conjugated Linoleic Acids (CLAs) and Anti-tumorigenesis. *Prostaglandins Leukot. Essent. Fatty Acids 67*, 183–186.
50. Marui, N., Offermann, M.K., Swerlick, R., Kunsch, C., Rosen, C.A., Ahmad, M., Alexander, R.W., and Medford, R.M. (1993) Vascular Cell Adhesion Molecule-1 (VCAM-1) Gene Transcription and Expression Are Regulated Through Antioxidant Sensitive Mechanisms in Human Vascular Endothelial Cells, *J. Clin. Invest. 92*, 1866–1874.
51. Crosby, A.J., Wahle, K.W.J., and Duthie, G.G. (1996). Modulation of Glutathione Peroxidase Activity in Human Vascular Endothelial Cells by Fatty Acids and the Cytokine Interleukin-1β, *Biochim. Biophys. Acta 1303*, 187–192.
52. Sen, C.K., and Packer, L. (1996) Antioxidant and Redox Regulation of Gene Transcription, *FASEB J. 10*, 709–720.
53. Faruqi, R.M., Poptic, J., Faruqi, T.R., De la motte, C., and Di Corleto, P.E. (1997). Distinct Mechanisms for *N*-Acetyl-Cysteine Inhibition of Cytokine-Induced E-Selectin and VCAM-1 Expression, *Am. J. Physiol. 273*, H817–H826.
54. Collie, E.S.R., Trayhurn, P., and Wahle, K.W.J. (1994) Investigation of the Action of Fatty Acids on the Expression of Endothelial Cell Adhesion Molecules *in vitro*, Abstract, 35th International Conference on the Bioscience of Lipids, Aberdeen, September, IVP5.
55. Collie-Duguid, E.S.R., and Wahle, K.W.J. (1995) Investigation of the Action of Fatty Acids on the Expression of Endothelial Cell Adhesion Molecules *in vitro*, Abstract, 2nd Meeting of International Society for the Study of Fatty Acids and Lipids, Washington, DC, June, Abstract 40.
56. Collie-Duguid, E.S.R., and Wahle, K.W.J. (1996) Inhibitory Effect of Fish Oil n-3 Long-chain Polyunsaturated Fatty Acids on the Expression of Endothelial Cell Adhesion Molecules, *Biochem. Biophys. Res. Comm. 220*, 969–974.
57. De Caterina, R., and Libby, P. (1996) Control of Endothelial Leukocyte Adhesion Molecule Expression by Fatty Acids, *Lipids 31*, S57–S63.
58. Hughes, D.A. (1998) *In vitro* and *in vivo* Effects of n-3 Polyunsaturated Fatty Acids on Human Monocyte Function, *Proc. Nutr. Soc. 57*, 521–525.
59. De Caterina, R., Liao, J.K., and Libby, P. (2000) Fatty Acid Modulation of Endothelial Activation, *Am. J. Clin. Nutr. 71*, 213S–223S.
60. Farquharson, A., Wu, H-C., Grant, I., Graf, B., Choung, J.J., Eremin, O., Heys, S.D., and Wahle, K.W.J. (1999). Possible Mechanisms for the Putative Anti-Atherogenic and Anti-Tumorigenic Effects of Conjugated Polyenoic Fatty Acids, *Lipids 34*, S343.
61. Graf, B. (1999) Regulation of Adhesion Molecule mRNA Levels in Cytokine Activated Human Endothelial Cells by Dietary Phenolic Acids and Conjugated Linoleic Acid, Diplomarbeit. Institut für Ernährungswissenschaft, Universität Giessen, Germany, and Rowett Research Institute, Aberdeen, United Kingdom.
62. Bertelli, A.A., Baccalini, R., Battaglia, E., Falchi, M., and Ferrero, M.E. (2001) Reseveratrol Inhibits TNF-α-Induced Endothelial Cell Activation, *Therapie 56*, 613–616.
63. Carluccio, M.A., Siculella, I., Ancora, M.A., Massaro, M., Scoditti, E., Storelli, C., Visioli, F., Distante, A., and De Caterina, R. (2003) Olive Oil and Red Wine Antioxidant Polyphenols Inhibit Endothelial Activation: Antiatherogenic Properties of Mediterranean Diet Phytochemicals, *Arterioscler. Thromb. Vasc. Biol. 23*, 622–629.
64. Collie-Duguid, E.S.R. (1999) Regulation of Human Endothelial ICAM-1, E-Selectin and VCAM-1 by Polyunsaturated Fatty Acids and Antioxidants, Ph.D. Thesis, Aberdeen University, Aberdeen, Scotland.
65. Willett, W.C. (1994) Diet and Health: What Should we Eat? *Science 264*, 532–537.
66. Lagiou, P., Trichopoulou, A., Hendrickx, H.K., Kellerher, C., Leonhauser, L.U., Moreiras, O., Nelson, M., Schmitt, A., Sekula, W., Trygg, K., and Zajkas, G. (1999) Household Budget Survey of Nutritional Data in Relation to Mortality from Coronary Heart Disease, Colorectal Cancer and Female Breast Cancer in European Countries. DAFNE I and II Projects of European Commission Data Food Network, *Eur. J. Clin. Nutr. 53*, 328–332.
67. Willett, W.C., and Trichopoulos, D. (1996) Nutrition and Cancer: A Survey of the Evidence, *Cancer Causes Control 7*, 178–180.
68. Karmali, R.A., Marsh, J., and Fuchs, L. (1984). Effect of Omega-3 Fatty Acids on Growth of a Rat Mammary Tumour, *J. Natl. Cancer Inst. 73*, 457–461.
69. Karmali, R.A. (1986) Eicosanoids and Cancer, *Proc. Clin. Biol. Res. 222*, 687–697.
70. Karmali, R.A. , Adams, L., and Trout, J.R. (1998) Plant and Marine n-3 Fatty Acids Inhibit Experimental Metastases of Rat Mammary Adenocrcinoma Cells, *Prostaglandins Leukotr. Essent. Fatty Acids 48*, 309–314.
71. Din, F.V., Dunlop, M.G., and Stark, L.A. (2004) Evidence for Colorectal Cancer Cell Specificity of Aspirin Effects on NF-κB Signalling and Apoptosis, *Br. J. Cancer 91*, 381–388.
72 Ochoa, J.J., Farquharson, A.J., Grant, I., Moffatt, L.E.F., Heys, S.D., and Wahle, K.W.J. (2004) Conjugated Linoleic Acids (CLAs) Decrease Prostate Cancer Cell Proliferation: Different Molecular Mechanisms for *cis*-9, *trans*-11 and *trans*-10, *cis*-12 Isomers, *Carcinogenesis 25*, 1185–1191.
73 Funck, C.D. (2001) Prostaglandins and Leukotrienes: Advances in Eicosanoid Biology, *Science 294*, 1871–1875.
74 Wahle, K.W.J., Eremin, O., and Heys, S.D. (1997). Nutrition and Cancer: Lipids and Antioxidants as Modulators of Malignancies, in *First Virtual Congress of Pharmacy*, Granada, Spain. Web address: http://www.ugr.es/~genfarm/bien.htm
75 Jenkinson, A.M., Collins, A.R., Duthie, S.J., Wahle, K.W.J., and Duthie, G.G. (1999) The Effect of Increased Intakes of Polyunsaturated Fatty Acids and Vitamin E on DNA Damage in Human Volunteers, *FASEB J. 13*, 2138–2142.
76 Quiles, J.L., Farquharson, A.J., Simpson, D.K., Grant, I., and Wahle, K.W.J. (2002) Olive Oil Phenolics: Effects on DNA Oxidation and Redox Enzyme mRNA in Prostate Cells, *Br. J. Nutr. 88*, 225–234.
77 Wahle, K.W.J., Rotondo, D., and Heys, S.D. (2003) Polyunsaturated Fatty Acids (PUFA) and Gene Expression in Mammalian Systems, *Proc. Nutr. Soc. 62*, 349–360.
78. Yaqoob, P., Newsholme, E.A., and Calder, P.C. (1994) The Effect of Dietary Lipid Manipulation on Rat Lymphocyte Subsets and Proliferation, *Immunology 82*, 603–610.
79. Jeffery, N.M., Yaqoob, P., Newsholme, E.A., and Calder, P.C. (1996) The Effects of Olive Oil Upon Rat Serum Lipid Levels and Lymphocyte Functions Are Due to Oleic Acid, *Ann. Nutr. Metab. 40*, 71–80.
80. Yaqoob, P., Knapper, J.A., Webb, D.H., Williams, C.M., New-

sholme, E.A., and Calder, P.C. (1998) The Effect of Olive Oil Consumption on Immune Function in Middle-Aged Men, *Am. J. Clin. Nutr. 67*, 129–135.
81. Yaqoob, P. (2002) Monounsaturated Fatty Acids and Immune Function, *Eur. J. Clin. Nutr. 56*, S9–S13.
82. de Caterina, R., Cybulsky, M.I., Clinton, S.K., Gimbrone, M.A. and Libby, P. (1994) The Omega-3 Fatty Acid Docosahexaenoate Reduces Cytokine-Induced Expression of Proatherogenic and Pro-inflammatory Proteins in Human Endothelial cells, *Arterioscler. Thromb. 14*, 1829–1836.
83. Sanderson, P., Yaqoob, P., and Calder, P.C. (1995) Effects of Dietary Lipid Manipulation on Graft Versus Host and Host Versus Graft Responses in the Rat, *Cell. Immunol. 164*, 240–247.
84. Mulrooney, H.M., and Grimble, R.E. (1993) Influence of Butter and of Corn, Coconut and Fish Oils on the Effects of Recombinant Human Tumour Necrosis Factor-α in Rats, *Clin. Sci. 84*, 105–112.
85. Linos, A., Kaklamanis, E., Kontomerkos, A., Koumantaki, Y., Gazi, S., Vaiopoulos, G., Tsokos, G.C., and Kaklamanis, P.H. (1991) The Effect of Olive Oil and Fish Oil and Fish Consumption on Rheumatoid Arthritis—A Case-Control Study, *Scand. J. Rheumatol. 20*, 419–426.
86 Kremer, J.M., Lawrence, D.A., Jubiz, W., DiGiacomo, R., Rynes, R., Bartholomew, L.E., and Sherman, M. (1990) Dietary Fish Oil and Olive Oil Supplementation in Patients with Rheumatoid Arthritis. Clinical and Immunologic Effects, *Arthritis Rheum. 33*, 810–820.

[Received September 21, 2004; accepted December 12, 2004]

Olive Oil Consumption and Reduced Incidence of Hypertension: The SUN Study

Alvaro Alonso[a,b] and Miguel Ángel Martínez-González[a,*]

[a]Department of Preventive Medicine and Public Health, School of Medicine, University of Navarra, 31008 Pamplona, Spain, and [b]Preventive Medicine and Quality Management Service, Virgen del Camino Hospital, 31008 Pamplona, Spain

ABSTRACT: Olive oil, a major component of the Mediterranean diet, has been associated in some small clinical trials and cross-sectional studies with a reduction in blood pressure. The objective of this study was to assess the association of olive oil consumption with the incidence of hypertension in an epidemiologic cohort, the Seguimiento Universidad de Navarra (SUN) study. The SUN Project is a prospective cohort study whose members are all university graduates. The recruitment and follow-up of participants is made using mailed questionnaires. Diet was assessed using a semiquantitative food frequency questionnaire previously validated in Spain, with 136 items. Outcomes of interest were newly diagnosed cases of hypertension, as reported by participants in the follow-up questionnaires. Logistic regression models were fit to assess the risk of hypertension associated with olive oil consumption. For the present analysis, we have taken in consideration the first 6,863 participants, with at least 2 yr of follow-up. After a median follow-up time of 28.5 mon, the cumulative incidence of hypertension was 4.7% in men and 1.7% in women. A lower risk of hypertension was observed among participants with a higher olive oil consumption at baseline, but the results were not statistically significant ($P = 0.13$ for the linear trend test in the multivariate model). However, among men, the adjusted odds ratios (OR) (95% confidence intervals) of hypertension for the second to fifth quintiles of olive oil consumption, compared with the first quintile, were 0.55 (0.28–1.10), 0.75 (0.39–1.43), 0.32 (0.15–0.70), and 0.46 (0.23–0.94), respectively ($P = 0.02$ for linear trend). No association was found between olive oil consumption and the risk of hypertension among women. In conclusion, in a Mediterranean population, we found olive oil consumption to be associated with a reduced risk of hypertension only among men. The lack of association observed among women might be attributed to the overall lower incidence of hypertension found among females and the resulting lower statistical power.

Paper no. L9573 in *Lipids 39*, 1233–1238 (December 2004).

The adherence to traditional Mediterranean dietary patterns (MDP) has been associated in some studies with a reduced risk of coronary heart disease (1,2). One plausible biological mechanism that may explain this benefit is the protective effect of some components of traditional MDP against hypertension, a major risk factor for cardiac disease. For example, high fruit and vegetable consumption has been linked with a lower risk of hypertension and reduced blood pressure (3,4).

Another characteristic of the typical MDP is the elevated consumption of olive oil as the main source of added lipids. There are, however, scarce data relating olive oil to blood pressure or to the risk of hypertension. Some small studies conducted in healthy volunteers and hypertensive patients suggest a beneficial effect of olive oil on blood pressure (5–7). Additionally, a small clinical trial has shown a reduced need for blood pressure lowering drugs in hypertensive subjects receiving extra-virgin olive oil (8). Nevertheless, no large epidemiological studies conducted in Mediterranean countries have assessed the association between olive oil consumption and the risk of hypertension.

Using data from the Seguimiento Universidad de Navarra (University of Navarra Follow-up, SUN) study, a prospective cohort study in Spain, we tried to assess whether olive oil consumption, independent of consumption of other foods, was associated with a lower risk of hypertension.

METHODS

The SUN Project. The SUN Project is a prospective cohort study conducted in Spain. A detailed description of its methods has been published elsewhere (9). The recruitment of participants began in 2000, and remains open (the study design corresponds to a dynamic cohort). All members of the cohort are university graduates, mainly former students of the University of Navarra. Other participants have been recruited from the Nurses Professional Association of Navarra and from an insurance company (ACUNSA, Inc.). Recruitment and follow-up of participants are done through biennial mailed questionnaires. The study protocol has been approved by the Institutional Review Board of the University of Navarra. For the present analysis, we have taken into consideration the first 6,863 participants, with at least two years of follow-up.

Dietary assessment. Diet was assessed in the baseline questionnaire using a semiquantitative food-frequency questionnaire, previously validated in Spain (10). The questionnaire has 136 food items, and open-labeled questions for dietary supplement intake and other food items not included in the questionnaire. The questionnaire offered nine frequency categories of intake for each food item (from 6+ per day to never or almost never). In addition to particular questions regarding consumption of olive oil consumption used in frying, as a spread, or to season

*To whom correspondence should be addressed at Department of Preventive Medicine and Public Health, School of Medicine, University of Navarra, Irunlarrea, 1, 31008 Pamplona, Spain. E-mail: mamartinez@unav.es

Abbreviations: CI, confidence interval; MDP, Mediterranean dietary patterns; MET, metabolic equivalents; MUFA, monounsaturated fatty acids; OR, odds ratio; SUN, Seguimiento Universidad de Navarra (University of Navarra Follow-up).

salads, the type of fat used in frying was specifically assessed. The biennial follow-up questionnaires also gathered information about changes in the habitual consumption of main components of the MDP, including olive oil. A dietitian updated the nutrient data bank using the latest available information included in the food composition tables for Spain (11).

Assessment of other covariates. The baseline questionnaire collected information about sociodemographic variables (age, sex, marital and occupational status), anthropometric measures (height, weight), smoking, physical activity during leisure time, sedentary lifestyle, and some clinical variables (medication use, past history of coronary heart disease, cancer, and other diseases).

Outcome ascertainment. In the baseline questionnaire, participants reported whether they had a history of medically diagnosed hypertension and their usual systolic and diastolic blood pressure (nine categories). In the follow-up questionnaire, individuals were asked to report whether they had received a physician's diagnosis of hypertension in the time between both questionnaires. Validity of self-reported hypertension has been shown to be appropriate in other similar settings (12, 13). In a sample of 63 participants of the SUN Study living in the metropolitan area of Pamplona, 31 reporting hypertension and 32 without a history of hypertension, there was a fair correlation between self-reported and measured systolic and diastolic blood pressure (Spearman's rho = 0.62 and 0.65, respectively). The negative predictive value was 94%, and the positive predictive value was 65%.

Statistical analysis. The main exposure of interest was olive oil consumption, adjusted for total energy intake using the residuals method (14) and taking total energy intake into account separately for women and men. Energy-adjusted olive oil consumption was divided into five categories, using quintiles as cutoff points. The main outcome variable was a new physician-made diagnosis of hypertension. This was defined as a self-reported physician-made diagnosis of hypertension in the follow-up questionnaire, with no report of a diagnosis of hypertension in the baseline questionnaire.

The cumulative incidence of hypertension was computed for each quintile of olive oil consumption. To avoid the confounding effect of other variables simultaneously associated with the outcome and the main exposure, we used nonconditional logistic regression modeling. The main known risk factors for hypertension were included in the final model. These potential confounders were age, gender, body mass index, physical activity during leisure time (metabolic equivalents [METS-h/week]), total energy intake, alcohol consumption, sodium intake, and calcium intake. In addition, models for each sex were run separately.

Tests for a linear trend in the relationship between olive oil consumption and risk of hypertension were obtained by assigning the median value for each quintile of olive oil consumption and modeling this variable as continuous in the logistic model.

RESULTS

The rate of follow-up for the first 7,650 participants in the cohort is 90%. The median follow-up time was 28.5 months. From the 6,863 respondents with data at baseline and at the first follow-up questionnaire, 658 were excluded due to prevalent hypertension at baseline and 632 because of extremely low or high caloric intakes (<400 kcal/day for women, <600 kcal/day for men, >3500 kcal/day for women, >4200 kcal/day for men). Finally, 5,573 participants were available for analysis, 3,384 women and 2,189 men. During the follow-up time, 161 incident cases of hypertension were identified among them (cumulative incidence 2.9%). The incidence was much lower in women than in men (1.7 vs. 4.7%). The characteristics of participants according to their quintiles of olive oil consumption are presented in Table 1, separately for men and women. Age and alcohol consumption were positively correlated with olive oil consumption, whereas sodium intake was inversely associated with it.

Odds ratios (OR) for incident hypertension in the whole sample are shown in Table 2. When we considered men and women together, in the age- and sex-adjusted analysis, olive oil was not associated with the incidence of hypertension. However, in the multivariate analysis, taking into consideration some known risk factors for hypertension, the fourth quintile of olive oil consumption was associated with a significantly decreased risk of hypertension, compared with the quintile with the lowest consumption.

Interestingly, after stratifying by sex, a clear inverse relationship between olive oil consumption and the risk of hypertension was apparent among male participants (Table 3). Men with the highest olive oil consumption, i.e., those in the fifth quintile, had a significantly lower risk of hypertension compared with those in the first quintile, as shown by the OR of 0.46 (95% confidence interval 0.23–0.94). Also, there was a significant linear trend for the association between olive oil consumption and the risk of hypertension ($P = 0.02$), suggesting a dose-response relationship between olive oil consumption and incidence of hypertension among men. In women, olive oil consumption was not associated with a change in the risk of hypertension. Further adjustment for fruit and vegetable consumption did not materially change the point estimates for the OR, and the linear trend continued to be statistically significant ($P = 0.03$).

DISCUSSION

In this prospective study, conducted in a Mediterranean population, those men with a higher olive oil consumption at baseline had a lower risk of developing hypertension, independently of other risk factors for this disorder. This relationship was not apparent among women. The lack of association observed among women could be attributed to the lower incidence of hypertension among females and consequently to lower statistical power. In fact, only 59 cases of incident hypertension were observed among women, thus hindering the ability to ascertain with confidence any association of weak magnitude.

To our knowledge, this is the first large epidemiological study showing an inverse association between olive oil consumption and the risk of hypertension. Some previous studies conducted in Mediterranean countries have shown a protective

TABLE 1
Distribution of Selected Variables Across Quintiles of Energy-Adjusted Olive Oil Consumption[a]

	Quintiles of energy-adjusted olive oil consumption					
Women	Q1 (lowest)	Q2	Q3	Q4	Q5 (highest)	*P* for trend
N	676	677	677	677	677	
Energy-adjusted olive oil consumption (g/d) (median)	5.3	11.2	16.8	25.1	36.2	
Age (yr) (mean)	34.5	36.2	37.3	36.8	38.5	<0.001
Total energy intake (kcal/d)	2594.3	2204.0	2090.4	2446.0	2313.1	0.18
BMI (mean)	21.5	21.8	21.8	21.9	22.0	<0.001
Physical activity during leisure time in METs-h/wk (mean)	14.6	15.9	15.9	17.1	15.1	0.27
Alcohol consumption (g/d) (mean)	3.6	3.4	4.1	3.8	4.0	0.04
Sodium consumption (g/d) (mean)	4.1	3.1	2.8	3.1	2.8	<0.001
Calcium consumption (g/d) (mean)	1.4	1.2	1.2	1.4	1.2	0.009
Fruit consumption (g/d) (mean)	391.9	397.0	383.5	387.8	355.8	0.04
Vegetable consumption (g/d) (mean)	512.6	585.8	594.8	623.0	602.3	<0.001
Dietary fiber consumption (g/d) (mean)	33.7	28.0	27.0	31.3	30.8	<0.001
	Quintiles of energy-adjusted olive oil consumption					
Men	Q1 (lowest)	Q2	Q3	Q4	Q5 (highest)	*P* for trend
N	437	438	438	438	438	
Energy-adjusted olive oil consumption (g/d) (median)	4.0	9.0	13.3	19.1	32.4	
Age (yr) (mean)	39.6	42.0	43.7	43.0	44.4	<0.001
Total energy intake (kcal/d)	2858.2	2516.0	2227.3	2407.9	2631.2	<0.001
BMI (mean)	24.6	25.0	25.3	25.3	25.3	<0.001
Physical activity during leisure time in MET-h/wk (mean)	23.8	23.8	22.5	22.5	24.4	0.83
Alcohol consumption (g/d) (mean)	8.7	9.7	9.1	10.1	10.8	0.03
Sodium consumption (g/d) (mean)	4.9	4.0	3.5	3.7	3.4	<0.001
Calcium consumption (g/d) (mean)	1.4	1.2	1.1	1.1	1.2	<0.001
Fruit consumption (g/d) (mean)	296.3	309.2	294.9	299.7	302.8	0.93
Vegetable consumption (g/d) (mean)	388.7	442.4	470.7	490.4	543.8	<0.001
Dietary fiber consumption (g/d) (mean)	29.0	25.9	23.2	25.8	29.7	0.45

[a]BMI, body mass index; MET, metabolic equivalent.

effect of olive oil in relation to the development of nonfatal myocardial infarction (15) or coronary death (1,16). A possible explanation for this favorable effect in studies of coronary heart disease is the beneficial effect of olive oil on blood pressure. In some small studies and clinical trials, olive oil has been shown to have a lowering effect on blood pressure. For example, in a crossover clinical trial conducted on 16 hypertensive women, olive oil but not a high-oleic sunflower oil, was associated with a significant reduction in systolic and diastolic blood pressure (7). In another study, a diet enriched with olive oil, followed during a period of 5 wk, was associated with a reduced mean blood pressure in 42 individuals (18 women and 24 men) (6). More interestingly, in a double-blind, randomized cross-over clinical trial conducted on 23 hypertensive patients, a diet rich in monounsaturated FA (MUFA) from extra-virgin olive oil was associated with lower systolic and diastolic blood pressure, and also with a reduced need for antihypertensive medication when compared with a diet rich in PUFA (8). The authors of the study suggested that the beneficial effect of olive oil on blood pressure was not only associated with its MUFA content,

TABLE 2
Odds Ratios (OR) and 95% Confidence Intervals (CI) of Self-Reported Incident Hypertension According to Quintiles of Olive Oil Consumption in the SUN Study

	Quintiles of energy-adjusted olive oil consumption					
	Q1	Q2	Q3	Q4	Q5	*P* for trend
Participants (*N*)	1113	1115	1115	1115	1115	
Median olive oil consumption (g/d)	4.8	10.2	15.0	23.5	34.6	
New cases of hypertension, *N* (%)	32 (2.9)	26 (2.3)	41 (3.7)	30 (2.7)	32 (2.9)	
Age- and sex-adjusted OR (95% CI)	1 (ref.)	0.69 (0.40–1.17)	1.01 (0.62–1.64)	0.77 (0.46–1.29)	0.75 (0.45–1.25)	0.39
Multivariate OR (95% CI)[a]	1 (ref.)	0.61 (0.35–1.07)	0.83 (0.49–1.41)	0.55 (0.31–0.98)	0.63 (0.36–1.07)	0.13

[a]Non-conditional logistic regression model adjusted for age (in years), sex, BMI (defined as weight in kilograms divided by the square of height in meters), energy intake, alcohol consumption (in g/d), sodium intake (in mg/d), calcium intake (in g/d), and physical activity during leisure time (in METs-h/wk). SUN, Seguimiento Universidad de Navarra; for other abbreviations see Table 1.

TABLE 3
OR and 95% CI of Self-Reported Incident Hypertension According to Quintiles of Olive Oil Consumption in the SUN Study

	Quintiles of energy-adjusted olive oil consumption					
Women	Q1	Q2	Q3	Q4	Q5	*P* for trend
Participants (*N*)	676	677	677	677	677	
Median olive oil consumption (g/d)	5.3	11.2	16.8	25.1	36.2	
New cases of hypertension, *N* (%)	9 (1.3)	8 (1.2)	12 (1.8)	15 (2.2)	15 (2.2)	
Age-adjusted OR (95% CI)	1 (ref.)	0.78 (0.30–2.06)	1.04 (0.43–2.51)	1.45 (0.62–3.35)	1.26 (0.54–2.93)	0.27
Multivariate OR (95% CI)[a]	1 (ref.)	0.74 (0.27–2.02)	0.97 (0.38–2.45)	1.14 (0.47–2.78)	0.97 (0.40–2.36)	0.74

	Quintiles of energy-adjusted olive oil consumption					
Men	Q1	Q2	Q3	Q4	Q5	*P* for trend
Participants (*N*)	437	438	438	438	438	
Median olive oil consumption (g/d)	4.0	9.0	13.3	19.1	32.4	
New cases of hypertension, *N* (%)	23 (5.3)	18 (4.1)	29 (6.6)	15 (3.4)	17 (3.9)	
Age-adjusted OR (95% CI)	1 (ref.)	0.65 (0.34–1.23)	1.00 (0.56–1.78)	0.52 (0.26–1.01)	0.55 (0.28–1.05)	0.05
Multivariate OR (95% CI)[a]	1 (ref.)	0.55 (0.28–1.10)	0.75 (0.39–1.43)	0.32 (0.15–0.70)	0.46 (0.23–0.94)	0.02

[a]Nonconditional logistic regression model adjusted for age (in years), BMI (defined as weight in kilograms divided by square of height in meters), energy intake, alcohol consumption (in g/d), sodium intake (in mg/d), calcium intake (in g/d), and physical activity during leisure time (in MET-h/wk). For abbreviations see Tables 1 and 2.

but also with the high content of antioxidant polyphenols. In this same study, patients supplemented with sunflower oil did not experience a beneficial effect.

The mechanisms behind the protective role of olive oil for hypertension are not clear. MUFA intake could be associated with an increased sensitivity to insulin, producing a reduction in blood pressure (17). However, some authors suggest that other components of olive oil, such as the polyphenols mentioned, could be associated with lower blood pressure and a reduced risk of hypertension. In fact, some studies have shown a reduction of blood pressure following supplementation with antioxidants (18), although there are some inconsistencies on this issue (19). Another explanation for the beneficial effect of olive oil on blood pressure is its greater resistance to denaturation during the process of frying, with a lower production of polar compounds. In a cross-sectional study conducted in southern Spain on 538 persons, the amount of polar compounds in cooking oil was associated with hypertension, and a lower concentration of polar compounds was found in olive oil used for frying when compared with sunflower oil from the same source. In that study, individuals using olive oil for frying had a higher concentration of MUFA in plasma phospholipids, and this variable was inversely associated with the prevalence of hypertension (20). Another possible explanation of olive oil's antihypertensive effect involves molecules closely related to the main FA contained in olive oil. A strong blood pressure-reducing effect has recently been observed for 2-hydroxy-oleic acid in an experimental model (21).

Our study has important strengths. Its prospective design avoids the reverse-causation bias. Also, the follow-up rate is high. Additionally, all participants are university graduates, allowing a better understanding of the food-frequency questionnaire and increasing the internal validity of our findings. Diet has been assessed with a comprehensive tool, previously validated and used in similar settings.

There are some limitations in this analysis. Statistically significant results, using the traditional cutoff point of $P < 0.05$, were found only after several analyses (whole sample, women, and men), increasing the possibility of a false positive result due to multiple comparisons.

Another potential limitation is the possible lower validity of the self-reported outcome. Although the validity of self-reported hypertension in the studied population is fair, the misclassification in the outcome could hide the studied associations. In fact, the correlation between self-reported and measured blood pressure was not very high. Similarly, the positive predictive value was only moderately good, due to false positive cases (i.e., those reporting hypertension but showing normal levels of blood pressure and not taking antihypertensive medication). The most likely explanation for these false positives is that the approach we used for the comparison (two measurements of blood pressure in the same day) is probably not good enough for a true "gold standard." Thus, our false positives are very likely those participants previously diagnosed with hypertension who had since undergone lifestyle changes that restored their blood pressure values to within normal limits. Interestingly, self-reported hypertension has been shown to result in enough accuracy in other epidemiological studies (12,13,22,23). We can assume that the same, if not better, validity can be applied to our population, given the higher educational level of our participants. Nevertheless, it could be probable that some degree of misclassification was associated with the exposure of interest, introducing an information bias. If olive oil consumption were associated with a lower awareness of hypertension, the observed beneficial relationship would be spurious. However, it has been previously reported that individuals in the SUN study following a Mediterranean diet, and therefore having higher olive oil consumption, had an overall healthier lifestyle and were more health-conscious (24). This fact suggests that the bias would go, in any case, in the opposite direction; that is, those with higher olive oil consumption would be more

aware of hypertension; thus the incidence of hypertension would be higher among them. This is contrary to our findings.

Finally, another potential problem is that dietary fat has a relatively quick turnover, and membranes and other cellular constituents might easily be affected after only a few weeks of feeding a diet different in FA composition (25). A short-term reduction in olive oil consumption is most likely to occur among people with a high baseline consumption of olive oil, because of regression to the mean. But that was not the case in our database, because a decrease in olive oil consumption was more likely (2.4%) among participants in the first quintile of baseline consumption than among those in the fourth and fifth quintiles (1.0 and 1.5%, respectively).

In conclusion, olive oil consumption seems to be associated with the incidence of hypertension among the highly educated males of our cohort, but we did not observe this association among women. With a longer follow-up period, it will be possible to confirm and strengthen the findings of this analysis. Olive oil appears to be a healthy food and a preferable substitute for other fats used for cooking.

ACKNOWLEDGMENTS

We are indebted to the participants of the SUN study for their continued participation and cooperation. This work has been funded by the Department of Health of the Navarra Regional Government and by the Spanish Ministry of Health (Fondo de Investigaciones Sanitarias, projects 01/0619, 03/0678, and G03/140, Red Tematica de Dieta y Enfermedad Cardiovascular). We would like to thank the other members of the SUN Study Group: J. de Irala, M. Seguí-Gómez, M. Bes-Rastrollo, R. Pajares, C. de la Fuente, M. Hernández, C. Rubio, A. Sánchez-Villegas, F. Guillén-Grima, J.A. Martínez, and A. Martí.

REFERENCES

1. Trichopoulou, A., Costacou, T., Barnia, C., and Trichopoulos, D. (2003) Adherence to a Mediterranean Diet and Survival in a Greek Population, *N. Engl. J. Med. 348*, 2599–2608.
2. Martínez-González, M.A., Fernández-Jarne, E., Serrano-Martínez, M., Martí, A., Martínez, J.A., and Martín-Moreno, J.M. (2002) Mediterranean Diet and Reduction in the Risk of a First Acute Myocardial Infarction: An Operational Healthy Dietary Score, *Eur. J. Nutr. 41*, 153–160.
3. Appel, L.J., Moore, T.J., Obarzanek, E., Vollmer, W.M., Svetkey, L.P., Sacks, F.M., Bray, G.A., Vogt, T.M., Cutler, J.A., Windhauser, M.M., Lin, P.H., and Karanja, N. (1997) A Clinical Trial of the Effects of Dietary Patterns on Blood Pressure, *N. Engl. J. Med. 336*, 1117–1124.
4. Alonso, A., de la Fuente, C., Martín-Arnau, A.M., de Irala, J., Martínez, J.A., and Martínez-González, M.A. (2004) Fruit and Vegetable Consumption Is Inversely Associated with Blood Pressure in a Mediterranean Population with a High Vegetable-Fat Intake: The Seguimiento Universidad de Navarra (SUN) Study, *Br. J. Nutr. 92*, 311–319.
5. Salas, J., López Miranda, J., Jansen, S., Zambrana, J.L., Castro, P., Paniagua, J.A., Blanco, A., López Segura, F., Jiménez Perepérez, J.A., Pérez-Jiménez, F., and Perepérez, J.A. (1999) La Dieta Rica en Grasa Monoinsaturada Modifica de Forma Beneficiosa el Metabolismo de los Hidratos de Carbono y la Presión arterial, *Med. Clin. (Barc.) 113*, 765–769.
6. Lahoz, C., Alonso, R., Porres, A., and Mata, P. (1999) Las Dietas Enriquecidas en Ácidos Grasos Monoinsaturados y Ácidos Grasos Poliinsaturados Omega 3 Disminuyen la Presión Arterial, sin Modificar la Concentración de Insulina Plasmática en Sujetos Sanos, *Med. Clin. (Barc.) 112*, 133–137.
7. Ruiz-Gutiérrez, V., Muriana, F.J., Guerrero, A., Cert, A.M., and Villar, J. (1996) Plasma Lipids, Erythrocyte Membrane Lipids and Blood Pressure of Hypertensive Women After Ingestion of Dietary Oleic Acid from Two Different Sources, *J. Hypertens. 14*, 1483–1490.
8. Ferrara, L.A., Raimondi, A.S., d'Episcopo, L., Guida, L., Dello Russo, A., and Marotta, T. (2000) Olive Oil and Reduced Need for Antihypertensive Medications, *Arch. Intern. Med. 160*, 837–842.
9. Martínez-González, M.A., Sánchez-Villegas, A., de Irala-Estévez, J., Martí, A., and Martínez, J.A. (2002) Mediterranean Diet and Stroke: Objectives and Design of the SUN Project, *Nutr. Neurosci. 5*, 65–73.
10. Martín-Moreno, J.M., Boyle, P., Gorgojo, L., Maisonneuve, P., Fernández-Rodríguez, J.C., Salvini, S., and Willett, W.C. (1993) Development and Validation of a Food Frequency Questionnaire in Spain, *Int. J. Epidemiol. 22*, 512–519.
11. Mataix Verdú, J. (2003) *Tabla de Composición de Alimentos Españoles*, 4th edn., Universidad de Granada, Granada, Spain.
12. Colditz, G.A., Martin, P., Stampfer, M.J., Willett, W.C., Sampson, L., Rosner, B., Hennekens, C.H., and Speizer, F.E. (1986) Validation of Questionnaire Information on Risk Factors and Disease Outcomes in a Prospective Cohort Study of Women, *Am. J. Epidemiol. 123*, 894–900.
13. Tormo, M.J., Navarro, C., Chirlaque, M.D., and Barber, X. (2000) Validation of Self Diagnosis of High Blood Pressure in a Sample of the Spanish EPIC Cohort: Overall Agreement and Predictive Values, *J. Epidemiol. Community Health 54*, 221–226.
14. Willett, W.C. (1998) *Nutritional Epidemiology*, 2nd edn., Oxford University Press, New York.
15. Fernández-Jarne, E., Martínez-Losa, E., Prado-Santamaría, M., Brugarolas-Brufau, C., Serrano-Martínez, M., and Martínez-González, M.A. (2002) Risk of First Non-fatal Myocardial Infarction Negatively Associated with Olive Oil Consumption: A Case–Control Study in Spain, *Int. J. Epidemiol. 31*, 474–480.
16. Barzi, F., Woodward, M., Marfisi, R.M., Tavazzi, L., Valagussa, F., and Marchioli, R. (2003) Mediterranean Diet and All-Causes Mortality After Myocardial Infarction: Results from the GISSI-Prevenzione Trial, *Eur. J. Clin. Nutr. 57*, 604–611.
17. Espino, A., López Miranda, J., Castro, P., Rodríguez, M., López Segura, F., and Blanco, A. (1996) Monounsaturated Fatty Acid Enriched Diets Lower Plasma Insulin Levels and Blood Pressure in Healthy Young Men, *Nutr. Metab. Cardiovasc. Dis. 6*, 147–152.
18. Esposito, K., Nappo, F., Giugliano, F., Giugliano, G., Marfella, R., and Giugliano, D. (2003) Effect of Dietary Antioxidants on Postprandial Endothelial Dysfunction Induced by a High-Fat Meal in Healthy Subjects, *Am. J. Clin. Nutr. 77*, 139–143.
19. Czernichow, S., Blacher, J., and Hercberg, S. (2004) Antioxidant Vitamins and Blood Pressure, *Curr. Hypertens. Rep. 6*, 27–30.
20. Soriguer, F., Rojo-Martínez, G., Dobarganes, M.C., García Almeida, J.M., Esteva, I., Beltrán, M., Ruiz de Adana, M.S., Tinahones, F., Gómez-Zumaquero, J.M., García-Fuentes, E., and González-Romero, S. (2003) Hypertension Is Related to the Degradation of Dietary Frying Oils, *Am. J. Clin. Nutr. 78*, 1092–1097.
21. Alemany, R., Terés, S., Baamonde, C., Benet, M., Vögler, O., and Escribá, P.V. (2004) 2-Hydroxyoleic Acid. A New Hypotensive Molecule, *Hypertension 43*, 249–254.
22. Martin, L.M., Leff, M., Calonge, N., Garrett, C., and Nelson, D.E. (2000) Validation of Self-Reported Chronic Conditions

and Health Services in a Managed Care Population, *Am. J. Prev. Med. 18*, 215–218.
23. Vargas, C.M., Burt, V.L., Gillum, R.F., and Pamuk, E.R. (1997) Validity of Self-Reported Hypertension in the National Health and Nutrition Examination Survey III, 1988–1991, *Prev. Med. 26*, 678–685.
24. Sánchez-Villegas, A., Delgado-Rodríguez, M., Martínez-González, M.A., and de Irala-Estévez, J. (2003) Gender, Age, Socio-demographic and Lifestyle Factors Associated with Major Dietary Patterns in the Spanish Project SUN (Seguimiento Universidad de Navarra), *Eur. J. Clin. Nutr. 57*, 285–292.
25. Vicario, I.M., Malkova, D., Lund, E.K., and Johnson, I.T. (1998) Olive Oil Supplementation in Healthy Adults: Effect on Cell Membrane Fatty Acid Composition and Platelet Function, *Ann. Nutr. Metab. 42*, 160–169.

[Received August 6, 2004; accepted October 20, 2004]

Hypochlorous Acid Scavenging Properties of Local Mediterranean Plant Foods

Sebastian Schaffer[a], Gunter P. Eckert[a], Walter E. Müller[a], Rafael Llorach[b], Diego Rivera[b], Simona Grande[c], Claudio Galli[c], and Francesco Visioli[c,*]

[a]Institute of Pharmacology (ZAFES), Biocenter Niederursel, University of Frankfurt, Frankfurt am Main, Germany; [b]Departamento de Biología Vegetal, University of Murcia, Spain; and [c]Department of Pharmacological Sciences, University of Milan, Italy

ABSTRACT: Oxidative modification of low density lipoprotein (LDL) is involved in the pathogenesis of atherosclerosis and coronary heart disease, which are low in the Mediterranean area possibly due to a high dietary proportion of plant foods. Ethanolic extracts were prepared from more than 120 Mediterranean edible plants collected in remote areas (which maintain their traditional diet) and their antioxidant potential was studied. Extracts derived from *Agaricus campestris*, *Cynara cardunculus*, *Thymus pulegioides*, and *Vicia faba* were subjected to further analysis in this study. The extracts' potential to scavenge the DPPH radical (2,2-diphenyl-1-picrylhydrazyl radical) and hypochlorous acid (HOCl), as well as their antioxidant capacity, was comparable to the those obtained for standard antioxidants (e.g., quercetin, Trolox). Myeloperoxidase (MPO) catalyzes the production of the highly chlorinating and oxidizing agent HOCl, which reacts with the LDL apoprotein moiety, leading to the derivatization of its aminoacidic residues. Coincubation with extracts significantly prevented HOCl-induced modification of the LDL residue tryptophan, whereas higher concentrations were required to retard lysine damage. Moreover, the extracts inhibited MPO-catalyzed guaiacol oxidation in a concentration-dependent manner in a cell-free assay but, in contrast, did not affect MPO activity in isolated human neutrophils. MPO is also known to facilitate nitric dioxide oxidation. The formation of 3-nitrotyrosine was significantly lower in bovine endothelial aortic cells incubated with *C. cardunculus* or *T. pulegioides*. In synthesis, our study shows that local Mediterranean plant foods prevent HOCl toxicity *in vitro* and, thus, suggests further mechanisms responsible for the reported health-beneficial effect of the Mediterranean diet.

Paper no. L9584 in *Lipids 39*, 1239–1247 (December 2004).

Oxidative modification of low density lipoprotein (LDL) plays a role in atherogenesis and, consequently, in coronary heart disease (CHD) mortality (1). Reactive oxygen and nitrogen species (ROS and RNS) have been hypothesized to be the main cause of LDL oxidation. Accordingly, a series of clinical trials have been undertaken to evaluate the effects of vitamin E, a lipid-soluble antioxidant, on CHD mortality. However, the majority of such trials failed to demonstrate any protective effect of vitamin E supplementation, in part questioning the true contribution of lipid peroxidation to the formation of atherosclerotic plaques (2,3). The enzyme myeloperoxidase (MPO; EC 1.11.1.7) catalyzes the formation of the chlorinating and oxidizing agent hypochlorous acid (HOCl) from hydrogen peroxide and chloride ions (4). This enzyme is activated, mostly in leukocytes, by inflammatory stimuli, which are known to strongly contribute to atherogenesis (5). Unlike "classic" reactions of lipid peroxidation, for example, those that are metal-dependent, HOCl reacts directly with the apoprotein moiety, derivatizing its aminoacidic residues (6). In addition, HOCl avidly reacts with other macromolecules such as thiols and nucleotides, enhancing tissue damage during inflammation, when HOCl concentrations can reach the high micromolar to low millimolar range (7). As vitamin E is unable to prevent HOCl-mediated lipoprotein modification (8), other antioxidants such as vitamin C and polyphenols are to be tested for their potential antiatherosclerotic effects, especially if MPO and HOCl are involved in atherogenesis and endothelial dysfunction, as indeed suggested by many investigators (9,10).

The incidence of atherosclerosis and CHD is low in the Mediterranean area, where plant foods contribute the majority of caloric intake (11). Vegetables, fruits, legumes, wine, and extra virgin olive oil, in particular, provide antioxidants both vitaminic and nonvitaminic in nature, which have been proposed to exert antiatherosclerotic and cardioprotective effects (12).

Within the EU-funded project "Local Food-Nutraceuticals" (www.biozentrum.uni-frankfurt.de/Pharmakologie/EU-Web/index.html) (13), local wild plant foods of the Mediterranean basin, namely Southern Spain and Southern Italy, were selected and tested for their *in vitro* ability to scavenge HOCl and, consequently, their potential protective role toward CHD and other degenerative and inflammatory diseases. Table 1 summarizes some of the characteristics of the plants used in this study.

*To whom correspondence should be addressed at Department of Pharmacological Sciences, University of Milan, Via Balzaretti 9, 20133 Milan, Italy. E-mail: francesco.visioli@unimi.it

Abbreviations: apoB, apdiprotein B, BAEC, bovine aortic endothelial cell; BHT, butylated hydroxytoluene; CHD, coronary heart disease; DPPH, 2,2-diphenyl-1-picrylhydrazyl radical; HOCl, hypochlorous acid; LDL, low density lipoprotein; MPO, myeloperoxidase; OxyHb, oxyhemoglobin; PBS, phosphate buffer saline; PMNL, polymorphonuclear leukocytes; REM, relative electrophoretic mobility; RNS, reactive nitrogen species; ROS, reactive oxygen species; SDS, sodium dodecyl sulfate.

TABLE 1
Parts of the Local Mediterranean Plant Foods Used in this Study and Polyphenol Content of Plant Extracts

Plant name	Abbreviation	Parts used for extraction	Polyphenol content (mg/g)
Agaricus campestris	*Agaricus c.*	Sporocarp	10.2
Cynara cardunculus	*Cynara c.*	Leaves	448.8
Thymus pulegioides	*Thymus p.*	Aerial parts	435.1
Vicia faba	*Vicia f.*	Young fruits	76.3

MATERIALS AND METHODS

Materials. Bovine aortic endothelial cells (BAEC) were purchased from Cambrex (Milan, Italy). The reagents for Western blot analysis were from Bio-Rad Laboratories (Hercules, CA) and the enhanced chemiluminescence (ECL) kit for Western blot analysis was from Amersham Biosciences (Milan, Italy). Mouse monoclonal anti-3-nitrotyrosine antibody was purchased from Calbiochem (Darmstadt, Germany); the secondary goat anti-mouse horseradish peroxidase-conjugate antibody was obtained from Bio-Rad (Hercules, CA); and the secondary fluorescent antibody, Alexa 594-conjugated goat anti-mouse antibody, was purchased from Molecular Probes (Eugene, OR). A dialysis membrane (20 × 32 mm) was purchased from MAGV (Rabenau-Londorf, Germany). Myeloperoxidase was obtained from Calbiochem (Darmstadt, Germany), Sephadex G-25 from Amersham Biosciences (Uppsala, Sweden), and hemoglobin from ICN (Eschwege, Germany). All other reagents were of the highest purity available and were purchased from Sigma Chemical (Milan, Italy, and Munich, Germany) or Merck (Darmstadt, Germany).

Plant samples were collected in Southern Italy (Castelmezzano) and Southern Spain (Rio Segura Valley, Murcia). Samples provided by the groups of Drs. Diego Rivera (Universidad de Murcia, Spain) and Michael Heinrich (The School of Pharmacy, University of London, UK) were dried and extracted with 90% hot ethanol under reflux. The extraction and characterization procedure will be fully reported elsewhere by those groups. The total polyphenolic content of the extracts was determined by the Folin-Ciocalteau method, using gallic acid as the reference compound (14).

DPPH scavenging test. A 15 μM ethanolic solution of 2,2-diphenyl-1-picrylhydrazyl radical (DPPH) was added to the compounds under investigation. After 15 min of incubation, the absorbance was read at 517 nm. EC_{50} was calculated by employing MacAllfit® as the software (15).

Total antioxidant potential. A validated assay (Bioxytech® AOP-490™; OXIS Research, Portland, OR) based upon the reduction of Cu^{2+} to Cu^{+} by antioxidants was employed (16,17). The results are shown as micromoles of Cu^{2+} reduced.

Oxyhemoglobin bleaching assay. Hemoglobin was reduced and oxygen-loaded according to manufacturer's instructions, with slight modifications. Briefly, a Sephadex G-25 column was equilibrated with phosphate buffer saline (PBS; 20 mM; pH 7.0) containing EDTA (1 mM). Sodium dithionite (200 mg) was added to the column and drained into the gel by adding 2 mL of PBS. After dissolving 100 mg of hemoglobin in 10 mL of PBS, the hemoglobin solution was applied to the column and eluted. The reduced hemoglobin was saturated with oxygen and dialyzed against oxygen-saturated PBS without EDTA to eliminate excess dithionite and to achieve complete conversion to oxyhemoglobin. Oxyhemoglobin (OxyHb) was stored at –20°C. Concentration of HOCl was determined at 292 nm, using a molar extinction coefficient of 142 (18).

Samples and OxyHb (10 μL) were added to 24- or 96-well plates and the bleaching reaction was started by adding a bolus of HOCl (400 μM). Change in absorbance was recorded at 405 nm by using a Wallac Victor^2 1420 Multilabel Counter (Perkin-Elmer, Rodgau-Jügesheim, Germany).

Isolation of LDL. Peripheral blood was drawn in evacuated tubes from healthy volunteers and LDL was isolated from plasma by sequential ultracentrifugation.

Total protein was estimated by the Lowry method (19), with bovine serum albumin as the standard. For all experiments, LDL was diluted to a concentration of 0.5 mg of protein/mL in PBS 10 mM.

Quantification of HOCl-mediated amino acid modifications. Freshly isolated LDL diluted in PBS (0.5 mg/mL; pH: 7.4) was incubated with or without the compounds under investigation at 37°C and exposed to 100 μM HOCl.

Tryptophan residues were evaluated directly by fluorescence (E_x 280 nm; E_m 335 nm). Lysine residues were also determined by fluorescence (E_x 390 nm; E_m 475 nm) after the addition of 163 μM fluorescamine (20).

Changes in relative electrophoretic mobility (REM) of LDL were determined by agarose-gel electrophoresis. LDL (100 μg) were loaded onto the gel, which was resolved at 50 V for 1.5 h. The bands were stained with Sudan Black.

Inhibition of MPO-catalyzed guaiacol oxidation. Lyophilized human MPO was reconstituted according to manufacturer's recommendation and aliquots were stored at –20°C. Compounds, guaiacol (5 mM in 20 mM phosphate buffer, pH 7.0), and MPO (0.2 μg/mL) were added to 24- or 96-well plates, and the reaction was initiated by addition of H_2O_2 (200 μM). Absorbance was read over time at 485 nm using a Wallac Victor^2 1420 Multilabel Counter (PerkinElmer, Germany).

MPO activity in human neutrophils. Human polymorphonuclear leukocytes (PMNL) were obtained from blood drawn from healthy donors using evacuated tubes with ACD (41 mM citric acid • H_2O, 100 mM sodium citrate • $2H_2O$, 136 mM glucose) as the anticoagulant. PMNL were separated by centrifugation on Ficoll cushions (density 1.077 g/mL), as described

by Sala *et al.* (21). This preparation contains more than 95% PMNL, based on the differential count of May-Grunwald/Giemsa-stained cytocentrifugates.

Aliquots of 2×10^6 cells, resuspended in 1 mL of PBS, were incubated with the individual compounds for 30 min. Cells were pelleted by centrifugation, resuspended in 700 μL of PBS with 0.5% hexadecyltrimethyl ammonium bromide, and sonicated on ice for 15 s. Following a further centrifugation to remove cellular debris, MPO activity was measured according to Kuebler *et al.* (22).

Western blot analysis. Confluent bovine aortic endothelial cells (BAEC; passage 4–8) grown in 22-mm wells were incubated with the compounds under investigation for 1 h. Following removal of the compounds, BAEC were incubated with hydrogen peroxide (50 μM) for 1 h. The reactions were stopped with cool PBS, cells were trypsinized until completely detached and centrifuged at 4°C for 18 min at 13,000 rpm. Pellets were resuspended in lysis buffer containing protease inhibitors, and supernatants were recovered and processed for Western blot analysis of 3-nitrotyrosine.

Total protein was estimated by using the Lowry method, with bovine serum albumin as a standard. Based on this, 100 μg of protein was dissolved in sodium dodecyl sulfate (SDS)-sample buffer (62.5 mM Tris-HCl, pH 6.8, containing 5% 2-mercaptoethanol, 2% SDS, 10% glycerol, and 0.01% bromophenol blue), separated by SDS-polyacrylamide gel electrophesis, and transferred onto a nitrocellulose membrane, which was blocked overnight with 5% dry milk in 100 mM Tris-buffered saline containing 0.1% Tween 20. The membrane was incubated with anti-nitrotyrosine antibody (1:1000) for 3 h at room temperature. Horseradish peroxidase-conjugated anti-mouse IgG (1:2500) was added for 1 h, followed by detection of the bands by enhanced chemiluminescence. Images were captured on a Nikon Eclipse TE2000-5 microscope equipped with Laser Scanning System Radiance 2100.

Immunocytochemistry. After incubation with the compounds under investigation and stimulation with hydrogen peroxide (50 μM; 1 h), confluent BAEC were washed twice with 0.01 M PBS at 37°C. Cell monolayers were fixed in 4% paraformaldehyde and then were permeabilized using 0.1% Triton X-100 in PBS and blocked for 2 h in 10% goat serum in PBS. The cells were incubated with primary antibody monoclonal mouse anti-nitrotyrosine (1:200) for 2 h at room temperature in 10% goat serum in PBS. Alexa 594-conjugated goat-anti mouse was used as a secondary antibody (1:100) for 45 min at room temperature. Images were acquired on a Nikon Eclipse TE2000-5 microscope equipped with the Laser Scanning System Radiance 2100.

Statistics. Results are expressed as means ± SD. Statistical analyses were performed on a personal computer by using Statistica® software (StatSoft Inc., Tulsa, OK). Data were compared by using one-way analysis of variance for repeated measures. Differences were considered significant if $P < 0.05$.

RESULTS

DPPH scavenging. The DPPH test showed that the local Mediterranean plant food extracts scavenge this stable radical with a potency similar to that of established antioxidants such as ascorbic acid and hydroxytyrosol, that is, EC_{50} values were in the range of 10^{-6} to 10^{-7} M. Moreover, their DPPH-scavenging activity was, by at least two orders of magnitude, higher than that of butylated hydroxytoluene (BHT) (Table 2).

TABLE 2
DPPH Scavenging Activity of Local Mediterranean Plant Food Extracts and Standard Antioxidants[a]

Compound	EC_{50}
Agaricus c.	6.50×10^{-6} M
Cynara c.	8.40×10^{-7} M
Thymus p.	3.20×10^{-7} M
Vicia f.	1.30×10^{-6} M
Ascorbic acid	1.31×10^{-5} M
Trolox	5.04×10^{-6} M
BHT	1.05×10^{-4} M
Hydroxytyrosol	2.60×10^{-7} M
Oleuropein	3.63×10^{-5} M

[a]Data for the local Mediterranean plant food extracts are expressed as moles of gallic acid equivalents. DPPH, 2,2-diphenyl-1-picryl-hydrazyl radical.

Total antioxidant capacity. The total antioxidant capacity of the extracts, evaluated as their ability to reduce Cu^{++} to Cu^{+}, is summarized in Table 3. The extracts exhibited antioxidant capacities that were similar to those of reference antioxidants, for example, vitamin C and quercetin.

Oxyhemoglobin bleaching. Figure 1 shows the HOCl scavenging activity of the extracts. At an extract concentration of 10^{-5} M, between 25 and 50% of HOCl is scavenged. The antioxidant potency declines in the order *Vicia f.* > *Thymus p.* > *Cynara c.* > *Agaricus c.* and the observed activities are in the same range as those obtained with the reference antioxidant Trolox. HOCl scavenging activity for quercetin at a concentration of up to 2×10^{-7} M was below 10% (data not shown). Higher concentrations interfered with the assay due to the precipitation of quercetin.

Amino acid modifications. Aminoacidic residues of apolipoprotein B (apoB) are susceptible to oxidation by HOCl, which leads to their uncontrolled uptake by macrophages. As shown in Figure 2, addition of HOCl to LDL samples caused the modification of apoB, in particular a loss of tryptophan (panel A) and lysine (panel B). Coincubation with local Mediterranean plant food extracts strongly protected LDL against the loss of tryptophan residues and partly—at higher concentrations—protected against the loss of lysine. These data compare with those of Carr *et al.* (23), who also reported differential aminoacidic protection by ascorbic acid.

Prevention of the HOCl-induced increase in REM (Fig. 3) was noted for *Cynara c.*, *Agaricus c.*, and resveratrol at 10^{-5} M, whereas *Cynara c.*, *Thymus p.*, lipoic acid, and resveratrol were effective at the concentration of 10^{-6} M.

Inhibition of guaiacol oxidation. The extracts inhibited guaiacol oxidation in a concentration-dependent manner (Fig. 4). In accordance with the data obtained in the DPPH assay, extract activity declines in the order *Thymus p.* ($EC_{50} = 9.66 \times 10^{-7}$ M) >

TABLE 3
Antioxidant Capacity (μM Cu^{2+} Reduced)[a]

Compound	10^{-7} M	10^{-6} M	5×10^{-6} M	10^{-5} M	5×10^{-5} M
Agaricus c.	119.36 ± 19.4	133.55 ± 1.3	192.28 ± 4.8	265.2 ± 2.2	231.68 ± 2.3
Cynara c.	109.76 ± 4.8	219.94 ± 5.3	283.13 ± 1.2	207.05 ± 8.4	217.37 ± 6.7
Thymus p.	248.31 ± 2.3	288.28 ± 7.5	267.65 ± 9.9	250.89 ± 12.7	218.07 ± 1.3
Vicia f.	188.41 ± 7.01	198.02 ± 1.66	252.31 ± 20.8	254.75 ± 3.01	231.54 ± 7.42
Ascorbic acid	136.84 ± 3.52	179.39 ± 1.4	161.34 ± 1.44	274.24 ± 2.44	280.68 ± 0.44
Trolox	134.84 ± 16.2	118.79 ± 12.2	155.47 ± 5.4	388.86 ± 5.32	288.97 ± 2.66
Quercetin	142.58 ± 2.83	165.79 ± 6.92	175.0 ± 0.42	476.55 ± 14.9	494.6 ± 13.3

[a]Data are means ± SD. Concentrations of local Mediterranean plant food extracts are expressed as moles of gallic acid equivalents.

Cynara c. ($EC_{50} = 1.30 \times 10^{-6}$ M) > *Vicia f.* ($EC_{50} = 1.98 \times 10^{-6}$ M) > *Agaricus c.* ($EC_{50} = 2.73 \times 10^{-6}$ M). The values for a 50% inhibition are of the same order of magnitude as those obtained for the standard antioxidant Trolox (1.20×10^{-6} M); quercetin, however, was the most potent agent (6.9×10^{-8} M) that prevented the MPO-catalyzed oxidation of guaiacol.

MPO activity in neutrophils. When the activity of MPO was assessed in neutrophils (Fig. 5), no inhibitory effect of the extracts was noted, as opposed to reference antioxidants such as quercetin, Trolox, and highly concentrated ascorbic acid (500 μM).

3-Nitrotyrosine formation. As activation of MPO has the potential to increase NO_2^- oxidation (24), 3-nitrotyrosine formation and its inhibition by selected extracts were investigated by Western blot analysis and by immunocytochemistry. As shown in Figure 6A, a significant reduction in 3-nitrotyrosine levels was detected in sonicates of cells that have been incubated with the extracts under investigation and stimulated with hydrogen peroxide. Accordingly, BAEC immunostaining for 3-nitrotyrosine was remarkably lower in cell supplemented with *Cynara c.* or *Thymus p.* extracts (Fig. 6B).

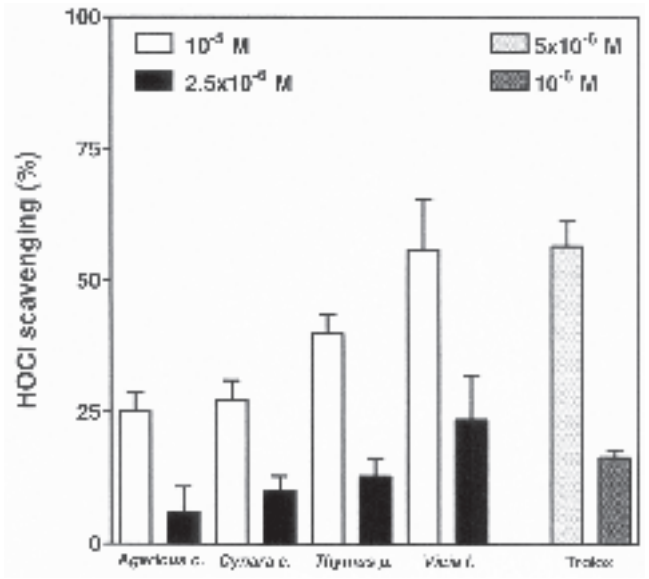

FIG. 1. HOCl scavenging activity (oxyhemoglobin bleaching test) of local Mediterranean plant food extracts in comparison with Trolox. Concentrations of the extracts are moles of gallic acid equivalents. Data are means ± SD.

DISCUSSION

We describe the preventive activities of selected local Mediterranean plant food extracts toward HOCl-mediated oxidation of LDL constituents. Even though the exact mechanisms for *in vivo* LDL oxidation are still elusive, a number of different cell types, for example, neutrophils, macrophages, monocytes, and endothelial cells, participate in this process and have the potential to release HOCl, especially during inflammatory episodes. Downstream, chlorine-modified LDL act as chemoattractants for blood cells and not only stimulate their adhesion to the endothelium but also trigger the formation of foam cells. Both events take place at the early stages of atherosclerosis (25)

Pathogens and inflammation stimulate neutrophils and macrophages to produce HOCl catalyzed by MPO, as follows (26):

$$H_2O_2 + Cl^- + H^+ \rightarrow HOCl + H_2O \quad [1]$$

Either an amplified activity of MPO or an overproduction of HOCl are highly cytotoxic, as they modify a wide variety of biological compounds by reacting with oxidizable groups. MPO and HOCl have been reported to not only modify LDL but also to hamper the physiological function of apoE, membrane cholesterol, high density lipoprotein, and the extracellular matrix (27–30). Moreover, oxidized LDL activate immune cells and contribute to the secretion of ROS, MPO, and HOCl into the extracellular medium, thus further exacerbating oxidative modification of LDL (25).

Antioxidants such as ascorbic acid and polyphenols effectively remove ROS by a direct scavenging process (31) or through the modulation of other defense mechanisms such as interactions with the antioxidant response element (32). Both vitamins and high amounts of other antioxidants, most of which are phenolic in nature, are found in foods of plant origin (33). This has been proposed as a potential explanation of the epidemiological data that show cardioprotective effects of the Mediterranean diet, which is characterized by a high intake of

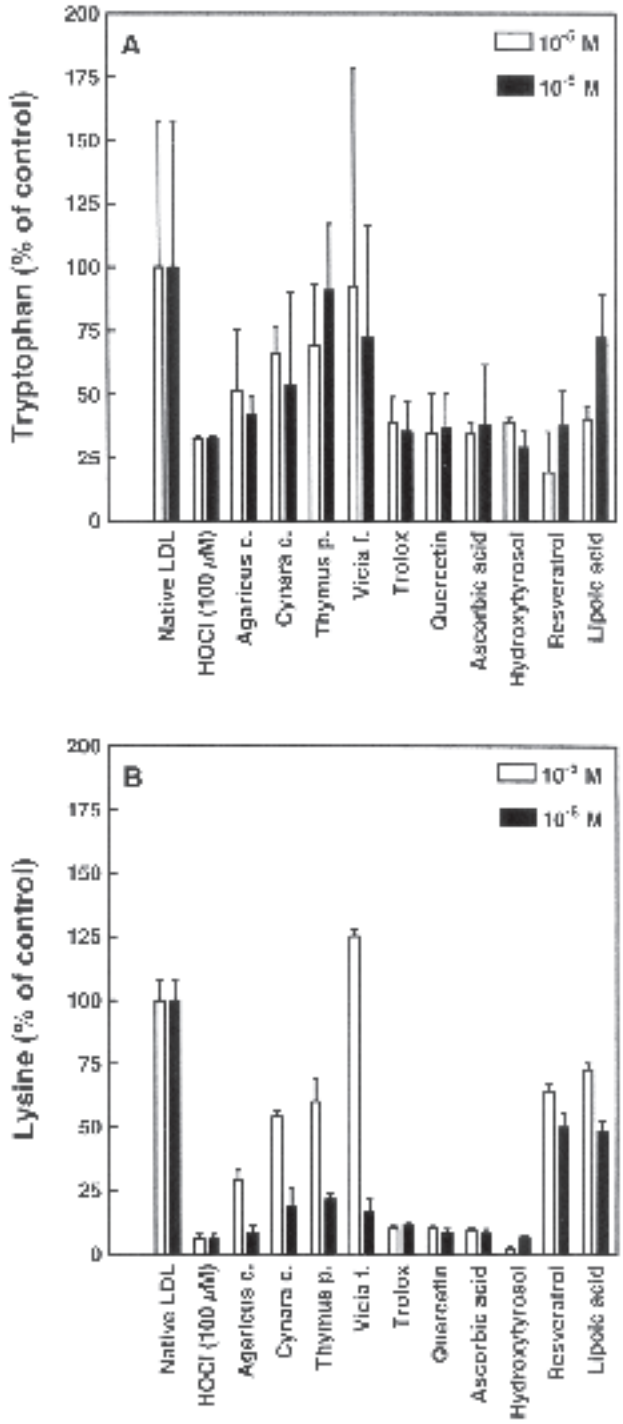

FIG. 2. Tryptophan (A) and lysine (B) loss after incubation of human low density lipoprotein (LDL) samples with hypochlorous acid (HOCl), in the presence or absence of local Mediterranean plant food extracts and standard antioxidants. Concentrations of the extracts are moles of gallic acid equivalents. Data are means ± SD.

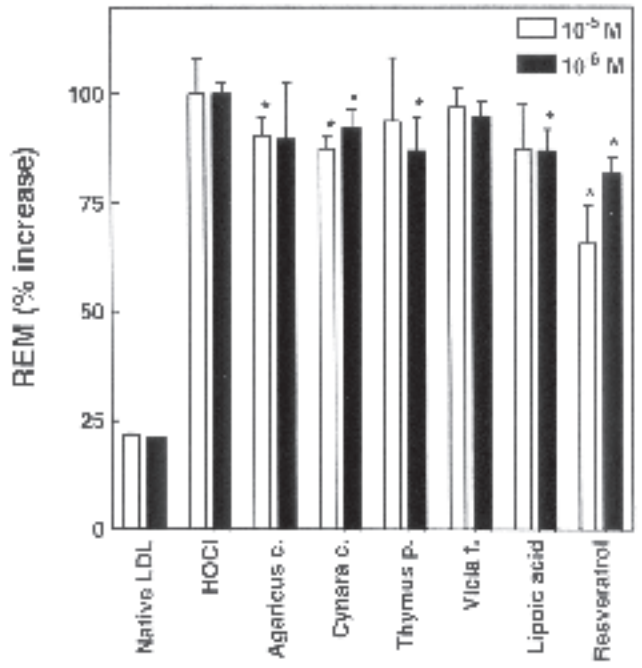

FIG. 3. Effect of local Mediterranean plant food extracts on hypochlorous acid (HOCl)-induced changes in relative electrophoretic mobility (REM) of human low density lipoprotein (LDL) in comparison with standard antioxidants. Concentrations of the extracts are moles of gallic acid equivalents. Data are means ± SD. *$P < 0.05$ vs. LDL oxidized with 100 μM HOCl.

vegetables and fruits (11,34). Pertinent to our study, a vitamin C-free, polyphenol-rich extract from *Rosa canina* shows high HOCl scavenging activity in cell-free and cell-based systems (35).

The direct *in vitro* DPPH and HOCl scavenging activities and the total antioxidant potential of *Agaricus campestris*, *Cynara cardunculus*, *Thymus pulegioides*, and *Vicia faba* extracts showed a moderate to high antioxidant power in all tests, though in variant order. Published data for comparison, however, are scarce for most extracts. Valentao *et al.* (36) reported that a lyophilized infusion of *Cynara cardunculus*, at a concentration of 0.25 mg/mL, scavenged HOCl less than 5%. Surprisingly, no concentration-dependent effect on the prevention of HOCl-mediated TNB to DTNB (5-thio-2nitrobenzoic acid to 5,5′-dithiobis[2-nitrobenzoic acid]) conversion was found in the range of 0–1 mg of extract/mL. These latter findings are in contrast with our observations. The superoxide radical- and hydroxyl radical-scavenging activity, however, was shown to be concentration-dependent and in agreement with our data. Likewise, extracts from a different artichoke source, *Cynara scolymus*, potently removed the DPPH and 2.2′-azinobis(3-ethylbenzthiazoline-6-sulfonic acid) radicals (37,38). In another study, LDL oxidation was inhibited by various oils obtained from different thyme species. Among such oils, that of wild thyme displayed the highest activity toward LDL oxidation. Furthermore, it has been demonstrated that thymol and carvacrol effectively prevented lipid peroxidation, whereas rather high concentrations of the two compounds were required to significantly scavenge DPPH (39). From the aerial parts of different thyme species, polyphenols such as apigenin, naringenin, and luteolin have been identified (40), and this also applies to

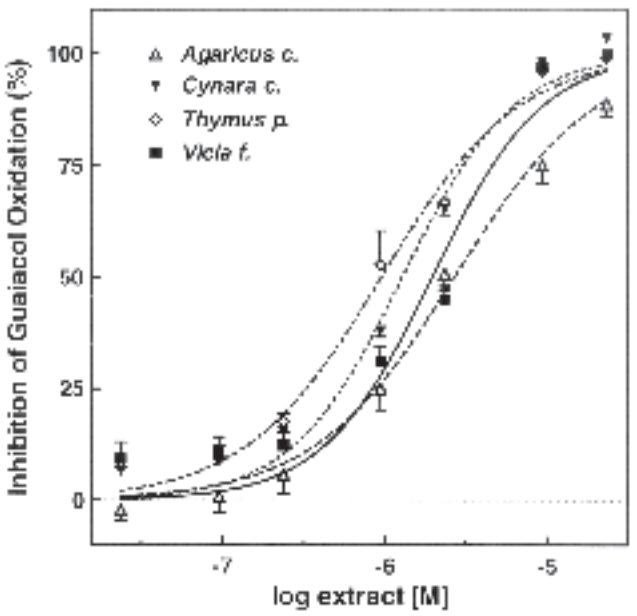

FIG. 4. Concentration-dependent inhibition of myeloperoxidase-catalyzed guaiacol oxidation in the presence of local Mediterranean plant food extracts. Concentrations of the extracts are moles of gallic acid equivalents. Methodological details are given in the Materials and Methods section. Data are means ± SD.

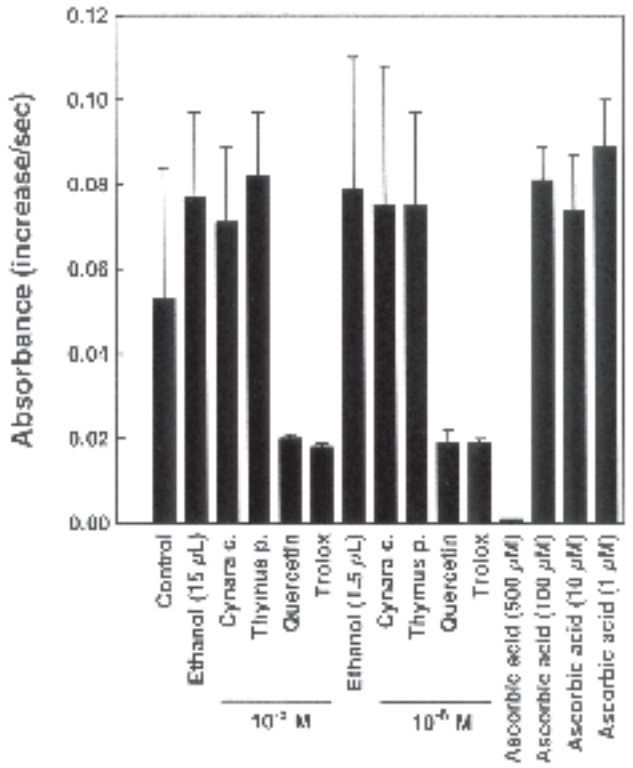

FIG. 5. Effect of local Mediterranean plant food extracts on myeloperoxidase activity of isolated human neutrophils in comparison to standard antioxidants. Concentrations of the extracts are moles of gallic acid equivalents. Data are means ± SD.

our extract (13). Some of these compounds were shown to effectively scavenge a variety of radicals (41,42) and might thus contribute to the observed antioxidant effects of *Thymus pulegioides* in the present study. Similarly, polyphenolic proanthocyanidins, which are known to possess high antioxidant activity, were isolated from the colored seed coats of *Vicia faba* (43,44). Whereas phenolic compounds were found to be low in the *Agaricus* species, such mushrooms contain moderately high amounts of vitamins such as riboflavin, niacin, and folates (45). Folic acid is known to act as a free radical scavenger and can be chlorinated by HOCl. Hence, it has been speculated that folate might protect cells from oxidative damage at sites of inflammation (46).

The polyphenolic content of fresh plant foods or plant extracts has often been utilized as an indicator for their antioxidant power (47). The data obtained in the Cu^{2+}-reducing and HOCl-scavenging assays, however, indicate that the polyphenol content is not always an accurate predictor of an extract's antioxidant capacity. In our particular case, an ethanol-based extraction process has been used to obtain the plant extracts. During this procedure, not only molecules of interest, that is, lipid-soluble vitamins and polyphenols, but also a variety of other lipophilic compounds, for example, fatty acids, are extracted. The latter are known to participate in the scavenging of HOCl and the redox reaction of Cu^{2+} (48,49), thus providing one possible explanation for the observed mismatch between polyphenol content and antioxidant activity.

At the molecular level, and relevant to CHD, it is noteworthy that the major targets of the MPO/H_2O_2/Cl^- system are the proteic components of LDL (6). The modification of protein residues, such as methionine, tryptophan, or lysine, is a widely used marker for monitoring HOCl toxicity (6). Our own data show a severe loss of lysine and tryptophan after the addition of HOCl to LDL and are in accordance with previous reports (50, 51). All four extracts prevented HOCl-mediated protein modifications, as was also confirmed by the observed maintenance of relative electrophoretic mobility. In general, the extracts' beneficial effect surpasses that of the reference antioxidants, except for resveratrol and lipoic acid, with regard to lysine protection. The *Vicia fava* extract showed the highest amino acid protective activity despite a more than six-fold lower polyphenol content compared with *Cynara cardunculus* and *Thymus pulegioides* (449 and 435 mg/g of extract, respectively).

The importance of MPO in cardiovascular disease has been brought forward by several studies (10,52–55), even though its precise role in human pathology has not been elucidated. However, inhibition of MPO is being considered as a potential therapeutic approach to inhibit HOCl production and, subsequently, to prevent LDL oxidation (56). In our study, modulation of MPO activity has been the subject of two assays leading to contrasting results. Whereas the addition of all four plant extracts and antioxidants lead to a concentration-dependent inhibition of human MPO-catalyzed guaiacol oxidation, no significant effect on MPO activity of neutrophils was observed. Various reports described an inhibitory effect of polyphenols on MPO activity.

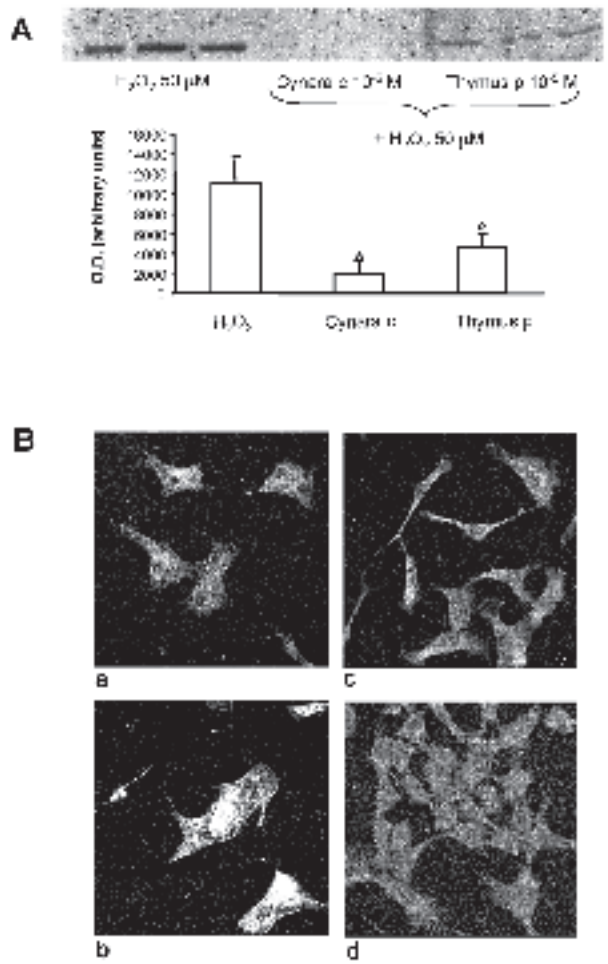

FIG. 6. Local Mediterranean plant food extracts reduce the formation of 3-nitrotyrosine by bovine aortic endothelial cell (BAEC) challenged with hydrogen peroxide. (A) Western blot analysis of cell homogenates, n = 3. (B) immunocytochemical analysis of BAEC control (a), incubated with H_2O_2 50 mL for 1 h (b), incubated with H_2O_2 and supplemented with *Cynara cardunculus* (c) or *Thymus pulegioides* (d) extracts 10^{-5} M.

Pincemail *et al.* (57) reported a concentration-dependent inhibitory effect of quercetin and rutin on purified human MPO and suggested a competitive inhibition mechanism for quercetin. Similarly, other flavonoids were identified as MPO substrates, thus leading to an inhibition of MPO/nitrite-mediated LDL oxidation (58). Also plant extracts, for example, prepared from *Hypericum perforatum* and *Rosa canina*, were found to effectively arrest MPO activity (35,59). Furthermore, Limasset *et al.* (60) described that most of 34 tested flavonoids and related compounds exhibited an inhibitory effect on the release of ROS by stimulated human neutrophils. Likewise, oleuropein and hydroxytyrosol have been reported to inhibit the respiratory burst of human neutrophils in a concentration-dependent manner (61). The lack of inhibition of MPO activity by challenged human neutrophils, as opposed to the inhibitory effects observed in the cell-free system, may be actually explained by the lack of cellular uptake of the extracts' phenolic constituents.

MPO can also utilize nitrite, the oxidation product of nitric oxide, as substrate to form RNS such as peroxynitrite or the nitrogen dioxide radical, both of which have been shown to nitrate proteins both *in vitro* and *in vivo* (24). Nitration of protein tyrosyl has been postulated to impair protein function (62). As *Cynara cardunculus* and *Thymus pulegioides* have been previously shown to increase NO release by aortic endothelial cells (13), the potential for increased 3-nitrotyrosine formation was investigated. However, Western blot and immunocytochemistry experiments in BAEC ruled out this possibility and, conversely, showed an inhibitory effect of *Cynara cardunculus* and *Thymus pulegioides* extracts toward the formation of 3-nitrotyrosine.

It is noteworthy that populations in the Mediterranean basin traditionally consume high amounts of wild greens, which strongly contribute to the overall high daily intake of foods of plant origin, a typical feature of the Mediterranean diet. The amount of polyphenols present in wild greens often exceeds that of food items such as red wine or black tea, which have been hypothesized to exert biological effects (63). In the past, wild greens have generally been considered minor dietary components. Yet, their possible contribution to the prevention of chronic diseases has been possibly overlooked and still needs to be elucidated.

In conclusion, these data showing HOCl-scavenging properties of some extracts from locally consumed wild plants increases our knowledge of the mechanism(s) by which Mediterranean diets exert their protective effects toward degenerative diseases.

ACKNOWLEDGMENTS

This project was funded by a grant from the European Commission (Local Food-Nutraceuticals, QLK-2001-00173). We thank the communities of Castelmezzano and Rio Segura Valley (Murcia) for their enthusiastic support.

REFERENCES

1. Witztum, J.L., and Steinberg, D. (2001) The Oxidative Modification Hypothesis of Atherosclerosis: Does It Hold for Humans? *Trends Cardiovasc. Med. 11,* 93–102.
2. Kritharides, L., and Stocker, R. (2002) The Use of Antioxidant Supplements in Coronary Heart Disease, *Atherosclerosis 164,* 211–219.
3. Vivekananthan, D.P., Penn, M.S., Sapp, S.K., Hsu, A., and Topol, E.J. (2003) Use of Antioxidant Vitamins for the Prevention of Cardiovascular Disease: Meta-analysis of Randomised Trials, *Lancet 361,* 2017–2023.
4. O'Brien, P.J. (2000) Peroxidases, *Chem. Biol. Interact. 129,* 113–139.
5. Kinlay, S., Libby, P., and Ganz, P. (2001) Endothelial Function and Coronary Artery Disease, *Curr. Opin. Lipidol. 12,* 383–389.
6. Carr, A., McCall, M.R., and Frei, B. (2000) Oxidation of LDL by Myeloperoxidase and Reactive Nitrogen Species, *Arterioscler. Thromb. Vasc. Biol. 20,* 1716–1723.
7. Aruoma, O.I., and Halliwell, B. (1987) Action of Hypochlorous Acid on the Antioxidant Protective Enzymes Superoxide Dismutase, Catalase and Glutathione Peroxidase, *Biochem. J. 248,* 973–976.

8. Hazell, L.J., and Stocker, R. (1997) Alpha-Tocopherol Does Not Inhibit Hypochlorite-Induced Oxidation of Apolipoprotein B-100 of Low-Density Lipoprotein, *FEBS Lett. 414,* 541–544.
9. Steinberg, D., and Witztum, J.L. (2002) Is the Oxidative Modification Hypothesis Relevant to Human Atherosclerosis? Do the Antioxidant Trials Conducted to Date Refute the Hypothesis? *Circulation 105,* 2107–2111.
10. Vita, J.A., Brennan, M.L., Gokce, N., Mann, S.A., Goormastic, M., Shishehbor, M.H., Penn, M.S., Keaney, J.F., Jr., and Hazen, S.L. (2004) Serum Myeloperoxidase Levels Independently Predict Endothelial Dysfunction in Humans, *Circulation 110,* 1134–1139.
11. Willett, W.C., Sacks, F., Trichopoulou, A., Drescher, G., Ferro-Luzzi, A., Helsing, E., and Trichopoulos, D. (1995) Mediterranean Diet Pyramid: A Cultural Model for Healthy Eating, *Am. J. Clin. Nutr. 61,* 1402S–1406S.
12. Kris-Etherton, P.M., Hecker, K.D., Bonanome, A., Coval, S.M., Binkoski, A.E., Hilpert, K.F., Griel, A.E., and Etherton, T.D. (2002) Bioactive Compounds in Foods: Their Role in the Prevention of Cardiovascular Disease and Cancer, *Am. J. Med. 113 (Suppl. 9B),* 71–88.
13. Grande, S., Bogani, P., de Saizieu, A., Schueler, G., Galli, C., and Visioli, F. (2004) Vasomodulating Potential of Mediterranean Wild Plant Extracts, *J. Agric. Food Chem. 52,* 5021–5026.
14. Visioli, F., Vincieri, F.F., and Galli, C. (1995) "Waste Waters" from Olive Oil Production Are Rich in Natural Antioxidants, *Experientia 51,* 32–34.
15. DeLean, A., Munson, P.J., and Rodbard, D. (1978) Simultaneous Analysis of Families of Sigmoidal Curves: Application to Bioassay, Radioligand Assay, and Physiological Dose-Response Curves, *Am. J. Physiol. 235,* E97–E102.
16. Visioli, F., Caruso, D., Plasmati, E., Patelli, R., Mulinacci, N., Romani, A., Galli, G., and Galli, C. (2001) Hydroxytyrosol, as a Component of Olive Mill Waste Water, Is Dose-Dependently Absorbed and Increases the Antioxidant Capacity of Rat Plasma, *Free Rad. Res. 34,* 301–305.
17. Visioli, F., Caruso, D., Grande, S., Bosisio, R., Villa, M., Galli, G., Sirtori, C.R., and Galli, C. (2004) Virgin Olive Oil Study (VOLOS): Vasoprotective Potential of Extra Virgin Olive Oil in Mildly Dyslipidemic Patients, *Eur. J. Nutr. May 6,* 1–7 (net link: http://springerlink.metapress.com, accessed December 13, 2004).
18. Cho, Y., Jang, Y.Y., Han, E.S., and Lee, C.S. (1999) The Inhibitory Effect of Ambroxol on Hypochlorous Acid-Induced Tissue Damage and Respiratory Burst of Phagocytic Cells, *Eur. J. Pharmacol. 383,* 83–91.
19. Lowry, O.H., Rosebrough, N.J., Farr, A.L., and Randall, R.J. (1957) Protein Measurement with Folin Phenol Reagent, *J. Biol. Chem. 193,* 265–275.
20. Carr, A., Hawkins, C.L., Thomas, S.R., Stocker, R., and Frei, B. (2001) Relative Reactivities of N-Chloramines and Hypochlorous Acid with Human Plasma Constituents, *Free Rad. Biol. Med. 30,* 526–536.
21. Sala, A., Zarini, S., Folco, G., Murphy, R.C., and Henson, P.M. (1999) Differential Metabolism of Exogenous and Endogenous Arachidonic Acid in Human Neutrophils, *J. Biol. Chem. 274,* 28264–28269.
22. Kuebler, W.M., Abels, C., Schuerer, L., and Goetz, A.E. (1996) Measurement of Neutrophil Content in Brain and Lung Tissue by a Modified Myeloperoxidase Assay, *Int. J. Microcirc. Clin. Exp. 16,* 89–97.
23. Carr, A.C., Tijerina, T., and Frei, B. (2000) Vitamin C Protects Against and Reverses Specific Hypochlorous Acid- and Chloramine-Dependent Modifications of Low-Density Lipoprotein, *Biochem. J. 346 (Pt. 2),* 491–9.
24. Hurst, J.K. (2002) Whence Nitrotyrosine? *J. Clin. Invest. 109*, 1287-1289.
25. Panasenko, O.M., and Sergienko, V.I. (2001) Hypochlorite, Oxidative Modification of Plasma Lipoproteins, and Atherosclerosis, *Bull. Exp. Biol. Med. 131,* 407–415.
26. Winterbourn, C.C., and Kettle, A.J. (2000) Biomarkers of Myeloperoxidase-Derived Hypochlorous Acid, *Free Rad. Biol. Med. 29,* 403–409.
27. Jolivalt, C., Leininger-Muller, B., Drozdz, R., Naskalski, J.W., and Siest, G. (1996) Apolipoprotein E Is Highly Susceptible to Oxidation by Myeloperoxidase, an Enzyme Present in the Brain, *Neurosci. Lett. 210,* 61–64.
28. Panzenboeck, U., Raitmayer, S., Reicher, H., Lindner, H., Glatter, O., Malle, E., and Sattler, W. (1997) Effects of Reagent and Enzymatically Generated Hypochlorite on Physicochemical and Metabolic Properties of High Density Lipoproteins, *J. Biol. Chem. 272,* 29711–29720.
29. Carr, A.C., van den Berg, J.J., and Winterbourn, C.C. (1996) Chlorination of Cholesterol in Cell Membranes by Hypochlorous Acid, *Arch. Biochem. Biophys. 332,* 63–69.
30. Woods, A.A., and Davies, M.J. (2003) Fragmentation of Extracellular Matrix by Hypochlorous Acid, *Biochem. J. 376,* 219–227.
31. Young, I.S., and Woodside, J.V. (2001) Antioxidants in Health and Disease, *J. Clin. Pathol. 54,* 176–186.
32. Nguyen, T., Sherratt, P.J., and Pickett, C.B. (2003) Regulatory Mechanisms Controlling Gene Expression Mediated by the Antioxidant Response Element, *Annu. Rev. Pharmacol. Toxicol. 43,* 233–260.
33. Iriti, M., and Faoro, F. (2004) Plant Defense & Human Nutrition: Phenylpropanoids on the Menu, *Curr. Top. Nutr. Res. 2,* 47–65.
34. Kok, F.J., and Kromhout, D. (2004) Atherosclerosis. Epidemiological Studies on the Health Effects of a Mediterranean Diet, *Eur. J. Nutr. 43 (Suppl. 1),* I2–I5.
35. Daels-Rakotoarison, D.A., Gressier, B., Trotin, F., Brunet, C., Luyckx, M., Dine, T., Bailleul, F., Cazin, M., and Cazin, J.C. (2002) Effects of *Rosa canina* Fruit Extract on Neutrophil Respiratory Burst, *Phytother. Res. 16,* 157–161.
36. Valentao, P., Fernandes, E., Carvalho, F., Andrade, P.B., Seabra, R.M., and Bastos, M.L. (2002) Antioxidative Properties of Cardoon (*Cynara cardunculus* L.) Infusion Against Superoxide Radical, Hydroxyl Radical, and Hypochlorous Acid, *J. Agric. Food Chem. 50,* 4989–4993.
37. Llorach, R., Espin, J.C., Tomas-Barberan, F.A., and Ferreres, F. (2002) Artichoke (*Cynara scolymus* L.) Byproducts as a Potential Source of Health-Promoting Antioxidant Phenolics, *J. Agric. Food Chem. 50,* 3458–3464.
38. Jimenez-Escrig, A., Dragsted, L.O., Daneshvar, B., Pulido, R., and Saura-Calixto, F. (2003) In Vitro Antioxidant Activities of Edible Artichoke (*Cynara scolymus* L.) and Effect on Biomarkers of Antioxidants in Rats, *J. Agric. Food Chem. 51,* 5540–5545.
39. Vardar-Unlu, G., Candan, F., Sokmen, A., Daferera, D., Polissiou, M., Sokmen, M., Donmez, E., and Tepe, B. (2003) Antimicrobial and Antioxidant Activity of the Essential Oil and Methanol Extracts of *Thymus pectinatus* Fisch et Mey Var. *pectinatus* (Lamiaceae), *J. Agric. Food Chem. 51,* 63–67.
40. Tomas-Barberan, F.A., Hernandez, L., Ferreres, F., and Tomas, F. (1985) Highly Methylated 6-Hydroxyflavones and Other Flavonoids from *Thymus piperella*, *Planta Med. 5,* 452–454.
41. Naderi, G.A., Asgary, S., Sarraf-Zadegan, N., and Shirvany, H. (2003) Anti-Oxidant Effect of Flavonoids on the Susceptibility of LDL Oxidation, *Mol. Cell. Biochem. 246,* 193–196.
42. Butkovic, V., Klasinc, L., and Bors, W. (2004) Kinetic Study of Flavonoid Reactions with Stable Radicals, *J. Agric. Food Chem. 52,* 2816–2820.
43. Cos, P., Hermans, N., Calomme, M., Maes, L., De Bruyne, T., Pieters, L., Vlietinck, A.J., and Vanden Berghe, D. (2003) Com-

parative Study of Eight Well-Known Polyphenolic Antioxidants, *J. Pharm. Pharmacol. 55,* 1291–1297.
44. Merghem, R., Jay, M., Brun, N., and Voirin, B. (2004) Qualitative Analysis and HPLC Isolation and Identification of Procyanidins from *Vicia faba*, *Phytochem. Anal. 15,* 95–99.
45. Mattila, P., Konko, K., Eurola, M., Pihlava, J.M., Astola, J., Vahteristo, L., Hietaniemi, V., Kumpulainen, J., Valtonen, M., and Piironen, V. (2001) Contents of Vitamins, Mineral Elements, and Some Phenolic Compounds in Cultivated Mushrooms, *J. Agric. Food Chem. 49,* 2343–2348.
46. Nakamura, M., Nagayoshi, R., Ijiri, K., Nakashima-Matsushita, N., Takeuchi, T., and Matsuyama, T. (2002) Nitration and Chlorination of Folic Acid by Peroxynitrite and Hypochlorous Acid, and the Selective Binding of 10-Nitro-Folate to Folate Receptor Beta, *Biochem. Biophys. Res. Commun. 297,* 1238–1244.
47. Proteggente, A.R., Pannala, A.S., Paganga, G., Van Buren, L., Wagner, E., Wiseman, S., Van De, P.F., Dacombe, C., and Rice-Evans, C.A. (2002) The Antioxidant Activity of Regularly Consumed Fruit and Vegetables Reflects Their Phenolic and Vitamin C Composition, *Free Rad. Res. 36,* 217–233.
48. Winterbourn, C.C., van den Berg, J.J., Roitman, E., and Kuypers, F.A. (1992) Chlorohydrin Formation from Unsaturated Fatty Acids Reacted with Hypochlorous Acid, *Arch. Biochem. Biophys. 296,* 547–555.
49. Bailey, A.L., and Southon, S. (1998) Determination of Total Long-Chain Fatty Acids in Human Plasma and Lipoproteins, Before and During Copper-Stimulated Oxidation, by High-Performance Liquid Chromatography, *Anal. Chem. 70,* 415–419.
50. Jerlich, A., Fabjan, J.S., Tschabuschnig, S., Smirnova, A.V., Horakova, L., Hayn, M., Auer, H., Guttenberger, H., Leis, H.J., Tatzber, F., Waeg, G., and Schaur, R.J. (1998) Human Low Density Lipoprotein as a Target of Hypochlorite Generated by Myeloperoxidase, *Free Rad. Biol. Med. 24,* 1139–1148.
51. McCall, M.R., Carr, A.C., Forte, T.M., and Frei, B. (2001) LDL Modified by Hypochlorous Acid Is a Potent Inhibitor of Lecithin-Cholesterol Acyltransferase Activity, *Arterioscler. Thromb. Vasc. Biol. 21,* 1040–1045.
52. Zhang, R., Brennan, M.L., Fu, X., Aviles, R.J., Pearce, G.L., Penn, M.S., Topol, E.J., Sprecher, D.L., and Hazen, S.L. (2001) Association Between Myeloperoxidase Levels and Risk of Coronary Artery Disease, *JAMA 286,* 2136–2142.
53. Brennan, M.L., Penn, M.S., Van Lente, F., Nambi, V., Shishehbor, M.H., Aviles, R.J., Goormastic, M., Pepoy, M.L., McErlean, E.S., Topol, E.J., Nissen, S.E., and Hazen, S.L. (2003) Prognostic Value of Myeloperoxidase in Patients with Chest Pain, *N. Engl. J. Med. 349,* 1595–1604.
54. Brennan, M.L., and Hazen, S.L. (2003) Emerging Role of Myeloperoxidase and Oxidant Stress Markers in Cardiovascular Risk Assessment, *Curr. Opin. Lipidol. 14,* 353–359.
55. Baldus, S., Heeschen, C., Meinertz, T., Zeiher, A.M., Eiserich, J.P., Munzel, T., Simoons, M.L., and Hamm, C.W. (2003) Myeloperoxidase Serum Levels Predict Risk in Patients with Acute Coronary Syndromes, *Circulation 108,* 1440–1445.
56. Jerlich, A., Fritz, G., Kharrazi, H., Hammel, M., Tschabuschnig, S., Glatter, O., and Schaur, R.J. (2000) Comparison of HOCl Traps with Myeloperoxidase Inhibitors in Prevention of Low Density Lipoprotein Oxidation, *Biochim. Biophys. Acta 1481,* 109–118.
57. Pincemail, J., Deby, C., Thirion, A., Bruyn-Dister, M., and Goutier, R. (1988) Human Myeloperoxidase Activity Is Inhibited In Vitro by Quercetin: Comparison with Three Related Compounds, *Experientia 44,* 450–453.
58. Kostyuk, V.A., Kraemer, T., Sies, H., and Schewe, T. (2003) Myeloperoxidase/Nitrite-Mediated Lipid Peroxidation of Low-Density Lipoprotein as Modulated by Flavonoids, *FEBS Lett. 537,* 146–150.
59. Pabuccuoglu, A., Konyalioglu, S., Bas, M., and Meral, G.E. (2003) The In Vitro Effects of Hypericum Species on Human Leukocyte Myeloperoxidase Activity, *J. Ethnopharmacol. 87,* 89–92.
60. Limasset, B., le Doucen, C., Dore, J.C., Ojasoo, T., Damon, M., and Crastes, d.P. (1993) Effects of Flavonoids on the Release of Reactive Oxygen Species by Stimulated Human Neutrophils: Multivariate Analysis of Structure-Activity Relationships (SAR), *Biochem. Pharmacol. 46,* 1257–1271.
61. Visioli, F., Bellomo, G., and Galli, C. (1998) Free Radical-Scavenging Properties of Olive Oil Polyphenols, *Biochem. Biophys. Res. Commun. 247,* 60–64.
62. Ischiropoulos, H., and Beckman, J.S. (2003) Oxidative Stress and Nitration in Neurodegeneration: Cause, Effect, or Association? *J. Clin. Invest. 111,* 163–169.
63. Manach, C., Scalbert, A., Morand, C., Remesy, C., and Jimenez, L. (2004) Polyphenols: Food Sources and Bioavailability, *Am. J. Clin. Nutr. 79,* 727–747.

[Received August 17, 2004; accepted October 17, 2004]